ASM HANDBOOK®

VOLUME

6

WELDING BRAZING AND SOLDERING

ASM INTERNATIONAL®

WELDING, BRAZING, AND SOLDERING WAS PUBLISHED IN 1993 AS VOLUME 6 OF THE ASM HANDBOOK. THE VOLUME WAS PREPARED UNDER THE DIRECTION OF THE ASM HANDBOOK COMMITTEE.

VOLUME CHAIRMEN

THE VOLUME CHAIRMEN WERE DAVID LEROY OLSON, THOMAS A. SIEWERT, STEPHEN LIU, AND GLEN R. EDWARDS.

AUTHORS

- **LAMET** UFRGS
- **BRUNO L. ALIA**
- **RICHARD L. ALLEY** AMERICAN WELDING SOCIETY
- **WILLIAM R. APBLETT, JR.**
- **WILLIAM A. BAESLACK III** THE OHIO STATE UNIVERSITY
- **WILLIAM BALLIS** COLUMBIA GAS OF OHIO
- **CLIFF C. BAMPTON** ROCKWELL INTERNATIONAL SCIENCE CENTER
- **PROBAL BANERJEE** AUBURN UNIVERSITY
- **JOHN G. BANKER** EXPLOSIVE FABRICATORS INC.
- **ROBERT G. BARTIFAY** ALUMINUM COMPANY OF AMERICA
- **ROY I. BATISTA**
- **ROY E. BEAL** AMALGAMATED TECHNOLOGIES INC.
- **RAYMOND E. BOHLMANN** MCDONNELL AIRCRAFT COMPANY
- **SÉRGIO D. BRANDI** ESCOLA POLITECNICA DA USP
- **JOHN A. BROOKS** SANDIA NATIONAL LABORATORIES
- **DONALD W. BUCHOLZ** IBM FEDERAL SYSTEMS CORPORATION
- **PAUL BURGARDT** EG&G ROCKY FLATS PLANT
- **ROGER A. BUSHEY** THE ESAB GROUP INC.
- **CHRIS CABLE** FEIN POWER TOOL
- **RICHARD D. CAMPBELL** JOINING SERVICES INC.
- **HOWARD CARY** HOBART BROTHERS COMPANY
- **HARVEY CASTNER** EDISON WELDING INSTITUTE
- **ALLEN CEDILOTE** INDUSTRIAL TESTING LABORATORY SERVICES
- **HARRY A. CHAMBERS** TRW NELSON STUD WELDING
- **C. CHRIS CHEN** MICROALLOYING INTERNATIONAL INC.
- **SHAOFENG CHEN** AUBURN UNIVERSITY
- **SHAO-PING CHEN** LOS ALAMOS NATIONAL LABORATORY
- **BRYAN A. CHIN** AUBURN UNIVERSITY
- **MICHAEL J. CIESLAK** SANDIA NATIONAL LABORATORIES
- **RODGER E. COOK** THE WILKINSON COMPANY
- **STEPHEN A. COUGHLIN** ACF INDUSTRIES INC.
- **MARK COWELL** METCAL INC.
- **RICHARD S. CREMISIO** RESCORP INTERNATIONAL INC.
- **CARL E. CROSS**
- **CRAIG DALLAM** THE LINCOLN ELECTRIC COMPANY
- **BRIAN DAMKROGER** SANDIA NATIONAL LABORATORIES
- **JOSEPH R. DAVIS** DAVIS AND ASSOCIATES

- **JANET DEVINE** SONOBOND ULTRASONICS
- **PAUL B. DICKERSON**
- **RAY DIXON** LOS ALAMOS NATIONAL LABORATORY
- **SUE DUNKERTON** THE WELDING INSTITUTE
- **KEVIN DUNN** TEXAS INSTRUMENTS INC.
- **CHUCK DVORAK** UNI-HYDRO, INC.
- **JIM DVORAK** UNI-HYDRO, INC.
- **ROBERT J. DYBAS** GENERAL ELECTRIC COMPANY
- **THOMAS W. EAGAR** MASSACHUSETTS INSTITUTE OF TECHNOLOGY
- **GLEN R. EDWARDS** COLORADO SCHOOL OF MINES
- **GRAHAM R. EDWARDS** THE WELDING INSTITUTE
- **W.H. ELLIOTT, JR.** OAK RIDGE NATIONAL LABORATORY
- **JOHN W. ELMER** LAWRENCE LIVERMORE NATIONAL LABORATORY
- **STEVEN C. ERNST** EASTMAN CHEMICAL COMPANY
- **WILLIAM FARRELL** FERRANTI-SCIAKY COMPANY
- **JOEL G. FELDSTEIN** FOSTER WHEELER ENERGY CORPORATION
- **DAVID A. FLEMING** COLORADO SCHOOL OF MINES
- **JAMES A. FORSTER** TEXAS INSTRUMENTS INC.
- **MICHAEL D. FREDERICKSON** ELECTRONICS MANUFACTURING PRODUCTIVITY FACILITY
- **EDWARD FRIEDMAN** WESTINGHOUSE ELECTRIC CORPORATION
- **R.H. FROST** COLORADO SCHOOL OF MINES
- **CHARLES E. FUERSTENAU** LUCAS-MILHAUPT INC.
- **EDWARD B. GEMPLER**
- **STANLEY S. GLICKSTEIN** WESTINGHOUSE ELECTRIC CORPORATION
- **JOHN A. GOLDAK** CARLETON UNIVERSITY
- **ROBIN GORDON** EDISON WELDING INSTITUTE
- **JERRY E. GOULD** EDISON WELDING INSTITUTE
- **JOHN B. GREAVES, JR.** ELECTRONICS MANUFACTURING PRODUCTIVITY FACILITY
- **F. JAMES GRIST**
- **JOHN F. GRUBB** ALLEGHENY LUDLUM STEEL
- **MAOSHI GU** CARLETON UNIVERSITY
- **IAN D. HARRIS** EDISON WELDING INSTITUTE
- **L.J. HART-SMITH** DOUGLAS AIRCRAFT COMPANY
- **DAN HAUSER** EDISON WELDING INSTITUTE
- **C.R. HEIPLE** METALLURGICAL CONSULTANT
- **HERBERT HERMAN** STATE UNIVERSITY OF NEW YORK
- **G. KEN HICKEN** SANDIA NATIONAL LABORATORIES
- **EVAN B. HINSHAW** INCO ALLOYS INTERNATIONAL INC.
- **D. BRUCE HOLLIDAY** WESTINGHOUSE MARINE DIVISION
- **S. IBARRA** AMOCO CORPORATION
- **J. ERNESTO INDACOCHEA** UNIVERSITY OF ILLINOIS AT CHICAGO
- **SUNIL JHA** TEXAS INSTRUMENTS INC.
- **JERALD E. JONES** COLORADO SCHOOL OF MINES
- **RAYMOND H. JUERS** NAVAL SURFACE WARFARE CENTER
- **WILLIAM R. KANNE, JR.** WESTINGHOUSE SAVANNAH RIVER COMPANY
- **MICHAEL J. KARAGOULIS** GENERAL MOTORS CORPORATION
- **MICHAEL KARAVOLIS** TEXAS INSTRUMENTS INC.
- **LENNART KARLSSON** LULEÅ UNIVERSITY OF TECHNOLOGY
- **MICHAEL E. KASSNER** OREGON STATE UNIVERSITY
- **DOUG D. KAUTZ** LAWRENCE LIVERMORE NATIONAL LABORATORY
- **W. DANIEL KAY** WALL COLMONOY CORPORATION
- **JAMES F. KEY** IDAHO NATIONAL ENGINEERING LABORATORY
- **H.-E. KIM** SEOUL NATIONAL UNIVERSITY

- **SAMUEL D. KISER** INCO ALLOYS INTERNATIONAL INC.
- **MARVIN L. KOHN** FMC CORPORATION
- **DAMIAN J. KOTECKI** THE LINCOLN ELECTRIC COMPANY
- **KENNETH KRYSIAC** HERCULES INC.
- **CHUCK LANDRY** THERMAL DYNAMICS
- **CHARLES LANE** DURALCAN
- **H.J. LATIMER** TAYLOR-WINFIELD CORPORATION
- **GLEN S. LAWRENCE** FERRANTI-SCIAKY COMPANY
- **KARL LAZAR**
- **WERNER LEHRHEUER** FORSCHUNGSZENTRUM JÜLICH GMBH
- **ALEXANDER LESNEWICH**
- **J.F. LIBSCH** LEPEL CORPORATION
- **TOM LIENERT** THE OHIO STATE UNIVERSITY
- **ALLEN C. LINGENFELTER** LAWRENCE LIVERMORE NATIONAL LABORATORY
- **DALE L. LINMAN** CENTECH CORPORATION
- **VONNE LINSE** EDISON WELDING INSTITUTE
- **JOHN C. LIPPOLD** EDISON WELDING INSTITUTE
- **JIAYAN LIU** AUBURN UNIVERSITY
- **STEPHEN LIU** COLORADO SCHOOL OF MINES
- **MATTHEW J. LUCAS, JR.** GENERAL ELECTRIC COMPANY
- **KEVIN A. LYTTLE** PRAXAIR INC.
- **KIM MAHIN** SANDIA NATIONAL LABORATORIES
- **MURRAY W. MAHONEY** ROCKWELL INTERNATIONAL SCIENCE CENTER
- **DARRELL MANENTE** VAC-AERO INTERNATIONAL INC.
- **RICHARD P. MARTUKANITZ** PENNSYLVANIA STATE UNIVERSITY
- **KOICHI MASUBUCHI** MASSACHUSETTS INSTITUTE OF TECHNOLOGY
- **DAVID K. MATLOCK** COLORADO SCHOOL OF MINES
- **R.B. MATTESON** TAYLOR-WINFIELD CORPORATION
- **STEVEN J. MATTHEWS** HAYNES INTERNATIONAL INC.
- **JYOTI MAZUMDER** UNIVERSITY OF ILLINOIS AT URBANA-CHAMPAIGN
- **C.N. MCCOWAN** NATIONAL INSTITUTE OF STANDARDS AND TECHNOLOGY
- **KRIS MEEKINS** LONG MANUFACTURING LTD.
- **GREGORY MELEKIAN** GENERAL MOTORS CORPORATION
- **ANTHONY R. MELLINI, SR.** MELLINI AND ASSOCIATES INC.
- **DAVID W. MEYER** THE ESAB GROUP INC.
- **JULE MILLER**
- **HOWARD MIZUHARA** WESGO INC.
- **ARTHUR G. MOORHEAD** OAK RIDGE NATIONAL LABORATORY
- **MILO NANCE** MARTIN MARIETTA ASTRONAUTICS GROUP
- **E.D. NICHOLAS** THE WELDING INSTITUTE
- **DAVID NOBLE** ARCO EXPLORATION AND PRODUCTION TECHNOLOGY
- **THOMAS NORTH** UNIVERSITY OF TORONTO
- **DAVID B. O'DONNELL** INCO ALLOYS INTERNATIONAL INC.
- **JONATHAN S. OGBORN** THE LINCOLN ELECTRIC COMPANY
- **DAVID L. OLSON** COLORADO SCHOOL OF MINES
- **TOSHI OYAMA** WESGO INC.
- **R. ALAN PATTERSON** LOS ALAMOS NATIONAL LABORATORY
- **LARRY PERKINS** WRIGHT LABORATORY
- **DARYL PETER** DARYL PETER AND ASSOCIATES
- **MANFRED PETRI** GERHARD PETRI GMBH & CO. KG
- **DAVID H. PHILLIPS** EDISON WELDING INSTITUTE
- **ABE POLLACK** MICROALLOYING INTERNATIONAL INC.
- **BARRY POLLARD**
- **ANATOL RABINKIN** ALLIEDSIGNAL AMORPHOUS METALS

- **GEETHA RAMARATHNAM** UNIVERSITY OF TORONTO
- **EDWARD G. REINEKE** EXPLOSIVE FABRICATORS INC.
- **JULIAN ROBERTS** THERMATOOL CORPORATION
- **M. NED ROGERS** BATESVILLE CASKET COMPANY
- **J.R. ROPER** EG&G ROCKY FLATS PLANT
- **ROBERT S. ROSEN** LAWRENCE LIVERMORE NATIONAL LABORATORY
- **JAMES E. ROTH** JAMES E. ROTH INC.
- **WILLIAM J. RUPRECHT** GENERAL ELECTRIC COMPANY
- **K. SAMPATH** CONCURRENT TECHNOLOGIES CORPORATION
- **BERNARD E. SCHALTENBRAND** ALUMINUM COMPANY OF AMERICA
- **BERNARD SCHWARTZ** NORFOLK SOUTHERN CORPORATION
- **MEL M. SCHWARTZ** SIKORSKY AIRCRAFT
- **ANN SEVERIN** LUCAS-MILHAUPT INC.
- **THOMAS A. SIEWERT** NATIONAL INSTITUTE OF STANDARDS AND TECHNOLOGY
- **HERSCHEL SMARTT** IDAHO NATIONAL ENGINEERING LABORATORY
- **RONALD B. SMITH** ALLOY RODS CORPORATION
- **WARREN F. SMITH** THERMATOOL CORPORATION
- **LANCE R. SOISSON** WELDING CONSULTANTS INC.
- **HARVEY D. SOLOMON** GENERAL ELECTRIC COMPANY
- **BRUCE R. SOMERS** LEHIGH UNIVERSITY
- **ROBERT E. SOMERS** SOMERS CONSULTANTS
- **ROGER K. STEELE** AAR TECHNICAL CENTER
- **FRANK STEIN** TAYLOR-WINFIELD CORPORATION
- **TIM STOTLER** EDISON WELDING INSTITUTE
- **ROBERT L. STROHL** TWECO/ARCAIR
- **ROBERT A. SULIT** SULIT ENGINEERING
- **VERN SUTTER** AMERICAN WELDING INSTITUTE
- **W.T. TACK** MARTIN MARIETTA
- **R. DAVID THOMAS, JR.** R.D. THOMAS & COMPANY
- **KARL THOMAS** TECHNISCHE UNIVERSITÄT, BRAUNSCHWEIG
- **RAYMOND G. THOMPSON** UNIVERSITY OF ALABAMA AT BIRMINGHAM
- **DONALD J. TILLACK** D.J. TILLACK & ASSOCIATES
- **CHON L. TSAI** THE OHIO STATE UNIVERSITY
- **SCHILLINGS TSANG** EG&G ROCKY FLATS PLANT
- **HENDRIKUS H. VANDERVELDT** AMERICAN WELDING INSTITUTE
- **RICCARDO VANZETTI** VANZETTI SYSTEMS INC.
- **PAUL T. VIANCO** SANDIA NATIONAL LABORATORIES
- **P. RAVI VISHNU** LULEÅ UNIVERSITY OF TECHNOLOGY
- **MARY B. VOLLARO** UNIVERSITY OF CONNECTICUT
- **A. WAHID** COLORADO SCHOOL OF MINES
- **DANIEL W. WALSH** CALIFORNIA POLYTECHNIC STATE UNIVERSITY
- **R. TERRENCE WEBSTER** CONSULTANT
- **JOHN R. WHALEN** CONTOUR SAWS INC.
- **NEVILLE T. WILLIAMS** BRITISH STEEL
- **FRED J. WINSOR** WELDING CONSULTANT
- **R. XU** UNIVERSITY OF ILLINOIS AT CHICAGO
- **XIAOSHU XU** AMERICAN WELDING INSTITUTE
- **PHILIP M. ZARROW** SYNERGISTEK ASSOCIATES

REVIEWERS

- **YONI ADONYI** U.S. STEEL TECHNICAL CENTER
- **RICHARD L. ALLEY** AMERICAN WELDING SOCIETY
- **BERNARD ALTSHULLER** ALCAN INTERNATIONAL LTD.

- **TED L. ANDERSON** TEXAS A&M UNIVERSITY
- **LLOYD ANDERSON** MARION-INDRESCO INC.
- **FRANK G. ARMAO** ALCOA TECHNICAL CENTER
- **DANIEL ARTHUR** TELEDYNE MCKAY
- **RICHARD E. AVERY** NICKEL DEVELOPMENT INSTITUTE
- **R.F. BACON** TECUMSEH PRODUCTS COMPANY
- **WALLY G. BADER**
- **WILLIAM A. BAESLACK III** THE OHIO STATE UNIVERSITY
- **CLIFF C. BAMPTON** ROCKWELL INTERNATIONAL SCIENCE CENTER
- **JOHN G. BANKER** EXPLOSIVE FABRICATORS INC.
- **GEORGE C. BARNES**
- **ROBERT G. BARTIFAY** ALUMINUM COMPANY OF AMERICA
- **ROY E. BEAL** AMALGAMATED TECHNOLOGIES INC.
- **GARY BECKA** ALLIEDSIGNAL AEROSPACE COMPANY
- **DAN BEESON** EXXON PRODUCTION MALAYSIA
- **DAVID M. BENETEAU** CENTERLINE (WINDSOR) LTD.
- **CHRISTOPHER C. BERNDT** THE THERMAL SPRAY LABORATORY
- **SURENDRA BHARGAVA** GENERAL MOTORS INC.
- **NORMAN C. BINKLEY** EDISON WELDING INSTITUTE
- **ROBERT A. BISHEL** INCO ALLOYS INTERNATIONAL INC.
- **R.A. BLACK** BLACKS EQUIPMENT LTD.
- **OMER W. BLODGETT** THE LINCOLN ELECTRIC COMPANY
- **RICHARD A. BRAINARD** GENERAL DYNAMICS LAND SYSTEMS DIVISION
- **GLENN H. BRAVE** ASSOCIATION OF AMERICAN RAILROADS
- **ROBERT S. BROWN** CARPENTER TECHNOLOGY CORPORATION
- **WILLIAM A. BRUCE** EDISON WELDING INSTITUTE
- **CHUCK CADDEN** GENERAL MOTORS
- **HARVEY R. CASTNER** EDISON WELDING INSTITUTE
- **ALLEN B. CEDILOTE** INDUSTRIAL TESTING LABORATORY SERVICES CORPORATION
- **KENNETH D. CHALLENGER** SAN JOSE STATE UNIVERSITY
- **P.R. CHIDAMBARAM** COLORADO SCHOOL OF MINES
- **BOB CHRISTOFFEL**
- **ROBIN CHURCHILL** ESCO CORPORATION
- **MICHAEL J. CIESLAK** SANDIA NATIONAL LABORATORIES
- **BRADLEY A. CLEVELAND** MTS SYSTEMS CORPORATION
- **NANCY C. COLE** OAK RIDGE NATIONAL LABORATORY
- **HAROLD R. CONAWAY** ROCKWELL INTERNATIONAL
- **RICHARD B. CORBIT** GENERAL PUBLIC UTILITIES NUCLEAR CORPORATION
- **MARK COWELL** METCAL INC.
- **NORM COX** RESEARCH INC.
- **JOHN A. CRAWFORD** NAVAL SURFACE WARFARE CENTER
- **DENNIS D. CROCKETT** THE LINCOLN ELECTRIC COMPANY
- **CARL E. CROSS**
- **NARENDRA B. DAHOTRE** UNIVERSITY OF TENNESSEE SPACE INSTITUTE
- **T. DEBROY** PENNSYLVANIA STATE UNIVERSITY
- **JOSEPH DEVITO** THE ESAB GROUP INC.
- **JOHN A. DEVORE** GENERAL ELECTRIC COMPANY
- **PAUL B. DICKERSON**
- **RAY DIXON** LOS ALAMOS NATIONAL LABORATORY
- **KARL E. DORSCHU** WELDRING COMPANY INC.
- **ROBERT J. DYBAS** GENERAL ELECTRIC COMPANY
- **THOMAS W. EAGAR** MASSACHUSETTS INSTITUTE OF TECHNOLOGY
- **BRUCE J. EBERHARD** WESTINGHOUSE SAVANNAH RIVER COMPANY
- **GLEN R. EDWARDS** COLORADO SCHOOL OF MINES

- **JOHN W. ELMER** LAWRENCE LIVERMORE NATIONAL LABORATORY
- **WERNER ENGELMAIER** ENGELMAIER ASSOCIATES INC.
- **CHRIS ENGLISH** GE AIRCRAFT ENGINES
- **ROBERT G. FAIRBANKS** SCARROTT METALLURGICAL COMPANY
- **HOWARD N. FARMER** CONSULTANT
- **DAVID A. FLEMING** COLORADO SCHOOL OF MINES
- **ROBERT FOLEY** COLORADO SCHOOL OF MINES
- **BOBBY FOLKENING** FMC GROUND SYSTEMS DIVISION
- **DARREL FREAR** SANDIA NATIONAL LABORATORIES
- **MICHAEL D. FREDERICKSON** ELECTRONICS MANUFACTURING PRODUCTIVITY FACILITY
- **EUGENE R. FREULER** SOUDRONIC NEFTENBACH AG
- **STEVEN A. GEDEON** WELDING INSTITUTE OF CANADA
- **BOB GIBBONS** PLS MATERIALS INC.
- **PAUL S. GILMAN** ALLIEDSIGNAL INC.
- **STANLEY S. GLICKSTEIN** WESTINGHOUSE ELECTRIC CORPORATION
- **JOHN A. GOLDAK** CARLETON UNIVERSITY
- **CARL GRAF** EDISON WELDING INSTITUTE
- **WILLIAM L. GREEN** THE OHIO STATE UNIVERSITY
- **CHUCK GREGOIRE** NATIONAL STEEL CORPORATION
- **ROBERT A. GRIMM** EDISON WELDING INSTITUTE
- **BRIAN GRINSELL** THOMPSON WELDING INC.
- **ROBIN GROSS-GOURLEY** WESTINGHOUSE
- **JOHN F. GRUBB** ALLEGHENY LUDLUM STEEL
- **BOB GUNOW, JR.** VAC-MET INC.
- **C. HOWARD HAMILTON** WASHINGTON STATE UNIVERSITY
- **JAMES R. HANNAHS** PMI FOOD EQUIPMENT GROUP
- **FRANK HANNEY** ABCO WELDING & INDUSTRIAL SUPPLY INC.
- **DAVID E. HARDT** MASSACHUSETTS INSTITUTE OF TECHNOLOGY
- **IAN D. HARRIS** EDISON WELDING INSTITUTE
- **MARK J. HATZENBELLER** KRUEGER INTERNATIONAL
- **DAN HAUSER** EDISON WELDING INSTITUTE
- **C.R. HEIPLE** METALLURGICAL CONSULTANT
- **J.S. HETHERINGTON** HETHERINGTON INC.
- **BARRY S. HEUER** NOOTER CORPORATION
- **ROGER B. HIRSCH** UNITROL ELECTRONICS INC.
- **TIM P. HIRTHE** LUCAS-MILHAUPT
- **HUGH B. HIX** INTERNATIONAL EXPLOSIVE METALWORKING ASSOCIATION
- **F. GALEN HODGE** HAYNES INTERNATIONAL INC.
- **RICHARD L. HOLDREN** WELDING CONSULTANTS INC.
- **ALAN B. HOPPER** ROBERTSHAW TENNESSEE DIVISION
- **CHARLES HUTCHINS** C. HUTCHINS AND ASSOCIATES
- **JENNIE S. HWANG** IEM-FUSION INC.
- **S. IBARRA** AMOCO CORPORATION
- **J. ERNESTO INDACOCHEA** UNIVERSITY OF ILLINOIS AT CHICAGO
- **GARY IRONS** HOBART TAFA TECHNOLOGIES INC.
- **JAMES R. JACHNA** MODINE MANUFACTURING COMPANY
- **ROBERT G. JAITE** WOLFENDEN INDUSTRIES INC.
- **JOHN C. JENKINS** CONSULTANT
- **KATHI JOHNSON** HEXACON ELECTRIC COMPANY
- **WILLIAM R. JONES** VACUUM FURNACE SYSTEMS CORPORATION
- **ROBERT W. JUD** CHRYSLER CORPORATION
- **WILLIAM F. KAUKLER** UNIVERSITY OF ALABAMA IN HUNTSVILLE
- **DOUG D. KAUTZ** LAWRENCE LIVERMORE NATIONAL LABORATORY

- **W. DANIEL KAY** WALL COLMONOY CORPORATION
- **JACQUE KENNEDY** WESTINGHOUSE
- **JAMES F. KING** OAK RIDGE NATIONAL LABORATORY
- **ANDREW G. KIRETA** COPPER DEVELOPMENT ASSOCIATION INC.
- **SAMUEL D. KISER** INCO ALLOYS INTERNATIONAL INC.
- **JOSEPH H. KISSEL** ITT STANDARD
- **FRED KOHLER** CONSULTANT
- **M.L. KOHN** FMC CORPORATION
- **DAMIAN J. KOTECKI** THE LINCOLN ELECTRIC COMPANY
- **SINDO KOU** UNIVERSITY OF WISCONSIN-MADISON
- **CURTIS W. KOVACH** TECHNICAL MARKETING RESOURCES INC.
- **LAWRENCE S. KRAMER** MARTIN MARIETTA LABORATORIES
- **RAYMOND B. KRIEGER** AMERICAN CYANAMID COMPANY
- **KENNETH KRYSIAC** HERCULES INC.
- **DANIEL KURUZAR** MANUFACTURING TECHNOLOGY INC.
- **RICHARD A. LAFAVE** ELLIOTT COMPANY
- **FRANK B. LAKE** THE ESAB GROUP INC.
- **JOHN D. LANDES** UNIVERSITY OF TENNESSEE
- **WERNER LEHRHEUER** FORSCHUNGSZENTRUM JÜLICH GMBH
- **J.F. LIBSCH** LEPEL CORPORATION
- **VONNE LINSE** EDISON WELDING INSTITUTE
- **JOHN C. LIPPOLD** EDISON WELDING INSTITUTE
- **STEPHEN LIU** COLORADO SCHOOL OF MINES
- **RONALD LOEHMAN** ADVANCED MATERIALS LABORATORY
- **PAUL T. LOVEJOY** ALLEGHENY LUDLUM STEEL
- **GEORGE LUCEY** U.S. ARMY LABORATORY COMMAND
- **KEVIN A. LYTTLE** PRAXAIR INC.
- **COLIN MACKAY** MICROELECTRONICS AND COMPUTER TECHNOLOGY CORPORATION
- **MICHAEL C. MAGUIRE** SANDIA NATIONAL LABORATORIES
- **KIM W. MAHIN** SANDIA NATIONAL LABORATORIES
- **WILLIAM E. MANCINI** DUPONT
- **DARRELL MANENTE** VAC-AERO INTERNATIONAL INC.
- **AUGUST F. MANZ** A.F. MANZ ASSOCIATES
- **RICHARD P. MARTUKANITZ** PENNSYLVANIA STATE UNIVERSITY
- **KOICHI MASUBUCHI** MASSACHUSETTS INSTITUTE OF TECHNOLOGY
- **STEVEN J. MATTHEWS** HAYNES INTERNATIONAL
- **JYOTI MAZUMDER** UNIVERSITY OF ILLINOIS AT URBANA-CHAMPAIGN
- **JIM MCMAHON** DOALL COMPANY
- **ALAN MEIER** COLORADO SCHOOL OF MINES
- **STANLEY MERRICK** TELEDYNE MCKAY
- **ROBERT W. MESSLER, JR.** RENSSELAER POLYTECHNIC INSTITUTE
- **E.A. METZBOWER** U.S. NAVAL RESEARCH LABORATORY
- **JOEL MILANO** DAVID TAYLOR MODEL BASIN
- **ROBERT A. MILLER** SULZER PLASMA TECHNIK INC.
- **HERBERT W. MISHLER** EDISON WELDING INSTITUTE
- **BRAJENDRA MISHRA** COLORADO SCHOOL OF MINES
- **HOWARD MIZUHARA** WESGO INC.
- **RICHARD MONTANA** MID-FLORIDA TECHNICAL INSTITUTE
- **JERRY MOODY** WORLD WIDE WELDING
- **RICHARD A. MORRIS** NAVAL SURFACE WARFARE CENTER
- **P.J. MUDGE** THE WELDING INSTITUTE
- **AMIYA MUKHERJEE** UNIVERSITY OF CALIFORNIA
- **BILL MYERS** DRESSER-RAND INC.

- **ERNEST F. NIPPES** CONSULTANT
- **DONG WON OH** COLORADO SCHOOL OF MINES
- **DAVID L. OLSON** COLORADO SCHOOL OF MINES
- **EDGAR D. OPPENHEIMER** CONSULTING ENGINEER
- **CARMEN PAPONETTI** HI TECMETAL GROUP INC.
- **MADHU PAREKH** HOBART BROTHERS COMPANY
- **SUBHASH R. PATI** INTERNATIONAL PAPER COMPANY
- **R. ALAN PATTERSON** LOS ALAMOS NATIONAL LABORATORIES
- **CHARLES C. PEASE** CP METALLURGICAL
- **ROBERT LEON PEASLEE** WALL COLMONOY CORPORATION
- **DARYL PETER** DARYL PETER & ASSOCIATES
- **LORENZ PFEIFER**
- **JOHN F. PFLZNIENSKI** KOLENE CORPORATION
- **DAVID H. PHILLIPS** EDISON WELDING INSTITUTE
- **EARL W. PICKERING, JR.** CONSULTANT
- **E.R. PIERRE** CONSULTING WELDING ADVISOR
- **JOHN PILLING** MICHIGAN TECHNOLOGICAL UNIVERSITY
- **ABE POLLACK** MICROALLOYING INTERNATIONAL INC.
- **BARRY POLLARD**
- **ALEXANDRE M. POPE** COLORADO SCHOOL OF MINES
- **JEFFREY W. POST** J.W. POST & ASSOCIATES INC.
- **TERRY PROFUGHI** HI TECMETAL GROUP INC.
- **ANATOL RABINKIN** ALLIEDSIGNAL AMORPHOUS METALS
- **JIM D. RABY** SOLDERING TECH INTERNATIONAL
- **TED RENSHAW** CONSULTANT
- **THERESA ROBERTS** SIKAMA INTERNATIONAL
- **DAVID E. ROBERTSON** PACE INC.
- **CHARLES ROBINO** SANDIA NATIONAL LABORATORIES
- **M.N. ROGERS** ABB POWER T&D COMPANY INC.
- **J.R. ROPER** EG&G ROCKY FLATS PLANT
- **N.V. ROSS** AJAX MAGNETHERMIC
- **DIETRICH K. ROTH** ROMAN MANUFACTURING INC.
- **JOHN RUFFING** 3M FLUIDS LABORATORY
- **WAYNE D. RUPERT** ENGLEHARD CORPORATION
- **J.D. RUSSELL** THE WELDING INSTITUTE
- **C.O. RUUD** PENNSYLVANIA STATE UNIVERSITY
- **EDMUND F. RYBICKI** UNIVERSITY OF TULSA
- **JONATHAN T. SALKIN** ARC APPLICATIONS INC.
- **MEL M. SCHWARTZ** SIKORSKY AIRCRAFT
- **JOE L. SCOTT** DEVASCO INTERNATIONAL INC.
- **ALAN P. SEIDLER** RMI TITANIUM COMPANY
- **OSCAR W. SETH** CHICAGO BRIDGE & IRON COMPANY
- **ANN SEVERIN** LUCAS-MILHAUPT INC.
- **LEWIS E. SHOEMAKER** INCO ALLOYS INTERNATIONAL INC.
- **LYNN E. SHOWALTER** NEWPORT NEWS SHIPBUILDING
- **THOMAS A. SIEWERT** NATIONAL INSTITUTE OF STANDARDS AND TECHNOLOGY
- **ALLEN W. SINDEL** BEGEMANN HEAVY INDUSTRIES INC.
- **MICHAEL H. SKILLINGBERG** REYNOLDS METALS COMPANY
- **GERALD M. SLAUGHTER** OAK RIDGE NATIONAL LABORATORY
- **HERSCHEL SMARTT** IDAHO NATIONAL ENGINEERING LABORATORY
- **JAMES P. SNYDER II** BETHLEHEM STEEL CORPORATION
- **LANCE R. SOISSON** WELDING CONSULTANTS INC.
- **HARVEY D. SOLOMON** GENERAL ELECTRIC
- **BRUCE R. SOMERS** LEHIGH UNIVERSITY

- **NARASI SRIDHAR** SOUTHWEST RESEARCH INSTITUTE
- **BOB STANLEY** NATIONAL TRAINING FUND
- **ROGER K. STEELE** ASSOCIATION OF AMERICAN RAILROADS
- **ARCHIE STEVENSON** MAGNESIUM ELEKRON INC.
- **VIJAY K. STOKES** GENERAL ELECTRIC
- **TIM STOTLER** EDISON WELDING INSTITUTE
- **M.A. STREICHER** CONSULTANT
- **ROBERT L. STROHL** TWECO/ARCAIR
- **LAWRENCE STRYKER** ALTECH INTERNATIONAL
- **MARK TARBY** WALL COLMONOY CORPORATION
- **CLAY TAYLOR** MERRICK AND COMPANY
- **J.R. TERRILL** CONSULTANT
- **RAYMOND G. THOMPSON** UNIVERSITY OF ALABAMA AT BIRMINGHAM
- **J.S. THROWER** GENERAL ELECTRIC POWER GENERATION
- **DONALD J. TILLACK** D.J. TILLACK & ASSOCIATES
- **FELIX TOMEI** TRUMPF INC.
- **CHON L. TSAI** THE OHIO STATE UNIVERSITY
- **SCHILLINGS TSANG** EG&G ROCKY FLATS PLANT
- **M. NASIM UDDIN** THYSSEN STEEL GROUP
- **ELMAR UPITIS** CBI TECHNICAL SERVICES COMPANY
- **JAMES VAN DEN AVYLE** SANDI NATIONAL LABORATORIES
- **CLARENCE VAN DYKE** LUCAS-MIHAUPT INC.
- **HENDRIKUS H. VANDERVELDT** AMERICAN WELDING INSTITUTE
- **DAVID B. VEVERKA** EDISON WELDING INSTITUTE
- **PAUL T. VIANCO** SANDIA NATIONAL LABORATORIES
- **ROBERT G. VOLLMER**
- **R. WALLACH** UNIVERSITY OF CAMBRIDGE
- **SANDRA J. WALMSLEY** WESTINGHOUSE ELECTRIC CORPORATION
- **RICHARD A. WATSON** THE P&LE CAR COMPANY
- **CHRIS WEHLUS** GENERAL MOTORS
- **C.E.T. WHITE** INDIUM CORPORATION OF AMERICA
- **ROGER N. WILD**
- **ELLIOTT WILLNER** LOCKHEED MISSILES & SPACE COMPANY
- **RICHARD WILSON** HOUSTON LIGHTING AND POWER COMPANY
- **W.L. WINTERBOTTOM** FORD MOTOR COMPANY
- **A.P. WOODFIELD** GENERAL ELECTRIC AIRCRAFT ENGINES
- **JAMES B.C. WU** STOODY COMPANY
- **THOMAS ZACHARIA** OAK RIDGE NATIONAL LABORATORY

FOREWORD

COVERAGE OF JOINING TECHNOLOGIES IN THE *ASM HANDBOOK* HAS GROWN DRAMATICALLY OVER THE YEARS. A SHORT CHAPTER ON WELDING--EQUAL IN SIZE TO ABOUT 5 PAGES OF TODAY'S *ASM HANDBOOK*--APPEARED IN THE 1933 EDITION OF THE *NATIONAL METALS HANDBOOK* PUBLISHED BY THE AMERICAN SOCIETY OF STEEL TREATERS, ASM'S PREDECESSOR. THAT MATERIAL WAS EXPANDED TO 13 PAGES IN THE CLASSIC 1948 EDITION OF *METALS HANDBOOK*. THE FIRST FULL VOLUME ON WELDING AND BRAZING IN THE SERIES APPEARED IN 1971, WITH PUBLICATION OF VOLUME 6 OF THE 8TH EDITION OF *METALS HANDBOOK*. VOLUME 6 OF THE 9TH EDITION, PUBLISHED IN 1983, WAS EXPANDED TO INCLUDE COVERAGE OF SOLDERING.

THE NEW VOLUME 6 OF THE *ASM HANDBOOK* BUILDS ON THE PROUD TRADITION ESTABLISHED BY THESE PREVIOUS VOLUMES, BUT IT ALSO REPRESENTS A BOLD NEW STEP FOR THE SERIES. THE HANDBOOK HAS NOT ONLY BEEN REVISED, BUT ALSO ENTIRELY

REFORMATTED TO MEET THE NEEDS OF TODAY'S MATERIALS COMMUNITY. OVER 90% OF THE ARTICLES IN THIS VOLUME ARE BRAND-NEW, AND THE REMAINDER HAVE BEEN SUBSTANTIALLY REVISED. MORE SPACE HAS BEEN DEVOTED TO COVERAGE OF SOLID-STATE WELDING PROCESSES, MATERIALS SELECTION FOR JOINED ASSEMBLIES, WELDING IN SPECIAL ENVIRONMENTS, QUALITY CONTROL, AND MODELING OF JOINING PROCESSES, TO NAME BUT A FEW. INFORMATION ALSO HAS BEEN ADDED FOR THE FIRST TIME ABOUT JOINING OF SELECTED NONMETALLIC MATERIALS.

WHILE A DELIBERATE ATTEMPT HAS BEEN MADE TO INCREASE THE AMOUNT OF CUTTING-EDGE INFORMATION PROVIDED, THE ORGANIZERS HAVE WORKED HARD TO ENSURE THAT THE HEART OF THE BOOK REMAINS PRACTICAL INFORMATION ABOUT JOINING PROCESSES, APPLICATIONS, AND MATERIALS WELDABILITY--THE TYPE OF INFORMATION THAT IS THE HALLMARK OF THE *ASM HANDBOOK* SERIES.

PUTTING TOGETHER A VOLUME OF THIS MAGNITUDE IS AN ENORMOUS EFFORT AND COULD NOT HAVE BEEN ACCOMPLISHED WITHOUT THE DEDICATED AND TIRELESS EFFORTS OF THE VOLUME CHAIRPERSONS: DAVID L. OLSON, THOMAS A. SIEWERT, STEPHEN LIU, AND GLEN R. EDWARDS. SPECIAL THANKS ARE ALSO DUE TO THE SECTION CHAIRPERSONS, TO THE MEMBERS OF THE ASM HANDBOOK COMMITTEE, AND TO THE ASM EDITORIAL STAFF. WE ARE ESPECIALLY GRATEFUL TO THE OVER 400 AUTHORS AND REVIEWERS WHO HAVE CONTRIBUTED THEIR TIME AND EXPERTISE IN ORDER TO MAKE THIS HANDBOOK A TRULY OUTSTANDING INFORMATION RESOURCE.

EDWARD H. KOTTCAMP, JR.
PRESIDENT
ASM INTERNATIONAL

EDWARD L. LANGER
MANAGING DIRECTOR
ASM INTERNATIONAL

PREFACE

THE *ASM HANDBOOK,* VOLUME 6, *WELDING, BRAZING, AND SOLDERING,* HAS BEEN ORGANIZED INTO A UNIQUE FORMAT THAT WE BELIEVE WILL PROVIDE HANDBOOK USERS WITH READY ACCESS TO NEEDED MATERIALS-ORIENTED JOINING INFORMATION AT A MINIMAL LEVEL OF FRUSTRATION AND STUDY TIME. WHEN WE DEVELOPED THE ORGANIZATIONAL STRUCTURE FOR THIS VOLUME, WE RECOGNIZED THAT ENGINEERS, TECHNICIANS, RESEARCHERS, DESIGNERS, STUDENTS, AND TEACHERS DO NOT SEEK OUT JOINING INFORMATION WITH THE SAME LEVEL OF UNDERSTANDING, OR WITH THE SAME NEEDS. THEREFORE, WE ESTABLISHED DISTINCT SECTIONS THAT WERE INTENDED TO MEET THE SPECIFIC NEEDS OF PARTICULAR USERS.

THE EXPERIENCED JOINING SPECIALIST CAN TURN TO THE SECTION "CONSUMABLE SELECTION, PROCEDURE DEVELOPMENT, AND PRACTICE CONSIDERATIONS" AND FIND DETAILED JOINING MATERIALS DATA ON A WELL-DEFINED PROBLEM. THIS HANDBOOK ALSO PROVIDES GUIDANCE FOR THOSE WHO NOT ONLY MUST SPECIFY THE JOINING PRACTICE, BUT ALSO THE MATERIALS TO BE JOINED. THE SECTION "MATERIALS SELECTION FOR JOINED ASSEMBLIES" CONTAINS COMPREHENSIVE INFORMATION ABOUT THE PROPERTIES, APPLICATIONS, AND WELDABILITIES OF THE MAJOR CLASSES OF STRUCTURAL MATERIALS. TOGETHER, THESE TWO MAJOR SECTIONS OF THE HANDBOOK SHOULD PROVIDE AN ENGINEER ASSIGNED A LOOSELY DEFINED DESIGN PROBLEM WITH THE MEANS TO MAKE INTELLIGENT CHOICES FOR COMPLETING AN ASSEMBLY.

FREQUENTLY, TECHNOLOGISTS ARE CALLED UPON TO INITIATE AND ADOPT WELDING PROCESSES WITHOUT IN-DEPTH KNOWLEDGE OF THESE PROCESSES OR THE SCIENTIFIC

PRINCIPLES THAT IMPACT THE PROPERTIES AND PERFORMANCE OF WELDMENTS. THE SECTIONS "FUNDAMENTALS OF JOINING" AND "JOINING PROCESSES" ARE DESIGNED TO MEET THE NEEDS OF THESE USERS, OR ANYONE WHO NEEDS BASIC BACKGROUND INFORMATION ABOUT JOINING PROCESSES AND PRINCIPLES.

WELDING, BRAZING, AND SOLDERING ARE TRULY INTERDISCIPLINARY ENTERPRISES; NO INDIVIDUAL CAN BE EXPECTED TO BE AN EXPERT IN ALL ASPECTS OF THESE TECHNOLOGIES. THEREFORE, WE HAVE ATTEMPTED TO PROVIDE A HANDBOOK THAT CAN BE USED AS A COMPREHENSIVE REFERENCE BY ANYONE NEEDING MATERIALS-RELATED JOINING INFORMATION.

MANY COLLEAGUES AND FRIENDS CONTRIBUTED THEIR TIME AND EXPERTISE TO THIS HANDBOOK, AND WE ARE VERY GRATEFUL FOR THEIR EFFORTS. WE WOULD ALSO LIKE TO EXPRESS OUR THANKS TO THE AMERICAN WELDING SOCIETY FOR THEIR COOPERATION AND ASSISTANCE IN THIS ENDEAVOR.

DAVID LEROY OLSON, COLORADO SCHOOL OF MINES

THOMAS A. SIEWERT, NATIONAL INSTITUTE OF STANDARDS AND TECHNOLOGY

STEPHEN LIU, COLORADO SCHOOL OF MINES

GLEN R. EDWARDS, COLORADO SCHOOL OF MINES

- **ROBERT J. BARNHURST** (1988-) NORANDA TECHNOLOGY CENTRE
- **TONI BRUGGER** (1993-) PHOENIX PIPE & TUBE COMPANY
- **STEPHEN J. BURDEN** (1989-)
- **CRAIG V. DARRAGH** (1989-) THE TIMKEN COMPANY
- **RUSSELL J. DIEFENDORF** (1990-) CLEMSON UNIVERSITY
- **AICHA EISHABINI-RIAD** (1990-) VIRGINIA POLYTECHNIC & STATE UNIVERSITY
- **GREGORY A. FETT** (1993-) DANA CORPORATION
- **MICHELLE M. GAUTHIER** (1990-) RAYTHEON COMPANY
- **TONI GROBSTEIN** (1990-) NASA LEWIS RESEARCH CENTER
- **SUSAN HOUSH** (1990-) DOW CHEMICAL U.S.A.
- **DENNIS D. HUFFMAN** (1982-) THE TIMKEN COMPANY
- **S. JIM LBARRA** (1991-) AMOCO RESEARCH CENTER
- **J. ERNESTO INDACOCHEA** (1987-) UNIVERSITY OF ILLINOIS AT CHICAGO
- **PETER W. LEE** (1990-) THE TIMKEN COMPANY
- **WILLIAM L. MANKINS** (1989-) INCO ALLOYS INTERNATIONAL, INC.
- **RICHARD E. ROBERTSON** (1990-) UNIVERSITY OF MICHIGAN
- **JOGENDER SINGH** (1993-) NASA GEORGE C. MARSHALL SPACE FLIGHT CENTER
- **JEREMY C. ST. PIERRE** (1990-) HAYES HEAT TREATING CORPORATION
- **EPHRAIM SUHIR** (1990-) AT&T BELL LABORATORIES
- **KENNETH TATOR** (1991-) KTA-TATOR, INC.
- **MALCOLM THOMAS** (1993-) ALLISON GAS TURBINES
- **WILLIAM B. YOUNG** (1991-) DANA CORPORATION

PREVIOUS CHAIRMEN OF THE ASM HANDBOOK COMMITTEE

- **R.S. ARCHER** (1940-1942) (MEMBER 1937-1942)
- **L.B. CASE** (1931-1933) (MEMBER 1927-1933)
- **T.D. COOPER** (1984-1986) (MEMBER 1981-1986)
- **E.O. DIXON** (1952-1954) (MEMBER 1947-1955)
- **R.L. DOWDELL** (1938-1939) (MEMBER 1935-1939)
- **J.P. GILL** (1937) (MEMBER 1934-1937)
- **J.D. GRAHAM** (1966-1968) (MEMBER 1961-1970)
- **J.F. HARPER** (1923-1926) (MEMBER 1923-1926)
- **C.H. HERTY, JR.** (1934-1936) (MEMBER 1930-1936)
- **D.D. HUFFMAN** (1986-1990) (MEMBER 1982-1990)
- **J.B. JOHNSON** (1948-1951) (MEMBER 1944-1951)
- **L.J. KORB** (1983) (MEMBER 1978-1983)
- **R.W.E. LEITER** (1962-1963) (MEMBER 1955-1958, 1960-1964)
- **G.V. LUERSSEN** (1943-1947) (MEMBER 1942-1947)
- **G.N. MANIAR** (1979-1980) (MEMBER 1974-1980)
- **J.L. MCCALL** (1982) (MEMBER 1977-1982)
- **W.J. MERTEN** (1927-1930) (MEMBER 1923-1933)
- **D.L. OLSON** (1990-1992) (MEMBER 1982-1988, 1989-1992)
- **N.E. PROMISEL** (1955-1961) (MEMBER 1954-1963)
- **G.J. SHUBAT** (1973-1975) (MEMBER 1966-1975)
- **W.A. STADTLER** (1969-1972) (MEMBER 1962-1972)
- **R. WARD** (1976-1978) (MEMBER 1972-1978)
- **M.G.H. WELLS** (1981) (MEMBER 1976-1981)
- **D.J. WRIGHT** (1964-1965) (MEMBER 1959-1967)

STAFF

ASM INTERNATIONAL STAFF WHO CONTRIBUTED TO THE DEVELOPMENT OF THE VOLUME INCLUDED WILLIAM W. SCOTT, JR., DIRECTOR OF TECHNICAL PUBLICATIONS; SCOTT D.

HENRY, MANAGER OF HANDBOOK DEVELOPMENT; SUZANNE E. HAMPSON, PRODUCTION PROJECT MANAGER; THEODORE B. ZORC, TECHNICAL EDITOR; FAITH REIDENBACH, CHIEF COPY EDITOR; LAURIE A. HARRISON, EDITORIAL ASSISTANT; NANCY M. SOBIE, PRODUCTION ASSISTANT. EDITORIAL ASSISTANCE WAS PROVIDED BY JOSEPH R. DAVIS, KELLY FERJUTZ, NIKKI D. WHEATON, AND MARA S. WOODS.

CONVERSION TO ELECTRONIC FILES

ASM HANDBOOK, VOLUME 6, WELDING, BRAZING, AND SOLDERING WAS CONVERTED TO ELECTRONIC FILES IN 1998. THE CONVERSION WAS BASED ON THE SECOND PRINTING (1994). NO SUBSTANTIVE CHANGES WERE MADE TO THE CONTENT OF THE VOLUME, BUT SOME MINOR CORRECTIONS AND CLARIFICATIONS WERE MADE AS NEEDED.

ASM INTERNATIONAL STAFF WHO CONTRIBUTED TO THE CONVERSION OF THE VOLUME INCLUDED SALLY FAHRENHOLZ-MANN, BONNIE SANDERS, SCOTT HENRY, ROBERT BRADDOCK, AND MARLENE SEUFFERT. THE ELECTRONIC VERSION WAS PREPARED UNDER THE DIRECTION OF WILLIAM W. SCOTT, JR., TECHNICAL DIRECTOR, AND MICHAEL J. DEHAEMER, MANAGING DIRECTOR.

COPYRIGHT INFORMATION (FOR PRINT VOLUME)

LIBRARY OF CONGRESS CATALOGING-IN-PUBLICATION DATA (FOR PRINT VOLUME)

ASM HANDBOOK (REVISED VOL. 6) METALS HANDBOOK. VOLS. 1-2 HAVE TITLE:

METALS HANDBOOK. VOL. 4 LACKS ED. STATEMENTS. INCLUDES BIBLIOGRAPHICAL REFERENCES AND INDEXES. CONTENTS: V. 1. PROPERTIES AND SELECTION-IRONS, STEELS, AND HIGH-PERFORMANCE ALLOYS-V. 2. PROPERTIES AND SELECTION-NONFERROUS ALLOYS

AND SPECIAL-PURPOSE MATERIALS-[ETC.]-V. 6. WELDING, BRAZING, AND SOLDERING. 1. METALS-HANDBOOKS, MANUALS, ETC. 2. METAL-WORK-HANDBOOKS, MANUALS, ETC. I. ASM INTERNATIONAL. HANDBOOK COMMITTEE. II. TITLE: METALS HANDBOOK.

TA459.M43 1990 620.1'6 90-115

ISBN 0-87170-377-7(V.1)

SAN 204-7586 ISBN 0-87170-382-3

PRINTED IN THE UNITED STATES OF AMERICA

Energy Sources Used for Fusion Welding

Thomas W. Eagar, Massachusetts Institute of Technology

Introduction

WELDING AND JOINING processes are essential for the development of virtually every manufactured product. However, these processes often appear to consume greater fractions of the product cost and to create more of the production difficulties than might be expected. There are a number of reasons that explain this situation.

First, welding and joining are multifaceted, both in terms of process variations (such as fastening, adhesive bonding, soldering, brazing, arc welding, diffusion bonding, and resistance welding) and in the disciplines needed for problem solving (such as mechanics, materials science, physics, chemistry, and electronics). An engineer with unusually broad and deep training is required to bring these disciplines together and to apply them effectively to a variety of processes.

Second, welding or joining difficulties usually occur far into the manufacturing process, where the relative value of scrapped parts is high.

Third, a very large percentage of product failures occur at joints because they are usually located at the highest stress points of an assembly and are therefore the weakest parts of that assembly. Careful attention to the joining processes can produce great rewards in manufacturing economy and product reliability.

The Section "Fusion Welding Processes" in this Volume provides details about equipment and systems for the major fusion welding processes. The purpose of this Section of the Volume is to discuss the fundamentals of fusion welding processes, with an emphasis on the underlying scientific principles.

Because there are many fusion welding processes, one of the greatest difficulties for the manufacturing engineer is to determine which process will produce acceptable properties at the lowest cost. There are no simple answers. Any change in the part geometry, material, value of the end product, or size of the production run, as well as the availability of joining equipment, can influence the choice of joining method. For small lots of complex parts, fastening may be preferable to welding, whereas for long production runs, welds can be stronger and less expensive.

The perfect joint is indistinguishable from the material surrounding it. Although some processes, such as diffusion bonding, can achieve results that are very close to this ideal, they are either expensive or restricted to use with just a few materials. There is no universal process that performs adequately on all materials in all geometries. Nevertheless, virtually any material can be joined in some way, although joint properties equal to those of the bulk material cannot always be achieved.

The economics of joining a material may limit its usefulness. For example, aluminum is used extensively in aircraft manufacturing and can be joined by using adhesives or fasteners, or by welding. However, none of these processes has proven economical enough to allow the extensive replacement of steel by aluminum in the frames of automobiles. An increased use of composites in aircrafts is limited by an inability to achieve adequate joint strength.

It is essential that the manufacturing engineer work with the designer from the point of product conception to ensure that compatible materials, processes, and properties are selected for the final assembly. Often, the designer leaves the problem of joining the parts to the manufacturing engineer. This can cause an escalation in cost and a decrease in reliability. If the design has been planned carefully and the parts have been produced accurately, the joining process becomes much easier and cheaper, and both the quality and reliability of the product are enhanced.

Generally, any two solids will bond if their surfaces are brought into intimate contact. One factor that generally inhibits this contact is surface contamination. Any freshly produced surface exposed to the atmosphere will absorb oxygen, water vapor, carbon dioxide, and hydrocarbons very rapidly. If it is assumed that each molecule that hits the surface will be absorbed, then the time-pressure value to produce a monolayer of contamination is approximately 0.001 Pa · s (10^{-8} atm · s). For example, at a pressure of 1 Pa (10^{-5} atm), the contamination time is 10^{-3} s, whereas at 0.1 MPa (1 atm), it is only 10×10^{-9} s.

In fusion welding, intimate interfacial contact is achieved by interposing a liquid of substantially similar composition as the base metal. If the surface contamination is soluble, then it is dissolved in the liquid. If it is insoluble, then it will float away from the liquid-solid interface.

Energy Sources Used for Fusion Welding

Thomas W. Eagar, Massachusetts Institute of Technology

Energy-Source Intensity

One distinguishing feature of all fusion welding processes is the intensity of the heat source used to melt the liquid. Virtually every concentrated heat source has been applied to the welding process. However, many of the characteristics of each type of heat source are determined by its intensity. For example, when considering a planar heat source diffusing into a very thick slab, the surface temperature will be a function of both the surface power density and the time.

Figure 1 shows how this temperature will vary on steel with power densities that range from 400 to 8000 W/cm^2. At the lower value, it takes 2 min to melt the surface. If that heat source were a point on the flat surface, then the heat flow would be divergent and might not melt the steel. Rather, the solid metal would be able to conduct away the heat as fast as it was being introduced. It is generally found that heat-source power densities of approximately 1000 W/cm^2 are necessary to melt most metals.

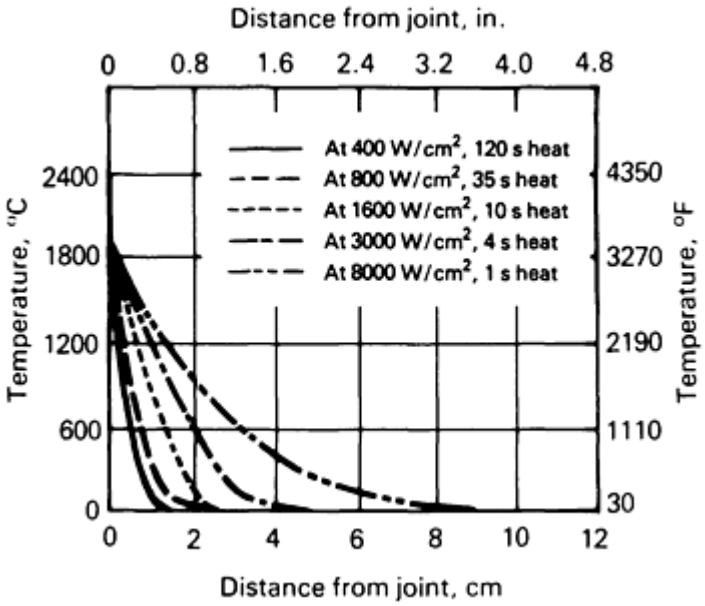

FIG. 1 TEMPERATURE DISTRIBUTION AFTER A SPECIFIC HEATING TIME IN A THICK STEEL PLATE HEATED

UNIFORMLY ON ONE SURFACE AS A FUNCTION OF APPLIED HEAT INTENSITY; INITIAL TEMPERATURE OF PLATE IS 25 °C (77 °F)

At the other end of the power-density spectrum, heat intensities of 10^6 or 10^7 W/cm^2 will vaporize most metals within a few microsecond. At levels above these values, all of the solid that interacts with the heat source will be vaporized, and no fusion welding can occur. Thus, the heat sources for all fusion welding processes should have power densities between approximately 0.001 and 1 MW/cm^2. This power-density spectrum is shown in Fig. 2, along with the points at which common joining processes are employed.

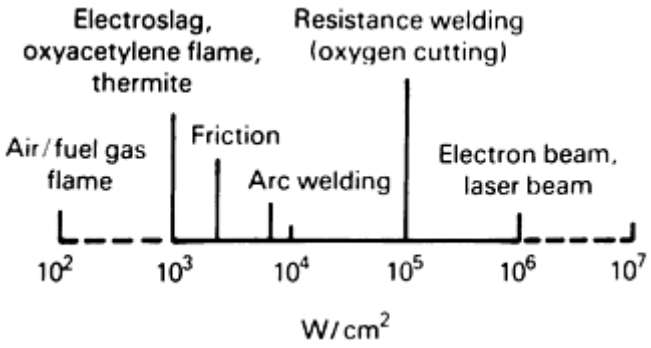

FIG. 2 SPECTRUM OF PRACTICAL HEAT INTENSITIES USED FOR FUSION WELDING

The fact that power density is inversely related to the interaction time of the heat source on the material is evident in Fig. 1. Because this represents a transient heat conduction problem, one can expect the heat to diffuse into the steel to a depth that increases as the square root of time, that is, from the Einstein equation:

$$X \sim \sqrt{a\,t} \qquad \textbf{(EQ 1)}$$

where x is the distance that the heat diffuses into the solid, in centimeters: α is the thermal diffusivity of the solid, in cm^2/s; and t is the time in seconds. Tables 1 and 2 give the thermal diffusivities of common elements and common alloys, respectively.

TABLE 1 THERMAL DIFFUSIVITIES OF COMMON ELEMENTS FROM 20 TO 100 °C (68 TO 212 °F)

ELEMENT	DENSITY		HEAT CAPACITY		THERMAL CONDUCTIVITY		mm^2/s	THERMAL DIFFUSIVITY cm^2/s
	g/cm^3	lb/in.^{3}	j/kg · k	cal$_{it}$/g · °c	w/m · k	cal$_{it}$/cm · s · °c		
ALUMINUM	2.699	0.098	900	0.215	221	0.53	91	0.91
ANTIMONY	6.62	0.239	205	0.049	19	0.045	14	0.14
BERYLLIUM	1.848	0.067	1880	0.45	147	0.35	42	0.42
BISMUTH	9.80	0.354	123	0.0294	8	0.020	7	0.09
CADMIUM	8.65	0.313	230	0.055	92	0.22	46	0.46
CARBON	2.25	0.081	691	0.165	24	0.057	15	0.15
COBALT	8.85	0.320	414	0.099	69	0.165	19	0.188
COPPER	8.96	0.324	385	0.092	394	0.941	114	1.14
GALLIUM	5.907	0.213	331	0.079	29-38	0.07-0.09	17	0.17
GERMANIUM	5.323	0.192	306	0.073	59	0.14	36	0.36
GOLD	19.32	0.698	131	0.0312	297	0.71	118	1.178
HAFNIUM	13.09	0.472	147	0.0351	22	0.053	12	0.12

INDIUM	7.31	0.264	239	0.057	24	0.057	14	0.137
IRIDIUM	22.5	0.813	129	0.0307	59	0.14	20	0.20
IRON	7.87	0.284	460	0.11	75	0.18	21	0.208
LEAD	11.36	0.410	129	0.0309	35	0.083	24	0.236
MAGNESIUM	1.74	0.063	1025	0.245	154	0.367	86	0.86
MOLYBDENUM	10.22	0.369	276	0.066	142	0.34	50	0.50
NICKEL	8.902	0.322	440	0.105	92	0.22	23.5	0.235
NIOBIUM	8.57	0.310	268	0.064	54	0.129	23.6	0.236
PALLADIUM	12.02	0.434	244	0.0584	70	0.168	24	0.24
PLATINUM	21.45	0.775	131	0.0314	69	0.165	24.5	0.245
PLUTONIUM	19.84	0.717	138	0.033	8	0.020	3.0	0.030
RHODIUM	12.44	0.449	247	0.059	88	0.21	29	0.286
SILICON	2.33	0.084	678	0.162	84	0.20	53	0.53
SILVER	10.49	0.379	234	0.0559	418	1.0	170	1.705
SODIUM	0.9712	0.035	1235	0.295	134	0.32	112	1.12
TANTALUM	16.6	0.600	142	0.034	54	0.130	23	0.23
TIN	7.2984	0.264	226	0.054	63	0.150	38	0.38
TITANIUM	4.507	0.163	519	0.124	22	0.052	9	0.092
TUNGSTEN	19.3	0.697	138	0.033	166	0.397	62	0.62
URANIUM	19.07	0.689	117	0.0279	30	0.071	13	0.13
VANADIUM	6.1	0.22	498	0.119	31	0.074	10	0.10
ZINC	7.133	0.258	383	0.0915	113	0.27	41	0.41
ZIRCONIUM	6.489	0.234	280	0.067	21	0.050	12	0.12

TABLE 2 THERMAL DIFFUSIVITIES OF COMMON ALLOYS FROM 20 TO 100 °C (68 TO 212 °F)

ALLOYS	**DENSITY**		**HEAT CAPACITY**		**THERMAL CONDUCTIVITY**		**THERMAL DIFFUSIVITY**	
	g/cm^3	**$lb/in.^3$**	**j/kg · k**	**$cal_{it}/g \cdot °c$**	**w/m · k**	**$cal_{it}/cm \cdot s \cdot °c$**	**mm^2/s**	**cm^2/s**
ALUMINUM ALLOYS								
1100	2.71	0.098	963	0.23	222	0.53	85	0.85
2014	2.80	0.101	963	0.23	193	0.46	71	0.71
5052	2.68	0.097	963	0.23	138	0.33	54	0.54
6061	2.70	0.098	963	0.23	172	0.41	66	0.66
7075	2.80	0.101	963	0.23	121	0.29	45	0.45
COPPER ALLOYS								
COMMERCIAL BRONZE	8.80	0.318	377	0.09	188	0.45	57	0.57
CARTRIDGE BRASS	8.53	0.308	377	0.09	121	0.29	38	0.38
NAVAL BRASS	8.41	0.303	377	0.09	117	0.28	37	0.37
BERYLLIUM COPPER	8.23	0.297	419	0.1	84	0.20	24	0.24
9% ALUMINUM BRONZE	7.58	0.273	435	0.104	60	0.144	18	0.18
MAGNESIUM ALLOYS								
AZ 31	1.78	0.064	1050	0.25	84	0.20	45	0.45
AZ 91	1.83	0.066	1005	0.24	84	0.20	46	0.46
ZW 1	1.8	0.065	1005	0.24	134	0.32	74	0.74
RZ 5	1.84	0.066	963	0.23	113	0.27	64	0.64
STAINLESS STEELS								

TYPE 301	7.9	0.285	502	0.12	16	0.039	4.1	0.041
TYPE 304	7.9	0.285	502	0.12	15.1	0.036	3.8	0.038
TYPE 316	8.0	0.289	502	0.12	15.5	0.037	3.9	0.039
TYPE 410	7.7	0.278	460	0.11	24	0.057	6.7	0.067
TYPE 430	7.7	0.278	460	0.11	26	0.062	7.3	0.073
TYPE 501	7.7	0.278	460	0.11	37	0.088	10	0.10
NICKEL-BASE ALLOYS								
NIMONIC 80A	8.19	0.296	460	0.11	11	0.027	3.0	0.030
INCONEL 600	8.42	0.304	460	0.11	15	0.035	3.8	0.038
MONEL 400	8.83	0.319	419	0.10	22	0.052	5.8	0.058
TITANIUM ALLOYS								
TI-6AL-4V	4.43	0.160	611	0.146	5.9	0.014	2.1	0.021
TI-5AL-2.5SN	4.46	0.161	460	0.11	6.3	0.015	3.1	0.031

For the planar heat source on a steel surface, as represented by Fig. 1, the time in seconds to produce melting on the surface, t_m, is given by:

$$T_M = (5000/\text{H.I.})^2 \qquad \textbf{(EQ 2)}$$

where H.I. is the net heat intensity (in W/cm^2) transferred to the workpiece.

Equation 2 provides a rough estimate of the time required to produce melting, and is based upon the thermal diffusivity of steel. Materials with higher thermal diffusivities--or the use of a local point heat source rather than a planar heat source--will increase the time to produce melting by a factor of up to two to five times. On the other hand, thin materials tend to heat more quickly.

If the time to melting is considered to be a characteristic interaction time, t_I, then the graph shown in Fig. 3 can be generated. Heat sources with power densities that are of the order of 1000 W/cm^2, such as oxyacetylene flames or electro-slag welding, require interaction times of 25 s with steel, whereas laser and electron beams, at 1 MW/cm^2, need interaction times on the order of only 25 μs. If this interaction time is divided into the heat-source diameter, d_H, then a maximum travel speed, V_{max}, is obtained for the welding process (Fig. 4).

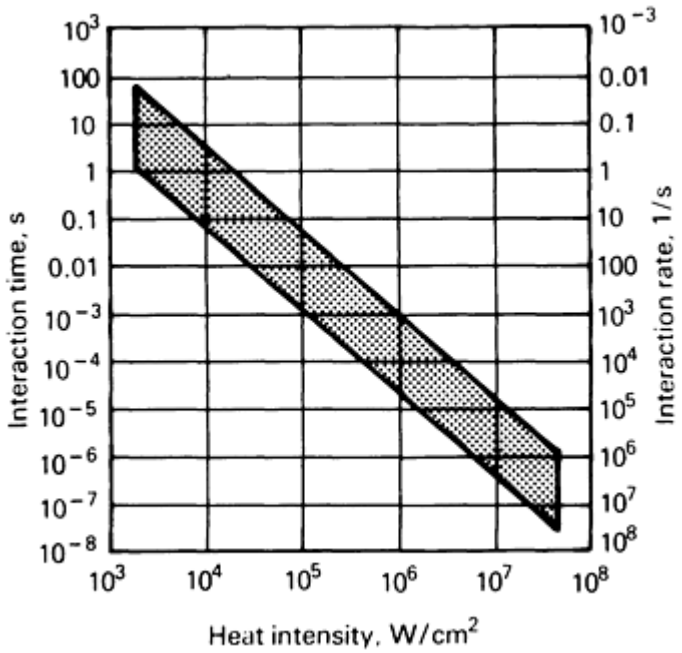

FIG. 3 TYPICAL WELD POOL-HEAT SOURCE INTERACTION TIMES AS FUNCTION OF HEAT-SOURCE INTENSITY.

MATERIALS WITH A HIGH THERMAL DIFFUSIVITY, SUCH AS COPPER OR ALUMINUM, WOULD LIE NEAR THE TOP OF THIS BAND, WHEREAS STEELS, NICKEL ALLOYS, OR TITANIUM WOULD LIE IN THE MIDDLE. URANIUM AND CERAMICS, WITH VERY LOW THERMAL DIFFUSIVITIES, WOULD LIE NEAR THE BOTTOM OF THE BAND.

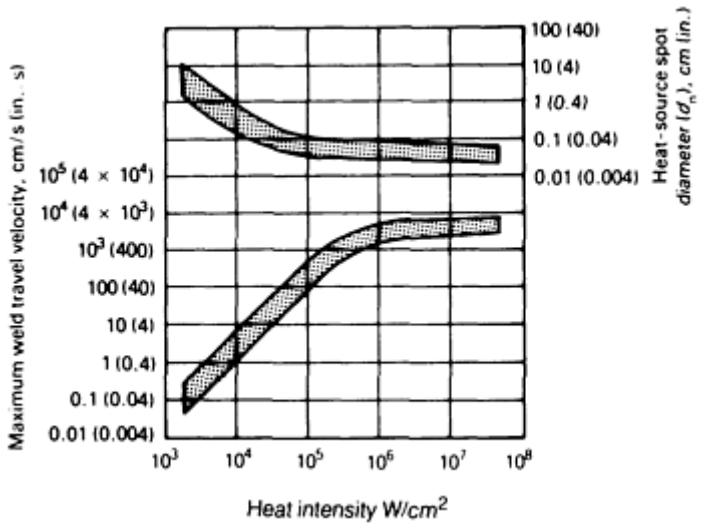

FIG. 4 MAXIMUM WELD TRAVEL VELOCITY AS A FUNCTION OF HEAT-SOURCE INTENSITY BASED ON TYPICAL HEAT-SOURCE SPOT DIAMETERS

The reason why welders begin their training with the oxyacetylene process should be clear: it is inherently slow and does not require rapid response time in order to control the size of the weld puddle. Greater skill is needed to control the more-rapid fluctuations in arc processes. The weld pool created by the high-heat-intensity processes, such as laser-beam and electron-beam welding, cannot be humanly controlled and must therefore be automated. This need to automate leads to increased capital costs. On an approximate basis, the W/cm^2 of a process can be substituted with the dollar cost of the capital equipment. With reference to Fig. 2, the cost of oxyacetylene welding equipment is nearly $1000, whereas a fully automated laser-beam or electron-beam system can cost $1 million. Note that the capital cost includes only the energy source, control system, fixturing, and materials handling equipment. It does not include operating maintenance or inspection costs, which can vary widely depending on the specific application.

For constant total power, a decrease in the spot size will produce a squared increase in the heat intensity. This is one of the reasons why the spot size decreases with increasing heat intensity (Fig. 4). It is easier to make the spot smaller than it is to increase the power rating of the equipment. In addition, only a small volume of material usually needs to be melted. If the spot size were kept constant and the input power were squared in order to obtain higher densities, then the volume of fused metal would increase dramatically, with no beneficial effect.

However, a decreasing spot size, coupled with a decreased interaction time at higher power densities, compounds the problem of controlling the higher-heat-intensity process. A shorter interaction time means that the sensors and controllers necessary for automation must operate at higher frequencies. The smaller spot size means that the positioning of the heat source must be even more precise, that is, on the order of the heat-source diameter, d_H. The control frequency must be greater than the travel velocity divided by the diameter of the heat source. For processes that operate near the maximum travel velocity, this is the inverse of the process interaction time, t_I (Fig. 3).

Thus, not only must the high-heat-intensity processes be automated because of an inherently high travel speed, but the fixturing requirements become greater, and the control systems and sensors must have ever-higher frequency responses. These factors lead to increased costs, which is one reason that the very productive laser-beam and electron-beam welding processes have not found wider use. The approximate productivity of selected welding processes, expressed as length of weld produced per second, to the relative capital cost of equipment is shown in Fig. 5.

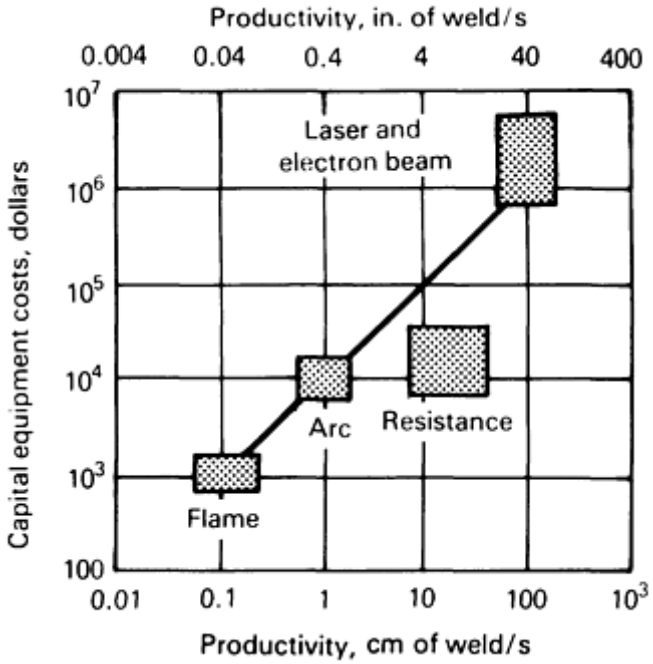

FIG. 5 APPROXIMATE RELATIONSHIP BETWEEN CAPITAL COST OF WELDING EQUIPMENT AND SPEED AT WHICH SHEET METAL JOINTS CAN BE PRODUCED

Another important welding process parameter that is related to the power density of the heat source is the width of the heat-affected zone (HAZ). This zone is adjacent to the weld metal and is not melted itself but is structurally changed because of the heat of welding. Using the Einstein equation, the HAZ width can be estimated from the process interaction time and the thermal diffusivity of the material. This is shown in Fig. 6, with one slight modification. At levels above approximately 10^4 W/cm^2, the HAZ width becomes roughly constant. This is due to the fact that the HAZ grows during the heating stage at power densities that are below 10^4 W/cm^2, but at higher power densities it grows during the cooling cycle. Thus, at low power densities, the HAZ width is controlled by the interaction time, whereas at high power densities, it is independent of the heat-source interaction time. In the latter case, the HAZ width grows during the cooling cycle as the heat of fusion is removed from the weld metal, and is proportional to the fusion zone width.

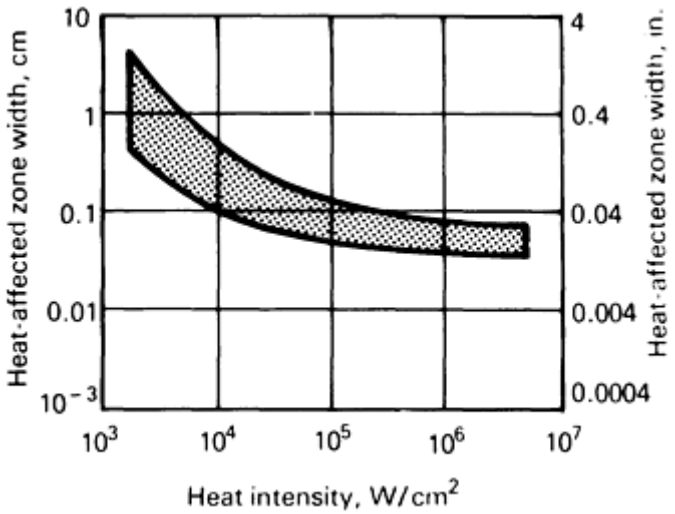

FIG. 6 RANGE OF WELD HAZ WIDTHS AS FUNCTION OF HEAT-SOURCE INTENSITY

The change of slope in Fig. 6 also represents the heat intensity at which the heat utilization efficiency of the process changes. At high heat intensities, nearly all of the heat is used to melt the material and little is wasted in preheating the surroundings. As heat intensity decreases, this efficiency is reduced. For arc welding, as little as half of the heat generated may enter the plate, and only 40% of this heat is used to fuse the metal. For oxyacetylene welding, the heat entering the metal may be 10% or less of the total heat, and the heat necessary to fuse the metal may be less than 2% of the total heat.

A final point is that the heat intensity also controls the depth-to-width ratio of the molten pool. This value can vary from 0.1 in low-heat-intensity processes to more than 10 in high-heat-intensity processes.

It should now be evident that all fusion welding processes can be characterized generally by heat-source intensity. The properties of any new heat source can be estimated readily from the figures in this article. Nonetheless, it is useful to more fully understand each of the common welding heat sources, such as flames, arcs, laser beams, electron beams, and electrical resistance. These are described in separate articles in the Section "Fusion Welding Processes" in this Volume.

Heat Flow in Fusion Welding

Chon L. Tsai and Chin M. Tso, The Ohio State University

Introduction

DURING FUSION WELDING, the thermal cycles produced by the moving heat source cause physical state changes, metallurgical phase transformation, and transient thermal stress and metal movement. After welding is completed, the finished product may contain physical discontinuities that are due to excessively rapid solidification, or adverse microstructures that are due to inappropriate cooling, or residual stress and distortion that are due to the existence of incompatible plastic strains.

In order to analyze these problems, this article presents an analysis of welding heat flow, focusing on the heat flow in the fusion welding process. The primary objective of welding heat flow modeling is to provide a mathematical tool for thermal data analysis, design iterations, or the systematic investigation of the thermal characteristics of any welding parameters. Exact comparisons with experimental measurements may not be feasible, unless some calibration through the experimental verification procedure is conducted.

Welding Thermal Process. A physical model of the welding system is shown in Fig. 1. The welding heat source moves at a constant speed along a straight path. The end result, after either initiating or terminating the heat source, is the formation of a transient thermal state in the weldment. At some point after heat-source initiation but before termination, the temperature distribution is stationary, or in thermal equilibrium, with respect to the moving coordinates. The origin of the moving coordinates coincides with the center of the heat source. The intense welding heat melts the metal and forms a molten pool. Some of the heat is conducted into the base metal and some is lost from either the arc column or the metal surface to the environment surrounding the plate. Three metallurgical zones are formed in the plate upon completion of the thermal cycle: the weld-metal (WM) zone, the heated-affected zone (HAZ), and the base-metal (BM) zone. The peak temperature and the subsequent cooling rates determine the HAZ structures, whereas the thermal gradients, the solidification rates, and the cooling rates at the liquid-solid pool boundary determine the solidification structure of the WM zone. The size and flow direction of the pool determines the amount of dilution and weld penetration. The material response in the temperature range near melting temperatures is primarily responsible for the metallurgical changes.

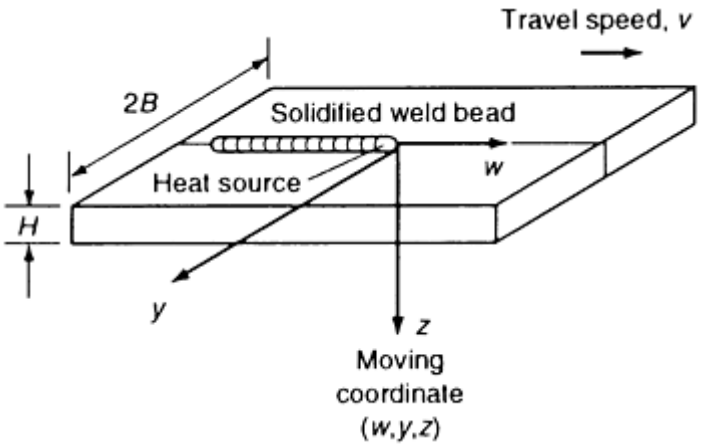

FIG. 1 SCHEMATIC OF THE WELDING THERMAL MODEL

Two thermal states, quasi-stationary and transient, are associated with the welding process. The transient thermal response occurs during the source initiation and termination stages of welding, the latter of which is of greater metallurgical interest. Hot cracking usually begins in the transient zone, because of the nonequilibrium solidification of the base material. A crack that forms in the source-initiation stage may propagate along the weld if the solidification strains sufficiently multiply in the wake of the welding heat source. During source termination, the weld pool solidifies several times faster than the weld metal in the quasi-stationary state. Cracks usually appear in the weld crater and may propagate along the weld. Another dominant transient phenomenon occurs when a short repair weld is made to a weldment. Rapid cooling results in a brittle HAZ structure and either causes cracking problems or creates a site for fatigue-crack initiation.

The quasi-stationary thermal state represents a steady thermal response of the weldment in respect to the moving heat source. The majority of the thermal expansion and shrinkage in the base material occurs during the quasi-stationary thermal cycles. Residual stress and weld distortion are the thermal stress and strain that remain in the weldment after completion of the thermal cycle.

Relation to Welding Engineering Problems. To model and analyze the thermal process, an understanding of thermally induced welding problems is important. A simplified modeling scheme, with adequate assumptions for specific problems, is possible for practical applications without using complex mathematical manipulations. The relationship between the thermal behavior of weldments and the metallurgy, control, and distortion associated with welding is summarized below.

Welding Metallurgy. As already noted, defective metallurgical structures in the HAZ and cracking in the WM usually occur under the transient thermal condition. Therefore, a transient thermal model is needed to analyze cracking and embrittlement problems.

To evaluate the various welding conditions for process qualification, the quasi-stationary thermal responses of the weld material need to be analyzed. The minimum required amount of welding heat input within the allowable welding speed range must be determined in order to avoid rapid solidification and cooling of the weldment Preheating may be necessary if the proper thermal conditions cannot be obtained under the specified welding procedure. A quasi-stationary thermal model is adequate for this type of analysis.

Hot cracking results from the combined effects of strain and metallurgy. The strain effect results from weld-metal displacement at near-melting temperatures, because of solidification shrinkage and weldment restraint. The metallurgical effect relates to the segregation of alloying elements and the formation of the eutectic during the high nonequilibrium solidification process. Using metallurgical theories, it is possible to determine the chemical segregation, the amounts and distributions of the eutectic, the magnitudes and directions of grain growth, and the weld-metal displacement at high temperatures. Using the heating and cooling rates, as well as the retention period predicted by modeling and analysis, hot-cracking tendencies can be determined. To analyze these tendencies, it is important to employ a more accurate numerical model that considers finite welding heat distribution, latent heat, and surface heat loss.

Welding Control. In-process welding control has been studied recently. Many of the investigations are aimed at developing sensing and control hardware. However, a link between weld-pool geometry and weld quality has not been fully established. A transient heat-flow analysis needs to be used to correlate the melted surface, which is considered to be the primary control variable, to the weld thermal response in a time domain.

Welding Distortion The temperature history and distortion caused by the welding thermal process creates nonlinear thermal strains in the weldment. Thermal stresses are induced if any incompatible strains exist in the weld. Plastic strains are formed when the thermal stresses are higher than the material yield stress. Incompatible plastic strains accumulate over the thermal process and result in residual stress and distortion of the final weldment. The material response in the lower temperature range during the cooling cycle is responsible for the residual stresses and weldment distortion. For this type of analysis, the temperature field away from the welding heat source is needed for the modeling of the heating and cooling cycle during and after welding. A quasi-stationary thermal model with a concentrated moving heat source can predict, with reasonable accuracy, the temperature information for the subsequent stress and distortion analysis.

Literature Review. Many investigators have analytically, numerically, and experimentally studied welding heat-flow modeling and analysis (Ref 1, 2, 3, 4, 5, 6, 7, 8, 9, 10, 11, 12, 13, 14, 15, 16, 17, 18). The majority of the studies were concerned with the quasi-stationary thermal state. Lance and Martin (Ref 1), Rosenthal and Schmerber (Ref 2) and Rykalin (Ref 3) independently obtained an analytical temperature solution for the quasi-stationary state using a point or line heat source moving along a straight line on a semi-infinite body. A solution for plates of finite thickness was later obtained by many investigators using the imaged heat source method (Ref 3, 4). Tsai (Ref 5) developed an analytical solution for a model that incorporated a welding heat source with a skewed Gaussian distribution and finite plate thickness. It was later called the "finite source theory" (Ref 6).

With the advancement of computer technology and the development of numerical techniques like the finite-difference and finite-element methods, more exact welding thermal models were studied and additional phenomena were considered, including nonlinear thermal properties, finite heat-source distributions, latent heat, and various joint geometries. Tsai (Ref 5), Pavelic (Ref 7), Kou (Ref 8), Kogan (Ref 9), and Brody (Ref 10) studied the simulation of the welding process using the finite-difference scheme. Hibbitt and Marcal (Ref 11), Friedman (Ref 12), and Paley (Ref 13) made some progress in welding simulation using the finite-element method.

Analytical solutions for transient welding heat flow in a plate were first studied by Naka (Ref 14), Rykalin (Ref 3), and Masubuchi and Kusuda (Ref 15) in the 1940s and 1950s. A point or line heat source, constant thermal properties, and adiabatic boundary conditions were assumed. Later, Tsai (Ref 16) extended the analytical solution to incorporate Gaussian heat distribution using the principle of superposition. The solution was used to investigate the effect of pulsed conditions on weld-pool formation and solidification without the consideration of latent heat and nonlinear thermal properties.

The analysis of the transient thermal behavior of weldments using numerical methods has been the focus of several investigations since 1980. Friedman (Ref 17) discussed the finite-element approach to the general transient thermal analysis of the welding process. Brody (Ref 10) developed a two-dimensional transient heat flow model using a finite-difference scheme and a simulated pulsed-current gas-tungsten arc welding process (GTAW). Tsai and Fan (Ref 18) modeled the two-dimensional transient welding heat flow using a finite-element scheme to study the transient welding thermal behavior of the weldment.

General Approach. The various modeling and analysis schemes summarized above can be used to investigate the thermal process of different welding applications. With adequate assumptions, analytical solutions for the simplified model can be used to analyze welding problems that show a linear response to the heat source if the solutions are properly calibrated by experimental tests. Numerical solutions that incorporate nonlinear thermal characteristics of weldments are usually required for investigating the weld-pool growth or solidification behavior. Numerical solutions can also be necessary for metallurgical studies in the weld HAZ if the rapid cooling phenomenon is significant under an adverse welding environment, such as welding under water.

Thermally related welding problems can be categorized as:

- SOLIDIFICATION RATES IN THE WELD POOL
- COOLING RATES IN THE HAZ AND ITS VICINITY
- THERMAL STRAINS IN THE GENERAL DOMAIN OF THE WELDMENT

The domain of concern in the weld pool solidification is within the molten pool area, in which the arc (or other heat source) phenomena and the liquid stirring effect are significant. A convective heat-transfer model with a moving boundary at the melting temperature is needed to study the first category, and numerical schemes are usually required, as well.

The HAZ is always bounded on one side by the liquid-solid interface during welding. This inner-boundary condition is the solidus temperature of the material. The liquid weld pool might be eliminated from thermal modeling if the interface could be identified. A conduction heat-transfer model would be sufficient for the analysis of the HAZ. Numerical methods are often employed and very accurate results can be obtained.

The thermal strains caused by welding thermal cycles are caused by the nonlinear temperature distribution in the general domain of the weldment. Because the temperature in the material near the welding heat source is high, very little stress can be accumulated from the thermal strains. This is due to low rigidity, that is, small modulus of elasticity and low yield strength. The domain for thermal strain study is less sensitive to the arc and fluid-flow phenomena and needs only a relatively simple thermal model. Analytical solutions with minor manipulations often provide satisfactory results.

In this article, only the analytical heat-flow solutions and their practical applications are addressed. The numerical conduction solutions and the convective models for fluid flow in a molten weld pool are not presented.

References

1. N.S. BOULTON AND H.E. LANCE-MARTIN, RESIDUAL STRESSES IN ARC WELDED PLATES, *PROC. INST. MECH. ENG.*, VOL 33, 1986, P 295
2. D. ROSENTHAL AND R. SCHMERBER, THERMAL STUDY OF ARC WELDING, *WELD. J.*, VOL 17 (NO. 4), 1983, P 2S
3. N.N. RYKALIN, "CALCULATIONS OF THERMAL PROCESSES IN WELDING," MASHGIZ, MOSCOW, 1951
4. K. MASUBUCHI, *ANALYSIS OF WELDED STRUCTURES*, PERGAMON PRESS, 1980
5. C.L. TSAI, "PARAMETRIC STUDY ON COOLING PHENOMENA IN UNDERWATER WELDING," PH.D THESIS, MIT, 1977
6. C.L. TSAI, FINITE SOURCE THEORY, *MODELING OF CASTING AND WELDING PROCESSES II*, ENGINEERING FOUNDATION MEETING, NEW ENGLAND COLLEGE (HENNIKER, NH), 31 JULY TO 5 AUG 1983, P 329
7. R. PAVELIC, R. TANAKUCHI, O. CZEHARA, AND P. MYERS, EXPERIMENTAL AND COMPUTED TEMPERATURE HISTORIES IN GAS TUNGSTEN ARC WELDING IN THIN PLATES, *WELD. J.*, VOL 48 (NO. 7), 1969, P 295S
8. S. KOU, 3-DIMENSIONAL HEAT FLOW DURING FUSION WELDING, *PROC. OF METALLURGICAL SOCIETY OF AIME*, AUG 1980, P 129-138
9. P.G. KOGAN, THE TEMPERATURE FIELD IN THE WELD ZONE, *AVE. SVARKA*, VOL 4 (NO. 9), 1979, P 8
10. G.M. ECER, H.D. DOWNS, H.D. BRODY, AND M.A. GOKHALE, HEAT FLOW SIMULATION OF PULSED CURRENT GAS TUNGSTEN ARC WELDING, *MODELING OF CASTING AND WELDING PROCESSES*, ENGINEERING FOUNDATION 1980 MEETING (RINDGE, NH), 3-8 AUG 1980, P 139-160
11. H. HIBBITT AND P. MARCAL, A NUMERICAL THERMOMECHANICAL MODEL FOR WELDING AND SUBSEQUENT LOADING OF A FABRICATED STRUCTURE, *COMPUT. STRUCT.*, VOL 3, 1973, P 1145
12. E. FRIEDMAN, THERMOMECHANICAL ANALYSIS OF THE WELDING PROCESS USING FINITE ELEMENT METHODS, *TRANS. ASME*, AUG 1975, P 206
13. Z. PALEY AND P. HIBBERT, COMPUTATION OF TEMPERATURE IN ACTUAL WELD DESIGN, *WELD. J.*, VOL 54 (NO. 11), 1975, P 385.S

14. T. NAKA, TEMPERATURE DISTRIBUTION DURING WELDING, *J. JPN. WELD. SOC.*, VOL 11 (NO. 1), 1941, P 4
15. K. MASUBUCHI AND T. KUSUDA, TEMPERATURE DISTRIBUTION OF WELDED PLATES, *J. JPN WELD. SOC.*, VOL 22 (NO. 5), 1953, P 14
16. C.L. TSAI AND C.A. HOU, THEORETICAL ANALYSIS OF WELD POLL BEHAVIOR IN THE PULSED CURRENT GTAW PROCESS, *TRANSPORT PHENOMENA IN MATERIALS PROCESSING,* ASME WINTER ANNUAL MEETING, 1983
17. E. FRIEDMAN, "FINITE ELEMENT ANALYSIS OF ARC WELDING," REPORT WAPD-TM-1438, DEPARTMENT OF ENERGY, 1980
18. J.S. FAN AND C.L. TSAI, "FINITE ELEMENT ANALYSIS OF WELDING THERMAL BEHAVIOR IN TRANSIENT CONDITIONS," 84-HT-80, ASME

Heat Flow in Fusion Welding

Chon L. Tsai and Chin M. Tso, The Ohio State University

Mathematical Formulations

Conduction Equation. A diagram of the welding thermal model is shown in Fig. 1. The origin of the moving coordinates (*w,x,z*) is fixed at the center of the welding heat source. The coordinates move with the source at the same speed. The conduction equation for heat flow in the weldments is:

$$\nabla.(l\nabla q) + rC_p v\frac{\partial q}{\partial w} + \dot{Q} = rC_p v\frac{\partial q}{\partial t} \qquad \textbf{(EQ 1)}$$

The initial condition is:

$$\theta = \theta_0, \text{ AT } T = 0 \qquad \textbf{(EQ 2)}$$

and the general boundary condition is:

$$l\frac{\partial q}{\partial w}I_w + \frac{\partial q}{\partial y}I_y + \frac{\partial q}{\partial z}I_z - \dot{q} + h(q - q_\infty) = 0 \qquad \textbf{(EQ 3)}$$

where ∇ is a differential operator; θ is the temperature; $\theta\ \infty$ is the environmental temperature; θ_0 is the initial temperature; λ is thermal conductivity; ρ is density; C_p is specific heat h is the surface heat-loss coefficient; l_w, l_y, and l_z are the direction cosines of the boundary surface; Q is the volumetric heat source, t is time, and v is welding speed.

The volumetric heat source represents the Joule heating in the weldment that is due to the electric current flow within that conducting medium. The total energy of such heating in welding is usually minimal, compared to the arc heat input. The majority of the energy is concentrated in a very small volume beneath the arc (Ref 5). In other words, a very high energy density generation exists in the weld pool, and it may have a significant effect on transient pool growth and solidification.

Heat-Source Formulation. The direction cosines on the surface that receive the heat flux from the welding source (z = 0) are $l_w = l_y = 0$ and $l_z = -1$. Within the significant heat-input area (to be defined later in this section), the heat loss coefficient, h, is zero.

The distribution of the welding heat flux on the weldment surface can be characterized, in a general form, by a skewed Gaussian function (Ref 19):

$$\dot{q}(r,w) = \dot{q}_0 \exp\left(-Cr^2 - \frac{bv}{2k}w\right) \qquad \textbf{(EQ 4)}$$

where β is a weight constant, κ is the thermal diffusivity of the base material, C is a shape constant, $\dot{q}$ is heat flux as a function of (*r*, *w*), $\dot{q}_0$ is heat flux at the source center, *r* is the radial coordinate from the source center, and *v* is welding speed.

The weight constant, β, indicates the significance of the welding travel speed. A normal distribution of the welding heat flux is obtained if the weight constant is zero.

In general, the total energy input to the weldment, which is a fraction of the total welding power generated by the welding machine, is the sum of the concentrated heat and the diffused heat (Ref 20). The concentrated heat is carried by the core of the energy transmission medium, for example, the arc plasma column. The diffused heat reaches the weld surface by radiation and convection energy transport from the core surface. The heat-flux distribution is a function of the proportional values between these two types of energy. The fraction of the total welding power reaching the weldment indicates the heating efficiency of the welding process, and the fraction percentage is defined as welding heat efficiency, η.

The shape constant, C, can be obtained in terms of the core diameter, *D*, and the concentration factor, *F*. The concentration factor is defined as the ratio of the concentrated heat to the net energy reaching the weldment. The core diameter can be assumed to be the diameter of the plasma column in the arc welding process. The concentration factor and welding heat efficiency are not fully understood and have been subjected to manipulation during the mathematical analyses in order to obtain a better correlation with the experimental data.

Assuming a normal heat-flux model, two concentrations are required to determine the shape constant and the heat flux at the source center, $\dot{q}_0$. By integrating Eq 4 over the core heat area and the entire heat input domain ($r = 0 \rightarrow \infty$), the shape factor can be determined by dividing the two integrals. The heat flux at the source center can then be determined from the second integral. The two constants are expressed as:

$$C = \frac{4l_{arc}[1/(1-F)]}{D^2} \qquad \textbf{(EQ 5)}$$

where l_{arc} is the length of the arc plasma column.

$$\frac{\dot{q}_0}{\dot{Q}} = \frac{C}{p} \qquad \textbf{(EQ 6)}$$

In the case of arc welding,

$$\frac{\dot{q}_0}{hEI} = \frac{C}{p} \qquad \textbf{(EQ 7)}$$

where *E* is the welding arc voltage and *I* is the welding current.

For practical purposes, the welding heat source can be considered to be restricted within a circle of radius r_a, where the heat flux drops to 1/100 of the center flux $\dot{q}_0$. The radius of the significant heat input area can be written as:

$$r_a = \left(\frac{I_{arc}100}{C}\right)^{0.5} \qquad \textbf{(EQ 8)}$$

Surface Heat Loss. The heat-loss coefficient, *h*, represents both radiation and convection heat loss from the boundary surfaces outside the significant heat input area. The formulation for both heat-loss mechanisms can be written as the radiation heat-loss coefficient (in air):

$$H_{RAD} = \varepsilon\sigma(\theta_w + \infty)(\theta_W{}^2 - \theta\infty^2)) \qquad \textbf{(EQ 9)}$$

or the natural convection heat-loss coefficient (in air):

$$H_{AC} = 0.00042\frac{q_W - q_\infty}{B} \qquad \textbf{(EQ 10)}$$

or the convection heat-loss coefficient (in water):

$$H_{CW} = 0.442(\theta_W - \theta\infty)^{0.25} \qquad \textbf{(EQ 11)}$$

where ε is emissivity, σ is the Stefan-Boltzmann constant, θ_w is the surface temperature, θ ∞, is the environmental temperature, and *B* is the characteristic surface dimension.

Natural convection is dominant at a temperature below 550 °C (1020 °F), whereas radiation becomes more important at temperatures above this level. The total heat-loss coefficient is the sum of Eq 9 and 10. The characteristic surface dimension is the effective distance from the source beyond which the temperature rises insignificantly during welding. The characteristic dimension for steel is about 150 mm (6 in.) (Ref 5). In underwater welding, heat losses are primarily due to heat transfer from the surface to the moving water environment. This motion is created by the rising gas column in the arc area (Ref 21).

For an insulated surface, no heat transfer into or out of the surface is assumed. The temperature gradient normal to the surface is zero, and can be represented by:

$$N \cdot \nabla q = 0 \qquad \textbf{(EQ 12)}$$

where *n* is a unit vector normal to the surface and equals $(l_w{}^2 + l_y{}^2 + l_z{}^2)^{0.5}$.

Other Boundary Conditions. There are several other possible boundary conditions in welding heat-flow modeling that depend on the assumptions used for model simplification. One is the condition at infinity:

$$q = q_\infty \text{ or } \lim_{r\to\infty}\frac{\partial q}{\partial r} = 0 \qquad \textbf{(EQ 13)}$$

Another is the condition near the heat source. In the case of a line source for a thin plate:

$$-2p\,l\,\mathrm{H}\lim_{r\to\infty} r\frac{\partial q}{\partial r} = h\,EI \qquad \textbf{(EQ 14)}$$

In the case of a point source for a thick plate:

$$-2p\,l\lim_{r\to\infty} r^2\frac{\partial q}{\partial r} = h\,EI \qquad \textbf{(EQ 15)}$$

In the case of a finite source for a thick plate:

$$N \cdot (-\lambda\nabla\theta) = \dot{q}\,;\; R \le R_A \qquad \textbf{(EQ 16)}$$

Another is represented by the conditions at the solid-liquid interface:

$$\theta_1 = \theta_S = \theta_M \qquad \textbf{(EQ 17)}$$

$$\text{n.}(l\nabla q)_s - n(l\nabla q)_1 = \pm r_s L\frac{ds}{dt} \qquad \textbf{(EQ 18)}$$

where + indicates the melting process and - indicates the solidification process. The subscripts s and l indicate the temperature and the properties in a solid and liquid, respectively. The *n* is a normal vector on the boundary surface or interface, r_a is the radius of the heat-input area, *L* is the latent heat of the base material, and the subscript m represents the melting temperature of the base material.

References cited in this section

5. C.L. TSAI, "PARAMETRIC STUDY ON COOLING PHENOMENA IN UNDERWATER WELDING," PH.D THESIS, MIT, 1977
19. R.L. APPS AND D.R. MILNER, HEAT FLOW IN ARGON-ARC WELDING, *BR. WELD. J.*, VOL 2 (NO. 10), 1955, P 475
20. H.S. CARSLAW AND J.C. JAEGER, *CONDUCTION OF HEAT IN SOLIDS*, OXFORD PRESS
21. C.L. TSAI AND J.H. WU, "AN INVESTIGATION OF HEAT TRANSPORT PHENOMENA IN UNDERWATER WELDING," PRESENTED AT THE ASME WINTER ANNUAL MEETING (MIAMI BEACH, FL), 1985

Chon L. Tsai and Chin M. Tso, The Ohio State University

Engineering Solutions and Empirical Correlation

General Solutions. The general (analytical) heat-flow solutions for fusion welding can be categorized by those appropriate for a thick plate, a thin plate, or a plate with finite thickness. In most cases, the boundary surfaces (except for the heat-input area) are assumed to be adiabatic, and the thermal properties are independent of temperature. The various metallurgical zones in the weldment are assumed to be homogeneous, and the thermal model is linear.

The solutions give the temperature for a specific point if the welding velocity, *v*, voltage, *E*, and current, *I*, as well as the physical properties of the plate material (ρ, λ, C_p) and the welding heat efficiency, η, are known. This specific point is defined by *r* and *w* in:

$$r = \sqrt{w^2 + y^2 + z^2} \qquad \textbf{(EQ 19)}$$

where $w = x - vt$. The heat-flow solutions are not accurate at points near the welding arc, because a point source or line source is assumed for thick and thin plates, respectively.

To approximate the transient temperature changes at the start and end of a weld, Fig. 2 shows a global coordinate system (*x,y,z*), the origin of which is fixed at the source initiation, where t_0 is the welding time and t_1 is the time after the welding heat-source termination. The temperature solutions at t_0 and t_1 are the temperature changes at the start and end of the weld, respectively.

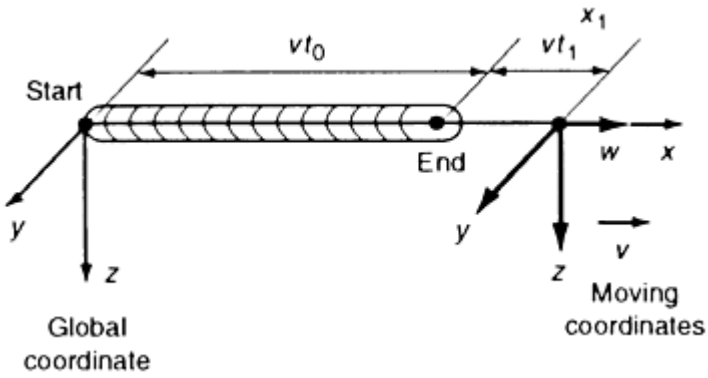

FIG. 2 GLOBAL AND MOVING COORDINATE SYSTEMS FOR WELDING HEAT CONDUCTION.

The temperature solution for thick plate at the arc start location is:

$$q - q_0 = \frac{h\,EI}{2p\,l\,vt_o} \qquad \textbf{(EQ 20)}$$

The quasi-stationary temperature distribution is:

$$q - q_0 = \frac{h\,EI}{2p\,l\,r}\exp\left[\frac{-v(w+r)}{2k}\right] \qquad \textbf{(EQ 21)}$$

At the arc termination location, the solution is:

$$q - q_0 = \frac{h\,EI}{2p\,l\,vt_1} \qquad \textbf{(EQ 22)}$$

The temperature solution for thin plate at the arc start location is:

$$q - q_0 = \frac{h\,EI}{2p\,l\,H}\exp\frac{v^2t_o}{2k}k_o\frac{v^2t_o}{2k} \qquad \textbf{(EQ 23)}$$

The quasi-stationary temperature distribution is:

$$q - q_0 = \frac{h\,EI}{2p\,l\,H}\exp\frac{-vw}{2k}k_o\frac{vr}{2k} \qquad \textbf{(EQ 24)}$$

For the arc termination location, the solution is:

$$q - q_0 = \frac{h\,EI}{2p\,l\,H}\exp\frac{v^2t_1}{2k}k_o\left(\frac{v^2t_1}{2k}\right) \qquad \textbf{(EQ 25)}$$

where K_0 is the modified Bessel function of the second kind of zeroth order and $\eta\,EI$ is the welding heat input rate.

Temperature for Plate With Finite Thickness. The image method enables the investigator to superimpose the solutions for an infinitely thick plate, the source of which is placed on imaginary surfaces until the proper boundary

conditions on the plate surfaces are obtained. This method is based on the premise that if a solution satisfies the governing equation and the boundary conditions, then it must be not only a correct solution, but the only solution (that is, the uniqueness of solution premise).

Using the image method, the solution for plates of finite thickness with a adiabatic surfaces can be modified from the respective temperature solutions described previously.

Let $f_0(w,y,z,t)$ be the initial solution for an infinitely thick plate. The temperature solution for a finite thick plate can be obtained by super imposing the imaginary solutions $f_{mn}(w,y_m, z_n, t)$ and $f'_{mn}(w,y'_m, z'_n, t)$ to the initial solution, and this can be written in a general form as:

$$q - q_0 = -f_0(w, y, z, f) + \sum_{m=0}^{\infty}\sum_{n=0}^{\infty}\left[f_{mn}(w, y_m, z_m, t] + f'_{mn}(w, y'_m, Z_m t)\right] \qquad \textbf{(EQ 26)}$$

where $y_m = 2mB - y$; $y'_m = 2mB + y$; $z_n = 2nH - z$; and $z'_n = 2nH + z$, in which B is the half width and H is the thickness of the plate. The subscripts m and n are integers that vary from zero to infinity.

For a plate with sufficient width, the subscript m is zero. The solution will coverage and reach the correct adiabatic surface condition in six to ten superposition steps, depending on the thickness of the plate. The two-dimensional solution (that is, thin plate) is generally used for any solution that requires more than ten superposition steps.

Equation 26 can be expressed as:

$$q - q_0 = -\frac{h\,EI\exp\left(\frac{-vw}{2k}\right)}{2p\,l}\left\{\frac{\exp\left(\frac{-vr}{2k}\right)}{r} + \sum_{n=1}^{\infty}\left[\frac{\exp\left(\frac{-vr_{2n}}{2k}\right)}{r_{2n}} + \right]\frac{\exp\left(\frac{-vr_{2n+1}}{2k}\right)}{r_{2n-1}}\right\} \qquad \textbf{(EQ 27)}$$

where

$$R_{2N} = W^2 + Y^2 + (2NH - Z)^2 \text{ AND}$$
$$R_{2N+1} = W^2 + Y^2 + (2NH + Z)^2 \qquad \textbf{(EQ 28)}$$

Cooling Rate. Frequently, it is desirable to know the cooling rate experienced at some location in a weldment to enable a prediction of the metallurgical structure in that area. A general methodology by which cooling rate equations are obtained from the temperature-distribution equations is discussed below.

Recall that the moving coordinate w is defined by $w = x - vt$. Using this definition, it is easily shown that:

$$\frac{\partial w}{\partial t} = -v \qquad \textbf{(EQ 29)}$$

Using the chain rule, the cooling-rate equation is:

$$\frac{\partial q}{\partial t} = -v\frac{\partial q}{\partial w} \qquad \textbf{(EQ 30)}$$

Because the temperature-distribution equations are a function of w and r, the cooling-rate equations can be obtained by differentiating the temperature-distribution equations with respect to w and multiplying by $-v$.

The cooling rate is defined as the slope of a tangent line drawn on the temperature-time curve. Because the cooling rate changes with temperature, when one speaks of a cooling rate, the specific temperature, θ_c, at which it occurs must also be

given. In a weldment, the variable of interest is the cooling rate at the critical temperature that ultimately defines what type of metallurgical structure will result (if the material is heat treatable). For steels, this critical temperature is the "nose" of the continuous cooling-transformation (CCT) curve. At this temperature, the cooling rate determines if upper transformation products (pearlite, upper bainite) or lower transformation products (martensite, lower bainite) will form. For many steels, this critical temperature ranges from approximately 200 to 540 °C (400 to 1000 °F).

The cooling rate in a weldment is also a function of location. In order to find a cooling-rate equation, the particular location in the weldment that is of interest must be defined. The resulting cooling-rate equation will be applicable only to that location.

The differentiation, $\partial\theta/\partial w$, of either Eq 21 or 27, which is required to obtain the cooling-rate expression, will result in a function of *w* and *r*. The variable *r* can be written in terms of *w* if the location of interest is defined by a given set of values of *y* and *z*. This relationship for *r*, once formulated, can then be substituted into $\partial\theta/\partial w$, the result being a function of *w* alone.

To determine *w* corresponding to the critical temperature, θ_c, a temperature-distribution equation is required (Eq 21 or 27). The aforementioned *r*-*w* relationship and temperature distribution equation (Eq 21 or 27) where θ is equal to θ_c, critical temperature, are used to determine *w*. Then *w* is substituted into the $d\theta/dw$ expression obtained previously. The end result will be an equation that defines the cooling rate for a particular location in the weldment, and, being a function of the critical temperature, the welding conditions and thermal conductivity of the base material.

To determine the cooling rate in a thick plate along the weld centerline (that is $y = 0$) for a particular critical temperature, the cooling-rate equation can be reduced to:

$$\frac{\partial q}{\partial t} = \frac{2p\,l\,v\left(q_c - q_0\right)^2}{h\,EI} \qquad \textbf{(EQ 31)}$$

This equation has been used to predict weld cooling rates in shop practices. Cooling rate is inversely (that is, $\dot{Q}/V$) and is proportional to thermal conductivity and the critical temperature at which the cooling rate needs to be evaluated.

On the basis of experimental results, a cooling-rate equation was developed for the HAZ of low-carbon steel weldments (Ref 25). This equation considers the combined effects of plate thickness, *H*, preheating temperature, θ_0, and welding conditions, and is given as:

$$\left.\frac{\partial q}{\partial t}\right|_{HAZ} = 0.35\left\{\left(\frac{q_c - q_0}{I/v}\right)^{1.7}\left[1 + \frac{2}{p}\tan^{-1}\left(\frac{H - H_o}{a}\right)\right]\right\}^{0.8} \qquad \textbf{(EQ 32)}$$

The variables α and H_0 depend on the critical temperature of interest. Several values are given in Table 1.

TABLE 1 SELECTED CRITICAL TEMPERATURE AND CORRESPONDING VALUES FOR α AND H_0

CRITICAL TEMPERATURE, θ_C		**H_0**		**α**	
°C	**°F**	**mm**	**in.**	**mm**	**in.**
700	1290	9.9	0.39	2.0	0.08
540	1000	14.2	0.56	4.1	0.16
300	570	19.8	0.78	9.9	0.39

The units used in Eq 32 are important, because the same units that were used in developing the equation must be employed in its application. The plate thickness, *H*, must be given in inches, and the travel speed, *v*, must be given in in./min. The temperatures θ_c and θ_0 must be given in °C, and the welding current, *I*, must be given in amperes. Using the

correct units, the application of Eq 32 will result in a predicted cooling rate (°C/s) for the HAZ of a low-carbon steel weldment.

For low-carbon steels welded by the shielded metal arc welding (SMAW), gas-metal arc welding (GMAW), and submerged arc welding (SAW) processes, an empirical equation has been developed that correlates the weld-metal cooling rate at 538 °C (1000 °F) with a 95 to 150 °C (200 to 300 °F) preheat, the weld nugget area (Ref 26):

$$°C/s = \left(\frac{2012}{\textit{nugget}\ \text{area}} \right)^{1.119} \qquad \textbf{(EQ 33)}$$

where the nugget area is in mm^2. For low-carbon steels, an empirical chart for determining nugget area for a given welding condition (Fig. 3) also has been developed (Ref 27). The straight line drawn to connect the current and travel speed intersects the nugget area at the calculated value. Welding voltage controls weld bead shape.

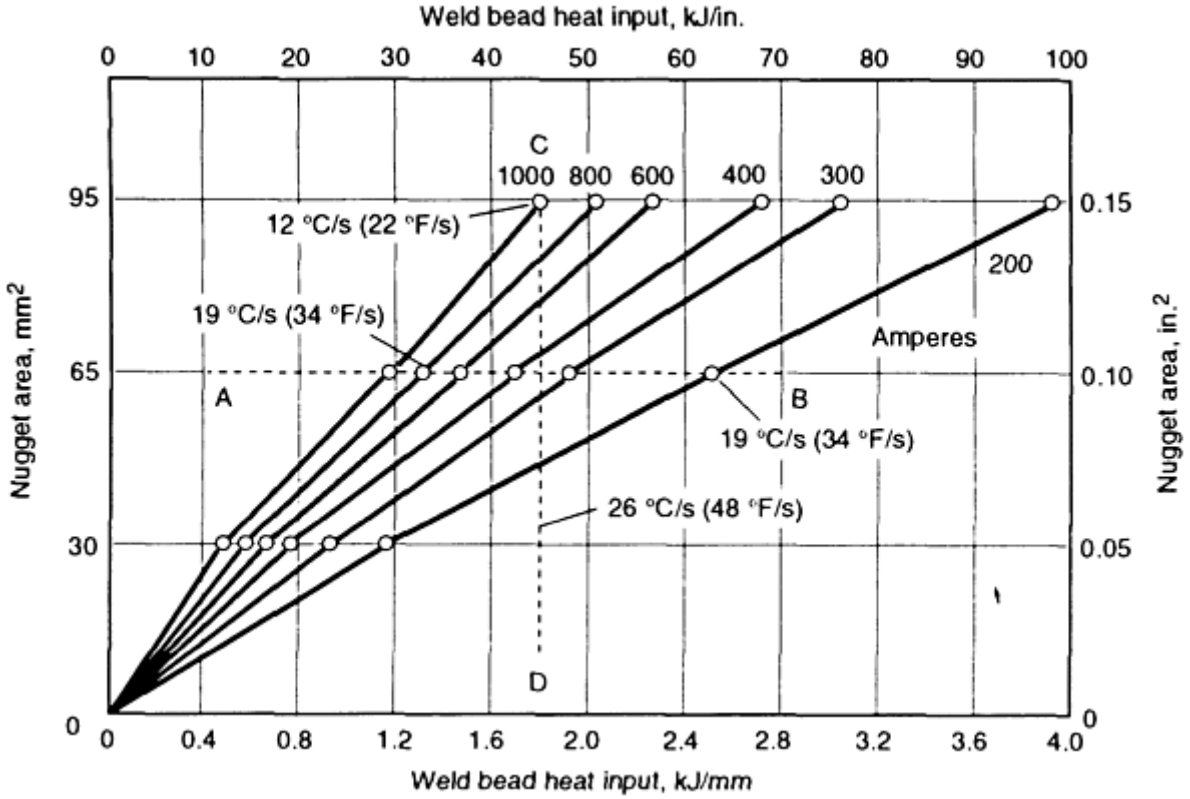

FIG. 3 RELATION BETWEEN NUGGET AREA, HEAT INPUT, AND CURRENT

Peak Temperature. An equation to determine the peak-temperature in a weldment at a given distance *y* from the weld centerline would enable the prediction of HAZ sizes, as well as weld bead widths. The general concept of obtaining a peak-temperature equation, as well as some results that have been obtained, are discussed below.

Consider Fig. 4 and note that the maximum, or peak, temperature is given when $\partial\theta/\partial t = 0$. For the thick-plate model, the cooling rate can be obtained by differentiating Eq 21 and multiplying by -*v*:

$$\frac{\partial q}{\partial t} = -v\frac{\partial q}{\partial w} = \frac{-vhEI}{2p\,l\,r}\exp\left[\frac{-v(w+r)}{2k}\right] x \left[\frac{-w}{r^2} - \frac{v}{2k}\left(1+\frac{w}{r}\right)\right] \qquad \textbf{(EQ 34)}$$

Clearly, the only way that $\partial\theta/\partial t$ can be equal to zero is if

$$\frac{-w}{r^2} - \frac{v}{2k}\left(1 + \frac{w}{r} = 0\right) \qquad \textbf{(EQ 35)}$$

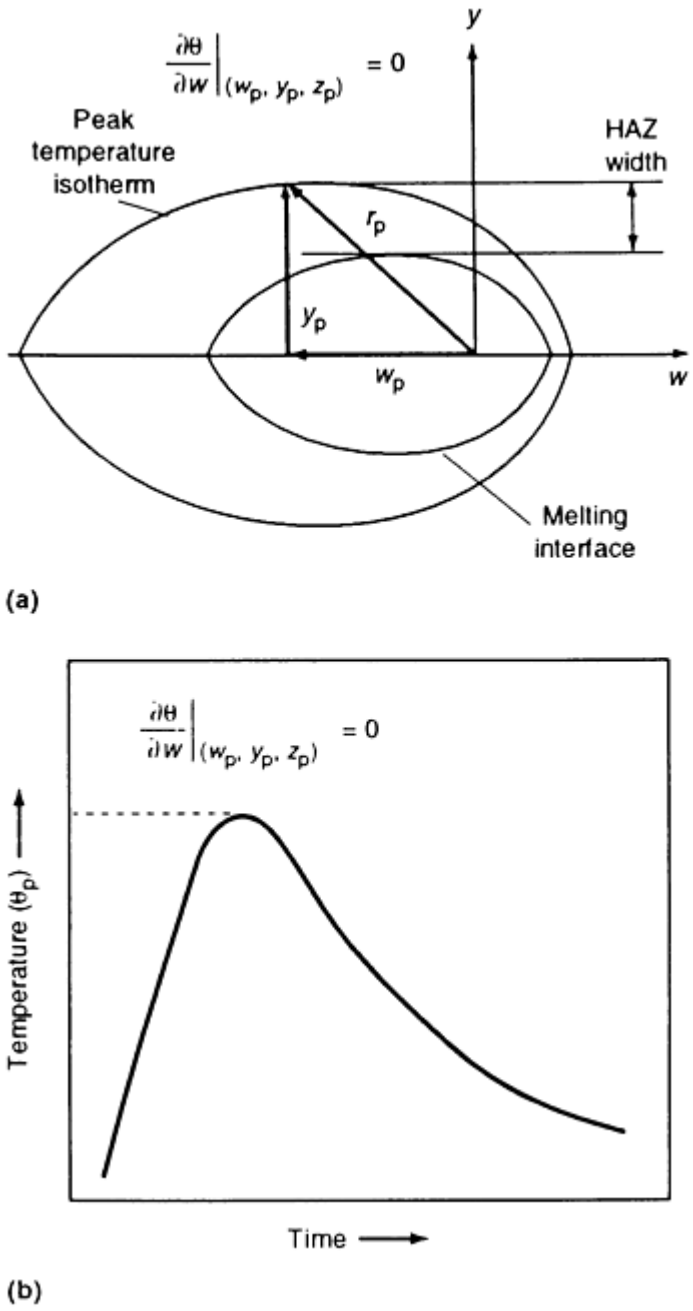

FIG. 4 SCHEMATIC SHOWING PEAK TEMPERATURE AT (W_P, Y_P, Z_P) WITH W_P TO BE DETERMINED FOR A GIVEN PEAK TEMPERATURE VALUE FOR A GIVEN (Y_P, Z_P) LOCATION. (A) ISOTHERMS. (B) TEMPERATURE HISTORY

Equation 35 describes the relationship that must exist between the two location variables, *r* and *w*, for the temperature at the point to be equal to the peak temperature. If this expression were to be substituted into the temperature distribution equation for thick plates (Eq 21) and solved for *w* and *r* (two equations and two unknowns), then the location of the peak temperature could be determined in terms of *w* and *r*. The location given by *r* and *w* would be easily converted to *y* and *z* as:

$$R^2 = W^2 + Y^2 + Z^2 \qquad \textbf{(EQ 36)}$$

Such a solution for r and w is not explicitly possible, however, because the equations for r and w that result are not explicit. Consequently, iterative techniques are required, resulting in a solution that is both cumbersome and time-consuming.

One method of obtaining a simpler thick-plate peak-temperature equation is to assume that the heat input is from an instantaneous line on the surface of the plate, rather than from a moving point source (that is, $v \to \infty$). This allows the elimination of the time dependency in the peak-temperature evaluation. Using this assumption, the temperature distribution is given by:

$$q - q_0 = \frac{h\,EI}{2p\,l\,t}\exp\left(\frac{r^2}{4kt}\right) \qquad \textbf{(EQ 37)}$$

Again, to find the peak-temperature location, $\partial\,\theta/\,\partial\,t$ is set equal to zero and the equation is solved for r. The result is:

$$\frac{r^2}{4kt} = 1 \qquad \textbf{(EQ 38)}$$

Substituting Eq 38 into Eq 37 yields the peak-temperature expression:

$$\frac{1}{q - q_0} = \left(\frac{e\,r\,C_p p\,r^2}{2}\right) / \left(\frac{h\,EI}{v}\right) \qquad \textbf{(EQ 39)}$$

It has been found that Eq 39 gives results that are too high, but that the slope of $1/(\theta_p - \theta_0)$ versus r^2 is accurate. To rectify this situation, Eq 39 is forced to fit experimental results by specifying a known temperature/location condition. When this is done, Eq 39 becomes:

$$\frac{1}{q_p - q_0} = \left(\frac{[e\,r\,C_p p\,(r^2 - r_t^2)]/2}{\left(\frac{h\,EI}{v}\right)}\right) + \frac{1}{q_r - q_0} \qquad \textbf{(EQ 40)}$$

where θ_r and r_r are the reference temperature and distance. If the peak temperature (θ_p) evaluation is restricted to locations on the plate surface ($z = 0$), and if the reference temperature and distance are assumed to be the melting temperature and the distance from the weld centerline to the fusion boundary (one half of the weld bead width), then Eq 40 can be written as:

$$\frac{1}{q_p - q_0} = \left(\frac{\frac{e\,r\,C_p p\,(y^2 - \left(\frac{d}{2}\right)^2}{2}}{\left(\frac{h\,EI}{v}\right)}\right) + \frac{1}{q_m - q_0} \qquad \textbf{(EQ 41)}$$

where θ_m is the melting temperature and d is the weld bead width. This equation gives the peak temperature θ_p in a thick plate at a distance y from the weld centerline.

Solidification Rate. The weld solidification structure can be determined by using the constitutional supercooling criterion. Three thermal parameters that influence the solidification structure are temperature gradient normal to the solid-liquid interface, G (°C/cm), solidification rate of the interface, R (cm/s), and cooling rate at the interface, $d\theta/dt$ at melting temperature (°C/s and equal to the product of GR). The microstructure may change from being planar to being cellular, a columnar dendrite, or an equiaxial structure if the G/R ratio becomes smaller. The dendrite arm spacing will decrease as the cooling rate increases. The solidification structure becomes refined at higher cooling rates.

At a quasi-steady state, the weld pool solidifies at a rate that is equal to the component of the electrode travel speed normal to the solid-liquid interface. Therefore, the solidification rate varies along the solid-liquid interface from the electrode travel speed, at the weld trailing edge, to zero, at the maximum pool width. The temperature gradient and the cooling rate at the solid-liquid interface can be determined from Eq 21, 24, and 27.

Modified Temperature Solution. The temperature solutions have a singularity at the center of the heat source. This singularity causes the predicted temperatures to be inaccurate in the area surrounding the heat source. However, a condition exists in which the peak temperature along the weld bead edge, that is, the solid-liquid interface location at the maximum pool width, is the melting temperature of the material. Using this temperature condition as a boundary condition for the temperature solutions, Eq 21 and 24 can be modified as shown below for thin plate:

$$q - q_0 = B_z \exp\left(\frac{-vw}{2k}\right) K_0\left(\frac{-vr}{2k}\right) \qquad \textbf{(EQ 42)}$$

where B_z is a heat input constant to be determined from the weld bead width, *d*.

$$B_z = \frac{q_m - q_0 \exp(vr_B / 2k)\left[\dfrac{K_0(vr_B / 2k)}{K_1(vr_B / 2k)}\right]}{K_0(vr_B / 2k)} \qquad \textbf{(EQ 43)}$$

with a bead width of:

$$d = 2r_B \left\{1 - \left[\frac{K_0(vr_B / 2k)}{K_1(vr_B / 2k)}\right]^2\right\}^{0.5} \qquad \textbf{(EQ 44)}$$

and for thick plate:

$$q_m - q_0 = B_z \exp\left[\frac{-v(w+r)}{2k}\right] / r \qquad \textbf{(EQ 45)}$$

$$B_z = (q_m - q_0) r_B \exp\left(\frac{-vr_B}{2k}\right)\left[\frac{1}{1+(2k / vr_B)} - 1\right] \qquad \textbf{(EQ 46)}$$

with a bead width of:

$$d = 2r_B \left[1 - \frac{1}{1+(2k / vr_B)}\right]^{0.5} \qquad \textbf{(EQ 47)}$$

The welding heat input, *Q*, is replaced by the weld bead width.

A Practical Application of Heat Flow Equations (Ref 22). The thermal condition in and near the weld metal must be established to control the metallurgical events in welding. The particular items of interests are the:

- DISTRIBUTION OF PEAK TEMPERATURE IN THE HAZ
- COOLING RATES IN THE WELD METAL AND IN THE HAZ
- SOLIDIFICATION RATE OF THE WELD METAL

Although the following discussion primarily focuses on manual are welding, certain general statements are applicable to all welding processes.

Peak Temperatures. The distribution of peak temperatures in the base metal adjacent to the weld is given by (Ref 23):

$$\frac{1}{T_p - T_0} = \frac{4.13 r C_p t Y}{H_{met}} + \frac{1}{T_m - T_0} \qquad \textbf{(EQ 48)}$$

where T_p is the peak temperature (°C) at distance Y (mm) from the weld fusion boundary, T_0 is the initial temperature (°C), T_m is the melting temperature (°C), H_{net} is the net energy input equal to $\eta EI/v$ (J/s · mm), ρ is the density of the material (g/mm^3), C_p is the specific heat of solid metal (J/g · °C), and t is the thickness of the base metal (mm).

Equation 48 can be used in order to determine the:

- PEAK TEMPERATURES AT SPECIFIC LOCATIONS IN THE HAZ
- WIDTH OF THE HAZ
- EFFECT OF PREHEAT ON THE WIDTH OF THE HAZ

In addition, determination of the peak temperature at specific locations in the HAZ and the width of the HAZ can be obtained by the procedure described from Eq 34, 35, 36, 37, 38, 39, 40, and 41.

Cooling Rate. Because the cooling rate varies with position and time, its calculation requires the careful specification of conditions. The most useful method is to determine the cooling rate on the weld centerline at the instant when the metal passes through a particular temperature of interest, T_c. At a temperature well below melting, the cooling rate in the weld and in its immediate HAZ is substantially independent of position. For carbon and low-alloy steels, T_c is the temperature near the pearlite "nose" temperature on the time-temperature transformation (TTT) diagram. The value of T_c = 550 °C (1020 °F) is satisfactory for most steels, although not critical.

The cooling rate for thick plate (Ref 23) is:

$$R = \frac{2\pi l (T_c - T_0)^2}{H_{met}} \qquad \textbf{(EQ 49)}$$

Equation 49 is comparable to Eq 31, which was obtained by the procedure described in the section "Cooling Rate" in this article. Adams (Ref 24) has developed a cooling rate equation for thin plate along the centerline from Eq 24.

The cooling rate for thin plate (Ref 24) is:

$$R = 2\pi l r C_p \left(\frac{t}{H_{met}} \right)^2 + (T_c - T_0)^3 \qquad \textbf{(EQ 50)}$$

where R is the cooling rate (°C/s) at a point on the weld centerline at just that moment when the point is cooling past the T_c, and λ is the thermal conductivity of the metal (J/mm · s · °C).

The dimensionless quantity t , called the "relative plate thickness," can be used to determine whether the plate is thick or thin:

$$t = t\sqrt{\frac{r C_p (T_c - T_0)}{H_{met}}} \qquad \textbf{(EQ 51)}$$

The thick-plate equation applies when t is greater than 0.75, and the thin-plate equation applies when t is less than that value.

Equations 49 and 50 are used to determine the cooling rate along the centerline for thick plate and thin plate, respectively. If one is interested in the cooling rate at the location at distance y (in mm) from the centerline, iterative techniques should be used to solve the cooling rate. First, w and r can be obtained by iteration of the simultaneous equation, which consists of Eq 21 or 27, where θ equals θ_c and $r^2 = w^2 + y^2$, where y is given. Then substitute w and r into the differentiation, $\partial\theta/\partial t = -v\partial\theta/\partial w$, from the temperature from Eq 21 or 27. The result will be the cooling rate for thick or thin plate located at y distance from the centerline:

$$\frac{\partial q}{\partial t}_{qc}$$

In addition, the cooling rate for HAZ of low-carbon steel weldments can be obtained from Eq 32 directly.

The solidification rate can have a significant effect on metallurgical structure, properties, response to heat treatment, and soundness. The solidification time, S_t, of weld metal, measured in seconds, is:

$$S_t = \frac{LH_{net}}{2p\,l\,C_p(T_m - T_o)^2} \qquad \textbf{(EQ 52)}$$

where L is the heat of fusion (J/mm^3).

Example 1: Welding of 5 mm (0.2 in.) Thick Low-Carbon Steels.

The thermal properties needed for heat flow analysis are assumed to be:

MELTING TEMPERATURE (T_M), °C (°F)	1510 (2750)
AUSTENIZATION TEMPERATURE, °C (°F)	730 (1350)
THERMAL CONDUCTIVITY (λ), W/M · K (J/MM · S · °C)	11.7 (0.028)
VOLUMETRIC SPECIFIC HEAT (ρC_P), J/MM^3 · °C	0.0044
HEAT OF FUSION (L), J/MM^3	2

The welding condition is assumed to be:

CURRENT (I), A	200
ARC VOLTAGE (E), V	20
TRAVEL SPEED (V), MM/S (IN./S)	5 (0.2)
PREHEAT (T_0), °C (°F)	25 (77)
HEAT-TRANSFER EFFICIENCY (η)	0.9
NET ENERGY INPUT, H_{NET}, J/MM (KJ/IN.)	720 (18.3)

Calculation of the HAZ Width. The value of Y at T_p = 730 °C (1345 °F) must be determined from Eq 48:

$$\frac{1}{730-25} = \frac{4.13(0.0044)5Y_z}{720}\frac{1}{1510-25} \qquad \textbf{(EQ 53)}$$

resulting in a value for Y_z (the width of the HAZ) of 5.9 mm (0.24 in.).

In addition, the HAZ width can be obtained by the procedure described in Eq 34, 35, 36, 37, 38, 39, 40, and 41. By substituting $w = w_p$, $r = r_p$, $y = y_p$, and $z = 0$ (on surface) into Eq 35 and 36, we obtain:

$$\frac{-w_p}{r_p^2} - \frac{v}{2k}\left(1 + \frac{w_p}{r_p}\right) = 0 \qquad \textbf{(EQ 54)}$$

$$r_p^2 = w_p^2 + y_p^2 \qquad \textbf{(EQ 55)}$$

The substitution of Eq 55 in Eq 54 yields:

$$\frac{-w_p}{w_p^2 + y_p^2} = \frac{v}{2k} 1 + \frac{w_p}{\sqrt{w_p^2 + y_p^2}} \qquad \textbf{(EQ 56)}$$

Inserting v = 5 mm/s, $\kappa = \lambda/\rho c_p = 0.028/0.004$ into Eq 56:

$$\frac{-w_p}{w_p^2 + y_p^2} = 0.3831 + \frac{w_p}{\sqrt{w_p^2 + y_p^2}} \qquad \textbf{(EQ 57)}$$

w_p and y_p should satisfy Eq 57.

From the temperature distribution equation (Eq 21) and E = 10V, I = 200 A, η= 0.9, λ= 0.028, θ_p = 730 °C, θ_0 = 25 °C, v = 5 mm/s, $\kappa = \lambda/\rho c_p = 0.028/0.044$:

$$730 - 25 = \frac{0.9x20x200/5}{2p\,x0.028r_p} x \exp\left[\frac{-5(w_p + r_p)}{2x0.028/0.0044}\right] \qquad \textbf{(EQ 58)}$$

$$-1.76 + \mathrm{LN}R_P = -0.393\,(W_P + R_P) \qquad \textbf{(EQ 59)}$$

Solving Eq 21 using the above values, by iteration:

- ASSUME R_P = 3.4 AND PUT THIS VALUE OF R_P INTO EQ 59 TO OBTAIN W_P = -2.036. SUBSTITUTE R_P = 3.4 AND W_P = -2.036 INTO EQ 55 AND SOLVE FOR Y_P: Y_P = 2.7. SUBSTITUTE Y_P AND W_P INTO EQ 56: THE LEFT SIDE OF EQ 56 = 0.176; THE RIGHT SIDE OF EQ 56 = 0.158. THE RESULTS DO NOT SATISFY EQ 56.
- ASSUME R_P = 3.5 AND PUT THIS VALUE OF R_P INTO EQ 59 TO OBTAIN W_P = -2.2. SUBSTITUTE R_P = 3.5 AND W_P = -2.2 INTO EQ 55 AND SOLVE FOR Y_P: Y_P = 2.72. SUBSTITUTE Y_P AND W_P INTO EQ 56: THE LEFT SIDE OF EQ 56 = 0.179; THE RIGHT SIDE OF EQ 56 = 0.146. THE RESULTS DO NOT SATISFY EQ 56.
- ASSUME R_P = 3.3 AND PUT THIS VALUE OF R_P INTO EQ 59 TO OBTAIN W_P = -1.86. SUBSTITUTE R_P = 3.3 AND W_P = -1.86 INTO EQ 55 AND SOLVE FOR Y_P: Y_P = 2.726. SUBSTITUTE Y_P AND W_P INTO EQ 56: THE LEFT SIDE OF EQ 56 = 0.170; THE RIGHT SIDE OF EQ 56 = 0.171. EQUATION 56 IS NOW SATISFIED.

The full HAZ width equals $2y_p = 2 \times 2.726 = 5.5$ mm. Comparing this result, 5.5 mm, with the result obtained with Eq 48 (that is, 5.9 mm), we know that Eq 48 can be used to obtain accurate results when calculating HAZ width and peak temperature.

Effect of Tempering Temperature on Quenched and Tempered (Q&T) Steels. If the plate had been quenched and then tempered to 430 °C (810 °F), then any region heated above that temperature will have been "over-tempered" and may exhibit modified properties. It would then be reasonable to consider the modified zone as being "heat affected," with its outer extremity located where T_p = 430 °C (810 °F):

$$\frac{1}{430-25}=\frac{4.13(0.0044)5Y_z}{720}+\frac{1}{1510-25} \qquad \textbf{(EQ 60)}$$

resulting in a value for Y_z of 14.2 mm (0.568 in.).

Effect of Preheating Temperature on Q&T Steels. Assume that the Q&T steel described above was preheated to a temperature, T_0, of 200 °C (390 °F):

$$\frac{1}{430-200}=\frac{4.13(0.0044)5Y_z}{720}+\frac{1}{1510-200} \qquad \textbf{(EQ 61)}$$

resulting in a value for Y_z of 28.4 mm > 14.2 mm (1.14 > 0.568 in.). Therefore, increasing the preheating temperature will increase the value of Y_z.

Effect of Energy Input on Q&T Steels. Assume that the energy input into the Q&T steel (without preheating) increases 50% (that is, 1.08 kJ/mm, or 27.4 kJ/in.):

$$\frac{1}{430-200}=\frac{4.13(0.0044)5Y_z}{1080}+\frac{1}{1510-25} \qquad \textbf{(EQ 62)}$$

resulting in a value for Y_z of 21.3 mm > 14.2 mm (0.839 > 0.568 in.). Therefore, increasing the energy input will increase the value of Y_z.

Example 2: Welding of 6 mm (0.24 in.) Thick Low-Carbon Steels.

The thermal properties needed for heat-flow analysis are assumed to be:

MELTING TEMPERATURE (T_M), °C (°F)	1510 (2750)
AUSTENIZATION TEMPERATURE, °C (°F)	730 (1346)
THERMAL CONDUCTIVITY (l), W/M · K (J/MM · S · °C)	11.7 (0.028)
VOLUMETRIC SPECIFIC HEAT (r C_P), J/MM^3 · °C	0.0044
HEAT OF FUSION (L), J/MM^3	2

The welding condition is assumed to be:

CURRENT (I), A	**300**
ARC VOLTAGE (E), V	**25**
PREHEAT (T_0), °C (°F)	**25 (77)**
HEAT-TRANSFER EFFICIENCY (η)	**0.9**

Critical Cooling Rate at 550 °C (1020 °F) (T_c). A critical cooling rate exists for each steel composition. If the actual cooling rate in the weld metal exceeds this critical value, then hard martensitic structures may develop in the HAZ, and there is a great risk of cracking under the influence of thermal stresses in the presence of hydrogen.

The best way to determine the critical cooling rate is to make a series of bead-on-plate weld passes in which all parameters, except the arc travel speed, are held constant. After the hardness tests on the weld passes deposited at travel speeds of 6, 7, 8, 9 and 10 mm/s (0.23, 0.28, 0.32, 0.35, and 0.39 in./s), it was found that at the latter two travel speeds, the weld HAZ had the highest hardness. Therefore, the critical cooling rate was encountered at a travel speed of approximately 8 mm/s (0.32 in.s). At this speed, the net energy input is:

$$H_{net} = \frac{25(300)0.9}{8} = 8.43.75 J/mm \qquad \textbf{(EQ 63)}$$

From Eq 51, the relative plate thickness is:

$$t = 6\sqrt{\frac{0.0044(550-25)}{843.75}} = 0.31 \qquad \textbf{(EQ 64)}$$

Because t is less than 0.75, the thin-plate equation (Eq 50) applies:

$$\frac{R}{2p\,l} = 0.0044\left(\frac{6}{843.75}\right)^2 (550-25)^3 = 32.2 \qquad \textbf{(EQ 65)}$$

resulting in R being equal to $2\pi(0.028)32.2$, which is equal to 5.7 °C/s (10.3 °F/s). This value is the maximum safe cooling rate for this steel and the actual cooling rate cannot exceed this value.

Preheating Temperature Requirement. Although the critical cooling rate cannot be exceeded, in the actual welding operation a preheat can be used to reduce the cooling rate to 5.7 °C/s (10.3 °F/s).

Assume that the welding condition is:

CURRENT (I), A	250
ARC VOLTAGE (E), V	25
HEAT-TRANSFER EFFICIENCY (η)	0.9
TRAVEL VELOCITY (V), MM/S (IN./S)	7 (0.3)
PLATE THICKNESS (T), MM (IN.)	9 (0.4)

The energy heat input, H_{net}, is:

$$H_{net} = \frac{25(250)0.9}{7} = 804 J/mm \qquad \textbf{(EQ 66)}$$

Assuming that the thin-plate equation (Eq 50) applies:

$$\left(\frac{R}{2p\,l}\right)_{max} = 32.2 = 0.0044\left(\frac{9}{804}\right)^2 (550-T_0)^3 \qquad \textbf{(EQ 67)}$$

resulting in a T_0 of 162 °C (325 °F).

The relative plate thickness should be checked:

$$t = 9\sqrt{\frac{0.0044(550-162)}{804}} = 0.41 \qquad \textbf{(EQ 68)}$$

Because t is less than 0.75, the thin-plate equation does apply. If the initial plate temperature is raised either to or above 162 °C (325 °F), then the cooling rate will not exceed 5.7 °C/s (10.3 °F/s).

Effect of Joint Thickness. If the plate thickness increases from 9 to 25 mm (0.36 to 1 in.), but there is the same level of energy input, then the calculation of the initial plate temperature would be as follows. First, using the thin-plate equation (Eq 50):

$$\left(\frac{R}{2pl}\right)_{\max} = 32.2 = 0.0044\left(\frac{25}{804}\right)^2 (550-T_0)^3 \qquad \textbf{(EQ 69)}$$

resulting in a value for T_0 of 354 °C (670 °F).

The relative plate thickness, t, should be checked:

$$t = 25\sqrt{\frac{0.0044(550-354)}{804}} = 0.82 \qquad \textbf{(EQ 70)}$$

Because t is greater than 0.75, the use of the thin-plate equation is inadequate. Using the thick-plate equation (Eq 49):

$$32.2 = \frac{(550-T_0)^2}{804} \qquad \textbf{(EQ 71)}$$

resulting in a value for T_0 of 389 °C (730 °F).

The relative plate thickness should be checked:

$$t = 25\sqrt{\frac{0.0044(550-389)}{804}} = 0.74 \qquad \textbf{(EQ 72)}$$

Although t is less than, but near to, 0.75, using the thin-plate equation is adequate. Therefore, the initial temperature should be raised to 389 °C (730 °F) to avoid exceeding the cooling rate of 5.7 °C/s (10.3 °F).

Now, if the plate thickness increases to 50 mm (2 in.), but there is the same level of energy input, then the thick-plate equation (Eq 49) applies and, again, the value for T_0 is 389 °C (730 °F).

The relative plate thickness should be checked:

$$t = 50\sqrt{\frac{0.0044(550-389)}{804}} = 1,48 \qquad \textbf{(EQ 73)}$$

Because t is greater than 0.75, the use of the thick-plate equation is adequate.

Under some welding conditions, it is not necessary to reduce the cooling rate by using a preheat. For example, if the plate thickness is 5 mm (0.2 in.) and there is the same level of energy input:

$$\left(\frac{R}{2p\,l}\right)_{\max} = 32.2 = 0.0044\left(\frac{5}{804}\right)^2 (550 - T_0)^3 \qquad \textbf{(EQ 74)}$$

resulting in a value for T_0 of -24 °C (-11 °F). Therefore, using a preheat is unnecessary.

Fillet-Welded "T" Joints. For a weld with a higher number of paths, as occurs in fillet-welded "T" joints, it is sometime necessary to modify the cooling-rate equation, because the cooling of a weld depends on the available paths for conducting heat into the surrounding cold base metal.

When joining 9 mm (0.35 in.) thick plate, where H_{net} = 804 J/mm (20.4 kJ/in.), and when there are three legs instead of two, the cooling-rate equation is modified by reducing the effective energy input by a factor of $\frac{2}{3}$:

$$H_{NET} = \frac{2}{3}\,(804) = 536 \text{ J/MM} \qquad \textbf{(EQ 75)}$$

Using the thin-plate equation (Eq 50):

$$\left(\frac{R}{2p\,l}\right)_{\max} = 32.2 = 0.0044\left(\frac{9}{536}\right)^2 (550 - T_0)^3 \qquad \textbf{(EQ 76)}$$

resulting in a value for T_0 of 254 °C (490 °F).

The relative plate thickness should be checked:

$$t = 9\sqrt{\frac{0.0044(550 - 254)}{536}} = 0,44 \qquad \textbf{(EQ 77)}$$

Because t is less than 0.75, using the thin-plate equation is adequate. Therefore, a higher preheat temperature is more necessary than a butt weld because of the enhanced cooling.

Example 3: Cooling Rate for the Location at Distance *y* (in cm) from the Centerline.

For a steel plate of 25 mm (1 in.) thickness, (*t*), the welding condition is assumed to be:

HEAT INPUT (ηEI), KW (CAL/S)	7.5 (1800)
TRAVEL SPEED (V), CM/S (IN./S)	0.1 (0.04)
PREHEAT (T_0), °C (°F)	20 (68)
NET ENERGY INPUT (H_{NET}), CAL/CM	18,000

The thermal properties needed for heat flow analysis are assumed to be:

MELTING TEMPERATURE (T_M), °C (°F)	1400 (2550)
THERMAL CONDUCTIVITY (λ), W/M · K (CAL_{IT}/CM · S · °C)	43.1 (0.103)
SPECIFIC HEAT (C_P), J/KG · C (BTU/LB · °F)	473 (0.113)
DENSITY (ρ), G/CM^3 (LB/$IN.^3$)	7.8 (0.28)

Assume that one is interested in the critical cooling rate at the location on the surface (z = 0) at distance y = 2 cm from the centerline at the instant when the metal passes through the specific temperature of 615 °C (1140 °F). Initially, the relative plate thickness should be checked. From Eq 51, the relative plate thickness (using English units) is:

$$t = 25\sqrt{\frac{7.8x0.113(615-20}{18,000}} = 4,267$$

Because t is greater than 0.75, this plate can be treated as a thick plate. From Eq 78, cooling rate for thick plate at the location where the variables are w and r and at critical temperature $\theta = \theta_c$ is:

$$\frac{\partial q}{\partial t} = -v\frac{\partial q}{\partial w} = \frac{-vhEI}{2p\,l\,r}\exp\left[\frac{-v(w+r)}{2k}\right]x\left[\frac{-w}{r^2} - \frac{v}{2k}\left(1+\frac{w}{r}\right)\right] \qquad \textbf{(EQ 78)}$$

To solve Eq 78, we need to calculate the value of w and r first. From Eq 21, the temperature distribution of thick plate, and Eq 36 where z = 0, we can get:

$$q - q_0 = \frac{hEI}{2p\,l\,r}\exp\left(\frac{-v(w+r)}{2k}\right) \qquad \textbf{(EQ 79)}$$

and $r=\sqrt{w^2+y^2}$

By substituting the welding condition and material properties into Eq 21, Eq 36, and $r = \sqrt{w^2+y^2}$, we can obtain the following simultaneous equations:

$$615-20 = \frac{1800}{22p\,x0.103r}\exp\left[\frac{-0.1(w+r)}{2x0.117}\right]$$

and $r=\sqrt{w^2+4}$

The value of w and r can be solved by using iteration techniques to solve the above simultaneous equation. The result is that w = -3 cm and r = 3.606 cm.

Substituting w and r into Eq 78:

$$\frac{\partial q}{\partial t}_{qC} = -v\frac{\partial q}{\partial w} = \frac{-0.1x1800}{2p\,x0.103x3.606}x\exp\left[\frac{-0.1(-3+3.606}{2x0.117}\right]x\left[\frac{-(-3)}{3.606^2} - \frac{0.1}{2x0.117}\left(1+\frac{-3}{3.606}\right)\right]$$

Therefore:

$$\left.\frac{\partial q}{\partial t}\right|_{qC} = -9.78°C/s$$

From Eq 49 we can calculate the cooling rate along the centerline at the same temperature (615 °C, or 1140 °F):

$$R = \frac{2p\,x0.103(615-20)^2}{18,000} = 12.7°C/s$$

Also from Eq 32, we can calculate the cooling rate in the heat-affected zone at a temperature of 615 °C (1140 °F):

$$\frac{\partial q}{\partial t}_{qC=615} = 0.35\left\{\left[\frac{615-20}{336/2.362}\right]^{1.7} x\left[1+\frac{2}{p}\tan^{-1}\left(\frac{0.9843-0.486}{0.125}\right)\right]\right\}^{0.8} = 4°C/s$$

Therefore, at the same temperature, the cooling rate at the centerline is greater than the cooling rate at the location a distance *y* from the centerline. In addition, the cooling rate of the heat-affected zone is less than the cooling rate in the weld pool at the same temperature.

Example 4: Solidification Rate.

A weld pass of 800 J/mm (20.3 kJ/in.) in net energy input is deposited on a steel plate. The initial temperature is 25 °C (75 °F). The solidification time would be:

$$S_t = \frac{2(800)}{2p\,(0.028)(0.0044)(1510-25)^2} = 0.94(s) \qquad \textbf{(EQ 80)}$$

References cited in this section

22. HEAT FLOW IN WELDING, CHAPTER 3, *WELDING HANDBOOK*, VOL 1, 7TH ED., AWS, 1976
23. C.M. ADAMS, JR. COOLING RATE AND PEAK TEMPERATURE IN FUSION WELDING, *WELD. J.*, VOL 37 (NO. 5), 1958, P 210S-215S
24. C.M. ADAMS, JR., COOLING RATES AND PEAK TEMPERATURES IN FUSION WELDING, *WELD. J.*, VOL 37 (NO. 5), P 210-S TO 215-S
25. H. KIHARA, H. SUZUKI, AND H. TAMURA, *RESEARCH ON WELDABLE HIGH-STRENGTH STEELS*, 60TH ANNIVERSARY SERIES, VOL 1, SOCIETY OF NAVAL ARCHITECTS OF JAPAN, TOKYO, 1957
26. C.E. JACKSON, DEPARTMENT OF WELDING ENGINEERING, THE OHIO STATE UNIVERSITY LECTURE NOTE, 1977
27. C.E. JACKSON AND W.J. GOODWIN, EFFECTS OF VARIATIONS IN WELDING TECHNIQUE ON THE TRANSITION BEHAVIOR OF WELDED SPECIMENS--PART II, *WELD. J.*, MAY 1948, P 253-S TO 266-S

Parametric Effects

To show the effects of material property and welding condition on the temperature distribution of weldments, the welding of 304 stainless steel, low-carbon steel, and aluminum are simulated for three different welding speeds: 1.0, 5.0, and 8.0 mm/s (0.04, 0.02, and 0.03 in./s). The thermal conductivity and thermal diffusivity of 304 stainless steel are 26 W/m · K (0.062 cal/cm · s · °C) and 4.6 mm^2/s (0.007 $in.^2/s$), respectively. For low-carbon steel, the respective values are 50 W/m K (0.12 cal/cm s °C) and 7.5 mm^2/s (0.012 $in.^2/s$), whereas for aluminum, the respective values are 347 W/m K (0.93 cal/cm · s · °C) and 80 mm^2 (0.12 $in.^2/s$). The heat input per unit weld length was kept constant, 4.2 kJ/s (1 kcal/s), for all cases. The parametric results are described below.

Effect of Material Type. Figures 5(a), 5(b), and 5(c) depict the effect of thermal properties on isotemperature contours for a heat input of 4.2 kJ/s (1 kcal/s) and travel speeds of 1.0, 5.0, and 8.0 mm/s (0.04, 0.02, and 0.3 in./s). The temperature spreads over a larger area and causes a larger weld pool (larger weld bead) for low-conductivity material. The isotemperature contours also elongate more toward the back of the arc for low-conductivity material. For aluminum, a larger heat input would be required to obtain the same weld size as the stainless steel weldment.

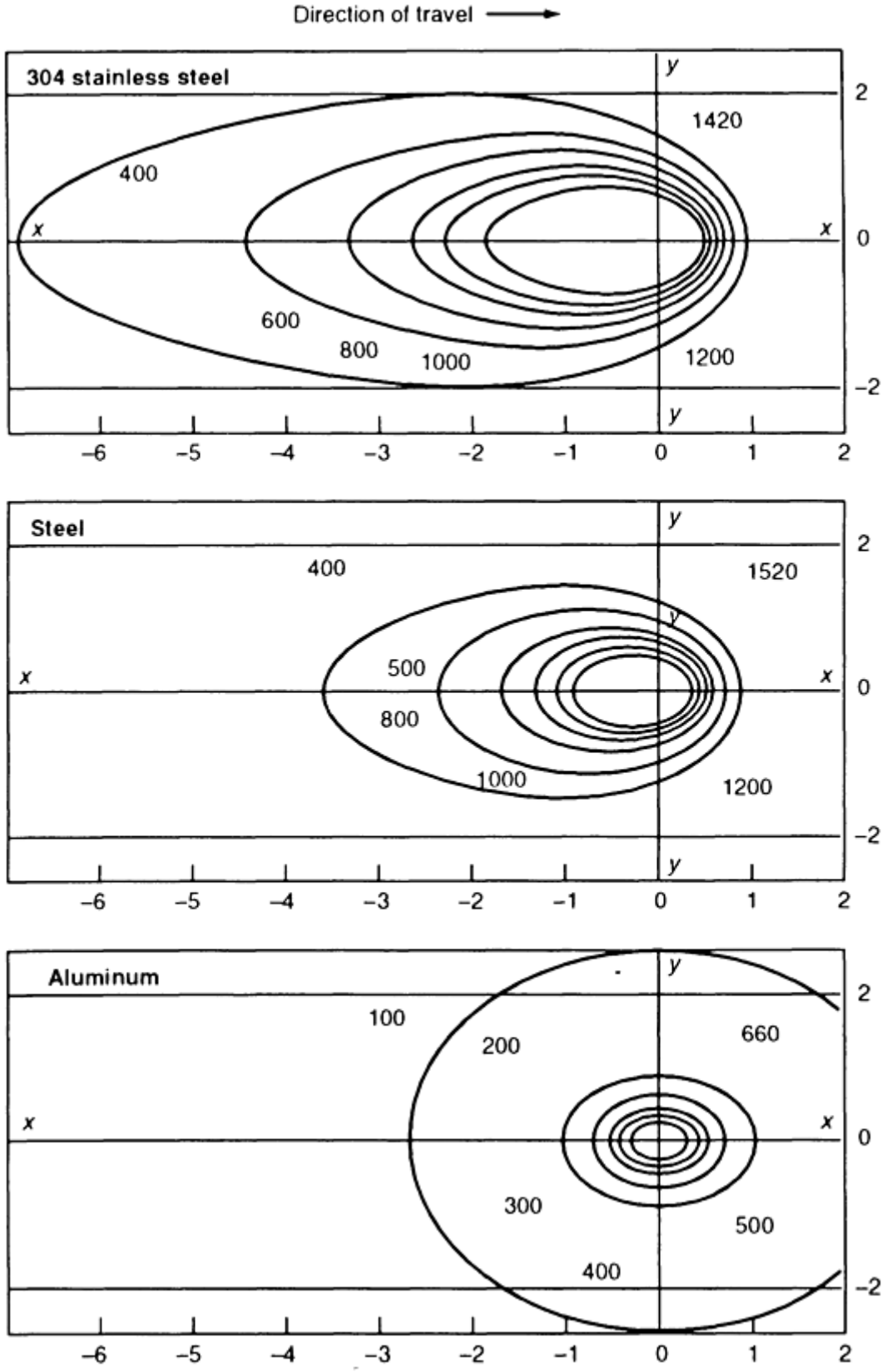

FIG. 5(A) EFFECT OF THERMAL PROPERTY ON ISOTEMPERATURE CONTOURS FOR A HEAT INPUT OF 4.2 KJ/S (1000 CAL/S) AT A WELDING SPEED, *V*, OF 1 MM/S (0.04 IN./S) AND THE RESPECTIVE THERMAL CONDUCTIVITIES OF EACH MATERIAL (REFER TO TEXT FOR VALUES). VALUES FOR *X* AND *Y* ARE GIVEN IN CM, AND TEMPERATURES ARE GIVEN IN °C.

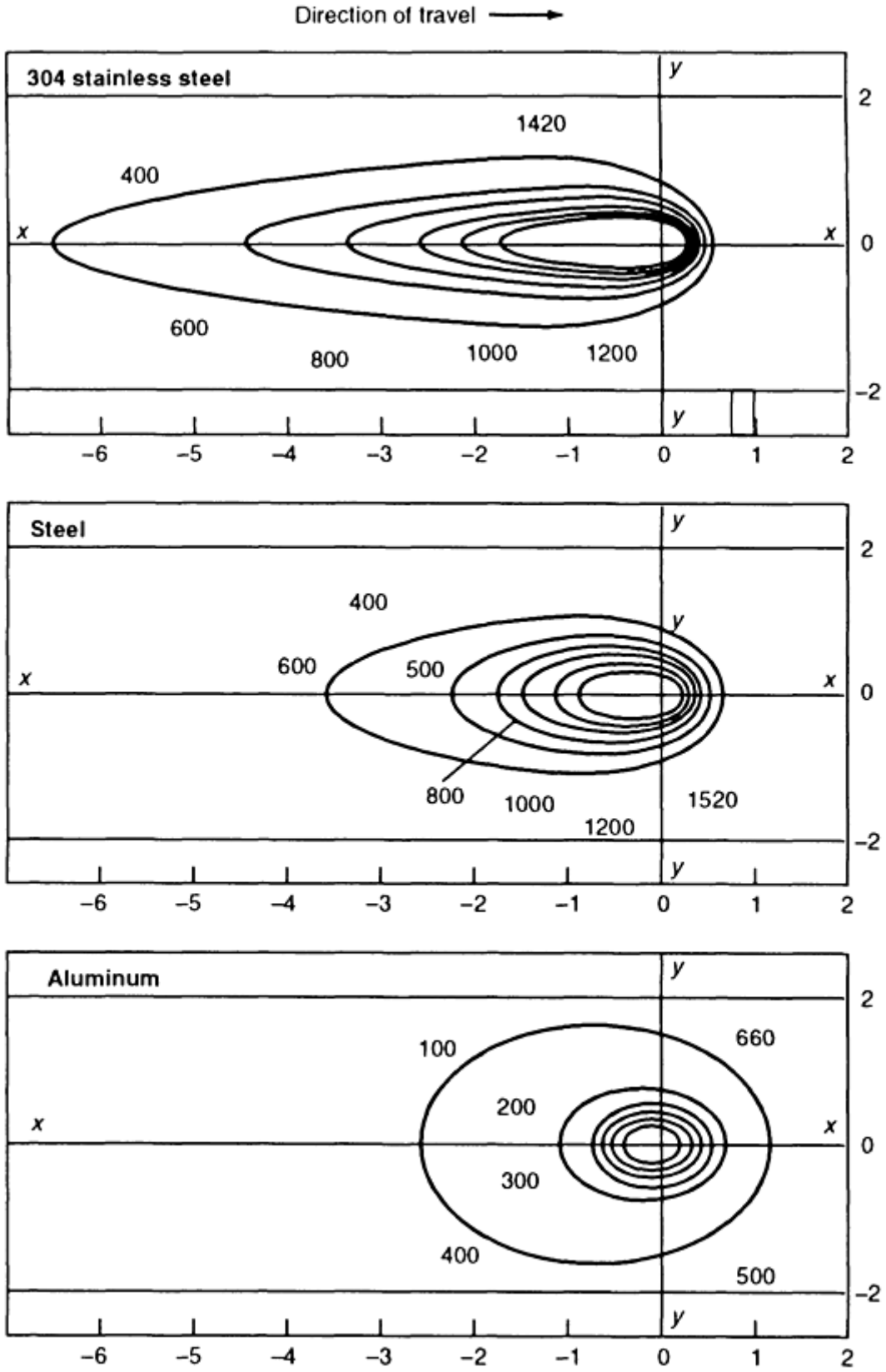

FIG. 5(B) EFFECT OF THERMAL PROPERTY ON ISOTEMPERATURE CONTOURS FOR A HEAT INPUT OF 4.2 KJ/S (1000 CAL/S) AT A WELDING SPEED, *V*, OF 5 MM/S (0.02 IN./S) AND THE RESPECTIVE THERMAL CONDUCTIVITIES OF EACH MATERIAL (REFER TO TEXT FOR VALUES). VALUES FOR *X* AND *Y* ARE GIVEN IN CM, AND TEMPERATURES ARE GIVEN IN °C.

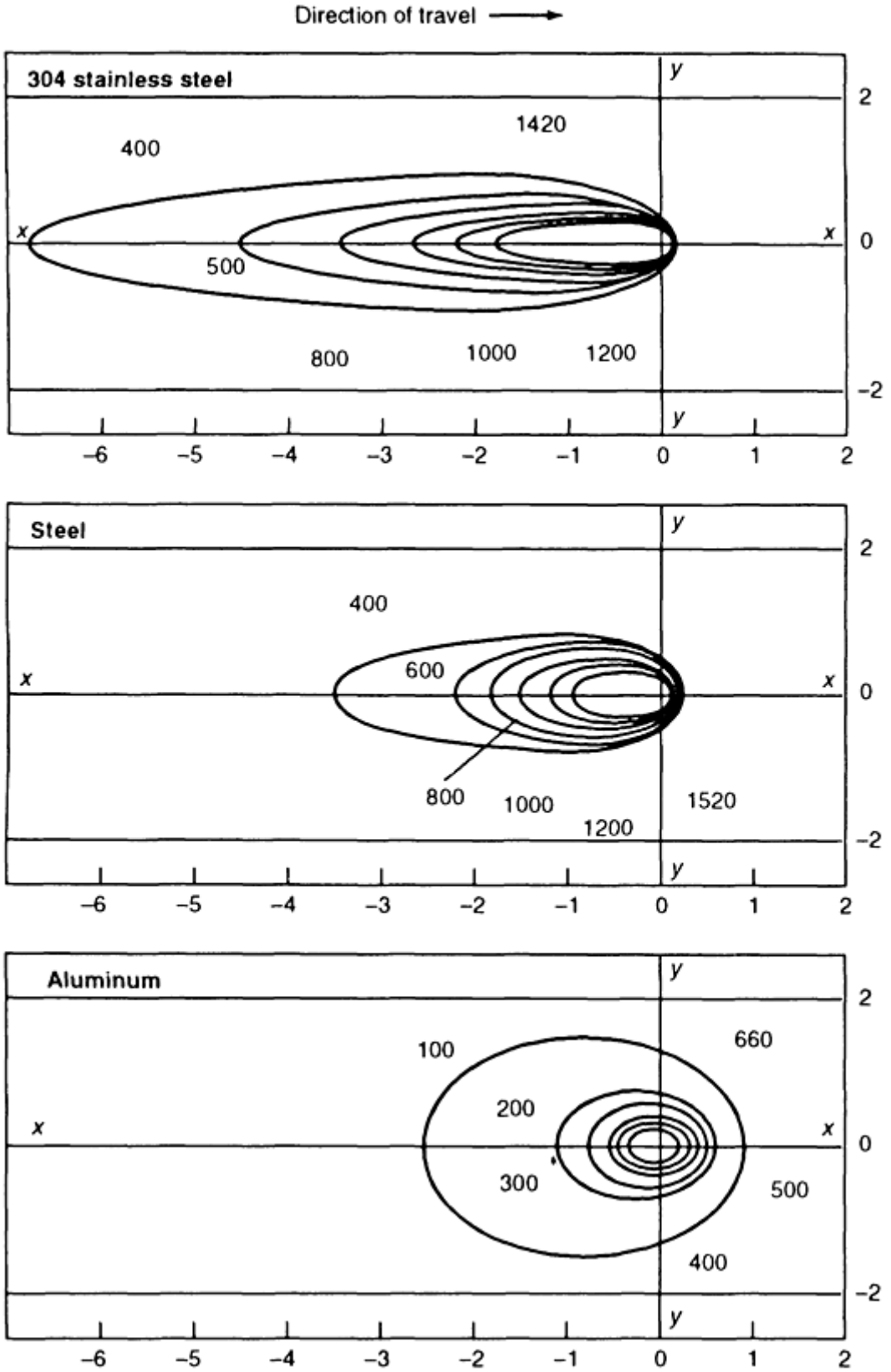

FIG. 5(C) EFFECT OF THERMAL PROPERTY ON ISOTEMPERATURE CONTOURS FOR A HEAT INPUT OF 4.2 KJ/S (1000 CAL/S) AT A WELDING SPEED, *V*, OF 8 MM/S (0.3 IN./S) AND THE RESPECTIVE THERMAL CONDUCTIVITIES OF EACH MATERIAL (REFER TO TEXT FOR VALUES). VALUES FOR *X* AND *Y* ARE GIVEN IN CM, AND TEMPERATURES ARE GIVEN IN °C.

Welding Speed. Figures 6(a), 6(b), and 6(c) show the effect of welding speed on isotemperature contours. When the travel speed increases, the weld size decreases and the isotemperature contours are more elongated toward the back of the arc. Larger heat inputs would be required for faster travel speeds in order to obtain the same weld size.

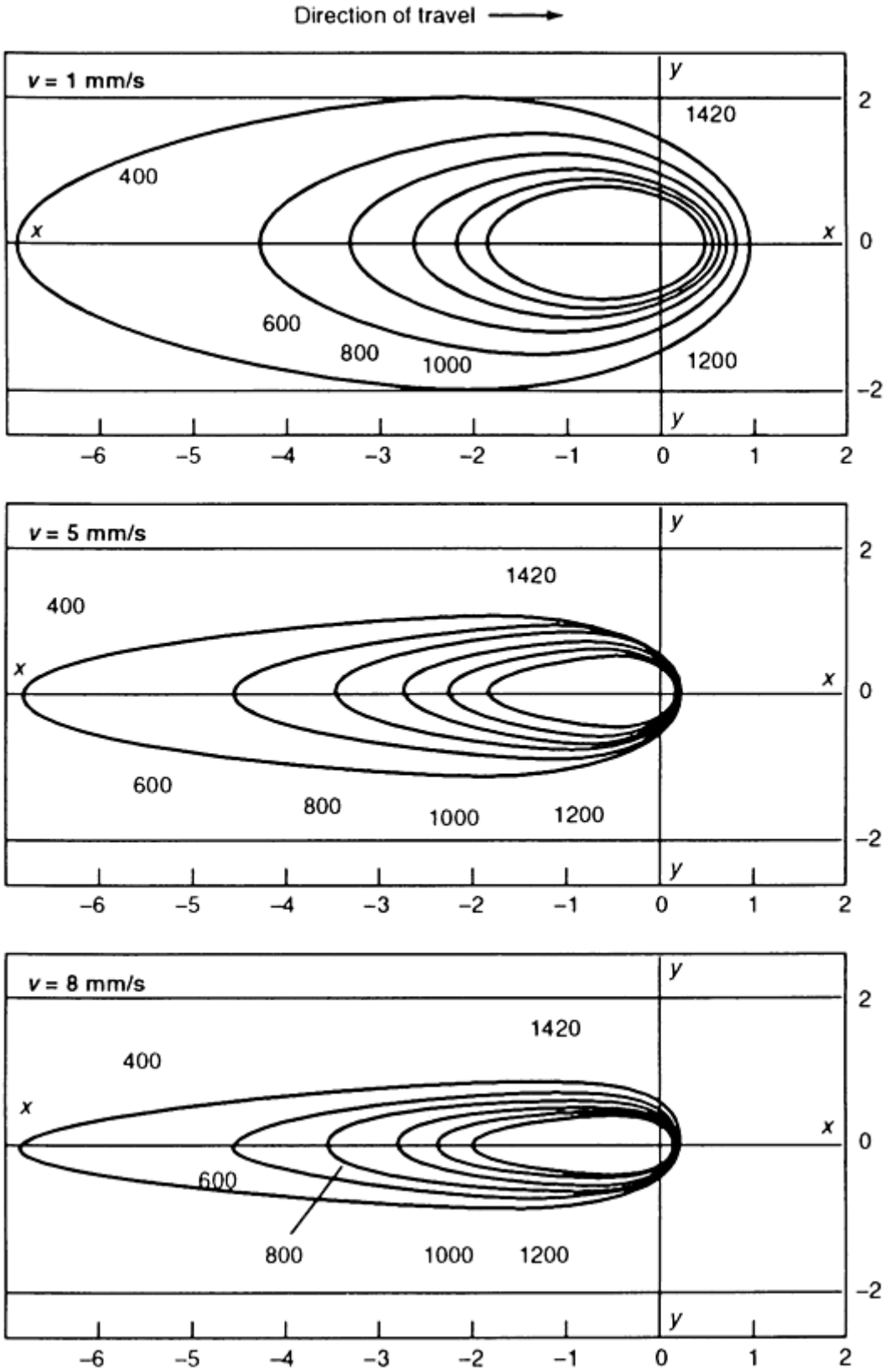

FIG. 6(A) EFFECT OF WELDING SPEED, *V*, ON ISOTEMPERATURE CONTOURS OF 304 STAINLESS STEEL FOR 4.2 KJ/S (1000 CAL/S) HEAT INPUT

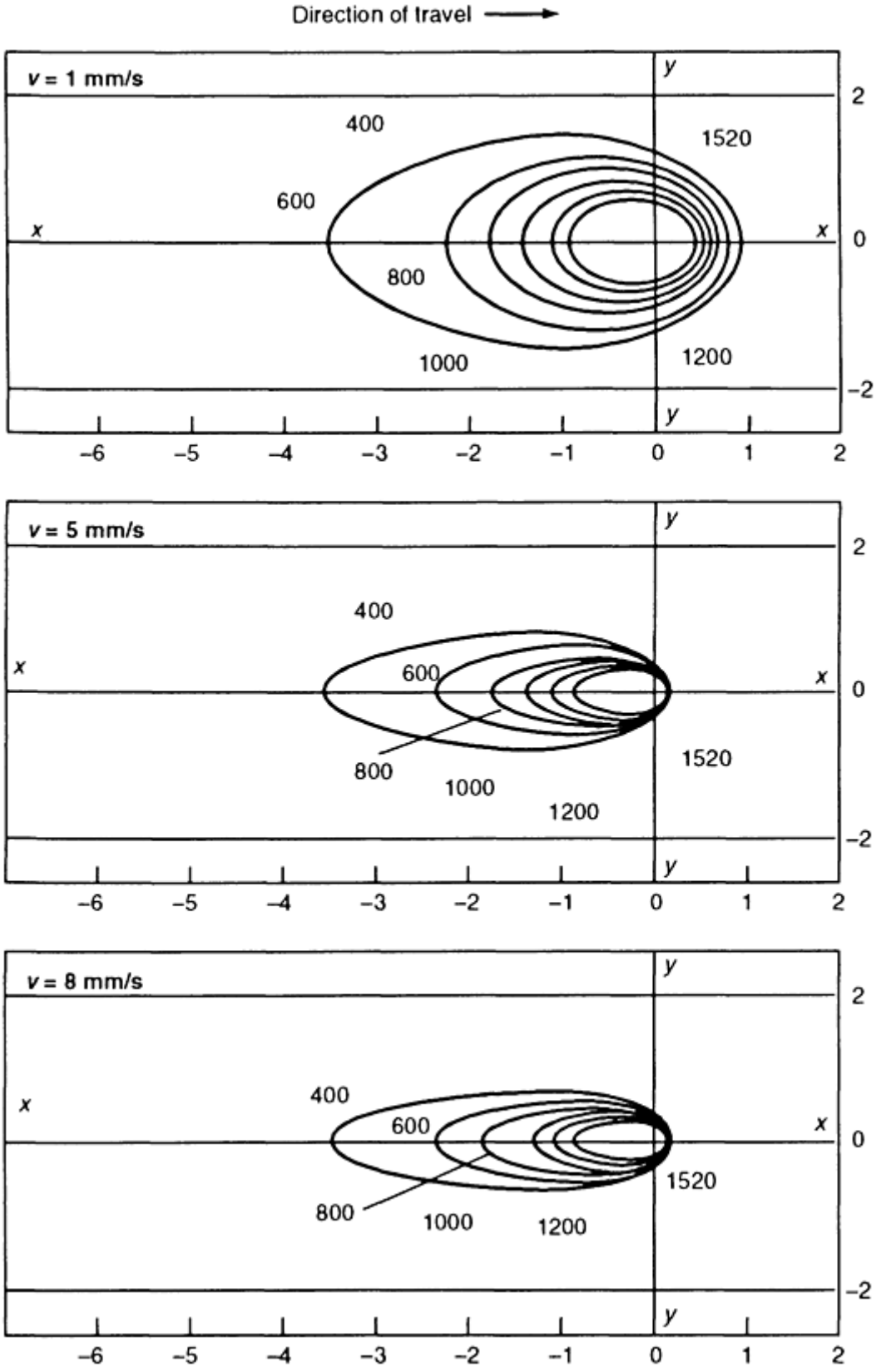

FIG. 6(B) EFFECT OF WELDING SPEED, *V*, ON ISOTEMPERATURE CONTOURS OF LOW-CARBON STEEL FOR 4.2 KJ/S (1000 CAL/S) HEAT INPUT

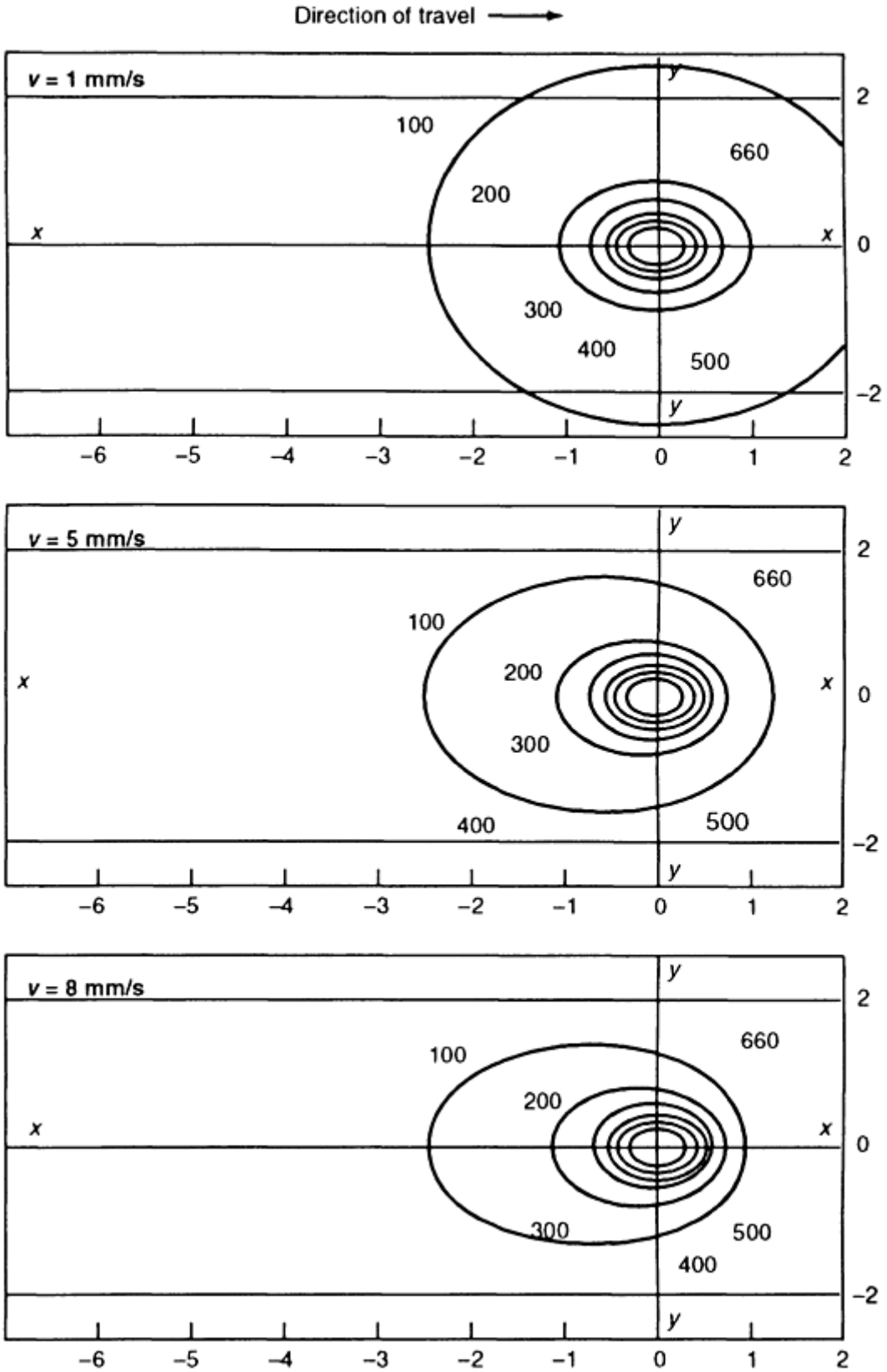

FIG. 6(C) EFFECT OF WELDING SPEED, *V*, ON ISOTEMPERATURE CONTOURS OF ALUMINUM FOR 4.2 KJ/S (1000 CAL/S) HEAT INPUT

Figure 7 shows the effect of welding heat input on the peak temperature at two locations, 6.4 mm ($\frac{1}{4}$ in.) and 13 mm ($\frac{1}{2}$ in.) from the weld centerline. (The material simulated in this illustration is low-carbon steel plate with a large thickness.) Within the practical range of welding conditions for the GMAW process of low-carbon steels, the peak temperature at both locations increases linearly, as the welding current increases, and decreases exponentially, with the travel speed. To increase welding current proportionally with travel speed for a constant heat input per unit weld length (that is. $\dot{Q}/V$ = constant), the peak temperature at two locations increases with the travel speed, which implies a larger weld size resulting from higher heat input. The welding current has a more significant effect on peak temperature than does the travel speed. However, the increase in peak temperature is more dominant at the 6.4 mm ($\frac{1}{4}$ in.) location. The influence of proportional increase in welding current and travel speed on peak temperature diminishes as the distance from the weld centerline increase and when the travel speed becomes high.

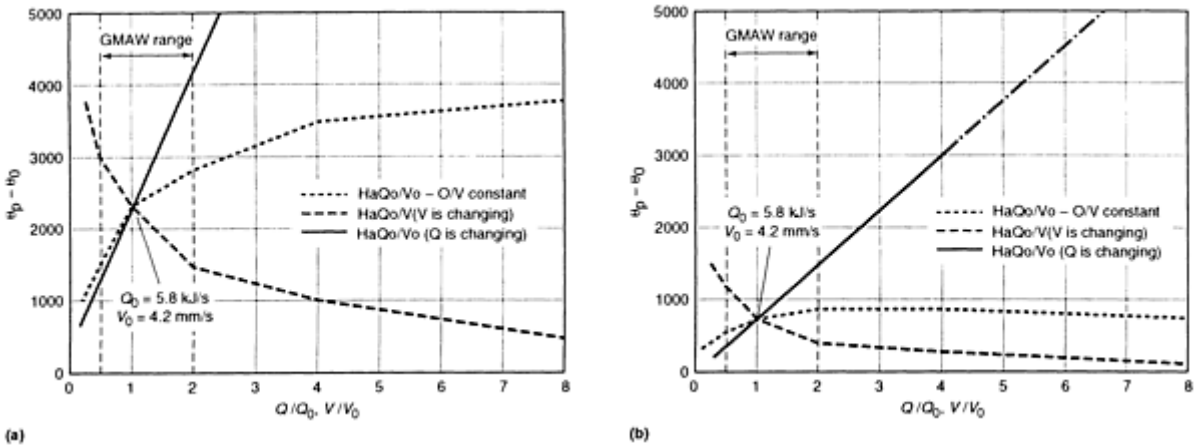

FIG. 7 PEAK TEMPERATURE DETERMINED BY THE POINT HEAT SOURCE SOLUTION. (A) AT 6.4 MM ($\frac{1}{2}$ IN.) FROM THE CENTER. (B) AT 13 MM ($\frac{1}{2}$ IN.) FROM THE CENTER

Heat Flow in Fusion Welding

Chon L. Tsai and Chin M. Tso, The Ohio State University

Thermophysical Properties of Selected Engineering Materials

For the sake of convenience when using heat-flow equations, the thermal properties of selected engineering materials are provided in Table 2.

TABLE 2 THERMAL PROPERTIES OF SELECTED ENGINEERING ALLOYS

ALLOY	DENSITY (ρ), AT 20 °C (68 °F), G/CM^3	SPECIFIC HEAT (CP), AT 20 °C (68 °F), KJ/KG · K	THERMAL CONDUCTIVITY (κ) AT 20 °C (68 °F, W/M · K)	COEFFICIENT OF THERMAL EXPANSION (α), AT 20 °C (68 °F), 10 $^{-5}$/°C
CARBON STEEL				
~0.5% C	7.833	0.465	54	1.474

~1.0% C	7.801	0.473	43	1.172
~1.5% C	7.753	0.486	36	0.970
ALUMINUM				
AL-CU (94-96 % AL, 3-5% CU)	2.787	0.883	164	6.676
AL-SI (86.5% AL. 1% CU)	2.659	0.867	137	5.933
AL-SI (78-80% AL, 20-22% SI)	2.627	0.854	161	7.172
AL-MG-SI (97% AL, 1% MG, 1% SI, 1% MN)	2.707	0.892	177	7.311
TITANIUM	4.500	0.52	16	0.84

ALLOY	**DENSITY (ρ), AT 100 °C (212 °F), G/CM^2**	**SPECIFIC HEAT (*C*P), AT 0-100 °C (32-212 °F), KJ/KG · K**	**THERMAL CONDUCTIVITY (κ), AT 100 °C (212 °F), W/M · K**	**COEFFICIENT OF THERMAL EXPANSION (α), AT 0-538 °C (32-1000 °F), 10 $^{-5}$/°C**
STAINLESS STEEL				
CHROMIUM-NICKEL AUSTENITIC	7.800-8.000	0.46-0.50	18.7-22.8	1.700-1.920
CHROMIUM FERRITIC	7.800	0.46-0.50	24.4-26.3	1.120-1.210
CHROMIUM MARTENSITIC	7.800	0.42-0.46	28.7	1.160-1.210
CARBON STEEL	7.800	0.48	60	1.17

Heat Flow in Fusion Welding

Chon L. Tsai and Chin M. Tso, The Ohio State University

References

1. N.S. BOULTON AND H.E. LANCE-MARTIN, RESIDUAL STRESSES IN ARC WELDED PLATES, *PROC. INST. MECH. ENG.*, VOL 33, 1986, P 295
2. D. ROSENTHAL AND R. SCHMERBER, THERMAL STUDY OF ARC WELDING, *WELD. J.*, VOL 17 (NO. 4), 1983, P 2S
3. N.N. RYKALIN, "CALCULATIONS OF THERMAL PROCESSES IN WELDING," MASHGIZ, MOSCOW, 1951
4. K. MASUBUCHI, *ANALYSIS OF WELDED STRUCTURES*, PERGAMON PRESS, 1980
5. C.L. TSAI, "PARAMETRIC STUDY ON COOLING PHENOMENA IN UNDERWATER WELDING," PH.D THESIS, MIT, 1977
6. C.L. TSAI, FINITE SOURCE THEORY, *MODELING OF CASTING AND WELDING PROCESSES II*, ENGINEERING FOUNDATION MEETING, NEW ENGLAND COLLEGE (HENNIKER, NH), 31 JULY TO 5 AUG 1983, P 329
7. R. PAVELIC, R. TANAKUCHI, O. CZEHARA, AND P. MYERS, EXPERIMENTAL AND COMPUTED TEMPERATURE HISTORIES IN GAS TUNGSTEN ARC WELDING IN THIN PLATES, *WELD. J.*, VOL 48 (NO. 7), 1969, P 295S
8. S. KOU, 3-DIMENSIONAL HEAT FLOW DURING FUSION WELDING, *PROC. OF METALLURGICAL SOCIETY OF AIME*, AUG 1980, P 129-138
9. P.G. KOGAN, THE TEMPERATURE FIELD IN THE WELD ZONE, *AVE. SVARKA*, VOL 4 (NO. 9), 1979, P 8
10. G.M. ECER, H.D. DOWNS, H.D. BRODY, AND M.A. GOKHALE, HEAT FLOW SIMULATION OF PULSED CURRENT GAS TUNGSTEN ARC WELDING, *MODELING OF CASTING AND WELDING PROCESSES*, ENGINEERING FOUNDATION 1980 MEETING (RINDGE, NH), 3-8 AUG 1980, P 139-160

11. H. HIBBITT AND P. MARCAL, A NUMERICAL THERMOMECHANICAL MODEL FOR WELDING AND SUBSEQUENT LOADING OF A FABRICATED STRUCTURE, *COMPUT. STRUCT.,* VOL 3, 1973, P 1145
12. E. FRIEDMAN, THERMOMECHANICAL ANALYSIS OF THE WELDING PROCESS USING FINITE ELEMENT METHODS, *TRANS. ASME,* AUG 1975, P 206
13. Z. PALEY AND P. HIBBERT, COMPUTATION OF TEMPERATURE IN ACTUAL WELD DESIGN, *WELD. J.,* VOL 54 (NO. 11), 1975, P 385.S
14. T. NAKA, TEMPERATURE DISTRIBUTION DURING WELDING, *J. JPN. WELD. SOC.,* VOL 11 (NO. 1), 1941, P 4
15. K. MASUBUCHI AND T. KUSUDA, TEMPERATURE DISTRIBUTION OF WELDED PLATES, *J. JPN WELD. SOC.,* VOL 22 (NO. 5), 1953, P 14
16. C.L. TSAI AND C.A. HOU, THEORETICAL ANALYSIS OF WELD POLL BEHAVIOR IN THE PULSED CURRENT GTAW PROCESS, *TRANSPORT PHENOMENA IN MATERIALS PROCESSING,* ASME WINTER ANNUAL MEETING, 1983
17. E. FRIEDMAN, "FINITE ELEMENT ANALYSIS OF ARC WELDING," REPORT WAPD-TM-1438, DEPARTMENT OF ENERGY, 1980
18. J.S. FAN AND C.L. TSAI, "FINITE ELEMENT ANALYSIS OF WELDING THERMAL BEHAVIOR IN TRANSIENT CONDITIONS," 84-HT-80, ASME
19. R.L. APPS AND D.R. MILNER, HEAT FLOW IN ARGON-ARC WELDING, *BR. WELD. J.,* VOL 2 (NO. 10), 1955, P 475
20. H.S. CARSLAW AND J.C. JAEGER, *CONDUCTION OF HEAT IN SOLIDS,* OXFORD PRESS
21. C.L. TSAI AND J.H. WU, "AN INVESTIGATION OF HEAT TRANSPORT PHENOMENA IN UNDERWATER WELDING," PRESENTED AT THE ASME WINTER ANNUAL MEETING (MIAMI BEACH, FL), 1985
22. HEAT FLOW IN WELDING, CHAPTER 3, *WELDING HANDBOOK,* VOL 1, 7TH ED., AWS, 1976
23. C.M. ADAMS, JR. COOLING RATE AND PEAK TEMPERATURE IN FUSION WELDING, *WELD. J.,* VOL 37 (NO. 5), 1958, P 210S-215S
24. C.M. ADAMS, JR., COOLING RATES AND PEAK TEMPERATURES IN FUSION WELDING, *WELD. J.,* VOL 37 (NO. 5), P 210-S TO 215-S
25. H. KIHARA, H. SUZUKI, AND H. TAMURA, *RESEARCH ON WELDABLE HIGH-STRENGTH STEELS,* 60TH ANNIVERSARY SERIES, VOL 1, SOCIETY OF NAVAL ARCHITECTS OF JAPAN, TOKYO, 1957
26. C.E. JACKSON, DEPARTMENT OF WELDING ENGINEERING, THE OHIO STATE UNIVERSITY LECTURE NOTE, 1977
27. C.E. JACKSON AND W.J. GOODWIN, EFFECTS OF VARIATIONS IN WELDING TECHNIQUE ON THE TRANSITION BEHAVIOR OF WELDED SPECIMENS--PART II, *WELD. J.,* MAY 1948, P 253-S TO 266-S

Fluid Flow Phenomena During Welding

C.R. Heiple and P. Burgardt, EG&G Rocky Flats

Introduction

MOLTEN WELD POOLS are dynamic. Liquid in the weld pool in acted on by several strong forces, which can result in high-velocity fluid motion. Fluid flow velocities exceeding 1 m/s (3.3 ft/s) have been observed in gas tungsten arc (GTA) welds under ordinary welding conditions, and higher velocities have been measured in submerged arc welds. Fluid flow is important because it affects weld shape and is related to the formation of a variety of weld defects. Moving liquid transports heat and often dominates heat transport in the weld pool. Because heat transport by mass flow depends on the

direction and speed of fluid motion, weld pool shape can differ dramatically from that predicted by conductive heat flow. Temperature gradients are also altered by fluid flow, which can affect weld microstructure. A number of defects in GTA welds have been attributed to fluid flow or changes in fluid flow, including lack of penetration, top bead roughness, humped beads, finger penetration, and undercutting. Instabilities in the liquid film around the keyhole in electron beam and laser welds are responsible for the uneven penetration (spiking) characteristic of these types of welds.

Mass Transport in the Arc

High-velocity gas motion occurs in and around the arc during welding. The gas motion is partially due to cover gas flow, but, more importantly, it is driven by electromagnetic forces associated with the arc itself. In gas metal arc (GMA) welds, liquid filler metal is also being transferred through the arc from the electrode to the workpiece. Both the mode and velocity of metal transfer have major effects on weld pool shape. Mass transport in and around the arc is important in GTA welding (GTAW) and even more so in GMA welding (GMAW); a detailed description of this phenomenon can be found in the articles on arc physics and metal transfer and weld behavior in this Volume. Only the effects of this transport on the weld pool will be discussed in this article.

Fluid Flow Phenomena During Welding

C.R. Heiple and P. Burgardt, EG&G Rocky Flats

Gas Tungsten Arc Welding

Most experimental and theoretical work on weld pool fluid flow and its effects has been directed toward GTAW. The motivation for much of this work was the observation of dramatically different weld pool shapes for GTA welds made using identical welding parameters on different heats of the same material with the same nominal composition. An extreme example of weld shape variability is shown in Fig. 1. Early observations of variable weld shape (often referred to as variable penetration) were not only an intellectual puzzle but also an indication of a growing practical problem. Gas tungsten arc welding is commonly used for high-precision, high-quality automated welding applications, where reproducibility of weld shape or penetration is critical.

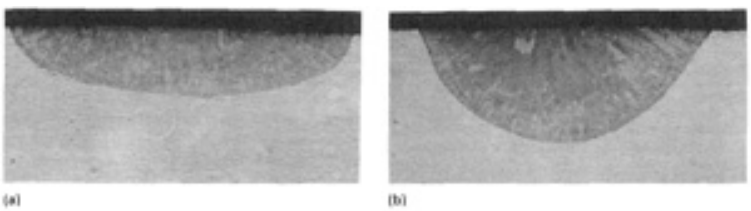

FIG. 1 PARTIAL-PENETRATION GTA WELDS MADE UNDER THE SAME WELDING CONDITIONS ON TWO HEATS OF TYPE 304L STAINLESS STEEL HAVING THE SAME NOMINAL COMPOSITION. (A) 3 PPM S, *D*/*W* = 0.2. (B) 160 PPM S, *D*/*W* = 0.40. 9×

The possibility that fluid flow in the weld pool could alter weld shape has been recognized for many years. For example, in 1965 Christensen *et al.* (Ref 1) proposed that convection is partially responsible for deviations in weld pool shapes from those predicted by conduction solutions. The forces driving fluid flow in GTA weld pools have also been long known. The four primary driving forces are surface tension gradients, electromagnetic or Lorentz forces, buoyancy forces, and aerodynamic drag forces caused by passage of the arc plasma over the weld pool surface.

Surface-Tension-Driven Fluid Flow Model. Surface tension gradients were first proposed by Ishizake *et al.* (Ref 2) as potential driving forces for weld pool fluid flow. Surface-tension-driven fluid flow was first described by Thomson (Ref 3) in 1855, but the phenomenon is commonly called Marangoni convection from the work of Carlo Marangoni (Ref 4).

In 1982, Heiple and Roper (Ref 5) proposed that surface tension gradients are commonly the dominant forces driving fluid flow in GTA welds and that these gradients could be drastically altered by very small concentrations of certain trace elements. Surface tension gradients exist on a weld pool surface because the surface tension is temperature dependent, and there are large temperature gradients on a weld pool surface. For pure metals and many alloys, the surface tension decreases as temperature increases; that is, the surface tension temperature coefficient is negative. For weld pools in such materials, the surface tension will be greatest on the coolest part of the pool surface at the edge and lowest on the hottest part under the arc near the center of the pool. Such a surface tension gradient produces outward surface fluid flow, as shown schematically in Fig. 2(a). This fluid flow pattern transfers heat efficiently from the hottest part of the weld pool (near the center) to the edge and produces a relatively wide and shallow weld.

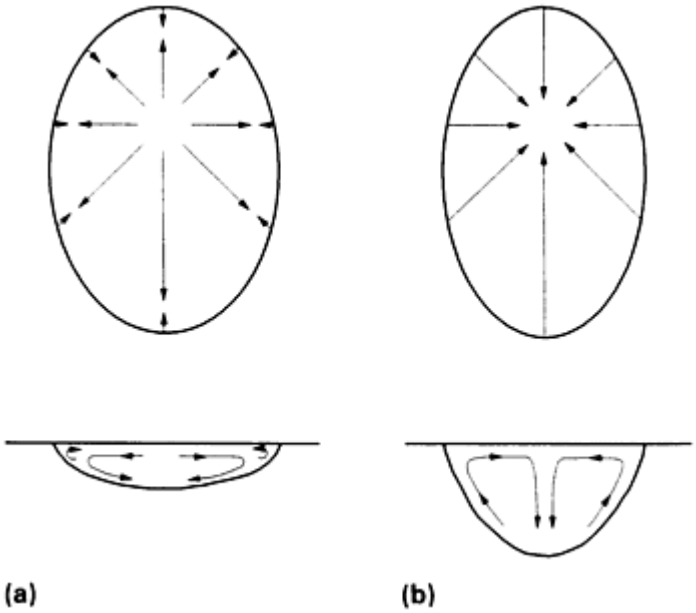

FIG. 2 SCHEMATIC SHOWING SURFACE FLUID FLOW (TOP) AND SUBSURFACE FLUID FLOW (BOTTOM) IN THE WELD POOL. (A) NEGATIVE SURFACE TENSION TEMPERATURE COEFFICIENT (PURE MATERIAL). (B) POSITIVE SURFACE TENSION TEMPERATURE COEFFICIENT (SURFACE-ACTIVE ELEMENTS PRESENT)

Certain elements are surface active in molten metals; that is, they segregate to the surface of the solvent liquid metal and lower the magnitude of the surface tension, often drastically. Small concentrations of surface-active additions can also change the temperature dependence of the surface tension of the solvent metal or alloy so that, for a limited range of temperature above the melting point, the surface tension increases with increasing temperature. With a positive surface tension temperature coefficient, the surface tension will be highest near the center of the weld pool. Such a surface tension gradient will produce fluid flow inward along the surface of the weld pool and then down, as indicated schematically in Fig. 2(b). This fluid flow pattern transfers heat efficiently to the bottom of the weld pool and produces a relatively deep, narrow weld.

Experimental Observations. This physical model was developed and verified with a series of experiments in which stainless steel base metal was doped with low concentrations of various elements and the effect of the doping on weld pool shape measured. High-speed motion pictures of the weld pool surface suggested the fluid flow patterns indicated in Fig. 2. The addition of sulfur, oxygen, selenium, and tellurium to stainless steel in low concentrations (less than 150 ppm) was shown to substantially increase GTA weld depth-to-width ratio (d/w). All these elements are known to be highly surface active in liquid iron. Measurements of the temperature dependence of the surface tension for steels with different GTA weld penetration characteristics produced an impressive correlation between a positive surface tension temperature coefficient arising from surface-active impurities and high d/w ratio welds (Fig. 3).

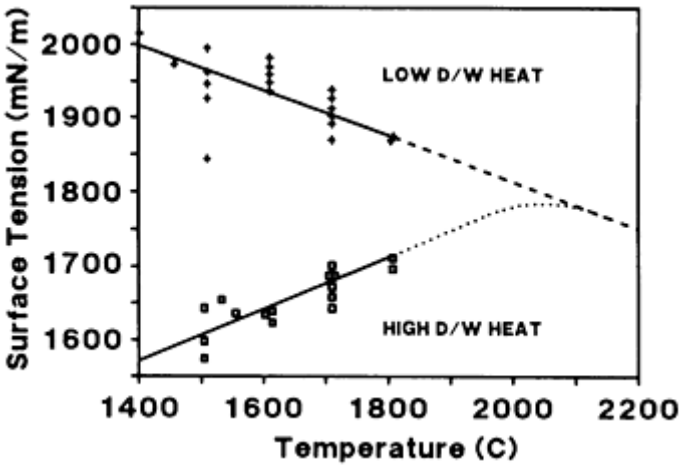

FIG. 3 PLOT OF SURFACE TENSION VERSUS TEMPERATURE FOR TWO LIQUID STEELS. THE DATA LABELED "HIGH *D/W* HEAT" ARE FROM MATERIAL HAVING APPROXIMATELY 160 PPM MORE SULFUR THAN THE MATERIAL LABELED "LOW *D/W* HEAT." THE DASHED LINES INDICATE THE EXPECTED BEHAVIOR OF THE SURFACE TENSION ABOVE THE MAXIMUM TEMPERATURE STUDIED. SOURCE: REF 6

When additions were made to the weld pool of elements known to react with surface-active elements already present in the steel to form compounds that are not surface active, the GTA weld *d*/*w* ratio decreased. Aluminum reacts with oxygen and produced wider, shallower welds in 21-6-9 stainless steel. Cerium reacts with both sulfur and oxygen and also produced lower *d*/*w* ratio welds. The effects of trace elements on weld shape have also been observed in a number of other alloys. These observations are summarized in Table 1.

TABLE 1 EFFECT OF TRACE ELEMENT IMPURITIES ON GTA WELD PENETRATION OF SELECTED ALLOYS

ALLOY SYSTEM	TRACE ELEMENT IMPURITY	
	INCREASES WELD PENETRATION	DECREASES WELD PENETRATION
ZIRCALOY-2	CHLORINE	. . .
IRON-BASE ALLOYS STAINLESS STEELS 304, 316, 21-6-9 JBK-75 AISI 8630 2.5CR-1MO	SULFUR, OXYGEN, SELENIUM(A), TELLURIUM(A)	CALCIUM, ALUMINUM, CERIUM(A), LANTHANUM(A), SILICON(B), TITANIUM(B)
NICKEL-BASE ALLOYS INCONEL 600, 718	SULFUR	OXYGEN

(A) UNCOMMON IMPURITIES

(B) EFFECT NEGLIGIBLE OR UNCERTAIN

The simple physical model illustrated in Fig. 2 has been remarkably successful in qualitatively explaining trace element effects. For example, changing GTA welding conditions alters the magnitude and distribution of arc energy input to the weld, which in turn changes temperature gradients on the weld pool surface. From Fig. 2, a change in welding conditions that makes the center of the weld hotter, such as increasing current, should drive the existing fluid flow pattern more strongly. As shown in Fig. 4, increasing current improves the *d/w* ratio of steel doped with surface-active elements and reduces it for high-purity base metal. If the center of the weld becomes so hot that there is a region where the temperature coefficient of the surface tension is no longer positive, then the fluid flow pattern necessary for deep penetration is disrupted and the *d/w* ratio decreases. This effect is seen at high currents in Fig. 4. Similar results have been obtained for other welding parameters. The surface temperature at which the change from positive to negative surface tension

temperature coefficient occurs for stainless steel is estimated by extrapolation in Fig. 3 to be about 2050 °C (3720 °F). Detailed thermodynamic calculations of the temperature dependence of the surface tension of iron-sulfur alloys predict that the transition from positive to negative $d\gamma/dT$ will occur at 2032 °C (3690 °F) for the high-sulfur alloy in Fig. 3. Recent spectrographic weld pool temperature measurements and numerical simulations have indicated that this temperature can be exceeded in stainless steel GTA weld pools under normal welding conditions.

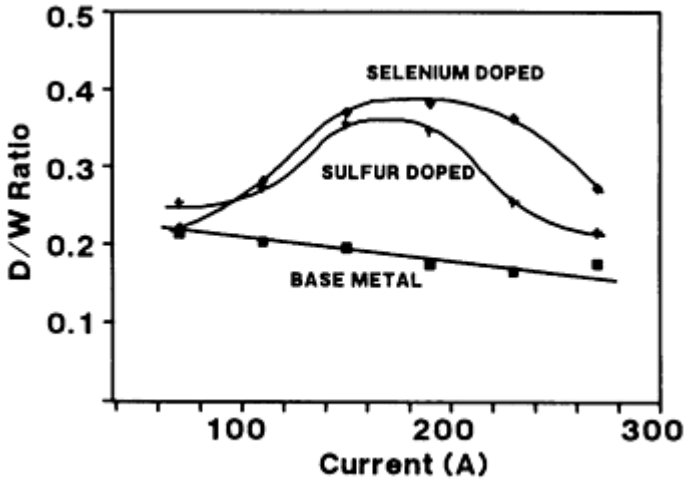

FIG. 4 PLOT OF WELD *D/W* RATIO VERSUS WELD CURRENT FOR THE STARTING BASE METAL (TYPE 304 STAINLESS STEEL WITH VERY LOW RESIDUAL IMPURITY CONTENT) AS WELL AS FOR ZONES DOPED WITH SULFUR AND SELENIUM. SOURCE: REF 7

The surface-tension-driven fluid flow model should be applicable to non-arc processes, provided the energy input distribution is similar to a GTA arc. This condition is satisfied for conduction-mode electron beam and laser welds. Dramatic increases in weld d/w ratio in selenium-doped zones in stainless steel have been observed for both traveling laser and electron beam conduction-mode welds. The weld shape changes were similar to those observed for GTA welds.

Conduction-mode electron beam welds can also be used to demonstrate that variations in weld shape with changes in welding parameters, as illustrated in Fig. 4, are not a result of some complex arc/weld pool interaction. One of the results of an investigation of the effect of changes in beam focus on weld shape in electron beam welds on low- and high-sulfur materials is shown in Fig. 5. The high-sulfur material exhibits a maximum in d/w ratio with increasing power density at a moderate power density away from sharp focus, which is analogous to that shown with increasing current in Fig. 4. (The low- and high-sulfur stainless steels have deep and nearly identical penetration near sharp focus. Near sharp focus, where the power density is high, penetration is by a keyhole mechanism in which average penetration is unrelated to surface-tension-driven fluid flow.) Measurements of the electron beam power-density distribution verified that there were no anomalous changes in the beam, such as a beam width maximum, with increasing peak power density. The d/w ratio maximum away from sharp focus is therefore proposed to originate from exactly the same mechanism as for increasing current with GTA welds.

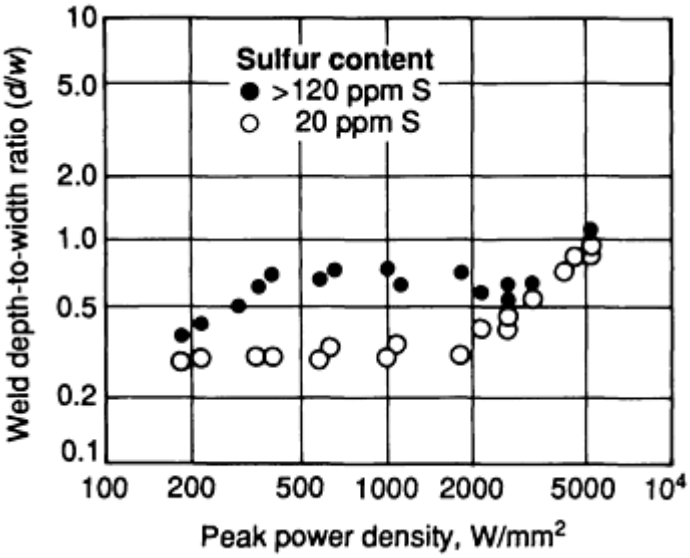

FIG. 5 PLOT OF ELECTRON BEAM WELD POOL RATIO (*D*/*W*) VERSUS ELECTRON BEAM POWER DENSITY FOR LOW-SULFUR (20 PPM) AND HIGH-SULFUR (>120 PPM) TYPE 304L STAINLESS STEEL. KEYHOLE FORMATION BEGINS AT ABOUT 2 × 10^3 W/MM^2.

Measurements of electron beam power distribution were made as a function of beam focus and were used to calculate the beam power density at the *d*/*w* maximum. The power density was also calculated at the *d*/*w* maximum for GTA welds. Calculation of weld pool surface temperatures using a traveling distributed heat source model showed the central surface temperatures to be essentially identical at the *d*/*w* maxima for the electron beam and GTA processes. The calculated surface temperatures using the traveling distributed heat source conduction approximation are much too high because, as indicated previously, most of the heat transport in the weld pool is by mass flow rather than by conduction. Nevertheless, the equality of the calculated weld pool peak temperatures at the *d*/*w* maxima provides strong confirmation that the mechanism responsible for the presence of the maximum in weld *d*/*w* with increasing input power density is independent of heat source and is not a result of an arc phenomenon.

A final example of the success of the fluid flow model in explaining GTA welding phenomena is provided by butt welding together two steels with large differences in weld penetration characteristics. The weld pool is not centered over the joint; rather, it is displaced toward the material with low *d*/*w* behavior (Ref 8), as indicated schematically in Fig. 6. The low *d*/*w* material has a low concentration of surface-active impurities and therefore a high surface tension. Thus, there is a net surface tension gradient across the weld pool toward the low *d*/*w* material, producing the fluid flow pattern and weld cross section indicated in Fig. 6. The actual fluid flow pattern is certain to be more complicated than that illustrated.

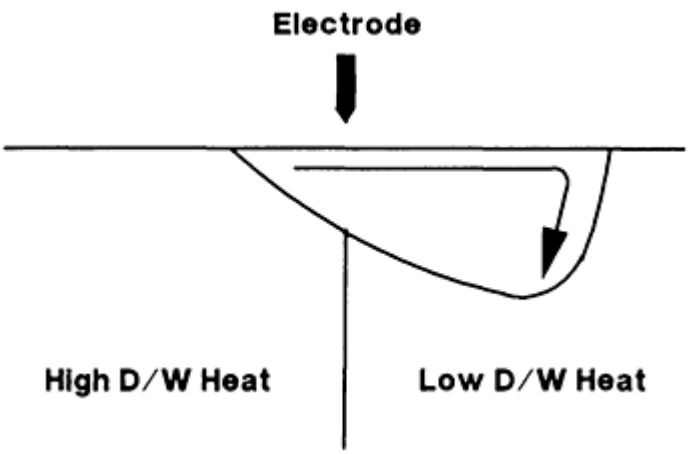

FIG. 6 SCHEMATIC SHOWING TYPICAL FLUID FLOW GENERATED WHEN BUTT WELDING TWO HEATS OF MATERIAL WITH DIFFERENT PENETRATION CHARACTERISTICS. SOURCE: REF 8

Numerical Simulations. Direct measurement of weld pool fluid flow is very difficult. Surface flow has been studied by observing the motion on the surface of slag or intentionally added particles, as has bulk flow in transparent liquid/solid systems using simulated welding heat sources. There are a number of numerical calculations of weld pool fluid flow and shape, the most comprehensive of which appears to be that of Zacharia *et al.* (Ref 9). These numerical fluid flow simulations agree in broad terms with the physical model illustrated in Fig. 2; however, they differ in detail with Fig. 2 and with one another. One result of the analysis of Zacharia is that the weld pool surface temperature reached in stationary welds exceeds that in traveling welds. Trace element effects should therefore be less pronounced in stationary welds, because a larger portion of the pool surface is above the temperature range where a positive surface tension temperature coefficient exists. This prediction is in agreement with experimental observations.

Interactions. Experiments in which low concentrations of various elements have been added to the base metal have demonstrated clear changes in weld pool shape. However, when weld *d*/*w* ratio is plotted versus chemical analysis for numerous heats of material, considerable scatter is observed. A comparison of weld *d*/*w* ratio in a standard weldability test versus sulfur content for about 200 lots of steel is shown in Fig. 7. There is a clear trend of increasing *d*/*w* with increasing sulfur, but the variability for a given sulfur content is substantial. Some of this variability is associated with imprecision in chemical analysis for sulfur and some with variations in oxygen content. However, it appears that much of the variability is related to interactions of the surface-active elements sulfur and oxygen with other components of the steel. Calcium is known to react with oxygen and, to a lesser extent, with sulfur to form stable compounds unlikely to be surface active. Aluminum and silicon also react with oxygen to form stable compounds. Thus, the amount of sulfur and oxygen available for segregation to the weld pool surface is a complicated function of the total weld pool chemistry.

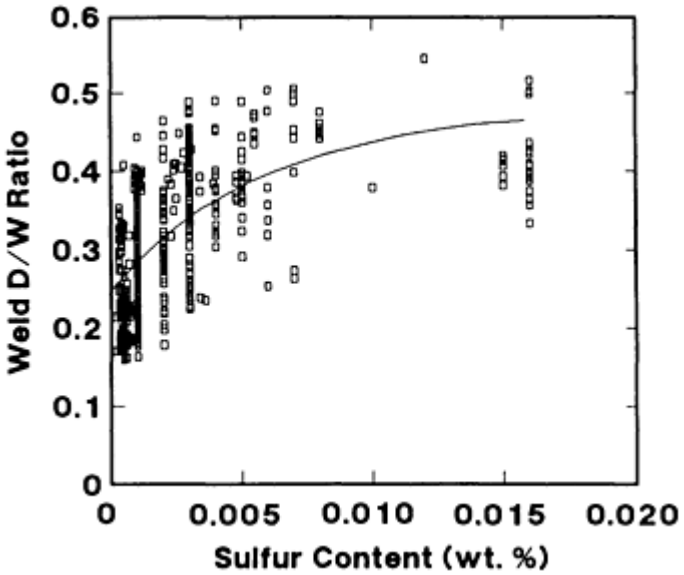

FIG. 7 PLOT OF WELD *D*/*W* RATIO VERSUS SULFUR CONTENT FOR APPROXIMATELY 200 HEATS OF TYPE 304L STAINLESS STEEL. EACH POINT IS AN AVERAGE OF MULTIPLE SULFUR ANALYSES AND WELD *D*/*W* RATIO MEASUREMENTS. IF SINGLE VALUES ARE USED, THE SCATTER IS GREATER. SOURCE: REF 10

There is an additional complication, illustrated in Fig. 8. When oxygen is added to the shielding gas, weld *d*/*w* ratio increases, passes through a maximum, and then declines with increasing oxygen content. Similar effects are seen with SO_2 additions. The surface of welds made with torch gas concentrations above the *d*/*w* maximum are heavily oxidized. A possible explanation for the decreasing *d*/*w* ratios at higher oxygen concentrations is that a liquid oxide film (slag) is formed on the weld pool surface, altering the surface tension gradients.

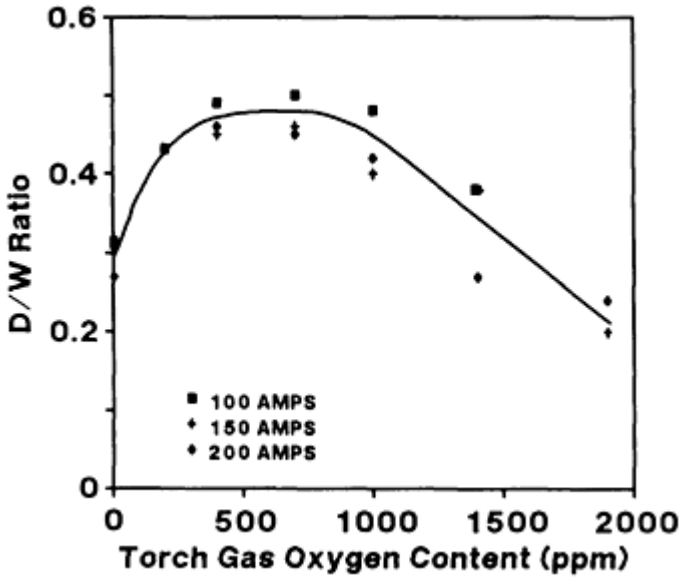

FIG. 8 PLOT OF WELD *D*/*W* RATIO VERSUS OXYGEN CONCENTRATION IN THE TORCH GAS FOR GTA BEAD-ON-PLATE WELDS ON 21-6-9 STAINLESS STEEL. SOURCE: REF 11

Oxygen can be added to the weld pool in other ways. Oxidizing the plate surface prior to welding adds oxygen to the weld pool and increases the weld *d*/*w* ratio. Wire brushing and grit blasting an originally clean surface increases both the surface oxide thickness and the surface area, thereby adding oxygen to the weld pool. The *d*/*w* ratio of JBK-75 stainless steel (a modification of ASTM A-286) GTA welds as a function of amount of wire brushing is similar in form to Fig. 8. Welds on plate brushed beyond the weld *d*/*w* maximum had extensive slag on the weld surface. The weld *d*/*w* ratio on JBK-75 stainless steel appears to be particularly sensitive to oxygen additions. Similar wire-brushing experiments on type 304 stainless steel showed smaller effects.

Although the origin of the difference in sensitivity between JBK-75 and type 304 is not known, one possibility is indicated by surface tension measurements on iron-silicon alloys in contact with carbon dioxide. The effect of CO_2 on the surface tension was a strong function of silicon content. For low-silicon alloys, the surface tension dropped sharply when contacted with CO_2. For alloys with more than 1.2% Si, the surface tension increased when contacted with CO_2. The different behavior was attributed to differences in slag formation on the liquid metal surface. Thus, silicon appears to interfere with the ability of oxygen to produce a positive surface tension temperature coefficient on liquid iron. The JBK-75 stainless steel used in the wire-brushing experiments contained only 0.06% Si, and the 21-6-9 used for the torch gas experiment (Fig. 8) contained only 0.16% Si. Type 304 stainless steel typically contains more than 0.5% Si. Thus, the high sensitivity of JBK-75 to oxygen additions may be related to its unusually low silicon content. Reports in the literature on the effect of oxygen on GTA weld penetration have been somewhat variable; differences in weld pool silicon content may be partially responsible for this variability.

Effects of High Current. Electromagnetic (Lorentz) stirring of the weld pool becomes more important at higher currents. The direction of the Lorentz force produces the deep penetration fluid flow pattern indicated in Fig. 2(b). At sufficiently high current, the Lorentz force dominates other forces that drive fluid flow, and the effects of trace elements become less important. In addition, the plasma jet becomes stronger with increasing current and at high enough currents produces a significant depression of the weld pool surface. The plasma jet forces are resisted by surface tension forces on the weld pool. Halmoy (Ref 12) has shown that for a traveling weld the radial pressure gradient from the plasma jet tends to transport liquid from the front to the rear of the weld (Fig. 9). For a sufficiently strong pressure gradient, p_B, the liquid level under the arc may be pushed down to the bottom of the pool, as shown in Fig. 9(c). High-speed motion pictures of the effect of sulfur additions on weld pool fluid flow in 21-6-9 stainless steel showed behavior similar to that in Fig. 9(c) after large sulfur additions. Sulfur additions substantially reduce the weld pool surface tension and thereby increase the effect of the plasma jet.

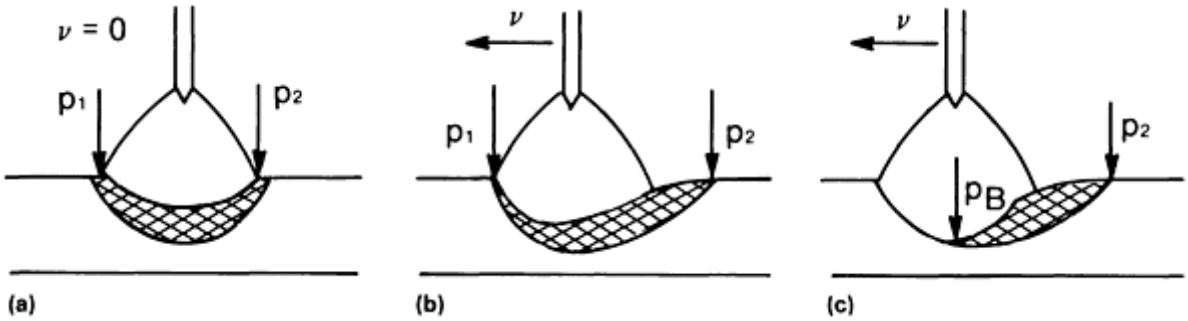

FIG. 9 EFFECT OF ARC PRESSURE ON THE WELD POOL FOR STATIONARY AND TRAVELING WELDS. (A) *V* = 0. (B) *V* > 0, WITH WEAK RADIAL PRESSURE GRADIENT, P_1. (C) *V* > 0, WITH STRONG RADIAL PRESSURE GRADIENT, P_B. SOURCE: REF 12

In addition, a surface depression almost certainly changes the energy distribution input to the weld pool by the arc compared with a flat weld pool surface. Finally, under some high-current conditions, a vortex has been observed near the center of weld pools.

Strategies for Controlling Poor and Variable Penetration. A number of techniques have been developed to reduce penetration variability and improve penetration. Sometimes the weld pool shift illustrated in Fig. 6, which occurs when heats with different penetration characteristics are welded together, can be minimized by very tight heat sinking. The sensitivity of weld shape to trace element differences is a function of welding parameters, as illustrated in Fig. 4 for current; thus, combinations of welding parameters can be chosen that minimize heat-to-heat penetration variability. For wire-fed joints, some joint designs are more tolerant of penetration variability than others. For example, joints with thinner, wider lands are less sensitive than narrower grooves with thicker lands.

Material control by selection or specification is another approach. It was originally anticipated that stainless steels with less than 20 ppm S would have poor, but consistent, penetration. However, the data illustrated in Fig. 7 demonstrate that penetration variability is substantial even at these very low sulfur levels. Stainless steels with more than about 100 ppm S generally have consistently good penetration. A related approach is to test incoming material for welding characteristics and then select material with desired welding behavior for critical applications.

Finally, the weld pool can be doped with enough surface-active elements to ensure good penetration. Sulfur and oxygen are the most practical dopants for ferrous alloys. The addition of oxygen or sulfur dioxide to the torch shielding gas has been shown to improve penetration and reduce penetration variability; however, this approach presents several practical problems. Oxygen can also be added to the weld pool by oxidizing the weld joint or by otherwise increasing the oxygen content of the weld groove surface--by wire brushing, for example. Probably the most useful approach is to dope the weld pool in the wire-fed joints by using a special filler wire. A group of defense contractors had a special heat of type 380L stainless steel produced with a sulfur content in the range of 100 to 150 ppm. The heat was then converted into weld wire. Welds made with this wire on a variety of stainless steel base metals have exhibited consistent and good penetration.

References cited in this section

1. N. CHRISTENSEN, V. DE L. DAVIES, AND K. GJERMUNDSEN, DISTRIBUTION OF TEMPERATURES IN ARC WELDING *BR. WELD.J.*, VOL 12, 1965, P 54-75
2. K. ISHIZAKE, K. MURAI, AND Y. KANBE, "PENETRATION IN ARC WELDING AND CONVECTION IN MOLTEN METAL," DOCUMENT 77-66, INTERNATIONAL INSTITUTE OF WELDING, STUDY GROUP 212, 1966
3. J. THOMSON, ON CERTAIN CURIOUS MOTIONS OBSERVABLE AT THE SURFACES OF WINE AND OTHER ALCOHOLIC LIQUORS, *PHILOS.MAG.*, VOL 10, 1855, P 330-333
4. C. MARANGONI, ÜBER DIE AUSBREITUNG DER TROPFEN EINER FLUESSIGKEIT AUF DER OBERFLAESCHE EINER ANDEREN, *ANN. PHYS. CHEM.*, VOL 143 (NO. 7), 1871, P 337-354

5. C.R. HEIPLE AND J.R. ROPER, MECHANISM FOR MINOR ELEMENT EFFECT ON GTA FUSION ZONE GEOMETRY, *WELD. J.*, VOL 61, 1982, P 97S-102S
6. B.J. KEENE, K.C. MILLS, AND R.F. BROOKS, SURFACE PROPERTIES OF LIQUID METALS AND THEIR EFFECTS ON WELDABILITY, *MATER. SCI.TECHNOL.*, VOL 1, 1985, P 568-571
7. P. BURGARDT AND C.R. HEIPLE, INTERACTION BETWEEN IMPURITIES AND WELDING PARAMETERS IN DETERMINING GTA WELD SHAPE, *WELD. J.*, VOL 65, 1986, P 150S-155S
8. M.J. TINKLER, I. GRANT, G. MIZUNO, AND C. GLUCK, WELDING 304L STAINLESS STEEL TUBING HAVING VARIABLE PENETRATION CHARACTERISTICS, *THE EFFECTS OF RESIDUAL, IMPURITY, AND MICRO-ALLOYING ELEMENTS ON WELDABILITY AND WELD PROPERTIES*, P.H.M. HART, ED., PAPER 29, THE WELDING INSTITUTE, CAMBRIDGE, 1984
9. T. ZACHARIA, S.A. DAVID, J.M. VITEK, AND T. DEBROY, WELD POOL DEVELOPMENT DURING GTA AND LASER BEAM WELDING OF TYPE 304 STAINLESS STEEL, PART 1--THEORETICAL ANALYSIS, *WELD. J.*, VOL 68, 1989, P 499S-509S
10. P. BURGARDT AND R.D. CAMPBELL, CHEMISTRY EFFECTS ON STAINLESS STEEL WELD PENETRATION, *FERROUS ALLOY WELDMENTS*, TRANS TECH PUBLICATIONS, SWITZERLAND, 1992, P 379-415
11. C.R. HEIPLE, P. BURGARDT, AND J.R. ROPER, THE EFFECT OF TRACE ELEMENTS ON GTA WELD PENETRATION, *MODELING OF CASTING AND WELDING PROCESSES II*, J.A. DANTZIG AND J.T. BERRY, ED., TMS-AIME, 1984, P 193-205
12. E. HALMOY, THE PRESSURE OF THE ARC ACTING ON THE WELD POOL, *ARC PHYSICS AND WELD POOL BEHAVIOR*, THE WELDING INSTITUTE, CAMBRIDGE, 1979, P 259-266

Fluid Flow Phenomena During Welding

C.R. Heiple and P. Burgardt, EG&G Rocky Flats

Deep-Penetration Electron Beam and Laser Welds

Keyhole Formation. A fundamental difference between arc heat sources and electron or laser beam heat sources is that electron and laser beams are capable of delivering heat over a small area at much higher power densities. As the power density of the welding heat source is increased, the peak surface temperature of the weld pool rises. For many metals, vapor pressure rises nearly exponentially with temperature and becomes appreciable (above 4000 Pa, or 30 torr, for an electron beam operating in a vacuum) near 0.8 T_b, where T_b is the material boiling point in degrees Kelvin. As the surface temperature approaches this value, the liquid surface under the power source is depressed by the vapor pressure. As the liquid moves away from the power source, the surface is depressed and a cavity is formed. This is the basic theory of keyhole formation by an electron or laser beam.

Fluid Flow in the Keyhole. The keyhole is a cavity having roughly the size and shape of the beam; that is, it is usually approximately cylindrical. Fluid flow in the thin layer around the cavity plays a major role in determining the behavior of deep-penetration, keyhole-mode electron beam and laser welds. The first flow required for a traveling weld is transport of metal melted at the front wall of the cavity to the rear (where it eventually solidifies). Because of the weld geometry, this liquid must move around the keyhole cavity as a thin, high-velocity layer on the walls of the cavity. The dominant driving force for this motion appears to be surface tension gradients. As in GTAW, these gradients arise because the surface tension is temperature dependent and there is a substantial temperature difference between the front and rear of the cavity.

Calculations of the fluid flow have been performed by Wei and Giedt (Ref 13). Their calculations for pure iron predict that liquid metal is moved from the front to the rear of a sharp focus keyhole in a film that is about 0.02 mm (0.0008 in.) thick and is moving at a velocity of about 250 mm/s (10 in./s). The fluid is driven by a temperature difference of about 400 °C (720 °F). These results are only nominal values from the calculations, but they change little with the assumptions used and are representative of electron beam welds in general.

There is an interesting potential problem with this model. As discussed previously, the surface tension temperature coefficient, $d\gamma/dT$, can be positive over a limited temperature range in steels and some other alloys if surface-active impurities are present in sufficient quantity. If $d\gamma/dT$ is positive, then it would appear that molten metal would not be transported around the cavity. The likely resolution of this difficulty is that the liquid dwells slightly longer in the front of the cavity and is heated by the beam above the temperature at which a transition to negative $d\gamma/dT$ occurs. Some perturbation of the normal fluid flow may occur under these circumstances. Effects of such a perturbation on weld characteristics appear to be uncommon. The only available evidence for such an effect comes from electron beam welds performed on a heat of type 304 stainless steel with very low residual impurity content, except for about 340 ppm S. These welds had very high porosity compared with identical welds in other heats of material.

Instability in Keyhole Fluid Flow. In addition to the steady-state flow of liquid around the keyhole, significant instability in the fluid motion has been seen. For example, Mara *et al.* (Ref 14) used side-view, self-illuminated X-ray films to show that the beam locations shifts between full penetration and nearly zero penetration in an irregular fashion. High-speed X-ray photographs show that the variable penetration is caused by a lump of metal that sags into the keyhole from high up on the cavity rear wall. The sequence of events that creates weld penetration irregularity was analyzed by Tong and Giedt (Ref 15) and is illustrated schematically in Fig. 10. First, the beam forms a keyhole and produces a lump of very hot displaced metal at the top rear of the traveling cavity (Fig. 10a). After some period of time, the weld reaches the full penetration allowed by heat flow (Fig. 10b). The lump of displaced metal is unstable and eventually falls into the cavity, partially filling it. The beam must now drill through this additional material. The sequence (a) to (c) in Fig. 10 occurs repeatedly, but irregularly, and produces weld penetration variability. When particularly severe, the irregular penetration is called spiking. Spiking also leads to a tendency for voids to become trapped in the root of the weld.

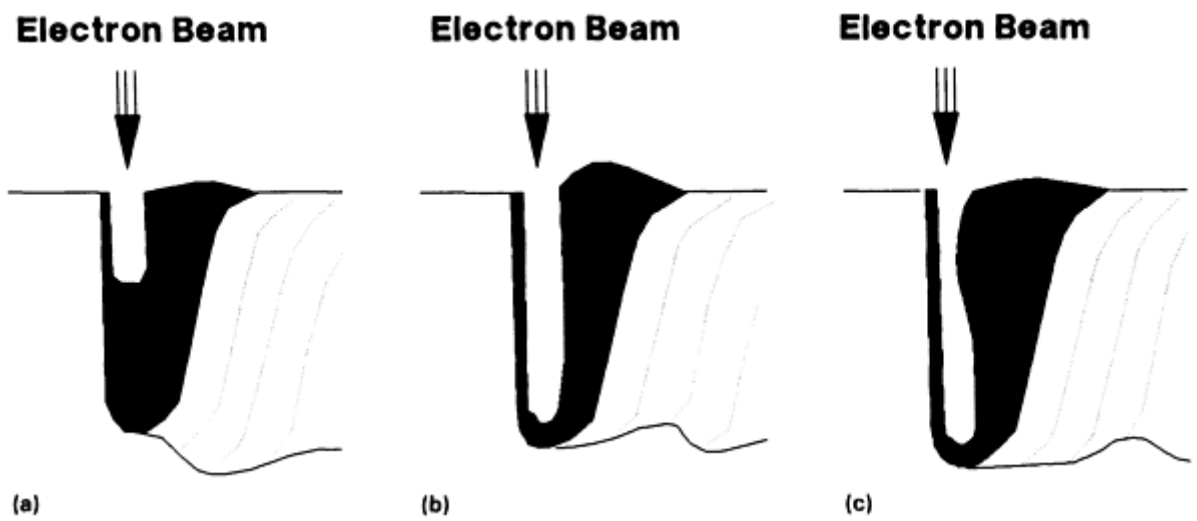

FIG. 10 SCHEMATIC SHOWING KEYHOLE INSTABILITY. (A) KEYHOLE IS FORMED BY HEAT GENERATED BY ELECTRON BEAM. (B) MAXIMUM PENETRATION THAT CAN BE PRODUCED BY HEAT FLOW. (C) LIQUID COOLS, CAUSING IMPENDING COLLAPSE OF DISPLACED METAL. THE KEYHOLE IS FILLED BY A LUMP OF COOLING MATERIAL AT THE END OF (C), WHICH RETURNS THE KEYHOLE TO CONDITION (A) TO RESTART THE SEQUENCE.

A mathematical model that is the basis for understanding this keyhole instability was developed by Giedt *et al.* (Ref 13, 15). Stability of the keyhole is basically a balance between vapor pressure, which keeps the cavity open, and surface tension, which tries to close the cavity. Vapor pressure and surface tension are both functions of temperature. Vapor pressure increases nearly exponentially with temperature for many materials, while surface tension generally decreases slowly with temperature. Because there is a substantial temperature gradient from the top to the bottom of the keyhole, both vapor pressure and surface tension vary with depth in the keyhole. Direct measurements of cavity wall temperatures for electron beam welds indicate that the temperature at the top is nearly equal to the melting temperature, while the temperature at the bottom is high enough that the vapor pressure there is large. In type 304 stainless steel, the temperature at the bottom of the cavity is about 2200 °C (1200 °F). The data indicate that the temperature profile is insensitive to welding variables and is determined primarily by material properties, that is, by the temperature where the vapor pressure exceeds about 1330 Pa (10 torr).

Based on temperature measurements of a typical keyhole, the vapor pressure decreases approximately exponentially with height from the bottom of the keyhole and approaches zero at the top of the keyhole. The vapor pressure is balanced primarily by surface tension. For pure iron and many other materials, the surface tension decreases approximately linearly with temperature. Thus, the inward surface tension pressure increases slowly from the bottom to the top of the keyhole. The balance of vapor pressure and surface tension is such that the cavity is stable near the bottom, where the vapor pressure tending to expand the cavity exceeds the surface tension tending to collapse it. At the top, the cavity is unstable because the surface tension tending to collapse it exceeds the vapor pressure tending to expand it. Thus, the cavity will always tend to be filled by liquid originating from above some height *H* in the keyhole, the pressure crossover height. This cavity filling produces weld penetration irregularity. Weld penetration irregularity is a consequence of the nature of the keyhole in deep-penetration welding and will not generally be solved by simple equipment or material modifications.

Penetration irregularity is usually less severe if *H* (as measured from the top) is a small fraction of the keyhole depth. In such cases the volume of the lump is small, and liquid tends to flow into the cavity relatively smoothly. If *H* is a large fraction of the keyhole depth, then the liquid lump has a relatively large volume and, when it falls into the keyhole at irregular times, it nearly fills the cavity and produces large penetration variations.

References cited in this section

13. P.S. WEI AND W.H. GIEDT, SURFACE TENSION GRADIENT-DRIVEN FLOW AROUND AN ELECTRON BEAM WELDING CAVITY, *WELD. J.*,VOL 64, 1985, P 251S-259S
14. G.L. MARA, E.R. FUNK, R.C. MCMASTER, AND P.E. PENCE, PENETRATION MECHANISMS OF ELECTRON BEAM WELDING AND THE SPIKING PHENOMENON, *WELD. J.*, VOL 53, 1974, P 246S-251S
15. H. TONG AND W.H. GIEDT, A DYNAMIC INTERPRETATION OF ELECTRON BEAM WELDING, *WELD. J.*, VOL 49, 1970, P 259S-266S

C.R. Heiple and P. Burgardt, EG&G Rocky Flats

Gas Metal Arc Welding

Fluid flow certainly occurs in GMA weld pools, but reports on the details of its nature and effects are quite limited. In the spray transfer mode, the impact of the stream of droplets from the electrode on the weld pool forms a substantial depression or crater. This is the mechanism responsible for the typical fingerlike penetration observed with argon as the torch gas. Thus, the depth of penetration is primarily dependent on the momentum of the stream of droplets. A plot of penetration versus the momentum of the droplet stream shows an excellent correlation (Fig. 11). Because the major force driving the droplets toward the weld is drag from the plasma jet, the kinematic viscosity (density times viscosity) of the shielding gas is important. For example, argon has a substantially higher kinematic viscosity than helium, so argon drives the droplet stream more effectively, resulting in a deeper, narrower penetration finger than with helium torch gas. The strength of the plasma jet can also be altered by changing the ambient pressure. For GMA welds on aluminum. Amson and Salter (Ref 17) saw a steady decrease in penetration with pressure until at 13,300 Pa (100 torr) there was essentially no penetration at all. Another way to modify the penetration depth is to spread the stream of droplets over the surface of the weld. This can be accomplished by applying a varying transverse magnetic field.

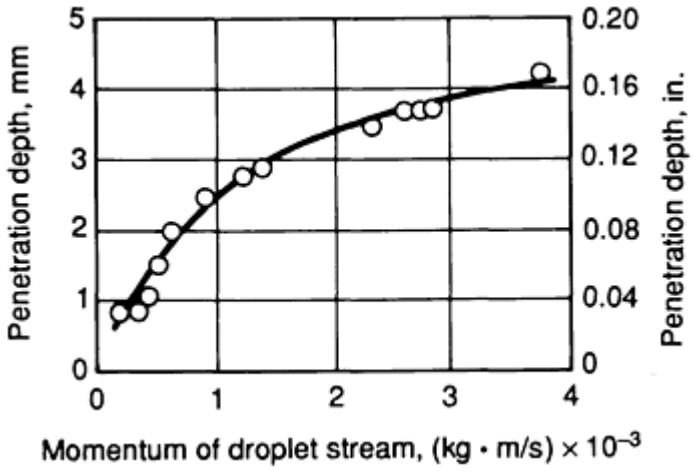

FIG. 11 PLOT OF GMA WELD PENETRATION IN MILD STEEL FOR SPRAY TRANSFER MODE VERSUS MOMENTUM OF DROPLET STREAM. SOURCE: REF 16

References cited in this section

16. W.G. ESSERS AND R. WALTER, HEAT TRANSFER AND PENETRATION MECHANISMS WITH GMA AND PLASMA-GMA WELDING, *WELD. J.*, VOL 62, 1981, P 37S-42S
17. J.C. AMSON AND G.R. SALTER, ANALYSIS OF THE GAS-SHIELDED CONSUMABLE METAL-ARC WELDING SYSTEM, *BR. WELD. J.*, VOL 10, 1963, P 472-483

Fluid Flow Phenomena During Welding

C.R. Heiple and P. Burgardt, EG&G Rocky Flats

Submerged Arc Welding

Currents commonly employed in submerged arc welding (SAW) are much higher than those used in GTAW or GMAW. Submerged arc welding currents often exceed 1000 A. Thus, the electromagnetic or Lorentz force combined with the tendency of the radial pressure gradient in the moving cavity to transport liquid to the rear of the cavity (Fig. 9) are likely the dominant forces driving fluid flow. The generally accepted flow pattern is indicated schematically in Fig. 12. A cavity is formed at the front of the moving weld pool by arc pressure and by the momentum of drops from the rapidly melting electrode. Metal that is melted at the front of the pool flows underneath and on either side of the cavity. At the rear of the pool, the flow reverses and metal flows back toward the cavity along and near the surface. Flow velocities can be very high; Eichhorn and Engel (Ref 19) measured 4 m/s (13 ft/s) at 720 A. The flow pattern was derived from observations of motion of marker elements, added to the weld pool, as determined from subsequent metallographic sections, and from the motion of radioactive tracer additions. The general features illustrated in Fig. 12 appear to be supported by X-ray fluoroscopy observations. Major perturbations in the indicated fluid flow have been demonstrated, including reversal of the flow direction. These perturbations have been associated with weld defects.

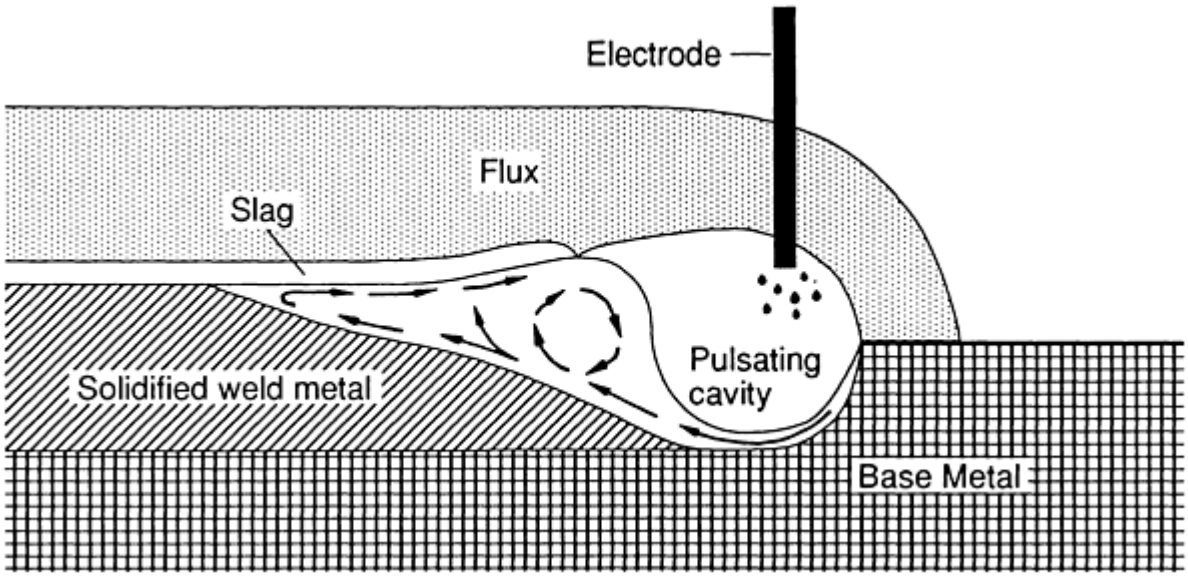

FIG. 12 SCHEMATIC SHOWING TYPICAL FLOW PATTERN IN A SUBMERGED ARC WELD POOL. SOURCE: REF 18

References cited in this section

18. J.F. LANCASTER, *THE PHYSICS OF WELDING*, INTERNATIONAL INSTITUTE OF WELDING, PERGAMON PRESS, OXFORD, 1984, P 243
19. F. EICHHORN AND A. ENGEL, "MASS TRANSFER IN THE WELD POOL," DOCUMENT 201-70, INTERNATIONAL INSTITUTE OF WELDING, STUDY GROUP 212, 1970

Fluid Flow Phenomena During Welding

C.R. Heiple and P. Burgardt, EG&G Rocky Flats

References

1. N. CHRISTENSEN, V. DE L. DAVIES, AND K. GJERMUNDSEN, DISTRIBUTION OF TEMPERATURES IN ARC WELDING *BR. WELD.J.*, VOL 12, 1965, P 54-75
2. K. ISHIZAKE, K. MURAI, AND Y. KANBE, "PENETRATION IN ARC WELDING AND CONVECTION IN MOLTEN METAL," DOCUMENT 77-66, INTERNATIONAL INSTITUTE OF WELDING, STUDY GROUP 212, 1966
3. J. THOMSON, ON CERTAIN CURIOUS MOTIONS OBSERVABLE AT THE SURFACES OF WINE AND OTHER ALCOHOLIC LIQUORS, *PHILOS.MAG.*, VOL 10, 1855, P 330-333
4. C. MARANGONI, ÜBER DIE AUSBREITUNG DER TROPFEN EINER FLUESSIGKEIT AUF DER OBERFLAESCHE EINER ANDEREN, *ANN. PHYS. CHEM.*, VOL 143 (NO. 7), 1871, P 337-354
5. C.R. HEIPLE AND J.R. ROPER, MECHANISM FOR MINOR ELEMENT EFFECT ON GTA FUSION ZONE GEOMETRY, *WELD. J.*, VOL 61, 1982, P 97S-102S
6. B.J. KEENE, K.C. MILLS, AND R.F. BROOKS, SURFACE PROPERTIES OF LIQUID METALS AND THEIR EFFECTS ON WELDABILITY, *MATER. SCI.TECHNOL.*, VOL 1, 1985, P 568-571
7. P. BURGARDT AND C.R. HEIPLE, INTERACTION BETWEEN IMPURITIES AND WELDING PARAMETERS IN DETERMINING GTA WELD SHAPE, *WELD. J.*, VOL 65, 1986, P 150S-155S
8. M.J. TINKLER, I. GRANT, G. MIZUNO, AND C. GLUCK, WELDING 304L STAINLESS STEEL

TUBING HAVING VARIABLE PENETRATION CHARACTERISTICS, *THE EFFECTS OF RESIDUAL, IMPURITY, AND MICRO-ALLOYING ELEMENTS ON WELDABILITY AND WELD PROPERTIES*, P.H.M. HART, ED., PAPER 29, THE WELDING INSTITUTE, CAMBRIDGE, 1984

9. T. ZACHARIA, S.A. DAVID, J.M. VITEK, AND T. DEBROY, WELD POOL DEVELOPMENT DURING GTA AND LASER BEAM WELDING OF TYPE 304 STAINLESS STEEL, PART 1--THEORETICAL ANALYSIS, *WELD. J.*, VOL 68, 1989, P 499S-509S
10. P. BURGARDT AND R.D. CAMPBELL, CHEMISTRY EFFECTS ON STAINLESS STEEL WELD PENETRATION, *FERROUS ALLOY WELDMENTS*, TRANS TECH PUBLICATIONS, SWITZERLAND, 1992, P 379-415
11. C.R. HEIPLE, P. BURGARDT, AND J.R. ROPER, THE EFFECT OF TRACE ELEMENTS ON GTA WELD PENETRATION, *MODELING OF CASTING AND WELDING PROCESSES II*, J.A. DANTZIG AND J.T. BERRY, ED., TMS-AIME, 1984, P 193-205
12. E. HALMOY, THE PRESSURE OF THE ARC ACTING ON THE WELD POOL, *ARC PHYSICS AND WELD POOL BEHAVIOR*, THE WELDING INSTITUTE, CAMBRIDGE, 1979, P 259-266
13. P.S. WEI AND W.H. GIEDT, SURFACE TENSION GRADIENT-DRIVEN FLOW AROUND AN ELECTRON BEAM WELDING CAVITY, *WELD. J.*,VOL 64, 1985, P 251S-259S
14. G.L. MARA, E.R. FUNK, R.C. MCMASTER, AND P.E. PENCE, PENETRATION MECHANISMS OF ELECTRON BEAM WELDING AND THE SPIKING PHENOMENON, *WELD. J.*, VOL 53, 1974, P 246S-251S
15. H. TONG AND W.H. GIEDT, A DYNAMIC INTERPRETATION OF ELECTRON BEAM WELDING, *WELD. J.*, VOL 49, 1970, P 259S-266S
16. W.G. ESSERS AND R. WALTER, HEAT TRANSFER AND PENETRATION MECHANISMS WITH GMA AND PLASMA-GMA WELDING, *WELD. J.*, VOL 62, 1981, P 37S-42S
17. J.C. AMSON AND G.R. SALTER, ANALYSIS OF THE GAS-SHIELDED CONSUMABLE METAL-ARC WELDING SYSTEM, *BR. WELD. J.*, VOL 10, 1963, P 472-483
18. J.F. LANCASTER, *THE PHYSICS OF WELDING*, INTERNATIONAL INSTITUTE OF WELDING, PERGAMON PRESS, OXFORD, 1984, P 243
19. F. EICHHORN AND A. ENGEL, "MASS TRANSFER IN THE WELD POOL," DOCUMENT 201-70, INTERNATIONAL INSTITUTE OF WELDING, STUDY GROUP 212, 1970

Fluid Flow Phenomena During Welding

C.R. Heiple and P. Burgardt, EG&G Rocky Flats

Selected References

- P. BURGARDT, WELDING VARIABLE EFFECTS ON WELD SHAPE IN ELECTRON BEAM WELDING OF STEELS, *FERROUS ALLOY WELDMENTS*, TRANS TECH PUBLICATIONS, SWITZERLAND, 1992, P 269-328
- P. BURGARDT AND R.D. CAMPBELL, CHEMISTRY EFFECTS ON STAINLESS STEEL WELD PENETRATION, *FERROUS ALLOY WELDMENTS*, TRANS TECH PUBLICATIONS, SWITZERLAND, 1992, P 379-415
- C.R. HEIPLE AND P. BURGARDT, PENETRATION IN GTA WELDING, *WELDABILITY OF MATERIALS*, R.A. PATTERSON AND K.W. MAHIN, ED., ASM INTERNATIONAL, 1990, P 73-80
- C.R. HEIPLE AND J.R. ROPER, THE GEOMETRY OF GAS TUNGSTEN ARC, GAS METAL ARC, AND SUBMERGED ARC WELD BEADS, *WELDING: THEORY AND PRACTICE*, D.L. OLSON, R.D. DIXON, AND A.L. LIBY, ED., NORTH-HOLLAND ELSEVIER SCIENCE PUBLISHERS, AMSTERDAM, 1990, 1-34
- K.C. MILLS AND B.J. KEENE, FACTORS AFFECTING VARIABLE WELD PENETRATION,

INT.MATER.REVIEW, VOL 35, 1990, P 185-216

Transfer of Heat and Mass to the Base Metal in Gas-Metal Arc Welding

Herschel B. Smartt, Idaho National Engineering Laboratory

Introduction

HEAT AND MASS TRANSFER in arc welding is normally studied from the standpoint of the weld pool and heat-affected zone (HAZ); however, it is also instructive to examine heat and mass transfer from the arc to the base metal. This article describes the latter topic in terms of the gas-metal arc welding (GMAW) process and provides practical information related to the development of welding procedures and the general operation of the process.

Welding procedures emphasize control of parameters such as electrode speed (or current), voltage, welding speed, contact tube-to-base metal distance, as well as current pulse parameters for out-of-position welding. It is therefore easy to overlook the fact that the process is simply a source of heat and mass inputs to the weldment. Melting of the base metal, dilution of the filler metal, solidification of the weld bead, microstructural development in the weld bead and HAZ, and thermomechanical distortion and residual stresses all follow from the heat and mass inputs. The conventional parameters identified above arc variables that control the heat and mass inputs. An example of the relationship between the conventional parameters of electrode speed and welding speed to heat and mass transferred to the weldment is shown in Fig. 1 for certain conditions, as applied to the welding of thick-section steel.

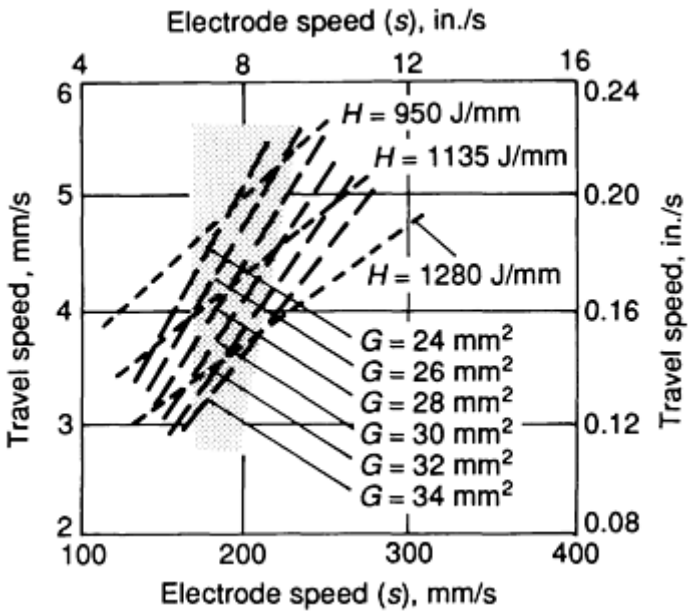

FIG. 1 PLOT OF WELDING SPEED VERSUS ELECTRODE SPEED AS FUNCTION OF HEAT TRANSFER PER LENGTH OF WELD, *H,* AND MASS TRANSFER EXPRESSED IN TERMS OF REINFORCEMENT, *G.* POWER SUPPLY OPEN-CIRCUIT VOLTAGE, E_0, IS 32 V; CONTACT TUBE-TO-BASE METAL DISTANCE, C_T, IS 15.9 MM (0.625 IN.). SHADED AREA DENOTES REGION IN WHICH SPRAY AND STREAMING TRANSFER MODES OCCUR; GLOBULAR TRANSFER OCCURS AT LOWER ELECTRODE SPEEDS, AND ELECTRODE CONTACTS THE WELD POOL AT HIGHER ELECTRODE SPEEDS. SOURCE: REF 1

The issues described in this article include the:

- TOTAL HEAT TRANSFERRED TO THE BASE METAL
- PARTITIONING OF HEAT TRANSFER BETWEEN THE ARC AND THE MOLTEN ELECTRODE

DROPLETS
- TRANSFER MODES OF THE DROPLETS
- ROLE OF THE ARC IN DROPLET TRANSFER
- SIMPLE MODEL FOR WELDING PROCEDURE DEVELOPMENT BASED ON AN UNDERSTANDING OF HEAT AND MASS TRANSFER TO THE BASE METAL

Reference

1. H.B. SMARTT, IDAHO NATIONAL ENGINEERING LABORATORY, 1992

Transfer of Heat and Mass to the Base Metal in Gas-Metal Arc Welding

Herschel B. Smartt, Idaho National Engineering Laboratory

Heat Transfer

The total transfer of heat, *H,* (neglecting preheating) from the GMAW process to the weldment per unit time is given by:

$$H = \eta EI \qquad \textbf{(EQ 1)}$$

where E is voltage, I is current, and η is the heat-transfer efficiency. The rate at which heat is transferred to the weldment per unit length of weld is given by:

$$H = \frac{h\,EI}{R} \qquad \textbf{(EQ 2)}$$

where R is welding speed. Calorimeter-based heat-transfer experiments reveal that the heat-transfer efficiency for welding thick-section steel is nominally 80 to 90%, as indicated in Fig. 2. The total heat-transfer efficiency is altered somewhat by changing other parameters. For example, it increases slightly as the power supply open-circuit voltage is decreased (for a silicon controlled rectifier regulated power supply and it increases slightly with increasing contact tube-to-base metal distance. However, 85% is a reasonable estimate for most conditions.

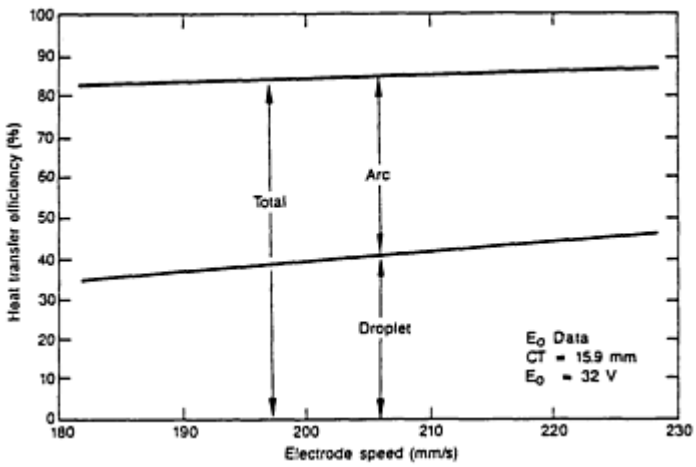

FIG. 2 PLOT OF HEAT-TRANSFER EFFICIENCY TO BASE METAL VERSUS ELECTRODE-SPEED FOR 0.89 MM (0.035 IN.) DIAMETER STEEL ELECTRODE IN AN AR-2% O_2 SHIELD GAS. TOTAL HEAT-TRANSFER EFFICIENCY

IS SHOWN PARTITIONED INTO ARC AND MOLTEN DROP COMPONENTS. POWER SUPPLY OPEN-CIRCUIT VOLTAGE, E_0, IS 32 V; CONTACT TUBE-TO-BASE METAL DISTANCE, C_T, IS 15.9 MM (0.625 IN.). SOURCE: REF 2

Partitioning of Heat Transfer. In the GMAW process, the molten droplets of electrode material carry a significant portion of the total heat transferred to the weld pool. This is seen in calorimetry experiments (Fig. 2), where the total heat-transfer efficiency of the GMAW process is partitioned into those portions associated with transfer by the arc and by the molten droplets. At low electrode speeds, about 60% of the total heat transferred is associated with the arc. As electrode speed increases, the fraction of total heat transferred associated with the droplets increases, reaching nominally 50% at current levels in excess of about 220 A (that is, at about 230 mm/s, or 9.1 in./s, electrode speed) for the conditions used.

Reference cited in this section

2. A.D. WATKINS, "HEAT TRANSFER EFFICIENCY IN GAS METAL ARC WELDING," MASTER'S THESIS, UNIVERSITY OF IDAHO, APRIL 1989

Transfer of Heat and Mass to the Base Metal in Gas-Metal Arc Welding

Herschel B. Smartt, Idaho National Engineering Laboratory

Mass Transfer

Droplet Transfer Modes. Although the International Institute of Welding (IIW) lists eight distinct metal transfer modes (Ref 3), the modes commonly used in U.S. welding practice are globular, spray, streaming, rotating, and short circuiting. The mode terms "drop" and "repelled" used by the IIW are often referred to as "globular," and the mode term "projected" is generally referred to as "spray." The globular, spray, streaming, and short-circuiting transfer modes are shown in Fig. 3, 4, 5, 6.

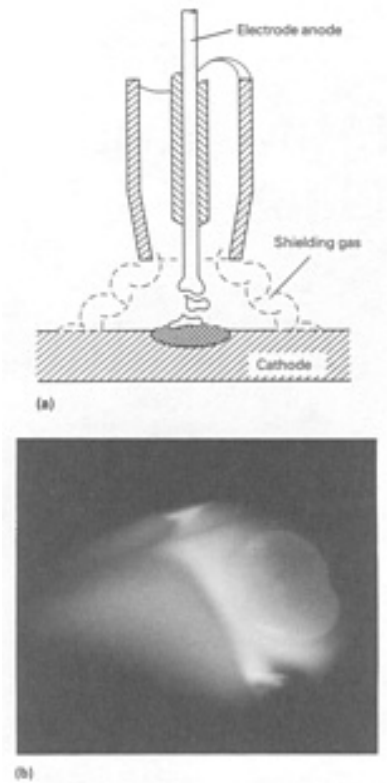

FIG. 3 GLOBULAR TRANSFER MODE IN GAS-METAL ARC WELDING OF STEEL. (A) SCHEMATIC SHOWING TRANSFER OF ELECTRODE MATERIAL GLOBULES ONTO CATHODE BASE METAL. (B) HIGH-SPEED PHOTOGRAPH OF GLOBULAR METAL TRANSFER

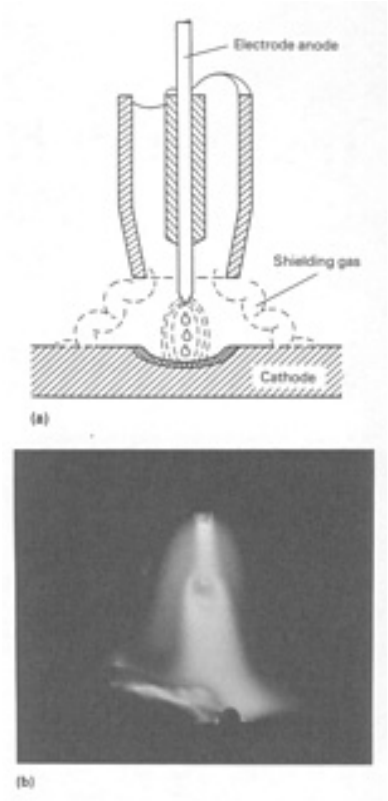

FIG. 4 SPRAY TRANSFER MODE IN GAS-METAL ARC WELDING OF STEEL. (A) SCHEMATIC SHOWING TRANSFER OF ELECTRODE MATERIAL DROPLETS ONTO CATHODE BASE METAL. (B) HIGH-SPEED PHOTOGRAPH OF SPRAY METAL TRANSFER MODE

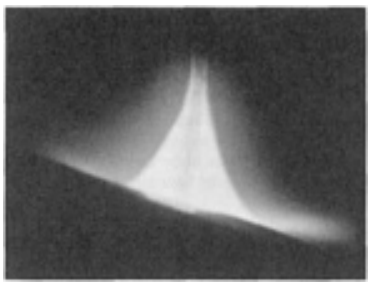

FIG. 5 HIGH-SPEED PHOTOGRAPH OF STREAMING TRANSFER MODE IN GAS-METAL ARC WELDING OF STEEL

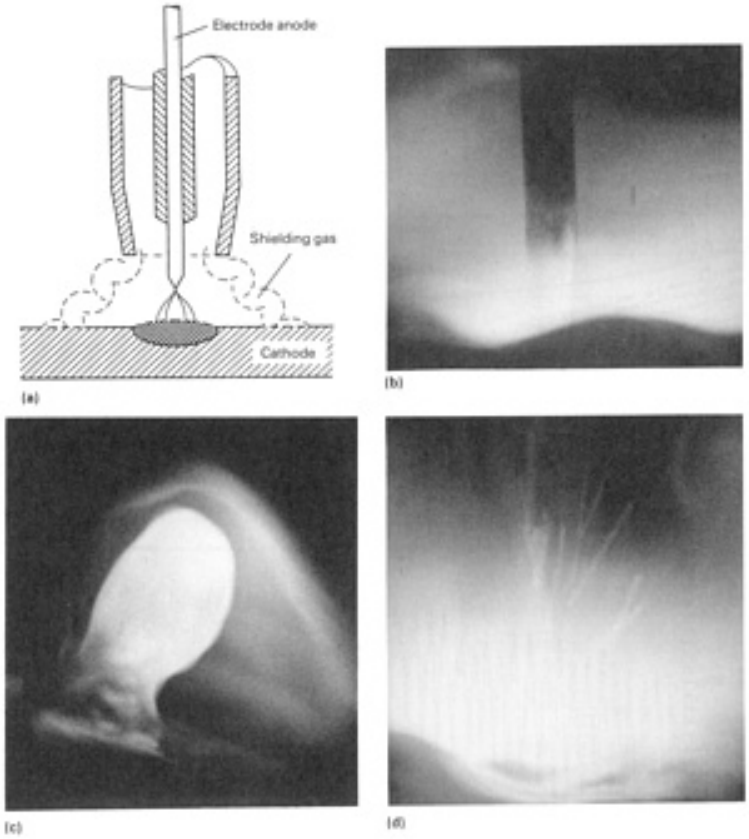

FIG. 6 SHORT-CIRCUITING TRANSFER MODE IN GAS-METAL ARC WELDING OF STEEL. (A) SCHEMATIC SHOWING TRANSFER OF ELECTRODE MATERIAL BY SURFACE TENSION OF WELD POOL ONTO CATHODE BASE METAL. (B) HIGH-SPEED PHOTOGRAPH OF MATERIAL TRANSFER WHEN ARC LENGTH IS VERY SHORT. (C) HIGH-SPEED PHOTOGRAPH OF CYCLIC SHORTING OF ARC BY THE ELECTRODE DURING METAL TRANSFER TO WELD POOL. (D) HIGH-SPEED PHOTOGRAPH OF VIOLENT ARC REIGNITION WITH ASSOCIATED SPATTER

When all other parameters are held constant, the metal transfer mode at the lowest wire feed speed (and associated current level) is globular. As wire speed (and therefore current) increases, the mode changes rapidly from globular to spray. With an additional increase in wire speed (and current), spray transfer becomes streaming transfer. Figure 7 shows the droplet sizes during the transition from globular to spray to streaming transfer for direct and pulsed current welding. If an adequately high current, contact tube-to-base metal distance, and voltage exist, then rotating transfer, wherein the lower part of the electrode becomes molten over a considerable length and rotates in a helical spiral under the influence of the magnetic field surrounding the arc, can occur. As it rotates, a controlled stream of droplets is transferred from the electrode tube to the weld pool over a relatively wide area. Additional increases in wire feed/current at low voltage shorten the arc length and, eventually, the wire stubs into the weld pool. In addition, with appropriate conditions (for example, carbon dioxide, argon-carbon dioxide mixtures, and helium-based shielding gases), droplets can be transferred directly, by surface tension forces, after contact of the drop with the weld pool, a condition called short-circuiting transfer.

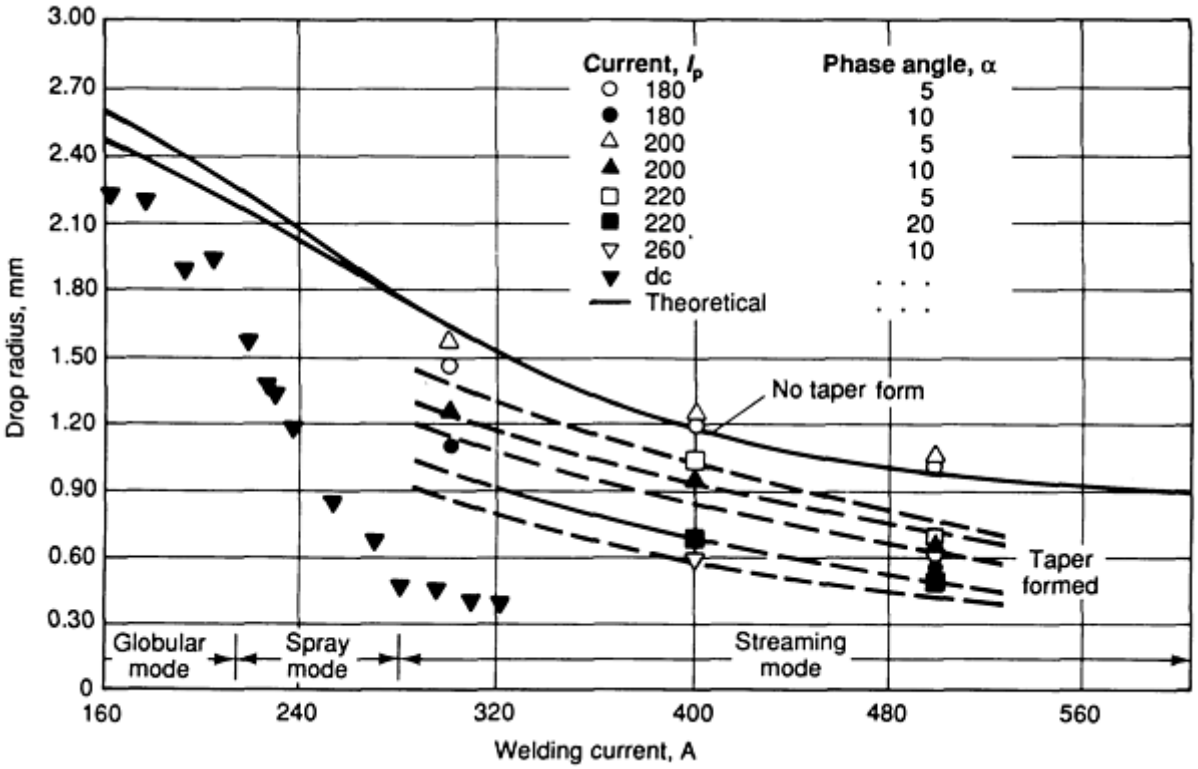

FIG. 7 DROPLET SIZES ATTAINABLE UNDER SELECTED CURRENT PULSING CONDITIONS IN GAS-METAL ARC WELDING OF STEEL. SOURCE: REF 4

In practical applications, the optimum transfer mode depends in part on the thickness of the base metal being welded. For example, very thin sections (in all positions) require the short-circuiting mode (with low current levels and appropriate settings of voltage and other operating parameters, including shielding gas composition). Thicker sections show best results with spray or streaming transfer. These transfer modes also produce high heat input, maximum penetration, and a high deposition rate. In welding steel, they are generally limited to welding that occurs in the flat position and the horizontal fillet position, except when pulsed current is used. Rotating transfer can be used in a deep groove in thick-section material. One- and two-pass heavy fillet welds are also a major area of application for this process variation.

Globular transfer (Fig. 3) involves a droplet that, generally, is much larger in diameter than the electrode wire. Globular transfer can involve a transfer rate of about 1 to 10 drops/s, and the arc has a soft, rounded appearance. Droplet detachment and transfer are mainly due to the gravitational force, which limits globular transfer to in-position welding. For spray transfer (Fig. 4), droplet and electrode diameters are roughly equivalent.

Spray transfer can involve 100 drops/s, and the arc noticeably contracts, or "stiffens." Drops usually travel in-line down the center of the arc, but several drops may be in flight at the same instant.

In streaming transfer (Fig. 5), a well-developed liquid column extends from the solid electrode down into the arc and breaks into small droplets before contacting the weld pool (see the discussion on spatter below). Streaming transfer can involve 1000 drops/s, and the arc has a characteristic "cone" shape, as shown in Fig. 5.

In short-circuiting transfer, the arc is very short (Fig. 6a). During metal transfer, the undetached molten droplet contacts the weld pool, shorting out the arc (Fig. 6b), which then extinguishes. Surface tension plays an important role in transferring the drop to the weld pool, but detachment of the drop from the electrode is due to electromagnetic pinch forces. Reignition of the arc is violent (Fig. 6c), resulting in considerable scatter.

As seen in Fig. 7, the transition from one mode to another actually involves continuous variations in droplet size. Because the product of droplet volume and transfer rate equals the electrode melting rate (in appropriate dimensions), there is also a continuous variation in droplet transfer rate. Detailed experimental studies have shown that rapid, cyclic transition from globular to spray to globular, and so on, occurs in the transition region between globular and spray transfer (Ref 5).

Although it is generally not possible for the welder to see droplet transfer events in the spray and streaming transfer modes (except under ideal conditions for spray transfer), the arc shape changes and associated changes in electrical and acoustic noise allow a trained welder to readily identify all of the transfer modes. The section "Electrical and Acoustic Signals" in this article describes this event more fully.

Weld Reinforcement. Assuming that mass is conserved as welding occurs, the transverse cross-sectional area of the weld bead added to the weldment for a single weld pass, which is called the reinforcement, *G*, is given by:

$$G = \frac{S}{R}\frac{p d^2}{4} \qquad \textbf{(EQ 3)}$$

where *S* is electrode speed, *R* is welding speed, and *d* is electrode diameter. For the spray and streaming transfer modes, the assumption that mass is conserved is reasonably good. However, because short circuiting and other conditions generate considerably spatter, the actual reinforcement will be slightly less than the value calculated by Eq 3.

Droplet Velocity and Temperature. In spray and streaming transfer, the droplets are accelerated rapidly through the arc to the weld pool. Velocities of 1 m/s (40 in./s) are typical, increasing with voltage (Fig. 8). Calorimetry-based experimental results indicate that steel droplets can reach temperatures of approximately 2600 K (4220 °F) (Ref 2). This explains why the droplets transport one-half of the total heat transferred to the base metal.

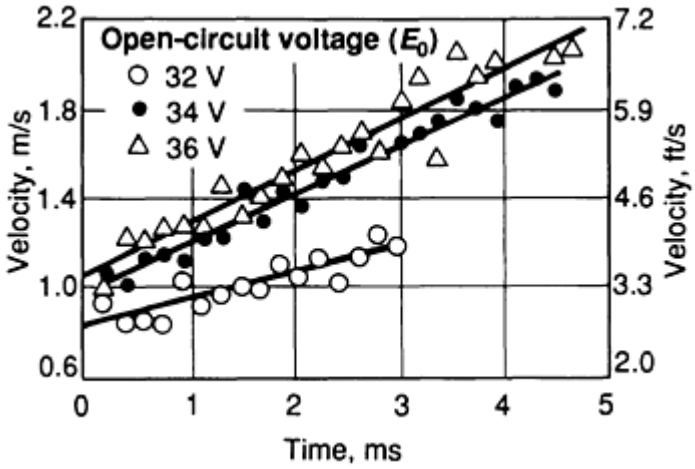

FIG. 8 DROPLET VELOCITIES FOR SPRAY TRANSFER IN GAS-METAL ARC WELDING OF STEEL AT THREE DIFFERENT OPEN-CIRCUIT VOLTAGES. SOURCE: REF 5

A result of the activity of molten electrode droplets in heat transfer to the base metal is that they also play an important role in convective heat transport in the weld pool and, thus, in weld penetration (Ref 6). This can be seen in Fig. 9, a transverse cross section of a gas-metal arc bead-on-plate weld on carbon steel. The region of deep penetration in the center of the weld bead is associated with the heat convected to the lower portion of the weld pool by the entering droplets.

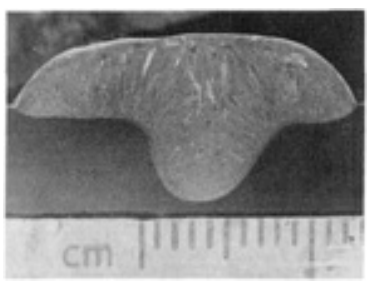

FIG. 9 TRANSVERSE CROSS SECTION OF GAS-METAL ARC BEAD-ON-PLATE WELD IN CARBON STEEL TO SHOW DEEP PENETRATION IN THE WELD BEAD CENTER GENERATED BY MOLTEN ELECTRODE DROPLETS

Electrical and Acoustic Signals. As the droplets of molten metal detach from the electrode, an almost instantaneous change occurs in the electrode extension, which results in a sudden, although small, change in the electrical resistance between the contact tube and the base metal. The results are spikes in the secondary circuit voltage and welding current, accompanied by pressure changes in the arc. Thus, both electrical and acoustic noise (Fig. 10) are generated by the GMAW process and are characteristic of the droplet transfer mode. The waveforms for globular transfer show prominent spikes associated with individual droplet transfer events. This can also be seen in Fig. 11, a plot of the computer-digitized current for a weld on carbon steel, where a change from globular to spray transfer has occurred at about 8 s into the weld. The power spectra of the current changes dramatically for the two transfer modes (Fig. 12), leading to a means of detecting transfer mode during welding.

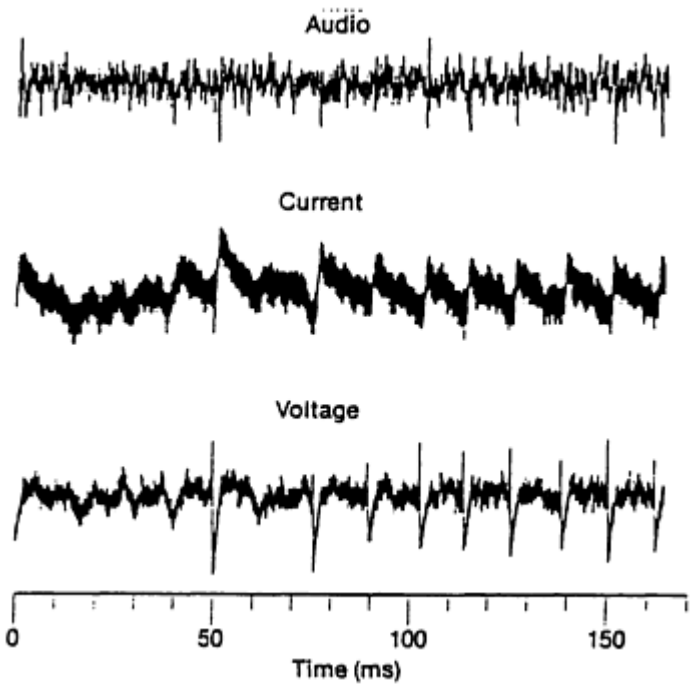

FIG. 10 AUDIO, CURRENT, AND VOLTAGE DURING GLOBULAR TRANSFER IN GAS-METAL ARC WELDING OF STEEL. SOURCE: REF 7

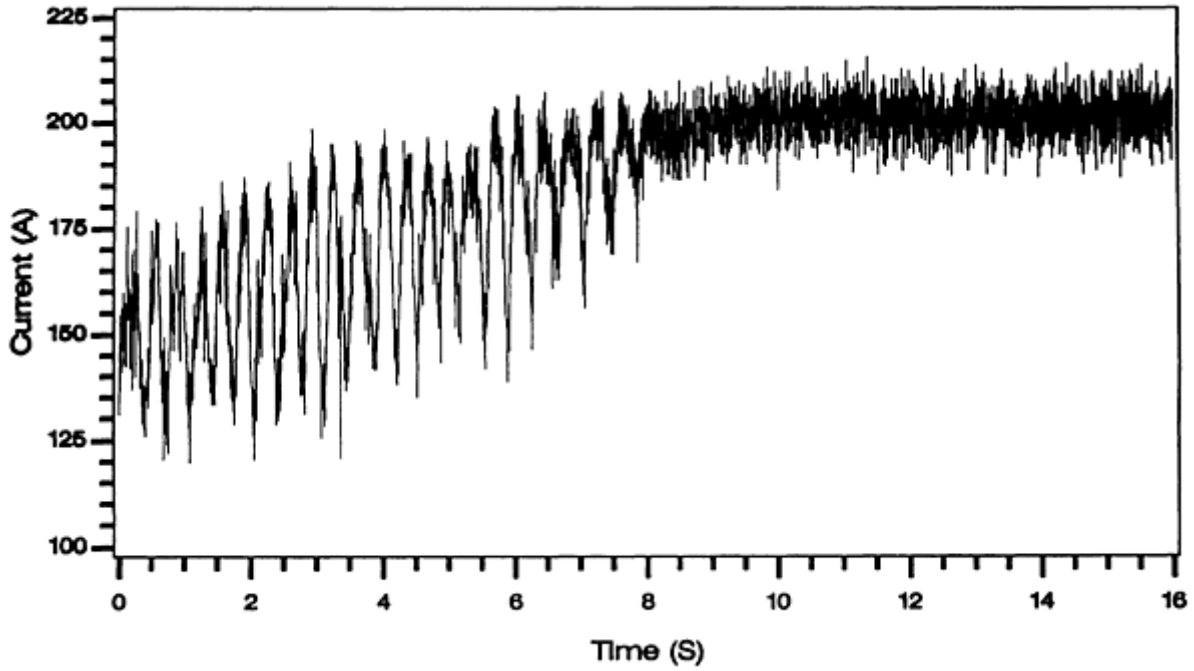

FIG. 11 PLOT OF DIGITIZED CURRENT VERSUS TIME DURING A GAS-METAL ARC WELD IN CARBON STEEL IN WHICH A TRANSITION FROM GLOBULAR TO SPRAY TRANSFER OCCURRED (AT ~*T* = 8 S) AS CURRENT WAS INCREASED. SOURCE: REF 1

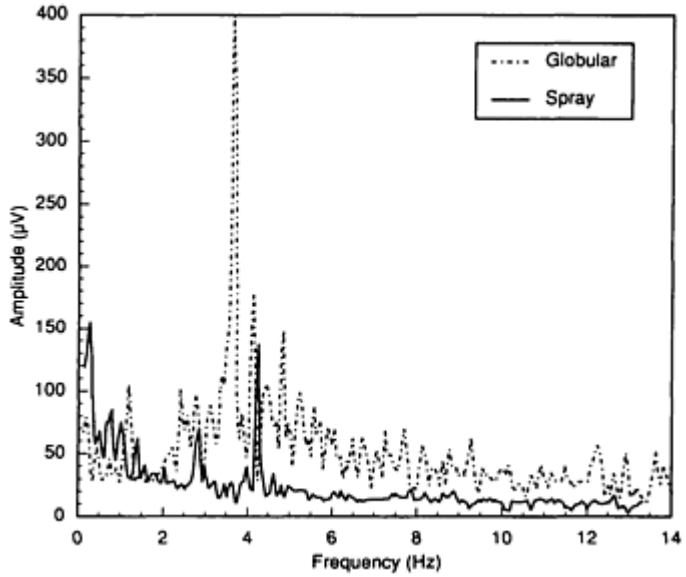

FIG. 12 WELDING CURRENT POWER SPECTRA FOR GLOBULAR TRANSFER AND SPRAY TRANSFER MODES DURING GAS-METAL ARC WELDING OF STEEL. SOURCE: REF 1

Several specific techniques have been identified (Ref 8) for detecting the mode of metal transfer: Fourier transform, standard deviation, peak ratios, and integrated amplitude of the current and voltage signal. In a similar manner, spatter, lack of shielding gas, and contact tube wear can also be detected. Similar power spectra changes also occur in the secondary circuit voltage and acoustic noise. The change in acoustic noise allows the aural detection of the transfer mode. An experienced welder can readily hear, for example, the difference between globular and spray transfer.

Contact of the molten droplet with the weld pool, while the droplet is still attached to the electrode, also results in a sudden change in electrical resistance. This is important, because spatter is generally produced when this electrode-to-

weld pool contact breaks. (Spatter can also be produced by rapid expansion of gas bubbles in the electrode as it melts.) The resulting electrical and acoustic noise can be used to detect that spatter is being produced.

References cited in this section

1. H.B. SMARTT, IDAHO NATIONAL ENGINEERING LABORATORY, 1992
2. A.D. WATKINS, "HEAT TRANSFER EFFICIENCY IN GAS METAL ARC WELDING," MASTER'S THESIS, UNIVERSITY OF IDAHO, APRIL 1989
3. J.F. LANCASTER, *THE PHYSICS OF WELDING*, 2ND ED., INTERNATIONAL INSTITUTE OF WELDING, PERGAMON PRESS, 1986, P 233
4. T.W. EAGAR, D.E. HARDT, H.B. SMARTT, AND J.A. JOHNSON, PROCESS CONTROLLABILITY IN GAS METAL ARC WELDING: MICRO AND MACROSCOPIC PROBLEMS, *PROC. EIGHTH SYMPOSIUM ON ENERGY SCIENCES*, CONF-9005183, U.S. DEPARTMENT OF ENERGY, ARGONNE NATIONAL LABORATORY, MAY 1990, P 51-67
5. D.E. CLARK, C. BUHRMASTER, AND H.B. SMARTT, DROPLET TRANSFER MECHANISMS IN GMAW, *PROC. 2ND INTERNATIONAL CONFERENCE ON TRENDS IN WELDING RESEARCH* (GATLINBURG, TN), 1989
6. W.G. ESSERS AND R. WALTER, HEAT TRANSFER AND PENETRATION MECHANISMS WITH GMA AND PLASMA-GMA WELDING, *WELD.J.*, VOL 60 (NO. 2), 1981, P 37-S TO 42-S
7. J.A. JOHNSON, N.M. CARLSON, AND H.B. SMARTT, DETECTION OF METAL TRANSFER MODE IN GMAW, *PROC. 2ND INTERNATIONAL CONFERENCE ON TRENDS IN WELDING RESEARCH* (GATLINBURG, TN), 1989
8. G. ADAM AND T.A. SIEWERT, SENSING OF GMAW DROPLET TRANSFER MODES USING AN ER100S-1 ELECTRODE, *WELD.J.*, VOL 69 (NO. 3), MARCH 1990, P 103-S TO 108-S

Herschel B. Smartt, Idaho National Engineering Laboratory

Procedure Development

The preceding discussion leads to a logical approach toward selecting welding parameters during the development of welding procedures. First, given a nominal power supply open-circuit voltage and contact tube-to-base metal distance, the electrode speed can be set to determine the welding current. It can be shown that:

$$S = \frac{4hGI}{Hpd^2}(E_0 + HI) \qquad \textbf{(EQ 4)}$$

where E_0 is the power supply open-circuit voltage. It is assumed that the proper selection of electrode type and shielding gas have been made, and that the electrode diameter is appropriate for the application.

Second, the open-circuit voltage is adjusted to give either an acceptable arc length or electrode extension. The objective is to prevent either burnback (transfer of the arc to the contact tube) or spatter caused by shorting of the molten electrode droplets with the weld pool prior to detachment from the electrode. Fine adjustment of voltage may be necessary to obtain a clean start of the process, thus avoiding a short period of spatter or globular transfer following arc ignition. The combination of current and voltage for a given contact tube-to-base metal distance determines the droplet transfer mode.

Third, the welding current determines the melting rate of the electrode. The electrode melting rate (M_{rp}) is a quadratic function of current (Ref 9):

$$M_{rp} = (C_1 + C_2 A)I + C_3 \frac{LI^2}{A^2} \qquad \textbf{(EQ 5)}$$

where A is the cross-sectional area of the electrode and C_1, C_2, C_3, and i are constants.

Another researcher (Ref 10) defines M_{rp} by:

$$M_{rp} = C_4 I + C_5 \frac{LI^2}{A} \qquad \textbf{(EQ 6)}$$

where C_4 and C_5 are constants.

Given a desired melting rate, the welding travel speed is set to obtain the desired weld bead reinforcement. The current, voltage, and weld travel speed have all now been set, thus determining the heat input per length of weld ($H = \eta EI/R$).

It should be noted that it is actually possible to independently vary heat input and mass input (in terms of weld bead reinforcement) to the weld, over at least a small range. This is shown in Fig. 13, where the same data presented in Fig. 1 are replotted in terms of reinforcement as a function of heat input per length of weld.

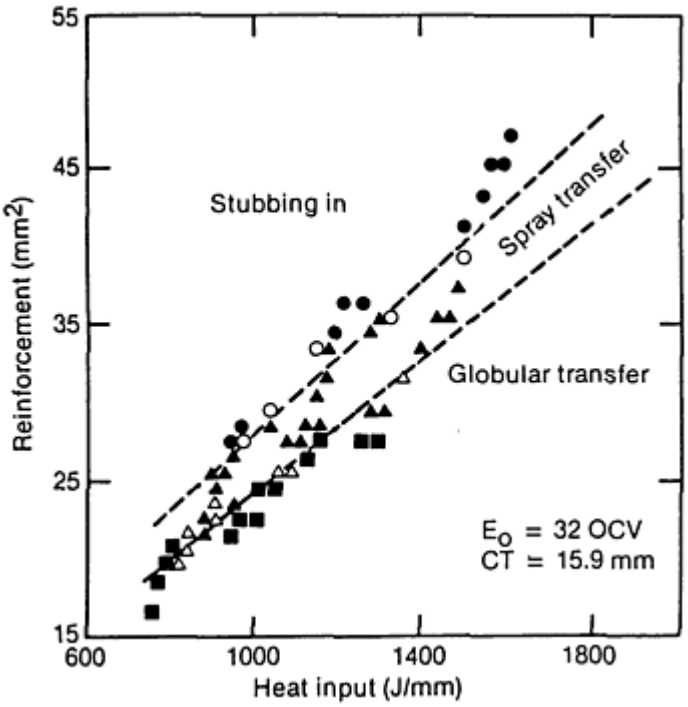

FIG. 13 PLOT OF REINFORCEMENT VERSUS HEAT INPUT TO SHOW PARAMETERS THAT FAVOR SPRAY TRANSFER MODE FOR GAS-METAL ARC WELDING OF STEEL. POWER SUPPLY OPEN-CIRCUIT VOLTAGE, E_0, IS 32 V; CONTACT TUBE-TO-BASE METAL DISTANCE, C_T, IS 15.9 MM (0.625 IN.).

The above discussion on procedure development ignores second-order effects, such as the dependence of arc length on weld travel speed. It should also be realized that several iterations through the steps defined above may be required for final parameter determination. Proper power supply settings must be used, and code requirements must be met.

References cited in this section

9. A. LESNEWICH, CONTROL OF MELTING RATE AND METAL TRANSFER IN GAS-SHIELDED

METAL-ARC WELDING, PART II--CONTROL OF METAL TRANSFER, *WELD.J.*, VOL 37 (NO. 9), SEPT 1958, P 418-S TO 425-S

10. J.H. WASZINK AND G.J.P.M. VAN DEN HEUVEL, HEAT GENERATION AND HEAT FLOW IN THE FILLER METAL IN GMA WELDING, *WELD.J.*, VOL 61 (NO. 8), AUG 1982, P 269-S TO 282-S

Transfer of Heat and Mass to the Base Metal in Gas-Metal Arc Welding

Herschel B. Smartt, Idaho National Engineering Laboratory

References

1. H.B. SMARTT, IDAHO NATIONAL ENGINEERING LABORATORY, 1992
2. A.D. WATKINS, "HEAT TRANSFER EFFICIENCY IN GAS METAL ARC WELDING," MASTER'S THESIS, UNIVERSITY OF IDAHO, APRIL 1989
3. J.F. LANCASTER, *THE PHYSICS OF WELDING*, 2ND ED., INTERNATIONAL INSTITUTE OF WELDING, PERGAMON PRESS, 1986, P 233
4. T.W. EAGAR, D.E. HARDT, H.B. SMARTT, AND J.A. JOHNSON, PROCESS CONTROLLABILITY IN GAS METAL ARC WELDING: MICRO AND MACROSCOPIC PROBLEMS, *PROC. EIGHTH SYMPOSIUM ON ENERGY SCIENCES*, CONF-9005183, U.S. DEPARTMENT OF ENERGY, ARGONNE NATIONAL LABORATORY, MAY 1990, P 51-67
5. D.E. CLARK, C. BUHRMASTER, AND H.B. SMARTT, DROPLET TRANSFER MECHANISMS IN GMAW, *PROC. 2ND INTERNATIONAL CONFERENCE ON TRENDS IN WELDING RESEARCH* (GATLINBURG, TN), 1989
6. W.G. ESSERS AND R. WALTER, HEAT TRANSFER AND PENETRATION MECHANISMS WITH GMA AND PLASMA-GMA WELDING, *WELD.J.*, VOL 60 (NO. 2), 1981, P 37-S TO 42-S
7. J.A. JOHNSON, N.M. CARLSON, AND H.B. SMARTT, DETECTION OF METAL TRANSFER MODE IN GMAW, *PROC. 2ND INTERNATIONAL CONFERENCE ON TRENDS IN WELDING RESEARCH* (GATLINBURG, TN), 1989
8. G. ADAM AND T.A. SIEWERT, SENSING OF GMAW DROPLET TRANSFER MODES USING AN ER100S-1 ELECTRODE, *WELD.J.*, VOL 69 (NO. 3), MARCH 1990, P 103-S TO 108-S
9. A. LESNEWICH, CONTROL OF MELTING RATE AND METAL TRANSFER IN GAS-SHIELDED METAL-ARC WELDING, PART II--CONTROL OF METAL TRANSFER, *WELD.J.*, VOL 37 (NO. 9), SEPT 1958, P 418-S TO 425-S
10. J.H. WASZINK AND G.J.P.M. VAN DEN HEUVEL, HEAT GENERATION AND HEAT FLOW IN THE FILLER METAL IN GMA WELDING, *WELD.J.*, VOL 61 (NO. 8), AUG 1982, P 269-S TO 282-S

Arc Physics of Gas-Tungsten Arc Welding

J.F. Key, EG&G Idaho, Inc.

Introduction

THE GAS-TUNGSTEN ARC WELDING (GTAW) process is performed using a welding arc between a nonconsumable tungsten-base electrode and the workpieces to be joined. C.E. Jackson defined a welding arc as "a sustained electrical discharge through a high-temperature conducting plasma producing sufficient thermal energy so as to be useful for the joining of metals by fusion." This definition is a good foundation for the discussion that follows.

The physics of GTAW are fundamental to all arc processes and are more straightforward, because the complications of materials (for example, filler and flux) transferred through and interacting with the arc can be avoided. Geometrically, the arc discharge in GTAW is between a rod-shaped tungsten electrode and a planar-shaped electrode, that is, the workpiece.

Pure tungsten electrodes are less expensive and, possibly, more environmentally compatible than those with rare earth or other oxide additions. They are used for lower-specification welds, where tungsten contamination that is caused by the molten electrode surface can be tolerated. They are also used for alternating current (ac) welding of aluminum, copper, magnesium, and thin sections of low-alloy and stainless steels.

Analysis of the arc discharge is separated into electrode regions and the arc column. The electrode regions are confined to very small distances from the electrode surfaces, have very high electrical and thermal fields, and have much higher current density, because of the contraction of the arc to a small spot. As a result, electrode regions for both the cathode and the anode are difficult to analyze by diagnostic measurements and theoretical computation. This situation must be remedied for a thorough understanding of the process, because the process parameters control the arc discharge at the cathode, with the anode serving as the connection to ground. The arc column, on the other hand, is relatively easy to analyze, but is important primarily as a means to deduce arc characteristics at the electrodes.

Polarity. The GTAW process generally utilizes a direct current (dc) arc, where the tungsten electrode has a negative polarity. The tungsten electrode thus becomes the cathode and the workpiece becomes the anode. The polarity is called straight polarity, or direct current electrode negative (DCEN).

Reverse polarity, or direct current electrode positive (DCEP), is literally the reverse of DCEN. The workpiece is the cathode and the tungsten electrode serves as the anode. Because most heat is generated at the anode in the GTAW process, DCEP is used for welding certain thin-section, low melting point materials when DCEN would be likely to cause excessive penetration or burn-through.

Either alternating current or DCEP is used for removing an oxide film from the surface of the weld pool or workpiece. The oxide film promotes emission during the half-cycle (ac) when the workpiece is negative polarity. As the oxide is depleted, the emission moves to a new location that has a high enough oxide content to sustain the discharge of electrons. The arc root or cathode spot where the emission occurs is highly mobile in ac or DCEP and, as a result, the arc is much less stable than in DCEN.

Gas Shielding. In all cases, the arc and both electrodes are shielding by gas, usually an inert gas or a gas mixture. Argon and argon-helium mixtures are used most often, although argon-hydrogen mixtures are used for some applications. The GTAW process may simply utilize the arc to fuse the workpieces together without the addition of filler materials (autogenous) or filler may be added to the molten pool to fill grooves in thicker weldments. A reasonable understanding of welding arc fundamentals and the GTAW process requires a more thorough discussion of the electrode regions of the arc and the arc column.

Arc Physics of Gas-Tungsten Arc Welding

J.F. Key, EG&G Idaho, Inc.

Electrode Regions and Arc Column

The cathode and anode are similar in several respects. Both exhibit a voltage drop caused by a space charge that covers a very thin region over their surfaces, and the arc is significantly contracted on the surfaces. Figure 1 shows that the total arc voltage is partitioned between the electrode drops and arc column. The relative magnitude of these drops depends on welding parameters and electrode material.

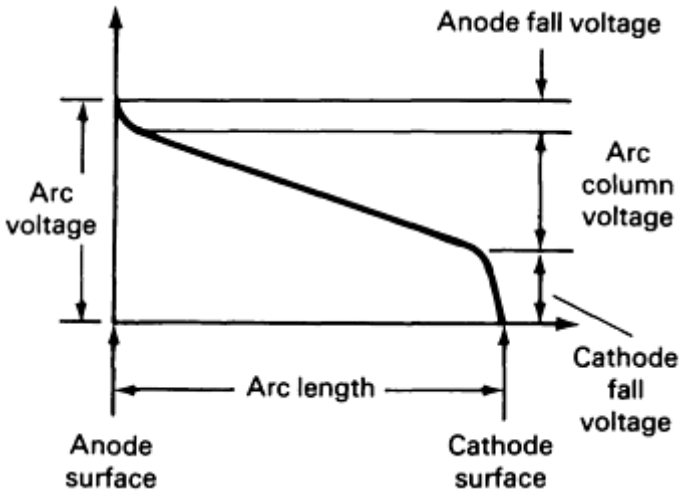

FIG. 1 PLOT OF RELATIVE ARC VOLTAGE DISTRIBUTION VERSUS RELATIVE ARC LENGTH BETWEEN ELECTRODES

The arc discharge requires a flow of electrons from the cathode through the arc column to the anode, regardless of polarity or whether ac or dc is used. Two cases of electron discharge at the cathode will be discussed: thermionic emission and nonthermionic emission, also called cold cathode, or field emission.

Thermionic emission results from joule heating (resistance) of the cathode by the imposed welding current until the electron energy at the cathode tip exceeds the work function (energy required to strip off an electron). This case applies to the general case of DCEN, where the tungsten electrode is the emitter, or cathode. Pure tungsten electrodes have to be heated to their melting point to achieve thermionic emission. Once molten, the equilibrium tip shape becomes a hemisphere, and a stable arc results from uniform emission over this surface. Thoria (ThO_2), zirconia (ZrO_2), or ceria (CeO_2) are added to pure tungsten in amounts up to 2.2 wt% ThO_2, 0.4 wt% ZrO_2, or 3.0 wt% CeO_2 to lower the work function, which results in thermionic emission at lower temperatures and avoids melting the cathode tip. These electrodes typically have a ground conical tip, and thermionic emission is localized to a cathode spot. Thermionic emission creates a cloud of electrons, called a space charge, around the cathode. If a second electrode at a higher potential is nearby (the workpiece, in this case), then the electrons will flow to it, thus establishing the arc.

Nonthermionic, or field, emission creates an electron discharge with a very high electric field, typically exceeding 10^9 V/m. This intense electric field literary pulls electrons out of a relatively cold or unheated cathode. This would not appear to be applicable to welding until one considers that for reverse polarity or DCEP, a condensation of positive ions from the arc column can build up in a very thin (1 nm, or 0.04 μin.) layer over the cathode surface, creating a very high localized electric field even though the cathode voltage drop may only amount to several volts.

An oxide layer, which is always present on the cathode surface in an actual weld, facilitates the discharge with a source of lower work function electrons. When the oxide layer is very thin (on the order of one atom layer), emission occurs via a tunneling mechanism through the film to an emitting site. Thicker oxide films exhibit locally conducting spots at the end of filamentary channels through the oxide. Large currents flow in these channels, which are on the order of 100 nm (4 μin.) in diameter and have lifetimes of 0.001 to 1 μs.

The cathode cleaning action, which is one of the principal reasons to use DCEP or ac, results from stripping away the oxide film at the emitting sites by very small and intense jets of metal vapor and debris. It becomes obvious that a practical implication of the short lifetime of these cathode spots is a generally unstable arc that is due to the necessity of continual movement of the cathode spot to undepleted regions of oxide film. Arc instability is undesirable and DCEP or ac is only used when cathodic cleaning or the minimizing of heat input to the workpiece is a higher priority than optimizing weld bead shape and location.

Anode. Welding process parameters (for example, current and voltage) control the arc discharge at the cathode. Although the electron flow enters the anode through the anode spot and constitutes 85% of the energy going into the weld pool, thus making current density the single most important welding parameter that determines pool shape, events at the anode can

only be controlled indirectly by controlling the cathode. Anode spot stability does depend somewhat on shielding gas composition and the shape of the anode (that is, weld groove).

Current density and heat input measurements at the anode have been made to better understand how process parameters that are largely controlling events at the cathode will, in turn, influence the shape and melting rate of the weld pool. The relative contributions of heat transfer to the workpiece, in terms of the GTAW process, are shown in Fig. 2.

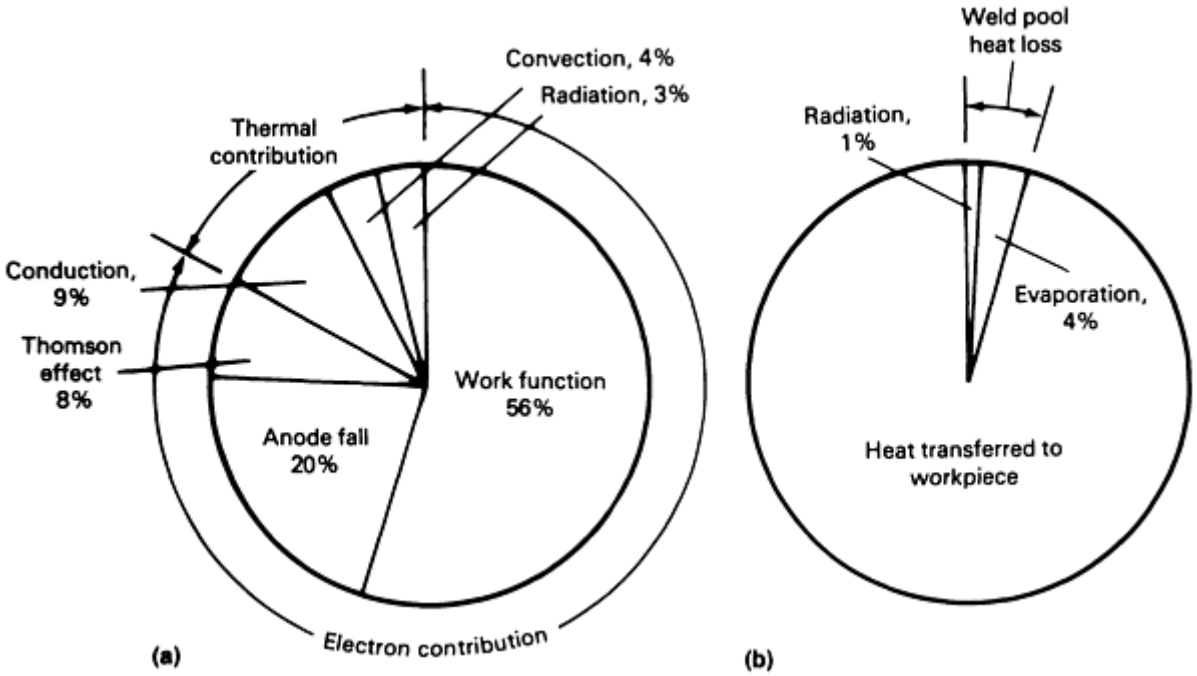

FIG. 2 RELATIVE HEAT TRANSFER CONTRIBUTIONS TO WORKPIECE WITH GTAW. (A) CONTRIBUTION OF INDIVIDUAL PARAMETERS TO ANODE HEAT INPUT. (B) HEAT OUTPUT AT CATHODE (WORKPIECE) RELATIVE TO WELD POOL HEAT LOSS

The Thomson effect represents the energy lost by electrons as they move from higher to lower temperatures. The sum of work function, Thomson effect, and anode fall gives an electron contribution to heat transfer of approximately 84%. The remaining 16% is due to thermal effects (that is, conduction, convection, and radiation). There are small heat losses from the pool that are due to evaporation of metal ions and radiation. Figure 3 shows that the energy distribution for this particular case approaches a Gaussian distribution (that is, normal distribution curve). High helium contents in the shielding gas have produced data that are typically better fit by a Lorentzian curve, indicating a narrower current density distribution (that is, a more-contracted arc at the anode spot).

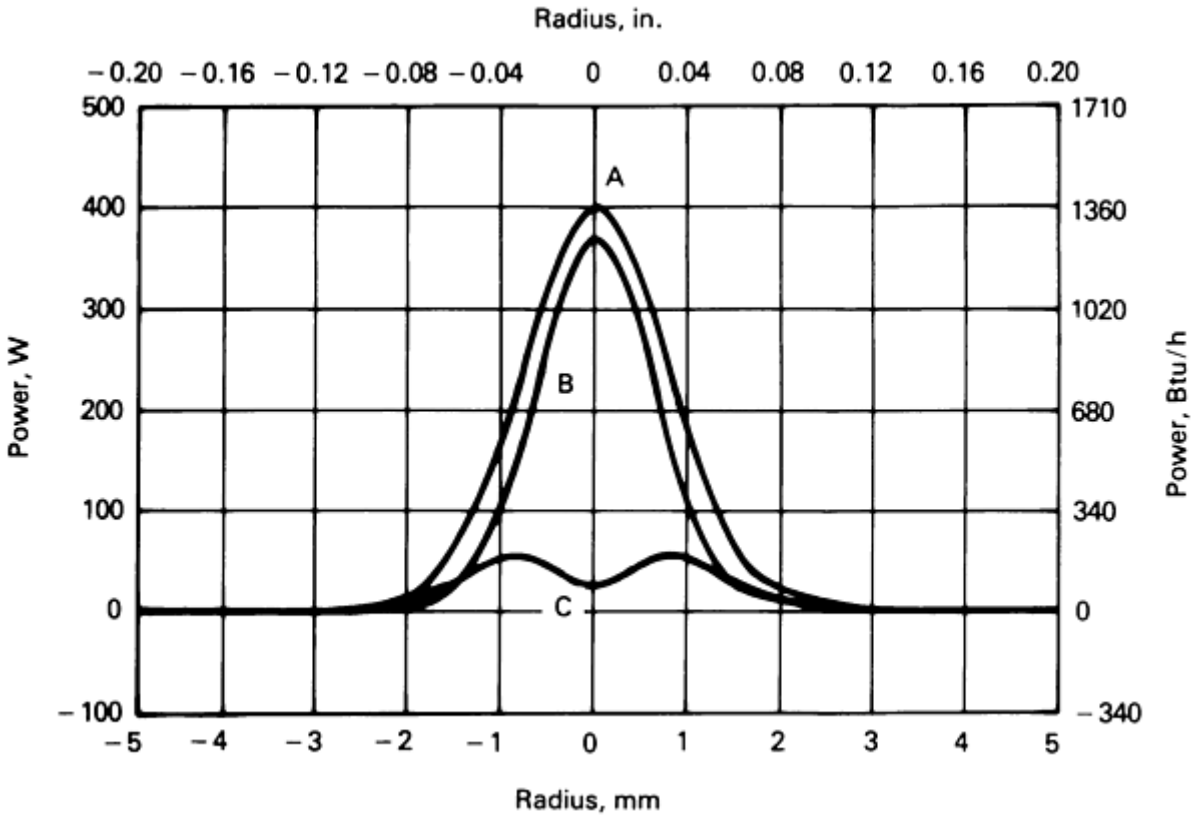

FIG. 3 PLOT OF ELECTRON AND THERMAL CONTRIBUTIONS TO HEAT TRANSFER. A, TOTAL ARC POWER (STANDARD DEVIATION, *s* , OF 0.8 MM, OR 0.031 IN.); B, ELECTRON CONTRIBUTION (σ = 0.7 MM OR 0.028 IN.); C, THERMAL CONTRIBUTION. WELD PARAMETERS: CURRENT, 10 A; VOLTAGE, 10 V; TIME, 10 S; SHIELDING GAS, ARGON; ELECTRODE ANGLE, 30°

Arc efficiency, in addition to those variables that have an effect on it, is an extremely important term in the heat transfer analysis of welding. It gives the percentage of heat dissipated in the arc that actually is captured by the workpieces and is available for melting. Arc efficiency, as a function of all GTAW welding parameters and many materials, has been determined experimentally and found to be nominally 75%. The variables having the greatest effect on arc efficiency are arc voltage and anode material. For those variables, the effect is usually no more than ±5%. Other parameters have a negligible effect.

Arc Column. The electron discharge between the electrodes partially ionizes the shielding gas in its path, thus making the arc column a conductor, or plasma. Overall, the arc column is neutral and is composed of electrons, positive gas and possibly metal ions, and neutral gas atoms.

Ironically, fundamental measurements of arc properties are most easily made in the arc column, although the actual effect of these properties on the electrode region of an actual weld must still be inferred. Nevertheless, it is useful to understand fundamentals of the arc that relate essential welding variables (for example, current, voltage, electrode gap, choice of shielding gas, and electrode shape) to arc temperature, current density distribution, and gas flow structure at the anode surface.

Effect of Cathode Tip Shape. For the general case of straight polarity, DCEN, the tip of the tungsten alloy cathode is ground to a point and then truncated somewhat to prevent the sharp tip from burning off and contaminating the weld. The included angle of the cone and the diameter of the truncation under some welding conditions have a significant effect on weld pool shape. Figure 4 shows examples of the effect of these two parameters on weld pool shape.

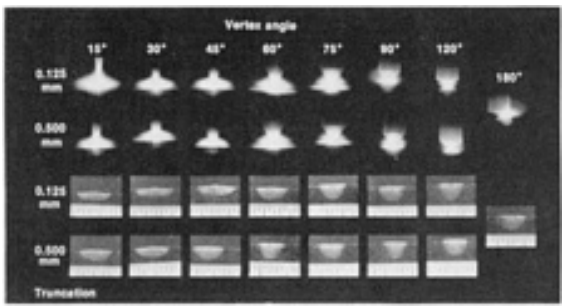

FIG. 4 FUSION ZONE PROFILE FOR SPOT-ON-PLATE WELDS AS A FUNCTION OF ELECTRODE TIP GEOMETRY USING 100% AR AS A SHIELDING GAS. WELD PARAMETERS: CURRENT, 150 A; DURATION, 2 S

For a stationary spot-on-plate weld shielded by pure argon, the weld depth-to-width ratio increased with an increasing vertex angle up to 90° and with an increasing truncation diameter. The arc became less "bell shaped" and more "ball shaped" as the vertex angle or truncation diameter increased. These results should be a valid indication of the effect of cathode tip shape for pulsed current welding, which produces a series of overlapping spot welds.

A study of bead-on-plate welds (Fig. 5) made with constant current and velocity indicated a similar but less pronounced trend. These conditions produce a tear-drop molten pool shape when viewed from above, compared to circular shape for spot or pulsed current welding. Fluid and heat flow within the pool is less uniform front-to-rear in a tear-drop-shaped pool and probably has a greater influence on pool shape than electrode tip shape.

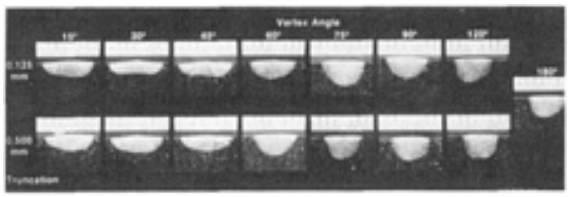

FIG. 5 FUSION ZONE PROFILE FOR BEAD-ON-PLATE WELDS AS A FUNCTION OF ELECTRODE TIP GEOMETRY USING 100% AR AS A SHIELDING GAS. WELD PARAMETERS: CURRENT, 150 A; WELDING SPEED, 3 MM/S (0.12 IN./S)

When the arc is used in a weld groove, the relative shapes of the cathode tip and the anode groove become more important. The arc discharge from the cathode will seek a path to ground with the lowest electrical resistance. For a stable arc properly centered in the groove (for example, a root pass), the shortest path to ground should be between the cathode tip and the bottom of the groove (Fig. 6). This will require the cathode vertex angle to be somewhat less than the included angle of the groove and/or a sufficiently wide groove to ensure that the shortest path to ground is from the cathode tip to the groove bottom and not, for example, from the electrode shoulder to the groove wall, as the case would be with a 90° electrode in a 10° narrow groove. Welding in a groove places a higher priority on arc stability and location than on maximum penetration.

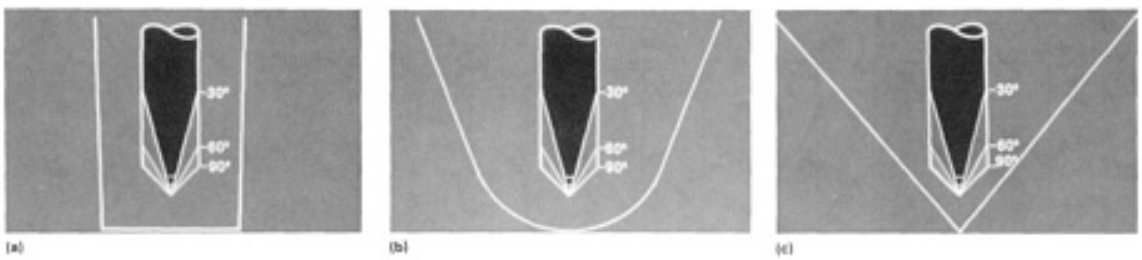

FIG. 6 EFFECTS OF ELECTRODE TIP GEOMETRY ON THE PATH LENGTH TO GROUND IN WELD GROOVES OF VARIOUS SHAPES. (A) 75° V-GROOVE. (B) 40° U-GROOVE. (C) 10° NARROW GROOVE

To understand the effects of tip shape, temperature distributions in the plasma were measured. Figure 7 shows that as the cathode vertex angle increases, the plasma radius of the arc column increases at mid-gap and becomes more constricted near the anode. The quantitative interpretation of these results requires theoretical modeling, which has yet to be completed.

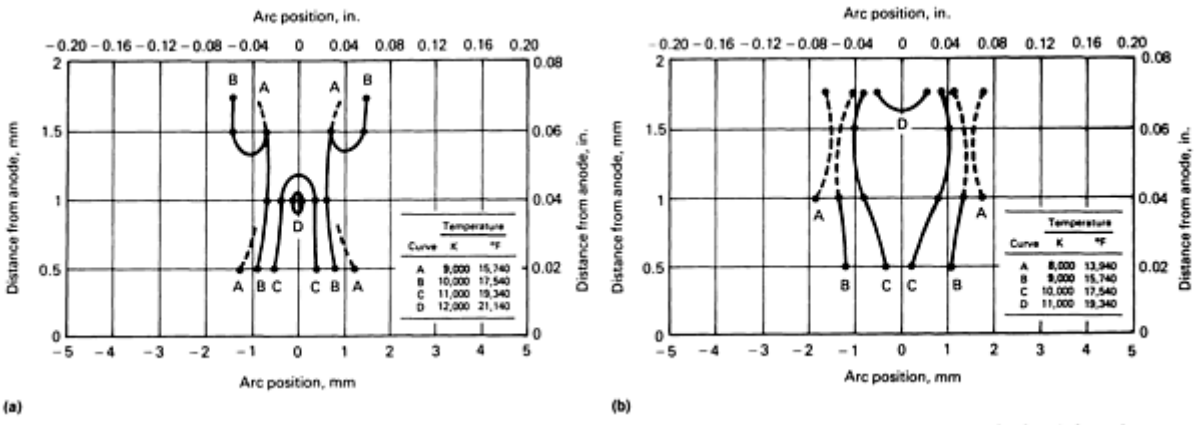

FIG. 7 EFFECT OF VERTEX ANGLE ON GTAW ARC COLUMN TEMPERATURE DISTRIBUTION WITH 100% AR USED AS SHIELDING GAS. (A) 30° ELECTRODE VERTEX ANGLE. (B) 90° ELECTRODE VERTEX ANGLE. WELDING CURRENT, 150 A

Effect of Shielding Gas Composition. The GTAW process typically uses either an inert gas, such as argon, or an inert gas mixture, such as argon and helium, to shield the arc and the weld from atmospheric contamination. Occasionally, a slightly reactive gas mixture, such as argon with up to 15 vol% H_2, is used. (The 15 vol% limit is based on safety considerations.) Shielding gas composition has a rather strong effect on arc temperature distribution and, under certain conditions, a significant effect on weld pool shape.

Figure 8 shows how shielding gas affects arc voltage. The curves would all be displaced downward for shorter arc lengths, but the relative positions would be maintained. Figure 9 shows the effects of both cathode vertex angle and shielding gas composition on weld pool shape for spot-on-plate welds. Increasing additions of helium to argon show a remarkable increase in penetration when using a 30° vertex angle. However, the effect is much less evident when using a 90° vertex angle.

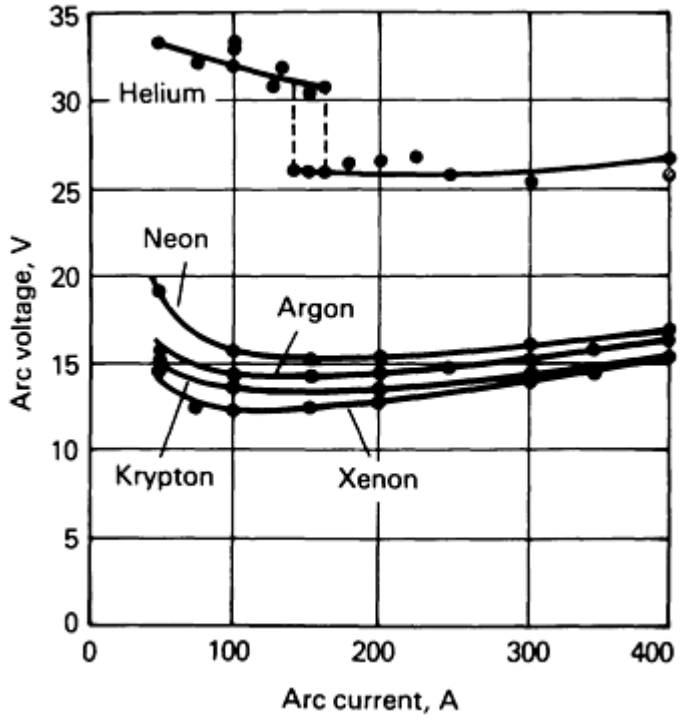

FIG. 8 PLOT OF ARC VOLTAGE VERSUS ARC CURRENT FOR SELECTED INERT SHIELDING GASES. WELDING PARAMETERS: ANODE, TITANIUM; CATHODE, TUNGSTEN; POLARITY, DCEN; ARC LENGTH, 12.7 MM (0.050 IN.)

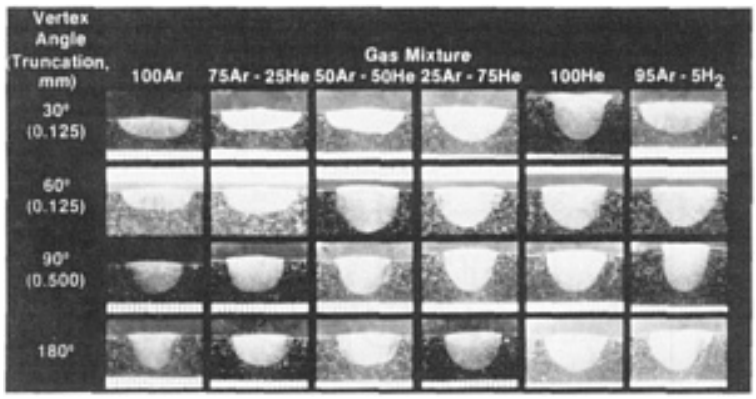

FIG. 9 EFFECT OF ELECTRODE TIP GEOMETRY AND SHIELDING GAS COMPOSITION ON WELD POOL SHAPE FOR SPOT-ON-PLATE WELDS. WELDING PARAMETERS: CURRENT, 150 A; DURATION, 2 S

To understand these phenomena, arc temperature distributions for a variety of shielding gases and mixtures, electrode shapes, current, arc voltages (electrode gaps), and anode materials have been measured in order to clarify welding arc fundamentals. Welding arcs are composed of electrons, positive gas ions, and neutral gas atoms. Some measurement techniques give the temperature of one species (electrons), whereas other techniques give the temperature of another species (neutral atoms). If the arc is in local thermodynamic equilibrium (LTE), all techniques should give the same temperature.

Although the assumption of LTE used to be considered completely valid, contemporary investigations have suggested that this is not always the case and that some of the older measurements may be somewhat in error. Absolute values of arc temperature are only needed to establish boundary conditions for detailed arc modeling of temperature-dependent properties. What is of more importance to the welding engineer or technologist is the relative effect of essential variables

on heat input to the workpiece. Arc temperature measurement is one useful indication of how these variables affect the arc.

When compared to Fig. 7(a), Fig. 10 shows that large additions of helium to argon decrease peak temperatures slightly and increase the plasma diameter in the plasma column. The arc appears to become a broader and more isothermal heat source. The lower peak temperature is reasonable, because a combination of the high ionization potential of helium and relatively low currents of welding arcs gives an arc column that is only slightly ionized. Figure 7 showed that a large vertex angle had a similar, but less pronounced, effect on arc temperature when adding helium to the shielding gas (that is, the axial peak temperature decreased and the plasma diameter increased).

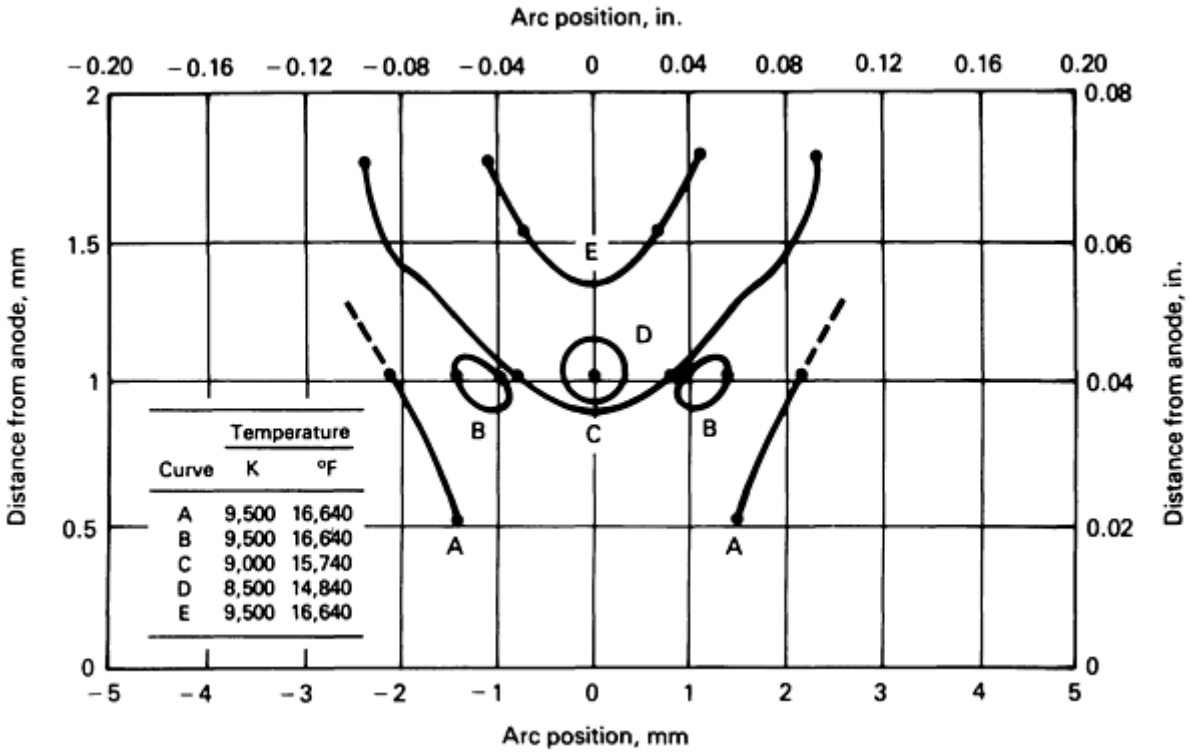

FIG. 10 PLOT OF GTAW ARC COLUMN TEMPERATURE DISTRIBUTION AS A FUNCTION OF ANODE DISTANCE AND ARC POSITION. WELDING PARAMETERS: ELECTRODE VERTEX ANGLE, 30°; CURRENT, 150 A; SHIELDING GAS, 10AR-90HE

Figure 11 shows that doubling the current from 150 to 300 A produces an increase in plasma diameter (that is, that portion of the arc above approximately 8000 K, or 13,900 °F). This effect occurs regardless of the shielding gas composition.

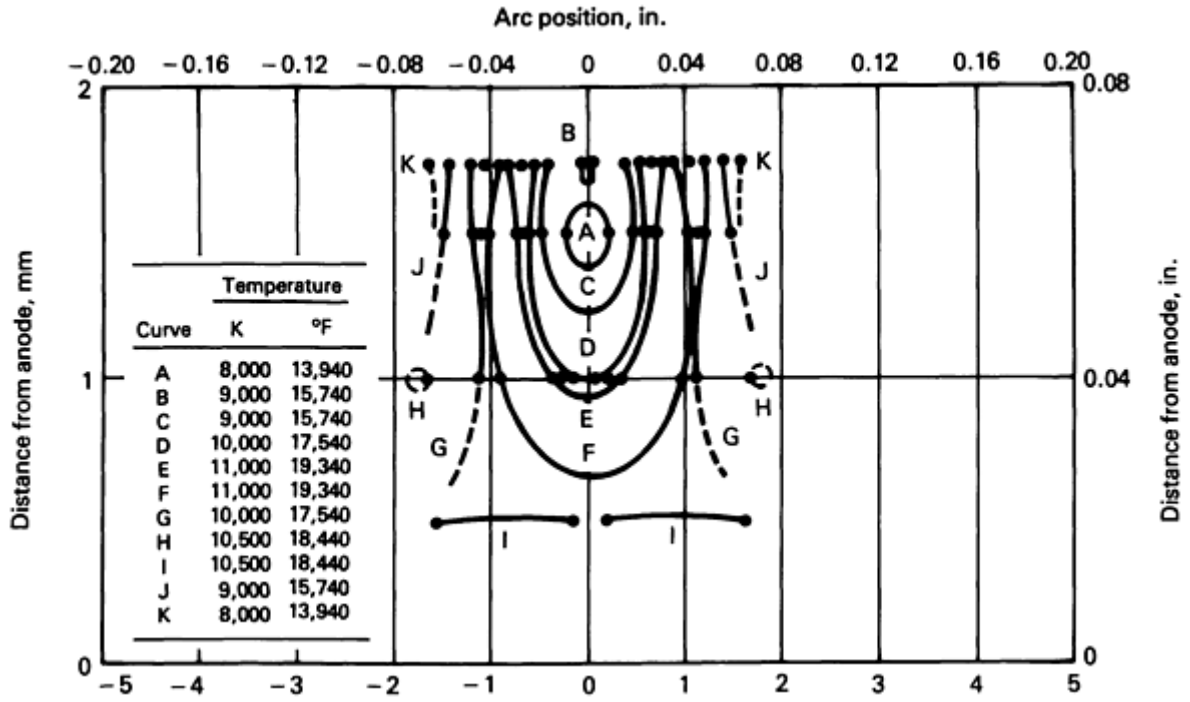

FIG. 11 PLOT OF GTAW ARC COLUMN TEMPERATURE DISTRIBUTION RELATIVE TO ANODE DISTANCE AND ARC POSITION. WELDING PARAMETERS: ELECTRODE VERTEX ANGLE, 30°; CURRENT, 300 A; SHIELDING GAS, 100% AR

The arc length or gap between the electrodes is yet another process parameter that must be considered, especially for mechanized welding, where it can be kept reasonably constant. Because arc length is proportional to arc voltage, longer arcs have higher arc voltages and consume more energy for the same current. However, this increased energy is generally lost through radiation to the environment surrounding the weld and does not effectively supply additional heat to the workpieces. Mechanized welding generally utilizes rather short arc lengths (2 to 3 mm, or 0.08 to 0.12 in.), whereas manual welding uses a longer arc length. Unfortunately, relationships that establish a direct correlation between the temperature distribution in the arc column and the weld pool shape still have not been established, primarily because weld pool shape depends on other factors, such as compositionally dependent molten metal properties.

Flow Structure. Shielding gas is used to displace reactive gases in the atmosphere from the vicinity of the weld. Inert gases are preferred for the GTAW process, because they minimize unwanted gas-metal reactions with the workpieces. A uniform laminar flow of gas from the gas cup would be ideal and, in fact, is usually achieved as long as there is no welding arc. However, the arc discharge rapidly heats the gas in the arc column, and thermal expansion causes plasma jets. The lower temperature near the cathode tip in Fig. 11 is an indication of a jet pumping in cooler gas. This becomes an important factor at high currents, because these jets can depress the surface of the weld pool and alter heat transfer to it. The rapid gas expansion can cause the flow to deviate from laminar and, in extreme cases, the flow can become turbulent. Turbulence tends to mix atmospheric contaminants into the arc, often where they can do the most harm: at the surface of the molten weld pool. Holographic interferometry and Schlieren photography have been used to characterize gas flow.

Figures 12, 13, and 14 show examples of laminar and turbulent flow. The flow from a commercial-design gas cup for three current levels is shown in Fig. 12. Laminar flow occurs where the fringes are generally straight and parallel. Turbulent flow is indicated by very wavy or circular fringes. Increasing current tends to make the laminar region somewhat broader and thicker, effectively increasing the area shielded from atmospheric contamination.

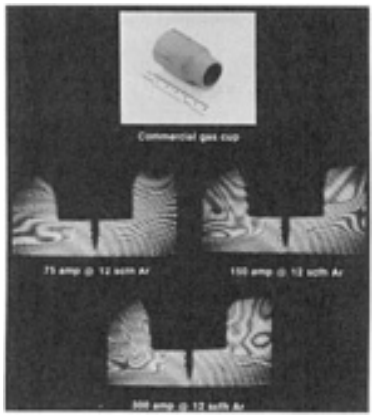

FIG. 12 EFFECT OF GEOMETRY ON COMMERCIAL GAS CUP LAMINAR AND TURBULENT FLOW AS DETECTED BY REAL-TIME HOLOGRAPHIC INTERFEROMETRY

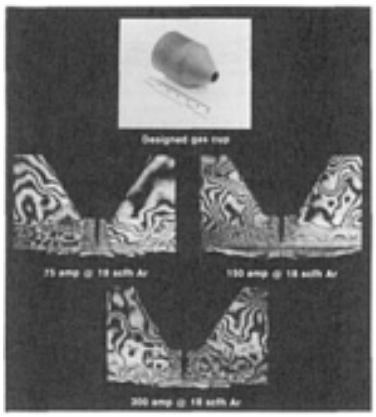

FIG. 13 EFFECT OF GEOMETRY ON CONVERGING CONE CUP LAMINAR AND TURBULENT FLOW AS DETECTED BY REAL-TIME HOLOGRAPHIC INTERFEROMETRY

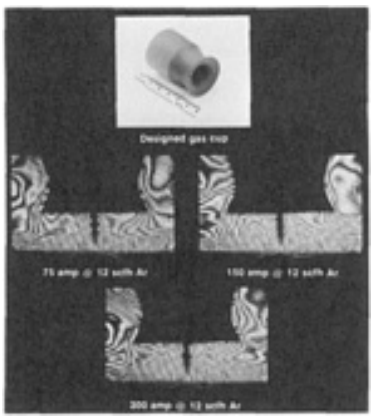

FIG. 14 EFFECT OF GEOMETRY ON VENTURI GAS CUP LAMINAR AND TURBULENT FLOW AS DETECTED BY REAL-TIME HOLOGRAPHIC INTERFEROMETRY

Figures 13 and 14 result from experiments with gas cup shapes that were designed to improve shielding. Figure 13 shows that a converging cone would be a very poor choice for the GTAW process, as indicated by the very small area of laminar flow and the extreme turbulence in the surrounding region.

Figure 14 is a venturi shape, which provides a large laminar flow region for all current levels and excellent shielding. This design may be somewhat better than commercial designs, but weld contamination studies should be conducted to verify this possibility.

Arc Physics of Gas-Tungsten Arc Welding

J.F. Key, EG&G Idaho, Inc.

Selected References

- S.S. GLICKSTEIN, "ARC-WELD POOL INTERACTIONS," DEPARTMENT OF ENERGY RESEARCH AND DEVELOPMENT REPORT WAPD-TM-1429, BETTIS ATOMIC POWER LABORATORY, AUG 1978
- C.E. JACKSON, THE SCIENCE OF ARC WELDING,*WELD. J.*, VOL 39, 1960, P 129S-140S, 177S-190S, 225S-230S
- J.F. KEY, H.B. SMARTT, J.W. CHAN, AND M.E. MCILWAIN, PROCESS PARAMETER EFFECTS ON ARC PHYSICS AND HEAT FLOW IN GTAW, *PROC. INT. CONF. ON WELDING TECHNOLOGY FOR ENERGY APPLICATIONS* (GATLINBURG, TN), 16-19 MAY, 1982, P 179-199
- J.F. KEY, J.W. CHAN, AND M.E. MCILWAIN, PROCESS VARIABLE INFLUENCE ON ARC TEMPERATURE DISTRIBUTION, *WELD. J./WELD. RES. SUPP.*, VOL 62 (NO. 7), P 179-S TO 184-S
- J.F. LANCASTER, ED., *THE PHYSICS OF WELDING*, 2ND ED., INTERNATIONAL INSTITUTE OF WELDING, PERGAMON PRESS, 1986
- H.B. SMARTT, J.A. STEWART, AND C.J. EINERSON, "HEAT TRANSFER IN GAS TUNGSTEN ARC WELDING," ASM METALS/MATERIALS TECHNOLOGY SERIES, ASM INTERNATIONAL WELDING CONGRESS (TORONTO), 14-17 OCT 1985

Power Sources for Welding

F. James Grist, Miller Electric Manufacturing Company, Inc.; William Farrell and Glen S. Lawrence, Ferranti Sciaky

Introduction

POWER SOURCES are apparatuses that are used to supply current and voltages that are suitable for particular welding processes. This article describes power sources for arc welding, resistance welding, and electron-beam welding.

Power Sources for Welding

F. James Grist, Miller Electric Manufacturing Company, Inc.; William Farrell and Glen S. Lawrence, Ferranti Sciaky

Arc Welding Power Sources

Arc welding requires that an electric arc be established between an electrode and the workpiece to produce the heat needed for melting the base plate. Because utility energy is not delivered at the proper voltage and current, it must be converted to the required levels by the welding power source.

Arc power sources convert the customary 240 or 480 V alternating current (ac) utility power to a range from 20 to 80 V and simultaneously increase the current proportionately. Galvanic isolation is also provided from the utility line voltage to ensure operator safety. Motor- or engine-driven welding generators are wound to deliver the correct voltage and current

directly; therefore, no transformer is necessary. Actual arc voltage is established by factors other than the power source (for example, electrode type, base-metal type, shielding gas, and standoff distance).

Ratings and Standards

The National Electrical Manufacturers Association (NEMA) categorizes arc welding power sources into three classes on the basis of duty cycle:

- CLASS I: RATED OUTPUT AT 60, 80, OR 100% DUTY CYCLE
- CLASS II: RATED OUTPUT AT 30, 40, OR 50% DUTY CYCLE
- CLASS III: RATED OUTPUT AT 20% DUTY CYCLE

Duty cycle is the ratio of arc time to total time based on a 10 min averaging period. A 60% machine will deliver 6 min of arc time and 4 min off time without overheating. In Fig. 1, curve A shows a NEMA class I (60%) 300 A rated machine that is capable of a maximum 375 A at reduced duty cycle (38%) and 232 A at 100% (continuous). Curve B represents a NEMA class II (50%) 250 A machine with a continuous duty of 176 A. Curve C represents an engine-driven machine rated at 225 A and 20% duty. It does not offer output in excess of its rating, because of a horsepower limitation of the engine.

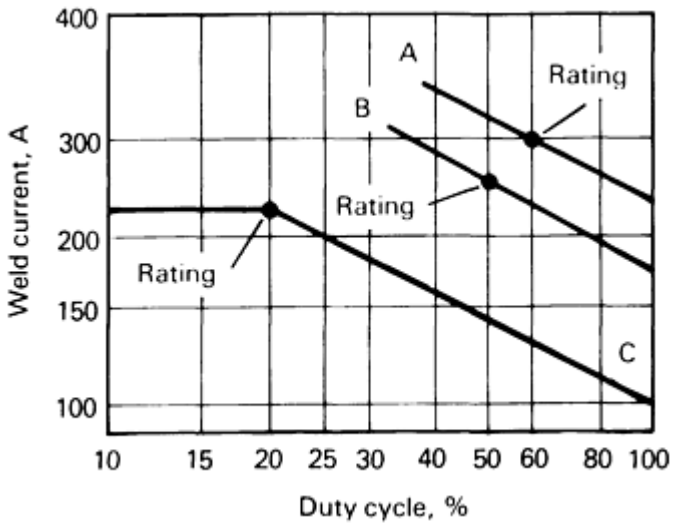

FIG. 1 SELECTED DUTY CYCLE CURVES. A, 300 A, 60% MACHINE; B, 250 A, 50% MACHINE; C, 225 A, 20% ENGINE-DRIVEN MACHINE WITH HORSEPOWER LIMITATION

NEMA requires most machines to produce a maximum of 125% of rated output current. No minimum current is specified, but 10% (of rating) is typical. Load voltage, *E*, for class I and II machines is defined by:

$$E = 20 + 0.04I \qquad \textbf{(EQ 1)}$$

where *I* is the current in amperes, below 600 A. Above 600 A, the rated load voltage remains at 44 V. Power sources intended for gas-tungsten arc welding (GTAW) service are defined by:

$$E_{GTAW} = 13 + 0.012I \qquad \textbf{(EQ 2)}$$

Class III machines are constant-current types limited to 20% duty cycle.

Efficiencies (that is, ratios of power output to power input) of 68% for line-frequency machines and 88% for inverters are typical. Line current draw can be reduced in certain machines by the addition of power factor correcting capacitors connected to the primary winding.

Input (line) voltages shown on the manufacturer nameplate are often multivoltage by means of tap changing for 200, 230, 460, or 575 V. Designed primarily for 60 Hz power, most systems will operate at 50 Hz, with minor changes in output. Input voltages for 50 Hz systems are typically 220, 380, and 415 V. Usual service conditions are temperature that range from 0 to 40 °C (32 to 105 °F) and altitudes of up to 1000 m (3300 ft). (Altitude is a factor because of fuel-air mixtures.)

The power source nameplate must include the following specifications:

- MANUFACTURER
- NEMA CLASS (I, II, OR III) AND DUTY CYCLE
- MAXIMUM OPEN-CIRCUIT VOLTAGE
- NUMBER OF PHASES
- MAXIMUM SPEED (IN REVOLUTIONS PER MINUTE) AT NO LOAD (ROTATING EQUIPMENT)
- RATED LOAD (IN VOLTS)
- RATED LOAD (IN AMPERES)
- FREQUENCY (OR FREQUENCIES) IN HERTZ
- INPUT VOLTAGE(S)

The National Electric Code (NEC) requires that a main disconnect switch be provided for each installed welding machine. Manufacturer installation instructions list the kVA and kW rating and recommend the correct fuse and conductor size. Local codes may differ from NEC requirements.

Proper grounding is a necessary safety consideration. Machines equipped with high-frequency arc stabilizers must be correctly grounded to prevent electromagnetic interference (EMI) to nearby equipment. The installer certifies (to the Federal Communications Commission) that the machine has been grounded according to manufacturer instructions. Most power sources are forced-air cooled by internal fans. Thermal sensors will interrupt output if airflow is impeded.

Power Source Selection

Because no single power source is right for all welding situations, it is necessary to know the processes to be used before selecting the best power source. Table 1 gives the more-common processes that use constant-current and constant-voltage power sources.

TABLE 1 SELECTION OF POWER SOURCE RELATIVE TO WELDING PROCESS TO BE EMPLOYED

WELDING PROCESS	POWER SOURCE	
	CONSTANT CURRENT	CONSTANT VOLTAGE
SHIELDED METAL ARC WELDING (SMAW)	•	. . .
GAS-TUNGSTEN ARC WELDING (GTAW)	•	. . .
GAS-METAL ARC WELDING (GMAW)	. . .	•
PULSED GAS-METAL ARC WELDING (GMAW-P)	•	. . .
FLUX-CORED ARC WELDING (FCAW)	. . .	•
SUBMERGED ARC WELDING (SAW)	. . .	•
ELECTROGAS WELDING (EGW)	•	•
ELECTROSLAG WELDING (ESW)	. . .	•
PLASMA ARC WELDING (PAW)	•	. . .

PLASMA ARC CUTTING (PAC)	•	. . .

Alternating current power sources for shielded metal arc welding (SMAW) and submerged arc welding (SAW) can be as simple as a single transformer (Fig. 2a). Low-voltage machines with open-circuit voltages of 50 V or less are transformer types. Output alternating current reflects the sinusoidal waveform of the utility input line (Fig. 3a).

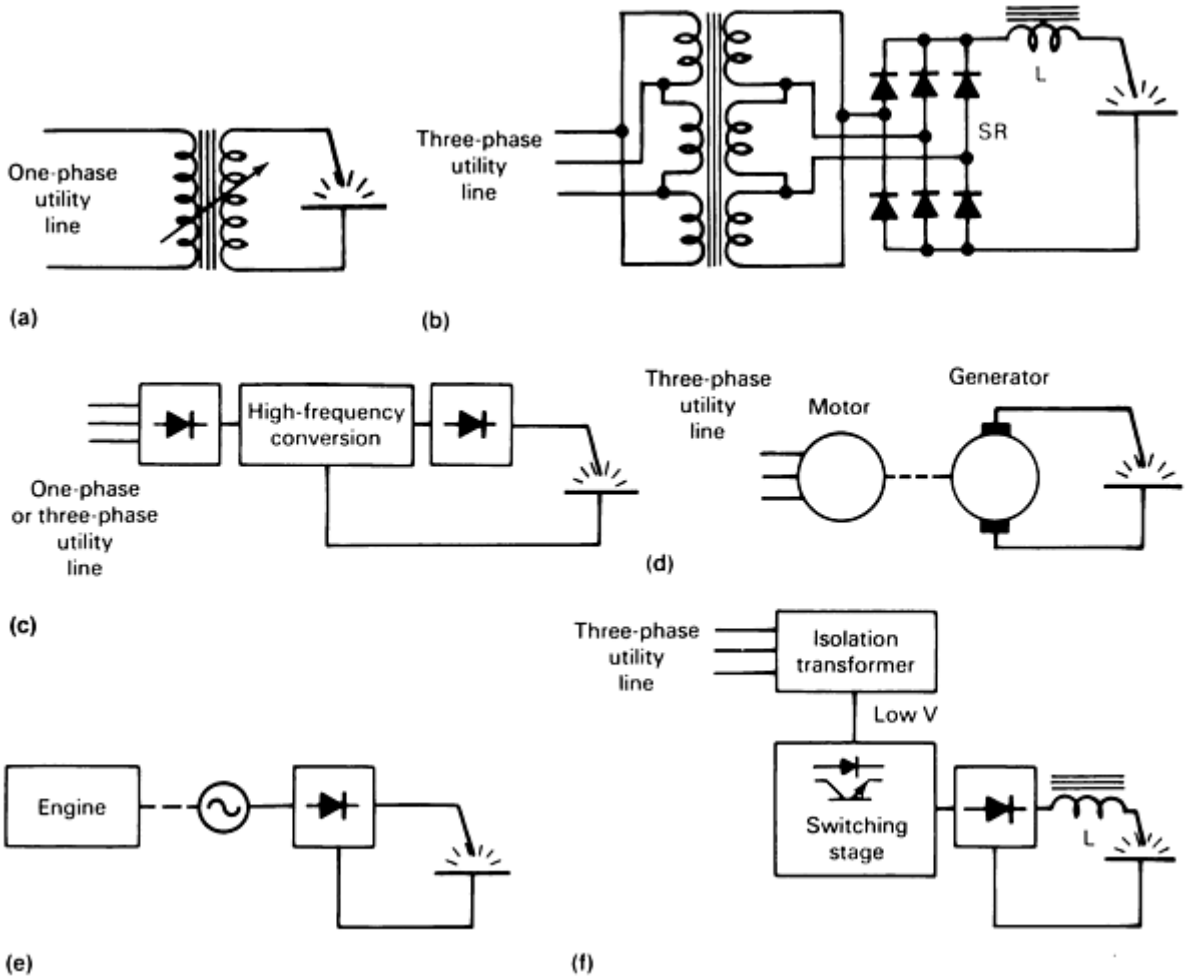

FIG. 2 SELECTED ALTERNATING CURRENT POWER SOURCES. (A) ALTERNATING CURRENT WELDING TRANSFORMER, ADJUSTABLE CORE OR WINDINGS. (B) THREE-PHASE SCR-CONTROLLED DC WELDING POWER SOURCE. (C) INVERTER BLOCK DIAGRAM. (D) MOTOR-GENERATOR SET. (E) ENGINE-DRIVEN ALTERNATOR WITH DC OUTPUT. (F) SECONDARY SWITCHING POWER SOURCE

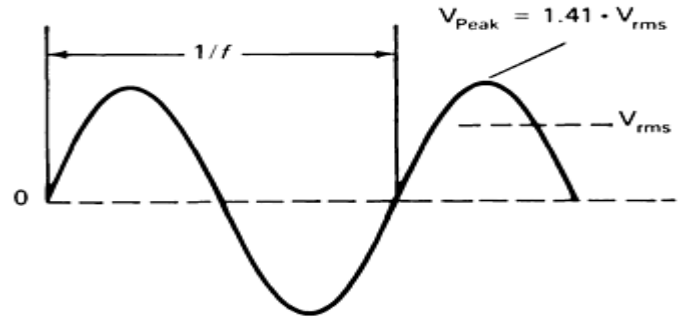
$V_{Peak} = 1.41 \cdot V_{rms}$
1/f
V_{rms}
0

(a)

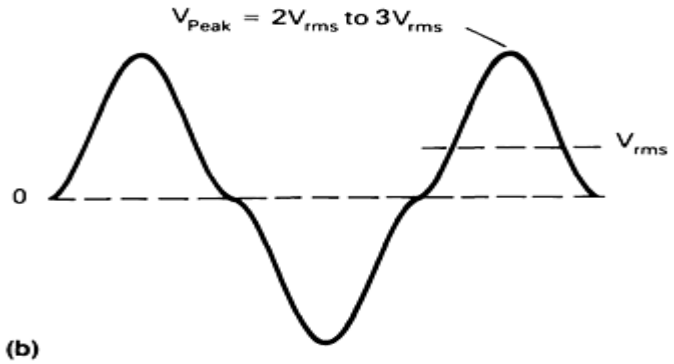
$V_{Peak} = 2V_{rms}$ to $3V_{rms}$
V_{rms}
0

(b)

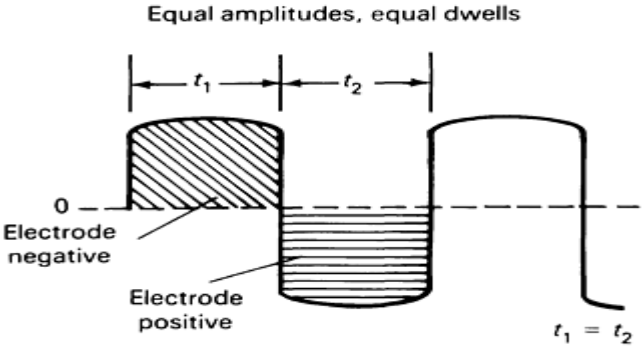
Equal amplitudes, equal dwells
t_1
t_2
0
Electrode negative
Electrode positive
$t_1 = t_2$

(c)

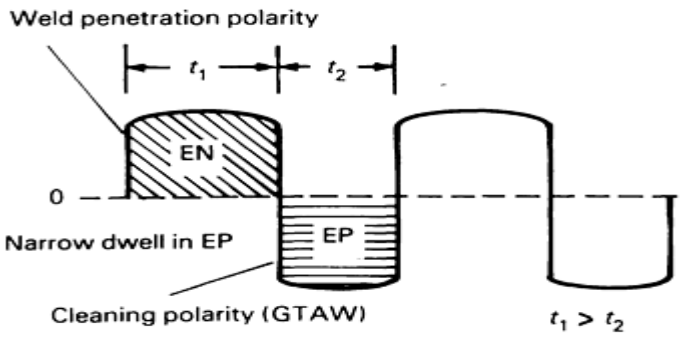
Weld penetration polarity
t_1
t_2
EN
0
Narrow dwell in EP
EP
Cleaning polarity (GTAW)
$t_1 > t_2$

(d)

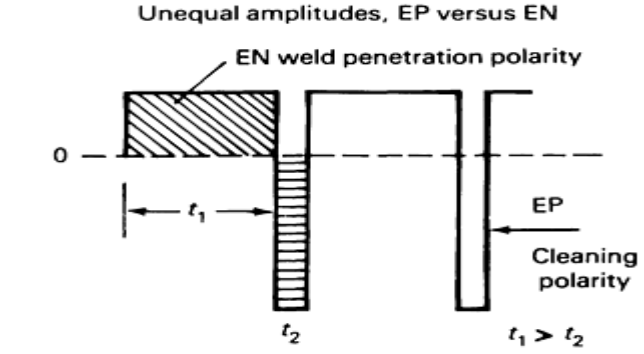
Unequal amplitudes, EP versus EN
EN weld penetration polarity
0
t_1
EP
Cleaning polarity
t_2
$t_1 > t_2$

(e)

FIG. 3 TYPICAL AC WELDING CURRENT WAVEFORMS. (A) SINE WAVE ALTERNATING CURRENT, SIMPLE TRANSFORMER WELDER. (B) MODIFIED SINE WAVE OBTAINED FROM MAGNETIC AMPLIFIER-TYPE WELDER. (C) SQUARE WAVE, LINE FREQUENCY, AND BALANCED DWELL. (D) SQUARE WAVE WITH UNBALANCED DWELLS, EP VERSUS EN. (E) VARIABLE-POLARITY AC WITH DWELL, AMPLITUDE, AND FREQUENCY ALL ADJUSTABLE

Magnetically controlled equipment (that is, a saturable reactor or magnetic amplifier) used for GTAW delivers a modified sinewave output (Fig. 3b). There is a risk of electrode (tungsten) migration to the workpiece if peak current greatly exceeds the average value. This technology exhibits moderate response.

Newer technologies deliver a square wave output at line frequency (Fig. 3c). A square wave eliminates peaking and provides a rapid transition through zero, which is important to cyclic reignition of the arc. Thyristors are employed in concert with magnetic cores to generate the square current waveform. Adjustable imbalance permits the operator to control the ratio of electrode positive (EP) to electrode negative (EN) current by dwell extension (Fig. 3d).

Direct current power sources can be classified as being constant-current sources or constant-voltage sources.

Constant-Current Sources. For the SMAW process, a family of "drooping" volt-ampere (V-A) curves (A, B, and C) is provided in Fig. 4(a). Often, a current boost or "dig" characteristic is made available (curve D in Fig. 4a). A burst of extra current during the brief period of metal transfer shorting tends to alleviate sticking during keyhole welding or when weaving or whipping the electrode, especially with the more-globular transfer electrodes.

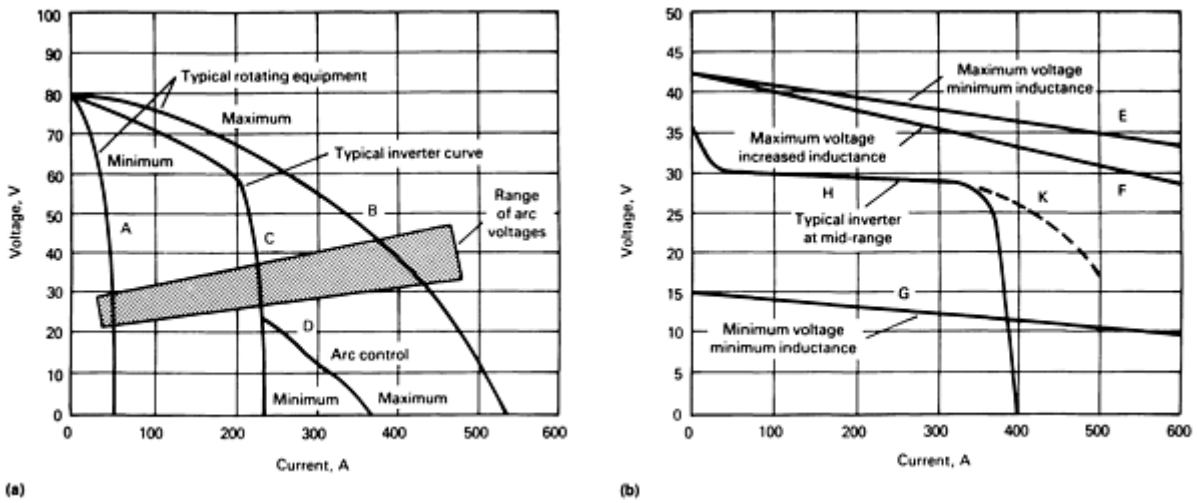

FIG. 4 VOLT-AMPERE CURVES OF TYPICAL DC POWER SOURCES. (A) CONSTANT-CURRENT SOURCE. (B) CONSTANT-VOLTAGE SOURCE

Power sources for dc GTAW processes are generally more critically constant-current than are the SMAW "stick droopers." Ripple content is lower and current regulation is tighter. Inverter types customarily regulate to ±1% or ±1 A, whichever is larger. Remote foot control is essential to ensure that both hands are free for manipulation. Response time need not be fast, except for pulsed programs. Programmable and pulse-capable units permit the automation of complex current profiles.

Power sources for GTAW processes include a high-frequency arc starting device that impresses a high radio frequency (RF) voltage on the electrode. This energy "jumps the gap" from the electrode to the workpiece, ionizing the shielding gas, and permits establishment of an arc. Thus, the electrode need not touch the workpiece.

Constant-Voltage Sources. Power sources intended for gas-metal arc welding (GMAW) exhibit a relatively flat V-A curve, as shown in Fig. 4(b) (curves E, F, and G). The self-correcting characteristic of GMAW regulates the electrode burn-off rate. As the wire feed rate is increased, additional current will be drawn, but terminal voltage will remain

essentially constant. Voltage feedback techniques are used in solid-state designs to hold long-term output close to a set value.

In the short-circuiting GMAW process, for example, drops of metal are transferred to the base metal through a pinch-off routine during a period of short circuiting of the electrode to the workpiece. Shorting time and arc time are determined by power source dynamics.

Source Characteristics

Whether utility fed or motor driven, all welding power sources have a characteristic that indicates their dynamic and steady-state response. In early machines, source characteristics were optimized for a single process and were relatively unchangeable. More recent designs can be programmed for a variety of characteristics that include multiple weld processes.

The welding arc process is a dynamic, fast-changing load, exhibiting short circuits (if shorting, then no arc) at high currents and momentary voltages from near zero to over 50 V. Changes occur in milliseconds, particularly when metal transfer takes place. The ability of the power source to respond properly to rapidly changing conditions at the arc is critical to good performance. Modern technology invariably includes a closed-loop feedback circuit in the control system.

Open-Circuit Voltage (OCV). When no load is connected to the output terminals of a welding power source, the voltage that appears at the terminals is at its maximum. A high OCV value generally aids in arc starting and stability. In transformer-type power sources. OCV is established by the incoming utility line voltage and the transformer primary-to-secondary turns ratio. The output winding turns, the flux, and the angular velocity (rev/min) will establish the OCV in generators.

In manual welding, the maximum OCV is 80 V_{rms} for machines with more than 10% ripple, or 100 V OCV for a ripple content of less than 10%. Power sources intended for automatic welding only are permitted 100 V OCV. The percentage ripple voltage is the ratio of rms ripple to average pulsating dc, expressed as:

$$\%ripple = \frac{V_{\max} - V_{\min}}{V_{rms}} \qquad \textbf{(EQ 3)}$$

Static V-A Curves. Two terms are commonly used to define the characteristics of a power source for welding: static output and dynamic response. Static characteristics are set forth by the manufacturer as a series of V-A curves (Fig. 4). The slope of the static V-A curve is the ratio of load voltage change to the change in load current, expressed in V/100 A. It indicates the achievable envelope of output limits, including the highest voltage the machine will support at a given current, and the highest current that can be drawn at a given voltage.

Dynamic Response. The static V-A curves discussed above do not take into account the dynamic interplay between the power source and the process. Instantaneous response of the power source to step changes in load voltage is important to welding performance. This is especially true in the case of certain GMAW processes, where the response to a metal transfer short circuit is instrumental in bead formation and the reduction of spatter generation.

Methods of Control or Electrical Conversation. Power source control methods are a key factor in the rate of current rise (d*I*/d*t*). Either increased reactance in the ac circuitry or inductance in the dc portion will slow the rate of rise (and fall) of current during changes at the arc. Some equipment incorporates an adjustment to select the proper number of turns for a given welding condition (with silicon-controlled rectifiers [SCR] and transistor controls, these characteristics can be synthesized). Because there is no industry-accepted method to quantify the dynamics, the user must obtain a power source with a satisfactory range of adjustment.

Another consideration is the frequency response of the power source, that is, its ability to "follow" a fast command signal, such as a pulse program. Magnetically based machines are generally not fast enough to faithfully reproduce a pulsed GMAW control signal and deliver it at high currents to the weld. When a better response is required, inverter-based SCR, transistorized sources with a high-frequency response are preferred.

Droopers. A constant-current, a drooper, power source displays V-A curves such as those in Fig.(a) (curves A and C). A considerable negative slope is evident. The internal impedance of the power source is said to be high. Large variations in

the arc (load) voltage (for example, below 40 V) do not appreciably affect the selected current. Droopers are noted for their use in the SMAW process, where the operator sets current to establish a suitable burn-off rate for the selected electrode. Manipulation, that is, shortening or lengthening the arc, does not greatly affect the arc current.

However, if welding is conducted on a flatter V-A curve (see curve B in Fig. 3a), then electrode manipulation may change the current considerably. Thus, the operator gains more local control of the current through eye-hand coordination. Increasing the arc length by "pulling back" on the electrode causes the operating point to shift up slightly in terms of voltage, but decrease considerably in terms of current.

Open-circuit voltage can be field adjusted in generator types, which provides the operator with a great degree of control through electrode manipulation. Skilled operators use this flexibility to their advantage when performing difficult out-of-position welds.

Constant-Voltage Sources. Equipment designed for constant-voltage processes will display a "stiff," nearly horizontal V-A curve (curve E, F, and G in Fig. 4b). The open-circuit voltage is 43 V for curve F. When serving a 300 A load, it falls to 35 V. This is expressed as:

$$\frac{(43-35)}{300A} = \frac{8V}{300A} = \frac{2.6V}{100A} \qquad \textbf{(EQ 4)}$$

Curve H of Fig. 4(b) is representative of an inverter source in the constant-voltage mode. When set to 30 V, the electronic regulation system keeps the output very constant out to 300 A under a static (resistive) load, beyond which it falls abruptly to 0 V at 400 A. Curve K in Fig. 4(b) represents an extended output that may be available on a short-term (dynamic) basis from inverters.

The term "constant" is taken to mean relatively constant. Some droop in voltage is permitted, and is even preferred in certain welding situations. Load current at a given voltage is responsive to the rate at which a consumable electrode is fed into the arc. The designer ensures that terminal voltage is maintained during heavy loads by providing tight coupling between the primary and secondary windings of the transformer, or by providing electronic regulation systems, or both.

Movable Magnetic Cores. Welding power must be delivered to the arc under complete control of the operator. In the simplest form, conversion to the lower voltage and selection of current are incorporated into a single, special welding transformer. Movable coils (varying the coupling between primary and secondary windings) and moving iron shunts provide stepless adjustment of the output (Fig. 2a).

Saturable Reactors. In heavy industrial equipment, control is imparted by saturable reactors. These reactors comprise laminated iron core assemblies fitted with power and control windings. A small control current varies the effective magnetic permeability of the iron core and controls flux to the power winding. Considerable gain is obtained. Typically, 5 A of control will command several hundred amperes of welding current. Both ac and dc outputs are available. Direct current output is obtained by the addition of secondary rectifiers. By combining rectifier diodes with self-saturating magnetic cores, a wider range is obtained, referred to as magamp control.

Alternating current and ac/dc power sources are manufactured in sizes that range from 180 A Class III "farm welders" to units designed for industrial use and rated in hundreds of amps. Principal attributes are low cost and simplicity. Alternating current is specified wherever arc blow is a concern. It is also preferred for welding aluminum. Direct current machines are favored for most SMAW and GTAW processes, and for essentially all GMAW processes.

Silicon-Controlled Rectifiers. In addition to the transformer taps, moving coils, moving shunts, and saturable reactors mentioned earlier, there are a number of other means by which output can be controlled. Thyristors, commonly known a SCRs, are frequently employed as control elements, replacing magnetic cores.

The SCR is similar to a rectifying diode, but is equipped with an additional gating element. With properly phased low-power gate signals, a configuration of SCRs will deliver hundreds of amperes of current.

The output of such a phase-controlled arrangement (Fig. 2b) can be tailored to perform as a stiff (that is, flat slope) constant-voltage source or as a drooping constant-current source through closed-loop feedback controls. When designed for three-phase operation, the dc output ripple frequency is either three times the line frequency (using three SCRs) or six

times, using six SCRs. Output ripple is "smoothed" with an appropriate inductor. Single-phase versions display the ripple of twice the line frequency and require a larger output inductor, *L*.

Because welding current is analog in nature, it has traditionally been adjusted with analog circuitry via rheostats and potentiometers. Recent advances allow digital control with microprocessors and dedicated software; tight-tolerance repeatability is the driving force.

Inverters. Inverter welding power sources are smaller and more efficient, and they offer better performance than their line-frequency counterparts. The size and weight of iron-core components are reduced when operating at higher frequencies (Fig. 5).

FIG. 5 300 A RATED CONVENTIONAL LINE-FREQUENCY POWER SOURCE (RIGHT) AND INVERTER POWER SOURCE WITH SAME RATING (LEFT). COURTESY OF MILLER ELECTRIC MANUFACTURING COMPANY, INC.

With reference to the inverted shown in Fig. 2(c), the incoming utility line directly feeds a rectifier for conversion to direct current, which powers an inverter stage operating in the range from 2 to 100 kHz. Various topologies include forward, buck, series capacitor, and series resonant inverters.

Control methods employ either pulse width modulation (PWM) or frequency modulation (FM). A variety of semiconductors are used as switching elements, including transistors (for example, field-effect transistors [FETs] and insulated-gate bipolar transistors [IGBTs]).

The transformer, which is often designed of ferrite core material, operates at high frequencies without introducing high losses. The turns ratio determines welding voltage, usually 80 V_{rms} ac at the secondary winding. A second rectifier converts it back to dc for welding. A small output inductor is required to smooth the high-frequency ripple.

Inverters have the greatest application where portability or advanced performance is required. Fast response permits current with fast transitions, low overshoot, and faithful reproduction of pulse programs.

Variable Polarity. High-technology power sources permit adjustment of the ac waveform to vary the ratio of EP to EN current and terms of both width and amplitude (Fig. 3e). Among these are switched dc types, wherein two dc constant-current power sources are alternately switched on and off, and arc current is of one polarity and then the other polarity. Almost unlimited frequencies can be generated, with rapid zero crossings.

Cycloconverter power sources constitute a family that uses three-phase inputs to generate low-frequency ac for the GTAW process. Through careful selection of specific portions of each line-frequency cycle, a pseudo square wave is assembled at a frequency lower than line frequency.

Rotating Equipment. For a variety of reasons, rotating generators and alternators are often used to supply welding power. In what is known as a motor-generator (M-G) set, an electric motor (Fig. 2d) drives the shaft of a generator, which also isolates weld power from the input utility power. The flywheel effect of the M-G set ensures stable output.

Where no electric utility power is readily available, engine-driven equipment can supply welding power (Fig. 2e). Gasoline and diesel fuels predominate. Both air- and water-cooled prime movers are available. Some include an auxiliary air compressor for air tool use.

Generators produce direct current. A wire-wound armature spins in a frame arranged with electromagnetic field poles. The armature windings cut through these fields cyclically, generating ac. This is collected by commutator, that is, copper segments fitted to the armature shaft and equipped with fixed carbon brushes. The commutator serves as a "mechanical rectifier," converting the armature currents to dc. Both the OCV and current can be user adjusted, providing good control of the V-A slopes. The output is relatively pure dc, with very little ripple content. Engine speed is governor controlled.

Most generators provide constant-current output for SMAW and GTAW processes, but adapters are often available for constant-voltage operation in the GMAW process. Auxiliary power for lights, tools, and so on derived from auxiliary stator windings.

Alternators (that is, ac generators) produce alternating current, as the name implies (Fig. 2e). A spinning rotor winding is charged with direct current obtained from the exciter and applied through slip rings, creating a rotating magnetic field. No commutator is required. The rotating field cuts through a surrounding stator assembly, the windings of which collectively produce alternating current, either single phase or three phase, as designed. In single-phase designs, the resulting current can be used for ac welding.

Output selection is provided in course ranges with reactor taps (Fig. 6), and fine adjustment is provided by rheostat-controlled current in the revolving field windings. Engine speeds are generally either 1800 or 3600 rev/min, corresponding with four-people and two-pole alternators, respectively. Some alternators eliminate the revolving field winding by employing rotating permanent magnets. If direct current is required, a static (silicon diode) rectifier is included. The combination is referred to as a dc generator-rectifier.

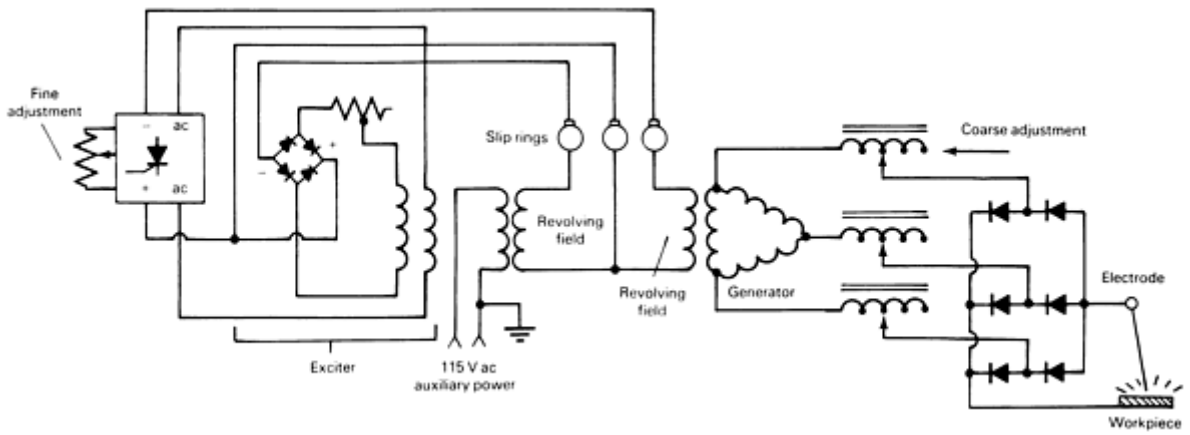

FIG. 6 SCHEMATIC SHOWING TYPICAL ENGINE-DRIVEN WELDING POWER SOURCE

The recent evolution to solid-state controls has raised the performance level of engine-driven machines. Accessories include remote controls, idle devices to reduce engine speed when not welding, battery charging capabilities, and high-frequency arc igniters.

Pulsed Power Supplies

Pulsed GTAW and GMAW processes require a power source with the ability to deliver precisely shaped current pulses superimposed on a lower background (arc-sustaining) level. In addition to thyristors in phase control, inverters are also used to generate pulses and are especially versatile for such applications. Add-on "pulse formers" have also been designed for attachment for conventional dc welding power sources.

Pulse Repetition Rates (PRR). For the GTAW process, PRRs (the number of times per second that a pulse is transmitted) are relatively low (typically, 1 to 10 PRR). Fast rise times are not essential. However, in the GMAW pulse

process, repetition rates typically range from 100 to 200 PRR. Rise (and fall) times must be short (50 to 500 μs) and overshoot must be low to preserve pulse fidelity.

The mean current of a train of rectangular pulses is given by:

$$I_{AV} = FT_P(I_P - I_B) + I_B \qquad \textbf{(EQ 5)}$$

where I_{av} is the average current, I_B is the background current, I_P is pulse peak current, f is frequency, and T_P is pulse width.

From Eq. 5, with background current, pulse width, and peak current selected, the average current will be proportional to frequency. Increasing and decreasing pulse frequency in proportion to wire feed speed will balance the current with the burn-off rate of the electrode, maintaining the proper arc length for the GMAW process. Individual droplet size will remain essentially constant.

Some pulse power sources generate pulses at line frequency or multiples thereof and stabilize the process by adjusting the power envelope of each pulse. (In a refined development, designated "one-knob control," the operator need only select a wire and gas type; pulse parameters are established by algorithms in the controller. As wire feed speed is adjusted, all other functions "track.")

Synergic Pulsed GMAW. A step higher in technology results in synergic pulsed GMAW. Inverters (Fig. 2c) and secondary switchers (Fig. 2f) ensure process stability by controlling melting rate through modulation of pulse shape and frequency. The relationship between digitally monitored wire feed speed and pulsation parameters is managed by microprocessor look-up tables and similar control strategies. The power source is simply required to exhibit fast response and high peak current capability.

Multiple Operator Power Sources

On large job sites with a number of arcs, a multiple operator (MO) power source can serve several operators. Diversity of use suggests that all arcs will not be operating simultaneously and that a 0.25 factor is typical. Accordingly, a single, large, 76 V constant potential power source can supply up to 20 SMAW operators. Each operator is equipped with a resistor "grid" to adjust arc current to his particular needs.

An alternative MO concept provides individual magamp control modules (typically, eight) fed from a single, large, multiwinding transformer. Each operator can select his preferred polarity and current. Modules can be connected in parallel for greater output.

Power Sources for Welding

F. James Grist, Miller Electric Manufacturing Company, Inc.; William Farrell and Glen S. Lawrence, Ferranti Sciaky

---

Resistance Welding Power Sources

The function of the power source for resistance welding (RW) is to deliver a predetermined amplitude of current to the welding electrodes that are clamping the workpiece. Current flows from the power source to one electrode, through the workpiece to the opposing electrode, and returns to the power source. The electrodes concentrate current into a small, usually circular area. The flow of this constricted current generates heat, concentrated largely at the interface(s) of the workpiece details to be joined.

Heat Input. The rate of heating must be sufficiently intense to cause local electrode/workpiece interface melting. The opposed electrodes apply a pressure and, when sufficient melting has been achieved, the current is interrupted. Electrode force is maintained while the molten metal solidifies, producing a sound, strong weld.

If both the local resistance of the workpiece and the welding current magnitude were constant, then the total quantity of heat, Q, developed in the workpiece would be given (in joules) by:

$$Q = I^2 RT \qquad \textbf{(EQ 6)}$$

where I is the effective value of current in amperes, R is the resistance of the workpiece in ohms, and t is the duration of flow of current in seconds.

However, the resistance is not constant. Contact resistances decrease in magnitude and the bulk resistance of the work column increases as its temperature rises. Furthermore, resistance variations of the workpiece may cause variations in the current amplitude, depending on the nature of the power source. Under these circumstances, the total quantity of heat, Q, is given by:

$$Q = \sum_{0}^{t} i^2 r.dt \qquad \textbf{(EQ 7)}$$

where i is the instantaneous value of current expressed as a function of time and r is the instantaneous resistance that is changing with time.

Equipment Selection. The design of resistance welding machines resembles that of a "C" frame press (Fig. 7). The power source transformer secondary winding is connected to the electrodes on cantilevered arms, one of which provides for adjustable electrode force. Throat depth is the distance from the frame to the electrodes. Throat gap is the vertical distance between the two parallel secondary conductors. The total area of the secondary circuit (throat depth times throat gap) exerts a profound influence on output performance. Any increase in inductance, whether due to geometry or magnetic materials within the secondary, will degrade performance and lower the power factor.

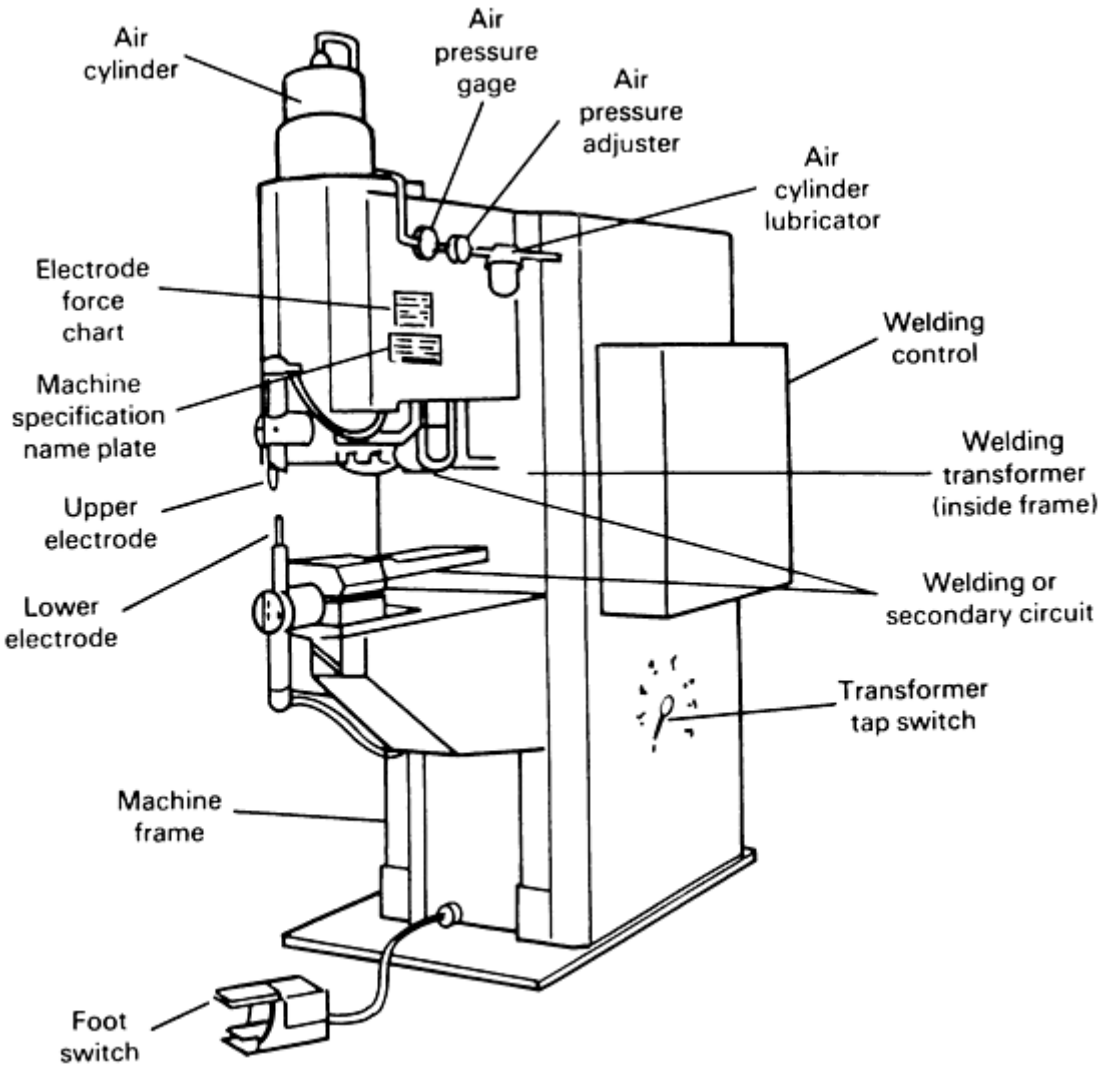

FIG. 7 SCHEMATIC SHOWING PRIMARY COMPONENTS OF A RESISTANCE WELDING MACHINE

The input to resistance welding power sources is usually 230 or 460 V utility power delivering single-phase or three-phase alternating current at 60 Hz. All systems require transformers to step down the line voltage to a relatively low value, with a proportional increase in current. The simplest systems consist of a transformer connected to single-phase power. More advanced sources produce a dc welding current through rectification.

Rectification Systems. In primary rectification systems, a special three-phase transformer is designed with a very large iron core. Each dc pulse is limited in duration and each is reversed in polarity to prevent saturation of the core. In the majority of applications, a weld is produced by a single impulse of direct current. For heavy gages, pulsation welding is used. A series of dc impulses of alternating polarity is separated by "cool time." The result is a very low frequency alternating current. Hence, the term frequency converter is commonly applied to this type of power source. Figure 8 shows a three-phase half-wave primary rectified power source.

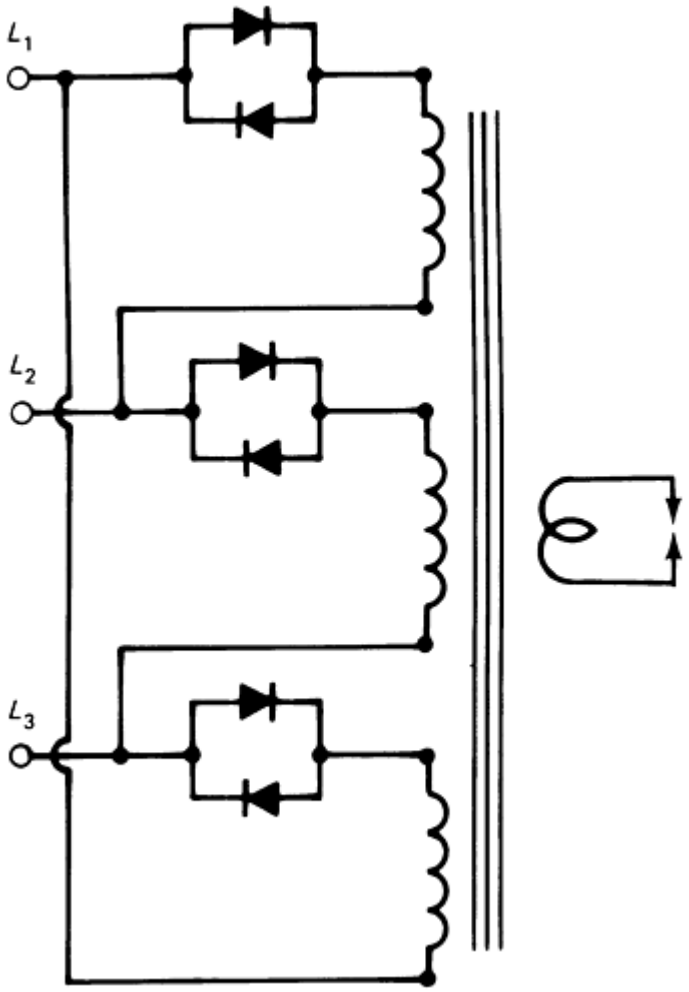

FIG. 8 CIRCUIT DIAGRAM OF THREE-PLATE HALF-WAVE RESISTANCE WELDING POWER SOURCE WITH PRIMARY RECTIFICATION

Secondary rectification systems are available in single-phase full-wave, three-phase half-wave, and three-phase full-wave forms; the latter is most commonly utilized. Three-phase full-wave systems consist of three single-phase transformers, with rectifiers connected to the secondary windings (Fig. 9). With this system, current pulse time is limited only by thermal considerations and polarity is fixed.

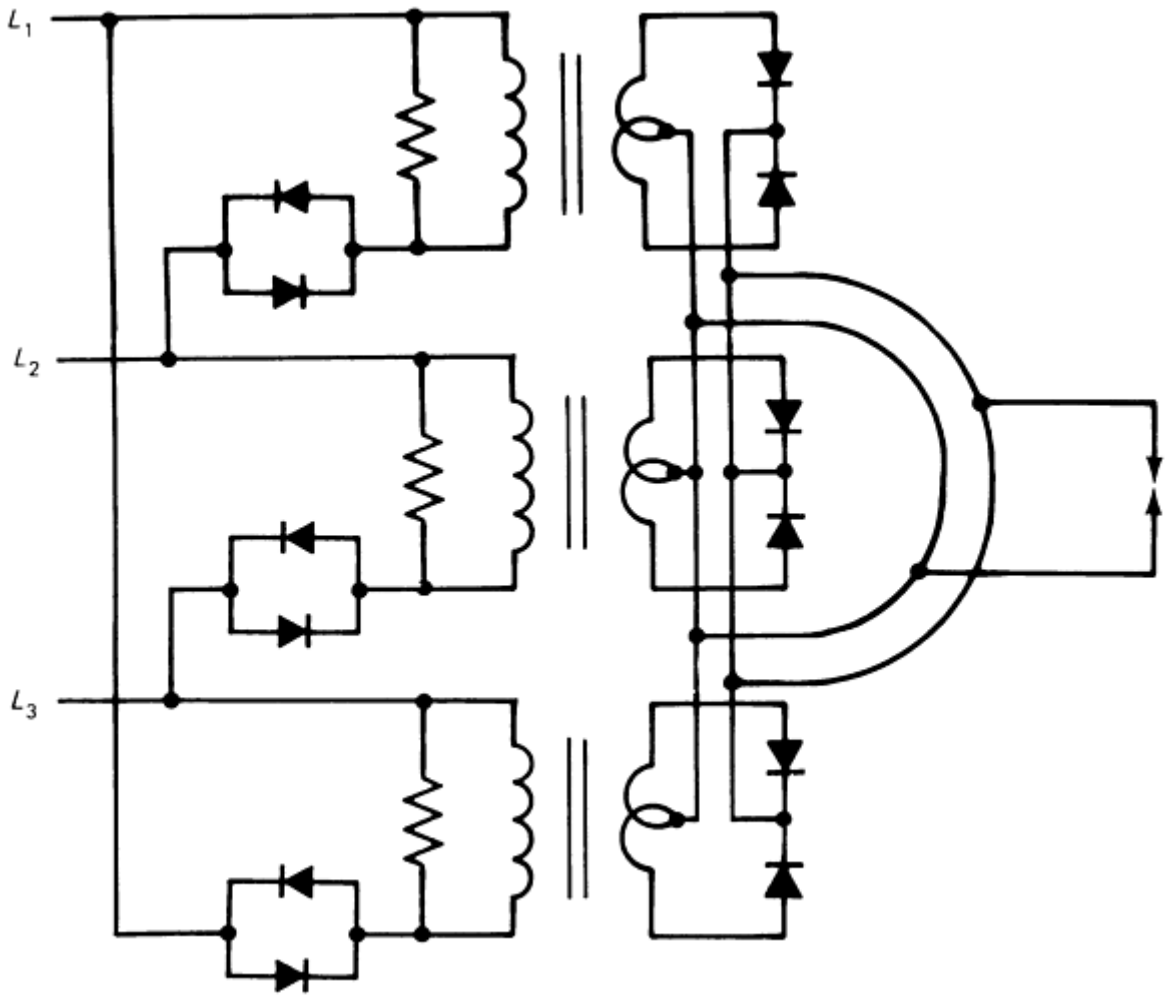

FIG. 9 CIRCUIT DIAGRAM OF THREE-PHASE FULL-WAVE RESISTANCE WELDING POWER SOURCE WITH SECONDARY RECTIFICATION

The energy efficiency of a resistance welder depends on the efficiency of delivered energy at the electrodes. Energy is dissipated in the form of heat, because of resistance in the conductors. The current, *I*, which produces the heat of welding, is simply the secondary voltage divided by the total machine impedance, *Z*, plus that of the weld:

$$i = \frac{E}{Z} \qquad \textbf{(EQ 8)}$$

where *Z* is the vector sum of the resistance and the reactance:

$$Z = \sqrt{R^2 + X^2} = \sqrt{R^2 + (wL)^2} \qquad \textbf{(EQ 9)}$$

where *R* is the total resistance of the circuit and $X = \omega L$ is the total reactance of the circuit (where ωequals $2\pi f$ and *L* is the inductance).

Resistance welders designed for single-phase utility power are lowest in investment cost, but highest in energy cost. The high-magnitude alternating current results in large inductive losses and a low power factor. Three-phase primary rectification and three-phase full-wave secondary rectification power sources reduce the power demand to about one half and operate at a higher power factor.

The rapidly pulsing weld zone temperature inherent with a single-phase source is least desirable from a welding standpoint. In addition, copper electrodes suffer from clamping impact, force, and heat, causing the occurrence of "mushrooming," which lowers current density.

Mushrooming also reduces resistance in the current path. Welding current will increase, because current is controlled indirectly in resistance welding machines by adjusting secondary voltage (that is, advancing or retarding the firing angle). From Eq 8, a decrease in impedance causes an increase in the current. Therefore, all resistance in the work path influences the current magnitude produced by a given secondary voltage. This influence is small if total system impedance is high, but significant if the system impedance is low.

A three-phase primary rectification system exhibits the greatest degree of this self-compensating effect, followed to a somewhat lesser degree by the three-phase secondary rectification category.

Finally, a thermoelectric effect is associated with passing current from a copper alloy electrode to a workpiece of a given material. This phenomenon is important when welding aluminum or magnesium alloys with a single impulse. Reversing the current polarity for each successive weld, an inherent characteristic of the three-phase primary rectification system, provides the maximum electrode life between dressings.

Duty Cycle. Resistance welding is inherently an intermittent process with a series of very short current periods followed by "off" or "cool" periods. Therefore, this type of power source is rated on a 50% duty cycle and a 1 min integrating period. The relationship between kVA rating at 50% duty cycle and kVA demand at actual duty cycle is as follows:

$$KVA_{50\%} = KVA_{Demand}\sqrt{2.(D.C.)} \qquad \textbf{(EQ 10)}$$

where D.C. is the duty cycle in %, entered in the form of a decimal. Duty cycle is defined by:

$$D.C. = \frac{N.T}{60.f} \qquad \textbf{(EQ 11)}$$

where N is the number of welds per minute, T is the weld time in cycles, and f is the frequency in hertz.

Heat Controls. Resistance welds are short and are measured in cycles. Because timing is very important, digital microprocessor controls abound. Electrochemical contactors have been replaced by SCRs or ignitrons connected in inverse parallel to handle the high currents. Coarse heat adjustment is accomplished by transformer tap switch setting, and fine adjustment is achieved through phase shifting, with digital circuitry providing the highest repeat accuracy.

Additional information on resistance welding is available in the Section "Joining Processes" in this Volume.

Power Sources for Welding

F. James Grist, Miller Electric Manufacturing Company, Inc.; William Farrell and Glen S. Lawrence, Ferranti Sciaky

---

Electron-Beam Welding Power Sources

Electron-beam welding (EBW) requires a variety of power supplies in two categories: those that generate and control beam position and those that control beam power. The outputs of various power supplies are coordinated by a machine control system.

Beam Position and Intensity. Beam position arrangements for alignment, deflection, and focus are dominated by magnetic devices in electron-beam welders. Because the magnetic field effect on the beam (the magnetomotive force) is directly proportional to the current in the windings of the device, these power supplies are typically current regulated.

$$MMF = N \cdot I \qquad \textbf{(EQ 12)}$$

where N is the number of turns in the coil and I is the current in the coil. The desired current value is programmed by potentiometer, computer, or function generator.

A second factor regarding the effectiveness of magnetic devices is the velocity of the electrons in the beam, as determined by the accelerating voltage. At the voltages used in EBW (typically, 50 to 150 kV), relativistic effects must be considered. In situations where the beam potential is changing, but it is desired to have the effect of the magnetic devices be constant, then the effective magnetic excitation, k, must be constant:

$$K^2 = \frac{(N.I)^2}{V^*} \qquad \textbf{(EQ 13)}$$

where NI is the magnetomotive force and V^* is the relativistic voltage. The relativistic voltage can be expressed in volts as:

$$V^* = V + (0.9785 \times 10^{-6})V^2 \qquad \textbf{(EQ 14)}$$

Sensors monitor the beam potential generated by the high-voltage (HV) supply and correct the control signal to the magnetic device power supply. Thus, the action of the device can be held constant as beam potential changes.

This correction can be achieved by using computer software or an analog circuit. Such correction is often called square root compensation, because of the relationship indicated in Eq 13.

Alignment coils are used for slight corrections to the x and y positions of the beam as it enters the magnetic focusing coil. Power supplies for these devices are typically potentiometer programmed by the operator in an alignment procedure. These supplies are characterized by a high degree of long-term stability, with minimal need for dynamic response. Selected installations employ alternate means for achieving alignment.

The magnetic focus coil acts very much as a glass focusing lens would for optics. It takes a divergent electron beam and converges it at a more distant point along the beam axis. The beam focus point from the magnetic lens is roughly inversely proportional to the square of the lens excitation:

$$f \propto \frac{V^*}{(N.I)^2} \qquad \textbf{(EQ 15)}$$

The magnetic lens supply is usually controlled by computer output in order to coordinate beam focus with the weld program. Manual control (operator offset) and square root compensation are also usually provided. These supplies are of high stability and moderate dynamic response.

The deflection coil moves the beam along the x and y axes to position the beam over the surface of the workpiece. Deflection rates can range from dc to high audio frequencies. Thus, the deflection supply is a high-quality current-regulated stereo amplifier.

Amplifier input controls allow computer input for coordinated movements of the part and beam, function generator inputs for beam deflection patterns (rasters, and so on), and dc offsets to patterns. These are highly stable current-regulated coils drivers with wide dynamic response.

High-Voltage Control. The electron beam is generated in an electron gun (resembling a diode or triode of cylindrical symmetry) that generates a paraxial flow of electrons. The power in an electron beam comes from the high-voltage supply that generates the large voltage difference between the anode and cathode of the gun. Electrons are emitted from the cathode and, accelerated by the voltage, fall to the anode. The beam passes through a central aperture in the anode and drifts through various alignment, focus, and deflection elements to strike the workpiece (Fig. 10). Both the workpiece and the anode are typically at ground potential, whereas the cathode is highly negative.

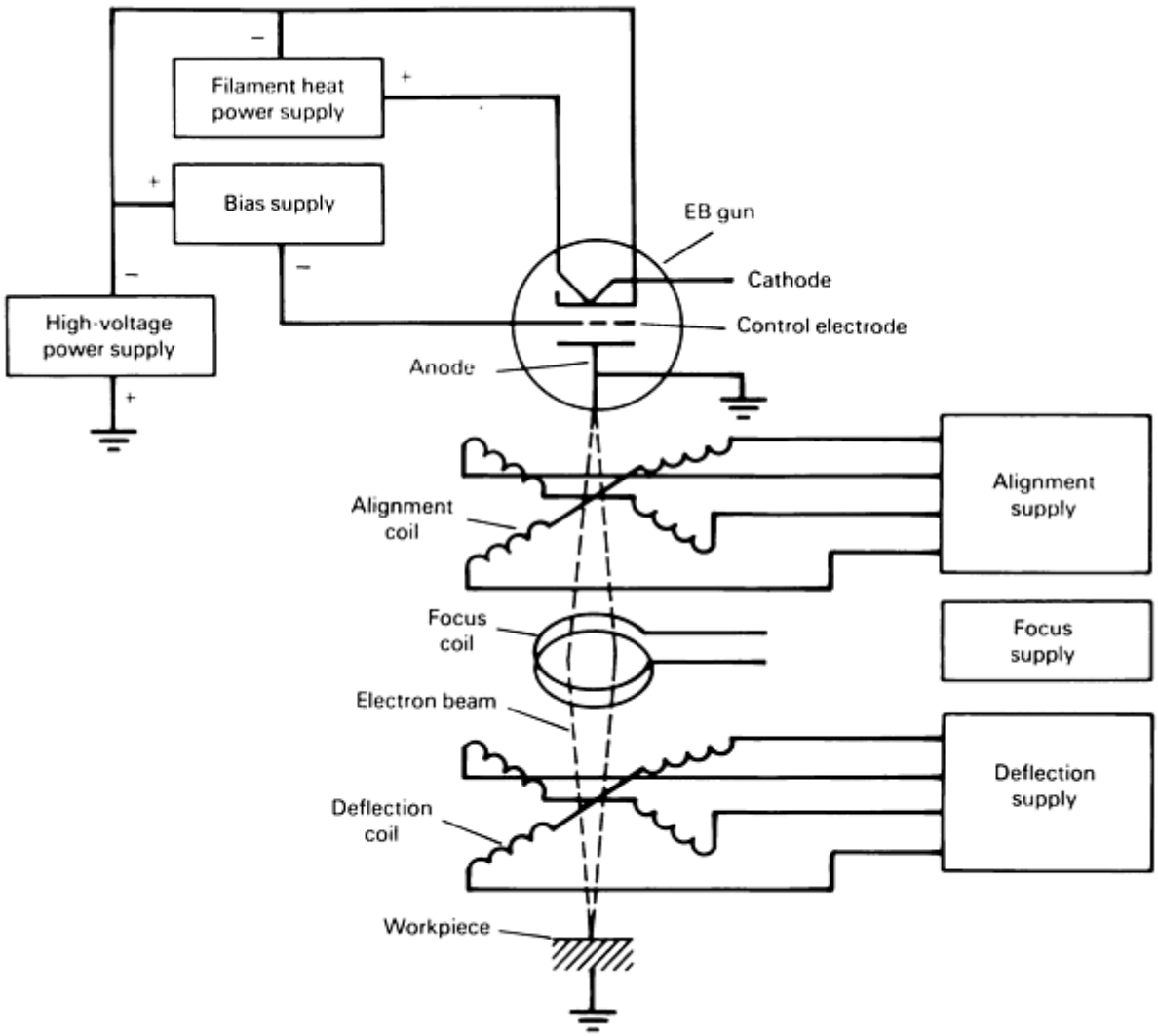

FIG. 10 SIX INDIVIDUAL POWER SUPPLIES THAT CONTROL POSITION AND INTENSITY OF THE BEAM IN EBW PROCESS

Control and regulation of the high voltage is usually done on the input to the high-voltage transformer/rectifier oil-filled tank. The input control installations range from motor-driven variable autotransformers, motor-alternators with field controls, SCR switching or phase control, to power MOSFET (metal-oxide semiconductor field-effect transistor) and IGBT devices in various switch mode regulators.

In a three-phase input unit, a standard technique is to place the switching control in the primary neutral conductor of the HV transformer (Fig. 11). The secondary circuitry is three-phase or six-phase, full-wave rectified, and filtered.

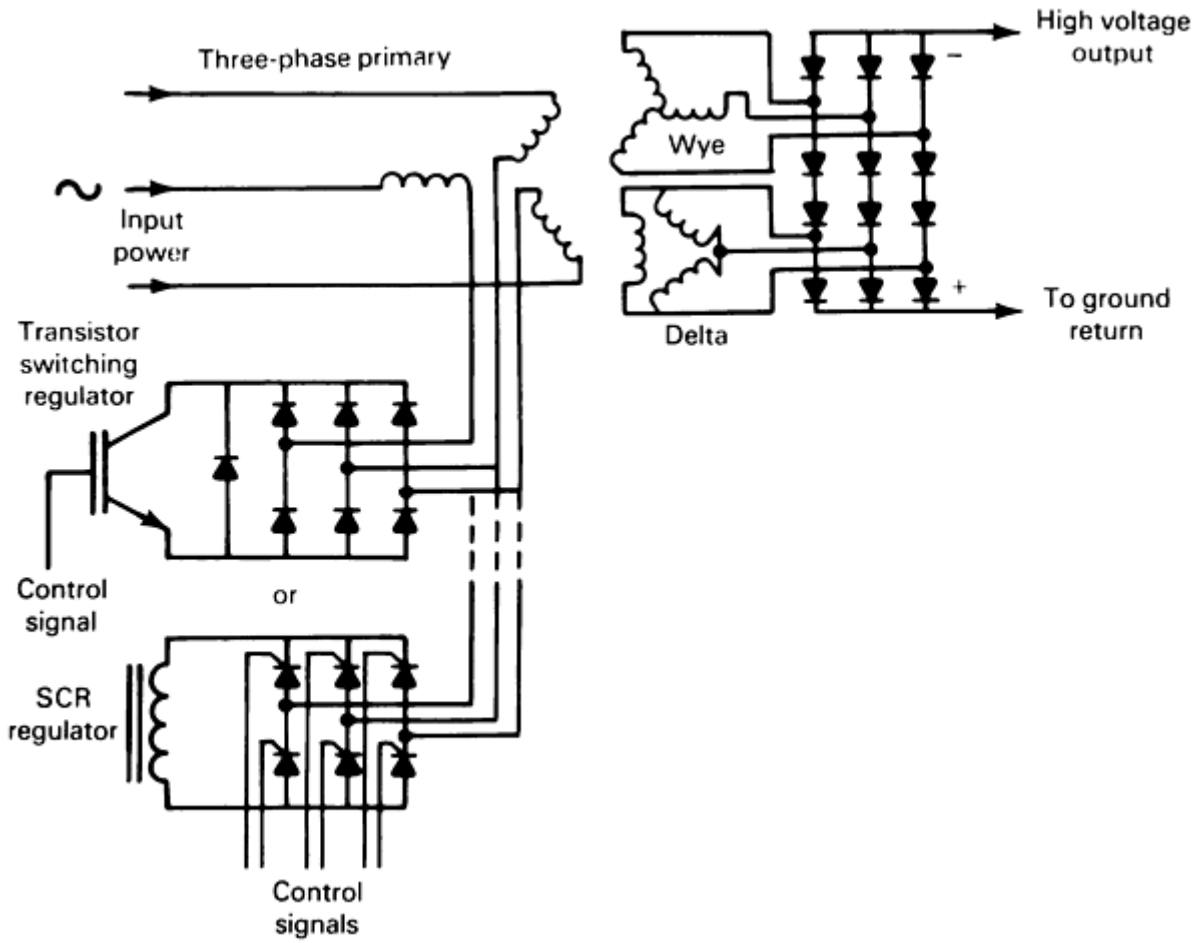

FIG. 11 CIRCUIT DIAGRAM OF A HIGH-VOLTAGE CONTROL IN NEUTRAL IN A THREE-PHASE INPUT UNIT

In an alternate arrangement, line voltage is converted to dc, which powers an inverter to produce high-frequency single-phase input to the high-voltage transformer. Control can be provided either by regulating the level of the dc supply or by controlling the inverter pulse width or frequency. The HV transformer can be a conventional step-up unit or a voltage multiplier. These supplies can be characterized as voltage regulated and input controlled, with a moderate response rate.

Thermionic Emission. The cathode heating unit provides the energy to raise the cathode to thermionic electron emission temperatures. This is usually a dc source. For beam-heated cathodes, discharge-heated cathodes, and others, it may be more complicated, to a point of supplying power to a second miniature gun.

In a space-charge limited electron beam, the cathode temperature must be held high enough that temperature-limited emission (Eq 16) is greater than space-charge limited flow (Eq 17):

$$I_P = AT^2 E^{-ef/kt} \qquad \textbf{(EQ 16)}$$

$$I_P = K(V_P + m V_G)^{3/2} \qquad \textbf{(EQ 17)}$$

In Eq 16 and 17, I_p is beam current, V_p is accelerating voltage, A is Dushman's constant, V_g is bias voltage, and T is temperature.

The bias supply provides voltage to the control electrode and regulates the magnitude of the beam current. Bias supplies can be input controlled with ground-level sensing of beam current on the return of the HV supply, or the beam can be sensed and regulated at high voltage using optical isolation (Fig. 12).

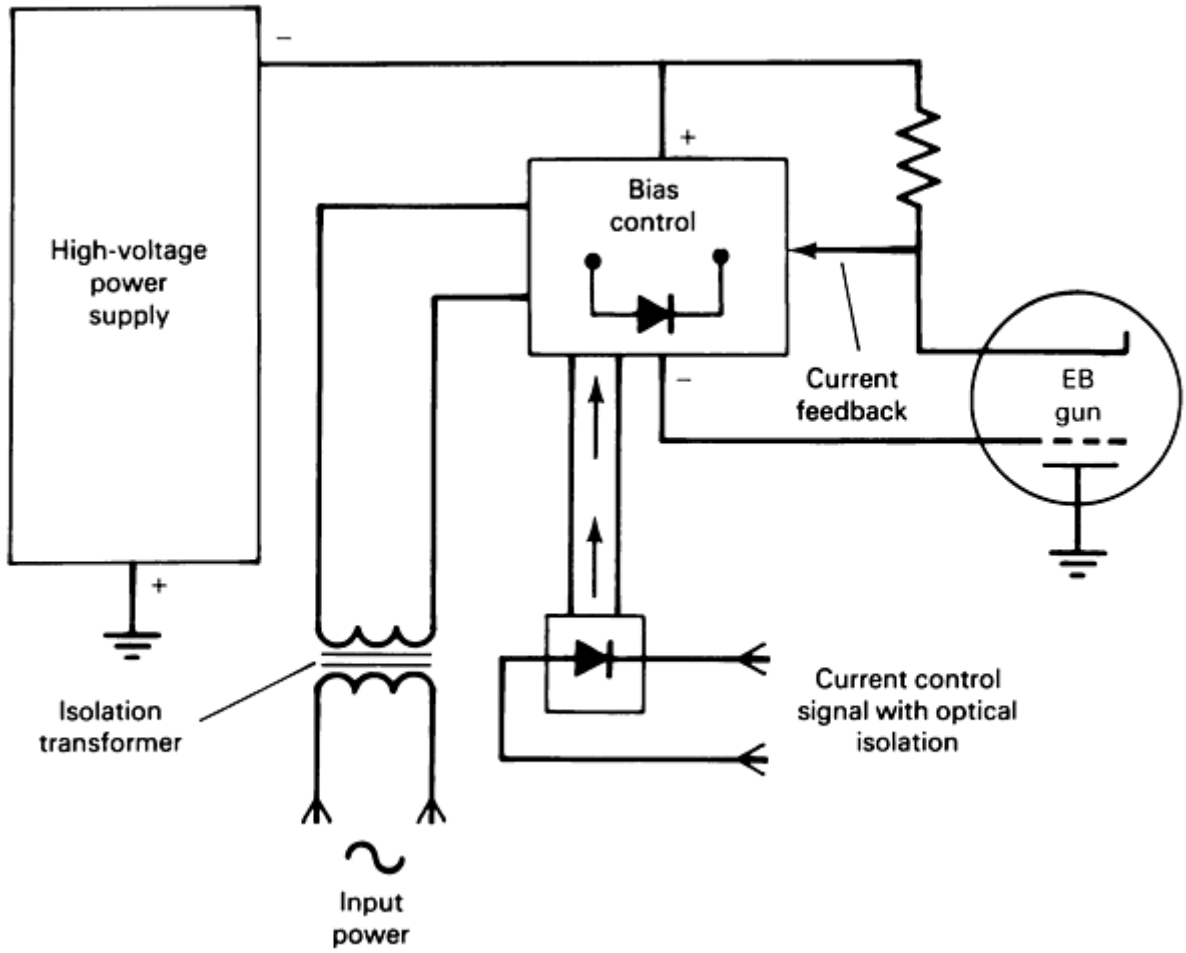

FIG. 12 CURRENT FEEDBACK AND BIAS CONTROL AT HIGH-VOLTAGE POTENTIAL

Ground-level sensing systems tend to use high-frequency inputs from linear amplifiers or switch mode inverters in order to achieve response on the order of a millisecond. Submillisecond response bias supplies are achieved by sensing and controlling the beam current at the high-voltage output. Because bias voltage is in the low kV range, vacuum tubes are used for output control.

Additional information on electron-beam welding is available in the article "Electron-Beam Welding" in this Volume.

Fundamentals of Weld Solidification

Harvey D. Solomon, General Electric Company

Introduction

OF ALL PHASE TRANSFORMATIONS, few have been more widely observed and studied than the transformation of a liquid to a solid (that is, solidification). The process of solidification is the same in all cases, whether it is the freezing of water on a windshield or in a freezer, or the solidification of metal in a casting or in the weld that joins two solids.

The process is controlled by the free energy of the liquid phase, G_l, relative to that of the solid, G_s. This is depicted in Fig. 1, which shows the behavior of a pure (single component) material. Above the freezing temperature, T_f, the liquid phase has the lower free energy and is therefore stable, but below T_f, the solid is the stable phase. At T_f, both phases are in equilibrium, that is, $G_l = G_s$.

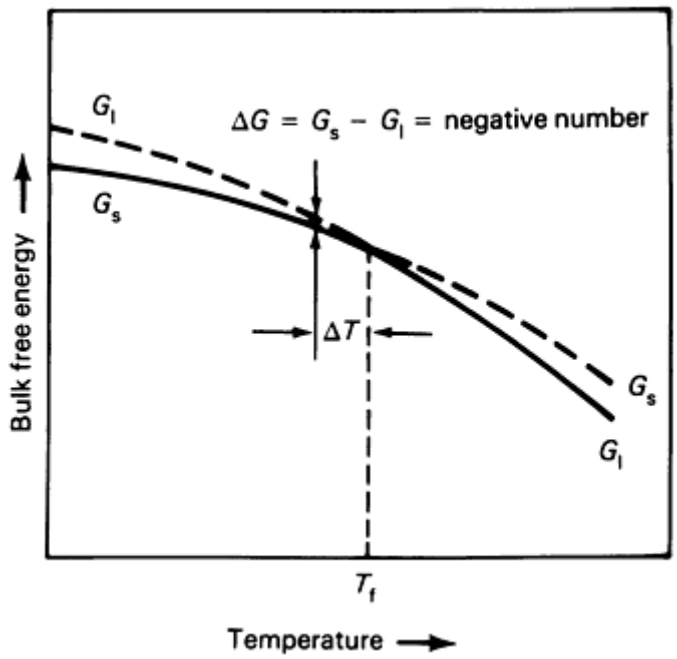

FIG. 1 TEMPERATURE DEPENDENCE OF BULK FREE ENERGY OF THE LIQUID AND SOLID PHASES IN SINGLE-COMPONENT SYSTEM. THE SOLID LINE PORTION AND THE DASHED LINE PORTION OF EACH G_L, AND G_S CURVE INDICATE THE STABLE AND UNSTABLE PHASES, RESPECTIVELY, OF THE FREE ENERGY ON EITHER SIDE OF T_F. SOURCE: REF 1

In the transition from one phase to another, the change in free energy, ΔG, is the difference in free energy of the product and the reactant. This free energy change can be expressed in terms of the enthalpy and the entropy changes, that is, for the transformation of a liquid to a solid during freezing:

$$\Delta G = G_S - G_L = (H_S - H_L) - T(S_S - S_L) = \Delta H - T\Delta S \qquad \textbf{(EQ 1)}$$

At the freezing temperature, T_f, $\Delta G = G_s - G_l = 0$, because the free energy of the two phases is the same, and $\Delta H = T_f \Delta S$, It is necessary to cool below T_f for solidification, because at T_f both the solid and liquid phases are present and in equilibrium. Below T_f, ΔG is not equal to zero (Fig. 1 shows that $G_s < G_l$) and is given by Eq 1 with $T = T'$, where $T' < T_f$.

Because the ΔH and ΔS are not strong functions of temperatures, they can be assumed to be temperature independent. Therefore, at any temperature, $\Delta H = \Delta H_f$ and $\Delta S = \Delta S_f$, where ΔH_f and ΔS_f are the values of the enthalpy and the entropy changes for the equilibrium reactions at T_f (that is, the latent heat of fusion and the entropy change on fusion, respectively). Combining these enthalpy and entropy expressions, the fact that $\Delta H = T_f \Delta S$, and Eq 1, then at T', one obtains:

$$\Delta G = (\Delta H_F / T_F)(T_F - T') \qquad \textbf{(EQ 2)}$$

where ΔH_f, the latent heat of fusion, is negative. Hence, in agreement with Fig. 1, ΔG is negative. The greater the amount of undercooling (supercooling) below T_f ($T_f - T'$), then the greater the thermodynamic driving force for solidification.

However, even when the conditions of Eq 2 are met, the liquid does not spontaneously transform to the solid below T_f. Rather, small amounts of solid nucleate and grow to produce complete solidification. Nucleation creates a new surface, that is, the surface between the solid and the liquid. The energy per unit are of this surface is the surface tension, γ, which is always positive. For solidification to occur, the increase in energy associated with the surface energy must be balanced by a greater decrease in the free energy of the solid relative to that of the liquid. This requires undercooling, as shown by Eq 2.

There are three ways in which a solid can form: homogeneous nucleation, heterogeneous nucleation, and epitaxial growth. Homogeneous nucleation occurs when there is no foreign body (mold wall, solid particle in the melt, etc.) on which to form the solid. Figure 2 shows the balance of the surface tension and the bulk free energy per unit volume, ΔG_v, as a function of the size of the nucleus that forms during homogeneous nucleation. The ΔG_v, value is just ΔG (as given by Eq 2) divided by the molar volume of the solid, V_s.

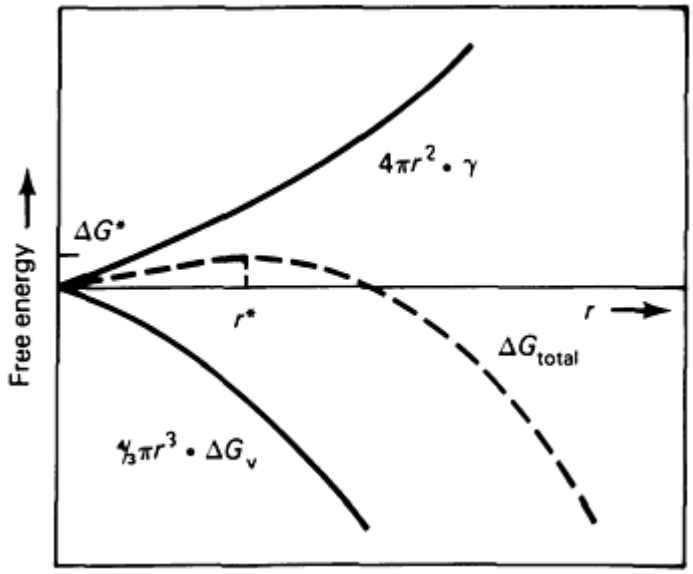

FIG. 2 FREE ENERGY OF FORMATION OF A NUCLEUS AS FUNCTION OF ITS RADIUS. SOURCE: REF 1

For a spherical nucleus of radius greater than r_c, the volume free energy decrease outweighs the increase in energy that is due to the surface energy, and the nucleus is stable. At $r = r^*$, the net energy is a maximum, but if additional atoms are added to the nucleus, then the energy decreases. The value r^* is thus the radius at which the spherical nucleus is just stable, because as additional atoms are added, the energy is decreased. The value r^* is given by:

$$R^* = -2\gamma/\Delta G_V \qquad \textbf{(EQ 3)}$$

which is a positive number, because ΔG_v is negative. Substituting into Eq 2, one gets:

$$R^* = -2\,\gamma T_F V_S/\Delta H_F(T_F - T) \qquad \textbf{(EQ 4)}$$

The r^* is positive because ΔH_f is negative and, for undercooling, $(T_f - T)$ is positive. This equation is a general expression relating the radius of curvature of a surface and the degree of undercooling that is required for solidification of that surface. The greater the degree of undercooling, the smaller the radius of curvature that is stable. This equation will be considered again when nonplanar solidification is discussed.

Nucleation requires a thermal energy either equal to or greater than ΔG^* in order for a spherical nucleus of radius r^* to form. The ΔG^* value is the activation energy, which, as Fig. 2 shows, is a positive quantity. The greater the degree of undercooling, the more negative the free energy, the less positive the ΔG^* value, and the greater the rate of nucleation of the solid. For homogeneous nucleation, ΔG^* is given by:

$$\Delta G^* = (16/3)(\pi\,\gamma^3 T_F^2 V_S^2)/(\Delta H_F^2 \Delta T^2) \qquad \textbf{(EQ 5)}$$

where $\Delta T = T_f - T$.

Heterogeneous nucleation develops when the solid forms on a foreign body. Now, the interaction of the nucleus and the foreign body must be considered. This interaction is defined in terms of the wetting angle between the nucleus and foreign body. The activation energy for heterogeneous nucleation is given by:

$$\Delta G^* = \frac{4p}{3}\frac{g^3 T_f^2 V_s^2}{\Delta H_f^2 \Delta T^2}(2 - 3\cos q + \cos^3 q) \qquad \textbf{(EQ 6)}$$

The angle is 180° if there is no wetting, and Eq 6 reduces to Eq 5, that is, with no wetting, there can only be homogeneous nucleation. With a wetting angle of 90°, ΔG^* is one half the value given by Eq 5. Instead of requiring a spherical nucleus of radius r^*, a hemispherical nucleus of the same radius is necessary, which requires one half the number of atoms and one half the activation energy. This is the sort of nucleation that develops in a casting, where the mold wall acts as the foreign body.

When the wetting angle is zero, Eq 6 shows that the activation energy is zero. This is the case for epitaxial growth on a substrate, where epitaxial derives from the Greek *epi*, upon, and *taxis*, to arrange, that is, to arrange upon. In effect, no new surface is being formed. Atoms are just being added to the substrate, thereby extending it. The important point is that no activation energy nor undercooling is required to add atoms onto an existing substrate. This is the situation that develops when a liquid solidifies on a substrate of the same material or one that is similar in composition and structure, as in the solidification of a weld.

Reference

1. J.D VERHOEVEN, *FUNDAMENTALS OF PHYSICAL METALLURGY*, JOHN WILEY & SONS, 1975

Fundamentals of Weld Solidification

Harvey D. Solomon, General Electric Company

Comparison of Casting and Welding Solidification

A weld can be thought of as a miniature casting. The fundamentals of weld solidification are the same as those of a casting, but with different boundary conditions. These differences and their effects are described below.

First, by its very nature, a sound weld *must* attach to the metals being joined, whereas a casting *must not* adhere to the mold wall. To achieve this, the mold is treated to prevent adherence, whereas the joint to be welded is prepared to promote adherence. The practical result of this preparation is that there is generally excellent heat transfer through a weld joint, but relatively poor heat transfer through the mold, because oxides are often used as mold materials or for mold coatings (the molten metal will not wet the oxide and therefore cannot adhere to it).

Second, heat is continually being added to the weld pool as it travels, whereas no heat is added to a casting after the pour, except for possibly modest heating of the mold. The practical result of this and of the first consideration described above is that the temperature of the casting is relatively uniform. In contrast, a very large temperature gradient develops in a weld. The center of a weld pool reaches a very high temperature (typically, 2000 to 2500 °C, or 3630 to 4530 °F), which is limited by the vaporization of the weld metal. At the sides of the weld pool, where solidification is taking place, the temperature is the solidification temperature, which is typically about 1000 °C (1800 °F) less than the temperature at the center on the weld pool. Thus, a positive temperature gradient is developed in a weld (that is, measured from the fusion line of the weld, the temperature increases going into the molten material). A casting will typically supercool to below the solidification temperature. Solidification will first develop by heterogeneous nucleation at the mold wall. The latent heat and the poor heat transfer through the mold wall will then cause a temperature rise at the mold wall. Thus, a small negative temperature gradient can develop briefly in a casting. The nature of this gradient is important, because it

promotes nonplanar solidification (to be discussed below) in the casting, whereas the positive gradient that develops in a weld helps to limit nonplanar solidification.

Third, solidification is developed at the mold wall of a casting by heterogeneous nucleation, whereas epitaxial growth develops at the weld fusion line. Thus, some supercooling is required for the casting, but only a vanishingly small degree of supercooling is required for the weld. (As was discussed, epitaxial growth requires no supercooling, but some slight degree of undercooling is required to shift the reaction from an equilibrium between the solid and liquid, to all solid.) This undercooling in a weld would typically be *less* than 1 °C (1.8 °F). In contrast, in castings when there is a lack of effective nuclei for hetergeneous nucleation, undercoolings of 100 °C (180 °F) or more are possible. In general, however, the undercooling in castings is typically only on the order of a few degrees centigrade.

Fourth, the generally larger volume of a casting, relative to that of a weld, and the poorer heat transfer makes the cooling rate and the solidification rate much lower for castings than for welds.

Fifth, as a casting solidifies, the volume of the remaining liquid decreases. Thus, the shape of the molten pool is continually changing. In a weld, the weld pool shape is generally kept constant as it travels (if the heat input and section geometry are constant).

Sixth, because of the stirring action of the arc and the action of Marongoni surface tension gradient induced convection forces, there is good mixing of the molten weld pool. In contrast, there is comparatively little mixing of the molten material of a casting.

As discussed in the section "Solidification of Alloy Welds (Constitutional Supercooling)" in this article, all of these factors influence the nature of weld solidification, relative to what is observed in a casting.

Solidification of Alloy Welds (Constitutional Supercooling)

The solidification of an alloy is much more complex than that of a pure metal, whether in a weld pool or in a casting. Figure 3 shows a simple binary isomorphous phase diagram. The temperatures of the liquidus and solidus lines of Fig. 3 can be approximated by straight lines (for a limited temperature range). (The liquidus defines the temperature above which only liquid is present and the solidus the temperature below which only solid is present. The liquidus and solidus lines bound the two-phase liquid plus solid region.) The liquidus line is given by:

$$T_L = T_{MA} + M_L C_L \qquad \textbf{(EQ 7)}$$

where T_{mA} is the melting point of pure A, M_L is the slope of the liquidus, and C_L is the composition of the liquid at T_L. The solidus is described by a similar expression.

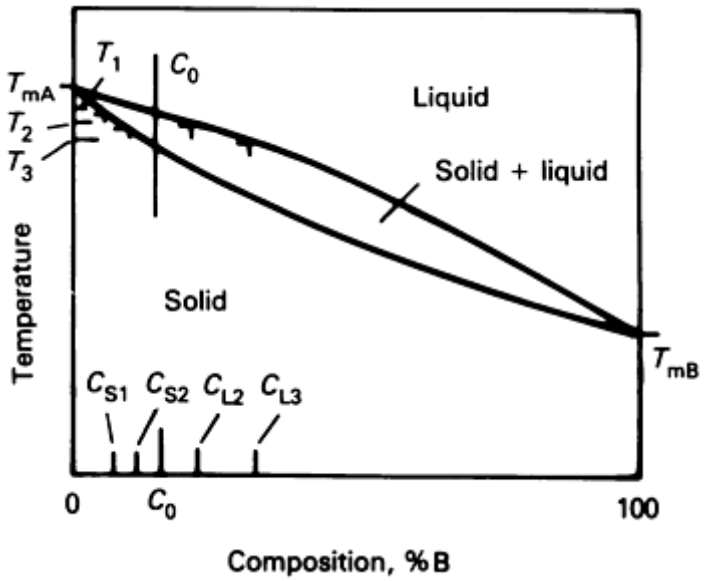

FIG. 3 BINARY ISOMORPHOUS PHASE DIAGRAM SHOWING THE LIQUID AND SOLID COMPOSITIONS AT SELECTED TEMPERATURES

Another important quantity that can be estimated from the phase diagram is the distribution coefficient, *K,* which is defined as:

$$K = C_S/C_L \qquad \textbf{(EQ 8)}$$

where C_S and C_L are the solidus and liquidus compositions, respectively, defined by equilibrium tie lines. Assuming that the solidus and liquidus lines are straight lines means that *K* is not a function of temperature. In general, the liquidus and solidus lines are curved, so that in actuality, *K* is a function of temperature. For simplicity, this curvature will be neglected and, instead, limited temperature ranges where *K* can correctly be assumed to be a constant will be considered. The use of a distribution coefficient defined by equilibrium tie lines implies that equilibrium exists between the liquid and the solid at the solid-liquid interface. This equilibrium need not exist elsewhere. Figure 3 and the following discussion are based on a *K* value of less than 1 and a negative M_L value. The following discussion is also true for diagrams where *K* is greater than 1 and M_L is positive.

The distribution coefficient defines how the solute is distributed or partitioned between the solidifying solid and the remaining liquid. The slope of the liquidus line and the distribution coefficient are important in defining the composition gradient that develops when alloys solidify. In general, the distribution coefficient, *K,* is a function of temperature, but as already noted, to simplify the analysis, it will be assumed that over a limited temperature range, it is a constant.

An equilibrium phase diagram, such as that of Fig. 3, assumes that equilibrium is maintained in all of the solid and liquid and that there are no composition gradients in the solid or liquid. It defines the equilibrium solid and liquid compositions at any temperature. Figure 3 shows that the solidification of an alloy of composition C_0 will begin when the temperature is reduced below T_1. If equilibrium is maintained, then solidification will be complete when the temperature is reduced below T_3. A two-phase mixture of solid plus liquid will be present between T_1 and T_3, with the relative amount of each phase given by the lever rule:

$$\%_{liquid} = \left(\frac{C_0 - C_{s2}}{C_{1.2} - C_{s2}} \right) 100\% \qquad \textbf{(EQ 9)}$$

at T_2. The free energy curves corresponding to this equilibrium are much more complex than those of Fig. 1, which is relevant for a pure material.

The equilibrium predicted by Fig. 3 is never realized in practice, because it would require an infinitely slow cooling rate. When considering castings, it is generally assumed that the equilibrium predicted by the phase diagram is maintained at the solid-liquid interface, but that no composition change occurs in the solid as the temperature is lowered. At T_1, a solid of composition C_{S1} forms. C_{S1} is equal to $C_{L1}K$, and because at the liquidus $C_{L1} = C_0$ the $C_{S1} = C_0K$. When the temperature drops to T_2, the solid that forms has a composition of C_{S2}, and so on. A composition gradient is thus developed in the solid. As the solid forms, solute is rejected into the liquid, and it is assumed that this solute is mixed into the liquid, raising its composition to that predicted by the phase diagram. This occurs even though the mixing action in a casting is relatively poor, because the cooling rate is generally low enough to provide enough time to allow for the required solute redistribution by diffusion in the liquid. As a result, no gradient is developed in the liquid. The composition of the solid at the solid-liquid interface is still given by the equilibrium phase diagram. However, the previously formed solid is deficient in solute. As a consequence, complete solidification does not occur at T_3. Further cooling is required, with solidification being completed only when the *average* solid composition is C_0.

The boundary conditions for a weld are somewhat different from those of a casting. The composition gradient that develops in the solid is assumed to be the same as that which forms in a casting, but the behavior of the liquid is assumed to be different. The mixing of the melt is greater than that developed in a casting, but the cooling rate is much higher. Thus, the solute that is rejected as the solid forms is not completely mixed into the liquid. Rather, the bulk liquid remains at the initial composition, C_0, with a solute gradient formed in the liquid near the solid-liquid interface. At the liquids, T_1, the solid that forms has a composition of $C_{S1} = C_0K$. At T_2, the solid composition is C_{S2}. As with castings, it is assumed that the solid-liquid equilibrium predicted by the equilibrium phase diagram is maintained at the solid-liquid interface. Therefore, the liquid in equilibrium with this solid is $C_{L2} = C_{S2}/K$. However, the lack of complete mixing means that the bulk liquid remains at C_0, and that a composition gradient forms directly ahead of the solid-liquid interface. This composition gradient is illustrated in Fig. 4, which shows the composition gradient developed by unidirectional solidification and the temperature gradient driving this solidification. The solidification is modeled by assuming that a bar is being unidirectionally solidified, but this approach is applicable to solidification in general.

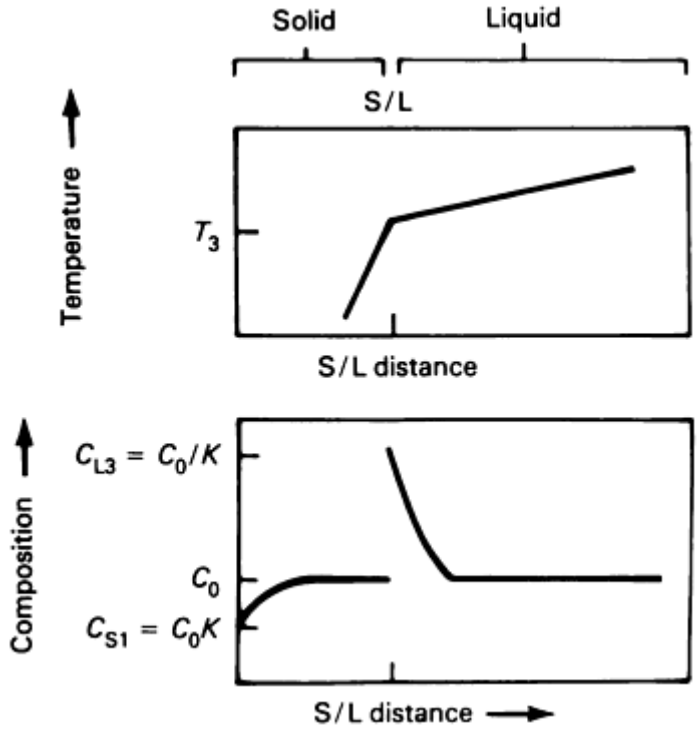

FIG. 4 INITIAL STAGE OF DIRECTIONAL SOLIDIFICATION OF A BAR, SHOWING THE TEMPERATURE PROFILE DRIVING THE SOLIDIFICATION AND THE COMPOSITION PROFILE ESTABLISHED FOR AN ALLOY WITH A SOLUTE CONTENT OF C_0. SOURCE: REF 4

At temperature T_3, the solid that forms has a composition of C_0. The solid that is forming now has the same composition as the bulk liquid. Thus, an equilibrium situation exists. Solidification can now continue *without* having to further reduce the temperature. For castings, however, the composition gradient in the solid and complete mixing of the solute into the

liquid leaves the liquid still present at T_3, thereby reducing the liquidus temperature. This means that, in a casting, the temperature must be lowered even more before further solidification can take place.

Figure 4 shows the situation *during* weld solidification, whereas Fig. 5 shows the composition when solidification is complete. For most of the solidification, the solid forms at C_0. The exceptions are at the start and at the end of solidification. The first solid that forms does so with a solute composition of C_{S1}, which the phase diagram shows is less than C_0. A composition gradient develops until temperature is lowered to T_3, when the solid composition reaches C_0 and an equilibrium is reached between the solid being formed and the composition of the bulk liquid. At the end of solidification, there is an increase in the solute content. This occurs to accommodate the solute buildup at the solid-liquid interface. At the end of the solidification, there is no longer any *bulk* liquid at C_0. The solute that is ahead of the solid-liquid interface raises the composition of the remaining liquid as it is rejected into this final small volume of liquid. This obviates the assumed boundary condition (a lack of mixing of the solute into the bulk liquid), and the situation becomes more like that of a casting (complete mixing in this small liquid volume). The final liquid composition of this final transient is the terminal composition predicted by the phase diagram, that is, the final liquid is driven to the composition of the lowest melting point. In the case of the simple binary isomorphous diagram used for this example, this is pure B. For a simple binary eutectic, it would be the eutectic composition.

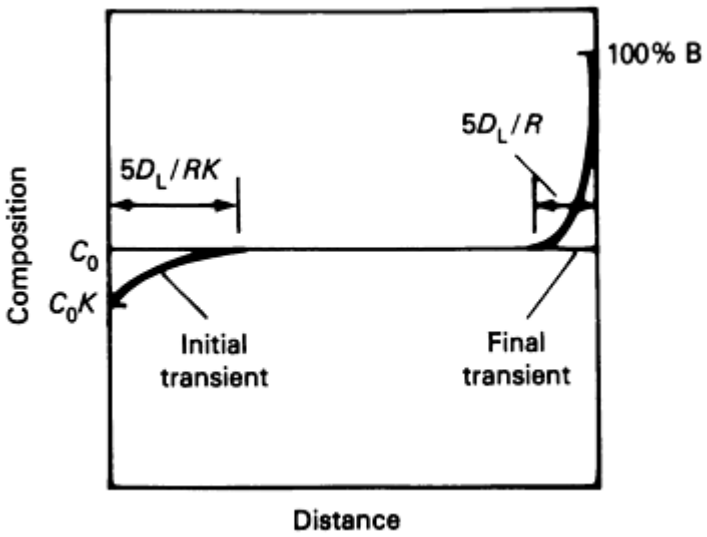

FIG. 5 FINAL COMPOSITION PROFILES FOR THE UNIDIRECTIONAL SOLIDIFIED BAR SHOWN IN FIG. 4. THE INITIAL AND FINAL TRANSIENT ARE SHOWN FOR $K < 1$. R, RATE OF SOLIDIFICATION; D_L, DIFFUSION RATE OF THE SOLUTE IN THE LIQUID. SOURCE: REF 4

The profile of the liquid composition gradient that is ahead of the solid-liquid interface is given by:

$$C_L = C_A e^{-[RX_L / D_L]} + C_0 \qquad \textbf{(EQ 10)}$$

where R is the rate of solidification. D_L, is the diffusion rate of the solute in the liquid, C_a is the increase in the composition of the liquid at the solid-liquid interface (relative to C_0), and X_L is the distance into the liquid that is ahead of the solid-liquid interface. The liquid at the solid-liquid interface has a composition of C_{L3}, which is in equilibrium with $C_{S3} = C_0$. Therefore, $C_{L3} = C_0/K$. The enrichment of the solute in the liquid, C_a, is thus $(C_0/K) - C_0$ or $C_0(1 - K)/K$. The distribution coefficient, K, is thus an important variable in determining the composition profile in the liquid and, as will be shown, in determining the nature of the solidified microstructure.

Substituting Eq 10 into Eq 7, one gets the expression describing the temperature variation of the liquidus that is ahead of the solid-liquid interface, namely:

$$T_L = T_{MA} + M_L C_A e^{-[RX_L / D_L]} + M_L C_0 \qquad \textbf{(EQ 11)}$$

Figure 6 illustrates this liquidus profile, along with three possible temperature gradients that could actually exist in the liquid. They are all positive, reflecting the positive gradient that develops in a weld. Gradient A is greater than the slope of the liquidus at the solid-liquid interface, but those of B and C are not. The slope of the liquidus can be found by differentiating Eq 11 at $X_L = 0$, that is, at the solid-liquid interface. For the temperature gradient to be less than this slope, the gradient G must be:

$$G < M_L R C_0 (K - 1)/D_L K \qquad \textbf{(EQ 12)}$$

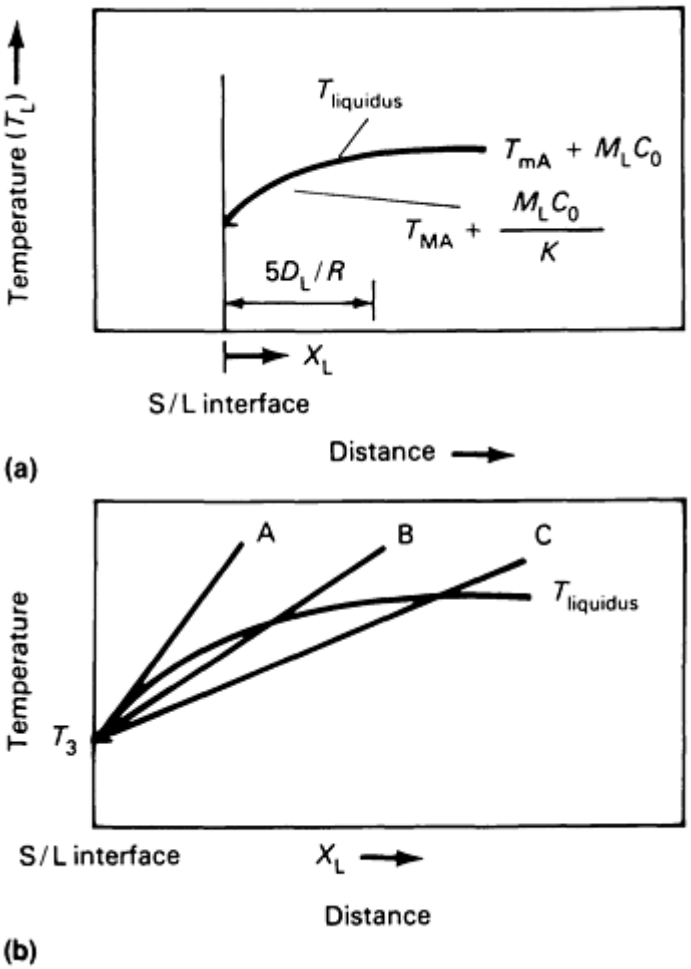

FIG. 6 LIQUIDUS PROFILE OF A SOLID-LIQUID INTERFACE. (A) LIQUIDUS PROFILE FOR STEADY-STATE CONSTITUTIONAL SUPERCOOLING. (B) THREE LIQUIDUS TEMPERATURE GRADIENTS (CURVES A, B, AND C) COMPARED TO THE LIQUIDUS PROFILE. SOURCE: REF 6

Equation 12 is important because it describes the temperature gradient required for constitutional supercooling (Ref 3, 4, 5). The establishment of the composition gradient in the liquid that is ahead of the solid-liquid interface produces a variation in the temperature of the liquidus. For curves B and C, this has allowed the actual temperature to be below the liquidus (that is, supercooling has developed, even though the temperature of the bulk liquid is above the bulk liquidus temperature). This is constitutional supercooling, and as will be shown, this promotes nonplanar solidification, even though there is a positive temperature gradient. The liquidus profile shown in Fig. 6 is correlated with the propensity for hot cracking. The greater the temperature difference between that of the solid-liquid interface and that of the bulk liquid, the greater the tendency for hot cracking. This is discussed in more detail in the article "Cracking Phenomena Associated with Welding" in this Volume.

The constitutional supercooling model for describing weld solidification is presented because it qualitatively describes the evolution of different microstructures (described in the section "Development of Weld Microstructures" in this article). Many newer nonequilibrium approaches to solidification give better quantitative results. These approaches will be

discussed in the section "Nonequilibrium Effects: High-Rate Weld Solidification and Composition Banding" in this article.

References cited in this section

3. J.A. BURTON, R.C. PRIM, AND J. SLICHTER, *J. CHEM. PHYS.*, VOL 21, 1953, P 1987-1991
4. W.A. TILLER, K.A. JACKSON, J.W. RUTTER, AND B. CHALMERS, *ACTA METALL.*, VOL 1, 1953, P 428-437
5. W.A. TILLER AND J.W. RUTTER, *CAN. J. PHYS.*, VOL 34, 1956, P 96-121
6. W.F. SAVAGE, E.F. NIPPES, AND T.W. MILLER, *WELD. J.*, VOL 55, 1976, P 165S-173S

Harvey D. Solomon, General Electric Company

Development of Weld Microstructures

Nonplanar solidification develops when a protrusion moves ahead of the rest of the solid-liquid interface and continues to grow in a stable manner. This increases the surface area. The stable radius is given by Eq 4, which shows that the protrusion must move into a supercooled region in order to be stable. This is possible in a casting, because a negative temperature gradient is developed (that is, the temperature decreases from the solid-liquid interface into the liquid). In a pure material (single-component system), the positive temperature gradient that is established in the liquid of a weld prevents this nonplanar growth. In an alloy, however, constitutional supercooling allows nonplanar solidification in a weld, even with a positive temperature gradient.

The lower the gradient, *G*, (compare curve C with curve B in Fig. 6), the greater the degree of constitutional supercooling. This is illustrated in Fig. 7, which shows several temperature gradients (Fig. 7f) compared to the variation in the liquidus and the nature of the solid-liquid interface (Ref 5, 6, 7). For a curve a, the temperature gradient is steeper than the liquidus temperature curve and only planar solidification is possible. For curve b, there is a shallower gradient and the solid-liquid interface can move by cellular growth. The gradient is successively lower for c and d, which allows larger protrusions and the development of cellular dendritic and columnar dendritic growth. At curve e, the gradient is so shallow and the resulting liquidus temperature is so far above the actual temperature in the liquid that equiaxed dendrites can form ahead of the solid-liquid interface.

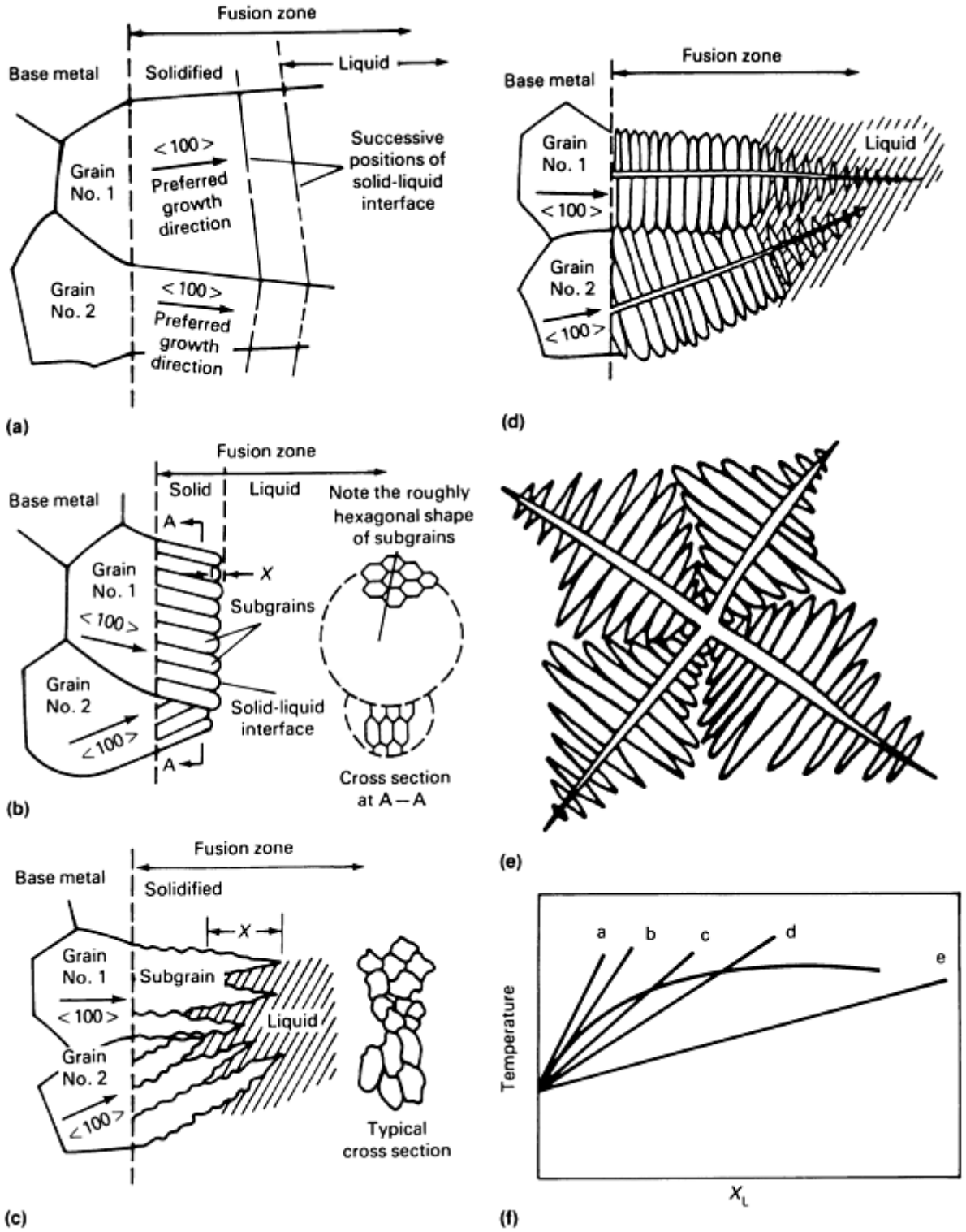

FIG. 7 SCHEMATICS SHOWING MICROSTRUCTURE OF SOLID-LIQUID INTERFACE FOR DIFFERENT MODES OF SOLIDIFICATION AND THE TEMPERATURE GRADIENTS THAT GENERATE EACH OF DIFFERENT MODES. (A) PLANAR GROWTH. (B) CELLULAR GROWTH. (C) CELLULAR DENDRITIC GROWTH. (D) COLUMNAR DENDRITIC GROWTH. (E) EQUIAXED DENDRITE. (F) FIVE TEMPERATURE GRADIENTS VERSUS CONSTITUTIONAL SUPERCOOLING. SOURCE: REF 6

Figure 8, which is based on experimental observations, relates the gradient, solidification rate, and composition to the type of structure developed (Ref 5, 6, 7). The basis for this figure lies in Eq 12. If R is moved to the left side of Eq 12, then the right side contains only material variables. For a given alloy system (where D_L, M_L, and K are fixed), the greater the C_0, the greater the tendency for constitutional super-cooling and nonplanar solidification. Equation 12 predicts that the

smaller the G/R, the more nonplanar the solidification. Figure 8 shows that, experimentally, the correlation is with $G/\sqrt{R}$, rather than G/R.

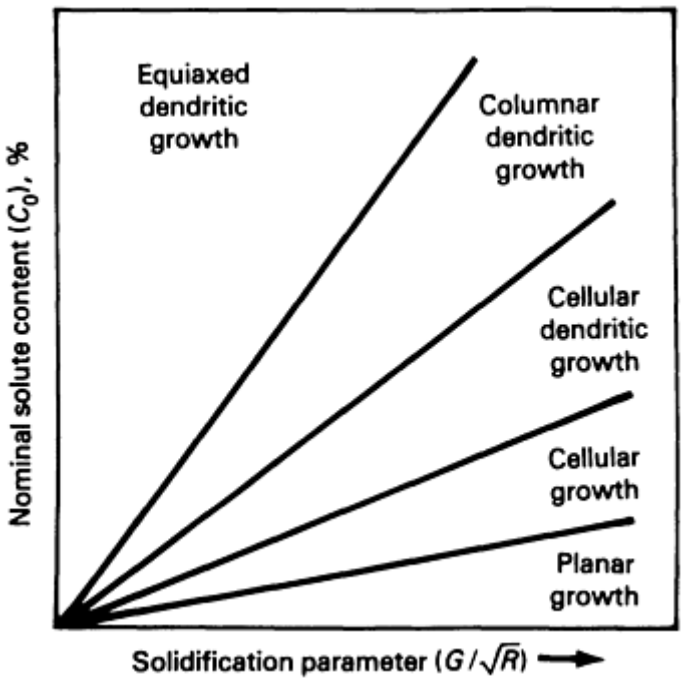

FIG. 8 PLOT OF SOLUTE CONTENT VERSUS SOLIDIFICATION PARAMETER TO SHOW THE NATURE OF SOLIDIFICATION. SOURCE: REF 6

As the dendrite, or columnar grain, grows into the liquid, it should follow the behavior shown in Fig. 5. (As will be discussed in the section "Nonequilibrium Effects: High-Rate Weld Solidification and Composition Banding" in this article, the experimentally determined compositions do not always exactly agree with that predicted by Fig. 5.) The center of each cell or dendrite behaves like the initial transient, that is, the solute content is low. The regions between the cells or dendrites behave like the final transients, that is, they are enriched in solute. This is illustrated schematically in Fig. 9. Cellular growth occurs for a smaller C_0 and/or for a larger $G/\sqrt{R}$ than that for dendritic growth (see Fig. 8).

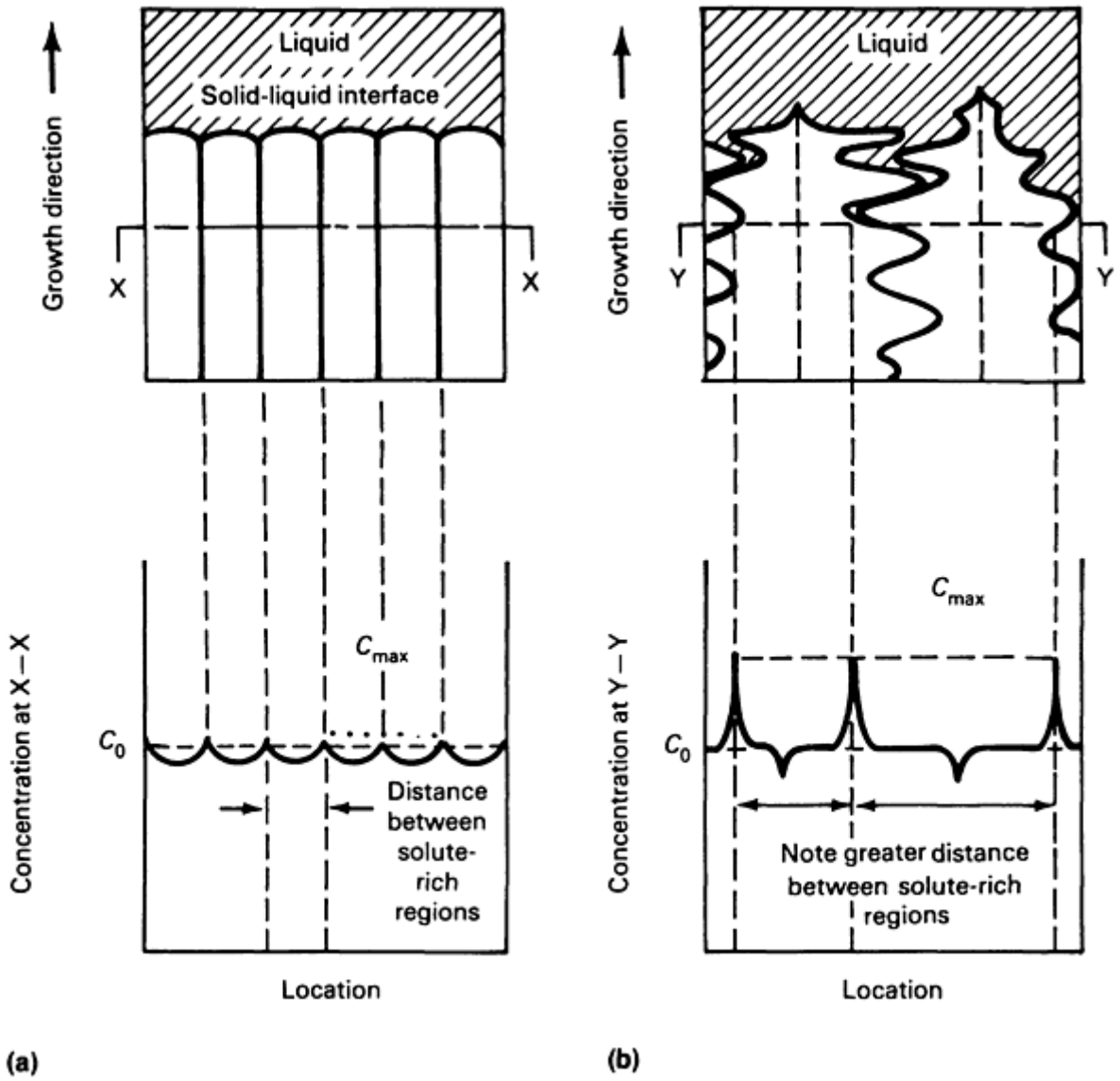

FIG. 9 SCHEMATIC SHOWING SOLUTE DISTRIBUTION AT THE DENDRITE OR CELL CORE AND IN THE INTERCELLULAR OR INTERDENDRITIC REGIONS. (A) CELLULAR GROWTH. (B) DENDRITIC GROWTH. SOURCE: REF 8

The constitutional cooling described by Fig. 4, 5, 6, 7, 8, and 9 occurs on a very fine scale. Solving Eq 10 shows that the solute composition that is ahead of the solid-liquid interface will decrease to almost C_0 when $X_L = 5D_L/R$. For a typical liquid diffusion rate of 5×10^{-5} cm^2/s (5×10^{-8} ft^2/s) and a solidification rate of 5 mm/s (0.2 in./s), the liquid composition drops to C_0 within about 5 μm (200 μin.). In the initial transient, the distance over which the solid composition increases to C_0 is given by $5D_L/RK$. Thus, for $K < 1$, this distance is greater than the region in the liquid just ahead of the solid-liquid interface. This is illustrated in Fig. 5. This difference is also important in defining the extent of the final transient, which is of the order of the length of the zone in the liquid where the composition drops to C_0. The length of the initial transient is thus $1/K$ larger than that of the final transient. The length of the solute-poor cell or dendrite core is thus $1/K$ larger than that of the solute-rich intercellular or interdendritic regions.

The solute-rich region between the cells or dendrites has a lower freezing temperature than that of the cellular or dendritic core. Thus, it is possible to have liquid films between impinging cells or dendrites. These films cannot support the thermally induced shrinkage stress that develops during solidification, and hot cracking can develop (see the article "Cracking Phenomena Associated with Welding" in this Volume). The hot cracking produced by nonplanar solidification can be minimized by reducing C_0 (that is, by using purer materials) and/or by increasing $G/\sqrt{R}$ (see Fig. 8).

The temperature gradient in the liquid, G, is *inversely* proportional to the heat input, Q, which is given by:

$$Q = FEI/V \qquad \textbf{(EQ 13)}$$

where f is the efficiency of the welding process, E is the arc voltage, I is the arc current, and V is the welding torch velocity. Thus, G can be increased by decreasing either the arc voltage or arc current, or by increasing the torch velocity. The influence of the velocity is counterbalanced by the fact that the solidification rate, R, is proportional to V (see the section "Effect of Welding Rate on Weld Pool Shape and Microstructure" in this article). Thus, increasing V increases R, which tends to increase the degree of constitutional supercooling.

References cited in this section

5. W.A. TILLER AND J.W. RUTTER, *CAN. J. PHYS.*, VOL 34, 1956, P 96-121
6. W.F. SAVAGE, E.F. NIPPES, AND T.W. MILLER, *WELD. J.*, VOL 55, 1976, P 165S-173S
7. F. MATSUDA, T. HASHIMOTO, AND T. SENDA, *TRANS. NATL. RES. INST. MET. (JPN)*, VOL 11, 1969, P 43
8. W.F. SAVAGE, C.D. LUNDIN, AND A.H. ARONSON, *WELD. J.*, VOL 44, 1965, P 420S-425S

Effect of Welding Rate on Weld Pool Shape and Microstructure

The velocity of the welding torch affects not only the rate of solidification, but the shape of the weld pool and the propensity to develop centerline hot cracks. The shape of the weld pool is dictated by the velocity, V, at which the welding torch moves and by the rate at which heat can be removed at the solid-liquid interface. To keep a constant shape, the rate of new melting must be exactly balanced by the solidification rate. On the average, this solidification occurs normal to the solid-liquid interface, because this is the direction of the maximum temperature gradient and, thus, the direction of the maximum heat removal. Simple geometry requires that for the weld pool shape to remain constant, the solidification rate, R, must be related to the torch velocity by:

$$R = V \cos f \qquad \textbf{(EQ 14)}$$

where f is the angle between the normal to the solid-liquid interface and the direction of motion of the torch (Fig. 10). At the back of the weld pool, where $f = 0$, $R = V$. If this were not so, then the weld pool would be elongating or shortening. At the side of the weld pool, where $f = 90°$, $R = 0$. If this were not the case, then the weld pool would be decreasing in diameter. With a constant weld pool shape, solidification at the side of the weld pool occurs as the region adjacent to where $f = 90°$ sweeps by, rather than by the motion normal to the weld pool velocity.

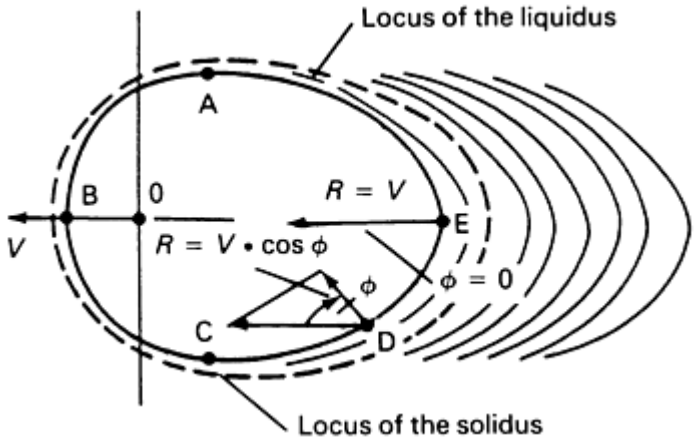

FIG. 10 SCHEMATIC OF A MOVING WELD POOL SHOWING THE RELATIONSHIP BETWEEN VELOCITY OF TRAVEL OF WELDING TORCH, *V*, AND THE RATE OF SOLIDIFICATION, *R*, AT SELECTED POINTS ALONG WELD POOL BOUNDARY. SOURCE: REF 9

Equation 14 predicts that *R* will vary around the weld pool. Figure 8 shows that as *R* varies, so does the microstructure. The result of these two effects is a variation of the microstructure around the weld pool (Ref 7). Planar solidification is to be expected at the sides of the weld pool, with the extent of the nonplanar solidification increasing towards the center of the weld pool. This is shown schematically in Fig. 11.

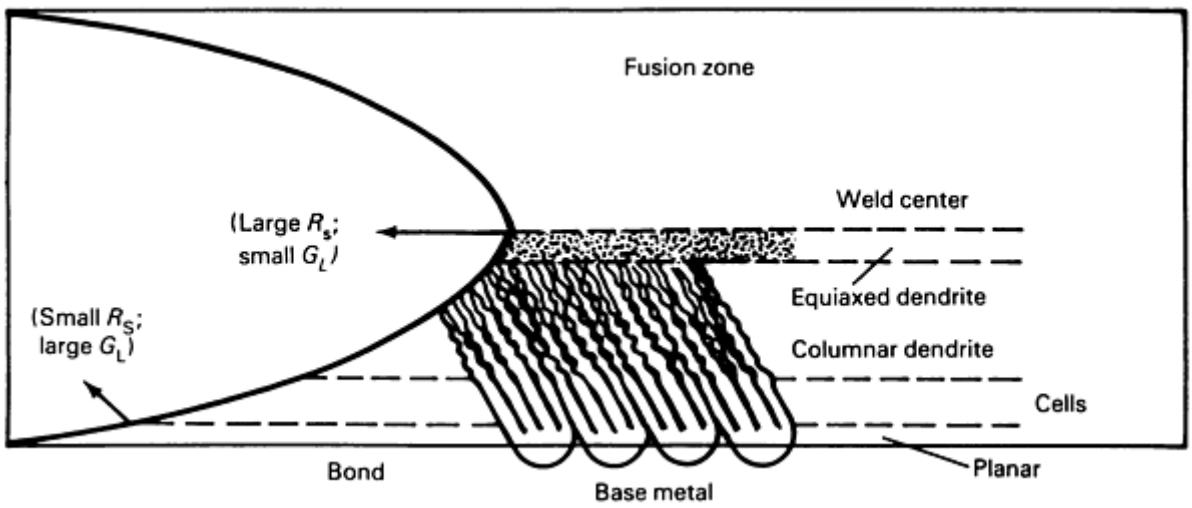

FIG. 11 SCHEMATIC SHOWING VARIATION OF MICROSTRUCTURES IN RESPONSE TO VARIATION OF THE SOLIDIFICATION RATE AROUND THE WELD POOL. SOURCE: REF 7

The coarseness of the nonplanar structure is also a function of *R.* The dendrite tip radius varies inversely with the square root of *R.* Not only does the dendrite tip radius become smaller as *R* increases, the dendrite arm spacing does also, although the exact form of the dependency is more complex. The same general inverse dependency with *R* is also true for the cell spacing when the solidification is cellular.

The ability of the solid-liquid interface to move at a velocity, *V*, depends on two factors: the maximum solidification rate, which is a function of the crystallographic orientation of the solid at the point in question, and the ability of the temperature gradient in the solid to remove the heat and establish the appropriate temperature for solidification to proceed. Consider first the influence of the orientation of the solid grain at the solid-liquid interface. For body-centered

cubic (bcc) and face-centered cubic (fcc) metals, the preferred growth direction for epitaxial solidification is the <100> direction. For hexagonal close-packed (hcp) metals, the preferred growth direction is <10**1**0>.

The planar growth of grains oriented with this direction normal to the solid-liquid interface is favored. This is illustrated in Fig. 12. Grains with the preferred orientation will grow at the expense of adjacent grains that are less favorably oriented (Ref 8, 9, 10, 11, 12). Because dendrites follow the same preferred growth directions, those with the proper orientation will be favored. The requirement for a constant weld pool size becomes somewhat more complex when the effect of crystallographic orientation is considered (Fig. 12). Equation 14 can be modified to become:

$$R' = V \cos f / \cos (f' - f) \qquad \textbf{(EQ 15)}$$

where R' is the growth rate in the preferred direction required to maintain a constant weld pool shape and f' is the angle between R' and V, and $(f' - f)$ is the angle between the local preferred growth direction and R, which is normal to the solid-liquid interface.

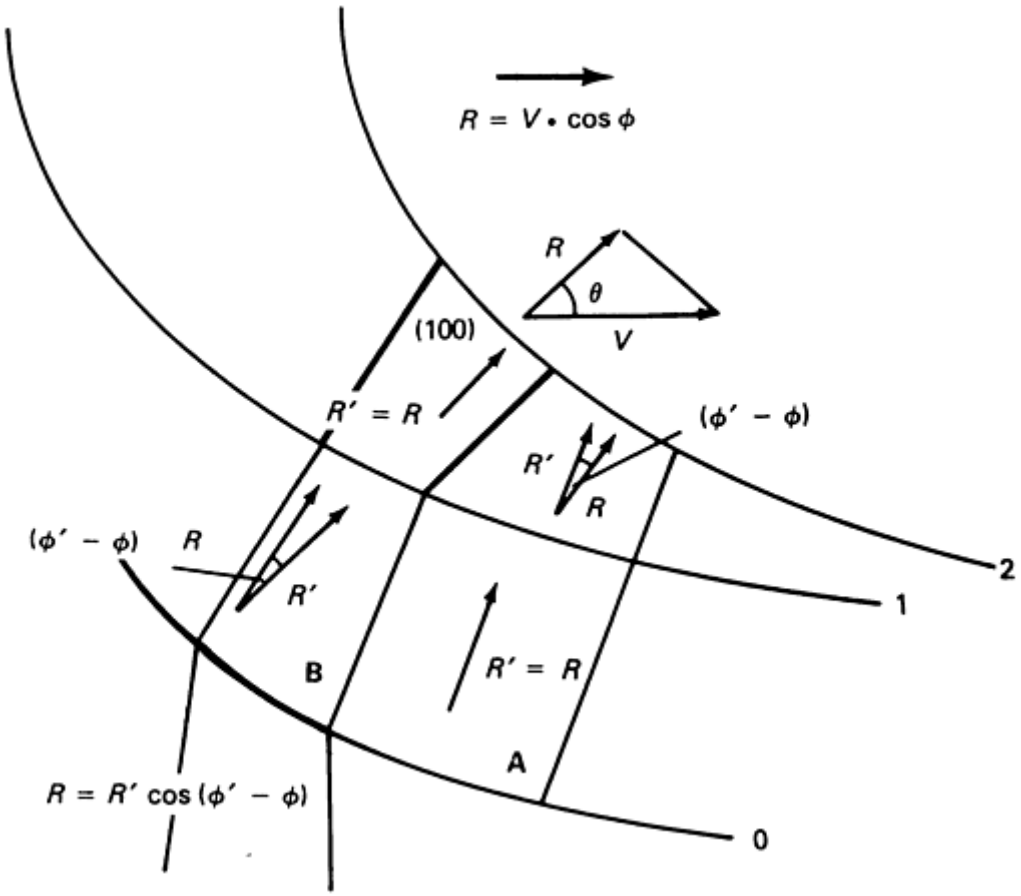

FIG. 12 SCHEMATIC SHOWING MOVEMENT OF A CURVED SOLID-LIQUID INTERFACE FOR SEVERAL GRAINS (A AND B), AND THE CHANGE IN THE RAPID GROWTH DIRECTION RELATIVE TO THE INTERFACE POSITION.

Figure 12 shows the situation at successive positions of the weld pool as it moves in the direction of V. The situation for the weld moving from position 1 to position 2 is shown. The weld pool is assumed to be elliptical in shape, so that at any point (except at the very back of the weld pool where $f = 0$) as the pool moves, the angle between R (or R') and V changes. If an adjacent grain becomes oriented such that R' becomes normal to the solid-liquid interface [that is, so that $(f' - f)$ is equal to zero], it will become most favored and will grow at the expense of adjacent grains. In Fig. 12, between positions 0 and 1, grain A is more favorably oriented than grain B. The reverse is true between positions 1 and 2. Figure 12 uses only a few widely spaced positions, but in reality there is a continuum of such positions.

Competitive growth causes grains to try to rotate into the direction of *V*. Figure 13(a) shows how the grains rotate in an elliptical weld pool. Dendrites will also try to rotate into the *R* direction, although the grains or dendrites do not actually rotate. Rather, the growth shifts to the most favored <100> (or <1010>) direction of the six present in the fcc, bcc, or hcp lattices. As grains are edged out by more favorably oriented grains, they get smaller and eventually can disappear. The solute that they were rejecting is spread out as this competitive process favors and disfavors different grains. Those grains or dendrites that eventually grow into the *V* direction will reject their solute into the weld pool, which gradually becomes solute enriched, contributing to possible crater cracking when the weld terminates. To combat this, the weld power should be gradually decreased in order to maintain a steep temperature gradient (minimizing the degree of constitutional supercooling). The use of a runoff weld tab could also be considered.

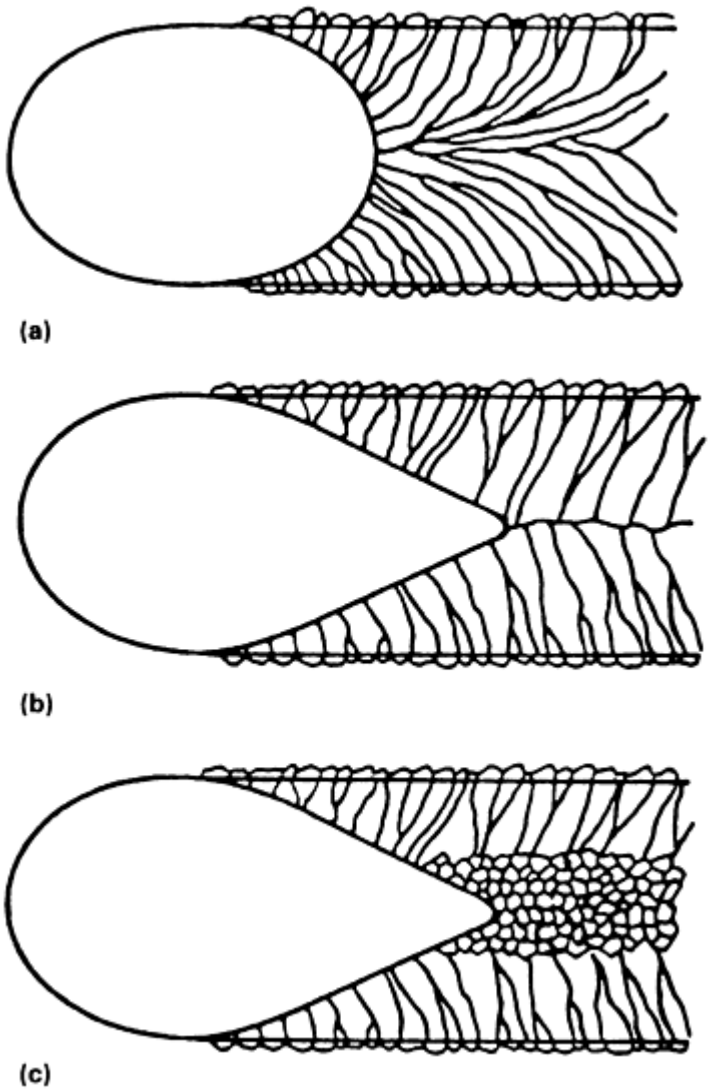

FIG. 13 SCHEMATIC SHOWING EFFECT OF HEAT INPUT AND WELDING SPEED VARIATIONS ON WELD GRAIN STRUCTURE. (A) LOW HEAT INPUT AND LOW WELDING SPEED, PRODUCING AN ELLIPTICAL WELD POOL. (B) HIGH HEAT INPUT AND HIGH WELDING SPEED, PRODUCING A TEAR-DROP-SHAPED WELD POOL. HERE, THE HEAT INPUT AND WELDING SPEED ARE NOT YET SUFFICIENT TO CAUSE HETEROGENEOUS NUCLEATION AT THE WELD POOL CENTERLINE. (C) HIGH HEAT INPUT AND HIGH WELDING SPEED, WITH HETEROGENEOUS NUCLEATION AT THE WELD POOL CENTERLINE. SOURCE: REF 13

The second factor to consider is the ability to extract heat at the solid-liquid interface. Heat is extracted by the temperature gradient of the solid. This gradient is a minimum at the back of the weld pool, where the temperature of the solid is the highest. Unfortunately, this is exactly where the solidification rate must be a maximum to keep up with *V*. The temperature gradient is a maximum at the side of the weld pool, where the least heat extraction is required, because here $R = 0$. As long as the maximum possible solidification rate, R_{max}, is equal to or greate than *V*, the weld pool can maintain an elliptical shape. If *V* is increased above R_{max}, then the solidification rate at the back of the weld pool cannot keep up, and

the weld pool elongates. Increasing V decreases the heat input, which shrinks the weld pool volume. With the weld elongating, this means that the diameter must decrease as the pool elongates. This causes the weld to take on a tear-drop shape, as shown in Fig. 13(b). The angle at the back of the weld pool will decrease until f_{critical} is reached. f_{critical} is given by:

$$f_{\text{CRITICAL}} = \text{COS}^{-1}\,(R_{\text{MAX}}/V) \qquad \textbf{(EQ 16)}$$

R_{max} is controlled by the thermal conductivity of the solid, the geometry of the part being welded (primarily the thickness), and the preferred direction growth rate.

When there is a shift to a tear-drop weld pool, the grain (or dendrite) rotation is limited to f_{critical}. When this situation is attained (Fig. 13b), the grains (or dendrites) will all grow together at the center of the weld pool. The solute that is being rejected into the terminal transient will build up at the centerline, which can lead to centerline cracking. This cracking is caused by the lower solidification temperature of this solute-rick centerline region. As the surrounding material solidifies, stresses are developed that cannot be supported by the liquid centerline material, causing centerline cracking. The obvious remedy is to reduce the welding rate, although this has a production rate penalty.

Figure 13(b) typifies what is to be expected from a pure material or one with a low solute content. In the case of alloys or in cases when the solute content is high, Fig. 8 predicts that when R is increased, not only does the weld pool become tear-drop shaped, but the nature of the structure changes, as shown in Fig. 11. If R is large enough, equiaxed grains can develop from heterogenous nucleation in the supercooled centerline material (Fig. 13c). Such behavior has indeed been observed in aluminum alloys (Ref 13, 14, 15). Figure 14 shows actual weld microstructures corresponding to the schematic structures of Fig. 13.

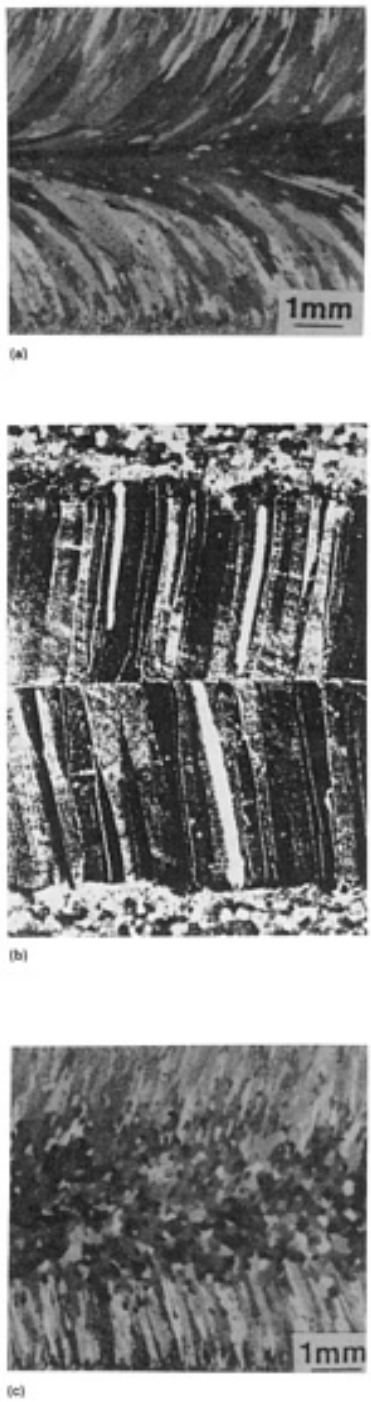

FIG. 14 ACTUAL WELD MICROSTRUCTURES CORRESPONDING TO SCHEMATICS OF FIG. 13. (A) GRAIN STRUCTURE OF A GTAW OF ALUMINUM ALLOY 6061, MADE WITH *Q* OF 700 W (200 BTU/H) AND *V* OF 5.1 MM/S (0.20 IN./S). (B) GRAIN STRUCTURE OF A GTAW OF PURE ALUMINUM, MADE WITH *V* OF 20.8 MM/S (0.819 IN./S). (C) GRAIN STRUCTURE OF A GTAW OF ALUMINUM ALLOY 6061, MADE WITH A HIGHER *Q* THAN THAT OF (A) (1320 W, OR 385 BTU/H) AND *V* OF 12.7 MM/S (0.500 IN./S). GTAW, GAS-TUNGSTEN ARC WELD. SOURCE: REF 13, 15

References cited in this section

7. F. MATSUDA, T. HASHIMOTO, AND T. SENDA, *TRANS. NATL. RES. INST. MET. (JPN),* VOL 11, 1969, P 43
8. W.F. SAVAGE, C.D. LUNDIN, AND A.H. ARONSON, *WELD. J.*, VOL 44, 1965, P 420S-425S

9. W.F. SAVAGE, *WELD. WORLD,* VOL 18, 1980, P 89-113
10. W.F. SAVAGE, C.D. LUNDIN, AND R.J. HRUBEC, *WELD. J.,* VOL 47, 1968, P 420S-425S
11. W.F. SAVAGE, C.D. LUNDIN, AND T.F. CHASE, *WELD. J.,* VOL 47, 1968, P 522S-526S
12. W.F. SAVAGE, E.F. NIPPES, AND J.S. ERICKSON, *WELD. J.,* VOL 55, 1976, P 213S-221S
13. S. KOU AND L. LE, *METALL. TRANS. A,* VOL 19, 1988, P 1075-1082
14. T. GANAHA, B.P. PEARCE, AND H.W. KERR, *METALL. TRANS. A,* VOL 11, 1980, P 1351-1359
15. H. NAKAGAWA, M. KATOH, F. MATSUDA, AND T. SENDA, *TRANS. JPN. WELD. SOC.,* VOL 4, 1973, P 11

Harvey D. Solomon, General Electric Company

Nonequilibrium Effects: High-Rate Weld Solidification and Composition Banding

As has been noted, while the constitutional supercooling model (described in previous sections of this article) gives valuable insights into the establishment of nonplanar structures, it does not necessarily give an exact depiction of the composition gradient develop within the dendrites or cells that may form and within the interdendritic or intercellular regions. This has been shown by Brooks and Baskes (Ref 16) in their study of gas-tungsten arc and electron-beam aluminum-copper and iron-niobium welds. For the aluminum-copper welds, the cell core compositions were about 2 to 3 times the KC_0 value expected for the first material to solidify (see Fig. 5) and almost 4 times KC_0 for the iron-niobium welds. This discrepancy was ascribed to the undercooling because of the curvature at the cell tip (see Eq 4), which is not considered in the constitutional supercooling model. Tip undercooling decreases the temperature at which the solidification occurs and, as Fig. 3 shows, increases the composition of the solid that is forming.

No initial transient of the sort shown in Fig. 5 was observed. This was explained by using the lower solidification rate at the side of a cell, rather than that at the dendrite tip in the calculation of the size of the initial transient. This increases the length of the transient (which is inversely proportional to the solidification rate, R) and eliminates the sharp composition variation of the initial transient shown in Fig. 5. Brooks and Baskes also incorporated postsolidification solid-state diffusion of solute (following the approach of Brody and Flemings, which is given in Ref 17) to explain the composition gradients that they measured. Such diffusion is also not considered in the conventional constitutional supercooling model.

In addition, the classical theory of constitutional supercooling, as described by Eq 10, 11, and 12, does not take into account the temperature gradient that develops in the solid, the thermal conductivity of the solid and the liquid, and, most importantly, the surface tension of the solid-liquid interface. These factors are considered in interface stability models (Ref 18, 19, 20, 21, 22, 23, 24, 25, 26), which describe the breakdown of a planar solid-liquid interface in terms of the stability of nonplanar perturbations. The importance of these models is that they explain the observed transition from nonplanar solidification *back* to planar solidification when the solidification rate is increased to very high levels.

As has already been shown, at low solidification rates there can be a transition from planar to nonplanar solidification, as described by constitutional supercooling (as shown in Fig. 8). As the solidification rate is increased, the radius of curvature and spacing of the dendrite arms will decrease, as does the cell spacing. What eventually occurs, at very high solidification rates, is that the very small radius that is required is not supportable, because of the increased surface energy. The stability models predict that there will be a solidification rate (the limiting stability rate) beyond which there will be a transition *back* to planar solidification. Figure 15 shows the calculated dendrite tip radius as a function of velocity of the solid-liquid interface. The increase in R at high rates defines the limiting stability rate.

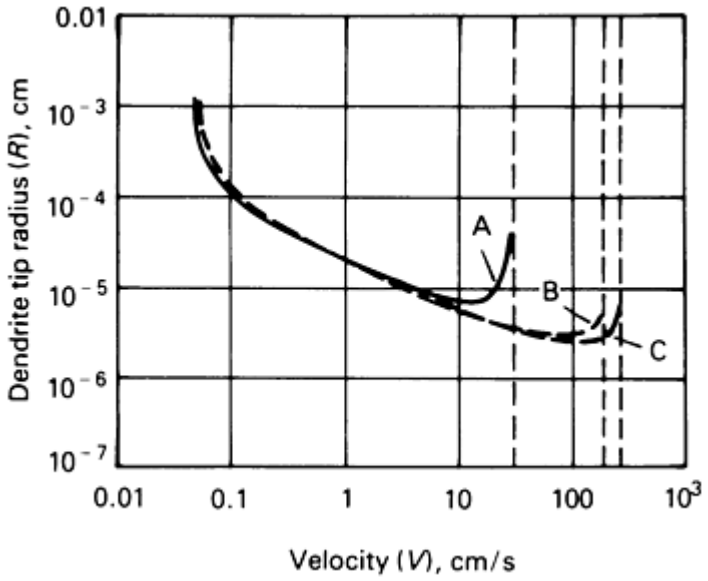

FIG. 15 PLOT OF DENDRITE TIP RADIUS, *R*, VERSUS VELOCITY, *V*, OF THE SOLID-LIQUID INTERFACE FOR AN AG-5% CU COMPOSITION WITH TEMPERATURE GRADIENT, *G*, OF 10^5 K/CM (5×10^5 °F/IN). CURVE A HAS $D_L(T)$ AND $K(V)$ WITH K_E AND M_L AS CONSTANTS; CURVE B, D_L (T) WITH K_E AND M_L AS CONSTANTS; CURVE C, WITH D_L, K_E, AND M_L AS CONSTANTS. THE VELOCITY WHERE THE TIP RADIUS INCREASES IS THE STABILITY LIMIT. THE CALCULATIONS ARE MADE USING THE CONVENTIONAL STABILITY LIMIT APPROACH, WITH THE ADDITION OF A TEMPERATURE-DEPENDENT DIFFUSION COEFFICIENT, AND WITH THE ADDITION OF BOTH A TEMPERATURE-DEPENDENT DIFFUSION COEFFICIENT AND A VELOCITY-DEPENDENT PARTITION COEFFICIENT. SOURCE: REF 21

Each of the three curves in Fig. 15 illustrates different assumptions. The right-most curve shows the result using the approach of Mullins and Sekerka (Ref 18), who developed the original interface stability model. Here, the solute diffusion rate in the liquid, D_L, the equilibrium distribution coefficient, K, and the liquidus slope, M_L, are all assumed to be constants. The middle curve takes into account the fact that the diffusion coefficient is temperature dependent. (Increasing the degree of undercooling that is due to rapid solidification decreases both the solute diffusion rate and the limiting velocity.) The left-most curve not only considers the temperature dependence of the diffusion coefficient, but also takes into account a dependency of the distribution coefficient on the solidification rate.

The preceding discussions have utilized the distribution coefficient, K, determined from equilibrium phase diagrams. At high solidification rates, this equilibrium is not achieved at the solid-liquid interface. Rather, K is a function of the solidification rate. One of several different expressions for the variation of K with V is given by (Ref 23):

$$K = [K_E + (V A_0/D_L)] / [1 + (VA_0/D_L)] \qquad \textbf{(EQ 17)}$$

where K_e is the equilibrium distribution coefficient (K in Eq 8 and 12), and a_0 is a distance that is related to the interatomic spacing. Different models use different definitions for a_0 and different functional relationships, but give similar results. When $V > D/a_0$, K will approach 1. For $D = 5 \times 10^{-5}$ cm^2/s, or 5×10^{-8} ft^2/s (a typical value for liquid diffusion), and $a_0 = 5 \times 10^{-8}$ cm, or 2.0×10^{-8} in., K will approach 1 for $V > 10^3$ cm/s, or 4×10^2 in./s. With $K = 1$, there is no partition of the solute, no constitutional supercooling, and the solidification will be planar for a positive temperature gradient. Figure 15 shows that the limiting velocity, as predicted by the stability model, is quite a bit lower than 10^3 cm/s (4×10^2 in./s). Thus, the reestablishment of planar solidification is not just the result of K approaching unity. Rather, it is due to the lack of the stability of nonplanar protrusions, which is influenced by this change in K. This development of planar solidification is important because it can arise in electron-beam and laser welds, and because the development of planar solidification lessens the tendency for hot cracking.

Figure 15 shows the results of calculations, whereas Fig. 16 shows the results of actual observations made on silver-copper electron-beam scans (passes of the electron beam). These results are in general agreement with the predictions of Fig. 15. Figure 16 shows the compositional dependence of the transition to segregation-free planar solidification. It is

analogous to Fig. 8, which describes the transition from planar to nonplanar solidification that occurs at lower solidification rates. Figure 16 also shows that just below the limiting solidification rate, a banded structure can develop. This banding develops at a constant solidification rate and is due to instabilities at the solid-liquid interface.

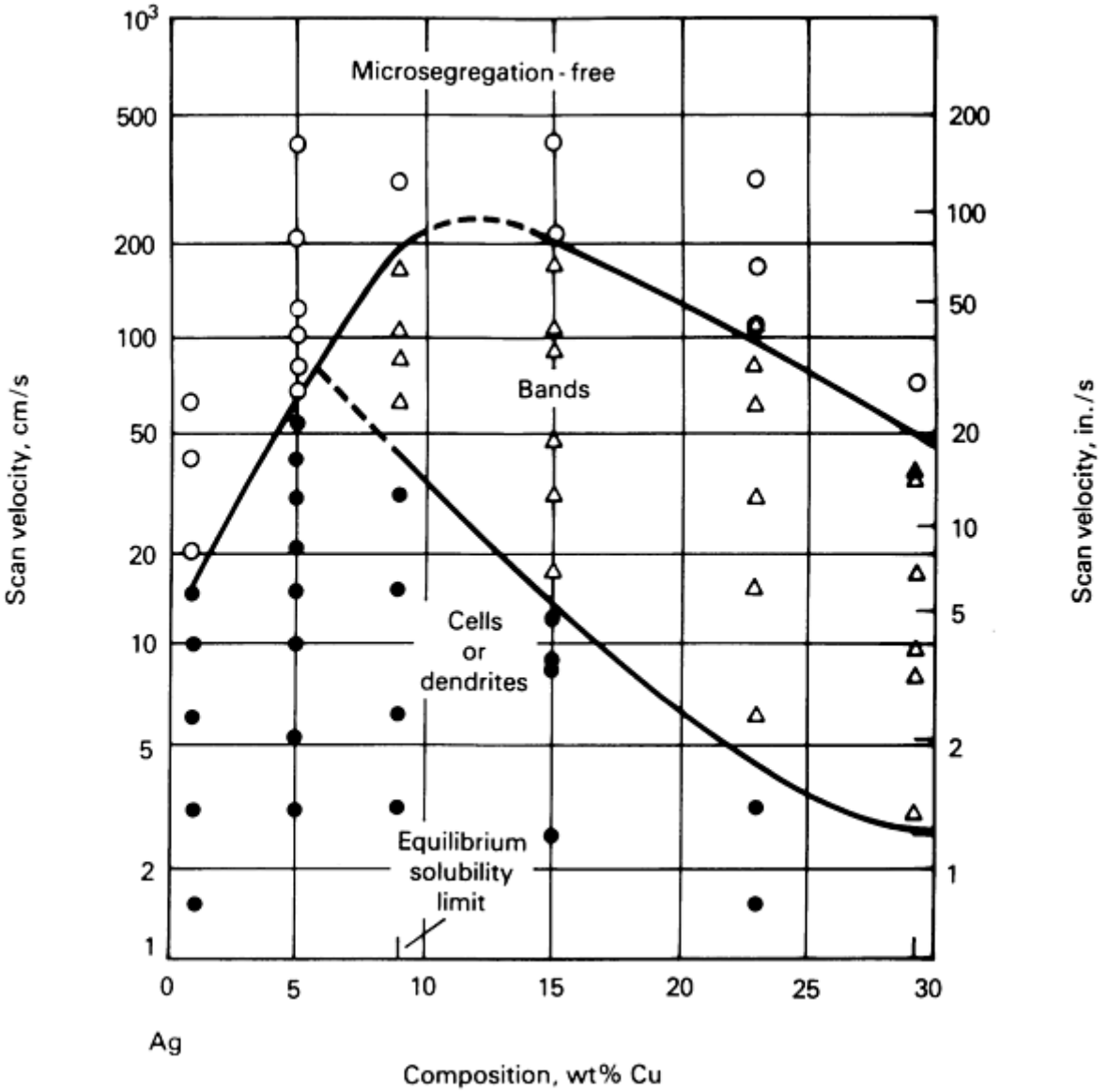

FIG. 16 OBSERVED MICROSTRUCTURES IN SILVER-COPPER ALLOYS AS A FUNCTION OF THE SCAN VELOCITY (BEAM TRANSLATION VELOCITY) FOR ELECTRON-BEAM WELDS. OPEN CIRCLES DENOTE MICROSEGREGATION-FREE STRUCTURE; CLOSED CIRCLES, A STRUCTURE CONSISTING OF CELLS OR DENDRITES; AND OPEN TRIANGLES, THE DEVELOPMENT OF A BANDED STRUCTURE. SOURCE: REF 24

A more common type of banding is associated with the ripples observed on the surface of most welds. Variations in the welding power will cause variations in the solidification rate. If the power decreases, then the solidification rate will increase. More solute will be incorporated into the solid and a solute-rich band will be created (for $K < 1$ and where M_L is negative). The reverse is true for an increase in the power (that is, the solidification rate will decrease), and this will cause a solute-poor band to form (for $K < 1$ and where M_L is negative). These power fluctuations can be deliberate, as in pulsed welding, or can result from unavoidable instabilities in the welding power supplies or fluctuations in primary voltage, mechanical (travel) motion, and so on. Solute banding and surface rippling are illustrated in Fig. 17.

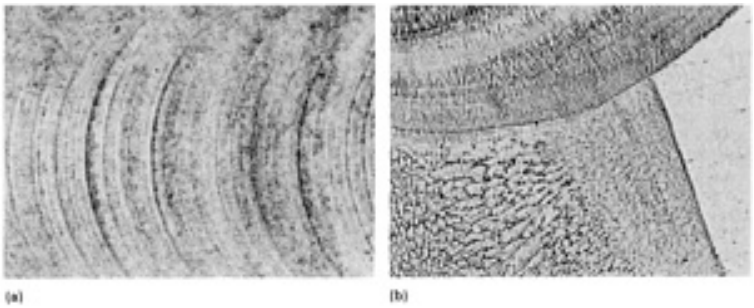

FIG. 17 SOLUTE BANDING AND SURFACE RIPPLING IN WELD BEADS. (A) SURFACE RIPPLES IN A TUNGSTEN-INERT GAS WELD MADE WITH AL-5SI FILLER. 6×. (B) SULFUR AND PHOSPHORUS SOLUTE BANDING AT THE FUSION BOUNDARY OF A MANUAL ARC WELD IN CARBON-MANGANESE STEEL. 26×. COURTESY OF THE WELDING INSTITUTE

Variations in the welding speed can also cause banding, as can the waves associated with the weld pool circulation, which can also influence the solidification rate. Special alternating magnetic fields have been used to supplement the surface tension forces, the usual electromagnetic forces, and the arc pressure and buoyancy forces, all of which affect the weld pool circulation (Ref 27). The aim is to induce interface fragmentation and cause grain refinement.

The solidified structure can also be influenced by several other factors, in addition to variations in the rate of movement of the solid-liquid interface (Ref 27). Inoculants have been used to nucleate equiaxed grains by heterogeneous nucleation on the inoculant particles. Ferro-titanium, ferro-niobium, titanium carbide, and titanium nitride have been used as grain refiners in steels. Zirconium and titanium have also been used as inoculants for aluminum. The effectiveness of inoculants depends not only on the type of inoculants used, but on the size of the inoculant particles, the method of introduction (where in the weld pool it is added), and welding conditions.

Arc motion and vibrations have also been used to suppress columnar growth and to produce a finer grain size (Ref 27). The effectiveness of arc vibration on the as-solidified grain size of an Al-2.5% Mg weld is illustrated in Fig. 18. The effectiveness of this approach depends on the frequency and amplitude of the arc motion, the heat input, arc length, and sheet thickness. In general, the greater the amplitude of vibration, the less the frequency required for grain refinement (Ref 28).

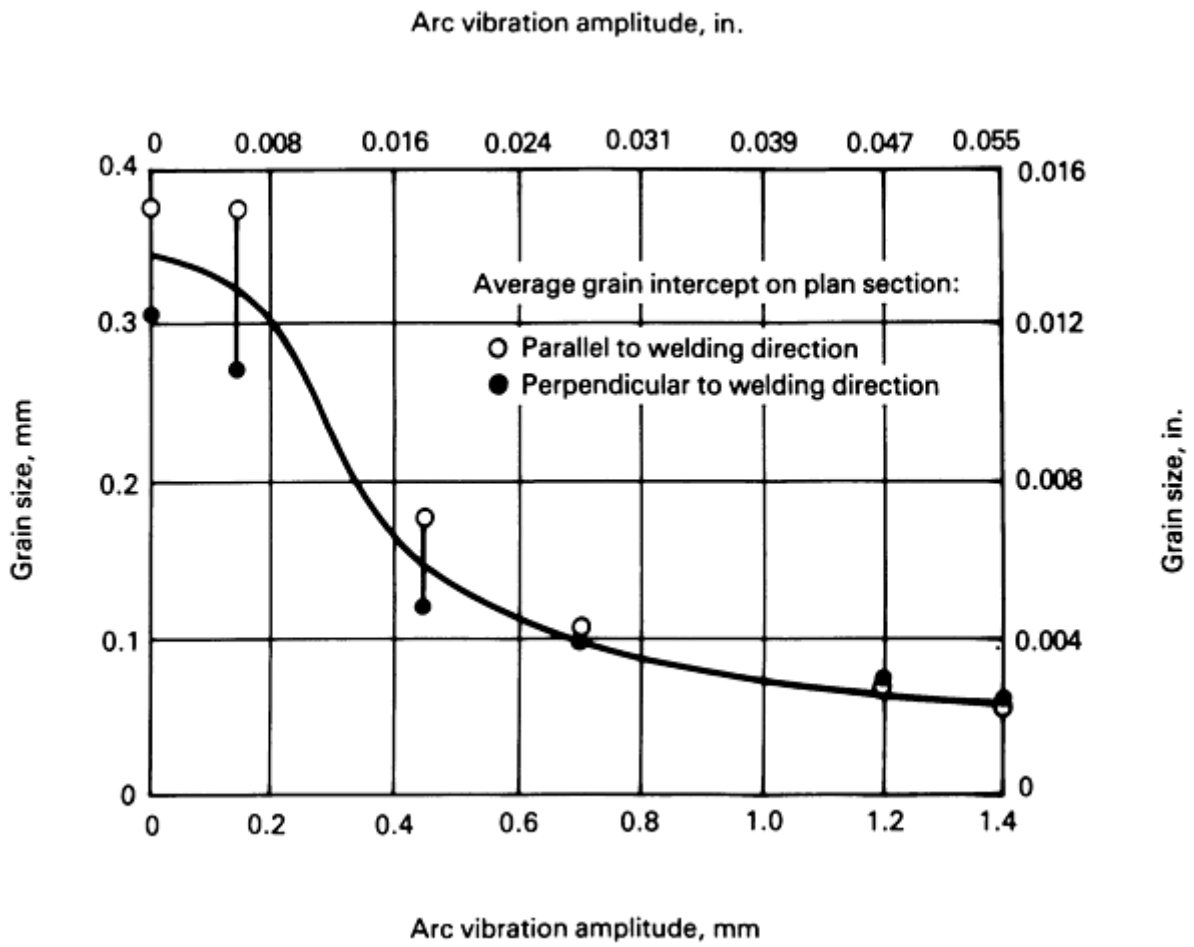

FIG. 18 PLOT OF GRAIN SIZE VERSUS ARC VIBRATION AMPLITUDE FOR AL-2.5MG WELD. WELD PARAMETERS: WELDING CURRENT, 150 A; WELDING SPEED, 200 MM/MIN (50 IN./MIN); ARC GAP, 2.4 MM (0.094 IN.); ARC VIBRATION FREQUENCY, 10 HZ. SOURCE: REF 27

Campbell (Ref 28) has developed frequency-amplitude maps that define several physical effects associated with the use of vibrations (that is, peak pressures generated, development of shearing stresses, power densities, laminar flow around dendrite arms, and the development of standing waves). These factors affect microstructural features, such as grain size, amount of microsegregation, and the development of porosity. For a given frequency of vibration, increasing the amplitude of vibration can cause a refinement of the grain size (Fig. 18), reduce microsegregation, and, unfortunately, increase the degree of porosity that is caused by vibration-induced cavitation. Vibrations can also cause splatter of the liquid weld metal; coarsen intragranular features, such as the secondary dendrite arm spacing; and promote hot tearing. Great care must therefore be taken when using vibratory motion and when determining the optimum amplitude and frequency of vibration.

Variations in the arc current can also help to refine the weld microstructure. Ultrasonic vibration of the weld pool has also been found to be effective in some cases. These vibrations have been added through the filler wire and through the use of water-cooled copper probes (in large weld pools, such as those developed in electro-slag welding). In some cases, variations in the nature of the weld pool circulation have also been found to be effective in refining the weld structure. The desire to produce a fine-grained equiaxed weld structure is driven by the improved mechanical properties and lessened hot cracking that this structure provides.

Torch weaving (Ref 29) (that is, moving the arc in a sinusoidal rather than linear fashion) has been used to break up the linear nature of the weld and to prevent hot cracks from propagating along the weld. A weld made with torch weaving is shown in Fig. 19. This weaved weld structure prevents cracks from running the length of the weld, but adds to the cost of the weld by decreasing the linear travel speed.

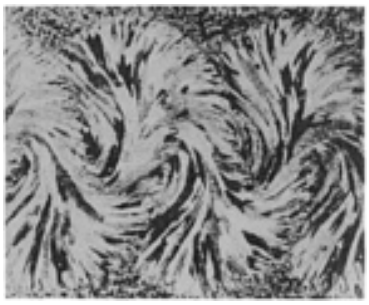

FIG. 19 TYPICAL GRAIN STRUCTURE OBTAINED WHEN TORCH WEAVING IS USED TO WELD ALUMINUM ALLOY 2014. WELD PARAMETERS: TRANSVERSE ARC FREQUENCY OSCILLATION, 1.0 HZ; AMPLITUDE OF OSCILLATION, 1.5 MM (0.059 IN.). SOURCE: REF 13, 30

Our understanding of weld solidification owes much to the more extensive study of the solidification of castings. The reader should refer to that subject area for a more in-depth treatment of solidification in general. However, it should be remembered that the boundary conditions for weld solidification and for that of a casting are not the same. Therefore, care must be taken in applying all that has been learned from casting metallurgy to the metallurgy of welds.

References cited in this section

13. S. KOU AND L. LE, *METALL. TRANS. A,* VOL 19, 1988, P 1075-1082
16. J.A. BROOKS AND M.I. BASKES, WELD MICROSTRUCTURE CHARACTERIZATION AND MODELING, *RECENT TRENDS IN WELDING SCIENCE AND TECHNOLOGY,* S.A. DAVID AND J.M. VITEK, ED., ASM INTERNATIONAL, 1990, P 93-99
17. H.D. BRODY AND M.C. FLEMINGS, *TRANS. AIME,* VOL 236, 1966, P 615-624
18. W.W. MULLINS AND R.F. SEKERKA, *J. APPL. PHYS.,* VOL 35, 1964, P 444-451
19. J.S. LANGER AND H. MULLER-KRUMBHAAR, *ACTA METALL.,* VOL 26, 1978, P 1681-1687
20. W. KURZ AND D.J. FISCHER, *ACTA METALL.,* VOL 29, 1981, P 11-20
21. W. KURZ, B. GIOVANOLA, AND R. TRIVEDI, *ACTA METALL.,* VOL 34, 1986, P 823-830
22. R. TRIVEDI AND W. KURZ, *ACTA METALL.,* VOL 34, 1986, P 1663-1670
23. M.J. AZIZ, *J. APPL. PHYS.,* VOL 53, 1982, P 1158-1168
24. W.J. BOETTINGER, D. SHECHTMAN, R.J. SCHAEFFER, AND BIANCANIELLO, *METALL. TRANS. A,* VOL 15, 1984, P 55-66
25. W.J. BOETTINGER AND S.R. CORIELL, *MATER. SCI. ENG.,* VOL 65, 1984, P 27-36
26. M. CARRARD, M. GREMAUD, M. ZIMMERMANN, AND W. KURZ, *ACTA METALL.,* VOL 40, 1992, P 983-996
27. G.J. DAVIES AND J.G. GARLAND, *INT. MET. REV.,* VOL 20, 1975, P 83-106
28. J. CAMPBELL, *INT. MET. REV.,* VOL 26 (NO. 2), 1981, P 71-108
29. S. KOU, *RECENT TRENDS IN WELDING SCIENCE AND TECHNOLOGY,* S.A. DAVID AND J.M. VITEK, ED., ASM INTERNATIONAL, 1989, P 137-147
30. S. KOU, *WELDING METALLURGY,* JOHN WILEY & SONS, 1987, P 161-162

Harvey D. Solomon, General Electric Company

References

1. J.D VERHOEVEN, *FUNDAMENTALS OF PHYSICAL METALLURGY,* JOHN WILEY & SONS, 1975
2. H.D. SOLOMON, IN *TREATISE ON MATERIALS SCIENCE AND TECHNOLOGY,* VOL 25, *EMBRITTLEMENT OF ENGINEERING ALLOYS,* C.L. BRIANT AND S.K. BANERJI, ED., ACADEMIC PRESS INC., 1983, P 525-599
3. J.A. BURTON, R.C. PRIM, AND J. SLICHTER, *J. CHEM. PHYS.,* VOL 21, 1953, P 1987-1991
4. W.A. TILLER, K.A. JACKSON, J.W. RUTTER, AND B. CHALMERS, *ACTA METALL.,* VOL 1, 1953, P 428-437
5. W.A. TILLER AND J.W. RUTTER, *CAN. J. PHYS.,* VOL 34, 1956, P 96-121
6. W.F. SAVAGE, E.F. NIPPES, AND T.W. MILLER, *WELD. J.,* VOL 55, 1976, P 165S-173S
7. F. MATSUDA, T. HASHIMOTO, AND T. SENDA, *TRANS. NATL. RES. INST. MET. (JPN),* VOL 11, 1969, P 43
8. W.F. SAVAGE, C.D. LUNDIN, AND A.H. ARONSON, *WELD. J.,* VOL 44, 1965, P 420S-425S
9. W.F. SAVAGE, *WELD. WORLD,* VOL 18, 1980, P 89-113
10. W.F. SAVAGE, C.D. LUNDIN, AND R.J. HRUBEC, *WELD. J.,* VOL 47, 1968, P 420S-425S
11. W.F. SAVAGE, C.D. LUNDIN, AND T.F. CHASE, *WELD. J.,* VOL 47, 1968, P 522S-526S
12. W.F. SAVAGE, E.F. NIPPES, AND J.S. ERICKSON, *WELD. J.,* VOL 55, 1976, P 213S-221S
13. S. KOU AND L. LE, *METALL. TRANS. A,* VOL 19, 1988, P 1075-1082
14. T. GANAHA, B.P. PEARCE, AND H.W. KERR, *METALL. TRANS. A,* VOL 11, 1980, P 1351-1359
15. H. NAKAGAWA, M. KATOH, F. MATSUDA, AND T. SENDA, *TRANS. JPN. WELD. SOC.,* VOL 4, 1973, P 11
16. J.A. BROOKS AND M.I. BASKES, WELD MICROSTRUCTURE CHARACTERIZATION AND MODELING, *RECENT TRENDS IN WELDING SCIENCE AND TECHNOLOGY,* S.A. DAVID AND J.M. VITEK, ED., ASM INTERNATIONAL, 1990, P 93-99
17. H.D. BRODY AND M.C. FLEMINGS, *TRANS. AIME,* VOL 236, 1966, P 615-624
18. W.W. MULLINS AND R.F. SEKERKA, *J. APPL. PHYS.,* VOL 35, 1964, P 444-451
19. J.S. LANGER AND H. MULLER-KRUMBHAAR, *ACTA METALL.,* VOL 26, 1978, P 1681-1687
20. W. KURZ AND D.J. FISCHER, *ACTA METALL.,* VOL 29, 1981, P 11-20
21. W. KURZ, B. GIOVANOLA, AND R. TRIVEDI, *ACTA METALL.,* VOL 34, 1986, P 823-830
22. R. TRIVEDI AND W. KURZ, *ACTA METALL.,* VOL 34, 1986, P 1663-1670
23. M.J. AZIZ, *J. APPL. PHYS.,* VOL 53, 1982, P 1158-1168
24. W.J. BOETTINGER, D. SHECHTMAN, R.J. SCHAEFFER, AND BIANCANIELLO, *METALL. TRANS. A,* VOL 15, 1984, P 55-66
25. W.J. BOETTINGER AND S.R. CORIELL, *MATER. SCI. ENG.,* VOL 65, 1984, P 27-36
26. M. CARRARD, M. GREMAUD, M. ZIMMERMANN, AND W. KURZ, *ACTA METALL.,* VOL 40, 1992, P 983-996
27. G.J. DAVIES AND J.G. GARLAND, *INT. MET. REV.,* VOL 20, 1975, P 83-106
28. J. CAMPBELL, *INT. MET. REV.,* VOL 26 (NO. 2), 1981, P 71-108
29. S. KOU, *RECENT TRENDS IN WELDING SCIENCE AND TECHNOLOGY,* S.A. DAVID AND J.M. VITEK, ED., ASM INTERNATIONAL, 1989, P 137-147
30. S. KOU, *WELDING METALLURGY,* JOHN WILEY & SONS, 1987, P 161-162

Selected References

• *CASTING,* VOL 15, *ASM HANDBOOK,* ASM INTERNATIONAL, 1988, P 100-181

- S.A. DAVID AND J.M. VITEK, *INT. MATER. REV.*, VOL 34, 1989, P 213-245
- J.H. DEVLETION AND W.E. WOOD, VOL 6, *METALS HANDBOOK*, 9TH ED., AMERICAN SOCIETY FOR METALS, 1983, P 21-49
- K. EASTERLING, *INTRODUCTION TO THE PHYSICAL METALLURGY OF WELDING*, BUTTERWORTHS, 1985
- M.C. FLEMINGS, *SOLIDIFICATION PROCESSING*, MCGRAW-HILL, 1974
- W. KURZ AND D.J. FISHER, *FUNDAMENTALS OF SOLIDIFICATION*, 3RD ED., TRANS TECH, 1989
- J.F. LANCASTER, *METALLURGY OF WELDING*, 3RD ED., GEORGE ALLEN & UNWIN, 1980
- M. RAPPAZ, *INT. MATER. REV.*, VOL 34, 1989, P 93-123

Nature and Behavior of Fluxes Used for Welding

D.L. Olson, S. Liu, R.H. Frost, G.R. Edwards, and D.A. Fleming, Colorado School of Mines

Introduction

FLUXES are added to the welding environment to improve arc stability, to provide a slag, to add alloying elements, and to refine the weld pool (Ref 1, 2). Different ingredients in the flux system will provide the process with different pyrometallurgical characteristics and thus different weld metal properties (Ref 3, 4).

The slag that forms during welding covers the hot weld metal and protects it from the atmosphere. Welding slag consists of the glass-forming components of the flux, as well as inclusions that form in the weld pool, coalesce, rise, and become incorporated into the slag.

The need to improve flux formulation to achieve optimal weld metal composition, and ultimately improve the properties of weldments, has led to fundamental studies of weld pyrochemistry. Understanding the thermodynamic and kinetic factors that are prevalent at the electrode, in the arc column, and in the weld pool, has led to more precise prediction of the final weld metal composition (Ref 5, 6, 7, 8, 9, 10, 11, 12, 13, 14, 15).

References

1. G.E. LINNERT, CHAPTER 8, *WELDING METALLURGY*, VOL 1, AWS, 1965, P 367-396
2. C.E. JACKSON, FLUXES AND SLAGS IN WELDING, *WELD. RES. BULL.*, NO. 190, 1973
3. T. LAU, G.C. WEATHERLY, AND A. MCLEAN, THE SOURCES OF OXYGEN AND NITROGEN CONTAMINATION IN SUBMERGED ARC WELDING USING CAO-AL_2O_3 BASED FLUXES, *WELD. J.*, VOL 64 (NO. 12), 1985, P 343S-347S
4. T.H. NORTH, H.B. BELL, A. NOWICKI, AND I. CRAIG, SLAG/METAL INTERACTION, OXYGEN, AND TOUGHNESS IN SUBMERGED ARC WELDING, *WELD. J.*, VOL 57 (NO. 3), 1978, P 63S-75S
5. N. CHRISTENSEN AND J. CHIPMAN, SLAG-METAL INTERACTION IN ARC WELDING, *WELD. RES. BULL.*, NO. 15, JAN 1953, P 1-14
6. R.H. FROST, D.L. OLSON, AND S. LIU, PYROCHEMICAL EVALUATION OF WELD METAL INCLUSION EVOLUTION, *PROC. 3RD INT. CONF. TRENDS IN WELDING*, ASM INTERNATIONAL, JUNE 1992
7. C.A. NATALIE, D.L. OLSON, AND M. BLANDER, PHYSICAL AND CHEMICAL BEHAVIOR OF WELDING FLUXES, *ANN. REV. MATER. SCI.*, VOL 16, 1986, P 389-413
8. J.E. INDACOCHEA, M. BLANDER, N. CHRISTENSEN, AND D.L. OLSON, CHEMICAL REACTIONS WITH FEO-MNO-SIO_2 *FLUXES, METALL. TRANS. B*, VOL 16, 1985, P 237-245
9. U. MITRA AND T.W. EAGAR, SLAG-METAL REACTIONS DURING WELDING, *METALL. TRANS. B*, VOL 22, 1991, P 65-100

10. C.S. CHAI AND T.W. EAGAR, SLAG-METAL EQUILIBRIUM DURING SUBMERGED ARC WELDING,*METALL. TRANS. B*, VOL 12, 1981, P 539-547
11. N. CHRISTENSEN, METALLURGICAL ASPECTS OF ARC WELDING, *WELD. J.*, VOL 27, 1949, P 373S-380S
12. O. GRONG, D.L. OLSON, AND N. CHRISTENSEN, CARBON OXIDATION IN HYPERBARIC MMA WELDING, *MET. CONSTRUCT.*, VOL 17. DEC 1985, P 810R-814R
13. U. MITRA AND T.W. EAGAR, SLAG-METAL REACTIONS DURING SUBMERGED ARC WELDING OF ALLOY STEELS, *METALL. TRANS. A*, VOL 15, 1984, P 217-227
14. T.W. EAGAR, SOURCES OF WELD METAL OXYGEN CONTAMINATION DURING SUBMERGED ARC WELDING, *WELD. J.*,VOL 57, 1978, P 76S-80S
15. N. CHRISTENSEN, *WELDING METALLURGY, LECTURE NOTES*, NTH, 1979

Nature and Behavior of Fluxes Used for Welding

D.L. Olson, S. Liu, R.H. Frost, G.R. Edwards, and D.A. Fleming, Colorado School of Mines

---

Equilibrium Parameters

Equilibrium is not achieved during welding, because of the very large temperature and density gradients, the short reaction times, and the large electric currents. Despite these expected departures from equilibrium, thermodynamic considerations can be used as a guide for constraining chemical reactions and mechanisms involved in welding (Ref 5, 7, 9). A common approach is to assume that extremely high temperatures and high surface-to-volume ratios allow thermodynamic equilibrium to be locally attained, in spite of the short reaction times available.

Further complicating the issue is the dependence on welding parameters of the chemical partitioning between the slag and the weld metal (Ref 3, 7). This dependence suggests that the pyrometallurgical reactions involved are influenced by the processes that occur at the electrode tip. As a specific example, the welding parameters affect metal-droplet size, which in turn alters the chemical kinetics. Nonetheless, thermodynamics will reveal the direction taken by the chemical reactions (but will not accurately predict weld metal composition).

The effective slag-metal reaction temperature has been estimated (by pyrochemical analysis of slag-metal compositions) to be approximately 1900 °C (3450 °F), a temperature intermediate between that of the hot spot at the arc root (2300 °C or 4170 °F) and the melting point of iron (1500 °C or 2730 °F). Thus, during the droplet lifetime, the average temperature is effectively 1900 °C (2730 °F). During this period, oxygen from the hot spot reactions is distributed throughout the droplet, and that oxygen reacts with the metallic elements to form oxides; these products of oxidation pass into the slag, and the slag-metal reactions tend toward equilibrium. Estimates of the time for which the molten slag and molten metal are in contact range from 3 to 8 s. During the process, the gaseous phase in the arc cavity contacts the metal for an estimated 0.5 to 1.0 s.

Effect of Oxygen

The most important chemical reagent in controlling weld metal composition, and thus microstructure and properties, is oxygen (Ref 3, 4, 14, 16, 17, 18, 19). Oxygen directly reacts with alloying elements to alter their effective role by:

- REDUCING HARDENABILITY
- PROMOTING POROSITY
- PRODUCING INCLUSIONS.

All three effects are significant to weld quality.

Oxygen is introduced into the weld pool at high temperatures by:

- THE PRESENCE OF OXIDE FLUXES THAT DISSOCIATE IN THE ARC
- THE SLAG-METAL REACTIONS IN THE WELD POOL
- THE OXIDES ON THE SURFACE OF BAKED METALLIC POWDERS MIXED WITH FLUX OR ON ELECTRODE
- THE ASPIRATION OF ATMOSPHERE (AIR) INTO THE ARC.

Shielding gas may contain oxidizing reagents; a common gas is 75Ar-25CO_2 or 100% CO_2. As a 100 to 1000 ppm, depending on the type of welding consumable used.

The weld metal oxygen measured directly at the molten electrode tip has been reported to be as high as 1400 ppm. Individual droplets have been found to contain as much as 2000 ppm O_2. There are two views concerning the genesis of the high oxygen content. One suggests that pyrochemical or electrochemical reactions (or both) provide oxygen to the electrode tip, and then further oxidation occurs within the droplet as it passes through the arc. The other view is that the high oxygen levels of the droplet represent the maximum buildup of oxygen in the electrode prior to detachment, with limited reaction during flight across the arc to the weld pool. In either case, high oxygen concentrations are introduced into the weld pool by the welding process.

At the melting point, the solubility of oxygen in pure liquid iron is approximately 1600 ppm at 100 kPa (1 atm) pressure. During solidification, solubility decreases to about 860 ppm at 1500 °C (2730 °F) in δ-Fe. Most of the alloying elements present in liquid steel reduce oxygen solubility through deoxidation equilibria. Steelmaking processes typically yield analytical oxygen levels ranging from 70 to 100 ppm. Welds typically pick up oxygen to levels of several hundred ppm, then deoxidize to oxygen levels of around 200 to 300 ppm. Deoxidation of the weld metal occurs in two separate steps, the first being the primary deoxidation of the weld pool (Ref 6). Secondary deoxidation occurs during solidification as solute concentrations increase within the intercellular or interdendritic regions. The secondary deoxidation will either form very small inclusions or will coat the interdendritically trapped primary inclusions.

The high oxygen concentrations added to the weld pool by the metal droplets significantly affect deoxidation. Figure 1 shows experimentally measured soluble oxygen concentrations for various deoxidants (solid lines), along with deoxidation curves predicted by the solubility products (broken lines). The experimental deviation is caused by interactions of the deoxidant with other alloy elements. If the oxygen and metallic element concentrations resulting from the welding process exceed the equilibrium concentration for a specific reaction, inclusions will result. The ability to form a specific inclusion will correspond directly to the position of the weld pool composition relative to the activity plot for this inclusion. Thus, the thermodynamic order for the formation of primary oxides would be: Al_2O_3 > Ti_2O_3 > SiO_2 > Cr_2O_4 > MnO.

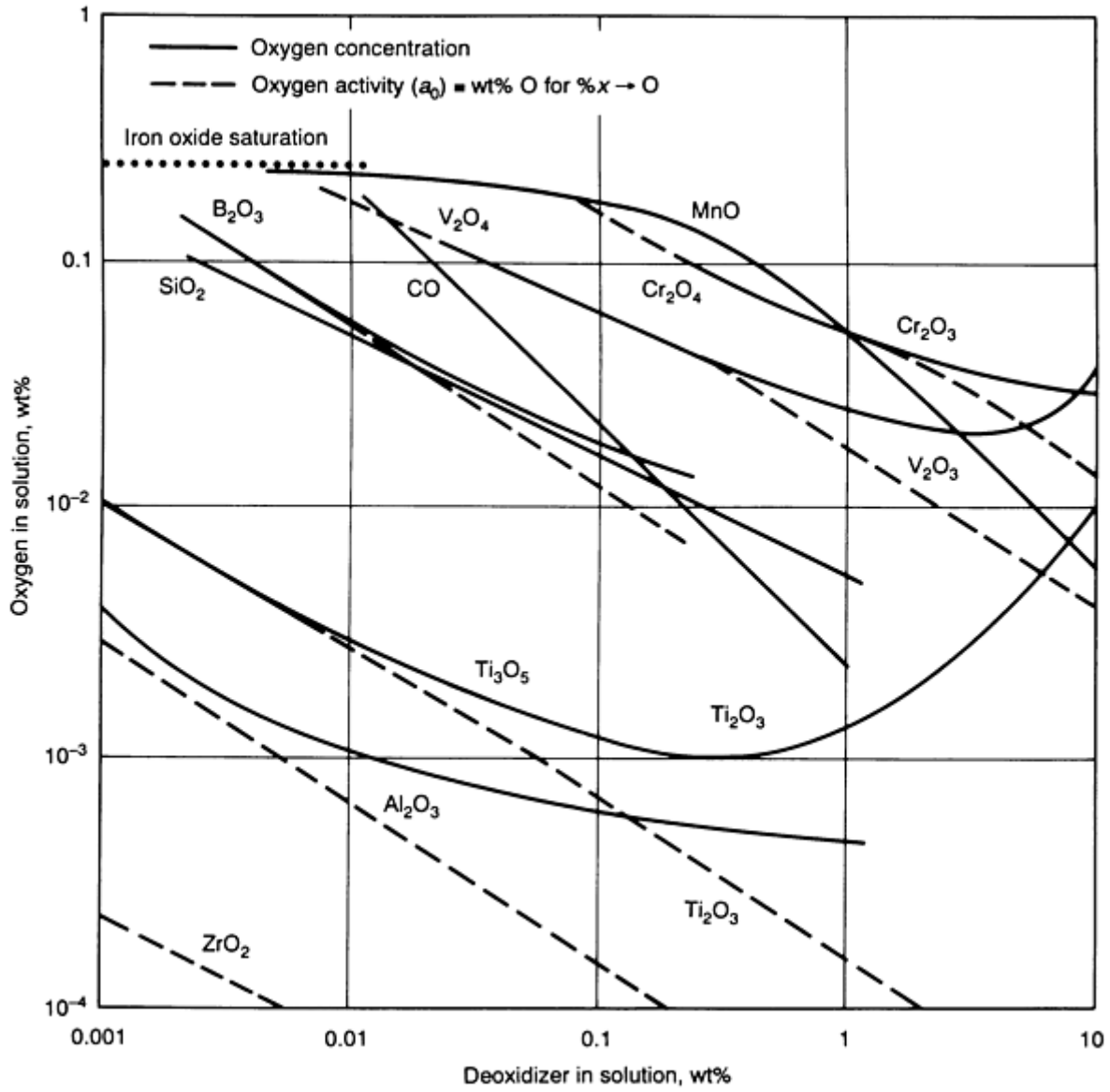

FIG. 1 DEOXIDATION EQUILIBRIA IN LIQUID IRON ALLOYS AT 1600 °C (2910 °F). THE BROKEN LINES SHOW DEOXIDATION EQUILIBRIA PREDICTED BY SOLUBILITY PRODUCT CALCULATIONS. THE SOLID LINES SHOW EXPERIMENTALLY DETERMINED SOLUBLE OXYGEN CONCENTRATIONS FOR VARIOUS DEOXIDANTS. THE EXPERIMENTAL DEVIATION IS CAUSED BY VARIATIONS IN THE ACTIVITY COEFFICIENTS WITH INCREASING DEOXIDANT CONCENTRATION. SOURCE: REF 20

Inclusion Formation. Inclusions form as a result of reactions between metallic alloy elements and nonmetallic tramp elements, or by mechanical entrapment of nonmetallic slag or refractory particles. Inclusions may include:

- OXIDES
- SULFIDES
- NITRIDES
- CARBIDES
- OTHER COMPOUNDS
- MULTIPLE PHASES

Among these, oxides and complex oxides occur most frequently in the size range known to influence weld metal microstructure.

Using only thermodynamic considerations in the analysis of slag-metal reactions, the following reactions may be considered as the ones that describe inclusion formation:

$$X\ \underline{M}\ + Y\ \underline{O}\ = (M_XO_Y) \qquad \textbf{(EQ 1)}$$

where the underlining of a component M ($\underline{M}$) and the component O ($\underline{O}$) indicate that M and O, respectively, are dissolved in the metal, and:

$$X\ \underline{M}\ + Y(FEO) = (M_XO_Y) + YFE \qquad \textbf{(EQ 2)}$$

The equilibrium constants (K_1 and K_2) for the above two reactions are:

$$K_1 = \frac{(A_{M_xO_y})}{[a_M]^x[a_o]^y} \qquad \textbf{(EQ 3)}$$

where a_i is the activity, a function of the concentration, for component *i*, and:

$$K_2 = \frac{(A_{M_xO_y})}{[a_M]^x[a_{FeO}]^y} \qquad \textbf{(EQ 4)}$$

Equilibrium compositions for the weld deposit can be estimated with Eq 1, 2, 3, and 4 and can be used to predict trends for the weld pool pyrochemical reactions. The actual compositions may, however, differ from the calculated values due to alloying-element partitioning during cellular or dendritic solidification, commonly observed in steel weldments.

During solidification of a weld metal, solute elements segregate to the liquid at the solid/liquid interface, and the solute concentrations can reach high levels in the interdendritic regions, as suggested in Fig. 2. Neglecting solid diffusion, the solute composition in the liquid at the solid/liquid interface can be modeled (Ref 6) by the nonequilibrium lever rule, or Scheil Equation:

$$C_L = C_0F_L^{K-1} \qquad \textbf{(EQ 5)}$$

where C_0 is the bulk concentration in the weld pool, C_L is the solute concentration in the liquid at the interface, and *k* is the equilibrium partition ratio.

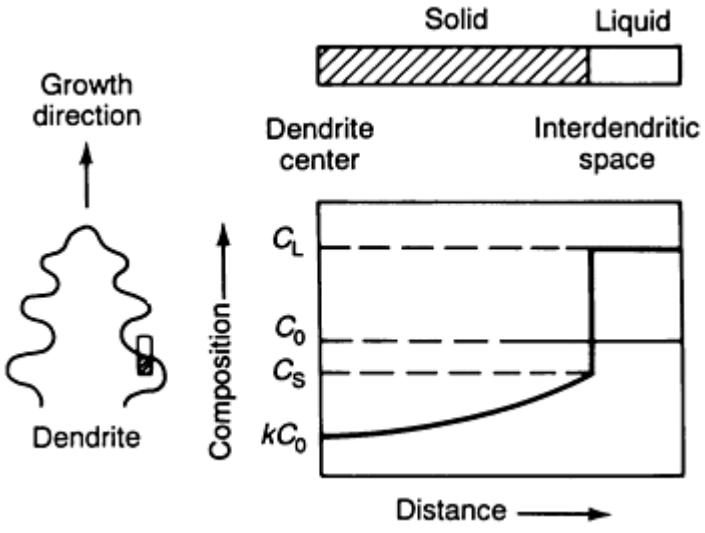

FIG. 2 SCHEMATIC SHOWING THE SOLID AND LIQUID COMPOSITION PROFILES MODELED BY EQ 5 BASED ON THE ASSUMPTION THAT THERE IS COMPLETE LIQUID DIFFUSION AND NO SOLID DIFFUSION. C_0, THE INITIAL ALLOY COMPOSITION; K, THE PARTITION RATIO OF THE SOLID TO LIQUID COMPOSITIONS ON THE EQUILIBRIUM PHASE DIAGRAM; KC_0, THE INITIAL COMPOSITION OF THE SOLID; AND C_S AND C_L, THE SOLID AND LIQUID COMPOSITIONS, RESPECTIVELY, AT THE SOLIDIFICATION INTERFACE. SOURCE: REF 4

The equilibrium partition ratio, *k*, controls the direction and the extent of segregation. For most alloy elements in steel, the partition ratio is less than one, and the element segregates to the interdendritic liquid.

Consider the deoxidation equilibrium as represented by the dissolution reaction for a complex oxide:

$$M_XN_YO_Z = X\ \underline{M}\ + Y\ \underline{N}\ + Z\ \underline{O} \qquad \textbf{(EQ 6)}$$

The free energy change associated with the dissolution of the $M_xN_yO_z$ can be written as:

$$\Delta G = \Delta G^\circ + RT \ln \frac{[M]^x[N]^y[O]^Z}{[M_xN_yO_z]} \qquad \textbf{(EQ 7)}$$

where [M], [N], and [O] are the solute activities in the liquid; and *x*, *y*, and *z* are the stoichiometric constants from Eq 6. The value $[M_xN_yO_z]$ is the activity for the specific inclusion and can be assumed to have the value of one.

The ratio of the activities of the reactants to that of the oxide can be termed the activity quotient (*Q*):

$$Q = \frac{[M]^x[N]^y[O]^Z}{[M_xN_yO_z]} \qquad \textbf{(EQ 8)}$$

With Eq 5 representing the extent of segregation, the solute activities in the interdendritic liquid can be written as:

$$[M]=[\gamma_M][M_O]f_L^{k_M-1} \qquad \textbf{(EQ 9A)}$$

$$[N]=[\gamma_N][N_0]f_L^{k_N-1} \qquad \textbf{(EQ 9B)}$$

$$[O] = [\gamma_O][O_0]f_L^{k_O-1} \qquad \textbf{(EQ 9C)}$$

In Eq 9a, 9b, and 9c, $[M_O]$, $[N_O]$, and $[O_O]$ are the bulk concentrations of M, N, and O in the melt; and $[\gamma_M]$, $[\gamma_N]$, and $[\gamma_O]$ are the activity coefficients for the solutes.

Substituting Eq 9a, 9b, and 9c into Eq 8 gives the free energy as a function of the remaining liquid fraction:

$$\Delta G = \Delta G^\circ + RT \ln \frac{[\gamma_M M_O f_L^{k_M-1}]^x [\gamma_N N_O f_L^{k_N-1}]^y [\gamma_O O_O f_L^{k_O-1}]^z}{[M_xN_yO_z]} \qquad \textbf{(EQ 10)}$$

Equation 10 expresses the free energy driving force for oxide dissolution. The first term on the right side, ΔG, represents equilibrium conditions. The second term represents the departure from equilibrium caused by changes in reactant concentrations or by segregation during solidification.

At equilibrium, the free energy driving force, ΔG, is zero, and the equilibrium concentrations can be found by equating the two terms on the right-hand side of Eq 10. At equilibrium, the activity quotient becomes the equilibrium constant, K_{eq}:

$$\Delta G^\circ = -RT \ln \frac{[M]^x[N]^y[O]^z}{[M_xN_yO_z]} = -RT \ln K_{eq} \qquad \textbf{(EQ 11)}$$

Inclusion precipitation is possible when the concentrations of oxygen and deoxidants exceed the equilibrium values for a particular oxide. This condition can be expressed with the ratio of the activity quotient to the equilibrium coefficient:

$$\text{Precipitation index} = \frac{Q}{K_{eq}} \qquad \textbf{(EQ 12)}$$

A precipitation index less than unity indicates that the concentrations of oxygen and deoxidants are below the equilibrium value, and the precipitation of the inclusions will not occur. A value greater than 1.0 indicates that concentrations are sufficiently high for precipitation according to the methodology described above. The compounds Al_2O_3, Ti_2O_3, and SiO_2 are some of the oxides that will form in a low-carbon low-alloy steel weld. Multiple reactions can occur, and different oxides may appear in the same weld when more than one of these deoxidizers is present.

Metal Transferability During Pyrochemical Reactions. The final weld metal concentration for a particular element is made up of contributions from the filler wire, flux, and base metal; however, losses caused by the welding process vary for each element.

Delta Quantity. The nominal composition of each weld can be calculated considering just the dilution effect of the filler wire and base metal. The extent of loss or transfer of a specific element can be evaluated by a quantity, which expresses the difference between the analytical and the nominal composition. These quantities, designated delta quantity in this article, indicate the effect of the flux on element transfer during welding. A positive delta quantity indicates an elemental transfer from the flux to the weld metal. A negative delta quantity suggests an elemental loss from the weld pool to the slag. A null delta quantity for a specific element suggests an apparent equilibrium condition, in which the flux and slag content for that element are the same. Flux compositions with null delta-quantity behavior have been used to make equilibrium calculations and thus achieve a better understanding of the chemical reactions involved in welding (Ref 8). Investigators have also quantified elemental transfer by measuring similar neutral points (null delta quantity) for various flux systems and have developed a thermodynamic model capable of predicting neutral points for some slag systems (Ref 10).

Arc Stabilizers. Arc welding fluxes are compositionally more complex than fluxes used in other metallurgical processes, such as steelmaking. Many of the additions to the flux are not designed to assist weld metal refinement. Some additions are present to promote arc stability, generate plasma and protective gases, control viscosity, support out-of-position welding, and promote slag detachability.

The welding arc requires an inert or chemically reducing plasma and shielding gas that can be easily ionized. Additions must be made to the flux to achieve the necessary current-carrying capacity and to maintain arc stability. Specific additions will be necessary for the various modes of current (direct current, dc, or alternating current, ac) and polarity.

Alkali metal, zirconium, and titanium additions to the arc affect the ionization process and the ease with which the welding is reinitiated (reinitiation is required 50 to 60 times per second with ac welding). These additions come to the welding flux as feldspar (alkali aluminum silicates), rutile, lithium carbonate, titanium aluminate, and potassium oxalate, and they play an especially important role when welding either in the dc electrode negative (DCEN) mode or in the alternate current (ac) mode. Arc stabilizers are also important in high-speed welding when the cathode and anode spots are less stable. These additions are part of the AWS classification of electrodes, as seen by the fourth digit (E XXX $\underline{X}$) in the classification standard for steel electrodes for shielded metal arc welding (SMAW) given in Table 1. The electrodes designed to perform with ac mode or in the DCEN mode current have been specified as containing high titania or alkali metal (potassium or sodium) additions. Special additions such as Li_2O have been used to achieve multipurpose results--for example, reducing the viscosity while increasing the arc stability.

TABLE 1 AWS CLASSIFICATION OF SELECTED SMAW ELECTRODES FOR WELDING MILD AND LOW-ALLOY STEELS

ELECTRODE DESIGNATION	CURRENT AND POLARITY[(A)]	PENETRATION	ARC STABILIZERS	% FE
EXX10	DCEP	DEEP	HIGH CELLULOSE-NA	0-10
EXXX1	AC, DCEP	DEEP	HIGH CELLULOSE-K	0
EXXX2	AC, DCEN	MEDIUM	HIGH RUTILE-NA	0-10
EXXX3	AC, DCEP, DCEN	LIGHT	HIGH RUTILE-K	0-10
EXXX4	AC, DCEP, DCEN	LIGHT	RUTILE-IRON POWDER	25-40
EXX24	AC, DCEP, DCEN	LIGHT	RUTILE-IRON POWDER	50
EXXX5	DCEP	MEDIUM	LOW H-NA	0
EXXX6	AC, DCEP	MEDIUM	LOW H-K	0
EXX27	AC, DCEN, DCEP	MEDIUM	IRON OXIDE-IRON POWDER	50
EXXX8	AC, DCEP	MEDIUM	LOW HYDROGEN-IRON POWDER	25-40
EXX28	AC, DCEP	MEDIUM	LOW HYDROGEN-IRON POWDER	50

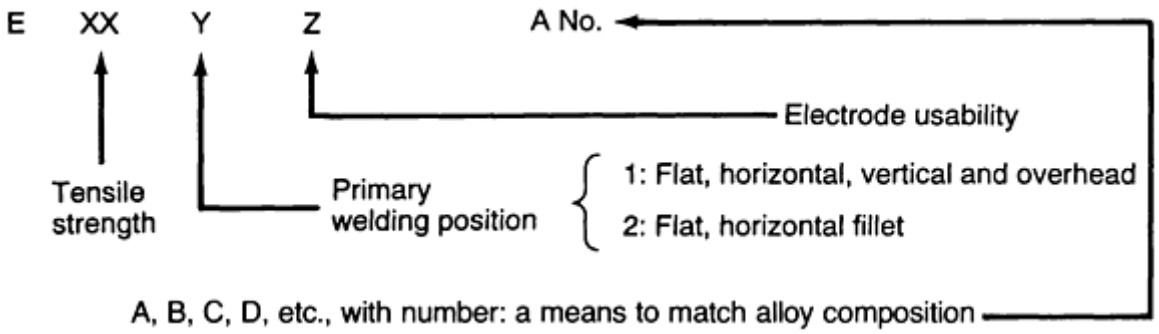

(A) DCEP, DC ELECTRODE POSITIVE, DCEN, DC ELECTRODE NEGATIVE

Changes in Flux Composition With Delta Quantity. Figure 3 shows a transfer of manganese for welds made with SiO_2-TiO_2-CaO-$1Na_2O$ flux at constant SiO_2 content in the flux. These values vary widely, depending on other alloy concentrations. The data imply that manganese is almost always lost to the slag, and that the activity of manganese varies considerably with changes in the amount of titania in the flux. Manganese is very important to weld metal hardenability and must be closely controlled to obtain the optimum weld microstructure. Controlling the weld metal manganese concentration in the titania-containing flux systems would require strict compositional control of the welding flux to ensure the correct manganese concentration in the weld metal.

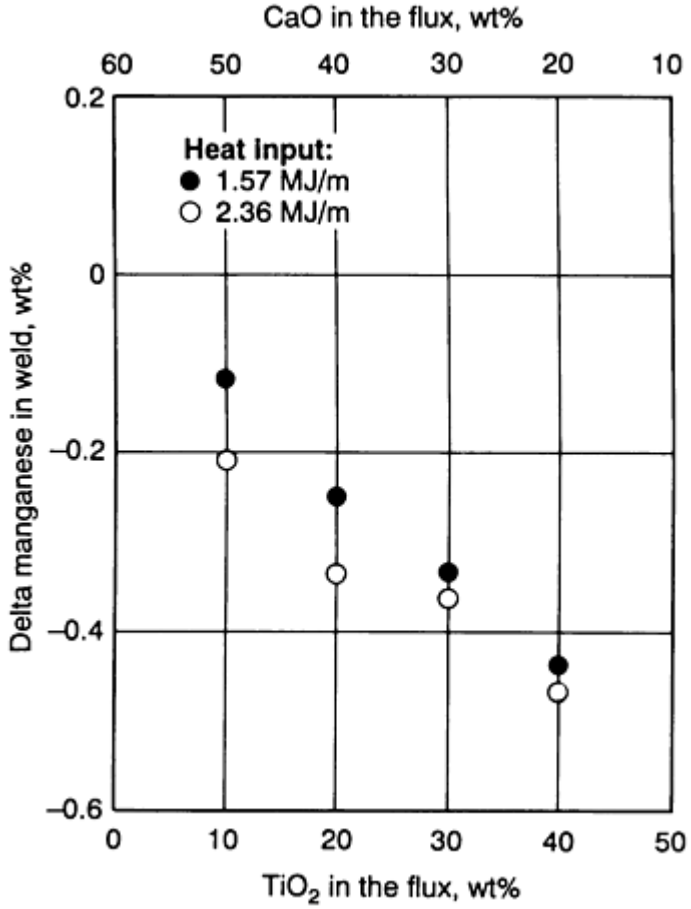

FIG. 3 PLOT OF CHANGES IN MANGANESE CONTENT IN THE WELD VERSUS THE VARIATION IN FLUX COMPOSITION AS A FUNCTION OF TWO-HEAT INPUTS. THE SIO_2 CONTENT WAS MAINTAINED AT 40% THROUGHOUT THE FLUX-CORED ARC WELDING PROCESS. SOURCE: REF 21

In the same system, the delta titanium showed a constant increase with increasing titania content of the flux (Fig. 4). Because of the large amounts of titania in the flux, it is not surprising that the welds show positive compositional deviations for titanium. These results also suggest that control of the weld metal titanium content will require tight control of the limits of the TiO_2 content of the flux.

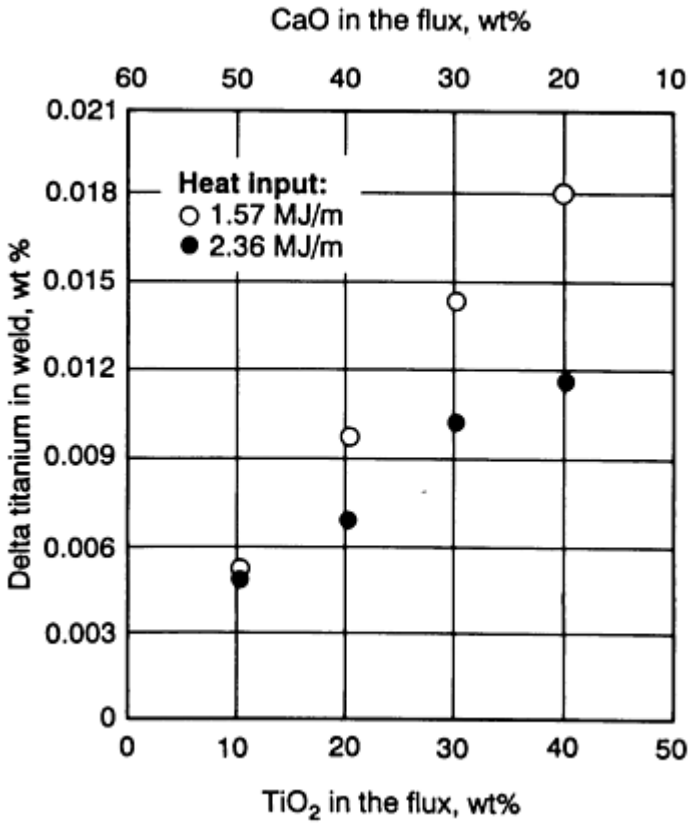

FIG. 4 PLOT OF CHANGES IN TITANIUM CONTENT IN THE WELD VERSUS THE VARIATION IN FLUX COMPOSITION AS A FUNCTION OF TWO HEAT INPUTS. THE SIO_2 CONTENT WAS MAINTAINED AT 40% THROUGHOUT THE FLUX-CORED ARC WELDING PROCESS. SOURCE: REF 21

If the delta quantity changes rapidly with flux composition, it may be difficult to maintain specific weld metal composition, microstructure, and properties with variation in flux composition. The magnitude of the delta quantity for specific elements is most often not as serious a concern as a rapid change in the delta quantity with variations in flux chemistry and welding parameters. The magnitude of the delta quantity can be adjusted by altering the alloy content of the welding wire or the amount of ferro-additions to the flux. Thus, a suitable combination of wire, flux, and welding parameters should achieve negligibly small delta quantities of major alloying elements.

Shielding Gas. When the shielding gas that protects the weld pool comes from the flux, it is necessary to understand the decomposition of specific flux components. Two common shielding gas atmospheres from flux dissociation are hydrogen and CO/CO_2. The hydrogen gas can be produced by the decomposition of cellulose (wood flour or similar hydrocarbons). A CO/CO_2 atmosphere results from the decomposition of carbonates such as limestone ($CaCO_3$) or dolomite [$CaMg(CO_3)_2$]. The CO/CO_2 atmosphere can be balanced to provide a reducing (and thus protective) atmosphere.

At high temperatures, CO_2 or CO will react with carbon to achieve equilibrium, which requires the presence of CO and CO_2. It is the relative amounts of CO and CO_2 that determine the reducing/oxidizing nature of the arc environment. The CO/CO_2 ratio also determines the recovery of specific alloying elements. Typical plasma atmospheres for both hydrogen-type and low-hydrogen-type electrodes are given in Table 2.

TABLE 2 GAS COMPOSITION OF WELDING ARC OBTAINED FROM SPECIFIC TYPES OF WELDING ELECTRODES

AWS DESIGNATION	TYPE	COMPOSITION, WT%			
		H_2O	H_2	CO_2	CO
6010	CELLULOSIC	16	41	3	40

6015	BASIC	2	2	19	77

Source: Ref 15

In submerged arc welding, the covering flux also produces the protective shielding gas and plasma. Other gaseous phases, including flourine-bearing components, are also part of the plasma.

The effect of arc environment (for example, amounts of CO and CO_2) on weld metal chemistry control for hyperbaric welding with a basic electrode is shown in Fig. 5. The high-pressure welding allows evaluation of the CO reaction. Considering the CO reaction:

$$C + O = CO \qquad \textbf{(EQ 13)}$$

the law of mass action gives:

$$k = \frac{P_{CO}}{[C][O]} \qquad \textbf{(EQ 14)}$$

where [C] and [O] are the weld metal carbon and oxygen contents, respectively. At equilibrium the partial pressure of CO is directly related to the total pressure by Dalton's Law.

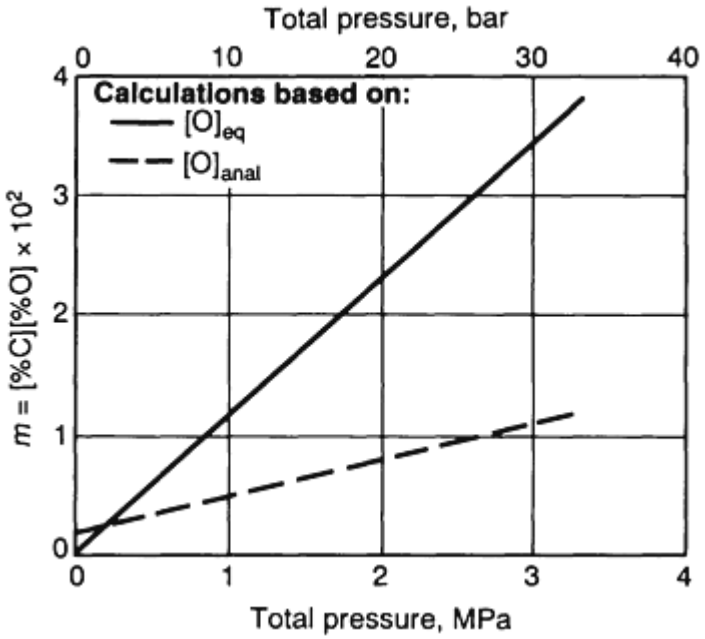

FIG. 5 EFFECT OF PRESSURE ON THE PRODUCT *M* = [%C][%O] FOR HYPERBARIC WELDING WITH A BASIC ELECTRODE. SOURCE: REF 12

In Fig. 5, two lines are indicated. The solid line plots the product of the weld metal oxygen and carbon as a function of total pressure when the analytical weld metal oxygen concentration, $[\%O]_{anal}$, was used. The broken line indicates a similar relationship; however, in this case, the weld metal oxygen concentration has been corrected for the displacement of oxygen because of the formation of manganese silicate inclusions during welding and its transport to the slag. The equilibrium oxygen content, $[\%O]_{eq}$, in the liquid steel at high temperatures is then given by the following expression:

$$[\%O]_{eq} = [\%O]_{anal} + \frac{32}{28}\Delta[\%Si] + \frac{16}{55}\Delta[\%Mn] \quad \textbf{(EQ 15)}$$

where Δ[%Si] and Δ[%Mn] represent the difference between the expected compositions of these elements (from knowledge of initial consumables and base plate compositions as well as dilution) and the actual compositions measured. The linearity of these lines in Fig. 5 is evidence of the strong influence of the CO reaction in arc welding.

The evidence of water reaction control for some electrodes (for example, cellulosic electrodes) can be seen in Fig. 6. With an increase in the degree of oxidation of the deposited metal, the weld metal hydrogen content decreases (Ref 22). The relationship between weld metal oxygen and hydrogen contents as seen in Fig. 6 is consistent with the functional form expected from the law of mass action for a H_2O reaction. It is apparent that with increasing weld metal oxygen content there is a significant reduction in weld metal hydrogen. The hydrogen content of the deposited metal can be reduced by increasing the $CaCO_3$ content of the coating. With the ever-increasing requirements of weld-deposit properties and the increasing need for higher productivity, pyrochemistry will play an important role for flux formulation and weld-property prediction.

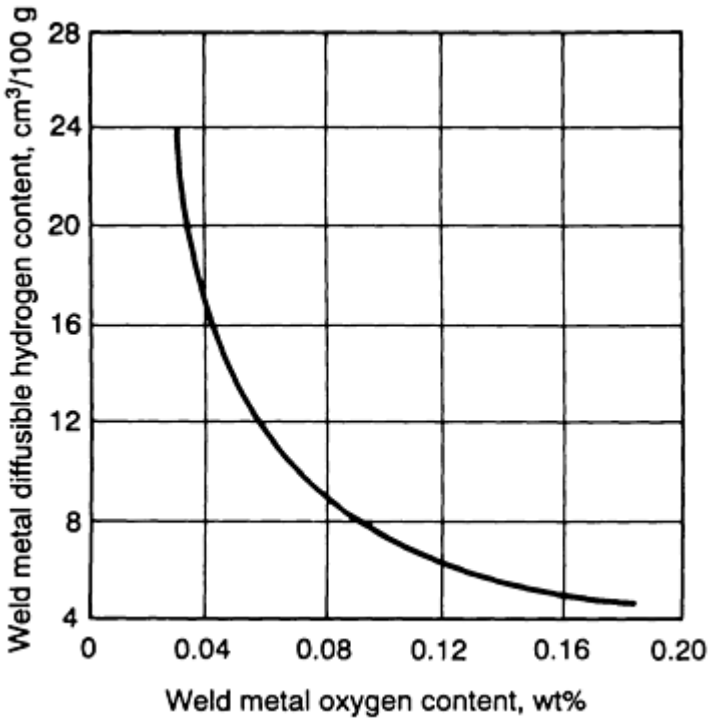

FIG. 6 PLOT OF WELD METAL OXYGEN CONTENT VERSUS WELD METAL HYDROGEN CONTENT WHEN WELDING WITH ELECTRODES THAT CONTAIN CHROMIUM AND NIOBIUM IN THEIR COATINGS. SOURCE: REF 22

Basicity Index

As indicated in the section "Metal Transferability During Pyrochemical Reactions" in this article, the transfer of alloying elements during welding depends strongly on the physical and chemical properties of the flux. The ability to correlate flux properties with weld metal chemical compositions and properties is essential to understand the interactions between weld metal and flux.

Because of the incomplete understanding of the thermodynamic properties of slags, the empirical concept of basicity has been applied to predict flux and weld properties. A basicity index, *BI,* for welding has been proposed:

$$BI = \frac{CaO + CaF_2 + MgO + K_2O + Na_2O + Li_2O + 1/2(MnO + FeO)}{SiO_2 + \frac{1}{2}(Al_2O_3 + TiO_2 + ZrO_2)} \quad \textbf{(EQ 16)}$$

where the chemical components are given in wt%. When the basicity index for a given flux is less than one, the flux is considered acidic. A flux with a *BI* between 1.0 and 1.2 can be classified as neutral. A flux with a *BI* greater than 1.2 is considered basic.

In general, the higher the basicity, the cleaner the weld with respect to nonmetallic inclusions (that is, lower weld metal oxygen content) (Ref 23). Figure 7 illustrates the correlation between weld metal oxygen and the basicity index for some flux systems. The weld metal oxygen content drops significantly as the *BI* is increased to 1.2 and then remains relatively constant at about 250 ppm O. The correlation between weld metal oxygen, which is an indication of weld metal toughness, and basicity is acceptable for some welding flux systems, especially those that are primarily based on CaO, MgO, and SiO_2. However, Eq 16 cannot be used to correlate the strength and toughness of welds made with high flux concentrations of Al_2O_3, TiO_2, ZrO_2, MnO, FeO, and CaF_2. Although numerous basicity formulas have been considered, none has been flexible enough to deal with high amphoteric oxide contents. There is still some concern over utilizing this index (which was primarily conceived by steelmakers for evaluating sulfur refinement) for predicting weld metal oxygen, or for use as a general criterion for weld metal quality (Ref 7). Additionally, the *BI* does not consider the physical properties of the fluxes, nor does it explain the kinetics of the flux-metal reactions.

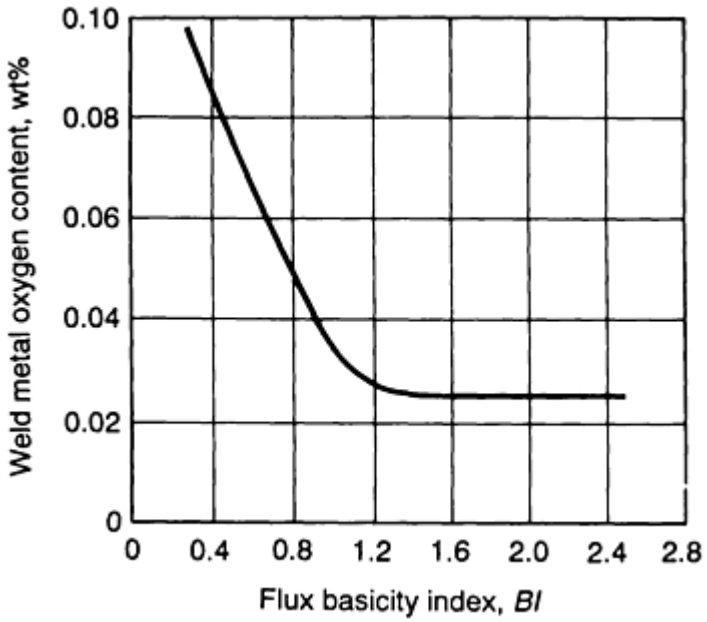

FIG. 7 EFFECT OF WELD METAL OXYGEN CONTENT ON FLUX BASICITY INDEX WHEN USING THE SUBMERGED ARC WELDING PROCESS. SOURCE: REF 23

Basicity index has been used by the welding industry as a measure of expected weld metal cleanliness and mechanical properties. Consequently, manufacturers of welding consumables have classified and advertised their fluxes with this index. It is believed that high basicity means high toughness, a quality of great interest to the engineer, while an acidic flux means excellent slag behavior, a characteristic of interest to the welder attempting to improve weld bead morphology and deposition rate. Table 3 classifies the various coating formulations for SMAW electrodes using the descriptors of cellulosic, basic, acid, and rutile (alternating current stabilizer and slag former).

TABLE 3 ELECTRODE COATING FORMULATIONS OF SELECTED SMAW ELECTRODES

Electrode		Coating formulation[(a)]										Comments
Type	AWS designation	Rutile	Cellulose	Quartz	Carbonates	Ferromanganese	Organics	Iron ore-manganese ore	Calcium carbonate	Complex silicates	Fluorspar	Ferroalloys	
Cellulosic	6010	20-60	10-50	15-30	0-15	5-10	. . .	. . .	. . .	. . .	. . .	. . .	Cellulose promotes gas shielding in the arc region. Hydrogen increases heat at weld. High hydrogen content (30-200 ppm). Deep penetration, fast cooling weld
Rutile	6012 6013	40-60 20-40	. . . . . .	15-25 15-25	0-15 5-25	10-12 1.4-14	2-6 0-5	. . . . . .	. . . . . .	. . . . . .	. . . . . .	. . . . . .	Slags mainly for slag shielding relatively high hydrogen content (15-30 ppm). High inclusion content in weld deposit
Acid-ore[(a)]	6020	. . .	. . .	X	X	X	. . .	X	. . .	X	. . .	. . .	Relatively high hydrogen content. High slag content in weld metal
Basic	7015	0-10	. . .	0-5	. . .	. . .	. . .	. . .	20-50	. . .	20-40	5-10	Relatively low hydrogen levels ($\leqslant$ 10 ppm), hence commonly used in welding low-alloy construction steels. Electrodes should be kept dry. Low inclusion content in weld deposit

Source: Ref 24

(A) X, DATA UNAVAILABLE.

Pyrochemical Kinetics During Welding

The ability of a flux to refine as well as protect the weld pool is related to the mass transport processes in the flux. The flux should melt approximately 200 °C (360 °F) below that of the alloy for proper flux coverage and for protection of the weld deposit. One of the most important physical properties of a flux is its slag viscosity, which not only governs the way the slag flows and covers the molten weld pool but also strongly affects the transport processes involved in pore removal, deoxidation, and retention of alloying additions. The chemical processing and refining by the flux to achieve a weld deposit with low concentrations of oxygen and sulfur and optimal concentration of hardenability agents (carbon, manganese, chromium, molybdenum, nickel, and so on) may not be achieved unless slag viscosity is also adequate. The viscosity is strongly temperature-dependent, so the use of various heat inputs during welding may require different flux compositions to produce the matching slag viscosity. For simple ionic melts, the viscosity has been shown to follow an Arrhenius-type temperature dependence:

$$\eta = \eta_0 \exp\left(\frac{E_\eta}{RT}\right) \qquad \textbf{(EQ 17)}$$

where ηis the viscosity, η_0 is a system constant, $E\eta$ is the viscous activation energy, RT is the gas constant, and T is the temperature.

For polymeric melts, Eq 17 often does not hold true. It has been shown that in certain cases a modified equation can be used:

$$\eta = \eta_0 \exp\left[\frac{E_\eta}{R(T - T_0)}\right] \qquad \textbf{(EQ 18)}$$

where T_0 is a constant for a given flux composition. The presence of entrapped particulates tends to increase the slag viscosity. Slag viscosity is also affected by composition. The compositional dependence is commonly reported by considering $E\eta$ to be a function of composition at constant temperature.

The slag must be fluid enough so that it flows and covers the molten weld pool but must be viscous enough so that it does not run away from the molten metal and flow in front of the arc, leading to possible overlapping by the weld metal. (For overhead welding, surface tension becomes a primary factor because fluidity reduces coverage [opposite gravitational vector].) It has been reported that if the manganese silicate flux viscosity at 1450 °C (2640 °F) is above 0.7 Pa · s (7 P), a definite increase in weld surface pocking will occur. Pock marks have been associated with easily reducible oxides in the flux, which contribute oxygen to the weld pool. The weld pool reacts with carbon to form carbon monoxide, which cannot be transported through a high-viscosity flux and is trapped at the liquid-metal/flux interface. The result is a weld metal surface blemished by surface defects or pocks. Because viscosity is sensitive to temperature and thus heat input, pocking can be the evidence that a flux formulated for high-current welding is being used at too low a current or too great a travel speed. The viscosity of most welding fluxes at 1400 °C (2550 °F) is in the range of 0.2 to 0.7 Pa · s (2 to 7 P).

Slag viscosity also affects the shape of the weld deposit and must be carefully controlled when covered electrodes are used out of position. The higher the slag viscosity, the greater the weld penetration in submerged arc welding. However, this benefit must be balanced, because if the viscosity is too high, the gaseous products cannot escape the weld pool, resulting in unacceptable porosity. This condition can be monitored by observing the density of pores trapped in the underside of the detached slag. Detached slags manifesting a honeycomb structure suggest a severe weld metal porosity problem. This condition usually means that a given flux has experienced an insufficient heat input for the effective transport of gas through the slag.

References cited in this section

3. T. LAU, G.C. WEATHERLY, AND A. MCLEAN, THE SOURCES OF OXYGEN AND NITROGEN CONTAMINATION IN SUBMERGED ARC WELDING USING CAO-AL_2O_3 BASED FLUXES, *WELD. J.*, VOL 64 (NO. 12), 1985, P 343S-347S

4. T.H. NORTH, H.B. BELL, A. NOWICKI, AND I. CRAIG, SLAG/METAL INTERACTION, OXYGEN, AND TOUGHNESS IN SUBMERGED ARC WELDING, *WELD. J.*, VOL 57 (NO. 3), 1978, P 63S-75S
5. N. CHRISTENSEN AND J. CHIPMAN, SLAG-METAL INTERACTION IN ARC WELDING, *WELD. RES. BULL.*, NO. 15, JAN 1953, P 1-14
6. R.H. FROST, D.L. OLSON, AND S. LIU, PYROCHEMICAL EVALUATION OF WELD METAL INCLUSION EVOLUTION, *PROC. 3RD INT. CONF. TRENDS IN WELDING*, ASM INTERNATIONAL, JUNE 1992
7. C.A. NATALIE, D.L. OLSON, AND M. BLANDER, PHYSICAL AND CHEMICAL BEHAVIOR OF WELDING FLUXES, *ANN. REV. MATER. SCI.*, VOL 16, 1986, P 389-413
8. J.E. INDACOCHEA, M. BLANDER, N. CHRISTENSEN, AND D.L. OLSON, CHEMICAL REACTIONS WITH FEO-MNO-SiO_2 *FLUXES*, *METALL. TRANS. B*, VOL 16, 1985, P 237-245
9. U. MITRA AND T.W. EAGAR, SLAG-METAL REACTIONS DURING WELDING, *METALL. TRANS. B*, VOL 22, 1991, P 65-100
10. C.S. CHAI AND T.W. EAGAR, SLAG-METAL EQUILIBRIUM DURING SUBMERGED ARC WELDING,*METALL. TRANS. B*, VOL 12, 1981, P 539-547
12. O. GRONG, D.L. OLSON, AND N. CHRISTENSEN, CARBON OXIDATION IN HYPERBARIC MMA WELDING, *MET. CONSTRUCT.*, VOL 17. DEC 1985, P 810R-814R
14. T.W. EAGAR, SOURCES OF WELD METAL OXYGEN CONTAMINATION DURING SUBMERGED ARC WELDING, *WELD. J.*,VOL 57, 1978, P 76S-80S
15. N. CHRISTENSEN, *WELDING METALLURGY*, *LECTURE NOTES*, NTH, 1979
16. O. GRONG, T.A. SIEWERT, T.A. MARTINS, AND D.L. OLSON, A MODEL FOR THE SILICON-MANGANESE DEOXIDATION OF STEEL WELD METAL, *METALL. TRANS. A*, VOL 17 (NO. 10), 1985, P 1797-1807
17. T.H. NORTH, THE DISTRIBUTION OF MANGANESE BETWEEN SLAG AND METAL DURING SUBMERGED ARC WELDING, *WELD. RES. ABROAD*, VOL 23 (NO. 1), 1977, P 2-40
18. T. BONISZEWSKI, BASIC FLUXES AND DEOXIDATION IN SUBMERGED ARC WELDING OF STEEL, *METAL. CONSTR. BRIT. WELD. J.*, VOL 6, 1974, P 128
19. L. DAVIS, *AN INTRODUCTION TO WELDING FLUXES FOR MILD AND LOW ALLOY STEELS*, WELDING INSTITUTE, 1981
20. *MAKING, SHAPING AND TREATING OF STEEL*, UNITED STATES STEEL CORPORATION, 1984
21. P.S. DUNN, C.A. NATALIE, AND D.L. OLSON, SOL-GEL FLUXES FOR FLUX CORED WELDING CONSUMABLES, *J. MATER. ENERGY SYSTEMS*, VOL 8 (NO. 2), 1986, P 176-184
22. L.I. SOROKIN AND Z.A. SIDLIN, THE EFFECT OF ALLOYING ELEMENTS AND OF MARBLE IN AN ELECTRODE COATING ON THE SUSCEPTIBILITY OF A DEPOSITED NICKEL CHROME METAL TO PORE FORMATION, *SVAR. PROIZVOD.*, NO. 11, 1974, P 7-9
23. S.S. TULIANI, T. BONISZEWSKI, AND N.F. EATON, NOTCH TOUGHNESS OF COMMERCIAL SUBMERGED ARC WELD METAL, *WELD. MET. FABR.*, VOL 37 (NO. 8), 1969, P 27
24. T.G.F. GRAY, J. SPENCE, AND T.H. NORTH, *RATIONAL WELDING DESIGN*, BUTTERWORTHS, 1975

Nature and Behavior of Fluxes Used for Welding

D.L. Olson, S. Liu, R.H. Frost, G.R. Edwards, and D.A. Fleming, Colorado School of Mines

---

Alloy Modification

Other additions to the welding consumables are required to make alloy additions to the weld pool, usually in the form of powder metal or ferro-additions (Ref 1). Often the composition of the wire that makes up the rod for the shielded metal arc electrode from a specific manufacturer is the same, regardless of the alloy to be welded. Alloying is achieved by

powder metal additions to the flux coating. Manganese, silicon, chromium, niobium, and other alloying additions are adjusted in the weld pool by ferroalloy powder additions. Specially prepared alloy additions of Fe-50Si, Fe-80Mn, Fe-60Mn-30Si, and others are used. One concern in formulating electrodes using ferro-additions is the alloying element recovery (that is, the amount of the element that is transferred across the arc and into the weld deposit). Values for the recovery of typical elements in steel welding are given in Table 4. The metal losses are either to the slag or to the fume.

TABLE 4 RECOVERY OF ELEMENTS FROM SELECTED ELECTRODE COVERINGS

ALLOY ELEMENT	FORM OF MATERIAL IN ELECTRODE COVERING	APPROXIMATE RECOVERY OF ELEMENT, WT%
ALUMINUM	FERROALUMINUM	20
BORON	FERROBORON	2
CARBON	GRAPHITE	75
CHROMIUM	FERROCHROMIUM	95
NIOBIUM	FERROCOLUMBIUM	70
COPPER	COPPER METAL	100
MANGANESE	FERROMANGANESE	75
MOLYBDENUM	FERROMOLYBDENUM	97
NICKEL	ELECTROLYTIC NICKEL	100
SILICON	FERROSILICON	45
TITANIUM	FERROTITANIUM	5
VANADIUM	FERROVANADIUM	80

Source: Ref 1

Slipping and Binding Agents. In the case of SMAW electrodes, slipping agents are also added to the green flux formulation to improve the extrudability of the flux onto the rod (Ref 1). Glycerin, china clay, kaolin, talc, bentonite, and mica have all been used as slipping agents. Binding agents can be classified into two types. The first type comprises binders that bond the flux components to the rod without introducing a hydrogen source. These low-hydrogen binders include sodium silicate and potassium silicate. The second type of binding agent does function as a hydrogen source. The binders used for high-hydrogen electrodes can be organic in nature and include gum arabic, sugar, dextrine, and other specialized synthetic organic binders.

Slag Formation. Slag, a mixture of glass and crystalline structure, must solidify on the already solidified weld deposit to protect the surface from oxidation during cooling. Specific physical properties are required of the slag. It must melt below the melting temperature of steel (~ 1450 °C, or 2640 °F), must have a density significantly less than steel to reduce slag entrapment in the weld deposit, must possess the proper viscosity in the temperature range of 1450 to 1550 °C (2640 to 2820 °F), and must easily detach from the weld deposit after welding.

Silicates, aluminates, and titanates are all primary slag formers. The high-valence cations of these compounds produce a bonding network that can promote glass formation. Most electrodes produce silicate or titanate slag. Silicates of such elements as manganese produce very workable glass deposits, but also produce weld deposits that are relatively high in weld metal oxygen content. These fluxes are said to range from acidic to neutral. The titanate and aluminate fluxes produce more rigid and stable oxide covers. The result is a lower concentration of weld metal oxygen, but a higher-viscosity slag. Aluminates and calcium-bearing compounds are common additions to basic fluxes for the submerged arc welding of high-toughness linepipe steels. Minerals used for slag formation include:

- RUTILE
- POTASSIUM TITANATE
- ILMENITE
- ALUMINA
- SILICA FLOUR

- IRON POWDER
- FLUORSPAR
- FELDSPAR
- MANGANESE DIOXIDE

Asbestos (up to 50%) was used as a slag former, but has been phased out by welding consumable manufacturers.

Slag detachability is a serious productivity concern for steel fabricators. The relative ease of slag detachability influences the economic advantages of flux-related welding processes. Residual slag on the weld deposit promotes slag stringers in multipass weldments, limits the effective use of narrow-gap flux-related welding processes, and may reduce the corrosion resistance of the weldment. Welding flux formulators have modified flux compositions to alleviate or reduce this hindrance (Ref 25).

Poor slag removal has been reported to occur when the flux contains fluorite. Slags containing spinels generally have been found to attach tenaciously to the weld deposit. Slags with cordierite and $(Cr,Mn,Mg)O \cdot (Cr,Mn,Al)_2O_3$ type spinel phases have been reported to be difficult to remove from stainless steel weldments. It has also been reported to be difficult to remove from stainless steel weldments. It has also been reported that if $(CaO)_2SiO_2$, Cr_2TiO_5, and $FeTiO_5$ are present, the slag readily detaches from the weld deposit (Ref 25). The compositional range for acceptable slag detachability has been reported for the $CaO \cdot CaF_2 \cdot SiO_2$ system and the $CaO \cdot TiO_2 \cdot SiO_2$ system. Easier slag removal has also been related to deoxidation with aluminum instead of titanium. Increasing the Al_2O_3 content in the flux has demonstrated improved detachability (Ref 25).

Differences in the coefficient of thermal expansion between the slag and the weld are also important.

References cited in this section

1. G.E. LINNERT, CHAPTER 8, *WELDING METALLURGY*, VOL 1, AWS, 1965, P 367-396
25. D.L. OLSON, G.R. EDWARDS, AND S.K. MARYA, THE PHYSICAL AND CHEMICAL BEHAVIOR ASSOCIATED WITH SLAG DETACHABILITY DURING WELDING, *FERROUS ALLOY WELDMENTS*, VOL 67-70, TRANS TECH, 1992, P 253-268

Nature and Behavior of Fluxes Used for Welding

D.L. Olson, S. Liu, R.H. Frost, G.R. Edwards, and D.A. Fleming, Colorado School of Mines

Types of Fluxes

Producing a weld deposit with high mechanical integrity and with high productivity requires many physical and chemical occurrences in the welding arc. These occurrences are achieved in flux-related arc welding processes by the careful formulation of the welding flux. The welding flux must:

- STABILIZE ARC AND CONTROL ARC RESISTIVITY
- PROVIDE SLAG WITH PROPER MELTING TEMPERATURE
- PROVIDE LOW-DENSITY SLAG
- PERMIT USE OF DIFFERENT TYPES OF CURRENT AND POLARITY
- ADD ALLOYING ELEMENTS
- REFINE THE WELD POOL (DEOXIDATION AND DESULFURIZATION)
- PROVIDE PROPER VISCOSITY FOR OUT-OF-POSITION WELDING
- PROMOTE SLAG DETACHABILITY
- PRODUCE SMOOTH WELD CONTOUR

- REDUCE SPATTER AND FUME

It is apparent, after considering the large number of necessary requirements, that a welding flux must be carefully and deliberately formulated to achieve an optimized performance.

A number of different arc welding processes depend on welding fluxes. Each of these processes requires a different formulation.

SMAW Fluxes. The typical constituents and their functions in electrode coatings for the SMAW process are given in Table 5. It should be noted that the flux ingredients are based on additions of refined minerals of the earth. Natural minerals offer an economical method of keeping welding consumables at a reasonable cost. Table 6 presents the elemental content of these minerals. Table 7 gives the typical chemical compositions for flux coatings for three different SMAW electrodes.

TABLE 5 TYPICAL FUNCTIONS AND COMPOSITIONS OF CONSTITUENTS FOR SELECTED MILD STEEL SMAW ELECTRODE COATINGS

COATING CONSTITUENT	FUNCTION OF CONSTITUENT		COMPOSITION RANGE OF COATING ON ELECTRODE				
	PRIMARY	SECONDARY	E6010, E6011	E6013	E7018	E7024	E7028
CELLULOSE	SHIELDING GAS	. . .	25-40	2-12	. . .	1-5	. . .
CALCIUM CARBONATE	SHIELDING GAS	FLUXING AGENT	. . .	0-5	15-30	0-5	0-5
FLUORSPAR	SLAG FORMER	FLUXING AGENT	. . .	. . .	15-30	. . .	5-10
DOLOMITE	SHIELDING GAS	FLUXING AGENT	. . .	. . .	. . .	. . .	5-10
TITANIUM DIOXIDE (RUTILE)	SLAG FORMER	ARC STABILIZER	10-20	30-55	0-5	20-35	10-20
POTASSIUM TITANATE	ARC STABILIZER	SLAG FORMER	(A)	(A)	0-5	. . .	0-5
FELDSPAR	SLAG FORMER	STABILIZER	. . .	0-20	0-5	. . .	0-5
MICA	EXTRUSION	STABILIZER	. . .	0-15	. . .	0-15	. . .
CLAY	EXTRUSION	SLAG FORMER	. . .	0-10	. . .	. . .	. . .
SILICA	SLAG FORMER	. . .	. . .	. . .	. . .	. . .	. . .
ASBESTOS	SLAG FORMER	EXTRUSION	10-20	. . .	. . .	. . .	. . .
MANGANESE OXIDE	SLAG FORMER	ALLOYING	. . .	. . .	. . .	. . .	. . .
IRON OXIDE	SLAG FORMER	. . .	. . .	. . .	. . .	. . .	
IRON POWDER	DEPOSITION RATE	CONTACT WELDING	. . .	. . .	25-40	40-55	40-55
FERROSILICON	DEOXIDIZER	. . .	. . .	. . .	5-10	0-5	2-6
FERROMANGANESE	ALLOYING	DEOXIDIZER	5-10	5-10	2-6	5-10	2-6
SODIUM SILICATE	BINDER	FLUXING	20-30	5-10	0-5	0-10	0-5

		AGENT					
POTASSIUM SILICATE	ARC STABILIZER	BINDER	(B)	5-15(B)	5-10	0-10	0-5

(A) REPLACES TITANIUM DIOXIDE (RUTILE) TO PERMIT USE WITH ALTERNATING CURRENT.

(B) REPLACES SODIUM SILICATE TO PERMIT USE WITH ALTERNATING CURRENT

TABLE 6 TYPICAL COMPOSITION OF COMMON MINERALS USED IN SMAW ELECTRODE COATINGS

MINERAL	**CHEMICAL COMPOSITION**
ILMENITE	$FEO \cdot TIO_2$
TALC	$3MGO \cdot 4SIO_2 \cdot H_2O$
BENTONITE	COMPLEX AL, MG, CA, FE HYDROXIDES
SILICA, QUARTZ	SIO_2
CELLULOSE	$(C_6H_{10}O_5)_X$
ALUMINA	AL_2O_3
MUSCOVITE, MICA(A)	$K_2O \cdot 3AL_2 \cdot 6SIO_2 \cdot 2H_2O$
ACTINOLITE	$CAO \cdot MGO \cdot 2FEO \cdot 4SIO_2$
MAGNETITE	FE_3O_4
HEMATITE	FE_2O_3
RUTILE, TITANIA	TIO_2
DOLOMITE	$MGO \cdot CAO \cdot (CO_2)_2$
FLUORSPAR, FLUORITE	CAF_2
CRYOLITE	NA_3ALF_4
LIME	CAO
LIMESTONE, CALCITE, MARBLE	$CACO_3$
ZIRCONIA	ZRO_2
FELDSPAR(A)	$K_2O \cdot AL_2O_3 \cdot 6SIO_2$
CLAY(A)	$AL_2O_3 \cdot 2SIO_2 \cdot 2H_2O$
SODIUM SILICATE	SIO_2/NA_2O (RATIO-3.22)
POTASSIUM SILICATE	SIO_2 K_2O (RATIO-2.11)
CHROMIC OXIDE	CR_2O_3

Source: Ref 1

(A) ALTHOUGH THESE SUBSTANCES CAN HAVE SEVERAL CHEMICAL COMPOSITIONS, ONLY TYPICAL COMPOSITION IS GIVEN.

TABLE 7 CHEMICAL COMPOSITION OF COVERINGS USED IN ELECTRODES FOR SMAW WELDING OF MILD STEELS AND LOW-ALLOY STEELS

ELECTRODE		COMPOSITION, WT%[A]														
DESCRIPTION	AWS DESIGNATION	CAO	TIO_2	CAF_2	SIO_2	AL_2O_3	MGO	NA_3ALF_3	N_3O	FEO	SI	MN	FE	$CO + CO_2$	VOLATILE MATTER	MOISTURE
HIGH-CELLULOSE, GAS SHIELDED	E6010	. . .	10.1	. . .	47.0	. . .	3.2	. . .	5.1	1.3	1.5	2.8	. . .	. . .	25.0	4.0
HIGH-TITANIUM GAS-SLAG SHIELD	E6012	. . .	46.0	. . .	23.6	5.0	2.0	. . .	2.4	7.0	1.5	2.5	. . .	. . .	5.0	2.0
LOW-HYDROGEN IRON POWDER	E7018	14.4	. . .	11.0	20.5	2.0	1.0	5.0	1.2	. . .	2.5	1.8	28.5	12.0	. . .	0.1

Source: Ref 1

(A) AFTER BAKING.

Flux-cored arc welding (FCAW) uses a hollow wire filled with flux reagents and ferro-additions. The two types of flux-cored electrodes are carbon-dioxide-shielded flux-cored electrodes and self-shielded flux-cored electrodes (Ref 26). Table 8 gives typical compositions for the three types of carbon-dioxide-shielded cored electrodes. Table 9 gives the typical compositions for the four types of self-shielded flux-cored electrodes.

TABLE 8 TYPICAL FLUX COMPOSITIONS OF AVAILABLE CO_2 SHIELDED FCAW ELECTRODES

ELECTRODE DESCRIPTION		AWS DESIGNATION	COMPOSITION, WT%											
TYPE NUMBER	FLUX TYPE		SiO_2	AL_2O_3	TiO_2	ZrO_2	CaO	Na_2O	K_2O	CO_2 (AS CARBONATE)	C	Fe	Mn	CaF_2
1	TITANIA (NONBASIC)	E70T-1, E70T-2	21.0	2.1	40.5	. . .	0.7	1.6	1.4	0.5	0.6	20.1	15.8	. . .
2	LIME-TITANIA (BASIC OR NEUTRAL)	E70T-1	17.8	4.3	9.8	6.2	9.7	1.9	1.5	. . .	0.3	24.7	13.0	18.0
3	LIME (BASIC)	E70T-1, E70T-5	7.5	0.5	. . .	. . .	3.2	. . .	0.5	2.5	1.1	55.0	7.2	20.5

Source: Ref 26

TABLE 9 TYPICAL FLUX COMPOSITIONS OF AVAILABLE SELF-SHIELDED FCAW ELECTRODES

ELECTRODE DESCRIPTION		AWS DESIGNATION	COMPOSITION, WT%													
TYPE NUMBER	FLUX TYPE		SiO_2	Al	AL_2O_3	TiO_2	CaO	MgO	K_2O	Na_2O	C	CO_2 (AS CARBONATE)	Fe	Mn	Ni	CaF_2
1	FLUORSPAR-ALUMINUM	E70T-4, E70T-7, E60T-8	0.5	15.4	. . .	. . .	. . .	12.6	0.4	0.2	1.2	0.4	0.4	3.0	. . .	63.5
2	FLUORSPAR-TITANIA	E70T-3	3.6	1.9	. . .	20.6	. . .	4.5	0.6	0.1	0.6	0.6	50.0	4.5	. . .	22.0
3	FLUORSPAR-LIME-TITANIA	E70T-6	4.2	1.4	. . .	14.7	4.0	2.2	. . .	. . .	0.6	2.1	50.5	2.0	2.4	15.3
4	FLUORSPAR-LIME	E70T-5	6.9	. . .	0.6	1.2	3.2	. . .	. . .	0.6	0.3	1.3	58.0	7.9	. . .	22.0

Source: Ref 26

Submerged Arc Welding (SAW). In the SAW process, the flux drops from a hopper onto the work such that the welding arc is submerged beneath the granular flux, producing an arc cavity that contains metal vapors, silicon monoxide, manganese oxide, gaseous fluorides, and other higher-vapor-pressure components of the flux. This arc welding process has been recognized as one that produces very little, if any, fume. Submerged arc welding is limited mainly to the flat or

horizontal position, and requires significant setup time. It is very successful in manufacturing numerous similar parts, such as producing welded steel pipe.

Submerged arc fluxes are made in three different forms:

- *BONDED FLUXES* MIX NONMETALLIC AND FERRO-ADDITIONS WITH A LOW-TEMPERATURE BINDER INTO MIXTURES OF SMALL PARTICLES.
- *AGGLOMERATED FLUXES* ARE SIMILAR TO THE BONDED FLUXES EXCEPT THAT A CERAMIC GLASS BINDER, CURED AT HIGH TEMPERATURE, IS USED.
- *FUSED FLUXES* ARE MADE BY POURING A HOMOGENEOUS GLASS MIXTURE OF THE PROPER FLUX COMPOSITION INTO WATER, RESULTING IN A FRIT.

Generally speaking, changing from bonded to agglomerated to fused fluxes improves control of the weld metal composition, especially with respect to such impurities as hydrogen and oxygen.

There are seven types of submerged arc fluxes (Table 10). Flux classification according to basicity is the result of observed correlations between weld metal oxygen concentration and flux composition. Table 11 gives some typical compositions for SAW fluxes.

TABLE 10 FLUXES USED FOR SAW APPLICATIONS

FLUX TYPE	CONSTITUENTS	BASICITY	FLUX FORM	ADVANTAGES	LIMITATIONS	COMMENTS
MANGANESE SILICATE	MNO + SIO_2 > 50%	ACID	FUSED	MODERATE STRENGTH; TOLERANT TO RUST; FAST WELDING SPEEDS; HIGH HEAT INPUT; GOOD STORAGE	LIMITED USE FOR MULTIPASS WELDING; USE WHERE NO TOUGHNESS REQUIREMENT; HIGH WELD METAL OXYGEN; INCREASE IN SILICON ON WELDING; LOW IN CARBON	ASSOCIATED MANGANESE GAIN; MAXIMUM CURRENT, 1100 A; HIGHER WELDING SPEEDS
CALCIUM-HIGH SILICA	CAO + MGO + SIO_2 > 60%	ACID	AGGLOMERATED, FUSED	HIGH WELDING CURRENT; TOLERANT TO RUST	POOR WELD TOUGHNESS; USE WHERE NO TOUGHNESS REQUIREMENT; HIGH WELD METAL OXYGEN	DIFFER IN SILICON GAIN; SOME CAPABLE OF 2500 A; WIRES WITH HIGH MANGANESE
CALCIUM SILICATE-NEUTRAL	CAO + MGO + SIO_2 > 60%	NEUTRAL	AGGLOMERATED, FUSED	MODERATE STRENGTH AND TOUGHNESS; ALL CURRENT TYPES; TOLERANT TO RUST; SINGLE- OR MULTIPLE-PASS WELD	. . .	. . .
CALCIUM SILICATE-LOW SILICA	CAO + MGO + SIO_2 > 60%	BASIC	AGGLOMERATED, FUSED	GOOD TOUGHNESS WITH MEDIUM STRENGTH; FAST WELDING SPEEDS; LESS CHANGE IN COMPOSITION AND LOWER OXYGEN	NOT TOLERANT TO RUST; NOT USED FOR MULTIWIRE WELDING	. . .
ALUMINATE	AL_2O_3 + CAO +	BASIC	AGGLOMERATED	GOOD STRENGTH	NOT TOLERANT TO	USUALLY

BASIC	MGO > 45%; AL_2O_3 > 20%			AND TOUGHNESS IN MULTIPASS WELDS; NO CHANGE IN CARBON; LOSS OF SULFUR AND SILICON	RUST, LIMITED TO DC ELECTRODE POSITIVE	MANGANESE GAIN; MAXIMUM CURRENT 1200 A; GOOD MECHANICAL PROPERTIES
ALUMINA	BAUXITE BASE	NEUTRAL	AGGLOMERATED, FUSED	LESS CHANGE IN WELD COMPOSITION AND LOWER OXYGEN THAN FOR ACID TYPE; MODERATE TO FAST WELDING SPEEDS	. . .	. . .
BASIC FLUORIDE	CAO + MGO + MNO + CAF_2 > 50%; $SIO_2 \leqslant$22%; $CAF_2 \leqslant$15%	BASIC	AGGLOMERATED, FUSED	VERY LOW OXYGEN; MODERATE TO GOOD LOW-TEMPERATURE TOUGHNESS	MAY PRESENT PROBLEMS OF SLAG DETACHABILITY; MAY PRESENT PROBLEM OF MOISTURE PICKUP	CAN BE USED WITH ALL WIRES, PREFERABLE DC WELDING; VERY GOOD WELD PROPERTIES

TABLE 11 TYPICAL COMPOSITIONS OF SMAW FLUXES

FLUX	COMPOSITION, WT%									BASICITY INDEX (*BI*)
	AL_2O_3	SIO_2	TIO_2	MGO	CAF_2	CAO	MNO	NA_2O	K_2O	
A	49.9	13.7	10.1	2.9	5.7	. . .	15.1	1.6	0.2	0.4
B	24.9	18.4	0.2	28.9	24.2	. . .	1.8	2.1	0.07	1.8
C	19.3	16.3	0.8	27.2	23.6	9.8	0.08	0.9	1.1	2.4
D	18.1	13.2	0.5	28.2	31.8	4.5	0.1	0.9	0.9	3.0
E	17.0	12.2	0.7	36.8	29.2	0.7	8.9	1.6	0.1	3.5

References cited in this section

1. G.E. LINNERT, CHAPTER 8, *WELDING METALLURGY*, VOL 1, AWS, 1965, P 367-396
26. *FUMES AND GASES IN THE WELDING ENVIRONMENT*, AWS, 1979

Nature and Behavior of Fluxes Used for Welding

D.L. Olson, S. Liu, R.H. Frost, G.R. Edwards, and D.A. Fleming, Colorado School of Mines

References

1. G.E. LINNERT, CHAPTER 8, *WELDING METALLURGY*, VOL 1, AWS, 1965, P 367-396
2. C.E. JACKSON, FLUXES AND SLAGS IN WELDING, *WELD. RES. BULL.*, NO. 190, 1973
3. T. LAU, G.C. WEATHERLY, AND A. MCLEAN, THE SOURCES OF OXYGEN AND NITROGEN CONTAMINATION IN SUBMERGED ARC WELDING USING CAO-AL_2O_3 BASED FLUXES, *WELD. J.*, VOL 64 (NO. 12), 1985, P 343S-347S
4. T.H. NORTH, H.B. BELL, A. NOWICKI, AND I. CRAIG, SLAG/METAL INTERACTION, OXYGEN, AND TOUGHNESS IN SUBMERGED ARC WELDING, *WELD. J.*, VOL 57 (NO. 3), 1978, P 63S-75S
5. N. CHRISTENSEN AND J. CHIPMAN, SLAG-METAL INTERACTION IN ARC WELDING, *WELD. RES. BULL.*, NO. 15, JAN 1953, P 1-14
6. R.H. FROST, D.L. OLSON, AND S. LIU, PYROCHEMICAL EVALUATION OF WELD METAL INCLUSION EVOLUTION, *PROC. 3RD INT. CONF. TRENDS IN WELDING*, ASM INTERNATIONAL, JUNE 1992
7. C.A. NATALIE, D.L. OLSON, AND M. BLANDER, PHYSICAL AND CHEMICAL BEHAVIOR OF WELDING FLUXES, *ANN. REV. MATER. SCI.*, VOL 16, 1986, P 389-413
8. J.E. INDACOCHEA, M. BLANDER, N. CHRISTENSEN, AND D.L. OLSON, CHEMICAL REACTIONS WITH FEO-MNO-SIO_2 *FLUXES*, *METALL. TRANS. B*, VOL 16, 1985, P 237-245
9. U. MITRA AND T.W. EAGAR, SLAG-METAL REACTIONS DURING WELDING, *METALL. TRANS. B*, VOL 22, 1991, P 65-100
10. C.S. CHAI AND T.W. EAGAR, SLAG-METAL EQUILIBRIUM DURING SUBMERGED ARC WELDING,*METALL. TRANS. B*, VOL 12, 1981, P 539-547
11. N. CHRISTENSEN, METALLURGICAL ASPECTS OF ARC WELDING, *WELD. J.*, VOL 27, 1949, P 373S-380S
12. O. GRONG, D.L. OLSON, AND N. CHRISTENSEN, CARBON OXIDATION IN HYPERBARIC MMA WELDING, *MET. CONSTRUCT.*, VOL 17. DEC 1985, P 810R-814R
13. U. MITRA AND T.W. EAGAR, SLAG-METAL REACTIONS DURING SUBMERGED ARC WELDING OF ALLOY STEELS, *METALL. TRANS. A*, VOL 15, 1984, P 217-227

14. T.W. EAGAR, SOURCES OF WELD METAL OXYGEN CONTAMINATION DURING SUBMERGED ARC WELDING, *WELD. J.*,VOL 57, 1978, P 76S-80S
15. N. CHRISTENSEN, *WELDING METALLURGY, LECTURE NOTES*, NTH, 1979
16. O. GRONG, T.A. SIEWERT, T.A. MARTINS, AND D.L. OLSON, A MODEL FOR THE SILICON-MANGANESE DEOXIDATION OF STEEL WELD METAL, *METALL. TRANS. A*, VOL 17 (NO. 10), 1985, P 1797-1807
17. T.H. NORTH, THE DISTRIBUTION OF MANGANESE BETWEEN SLAG AND METAL DURING SUBMERGED ARC WELDING, *WELD. RES. ABROAD*, VOL 23 (NO. 1), 1977, P 2-40
18. T. BONISZEWSKI, BASIC FLUXES AND DEOXIDATION IN SUBMERGED ARC WELDING OF STEEL, *METAL. CONSTR. BRIT. WELD. J.*, VOL 6, 1974, P 128
19. L. DAVIS, *AN INTRODUCTION TO WELDING FLUXES FOR MILD AND LOW ALLOY STEELS*, WELDING INSTITUTE, 1981
20. *MAKING, SHAPING AND TREATING OF STEEL*, UNITED STATES STEEL CORPORATION, 1984
21. P.S. DUNN, C.A. NATALIE, AND D.L. OLSON, SOL-GEL FLUXES FOR FLUX CORED WELDING CONSUMABLES, *J. MATER. ENERGY SYSTEMS*, VOL 8 (NO. 2), 1986, P 176-184
22. L.I. SOROKIN AND Z.A. SIDLIN, THE EFFECT OF ALLOYING ELEMENTS AND OF MARBLE IN AN ELECTRODE COATING ON THE SUSCEPTIBILITY OF A DEPOSITED NICKEL CHROME METAL TO PORE FORMATION, *SVAR. PROIZVOD.*, NO. 11, 1974, P 7-9
23. S.S. TULIANI, T. BONISZEWSKI, AND N.F. EATON, NOTCH TOUGHNESS OF COMMERCIAL SUBMERGED ARC WELD METAL, *WELD. MET. FABR.*, VOL 37 (NO. 8), 1969, P 27
24. T.G.F. GRAY, J. SPENCE, AND T.H. NORTH, *RATIONAL WELDING DESIGN*, BUTTERWORTHS, 1975
25. D.L. OLSON, G.R. EDWARDS, AND S.K. MARYA, THE PHYSICAL AND CHEMICAL BEHAVIOR ASSOCIATED WITH SLAG DETACHABILITY DURING WELDING, *FERROUS ALLOY WELDMENTS*, VOL 67-70, TRANS TECH, 1992, P 253-268
26. *FUMES AND GASES IN THE WELDING ENVIRONMENT*, AWS, 1979

Shielding Gases for Welding

Kevin A. Lyttle, Praxair, Inc.

Introduction

THE SHIELDING GAS used in a welding process has a significant influence on the overall performance of the welding system. Its primary function is to protect the molten metal from atmospheric nitrogen and oxygen as the weld pool is being formed. The shielding gas also promotes a stable arc and uniform metal transfer. In gas-metal arc welding (GMAW) and flux-cored arc welding (FCAW), the gas used has a substantial influence on the form of metal transfer during welding. This, in turn, affects the efficiency, quality, and overall operator acceptance of the welding operation.

The shielding gas interacts with the base material and with the filler material, if any, to produce the basic strength, toughness, and corrosion resistance of the weld. It can also affect the weld bead shape and the penetration pattern.

Understanding the basic properties of a shielding gas will aid in the selection of the right shielding gas or gases for a welding application. Use of the best gas blend will improve the quality and may reduce the overall cost of the welding operation as well.

Shielding Gases for Welding

Kevin A. Lyttle, Praxair, Inc.

Basic Properties of a Shielding Gas

The "controlled electrical discharge" known as the welding arc is formed and sustained by the establishment of a conductive medium called the arc plasma. This plasma consists of ionized gas, molten metals, slags, vapors, and gaseous atoms and molecules. The formation and structure of the arc plasma is dependent on the properties of the shielding gases used for welding. Table 1 lists the basic properties of gases used for welding (Ref 1).

TABLE 1 PROPERTIES OF SHIELDING GASES USED FOR WELDING

GAS	CHEMICAL SYMBOL	MOLECULAR WEIGHT	SPECIFIC GRAVITY(A)	DENSITY		IONIZATION POTENTIAL	
				g/ft^3	g/l	aj(b)	eV
ARGON	AR	39.95	1.38	0.1114	1.784	2.52	15.7
CARBON DIOXIDE	CO_2	44.01	1.53	0.1235	1.978	2.26	14.4
HELIUM	HE	4.00	0.1368	0.0111	0.178	3.92	24.5
HYDROGEN	H_2	2.016	0.0695	0.0056	0.090	2.16	13.5
NITROGEN	N_2	28.01	0.967	0.782	12.5	2.32	14.5
OXYGEN	O_2	32.00	1.105	0.0892	1.43	2.11	13.2

Source: Ref 1

(A) AT 100 KPA (1 ATM) AND 0 °C (32 °F); AIR = 1.

(B) 10^{-18} J.

The ionization potential is the energy, expressed in electron volts, necessary to remove an electron from a gas atom--making it an ion, or an electrically charged gas atom. All other factors held constant, the value of the ionization potential decreases as the molecular weight of the gas increases. Arc starting and arc stability are greatly influenced by the ionization potentials of the component shielding gases used in welding process. A gas with a low ionization potential,

such as argon, can atoms into ions easily. Helium, with its significantly higher ionization potential, produces a harder to start, less stable arc.

Although other factors are involved in sustaining the plasma, the respective energy levels required to ionize these gases must be maintained; as a consequence, the arc voltage is directly influenced. For equivalent arc lengths and welding currents, the voltage obtained with helium is appreciably higher than is with argon. This translates into more available heat input to the base material with helium than with argon.

The thermal conductivity of a gas is a measure of how well it is able to conduct heat. It influences the radial heat loss from the center to the periphery of the arc column as well as heat transfer between the plasma and the liquid metal. Argon, which has a low thermal conductivity, produces an arc that has two zones: a narrow hot core and a considerably cooler outer zone. The penetration profile of the weld fusion area then exhibits a narrow "finger" at the root and a wider top. A gas with a high thermal conductivity conducts heat outward from the core; this results in a wider, hotter arc core. This type of heat distribution occurs with helium, argon-hydrogen, and argon-carbon dioxide blends; it gives a more even distribution of heat to the work surface and produces a wider fusion area.

Dissociation and Recombination. Shielding gases such as carbon dioxide, hydrogen, and oxygen are multiatom molecules. When heated to high temperatures within the arc plasma, these gases break down, or dissociate, into their component atoms. They are then at least partially ionized, producing free electrons and current flow. As the dissociated gas comes into contact with the relatively cool work surface, the atoms recombine and release heat at that point. This heat of recombination causes multiatomic gases to behave as if they have a higher thermal conductivity, similar to that of helium. Dissociation and recombination do not occur with gases, such as argon, that consist of a single atom. Thus, at the same arc temperature, the heat generated at the work surface can be considerably greater with gases such as carbon dioxide and hydrogen.

Reactivity/Oxidation Potential. The oxidizing nature of the shielding gas affects both welding performance and the properties of the resultant weld deposit. Argon and helium are completely nonreactive, or inert, and thus have no direct chemical affect on the weld metal. Oxidizing or active gases, such as CO_2 and oxygen, will react with elements in the filler metal or baseplate and will form a slag on the surface of the weld deposit. The loss of elements, such as manganese and silicon, from steel can affect the quality and cost of the weldment produced. Both weld strength and toughness generally decline as the oxidizing nature of the shielding gas increases.

Additions of reactive gases such as oxygen or carbon dioxide enhance the stability of the arc and affect the type of metal transfer obtained. Metal droplet size is decreased, and the number of droplets transferred per unit time increases as the level of oxygen in the shielding gas increases. Oxygen reduces the molten weld bead surface tension, promoting better bead wetting and higher welding travel speeds. Small additions of CO_2 work in a similar manner.

The surface tension between the molten metal and its surrounding atmosphere has a pronounced influence on bead shape. If the surface energy is high, a convex, irregular bead will result. Low values promote flatter beads with minimal susceptibility for undercutting.

Pure argon is generally associated with high interfacial energy, producing a sluggish weld puddle and high, crowned bead. The addition of a small amount of a reactive gas, such as oxygen, lowers this surface tension and promote fluidity and better wetting of the base material; it does this without creating excessive oxidation of the weld metal.

Gas Purity. Some metals, such as carbon steel and copper, have a relatively high tolerance for contaminants in the shielding gas; others, such as aluminum and magnesium, are fairly sensitive to particular contaminants. Still others, such as titanium and zirconium, have an extremely low tolerance for any foreign constituent in the shielding gas.

Depending on the metal being welded and the welding process used, very small quantities of gas impurities can significantly affect welding speed, weld surface appearance, weld bead solidification, and porosity levels. The effects of any given impurity are wide ranging, but weld quality and eventual fitness for purpose are major areas of concern.

There is always a possibility that the gas, as delivered, is contaminated; however, it is far more likely that impurities will enters somewhere between the supply and the end-use points. For this reason, property designed piping systems and high-quality hose are recommended for use with welding shielding gases. Typical industry minimum purity levels for welding gases are listed in Table 2 (Ref 2).

TABLE 2 TYPICAL GASES PURITY AND MOISTURE CONTENT OF SHIELDING

GAS	PRODUCT STATE	MINIMUM PURITY, %	MAXIMUM MOISTURE, PPM(A)	APPROXIMATE DEW POINT AT MAXIMUM MOISTURE CONTENT	
				°C	°F
ARGON	GAS	99.995	10	-60	-77
	LIQUID	99.997	6	-64	-83
CARBON DIOXIDE	GAS	99.5	19	-51	-60
	LIQUID	99.8	50	-58	-73
HELIUM	GAS	99.95	32	-51	-61
	LIQUID	99.995	3	-69	-92
HYDROGEN	GAS	99.95	8	-63	-80
	LIQUID	99.995	5	-65	-86
NITROGEN	GAS	99.7	32	-51	-61
	LIQUID	99.997	5	-65	-86
OXYGEN	INDUSTRIAL	99.5	50	-48	-54
	LIQUID	99.5	6	-64	-83

Source: Ref 2

(A) MOISTURE SPECIFICATIONS ARE MEASURED AT FULL CYLINDER PRESSURE, THE PRESSURE AT WHICH THE CYLINDER IS ANALYZED.

Gas density is the weight of the gas per unit volume. Density is one of the chief factors that influence shielding gas effectiveness. Basically, gases heavier than air, such as argon and carbon dioxide, require lower flow rates in use than do the lighter gases, such as helium, to ensure adequate protection of the weld puddle.

References cited in this section

1. N.E. LARSON AND W.F. MEREDITH, *SHIELDING GAS SELECTION MANUAL*, UNION CARBIDE INDUSTRIAL GASES TECHNOLOGY CORP., 1990, P 10
2. N.E. LARSON AND W.F. MEREDITH, *SHIELDING GAS SELECTION MANUAL*, UNION CARBIDE INDUSTRIAL GASES TECHNOLOGY CORP., 1990, P 11

Shielding Gases for Welding

Kevin A. Lyttle, Praxair, Inc.

Characteristics of the Components of a Shielding Gas Blend

To obtain a shielding gas that is suited to a specific application, a mix of gases is generally needed. Each basic gas contributes certain characteristics to the performance of the overall mix. Some gas blends have relatively specific areas of application and limited operating ranges; others can be used on many materials under a variety of welding conditions. Each component of the blend brings with it properties that are supplemented by the others to produce an enhanced level of performance.

Argon is inert or unreactive with respect to the materials present in the welding electrode. With its low ionization potential, argon promotes easy arc starting and stable arc operation. Its lower thermal conductivity promotes the development of axial "spray" transfer in certain forms of GMAW. It is also used in applications where base material distortion must be controlled or where good gap-bridging ability is required.

Helium. Unlike argon, helium is lighter than air and has a low density. Like argon, it is chemically inert and does not react with other elements or compounds. Because of its high thermal conductivity and high ionization potential, more heat is transferred to the base material, thus enhancing the penetration characteristics of the arc. In many applications, it also allows higher weld travel speeds to be obtained. Because of its higher cost, helium is frequently combined with argon or argon mixtures to enhance the overall performance of the blend while minimizing its cost.

Oxygen combines with almost all known elements except rare and inert gases; it vigorously support combustion. Small amounts of oxygen are added to some inert mixtures to improve the stability of the welding arc developed as well as to increase the fluidity of the weld puddle.

In the spray-transfer mode of GMAW, small additions of oxygen enhance the range over which this spatterless form of welding can be performed. The droplet size decreases and the number of drops transferred per unit time increases as oxygen is added to the blend.

Carbon dioxide is a reactive gas that is commonly used alone in certain types of GMAW. Oxidation of the base material and any filler electrode occurs readily. Carbon dioxide is added to argon blends to improve are stability, enhance penetration, and improve weld puddle flow characteristics. The higher thermal conductivity of carbon dioxide (because of the dissociation and recombination of its component parts) transfer more heat to the base material than does argon alone. A broader penetration pattern versus argon is obtained; however, base material distortion and lack of gap-bridging ability are possible problems.

Hydrogen is the lightest known element and is a flammable gas. Explosive mixtures can be formed when certain concentration of hydrogen are mixed with oxygen or air. It is added to inert gases to increase the heat input to the base material or for operations involving cutting and gouging. Because some materials are especially sensitive to hydrogen-related contamination, its use is generally limited to special applications, such as the joining of stainless steels, and to plasma are cutting and gouging.

Nitrogen is generally considered to be inert except at high temperatures. At arc welding temperatures, it will react with some metals (e.g., aluminum, magnesium, steel, and titanium), so it is not used as a primary shielding gas. It can be used with other gases for some welding applications (e.g., copper) and is also widely used in plasma cutting.

Shielding Gases for Welding

Kevin A. Lyttle, Praxair, Inc.

Shielding Gas Selection

In most welding applications, more than one shielding gas or gas blend can be used successfully. For example, there is no one optimal gas blend for joining carbon steels, but a considerable array of mixes are available depending on the specific requirements of the application. For some processes, such as gas-tungsten arc welding (GTAW) and plasma arc welding (PAW), the choices may be somewhat limited by the nature of the electrodes used and the materials being welded. However, for applications involving GMAW, a multitude of blends can be selected from when carbon steels are being joined. Determination of the best blend depends on a number of specific job-related needs.

Accuracy of Gas Blends

The accuracy with which gases are blended is a function of the way in which they are supplied. If the source of the gas is a high-pressure cylinder, the following generally applies:

1. ±10% RELATIVE, MINOR COMPONENT (REF 3)

2. ±0.5% ABSOLUTE FOR CONCENTRATIONS UP TO 5%; ±10% RELATIVE FOR CONCENTRATIONS BETWEEN 5 AND 50% (REF 4)

For example, the mix accuracy of an Ar-2O_2 blend would be Ar/1.8-2.2O_2 (method 1) or Ar/1.5-2.5O_2 (method 2). A blend of Ar-25CO_2 would yield Ar/22.5-27.5CO_2 by their method of calculation.

When gas cylinders are properly filled with the appropriate blend, the components of that mixture will not separate unless the temperature of the environment is reduced far below normal working temperatures. If the gases are supplied from a liquid source, such as a bulk tank, the accuracy of the blend is a function of the mixing equipment used, but most likely falls within the ±10% minor component range.

Shielding Gases for GMAW

By far, the largest number of gas blends have been developed for GMAW, especially for joining carbon steel. These can be roughly divided into four categories: pure gases, argon-oxygen mixes, argon/carbon dioxide mixes, and three-part gas blends composed of either argon, helium, oxygen, carbon dioxide, or hydrogen. Table 3 contains suggestions for shielding gas selection based on material type, thickness, and mode of metal transfer.

TABLE 3 RECOMMENDED SHIELDING GAS SELECTION FOR GMAW

MATERIAL	THICKNESS		TRANSFER MODE	RECOMMENDED SHIELDING GAS	ADVANTAGES AND LIMITATIONS
	MM	IN.			
CARBON STEEL	<2.0	<0.080	SHORT CIRCUITING	AR-25CO_2 AR-15CO_2 AR-8CO_2	GOOD PENETRATION AND DISTORTION CONTROL TO REDUCE POTENTIAL BURNTHROUGH
	2.0-3.2	0.080-0.125	SHORT CIRCUITING	AR-8CO_2 AR-15CO_2 AR-25CO_2	HIGHER DEPOSITION RATES WITHOUT BURNTHROUGH: MINIMUM DISTORTION AND SPATTER; GOOD PUDDLE CONTROL FOR OUT-OF-POSITION WELDING
	>3.2	>0.125	SHORT CIRCUITING	AR-15CO_2 AR-25CO_2 CO_2	HIGH WELDING SPEEDS, GOOD PENETRATION AND PUDDLE CONTROL; APPLICABLE LOT OUT-OF-POSITION WELDS
			GLOBULAR	AR-25CO_2 CO_2	SUITABLE FOR HIGH-CURRENT AND HIGH-SPEED WELDING; DEEP PENETRATION AND FAST TRAVEL SPEEDS, BUT WITH GREATER BURNTHROUGH POTENTIAL
			CONVENTIONAL SPRAY ARC	AR-1O_2 AR-2O_2 AR-5CO_2	GOOD ARC STABILITY; PRODUCES A MORE FLUID PUDDLE AS O_2

				AR-8CO_2 AR-10CO_2 AR-15CO_2 AR-CO_2-O_2 BLENDS	INCREASES; GOOD COALESCENCE AND BEAD CONTOUR, GOOD WELD APPEARANCE AND PUDDLE CONTROL
			PULSED SPRAY	ARGON-5CO_2 AR-HE-CO_2 BLENDS AR-CO_2-O_2 BLENDS	USED FOR BOTH GAGE AND OUT-OF-POSITION WELDMENTS; ACHIEVES GOOD PULSED SPRAY STABILITY OVER A WIDE RANGE OF ARC CHARACTERISTICS AND DEPOSITION RANGES
ALLOY STEEL	ALL SIZES		SHORT CIRCUITING	AR-8CO_2 AR-15CO_2 AR-CO_2-O_2 BLEND	HIGH WELDING SPEEDS; GOOD PENETRATION AND PUDDLE CONTROL; APPLICABLE FOR OUT-OF-POSITION WELDS; SUITABLE FOR HIGH-CURRENT AND HIGH-SPEED WELDING
			SPRAY ARC (HIGH-CURRENT DENSITY AND ROTATIONAL)	AR-2O_2 AR-5O_2 AR-CO_2-O_2 BLENDS AR-HE-CO_2 BLENDS	REDUCES UNDERCUTTING; HIGHER DEPOSITION RATES AND IMPROVED BEAD WETTING; DEEP PENETRATION AND GOOD MECHANICAL PROPERTIES
			PULSED SPRAY	AR-5CO_2 AR-8CO_2 AR-2O_2	USED FOR BOTH LIGHT-GAGE AND HEAVY OUT-OF-POSITION WELDMENTS; ACHIEVES GOOD PULSED SPRAY STABILITY OVER A WIDE RANGE OF ARC CHARACTERISTICS AND DEPOSITION RANGES
STAINLESS STEEL, COPPER, NICKEL, AND CU-NI ALLOYS	ALL SIZES		SHORT-CIRCUITING TRANSFER	AR-HE-CO_2 BLENDS HE-AR-CO_2 BLENDS AR-1O_2 AR-2O_2	LOW CO_2 CONTENTS IN HELIUM MIX MINIMIZE CARBON PICKUP, WHICH CAN CAUSE INTERGRANULAR CORROSION WITH SOME ALLOYS; HELIUM IMPROVES WETTING ACTION; CO_2 CONTENTS >5% SHOULD BE USED WITH CAUTION ON

					SOME ALLOYS; APPLICABLE FOR ALL POSITION WELDING
			SPRAY ARC	AR-HE-CO_2 BLENDS AR-1O_2 AR-2O_2	GOOD ARC STABILITY; PRODUCES A FLUID BUT CONTROLLABLE WELD PUDDLE; GOOD COALESCENCE AND BEAD CONTOUR; MINIMIZES UNDERCUTTING ON HEAVIER THICKNESSES
			PULSED SPRAY	AR-HE-CO_2BLENDS AR-1O_2 AR-2O_2	USED FOR BOTH LIGHT-GAGE AND HEAVY OUT-OF-POSITION WELDMENTS; ACHIEVES GOOD PULSED SPRAY STABILITY OVER A WIDE RANGE OF ARC CHARACTERISTICS AND DEPOSITION RANGES
ALUMINUM, TITANIUM, AND OTHER REACTIVE METALS	≤ 13	$\leq \frac{1}{2}$	SPRAY ARC	ARGON	BEST METAL TRANSFER, ARC STABILITY, AND PLATE CLEANING; LITTLE OR NO SPATTER; REMOVES OXIDES WHEN USED WITH DCEP (REVERSE POLARITY)
			SPRAY ARC	75HE-25AR 50HE-50AR	HIGH HEAT INPUT; PRODUCES FLUID PUDDLE, FLAT BEAD CONTOUR, AND DEEP PENETRATION; MINIMIZES POROSITY
	>13	$> \frac{1}{2}$	SPRAY ARC	HELIUM 50HE-25AR	HIGH HEAT INPUT; GOOD FOR MECHANIZED WELDING AND OVERHEAD; APPLICABLE TO HEAVY SECTION WELDING
			PULSED SPRAY	ARGON	GOOD WETTING; GOOD PUDDLE CONTROL

Argon. Pure argon is generally used on nonferrous base metal, such as aluminum, nickel, copper, and magnesium alloys, and on reactive metals, such as titanium. Argon provides excellent arc stability, penetration, and bead profile when joining these materials. Its low ionization potential results in easy arc starting. Argon produces a constricted arc column with high current density, which concentrates the arc energy over a small area; deep, fingerlike penetration results.

Carbon Dioxide. A reactive gas, carbon dioxide is generally used only for joining carbon steel. It is readily available and relatively inexpensive. Because CO_2 will not support spray transfer, deposition efficiency is lower and spatter and fume

levels are higher than with argon blends. Weld bead surfaces are more oxidized and irregular in shape. The higher ionization potential of CO_2 and its characteristic dissociation upon heating provide greater weld fusion and penetration while still achieving acceptable mechanical properties.

Helium. Because of its higher thermal conductivity, helium can provide additional heat input to the base material while still maintaining an inert atmosphere. Wetting action, depth of fusion, and travel speed can be improved over comparable argon levels. This advantage is most frequently utilized in the welding of heavier sections of aluminum, magnesium, and copper alloys.

Argon-Oxygen. The addition of a small amount of oxygen to a argon greatly stabilizes the welding arc, increases the filler metal droplet rate, lowers the spray transition current, and influences bead shape. The weld pool is more fluid and stays molten longer, allowing the metal to flow out toward the edges of the weld (Fig. 1a).

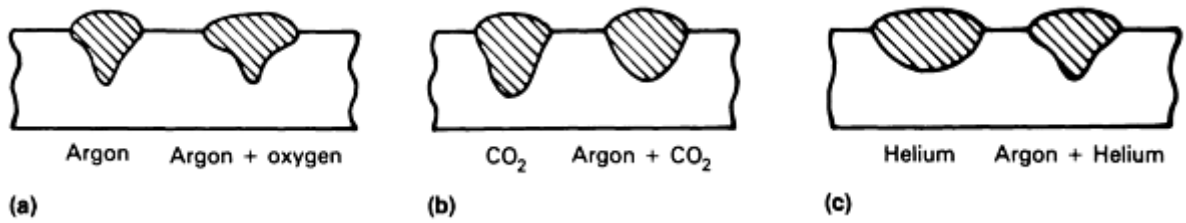

FIG. 1 EFFECT OF SHIELDING GAS BLENDS ON WELD PROFILE USING DIRECT CURRENT ELECTRODE POSITIVE (DCEP). (A) ARGON VERSUS ARGON-OXYGEN. (B) CARBON DIOXIDE VERSUS ARGON/CARBON DIOXIDE. (C) HELIUM VERSUS ARGON-HELIUM. SOURCE: REF 5

The most common blends contain 1, 2, 5, or 8% O_2 in argon. Increasing oxygen improves arc stability and makes higher travel speeds possible by enhanced puddle fluidity. Some increased alloy loss and a greater chance of undercut occur as the oxygen level is increased, especially beyond 5%.

Argon/carbon dioxide blends are primarily used for carbon and low-alloy steels and have limited use for stainless steels. The addition of CO_2 to argon produces results similar to the addition of oxygen, but is also broadens the penetration pattern as the CO_2 content is increased (Fig. 1b). Above a range of 18 to 20% CO_2, spraylike transfer can no longer be obtained; short-circuiting/globular transfer with somewhat increased spatter levels is found from this point up to approximately 50% CO_2 in argon.

The most common blends for spray transfer are argon plus 5, 8, 10, or 13 to 18% CO_2. With increased CO_2 content, the more fluid weld puddle permits higher weld travel speeds.

Mixes with higher carbon dioxide levels can also be used for short-circuiting transfer--commonly, argon plus 20 or 25% CO_2. Mixtures in this range provide an optimum droplet frequency for minimum spatter when small-diameter (0.9 and 1.2 mm, or 0.035 and 0.045 in.) wire is used.

Argon-Helium. Helium is often mixed with argon to obtain the advantages of both gases. These blends are primarily used for nonferrous base materials, such as aluminum, copper, and nickel alloys. Helium increases the heat input to the base material and thus is used for joining thick, thermally conductive plates. As the helium percentage increases, the arc voltage, spatter, and weld width-to-depth ratio increase (Fig. 1c).

The most common blends contain 25, 50, or 75% He in argon. The highest percentage of helium is used for joining thick (>50 mm, or 2 in.) plate material, especially aluminum and copper. Higher travel speeds can be obtained using helium-enhanced blends.

Argon/Oxygen/Carbon Dioxide. Mixtures containing three gas components are versatile because of their ability to operate in short-circuiting, globular, and spray-transfer modes. These blends are generally proprietary, and manufacturers' recommendations should be followed for their proper use. Blends of argon, carbon dioxide, and oxygen are generally used to join carbon and alloy steels.

Argon/Helium/Carbon Dioxide. Helium and carbon dioxide additions to argon increase the heat input to the base metal, which improves wetting, puddle fluidity, and weld bead profile. With helium plus CO_2 additions less than 40%, good spray transfer is obtained for carbon and low-alloy steel welding. Some increase in tolerance of base material surface contamination is also noted.

When the helium content exceeds 50 to 60%, transfer is restricted to short-circuiting and globular. Blends in which the CO_2 content is relatively low ($\leq 5\%$) are generally used for the joining of stainless steels without any loss in corrosion resistance.

Argon/Carbon Dioxide/Hydrogen. Three-part blends of this design are intended for the joining of austenitic stainless in the spray or short-circuiting transfer modes. Because of the addition of hydrogen, these blends should not be used for carbon steel. The carbon dioxide and hydrogen increase the heat input to the base material and improve bead shape characteristics, as well as promote higher welding travel speeds.

Shielding Gas Selection for FCAW

Carbon Dioxide. The majority of large-diameter (>1.6 mm, or $\frac{1}{16}$ in.) wires that use a shielding gas use carbon dioxide. Some smaller diameter wires are formulated to operate in 100% CO_2. The arcs are generally stable and provide a globular transfer over the usable operating range. Good performance over rust and mill scale on the plate surface is obtained with these large-diameter wires and CO_2 shielding.

Argon/Carbon Dioxide. A significant number of small-diameter (≤ 1.6 mm, or $\frac{1}{16}$ in.) cored wires are shielded with the blends of argon with 15 to 50% CO_2. These blends provide better out-of-position weld puddle control versus that of CO_2. To obtain the best performance from a particular cored wire, check the manufacturer's product literature for the recommended gas blend.

Shielding Gas Selection for GTAW

Argon. The most commonly used gas for GTAW, argon exhibits low thermal conductivity, which produces a narrow, constricted arc column; this allows greater variations in arc length with minimal influence on arc power or weld bead shape. Its low ionization potential provides good arc starting characteristics and good arc stability using the direct current electrode negative (DCEN) power connection plus superior arc cleaning action and bead appearance when ac power is used. Argon is the most commonly selected gas for DCEN welding of most materials and ac manual welding of aluminum.

Helium. The high thermal conductivity and ionization potential of helium make it suitable for the high-current joining of heavy sections of heat-conductive materials such as aluminum. Helium increases the penetration of the weld as well as its width. It also allows the use of higher weld travel speeds.

Argon-Helium. Blends of argon and helium are selected to increase the heat input to the base material while maintaining favorable arc stability and superior arc starting characteristics. Blends of 25, 50, and 75% He in argon are commonly used.

Argon-Hydrogen. Hydrogen is added to argon to enhance its thermal properties. The slightly reducing atmosphere improves weld puddle wetting and reduces some surface oxides to produce a cleaner weld surface. To minimize problems associated with arc starting, additions of hydrogen are generally limited to 5 to 15%. These blends are primarily used to join some stainless steels, nickel, and nickel alloys. These mixtures should not be used to join alloy steels; delayed weld cracking may result.

Argon/2-5H_2 is used in manual welding applications on materials thicker than 1.6 mm ($\frac{1}{16}$ in.). Additions of 10 to 15% H_2 are used in mechanized applications, such as those found in the manufacture of stainless steel tubing.

Caution: Special safety precautions are required when mixing argon and hydrogen. Do not attempt to mix argon and hydrogen from separate cylinders. Always purchase ready-mixed hydrogen blends from a qualified supplier.

Shielding Gas Selection for PAW

The physical configuration of the PAW system requires the use of two gases: a "plasma" or orifice gas and a shielding gas. The primary role of the plasma gas, which exits the torch through the center orifice, is to control arc characteristics and shield the electrode. The shielding gas, introduced around the periphery of the arc, shields or protects the weld area. In many applications, the shielding gas is also partially ionized to enhance the performance of the plasma gas.

Low-Current (<100 A) PAW. Argon is the preferred plasma gas for low-current PAW because of its low ionization potential, which ensures easy and reliable arc starting. Argon-hellium mixtures are used for some applications requiring higher heat inputs. The choice of the shielding gas depends on the type and thickness of the base material. Recommendations can be found in Table 4.

TABLE 4 RECOMMENDED GUIDELINES FOR SELECTING PAW SHIELDING GASES

MATERIAL	THICKNESS		MODE OF PENETRATION	
	MM	IN.	KEYHOLE TECHNIQUE[C]	MELT-IN TECHNIQUE[D]
LOW-CURRENT PAW[A]				
ALUMINUM COPPER	<1.6	$<\frac{1}{16}$	NOT RECOMMENDED	ARGON HELIUM
	[GES]1.6	[GES] $\frac{1}{16}$	HELIUM	HELIUM
CARBON STEEL	<1.6	$<\frac{1}{16}$	NOT RECOMMENDED	ARGON HELIUM 75AR-25HE
	[GES]1.6	[GES] $\frac{1}{16}$	ARGON 75HE-25AR	ARGON 75HE-25AR
LOW-ALLOY STEEL	<1.6	$<\frac{1}{16}$	NOT RECOMMENDED	ARGON HELIUM AR-1.5H_2
	[GES]1.6	[GES] $\frac{1}{16}$	ARGON 75HE-25AR AR-1.5H_2	ARGON HELIUM AR-1.5H_2
STAINLESS STEEL, NICKEL ALLOYS	<1.6	$<\frac{1}{16}$	ARGON 75HE-25AR AR-1.5H_2	ARGON HELIUM AR-1.5H_2
	[GES]1.6	[GES] $\frac{1}{16}$	ARGON 75HE-25AR AR-1.5H_2	ARGON HELIUM AR-1.5H_2
HIGH-CURRENT PAW[B]				
ALUMINUM	<6.4	$<\frac{1}{4}$	ARGON	ARGON 75-25AR
	[GES]6.4	[GES] $\frac{1}{4}$	HELIUM	HELIUM 75-25AR
COPPER	<2.4	$<\frac{3}{32}$	NOT RECOMMENDED	HELIUM
CARBON STEEL; LOW-ALLOY STEEL	<3.2	$<\frac{1}{8}$	ARGON	ARGON
	[GES]3.2	[GES]	ARGON	75HE-25AR

		$\frac{1}{8}$		
STAINLESS STEEL; NICKEL ALLOYS	<3.2	$<\frac{1}{8}$	ARGON AR-5H_2	ARGON
	[GES]3.2	[GES] $\frac{1}{8}$	ARGON AR-5H_2	75-HE-25AR

Source: Ref 6, 7

(A) GAS SELECTIONS SHOWN ARE FOR SHIELDING GAS ONLY. ORIFICE GAS IN ALL CASES IS ARGON.

(B) GAS SELECTIONS SHOWN ARE FOR BOTH THE ORIFICE AND SHIELDING GAS.

(C) PROPERLY BALANCED GAS FLOW RATES PRODUCE COMPLETE JOINT PENETRATION BY FORMING A SMALL WELD POOL WITH A HOLE PENETRATING COMPLETELY THROUGH THE BASE METAL. AS THE PLASMA TORCH IS MOVED, METAL MELTED BY THE ARC IS FORCED TO FLOW AROUND THE PLASMA STEAM PRODUCING THE "KEYHOLE" TO THE REAR WHERE THE WELD POOL IS FORMED AND SOLIDIFIED.

(D) CONVENTIONAL FUSION WELDING SIMILAR TO THAT DONE WITH GTAW.

High-Current ([ges]100 A) PAW. The choice of gas used for high-current PAW also depends on the material to be welded. In almost all cases, the shielding gas is the same as the orifice gas. Again, argon is suitable for welding all metals, but it does not necessarily produce optimum results. Depending on the welding mode used (keyhole or melt-in), the optimum gas blend will vary. Table 4 lists gases recommended on the basis of materials joined.

References cited in this section

3. "SPECIFICATION FOR SHIELDING GASES," AWS A5.32-9X, JULY 1991 (DRAFT)
4. "GASES FOR GAS-SHIELDED ARC WELDING AND CUTTING," EUROPEAN STANDARD EN 439, DEC 1990 (DRAFT)
5. H.B. CARY, *MODERN WELDING TECHNOLOGY*, 2ND ED., PRENTICE-HALL, 1989
6. N.E. LARSON AND W.F. MEREDITH, *SHIELDING GAS SELECTION MANUAL*, UNION CARBIDE INDUSTRIAL GASES TECHNOLOGY CORP., 1990, P 30-32
7. N.E. LARSON AND W.F. MEREDITH, *SHIELDING GAS SELECTION MANUAL*, UNION CARBIDE INDUSTRIAL GASES TECHNOLOGY CORP., 1990, P 18-19

Shielding Gases for Welding

Kevin A. Lyttle, Praxair, Inc.

Influence of Shielding Gas on Weld Mechanical Properties

The mechanical properties of a weld are dependent on specific characteristics of the shielding gas. When the gas blend is totally inert, the effects are less pronounced and are derived more indirectly. In this case, the shielding gas affects penetration and solidification, which can influence the microstructure of the resulting weld.

When the shielding gas contains active components, such as oxygen or carbon dioxide, the influence is direct and more substantial. The oxygen potential of the shielding gas influences the amount of surface slag, the fume emission rate, the fluidity of the weld puddle, and the mechanical properties (both strength and toughness) of the weld metal. A number of empirical formulas have been developed to estimate the oxygen potential of a gas blend (Ref 8); the differences lie in their treatment of the CO_2 component of the gas mix. Because parameters other than gas composition can affect the

oxygen level of the weld metal (e.g., welding speed), most of the recently developed formulas are also welding parameter and material specific. Their importance centers on how the oxidation potential is linked to elemental loss of silicon and manganese in the weld metal, to weld metal oxygen content, and to weld mechanical properties.

Because a relatively complex relationship exists between the loss of alloying elements, the composition of the shielding gas, and the mechanical properties of the resulting weld metal it is difficult to select an optimum gas blend that will work well with all types of wires. This influence is most noticeable in the gas metal-arc welding of carbon steel. Figure 2 (Ref 8) and Table 5 (Ref 9) illustrate the effect of the shielding gas on impact strength and tensile strength. In general, as the oxidation potential of the shielding gas increases, the toughness and the tensile strength of the weld deposit decrease. Because of their lower oxidizing gas content, argon blends will generally produce weld properties superior to those obtained by shielding with CO_2 only. There appears to be an "optimum" oxygen content, as too low an oxygen level can also be detrimental to toughness.

TABLE 5 EFFECT OF SHIELDING GAS ON CARBON, MANGANESE, AND SILICON LOSSES AND ON WELD STRENGTH VALUES

SHIELDING GAS[A]	ULTIMATE TENSILE STRENGTH		YIELD STRENGTH		ELONGATION, %	WELD METAL COMPOSITION, %[B]		
	MPA	KSI	MPA	KSI		C	MN	SI
AR-10CO_2	640	92.9	544	79.0	25.7	0.09	1.43	0.72
AR-18CO_2	620	90.0	522	75.8	26.8	0.09	1.37	0.70
AR-5CO_2-4O_2	610	88.5	472	68.5	28.1	0.08	1.32	0.67
AR-25CO_2	601	87.2	505	73.3	29.3	0.09	1.30	0.65
AR-12O_2	591	85.8	510	74.0	27.5	0.06	1.20	0.60
CO_2	594	86.2	487	70.7	27.8	0.10	1.21	0.62

Source: Ref 9

(A) GASES LISTED IN ORDER OF INCREASING OXIDATION POTENTIAL.

(B) BASE WIRE COMPOSITION: 0.115% C, 1.53% MN, 0.98% SI.

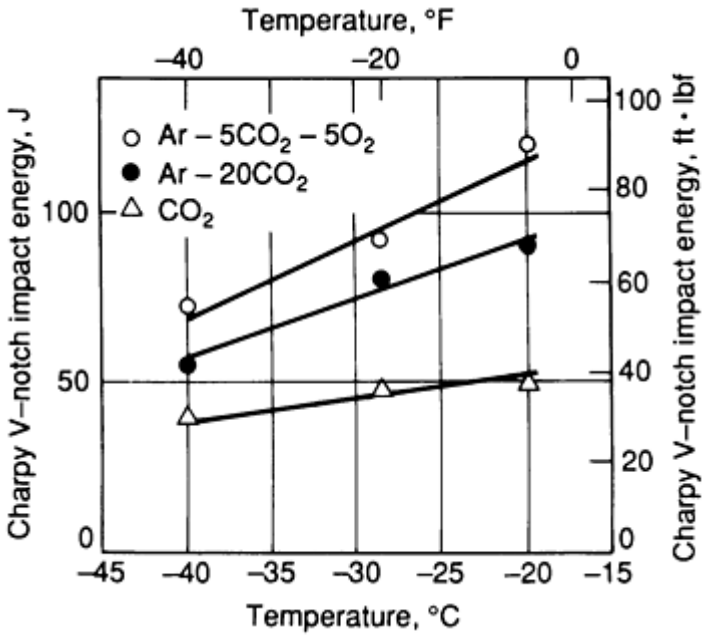

FIG. 2 PLOT OF WELD METAL IMPACT ENERGY VERSUS TEST TEMPERATURE AS A FUNCTION OF SHIELDING GAS COMPOSITION. SOURCE: REF 8

References cited in this section

8. N. STENBACKA AND K.A. PERSSON, SHIELDING GASES FOR GAS METAL ARC WELDING, *WELD.J.*, VOL 68, NOV 1989, P 41-47
9. H.U. POMASKA, "SHIELDING GASES FOR ARC WELDING AND CUTTING," SONDERDRUCK 48, LINDE AG, LINDE TECHNISCHE GASES, HOLRIEGELSKREUTH, GERMANY

Shielding Gases for Welding

Kevin A. Lyttle, Praxair, Inc.

Shielding Gas and Fume Generation

The shielding gas used in solid and flux-cored wire welding affects the rate at which fumes are produced during welding, as well as the composition of the fumes. The type of shielding gas also affects the composition of the pollutant gases in the welding area. The fumes and gases generated in some welding applications impact on health and safety; therefore, it is important for the user to review the Material Safety Data Sheets and precautionary labeling provided by the manufacturers and suppliers of welding consumables. Welding safety and health information can be also be found in this Handbook and in ANSI Z49.1, "Safety in Welding and Cutting."

Fume generation rates are generally highest when CO_2 shielding is used. Inert gas blends containing CO_2 produce higher fume levels than those containing only oxygen additions. For solid wire welding at the same weld metal deposition rate, argon blends typically generate significantly less fumes than when CO_2 only is used (Ref 10, 11, 12). Figure 3 (Ref 13) illustrates the dependence of the fume generation rate on shielding gas composition as a function of current level in GMAW. Similar trends can be seen when using gas-shielded flux-cored wires.

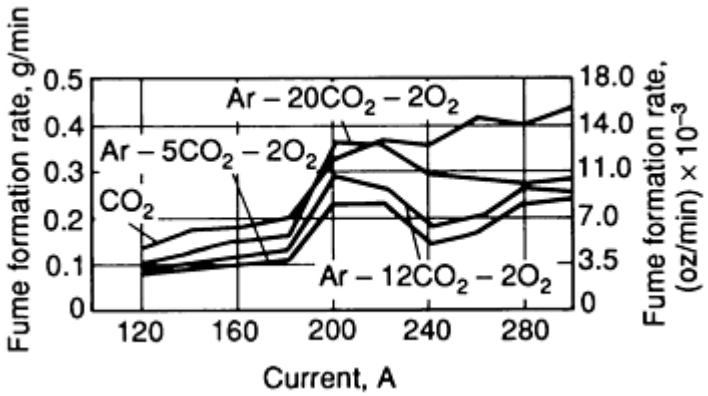

FIG. 3 PLOT OF FUME FORMATION RATE VERSUS CURRENT FOR MILD STEEL SOLID WIRE USING SELECTED SHIELDING GASES. SOURCE: REF 13

Pollutant gases must be considered when arc welding. The gases of greatest interest arc carbon monoxide, ozone, and nitrogen oxides. When CO_2 is used for shielding in confined spaces, CO can be a potential problem. Ozone can be a concern when high-energy gas-shielded welding is conducted, particularly on aluminum and stainless steel plate. It is produced in the immediate arc area as well as in the surrounding environment. Oxides of nitrogen can be present in some plasma welding and cutting applications (Ref 14).

References cited in this section

10. R.F. HEILE AND D.C. HILL, PARTICULATE FUME GENERATION IN ARC WELDING PROCESSES, *WELD.J.*, VOL 54, JULY 1975, P 201S-210S
11. H. PRESS AND W. FLORIAN, CONTRIBUTION ON THE FORMATION OF TOXIC SUBSTANCES IN GAS SHIELDED ARC WELDING AND DETERMINATION OF DESIRED EXHAUSTION CAPACITY, *IIW PROCEEDINGS OF COLLOQUIUM ON WELDING AND HEALTH*, PORTUGAL, JULY 1980
12. B. HAAS, INFLUENCE OF PROCESS SPECIFIC WELDING PARAMETERS IN FUME GENERATION IN SOLID WIRE, GMA/MAG WELDING, *IIW PROCEEDINGS OF COLLOQUIUM ON WELDING SAFETY AND HEALTH*, PORTUGAL, JULY 1980
13. D.E. HILTON AND P.N. PLUMRIDGE, PARTICULATE FUME GENERATION DURING GMAW AND GTAW, *WELD. MET. FABR.*, VOL 59 (NO. 10), DEC 1991, P 555-560
14. N. JENKINS, J. MORETON, P.J. OAKLEY, AND S.M. STEVENS, *WELDING FUMES SOURCES, CHARACTERISTICS, CONTROL*, VOL 2, THE WELDING INSTITUTE, CAMBRIDGE, UNITED KINGDOM, 1981, P 272

Shielding Gases for Welding

Kevin A. Lyttle, Praxair, Inc.

Self-Shielded Flux-Cored Arc Welding

The self-shielded flux-cored wire welding process employs a continuous wire electrode that requires no external shielding. These cored wires generate protective shielding gases from components in the core material similar to those found in coated electrodes. The unique feature of this class of consumables is that they rely only partly on the exclusion of air from the molten electrode and weld pool to produce a quality deposit. In addition to deoxidizers, they contain denitriders to react with nitrogen that may be entrained in the molten metal. The less a given consumable relies on shielding and the more it relies on "killing" to control nitrogen and produce sound weld metal, the less that consumable will be affected by cross air currents and side winds.

Through careful control of welding parameters and the proper balance of core constituents, good-quality weld metal can be obtained under poor welding conditions. Self-shielded flux-cored wires are especially suited to welding outdoors, where it is difficult to provide acceptable external gas shielding. Both light- and heavy-gage materials have been successfully joined with these electrodes.

Shielding Gases for Welding

Kevin A. Lyttle, Praxair, Inc.

References

1. N.E. LARSON AND W.F. MEREDITH, *SHIELDING GAS SELECTION MANUAL*, UNION CARBIDE INDUSTRIAL GASES TECHNOLOGY CORP., 1990, P 10
2. N.E. LARSON AND W.F. MEREDITH, *SHIELDING GAS SELECTION MANUAL*, UNION CARBIDE INDUSTRIAL GASES TECHNOLOGY CORP., 1990, P 11
3. "SPECIFICATION FOR SHIELDING GASES," AWS A5.32-9X, JULY 1991 (DRAFT)
4. "GASES FOR GAS-SHIELDED ARC WELDING AND CUTTING," EUROPEAN STANDARD EN 439, DEC 1990 (DRAFT)

5. H.B. CARY, *MODERN WELDING TECHNOLOGY*, 2ND ED., PRENTICE-HALL, 1989
6. N.E. LARSON AND W.F. MEREDITH, *SHIELDING GAS SELECTION MANUAL*, UNION CARBIDE INDUSTRIAL GASES TECHNOLOGY CORP., 1990, P 30-32
7. N.E. LARSON AND W.F. MEREDITH, *SHIELDING GAS SELECTION MANUAL*, UNION CARBIDE INDUSTRIAL GASES TECHNOLOGY CORP., 1990, P 18-19
8. N. STENBACKA AND K.A. PERSSON, SHIELDING GASES FOR GAS METAL ARC WELDING, *WELD.J.*, VOL 68, NOV 1989, P 41-47
9. H.U. POMASKA, "SHIELDING GASES FOR ARC WELDING AND CUTTING," SONDERDRUCK 48, LINDE AG, LINDE TECHNISCHE GASES, HOLRIEGELSKREUTH, GERMANY
10. R.F. HEILE AND D.C. HILL, PARTICULATE FUME GENERATION IN ARC WELDING PROCESSES, *WELD.J.*, VOL 54, JULY 1975, P 201S-210S
11. H. PRESS AND W. FLORIAN, CONTRIBUTION ON THE FORMATION OF TOXIC SUBSTANCES IN GAS SHIELDED ARC WELDING AND DETERMINATION OF DESIRED EXHAUSTION CAPACITY, *IIW PROCEEDINGS OF COLLOQUIUM ON WELDING AND HEALTH*, PORTUGAL, JULY 1980
12. B. HAAS, INFLUENCE OF PROCESS SPECIFIC WELDING PARAMETERS IN FUME GENERATION IN SOLID WIRE, GMA/MAG WELDING, *IIW PROCEEDINGS OF COLLOQUIUM ON WELDING SAFETY AND HEALTH*, PORTUGAL, JULY 1980
13. D.E. HILTON AND P.N. PLUMRIDGE, PARTICULATE FUME GENERATION DURING GMAW AND GTAW, *WELD. MET. FABR.*, VOL 59 (NO. 10), DEC 1991, P 555-560
14. N. JENKINS, J. MORETON, P.J. OAKLEY, AND S.M. STEVENS, *WELDING FUMES SOURCES, CHARACTERISTICS, CONTROL*, VOL 2, THE WELDING INSTITUTE, CAMBRIDGE, UNITED KINGDOM, 1981, P 272

Solid-State Transformations in Weldments

P. Ravi Vishnu, Luleå University of Technology, Sweden

Introduction

SOLID-STATE TRANSFORMATIONS occurring in a weld are highly nonequilibrium in nature and differ distinctly from those experienced during casting, thermomechanical processing, and heat treatment. This discussion will primarily focus on the welding metallurgy of fusion welding of steels and attempt to highlight the fundamental principles that form the basis of many of the recent developments in steels and consumables for welding. Accordingly, examples are largely drawn from the well-known and relatively well-studied case of ferritic steel weldments to illustrate the special physical metallurgical considerations brought about by the weld thermal cycles and by the welding environment. Because of space limitations, only a very brief discussion is included on welds in other alloy systems such as stainless steels and aluminum-base, nickel-base, and titanium-base alloys. For detailed information on how the principles explained in the first part of this article (using steel weldments as an example) are applicable to other materials, the reader is referred to the Sections where individual alloy systems are discussed (see "Selection of Stainless Steels," "Selection of Nonferrous Low-Temperature Materials," "Selection of Nonferrous High-Temperature Materials," and "Selection of Nonferrous Corrosion-Resistant Materials" in this Volume).

A concise method of describing the transformation behavior of a steel is by a continuous cooling transformation (CCT) diagram (Fig. 1). However, a conventional CCT diagram such as the one shown in Fig. 1 cannot be used to accurately describe the transformation behavior in a weldment of the same material because weld thermal cycles are very different from those used for generating conventional CCT diagrams.

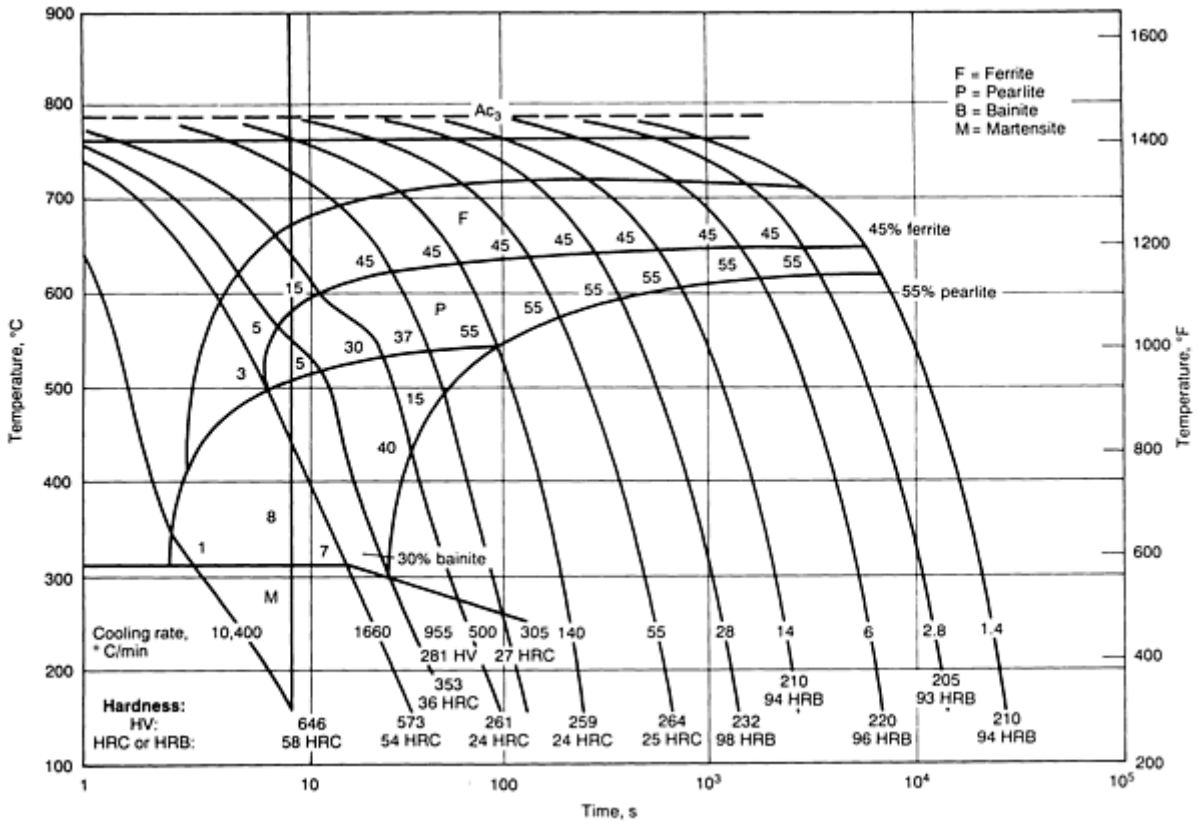

FIG. 1 CONVENTIONAL CCT DIAGRAM FOR AISI 1541 (0.39C-1.56MN-0.21SI-0.24S-0.010P) PLAIN CARBON STEEL WITH ASTM NUMBER 8 GRAIN SIZE AND AUSTENITIZATION AT 980 °C (1800 °F). FOR EACH OF THE COOLING CURVES IN THE PLOT (GIVEN IN TERMS OF °C/MIN), THE TRANSFORMATION START AND END TEMPERATURES GIVEN BY THE CCT CURVES, THE AMOUNT OF EACH TRANSFORMATION PRODUCT, AND THE HARDNESS OF THE FINAL STRUCTURE ARE SHOWN. AC_3, 788 °C (1450 °F); AC_1, 716 °C (1321 °F). F, FERRITE; P, PEARLITE; B, BAINITE; M, MARTENSITE. SOURCE: REF 1

Acknowledgements

The author would like to convey his immense gratitude to the late Professor K. Easterling, University of Exeter, U.K., for giving him the opportunity to write this article and for his constant support and encouragement. The author thanks Dr. Bengt Loberg and Professor Richard Warren of the Department of Engineering Materials, University of Luleå, for their active encouragement. The author would also like to thank Dr. H.K.D.H. Bhadeshia, University of Cambridge, U.K., and Dr. K. Sampath, Concurrent Technologies Corporation, Johnstown, PA, for valuable technical consultation.

Reference

1. *ATLAS OF ISOTHERMAL TRANSFORMATION AND COOLING TRANSFORMATION DIAGRAMS* AMERICAN SOCIETY FOR METALS, 1977

P. Ravi Vishnu, Luleå University of Technology, Sweden

Special Factors Affecting Transformation Behavior in a Weldment

Several aspects of the weld thermal cycle and weld segregation should be considered because of their effect on the transformation upon cooling:

- PEAK TEMPERATURES REACHED IN THE HEAT-AFFECTED ZONE (HAZ) CAN BE VERY MUCH HIGHER THAN THE AC_3 TEMPERATURE (THAT IS, THE TEMPERATURE AT WHICH TRANSFORMATION OF FERRITE TO AUSTENITE IS COMPLETED DURING HEATING). THE HEATING RATES ARE VERY HIGH, AND THE TIMES SPENT AT HIGH TEMPERATURE ARE ONLY OF THE ORDER OF A FEW SECONDS.
- THE TEMPERATURE GRADIENT IN THE HAZ IS VERY STEEP, AND THIS COMPLICATES THE PROBLEM OF STUDYING IN *IN SITU* TRANSFORMATIONS IN THE HAZ DURING WELDING (REF 2).
- DURING SOLIDIFICATION OF THE WELD METAL, ALLOYING AND IMPURITY ELEMENTS TEND TO SEGREGATE EXTENSIVELY TO THE INTERDENDRITIC OR INTERCELLULAR REGIONS UNDER THE CONDITIONS OF RAPID COOLING. ALSO, THE PICKUP OF ELEMENTS LIKE OXYGEN BY THE MOLTEN WELD POOL LEADS TO THE ENTRAPMENT OF OXIDE INCLUSIONS IN THE SOLIDIFIED WELD. THESE INCLUSIONS THEN SERVE AS HETEROGENEOUS NUCLEATION SITES AND CAN SUBSTANTIALLY INFLUENCE THE KINETICS OF SUBSEQUENT SOLID STATE TRANSFORMATIONS. ACCORDINGLY, THE WELD METAL TRANSFORMATION BEHAVIOR IS QUITE DIFFERENT FROM THAT OF THE BASE METAL, EVEN THOUGH THE NOMINAL CHEMICAL COMPOSITION HAS NOT BEEN SIGNIFICANTLY CHANGED BY THE WELDING PROCESS (REF 3). MOST OF THE CCT DIAGRAMS (APPLICABLE TO THE WELD METAL) HAVE BEEN GENERATED BY REHEATING THE AS-DEPOSITED WELD METAL (REF 4). ONE OF THE LIMITATIONS OF THESE DIAGRAMS IS THAT THEY ARE STRICTLY APPLICABLE ONLY TO THE HIGH-TEMPERATURE REHEATED ZONE OF MULTIPASS WELDS, BECAUSE THE INITIAL MICROSTRUCTURE AT HIGH TEMPERATURES IS NOT CHARACTERISTIC OF THAT DEVELOPED FROM THE LIQUID PHASE.
- WELDING MAY BE CARRIED OUT IN SEVERAL PASSES, AND THIS MAY RESULT IN THE SUPERPOSITION OF SEVERAL DIFFERENT HEATING AND COOLING CYCLES AT ONE POINT, EACH OF THESE CYCLES HAVING THE CHARACTERISTICS NOTED ABOVE.
- SOLIDIFICATION OF THE WELD METAL IS ACCOMPANIED BY SHRINKAGE, AND THE ANISOTHERMAL CONDITIONS ALREADY EMPHASIZED CAUSE DEFORMATION. THE THERMAL CYCLES ARE THEREFORE ACTING ON METAL THAT IS SUBJECTED TO MECHANICAL STRESSES AT THE SAME TIME.

The essential differences between weld thermal cycles and then thermal cycles used for generating a conventional CCT diagram are summarized in Fig. 2. Figure 2(a) shows thermal cycles which involve a slow heating rate, soak at a temperature just above the Ac_3 temperature, and various constant cooling rates. Instead of a constant cooling rate, some investigators (Ref 5) have used cooling curves according to Newton's law of cooling:

$$T \propto E^{-T} \qquad \textbf{(EQ 1)}$$

where T is the temperature and t is the time. Others have used cooling curves corresponding to the mid-radial position of cylindrical bars of different diameters when cooled in air or when quenched in different media. The weld thermal cycles shown in Fig. 2(b) are very different, and this is why a conventional CCT diagram can give only an approximate idea of the transformation behavior in the HAZ of a weldment.

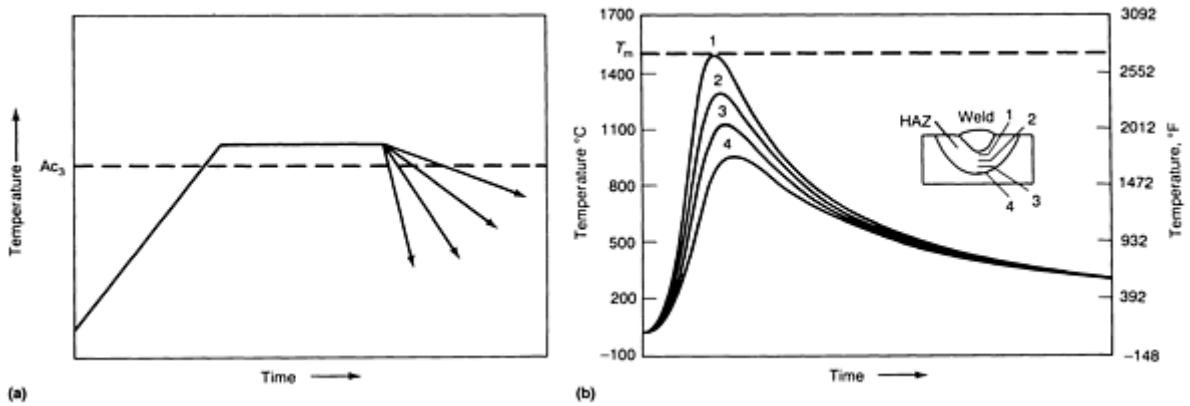

FIG. 2 GRAPHS TO SHOW DIFFERENCES IN THERMAL CYCLES. (A) THERMAL CYCLES USED TO GENERATE A CONVENTIONAL CCT DIAGRAM. (B) WELD THERMAL CYCLES. THE NUMBERS IN (B) CORRESPOND TO LOCATIONS INDICATED IN THE HAZ. NOTE THE CORRESPONDENCE BETWEEN THE THERMAL CYCLES IN (A) AND THOSE IN FIG. 1

References cited in this section

2. O.M. AKSELSEN AND T. SIMONSEN, TECHNIQUES FOR EXAMINING TRANSFORMATION BEHAVIOUR IN WELD METAL AND HAZ--A STATE OF ART REVIEW, *WELD. WORLD*, VOL 25 (NO. 1/2), 1987, P 26-34
3. O. GRONG AND D.K. MATLOCK, MICROSTRUCTURAL DEVELOPMENT IN MILD AND LOW ALLOY STEEL WELD METALS, *INT. MET. REV.*, VOL 31 (NO. 1), 1986, P 27-48
4. P.L. HARRISON AND R.A. FARRAR, APPLICATION OF CONTINUOUS COOLING TRANSFORMATION DIAGRAMS FOR WELDING OF STEELS, *INT. MATER. REV.*, VOL 34 (NO. 1), 1989, P 35-51
5. G.T. ELDIS, A CRITICAL REVIEW OF DATA SOURCES FOR ISOTHERMAL TRANSFORMATION AND CONTINUOUS COOLING TRANSFORMATION DIAGRAMS, *HARDENABILITY CONCEPTS WITH APPLICATION TO STEEL*, D.V. DOANE AND J.S. KIRKALDY, ED., TMS-AIME, 1978, P 126-157

Solid-State Transformations in Weldments

P. Ravi Vishnu, Luleå University of Technology, Sweden

HAZ of a Single-Pass Weld

Peak Temperature-Cooling Time Diagrams. The gradient in microstructure than can be obtained in a single-pass weld is shown in Fig. 3. High peak temperatures in the HAZ just adjacent to the fusion line cause coarsening of the austenite (γ) grains, and this in turn increases the hardenability of this region compared to other regions. Because each of the subzones shown in Fig. 3 occurs in a small volume, it is difficult to study the transformation behavior of individual regions by *in situ* methods (Ref 2). It is more convenient to obtain information about the microstructural and property changes in the HAZ by weld simulation (Ref 6, 7). A thermal cycle simulator (TCS) is used to reproduce the thermal cycle corresponding to a point in the HAZ in a large volume (usually a specimen has the Charpy test specimen dimensions). It is possible to program the required thermal cycle in the TCS so that the peak temperature and the cooling rate can be varied independently. It is thus possible to obtain information about the microstructural changes in the HAZ for a wide range of welding parameters.

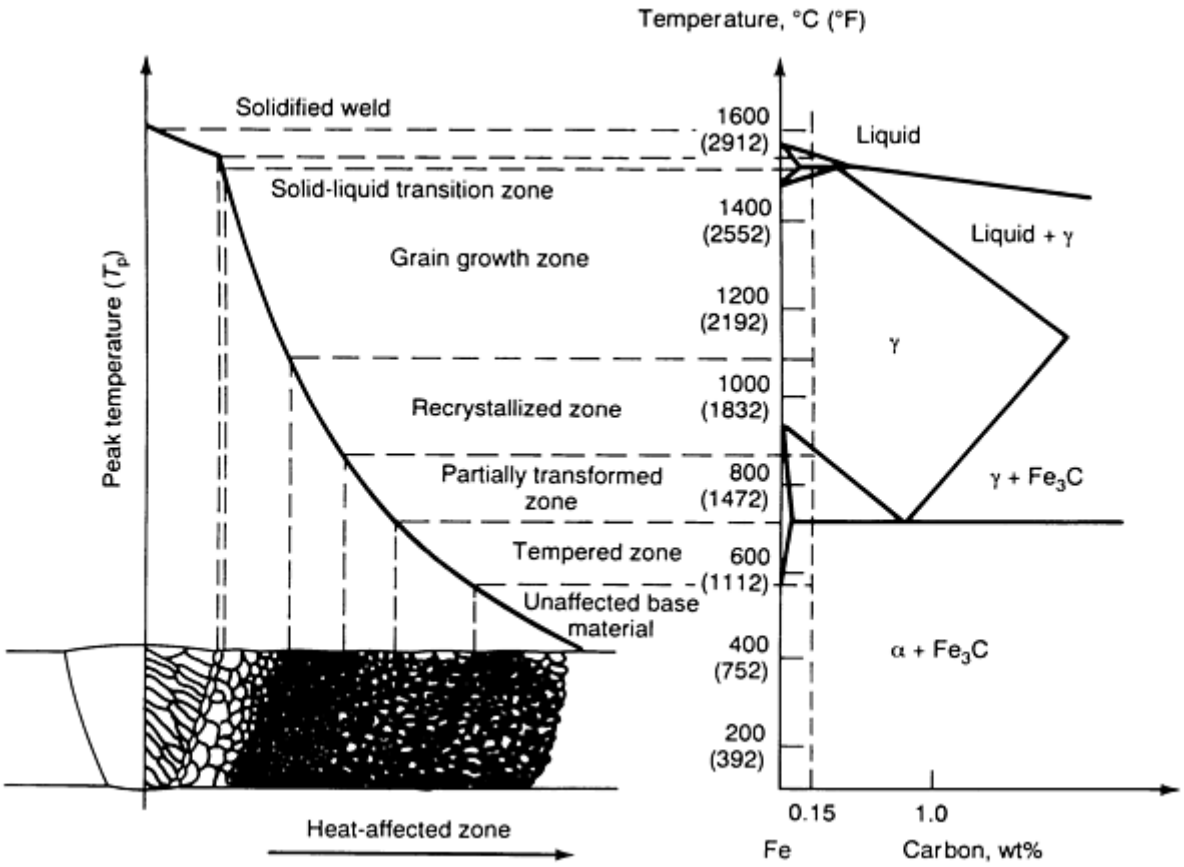

FIG. 3 SCHEMATIC SHOWING VARIOUS SUBZONES THAT CAN FORM IN THE HAZ OF A CARBON STEEL CONTAINING 0.15% C. SOURCE: REF 6

Figure 4 shows how a change in the peak temperature of the thermal cycle affects the CCT characteristics of a steel. The well-known effect of a larger γ grain size (due to a higher peak temperature) in increasing the hardenability of the steel is seen. To present the information about the CCT behavior for a number of peak temperatures (see Fig. 2b and 3), it is more convenient to adopt the scheme shown in Fig. 5. In this peak temperature-cooling time (PTCT) diagram (Ref 8, 9), each point represents a weld thermal cycle with a peak temperature, T_p, given by the ordinate and the cooling time, $\Delta t_{8\text{-}5}$ (that is, required for cooling from 800 to 500 °C, or 1470 to 930 °F), given by the abscissa. A microstructural constituent or a combination of two or more constituents is shown to occur over an area in the diagram. The upward slope in the boundary between two areas is consistent with the information presented earlier in Fig. 4 that the hardenability increases with an increase in the peak temperature of the thermal cycle. Hardness and C_v transition temperatures are also shown in the diagram corresponding to different thermal cycles.

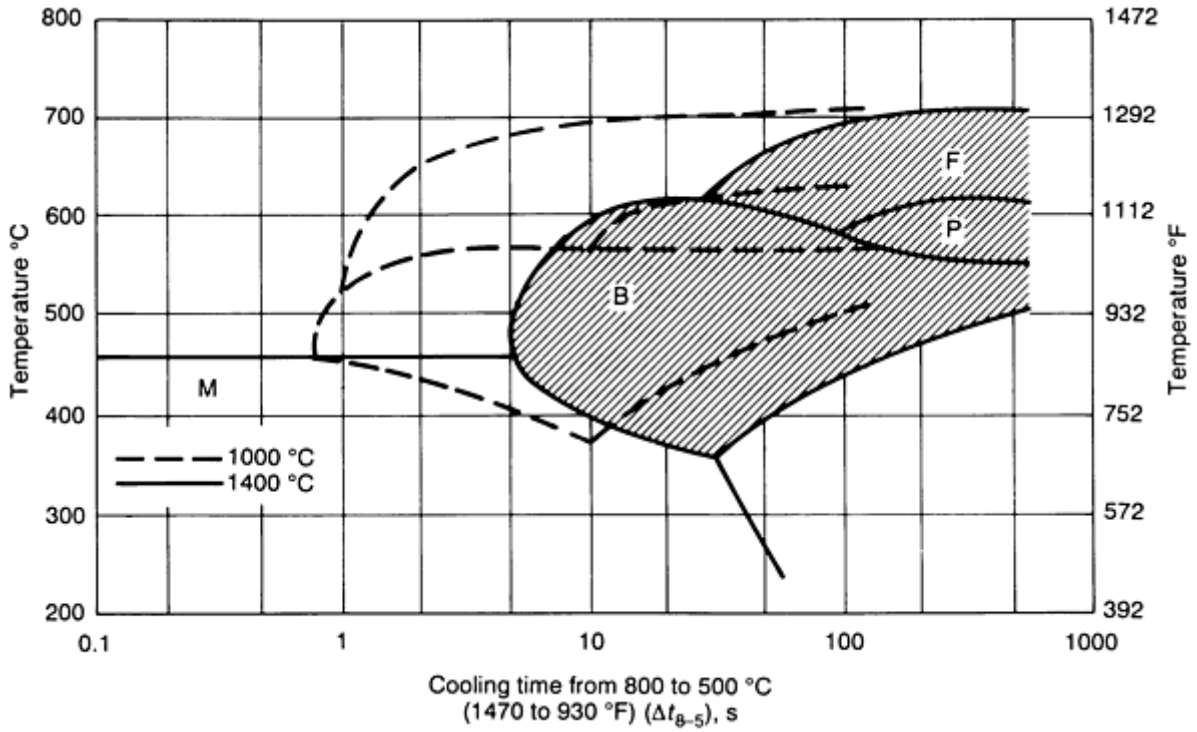

FIG. 4 EFFECT OF A CHANGE IN THE PEAK TEMPERATURE OF THE WELD THERMAL CYCLE (FROM 1000 TO 1400 °C, OR 1830 TO 2550 °F) ON THE CCT CHARACTERISTICS. M, MARTENSITE; B, BAINITE; P, PEARLITE; F, FERRITE. SOURCE: REF 8

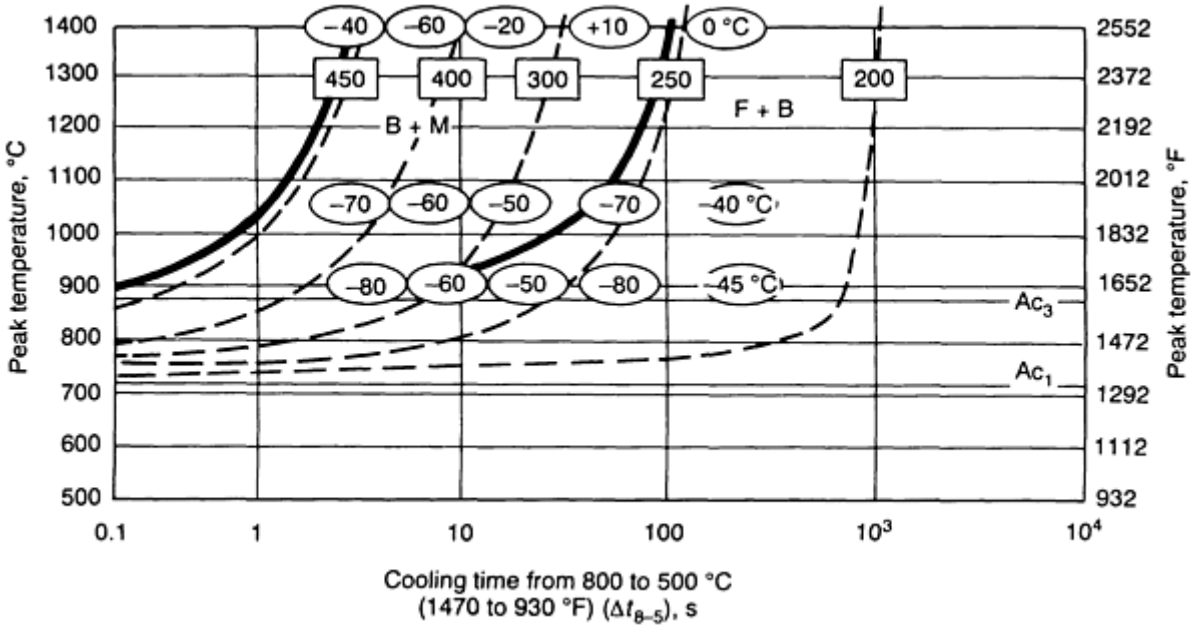

FIG. 5 TYPICAL PEAK TEMPERATURE VERSUS COOLING TIME DIAGRAM, SHOWING THE EFFECTS OF THESE PARAMETERS OF A WELD THERMAL CYCLE ON THE FINAL TRANSFORMATION PRODUCTS, ON HARDNESS, AND CHARPY V-NOTCH IMPACT ENERGY. M, MARTENSITE; B, BAINITE; F, FERRITE. FIGURES IN SQUARES INDICATE THE HARDNESS (30 HV); FIGURES IN OVALS INDICATE THE 21 J (16 FT · LBF) TRANSITION TEMPERATURES FOR CHARPY V-NOTCH IMPACT SPECIMENS SUBJECTED TO A SPECIFIC THERMAL CYCLE. SOURCE: REF 9

It may appear strange that the CCT diagram shown in Fig. 4 is plotted with $\Delta t_{8\text{-}5}$ as the abscissa instead of time as in Fig. 1. Historically, the practice of thinking in terms of a cooling time began when a need was recognized (Ref 5) to compare the CCT behavior of specimens subjected to different types of cooling curves--Jominy specimens; cylindrical bars cooled in air, water, or oil; dilatometer specimens cooled at a constant or a Newtonian rate; and so on. Initially, the cooling rate at 704 °C (1300 °F) was used as a criterion to judge the equivalency of these specimens in terms of microstructure and hardness. Because transformation takes place at lower temperatures in many steels, the half cooling time (Ref 5) was found to be a better equivalency criterion. The half cooling time was defined as the time to cool from Ac_3 to a temperature that lies midway between Ac_3 and room temperature. For the sake of general applicability, this was later modified to the $\Delta t_{8\text{-}5}$ criterion, and CCT diagrams began to be plotted with $\Delta t_{8\text{-}5}$ as the abscissa. It must be noted that using $\Delta t_{8\text{-}5}$ as an equivalency criterion is just an expedient solution that does not have strict theoretical justification (refer, for example, to the additivity principle in Ref 5).

A special significance of using $\Delta t_{8\text{-}5}$ as the abscissa in Fig. 5 is that it is almost constant (for T_p > 900 °C, or 1650 °F) in the whole of the HAZ. This can be seen from Ref 6, where the expressions given for $\Delta t_{8\text{-}5}$ do not contain the distance from the weld centerline as a factor. The derivation of these expressions is based on the assumption that the time to cool to 800 °C (1470 °F) is far greater than the time to reach the peak temperature, so the $\Delta t_{8\text{-}5}$ can be taken to be the same for the whole of the weld and the HAZ. This can be intuitively rationalized by observing that the thermal cycles in Fig. 2(b) are such that the curves are approximately parallel below 800 °C (1470 °F). The constancy of $\Delta t_{8\text{-}5}$ in the HAZ means that the gradient in microstructure (in terms of the final transformation products from austenite) is mainly due to a variation in the peak temperature. By drawing a vertical line in Fig. 5 at a value of $\Delta t_{8\text{-}5}$ corresponding to a given heat input and preheating temperature, it is possible to get information about the type of microstructural gradient in the HAZ. An idea of property changes like hardness and toughness can also be obtained from Fig. 5.

A fairly satisfactory correlation between real welds and simulation studies has been observed with respect to microstructure and property measurements. However, it has frequently been observed that the maximum prior to austenite grain size in real welds is less than that in corresponding simulation specimens (Ref 2, 6, 7). It is believed that this is due to the growth of large grains in the HAZ of real welds being hindered by the adjacent smaller grains. The constraint arises from the fact that grain growth in real welds is in some sense directional, occurring from the fusion line toward lower temperatures, while under the simulation condition the austenite grains can grow in all directions.

The above discussion shows that the PTCT diagram (along with property measurements, as in Fig. 5) can alert the user to the possibility of local brittle zones in actual weldments, and that any error in the property being assessed will be on the conservative side.

While the expressions for $\Delta t_{8\text{-}5}$ given Ref 6 (to determine the point at which a vertical line is to be drawn in the PTCT diagram) are reasonably accurate, those for T_p may be grossly in error because they are derived from a model with many simplistic assumptions (Ref 10, 11). For this reason, although an idea of the type of microstructural gradient in the HAZ can be obtained from the PTCT diagram, it is not possible to calculate the width of each region using simple closed form solutions of the type given in Ref 6 (derived from Rosenthal's equations). Moreover, T_p and $\Delta t_{8\text{-}5}$ are alone not enough to completely characterize a weld thermal cycle. To improve the accuracy of simulation, it would be necessary to program the thermal cycle with heating rates and the shape of the thermal cycle at higher temperatures, as in the HAZ of real welds. The significance of these additional factors is discussed below.

Continuous Heating Transformation Diagrams. The heating rate in many welding processes can be very high. The implication is that considerable superheating may be required for the transformation to austenite on heating. That is, the Ac_1 and Ac_3 temperatures will be raised with an increase in the heating rate (Ref 11). This is seen in Fig. 6, a continuous heating transformation (CHT) diagram, which is analogous to a CCT diagram. It is seen that grain growth begins only after the carbides have dissolved and after a homogeneous austenite (with respect to the distribution of carbon, at least) is formed.

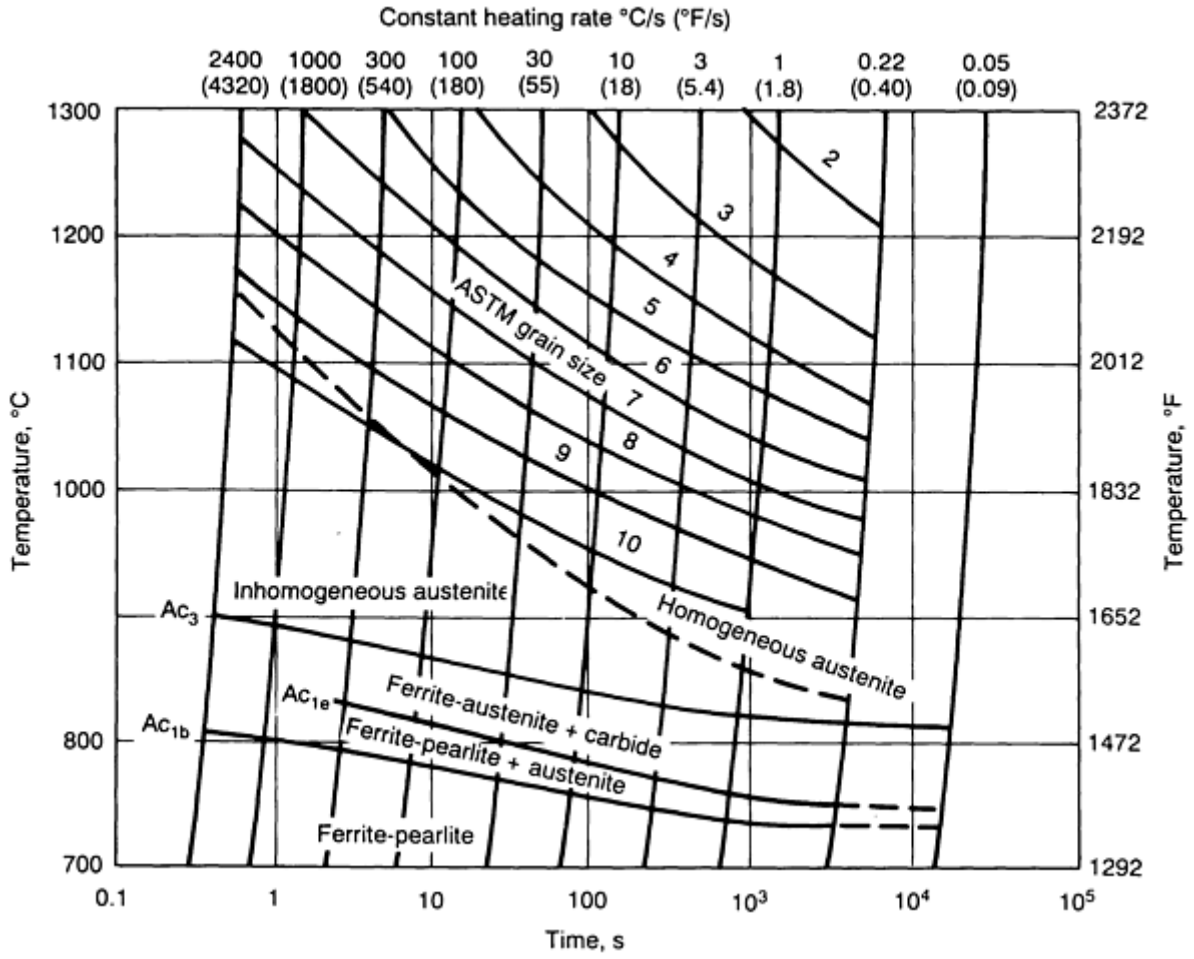

FIG. 6 CONTINUOUS HEATING TRANSFORMATION DIAGRAM FOR 34CRMO4STEEL. IN THE REGION OF HOMOGENEOUS AUSTENITE THERE ARE LINES OF CONSTANT AUSTENITE GRAIN SIZE (ASTM NUMBERS). BECAUSE OF THE MEASURING PROCEDURE, THE DIAGRAMS CAN ONLY BE INTERPRETED ALONG LINES OF CONSTANT HEATING RATE. TO SHOW THE HEATING TIME MORE CLEARLY, A TIME SCALE IS ADDED. SOURCE: REF 12

Precipitate Stability and Grain Boundary Pinning. In the last three decades, there has been a surge in the development of microalloyed or high-strength low-alloy (HSLA) steels (base metals). Almost the entire thrust behind this effort has been to tailor the thermomechanical processing of these steels to produce a fine grain size (Ref 13). Previously, higher strength was obtained by alloying the steel sufficiently to increase the hardenability and then heat treating to obtain a tempered martensitic structure. The higher carbon equivalent (Ref 6, 14) in these alloy steels led to an increased susceptibility to cold cracking or hydrogen-induced cracking. In the microalloyed steels, however, alloying additions are kept to a minimum, and higher strength is achieved primarily by a reduction in the grain size and by precipitation strengthening. A reduction in grain size is the only known method of increasing the strength and toughness at the same time. Because strengthening is obtained by other means, both carbon and carbon equivalent can be decreased to significantly reduce the susceptibility to cold cracking in these new HSLA steels (Fig. 7).

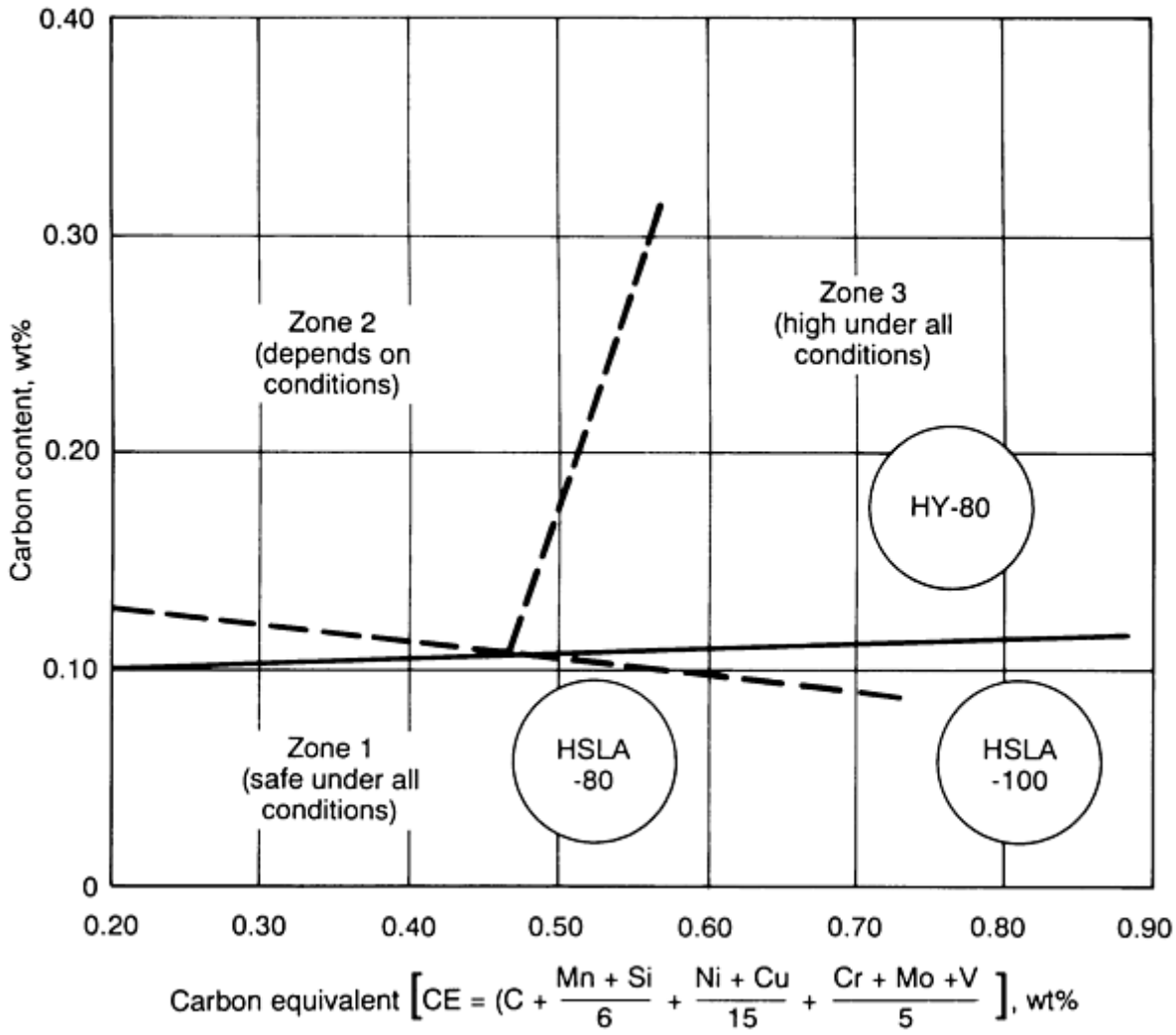

FIG. 7 EFFECT OF STEEL COMPOSITION (HY-80, HSLA-80, HSLA-100) ON THE SUSCEPTIBILITY TO COLD CRACKING IN THE HAZ. SOURCE: REF 13

A fine ferrite grain size in these steels is best achieved (after thermomechanical processing) by obtaining a fine austenite grain size before the γ-α transformation (Ref 13). To realize this goal, it is essential that microalloy additions such as niobium, vanadium, titanium, and aluminum are present so that the fine precipitate particles they form with nitrogen, carbon, or oxygen can "pin" the austenite grain boundaries and inhibit grain coarsening. The pinning effect arises from the fact that when a short length of grain boundary is replaced by a precipitate particle, the effective grain boundary energy is lowered. When the grain boundary attempts to migrate away from the particles, the local energy increases and a drag is exerted on the boundary by the particles.

In the HAZs of welds in these microalloyed steels, it is not possible to get the same optimum microstructure and microalloy precipitation obtained in the parent material by controlled thermomechanical processing. Because peak temperatures are much higher in the HAZ, the precipitate particles coarsen and dissolve, resulting in reduced pinning forces and therefore coarser austenite grains. This effect can be minimized by having precipitate particles that do not dissolve, even at higher temperatures. An idea of the stability of precipitate particles can be obtained from the plot shown in Fig. 8. It is seen that TiN has maximum stability, and this has been used to advantage in many steel. The other carbides and nitrides are not as effective as titanium nitride in limiting the extent of grain coarsening; they play a bigger role during thermomechanical processing (Ref 13).

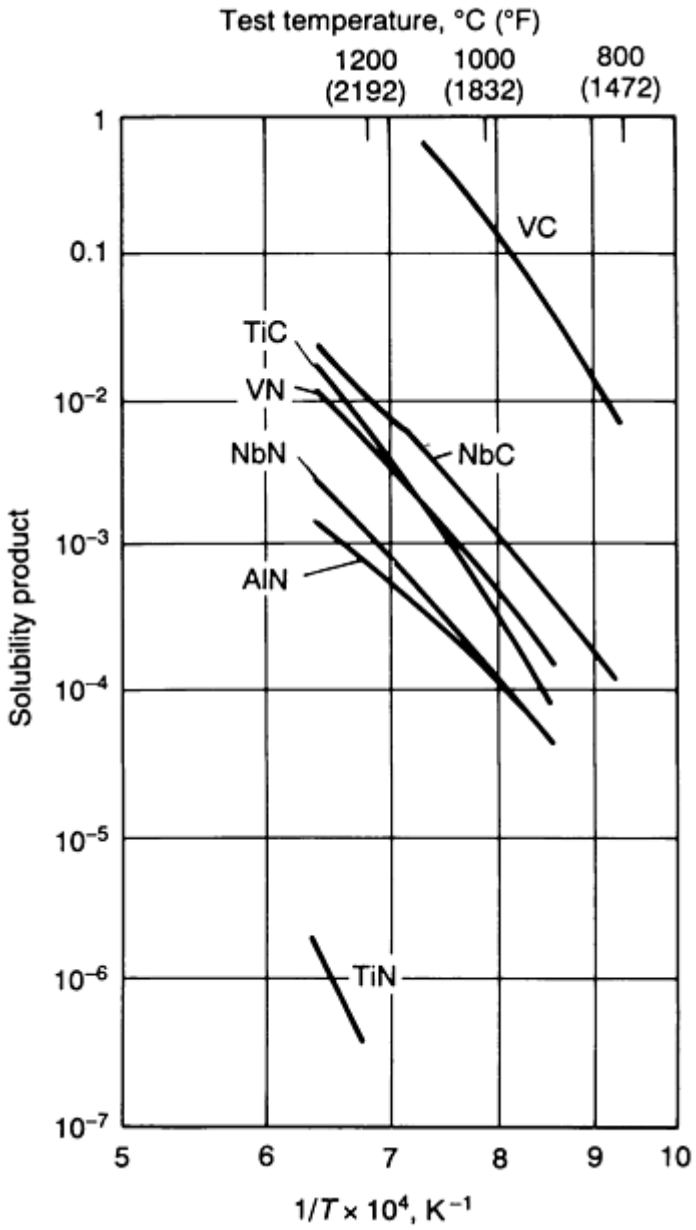

FIG. 8 SOLUBILITY PRODUCTS OF CARBIDES AND NITRIDES AS A FUNCTION OF TEMPERATURE. SOURCE: REF 15

Figure 9 shows how a high volume fraction of fine precipitate particles is needed to maximize the pinning effect. It also shows that heating to high temperatures increases the size of the particles, by a process known as Ostwald ripening (Ref 6), and decreases their volume fraction due to dissolution. This means that it is only possible to limit, and not to totally stop, grain coarsening in the HAZ, especially in high heat input welds. This inevitable grain coarsening is actually used to advantage in titanium, oxide steels (see the section "Titanium Oxide Steels" in this article).

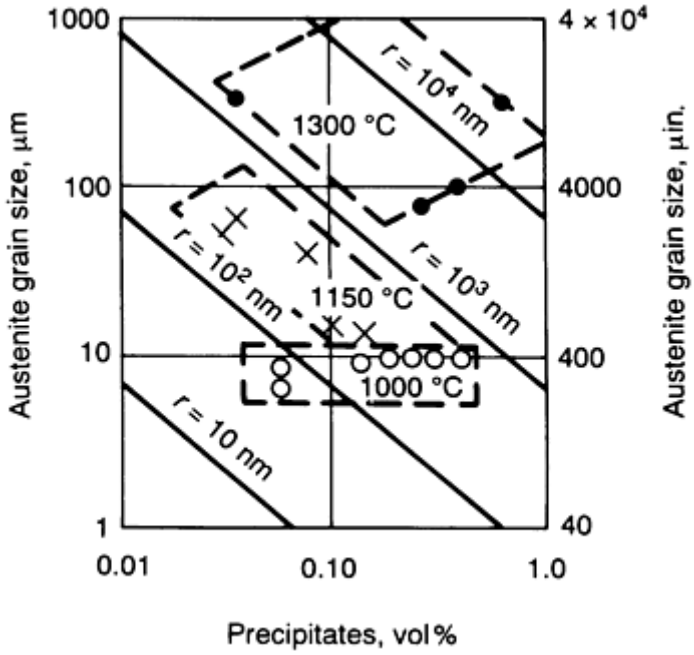

FIG. 9 EFFECT OF PARTICLE RADIUS, *R,* AND AMOUNT OF PRECIPITATE ON AUSTENITE GRAIN SIZE. SOURCE: REF 16

Unmixed and Partially Melted Zones in a Weldment. It is common to think of a single-pass weld as consisting of two zones: weld metal and HAZ. Careful metallographic examination has shown that a weld can in fact be divided into four regions (Fig. 10):

- *THE COMPOSITE ZONE,* IN WHICH A VOLUME OF BASE METAL MELTED BY THE SUPERHEATED FILLER METAL EXPERIENCES COMPLETE MIXING TO PRODUCE AN ALLOY WITH NOMINAL COMPOSITION INTERMEDIATE BETWEEN THAT OF THE BASE METAL AND THAT OF THE FILLER METAL.
- *THE UNMIXED ZONE,* WHICH FORMS FROM THE STAGNANT MOLTEN BOUNDARY LAYER REGION (ABOUT 100 TO 1000 μM, OR 0.004 TO 0.040 IN., THICK) AT THE OUTER EXTREMITIES OF THE COMPOSITE REGION. BECAUSE NO MECHANICAL MIXING WITH THE FILLER METAL OCCURS HERE, THE COMPOSITION OF THE METAL IN THIS REGION IS IDENTICAL TO THAT OF THE BASE METAL, EXCEPT FOR MINOR CHANGES PRODUCED BY DIFFUSION.
- *THE PARTIALLY MELTED ZONE,* WHICH IS A REGION AT THE FUSION BOUNDARY WHERE THE PEAK TEMPERATURES FALL BETWEEN THE LIQUIDUS AND SOLIDUS SO THAT MELTING IS INCOMPLETE.
- *THE TRUE HEAT-AFFECTED ZONE,* WHICH IS THAT PORTION OF THE BASE METAL WHERE ALL MICROSTRUCTURAL CHANGES INDUCED BY WELDING OCCUR IN THE SOLID STATE.

Special metallographic procedures are needed to reveal the existence of these special zones, as shown in Fig. 11.

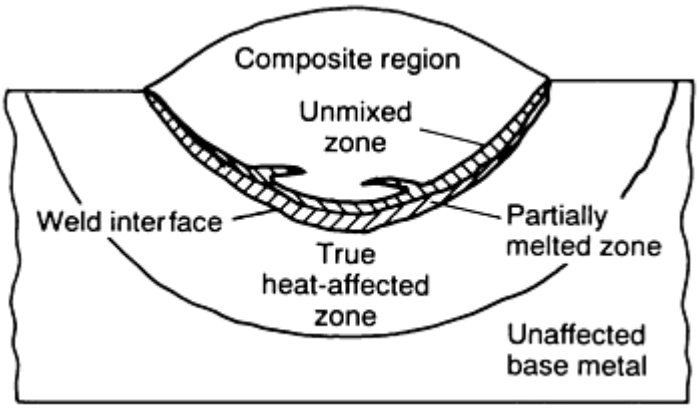

FIG. 10 SCHEMATIC SHOWING THE DIFFERENT DISCRETE REGIONS PRESENT IN A SINGLE-PASS WELD. SOURCE: REF 17

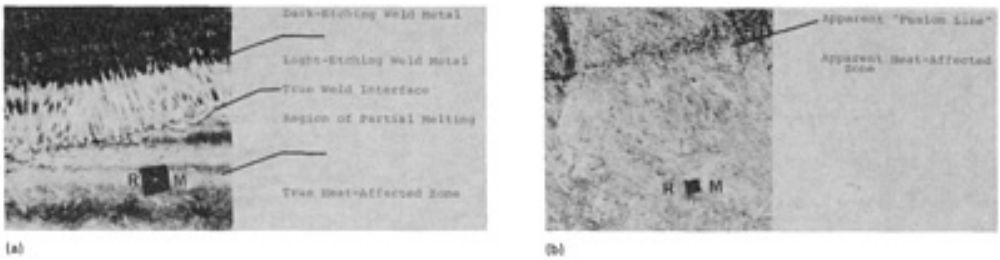

FIG. 11 SPECIAL METALLOGRAPHIC PROCEDURES SHOW THE MICROSTRUCTURE OF DISCRETE REGIONS (SEE FIG. 10) IN AN HY-80 WELD. (A) MICROSTRUCTURE OBTAINED NEAR A REFERENCE MARK (INDICATED BY "RM") USING A TWO-STAGE NITAL AND SODIUM BISULFITE PROCEDURE. (B) MICROSTRUCTURE AT IDENTICAL LOCATION REPOLISHED AND ETCHED WITH NITAL ONLY. TWO-STAGE PROCEDURE SHOWS MUCH GREATER DETAIL. SOURCE: REF 17

The width of the partially melted zone can be extended by a phenomenon known as constitutional liquation (Ref 18), whereby melting can occur even when the peak temperature is less than the solidus temperature. This can be understood by referring to a phase diagram for a simple binary system A and B (Fig. 12). Consider an alloy of composition C. Its equilibrium structures at temperatures T_1, T_2, T_3 and T_4 are α+ β, α, α, and L + α, respectively (Fig. 12a). On heating from room temperature to T_3 and holding at this temperature for a long time, the βparticles will dissolve and give a homogeneous α of composition C. However, under conditions of rapid heating in the HAZ, the dissolution of β will give rise to a solute concentration gradient around each particle, as shown in Fig. 12(b). In the region surrounding each particle, the concentration of the solute B will correspond to that of liquid because, as the phase diagram shows, a liquid phase must exist between α and β at T_3. This phenomenon of localized melting due to a nonequilibrium distribution of phases during rapid heating is called constitutional liquation.

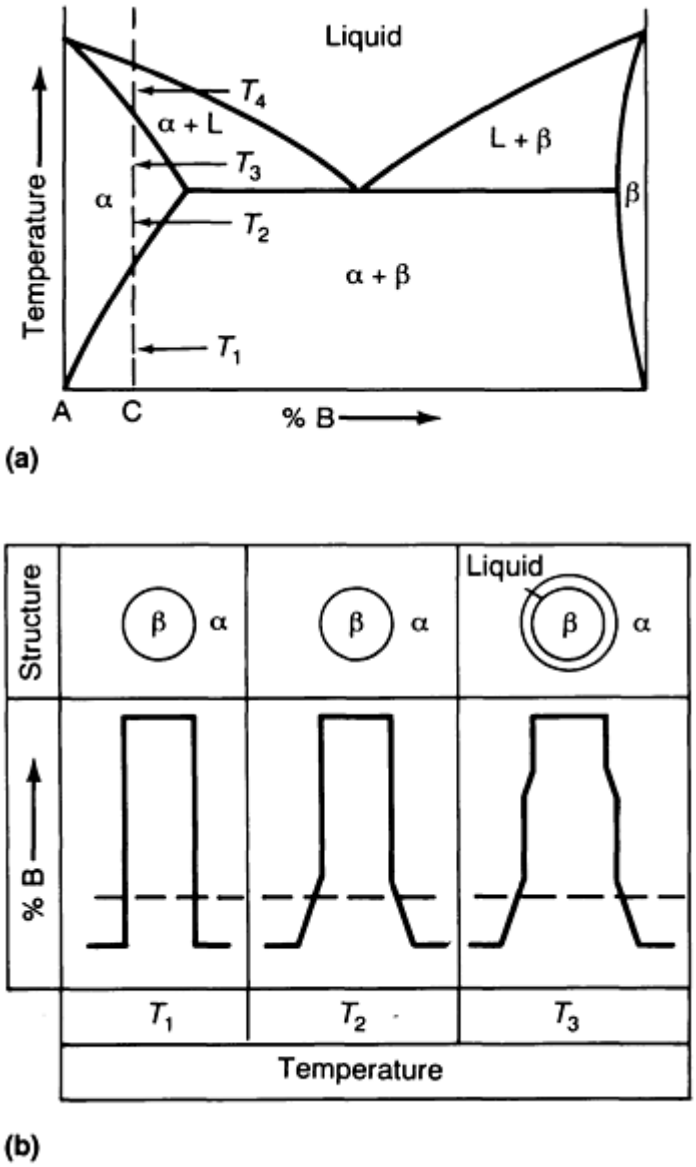

FIG. 12 EXTENSION OF PARTIALLY MELTED ZONE BY CONSTITUTIONAL LIQUATION. (A) PHASE DIAGRAM FOR A SIMPLE BINARY ALLOY. (B) STRUCTURES AND DISTRIBUTION OF CONSTITUENT B IN ALLOY C AT THREE TEMPERATURES SHOWN IN (A) WHEN RAPID HEATING IS APPLIED. SOURCE: REF 19

The partially melted zone is the region where liquation cracks have been known to occur in maraging steels, austenitic stainless steels, heat-treatable aluminum alloys, and nickel-base superalloys. It can also be a site where hydrogen-induced cracking is initiated (Ref 17), because it can act as a pipeline for the diffusion of hydrogen picked up by the molten weld metal and also because of the higher hardenability at these segregated regions.

While the phenomenon of constitutional liquation is usually discussed in connection with liquation cracking of aluminum- and nickel-base alloys (Ref 14, 18, 19), a more dramatic example can actually be found in the case of cast iron welds (Ref 20). Figure 13 shows the micro structure of the HAZ in a cast iron weld deposited using a "quench welding" technique (Ref 21). This procedure involves welding without any preheat by intermittently depositing a series of small stringer beads and strictly maintaining the interpass temperature below about 80 °C (175 °F). The idea is to limit the size of the hard and brittle white iron colonies forming by constitutional liquation around the graphite nodules and to see that they do not interconnect. By contrast, a procedure involving a preheat of about 200 °C (390 °F) can prevent the formation of martensite but not the formation of ledeburite (the structure of white iron). Because ledeburite forms at higher temperatures than martensite (≈1100 °C, or 2010 °F), a much higher preheat temperature of about 600 °C (1110 °F) is required to significantly reduce the cooling rate at the higher temperatures, thereby preventing the formation of white iron. This high level of preheat is impractical. While cast iron appears to have been successfully welded with preheats of

about 200 °C (390 °F), it has sometimes been found that weld repair is most effective using the quench welding technique, by which it is possible to limit both the amount of ledeburite formed and the width of the HAZ.

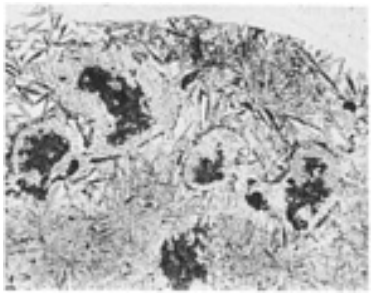

FIG. 13 DISCONTINUOUS WHITE IRON COLONIES OBTAINED IN THE HAZ OF BLACKHEART MALLEABLE IRON WELDED USING A "QUENCH WELDING" TECHNIQUE WITH A NICKEL-BASE ELECTRODE. 180×. SOURCE: REF 21

References cited in this section

2. O.M. AKSELSEN AND T. SIMONSEN, TECHNIQUES FOR EXAMINING TRANSFORMATION BEHAVIOUR IN WELD METAL AND HAZ--A STATE OF ART REVIEW, *WELD. WORLD,* VOL 25 (NO. 1/2), 1987, P 26-34
5. G.T. ELDIS, A CRITICAL REVIEW OF DATA SOURCES FOR ISOTHERMAL TRANSFORMATION AND CONTINUOUS COOLING TRANSFORMATION DIAGRAMS, *HARDENABILITY CONCEPTS WITH APPLICATION TO STEEL,* D.V. DOANE AND J.S. KIRKALDY, ED., TMS-AIME, 1978, P 126-157
6. K. EASTERLING, *INTRODUCTION TO THE PHYSICAL METALLURGY OF WELDING,* BUTTERWORTHS, 1983
7. *WELD THERMAL SIMULATORS FOR RESEARCH AND PROBLEM SOLVING,* THE WELDING INSTITUTE, U.K., 1972
8. C.F. BERKHOUT AND P.H. VAN LENT, THE USE OF PEAK TEMPERATURE-COOLING TIME DIAGRAMS IN THE WELDING OF HIGH STRENGTH STEELS (IN GERMAN), *SCHWEISS. SCHNEID.,* VOL 20 (NO. 6), 1968, P 256-260
9. TH.J. VAN ADRICHEM AND J. KAS, *CALCULATION, MEASUREMENT AND SIMULATION OF WELD THERMAL CYCLES,* SMITWELD N.V., NIJMEGEN, THE NETHERLANDS
10. P. RAVI VISHNU, W.B. LI, AND K. EASTERLING, HEAT FLOW MODEL FOR PULSED WELDING, *MATER. SCI. TECH.,* VOL 7 (NO. 7), 1991, P 649-659
11. P. RAVI VISHNU AND K. EASTERLING, PHENOMENOLOGICAL MODELLING OF HEAT FLOW AND MICROSTRUCTURAL CHANGES IN PULSED GTAW WELDS OF A QT STEEL, *MATHEMATICAL MODELING OF WELD PHENOMENA,* H. CERJAK AND K. EASTERLING, ED., THE INSTITUTE OF METALS, 1993
12. VEREIN DEUTSCHER EISENHÜTTENLEUTE, ED., *STEEL--A HANDBOOK FOR MATERIALS RESEARCH AND ENGINEERING, VOLUME 1: FUNDAMENTALS,* SPRINGER VERLAG, 1992, P 175
13. A.J. DEARDO, C.I. GARCIA, AND E.J. PALMIERE, THERMOMECHANICAL PROCESSING OF STEELS, *HEAT TREATING,* VOL 4, *ASM HANDBOOK,* 1991, P 237-255
14. S. KOU, *WELDING METALLURGY,* JOHN WILEY & SONS, 1987
15. K. NARITA, PHYSICAL CHEMISTRY OF THE GROUPS IVA (TI, ZR), VA (V, NB, TA) AND THE RARE EARTH ELEMENTS IN STEEL, *TRANS. ISIJ,* VOL 15, 1975, P 145-152
16. R.K. AMIN AND F.B. PICKERING, AUSTENITE GRAIN COARSENING AND THE EFFECT OF

THERMOMECHANICAL PROCESSING ON AUSTENITE RECRYSTALLIZATION, *THERMOMECHANICAL PROCESSING OF MICROALLOYED AUSTENITE,* A.J. DEARDO, G.A. RATZ, AND P.J. WRAY, ED., TMS-AIME, 1982, P 14

17. W.F. SAVAGE, E.F. NIPPES, AND E.S SZEKERES, A STUDY OF WELD INTERFACE PHENOMENA IN A LOW ALLOY STEEL, *WELD. J.*, SEPT 1976, P 260S-268S, AND HYDROGEN INDUCED COLD CRACKING IN A LOW ALLOY STEEL, *WELD. J.*, SEPT 1976, P 276S-283S
18. J.J. PEPE AND W.F. SAVAGE, EFFECTS OF CONSTITUTIONAL LIQUATION IN 18-NI MARAGING STEEL WELDMENTS, *WELD J.*, SEPT 1967, P 411S-422S
19. W. YENISCAVITCH, JOINING, *SUPERALLOYS II,* C.T. SIMS, N.S. STOLOFF, AND W.C. HAGEL, ED., JOHN WILEY & SONS, 1987, P 495-516
20. E.E. HUCKE AND H. UDIN, WELDING METALLURGY OF NODULAR CAST IRON, *WELD. J.*, AUG 1953, P 378S-385S
21. E.N. GREGORY AND S.B. JONES, WELDING CAST IRONS, *WELDING OF CASTINGS,* THE WELDING INSTITUTE, U.K., 1977, P 145-156

Solid-State Transformations in Weldments

P. Ravi Vishnu, Luleå University of Technology, Sweden

Fusion Zone of a Single-Pass Weld

Transformations in Single-Pass Weld Metal. It is usually not necessary to select a filler metal that has exactly the same composition as the base metal; it is more important that the weld metal has the same strength and other properties (such as toughness or corrosion resistance). Because these properties are governed by the microstructure, it is important to understand the influence of different factors on phase transformations in the weld metal. But first, for a meaningful communication of the different features in a microstructure, the various phases and microconstituents must be identified using a system of nomenclature that is both widely accepted and well understood. In wrought steels, this need has been satisfied to a large degree by the Dubé scheme (Ref 22) for classifying the different morphologies of ferrite, as shown in Fig. 14. Similarly, confusion and controversy in the terminology for describing the microstructures in ferritic steel weld metals have been largely resolved by the classification scheme shown in Fig. 15. This scheme (Ref 23) was the result of several collaborative exercises undertaken under the auspices of the International Institute of Welding (IIW). Typical micrographs illustrating some of the microstructural constituents are shown in Fig. 16.

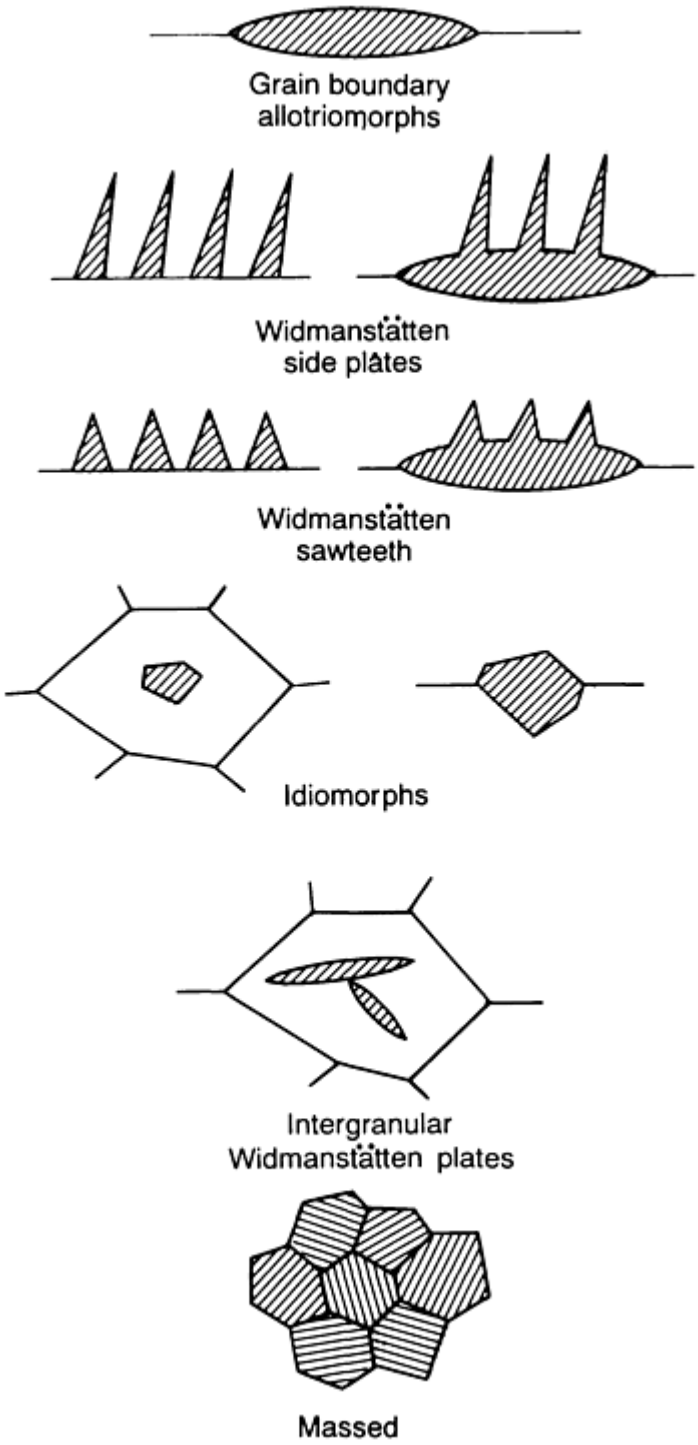

FIG. 14 SCHEMATICS SHOWING THE DUBÉ CLASSIFICATION OF FERRITE MORPHOLOGIES. SOURCE: REF 22

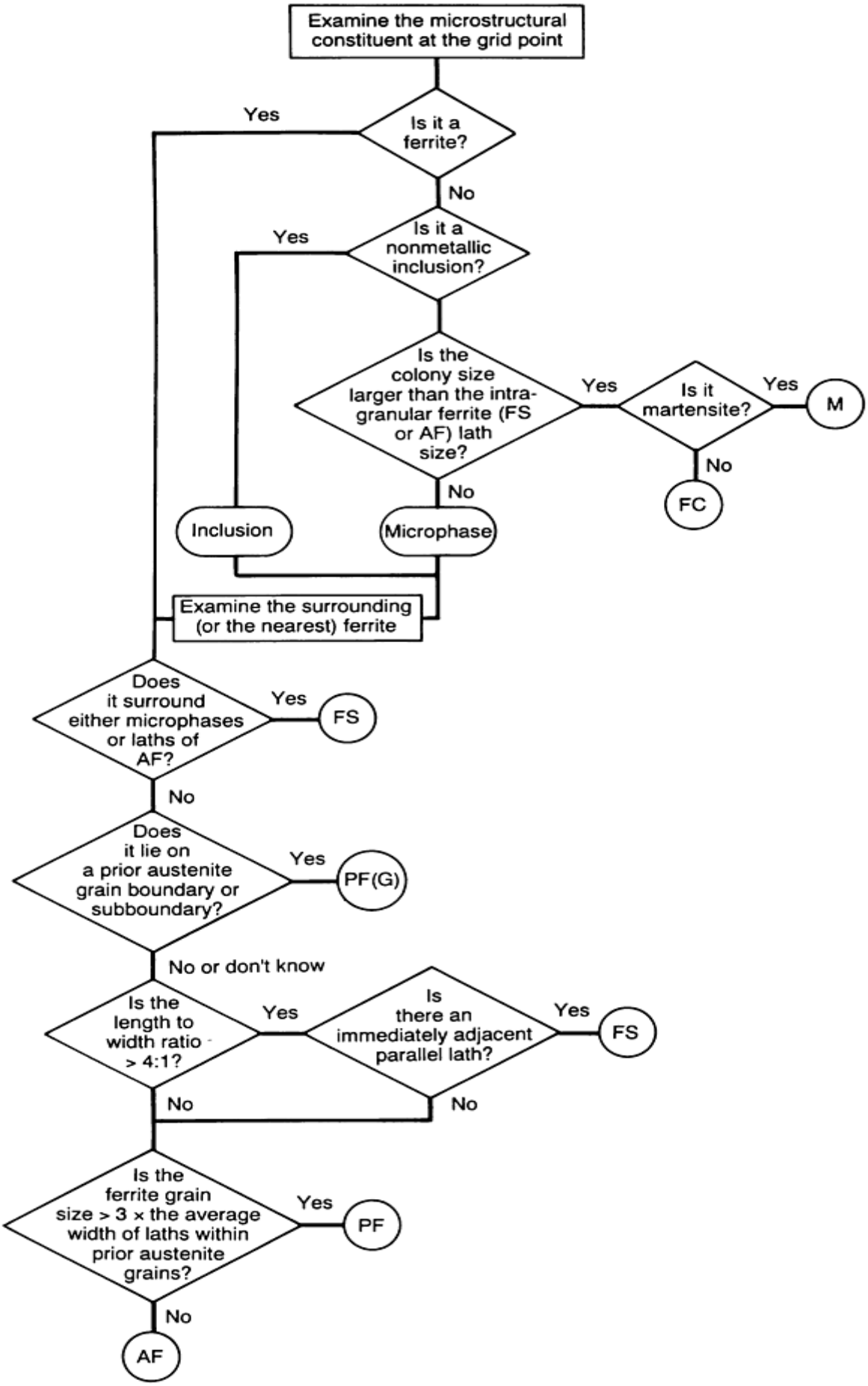
Examine the microstructural constituent at the grid point
Is it a ferrite?
Yes
No
Is it a nonmetallic inclusion?
Yes
Is the colony size larger than the intra-granular ferrite (FS or AF) lath size?
Yes
Is it martensite?
Yes
M
No
FC
No
Inclusion
Microphase
Examine the surrounding (or the nearest) ferrite
Does it surround either microphases or laths of AF?
Yes
FS
No
Does it lie on a prior austenite grain boundary or subboundary?
Yes
PF(G)
No or don't know
Is the length to width ratio > 4:1?
Yes
Is there an immediately adjacent parallel lath?
Yes
FS
No
No
Is the ferrite grain size > 3 × the average width of laths within prior austenite grains?
Yes
PF
No
AF

CATEGORY	ABBREVIATION
PRIMARY FERRITE	PF
GRAIN BOUNDARY FERRITE	PF(G)
INTRAGRANULAR POLYGONAL FERRITE	PF(I)
FERRITE WITH SECOND PHASE	FS
FERRITE WITH NONALIGNED SECOND PHASE	FS(NA)
FERRITE WITH ALIGNED SECOND PHASE	FS(A)
FERRITE SIDE PLATES	FS(SP)
BAINITE	FS(B)
UPPER BAINITE	FS(UB)
LOWER BAINITE	FS(LB)
ACICULAR FERRITE	AF
FERRITE-CARBIDE AGGREGATE	FC
PEARLITE	FC(P)
MARTENSITE	M
LATH MARTENSITE	M(L)
TWIN MARTENSITE	M(T)

FIG. 15 INTERNATIONAL INSTITUTE OF WELDING SCHEME FOR CLASSIFYING MICROSTRUCTURAL CONSTITUENTS IN FERRITIC STEEL WELD METALS WITH THE OPTICAL MICROSCOPE. SOURCE: REF 23

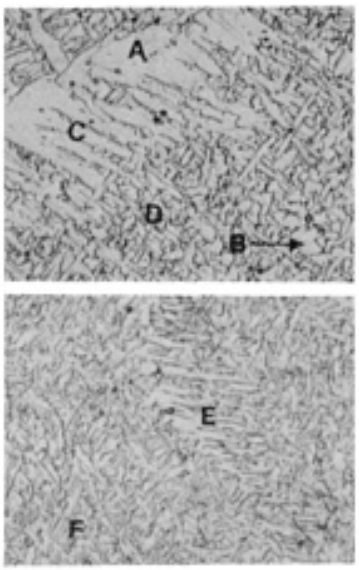

FIG. 16 MICROGRAPHS SHOWING TYPICAL MICROSTRUCTURES IN LOW-CARBON STEEL WELD METAL (NITAL ETCH). A, GRAIN BOUNDARY FERRITE [PF(G)]; B, POLYGONAL FERRITE [PF(I)]; C, WIDMANSTÄTTEN FERRITE [FS(SP)]; D, ACICULAR FERRITE (AF); E, UPPER BAINITE [FS(UB)]; F, LOWER BAINITE [FS(LB)] AND/OR MARTENSITE (M). SOURCE: REF 3

The transformation behavior in ferritic steel weld metals is best understood by first noting that ferrite is nucleated heterogeneously and that for all practical purposes, it is necessary to consider the competitive nucleation behavior only at grain boundaries and at inclusions. Figure 17 shows that inclusions have to be larger than a certain size (0.2 to 0.5 μm, or 8 to 20 μin., the typical size range of most weld metal inclusions) for their potency as nucleation sites to reach a maximum. It also shows that nucleation of ferrite is always energetically more favorable at grain boundaries than at inclusions. Based on additional considerations, like thermal contraction strains and lattice matching at inclusion-austenite-

ferrite interfaces (not taken into account to get the results in Fig. 17), a discussion of why certain inclusions are more potent nucleation sites than others is found in Ref 3, 24, and 25.

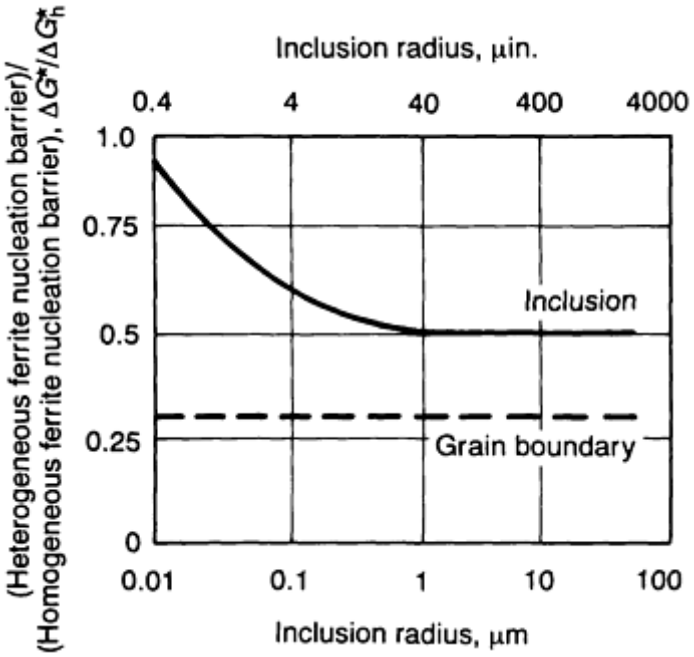

FIG. 17 EFFECT OF PARTICLE RADIUS ON ENERGY BARRIER TO FERRITE NUCLEATION AT INCLUSIONS, ΔG^* (HETEROGENEOUS), NORMALIZED RELATIVE TO THE HOMOGENEOUS NUCLEATION BARRIER, ΔG^*_H (HOMOGENEOUS). CORRESPONDING ENERGY BARRIER TO NUCLEATION OF FERRITE AT AUSTENITE GRAIN BOUNDARIES IS INDICATED BY HORIZONTAL BROKEN LINE. SOURCE: REF 6

Broadly, the major factors affecting transformation behavior in ferritic steel weld metals are alloy composition, weld heat input (by its effect on γ grain size and $\Delta t_{8\text{-}5}$), oxygen content (that is, the inclusion content), and the nature of segregation in the weld metal. A typical weld CCT diagram is shown in Fig. 18. For the cooling curve shown in the figure, the first phase that forms is allotriomorphic ferrite, or grain boundary ferrite in the IIW scheme. The term "allotriomorphic" means a "particle of a phase that does not have a regular external shape" and in the present context means that ferrite grows on the grain boundary surfaces and does not have a regular faceted shape reflecting the symmetry of its internal crystalline structure. At lower temperatures, the mobility of the curved or random γ/α-allotriomorph boundaries decreases, and Widmanstätten side plates (ferrite side plates in the IIW scheme) form. Growth of these side plates is rapid because carbon is efficiently redistributed to the sides of the growing tips, thus avoiding solute pile-up problems. In addition, substitutional atoms do not diffuse during the growth of Widmanstätten ferrite.

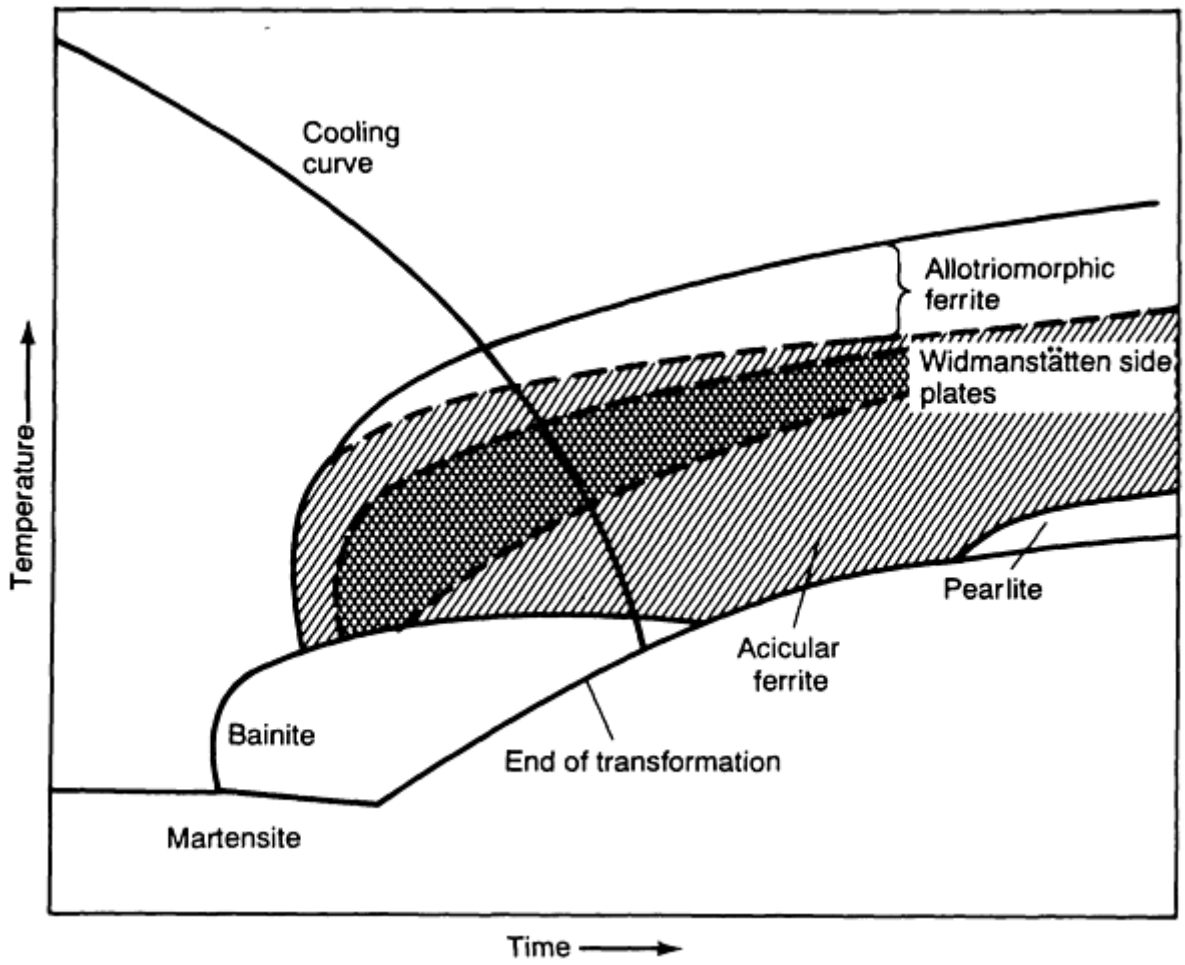

FIG. 18 SCHEMATIC OF WELD CCT DIAGRAM SHOWING SELECTED MICROSTRUCTURES

After all the grain boundary sites are saturated with allotriomorphic or Widmanstätten ferrite and their growth rate is not sufficient to extend to the interior of the grains, the nucleation of ferrite at inclusions within the γ grains becomes competitive. Acicular ferrite forms, a structure resulting from ferrite laths growing in different directions from inclusions and from laths already nucleated. Upon impingement, high-angle grain boundaries and a very fine dispersion of microphases are obtained between ferrite laths. "Microphases" in this context means the transformation structures resulting from the carbon-enriched regions between the ferrite laths and could be the martensite-austenite constituent, bainite, or pearlite (see the section "HAZ in Multipass Weldments" in this article). An example of the microstructure of acicular ferrite is shown in Fig. 19. Acicular ferrite does not figure in the Dubé scheme because it is rarely observed in wrought steels. When the cooling rate is higher or when the inclusion content is very low, bainite can be nucleated directly at the γ grain boundaries. Bainite can form as upper or lower bainite; the difference between the two is illustrated in Fig. 20. Examination with transmission electron microscopy (TEM) is usually required for a firm identification of the type of bainite formed. In the case of the highest cooling rates, martensite is obtained.

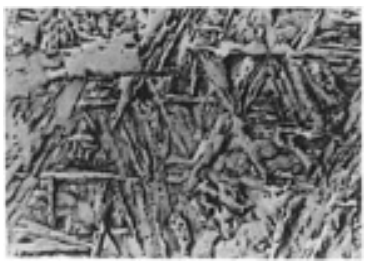

FIG. 19 SCANNING ELECTRON MICROGRAPH SHOWING MORPHOLOGY OF ACICULAR FERRITE. SOURCE: REF 24

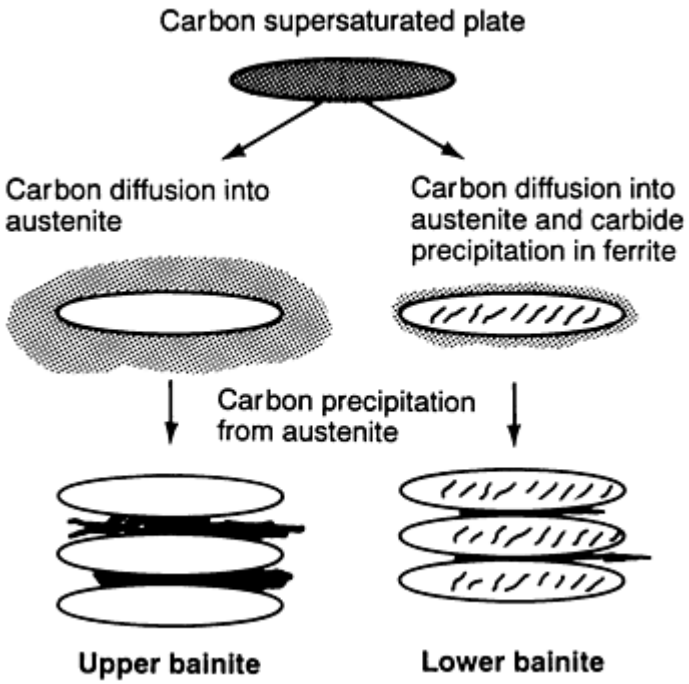

FIG. 20 SCHEMATIC SHOWING THE DIFFERENCES IN THE TRANSFORMATION MECHANISM FOR UPPER AND LOWER BAINITE AND THE EFFECT OF THESE MECHANISMS ON THE FINAL MORPHOLOGY. SOURCE: REF 24

Figure 21 shows the effect of alloying additions, $\Delta t_{8\text{-}5}$, oxygen content, and the γ grain size on the sequence and relative amounts of allotriomorphic ferrite, Widmanstätten ferrite, and bainite in the weld metal. Broadly, the trends shown can be understood in terms of the wellknown observation that an increase in γ grain size, a decrease in inclusion content, and an increase in alloying additions will shift the CCT curves to lower temperatures and to longer times. While Fig. 21 can generally be interpreted by assuming that the individual factors act independently of each other, the transition from (b) to (a) with an increase in the inclusion content must be understood in terms of its effect of the γ grain size. It has been observed that the γ grain size decreases with an increase in the inclusion content, and this has been explained by the higher magnitude of pinning forces at higher inclusion contents (Ref 25). The smaller grain size implies a greater grain boundary surface area, and this increases the amount of grain boundary ferrite and sideplate structures formed at the expense of acicular ferrite in Fig. 21(a). The role of the initial formation or non-formation of allotriomorphic ferrite at γ grain boundaries in bringing about the transition from Fig. 21(b) to Fig. 21(c) in Fig. 21 is discussed in the next section of this article.

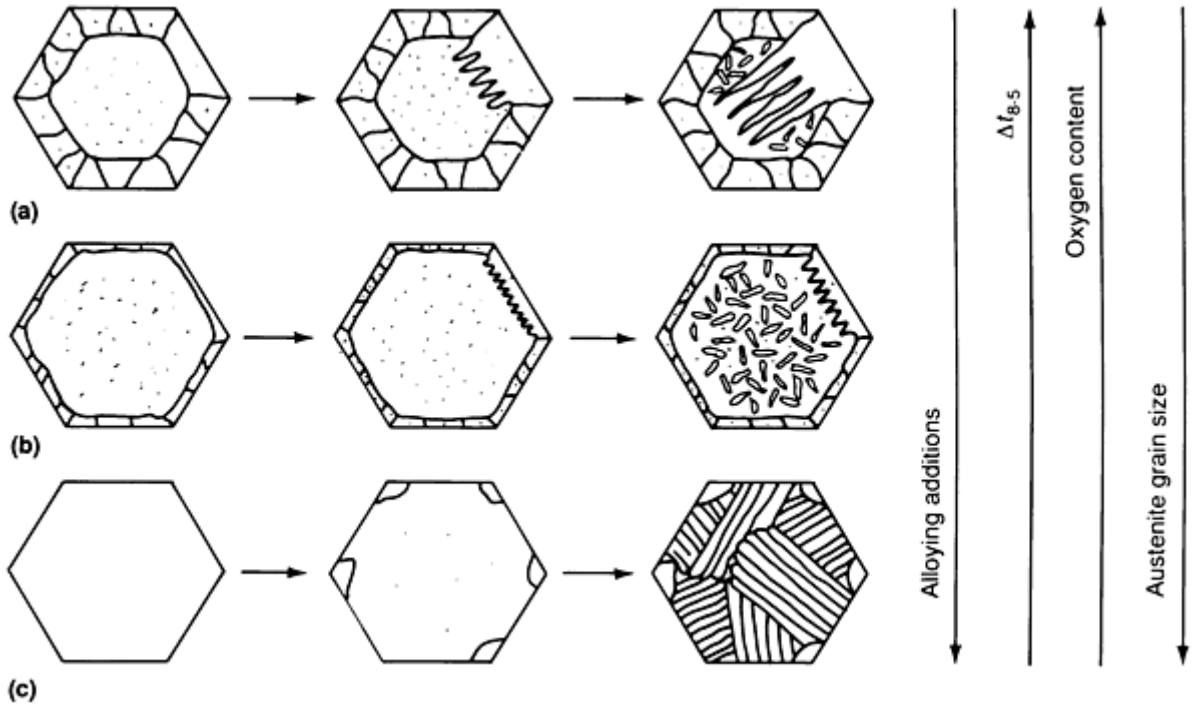

FIG. 21 SCHEMATIC SHOWING THE EFFECT OF ALLOY COMPOSITION, $\Delta T_{8\text{-}5}$, OXYGEN CONTENT, AND γ GRAIN SIZE ON THE DEVELOPMENT OF MICROSTRUCTURE IN FERRITIC STEEL WELD METALS. THE HEXAGONS REPRESENT CROSS SECTIONS OF COLUMNAR γ GRAINS. (A) THE GRAIN BOUNDARIES BECOME DECORATED FIRST WITH A UNIFORM, POLYCRYSTALLINE LAYER OF ALLOTRIOMORPHIC FERRITE, FOLLOWED BY FORMATION OF WIDMANSTÄTTEN FERRITE, AND THEN BY FORMATION OF ACICULAR FERRITE. (B) THE GROWTH RATE OF WIDMANSTÄTTEN FERRITE IS NOT SUFFICIENTLY HIGH TO EXTEND ENTIRELY ACROSS γ GRAINS. NUCLEATION OF FERRITE AT INCLUSIONS WITHIN THE γ GRAINS LEADS TO AN INCREASE IN THE AMOUNT OF ACICULAR FERRITE WHEN COMPARED WITH CASE (A). (C) THE HIGHER ALLOY CONTENT OR THE HIGHER COOLING RATE SUPPRESSES THE FORMATION OF ALLOTRIOMORPHIC FERRITE. THIS LEAVES THE γ GRAIN BOUNDARIES FREE TO NUCLEATE UPPER BAINITE. SOURCE: REF 24

Although the IIW classification is the result of a consensus viewpoint, some researchers (Ref 24) still feel that it places an exaggerated emphasis on morphological features observed with the light microscope. They believe that it is more important that the terminology reflect the mechanism of transformation. For example, it can be difficult to differentiate between Widmanstätten ferrite and upper bainite when using the light microscope, and both are identified as FS in the IIW classification. For a more fundamental understanding and to clearly interpret the trends in microstructural development, it is essential to make a distinction between the two. In addition, the subclassification of grain boundary ferrite in the IIW classification is not unequivocal in its meaning--it could refer to ferrite that forms by diffusion, Widmanstätten ferrite, or the ferrite in upper bainite. By contrast, the term "allotriomorphic ferrite" clearly identifies the mechanism by which it is formed. On the other hand, the IIW classification is easy to use and allows a more detailed identification, either by judgment or by further TEM examination, for example, to determine whether FS is FS(SP) or FS(UB). At least, it decreases the tendency for a wrong identification of the transformation mechanism with insufficient data. For a microstructure-toughness correlation, it is sufficient to characterize the morphological features.

Relating Weld Metal Toughness to the Microstructure. A good insight into the subject of toughness in ferrite steel weld metal is obtained by examining the data shown in Fig. 22. It is seen from Fig. 22(a) that the upper-shelf Charpy V-notch (CVN) energy monotonically decreases with an increase in oxygen content. In the upper-shelf temperature region, ductile fracture occurs by a process of microvoid coalescence, and because microvoids are initiated at the inclusion-matrix interface, the upper-shelf impact energy decreases with an increase in the inclusion content. By contrast, from Fig. 22(b) it is seen that an optimum inclusion content is required to obtain the lowest CVN transition temperature. The transition temperature is mainly governed by cleavage fracture, and this in turn depends on how effectively a propagating cleavage crack is forced to change direction as it traverses the microstructure. At low inclusion contents, an upper bainitic structure is obtained, and this consists of parallel platelets of ferrite (in a single packet) growing from the grain boundary surfaces. With an optimum inclusion content, a predominantly acicular ferrite structure is obtained, and here the adjacent

ferrite platelets tend to radiate in many different directions from inclusion nucleation site. At higher inclusion contents, the amount of ferrite sideplate structures increases, again having nearly parallel ferrite platelets. The highest toughness (that is, the lowest transition temperature) is obtained only in the "chaotic" microstructure of acicular ferrite because it has the smallest effective ferrite grain size.

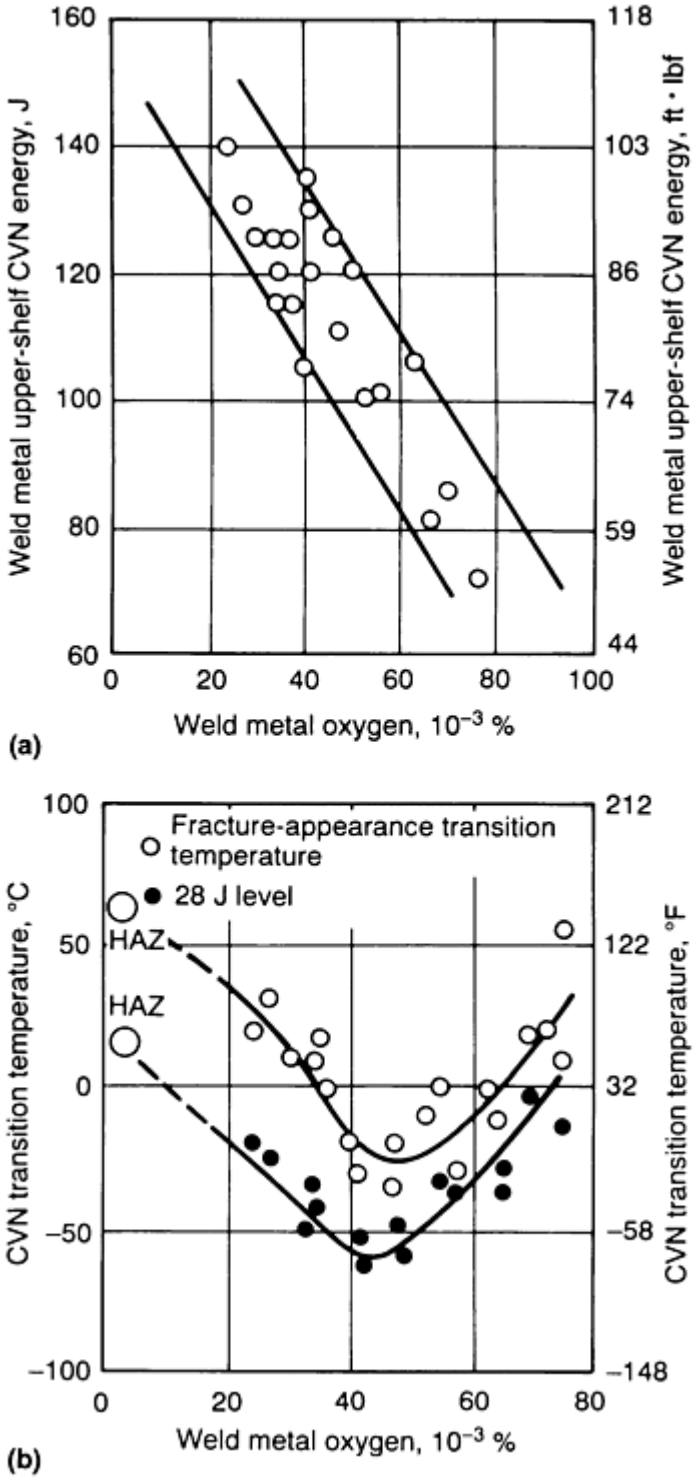

FIG. 22 TYPICAL VARIATION OF SELECTED WELD METAL PROPERTIES WITH OXYGEN CONTENT IN FERRITIC STEEL WELD METALS. (A) PLOT OF CHARPY V-NOTCH (CVN) IMPACT TEST UPPER-SHELF ENERGY VERSUS OXYGEN CONTENT. (B) PLOT OF CVN TRANSITION TEMPERATURE VERSUS OXYGEN CONTENT. SOURCE: REF 26

In recognition of the latter fact, most of the work in consumables development in the recent past has concentrated on increasing the amount of acicular ferrite in the microstructure. In line with the trends shown in Fig. 21(a) and 21(b), it has been found that decreasing the amount of grain boundary ferrite and ferrite sideplate structures increases the acicular ferrite content. This is shown more clearly in Fig. 23.

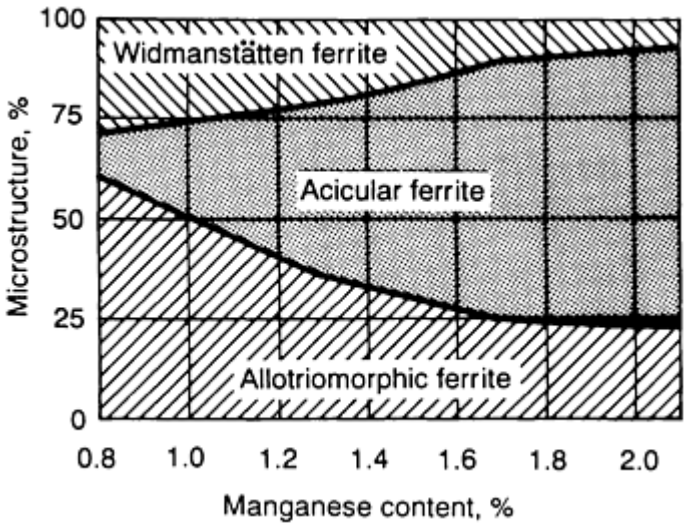

FIG. 23 EFFECT OF MANGANESE CONTENT OF WELD METAL ON THE RELATIVE AMOUNTS OF THE MICROSTRUCTURAL CONSTITUENTS PRESENT. CARBON CONTENT MAINTAINED AT 0.03%. SOURCE: REF 27

Recent work (Ref 24, 25, 27), however, has shown that a 100% acicular ferritic structure is neither desirable nor, in most cases, achievable. Figure 24 shows that the impact toughness peaks at about 70% acicular ferrite and then falls. This was attributed to the formation of segregated bands of brittle microphases in the alloy compositions giving the highest acicular ferrite contents. Moreover, when the alloying additions are increased still further, the transformation behavior becomes such that allotriomorphic ferrite formation is totally suppressed, leaving the γ grain boundaries free to nucleate upper bainite at lower temperatures (see Fig. 21c). It appears that a small layer of allotriomorphic ferrite is essential to obtain high acicular ferrite contents. When it forms, it saturates the γ grain boundary sites, and bainite nucleation at the γ/α-allotriomorphic interface is inhibited by the high carbon content there as a result of its rejection from the ferrite (Ref 24). Conditions are then favorable for intragranular nucleation at inclusion sites and thus the formation of acicular ferrite.

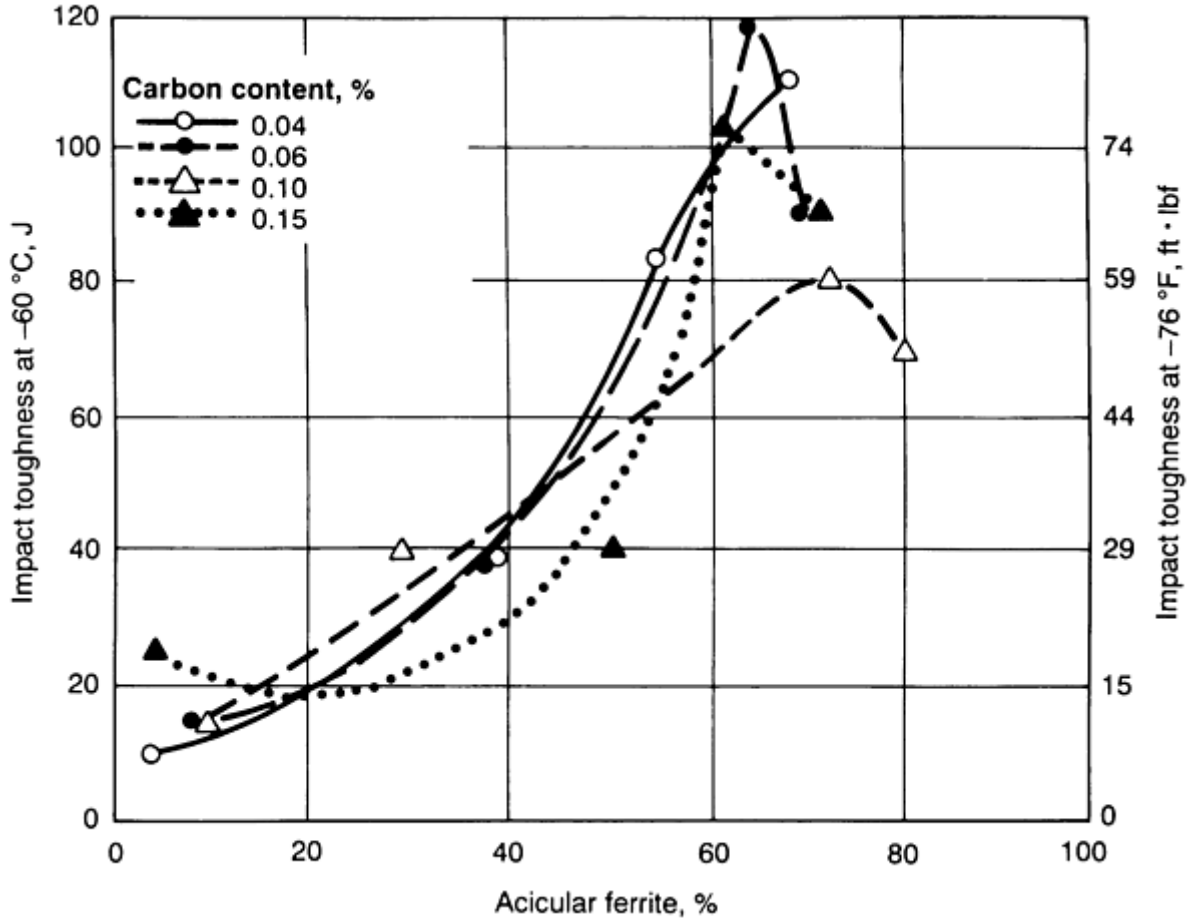

FIG. 24 PLOT OF IMPACT ENERGY VERSUS ACICULAR FERRITE CONTENT FOR SELECTED CARBON CONTENTS AT -60 °C (-78 °F). SOURCE: REF 27

For the welding of steels with yield strengths less than 600 MPa (85 ksi), it has been possible to develop weld metals with matching strength and toughness by having high acicular ferrite contents in them. A yield strength of about 600 MPa (85 ksi) seems to be the ceiling for weld metals based on acicular ferrite. Attempting to obtain additional strength by additional alloying to increase the amount of solid solution hardening and precipitation hardening in fact only results in increasing amounts of martensite and bainite. These structures are associated with a lower toughness. This has been observed in the case of HSLA-100 steels, for example, where attempts to get a matching strength in the weld metal have resulted in a drop in toughness (Ref 25, 28). Work on consumables development for high-strength steels is still in progress to match the base metal in strength and toughness (Ref 25, 28). However, current thinking appears to favor resorting to a slightly undermatching weld metal (in terms of strength) so that the already available lower-strength, high-toughness, consumables having high acicular ferrite contents (Ref 29) can be used. These weld metal compositions have the additional benefit of requiring less stringent measures for avoiding hydrogen-induced cracking.

Titanium Oxide Steels. In the discussion of the role of pinning by precipitate particles (for example, TiN) in limiting grain growth in the HAZ (in the section "Precipitate Stability and Grain Boundary Pinning" in this article), it was pointed out that at high heat inputs the particles dissolve and are not able to prevent coarse γ grains from forming. The low toughness in these coarse-grained regions is of some concern. The fact that a coarse γ grain size will lead to a higher acicular ferrite content (see Fig. 21b) with improved toughness has been used to advantage in the development of titanium-oxide-containing steels (Ref 30, 31). Ti_2O_3 is more stable than titanium nitride and does not dissolve, even at the highest heat inputs. The undissolved, Ti_2O_3 particles do not stop grain growth, but their survival after the heating cycle means that they can be effective in nucleating acicular ferrite within the coarse γ grains. The precise reasons why they are more effective than other undissolved inclusions, such as Al_2O_3 in nucleating acicular ferrite are not well understood (Ref 24). The improved HAZ microstructure and toughness obtained with titanium oxide steels over titanium nitride steels at high heat inputs are shown in Fig. 25 and 26, respectively.

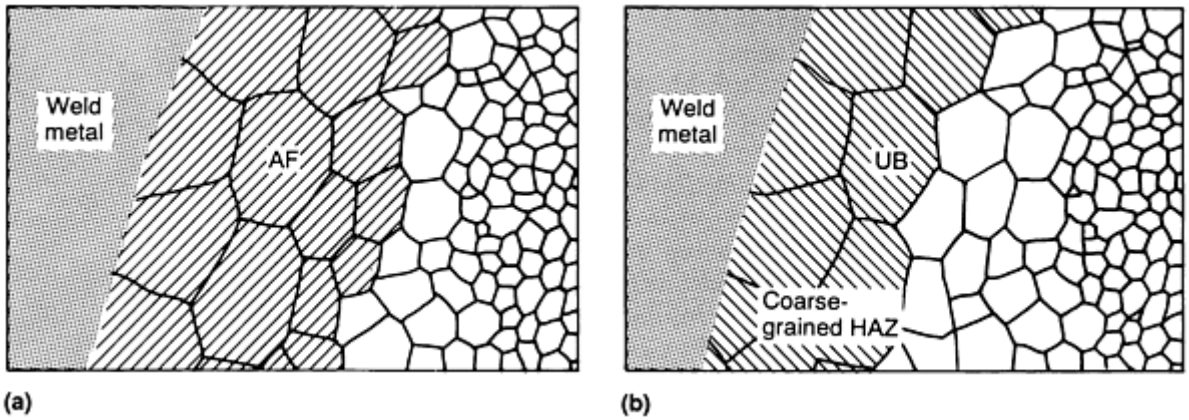

FIG. 25 SCHEMATIC SHOWING HAZ MICROSTRUCTURE IN SELECTED HIGH HEAT INPUT WELDS. (A) TITANIUM OXIDE STEEL. (B) TITANIUM NITRIDE STEEL. AF, ACICULAR FERRITE; UB, UPPER BAINITE. SOURCE: REF 30

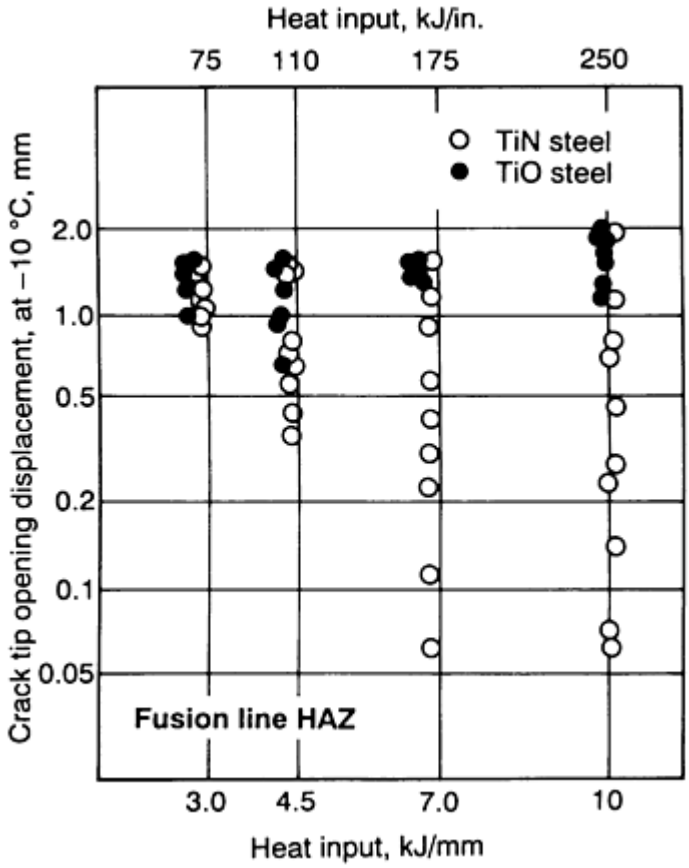

FIG. 26 HAZ TOUGHNESS OF TITANIUM NITRIDE AND TITANIUM OXIDE STEELS WITH 420 MPA (60 KSI) YIELD STRENGTH. SOURCE: REF 31

Effect of Transformations on Transient Weld Stresses. The effect of transformations on weld stresses (and vice versa) is best illustrated by introducing an apparently little-known proposal (Ref 32) about the use of a duplex austenite-martensite weld metal for welding high-strength steels. First, to prepare the background, the way in which transient stresses develop in a weld and the effect of transformations on weld stresses will be discussed.

Four uniaxial specimens using an HAZ simulation technique, the manner in which residual stress is accumulated during a weld thermal cycle was investigated (Ref 33), and the results are shown in Fig. 27. Initially, when a material is austenite at high temperature, its yield strength is low and only a small tensile stress can develop. On cooling, the tensile stress increases. When a phase transformation occurs, the resulting volume expansion opposes the contraction due to cooling and decreases the stress. Once the transformation is complete, the tensile stress increases again. As seen in Fig. 27, if the transformation occurs at a lower temperature (for example, in the case of 9Cr1Mo or 12CrMo steels), the magnitude of the final residual stress is less. The dotted line in the plot shows the expected variation for a material with an austenite-martensite structure. The greater the amount of martensite, the lower the final residual stress.

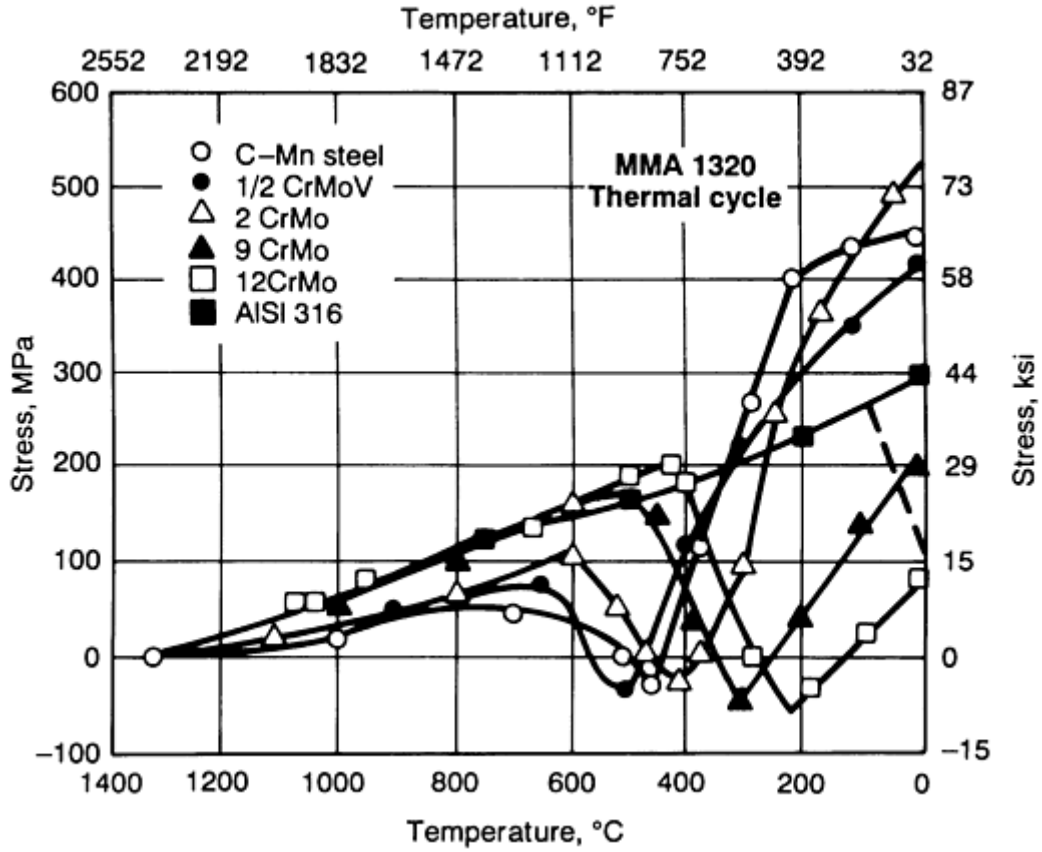

FIG. 27 STRESS ACCUMULATED DURING COOLING UNDER RESTRAINT FOR SELECTED STEELS. THE DOTTED LINE SHOWS THE EXPECTED VARIATION IN STRESS FOR A DUPLEX AUSTENITE-MARTENSITE WELD METAL WHERE TRANSFORMATION BELOW ABOUT 100 °C (212 °F) GREATLY REDUCES THE FINAL STRESS. (MMA 1320 INDICATES THE PEAK TEMPERATURE OF THE SIMULATED WELD THERMAL CYCLE AND CORRESPONDS TO THE TEMPERATURE AT THE START OF THE COOLING CYCLE.) SOURCE: REF 33

As discussed in the section "Weld Metal Toughness Relative to the Microstructure" in this article, the main problems in the welding of high-strength steels (with yield strengths of 600 to 1000 MPa, or 85 to 145 ksi) are hydrogen-induced cracking (HIC) and low toughness in the weld metal. Both problems can be addressed (in principle at least) by the use of a duplex austenite-martensite weld metal. Austenite can contribute by increasing the toughness and by minimizing the risk for HIC (Ref 14). The role of martensite will be to increase the strength and to decrease the final residual tensile stress, which also makes conditions less favorable for HIC. An additional benefit will be that the higher tensile residual stress in the weld metal before martensite forms will induce the transformations in the HAZ to occur at a slightly higher temperature, by Le Chatelier's principle (Ref 34), and thereby cause a microstructure less susceptible to HIC to form in the HAZ. The results of this effect are shown in Fig. 28, where it is seen that a tensile stress in the 500 to 300 °C (930 to 570 °F) temperature range on a ferrite-pearlite weld increased the stresses for failure (Ref 35).

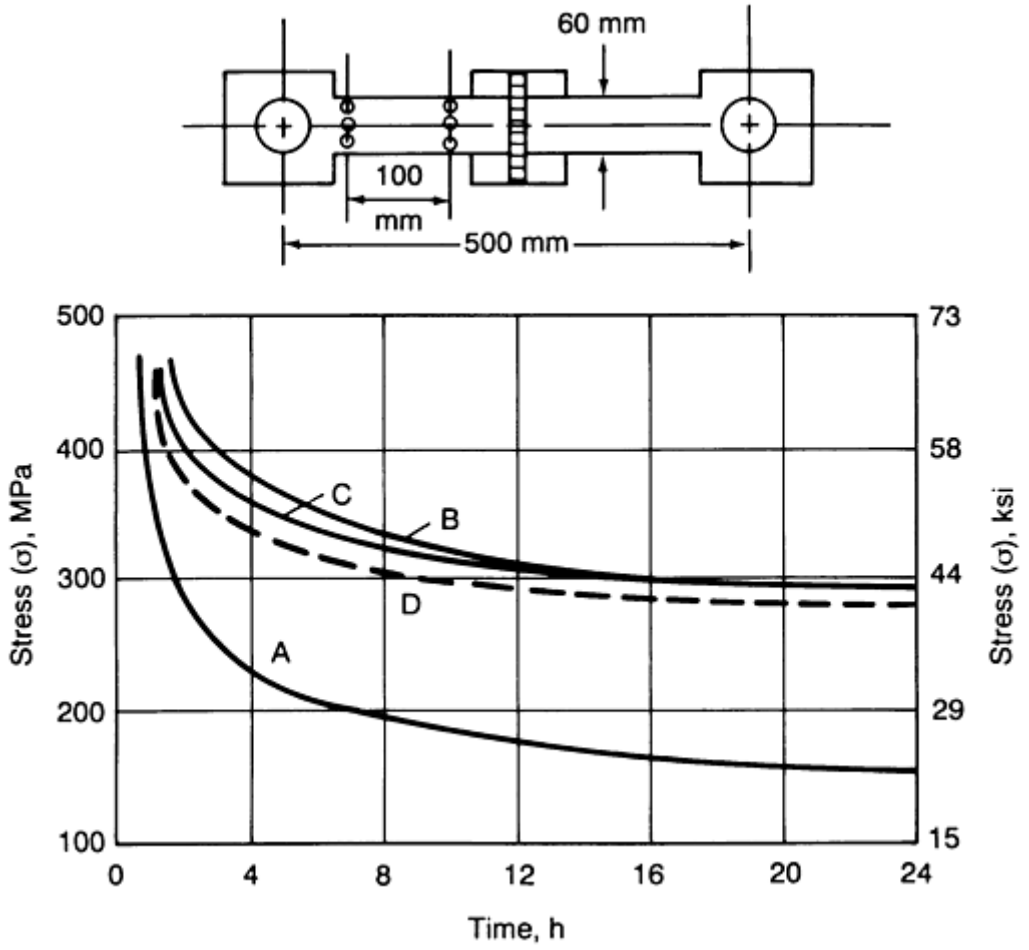

FIG. 28 DELAYED FRACTURE CURVES FOR TENSILE TESTS ON WELDED JOINTS IN 35KH3N3M (A RUSSIAN SPECIFICATION) STEEL. A, FERRITIC-PEARLITIC WELD; B, BAINITIC-MARTENSITIC WELD; C, AUSTENITIC WELD; D, FERRITIC-PEARLITIC WELD PLUS DEFORMATION AT 500 TO 300 °C (930 TO 570 °F). THE SCHEMATIC SHOWS THE SPECIMEN DIMENSIONS FOR THE DELAYED FRACTURE TENSILE TESTS ON WELDED JOINTS. SOURCE: REF 35

It must be mentioned that the idea of using an austenite-martensite weld metal represents a considerable departure from conventional thinking. For example, for certain overlaying applications of stainless steel deposits on low-alloy steel, an overalloyed electrode like E310 or E312 is preferred to E309. Even though the weld metal composition with any of the three electrodes would be acceptable, the use of overalloyed electrodes will minimize the width of the martensitic layer in the unmixed zone at the weld-HAZ interface (Ref 36). By contrast, an austenite-martensite weld metal implies that the choice of consumable will have to be such that the width of the martensitic layer will increase. However, because the proposal is meant for the recently developed high-strength steels that have a low carbon content, only a low-carbon martensite will form, which will not be that harmful. The benefits already discussed could override conventional concerns about having martensite in the weld metal in this case.

To sum up, even though the idea of using an austenite-martensite weld metal for high-strength steels does not seem to have been taken up for serious investigation so far, it has been included here because it is a nice way of illustrating the principles discussed. In addition, it shows that a fundamental knowledge of different effects on phase transformations can lead to unconventional solutions to practical problems.

References cited in this section

3. O. GRONG AND D.K. MATLOCK, MICROSTRUCTURAL DEVELOPMENT IN MILD AND LOW ALLOY STEEL WELD METALS, *INT. MET. REV.,* VOL 31 (NO. 1), 1986, P 27-48

6. K. EASTERLING, *INTRODUCTION TO THE PHYSICAL METALLURGY OF WELDING,* BUTTERWORTHS, 1983

14. S. KOU, *WELDING METALLURGY,* JOHN WILEY & SONS, 1987

22. L.E. SAMUELS, *OPTICAL MICROSCOPY OF CARBON STEELS,* AMERICAN SOCIETY FOR METALS, 1980

23. "GUIDE TO THE LIGHT MICROSCOPE EXAMINATION OF FERRITIC STEEL WELD METALS," DOC. NO. IX-1533-88, INTERNATIONAL INSTITUTE OF WELDING, 1988

24. H.K.D.H. BHADESHIA AND L.E. SVENSSON, MODELLING THE EVOLUTION OF MICROSTRUCTURE OF STEEL WELD METAL, *MATHEMATICAL MODELLING OF WELD PHENOMENA,* H. CERJAK AND K. EASTERLING, ED., THE INSTITUTE OF MATERIALS, 1993

25. G.R. EDWARDS AND S. LIU, RECENT DEVELOPMENTS IN HSLA STEEL WELDING, *ADVANCES IN WELDING METALLURGY,* FIRST U.S.-JAPAN SYMPOSIUM, AMERICAN WELDING SOCIETY AND OTHERS, JUNE 1990, P 215-293

26. B. AHLBLOM, "OXYGEN AND ITS ROLE IN DETERMINING WELD METAL MICROSTRUCTURE AND TOUGHNESS--A STATE OF THE ART REVIEW," DOC. NO. IX-1322-84, INTERNATIONAL INSTITUTE OF WELDING, 1984

27. L.-E. SVENSSON AND B. GRETOFT, MICROSTRUCTURE AND IMPACT TOUGHNESS OF C-MN WELD METALS. *WELD. J.,* DEC 1990, P 454S-461S

28. P.W. HOLSBERG AND R.J. WONG, WELDING OF HSLA-100 STEEL FOR NAVAL APPLICATIONS, *WELDABILITY OF MATERIALS,* R.A. PATTERSON AND K.W. MAHIN, ED., ASM INTERNATIONAL, 1990

29. J.M.B. LOSZ AND K.D. CHALLENGER, MICROSTRUCTURE AND PROPERTIES OF A COPPER PRECIPITATION STRENGTHENED HSLA STEEL WELDMENT, *RECENT TRENDS IN WELDING SCIENCE AND TECHNOLOGY,* S.A. DAVID AND J.M. VITEK, ED., ASM INTERNATIONAL, 1990

30. H. HOMMA, S. OHKITA, S. MATSUDA, AND K. YAMAMOTO, IMPROVEMENTS OF HAZ TOUGHNESS IN HSLA STEEL BY INTRODUCING FINELY DISPERSED TI-OXIDE, *WELD. J.,* OCT 1987, P 301S-309S

31. N. YURIOKA, "MODERN HIGH STRENGTH STEEL IN JAPAN," FIFTH INTERNATIONAL SYMPOSIUM, JAPAN WELDING SOCIETY, APRIL 1990 (TOKYO)

32. YU.N. GOTALSKII, THE PROBLEM OF WELDING HIGH STRENGTH STEELS, *AUTOM. WELD.,* JUNE 1984, P 37-40

33. W.K.C. JONES AND P.J. ALBERRY, THE ROLE OF PHASE TRANSFORMATIONS IN THE DEVELOPMENT OF RESIDUAL STRESSES DURING THE WELDING OF SOME FAST REACTOR STEELS, *PROC. CONF. FERRITIC STEELS FOR FAST REACTOR STEAM GENERATORS,* BRITISH NUCLEAR ENERGY SOCIETY, 1977

34. *MCGRAW-HILL ENCYCLOPEDIA OF SCIENCE AND TECHNOLOGY,* VOL 9, P 685

35. A.M. MAKARA AND N.A. MOSENDZ, EFFECTS OF THE WELD METAL ON CRACKING IN HAZ, *WELD. RES. ABROAD,* NOV 1965, P 78-86

36. H. IKAWA, S. SHIN, M. INUI, Y. TAKEDA, AND A. NAKANO, "ON THE MARTENSITE-LIKE STRUCTURE AT WELD BOND AND THE MACROSCOPIC SEGREGATION IN WELD METAL IN THE WELDED DISSIMILAR METALS OF α-STEELS AND γ-STEELS," DOC. NO. IX-785-72, INTERNATIONAL INSTITUTE OF WELDING, 1972

Solid-State Transformations in Weldments

P. Ravi Vishnu, Luleå University of Technology, Sweden

HAZ in Multipass Weldments

In the HAZ of a single-pass weld, the grain-coarsened zone (GC HAZ) is normally the region having the lowest toughness. Turning to a multipass weld, Fig. 29 (compare with Fig. 3) shows how the GC HAZ can be modified by subsequent passes and can be categorized into four regions, depending on the reheating temperature (Ref 37):

- SUBCRITICALLY REHEATED GRAIN-COARSENED (SCGC) ZONE, THE ZONE REHEATED BELOW AC_1
- INTERCRITICALLY REHEATED GRAIN-COARSENED (ICGC) ZONE, THE ZONE REHEATED BETWEEN AC_1 AND AC_3
- SUPERCRITICALLY REHEATED GRAIN-REFINED (SCGR) ZONE, THE ZONE REHEATED ABOVE AC_3 AND BELOW ABOUT 1200 °C (2190 °F)
- UNALTERED GRAIN-COARSENED (UAGC) ZONE, THE ZONE THAT IS NOT REHEATED ABOVE ABOUT 200 °C (390 °F) OR THE ZONE THAT IS AGAIN REHEATED ABOVE ABOUT 1200 °C (2190 °F)

Figure 30 shows how the crack tip opening displacement (CTOD) value of simulated specimens varies with the peak temperature of the second thermal cycle, T_{p2} (T_{p1} = 1400 °C, or 2550 °F). It is seen that the ICGC, UAGC, and SCGC regions have CTOD values less than about 0.1 mm (0.004 in.). Similar low values have been obtained by locating the crack tip in the CTOD tests at corresponding locations in the HAZ of actual multipass weldments. These low toughness regions are commonly known as local brittle zones (LBZs).

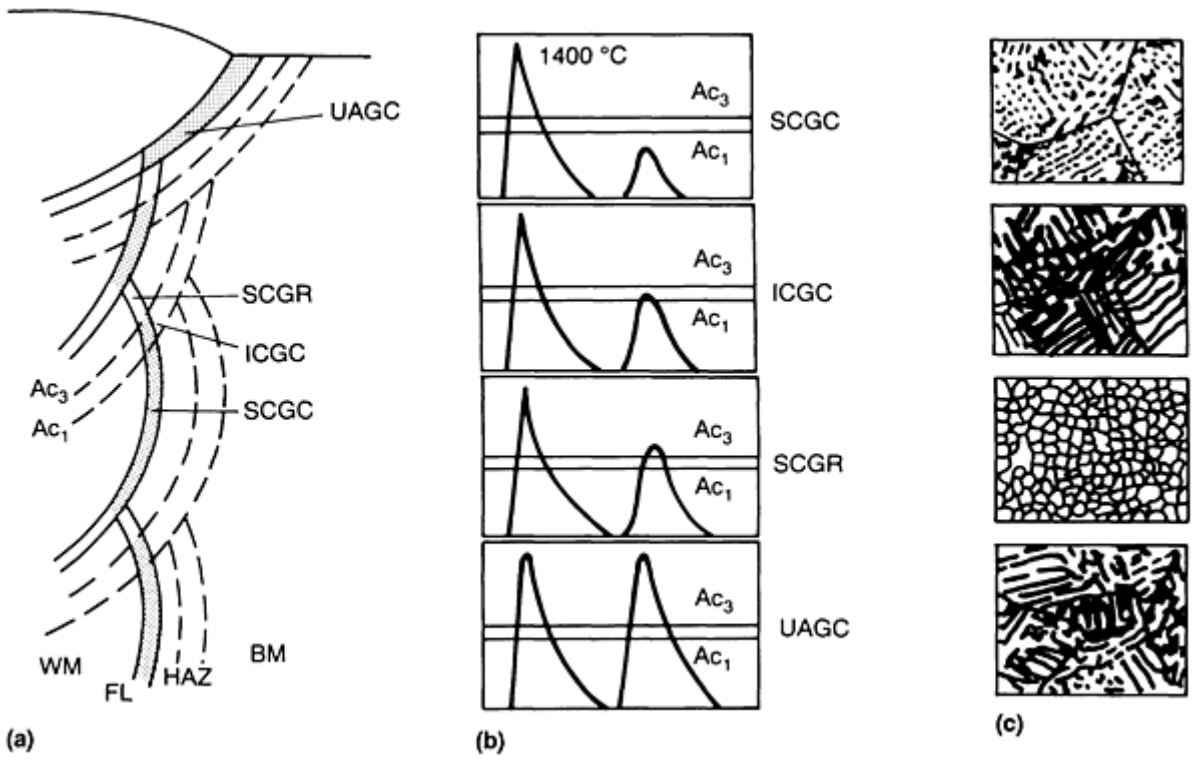

FIG. 29 SCHEMATIC SHOWING THE DIFFERENT SUBZONES THAT CAN FORM IN THE COARSE-GRAINED REGION OF THE HAZ IN A MULTIPASS WELD. (A) POSITION OF SUBZONES RELATIVE TO BASE METAL (BM) AND WELD METAL (WM). (B) PLOT OF THERMAL CYCLES RELATIVE TO AC_3 AND AC_1. (C) MICROSTRUCTURES AT THE DIFFERENT ZONES. FL REFERS TO THE FUSION LINE. SEE TEXT FOR DETAILS. SOURCE: REF 37

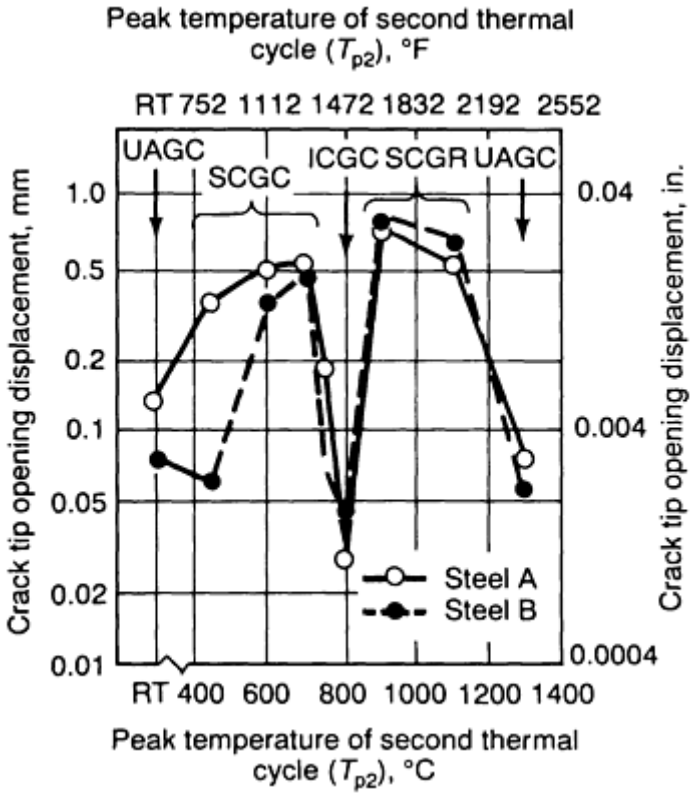

FIG. 30 PLOT OF CRACK TIP OPENING DISPLACEMENT VERSUS PEAK TEMPERATURE OF THE SECOND THERMAL CYCLE FOR SIMULATED SPECIMENS SUBJECTED TO A DOUBLE THERMAL CYCLE. (T_{P1} = 1400 °C = 2550 °F; $\Delta T_{8\text{-}5}$ = 20 S). THE HAZ ZONES (FIG. 29) CORRESPONDING TO THE SIMULATION TRIALS ARE ALSO SHOWN IN THE FIGURE. SOURCE: REF 37

The low CTOD values have been obtained only in tests on modern structural steels, whereas no actual structural failure attributable to the LBZs has been reported so far (Ref 38). Because the structural significance of the low toughness test results is still largely unresolved, the present conservative strategies are to choose a steel whose tendency to form LBZs is less or to choose a welding procedure by which the size of the LBZs can be reduced.

The ICGC HAZ usually has a lower toughness than the SCGC or UAGC regions, even though all of them have nearly the same γ grain size. This is due to the higher amount of highcarbon martensite-austenite (M-A) constituent in the ICGC HAZ. When the GC HAZ is reheated to a temperature between Ac_1 and Ac_3, austenite is nucleated at the high carbon areas. Upon cooling, these local high-carbon areas can transform to give twinned martensite with every thin regions of retained austenite in between. (See Ref 39 for detailed metallographic procedures for identifying the M-A constituent.) The carbon content in the M-A islands can range from about 0.3 to 0.5% C. The significance of this is that, for a given nominal carbon content in the steel, the volume fraction of the M-A constituent will be much higher than if most of the carbon formed carbides (by the lever rule). This will increase the number of crack nucleation sites and thereby contribute to the inferior toughness of ICGC HAZ. As is to be expected, the volume fraction of the M-A constituent also depends on the hardenability of the steel, which in turn depends on the alloying content. It has been shown that if the development of pearlitic microphases could be promoted instead of the development of M-A, by decreasing the alloy content, the toughness of the ICGC HAZ could be improved (Ref 40). However, this would have penalties in terms of achievement of parent plate strength. A more feasible solution would be to inhibit grain growth in the HAZ.

The multipass welding procedure can alternatively be controlled to limit the size of the LBZs. Figure 31 shows how this can be done with a tandem three-wire high current gas-metal arc welding procedure by adjusting the distance between the three arcs. Special "temper-bead" procedures (Ref 42) have been developed for controlling the microstructure in the HAZ, and a need for these procedures arises in the following way. Low-alloy steel weldments for critical applications (for example, pressure vessels) require a postweld heat treatment (PWHT) in a furnace. This is done to temper the hard regions in the HAZ and to relieve residual stresses. If repairs become necessary on site after the component has been in service, PWHT is usually not feasible. The heat of the arc can then be used to achieve the tempering function of PWHT

by suitable spatial positioning and sequencing of the individual passes. Grain refinement in he HAZ is also sought to increase the toughness and thereby offset the harmful effects of residual stresses that would remain in the absence of PWHT.

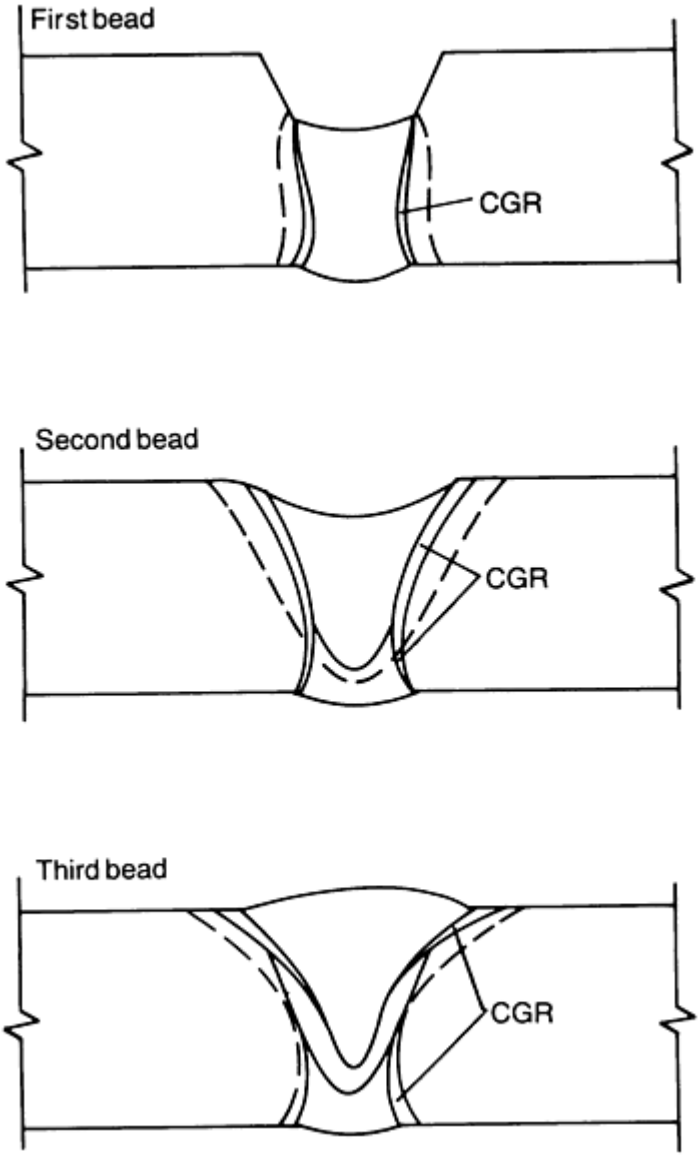

FIG. 31 SCHEMATIC SHOWING THAT THE HAZ ISOTHERMS AND THE SIZE AND LOCATION OF THE COARSE-GRAINED REGION (CGR) CAN BE CONTROLLED IN A TANDEM THREE-WIRE HIGH CURRENT GAS-METAL ARC WELDING PROCEDURE. GRAIN REFINEMENT OF COARSE-GRAINED REGIONS INITIALLY FORMED IS OBTAINED BY OPTIMIZING THE DISTANCES BETWEEN THE THREE ARCS. SOURCE: REF 41

An example of a two-layer temper bead procedure is shown in Fig. 32. The heat inputs of the first and second layer are carefully controlled, so that the heat from the second layer is used to refine the coarse-grained region in the HAZ of the base metal due to the first layer. This ideas can be extended one step further by using a pulsed gas-tungsten arc welding procedure whereby a given pulse in a pulsed weldment can be used to successively refine and temper the preceding pulse pitch regions (Ref 11). The degree of microstructural refinement depends primarily on the welding speed and pulsing frequency, and these parameters can be controlled with great precision. By contrast, an important variable to be controlled in the temper-bead procedure is the weld deposit height, and it is difficult to exercise the same degree of control on this. For this reason, it is argued that the maximum possible control on the microstructural changes in the repair weldment is possible with the pulsing procedure.

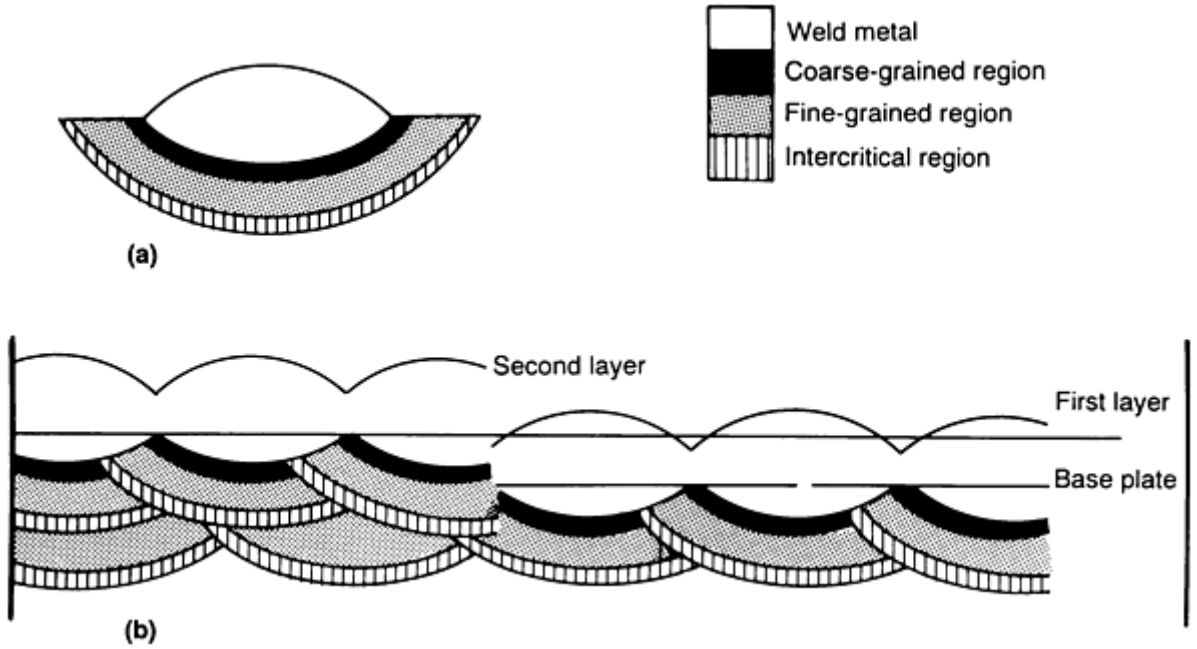

FIG. 32 SCHEMATIC SHOWING A TWO-LAYER REPAIR PROCEDURE. (A) HEAT-AFFECTED AREAS OF A SINGLE WELD BEAD. (B) FIRST LAYER CAUSES COARSE-GRAINED REGIONS TO FORM IN THE HAZ OF THE BASE METAL (RIGHT PORTION OF THE FIGURE). DEPOSITION OF THE SECOND LAYER REFINES THESE INITIAL COARSE-GRAINED REGIONS (LEFT PORTION OF FIGURE). SOURCE: REF 42

References cited in this section

11. P. RAVI VISHNU AND K. EASTERLING, PHENOMENOLOGICAL MODELLING OF HEAT FLOW AND MICROSTRUCTURAL CHANGES IN PULSED GTAW WELDS OF A QT STEEL, *MATHEMATICAL MODELING OF WELD PHENOMENA,* H. CERJAK AND K. EASTERLING, ED., THE INSTITUTE OF METALS, 1993
37. T. HAZE AND S. AIHARA, "INFLUENCE OF TOUGHNESS AND SIZE OF LOCAL BRITTLE ZONES ON HAZ TOUGHNESS OF HSLA STEELS," SEVENTH INTERNATIONAL CONFERENCE ON OFFSHORE MECHANICS AND ARCTIC ENGINEERING, HOUSTON, 1988
38. C.P. ROYER, A USER'S PERSPECTIVE ON HEAT AFFECTED ZONE TOUGHNESS, *WELDING METALLURGY OF STRUCTURAL STEELS,* J.Y. KOO, ED., TMS-AIME, 1987
39. F. MATSUDA, Z. LI, P. BERNASOVSKY, K. ISHIHARA, AND H. OKADA, "AN INVESTIGATION OF THE BEHAVIOUR OF M-A CONSTITUENT IN SIMULATED HAZ OF HSLA STEELS," DOC. NO. IX-B-1591-90, INTERNATIONAL INSTITUTE OF WELDING, 1990
40. P.L. HARRISON AND P.H.M. HART, RELATIONSHIPS BETWEEN HAZ MICROSTRUCTURE AND CTOD TRANSITION BEHAVIOUR IN MULTIPASS C-MN STEEL WELDS, *RECENT TRENDS IN WELDING SCIENCE AND TECHNOLOGY,* S.A. DAVID AND J.M. VITEK, ED., ASM INTERNATIONAL, 1990
41. H. ONOE, J. TANAKA, AND I. WATANABE, JAPANESE LNG TANKER CONSTRUCTED USING A NEW WELDING PROCESS AND IMPROVED AL-KILLED STEELS, *MET. CONSTR.,* JAN 1979, P 26-31
42. P.J. ALBERRY, SENSITIVITY ANALYSIS OF HALF-BEAD AND ALTERNATIVE GTAW TECHNIQUES, *WELD. J.,* NOV 1989, P 442S-451S

Fusion Zone in Multipass Weldments

In the weld metal of a multipass weld, reheating effects will lead to a gradient in microstructure similar to the case of the HAZ. However, instead of a detailed classification, the multipass weld metal is usually considered to consist of just two regions (Fig. 33):

- *AS-DEPOSITED OR PRIMARY REGION,* WHERE THE MICROSTRUCTURE DEVELOPS AS THE WELD COOLS FROM THE LIQUID PHASE TO AMBIENT TEMPERATURE
- *REHEATED OR SECONDARY REGION,* WHERE REGIONS WITH THE ORIGINAL PRIMARY MICROSTRUCTURE ARE REHEATED TO TEMPERATURES ABOVE THE AC_1 TEMPERATURE. THE TEMPERED REGIONS WHICH ARE REHEATED TO SLIGHTLY LOWER TEMPERATURES ARE ALSO GENERALLY CONSIDERED TO BELONG TO THIS CATEGORY

The properties of the weld metal depend on the relative area or volume fractions of the two regions, which in turn depend on the welding procedure, so the properties are procedure-specific. Hence arises the need for welding procedure qualification as per codes and standards in addition to the qualification of consumables (for which is standard procedure is specified).

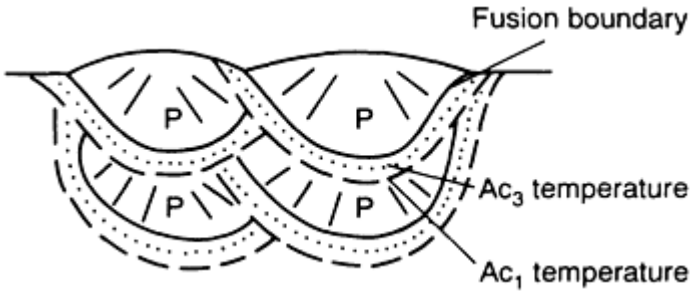

FIG. 33 PRIMARY (P) AND REAUSTENITIZED REGIONS IN THE WELD METAL REGION OF A MULTIPASS WELD. THE REAUSTENITIZED REGION IS WHERE THE COLUMNAR STRUCTURE IS NOT CLEARLY DETECTED. SOURCE: REF 23

Reference cited in this section

23. "GUIDE TO THE LIGHT MICROSCOPE EXAMINATION OF FERRITIC STEEL WELD METALS," DOC. NO. IX-1533-88, INTERNATIONAL INSTITUTE OF WELDING, 1988

Solid-State Transformations in Weldments

P. Ravi Vishnu, Luleå University of Technology, Sweden

Stainless Steels

It has long been known that solidification cracking can be avoided in austenitic stainless steel welds by having a small concentration of ferrite in them. Recent work has shown, however, that residual ferrite content at room temperature is no

more than a symptom and that it is really the solidification mode (whether the weld metal solidifies as primary austenite or ferrite) that is the deciding criterion (Ref 43). It has been found that susceptibility to solidification cracking is least for a primary ferrite solidification mode (more specifically, when the solidification mode corresponds to the types shown in Fig. 34c and 34d). It is believed that low-melting-point liquid phases (formed by the segregation of impurities like sulfur and phosphorus, for example) solidifying in the intercellular regions do not wet the δ-γ interphase boundaries as easily as they would δ-δ or γ-γ boundaries. In the ferritic-austenitic solidification mode (Fig. 34c and 34d), the δ-γ interphase boundary area is greater at temperatures just below the nominal solidus temperature, and this is the reason for a greater resistance to solidification cracking.

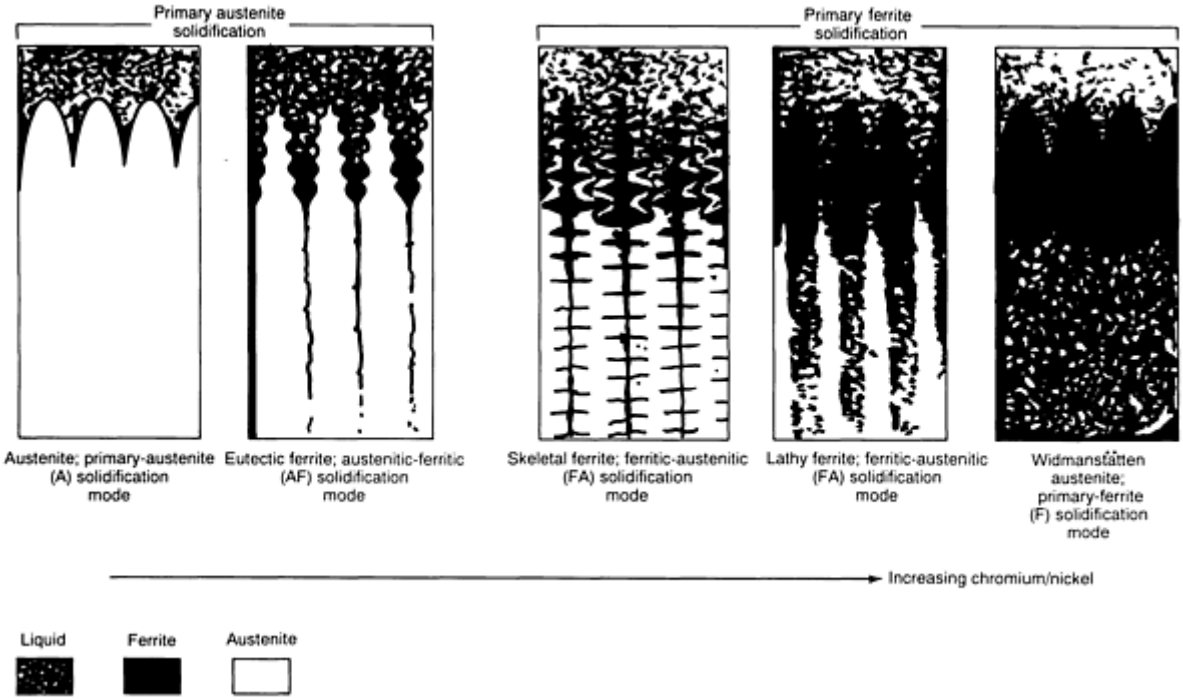

FIG. 34 SCHEMATIC SHOWING SOLIDIFICATION AND TRANSFORMATION BEHAVIOR RESULTING IN A RANGE OF FERRITE MORPHOLOGIES IN AUSTENITIC STAINLESS STEEL WELDS. SOURCE: REF 43

Information about the solidification mode can be obtained from the chemical composition of the weld metal by referring to the WRC-1992 diagram (Fig. 35). It has been found that this diagram is more accurate than the Schaeffler (for duplex stainless steel welds) and Delong (for 300 series austenitic steel welds) diagrams developed earlier. All of these diagrams are strictly applicable only for the cooling rates obtained in manual metal arc (MMA) welding because the data for establishing the statistical correlations have been taken from MMA welds. The dotted lines in Fig. 35 are the demarcation lines between the different solidification modes shown (that is, A, AF, FA, and F) corresponding to the types in Fig. 34(a), 34(b), 34(c), 34(d), and 34(e), respectively. The AF-FA boundary in Fig. 35 (which, as discussed earlier, corresponds to the onset of cracking) intersects the iso-ferrite number lines at an angle. This is consistent with the findings of several investigators that the minimum ferrite content necessary to avoid hot cracking is different for different weld metal compositions (that is, for weld metals deposited with E 316, E 308L, E 309, and so on).

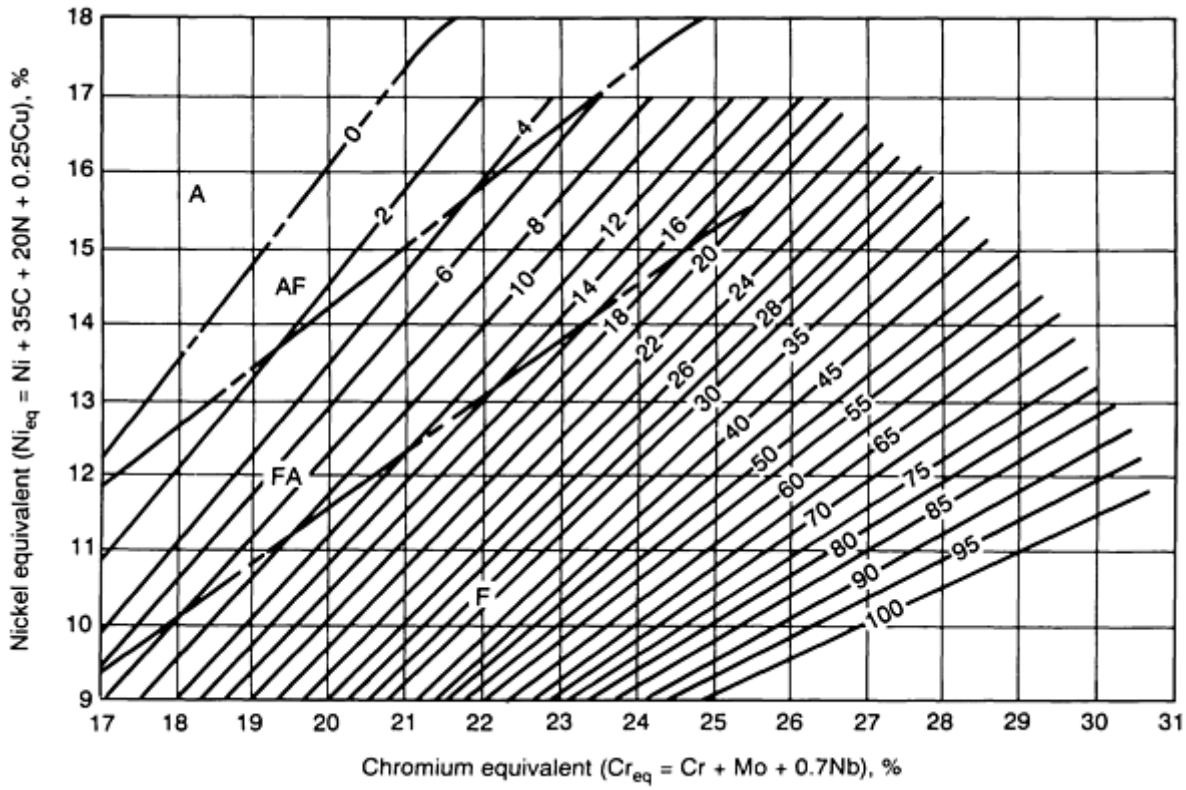

FIG. 35 WRC-1992 DIAGRAM PREDICTING FERRITE CONTENT IN STAINLESS STEELS. FERRITE CONTENT IS GIVEN BY THE FERRITE NUMBER (FN), WHERE 100 FN IS APPROXIMATELY EQUAL TO 65 VOL% FERRITE. BOUNDARIES DENOTING A CHANGE IN SOLIDIFICATION MODE (A, AF, FA AND F PER FIG. 34) ARE ALSO SHOWN (INDICATED BY DOTTED LINES). SOURCE: REF 45

It is a fortunate coincidence that the coefficients in the Cr_{eq} and Ni_{eq} expressions (see Fig. 35), which have been obtained by statistical fitting methods, result in satisfactory correlations with both the solidification mode and the ferrite number (a precisely measurable quantity that is roughly proportional to the actual volume percentage of ferrite at room temperature) (Ref 44). Indeed, it has been found that the same Cr_{eq} and Ni_{eq} expressions (that is, with the same elements and coefficients) are not able to satisfactorily fix the locations of the martensite and martensite-austenite phase fields seen in the lower left region of the Schaeffler diagram. For this reason, such regions of Cr_{eq} and Ni_{eq} are excluded in the WRC-1992 diagram.

A discussion of weld decay due to sensitization and knife line attack in the HAZ of austenitic stainless steels can be found in Ref 14 and 46.

References cited in this section

14. S. KOU, *WELDING METALLURGY,* JOHN WILEY & SONS, 1987
43. J.A. BROOKS AND A.W. THOMPSON, MICROSTRUCTURAL DEVELOPMENT AND SOLIDIFICATION CRACKING SUSCEPTIBILITY OF AUSTENITIC STAINLESS STEEL WELDS, *INT. MATER. REV.,* VOL 36 (NO. 1), 1991
44. T.A. SIEWERT, C.N. MCCOWAN, AND D.L. OLSON, FERRITE NUMBER PREDICTION TO 100 FN IN STAINLESS STEEL WELD METAL, *WELD. J.,* DEC 1988, P 289S-298S
45. D.J. KOTECKI AND T.A. SIEWERT, WRC-1992 CONSTITUTION DIAGRAM FOR STAINLESS STEEL WELD METALS: A MODIFICATION OF THE WRC-1988 DIAGRAM, *WELD. J.,* MAY 1992, P 171S-178S
46. T.G. GOOCH AND D.C. WILLINGHAM, *WELD DECAY IN AUSTENITIC STAINLESS STEELS,* THE

P. Ravi Vishnu, Luleå University of Technology, Sweden

Aluminum Alloys

The main problems in the welding of heat-treatable aluminum alloys are liquation cracking in the partially melted zone (see the section "Unmixed and Partially Melted Zones in a Weldment" in this article) and softening in the HAZ (Ref 14, 47). The latter means that the weld joint strength can be reduced. Reasons for the softening can be understood by referring to Fig. 36. The parent material is assumed to be a 2000- or 6000-series aluminum alloy, artificially aged to contain the metastable phase of θ' (in aluminum-copper alloys), S' (in aluminum-copper-magnesium alloys), or β' (in aluminum-magnesium-silicon alloys). A very fine dispersion of precipitate particles is obtained in the parent material by a solution heat treatment followed by aging, and this is the reason for the high strength in the materials. Figure 36(b) shows that a gradient in hardness is obtained in the HAZ immediately after welding. At location 1, the high peak temperature causes the precipitate particles to go into solution, and the cooling rate is too high for reprecipitation. At locations 2 and 3, the precipitate particles partially dissolve and coarsen. After postweld artificial aging, fine precipitate particles are again formed at location 1, causing the hardness to increase to the parent material level. However, at locations 2 and 3, only a lower hardness can be obtained because of the formation of coarse precipitate particles. For increasing weld heat inputs, the width of the softened zone increases. A good discussion of how the above phenomenon can be modeled is found in Ref 48.

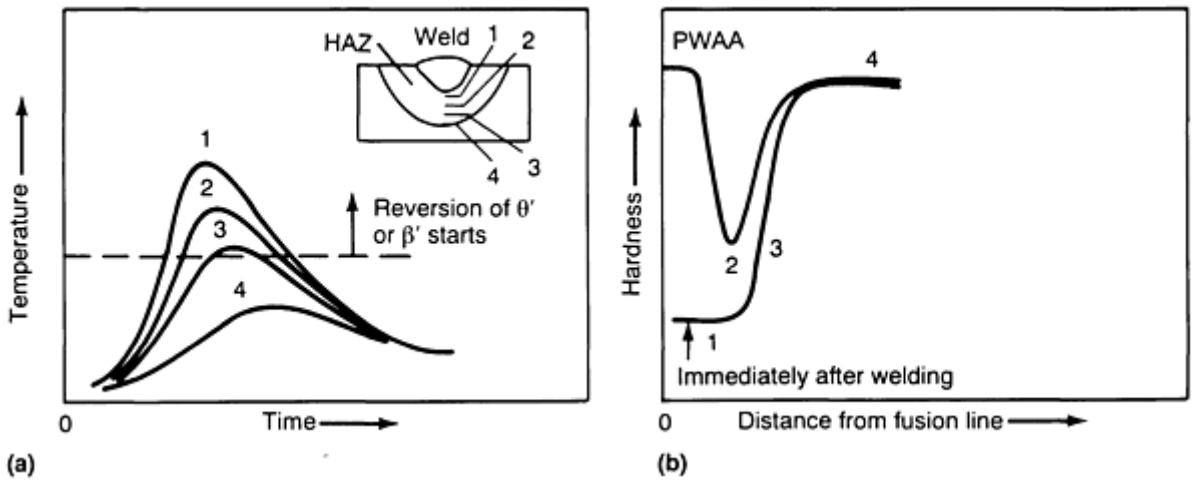

FIG. 36 SCHEMATIC SHOWING THE EFFECT OF WELD THERMAL CYCLES ON THE SOFTENING IN THE HAZ IN AGE-HARDENABLE ALUMINUM ALLOYS. (A) THERMAL CYCLES IN THE HAZ (FOR CORRESPONDING LOCATIONS IN WELD, SEE INSET. (B) HAZ HARDNESS PROFILES BEFORE AND AFTER AGING. PWAA, POSTWELD ARTIFICIAL AGING. SOURCE: REF 14

References cited in this section

14. S. KOU, *WELDING METALLURGY*, JOHN WILEY & SONS, 1987

47. S. KOU, WELDING METALLURGY AND WELDABILITY OF HIGH STRENGTH ALUMINUM ALLOYS, *WELD. RES. COUNC. BULL.*, NO. 320, DEC 1986

48. H. SHERCLIFF AND M.F. ASHBY, A PROCESS MODEL FOR AGE HARDENING OF AL ALLOYS--I. MODEL AND II. APPLICATIONS OF THE MODEL, *ACTA METALL. MATER.*, VOL 38 (NO. 10), 1990, P 1789-1812

Nickel-Base Superalloys

Nickel-base superalloys have a very high creep resistance, making them attractive for critical high-temperature applications such as gas turbines. Yet it is this very characteristic that gives rise to the problem of strain age cracking in the weld HAZ (Ref 14, 19, 49). The high-temperature creep strength in the parent materials is obtained by forming fine precipitates of γ' (Ni_3(Al, Ti)) or γ" (Ni_3Nb) in them. In the region of the weld HAZ subjected to high peak temperatures, these precipitates dissolve, similar to the case of aluminum alloys. After welding, the weldments are again solution heat-treated and aged (note the difference between aluminum alloys and the nickel-base superalloys in this respect). The purposes of this treatment are to obtain the same uniform and fine precipitation in the weld as in the parent material and to relieve the weld residual stresses.

Normally (for example, in the case of low-alloy or carbon steel welds), PWHT in a furnace relieves the residual stresses because the yield stress at the PWHT temperature is very low. A residual stress greater than the yield stress cannot be supported, and stress relief is brought about by a process of creep and plastic deformation. This process is difficult in nickel-base superalloy weldments, however, because of their high creep strength and low creep ductility. Reprecipitation in the solutionized regions of the HAZ (during the heating-up to the PWHT temperature) strengthens the matrix and does not allow any creep or plastic deformation (necessary for the relief of residual stress) to take place. Cracking can occur in this condition at the grain boundaries in the grain-coarsened region of the HAZ. Cracks initiated here have been known to run far into the base material. This problem is very difficult to solve, and the best solution has been found to be to switch over to materials such as Inconel 718 alloy that are inherently less susceptible to cracking, even though their creep strength is somewhat lower. Inconel 718 alloy contains γ" precipitate, and the slow kinetics of precipitation in this alloy allow substantial stress relief to be achieved before precipitation increases the creep strength in the HAZ.

References cited in this section

14. S. KOU, *WELDING METALLURGY,* JOHN WILEY & SONS, 1987

19. W. YENISCAVITCH, JOINING, *SUPERALLOYS II,* C.T. SIMS, N.S. STOLOFF, AND W.C. HAGEL, ED., JOHN WILEY & SONS, 1987, P 495-516

49. W.A. OWCZARSKI, PROCESS AND METALLURGICAL FACTORS IN JOINING SUPERALLOYS AND OTHER HIGH SERVICE TEMPERATURE MATERIALS, *PHYSICAL METALLURGY OF JOINING,* R. KOSSOWSKY AND M.E. GLICKSMAN, ED., TMS-AIME, 1980

Solid-State Transformations in Weldments

P. Ravi Vishnu, Luleå University of Technology, Sweden

Titanium Alloys

Titanium alloys find use in aerospace applications, pressure vessels, and so on because of their high strength-to-weight ratio, high corrosion resistance, and high fracture toughness. Pure titanium has two allotropic forms: low-temperature hexagonal close-packed (hcp) α-phase and elevated-temperature body-centered cubic (bcc) β-phase. Various alloying elements tend to preferentially stabilize one or the other of these phases. As a result, titanium alloys are generally classified as α, α+ β, metastable β, and β alloys (Fig. 37).

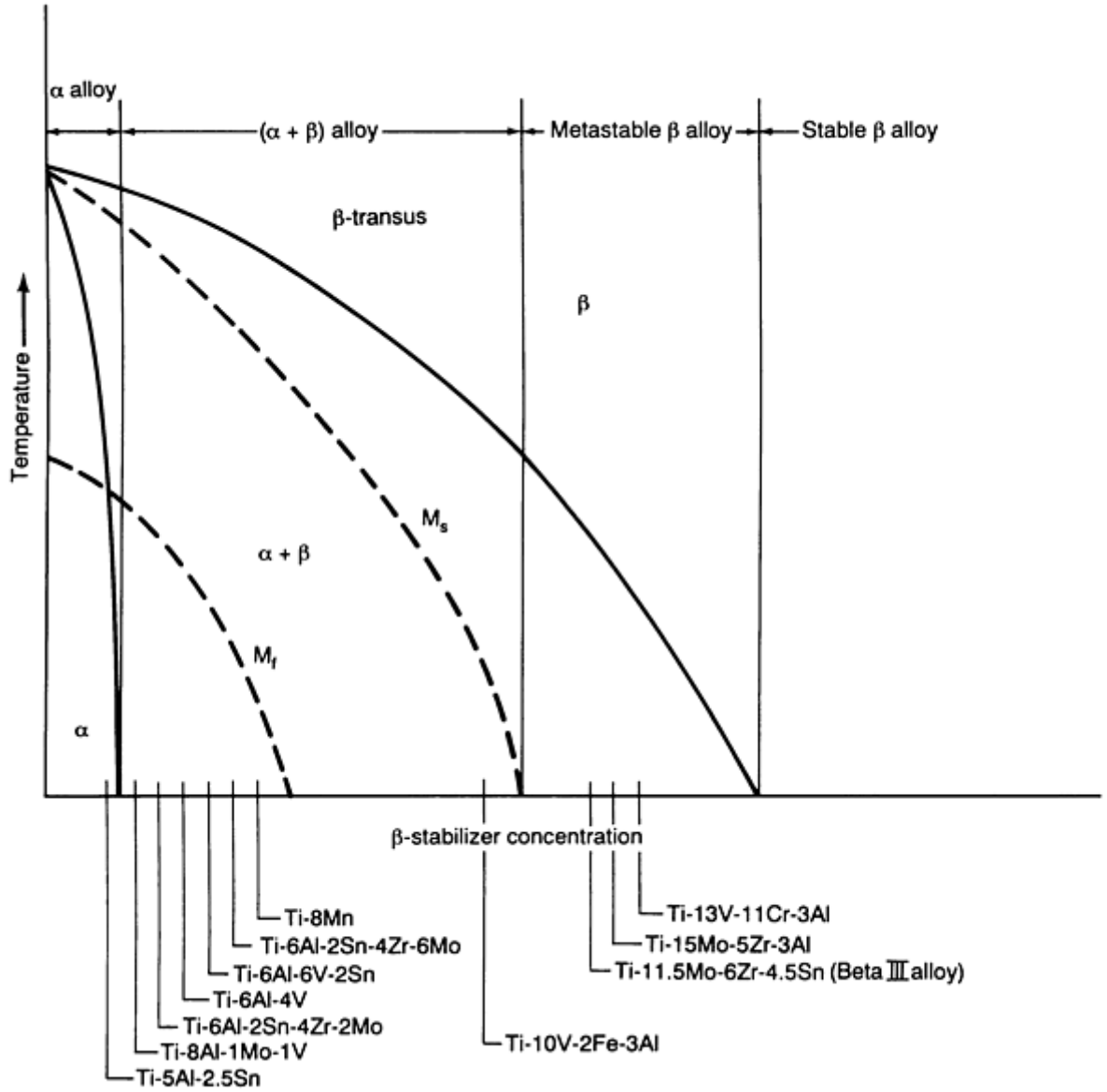

FIG. 37 HYPOTHETICAL β ISOMORPHOUS PHASE DIAGRAM THAT SHOWS RELATION BETWEEN β -STABILIZER SOLUTE CONTENT AND TITANIUM ALLOY FAMILY DESCRIPTION. SELECTED COMMON ALLOYS ARE LISTED ALONG THE *X*-AXIS OF THE DIAGRAM BASED ON THEIR COMPOSITIONS. SOURCE: REF 50

The α-alloys are not heat-treatable (that is, a significant increase in strength and toughness cannot be obtained by heat treatment), and they have the lowest strength of the four titanium alloy families. Interestingly enough, these alloys are thus considered to have excellent weldability. What this means in practice is that there is no significant degradation in the properties of the weld and HAZ with regard to the parent material due to the weld thermal cycles. Also, the β ↔ α transformation in the weld and near HAZ means that the extent of grain coarsening will not be so high as in other single-phase materials in which no phase transformation occurs upon heating or cooling, such as stabilized ferritic stainless steels (Ref 51), pure aluminum, and so on.

In the α+ β alloys, a higher strength is obtained with a higher volume fraction of the β phase, which in turn is obtained with a higher β -stabilizing alloy content (Fig. 37). The effect of cooling rate on the phase transformations in two α+ β alloys is shown schematically in Fig. 38. As in the case of steels, it is seen that the β ↔ αtransformation can occur either by nucleation and growth at slower cooling rates or martensitically at higher cooling rates. The martensitic product in the lean α+ β alloys has an hcp crystal structure (designated as α') or an orthorhombic one (designated as α") in the β-stabilized α+ β alloys. It is seen that the C-curve for the β ↔ intergranular α transformation is shifted to the right for alloys with increasing β-stabilizing alloy content, while that for the allotriomorphic α (more commonly referred to as GB

α) is relatively insensitive to alloy concentration (Ref 52). As a result, alloys that are fairly rich in β-stabilizing additions exhibit a stronger tendency to form a continuous network of GB α than do leaner α + β alloys.

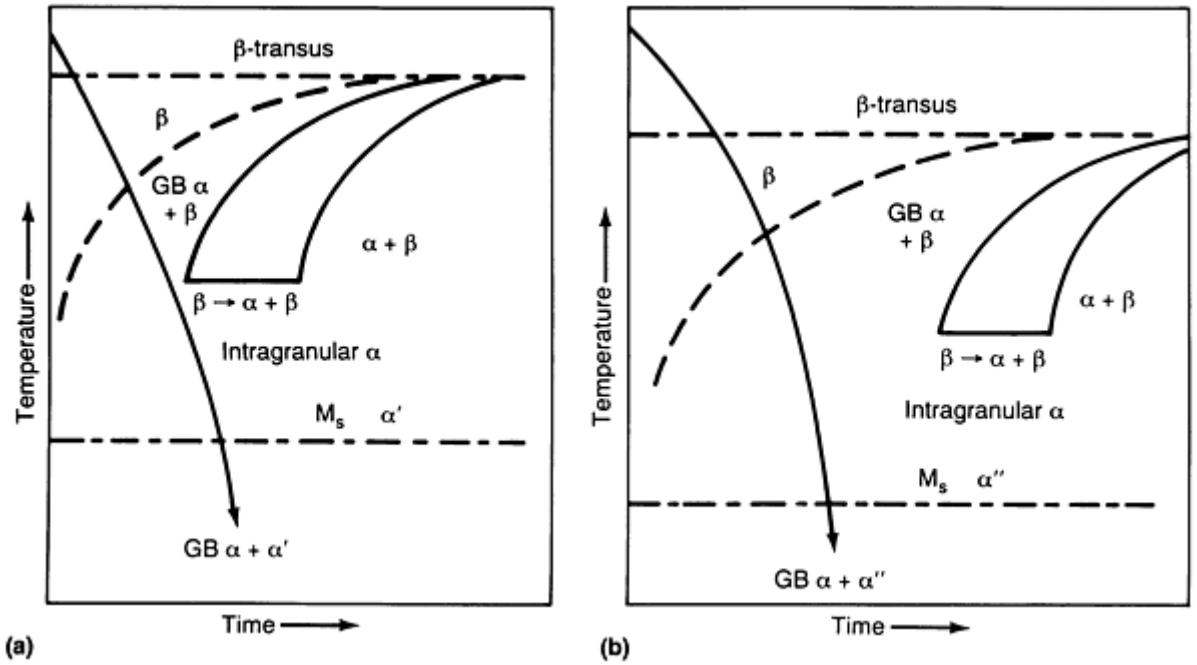

FIG. 38 SCHEMATIC CCT DIAGRAMS FOR TWO α + β TITANIUM ALLOYS WITH DIFFERENT β -STABILIZER SOLUTE CONTENTS. (A) LEAN α + β ALLOY (FOR EXAMPLE, TI-6AL-4V). (B) α + β ALLOY (FOR EXAMPLE, CORONA 5 [TI-4.5AL-5MO-1.5CR]) RICHER IN β -STABILIZING SOLUTE CONTENT

The morphology of the α and β phases in the α + β base materials is strongly dependent on thermomechanical processing (TMP) and heat treatment, which are performed either in the β-phase field or in the two-phase α + β phase field. When TMP is done in the α+ β phase field, the α that forms on cooling is continuously deformed. After recrystallization, a near-equiaxed α structure is obtained after this α + β processing. Very little GB α is formed because deformation introduces sufficient alternate heterogeneous nucleation sites in the form of dislocations. On the other hand, if TMP is done above the β-transus temperature (β-processing) and cooled, α forms at grain boundaries (giving GB α) and in the interior of grains as a Widmanstätten structure (also referred to as an acicular, lenticular, or basketweave structure). The microstructure in the weld and the near HAZ is closer to that obtained after β-processing.

Figure 39 shows the effect of α + β processing and β-processing on the strength and toughness of α + β alloys with increasing β-stabilizing alloy content. At the lower strength levels obtained with a lower β-stabilizing alloy content (because of a lower volume fraction of β-phase present), the finer Widmanstätten structure obtained after β-processing has a higher toughness than the coarser structure obtained by α + β processing. At higher strength levels, the trend reverses with the α + β processed structure having a higher toughness. This result can be understood in terms of the strength differences between GB α and the interior of the prior β grains (Fig. 40). At lower strengths, when the grain interiors are relatively weak, the crack tip plastic zone is distributed between the GB α and the grain interiors. However, as the α-phase precipitates are refined by lower aging temperatures, as in the case of the metastable β alloys, the grain interiors are strengthened considerably. Under such circumstances, the cracks are essentially constrained to follow the GB α layer. This results in a contraction of the plastic zone, a reduction in the crack tip opening displacement for crack extension, and an attendant drop in the toughness.

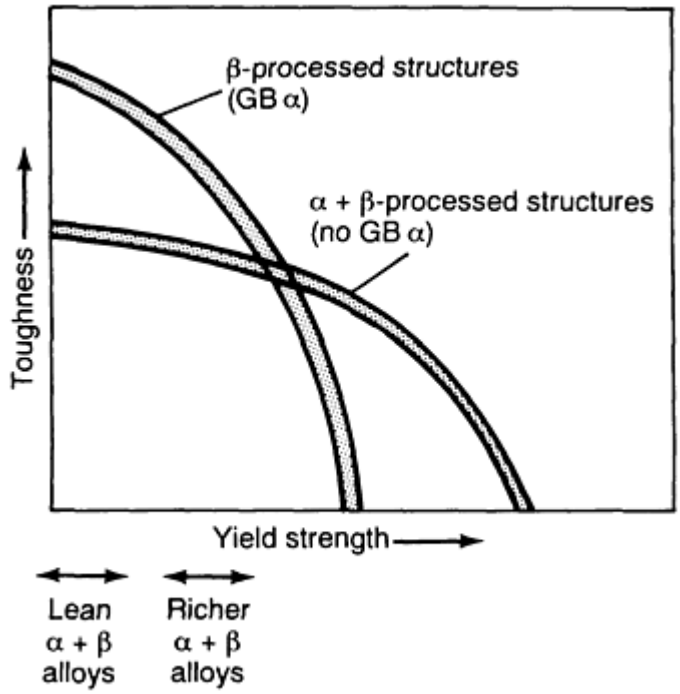

FIG. 39 SCHEMATIC PLOT OF TOUGHNESS VERSUS YIELD STRENGTH FOR α + β AND β-PROCESSED STRUCTURES. APPROXIMATE LOCATIONS OF LEAN (FOR EXAMPLE, TI-6AL-4V) AND RICHER β STABILIZED α + β ALLOYS (FOR EXAMPLE, CORONA 5 [TI-4.5AL-5MO-1.5CR]) ARE SHOWN. SOURCE: REF 52

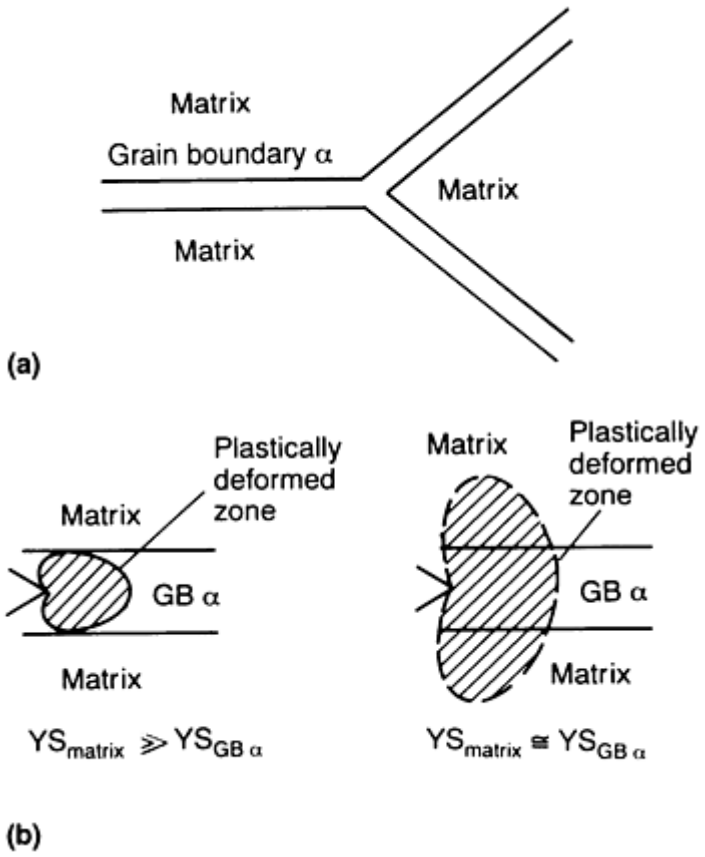

FIG. 40 SCHEMATIC SHOWING THE EFFECT OF THE RELATIVE STRENGTHS OF GB α AND MATRIX ON THE

PLASTIC ZONE SIZE. (A) GB α LOCATION RELATIVE TO MATRIX. (B) EFFECT OF PLASTIC ZONE SIZE ON YIELD STRENGTHS OF MATRIX AND GB α. SOURCE: REF 52

The microstructures in the weld metal and the near HAZ (the region where the peak temperature exceeds the β-transus temperature) resemble those obtained after β-processing. This means that it is easier to get a matching toughness in the weld metal at the lower strength levels referred to in Fig. 39. Even this is made somewhat difficult by the coarser β grain size in the weld and HAZ. Grain coarsening in the HAZ induces coarse β grains to form in the weld also, because solidification in the weld metal occurs by epitaxial growth from the HAZ. The extent of grain coarsening is such that it is not uncommon to find a single columnar β grain traversing the entire thickness in gas-tungsten arc welds on thin sheet (Ref 53). If high energy density welding processes are used (for example, electron-beam welding or laser-beam welding), it is possible to limit the extent of β grain coarsening. However, the high cooling rates in the weld and HAZ will mean that a martensitic structure will be obtained.

To obtain adequate ductility and toughness, PWHT will have to be done at temperatures close to the β-transus temperature. This can be a problem because the low strength at these temperatures can cause sagging in large welded structures, and complex fixturing will be necessary to maintain dimensional tolerances. It can also be expensive, because inert gas shielding is required for almost the entire time of PWHT (it is assumed in the present discussion that adequate care is taken to maintain proper shielding during welding). Moreover, it can be difficult to increase the ductility in the weld metal and HAZ to a level equal to that in an α+ β processed base material (Fig. 41). The trends seen in Fig. 39 and 41 can be understood by noting that crack nucleation is more difficult in an equaixed structure (because the strain concentration effects are less) and that the plastic zone sizes are bigger (Table 1). This results in a higher tensile ductility. However, because crack propagation follows a less tortuous path, the toughness is lower. The reverse is true for a Widmanstätten structure (referred to as a lenticular structure in Table 1). Table 1 explains the apparently strange observation in titanium alloys that a structure having a high strength and toughness is not necessarily the one having a high tensile ductility. The implication of this for weldments is that for many applications it may be more important to optimize the welding and PWHT procedure with respect to the toughness than with respect to the ductility.

TABLE 1 EFFECT OF MORPHOLOGICAL FEATURES OF THE MICROSTRUCTURE ON CRACK NUCLEATION AND PROPAGATION IN α + β TITANIUM ALLOYS

Note: Voids initiated at the α -β interfaces are shown as black regions. Source: Ref 54

Structure	Crack nucleation	Crack growth	Tensile ductility as a function of plastic zone size	Toughness as a function of crack propagation
Lenticular (Widmanstätten)	Easy	Difficult	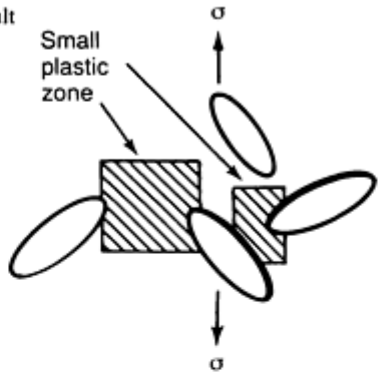 Low ductility	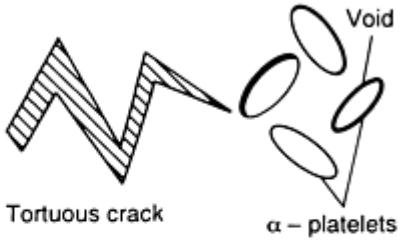 High toughness
Globular (equiaxed)	Difficult	Easy	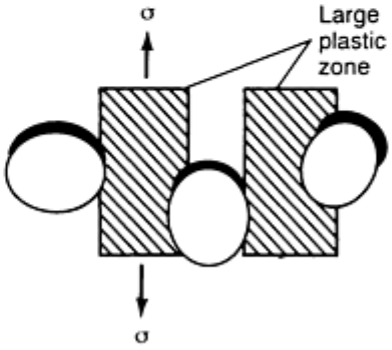 High ductility	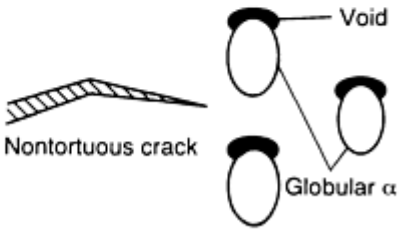 Low toughness

Note: Voids initiated at the α-β interfaces are shown as black regions. Source: Ref 54

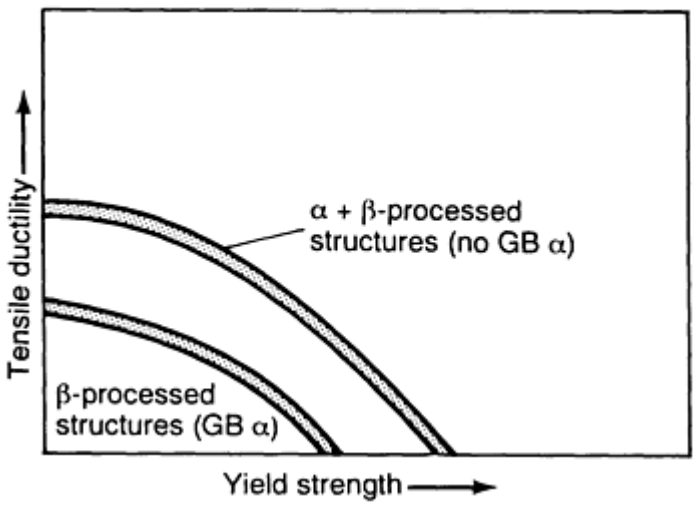

FIG. 41 SCHEMATIC PLOT OF DUCTILITY VERSUS STRENGTH FOR α + β AND β -PROCESSED STRUCTURES. SOURCE: REF 52

A more detailed discussion of the welding metallurgy of titanium alloys can be found in Ref 53, 55, and 56.

References cited in this section

50. E.W. COLLINGS, INTRODUCTION TO TITANIUM ALLOY DESIGN, *ALLOYING*, J.L. WALTER,

M.R. JACKSON, AND C.T. SIMS, ED., ASM INTERNATIONAL, 1988, P 267

51. C.R. THOMAS AND F.P.A. ROBINSON, KINETICS AND MECHANISM OF GRAIN GROWTH DURING WELDING IN NIOBIUM STABILISED 17% CHROMIUM STAINLESS STEELS, *MET. TECHNOL.*, APRIL 1978, P 133-138
52. J.C. WILLIAMS AND E.A. STARKE, JR., THE ROLE OF THERMOMECHANICAL PROCESSING IN TAILORING THE PROPERTIES OF ALUMINUM AND TITANIUM ALLOYS, *DEFORMATION, PROCESSING AND STRUCTURE,* G. KRAUSS, ED., AMERICAN SOCIETY FOR METALS, 1984, P 279-354
53. W.A. BAESLACK III, D.W. BECKER, AND F.H. FROES, ADVANCES IN TITANIUM ALLOY WELDING METALLURGY, *J. MET.*, MAY 1984, P 46-58
54. J.P. HIRTH AND F.H. FROES, INTERRELATIONS BETWEEN FRACTURE TOUGHNESS AND OTHER MECHANICAL PROPERTIES IN TITANIUM ALLOYS, *METALL. TRANS. A,* VOL 8, JULY 1977, P 1165-1176
55. C.G. RHODES, MICROSCOPY AND TITANIUM ALLOY DEVELOPMENT, *APPLIED METALLOGRAPHY,* G.F. VANDER VOORT, ED., VAN NOSTRAND REINHOLD, 1986
56. W.A. BAESLACK III, METALLOGRAPHY OF TITANIUM ALLOY WELDMENTS, *METALLOGRAPHY AND INTERPRETATION OF WELD MICROSTRUCTURES,* J.L. MCCALL, D.L. OLSON, AND I. LEMAY, ED., ASM INTERNATIONAL, 1987, P 23-60

Solid-State Transformations in Weldments

P. Ravi Vishnu, Luleå University of Technology, Sweden

Titanium Alloys

Titanium alloys find use in aerospace applications, pressure vessels, and so on because of their high strength-to-weight ratio, high corrosion resistance, and high fracture toughness. Pure titanium has two allotropic forms: low-temperature hexagonal close-packed (hcp) α-phase and elevated-temperature body-centered cubic (bcc) β-phase. Various alloying elements tend to preferentially stabilize one or the other of these phases. As a result, titanium alloys are generally classified as α, α+ β, metastable β, and βalloys (Fig. 37).

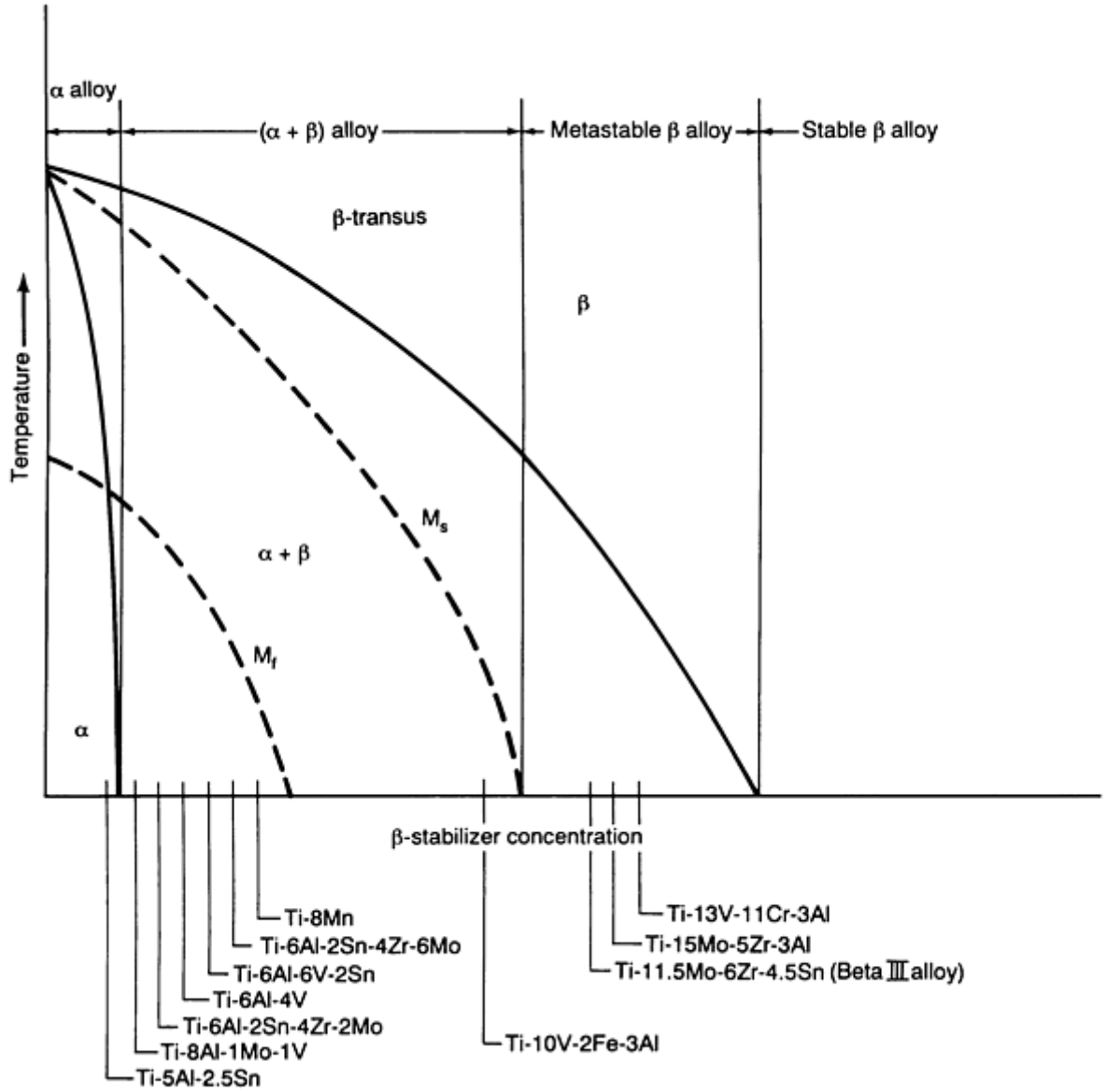

FIG. 37 HYPOTHETICAL β ISOMORPHOUS PHASE DIAGRAM THAT SHOWS RELATION BETWEEN β -STABILIZER SOLUTE CONTENT AND TITANIUM ALLOY FAMILY DESCRIPTION. SELECTED COMMON ALLOYS ARE LISTED ALONG THE *X*-AXIS OF THE DIAGRAM BASED ON THEIR COMPOSITIONS. SOURCE: REF 50

The α-alloys are not heat-treatable (that is, a significant increase in strength and toughness cannot be obtained by heat treatment), and they have the lowest strength of the four titanium alloy families. Interestingly enough, these alloys are thus considered to have excellent weldability. What this means in practice is that there is no significant degradation in the properties of the weld and HAZ with regard to the parent material due to the weld thermal cycles. Also, the β ↔ α transformation in the weld and near HAZ means that the extent of grain coarsening will not be so high as in other single-phase materials in which no phase transformation occurs upon heating or cooling, such as stabilized ferritic stainless steels (Ref 51), pure aluminum, and so on.

In the α+ β alloys, a higher strength is obtained with a higher volume fraction of the β phase, which in turn is obtained with a higher β-stabilizing alloy content (Fig. 37). The effect of cooling rate on the phase transformations in two α + β alloys is shown schematically in Fig. 38. As in the case of steels, it is seen that the β ↔ α transformation can occur either by nucleation and growth at slower cooling rates or martensitically at higher cooling rates. The martensitic product in the lean α + β alloys has an hcp crystal structure (designated as α') or an orthorhombic one (designated as α ") in the β-stabilized α + β alloys. It is seen that the C-curve for the β ↔ intergranular α transformation is shifted to the right for alloys with increasing β-stabilizing alloy content, while that for the allotriomorphic α(more commonly referred to as GB

α) is relatively insensitive to alloy concentration (Ref 52). As a result, alloys that are fairly rich in β-stabilizing additions exhibit a stronger tendency to form a continuous network of GB α than do leaner α + β alloys.

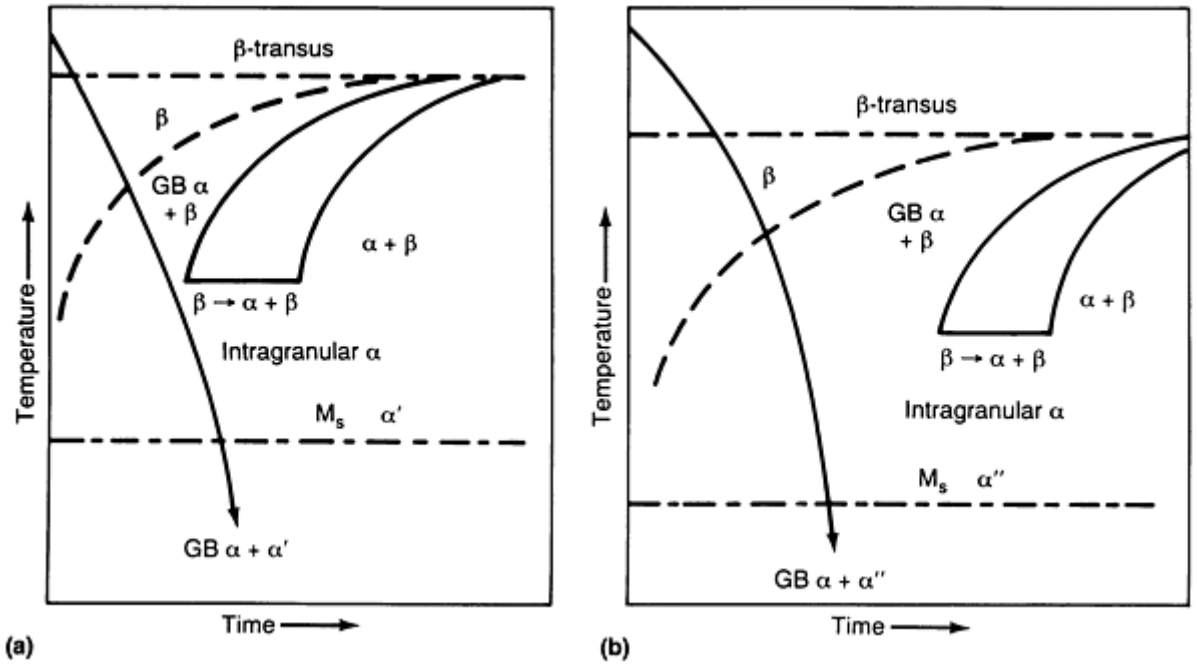

FIG. 38 SCHEMATIC CCT DIAGRAMS FOR TWO α + β TITANIUM ALLOYS WITH DIFFERENT β -STABILIZER SOLUTE CONTENTS. (A) LEAN α + β ALLOY (FOR EXAMPLE, TI-6AL-4V). (B) α + β ALLOY (FOR EXAMPLE, CORONA 5 [TI-4.5AL-5MO-1.5CR]) RICHER IN β -STABILIZING SOLUTE CONTENT

The morphology of the α and β phases in the α + β base materials is strongly dependent on thermomechanical processing (TMP) and heat treatment, which are performed either in the β-phase field or in the two-phase α+ β phase field. When TMP is done in the α+ β phase field, the α that forms on cooling is continuously deformed. After recrystallization, a near-equiaxed α structure is obtained after this α + β processing. Very little GB α is formed because deformation introduces sufficient alternate heterogeneous nucleation sites in the form of dislocations. On the other hand, if TMP is done above the β-transus temperature (β-processing) and cooled, α forms at grain boundaries (giving GB α) and in the interior of grains as a Widmanstätten structure (also referred to as an acicular, lenticular, or basketweave structure). The microstructure in the weld and the near HAZ is closer to that obtained after β-processing.

Figure 39 shows the effect of α + β processing and β-processing on the strength and toughness of α + β alloys with increasing β-stabilizing alloy content. At the lower strength levels obtained with a lower β-stabilizing alloy content (because of a lower volume fraction of β-phase present), the finer Widmanstätten structure obtained after β-processing has a higher toughness than the coarser structure obtained by α + β processing. At higher strength levels, the trend reverses with the α + β processed structure having a higher toughness. This result can be understood in terms of the strength differences between GB α and the interior of the prior β grains (Fig. 40). At lower strengths, when the grain interiors are relatively weak, the crack tip plastic zone is distributed between the GB α and the grain interiors. However, as the α-phase precipitates are refined by lower aging temperatures, as in the case of the metastable β alloys, the grain interiors are strengthened considerably. Under such circumstances, the cracks are essentially constrained to follow the GB α layer. This results in a contraction of the plastic zone, a reduction in the crack tip opening displacement for crack extension, and an attendant drop in the toughness.

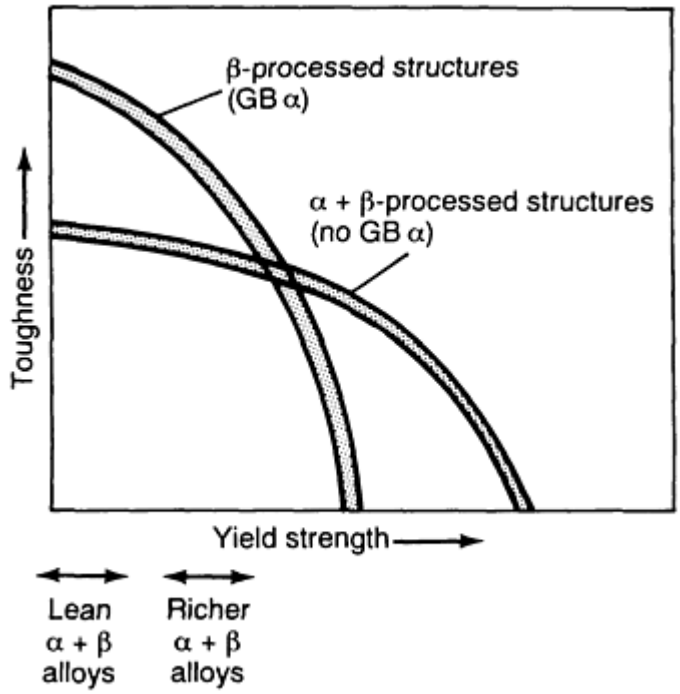

FIG. 39 SCHEMATIC PLOT OF TOUGHNESS VERSUS YIELD STRENGTH FOR α + β AND β -PROCESSED STRUCTURES. APPROXIMATE LOCATIONS OF LEAN (FOR EXAMPLE, TI-6AL-4V) AND RICHER β STABILIZED α + β ALLOYS (FOR EXAMPLE, CORONA 5 [TI-4.5AL-5MO-1.5CR]) ARE SHOWN. SOURCE: REF 52

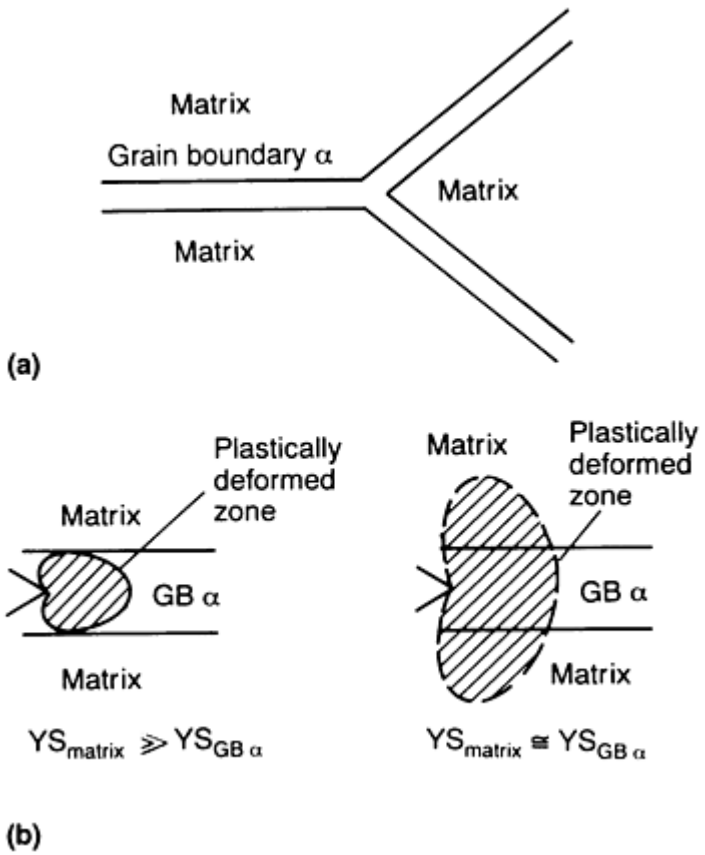

FIG. 40 SCHEMATIC SHOWING THE EFFECT OF THE RELATIVE STRENGTHS OF GB α AND MATRIX ON THE PLASTIC ZONE SIZE. (A) GB α LOCATION RELATIVE TO MATRIX. (B) EFFECT OF PLASTIC ZONE SIZE ON YIELD

STRENGTHS OF MATRIX AND GB α. SOURCE: REF 52

The microstructures in the weld metal and the near HAZ (the region where the peak temperature exceeds the β-transus temperature) resemble those obtained after β-processing. This means that it is easier to get a matching toughness in the weld metal at the lower strength levels referred to in Fig. 39. Even this is made somewhat difficult by the coarser β grain size in the weld and HAZ. Grain coarsening in the HAZ induces coarse β grains to form in the weld also, because solidification in the weld metal occurs by epitaxial growth from the HAZ. The extent of grain coarsening is such that it is not uncommon to find a single columnar β grain traversing the entire thickness in gas-tungsten arc welds on thin sheet (Ref 53). If high energy density welding processes are used (for example, electron-beam welding or laser-beam welding), it is possible to limit the extent of β grain coarsening. However, the high cooling rates in the weld and HAZ will mean that a martensitic structure will be obtained.

To obtain adequate ductility and toughness, PWHT will have to be done at temperatures close to the β-transus temperature. This can be a problem because the low strength at these temperatures can cause sagging in large welded structures, and complex fixturing will be necessary to maintain dimensional tolerances. It can also be expensive, because inert gas shielding is required for almost the entire time of PWHT (it is assumed in the present discussion that adequate care is taken to maintain proper shielding during welding). Moreover, it can be difficult to increase the ductility in the weld metal and HAZ to a level equal to that in an α + β processed base material (Fig. 41). The trends seen in Fig. 39 and 41 can be understood by noting that crack nucleation is more difficult in an equaixed structure (because the strain concentration effects are less) and that the plastic zone sizes are bigger (Table 1). This results in a higher tensile ductility. However, because crack propagation follows a less tortuous path, the toughness is lower. The reverse is true for a Widmanstätten structure (referred to as a lenticular structure in Table 1). Table 1 explains the apparently strange observation in titanium alloys that a structure having a high strength and toughness is not necessarily the one having a high tensile ductility. The implication of this for weldments is that for many applications it may be more important to optimize the welding and PWHT procedure with respect to the toughness than with respect to the ductility.

TABLE 1 EFFECT OF MORPHOLOGICAL FEATURES OF THE MICROSTRUCTURE ON CRACK NUCLEATION AND PROPAGATION IN α+ β TITANIUM ALLOYS

Note: Voids initiated at the α-β interfaces are shown as black regions. Source: Ref 54

Structure	Crack nucleation	Crack growth	Tensile ductility as a function of plastic zone size	Toughness as a function of crack propagation
Lenticular (Widmanstätten)	Easy	Difficult	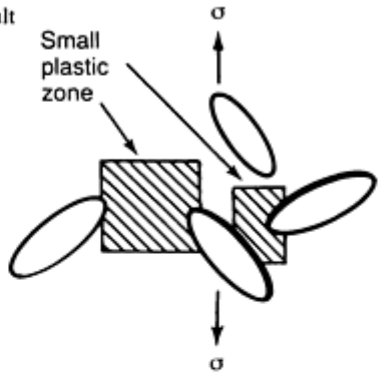 Low ductility	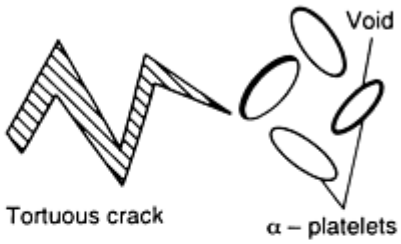 High toughness
Globular (equiaxed)	Difficult	Easy	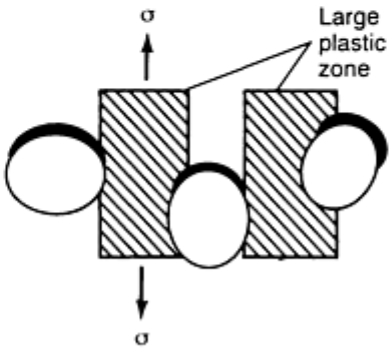 High ductility	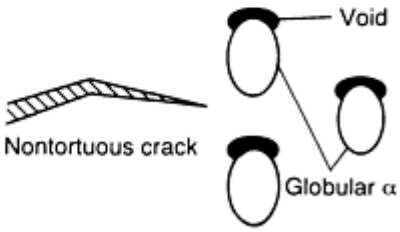 Low toughness

Note: Voids initiated at the α-β interfaces are shown as black regions. Source: Ref 54

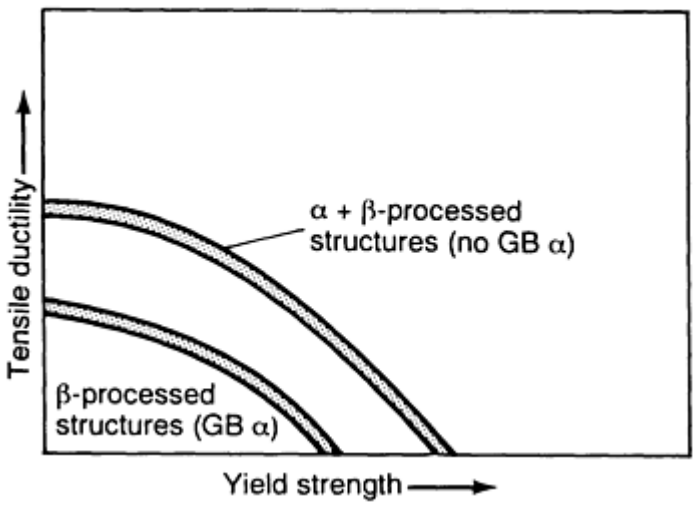

FIG. 41 SCHEMATIC PLOT OF DUCTILITY VERSUS STRENGTH FOR α+β AND β -PROCESSED STRUCTURES. SOURCE: REF 52

A more detailed discussion of the welding metallurgy of titanium alloys can be found in Ref 53, 55, and 56.

References cited in this section

50. E.W. COLLINGS, INTRODUCTION TO TITANIUM ALLOY DESIGN, *ALLOYING*, J.L. WALTER,

M.R. JACKSON, AND C.T. SIMS, ED., ASM INTERNATIONAL, 1988, P 267

51. C.R. THOMAS AND F.P.A. ROBINSON, KINETICS AND MECHANISM OF GRAIN GROWTH DURING WELDING IN NIOBIUM STABILISED 17% CHROMIUM STAINLESS STEELS, *MET. TECHNOL.*, APRIL 1978, P 133-138
52. J.C. WILLIAMS AND E.A. STARKE, JR., THE ROLE OF THERMOMECHANICAL PROCESSING IN TAILORING THE PROPERTIES OF ALUMINUM AND TITANIUM ALLOYS, *DEFORMATION, PROCESSING AND STRUCTURE,* G. KRAUSS, ED., AMERICAN SOCIETY FOR METALS, 1984, P 279-354
53. W.A. BAESLACK III, D.W. BECKER, AND F.H. FROES, ADVANCES IN TITANIUM ALLOY WELDING METALLURGY, *J. MET.*, MAY 1984, P 46-58
54. J.P. HIRTH AND F.H. FROES, INTERRELATIONS BETWEEN FRACTURE TOUGHNESS AND OTHER MECHANICAL PROPERTIES IN TITANIUM ALLOYS, *METALL. TRANS. A,* VOL 8, JULY 1977, P 1165-1176
55. C.G. RHODES, MICROSCOPY AND TITANIUM ALLOY DEVELOPMENT, *APPLIED METALLOGRAPHY,* G.F. VANDER VOORT, ED., VAN NOSTRAND REINHOLD, 1986
56. W.A. BAESLACK III, METALLOGRAPHY OF TITANIUM ALLOY WELDMENTS, *METALLOGRAPHY AND INTERPRETATION OF WELD MICROSTRUCTURES,* J.L. MCCALL, D.L. OLSON, AND I. LEMAY, ED., ASM INTERNATIONAL, 1987, P 23-60

Solid-State Transformations in Weldments

P. Ravi Vishnu, Luleå University of Technology, Sweden

References

1. *ATLAS OF ISOTHERMAL TRANSFORMATION AND COOLING TRANSFORMATION DIAGRAMS* AMERICAN SOCIETY FOR METALS, 1977
2. O.M. AKSELSEN AND T. SIMONSEN, TECHNIQUES FOR EXAMINING TRANSFORMATION BEHAVIOUR IN WELD METAL AND HAZ--A STATE OF ART REVIEW, *WELD. WORLD,* VOL 25 (NO. 1/2), 1987, P 26-34
3. O. GRONG AND D.K. MATLOCK, MICROSTRUCTURAL DEVELOPMENT IN MILD AND LOW ALLOY STEEL WELD METALS, *INT. MET. REV.,* VOL 31 (NO. 1), 1986, P 27-48
4. P.L. HARRISON AND R.A. FARRAR, APPLICATION OF CONTINUOUS COOLING TRANSFORMATION DIAGRAMS FOR WELDING OF STEELS, *INT. MATER. REV.,* VOL 34 (NO. 1), 1989, P 35-51
5. G.T. ELDIS, A CRITICAL REVIEW OF DATA SOURCES FOR ISOTHERMAL TRANSFORMATION AND CONTINUOUS COOLING TRANSFORMATION DIAGRAMS, *HARDENABILITY CONCEPTS WITH APPLICATION TO STEEL,* D.V. DOANE AND J.S. KIRKALDY, ED., TMS-AIME, 1978, P 126-157
6. K. EASTERLING, *INTRODUCTION TO THE PHYSICAL METALLURGY OF WELDING,* BUTTERWORTHS, 1983
7. *WELD THERMAL SIMULATORS FOR RESEARCH AND PROBLEM SOLVING,* THE WELDING INSTITUTE, U.K., 1972
8. C.F. BERKHOUT AND P.H. VAN LENT, THE USE OF PEAK TEMPERATURE-COOLING TIME DIAGRAMS IN THE WELDING OF HIGH STRENGTH STEELS (IN GERMAN), *SCHWEISS. SCHNEID.,* VOL 20 (NO. 6), 1968, P 256-260
9. TH.J. VAN ADRICHEM AND J. KAS, *CALCULATION, MEASUREMENT AND SIMULATION OF WELD THERMAL CYCLES,* SMITWELD N.V., NIJMEGEN, THE NETHERLANDS

10. P. RAVI VISHNU, W.B. LI, AND K. EASTERLING, HEAT FLOW MODEL FOR PULSED WELDING, *MATER. SCI. TECH.,* VOL 7 (NO. 7), 1991, P 649-659
11. P. RAVI VISHNU AND K. EASTERLING, PHENOMENOLOGICAL MODELLING OF HEAT FLOW AND MICROSTRUCTURAL CHANGES IN PULSED GTAW WELDS OF A QT STEEL, *MATHEMATICAL MODELING OF WELD PHENOMENA,* H. CERJAK AND K. EASTERLING, ED., THE INSTITUTE OF METALS, 1993
12. VEREIN DEUTSCHER EISENHÜTTENLEUTE, ED., *STEEL--A HANDBOOK FOR MATERIALS RESEARCH AND ENGINEERING, VOLUME 1: FUNDAMENTALS*, SPRINGER VERLAG, 1992, P 175
13. A.J. DEARDO, C.I. GARCIA, AND E.J. PALMIERE, THERMOMECHANICAL PROCESSING OF STEELS, *HEAT TREATING,* VOL 4, *ASM HANDBOOK,* 1991, P 237-255
14. S. KOU, *WELDING METALLURGY,* JOHN WILEY & SONS, 1987
15. K. NARITA, PHYSICAL CHEMISTRY OF THE GROUPS IVA (TI, ZR), VA (V, NB, TA) AND THE RARE EARTH ELEMENTS IN STEEL, *TRANS. ISIJ,* VOL 15, 1975, P 145-152
16. R.K. AMIN AND F.B. PICKERING, AUSTENITE GRAIN COARSENING AND THE EFFECT OF THERMOMECHANICAL PROCESSING ON AUSTENITE RECRYSTALLIZATION, *THERMOMECHANICAL PROCESSING OF MICROALLOYED AUSTENITE,* A.J. DEARDO, G.A. RATZ, AND P.J. WRAY, ED., TMS-AIME, 1982, P 14
17. W.F. SAVAGE, E.F. NIPPES, AND E.S SZEKERES, A STUDY OF WELD INTERFACE PHENOMENA IN A LOW ALLOY STEEL, *WELD. J.,* SEPT 1976, P 260S-268S, AND HYDROGEN INDUCED COLD CRACKING IN A LOW ALLOY STEEL, *WELD. J.,* SEPT 1976, P 276S-283S
18. J.J. PEPE AND W.F. SAVAGE, EFFECTS OF CONSTITUTIONAL LIQUATION IN 18-NI MARAGING STEEL WELDMENTS, *WELD J.,* SEPT 1967, P 411S-422S
19. W. YENISCAVITCH, JOINING, *SUPERALLOYS II,* C.T. SIMS, N.S. STOLOFF, AND W.C. HAGEL, ED., JOHN WILEY & SONS, 1987, P 495-516
20. E.E. HUCKE AND H. UDIN, WELDING METALLURGY OF NODULAR CAST IRON, *WELD. J.,* AUG 1953, P 378S-385S
21. E.N. GREGORY AND S.B. JONES, WELDING CAST IRONS, *WELDING OF CASTINGS,* THE WELDING INSTITUTE, U.K., 1977, P 145-156
22. L.E. SAMUELS, *OPTICAL MICROSCOPY OF CARBON STEELS,* AMERICAN SOCIETY FOR METALS, 1980
23. "GUIDE TO THE LIGHT MICROSCOPE EXAMINATION OF FERRITIC STEEL WELD METALS," DOC. NO. IX-1533-88, INTERNATIONAL INSTITUTE OF WELDING, 1988
24. H.K.D.H. BHADESHIA AND L.E. SVENSSON, MODELLING THE EVOLUTION OF MICROSTRUCTURE OF STEEL WELD METAL, *MATHEMATICAL MODELLING OF WELD PHENOMENA,* H. CERJAK AND K. EASTERLING, ED., THE INSTITUTE OF MATERIALS, 1993
25. G.R. EDWARDS AND S. LIU, RECENT DEVELOPMENTS IN HSLA STEEL WELDING, *ADVANCES IN WELDING METALLURGY,* FIRST U.S.-JAPAN SYMPOSIUM, AMERICAN WELDING SOCIETY AND OTHERS, JUNE 1990, P 215-293
26. B. AHLBLOM, "OXYGEN AND ITS ROLE IN DETERMINING WELD METAL MICROSTRUCTURE AND TOUGHNESS--A STATE OF THE ART REVIEW," DOC. NO. IX-1322-84, INTERNATIONAL INSTITUTE OF WELDING, 1984
27. L.-E. SVENSSON AND B. GRETOFT, MICROSTRUCTURE AND IMPACT TOUGHNESS OF C-MN WELD METALS. *WELD. J.,* DEC 1990, P 454S-461S
28. P.W. HOLSBERG AND R.J. WONG, WELDING OF HSLA-100 STEEL FOR NAVAL APPLICATIONS, *WELDABILITY OF MATERIALS,* R.A. PATTERSON AND K.W. MAHIN, ED., ASM INTERNATIONAL, 1990
29. J.M.B. LOSZ AND K.D. CHALLENGER, MICROSTRUCTURE AND PROPERTIES OF A COPPER PRECIPITATION STRENGTHENED HSLA STEEL WELDMENT, *RECENT TRENDS IN WELDING SCIENCE AND TECHNOLOGY,* S.A. DAVID AND J.M. VITEK, ED., ASM INTERNATIONAL, 1990
30. H. HOMMA, S. OHKITA, S. MATSUDA, AND K. YAMAMOTO, IMPROVEMENTS OF HAZ

TOUGHNESS IN HSLA STEEL BY INTRODUCING FINELY DISPERSED TI-OXIDE, *WELD. J.,* OCT 1987, P 301S-309S

31. N. YURIOKA, "MODERN HIGH STRENGTH STEEL IN JAPAN," FIFTH INTERNATIONAL SYMPOSIUM, JAPAN WELDING SOCIETY, APRIL 1990 (TOKYO)
32. YU.N. GOTALSKII, THE PROBLEM OF WELDING HIGH STRENGTH STEELS, *AUTOM. WELD.,* JUNE 1984, P 37-40
33. W.K.C. JONES AND P.J. ALBERRY, THE ROLE OF PHASE TRANSFORMATIONS IN THE DEVELOPMENT OF RESIDUAL STRESSES DURING THE WELDING OF SOME FAST REACTOR STEELS, *PROC. CONF. FERRITIC STEELS FOR FAST REACTOR STEAM GENERATORS,* BRITISH NUCLEAR ENERGY SOCIETY, 1977
34. *MCGRAW-HILL ENCYCLOPEDIA OF SCIENCE AND TECHNOLOGY,* VOL 9, P 685
35. A.M. MAKARA AND N.A. MOSENDZ, EFFECTS OF THE WELD METAL ON CRACKING IN HAZ, *WELD. RES. ABROAD,* NOV 1965, P 78-86
36. H. IKAWA, S. SHIN, M. INUI, Y. TAKEDA, AND A. NAKANO, "ON THE MARTENSITE-LIKE STRUCTURE AT WELD BOND AND THE MACROSCOPIC SEGREGATION IN WELD METAL IN THE WELDED DISSIMILAR METALS OF α-STEELS AND γ-STEELS," DOC. NO. IX-785-72, INTERNATIONAL INSTITUTE OF WELDING, 1972
37. T. HAZE AND S. AIHARA, "INFLUENCE OF TOUGHNESS AND SIZE OF LOCAL BRITTLE ZONES ON HAZ TOUGHNESS OF HSLA STEELS," SEVENTH INTERNATIONAL CONFERENCE ON OFFSHORE MECHANICS AND ARCTIC ENGINEERING, HOUSTON, 1988
38. C.P. ROYER, A USER'S PERSPECTIVE ON HEAT AFFECTED ZONE TOUGHNESS, *WELDING METALLURGY OF STRUCTURAL STEELS,* J.Y. KOO, ED., TMS-AIME, 1987
39. F. MATSUDA, Z. LI, P. BERNASOVSKY, K. ISHIHARA, AND H. OKADA, "AN INVESTIGATION OF THE BEHAVIOUR OF M-A CONSTITUENT IN SIMULATED HAZ OF HSLA STEELS," DOC. NO. IX-B-1591-90, INTERNATIONAL INSTITUTE OF WELDING, 1990
40. P.L. HARRISON AND P.H.M. HART, RELATIONSHIPS BETWEEN HAZ MICROSTRUCTURE AND CTOD TRANSITION BEHAVIOUR IN MULTIPASS C-MN STEEL WELDS, *RECENT TRENDS IN WELDING SCIENCE AND TECHNOLOGY,* S.A. DAVID AND J.M. VITEK, ED., ASM INTERNATIONAL, 1990
41. H. ONOE, J. TANAKA, AND I. WATANABE, JAPANESE LNG TANKER CONSTRUCTED USING A NEW WELDING PROCESS AND IMPROVED AL-KILLED STEELS, *MET. CONSTR.,* JAN 1979, P 26-31
42. P.J. ALBERRY, SENSITIVITY ANALYSIS OF HALF-BEAD AND ALTERNATIVE GTAW TECHNIQUES, *WELD. J.,* NOV 1989, P 442S-451S
43. J.A. BROOKS AND A.W. THOMPSON, MICROSTRUCTURAL DEVELOPMENT AND SOLIDIFICATION CRACKING SUSCEPTIBILITY OF AUSTENITIC STAINLESS STEEL WELDS, *INT. MATER. REV.,* VOL 36 (NO. 1), 1991
44. T.A. SIEWERT, C.N. MCCOWAN, AND D.L. OLSON, FERRITE NUMBER PREDICTION TO 100 FN IN STAINLESS STEEL WELD METAL, *WELD. J.,* DEC 1988, P 289S-298S
45. D.J. KOTECKI AND T.A. SIEWERT, WRC-1992 CONSTITUTION DIAGRAM FOR STAINLESS STEEL WELD METALS: A MODIFICATION OF THE WRC-1988 DIAGRAM, *WELD. J.,* MAY 1992, P 171S-178S
46. T.G. GOOCH AND D.C. WILLINGHAM, *WELD DECAY IN AUSTENITIC STAINLESS STEELS,* THE WELDING INSTITUTE, UK, 1975
47. S. KOU, WELDING METALLURGY AND WELDABILITY OF HIGH STRENGTH ALUMINUM ALLOYS, *WELD. RES. COUNC. BULL.,* NO. 320, DEC 1986
48. H. SHERCLIFF AND M.F. ASHBY, A PROCESS MODEL FOR AGE HARDENING OF AL ALLOYS--I. MODEL AND II. APPLICATIONS OF THE MODEL, *ACTA METALL. MATER.,* VOL 38 (NO. 10), 1990, P 1789-1812
49. W.A. OWCZARSKI, PROCESS AND METALLURGICAL FACTORS IN JOINING SUPERALLOYS

AND OTHER HIGH SERVICE TEMPERATURE MATERIALS, *PHYSICAL METALLURGY OF JOINING*, R. KOSSOWSKY AND M.E. GLICKSMAN, ED., TMS-AIME, 1980

50. E.W. COLLINGS, INTRODUCTION TO TITANIUM ALLOY DESIGN, *ALLOYING*, J.L. WALTER, M.R. JACKSON, AND C.T. SIMS, ED., ASM INTERNATIONAL, 1988, P 267
51. C.R. THOMAS AND F.P.A. ROBINSON, KINETICS AND MECHANISM OF GRAIN GROWTH DURING WELDING IN NIOBIUM STABILISED 17% CHROMIUM STAINLESS STEELS, *MET. TECHNOL.*, APRIL 1978, P 133-138
52. J.C. WILLIAMS AND E.A. STARKE, JR., THE ROLE OF THERMOMECHANICAL PROCESSING IN TAILORING THE PROPERTIES OF ALUMINUM AND TITANIUM ALLOYS, *DEFORMATION, PROCESSING AND STRUCTURE*, G. KRAUSS, ED., AMERICAN SOCIETY FOR METALS, 1984, P 279-354
53. W.A. BAESLACK III, D.W. BECKER, AND F.H. FROES, ADVANCES IN TITANIUM ALLOY WELDING METALLURGY, *J. MET.*, MAY 1984, P 46-58
54. J.P. HIRTH AND F.H. FROES, INTERRELATIONS BETWEEN FRACTURE TOUGHNESS AND OTHER MECHANICAL PROPERTIES IN TITANIUM ALLOYS, *METALL. TRANS. A*, VOL 8, JULY 1977, P 1165-1176
55. C.G. RHODES, MICROSCOPY AND TITANIUM ALLOY DEVELOPMENT, *APPLIED METALLOGRAPHY*, G.F. VANDER VOORT, ED., VAN NOSTRAND REINHOLD, 1986
56. W.A. BAESLACK III, METALLOGRAPHY OF TITANIUM ALLOY WELDMENTS, *METALLOGRAPHY AND INTERPRETATION OF WELD MICROSTRUCTURES*, J.L. MCCALL, D.L. OLSON, AND I. LEMAY, ED., ASM INTERNATIONAL, 1987, P 23-60

Cracking Phenomena Associated With Welding

Michael J. Cieslak, Physical and Joining Metallurgy Department, Sandia National Laboratories

Introduction

THE FORMATION OF DEFECTS in materials that have been fusion welded is a major concern in the design of welded assemblies. Four types of defects in particular have been the focus of much attention because of the magnitude of their impact on product quality. These defects, all of which manifest themselves as cracks, are characteristic of phenomena that occur at certain temperature intervals specific to a given alloy. Colloquially, these four defect types are known as hot cracks, heat-affected zone (HAZ) microfissures, cold cracks, and lamellar tearing.

Acknowledgements

This work was performed at Sandia National Laboratories, supported by the U.S. Department of Energy under Contract No. DE-AC04-76DP00789.

Cracking Phenomena Associated With Welding

Michael J. Cieslak, Physical and Joining Metallurgy Department, Sandia National Laboratories

Solidification Cracking (Hot Cracking)

Hot cracks are solidification cracks that occur in the fusion zone near the end of solidification. Simplistically, they result from the inability of the semisolid material to accommodate the thermal shrinkage strains associated with weld solidification and cooling. Cracks then form at susceptible sites to relieves the accumulating strain. Susceptible sites are interfaces, such as solidification grain boundaries and interdendritic regions, that are at least partially wetted.

Figure 1 is a photomicrograph of a metallographic section showing the appearance of a typical solidification crack in a fusion weld. Note the intergranular nature of the crack path. Figure 2 shows the surface morphology of a solidification crack, reflecting the nearly solidified nature of the interface at the time of failure. Note the smooth dendritic appearance of this surface.

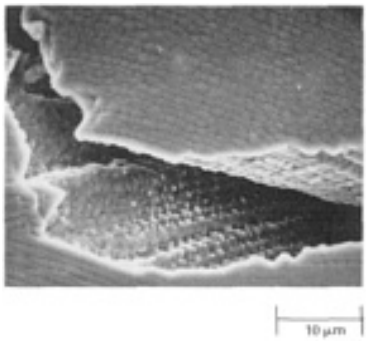

FIG. 1 SOLIDIFICATION CRACK IN A PULSED ND:YAG LASER WELD JOINING HASTELLOY C-276 TO 17-4 PH STAINLESS STEEL. YAG, YTTRIUM-ALUMINUM-GARNET

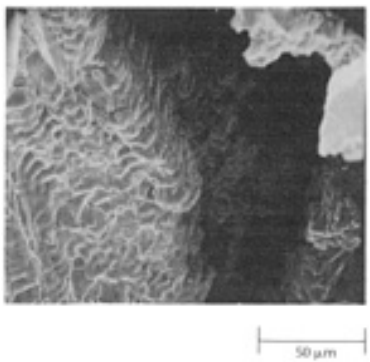

FIG. 2 SURFACE OF A SOLIDIFICATION CRACK IN AN ALLOY 214 VARESTRAINT TEST SPECIMEN

Solidification cracking requires both a sufficient amount of mechanical restraint (strain) and a susceptible microstructure. Knowledge regarding the development of shrinkage strains at the microstructural scale of a solidifying dendrite is still quite limited, making it nearly impossible to quantify *a priori* the amount of local strain required to initiate solidification cracks. Furthermore, the rate at which the strain is applied can influence the ability of an alloy to survive the solidification process without cracking. At temperatures near their melting points, metal alloys can readily dissipate applied loads by time-dependent deformation processes (i.e., creep processes). At high rates of applied stress, both the fusion zone and the HAZ have limited time to accommodate this mechanical imposition. Under conditions of rapid solidification and cooling, the rate of strain accumulation is rapid, leading to an increased cracking susceptibility. Inherently, then, requisite strains for solidification cracking are more likely to be experienced with welding processes that promote rapid solidification and cooling.

Because of the limited quantitative understanding of strain development in a solidifying weld, the practical approach taken to minimize the mechanical factor is to reduce the overall weld restraint through judicious joint design and appropriate choice of welding parameters. A simple way to minimize the restraint on a solidifying weld joint is to keep the joint gap to a minimum by designing hardware with good fit-up. Another approach, particularly attractive for small parts, is to design the weld joint as a standing edge. Welding parameters can have a profound influence on the occurrence of solidification cracking. The natural tendency to use high-speed welding to improve productivity can have detrimental effects. Formation of a teardrop-shaped weld pool, which may occur as the weld travel speed increases, can result in centerline solidification cracks. The solidification pattern associated with this type of weld pool is such that solidifying grains meet at the weld centerline, forming a particularly susceptible site for solidification crack initiation.

The manner in which a fusion weld is terminated can also influence cracking behavior. In a closure weld, simply extinguishing the power can result in the formation of "crater cracks" as the final weld pool rapidly solidifies in on itself. A common method used to minimize this problem is to ramp down the power slowly, either while the workpiece remains stationary or as it continues to travel a short length under the heat source. In some cases, the use of a runoff tab as a site for weld termination may be appropriate.

The extent to which special joint designs or precisely controlled welding parameters can be used to produce welds without solidification cracks is specific for a given alloy. Alloys that are microstructurally susceptible to cracking will necessarily have a more limited set of joint designs and processing parameters around which defect-free welds can be produced.

Alloys with a wide solidification temperature range are more susceptible to solidification cracking than alloys that solidify over a narrow temperature range. Simply described, this is because accumulated thermal strain is proportional to the temperature range over which a material solidifies. This temperature range is determined primarily by chemical composition. For many binary alloy systems and a few ternary alloy systems, the equilibrium solidification (or melting) temperature range has been established in phase diagram studies. For the vast majority of commercial alloys, however, these data are not precisely known.

Borland (Ref 1, 2) attempted to establish a general quantitative method for comparing the effects of various alloying elements on the melting temperature range of a given solvent element. Figure 3 shows a schematic binary alloy phase diagram having linear liquidus and solidus boundaries. For an alloy of composition C_0, T_L is the liquidus composition and T_S is the solidus composition, where the alloy would be completely solidified under conditions of equilibrium cooling. T_M is the invariant melting temperature of the solvent element. The slope of the liquidus is m_L, and the slope of the solidus is m_S. The equilibrium distribution coefficient, k, is defined as the ratio of the composition of the solid, C_S, to the composition of the liquid, C_L, at a given temperature (i.e., $k = C_S/C_L|_T$). For a linear liquidus and solidus, this value is constant and also equal to m_L/m_S.

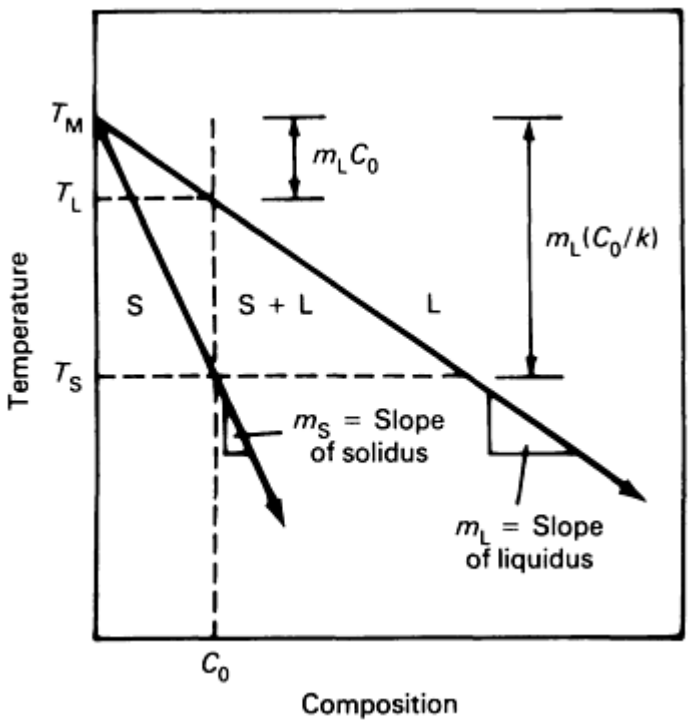

FIG. 3 HYPOTHETICAL BINARY ALLOY PHASE DIAGRAM SHOWING KEY PARAMETERS REQUIRED TO DERIVE THE RELATIVE POTENCY FACTOR (RPF)

With these terms thus defined, a derivation of the relative potency factor (RPF), after Borland (Ref 2), follows:

$$T_L = T_M - M_L C_0 \quad \textbf{(EQ 1)}$$

$$T_S = T_M - M_S C_0 \quad \textbf{(EQ 2)}$$

However, $m_S = m_L/k$:

$$T_s = T_M - \frac{M_L}{K} C_o \quad \textbf{(EQ 3)}$$

Then:

$$T_L - T_S = \frac{m_L C_o (K-1)}{K} \quad \textbf{(EQ 4)}$$

The RPF, always a positive number, is defined as the change in melting temperature ranger per weight percent of solute added, or:

$$RPF = \frac{T1 - Ts}{C_o} = \frac{M_L (k-1)}{K} \quad \textbf{(EQ 5)}$$

where for $k < 1$, $m_L < 0$; and for $k > 1$,$m_L > 0$. The larger the RPF, the wider the melting temperature range and the higher the solidification cracking susceptibility. The final form of Eq 5 indicates that as k becomes very small (indicating a high level of microsegregation), the solidification cracking sensitivity increases. Similarly, as the magnitude of m_L increases (that is, becomes more highly negative), indicating a rapid decrease in liquidus with alloying concentration, the cracking propensity also increases.

Table 1 lists RPF values for various alloying elements in binary iron (Ref 2), nickel-base alloys (Ref 3), and aluminum alloys. It is clear that certain alloying elements, such as sulfur, phosphorus, and boron, are detrimental to the weldability of these alloy systems. This has been borne out by field experience.

TABLE 1 RELATIVE POTENCY FACTORS FOR SELECTED ALLOYING ELEMENTS IN BINARY IRON, NICKEL, AND ALUMINUM SYSTEMS

SYSTEM	RPF FOR:										
	Al	**B**	**C**	**Co**	**Mn**	**Nb**	**Ni**	**P**	**S**	**Si**	**Ti**
BINARY IRON	1.5	. . .	322	0.3	26.2	28.8	2.9	121	925	1.8	13.8
BINARY NICKEL	1.7	22700	330	. . .	0.7	. . .	. . .	556	244000	11	5.4

	Cu	**Li**	**Mg**	**Si**	**Zn**
BINARY ALUMINUM	16.6	9.0	8.0	42.4	2.3

Source: Ref 2, 3

Although the exact derivation of the RPF is specific to a very simple binary system solidifying under equilibrium conditions, the methodology provides general insight that can be applied to commercial alloys. The association of cracking susceptibility with solidification temperature range has implications for alloy design and primary melt processing. An extended melting/solidification temperature range can be the result of either intentional alloying or impurities present after refining.

An example (Ref 4) of the application of Borland's concepts to the solidification cracking propensity of a commercial alloy system involves alloy 625. This alloy is derived from the ternary Ni-Cr-Mo system, a very common base system for alloys designed to survive aggressive corrosive or high-temperature environments. A factorially designed set of alloys was produced to identify the effects of the alloying elements niobium, silicon, and carbon on the temperature range of

two-phase coexistence of liquid and solid (equilibrium melting/solidification temperature range) and on solidification cracking susceptibility.

Solidification cracking susceptibility was measured with the varestraint test, using the maximum crack length (MCL) parameter as the quantitative measurement (Ref 5). The melting temperature ranges of these same alloys were measured using differential thermal analysis (DTA). Table 2 lists the compositions of the alloys examined.

TABLE 2 SELECTED ALLOY 625 COMPOSITIONS USED IN WELDABILITY STUDY

ALLOY NO.	COMPOSITION, %										
	C	Cr	Fe	Mn	Mo	Nb	Ni	P	S	Si	Ti
NIOBIUM-FREE											
1	0.006	22.10	2.56	0.02	9.54	0.01	BAL	0.005	0.002	0.03	0.06
2	0.031	21.95	2.55	0.02	9.61	0.01	BAL	0.005	0.002	0.03	0.06
3	0.006	21.63	2.18	0.02	9.60	0.02	BAL	0.005	0.002	0.35	0.06
4	0.036	21.57	2.59	0.03	9.63	0.02	BAL	0.005	0.003	0.39	0.06
NIOBIUM ALLOYED											
5	0.009	21.81	2.30	0.03	9.81	3.61	BAL	0.006	0.003	0.03	0.06
6	0.038	21.83	2.31	0.03	9.81	3.60	BAL	0.006	0.003	0.03	0.06
7	0.008	21.65	2.26	0.03	9.68	3.57	BAL	0.006	0.004	0.38	0.06
8	0.035	21.68	2.29	0.03	9.67	3.53	BAL	0.006	0.003	0.46	0.06

The results of the varestraint testing are shown in Fig. 4. These data clearly show that the alloys that contain intentionally alloyed niobium (alloys 5 to 8) are more susceptible to solidification cracking (larger MCL) than niobium-free alloys (1 to 4). Furthermore, the alloy with no intentionally alloyed carbon, silicon, or niobium (alloy 1) is the least susceptible to cracking.

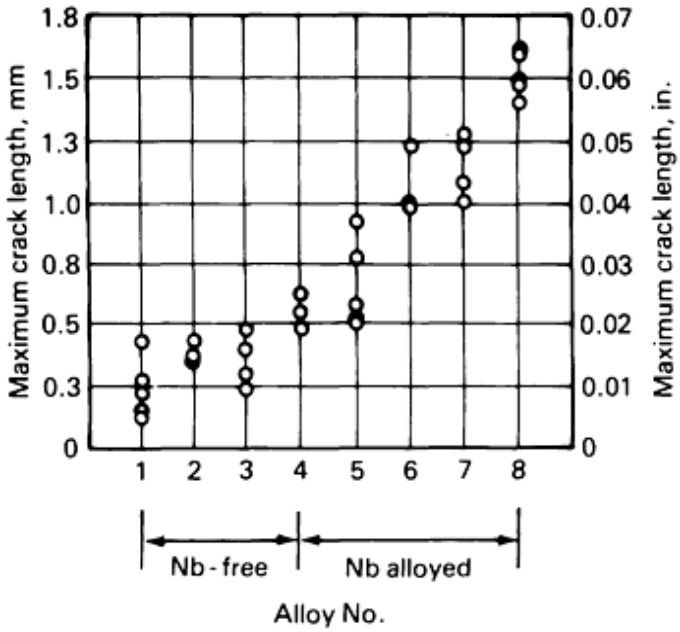

FIG. 4 MAXIMUM CRACK LENGTH DATA OBTAINED FROM VARESTRAINT TEST FOR ALLOY 625 WELDABILITY STUDY

The results of the DTA testing are given in Table 3. Listed are the liquidus (T_L), solidus (T_S), and melting temperature range (ΔT) data obtained from multiple tests. The baseline ΔT of an alloy without intentionally alloyed carbon, silicon,

and niobium (alloy 1) is 26.5 °C (79.7 °F). Increases in ΔT are observed when carbon or silicon is added (alloys 2 and 3) at levels that would be considered high for commercial alloys. When niobium is added (alloy 5) at a level that would be considered nominal for alloy 625 (~3.6 wt%), the melting temperature range effectively doubles to 55.3 °C (131.5 °F). Additions of carbon and silicon to the high-niobium alloys (alloys 6 to 8) further increase this value.

TABLE 3 MELTING TEMPERATURE DATA FOR ALLOY 625 WELDABILITY STUDY

σ is the standard deviation.

ALLOY NO.	ALLOY ADDITION			LIQUIDUS, $T_L \pm \sigma T_L$				SOLIDUS, $T_S \pm \sigma T_S$				MELTING TEMPERATURE RANGE, $\Delta T \pm \sigma \Delta T$			
				T_L		σT_L		T_S		σT_S		ΔT		$\sigma \Delta T$	
	C	NB	SI	°C	°F	°C	°F	°C	°F	°C	°F	°C	°F	°C	°F
1				1406.5	2563.7	1.3	2.3	1380.0	2516.0	1.4	2.5	26.5	47.7	0.6	1.1
2	X			1403.0	2557.4	1.0	1.8	1369.3	249.7	2.5	4.5	33.7	60.7	1.5	2.7
3			X	1395.5	2543.9	1.3	2.3	1366.5	2491.7	1.3	2.3	29.0	52.2	1.6	2.9
4	X		X	1390.8	2535.4	0.5	0.9	1347.5	2457.5	1.7	3.1	43.3	77.9	1.3	2.3
5		X		1363.3	2485.9	0.5	0.9	1308.0	2386.4	2.2	4.0	55.3	99.5	2.4	4.3
6	X	X		1362.0	2483.6	0.8	1.4	1289.3	2352.7	2.6	4.7	72.8	131.0	3.2	5.8
7		X	X	1356.0	2472.8	0.8	1.4	1287.8	2350.0	2.4	4.3	68.3	122.9	2.5	4.5
8	X	X	X	1352.0	2465.6	0.0	0.0	1275.7	2328.3	0.6	1.1	76.3	137.3	0.6	1.1

The correlation of cracking susceptibility with melting temperature range is shown in Fig. 5. Linear regression analysis performed on the data set resulted in the following functional relationship:

$$MCL = 0.00087(\Delta T) - 0.015 \qquad \textbf{(EQ 6)}$$

The incomplete statistical correlation ($R^2 = 0.86$) suggests that other factors are necessarily involved.

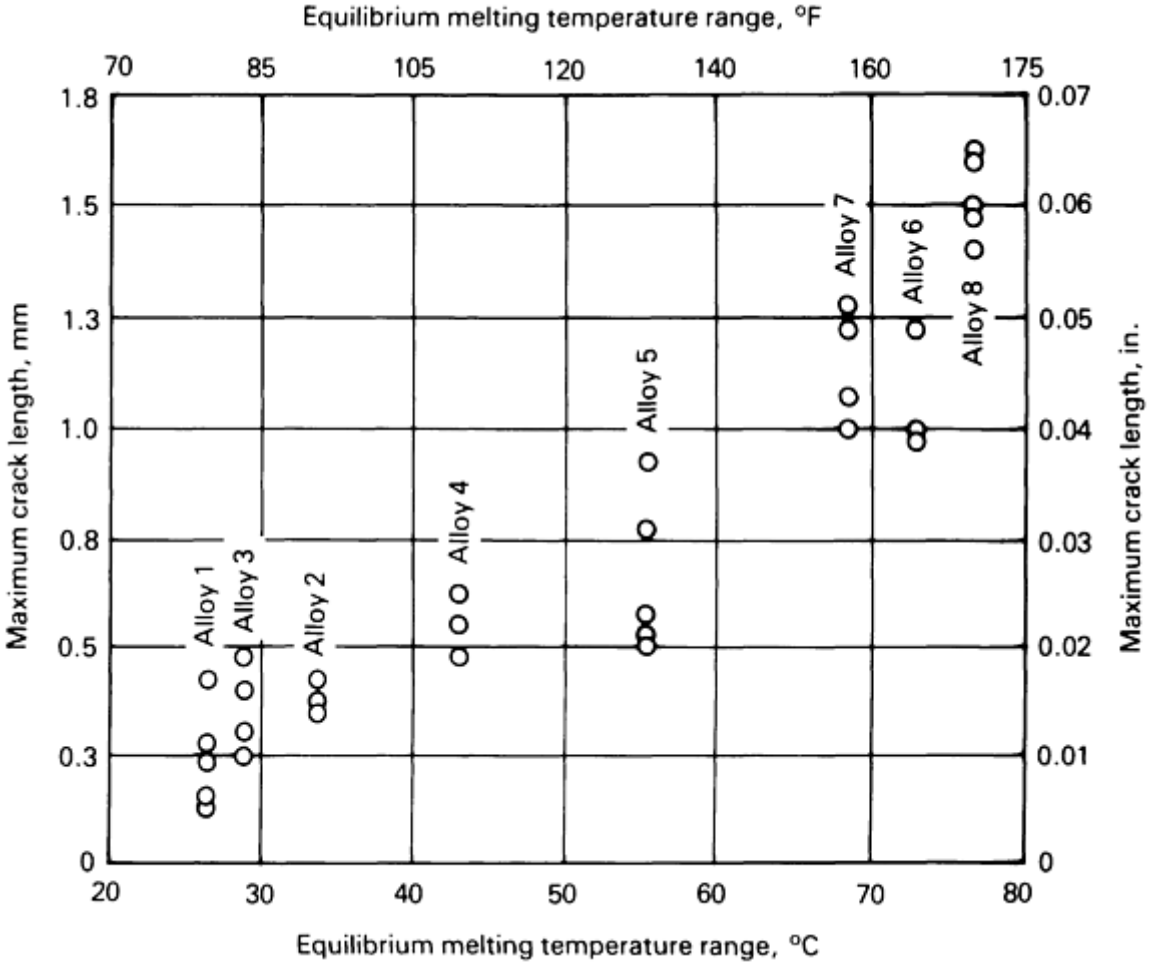

FIG. 5 RELATIONSHIP BETWEEN MAXIMUM CRACK LENGTH AND EQUILIBRIUM MELTING TEMPERATURE RANGE IN ALLOY 625 WELDABILITY STUDY

The solidification behavior of fusion welds is nonequilibrium in nature and may result in an extension of the solidification temperature range significantly beyond that measured under "equilibrium" conditions. Indeed, the niobium-bearing alloys terminate weld solidification below the equilibrium solidus with the formation of nonequilibrium eutecticlike constituents involving niobium carbides and Laves-type phases. Nonetheless, it is clear from an engineering perspective that Borland's concepts are valid enough to allow the establishment of a useful alloy ranking system from a solidification cracking perspective.

In addition to the effect of melting temperature range. Borland realized that the distribution of liquid along solidifying grain boundaries plays an important role in determining the solidification cracking susceptibility on an alloy (Ref 1). If the terminal solidification liquid easily wets the solidifying grain boundary (that is, has a low solid/liquid surface tension), it will tend to be spread out over a wider area, easing separation of the grains under a mechanical imposition. Conversely, if the liquid does not readily wet these boundaries, it will be more localized, creating a smaller area of liquid-solid contact and more solid-solid bridging, resulting in a more robust mechanical structure with increased cracking resistance. Elements such as sulfur and boron have been suggested as providing this surfactant property to terminal solidification liquids in iron and nickel alloys. Manganese may serve to increase the surface tension of terminal solidification fluids.

Figure 6 shows the results (Ref 6) of varestraint testing on two heats of Cabot alloy 214, a Ni-16Cr-4.5Al-2.5Fe alloy designed for use in high-temperature environments. The two alloys differ primarily in their boron content. With no boron intentionally added (0.0002 wt%), the alloy is extremely resistant to solidification cracking. With boron intentionally added at a level of 0.003 wt%, the solidification cracking propensity is much greater. Figures 7 and 8 are surface images of pulsed Nd:YAG laser welds made on the two alloys. Extensive cracking is evident in the high-boron alloy. Figure 7(b) is a good example of the extensive terminal "crater cracking" discussed above.

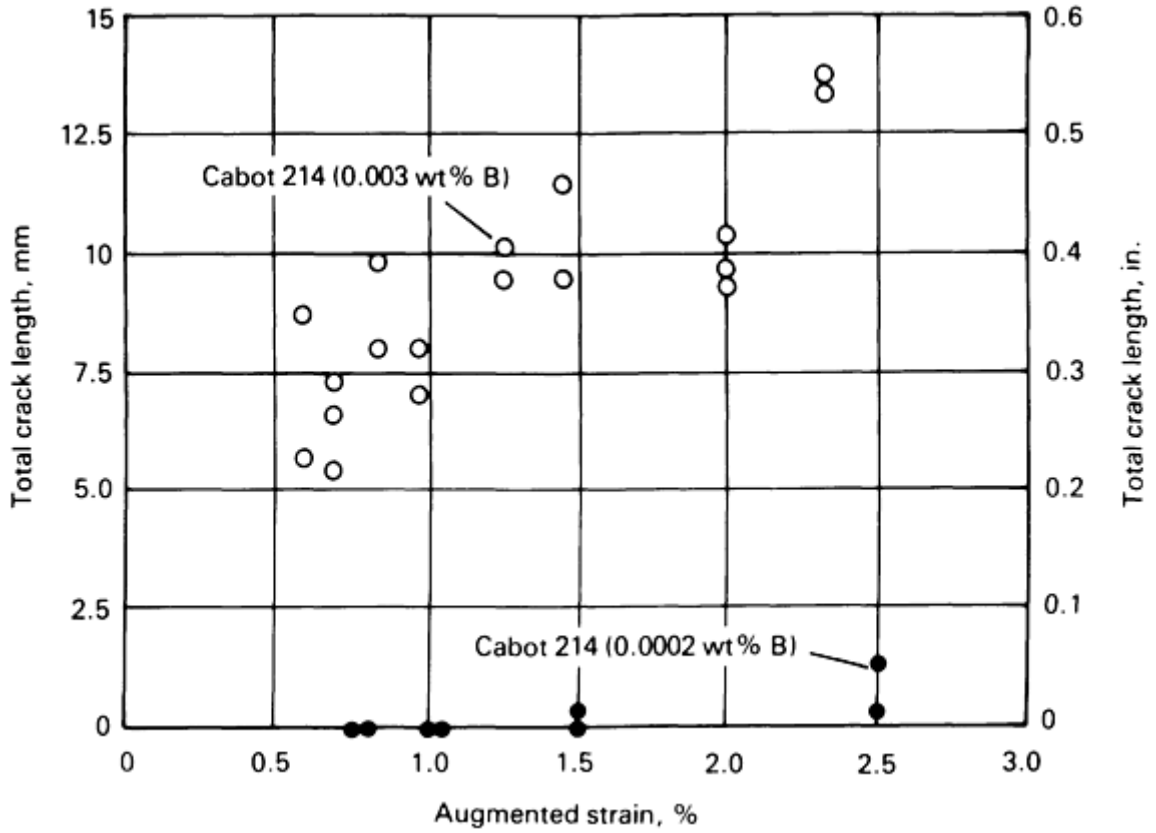

FIG. 6 VARESTRAINT TEST WELDABILITY DATA FOR CABOT ALLOY 214 WITH VARYING BORON CONCENTRATIONS

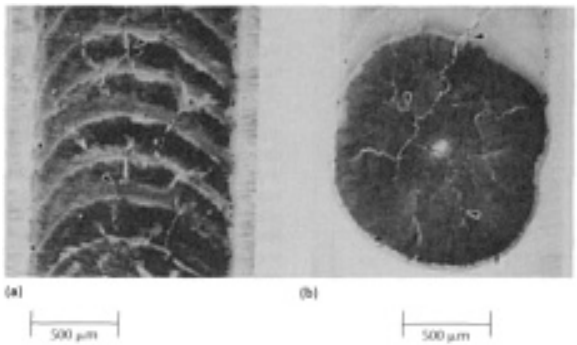

FIG. 7 SEM SURFACE IMAGE OF PULSED ND:YAG LASER WELDS IN HIGH-BORON ALLOY 214. (A) SOLIDIFICATION CRACKING. (B) CRATER CRACKING

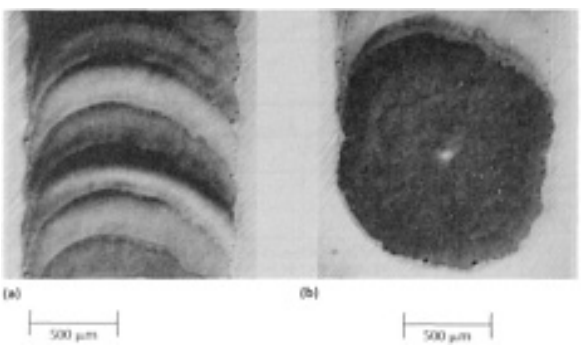

FIG. 8 SEM SURFACE IMAGE OF PULSED ND:YAG LASER WELDS IN LOW-BORON CONTENT ALLOY 214. (A) SOLIDIFICATION CRACKING. (B) CRATER CRACKING

Figures 9 and 10 summarize parameters that affect hot cracking in the weld metal and in the base metal HAZ, respectively. For most alloys that are highly susceptible to solidification cracking, filler metals of different composition have been developed to minimize the cracking that accompanies fusion welding.

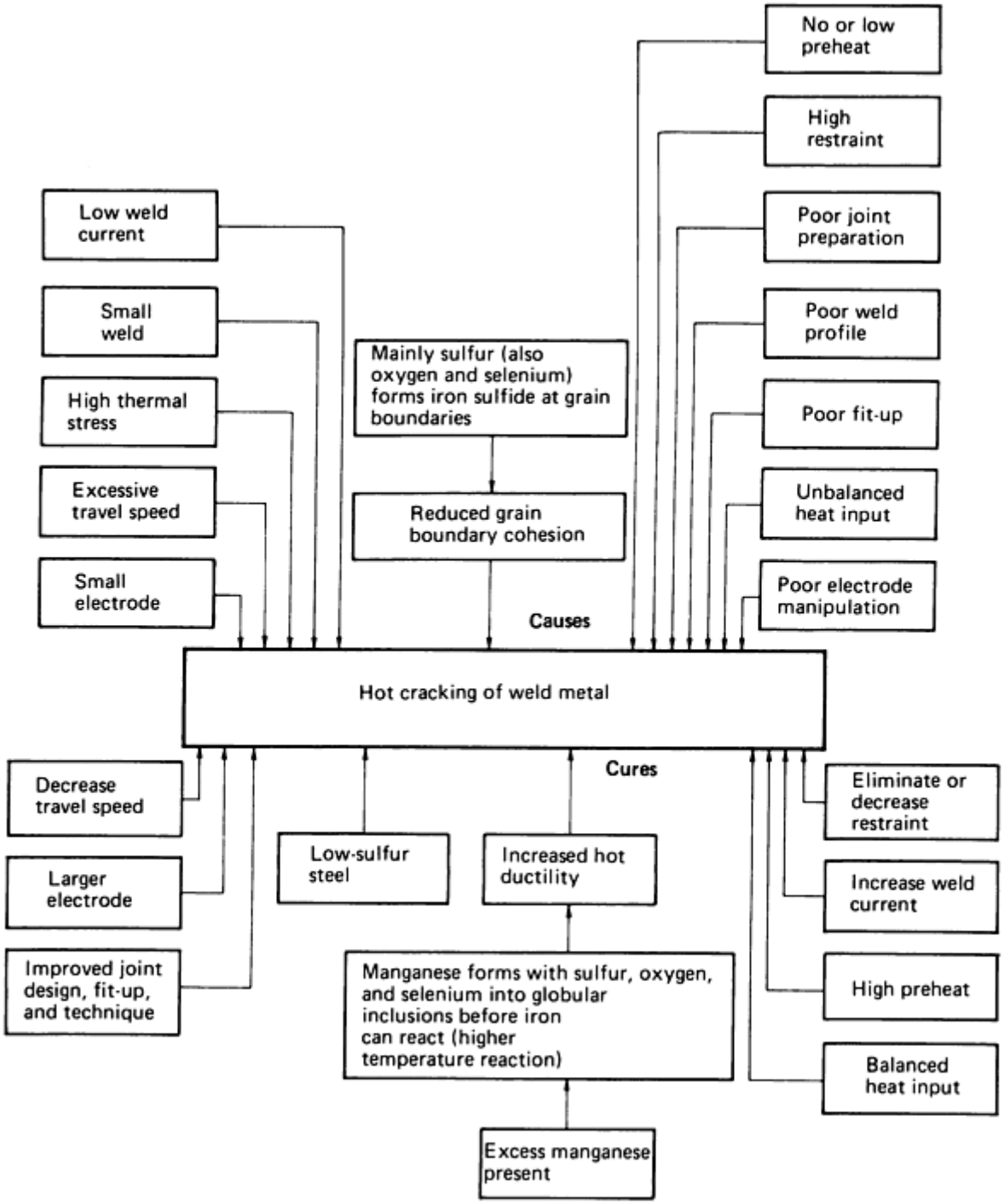

FIG. 9 FACTORS AFFECTING HOT CRACKING IN WELD METAL

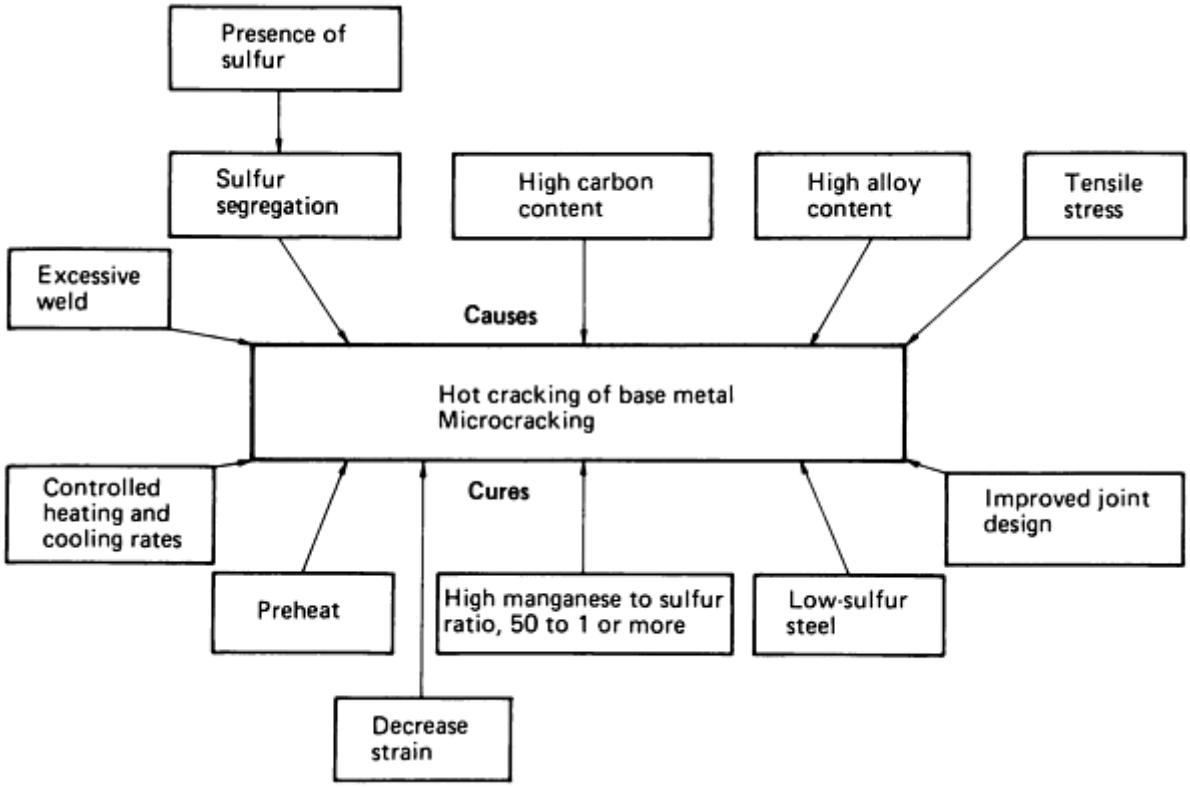

FIG. 10 FACTORS AFFECTING HOT CRACKING IN BASE METAL HAZ

References cited in this section

1. J.C. BORLAND, GENERALIZED THEORY OF SUPER-SOLIDUS CRACKING IN WELDS (AND CASTINGS), *BR. WELD. J.*, VOL 7 (NO. 8), 1960, P 508-512
2. J.C. BORLAND, HOT CRACKING IN WELDS, *BR. WELD. J.*, VOL 7 (NO. 9), 1960, P 558-559
3. D.A. CANONICO, W.F. SAVAGE, W.J. WERNER, AND G.M. GOODWIN, EFFECTS OF MINOR ADDITIONS ON THE WELDABILITY OF INCOLOY 800, *EFFECTS OF MINOR ELEMENTS ON THE WELDABILITY OF HIGH-NICKEL ALLOYS*, WRC, JULY 1969, P 68-92
4. M.J. CIESLAK, THE WELDING AND SOLIDIFICATION METALLURGY OF ALLOY 625, *WELD. J.*, FEB 1991, P 49S-56S
5. W.F. SAVAGE AND C.D. LUNDIN, APPLICATION OF THE VARESTRAINT TECHNIQUE TO THE STUDY OF WELDABILITY, *WELD. J.*, NOV 1966, P 497S-503S
6. M.J. CIESLAK, J.J. STEPHENS, AND M.J. CARR, A STUDY OF THE WELDABILITY AND WELD RELATED MICROSTRUCTURE OF CABOT ALLOY 214, *METALL. TRANS. A*, MARCH 1988, P 657-667

Cracking Phenomena Associated With Welding

Michael J. Cieslak, Physical and Joining Metallurgy Department, Sandia National Laboratories

Heat-Affected-Zone Cracks

Microfissures are cracks that occur in the area of partial melting and the HAZ adjacent to the fusion line. Because no material can be purified to the state where it solidifies truly as an invariant, all materials have a temperature region of stable two-phase coexistence of solid and liquid. In fusion welding, this manifests itself in the formation of a zone of

partial melting at temperatures below the alloy liquidus. The extent of this zone may be enlarged by the presence of chemical inhomogeneity in a material. Local chemical variations will result in local variations in the melting point. Segregation of specific alloying elements to grain boundaries may cause a reduction in the melting temperatures of these areas.

Many microfissures form in a manner somewhat analogous to the formation of solidification cracks in that susceptible sites, generally grain boundaries that intersect the fusion zone, are wetted with liquid from one of various sources. shrinkage strains accumulating as the weld pool advances past the liquated boundary can develop to a level sufficient to cause boundary separation (i.e., cracking). Figure 11 is a photomicrograph of an HAZ microfissure in a cast austenitic stainless steel (this crack also extends into the fusion zone as a solidification crack). Cast microstructures are highly inhomogeneous, raising the possibility of extensive partial melting. Note the melting associated with interdendritic constituents in Fig. 11.

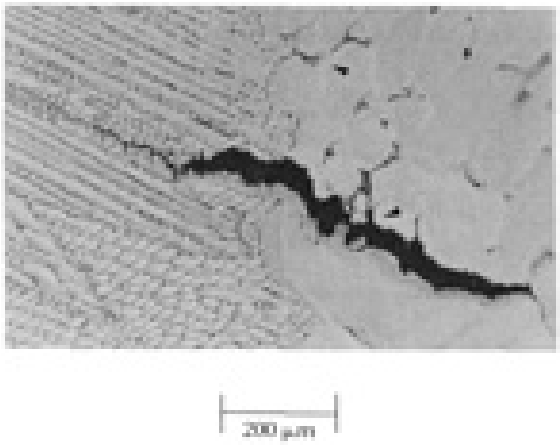

FIG. 11 HAZ MICROFISSURE IN A CAST STAINLESS STEEL. NOTE EXTENSIVE REGION OF PARTIAL MELTING.

Castings represent a special case of inhomogeneity on a continuous scale. Chemical inhomogeneities in wrought products are more discrete, generally involving minor phase particles. In many cases, these minor phases arise from thermomechanical processing of alloys well below the solidus, where the solubility for specific alloying elements can be lower. Because of the potential for extremely rapid rates of heating and cooling (especially heating) in the HAZ of fusion welds, it is entirely possible that minor phases not thermodynamically stable under equilibrium conditions may continue to exist at near-solidus temperatures. Under these conditions, the minor phases may interact with the matrix to form a liquid product. This reaction, often referred to as constitutional liquation (Ref 7), can provide the liquid required to wet grain boundaries producing a microstructure that may be susceptible to cracking.

Hot ductility testing is a common method of assessing the susceptibility of an alloy to this form of cracking. In this test, a laboratory-scale specimen is subjected to a thermal cycle representative of what the material would experience in the HAZ during fusion welding. At various temperatures during both the heating and cooling portions of the cycle, samples are strained to failure. The ductility response (usually expressed in terms of reduction of area) as the alloy progresses through the thermal cycle simulates the response of the alloy to an actual welding situation. In particular, the ability of the material to reestablish ductility after experiencing the peak temperature is a critical measure of sensitivity to this form of cracking.

Figures 12(a) and 12(b) show the hot ductility response of two heats of Cabot alloy 214 containing two different concentrations of boron. The return of ductility in the low-boron alloy after cooling from a peak temperature of 1345 °C (2453 °F) indicates that this alloy should be virtually immune to this form of cracking, as weldability tests confirmed (Ref 6). The high-boron heat showed no appreciable recovery of ductility until a temperature approximately 250 °C (450 °F) below the thermal peak temperature. This alloy should be quite susceptible to this form of cracking, as weldability tests also confirmed (Ref 6). Figure 13 is a fractograph of a hot ductility test specimen from the high-boron alloy taken from the sample strained at 1150 °C (2102 °F) on cooling from the peak temperature. The smooth, intergranular appearance is characteristic of this type of cracking. Although the presence of a liquid phase along this fracture surface could not be

unequivocally established by fractographic techniques, it was noted that the failure occurred at an exceedingly low load (Ref 6), consistent with the presence of a liquid film.

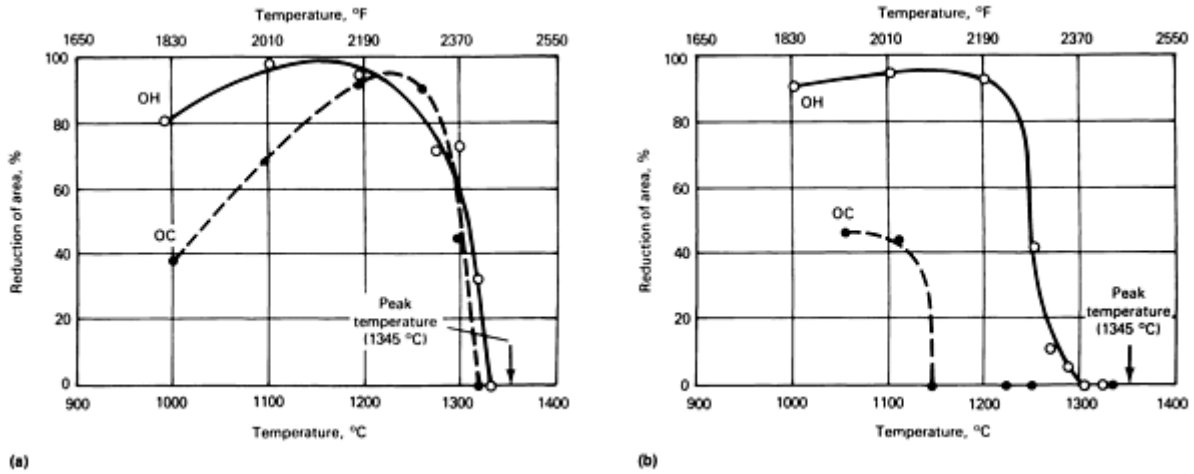

FIG. 12 HOT DUCTILITY RESPONSE OF CABOT ALLOY 214 WITH VARYING BORON CONCENTRATIONS. (A) LOW-BORON CONTENT (0.0002 WT% B). (B) HIGH-BORON CONTENT (0.003 WT% B). (OH, TESTING DONE ON HEATING; OC, TESTING DONE ON COOLING FROM 1345 °C (2455 °F)

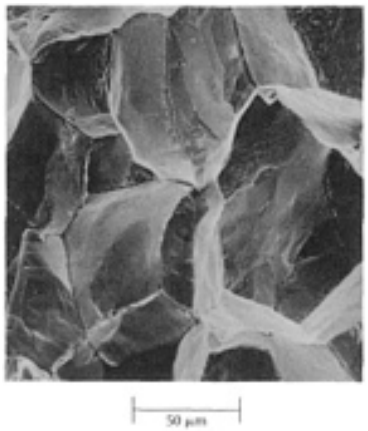

FIG. 13 FRACTURE SURFACE OF A HOT DUCTILITY SAMPLE OF HIGH-BORON ALLOY 214 TESTED AT 1150 °C (2100 °F) ON COOLING FROM 1345 °C (2455 °F)

The presence of a liquid is not essential to the formation of HAZ cracks, as they may occur at temperatures well below the solidus. Poor ductility inherent in certain materials, such as intermetallics, can lead to solid-state failure during welding if the thermal stresses associated with the weld thermal cycle exceed the local tensile strength.

Cracks may also occur in alloys that undergo polymorphic transformations during the weld thermal cycle. The act of fusion welding subjects the fusion zone and the HAZ to temperatures above those normally encountered during prior deformation processing. The resultant HAZ microstructure may be substantially different from that of the base material. In the case of martensitic-type transformations, there is often a relatively large, discontinuous change in the molar volume occurring very rapidly with decreasing temperature below the M_s. If that event causes a local shrinkage, then large, localized tensile stresses can develop. If the newly transformations microstructure has limited ductility (not uncommon in shear transformations or in transformations that result in ordered structures), the likelihood of cracks forming at susceptible sites, such as grain boundaries, matrix/minor phase interfaces, and slip band intersections, is increased.

Reheat cracking, also referred to as stress-relief of strain-age cracking, is another defect type observed in certain alloys that undergo precipitation reactions. Historically observed in several nickel-base superalloys and creep-resistant steels, this type of defect manifests itself during postweld heat treatment, generally as intergranular HAZ cracks.

Postweld heat treatment is often a recommended practice for high-strength thick-section welded steels, where reduction of residual stresses developed as a result of welding is desired. In the case of welded nickel-base superalloys, postweld heat treatment is used both to relieve residual stresses and to achieve optimum mechanical properties through precipitation-hardening reactions.

In alloys that undergo precipitation reactions, the rate at which the alloy strengthens may greatly exceed the rate at which residual stresses are thermally diminished. This can be especially true in the case of heavy-section welds or in alloys with relatively poor thermal conductivity. (That is, before the alloy can reach the temperature at which residual stresses begin to be eliminated, it has aged and lost ductility relative to its as-welded state.) At this new lower level of ductility, the residual stresses present may induce cracks to eliminate the accumulated strain energy.

In principle, the problem of reheat cracking could be largely eliminated if the rate of heating through the precipitation temperature range was rapid enough to prevent precipitate formation. However, extremely rapid rates of heating in welded hardware would likely lead to problems such as excessive distortion; therefore, improved alloys (e.g., alloy 718 among the nickel-base superalloys) have been developed in which the kinetics of precipitate formation have been sufficiently retarded to allow for successful postweld heat treatment.

Dealing with HAZ cracks, however they might form, is generally more difficult than attending to the problem of solidification cracking. Modifying the composition in the HAZ through the addition of consumables is not a viable option. Prior heat treatment may allow the production of a less susceptible starting microstructure, but this option generally is quite limited. Optimization of weld process parameters to minimize the extent of tensile stress and strain development should always be considered, as should optimizing weld joint design as discussed above.

References cited in this section

6. M.J. CIESLAK, J.J. STEPHENS, AND M.J. CARR, A STUDY OF THE WELDABILITY AND WELD RELATED MICROSTRUCTURE OF CABOT ALLOY 214, *METALL. TRANS. A,* MARCH 1988, P 657-667
7. J.J. PEPE AND W.F. SAVAGE, EFFECTS OF CONSTITUTIONAL LIQUATION IN 18-NI MARAGING STEEL WELDMENTS, *WELD. J.,* SEPT 1967, P 411S-422S

Cracking Phenomena Associated With Welding

Michael J. Cieslak, Physical and Joining Metallurgy Department, Sandia National Laboratories

Hydrogen-Induced Cracking (Cold Cracking)

Cold cracks are defects that form as the result of the contamination of the weld microstructure by hydrogen. Whereas solidification cracking and HAZ cracking occur during or soon after the actual welding process, hydrogen-induced cracking is usually a delayed phenomenon, occurring possibly weeks or even months after the welding operation. The temperature at which these defects tend to form ranges from -50 to 150 °C (-60 to 300 °F) in steels. The fracture is either intergranular or transgranular cleavage.

As with other forms of cracking, hydrogen-induced cracking involves both a requisite microstructure and a threshold level of stress. It also involves a critical level of hydrogen, which is alloy and microstructure dependent.

In the case of ideal weld processing, hydrogen-induced cracking would be at most a minor welding engineering concern. However, excluding hydrogen from structures during welding is exceedingly difficult. Although the primary source of hydrogen in weld metal is considered to be the disassociation of water vapor in the arc and absorption of gaseous or ionized hydrogen into the liquid, other sources are also available. All organic compounds contain hydrogen in their

molecular structure, and all may be broken down in the intense thermal environment of a welding heat source. Organic compounds are ubiquitous in the welding environment, from lubricants in assembly areas to body oils on the hands of welding operators. Plated hardware may also contain high levels of residual hydrogen.

The mechanism of hydrogen-induced crack formation is still being investigated. An early hypothesis, involving the buildup of hydrogen gas pressure in voids, is now generally discredited. Currently, the most widely accepted model involves the presence of preexisting defect sites in the material--small cracks or discontinuities caused by minor phase particles or inclusions. In the presence of existing stress, these sites may develop high local areas of biaxial or triaxial tensile stress. Hydrogen diffuses preferentially to these sites of dilated lattice structure. As the local hydrogen concentration increases, the cohesive energy and stress of the lattice decrease. When the cohesive stress falls below the local intensified stress level, fracture occurs spontaneously. Hydrogen then evolves in the crack volume, and the process is repeated. This model of hydrogen-induced cracking is consistent with the relatively slow and discontinuous nature of the process.

In steels, where the problem of hydrogen-induced cracking is extremely significant, cracking susceptibility has been correlated both with material hardness and strength, and with specific microstructure. Higher-strength steels are more susceptible to hydrogen-induced cracking than low-strength steels. Steels that transform martensitically are particularly susceptible, especially the higher-carbon alloys with twinned martensitic structures. The desire to avoid martensite formation has driven the development of high-strength structural steels for welded applications.

Production of the newer high-strength low-alloy (HSLA) steels uses a variety of precisely controlled alloying additions (for example, aluminum, titanium, vanadium, and niobium) along with meticulous thermomechanical processing to develop a very fine-grained ferrite microstructure possessing substantial strength and fracture toughness with a high degree of resistance to hydrogen-induced cracking. The form of the ferrite produced during transformation on cooling from the austenite phase field is also critical, with acicular ferrite resulting in improved properties compared with grain-boundary, polygonal, or Widmanstätten ferrite. Acicular ferrite is often nucleated on minor phase particles, such as specific oxides or borides. Acknowledgement of the beneficial effect of certain oxides in providing sites for acicular ferrite nucleation in modern steels is in sharp contrast to steel design of earlier decades, when elimination of oxygen to the greatest extent possible was considered essential to the development of optimal fracture behavior.

A useful concept for understanding the susceptibility of carbon and alloy steels to hydrogen-induced cracking is the carbon equivalent (CE), an empirical relationship that attempts to reduce the number of significant compositional variables affecting the weldability of steels into a single quantity. Several carbon equivalent relationships have been developed for different classes of steels. An example is:

$$CE = \%C + \frac{\%Mn}{6} + \frac{\%Cr + \%Mo + \%V}{5} + \frac{\%Si + \%Ni + \%Cu}{15} \qquad \textbf{(EQ 7)}$$

From a metallurgical perspective, the carbon equivalent can be related to the development of hydrogen-sensitive microstructures. That is, as the carbon equivalent increases, microstructures are evolved during cooling through the transformation temperature range that are increasingly more susceptible to hydrogen-induced cracking. At high carbon equivalent values, martensitic structures can be expected.

Carbon equivalent formulas are usually developed from large databases of critical hydrogen concentrations and weld joint restraints that will result in hydrogen-induced cracking in the steels under consideration. At various levels of carbon equivalent, certain weld preheat requirements are often established. In the example of Eq 7, when the carbon equivalent exceeds 0.35%, preheats are recommended to minimize susceptibility to hydrogen cracking. At higher levels of carbon equivalent, both preheats and postheats may be required.

Most structural carbon and low-alloy steels that may be susceptible to hydrogen-induced cracking transform from austenite during cooling through the temperature range of 800 to 500 °C (1470 to 930 °F). The length of time a steel spends in this temperature range during cooling will establish its microstructure and hence its cracking sensitivity. This time segment is generally referred to as $t_{8/5}$ (in seconds). To maximize cracking resistance, a microstructure free of untempered martensite is desired.

Using a specifically developed carbon equivalent, Yurioka (Ref 8) formulated a relationship to establish the critical $t_{8/5}$ for a martensite-free HAZ in low-carbon alloy steels. The carbon equivalent is defined as:

$$CE = \%C^* + \frac{\%Mn}{3.6} + \frac{\%Cu}{20} + \frac{\%Ni}{9} + \frac{\%Cr}{5} + \frac{\%Mo}{4} \qquad \textbf{(EQ 8)}$$

where %C* = %C for C $\leq$ 0.3% and %C* = %C/6 + 0.25 for %C > 0.3%. The critical time length in seconds, $t_{8/5}$, for the avoidance of martensitic transformation is given as:

$$\text{LOG } t_{8/5} = 2.69\ CE^* + 0.321 \qquad \textbf{(EQ 9)}$$

When this quantity is known, welding parameters and preheat temperature for the given thickness of material being welded can be established to produce cooling rates that avoid formation of a martensitic constituent in the HAZ.

The use of preheating and postheating to minimize the susceptibility to hydrogen-induced cracking is an accepted welding procedure for many steels. Preheating controls the cooling rate through the transformation temperature range; a higher base metal temperature in a slower cooling rate through the transformation temperature range and thus a larger $\tau_{8/5}$. Thicker sections often require preheating because of the greater heat-sinking capability of a thick section, for which a given set of welding parameters will produce a faster cooling rate and a smaller $t_{8/5}$. Preheating may also reduce the level of residual stress in the welded assembly.

There are, of course, practical limits to the use of preheating. Excessively high base metal temperatures can make welding difficult, especially manual welding. A high preheat temperature will result in the flattening of temperature gradients, increasing the spatial extent of and the time spent in the austenite phase field. This may result in excessive grain growth in the HAZ, which can lead to a loss of fracture toughness independent of hydrogen content. Preheat temperatures up to 150 °C (300 °F) are not uncommon for low-alloy steels and may increase up to 425 °C (800 °F) for higher-carbon equivalent martensitic steels.

Several benefits can be realized by postheating. At high enough temperatures (550 to 600 °C, or 1020 to 1110 °F), postheating can diminish residual stresses present in the as-welded structure. Microstructural modifications such as tempering can also occur, producing a microstructure less susceptible to hydrogen-induced cracking. Finally, the higher temperature may allow hydrogen to diffuse into the bulk of the structure or even to the surface, where it may recombine and exit as a gas. In either case, the level of hydrogen concentration may be reduced below that required to initiate cracks.

The following guidelines should be followed to minimize the occurrence of hydrogen-induced cracking. For a given level of required strength, the steel with the lowest carbon equivalent should be considered. Low-hydrogen welding practice should be followed. This involves elimination of possible sources of hydrogen by using ultrahigh-purity gases and moisture-free gas lines and by baking coated electrodes following the manufacturer's recommendations to ensure removal of nascent water. Finally, preheating and postheating requirements should be followed assiduously. Figures 14 and 15 summarize the causes and cures of hydrogen-induced cracking in the weld metal and in the base metal, respectively.

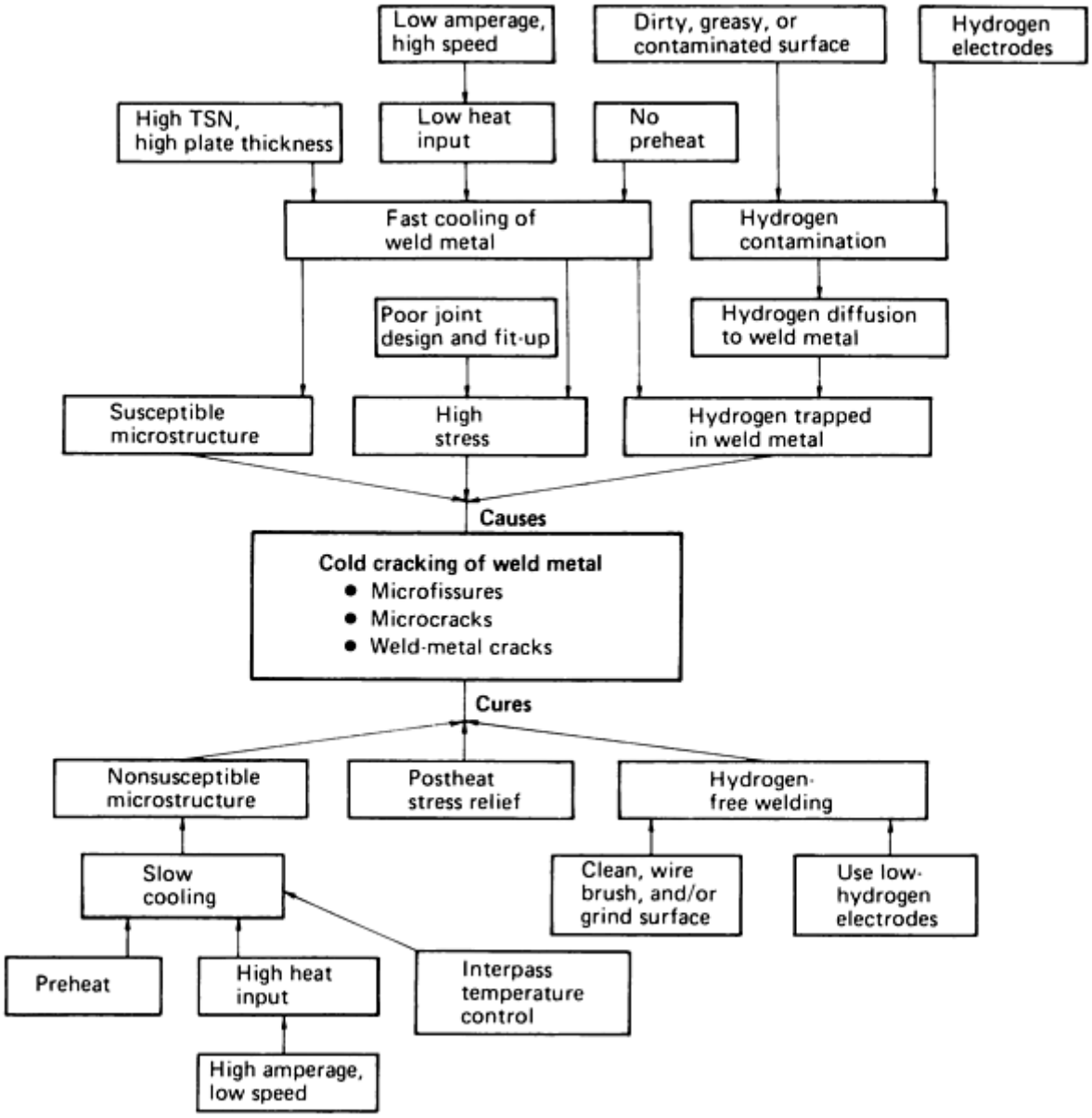

FIG. 14 CAUSES AND CURES OF HYDROGEN-INDUCED CRACKING IN WELD METAL. THERMAL SEVERITY NUMBER (TSN), WHICH IS FOUR TIMES THE TOTAL PLATE THICKNESS CAPABLE OF REMOVING HEAT FROM THE JOINT, IS A MEASURE OF THE ABILITY OF THE MEMBER TO SERVE AS A HEAT SINK.

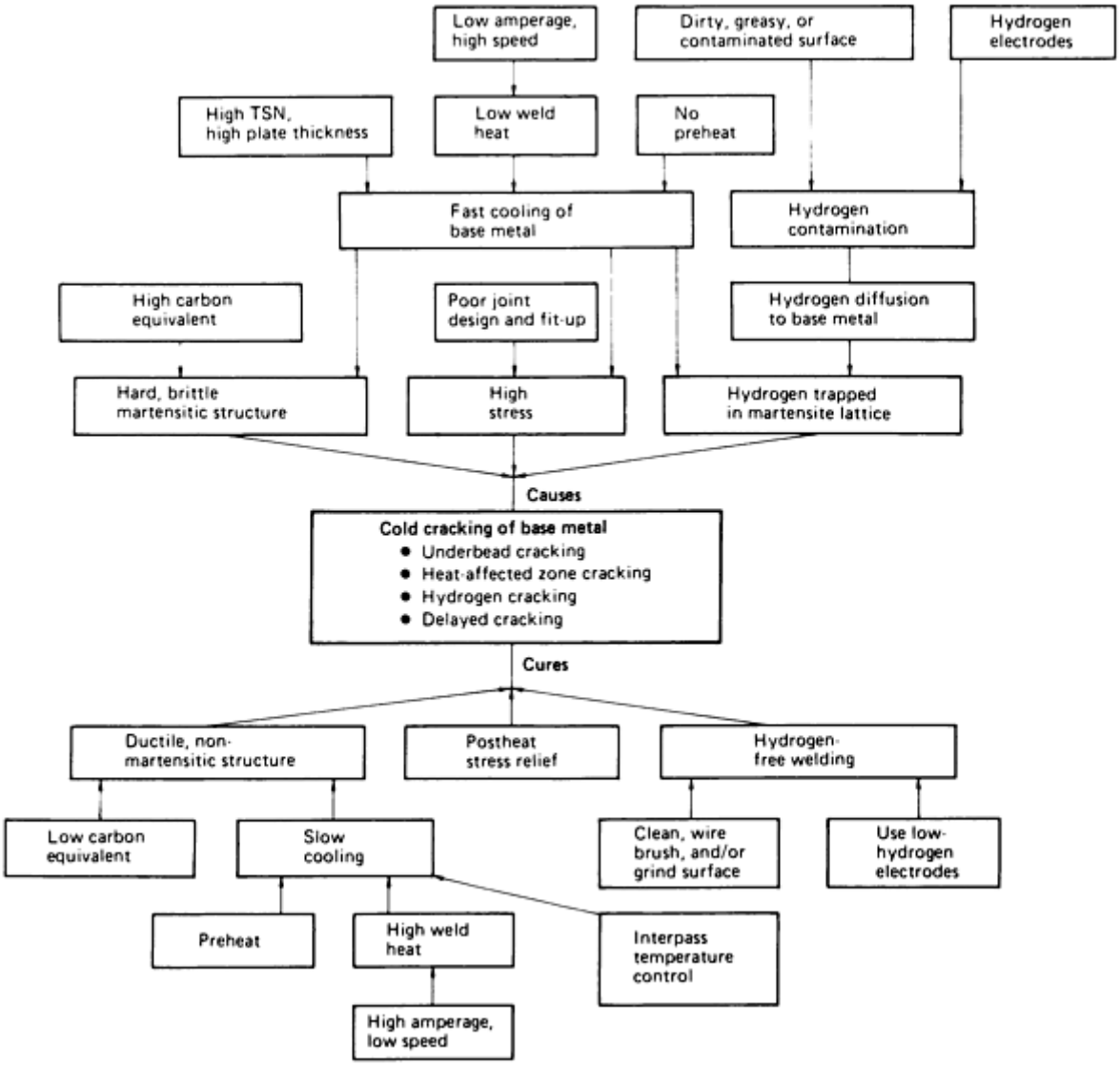

FIG. 15 CAUSES AND CURES OF HYDROGEN-INDUCED CRACKING IN BASE METAL

Reference cited in this section

8. N. YURIOKA, WELDABILITY OF MODERN HIGH STRENGTH STEELS, *1ST U.S.-JAPAN SYMP. ADVANCES IN WELDING METALLURGY,* AWS, 1990, P 79-100

Cracking Phenomena Associated With Welding

Michael J. Cieslak, Physical and Joining Metallurgy Department, Sandia National Laboratories

Lamellar Tearing (Ref 9)

Lamellar tearing is cracking that occurs beneath welds. It is found in rolled steel plate weldments. The tearing always lies within the base metal, generally outside the HAZ and parallel to the weld fusion boundary. The problem is caused by welds that subject the base metal to tensile loads in the *z*, or through, direction of the rolled steel. Occasionally the tearing comes to the surface of the metal, but more commonly remains under the weld (Fig. 16) and is detectable only by ultrasonic testing. Lamellar tearing occurs when three conditions are simultaneously present:

- STRAINS DEVELOP IN THE THROUGH DIRECTION OF THE PLATE. THEY ARE CAUSED BY WELD METAL SHRINKAGE IN THE JOINT AND CAN BE INCREASED BY RESIDUAL STRESSES AND BY LOADING.
- THE WELD ORIENTATION IS SUCH THAT THE STRESS ACTS THROUGH THE JOINT ACROSS THE PLATE THICKNESS (THE *Z* DIRECTION). THE FUSION LINE BENEATH THE WELD IS ROUGHLY PARALLEL TO THE LAMELLAR SEPARATION.
- THE MATERIAL HAS POOR DUCTILITY IN THE *Z* DIRECTION.

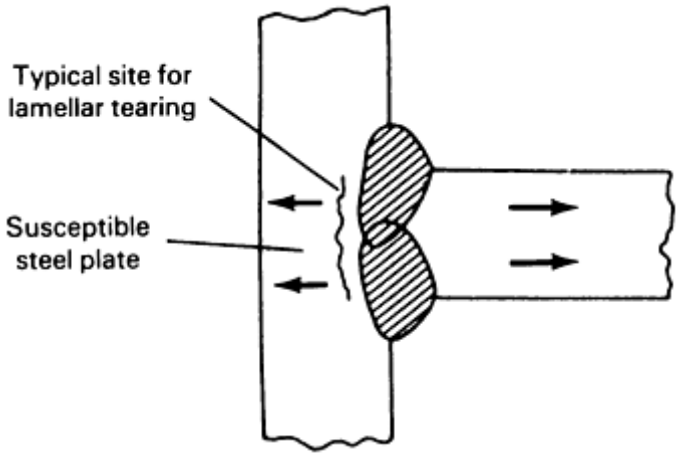

FIG. 16 TYPICAL LOCATION FOR LAMELLAR TEARING IN A T-JOINT

Lamellar tearing can occur during flame cutting and cold shearing operations. Low material strength in the *z* direction is the primary cause, with stress in that direction initiating the tearing. Thermal heating and stresses from weld shrinking create the fracture. Lamellar tearing can take place shortly after welding or occasionally months later. Thicker, higher-strength materials appear to be more susceptible. However, the phenomenon affects only a very small percentage of steel plates, as all three of the above conditions rarely occur in combination.

The problem can be avoided by proper attention to joint details. In T-joints (Fig. 16), double-fillet welds appear to be less susceptible than full-penetration welds. Also, balanced welds on both sides of the joint appear to present less risk than large, single-sided welds. In corner joints, common in box columns, lamellar tearing can be readily detected on the exposed edge of the plate (Fig. 17a). The problem can be overcome by placing the bevel for the joint on the edge of the plate that would exhibit the tearing rather than on the other plate (Fig. 17b). Butt joints rarely exhibit lamellar tearing, because weld shrinkage does not set up a tensile stress in the thickness direction of the plates.

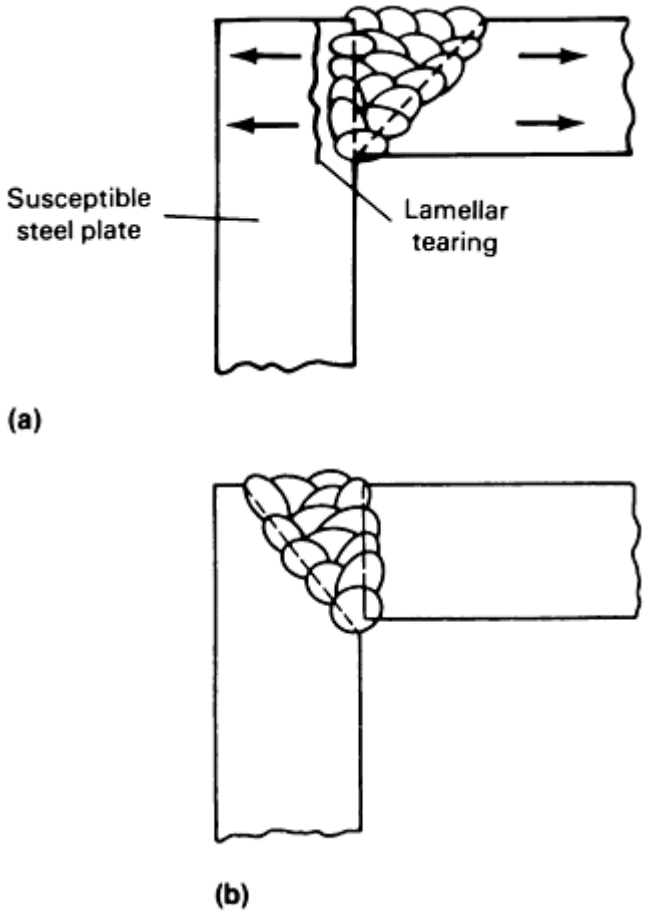

FIG. 17 CORNER JOINT. (A) LAMELLAR TEARING SURFACES AT THE EXPOSED PLATE EDGE. (B) REDESIGNED JOINT

Arc welding processes with high heat input are less likely to create lamellar tearing, perhaps because of the fewer number of applications of heat and the lesser number of shrinkage cycles involved in making a weld. Also, filler metal with lower yield strength and high ductility appears to lessen the possibility of tearing. Preheating does not appear to be particularly advantageous, nor does stress relieving. The "buttering" technique of laying one or more layers of low-strength, high-ductility weld metal deposit on the surface of the plate stressed in the *z* direction will reduce the possibility of lamellar tearing. However, this is an extreme solution and should be used only as a last resort.

Reference cited in this section

9. H.B. CARY, *MODERN WELDING TECHNOLOGY*, 2ND ED., PRENTICE-HALL, 1989, P 702-703

Cracking Phenomena Associated With Welding

Michael J. Cieslak, Physical and Joining Metallurgy Department, Sandia National Laboratories

References

1. J.C. BORLAND, GENERALIZED THEORY OF SUPER-SOLIDUS CRACKING IN WELDS (AND CASTINGS), *BR. WELD. J.*, VOL 7 (NO. 8), 1960, P 508-512

2. J.C. BORLAND, HOT CRACKING IN WELDS, *BR. WELD. J.*, VOL 7 (NO. 9), 1960, P 558-559
3. D.A. CANONICO, W.F. SAVAGE, W.J. WERNER, AND G.M. GOODWIN, EFFECTS OF MINOR ADDITIONS ON THE WELDABILITY OF INCOLOY 800, *EFFECTS OF MINOR ELEMENTS ON THE WELDABILITY OF HIGH-NICKEL ALLOYS*, WRC, JULY 1969, P 68-92
4. M.J. CIESLAK, THE WELDING AND SOLIDIFICATION METALLURGY OF ALLOY 625, *WELD. J.*, FEB 1991, P 49S-56S
5. W.F. SAVAGE AND C.D. LUNDIN, APPLICATION OF THE VARESTRAINT TECHNIQUE TO THE STUDY OF WELDABILITY, *WELD. J.*, NOV 1966, P 497S-503S
6. M.J. CIESLAK, J.J. STEPHENS, AND M.J. CARR, A STUDY OF THE WELDABILITY AND WELD RELATED MICROSTRUCTURE OF CABOT ALLOY 214, *METALL. TRANS. A*, MARCH 1988, P 657-667
7. J.J. PEPE AND W.F. SAVAGE, EFFECTS OF CONSTITUTIONAL LIQUATION IN 18-NI MARAGING STEEL WELDMENTS, *WELD. J.*, SEPT 1967, P 411S-422S
8. N. YURIOKA, WELDABILITY OF MODERN HIGH STRENGTH STEELS, *1ST U.S.-JAPAN SYMP. ADVANCES IN WELDING METALLURGY*, AWS, 1990, P 79-100
9. H.B. CARY, *MODERN WELDING TECHNOLOGY*, 2ND ED., PRENTICE-HALL, 1989, P 702-703

Characterization of Welds

Craig B. Dallam, The Lincoln Electric Company; Brian K. Damkroger, Sandia National Laboratories

Introduction

WELDS CAN BE CHARACTERIZED according to a number of criteria, including the welding process used, size, shape, mechanical properties, chemical composition, and a number of others. The appropriate methods of characterization depend on the weld's function and the particular set of properties required for the application. In some instances, the ability of a weld to function successfully can be addressed by characterizing the size or shape of the weld. An example of this is where factors related to the welding procedure, such as inadequate weld size, convexity of the bead, or lack of penetration, may cause a weld to fail. In other cases, it is important to characterize metallurgical factors such as weld metal composition and microstructure. Examples might include welds for which the goal is to avoid failures due to inadequate strength, ductility, toughness, or corrosion resistance. In general, the goals of weld characterization are to assess the ability of a weld to successfully perform its function, to thoroughly document a weld and welding procedure that have been demonstrated to be adequate, or to determine why a weld failed.

In the first part of this article, characterization of welds will be treated as a sequence of procedures, each more involved than the last and concerned with a finer scale of detail. Initially, non-destructive characterization procedures will be the focus. The first level of characterization involves information that may be obtained by direct visual inspection and measurement of the weld. A discussion of nondestructive evaluation follows. This encompasses techniques used to characterize the locations and structure of internal and surface defects, including radiography, ultrasonic testing, and liquid penetrant inspection.

The next group of characterization procedures discussed are destructive, requiring the removal of specimens from the weld. The first of these is macrostructural characterization of a sectioned weld, including features such as number of passes; weld bead size, shape, and homogeneity; and the orientation of beads in a multipass weld. Macroscopic characterization is followed by microstructural analysis, including microsegregation, grain size and structure, the phase makeup of the weld, and compositional analysis.

The third component of weld characterization is the measurement of mechanical and corrosion properties. The goal of any weld is to create a structure that can meet all the demands of its service environment. In many cases, the best way of assessing the performance of a weld is to establish its mechanical properties. In addition to a number of standard material tests, many mechanical tests are directed specifically at determining a weld's capabilities. Examples of mechanical properties typically characterized for welds include yield and tensile strength, ductility, hardness, and impact or fracture toughness. Corrosion testing is often employed in situations where a welding operation is performed on a corrosion-

resistant material, or in a structure exposed to a hostile environment. Although absolute corrosion performance is important, a major concern is to ensure that a weld and its heat-affected zone (HAZ) are cathodic to the surrounding metal.

Following the discussion of the characterization procedures, the second part of this article will give examples of how two particular welds were characterized according to these procedures.

Acknowledgement

Support for the portion of this work performed at Sandia National Laboratories was provided by the U.S. Department of Energy under contract number DE-AC0476DP00789.

Characterization of Welds

Craig B. Dallam, The Lincoln Electric Company; Brian K. Damkroger, Sandia National Laboratories

---

Nondestructive Characterization Techniques

Externally Observed Macroscopic Features. Several factors associated with the production and performance of welds are macroscopic and easily observed. The most obvious of these are the size, shape, and general appearance of the weld. To a large extent, these parameters depend on the geometry of the weld joint and the welding process selected. Figure 1 shows schematic representations of fillet, lap, butt, and groove welds, in which a number of features (defined in Table 1) are labeled.

TABLE 1 NONMENCLATURE FOR FILLET, LAP, BUTT, AND GROOVE WELDS

FEATURE	DEFINITION
FACE	EXPOSED SURFACE OF A WELD ON THE SIDE FROM WHICH THE WELDING WAS PERFORMED
ROOT	POINTS, AS SHOWN IN CROSS SECTION, AT WHICH THE BACK OF THE WELD INTERSECTS THE BASE METAL SURFACE
LEG	SHORTEST DISTANCE FROM ROOT TO TOE IN A FILLET WELD
TOE	JUNCTION BETWEEN THE WELD FACE AND THE BASE METAL
THROAT	SHORTEST DISTANCE FROM ROOT TO FACE IN A FILLET WELD
PENETRATION	DEPTH A GROOVE WELD EXTENDS INTO THE ROOT OF A JOINT, MEASURED ON THE CENTERLINE OF A ROOT CROSS SECTION
REINFORCEMENT	WELD METAL IN EXCESS OF THE SPECIFIED WELD SIZE
FACE REINFORCEMENT	REINFORCEMENT AT THE SIDE OF THE WELD FROM WHICH WELDING WAS PERFORMED
SIZE (GROOVE WELD)	JOINT PENETRATION (DEPTH OF ROOT PREPARATION) PLUS THE ROOT PENETRATION (WHEN SPECIFIED)
SIZE (FILLET WELD)	LEG OF THE LARGEST ISOSCELES RIGHT TRIANGLE THAT CAN BE INSCRIBED WITHIN THE FILLET WELD CROSS SECTION

Source: Ref 1

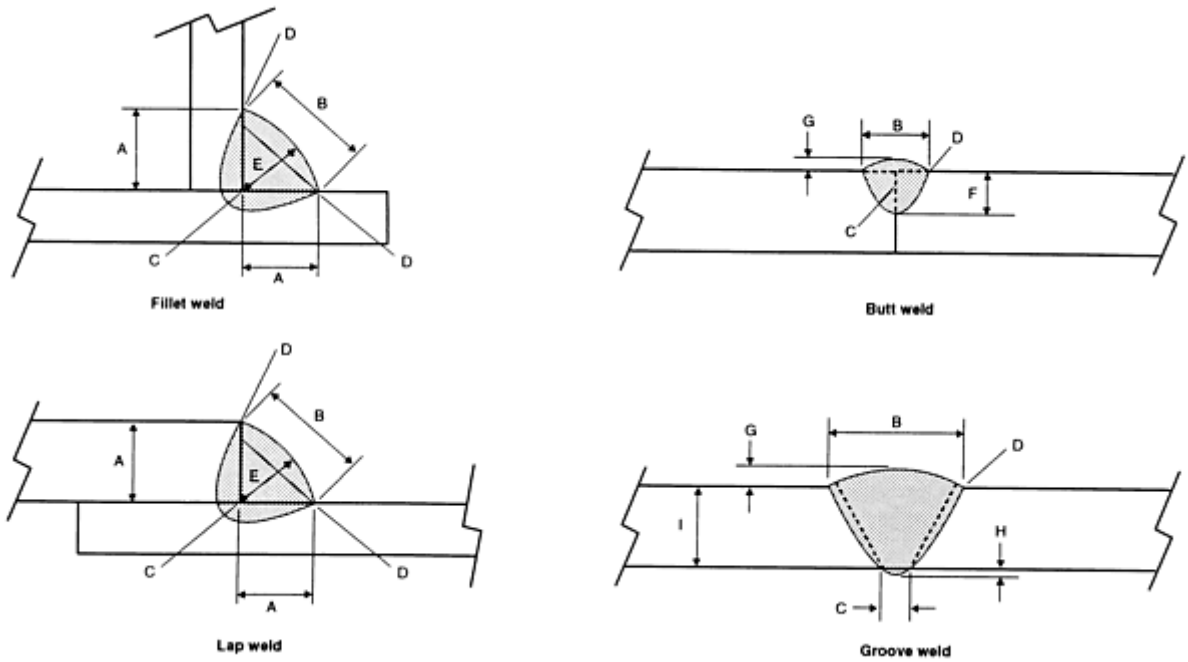

FIG. 1 SCHEMATICS SHOWING PARAMETERS OF COMMONLY USED JOINT GEOMETRIES. A, LEG; A', SMALLER LEG SIZE (EQUAL TO SIZE OF WELD); B, FACE, C, ROOT; D, TOE; E, THROAT; F, PENETRATION (EQUAL TO SIZE OF WELD); G, FACE REINFORCEMENT; H, ROOT REINFORCEMENT; I, SIZE OF WELD

Methods of Characterization. The primary tools used in the external macrocharacterization of a weld are the unaided eye and a hand lens. A number of macrocharacterization parameters (for example, weld location, size, shape, and general uniformity) can be assessed by visual inspection. Figure 2 shows top-view macrographs of two welds that illustrate several of these considerations. In many cases, the presence of gross defects such as hot cracking or porosity may also be detected by visual inspection and a top-view photograph. Additional examples of factors included in overall weld bead appearance include distortion, discoloration due to inadequate shielding or excessive heat, undercut, excessive crater size, and uneven bead width. In fillet welds, a number of performance aspects can be affected by the relative geometry of the joint. Fillet gages can be used to determine the size of a weld, the curvature of the face, and the length of the weld legs.

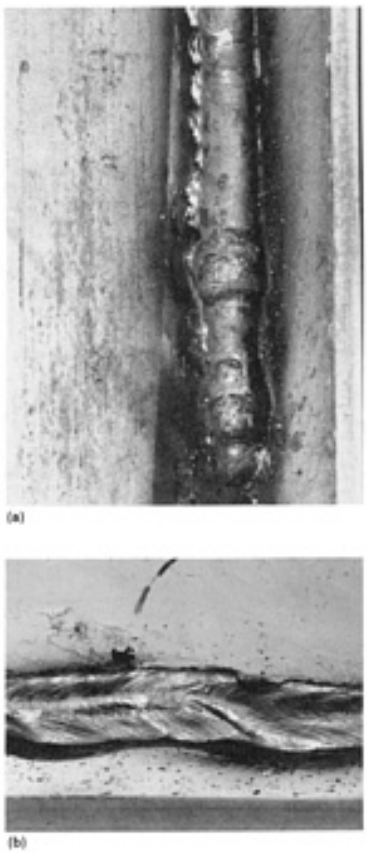

FIG. 2 MACROGRAPHS SHOWING TOP VIEW OF FILLET WELDS. (A) VERTICAL WELD IN TYPE 304L STAINLESS STEEL (NOTE CONVEXITY OF BEAD AND NONUNIFORM REGIONS). (B) HORIZONTAL E 7024 WELD (NOTE WELD PLACEMENT AND LACK OF UNIFORMITY)

General Considerations. Most types of welds will be evaluated with respect to specific macrocharacteristics deemed to be either desirable or undesirable. However, a number of general considerations apply to most types of welds. These include:

- *SIZE:* THE SIZE OF THE WELD SHOULD BE APPROPRIATE FOR THE PART (AS AN EXAMPLE, A GENERAL RULE FOR FILLET WELDS IS THAT THE RATIO OF LEG SIZE/PLATE THICKNESS SHOULD BE BETWEEN 3:4 AND 1:1.
- *LOCATION:* AN INCORRECTLY LOCATED BUTT WELD MAY NOT ALLOW THE PART TO FUNCTION CORRECTLY. A LESS EXTREME EXAMPLE IS A FILLET WELD WITH UNEQUAL LEG LENGTHS, LEADING TO AN UNEVEN STRESS DISTRIBUTION AND PERHAPS LAMELLAR TEARING.
- *UNIFORMITY:* DISTORTION, THE PROBABILITY OF SLAG ENTRAPMENT ON MULTIPASS WELDS, AND UNIFORMITY OF LOAD-CARRYING ABILITY ALL DEPEND ON THE RELATIVE UNIFORMITY OF THE WELD.
- *DEFECTS:* IDEALLY, A WELD SHOULD BE FREE OF MACROSCOPIC DEFECTS. COMMON DEFECTS INCLUDE UNDERCUTTING, LACK OF FUSION, PINHOLE POROSITY, AND SLAG ENTRAPMENT.
- *FACE SHAPE:* A WELD SHOULD HAVE A RELATIVELY FLAT FACE. IF THE WELD IS TOO CONVEX, STRESS WILL BE CONCENTRATED ALONG THE TOE OF THE WELD. CONVERSELY, A HIGHLY CONCAVE WELD FACE WILL RESULT IN LOCALLY HIGH STRESSES IN THE THROAT REGION OF THE WELD.

Defects. The presence of surface or internal defects can degrade the performance of a weld that may appear to be sound in a cursory examination. The causes and means of preventing defects are covered in Ref 2, 3, and 4. Typical defects found in welds include:

- POROSITY
- UNDERCUT
- OVERLAP
- LACK OF PENETRATION
- LACK OF FUSION
- SHRINKAGE VOIDS
- CRATER CRACKING
- MELT-THROUGH OR BURN-THROUGH
- SUBSOLIDUS OR HOT CRACKING
- INCLUSIONS DUE TO ENTRAPPED SLAG, TUNGSTEN ELECTRODE PIECES, OR DEFECTS PRESENT IN THE STARTING MATERIAL

A number of techniques are widely used to assess the presence of surface and subsurface defects in welds. The most common of these are liquid penetrant inspection for surface cracks, magnetic particle inspection, x-ray radiography, and ultrasonic inspection. Penetrant inspection involves the application of an indicator fluid that has a surface tension sufficiently low to be drawn into surface cracks too small to be detected visually. The excess dye or fluorescent material is then removed from the surface, but it remains in and highlights the cracks when a developer is applied. Figure 3 shows cracks in a flux-cored are weld highlighted by dye penetrant inspection. Table 2 lists the characteristics of several types of nondestructive inspection techniques. Additional information is available in the article "Inspection of Welded Joints" in this Volume.

TABLE 2 GUIDELINES FOR SELECTING TECHNIQUES

Technique	Equipment Requirements	Defects Detected	Advantages	Limitations	Comments
liquid-penetrant or fluorescent-penetrant inspection	fluorescent or visible penetration liquids and developers; ultraviolet light for fluorescent dyes	defects open to the surface only; good for leak detection	detects small surface imperfections; easy application; inexpensive; use on magnetic or nonmagnetic material; low cost	time-consuming; not permanent	used on root pass of highly critical pipe welds; indications may be misleading on poorly prepared surfaces
magnetic particle inspection	wet or dry iron particles, or fluorescent; special power source; ultraviolet light for fluorescent dyes	surface and near-surface discontinuities: cracks, porosity, slag	indicates discontinuities not visible to the naked eye; useful for checking edges before welding; no size limitations	for magnetic materials; surface roughness may distort magnetic field; not permanent	test from two perpendicular directions to detect any indications parallel to one set of magnetic lines
radiographic inspection	x-ray or γ ray; film processing and viewing equipment	most internal discontinuities and flaws; limited by direction of discontinuity	provides permanent record of surface and internal flaws; applicable to any alloy	usually not suitable for fillet weld inspection; film exposure and processing	popular technique for sub-surface inspection

				critical; slow and expensive	
ultrasonic inspection	ultrasonic units and probes; reference patterns	can locate all internal flaws located by other methods, as well as small flaws	extremely sensitive; complex weldments restrict usage; can be used on all materials	highly skilled interpretor required; not permanent	required by some specifications and codes

Source: Ref 5

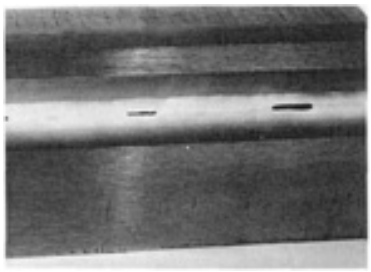

FIG. 3 SURFACE CRACKS IN A FLUX-CORED ARC WELD HIGHLIGHTED BY DYE PENETRANT INSPECTION

X-ray radiography is used to detect internal defects such as porosity or inclusions: these defects show up because of the difference in x-ray absorption between the matrix and defect materials. Although a number of factors affect the resolution level of radiographic techniques (Ref 5, 6), the minimum size of defects considered in AWS specifications is 0.4 mm (0.0156 in.). In practice, this refers to slag entrapment and large inclusions that were present in the starting material. Defect structures are usually quantified by comparison with an existing standard, of which several exist. An example of such a standard is American Petroleum Institute (API) 1104 (Ref 7), a pipeline welding specification. The API 1104 standard includes criteria for acceptance of steel welds based on a number of defects, including inadequate penetration, incomplete fusion, internal concavity, burn-through, slag inclusions, and porosity. For example, one section of API 1104 can be summarized as follows:

> Slag inclusions--50 mm (2 in.) maximum length for elongated slag inclusions, 50 mm (2 in.) limit per 305 mm (12 in.) of weld, 1.6 mm ($\frac{1}{16}$ in.) width limit per elongated slag inclusion. Isolated slag inclusions, 13 mm ($\frac{1}{2}$ in.) per 305 mm (12 in.) of weld, width greater than 3.2 mm ($\frac{1}{8}$ in.), 105 mm ($4\frac{1}{8}$ in.) isolated slag inclusions per 305 mm (12 in.) of weld. Aggregate length of isolated slag inclusion indications may not exceed two times the thinner of the nominal wall thickness and the width may not exceed one-half the thinner of the wall thicknesses joined.

Other examples include ASTM E 390 (Ref 8), which contains reference radiographs for steel welds and the *Structural Welding Code* (Ref 9), which includes a group of radiographic plates showing defect patterns for rounded inclusions corresponding to grade 1 and grade 2 quality levels. Several industries and product categories have applicable specifications and standards. A number of these are given in Ref 5.

Ultrasonic testing can also be used to locate internal defects, including porosity and inclusions. Ultrasonic testing involves transmitting mechanical vibrations through a piece of metal and analyzing both reflected and transmitted vibrations. Vibrations interact with discontinuities in the media through which they are passing, so the operator can detect voids, inclusions, and other internal interfaces. Table 2 includes ultrasonic testing, and Ref 5 lists a number of example specifications and detailed references.

References cited in this section

1. STANDARD WELDING TERMS AND DEFINITIONS, ANSI/AWS A3.0-89, AWS, 1989
2. WELD DISCONTINUITIES, *METALS HANDBOOK*, 9TH ED., VOL 6, AMERICAN SOCIETY FOR METALS, 1983, P 829-855
3. *WELDING HANDBOOK*, 8TH ED., VOL 2, AWS, 1987
4. *PROCEDURE HANDBOOK OF ARC WELDING*, 12TH ED., LINCOLN ELECTRIC CO., 1973
5. CODES, STANDARDS, AND INSPECTION, *METALS HANDBOOK*, 9TH ED., VOL 6, AMERICAN SOCIETY FOR METALS, 1983, P 823-838
6. *RADIOGRAPHY IN MODERN INDUSTRY*, 4TH ED., EASTMAN KODAK CO., 1980
7. WELDING OF PIPELINES AND RELATED FACILITIES, API STANDARD 1104, 17TH ED., AMERICAN PETROLEUM INSTITUTE, 1988
8. REFERENCE RADIOGRAPHS FOR STEEL WELDMENTS, ASTM E 390, ASTM
9. *STRUCTURAL WELDING CODE--STEEL*, ANSI/AWS D1.1-92, AWS, 1992

Characterization of Welds

Craig B. Dallam, The Lincoln Electric Company; Brian K. Damkroger, Sandia National Laboratories

Internal Characterization Requiring Destructive Procedures

This section briefly covers macrostructural and microstructural characterization and compositional analysis. These procedures are usually based on a cross section of the weld, referred to as a transverse section. The transverse section may be supplemented by the top-view photograph, the longitudinal section, and the normal section (Fig. 4). In particular, the top-view photograph will depict the general appearance of the weld, illustrating surface irregularities, spatter, or macroscopic defects such as hot cracking or porosity.

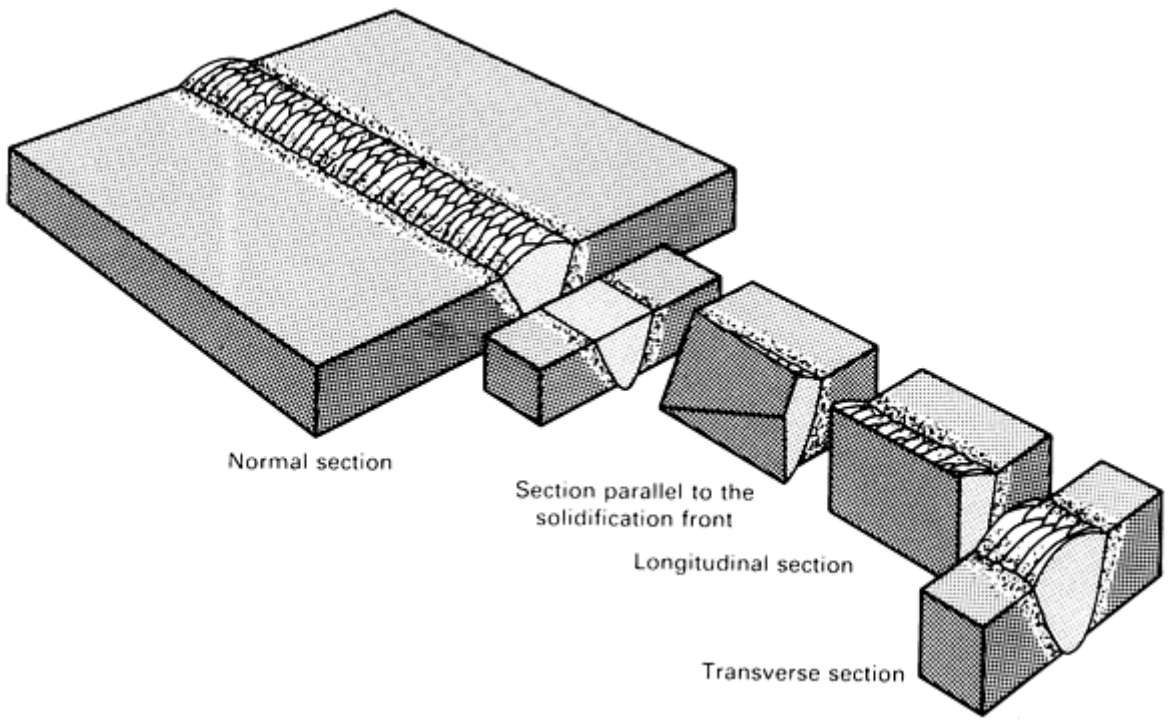

FIG. 4 TYPICAL SECTIONS USED IN THE METALLOGRAPHIC EXAMINATION OF WELDED JOINTS

Weld Macrostructure

Figures 5(a) and 5(b) show transverse sections of two welds, a submerged arc weld made on a 25 mm (1 in.) thick ASTM A 36 steel and a flux-cored weld made on a 50 mm (2 in.) thick ASTM A 537 steel. Readily apparent features include the number of passes and number of layers, fusion zone area, weld aspect ratio, extent of penetration, face width, and the reinforcement and curvature of the top bead. A transverse macrosection will also show any gross porosity or large inclusions present in a weld and the extent of the HAZ. It is important to note that quantitative measurements of weld features made based on a transverse section will be accurate only if the section is properly done. Potential errors, sectioning procedures, and sample preparation techniques are discussed in Ref 10.

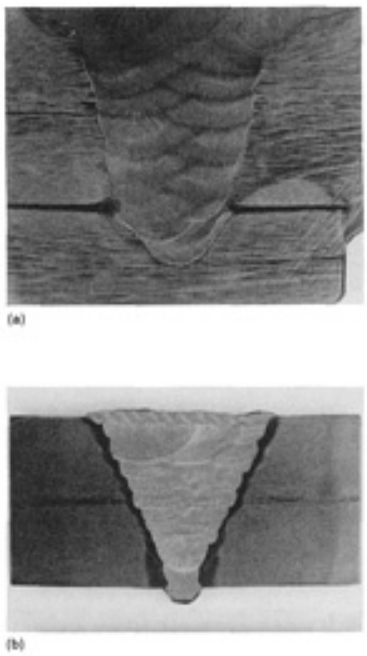

FIG. 5 TYPICAL MULTIPASS ARC WELDS IN STEELS USED IN STRUCTURAL APPLICATIONS. (A) SUBMERGED ARC WELD ON A 25 MM (1 IN.) THICK A 36 STRUCTURAL STEEL; THE MUSHROOM SHAPE OF THE LAST BEAD IS TYPICAL OF WELDS PRODUCED BY THIS PROCESS. (B) FLUX-CORED ARC WELD ON A 50 MM (2 IN.) THICK A 537 STEEL USED IN PRESSURE VESSEL AND STRUCTURE APPLICATIONS (THE LAST LAYER WAS MADE WITH SEVERAL SMALL PASSES TO IMPROVE MECHANICAL PROPERTIES)

Weld Microstructure

In many cases, it is important to examine and characterize the weldment microstructure and to understand its formation and effects on properties. This is the case when the materials and processes involved are not well characterized, so specifications have not been established. Other problems arise where the potential exists for the formation of detrimental microconstituents and/or where the consequences of weld failure are severe. Welding of high-strength or brittle materials are typical examples.

The microstructure of a weld consists of three regions: a fusion zone (material that has been melted); a heat affected zone (material that was not melted, but whose microstructure has been altered); and the base metal. These three regions can be seen in the transverse section shown in Fig. 5(b). Weld microstructures are examined using standard specimen removal and preparation techniques, with some concessions made for their inhomogeneous nature (Ref 10). Similarly, the parameters used to characterize the weld microstructures, such as grain size, grain morphology, and the amount of the various phases or microconstituents present, are those used to characterize monolithic materials. The equipment, procedures, and techniques used are well described in Ref 10.

Special importance may be attached to one or more specific features of a weld microstructure. An example is the classification of ferrite and carbide microconstituents in a low-ally steel weld. The various morphologies included in a characterization of a low-alloy steel weld are listed in Table 3. In these welds, a large amount of acicular ferrite is associated with high toughness levels, whereas martensitic or bainitic microstructures have much lower toughness levels. Bainite and martensite are also associated with higher effective cooling rates, so decreasing the weld metal manganese content, or reducing the cooling rate with increased heat input or preheat, will increase the amount of acicular ferrite and improve weld metal toughness.

TABLE 3 DESCRIPTION OF FERRITE/CARBIDE MICROCONSTITUENTS IN LOW-CARBON STEEL WELDS

Microconstituent	Description
Primary ferrite	
Grain boundry ferrite	Proeutectoid ferrite that grows along the prior austenite grain boundaries. It is equiaxed or polygonal, and it may occur in veins
Intragranular polygonal ferrite	Polygonal ferrite that is not associated with the prior austenite grain boundaries. Much larger than the average width of the surrounding acicular ferrite laths
Ferrite with second phase	
With aligned second phase	Parallel ferrite laths. Further classifications are widmanstätten ferrite and upper/lower bainite
With nonaligned second phase	Ferrite that completely surrounds either equiaxed, randomly distributed microphases, or solitary ferrite laths
Ferrite/carbide aggregate	Fine ferrite/carbide structures, including pearlite
Acicular ferrite	Small nonaligned ferrite grains found within prior austenite grains
Martensite	Martensite colony larger than adjacent ferrite laths

Microstructural characterization of welds has two purposes: to evaluate the microstructure with respect to properties and to relate the microstructure to the process used. The ultimate goal is to optimize the process to produce the most desirable microstructure. In general, the effects of a process and parameters on microstructure are due to the compositional and thermal effects. The compositional effects are largely limited to the fusion zone and will be discussed in the next section. Thermal cycles affect both the fusion zone and HAZ. Microstructural development in the HAZ has been the subject of much study, and a number of computational tools have been developed specifically for the prediction of HAZ microstructures (Ref 11).

Composition of a Weld

The composition of a weld will have a significant effect on its performance, contributing to both the mechanical and corrosion properties of the weld. In some instances, the effects can be drastic, such as sensitization of stainless steel or changing the ductile-to-brittle transition temperature of ferritic steels by an amount sufficient to cause brittle failure under normal use. In a number of cases, particular elements will govern the propensity toward certain defects or behavior. For example, a low-alloy steel weld with a carbon equivalent of over 0.4% is considered to be a high-carbon deposit, and it is treated differently than a low-carbon weld. Similarly, deposit silicon levels in excess of approximately 0.4% are often associated with a defect called "hollow bead," where the root pass in a pipe weld made with a cellulosic electrode has a continuous pore. In general, care must be taken to either minimize the compositional changes associated with welding or to factor the composition and property changes into the design.

Factors Affecting Weld Composition. The composition of a weld is affected by the base metal composition, the composition of any filler metal used (and dilution between the two), reactions with flux or shielding gas, and any material losses associated with the process. These factors are, in turn, largely controlled by the welding setup, process selection, parameters, and stability. The Schaeffler diagram (Ref 12) for stainless steels is an example of composition being controlled by dilution. The weld metal composition and microstructure are predicted based on the "ferrite stabilizer" and the "austenite stabilizer" content of the base metal, the nickel equivalent and chromium equivalent of the filler metal, and the level of dilution. The microstructure will be predicted as martensitic, ferritic, or austenitic, and the level of ferrite in the weldment will be estimated. In these welds, ferrite numbers below 4 indicate microstructures in which low-melting-

point compounds may be formed at the grain boundaries, and the welds can be prone to hot cracking. Conversely, welds with ferrite numbers above 10 have reduced corrosion resistance and can be susceptible to the formation of σ phase at high temperatures (Ref 13). The Schaeffler diagram has been revised many times for adaptation to different alloy modifications. An example is the inclusion of nitrogen in the nickel equivalent. Many stainless steels often contain small amounts of nitrogen, and in fact some stainless steels are deliberately strengthened with nitrogen additions. Other modifications include copper in the nickel equivalent and vanadium and aluminum in the chromium equivalent (Ref 14). Additional information is available in the Section "Selection of Stainless Steels" and in the article "Welding of Stainless Steels" in this Volume.

An example of the effect of flux on weld metal composition is seen when low-carbon steel is welded with E6010 and E7018 electrodes, using identical parameters. Although the core wire composition of the two electrodes is identical, the E6010 electrode will produce a deposit with approximately 0.15 to 0.25% Si, and the E7018 electrode will produce a deposit with 0.5 to 0.6% Si. An example of a procedure-related effect is seen when the arc length is changed for welds made with an E7018 electrode. Arc length changes can alter the silicon content from 0.3 to 0.6%, and they can alter the manganese content from 0.8 to 1.3%.

Measurement Techniques and Procedures. The usual techniques for compositional analysis of metallic samples can be used on welds and are covered in Ref 15. However, some considerations must be made when dealing with welds, because of their inhomogeneity. The most commonly used method for compositional analysis of welds is optical emission spectroscopy, where a spot of material (typically 6 mm, or $\frac{1}{4}$ in., in diameter) is ablated off the surface of the specimen and the light emissions are analyzed. In many welds, a spot this size will encompass several passes in a multipass weld, and it will perhaps encompass weld metal, HAZ, and base metal in a single-pass weld. An average composition over this large an area may not address local effects, for example, sensitization of stainless steel.

Welds are prone to both macrosegregation and microsegregation, and the properties may be governed by the composition in a very local region. A thorough characterization of welds requires techniques with sufficient spatial resolution to characterize their inhomogeneity. Scanning electron microscopy with wavelength or energy dispersive x-ray analysis systems, electron microprobes, and x-ray fluorescence techniques are often employed. Often, a number of closely spaced analyses are made along a line traversing a weld. This data may then be coupled with a similar microhardness traverse and microstructural analyses to characterize the variation across the weld. Thorough treatments of a number of microanalytical techniques are contained in Ref 16.

Mechanical Testing

A number of mechanical properties are used to characterize welds, including strength, ductility, hardness, and toughness. In general, the same samples and procedures are used in other areas of metallurgy (Ref 17). However, a prominent concern regarding the mechanical performance of welds is the direct comparison with base material. The goal is to ensure that the weld is not the weakest component of a structure, or if it is, to compensate for this in the design.

Strength. Yield and tensile strength are measured for all-weld-metal specimens using a standard tensile test (Ref 18), but with specimens removed from test plates welded according to AWS-specified procedures (Ref 19). These tests form the basis for the assignment of yield and ultimate strength values to welds made using a specific electrode and according to a set procedure. Additional tests are sometimes performed to compare the base metal and weld metal strengths. An example of this type of test is the transverse tensile test, in which the specimen is removed from the weld so that the loading axis is perpendicular to the weld bead and the weld reinforcement is left intact. The goal of this test is to verify that overload failure will occur in the base metal rather than in the weld metal or HAZ.

Ductility is another critical weld property. In addition to defects, many welding processes can produce hard, brittle microstructures. The standard measures of ductility--percent reduction in area and percent elongation--are obtained in a uniaxial tensile test. Another test often specified for welds is a bend test (face bends, roof bends, and side bends). In this test, a strip of material containing a weld is deformed around a specified radius and its surface is examined. The criteria for success or failure are the number and size of defects seen on the outer surface of the bend. An example of bend test criteria is the AWS *Structural Welding Code* (Ref 9), which calls for bending around a 19 mm (0.75 in.) radius for materials with yield strengths less than or equal to 345 MPa (50 ksi), a 25 mm (1 in.) radius for 345 to 620 MPa (50 to 90 ksi) materials, and a 32 mm (1.25 in.) radius for materials with yield strengths greater than or equal to 620 MPa (90 ksi).

Hardness. One common use of hardness values in weld specifications is as a check for the formation of microstructures that might have low ductility and toughness and thus are prone to cracking. For example, in pipeline steels, the formation of martensite in the HAZ is a cause for concern because of the potential for cracking. This is addressed by specifying maximum values for microhardness traverses across several sections of the weld. Hardness values are also used as an indicator of susceptibility to some forms of stress-corrosion cracking.

Toughness is the ability of a material to absorb energy during fracture. There are two approaches to toughness testing: impact toughness testing and fracture mechanics testing.

Impact Toughness Testing. To test impact toughness, a sample of specified geometry is subjected to an impact load, and the amount of energy absorbed during fracture is recorded. Usually the specimen is oriented so that the notch and expected plane of fracture run longitudinally through the weld metal. Charpy tests do not measure an inherent material property, but they result in a relative measure of impact toughness between materials. A very common use of the Charpy test is to determine a material's ductile-to-brittle transition temperature by performing tests at several different temperatures. AWS A5.1 (Ref 19) gives minimum Charpy impact values, at several temperatures, for welds made on carbon steel using a number of different electrodes.

Fracture Mechanics Testing. The second type of toughness testing is based on fracture mechanics, and it can use either linear elastic or elastic-plastic methodologies. Although elastic-plastic behavior (J_{Ic}) is becoming of interest in some cases, the bulk of fracture mechanics testing is based on linear elastic considerations. These tests, using specimens and procedures given in ASTM E 399 (Ref 20), are used to measure a material's fracture toughness (K_{Ic}), which is a material property. In the case of welding, fracture toughness is usually expressed using a value for crack tip opening displacement (Ref 21). Fracture toughness testing has only recently begun gaining acceptance as applicable to welds. The major shortcomings of this approach include the complexity and cost of testing and the wide variability in fracture toughness values for weld metal, due largely to the inhomogeneous nature of welds and residual stress effects.

References cited in this section

9. *STRUCTURAL WELDING CODE--STEEL,* ANSI/AWS D1.1-92, AWS, 1992
10. METALLOGRAPHY OF WELDMENTS, *METALS HANDBOOK,* 9TH ED., VOL 9, AMERICAN SOCIETY FOR METALS, 1985, P 577-586
11. K.E. EASTERLING, MICROSTRUCTURE AND PROPERTIES OF THE HAZ, *RECENT TRENDS IN WELDING SCIENCE AND TECHNOLOGY,* S. DAVID AND J. VITEK, ED., ASM INTERNATIONAL, 1990, P 177-188
12. WRC 1992 DIAGRAM, *WELD. J.*, MAY 1992, P 171
13. T.G.F. GRAY, J. SPENCE, AND T.H. NORTH, *RATIONAL WELDING DESIGN,* NEWNES-BUTTERWORTHS, 1975, P 111
14. R.H. ESPY, WELDABILITY OF NITROGEN-STRENGTHENED STAINLESS STEELS, *WELD. J. RES. SUPPL.*, VOL 61 (NO. 5), MAY 1982, P 149S-156S
15. METAL TEST METHODS AND ANALYTICAL PROCEDURES, *1991 ANNUAL BOOK OF ASTM STANDARDS,* VOL 03.05 AND 03.06, ASTM, 1991
16. *MATERIALS CHARACTERIZATION,* 9TH ED., VOL 10, *METALS HANDBOOK,* AMERICAN SOCIETY FOR METALS, 1986
17. *MECHANICAL TESTING,* 9TH ED., VOL 8, *METALS HANDBOOK,* AMERICAN SOCIETY FOR METALS, 1985
18. STANDARD METHODS OF TENSION TESTING OF METALLIC MATERIALS, ASTM E 8, *ANNUAL BOOK OF ASTM STANDARDS,* VOL 03.01, ASTM, 1984
19. *SPECIFICATION FOR CARBON STEEL ELECTRODES FOR SHIELDED METAL ARC WELDING,* ANSI/AWS A5.1-91, AWS, 1991
20. STANDARD TEST METHOD FOR PLANE-STRAIN FRACTURE TOUGHNESS OF METALLIC MATERIALS, ASTM E 399, *ANNUAL BOOK OF ASTM STANDARDS,* ASTM, 1984
21. STANDARD TEST METHOD FOR CRACK TIP OPENING DISPLACEMENT (CTOD) FRACTURE

Characterization of Welds

Craig B. Dallam, The Lincoln Electric Company; Brian K. Damkroger, Sandia National Laboratories

Weld Characterization Examples

In this section, two weld will be analyzed to serve as examples of techniques discussed thus far in this article. The first of these welds is a multipass shielded metal arc weld/flux-cored arc weld made on pipe steel for an industrial application. This type of weld would typically be made in great quantity. In practice, it would be characterized largely on the basis of its external appearance, perhaps supplemented by nondestructive testing. The initial characterization of a weld and procedure, however, would be based on chemical composition and mechanical properties. Primary concerns are whether the weld being examined is representative of a normal weld of this type and can thus be reasonably well described based on the materials, process, and specifications involved in its production. The bulk of the actual characterization of such a weld would be done during the development and certification of the initial process to determine its suitability for the intended application.

The second example is a weld used for a very specific application. This weld is a butt weld made on Ti-6Al-4V, with a tantalum shim inserted between the base metal sections. Among the requirements for this weld are that it have microstructural and property homogeneity and stability at elevated temperatures and that it be cathodic to the base metal under unusual and extremely severe environmental conditions. In this case, the concerns center less on the eventual application and more on building a thorough database regarding the metallurgical and microstructural characteristics of the weld.

Example 1: Multipass Weld in a 1.07 m (42 in.) Diameter X-65 Pipe.

This weld is a circumferential weld on a 12.7 mm (0.50 in.) thick, 1.07 m (42 in.) diameter X-65 pipe. The X-65 materials is designated by API as a pipe steel with at least 448 MPa (65 ksi) yield strength and 566 MPa (82 ksi) tensile strength. This type of weld is typical for a large oil or gas pipeline. However, for this example, procedures were deliberately selected to produce a weld with a range of defects. These procedures, given by Table 4, are not representative of standard practice.

TABLE 4 PARAMETERS (NOT STANDARD PROCEDURE) USED TO OBTAIN MULTIPASS WELD IN 1.07 M (42 IN.) DIAMETER X-65 STEEL PIPE

PROCESS	PASS NO.	ELECTRODE	DIAMETER		WIRE FEED		CURRENT, A	VOLTAGE, V	TRAVEL SPEED	
			mm	in.	mm/s	in./s			mm/s	in./s
SMAW	1	E8010-G	4.0	0.16	. . .	. . .	150	26-28	5.9-7.2	2.3-2.8
	2	E8010-G	4.0	0.16	. . .	. . .	180	26-28	5.9-7.2	2.3-2.8
FCAW	3	E71T8-K6	1.73	0.068	47	1.9	200	19	4.5	1.8
	4	E71T8-K6	1.73	0.068	47	1.9	200	19	4.0	1.6
	5	E71T8-K6	1.73	0.068	47	1.9	200	19	4.0	1.6
	6	E71T8-K6	1.73	0.068	47	1.9	200	19	4.7	1.9
	7	E71T8-K6	1.73	0.068	47	1.9	200	19	5.9	2.3
	8	E71T8-K6	1.73	0.068	42	1.7	180	18	4.2	1.7
	9	E71T8-K6	1.73	0.068	42	1.7	180	18	4.5	1.8

Additional specifications include: 12.7 mm (0.50 in.) wall thickness; 1.59 mm (0.0625 in.) land; 1.59 mm (0.0625 in.) gap; 60° bevel in groove; vertical down position; preheat and interpass temperature of 150 °C (300 °F)

Visual Observation. The weld was initially characterized by visual observation. From the top of the joint, the size and uniformity of the weld and undercut can be observed (Fig. 6a). From the underside, spatter, lack of penetration, and internal undercut can be seen (Fig. 6b).

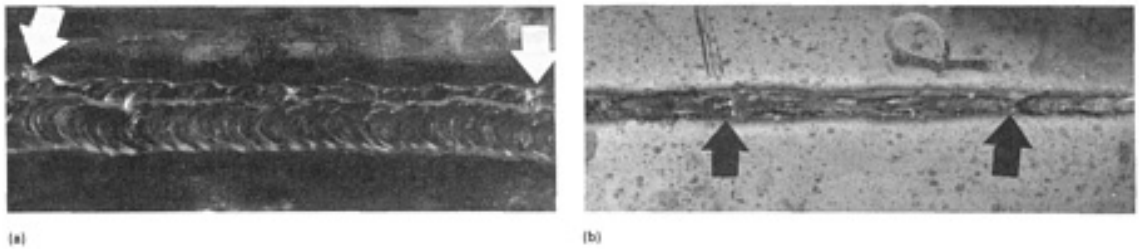

FIG. 6 DEFECTS IN A MULTIPASS WELD MADE ON A 1.07 M (42 IN.) DIAMETER X-65 STEEL PIPE. (A) EXTERIOR VIEW SHOWING LACK OF UNIFORMITY (RIGHT ARROW) AND UNDERCUT (LEFT ARROW). (B) INTERIOR VIEW SHOWING LACK OF PENETRATION (RIGHT ARROW) AND BURN-THROUGH (LEFT ARROW)

Nondestructive evaluation was then used to examine the weld for internal and surface defects. Slag entrapment and lack of fusion are typical internal defects for this type of weld, and they can be seen in the radiograph shown in Fig. 7. Figure 7 also shows the external defects noted during visual observation. In addition to nondestructive evaluation, other tests that highlight defects (for example, "nick-break" tests and face or root bend tests) can be run, but these were not used in this case. Similarly, ultrasonic testing, magnetic particle testing, and penetrant testing were not used in this characterization.

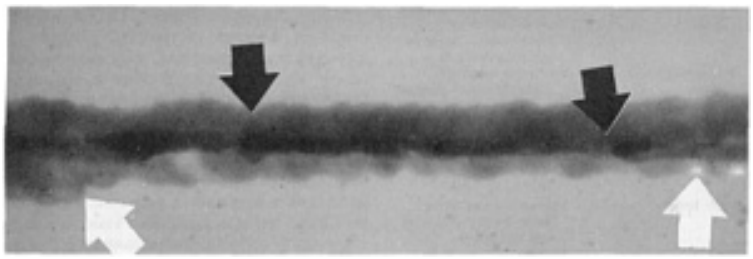

FIG. 7 RADIOGRAPH SHOWING POSITIVE IMAGE OF MACROSCOPICALLY VISIBLE DEFECTS IN THE X-65 PIPE STEEL OF FIG. 6. SEE FIG. 6 FOR DESIGNATION OF SPECIFIC DEFECTS.

Weld Macrostructure. Destructive evaluation begins by removing a transverse section from the weld and preparing it for metallographic examination (Fig. 8). The welding pass sequence (that is, number and size of passes, number of passes per layer, amount of penetration, and extent of HAZ) is apparent. In addition, any gross defects present in the sectioning plane are visible. In this example, nine passes were made, three layers with one pass and three with two passes. Figure 8 also shows four small pores, one each in the third, fourth, sixth, and ninth passes. In this case, the porosity was induced by deliberately varying the electrode stickout.

FIG. 8 TRAVERSE SECTION OF THE X-65 PIPE STEEL SHOWN IN FIG. 6 AND 7. PORES IN PASSES 3, 4, 6, AND

8 WERE CAUSED BY INTENTIONALLY VARYING THE ELECTRODE STICKOUT.

Weld Metal Composition. Compositional analysis of the weld was performed at this point. For this application, the bulk, or average, composition of the weld is of the most interest. The bulk composition of the weld was measured using an emission spectrometer, and the results are given in Table 5. The interstitial content of the weld is also of interest, and the levels of oxygen and nitrogen were measured with dedicated instruments. The oxygen level of the weld was found to be 110 ppm and the nitrogen level, 330 ppm. For some welds, techniques can be used to map compositional variations within the weld. In this case, the bulk composition, measured at the weld center, is considered adequate to characterize the weld.

TABLE 5 BULK COMPOSITION OF WELD IN 1.07 M (42 IN.) DIAMETER X-65 STEEL PIPE

SAMPLE	COMPOSITION, WT. %									
	C	Mn	Si	Al	Ni	Cr	Mo	Ti	V	Nb
WELD METAL	0.062	0.85	0.22	0.76	0.65	0.02	0.02	0.011	0.008	0.003
BASE METAL	0.093	1.35	0.21	0.02	0.02	0.04	0.00	0.002	0.069	0.033
ELECTRODES:										
E8010-G	0.14	0.70	0.20	0.01	0.73	0.02	0.07	0.008	0	0
E71T8-K6	0.056	0.91	0.24	0.95	0.97	0.02	0.01	0.002	0	0

Weld Microstructure. The transverse section was also used for examination and characterization of the microstructure of the weld. Figure 9 shows micrographs of different regions of the weld. Figure 9(a) shows weld metal that has not been reheated by successive passes. Figure 9(b) shows weld metal that has been reheated and has a finer structure than the non-reheated weld metal. Figure 9(c) shows a location in the HAZ that closely resembles the structure seen in the reheat zone. The important parameters to characterize for this type of weld are the percentage of reheat zone, the relative amount of various microconstituents, and the average grain size. In the example weld, the weld metal is approximately 80% reheat zone. In the non-reheated zone (Fig. 9a), quantitative microstructural analysis showed that the structure consisted of 20% grain boundary ferrite, 20% intergranular polygonal ferrite, 16% acicular ferrite, 32% ferrite with an aligned second phase, and 12% ferrite with a nonaligned second phase. No martensite or ferrite-carbide aggregate was found.

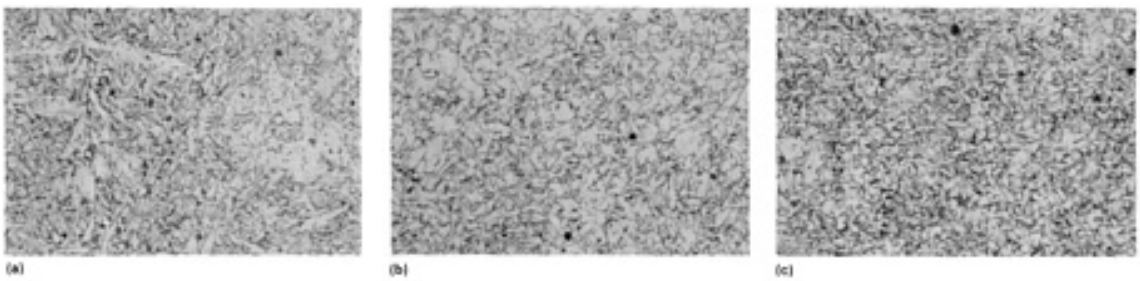

FIG. 9 MICROSTRUCTURE OBTAINED IN SELECTED REGIONS OF THE TRAVERSE SECTION OF THE X-65 PIPE STEEL OF FIG. 8. (A) NON-REHEATED WELD METAL. (B) REHEATED WELD METAL. (C) HEAT-AFFECTED ZONE. ALL 250×

Mechanical Testing. Following the characterization of the microstructure, specimens were removed and used for mechanical testing. For this application, the pertinent mechanical tests are tension tests (transverse and all-weld-metal), Charpy impact tests, fracture toughness tests, and a microhardness traverse. A transverse tensile test is primarily used to ensure that the welded joint is not the weak link in the final structure. In this case, a 305 × 32 mm (12.0 × 1.25 in.) specimen was removed from the pipe, the long axis perpendicular to the weld bead. The specimen was loaded to 247 kN (27.8 tonf) and failed in the base metal. Based on a weld cross-sectional area of 5.08 cm^2 (0.787 $in.^2$), a minimum weld tensile strength was calculated as 487 MPa (70.6 ksi).

An all-weld-metal tensile test was run using a specimen removed from the bead so that its loading axis was parallel to the weld direction. In this case, the weld was aged prior to testing, with the heat treatment being 48 h at 104 °C (220 °F). The results of the tensile test are shown in Fig. 10. The yield strength was found to be 520 MPa (75.4 ksi), the ultimate strength 594 MPa (86.1 ksi), and the percent elongation 30%. With respect to a typical vendor specification for this type of weld, these values indicate that the weld is adequate.

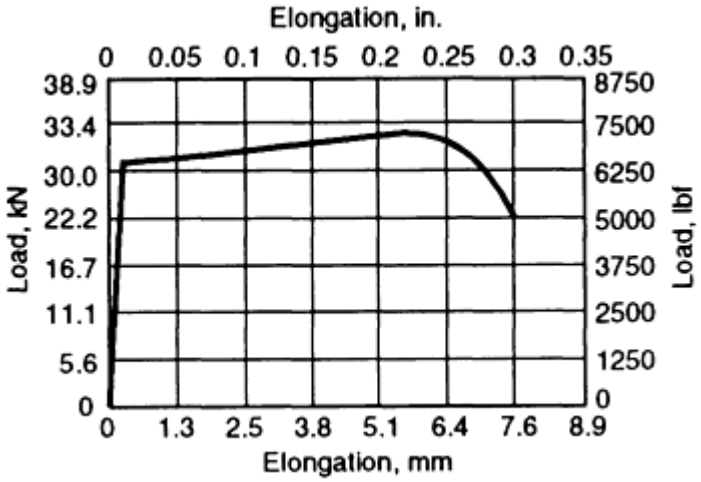

FIG. 10 PLOT OF LOAD VERSUS ELONGATION FOR ALL-WELD-METAL TENSILE TEST OF A 6.4 MM (0.25 IN.) DIAMETER SPECIMEN TAKEN FROM THE 1.07 M (42 IN.) DIAMETER X-65 STEEL PIPE

Charpy V-notch impact specimens were removed from the weld as shown in Fig. 11. For this type of application, tests are usually run at only one temperature, dictated by a specification and/or past experience. For a full characterization, however, tests will be run over a broad enough range to clearly establish the upper- and lower-shelf energy levels and to identify the ductile-to-brittle transition temperature (DBTT). For this example, tests were run at several temperatures, and the results are shown in Fig. 12. This figure clearly shows that the upper shelf energy is approximately 200 J (150 ft · lbf), the lower shelf 2 J (1.5 ft · lbf), and the DBTT -10 °C (14 °F).

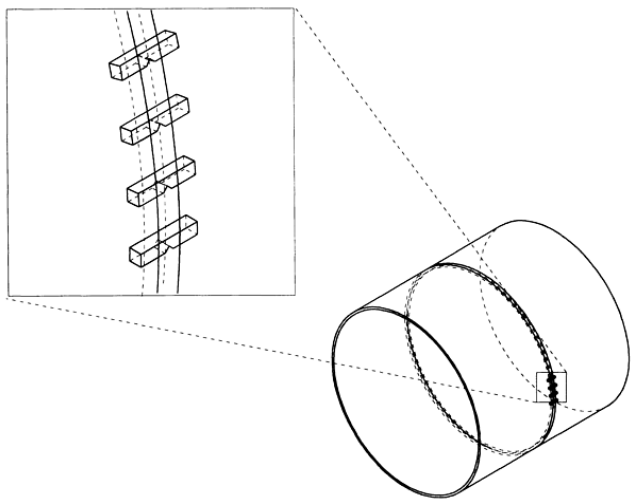

FIG. 11 SCHEMATIC SHOWING LOCATION AND ORIENTATION OF CHARPY V-NOTCH SPECIMENS TAKEN FROM THE 1.07 M (42 IN.) DIAMETER X-65 STEEL PIPE. ALTHOUGH INSET SHOWS WIDELY SPACED SAMPLES FOR THE SAKE OF CLARITY, ACTUAL SAMPLES REMOVED ARE TYPICALLY ADJACENT TO ONE ANOTHER.

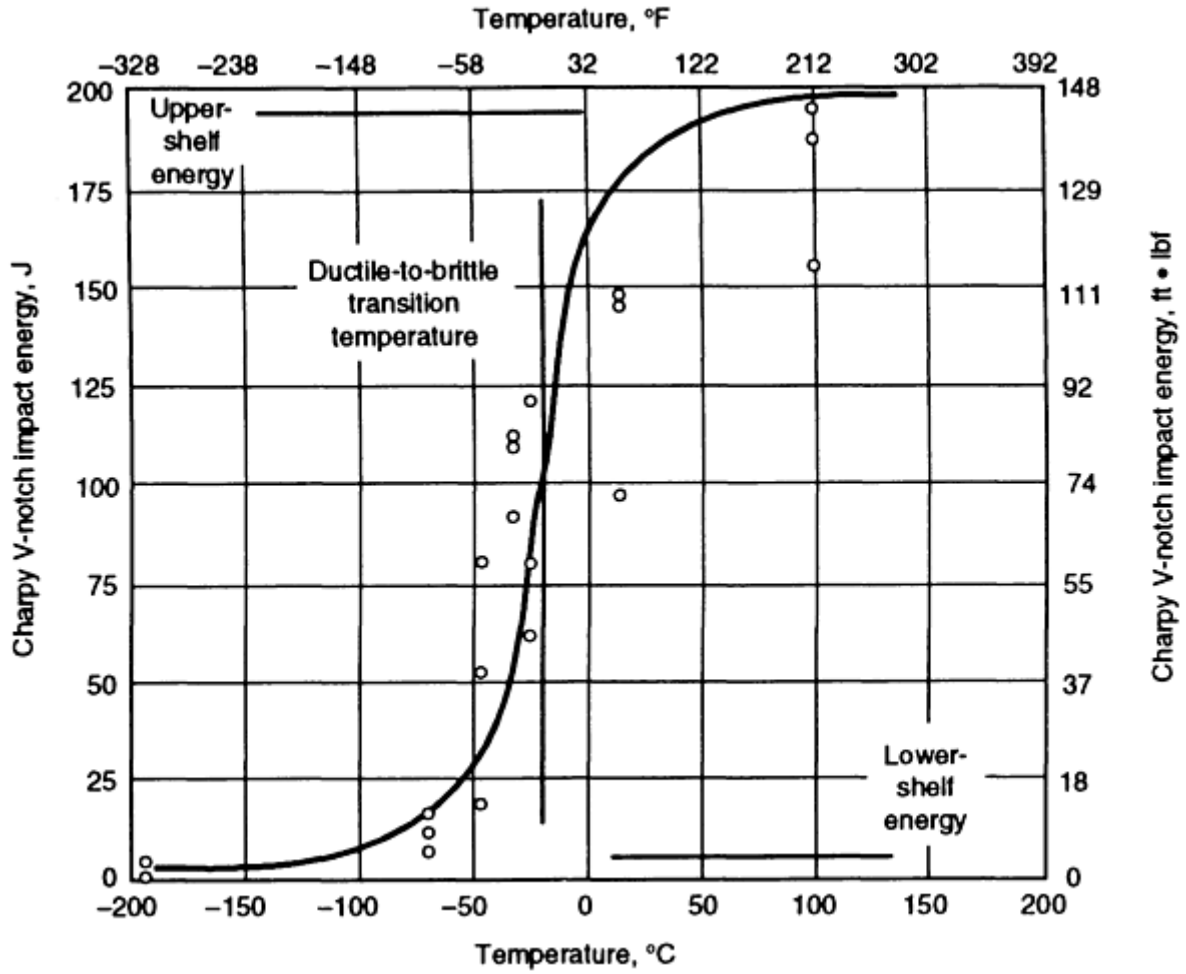

FIG. 12 CHARPY V-NOTCH IMPACT ENERGY TEST RESULTS USED TO OBTAIN DUCTILE-TO-BRITTLE TRANSITION TEMPERATURE (-10 °C, OR 14 °F) FOR THE 1.07 M (42 IN.) DIAMETER X-65 STEEL PIPE

Fracture toughness specimens were removed from the weld in an orientation similar to that of the Charpy specimens. As with Charpy tests, fracture toughness specifications usually require a certain value at a given temperature, usually the minimum service temperature. Crack tip opening displacement tests were conducted at -45 °C (-50 °F) on three specimens removed from the example weld. The results were found to vary from 0.137 to 0.322 mm (0.005 to 0.013 in.), with the average being 0.229 mm (0.009 in.). Figure 13 shows the fracture surface of one of the test specimens, on which the ductile fracture mode and overload zone can be clearly seen.

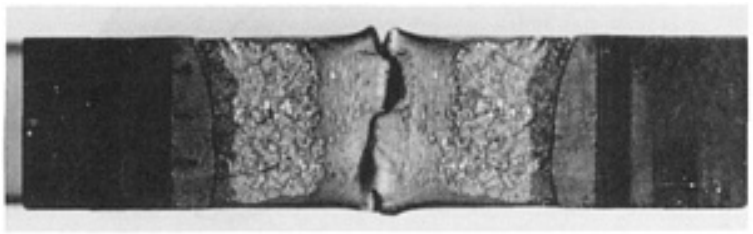

FIG. 13 MACROGRAPH OF THE FRACTURE SURFACE OF A CRACK TIP OPENING DISPLACEMENT TEST SPECIMEN REMOVED FROM THE 1.07 M (42 IN.) X-65 STEEL PIPE. THE REGIONS OF THE SURFACE SHOWN CORRESPOND WITH THE NOTCH, PRECRACK, STABLE CRACK GROWTH, FAST FRACTURE, AND OVERLOAD ZONES.

In addition to the previous mechanical tests, microhardness testing is often used for this type of weld. The primary purpose of microhardness testing is to check for the presence of martensite in the HAZ. Figure 14 shows a schematic of the example weld and the location and values of several microhardness tests. In this case, none of the values exceeded 240 HV, the level associated with the presence of martensite.

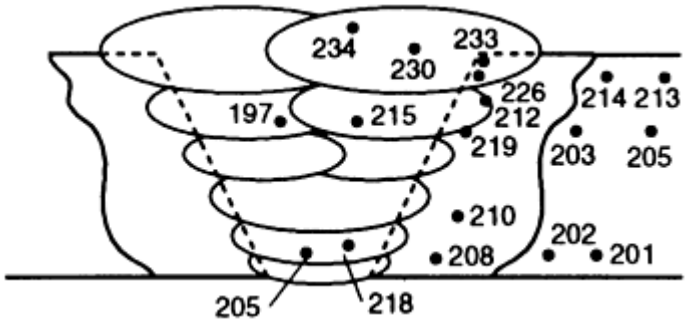

FIG. 14 MICROHARDNESS READINGS (LOCATION IN MULTI-PASS WELD INDICATED BY DOTS) BELOW 240 HV INDICATING THAT NO MARTENSITE STRUCTURE IS PRESENT IN THE 1.07 M (42 IN.) X-65 STEEL PIPE

Typically, this type of pipe weld is characterized with respect to stress-corrosion cracking resistance. In addition, testing is often performed to characterize the HAZ toughness.

Example 2: Welding of 2.5 mm (0.100 in.) Thick Ti-6Al-4V Sheet using a 0.127 mm (0.005 in.) Thick Tantalum Shim.

Figure 15 shows a transverse section of a butt weld, where the base metal is 2.5 mm (0.100 in.) thick Ti-6Al-4V and a 0.127 mm (0.005 in.) thick tantalum shim has been placed in the joint. This weld geometry was used in a study of the effect of dilution on the microstructures and properties of dissimilar metal welds of titanium to refractory metals. The questions to be answered in the characterization of this weld were:

- HOW UNIFORMLY WOULD THE TANTALUM BE DISTRIBUTED IN THE WELD POOL?
- HOW ACCURATELY COULD THE COMPOSITION OF THE WELD POOL BE PREDICTED BASED ON DILUTION CALCULATIONS?
- WHAT PHASES AND MICROCONSTITUENTS ARE PRESENT IN THE WELD METAL?
- WHAT ARE THE MECHANICAL PROPERTIES OF THE WELD METAL?

In addition, a number of very application-specific corrosion and elevated-temperature tests were performed on the dissimilar metal welds. In contrast with the pipe weld of the first example, the primary tools used in this characterization were macrostructural examination, compositional mapping, x-ray diffraction, tension testing of all weld metal specimens, and microhardness traverses.

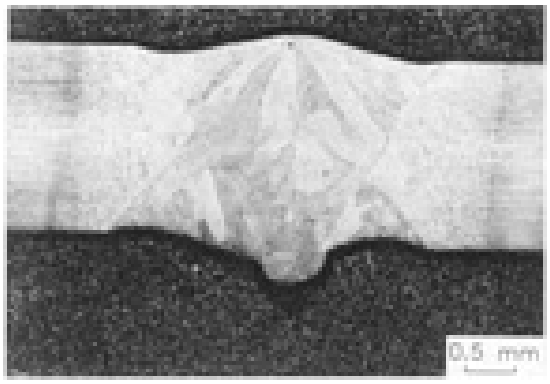

FIG. 15 MICROGRAPH OF TRANSVERSE SECTION OF AN ELECTRON-BEAM WELDED BUTT WELD JOINING 2.5 MM (0.100 IN.) THICK TI-6AL-4V SHEET USING A 0.127 MM (0.005 IN.) THICK TANTALUM SHIM PLACED IN THE JOINT. KROLL'S REAGENT WAS USED AS ETCHANT.

Weld Macrostructure. The weld shown in Fig. 15 was made with the electron-beam welding process, using sharp focus, 100 kV power, 16 to 25 mA current, and a travel speed of 12.7 mm/s (30 in./min). As can be seen in the transverse section, a full penetration weld was achieved using one pass from each side of the weld. The transverse section also shows that no obvious discontinuities exist in the weld pool and that the weld metal microstructure is fairly uniform. Figure 15 also suggests that the tantalum shim was completely melted.

Weld Metal Composition. An initial examination of the weld metal composition was performed to help assess the uniformity of the weld macrostructure. Figure 16 shows tantalum, titanium, vanadium, and aluminum elemental scan lines traversing the weld. These data were generated using a scanning electron microscope with energy-dispersive spectroscopy capability, and they confirm that the elements in question are uniformly distributed throughout the weld pool. Based on these analyses and the macrostructural characterization, it was determined that this combination of welding processes and parameters was successful in producing a full-penetration weld and a macroscopically homogeneous and defect-free weld pool.

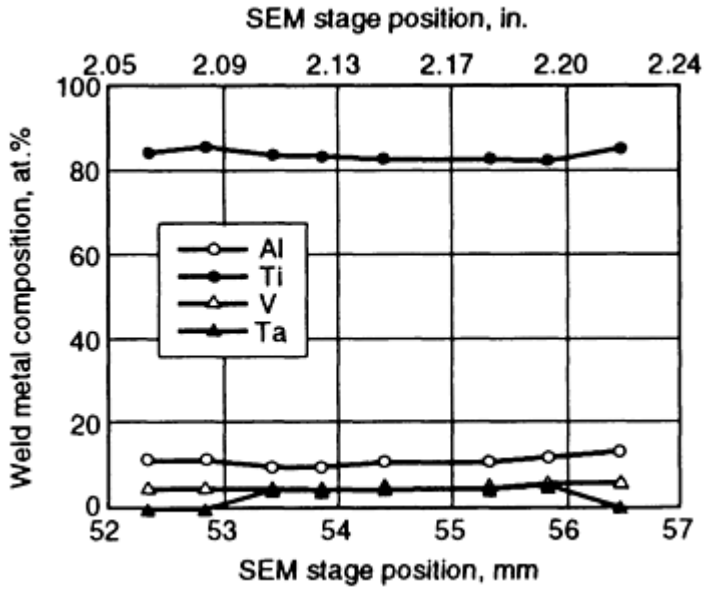

FIG. 16 ELEMENTAL LINE SCANS OF TITANIUM, ALUMINUM, VANADIUM, AND TANTALUM SPANNING THE HAZ AND FUSION ZONE OF THE 2.5 MM (0.100 IN.) THICK TI-6AL-4V SHEET WELDED USING A 0.127 MM (0.005 IN.) THICK TANTALUM SHIM.

The properties of titanium alloys can be strongly affected by the phases present in the microstructure, which are largely controlled by the weld metal composition. In this example, aluminum stabilizes the hexagonal close-packed (hcp) α and/or α' phases, and vanadium and tantalum, the body-centered cubic (bcc) β phase. In titanium alloys, the composition can be expressed as an electron/atom (*e*/*a*) ratio, which allows the phase stabilization effects of different elements to be combined. Table 6 lists the calculated (based on dilution) and measured compositions of the weld. This table shows that the measured and calculated compositions agree reasonably well. The measured aluminum values are somewhat lower than the calculations predict, perhaps due to some loss of aluminum during the welding process. Of most interest is that the measured and calculated *e*/*a* ratios are 3.96 to 3.98. This compositional range indicates that the weld metal microstructure should be α', a hexagonal martensite structure associated with good mechanical properties (Ref 20).

TABLE 6 COMPOSITION OF TI-6AL-4V RELATIVE TO THAT OF TI-6AL-4V PLUS TANTALUM WELD METAL

SAMPLE	COMPOSITION, AT.%				
	Ti	V	Al	Ta	*E/A* RATIO
TI-6AL-4V	86.2	3.6	10.2	. . .	3.93
TI-6AL-4V WELDED TO TA SHIM:					
CALCULATED	83.9	3.5	9.9	2.7	3.96
MEASURED	83.0	3.9	9.5	3.6	3.98

Weld Microstructure. The microstructure of the weld was analyzed using optical microscopy, transmission electron microscopy, and x-ray diffraction. Of particular interest were the structure of any martensitic phase present and the possible existence of ω, an ordered phase that can severely embrittle the material. The composition of the weld metal suggests that the structure will be α' hexagonal martensite. Figure 17 shows an optical micrograph of the fusion zone. Examination of Fig. 17 and comparison with Ti-6Al-4V (no tantalum shim) welds further suggest that the weld metal microstructure is α'. This was further supported by x-ray diffraction and TEM data. Figure 18 shows an x-ray diffraction trace for the weld metal. Aside from peaks from the specimen-mounting material, only peaks associated with a hexagonal structure were detected.

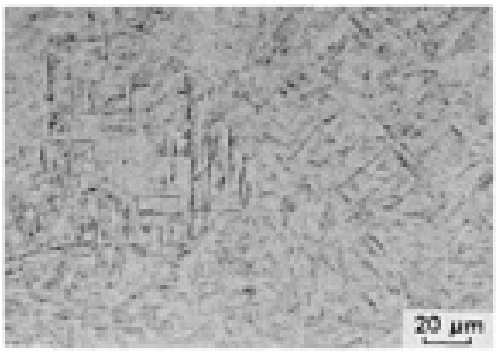

FIG. 17 OPTICAL MICROGRAPH OF FUSION ZONE OBTAINED WITH THE TI-6AL-4V SHEET WELDED USING A TANTALUM SHIM. KROLL'S REAGENT WAS USED AS THE ETCHANT. MICROSTRUCTURE CONSISTS OF WIDMANSTÄTTEN α+ β AND α' MARTENSITE.

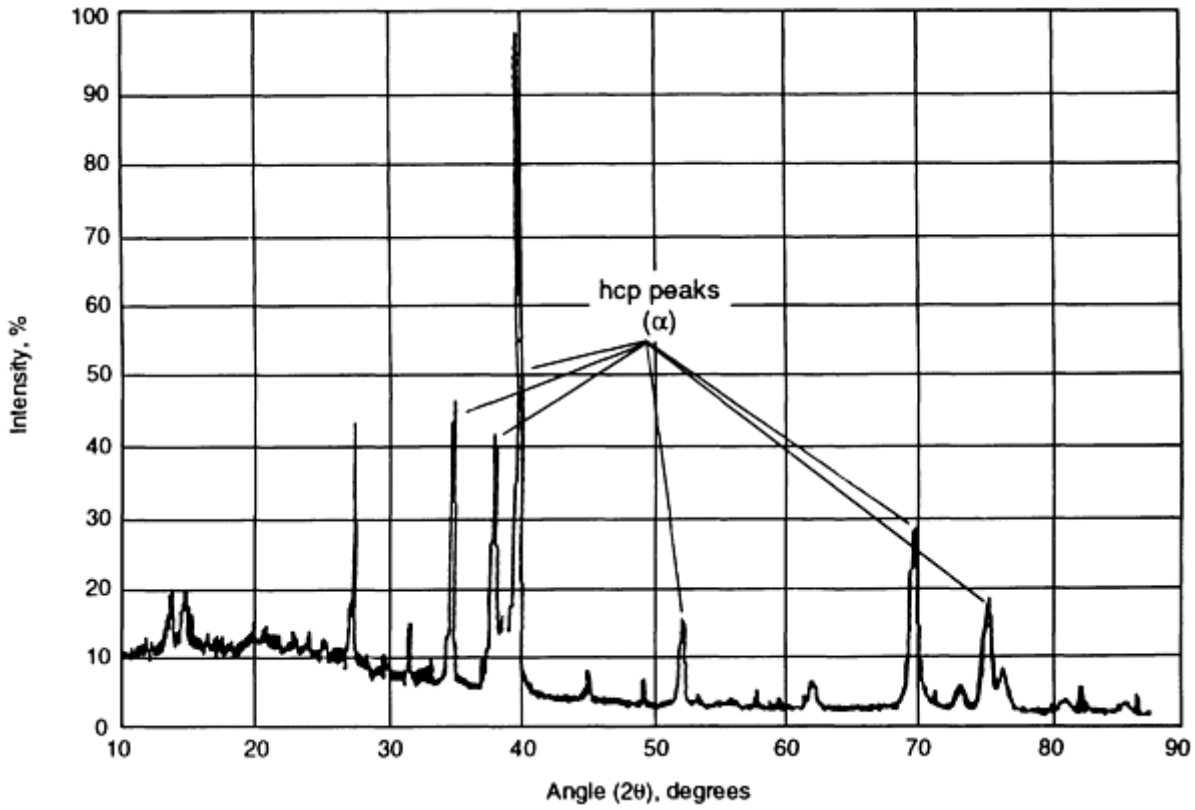

FIG. 18 X-RAY DIFFRACTION TRACE OF FUSION ZONE IN TI-6AL-4V SHEET WELDED USING A TANTALUM SHIM, SHOWING PEAKS THAT IDENTIFY HEXAGONAL STRUCTURES

Based on the compositional analysis, diffraction results, and microstructural analysis, the weld metal can be characterized as α' hexagonal martensite. By comparison with Ti-6Al-4V base metal and (no shim) weld metal, it was determined that the weld metal could be treated as a slightly more heavily stabilized variant of Ti-6Al-4V. This analysis allowed its properties and performance to be reasonably predicted.

Mechanical Testing. Microhardness traverses and all-weld-metal tension tests were performed on this weld. Figure 19 shows the results of two microhardness traverses, one across the second pass only, and one across the middle of the weld where the two passes overlap. Both traces are very similar, and the hardness is fairly constant across the fusion zone. These data confirm that the weld metal is relatively homogeneous. The hardness of the fusion zone is slightly higher than that of the base metal, as would be expected because of the martensitic structure and slightly higher β-stabilizer content.

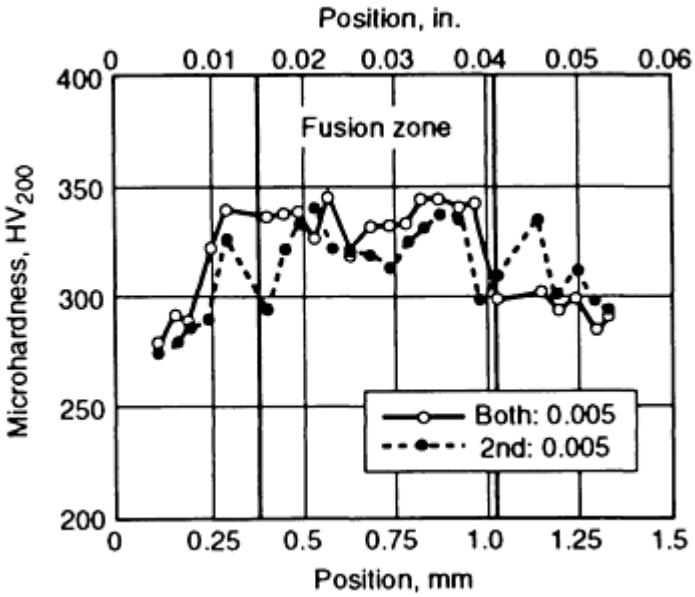

FIG. 19 MICROHARDNESS TRAVERSE DATA IN TWO LOCATIONS FOR THE TI-6AL-4V SHEET WELDED USING A TANTALUM SHIM. DATA LABELED "2ND" REFER TO TRAVERSE OVER SECOND PASS OF WELD ONLY. DATA LABELED "BOTH" INDICATE TRAVERSE ACROSS CENTER OF WELD WHERE TWO PASSES OVERLAP (SEE FIG. 15).

The tensile testing further confirmed that the weld metal could be considered to be a more heavily stabilized variant of Ti-6Al-4V. Table 7 compares the results of tensile tests performed on a baseline Ti-6Al-4V (no shim) weld with those of tests performed on the example weld. As the data show, the tantalum-containing weld had slightly higher strength and lower ductility than the baseline weld. Again these data are consistent with a slightly higher β-stabilizer content. However, the differences were not as great as in the microhardness testing, because in the case of the tensile tests, both structures were α' martensite.

TABLE 7 TENSILE PROPERTIES OF BASELINE TI-6AL-4V WELD COMPARED TO TI-6AL-4V WELDED USING TANTALUM SHIM

SAMPLE	YIELD STRENGTH		ULTIMATE TENSILE STRENGTH		YOUNG'S MODULUS		MAXIMUM STRAIN, %
	MPA	KSI	MPA	KSI	GPA	10^6 PSI	
BASELINE 1	828	120	970	141	114	16.5	12.7
BASELINE 2	787	114	960	139	127	18.4	12.3
BASELINE AVERAGE	807	117	965	140	121	17.5	12.5
TA WELD 1(A)	839	121.7	983	143	105	15.2	4.7
TA WELD 2(A)	838	121.5	971	141	103	14.9	10.5
TA WELD 3(A)	837	121.4	981	142	107	15.5	14.3
TA WELD AVERAGE	838	121.5	978	142	105	15.2	9.8

(A) REPLICANTS OF TI-6AL-4V WELDED TO TANTALUM SHIM

Test Results. The goal of the Ti-6Al-4V/tantalum dissimilar metal weld study was to thoroughly characterize the homogeneity, structure, and properties of the weld, relative to a baseline Ti-6Al-4V weld, and to determine the effect of the tantalum additions. The study showed that the tantalum shim could be completely melted using the chosen welding procedure and that a uniform weld bead could be produced. The compositional and microstructural analyses showed that the weld was very similar to the baseline weld. The tantalum-alloyed weld metal appeared to be consistent with standard principles regarding titanium alloy compositions and structure, and it was what would be expected in a weld made on slightly more heavily alloyed material. The mechanical test results confirmed this interpretation as well. In total, the

characterization showed that this weld could be made and that its properties could be predicted and/or interpreted accurately as an extrapolation of the baseline weld.

Characterization Objectives. A number of characterization techniques have been briefly discussed with respect to their application to welds. Examples 1 and 2 show that the choice and emphasis of the characterization procedure are largely determined by the intended application of the weld and the goals to be accomplished by the characterization. Each of the procedures in Examples 1 and 2 are discussed in great detail in the cited references. Additional information is available in the Section "Joint Evaluation and Quality Control" in this Volume and in Ref 16, 17, and 22

References cited in this section

16. *MATERIALS CHARACTERIZATION,* 9TH ED., VOL 10, *METALS HANDBOOK,* AMERICAN SOCIETY FOR METALS, 1986
17. *MECHANICAL TESTING,* 9TH ED., VOL 8, *METALS HANDBOOK,* AMERICAN SOCIETY FOR METALS, 1985
20. STANDARD TEST METHOD FOR PLANE-STRAIN FRACTURE TOUGHNESS OF METALLIC MATERIALS, ASTM E 399, *ANNUAL BOOK OF ASTM STANDARDS,* ASTM, 1984
22. *WELDING, BRAZING, AND SOLDERING,* 9TH ED., VOL 6, *METALS HANDBOOK,* AMERICAN SOCIETY FOR METALS, 1983

Characterization of Welds

Craig B. Dallam, The Lincoln Electric Company; Brian K. Damkroger, Sandia National Laboratories

References

1. STANDARD WELDING TERMS AND DEFINITIONS, ANSI/AWS A3.0-89, AWS, 1989
2. WELD DISCONTINUITIES, *METALS HANDBOOK,* 9TH ED., VOL 6, AMERICAN SOCIETY FOR METALS, 1983, P 829-855
3. *WELDING HANDBOOK,* 8TH ED., VOL 2, AWS, 1987
4. *PROCEDURE HANDBOOK OF ARC WELDING,* 12TH ED., LINCOLN ELECTRIC CO., 1973
5. CODES, STANDARDS, AND INSPECTION, *METALS HANDBOOK,* 9TH ED., VOL 6, AMERICAN SOCIETY FOR METALS, 1983, P 823-838
6. *RADIOGRAPHY IN MODERN INDUSTRY,* 4TH ED., EASTMAN KODAK CO., 1980
7. WELDING OF PIPELINES AND RELATED FACILITIES, API STANDARD 1104, 17TH ED., AMERICAN PETROLEUM INSTITUTE, 1988
8. REFERENCE RADIOGRAPHS FOR STEEL WELDMENTS, ASTM E 390, ASTM
9. *STRUCTURAL WELDING CODE--STEEL,* ANSI/AWS D1.1-92, AWS, 1992
10. METALLOGRAPHY OF WELDMENTS, *METALS HANDBOOK,* 9TH ED., VOL 9, AMERICAN SOCIETY FOR METALS, 1985, P 577-586
11. K.E. EASTERLING, MICROSTRUCTURE AND PROPERTIES OF THE HAZ, *RECENT TRENDS IN WELDING SCIENCE AND TECHNOLOGY,* S. DAVID AND J. VITEK, ED., ASM INTERNATIONAL, 1990, P 177-188
12. WRC 1992 DIAGRAM, *WELD. J.,* MAY 1992, P 171
13. T.G.F. GRAY, J. SPENCE, AND T.H. NORTH, *RATIONAL WELDING DESIGN,* NEWNES-BUTTERWORTHS, 1975, P 111
14. R.H. ESPY, WELDABILITY OF NITROGEN-STRENGTHENED STAINLESS STEELS, *WELD. J. RES. SUPPL.,* VOL 61 (NO. 5), MAY 1982, P 149S-156S

15. METAL TEST METHODS AND ANALYTICAL PROCEDURES, *1991 ANNUAL BOOK OF ASTM STANDARDS,* VOL 03.05 AND 03.06, ASTM, 1991
16. *MATERIALS CHARACTERIZATION,* 9TH ED., VOL 10, *METALS HANDBOOK,* AMERICAN SOCIETY FOR METALS, 1986
17. *MECHANICAL TESTING,* 9TH ED., VOL 8, *METALS HANDBOOK,* AMERICAN SOCIETY FOR METALS, 1985
18. STANDARD METHODS OF TENSION TESTING OF METALLIC MATERIALS, ASTM E 8, *ANNUAL BOOK OF ASTM STANDARDS,* VOL 03.01, ASTM, 1984
19. *SPECIFICATION FOR CARBON STEEL ELECTRODES FOR SHIELDED METAL ARC WELDING,* ANSI/AWS A5.1-91, AWS, 1991
20. STANDARD TEST METHOD FOR PLANE-STRAIN FRACTURE TOUGHNESS OF METALLIC MATERIALS, ASTM E 399, *ANNUAL BOOK OF ASTM STANDARDS,* ASTM, 1984
21. STANDARD TEST METHOD FOR CRACK TIP OPENING DISPLACEMENT (CTOD) FRACTURE TOUGHNESS MEASUREMENT, ASTM E 1290, VOL 03.01, ASTM, 1989
22. *WELDING, BRAZING, AND SOLDERING,* 9TH ED., VOL 6, *METALS HANDBOOK,* AMERICAN SOCIETY FOR METALS, 1983

Introduction to Brazing and Soldering

Melvin M. Schwartz, Sikorsky Aircraft

Introduction

BRAZING AND SOLDERING require the application of a number of scientific and engineering skills to produce joints of satisfactory quality and reliability. Brazing employs higher temperatures than soldering, but the fundamental concepts are similar, particularly with respect to metallurgy and surface chemistry (Table 1). However, joint design, materials to be joined, filler metal and flux selection, heating methods, and joint preparation can vary widely between the two processes. Economic considerations involving filler metal and process technology are also varied, particularly in relation to automated techniques and inspection and testing. Brazing and soldering are performed in many industries, from exotic applications in the electronics and aerospace field to everyday plumbing applications.

TABLE 1 COMPARISON OF SOLDERING, BRAZING, AND WELDING

Parameter	**Process**		
	Soldering	**Brazing**	**Welding**
Joint formed	Mechanical	Metallurgical	Metallurgical
Filler metal melt temperature, °c (°f)	<450 (<840)	>450 (>840)[(a)]	>450 (>840)[(b)]
Base metal	Does not melt	Does not melt	. . .
Fluxes used to protect and to assist in wetting of base-metal surfaces	Required	Optional	Optional
Typical heat sources	Soldering iron; ultrasonics; resistance; oven	Furnace; chemical reaction; induction; torch; infared	Plasma; electron beam; tungsten and submerged arc; resistance; laser
Tendency to warp or burn	Atypical	Atypical	Potential distortion and warpage of base-metal likely
Residual stresses	. . .	. . .	Likely around weld area

(A) LESS THAN MELTING POINT OF BASE METAL.

Introduction to Brazing and Soldering

Melvin M. Schwartz, Sikorsky Aircraft

Brazing

Many products are assembled from two or more individual components that are often permanently joined to produce structurally sound assemblies. Joining methods include various fasteners, interference-type joints, adhesives, and, for the highest-integrity joints, the many techniques classified under welding. Brazing, although fundamentally indifferent from welding, is one such technique.

Early metalworkers, stimulated by a desire to produce structures that were difficult or impossible to build using methods then in existence, realized that it was possible to fill the joint between two metal pieces with molten metal and allow it to solidify. These artisans soon learned by experience that, in order to achieve adherence, the metals to be joined and the brazing filler metal had to be kept free of oxides and the filler metal had to have a lower melting point, and, furthermore, that a given filler metal would not necessarily adhere to all metals. From these basic requirements, brazing grew into a craft whose practitioners were well versed in what to do and what not to do in order to produce sound joints.

Just as the technique of brazing developed empirically, so did the lower-melting point filler metals. Workers first used lead and tin solders as well as silver and copper-arsenic ores, which were readily available and had low melting points. Later, the alloy brass was developed and found to be more desirable for joining copper, silver, and steel structures, because it provided higher-strength joints and could withstand higher temperatures.

Early silversmiths, probably wanting to produce white solder joints for aesthetic reasons, melted brass and silver together and found it to have an even lower melting point than brass, good adherence, and better corrosion resistance. Although innumerable combinations of silver, copper, and zinc subsequently evolved, primarily to meet melting-point requirements, these silver-brass, brass, and lead-tin alloys were essentially the only brazing and soldering filler materials available for generations.

Advantages of Brazing. Brazing has many distinct advantages, including the following:

- ECONOMICAL FABRICATION OF COMPLEX AND MULTI-COMPONENT ASSEMBLIES
- SIMPLE METHOD TO OBTAIN EXTENSIVE JOINT AREA OR JOINT LENGTH
- JOINT TEMPERATURE CAPABILITY APPROACHING THAT OF BASE METAL
- EXCELLENT STRESS DISTRIBUTION AND HEAT-TRANSFER PROPERTIES
- ABILITY TO PRESERVE PROTECTIVE METAL COATING OR CLADDING
- ABILITY TO JOIN CAST MATERIALS TO WROUGHT METALS
- ABILITY TO JOIN NONMETALS TO METALS
- ABILITY TO JOIN METAL THICKNESSES THAT VARY WIDELY IN SIZE
- ABILITY TO JOIN DISSIMILAR METALS
- ABILITY TO JOIN POROUS METAL COMPONENTS
- ABILITY TO FABRICATE LARGE ASSEMBLIES IN A STRESS-FREE CONDITION
- ABILITY TO PRESERVE SPECIAL METALLURGICAL CHARACTERISTICS OF METALS
- ABILITY TO JOIN FIBER- AND DISPERSION-STRENGTHENED COMPOSITES
- CAPABILITY FOR PRECISION PRODUCTION TOLERANCE
- REPRODUCIBLE AND RELIABLE QUALITY CONTROL TECHNIQUES

Strong, uniform, leakproof joints can be made rapidly, inexpensively, and even simultaneously. Joints that are inaccessible and parts that may not be joinable at all by other methods often can be joined by brazing. Complicated assemblies comprising thick and thin sections, odd shapes, and differing wrought and cast alloys can be turned into

integral components by a single trip through a brazing furnace or a dip pot. Metal as thin as 0.01 mm (0.0004 in.) and as thick as 150 mm (6 in.) can be brazed.

Brazed joint strength is high. The nature of the interatomic (metallic) bond is such that even a simple joint, when properly designed and made, will have strength equal to or greater than that of the as-brazed parent metal. The natural shapes of brazing fillets are excellent. The meniscus surface formed by the fillet metal as it curves across corners and adjoining sections is ideally shaped to resist fatigue. (It should be noted that in brazed joints using eutectic-type filler metal, fillets often contain an excessive amount of brittle intermetallic compounds. In fact, fillets are 5 to 10 times thicker than the joint and thus have a much higher volume of the liquid phase from which these brittle phases crystallize. Therefore, crack nucleation often originates in fillets.)

Complex shapes with greatly varied sections can be brazed with little distortion, and precise joining is comparatively simple. Unlike welding, in which the application of intense heat to small areas acts to move the parts out of alignment and introduces residual stresses, brazing involves fairly even heating and thus part alignment is easier.

Limitations of Brazing. A brazed joint is not a homologous body but rather is heterogeneous, composed of different phases with differing physical and chemical properties. In the simplest case, it consists of the base metal parts to be joined and the added filler metal. However, partial dissolution of the base metal, combined with diffusion processes, can change the composition and therefore the chemical and physical properties of the boundary zone formed at the interface between base metal and filler metal and often of the entire joint. Thus, in addition to the two different materials present in the simplest example given above, a complicated transitional or even completely different zone must be considered.

In determining the strength of such heterogeneous joints, the simplified concepts of elasticity and plasticity theory--valid for a homogeneous metallic body where imposed stresses are uniformly transmitted from one surface or space element to the adjacent ones--no longer apply. In a brazed joint formed of several materials with different characteristics of deformation resistance and deformation speed, the stresses caused by externally applied loads are nonuniformly distributed.

Mechanics of Brazing. Brazing involves a limited dissolution or plastic deformation of the base metal (Ref 1). Brazing comprises a group of joining processes in which coalescence is produced by heating to a suitable temperature above 450 °C (840 °F) and by using a ferrous or nonferrous filler metal that must have a liquidus temperature above 450 °C (840 °F) and below the solidus temperature(s) of the base metal(s). The filler metal is distributed between the closely fitted surfaces of the joint. Brazing is distinguished from soldering in that soldering employs a filler metal having a liquidus below 450 °C (840 °F) (Table 1).

Brazing proceeds through four distinct steps:

- THE ASSEMBLY OR THE REGION OF THE PARTS TO BE JOINED IS HEATED TO A TEMPERATURE OF AT LEAST 450 °C (840 °F).
- THE ASSEMBLED PARTS AND BRAZING FILLER METAL REACH A TEMPERATURE HIGH ENOUGH TO MELT THE FILLER METAL (FOIL, WIRE, PASTE, PLATINGS, ETC.) BUT NOT THE PARTS.
- THE MOLTEN FILLER METAL, HELD IN THE JOINT BY SURFACE TENSION, SPREADS INTO THE JOINT AND WETS THE BASE METAL SURFACES.
- THE PARTS ARE COOLED TO SOLIDITY, OR "FREEZE," THE FILLER METAL, WHICH IS HELD IN THE JOINT BY CAPILLARY ATTRACTION AND ANCHORS THE PARTS TOGETHER BY METALLURGICAL REACTION AND ATOMIC BONDING.

Brazing Versus Other Welding Processes. The mere fact that brazing does not involve any substantial melting of the base metals offers several advantages over other welding processes. It is generally possible to maintain closer assembly tolerances and to produce a cosmetically neater joint without costly secondary operations. Even more important, however, is that brazing makes it possible to join dissimilar metals (or metals to ceramics) that, because of metallurgical incompatibilities, cannot be joined by traditional fusion welding processes. If the base metals do not have to be melted to be joined, it does not matter that they have widely different melting points. Therefore, steel can be brazed to copper as easily as to another steel.

Brazing also generally produces less thermally induced distortion, or warping, than fusion welding. An entire part can be brought up to the same brazing temperature, thereby preventing the kind of localized heating that causes distortion in welding.

Finally, and perhaps most important to the manufacturing engineer, brazing readily lends itself to mass production techniques. It is relatively easy to automate, because the application of heat does not have to be localized, as in fusion welding, and the application of filler metal is less critical. In fact, given the proper clearance conditions and heat, a brazed joint tends to "make itself" and is not dependent on operator skill, as are most fusion welding processes.

Automation is also simplified by the fact that there are many means of applying heat to the joint, including torches, furnaces, induction coils, electrical resistance, and dipping. Several joints in one assembly often can be produced in one multiple-braze operation during one heating cycle, further enhancing production automation.

As noted in Table 1, essentially no melting of the base metal occurs in brazing; however, the temperatures involved can affect the properties of the metals being joined. For example, base metals whose mechanical properties were obtained by cold working may soften or undergo grain growth if the brazing temperature is above their recrystallization temperatures. Mechanical properties obtained by heat treatment may be altered by the heat of brazing. On the other hand, materials in the annealed condition are usually not altered by brazing.

As with other welding processes, brazing produces a heat-affected zone (HAZ) with a strongly altered microstructure due to intensive mutual mass transfer between base metal and filler metal. The width of this zone varies with the heating process used. In torch and induction brazing, for example, only a localized zone is heated; in france and dip brazing, the entire part is subjected to the brazing temperature. As a rule, the HAZ produced during brazing is wider and less sharply defined than those resulting from other fusion-related processes.

Several elements of the brazing process must be understood in order to produce satisfactory brazed joints:

- FILLER METAL FLOW
- BASE METAL CHARACTERISTICS
- FILLER METAL CHARACTERISTICS
- SURFACE PREPARATION
- JOINT DESIGN AND CLEARANCE
- TEMPERATURE AND TIME
- RATE AND SOURCE OF HEATING

Each of these topics is discussed in detail in the article "Fundamentals of Brazing" in this Volume.

Reference cited in this section

1. E. LIEBERMAN, *MODERN SOLDERING AND BRAZING TECHNIQUES*, BUSINESS NEWS PUBLICATIONS, 1988

Introduction to Brazing and Soldering

Melvin M. Schwartz, Sikorsky Aircraft

Soldering

Like brazing and other joining processes, soldering involves several fields of science, including mechanics, chemistry, and metallurgy. Soldering is a simple operation (Ref 2), consisting of the relative placement of the parts to be joined, wetting the surfaces with molten solder, and allowing the solder to cool until it has solidified.

Soldering in the field of electronics is in many respects different from soldering in other branches of industry. Although the physical principles of all soldering (and brazing) processes are the same, the features specific to their use in electronics are so numerous that it is possible to speak of soldering in electronics as a separate subject.

Soldering Versus Other Joining Technologies. Soldering has several clear advantages over competitive joining techniques, such as welding or bonding with conductive adhesives:

- THE SOLDER JOINT FORMS ITSELF BY THE NATURE OF THE FLOW, WETTING, AND SUBSEQUENT CRYSTALLIZATION PROCESS, EVEN WHEN THE HEAT AND THE SOLDER ARE NOT DIRECTED PRECISELY TO THE PLACES TO BE SOLDERED. BECAUSE SOLDER DOES NOT ADHERE TO INSULATING MATERIALS, IT OFTEN CAN BE APPLIED IN EXCESS QUANTITIES, IN CONTRAST TO CONDUCTIVE ADHESIVES. THE SOLDERING TEMPERATURE IS RELATIVELY LOW, SO THERE IS NO NEED FOR THE HEAT TO BE APPLIED LOCALLY AS IN WELDING.
- SOLDERING ALLOWS CONSIDERABLE FREEDOM IN THE DIMENSIONING OF JOINTS, SO THAT IT IS POSSIBLE TO OBTAIN GOOD RESULTS EVEN IF A VARIETY OF COMPONENTS ARE USED ON THE SAME PRODUCT.
- THE SOLDERED CONNECTIONS CAN BE DISCONNECTED IF NECESSARY, THUS FACILITATING REPAIR.
- THE EQUIPMENT FOR BOTH MANUAL SOLDERING AND MACHINE SOLDERING IS RELATIVELY SIMPLE.
- THE SOLDERING PROCESS CAN BE EASILY AUTOMATED, OFFERING THE POSSIBILITY OF IN-LINE ARRANGEMENTS OF SOLDERING MACHINES WITH OTHER EQUIPMENT.

Mass soldering by wave, drag, or dip machines has been the preferred method for making high-quality, reliable connections for many decades. Despite the appearance of new connecting systems, it still retains this position. Correctly controlled, soldering is one of the least expensive methods for fabricating electrical connections. Incorrectly controlled, it can be one of the most costly processes--not because of the initial cost, but because of the many far-reaching effects of poor workmanship.

Chronology of Soldering. Soldering is not a new process (Ref 2). It probably dates to the Bronze Age, when some metalworker discovered the affinity of a tin-lead mixture for a clean copper surface. As recorded in the writings of Pliny, the Romans used 60Sn-40Pb mixture to solder their lead water pipes.

During the late 19th and early 20th centuries, a great deal of work was devoted to the development and improvement of the soldering process and to the determination of the fundamental principles involved. Examination of the books, papers, and especially the patents of the era shows that soldering as a science was clearly understood long before the start of the electronics industry. There has certainly been a great improvement in the materials and machines used in the process, but the basics have changed little since the early part of this century.

Soldering in the electronics field has undergone many dramatic changes since the first radios were built. Between the 1920s and the 1940s, all interconnections were made using the point-to-point wiring method, and the solder joints were made using soldering irons. After World War II (Ref 3, 4), the demand for consumer electronics began to increase, and by the 1950s a mass market had developed. To meet this demand, the first mass soldering technique, dip soldering, was used with boards that were the precursors of printed wiring boards (PWBs). By the late 1950s, wave soldering had been developed in England and soon thereafter reached the United States. This development was necessitated by the introduction of PWBs. Wave soldering continued to be the method of choice through the 1980s and is still widely used.

The development and maturation of the multi-layer PWB and the first major effort toward miniaturization occurred in the 1970s. The dual inline integrated circuit package replaced many discrete components. By the early 1980s, the pressure to increase component densities had grown to such a degree that a new technique for attachment was needed, and surface mounting was developed. Surface mount technology in turn required new ways to make solder joints, prompting the development of vapor phase, infrared, hot gas, and other reflow soldering techniques.

Soldering remains the attachment method of choice in the evolving electronics industry. It is the only metallurgical joining technique suitable for the mass manufacture of electronic and electrical interconnections within the temperature restrictions of electronic components and substrates.

Solder Metals. The solder metal business has changed dramatically, having moved from merely producing wire to producing bulk, preform, and paste in order to meet the needs of soldering techniques. Solder can be applied in several ways (Ref 2, 3):

- A MIXTURE OF SOLDER POWDER AND FLUX, KNOWN AS SOLDER PASTE (REF 5), CAN BE APPLIED TO THE JOINTS BY SCREENING, STENCILING, OR USING ONE OF THE MACHINES THAT APPLIES DOTS OF THE PASTE BY A SIMPLE PNEUMATIC SYSTEM. THIS METHOD IS ESPECIALLY USEFUL WHERE SURFACE-MOUNTED COMPONENTS ARE TO BE SOLDERED AND CANNOT BE PASSED THROUGH THE SOLDER WAVE.
- PARTS CAN BE PRETINNED, THAT IS, COATED WITH A LAYER OF SOLDER BY FLUXING AND DIPPING INTO A BATH OF THE MOLTEN METAL.
- SOLDER CAN BE OBTAINED IN THE SHAPE OF RINGS, WASHERS, OR TUBES, WHICH ARE PLACED ON OR ADJACENT TO THE PARTS TO BE JOINED. THESE SOLDER PREFORMS CAN BE OBTAINED WITH OR WITHOUT A FLUX COATING.

The two latter methods of providing solder for the joint are used in many areas of the electronics industry where machine soldering is not possible. Tiny solder rings are placed over long wire wrap pins on a mother board, where the gold plating of the pins in the wrapping area must not be coated with solder. Solder washers are fitted under bolts that must be soldered to a ground plane. Wires and tinned before soldering into a pretinned wiring lug. The possibilities are seemingly limitless (Ref 6).

Solder filler metals have also changed. The first electronic soldering was done with the 50Sn-50Pb solder material used by plumbers. By the 1950s, the choice of materials had switched to eutectic tin-lead solders to counter the problems created by a vibrating wave solder machine conveyor. Today a wide range of filler materials is used in the electronics industry. With the spread of electronics technology into every facet of life, the environmental and materials demands have grown substantially, requiring the use of such specialized materials as indium and gold-tin fillers.

Flux technology has also evolved (Ref 3, 5). As a result of the restraints of military and government specifications, the emphasis has been on the addition of new flux types rather than on the replacement of old ones. Extensive work has been done with organic acids, which enlarge the processing windows. Other categories include synthetic activated materials, which are non-rosin fluorocarbon solvent-removable types, and low solids fluxes for surface mounting that can be used instead of the classic fully activated rosin formulations.

Other materials, such as adhesives for the surface mounting of components intended for wave soldering, are new to soldering technology. These materials must be specially designed to avoid interference with the soldering process, yet must remain intact through the solvent action of fluxes and, often, flux removal.

Mass Soldering. With the introduction of mass soldering techniques (Ref 1, 6), the issue of solderability has become one of the major interest. Mass production processes are not as tolerant as the hand soldering process. In addition, modern components cannot withstand as much heat, as for example, a tube socket. Lower soldering temperatures and less mechanical working have made it necessary to attain the highest solderability to ensure a metallurgically sound and reliably solder joint.

Machine or mass soldering (Ref 2, 4, 6) can make thousands of joints in a few seconds, providing the electrical connections and simultaneously mechanically fastening the components. No other process has yet been developed that can so economically interconnect electronic circuitry.

Wave Soldering. From the original concept of hand dipping boards came the idea of pumping solder through a slot or nozzle to form a wave, or mound, of constantly moving, dross-free metal through which the board could be passed. This offered several advantages: the surface of the solder was always clean and did not require skimming, the pumping action maintained an even temperature, and the raised wave provided an easy form for adding a conveyor system for automatic movement of the board over the solder.

Once the idea of the solder wave had been born, it was logical to use a similar method to apply the flux, and the basic soldering machine appeared. These original machines were quite crude, consisting of individual modules with a freestanding conveyor (often added by the user) placed over them. There was little attempt to integrate the parts into one system, and the smoke and fumes were left to escape into the factory exhaust, aided by a makeshift canopy hung over the machine.

Much work was done on the development of the actual wave in an attempt to improve the speed of soldering and to reduce the incidence of shorts and icicles. The solder weir, the double wave, and the cascade all experienced brief popularity. The cascade wave, which consists of several waves in series, was one of the more interesting of these developments. It was used with an inclined conveyor and was the basis of machines built for in-house use by several manufacturers. However, it never achieved great popularity.

Another development was the use of ultrasonics to form a wave, with the intention of causing cavitation at the joint of avoiding the use of flux, or at least reducing the activity required. Some experimental machines were built, but the cost was excessive, the soldering results were no better than those produced with the conventional pumped wave, and the power of the ultrasonic energy had to be so high that the matching horns used to energize the pot were quickly eroded away. With the advent of the semiconductor, ulrasonics were found to cause occasional damage to the devices. Today the main use for ultrasonics in the soldering industry is to be found in the pots used for tinning components prior to assembly. This era also saw the introduction of oil into the solder wave. This idea worked extremely well and has been a feature of some soldering machines for many years (Fig. 1) (Ref 2, 3, 4, 5, 6, 7).

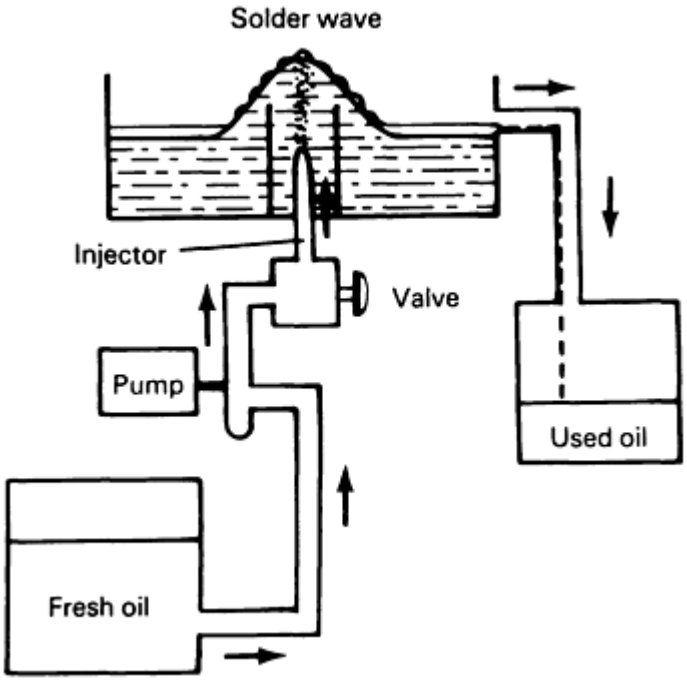

FIG. 1 SCHEMATIC SHOWING SIMPLE OIL INJECTION OF A SOLDER WAVE

Drag Soldering. In a totally different direction, the static solder bath soldering process, or drag soldering, was developed, and machines were designed using this principle (Fig. 2). These machines have been developed to a high level of sophistication, initially in Europe and Japan and later in the United States. As has often been the case in the growth of the soldering machine industry, initial developments were prompted because of patent restrictions that at the time prevented the free use of the more conventional solder wave. These restrictions have often proved beneficial to the industry by forcing creative thinking that has eventually resulted in improved products (Ref 2, 3, 4, 5, 6).

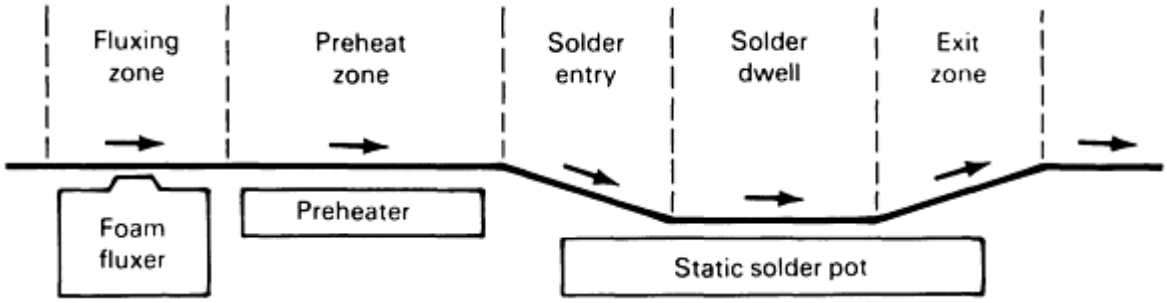

FIG. 2 SCHEMATIC SHOWING SEQUENCE OF OPERATIONS FOR A DRAG SOLDERING MACHINE

Current Technology. Today machines are available from many different manufacturers, each with its own particular features. These machines have various levels of sophistication and capability, ranging from small laboratory units to high-production systems, often complete with in-line cleaning and assembly and return conveyors. Machines in use today are generally self-contained, with a high degree of control, optional auxiliary systems, and exhaust venting. Coming onto the market are systems with computer-controlled operation and setup, which practically eliminate human error from the machine soldering process.

Soldering processes have evolved dramatically since the introduction of mass soldering techniques. Wave machines have become highly specialized, especially since the introduction of surface-mount technology. Reflow techniques (Ref 8), which were once limited to hybrid technology and leaded flatpacks, have grown remarkably. Vapor phase, infrared, and hot gas soldering equipment have initiated a new process of evolution.

The performance of a solder joint in its service environment is a strong consideration in modern electronics. Many applications, such as jet engines, dishwashers, and automobiles, impose a repeated cyclic thermal cycle on the equipment. This produces thermomechanical strains, which result in fatigue or creep failure if the joint design is poor or if life predictions have been incorrectly calculated. Each situation must be carefully analyzed and the correct design employed for the equipment to fulfill its intended service life.

Thermally induced fatigue and creep failures, virtually unknown in the 1950s but common today, are illustrative of the added stresses and strains placed on joints. It should be emphasized that miniaturization of electronic parts, particularly current paths, results in a dramatic increase in current density, which generates strong thermal and mechanical shocks upon switching. Proper design can minimize these strains and make the joints more highly producible. Design has become even more critical with the introduction of surface-mount technology.

Quality Control. Once a joint is made, its quality must be assessed through inspection. Advanced technology has produced some electronic assembly designs that are impossible to inspect visually, and an entire group of automated inspection tools has thus evolved. These tools include radiography, infrared signature, and two- or three-dimensional vision systems. Most of these are aided with very sophisticated computer software. The role of inspection, which historically was to locate those joints that needed rework, is changing along with the technology. Inspection is now used as a process-control audit to locate those portions of the process that need improvement or should returned to a position within the control limits. Therefore, the emphasis has shifted from merely shipping an acceptable product to manufacturing it correctly the first time.

Future Trends. Several other technologies and materials for soldering are being developed and tested (Ref 2, 3, 4, 5). One process that is becoming widely used is condensation, or vapor phase, soldering. In this process, the vapor from a liquid with a high-temperature boiling point is allowed to condense on the items to be soldered and, in giving up the latent heat of vaporization, quickly and evenly raises their temperature and produces a sound soldered joint. The method is simple, clean, and extremely well controlled. It requires-special equipment, and, of course, the parts are all exposed to the same temperature.

In another method, the parts are dipped into an oil heated above the melting point of the solder. Peanut oil can be used, although several excellent synthetic products are available. Here again, the component parts are subjected to the same temperature as the joint. This is a messy process, and the parts must be cleaned after soldering to remove the oil.

Infrared heating is a useful method for producing the temperature necessary for soldering. The shorter wavelengths can be focused onto very small areas, allowing selective heating of the joints to be soldered, without subjecting nearby components to the soldering temperature. Equipment and tooling are expensive if complex assemblies have to be soldered, and the relative emissivity of the joint metals and the adjacent materials can cause processing problems. For example, the base laminate of a PWB can be burned before the joint to be soldered has even reached the soldering temperature. This process thus requires very careful control.

Resistance heating can be used for soldering in two ways. The first method passes a current through the parts of the joint, causing their temperature to rise by virtue of the resistance existing in the joint structure. This is not a very controllable process and is primarily used for less critical applications on large connections. The second method passes a current through a wire that is shaped to touch the parts to be heated. Despite the lack of precise control, the process is often used to solder the leads on surface-mounted components.

Lasers have been used to provide the heat for soldering, although this is not yet a common method. A laser can provide a very high-energy, small-area beam, and heating is therefore extremely fast, localized, and limited only by the ability of the joint materials to absorb this energy. However, the shiny metal surfaces in the joint reflect most of the energy of the commonly used lasers, and coupling the laser and the joint is a major problem. The soldering flux is often used as a coupling medium. When correctly set up, laser soldering offers a fast, clean method of making joints. The cost of the equipment is quite high.

Since 1980, significant improvements and innovations in the soldering arena with respect to materials, equipment, and processes have occurred. However, two main tasks remain: developing environmentally friendly solder materials and establishing failure-free solder joint technology (Ref 2, 3, 4, 6, 7, 8).

For solders and soldering, two issues that are directly related to environmental concerns are the replacement of chlorofluorocarbon (CFCs) as the primary cleaning agent for electronic assemblies and the feasibility of using alternatives to lead-containing solders. For electronic assembly solders (Ref 4), in addition to using CFC substitutes and other solvents (e.g., hydrocarbon-based systems), aqueous cleaning and "no-clean" setups are two viable solutions.

The other task to be accomplished is the development of failure-free solder joint technology. Strengthened solder materials are expected to possess the properties that impede the occurrence of undesirable metallurgical phenomena during their service life under various in-circuit and external conditions, particularly temperature and induced stresses. Three approaches are being examined: macroscopic blends of selected fillers in a tin-rich matrix (composite solder), microscopic incorporation of doping additives to tin-rich base material, and atomic-level interaction. Preliminary experiments have been carried out to accomplish the first approach. Figure 3 demonstrates the increased yield strength of the 63Sn-37Pb composite solder with various amounts of filler (Ref 9).

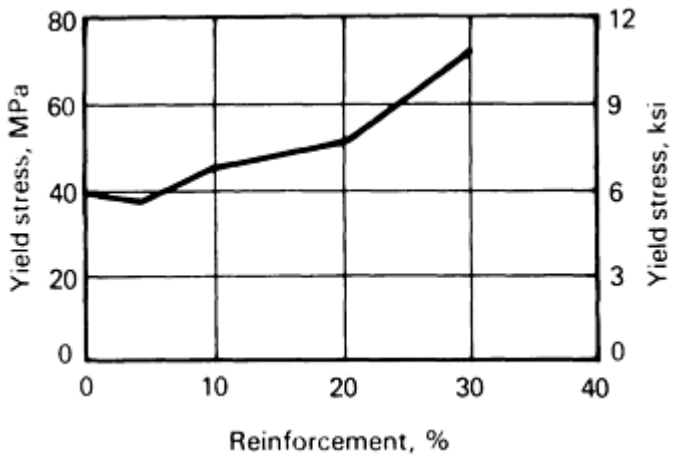

FIG. 3 EFFECT OF FILLER REINFORCEMENT ON THE YIELD STRENGTH OF 63SN-37PB COMPOSITE SOLDER. SOURCE: REF 9

The intrinsic properties of the new materials are expected to possess the following characteristics, while maintaining thermal and electrical conductivities:

- STABLE MICROSTRUCTURE
- INCREASED THERMAL AND MECHANICAL FATIGUE RESISTANCE
- HIGH CREEP RESISTANCE
- DECREASED THERMAL EXPANSION COEFFICIENT

These aggregate characteristics constitute the "strengthened" solder materials that are able to withstand harsher application conditions. The reduced thermal expansion coefficient of these new solders is expected to be more compatible with that of state-of-the-art electronic components and with ceramic substrates.

With respect to quality, solder joints have historically been judged by visual criteria. However, due to the nature of solder materials and the effect of the solder joint-forming process on appearance, many serviceable solder joints are often rejected, while other potentially questionable joints are accepted to carry out critical missions. This not only adds to manufacturing costs, but can also jeopardize service performance. Strengthened solder joints are expected to relieve the necessity of on-line inspection and rework while also reducing manufacturing costs and enhancing life span and tolerance of harsh service conditions in many military applications.

References cited in this section

1. E. LIEBERMAN, *MODERN SOLDERING AND BRAZING TECHNIQUES,* BUSINESS NEWS PUBLICATIONS, 1988
2. R.J. KLEIN WASSINK, *SOLDERING IN ELECTRONICS,* ELECTROCHEMICAL PUBLICATIONS, 1989
3. H.H. MANKO, *SOLDERS AND SOLDERING,* 2ND ED., MCGRAW-HILL 1964
4. L.P. LAMBERT, *SOLDERING FOR ELECTRONIC ASSEMBLIES,* MARCEL DEKKER, 1987
5. H.H. MANKO, SOLDERING FLUXES--PAST AND PRESENT *WELD. J.*, VOL 52 (NO. 3), 1973, P 163-166
6. R.W. WOODGATE, *THE HANDBOOK OF MACHINE SOLDERING,* 2ND ED., JOHN WILEY & SONS, 1988
7. T.J. NEILLO, "AN APPROACH TO SOLDERING IN THE AUTOMATED FACTORY," SME SOLDERING TECH. CONF., SME MS 91-288, MAY 1991
8. T. ROBERTS, "CONDUCTIVE REFLOW SOLDERING," SME SOLDERING TECH. CONF., SME MS 91-290, MAY 1991
9. J.S. HWANG, *ET AL.,* FUTURISTIC SOLDERS, *SURF. MOUNT. TECHNOL.,* SEPT 1991, P 40-43

Introduction to Brazing and Soldering

Melvin M. Schwartz, Sikorsky Aircraft

References

1. E. LIEBERMAN, *MODERN SOLDERING AND BRAZING TECHNIQUES,* BUSINESS NEWS PUBLICATIONS, 1988
2. R.J. KLEIN WASSINK, *SOLDERING IN ELECTRONICS,* ELECTROCHEMICAL PUBLICATIONS, 1989
3. H.H. MANKO, *SOLDERS AND SOLDERING,* 2ND ED., MCGRAW-HILL 1964
4. L.P. LAMBERT, *SOLDERING FOR ELECTRONIC ASSEMBLIES,* MARCEL DEKKER, 1987
5. H.H. MANKO, SOLDERING FLUXES--PAST AND PRESENT *WELD. J.*, VOL 52 (NO. 3), 1973, P 163-166
6. R.W. WOODGATE, *THE HANDBOOK OF MACHINE SOLDERING,* 2ND ED., JOHN WILEY & SONS,

1988
7. T.J. NEILLO, "AN APPROACH TO SOLDERING IN THE AUTOMATED FACTORY," SME SOLDERING TECH. CONF., SME MS 91-288, MAY 1991
8. T. ROBERTS, "CONDUCTIVE REFLOW SOLDERING," SME SOLDERING TECH. CONF., SME MS 91-290, MAY 1991
9. J.S. HWANG, *ET AL.*, FUTURISTIC SOLDERS, *SURF. MOUNT. TECHNOL.*, SEPT 1991, P 40-43

Fundamentals of Brazing

Mel M. Schwartz, Sikorsky Aircraft

Introduction

BRAZING is a process for joining solid metals in close proximity by introducing a liquid metal that melts above 450 °C (840 °F). A sound brazed joint generally results when an appropriate filler alloy is selected, the parent metal surfaces are clean and remain clean during heating to the flow temperature of the brazing alloy, and a suitable joint design is used. Like the other joining processes, brazing encompasses a variety of scientific disciplines (for example, mechanics, physics, and chemistry).

Recently, the demands of more-sophisticated structures have forced technicians and engineers to encourage metal producers to apply their metallurgical knowledge to produce brazing filler metals that meet more-specific needs. To ensure the production of good brazed joints, the technicians and engineers also had to appeal to mechanical engineers for improved joint design, to chemical engineers for solutions to corrosion problems, and to metallurgists and ceramists for proper material selection.

Brazing has been embraced by the engineering community and has now reached a very successful plateau within the joining field. This has come about because of the:

- DEVELOPMENT OF NEW TYPES OF BRAZING FILLER METALS (RAPID SOLIDIFICATION AMORPHOUS FOILS AND TITANIUM-ADDED FILLER METALS FOR CERAMIC JOINING
- AVAILABILITY OF NEW FORMS AND SHAPES OF FILLER METALS
- INTRODUCTION OF AUTOMATION THAT HAS BROUGHT BRAZING PROCESSES TO THE FOREFRONT IN HIGH-PRODUCTION SITUATIONS
- INCREASED USE OF FURNACE BRAZING IN A VACUUM, AS WELL AS ACTIVE AND INERT-GAS ATMOSPHERES

Since the early 1980s, other developments, such as aluminum-clad foils for fluxless aluminum brazing, copper-nickel-titanium filler metals for brazing titanium and some of its alloys, cadmium-free silver filler metals, and vacuum-grade metal brazing foils, have evolved to be used in production applications.

Fundamentals of Brazing

Mel M. Schwartz, Sikorsky Aircraft

Physical Principles

Capillary flow is the dominant physical phenomenon that ensures good brazements when both faying surfaces to be joined are wet by the molten filter metal. The joint must be properly spaced to permit efficient capillary action and coalescence. More specifically, capillarity is a result of the relative attraction of the molecules of the liquid to each other and to those of the solid. In actual practice, brazing filler metal flow characteristics are also influenced by dynamic considerations involving fluidity, viscosity, vapor pressure, gravity, and, especially, by the effects of any metallurgical reasons between the filler metal and the base metal.

Capillary attraction makes the brazing of leak-tight joints a simple proposition. In a properly designed joint, the molten brazing filler metal is normally drawn completely through the joint area without any voids gaps when processed in a protective atmosphere. Solidified joints will remain intact and gas will remain tight under heavy pressures, even when the joint is subjected to shock or vibrational type of loading. Capillary attraction is also the physical force that governs the action of a liquid against solid surfaces in small, confined areas.

The phenomena of wetting and spreading are very important to the formation of brazed joints. Other significant factors that also must be considered include the condition of the solid surface in terms of the presence of oxide films and their effects on wetting and spreading, surface roughness, alloying with between the brazing filler metal and base metal, and the extent to which alloying is affected by the thermodynamic properties of the brazing atmosphere. A number of studies (Ref 1, 2) have been conducted on surface activation, contact angle, equilibrium, and surface energies. Some of these alloy systems have a finite contact angle that is thermodynamically unstable, because the solid-vapor surface energy exceeds the sum of the liquid-solid surface energies, that is, an alloy system in which thermodynamics would predict complete spreading. In actual fact, spreading may or may not occur in this type of alloy system, and the rate of spreading can be markedly dependent on surface chemistry.

Wetting is, perhaps, best explained by the following example. If a solid is immersed in a liquid bath and wetting occurs, then a thin continuous layer of liquid adheres to the solid when it is removed from the liquid (Fig. 1). Technically, the force of adhesion between the solid and liquid (during the wetting process) is greater than the cohesive force of the liquid. In practical terms, with respect to brazing, wetting implies that the liquid brazing filler metal spreads on the solid base metal, instead of balling up on its surface. It has been demonstrated that wetting actually depends on a slight surface alloying of the base metal with the brazing filler metal. Lead, for example, does not alloy with iron and will not wet it. Tin, on the other hand, does form an alloy with iron, and, therefore, a tin-lead solder will wet steel.

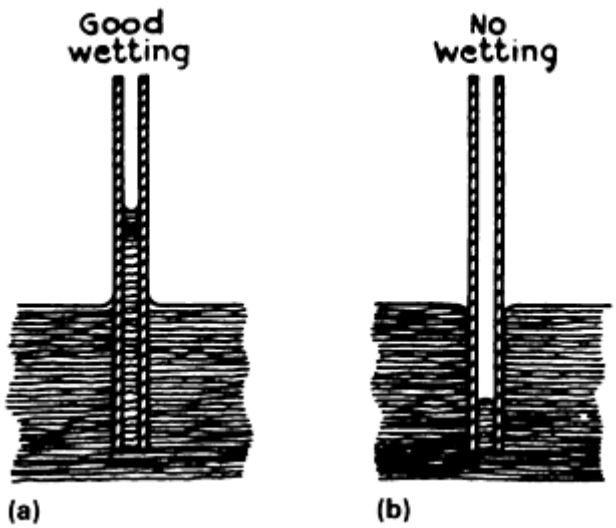

FIG. 1 SCHEMATIC SHOWING PRINCIPLE OF CAPILLARY ATTRACTION FOR SELECTED LIQUIDS WHEN THE LIQUID IS SANDWICHED BETWEEN TWO CLEAN GLASS PLATES. (A) WHEN IMMERSED IN WATER OR INK, A COLUMN WILL RISE BETWEEN THE PLATES BECAUSE OF WETTING. (B) WHEN THE PLATES ARE IMMERSED IN MERCURY, NO WETTING OCCURS AND THE COLUMN IS DEPRESSED. IF PARAFFIN PLATES ARE USED IN PLACE OF THE GLASS PLATES, IMMERSION OF THE PLATES IN MERCURY WILL PRODUCE WETTING.

A comprehensive theory of the wetting or spreading of liquids on solid surfaces and a complete and detailed derivation of the quantitative relationships are presented by Harkins (Ref 3) and Schwartz (Ref 4).

Experimentally, it has been observed that liquids placed on solid surfaces usually do not completely wet, but, rather, remain as a drop that has a definite contact angle between the liquid and solid phases (Ref 5). This condition is illustrated in Fig. 2. The Young and Dupré equation (Eq 1) permits the determination of change in surface free energy, ΔF, accompanying a small change in solid surface covered, ΔA (Ref 5). Thus,

$$\frac{\partial F}{\partial A}_{p,T} = g_{LV} + g_{SL} - g_{SV} \qquad \textbf{(EQ 1)}$$

where γ_{LV} is the liquid-vapor surface energy, γ_{SL} is the solid-liquid surface energy, and γ_{SV} is the solid-vapor surface energy.

$$\Delta F = \Delta A\,(\gamma_{SL} - \gamma_{SV}) + \Delta A \gamma_{LV}\,\mathrm{COS}\,(\theta - \Delta\theta) \qquad \textbf{(EQ 2)}$$

At equilibrium,

$$\lim_{\Delta A \to \Delta 0} \frac{\Delta F}{\Delta A} = 0 \qquad \textbf{(EQ 3)}$$

and

$$\gamma_{SL} - \gamma_{SV} + \gamma_{LV}\,\mathrm{COS}\,\theta = 0 \qquad \textbf{(EQ 4)}$$

or

$$\gamma_{SL} = \gamma_{SV} - \gamma_{LV}\,\mathrm{COS}\,\theta \qquad \textbf{(EQ 5)}$$

In Eq 4 and 5, it can be seen that θ is greater than 90° (1.6 rad) when γ_{SL} is larger than γ_{SV}, as shown in Fig. 3, and the liquid drop tends to spheroidize.

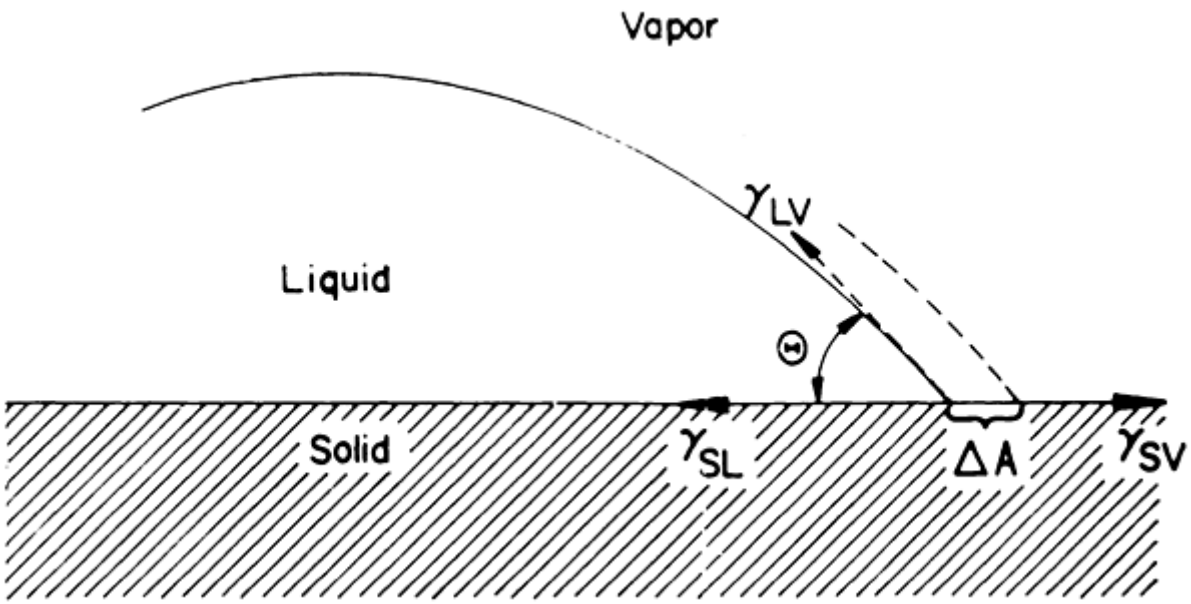

FIG. 2 SESSILE DROP LOCATED ON A SURFACE AND DIRECTIONS OF VECTORS OF THE SURFACE ENERGIES FOR THE SYSTEM

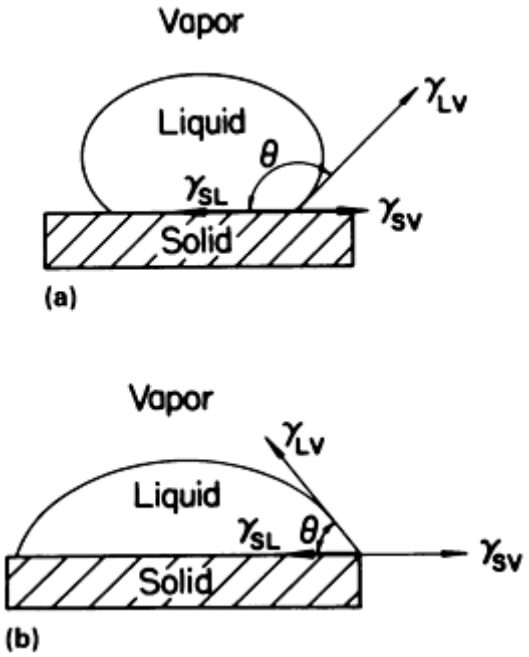

FIG. 3 EFFECT OF INTERFACIAL ENERGIES ON SESSILE DROPS. (A) NO WETTING TAKES PLACE WHEN CONTACT ANGLE IS > 90°. (B) WETTING OCCURS WHEN CONTACT ANGLE IS < 90°.

The contact angle, θ, is less than 90° (1.6 rad) when the reverse is true, as shown at right in Fig. 3, and the liquid drop flattens out and wets the solid. If the balance in such that θ is zero (0 rad) and greater wetting is desired, θ should be as small as possible so that cos θ approaches unity and the liquid spreads over the solid surface.

These considerations show the importance of surface energies in brazing. If brazing filler metal is to successfully form a joint, it must wet the solid material. The surface-energy balance must be such that the contact angle is less than 90° (1.6 rad). The energy equation shows that if θ is to be less than 90° (1.6 rad) (cos θ > 0), then γ_{SV} must be greater than γ_{SL}. This is demonstrated in Table 1, which gives contact-angle measurements of several liquid metals on beryllium at various test temperatures in argon and vacuum.

TABLE 1 CONTACT ANGLES OF SELECTED LIQUID METALS ON BERYLLIUM AT VARIOUS TEST TEMPERATURES IN ARGON AND VACUUM ATMOSPHERES

SYSTEM	ATMOSPHERE	TEMPERATURE		CONTACT ANGLE, DEGREES, AT INDICATED ELAPSED TIME				
		°C	°F	0 s	15 s	45 s	90 s	150 s
AG	VACUUM	1010	1850	142.2	141.1	140.6	141.2	140.2
		1060	1940	135.4	135.6	131.4	133.2	127.9
	ARGON	1010	1850	148.1	148.9	150.7	147.3	143.3
		1060	1940	61.0	59.9	57.2	54.4	52.6
AU	VACUUM	1070	1958	58.6	58.0	57.2	55.7	54.6
	ARGON	1070	1958	57.3	56.6	57.9	56.9	55.9
CU	VACUUM	1108	2026	129.0	128.5	124.2	124.1	123.6
		1133	2071	126.6	122.5	121.8	120.0	120.0
	ARGON	1108	2026	EXTREME BASE-METAL SOLUTION				
		1133	2071	EXTREME BASE-METAL SOLUTION				
GE	VACUUM	1000	1832	145.5	145.3	144.3	143.7	143.6
		1050	1922	102.9	100.0	100.9	96.1	95.4
	ARGON	1000	1832	99.3	99.6	98.8	98.2	97.1

		1050	1922	89.2	89.2	88.9	87.1	87.1
PD-2.1BE	VACUUM	980	1796	77.0	74.0	73.2	70.8	69.9
		1030	1886	74.2	73.2	68.7	66.5	65.6
	ARGON	980	1796	77.2	76.5	76.0	75.0	72.7
		1030	1886	70.2	63.1	61.7	57.2	57.2
AL	VACUUM	710	1310	155.1	154.1	151.3	146.6	142.0
		760	1400	140.0	138.8	136.6	134.1	132.0
	ARGON	710	1310	146.2	139.6	130.5	120.1	116.6
		760	1400	108.2	106.6	102.3	100.0	99.9
ZR-5BE	VACUUM	1030	1886	88.0	85.6	83.9	81.8	80.9
		1080	1976	69.8	67.7	67.3	66.5	64.7
	ARGON	1030	1886	101.4	98.8	99.2	98.3	96.2
		1080	1976	83.6	84.2	84.9	82.4	79.7
TI-6BE	VACUUM	1075	1967	15.8	14.8	14.5	14.0	13.2
		1125	2057	14.2	13.4	12.1	11.2	10.7
	ARGON	1075	1967	13.4	12.0	11.9	9.7	8.6
		1125	2057	10.0	7.9	7.8	6.8	5.6

Although during the testing period minor fluctuations in angle were noted, the overall tendency was for the contact angles to decrease with increasing time at test temperature. This behavior is reflected in the data presented in Table 2. The fluctuations can be attributed to alloying effects, because as alloying progresses, composition and temperature variations change the interfacial energies.

TABLE 2 EFFECT OF TEST CONDITIONS ON INTERFACIAL ENERGIES

SYSTEM	ATMOSPHERE	TEMPERATURE		CONTACT ANGLE[A]		γ_{LV}, DYNES/CM	γ_{LS}, DYNES/CM	FINAL SPREADING COEFFICIENT S_{LS}, DYNES/CM	WORK OF ADHESION (W_{AD}), DYNES/CM
		°C	°F	DEGREES	RADIANS				
AL	VACUUM	710	1310	142.5	2.5	831	2520	-1490	176
		760	1400	132.0	2.3	726	2350	-1210	239
	ARGON	710	1310	116.7	2.0	787	2220	-1140	434
		760	1400	99.9	1.7	561	1960	-658	464
ZR-5BE	VACUUM	1030	1886	79.8	1.4	625	1940	-702	549
		1080	1976	64.6	1.1	520	1770	-427	614
	ARGON	1030	1886	97.0	1.7	488	1780	-405	576
		1080	1976	79.8	1.4	172	1690	-225	569
TI-6BE	VACUUM	1075	1967	13.2	0.2	492[A]	1380	-9.00	970
		1125	2057	10.8	0.2	277	1590	-4.00	548
	ARGON	1075	1967	8.6	0.2	424	1440	-1.00	844
		1125	2057	5.6	0.01	329[B]	1530	+3.00	660

(A) AVERAGE OF TWO TESTS.

(B) ONE TEST ONLY

These data provide a means of comparing the wettability of beryllium by various liquids. If one assumes wettability for contact angles less than 90° and nonwetting for angles greater than 90°, then these data permit qualitative separation of the systems into two classes: those with contact angles less than 90°, and those with contact angles greater than 90°. Gold, Pd-2.1Be, and Ti-6Be were found to wet beryllium at both temperatures. The latter two brazing filler metals, as well as silver and gold, did not wet when tested in argon atmospheres at the lower temperature. However, it was found that an increase of 50 °C (90 °F) resulted in wetting. Aluminum exhibited a nonwetting behavior at both temperatures and in both atmospheres. Copper was nonwetting at both temperatures in vacuum, but underwent extensive alloying with the solid

beryllium at these temperatures in argon. From these data it appears that the binary alloys have the greatest tendency to wet beryllium (Ref 6).

Surface-energy calculations have been performed on beryllium-base metals brazed with Al, Zr-5Be, and Ti-6Be filler metals. The calculated spreading coefficient were negative for all system test conditions, except with Ti-6Be. Negative spreading coefficients indicated a very definite trend. The greater the system wettability, as indicated by lower contact angles and liquid-vapor surface tensions, the greater the numerical magnitude of the spreading coefficient.

Of the three systems used, Ti-6Be was observed to provide the best wetting of beryllium, followed by Zr-5Be. Although no basic significance can be given to the absolute values of the calculated surface-tension properties, they are useful in indicating the relative tendencies for these liquids to wet beryllium.

The above observations indicate that some liquid-metal systems will wet beryllium, whereas some system that should wet it do not, in actual practice. The problem is more complex than it seems at first.

Recent work in Japan (Ref 7) and the United States (Ref 8) has shown that the effects of the base-metal/filler-metal reaction on the wetting of silicon nitride (Si_3N_4) and titanium-added active filler metals vary with reaction-layer thickness and morphology, as well as with the composition of the reaction layer. Several results of thermodynamic studies on the formation of the compound by the interfacial reaction are reported (Ref 7, 9). Moreover, kinetic studies (Ref 7) were also performed to achieve a quantitative understanding of the formation of the reaction layer.

It can be concluded that wetting is the ability of the molten brazing filler metal to adhere to the surface of a metal in the solid state and, when cooled below its solidus temperature, to make a strong bond with that metal. Wetting is a function not only of the nature of the brazing filler metal (Table 3), but of the degree of interaction between materials (ceramics, and so on) to be joined. There is considerable evidence that in order to wet well, a molten metal must be capable of dissolving, or alloying with, some of the metal on which it flows.

TABLE 3 COMPOSITION OF SELECTED FILLER METALS USED FOR BRAZING APPLICATIONS

FILLER METAL	COMPOSITION	LIQUIDUS		SOLIDUS	
		°C	°F	°C	°F
SILVER	99.99AG	961	1762	961	1762
CUSIL	72AG-28CU	780	1436	780	1436
PALCUSIL 5	68AG-27CU-5PD	810	1490	807	1485
PALCUSIL 10	58AG-32CU-10PD	852	1566	824	1515
PALCUSIL 15	65AG-20CU-15PD	900	1650	850	1560
PALCUSIL 25	54AG-21CU-25PD	950	1740	900	1650
GAPASIL 9	82AG-9GA-9PD	880	1615	845	1555
NICUSIL 3	71.5AG-28.1CU-0.75NI	795	1465	780	1435
NICUSIL 8	56AG-42CU-2NI	893	1639	771	1420
T50	62.5AG-32.5CU-5NI	866	1591	780	1435
T51	75AG-24.5CU-0.5NI	802	1476	780	1435
T52	77AG-21CU-2NI	830	1525	780	1435
CUSILTIN 5	68AG-27CU-5SN	760	1400	743	1369
CUSILTIN 10	60AG-30CU-10SN	718	1324	602	1116
BRAZE 630	63AG-28CU-6SN-3NI	800	1472	690	1275
BRAZE 580	57AG-33CU-7SN-3MN	730	1345	605	1120
BRAZE 655	65AG-28CU-5MN-2NI	850	1560	750	1380
SILCORO 60	60AU-20AG-20CU	845	1550	835	1535
NIORO	82AU-18NI	950	1740	950	1740
PALNIRO 7	70AU-22NI-8PD	1037	1899	1005	1840
INCURO 60	60AU-37CU-3IN	900	1650	860	1580
SILCORO 75	75AU-20CU-5AG	895	1645	885	1625

NICORO 80	81.5AU-16.5CU-2NI	925	1695	910	1670
PALCUSIL 20	52AU-28CU-20PD	925	1695	875	1605
GOLD	99.99AU	1064	1947	1064	1947
PALNIRO 4	30AU-36NI-34PD	1169	2136	1135	2075
PALNIRO 1	50AU-25NI-25PD	1121	2050	1102	2016
TICUSIL	68.8AG-26.7CU-4.5TI	850	1560	830	1525
PALNICUSIL	48AG-18.9CU-10NI-22.5PD	1179	2154	910	1670
PALCO	65PD-35CO	1235	2255	1230	2245
INCUSIL15	62AG-24CU-15IN	705	1300	630	1165
INCUSIL 10	63AG-27CU-10IN	730	1345	685	1265
BAG-8A	71.8AG-28CU-0.2LI	760	1400	760	1400
BAG-19	92.5AG-7.3CU-0.2LI	890	1635	760	1400
BRAZE 071	85CU-7AG-8SN	986	1807	665	1230
BRAZE 852	85AG-15MN	970	1780	960	1760
NIORONI	73.8AU-26.2NI	1010	1850	980	1795
NICUMAN 23	67.5CU-23.5MN-9NI	955	1750	925	1695
PALSIL 10	90AG-10PD	1065	1950	1002	1836
PALNI	60PD-40NI	1238	2260	1238	2260

Wetting is only one facet of the brazing process. Another factor that affects wetting is the cleanliness of the surface to be wetted. Oxide layers inhibit wetting and spreading, as do grease, dirt, and other contaminants that prevent good contact between the brazing filler metal and the base metal. One of the functions of a flux the oxide layer on the joint area and thereby expose clean base metal.

Good wetting and spreading of the liquid filler metal on the base metal are necessary in brazing because the mechanics of the process demand that the filler metal be brought smoothly, rapidly, and continuously to the joint opening. If the conditions within the capillary space of the joint do not promote good wetting, then the filler metal will not be drawn into the space by capillary attraction.

Kim *et al.* (Ref 10) investigated the wettability and reactivity of pressureless sintered Si_3N_4 with powdered copper-titanium filler metal using sessile drop tests conducted in a vacuum where Si_3N_4 was bonded to itself and joint strength was evaluated by shear testing. The wettability of Si_3N_4 on copper-titanium base filler metals was improved greatly by adding up to 50 wt% titanium. However, the reaction-layer thickness was increased up to 10% and, thereafter, decreased up to 50 wt%.

Wettability improved with the increment of titanium concentration, and no linear proportionality was found between the reaction and the wettability. As titanium concentration increased, a continuous thin layer tended to form at the interface and markedly improved wettability.

The thickness of the reaction layer was not in proportion to the titanium concentration. For a copper-titanium filler metal with a low titanium concentration (less than 5 wt%), the initial reaction layer tended to form discontinuously, whereas the reaction layer thickness increased with titanium concentration. On the contrary, in the filler metal with a high titanium concentration (15 wt%) the reaction-layer thickness decreased as titanium concentration increased because a continuous thin reaction layer tended to form (Ref 10).

The shear strength of the Si_3N_4-Si_3N_4 joint using copper-titanium filler metal is influenced by reaction-layer thickness and morphology. Strength increased with the increment of titanium concentration, and was accompanied by improved wettability, because the tendency of the continuous thin reaction layer to form increased.

With the development of new steels, Keller *et al.* (Ref 11) undertook an extensive study of the wettability of commercial braze filler metals on type 304 stainless steel, the most common of the austenitic stainless steels; type 316 stainless steel, which is often substituted for type 304 when increased corrosion resistance is desired; and 21-6-9, a new high-manganese stainless steel that is an attractive alternative to types 304 or 316 for certain applications. Because the 21-6-9 steel has a very stable austenitic structure, it is attractive for cryogenic applications (Ref 12).

Because high wettability means that the thermocapillary attraction that fills the braze joint is strong, wettability is an important component of braze performance. The wettability index (WI) developed by Feduska (Ref 13) is used as the measure of wettability. The WI is defined as the area covered by the braze metal filler times the cosine of the contact angle between the braze and the base metal. Therefore, the higher the WI, the better the braze filler metal wets the base metal. It should be emphasized that the WI, as defined, is a relative measure, and depends on the volume of filler metal used (Table 4).

TABLE 4 WETTABILITY INDICES OF BRAZE FILLER METALS ON SELECTED STAINLESS STEEL BASE METALS

FILLER METAL	TEST TEMPERATURE		WETTABILITY INDEX FOR INDICATED STAINLESS STEEL BASE METAL		
	°C	°F	TYPE 316	21-6-9	TYPE 304
SILVER	975	1785	. . .	. . .	. . .
	1000	1830	0.008	. . .	0.015
	1050	1920	0.041	. . .	0.023
	1100	2010	0.053	. . .	0.020
	1150	2100	. . .	. . .	. . .
CUSIL	800	1470	. . .	0.013	. . .
	850	1560	. . .	0.007	. . .
	900	1650	0.022	0.016	0.003
	925	1695	0.032	. . .	. . .
	950	1740	0.037	. . .	. . .
PALCUSIL 5	800	1470	0.027	. . .	. . .
	850	1560	. . .	0.014	. . .
	900	1650	0.047	0.020	0.011
	950	1740	0.080	0.061	0.035
PALCUSIL 10	850	1560	0.035	0.020	0.015
	900	1650	0.057	0.050	0.025
	950	1740	0.107	0.101	0.062
PALCUSIL 15	900	1650	0.107	0.092	0.068
	950	1740	0.152	0.170	0.119
	1000	1830	0.754	0.263	0.212
PALCUSIL 25	950	1740	0.104	0.107	0.096
	975	1785	0.225	. . .	. . .
	1000	1830	. . .	0.283	0.226
GAPASIL 9	900	1650	0.023	. . .	. . .
	950	1740	0.068	. . .	. . .
	1000	1830	0.269	. . .	. . .
NICUSIL 3	800	1470	0.006	0.000	0.012
	850	1560	0.027	0.017	0.008
	900	1650	0.041	0.039	0.021
	925	1695	0.051	. . .	. . .
	950	1740	0.064	. . .	. . .
NICUSIL 8	850	1560	0.024	. . .	. . .
	900	1650	0.052	. . .	0.033
	950	1740	0.085	. . .	0.064
	1000	1830	. . .	. . .	0.229
T-50	850	1560	0.024	. . .	. . .
	900	1650	0.038	. . .	0.026

FILLER METAL	TEST TEMPERATURE		WETTABILITY INDEX FOR INDICATED STAINLESS STEEL BASE METAL		
	°C	°F	TYPE 316	21-6-9	TYPE 304
	950	1740	0.062	. . .	0.057
	1000	1830	. . .	. . .	. . .
T-51	800	1470	0.007	. . .	. . .
	850	1560	0.029	. . .	. . .
	900	1650	0.039	. . .	. . .
	950	1740	. . .	. . .	0.029
	1000	1830	. . .	. . .	0.082
T-52	850	1560	0.027	. . .	0.001
	900	1650	0.045	. . .	0.014
	950	1740	0.063	. . .	0.045
	1000	1830	. . .	. . .	0.090
CUSILTIN 5	850	1560	0.015	. . .	0.000
	875	1605	0.043	. . .	. . .
	900	1650	0.047	. . .	0.013
	950	1740	. . .	. . .	0.033
	1000	1830	. . .	. . .	. . .
CUSILTIN 10	750	1380	. . .	0.025	0.000
	800	1470	. . .	0.017	0.023
	825	1515	0.021	. . .	. . .
	850	1560	0.034	0.051	0.050
	875	1605	0.043	. . .	. . .
BRAZE 630	800	1470	0.014	0.037	0.023
	850	1560	0.046	0.065	0.024
	900	1650	0.064	. . .	. . .
BRAZE 580	750	1380	0.020	0.060	0.060
	800	1470	0.051	0.056	0.089
	850	1560	0.073	0.120	0.102
	875	1605	0.078	. . .	. . .
BRAZE 655	825	1515	0.080	. . .	. . .
	850	1560	0.110	0.037	0.074
	875	1605	0.116	. . .	. . .
	900	1650	. . .	0.137	0.124
SILCORO 60	850	1560	. . .	0.005	0.004
	900	1650	0.039	0.007	0.011
	925	1695	0.051	. . .	. . .
	950	1740	0.073	0.025	0.016
	1000	1830	. . .	0.055	0.037
NIORO	950	1740	. . .	0.000	0.000
	975	1785	0.049	. . .	. . .
	1000	1830	0.061	0.060	0.065
PALNIRO 7	1025	1875	. . .	. . .	. . .
	1050	1920	0.053	. . .	. . .
	1075	1965	0.073	. . .	. . .
INCURO 60	900	1650	0.010	. . .	. . .
	950	1740	0.025	. . .	. . .
	1000	1830	0.091	. . .	. . .
SILCORO 75	900	1650	0.006	. . .	. . .

FILLER METAL	TEST TEMPERATURE		WETTABILITY INDEX FOR INDICATED STAINLESS STEEL BASE METAL		
	°C	°F	TYPE 316	21-6-9	TYPE 304
	950	1740	0.057	. . .	. . .
	1000	1830	0.170	. . .	. . .
NICORO 80	950	1740	0.041	0.019	0.016
	1000	1830	0.163	0.126	0.070
	1050	1920	0.413	0.190	0.084
PALCUSIL 20	875	1610	0.061	. . .	. . .
	900	1650	0.110	. . .	. . .
	925	1695	0.122	. . .	. . .
GOLD	1070	1960	. . .	. . .	0.088
	1075	1965	0.087	. . .	. . .
	1100	2010	0.358	. . .	0.238
	1150	2100	. . .	. . .	0.355
PALNIRO 4	1175	2145	0.036	. . .	. . .
	1200	2190	0.061	. . .	. . .
	1225	2235	0.078	. . .	. . .
PALNIRO 1	1125	2055	0.041	. . .	. . .
	1150	2100	0.063	. . .	. . .
	1175	2145	0.075	. . .	. . .
TICUSIL	875	1605	0.032	. . .	. . .
	900	1650	0.057	. . .	. . .
	950	1740	0.083	. . .	. . .
PALNICUSIL	950	1740	0.025	. . .	0.038
	975	1785	0.213	. . .	. . .
	1000	1830	. . .	. . .	. . .
	1025	1875	0.362	. . .	. . .
	1050	1920	. . .	. . .	. . .
	1075	1965	0.336	. . .	. . .
	1100	2010	. . .	. . .	. . .
PALCO	1250	2280	0.000	. . .	. . .
	1275	2325	0.073	. . .	. . .
	1300	2370	0.159	. . .	. . .
INCUSIL 15	750	1380	. . .	. . .	. . .
	800	1470	. . .	. . .	. . .
	850	1560	. . .	. . .	. . .
INCUSIL 10	750	1380	. . .	. . .	. . .
	800	1470	. . .	. . .	. . .
	850	1560	0.008	. . .	. . .
BAG-8A	800	1470	0.005	. . .	. . .
	850	1560	0.008	. . .	. . .
	900	1650	0.032	. . .	. . .
	950	1740	0.045	. . .	. . .
BAG-19	950	1740	0.016	. . .	. . .
	1000	1830	0.016	. . .	. . .
	1050	1920	0.034	. . .	. . .
BRAZE 071	1000	1830	0.066	0.106	0.101
	1050	1920	. . .	0.125	0.101
BRAZE 852	1000	1830	0.039	0.037	0.038

FILLER METAL	TEST TEMPERATURE		WETTABILITY INDEX FOR INDICATED STAINLESS STEEL BASE METAL		
	°C	°F	TYPE 316	21-6-9	TYPE 304
	1050	1920	0.029	0.038	0.042
	1100	2010	0.043	0.037	0.020
NIORONI	1000	1830	0.068	. . .	. . .
	1025	1875	0.070	. . .	. . .
	1100	2010	0.116	. . .	. . .
NICUMAN 23	950	1740	0.026	. . .	. . .
	975	1785	0.099	. . .	. . .
	1000	1830	0.091	. . .	. . .
	1025	1875	0.091	. . .	. . .
PALSIL 10	1050	1920	0.113	. . .	. . .
	1075	1965	0.113	. . .	. . .
	1100	2010	0.126	. . .	. . .
PALNI	1225	2235	. . .	. . .	. . .
	1250	2280	0.068	. . .	. . .
	1275	2325	0.078	. . .	. . .
	1300	2370	0.107	. . .	. . .
PALMANSIL 5	950	1740	. . .	. . .	0.057
	1000	1830	. . .	. . .	. . .
	1050	1920	. . .	. . .	. . .
	1100	2010	. . .	. . .	. . .

The WIs for each braze filler metal at each temperature on type 316 stainless steel, type 304L stainless steel, and 21-6-9 stainless steel are provided in Table 4. Wetting indices greater than 0.05 are indicative of good performance during brazing, whereas WI values greater than 0.10 are indicative of excellent performance during brazing (Ref 13).

A comparison of the WI of the braze filler metals on the three stainless steels revealed these trends:

- FILLER METALS GENERALLY WET TYPE 316 STAINLESS STEEL BETTER THAN TYPE 304 STAINLESS STEEL AND GENERALLY WET TYPE 316 STAINLESS BETTER THAN 21-6-9 STAINLESS.
- THE DEGREE OF WETTING OF MOST BRAZE FILLER METALS ON 21-6-9 STAINLESS WAS EQUAL TO OR BETTER THAN IT WAS ON TYPE 304 STAINLESS (REF 12).
- THE IMPROVED WETTABILITY OF BRAZE FILLER METALS ON TYPE 316 STAINLESS IS BELIEVED TO BE DUE TO THE PRESENCE OF MOLYBDENUM IN THE SURFACE OXIDE, WHEREAS THE ENHANCED WETTING ON 21-6-9 STAINLESS VERSUS TYPE 304 STAINLESS IS BELIEVED TO BE DUE TO THE HIGHER MANGANESE CONTENT OF THE SURFACE OXIDE.

Essentially, the successful joining of components by the brazing process depends on the selected brazing filler metal having a melting point above 450 °C (840 °F) and wetting the base metal without melting it. Furthermore, the joint must be designed to ensure that the mating surfaces of the components are parallel and close enough together to cause capillary attraction.

Mel M. Schwartz, Sikorsky Aircraft

Elements of the Brazing Process

An engineer must consider reliability and cost when designing the braze joint. Joint strength, fatigue resistance, corrosion susceptibility, and high-temperature stability are additional concerns that determine the selection of joint design, braze filler materials, and processing parameters.

A careful and intelligent appraisal of the following elements is required in order to produce satisfactory brazed joints:

- FILLER-METAL FLOW
- BASE-METAL CHARACTERISTICS
- FILLER-METAL CHARACTERISTICS
- SURFACE PREPARATION
- JOINT DESIGN AND CLEARANCE
- TEMPERATURE AND TIME
- RATE AND SOURCE OF HEATING
- PROTECTION BY AN ATMOSPHERE OR FLUX

Filler-Metal Flow. As mentioned previously, wetting is only one important facet of the brazing process. A low contact angle, which implies wetting, is also necessary, but is not a sufficient condition itself for flow. Viscosity is also important. Brazing filler metals with narrow melting ranges that are close to the eutectic composition generally have lower viscosities than those with wide melting ranges. Thus, a high surface tension of liquid filler metal, a low contact angle, and low viscosity are all desirable.

Flowability is the property of a brazing filler metal that determines the distance it will travel away from its original position, because of the action of capillary forces. To flow well, a filler metal must not gain an appreciable increase in its liquidus temperature even though its composition is altered by the addition of the metal it has dissolved. This is important because the brazing operation is carried out at temperatures just above the liquidus of the filler metal.

The composition and surface energy of liquids and solids are assumed to remain constant. In real systems, however, these interactions occur (Ref 14):

- ALLOY FORMATION BETWEEN LIQUID AND BASE METAL
- DIFFUSION OF BASE METAL INTO BRAZING FILLER METAL
- DIFFUSION OF FILLER METAL INTO GRAINS OF BASE METAL
- PENETRATION OF FILLER METAL ALONG GRAIN BOUNDARIES
- FORMATION OF INTERMETALLIC COMPOUNDS

In practice, interactions are usually minimized by selecting the proper brazing filler metal; keeping the brazing temperature as low as possible, but high enough to produce flow; and keeping the time of brazing temperature short and cooling the brazed joint as quickly as possible without causing cracking or distortion. When diffusion brazing is desired, higher brazing temperatures and longer times at brazing temperatures are employed.

Base-Metal Characteristics. The base metal has a prime effect on joint strength. A high-strength base metal produces joints of greater strength than those made with softer base metals (other factors being equal). When hardenable metals are brazed, joint strength becomes less predictable. This is because more-complex metallurgical reactions between hardenable base metals and the brazing filler metals are involved. These reactions can cause changes in the base-metal hardenability and can create residual stresses (Ref 15).

In cases where different materials make up the assembly and gaps may open or close as heating proceeds to the joining temperature, the coefficient of thermal expansion becomes vitally important.

Several metallurgical phenomena influence the behavior of brazed joints and, in some instances, necessitate special procedures. These base-metal effects include alloying by brazing filler; carbide precipitation; stress cracking; hydrogen, sulfur, and phosphorus embrittlement; and oxidation stability.

The extent of interaction varies greatly, depending on compositions (base metal and brazing filler metal) and thermal cycles. There is always some interaction, except in cases of mutual insolubility.

The strength of the base metal has a profound effect on the strength of the brazed joint. Therefore, this property must be carefully considered when designing the joint to have specific properties. Some base metals also are easier to braze than others, particularly by specific brazing processes.

Filler-Metal Characteristics. The second material involved in joint structures is the brazing filler metal. Unfortunately, it cannot be chosen to provide a specific joint strength. Actually, strong joints can be brazed with almost any good commercial brazing filler metal if correct brazing methods and joint design are implemented.

Necessary characteristics of brazing filler metals are:

- PROPER FLUIDITY AT BRAZING TEMPERATURES TO ENSURE FLOW BY CAPILLARY ACTION AND TO PROVIDE FULL ALLOY DISTRIBUTION
- STABILITY TO AVOID PREMATURE RELEASE OF LOW-MELTING-POINT ELEMENTS IN THE BRAZING FILLER METAL
- ABILITY TO WET THE BASE-METAL JOINT SURFACE
- LOW VOLATILIZATION OF ALLOYING ELEMENTS OF THE BRAZING FILLER METAL AT BRAZING TEMPERATURES
- ABILITY TO ALLOY OR COMBINE WITH THE BASE METAL TO FORM AN ALLOY WITH A HIGHER MELTING TEMPERATURE
- CONTROL OF WASHING OR CONTROL OF EROSION BETWEEN THE BRAZING FILLER METAL AND THE BASE METAL WITHIN THE LIMITS REQUIRED FOR THE BRAZING OPERATION

It should be noted that the strength of the brazed joint is not directly related to the method of filler-metal melting. For example, if constructional metals are produced by vacuum melting, then there is a definite relationship between the vacuum-melting practice and the final strength of the ingot, bar, or rolled sheet. With a brazing filler metal, however, joint strength is dependent on joint design, brazing temperature, amount of brazing filler metal applied, location and method of application, heating rate, and many other factors that constitute the brazing technique.

The degree to which brazing filler metal interacts with and penetrates the base metal during brazing depends on the intensity of mutual diffusion processes that occur between both those materials. In applications that require strong joints for high-temperature, high-stress service conditions (such as turbine rotor assemblies and jet-engine components), it is generally wise to specify a brazing filler metal that has high diffusion and solution properties with the base metal. When the assembly is constructed of extremely thin base metals (as in honeycomb structures and some heat exchangers), good practice entails specifying a brazing filler metal that contains elements with a low-diffusion characteristic relative to the base metal being used. Diffusion, a normal part of the metallurgical process, can contribute to good brazed joints when brazing, for example, high-temperature metals with nickel-base brazing filler metals.

Brazing Temperature. When choosing a brazing filler metal, the first selection criterion is the brazing temperature. Some brazing-temperature ranges are given in Table 5. Very few brazing filler metals possess narrow melting ranges. Brazing filler metals in which the solidus and liquidus temperatures are close together do not usually exhibit a strong tendency to coexist as a mixture of liquid and solid phases or to liquate. They flow readily and should be used with small joint clearances. As the solidus and liquidus temperatures diverge, the tendency to liquate increases, requiring greater precautions in brazing filler metal application. The mixture of solid and liquid metal can aid gap filling.

TABLE 5 JOINING TEMPERATURES FOR FILLER METALS USED IN BRAZING APPLICATIONS

BRAZING FILLER-METAL GROUPS	JOINING TEMPERATURE	
	°C	°F
NI, CO, AND PD ALLOYS	[GES]1100	[GES]2012
CU, NI, AND AU ALLOYS	[GES]1100	[GES]2012
CU-ZN, CU-SN, NI-P, NI-CR-P, PD-AG-CU	[GES]900	[GES]1652
CU-P, CU-AG-P	600-800	1112-1472
AG-CU-ZN, AG-CU-ZN-CD	600-800	1112-1472
AL-SI	580-600	1076-1112
MG-AL-ZN	585-615	1085-1139

The necessity for the brazing filler metal to melt below the solidus of the base metal is just one of several factors that affect its selection. It may be necessary for the brazing filler metal to melt below the temperature at which parts to be brazed lose strength or above the temperature at which oxides are reduced or dissociated. Joining may have to be carried out above the solution-treatment temperature of the base metal, or at a structure refining temperature, or below the remelt temperature of a brazing filler metal used previously in the production of a brazed subassembly.

Liquidation. During melting, the composition of the liquid and solid filler metal phases changes as the temperature increases from the solidus to the liquidus point. If the portion that melts first is allowed to flow out, then the remaining solid phases have higher melting points than the original composition and may never melt, remaining behind as a residue, or "skull." Filler metals with narrow melting ranges do not tend to separate, but flow quite freely in joints of extremely narrow clearance as long as the solution and diffusion rates of the filler metal with the base metal are low (as in aluminum brazing, the use of silver filler metal on copper, and so on). The rapid heating of filler metals with wide melting ranges or their application to the joint after the base metal reaches brazing temperature will minimize the separation, or liquation. However, liquation cannot be entirely eliminated and wide-melting-range filler metals, which tend to have more sluggish flow, will require wider joint clearances and will form larger fillets at the joint extremities. A few brazing filler metals become sufficiently fluid below the actual liquidus temperature, and satisfactory joints are achieved, even though the liquidus temperature has not been reached.

When sluggish behavior is needed, such as in filling large gaps, brazing can be accomplished within the melting range of the filler metal. However, the brazing temperature is usually 10 to 93 °C (20 to 170 °F) above the liquidus of the filler metal. The actual temperature required to produce a good joint filling is influenced by factors such as heating rate, brazing environment (atmosphere or flux), thickness of parts, thermal conductivity of the metals being joined, and type of joint to be made.

Large-scale mechanical properties of brazing filler metals can be a guideline for their suitability (in terms of strength, oxidation resistance, and so on) for use in different capillary joining applications. However, designers cannot use the mechanical properties of brazed assemblies that are related to different joint configurations brazed at given cycles of time and temperatures.

The placement of the brazing filler metal is an important design consideration, not only because the joint must be accessible to the method chosen, but because, in automatic heating setups, the filler metal must be retained in its location until molten. Brazing filler metals are available in different forms (Table 6) and filler-metal selection may depend on which form is suitable for a particular joint design.

TABLE 6 AVAILABLE PRODUCT FORMS OF BRAZING FILLER METALS CATEGORIZED BY GROUP

BRAZING FILLER-METAL GROUPS	AVAILABLE FORMS[A]											
	AD	CL	FL	FO	PA	PB	PO	PR	SH	RD	SP	WI
NI AND CO ALLOYS	X	. . .	X	[B]	X	X	X	[B]	X	[B]	. . .	[C]
PD ALLOYS	. . .	. . .	X	X	. . .	. . .	X	X	X	. . .	X	X
CU AND AU ALLOYS	. . .	. . .	X	X	X	. . .	X	X	X	. . .	X	X

NI ALLOYS	X	. . .	X	(B)	X	X	X	(B)	X	(B)	. . .	(C)
CU-SN, CU-ZN, PD-AG-CU	. . .	. . .	X	X	. . .	. . .	X	X	X	. . .	X	X
NI-P, NI-CR-P	X	. . .	. . .	. . .	X	X	X	. . .	. . .	. . .	. . .	. . .
CU-P, CU-AG-P	. . .	. . .	. . .	. . .	X	. . .	X	. . .	. . .	. . .	X	X
AG-CU-ZN, AG-CU-ZN-CD	. . .	. . .	X	X	. . .	. . .	X	X	X	. . .	X	X
AL-SI	. . .	X	. . .	. . .	. . .	. . .	X	. . .	X	. . .	. . .	X
MG-AL-ZN	. . .	. . .	. . .	. . .	. . .	. . .	. . .	. . .	X	. . .	X	X

(A) AD, ADHESIVE SHEET; CL, CLADDING; FL, FLUX PASTE; FO, FOIL; PA, PASTE (NONFLUXING); PB, PLASTIC-BONDED SHEET; PO, POWDER; PR, PREFORM; SH, SHIM; RD, ROD; SP, STRIP; WI, WIRE.

(B) A FEW ALLOYS ONLY.

(C) PLASTIC BOND

Several general rules apply in the filler-metal placement. Wherever possible, the filler metal should be placed on the most slowly heated part of the assembly in order to ensure complete melting. Although brazing is independent of gravity, gravity can be used to assist filler-metal flow, particularly for those filler metals having wide ranges between their solidus and liquidus temperatures. Brazing filler metals can be chosen to fill wide gaps or to flow through joint configurations where the gap may vary, for example, around a corner. Unless movement between the components being joined is unimportant or can be corrected manually (through self-jigging or by using fixtures after the filler metal is molten), the filler metal should be placed outside the joint and allowed to flow into it. It should not be placed between the joint members. If erosion of thin members is possible, then the brazing filler metal should be placed on the heavier sections, which heat up more slowly, so that flow proceeds toward the thin sections. Apart from suiting the placement method selected for the joint, the form chosen for the brazing filler metal may be needed to accurately gage the amount applied, not just for economy and reproducibility, but to regulate and maintain joint properties and configuration.

Surface Preparation. A clean, oxide-free surface is imperative to ensure uniform quality and sound brazed joints. All grease, oil, dirt, and oxides must be carefully removed from the base and filler metals before brazing, because only then can uniform capillary attraction be obtained. Brazing should be done as soon as possible after the material has been cleaned. The length of time that the cleaning remains effective depends on the metals involved, atmospheric conditions, storage and handling practices, and other factors. Cleaning operations are commonly categorized as being either chemical or mechanical. Chemical cleaning is the most effective means of removing all traces of oil or grease. Trichloroethylene and trisodium phosphate are the usual cleaning agents employed. Oxides and scale that cannot be eliminated by these cleaners should be removed by other chemical means.

The selection of the chemical cleaning agent depends on the nature of the contaminant, the base metal, the surface condition, and the joint design. Regardless of the nature of the cleaning agent or the cleaning method used, it is important that all residue or surface film be adequately rinsed from the cleaned parts to prevent the formation of other equally undesirable films on the faying surfaces.

Objectionable surface conditions can be removed by mechanical means, such as grinding, filing, wire brushing, or any form of machining, provided that joint clearances are not disturbed. When grinding the surfaces of the parts to be brazed, care should be exercised to ensure that the coolant is clean and free from impurities to avoid grinding these impurities into the finished surfaces.

When faying surfaces of parts to be brazed are prepared by blasting techniques, several factors should be considered. There are two purposes behind the blasting of parts to be brazed. One is to remove any oxide film and the other is to roughen the mating surfaces in order to increase capillary attraction of the brazing filler metal. The blasting material must be clean and must not leave any deposit on the surfaces to be joined that restricts filler-metal flow or impairs brazing. The particles of the blasting material should be angular rather than spherical, so that the blasted parts are lightly roughened, rather than peened, after the scale is removed. The operation should not distort or otherwise harm delicate parts. Vapor blasting and similar wet blasting methods require care, because of the possibility of surface contamination.

Mechanical cleaning may be adequate, in which case it should be permitted (by the design) during manufacture. In those cases that require chemical cleaning, the cleaning operation may be followed by protective electroplating, which necessitates access to the faying surface by the liquids involved.

Another surface protection technique is the use of solid and liquid brazing fluxes. At temperatures up to about 1000 °C (1830 °F), fluxes often provide the easiest method of maintaining or producing surface cleanliness. In such cases, the design must not only permit easy ingress of the flux, but should allow the filler metal to wash it through the joint. Above 1000 °C (1830 °F), the flux residues can be difficult to remove, and surface cleaning can be accompanied by brazing in furnaces with protective atmospheres. However, the design must permit the gas to penetrate the joint.

In addition to cleanliness and freedom from oxides, another important factor in determining the ease and evenness of brazing filler metal flow is surface roughness. Generally, a liquid that wets a smooth surface will wet a rough one even more. A rough surface will modify filler-metal flow from laminar to turbulent, prolonging flow time and increasing the possibility of alloying and other interactions. Surfaces often are not truly planar, and, in some instances, surface roughening will improve the uniformity of the joint clearance. A rough surface features a series of crests and troughs that produce turbulent flow. These irregularities on the surface simulate grips to prevent the flow of the filler metal.

Conversely, there may be a requirement that brazing filler metal not flow onto some surfaces. Stop-off materials will often avoid flow, but the design must permit easy application of the stop-off material without contaminating the surfaces to be joined.

Self-fluxing filler metals, in a suitably protective environment such as vacuum, may provide the essential surface wetting.

Joint Design and Clearance. A brazed joint is not a homogeneous body. Rather, it is a heterogeneous area that is composed of different phases with different physical and chemical properties. In the simplest case, it consists of the base-metal parts to be joined and the added brazing filler metal. However, dissimilar materials must also be considered.

Small clearances are used because the smaller the clearance, the easier it is for capillarity to distribute the brazing filler metal throughout the joint area and the less likely it is that voids or shrinkage cavities will form as the brazing filler metal solidifies. The optimum joints are those in which the entire joint area is wetted and filled by the brazing filler metal. Typically, brazing clearances that range from 0.03 to 0.08 mm (0.001 to 0.003 in.) are designed for the best capillary action and greatest joint strength.

Because brazing relies on capillary attraction, the design of a point must provide an unobstructed and unbroken capillary path to enable the escape of flux, if used, as well as allow the brazing filler metal into the joint. In cases where filler metal is added to a joint by hand, such as by feeding in a rod or wire, the joint entry must be visible and accessible.

Some of the more-important factors influencing joint design are the required strength and corrosion resistance, the necessary electrical and thermal conductivity, the materials to be joined, the mode of application of the brazing filler metal, and the postjoining inspection needs.

Consideration also should be given to the ductility of the base metal, the stress distribution in the joint, and the relative movements of the two surfaces during joining, which may introduce distortion in dimensions of the work to be brazed.

Viscosity, surface tension, and specific gravity of the brazing filler metal are not the only factors that determine the gap-filling capability of a given filler metal. Joint strength increases as joint gap decreases, down to a minimum. Table 7 gives the allowable joint clearances for various filler-metal systems. Other factors that influence optimum joint gap with a specific brazing filler metal are joint length, brazing temperature, and base-metal/filler-metal metallurgical reactions.

TABLE 7 RECOMMENDED GAP FOR SELECTED BRAZE FILLER METALS

BRAZING FILLER-METAL SYSTEM	JOINT CLEARANCE	
	mm	in.
AL-SI ALLOYS[(A)]	0.15-0.61	0.006-0.024
MG ALLOYS	0.10-0.25	0.004-0.010
CU	0.00-0.05	0.000-0.002
CU-P	0.03-0.13	0.001-0.005
CU-ZN	0.05-0.13	0.002-0.005
AG ALLOYS	0.05-0.13	0.002-0.005

AU ALLOYS	0.03-0.13	0.001-0.005
NI-P ALLOYS	0.00-0.03	0.000-0.001
NI-CR ALLOYS(B)	0.03-0.61	0.001-0.024
PD ALLOYS	0.03-0.10	0.001-0.004

(A) IF JOINT LENGTH IS LESS THAN 6 MM (0.240 IN.), GAP IS 0.12 TO 0.75 MM (0.005 TO 0.030 IN.). IF JOINT LENGTH EXCEEDS 6 MM (0.240 IN.), GAP IS 0.25 TO 0.60 MM (0.010 TO 0.24 IN.).

(B) MANY DIFFERENT NICKEL BRAZING FILLER METALS ARE AVAILABLE, AND JOINT GAP REQUIREMENTS MAY VARY GREATLY FROM ONE FILLER METAL TO ANOTHER

It is important to remember that an assembly expands during heating and that the joint gap can either widen or close by the time the brazing filler metal starts to melt and move. It is desirable to design the joint to expose the solidifying filler metal to compressive, rather than tensile, stress. This is much more important in brazing than in soldering, because brazing temperatures are higher, increasing the total thermal expansion. With cylindrical joints, the components with the larger coefficient of expansion should be on the outside, whenever possible.

Joint clearance is probably one of the most significant factors in vacuum brazing operations. Naturally, it receives special consideration when joint are designed at room temperature. Actually, joint clearance is not the same at all phases of brazing. It will have one value before brazing, another value at the brazing temperature, and still another value after brazing, especially if there has been a substantial interaction between the brazing filler metal and the base metal. To avoid confusion, it has become general practice to specify joint clearance as the value at room temperature before brazing.

The recommended joint clearances given in Table 7 are based on joints that have members of similar metals and equal mass. When dissimilar metals and/or metals of widely differing masses are joined by brazing, special problems arise. These problems necessitate specialized selection of brazing filler metals. Furthermore, the most suitable joint clearance for the specific job must be carefully determined. Thus, clearances given in Table 7 are the clearances that must be attained at the brazing temperature.

Although there are many kinds of brazed joints, the selection of joint type is not as complicated as it may seem, because butt and lap joints are the two fundamental types used. All other types, such as the scarf joint, are modifications of these two. The scarf joint of the scarf angle. It approaches the lap joint at the other extreme of the scarf angle.

Selection of joint type is influenced by the configuration of the parts, as well as by joint strength and other service requirements, such as electrical conductivity, pressure tightness, and appearance. Also influential in the selection of joint type are fabrication techniques, production quantities, and methods of feeding brazing filler metal. Lap joints are generally preferred for brazing operations, particularly when it is important that the joints be at least as strong as the weaker member. For maximum strength, lap-joint length should equal three to four times the thickness of the thinner member.

Temperature and Time. The temperature of the brazing filler metal has an important effect on the wetting and alloying action, which increases with increasing temperature. The temperature must be above the melting point of the brazing filler metal and below the melting point of the parent metal. Within this range, a brazing temperature that is most satisfactory overall is generally selected.

Usually, low brazing temperatures are preferred in order to economize on the heat energy required, minimize the heat effect on the base metal (annealing, grain growth, or warpage, for example), minimize base-metal/filler-metal interactions, and increase the life of fixtures, jigs, or other tools.

Higher brazing temperatures may be desirable so as to:

- ENABLE THE USE OF A HIGHER-MELTING, BUT MORE ECONOMICAL, BRAZING FILLER METAL
- COMBINE ANNEALING, STRESS RELIEF, OR HEAT TREATMENT OF THE BASE METAL WITH BRAZING
- PERMIT SUBSEQUENT PROCESSING AT ELEVATED TEMPERATURES
- PROMOTE BASE-METAL/FILLER-METAL INTERACTIONS IN ORDER TO CHANGE THE

COMPOSITION OF THE BRAZING FILLER METAL (THIS TECHNIQUE IS USUALLY USED TO INCREASE THE REMELT TEMPERATURE AND DUCTILITY OF THE JOINT)

- EFFECTIVELY REMOVE SURFACE CONTAMINANTS AND OXIDES WITHIN PROTECTIVE ATMOSPHERES BRAZING (ALSO APPLIES TO PURE DRY HYDROGEN, TO ARGON, AND TO VACUUM)
- AVOID STRESS CRACKING

The time at brazing temperature also affects the wetting action. If the brazing filler metal has a tendency to creep, the distance generally increases with time. The alloying action between filler metal and parent metal is, of course, a function of temperature, time, and quantity of filler metal. For production work, temperature, time, and quantity of filler metal are generally kept at a minimum, consistent with good quality, where diffusion is not required.

References cited in this section

14. W.H. KOHL, SOLDERING AND BRAZING, *VACUUM*, VOL 14, 1964, P 175-198
15. *METALS HANDBOOK*, 9TH ED., *WELDING, BRAZING, AND SOLDERING*, VOL 6, AMERICAN SOCIETY FOR METALS, 1983, P 929-995

Mel M. Schwartz, Sikorsky Aircraft

Heating Methods

The numerous heating methods available for brazing often represent constraints on the designer or engineer when selecting the best type of capillary joint (Table 8). However, because effective capillary joining requires the efficient transfer of heat from the heat source into the joint, one cannot braze a 0.025 mm (0.001 in.) diam wire to a 2.3 kg (5.1 lb) lump of copper with a small torch.

TABLE 8 RELATIVE RATING OF SELECTED BRAZING PROCESS HEATING METHODS

METHOD	CHARACTERISTICS[(A)]					
	CAPITAL COST	RUNNING COST	BASIC OUTPUT	FLUX REQUIRED	VERSATILITY	OPERATOR SKILL REQUIRED
Torch (flame)	L/M	M/H	L	YES	H	YES
Electrical resistance	M	M	M/H	YES	L	NO
Induction	M/H	M	M/H	Y/N	M	NO
Furnace (atmosphere)	M/H	M/H	H	Y/N	M	NO
Furnace (vacuum)	H	L	H	NO	M	NO
Dip (flux bath)	L/M	M/H	L/M	YES	L	YES
Infrared	M	L	M	Y/N	L	NO

(A) H, HIGH; M, MEDIUM; L, LOW

The size and value of individual assemblies, the numbers required, and the required rate of production will influence the selection of heating method. Other factors that also must be considered include the rate of heating, differential thermal gradients, and both external and internal cooling rates. These factors vary tremendously with different methods of heating, and their effects on dimensional stability, distortion, and joint structure must be considered.

Manual torch brazing is the method most frequently used for repairs, one-of-a-kind brazing jobs, and short production runs, as an alternative to fusion welding. Any joint that can be accessed by a torch and brought to brazing temperature (by the torch alone or in conjunction with auxiliary heating) can be readily brazed by this technique.

Although any flame-producing device can be used for torch brazing, commercial applications are accomplished with the same type of torch, controls, and gases used for torch fusion welding. Conversion to brazing merely requires changes in torch nozzles and goggle lenses.

The torch brazing technique is relatively simple and can be mastered by the mechanically adept in a short time. Those already experienced in torch welding and the brazing of other metals generally encounter little difficulty learning torch brazing.

Depending on the temperature and heat required, all commercial gas mixtures can be used to fuel the torch: oxyacetylene, oxyhydrogen, oxy-natural gas, acetylene and air, hydrogen and air, propane, methane, and natural gas and air. Oxyacetylene and oxy-natural gas are the mixtures most often used commercially and are preferred in that order. Flame adjustment is very important. Generally, a slightly reducing flame is desirable in order to preserve part surfaces from oxidation.

The oxyacetylene combination produces the highest temperature. The other gases are cooler and their flames have relatively lower intensity. Thus, they are easier to use and are applied advantageously to light-gage material.

Manual torch brazing is particularly useful on assemblies with sections of unequal mass. As warranted by the rate of production, machine operations can be set up using one or more torches equipped with single or multiple flame tips. The machine can be designed to move either the work or the torches.

Torch brazing can be rather easily automated with appropriate gas supplies, indexing fixtures, and cycle controls. Usually, such systems involve multiple-station rotary indexing tables. The part is fed into a holding fixture at the first station and is then indexed to one or more preheating stations, depending on the heating time required. A brazing station is next, followed by a cooling station and an ejection station (see Fig. 4).

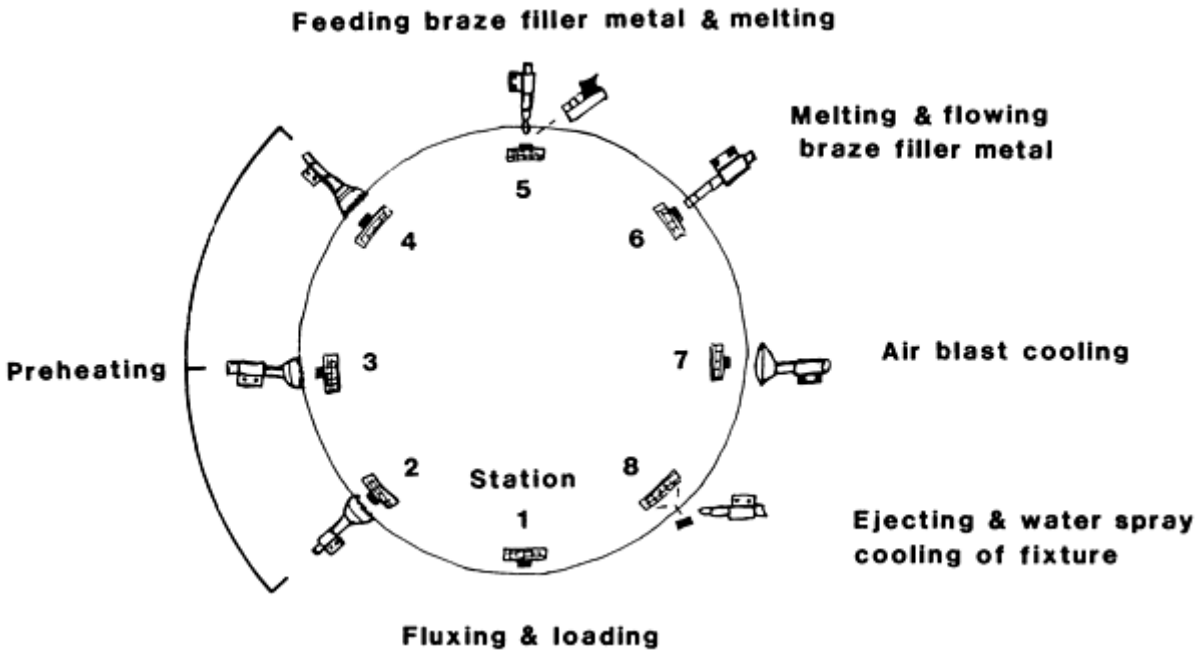

FIG. 4 SCHEMATIC OF AN EIGHT-STATION AUTOMATIC TORCH BRAZING OPERATION THAT PRODUCES MAGNET ARMATURE ASSEMBLIES (230 PIECES/H) USED AS STRIKING MEMBERS OF A PRINTING MACHINE

Additional information is available in the article "Torch Brazing" in this Volume.

Furnace brazing is popular because of its comparatively low equipment cost, furnace adaptability, and minimal required jigging. Furnace brazing is a low-cost process relative to other processes such as torch brazing, induction brazing, or salt-bath brazing when high-volume production output is a primary factor. Secondary factors include tooling requirements, fluxing, and cleaning requirements. With many brazing assemblies, the weight of the parts alone is sufficient to hold them together. Other configurations require only one or two rectangular fixturing blocks of metal.

Four basic types of furnaces are used:

- BATCH, WITH EITHER AIR OR CONTROLLED ATMOSPHERE (FIG. 5)
- CONTINUOUS, WITH EITHER AIR OR CONTROLLED ATMOSPHERE (FIG. 6)
- RETORT, WITH CONTROLLED ATMOSPHERE
- VACUUM

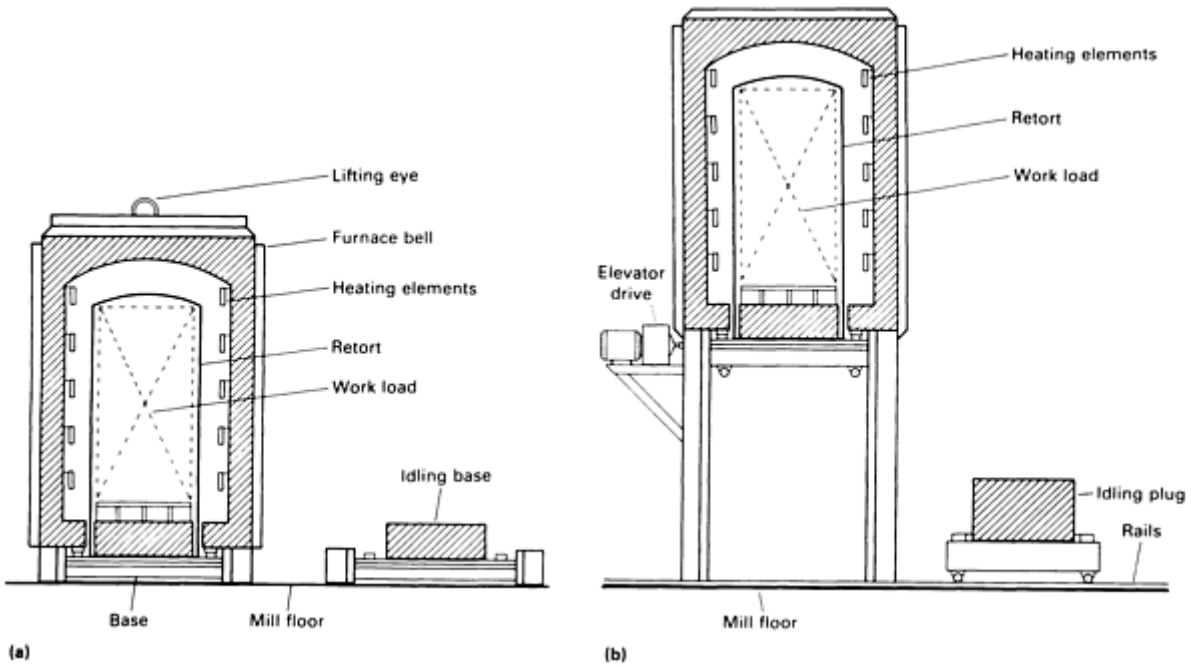

FIG. 5 BATCH-TYPE BRAZING FURNACES. (A) BELL FURNACE. (B) ELEVATOR FURNACE

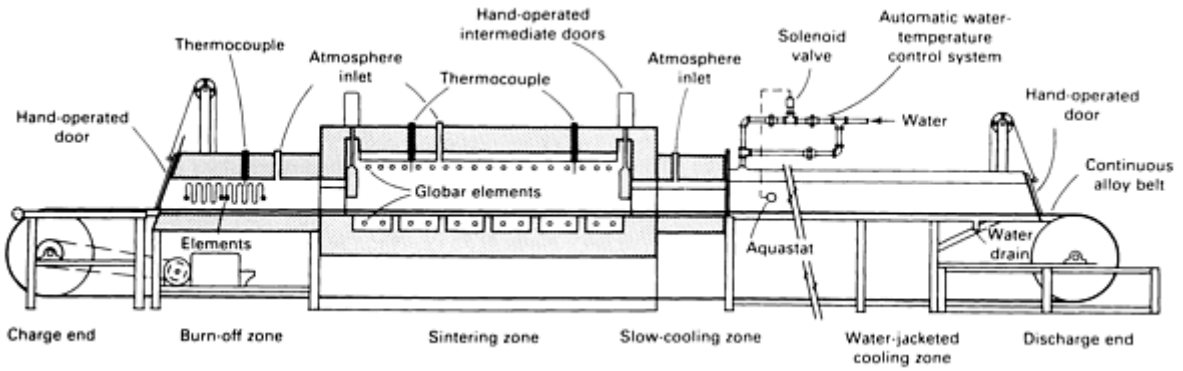

FIG. 6 CONTINUOUS-TYPE BRAZING FURNACE WITH WATER-JACKETED COOLING CHAMBER FOR USE IN AIR OR CONTROLLED ATMOSPHERES

Furnace brazing is used extensively where the parts to be brazed can be assembled with the brazing filler metal preplaced near or in the joint. Furnace brazing is particularly applicable for high-production applications in which continuous

conveyor-type furnaces are used. For medium-production work, batch-type furnaces are best. Regardless of furnace type, heating is usually produced by electrical resistance, although other types of fuel can be used in muffle-type furnaces.

The parts should be self jigged or fixtured and assembled, with brazing filler metal preplaced near or in the joint. Fluxing is used, except in cases where a reducing atmosphere, such as hydrogen, and either exothermic or endothermic combusted gas can be introduced into the furnace. Sometimes, both flux and a reducing atmosphere are necessary. Pure and dry inert gases, such as argon and helium, are used to obtain special atmosphere properties. Fluxes should never be used when furnace brazing with a vacuum atmosphere.

When continuous-type furnaces are used (Ref 16, 17), several different temperature zones can be set up to provide the proper preheating, brazing, and cooling temperatures. The speed through a conveyor-type furnace must be controlled to provide the appropriate time at the brazing temperature. It is also necessary to properly support the assembly so that it does not move while traveling on the belt (Ref 18).

A large volume of furnace brazing is performed in a vacuum atmosphere, which prevents oxidation during the heating cycle and eliminates the need for flux (Ref 19) (Fig. 7). Vacuum brazing has found wide application in the aerospace and nuclear fields, where reactive metals are joined or where entrapped fluxes would not be tolerable. Vacuum brazing does not allow as wide a choice of brazing filler metals as does atmosphere brazing (Ref 20, 21).

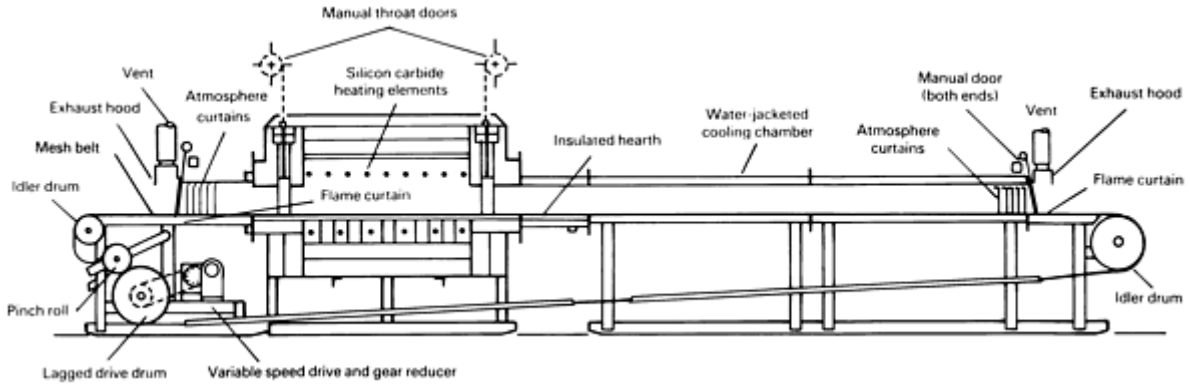

FIG. 7 HIGH-VACUUM BOTTOM-LOADING VACUUM FURNACE FOR MEDIUM-PRODUCTION APPLICATIONS

In most cases, vacuum furnaces are heated by electrical resistance heaters in a numbers of different forms. The overall time of a vacuum brazing operation is usually much longer than that of other batch brazing techniques and involves typing up expensive equipment for long periods to process comparatively small workloads. However, most of the metals on which vacuum brazing excels are also costly, the use of a process that permits material economics through fabrication while ensuring the necessary joint properties often can be justified (Ref 22, 23, 24).

Detailed information is available in the article "Furnace Brazing" in this Volume.

Induction Brazing. The high-frequency induction heating method for brazing is clean and rapid, lends itself to close control of temperature and location, and requires little operator skill.

The workpiece is placed in or near a coil carrying alternating current (ac), which induces the heating current in the desired area (Fig. 8). The coils, which are water cooled, are designed specifically for each part. Therefore, heating efficiency relies on establishing the best coil design and power frequency for each application. In most cases, the coils provide heat only to the joint area.

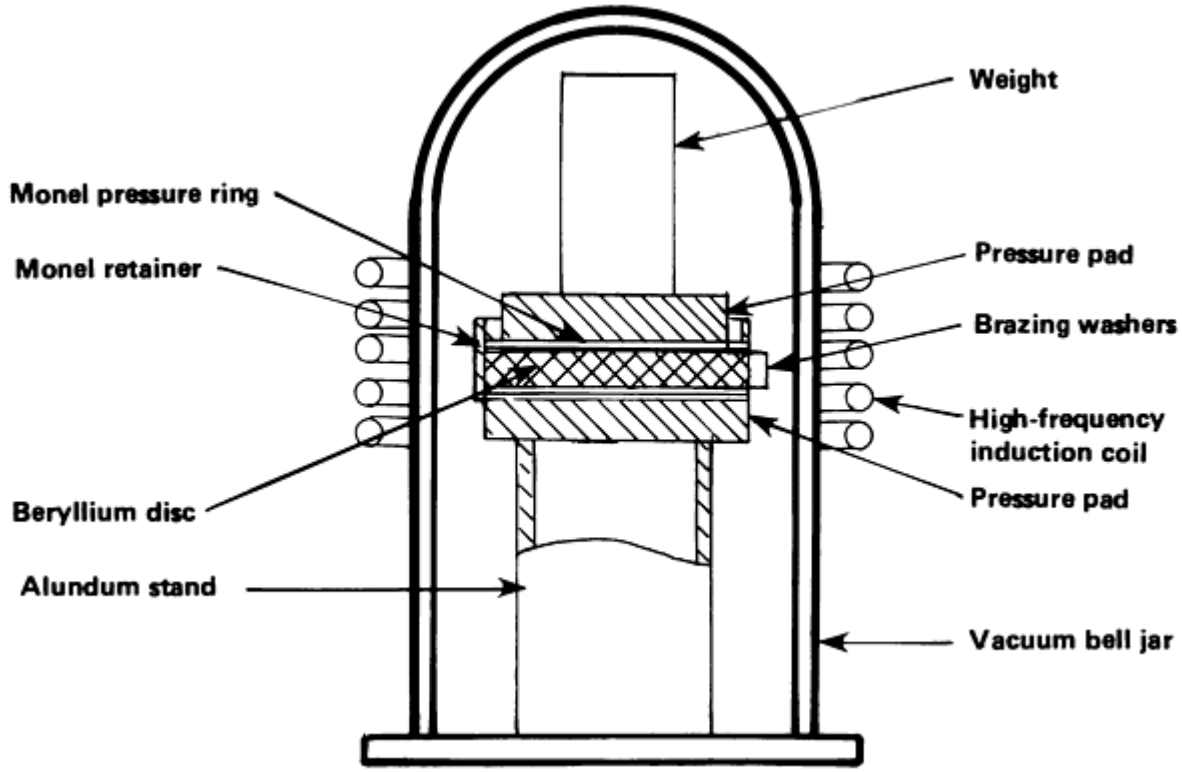

FIG. 8 INDUCTION HEATING APPARATUS USED TO VACUUM BRAZE BERYLLIUM AND MONEL COMPONENTS

The capability to heat selectively enables the induction method to be used when the nature of the brazement demands localized brazing.

There are several types of high-frequency sources to supply power to induction coils, each with a different range of frequencies:

- MOTOR GENERATORS (5 TO 10 KHZ)
- SPARK-GAP OSCILLATORS (20 TO 30 KHZ)
- VACUUM-TUBE OSCILLATORS (20 TO 5000 KHZ)
- SOLID-STATE POWER SUPPLIES (VARIABLE HZ)

The frequency of the power source determines the type of heat that will be induced in the part: high-frequency sources produce "skin" heating, whereas lower-frequency sources provide heating in thicker areas. The brazing heat usually develops within 10 to 60 s.

Induction brazing is well suited for mass production. Mechanized brazing lines for moving assemblies to and from the coils are very common. Brazing filler metals is normally preplaced in the joint, and the brazing can be done in air with the use of a flux, in an inert atmosphere, or in a vacuum atmosphere. The rapid heating rates available with induction heating are a major advantage when using brazing filler metals that tend to vaporize or segregate. The heating cycle for induction brazing is invariably automated, even when manual loading of assemblies is used.

Additional information is available in the article "Induction Brazing" in this Volume.

Dip brazing involves immersion of assembled parts into a suitable molten bath to effect brazing. The bath can be molten brazing filler metal, molten chemical flux, or molten chemical salts. The molten material is contained in a "pot" furnace heated by oil, gas, or electricity. In some instances, electrical-resistance heaters are used in the bath (Fig. 9). In the first type of bath, the parts being joined are held together and immersed in flux-covered molten filler metal, which flows into

the joints when the parts reach the bath temperature. The flux cleans the workpiece as it is introduced and protects the brazing filler metal by preventing oxidation and the loss of volatile elements from the bath.

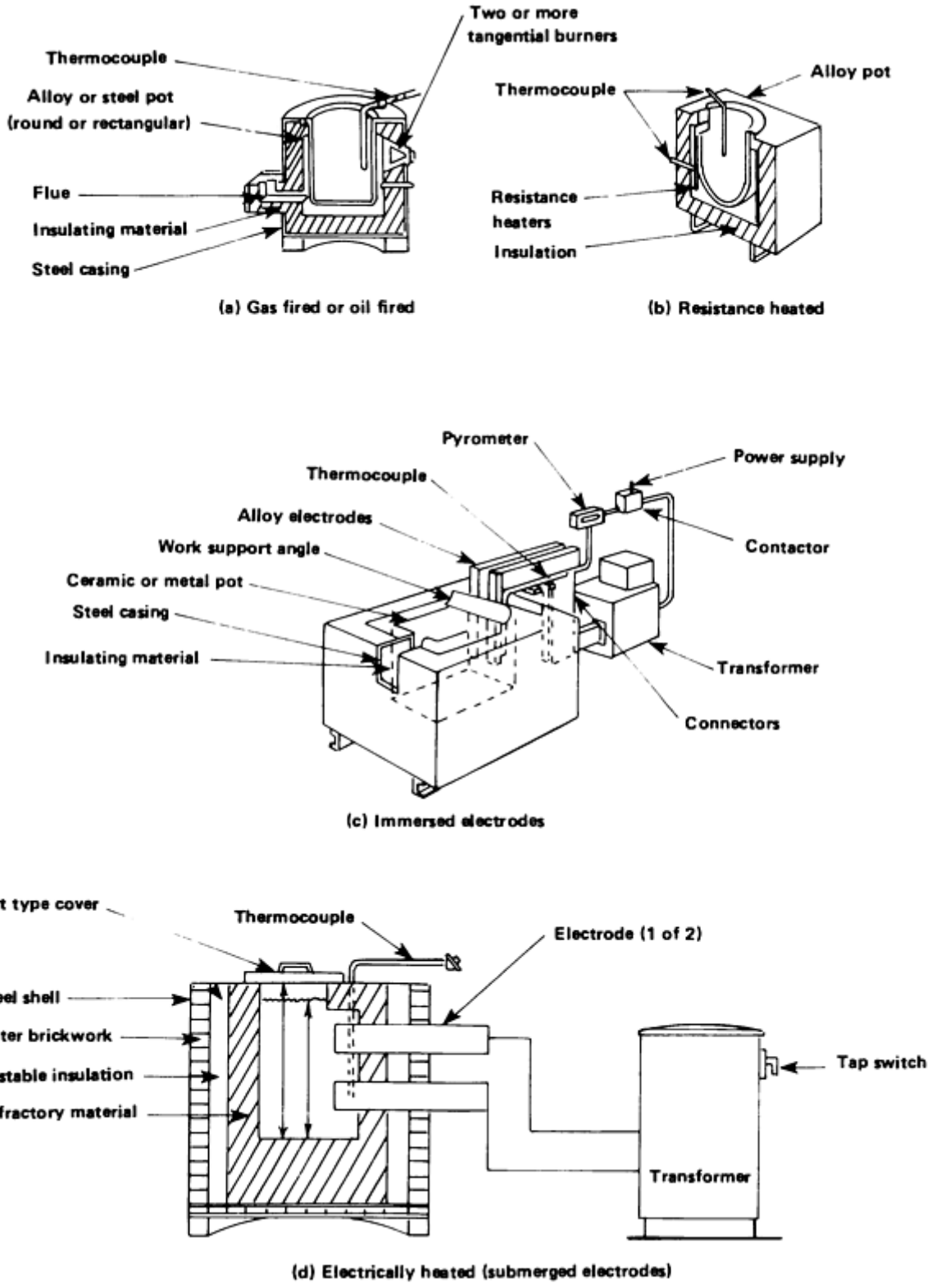

FIG. 9 EXTERNALLY AND INTERNALLY HEATED FURNACES USED FOR DIP BRAZING APPLICATIONS

The pot, or crucible, used in the molten-metal method is usually made of graphite. Jigging to maintain alignment is generally necessary. Because of the difficulties of heating and containing metals at high temperatures, filler metals that

require a brazing temperature above 1000 °C (1830 °F) are rarely used. Therefore, the choice of brazing filler metal is restricted to straight brasses and silver-base filler metals.

In the molten-flux method, the brazing filler metal is located in or near the joints and is heated to the required temperature by immersion in a bath of molten flux. Molten salt bath brazing has a greater scope than any other single brazing process. It can be used on as wide a range of parent metals as torch brazing, but is not subject to the same maximum temperature limitations. Unfortunately, it is an inflexible process. The type of salt used for a particular application depends on the ease with which the parent-metal surface oxides can be removed and on the temperature required for brazing.

The molten-flux method is used extensively for brazing aluminum and its alloys. The flux bath provides excellent protection against metal reoxidation, which can occur quite easily with aluminum.

The dip brazing method generally causes less distortion than torch brazing, because of its uniform heating. However, it may require relatively complex tooling and is therefore best used in medium- to high-production runs. This process is particularly well suited for small- to medium-sized parts with multiple hidden joints.

Detailed information is available in the article "Dip Brazing" in this Volume.

Resistance brazing is most applicable to relatively simple joints in metals that have high electrical conductivity. In this process, the workpieces are heated locally. Brazing filler metal that is preplaced between the workpieces is melted by the heat obtained from its resistance to the flow of electric current through the electrodes and the work. Usually, the heating current, which is normally ac, is passed through the joint itself. The joint becomes part of an electrical circuit, and the brazing heat is generated by the resistance at the joint.

Equipment is the same as that used for resistance welding, and the pressure needed for establishing electrical contact across the joint is ordinarily applied through the electrodes. The electrode pressure also in the usual means for providing the tight fit needed for capillary behavior in the joint. The component parts are generally held between copper or carbon-graphite electrodes.

The flux that is used must be conductive. Normally, fluxes are insulators when cool and dry, but are conductive when wet. The process is generally used for low-volume production in joining electrical contacts, related electrical elements, copper commutator segments, stainless steel tube to fittings, and so on.

Additional information is available in the article "Resistance Brazing" in this Volume.

Infrared (Quartz) Brazing. The development of high-intensity quartz lamps and the availability of suitable reflectors have made the infrared heat technique commercially important for brazing. Infrared heat is radiant heat that is obtained with the sources having energy frequency below the red rays in the light spectrum. Although there is some visible light with every "black" source, heating is principally done by the invisible radiation. Heat sources (lamps) capable of delivering up to 5000 W of radiant energy are commercially available. The lamps do not need to follow the contour of the part in order to hear the joint area, even though the heat input varies inversely as the square of the distance from the source, unless reflectors are used to concentrate the heat.

Lamps are often arranged in a toaster-like configuration, with parts traveling between two banks of lamps (Fig. 10). Infrared brazing can concentrate large amounts of heat in small areas, which can be advantageous in certain applications. Infrared brazing setups are generally not as fast as induction brazing, but the equipment is less expensive.

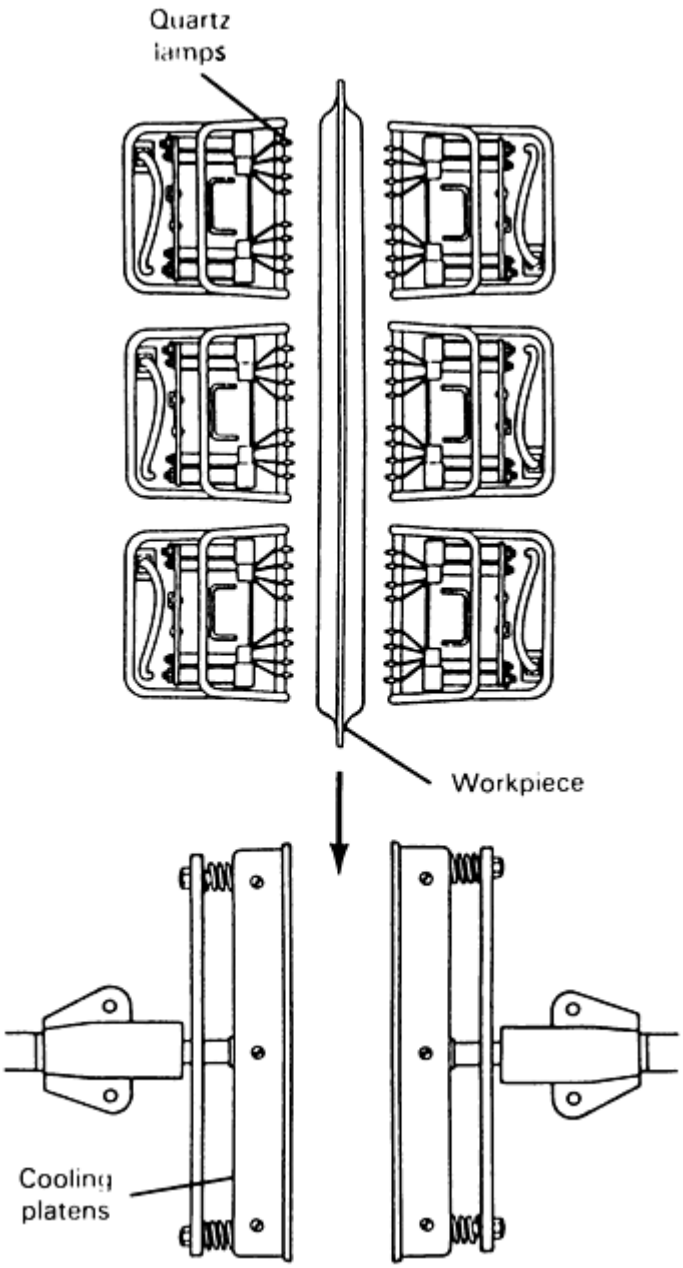

FIG. 10 WORKPIECE SUBJECTED TO INFRARED BRAZING PROCESS PRIOR TO BEING MOVED TO COOLING PLATENS

Exothermic brazing is a special process, but is rarely used because there are more-economical production methods. In this process, the heat required to melt and flow the brazing filler metal is produced by a solid-state exothermic chemical reaction, which is defined as any reaction between two or more reactants that involves the free energy of the system. Although nature provides countless numbers of these reactions, only the solid-state or nearly solid-state metal/metal-oxide reactions are suitable for use in exothermic brazing units.

Additional information is available in the article "Exothermic Brazing" in this Volume.

Electron-beam and laser brazing have been used in a limited number of applications. A laser can be used when a very small localized area of heat is required, such as for brazing small carbide tips on printer heads for electronic printers. The electron beam can be used for brazing by defocusing the beam to provide a wider area of heating. Because this is done in a vacuum, fluxes cannot be used and the brazing filler metal must be selected so that there is little or no vaporization during brazing.

Microwave Brazing. One of the newest heating methods to be developed is the use of microwaves. This technique is being used to join ceramics in high-temperature, corrosion-resistant, and high-performance applications. These applications require complex ceramics parts with strong, durable joints (Ref 25, 26).

The technique uses a single-mode microwave cavity. An iris controls the percent of microwaves reflected in the cavity, and a plunger adjusts the frequency. Together, they focus microwaves on the joint. The major advantage of this technique in terms of ceramic parts is that the entire part does not have to be heated in order to make a joint. Reheating finished ceramic parts can subject them to thermal stresses and cause cracking, which weakens the part. With microwave joining, only the interface between the pieces is heated. The technique is faster than conventional joining, which requires long times to heat ceramics uniformly. Large pieces, can, in principle, be joined at a lower cost.

One disadvantage of microwave joining is that commercial equipment is only produced by a few companies, mostly for research and development purposes.

Some microwave units feature 2.45 GHz single-mode or controlled multimode operation. Their cavity is designed to provide controlled-mode patterns that can focus high-energy microwave fields to heat a part only where it is needed, such as at a joint. The joint or part can be heated up to 2200 °C (3990 °F). Researchers have joined 92% Al_2O_3 ceramic parts in a 6 GHz single-mode microwave cavity at various temperatures and times. The bending strength of this joint gradually increased from the solidus temperature of 1400 °C (2550 °F) and reached a peak of 420 MPa (60 ksi) at about 1750 °C (3180 °F).

Braze welding is a joining process in which a filler metal is melted and deposited in a specific joint configuration, and a metallurgical bond is obtained by a wetting action that is often accompanied by some degree of diffusion with the base metals. Braze welding requires heating and melting of the filler metal that has a melting (liquidus) temperature above 450 °C (840 °F).

Stringent fit-up is not critical, because the filler metal is deposited in grooves and spaces and flows into gaps wider than those used for brazing. Fabricators use braze welding as a low-temperature substitute for oxyfuel welding or as a low-cost substitute for brazing. Joint designs for braze welding are the same as for oxyfuel welding (OFW). Braze welding has been used to join cast iron, steels, copper, nickel, and nickel alloys.

Compared to conventional fusion-welding processes, braze welding requires less heat input, permits higher travel speeds, and causes less distortion. Deposited filler metal is soft and ductile, providing good machinability, and residual stresses are low. The process joins brittle cast irons without extensive preheating.

Although most braze welding initially used an OFW torch, copper filler metal brazing rod, and a suitable flux, present applications use carbon arc welding (CAW), gas-tungsten arc welding (GTAW), gas-metal arc welding (GMAW), or plasma arc welding (PAW) without flux in the manual, semiautomatic, or automatic modes to economically bond and deposit the filler metal in the braze weld joints. OFW is, however, still widely used in machinery repair applications. Filler metal selection, proper wetting and compatibility with the base metals, and shielding from air are important to the effective use of the process with any suitable heating method.

A wide variety of parts can be braze welded using typical weld joint designs. Groove, fillet, and edge welds can be used to join simple and complex assemblies made from sheet, plate, pipe, tubing, rods, bars, castings, and forgings. Sharp corners that are easily overheated and may become points of stress concentrations should be avoided. To obtain good strength, an adequate bond area is required between filler metal and the base metal. Weld groove geometry should provide an adequate groove face area, so that the joint will not fail along the interfaces. Proper joint design selection will produce deposited filler-metal strengths that may meet or exceed the minimum base-metal tensile strengths. Because of the inert shielding gas, electrical arc methods have fewer included flux compounds and oxides at the faying surfaces. The result is higher joint strength and improved corrosion resistance. Original surfaces are restored by overlayments and subsequent machining.

References cited in this section

16. W.S. STEFFAN, NITROGEN-BASED ATMOSPHERE FURNACE BRAZING SYSTEM PROVIDES STRENGTH AND LEAK-PROOF PERFORMANCE OF NEWLY DESIGNED FUEL INJECTION RAIL,

IND. HEAT., AUG 1989, P 21-23
17. *METALS HANDBOOK,* 9TH ED., *POWDER METALLURGY,* VOL 7, 1984, P 358
18. *METALS HANDBOOK,* 8TH ED., VOL 6, 1971, P 595
19. PRODUCT LITERATURE, SECO-WARWICK CORP. (SUNBEAM), SEPT 1977
20. A. SAKAMOTO, STUDY OF FURNACE ATMOSPHERE FOR VACUUM-INERT GAS PARTIAL-PRESSURE BRAZING, *WELD. J.,* NOV 1991, P 311S-320S
21. NEW GENERATION OF VACUUM HEAT-TREATMENT FURNACES FEATURE HIGH GAS PRESSURE QUENCHING AND OIL QUENCH VACUUM FURNACE, *METALLURGIA,* MAY 1989, P 205
22. W.R. JONES, VACUUM--ANOTHER ATMOSPHERE?, *HEAT TREAT.,* OCT 1986, P 39-41
23. W.T. HOOVEN AND K.W. NOKES, MAKE YOUR VACUUM BRAZING FURNACES USER FRIENDLY, *WELD. J.,* OCT 1990, P 25-29
24. S. DRESSLER, ROLE OF HOT WALL VACUUM FURNACES IN PLASMA-ASSISTED SURFACE TREATMENT: PART II, OPERATING INFLUENCES, *IND. HEAT.,* SEPT 1989, P 31-33
25. "ADVANCED STRUCTURAL CERAMICS: TECHNOLOGIES, ECONOMICS AND MARKET OPPORTUNITIES," GB-107, BCC INC., DEC 1987
26. E.J. KUBEL, JR., STRUCTURAL CERAMICS; MATERIALS OF THE FUTURE, *ADV. MATER. PROCESS.,* VOL 134, AUG 1988, P 25-33

Fundamentals of Brazing

Mel M. Schwartz, Sikorsky Aircraft

References

1. C.M. ADAMS, JR., "DYNAMICS OF WETTING IN BRAZING AND SOLDERING," TECHNICAL REPORT WAL TR 650/1, ARMY MATERIALS RESEARCH AGENCY, WATERTOWN ARSENAL, JULY 1962
2. S. WEISS AND C.M. ADAMS, JR., THE PROMOTION OF WETTING, *WELD. J.,* VOL 46 (NO. 2), FEB 1967, P 49S-57S
3. W.D. HARKINS, *PHYSICAL CHEMISTRY OF SURFACE FILMS,* REINHOLD, 1952
4. M.M. SCHWARTZ, *MODERN METAL JOINING TECHNIQUES,* WILEY, 1969
5. A. BONDI, SPREADING OF LIQUID METALS ON SOLID SURFACE CHEMISTRY OF HIGH ENERGY SUBSTANCES, *CHEM. REV.,* VOL 52 (NO. 2), 1953, P 417-458
6. R.G. GILLILAND, WETTING OF BERYLLIUM BY VARIOUS PURE METALS AND ALLOYS, *WELD. J.,* VOL 43, JUNE 1964, P 248S-258S
7. M. NAKA, T. TANAKA, AND I. OKAMOTO, *Q. J. JPN. WELD. SOC.,* VOL 4, 1986, P 597
8. R.R. KAPOOR AND T.W. EAGER, *J. AM. CERAM. SOC.,* VOL 72, 1989, P 448
9. R.E. LOCHMAN, *CERAM. BULL.,* VOL 68, 1989, P 891
10. D.H. KIM, S.H. HWANG, AND S.S. CHUN, THE WETTING, REACTION, AND BONDING OF SILICON NITRIDE BY CU-TI ALLOYS, *J. MATER. SCI.,* VOL 26, 1991, P 3223-3234
11. D.L. KELLER *ET AL.,* WETTABILITY OF BRAZING FILLER METALS, *WELD. J.,* VOL 69 (NO. 10), 1990, P 31-34
12. W.S. BENNETT *ET AL.,* VACUUM BRAZING STUDIES ON HIGH-MANGANESE STAINLESS STEEL, *WELD. J.,* VOL 53, 1974, P 510S-516S
13. W. FEDUSKA, HIGH-TEMPERATURE BRAZING ALLOY--BASE METAL WETTING REACTIONS, *WELD. J.,* VOL 38 (NO. 3) 1959, P 122S-130S

14. W.H. KOHL, SOLDERING AND BRAZING, *VACUUM*, VOL 14, 1964, P 175-198
15. *METALS HANDBOOK*, 9TH ED., *WELDING, BRAZING, AND SOLDERING*, VOL 6, AMERICAN SOCIETY FOR METALS, 1983, P 929-995
16. W.S. STEFFAN, NITROGEN-BASED ATMOSPHERE FURNACE BRAZING SYSTEM PROVIDES STRENGTH AND LEAK-PROOF PERFORMANCE OF NEWLY DESIGNED FUEL INJECTION RAIL, *IND. HEAT.*, AUG 1989, P 21-23
17. *METALS HANDBOOK*, 9TH ED., *POWDER METALLURGY*, VOL 7, 1984, P 358
18. *METALS HANDBOOK*, 8TH ED., VOL 6, 1971, P 595
19. PRODUCT LITERATURE, SECO-WARWICK CORP. (SUNBEAM), SEPT 1977
20. A. SAKAMOTO, STUDY OF FURNACE ATMOSPHERE FOR VACUUM-INERT GAS PARTIAL-PRESSURE BRAZING, *WELD. J.*, NOV 1991, P 311S-320S
21. NEW GENERATION OF VACUUM HEAT-TREATMENT FURNACES FEATURE HIGH GAS PRESSURE QUENCHING AND OIL QUENCH VACUUM FURNACE, *METALLURGIA*, MAY 1989, P 205
22. W.R. JONES, VACUUM--ANOTHER ATMOSPHERE?, *HEAT TREAT.*, OCT 1986, P 39-41
23. W.T. HOOVEN AND K.W. NOKES, MAKE YOUR VACUUM BRAZING FURNACES USER FRIENDLY, *WELD. J.*, OCT 1990, P 25-29
24. S. DRESSLER, ROLE OF HOT WALL VACUUM FURNACES IN PLASMA-ASSISTED SURFACE TREATMENT: PART II, OPERATING INFLUENCES, *IND. HEAT.*, SEPT 1989, P 31-33
25. "ADVANCED STRUCTURAL CERAMICS: TECHNOLOGIES, ECONOMICS AND MARKET OPPORTUNITIES," GB-107, BCC INC., DEC 1987
26. E.J. KUBEL, JR., STRUCTURAL CERAMICS; MATERIALS OF THE FUTURE, *ADV. MATER. PROCESS.*, VOL 134, AUG 1988, P 25-33

Fundamentals of Brazing

Mel M. Schwartz, Sikorsky Aircraft

Selected References

- *BRAZING HANDBOOK*, 4TH ED., AWS, 1991
- M.M. SCHWARTZ, *BRAZING*, ASM INTERNATIONAL, 1987
- M.M. SCHWARTZ, *CERAMIC JOINING*, ASM INTERNATIONAL, 1990

Shielding Gases for Welding

Kevin A. Lyttle, Praxair, Inc.

Introduction

THE SHIELDING GAS used in a welding process has a significant influence on the overall performance of the welding system. Its primary function is to protect the molten metal from atmospheric nitrogen and oxygen as the weld pool is being formed. The shielding gas also promotes a stable arc and uniform metal transfer. In gas-metal arc welding (GMAW) and flux-cored arc welding (FCAW), the gas used has a substantial influence on the form of metal transfer during welding. This, in turn, affects the efficiency, quality, and overall operator acceptance of the welding operation.

The shielding gas interacts with the base material and with the filler material, if any, to produce the basic strength, toughness, and corrosion resistance of the weld. It can also affect the weld bead shape and the penetration pattern.

Understanding the basic properties of a shielding gas will aid in the selection of the right shielding gas or gases for a welding application. Use of the best gas blend will improve the quality and may reduce the overall cost of the welding operation as well.

Shielding Gases for Welding

Kevin A. Lyttle, Praxair, Inc.

Basic Properties of a Shielding Gas

The "controlled electrical discharge" known as the welding arc is formed and sustained by the establishment of a conductive medium called the arc plasma. This plasma consists of ionized gas, molten metals, slags, vapors, and gaseous atoms and molecules. The formation and structure of the arc plasma is dependent on the properties of the shielding gases used for welding. Table 1 lists the basic properties of gases used for welding (Ref 1).

TABLE 1 PROPERTIES OF SHIELDING GASES USED FOR WELDING

GAS	CHEMICAL SYMBOL	MOLECULAR WEIGHT	SPECIFIC GRAVITY(A)	DENSITY		IONIZATION POTENTIAL	
				g/ft^3	g/l	aj(b)	eV
ARGON	AR	39.95	1.38	0.1114	1.784	2.52	15.7
CARBON DIOXIDE	CO_2	44.01	1.53	0.1235	1.978	2.26	14.4
HELIUM	HE	4.00	0.1368	0.0111	0.178	3.92	24.5
HYDROGEN	H_2	2.016	0.0695	0.0056	0.090	2.16	13.5
NITROGEN	N_2	28.01	0.967	0.782	12.5	2.32	14.5
OXYGEN	O_2	32.00	1.105	0.0892	1.43	2.11	13.2

Source: Ref 1

(A) AT 100 KPA (1 ATM) AND 0 °C (32 °F); AIR = 1.

(B) 10^{-18} J.

The ionization potential is the energy, expressed in electron volts, necessary to remove an electron from a gas atom--making it an ion, or an electrically charged gas atom. All other factors held constant, the value of the ionization potential decreases as the molecular weight of the gas increases. Arc starting and arc stability are greatly influenced by the ionization potentials of the component shielding gases used in welding process. A gas with a low ionization potential,

such as argon, can atoms into ions easily. Helium, with its significantly higher ionization potential, produces a harder to start, less stable arc.

Although other factors are involved in sustaining the plasma, the respective energy levels required to ionize these gases must be maintained; as a consequence, the arc voltage is directly influenced. For equivalent arc lengths and welding currents, the voltage obtained with helium is appreciably higher than is with argon. This translates into more available heat input to the base material with helium than with argon.

The thermal conductivity of a gas is a measure of how well it is able to conduct heat. It influences the radial heat loss from the center to the periphery of the arc column as well as heat transfer between the plasma and the liquid metal. Argon, which has a low thermal conductivity, produces an arc that has two zones: a narrow hot core and a considerably cooler outer zone. The penetration profile of the weld fusion area then exhibits a narrow "finger" at the root and a wider top. A gas with a high thermal conductivity conducts heat outward from the core; this results in a wider, hotter arc core. This type of heat distribution occurs with helium, argon-hydrogen, and argon-carbon dioxide blends; it gives a more even distribution of heat to the work surface and produces a wider fusion area.

Dissociation and Recombination. Shielding gases such as carbon dioxide, hydrogen, and oxygen are multiatom molecules. When heated to high temperatures within the arc plasma, these gases break down, or dissociate, into their component atoms. They are then at least partially ionized, producing free electrons and current flow. As the dissociated gas comes into contact with the relatively cool work surface, the atoms recombine and release heat at that point. This heat of recombination causes multiatomic gases to behave as if they have a higher thermal conductivity, similar to that of helium. Dissociation and recombination do not occur with gases, such as argon, that consist of a single atom. Thus, at the same arc temperature, the heat generated at the work surface can be considerably greater with gases such as carbon dioxide and hydrogen.

Reactivity/Oxidation Potential. The oxidizing nature of the shielding gas affects both welding performance and the properties of the resultant weld deposit. Argon and helium are completely nonreactive, or inert, and thus have no direct chemical affect on the weld metal. Oxidizing or active gases, such as CO_2 and oxygen, will react with elements in the filler metal or baseplate and will form a slag on the surface of the weld deposit. The loss of elements, such as manganese and silicon, from steel can affect the quality and cost of the weldment produced. Both weld strength and toughness generally decline as the oxidizing nature of the shielding gas increases.

Additions of reactive gases such as oxygen or carbon dioxide enhance the stability of the arc and affect the type of metal transfer obtained. Metal droplet size is decreased, and the number of droplets transferred per unit time increases as the level of oxygen in the shielding gas increases. Oxygen reduces the molten weld bead surface tension, promoting better bead wetting and higher welding travel speeds. Small additions of CO_2 work in a similar manner.

The surface tension between the molten metal and its surrounding atmosphere has a pronounced influence on bead shape. If the surface energy is high, a convex, irregular bead will result. Low values promote flatter beads with minimal susceptibility for undercutting.

Pure argon is generally associated with high interfacial energy, producing a sluggish weld puddle and high, crowned bead. The addition of a small amount of a reactive gas, such as oxygen, lowers this surface tension and promote fluidity and better wetting of the base material; it does this without creating excessive oxidation of the weld metal.

Gas Purity. Some metals, such as carbon steel and copper, have a relatively high tolerance for contaminants in the shielding gas; others, such as aluminum and magnesium, are fairly sensitive to particular contaminants. Still others, such as titanium and zirconium, have an extremely low tolerance for any foreign constituent in the shielding gas.

Depending on the metal being welded and the welding process used, very small quantities of gas impurities can significantly affect welding speed, weld surface appearance, weld bead solidification, and porosity levels. The effects of any given impurity are wide ranging, but weld quality and eventual fitness for purpose are major areas of concern.

There is always a possibility that the gas, as delivered, is contaminated; however, it is far more likely that impurities will enters somewhere between the supply and the end-use points. For this reason, property designed piping systems and high-quality hose are recommended for use with welding shielding gases. Typical industry minimum purity levels for welding gases are listed in Table 2 (Ref 2).

TABLE 2 TYPICAL GASES PURITY AND MOISTURE CONTENT OF SHIELDING

GAS	PRODUCT STATE	MINIMUM PURITY, %	MAXIMUM MOISTURE, PPM(A)	APPROXIMATE DEW POINT AT MAXIMUM MOISTURE CONTENT	
				°C	°F
ARGON	GAS	99.995	10	-60	-77
	LIQUID	99.997	6	-64	-83
CARBON DIOXIDE	GAS	99.5	19	-51	-60
	LIQUID	99.8	50	-58	-73
HELIUM	GAS	99.95	32	-51	-61
	LIQUID	99.995	3	-69	-92
HYDROGEN	GAS	99.95	8	-63	-80
	LIQUID	99.995	5	-65	-86
NITROGEN	GAS	99.7	32	-51	-61
	LIQUID	99.997	5	-65	-86
OXYGEN	INDUSTRIAL	99.5	50	-48	-54
	LIQUID	99.5	6	-64	-83

Source: Ref 2

(A) MOISTURE SPECIFICATIONS ARE MEASURED AT FULL CYLINDER PRESSURE, THE PRESSURE AT WHICH THE CYLINDER IS ANALYZED.

Gas density is the weight of the gas per unit volume. Density is one of the chief factors that influence shielding gas effectiveness. Basically, gases heavier than air, such as argon and carbon dioxide, require lower flow rates in use than do the lighter gases, such as helium, to ensure adequate protection of the weld puddle.

References cited in this section

1. N.E. LARSON AND W.F. MEREDITH, *SHIELDING GAS SELECTION MANUAL*, UNION CARBIDE INDUSTRIAL GASES TECHNOLOGY CORP., 1990, P 10
2. N.E. LARSON AND W.F. MEREDITH, *SHIELDING GAS SELECTION MANUAL*, UNION CARBIDE INDUSTRIAL GASES TECHNOLOGY CORP., 1990, P 11

Shielding Gases for Welding

Kevin A. Lyttle, Praxair, Inc.

Characteristics of the Components of a Shielding Gas Blend

To obtain a shielding gas that is suited to a specific application, a mix of gases is generally needed. Each basic gas contributes certain characteristics to the performance of the overall mix. Some gas blends have relatively specific areas of application and limited operating ranges; others can be used on many materials under a variety of welding conditions. Each component of the blend brings with it properties that are supplemented by the others to produce an enhanced level of performance.

Argon is inert or unreactive with respect to the materials present in the welding electrode. With its low ionization potential, argon promotes easy arc starting and stable arc operation. Its lower thermal conductivity promotes the development of axial "spray" transfer in certain forms of GMAW. It is also used in applications where base material distortion must be controlled or where good gap-bridging ability is required.

Helium. Unlike argon, helium is lighter than air and has a low density. Like argon, it is chemically inert and does not react with other elements or compounds. Because of its high thermal conductivity and high ionization potential, more heat is transferred to the base material, thus enhancing the penetration characteristics of the arc. In many applications, it also allows higher weld travel speeds to be obtained. Because of its higher cost, helium is frequently combined with argon or argon mixtures to enhance the overall performance of the blend while minimizing its cost.

Oxygen combines with almost all known elements except rare and inert gases; it vigorously support combustion. Small amounts of oxygen are added to some inert mixtures to improve the stability of the welding arc developed as well as to increase the fluidity of the weld puddle.

In the spray-transfer mode of GMAW, small additions of oxygen enhance the range over which this spatterless form of welding can be performed. The droplet size decreases and the number of drops transferred per unit time increases as oxygen is added to the blend.

Carbon dioxide is a reactive gas that is commonly used alone in certain types of GMAW. Oxidation of the base material and any filler electrode occurs readily. Carbon dioxide is added to argon blends to improve are stability, enhance penetration, and improve weld puddle flow characteristics. The higher thermal conductivity of carbon dioxide (because of the dissociation and recombination of its component parts) transfer more heat to the base material than does argon alone. A broader penetration pattern versus argon is obtained; however, base material distortion and lack of gap-bridging ability are possible problems.

Hydrogen is the lightest known element and is a flammable gas. Explosive mixtures can be formed when certain concentration of hydrogen are mixed with oxygen or air. It is added to inert gases to increase the heat input to the base material or for operations involving cutting and gouging. Because some materials are especially sensitive to hydrogen-related contamination, its use is generally limited to special applications, such as the joining of stainless steels, and to plasma are cutting and gouging.

Nitrogen is generally considered to be inert except at high temperatures. At arc welding temperatures, it will react with some metals (e.g., aluminum, magnesium, steel, and titanium), so it is not used as a primary shielding gas. It can be used with other gases for some welding applications (e.g., copper) and is also widely used in plasma cutting.

Shielding Gases for Welding

Kevin A. Lyttle, Praxair, Inc.

Shielding Gas Selection

In most welding applications, more than one shielding gas or gas blend can be used successfully. For example, there is no one optimal gas blend for joining carbon steels, but a considerable array of mixes are available depending on the specific requirements of the application. For some processes, such as gas-tungsten arc welding (GTAW) and plasma arc welding (PAW), the choices may be somewhat limited by the nature of the electrodes used and the materials being welded. However, for applications involving GMAW, a multitude of blends can be selected from when carbon steels are being joined. Determination of the best blend depends on a number of specific job-related needs.

Accuracy of Gas Blends

The accuracy with which gases are blended is a function of the way in which they are supplied. If the source of the gas is a high-pressure cylinder, the following generally applies:

1. ±10% RELATIVE, MINOR COMPONENT (REF 3)

2. ±0.5% ABSOLUTE FOR CONCENTRATIONS UP TO 5%; ±10% RELATIVE FOR CONCENTRATIONS BETWEEN 5 AND 50% (REF 4)

For example, the mix accuracy of an Ar-2O_2 blend would be Ar/1.8-2.2O_2 (method 1) or Ar/1.5-2.5O_2 (method 2). A blend of Ar-25CO_2 would yield Ar/22.5-27.5CO_2 by their method of calculation.

When gas cylinders are properly filled with the appropriate blend, the components of that mixture will not separate unless the temperature of the environment is reduced far below normal working temperatures. If the gases are supplied from a liquid source, such as a bulk tank, the accuracy of the blend is a function of the mixing equipment used, but most likely falls within the ±10% minor component range.

Shielding Gases for GMAW

By far, the largest number of gas blends have been developed for GMAW, especially for joining carbon steel. These can be roughly divided into four categories: pure gases, argon-oxygen mixes, argon/carbon dioxide mixes, and three-part gas blends composed of either argon, helium, oxygen, carbon dioxide, or hydrogen. Table 3 contains suggestions for shielding gas selection based on material type, thickness, and mode of metal transfer.

TABLE 3 RECOMMENDED SHIELDING GAS SELECTION FOR GMAW

MATERIAL	THICKNESS		TRANSFER MODE	RECOMMENDED SHIELDING GAS	ADVANTAGES AND LIMITATIONS
	MM	IN.			
CARBON STEEL	<2.0	<0.080	SHORT CIRCUITING	AR-25CO_2 AR-15CO_2 AR-8CO_2	GOOD PENETRATION AND DISTORTION CONTROL TO REDUCE POTENTIAL BURNTHROUGH
	2.0-3.2	0.080-0.125	SHORT CIRCUITING	AR-8CO_2 AR-15CO_2 AR-25CO_2	HIGHER DEPOSITION RATES WITHOUT BURNTHROUGH: MINIMUM DISTORTION AND SPATTER; GOOD PUDDLE CONTROL FOR OUT-OF-POSITION WELDING
	>3.2	>0.125	SHORT CIRCUITING	AR-15CO_2 AR-25CO_2 CO_2	HIGH WELDING SPEEDS, GOOD PENETRATION AND PUDDLE CONTROL; APPLICABLE LOT OUT-OF-POSITION WELDS
			GLOBULAR	AR-25CO_2 CO_2	SUITABLE FOR HIGH-CURRENT AND HIGH-SPEED WELDING; DEEP PENETRATION AND FAST TRAVEL SPEEDS, BUT WITH GREATER BURNTHROUGH POTENTIAL
			CONVENTIONAL SPRAY ARC	AR-1O_2 AR-2O_2 AR-5CO_2	GOOD ARC STABILITY; PRODUCES A MORE FLUID PUDDLE AS O_2

				AR-8CO_2 AR-10CO_2 AR-15CO_2 AR-CO_2-O_2 BLENDS	INCREASES; GOOD COALESCENCE AND BEAD CONTOUR, GOOD WELD APPEARANCE AND PUDDLE CONTROL
			PULSED SPRAY	ARGON-5CO_2 AR-HE-CO_2 BLENDS AR-CO_2-O_2 BLENDS	USED FOR BOTH GAGE AND OUT-OF-POSITION WELDMENTS; ACHIEVES GOOD PULSED SPRAY STABILITY OVER A WIDE RANGE OF ARC CHARACTERISTICS AND DEPOSITION RANGES
ALLOY STEEL	ALL SIZES		SHORT CIRCUITING	AR-8CO_2 AR-15CO_2 AR-CO_2-O_2 BLEND	HIGH WELDING SPEEDS; GOOD PENETRATION AND PUDDLE CONTROL; APPLICABLE FOR OUT-OF-POSITION WELDS; SUITABLE FOR HIGH-CURRENT AND HIGH-SPEED WELDING
			SPRAY ARC (HIGH-CURRENT DENSITY AND ROTATIONAL)	AR-2O_2 AR-5O_2 AR-CO_2-O_2 BLENDS AR-HE-CO_2 BLENDS	REDUCES UNDERCUTTING; HIGHER DEPOSITION RATES AND IMPROVED BEAD WETTING; DEEP PENETRATION AND GOOD MECHANICAL PROPERTIES
			PULSED SPRAY	AR-5CO_2 AR-8CO_2 AR-2O_2	USED FOR BOTH LIGHT-GAGE AND HEAVY OUT-OF-POSITION WELDMENTS; ACHIEVES GOOD PULSED SPRAY STABILITY OVER A WIDE RANGE OF ARC CHARACTERISTICS AND DEPOSITION RANGES
STAINLESS STEEL, COPPER, NICKEL, AND CU-NI ALLOYS	ALL SIZES		SHORT-CIRCUITING TRANSFER	AR-HE-CO_2 BLENDS HE-AR-CO_2 BLENDS AR-1O_2 AR-2O_2	LOW CO_2 CONTENTS IN HELIUM MIX MINIMIZE CARBON PICKUP, WHICH CAN CAUSE INTERGRANULAR CORROSION WITH SOME ALLOYS; HELIUM IMPROVES WETTING ACTION; CO_2 CONTENTS >5% SHOULD BE USED WITH CAUTION ON

					SOME ALLOYS; APPLICABLE FOR ALL POSITION WELDING
			SPRAY ARC	AR-HE-CO_2 BLENDS AR-1O_2 AR-2O_2	GOOD ARC STABILITY; PRODUCES A FLUID BUT CONTROLLABLE WELD PUDDLE; GOOD COALESCENCE AND BEAD CONTOUR; MINIMIZES UNDERCUTTING ON HEAVIER THICKNESSES
			PULSED SPRAY	AR-HE-CO_2BLENDS AR-1O_2 AR-2O_2	USED FOR BOTH LIGHT-GAGE AND HEAVY OUT-OF-POSITION WELDMENTS; ACHIEVES GOOD PULSED SPRAY STABILITY OVER A WIDE RANGE OF ARC CHARACTERISTICS AND DEPOSITION RANGES
ALUMINUM, TITANIUM, AND OTHER REACTIVE METALS	≤ 13	$\leq \frac{1}{2}$	SPRAY ARC	ARGON	BEST METAL TRANSFER, ARC STABILITY, AND PLATE CLEANING; LITTLE OR NO SPATTER; REMOVES OXIDES WHEN USED WITH DCEP (REVERSE POLARITY)
			SPRAY ARC	75HE-25AR 50HE-50AR	HIGH HEAT INPUT; PRODUCES FLUID PUDDLE, FLAT BEAD CONTOUR, AND DEEP PENETRATION; MINIMIZES POROSITY
	>13	$> \frac{1}{2}$	SPRAY ARC	HELIUM 50HE-25AR	HIGH HEAT INPUT; GOOD FOR MECHANIZED WELDING AND OVERHEAD; APPLICABLE TO HEAVY SECTION WELDING
			PULSED SPRAY	ARGON	GOOD WETTING; GOOD PUDDLE CONTROL

Argon. Pure argon is generally used on nonferrous base metal, such as aluminum, nickel, copper, and magnesium alloys, and on reactive metals, such as titanium. Argon provides excellent arc stability, penetration, and bead profile when joining these materials. Its low ionization potential results in easy arc starting. Argon produces a constricted arc column with high current density, which concentrates the arc energy over a small area; deep, fingerlike penetration results.

Carbon Dioxide. A reactive gas, carbon dioxide is generally used only for joining carbon steel. It is readily available and relatively inexpensive. Because CO_2 will not support spray transfer, deposition efficiency is lower and spatter and fume

levels are higher than with argon blends. Weld bead surfaces are more oxidized and irregular in shape. The higher ionization potential of CO_2 and its characteristic dissociation upon heating provide greater weld fusion and penetration while still achieving acceptable mechanical properties.

Helium. Because of its higher thermal conductivity, helium can provide additional heat input to the base material while still maintaining an inert atmosphere. Wetting action, depth of fusion, and travel speed can be improved over comparable argon levels. This advantage is most frequently utilized in the welding of heavier sections of aluminum, magnesium, and copper alloys.

Argon-Oxygen. The addition of a small amount of oxygen to a argon greatly stabilizes the welding arc, increases the filler metal droplet rate, lowers the spray transition current, and influences bead shape. The weld pool is more fluid and stays molten longer, allowing the metal to flow out toward the edges of the weld (Fig. 1a).

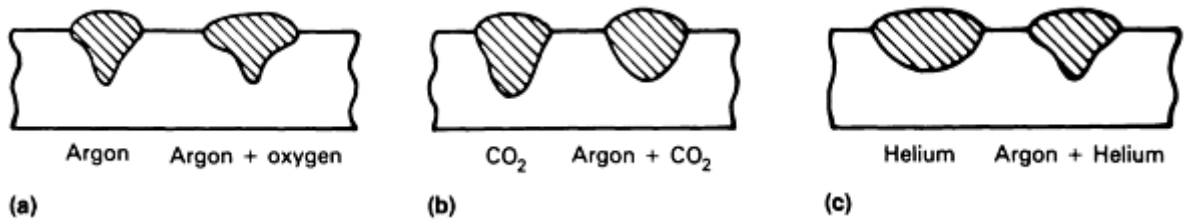

FIG. 1 EFFECT OF SHIELDING GAS BLENDS ON WELD PROFILE USING DIRECT CURRENT ELECTRODE POSITIVE (DCEP). (A) ARGON VERSUS ARGON-OXYGEN. (B) CARBON DIOXIDE VERSUS ARGON/CARBON DIOXIDE. (C) HELIUM VERSUS ARGON-HELIUM. SOURCE: REF 5

The most common blends contain 1, 2, 5, or 8% O_2 in argon. Increasing oxygen improves arc stability and makes higher travel speeds possible by enhanced puddle fluidity. Some increased alloy loss and a greater chance of undercut occur as the oxygen level is increased, especially beyond 5%.

Argon/carbon dioxide blends are primarily used for carbon and low-alloy steels and have limited use for stainless steels. The addition of CO_2 to argon produces results similar to the addition of oxygen, but is also broadens the penetration pattern as the CO_2 content is increased (Fig. 1b). Above a range of 18 to 20% CO_2, spraylike transfer can no longer be obtained; short-circuiting/globular transfer with somewhat increased spatter levels is found from this point up to approximately 50% CO_2 in argon.

The most common blends for spray transfer are argon plus 5, 8, 10, or 13 to 18% CO_2. With increased CO_2 content, the more fluid weld puddle permits higher weld travel speeds.

Mixes with higher carbon dioxide levels can also be used for short-circuiting transfer--commonly, argon plus 20 or 25% CO_2. Mixtures in this range provide an optimum droplet frequency for minimum spatter when small-diameter (0.9 and 1.2 mm, or 0.035 and 0.045 in.) wire is used.

Argon-Helium. Helium is often mixed with argon to obtain the advantages of both gases. These blends are primarily used for nonferrous base materials, such as aluminum, copper, and nickel alloys. Helium increases the heat input to the base material and thus is used for joining thick, thermally conductive plates. As the helium percentage increases, the arc voltage, spatter, and weld width-to-depth ratio increase (Fig. 1c).

The most common blends contain 25, 50, or 75% He in argon. The highest percentage of helium is used for joining thick (>50 mm, or 2 in.) plate material, especially aluminum and copper. Higher travel speeds can be obtained using helium-enhanced blends.

Argon/Oxygen/Carbon Dioxide. Mixtures containing three gas components are versatile because of their ability to operate in short-circuiting, globular, and spray-transfer modes. These blends are generally proprietary, and manufacturers' recommendations should be followed for their proper use. Blends of argon, carbon dioxide, and oxygen are generally used to join carbon and alloy steels.

Argon/Helium/Carbon Dioxide. Helium and carbon dioxide additions to argon increase the heat input to the base metal, which improves wetting, puddle fluidity, and weld bead profile. With helium plus CO_2 additions less than 40%, good spray transfer is obtained for carbon and low-alloy steel welding. Some increase in tolerance of base material surface contamination is also noted.

When the helium content exceeds 50 to 60%, transfer is restricted to short-circuiting and globular. Blends in which the CO_2 content is relatively low ($\leq 5\%$) are generally used for the joining of stainless steels without any loss in corrosion resistance.

Argon/Carbon Dioxide/Hydrogen. Three-part blends of this design are intended for the joining of austenitic stainless in the spray or short-circuiting transfer modes. Because of the addition of hydrogen, these blends should not be used for carbon steel. The carbon dioxide and hydrogen increase the heat input to the base material and improve bead shape characteristics, as well as promote higher welding travel speeds.

Shielding Gas Selection for FCAW

Carbon Dioxide. The majority of large-diameter (>1.6 mm, or $\frac{1}{16}$ in.) wires that use a shielding gas use carbon dioxide. Some smaller diameter wires are formulated to operate in 100% CO_2. The arcs are generally stable and provide a globular transfer over the usable operating range. Good performance over rust and mill scale on the plate surface is obtained with these large-diameter wires and CO_2 shielding.

Argon/Carbon Dioxide. A significant number of small-diameter (≤ 1.6 mm, or $\frac{1}{16}$ in.) cored wires are shielded with the blends of argon with 15 to 50% CO_2. These blends provide better out-of-position weld puddle control versus that of CO_2. To obtain the best performance from a particular cored wire, check the manufacturer's product literature for the recommended gas blend.

Shielding Gas Selection for GTAW

Argon. The most commonly used gas for GTAW, argon exhibits low thermal conductivity, which produces a narrow, constricted arc column; this allows greater variations in arc length with minimal influence on arc power or weld bead shape. Its low ionization potential provides good arc starting characteristics and good arc stability using the direct current electrode negative (DCEN) power connection plus superior arc cleaning action and bead appearance when ac power is used. Argon is the most commonly selected gas for DCEN welding of most materials and ac manual welding of aluminum.

Helium. The high thermal conductivity and ionization potential of helium make it suitable for the high-current joining of heavy sections of heat-conductive materials such as aluminum. Helium increases the penetration of the weld as well as its width. It also allows the use of higher weld travel speeds.

Argon-Helium. Blends of argon and helium are selected to increase the heat input to the base material while maintaining favorable arc stability and superior arc starting characteristics. Blends of 25, 50, and 75% He in argon are commonly used.

Argon-Hydrogen. Hydrogen is added to argon to enhance its thermal properties. The slightly reducing atmosphere improves weld puddle wetting and reduces some surface oxides to produce a cleaner weld surface. To minimize problems associated with arc starting, additions of hydrogen are generally limited to 5 to 15%. These blends are primarily used to join some stainless steels, nickel, and nickel alloys. These mixtures should not be used to join alloy steels; delayed weld cracking may result.

Argon/2-5H_2 is used in manual welding applications on materials thicker than 1.6 mm ($\frac{1}{16}$ in.). Additions of 10 to 15% H_2 are used in mechanized applications, such as those found in the manufacture of stainless steel tubing.

Caution: Special safety precautions are required when mixing argon and hydrogen. Do not attempt to mix argon and hydrogen from separate cylinders. Always purchase ready-mixed hydrogen blends from a qualified supplier.

Shielding Gas Selection for PAW

The physical configuration of the PAW system requires the use of two gases: a "plasma" or orifice gas and a shielding gas. The primary role of the plasma gas, which exits the torch through the center orifice, is to control arc characteristics and shield the electrode. The shielding gas, introduced around the periphery of the arc, shields or protects the weld area. In many applications, the shielding gas is also partially ionized to enhance the performance of the plasma gas.

Low-Current (<100 A) PAW. Argon is the preferred plasma gas for low-current PAW because of its low ionization potential, which ensures easy and reliable arc starting. Argon-hellium mixtures are used for some applications requiring higher heat inputs. The choice of the shielding gas depends on the type and thickness of the base material. Recommendations can be found in Table 4.

TABLE 4 RECOMMENDED GUIDELINES FOR SELECTING PAW SHIELDING GASES

MATERIAL	THICKNESS		MODE OF PENETRATION	
	MM	IN.	KEYHOLE TECHNIQUE[C]	MELT-IN TECHNIQUE[D]
LOW-CURRENT PAW[A]				
ALUMINUM COPPER	<1.6	$<\frac{1}{16}$	NOT RECOMMENDED	ARGON HELIUM
	[GES]1.6	[GES] $\frac{1}{16}$	HELIUM	HELIUM
CARBON STEEL	<1.6	$<\frac{1}{16}$	NOT RECOMMENDED	ARGON HELIUM 75AR-25HE
	[GES]1.6	[GES] $\frac{1}{16}$	ARGON 75HE-25AR	ARGON 75HE-25AR
LOW-ALLOY STEEL	<1.6	$<\frac{1}{16}$	NOT RECOMMENDED	ARGON HELIUM AR-1.5H_2
	[GES]1.6	[GES] $\frac{1}{16}$	ARGON 75HE-25AR AR-1.5H_2	ARGON HELIUM AR-1.5H_2
STAINLESS STEEL, NICKEL ALLOYS	<1.6	$<\frac{1}{16}$	ARGON 75HE-25AR AR-1.5H_2	ARGON HELIUM AR-1.5H_2
	[GES]1.6	[GES] $\frac{1}{16}$	ARGON 75HE-25AR AR-1.5H_2	ARGON HELIUM AR-1.5H_2
HIGH-CURRENT PAW[B]				
ALUMINUM	<6.4	$<\frac{1}{4}$	ARGON	ARGON 75-25AR
	[GES]6.4	[GES] $\frac{1}{4}$	HELIUM	HELIUM 75-25AR
COPPER	<2.4	$<\frac{3}{32}$	NOT RECOMMENDED	HELIUM
CARBON STEEL; LOW-ALLOY STEEL	<3.2	$<\frac{1}{8}$	ARGON	ARGON
	[GES]3.2	[GES]	ARGON	75HE-25AR

		$\frac{1}{8}$		
STAINLESS STEEL; NICKEL ALLOYS	<3.2	$<\frac{1}{8}$	ARGON AR-5H_2	ARGON
	[GES]3.2	[GES] $\frac{1}{8}$	ARGON AR-5H_2	75-HE-25AR

Source: Ref 6, 7

(A) GAS SELECTIONS SHOWN ARE FOR SHIELDING GAS ONLY. ORIFICE GAS IN ALL CASES IS ARGON.

(B) GAS SELECTIONS SHOWN ARE FOR BOTH THE ORIFICE AND SHIELDING GAS.

(C) PROPERLY BALANCED GAS FLOW RATES PRODUCE COMPLETE JOINT PENETRATION BY FORMING A SMALL WELD POOL WITH A HOLE PENETRATING COMPLETELY THROUGH THE BASE METAL. AS THE PLASMA TORCH IS MOVED, METAL MELTED BY THE ARC IS FORCED TO FLOW AROUND THE PLASMA STEAM PRODUCING THE "KEYHOLE" TO THE REAR WHERE THE WELD POOL IS FORMED AND SOLIDIFIED.

(D) CONVENTIONAL FUSION WELDING SIMILAR TO THAT DONE WITH GTAW.

High-Current ([ges]100 A) PAW. The choice of gas used for high-current PAW also depends on the material to be welded. In almost all cases, the shielding gas is the same as the orifice gas. Again, argon is suitable for welding all metals, but it does not necessarily produce optimum results. Depending on the welding mode used (keyhole or melt-in), the optimum gas blend will vary. Table 4 lists gases recommended on the basis of materials joined.

References cited in this section

3. "SPECIFICATION FOR SHIELDING GASES," AWS A5.32-9X, JULY 1991 (DRAFT)
4. "GASES FOR GAS-SHIELDED ARC WELDING AND CUTTING," EUROPEAN STANDARD EN 439, DEC 1990 (DRAFT)
5. H.B. CARY, *MODERN WELDING TECHNOLOGY*, 2ND ED., PRENTICE-HALL, 1989
6. N.E. LARSON AND W.F. MEREDITH, *SHIELDING GAS SELECTION MANUAL*, UNION CARBIDE INDUSTRIAL GASES TECHNOLOGY CORP., 1990, P 30-32
7. N.E. LARSON AND W.F. MEREDITH, *SHIELDING GAS SELECTION MANUAL*, UNION CARBIDE INDUSTRIAL GASES TECHNOLOGY CORP., 1990, P 18-19

Shielding Gases for Welding

Kevin A. Lyttle, Praxair, Inc.

Influence of Shielding Gas on Weld Mechanical Properties

The mechanical properties of a weld are dependent on specific characteristics of the shielding gas. When the gas blend is totally inert, the effects are less pronounced and are derived more indirectly. In this case, the shielding gas affects penetration and solidification, which can influence the microstructure of the resulting weld.

When the shielding gas contains active components, such as oxygen or carbon dioxide, the influence is direct and more substantial. The oxygen potential of the shielding gas influences the amount of surface slag, the fume emission rate, the fluidity of the weld puddle, and the mechanical properties (both strength and toughness) of the weld metal. A number of empirical formulas have been developed to estimate the oxygen potential of a gas blend (Ref 8); the differences lie in their treatment of the CO_2 component of the gas mix. Because parameters other than gas composition can affect the

oxygen level of the weld metal (e.g., welding speed), most of the recently developed formulas are also welding parameter and material specific. Their importance centers on how the oxidation potential is linked to elemental loss of silicon and manganese in the weld metal, to weld metal oxygen content, and to weld mechanical properties.

Because a relatively complex relationship exists between the loss of alloying elements, the composition of the shielding gas, and the mechanical properties of the resulting weld metal it is difficult to select an optimum gas blend that will work well with all types of wires. This influence is most noticeable in the gas metal-arc welding of carbon steel. Figure 2 (Ref 8) and Table 5 (Ref 9) illustrate the effect of the shielding gas on impact strength and tensile strength. In general, as the oxidation potential of the shielding gas increases, the toughness and the tensile strength of the weld deposit decrease. Because of their lower oxidizing gas content, argon blends will generally produce weld properties superior to those obtained by shielding with CO_2 only. There appears to be an "optimum" oxygen content, as too low an oxygen level can also be detrimental to toughness.

TABLE 5 EFFECT OF SHIELDING GAS ON CARBON, MANGANESE, AND SILICON LOSSES AND ON WELD STRENGTH VALUES

SHIELDING GAS[A]	ULTIMATE TENSILE STRENGTH		YIELD STRENGTH		ELONGATION, %	WELD METAL COMPOSITION, %[B]		
	MPA	KSI	MPA	KSI		C	MN	SI
AR-10CO_2	640	92.9	544	79.0	25.7	0.09	1.43	0.72
AR-18CO_2	620	90.0	522	75.8	26.8	0.09	1.37	0.70
AR-5CO_2-4O_2	610	88.5	472	68.5	28.1	0.08	1.32	0.67
AR-25CO_2	601	87.2	505	73.3	29.3	0.09	1.30	0.65
AR-12O_2	591	85.8	510	74.0	27.5	0.06	1.20	0.60
CO_2	594	86.2	487	70.7	27.8	0.10	1.21	0.62

Source: Ref 9

(A) GASES LISTED IN ORDER OF INCREASING OXIDATION POTENTIAL.

(B) BASE WIRE COMPOSITION: 0.115% C, 1.53% MN, 0.98% SI.

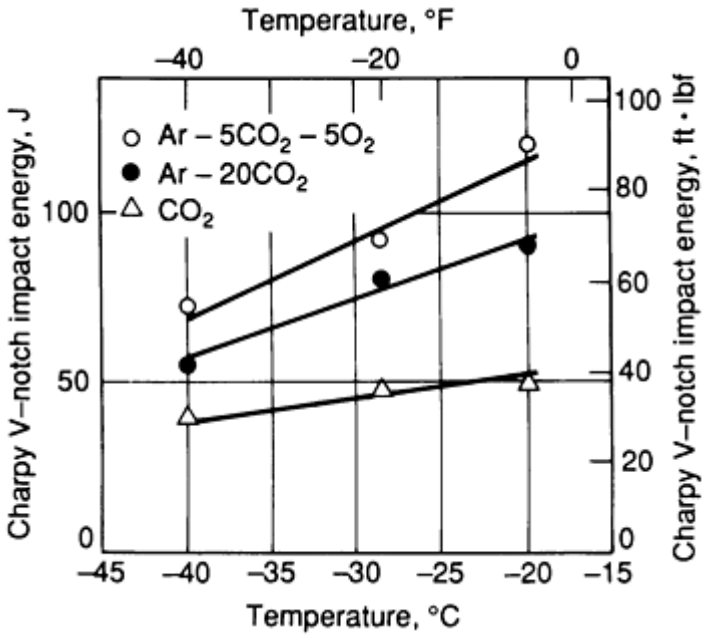

FIG. 2 PLOT OF WELD METAL IMPACT ENERGY VERSUS TEST TEMPERATURE AS A FUNCTION OF SHIELDING GAS COMPOSITION. SOURCE: REF 8

References cited in this section

8. N. STENBACKA AND K.A. PERSSON, SHIELDING GASES FOR GAS METAL ARC WELDING, *WELD.J.*, VOL 68, NOV 1989, P 41-47
9. H.U. POMASKA, "SHIELDING GASES FOR ARC WELDING AND CUTTING," SONDERDRUCK 48, LINDE AG, LINDE TECHNISCHE GASES, HOLRIEGELSKREUTH, GERMANY

Shielding Gases for Welding

Kevin A. Lyttle, Praxair, Inc.

Shielding Gas and Fume Generation

The shielding gas used in solid and flux-cored wire welding affects the rate at which fumes are produced during welding, as well as the composition of the fumes. The type of shielding gas also affects the composition of the pollutant gases in the welding area. The fumes and gases generated in some welding applications impact on health and safety; therefore, it is important for the user to review the Material Safety Data Sheets and precautionary labeling provided by the manufacturers and suppliers of welding consumables. Welding safety and health information can be also be found in this Handbook and in ANSI Z49.1, "Safety in Welding and Cutting."

Fume generation rates are generally highest when CO_2 shielding is used. Inert gas blends containing CO_2 produce higher fume levels than those containing only oxygen additions. For solid wire welding at the same weld metal deposition rate, argon blends typically generate significantly less fumes than when CO_2 only is used (Ref 10, 11, 12). Figure 3 (Ref 13) illustrates the dependence of the fume generation rate on shielding gas composition as a function of current level in GMAW. Similar trends can be seen when using gas-shielded flux-cored wires.

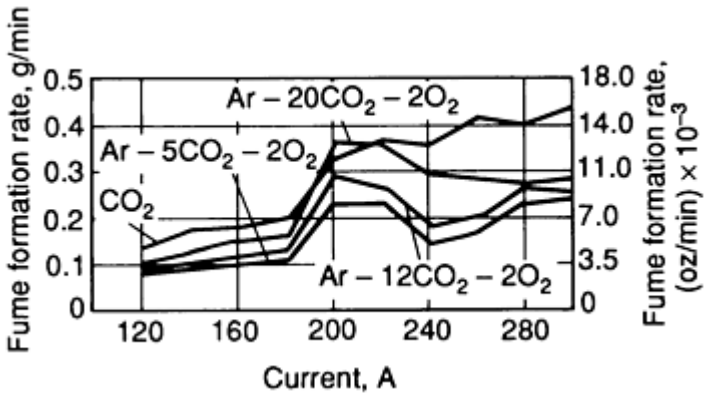

FIG. 3 PLOT OF FUME FORMATION RATE VERSUS CURRENT FOR MILD STEEL SOLID WIRE USING SELECTED SHIELDING GASES. SOURCE: REF 13

Pollutant gases must be considered when arc welding. The gases of greatest interest arc carbon monoxide, ozone, and nitrogen oxides. When CO_2 is used for shielding in confined spaces, CO can be a potential problem. Ozone can be a concern when high-energy gas-shielded welding is conducted, particularly on aluminum and stainless steel plate. It is produced in the immediate arc area as well as in the surrounding environment. Oxides of nitrogen can be present in some plasma welding and cutting applications (Ref 14).

References cited in this section

10. R.F. HEILE AND D.C. HILL, PARTICULATE FUME GENERATION IN ARC WELDING PROCESSES, *WELD.J.*, VOL 54, JULY 1975, P 201S-210S
11. H. PRESS AND W. FLORIAN, CONTRIBUTION ON THE FORMATION OF TOXIC SUBSTANCES IN GAS SHIELDED ARC WELDING AND DETERMINATION OF DESIRED EXHAUSTION CAPACITY, *IIW PROCEEDINGS OF COLLOQUIUM ON WELDING AND HEALTH*, PORTUGAL, JULY 1980
12. B. HAAS, INFLUENCE OF PROCESS SPECIFIC WELDING PARAMETERS IN FUME GENERATION IN SOLID WIRE, GMA/MAG WELDING, *IIW PROCEEDINGS OF COLLOQUIUM ON WELDING SAFETY AND HEALTH*, PORTUGAL, JULY 1980
13. D.E. HILTON AND P.N. PLUMRIDGE, PARTICULATE FUME GENERATION DURING GMAW AND GTAW, *WELD. MET. FABR.*, VOL 59 (NO. 10), DEC 1991, P 555-560
14. N. JENKINS, J. MORETON, P.J. OAKLEY, AND S.M. STEVENS, *WELDING FUMES SOURCES, CHARACTERISTICS, CONTROL*, VOL 2, THE WELDING INSTITUTE, CAMBRIDGE, UNITED KINGDOM, 1981, P 272

Shielding Gases for Welding

Kevin A. Lyttle, Praxair, Inc.

Self-Shielded Flux-Cored Arc Welding

The self-shielded flux-cored wire welding process employs a continuous wire electrode that requires no external shielding. These cored wires generate protective shielding gases from components in the core material similar to those found in coated electrodes. The unique feature of this class of consumables is that they rely only partly on the exclusion of air from the molten electrode and weld pool to produce a quality deposit. In addition to deoxidizers, they contain denitriders to react with nitrogen that may be entrained in the molten metal. The less a given consumable relies on shielding and the more it relies on "killing" to control nitrogen and produce sound weld metal, the less that consumable will be affected by cross air currents and side winds.

Through careful control of welding parameters and the proper balance of core constituents, good-quality weld metal can be obtained under poor welding conditions. Self-shielded flux-cored wires are especially suited to welding outdoors, where it is difficult to provide acceptable external gas shielding. Both light- and heavy-gage materials have been successfully joined with these electrodes.

Shielding Gases for Welding

Kevin A. Lyttle, Praxair, Inc.

References

1. N.E. LARSON AND W.F. MEREDITH, *SHIELDING GAS SELECTION MANUAL*, UNION CARBIDE INDUSTRIAL GASES TECHNOLOGY CORP., 1990, P 10
2. N.E. LARSON AND W.F. MEREDITH, *SHIELDING GAS SELECTION MANUAL*, UNION CARBIDE INDUSTRIAL GASES TECHNOLOGY CORP., 1990, P 11
3. "SPECIFICATION FOR SHIELDING GASES," AWS A5.32-9X, JULY 1991 (DRAFT)
4. "GASES FOR GAS-SHIELDED ARC WELDING AND CUTTING," EUROPEAN STANDARD EN 439, DEC 1990 (DRAFT)

5. H.B. CARY, *MODERN WELDING TECHNOLOGY*, 2ND ED., PRENTICE-HALL, 1989
6. N.E. LARSON AND W.F. MEREDITH, *SHIELDING GAS SELECTION MANUAL*, UNION CARBIDE INDUSTRIAL GASES TECHNOLOGY CORP., 1990, P 30-32
7. N.E. LARSON AND W.F. MEREDITH, *SHIELDING GAS SELECTION MANUAL*, UNION CARBIDE INDUSTRIAL GASES TECHNOLOGY CORP., 1990, P 18-19
8. N. STENBACKA AND K.A. PERSSON, SHIELDING GASES FOR GAS METAL ARC WELDING, *WELD.J.*, VOL 68, NOV 1989, P 41-47
9. H.U. POMASKA, "SHIELDING GASES FOR ARC WELDING AND CUTTING," SONDERDRUCK 48, LINDE AG, LINDE TECHNISCHE GASES, HOLRIEGELSKREUTH, GERMANY
10. R.F. HEILE AND D.C. HILL, PARTICULATE FUME GENERATION IN ARC WELDING PROCESSES, *WELD.J.*, VOL 54, JULY 1975, P 201S-210S
11. H. PRESS AND W. FLORIAN, CONTRIBUTION ON THE FORMATION OF TOXIC SUBSTANCES IN GAS SHIELDED ARC WELDING AND DETERMINATION OF DESIRED EXHAUSTION CAPACITY, *IIW PROCEEDINGS OF COLLOQUIUM ON WELDING AND HEALTH*, PORTUGAL, JULY 1980
12. B. HAAS, INFLUENCE OF PROCESS SPECIFIC WELDING PARAMETERS IN FUME GENERATION IN SOLID WIRE, GMA/MAG WELDING, *IIW PROCEEDINGS OF COLLOQUIUM ON WELDING SAFETY AND HEALTH*, PORTUGAL, JULY 1980
13. D.E. HILTON AND P.N. PLUMRIDGE, PARTICULATE FUME GENERATION DURING GMAW AND GTAW, *WELD. MET. FABR.*, VOL 59 (NO. 10), DEC 1991, P 555-560
14. N. JENKINS, J. MORETON, P.J. OAKLEY, AND S.M. STEVENS, *WELDING FUMES SOURCES, CHARACTERISTICS, CONTROL*, VOL 2, THE WELDING INSTITUTE, CAMBRIDGE, UNITED KINGDOM, 1981, P 272

Solid-State Transformations in Weldments

P. Ravi Vishnu, Luleå University of Technology, Sweden

Introduction

SOLID-STATE TRANSFORMATIONS occurring in a weld are highly nonequilibrium in nature and differ distinctly from those experienced during casting, thermomechanical processing, and heat treatment. This discussion will primarily focus on the welding metallurgy of fusion welding of steels and attempt to highlight the fundamental principles that form the basis of many of the recent developments in steels and consumables for welding. Accordingly, examples are largely drawn from the well-known and relatively well-studied case of ferritic steel weldments to illustrate the special physical metallurgical considerations brought about by the weld thermal cycles and by the welding environment. Because of space limitations, only a very brief discussion is included on welds in other alloy systems such as stainless steels and aluminum-base, nickel-base, and titanium-base alloys. For detailed information on how the principles explained in the first part of this article (using steel weldments as an example) are applicable to other materials, the reader is referred to the Sections where individual alloy systems are discussed (see "Selection of Stainless Steels," "Selection of Nonferrous Low-Temperature Materials," "Selection of Nonferrous High-Temperature Materials," and "Selection of Nonferrous Corrosion-Resistant Materials" in this Volume).

A concise method of describing the transformation behavior of a steel is by a continuous cooling transformation (CCT) diagram (Fig. 1). However, a conventional CCT diagram such as the one shown in Fig. 1 cannot be used to accurately describe the transformation behavior in a weldment of the same material because weld thermal cycles are very different from those used for generating conventional CCT diagrams.

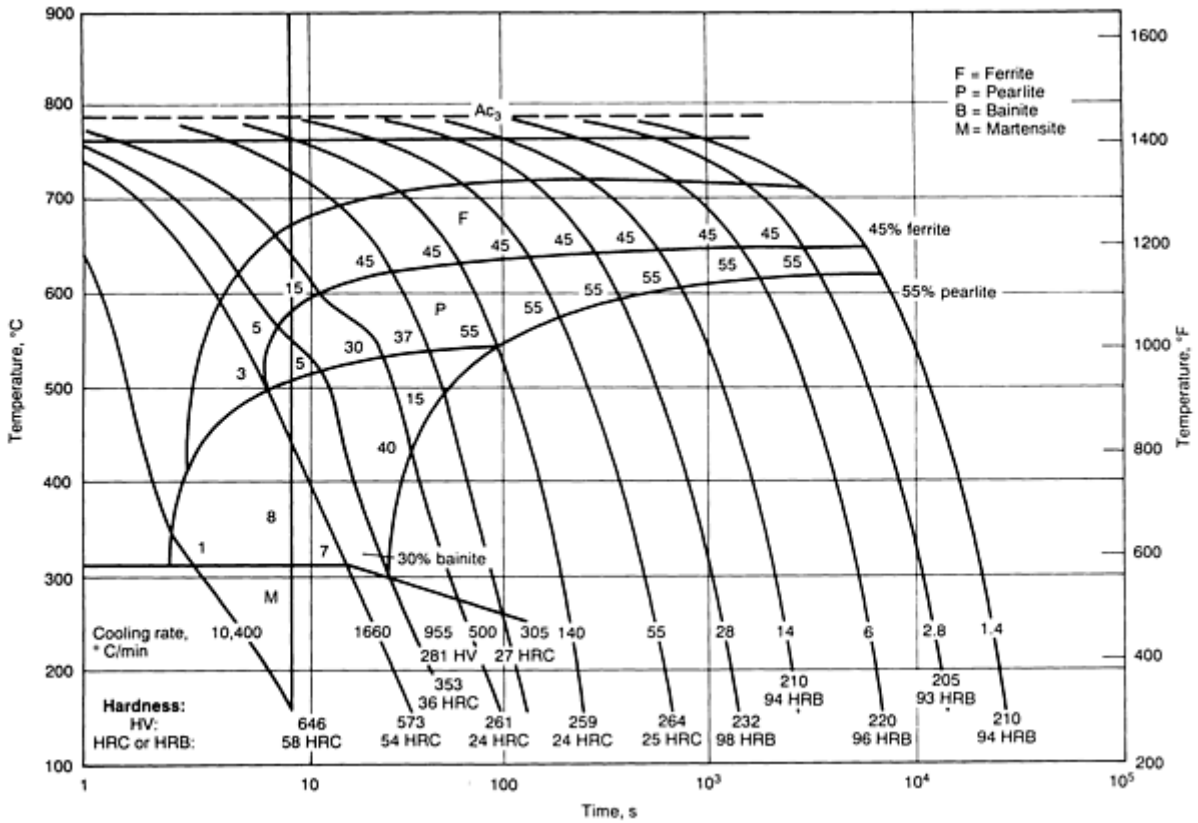

FIG. 1 CONVENTIONAL CCT DIAGRAM FOR AISI 1541 (0.39C-1.56MN-0.21SI-0.24S-0.010P) PLAIN CARBON STEEL WITH ASTM NUMBER 8 GRAIN SIZE AND AUSTENITIZATION AT 980 °C (1800 °F). FOR EACH OF THE COOLING CURVES IN THE PLOT (GIVEN IN TERMS OF °C/MIN), THE TRANSFORMATION START AND END TEMPERATURES GIVEN BY THE CCT CURVES, THE AMOUNT OF EACH TRANSFORMATION PRODUCT, AND THE HARDNESS OF THE FINAL STRUCTURE ARE SHOWN. AC_3, 788 °C (1450 °F); AC_1, 716 °C (1321 °F). F, FERRITE; P, PEARLITE; B, BAINITE; M, MARTENSITE. SOURCE: REF 1

Acknowledgements

The author would like to convey his immense gratitude to the late Professor K. Easterling, University of Exeter, U.K., for giving him the opportunity to write this article and for his constant support and encouragement. The author thanks Dr. Bengt Loberg and Professor Richard Warren of the Department of Engineering Materials, University of Luleå, for their active encouragement. The author would also like to thank Dr. H.K.D.H. Bhadeshia, University of Cambridge, U.K., and Dr. K. Sampath, Concurrent Technologies Corporation, Johnstown, PA, for valuable technical consultation.

Reference

1. *ATLAS OF ISOTHERMAL TRANSFORMATION AND COOLING TRANSFORMATION DIAGRAMS* AMERICAN SOCIETY FOR METALS, 1977

P. Ravi Vishnu, Luleå University of Technology, Sweden

Special Factors Affecting Transformation Behavior in a Weldment

Several aspects of the weld thermal cycle and weld segregation should be considered because of their effect on the transformation upon cooling:

- PEAK TEMPERATURES REACHED IN THE HEAT-AFFECTED ZONE (HAZ) CAN BE VERY MUCH HIGHER THAN THE AC_3 TEMPERATURE (THAT IS, THE TEMPERATURE AT WHICH TRANSFORMATION OF FERRITE TO AUSTENITE IS COMPLETED DURING HEATING). THE HEATING RATES ARE VERY HIGH, AND THE TIMES SPENT AT HIGH TEMPERATURE ARE ONLY OF THE ORDER OF A FEW SECONDS.
- THE TEMPERATURE GRADIENT IN THE HAZ IS VERY STEEP, AND THIS COMPLICATES THE PROBLEM OF STUDYING IN *IN SITU* TRANSFORMATIONS IN THE HAZ DURING WELDING (REF 2).
- DURING SOLIDIFICATION OF THE WELD METAL, ALLOYING AND IMPURITY ELEMENTS TEND TO SEGREGATE EXTENSIVELY TO THE INTERDENDRITIC OR INTERCELLULAR REGIONS UNDER THE CONDITIONS OF RAPID COOLING. ALSO, THE PICKUP OF ELEMENTS LIKE OXYGEN BY THE MOLTEN WELD POOL LEADS TO THE ENTRAPMENT OF OXIDE INCLUSIONS IN THE SOLIDIFIED WELD. THESE INCLUSIONS THEN SERVE AS HETEROGENEOUS NUCLEATION SITES AND CAN SUBSTANTIALLY INFLUENCE THE KINETICS OF SUBSEQUENT SOLID STATE TRANSFORMATIONS. ACCORDINGLY, THE WELD METAL TRANSFORMATION BEHAVIOR IS QUITE DIFFERENT FROM THAT OF THE BASE METAL, EVEN THOUGH THE NOMINAL CHEMICAL COMPOSITION HAS NOT BEEN SIGNIFICANTLY CHANGED BY THE WELDING PROCESS (REF 3). MOST OF THE CCT DIAGRAMS (APPLICABLE TO THE WELD METAL) HAVE BEEN GENERATED BY REHEATING THE AS-DEPOSITED WELD METAL (REF 4). ONE OF THE LIMITATIONS OF THESE DIAGRAMS IS THAT THEY ARE STRICTLY APPLICABLE ONLY TO THE HIGH-TEMPERATURE REHEATED ZONE OF MULTIPASS WELDS, BECAUSE THE INITIAL MICROSTRUCTURE AT HIGH TEMPERATURES IS NOT CHARACTERISTIC OF THAT DEVELOPED FROM THE LIQUID PHASE.
- WELDING MAY BE CARRIED OUT IN SEVERAL PASSES, AND THIS MAY RESULT IN THE SUPERPOSITION OF SEVERAL DIFFERENT HEATING AND COOLING CYCLES AT ONE POINT, EACH OF THESE CYCLES HAVING THE CHARACTERISTICS NOTED ABOVE.
- SOLIDIFICATION OF THE WELD METAL IS ACCOMPANIED BY SHRINKAGE, AND THE ANISOTHERMAL CONDITIONS ALREADY EMPHASIZED CAUSE DEFORMATION. THE THERMAL CYCLES ARE THEREFORE ACTING ON METAL THAT IS SUBJECTED TO MECHANICAL STRESSES AT THE SAME TIME.

The essential differences between weld thermal cycles and then thermal cycles used for generating a conventional CCT diagram are summarized in Fig. 2. Figure 2(a) shows thermal cycles which involve a slow heating rate, soak at a temperature just above the Ac_3 temperature, and various constant cooling rates. Instead of a constant cooling rate, some investigators (Ref 5) have used cooling curves according to Newton's law of cooling:

$$T \propto E^{-T} \qquad \textbf{(EQ 1)}$$

where T is the temperature and t is the time. Others have used cooling curves corresponding to the mid-radial position of cylindrical bars of different diameters when cooled in air or when quenched in different media. The weld thermal cycles shown in Fig. 2(b) are very different, and this is why a conventional CCT diagram can give only an approximate idea of the transformation behavior in the HAZ of a weldment.

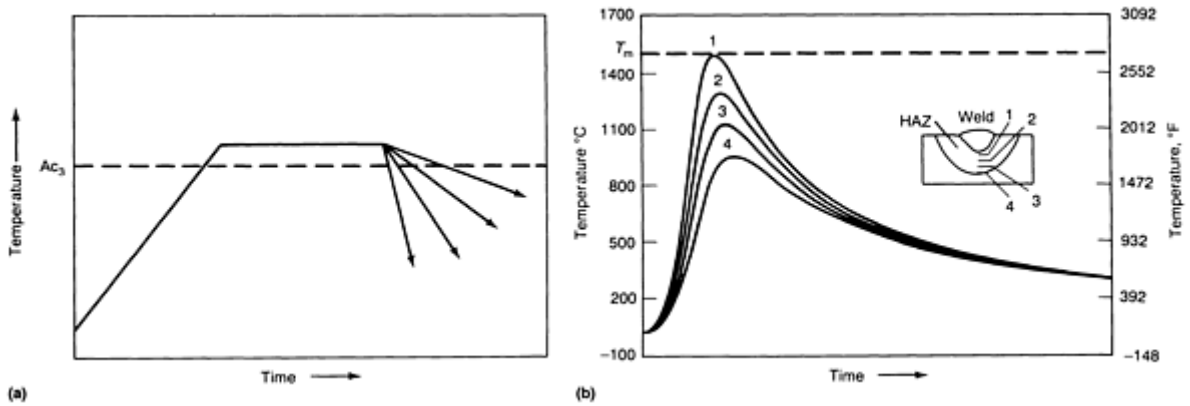

FIG. 2 GRAPHS TO SHOW DIFFERENCES IN THERMAL CYCLES. (A) THERMAL CYCLES USED TO GENERATE A CONVENTIONAL CCT DIAGRAM. (B) WELD THERMAL CYCLES. THE NUMBERS IN (B) CORRESPOND TO LOCATIONS INDICATED IN THE HAZ. NOTE THE CORRESPONDENCE BETWEEN THE THERMAL CYCLES IN (A) AND THOSE IN FIG. 1

References cited in this section

2. O.M. AKSELSEN AND T. SIMONSEN, TECHNIQUES FOR EXAMINING TRANSFORMATION BEHAVIOUR IN WELD METAL AND HAZ--A STATE OF ART REVIEW, *WELD. WORLD*, VOL 25 (NO. 1/2), 1987, P 26-34
3. O. GRONG AND D.K. MATLOCK, MICROSTRUCTURAL DEVELOPMENT IN MILD AND LOW ALLOY STEEL WELD METALS, *INT. MET. REV.*, VOL 31 (NO. 1), 1986, P 27-48
4. P.L. HARRISON AND R.A. FARRAR, APPLICATION OF CONTINUOUS COOLING TRANSFORMATION DIAGRAMS FOR WELDING OF STEELS, *INT. MATER. REV.*, VOL 34 (NO. 1), 1989, P 35-51
5. G.T. ELDIS, A CRITICAL REVIEW OF DATA SOURCES FOR ISOTHERMAL TRANSFORMATION AND CONTINUOUS COOLING TRANSFORMATION DIAGRAMS, *HARDENABILITY CONCEPTS WITH APPLICATION TO STEEL*, D.V. DOANE AND J.S. KIRKALDY, ED., TMS-AIME, 1978, P 126-157

Solid-State Transformations in Weldments

P. Ravi Vishnu, Luleå University of Technology, Sweden

HAZ of a Single-Pass Weld

Peak Temperature-Cooling Time Diagrams. The gradient in microstructure than can be obtained in a single-pass weld is shown in Fig. 3. High peak temperatures in the HAZ just adjacent to the fusion line cause coarsening of the austenite (γ) grains, and this in turn increases the hardenability of this region compared to other regions. Because each of the subzones shown in Fig. 3 occurs in a small volume, it is difficult to study the transformation behavior of individual regions by *in situ* methods (Ref 2). It is more convenient to obtain information about the microstructural and property changes in the HAZ by weld simulation (Ref 6, 7). A thermal cycle simulator (TCS) is used to reproduce the thermal cycle corresponding to a point in the HAZ in a large volume (usually a specimen has the Charpy test specimen dimensions). It is possible to program the required thermal cycle in the TCS so that the peak temperature and the cooling rate can be varied independently. It is thus possible to obtain information about the microstructural changes in the HAZ for a wide range of welding parameters.

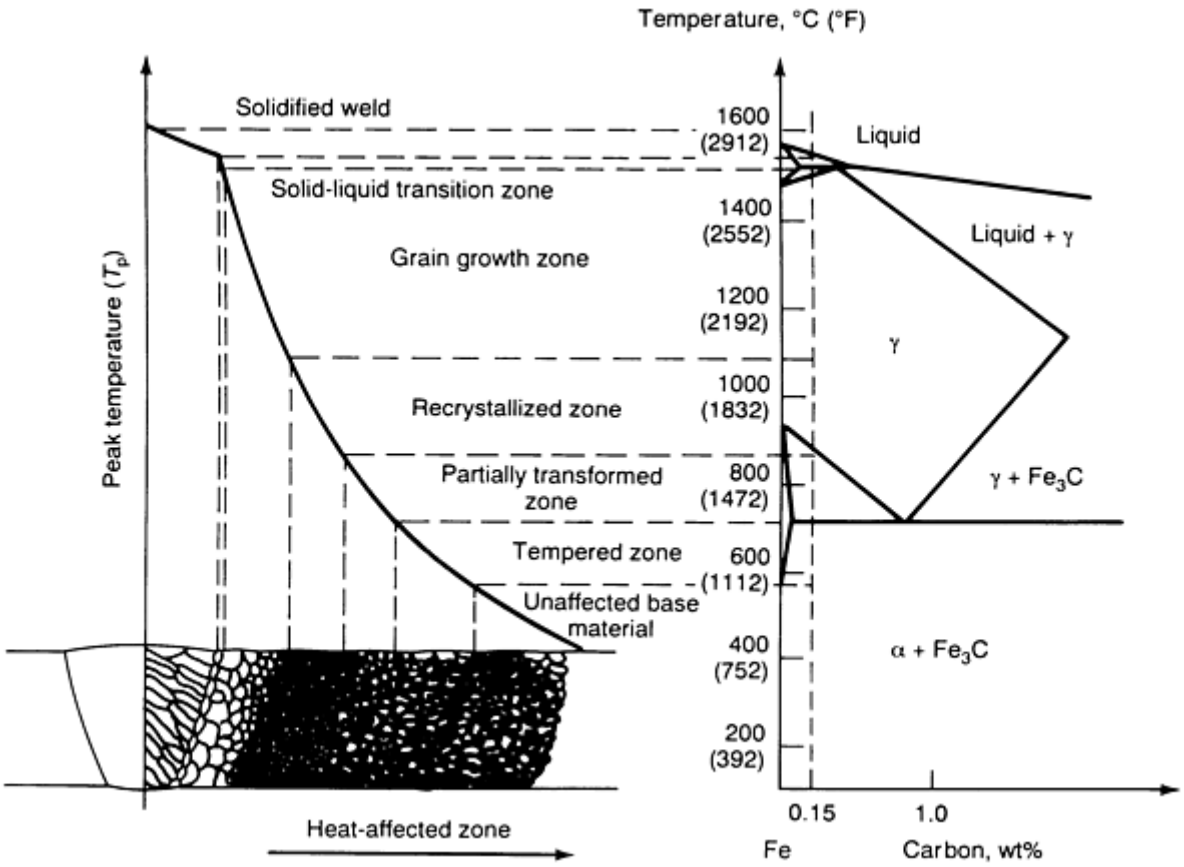

FIG. 3 SCHEMATIC SHOWING VARIOUS SUBZONES THAT CAN FORM IN THE HAZ OF A CARBON STEEL CONTAINING 0.15% C. SOURCE: REF 6

Figure 4 shows how a change in the peak temperature of the thermal cycle affects the CCT characteristics of a steel. The well-known effect of a larger γ grain size (due to a higher peak temperature) in increasing the hardenability of the steel is seen. To present the information about the CCT behavior for a number of peak temperatures (see Fig. 2b and 3), it is more convenient to adopt the scheme shown in Fig. 5. In this peak temperature-cooling time (PTCT) diagram (Ref 8, 9), each point represents a weld thermal cycle with a peak temperature, T_p, given by the ordinate and the cooling time, $\Delta t_{8\text{-}5}$ (that is, required for cooling from 800 to 500 °C, or 1470 to 930 °F), given by the abscissa. A microstructural constituent or a combination of two or more constituents is shown to occur over an area in the diagram. The upward slope in the boundary between two areas is consistent with the information presented earlier in Fig. 4 that the hardenability increases with an increase in the peak temperature of the thermal cycle. Hardness and C_v transition temperatures are also shown in the diagram corresponding to different thermal cycles.

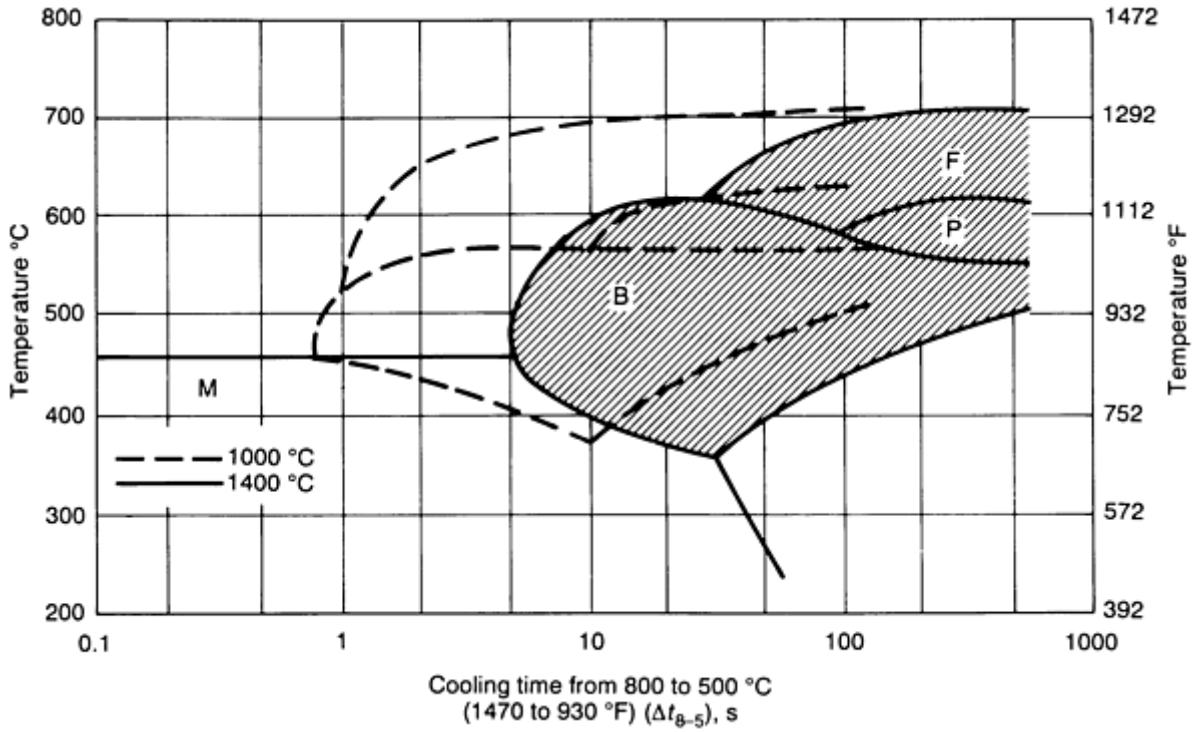

FIG. 4 EFFECT OF A CHANGE IN THE PEAK TEMPERATURE OF THE WELD THERMAL CYCLE (FROM 1000 TO 1400 °C, OR 1830 TO 2550 °F) ON THE CCT CHARACTERISTICS. M, MARTENSITE; B, BAINITE; P, PEARLITE; F, FERRITE. SOURCE: REF 8

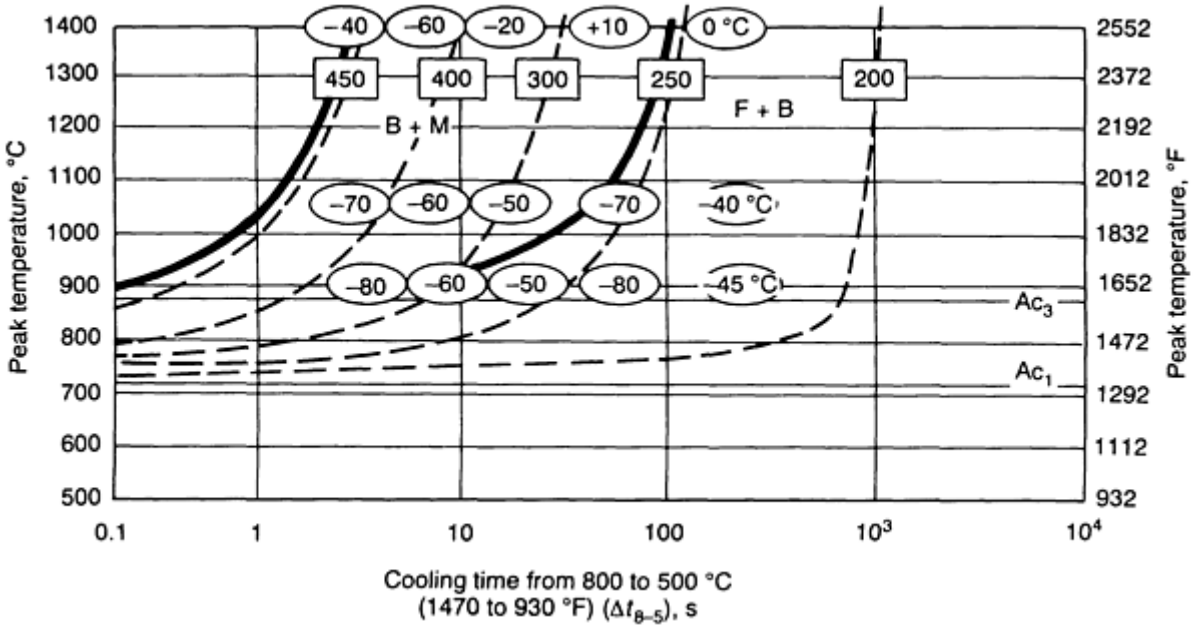

FIG. 5 TYPICAL PEAK TEMPERATURE VERSUS COOLING TIME DIAGRAM, SHOWING THE EFFECTS OF THESE PARAMETERS OF A WELD THERMAL CYCLE ON THE FINAL TRANSFORMATION PRODUCTS, ON HARDNESS, AND CHARPY V-NOTCH IMPACT ENERGY. M, MARTENSITE; B, BAINITE; F, FERRITE. FIGURES IN SQUARES INDICATE THE HARDNESS (30 HV); FIGURES IN OVALS INDICATE THE 21 J (16 FT · LBF) TRANSITION TEMPERATURES FOR CHARPY V-NOTCH IMPACT SPECIMENS SUBJECTED TO A SPECIFIC THERMAL CYCLE. SOURCE: REF 9

It may appear strange that the CCT diagram shown in Fig. 4 is plotted with $\Delta t_{8\text{-}5}$ as the abscissa instead of time as in Fig. 1. Historically, the practice of thinking in terms of a cooling time began when a need was recognized (Ref 5) to compare the CCT behavior of specimens subjected to different types of cooling curves--Jominy specimens; cylindrical bars cooled in air, water, or oil; dilatometer specimens cooled at a constant or a Newtonian rate; and so on. Initially, the cooling rate at 704 °C (1300 °F) was used as a criterion to judge the equivalency of these specimens in terms of microstructure and hardness. Because transformation takes place at lower temperatures in many steels, the half cooling time (Ref 5) was found to be a better equivalency criterion. The half cooling time was defined as the time to cool from Ac_3 to a temperature that lies midway between Ac_3 and room temperature. For the sake of general applicability, this was later modified to the $\Delta t_{8\text{-}5}$ criterion, and CCT diagrams began to be plotted with $\Delta t_{8\text{-}5}$ as the abscissa. It must be noted that using $\Delta t_{8\text{-}5}$ as an equivalency criterion is just an expedient solution that does not have strict theoretical justification (refer, for example, to the additivity principle in Ref 5).

A special significance of using $\Delta t_{8\text{-}5}$ as the abscissa in Fig. 5 is that it is almost constant (for T_p > 900 °C, or 1650 °F) in the whole of the HAZ. This can be seen from Ref 6, where the expressions given for $\Delta t_{8\text{-}5}$ do not contain the distance from the weld centerline as a factor. The derivation of these expressions is based on the assumption that the time to cool to 800 °C (1470 °F) is far greater than the time to reach the peak temperature, so the $\Delta t_{8\text{-}5}$ can be taken to be the same for the whole of the weld and the HAZ. This can be intuitively rationalized by observing that the thermal cycles in Fig. 2(b) are such that the curves are approximately parallel below 800 °C (1470 °F). The constancy of $\Delta t_{8\text{-}5}$ in the HAZ means that the gradient in microstructure (in terms of the final transformation products from austenite) is mainly due to a variation in the peak temperature. By drawing a vertical line in Fig. 5 at a value of $\Delta t_{8\text{-}5}$ corresponding to a given heat input and preheating temperature, it is possible to get information about the type of microstructural gradient in the HAZ. An idea of property changes like hardness and toughness can also be obtained from Fig. 5.

A fairly satisfactory correlation between real welds and simulation studies has been observed with respect to microstructure and property measurements. However, it has frequently been observed that the maximum prior to austenite grain size in real welds is less than that in corresponding simulation specimens (Ref 2, 6, 7). It is believed that this is due to the growth of large grains in the HAZ of real welds being hindered by the adjacent smaller grains. The constraint arises from the fact that grain growth in real welds is in some sense directional, occurring from the fusion line toward lower temperatures, while under the simulation condition the austenite grains can grow in all directions.

The above discussion shows that the PTCT diagram (along with property measurements, as in Fig. 5) can alert the user to the possibility of local brittle zones in actual weldments, and that any error in the property being assessed will be on the conservative side.

While the expressions for $\Delta t_{8\text{-}5}$ given Ref 6 (to determine the point at which a vertical line is to be drawn in the PTCT diagram) are reasonably accurate, those for T_p may be grossly in error because they are derived from a model with many simplistic assumptions (Ref 10, 11). For this reason, although an idea of the type of microstructural gradient in the HAZ can be obtained from the PTCT diagram, it is not possible to calculate the width of each region using simple closed form solutions of the type given in Ref 6 (derived from Rosenthal's equations). Moreover, T_p and $\Delta t_{8\text{-}5}$ are alone not enough to completely characterize a weld thermal cycle. To improve the accuracy of simulation, it would be necessary to program the thermal cycle with heating rates and the shape of the thermal cycle at higher temperatures, as in the HAZ of real welds. The significance of these additional factors is discussed below.

Continuous Heating Transformation Diagrams. The heating rate in many welding processes can be very high. The implication is that considerable superheating may be required for the transformation to austenite on heating. That is, the Ac_1 and Ac_3 temperatures will be raised with an increase in the heating rate (Ref 11). This is seen in Fig. 6, a continuous heating transformation (CHT) diagram, which is analogous to a CCT diagram. It is seen that grain growth begins only after the carbides have dissolved and after a homogeneous austenite (with respect to the distribution of carbon, at least) is formed.

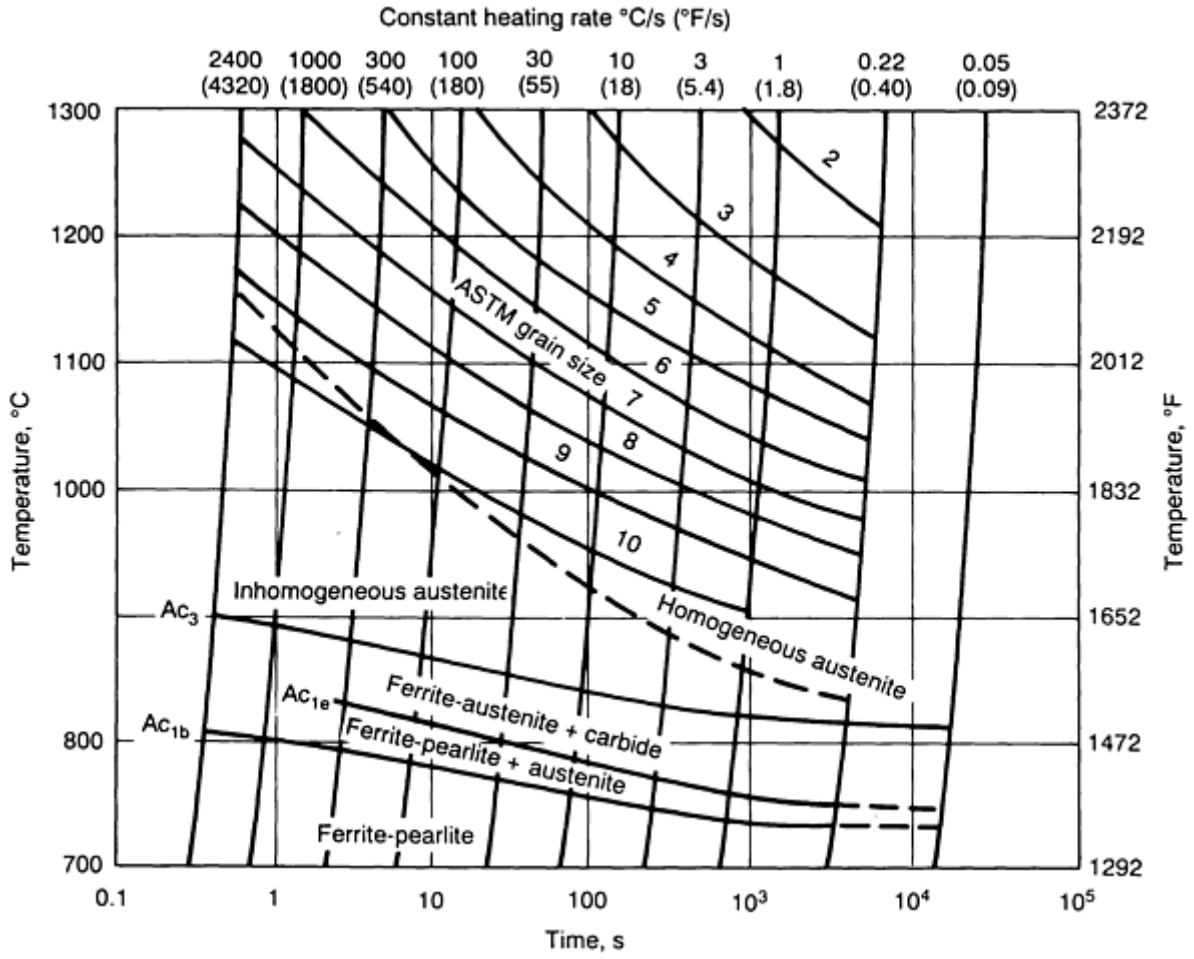

FIG. 6 CONTINUOUS HEATING TRANSFORMATION DIAGRAM FOR 34CRMO4STEEL. IN THE REGION OF HOMOGENEOUS AUSTENITE THERE ARE LINES OF CONSTANT AUSTENITE GRAIN SIZE (ASTM NUMBERS). BECAUSE OF THE MEASURING PROCEDURE, THE DIAGRAMS CAN ONLY BE INTERPRETED ALONG LINES OF CONSTANT HEATING RATE. TO SHOW THE HEATING TIME MORE CLEARLY, A TIME SCALE IS ADDED. SOURCE: REF 12

Precipitate Stability and Grain Boundary Pinning. In the last three decades, there has been a surge in the development of microalloyed or high-strength low-alloy (HSLA) steels (base metals). Almost the entire thrust behind this effort has been to tailor the thermomechanical processing of these steels to produce a fine grain size (Ref 13). Previously, higher strength was obtained by alloying the steel sufficiently to increase the hardenability and then heat treating to obtain a tempered martensitic structure. The higher carbon equivalent (Ref 6, 14) in these alloy steels led to an increased susceptibility to cold cracking or hydrogen-induced cracking. In the microalloyed steels, however, alloying additions are kept to a minimum, and higher strength is achieved primarily by a reduction in the grain size and by precipitation strengthening. A reduction in grain size is the only known method of increasing the strength and toughness at the same time. Because strengthening is obtained by other means, both carbon and carbon equivalent can be decreased to significantly reduce the susceptibility to cold cracking in these new HSLA steels (Fig. 7).

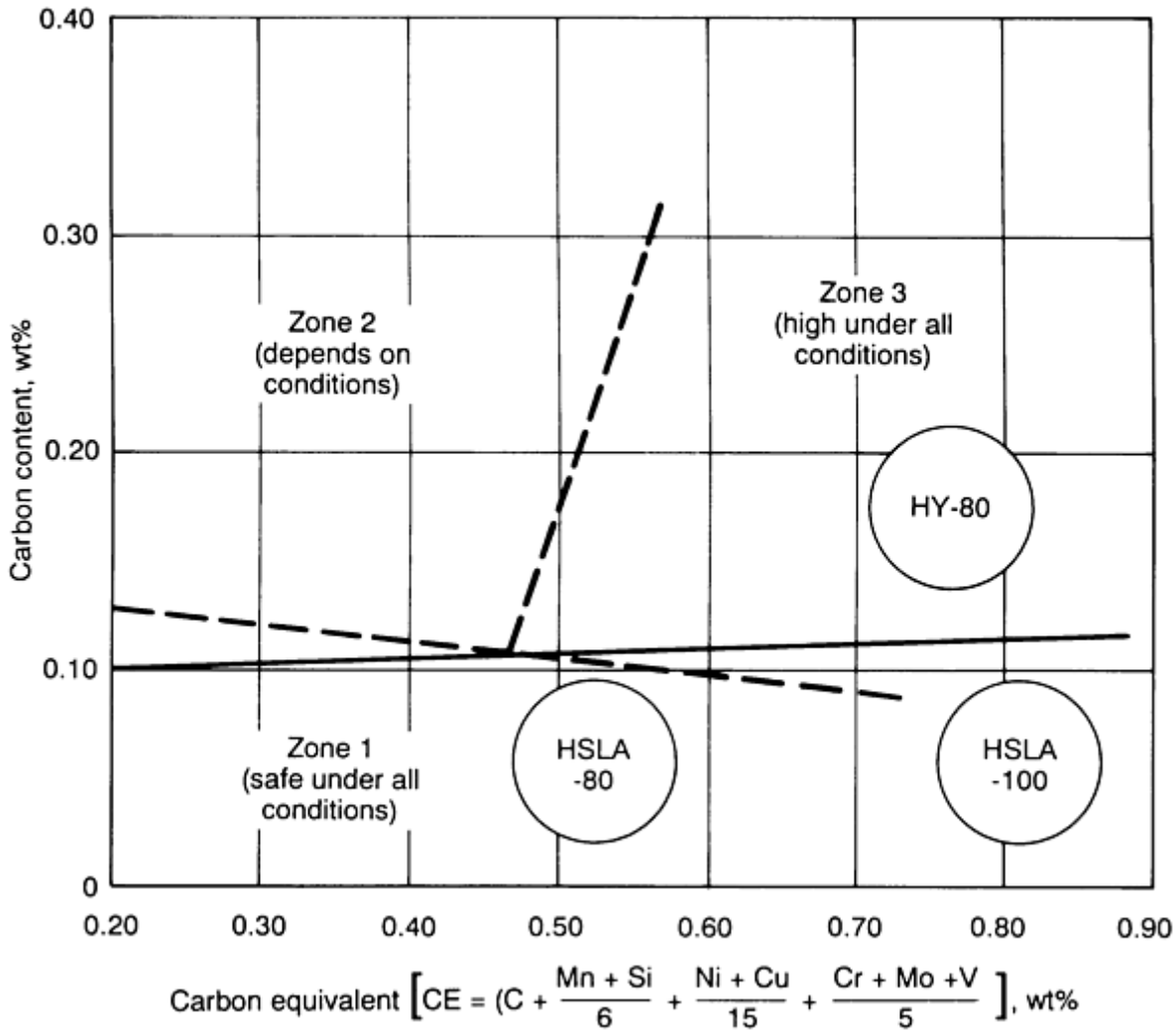

FIG. 7 EFFECT OF STEEL COMPOSITION (HY-80, HSLA-80, HSLA-100) ON THE SUSCEPTIBILITY TO COLD CRACKING IN THE HAZ. SOURCE: REF 13

A fine ferrite grain size in these steels is best achieved (after thermomechanical processing) by obtaining a fine austenite grain size before the γ-α transformation (Ref 13). To realize this goal, it is essential that microalloy additions such as niobium, vanadium, titanium, and aluminum are present so that the fine precipitate particles they form with nitrogen, carbon, or oxygen can "pin" the austenite grain boundaries and inhibit grain coarsening. The pinning effect arises from the fact that when a short length of grain boundary is replaced by a precipitate particle, the effective grain boundary energy is lowered. When the grain boundary attempts to migrate away from the particles, the local energy increases and a drag is exerted on the boundary by the particles.

In the HAZs of welds in these microalloyed steels, it is not possible to get the same optimum microstructure and microalloy precipitation obtained in the parent material by controlled thermomechanical processing. Because peak temperatures are much higher in the HAZ, the precipitate particles coarsen and dissolve, resulting in reduced pinning forces and therefore coarser austenite grains. This effect can be minimized by having precipitate particles that do not dissolve, even at higher temperatures. An idea of the stability of precipitate particles can be obtained from the plot shown in Fig. 8. It is seen that TiN has maximum stability, and this has been used to advantage in many steel. The other carbides and nitrides are not as effective as titanium nitride in limiting the extent of grain coarsening; they play a bigger role during thermomechanical processing (Ref 13).

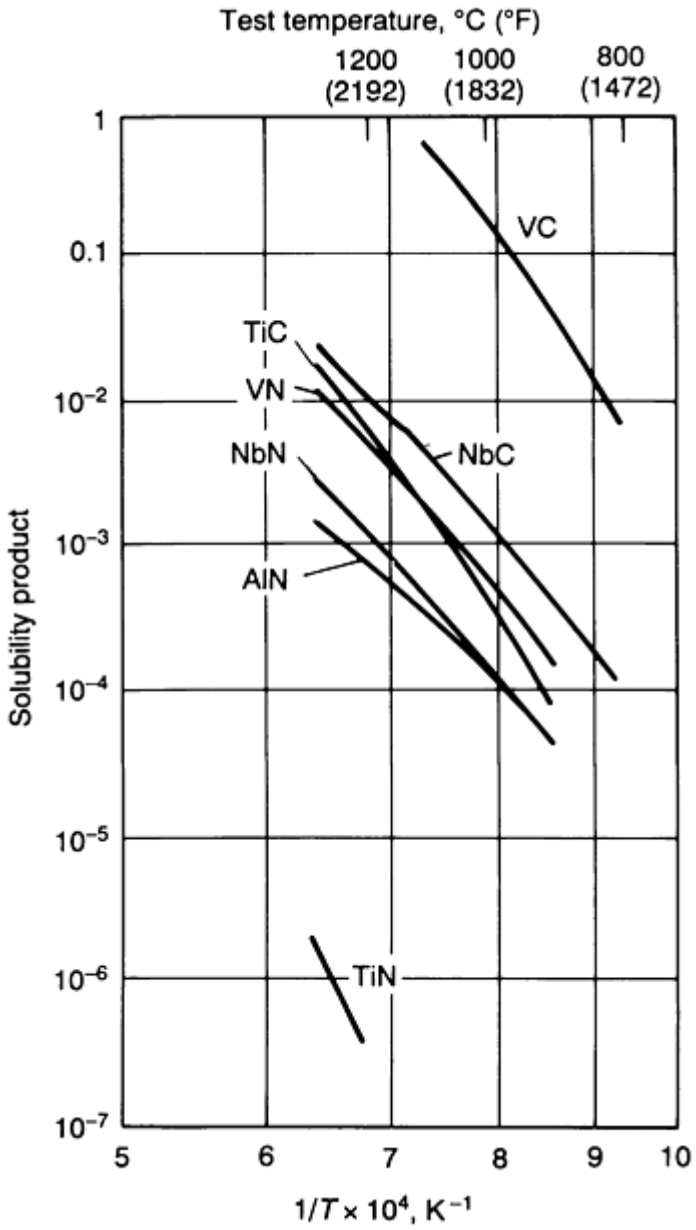

FIG. 8 SOLUBILITY PRODUCTS OF CARBIDES AND NITRIDES AS A FUNCTION OF TEMPERATURE. SOURCE: REF 15

Figure 9 shows how a high volume fraction of fine precipitate particles is needed to maximize the pinning effect. It also shows that heating to high temperatures increases the size of the particles, by a process known as Ostwald ripening (Ref 6), and decreases their volume fraction due to dissolution. This means that it is only possible to limit, and not to totally stop, grain coarsening in the HAZ, especially in high heat input welds. This inevitable grain coarsening is actually used to advantage in titanium, oxide steels (see the section "Titanium Oxide Steels" in this article).

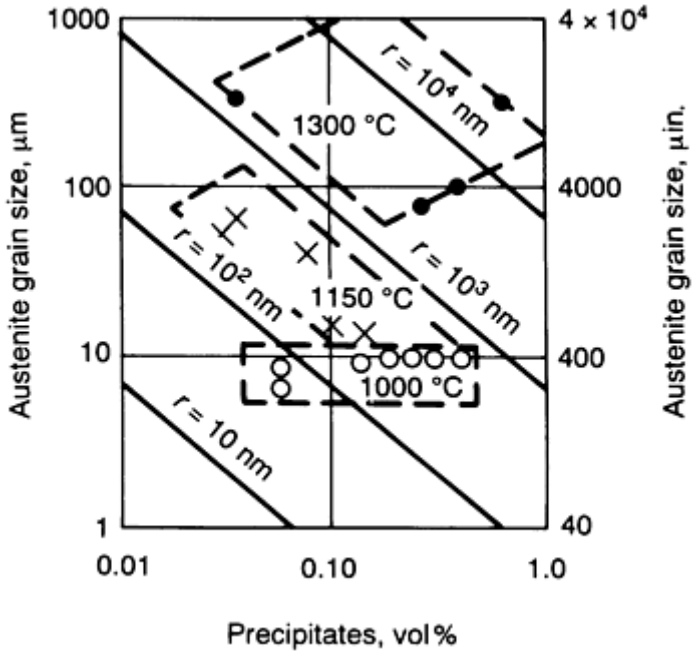

FIG. 9 EFFECT OF PARTICLE RADIUS, *R,* AND AMOUNT OF PRECIPITATE ON AUSTENITE GRAIN SIZE. SOURCE: REF 16

Unmixed and Partially Melted Zones in a Weldment. It is common to think of a single-pass weld as consisting of two zones: weld metal and HAZ. Careful metallographic examination has shown that a weld can in fact be divided into four regions (Fig. 10):

- *THE COMPOSITE ZONE,* IN WHICH A VOLUME OF BASE METAL MELTED BY THE SUPERHEATED FILLER METAL EXPERIENCES COMPLETE MIXING TO PRODUCE AN ALLOY WITH NOMINAL COMPOSITION INTERMEDIATE BETWEEN THAT OF THE BASE METAL AND THAT OF THE FILLER METAL.
- *THE UNMIXED ZONE,* WHICH FORMS FROM THE STAGNANT MOLTEN BOUNDARY LAYER REGION (ABOUT 100 TO 1000 μM, OR 0.004 TO 0.040 IN., THICK) AT THE OUTER EXTREMITIES OF THE COMPOSITE REGION. BECAUSE NO MECHANICAL MIXING WITH THE FILLER METAL OCCURS HERE, THE COMPOSITION OF THE METAL IN THIS REGION IS IDENTICAL TO THAT OF THE BASE METAL, EXCEPT FOR MINOR CHANGES PRODUCED BY DIFFUSION.
- *THE PARTIALLY MELTED ZONE,* WHICH IS A REGION AT THE FUSION BOUNDARY WHERE THE PEAK TEMPERATURES FALL BETWEEN THE LIQUIDUS AND SOLIDUS SO THAT MELTING IS INCOMPLETE.
- *THE TRUE HEAT-AFFECTED ZONE,* WHICH IS THAT PORTION OF THE BASE METAL WHERE ALL MICROSTRUCTURAL CHANGES INDUCED BY WELDING OCCUR IN THE SOLID STATE.

Special metallographic procedures are needed to reveal the existence of these special zones, as shown in Fig. 11.

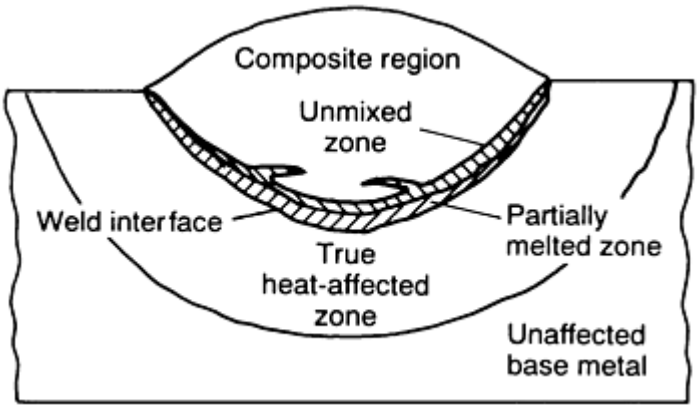

FIG. 10 SCHEMATIC SHOWING THE DIFFERENT DISCRETE REGIONS PRESENT IN A SINGLE-PASS WELD. SOURCE: REF 17

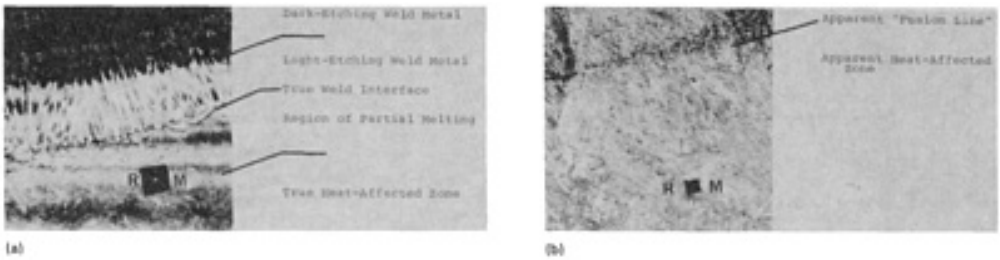

FIG. 11 SPECIAL METALLOGRAPHIC PROCEDURES SHOW THE MICROSTRUCTURE OF DISCRETE REGIONS (SEE FIG. 10) IN AN HY-80 WELD. (A) MICROSTRUCTURE OBTAINED NEAR A REFERENCE MARK (INDICATED BY "RM") USING A TWO-STAGE NITAL AND SODIUM BISULFITE PROCEDURE. (B) MICROSTRUCTURE AT IDENTICAL LOCATION REPOLISHED AND ETCHED WITH NITAL ONLY. TWO-STAGE PROCEDURE SHOWS MUCH GREATER DETAIL. SOURCE: REF 17

The width of the partially melted zone can be extended by a phenomenon known as constitutional liquation (Ref 18), whereby melting can occur even when the peak temperature is less than the solidus temperature. This can be understood by referring to a phase diagram for a simple binary system A and B (Fig. 12). Consider an alloy of composition C. Its equilibrium structures at temperatures T_1, T_2, T_3 and T_4 are α+ β, α, α, and L + α, respectively (Fig. 12a). On heating from room temperature to T_3 and holding at this temperature for a long time, the βparticles will dissolve and give a homogeneous α of composition C. However, under conditions of rapid heating in the HAZ, the dissolution of β will give rise to a solute concentration gradient around each particle, as shown in Fig. 12(b). In the region surrounding each particle, the concentration of the solute B will correspond to that of liquid because, as the phase diagram shows, a liquid phase must exist between α and β at T_3. This phenomenon of localized melting due to a nonequilibrium distribution of phases during rapid heating is called constitutional liquation.

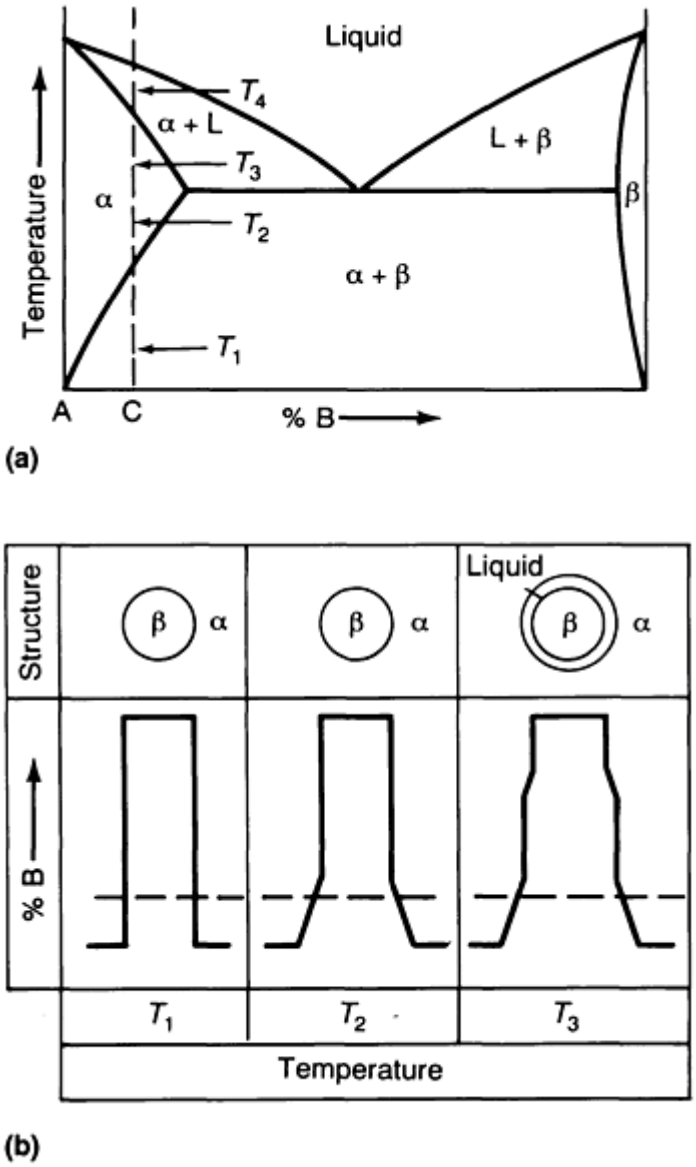

FIG. 12 EXTENSION OF PARTIALLY MELTED ZONE BY CONSTITUTIONAL LIQUATION. (A) PHASE DIAGRAM FOR A SIMPLE BINARY ALLOY. (B) STRUCTURES AND DISTRIBUTION OF CONSTITUENT B IN ALLOY C AT THREE TEMPERATURES SHOWN IN (A) WHEN RAPID HEATING IS APPLIED. SOURCE: REF 19

The partially melted zone is the region where liquation cracks have been known to occur in maraging steels, austenitic stainless steels, heat-treatable aluminum alloys, and nickel-base superalloys. It can also be a site where hydrogen-induced cracking is initiated (Ref 17), because it can act as a pipeline for the diffusion of hydrogen picked up by the molten weld metal and also because of the higher hardenability at these segregated regions.

While the phenomenon of constitutional liquation is usually discussed in connection with liquation cracking of aluminum- and nickel-base alloys (Ref 14, 18, 19), a more dramatic example can actually be found in the case of cast iron welds (Ref 20). Figure 13 shows the micro structure of the HAZ in a cast iron weld deposited using a "quench welding" technique (Ref 21). This procedure involves welding without any preheat by intermittently depositing a series of small stringer beads and strictly maintaining the interpass temperature below about 80 °C (175 °F). The idea is to limit the size of the hard and brittle white iron colonies forming by constitutional liquation around the graphite nodules and to see that they do not interconnect. By contrast, a procedure involving a preheat of about 200 °C (390 °F) can prevent the formation of martensite but not the formation of ledeburite (the structure of white iron). Because ledeburite forms at higher temperatures than martensite (≈1100 °C, or 2010 °F), a much higher preheat temperature of about 600 °C (1110 °F) is required to significantly reduce the cooling rate at the higher temperatures, thereby preventing the formation of white iron. This high level of preheat is impractical. While cast iron appears to have been successfully welded with preheats of

about 200 °C (390 °F), it has sometimes been found that weld repair is most effective using the quench welding technique, by which it is possible to limit both the amount of ledeburite formed and the width of the HAZ.

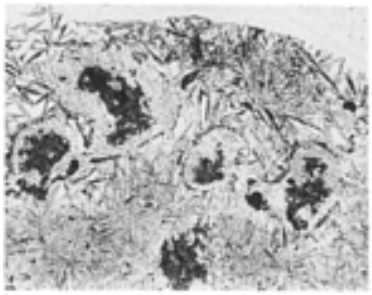

FIG. 13 DISCONTINUOUS WHITE IRON COLONIES OBTAINED IN THE HAZ OF BLACKHEART MALLEABLE IRON WELDED USING A "QUENCH WELDING" TECHNIQUE WITH A NICKEL-BASE ELECTRODE. 180×. SOURCE: REF 21

References cited in this section

2. O.M. AKSELSEN AND T. SIMONSEN, TECHNIQUES FOR EXAMINING TRANSFORMATION BEHAVIOUR IN WELD METAL AND HAZ--A STATE OF ART REVIEW, *WELD. WORLD,* VOL 25 (NO. 1/2), 1987, P 26-34
5. G.T. ELDIS, A CRITICAL REVIEW OF DATA SOURCES FOR ISOTHERMAL TRANSFORMATION AND CONTINUOUS COOLING TRANSFORMATION DIAGRAMS, *HARDENABILITY CONCEPTS WITH APPLICATION TO STEEL,* D.V. DOANE AND J.S. KIRKALDY, ED., TMS-AIME, 1978, P 126-157
6. K. EASTERLING, *INTRODUCTION TO THE PHYSICAL METALLURGY OF WELDING,* BUTTERWORTHS, 1983
7. *WELD THERMAL SIMULATORS FOR RESEARCH AND PROBLEM SOLVING,* THE WELDING INSTITUTE, U.K., 1972
8. C.F. BERKHOUT AND P.H. VAN LENT, THE USE OF PEAK TEMPERATURE-COOLING TIME DIAGRAMS IN THE WELDING OF HIGH STRENGTH STEELS (IN GERMAN), *SCHWEISS. SCHNEID.,* VOL 20 (NO. 6), 1968, P 256-260
9. TH.J. VAN ADRICHEM AND J. KAS, *CALCULATION, MEASUREMENT AND SIMULATION OF WELD THERMAL CYCLES,* SMITWELD N.V., NIJMEGEN, THE NETHERLANDS
10. P. RAVI VISHNU, W.B. LI, AND K. EASTERLING, HEAT FLOW MODEL FOR PULSED WELDING, *MATER. SCI. TECH.,* VOL 7 (NO. 7), 1991, P 649-659
11. P. RAVI VISHNU AND K. EASTERLING, PHENOMENOLOGICAL MODELLING OF HEAT FLOW AND MICROSTRUCTURAL CHANGES IN PULSED GTAW WELDS OF A QT STEEL, *MATHEMATICAL MODELING OF WELD PHENOMENA,* H. CERJAK AND K. EASTERLING, ED., THE INSTITUTE OF METALS, 1993
12. VEREIN DEUTSCHER EISENHÜTTENLEUTE, ED., *STEEL--A HANDBOOK FOR MATERIALS RESEARCH AND ENGINEERING, VOLUME 1: FUNDAMENTALS,* SPRINGER VERLAG, 1992, P 175
13. A.J. DEARDO, C.I. GARCIA, AND E.J. PALMIERE, THERMOMECHANICAL PROCESSING OF STEELS, *HEAT TREATING,* VOL 4, *ASM HANDBOOK,* 1991, P 237-255
14. S. KOU, *WELDING METALLURGY,* JOHN WILEY & SONS, 1987
15. K. NARITA, PHYSICAL CHEMISTRY OF THE GROUPS IVA (TI, ZR), VA (V, NB, TA) AND THE RARE EARTH ELEMENTS IN STEEL, *TRANS. ISIJ,* VOL 15, 1975, P 145-152
16. R.K. AMIN AND F.B. PICKERING, AUSTENITE GRAIN COARSENING AND THE EFFECT OF

THERMOMECHANICAL PROCESSING ON AUSTENITE RECRYSTALLIZATION, *THERMOMECHANICAL PROCESSING OF MICROALLOYED AUSTENITE,* A.J. DEARDO, G.A. RATZ, AND P.J. WRAY, ED., TMS-AIME, 1982, P 14

17. W.F. SAVAGE, E.F. NIPPES, AND E.S SZEKERES, A STUDY OF WELD INTERFACE PHENOMENA IN A LOW ALLOY STEEL, *WELD. J.*, SEPT 1976, P 260S-268S, AND HYDROGEN INDUCED COLD CRACKING IN A LOW ALLOY STEEL, *WELD. J.*, SEPT 1976, P 276S-283S
18. J.J. PEPE AND W.F. SAVAGE, EFFECTS OF CONSTITUTIONAL LIQUATION IN 18-NI MARAGING STEEL WELDMENTS, *WELD J.*, SEPT 1967, P 411S-422S
19. W. YENISCAVITCH, JOINING, *SUPERALLOYS II,* C.T. SIMS, N.S. STOLOFF, AND W.C. HAGEL, ED., JOHN WILEY & SONS, 1987, P 495-516
20. E.E. HUCKE AND H. UDIN, WELDING METALLURGY OF NODULAR CAST IRON, *WELD. J.*, AUG 1953, P 378S-385S
21. E.N. GREGORY AND S.B. JONES, WELDING CAST IRONS, *WELDING OF CASTINGS,* THE WELDING INSTITUTE, U.K., 1977, P 145-156

Solid-State Transformations in Weldments

P. Ravi Vishnu, Luleå University of Technology, Sweden

Fusion Zone of a Single-Pass Weld

Transformations in Single-Pass Weld Metal. It is usually not necessary to select a filler metal that has exactly the same composition as the base metal; it is more important that the weld metal has the same strength and other properties (such as toughness or corrosion resistance). Because these properties are governed by the microstructure, it is important to understand the influence of different factors on phase transformations in the weld metal. But first, for a meaningful communication of the different features in a microstructure, the various phases and microconstituents must be identified using a system of nomenclature that is both widely accepted and well understood. In wrought steels, this need has been satisfied to a large degree by the Dubé scheme (Ref 22) for classifying the different morphologies of ferrite, as shown in Fig. 14. Similarly, confusion and controversy in the terminology for describing the microstructures in ferritic steel weld metals have been largely resolved by the classification scheme shown in Fig. 15. This scheme (Ref 23) was the result of several collaborative exercises undertaken under the auspices of the International Institute of Welding (IIW). Typical micrographs illustrating some of the microstructural constituents are shown in Fig. 16.

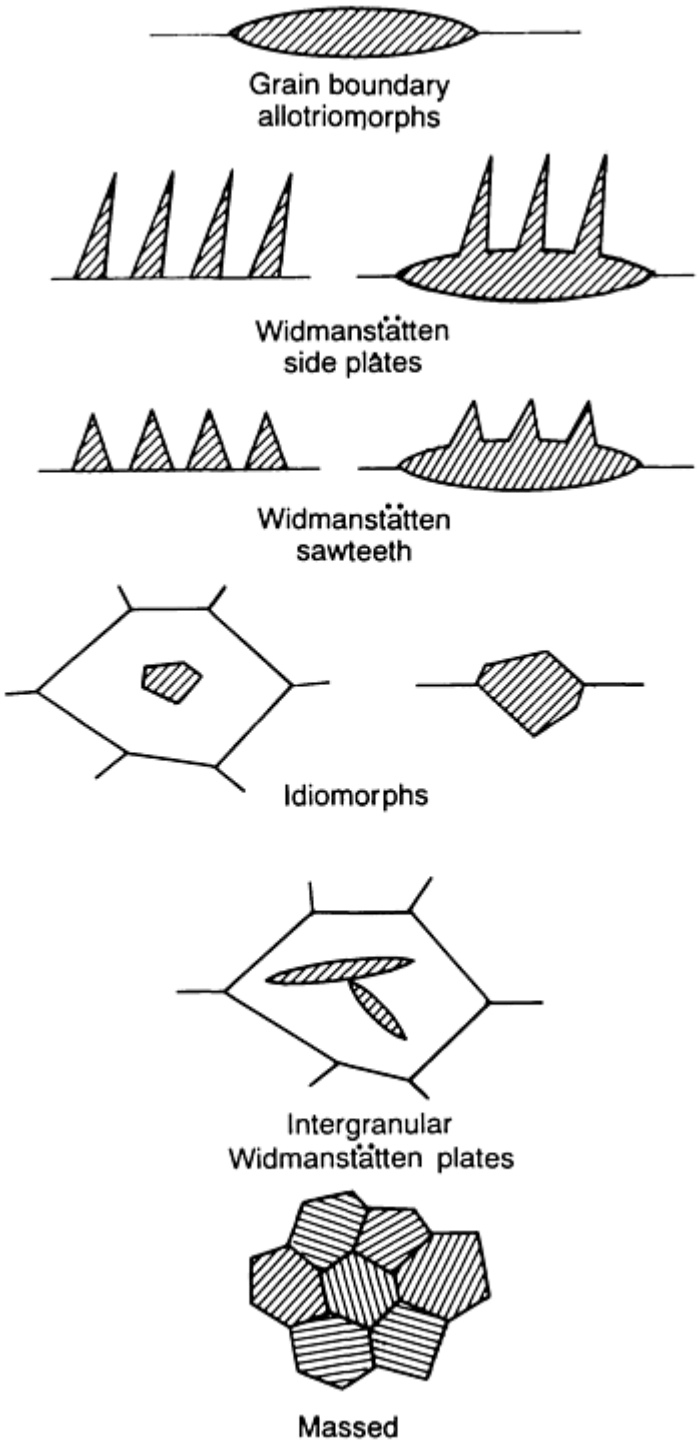

FIG. 14 SCHEMATICS SHOWING THE DUBÉ CLASSIFICATION OF FERRITE MORPHOLOGIES. SOURCE: REF 22

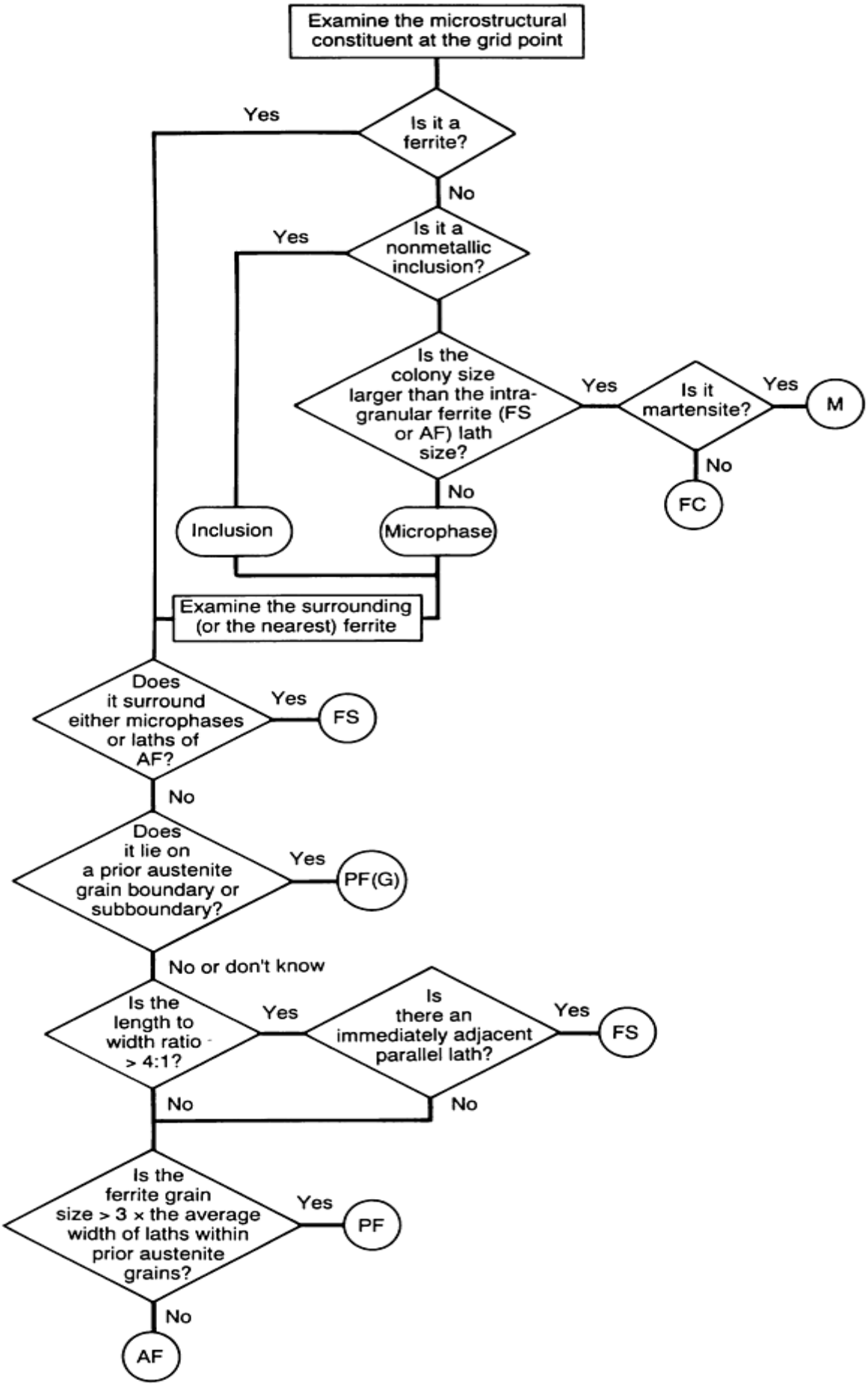
Examine the microstructural constituent at the grid point
Is it a ferrite?
Yes
No
Is it a nonmetallic inclusion?
Yes
Is the colony size larger than the intra-granular ferrite (FS or AF) lath size?
Yes
Is it martensite?
Yes
M
No
FC
No
Inclusion
Microphase
Examine the surrounding (or the nearest) ferrite
Does it surround either microphases or laths of AF?
Yes
FS
No
Does it lie on a prior austenite grain boundary or subboundary?
Yes
PF(G)
No or don't know
Is the length to width ratio > 4:1?
Yes
Is there an immediately adjacent parallel lath?
Yes
FS
No
No
Is the ferrite grain size > 3 × the average width of laths within prior austenite grains?
Yes
PF
No
AF

CATEGORY	ABBREVIATION
PRIMARY FERRITE	PF
GRAIN BOUNDARY FERRITE	PF(G)
INTRAGRANULAR POLYGONAL FERRITE	PF(I)
FERRITE WITH SECOND PHASE	FS
FERRITE WITH NONALIGNED SECOND PHASE	FS(NA)
FERRITE WITH ALIGNED SECOND PHASE	FS(A)
FERRITE SIDE PLATES	FS(SP)
BAINITE	FS(B)
UPPER BAINITE	FS(UB)
LOWER BAINITE	FS(LB)
ACICULAR FERRITE	AF
FERRITE-CARBIDE AGGREGATE	FC
PEARLITE	FC(P)
MARTENSITE	M
LATH MARTENSITE	M(L)
TWIN MARTENSITE	M(T)

FIG. 15 INTERNATIONAL INSTITUTE OF WELDING SCHEME FOR CLASSIFYING MICROSTRUCTURAL CONSTITUENTS IN FERRITIC STEEL WELD METALS WITH THE OPTICAL MICROSCOPE. SOURCE: REF 23

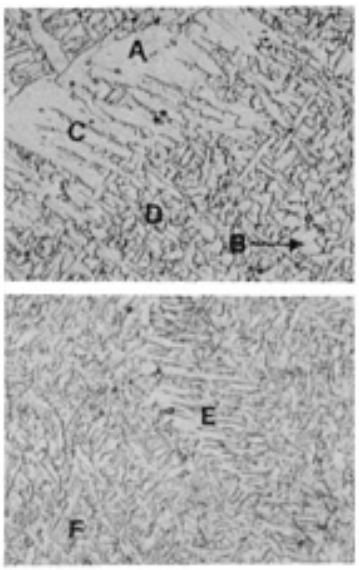

FIG. 16 MICROGRAPHS SHOWING TYPICAL MICROSTRUCTURES IN LOW-CARBON STEEL WELD METAL (NITAL ETCH). A, GRAIN BOUNDARY FERRITE [PF(G)]; B, POLYGONAL FERRITE [PF(I)]; C, WIDMANSTÄTTEN FERRITE [FS(SP)]; D, ACICULAR FERRITE (AF); E, UPPER BAINITE [FS(UB)]; F, LOWER BAINITE [FS(LB)] AND/OR MARTENSITE (M). SOURCE: REF 3

The transformation behavior in ferritic steel weld metals is best understood by first noting that ferrite is nucleated heterogeneously and that for all practical purposes, it is necessary to consider the competitive nucleation behavior only at grain boundaries and at inclusions. Figure 17 shows that inclusions have to be larger than a certain size (0.2 to 0.5 μm, or 8 to 20 μin., the typical size range of most weld metal inclusions) for their potency as nucleation sites to reach a maximum. It also shows that nucleation of ferrite is always energetically more favorable at grain boundaries than at inclusions. Based on additional considerations, like thermal contraction strains and lattice matching at inclusion-austenite-

ferrite interfaces (not taken into account to get the results in Fig. 17), a discussion of why certain inclusions are more potent nucleation sites than others is found in Ref 3, 24, and 25.

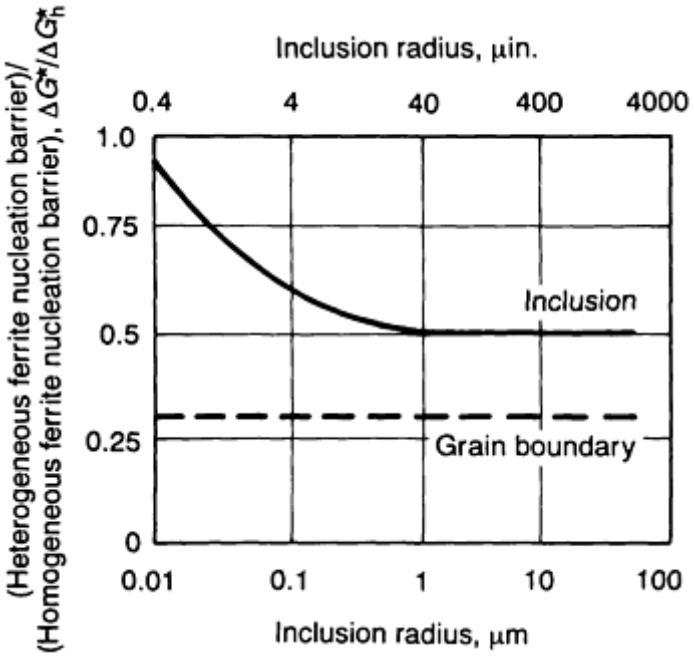

FIG. 17 EFFECT OF PARTICLE RADIUS ON ENERGY BARRIER TO FERRITE NUCLEATION AT INCLUSIONS, ΔG^* (HETEROGENEOUS), NORMALIZED RELATIVE TO THE HOMOGENEOUS NUCLEATION BARRIER, ΔG^*_H (HOMOGENEOUS). CORRESPONDING ENERGY BARRIER TO NUCLEATION OF FERRITE AT AUSTENITE GRAIN BOUNDARIES IS INDICATED BY HORIZONTAL BROKEN LINE. SOURCE: REF 6

Broadly, the major factors affecting transformation behavior in ferritic steel weld metals are alloy composition, weld heat input (by its effect on γ grain size and $\Delta t_{8\text{-}5}$), oxygen content (that is, the inclusion content), and the nature of segregation in the weld metal. A typical weld CCT diagram is shown in Fig. 18. For the cooling curve shown in the figure, the first phase that forms is allotriomorphic ferrite, or grain boundary ferrite in the IIW scheme. The term "allotriomorphic" means a "particle of a phase that does not have a regular external shape" and in the present context means that ferrite grows on the grain boundary surfaces and does not have a regular faceted shape reflecting the symmetry of its internal crystalline structure. At lower temperatures, the mobility of the curved or random γ/α-allotriomorph boundaries decreases, and Widmanstätten side plates (ferrite side plates in the IIW scheme) form. Growth of these side plates is rapid because carbon is efficiently redistributed to the sides of the growing tips, thus avoiding solute pile-up problems. In addition, substitutional atoms do not diffuse during the growth of Widmanstätten ferrite.

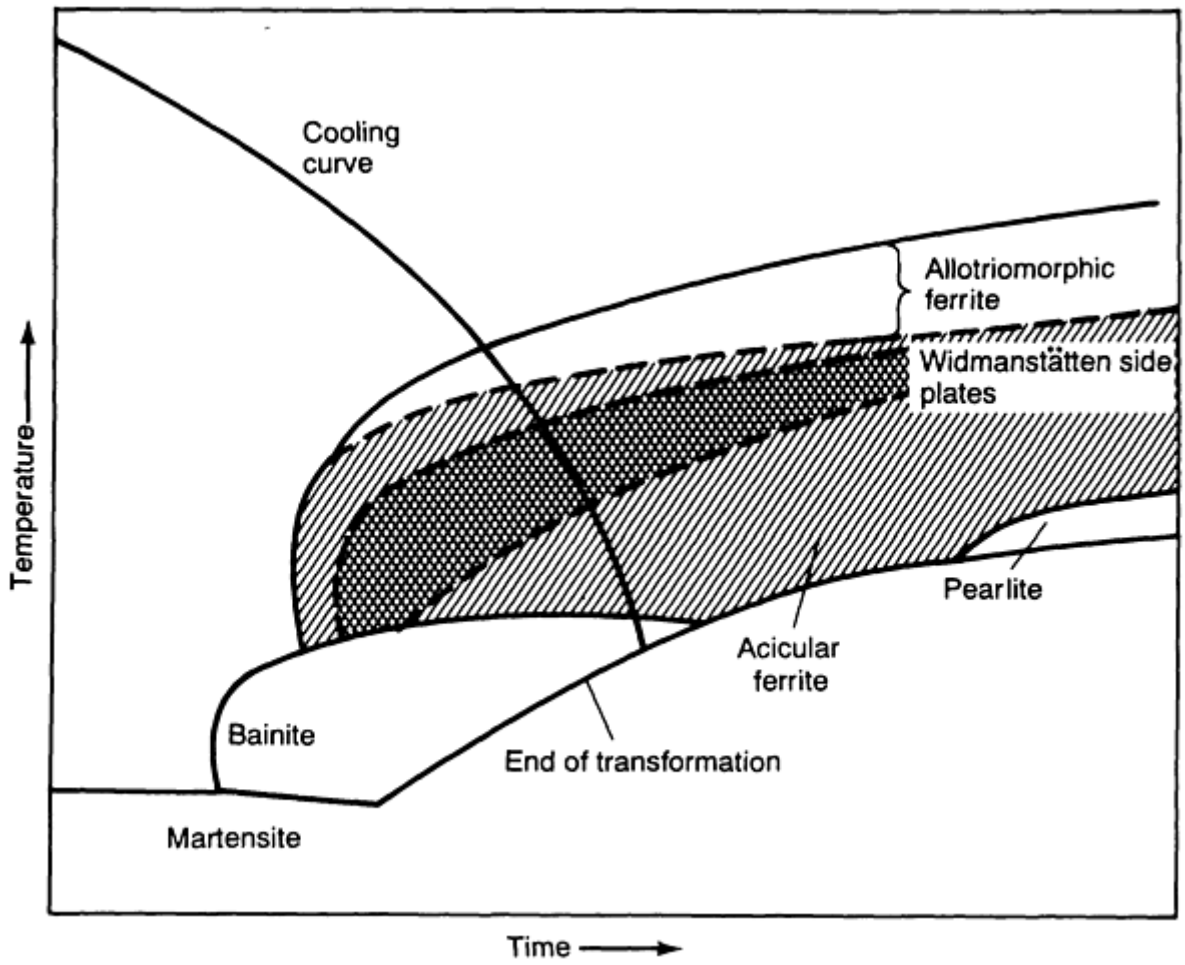

FIG. 18 SCHEMATIC OF WELD CCT DIAGRAM SHOWING SELECTED MICROSTRUCTURES

After all the grain boundary sites are saturated with allotriomorphic or Widmanstätten ferrite and their growth rate is not sufficient to extend to the interior of the grains, the nucleation of ferrite at inclusions within the γ grains becomes competitive. Acicular ferrite forms, a structure resulting from ferrite laths growing in different directions from inclusions and from laths already nucleated. Upon impingement, high-angle grain boundaries and a very fine dispersion of microphases are obtained between ferrite laths. "Microphases" in this context means the transformation structures resulting from the carbon-enriched regions between the ferrite laths and could be the martensite-austenite constituent, bainite, or pearlite (see the section "HAZ in Multipass Weldments" in this article). An example of the microstructure of acicular ferrite is shown in Fig. 19. Acicular ferrite does not figure in the Dubé scheme because it is rarely observed in wrought steels. When the cooling rate is higher or when the inclusion content is very low, bainite can be nucleated directly at the γ grain boundaries. Bainite can form as upper or lower bainite; the difference between the two is illustrated in Fig. 20. Examination with transmission electron microscopy (TEM) is usually required for a firm identification of the type of bainite formed. In the case of the highest cooling rates, martensite is obtained.

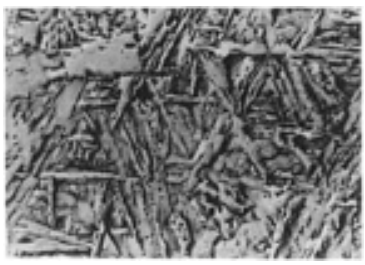

FIG. 19 SCANNING ELECTRON MICROGRAPH SHOWING MORPHOLOGY OF ACICULAR FERRITE. SOURCE: REF 24

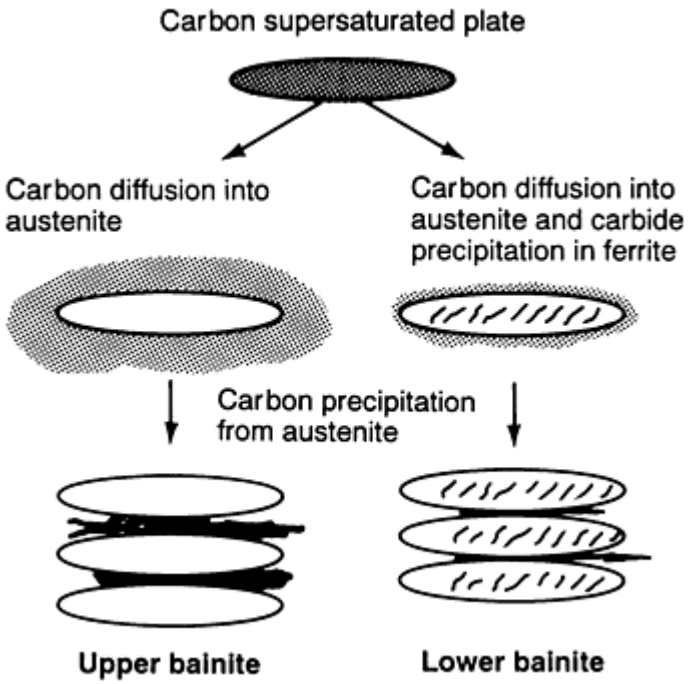

FIG. 20 SCHEMATIC SHOWING THE DIFFERENCES IN THE TRANSFORMATION MECHANISM FOR UPPER AND LOWER BAINITE AND THE EFFECT OF THESE MECHANISMS ON THE FINAL MORPHOLOGY. SOURCE: REF 24

Figure 21 shows the effect of alloying additions, $\Delta t_{8\text{-}5}$, oxygen content, and the γ grain size on the sequence and relative amounts of allotriomorphic ferrite, Widmanstätten ferrite, and bainite in the weld metal. Broadly, the trends shown can be understood in terms of the wellknown observation that an increase in γ grain size, a decrease in inclusion content, and an increase in alloying additions will shift the CCT curves to lower temperatures and to longer times. While Fig. 21 can generally be interpreted by assuming that the individual factors act independently of each other, the transition from (b) to (a) with an increase in the inclusion content must be understood in terms of its effect of the γ grain size. It has been observed that the γ grain size decreases with an increase in the inclusion content, and this has been explained by the higher magnitude of pinning forces at higher inclusion contents (Ref 25). The smaller grain size implies a greater grain boundary surface area, and this increases the amount of grain boundary ferrite and sideplate structures formed at the expense of acicular ferrite in Fig. 21(a). The role of the initial formation or non-formation of allotriomorphic ferrite at γ grain boundaries in bringing about the transition from Fig. 21(b) to Fig. 21(c) in Fig. 21 is discussed in the next section of this article.

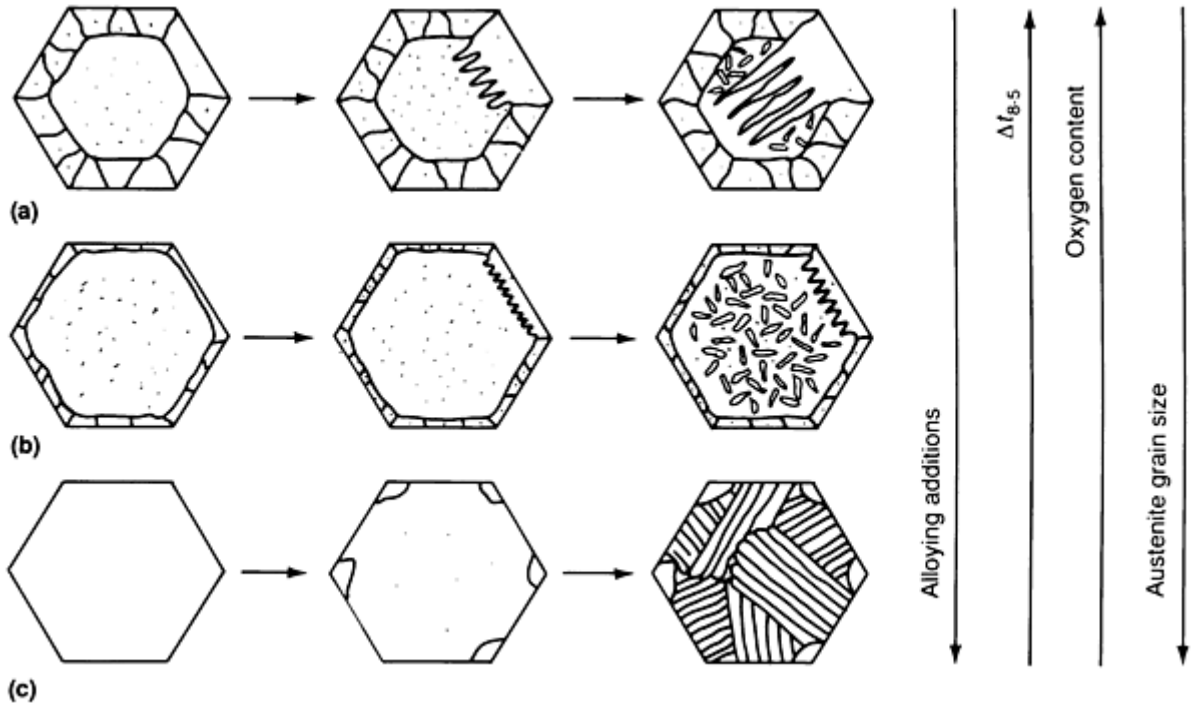

FIG. 21 SCHEMATIC SHOWING THE EFFECT OF ALLOY COMPOSITION, $\Delta T_{8\text{-}5}$, OXYGEN CONTENT, AND γ GRAIN SIZE ON THE DEVELOPMENT OF MICROSTRUCTURE IN FERRITIC STEEL WELD METALS. THE HEXAGONS REPRESENT CROSS SECTIONS OF COLUMNAR γ GRAINS. (A) THE GRAIN BOUNDARIES BECOME DECORATED FIRST WITH A UNIFORM, POLYCRYSTALLINE LAYER OF ALLOTRIOMORPHIC FERRITE, FOLLOWED BY FORMATION OF WIDMANSTÄTTEN FERRITE, AND THEN BY FORMATION OF ACICULAR FERRITE. (B) THE GROWTH RATE OF WIDMANSTÄTTEN FERRITE IS NOT SUFFICIENTLY HIGH TO EXTEND ENTIRELY ACROSS γ GRAINS. NUCLEATION OF FERRITE AT INCLUSIONS WITHIN THE γ GRAINS LEADS TO AN INCREASE IN THE AMOUNT OF ACICULAR FERRITE WHEN COMPARED WITH CASE (A). (C) THE HIGHER ALLOY CONTENT OR THE HIGHER COOLING RATE SUPPRESSES THE FORMATION OF ALLOTRIOMORPHIC FERRITE. THIS LEAVES THE γ GRAIN BOUNDARIES FREE TO NUCLEATE UPPER BAINITE. SOURCE: REF 24

Although the IIW classification is the result of a consensus viewpoint, some researchers (Ref 24) still feel that it places an exaggerated emphasis on morphological features observed with the light microscope. They believe that it is more important that the terminology reflect the mechanism of transformation. For example, it can be difficult to differentiate between Widmanstätten ferrite and upper bainite when using the light microscope, and both are identified as FS in the IIW classification. For a more fundamental understanding and to clearly interpret the trends in microstructural development, it is essential to make a distinction between the two. In addition, the subclassification of grain boundary ferrite in the IIW classification is not unequivocal in its meaning--it could refer to ferrite that forms by diffusion, Widmanstätten ferrite, or the ferrite in upper bainite. By contrast, the term "allotriomorphic ferrite" clearly identifies the mechanism by which it is formed. On the other hand, the IIW classification is easy to use and allows a more detailed identification, either by judgment or by further TEM examination, for example, to determine whether FS is FS(SP) or FS(UB). At least, it decreases the tendency for a wrong identification of the transformation mechanism with insufficient data. For a microstructure-toughness correlation, it is sufficient to characterize the morphological features.

Relating Weld Metal Toughness to the Microstructure. A good insight into the subject of toughness in ferrite steel weld metal is obtained by examining the data shown in Fig. 22. It is seen from Fig. 22(a) that the upper-shelf Charpy V-notch (CVN) energy monotonically decreases with an increase in oxygen content. In the upper-shelf temperature region, ductile fracture occurs by a process of microvoid coalescence, and because microvoids are initiated at the inclusion-matrix interface, the upper-shelf impact energy decreases with an increase in the inclusion content. By contrast, from Fig. 22(b) it is seen that an optimum inclusion content is required to obtain the lowest CVN transition temperature. The transition temperature is mainly governed by cleavage fracture, and this in turn depends on how effectively a propagating cleavage crack is forced to change direction as it traverses the microstructure. At low inclusion contents, an upper bainitic structure is obtained, and this consists of parallel platelets of ferrite (in a single packet) growing from the grain boundary surfaces. With an optimum inclusion content, a predominantly acicular ferrite structure is obtained, and here the adjacent

ferrite platelets tend to radiate in many different directions from inclusion nucleation site. At higher inclusion contents, the amount of ferrite sideplate structures increases, again having nearly parallel ferrite platelets. The highest toughness (that is, the lowest transition temperature) is obtained only in the "chaotic" microstructure of acicular ferrite because it has the smallest effective ferrite grain size.

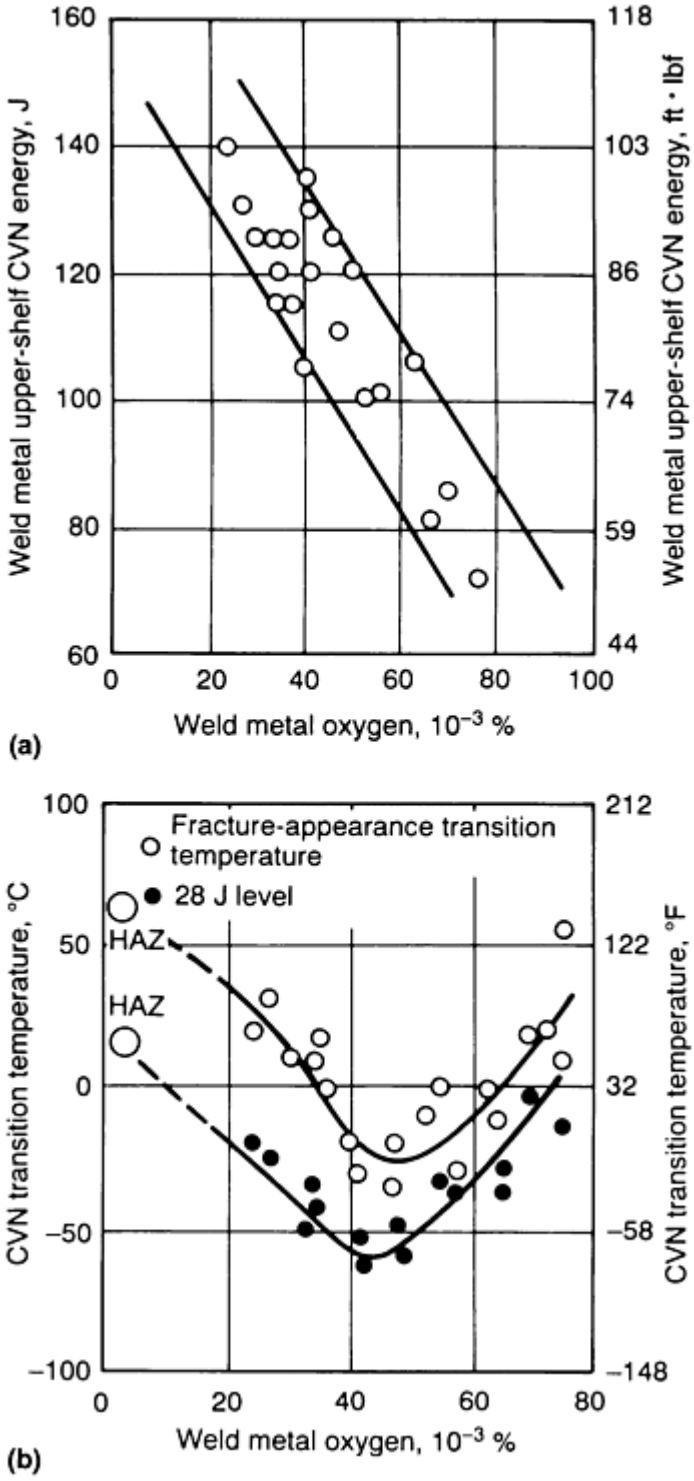

FIG. 22 TYPICAL VARIATION OF SELECTED WELD METAL PROPERTIES WITH OXYGEN CONTENT IN FERRITIC STEEL WELD METALS. (A) PLOT OF CHARPY V-NOTCH (CVN) IMPACT TEST UPPER-SHELF ENERGY VERSUS OXYGEN CONTENT. (B) PLOT OF CVN TRANSITION TEMPERATURE VERSUS OXYGEN CONTENT. SOURCE: REF 26

In recognition of the latter fact, most of the work in consumables development in the recent past has concentrated on increasing the amount of acicular ferrite in the microstructure. In line with the trends shown in Fig. 21(a) and 21(b), it has been found that decreasing the amount of grain boundary ferrite and ferrite sideplate structures increases the acicular ferrite content. This is shown more clearly in Fig. 23.

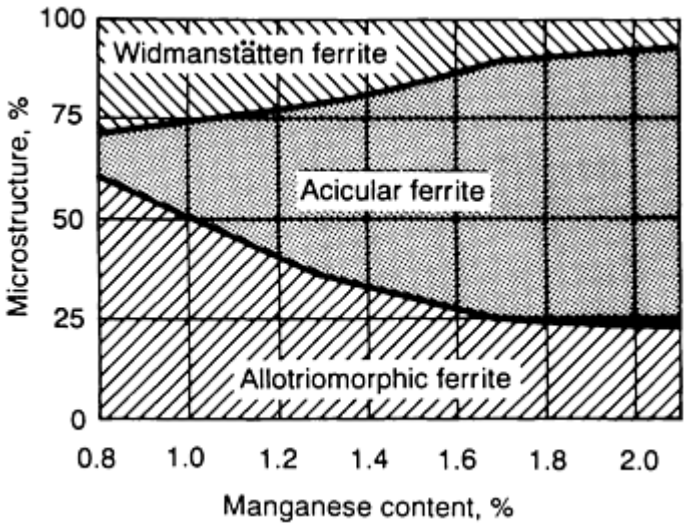

FIG. 23 EFFECT OF MANGANESE CONTENT OF WELD METAL ON THE RELATIVE AMOUNTS OF THE MICROSTRUCTURAL CONSTITUENTS PRESENT. CARBON CONTENT MAINTAINED AT 0.03%. SOURCE: REF 27

Recent work (Ref 24, 25, 27), however, has shown that a 100% acicular ferritic structure is neither desirable nor, in most cases, achievable. Figure 24 shows that the impact toughness peaks at about 70% acicular ferrite and then falls. This was attributed to the formation of segregated bands of brittle microphases in the alloy compositions giving the highest acicular ferrite contents. Moreover, when the alloying additions are increased still further, the transformation behavior becomes such that allotriomorphic ferrite formation is totally suppressed, leaving the γ grain boundaries free to nucleate upper bainite at lower temperatures (see Fig. 21c). It appears that a small layer of allotriomorphic ferrite is essential to obtain high acicular ferrite contents. When it forms, it saturates the γ grain boundary sites, and bainite nucleation at the γ/α-allotriomorphic interface is inhibited by the high carbon content there as a result of its rejection from the ferrite (Ref 24). Conditions are then favorable for intragranular nucleation at inclusion sites and thus the formation of acicular ferrite.

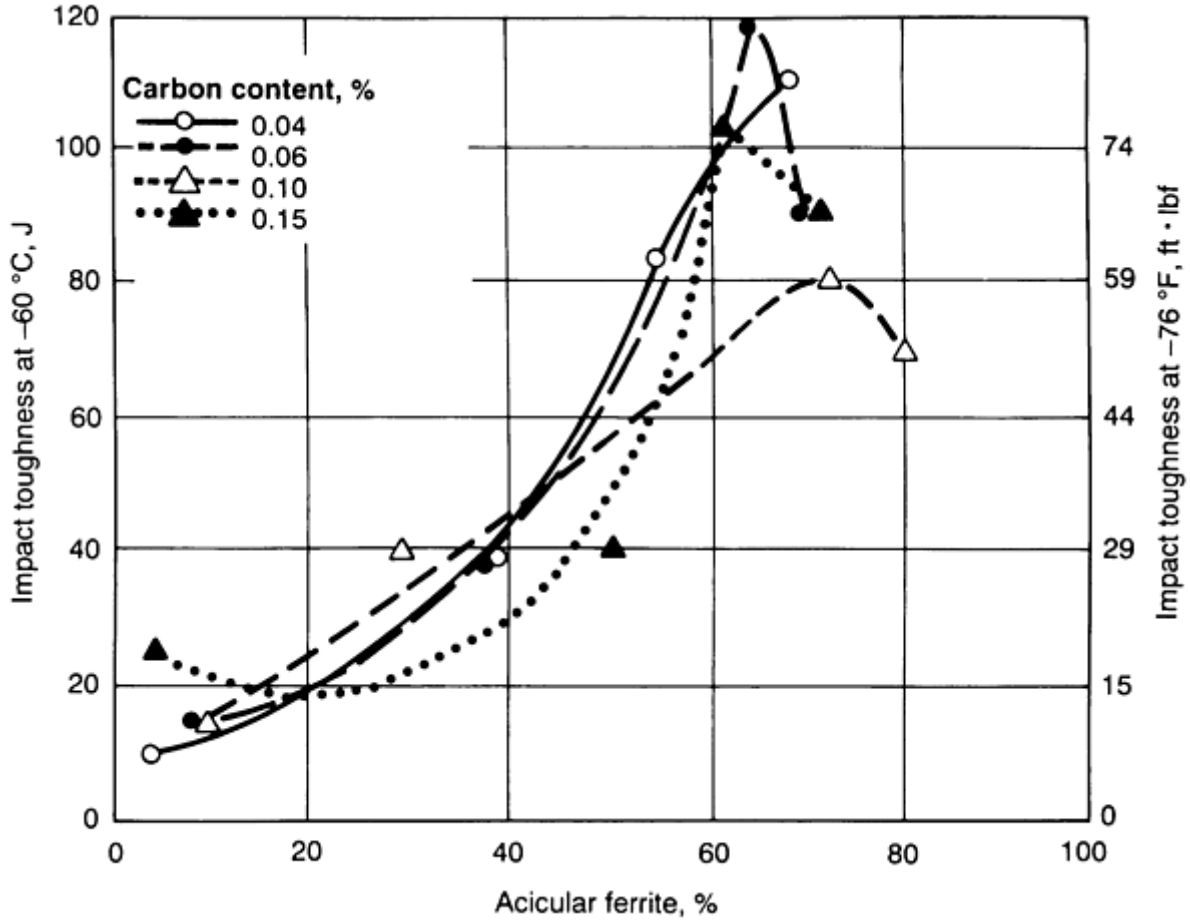

FIG. 24 PLOT OF IMPACT ENERGY VERSUS ACICULAR FERRITE CONTENT FOR SELECTED CARBON CONTENTS AT -60 °C (-78 °F). SOURCE: REF 27

For the welding of steels with yield strengths less than 600 MPa (85 ksi), it has been possible to develop weld metals with matching strength and toughness by having high acicular ferrite contents in them. A yield strength of about 600 MPa (85 ksi) seems to be the ceiling for weld metals based on acicular ferrite. Attempting to obtain additional strength by additional alloying to increase the amount of solid solution hardening and precipitation hardening in fact only results in increasing amounts of martensite and bainite. These structures are associated with a lower toughness. This has been observed in the case of HSLA-100 steels, for example, where attempts to get a matching strength in the weld metal have resulted in a drop in toughness (Ref 25, 28). Work on consumables development for high-strength steels is still in progress to match the base metal in strength and toughness (Ref 25, 28). However, current thinking appears to favor resorting to a slightly undermatching weld metal (in terms of strength) so that the already available lower-strength, high-toughness, consumables having high acicular ferrite contents (Ref 29) can be used. These weld metal compositions have the additional benefit of requiring less stringent measures for avoiding hydrogen-induced cracking.

Titanium Oxide Steels. In the discussion of the role of pinning by precipitate particles (for example, TiN) in limiting grain growth in the HAZ (in the section "Precipitate Stability and Grain Boundary Pinning" in this article), it was pointed out that at high heat inputs the particles dissolve and are not able to prevent coarse γ grains from forming. The low toughness in these coarse-grained regions is of some concern. The fact that a coarse γ grain size will lead to a higher acicular ferrite content (see Fig. 21b) with improved toughness has been used to advantage in the development of titanium-oxide-containing steels (Ref 30, 31). Ti_2O_3 is more stable than titanium nitride and does not dissolve, even at the highest heat inputs. The undissolved, Ti_2O_3 particles do not stop grain growth, but their survival after the heating cycle means that they can be effective in nucleating acicular ferrite within the coarse γ grains. The precise reasons why they are more effective than other undissolved inclusions, such as Al_2O_3 in nucleating acicular ferrite are not well understood (Ref 24). The improved HAZ microstructure and toughness obtained with titanium oxide steels over titanium nitride steels at high heat inputs are shown in Fig. 25 and 26, respectively.

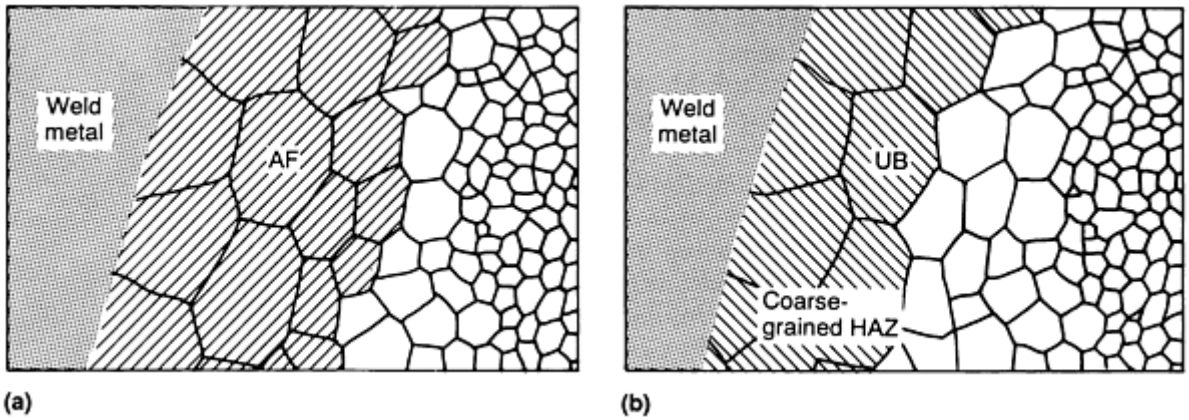

FIG. 25 SCHEMATIC SHOWING HAZ MICROSTRUCTURE IN SELECTED HIGH HEAT INPUT WELDS. (A) TITANIUM OXIDE STEEL. (B) TITANIUM NITRIDE STEEL. AF, ACICULAR FERRITE; UB, UPPER BAINITE. SOURCE: REF 30

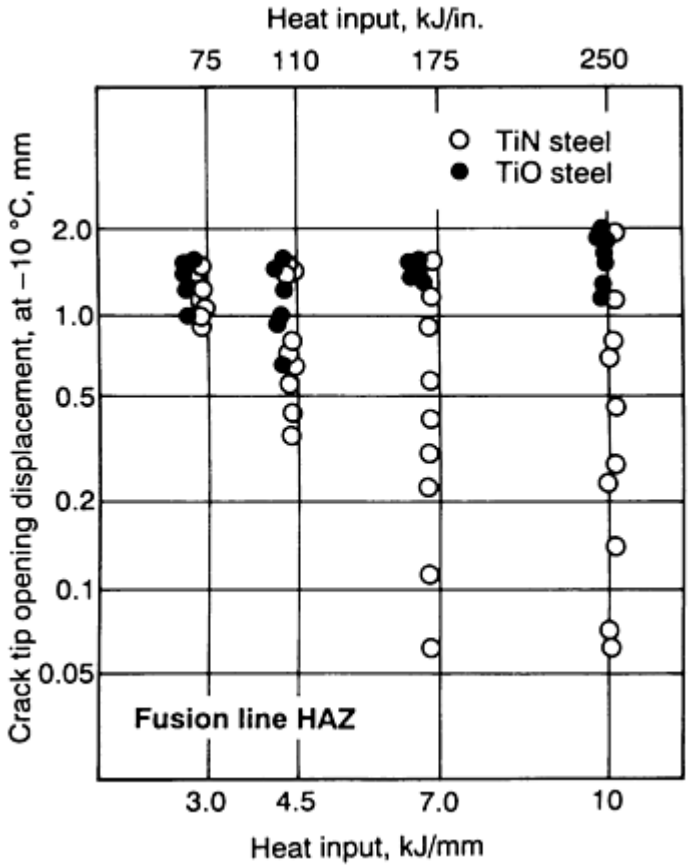

FIG. 26 HAZ TOUGHNESS OF TITANIUM NITRIDE AND TITANIUM OXIDE STEELS WITH 420 MPA (60 KSI) YIELD STRENGTH. SOURCE: REF 31

Effect of Transformations on Transient Weld Stresses. The effect of transformations on weld stresses (and vice versa) is best illustrated by introducing an apparently little-known proposal (Ref 32) about the use of a duplex austenite-martensite weld metal for welding high-strength steels. First, to prepare the background, the way in which transient stresses develop in a weld and the effect of transformations on weld stresses will be discussed.

Four uniaxial specimens using an HAZ simulation technique, the manner in which residual stress is accumulated during a weld thermal cycle was investigated (Ref 33), and the results are shown in Fig. 27. Initially, when a material is austenite at high temperature, its yield strength is low and only a small tensile stress can develop. On cooling, the tensile stress increases. When a phase transformation occurs, the resulting volume expansion opposes the contraction due to cooling and decreases the stress. Once the transformation is complete, the tensile stress increases again. As seen in Fig. 27, if the transformation occurs at a lower temperature (for example, in the case of 9Cr1Mo or 12CrMo steels), the magnitude of the final residual stress is less. The dotted line in the plot shows the expected variation for a material with an austenite-martensite structure. The greater the amount of martensite, the lower the final residual stress.

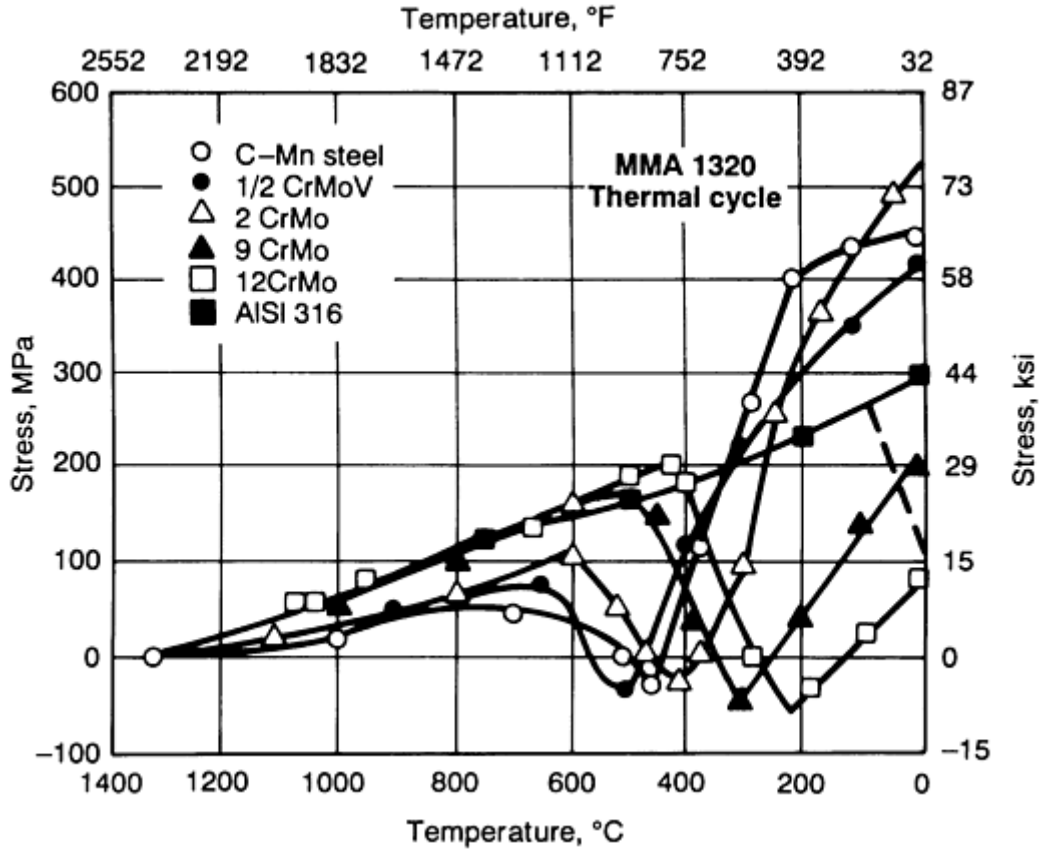

FIG. 27 STRESS ACCUMULATED DURING COOLING UNDER RESTRAINT FOR SELECTED STEELS. THE DOTTED LINE SHOWS THE EXPECTED VARIATION IN STRESS FOR A DUPLEX AUSTENITE-MARTENSITE WELD METAL WHERE TRANSFORMATION BELOW ABOUT 100 °C (212 °F) GREATLY REDUCES THE FINAL STRESS. (MMA 1320 INDICATES THE PEAK TEMPERATURE OF THE SIMULATED WELD THERMAL CYCLE AND CORRESPONDS TO THE TEMPERATURE AT THE START OF THE COOLING CYCLE.) SOURCE: REF 33

As discussed in the section "Weld Metal Toughness Relative to the Microstructure" in this article, the main problems in the welding of high-strength steels (with yield strengths of 600 to 1000 MPa, or 85 to 145 ksi) are hydrogen-induced cracking (HIC) and low toughness in the weld metal. Both problems can be addressed (in principle at least) by the use of a duplex austenite-martensite weld metal. Austenite can contribute by increasing the toughness and by minimizing the risk for HIC (Ref 14). The role of martensite will be to increase the strength and to decrease the final residual tensile stress, which also makes conditions less favorable for HIC. An additional benefit will be that the higher tensile residual stress in the weld metal before martensite forms will induce the transformations in the HAZ to occur at a slightly higher temperature, by Le Chatelier's principle (Ref 34), and thereby cause a microstructure less susceptible to HIC to form in the HAZ. The results of this effect are shown in Fig. 28, where it is seen that a tensile stress in the 500 to 300 °C (930 to 570 °F) temperature range on a ferrite-pearlite weld increased the stresses for failure (Ref 35).

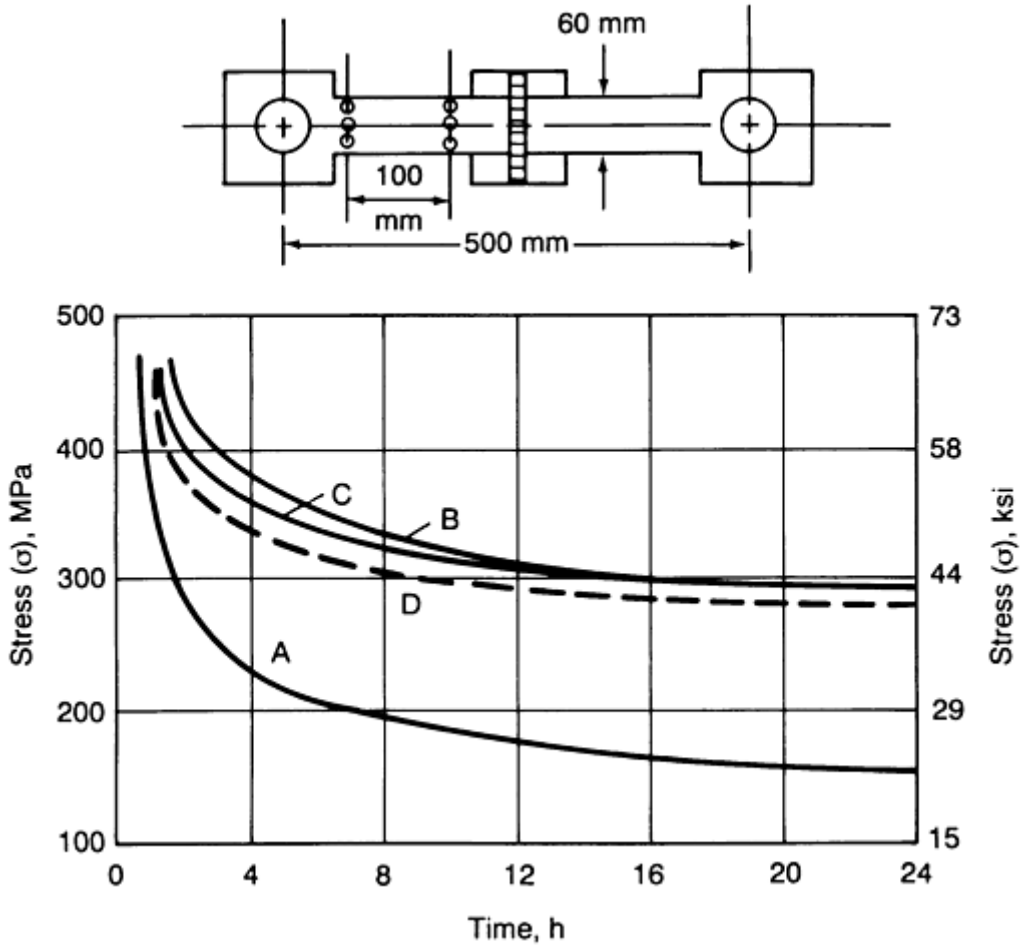

FIG. 28 DELAYED FRACTURE CURVES FOR TENSILE TESTS ON WELDED JOINTS IN 35KH3N3M (A RUSSIAN SPECIFICATION) STEEL. A, FERRITIC-PEARLITIC WELD; B, BAINITIC-MARTENSITIC WELD; C, AUSTENITIC WELD; D, FERRITIC-PEARLITIC WELD PLUS DEFORMATION AT 500 TO 300 °C (930 TO 570 °F). THE SCHEMATIC SHOWS THE SPECIMEN DIMENSIONS FOR THE DELAYED FRACTURE TENSILE TESTS ON WELDED JOINTS. SOURCE: REF 35

It must be mentioned that the idea of using an austenite-martensite weld metal represents a considerable departure from conventional thinking. For example, for certain overlaying applications of stainless steel deposits on low-alloy steel, an overalloyed electrode like E310 or E312 is preferred to E309. Even though the weld metal composition with any of the three electrodes would be acceptable, the use of overalloyed electrodes will minimize the width of the martensitic layer in the unmixed zone at the weld-HAZ interface (Ref 36). By contrast, an austenite-martensite weld metal implies that the choice of consumable will have to be such that the width of the martensitic layer will increase. However, because the proposal is meant for the recently developed high-strength steels that have a low carbon content, only a low-carbon martensite will form, which will not be that harmful. The benefits already discussed could override conventional concerns about having martensite in the weld metal in this case.

To sum up, even though the idea of using an austenite-martensite weld metal for high-strength steels does not seem to have been taken up for serious investigation so far, it has been included here because it is a nice way of illustrating the principles discussed. In addition, it shows that a fundamental knowledge of different effects on phase transformations can lead to unconventional solutions to practical problems.

References cited in this section

3. O. GRONG AND D.K. MATLOCK, MICROSTRUCTURAL DEVELOPMENT IN MILD AND LOW ALLOY STEEL WELD METALS, *INT. MET. REV.,* VOL 31 (NO. 1), 1986, P 27-48

6. K. EASTERLING, *INTRODUCTION TO THE PHYSICAL METALLURGY OF WELDING,* BUTTERWORTHS, 1983

14. S. KOU, *WELDING METALLURGY,* JOHN WILEY & SONS, 1987

22. L.E. SAMUELS, *OPTICAL MICROSCOPY OF CARBON STEELS,* AMERICAN SOCIETY FOR METALS, 1980

23. "GUIDE TO THE LIGHT MICROSCOPE EXAMINATION OF FERRITIC STEEL WELD METALS," DOC. NO. IX-1533-88, INTERNATIONAL INSTITUTE OF WELDING, 1988

24. H.K.D.H. BHADESHIA AND L.E. SVENSSON, MODELLING THE EVOLUTION OF MICROSTRUCTURE OF STEEL WELD METAL, *MATHEMATICAL MODELLING OF WELD PHENOMENA,* H. CERJAK AND K. EASTERLING, ED., THE INSTITUTE OF MATERIALS, 1993

25. G.R. EDWARDS AND S. LIU, RECENT DEVELOPMENTS IN HSLA STEEL WELDING, *ADVANCES IN WELDING METALLURGY,* FIRST U.S.-JAPAN SYMPOSIUM, AMERICAN WELDING SOCIETY AND OTHERS, JUNE 1990, P 215-293

26. B. AHLBLOM, "OXYGEN AND ITS ROLE IN DETERMINING WELD METAL MICROSTRUCTURE AND TOUGHNESS--A STATE OF THE ART REVIEW," DOC. NO. IX-1322-84, INTERNATIONAL INSTITUTE OF WELDING, 1984

27. L.-E. SVENSSON AND B. GRETOFT, MICROSTRUCTURE AND IMPACT TOUGHNESS OF C-MN WELD METALS. *WELD. J.,* DEC 1990, P 454S-461S

28. P.W. HOLSBERG AND R.J. WONG, WELDING OF HSLA-100 STEEL FOR NAVAL APPLICATIONS, *WELDABILITY OF MATERIALS,* R.A. PATTERSON AND K.W. MAHIN, ED., ASM INTERNATIONAL, 1990

29. J.M.B. LOSZ AND K.D. CHALLENGER, MICROSTRUCTURE AND PROPERTIES OF A COPPER PRECIPITATION STRENGTHENED HSLA STEEL WELDMENT, *RECENT TRENDS IN WELDING SCIENCE AND TECHNOLOGY,* S.A. DAVID AND J.M. VITEK, ED., ASM INTERNATIONAL, 1990

30. H. HOMMA, S. OHKITA, S. MATSUDA, AND K. YAMAMOTO, IMPROVEMENTS OF HAZ TOUGHNESS IN HSLA STEEL BY INTRODUCING FINELY DISPERSED TI-OXIDE, *WELD. J.,* OCT 1987, P 301S-309S

31. N. YURIOKA, "MODERN HIGH STRENGTH STEEL IN JAPAN," FIFTH INTERNATIONAL SYMPOSIUM, JAPAN WELDING SOCIETY, APRIL 1990 (TOKYO)

32. YU.N. GOTALSKII, THE PROBLEM OF WELDING HIGH STRENGTH STEELS, *AUTOM. WELD.,* JUNE 1984, P 37-40

33. W.K.C. JONES AND P.J. ALBERRY, THE ROLE OF PHASE TRANSFORMATIONS IN THE DEVELOPMENT OF RESIDUAL STRESSES DURING THE WELDING OF SOME FAST REACTOR STEELS, *PROC. CONF. FERRITIC STEELS FOR FAST REACTOR STEAM GENERATORS,* BRITISH NUCLEAR ENERGY SOCIETY, 1977

34. *MCGRAW-HILL ENCYCLOPEDIA OF SCIENCE AND TECHNOLOGY,* VOL 9, P 685

35. A.M. MAKARA AND N.A. MOSENDZ, EFFECTS OF THE WELD METAL ON CRACKING IN HAZ, *WELD. RES. ABROAD,* NOV 1965, P 78-86

36. H. IKAWA, S. SHIN, M. INUI, Y. TAKEDA, AND A. NAKANO, "ON THE MARTENSITE-LIKE STRUCTURE AT WELD BOND AND THE MACROSCOPIC SEGREGATION IN WELD METAL IN THE WELDED DISSIMILAR METALS OF α-STEELS AND γ-STEELS," DOC. NO. IX-785-72, INTERNATIONAL INSTITUTE OF WELDING, 1972

Solid-State Transformations in Weldments

P. Ravi Vishnu, Luleå University of Technology, Sweden

HAZ in Multipass Weldments

In the HAZ of a single-pass weld, the grain-coarsened zone (GC HAZ) is normally the region having the lowest toughness. Turning to a multipass weld, Fig. 29 (compare with Fig. 3) shows how the GC HAZ can be modified by subsequent passes and can be categorized into four regions, depending on the reheating temperature (Ref 37):

- SUBCRITICALLY REHEATED GRAIN-COARSENED (SCGC) ZONE, THE ZONE REHEATED BELOW AC_1
- INTERCRITICALLY REHEATED GRAIN-COARSENED (ICGC) ZONE, THE ZONE REHEATED BETWEEN AC_1 AND AC_3
- SUPERCRITICALLY REHEATED GRAIN-REFINED (SCGR) ZONE, THE ZONE REHEATED ABOVE AC_3 AND BELOW ABOUT 1200 °C (2190 °F)
- UNALTERED GRAIN-COARSENED (UAGC) ZONE, THE ZONE THAT IS NOT REHEATED ABOVE ABOUT 200 °C (390 °F) OR THE ZONE THAT IS AGAIN REHEATED ABOVE ABOUT 1200 °C (2190 °F)

Figure 30 shows how the crack tip opening displacement (CTOD) value of simulated specimens varies with the peak temperature of the second thermal cycle, T_{p2} (T_{p1} = 1400 °C, or 2550 °F). It is seen that the ICGC, UAGC, and SCGC regions have CTOD values less than about 0.1 mm (0.004 in.). Similar low values have been obtained by locating the crack tip in the CTOD tests at corresponding locations in the HAZ of actual multipass weldments. These low toughness regions are commonly known as local brittle zones (LBZs).

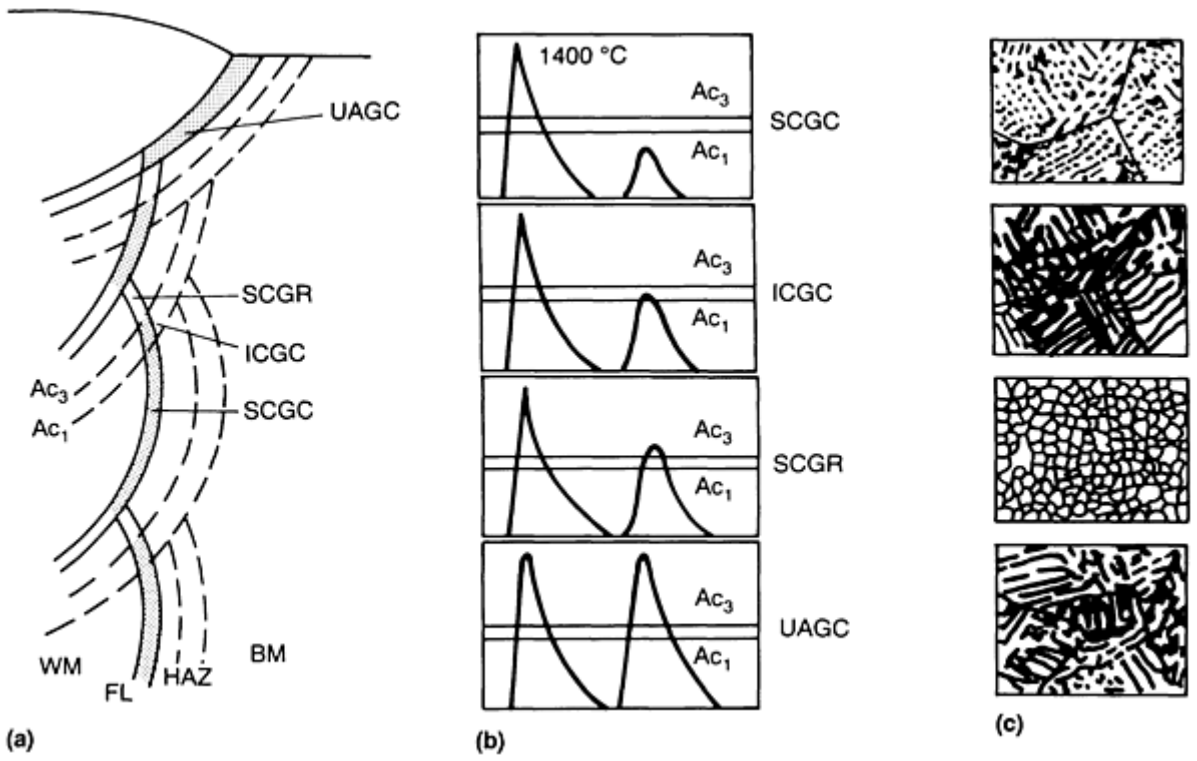

FIG. 29 SCHEMATIC SHOWING THE DIFFERENT SUBZONES THAT CAN FORM IN THE COARSE-GRAINED REGION OF THE HAZ IN A MULTIPASS WELD. (A) POSITION OF SUBZONES RELATIVE TO BASE METAL (BM) AND WELD METAL (WM). (B) PLOT OF THERMAL CYCLES RELATIVE TO AC_3 AND AC_1. (C) MICROSTRUCTURES AT THE DIFFERENT ZONES. FL REFERS TO THE FUSION LINE. SEE TEXT FOR DETAILS. SOURCE: REF 37

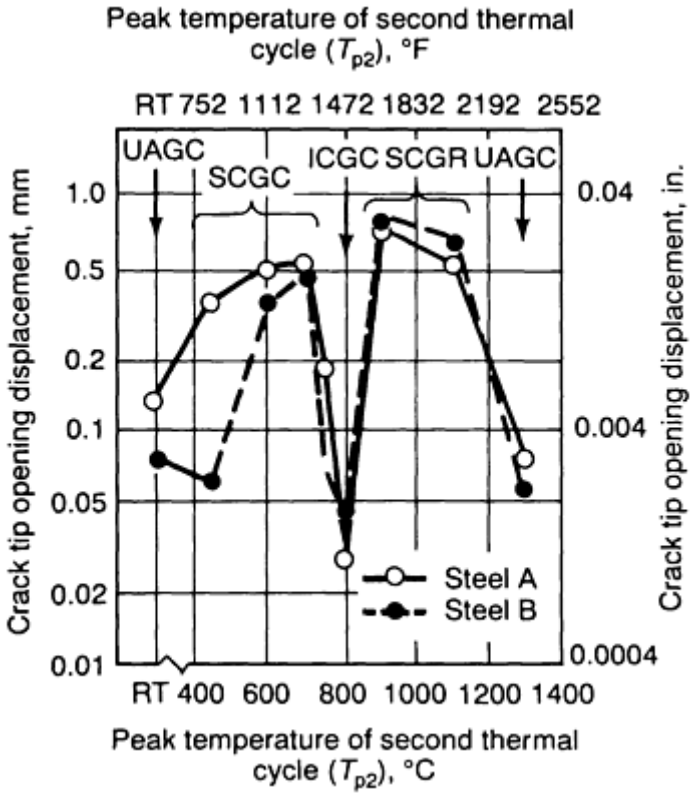

FIG. 30 PLOT OF CRACK TIP OPENING DISPLACEMENT VERSUS PEAK TEMPERATURE OF THE SECOND THERMAL CYCLE FOR SIMULATED SPECIMENS SUBJECTED TO A DOUBLE THERMAL CYCLE. (T_{P1} = 1400 °C = 2550 °F; $\Delta T_{8\text{-}5}$ = 20 S). THE HAZ ZONES (FIG. 29) CORRESPONDING TO THE SIMULATION TRIALS ARE ALSO SHOWN IN THE FIGURE. SOURCE: REF 37

The low CTOD values have been obtained only in tests on modern structural steels, whereas no actual structural failure attributable to the LBZs has been reported so far (Ref 38). Because the structural significance of the low toughness test results is still largely unresolved, the present conservative strategies are to choose a steel whose tendency to form LBZs is less or to choose a welding procedure by which the size of the LBZs can be reduced.

The ICGC HAZ usually has a lower toughness than the SCGC or UAGC regions, even though all of them have nearly the same γ grain size. This is due to the higher amount of highcarbon martensite-austenite (M-A) constituent in the ICGC HAZ. When the GC HAZ is reheated to a temperature between Ac_1 and Ac_3, austenite is nucleated at the high carbon areas. Upon cooling, these local high-carbon areas can transform to give twinned martensite with every thin regions of retained austenite in between. (See Ref 39 for detailed metallographic procedures for identifying the M-A constituent.) The carbon content in the M-A islands can range from about 0.3 to 0.5% C. The significance of this is that, for a given nominal carbon content in the steel, the volume fraction of the M-A constituent will be much higher than if most of the carbon formed carbides (by the lever rule). This will increase the number of crack nucleation sites and thereby contribute to the inferior toughness of ICGC HAZ. As is to be expected, the volume fraction of the M-A constituent also depends on the hardenability of the steel, which in turn depends on the alloying content. It has been shown that if the development of pearlitic microphases could be promoted instead of the development of M-A, by decreasing the alloy content, the toughness of the ICGC HAZ could be improved (Ref 40). However, this would have penalties in terms of achievement of parent plate strength. A more feasible solution would be to inhibit grain growth in the HAZ.

The multipass welding procedure can alternatively be controlled to limit the size of the LBZs. Figure 31 shows how this can be done with a tandem three-wire high current gas-metal arc welding procedure by adjusting the distance between the three arcs. Special "temper-bead" procedures (Ref 42) have been developed for controlling the microstructure in the HAZ, and a need for these procedures arises in the following way. Low-alloy steel weldments for critical applications (for example, pressure vessels) require a postweld heat treatment (PWHT) in a furnace. This is done to temper the hard regions in the HAZ and to relieve residual stresses. If repairs become necessary on site after the component has been in service, PWHT is usually not feasible. The heat of the arc can then be used to achieve the tempering function of PWHT

by suitable spatial positioning and sequencing of the individual passes. Grain refinement in he HAZ is also sought to increase the toughness and thereby offset the harmful effects of residual stresses that would remain in the absence of PWHT.

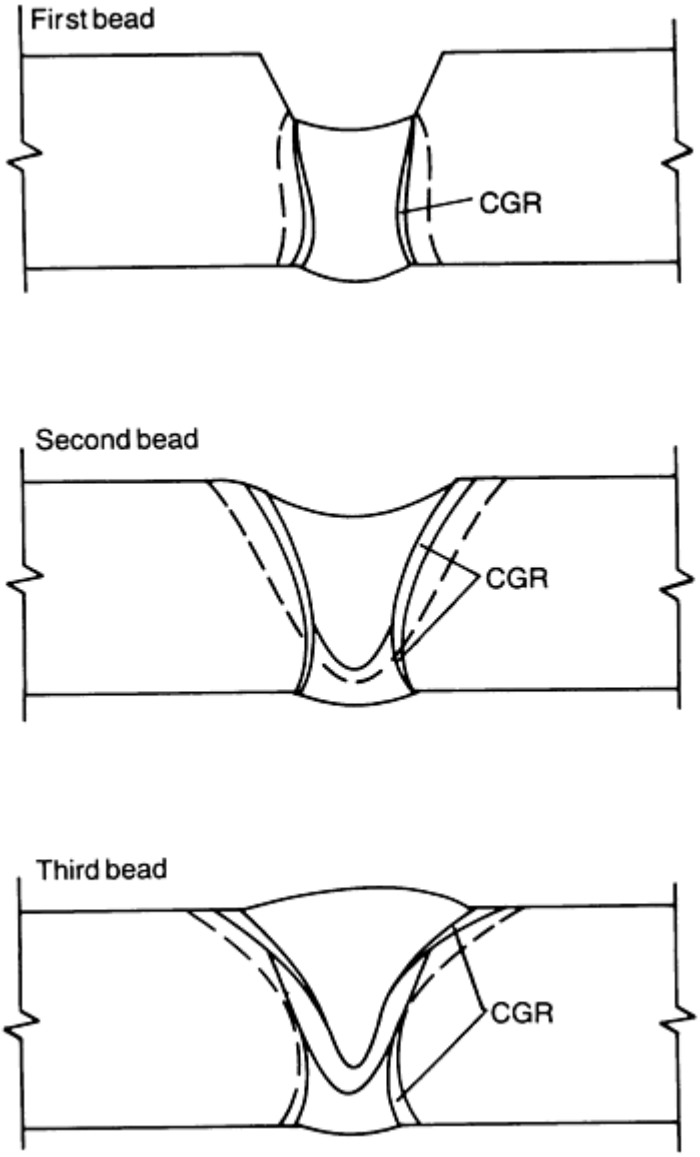

FIG. 31 SCHEMATIC SHOWING THAT THE HAZ ISOTHERMS AND THE SIZE AND LOCATION OF THE COARSE-GRAINED REGION (CGR) CAN BE CONTROLLED IN A TANDEM THREE-WIRE HIGH CURRENT GAS-METAL ARC WELDING PROCEDURE. GRAIN REFINEMENT OF COARSE-GRAINED REGIONS INITIALLY FORMED IS OBTAINED BY OPTIMIZING THE DISTANCES BETWEEN THE THREE ARCS. SOURCE: REF 41

An example of a two-layer temper bead procedure is shown in Fig. 32. The heat inputs of the first and second layer are carefully controlled, so that the heat from the second layer is used to refine the coarse-grained region in the HAZ of the base metal due to the first layer. This ideas can be extended one step further by using a pulsed gas-tungsten arc welding procedure whereby a given pulse in a pulsed weldment can be used to successively refine and temper the preceding pulse pitch regions (Ref 11). The degree of microstructural refinement depends primarily on the welding speed and pulsing frequency, and these parameters can be controlled with great precision. By contrast, an important variable to be controlled in the temper-bead procedure is the weld deposit height, and it is difficult to exercise the same degree of control on this. For this reason, it is argued that the maximum possible control on the microstructural changes in the repair weldment is possible with the pulsing procedure.

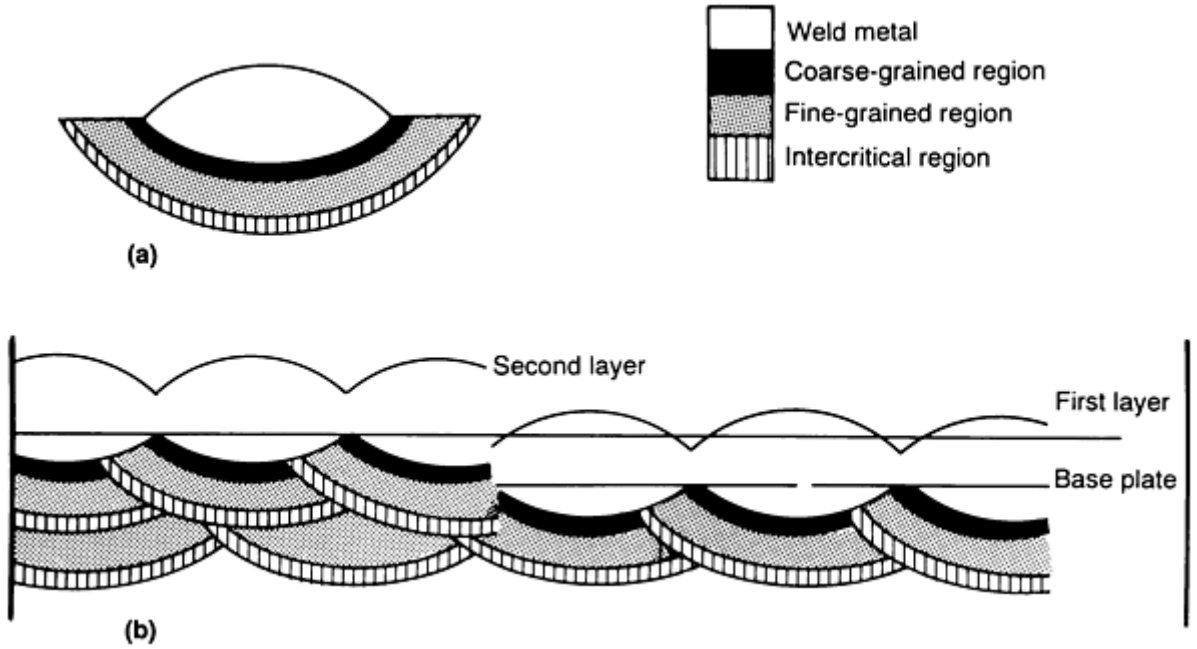

FIG. 32 SCHEMATIC SHOWING A TWO-LAYER REPAIR PROCEDURE. (A) HEAT-AFFECTED AREAS OF A SINGLE WELD BEAD. (B) FIRST LAYER CAUSES COARSE-GRAINED REGIONS TO FORM IN THE HAZ OF THE BASE METAL (RIGHT PORTION OF THE FIGURE). DEPOSITION OF THE SECOND LAYER REFINES THESE INITIAL COARSE-GRAINED REGIONS (LEFT PORTION OF FIGURE). SOURCE: REF 42

References cited in this section

11. P. RAVI VISHNU AND K. EASTERLING, PHENOMENOLOGICAL MODELLING OF HEAT FLOW AND MICROSTRUCTURAL CHANGES IN PULSED GTAW WELDS OF A QT STEEL, *MATHEMATICAL MODELING OF WELD PHENOMENA,* H. CERJAK AND K. EASTERLING, ED., THE INSTITUTE OF METALS, 1993
37. T. HAZE AND S. AIHARA, "INFLUENCE OF TOUGHNESS AND SIZE OF LOCAL BRITTLE ZONES ON HAZ TOUGHNESS OF HSLA STEELS," SEVENTH INTERNATIONAL CONFERENCE ON OFFSHORE MECHANICS AND ARCTIC ENGINEERING, HOUSTON, 1988
38. C.P. ROYER, A USER'S PERSPECTIVE ON HEAT AFFECTED ZONE TOUGHNESS, *WELDING METALLURGY OF STRUCTURAL STEELS,* J.Y. KOO, ED., TMS-AIME, 1987
39. F. MATSUDA, Z. LI, P. BERNASOVSKY, K. ISHIHARA, AND H. OKADA, "AN INVESTIGATION OF THE BEHAVIOUR OF M-A CONSTITUENT IN SIMULATED HAZ OF HSLA STEELS," DOC. NO. IX-B-1591-90, INTERNATIONAL INSTITUTE OF WELDING, 1990
40. P.L. HARRISON AND P.H.M. HART, RELATIONSHIPS BETWEEN HAZ MICROSTRUCTURE AND CTOD TRANSITION BEHAVIOUR IN MULTIPASS C-MN STEEL WELDS, *RECENT TRENDS IN WELDING SCIENCE AND TECHNOLOGY,* S.A. DAVID AND J.M. VITEK, ED., ASM INTERNATIONAL, 1990
41. H. ONOE, J. TANAKA, AND I. WATANABE, JAPANESE LNG TANKER CONSTRUCTED USING A NEW WELDING PROCESS AND IMPROVED AL-KILLED STEELS, *MET. CONSTR.,* JAN 1979, P 26-31
42. P.J. ALBERRY, SENSITIVITY ANALYSIS OF HALF-BEAD AND ALTERNATIVE GTAW TECHNIQUES, *WELD. J.,* NOV 1989, P 442S-451S

Fusion Zone in Multipass Weldments

In the weld metal of a multipass weld, reheating effects will lead to a gradient in microstructure similar to the case of the HAZ. However, instead of a detailed classification, the multipass weld metal is usually considered to consist of just two regions (Fig. 33):

- *AS-DEPOSITED OR PRIMARY REGION,* WHERE THE MICROSTRUCTURE DEVELOPS AS THE WELD COOLS FROM THE LIQUID PHASE TO AMBIENT TEMPERATURE
- *REHEATED OR SECONDARY REGION,* WHERE REGIONS WITH THE ORIGINAL PRIMARY MICROSTRUCTURE ARE REHEATED TO TEMPERATURES ABOVE THE AC_1 TEMPERATURE. THE TEMPERED REGIONS WHICH ARE REHEATED TO SLIGHTLY LOWER TEMPERATURES ARE ALSO GENERALLY CONSIDERED TO BELONG TO THIS CATEGORY

The properties of the weld metal depend on the relative area or volume fractions of the two regions, which in turn depend on the welding procedure, so the properties are procedure-specific. Hence arises the need for welding procedure qualification as per codes and standards in addition to the qualification of consumables (for which is standard procedure is specified).

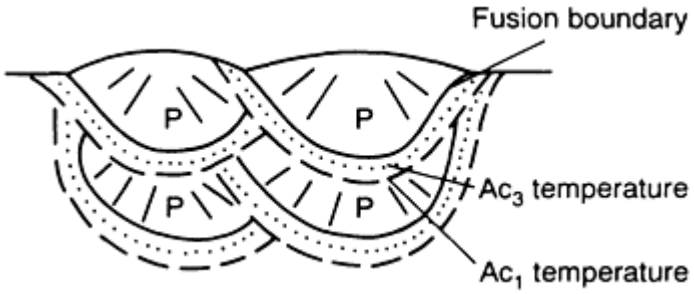

FIG. 33 PRIMARY (P) AND REAUSTENITIZED REGIONS IN THE WELD METAL REGION OF A MULTIPASS WELD. THE REAUSTENITIZED REGION IS WHERE THE COLUMNAR STRUCTURE IS NOT CLEARLY DETECTED. SOURCE: REF 23

Reference cited in this section

23. "GUIDE TO THE LIGHT MICROSCOPE EXAMINATION OF FERRITIC STEEL WELD METALS," DOC. NO. IX-1533-88, INTERNATIONAL INSTITUTE OF WELDING, 1988

Solid-State Transformations in Weldments

P. Ravi Vishnu, Luleå University of Technology, Sweden

Stainless Steels

It has long been known that solidification cracking can be avoided in austenitic stainless steel welds by having a small concentration of ferrite in them. Recent work has shown, however, that residual ferrite content at room temperature is no

more than a symptom and that it is really the solidification mode (whether the weld metal solidifies as primary austenite or ferrite) that is the deciding criterion (Ref 43). It has been found that susceptibility to solidification cracking is least for a primary ferrite solidification mode (more specifically, when the solidification mode corresponds to the types shown in Fig. 34c and 34d). It is believed that low-melting-point liquid phases (formed by the segregation of impurities like sulfur and phosphorus, for example) solidifying in the intercellular regions do not wet the δ-γ interphase boundaries as easily as they would δ-δ or γ-γ boundaries. In the ferritic-austenitic solidification mode (Fig. 34c and 34d), the δ-γ interphase boundary area is greater at temperatures just below the nominal solidus temperature, and this is the reason for a greater resistance to solidification cracking.

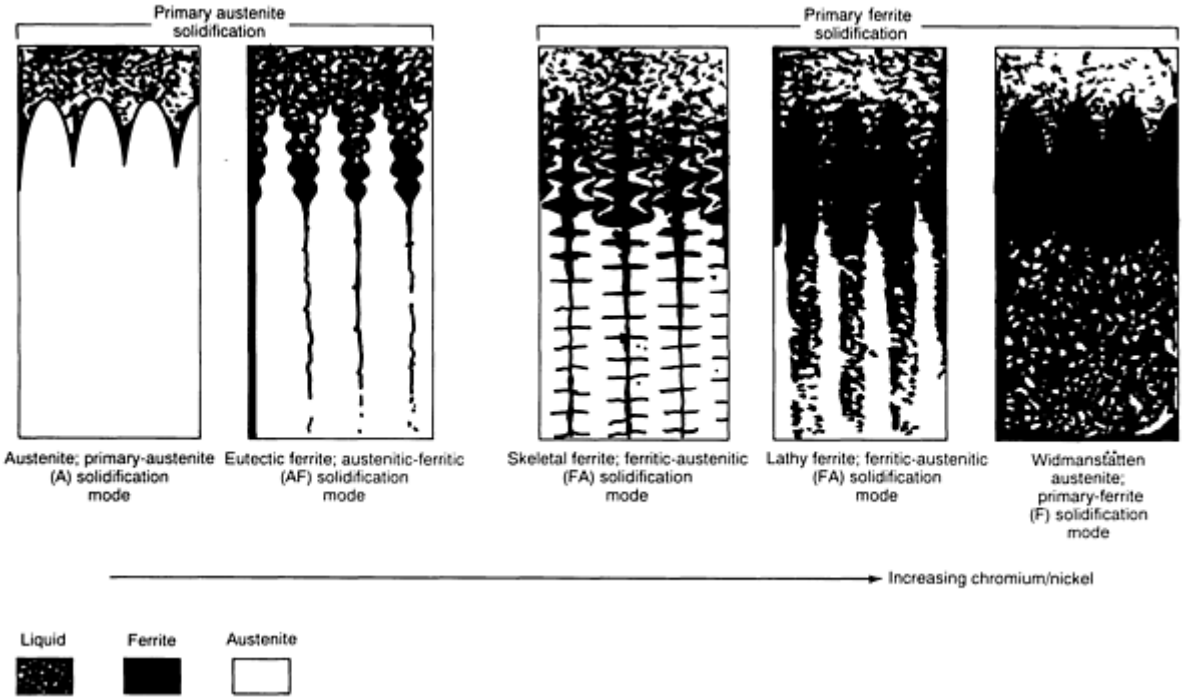

FIG. 34 SCHEMATIC SHOWING SOLIDIFICATION AND TRANSFORMATION BEHAVIOR RESULTING IN A RANGE OF FERRITE MORPHOLOGIES IN AUSTENITIC STAINLESS STEEL WELDS. SOURCE: REF 43

Information about the solidification mode can be obtained from the chemical composition of the weld metal by referring to the WRC-1992 diagram (Fig. 35). It has been found that this diagram is more accurate than the Schaeffler (for duplex stainless steel welds) and Delong (for 300 series austenitic steel welds) diagrams developed earlier. All of these diagrams are strictly applicable only for the cooling rates obtained in manual metal arc (MMA) welding because the data for establishing the statistical correlations have been taken from MMA welds. The dotted lines in Fig. 35 are the demarcation lines between the different solidification modes shown (that is, A, AF, FA, and F) corresponding to the types in Fig. 34(a), 34(b), 34(c), 34(d), and 34(e), respectively. The AF-FA boundary in Fig. 35 (which, as discussed earlier, corresponds to the onset of cracking) intersects the iso-ferrite number lines at an angle. This is consistent with the findings of several investigators that the minimum ferrite content necessary to avoid hot cracking is different for different weld metal compositions (that is, for weld metals deposited with E 316, E 308L, E 309, and so on).

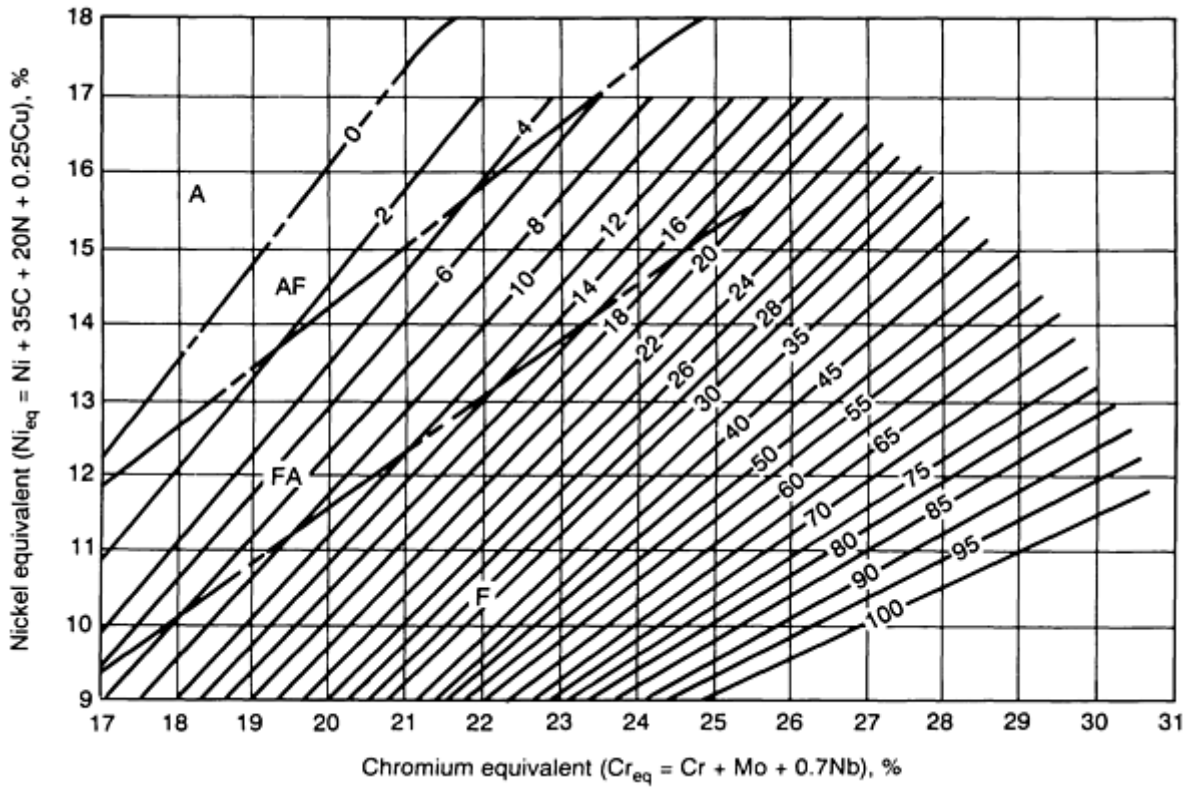

FIG. 35 WRC-1992 DIAGRAM PREDICTING FERRITE CONTENT IN STAINLESS STEELS. FERRITE CONTENT IS GIVEN BY THE FERRITE NUMBER (FN), WHERE 100 FN IS APPROXIMATELY EQUAL TO 65 VOL% FERRITE. BOUNDARIES DENOTING A CHANGE IN SOLIDIFICATION MODE (A, AF, FA AND F PER FIG. 34) ARE ALSO SHOWN (INDICATED BY DOTTED LINES). SOURCE: REF 45

It is a fortunate coincidence that the coefficients in the Cr_{eq} and Ni_{eq} expressions (see Fig. 35), which have been obtained by statistical fitting methods, result in satisfactory correlations with both the solidification mode and the ferrite number (a precisely measurable quantity that is roughly proportional to the actual volume percentage of ferrite at room temperature) (Ref 44). Indeed, it has been found that the same Cr_{eq} and Ni_{eq} expressions (that is, with the same elements and coefficients) are not able to satisfactorily fix the locations of the martensite and martensite-austenite phase fields seen in the lower left region of the Schaeffler diagram. For this reason, such regions of Cr_{eq} and Ni_{eq} are excluded in the WRC-1992 diagram.

A discussion of weld decay due to sensitization and knife line attack in the HAZ of austenitic stainless steels can be found in Ref 14 and 46.

References cited in this section

14. S. KOU, *WELDING METALLURGY,* JOHN WILEY & SONS, 1987
43. J.A. BROOKS AND A.W. THOMPSON, MICROSTRUCTURAL DEVELOPMENT AND SOLIDIFICATION CRACKING SUSCEPTIBILITY OF AUSTENITIC STAINLESS STEEL WELDS, *INT. MATER. REV.,* VOL 36 (NO. 1), 1991
44. T.A. SIEWERT, C.N. MCCOWAN, AND D.L. OLSON, FERRITE NUMBER PREDICTION TO 100 FN IN STAINLESS STEEL WELD METAL, *WELD. J.,* DEC 1988, P 289S-298S
45. D.J. KOTECKI AND T.A. SIEWERT, WRC-1992 CONSTITUTION DIAGRAM FOR STAINLESS STEEL WELD METALS: A MODIFICATION OF THE WRC-1988 DIAGRAM, *WELD. J.,* MAY 1992, P 171S-178S
46. T.G. GOOCH AND D.C. WILLINGHAM, *WELD DECAY IN AUSTENITIC STAINLESS STEELS,* THE

P. Ravi Vishnu, Luleå University of Technology, Sweden

Aluminum Alloys

The main problems in the welding of heat-treatable aluminum alloys are liquation cracking in the partially melted zone (see the section "Unmixed and Partially Melted Zones in a Weldment" in this article) and softening in the HAZ (Ref 14, 47). The latter means that the weld joint strength can be reduced. Reasons for the softening can be understood by referring to Fig. 36. The parent material is assumed to be a 2000- or 6000-series aluminum alloy, artificially aged to contain the metastable phase of θ' (in aluminum-copper alloys), S' (in aluminum-copper-magnesium alloys), or β' (in aluminum-magnesium-silicon alloys). A very fine dispersion of precipitate particles is obtained in the parent material by a solution heat treatment followed by aging, and this is the reason for the high strength in the materials. Figure 36(b) shows that a gradient in hardness is obtained in the HAZ immediately after welding. At location 1, the high peak temperature causes the precipitate particles to go into solution, and the cooling rate is too high for reprecipitation. At locations 2 and 3, the precipitate particles partially dissolve and coarsen. After postweld artificial aging, fine precipitate particles are again formed at location 1, causing the hardness to increase to the parent material level. However, at locations 2 and 3, only a lower hardness can be obtained because of the formation of coarse precipitate particles. For increasing weld heat inputs, the width of the softened zone increases. A good discussion of how the above phenomenon can be modeled is found in Ref 48.

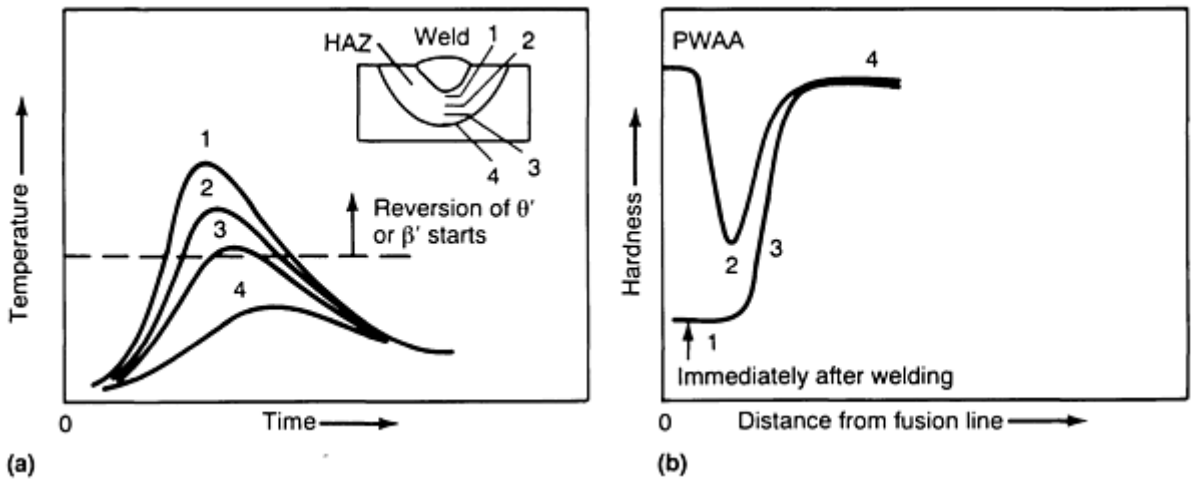

FIG. 36 SCHEMATIC SHOWING THE EFFECT OF WELD THERMAL CYCLES ON THE SOFTENING IN THE HAZ IN AGE-HARDENABLE ALUMINUM ALLOYS. (A) THERMAL CYCLES IN THE HAZ (FOR CORRESPONDING LOCATIONS IN WELD, SEE INSET. (B) HAZ HARDNESS PROFILES BEFORE AND AFTER AGING. PWAA, POSTWELD ARTIFICIAL AGING. SOURCE: REF 14

References cited in this section

14. S. KOU, *WELDING METALLURGY*, JOHN WILEY & SONS, 1987

47. S. KOU, WELDING METALLURGY AND WELDABILITY OF HIGH STRENGTH ALUMINUM ALLOYS, *WELD. RES. COUNC. BULL.*, NO. 320, DEC 1986

48. H. SHERCLIFF AND M.F. ASHBY, A PROCESS MODEL FOR AGE HARDENING OF AL ALLOYS--I. MODEL AND II. APPLICATIONS OF THE MODEL, *ACTA METALL. MATER.*, VOL 38 (NO. 10), 1990, P 1789-1812

Nickel-Base Superalloys

Nickel-base superalloys have a very high creep resistance, making them attractive for critical high-temperature applications such as gas turbines. Yet it is this very characteristic that gives rise to the problem of strain age cracking in the weld HAZ (Ref 14, 19, 49). The high-temperature creep strength in the parent materials is obtained by forming fine precipitates of γ' (Ni_3(Al, Ti)) or γ" (Ni_3Nb) in them. In the region of the weld HAZ subjected to high peak temperatures, these precipitates dissolve, similar to the case of aluminum alloys. After welding, the weldments are again solution heat-treated and aged (note the difference between aluminum alloys and the nickel-base superalloys in this respect). The purposes of this treatment are to obtain the same uniform and fine precipitation in the weld as in the parent material and to relieve the weld residual stresses.

Normally (for example, in the case of low-alloy or carbon steel welds), PWHT in a furnace relieves the residual stresses because the yield stress at the PWHT temperature is very low. A residual stress greater than the yield stress cannot be supported, and stress relief is brought about by a process of creep and plastic deformation. This process is difficult in nickel-base superalloy weldments, however, because of their high creep strength and low creep ductility. Reprecipitation in the solutionized regions of the HAZ (during the heating-up to the PWHT temperature) strengthens the matrix and does not allow any creep or plastic deformation (necessary for the relief of residual stress) to take place. Cracking can occur in this condition at the grain boundaries in the grain-coarsened region of the HAZ. Cracks initiated here have been known to run far into the base material. This problem is very difficult to solve, and the best solution has been found to be to switch over to materials such as Inconel 718 alloy that are inherently less susceptible to cracking, even though their creep strength is somewhat lower. Inconel 718 alloy contains γ" precipitate, and the slow kinetics of precipitation in this alloy allow substantial stress relief to be achieved before precipitation increases the creep strength in the HAZ.

References cited in this section

14. S. KOU, *WELDING METALLURGY,* JOHN WILEY & SONS, 1987

19. W. YENISCAVITCH, JOINING, *SUPERALLOYS II,* C.T. SIMS, N.S. STOLOFF, AND W.C. HAGEL, ED., JOHN WILEY & SONS, 1987, P 495-516

49. W.A. OWCZARSKI, PROCESS AND METALLURGICAL FACTORS IN JOINING SUPERALLOYS AND OTHER HIGH SERVICE TEMPERATURE MATERIALS, *PHYSICAL METALLURGY OF JOINING,* R. KOSSOWSKY AND M.E. GLICKSMAN, ED., TMS-AIME, 1980

Solid-State Transformations in Weldments

P. Ravi Vishnu, Luleå University of Technology, Sweden

Titanium Alloys

Titanium alloys find use in aerospace applications, pressure vessels, and so on because of their high strength-to-weight ratio, high corrosion resistance, and high fracture toughness. Pure titanium has two allotropic forms: low-temperature hexagonal close-packed (hcp) α-phase and elevated-temperature body-centered cubic (bcc) β-phase. Various alloying elements tend to preferentially stabilize one or the other of these phases. As a result, titanium alloys are generally classified as α, α+ β, metastable β, and β alloys (Fig. 37).

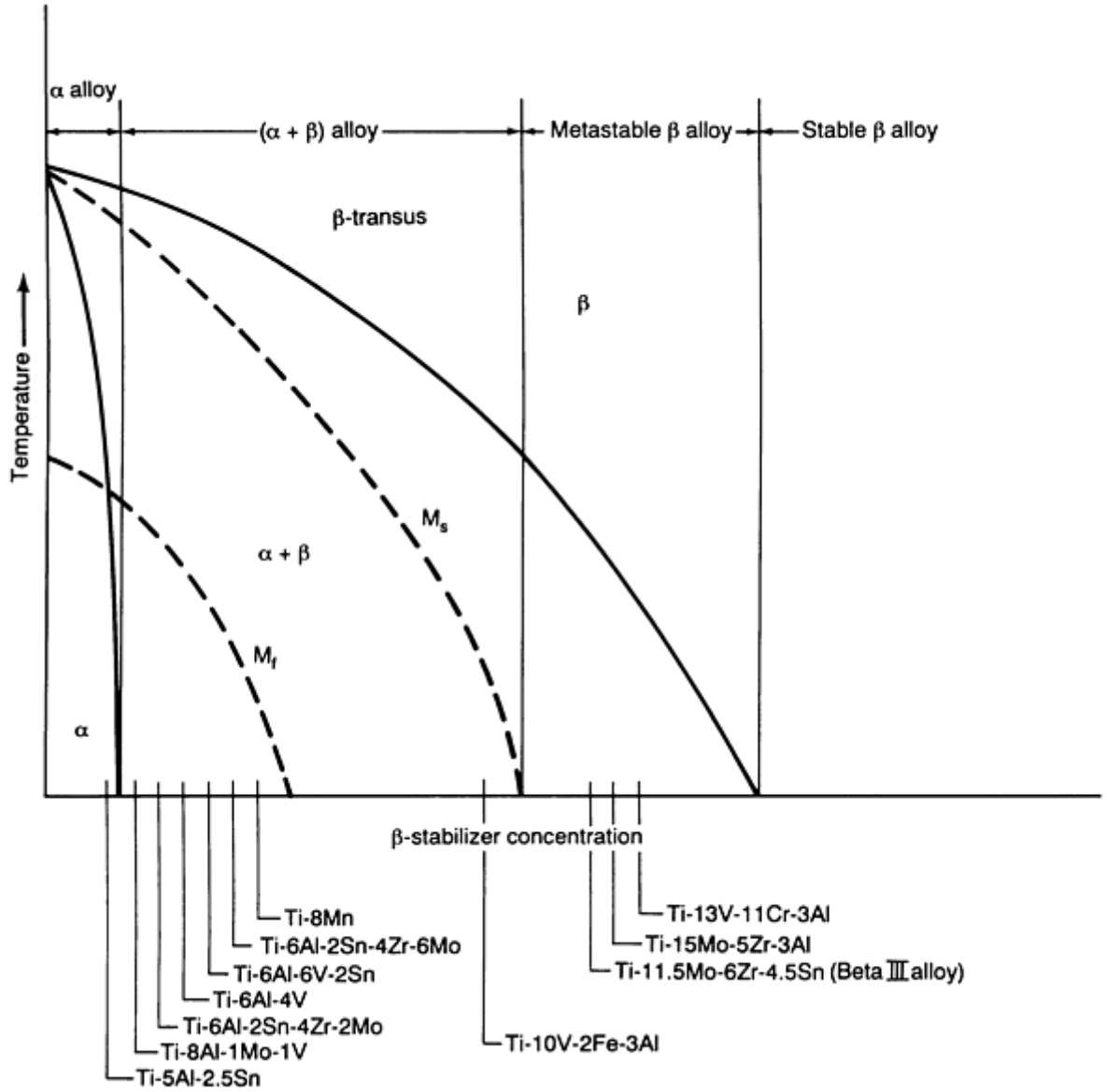

FIG. 37 HYPOTHETICAL β ISOMORPHOUS PHASE DIAGRAM THAT SHOWS RELATION BETWEEN β -STABILIZER SOLUTE CONTENT AND TITANIUM ALLOY FAMILY DESCRIPTION. SELECTED COMMON ALLOYS ARE LISTED ALONG THE *X*-AXIS OF THE DIAGRAM BASED ON THEIR COMPOSITIONS. SOURCE: REF 50

The α-alloys are not heat-treatable (that is, a significant increase in strength and toughness cannot be obtained by heat treatment), and they have the lowest strength of the four titanium alloy families. Interestingly enough, these alloys are thus considered to have excellent weldability. What this means in practice is that there is no significant degradation in the properties of the weld and HAZ with regard to the parent material due to the weld thermal cycles. Also, the β ↔ α transformation in the weld and near HAZ means that the extent of grain coarsening will not be so high as in other single-phase materials in which no phase transformation occurs upon heating or cooling, such as stabilized ferritic stainless steels (Ref 51), pure aluminum, and so on.

In the α+ β alloys, a higher strength is obtained with a higher volume fraction of the β phase, which in turn is obtained with a higher β -stabilizing alloy content (Fig. 37). The effect of cooling rate on the phase transformations in two α+ β alloys is shown schematically in Fig. 38. As in the case of steels, it is seen that the β ↔ αtransformation can occur either by nucleation and growth at slower cooling rates or martensitically at higher cooling rates. The martensitic product in the lean α+ β alloys has an hcp crystal structure (designated as α') or an orthorhombic one (designated as α") in the β-stabilized α+ β alloys. It is seen that the C-curve for the β ↔ intergranular α transformation is shifted to the right for alloys with increasing β-stabilizing alloy content, while that for the allotriomorphic α (more commonly referred to as GB

α) is relatively insensitive to alloy concentration (Ref 52). As a result, alloys that are fairly rich in β-stabilizing additions exhibit a stronger tendency to form a continuous network of GB α than do leaner α + β alloys.

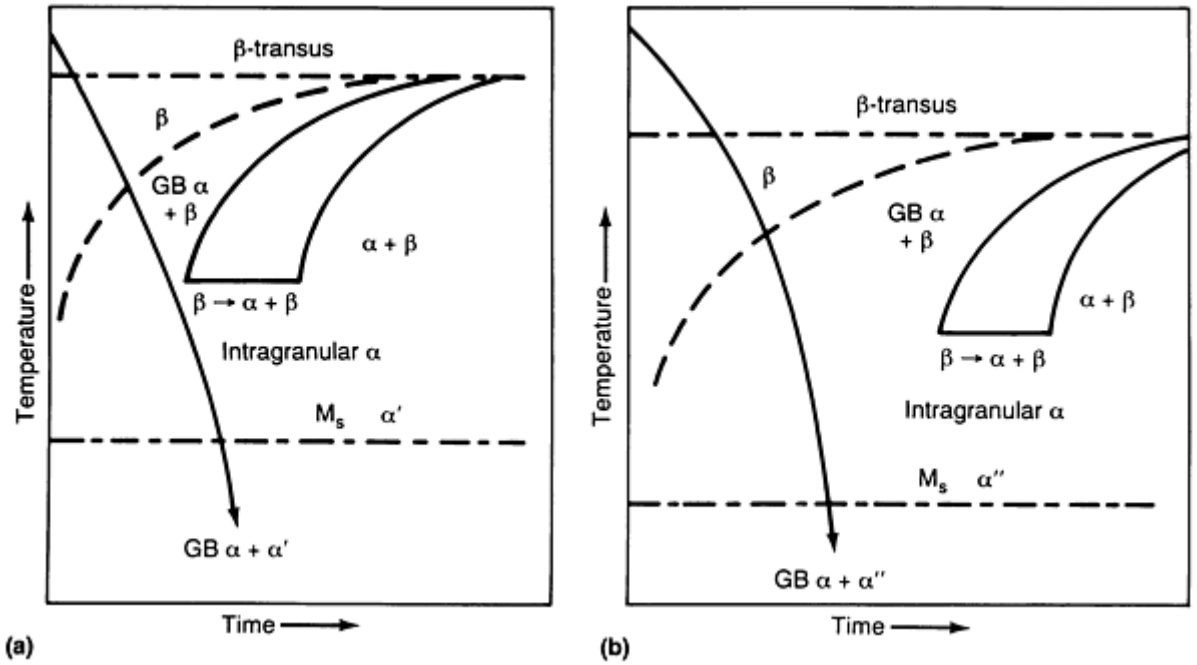

FIG. 38 SCHEMATIC CCT DIAGRAMS FOR TWO α + β TITANIUM ALLOYS WITH DIFFERENT β -STABILIZER SOLUTE CONTENTS. (A) LEAN α + β ALLOY (FOR EXAMPLE, TI-6AL-4V). (B) α + β ALLOY (FOR EXAMPLE, CORONA 5 [TI-4.5AL-5MO-1.5CR]) RICHER IN β -STABILIZING SOLUTE CONTENT

The morphology of the α and β phases in the α + β base materials is strongly dependent on thermomechanical processing (TMP) and heat treatment, which are performed either in the β-phase field or in the two-phase α + β phase field. When TMP is done in the α+ β phase field, the α that forms on cooling is continuously deformed. After recrystallization, a near-equiaxed α structure is obtained after this α + β processing. Very little GB α is formed because deformation introduces sufficient alternate heterogeneous nucleation sites in the form of dislocations. On the other hand, if TMP is done above the β-transus temperature (β-processing) and cooled, α forms at grain boundaries (giving GB α) and in the interior of grains as a Widmanstätten structure (also referred to as an acicular, lenticular, or basketweave structure). The microstructure in the weld and the near HAZ is closer to that obtained after β-processing.

Figure 39 shows the effect of α + β processing and β-processing on the strength and toughness of α + β alloys with increasing β-stabilizing alloy content. At the lower strength levels obtained with a lower β-stabilizing alloy content (because of a lower volume fraction of β-phase present), the finer Widmanstätten structure obtained after β-processing has a higher toughness than the coarser structure obtained by α + β processing. At higher strength levels, the trend reverses with the α + β processed structure having a higher toughness. This result can be understood in terms of the strength differences between GB α and the interior of the prior β grains (Fig. 40). At lower strengths, when the grain interiors are relatively weak, the crack tip plastic zone is distributed between the GB α and the grain interiors. However, as the α-phase precipitates are refined by lower aging temperatures, as in the case of the metastable β alloys, the grain interiors are strengthened considerably. Under such circumstances, the cracks are essentially constrained to follow the GB α layer. This results in a contraction of the plastic zone, a reduction in the crack tip opening displacement for crack extension, and an attendant drop in the toughness.

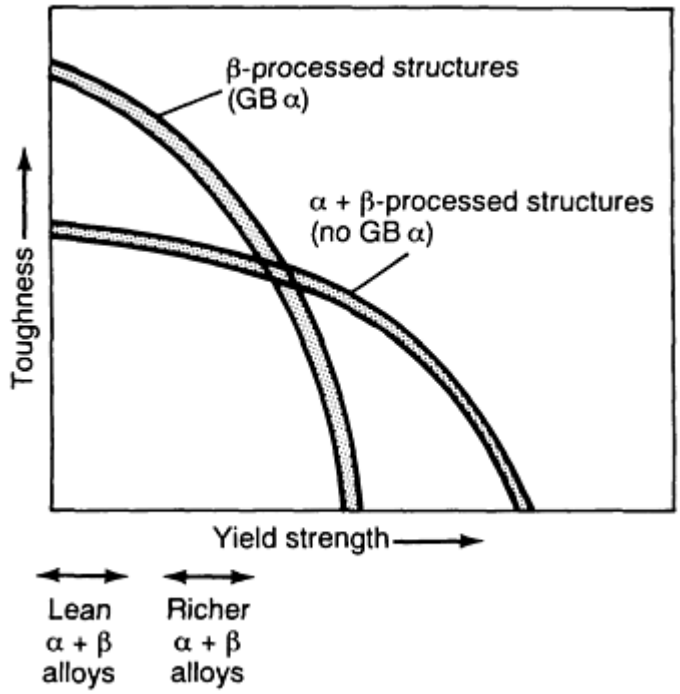

FIG. 39 SCHEMATIC PLOT OF TOUGHNESS VERSUS YIELD STRENGTH FOR α + β AND β-PROCESSED STRUCTURES. APPROXIMATE LOCATIONS OF LEAN (FOR EXAMPLE, TI-6AL-4V) AND RICHER β STABILIZED α + β ALLOYS (FOR EXAMPLE, CORONA 5 [TI-4.5AL-5MO-1.5CR]) ARE SHOWN. SOURCE: REF 52

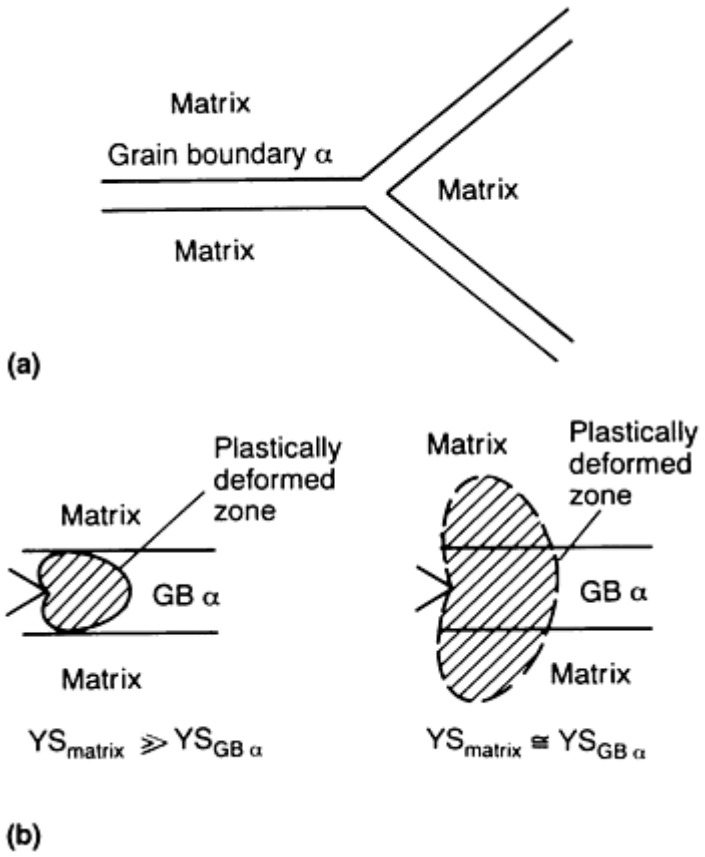

FIG. 40 SCHEMATIC SHOWING THE EFFECT OF THE RELATIVE STRENGTHS OF GB α AND MATRIX ON THE

PLASTIC ZONE SIZE. (A) GB α LOCATION RELATIVE TO MATRIX. (B) EFFECT OF PLASTIC ZONE SIZE ON YIELD STRENGTHS OF MATRIX AND GB α. SOURCE: REF 52

The microstructures in the weld metal and the near HAZ (the region where the peak temperature exceeds the β-transus temperature) resemble those obtained after β-processing. This means that it is easier to get a matching toughness in the weld metal at the lower strength levels referred to in Fig. 39. Even this is made somewhat difficult by the coarser β grain size in the weld and HAZ. Grain coarsening in the HAZ induces coarse β grains to form in the weld also, because solidification in the weld metal occurs by epitaxial growth from the HAZ. The extent of grain coarsening is such that it is not uncommon to find a single columnar β grain traversing the entire thickness in gas-tungsten arc welds on thin sheet (Ref 53). If high energy density welding processes are used (for example, electron-beam welding or laser-beam welding), it is possible to limit the extent of β grain coarsening. However, the high cooling rates in the weld and HAZ will mean that a martensitic structure will be obtained.

To obtain adequate ductility and toughness, PWHT will have to be done at temperatures close to the β-transus temperature. This can be a problem because the low strength at these temperatures can cause sagging in large welded structures, and complex fixturing will be necessary to maintain dimensional tolerances. It can also be expensive, because inert gas shielding is required for almost the entire time of PWHT (it is assumed in the present discussion that adequate care is taken to maintain proper shielding during welding). Moreover, it can be difficult to increase the ductility in the weld metal and HAZ to a level equal to that in an α+ β processed base material (Fig. 41). The trends seen in Fig. 39 and 41 can be understood by noting that crack nucleation is more difficult in an equaixed structure (because the strain concentration effects are less) and that the plastic zone sizes are bigger (Table 1). This results in a higher tensile ductility. However, because crack propagation follows a less tortuous path, the toughness is lower. The reverse is true for a Widmanstätten structure (referred to as a lenticular structure in Table 1). Table 1 explains the apparently strange observation in titanium alloys that a structure having a high strength and toughness is not necessarily the one having a high tensile ductility. The implication of this for weldments is that for many applications it may be more important to optimize the welding and PWHT procedure with respect to the toughness than with respect to the ductility.

TABLE 1 EFFECT OF MORPHOLOGICAL FEATURES OF THE MICROSTRUCTURE ON CRACK NUCLEATION AND PROPAGATION IN α + β TITANIUM ALLOYS

Note: Voids initiated at the α -β interfaces are shown as black regions. Source: Ref 54

Structure	Crack nucleation	Crack growth	Tensile ductility as a function of plastic zone size	Toughness as a function of crack propagation
Lenticular (Widmanstätten)	Easy	Difficult	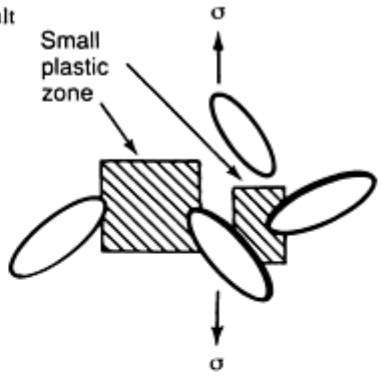 Low ductility	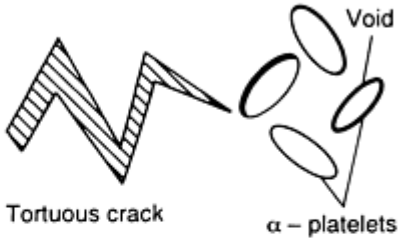 High toughness
Globular (equiaxed)	Difficult	Easy	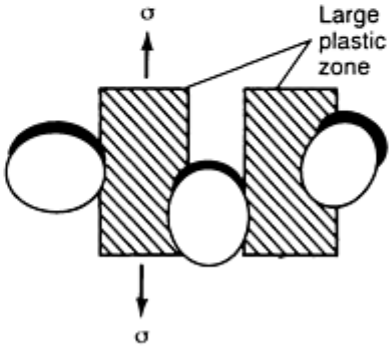 High ductility	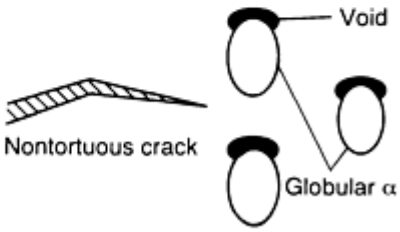 Low toughness

Note: Voids initiated at the α-β interfaces are shown as black regions. Source: Ref 54

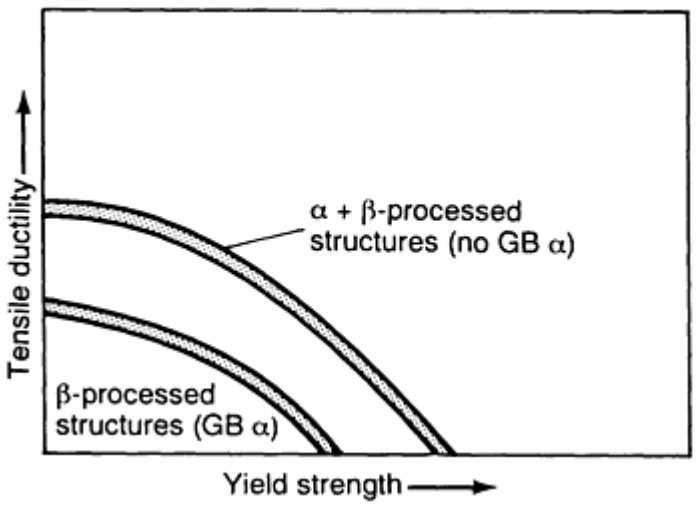

FIG. 41 SCHEMATIC PLOT OF DUCTILITY VERSUS STRENGTH FOR α + β AND β -PROCESSED STRUCTURES. SOURCE: REF 52

A more detailed discussion of the welding metallurgy of titanium alloys can be found in Ref 53, 55, and 56.

References cited in this section

50. E.W. COLLINGS, INTRODUCTION TO TITANIUM ALLOY DESIGN, *ALLOYING*, J.L. WALTER,

M.R. JACKSON, AND C.T. SIMS, ED., ASM INTERNATIONAL, 1988, P 267

51. C.R. THOMAS AND F.P.A. ROBINSON, KINETICS AND MECHANISM OF GRAIN GROWTH DURING WELDING IN NIOBIUM STABILISED 17% CHROMIUM STAINLESS STEELS, *MET. TECHNOL.*, APRIL 1978, P 133-138
52. J.C. WILLIAMS AND E.A. STARKE, JR., THE ROLE OF THERMOMECHANICAL PROCESSING IN TAILORING THE PROPERTIES OF ALUMINUM AND TITANIUM ALLOYS, *DEFORMATION, PROCESSING AND STRUCTURE,* G. KRAUSS, ED., AMERICAN SOCIETY FOR METALS, 1984, P 279-354
53. W.A. BAESLACK III, D.W. BECKER, AND F.H. FROES, ADVANCES IN TITANIUM ALLOY WELDING METALLURGY, *J. MET.*, MAY 1984, P 46-58
54. J.P. HIRTH AND F.H. FROES, INTERRELATIONS BETWEEN FRACTURE TOUGHNESS AND OTHER MECHANICAL PROPERTIES IN TITANIUM ALLOYS, *METALL. TRANS. A,* VOL 8, JULY 1977, P 1165-1176
55. C.G. RHODES, MICROSCOPY AND TITANIUM ALLOY DEVELOPMENT, *APPLIED METALLOGRAPHY,* G.F. VANDER VOORT, ED., VAN NOSTRAND REINHOLD, 1986
56. W.A. BAESLACK III, METALLOGRAPHY OF TITANIUM ALLOY WELDMENTS, *METALLOGRAPHY AND INTERPRETATION OF WELD MICROSTRUCTURES,* J.L. MCCALL, D.L. OLSON, AND I. LEMAY, ED., ASM INTERNATIONAL, 1987, P 23-60

Solid-State Transformations in Weldments

P. Ravi Vishnu, Luleå University of Technology, Sweden

Titanium Alloys

Titanium alloys find use in aerospace applications, pressure vessels, and so on because of their high strength-to-weight ratio, high corrosion resistance, and high fracture toughness. Pure titanium has two allotropic forms: low-temperature hexagonal close-packed (hcp) α-phase and elevated-temperature body-centered cubic (bcc) β-phase. Various alloying elements tend to preferentially stabilize one or the other of these phases. As a result, titanium alloys are generally classified as α, α+ β, metastable β, and βalloys (Fig. 37).

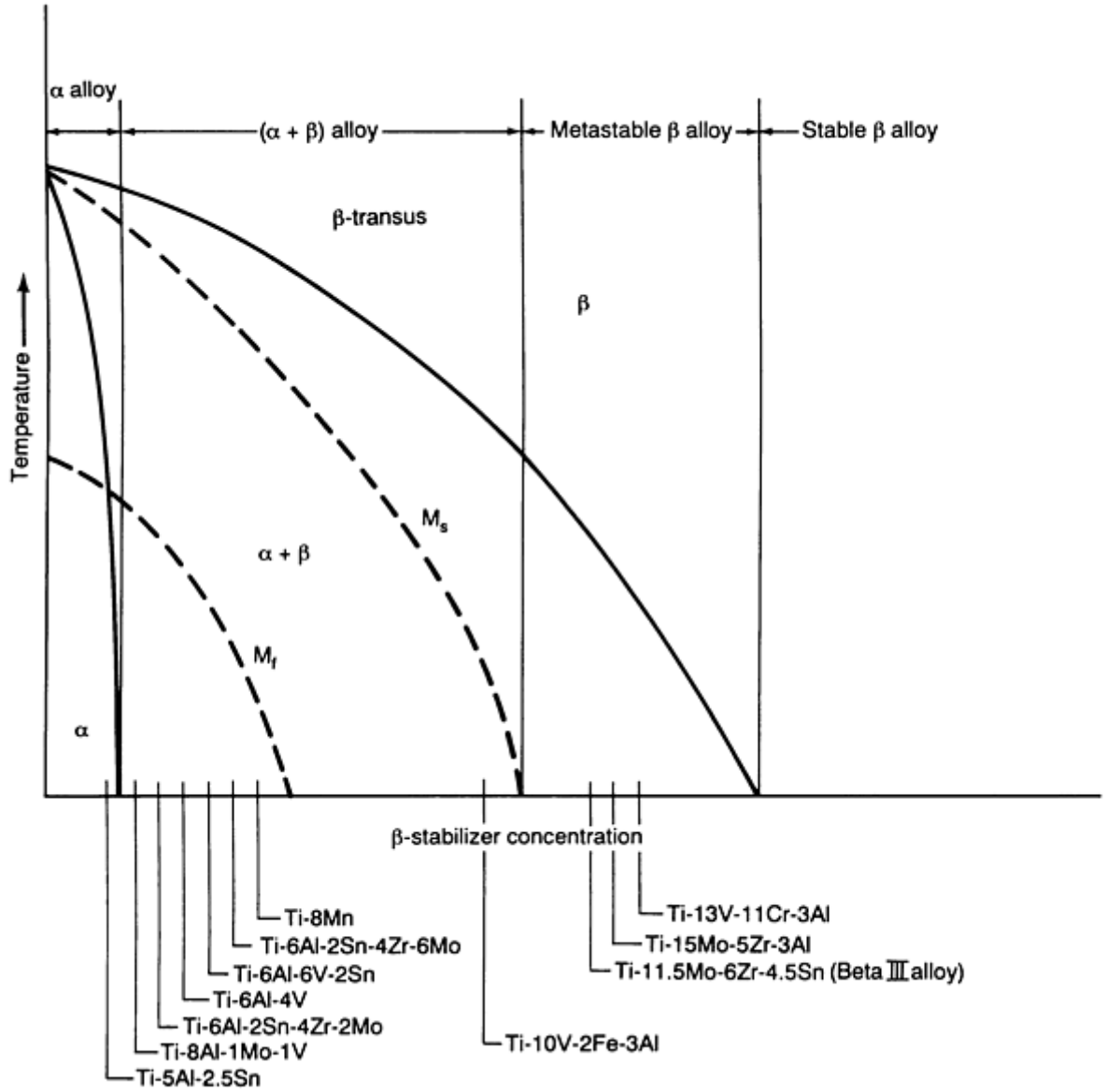

FIG. 37 HYPOTHETICAL β ISOMORPHOUS PHASE DIAGRAM THAT SHOWS RELATION BETWEEN β -STABILIZER SOLUTE CONTENT AND TITANIUM ALLOY FAMILY DESCRIPTION. SELECTED COMMON ALLOYS ARE LISTED ALONG THE *X*-AXIS OF THE DIAGRAM BASED ON THEIR COMPOSITIONS. SOURCE: REF 50

The α-alloys are not heat-treatable (that is, a significant increase in strength and toughness cannot be obtained by heat treatment), and they have the lowest strength of the four titanium alloy families. Interestingly enough, these alloys are thus considered to have excellent weldability. What this means in practice is that there is no significant degradation in the properties of the weld and HAZ with regard to the parent material due to the weld thermal cycles. Also, the β ↔ α transformation in the weld and near HAZ means that the extent of grain coarsening will not be so high as in other single-phase materials in which no phase transformation occurs upon heating or cooling, such as stabilized ferritic stainless steels (Ref 51), pure aluminum, and so on.

In the α+ β alloys, a higher strength is obtained with a higher volume fraction of the β phase, which in turn is obtained with a higher β-stabilizing alloy content (Fig. 37). The effect of cooling rate on the phase transformations in two α + β alloys is shown schematically in Fig. 38. As in the case of steels, it is seen that the β ↔ α transformation can occur either by nucleation and growth at slower cooling rates or martensitically at higher cooling rates. The martensitic product in the lean α + β alloys has an hcp crystal structure (designated as α') or an orthorhombic one (designated as α ") in the β-stabilized α + β alloys. It is seen that the C-curve for the β ↔ intergranular α transformation is shifted to the right for alloys with increasing β-stabilizing alloy content, while that for the allotriomorphic α(more commonly referred to as GB

α) is relatively insensitive to alloy concentration (Ref 52). As a result, alloys that are fairly rich in β-stabilizing additions exhibit a stronger tendency to form a continuous network of GB α than do leaner α + β alloys.

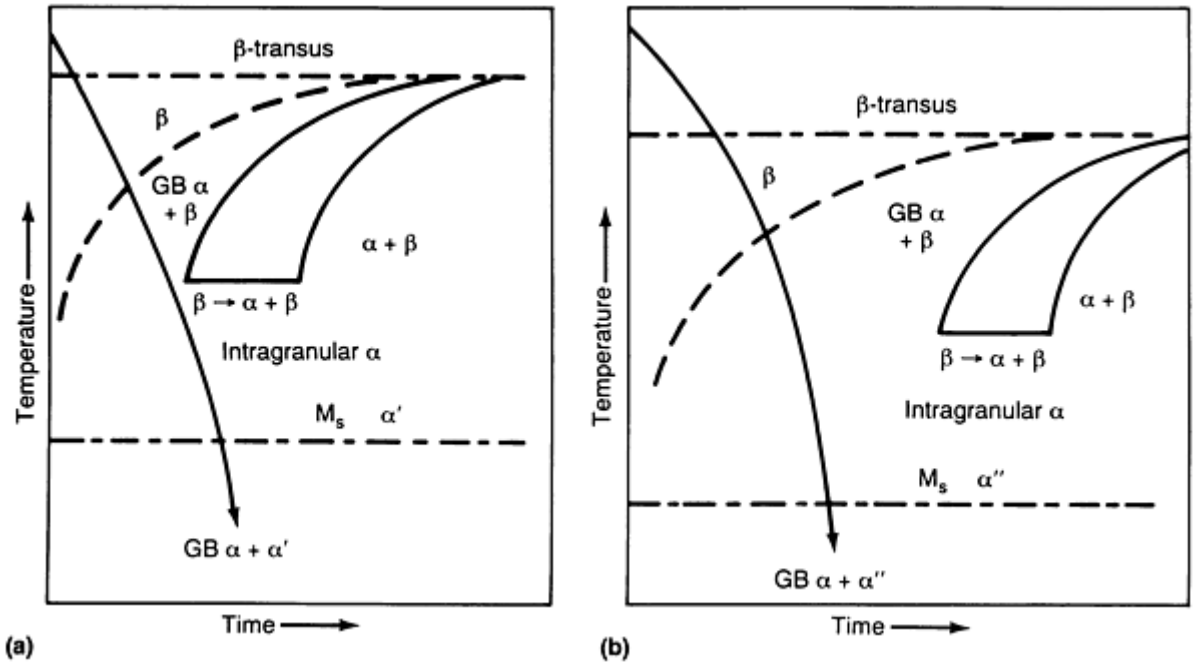

FIG. 38 SCHEMATIC CCT DIAGRAMS FOR TWO α + β TITANIUM ALLOYS WITH DIFFERENT β -STABILIZER SOLUTE CONTENTS. (A) LEAN α + β ALLOY (FOR EXAMPLE, TI-6AL-4V). (B) α + β ALLOY (FOR EXAMPLE, CORONA 5 [TI-4.5AL-5MO-1.5CR]) RICHER IN β -STABILIZING SOLUTE CONTENT

The morphology of the α and β phases in the α + β base materials is strongly dependent on thermomechanical processing (TMP) and heat treatment, which are performed either in the β-phase field or in the two-phase α+ β phase field. When TMP is done in the α+ β phase field, the α that forms on cooling is continuously deformed. After recrystallization, a near-equiaxed α structure is obtained after this α + β processing. Very little GB α is formed because deformation introduces sufficient alternate heterogeneous nucleation sites in the form of dislocations. On the other hand, if TMP is done above the β-transus temperature (β-processing) and cooled, α forms at grain boundaries (giving GB α) and in the interior of grains as a Widmanstätten structure (also referred to as an acicular, lenticular, or basketweave structure). The microstructure in the weld and the near HAZ is closer to that obtained after β-processing.

Figure 39 shows the effect of α + β processing and β-processing on the strength and toughness of α + β alloys with increasing β-stabilizing alloy content. At the lower strength levels obtained with a lower β-stabilizing alloy content (because of a lower volume fraction of β-phase present), the finer Widmanstätten structure obtained after β-processing has a higher toughness than the coarser structure obtained by α + β processing. At higher strength levels, the trend reverses with the α + β processed structure having a higher toughness. This result can be understood in terms of the strength differences between GB α and the interior of the prior β grains (Fig. 40). At lower strengths, when the grain interiors are relatively weak, the crack tip plastic zone is distributed between the GB α and the grain interiors. However, as the α-phase precipitates are refined by lower aging temperatures, as in the case of the metastable β alloys, the grain interiors are strengthened considerably. Under such circumstances, the cracks are essentially constrained to follow the GB α layer. This results in a contraction of the plastic zone, a reduction in the crack tip opening displacement for crack extension, and an attendant drop in the toughness.

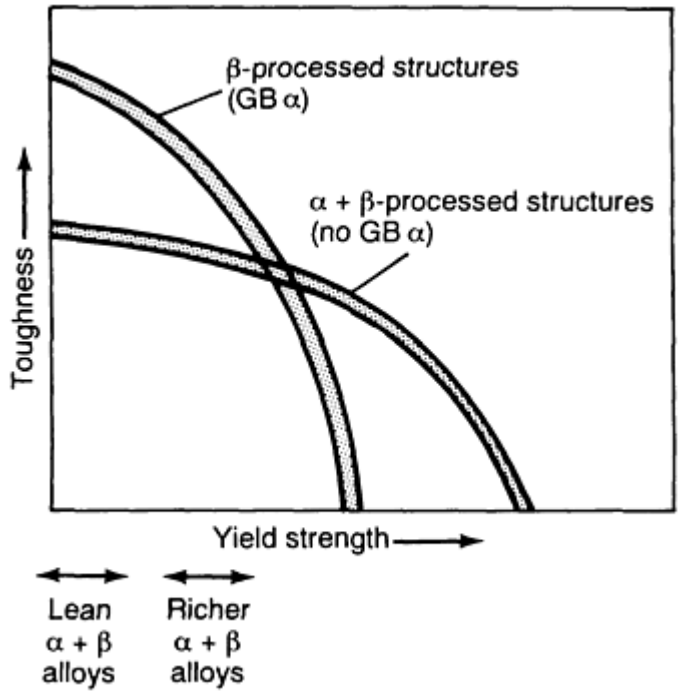

FIG. 39 SCHEMATIC PLOT OF TOUGHNESS VERSUS YIELD STRENGTH FOR α + β AND β -PROCESSED STRUCTURES. APPROXIMATE LOCATIONS OF LEAN (FOR EXAMPLE, TI-6AL-4V) AND RICHER β STABILIZED α + β ALLOYS (FOR EXAMPLE, CORONA 5 [TI-4.5AL-5MO-1.5CR]) ARE SHOWN. SOURCE: REF 52

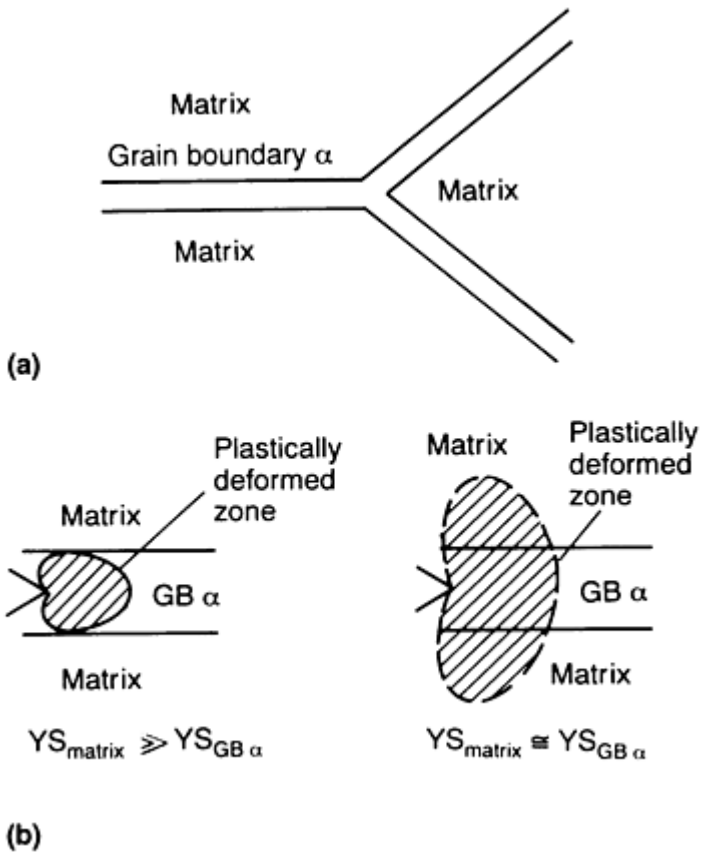

FIG. 40 SCHEMATIC SHOWING THE EFFECT OF THE RELATIVE STRENGTHS OF GB α AND MATRIX ON THE PLASTIC ZONE SIZE. (A) GB α LOCATION RELATIVE TO MATRIX. (B) EFFECT OF PLASTIC ZONE SIZE ON YIELD

STRENGTHS OF MATRIX AND GB α. SOURCE: REF 52

The microstructures in the weld metal and the near HAZ (the region where the peak temperature exceeds the β-transus temperature) resemble those obtained after β-processing. This means that it is easier to get a matching toughness in the weld metal at the lower strength levels referred to in Fig. 39. Even this is made somewhat difficult by the coarser β grain size in the weld and HAZ. Grain coarsening in the HAZ induces coarse β grains to form in the weld also, because solidification in the weld metal occurs by epitaxial growth from the HAZ. The extent of grain coarsening is such that it is not uncommon to find a single columnar β grain traversing the entire thickness in gas-tungsten arc welds on thin sheet (Ref 53). If high energy density welding processes are used (for example, electron-beam welding or laser-beam welding), it is possible to limit the extent of β grain coarsening. However, the high cooling rates in the weld and HAZ will mean that a martensitic structure will be obtained.

To obtain adequate ductility and toughness, PWHT will have to be done at temperatures close to the β-transus temperature. This can be a problem because the low strength at these temperatures can cause sagging in large welded structures, and complex fixturing will be necessary to maintain dimensional tolerances. It can also be expensive, because inert gas shielding is required for almost the entire time of PWHT (it is assumed in the present discussion that adequate care is taken to maintain proper shielding during welding). Moreover, it can be difficult to increase the ductility in the weld metal and HAZ to a level equal to that in an α + β processed base material (Fig. 41). The trends seen in Fig. 39 and 41 can be understood by noting that crack nucleation is more difficult in an equaixed structure (because the strain concentration effects are less) and that the plastic zone sizes are bigger (Table 1). This results in a higher tensile ductility. However, because crack propagation follows a less tortuous path, the toughness is lower. The reverse is true for a Widmanstätten structure (referred to as a lenticular structure in Table 1). Table 1 explains the apparently strange observation in titanium alloys that a structure having a high strength and toughness is not necessarily the one having a high tensile ductility. The implication of this for weldments is that for many applications it may be more important to optimize the welding and PWHT procedure with respect to the toughness than with respect to the ductility.

TABLE 1 EFFECT OF MORPHOLOGICAL FEATURES OF THE MICROSTRUCTURE ON CRACK NUCLEATION AND PROPAGATION IN α+ β TITANIUM ALLOYS

Note: Voids initiated at the α-β interfaces are shown as black regions. Source: Ref 54

Structure	Crack nucleation	Crack growth	Tensile ductility as a function of plastic zone size	Toughness as a function of crack propagation
Lenticular (Widmanstätten)	Easy	Difficult	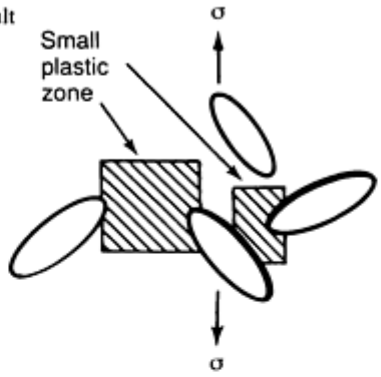 Low ductility	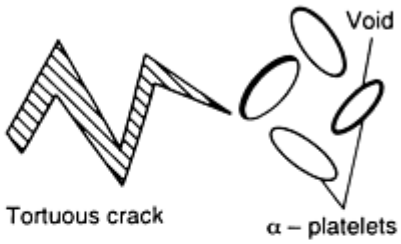 High toughness
Globular (equiaxed)	Difficult	Easy	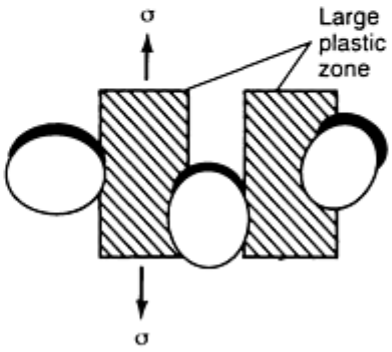 High ductility	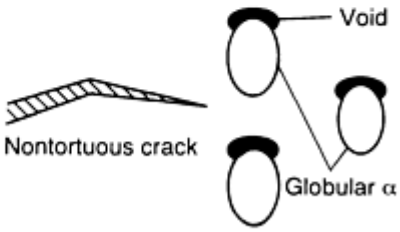 Low toughness

Note: Voids initiated at the α-β interfaces are shown as black regions. Source: Ref 54

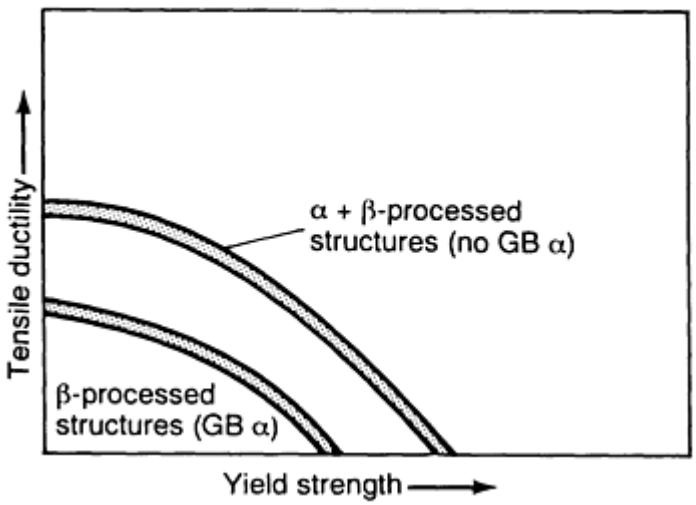

FIG. 41 SCHEMATIC PLOT OF DUCTILITY VERSUS STRENGTH FOR α+β AND β -PROCESSED STRUCTURES. SOURCE: REF 52

A more detailed discussion of the welding metallurgy of titanium alloys can be found in Ref 53, 55, and 56.

References cited in this section

50. E.W. COLLINGS, INTRODUCTION TO TITANIUM ALLOY DESIGN, *ALLOYING*, J.L. WALTER,

M.R. JACKSON, AND C.T. SIMS, ED., ASM INTERNATIONAL, 1988, P 267

51. C.R. THOMAS AND F.P.A. ROBINSON, KINETICS AND MECHANISM OF GRAIN GROWTH DURING WELDING IN NIOBIUM STABILISED 17% CHROMIUM STAINLESS STEELS, *MET. TECHNOL.*, APRIL 1978, P 133-138
52. J.C. WILLIAMS AND E.A. STARKE, JR., THE ROLE OF THERMOMECHANICAL PROCESSING IN TAILORING THE PROPERTIES OF ALUMINUM AND TITANIUM ALLOYS, *DEFORMATION, PROCESSING AND STRUCTURE,* G. KRAUSS, ED., AMERICAN SOCIETY FOR METALS, 1984, P 279-354
53. W.A. BAESLACK III, D.W. BECKER, AND F.H. FROES, ADVANCES IN TITANIUM ALLOY WELDING METALLURGY, *J. MET.*, MAY 1984, P 46-58
54. J.P. HIRTH AND F.H. FROES, INTERRELATIONS BETWEEN FRACTURE TOUGHNESS AND OTHER MECHANICAL PROPERTIES IN TITANIUM ALLOYS, *METALL. TRANS. A,* VOL 8, JULY 1977, P 1165-1176
55. C.G. RHODES, MICROSCOPY AND TITANIUM ALLOY DEVELOPMENT, *APPLIED METALLOGRAPHY,* G.F. VANDER VOORT, ED., VAN NOSTRAND REINHOLD, 1986
56. W.A. BAESLACK III, METALLOGRAPHY OF TITANIUM ALLOY WELDMENTS, *METALLOGRAPHY AND INTERPRETATION OF WELD MICROSTRUCTURES,* J.L. MCCALL, D.L. OLSON, AND I. LEMAY, ED., ASM INTERNATIONAL, 1987, P 23-60

Solid-State Transformations in Weldments

P. Ravi Vishnu, Luleå University of Technology, Sweden

References

1. *ATLAS OF ISOTHERMAL TRANSFORMATION AND COOLING TRANSFORMATION DIAGRAMS* AMERICAN SOCIETY FOR METALS, 1977
2. O.M. AKSELSEN AND T. SIMONSEN, TECHNIQUES FOR EXAMINING TRANSFORMATION BEHAVIOUR IN WELD METAL AND HAZ--A STATE OF ART REVIEW, *WELD. WORLD,* VOL 25 (NO. 1/2), 1987, P 26-34
3. O. GRONG AND D.K. MATLOCK, MICROSTRUCTURAL DEVELOPMENT IN MILD AND LOW ALLOY STEEL WELD METALS, *INT. MET. REV.,* VOL 31 (NO. 1), 1986, P 27-48
4. P.L. HARRISON AND R.A. FARRAR, APPLICATION OF CONTINUOUS COOLING TRANSFORMATION DIAGRAMS FOR WELDING OF STEELS, *INT. MATER. REV.,* VOL 34 (NO. 1), 1989, P 35-51
5. G.T. ELDIS, A CRITICAL REVIEW OF DATA SOURCES FOR ISOTHERMAL TRANSFORMATION AND CONTINUOUS COOLING TRANSFORMATION DIAGRAMS, *HARDENABILITY CONCEPTS WITH APPLICATION TO STEEL,* D.V. DOANE AND J.S. KIRKALDY, ED., TMS-AIME, 1978, P 126-157
6. K. EASTERLING, *INTRODUCTION TO THE PHYSICAL METALLURGY OF WELDING,* BUTTERWORTHS, 1983
7. *WELD THERMAL SIMULATORS FOR RESEARCH AND PROBLEM SOLVING,* THE WELDING INSTITUTE, U.K., 1972
8. C.F. BERKHOUT AND P.H. VAN LENT, THE USE OF PEAK TEMPERATURE-COOLING TIME DIAGRAMS IN THE WELDING OF HIGH STRENGTH STEELS (IN GERMAN), *SCHWEISS. SCHNEID.,* VOL 20 (NO. 6), 1968, P 256-260
9. TH.J. VAN ADRICHEM AND J. KAS, *CALCULATION, MEASUREMENT AND SIMULATION OF WELD THERMAL CYCLES,* SMITWELD N.V., NIJMEGEN, THE NETHERLANDS

10. P. RAVI VISHNU, W.B. LI, AND K. EASTERLING, HEAT FLOW MODEL FOR PULSED WELDING, *MATER. SCI. TECH.,* VOL 7 (NO. 7), 1991, P 649-659
11. P. RAVI VISHNU AND K. EASTERLING, PHENOMENOLOGICAL MODELLING OF HEAT FLOW AND MICROSTRUCTURAL CHANGES IN PULSED GTAW WELDS OF A QT STEEL, *MATHEMATICAL MODELING OF WELD PHENOMENA,* H. CERJAK AND K. EASTERLING, ED., THE INSTITUTE OF METALS, 1993
12. VEREIN DEUTSCHER EISENHÜTTENLEUTE, ED., *STEEL--A HANDBOOK FOR MATERIALS RESEARCH AND ENGINEERING, VOLUME 1: FUNDAMENTALS*, SPRINGER VERLAG, 1992, P 175
13. A.J. DEARDO, C.I. GARCIA, AND E.J. PALMIERE, THERMOMECHANICAL PROCESSING OF STEELS, *HEAT TREATING,* VOL 4, *ASM HANDBOOK,* 1991, P 237-255
14. S. KOU, *WELDING METALLURGY,* JOHN WILEY & SONS, 1987
15. K. NARITA, PHYSICAL CHEMISTRY OF THE GROUPS IVA (TI, ZR), VA (V, NB, TA) AND THE RARE EARTH ELEMENTS IN STEEL, *TRANS. ISIJ,* VOL 15, 1975, P 145-152
16. R.K. AMIN AND F.B. PICKERING, AUSTENITE GRAIN COARSENING AND THE EFFECT OF THERMOMECHANICAL PROCESSING ON AUSTENITE RECRYSTALLIZATION, *THERMOMECHANICAL PROCESSING OF MICROALLOYED AUSTENITE,* A.J. DEARDO, G.A. RATZ, AND P.J. WRAY, ED., TMS-AIME, 1982, P 14
17. W.F. SAVAGE, E.F. NIPPES, AND E.S SZEKERES, A STUDY OF WELD INTERFACE PHENOMENA IN A LOW ALLOY STEEL, *WELD. J.,* SEPT 1976, P 260S-268S, AND HYDROGEN INDUCED COLD CRACKING IN A LOW ALLOY STEEL, *WELD. J.,* SEPT 1976, P 276S-283S
18. J.J. PEPE AND W.F. SAVAGE, EFFECTS OF CONSTITUTIONAL LIQUATION IN 18-NI MARAGING STEEL WELDMENTS, *WELD J.,* SEPT 1967, P 411S-422S
19. W. YENISCAVITCH, JOINING, *SUPERALLOYS II,* C.T. SIMS, N.S. STOLOFF, AND W.C. HAGEL, ED., JOHN WILEY & SONS, 1987, P 495-516
20. E.E. HUCKE AND H. UDIN, WELDING METALLURGY OF NODULAR CAST IRON, *WELD. J.,* AUG 1953, P 378S-385S
21. E.N. GREGORY AND S.B. JONES, WELDING CAST IRONS, *WELDING OF CASTINGS,* THE WELDING INSTITUTE, U.K., 1977, P 145-156
22. L.E. SAMUELS, *OPTICAL MICROSCOPY OF CARBON STEELS,* AMERICAN SOCIETY FOR METALS, 1980
23. "GUIDE TO THE LIGHT MICROSCOPE EXAMINATION OF FERRITIC STEEL WELD METALS," DOC. NO. IX-1533-88, INTERNATIONAL INSTITUTE OF WELDING, 1988
24. H.K.D.H. BHADESHIA AND L.E. SVENSSON, MODELLING THE EVOLUTION OF MICROSTRUCTURE OF STEEL WELD METAL, *MATHEMATICAL MODELLING OF WELD PHENOMENA,* H. CERJAK AND K. EASTERLING, ED., THE INSTITUTE OF MATERIALS, 1993
25. G.R. EDWARDS AND S. LIU, RECENT DEVELOPMENTS IN HSLA STEEL WELDING, *ADVANCES IN WELDING METALLURGY,* FIRST U.S.-JAPAN SYMPOSIUM, AMERICAN WELDING SOCIETY AND OTHERS, JUNE 1990, P 215-293
26. B. AHLBLOM, "OXYGEN AND ITS ROLE IN DETERMINING WELD METAL MICROSTRUCTURE AND TOUGHNESS--A STATE OF THE ART REVIEW," DOC. NO. IX-1322-84, INTERNATIONAL INSTITUTE OF WELDING, 1984
27. L.-E. SVENSSON AND B. GRETOFT, MICROSTRUCTURE AND IMPACT TOUGHNESS OF C-MN WELD METALS. *WELD. J.,* DEC 1990, P 454S-461S
28. P.W. HOLSBERG AND R.J. WONG, WELDING OF HSLA-100 STEEL FOR NAVAL APPLICATIONS, *WELDABILITY OF MATERIALS,* R.A. PATTERSON AND K.W. MAHIN, ED., ASM INTERNATIONAL, 1990
29. J.M.B. LOSZ AND K.D. CHALLENGER, MICROSTRUCTURE AND PROPERTIES OF A COPPER PRECIPITATION STRENGTHENED HSLA STEEL WELDMENT, *RECENT TRENDS IN WELDING SCIENCE AND TECHNOLOGY,* S.A. DAVID AND J.M. VITEK, ED., ASM INTERNATIONAL, 1990
30. H. HOMMA, S. OHKITA, S. MATSUDA, AND K. YAMAMOTO, IMPROVEMENTS OF HAZ

TOUGHNESS IN HSLA STEEL BY INTRODUCING FINELY DISPERSED TI-OXIDE, *WELD. J.,* OCT 1987, P 301S-309S

31. N. YURIOKA, "MODERN HIGH STRENGTH STEEL IN JAPAN," FIFTH INTERNATIONAL SYMPOSIUM, JAPAN WELDING SOCIETY, APRIL 1990 (TOKYO)
32. YU.N. GOTALSKII, THE PROBLEM OF WELDING HIGH STRENGTH STEELS, *AUTOM. WELD.,* JUNE 1984, P 37-40
33. W.K.C. JONES AND P.J. ALBERRY, THE ROLE OF PHASE TRANSFORMATIONS IN THE DEVELOPMENT OF RESIDUAL STRESSES DURING THE WELDING OF SOME FAST REACTOR STEELS, *PROC. CONF. FERRITIC STEELS FOR FAST REACTOR STEAM GENERATORS,* BRITISH NUCLEAR ENERGY SOCIETY, 1977
34. *MCGRAW-HILL ENCYCLOPEDIA OF SCIENCE AND TECHNOLOGY,* VOL 9, P 685
35. A.M. MAKARA AND N.A. MOSENDZ, EFFECTS OF THE WELD METAL ON CRACKING IN HAZ, *WELD. RES. ABROAD,* NOV 1965, P 78-86
36. H. IKAWA, S. SHIN, M. INUI, Y. TAKEDA, AND A. NAKANO, "ON THE MARTENSITE-LIKE STRUCTURE AT WELD BOND AND THE MACROSCOPIC SEGREGATION IN WELD METAL IN THE WELDED DISSIMILAR METALS OF α-STEELS AND γ-STEELS," DOC. NO. IX-785-72, INTERNATIONAL INSTITUTE OF WELDING, 1972
37. T. HAZE AND S. AIHARA, "INFLUENCE OF TOUGHNESS AND SIZE OF LOCAL BRITTLE ZONES ON HAZ TOUGHNESS OF HSLA STEELS," SEVENTH INTERNATIONAL CONFERENCE ON OFFSHORE MECHANICS AND ARCTIC ENGINEERING, HOUSTON, 1988
38. C.P. ROYER, A USER'S PERSPECTIVE ON HEAT AFFECTED ZONE TOUGHNESS, *WELDING METALLURGY OF STRUCTURAL STEELS,* J.Y. KOO, ED., TMS-AIME, 1987
39. F. MATSUDA, Z. LI, P. BERNASOVSKY, K. ISHIHARA, AND H. OKADA, "AN INVESTIGATION OF THE BEHAVIOUR OF M-A CONSTITUENT IN SIMULATED HAZ OF HSLA STEELS," DOC. NO. IX-B-1591-90, INTERNATIONAL INSTITUTE OF WELDING, 1990
40. P.L. HARRISON AND P.H.M. HART, RELATIONSHIPS BETWEEN HAZ MICROSTRUCTURE AND CTOD TRANSITION BEHAVIOUR IN MULTIPASS C-MN STEEL WELDS, *RECENT TRENDS IN WELDING SCIENCE AND TECHNOLOGY,* S.A. DAVID AND J.M. VITEK, ED., ASM INTERNATIONAL, 1990
41. H. ONOE, J. TANAKA, AND I. WATANABE, JAPANESE LNG TANKER CONSTRUCTED USING A NEW WELDING PROCESS AND IMPROVED AL-KILLED STEELS, *MET. CONSTR.,* JAN 1979, P 26-31
42. P.J. ALBERRY, SENSITIVITY ANALYSIS OF HALF-BEAD AND ALTERNATIVE GTAW TECHNIQUES, *WELD. J.,* NOV 1989, P 442S-451S
43. J.A. BROOKS AND A.W. THOMPSON, MICROSTRUCTURAL DEVELOPMENT AND SOLIDIFICATION CRACKING SUSCEPTIBILITY OF AUSTENITIC STAINLESS STEEL WELDS, *INT. MATER. REV.,* VOL 36 (NO. 1), 1991
44. T.A. SIEWERT, C.N. MCCOWAN, AND D.L. OLSON, FERRITE NUMBER PREDICTION TO 100 FN IN STAINLESS STEEL WELD METAL, *WELD. J.,* DEC 1988, P 289S-298S
45. D.J. KOTECKI AND T.A. SIEWERT, WRC-1992 CONSTITUTION DIAGRAM FOR STAINLESS STEEL WELD METALS: A MODIFICATION OF THE WRC-1988 DIAGRAM, *WELD. J.,* MAY 1992, P 171S-178S
46. T.G. GOOCH AND D.C. WILLINGHAM, *WELD DECAY IN AUSTENITIC STAINLESS STEELS,* THE WELDING INSTITUTE, UK, 1975
47. S. KOU, WELDING METALLURGY AND WELDABILITY OF HIGH STRENGTH ALUMINUM ALLOYS, *WELD. RES. COUNC. BULL.,* NO. 320, DEC 1986
48. H. SHERCLIFF AND M.F. ASHBY, A PROCESS MODEL FOR AGE HARDENING OF AL ALLOYS--I. MODEL AND II. APPLICATIONS OF THE MODEL, *ACTA METALL. MATER.,* VOL 38 (NO. 10), 1990, P 1789-1812
49. W.A. OWCZARSKI, PROCESS AND METALLURGICAL FACTORS IN JOINING SUPERALLOYS

AND OTHER HIGH SERVICE TEMPERATURE MATERIALS, *PHYSICAL METALLURGY OF JOINING*, R. KOSSOWSKY AND M.E. GLICKSMAN, ED., TMS-AIME, 1980

50. E.W. COLLINGS, INTRODUCTION TO TITANIUM ALLOY DESIGN, *ALLOYING*, J.L. WALTER, M.R. JACKSON, AND C.T. SIMS, ED., ASM INTERNATIONAL, 1988, P 267
51. C.R. THOMAS AND F.P.A. ROBINSON, KINETICS AND MECHANISM OF GRAIN GROWTH DURING WELDING IN NIOBIUM STABILISED 17% CHROMIUM STAINLESS STEELS, *MET. TECHNOL.*, APRIL 1978, P 133-138
52. J.C. WILLIAMS AND E.A. STARKE, JR., THE ROLE OF THERMOMECHANICAL PROCESSING IN TAILORING THE PROPERTIES OF ALUMINUM AND TITANIUM ALLOYS, *DEFORMATION, PROCESSING AND STRUCTURE*, G. KRAUSS, ED., AMERICAN SOCIETY FOR METALS, 1984, P 279-354
53. W.A. BAESLACK III, D.W. BECKER, AND F.H. FROES, ADVANCES IN TITANIUM ALLOY WELDING METALLURGY, *J. MET.*, MAY 1984, P 46-58
54. J.P. HIRTH AND F.H. FROES, INTERRELATIONS BETWEEN FRACTURE TOUGHNESS AND OTHER MECHANICAL PROPERTIES IN TITANIUM ALLOYS, *METALL. TRANS. A*, VOL 8, JULY 1977, P 1165-1176
55. C.G. RHODES, MICROSCOPY AND TITANIUM ALLOY DEVELOPMENT, *APPLIED METALLOGRAPHY*, G.F. VANDER VOORT, ED., VAN NOSTRAND REINHOLD, 1986
56. W.A. BAESLACK III, METALLOGRAPHY OF TITANIUM ALLOY WELDMENTS, *METALLOGRAPHY AND INTERPRETATION OF WELD MICROSTRUCTURES*, J.L. MCCALL, D.L. OLSON, AND I. LEMAY, ED., ASM INTERNATIONAL, 1987, P 23-60

Cracking Phenomena Associated With Welding

Michael J. Cieslak, Physical and Joining Metallurgy Department, Sandia National Laboratories

Introduction

THE FORMATION OF DEFECTS in materials that have been fusion welded is a major concern in the design of welded assemblies. Four types of defects in particular have been the focus of much attention because of the magnitude of their impact on product quality. These defects, all of which manifest themselves as cracks, are characteristic of phenomena that occur at certain temperature intervals specific to a given alloy. Colloquially, these four defect types are known as hot cracks, heat-affected zone (HAZ) microfissures, cold cracks, and lamellar tearing.

Acknowledgements

This work was performed at Sandia National Laboratories, supported by the U.S. Department of Energy under Contract No. DE-AC04-76DP00789.

Cracking Phenomena Associated With Welding

Michael J. Cieslak, Physical and Joining Metallurgy Department, Sandia National Laboratories

Solidification Cracking (Hot Cracking)

Hot cracks are solidification cracks that occur in the fusion zone near the end of solidification. Simplistically, they result from the inability of the semisolid material to accommodate the thermal shrinkage strains associated with weld solidification and cooling. Cracks then form at susceptible sites to relieves the accumulating strain. Susceptible sites are interfaces, such as solidification grain boundaries and interdendritic regions, that are at least partially wetted.

Figure 1 is a photomicrograph of a metallographic section showing the appearance of a typical solidification crack in a fusion weld. Note the intergranular nature of the crack path. Figure 2 shows the surface morphology of a solidification crack, reflecting the nearly solidified nature of the interface at the time of failure. Note the smooth dendritic appearance of this surface.

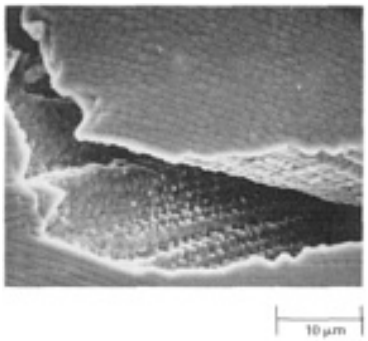

FIG. 1 SOLIDIFICATION CRACK IN A PULSED ND:YAG LASER WELD JOINING HASTELLOY C-276 TO 17-4 PH STAINLESS STEEL. YAG, YTTRIUM-ALUMINUM-GARNET

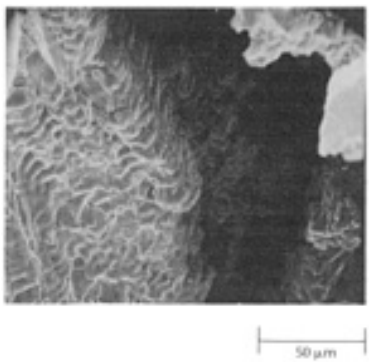

FIG. 2 SURFACE OF A SOLIDIFICATION CRACK IN AN ALLOY 214 VARESTRAINT TEST SPECIMEN

Solidification cracking requires both a sufficient amount of mechanical restraint (strain) and a susceptible microstructure. Knowledge regarding the development of shrinkage strains at the microstructural scale of a solidifying dendrite is still quite limited, making it nearly impossible to quantify *a priori* the amount of local strain required to initiate solidification cracks. Furthermore, the rate at which the strain is applied can influence the ability of an alloy to survive the solidification process without cracking. At temperatures near their melting points, metal alloys can readily dissipate applied loads by time-dependent deformation processes (i.e., creep processes). At high rates of applied stress, both the fusion zone and the HAZ have limited time to accommodate this mechanical imposition. Under conditions of rapid solidification and cooling, the rate of strain accumulation is rapid, leading to an increased cracking susceptibility. Inherently, then, requisite strains for solidification cracking are more likely to be experienced with welding processes that promote rapid solidification and cooling.

Because of the limited quantitative understanding of strain development in a solidifying weld, the practical approach taken to minimize the mechanical factor is to reduce the overall weld restraint through judicious joint design and appropriate choice of welding parameters. A simple way to minimize the restraint on a solidifying weld joint is to keep the joint gap to a minimum by designing hardware with good fit-up. Another approach, particularly attractive for small parts, is to design the weld joint as a standing edge. Welding parameters can have a profound influence on the occurrence of solidification cracking. The natural tendency to use high-speed welding to improve productivity can have detrimental effects. Formation of a teardrop-shaped weld pool, which may occur as the weld travel speed increases, can result in centerline solidification cracks. The solidification pattern associated with this type of weld pool is such that solidifying grains meet at the weld centerline, forming a particularly susceptible site for solidification crack initiation.

The manner in which a fusion weld is terminated can also influence cracking behavior. In a closure weld, simply extinguishing the power can result in the formation of "crater cracks" as the final weld pool rapidly solidifies in on itself. A common method used to minimize this problem is to ramp down the power slowly, either while the workpiece remains stationary or as it continues to travel a short length under the heat source. In some cases, the use of a runoff tab as a site for weld termination may be appropriate.

The extent to which special joint designs or precisely controlled welding parameters can be used to produce welds without solidification cracks is specific for a given alloy. Alloys that are microstructurally susceptible to cracking will necessarily have a more limited set of joint designs and processing parameters around which defect-free welds can be produced.

Alloys with a wide solidification temperature range are more susceptible to solidification cracking than alloys that solidify over a narrow temperature range. Simply described, this is because accumulated thermal strain is proportional to the temperature range over which a material solidifies. This temperature range is determined primarily by chemical composition. For many binary alloy systems and a few ternary alloy systems, the equilibrium solidification (or melting) temperature range has been established in phase diagram studies. For the vast majority of commercial alloys, however, these data are not precisely known.

Borland (Ref 1, 2) attempted to establish a general quantitative method for comparing the effects of various alloying elements on the melting temperature range of a given solvent element. Figure 3 shows a schematic binary alloy phase diagram having linear liquidus and solidus boundaries. For an alloy of composition C_0, T_L is the liquidus composition and T_S is the solidus composition, where the alloy would be completely solidified under conditions of equilibrium cooling. T_M is the invariant melting temperature of the solvent element. The slope of the liquidus is m_L, and the slope of the solidus is m_S. The equilibrium distribution coefficient, k, is defined as the ratio of the composition of the solid, C_S, to the composition of the liquid, C_L, at a given temperature (i.e., $k = C_S/C_L|_T$). For a linear liquidus and solidus, this value is constant and also equal to m_L/m_S.

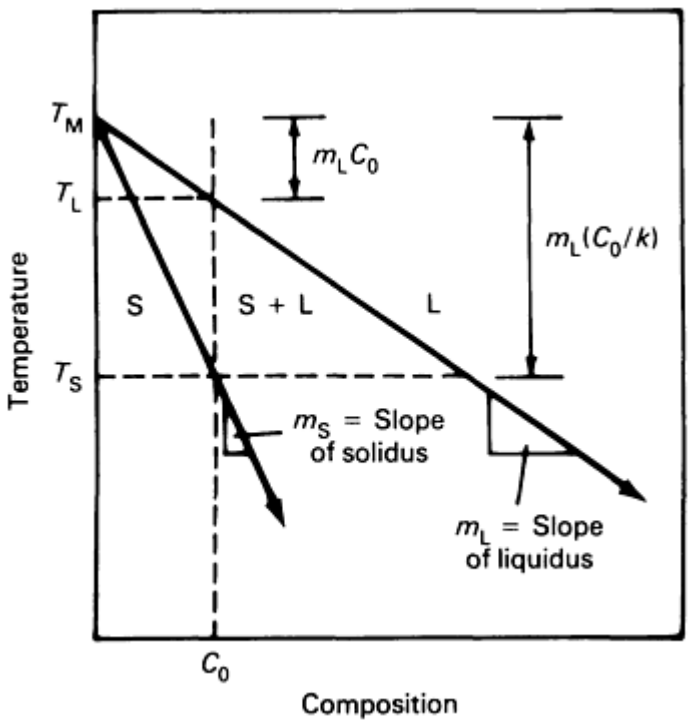

FIG. 3 HYPOTHETICAL BINARY ALLOY PHASE DIAGRAM SHOWING KEY PARAMETERS REQUIRED TO DERIVE THE RELATIVE POTENCY FACTOR (RPF)

With these terms thus defined, a derivation of the relative potency factor (RPF), after Borland (Ref 2), follows:

$$T_L = T_M - M_L C_0 \quad \textbf{(EQ 1)}$$

$$T_S = T_M - M_S C_0 \quad \textbf{(EQ 2)}$$

However, $m_S = m_L/k$:

$$T_s = T_M - \frac{M_L}{K} C_o \quad \textbf{(EQ 3)}$$

Then:

$$T_L - T_S = \frac{m_L C_o (K-1)}{K} \quad \textbf{(EQ 4)}$$

The RPF, always a positive number, is defined as the change in melting temperature ranger per weight percent of solute added, or:

$$RPF = \frac{T1 - Ts}{C_o} = \frac{M_L (k-1)}{K} \quad \textbf{(EQ 5)}$$

where for $k < 1$, $m_L < 0$; and for $k > 1$,$m_L > 0$. The larger the RPF, the wider the melting temperature range and the higher the solidification cracking susceptibility. The final form of Eq 5 indicates that as k becomes very small (indicating a high level of microsegregation), the solidification cracking sensitivity increases. Similarly, as the magnitude of m_L increases (that is, becomes more highly negative), indicating a rapid decrease in liquidus with alloying concentration, the cracking propensity also increases.

Table 1 lists RPF values for various alloying elements in binary iron (Ref 2), nickel-base alloys (Ref 3), and aluminum alloys. It is clear that certain alloying elements, such as sulfur, phosphorus, and boron, are detrimental to the weldability of these alloy systems. This has been borne out by field experience.

TABLE 1 RELATIVE POTENCY FACTORS FOR SELECTED ALLOYING ELEMENTS IN BINARY IRON, NICKEL, AND ALUMINUM SYSTEMS

SYSTEM	RPF FOR:										
	Al	**B**	**C**	**Co**	**Mn**	**Nb**	**Ni**	**P**	**S**	**Si**	**Ti**
BINARY IRON	1.5	. . .	322	0.3	26.2	28.8	2.9	121	925	1.8	13.8
BINARY NICKEL	1.7	22700	330	. . .	0.7	. . .	. . .	556	244000	11	5.4

	Cu	**Li**	**Mg**	**Si**	**Zn**
BINARY ALUMINUM	16.6	9.0	8.0	42.4	2.3

Source: Ref 2, 3

Although the exact derivation of the RPF is specific to a very simple binary system solidifying under equilibrium conditions, the methodology provides general insight that can be applied to commercial alloys. The association of cracking susceptibility with solidification temperature range has implications for alloy design and primary melt processing. An extended melting/solidification temperature range can be the result of either intentional alloying or impurities present after refining.

An example (Ref 4) of the application of Borland's concepts to the solidification cracking propensity of a commercial alloy system involves alloy 625. This alloy is derived from the ternary Ni-Cr-Mo system, a very common base system for alloys designed to survive aggressive corrosive or high-temperature environments. A factorially designed set of alloys was produced to identify the effects of the alloying elements niobium, silicon, and carbon on the temperature range of

two-phase coexistence of liquid and solid (equilibrium melting/solidification temperature range) and on solidification cracking susceptibility.

Solidification cracking susceptibility was measured with the varestraint test, using the maximum crack length (MCL) parameter as the quantitative measurement (Ref 5). The melting temperature ranges of these same alloys were measured using differential thermal analysis (DTA). Table 2 lists the compositions of the alloys examined.

TABLE 2 SELECTED ALLOY 625 COMPOSITIONS USED IN WELDABILITY STUDY

ALLOY NO.	COMPOSITION, %										
	C	Cr	Fe	Mn	Mo	Nb	Ni	P	S	Si	Ti
NIOBIUM-FREE											
1	0.006	22.10	2.56	0.02	9.54	0.01	BAL	0.005	0.002	0.03	0.06
2	0.031	21.95	2.55	0.02	9.61	0.01	BAL	0.005	0.002	0.03	0.06
3	0.006	21.63	2.18	0.02	9.60	0.02	BAL	0.005	0.002	0.35	0.06
4	0.036	21.57	2.59	0.03	9.63	0.02	BAL	0.005	0.003	0.39	0.06
NIOBIUM ALLOYED											
5	0.009	21.81	2.30	0.03	9.81	3.61	BAL	0.006	0.003	0.03	0.06
6	0.038	21.83	2.31	0.03	9.81	3.60	BAL	0.006	0.003	0.03	0.06
7	0.008	21.65	2.26	0.03	9.68	3.57	BAL	0.006	0.004	0.38	0.06
8	0.035	21.68	2.29	0.03	9.67	3.53	BAL	0.006	0.003	0.46	0.06

The results of the varestraint testing are shown in Fig. 4. These data clearly show that the alloys that contain intentionally alloyed niobium (alloys 5 to 8) are more susceptible to solidification cracking (larger MCL) than niobium-free alloys (1 to 4). Furthermore, the alloy with no intentionally alloyed carbon, silicon, or niobium (alloy 1) is the least susceptible to cracking.

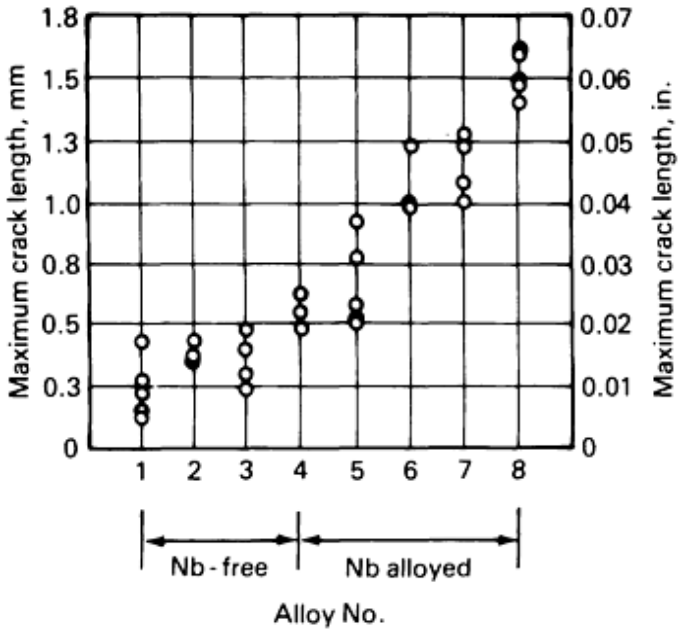

FIG. 4 MAXIMUM CRACK LENGTH DATA OBTAINED FROM VARESTRAINT TEST FOR ALLOY 625 WELDABILITY STUDY

The results of the DTA testing are given in Table 3. Listed are the liquidus (T_L), solidus (T_S), and melting temperature range (ΔT) data obtained from multiple tests. The baseline ΔT of an alloy without intentionally alloyed carbon, silicon,

and niobium (alloy 1) is 26.5 °C (79.7 °F). Increases in ΔT are observed when carbon or silicon is added (alloys 2 and 3) at levels that would be considered high for commercial alloys. When niobium is added (alloy 5) at a level that would be considered nominal for alloy 625 (~3.6 wt%), the melting temperature range effectively doubles to 55.3 °C (131.5 °F). Additions of carbon and silicon to the high-niobium alloys (alloys 6 to 8) further increase this value.

TABLE 3 MELTING TEMPERATURE DATA FOR ALLOY 625 WELDABILITY STUDY

σ is the standard deviation.

ALLOY NO.	ALLOY ADDITION			LIQUIDUS, $T_L \pm \sigma T_L$				SOLIDUS, $T_S \pm \sigma T_S$				MELTING TEMPERATURE RANGE, $\Delta T \pm \sigma \Delta T$			
				T_L		σT_L		T_S		σT_S		ΔT		$\sigma \Delta T$	
	C	NB	SI	°C	°F	°C	°F	°C	°F	°C	°F	°C	°F	°C	°F
1				1406.5	2563.7	1.3	2.3	1380.0	2516.0	1.4	2.5	26.5	47.7	0.6	1.1
2	X			1403.0	2557.4	1.0	1.8	1369.3	249.7	2.5	4.5	33.7	60.7	1.5	2.7
3			X	1395.5	2543.9	1.3	2.3	1366.5	2491.7	1.3	2.3	29.0	52.2	1.6	2.9
4	X		X	1390.8	2535.4	0.5	0.9	1347.5	2457.5	1.7	3.1	43.3	77.9	1.3	2.3
5		X		1363.3	2485.9	0.5	0.9	1308.0	2386.4	2.2	4.0	55.3	99.5	2.4	4.3
6	X	X		1362.0	2483.6	0.8	1.4	1289.3	2352.7	2.6	4.7	72.8	131.0	3.2	5.8
7		X	X	1356.0	2472.8	0.8	1.4	1287.8	2350.0	2.4	4.3	68.3	122.9	2.5	4.5
8	X	X	X	1352.0	2465.6	0.0	0.0	1275.7	2328.3	0.6	1.1	76.3	137.3	0.6	1.1

The correlation of cracking susceptibility with melting temperature range is shown in Fig. 5. Linear regression analysis performed on the data set resulted in the following functional relationship:

$$MCL = 0.00087(\Delta T) - 0.015 \qquad \textbf{(EQ 6)}$$

The incomplete statistical correlation ($R^2 = 0.86$) suggests that other factors are necessarily involved.

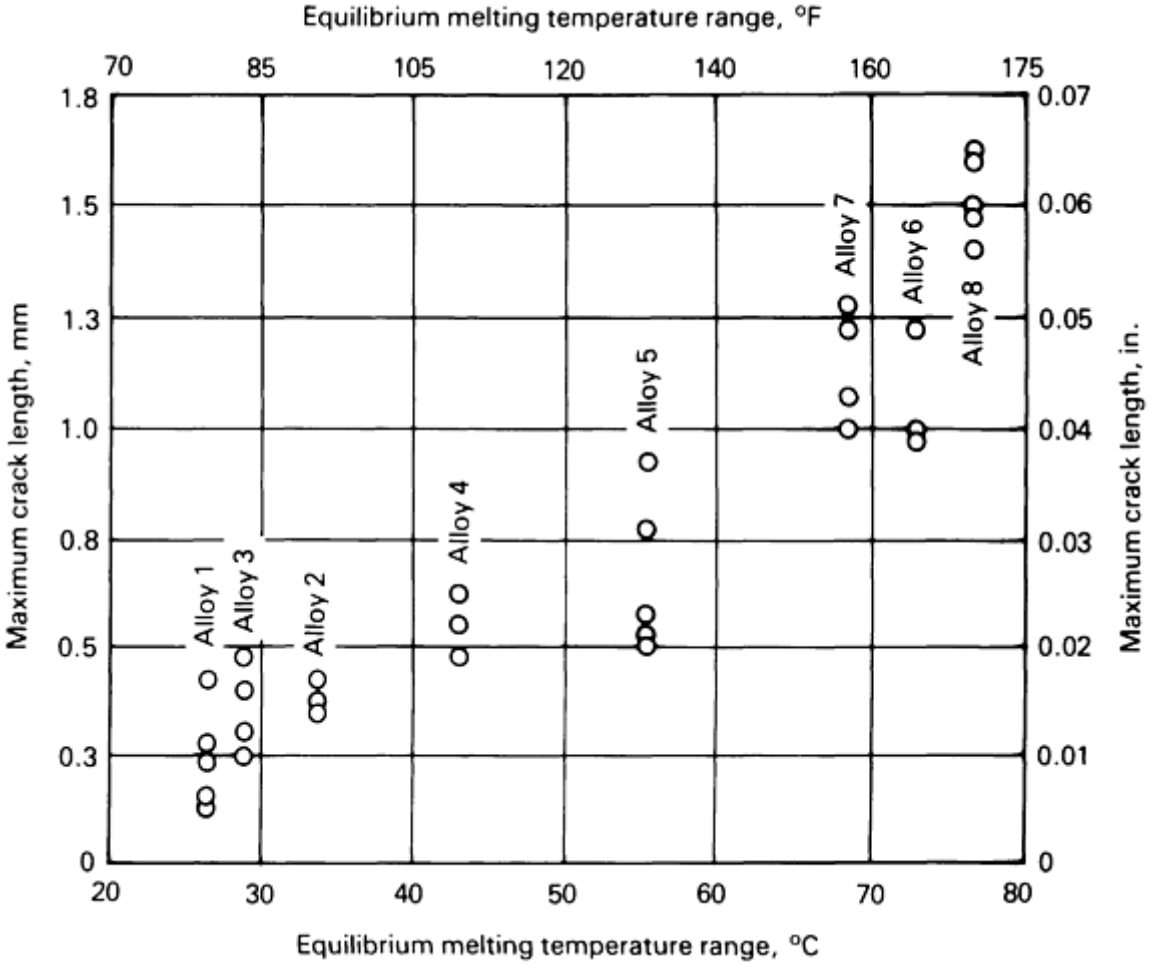

FIG. 5 RELATIONSHIP BETWEEN MAXIMUM CRACK LENGTH AND EQUILIBRIUM MELTING TEMPERATURE RANGE IN ALLOY 625 WELDABILITY STUDY

The solidification behavior of fusion welds is nonequilibrium in nature and may result in an extension of the solidification temperature range significantly beyond that measured under "equilibrium" conditions. Indeed, the niobium-bearing alloys terminate weld solidification below the equilibrium solidus with the formation of nonequilibrium eutecticlike constituents involving niobium carbides and Laves-type phases. Nonetheless, it is clear from an engineering perspective that Borland's concepts are valid enough to allow the establishment of a useful alloy ranking system from a solidification cracking perspective.

In addition to the effect of melting temperature range. Borland realized that the distribution of liquid along solidifying grain boundaries plays an important role in determining the solidification cracking susceptibility on an alloy (Ref 1). If the terminal solidification liquid easily wets the solidifying grain boundary (that is, has a low solid/liquid surface tension), it will tend to be spread out over a wider area, easing separation of the grains under a mechanical imposition. Conversely, if the liquid does not readily wet these boundaries, it will be more localized, creating a smaller area of liquid-solid contact and more solid-solid bridging, resulting in a more robust mechanical structure with increased cracking resistance. Elements such as sulfur and boron have been suggested as providing this surfactant property to terminal solidification liquids in iron and nickel alloys. Manganese may serve to increase the surface tension of terminal solidification fluids.

Figure 6 shows the results (Ref 6) of varestraint testing on two heats of Cabot alloy 214, a Ni-16Cr-4.5Al-2.5Fe alloy designed for use in high-temperature environments. The two alloys differ primarily in their boron content. With no boron intentionally added (0.0002 wt%), the alloy is extremely resistant to solidification cracking. With boron intentionally added at a level of 0.003 wt%, the solidification cracking propensity is much greater. Figures 7 and 8 are surface images of pulsed Nd:YAG laser welds made on the two alloys. Extensive cracking is evident in the high-boron alloy. Figure 7(b) is a good example of the extensive terminal "crater cracking" discussed above.

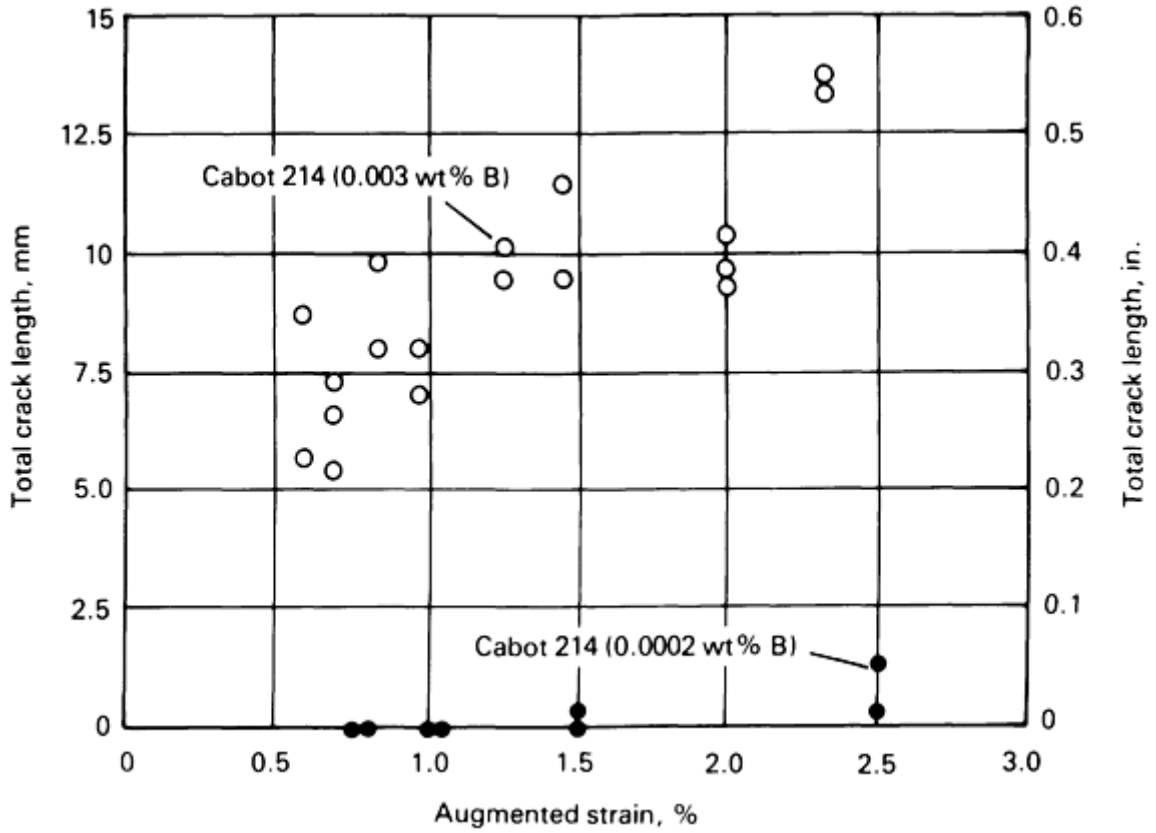

FIG. 6 VARESTRAINT TEST WELDABILITY DATA FOR CABOT ALLOY 214 WITH VARYING BORON CONCENTRATIONS

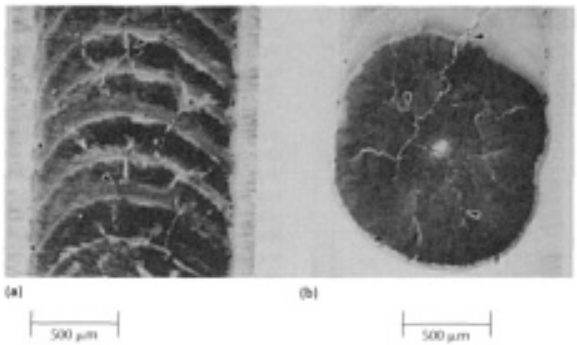

FIG. 7 SEM SURFACE IMAGE OF PULSED ND:YAG LASER WELDS IN HIGH-BORON ALLOY 214. (A) SOLIDIFICATION CRACKING. (B) CRATER CRACKING

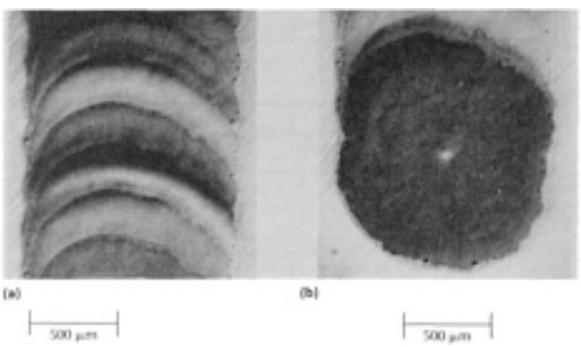

FIG. 8 SEM SURFACE IMAGE OF PULSED ND:YAG LASER WELDS IN LOW-BORON CONTENT ALLOY 214. (A) SOLIDIFICATION CRACKING. (B) CRATER CRACKING

Figures 9 and 10 summarize parameters that affect hot cracking in the weld metal and in the base metal HAZ, respectively. For most alloys that are highly susceptible to solidification cracking, filler metals of different composition have been developed to minimize the cracking that accompanies fusion welding.

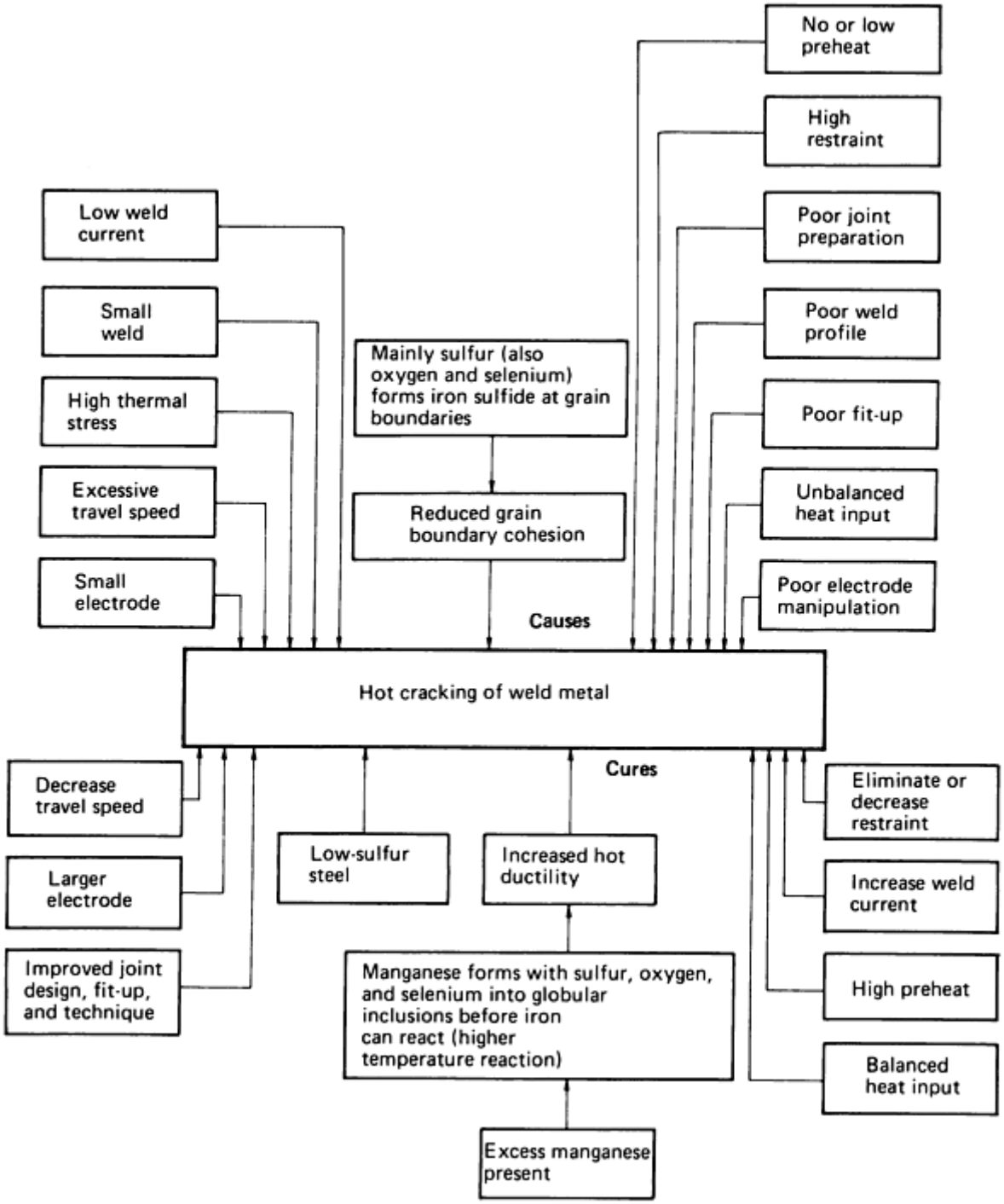

FIG. 9 FACTORS AFFECTING HOT CRACKING IN WELD METAL

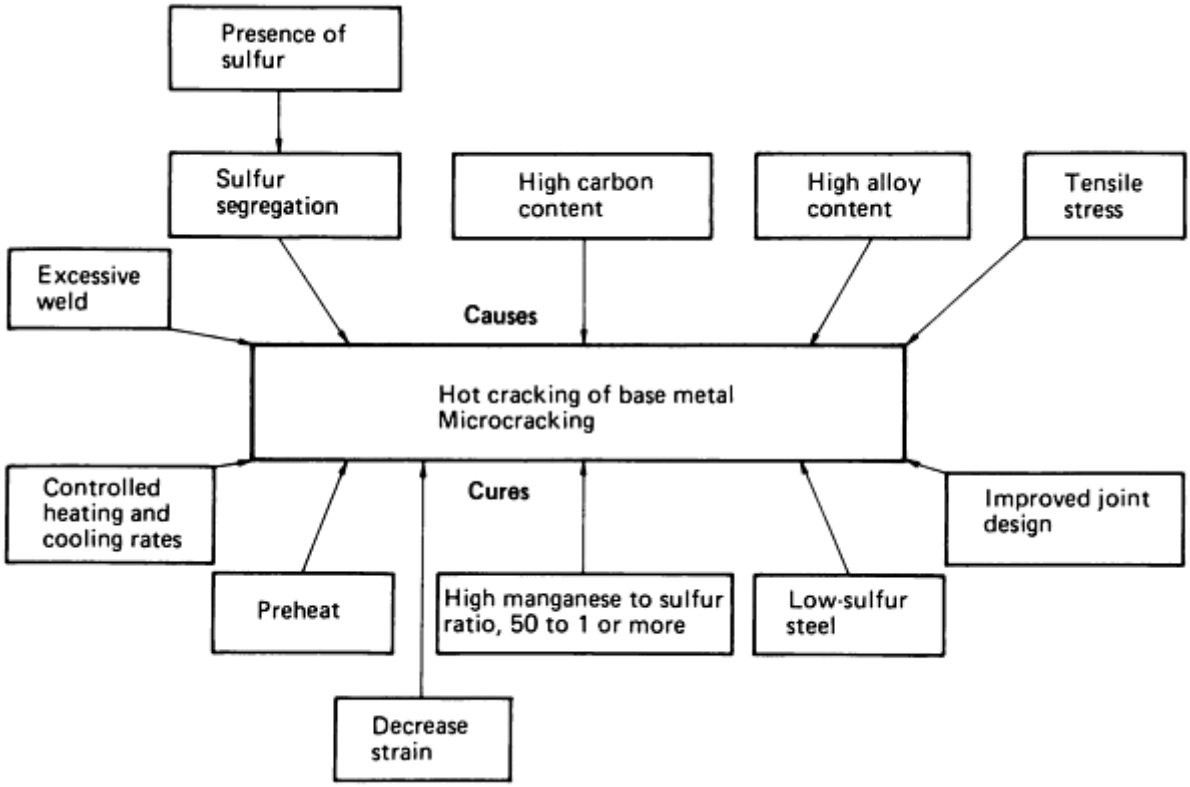

FIG. 10 FACTORS AFFECTING HOT CRACKING IN BASE METAL HAZ

References cited in this section

1. J.C. BORLAND, GENERALIZED THEORY OF SUPER-SOLIDUS CRACKING IN WELDS (AND CASTINGS), *BR. WELD. J.*, VOL 7 (NO. 8), 1960, P 508-512
2. J.C. BORLAND, HOT CRACKING IN WELDS, *BR. WELD. J.*, VOL 7 (NO. 9), 1960, P 558-559
3. D.A. CANONICO, W.F. SAVAGE, W.J. WERNER, AND G.M. GOODWIN, EFFECTS OF MINOR ADDITIONS ON THE WELDABILITY OF INCOLOY 800, *EFFECTS OF MINOR ELEMENTS ON THE WELDABILITY OF HIGH-NICKEL ALLOYS*, WRC, JULY 1969, P 68-92
4. M.J. CIESLAK, THE WELDING AND SOLIDIFICATION METALLURGY OF ALLOY 625, *WELD. J.*, FEB 1991, P 49S-56S
5. W.F. SAVAGE AND C.D. LUNDIN, APPLICATION OF THE VARESTRAINT TECHNIQUE TO THE STUDY OF WELDABILITY, *WELD. J.*, NOV 1966, P 497S-503S
6. M.J. CIESLAK, J.J. STEPHENS, AND M.J. CARR, A STUDY OF THE WELDABILITY AND WELD RELATED MICROSTRUCTURE OF CABOT ALLOY 214, *METALL. TRANS. A*, MARCH 1988, P 657-667

Cracking Phenomena Associated With Welding

Michael J. Cieslak, Physical and Joining Metallurgy Department, Sandia National Laboratories

Heat-Affected-Zone Cracks

Microfissures are cracks that occur in the area of partial melting and the HAZ adjacent to the fusion line. Because no material can be purified to the state where it solidifies truly as an invariant, all materials have a temperature region of stable two-phase coexistence of solid and liquid. In fusion welding, this manifests itself in the formation of a zone of

partial melting at temperatures below the alloy liquidus. The extent of this zone may be enlarged by the presence of chemical inhomogeneity in a material. Local chemical variations will result in local variations in the melting point. Segregation of specific alloying elements to grain boundaries may cause a reduction in the melting temperatures of these areas.

Many microfissures form in a manner somewhat analogous to the formation of solidification cracks in that susceptible sites, generally grain boundaries that intersect the fusion zone, are wetted with liquid from one of various sources. shrinkage strains accumulating as the weld pool advances past the liquated boundary can develop to a level sufficient to cause boundary separation (i.e., cracking). Figure 11 is a photomicrograph of an HAZ microfissure in a cast austenitic stainless steel (this crack also extends into the fusion zone as a solidification crack). Cast microstructures are highly inhomogeneous, raising the possibility of extensive partial melting. Note the melting associated with interdendritic constituents in Fig. 11.

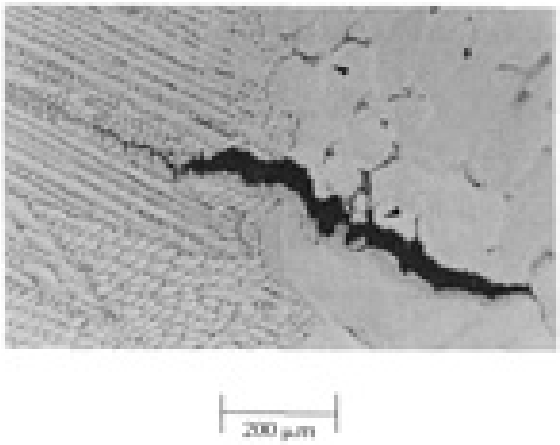

FIG. 11 HAZ MICROFISSURE IN A CAST STAINLESS STEEL. NOTE EXTENSIVE REGION OF PARTIAL MELTING.

Castings represent a special case of inhomogeneity on a continuous scale. Chemical inhomogeneities in wrought products are more discrete, generally involving minor phase particles. In many cases, these minor phases arise from thermomechanical processing of alloys well below the solidus, where the solubility for specific alloying elements can be lower. Because of the potential for extremely rapid rates of heating and cooling (especially heating) in the HAZ of fusion welds, it is entirely possible that minor phases not thermodynamically stable under equilibrium conditions may continue to exist at near-solidus temperatures. Under these conditions, the minor phases may interact with the matrix to form a liquid product. This reaction, often referred to as constitutional liquation (Ref 7), can provide the liquid required to wet grain boundaries producing a microstructure that may be susceptible to cracking.

Hot ductility testing is a common method of assessing the susceptibility of an alloy to this form of cracking. In this test, a laboratory-scale specimen is subjected to a thermal cycle representative of what the material would experience in the HAZ during fusion welding. At various temperatures during both the heating and cooling portions of the cycle, samples are strained to failure. The ductility response (usually expressed in terms of reduction of area) as the alloy progresses through the thermal cycle simulates the response of the alloy to an actual welding situation. In particular, the ability of the material to reestablish ductility after experiencing the peak temperature is a critical measure of sensitivity to this form of cracking.

Figures 12(a) and 12(b) show the hot ductility response of two heats of Cabot alloy 214 containing two different concentrations of boron. The return of ductility in the low-boron alloy after cooling from a peak temperature of 1345 °C (2453 °F) indicates that this alloy should be virtually immune to this form of cracking, as weldability tests confirmed (Ref 6). The high-boron heat showed no appreciable recovery of ductility until a temperature approximately 250 °C (450 °F) below the thermal peak temperature. This alloy should be quite susceptible to this form of cracking, as weldability tests also confirmed (Ref 6). Figure 13 is a fractograph of a hot ductility test specimen from the high-boron alloy taken from the sample strained at 1150 °C (2102 °F) on cooling from the peak temperature. The smooth, intergranular appearance is characteristic of this type of cracking. Although the presence of a liquid phase along this fracture surface could not be

unequivocally established by fractographic techniques, it was noted that the failure occurred at an exceedingly low load (Ref 6), consistent with the presence of a liquid film.

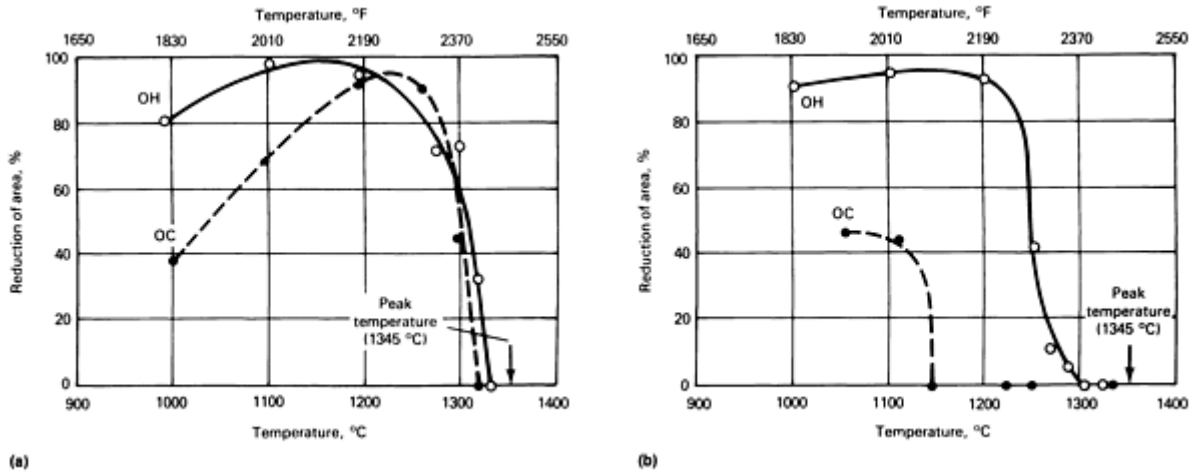

FIG. 12 HOT DUCTILITY RESPONSE OF CABOT ALLOY 214 WITH VARYING BORON CONCENTRATIONS. (A) LOW-BORON CONTENT (0.0002 WT% B). (B) HIGH-BORON CONTENT (0.003 WT% B). (OH, TESTING DONE ON HEATING; OC, TESTING DONE ON COOLING FROM 1345 °C (2455 °F)

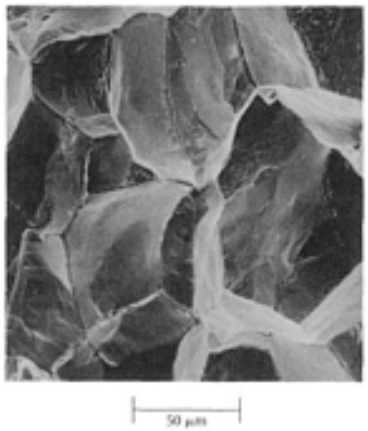

FIG. 13 FRACTURE SURFACE OF A HOT DUCTILITY SAMPLE OF HIGH-BORON ALLOY 214 TESTED AT 1150 °C (2100 °F) ON COOLING FROM 1345 °C (2455 °F)

The presence of a liquid is not essential to the formation of HAZ cracks, as they may occur at temperatures well below the solidus. Poor ductility inherent in certain materials, such as intermetallics, can lead to solid-state failure during welding if the thermal stresses associated with the weld thermal cycle exceed the local tensile strength.

Cracks may also occur in alloys that undergo polymorphic transformations during the weld thermal cycle. The act of fusion welding subjects the fusion zone and the HAZ to temperatures above those normally encountered during prior deformation processing. The resultant HAZ microstructure may be substantially different from that of the base material. In the case of martensitic-type transformations, there is often a relatively large, discontinuous change in the molar volume occurring very rapidly with decreasing temperature below the M_s. If that event causes a local shrinkage, then large, localized tensile stresses can develop. If the newly transformations microstructure has limited ductility (not uncommon in shear transformations or in transformations that result in ordered structures), the likelihood of cracks forming at susceptible sites, such as grain boundaries, matrix/minor phase interfaces, and slip band intersections, is increased.

Reheat cracking, also referred to as stress-relief of strain-age cracking, is another defect type observed in certain alloys that undergo precipitation reactions. Historically observed in several nickel-base superalloys and creep-resistant steels, this type of defect manifests itself during postweld heat treatment, generally as intergranular HAZ cracks.

Postweld heat treatment is often a recommended practice for high-strength thick-section welded steels, where reduction of residual stresses developed as a result of welding is desired. In the case of welded nickel-base superalloys, postweld heat treatment is used both to relieve residual stresses and to achieve optimum mechanical properties through precipitation-hardening reactions.

In alloys that undergo precipitation reactions, the rate at which the alloy strengthens may greatly exceed the rate at which residual stresses are thermally diminished. This can be especially true in the case of heavy-section welds or in alloys with relatively poor thermal conductivity. (That is, before the alloy can reach the temperature at which residual stresses begin to be eliminated, it has aged and lost ductility relative to its as-welded state.) At this new lower level of ductility, the residual stresses present may induce cracks to eliminate the accumulated strain energy.

In principle, the problem of reheat cracking could be largely eliminated if the rate of heating through the precipitation temperature range was rapid enough to prevent precipitate formation. However, extremely rapid rates of heating in welded hardware would likely lead to problems such as excessive distortion; therefore, improved alloys (e.g., alloy 718 among the nickel-base superalloys) have been developed in which the kinetics of precipitate formation have been sufficiently retarded to allow for successful postweld heat treatment.

Dealing with HAZ cracks, however they might form, is generally more difficult than attending to the problem of solidification cracking. Modifying the composition in the HAZ through the addition of consumables is not a viable option. Prior heat treatment may allow the production of a less susceptible starting microstructure, but this option generally is quite limited. Optimization of weld process parameters to minimize the extent of tensile stress and strain development should always be considered, as should optimizing weld joint design as discussed above.

References cited in this section

6. M.J. CIESLAK, J.J. STEPHENS, AND M.J. CARR, A STUDY OF THE WELDABILITY AND WELD RELATED MICROSTRUCTURE OF CABOT ALLOY 214, *METALL. TRANS. A,* MARCH 1988, P 657-667
7. J.J. PEPE AND W.F. SAVAGE, EFFECTS OF CONSTITUTIONAL LIQUATION IN 18-NI MARAGING STEEL WELDMENTS, *WELD. J.,* SEPT 1967, P 411S-422S

Cracking Phenomena Associated With Welding

Michael J. Cieslak, Physical and Joining Metallurgy Department, Sandia National Laboratories

Hydrogen-Induced Cracking (Cold Cracking)

Cold cracks are defects that form as the result of the contamination of the weld microstructure by hydrogen. Whereas solidification cracking and HAZ cracking occur during or soon after the actual welding process, hydrogen-induced cracking is usually a delayed phenomenon, occurring possibly weeks or even months after the welding operation. The temperature at which these defects tend to form ranges from -50 to 150 °C (-60 to 300 °F) in steels. The fracture is either intergranular or transgranular cleavage.

As with other forms of cracking, hydrogen-induced cracking involves both a requisite microstructure and a threshold level of stress. It also involves a critical level of hydrogen, which is alloy and microstructure dependent.

In the case of ideal weld processing, hydrogen-induced cracking would be at most a minor welding engineering concern. However, excluding hydrogen from structures during welding is exceedingly difficult. Although the primary source of hydrogen in weld metal is considered to be the disassociation of water vapor in the arc and absorption of gaseous or ionized hydrogen into the liquid, other sources are also available. All organic compounds contain hydrogen in their

molecular structure, and all may be broken down in the intense thermal environment of a welding heat source. Organic compounds are ubiquitous in the welding environment, from lubricants in assembly areas to body oils on the hands of welding operators. Plated hardware may also contain high levels of residual hydrogen.

The mechanism of hydrogen-induced crack formation is still being investigated. An early hypothesis, involving the buildup of hydrogen gas pressure in voids, is now generally discredited. Currently, the most widely accepted model involves the presence of preexisting defect sites in the material--small cracks or discontinuities caused by minor phase particles or inclusions. In the presence of existing stress, these sites may develop high local areas of biaxial or triaxial tensile stress. Hydrogen diffuses preferentially to these sites of dilated lattice structure. As the local hydrogen concentration increases, the cohesive energy and stress of the lattice decrease. When the cohesive stress falls below the local intensified stress level, fracture occurs spontaneously. Hydrogen then evolves in the crack volume, and the process is repeated. This model of hydrogen-induced cracking is consistent with the relatively slow and discontinuous nature of the process.

In steels, where the problem of hydrogen-induced cracking is extremely significant, cracking susceptibility has been correlated both with material hardness and strength, and with specific microstructure. Higher-strength steels are more susceptible to hydrogen-induced cracking than low-strength steels. Steels that transform martensitically are particularly susceptible, especially the higher-carbon alloys with twinned martensitic structures. The desire to avoid martensite formation has driven the development of high-strength structural steels for welded applications.

Production of the newer high-strength low-alloy (HSLA) steels uses a variety of precisely controlled alloying additions (for example, aluminum, titanium, vanadium, and niobium) along with meticulous thermomechanical processing to develop a very fine-grained ferrite microstructure possessing substantial strength and fracture toughness with a high degree of resistance to hydrogen-induced cracking. The form of the ferrite produced during transformation on cooling from the austenite phase field is also critical, with acicular ferrite resulting in improved properties compared with grain-boundary, polygonal, or Widmanstätten ferrite. Acicular ferrite is often nucleated on minor phase particles, such as specific oxides or borides. Acknowledgement of the beneficial effect of certain oxides in providing sites for acicular ferrite nucleation in modern steels is in sharp contrast to steel design of earlier decades, when elimination of oxygen to the greatest extent possible was considered essential to the development of optimal fracture behavior.

A useful concept for understanding the susceptibility of carbon and alloy steels to hydrogen-induced cracking is the carbon equivalent (CE), an empirical relationship that attempts to reduce the number of significant compositional variables affecting the weldability of steels into a single quantity. Several carbon equivalent relationships have been developed for different classes of steels. An example is:

$$CE = \%C + \frac{\%Mn}{6} + \frac{\%Cr + \%Mo + \%V}{5} + \frac{\%Si + \%Ni + \%Cu}{15} \qquad \textbf{(EQ 7)}$$

From a metallurgical perspective, the carbon equivalent can be related to the development of hydrogen-sensitive microstructures. That is, as the carbon equivalent increases, microstructures are evolved during cooling through the transformation temperature range that are increasingly more susceptible to hydrogen-induced cracking. At high carbon equivalent values, martensitic structures can be expected.

Carbon equivalent formulas are usually developed from large databases of critical hydrogen concentrations and weld joint restraints that will result in hydrogen-induced cracking in the steels under consideration. At various levels of carbon equivalent, certain weld preheat requirements are often established. In the example of Eq 7, when the carbon equivalent exceeds 0.35%, preheats are recommended to minimize susceptibility to hydrogen cracking. At higher levels of carbon equivalent, both preheats and postheats may be required.

Most structural carbon and low-alloy steels that may be susceptible to hydrogen-induced cracking transform from austenite during cooling through the temperature range of 800 to 500 °C (1470 to 930 °F). The length of time a steel spends in this temperature range during cooling will establish its microstructure and hence its cracking sensitivity. This time segment is generally referred to as $t_{8/5}$ (in seconds). To maximize cracking resistance, a microstructure free of untempered martensite is desired.

Using a specifically developed carbon equivalent, Yurioka (Ref 8) formulated a relationship to establish the critical $t_{8/5}$ for a martensite-free HAZ in low-carbon alloy steels. The carbon equivalent is defined as:

$$CE = \%C^* + \frac{\%Mn}{3.6} + \frac{\%Cu}{20} + \frac{\%Ni}{9} + \frac{\%Cr}{5} + \frac{\%Mo}{4} \qquad \textbf{(EQ 8)}$$

where %C* = %C for C $\leq$ 0.3% and %C* = %C/6 + 0.25 for %C > 0.3%. The critical time length in seconds, $t_{8/5}$, for the avoidance of martensitic transformation is given as:

$$\text{LOG } t_{8/5} = 2.69\ CE^* + 0.321 \qquad \textbf{(EQ 9)}$$

When this quantity is known, welding parameters and preheat temperature for the given thickness of material being welded can be established to produce cooling rates that avoid formation of a martensitic constituent in the HAZ.

The use of preheating and postheating to minimize the susceptibility to hydrogen-induced cracking is an accepted welding procedure for many steels. Preheating controls the cooling rate through the transformation temperature range; a higher base metal temperature in a slower cooling rate through the transformation temperature range and thus a larger $\tau_{8/5}$. Thicker sections often require preheating because of the greater heat-sinking capability of a thick section, for which a given set of welding parameters will produce a faster cooling rate and a smaller $t_{8/5}$. Preheating may also reduce the level of residual stress in the welded assembly.

There are, of course, practical limits to the use of preheating. Excessively high base metal temperatures can make welding difficult, especially manual welding. A high preheat temperature will result in the flattening of temperature gradients, increasing the spatial extent of and the time spent in the austenite phase field. This may result in excessive grain growth in the HAZ, which can lead to a loss of fracture toughness independent of hydrogen content. Preheat temperatures up to 150 °C (300 °F) are not uncommon for low-alloy steels and may increase up to 425 °C (800 °F) for higher-carbon equivalent martensitic steels.

Several benefits can be realized by postheating. At high enough temperatures (550 to 600 °C, or 1020 to 1110 °F), postheating can diminish residual stresses present in the as-welded structure. Microstructural modifications such as tempering can also occur, producing a microstructure less susceptible to hydrogen-induced cracking. Finally, the higher temperature may allow hydrogen to diffuse into the bulk of the structure or even to the surface, where it may recombine and exit as a gas. In either case, the level of hydrogen concentration may be reduced below that required to initiate cracks.

The following guidelines should be followed to minimize the occurrence of hydrogen-induced cracking. For a given level of required strength, the steel with the lowest carbon equivalent should be considered. Low-hydrogen welding practice should be followed. This involves elimination of possible sources of hydrogen by using ultrahigh-purity gases and moisture-free gas lines and by baking coated electrodes following the manufacturer's recommendations to ensure removal of nascent water. Finally, preheating and postheating requirements should be followed assiduously. Figures 14 and 15 summarize the causes and cures of hydrogen-induced cracking in the weld metal and in the base metal, respectively.

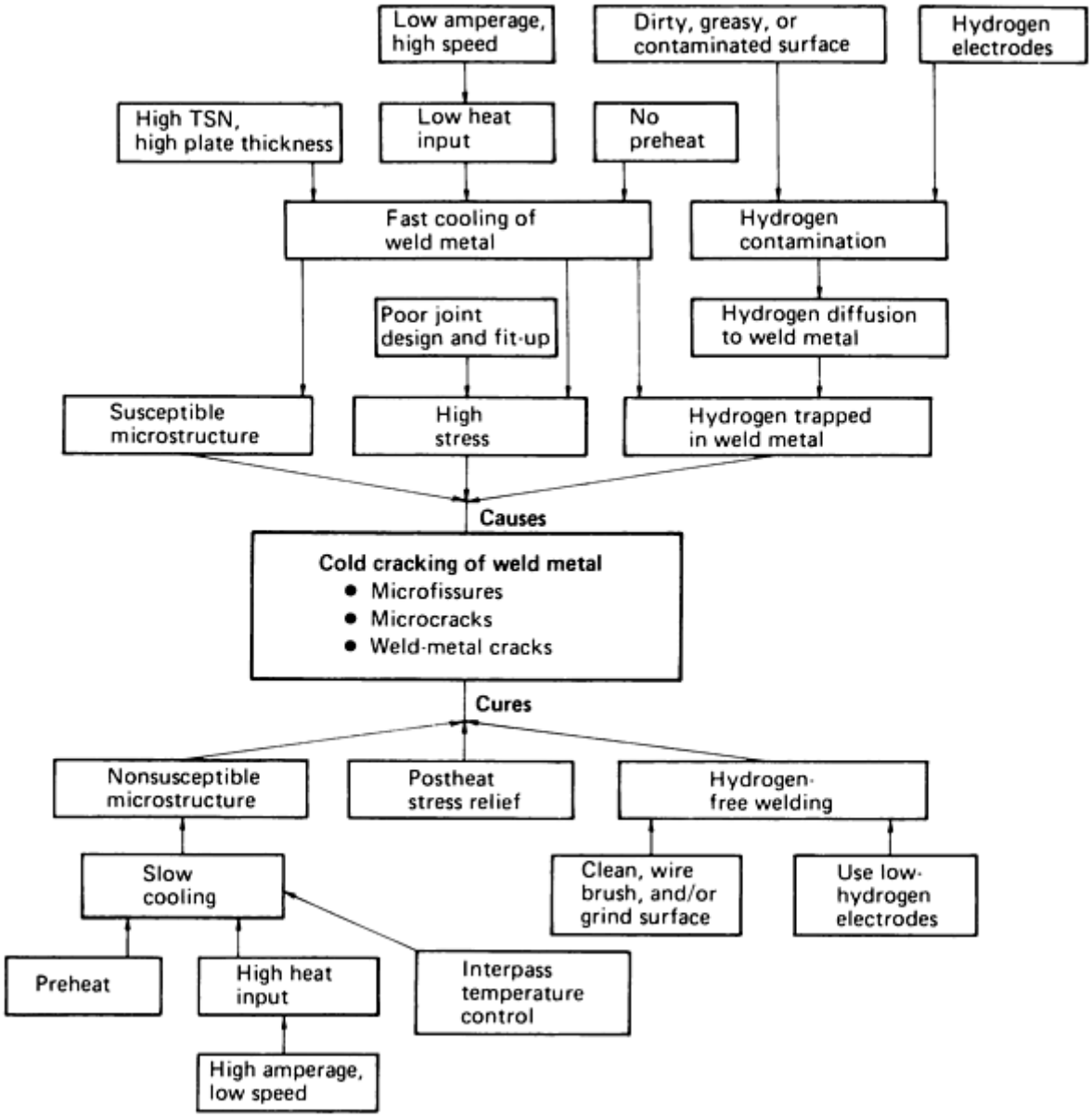

FIG. 14 CAUSES AND CURES OF HYDROGEN-INDUCED CRACKING IN WELD METAL. THERMAL SEVERITY NUMBER (TSN), WHICH IS FOUR TIMES THE TOTAL PLATE THICKNESS CAPABLE OF REMOVING HEAT FROM THE JOINT, IS A MEASURE OF THE ABILITY OF THE MEMBER TO SERVE AS A HEAT SINK.

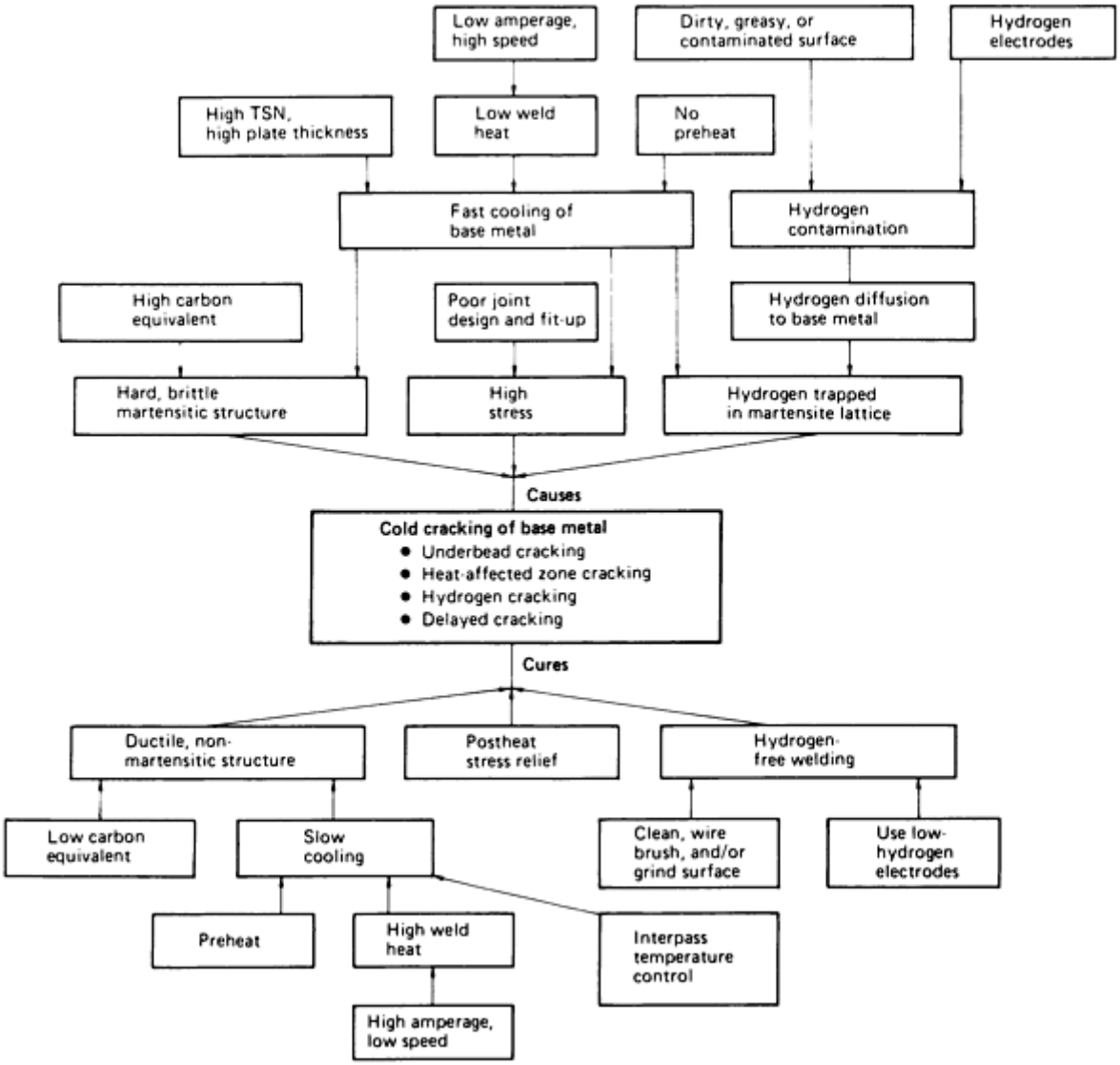

FIG. 15 CAUSES AND CURES OF HYDROGEN-INDUCED CRACKING IN BASE METAL

Reference cited in this section

8. N. YURIOKA, WELDABILITY OF MODERN HIGH STRENGTH STEELS, *1ST U.S.-JAPAN SYMP. ADVANCES IN WELDING METALLURGY,* AWS, 1990, P 79-100

Cracking Phenomena Associated With Welding

Michael J. Cieslak, Physical and Joining Metallurgy Department, Sandia National Laboratories

Lamellar Tearing (Ref 9)

Lamellar tearing is cracking that occurs beneath welds. It is found in rolled steel plate weldments. The tearing always lies within the base metal, generally outside the HAZ and parallel to the weld fusion boundary. The problem is caused by welds that subject the base metal to tensile loads in the *z*, or through, direction of the rolled steel. Occasionally the tearing comes to the surface of the metal, but more commonly remains under the weld (Fig. 16) and is detectable only by ultrasonic testing. Lamellar tearing occurs when three conditions are simultaneously present:

- STRAINS DEVELOP IN THE THROUGH DIRECTION OF THE PLATE. THEY ARE CAUSED BY WELD METAL SHRINKAGE IN THE JOINT AND CAN BE INCREASED BY RESIDUAL STRESSES AND BY LOADING.
- THE WELD ORIENTATION IS SUCH THAT THE STRESS ACTS THROUGH THE JOINT ACROSS THE PLATE THICKNESS (THE *Z* DIRECTION). THE FUSION LINE BENEATH THE WELD IS ROUGHLY PARALLEL TO THE LAMELLAR SEPARATION.
- THE MATERIAL HAS POOR DUCTILITY IN THE *Z* DIRECTION.

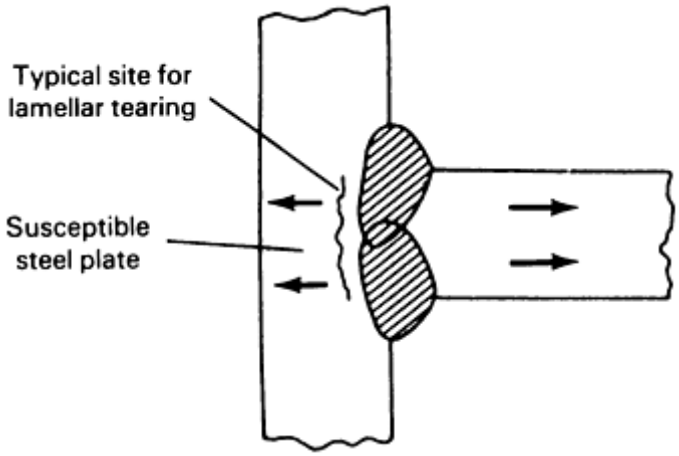

FIG. 16 TYPICAL LOCATION FOR LAMELLAR TEARING IN A T-JOINT

Lamellar tearing can occur during flame cutting and cold shearing operations. Low material strength in the *z* direction is the primary cause, with stress in that direction initiating the tearing. Thermal heating and stresses from weld shrinking create the fracture. Lamellar tearing can take place shortly after welding or occasionally months later. Thicker, higher-strength materials appear to be more susceptible. However, the phenomenon affects only a very small percentage of steel plates, as all three of the above conditions rarely occur in combination.

The problem can be avoided by proper attention to joint details. In T-joints (Fig. 16), double-fillet welds appear to be less susceptible than full-penetration welds. Also, balanced welds on both sides of the joint appear to present less risk than large, single-sided welds. In corner joints, common in box columns, lamellar tearing can be readily detected on the exposed edge of the plate (Fig. 17a). The problem can be overcome by placing the bevel for the joint on the edge of the plate that would exhibit the tearing rather than on the other plate (Fig. 17b). Butt joints rarely exhibit lamellar tearing, because weld shrinkage does not set up a tensile stress in the thickness direction of the plates.

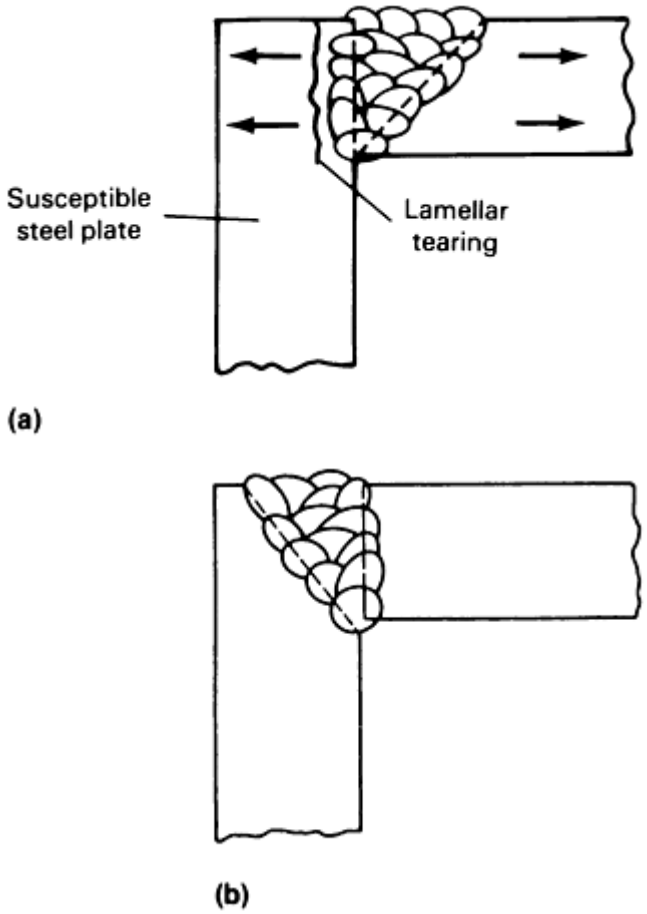

FIG. 17 CORNER JOINT. (A) LAMELLAR TEARING SURFACES AT THE EXPOSED PLATE EDGE. (B) REDESIGNED JOINT

Arc welding processes with high heat input are less likely to create lamellar tearing, perhaps because of the fewer number of applications of heat and the lesser number of shrinkage cycles involved in making a weld. Also, filler metal with lower yield strength and high ductility appears to lessen the possibility of tearing. Preheating does not appear to be particularly advantageous, nor does stress relieving. The "buttering" technique of laying one or more layers of low-strength, high-ductility weld metal deposit on the surface of the plate stressed in the *z* direction will reduce the possibility of lamellar tearing. However, this is an extreme solution and should be used only as a last resort.

Reference cited in this section

9. H.B. CARY, *MODERN WELDING TECHNOLOGY*, 2ND ED., PRENTICE-HALL, 1989, P 702-703

Cracking Phenomena Associated With Welding

Michael J. Cieslak, Physical and Joining Metallurgy Department, Sandia National Laboratories

References

1. J.C. BORLAND, GENERALIZED THEORY OF SUPER-SOLIDUS CRACKING IN WELDS (AND CASTINGS), *BR. WELD. J.*, VOL 7 (NO. 8), 1960, P 508-512

2. J.C. BORLAND, HOT CRACKING IN WELDS, *BR. WELD. J.*, VOL 7 (NO. 9), 1960, P 558-559
3. D.A. CANONICO, W.F. SAVAGE, W.J. WERNER, AND G.M. GOODWIN, EFFECTS OF MINOR ADDITIONS ON THE WELDABILITY OF INCOLOY 800, *EFFECTS OF MINOR ELEMENTS ON THE WELDABILITY OF HIGH-NICKEL ALLOYS*, WRC, JULY 1969, P 68-92
4. M.J. CIESLAK, THE WELDING AND SOLIDIFICATION METALLURGY OF ALLOY 625, *WELD. J.*, FEB 1991, P 49S-56S
5. W.F. SAVAGE AND C.D. LUNDIN, APPLICATION OF THE VARESTRAINT TECHNIQUE TO THE STUDY OF WELDABILITY, *WELD. J.*, NOV 1966, P 497S-503S
6. M.J. CIESLAK, J.J. STEPHENS, AND M.J. CARR, A STUDY OF THE WELDABILITY AND WELD RELATED MICROSTRUCTURE OF CABOT ALLOY 214, *METALL. TRANS. A*, MARCH 1988, P 657-667
7. J.J. PEPE AND W.F. SAVAGE, EFFECTS OF CONSTITUTIONAL LIQUATION IN 18-NI MARAGING STEEL WELDMENTS, *WELD. J.*, SEPT 1967, P 411S-422S
8. N. YURIOKA, WELDABILITY OF MODERN HIGH STRENGTH STEELS, *1ST U.S.-JAPAN SYMP. ADVANCES IN WELDING METALLURGY*, AWS, 1990, P 79-100
9. H.B. CARY, *MODERN WELDING TECHNOLOGY*, 2ND ED., PRENTICE-HALL, 1989, P 702-703

Characterization of Welds

Craig B. Dallam, The Lincoln Electric Company; Brian K. Damkroger, Sandia National Laboratories

Introduction

WELDS CAN BE CHARACTERIZED according to a number of criteria, including the welding process used, size, shape, mechanical properties, chemical composition, and a number of others. The appropriate methods of characterization depend on the weld's function and the particular set of properties required for the application. In some instances, the ability of a weld to function successfully can be addressed by characterizing the size or shape of the weld. An example of this is where factors related to the welding procedure, such as inadequate weld size, convexity of the bead, or lack of penetration, may cause a weld to fail. In other cases, it is important to characterize metallurgical factors such as weld metal composition and microstructure. Examples might include welds for which the goal is to avoid failures due to inadequate strength, ductility, toughness, or corrosion resistance. In general, the goals of weld characterization are to assess the ability of a weld to successfully perform its function, to thoroughly document a weld and welding procedure that have been demonstrated to be adequate, or to determine why a weld failed.

In the first part of this article, characterization of welds will be treated as a sequence of procedures, each more involved than the last and concerned with a finer scale of detail. Initially, non-destructive characterization procedures will be the focus. The first level of characterization involves information that may be obtained by direct visual inspection and measurement of the weld. A discussion of nondestructive evaluation follows. This encompasses techniques used to characterize the locations and structure of internal and surface defects, including radiography, ultrasonic testing, and liquid penetrant inspection.

The next group of characterization procedures discussed are destructive, requiring the removal of specimens from the weld. The first of these is macrostructural characterization of a sectioned weld, including features such as number of passes; weld bead size, shape, and homogeneity; and the orientation of beads in a multipass weld. Macroscopic characterization is followed by microstructural analysis, including microsegregation, grain size and structure, the phase makeup of the weld, and compositional analysis.

The third component of weld characterization is the measurement of mechanical and corrosion properties. The goal of any weld is to create a structure that can meet all the demands of its service environment. In many cases, the best way of assessing the performance of a weld is to establish its mechanical properties. In addition to a number of standard material tests, many mechanical tests are directed specifically at determining a weld's capabilities. Examples of mechanical properties typically characterized for welds include yield and tensile strength, ductility, hardness, and impact or fracture toughness. Corrosion testing is often employed in situations where a welding operation is performed on a corrosion-

resistant material, or in a structure exposed to a hostile environment. Although absolute corrosion performance is important, a major concern is to ensure that a weld and its heat-affected zone (HAZ) are cathodic to the surrounding metal.

Following the discussion of the characterization procedures, the second part of this article will give examples of how two particular welds were characterized according to these procedures.

Acknowledgement

Support for the portion of this work performed at Sandia National Laboratories was provided by the U.S. Department of Energy under contract number DE-AC0476DP00789.

Characterization of Welds

Craig B. Dallam, The Lincoln Electric Company; Brian K. Damkroger, Sandia National Laboratories

---

Nondestructive Characterization Techniques

Externally Observed Macroscopic Features. Several factors associated with the production and performance of welds are macroscopic and easily observed. The most obvious of these are the size, shape, and general appearance of the weld. To a large extent, these parameters depend on the geometry of the weld joint and the welding process selected. Figure 1 shows schematic representations of fillet, lap, butt, and groove welds, in which a number of features (defined in Table 1) are labeled.

TABLE 1 NONMENCLATURE FOR FILLET, LAP, BUTT, AND GROOVE WELDS

FEATURE	DEFINITION
FACE	EXPOSED SURFACE OF A WELD ON THE SIDE FROM WHICH THE WELDING WAS PERFORMED
ROOT	POINTS, AS SHOWN IN CROSS SECTION, AT WHICH THE BACK OF THE WELD INTERSECTS THE BASE METAL SURFACE
LEG	SHORTEST DISTANCE FROM ROOT TO TOE IN A FILLET WELD
TOE	JUNCTION BETWEEN THE WELD FACE AND THE BASE METAL
THROAT	SHORTEST DISTANCE FROM ROOT TO FACE IN A FILLET WELD
PENETRATION	DEPTH A GROOVE WELD EXTENDS INTO THE ROOT OF A JOINT, MEASURED ON THE CENTERLINE OF A ROOT CROSS SECTION
REINFORCEMENT	WELD METAL IN EXCESS OF THE SPECIFIED WELD SIZE
FACE REINFORCEMENT	REINFORCEMENT AT THE SIDE OF THE WELD FROM WHICH WELDING WAS PERFORMED
SIZE (GROOVE WELD)	JOINT PENETRATION (DEPTH OF ROOT PREPARATION) PLUS THE ROOT PENETRATION (WHEN SPECIFIED)
SIZE (FILLET WELD)	LEG OF THE LARGEST ISOSCELES RIGHT TRIANGLE THAT CAN BE INSCRIBED WITHIN THE FILLET WELD CROSS SECTION

Source: Ref 1

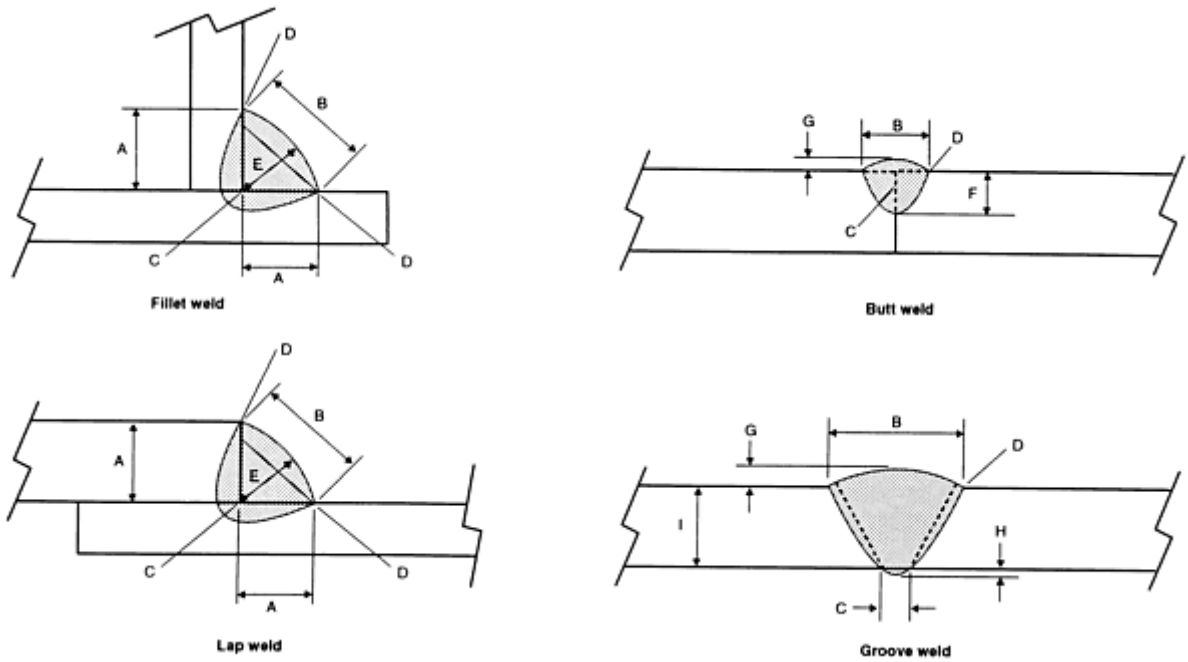

FIG. 1 SCHEMATICS SHOWING PARAMETERS OF COMMONLY USED JOINT GEOMETRIES. A, LEG; A', SMALLER LEG SIZE (EQUAL TO SIZE OF WELD); B, FACE, C, ROOT; D, TOE; E, THROAT; F, PENETRATION (EQUAL TO SIZE OF WELD); G, FACE REINFORCEMENT; H, ROOT REINFORCEMENT; I, SIZE OF WELD

Methods of Characterization. The primary tools used in the external macrocharacterization of a weld are the unaided eye and a hand lens. A number of macrocharacterization parameters (for example, weld location, size, shape, and general uniformity) can be assessed by visual inspection. Figure 2 shows top-view macrographs of two welds that illustrate several of these considerations. In many cases, the presence of gross defects such as hot cracking or porosity may also be detected by visual inspection and a top-view photograph. Additional examples of factors included in overall weld bead appearance include distortion, discoloration due to inadequate shielding or excessive heat, undercut, excessive crater size, and uneven bead width. In fillet welds, a number of performance aspects can be affected by the relative geometry of the joint. Fillet gages can be used to determine the size of a weld, the curvature of the face, and the length of the weld legs.

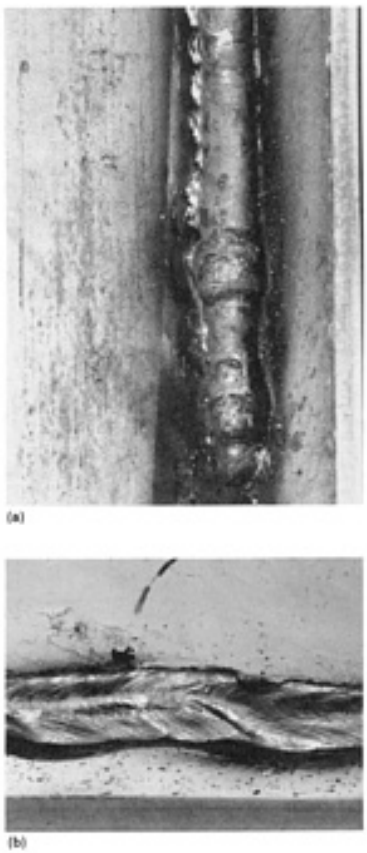

FIG. 2 MACROGRAPHS SHOWING TOP VIEW OF FILLET WELDS. (A) VERTICAL WELD IN TYPE 304L STAINLESS STEEL (NOTE CONVEXITY OF BEAD AND NONUNIFORM REGIONS). (B) HORIZONTAL E 7024 WELD (NOTE WELD PLACEMENT AND LACK OF UNIFORMITY)

General Considerations. Most types of welds will be evaluated with respect to specific macrocharacteristics deemed to be either desirable or undesirable. However, a number of general considerations apply to most types of welds. These include:

- *SIZE:* THE SIZE OF THE WELD SHOULD BE APPROPRIATE FOR THE PART (AS AN EXAMPLE, A GENERAL RULE FOR FILLET WELDS IS THAT THE RATIO OF LEG SIZE/PLATE THICKNESS SHOULD BE BETWEEN 3:4 AND 1:1.
- *LOCATION:* AN INCORRECTLY LOCATED BUTT WELD MAY NOT ALLOW THE PART TO FUNCTION CORRECTLY. A LESS EXTREME EXAMPLE IS A FILLET WELD WITH UNEQUAL LEG LENGTHS, LEADING TO AN UNEVEN STRESS DISTRIBUTION AND PERHAPS LAMELLAR TEARING.
- *UNIFORMITY:* DISTORTION, THE PROBABILITY OF SLAG ENTRAPMENT ON MULTIPASS WELDS, AND UNIFORMITY OF LOAD-CARRYING ABILITY ALL DEPEND ON THE RELATIVE UNIFORMITY OF THE WELD.
- *DEFECTS:* IDEALLY, A WELD SHOULD BE FREE OF MACROSCOPIC DEFECTS. COMMON DEFECTS INCLUDE UNDERCUTTING, LACK OF FUSION, PINHOLE POROSITY, AND SLAG ENTRAPMENT.
- *FACE SHAPE:* A WELD SHOULD HAVE A RELATIVELY FLAT FACE. IF THE WELD IS TOO CONVEX, STRESS WILL BE CONCENTRATED ALONG THE TOE OF THE WELD. CONVERSELY, A HIGHLY CONCAVE WELD FACE WILL RESULT IN LOCALLY HIGH STRESSES IN THE THROAT REGION OF THE WELD.

Defects. The presence of surface or internal defects can degrade the performance of a weld that may appear to be sound in a cursory examination. The causes and means of preventing defects are covered in Ref 2, 3, and 4. Typical defects found in welds include:

- POROSITY
- UNDERCUT
- OVERLAP
- LACK OF PENETRATION
- LACK OF FUSION
- SHRINKAGE VOIDS
- CRATER CRACKING
- MELT-THROUGH OR BURN-THROUGH
- SUBSOLIDUS OR HOT CRACKING
- INCLUSIONS DUE TO ENTRAPPED SLAG, TUNGSTEN ELECTRODE PIECES, OR DEFECTS PRESENT IN THE STARTING MATERIAL

A number of techniques are widely used to assess the presence of surface and subsurface defects in welds. The most common of these are liquid penetrant inspection for surface cracks, magnetic particle inspection, x-ray radiography, and ultrasonic inspection. Penetrant inspection involves the application of an indicator fluid that has a surface tension sufficiently low to be drawn into surface cracks too small to be detected visually. The excess dye or fluorescent material is then removed from the surface, but it remains in and highlights the cracks when a developer is applied. Figure 3 shows cracks in a flux-cored are weld highlighted by dye penetrant inspection. Table 2 lists the characteristics of several types of nondestructive inspection techniques. Additional information is available in the article "Inspection of Welded Joints" in this Volume.

TABLE 2 GUIDELINES FOR SELECTING TECHNIQUES

Technique	Equipment Requirements	Defects Detected	Advantages	Limitations	Comments
liquid-penetrant or fluorescent-penetrant inspection	fluorescent or visible penetration liquids and developers; ultraviolet light for fluorescent dyes	defects open to the surface only; good for leak detection	detects small surface imperfections; easy application; inexpensive; use on magnetic or nonmagnetic material; low cost	time-consuming; not permanent	used on root pass of highly critical pipe welds; indications may be misleading on poorly prepared surfaces
magnetic particle inspection	wet or dry iron particles, or fluorescent; special power source; ultraviolet light for fluorescent dyes	surface and near-surface discontinuities: cracks, porosity, slag	indicates discontinuities not visible to the naked eye; useful for checking edges before welding; no size limitations	for magnetic materials; surface roughness may distort magnetic field; not permanent	test from two perpendicular directions to detect any indications parallel to one set of magnetic lines
radiographic inspection	x-ray or γ ray; film processing and viewing equipment	most internal discontinuities and flaws; limited by direction of discontinuity	provides permanent record of surface and internal flaws; applicable to any alloy	usually not suitable for fillet weld inspection; film exposure and processing	popular technique for sub-surface inspection

				critical; slow and expensive	
ultrasonic inspection	ultrasonic units and probes; reference patterns	can locate all internal flaws located by other methods, as well as small flaws	extremely sensitive; complex weldments restrict usage; can be used on all materials	highly skilled interpretor required; not permanent	required by some specifications and codes

Source: Ref 5

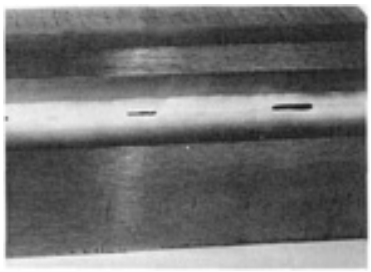

FIG. 3 SURFACE CRACKS IN A FLUX-CORED ARC WELD HIGHLIGHTED BY DYE PENETRANT INSPECTION

X-ray radiography is used to detect internal defects such as porosity or inclusions: these defects show up because of the difference in x-ray absorption between the matrix and defect materials. Although a number of factors affect the resolution level of radiographic techniques (Ref 5, 6), the minimum size of defects considered in AWS specifications is 0.4 mm (0.0156 in.). In practice, this refers to slag entrapment and large inclusions that were present in the starting material. Defect structures are usually quantified by comparison with an existing standard, of which several exist. An example of such a standard is American Petroleum Institute (API) 1104 (Ref 7), a pipeline welding specification. The API 1104 standard includes criteria for acceptance of steel welds based on a number of defects, including inadequate penetration, incomplete fusion, internal concavity, burn-through, slag inclusions, and porosity. For example, one section of API 1104 can be summarized as follows:

> Slag inclusions--50 mm (2 in.) maximum length for elongated slag inclusions, 50 mm (2 in.) limit per 305 mm (12 in.) of weld, 1.6 mm ($\frac{1}{16}$ in.) width limit per elongated slag inclusion. Isolated slag inclusions, 13 mm ($\frac{1}{2}$ in.) per 305 mm (12 in.) of weld, width greater than 3.2 mm ($\frac{1}{8}$ in.), 105 mm ($4\frac{1}{8}$ in.) isolated slag inclusions per 305 mm (12 in.) of weld. Aggregate length of isolated slag inclusion indications may not exceed two times the thinner of the nominal wall thickness and the width may not exceed one-half the thinner of the wall thicknesses joined.

Other examples include ASTM E 390 (Ref 8), which contains reference radiographs for steel welds and the *Structural Welding Code* (Ref 9), which includes a group of radiographic plates showing defect patterns for rounded inclusions corresponding to grade 1 and grade 2 quality levels. Several industries and product categories have applicable specifications and standards. A number of these are given in Ref 5.

Ultrasonic testing can also be used to locate internal defects, including porosity and inclusions. Ultrasonic testing involves transmitting mechanical vibrations through a piece of metal and analyzing both reflected and transmitted vibrations. Vibrations interact with discontinuities in the media through which they are passing, so the operator can detect voids, inclusions, and other internal interfaces. Table 2 includes ultrasonic testing, and Ref 5 lists a number of example specifications and detailed references.

References cited in this section

1. STANDARD WELDING TERMS AND DEFINITIONS, ANSI/AWS A3.0-89, AWS, 1989
2. WELD DISCONTINUITIES, *METALS HANDBOOK*, 9TH ED., VOL 6, AMERICAN SOCIETY FOR METALS, 1983, P 829-855
3. *WELDING HANDBOOK*, 8TH ED., VOL 2, AWS, 1987
4. *PROCEDURE HANDBOOK OF ARC WELDING*, 12TH ED., LINCOLN ELECTRIC CO., 1973
5. CODES, STANDARDS, AND INSPECTION, *METALS HANDBOOK*, 9TH ED., VOL 6, AMERICAN SOCIETY FOR METALS, 1983, P 823-838
6. *RADIOGRAPHY IN MODERN INDUSTRY*, 4TH ED., EASTMAN KODAK CO., 1980
7. WELDING OF PIPELINES AND RELATED FACILITIES, API STANDARD 1104, 17TH ED., AMERICAN PETROLEUM INSTITUTE, 1988
8. REFERENCE RADIOGRAPHS FOR STEEL WELDMENTS, ASTM E 390, ASTM
9. *STRUCTURAL WELDING CODE--STEEL*, ANSI/AWS D1.1-92, AWS, 1992

Characterization of Welds

Craig B. Dallam, The Lincoln Electric Company; Brian K. Damkroger, Sandia National Laboratories

Internal Characterization Requiring Destructive Procedures

This section briefly covers macrostructural and microstructural characterization and compositional analysis. These procedures are usually based on a cross section of the weld, referred to as a transverse section. The transverse section may be supplemented by the top-view photograph, the longitudinal section, and the normal section (Fig. 4). In particular, the top-view photograph will depict the general appearance of the weld, illustrating surface irregularities, spatter, or macroscopic defects such as hot cracking or porosity.

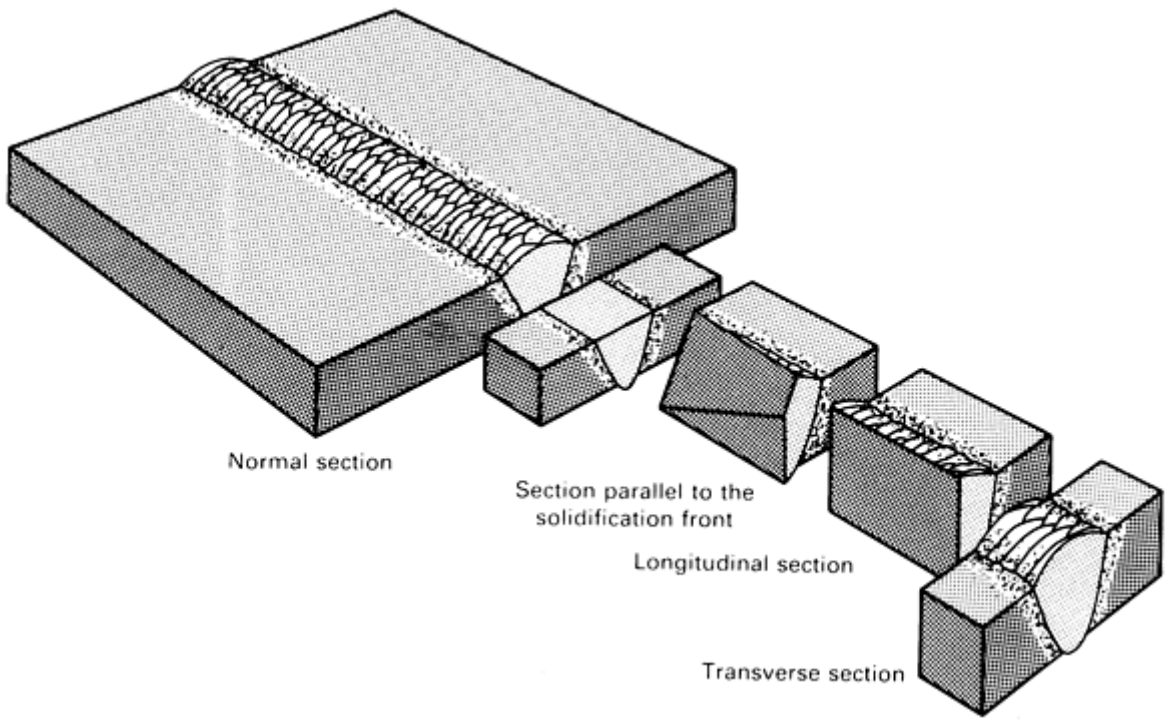

FIG. 4 TYPICAL SECTIONS USED IN THE METALLOGRAPHIC EXAMINATION OF WELDED JOINTS

Weld Macrostructure

Figures 5(a) and 5(b) show transverse sections of two welds, a submerged arc weld made on a 25 mm (1 in.) thick ASTM A 36 steel and a flux-cored weld made on a 50 mm (2 in.) thick ASTM A 537 steel. Readily apparent features include the number of passes and number of layers, fusion zone area, weld aspect ratio, extent of penetration, face width, and the reinforcement and curvature of the top bead. A transverse macrosection will also show any gross porosity or large inclusions present in a weld and the extent of the HAZ. It is important to note that quantitative measurements of weld features made based on a transverse section will be accurate only if the section is properly done. Potential errors, sectioning procedures, and sample preparation techniques are discussed in Ref 10.

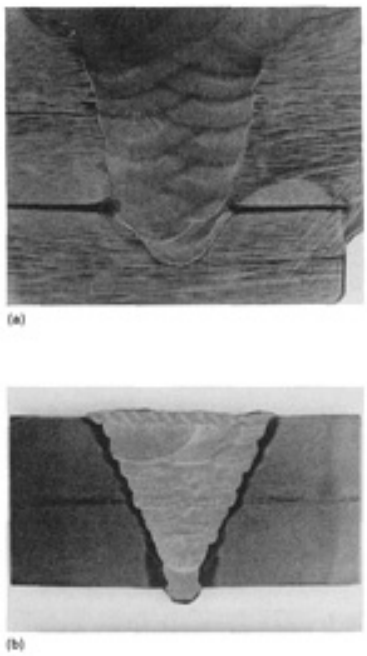

FIG. 5 TYPICAL MULTIPASS ARC WELDS IN STEELS USED IN STRUCTURAL APPLICATIONS. (A) SUBMERGED ARC WELD ON A 25 MM (1 IN.) THICK A 36 STRUCTURAL STEEL; THE MUSHROOM SHAPE OF THE LAST BEAD IS TYPICAL OF WELDS PRODUCED BY THIS PROCESS. (B) FLUX-CORED ARC WELD ON A 50 MM (2 IN.) THICK A 537 STEEL USED IN PRESSURE VESSEL AND STRUCTURE APPLICATIONS (THE LAST LAYER WAS MADE WITH SEVERAL SMALL PASSES TO IMPROVE MECHANICAL PROPERTIES)

Weld Microstructure

In many cases, it is important to examine and characterize the weldment microstructure and to understand its formation and effects on properties. This is the case when the materials and processes involved are not well characterized, so specifications have not been established. Other problems arise where the potential exists for the formation of detrimental microconstituents and/or where the consequences of weld failure are severe. Welding of high-strength or brittle materials are typical examples.

The microstructure of a weld consists of three regions: a fusion zone (material that has been melted); a heat affected zone (material that was not melted, but whose microstructure has been altered); and the base metal. These three regions can be seen in the transverse section shown in Fig. 5(b). Weld microstructures are examined using standard specimen removal and preparation techniques, with some concessions made for their inhomogeneous nature (Ref 10). Similarly, the parameters used to characterize the weld microstructures, such as grain size, grain morphology, and the amount of the various phases or microconstituents present, are those used to characterize monolithic materials. The equipment, procedures, and techniques used are well described in Ref 10.

Special importance may be attached to one or more specific features of a weld microstructure. An example is the classification of ferrite and carbide microconstituents in a low-ally steel weld. The various morphologies included in a characterization of a low-alloy steel weld are listed in Table 3. In these welds, a large amount of acicular ferrite is associated with high toughness levels, whereas martensitic or bainitic microstructures have much lower toughness levels. Bainite and martensite are also associated with higher effective cooling rates, so decreasing the weld metal manganese content, or reducing the cooling rate with increased heat input or preheat, will increase the amount of acicular ferrite and improve weld metal toughness.

TABLE 3 DESCRIPTION OF FERRITE/CARBIDE MICROCONSTITUENTS IN LOW-CARBON STEEL WELDS

Microconstituent	Description
Primary ferrite	
Grain boundry ferrite	Proeutectoid ferrite that grows along the prior austenite grain boundaries. It is equiaxed or polygonal, and it may occur in veins
Intragranular polygonal ferrite	Polygonal ferrite that is not associated with the prior austenite grain boundaries. Much larger than the average width of the surrounding acicular ferrite laths
Ferrite with second phase	
With aligned second phase	Parallel ferrite laths. Further classifications are widmanstätten ferrite and upper/lower bainite
With nonaligned second phase	Ferrite that completely surrounds either equiaxed, randomly distributed microphases, or solitary ferrite laths
Ferrite/carbide aggregate	Fine ferrite/carbide structures, including pearlite
Acicular ferrite	Small nonaligned ferrite grains found within prior austenite grains
Martensite	Martensite colony larger than adjacent ferrite laths

Microstructural characterization of welds has two purposes: to evaluate the microstructure with respect to properties and to relate the microstructure to the process used. The ultimate goal is to optimize the process to produce the most desirable microstructure. In general, the effects of a process and parameters on microstructure are due to the compositional and thermal effects. The compositional effects are largely limited to the fusion zone and will be discussed in the next section. Thermal cycles affect both the fusion zone and HAZ. Microstructural development in the HAZ has been the subject of much study, and a number of computational tools have been developed specifically for the prediction of HAZ microstructures (Ref 11).

Composition of a Weld

The composition of a weld will have a significant effect on its performance, contributing to both the mechanical and corrosion properties of the weld. In some instances, the effects can be drastic, such as sensitization of stainless steel or changing the ductile-to-brittle transition temperature of ferritic steels by an amount sufficient to cause brittle failure under normal use. In a number of cases, particular elements will govern the propensity toward certain defects or behavior. For example, a low-alloy steel weld with a carbon equivalent of over 0.4% is considered to be a high-carbon deposit, and it is treated differently than a low-carbon weld. Similarly, deposit silicon levels in excess of approximately 0.4% are often associated with a defect called "hollow bead," where the root pass in a pipe weld made with a cellulosic electrode has a continuous pore. In general, care must be taken to either minimize the compositional changes associated with welding or to factor the composition and property changes into the design.

Factors Affecting Weld Composition. The composition of a weld is affected by the base metal composition, the composition of any filler metal used (and dilution between the two), reactions with flux or shielding gas, and any material losses associated with the process. These factors are, in turn, largely controlled by the welding setup, process selection, parameters, and stability. The Schaeffler diagram (Ref 12) for stainless steels is an example of composition being controlled by dilution. The weld metal composition and microstructure are predicted based on the "ferrite stabilizer" and the "austenite stabilizer" content of the base metal, the nickel equivalent and chromium equivalent of the filler metal, and the level of dilution. The microstructure will be predicted as martensitic, ferritic, or austenitic, and the level of ferrite in the weldment will be estimated. In these welds, ferrite numbers below 4 indicate microstructures in which low-melting-

point compounds may be formed at the grain boundaries, and the welds can be prone to hot cracking. Conversely, welds with ferrite numbers above 10 have reduced corrosion resistance and can be susceptible to the formation of σ phase at high temperatures (Ref 13). The Schaeffler diagram has been revised many times for adaptation to different alloy modifications. An example is the inclusion of nitrogen in the nickel equivalent. Many stainless steels often contain small amounts of nitrogen, and in fact some stainless steels are deliberately strengthened with nitrogen additions. Other modifications include copper in the nickel equivalent and vanadium and aluminum in the chromium equivalent (Ref 14). Additional information is available in the Section "Selection of Stainless Steels" and in the article "Welding of Stainless Steels" in this Volume.

An example of the effect of flux on weld metal composition is seen when low-carbon steel is welded with E6010 and E7018 electrodes, using identical parameters. Although the core wire composition of the two electrodes is identical, the E6010 electrode will produce a deposit with approximately 0.15 to 0.25% Si, and the E7018 electrode will produce a deposit with 0.5 to 0.6% Si. An example of a procedure-related effect is seen when the arc length is changed for welds made with an E7018 electrode. Arc length changes can alter the silicon content from 0.3 to 0.6%, and they can alter the manganese content from 0.8 to 1.3%.

Measurement Techniques and Procedures. The usual techniques for compositional analysis of metallic samples can be used on welds and are covered in Ref 15. However, some considerations must be made when dealing with welds, because of their inhomogeneity. The most commonly used method for compositional analysis of welds is optical emission spectroscopy, where a spot of material (typically 6 mm, or $\frac{1}{4}$ in., in diameter) is ablated off the surface of the specimen and the light emissions are analyzed. In many welds, a spot this size will encompass several passes in a multipass weld, and it will perhaps encompass weld metal, HAZ, and base metal in a single-pass weld. An average composition over this large an area may not address local effects, for example, sensitization of stainless steel.

Welds are prone to both macrosegregation and microsegregation, and the properties may be governed by the composition in a very local region. A thorough characterization of welds requires techniques with sufficient spatial resolution to characterize their inhomogeneity. Scanning electron microscopy with wavelength or energy dispersive x-ray analysis systems, electron microprobes, and x-ray fluorescence techniques are often employed. Often, a number of closely spaced analyses are made along a line traversing a weld. This data may then be coupled with a similar microhardness traverse and microstructural analyses to characterize the variation across the weld. Thorough treatments of a number of microanalytical techniques are contained in Ref 16.

Mechanical Testing

A number of mechanical properties are used to characterize welds, including strength, ductility, hardness, and toughness. In general, the same samples and procedures are used in other areas of metallurgy (Ref 17). However, a prominent concern regarding the mechanical performance of welds is the direct comparison with base material. The goal is to ensure that the weld is not the weakest component of a structure, or if it is, to compensate for this in the design.

Strength. Yield and tensile strength are measured for all-weld-metal specimens using a standard tensile test (Ref 18), but with specimens removed from test plates welded according to AWS-specified procedures (Ref 19). These tests form the basis for the assignment of yield and ultimate strength values to welds made using a specific electrode and according to a set procedure. Additional tests are sometimes performed to compare the base metal and weld metal strengths. An example of this type of test is the transverse tensile test, in which the specimen is removed from the weld so that the loading axis is perpendicular to the weld bead and the weld reinforcement is left intact. The goal of this test is to verify that overload failure will occur in the base metal rather than in the weld metal or HAZ.

Ductility is another critical weld property. In addition to defects, many welding processes can produce hard, brittle microstructures. The standard measures of ductility--percent reduction in area and percent elongation--are obtained in a uniaxial tensile test. Another test often specified for welds is a bend test (face bends, roof bends, and side bends). In this test, a strip of material containing a weld is deformed around a specified radius and its surface is examined. The criteria for success or failure are the number and size of defects seen on the outer surface of the bend. An example of bend test criteria is the AWS *Structural Welding Code* (Ref 9), which calls for bending around a 19 mm (0.75 in.) radius for materials with yield strengths less than or equal to 345 MPa (50 ksi), a 25 mm (1 in.) radius for 345 to 620 MPa (50 to 90 ksi) materials, and a 32 mm (1.25 in.) radius for materials with yield strengths greater than or equal to 620 MPa (90 ksi).

Hardness. One common use of hardness values in weld specifications is as a check for the formation of microstructures that might have low ductility and toughness and thus are prone to cracking. For example, in pipeline steels, the formation of martensite in the HAZ is a cause for concern because of the potential for cracking. This is addressed by specifying maximum values for microhardness traverses across several sections of the weld. Hardness values are also used as an indicator of susceptibility to some forms of stress-corrosion cracking.

Toughness is the ability of a material to absorb energy during fracture. There are two approaches to toughness testing: impact toughness testing and fracture mechanics testing.

Impact Toughness Testing. To test impact toughness, a sample of specified geometry is subjected to an impact load, and the amount of energy absorbed during fracture is recorded. Usually the specimen is oriented so that the notch and expected plane of fracture run longitudinally through the weld metal. Charpy tests do not measure an inherent material property, but they result in a relative measure of impact toughness between materials. A very common use of the Charpy test is to determine a material's ductile-to-brittle transition temperature by performing tests at several different temperatures. AWS A5.1 (Ref 19) gives minimum Charpy impact values, at several temperatures, for welds made on carbon steel using a number of different electrodes.

Fracture Mechanics Testing. The second type of toughness testing is based on fracture mechanics, and it can use either linear elastic or elastic-plastic methodologies. Although elastic-plastic behavior (J_{Ic}) is becoming of interest in some cases, the bulk of fracture mechanics testing is based on linear elastic considerations. These tests, using specimens and procedures given in ASTM E 399 (Ref 20), are used to measure a material's fracture toughness (K_{Ic}), which is a material property. In the case of welding, fracture toughness is usually expressed using a value for crack tip opening displacement (Ref 21). Fracture toughness testing has only recently begun gaining acceptance as applicable to welds. The major shortcomings of this approach include the complexity and cost of testing and the wide variability in fracture toughness values for weld metal, due largely to the inhomogeneous nature of welds and residual stress effects.

References cited in this section

9. *STRUCTURAL WELDING CODE--STEEL,* ANSI/AWS D1.1-92, AWS, 1992
10. METALLOGRAPHY OF WELDMENTS, *METALS HANDBOOK,* 9TH ED., VOL 9, AMERICAN SOCIETY FOR METALS, 1985, P 577-586
11. K.E. EASTERLING, MICROSTRUCTURE AND PROPERTIES OF THE HAZ, *RECENT TRENDS IN WELDING SCIENCE AND TECHNOLOGY,* S. DAVID AND J. VITEK, ED., ASM INTERNATIONAL, 1990, P 177-188
12. WRC 1992 DIAGRAM, *WELD. J.*, MAY 1992, P 171
13. T.G.F. GRAY, J. SPENCE, AND T.H. NORTH, *RATIONAL WELDING DESIGN,* NEWNES-BUTTERWORTHS, 1975, P 111
14. R.H. ESPY, WELDABILITY OF NITROGEN-STRENGTHENED STAINLESS STEELS, *WELD. J. RES. SUPPL.*, VOL 61 (NO. 5), MAY 1982, P 149S-156S
15. METAL TEST METHODS AND ANALYTICAL PROCEDURES, *1991 ANNUAL BOOK OF ASTM STANDARDS,* VOL 03.05 AND 03.06, ASTM, 1991
16. *MATERIALS CHARACTERIZATION,* 9TH ED., VOL 10, *METALS HANDBOOK,* AMERICAN SOCIETY FOR METALS, 1986
17. *MECHANICAL TESTING,* 9TH ED., VOL 8, *METALS HANDBOOK,* AMERICAN SOCIETY FOR METALS, 1985
18. STANDARD METHODS OF TENSION TESTING OF METALLIC MATERIALS, ASTM E 8, *ANNUAL BOOK OF ASTM STANDARDS,* VOL 03.01, ASTM, 1984
19. *SPECIFICATION FOR CARBON STEEL ELECTRODES FOR SHIELDED METAL ARC WELDING,* ANSI/AWS A5.1-91, AWS, 1991
20. STANDARD TEST METHOD FOR PLANE-STRAIN FRACTURE TOUGHNESS OF METALLIC MATERIALS, ASTM E 399, *ANNUAL BOOK OF ASTM STANDARDS,* ASTM, 1984
21. STANDARD TEST METHOD FOR CRACK TIP OPENING DISPLACEMENT (CTOD) FRACTURE

Characterization of Welds

Craig B. Dallam, The Lincoln Electric Company; Brian K. Damkroger, Sandia National Laboratories

Weld Characterization Examples

In this section, two weld will be analyzed to serve as examples of techniques discussed thus far in this article. The first of these welds is a multipass shielded metal arc weld/flux-cored arc weld made on pipe steel for an industrial application. This type of weld would typically be made in great quantity. In practice, it would be characterized largely on the basis of its external appearance, perhaps supplemented by nondestructive testing. The initial characterization of a weld and procedure, however, would be based on chemical composition and mechanical properties. Primary concerns are whether the weld being examined is representative of a normal weld of this type and can thus be reasonably well described based on the materials, process, and specifications involved in its production. The bulk of the actual characterization of such a weld would be done during the development and certification of the initial process to determine its suitability for the intended application.

The second example is a weld used for a very specific application. This weld is a butt weld made on Ti-6Al-4V, with a tantalum shim inserted between the base metal sections. Among the requirements for this weld are that it have microstructural and property homogeneity and stability at elevated temperatures and that it be cathodic to the base metal under unusual and extremely severe environmental conditions. In this case, the concerns center less on the eventual application and more on building a thorough database regarding the metallurgical and microstructural characteristics of the weld.

Example 1: Multipass Weld in a 1.07 m (42 in.) Diameter X-65 Pipe.

This weld is a circumferential weld on a 12.7 mm (0.50 in.) thick, 1.07 m (42 in.) diameter X-65 pipe. The X-65 materials is designated by API as a pipe steel with at least 448 MPa (65 ksi) yield strength and 566 MPa (82 ksi) tensile strength. This type of weld is typical for a large oil or gas pipeline. However, for this example, procedures were deliberately selected to produce a weld with a range of defects. These procedures, given by Table 4, are not representative of standard practice.

TABLE 4 PARAMETERS (NOT STANDARD PROCEDURE) USED TO OBTAIN MULTIPASS WELD IN 1.07 M (42 IN.) DIAMETER X-65 STEEL PIPE

PROCESS	PASS NO.	ELECTRODE	DIAMETER		WIRE FEED		CURRENT, A	VOLTAGE, V	TRAVEL SPEED	
			mm	in.	mm/s	in./s			mm/s	in./s
SMAW	1	E8010-G	4.0	0.16	. . .	. . .	150	26-28	5.9-7.2	2.3-2.8
	2	E8010-G	4.0	0.16	. . .	. . .	180	26-28	5.9-7.2	2.3-2.8
FCAW	3	E71T8-K6	1.73	0.068	47	1.9	200	19	4.5	1.8
	4	E71T8-K6	1.73	0.068	47	1.9	200	19	4.0	1.6
	5	E71T8-K6	1.73	0.068	47	1.9	200	19	4.0	1.6
	6	E71T8-K6	1.73	0.068	47	1.9	200	19	4.7	1.9
	7	E71T8-K6	1.73	0.068	47	1.9	200	19	5.9	2.3
	8	E71T8-K6	1.73	0.068	42	1.7	180	18	4.2	1.7
	9	E71T8-K6	1.73	0.068	42	1.7	180	18	4.5	1.8

Additional specifications include: 12.7 mm (0.50 in.) wall thickness; 1.59 mm (0.0625 in.) land; 1.59 mm (0.0625 in.) gap; 60° bevel in groove; vertical down position; preheat and interpass temperature of 150 °C (300 °F)

Visual Observation. The weld was initially characterized by visual observation. From the top of the joint, the size and uniformity of the weld and undercut can be observed (Fig. 6a). From the underside, spatter, lack of penetration, and internal undercut can be seen (Fig. 6b).

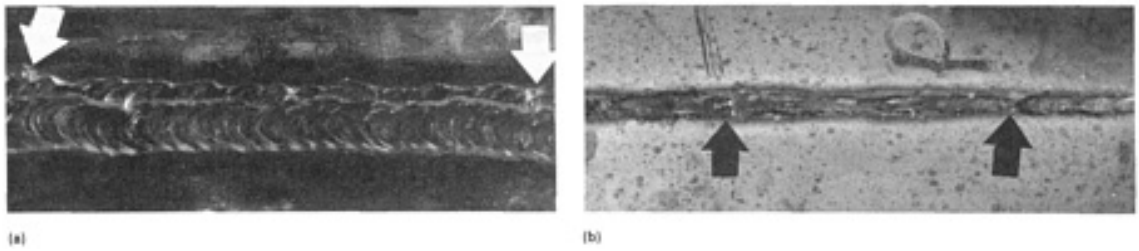

FIG. 6 DEFECTS IN A MULTIPASS WELD MADE ON A 1.07 M (42 IN.) DIAMETER X-65 STEEL PIPE. (A) EXTERIOR VIEW SHOWING LACK OF UNIFORMITY (RIGHT ARROW) AND UNDERCUT (LEFT ARROW). (B) INTERIOR VIEW SHOWING LACK OF PENETRATION (RIGHT ARROW) AND BURN-THROUGH (LEFT ARROW)

Nondestructive evaluation was then used to examine the weld for internal and surface defects. Slag entrapment and lack of fusion are typical internal defects for this type of weld, and they can be seen in the radiograph shown in Fig. 7. Figure 7 also shows the external defects noted during visual observation. In addition to nondestructive evaluation, other tests that highlight defects (for example, "nick-break" tests and face or root bend tests) can be run, but these were not used in this case. Similarly, ultrasonic testing, magnetic particle testing, and penetrant testing were not used in this characterization.

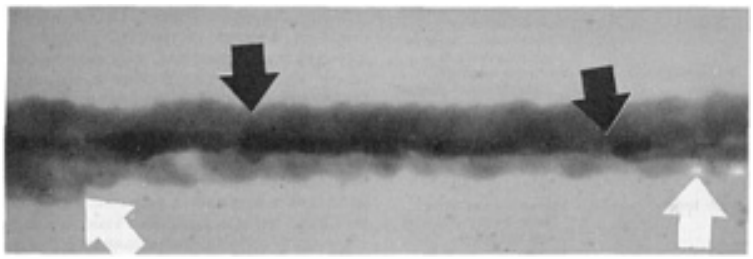

FIG. 7 RADIOGRAPH SHOWING POSITIVE IMAGE OF MACROSCOPICALLY VISIBLE DEFECTS IN THE X-65 PIPE STEEL OF FIG. 6. SEE FIG. 6 FOR DESIGNATION OF SPECIFIC DEFECTS.

Weld Macrostructure. Destructive evaluation begins by removing a transverse section from the weld and preparing it for metallographic examination (Fig. 8). The welding pass sequence (that is, number and size of passes, number of passes per layer, amount of penetration, and extent of HAZ) is apparent. In addition, any gross defects present in the sectioning plane are visible. In this example, nine passes were made, three layers with one pass and three with two passes. Figure 8 also shows four small pores, one each in the third, fourth, sixth, and ninth passes. In this case, the porosity was induced by deliberately varying the electrode stickout.

FIG. 8 TRAVERSE SECTION OF THE X-65 PIPE STEEL SHOWN IN FIG. 6 AND 7. PORES IN PASSES 3, 4, 6, AND

8 WERE CAUSED BY INTENTIONALLY VARYING THE ELECTRODE STICKOUT.

Weld Metal Composition. Compositional analysis of the weld was performed at this point. For this application, the bulk, or average, composition of the weld is of the most interest. The bulk composition of the weld was measured using an emission spectrometer, and the results are given in Table 5. The interstitial content of the weld is also of interest, and the levels of oxygen and nitrogen were measured with dedicated instruments. The oxygen level of the weld was found to be 110 ppm and the nitrogen level, 330 ppm. For some welds, techniques can be used to map compositional variations within the weld. In this case, the bulk composition, measured at the weld center, is considered adequate to characterize the weld.

TABLE 5 BULK COMPOSITION OF WELD IN 1.07 M (42 IN.) DIAMETER X-65 STEEL PIPE

SAMPLE	COMPOSITION, WT. %									
	C	Mn	Si	Al	Ni	Cr	Mo	Ti	V	Nb
WELD METAL	0.062	0.85	0.22	0.76	0.65	0.02	0.02	0.011	0.008	0.003
BASE METAL	0.093	1.35	0.21	0.02	0.02	0.04	0.00	0.002	0.069	0.033
ELECTRODES:										
E8010-G	0.14	0.70	0.20	0.01	0.73	0.02	0.07	0.008	0	0
E71T8-K6	0.056	0.91	0.24	0.95	0.97	0.02	0.01	0.002	0	0

Weld Microstructure. The transverse section was also used for examination and characterization of the microstructure of the weld. Figure 9 shows micrographs of different regions of the weld. Figure 9(a) shows weld metal that has not been reheated by successive passes. Figure 9(b) shows weld metal that has been reheated and has a finer structure than the non-reheated weld metal. Figure 9(c) shows a location in the HAZ that closely resembles the structure seen in the reheat zone. The important parameters to characterize for this type of weld are the percentage of reheat zone, the relative amount of various microconstituents, and the average grain size. In the example weld, the weld metal is approximately 80% reheat zone. In the non-reheated zone (Fig. 9a), quantitative microstructural analysis showed that the structure consisted of 20% grain boundary ferrite, 20% intergranular polygonal ferrite, 16% acicular ferrite, 32% ferrite with an aligned second phase, and 12% ferrite with a nonaligned second phase. No martensite or ferrite-carbide aggregate was found.

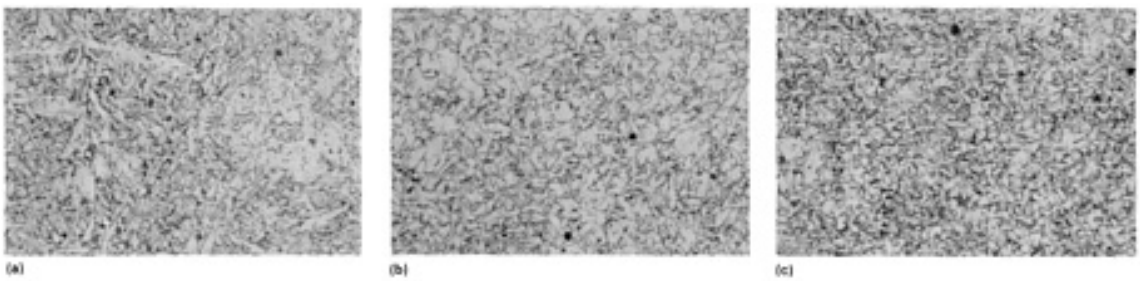

FIG. 9 MICROSTRUCTURE OBTAINED IN SELECTED REGIONS OF THE TRAVERSE SECTION OF THE X-65 PIPE STEEL OF FIG. 8. (A) NON-REHEATED WELD METAL. (B) REHEATED WELD METAL. (C) HEAT-AFFECTED ZONE. ALL 250×

Mechanical Testing. Following the characterization of the microstructure, specimens were removed and used for mechanical testing. For this application, the pertinent mechanical tests are tension tests (transverse and all-weld-metal), Charpy impact tests, fracture toughness tests, and a microhardness traverse. A transverse tensile test is primarily used to ensure that the welded joint is not the weak link in the final structure. In this case, a 305 × 32 mm (12.0 × 1.25 in.) specimen was removed from the pipe, the long axis perpendicular to the weld bead. The specimen was loaded to 247 kN (27.8 tonf) and failed in the base metal. Based on a weld cross-sectional area of 5.08 cm^2 (0.787 $in.^2$), a minimum weld tensile strength was calculated as 487 MPa (70.6 ksi).

An all-weld-metal tensile test was run using a specimen removed from the bead so that its loading axis was parallel to the weld direction. In this case, the weld was aged prior to testing, with the heat treatment being 48 h at 104 °C (220 °F). The results of the tensile test are shown in Fig. 10. The yield strength was found to be 520 MPa (75.4 ksi), the ultimate strength 594 MPa (86.1 ksi), and the percent elongation 30%. With respect to a typical vendor specification for this type of weld, these values indicate that the weld is adequate.

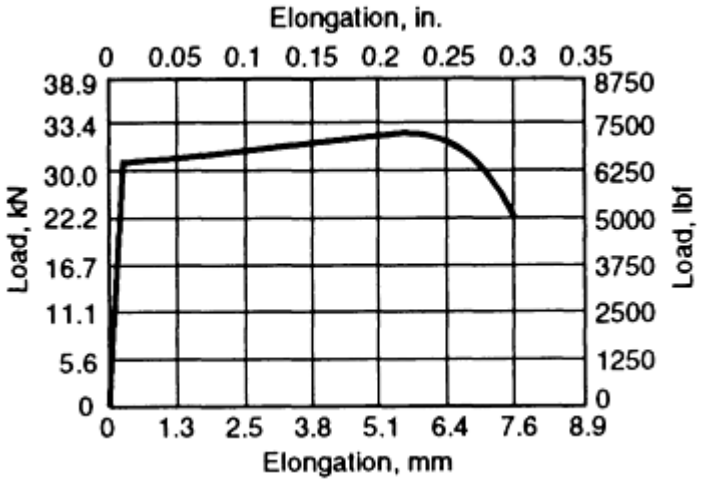

FIG. 10 PLOT OF LOAD VERSUS ELONGATION FOR ALL-WELD-METAL TENSILE TEST OF A 6.4 MM (0.25 IN.) DIAMETER SPECIMEN TAKEN FROM THE 1.07 M (42 IN.) DIAMETER X-65 STEEL PIPE

Charpy V-notch impact specimens were removed from the weld as shown in Fig. 11. For this type of application, tests are usually run at only one temperature, dictated by a specification and/or past experience. For a full characterization, however, tests will be run over a broad enough range to clearly establish the upper- and lower-shelf energy levels and to identify the ductile-to-brittle transition temperature (DBTT). For this example, tests were run at several temperatures, and the results are shown in Fig. 12. This figure clearly shows that the upper shelf energy is approximately 200 J (150 ft · lbf), the lower shelf 2 J (1.5 ft · lbf), and the DBTT -10 °C (14 °F).

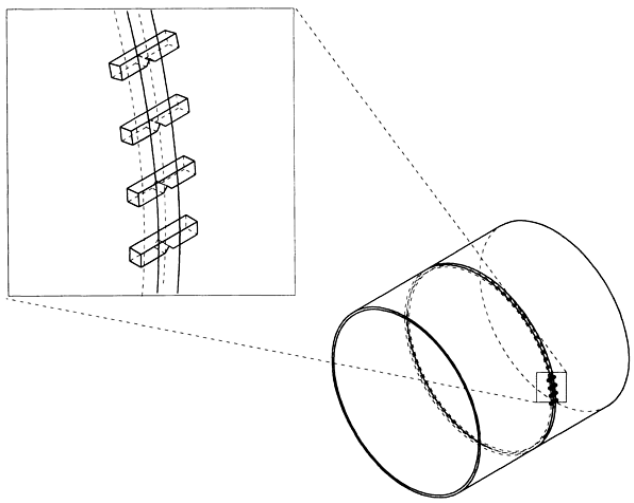

FIG. 11 SCHEMATIC SHOWING LOCATION AND ORIENTATION OF CHARPY V-NOTCH SPECIMENS TAKEN FROM THE 1.07 M (42 IN.) DIAMETER X-65 STEEL PIPE. ALTHOUGH INSET SHOWS WIDELY SPACED SAMPLES FOR THE SAKE OF CLARITY, ACTUAL SAMPLES REMOVED ARE TYPICALLY ADJACENT TO ONE ANOTHER.

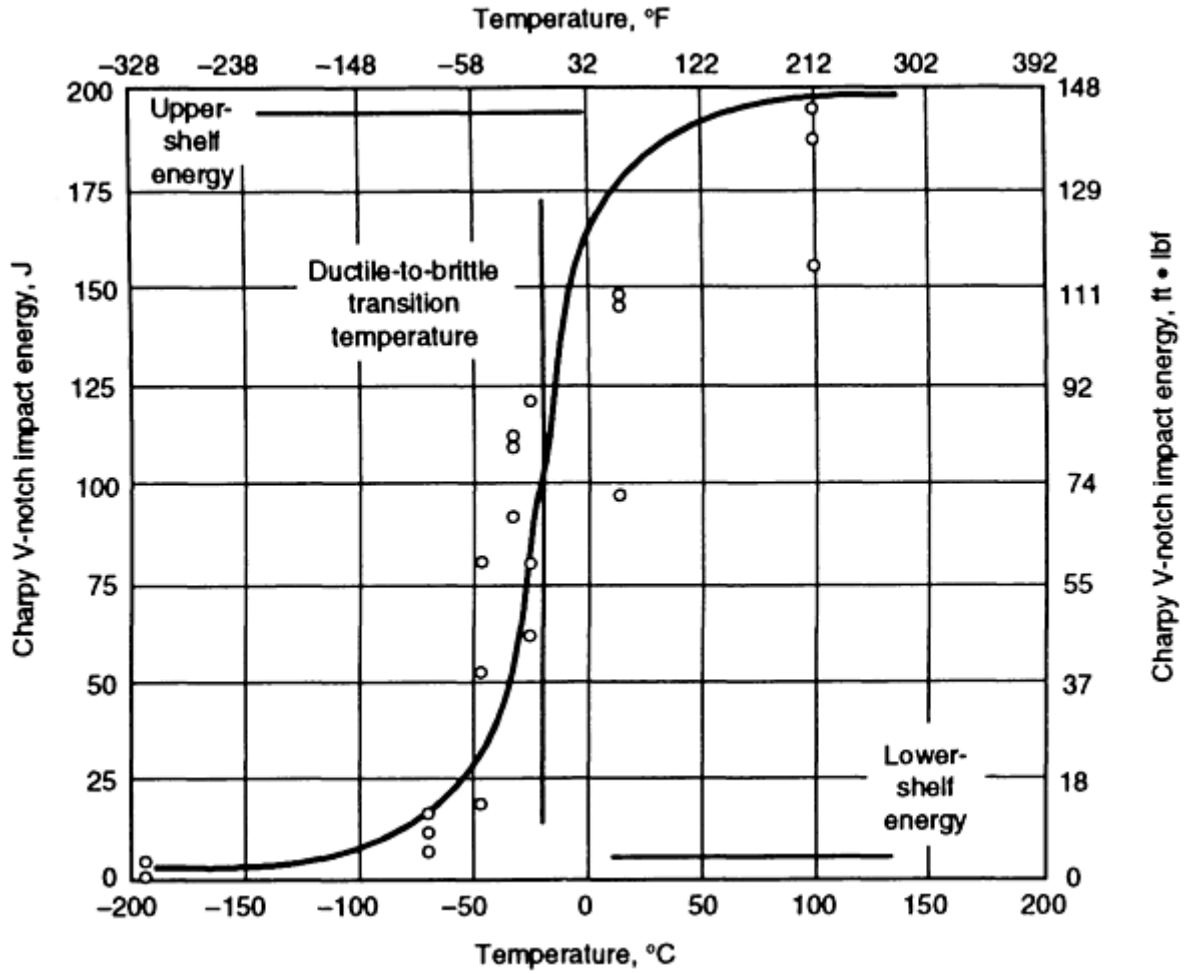

FIG. 12 CHARPY V-NOTCH IMPACT ENERGY TEST RESULTS USED TO OBTAIN DUCTILE-TO-BRITTLE TRANSITION TEMPERATURE (-10 °C, OR 14 °F) FOR THE 1.07 M (42 IN.) DIAMETER X-65 STEEL PIPE

Fracture toughness specimens were removed from the weld in an orientation similar to that of the Charpy specimens. As with Charpy tests, fracture toughness specifications usually require a certain value at a given temperature, usually the minimum service temperature. Crack tip opening displacement tests were conducted at -45 °C (-50 °F) on three specimens removed from the example weld. The results were found to vary from 0.137 to 0.322 mm (0.005 to 0.013 in.), with the average being 0.229 mm (0.009 in.). Figure 13 shows the fracture surface of one of the test specimens, on which the ductile fracture mode and overload zone can be clearly seen.

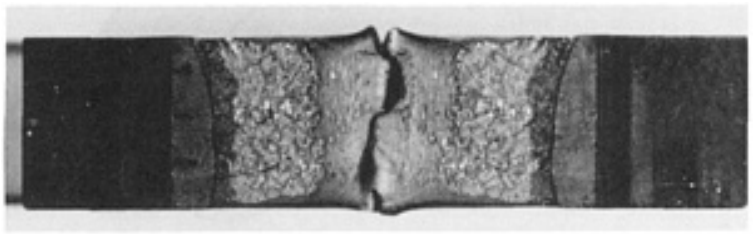

FIG. 13 MACROGRAPH OF THE FRACTURE SURFACE OF A CRACK TIP OPENING DISPLACEMENT TEST SPECIMEN REMOVED FROM THE 1.07 M (42 IN.) X-65 STEEL PIPE. THE REGIONS OF THE SURFACE SHOWN CORRESPOND WITH THE NOTCH, PRECRACK, STABLE CRACK GROWTH, FAST FRACTURE, AND OVERLOAD ZONES.

In addition to the previous mechanical tests, microhardness testing is often used for this type of weld. The primary purpose of microhardness testing is to check for the presence of martensite in the HAZ. Figure 14 shows a schematic of the example weld and the location and values of several microhardness tests. In this case, none of the values exceeded 240 HV, the level associated with the presence of martensite.

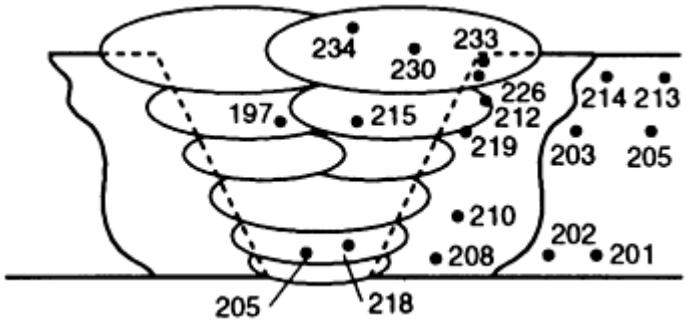

FIG. 14 MICROHARDNESS READINGS (LOCATION IN MULTI-PASS WELD INDICATED BY DOTS) BELOW 240 HV INDICATING THAT NO MARTENSITE STRUCTURE IS PRESENT IN THE 1.07 M (42 IN.) X-65 STEEL PIPE

Typically, this type of pipe weld is characterized with respect to stress-corrosion cracking resistance. In addition, testing is often performed to characterize the HAZ toughness.

Example 2: Welding of 2.5 mm (0.100 in.) Thick Ti-6Al-4V Sheet using a 0.127 mm (0.005 in.) Thick Tantalum Shim.

Figure 15 shows a transverse section of a butt weld, where the base metal is 2.5 mm (0.100 in.) thick Ti-6Al-4V and a 0.127 mm (0.005 in.) thick tantalum shim has been placed in the joint. This weld geometry was used in a study of the effect of dilution on the microstructures and properties of dissimilar metal welds of titanium to refractory metals. The questions to be answered in the characterization of this weld were:

- HOW UNIFORMLY WOULD THE TANTALUM BE DISTRIBUTED IN THE WELD POOL?
- HOW ACCURATELY COULD THE COMPOSITION OF THE WELD POOL BE PREDICTED BASED ON DILUTION CALCULATIONS?
- WHAT PHASES AND MICROCONSTITUENTS ARE PRESENT IN THE WELD METAL?
- WHAT ARE THE MECHANICAL PROPERTIES OF THE WELD METAL?

In addition, a number of very application-specific corrosion and elevated-temperature tests were performed on the dissimilar metal welds. In contrast with the pipe weld of the first example, the primary tools used in this characterization were macrostructural examination, compositional mapping, x-ray diffraction, tension testing of all weld metal specimens, and microhardness traverses.

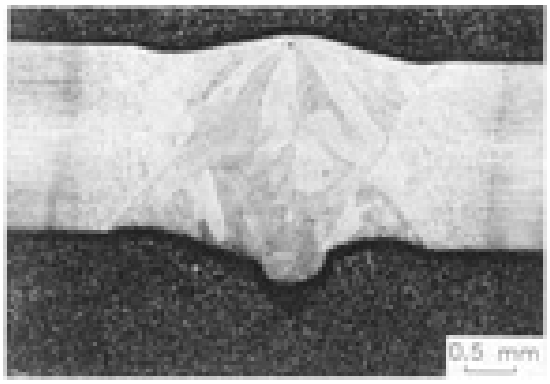

FIG. 15 MICROGRAPH OF TRANSVERSE SECTION OF AN ELECTRON-BEAM WELDED BUTT WELD JOINING 2.5 MM (0.100 IN.) THICK TI-6AL-4V SHEET USING A 0.127 MM (0.005 IN.) THICK TANTALUM SHIM PLACED IN THE JOINT. KROLL'S REAGENT WAS USED AS ETCHANT.

Weld Macrostructure. The weld shown in Fig. 15 was made with the electron-beam welding process, using sharp focus, 100 kV power, 16 to 25 mA current, and a travel speed of 12.7 mm/s (30 in./min). As can be seen in the transverse section, a full penetration weld was achieved using one pass from each side of the weld. The transverse section also shows that no obvious discontinuities exist in the weld pool and that the weld metal microstructure is fairly uniform. Figure 15 also suggests that the tantalum shim was completely melted.

Weld Metal Composition. An initial examination of the weld metal composition was performed to help assess the uniformity of the weld macrostructure. Figure 16 shows tantalum, titanium, vanadium, and aluminum elemental scan lines traversing the weld. These data were generated using a scanning electron microscope with energy-dispersive spectroscopy capability, and they confirm that the elements in question are uniformly distributed throughout the weld pool. Based on these analyses and the macrostructural characterization, it was determined that this combination of welding processes and parameters was successful in producing a full-penetration weld and a macroscopically homogeneous and defect-free weld pool.

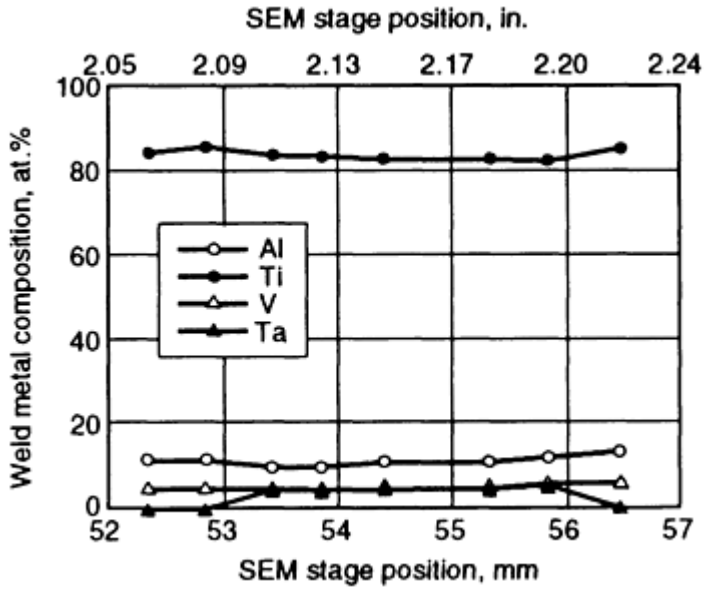

FIG. 16 ELEMENTAL LINE SCANS OF TITANIUM, ALUMINUM, VANADIUM, AND TANTALUM SPANNING THE HAZ AND FUSION ZONE OF THE 2.5 MM (0.100 IN.) THICK TI-6AL-4V SHEET WELDED USING A 0.127 MM (0.005 IN.) THICK TANTALUM SHIM.

The properties of titanium alloys can be strongly affected by the phases present in the microstructure, which are largely controlled by the weld metal composition. In this example, aluminum stabilizes the hexagonal close-packed (hcp) α and/or α' phases, and vanadium and tantalum, the body-centered cubic (bcc) β phase. In titanium alloys, the composition can be expressed as an electron/atom (*e*/*a*) ratio, which allows the phase stabilization effects of different elements to be combined. Table 6 lists the calculated (based on dilution) and measured compositions of the weld. This table shows that the measured and calculated compositions agree reasonably well. The measured aluminum values are somewhat lower than the calculations predict, perhaps due to some loss of aluminum during the welding process. Of most interest is that the measured and calculated *e*/*a* ratios are 3.96 to 3.98. This compositional range indicates that the weld metal microstructure should be α', a hexagonal martensite structure associated with good mechanical properties (Ref 20).

TABLE 6 COMPOSITION OF TI-6AL-4V RELATIVE TO THAT OF TI-6AL-4V PLUS TANTALUM WELD METAL

SAMPLE	COMPOSITION, AT.%				
	Ti	V	Al	Ta	*E/A* RATIO
TI-6AL-4V	86.2	3.6	10.2	. . .	3.93
TI-6AL-4V WELDED TO TA SHIM:					
CALCULATED	83.9	3.5	9.9	2.7	3.96
MEASURED	83.0	3.9	9.5	3.6	3.98

Weld Microstructure. The microstructure of the weld was analyzed using optical microscopy, transmission electron microscopy, and x-ray diffraction. Of particular interest were the structure of any martensitic phase present and the possible existence of ω, an ordered phase that can severely embrittle the material. The composition of the weld metal suggests that the structure will be α' hexagonal martensite. Figure 17 shows an optical micrograph of the fusion zone. Examination of Fig. 17 and comparison with Ti-6Al-4V (no tantalum shim) welds further suggest that the weld metal microstructure is α'. This was further supported by x-ray diffraction and TEM data. Figure 18 shows an x-ray diffraction trace for the weld metal. Aside from peaks from the specimen-mounting material, only peaks associated with a hexagonal structure were detected.

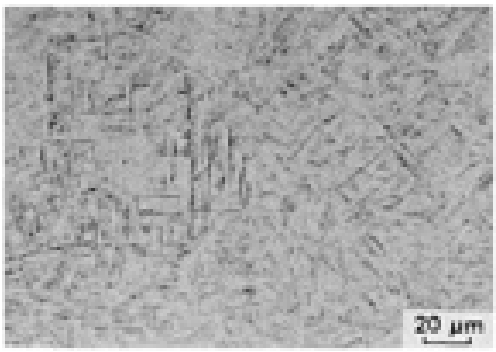

FIG. 17 OPTICAL MICROGRAPH OF FUSION ZONE OBTAINED WITH THE TI-6AL-4V SHEET WELDED USING A TANTALUM SHIM. KROLL'S REAGENT WAS USED AS THE ETCHANT. MICROSTRUCTURE CONSISTS OF WIDMANSTÄTTEN α+ β AND α' MARTENSITE.

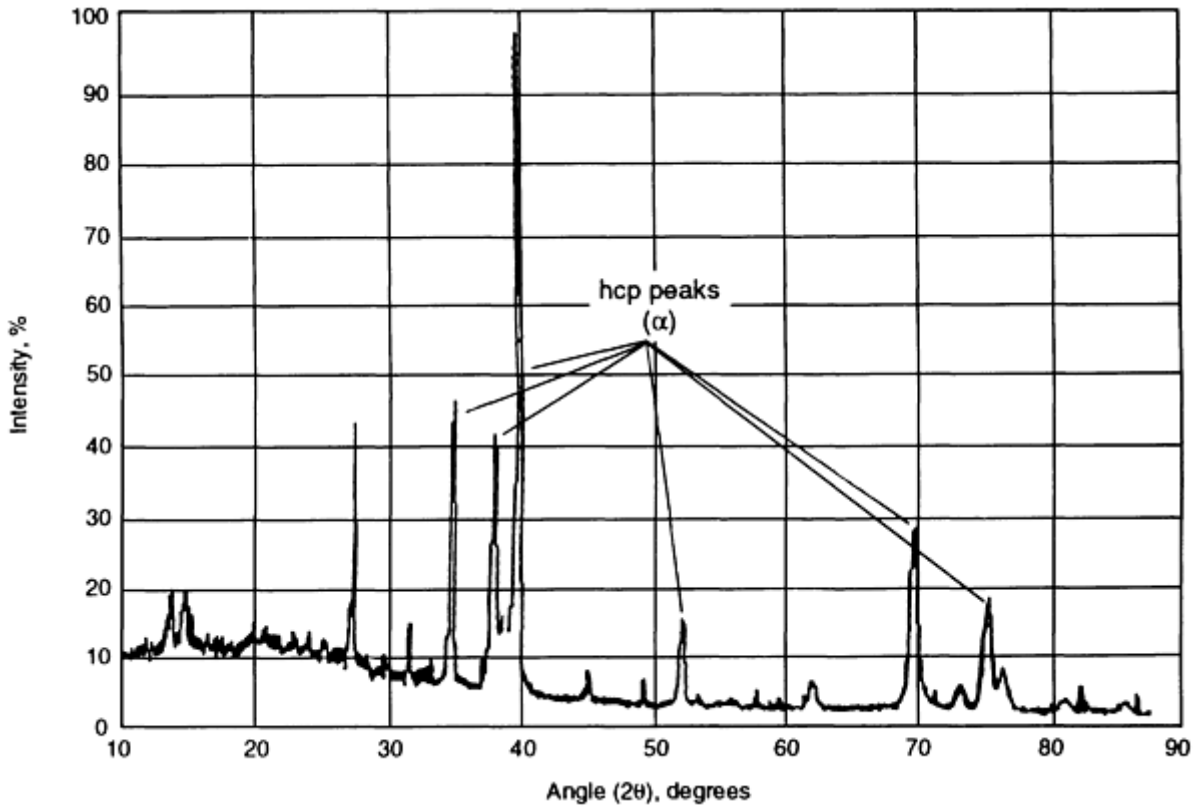

FIG. 18 X-RAY DIFFRACTION TRACE OF FUSION ZONE IN TI-6AL-4V SHEET WELDED USING A TANTALUM SHIM, SHOWING PEAKS THAT IDENTIFY HEXAGONAL STRUCTURES

Based on the compositional analysis, diffraction results, and microstructural analysis, the weld metal can be characterized as α' hexagonal martensite. By comparison with Ti-6Al-4V base metal and (no shim) weld metal, it was determined that the weld metal could be treated as a slightly more heavily stabilized variant of Ti-6Al-4V. This analysis allowed its properties and performance to be reasonably predicted.

Mechanical Testing. Microhardness traverses and all-weld-metal tension tests were performed on this weld. Figure 19 shows the results of two microhardness traverses, one across the second pass only, and one across the middle of the weld where the two passes overlap. Both traces are very similar, and the hardness is fairly constant across the fusion zone. These data confirm that the weld metal is relatively homogeneous. The hardness of the fusion zone is slightly higher than that of the base metal, as would be expected because of the martensitic structure and slightly higher β-stabilizer content.

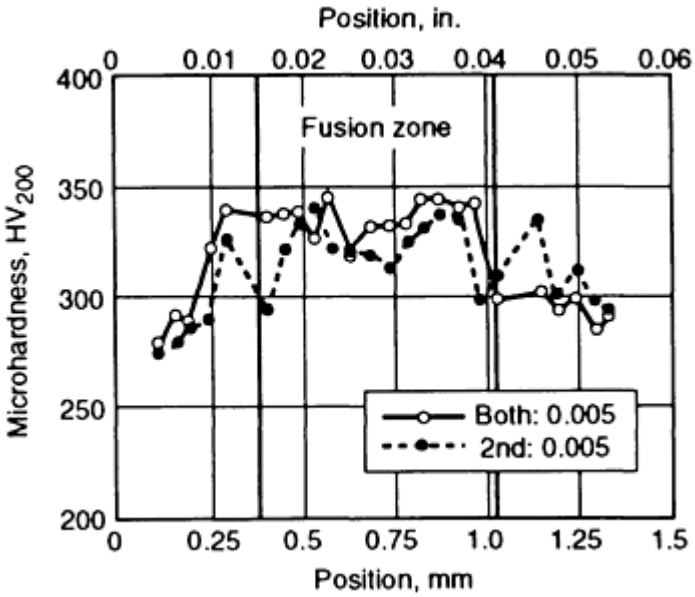

FIG. 19 MICROHARDNESS TRAVERSE DATA IN TWO LOCATIONS FOR THE TI-6AL-4V SHEET WELDED USING A TANTALUM SHIM. DATA LABELED "2ND" REFER TO TRAVERSE OVER SECOND PASS OF WELD ONLY. DATA LABELED "BOTH" INDICATE TRAVERSE ACROSS CENTER OF WELD WHERE TWO PASSES OVERLAP (SEE FIG. 15).

The tensile testing further confirmed that the weld metal could be considered to be a more heavily stabilized variant of Ti-6Al-4V. Table 7 compares the results of tensile tests performed on a baseline Ti-6Al-4V (no shim) weld with those of tests performed on the example weld. As the data show, the tantalum-containing weld had slightly higher strength and lower ductility than the baseline weld. Again these data are consistent with a slightly higher β-stabilizer content. However, the differences were not as great as in the microhardness testing, because in the case of the tensile tests, both structures were α' martensite.

TABLE 7 TENSILE PROPERTIES OF BASELINE TI-6AL-4V WELD COMPARED TO TI-6AL-4V WELDED USING TANTALUM SHIM

SAMPLE	YIELD STRENGTH		ULTIMATE TENSILE STRENGTH		YOUNG'S MODULUS		MAXIMUM STRAIN, %
	MPA	KSI	MPA	KSI	GPA	10^6 PSI	
BASELINE 1	828	120	970	141	114	16.5	12.7
BASELINE 2	787	114	960	139	127	18.4	12.3
BASELINE AVERAGE	807	117	965	140	121	17.5	12.5
TA WELD 1(A)	839	121.7	983	143	105	15.2	4.7
TA WELD 2(A)	838	121.5	971	141	103	14.9	10.5
TA WELD 3(A)	837	121.4	981	142	107	15.5	14.3
TA WELD AVERAGE	838	121.5	978	142	105	15.2	9.8

(A) REPLICANTS OF TI-6AL-4V WELDED TO TANTALUM SHIM

Test Results. The goal of the Ti-6Al-4V/tantalum dissimilar metal weld study was to thoroughly characterize the homogeneity, structure, and properties of the weld, relative to a baseline Ti-6Al-4V weld, and to determine the effect of the tantalum additions. The study showed that the tantalum shim could be completely melted using the chosen welding procedure and that a uniform weld bead could be produced. The compositional and microstructural analyses showed that the weld was very similar to the baseline weld. The tantalum-alloyed weld metal appeared to be consistent with standard principles regarding titanium alloy compositions and structure, and it was what would be expected in a weld made on slightly more heavily alloyed material. The mechanical test results confirmed this interpretation as well. In total, the

characterization showed that this weld could be made and that its properties could be predicted and/or interpreted accurately as an extrapolation of the baseline weld.

Characterization Objectives. A number of characterization techniques have been briefly discussed with respect to their application to welds. Examples 1 and 2 show that the choice and emphasis of the characterization procedure are largely determined by the intended application of the weld and the goals to be accomplished by the characterization. Each of the procedures in Examples 1 and 2 are discussed in great detail in the cited references. Additional information is available in the Section "Joint Evaluation and Quality Control" in this Volume and in Ref 16, 17, and 22

References cited in this section

16. *MATERIALS CHARACTERIZATION,* 9TH ED., VOL 10, *METALS HANDBOOK,* AMERICAN SOCIETY FOR METALS, 1986
17. *MECHANICAL TESTING,* 9TH ED., VOL 8, *METALS HANDBOOK,* AMERICAN SOCIETY FOR METALS, 1985
20. STANDARD TEST METHOD FOR PLANE-STRAIN FRACTURE TOUGHNESS OF METALLIC MATERIALS, ASTM E 399, *ANNUAL BOOK OF ASTM STANDARDS,* ASTM, 1984
22. *WELDING, BRAZING, AND SOLDERING,* 9TH ED., VOL 6, *METALS HANDBOOK,* AMERICAN SOCIETY FOR METALS, 1983

Characterization of Welds

Craig B. Dallam, The Lincoln Electric Company; Brian K. Damkroger, Sandia National Laboratories

References

1. STANDARD WELDING TERMS AND DEFINITIONS, ANSI/AWS A3.0-89, AWS, 1989
2. WELD DISCONTINUITIES, *METALS HANDBOOK,* 9TH ED., VOL 6, AMERICAN SOCIETY FOR METALS, 1983, P 829-855
3. *WELDING HANDBOOK,* 8TH ED., VOL 2, AWS, 1987
4. *PROCEDURE HANDBOOK OF ARC WELDING,* 12TH ED., LINCOLN ELECTRIC CO., 1973
5. CODES, STANDARDS, AND INSPECTION, *METALS HANDBOOK,* 9TH ED., VOL 6, AMERICAN SOCIETY FOR METALS, 1983, P 823-838
6. *RADIOGRAPHY IN MODERN INDUSTRY,* 4TH ED., EASTMAN KODAK CO., 1980
7. WELDING OF PIPELINES AND RELATED FACILITIES, API STANDARD 1104, 17TH ED., AMERICAN PETROLEUM INSTITUTE, 1988
8. REFERENCE RADIOGRAPHS FOR STEEL WELDMENTS, ASTM E 390, ASTM
9. *STRUCTURAL WELDING CODE--STEEL,* ANSI/AWS D1.1-92, AWS, 1992
10. METALLOGRAPHY OF WELDMENTS, *METALS HANDBOOK,* 9TH ED., VOL 9, AMERICAN SOCIETY FOR METALS, 1985, P 577-586
11. K.E. EASTERLING, MICROSTRUCTURE AND PROPERTIES OF THE HAZ, *RECENT TRENDS IN WELDING SCIENCE AND TECHNOLOGY,* S. DAVID AND J. VITEK, ED., ASM INTERNATIONAL, 1990, P 177-188
12. WRC 1992 DIAGRAM, *WELD. J.,* MAY 1992, P 171
13. T.G.F. GRAY, J. SPENCE, AND T.H. NORTH, *RATIONAL WELDING DESIGN,* NEWNES-BUTTERWORTHS, 1975, P 111
14. R.H. ESPY, WELDABILITY OF NITROGEN-STRENGTHENED STAINLESS STEELS, *WELD. J. RES. SUPPL.,* VOL 61 (NO. 5), MAY 1982, P 149S-156S

15. METAL TEST METHODS AND ANALYTICAL PROCEDURES, *1991 ANNUAL BOOK OF ASTM STANDARDS,* VOL 03.05 AND 03.06, ASTM, 1991
16. *MATERIALS CHARACTERIZATION,* 9TH ED., VOL 10, *METALS HANDBOOK,* AMERICAN SOCIETY FOR METALS, 1986
17. *MECHANICAL TESTING,* 9TH ED., VOL 8, *METALS HANDBOOK,* AMERICAN SOCIETY FOR METALS, 1985
18. STANDARD METHODS OF TENSION TESTING OF METALLIC MATERIALS, ASTM E 8, *ANNUAL BOOK OF ASTM STANDARDS,* VOL 03.01, ASTM, 1984
19. *SPECIFICATION FOR CARBON STEEL ELECTRODES FOR SHIELDED METAL ARC WELDING,* ANSI/AWS A5.1-91, AWS, 1991
20. STANDARD TEST METHOD FOR PLANE-STRAIN FRACTURE TOUGHNESS OF METALLIC MATERIALS, ASTM E 399, *ANNUAL BOOK OF ASTM STANDARDS,* ASTM, 1984
21. STANDARD TEST METHOD FOR CRACK TIP OPENING DISPLACEMENT (CTOD) FRACTURE TOUGHNESS MEASUREMENT, ASTM E 1290, VOL 03.01, ASTM, 1989
22. *WELDING, BRAZING, AND SOLDERING,* 9TH ED., VOL 6, *METALS HANDBOOK,* AMERICAN SOCIETY FOR METALS, 1983

Introduction to Brazing and Soldering

Melvin M. Schwartz, Sikorsky Aircraft

Introduction

BRAZING AND SOLDERING require the application of a number of scientific and engineering skills to produce joints of satisfactory quality and reliability. Brazing employs higher temperatures than soldering, but the fundamental concepts are similar, particularly with respect to metallurgy and surface chemistry (Table 1). However, joint design, materials to be joined, filler metal and flux selection, heating methods, and joint preparation can vary widely between the two processes. Economic considerations involving filler metal and process technology are also varied, particularly in relation to automated techniques and inspection and testing. Brazing and soldering are performed in many industries, from exotic applications in the electronics and aerospace field to everyday plumbing applications.

TABLE 1 COMPARISON OF SOLDERING, BRAZING, AND WELDING

Parameter	**Process**		
	Soldering	**Brazing**	**Welding**
Joint formed	Mechanical	Metallurgical	Metallurgical
Filler metal melt temperature, °c (°f)	<450 (<840)	>450 (>840)[(a)]	>450 (>840)[(b)]
Base metal	Does not melt	Does not melt	. . .
Fluxes used to protect and to assist in wetting of base-metal surfaces	Required	Optional	Optional
Typical heat sources	Soldering iron; ultrasonics; resistance; oven	Furnace; chemical reaction; induction; torch; infared	Plasma; electron beam; tungsten and submerged arc; resistance; laser
Tendency to warp or burn	Atypical	Atypical	Potential distortion and warpage of base-metal likely
Residual stresses	. . .	. . .	Likely around weld area

(A) LESS THAN MELTING POINT OF BASE METAL.

Introduction to Brazing and Soldering

Melvin M. Schwartz, Sikorsky Aircraft

Brazing

Many products are assembled from two or more individual components that are often permanently joined to produce structurally sound assemblies. Joining methods include various fasteners, interference-type joints, adhesives, and, for the highest-integrity joints, the many techniques classified under welding. Brazing, although fundamentally indifferent from welding, is one such technique.

Early metalworkers, stimulated by a desire to produce structures that were difficult or impossible to build using methods then in existence, realized that it was possible to fill the joint between two metal pieces with molten metal and allow it to solidify. These artisans soon learned by experience that, in order to achieve adherence, the metals to be joined and the brazing filler metal had to be kept free of oxides and the filler metal had to have a lower melting point, and, furthermore, that a given filler metal would not necessarily adhere to all metals. From these basic requirements, brazing grew into a craft whose practitioners were well versed in what to do and what not to do in order to produce sound joints.

Just as the technique of brazing developed empirically, so did the lower-melting point filler metals. Workers first used lead and tin solders as well as silver and copper-arsenic ores, which were readily available and had low melting points. Later, the alloy brass was developed and found to be more desirable for joining copper, silver, and steel structures, because it provided higher-strength joints and could withstand higher temperatures.

Early silversmiths, probably wanting to produce white solder joints for aesthetic reasons, melted brass and silver together and found it to have an even lower melting point than brass, good adherence, and better corrosion resistance. Although innumerable combinations of silver, copper, and zinc subsequently evolved, primarily to meet melting-point requirements, these silver-brass, brass, and lead-tin alloys were essentially the only brazing and soldering filler materials available for generations.

Advantages of Brazing. Brazing has many distinct advantages, including the following:

- ECONOMICAL FABRICATION OF COMPLEX AND MULTI-COMPONENT ASSEMBLIES
- SIMPLE METHOD TO OBTAIN EXTENSIVE JOINT AREA OR JOINT LENGTH
- JOINT TEMPERATURE CAPABILITY APPROACHING THAT OF BASE METAL
- EXCELLENT STRESS DISTRIBUTION AND HEAT-TRANSFER PROPERTIES
- ABILITY TO PRESERVE PROTECTIVE METAL COATING OR CLADDING
- ABILITY TO JOIN CAST MATERIALS TO WROUGHT METALS
- ABILITY TO JOIN NONMETALS TO METALS
- ABILITY TO JOIN METAL THICKNESSES THAT VARY WIDELY IN SIZE
- ABILITY TO JOIN DISSIMILAR METALS
- ABILITY TO JOIN POROUS METAL COMPONENTS
- ABILITY TO FABRICATE LARGE ASSEMBLIES IN A STRESS-FREE CONDITION
- ABILITY TO PRESERVE SPECIAL METALLURGICAL CHARACTERISTICS OF METALS
- ABILITY TO JOIN FIBER- AND DISPERSION-STRENGTHENED COMPOSITES
- CAPABILITY FOR PRECISION PRODUCTION TOLERANCE
- REPRODUCIBLE AND RELIABLE QUALITY CONTROL TECHNIQUES

Strong, uniform, leakproof joints can be made rapidly, inexpensively, and even simultaneously. Joints that are inaccessible and parts that may not be joinable at all by other methods often can be joined by brazing. Complicated assemblies comprising thick and thin sections, odd shapes, and differing wrought and cast alloys can be turned into

integral components by a single trip through a brazing furnace or a dip pot. Metal as thin as 0.01 mm (0.0004 in.) and as thick as 150 mm (6 in.) can be brazed.

Brazed joint strength is high. The nature of the interatomic (metallic) bond is such that even a simple joint, when properly designed and made, will have strength equal to or greater than that of the as-brazed parent metal. The natural shapes of brazing fillets are excellent. The meniscus surface formed by the fillet metal as it curves across corners and adjoining sections is ideally shaped to resist fatigue. (It should be noted that in brazed joints using eutectic-type filler metal, fillets often contain an excessive amount of brittle intermetallic compounds. In fact, fillets are 5 to 10 times thicker than the joint and thus have a much higher volume of the liquid phase from which these brittle phases crystallize. Therefore, crack nucleation often originates in fillets.)

Complex shapes with greatly varied sections can be brazed with little distortion, and precise joining is comparatively simple. Unlike welding, in which the application of intense heat to small areas acts to move the parts out of alignment and introduces residual stresses, brazing involves fairly even heating and thus part alignment is easier.

Limitations of Brazing. A brazed joint is not a homologous body but rather is heterogeneous, composed of different phases with differing physical and chemical properties. In the simplest case, it consists of the base metal parts to be joined and the added filler metal. However, partial dissolution of the base metal, combined with diffusion processes, can change the composition and therefore the chemical and physical properties of the boundary zone formed at the interface between base metal and filler metal and often of the entire joint. Thus, in addition to the two different materials present in the simplest example given above, a complicated transitional or even completely different zone must be considered.

In determining the strength of such heterogeneous joints, the simplified concepts of elasticity and plasticity theory--valid for a homogeneous metallic body where imposed stresses are uniformly transmitted from one surface or space element to the adjacent ones--no longer apply. In a brazed joint formed of several materials with different characteristics of deformation resistance and deformation speed, the stresses caused by externally applied loads are nonuniformly distributed.

Mechanics of Brazing. Brazing involves a limited dissolution or plastic deformation of the base metal (Ref 1). Brazing comprises a group of joining processes in which coalescence is produced by heating to a suitable temperature above 450 °C (840 °F) and by using a ferrous or nonferrous filler metal that must have a liquidus temperature above 450 °C (840 °F) and below the solidus temperature(s) of the base metal(s). The filler metal is distributed between the closely fitted surfaces of the joint. Brazing is distinguished from soldering in that soldering employs a filler metal having a liquidus below 450 °C (840 °F) (Table 1).

Brazing proceeds through four distinct steps:

- THE ASSEMBLY OR THE REGION OF THE PARTS TO BE JOINED IS HEATED TO A TEMPERATURE OF AT LEAST 450 °C (840 °F).
- THE ASSEMBLED PARTS AND BRAZING FILLER METAL REACH A TEMPERATURE HIGH ENOUGH TO MELT THE FILLER METAL (FOIL, WIRE, PASTE, PLATINGS, ETC.) BUT NOT THE PARTS.
- THE MOLTEN FILLER METAL, HELD IN THE JOINT BY SURFACE TENSION, SPREADS INTO THE JOINT AND WETS THE BASE METAL SURFACES.
- THE PARTS ARE COOLED TO SOLIDITY, OR "FREEZE," THE FILLER METAL, WHICH IS HELD IN THE JOINT BY CAPILLARY ATTRACTION AND ANCHORS THE PARTS TOGETHER BY METALLURGICAL REACTION AND ATOMIC BONDING.

Brazing Versus Other Welding Processes. The mere fact that brazing does not involve any substantial melting of the base metals offers several advantages over other welding processes. It is generally possible to maintain closer assembly tolerances and to produce a cosmetically neater joint without costly secondary operations. Even more important, however, is that brazing makes it possible to join dissimilar metals (or metals to ceramics) that, because of metallurgical incompatibilities, cannot be joined by traditional fusion welding processes. If the base metals do not have to be melted to be joined, it does not matter that they have widely different melting points. Therefore, steel can be brazed to copper as easily as to another steel.

Brazing also generally produces less thermally induced distortion, or warping, than fusion welding. An entire part can be brought up to the same brazing temperature, thereby preventing the kind of localized heating that causes distortion in welding.

Finally, and perhaps most important to the manufacturing engineer, brazing readily lends itself to mass production techniques. It is relatively easy to automate, because the application of heat does not have to be localized, as in fusion welding, and the application of filler metal is less critical. In fact, given the proper clearance conditions and heat, a brazed joint tends to "make itself" and is not dependent on operator skill, as are most fusion welding processes.

Automation is also simplified by the fact that there are many means of applying heat to the joint, including torches, furnaces, induction coils, electrical resistance, and dipping. Several joints in one assembly often can be produced in one multiple-braze operation during one heating cycle, further enhancing production automation.

As noted in Table 1, essentially no melting of the base metal occurs in brazing; however, the temperatures involved can affect the properties of the metals being joined. For example, base metals whose mechanical properties were obtained by cold working may soften or undergo grain growth if the brazing temperature is above their recrystallization temperatures. Mechanical properties obtained by heat treatment may be altered by the heat of brazing. On the other hand, materials in the annealed condition are usually not altered by brazing.

As with other welding processes, brazing produces a heat-affected zone (HAZ) with a strongly altered microstructure due to intensive mutual mass transfer between base metal and filler metal. The width of this zone varies with the heating process used. In torch and induction brazing, for example, only a localized zone is heated; in france and dip brazing, the entire part is subjected to the brazing temperature. As a rule, the HAZ produced during brazing is wider and less sharply defined than those resulting from other fusion-related processes.

Several elements of the brazing process must be understood in order to produce satisfactory brazed joints:

- FILLER METAL FLOW
- BASE METAL CHARACTERISTICS
- FILLER METAL CHARACTERISTICS
- SURFACE PREPARATION
- JOINT DESIGN AND CLEARANCE
- TEMPERATURE AND TIME
- RATE AND SOURCE OF HEATING

Each of these topics is discussed in detail in the article "Fundamentals of Brazing" in this Volume.

Reference cited in this section

1. E. LIEBERMAN, *MODERN SOLDERING AND BRAZING TECHNIQUES*, BUSINESS NEWS PUBLICATIONS, 1988

Introduction to Brazing and Soldering

Melvin M. Schwartz, Sikorsky Aircraft

Soldering

Like brazing and other joining processes, soldering involves several fields of science, including mechanics, chemistry, and metallurgy. Soldering is a simple operation (Ref 2), consisting of the relative placement of the parts to be joined, wetting the surfaces with molten solder, and allowing the solder to cool until it has solidified.

Soldering in the field of electronics is in many respects different from soldering in other branches of industry. Although the physical principles of all soldering (and brazing) processes are the same, the features specific to their use in electronics are so numerous that it is possible to speak of soldering in electronics as a separate subject.

Soldering Versus Other Joining Technologies. Soldering has several clear advantages over competitive joining techniques, such as welding or bonding with conductive adhesives:

- THE SOLDER JOINT FORMS ITSELF BY THE NATURE OF THE FLOW, WETTING, AND SUBSEQUENT CRYSTALLIZATION PROCESS, EVEN WHEN THE HEAT AND THE SOLDER ARE NOT DIRECTED PRECISELY TO THE PLACES TO BE SOLDERED. BECAUSE SOLDER DOES NOT ADHERE TO INSULATING MATERIALS, IT OFTEN CAN BE APPLIED IN EXCESS QUANTITIES, IN CONTRAST TO CONDUCTIVE ADHESIVES. THE SOLDERING TEMPERATURE IS RELATIVELY LOW, SO THERE IS NO NEED FOR THE HEAT TO BE APPLIED LOCALLY AS IN WELDING.
- SOLDERING ALLOWS CONSIDERABLE FREEDOM IN THE DIMENSIONING OF JOINTS, SO THAT IT IS POSSIBLE TO OBTAIN GOOD RESULTS EVEN IF A VARIETY OF COMPONENTS ARE USED ON THE SAME PRODUCT.
- THE SOLDERED CONNECTIONS CAN BE DISCONNECTED IF NECESSARY, THUS FACILITATING REPAIR.
- THE EQUIPMENT FOR BOTH MANUAL SOLDERING AND MACHINE SOLDERING IS RELATIVELY SIMPLE.
- THE SOLDERING PROCESS CAN BE EASILY AUTOMATED, OFFERING THE POSSIBILITY OF IN-LINE ARRANGEMENTS OF SOLDERING MACHINES WITH OTHER EQUIPMENT.

Mass soldering by wave, drag, or dip machines has been the preferred method for making high-quality, reliable connections for many decades. Despite the appearance of new connecting systems, it still retains this position. Correctly controlled, soldering is one of the least expensive methods for fabricating electrical connections. Incorrectly controlled, it can be one of the most costly processes--not because of the initial cost, but because of the many far-reaching effects of poor workmanship.

Chronology of Soldering. Soldering is not a new process (Ref 2). It probably dates to the Bronze Age, when some metalworker discovered the affinity of a tin-lead mixture for a clean copper surface. As recorded in the writings of Pliny, the Romans used 60Sn-40Pb mixture to solder their lead water pipes.

During the late 19th and early 20th centuries, a great deal of work was devoted to the development and improvement of the soldering process and to the determination of the fundamental principles involved. Examination of the books, papers, and especially the patents of the era shows that soldering as a science was clearly understood long before the start of the electronics industry. There has certainly been a great improvement in the materials and machines used in the process, but the basics have changed little since the early part of this century.

Soldering in the electronics field has undergone many dramatic changes since the first radios were built. Between the 1920s and the 1940s, all interconnections were made using the point-to-point wiring method, and the solder joints were made using soldering irons. After World War II (Ref 3, 4), the demand for consumer electronics began to increase, and by the 1950s a mass market had developed. To meet this demand, the first mass soldering technique, dip soldering, was used with boards that were the precursors of printed wiring boards (PWBs). By the late 1950s, wave soldering had been developed in England and soon thereafter reached the United States. This development was necessitated by the introduction of PWBs. Wave soldering continued to be the method of choice through the 1980s and is still widely used.

The development and maturation of the multi-layer PWB and the first major effort toward miniaturization occurred in the 1970s. The dual inline integrated circuit package replaced many discrete components. By the early 1980s, the pressure to increase component densities had grown to such a degree that a new technique for attachment was needed, and surface mounting was developed. Surface mount technology in turn required new ways to make solder joints, prompting the development of vapor phase, infrared, hot gas, and other reflow soldering techniques.

Soldering remains the attachment method of choice in the evolving electronics industry. It is the only metallurgical joining technique suitable for the mass manufacture of electronic and electrical interconnections within the temperature restrictions of electronic components and substrates.

Solder Metals. The solder metal business has changed dramatically, having moved from merely producing wire to producing bulk, preform, and paste in order to meet the needs of soldering techniques. Solder can be applied in several ways (Ref 2, 3):

- A MIXTURE OF SOLDER POWDER AND FLUX, KNOWN AS SOLDER PASTE (REF 5), CAN BE APPLIED TO THE JOINTS BY SCREENING, STENCILING, OR USING ONE OF THE MACHINES THAT APPLIES DOTS OF THE PASTE BY A SIMPLE PNEUMATIC SYSTEM. THIS METHOD IS ESPECIALLY USEFUL WHERE SURFACE-MOUNTED COMPONENTS ARE TO BE SOLDERED AND CANNOT BE PASSED THROUGH THE SOLDER WAVE.
- PARTS CAN BE PRETINNED, THAT IS, COATED WITH A LAYER OF SOLDER BY FLUXING AND DIPPING INTO A BATH OF THE MOLTEN METAL.
- SOLDER CAN BE OBTAINED IN THE SHAPE OF RINGS, WASHERS, OR TUBES, WHICH ARE PLACED ON OR ADJACENT TO THE PARTS TO BE JOINED. THESE SOLDER PREFORMS CAN BE OBTAINED WITH OR WITHOUT A FLUX COATING.

The two latter methods of providing solder for the joint are used in many areas of the electronics industry where machine soldering is not possible. Tiny solder rings are placed over long wire wrap pins on a mother board, where the gold plating of the pins in the wrapping area must not be coated with solder. Solder washers are fitted under bolts that must be soldered to a ground plane. Wires and tinned before soldering into a pretinned wiring lug. The possibilities are seemingly limitless (Ref 6).

Solder filler metals have also changed. The first electronic soldering was done with the 50Sn-50Pb solder material used by plumbers. By the 1950s, the choice of materials had switched to eutectic tin-lead solders to counter the problems created by a vibrating wave solder machine conveyor. Today a wide range of filler materials is used in the electronics industry. With the spread of electronics technology into every facet of life, the environmental and materials demands have grown substantially, requiring the use of such specialized materials as indium and gold-tin fillers.

Flux technology has also evolved (Ref 3, 5). As a result of the restraints of military and government specifications, the emphasis has been on the addition of new flux types rather than on the replacement of old ones. Extensive work has been done with organic acids, which enlarge the processing windows. Other categories include synthetic activated materials, which are non-rosin fluorocarbon solvent-removable types, and low solids fluxes for surface mounting that can be used instead of the classic fully activated rosin formulations.

Other materials, such as adhesives for the surface mounting of components intended for wave soldering, are new to soldering technology. These materials must be specially designed to avoid interference with the soldering process, yet must remain intact through the solvent action of fluxes and, often, flux removal.

Mass Soldering. With the introduction of mass soldering techniques (Ref 1, 6), the issue of solderability has become one of the major interest. Mass production processes are not as tolerant as the hand soldering process. In addition, modern components cannot withstand as much heat, as for example, a tube socket. Lower soldering temperatures and less mechanical working have made it necessary to attain the highest solderability to ensure a metallurgically sound and reliably solder joint.

Machine or mass soldering (Ref 2, 4, 6) can make thousands of joints in a few seconds, providing the electrical connections and simultaneously mechanically fastening the components. No other process has yet been developed that can so economically interconnect electronic circuitry.

Wave Soldering. From the original concept of hand dipping boards came the idea of pumping solder through a slot or nozzle to form a wave, or mound, of constantly moving, dross-free metal through which the board could be passed. This offered several advantages: the surface of the solder was always clean and did not require skimming, the pumping action maintained an even temperature, and the raised wave provided an easy form for adding a conveyor system for automatic movement of the board over the solder.

Once the idea of the solder wave had been born, it was logical to use a similar method to apply the flux, and the basic soldering machine appeared. These original machines were quite crude, consisting of individual modules with a freestanding conveyor (often added by the user) placed over them. There was little attempt to integrate the parts into one system, and the smoke and fumes were left to escape into the factory exhaust, aided by a makeshift canopy hung over the machine.

Much work was done on the development of the actual wave in an attempt to improve the speed of soldering and to reduce the incidence of shorts and icicles. The solder weir, the double wave, and the cascade all experienced brief popularity. The cascade wave, which consists of several waves in series, was one of the more interesting of these developments. It was used with an inclined conveyor and was the basis of machines built for in-house use by several manufacturers. However, it never achieved great popularity.

Another development was the use of ultrasonics to form a wave, with the intention of causing cavitation at the joint of avoiding the use of flux, or at least reducing the activity required. Some experimental machines were built, but the cost was excessive, the soldering results were no better than those produced with the conventional pumped wave, and the power of the ultrasonic energy had to be so high that the matching horns used to energize the pot were quickly eroded away. With the advent of the semiconductor, ulrasonics were found to cause occasional damage to the devices. Today the main use for ultrasonics in the soldering industry is to be found in the pots used for tinning components prior to assembly. This era also saw the introduction of oil into the solder wave. This idea worked extremely well and has been a feature of some soldering machines for many years (Fig. 1) (Ref 2, 3, 4, 5, 6, 7).

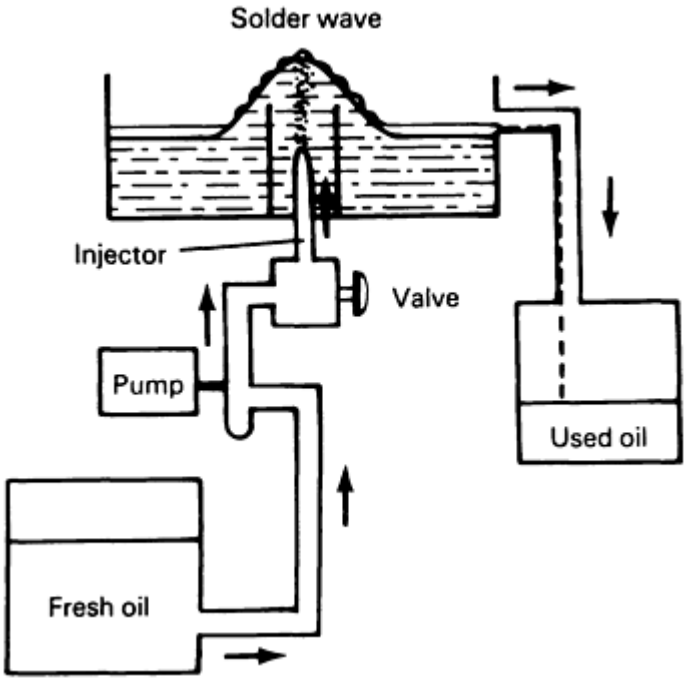

FIG. 1 SCHEMATIC SHOWING SIMPLE OIL INJECTION OF A SOLDER WAVE

Drag Soldering. In a totally different direction, the static solder bath soldering process, or drag soldering, was developed, and machines were designed using this principle (Fig. 2). These machines have been developed to a high level of sophistication, initially in Europe and Japan and later in the United States. As has often been the case in the growth of the soldering machine industry, initial developments were prompted because of patent restrictions that at the time prevented the free use of the more conventional solder wave. These restrictions have often proved beneficial to the industry by forcing creative thinking that has eventually resulted in improved products (Ref 2, 3, 4, 5, 6).

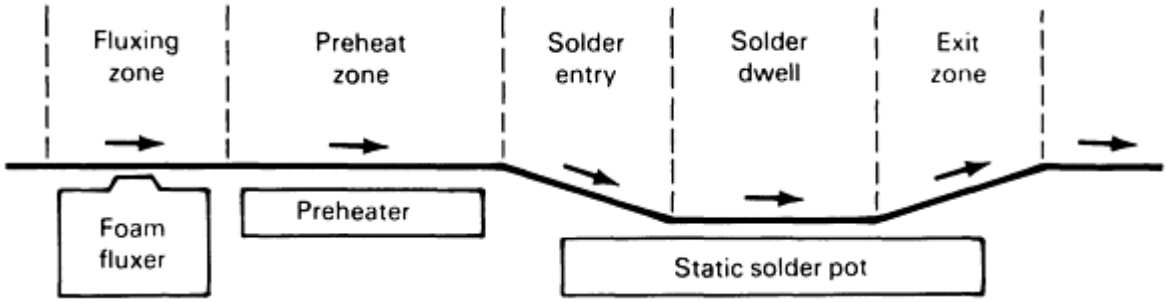

FIG. 2 SCHEMATIC SHOWING SEQUENCE OF OPERATIONS FOR A DRAG SOLDERING MACHINE

Current Technology. Today machines are available from many different manufacturers, each with its own particular features. These machines have various levels of sophistication and capability, ranging from small laboratory units to high-production systems, often complete with in-line cleaning and assembly and return conveyors. Machines in use today are generally self-contained, with a high degree of control, optional auxiliary systems, and exhaust venting. Coming onto the market are systems with computer-controlled operation and setup, which practically eliminate human error from the machine soldering process.

Soldering processes have evolved dramatically since the introduction of mass soldering techniques. Wave machines have become highly specialized, especially since the introduction of surface-mount technology. Reflow techniques (Ref 8), which were once limited to hybrid technology and leaded flatpacks, have grown remarkably. Vapor phase, infrared, and hot gas soldering equipment have initiated a new process of evolution.

The performance of a solder joint in its service environment is a strong consideration in modern electronics. Many applications, such as jet engines, dishwashers, and automobiles, impose a repeated cyclic thermal cycle on the equipment. This produces thermomechanical strains, which result in fatigue or creep failure if the joint design is poor or if life predictions have been incorrectly calculated. Each situation must be carefully analyzed and the correct design employed for the equipment to fulfill its intended service life.

Thermally induced fatigue and creep failures, virtually unknown in the 1950s but common today, are illustrative of the added stresses and strains placed on joints. It should be emphasized that miniaturization of electronic parts, particularly current paths, results in a dramatic increase in current density, which generates strong thermal and mechanical shocks upon switching. Proper design can minimize these strains and make the joints more highly producible. Design has become even more critical with the introduction of surface-mount technology.

Quality Control. Once a joint is made, its quality must be assessed through inspection. Advanced technology has produced some electronic assembly designs that are impossible to inspect visually, and an entire group of automated inspection tools has thus evolved. These tools include radiography, infrared signature, and two- or three-dimensional vision systems. Most of these are aided with very sophisticated computer software. The role of inspection, which historically was to locate those joints that needed rework, is changing along with the technology. Inspection is now used as a process-control audit to locate those portions of the process that need improvement or should returned to a position within the control limits. Therefore, the emphasis has shifted from merely shipping an acceptable product to manufacturing it correctly the first time.

Future Trends. Several other technologies and materials for soldering are being developed and tested (Ref 2, 3, 4, 5). One process that is becoming widely used is condensation, or vapor phase, soldering. In this process, the vapor from a liquid with a high-temperature boiling point is allowed to condense on the items to be soldered and, in giving up the latent heat of vaporization, quickly and evenly raises their temperature and produces a sound soldered joint. The method is simple, clean, and extremely well controlled. It requires-special equipment, and, of course, the parts are all exposed to the same temperature.

In another method, the parts are dipped into an oil heated above the melting point of the solder. Peanut oil can be used, although several excellent synthetic products are available. Here again, the component parts are subjected to the same temperature as the joint. This is a messy process, and the parts must be cleaned after soldering to remove the oil.

Infrared heating is a useful method for producing the temperature necessary for soldering. The shorter wavelengths can be focused onto very small areas, allowing selective heating of the joints to be soldered, without subjecting nearby components to the soldering temperature. Equipment and tooling are expensive if complex assemblies have to be soldered, and the relative emissivity of the joint metals and the adjacent materials can cause processing problems. For example, the base laminate of a PWB can be burned before the joint to be soldered has even reached the soldering temperature. This process thus requires very careful control.

Resistance heating can be used for soldering in two ways. The first method passes a current through the parts of the joint, causing their temperature to rise by virtue of the resistance existing in the joint structure. This is not a very controllable process and is primarily used for less critical applications on large connections. The second method passes a current through a wire that is shaped to touch the parts to be heated. Despite the lack of precise control, the process is often used to solder the leads on surface-mounted components.

Lasers have been used to provide the heat for soldering, although this is not yet a common method. A laser can provide a very high-energy, small-area beam, and heating is therefore extremely fast, localized, and limited only by the ability of the joint materials to absorb this energy. However, the shiny metal surfaces in the joint reflect most of the energy of the commonly used lasers, and coupling the laser and the joint is a major problem. The soldering flux is often used as a coupling medium. When correctly set up, laser soldering offers a fast, clean method of making joints. The cost of the equipment is quite high.

Since 1980, significant improvements and innovations in the soldering arena with respect to materials, equipment, and processes have occurred. However, two main tasks remain: developing environmentally friendly solder materials and establishing failure-free solder joint technology (Ref 2, 3, 4, 6, 7, 8).

For solders and soldering, two issues that are directly related to environmental concerns are the replacement of chlorofluorocarbon (CFCs) as the primary cleaning agent for electronic assemblies and the feasibility of using alternatives to lead-containing solders. For electronic assembly solders (Ref 4), in addition to using CFC substitutes and other solvents (e.g., hydrocarbon-based systems), aqueous cleaning and "no-clean" setups are two viable solutions.

The other task to be accomplished is the development of failure-free solder joint technology. Strengthened solder materials are expected to possess the properties that impede the occurrence of undesirable metallurgical phenomena during their service life under various in-circuit and external conditions, particularly temperature and induced stresses. Three approaches are being examined: macroscopic blends of selected fillers in a tin-rich matrix (composite solder), microscopic incorporation of doping additives to tin-rich base material, and atomic-level interaction. Preliminary experiments have been carried out to accomplish the first approach. Figure 3 demonstrates the increased yield strength of the 63Sn-37Pb composite solder with various amounts of filler (Ref 9).

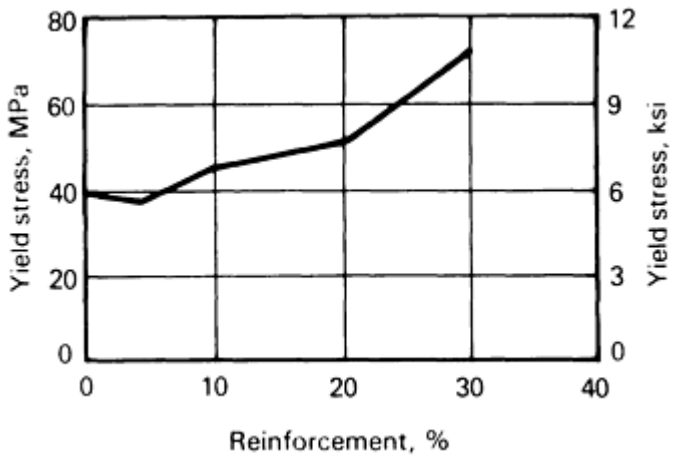

FIG. 3 EFFECT OF FILLER REINFORCEMENT ON THE YIELD STRENGTH OF 63SN-37PB COMPOSITE SOLDER. SOURCE: REF 9

The intrinsic properties of the new materials are expected to possess the following characteristics, while maintaining thermal and electrical conductivities:

- STABLE MICROSTRUCTURE
- INCREASED THERMAL AND MECHANICAL FATIGUE RESISTANCE
- HIGH CREEP RESISTANCE
- DECREASED THERMAL EXPANSION COEFFICIENT

These aggregate characteristics constitute the "strengthened" solder materials that are able to withstand harsher application conditions. The reduced thermal expansion coefficient of these new solders is expected to be more compatible with that of state-of-the-art electronic components and with ceramic substrates.

With respect to quality, solder joints have historically been judged by visual criteria. However, due to the nature of solder materials and the effect of the solder joint-forming process on appearance, many serviceable solder joints are often rejected, while other potentially questionable joints are accepted to carry out critical missions. This not only adds to manufacturing costs, but can also jeopardize service performance. Strengthened solder joints are expected to relieve the necessity of on-line inspection and rework while also reducing manufacturing costs and enhancing life span and tolerance of harsh service conditions in many military applications.

References cited in this section

1. E. LIEBERMAN, *MODERN SOLDERING AND BRAZING TECHNIQUES,* BUSINESS NEWS PUBLICATIONS, 1988
2. R.J. KLEIN WASSINK, *SOLDERING IN ELECTRONICS,* ELECTROCHEMICAL PUBLICATIONS, 1989
3. H.H. MANKO, *SOLDERS AND SOLDERING,* 2ND ED., MCGRAW-HILL 1964
4. L.P. LAMBERT, *SOLDERING FOR ELECTRONIC ASSEMBLIES,* MARCEL DEKKER, 1987
5. H.H. MANKO, SOLDERING FLUXES--PAST AND PRESENT *WELD. J.*, VOL 52 (NO. 3), 1973, P 163-166
6. R.W. WOODGATE, *THE HANDBOOK OF MACHINE SOLDERING,* 2ND ED., JOHN WILEY & SONS, 1988
7. T.J. NEILLO, "AN APPROACH TO SOLDERING IN THE AUTOMATED FACTORY," SME SOLDERING TECH. CONF., SME MS 91-288, MAY 1991
8. T. ROBERTS, "CONDUCTIVE REFLOW SOLDERING," SME SOLDERING TECH. CONF., SME MS 91-290, MAY 1991
9. J.S. HWANG, *ET AL.,* FUTURISTIC SOLDERS, *SURF. MOUNT. TECHNOL.,* SEPT 1991, P 40-43

Introduction to Brazing and Soldering

Melvin M. Schwartz, Sikorsky Aircraft

References

1. E. LIEBERMAN, *MODERN SOLDERING AND BRAZING TECHNIQUES,* BUSINESS NEWS PUBLICATIONS, 1988
2. R.J. KLEIN WASSINK, *SOLDERING IN ELECTRONICS,* ELECTROCHEMICAL PUBLICATIONS, 1989
3. H.H. MANKO, *SOLDERS AND SOLDERING,* 2ND ED., MCGRAW-HILL 1964
4. L.P. LAMBERT, *SOLDERING FOR ELECTRONIC ASSEMBLIES,* MARCEL DEKKER, 1987
5. H.H. MANKO, SOLDERING FLUXES--PAST AND PRESENT *WELD. J.*, VOL 52 (NO. 3), 1973, P 163-166
6. R.W. WOODGATE, *THE HANDBOOK OF MACHINE SOLDERING,* 2ND ED., JOHN WILEY & SONS,

1988
7. T.J. NEILLO, "AN APPROACH TO SOLDERING IN THE AUTOMATED FACTORY," SME SOLDERING TECH. CONF., SME MS 91-288, MAY 1991
8. T. ROBERTS, "CONDUCTIVE REFLOW SOLDERING," SME SOLDERING TECH. CONF., SME MS 91-290, MAY 1991
9. J.S. HWANG, *ET AL.*, FUTURISTIC SOLDERS, *SURF. MOUNT. TECHNOL.*, SEPT 1991, P 40-43

Fundamentals of Brazing

Mel M. Schwartz, Sikorsky Aircraft

Introduction

BRAZING is a process for joining solid metals in close proximity by introducing a liquid metal that melts above 450 °C (840 °F). A sound brazed joint generally results when an appropriate filler alloy is selected, the parent metal surfaces are clean and remain clean during heating to the flow temperature of the brazing alloy, and a suitable joint design is used. Like the other joining processes, brazing encompasses a variety of scientific disciplines (for example, mechanics, physics, and chemistry).

Recently, the demands of more-sophisticated structures have forced technicians and engineers to encourage metal producers to apply their metallurgical knowledge to produce brazing filler metals that meet more-specific needs. To ensure the production of good brazed joints, the technicians and engineers also had to appeal to mechanical engineers for improved joint design, to chemical engineers for solutions to corrosion problems, and to metallurgists and ceramists for proper material selection.

Brazing has been embraced by the engineering community and has now reached a very successful plateau within the joining field. This has come about because of the:

- DEVELOPMENT OF NEW TYPES OF BRAZING FILLER METALS (RAPID SOLIDIFICATION AMORPHOUS FOILS AND TITANIUM-ADDED FILLER METALS FOR CERAMIC JOINING
- AVAILABILITY OF NEW FORMS AND SHAPES OF FILLER METALS
- INTRODUCTION OF AUTOMATION THAT HAS BROUGHT BRAZING PROCESSES TO THE FOREFRONT IN HIGH-PRODUCTION SITUATIONS
- INCREASED USE OF FURNACE BRAZING IN A VACUUM, AS WELL AS ACTIVE AND INERT-GAS ATMOSPHERES

Since the early 1980s, other developments, such as aluminum-clad foils for fluxless aluminum brazing, copper-nickel-titanium filler metals for brazing titanium and some of its alloys, cadmium-free silver filler metals, and vacuum-grade metal brazing foils, have evolved to be used in production applications.

Fundamentals of Brazing

Mel M. Schwartz, Sikorsky Aircraft

Physical Principles

Capillary flow is the dominant physical phenomenon that ensures good brazements when both faying surfaces to be joined are wet by the molten filter metal. The joint must be properly spaced to permit efficient capillary action and coalescence. More specifically, capillarity is a result of the relative attraction of the molecules of the liquid to each other and to those of the solid. In actual practice, brazing filler metal flow characteristics are also influenced by dynamic considerations involving fluidity, viscosity, vapor pressure, gravity, and, especially, by the effects of any metallurgical reasons between the filler metal and the base metal.

Capillary attraction makes the brazing of leak-tight joints a simple proposition. In a properly designed joint, the molten brazing filler metal is normally drawn completely through the joint area without any voids gaps when processed in a protective atmosphere. Solidified joints will remain intact and gas will remain tight under heavy pressures, even when the joint is subjected to shock or vibrational type of loading. Capillary attraction is also the physical force that governs the action of a liquid against solid surfaces in small, confined areas.

The phenomena of wetting and spreading are very important to the formation of brazed joints. Other significant factors that also must be considered include the condition of the solid surface in terms of the presence of oxide films and their effects on wetting and spreading, surface roughness, alloying with between the brazing filler metal and base metal, and the extent to which alloying is affected by the thermodynamic properties of the brazing atmosphere. A number of studies (Ref 1, 2) have been conducted on surface activation, contact angle, equilibrium, and surface energies. Some of these alloy systems have a finite contact angle that is thermodynamically unstable, because the solid-vapor surface energy exceeds the sum of the liquid-solid surface energies, that is, an alloy system in which thermodynamics would predict complete spreading. In actual fact, spreading may or may not occur in this type of alloy system, and the rate of spreading can be markedly dependent on surface chemistry.

Wetting is, perhaps, best explained by the following example. If a solid is immersed in a liquid bath and wetting occurs, then a thin continuous layer of liquid adheres to the solid when it is removed from the liquid (Fig. 1). Technically, the force of adhesion between the solid and liquid (during the wetting process) is greater than the cohesive force of the liquid. In practical terms, with respect to brazing, wetting implies that the liquid brazing filler metal spreads on the solid base metal, instead of balling up on its surface. It has been demonstrated that wetting actually depends on a slight surface alloying of the base metal with the brazing filler metal. Lead, for example, does not alloy with iron and will not wet it. Tin, on the other hand, does form an alloy with iron, and, therefore, a tin-lead solder will wet steel.

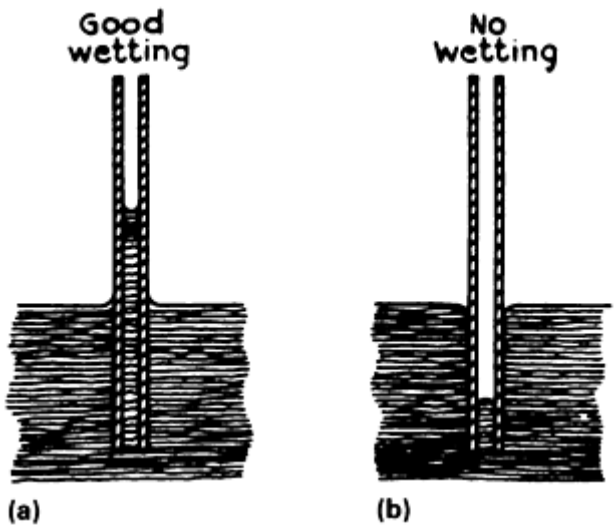

FIG. 1 SCHEMATIC SHOWING PRINCIPLE OF CAPILLARY ATTRACTION FOR SELECTED LIQUIDS WHEN THE LIQUID IS SANDWICHED BETWEEN TWO CLEAN GLASS PLATES. (A) WHEN IMMERSED IN WATER OR INK, A COLUMN WILL RISE BETWEEN THE PLATES BECAUSE OF WETTING. (B) WHEN THE PLATES ARE IMMERSED IN MERCURY, NO WETTING OCCURS AND THE COLUMN IS DEPRESSED. IF PARAFFIN PLATES ARE USED IN PLACE OF THE GLASS PLATES, IMMERSION OF THE PLATES IN MERCURY WILL PRODUCE WETTING.

A comprehensive theory of the wetting or spreading of liquids on solid surfaces and a complete and detailed derivation of the quantitative relationships are presented by Harkins (Ref 3) and Schwartz (Ref 4).

Experimentally, it has been observed that liquids placed on solid surfaces usually do not completely wet, but, rather, remain as a drop that has a definite contact angle between the liquid and solid phases (Ref 5). This condition is illustrated in Fig. 2. The Young and Dupré equation (Eq 1) permits the determination of change in surface free energy, ΔF, accompanying a small change in solid surface covered, ΔA (Ref 5). Thus,

$$\frac{\partial F}{\partial A}_{p,T} = g_{LV} + g_{SL} - g_{SV} \qquad \textbf{(EQ 1)}$$

where γ_{LV} is the liquid-vapor surface energy, γ_{SL} is the solid-liquid surface energy, and γ_{SV} is the solid-vapor surface energy.

$$\Delta F = \Delta A\,(\gamma_{SL} - \gamma_{SV}) + \Delta A \gamma_{LV}\,\mathrm{COS}\,(\theta - \Delta\theta) \qquad \textbf{(EQ 2)}$$

At equilibrium,

$$\lim_{\Delta A \to \Delta 0} \frac{\Delta F}{\Delta A} = 0 \qquad \textbf{(EQ 3)}$$

and

$$\gamma_{SL} - \gamma_{SV} + \gamma_{LV}\,\mathrm{COS}\,\theta = 0 \qquad \textbf{(EQ 4)}$$

or

$$\gamma_{SL} = \gamma_{SV} - \gamma_{LV}\,\mathrm{COS}\,\theta \qquad \textbf{(EQ 5)}$$

In Eq 4 and 5, it can be seen that θ is greater than 90° (1.6 rad) when γ_{SL} is larger than γ_{SV}, as shown in Fig. 3, and the liquid drop tends to spheroidize.

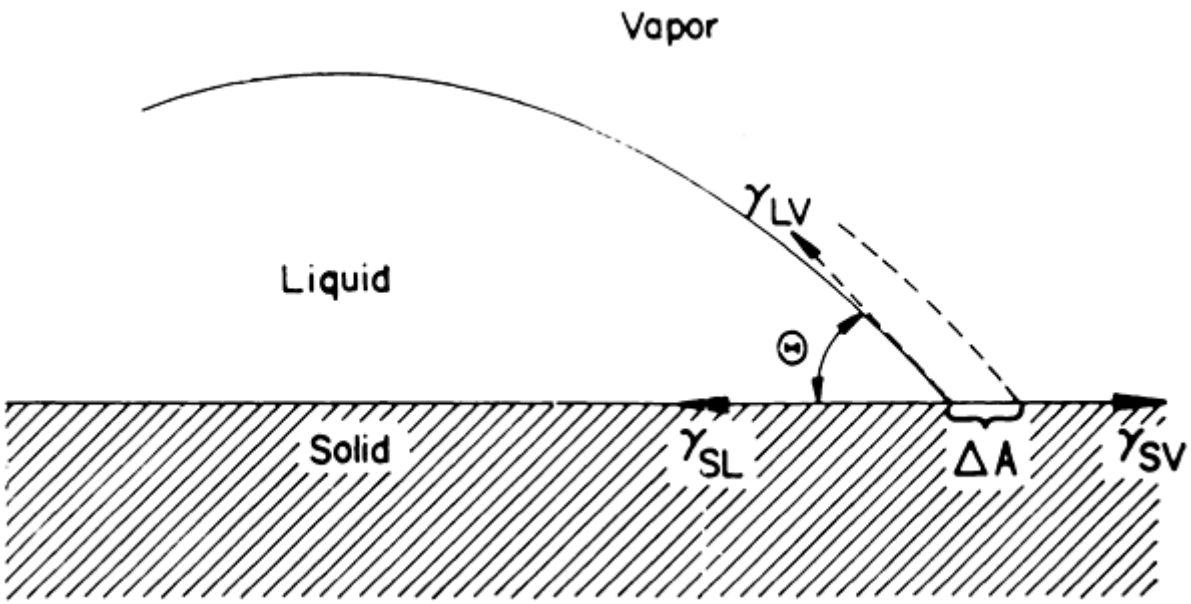

FIG. 2 SESSILE DROP LOCATED ON A SURFACE AND DIRECTIONS OF VECTORS OF THE SURFACE ENERGIES FOR THE SYSTEM

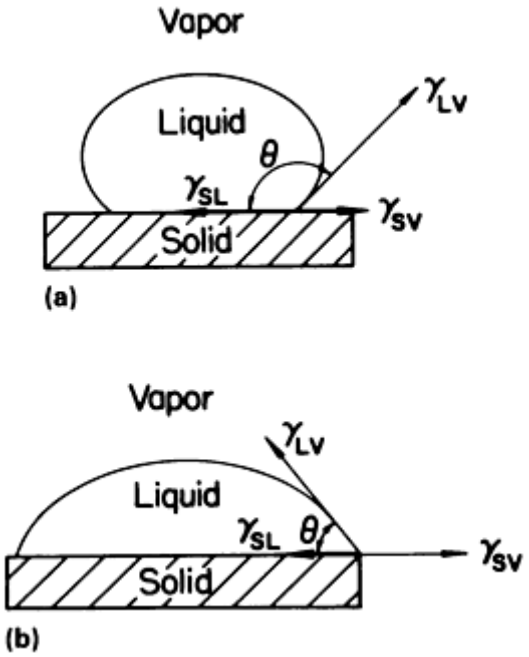

FIG. 3 EFFECT OF INTERFACIAL ENERGIES ON SESSILE DROPS. (A) NO WETTING TAKES PLACE WHEN CONTACT ANGLE IS > 90°. (B) WETTING OCCURS WHEN CONTACT ANGLE IS < 90°.

The contact angle, θ, is less than 90° (1.6 rad) when the reverse is true, as shown at right in Fig. 3, and the liquid drop flattens out and wets the solid. If the balance in such that θ is zero (0 rad) and greater wetting is desired, θ should be as small as possible so that cos θ approaches unity and the liquid spreads over the solid surface.

These considerations show the importance of surface energies in brazing. If brazing filler metal is to successfully form a joint, it must wet the solid material. The surface-energy balance must be such that the contact angle is less than 90° (1.6 rad). The energy equation shows that if θ is to be less than 90° (1.6 rad) (cos θ > 0), then γ_{SV} must be greater than γ_{SL}. This is demonstrated in Table 1, which gives contact-angle measurements of several liquid metals on beryllium at various test temperatures in argon and vacuum.

TABLE 1 CONTACT ANGLES OF SELECTED LIQUID METALS ON BERYLLIUM AT VARIOUS TEST TEMPERATURES IN ARGON AND VACUUM ATMOSPHERES

SYSTEM	ATMOSPHERE	TEMPERATURE		CONTACT ANGLE, DEGREES, AT INDICATED ELAPSED TIME				
		°C	°F	0 s	15 s	45 s	90 s	150 s
AG	VACUUM	1010	1850	142.2	141.1	140.6	141.2	140.2
		1060	1940	135.4	135.6	131.4	133.2	127.9
	ARGON	1010	1850	148.1	148.9	150.7	147.3	143.3
		1060	1940	61.0	59.9	57.2	54.4	52.6
AU	VACUUM	1070	1958	58.6	58.0	57.2	55.7	54.6
	ARGON	1070	1958	57.3	56.6	57.9	56.9	55.9
CU	VACUUM	1108	2026	129.0	128.5	124.2	124.1	123.6
		1133	2071	126.6	122.5	121.8	120.0	120.0
	ARGON	1108	2026	EXTREME BASE-METAL SOLUTION				
		1133	2071	EXTREME BASE-METAL SOLUTION				
GE	VACUUM	1000	1832	145.5	145.3	144.3	143.7	143.6
		1050	1922	102.9	100.0	100.9	96.1	95.4
	ARGON	1000	1832	99.3	99.6	98.8	98.2	97.1

		1050	1922	89.2	89.2	88.9	87.1	87.1
PD-2.1BE	VACUUM	980	1796	77.0	74.0	73.2	70.8	69.9
		1030	1886	74.2	73.2	68.7	66.5	65.6
	ARGON	980	1796	77.2	76.5	76.0	75.0	72.7
		1030	1886	70.2	63.1	61.7	57.2	57.2
AL	VACUUM	710	1310	155.1	154.1	151.3	146.6	142.0
		760	1400	140.0	138.8	136.6	134.1	132.0
	ARGON	710	1310	146.2	139.6	130.5	120.1	116.6
		760	1400	108.2	106.6	102.3	100.0	99.9
ZR-5BE	VACUUM	1030	1886	88.0	85.6	83.9	81.8	80.9
		1080	1976	69.8	67.7	67.3	66.5	64.7
	ARGON	1030	1886	101.4	98.8	99.2	98.3	96.2
		1080	1976	83.6	84.2	84.9	82.4	79.7
TI-6BE	VACUUM	1075	1967	15.8	14.8	14.5	14.0	13.2
		1125	2057	14.2	13.4	12.1	11.2	10.7
	ARGON	1075	1967	13.4	12.0	11.9	9.7	8.6
		1125	2057	10.0	7.9	7.8	6.8	5.6

Although during the testing period minor fluctuations in angle were noted, the overall tendency was for the contact angles to decrease with increasing time at test temperature. This behavior is reflected in the data presented in Table 2. The fluctuations can be attributed to alloying effects, because as alloying progresses, composition and temperature variations change the interfacial energies.

TABLE 2 EFFECT OF TEST CONDITIONS ON INTERFACIAL ENERGIES

SYSTEM	ATMOSPHERE	TEMPERATURE		CONTACT ANGLE[A]		γ_{LV}, DYNES/CM	γ_{LS}, DYNES/CM	FINAL SPREADING COEFFICIENT S_{LS}, DYNES/CM	WORK OF ADHESION (W_{AD}), DYNES/CM
		°C	°F	DEGREES	RADIANS				
AL	VACUUM	710	1310	142.5	2.5	831	2520	-1490	176
		760	1400	132.0	2.3	726	2350	-1210	239
	ARGON	710	1310	116.7	2.0	787	2220	-1140	434
		760	1400	99.9	1.7	561	1960	-658	464
ZR-5BE	VACUUM	1030	1886	79.8	1.4	625	1940	-702	549
		1080	1976	64.6	1.1	520	1770	-427	614
	ARGON	1030	1886	97.0	1.7	488	1780	-405	576
		1080	1976	79.8	1.4	172	1690	-225	569
TI-6BE	VACUUM	1075	1967	13.2	0.2	492[A]	1380	-9.00	970
		1125	2057	10.8	0.2	277	1590	-4.00	548
	ARGON	1075	1967	8.6	0.2	424	1440	-1.00	844
		1125	2057	5.6	0.01	329[B]	1530	+3.00	660

(A) AVERAGE OF TWO TESTS.

(B) ONE TEST ONLY

These data provide a means of comparing the wettability of beryllium by various liquids. If one assumes wettability for contact angles less than 90° and nonwetting for angles greater than 90°, then these data permit qualitative separation of the systems into two classes: those with contact angles less than 90°, and those with contact angles greater than 90°. Gold, Pd-2.1Be, and Ti-6Be were found to wet beryllium at both temperatures. The latter two brazing filler metals, as well as silver and gold, did not wet when tested in argon atmospheres at the lower temperature. However, it was found that an increase of 50 °C (90 °F) resulted in wetting. Aluminum exhibited a nonwetting behavior at both temperatures and in both atmospheres. Copper was nonwetting at both temperatures in vacuum, but underwent extensive alloying with the solid

beryllium at these temperatures in argon. From these data it appears that the binary alloys have the greatest tendency to wet beryllium (Ref 6).

Surface-energy calculations have been performed on beryllium-base metals brazed with Al, Zr-5Be, and Ti-6Be filler metals. The calculated spreading coefficient were negative for all system test conditions, except with Ti-6Be. Negative spreading coefficients indicated a very definite trend. The greater the system wettability, as indicated by lower contact angles and liquid-vapor surface tensions, the greater the numerical magnitude of the spreading coefficient.

Of the three systems used, Ti-6Be was observed to provide the best wetting of beryllium, followed by Zr-5Be. Although no basic significance can be given to the absolute values of the calculated surface-tension properties, they are useful in indicating the relative tendencies for these liquids to wet beryllium.

The above observations indicate that some liquid-metal systems will wet beryllium, whereas some system that should wet it do not, in actual practice. The problem is more complex than it seems at first.

Recent work in Japan (Ref 7) and the United States (Ref 8) has shown that the effects of the base-metal/filler-metal reaction on the wetting of silicon nitride (Si_3N_4) and titanium-added active filler metals vary with reaction-layer thickness and morphology, as well as with the composition of the reaction layer. Several results of thermodynamic studies on the formation of the compound by the interfacial reaction are reported (Ref 7, 9). Moreover, kinetic studies (Ref 7) were also performed to achieve a quantitative understanding of the formation of the reaction layer.

It can be concluded that wetting is the ability of the molten brazing filler metal to adhere to the surface of a metal in the solid state and, when cooled below its solidus temperature, to make a strong bond with that metal. Wetting is a function not only of the nature of the brazing filler metal (Table 3), but of the degree of interaction between materials (ceramics, and so on) to be joined. There is considerable evidence that in order to wet well, a molten metal must be capable of dissolving, or alloying with, some of the metal on which it flows.

TABLE 3 COMPOSITION OF SELECTED FILLER METALS USED FOR BRAZING APPLICATIONS

FILLER METAL	COMPOSITION	LIQUIDUS		SOLIDUS	
		°C	°F	°C	°F
SILVER	99.99AG	961	1762	961	1762
CUSIL	72AG-28CU	780	1436	780	1436
PALCUSIL 5	68AG-27CU-5PD	810	1490	807	1485
PALCUSIL 10	58AG-32CU-10PD	852	1566	824	1515
PALCUSIL 15	65AG-20CU-15PD	900	1650	850	1560
PALCUSIL 25	54AG-21CU-25PD	950	1740	900	1650
GAPASIL 9	82AG-9GA-9PD	880	1615	845	1555
NICUSIL 3	71.5AG-28.1CU-0.75NI	795	1465	780	1435
NICUSIL 8	56AG-42CU-2NI	893	1639	771	1420
T50	62.5AG-32.5CU-5NI	866	1591	780	1435
T51	75AG-24.5CU-0.5NI	802	1476	780	1435
T52	77AG-21CU-2NI	830	1525	780	1435
CUSILTIN 5	68AG-27CU-5SN	760	1400	743	1369
CUSILTIN 10	60AG-30CU-10SN	718	1324	602	1116
BRAZE 630	63AG-28CU-6SN-3NI	800	1472	690	1275
BRAZE 580	57AG-33CU-7SN-3MN	730	1345	605	1120
BRAZE 655	65AG-28CU-5MN-2NI	850	1560	750	1380
SILCORO 60	60AU-20AG-20CU	845	1550	835	1535
NIORO	82AU-18NI	950	1740	950	1740
PALNIRO 7	70AU-22NI-8PD	1037	1899	1005	1840
INCURO 60	60AU-37CU-3IN	900	1650	860	1580
SILCORO 75	75AU-20CU-5AG	895	1645	885	1625

NICORO 80	81.5AU-16.5CU-2NI	925	1695	910	1670
PALCUSIL 20	52AU-28CU-20PD	925	1695	875	1605
GOLD	99.99AU	1064	1947	1064	1947
PALNIRO 4	30AU-36NI-34PD	1169	2136	1135	2075
PALNIRO 1	50AU-25NI-25PD	1121	2050	1102	2016
TICUSIL	68.8AG-26.7CU-4.5TI	850	1560	830	1525
PALNICUSIL	48AG-18.9CU-10NI-22.5PD	1179	2154	910	1670
PALCO	65PD-35CO	1235	2255	1230	2245
INCUSIL15	62AG-24CU-15IN	705	1300	630	1165
INCUSIL 10	63AG-27CU-10IN	730	1345	685	1265
BAG-8A	71.8AG-28CU-0.2LI	760	1400	760	1400
BAG-19	92.5AG-7.3CU-0.2LI	890	1635	760	1400
BRAZE 071	85CU-7AG-8SN	986	1807	665	1230
BRAZE 852	85AG-15MN	970	1780	960	1760
NIORONI	73.8AU-26.2NI	1010	1850	980	1795
NICUMAN 23	67.5CU-23.5MN-9NI	955	1750	925	1695
PALSIL 10	90AG-10PD	1065	1950	1002	1836
PALNI	60PD-40NI	1238	2260	1238	2260

Wetting is only one facet of the brazing process. Another factor that affects wetting is the cleanliness of the surface to be wetted. Oxide layers inhibit wetting and spreading, as do grease, dirt, and other contaminants that prevent good contact between the brazing filler metal and the base metal. One of the functions of a flux the oxide layer on the joint area and thereby expose clean base metal.

Good wetting and spreading of the liquid filler metal on the base metal are necessary in brazing because the mechanics of the process demand that the filler metal be brought smoothly, rapidly, and continuously to the joint opening. If the conditions within the capillary space of the joint do not promote good wetting, then the filler metal will not be drawn into the space by capillary attraction.

Kim *et al.* (Ref 10) investigated the wettability and reactivity of pressureless sintered Si_3N_4 with powdered copper-titanium filler metal using sessile drop tests conducted in a vacuum where Si_3N_4 was bonded to itself and joint strength was evaluated by shear testing. The wettability of Si_3N_4 on copper-titanium base filler metals was improved greatly by adding up to 50 wt% titanium. However, the reaction-layer thickness was increased up to 10% and, thereafter, decreased up to 50 wt%.

Wettability improved with the increment of titanium concentration, and no linear proportionality was found between the reaction and the wettability. As titanium concentration increased, a continuous thin layer tended to form at the interface and markedly improved wettability.

The thickness of the reaction layer was not in proportion to the titanium concentration. For a copper-titanium filler metal with a low titanium concentration (less than 5 wt%), the initial reaction layer tended to form discontinuously, whereas the reaction layer thickness increased with titanium concentration. On the contrary, in the filler metal with a high titanium concentration (15 wt%) the reaction-layer thickness decreased as titanium concentration increased because a continuous thin reaction layer tended to form (Ref 10).

The shear strength of the Si_3N_4-Si_3N_4 joint using copper-titanium filler metal is influenced by reaction-layer thickness and morphology. Strength increased with the increment of titanium concentration, and was accompanied by improved wettability, because the tendency of the continuous thin reaction layer to form increased.

With the development of new steels, Keller *et al.* (Ref 11) undertook an extensive study of the wettability of commercial braze filler metals on type 304 stainless steel, the most common of the austenitic stainless steels; type 316 stainless steel, which is often substituted for type 304 when increased corrosion resistance is desired; and 21-6-9, a new high-manganese stainless steel that is an attractive alternative to types 304 or 316 for certain applications. Because the 21-6-9 steel has a very stable austenitic structure, it is attractive for cryogenic applications (Ref 12).

Because high wettability means that the thermocapillary attraction that fills the braze joint is strong, wettability is an important component of braze performance. The wettability index (WI) developed by Feduska (Ref 13) is used as the measure of wettability. The WI is defined as the area covered by the braze metal filler times the cosine of the contact angle between the braze and the base metal. Therefore, the higher the WI, the better the braze filler metal wets the base metal. It should be emphasized that the WI, as defined, is a relative measure, and depends on the volume of filler metal used (Table 4).

TABLE 4 WETTABILITY INDICES OF BRAZE FILLER METALS ON SELECTED STAINLESS STEEL BASE METALS

FILLER METAL	TEST TEMPERATURE		WETTABILITY INDEX FOR INDICATED STAINLESS STEEL BASE METAL		
	°C	°F	TYPE 316	21-6-9	TYPE 304
SILVER	975	1785	. . .	. . .	. . .
	1000	1830	0.008	. . .	0.015
	1050	1920	0.041	. . .	0.023
	1100	2010	0.053	. . .	0.020
	1150	2100	. . .	. . .	. . .
CUSIL	800	1470	. . .	0.013	. . .
	850	1560	. . .	0.007	. . .
	900	1650	0.022	0.016	0.003
	925	1695	0.032	. . .	. . .
	950	1740	0.037	. . .	. . .
PALCUSIL 5	800	1470	0.027	. . .	. . .
	850	1560	. . .	0.014	. . .
	900	1650	0.047	0.020	0.011
	950	1740	0.080	0.061	0.035
PALCUSIL 10	850	1560	0.035	0.020	0.015
	900	1650	0.057	0.050	0.025
	950	1740	0.107	0.101	0.062
PALCUSIL 15	900	1650	0.107	0.092	0.068
	950	1740	0.152	0.170	0.119
	1000	1830	0.754	0.263	0.212
PALCUSIL 25	950	1740	0.104	0.107	0.096
	975	1785	0.225	. . .	. . .
	1000	1830	. . .	0.283	0.226
GAPASIL 9	900	1650	0.023	. . .	. . .
	950	1740	0.068	. . .	. . .
	1000	1830	0.269	. . .	. . .
NICUSIL 3	800	1470	0.006	0.000	0.012
	850	1560	0.027	0.017	0.008
	900	1650	0.041	0.039	0.021
	925	1695	0.051	. . .	. . .
	950	1740	0.064	. . .	. . .
NICUSIL 8	850	1560	0.024	. . .	. . .
	900	1650	0.052	. . .	0.033
	950	1740	0.085	. . .	0.064
	1000	1830	. . .	. . .	0.229
T-50	850	1560	0.024	. . .	. . .
	900	1650	0.038	. . .	0.026

FILLER METAL	TEST TEMPERATURE		WETTABILITY INDEX FOR INDICATED STAINLESS STEEL BASE METAL		
	°C	°F	TYPE 316	21-6-9	TYPE 304
	950	1740	0.062	. . .	0.057
	1000	1830	. . .	. . .	. . .
T-51	800	1470	0.007	. . .	. . .
	850	1560	0.029	. . .	. . .
	900	1650	0.039	. . .	. . .
	950	1740	. . .	. . .	0.029
	1000	1830	. . .	. . .	0.082
T-52	850	1560	0.027	. . .	0.001
	900	1650	0.045	. . .	0.014
	950	1740	0.063	. . .	0.045
	1000	1830	. . .	. . .	0.090
CUSILTIN 5	850	1560	0.015	. . .	0.000
	875	1605	0.043	. . .	. . .
	900	1650	0.047	. . .	0.013
	950	1740	. . .	. . .	0.033
	1000	1830	. . .	. . .	. . .
CUSILTIN 10	750	1380	. . .	0.025	0.000
	800	1470	. . .	0.017	0.023
	825	1515	0.021	. . .	. . .
	850	1560	0.034	0.051	0.050
	875	1605	0.043	. . .	. . .
BRAZE 630	800	1470	0.014	0.037	0.023
	850	1560	0.046	0.065	0.024
	900	1650	0.064	. . .	. . .
BRAZE 580	750	1380	0.020	0.060	0.060
	800	1470	0.051	0.056	0.089
	850	1560	0.073	0.120	0.102
	875	1605	0.078	. . .	. . .
BRAZE 655	825	1515	0.080	. . .	. . .
	850	1560	0.110	0.037	0.074
	875	1605	0.116	. . .	. . .
	900	1650	. . .	0.137	0.124
SILCORO 60	850	1560	. . .	0.005	0.004
	900	1650	0.039	0.007	0.011
	925	1695	0.051	. . .	. . .
	950	1740	0.073	0.025	0.016
	1000	1830	. . .	0.055	0.037
NIORO	950	1740	. . .	0.000	0.000
	975	1785	0.049	. . .	. . .
	1000	1830	0.061	0.060	0.065
PALNIRO 7	1025	1875	. . .	. . .	. . .
	1050	1920	0.053	. . .	. . .
	1075	1965	0.073	. . .	. . .
INCURO 60	900	1650	0.010	. . .	. . .
	950	1740	0.025	. . .	. . .
	1000	1830	0.091	. . .	. . .
SILCORO 75	900	1650	0.006	. . .	. . .

FILLER METAL	TEST TEMPERATURE		WETTABILITY INDEX FOR INDICATED STAINLESS STEEL BASE METAL		
	°C	°F	TYPE 316	21-6-9	TYPE 304
	950	1740	0.057	. . .	. . .
	1000	1830	0.170	. . .	. . .
NICORO 80	950	1740	0.041	0.019	0.016
	1000	1830	0.163	0.126	0.070
	1050	1920	0.413	0.190	0.084
PALCUSIL 20	875	1610	0.061	. . .	. . .
	900	1650	0.110	. . .	. . .
	925	1695	0.122	. . .	. . .
GOLD	1070	1960	. . .	. . .	0.088
	1075	1965	0.087	. . .	. . .
	1100	2010	0.358	. . .	0.238
	1150	2100	. . .	. . .	0.355
PALNIRO 4	1175	2145	0.036	. . .	. . .
	1200	2190	0.061	. . .	. . .
	1225	2235	0.078	. . .	. . .
PALNIRO 1	1125	2055	0.041	. . .	. . .
	1150	2100	0.063	. . .	. . .
	1175	2145	0.075	. . .	. . .
TICUSIL	875	1605	0.032	. . .	. . .
	900	1650	0.057	. . .	. . .
	950	1740	0.083	. . .	. . .
PALNICUSIL	950	1740	0.025	. . .	0.038
	975	1785	0.213	. . .	. . .
	1000	1830	. . .	. . .	. . .
	1025	1875	0.362	. . .	. . .
	1050	1920	. . .	. . .	. . .
	1075	1965	0.336	. . .	. . .
	1100	2010	. . .	. . .	. . .
PALCO	1250	2280	0.000	. . .	. . .
	1275	2325	0.073	. . .	. . .
	1300	2370	0.159	. . .	. . .
INCUSIL 15	750	1380	. . .	. . .	. . .
	800	1470	. . .	. . .	. . .
	850	1560	. . .	. . .	. . .
INCUSIL 10	750	1380	. . .	. . .	. . .
	800	1470	. . .	. . .	. . .
	850	1560	0.008	. . .	. . .
BAG-8A	800	1470	0.005	. . .	. . .
	850	1560	0.008	. . .	. . .
	900	1650	0.032	. . .	. . .
	950	1740	0.045	. . .	. . .
BAG-19	950	1740	0.016	. . .	. . .
	1000	1830	0.016	. . .	. . .
	1050	1920	0.034	. . .	. . .
BRAZE 071	1000	1830	0.066	0.106	0.101
	1050	1920	. . .	0.125	0.101
BRAZE 852	1000	1830	0.039	0.037	0.038

FILLER METAL	TEST TEMPERATURE		WETTABILITY INDEX FOR INDICATED STAINLESS STEEL BASE METAL		
	°C	°F	TYPE 316	21-6-9	TYPE 304
	1050	1920	0.029	0.038	0.042
	1100	2010	0.043	0.037	0.020
NIORONI	1000	1830	0.068	. . .	. . .
	1025	1875	0.070	. . .	. . .
	1100	2010	0.116	. . .	. . .
NICUMAN 23	950	1740	0.026	. . .	. . .
	975	1785	0.099	. . .	. . .
	1000	1830	0.091	. . .	. . .
	1025	1875	0.091	. . .	. . .
PALSIL 10	1050	1920	0.113	. . .	. . .
	1075	1965	0.113	. . .	. . .
	1100	2010	0.126	. . .	. . .
PALNI	1225	2235	. . .	. . .	. . .
	1250	2280	0.068	. . .	. . .
	1275	2325	0.078	. . .	. . .
	1300	2370	0.107	. . .	. . .
PALMANSIL 5	950	1740	. . .	. . .	0.057
	1000	1830	. . .	. . .	. . .
	1050	1920	. . .	. . .	. . .
	1100	2010	. . .	. . .	. . .

The WIs for each braze filler metal at each temperature on type 316 stainless steel, type 304L stainless steel, and 21-6-9 stainless steel are provided in Table 4. Wetting indices greater than 0.05 are indicative of good performance during brazing, whereas WI values greater than 0.10 are indicative of excellent performance during brazing (Ref 13).

A comparison of the WI of the braze filler metals on the three stainless steels revealed these trends:

- FILLER METALS GENERALLY WET TYPE 316 STAINLESS STEEL BETTER THAN TYPE 304 STAINLESS STEEL AND GENERALLY WET TYPE 316 STAINLESS BETTER THAN 21-6-9 STAINLESS.
- THE DEGREE OF WETTING OF MOST BRAZE FILLER METALS ON 21-6-9 STAINLESS WAS EQUAL TO OR BETTER THAN IT WAS ON TYPE 304 STAINLESS (REF 12).
- THE IMPROVED WETTABILITY OF BRAZE FILLER METALS ON TYPE 316 STAINLESS IS BELIEVED TO BE DUE TO THE PRESENCE OF MOLYBDENUM IN THE SURFACE OXIDE, WHEREAS THE ENHANCED WETTING ON 21-6-9 STAINLESS VERSUS TYPE 304 STAINLESS IS BELIEVED TO BE DUE TO THE HIGHER MANGANESE CONTENT OF THE SURFACE OXIDE.

Essentially, the successful joining of components by the brazing process depends on the selected brazing filler metal having a melting point above 450 °C (840 °F) and wetting the base metal without melting it. Furthermore, the joint must be designed to ensure that the mating surfaces of the components are parallel and close enough together to cause capillary attraction.

Mel M. Schwartz, Sikorsky Aircraft

Elements of the Brazing Process

An engineer must consider reliability and cost when designing the braze joint. Joint strength, fatigue resistance, corrosion susceptibility, and high-temperature stability are additional concerns that determine the selection of joint design, braze filler materials, and processing parameters.

A careful and intelligent appraisal of the following elements is required in order to produce satisfactory brazed joints:

- FILLER-METAL FLOW
- BASE-METAL CHARACTERISTICS
- FILLER-METAL CHARACTERISTICS
- SURFACE PREPARATION
- JOINT DESIGN AND CLEARANCE
- TEMPERATURE AND TIME
- RATE AND SOURCE OF HEATING
- PROTECTION BY AN ATMOSPHERE OR FLUX

Filler-Metal Flow. As mentioned previously, wetting is only one important facet of the brazing process. A low contact angle, which implies wetting, is also necessary, but is not a sufficient condition itself for flow. Viscosity is also important. Brazing filler metals with narrow melting ranges that are close to the eutectic composition generally have lower viscosities than those with wide melting ranges. Thus, a high surface tension of liquid filler metal, a low contact angle, and low viscosity are all desirable.

Flowability is the property of a brazing filler metal that determines the distance it will travel away from its original position, because of the action of capillary forces. To flow well, a filler metal must not gain an appreciable increase in its liquidus temperature even though its composition is altered by the addition of the metal it has dissolved. This is important because the brazing operation is carried out at temperatures just above the liquidus of the filler metal.

The composition and surface energy of liquids and solids are assumed to remain constant. In real systems, however, these interactions occur (Ref 14):

- ALLOY FORMATION BETWEEN LIQUID AND BASE METAL
- DIFFUSION OF BASE METAL INTO BRAZING FILLER METAL
- DIFFUSION OF FILLER METAL INTO GRAINS OF BASE METAL
- PENETRATION OF FILLER METAL ALONG GRAIN BOUNDARIES
- FORMATION OF INTERMETALLIC COMPOUNDS

In practice, interactions are usually minimized by selecting the proper brazing filler metal; keeping the brazing temperature as low as possible, but high enough to produce flow; and keeping the time of brazing temperature short and cooling the brazed joint as quickly as possible without causing cracking or distortion. When diffusion brazing is desired, higher brazing temperatures and longer times at brazing temperatures are employed.

Base-Metal Characteristics. The base metal has a prime effect on joint strength. A high-strength base metal produces joints of greater strength than those made with softer base metals (other factors being equal). When hardenable metals are brazed, joint strength becomes less predictable. This is because more-complex metallurgical reactions between hardenable base metals and the brazing filler metals are involved. These reactions can cause changes in the base-metal hardenability and can create residual stresses (Ref 15).

In cases where different materials make up the assembly and gaps may open or close as heating proceeds to the joining temperature, the coefficient of thermal expansion becomes vitally important.

Several metallurgical phenomena influence the behavior of brazed joints and, in some instances, necessitate special procedures. These base-metal effects include alloying by brazing filler; carbide precipitation; stress cracking; hydrogen, sulfur, and phosphorus embrittlement; and oxidation stability.

The extent of interaction varies greatly, depending on compositions (base metal and brazing filler metal) and thermal cycles. There is always some interaction, except in cases of mutual insolubility.

The strength of the base metal has a profound effect on the strength of the brazed joint. Therefore, this property must be carefully considered when designing the joint to have specific properties. Some base metals also are easier to braze than others, particularly by specific brazing processes.

Filler-Metal Characteristics. The second material involved in joint structures is the brazing filler metal. Unfortunately, it cannot be chosen to provide a specific joint strength. Actually, strong joints can be brazed with almost any good commercial brazing filler metal if correct brazing methods and joint design are implemented.

Necessary characteristics of brazing filler metals are:

- PROPER FLUIDITY AT BRAZING TEMPERATURES TO ENSURE FLOW BY CAPILLARY ACTION AND TO PROVIDE FULL ALLOY DISTRIBUTION
- STABILITY TO AVOID PREMATURE RELEASE OF LOW-MELTING-POINT ELEMENTS IN THE BRAZING FILLER METAL
- ABILITY TO WET THE BASE-METAL JOINT SURFACE
- LOW VOLATILIZATION OF ALLOYING ELEMENTS OF THE BRAZING FILLER METAL AT BRAZING TEMPERATURES
- ABILITY TO ALLOY OR COMBINE WITH THE BASE METAL TO FORM AN ALLOY WITH A HIGHER MELTING TEMPERATURE
- CONTROL OF WASHING OR CONTROL OF EROSION BETWEEN THE BRAZING FILLER METAL AND THE BASE METAL WITHIN THE LIMITS REQUIRED FOR THE BRAZING OPERATION

It should be noted that the strength of the brazed joint is not directly related to the method of filler-metal melting. For example, if constructional metals are produced by vacuum melting, then there is a definite relationship between the vacuum-melting practice and the final strength of the ingot, bar, or rolled sheet. With a brazing filler metal, however, joint strength is dependent on joint design, brazing temperature, amount of brazing filler metal applied, location and method of application, heating rate, and many other factors that constitute the brazing technique.

The degree to which brazing filler metal interacts with and penetrates the base metal during brazing depends on the intensity of mutual diffusion processes that occur between both those materials. In applications that require strong joints for high-temperature, high-stress service conditions (such as turbine rotor assemblies and jet-engine components), it is generally wise to specify a brazing filler metal that has high diffusion and solution properties with the base metal. When the assembly is constructed of extremely thin base metals (as in honeycomb structures and some heat exchangers), good practice entails specifying a brazing filler metal that contains elements with a low-diffusion characteristic relative to the base metal being used. Diffusion, a normal part of the metallurgical process, can contribute to good brazed joints when brazing, for example, high-temperature metals with nickel-base brazing filler metals.

Brazing Temperature. When choosing a brazing filler metal, the first selection criterion is the brazing temperature. Some brazing-temperature ranges are given in Table 5. Very few brazing filler metals possess narrow melting ranges. Brazing filler metals in which the solidus and liquidus temperatures are close together do not usually exhibit a strong tendency to coexist as a mixture of liquid and solid phases or to liquate. They flow readily and should be used with small joint clearances. As the solidus and liquidus temperatures diverge, the tendency to liquate increases, requiring greater precautions in brazing filler metal application. The mixture of solid and liquid metal can aid gap filling.

TABLE 5 JOINING TEMPERATURES FOR FILLER METALS USED IN BRAZING APPLICATIONS

BRAZING FILLER-METAL GROUPS	JOINING TEMPERATURE	
	°C	°F
NI, CO, AND PD ALLOYS	[GES]1100	[GES]2012
CU, NI, AND AU ALLOYS	[GES]1100	[GES]2012
CU-ZN, CU-SN, NI-P, NI-CR-P, PD-AG-CU	[GES]900	[GES]1652
CU-P, CU-AG-P	600-800	1112-1472
AG-CU-ZN, AG-CU-ZN-CD	600-800	1112-1472
AL-SI	580-600	1076-1112
MG-AL-ZN	585-615	1085-1139

The necessity for the brazing filler metal to melt below the solidus of the base metal is just one of several factors that affect its selection. It may be necessary for the brazing filler metal to melt below the temperature at which parts to be brazed lose strength or above the temperature at which oxides are reduced or dissociated. Joining may have to be carried out above the solution-treatment temperature of the base metal, or at a structure refining temperature, or below the remelt temperature of a brazing filler metal used previously in the production of a brazed subassembly.

Liquidation. During melting, the composition of the liquid and solid filler metal phases changes as the temperature increases from the solidus to the liquidus point. If the portion that melts first is allowed to flow out, then the remaining solid phases have higher melting points than the original composition and may never melt, remaining behind as a residue, or "skull." Filler metals with narrow melting ranges do not tend to separate, but flow quite freely in joints of extremely narrow clearance as long as the solution and diffusion rates of the filler metal with the base metal are low (as in aluminum brazing, the use of silver filler metal on copper, and so on). The rapid heating of filler metals with wide melting ranges or their application to the joint after the base metal reaches brazing temperature will minimize the separation, or liquation. However, liquation cannot be entirely eliminated and wide-melting-range filler metals, which tend to have more sluggish flow, will require wider joint clearances and will form larger fillets at the joint extremities. A few brazing filler metals become sufficiently fluid below the actual liquidus temperature, and satisfactory joints are achieved, even though the liquidus temperature has not been reached.

When sluggish behavior is needed, such as in filling large gaps, brazing can be accomplished within the melting range of the filler metal. However, the brazing temperature is usually 10 to 93 °C (20 to 170 °F) above the liquidus of the filler metal. The actual temperature required to produce a good joint filling is influenced by factors such as heating rate, brazing environment (atmosphere or flux), thickness of parts, thermal conductivity of the metals being joined, and type of joint to be made.

Large-scale mechanical properties of brazing filler metals can be a guideline for their suitability (in terms of strength, oxidation resistance, and so on) for use in different capillary joining applications. However, designers cannot use the mechanical properties of brazed assemblies that are related to different joint configurations brazed at given cycles of time and temperatures.

The placement of the brazing filler metal is an important design consideration, not only because the joint must be accessible to the method chosen, but because, in automatic heating setups, the filler metal must be retained in its location until molten. Brazing filler metals are available in different forms (Table 6) and filler-metal selection may depend on which form is suitable for a particular joint design.

TABLE 6 AVAILABLE PRODUCT FORMS OF BRAZING FILLER METALS CATEGORIZED BY GROUP

BRAZING FILLER-METAL GROUPS	AVAILABLE FORMS[A]											
	AD	CL	FL	FO	PA	PB	PO	PR	SH	RD	SP	WI
NI AND CO ALLOYS	X	. . .	X	[B]	X	X	X	[B]	X	[B]	. . .	[C]
PD ALLOYS	. . .	. . .	X	X	. . .	. . .	X	X	X	. . .	X	X
CU AND AU ALLOYS	. . .	. . .	X	X	X	. . .	X	X	X	. . .	X	X

NI ALLOYS	X	. . .	X	(B)	X	X	X	(B)	X	(B)	. . .	(C)
CU-SN, CU-ZN, PD-AG-CU	. . .	. . .	X	X	. . .	. . .	X	X	X	. . .	X	X
NI-P, NI-CR-P	X	. . .	. . .	. . .	X	X	X	. . .	. . .	. . .	. . .	. . .
CU-P, CU-AG-P	. . .	. . .	. . .	. . .	X	. . .	X	. . .	. . .	. . .	X	X
AG-CU-ZN, AG-CU-ZN-CD	. . .	. . .	X	X	. . .	. . .	X	X	X	. . .	X	X
AL-SI	. . .	X	. . .	. . .	. . .	. . .	X	. . .	X	. . .	. . .	X
MG-AL-ZN	. . .	. . .	. . .	. . .	. . .	. . .	. . .	. . .	X	. . .	X	X

(A) AD, ADHESIVE SHEET; CL, CLADDING; FL, FLUX PASTE; FO, FOIL; PA, PASTE (NONFLUXING); PB, PLASTIC-BONDED SHEET; PO, POWDER; PR, PREFORM; SH, SHIM; RD, ROD; SP, STRIP; WI, WIRE.

(B) A FEW ALLOYS ONLY.

(C) PLASTIC BOND

Several general rules apply in the filler-metal placement. Wherever possible, the filler metal should be placed on the most slowly heated part of the assembly in order to ensure complete melting. Although brazing is independent of gravity, gravity can be used to assist filler-metal flow, particularly for those filler metals having wide ranges between their solidus and liquidus temperatures. Brazing filler metals can be chosen to fill wide gaps or to flow through joint configurations where the gap may vary, for example, around a corner. Unless movement between the components being joined is unimportant or can be corrected manually (through self-jigging or by using fixtures after the filler metal is molten), the filler metal should be placed outside the joint and allowed to flow into it. It should not be placed between the joint members. If erosion of thin members is possible, then the brazing filler metal should be placed on the heavier sections, which heat up more slowly, so that flow proceeds toward the thin sections. Apart from suiting the placement method selected for the joint, the form chosen for the brazing filler metal may be needed to accurately gage the amount applied, not just for economy and reproducibility, but to regulate and maintain joint properties and configuration.

Surface Preparation. A clean, oxide-free surface is imperative to ensure uniform quality and sound brazed joints. All grease, oil, dirt, and oxides must be carefully removed from the base and filler metals before brazing, because only then can uniform capillary attraction be obtained. Brazing should be done as soon as possible after the material has been cleaned. The length of time that the cleaning remains effective depends on the metals involved, atmospheric conditions, storage and handling practices, and other factors. Cleaning operations are commonly categorized as being either chemical or mechanical. Chemical cleaning is the most effective means of removing all traces of oil or grease. Trichloroethylene and trisodium phosphate are the usual cleaning agents employed. Oxides and scale that cannot be eliminated by these cleaners should be removed by other chemical means.

The selection of the chemical cleaning agent depends on the nature of the contaminant, the base metal, the surface condition, and the joint design. Regardless of the nature of the cleaning agent or the cleaning method used, it is important that all residue or surface film be adequately rinsed from the cleaned parts to prevent the formation of other equally undesirable films on the faying surfaces.

Objectionable surface conditions can be removed by mechanical means, such as grinding, filing, wire brushing, or any form of machining, provided that joint clearances are not disturbed. When grinding the surfaces of the parts to be brazed, care should be exercised to ensure that the coolant is clean and free from impurities to avoid grinding these impurities into the finished surfaces.

When faying surfaces of parts to be brazed are prepared by blasting techniques, several factors should be considered. There are two purposes behind the blasting of parts to be brazed. One is to remove any oxide film and the other is to roughen the mating surfaces in order to increase capillary attraction of the brazing filler metal. The blasting material must be clean and must not leave any deposit on the surfaces to be joined that restricts filler-metal flow or impairs brazing. The particles of the blasting material should be angular rather than spherical, so that the blasted parts are lightly roughened, rather than peened, after the scale is removed. The operation should not distort or otherwise harm delicate parts. Vapor blasting and similar wet blasting methods require care, because of the possibility of surface contamination.

Mechanical cleaning may be adequate, in which case it should be permitted (by the design) during manufacture. In those cases that require chemical cleaning, the cleaning operation may be followed by protective electroplating, which necessitates access to the faying surface by the liquids involved.

Another surface protection technique is the use of solid and liquid brazing fluxes. At temperatures up to about 1000 °C (1830 °F), fluxes often provide the easiest method of maintaining or producing surface cleanliness. In such cases, the design must not only permit easy ingress of the flux, but should allow the filler metal to wash it through the joint. Above 1000 °C (1830 °F), the flux residues can be difficult to remove, and surface cleaning can be accompanied by brazing in furnaces with protective atmospheres. However, the design must permit the gas to penetrate the joint.

In addition to cleanliness and freedom from oxides, another important factor in determining the ease and evenness of brazing filler metal flow is surface roughness. Generally, a liquid that wets a smooth surface will wet a rough one even more. A rough surface will modify filler-metal flow from laminar to turbulent, prolonging flow time and increasing the possibility of alloying and other interactions. Surfaces often are not truly planar, and, in some instances, surface roughening will improve the uniformity of the joint clearance. A rough surface features a series of crests and troughs that produce turbulent flow. These irregularities on the surface simulate grips to prevent the flow of the filler metal.

Conversely, there may be a requirement that brazing filler metal not flow onto some surfaces. Stop-off materials will often avoid flow, but the design must permit easy application of the stop-off material without contaminating the surfaces to be joined.

Self-fluxing filler metals, in a suitably protective environment such as vacuum, may provide the essential surface wetting.

Joint Design and Clearance. A brazed joint is not a homogeneous body. Rather, it is a heterogeneous area that is composed of different phases with different physical and chemical properties. In the simplest case, it consists of the base-metal parts to be joined and the added brazing filler metal. However, dissimilar materials must also be considered.

Small clearances are used because the smaller the clearance, the easier it is for capillarity to distribute the brazing filler metal throughout the joint area and the less likely it is that voids or shrinkage cavities will form as the brazing filler metal solidifies. The optimum joints are those in which the entire joint area is wetted and filled by the brazing filler metal. Typically, brazing clearances that range from 0.03 to 0.08 mm (0.001 to 0.003 in.) are designed for the best capillary action and greatest joint strength.

Because brazing relies on capillary attraction, the design of a point must provide an unobstructed and unbroken capillary path to enable the escape of flux, if used, as well as allow the brazing filler metal into the joint. In cases where filler metal is added to a joint by hand, such as by feeding in a rod or wire, the joint entry must be visible and accessible.

Some of the more-important factors influencing joint design are the required strength and corrosion resistance, the necessary electrical and thermal conductivity, the materials to be joined, the mode of application of the brazing filler metal, and the postjoining inspection needs.

Consideration also should be given to the ductility of the base metal, the stress distribution in the joint, and the relative movements of the two surfaces during joining, which may introduce distortion in dimensions of the work to be brazed.

Viscosity, surface tension, and specific gravity of the brazing filler metal are not the only factors that determine the gap-filling capability of a given filler metal. Joint strength increases as joint gap decreases, down to a minimum. Table 7 gives the allowable joint clearances for various filler-metal systems. Other factors that influence optimum joint gap with a specific brazing filler metal are joint length, brazing temperature, and base-metal/filler-metal metallurgical reactions.

TABLE 7 RECOMMENDED GAP FOR SELECTED BRAZE FILLER METALS

BRAZING FILLER-METAL SYSTEM	JOINT CLEARANCE	
	mm	in.
AL-SI ALLOYS[(A)]	0.15-0.61	0.006-0.024
MG ALLOYS	0.10-0.25	0.004-0.010
CU	0.00-0.05	0.000-0.002
CU-P	0.03-0.13	0.001-0.005
CU-ZN	0.05-0.13	0.002-0.005
AG ALLOYS	0.05-0.13	0.002-0.005

AU ALLOYS	0.03-0.13	0.001-0.005
NI-P ALLOYS	0.00-0.03	0.000-0.001
NI-CR ALLOYS(B)	0.03-0.61	0.001-0.024
PD ALLOYS	0.03-0.10	0.001-0.004

(A) IF JOINT LENGTH IS LESS THAN 6 MM (0.240 IN.), GAP IS 0.12 TO 0.75 MM (0.005 TO 0.030 IN.). IF JOINT LENGTH EXCEEDS 6 MM (0.240 IN.), GAP IS 0.25 TO 0.60 MM (0.010 TO 0.24 IN.).

(B) MANY DIFFERENT NICKEL BRAZING FILLER METALS ARE AVAILABLE, AND JOINT GAP REQUIREMENTS MAY VARY GREATLY FROM ONE FILLER METAL TO ANOTHER

It is important to remember that an assembly expands during heating and that the joint gap can either widen or close by the time the brazing filler metal starts to melt and move. It is desirable to design the joint to expose the solidifying filler metal to compressive, rather than tensile, stress. This is much more important in brazing than in soldering, because brazing temperatures are higher, increasing the total thermal expansion. With cylindrical joints, the components with the larger coefficient of expansion should be on the outside, whenever possible.

Joint clearance is probably one of the most significant factors in vacuum brazing operations. Naturally, it receives special consideration when joint are designed at room temperature. Actually, joint clearance is not the same at all phases of brazing. It will have one value before brazing, another value at the brazing temperature, and still another value after brazing, especially if there has been a substantial interaction between the brazing filler metal and the base metal. To avoid confusion, it has become general practice to specify joint clearance as the value at room temperature before brazing.

The recommended joint clearances given in Table 7 are based on joints that have members of similar metals and equal mass. When dissimilar metals and/or metals of widely differing masses are joined by brazing, special problems arise. These problems necessitate specialized selection of brazing filler metals. Furthermore, the most suitable joint clearance for the specific job must be carefully determined. Thus, clearances given in Table 7 are the clearances that must be attained at the brazing temperature.

Although there are many kinds of brazed joints, the selection of joint type is not as complicated as it may seem, because butt and lap joints are the two fundamental types used. All other types, such as the scarf joint, are modifications of these two. The scarf joint of the scarf angle. It approaches the lap joint at the other extreme of the scarf angle.

Selection of joint type is influenced by the configuration of the parts, as well as by joint strength and other service requirements, such as electrical conductivity, pressure tightness, and appearance. Also influential in the selection of joint type are fabrication techniques, production quantities, and methods of feeding brazing filler metal. Lap joints are generally preferred for brazing operations, particularly when it is important that the joints be at least as strong as the weaker member. For maximum strength, lap-joint length should equal three to four times the thickness of the thinner member.

Temperature and Time. The temperature of the brazing filler metal has an important effect on the wetting and alloying action, which increases with increasing temperature. The temperature must be above the melting point of the brazing filler metal and below the melting point of the parent metal. Within this range, a brazing temperature that is most satisfactory overall is generally selected.

Usually, low brazing temperatures are preferred in order to economize on the heat energy required, minimize the heat effect on the base metal (annealing, grain growth, or warpage, for example), minimize base-metal/filler-metal interactions, and increase the life of fixtures, jigs, or other tools.

Higher brazing temperatures may be desirable so as to:

- ENABLE THE USE OF A HIGHER-MELTING, BUT MORE ECONOMICAL, BRAZING FILLER METAL
- COMBINE ANNEALING, STRESS RELIEF, OR HEAT TREATMENT OF THE BASE METAL WITH BRAZING
- PERMIT SUBSEQUENT PROCESSING AT ELEVATED TEMPERATURES
- PROMOTE BASE-METAL/FILLER-METAL INTERACTIONS IN ORDER TO CHANGE THE

COMPOSITION OF THE BRAZING FILLER METAL (THIS TECHNIQUE IS USUALLY USED TO INCREASE THE REMELT TEMPERATURE AND DUCTILITY OF THE JOINT)

- EFFECTIVELY REMOVE SURFACE CONTAMINANTS AND OXIDES WITHIN PROTECTIVE ATMOSPHERES BRAZING (ALSO APPLIES TO PURE DRY HYDROGEN, TO ARGON, AND TO VACUUM)
- AVOID STRESS CRACKING

The time at brazing temperature also affects the wetting action. If the brazing filler metal has a tendency to creep, the distance generally increases with time. The alloying action between filler metal and parent metal is, of course, a function of temperature, time, and quantity of filler metal. For production work, temperature, time, and quantity of filler metal are generally kept at a minimum, consistent with good quality, where diffusion is not required.

References cited in this section

14. W.H. KOHL, SOLDERING AND BRAZING, *VACUUM*, VOL 14, 1964, P 175-198
15. *METALS HANDBOOK*, 9TH ED., *WELDING, BRAZING, AND SOLDERING*, VOL 6, AMERICAN SOCIETY FOR METALS, 1983, P 929-995

Mel M. Schwartz, Sikorsky Aircraft

Heating Methods

The numerous heating methods available for brazing often represent constraints on the designer or engineer when selecting the best type of capillary joint (Table 8). However, because effective capillary joining requires the efficient transfer of heat from the heat source into the joint, one cannot braze a 0.025 mm (0.001 in.) diam wire to a 2.3 kg (5.1 lb) lump of copper with a small torch.

TABLE 8 RELATIVE RATING OF SELECTED BRAZING PROCESS HEATING METHODS

METHOD	CHARACTERISTICS[(A)]					
	CAPITAL COST	RUNNING COST	BASIC OUTPUT	FLUX REQUIRED	VERSATILITY	OPERATOR SKILL REQUIRED
Torch (flame)	L/M	M/H	L	YES	H	YES
Electrical resistance	M	M	M/H	YES	L	NO
Induction	M/H	M	M/H	Y/N	M	NO
Furnace (atmosphere)	M/H	M/H	H	Y/N	M	NO
Furnace (vacuum)	H	L	H	NO	M	NO
Dip (flux bath)	L/M	M/H	L/M	YES	L	YES
Infrared	M	L	M	Y/N	L	NO

(A) H, HIGH; M, MEDIUM; L, LOW

The size and value of individual assemblies, the numbers required, and the required rate of production will influence the selection of heating method. Other factors that also must be considered include the rate of heating, differential thermal gradients, and both external and internal cooling rates. These factors vary tremendously with different methods of heating, and their effects on dimensional stability, distortion, and joint structure must be considered.

Manual torch brazing is the method most frequently used for repairs, one-of-a-kind brazing jobs, and short production runs, as an alternative to fusion welding. Any joint that can be accessed by a torch and brought to brazing temperature (by the torch alone or in conjunction with auxiliary heating) can be readily brazed by this technique.

Although any flame-producing device can be used for torch brazing, commercial applications are accomplished with the same type of torch, controls, and gases used for torch fusion welding. Conversion to brazing merely requires changes in torch nozzles and goggle lenses.

The torch brazing technique is relatively simple and can be mastered by the mechanically adept in a short time. Those already experienced in torch welding and the brazing of other metals generally encounter little difficulty learning torch brazing.

Depending on the temperature and heat required, all commercial gas mixtures can be used to fuel the torch: oxyacetylene, oxyhydrogen, oxy-natural gas, acetylene and air, hydrogen and air, propane, methane, and natural gas and air. Oxyacetylene and oxy-natural gas are the mixtures most often used commercially and are preferred in that order. Flame adjustment is very important. Generally, a slightly reducing flame is desirable in order to preserve part surfaces from oxidation.

The oxyacetylene combination produces the highest temperature. The other gases are cooler and their flames have relatively lower intensity. Thus, they are easier to use and are applied advantageously to light-gage material.

Manual torch brazing is particularly useful on assemblies with sections of unequal mass. As warranted by the rate of production, machine operations can be set up using one or more torches equipped with single or multiple flame tips. The machine can be designed to move either the work or the torches.

Torch brazing can be rather easily automated with appropriate gas supplies, indexing fixtures, and cycle controls. Usually, such systems involve multiple-station rotary indexing tables. The part is fed into a holding fixture at the first station and is then indexed to one or more preheating stations, depending on the heating time required. A brazing station is next, followed by a cooling station and an ejection station (see Fig. 4).

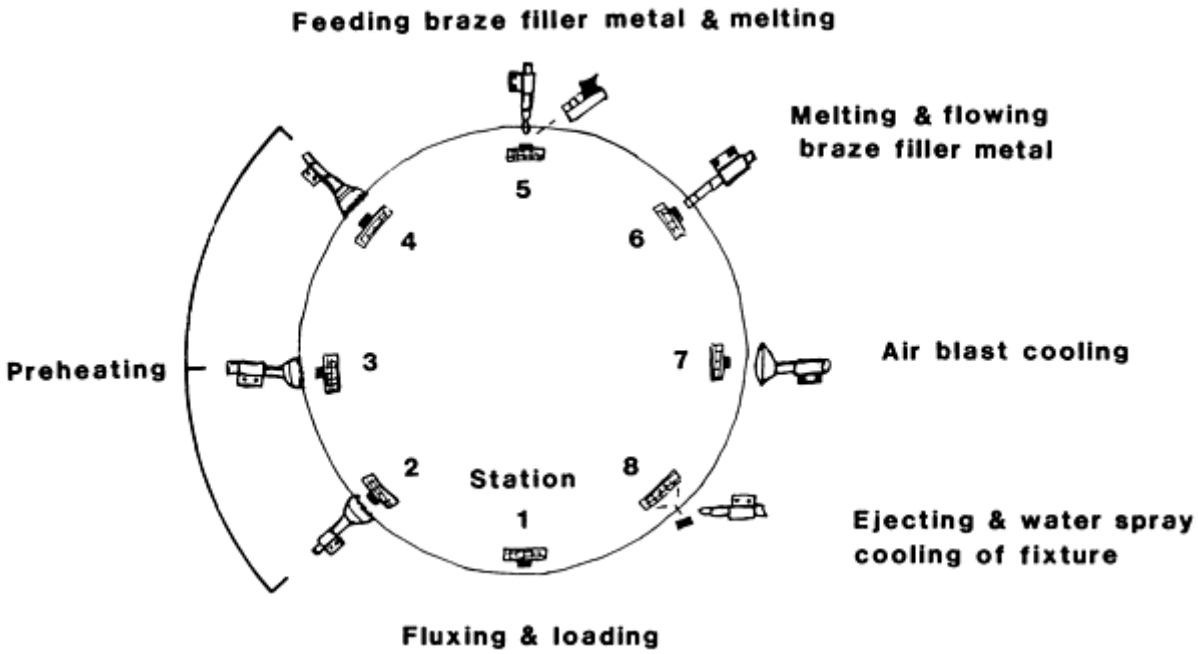

FIG. 4 SCHEMATIC OF AN EIGHT-STATION AUTOMATIC TORCH BRAZING OPERATION THAT PRODUCES MAGNET ARMATURE ASSEMBLIES (230 PIECES/H) USED AS STRIKING MEMBERS OF A PRINTING MACHINE

Additional information is available in the article "Torch Brazing" in this Volume.

Furnace brazing is popular because of its comparatively low equipment cost, furnace adaptability, and minimal required jigging. Furnace brazing is a low-cost process relative to other processes such as torch brazing, induction brazing, or salt-bath brazing when high-volume production output is a primary factor. Secondary factors include tooling requirements, fluxing, and cleaning requirements. With many brazing assemblies, the weight of the parts alone is sufficient to hold them together. Other configurations require only one or two rectangular fixturing blocks of metal.

Four basic types of furnaces are used:

- BATCH, WITH EITHER AIR OR CONTROLLED ATMOSPHERE (FIG. 5)
- CONTINUOUS, WITH EITHER AIR OR CONTROLLED ATMOSPHERE (FIG. 6)
- RETORT, WITH CONTROLLED ATMOSPHERE
- VACUUM

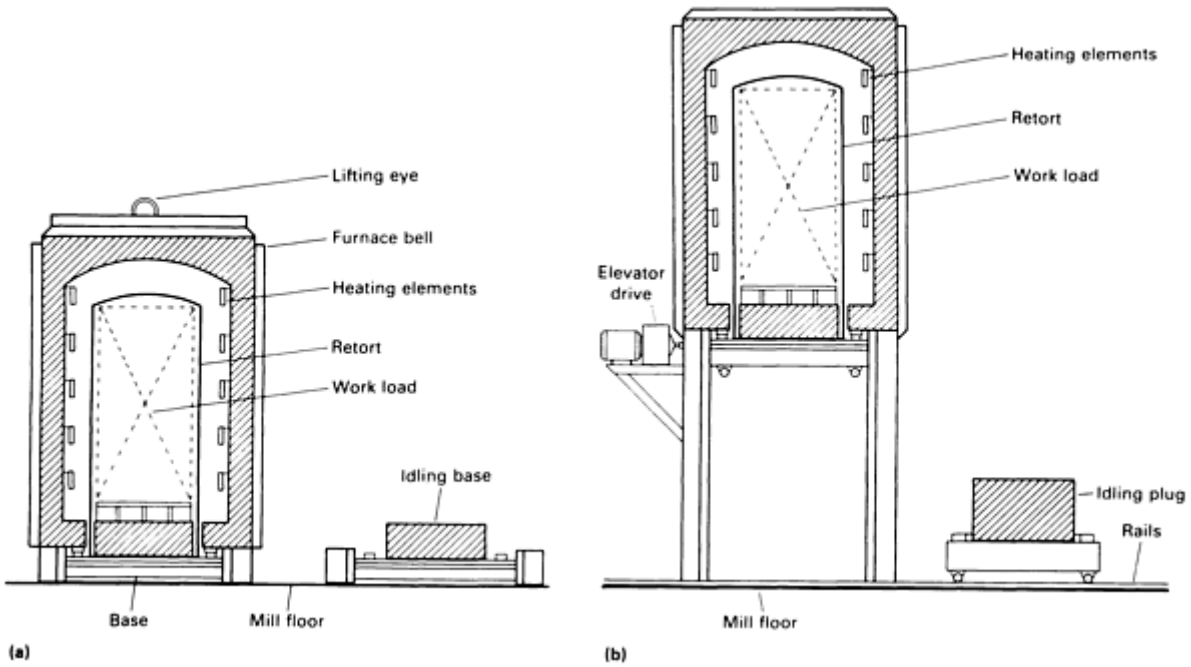

FIG. 5 BATCH-TYPE BRAZING FURNACES. (A) BELL FURNACE. (B) ELEVATOR FURNACE

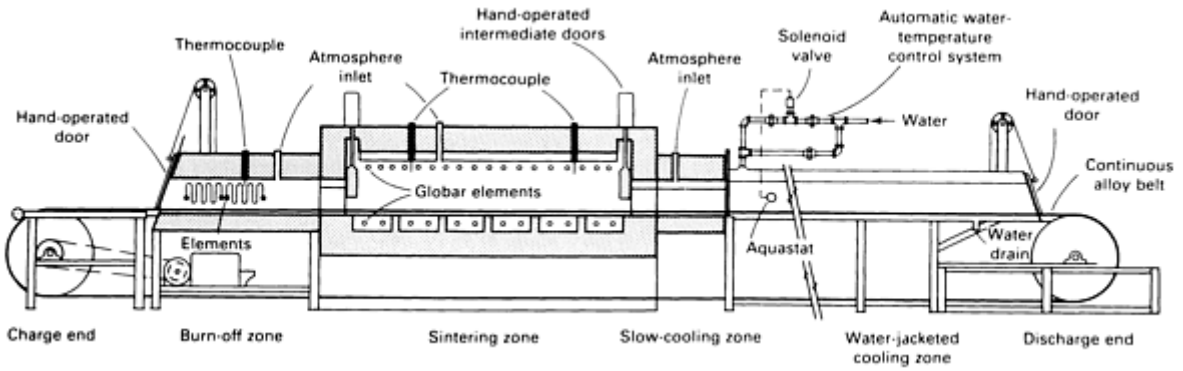

FIG. 6 CONTINUOUS-TYPE BRAZING FURNACE WITH WATER-JACKETED COOLING CHAMBER FOR USE IN AIR OR CONTROLLED ATMOSPHERES

Furnace brazing is used extensively where the parts to be brazed can be assembled with the brazing filler metal preplaced near or in the joint. Furnace brazing is particularly applicable for high-production applications in which continuous

conveyor-type furnaces are used. For medium-production work, batch-type furnaces are best. Regardless of furnace type, heating is usually produced by electrical resistance, although other types of fuel can be used in muffle-type furnaces.

The parts should be self jigged or fixtured and assembled, with brazing filler metal preplaced near or in the joint. Fluxing is used, except in cases where a reducing atmosphere, such as hydrogen, and either exothermic or endothermic combusted gas can be introduced into the furnace. Sometimes, both flux and a reducing atmosphere are necessary. Pure and dry inert gases, such as argon and helium, are used to obtain special atmosphere properties. Fluxes should never be used when furnace brazing with a vacuum atmosphere.

When continuous-type furnaces are used (Ref 16, 17), several different temperature zones can be set up to provide the proper preheating, brazing, and cooling temperatures. The speed through a conveyor-type furnace must be controlled to provide the appropriate time at the brazing temperature. It is also necessary to properly support the assembly so that it does not move while traveling on the belt (Ref 18).

A large volume of furnace brazing is performed in a vacuum atmosphere, which prevents oxidation during the heating cycle and eliminates the need for flux (Ref 19) (Fig. 7). Vacuum brazing has found wide application in the aerospace and nuclear fields, where reactive metals are joined or where entrapped fluxes would not be tolerable. Vacuum brazing does not allow as wide a choice of brazing filler metals as does atmosphere brazing (Ref 20, 21).

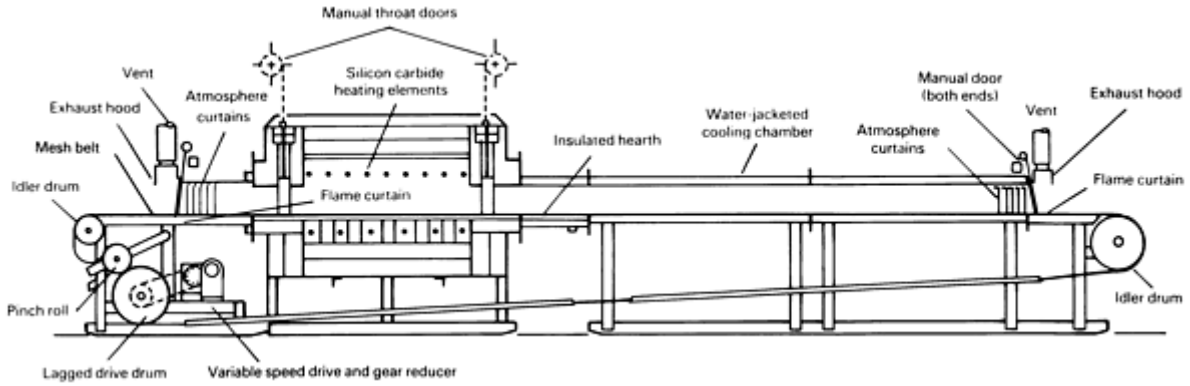

FIG. 7 HIGH-VACUUM BOTTOM-LOADING VACUUM FURNACE FOR MEDIUM-PRODUCTION APPLICATIONS

In most cases, vacuum furnaces are heated by electrical resistance heaters in a numbers of different forms. The overall time of a vacuum brazing operation is usually much longer than that of other batch brazing techniques and involves typing up expensive equipment for long periods to process comparatively small workloads. However, most of the metals on which vacuum brazing excels are also costly, the use of a process that permits material economics through fabrication while ensuring the necessary joint properties often can be justified (Ref 22, 23, 24).

Detailed information is available in the article "Furnace Brazing" in this Volume.

Induction Brazing. The high-frequency induction heating method for brazing is clean and rapid, lends itself to close control of temperature and location, and requires little operator skill.

The workpiece is placed in or near a coil carrying alternating current (ac), which induces the heating current in the desired area (Fig. 8). The coils, which are water cooled, are designed specifically for each part. Therefore, heating efficiency relies on establishing the best coil design and power frequency for each application. In most cases, the coils provide heat only to the joint area.

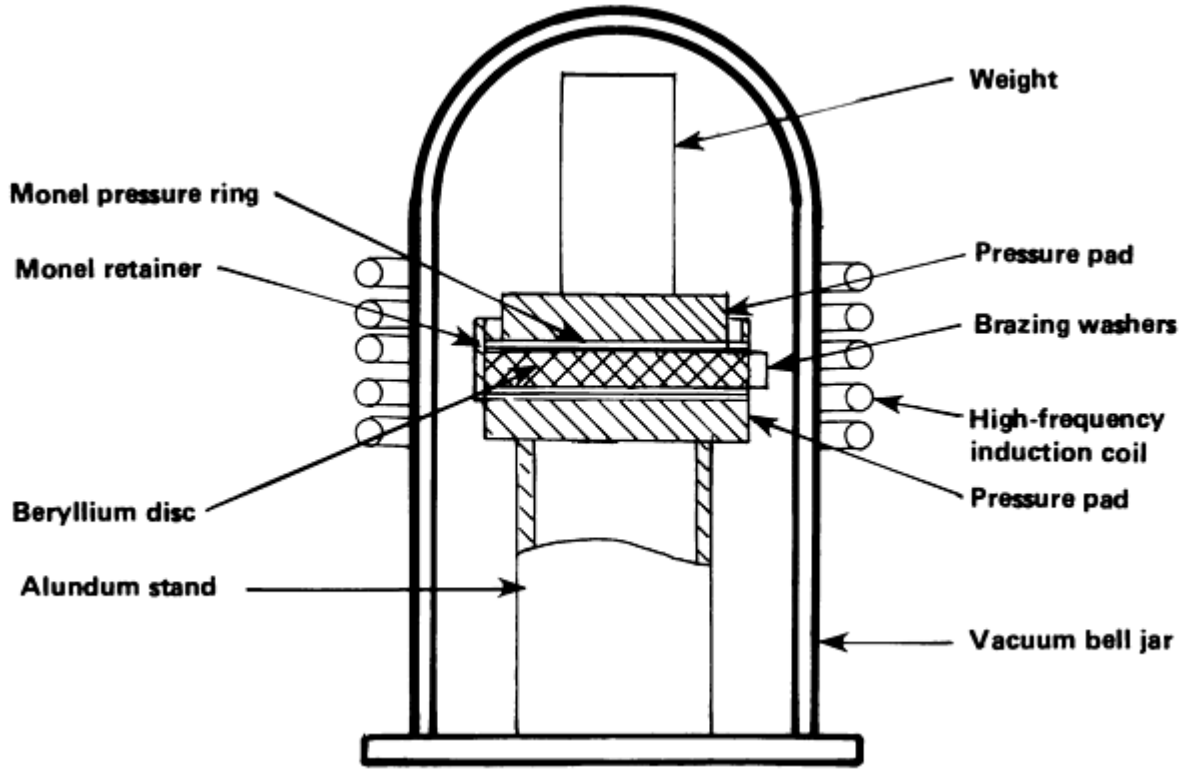

FIG. 8 INDUCTION HEATING APPARATUS USED TO VACUUM BRAZE BERYLLIUM AND MONEL COMPONENTS

The capability to heat selectively enables the induction method to be used when the nature of the brazement demands localized brazing.

There are several types of high-frequency sources to supply power to induction coils, each with a different range of frequencies:

- MOTOR GENERATORS (5 TO 10 KHZ)
- SPARK-GAP OSCILLATORS (20 TO 30 KHZ)
- VACUUM-TUBE OSCILLATORS (20 TO 5000 KHZ)
- SOLID-STATE POWER SUPPLIES (VARIABLE HZ)

The frequency of the power source determines the type of heat that will be induced in the part: high-frequency sources produce "skin" heating, whereas lower-frequency sources provide heating in thicker areas. The brazing heat usually develops within 10 to 60 s.

Induction brazing is well suited for mass production. Mechanized brazing lines for moving assemblies to and from the coils are very common. Brazing filler metals is normally preplaced in the joint, and the brazing can be done in air with the use of a flux, in an inert atmosphere, or in a vacuum atmosphere. The rapid heating rates available with induction heating are a major advantage when using brazing filler metals that tend to vaporize or segregate. The heating cycle for induction brazing is invariably automated, even when manual loading of assemblies is used.

Additional information is available in the article "Induction Brazing" in this Volume.

Dip brazing involves immersion of assembled parts into a suitable molten bath to effect brazing. The bath can be molten brazing filler metal, molten chemical flux, or molten chemical salts. The molten material is contained in a "pot" furnace heated by oil, gas, or electricity. In some instances, electrical-resistance heaters are used in the bath (Fig. 9). In the first type of bath, the parts being joined are held together and immersed in flux-covered molten filler metal, which flows into

the joints when the parts reach the bath temperature. The flux cleans the workpiece as it is introduced and protects the brazing filler metal by preventing oxidation and the loss of volatile elements from the bath.

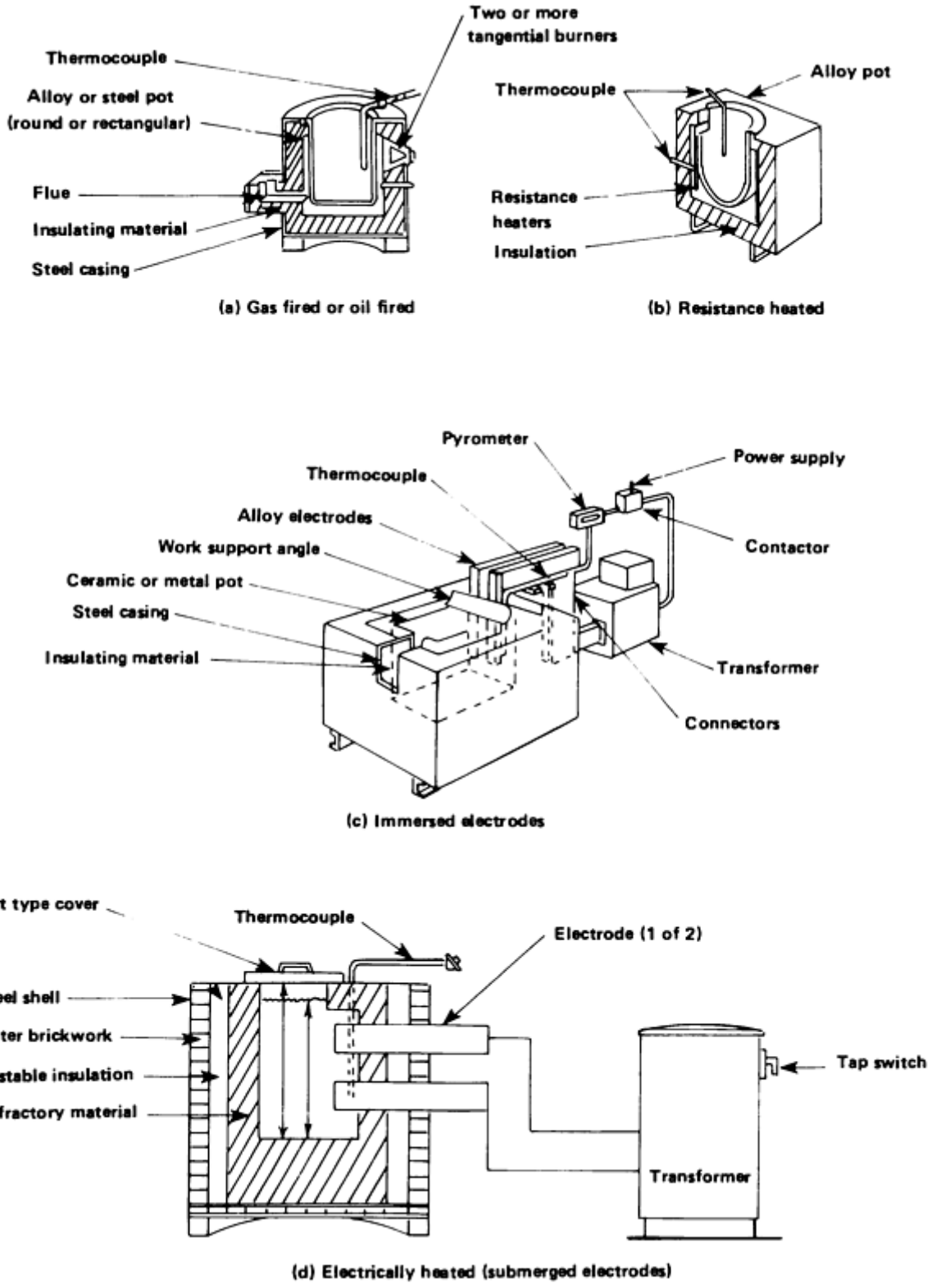

FIG. 9 EXTERNALLY AND INTERNALLY HEATED FURNACES USED FOR DIP BRAZING APPLICATIONS

The pot, or crucible, used in the molten-metal method is usually made of graphite. Jigging to maintain alignment is generally necessary. Because of the difficulties of heating and containing metals at high temperatures, filler metals that

require a brazing temperature above 1000 °C (1830 °F) are rarely used. Therefore, the choice of brazing filler metal is restricted to straight brasses and silver-base filler metals.

In the molten-flux method, the brazing filler metal is located in or near the joints and is heated to the required temperature by immersion in a bath of molten flux. Molten salt bath brazing has a greater scope than any other single brazing process. It can be used on as wide a range of parent metals as torch brazing, but is not subject to the same maximum temperature limitations. Unfortunately, it is an inflexible process. The type of salt used for a particular application depends on the ease with which the parent-metal surface oxides can be removed and on the temperature required for brazing.

The molten-flux method is used extensively for brazing aluminum and its alloys. The flux bath provides excellent protection against metal reoxidation, which can occur quite easily with aluminum.

The dip brazing method generally causes less distortion than torch brazing, because of its uniform heating. However, it may require relatively complex tooling and is therefore best used in medium- to high-production runs. This process is particularly well suited for small- to medium-sized parts with multiple hidden joints.

Detailed information is available in the article "Dip Brazing" in this Volume.

Resistance brazing is most applicable to relatively simple joints in metals that have high electrical conductivity. In this process, the workpieces are heated locally. Brazing filler metal that is preplaced between the workpieces is melted by the heat obtained from its resistance to the flow of electric current through the electrodes and the work. Usually, the heating current, which is normally ac, is passed through the joint itself. The joint becomes part of an electrical circuit, and the brazing heat is generated by the resistance at the joint.

Equipment is the same as that used for resistance welding, and the pressure needed for establishing electrical contact across the joint is ordinarily applied through the electrodes. The electrode pressure also in the usual means for providing the tight fit needed for capillary behavior in the joint. The component parts are generally held between copper or carbon-graphite electrodes.

The flux that is used must be conductive. Normally, fluxes are insulators when cool and dry, but are conductive when wet. The process is generally used for low-volume production in joining electrical contacts, related electrical elements, copper commutator segments, stainless steel tube to fittings, and so on.

Additional information is available in the article "Resistance Brazing" in this Volume.

Infrared (Quartz) Brazing. The development of high-intensity quartz lamps and the availability of suitable reflectors have made the infrared heat technique commercially important for brazing. Infrared heat is radiant heat that is obtained with the sources having energy frequency below the red rays in the light spectrum. Although there is some visible light with every "black" source, heating is principally done by the invisible radiation. Heat sources (lamps) capable of delivering up to 5000 W of radiant energy are commercially available. The lamps do not need to follow the contour of the part in order to hear the joint area, even though the heat input varies inversely as the square of the distance from the source, unless reflectors are used to concentrate the heat.

Lamps are often arranged in a toaster-like configuration, with parts traveling between two banks of lamps (Fig. 10). Infrared brazing can concentrate large amounts of heat in small areas, which can be advantageous in certain applications. Infrared brazing setups are generally not as fast as induction brazing, but the equipment is less expensive.

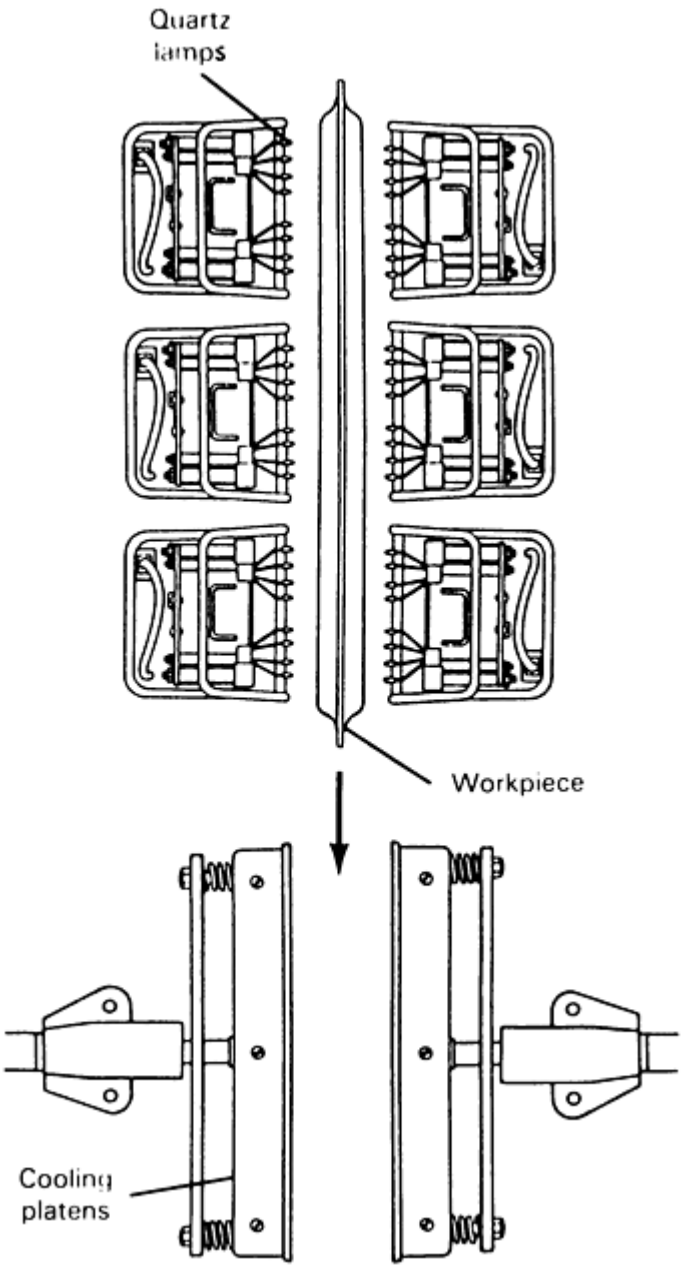

FIG. 10 WORKPIECE SUBJECTED TO INFRARED BRAZING PROCESS PRIOR TO BEING MOVED TO COOLING PLATENS

Exothermic brazing is a special process, but is rarely used because there are more-economical production methods. In this process, the heat required to melt and flow the brazing filler metal is produced by a solid-state exothermic chemical reaction, which is defined as any reaction between two or more reactants that involves the free energy of the system. Although nature provides countless numbers of these reactions, only the solid-state or nearly solid-state metal/metal-oxide reactions are suitable for use in exothermic brazing units.

Additional information is available in the article "Exothermic Brazing" in this Volume.

Electron-beam and laser brazing have been used in a limited number of applications. A laser can be used when a very small localized area of heat is required, such as for brazing small carbide tips on printer heads for electronic printers. The electron beam can be used for brazing by defocusing the beam to provide a wider area of heating. Because this is done in a vacuum, fluxes cannot be used and the brazing filler metal must be selected so that there is little or no vaporization during brazing.

Microwave Brazing. One of the newest heating methods to be developed is the use of microwaves. This technique is being used to join ceramics in high-temperature, corrosion-resistant, and high-performance applications. These applications require complex ceramics parts with strong, durable joints (Ref 25, 26).

The technique uses a single-mode microwave cavity. An iris controls the percent of microwaves reflected in the cavity, and a plunger adjusts the frequency. Together, they focus microwaves on the joint. The major advantage of this technique in terms of ceramic parts is that the entire part does not have to be heated in order to make a joint. Reheating finished ceramic parts can subject them to thermal stresses and cause cracking, which weakens the part. With microwave joining, only the interface between the pieces is heated. The technique is faster than conventional joining, which requires long times to heat ceramics uniformly. Large pieces, can, in principle, be joined at a lower cost.

One disadvantage of microwave joining is that commercial equipment is only produced by a few companies, mostly for research and development purposes.

Some microwave units feature 2.45 GHz single-mode or controlled multimode operation. Their cavity is designed to provide controlled-mode patterns that can focus high-energy microwave fields to heat a part only where it is needed, such as at a joint. The joint or part can be heated up to 2200 °C (3990 °F). Researchers have joined 92% Al_2O_3 ceramic parts in a 6 GHz single-mode microwave cavity at various temperatures and times. The bending strength of this joint gradually increased from the solidus temperature of 1400 °C (2550 °F) and reached a peak of 420 MPa (60 ksi) at about 1750 °C (3180 °F).

Braze welding is a joining process in which a filler metal is melted and deposited in a specific joint configuration, and a metallurgical bond is obtained by a wetting action that is often accompanied by some degree of diffusion with the base metals. Braze welding requires heating and melting of the filler metal that has a melting (liquidus) temperature above 450 °C (840 °F).

Stringent fit-up is not critical, because the filler metal is deposited in grooves and spaces and flows into gaps wider than those used for brazing. Fabricators use braze welding as a low-temperature substitute for oxyfuel welding or as a low-cost substitute for brazing. Joint designs for braze welding are the same as for oxyfuel welding (OFW). Braze welding has been used to join cast iron, steels, copper, nickel, and nickel alloys.

Compared to conventional fusion-welding processes, braze welding requires less heat input, permits higher travel speeds, and causes less distortion. Deposited filler metal is soft and ductile, providing good machinability, and residual stresses are low. The process joins brittle cast irons without extensive preheating.

Although most braze welding initially used an OFW torch, copper filler metal brazing rod, and a suitable flux, present applications use carbon arc welding (CAW), gas-tungsten arc welding (GTAW), gas-metal arc welding (GMAW), or plasma arc welding (PAW) without flux in the manual, semiautomatic, or automatic modes to economically bond and deposit the filler metal in the braze weld joints. OFW is, however, still widely used in machinery repair applications. Filler metal selection, proper wetting and compatibility with the base metals, and shielding from air are important to the effective use of the process with any suitable heating method.

A wide variety of parts can be braze welded using typical weld joint designs. Groove, fillet, and edge welds can be used to join simple and complex assemblies made from sheet, plate, pipe, tubing, rods, bars, castings, and forgings. Sharp corners that are easily overheated and may become points of stress concentrations should be avoided. To obtain good strength, an adequate bond area is required between filler metal and the base metal. Weld groove geometry should provide an adequate groove face area, so that the joint will not fail along the interfaces. Proper joint design selection will produce deposited filler-metal strengths that may meet or exceed the minimum base-metal tensile strengths. Because of the inert shielding gas, electrical arc methods have fewer included flux compounds and oxides at the faying surfaces. The result is higher joint strength and improved corrosion resistance. Original surfaces are restored by overlayments and subsequent machining.

References cited in this section

16. W.S. STEFFAN, NITROGEN-BASED ATMOSPHERE FURNACE BRAZING SYSTEM PROVIDES STRENGTH AND LEAK-PROOF PERFORMANCE OF NEWLY DESIGNED FUEL INJECTION RAIL,

IND. HEAT., AUG 1989, P 21-23
17. *METALS HANDBOOK,* 9TH ED., *POWDER METALLURGY,* VOL 7, 1984, P 358
18. *METALS HANDBOOK,* 8TH ED., VOL 6, 1971, P 595
19. PRODUCT LITERATURE, SECO-WARWICK CORP. (SUNBEAM), SEPT 1977
20. A. SAKAMOTO, STUDY OF FURNACE ATMOSPHERE FOR VACUUM-INERT GAS PARTIAL-PRESSURE BRAZING, *WELD. J.,* NOV 1991, P 311S-320S
21. NEW GENERATION OF VACUUM HEAT-TREATMENT FURNACES FEATURE HIGH GAS PRESSURE QUENCHING AND OIL QUENCH VACUUM FURNACE, *METALLURGIA,* MAY 1989, P 205
22. W.R. JONES, VACUUM--ANOTHER ATMOSPHERE?, *HEAT TREAT.,* OCT 1986, P 39-41
23. W.T. HOOVEN AND K.W. NOKES, MAKE YOUR VACUUM BRAZING FURNACES USER FRIENDLY, *WELD. J.,* OCT 1990, P 25-29
24. S. DRESSLER, ROLE OF HOT WALL VACUUM FURNACES IN PLASMA-ASSISTED SURFACE TREATMENT: PART II, OPERATING INFLUENCES, *IND. HEAT.,* SEPT 1989, P 31-33
25. "ADVANCED STRUCTURAL CERAMICS: TECHNOLOGIES, ECONOMICS AND MARKET OPPORTUNITIES," GB-107, BCC INC., DEC 1987
26. E.J. KUBEL, JR., STRUCTURAL CERAMICS; MATERIALS OF THE FUTURE, *ADV. MATER. PROCESS.,* VOL 134, AUG 1988, P 25-33

Fundamentals of Brazing

Mel M. Schwartz, Sikorsky Aircraft

References

1. C.M. ADAMS, JR., "DYNAMICS OF WETTING IN BRAZING AND SOLDERING," TECHNICAL REPORT WAL TR 650/1, ARMY MATERIALS RESEARCH AGENCY, WATERTOWN ARSENAL, JULY 1962
2. S. WEISS AND C.M. ADAMS, JR., THE PROMOTION OF WETTING, *WELD. J.,* VOL 46 (NO. 2), FEB 1967, P 49S-57S
3. W.D. HARKINS, *PHYSICAL CHEMISTRY OF SURFACE FILMS,* REINHOLD, 1952
4. M.M. SCHWARTZ, *MODERN METAL JOINING TECHNIQUES,* WILEY, 1969
5. A. BONDI, SPREADING OF LIQUID METALS ON SOLID SURFACE CHEMISTRY OF HIGH ENERGY SUBSTANCES, *CHEM. REV.,* VOL 52 (NO. 2), 1953, P 417-458
6. R.G. GILLILAND, WETTING OF BERYLLIUM BY VARIOUS PURE METALS AND ALLOYS, *WELD. J.,* VOL 43, JUNE 1964, P 248S-258S
7. M. NAKA, T. TANAKA, AND I. OKAMOTO, *Q. J. JPN. WELD. SOC.,* VOL 4, 1986, P 597
8. R.R. KAPOOR AND T.W. EAGER, *J. AM. CERAM. SOC.,* VOL 72, 1989, P 448
9. R.E. LOCHMAN, *CERAM. BULL.,* VOL 68, 1989, P 891
10. D.H. KIM, S.H. HWANG, AND S.S. CHUN, THE WETTING, REACTION, AND BONDING OF SILICON NITRIDE BY CU-TI ALLOYS, *J. MATER. SCI.,* VOL 26, 1991, P 3223-3234
11. D.L. KELLER *ET AL.,* WETTABILITY OF BRAZING FILLER METALS, *WELD. J.,* VOL 69 (NO. 10), 1990, P 31-34
12. W.S. BENNETT *ET AL.,* VACUUM BRAZING STUDIES ON HIGH-MANGANESE STAINLESS STEEL, *WELD. J.,* VOL 53, 1974, P 510S-516S
13. W. FEDUSKA, HIGH-TEMPERATURE BRAZING ALLOY--BASE METAL WETTING REACTIONS, *WELD. J.,* VOL 38 (NO. 3) 1959, P 122S-130S

14. W.H. KOHL, SOLDERING AND BRAZING, *VACUUM*, VOL 14, 1964, P 175-198
15. *METALS HANDBOOK*, 9TH ED., *WELDING, BRAZING, AND SOLDERING*, VOL 6, AMERICAN SOCIETY FOR METALS, 1983, P 929-995
16. W.S. STEFFAN, NITROGEN-BASED ATMOSPHERE FURNACE BRAZING SYSTEM PROVIDES STRENGTH AND LEAK-PROOF PERFORMANCE OF NEWLY DESIGNED FUEL INJECTION RAIL, *IND. HEAT.*, AUG 1989, P 21-23
17. *METALS HANDBOOK*, 9TH ED., *POWDER METALLURGY*, VOL 7, 1984, P 358
18. *METALS HANDBOOK*, 8TH ED., VOL 6, 1971, P 595
19. PRODUCT LITERATURE, SECO-WARWICK CORP. (SUNBEAM), SEPT 1977
20. A. SAKAMOTO, STUDY OF FURNACE ATMOSPHERE FOR VACUUM-INERT GAS PARTIAL-PRESSURE BRAZING, *WELD. J.*, NOV 1991, P 311S-320S
21. NEW GENERATION OF VACUUM HEAT-TREATMENT FURNACES FEATURE HIGH GAS PRESSURE QUENCHING AND OIL QUENCH VACUUM FURNACE, *METALLURGIA*, MAY 1989, P 205
22. W.R. JONES, VACUUM--ANOTHER ATMOSPHERE?, *HEAT TREAT.*, OCT 1986, P 39-41
23. W.T. HOOVEN AND K.W. NOKES, MAKE YOUR VACUUM BRAZING FURNACES USER FRIENDLY, *WELD. J.*, OCT 1990, P 25-29
24. S. DRESSLER, ROLE OF HOT WALL VACUUM FURNACES IN PLASMA-ASSISTED SURFACE TREATMENT: PART II, OPERATING INFLUENCES, *IND. HEAT.*, SEPT 1989, P 31-33
25. "ADVANCED STRUCTURAL CERAMICS: TECHNOLOGIES, ECONOMICS AND MARKET OPPORTUNITIES," GB-107, BCC INC., DEC 1987
26. E.J. KUBEL, JR., STRUCTURAL CERAMICS; MATERIALS OF THE FUTURE, *ADV. MATER. PROCESS.*, VOL 134, AUG 1988, P 25-33

Fundamentals of Brazing

Mel M. Schwartz, Sikorsky Aircraft

Selected References

- *BRAZING HANDBOOK*, 4TH ED., AWS, 1991
- M.M. SCHWARTZ, *BRAZING*, ASM INTERNATIONAL, 1987
- M.M. SCHWARTZ, *CERAMIC JOINING*, ASM INTERNATIONAL, 1990

Mel M. Schwartz, Sikorsky Aircraft

Introduction

SOLDERING is an ancient joining method. It is mentioned in the Bible (Isaiah, 41:7), and there is evidence of its use in Mesopotamia 5000 years ago, well before the time of Cleopatra, as well as later, in Egypt, Greece, and Rome (Ref 1). Pliny the Elder, in his *Historia Naturalis,* written 2000 years ago, mentions (in Chapter XLVIII of Book XXXIV) that the soldered connections of the pipes of the Roman aqueducts were made with a so-called "tertiarium" mixture, an alloy of two parts lead and one part tin. The earliest solders were alloys found in nature, which meant that only a few solders, with a severely limited range of properties, were available. Because these early solders were generally used to join jewelry parts or to attach handles to decorative vessels, the primary concerns were appearance, melting point, and, to a lesser degree, strength. The materials were rare and costly, and the work was done by highly skilled artisans. Therefore, only the wealthy could hope to own such articles.

It has only been in the last two centuries that some metals have become cheap and that strictly utilitarian parts are soldered. In the 1800s, low-cost steels made household tinware practical for most families, and the "tinner" became the common solder practitioner. The emergence of electrical technology required the attachment of electrical leads, which became a most common use of solders. This meant that the electrical properties of solders became a consideration, and the electrical continuity of the joint was of paramount importance, rather than strength or appearance, as had been the case with jewelry or utensils. The use of solders for electrical attachments also involved simple mechanical joints and repetitive operations. The cost of the materials was generally much less, because lead-tin solders were usually used. Even today, it is customary to give the tin content first when designating a solder (for example, 40/60 solder refers to a solder that is 40% Sn and 60% Pb). These new criteria promoted a new type of artisan whose skills were more oriented to engineering and production than to aesthetics, although most of the work was still done manually.

By the 20th century, metallurgical science had developed to the point that new solders could be tailored specifically for electrical, plumbing, or structural applications. The emerging electronics industry required solders having the following properties:

- COMPATIBILITY WITH COPPER (ESPECIALLY WITH RESPECT TO ALLOYING BEHAVIOR AND MELTING TEMPERATURES)
- GOOD ELECTRICAL CONDUCTIVITY
- WORKABILITY TO ENABLE FACTORY WORKERS TO RAPIDLY FORM LOW-COST, RELIABLE SOLDER JOINTS

Engineers now had formal rules to govern the design of joints used in various applications to ensure the required levels of strength. The materials and processes involved in soldering were now becoming established in engineering practice (Ref 2, 3, 4, 5).

References

1. J. WOLTERS, *ZUR GESEHICHTE DER LOTTECHNIK*, DEGUSSA, WEST GERMANY, 1977
2. H.H. MANKO, *SOLDERS AND SOLDERING,* 2ND ED., MCGRAW-HILL, 1964
3. R.J. KLEIN WASSINK, *SOLDERING IN ELECTRONICS*, ELECTROCHEMICAL PUBLICATIONS LTD., 1989
4. L.P. LAMBERT, *SOLDERING FOR ELECTRONIC ASSEMBLIES,* MARCEL DEKKER, 1987
5. *SOLDERING MANUAL*, AWS, 1978

Mel M. Schwartz, Sikorsky Aircraft

Process Overview

Soldering is defined as a joining process by which two substrates are bonded together using a filler metal (solder) with a liquidus temperature that does not exceed 450 °C (840 °F). The substrate materials remain solid during the bonding process. The solder is usually distributed between the properly fitted surfaces of the joint by capillary attraction.

The bond between solder and base metal is more than adhesion or mechanical attachment, although these do contribute to bond strength. Rather, the essential feature of the soldered joint is that a metallurgical bond is produced at the filler-metal/base-metal interface. The solder reacts with a small amount of the base metal and wets the metal by intermetallic compound formation. Upon solidification, the joint is held together by the same attraction, between adjacent atoms, that holds a piece of solid metal together. The ease of wetting is related to the ease with which this solvent action occurs. The presence of the base-metal/filler-metal reaction is one factor in the wetting action of the solder. Other factors include surface cleanliness and solder surface tension (that is, capillary flow).

Fundamentals of Soldering

Mel M. Schwartz, Sikorsky Aircraft

Fundamentals of Soldering

Pure metals have a crystalline state and a well-defined melting temperature. They also possess reasonable ductility and strength. Metals are excellent electrical conductors, when compared with ceramics or plastic polymer materials. Thermal conductivity generally follows electrical conductivity (that is, a good electrical conductor also is a good thermal conductor).

Melting and Solidification of Pure Metals. The melting behavior of pure lead is plotted in Fig. 1. From point A, which is room temperature, heat is applied to raise the temperature to 327 °C (621 °F), the melting point of lead, represented as point B, whereupon the heat of fusion is absorbed and the temperature remains constant until all the lead becomes liquid. At point C, when all of the solid is molten, the temperature of the liquid will again rise (to point D) upon the application of heat.

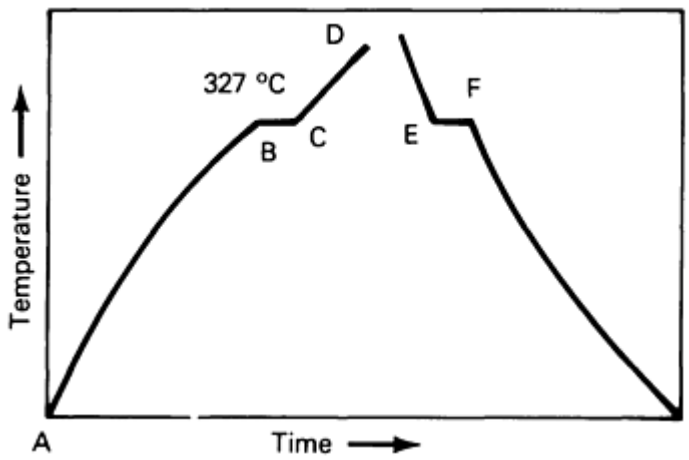

FIG. 1 PLOT OF THE HEATING AND COOLING CURVES OF PURE LEAD. SEE TEXT FOR DETAILS.

If the process is reversed and the heat source is turned off, then the temperature will fall from point D to E, where the liquid will begin to give off its heat of fusion, as atoms assume a solid crystalline form. A nucleus is formed and gradually grows as the atoms attach themselves in a regular crystalline pattern, forming dendritic crystals, which have a main trunk

and branches. As the solid forms, the release of the heat of fusion causes the temperature to remain constant (point E to F) at 327 °C (621 °F), until all the lead has solidified. Then, the solid cools back to room temperature. Under equilibrium conditions, lead will always be in the liquid phase at temperatures above 327 °C (621 °F), and will always be in the solid phase below that temperature. This behavior is observed for all pure metals, although each has a specific melting temperature. The solidification and cooling curve for pure tin is shown in Fig. 2. The cooling arrest at the solidification temperature is typical of all pure metals (Ref 3).

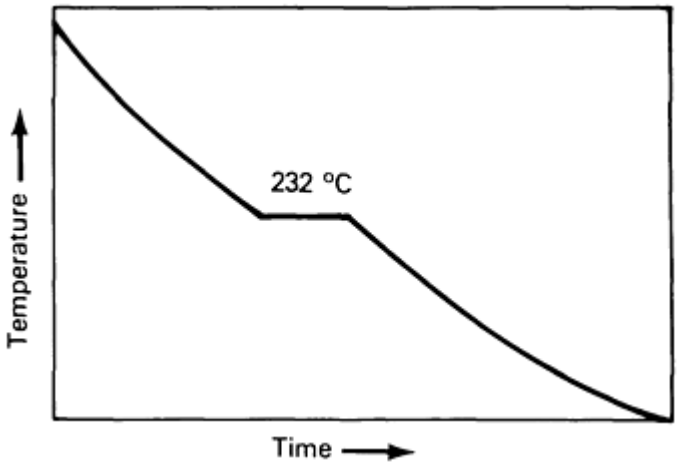

FIG. 2 COOLING CURVE FOR PURE TIN

Alloy Formation and Phase Diagrams. The best vehicle for portraying the behavior of alloys is the equilibrium phase diagram (also called equilibrium or constitution diagram), which represents the phases present under equilibrium conditions in a given alloy system. Phase diagrams are plots of alloy equilibrium composition versus temperature. The diagrams are generally worked out by measuring the melting and solidification behaviors of alloys of different compositions and then observing the resultant microstuctures. Understanding phase diagrams is essential to working effectively with solders, because they are used to predict solder microstructure and behavior.

When two or more metals are melted together, they form an alloy that behaves as a unique material with specific properties that can significantly differ from the properties of the individual pure metals. Alloy properties depend on the atomic structure and thermal-physical properties of its constituent elements. For example, the addition of tin to lead will result in an alloy that has a lower melting point than either tin or lead. Perhaps more surprising is that the addition of lead to tin will also result in an alloy with a lower melting point. The physical and mechanical properties of the alloys will also differ from the properties of the pure metals.

In Fig. 3, 327 °C (621 °F) is the melting point of pure lead (point A) and 232 °C (450 °F) is the melting point of pure tin (point B). The line AEB, which separates the liquid field from the rest of the diagram, represents the "liquidus." For any given composition in this system, the alloy is completely molten at any temperature above that line. The line below which any lead-tin alloy will be solid is called the "solidus" (represented by ACEDB).

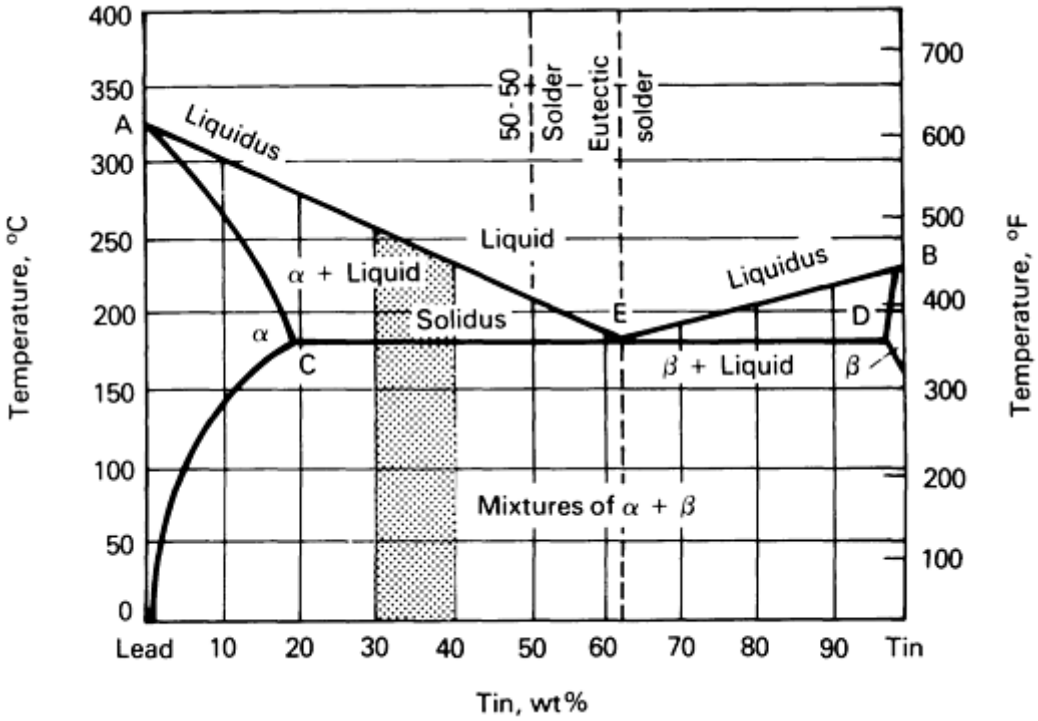

FIG. 3 CONSTITUTIONAL DIAGRAM FOR THE TIN-LEAD ALLOY SYSTEM

The CEB segment of this line is a special case known as the "eutectic" temperature. It should be noted that the fields on the phase diagram are labeled to indicate the phases existing in those regions, which enables the quick determination of the state of an alloy or the phases present at a temperature in that region.

Some metals, such as gold and silver, form alloys simply because of their mutual solubility. Such alloy formation is called a solid solution.

Two metals that have somewhat greater differences in their basic properties may not dissolve completely, that is, they have limited solubility in one another. The combination of silver and copper, however, causes a large drop in the melting temperatures, forming a eutectic (low melting) alloy system. In addition, the eutectic alloy composition itself exhibits a unique type of melting and solidification behavior, melting and solidifying at a single, specific temperature just as a pure metal does. The solid eutectic alloy is a mixture comprising two phases, rather than a solid solution. Eutectic alloy structures and behavior are of critical importance in soldering.

Wettability of Metals by Solder. Solder wetting necessarily involves the metallurgical reactions between the filler metal and the base metal. This interaction at the solder/base-metal interface can result in a covalently bonded layer of material, referred to as an intermetallic compound. Examples include tin and gold ($AuSn_4$), copper and tin (Cu_6Sn_5 and Cu_3Sn), or nickel and tin (Ni_3Sn_4). As opposed to the metallic bond of metals and alloys, the covalently bonded structure causes the intermetallic to be hard and brittle, to have a high melting point, and to be resistant to chemical attack. Excessively hard intermetallic layers can jeopardize the physical and mechanical integrity of solder joints.

All electrical/electronic applications require soldering to a base metal. This base metal can be the metal that makes up the physical structure of the electrical/electronic lead or it can constitute an underplate or a barrier metallization. In all cases, the metal must be metallurgically wettable by the solder.

Intermetallic compounds are more similar to chemical compounds than they are to metallic alloys. In soldering, intermetallic compounds in thin and uniform layers represent the "glue" that forms the structural bond between the solder and the metal being soldered. Therefore, the base metal must be metallurgically compatible with at least one of the metallic components in the solder.

This intermetallic compound formation can occur by a solid/liquid reaction (molten solder against a solid base metal) or a solid-state diffusion reaction (solder plate against a solid base metal). In either case, the solder and base metal react to form a film of intermetallic compound between the two metals, which holds them together. When tin-lead solders are used with copper, a widely used base metal, the tin reacts with the copper.

Two intermetallics discussed previously in this article can form in this metallurgical system. The compound Cu_6Sn_5 will primarily form during liquid/solid reactions. In addition, Cu_6Sn_5 continues to grow in the solid state at elevated temperatures. The compound Cu_3Sn will be present during any solid-state reactions. All base-metal solder systems form one or more such compounds. For example, soldering to nickel instead of copper will result in tin-nickel intermetallics (Ni_3Sn_4) at the interface. The Ni_3Sn_4 layer grows very slowly in the solid state and is typically difficult to observe.

The ability of base metal to form a stable intermetallic compound layer with a solder limits the number of base-metal/solder combinations that are suitable for the majority of applications. The formation kinetics of intermetallic layers must permit the thorough wetting of the solder for efficient processing. Therefore, some metals are more readily soldered than others.

Another factor is the passivation characteristic of the base metal. Passivation layers form a physical barrier to metallurgical wetting. Before the base metal can be metallurgically wet by the solder, the solder must make intimate contact, on an atomic scale, with clean base metal. Passivation layers are normally oxide films that may be only a few atomic layers thick. Even so, they affect the ability of the solder to contact the base metals underneath them. Many metals will passivate extremely rapidly. Stainless steel becomes unwettable, even with the use of very active fluxes after a short exposure in the atmosphere at room temperature.

Another issue that relates to passivation layers is their chemical and mechanical stability. Because the passivation layer that forms on solder is chemically weak, it can be reduced by weak fluxes. Nickel, on the other hand, forms a passivation film that is strong both chemically and mechanically. It is adherent to the base metal and requires much stronger fluxes to remove chemically.

Figure 4 shows the phase diagram for lead-tin. The solid solution of tin in lead is designated by α, whereas the solution of lead in tin at the other extreme of the diagram is designated by β. The line ADF, which separates the α from the rest of the diagram, is the solvus, as is the similar line (CEG) isolating the β phase.

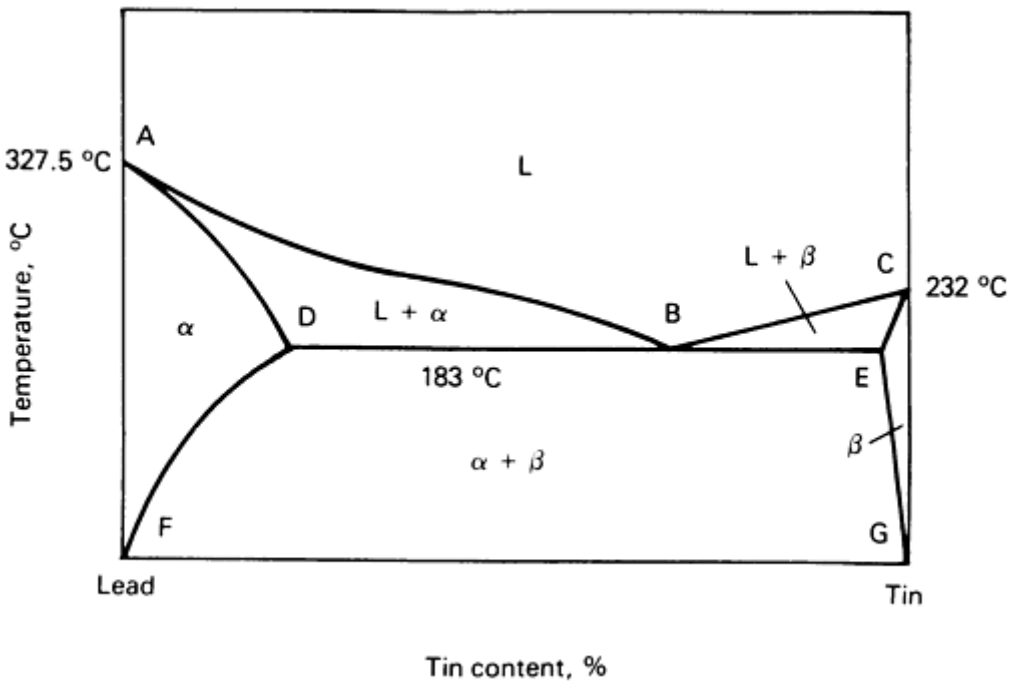

FIG. 4 LEAD-TIN PHASE DIAGRAM SHOWING EUTECTIC TEMPERATURE AT POINT B WITH 63SN-37PB

The segments D-F and E-G denote the limits of solid solubility of tin or lead in the α or the β solid solution, respectively. If the amount of tin in an alloy exceeds the solid solubility as shown by D-F, then a second phase, β, will precipitate. The amount of precipitation depends on the amount by which the Sn exceeds the solubility limit at that temperature.

Effect of Wetting Phenomena on Solderability. Solderability is a property of electronic and other components that is crucial both to the efficiency of manufacture and the reliability of the product (Ref 6). Good component solderability is important for three basic reasons:

- IT ALLOWS THE USE OF LESS-ACTIVE FLUXES, THEREBY REDUCING THE REQUIREMENT FOR CLEANING FLUX RESIDUES. (THIS IS AN ENVIRONMENTAL BENEFIT. IN ADDITION, THE REMOVAL OF FLUX RESIDUE ELIMINATES POTENTIAL CORROSION PROBLEMS THAT ARE DUE TO THAT RESIDUE.)
- IT PRODUCES GREATER "FIRST-PASS" SOLDERING YIELDS AND, CONSEQUENTLY, LESS HAND WORKING OF THE SOLDER JOINTS (IMPORTANT BECAUSE REWORKING CAN REDUCE THE FATIGUE PERFORMANCE OF A JOINT, COMPARED WITH A SUCCESSFUL FIRST-PASS JOINT).
- IT RESULTS IN A GREATER UNIFORMITY OF SOLDER FILLET, WITH A GEOMETRY THAT IS CLOSE TO THE IDEAL FOR MAXIMUM FATIGUE PERFORMANCE.

Solderability depends on the wettability of the two surfaces being joined. Poor component solderability can, to some extent, be overcome by using more-active fluxes, but the trend toward denser component packing makes it difficult to remove flux residue after assembly. Therefore, less-active fluxes are preferred. Environmental concerns (such as those about the use of chlorofluorinated carbon solvents) are also becoming important. The cost of inspection, testing, and component replacement or solder fillet rework increases the desirability of defect-free soldering. Therefore, solderability is an increasingly important manufacturing issue.

The solderability of a component, defined as its suitability to be soldered by a given method, is a complex processing parameter. The relationship between wettability and solderability represents a major unresolved gap in the understanding of the soldering process. As described in the section "Physics of Wetting," wettability can be measured directly. Solderability, however, cannot be directly measured in a quantifiable way, and its relationship to wettability has not yet been explicitly defined.

There are three important aspects to solderability:

- THERMAL DEMAND
- WETTABILITY
- RESISTANCE TO SOLDERING HEAT

The thermal characteristics of the component must allow the joint to be heated to the soldering temperature within the specified time. The solderable surfaces must allow the molten solder to wet and spread during the available time without subsequent dewetting. The soldering heat and the induced thermal stresses associated with it must not affect the functioning of the components. Each of these solderability aspects can be engineered to fit a particular application by the suitable choice of solder alloys and process control parameters. The most restraining of the solderability aspects, in regard to design for performance, is component wettability.

Wettability. When discussing the wetting characteristics of a surface by molten solder, there are two important factors to consider: the extent of wetting and the rate of wetting (Ref 6). The extent of wetting (as indicated by the contact angle) is an equilibrium governed by the laws of thermodynamics and depends on the surface and interfacial energies involved at the liquid/solid interface (Fig. 5). The rate of wetting (that is, how rapidly the solder wets and spreads) is governed by the thermal demand of the system, the ability of the heat source to supply heat, the efficacy of the flux, the viscosity of the solder, and the chemical reactions that occur at the interfaces.

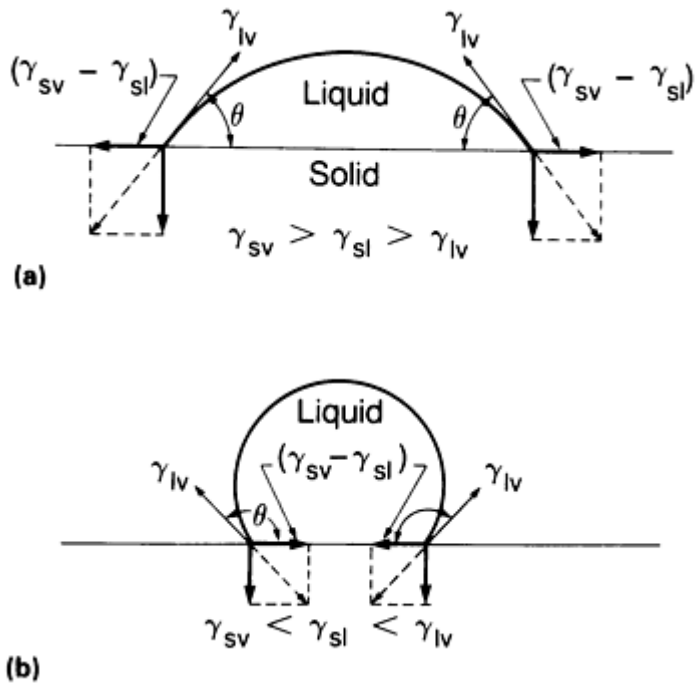

FIG. 5 LIQUID SOLDER DROPLETS ON A SOLID SURFACE UNDER TWO CONDITIONS. (A) WETTING. (B) NONWETTING. ARROWS INDICATE SURFACE TENSION.

The physics of wetting is the governed by Young's equation (also known as Young-Depre equation because Young described the problem quantitatively in 1805 and Depre put it in mathematical terms in 1869):

$$\gamma_{SV} = \gamma_{SL} - \gamma_{LV} \cos \theta \qquad \textbf{(EQ 1)}$$

where γ_{sv}, γ_{sl}, and γ_{lv} refer to the solid-vapor, solid-liquid, and liquid-vapor surface tensions, respectively. Relative to each other, these parameters can be defined by:

$$\gamma_{SV} > \gamma_{SL} > \gamma_{LV} \qquad \textbf{(EQ 2)}$$

For soldering, the vapor phase will be replaced in nearly all processes by flux (that is, γ_{sv} is replaced by γ_{sf} and γ_{lv} is replaced by γ_{lf}).

For optimum wetting, the contact angle, θ, must be minimized and, therefore, γ_{sv} must be maximized. Oxides and contamination lower the value of γ_{sv} (or γ_{sf}). A function of the flux is to remove or disperse oxides and contaminants, thereby increasingly γ_{sv}. An important function of flux is to lower the value of γ_{lf} (or γ_{lv}). The flux also maintains a local environment around the surfaces being joined, protecting them from reoxidation during soldering, as well as enhancing heat transfer from the heating source to the substrate and the solder.

Equation 1 shows that wetting is also enhanced by minimizing γ_{lv}, a value commonly referred to as the surface tension of the solder. Although γ_{lv} is a function of the solder composition, the flux covering the liquid solder, and the temperature, it is normally close to 0.4 J/m^2 (4×10^{-5} Btu/ft^2).

A typical example of nonwetting occurs when a liquid metal droplet is placed on a nonmetallic surface, such as copper oxide. Because there are no metallic bonds at the oxide surface, the liquid metal will have little tendency to interact with that surface. The metal droplet will behave as though it is repelled, and will try to ball up to minimize the area of contact with the nonmetallic surface. One method for quantifying wettability is to observe the behavior of solder droplets on the metal surface. The contact angle formed between the surface of the liquid solder and the surface of the solid can be

measured (Fig. 5). If the solder droplet forms an angle, θ, of less than 90°, then the solder is said to wet the metal. If the angle is greater than 90°, the solder is nonwetting. This is one method used to qualitatively assess solderability.

The formation of intermetallic compounds can affect Young's equation because it alters the value of γ_{sl}. The influence of this term has been recognized (Ref 6), but the magnitude has not yet been calculated quantitatively.

Surfaces of a metal crystal have a higher free energy than the bulk of the crystal because of the existence of unsatisfied metallic bonds. When a liquid metal or alloy is brought into contact with this solid surface, the liquid will proceed to interact with the solid to satisfy those dangling surface bonds and thus reduce the surface free energy of the system. To the extent that a liquid solder can satisfy these surface bonds, it will wet the solid metal and spread across its surface. If no exchange of bonding energy takes place, then wetting will not occur and the solder will tend to ball up on the surface of the solid, minimizing the area of contact between liquid and solid.

Information about selecting solders for specific applications is provided in the article "General Soldering" in this Volume.

References cited in this section

3. R.J. KLEIN WASSINK, *SOLDERING IN ELECTRONICS,* ELECTROCHEMICAL PUBLICATIONS LTD., 1989
6. A.D. ROMIG, JR., Y.A. CHANG, J.J. STEPHENS, *ET AL.*, PHYSICAL METALLURGY OF SOLDER-SUBSTRATE REACTIONS, *SOLDER MECHANICS,* THE MINERALS, METALS, & MATERIALS SOCIETY, 1991, P 30-32

Mel M. Schwartz, Sikorsky Aircraft

Guidelines for Flux Selection

A flux promotes solder wetting of the base materials by:

- REMOVING TARNISH FILMS FROM PRECLEANED SURFACES
- PREVENTING OXIDATION DURING THE SOLDERING OPERATION
- LOWERING THE SURFACE TENSION OF THE SOLDER

Successful establishment of a solder joint requires that the liquid solder make contact with the metal to which it is to be joined, so that wetting can be initiated. Unfortunately, almost all of the metals involved in soldering are oxidized during exposure to elevated temperatures in air. This prevents metal-to-metal contact, as well as the wetting and formation of a metallurgical bond, unless the oxides are removed. Fluxes are used in soldering to remove such films and to protect the surfaces against reoxidation during soldering.

In addition to cleaning metal surfaces, a flux also:

- AIDS IN THE WETTING PROCESS
- IMPROVES HEAT TRANSFER (ESPECIALLY IN SOLDER PASTES)
- CARRIES OXIDES AND SOLID DEBRIS AWAY FROM THE JOINT

Fluxes are chemical (liquid, solid, or gaseous materials) that remove oxide layers from the base metal and solder. When heated, fluxes either promote or accelerate the wetting of metals by solder. Flux selection usually depends on the ease with which a material can be soldered. Rosin fluxes are used with solderable base metals or with metals that are precoated

with a solderable base metal or with metals that are precoated with a solderable finish. Inorganic fluxes are often used on metals such as stainless steel. Table 1 indicates the relative ease with which a number of alloys and metals can be soldered, based on flux requirements.

TABLE 1 RELATIVE SOLDERABILITY OF SELECTED METALS AND ALLOYS AS A FUNCTION OF FLUX TYPE USED

Base Metal, Alloy, Or Applied Finish	Flux Type				Soldering Not Recommended[(A)]
	ROSIN	ORGANIC	INORGANIC	SPECIAL FLUX AND SOLDER	
Aluminum	. . .	. . .	. . .	X	. . .
Aluminum-Bronze	. . .	. . .	. . .	X	. . .
Beryllium	. . .	. . .	. . .	. . .	X
Beryllium-Copper	X	X	X	. . .	. . .
Brass	X	X	X	. . .	. . .
Cadmium	X	X	X	. . .	. . .
Cast Iron	. . .	. . .	. . .	X	. . .
Chromium	. . .	. . .	. . .	. . .	X
Copper	X	X	X	. . .	. . .
Copper-Chromium	. . .	. . .	X	. . .	. . .
Copper-Nickel	X	X	X	. . .	. . .
Copper-Silicon	. . .	. . .	X	. . .	. . .
Gold	X	X	X	. . .	. . .
Inconel	. . .	. . .	. . .	X	. . .
Lead	X	X	X	. . .	. . .
Magnesium	. . .	. . .	. . .	. . .	X
Manganese-Bronze (High Tensile)	. . .	. . .	. . .	. . .	X
Monel	. . .	X	X	. . .	. . .
Nickel	. . .	X	X	. . .	. . .
Nickel-Iron	. . .	X	X	. . .	. . .
Nichrome	. . .	. . .	. . .	X	. . .
Palladium	X	X	X	. . .	. . .
Platinum	X	X	X	. . .	. . .
Rhodium	. . .	. . .	X	. . .	. . .
Silver	X	X	X	. . .	. . .
Stainless Steel	. . .	X	X	. . .	. . .
Steel	. . .	. . .	X	. . .	. . .
Tin	X	X	X	. . .	. . .
Tin-Bronze	X	X	X	. . .	. . .
Tin-Lead	X	X	X	. . .	. . .
Tin-Nickel	. . .	X	X	. . .	. . .
Tin-Zinc	X	X	X	. . .	. . .
Titanium	. . .	. . .	. . .	. . .	X
Zinc	. . .	X	X	. . .	. . .
Zinc Die Castings	. . .	. . .	. . .	. . .	X

(A) WITH PROPER PROCEDURES, SUCH AS PRECOATING, MOST METALS CAN BE SOLDERED

Mel M. Schwartz, Sikorsky Aircraft

Types of Fluxes

Fluxes can be categorized by their chemical makeup (Ref 2, 3, 9, 10, 11):

- ROSIN-BASE FLUXES
- ORGANIC FLUXES
- INORGANIC FLUXES
- SYNTHETICALLY ACTIVATED FLUXES (RESINS)

These materials vary in their activity (that is, aggressiveness). Rosin-base fluxes are very mild, whereas inorganic fluxes can be extremely active and corrosive. Because of the potential for corrosion by inorganic fluxes in electronic assemblies, the rosin-base fluxes (with their low flux activity) are favored by the electronics industry.

Rosin Fluxes. Water-white rosin dissolved in a suitable organic solvent is the closest model of a flux with noncorrosive residue. Rosin fluxes possess important physical and chemical properties that make them particularly suitable for use in the electrical industry. They are solid and inactive chemically at room temperature, but at soldering temperatures they gain sufficient activity to remove weakly adherent oxides from the noble metals gold and silver, as well as copper.

Nonactivated Rosin Flux. Although its noncorrosive nature has led to its widespread use in microelectronics, rosin-base flux is lacking in chemical activity, which essentially limits its use to precleaned parts and to only a few metals that do not have adherent oxides. The active constituent, abietic acid ($C_{20}H_{30}O_2$), with a melting point of 173 °C (343 °F), becomes mildly active at soldering temperatures ranging from 177 to 316 °C (350 to 601 °F). The residue is hard, nonhygroscopic, electrically nonconductive, and noncorrosive.

Mildly Activated Rosin Flux. The very low chemical activity of rosin-base flux can be countered by the addition of activators, usually organic acids or amines. The end product, rosin mildly activated (RMA) flux, is still essentially noncorrosive, but is sufficiently active to remove oxides more reliably than the rosin-base flux. In addition, the residues are noncorrosive. However, care must be exercised in cases of high-reliability applications. It is advisable to specify that these fluxes be halide-free, in order to ensure that specific safety requirements are met in critical components. Even so, cleaning is now required to remove the flux residue. Both polar and nonpolar solvents have been used. These RMA fluxes are preferred for military, telephone, and other high-reliability electronic products.

Activated rosin fluxes were developed to provide more chemically active fluxes for mass-produced electronics, such as packaged components. Most mass-produced electronics are manufactured using RMA fluxes. The use of chlorides in these fluxes requires effective cleaning after soldering to prevent corrosion and electrical leakage, because the presence of chloride ions in flux residue makes it conductive. Because of the chemistry of the activators, a double solvent cleaning is normally required. Activated rosin fluxes are widely used in commercial electronics and in high-reliability applications where the residue can be completely removed after soldering.

Inorganic Fluxes. Inorganic acids and salts that are highly corrosive and extremely active compose this class of fluxes. In many instances, they are not acceptable for use on electronics, but are suitable for plumbing and industrial applications. Inorganic fluxes do enable the soldering of ferrous alloys and high-nickel alloys used in electronic packages and hermetic enclosures. The difficulty of chloride ion removal has led to the gradual abandonment of inorganic fluxes, even for tinning purposes.

Inorganic fluxes are used to optimum advantage where conditions require rapid and highly active fluxing action. They can be applied as solutions, pastes, or dry salts in many general soldering applications. They function equally well with torch, oven, resistance, or induction soldering methods, because they neither char nor burn. These fluxes can be formulated to provide stability over the entire soldering temperature range.

One distinct disadvantage of inorganic fluxes is that their residue remains chemically active after soldering. If this residue is not removed, then severe corrosion can occur at the joint. Adjoining areas can also be attacked by residues from the spray of flux and from flux vapors. Fluxes that contain ammonium salts can cause stress-corrosion cracking (SCC) when soldering brass, as well as most iron-nickel alloys.

Organic acid fluxes, although less active than inorganic fluxes, are effective at soldering temperatures ranging from 90 to 320 °C (195 to 610 °F). They consist of organic acids and bases and, often, hydrohalides. They are active at soldering temperatures, but the period of activity is short because of their susceptibility to thermal decomposition. Their tendency to volatilize, char, or burn when heated limits their use with torch or flame heating. When these fluxes are properly used, their residues are relatively inert and can be removed with water.

Organic acid fluxes are particularly useful in applications where controlled quantities of flux can be applied and where sufficient heat can be used to fully decompose or volatilize the corrosive constituents. Caution is necessary to prevent undecomposed flux from spreading to insulating sleeving. Care must also be taken when soldering in closed systems where corrosive fumes can condense on critical parts of the assembly.

References cited in this section

2. H.H. MANKO, *SOLDERS AND SOLDERING,* 2ND ED., MCGRAW-HILL, 1964
3. R.J. KLEIN WASSINK, *SOLDERING IN ELECTRONICS,* ELECTROCHEMICAL PUBLICATIONS LTD., 1989
9. J.F. SHIPLEY, INFLUENCE OF FLUX, SUBSTRATE AND SOLDER COMPOSITION ON SOLDER WETTING, *WELD. J.,* VOL 54 (NO. 10), OCT 1975, P 357S-362S
10. H.H. MANKO, SOLDERING FLUXES--PAST AND PRESENT, *WELD. J.*, VOL 52 (NO. 3), MARCH 1973, P 163-166
11. R.W. WOODGATE, *THE HANDBOOK OF MACHINE SOLDERING,* 2ND ED., JOHN WILEY & SONS, 1988

Flux Evaluation

Several tests are used to evaluate the relative activity of fluxes. The most common are the copper mirror test, the halide test, a surface conductivity test, and a test based on the resistivity of a water extract present in the flux. In all cases, a measure of the chemical activity of the flux is obtained.

Because the fluxes all depend on other properties (for example, viscosity, ease of removal, and thermal behavior), chemical activity is only one factor in flux selection for a given application. Information about selecting fluxes for specific applications is provided in the article "General Soldering" in this Volume.

Fundamentals of Soldering

Mel M. Schwartz, Sikorsky Aircraft

Joint Design

Joints should be designed to fulfill the requirements of the finished assembly, as well as to permit the application of the flux and solder. Joint design should maintain proper clearance during heating and upon solidification of the filler metal. Special fixtures may be necessary or the units can be crimped, clinched, wrapped, or otherwise held together.

The selection of a joint design for a specific application will primarily depend on the service requirements of the assembly. It may also depend on such factors as the heating method to be used, the fabrication techniques utilized prior to soldering, the number of items to be soldered, and the method used to apply the solder. In general, solders have low

strength when compared with the metals for which they are used to join. Therefore, the soldered joint should be designed to avoid dependence on solder strength. The necessary strength can be provided by shaping the parts to be joined so that they engage or interlock, requiring the solder only to bond, seal, and stiffen the assembly.

Figure 6 shows joint designs commonly used for soldering applications. The lap joint and the lock seam joint are used when soldering sheets. Lap joints are also applied to join pipes. Actually, the lap type of joint should be used whenever possible because it offers the best chance to obtain joints with maximum strength. It should also be used whenever a seal is required. Butt joints should be avoided whenever possible.

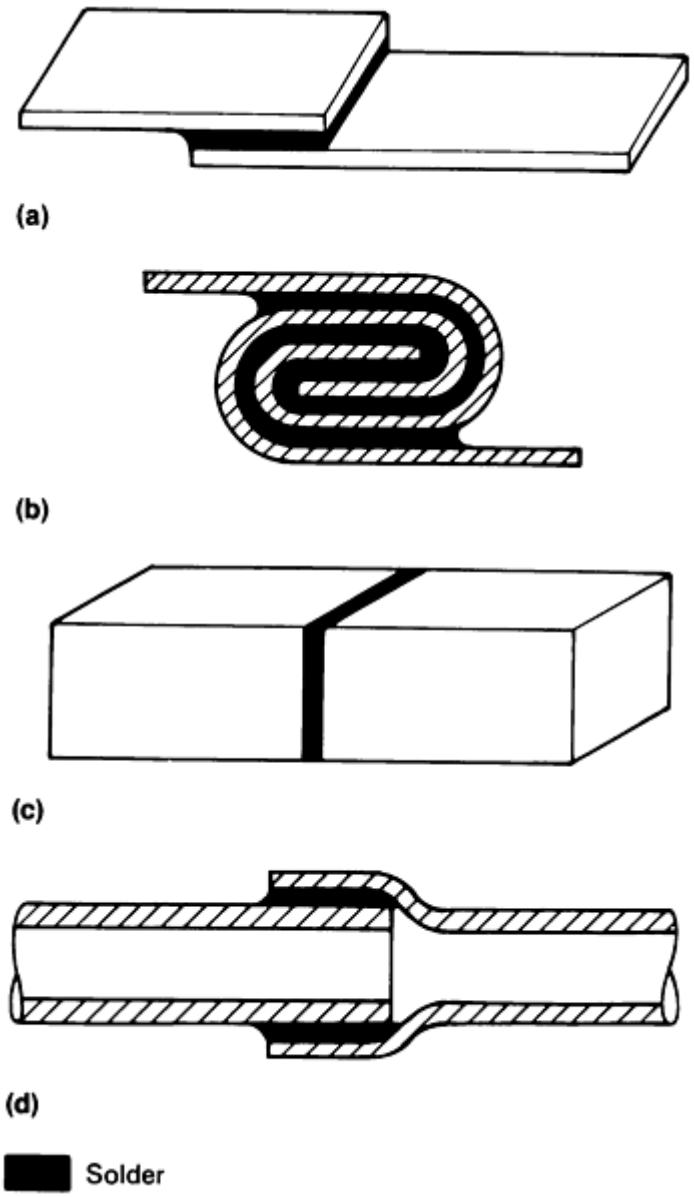

FIG. 6 BASIC JOINT CONFIGURATIONS USED FOR SOLDERING APPLICATIONS. (A) LAP JOINT. (B) LOCK SEAM JOINT. (C) BUTT JOINT. (D) PIPE JOINT

An important factor in joint design is the manner in which the solder will be applied to the joint. The designer must consider the number of joints per assembly and the number of assemblies to be manufactured. For limited production using a manual soldering process, the solder can be face-fed into the joint with few problems. However, for a large production lot of assemblies containing multiple joints, an automated process such as condensation/vapor-phase reflow soldering can be advantageous (Ref 12, 13, 14). In this case, the design must provide for accessible joints that are suitable for automated fluxing, soldering, and cleaning.

There should be enough clearance between the parts being joined to allow the solder to be drawn into the space by capillary action, but not so much that the solder is unable to fill the gap. Joint clearances ranging from 0.075 to 0.150 mm (0.0030 to 0.059 in.) are preferred for optimum strength, but variations are allowed in specific cases. It is often necessary to fabricate sample parts and to test the joints to ensure their producibility and capability regarding strength properties (Ref 2, 3, 10, 15, 16, 17).

Other commonly used soldered joints are shown in Fig. 7; self-jigging joints are shown in Fig. 8. The most definitive work available on the loading of soldered joints is that used for the load-carrying capabilities of copper tube with sleeve-type joints or fittings. Conservative joint design requires that only 50% of the joint be considered filled. Under normal conditions, it would be considered good soldering practice if 70% or more of the joint consists of sound joint material (Ref 2, 3, 4, 5, 6, 11, 15, 18). Additional information about joint configurations is provided in the article "General Soldering" in this Volume.

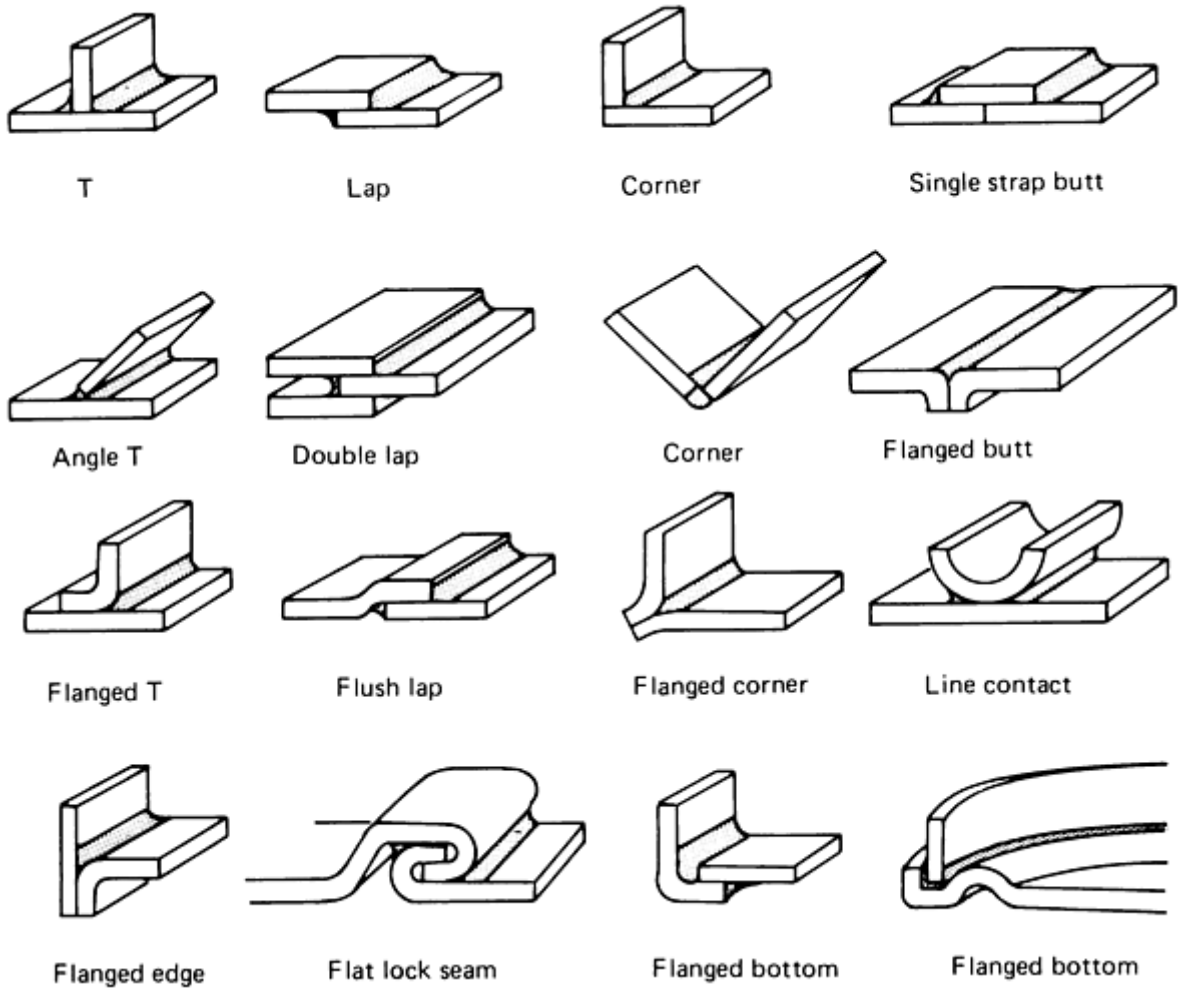

FIG. 7 JOINT DESIGNS FREQUENTLY USED IN SOLDERING OPERATIONS. SOURCE: REF 5

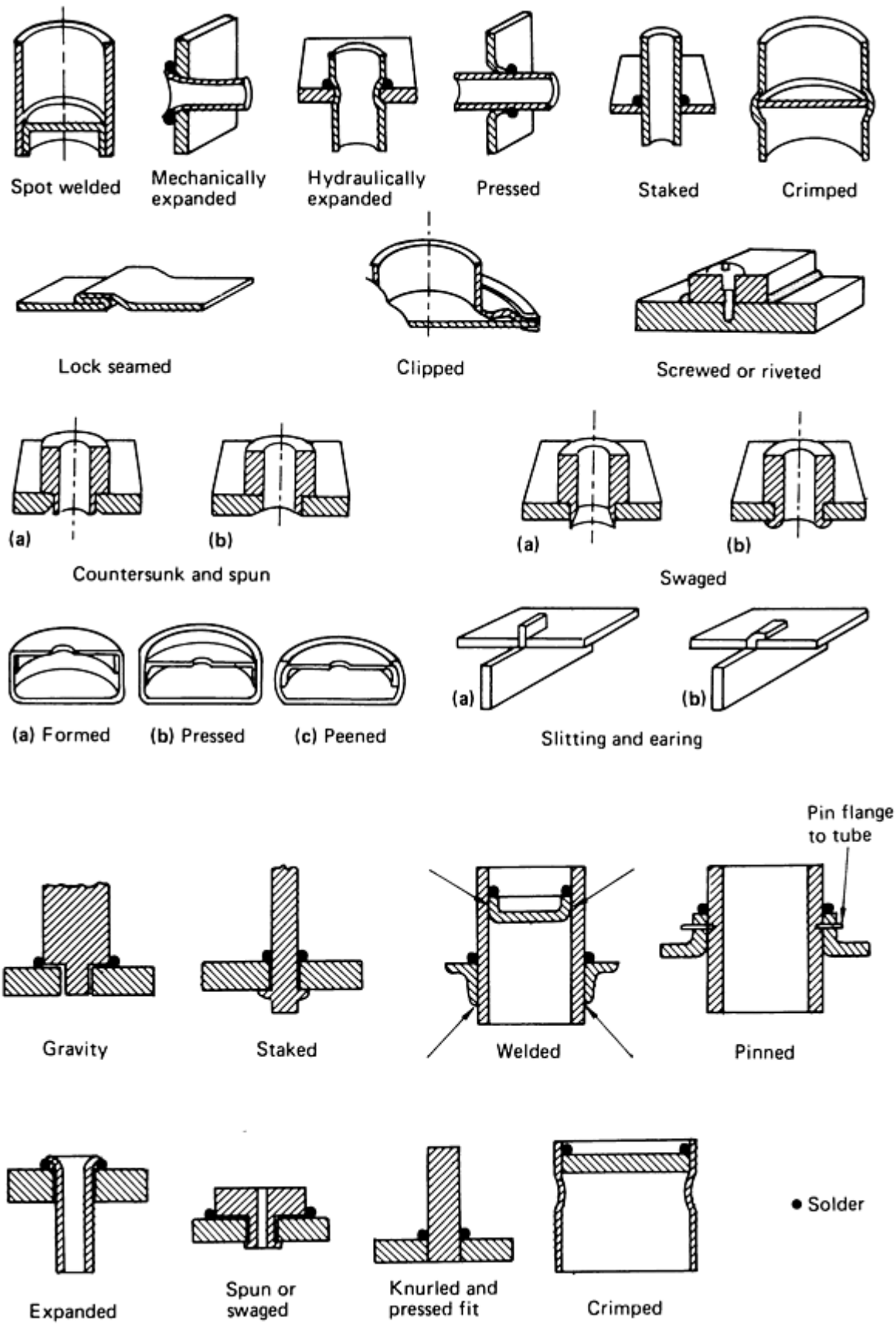

FIG. 8 METHODS THAT CAN BE USED TO MAKE SOLDER JOINTS SELF-JIGGING. SOURCE: REF 5

References cited in this section

2. H.H. MANKO, *SOLDERS AND SOLDERING,* 2ND ED., MCGRAW-HILL, 1964
3. R.J. KLEIN WASSINK, *SOLDERING IN ELECTRONICS,* ELECTROCHEMICAL PUBLICATIONS LTD., 1989
4. L.P. LAMBERT, *SOLDERING FOR ELECTRONIC ASSEMBLIES,* MARCEL DEKKER, 1987
5. *SOLDERING MANUAL,* AWS, 1978
6. A.D. ROMIG, JR., Y.A. CHANG, J.J. STEPHENS, *ET AL.,* PHYSICAL METALLURGY OF SOLDER-SUBSTRATE REACTIONS, *SOLDER MECHANICS,* THE MINERALS, METALS, & MATERIALS SOCIETY, 1991, P 30-32
10. H.H. MANKO, SOLDERING FLUXES--PAST AND PRESENT, *WELD. J.,* VOL 52 (NO. 3), MARCH 1973, P 163-166
11. R.W. WOODGATE, *THE HANDBOOK OF MACHINE SOLDERING,* 2ND ED., JOHN WILEY & SONS, 1988
12. T. THOMPSON, CONDENSATION/VAPOR-PHASE REFLOW SOLDERING, *ASS. ENG.,* JUNE 1977, P 44-47
13. T.Y. CHU, A GENERAL REVIEW OF MASS SOLDERING METHODS, *INS. CIRC.,* NOV 1976
14. R.C. PFAHL, JR., J.C. MOLLENDORF, AND T.Y. CHU, CONDENSATION SOLDERING, *WELD. J.,* VOL 54 (NO. 1), 1975
15. E. LIEBERMAN, *MODERN SOLDERING AND BRAZING TECHNIQUES,* BUSINESS NEWS PUBLISHING CO., 1988
16. "SOLDER METAL SPECIFICATION," ASTM B 32, *ANNUAL BOOK OF ASTM STANDARDS,* PART B, ASTM
17. D.R. FREAR, W.B. JONES, AND K.R. KINSMAN, ED., *SOLDER MECHANICS,* TMS, 1991, P 30-41
18. *PROC. IEEE 41ST ELECT. COMP. & TECH. CONF.,* IEEE, 1991

Fundamentals of Soldering

Mel M. Schwartz, Sikorsky Aircraft

Precleaning and Surface Preparation

An unclean surface will not permit the solder to flow, which makes soldering either difficult or impossible and contributes to the formation of a poor joint. Materials such as oil, grease, paint, pencil markings, drawing, and cutting lubricants, general atmospheric dirt, oxide, and rust films must be removed before soldering. The importance of cleanliness cannot be overemphasized in ensuring sound soldered joints. Fluxing alone cannot substitute for adequate precleaning (Ref 19). Because cleaning methods are often designed for a specific soldering operation, their suitability for a particular application should be investigated thoroughly.

Degreasing. Either solvent or alkaline degreasing is recommended for the cleaning of oily or greasy surfaces. Of the solvent degreasing methods, the vapor condensation of the trichloroethylene-type solvents probably minimizes residual film on the surface. In the absence of vapor degreasing apparatus, immersion in liquid solvents or in detergent solutions is a suitable procedure. Hot alkali detergents are widely used for degreasing. All cleaning solutions must be thoroughly removed before soldering. Residues from hard-water rinses can interfere with soldering. Material compatibility is a prime consideration.

Pickling. The purpose of pickling, or acid cleaning, is to remove rust, scale and oxides, or sulfides from the metal in order to provide a clean surface for soldering. All of the inorganic acids (that is, hydrochloric, sulfuric, phosphoric, nitric, and hydrofluoric acids), singly or mixed, will fulfill this function, although hydrochloric and sulfuric acids are the most widely used. The pieces should be washed thoroughly in hot water after pickling and then dried as quickly as possible.

Mechanical cleaning includes the following methods:

- GRIT AND SHOTBLASTING
- MECHANICAL SANDING AND GRINDING
- FILING AND HAND SANDING
- CLEANING WITH STEEL WOOL
- WIRE BRUSHING AND SCRAPING

For best results, cleaning should extend beyond the joint area. Shot or steel gritblasting is often effective and is preferable to sandblasting because it avoids the embedding of silica particles on the surface, which interferes with the flow of solder. Mechanical cleaning is not recommended for softer metals, such as copper.

Precoating. The coating of the base metal surfaces with a more-solderable metal or alloy prior to the soldering operation can facilitate soldering. Coatings of tin, copper, silver, cadmium, iron, nickel, and the alloys of tin-lead, tin-zinc, tin-copper, and tin-nickel are used for this purpose. The advantages of precoating include the following:

- SOLDERING IS MORE RAPID AND UNIFORM.
- STRONG ACIDIC FLUXES CAN BE AVOIDED DURING SOLDERING.

The precoating of metals that have tenacious oxide films (for example, aluminum, aluminum bronzes, highly alloyed steels, and cast iron) is almost mandatory. The precoating of steel, brass, and copper, although not entirely essential, is of great value in some applications.

A number of different methods are used to precoat the metal surfaces. Solder or tin can be applied using a soldering iron or an abrasive wheel, ultrasonic soldering, immersion in molten metal, electrodeposition, or chemical displacement.

Hot dipping can be accomplished by fluxing and dipping the parts in molten tin or solder. Often, small parts are initially placed in wire baskets and then cleaned, fluxed, and dipped in the molten metal. Finally, they are centrifuged to remove the excess metal. Coating by hot dipping is applicable to carbon steel, alloy steel, cast iron, copper, and certain copper alloys. Prolonged immersion in molten tin or solder should be avoided to prevent the excessive formation of intermetallic compounds at the coating/base-metal interface.

Electrodeposition. Precoating by electrodeposition can be accomplished in stationary tanks, in conveyorized plating units, or in barrels. This method is applicable to all steels, copper alloys, and nickel alloys. The coating metals are not limited to tin and solder. Copper, cadmium, silver, precious metals, nickel, iron, and alloy platings such as tin-copper, tin-zinc, and tin-nickel are also commonly used.

Certain combinations of electrodeposited metals (that is, duplex coatings), where one metal is plated over another, are becoming more popular as an aid to soldering. A coating of 0.005 mm (0.0002 in.) of copper plus 0.0075 mm (0.0003 in.) of tin is particularly useful for brass. The solderability of aluminum is enhanced by a coating of 0.013 mm (0.0005 in.) of nickel, followed by 0.008 mm (0.0003 in.) of tin or by a combination of zincate (zinc), 0.005 mm (0.0002 in.) copper, and tin. An iron plating followed by tin plating is extremely useful over a cast iron surface.

Immersion coatings (that is, chemical displacement coatings) of tin, silver, or nickel can be applied to some of the common base metals. These coatings are usually very thin and generally have a poor shelf life.

The shelf life of a coating is defined as its ability to withstand storage conditions without impairing solderability. Hot tinned and brightened electrotin coatings have an excellent shelf life. Inadequate thicknesses of electrotinned or immersion-tinned coatings have a limited shelf life. Tin or solder coating thicknesses ranging from 0.003 to 0.008 (0.0001 to 0.0003 in.) are recommended to ensure maximum solderability after prolonged storage.

Reference cited in this section

19. J. BROUS, EVALUATION OF POST-SOLDER FLUX REMOVAL, *WELD. J.,* VOL 54 (NO. 12), 1975, P 444S-448S

Mel M. Schwartz, Sikorsky Aircraft

Soldering in Electronic Applications

This section addresses some general considerations in the soldering of electronic devices. More detailed information is provided in the article "Soldering in Electronic Applications," in this Volume.

Substrates for Electronic Component Applications

A substrate is the platform on which the electrical/electronic circuitry is built. Many different types of substrates are used in the electronics field. Early substrates were sheets of material to which insulated, stand-off terminals were attached by bolting or riveting. The circuitry was then obtained by point-to-point wiring between these terminals. Although this approach is still used, the most common substrate in use today has circuitry that is laid on it in planar form, with the components already attached. Attachment is normally accomplished through the soldering process. The most common form of this substrate is the printed wiring board (PWB).

A substrate can actually have numerous forms:

- CIRCUITRY CAN BE LAID ON ONE SIDE OF THE SUBSTRATE OR ON BOTH SIDES.
- CIRCUITRY CAN BE NOT ONLY ON THE OUTER SURFACES OF THE SUBSTRATE, BUT IN LAYERS WITHIN THE SUBSTRATE MATERIAL (MULTILAYERING).
- THE SUBSTRATE CAN BE RIGID OR FLEXIBLE.

There are many methods of applying the conductive patterns that make up the circuitry and each has its own specific soldering solutions.

Many different materials are used for substrates. Substrates used for electrical/electronic applications must be insulators to allow the conductive circuitry to function in the manner of a network made from separate insulated wires. Common substrate materials for this application include ceramics and organic laminates. Metals can also be used as substrates if they are coated with a substantial insulating material that can withstand the rigors of assembly.

Ceramic Substrates. Many types of ceramics can be used as substrates, but the most common is a high-fired alumina that is either 96 or 99% Al_2O_3. The 96% Al_2O_3 material is usually employed when thick-film materials are placed on the surface to form the circuitry. The 99% Al_2O_3 material is most often used for the evaporation or sputtering of thin materials. The materials that are laid down for terminal and component bonding pads are usually gold (or alloys high in gold), silver, and copper. Because these metals are laid down in thin layers, a soldering problem called leaching occurs. Leaching is the migration of the components of a substrate into a working solution. The process must be controlled because soldering results in bonding between the solder and the metals being attached. If the soldering process is not controlled, it can literally dissolve the metallization from the surface of the substrate. A gold-platinum alloy is more resistant to leaching than pure gold.

Thin-film (10 to 500 nm, or 100 to 5000 Å) deposits are more susceptible to leaching than are thick-film (10 to 25 μm, or 400 to 1000 μin.) deposits, because the thin layer is more susceptible to being consumed by the leaching. Therefore, the time at temperature and the maximum temperature become very important. In leaching, temperature is more important than time. Significantly, more leaching will be generated by a small increase in temperature than would be produced with even a moderate increase in time.

Composite Laminates. The most popular composites are the copper-clad laminates used for PWB substrates. The metal cladding is usually copper, but could be nickel or some other metal. Copper cladding can be either a plated material or wrought rolled foil. From a soldering standpoint, the rolled material is preferable, but it is more costly and more difficult to bond to the laminate material. Many PWBs are passed through numerous heat cycles during the manufacturing process. In addition, the use of multilayer designs is increasing dramatically. Plated foil, contaminated with codeposited organics,

can become brittle at elevated temperatures. Hence, foil coppers are available in several classes, depending on their application.

Printed Wiring Laminate Materials. The laminate upon which the metal cladding is applied is available in many composite forms. Originally, layers of paper or cloth impregnated with a phenolic resin and designated XP, XXP, or XXXP were used. The latter became the standard in the mid-1950s.

The selection of organic-based laminate materials as electronic substrates has certain limitations, the most common of which is temperature. In addition, soldering must not degrade the material by burning or charring. Laminate selection should depend on the application of the electronic hardware. A glass-epoxy laminate material known as FR-4 is commonly used in consumer and industrial electronics. The "FR" designation indicates that the material is fire resistant.

Metal Substrates. There are some applications in which metals can be used as base substrates. Because the presence of an insulating material is required, the metal must be coated with a suitable material (for example, porcelain enamel).

Solder Application

Because of the small distances between components, when soldering electronics, it is often necessary to measure carefully the amount of solder that must be applied to form a satisfactory joint. It is not only a matter of providing a sufficient amount of solder for a good fillet, but it is also important to not have excess solder in the joint. This can sometimes be accomplished by plating the area to be soldered to a predetermined solder thickness, so that the solder forms a good fillet when it is reflowed. This is often the method used to accomplish "flip-chip" bonding to produce tape automated bonding (TAB) assemblies (Ref 20).

Solder can also be apportioned in proper amounts to individual joints by using preforms. In the case of surface-mount technology (SMT), the solder is often screened onto the substrate in the form of solder paste or it is dispersed in small quantities in precise locations by using tiny nozzles or tubes.

Preforms. When a square or round lid is attached to a device, but solder is not desired in the enclosed area, the solder application is often accomplished by using squares or annular rings that are punched from solder sheet. The solder quantity is usually sufficient to fill the asperities in the surfaces. The thickness and the lateral dimensions are determined by the location and the amount of solder needed to make a satisfactory joint. The solder preform is placed in the space between the parts to be joined, and then this assembly is subjected to sufficient heat to fuse the solder and hermetically seal the assembly. The entire body is then cooled. If the parts were clean and the proper amount of solder was supplied, a good solder joint results.

Heat for soldering can be applied in a number of different ways. In automated processing, the parts to be soldered are often passed through the hot zone of a furnace on a belt. This makes it possible to provide adequate preheating of the parts, the proper maximum temperature, and a gentle cooling cycle to minimize stresses. This method is fast and allows easy control of the measured amounts of solder to precise locations in a variety of geometric shapes. However, the cost of the preforms is a drawback.

Solder Pastes. The rapid development of SMT processing, which can involve very dense populations of devices and leads, necessitated a method to precisely place controlled amounts of solder on a substrate, either for lead attachment or for bonding of the device to attain more-effective heat transfer. Solder pastes that are applied by screening or printing through a mask or by application through a fine tube can fulfill these needs.

The screening method, although ancient, has been modernized by the development of new high-precision screens, solder pastes, and equipment for screening and curing the screened materials.

Solder paste also can be applied through a metal mask, or stencil. Although the location of the solder is not as precise as that obtained with screening, the metal masks are more durable and provide better control of solder thickness as it is applied.

Another paste placement method is to use fine tubes or nozzles to deliver the paste to precise locations. This method is ideal for placing discrete dots of paste, rather than covering large areas.

Paste Composition. A solder paste must contain solder particles of the desired composition to yield the melting and joining requirements of the application. The metal particles must be sized to provide good screenability and to avoid excessive oxide content. The shape of the particles is important. Spherical particles are lower in oxide content because there is less surface area and they are able to flow more freely in screening applications.

A paste must also contain a vehicle to control its rheological, or flow, properties; its drying behavior; its surface activity (wetting behavior); and the solubility of the residues left after reflow. The vehicle usually consists of a rosin (pine derivative) or a synthetic resin, solvents to adjust drying time and temperature, modifiers to control rheological behavior, and an activator, or flux, to remove oxides from the solder and to protect the liquefied solder from oxidation.

Paste Properties. The paste must set and hold its shape and location after screening so that subsequent processing maintains the solder in the desired locations and amounts. The assembly is then subjected to heat and the solder is melted and joined to the part being soldered. This reflow can be conducted either as the final step in soldering or as a separate step. The parts must generally be cleaned after soldering.

Solder resists enable control over the PWB areas that will be wet by the solder. The resist, or mask, is an organic coating placed selectively on the board. Only the uncoated areas are exposed to and are wettable by the solder. The higher interconnect densities now being attained by SMT processing make solder resists a valuable method.

Solder resists can be either permanent or temporary, depending on the application. The permanent resists must resist not only the solder, but any fluxes or solvents applied later in the manufacturing sequence. Compatibility with the process and the circuit materials is a consideration, as is the ability to withstand soldering temperatures. In addition, the solder resist offers the circuits some protection against dirt and contamination. Commonly used resist materials are polystyrene, epoxides, and acrylics, although more-costly materials, such as polyimides, are sometimes used because of their greater thermal resistance.

Screened Materials. Solder masks are commonly applied by screening. The films are subsequently dried and cured thermally. The elevated temperatures involved in the curing cycle can cause oxidation of the conductors on the PWB, resulting in a loss of solderability. Lower curing temperatures are desirable. Some of the resists are cured by exposure to ultraviolet light, rather than by heating. This approach is very fast, involves less emission of volatile pollutants, and does not cause oxidation of the metal surfaces.

Photographic Films. A second method of applying solder resists is to use sheets of photosensitive material laminated to the surface of the circuit. Although these are more expensive than screened materials, the photographic films enable much higher pattern resolution. Dry film resists are much stronger and more resistant to damage during soldering and cleaning operations. The use of these photosensitive materials increases the complexity of the process.

Temporary solder masks are often used as production aids, offering local protection from solder at locations such as:

- CONTACT PADS THAT HAVE BEEN GOLD PLATED
- PLATED-THROUGH HOLES THAT MUST BE SOLDERED IN A LATER OPERATION
- PADS THAT MUST BE KEPT FREE OF SOLDER

Adhesive solder-mask tapes that specifically protect edge connectors on PWBs are also available, and numerous mechanical approaches to limiting solder contact exists (Ref 18).

References cited in this section

18. *PROC. IEEE 41ST ELECT. COMP. & TECH. CONF.,* IEEE, 1991

20. J.H. LAU, *HANDBOOK OF TAPE AUTOMATED BONDING,* VAN NOSTRAND REINHOLD, 1992

Soldering Process Parameters

The parameters that affect wetting and spreading phenomena include:

- TEMPERATURE
- TIME
- VAPOR PRESSURE
- METALLURGICAL AND CHEMICAL NATURE OF THE SURFACES
- GEOMETRY OF THE SOLID

The manipulation of each parameter can result in some control of the wetting and soldering processes.

Temperature is important to wetting and spreading for several reasons. Higher temperatures result in greater atomic activity and provide some of the energy needed to overcome surface barriers. Higher temperatures also increase reaction rates exponentially. Temperature determines phase relationships for a given alloy composition, whether for the formation of a solid solution or for that of an intermetallic compound. The fluidity of the liquid solder is also increased with increasing temperature. In addition, higher temperatures promote the formation of oxides, which can be troublesome when soldering.

Time. Wetting is time dependent because of the rate of kinetics of the solder-substrate interaction, the flux action, and the heat conduction of the substrate. The soldering process is time sensitive, because time is needed to provide sufficient opportunity for the solder to wet, penetrate, or "wick up" into the various areas of the substrate that must be incorporated into the solder joint. It is clear that measures of the time to initiate wetting and of the time it takes for spreading to occur are needed.

Vapor pressure is considered to be negligible for lead-tin solders, but it can be a significant factor when working with certain solders. Caution must be exercised when selecting and working with alloys that have appreciable vapor pressures.

The chemical and metallurgical nature of a surface affects wetting and spreading in several ways. Alloy content, as well as the fluidity of the liquid, both affect wetting and, thus, the rate of spreading. Grain boundaries are wet differently than the bulk of the metal. The formation of solid solutions or intermetallic compounds also can have a considerable effect on wetting and spreading.

The presence of oxide skins will prevent wetting and spreading, because the solder generally will not wet oxides. Likewise, films or particles of organic matter will interfere with wetting. Oils and silicones are frequent offenders and usually require different types of cleaning materials for their removal than the types used for oxides.

Surface Geometry. Because contact angle is a critical measure of wetting and spreading behavior, surface geometry is an important factor in the control of spreading. Soldering artisans have long used a wire brush not only to clean the surface to be soldered, but also to aid the spreading of the solder by providing sharp grooves that act as small capillaries to assist wetting. Isotropic spreading is actually what is needed.

Another condition of surface interaction that is sometimes encountered in soldering is dewetting, where a metal surface is initially wet by solder, but as the solder cools, its cohesive forces exceed the forces involved in wetting, and the solder balls up on the metal surface. This usually results from surface contamination of the metal or from the entrapment of foreign particles in the metal surface, leading to weak wetting or, possibly, only local wetting.

Base-Metal Selection. A sound soldered joint is achieved by selecting and using the proper materials and processes. Base metals are usually selected to achieve the specific property requirements of a component. These properties can include strength, ductility, electrical conductivity, weight, corrosion resistance, and others. When soldering is required, the solderability of the base materials should also be a selection factor. Both flux selection and surface preparation will be affected by the solderability of the base materials to be joined.

The solderability of metals and alloys is not simply a matter of chemical nobility, as might be supposed when regarding the good solderability of the noble metals, which do not readily form oxide or tarnish films. Although cadmium and tin both form oxides readily, they are considered easy to solder. On the other hand, chromium, nickel, and aluminum also form oxide films readily, but are difficult to solder. The difference is in the extremely adherent, protective nature of the oxides formed on chromium, nickel, and aluminum, compared with the oxides that form on tin and cadmium (Table 2).

TABLE 2 RELATIVE SOLDERABILITY OF SELECTED METALS AND ALLOYS

EASY TO SOLDER • PLATINUM • GOLD • COPPER • SILVER • CADMIUM PLATE • TIN • SOLDER PLATE
LESS EASY TO SOLDER • LEAD • NICKEL PLATE • BRASS • BRONZE • RHODIUM • BERYLLIUM COPPER
DIFFICULT TO SOLDER • GLAVANIZED IRON • TIN-NICKEL • NICKEL-IRON • MILD STEEL
VERY DIFFICULT TO SOLDER • CHROMIUM • NICKEL-CHROMIUM • NICKEL-COPPER • STAINLESS STEEL
MOST DIFFICULT TO SOLDER • ALUMINUM • ALUMINUM BRONZE
NOT SOLDERABLE • BERYLLIUM • TITANIUM

It should be noted that chromium, nickel, and aluminum are all soldered regularly with good results, but that special attention must be given to the selection of fluxes, which must be very active. In many cases, the use of active fluxes is either restricted or not allowed. Therefore, these hard-to-solder metals and alloys always require special consideration in order to provide reproducible soldering.

Numerous tests and methods to measure solderability are available. The tendencies of solder to either wet or spread on a given material are critical when evaluating candidate soldering systems. When hand soldering on single, large-dimension bodies prevailed, the skilled artisan could adjust parameters while watching the results develop. In most cases, visual determinations of wetting and spreading characteristics provided a sufficient basis for process control.

Today, operating parameters must be controlled very carefully, because the soldering of components and/or electronic assemblies can involve many joints that are soldered at one time, or joints that are often hidden, or dimensions that are extremely small, or situations where joint-to-joint accommodations cannot be made. This necessitates the use of automatic soldering systems. Moreover, conditions must be uniform over the whole structure being soldered. In this environment, it is essential that the processes be based on measurements of wetting and spreading behavior, so that the controlling parameters can be accurately set.

Additional information is available in the articles "Brazeability and Solderability of Engineered Materials," "General Soldering," and "Soldering in Electronic Applications" in this Volume.

Fundamentals of Soldering

Mel M. Schwartz, Sikorsky Aircraft

Soldering Equipment

The proper application of heat is of paramount importance in any soldering operation. The solder should melt while the surface is heated to permit the molten solder to wet and flow over the surface. The best heating method is therefore another important consideration.

Soldering Irons. The traditional soldering tool is the soldering iron, or bit, with a copper tip than can be heated electrically, by direct flame, or in an oven. Because soldering is a heat-transfer process, the maximum surface area of the heated tip should contact the base metal. The solder itself should not be melted upon the tip of the iron when a joint is being made. To lengthen the usable life of a copper tip, a coating of solder-wettable metal, such as iron with or without additional coatings, is applied to the surface of the copper. The rate of dissolution of the iron coating in molten solder is substantially less than the rate for copper. The iron coating also shows less wear, oxidation, and pitting than uncoated copper.

Soldering irons are available in a large variety of sizes and designs, ranging from a small pencil to special irons or bits that weigh 2 kg (5 lb) or more. The selection of the iron depends on the application and the quantity of heat needed at the joint. The heat recovery time of the iron should be fast enough to keep up with the job.

Regardless of the heating method, the tip performs the following functions:

- STORING AND CONDUCTING HEAT FROM THE HEAT SOURCE TO THE PARTS BEING SOLDERED
- STORING MOLTEN SOLDER
- CONVEYING MOLTEN SOLDER
- WITHDRAWING SURPLUS MOLTEN SOLDER
- BRINGING THE WORKPIECE JOINT AREA TO THE SOLDERING TEMPERATURE

The angle at which the copper tip is applied to the work is important in terms of delivering maximum heat. The flat side of the tip should be applied to the work to obtain the maximum area of contact. Flux-cored solders should not be melted on the soldering tip, because this destroys the effectiveness of the flux. The cored solder should be touched to the

soldering tip to initiate good heat transfer, and then the solder should be melted on the work parts to complete the solder joint (Ref 11).

Additional information is available in the article "Iron Soldering" in this Volume.

Torch Soldering (TS). The selection of a gas torch is controlled by the size, mass, and configuration of the assembly to be soldered. When fast soldering is necessary, a flame is frequently used. The flame temperature is controlled by the fuel mixture used. Fuel gas burned with oxygen gives the highest flame temperature possible with that gas. The highest flame temperatures are attained with acetylene. Lower temperatures are obtained with propane, butane, natural gas, and manufactured gas.

Multiple flame tips, or burners, often have shapes that are suitable to the work. They can be designed to operate on oxygen and fuel gas, compressed air and fuel gas, or Bunsen-type torches.

When adjusting tips or torches, care should be taken to avoid adjustments that result in a "sooty" flame, because the carbon deposited on the work will prevent the flow of solder (Ref 11, 15).

Detailed information is available in the article "Torch Soldering" in this Volume.

Dip soldering (DS) utilizes a molten bath of solder to supply both the heat and solder required to produce the joints (Fig. 9a). This method is useful and economical, because an entire unit comprising any number of joints can be soldered in one operation after proper cleaning and fluxing. Fixtures are required to contain the unit and maintain proper joint clearances during solder solidification. The soldering pot should be large enough so that, at a given rate of production, the units being dipped will not appreciably lower the temperature of the solder bath.

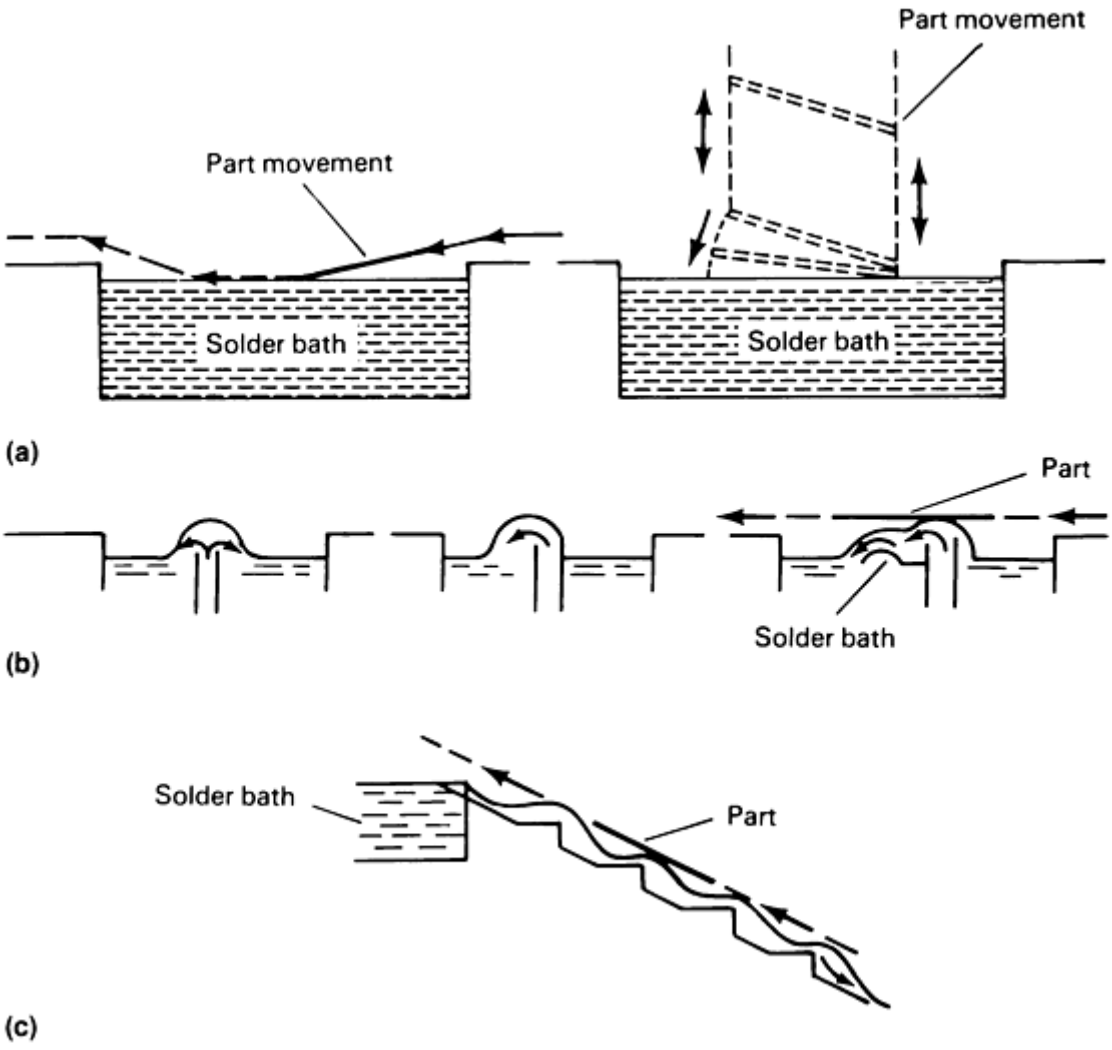

FIG. 9 SELECTED SOLDERING TECHNIQUES USED FOR HIGH-VOLUME PRODUCTION APPLICATIONS. (A) DIPPING ON A STATIC BATH. (B) WAVE SOLDERING SYSTEM. (C) CASCADE SOLDERING SYSTEM

Additional information is available in the article "Dip Soldering" in this Volume.

Wave Soldering (WS). Electronic components are commonly soldered to PWBs by wave soldering (Fig. 9b). The solder is pumped out of a narrow slot to produce a wave or series of waves. This approach, which lends itself to automatic soldering, involves a continuously pumped crest of solder that peaks at the PWB. Another method is "drag," or planar, soldering. This method uses a bath, into which the board is automatically dipped with controlled conveyorization (Ref 21, 22).

In cascade soldering (Fig. 9c), the solder flows down a trough because of gravity and is returned by pump to the upper reservoir. Both of these wave solder systems are excellent in that a virtually oxide-free solder surface is presented to the part, and the flux and vapors are dislodged by the flow of the solder.

Integrated wave soldering systems for printed wiring assemblies provide units that can apply the flux, dry and preheat the board, solder components, and clean the completed assembly. Some systems have special features that apply the flux by passing the assemblies through a wave, by spraying, by rolling, or by dipping. Several systems use oil mixed with the solder to aid in eliminating icicles and bridging between conductor paths. Another system features dual waves that flow in the opposite direction to the travel of the board.

Additional information is available in the article "Wave Soldering" in this Volume.

Induction Soldering (IS). The only requirement for a material that is to be induction soldered is that it be an electrical conductor. The rate of heating depends on the induced current flow. The distribution of heat obtained with induction heating is a function of the induced current frequency. The higher frequencies concentrate the heat at the surface of the workpiece.

Several types of equipment are available for induction heating: the vacuum tube oscillator, the resonant spark gap, the motor-generator unit, and solid-state units.

Induction heating is generally applicable for soldering operations, with the following requirements and attributes:

- LARGE-SCALE PRODUCTION
- APPLICATION OF HEAT TO A LOCALIZED AREA
- MINIMUM OXIDATION OF SURFACE ADJACENT TO THE JOINT
- GOOD APPEARANCE AND CONSISTENTLY HIGH JOINT QUALITY
- SIMPLE JOINT DESIGN THAT LENDS ITSELF TO MECHANIZATION

The induction technique requires that the parts being joined have clean surfaces and that joint clearances be maintained accurately. High-grade solders are generally required to obtain rapid spreading and good capillary flow. Preforms often afford the best means of supplying the correct amount of solder and flux to the joint.

When induction soldering dissimilar metals (particularly joints composed of both magnetic and nonmagnetic components), attention must be given to the design of the induction coil in order to bring both parts to approximately the same temperature.

Additional information is available in the article "Induction Soldering" in this Volume.

Furnace Soldering. There are many applications, especially in high-production soldering, where a furnace will produce consistent and satisfactory soldering. Although this method is not widely used, furnace heating should be considered under the following circumstances:

- WHEN ENTIRE ASSEMBLIES CAN BE BROUGHT TO THE SOLDERING TEMPERATURE WITHOUT DAMAGE TO ANY OF THE COMPONENTS
- WHEN PRODUCTION IS SUFFICIENTLY LARGE TO ALLOW EXPENDITURES FOR JIGS AND FIXTURES TO HOLD THE PARTS DURING THE SOLDERING PROCESS
- WHEN THE ASSEMBLY IS COMPLICATED IN NATURE, MAKING OTHER HEATING METHODS IMPRACTICAL

The proper clamping fixtures are very important during furnace soldering. Movement of the joint during solder solidification can result in a poor joint.

Another important consideration in furnace soldering is flux selection. Rosin and organic fluxes are subject to decomposition when maintained at elevated temperatures for an extended period of time. When either rosin or organic flux is used, the part must be brought rapidly to the liquidus temperature of the solder. It is sometimes beneficial to dip the parts in a hot flux solution before placing them in the oven. When using rosin-base flux, it is generally necessary to use a solder with a tin content of 50% or more.

The reducing atmosphere used in the furnace does not allow joints to be made without flux, because the temperatures at which these atmospheres become reducing are far above the liquidus temperature of the solders. The use of inert atmospheres will prevent further oxidation of the parts, but flux must be used to remove the oxide that is already present.

The furnaces should be equipped with adequate temperature controls because solder flow begins at approximately 45 to 50 °C (80 to 90 °F) above the solder liquidus temperature. The optimum condition exists when the heating capacity of the furnace is sufficient to heat the parts rapidly to the liquidus temperature of the solder.

Detailed information is available in the article "Furnace and Infrared Soldering" in this Volume.

Resistance soldering (RS) involves placing the workpiece either between a ground and a movable electrode or between two movable electrodes as part of an electrical circuit. Heat is applied to the joint both by the electrical resistance of the metal being soldered and by conduction from the electrode, which is usually carbon. Production assemblies can utilize multiple electrodes, rolling electrodes, or special electrodes, depending on which setup offers the most advantageous soldering speed, localized heating, and power consumption. Resistance soldering electrode bits generally cannot be tinned, and the solder must be fed directly into the joint.

Additional information is available in the article "Resistance Soldering" in this Volume.

Infrared Soldering (IRS). Optical soldering systems that focus infrared light (radiant energy) on the joint by means of a lens are available. Lamps with power ratings that range from 45 to 1500 W (140 to 4700 Btu/h) can be used for different application requirements. The devices can be programmed through a silicon-controlled rectifier (SCR) power supply with an internal timer.

The most common sources of infrared heating for soldering applications are heated filaments. The quartz-iodine tungsten-filament lamp is widely used because it is very stable and reliable over a wide range of temperatures.

In general, infrared soldering systems are simple and inexpensive to operate. One of the most critical operating parameters is surface condition. Variations in the condition of the solder surface can be compensated for, to some extent, by adjusting the heating power. Advantages are process repeatability, ability to concentrate or focus the energy with reflectors and lenses, economy of operation, and absence of contact with the workpiece.

Detailed information is available in the article "Furnace and Infrared Soldering" in this Volume.

Ultrasonic Soldering. This process uses a transducer as the source of ultrasonic energy. The transducer is energized in a bath of molten solder, and sound waves are coupled between the transducer and the workpiece, allowing the oxides in the base metal to be disrupted so that the solder melts the base metal. Sound waves are transmitted throughout the base metal, permitting wetting to occur on surfaces that are "blind" to the source. Ultrasonic soldering is also used to apply solderable coatings on difficult-to-solder metals.

Additional Soldering Processes. In addition to the above-mentioned processes, hot-gas soldering, spray-gun soldering, and condensation soldering are also used.

Hot gas soldering utilizes a fine jet of inert gas, heated to above the liquidus of the solder. The gas acts as a heat-transfer medium and as a blanket to reduce access of air at the joint.

Additional information is available in the article "Hot Gas Soldering" in this Volume.

Spray gun soldering is a heating method used when the contour of the part to be soldered is difficult to follow with either a wiping or drop method or when the part is placed in the assembly in such a way that the solder cannot be applied after the parts are assembled.

Gas-fired or electrically heated guns are available. Each type is designed to spray molten or semimolten solder on the work from a continuously fed solid solder wire. Soldering guns use either propane mixed with oxygen or natural gas mixed with air to heat and to spray a continuously fed solid solder wire of approximately 3.2 mm (0.12 in.) diameter. About 90% of the solder wire is melted by the flame of the gun. The solder contacts the workpiece in a semiliquid form. The workpiece then supplies the balance of the heat required to melt and flow the solder. Adjustments can be made within the spray gun to control the solder spray.

Vapor-phase soldering (also known as condensation soldering) utilizes the latent heat of vaporization of a condensing saturated liquid to provide the heat required for soldering. A reservoir of saturated vapor over a boiling liquid provides a constant controlled temperature with rapid heat transfer. This method is useful for large assemblies, as well as for temperature-sensitive parts.

Detailed information is available in the article "Vapor-Phase Soldering" in this Volume.

References cited in this section

11. R.W. WOODGATE, *THE HANDBOOK OF MACHINE SOLDERING,* 2ND ED., JOHN WILEY & SONS, 1988
15. E. LIEBERMAN, *MODERN SOLDERING AND BRAZING TECHNIQUES,* BUSINESS NEWS PUBLISHING CO., 1988
21. P.J. BUD, MASS PRODUCTION TECHNIQUES USING THE PRINCIPLE OF WAVE SOLDERING, *WELD. J.*, VOL 52 (NO. 7), JULY 1973, P 431-439
22. P.J. BUD AND D.A. ELLIOT, WAVESOLDERING AT ELEVATED TEMPERATURES, *WELD. J.*, VOL 53 (NO. 2), FEB 1974, P 79-87

Fundamentals of Soldering

Mel M. Schwartz, Sikorsky Aircraft

Quality Control

Table 3 lists that are commonly used to evaluate the solderability properties of selected soldered components.

TABLE 3 TEST STANDARDS USED TO EVALUATE SOLDERABILITY

BASIC METHOD	TEST STANDARD
DIP AND LOOK	ANSI/IPC-S-804 (BOARDS)
	ANSI/IPC-S-805 (COMPONENTS)

	IEC 68-2-20
	MIL-STD-202, 750, 883
	EIA RS-186-9E
ROTARY DIP	ANSI-IPC-S-804 (BOARDS)
	IEC 68-2-20
	BS4025 (BRITISH STANDARD)
WETTING BALANCE	ANSI-IPC-S-805 (COMPONENTS)
	IEC-68-2-20
	MIL-STD-883
GLOBULE TEST	ANSI-IPC-S-805 (COMPONENTS)
	IEC 68-2-20
	BS 2011 (BRITISH STANDARD)
	DIN 40046 (GERMAN STANDARD)
MENISCUS RISE	NO STANDARDS TO DATE
TIMED SOLDER RISE	ANSI/IPC-S-804 (BOARDS)

Dip Test. The most useful test for assessing solderability is the dip test, because of its accuracy and simplicity. It is conducted with the additions of cams and timers so that standardized conditions are established. The dip test is a reasonable simulation of practical soldering conditions and starts with a test specimen that has been dipped in a mild flux, as is usually the case with soldering tests. The dip test involves immersing the test specimen into a clean solder bath, waiting an appropriate length of time, and then withdrawing the specimen from the bath. In most cases, the test is automated to ensure reproducibility. The results are evaluated by means of visual inspection and comparison with a set of standards. Thus, the dip test is operator sensitive, somewhat subjective, and of limited value, because it is not quantitative.

Rotary Dip Test. This test was devised to provide a better simulation of the dynamic conditions that exist in machine soldering operations. It is used to evaluate the solderability of PWBs, and involves bringing the specimen into moving contact with the molten solder for a specified period of time. This is a "go/no-go" test that requires complete wetting of the specimen surface within a set time, and is thus dependent on visual inspection of the test specimen.

Wetting Balance (Meniscograph). Another common test employs the wetting balance, which gives a numerical result. The equipment consists of a balance that records the forces exerted on a fluxed test specimen during a controlled dipping cycle in a clean solder bath. From the values obtained, it is possible to compare the rate of wetting, as well as the forces involved for various flux formulations.

The speed of wetting is an especially important factor in the wave soldering process, where automation requires a time-based response of flux and solder as the work moves through the process machine at a constant speed.

The wetting balance test cannot be used on finished, etched printed circuits or on single-sided circuits. It is often used on specimens cut from double-sided clad materials prior to etching.

Although this test gives numerical results, they are not strictly quantitative. However, the results do provide the basis for a meaningful comparison among fluxes.

Additional Tests. There are several other tests that provide practical information for special purposes, such as the spreading test and the globule test. These tests are sometimes used to evaluate incoming materials or to aid in the selection of materials. They are not universally employed.

The spreading test is used to provide a numerical rating for both fluxes and solders. It is described in detail in MIL-F-14256, "Flux, Soldering, Liquid (Rosin Base)," and in QQ-S-571, "Solder, Electronic," which are national-level specifications.

The globule test was once widely applied, but is now limited to being used to determine the wetting of component leads and wires (Ref 24).

Additional information is available in the article "Evaluation and Quality Control of Soldered Joints" in this Volume.

Reference cited in this section

24. IEC-68-2-20, INTERNATIONAL ELECTROCHEMICAL COMMISSION, GENEVA

Future Outlook

The quality soldered joints obtained by automation have resulted in the widespread use of automated equipment throughout the electronics industry, as well as throughout the world (Ref 25).

When compared to processes such as adhesive bonding, welding, brazing, or mechanical joining, soldering offers many advantages. Automated soldering equipment for wave or planar soldering can be easily and economically installed. The high reliability that can be achieved with soldering results in a quality end product. Soldering offers the additional benefit of providing sequential assembly, a common practice in the electronics industry.

Reference cited in this section

25. REFLOW SOLDERING, *WELD. J.*, VOL 52 (NO. 1), JAN 1973, P 22-30

References

1. J. WOLTERS, *ZUR GESEHICHTE DER LOTTECHNIK,* DEGUSSA, WEST GERMANY, 1977
2. H.H. MANKO, *SOLDERS AND SOLDERING,* 2ND ED., MCGRAW-HILL, 1964
3. R.J. KLEIN WASSINK, *SOLDERING IN ELECTRONICS,* ELECTROCHEMICAL PUBLICATIONS LTD., 1989
4. L.P. LAMBERT, *SOLDERING FOR ELECTRONIC ASSEMBLIES,* MARCEL DEKKER, 1987
5. *SOLDERING MANUAL,* AWS, 1978
6. A.D. ROMIG, JR., Y.A. CHANG, J.J. STEPHENS, *ET AL.,* PHYSICAL METALLURGY OF SOLDER-SUBSTRATE REACTIONS, *SOLDER MECHANICS,* THE MINERALS, METALS, & MATERIALS SOCIETY, 1991, P 30-32
7. "SOFT SOLDER ALLOYS--CHEMICAL COMPOSITIONS AND FORMS," ISO 9453, 1ST ED., 1990
8. "SOFT SOLDERING FLUXES--CLASSIFICATION AND REQUIREMENTS--PART I: CLASSIFICATION, LABELING AND PACKAGING," ISO 9454-1, 1990
9. J.F. SHIPLEY, INFLUENCE OF FLUX, SUBSTRATE AND SOLDER COMPOSITION ON SOLDER WETTING, *WELD. J.,* VOL 54 (NO. 10), OCT 1975, P 357S-362S
10. H.H. MANKO, SOLDERING FLUXES--PAST AND PRESENT, *WELD. J.,* VOL 52 (NO. 3), MARCH 1973, P 163-166
11. R.W. WOODGATE, *THE HANDBOOK OF MACHINE SOLDERING,* 2ND ED., JOHN WILEY & SONS, 1988

12. T. THOMPSON, CONDENSATION/VAPOR-PHASE REFLOW SOLDERING, *ASS. ENG.*, JUNE 1977, P 44-47
13. T.Y. CHU, A GENERAL REVIEW OF MASS SOLDERING METHODS, *INS. CIRC.*, NOV 1976
14. R.C. PFAHL, JR., J.C. MOLLENDORF, AND T.Y. CHU, CONDENSATION SOLDERING, *WELD. J.*, VOL 54 (NO. 1), 1975
15. E. LIEBERMAN, *MODERN SOLDERING AND BRAZING TECHNIQUES*, BUSINESS NEWS PUBLISHING CO., 1988
16. "SOLDER METAL SPECIFICATION," ASTM B 32, *ANNUAL BOOK OF ASTM STANDARDS*, PART B, ASTM
17. D.R. FREAR, W.B. JONES, AND K.R. KINSMAN, ED., *SOLDER MECHANICS*, TMS, 1991, P 30-41
18. *PROC. IEEE 41ST ELECT. COMP. & TECH. CONF.*, IEEE, 1991
19. J. BROUS, EVALUATION OF POST-SOLDER FLUX REMOVAL, *WELD. J.*, VOL 54 (NO. 12), 1975, P 444S-448S
20. J.H. LAU, *HANDBOOK OF TAPE AUTOMATED BONDING*, VAN NOSTRAND REINHOLD, 1992
21. P.J. BUD, MASS PRODUCTION TECHNIQUES USING THE PRINCIPLE OF WAVE SOLDERING, *WELD. J.*, VOL 52 (NO. 7), JULY 1973, P 431-439
22. P.J. BUD AND D.A. ELLIOT, WAVESOLDERING AT ELEVATED TEMPERATURES, *WELD. J.*, VOL 53 (NO. 2), FEB 1974, P 79-87
23. *ELECTRONIC MATERIALS HANDBOOK*, VOL 1, *PACKAGING*, ASM INTERNATIONAL, 1989
24. IEC-68-2-20, INTERNATIONAL ELECTROCHEMICAL COMMISSION, GENEVA
25. REFLOW SOLDERING, *WELD. J.*, VOL 52 (NO. 1), JAN 1973, P 22-30

Introduction to Solid-State Welding

Ray Dixon, Los Alamos National Laboratory

Solid-State Welding

(SSW) processes are those that produce coalescence of the faying surfaces at temperatures below the melting point of the base metal being joined without the addition of brazing or solder filler metal. Pressure may or may not be applied. These processes involve either the use of deformation or of diffusion and limited deformation in order to produce high-quality joints between both similar and dissimilar materials.

Dissimilar metal joints are necessary in applications that require a variety of material properties within the same component. For example, heat exchangers often require different types of stainless steels at each end, because of temperature-induced corrosion. Under laboratory conditions, dissimilar materials can be chosen based on physical or material properties that influence the phenomenon being studied. For whatever reason, and appropriate method of producing dissimilar metal joints can usually be determined (assuming it is even possible) by examining the phase diagram. If the diagram indicates difficulty in joining the materials (intermetallics, and so on), then a solid-state (nonmelting) process may be applicable. When a nonmelting process is chosen, it is only successful if a relatively strong joint is produced.

There is considerable interest is quantifying joint strength, and extensive literature (Ref 1, 2, 3, 4, 5, 6, 7, 8, 9, 10, 11, 12, 13, 14) exists to help design and evaluate various specimen geometries. This experience includes not only techniques for conducting the tests, but analysis and interpretation of the data with respect to the physical properties of individual materials.

The study of dissimilar welds necessarily leads to studies of the interfacial region, because it is the most likely site of part failures. In a two-component system (materials A and B), interfacial failure can be a result of the individual properties of either A and B, but they are by necessity synergistic. These synergisms and the resulting complex interactions that they produce are what is significant. From an engineering and processing standpoint, an interfacial "cookbook" that provides

all the answers would be ideal. However, this capability is not yet available, and, as explained in this Section, researchers are still far from reaching that goal. This is the case even for simple systems, such as metal pair that form solid solutions.

The opportunities for understanding interfacial behavior come from studies conducted at the atomic level (for example, using scanning tunneling microscopy, transmission electron microscopy, first principles energy band calculations, and embedded atom potential calculations) with appropriate correlations to both micromechanics and a macroscopic level, and vice versa. The computational and experimental tools that begin to provide insight at these levels have only recently been developed.

Because the interest in interfaces is so diverse (all combinations of metals, ceramics, semiconductors, glasses, and conducting polymers), the advances in interfacial science encompass the creative efforts of a large number of people and organizations. Thus, the quantity of available literature seems overwhelming, and perhaps, disjointed. It will become apparent that there is no preferred approach to the treatment of dissimilar welds or welding. It really depends on the interests and objectives of each engineer.

For example, if you know that what you are doing actually works (that is, produces a joint) and are searching for understanding, then this Section of the Handbook will guide you to the appropriate technical literature. If you have an idea and need guidance for bonding, testing, processing, or interpreting the data, then this Section should also provide that direction. Lastly, if the reader wants state-of-the-art research and development topics, then those can be found in this Section, as well. This should provide the reader with a comprehensive overview of the welding of dissimilar metals.

Therefore, this Section is concerned with the fundamentals of welding and joining materials via the application of a nonmelting process. The specific processes usually associated with this technology are also discussed. Before considering nonmelting processes in detail, however, a brief discussion of adhesion is presented. This is followed by articles that discuss the fundamentals of the major solid-state welding techniques.

References

1. P.G. CHARALAMBIDES, J. LUND, A.G. EVANS, AND R.M. MCMEEKING, "A TEST FOR DETERMINING THE FRACTURE RESISTANCE OF BIMATERIAL INTERFACES," REPORT M87-4, MATERIALS DEPARTMENT, COLLEGE OF ENGINEERING, UC SANTA BARBARA
2. Z. SUO AND J.W. HUTCHINSON, "INTERFACE CRACK BETWEEN TWO ELASTIC LAYERS," REPORT MECH-118, DIVISION OF APPLIED SCIENCES, HARVARD UNIVERSITY, MARCH 1988
3. N.P. O'DOWD, C.F. SHIH, AND M.G. STOUT, TEST GEOMETRIES FOR MEASURING INTERFACIAL FRACTURE TOUGHNESS, FOR *INT. J. SOLIDS STRUCT.*, VOL 29, 1992, P 571-589
4. J.W. HUTCHINSON AND Z. SUO, MIXED MODE CRACKING IN LAYERED MATERIALS, *ADV. IN APPL. MECH.*, VOL 28, J.W. HUTCHINSON AND T.Y. WU, ED., ACADEMIC PRESS, 1990
5. H.M. JENSEN, MIXED MODE INTERFACE FRACTURE CRITERIA, *ACTA METALL. MATER.*, VOL 38 (NO. 12), 1990, P 2637-2644
6. R.L. BRADY, R.S. PORTER, AND J.A. DONOVAN, A BUCKLED PLATE TEST TO MEASURE INTERFACIAL TOUGHNESS IN COMPOSITES, *J. MATER. SCI.*, VOL 24, 1989, P 4138-4143
7. M.-Y. HE AND J.W. HUTCHINSON, "KINKING OF A CRACK OUT OF AN INTERFACE," REPORT MECH-113, DIVISION OF APPLIED SCIENCE, HARVARD UNIVERSITY, FEB 1988
8. J.J. MECHOLSKY AND L.M. BAKER, A CHEVRON-NOTCHED SPECIMEN FOR FRACTURE TOUGHNESS MEASUREMENTS OF CERAMIC-METAL INTERFACES, *CHEVRON-NOTCHED SPECIMENS: TESTING AND STRESS ANALYSIS*, STP 855, J.H. UNDERWOOD, S.W. FREIMAN, AND F.I. BARATTA, ED., ASTM, 1984, P 324-336
9. W.W. GERBERICH, D.L. DAVIDSON, AND M. KACZOROWSKI, EXPERIMENTAL AND THEORETICAL STRAIN DISTRIBUTIONS FOR STATIONARY AND GROWING CRACKS, *J. MECH. PHYS. SOLIDS*, VOL 38 (NO. 1), 1990, P 87-113
10. J. QU AND Q. LI, INTERFACIAL DISLOCATION AND ITS APPLICATIONS TO INTERFACE CRACKS IN ANISOTROPIC BIMATERIALS, *J. ELAST.*, VOL 26, 1991, P 169-195

11. A.N. STROH, DISLOCATIONS AND CRACKS IN ANISOTROPIC ELASTICITY, *PHILOS. MAG.,* VOL 7, 1958, P 625-646
12. Q.Q. LI AND T.C.T. TING, LINE INCLUSION IN ANISOTROPIC ELASTIC SOLIDS, *J. APPL. MECH.,* VOL 56, 1989, P 556-563
13. T.C.T. TING, EXPLICIT SOLUTION AND INVARIANCE OF THE SINGULARITIES AT AN INTERFACE CRACK IN ANISOTROPIC COMPOSITES, *INT. J. SOLIDS STRUCT.,* VOL 22, 1986, P 965-983
14. M.D. PASHLEY AND D. TABOR, ADHESION AND DEFORMATION PROPERTIES OF CLEAN AND CHARACTERIZED METAL MICRO-CONTACTS, *VACUUM,* VOL 10-12, 1981, P 619-623

Introduction to Solid-State Welding

Ray Dixon, Los Alamos National Laboratory

References

1. P.G. CHARALAMBIDES, J. LUND, A.G. EVANS, AND R.M. MCMEEKING, "A TEST FOR DETERMINING THE FRACTURE RESISTANCE OF BIMATERIAL INTERFACES," REPORT M87-4, MATERIALS DEPARTMENT, COLLEGE OF ENGINEERING, UC SANTA BARBARA
2. Z. SUO AND J.W. HUTCHINSON, "INTERFACE CRACK BETWEEN TWO ELASTIC LAYERS," REPORT MECH-118, DIVISION OF APPLIED SCIENCES, HARVARD UNIVERSITY, MARCH 1988
3. N.P. O'DOWD, C.F. SHIH, AND M.G. STOUT, TEST GEOMETRIES FOR MEASURING INTERFACIAL FRACTURE TOUGHNESS, FOR *INT. J. SOLIDS STRUCT.,* VOL 29, 1992, P 571-589
4. J.W. HUTCHINSON AND Z. SUO, MIXED MODE CRACKING IN LAYERED MATERIALS, *ADV. IN APPL. MECH.,* VOL 28, J.W. HUTCHINSON AND T.Y. WU, ED., ACADEMIC PRESS, 1990
5. H.M. JENSEN, MIXED MODE INTERFACE FRACTURE CRITERIA, *ACTA METALL. MATER.,* VOL 38 (NO. 12), 1990, P 2637-2644
6. R.L. BRADY, R.S. PORTER, AND J.A. DONOVAN, A BUCKLED PLATE TEST TO MEASURE INTERFACIAL TOUGHNESS IN COMPOSITES, *J. MATER. SCI.,* VOL 24, 1989, P 4138-4143
7. M.-Y. HE AND J.W. HUTCHINSON, "KINKING OF A CRACK OUT OF AN INTERFACE," REPORT MECH-113, DIVISION OF APPLIED SCIENCE, HARVARD UNIVERSITY, FEB 1988
8. J.J. MECHOLSKY AND L.M. BAKER, A CHEVRON-NOTCHED SPECIMEN FOR FRACTURE TOUGHNESS MEASUREMENTS OF CERAMIC-METAL INTERFACES, *CHEVRON-NOTCHED SPECIMENS: TESTING AND STRESS ANALYSIS,* STP 855, J.H. UNDERWOOD, S.W. FREIMAN, AND F.I. BARATTA, ED., ASTM, 1984, P 324-336
9. W.W. GERBERICH, D.L. DAVIDSON, AND M. KACZOROWSKI, EXPERIMENTAL AND THEORETICAL STRAIN DISTRIBUTIONS FOR STATIONARY AND GROWING CRACKS, *J. MECH. PHYS. SOLIDS,* VOL 38 (NO. 1), 1990, P 87-113
10. J. QU AND Q. LI, INTERFACIAL DISLOCATION AND ITS APPLICATIONS TO INTERFACE CRACKS IN ANISOTROPIC BIMATERIALS, *J. ELAST.,* VOL 26, 1991, P 169-195
11. A.N. STROH, DISLOCATIONS AND CRACKS IN ANISOTROPIC ELASTICITY, *PHILOS. MAG.,* VOL 7, 1958, P 625-646
12. Q.Q. LI AND T.C.T. TING, LINE INCLUSION IN ANISOTROPIC ELASTIC SOLIDS, *J. APPL. MECH.,* VOL 56, 1989, P 556-563
13. T.C.T. TING, EXPLICIT SOLUTION AND INVARIANCE OF THE SINGULARITIES AT AN INTERFACE CRACK IN ANISOTROPIC COMPOSITES, *INT. J. SOLIDS STRUCT.,* VOL 22, 1986, P 965-983
14. M.D. PASHLEY AND D. TABOR, ADHESION AND DEFORMATION PROPERTIES OF CLEAN AND CHARACTERIZED METAL MICRO-CONTACTS, *VACUUM,* VOL 10-12, 1981, P 619-623

Introduction

IN ANY SOLID-STATE (NONMELTING) WELDING PROCESS, there are two primary areas of concern: Will the material bond and how strong is the bond? Literature that deals with the science and technology of material compatibility and bond strength is readily available. This article will review recent work in quantifying adhesion, bonding, and interfacial characterization and strength. Subsequent articles in this Section of the Handbook focus on the engineering principles associated with the formation of welds using these techniques. This discussion concentrates on metal-metal configurations, with only passing comments on metal-ceramic and metal/ceramic-semiconductor interfaces. This restriction is necessary to limit the length of this article. Wherever appropriate, applications of thin films on substrates will also be used.

Fundamentals of Metal and Metal-to-Ceramic Adhesion

Ray Dixon and S.P. Chen, Los Alamos National Laboratory

Adhesion Energy

Surface energy, Γ_{surf}, is defined as the increase in energy, ΔE, of a system divided by the area, A, caused by the creation of the surface:

$$\Gamma_{SURF} = \Sigma \Delta E_I / A \qquad \textbf{(EQ 1)}$$

The atoms that contribute to the extra energy, ΔE_i, are usually within 10 lattice parameters or less of the surface (or interface) (Ref 1, 2, 3). A freshly created surface has a high surface energy, whereas a relaxed or reconstructed one is lower, by about 3 to 5%. At 0 K (-459 °F), surface energies vary about 15 to 25% for planes of various indices. The variation is less at higher temperatures, because of entropy. For example, the (111) surface of a face-centered cubic (fcc) structure has the lowest energy, whereas the (210) surface is about 15% higher (Ref 1, 2, 3). The ideal fracture energy, Γ_{coh}, which is used in estimating the Griffith criterion, is twice the surface energy:

$$\Gamma_{COH}\,(HKL) = 2 \cdot \Gamma_{SURF}\,(HKL) \qquad \textbf{(EQ 2)}$$

where (hkl) are the indices of the plane. The actual energy consumed in fracture or crack propagation is composed of two terms: one is the Γ_{coh} and the other is the plastic work consumed per unit area $\Gamma_{plastic}$ (Ref 4, 5, 6, 7, 8). For ionic crystals, $\Gamma_{plastic}$ is usually a few times Γ_{coh}; for metals, Γ_{coh} is about 1 to 4 J/m^2 (2×10^{-5} to 1×10^{-4} cal/cm^2); and $\Gamma_{plastic}$ is about 1000 J/m^2 (2×10^{-2} cal/cm^2). For ceramic systems, Γ_{coh} is about the same, but $\Gamma_{plastic}$ is about 10 to 100 J/m^2 (2×10^{-4} to 2×10^{-3} cal/cm^2) (Ref 7). $\Gamma_{plastic}$ and Γ_{coh} are related, because when Γ_{coh} is zero, no plastic work ($\Gamma_{plastic}$) will be consumed. The exact form of this dependence is not known, although some attempts have been made (Ref 4, 5, 6) to correlate the two terms.

References cited in this section

1. S.P. CHEN, D.J. SROLOVITZ, AND A.F. VOTER, COMPUTER SIMULATION ON SURFACES AND [001] TILT GRAIN BOUNDARIES IN NI, AL, AND NI_3AL, *J. MATER. RES.*, VOL 4, 1989, P 62-77
2. S.P. CHEN AND A.F. VOTER, RECONSTRUCTION OF THE (310), (210), AND (110) SURFACES IN FCC METALS, *SURF. SCI. LETT.*, VOL 244, 1991, P L107-L112
3. S.P. CHEN, THEORETICAL STUDIES OF METALLIC INTERFACES, *MATER. SCI. ENG. B*, VOL 6, 1990, P 113-121

4. M.L. JOKL, V. VITEK, AND C.J. MCMAHON, JR., A MICROSCOPIC THEORY OF BRITTLE FRACTURE IN DEFORMABLE SOLIDS: A RELATION BETWEEN IDEAL WORK TO FRACTURE AND PLASTIC WORK, *ACTA METALL.*, VOL 28, 1980, P 1479-1488
5. M.L. JOKL, V. VITEK, AND C.J. MCMAHON, JR., ON THE MICROMECHANICS OF BRITTLE FRACTURE: EXISTING VS INJECTED CRACKS, *ACTA METALL.*, VOL 37, 1989, P 87-97
6. J. HACK, S.P. CHEN, AND D. SROLOVITZ, A KINETIC CRITERION FOR QUASI-BRITTLE FRACTURE, *ACTA METALL.*, VOL 37, 1989, P 1957-1970
7. A. KELLY AND N.H. MACMILLAN, *STRONG SOLIDS*, 3RD ED., OXFORD SCIENCE PUBLICATIONS, 1986
8. V. VITEK, MICROMECHANISMS OF INTERGRANULAR BRITTLE FRACTURE IN INTERMETALLIC COMPOUND, *J. PHYS. III*, VOL 1, 1991, P 1085-1097

Grain Boundary Energy

The grain boundary energy, Γ_{gb}, is defined the same way as surface energy is, but it depends on the relative orientation of the adjacent grains (Ref 1):

$$\Gamma_{GB} = \Sigma \Delta E_I / A_I \text{ (GB)} \qquad \textbf{(EQ 3)}$$

At misorientation angles of greater than 25°, Γ_{gb} usually reaches a plateau that characterizes random grain boundaries. Special grain boundaries, like Σ5 (210) or (310), tend to have slightly lower energies (Ref 1, 2, 3, 9). Twin boundary energies are even lower than special grain boundaries. For metals, Γ_{gb} usually ranges from 40 to 60% of the surface energy (Ref 10), whereas the twin energy is only about 5 to 15%. Grain boundary cohesive energy is defined as (Ref 1):

$$\Gamma_{COH} \text{ (GB)} = \Gamma_{SURF} \text{ (GRAIN A)} + \Gamma_{SURF} \text{ (GRAIN B)} - \Gamma_{GB} \qquad \textbf{(EQ 4)}$$

For general and random grain boundaries, grain boundary cohesive energy is smaller. General grain boundaries tend to be weaker than the small angle boundaries.

References cited in this section

1. S.P. CHEN, D.J. SROLOVITZ, AND A.F. VOTER, COMPUTER SIMULATION ON SURFACES AND [001] TILT GRAIN BOUNDARIES IN NI, AL, AND NI_3AL, *J. MATER. RES.*, VOL 4, 1989, P 62-77
2. S.P. CHEN AND A.F. VOTER, RECONSTRUCTION OF THE (310), (210), AND (110) SURFACES IN FCC METALS, *SURF. SCI. LETT.*, VOL 244, 1991, P L107-L112
3. S.P. CHEN, THEORETICAL STUDIES OF METALLIC INTERFACES, *MATER. SCI. ENG. B*, VOL 6, 1990, P 113-121
9. S.P. CHEN, STUDIES OF IRIDIUM SURFACES AND GRAIN BOUNDARIES, *PHIL. MAG. A*, VOL 65, 1992, TO BE PUBLISHED
10. L.E. MURR, *INTERFACIAL PHENOMENA IN METALS AND ALLOYS*, ADDISON-WESLEY, 1975

Interfacial Energy

By definition, the interfacial energy (Ref 2, 3) between two bulk materials (A and B) is the same as the grain boundary energy, except that there are two reference states:

$$\Gamma_{INTERFACE} = [\Sigma\Delta E_I\,(A) + \Sigma\Delta E_J(B)]/A \qquad \textbf{(EQ 5)}$$

where $\Delta E_i(A) \cdot [(\Delta E_j(B)]$ is the extra energy of atom *i* of A (B) type, compared to its bulk state of A (B) materials. The interfacial energy between similar metals tends to be small. For dissimilar materials, however, interfacial energies tend toward large positive values if they do not form compounds and large negative values if they do form compounds. The ideal adhesion energy is similar to grain boundary cohesion and is the difference between the two surfaces and the interfacial energies:

$$\Gamma_{ADHESION} = \Gamma_{SURFACE}\,(A) + \Gamma_{SURFACE}\,(B) - \Gamma_{INTERFACE}\,(A/B) \qquad \textbf{(EQ 6)}$$

References cited in this section

2. S.P. CHEN AND A.F. VOTER, RECONSTRUCTION OF THE (310), (210), AND (110) SURFACES IN FCC METALS, *SURF. SCI. LETT.*, VOL 244, 1991, P L107-L112
3. S.P. CHEN, THEORETICAL STUDIES OF METALLIC INTERFACES, *MATER. SCI. ENG. B,* VOL 6, 1990, P 113-121

Ray Dixon and S.P. Chen, Los Alamos National Laboratory

Theory of Adhesion

Rose *et al.* (Ref 11) have calculated the bimaterial interfacial cohesion for many combinations of elements using band structure methods. They found a universal scaling relationship for the adhesion of different materials that extends beyond metal-metal interfaces to nonmetal systems. A few calculations are necessary to identify the adhesion behavior of the system and set the appropriate energy, length, and elastic constant scales. Plastic contributions are not treated in this formalism. The plastic work is more likely to be solved by incorporating the atomistic simulation and continuum analysis of Jokl *et al.* (Ref 4, 5) and Hack *et al.* (Ref 6).

The tight binding method give qualitative trends as the energy band is filled for calculations using the elements in the periodic table (Ref 12, 13, 14). The correct trend seems to be captured by the band-filling argument pioneered in the original work of Friedel (Ref 15). For noble metals, a rigid band picture is preferred (Ref 14). Another useful tool is the Pettifor structure map. By using the Mendelev number for each of the 103 elements (Ref 13, 16), Pettifor found that alloying tendencies can be grouped into separate regions. If the interfacial chemistry and average Mendelev number are known, then the interfacial structure can be found from the Pettifor map.

Extensive atomistic simulation work, using effective medium theory (Ref 17, 18), embedded atom potentials (Ref 19), or local volume potentials (Ref 1, 2, 3, 8, 9, 20, 21, 22, 23) had been very useful in describing the properties of many metals and compounds and their interactions with impurities such as boron and sulfur in Ni_3Al and NiAl (Ref 20, 21). These atomic interaction descriptions include pair potential and many body interactions and have been obtained for systems that include Ni_3Al, Cu_3Au, NiAl, nickel, aluminum, iridium, gold, platinum, silver, copper, molybdenum, tantalum, iron, tungsten, niobium, beryllium, titanium, hafnium, zirconium, and rhenium (Ref 1, 2, 3, 9, 20, 21, 22, 23, 24, 25, 26, 27). These studies indicate that stoichiometry (Ref 1, 20, 21) and impurities (Ref 20, 21) can be crucial in determining ideal and realistic adhesion, including effects induced by boron and sulfur. They represent the fundamentals for future work,

which is expected to have significant impact on the theory using atomistic simulation under well-controlled situations for all conditions of stress, temperature, and chemical environments. These calculations should enable direct linking of theoretical studies and materials by design concepts, as applied in NiAl microalloyed with boron or iron (Ref 24, 25, 26, 27).

DeBoer *et al.* (Ref 28) have developed excellent tools for screening bonding materials, based on two properties of the elements: electronegativity and electron density. One can use the Miedema formula for the adhesion of a bimetallic interface, based on the work function (closely related to the Pauling electronegativity), Φ, and the electron density, *n*, at the Wigner-Seitz radius, as described in Ref 28.

References cited in this section

1. S.P. CHEN, D.J. SROLOVITZ, AND A.F. VOTER, COMPUTER SIMULATION ON SURFACES AND [001] TILT GRAIN BOUNDARIES IN NI, AL, AND NI_3AL, *J. MATER. RES.*, VOL 4, 1989, P 62-77
2. S.P. CHEN AND A.F. VOTER, RECONSTRUCTION OF THE (310), (210), AND (110) SURFACES IN FCC METALS, *SURF. SCI. LETT.*, VOL 244, 1991, P L107-L112
3. S.P. CHEN, THEORETICAL STUDIES OF METALLIC INTERFACES, *MATER. SCI. ENG. B*, VOL 6, 1990, P 113-121
4. M.L. JOKL, V. VITEK, AND C.J. MCMAHON, JR., A MICROSCOPIC THEORY OF BRITTLE FRACTURE IN DEFORMABLE SOLIDS: A RELATION BETWEEN IDEAL WORK TO FRACTURE AND PLASTIC WORK, *ACTA METALL.*, VOL 28, 1980, P 1479-1488
5. M.L. JOKL, V. VITEK, AND C.J. MCMAHON, JR., ON THE MICROMECHANICS OF BRITTLE FRACTURE: EXISTING VS INJECTED CRACKS, *ACTA METALL.*, VOL 37, 1989, P 87-97
6. J. HACK, S.P. CHEN, AND D. SROLOVITZ, A KINETIC CRITERION FOR QUASI-BRITTLE FRACTURE, *ACTA METALL.*, VOL 37, 1989, P 1957-1970
8. V. VITEK, MICROMECHANISMS OF INTERGRANULAR BRITTLE FRACTURE IN INTERMETALLIC COMPOUND, *J. PHYS. III*, VOL 1, 1991, P 1085-1097
9. S.P. CHEN, STUDIES OF IRIDIUM SURFACES AND GRAIN BOUNDARIES, *PHIL. MAG. A*, VOL 65, 1992, TO BE PUBLISHED
11. J.H. ROSE, J.R. SMITH, F. GUINEA, AND J. FERRANTE, UNIVERSAL FEATURES OF THE EQUATION OF STATE OF METALS, *PHYS. REV. B*, VOL 29, 1984, P 2963-2969
12. T.B. MASSALSKI, ED., *BINARY ALLOYS PHASE DIAGRAMS*, ASM, 1986, P 2176-2181
13. D.G. PETTIFOR, ELECTRON THEORY OF METALS, *PHYSICAL METALLURGY*, R.W. CAHN AND P. HAASEN, ED., NORTH-HOLLAND, AMSTERDAM, 1983, P 73-152
14. J.S. FAULKNER, THE MODERN THEORY OF ALLOYS, *PROG. MATER. SCI.*, VOL 27, 1982, P 1-187
15. J. FRIEDEL, TRANSITION METALS, ELECTRONIC STRUCTURE OF THE D-BAND, ITS ROLE IN THE CRYSTALLINE AND MAGNETIC STRUCTURES, *THE PHYSICS OF METALS*, J.M. ZIMAN, ED., CAMBRIDGE UNIVERSITY PRESS, 1969, P 340-408
16. D.G. PETTIFOR, NEW MANY-BODY POTENTIAL FOR THE BOND ORDER, *PHYS. REV. LETT.*, VOL 63, 1989, P 2480-2483
17. J.K. NORSKOV AND N.D. LANG, EFFECTIVE-MEDIUM THEORY OF CHEMICAL BINDING: APPLICATION TO CHEMISORPTION, *PHYS. REV. B*, VOL 21, 1980, P 2131-2136
18. M.J. STOTT AND E. ZAREMBA, QUASIATOMS: AN APPROACH TO ATOMS IN NONUNIFORM ELECTRONIC SYSTEMS, *PHYS. REV. B*, VOL 22, 1980, P 1564-1583
19. M.S. DAW AND M.I. BASKES, EMBEDDED-ATOM METHOD: DERIVATION AND APPLICATION TO IMPURITIES, SURFACES, AND OTHER DEFECTS IN METALS, *PHYS. REV. B*, VOL 29, 1984, P 6443-6453
20. S.P. CHEN, A.F. VOTER, R.C. ALBERS, A.M. BORING, AND P.J. HAY, INVESTIGATION OF BORON EFFECT ON NI AND NI_3AL GRAIN BOUNDARIES, *J. MATER. RES.*, VOL 5, 1990, P 955-970

21. S.P. CHEN, A.F. VOTER, R.C. ALBERS, A.M. BORING, AND P.J. HAY, THEORETICAL STUDIES OF GRAIN BOUNDARIES IN NI_3AL WITH BORON OR SULFUR, *SCR. METALL.*, VOL 23, 1989, P 217-222
22. A.F. VOTER AND S.P. CHEN, ACCURATE INTERATOMIC POTENTIALS FOR NI, AL, AND NI_3AL, *MATER. RES. SOC. PROC.*, VOL 82, 1987, P 175-180
23. S.P. CHEN, ANOMALOUS RELAXATIONS OF (0001) AND $(10\bar{1}0)$ SURFACES IN HCP METALS, *SURF. SCI. LETT.*, VOL 264, 1992, P L162-L168
24. R.J. HARRISON, A.F. VOTER, AND S.P. CHEN, *ATOMISTIC MODELING OF MATERIALS: BEYOND PAIR POTENTIALS*, V. VITEK AND D.J. SROLOVITZ, ED., PLENUM PRESS, 1989, P 219-222
25. R.J. HARRISON, F. SPAEPEN, A.F. VOTER, AND S P. CHEN, STRUCTURE OF GRAIN BOUNDARIES IN IRON, *PROC. 34TH SAGAMORE ARMY MATERIALS RESEARCH CONFERENCE* (LAKE GEORGE, NY), 1990, P 651-675 (FOR FE)
26. S.P. CHEN, LOCAL VOLUME POTENTIALS FOR BCC METALS, TO BE PUBLISHED (FOR FE, NB, CR, W, AND MO)
27. S.P. CHEN, A.M. BORING, R.C. ALBER, AND P.J. HAY, THEORETICAL STUDIES OF NI_3AL AND NIAL WITH IMPURITIES, *HIGH TEMPERATURE ORDERED INTERMETALLIC ALLOYS III*, C.C. KOCH, C.T. LIU, N.S. STOLOFF, AND A.I. TAUB, ED., *PROC. MATER. RES. SOC.*, VOL 133, 1989, P 149-154
28. F.R. DEBOER, R. BOOM, W.C.M. MATTENS, A.R. MIEDEMA, AND A.K. NIESSEN, *COHESION IN METALS: TRANSITION METAL ALLOYS*, NORTH-HOLLAND, 1989

Fundamentals of Metal and Metal-to-Ceramic Adhesion

Ray Dixon and S.P. Chen, Los Alamos National Laboratory

Properties Affecting Adhesion

Large impurities, such as bismuth, sulfur, phosphorus, and so on, tend to lower grain boundary adhesion, whereas small interstitial atoms, such as boron, carbon, and beryllium tend to increase cohesion in nickel, Ni_3Al, and Ni_3Si (Ref 1, 20, 21). Deviations from stoichiometry can either increase or decrease cohesion, depending on whether amounts of strong bonding elements, like nickel in Ni_3Al, are increased or decreased. Although stoichiometry may slightly affect the ideal cohesion energy, its effect on the consumption of plastic work is potentially higher, as demonstrated in Co_3Ti. Researchers (Ref 29) found that excess cobalt suppressed intergranular brittleness and rendered the material ductile, without adding strengtheners such as boron or beryllium. Sometimes impurity effects only work in off-stoichiometric compounds, such as boron in Ni_3Al. Quantitative analysis of these kinds of effects have been attempted for impurity-controlled fracture properties in iron, which has been studied extensively by Hondros and Seah (Ref 30). A simple linear formula linking cohesion and level of impurities has been extracted from many experiments (Ref 30).

References cited in this section

1. S.P. CHEN, D.J. SROLOVITZ, AND A.F. VOTER, COMPUTER SIMULATION ON SURFACES AND [001] TILT GRAIN BOUNDARIES IN NI, AL, AND NI_3AL, *J. MATER. RES.*, VOL 4, 1989, P 62-77
20. S.P. CHEN, A.F. VOTER, R.C. ALBERS, A.M. BORING, AND P.J. HAY, INVESTIGATION OF BORON EFFECT ON NI AND NI_3AL GRAIN BOUNDARIES, *J. MATER. RES.*, VOL 5, 1990, P 955-970
21. S.P. CHEN, A.F. VOTER, R.C. ALBERS, A.M. BORING, AND P.J. HAY, THEORETICAL STUDIES OF GRAIN BOUNDARIES IN NI_3AL WITH BORON OR SULFUR, *SCR. METALL.*, VOL 23, 1989, P 217-222
29. J.E. HACK, D.J. STROLOVITZ, AND S.P. CHEN, A MODEL FOR THE FRACTURE BEHAVIOR OF POLYCRYSTALLINE NI_3AL, *SCR. METALL.*, VOL 20, 1986, P 1699-1704

30. E.D. HONDROS AND M.P. SEAH, INTERFACIAL AND SURFACE MICROCHEMISTRY, *PHYSICAL METALLURGY,* 3RD ED., R.W. CAHN AND P. HAASEN, ED., ELSEVIER SCIENCE PUBLISHER, 1983, P 855-931

Ray Dixon and S.P. Chen, Los Alamos National Laboratory

Adhesion Measurement

Sikorski (Ref 31) describes two modifications of the twist-compression bonding method for adhesion testing and concludes that the measured coefficient of friction supports the adhesion theory of friction. This correlation implies that a large coefficient of adhesion (ratio of the force necessary to break a bond to the normal loading force used to produce the bond) corresponds to a large coefficient of friction.

Experimentally, he showed that the coefficient of adhesion was inversely proportional to the melting point, which meant that higher melting point materials had lower adhesion. This agress with the observation that higher melting point materials have higher hardness, which also corresponds to lower adhesion coefficients. Gerkema and Miedema (Ref 32) considered lubrication of iron substrates by thin films of lead and silver with copper, platinum, or molybdenum additions by calculating surface adhesion using heats of solution and surface energies. Their predictions agree well with sliding wear experiments.

Pashley and Tabor (Ref 33) measured adhesion between tungsten and nickel using techniques similar to those used in atomic force microscopy (AFM). They were able to verify surface cleanliness and ensure that the adhesion measured was between clean tungsten and nickel by using Auger spectroscopy (AES). In a subsequent publication, Pashley and Pethia again measured the surface energy of adhesion between tungsten and nickel (Ref 34). This work was done between a tungsten tip and a nickel flat in high vacuum and showed that surface forces alone could cause plastic flow. The loading/unloading curves provide information on the elastic/plastic response of the material. This in turn determines the interpretation of the adhesion.

Johnson and Keller (Ref 35) used a torsion balance with a 3 mm (0.12 in.) diameter ball against a flat plate to measure the force of adhesion between silver-silver, copper-nickel, and silver-nickel couples. They concluded that mutual solubility did not affect the tendency for adhesion. However, surface contaminants did have a significant effect on the adhesion (joint strength) between silver-silver couples when the vacuum varied. The difference in joint strength for a clean surface at 130 μPa (5×10^{-10} torr) and for the same surface after a few microns of argon was 50 GPa (5×10^{8} dynes/cm^2).

Conrad and Rice (Ref 36) studied the cohesion of fcc metals (silver, aluminum, copper, and nickel) by fracturing the metals in high vacuum, rewelding the metals by compressing the fractured surfaces, and retesting the metals by fracturing. They found that the cohesive strength of the weld increased with compressive load when both were normalized to the initial fracture strength. Results for all materials fell on a single curve. They proposed that the essentially constant cohesion coefficient was due to the fact that the contact area produced by a given compressive load was inversely proportional to the fracture stress of the metal, whereas the cohesive strength was directly proportional to the fracture stress.

Acoustic emission was used to measure and monitor cohesion. In one case, this technique was used to signal the onset of fiber debonding and to determine crack initiation locations in fiber-reinforced ceramic-matrix composites (Ref 37). This approach is a valuable and viable technique for monitoring debonding, but cannot be used to provide quantitative information on either bond strength or fundamental material parameters. It can be used to locate the origin of the debonding, but the error is on the order of the dimensions used for continuum calculations, which are much larger than the atomic dimensions.

In another study (Ref 38), acoustic measurements were used to monitor fatigue cracks and interfaces by defining a spring stiffness (for continuous and discontinuous spring models) that represented the degree of contact across an interface. A measured acoustic reflection coefficient was found to be in good agreement with one predicted for the same geometry. In addition, a single stress-intensity factor was found to determine bond strength.

In a similar vein, Neid (Ref 39) developed a technique for measuring bond integrity by propagating a planar shock were through the bond region. Depending on the shock energy, defects developed in the bond. The change in density was used to detect defects created at the interface, because other nondestructive test (NDT) methods were not sensitive enough to detect the small defects created. The defects were subsequently verified using optical microscopy.

Itou (Ref 40) used electrical resistance to monitor crack tip contact in order to verify crack tip shielding in aluminum, steel, and cork. The results were inconclusive, although he found that there was no oscillating stress singularity around the crack tip. From this discussion, one can see that no generally quick, accurate, and easy-to-use technique has been developed to measure adhesion.

References cited in this section

31. M.E. SIKORSKI, THE ADHESION OF METALS AND FACTORS THAT INFLUENCE IT, *WEAR*, VOL 7, 1964, P 144-162
32. J. GERKEMA AND A.R. MIEDEMA, ADHESION BETWEEN SOLID METALS: OBSERVATIONS OF INTERFACIAL SEGREGATION EFFECTS IN METAL FILM LUBRICATION EXPERIMENTS, *SURF. SCI.*, VOL 124, 1983, P 351-371
33. M.D. PASHLEY AND D. TABOR, ADHESION AND DEFORMATION PROPERTIES OF CLEAN AND CHARACTERIZED METAL MICRO-CONTACTS, *VACUUM*, VOL 10-12, 1981, P 619-623
34. M.D. PASHLEY AND J.B. PETHICA, THE ROLE OF SURFACE FORCES IN METAL-METAL CONTACTS, *J. VAC. SCI. TECHNOL. A*, VOL 3 (NO. 3), MAY/JUNE 1985, P 757-761
35. K.I. JOHNSON AND D.V. KELLER, JR., EFFECT OF CONTAMINATION ON THE ADHESION OF METALLIC COUPLES IN ULTRA-HIGH VACUUM, *J. APPL. PHYS.*, VOL 38 (NO. 4), JAN 1967, P 1896-1904
36. H. CONRAD AND L. RICE, THE COHESION OF PREVIOUSLY FRACTURED FCC METALS IN ULTRA-HIGH VACUUM, *METALL. TRANS.*, VOL 1, NOV 1970, P 3019-3029
37. T. KISHI, M. ENOKI, AND H. TSUDA, INTERFACE AND STRENGTH IN CERAMIC MATRIX COMPOSITES, *MATER. SCI. ENG.*, VOL A143, 1991, P 103-110
38. O. BUCK, R.B. THOMPSON, D.K. REHBEIN, D.D. PALMER, AND L.J.H. BRASCHE, CONTACTING SURFACES: A PROBLEM IN FATIGUE AND DIFFUSION BONDING, *METALL. TRANS. A*, VOL 20, APRIL 1989, P 627-635
39. H.A. NIED, "DETERMINATION OF THE STRUCTURAL INTEGRITY OF METALLURGICALLY BONDED PLATES BY HIGH ENERGY IMPULSE TEST," *SIXTH INT. CONF. ON EXP. STRESS ANALYSIS* (MUNICH), SEPT 1978
40. S. ITOU, AN EXPERIMENT ON THE BEHAVIOUR AROUND THE TIPS OF AN INTERFACE CRACK, *ENG. FRACT. MECH.*, VOL 37 (NO. 1), 1990, P 145-150

Fundamentals of Metal and Metal-to-Ceramic Adhesion

Ray Dixon and S.P. Chen, Los Alamos National Laboratory

Interfacial Analysis

Electron spectroscopies are extremely valuable for the quantitative and qualitative analysis of surfaces. Fundamental information about the atomic forces and energies of the regions being probed, as well as their geometry, can be obtained. The shortcoming of these techniques in analyzing interfaces is that the interfacial volume is a small fraction of the probed volume and the effects of the interface cannot be separated from the signal. This condition can be overcome by using scanning tunneling microscopy (STM) or AFM. However, preparation of the surface is extremely difficult, the equipment requires a skilled and trained operator, the data are fundamental, and engineering information is not obtained. The crux of the problem is that there is no simple connection between condensed matter theory, micromechanics, and continuum

mechanics. The following discussion briefly reviews some of the available technical literature that describes the use of these spectroscopies and their application to bimaterial systems.

Photoelectron spectroscopy has been used to study electron core-level shifts for ytterbium, aluminum, and silicon grown on molybdenum (110) (Ref 41, 42). The core-level shifts between the film and the substrate are expressed in terms of adhesion energy. In this case, the adhesion energy is the difference between the energy of the neutral and excited atoms per atom, which is readily found from the spectra. The measured adhesion energy is in good agreement with the adhesion energy determined using the Miedema technique (Ref 28). High-resolution electron microscopy (HREM), electron energy loss spectroscopy (EELS), microspectroscopy, and microdiffraction have been used to analyzed the chemical distributions on or near interface planes (Ref 43). This information can be used to support models requiring detailed stoichiometry, but does not yield adhesion values.

Gerberich *et al.* (Ref 44) used selected-area-electron channeling patterns (SACP) and stereoimaging to quantify the strain in grains. The work was carried out under plane strain and plane stress conditions. The researchers determined strain distributions within 1 μm (40 μin.) of a stationary or growing crack in Fe-3Si single crystals with a {100}<010> crack. Although this arrangement is not a bimaterial interface, the results reflect the effort needed to obtain fundamental materials information.

Optical techniques, such as reflection (Ref 45), have also been used to probe interfaces and to aid in determining interfacial electronic structure. The data, in turn, are related to adhesion and segregation. For example, Lanning *et al.* (Ref 46) recently correlated reflectance spectra with surface free energy. This was then used as a measure of surface energy and the work of decohesion was calculated.

The most promising technology for understanding interfaces is probably STM and associated techniques. Advances in the science and technology of scanning tunneling microscopy/spectroscopy (STM/S), AFM, photon scanning tunneling microscopy (PSTM), scanning chemical potential microscopy (SCPM), and related spectroscopies/microscopies offer new insight into interfaces (Ref 47). Low-energy electron diffraction (LEED), LEED-spot profile analysis (SPA-LEED), scanning low-energy electron microscopy (SLEEM), and photoemission electron microscopy (PEEM) are also being applied to surface analysis and adhesion. These technologies, although currently applied to the vacuum-surface interface, are appropriate tools for the study of grain boundaries and dissimilar metal surfaces. They provide excellent methods for measuring the electronic behavior at interfaces and, thus, the fundamental interactions that occur at these interfaces. This information must then be correlated to engineering properties predicted by micromechanical and continuum mechanics methods, as well as experiments.

References cited in this section

28. F.R. DEBOER, R. BOOM, W.C.M. MATTENS, A.R. MIEDEMA, AND A.K. NIESSEN, *COHESION IN METALS: TRANSITION METAL ALLOYS,* NORTH-HOLLAND, 1989
41. N. MARTENSSON, A. STENBORG, O. BJORNEHOLM, A. NILSSON, AND J.N. ANDERSON, QUANTITATIVE STUDIES OF METAL-METAL ADHESION AND INTERFACE SEGREGATION ENERGIES USING PHOTOELECTRON SPECTROSCOPY, *PHYS. REV. LETT.*, VOL 60 (NO. 17), APRIL 1988, P 1731-1734
42. J.N. ANDERSON, O. BJORNEHOLM, A. STENBORG, A. NILSSON, C. WIGREN, AND N. MARTENSSON, MEASUREMENT OF METAL-METAL ADHESION AND INTERFACE SEGREGATION ENERGIES BY CORE-LEVEL PHOTOELECTRON SPECTROSCOPY. AL AND SI ON MO(110), *J. PHYS., CONDENS. MATTER,* VOL 1, 1989, P 7309-7313
43. R.W. CARPENTER, HIGH RESOLUTION INTERFACE ANALYSIS, *MATER. SCI. ENG.,* VOL A107, 1989, P 207-216
44. W.W. GERBERICH, D.L. DAVIDSON, AND M. KACZOROWSKI, EXPERIMENTAL AND THEORETICAL STRAIN DISTRIBUTIONS FOR STATIONARY AND GROWING CRACKS, *J. MECH. PHYS. SOLIDS,* VOL 38 (NO. 1), 1990
45. A. JOHNER AND P. SCHAAF, CALCULATION OF THE REFLECTION COEFFICIENTS OF INTERFACES: A SCATTERING APPROACH, *PHYS. REV. B,* VOL 42 (NO. 9), SEPT 1990, P 5516-5526

46. B.R. LANNING, T. FURTAK, AND G.R. EDWARDS, A METHOD FOR PREDICTION OF METAL-CERAMIC INTERFACIAL BOND ENERGIES, SUBMITTED FOR PUBLICATION IN *J. MATER. RES.*
47. R.J. COLTON, C.R.K. MARRIAN, AND J.A. STROSCIO, ED., *PROC. FIFTH INT. CONF. SCANNING TUNNELING MICROSCOPY/SPECTROSCOPY (SAM '90)* AND *THE FIRST INT. CONF. NANOMETER SCALE SCIENCE AND TECHNOLOGY (NANO I)* (BALTIMORE, MD), JUNE 1990, AND *J. VAC. SCI. TECH. B,* SECOND SERIES, VOL 9 (NO. 2), PART II, MARCH/APRIL 1991

Fundamentals of Metal and Metal-to-Ceramic Adhesion

Ray Dixon and S.P. Chen, Los Alamos National Laboratory

Welding (Bonding)

An extensive review of diffusion bonding is given by Gerken and Owczarski (Ref 48). This treatise reviewed the status of theory at that time (1965) and cited numerous examples. Eleven years later, Williams and Crossland (Ref 49, 50) highlighted cold and diffusion welding. They pointed out that the major technical concerns for these processes had not significantly changed in the interim. As recently as 1986, there was concern over the knowledge base of bonding and adhesion at interfaces (Ref 51). This group felt that detailed mechanisms of adhesion were largely missing, but that first-principle theories were beginning to appear. A strong need for collaboration between theorists and experimentalists was indicated. Furthermore, much information was still unknown about interfaces, and the field was ripe for expansion. This situation still applies. Described below are examples of some of the proposed models for bonding.

Several mechanisms have been proposed to explain the formation of solid-state welds (Ref 52, 53). Mohamed and Washburn (Ref 52) proposed a two-stage mechanism that depends on breaking the surface oxide. Their work is supported by the work of Bay. (Ref 54), who developed a theoretical model for oxide breakage and bond formation on aluminum. Kawakatsu and Kitayama (Ref 53) describe bonding as being controlled by three metallurgical factors, which have been identified as bonds between solid-solution, two-phase, or intermetallic materials. Their studies involved bond-strength measurements and microstructural examination as a function of bonding conditions for copper-nickel, copper-silver, and iron-aluminum couples. They concluded that a minimum bonding temperature occurs at about the softening temperature of one of the materials. They also found that bond strength depends on recrystallization temperature. In the case of solid-solution materials, the interfaces tend to disappear after sufficient time above the recrystallization temperature, whereas this does not occur in two-phase and intermetallic materials.

Excellent treatises on surface and interfacial segregation are provided by Dowben and Miller (Ref 55) and Hondros and Seah (Ref 30). The concept of migration or segregation of one component of a system to a surface or interface is considered in detail. This work provides insight into the behavior that must be considered when determining the possibility of adhesion between two dissimilar materials.

Garmong *et al.* (Ref 56) describe the rate-limiting step in bonding as the complete elimination of porosity from the bond line and have developed a time-prediction model to support it. The model proceeds in two stages. First, long-wavelength asperities (roughness) are eliminated by plastic flow. Second, voids are eliminated by plastic flow and vacancy diffusion. This model is similar to that proposed by Hill and Wallach (Ref 57), who consider void elimination at the bond line. In this case, voids are created by surface asperities on the mating surfaces and pressure sintering is invoked for its elimination. The effect of grain size is also considered.

Cahn (Ref 58) derived interfacial energy from thermodynamic considerations. He considered how the order parameter changes surface tension, elastic energy, and excess free energy when it affects the lattice parameter of an ordered material at an antiphase boundary. The work is not only appropriate for grain boundary interfaces in ordered materials, but is also relevant for dissimilar materials.

Cline (Ref 59) reviews the difference between deformation and diffusion bonding. He defines diffusion bonding as not requiring significant deformation for bond formation. With respect to deformation bonding, Cline discusses the "film" and "energy barrier" theories and reviews the factors affecting the resultant bond. With respect to diffusion bonding, he defines two stages for bonding: microscopic deformation and diffusion. He then reviews the results for bonding aluminum and titanium and shows that both can be readily deformation bonded. The diffusion bonding of aluminum was simplified

by using a silver interlayer, whereas titanium required smooth, clean surfaces and protection from atmospheric contaminants.

Derby and Wallach (Ref 60, 61) developed a thorough model for diffusion welding which accounts for:

- SURFACE DIFFUSION FROM SURFACE SOURCES TO A NECK
- VOLUME DIFFUSION FROM SURFACE SOURCES TO A NECK
- DIFFUSION ALONG THE BOND INTERFACE FROM INTERFACIAL SOURCES TO A NECK
- VOLUME DIFFUSION FROM INTERFACIAL SOURCES TO A NECK
- POWER-LAW CREEP DEFORMING THE RIDGE (SURFACE ROUGHNESS)
- PLASTIC YIELDING DEFORMING THE RIDGE
- VAPOR PHASE MASS TRANSPORT

Mass transport rate equations were developed in terms of the process variables (time, temperature, pressure, and material properties). The model is in reasonable agreement with experiment (Ref 62, 63).

Guo and Ridley (Ref 64) consider the rate-limiting step in bonding to be the removal of interfacial voids that are due to the surface roughness and have developed a model to support this position. The main difference between their model and that of Derby and Wallach (Ref 60) is the void geometry used. Guo and Ridley use a lenticular-shaped cavity and have developed a model that agrees reasonably with the experimental data.

References cited in this section

30. E.D. HONDROS AND M.P. SEAH, INTERFACIAL AND SURFACE MICROCHEMISTRY, *PHYSICAL METALLURGY,* 3RD ED., R.W. CAHN AND P. HAASEN, ED., ELSEVIER SCIENCE PUBLISHER, 1983, P 855-931
48. J.M. GERKEN AND W.A. OWCZARSKI, "A REVIEW OF DIFFUSION WELDING," WELDING RESEARCH COUNCIL BULLETIN NO. 109, OCT 1965
49. J.D. WILLIAMS AND B. CROSSLAND, PART 1 COLD PRESSURE WELDING, *CME,* MARCH 1976, P 65-67
50. J.D. WILLIAMS AND B. CROSSLAND, PART 2 DIFFUSION BONDING, *CME,* APRIL 1976, P 73-75
51. J.R. SMITH, PANEL REPORT ON INTERFACIAL BONDING AND ADHESION, *MATER. SCI. ENG.,* VOL 83, 1986
52. H.A. MOHAMED AND J. WASHBURN, MECHANISM OF SOLID STATE PRESSURE WELDING, *WELD. J. RES. SUPP.,* SEPT 1975, P 302S-310S
53. I. KAWAKATSU AND S. KITAYAMA, STUDY ON DIFFUSION BONDING OF METALS, *TRANS. JIM,* VOL 18, 1977, P 455-465
54. N. BAY, MECHANISMS PRODUCING METALLIC BONDS IN COLD WELDING, *WELD. J. RES. SUPP.,* MAY 1983, P 137S-142S
55. P.A. DOWBEN AND A. MILLER, ED., *SURFACE SEGREGATION PHENOMENA,* CRC PRESS, 1990
56. G. GARMONG, N.E. PATON, AND A.S. ARGON, ATTAINMENT OF FULL INTERFACIAL CONTACT DURING DIFFUSION BONDING, *METALL. TRANS. A,* VOL 6, JUNE 1975, P 1269-1279
57. A. HILL AND E.R. WALLACH, MODELLING SOLID-STATE DIFFUSION BONDING, *ACTA METALL.,* VOL 37 (NO. 9), 1989, P 2425-2437
58. J.W. CAHN, INTERFACIAL FREE ENERGY AND INTERFACIAL STRESS: THE CASE OF AN INTERNAL INTERFACE IN A SOLID, *ACTA METALL.,* VOL 37 (NO. 3), 1989, P 773-776
59. C.L. CLINE, AN ANALYTICAL AND EXPERIMENTAL STUDY OF DIFFUSION BONDING, *WELD. J.,* NOV 1966, P 481-S TO 489-S
60. D. DERBY AND E.R. WALLACH, THEORETICAL MODEL FOR DIFFUSION BONDING, *MET. SCI.,*

VOL 16, JAN 1982, P 49-56

61. D. DERBY AND E.R. WALLACH, DIFFUSION BONDING: DEVELOPMENT OF THEORETICAL MODEL, *MET. SCI.*, VOL 18, SEPT 1984, P 427-431
62. D. DERBY AND E.R. WALLACH, DIFFUSION BONDS IN IRON AND A LOW-ALLOY STEEL, *J. MATER. SCI.*, VOL 19, 1984, P 3149-3158
63. D. DERBY AND E.R. WALLACH, DIFFUSION BONDS IN COPPER, *J. MATER. SCI.*, VOL 19, 1984, P 3140-3148
64. Z.X. GUO AND N. RIDLEY, MODELLING OF DIFFUSION BONDING OF METALS, *MATER. SCI. TECH.*, VOL 3, NOV 1987, P 945-953

Fundamentals of Metal and Metal-to-Ceramic Adhesion

Ray Dixon and S.P. Chen, Los Alamos National Laboratory

Interface Formation

When considering the compression needed to bond dissimilar materials, the deformation-mechanism map work of Frost and Ashby (Ref 65) is helpful. The maps are in a stress/temperature space in which a single deformation mechanism is dominant. The stress used is a normalized tensile stress (tensile stress/shear modulus), and the temperature is the homologous temperature T/T_m, where T is the test temperature and T_m is the melting point of the material being tested, where both temperatures are expressed in degrees K. From these maps and the corresponding constitutive equations, contour plots of constant strain rate can be plotted. At this point, knowing any two values of strain rate, stress, or temperature, a point on the map will give the third variable and thee dominant deformation mechanism. This information can be a guide to determining the bonding mechanism when considering one of the previously discussed mechanisms that requires elimination of defects at the interface.

Dammer *et al.* (Ref 66) describe a study where type 347 stainless steel was bonded to itself with several different interlayers. The interlayers were electrolytic-grade copper foil, electrolytic tough pitch (ETP) copper sheet, 80Au-20Cu foil, 72Ag-28Cu foil, and several combinations of silver, copper, and gold electroplates. They successfully bonded the specimens at temperatures below 540 °C (1005 °F), but found that the intermediate materials were essential to forming the weld.

Bachin (Ref 67) discusses the interactions of metals and oxides when diffusion welding metals to metals and to ceramics. He discusses the reactions and exchanges at the interface by considering the formation of spinels and oxides. This leads to the conditions under which each is known to be operative and to the possibility of diffusion across the resulting interface. For example, Al + SiO_2 proceeds by exchange:

$$4AL + 3SIO_2 \rightarrow 2AL_2O_3 + 3SI \qquad \textbf{(EQ 7)}$$

When thin silicon dioxide is joined through a thin intermediate interlayer of aluminum, new phases precipitate at the dividing boundaries and the solid solution is decomposed when the limit of solubility is reached for the reaction products. This behavior results in high internal stresses and resultant microcracks. Caution is therefore required when welding these systems. A thorough review of the thermodynamics involved for the systems being considered is essential.

Munir (Ref 68) developed equations that predict the amount of time required to dissolve oxides into their host metals for systems that have unstable oxides with respect to dissolution. He considered niobium, zirconium, titanium, copper, tantalum, cobalt, nickel, and iron and found reasonable agreement with the theory.

Wang and Vehoff (Ref 69) discuss the segregation of atoms to interfaces. Their work deals with grain boundaries as interfaces, and they conclude that the cohesive energy of the interface at a fixed chemical potential is always less than the cohesive energy at a fixed concentration. The concept of segregation to the interface is probably important for bimaterial interfaces because of the different chemical potentials, diffusion rates, and, thus, concentrations that can exist. Because

these parameters are all temperature dependent, the bonding process and the service temperature will affect the interface segregation and, thus, its performance. This work provides a way to consider these effects.

References cited in this section

65. H.J. FROST AND M.F. ASHBY, *DEFORMATION MECHANISM MAPS*, PERGAMON PRESS, 1982
66. P.A. DAMMER, R.E. MONROE, AND D.C. MARTIN, FURTHER STUDIES OF DIFFUSION BONDING BELOW 1000 °F, *WELD. J.*, MARCH 1969, P 116-S TO 124-S
67. V.A. BACHIN, INTERACTION BETWEEN METALS AND THE OXIDES OF CERAMIC MATERIALS DURING DIFFUSION WELDING, *AVT. SVARKA*, NO. 10, 1982, P 15-17
68. Z.A. MUNIR, A THEORETICAL ANALYSIS OF THE STABILITY OF SURFACE OXIDES DURING DIFFUSION WELDING OF METALS, *WELD. J.*, DEC 1983, P 333-S TO 336-S
69. J.-S. WANG AND H. VEHOFF, THE EFFECT OF THE MOBILITY OF SEGREGATED ATOMS ON INTERFACIAL EMBRITTLEMENT, *SCR. METALL.*, VOL 25, 1991, P 1339-1344

Fundamentals of Metal and Metal-to-Ceramic Adhesion

Ray Dixon and S.P. Chen, Los Alamos National Laboratory

Strength of Interfaces

One of the most important and probably the most frequent questions: What is the strength of the interfacial bond? This question has often been answered by tensile testing. The difficulty is that the failure is often not at the interface and that it must be forced there. Additionally, there is concern that the strain is not one-dimensional across the bond and that the bond experiences triaxial strain in service. For these reasons, there has been considerable interests in determining fracture toughness and in detecting the failure of interfaces.

Several reviews on the importance and extent of interfacial science were recently presented in one technical journal (Ref 70). Three reviews are noteworthy because they discuss the mechanical properties of interfaces (Ref 71, 72, 73). The efforts of Hutchinson and Suo (Ref 71) bring together much of the recent work on elastic fracture phenomena for bimetallic systems and builds on it to support work being done to understand mixed-mode failure in systems with interfaces. Shih (Ref 72) summarizes progress on interfacial mechanics and points out that fracture toughness, at various mode mixities, is needed to characterize fracture resistance of a weak plane in a composite. An application of this analysis has been demonstrated on the alumina/niobium metal-ceramic system by Stout *et al.* (Ref 74). Comninou (Ref 73) reviews the interface crack problem from the standpoint of open and closed crack tips and describes preliminary experimental results on fatigue and fracture of interface cracks in aluminum bonded by epoxy.

Interface Strength Models. There has been considerable progress in analyzing the fracture behavior of interfaces with various configurations. This work has led to the development of specimen geometries for systems with differing physical and mechanical properties. The analysis work is reviewed in this section and the experimental work is described in the section "Interface Strength Measurements" of this article.

Suo and Hutchinson (Ref 75) have provided a complete solution to the semi-infinite crack lying along the interface of two infinite elastic layers under edge loads. This solution allows the determination of material properties for complex geometries, as well as the effect of welding two dissimilar materials. Jensen (Ref 76) demonstrates that shielding the full effect of mode II and III loading is important for interface cracks in brittle materials and that a proper interface fracture criteria needs to be modeled. He discusses a method for comparing different phenomenological fracture criteria and sets up micromechanical models describing shielding for interface geometries with kinks.

The models of He and Hutchinson (Ref 77) explain conditions for interfacial crack propagation (kinking) into material on either side of the interface. Their models suggest that a crack propagates along an interface as long as the compliant material is tough and that the stiff material is at least as tough as the interface. They also show that the energy release rate is increased if the crack kinks into the more-compliant material and is diminished if it kinks into the stiff material.

Qu and Li (Ref 78) also analyzed cracks and dislocations at the interface between two anisotropic elastic half spaces. They obtained an explicit and real solution to the dislocation problem in the Stroh (Ref 79) formalism and showed that a planar interface between dissimilar anisotropic solids is completely characterized by no more than nine independent parameters. The work by Li and Ting (Ref 80, 81) is also relevant.

Evans *et al.* (Ref 82, 83) concluded that fracture energy is not unique and is usually greater than the thermodynamic work of adhesion. The nonuniqueness is related to the mixity experienced by interface cracks. As a result, the fracture energy is influenced by the choice of test specimen. This result implies that when considering fracture energy for specific material combinations, the test geometry must be known, reported, and maintained. This also means that it is now possible to systematically study interfacial mechanical behavior and produce meaningful data on interface fracture toughness.

Fischmeister *et al.* (Ref 84) modeled simple crack propagation, dislocation emission from crack tips, and twinning using atomistic calculations (molecular dynamics) embedded in a finite-element continuum. They also studied the behavior of cracks propagating in tungsten and iron on different planes and in different directions within these planes. Their results confirm that {100} should be the easiest cleavage plane in these body-centered cubic (bcc) tungsten and iron crystals. They further studied the propagation direction restrictions for cracks on particular planes. The modeling work was supported by experiments to verify the crack propagation behavior in WC-Co alloy, high-speed steel consolidated with nickel particles, and nickel coated on high-speed steel.

Chen *et al.* (Ref 1, 9, 20, 21) studied crack growth in nickel, Ni_3Al, Ni_3Al plus boron, Ni_3Al plus sulfur, and iridium grain boundaries using local volume potentials. They found that cohesive strength is important in determining grain boundary fracture and can be strongly affected by impurities and stoichiometry.

Another approach to modeling fracture is given by Needleman (Ref 85), who used a cohesive zone-type interface model. His model takes full account of finite geometry changes and is used to study decohesion of a viscoplastic block from a rigid substrate. He found that the normal traction versus separation relation had an exponential form consistent with the universal binding energy relationship of Rose *et al.* (Ref 86) and of Ferrante and Smith (Ref 87).

Ting (Ref 88) showed that oscillatory displacement at the interfacial crack surface in a bimaterial under a two-dimensional deformation depends only on the material properties and is independent of specimen orientation. The exception is that bimaterials always produce oscillation and that there is an exception for one choice of relative orientation in one material combination. He also shows that for two different orthotropic materials, the oscillation depends on whether or not the Voigt elastic constants combinations, $\sqrt{C_{11}+C_{22}+C_{12}}$, for the two materials are different.

Cook (Ref 89) explains crack propagation threshold in brittle materials through the work done by the applied loading and that which is needed to create new surfaces during crack propagation. He showed that the mechanical energy release rate was a measure of the equilibrium surface energy of the material and the chemical environment. The latter affects the surface tension of both the fresh and aged crack.

Reynolds *et al.* (Ref 90) investigated the difference between the concepts of cracks with zero normal and shear traction over the entire face of the crack and cracks with normal and shear traction specified at zero on the crack surface, except near the tip, where zero shear fraction and continuity of displacements normal to the crack were required. Of these two approaches, the first leads to oscillatory stress singularities and interpenetration of the material near the crack tip, whereas the second shows that a small region of contact exists at the tip, regardless, of the loading. The two methods require different treatments in terms of stress intensity, but predict the same strain-energy release rate. The work was done using the finite-element method (FEM) and, thus, also served to verify the formulation of each problem by FEM analysis. The results showed that the two formulations could be modeled by the absence or presence of interface elements that prevent interpenetration of the crack surfaces. Additionally, fracture parameters were calculated and compared well with previous analytic solutions.

Interface Strength Measurements. Based on the theoretical analysis described above, as well as their own models, the authors identified below have carried out excellent experimental work in measuring the mechanical properties of interfaces.

Charalambides *et al.* (Ref 91) developed a test procedure to measure interface fracture resistance under mixed-mode conditions. Strain-energy release rates and stress-intensity factors can be obtained using this test. O'Dowd *et al.* (Ref 92) developed FEM model solutions and tested several geometries to determine interfacial fracture toughness as a function of mixity. They were able to explain near-tip contact and variation of mixity with distance. They also developed a procedure

for determining the effect of residual stress on the stress-intensity factor. Brady *et al.* (Ref 93) developed a buckled plate test to determine the transverse fracture toughness of unidirectional continuous-fiber composites. Their test was found to be independent of sample geometry and testing conditions. Mecholsky and Baker (Ref 94) developed a double cantilever beam specimen with a chevron notch to measure fracture toughness of ceramic-metal interfaces. The specimen is easy to make and introduces its own crack, and the test is easy to perform. Zhu and Byrne (Ref 95) looked at the effect of interfacial defects by bonding and subsequent tensile, fatigue, and photomicroscopy tests. They measured void ratios at the bond line and found the defects smaller than those detectable by current nondestructive test methods (~0.2 to 0.5 mm^2 by 1 to 3 μm, or 3×10^{-4} to 8×10^{-4} $in.^2$, or 40 to 120 μin., thick) could still significantly affect bond strength. They concluded that fatigue testing is a better test method than tensile testing because it is sensitive to a void ratio of approximately 27%, whereas tensile tests were not.

Thouless (Ref 96) used epoxy-bonded glass slides to investigate interfacial failure under mixed-mode loading. He found that when the scale is sufficiently large, the sample could be considered homogeneous with a weak planar interface. This result produced a correlation between apparent fracture resistance and the degree of mixity. At a very detailed scale, the lack of homogeneity required that the crack-tip stress be determined by the position of the crack within the interface (epoxy). This condition leads to a change in failure mechanisms, whereby under pure mode-I conditions, the crack propagates entirely within the interfacial layer, whereas mode-II effects drive the crack toward the glass-epoxy interface.

Nickel specimens with known surface roughnesses were diffusion welded under controlled conditions of temperature and pressure (Ref 97). The welds were interrupted at several different time intervals and the resulting interface was examined. The defect sizes were successfully related to surface tension and diffusion. It was also found that temperature increases produced a greater effect on reducing interfacial defects than did pressure. Meriin and Sliozberg (Ref 98) make the point that sound welds (bonds) cannot be obtained unless the voids are eliminated at the interface, which requires high temperatures and pressures. It further requires that mechanical tests be used as the principal detection method.

This article has shown that there has been and continues to be active interest in interfacial behavior. The science is sufficiently complex that numerous approaches are useful to evaluate interfacial behavior, depending on the specific goal. However, it is obvious that the seemingly unrelated approaches all seek to understand the interface. It is therefore incumbent upon scientists in this field to be familiar with all developments concerning adhesion so that they can contribute to its understanding and future advancement.

References cited in this section

1. S.P. CHEN, D.J. SROLOVITZ, AND A.F. VOTER, COMPUTER SIMULATION ON SURFACES AND [001] TILT GRAIN BOUNDARIES IN NI, AL, AND NI_3AL, *J. MATER. RES.*, VOL 4, 1989, P 62-77
9. S.P. CHEN, STUDIES OF IRIDIUM SURFACES AND GRAIN BOUNDARIES, *PHIL. MAG. A*, VOL 65, 1992, TO BE PUBLISHED
20. S.P. CHEN, A.F. VOTER, R.C. ALBERS, A.M. BORING, AND P.J. HAY, INVESTIGATION OF BORON EFFECT ON NI AND NI_3AL GRAIN BOUNDARIES, *J. MATER. RES.*, VOL 5, 1990, P 955-970
21. S.P. CHEN, A.F. VOTER, R.C. ALBERS, A.M. BORING, AND P.J. HAY, THEORETICAL STUDIES OF GRAIN BOUNDARIES IN NI_3AL WITH BORON OR SULFUR, *SCR. METALL.*, VOL 23, 1989, P 217-222
70. T. TSAKALAKOS, ED., *MATER. SCI. ENG. B*, VOL 6, 1990, P 69-210
71. J.W. HUTCHINSON AND Z. SUO, MIXED MODE CRACKING IN LAYERED MATERIALS, *ADVANCES IN APPLIED MECHANICS*, VOL 28, J.W. HUTCHINSON AND T.Y. WU, ED., ACADEMIC PRESS, 1990
72. C.F. SHIH, CRACKS ON BIMATERIAL INTERFACES: ELASTICITY AND PLASTICITY ASPECTS, *MATER. SCI. ENG. A*, VOL 143, 1991, P 77-90
73. M. COMNINOU, AN OVERVIEW OF INTERFACE CRACKS, *ENG. FRACT. MECH.*, VOL 37 (NO. 1), 1990, P 197-208
74. M.G. STOUT, N.P. O'DOWD, AND C.F. SHIH, "INTERFACIAL FRACTURE TOUGHNESS OF ALUMINA/NIOBIUM SYSTEMS," SYMPOSIUM ON EXPERIMENTS IN MICROMECHANICS OF

FAILURE RESISTANT MATERIALS, ASME WINTER ANNUAL MEETING (ATLANTA, GA), DEC 1991

75. Z. SUO AND J.W. HUTCHINSON, "INTERFACE CRACK BETWEEN TWO ELASTIC LAYERS," REPORT MECH-118, HARVARD UNIVERSITY, DIVISION OF APPLIED SCIENCES, MARCH 1988
76. H.M. JENSEN, MIXED MODE INTERFACE FRACTURE CRITERIA, *ACTA METALL. MATER.,* VOL 38 (NO. 12), 1990, P 2637-2644
77. M.-Y. HE AND J.W. HUTCHINSON, "KINKING OF A CRACK OUT OF AN INTERFACE," REPORT MECH-113, HARVARD UNIVERSITY, DIVISION OF APPLIED SCIENCES, FEB 1988
78. J. QU AND Q. LI, INTERFACIAL DISLOCATION AND ITS APPLICATIONS TO INTERFACE CRACKS IN ANISOTROPIC BIMATERIALS, *J. ELASTICITY,* VOL 26, 1991, P 169-195
79. A.N. STROH, DISLOCATIONS AND CRACKS IN ANISOTROPIC ELASTICITY, *PHILOS. MAG.,* VOL 7, 1958, P 625-646
80. Q.Q. LI AND T.C.T. TING, LINE INCLUSION IN ANISOTROPIC ELASTIC SOLIDS, *J. APPL. MECH.,* VOL 56, 1989, P 556-563
81. T.C.T. TING, EXPLICIT SOLUTION AND INVARIANCE OF THE SINGULARITIES AT AN INTERFACE CRACK IN ANISOTROPIC COMPOSITES, *INT. J. SOLIDS STRUCT.,* VOL 22, 1986, P 965-983
82. A.G. EVANS, M. RUHLE, B.J. DALGLEISH, AND P.G. CHARALAMBIDES, THE FRACTURE ENERGY OF BIMATERIAL INTERFACES, *MATER. SCI. ENG.,* VOL A 126, 1990, P 53-64
83. A.G. EVANS, M. RUHLE, B.J. DALGLEISH, AND P.G. CHARALAMBIDES, THE FRACTURE ENERGY OF BIMATERIAL INTERFACES, *METALL. TRANS. A,* VOL 21, SEPT 1990, P 2419-2429
84. H.F. FISCHMEISTER, H.E. EXNER, M.-H. POECH, S. KOHLHOFF, P. GUMBSCH, S. SCHMAUDER, L.S. SIGL, AND R. SPEIGLER, MODELING FRACTURE PROCESSES IN METALS AND COMPOSITE MATERIALS, *Z. METALLKDE,* BD 80, 1989, P 839-846
85. A. NEEDLEMAN, AN ANALYSIS OF TENSILE DECOHESION ALONG AN INTERFACE, *J. MECH. PHYS. SOLIDS,* VOL 38 (NO. 3), 1990, P 289-324
86. J.H. ROSE, J. FERRANTE, AND J.R. SMITH, UNIVERSAL BINDING ENERGY CURVES FOR METALS AND BIMETALLIC INTERFACES, *PHYS. REV. LETT.,* VOL 47 (NO. 9), AUG 1981, P 675-678
87. J. FERRANTE AND J.R. SMITH, THEORY OF THE BIMETALLIC INTERFACE, *PHYS. REV. B,* VOL 31 (NO. 6), MARCH 1985, P 3427-3434
88. T.C.T. TING, INTERFACE CRACKS IN ANISOTROPIC BIMATERIALS, *J. MECH. PHYS. SOLIDS,* VOL 38 (NO. 4), 1990, P 505-513
89. R.F. COOK, CRACK PROPAGATION THRESHOLDS: A MEASURE OF SURFACE ENERGY, *J. MATER. RES.,* VOL 1 (NO. 6), NOV/DEC 1986, P 852-860
90. R.R. REYNOLDS, K. KOKINI, AND G. CHEN, THE MECHANICS OF THE INTERFACE CRACK USING THE FINITE ELEMENT METHOD, *J. ENG. MATER. TECHNOL.,* VOL 112, JAN 1990, P 38-43
91. P.G. CHARALAMBIDES, J. LUND, A.G. EVANS, AND R.M. MCMEEKING, "A TEST FOR DETERMINING THE FRACTURE RESISTANCE OF BIMATERIAL INTERFACES," REPORT M87-4, MATERIALS DEPARTMENT, COLLEGE OF ENGINEERING, UC SANTA BARBARA
92. N.P. O'DOWD, C.F. SHIH, AND M.G. STOUT, TEST GEOMETRIES FOR MEASURING INTERFACIAL FRACTURE TOUGHNESS, *INT. J. SOLIDS AND STRUCT.,* VOL 29, 1992, P 571-589
93. R.L. BRADY, R.S. PORTER, AND J.A. DONOVAN, A BUCKLED PLATE TEST TO MEASURE INTERFACIAL TOUGHNESS IN COMPOSITES, *J. MATER. SCI.,* VOL 24, 1989, P 4138-4143
94. J.J. MECHOLSKY AND L.M. BAKER, A CHEVRON-NOTCHED SPECIMEN FOR FRACTURE TOUGHNESS MEASUREMENTS OF CERAMIC-METAL INTERFACES, *CHEVRON-NOTCHED SPECIMENS: TESTING AND STRESS ANALYSIS,* STP 855, J.H. UNDERWOOD, S.W. FREIMAN, AND F.I. BARATTA, ED., ASTM, 1984, P 324-336
95. X. ZHU AND J.G. BYRNE, EFFECT OF INTERFACE DEFECTS ON THE MECHANICAL PROPERTIES OF AUTOGENOUS DIFFUSION BONDED JOINTS, *J. MATER. ENG.,* VOL 13, 1991, P

207-211

96. M.D. THOULESS, FRACTURE OF A MODEL INTERFACE UNDER MIXED-MODE LOADING, *ACTA METALL. MATER.,* VOL 38 (NO. 6), 1990, P 1135-1140
97. V.S. GOSTOMEL'SKII, E.S. KARAKOZOV, AND A.P. TERNOVSKII, THE IMPORTANCE OF DIFFUSION AND SURFACE TENSION IN THE FORMATION OF CONTACT DURING DIFFUSION WELDING, *AVT. SVARKA,* NO. 4, 1980, P 28-31
98. A.V. MERIIN AND S.K. SLIOZBERG, SOME CHARACTERISTICS OF JOINTS IN THE SOLID-PHASE WELDING OF METALS, *SVAR. PROIZ.,* NO. 5, 1973, P 22-23

Fundamentals of Metal and Metal-to-Ceramic Adhesion

Ray Dixon and S.P. Chen, Los Alamos National Laboratory

References

1. S.P. CHEN, D.J. SROLOVITZ, AND A.F. VOTER, COMPUTER SIMULATION ON SURFACES AND [001] TILT GRAIN BOUNDARIES IN NI, AL, AND NI_3AL, *J. MATER. RES.,* VOL 4, 1989, P 62-77
2. S.P. CHEN AND A.F. VOTER, RECONSTRUCTION OF THE (310), (210), AND (110) SURFACES IN FCC METALS, *SURF. SCI. LETT.,* VOL 244, 1991, P L107-L112
3. S.P. CHEN, THEORETICAL STUDIES OF METALLIC INTERFACES, *MATER. SCI. ENG. B,* VOL 6, 1990, P 113-121
4. M.L. JOKL, V. VITEK, AND C.J. MCMAHON, JR., A MICROSCOPIC THEORY OF BRITTLE FRACTURE IN DEFORMABLE SOLIDS: A RELATION BETWEEN IDEAL WORK TO FRACTURE AND PLASTIC WORK, *ACTA METALL.,* VOL 28, 1980, P 1479-1488
5. M.L. JOKL, V. VITEK, AND C.J. MCMAHON, JR., ON THE MICROMECHANICS OF BRITTLE FRACTURE: EXISTING VS INJECTED CRACKS, *ACTA METALL.,* VOL 37, 1989, P 87-97
6. J. HACK, S.P. CHEN, AND D. SROLOVITZ, A KINETIC CRITERION FOR QUASI-BRITTLE FRACTURE, *ACTA METALL.,* VOL 37, 1989, P 1957-1970
7. A. KELLY AND N.H. MACMILLAN, *STRONG SOLIDS,* 3RD ED., OXFORD SCIENCE PUBLICATIONS, 1986
8. V. VITEK, MICROMECHANISMS OF INTERGRANULAR BRITTLE FRACTURE IN INTERMETALLIC COMPOUND, *J. PHYS. III,* VOL 1, 1991, P 1085-1097
9. S.P. CHEN, STUDIES OF IRIDIUM SURFACES AND GRAIN BOUNDARIES, *PHIL. MAG. A,* VOL 65, 1992, TO BE PUBLISHED
10. L.E. MURR, *INTERFACIAL PHENOMENA IN METALS AND ALLOYS,* ADDISON-WESLEY, 1975
11. J.H. ROSE, J.R. SMITH, F. GUINEA, AND J. FERRANTE, UNIVERSAL FEATURES OF THE EQUATION OF STATE OF METALS, *PHYS. REV. B,* VOL 29, 1984, P 2963-2969
12. T.B. MASSALSKI, ED., *BINARY ALLOYS PHASE DIAGRAMS,* ASM, 1986, P 2176-2181
13. D.G. PETTIFOR, ELECTRON THEORY OF METALS, *PHYSICAL METALLURGY,* R.W. CAHN AND P. HAASEN, ED., NORTH-HOLLAND, AMSTERDAM, 1983, P 73-152
14. J.S. FAULKNER, THE MODERN THEORY OF ALLOYS, *PROG. MATER. SCI.,* VOL 27, 1982, P 1-187
15. J. FRIEDEL, TRANSITION METALS, ELECTRONIC STRUCTURE OF THE D-BAND, ITS ROLE IN THE CRYSTALLINE AND MAGNETIC STRUCTURES, *THE PHYSICS OF METALS,* J.M. ZIMAN, ED., CAMBRIDGE UNIVERSITY PRESS, 1969, P 340-408
16. D.G. PETTIFOR, NEW MANY-BODY POTENTIAL FOR THE BOND ORDER, *PHYS. REV. LETT.,* VOL 63, 1989, P 2480-2483
17. J.K. NORSKOV AND N.D. LANG, EFFECTIVE-MEDIUM THEORY OF CHEMICAL BINDING: APPLICATION TO CHEMISORPTION, *PHYS. REV. B,* VOL 21, 1980, P 2131-2136

18. M.J. STOTT AND E. ZAREMBA, QUASIATOMS: AN APPROACH TO ATOMS IN NONUNIFORM ELECTRONIC SYSTEMS, *PHYS. REV. B,* VOL 22, 1980, P 1564-1583
19. M.S. DAW AND M.I. BASKES, EMBEDDED-ATOM METHOD: DERIVATION AND APPLICATION TO IMPURITIES, SURFACES, AND OTHER DEFECTS IN METALS, *PHYS. REV. B,* VOL 29, 1984, P 6443-6453
20. S.P. CHEN, A.F. VOTER, R.C. ALBERS, A.M. BORING, AND P.J. HAY, INVESTIGATION OF BORON EFFECT ON NI AND NI_3AL GRAIN BOUNDARIES, *J. MATER. RES.,* VOL 5, 1990, P 955-970
21. S.P. CHEN, A.F. VOTER, R.C. ALBERS, A.M. BORING, AND P.J. HAY, THEORETICAL STUDIES OF GRAIN BOUNDARIES IN NI_3AL WITH BORON OR SULFUR, *SCR. METALL.,* VOL 23, 1989, P 217-222
22. A.F. VOTER AND S.P. CHEN, ACCURATE INTERATOMIC POTENTIALS FOR NI, AL, AND NI_3AL, *MATER. RES. SOC. PROC.,* VOL 82, 1987, P 175-180
23. S.P. CHEN, ANOMALOUS RELAXATIONS OF (0001) AND $(10\bar{1}0)$ SURFACES IN HCP METALS, *SURF. SCI. LETT.,* VOL 264, 1992, P L162-L168
24. R.J. HARRISON, A.F. VOTER, AND S.P. CHEN, *ATOMISTIC MODELING OF MATERIALS: BEYOND PAIR POTENTIALS,* V. VITEK AND D.J. SROLOVITZ, ED., PLENUM PRESS, 1989, P 219-222
25. R.J. HARRISON, F. SPAEPEN, A.F. VOTER, AND S P. CHEN, STRUCTURE OF GRAIN BOUNDARIES IN IRON, *PROC. 34TH SAGAMORE ARMY MATERIALS RESEARCH CONFERENCE* (LAKE GEORGE, NY), 1990, P 651-675 (FOR FE)
26. S.P. CHEN, LOCAL VOLUME POTENTIALS FOR BCC METALS, TO BE PUBLISHED (FOR FE, NB, CR, W, AND MO)
27. S.P. CHEN, A.M. BORING, R.C. ALBER, AND P.J. HAY, THEORETICAL STUDIES OF NI_3AL AND NIAL WITH IMPURITIES, *HIGH TEMPERATURE ORDERED INTERMETALLIC ALLOYS III,* C.C. KOCH, C.T. LIU, N.S. STOLOFF, AND A.I. TAUB, ED., *PROC. MATER. RES. SOC.,* VOL 133, 1989, P 149-154
28. F.R. DEBOER, R. BOOM, W.C.M. MATTENS, A.R. MIEDEMA, AND A.K. NIESSEN, *COHESION IN METALS: TRANSITION METAL ALLOYS,* NORTH-HOLLAND, 1989
29. J.E. HACK, D.J. STROLOVITZ, AND S.P. CHEN, A MODEL FOR THE FRACTURE BEHAVIOR OF POLYCRYSTALLINE NI_3AL, *SCR. METALL.,* VOL 20, 1986, P 1699-1704
30. E.D. HONDROS AND M.P. SEAH, INTERFACIAL AND SURFACE MICROCHEMISTRY, *PHYSICAL METALLURGY,* 3RD ED., R.W. CAHN AND P. HAASEN, ED., ELSEVIER SCIENCE PUBLISHER, 1983, P 855-931
31. M.E. SIKORSKI, THE ADHESION OF METALS AND FACTORS THAT INFLUENCE IT, *WEAR,* VOL 7, 1964, P 144-162
32. J. GERKEMA AND A.R. MIEDEMA, ADHESION BETWEEN SOLID METALS: OBSERVATIONS OF INTERFACIAL SEGREGATION EFFECTS IN METAL FILM LUBRICATION EXPERIMENTS, *SURF. SCI.,* VOL 124, 1983, P 351-371
33. M.D. PASHLEY AND D. TABOR, ADHESION AND DEFORMATION PROPERTIES OF CLEAN AND CHARACTERIZED METAL MICRO-CONTACTS, *VACUUM,* VOL 10-12, 1981, P 619-623
34. M.D. PASHLEY AND J.B. PETHICA, THE ROLE OF SURFACE FORCES IN METAL-METAL CONTACTS, *J. VAC. SCI. TECHNOL. A,* VOL 3 (NO. 3), MAY/JUNE 1985, P 757-761
35. K.I. JOHNSON AND D.V. KELLER, JR., EFFECT OF CONTAMINATION ON THE ADHESION OF METALLIC COUPLES IN ULTRA-HIGH VACUUM, *J. APPL. PHYS.,* VOL 38 (NO. 4), JAN 1967, P 1896-1904
36. H. CONRAD AND L. RICE, THE COHESION OF PREVIOUSLY FRACTURED FCC METALS IN ULTRA-HIGH VACUUM, *METALL. TRANS.,* VOL 1, NOV 1970, P 3019-3029
37. T. KISHI, M. ENOKI, AND H. TSUDA, INTERFACE AND STRENGTH IN CERAMIC MATRIX COMPOSITES, *MATER. SCI. ENG.,* VOL A143, 1991, P 103-110
38. O. BUCK, R.B. THOMPSON, D.K. REHBEIN, D.D. PALMER, AND L.J.H. BRASCHE, CONTACTING

SURFACES: A PROBLEM IN FATIGUE AND DIFFUSION BONDING, *METALL. TRANS. A,* VOL 20, APRIL 1989, P 627-635

39. H.A. NIED, "DETERMINATION OF THE STRUCTURAL INTEGRITY OF METALLURGICALLY BONDED PLATES BY HIGH ENERGY IMPULSE TEST," *SIXTH INT. CONF. ON EXP. STRESS ANALYSIS* (MUNICH), SEPT 1978
40. S. ITOU, AN EXPERIMENT ON THE BEHAVIOUR AROUND THE TIPS OF AN INTERFACE CRACK, *ENG. FRACT. MECH.,* VOL 37 (NO. 1), 1990, P 145-150
41. N. MARTENSSON, A. STENBORG, O. BJORNEHOLM, A. NILSSON, AND J.N. ANDERSON, QUANTITATIVE STUDIES OF METAL-METAL ADHESION AND INTERFACE SEGREGATION ENERGIES USING PHOTOELECTRON SPECTROSCOPY, *PHYS. REV. LETT.,* VOL 60 (NO. 17), APRIL 1988, P 1731-1734
42. J.N. ANDERSON, O. BJORNEHOLM, A. STENBORG, A. NILSSON, C. WIGREN, AND N. MARTENSSON, MEASUREMENT OF METAL-METAL ADHESION AND INTERFACE SEGREGATION ENERGIES BY CORE-LEVEL PHOTOELECTRON SPECTROSCOPY. AL AND SI ON MO(110), *J. PHYS., CONDENS. MATTER,* VOL 1, 1989, P 7309-7313
43. R.W. CARPENTER, HIGH RESOLUTION INTERFACE ANALYSIS, *MATER. SCI. ENG.,* VOL A107, 1989, P 207-216
44. W.W. GERBERICH, D.L. DAVIDSON, AND M. KACZOROWSKI, EXPERIMENTAL AND THEORETICAL STRAIN DISTRIBUTIONS FOR STATIONARY AND GROWING CRACKS, *J. MECH. PHYS. SOLIDS,* VOL 38 (NO. 1), 1990
45. A. JOHNER AND P. SCHAAF, CALCULATION OF THE REFLECTION COEFFICIENTS OF INTERFACES: A SCATTERING APPROACH, *PHYS. REV. B,* VOL 42 (NO. 9), SEPT 1990, P 5516-5526
46. B.R. LANNING, T. FURTAK, AND G.R. EDWARDS, A METHOD FOR PREDICTION OF METAL-CERAMIC INTERFACIAL BOND ENERGIES, SUBMITTED FOR PUBLICATION IN *J. MATER. RES.*
47. R.J. COLTON, C.R.K. MARRIAN, AND J.A. STROSCIO, ED., *PROC. FIFTH INT. CONF. SCANNING TUNNELING MICROSCOPY/SPECTROSCOPY (SAM '90)* AND *THE FIRST INT. CONF. NANOMETER SCALE SCIENCE AND TECHNOLOGY (NANO I)* (BALTIMORE, MD), JUNE 1990, AND *J. VAC. SCI. TECH. B,* SECOND SERIES, VOL 9 (NO. 2), PART II, MARCH/APRIL 1991
48. J.M. GERKEN AND W.A. OWCZARSKI, "A REVIEW OF DIFFUSION WELDING," WELDING RESEARCH COUNCIL BULLETIN NO. 109, OCT 1965
49. J.D. WILLIAMS AND B. CROSSLAND, PART 1 COLD PRESSURE WELDING, *CME,* MARCH 1976, P 65-67
50. J.D. WILLIAMS AND B. CROSSLAND, PART 2 DIFFUSION BONDING, *CME,* APRIL 1976, P 73-75
51. J.R. SMITH, PANEL REPORT ON INTERFACIAL BONDING AND ADHESION, *MATER. SCI. ENG.,* VOL 83, 1986
52. H.A. MOHAMED AND J. WASHBURN, MECHANISM OF SOLID STATE PRESSURE WELDING, *WELD. J. RES. SUPP.,* SEPT 1975, P 302S-310S
53. I. KAWAKATSU AND S. KITAYAMA, STUDY ON DIFFUSION BONDING OF METALS, *TRANS. JIM,* VOL 18, 1977, P 455-465
54. N. BAY, MECHANISMS PRODUCING METALLIC BONDS IN COLD WELDING, *WELD. J. RES. SUPP.,* MAY 1983, P 137S-142S
55. P.A. DOWBEN AND A. MILLER, ED., *SURFACE SEGREGATION PHENOMENA,* CRC PRESS, 1990
56. G. GARMONG, N.E. PATON, AND A.S. ARGON, ATTAINMENT OF FULL INTERFACIAL CONTACT DURING DIFFUSION BONDING, *METALL. TRANS. A,* VOL 6, JUNE 1975, P 1269-1279
57. A. HILL AND E.R. WALLACH, MODELLING SOLID-STATE DIFFUSION BONDING, *ACTA METALL.,* VOL 37 (NO. 9), 1989, P 2425-2437
58. J.W. CAHN, INTERFACIAL FREE ENERGY AND INTERFACIAL STRESS: THE CASE OF AN INTERNAL INTERFACE IN A SOLID, *ACTA METALL.,* VOL 37 (NO. 3), 1989, P 773-776
59. C.L. CLINE, AN ANALYTICAL AND EXPERIMENTAL STUDY OF DIFFUSION BONDING, *WELD.*

J., NOV 1966, P 481-S TO 489-S

60. D. DERBY AND E.R. WALLACH, THEORETICAL MODEL FOR DIFFUSION BONDING, *MET. SCI.*, VOL 16, JAN 1982, P 49-56
61. D. DERBY AND E.R. WALLACH, DIFFUSION BONDING: DEVELOPMENT OF THEORETICAL MODEL, *MET. SCI.*, VOL 18, SEPT 1984, P 427-431
62. D. DERBY AND E.R. WALLACH, DIFFUSION BONDS IN IRON AND A LOW-ALLOY STEEL, *J. MATER. SCI.*, VOL 19, 1984, P 3149-3158
63. D. DERBY AND E.R. WALLACH, DIFFUSION BONDS IN COPPER, *J. MATER. SCI.*, VOL 19, 1984, P 3140-3148
64. Z.X. GUO AND N. RIDLEY, MODELLING OF DIFFUSION BONDING OF METALS, *MATER. SCI. TECH.*, VOL 3, NOV 1987, P 945-953
65. H.J. FROST AND M.F. ASHBY, *DEFORMATION MECHANISM MAPS*, PERGAMON PRESS, 1982
66. P.A. DAMMER, R.E. MONROE, AND D.C. MARTIN, FURTHER STUDIES OF DIFFUSION BONDING BELOW 1000 °F, *WELD. J.*, MARCH 1969, P 116-S TO 124-S
67. V.A. BACHIN, INTERACTION BETWEEN METALS AND THE OXIDES OF CERAMIC MATERIALS DURING DIFFUSION WELDING, *AVT. SVARKA*, NO. 10, 1982, P 15-17
68. Z.A. MUNIR, A THEORETICAL ANALYSIS OF THE STABILITY OF SURFACE OXIDES DURING DIFFUSION WELDING OF METALS, *WELD. J.*, DEC 1983, P 333-S TO 336-S
69. J.-S. WANG AND H. VEHOFF, THE EFFECT OF THE MOBILITY OF SEGREGATED ATOMS ON INTERFACIAL EMBRITTLEMENT, *SCR. METALL.*, VOL 25, 1991, P 1339-1344
70. T. TSAKALAKOS, ED., *MATER. SCI. ENG. B*, VOL 6, 1990, P 69-210
71. J.W. HUTCHINSON AND Z. SUO, MIXED MODE CRACKING IN LAYERED MATERIALS, *ADVANCES IN APPLIED MECHANICS*, VOL 28, J.W. HUTCHINSON AND T.Y. WU, ED., ACADEMIC PRESS, 1990
72. C.F. SHIH, CRACKS ON BIMATERIAL INTERFACES: ELASTICITY AND PLASTICITY ASPECTS, *MATER. SCI. ENG. A*, VOL 143, 1991, P 77-90
73. M. COMNINOU, AN OVERVIEW OF INTERFACE CRACKS, *ENG. FRACT. MECH.*, VOL 37 (NO. 1), 1990, P 197-208
74. M.G. STOUT, N.P. O'DOWD, AND C.F. SHIH, "INTERFACIAL FRACTURE TOUGHNESS OF ALUMINA/NIOBIUM SYSTEMS," SYMPOSIUM ON EXPERIMENTS IN MICROMECHANICS OF FAILURE RESISTANT MATERIALS, ASME WINTER ANNUAL MEETING (ATLANTA, GA), DEC 1991
75. Z. SUO AND J.W. HUTCHINSON, "INTERFACE CRACK BETWEEN TWO ELASTIC LAYERS," REPORT MECH-118, HARVARD UNIVERSITY, DIVISION OF APPLIED SCIENCES, MARCH 1988
76. H.M. JENSEN, MIXED MODE INTERFACE FRACTURE CRITERIA, *ACTA METALL. MATER.*, VOL 38 (NO. 12), 1990, P 2637-2644
77. M.-Y. HE AND J.W. HUTCHINSON, "KINKING OF A CRACK OUT OF AN INTERFACE," REPORT MECH-113, HARVARD UNIVERSITY, DIVISION OF APPLIED SCIENCES, FEB 1988
78. J. QU AND Q. LI, INTERFACIAL DISLOCATION AND ITS APPLICATIONS TO INTERFACE CRACKS IN ANISOTROPIC BIMATERIALS, *J. ELASTICITY*, VOL 26, 1991, P 169-195
79. A.N. STROH, DISLOCATIONS AND CRACKS IN ANISOTROPIC ELASTICITY, *PHILOS. MAG.*, VOL 7, 1958, P 625-646
80. Q.Q. LI AND T.C.T. TING, LINE INCLUSION IN ANISOTROPIC ELASTIC SOLIDS, *J. APPL. MECH.*, VOL 56, 1989, P 556-563
81. T.C.T. TING, EXPLICIT SOLUTION AND INVARIANCE OF THE SINGULARITIES AT AN INTERFACE CRACK IN ANISOTROPIC COMPOSITES, *INT. J. SOLIDS STRUCT.*, VOL 22, 1986, P 965-983
82. A.G. EVANS, M. RUHLE, B.J. DALGLEISH, AND P.G. CHARALAMBIDES, THE FRACTURE ENERGY OF BIMATERIAL INTERFACES, *MATER. SCI. ENG.*, VOL A 126, 1990, P 53-64

83. A.G. EVANS, M. RUHLE, B.J. DALGLEISH, AND P.G. CHARALAMBIDES, THE FRACTURE ENERGY OF BIMATERIAL INTERFACES, *METALL. TRANS. A*, VOL 21, SEPT 1990, P 2419-2429
84. H.F. FISCHMEISTER, H.E. EXNER, M.-H. POECH, S. KOHLHOFF, P. GUMBSCH, S. SCHMAUDER, L.S. SIGL, AND R. SPEIGLER, MODELING FRACTURE PROCESSES IN METALS AND COMPOSITE MATERIALS, *Z. METALLKDE*, BD 80, 1989, P 839-846
85. A. NEEDLEMAN, AN ANALYSIS OF TENSILE DECOHESION ALONG AN INTERFACE, *J. MECH. PHYS. SOLIDS*, VOL 38 (NO. 3), 1990, P 289-324
86. J.H. ROSE, J. FERRANTE, AND J.R. SMITH, UNIVERSAL BINDING ENERGY CURVES FOR METALS AND BIMETALLIC INTERFACES, *PHYS. REV. LETT.*, VOL 47 (NO. 9), AUG 1981, P 675-678
87. J. FERRANTE AND J.R. SMITH, THEORY OF THE BIMETALLIC INTERFACE, *PHYS. REV. B*, VOL 31 (NO. 6), MARCH 1985, P 3427-3434
88. T.C.T. TING, INTERFACE CRACKS IN ANISOTROPIC BIMATERIALS, *J. MECH. PHYS. SOLIDS*, VOL 38 (NO. 4), 1990, P 505-513
89. R.F. COOK, CRACK PROPAGATION THRESHOLDS: A MEASURE OF SURFACE ENERGY, *J. MATER. RES.*, VOL 1 (NO. 6), NOV/DEC 1986, P 852-860
90. R.R. REYNOLDS, K. KOKINI, AND G. CHEN, THE MECHANICS OF THE INTERFACE CRACK USING THE FINITE ELEMENT METHOD, *J. ENG. MATER. TECHNOL.*, VOL 112, JAN 1990, P 38-43
91. P.G. CHARALAMBIDES, J. LUND, A.G. EVANS, AND R.M. MCMEEKING, "A TEST FOR DETERMINING THE FRACTURE RESISTANCE OF BIMATERIAL INTERFACES," REPORT M87-4, MATERIALS DEPARTMENT, COLLEGE OF ENGINEERING, UC SANTA BARBARA
92. N.P. O'DOWD, C.F. SHIH, AND M.G. STOUT, TEST GEOMETRIES FOR MEASURING INTERFACIAL FRACTURE TOUGHNESS, *INT. J. SOLIDS AND STRUCT.*, VOL 29, 1992, P 571-589
93. R.L. BRADY, R.S. PORTER, AND J.A. DONOVAN, A BUCKLED PLATE TEST TO MEASURE INTERFACIAL TOUGHNESS IN COMPOSITES, *J. MATER. SCI.*, VOL 24, 1989, P 4138-4143
94. J.J. MECHOLSKY AND L.M. BAKER, A CHEVRON-NOTCHED SPECIMEN FOR FRACTURE TOUGHNESS MEASUREMENTS OF CERAMIC-METAL INTERFACES, *CHEVRON-NOTCHED SPECIMENS: TESTING AND STRESS ANALYSIS*, STP 855, J.H. UNDERWOOD, S.W. FREIMAN, AND F.I. BARATTA, ED., ASTM, 1984, P 324-336
95. X. ZHU AND J.G. BYRNE, EFFECT OF INTERFACE DEFECTS ON THE MECHANICAL PROPERTIES OF AUTOGENOUS DIFFUSION BONDED JOINTS, *J. MATER. ENG.*, VOL 13, 1991, P 207-211
96. M.D. THOULESS, FRACTURE OF A MODEL INTERFACE UNDER MIXED-MODE LOADING, *ACTA METALL. MATER.*, VOL 38 (NO. 6), 1990, P 1135-1140
97. V.S. GOSTOMEL'SKII, E.S. KARAKOZOV, AND A.P. TERNOVSKII, THE IMPORTANCE OF DIFFUSION AND SURFACE TENSION IN THE FORMATION OF CONTACT DURING DIFFUSION WELDING, *AVT. SVARKA*, NO. 4, 1980, P 28-31
98. A.V. MERIIN AND S.K. SLIOZBERG, SOME CHARACTERISTICS OF JOINTS IN THE SOLID-PHASE WELDING OF METALS, *SVAR. PROIZ.*, NO. 5, 1973, P 22-23

Fundamentals of Friction Welding

J.W. Elmer and D.D. Kautz, Lawrence Livermore National Laboratory

Introduction

FRICTION WELDING (FRW) is a solid-state welding process in which the heat for welding is produced by the relative motion of the two interfaces being joined. This method relies on the direct conversion of mechanical energy to thermal energy to form the weld, without the application of heat from any other source. Under normal conditions no melting

occurs at the interface. Figure 1 shows a typical friction weld, in which a nonrotating workpiece is held in contract with a rotating workpiece under constant or gradually increasing pressure until the interface reaches the welding temperature. The rotational speed, the axial pressure, and the welding time are the principal variables that are controlled in order to provide the necessary combination of heat and pressure to form the weld. These parameters are adjusted so that the interface is heated into the plastic temperature range where welding can take place. Once the interface is heated, axial pressure is used to bring the weld interfaces into intimate contact. During this last stage of the welding process, atomic diffusion occurs while the interfaces are in contact, allowing a metallurgical bond to form between the two materials.

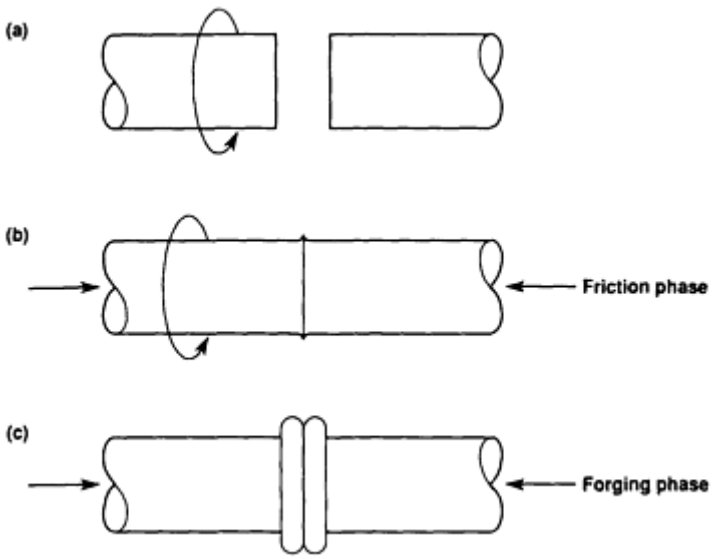

FIG. 1 SCHEMATIC SHOWING FUNDAMENTAL STEPS IN THE FRICTION WELDING PROCESS. (A) ONE WORKPIECE IS ROTATED, AND THE OTHER WORKPIECE IS HELD STATIONARY. (B) BOTH WORKPIECES ARE BROUGHT TOGETHER, AND AXIAL FORCE IS APPLIED TO BEGIN THE UPSETTING PROCESS. (C) WORKPIECE ROTATION IS STOPPED, AND THE UPSETTING PROCESS IS COMPLETED

Friction welding involves heat generation through friction abrasion (Ref 1, 2, 3), heat dissipation, plastic deformation, and chemical interdiffusion. The interrelation among these factors during FRW to complications when trying to develop predictive models of the friction welding process. However, from a qualitative standpoint the process is well understood through empirical FRW studies that have been performed on a wide variety of materials. Five qualitative factors influence the quality of a friction weld (Ref 4):

- RELATIVE VELOCITY OF THE SURFACES
- APPLIED PRESSURE
- SURFACE TEMPERATURE
- BULK MATERIAL PROPERTIES
- SURFACE CONDITION AND PRESENCE OF SURFACE FILMS

The first three factors are related to FRW, while the last two are related to the properties of the materials being joined.

During FRW, the relative velocity, the applied pressure, and the duration of the force are the three variables that are controlled. The effect of these variables on weld quality will be discussed for the two basic friction welding processes: direct-drive welding and inertia-drive welding. The surface temperature is the critical parameter for ensuring good welds and is dependent on the processing conditions and the materials being joined. Although the surface temperature is not measured or directly controlled the effects of insufficient or excessive temperature are generally apparent through visual examination of the finished weld. The bulk material properties and the condition of the surfaces being joined affect both the frictional forces and the forging characteristics of the materials being joined. These factors will be discussed for the friction welding of both similar-material and dissimilar-material combinations.

Commercial FRW applications employ a number of variations on the basic FRW concepts. These variations were developed to accommodate different part geometries and to produce different metallurgical effects (Ref 5) and will not be discussed in this article.

References

1. T.H. HAZLET, FUNDAMENTALS OF FRICTION WELDING, *SOURCE BOOK ON INNOVATIVE WELDING PROCESSES,* AMERICAN SOCIETY FOR METALS, 1981, P 11-36
2. F.P. BOWDEN AND D. TABOR, *THE FRICTION AND LUBRICATION OF SOLIDS,* PART I, OXFORD UNIVERSITY PRESS, 1954
3. J. GODDARD AND H. WILMAN, A THEORY OF FRICTION AND WEAR DURING THE ABRASION OF METALS, *WEAR,* VOL 5, 1962
4. V.I. VILL, *FRICTION WELDING OF METALS,* TRANSLATED FROM THE RUSSIAN, AMERICAN WELDING SOCIETY, 1962
5. *WELDING HANDBOOK,* 8TH ED., VOL 2, AMERICAN WELDING SOCIETY, 1991, P 739-763

Fundamentals of Friction Welding

J.W. Elmer and D.D. Kautz, Lawrence Livermore National Laboratory

Friction Welding Technology

There are two principal FRW methods: direct-drive welding and inertia-drive welding. Direct-drive FRW, sometimes called conventional friction welding, uses a motor running at constant speed to input energy to the weld. Inertia-drive friction welding, sometimes called flywheel friction welding, uses the energy stored in a flywheel to input energy to the weld. These two FRW technologies produce inherently different metallurgical effects at the joint interface.

Both FRW technologies can be applied through different types of relative motion in order to generate the friction necessary to form the weld. The most common FRW geometry is that shown in Fig. 1, in which one cylindrical component is held stationary and the other is rotated. However, in other methods, both components are rotated in opposite directions, or two-stationary components are pushed against a rotating piece positioned between them. Additional forms of FRW, such as radial, orbital, and linear reciprocating motions, have been developed for special part geometries. These alternate methods are discussed elsewhere (Ref 5, 6).

Direct Drive Welding

In direct-drive FRW, a machine resembling a lathe is equipped with a brake and clutch, a means of applying and controlling axial pressure, and a weld-cycle timer and displacement controller. The operation of a direct-drive machine consists of a friction phase where heat is generated, a stopping phase where the rotation is terminated, and a forging phase where the pressure is applied to join the pieces. The relationships among the process variables are shown in Fig. 2, which plots the rotational speed and the axial pressure as a function of time for typical weld. The time required to stop the spindle is also an important variable because it affects the weld temperature and the timing of the forging force.

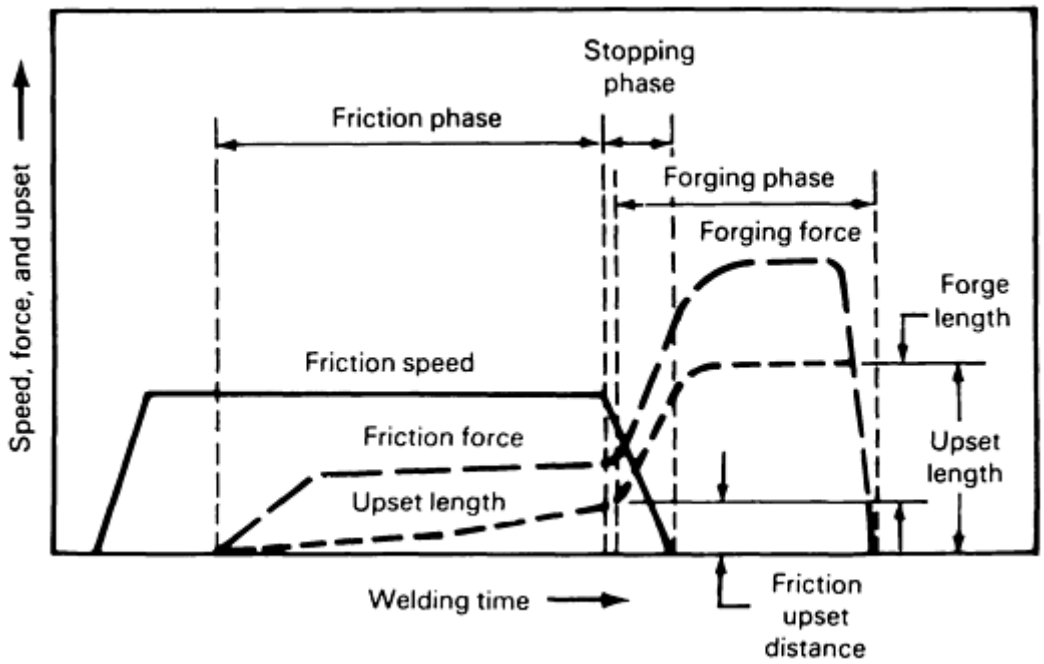

FIG. 2 PLOT OF SELECTED PARAMETERS VERSUS TIME RELATIVE TO THE THREE PHASES OF THE DIRECT-DRIVE FRW PROCESS

The forging phase starts at the instant when higher pressure (that is, a larger forging force) is applied in the weld cycle. Thus, the forging phase actually starts somewhere in the stopping phase. In general, the larger forging force can be applied (case 1) while the spindle is decelerating in the stopping phase (Fig. 2) or (case 2) after the spindle has stopped rotating at the end of the stopping phase. The difference in the two applications of the larger forging force is the presence of a second friction peak. In case 1, the torque will rise again to reach a second peak before dropping. This produces a torsional force. In case 2, especially when the stopping phase is very short due to rapid braking, frictional torque does not rise but actually starts to decrease at the onset of the forging phase. In this case, there is no torsional force, and forging is affected only by the upsetting force.

The speed of rotation is the least sensitive process variable in that it can be varied over a wide range if heating time and pressure are properly controlled. For steels, the recommended peripheral velocity varies from 75 to 215 m/min (250 to 700 ft/min) (Ref 7). In general, higher speeds correspond to low weld heat inputs and are used to weld heat-sensitive materials such as hardenable steels.

The friction force is generally applied gradually to the weld to help overcome the initial contact-torque peak. For carbon steels, a friction pressure of about 70 MPa (10 ksi) at the interface area is required to form a good joint. After the drive motor is disengaged from the workpiece, the forging force is applied to complete the weld. Typical forging forces for carbon steel are of 140 MPa (20 ksi) at the weld interface.

Inertia-Drive Welding

The inertia-drive FRW method uses a similar type of machine except that the spindle holding the rotating piece is attached to a flywheel. The flywheel controls the energy input to the weld. The moment of inertia of the flywheel is an important variable that is adjusted by adding or removing flywheels. The amount of energy stored in the flywheel is controlled by its speed. Once the spindle is at the correct speed, the drive system is disengaged, leaving a rotating flywheel mass. Axial pressure is then applied and held constant throughout the welding process. The applied pressure results in a decrease in the rotational speed, typically referred to as deceleration. In some cases, when the spindle has either nearly stopped or come to a complete stop, a higher forging force may be used.

Figure 3 illustrates the inertia-drive FRW process, which is similar to the direct-drive method in that the weld typically takes place in two stages: friction and forging. However, some weld schedules do not require a forging stage.

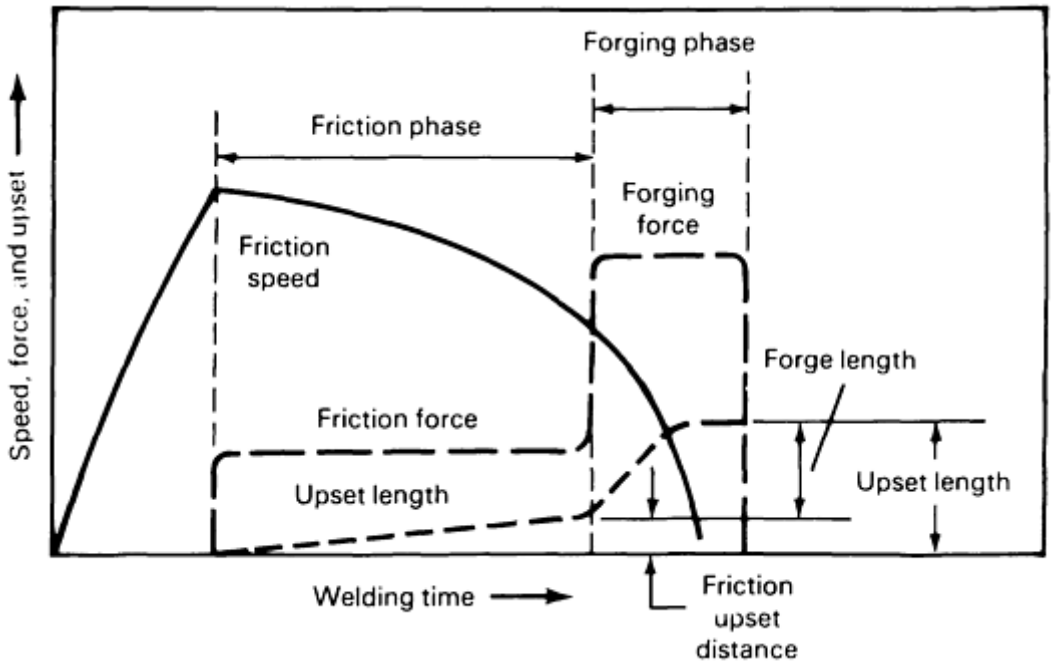

FIG. 3 PLOT OF SELECTED PARAMETERS VERSUS TIME RELATIVE TO THE TWO PHASES OF THE INERTIA-DRIVE FRW PROCESS

The major difference between the direct-drive and inertia-drive methods is the friction speed. In inertia welding, the friction speed continuously decreases during the friction stage, while in direct welding the friction speed stays constant.

The heat generated by the plastic deformation of materials at the faying surfaces, not the heat generated by friction in the friction phase, is the primary source in the forging phase of preventing rapid decrease of the temperature at the interface.

The process variables that control the characteristics of an inertia weld are the flywheel size (moment of inertia), the flywheel speed, and the axial pressure. The weld energy is related to the first two variables and is a fixed quantity once they have been determined. The kinetic energy in the flywheel at any time during the weld is given by:

$$E = \frac{S^2.1}{C}$$

where E is the energy (ft · lbf, or J), I is the moment of inertia (lb/ft^2, or kg/m^2), S is the flywheel speed (rev/min), and C is a conversion constant that is equal to 5873 for English units or 182.4 for metric units.

The constant C is derived from:

$$E = \frac{1}{2}mv^2$$

where $v = \omega r$. Because $\omega = 2\pi s$, $v = 2\pi sr$:

$$E = \frac{1}{2}m(2p)^2s^2r^2$$

$$E = \frac{1}{2}mr^2(2p)^2s^2$$

Making $mr^2 = I$, the previous equation becomes:

$$E = \frac{1}{2} I (2p)^2 s^2$$

In SI units, the previous equation becomes:

$$E = \left[\frac{m^2.Kg}{s^2}\right] = \frac{1}{2}(2p)^2 s^2 \left[\frac{1}{\min^2}\right] I \left[m^2.Kg\right] \left[\frac{\min}{60s}\right]^2$$

$$E = \frac{1}{2}\frac{(2p)^2}{60^2} s^2 I$$

$$E = \frac{Is^2}{C}$$

Solving for C in the previous equation:

$$C = \frac{2*60^2}{(2p)^2} = \frac{60^2}{2p^2} = 182.378$$

The energy stored in the flywheel is proportional to its speed of rotation squared, S^2. Therefore, a wide range of energy levels can be obtained without changing the flywheel to accommodate changes in part geometries. For large changes in the parts being joined, the capacity of an inertia welding machine can be modified by changing the flywheel moment of inertia if necessary.

Flywheel Energy. The moment of inertia of the flywheel is selected to produce both the desired amount of kinetic energy and the desired amount of forging. Forging results from the characteristic increase in torque that occurs at the weld interface as the flywheel slows and comes to rest. This increased torque, in combination with the axial pressure, produces forging. Because forging begins at some critical velocity, the amount of forging depends on the amount of energy remaining in the flywheel, which is a linear function of the flywheel moment of inertia. Large, low-speed flywheels produce greater forging force than small, high-speed flywheels even though they contain the same amount of kinetic energy. Although small, medium, and large amounts of flywheel energy produce similar heating patterns, the amount of energy greatly affects the size and shape of the weld upset, as shown in Fig. 4(a) for similar-metal joints.

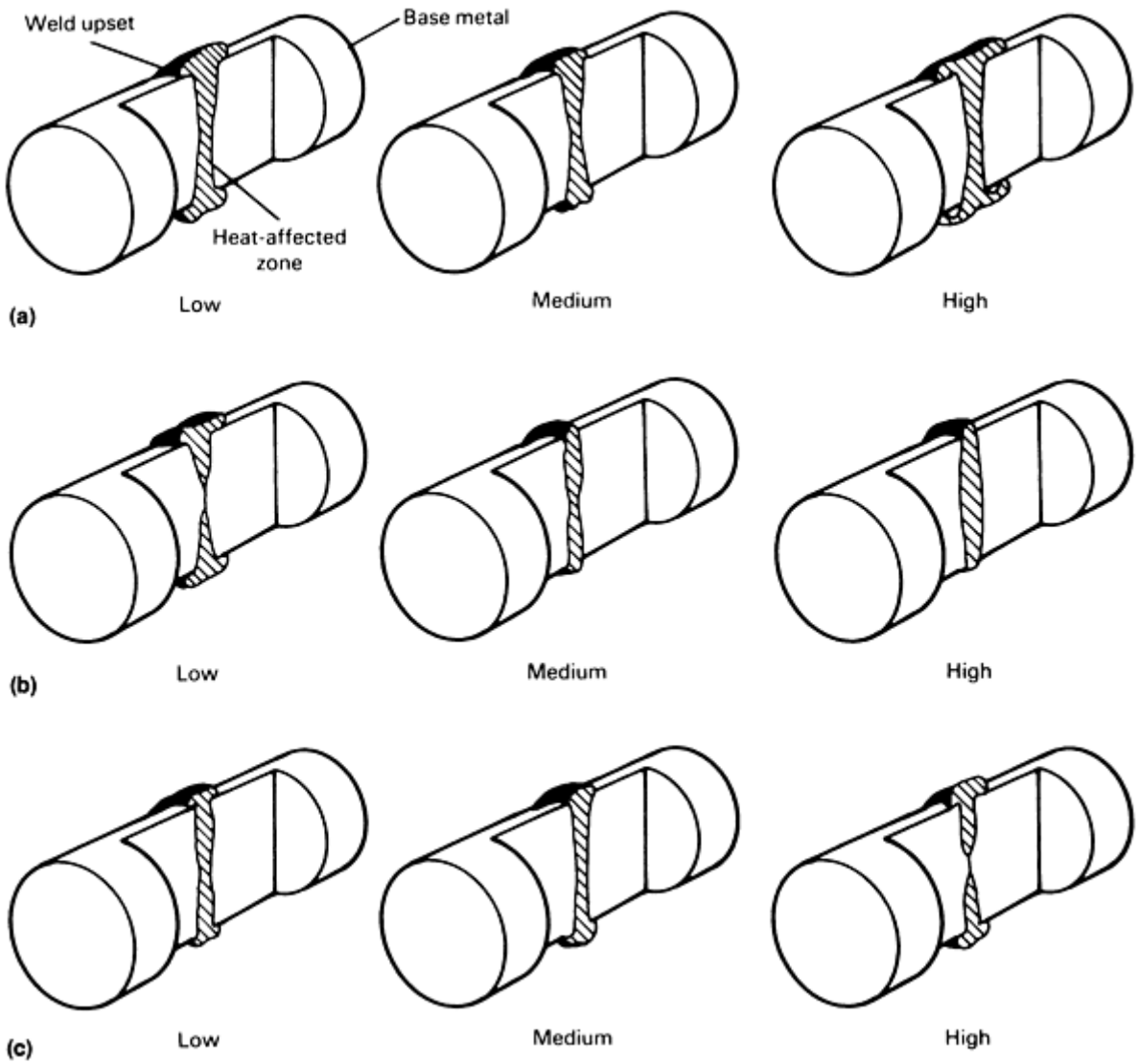

FIG. 4 SCHEMATIC SHOWING EFFECT OF WELDING PARAMETERS ON THE FINISHED WELD NUGGET OBTAINED WHEN SIMILAR METALS ARE WELDED USING INERTIA-DRIVE FRW EQUIPMENT. (A) FLYWHEEL ENERGY. (B) INITIAL PERIPHERAL VELOCITY OF WORKPIECE. (C) AXIAL PRESSURE. SOURCE: REF 7

Peripheral Velocities. There is an optimum range of peripheral or linear surface velocities for each combination of metals being joined. For welding steel to steel, the recommended initial peripheral velocity ranges from 90 to 460 m/min (300 to 1500 ft/min). However, welds can be made at velocities as low as 85 m/min (275 ft/min). Figure 4(b) shows the effect of initial peripheral velocity on weld shape for similar-metal welds.

Axial Pressure Versus Peripheral Velocities. The effect of varying the axial pressure is opposite to the effect of varying the velocity. Welds made at low axial pressure resemble welds made at medium velocity relative to the formation of weld upset and heat-affected zones (HAZ), as shown in Fig. 4(c). Excessive pressure produces a weld that has poor quality at the center and has a large amount of weld upset, similar to a weld made at a low velocity.

References cited in this section

5. *WELDING HANDBOOK*, 8TH ED., VOL 2, AMERICAN WELDING SOCIETY, 1991, P 739-763
6. *RECOMMENDED PRACTICES FOR FRICTION WELDING*, ANSI/AWS C6. 1-89, AMERICAN WELDING SOCIETY, 1989

7. *METALS HANDBOOK,* 9TH ED., VOL 6, AMERICAN SOCIETY FOR METALS, 1983

Fundamentals of Friction Welding

J.W. Elmer and D.D. Kautz, Lawrence Livermore National Laboratory

Metallurgical Parameters

Friction welding can be used to join a wide range of similar and dissimilar materials. Metals, ceramics, metal-matrix composites (MMC), and polymers have all been joined by FRW, and many of the dissimilar-metal combinations that cannot be joined by conventional fusion welding techniques are readily joined by FRW methods. This section summarizes some of the metals that have been joined by FRW and discusses the metallurgical considerations that govern the properties of the resulting weld.

Joining of Similar Metals

The two general requirements for forming good friction welds are, first, that the materials to be joined can be forged and, second, that the materials can generate friction at the weld interface. The first requirement eliminates similar-metal welds in brittle materials such as ceramics, cast irons, and cemented carbides. However, ductile materials can sometimes be joined to these materials. The second requirements eliminates materials that contain alloying that provide dry lubrication. Free-machining additives to steel, graphite-containing alloys such as cast iron, and lead alloys may suffer from this requirement.

Almost all other metal alloys can be welded to themselves by FRW techniques. Table 1 summarizes a number of common similar-metal weld joints that have been made using inertia-drive FRW. Metallic alloys known to form high-quality FRW joints include alloys based on aluminum, copper (copper-nickel, brass, bronze), iron (low-alloy steel, tool steel, stainless steel, maraging steel), nickel, titanium, tantalum, and many others (Ref 5, 6). Near full-strength metallurgical bonds can be produced for a very wide range of similar-metal alloy friction welds. The microstructure and mechanical properties of inertia-welded similar-metal joints for the following alloys can be found in the sources listed:

TABLE 1 PARAMETERS FOR INERTIA-DRIVE FRICTION WELDING OF TWO 25 MM (1 IN.) DIAM BARS MADE OF SIMILAR METALS

WORK METAL	SPINDLE SPEED, REV/MIN	AXIAL FORCE		FLYWHEEL SIZE[A]		WELD ENERGY		METAL LOSS[B]		TOTAL TIME[C], S
		KN	LBF × 10^3	KG · M^2	LB · FT^2	KJ	FT · LBF × 10^3	MM	IN.	
1018 STEEL	4600	53	12	0.28	6.7	33	24	2.5	0.10	2.0
1045 STEEL	4600	62	14	0.33	7.8	38	28	2.5	0.10	2.0
4140 STEEL	4600	67	15	0.35	8.3	41	30	2.5	0.10	2.0
INCONEL 718	1500	220	50	5.48	130.0	68	50	3.8	0.15	3.0
MARAGING STEEL	3000	90	20	0.84	20.0	41	30	2.5	0.10	2.5
TYPE 410 STAINLESS	3000	80	18	0.84	20.0	41	30	2.5	0.10	2.5
TYPE 302 STAINLESS	3500	80	18	0.59	14.0	41	30	2.5	0.10	2.5
COPPER (COMMERCIALLY PURE)	8000	22	5	0.04	1.0	14	10	3.8	0.15	0.5
COPPER ALLOY 260 (CARTRIDGE BRASS, 70%)	7000	22	5	0.05	1.2	14	10	3.8	0.15	0.7
TITANIUM ALLOY, TI-6AL-4V	6000	36	8	0.07	1.7	22	16	2.5	0.10	2.0
ALUMINUM ALLOY 1100	5700	27	6	0.11	2.7	20	15	3.8	0.15	1.0

ALUMINUM ALLOY 6061	5700	31	7	0.13	3.0	23	17	3.8	0.15	1.0

Source: Ref 7

(A) MOMENT OF INERTIA OF THE FLYWHEEL.

(B) TOTAL SHORTENING OF THE WORKPIECES DURING WELDING.

(C) SUM OF HEATING TIME PLUS WELDING TIME.

The relative ease of friction welding metals to themselves is related to the matching properties at the weld interface. Because the materials properties are matched, heat is distributed uniformly on both sides of the joint, and the deformation characteristics are identical on both sides of the joint. This results in symmetric welds with good properties. In general, the process variables do not vary significantly for different alloys within a given class of materials. However, there can be a significant variation in processing variables between different classes of materials (Table 1).

Because FRW generates localized heating at the interface, the HAZ is subject to rapid cooling due to heat transfer to the cold base metal. This rapid quenching may sufficiently alter the mechanical properties of the base metal in the HAZ region to require postweld heat treatment. For example, in order to restore ductility, stress relieving or tempering may be required to friction weld steels with hardenability greater than that of AISI 1035 (Ref 5, 6). In addition, age-hardenable alloys will lose strength in the HAZ during welding and may require postweld solution heat treating and/or postweld aging to restore their strength. Other alloys, such as those that obtain their strength from cold working, will lose strength in the HAZ of the weld, and their properties cannot be restored with postweld treatments.

Joining of Dissimilar Metals

While many similar-metal FRW joints are produced because of economic considerations, many dissimilar-metal FRW joints are produced because there are no alternative welding methods that can be used. Examples of these types of joints include dissimilar-metal combinations with widely different melting points and dissimilar-metal combinations that form incompatible phases when fusion welded. Table 2 gives parameters used for inertia welding several common dissimilar-material combinations.

TABLE 2 PARAMETERS FOR INERTIA-DRIVE FRICTION WELDING OF TWO 25-MM (1-IN.) DIAM BARS MADE OF DISSIMILAR METALS

WORK METAL	SPINDLE SPEED, REV/MIN	AXIAL FORCE		FLYWHEEL SIZE[A]		WELD ENERGY		METAL LOSS[B]		TOTAL TIME[C], S
		KN	LBF × 10^3	KG · M^2	LB · FT^2	KJ	FT · LBF × 10^3	MM	IN.	
Copper to 1018 steel	8000	22	5	0.06	1.4	20	15	3.8	0.15	1.0
M2 tool steel to 1045 steel	3000	180	40	1.14	27.0	54	40	2.5	0.10	3.0
Nickel alloy 718 to 1045 steel	1500	180	40	5.48	130.0	68	50	3.8	0.15	2.5
Type 302 stainless to 1020 steel	3000	80	18	0.84	20.0	41	30	2.5	0.10	2.5
Sintered high-carbon steel to 1018	4600	53	12	0.35	8.3	41	30	2.5	0.10	2.5
Aluminum 6061 to type 302 stainless	5500	22 67[D]	5 15[D]	0.16 . . .	3.9 . . .	27 . . .	20 . . .	5.1 . . .	0.20 . . .	3.0 . . .
Copper to aluminum alloy 1100	2000	33	7.5	0.46	11.0	10	7.5	5.1	0.20	1.0

(A) MOMENT OF INERTIA OF THE FLYWHEEL.

(B) TOTAL SHORTENING OF THE WORKPIECES DURING WELDING.

(C) SUM OF HEATING TIME PLUS WELDING TIME.

(D) THE 22 KN (5000 LBF) FORCE IS APPLIED DURING THE HEATING STAGE OF THE WELD; FORCE IS SUBSEQUENTLY INCREASED TO 67 KN (15000 LBF) NEAR THE END OF THE WELD.

Low-Carbon Steels to Medium-Carbon Steels. In general, low- and medium-carbon steels are joined to each other under a wide range of conditions, and high-carbon steels are readily joined to alloy steels (Ref 7) using friction welding. High-speed tool steels are welded to alloy steel shanks for numerous machine-tool applications. Steel with carbon contents as high as 1.0%, such as 52100 steel, can be joined to lower-carbon alloys. Preweld heat treating may be required in some cases to better match the properties at the interface, and postweld heat treatment may be required in some cases to temper the interface region of the high-carbon steel grades.

Stainless Steels to Other Selected Metals. Stainless steel alloys are comparatively easy to friction weld to other metals. For example, austenitic stainless steel to low-alloy steel (Ref 15), titanium and copper to stainless steel (Ref 16), and 1100 aluminum to stainless steel (Ref 17) are examples of transition joints that are made by FRW.

Titanium can be welded to stainless steel with extreme care (Ref 18), and other incompatible dissimilar combinations may be successfully welded using interlayer techniques (Ref 19). Figure 5 shows a micrograph of the interfacial region of an inertia weld between Monel 400 and 21-6-9 stainless steel. The joint properties are excellent, with plastic flow occurring in Monel 400 before joint failure during bend testing.

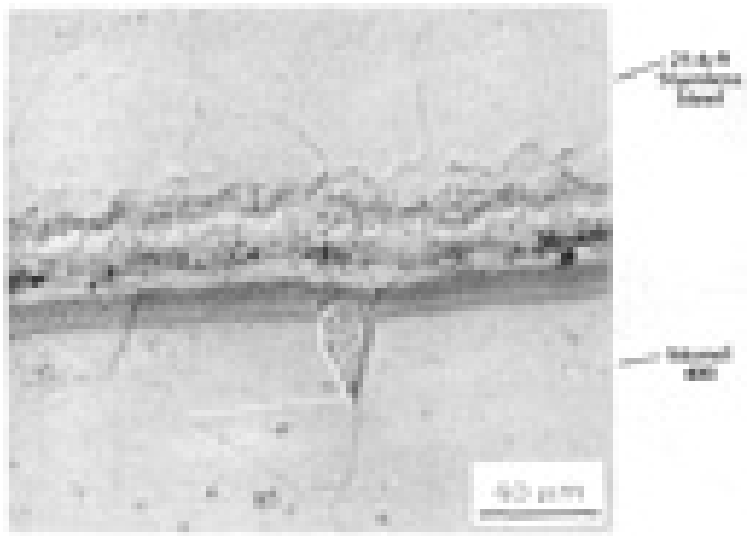

FIG. 5 METALLOGRAPHIC CROSS SECTION OF THE INTERFACE OF A MONEL 400 TO 21-6-9 STAINLESS STEEL WELD PRODUCED BY INERTIA-DRIVE FRW. NOTE THE FINE GRAIN SIZE PRESENT AT THE INTERFACE.

Such transition joints can often be used as interlayers for the friction welding of incompatible materials. For example, it is difficult to weld 5083 aluminum directly to stainless steel. However, by first friction welding aluminum alloy 1100 to the stainless steel, and machining the 1100 aluminum alloy back to an interlayer thickness of about 1 mm (0.04 in.), the 5083 aluminum alloy can be joined to the stainless steel via this 1100 interlayer with high joint efficiencies (Ref 20).

Figure 6(a) shows an example of an aluminum-base MMC that was friction welded to 1100 aluminum. The MMC is a 2024 aluminum alloy with 15 vol% Al_2O_3 particles. The interface region between these materials is shown at higher magnification in Fig. 6(b), where intermixing of both the materials is shown to occur.

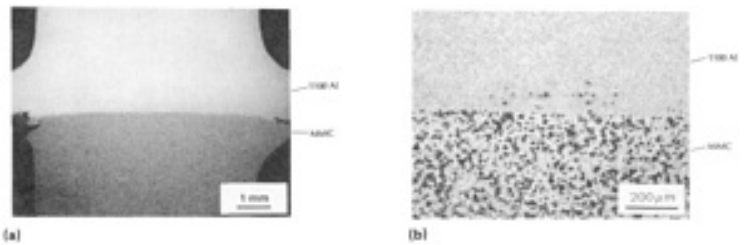

FIG. 6 CROSS SECTION OF THE INTERFACE OF A DIRECT-DRIVE FRICTION WELD JOINING 1100 ALUMINUM TO A 2024 ALUMINUM ALLOY WITH 15 VOL% AL_2O_3 PARTICLES. (B) HIGHER MAGNIFICATION OF THE SAME WELD SHOWING THE EXCELLENT WELD FORMED AT THE INTERFACE

Problems Common to Welding of Dissimilar Materials. In general, the same problems encountered when welding similar materials must be addressed when welding dissimilar materials. However, some problems are associated only with the welding of dissimilar materials or are greatly magnified during the welding of dissimilar materials. These factors include joint interfaces, low-melting phases, brittle phases, and different thermal expansions.

Joint Interfaces. While most similar-material welds are made with little concern for surface preparation, highly dissimilar-metal combinations are more sensitive. This happens for various reasons. In stainless steel to aluminum alloy welds, the oxide surface that forms on the aluminum picks up contaminants such as water and hydrocarbons, forming extremely tenacious surface layers (Ref 21). If this layer is not removed prior to welding, poor structural welds may occur. In stainless steel to refractory metal alloy welds, the oxide on the faying surfaces again contain contaminants such as water and hydrocarbons. The contaminants in this case are likely to alloy into the finished weldment. This alloying causes a reduction of structural integrity through the formation of low-melting or brittle phases at the weld interface.

Surface-treated interfaces frequently cause problems during FRW. Steels that have been carburized or nitrided, titanium alloys that have been nitrided, and other hardfaced alloys are difficult to friction weld due to the inherently low friction coefficient and low forgeability. The repeatability of welds made on materials with hard surface layers is difficult to characterize due to several factors, including coating thickness, coating quality, and physical properties of the coating. In most instances, weldability is improved if the surface-treated area is removed from the faying surface before welding.

Low-Melting Phase Formation. Some material combinations have very low melting point phases associated with mixing of constituents at the weld interface. The formation of these phases during the welding cycle is deleterious to the finished weld properties. Examples of combinations that fall into this category include iron-base alloys to titanium alloys and aluminum alloys to magnesium alloys. Low melting point eutectics are found in both of these metallurgical systems, and great care must be exercised during parameter development to prevent the formation of liquid phases during the completion of successful welds.

Other weld combinations may be affected by contaminants at the weld interface. Examples include sulfur and phosphorus in iron-base alloys and bismuth in copper alloys. These contaminants may cause problems with hot shortness in very low concentrations. It is imperative that good cleaning practices be implemented when materials may have been contaminated with these elements or with material containing these elements.

Brittle Phase Formation. Many materials, when combined, are susceptible to the formation of brittle phases. In some combinations, this occurs during the welding cycle; in others, service conditions after welding cause the problem. Two main reasons exist for brittle phase formation in friction welds:

- SURFACE CONTAMINANTS THAT EMBRITTLE THE WELD INTERFACE (SEE THE SECTION "JOINT INTERFACES" IN THIS ARTICLE)
- FORMATION OF INTERMETALLIC PHASES BETWEEN NORMAL CONSTITUENTS OF THE ALLOYS BEING WELDED

Intermetallic phase formation is common when welding refractory metal alloys to stainless steel alloys and in several other systems. In the case of stainless steels to refractory metals, σ phase or similar phases may occur upon welding at the interface. Proper weld procedure development reduces the amount of brittle phases that are formed, but typically does not eliminate their formation completely. Properly developed welds have satisfactory structural properties, because only small, noncontinuous areas of the brittle phase are present at the weld interface. Figure 7(a) shows an inertia-drive welded joint between vanadium and 21-6-9 stainless steel. The interface is smooth and shows no areas of brittle phases. Electron microscopy techniques are needed to find the small areas of σ phase present at the weld interfaces.

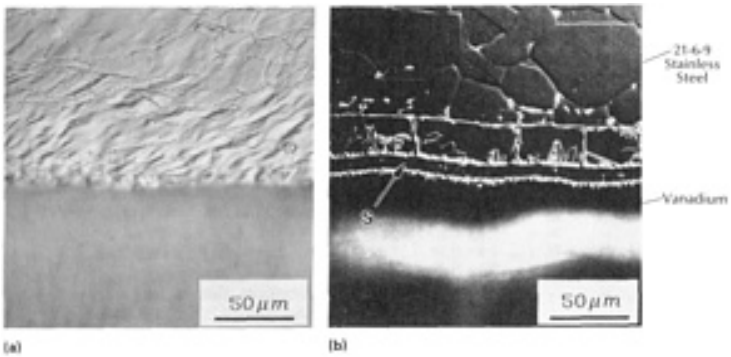

FIG. 7 METALLOGRAPHIC CROSS SECTION OF AN INERTIA-DRIVE FRW JOINT BETWEEN VANADIUM AND A 21-6-9 STAINLESS STEEL. NOTE THE EXCELLENT WELD QUALITY AT THE INTERFACE. (A) WELD INTERFACE WITH NO σ-PHASE GROWTH. (B) WELD INTERFACE WITH σ-PHASE GROWTH (INDICATED BY S) AND A SOLID-SOLUTION MIXING CAUSED BY CHEMICAL DIFFUSION AFTER EXPOSURE TO A 1000 °C (1830 °F) THERMAL CYCLE

Caution must be used when designing components for use at elevated-temperature extremes. In many instances, material combinations in which no brittle phases form during welding are susceptible to brittle phase formation at the interface during high-temperature use. This is not a design issue when the welds are used for near-room-temperature applications. Figure 7(b) shows the vanadium to 21-6-9 stainless steel inertia-drive weld after a severe thermal cycle of 1000 °C (1830 °F) for 2 h with σ-phase and solid-solution growth at the weld interface. The thick layer next to the stainless steel is a solid solution of iron and vanadium. The thin layer next to the vanadium is σphase and forms a continuous brittle fracture path across the weld interface.

Differential Thermal Expansion. Some material combinations are difficult to weld because of the large differences in thermal expansion. Low-expansion materials such as refractory metals, ceramics, and low-expansion iron-nickel and iron-nickel-cobalt alloys may fail or be highly stressed during cooling when welded to high-expansion material such as austenitic stainless steels and nickel-base and cobalt-base superalloys. Use of these combinations requires the designer to consider the large stresses developed within the fabricated structure if the welds are restrained when exposed to large temperature changes. Intermediate expansion materials and multiple friction welds may be required to allow for the transition from high to low thermal expansion materials.

References cited in this section

5. *WELDING HANDBOOK*, 8TH ED., VOL 2, AMERICAN WELDING SOCIETY, 1991, P 739-763
6. *RECOMMENDED PRACTICES FOR FRICTION WELDING*, ANSI/AWS C6. 1-89, AMERICAN WELDING SOCIETY, 1989
7. *METALS HANDBOOK*, 9TH ED., VOL 6, AMERICAN SOCIETY FOR METALS, 1983
8. T.N. HAZLET, PROPERTIES OF FRICTION WELDED PLAIN CARBON AND LOW ALLOY STEELS, *WELD. J.*, VOL 41, 1962, P 49-S TO 52-S
9. S.B. DUNKERTON, TOUGHNESS PROPERTIES OF FRICTION WELDS IN STEELS, *WELD. J.*, VOL 65, 1986, P 193-S TO 202-S
10. J.C. LIPPOLD AND B.C. ODEGARD, TECHNICAL NOTE: MICROSTRUCTURAL EVOLUTION

DURING INERTIA FRICTION WELDING OF AUSTENITIC STAINLESS STEELS, *WELD. J.*, VOL 63, 1984, P 35-S TO 38-S

11. W.A. BAESLACK III AND K.S. HAGEY, INERTIA FRICTION WELDING OF RAPIDLY SOLIDIFIED POWDER METALLURGY ALUMINUM, *WELD. J.*, VOL 67, 1988, P 139-S TO 149-S
12. H.H. KOO AND W.A. BAESLACK III, FRICTION WELDING OF A RAPIDLY SOLIDIFIED AL-FE-V-SI ALLOY, *WELD. J.*, VOL 71, 1992, P 147-S TO 169-S
13. K. OGAWA, H. YAMAGUCHI, T. MORIMOTO, K. TAKEMATA, H. SUDO, AND A. HIRATSUKA, SHEAR STRENGTH CHARACTERISTICS OF ALUMINUM ALLOY FRICTION WELDS, *WELD. J.*, VOL 5, 1991, P 860-866
14. C.G. NESSLAR *ET AL.*, FRICTION WELDING OF TITANIUM ALLOYS, *WELD. J.*, VOL 50, 1971, P 379-S TO 385-S
15. K.G.K. MURTI AND S. SANDARESAN, THERMAL BEHAVIOR OF AUSTENITIC-FERRITIC JOINTS MADE BY FRICTION WELDING, *WELD. J.*, VOL 64, 1985, P 327-S TO 334-S
16. R.A. BELL, J.C. LIPPOLD, AND D.R. ADOLPHSON, AN EVALUATION OF COPPER-STAINLESS STEEL FRICTION WELDS, *WELD. J.*, VOL 63, 1984, P 325-2 TO 332-S
17. D. YASHAN, S. TSANG, W.L. JOHNS, AND M.W. DOUGHTY, INERTIA FRICTION WELDING OF 1100 ALUMINUM TO TYPE 316 STAINLESS STEEL, *WELD. J.*, VOL 66, 1987, P 27-37
18. M. FUTAMATA AND A. FUJI, FRICTION WELDING OF TITANIUM AND SUS 304L AUSTENITIC STAINLESS STEEL, *WELD. INT.*, VOL 4, 1990, P 768-774
19. F. SASSANI AND J.R. NEELAN, FRICTION WELDING OF INCOMPATIBLE MATERIALS, *WELD. J.*, VOL 67, 1988, P 264-S TO 270-S
20. R. ARMSTRONG, PRIVATE COMMUNICATION AND INTERNAL REPORTS, LAWRENCE LIVERMORE NATIONAL LABORATORY, 1991
21. *METALS HANDBOOK*, 9TH ED., VOL 2, AMERICAN SOCIETY FOR METALS, 1979, P 204-209

Fundamentals of Friction Welding

J.W. Elmer and D.D. Kautz, Lawrence Livermore National Laboratory

---

References

1. T.H. HAZLET, FUNDAMENTALS OF FRICTION WELDING, *SOURCE BOOK ON INNOVATIVE WELDING PROCESSES*, AMERICAN SOCIETY FOR METALS, 1981, P 11-36
2. F.P. BOWDEN AND D. TABOR, *THE FRICTION AND LUBRICATION OF SOLIDS*, PART I, OXFORD UNIVERSITY PRESS, 1954
3. J. GODDARD AND H. WILMAN, A THEORY OF FRICTION AND WEAR DURING THE ABRASION OF METALS, *WEAR*, VOL 5, 1962
4. V.I. VILL, *FRICTION WELDING OF METALS*, TRANSLATED FROM THE RUSSIAN, AMERICAN WELDING SOCIETY, 1962
5. *WELDING HANDBOOK*, 8TH ED., VOL 2, AMERICAN WELDING SOCIETY, 1991, P 739-763
6. *RECOMMENDED PRACTICES FOR FRICTION WELDING*, ANSI/AWS C6. 1-89, AMERICAN WELDING SOCIETY, 1989
7. *METALS HANDBOOK*, 9TH ED., VOL 6, AMERICAN SOCIETY FOR METALS, 1983
8. T.N. HAZLET, PROPERTIES OF FRICTION WELDED PLAIN CARBON AND LOW ALLOY STEELS, *WELD. J.*, VOL 41, 1962, P 49-S TO 52-S
9. S.B. DUNKERTON, TOUGHNESS PROPERTIES OF FRICTION WELDS IN STEELS, *WELD. J.*, VOL 65, 1986, P 193-S TO 202-S
10. J.C. LIPPOLD AND B.C. ODEGARD, TECHNICAL NOTE: MICROSTRUCTURAL EVOLUTION

DURING INERTIA FRICTION WELDING OF AUSTENITIC STAINLESS STEELS, *WELD. J.*, VOL 63, 1984, P 35-S TO 38-S

11. W.A. BAESLACK III AND K.S. HAGEY, INERTIA FRICTION WELDING OF RAPIDLY SOLIDIFIED POWDER METALLURGY ALUMINUM, *WELD. J.*, VOL 67, 1988, P 139-S TO 149-S
12. H.H. KOO AND W.A. BAESLACK III, FRICTION WELDING OF A RAPIDLY SOLIDIFIED AL-FE-V-SI ALLOY, *WELD. J.*, VOL 71, 1992, P 147-S TO 169-S
13. K. OGAWA, H. YAMAGUCHI, T. MORIMOTO, K. TAKEMATA, H. SUDO, AND A. HIRATSUKA, SHEAR STRENGTH CHARACTERISTICS OF ALUMINUM ALLOY FRICTION WELDS, *WELD. J.*, VOL 5, 1991, P 860-866
14. C.G. NESSLAR *ET AL.*, FRICTION WELDING OF TITANIUM ALLOYS, *WELD. J.*, VOL 50, 1971, P 379-S TO 385-S
15. K.G.K. MURTI AND S. SANDARESAN, THERMAL BEHAVIOR OF AUSTENITIC-FERRITIC JOINTS MADE BY FRICTION WELDING, *WELD. J.*, VOL 64, 1985, P 327-S TO 334-S
16. R.A. BELL, J.C. LIPPOLD, AND D.R. ADOLPHSON, AN EVALUATION OF COPPER-STAINLESS STEEL FRICTION WELDS, *WELD. J.*, VOL 63, 1984, P 325-2 TO 332-S
17. D. YASHAN, S. TSANG, W.L. JOHNS, AND M.W. DOUGHTY, INERTIA FRICTION WELDING OF 1100 ALUMINUM TO TYPE 316 STAINLESS STEEL, *WELD. J.*, VOL 66, 1987, P 27-37
18. M. FUTAMATA AND A. FUJI, FRICTION WELDING OF TITANIUM AND SUS 304L AUSTENITIC STAINLESS STEEL, *WELD. INT.*, VOL 4, 1990, P 768-774
19. F. SASSANI AND J.R. NEELAN, FRICTION WELDING OF INCOMPATIBLE MATERIALS, *WELD. J.*, VOL 67, 1988, P 264-S TO 270-S
20. R. ARMSTRONG, PRIVATE COMMUNICATION AND INTERNAL REPORTS, LAWRENCE LIVERMORE NATIONAL LABORATORY, 1991
21. *METALS HANDBOOK*, 9TH ED., VOL 2, AMERICAN SOCIETY FOR METALS, 1979, P 204-209

Fundamentals of Diffusion Bonding

Murray W. Mahoney and Cliff C. Bampton, Rockwell International Science Center

Introduction

DIFFUSION BONDING is only one of many solid-state joining processes wherein joining is accomplished without the need for a liquid interface (brazing) or the creation of a cast product via melting and resolidification (welding). In its most narrow definition, which is used to differentiate it from other joining processes such as deformation bonding or transient liquid phase joining, diffusion bonding (DB) is a process that produces solid-state coalescence between two materials under the following conditions:

- JOINING OCCURS AT A TEMPERATURE BELOW THE MELTING POINT, T_M, OF THE MATERIALS TO BE JOINED (USUALLY $>1/2T_M$).
- COALESCENCE OF CONTACTING SURFACES IS PRODUCED WITH LOADS BELOW THOSE THAT WOULD CAUSE MACROSCOPIC DEFORMATION TO THE PART.
- A BONDING AID CAN BE USED, SUCH AS AN INTERFACE FOIL OR COATING, TO EITHER FACILITATE BONDING OR PREVENT THE CREATION OF BRITTLE PHASES BETWEEN DISSIMILAR MATERIALS, BUT THE MATERIAL SHOULD NOT PRODUCE A LOW-TEMPERATURE LIQUID EUTECTIC UPON REACTION WITH THE MATERIALS TO BE JOINED.

Thus, diffusion bonding facilitates the joining of materials to produce components with no abrupt discontinuity in the microstructure and with a minimum of deformation.

Within the confines of this definition, the DB process, in practice, is limited to either press or gas pressure or bonding approaches. Illustrations and discussions of equipment and systems are presented elsewhere within this Handbook (see the Section "Solid-State Welding, Brazing, and Soldering Processes"). This article offers a qualitative summary of the theory of diffusion bonding. For those who require a more quantitative assessment, refer to the Selected References at the end of the article.

It should be noted that the preferred term for this process, according to the American Welding Society, is diffusion *welding.* However, because diffusion *bonding* is used more commonly in industry, it is the term that will be used in this article.

Fundamentals of Diffusion Bonding

Murray W. Mahoney and Cliff C. Bampton, Rockwell International Science Center

Diffusion Bonding Process

The DB process, that is, the application of pressure and temperature to an interface for a prescribed period of time, is generally considered complete when cavities fully close at the faying surfaces. Relative agreement is found for the mechanisms and sequence of events that lead to the collapse of interface voids, and the discussion below describes these metallurgical processes. Although this theoretical understanding of the DB process is universally applicable, it should be understood that parent metal strength is only approached for materials with surface conditions that do not have barriers to impede atomic bonding such as the absence of surface oxides or absorbed gases at the bonding interface.

In practice, oxide-free conditions exist only for a limited number of materials. Accordingly, the properties of real surfaces limit and impede the extent of diffusion bonding. The most notable exception is titanium alloys, which, at DB temperatures greater than 850 °C (1560 °F), can readily dissolve minor amounts of adsorbed gases and thin surface oxide films and diffuse them away from the bonding surfaces, so that they will not impede the formation of the required metallic bonds across the bond interface, as shown in Fig. 1(a). An example of a successful diffusion bond in a titanium alloy is illustrated in Fig. 1(b), where the integrity of the bonded interfaces was demonstrated with subsequent superplastic expansion without interface failure.

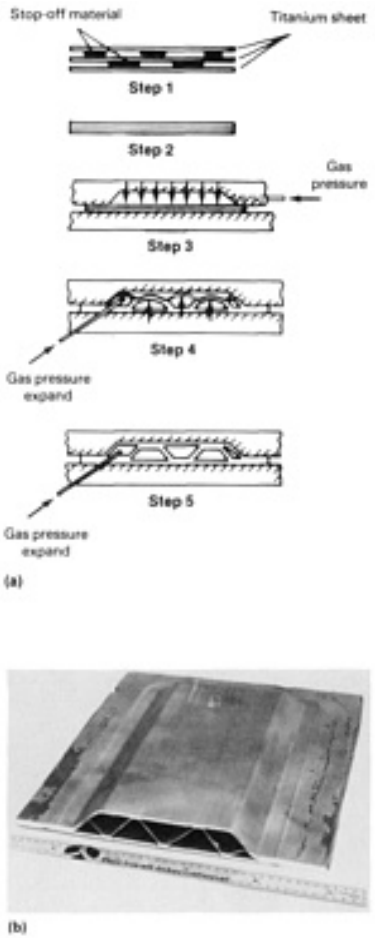

FIG. 1 SUPERPLASTIC FORMING/DIFFUSION BONDING (SPF/DB) OF TITANIUM SHEET. (A) SEQUENCE OF OPERATIONS REQUIRED TO JOIN THREE SHEETS OF SUPERPLASTIC TITANIUM ALLOY USING SPF/DB PROCESS. (B) TYPICAL THREE-SHEET TITANIUM ALLOY COMPONENT SUPERPLASTICALLY FORMED FOLLOWING DIFFUSION BONDING.

Similarly, the joining of silver at 200 °C (390 °F) requires no deformation to break up and disperse oxides, because silver oxide dissociates completely at 190 °C (375 °F). Above this temperature, silver dissolves its oxide and also scavenges many surface contaminants. Other examples of metals that have a high solubility for interstitial contaminants include tantalum, tungsten, copper, iron, zirconium, and niobium. Accordingly, this class of alloy is easiest to diffusion bond.

A second class of material, that is, metals and alloys that exhibit very low solubility for interstitials (such as aluminum-, iron-, nickel-, and cobalt-base alloys) are not readily diffusion bondable. Special consideration must be given to remove surface barriers to atomic diffusion prior to joining and subsequently prevent their reformation during the joining process. This is not an easy processing matter. Accordingly, the potential for high-strength bond interfaces for alloys with low interstitial solubility should be considered on an individual alloy basis.

Fundamentals of Diffusion Bonding

Murray W. Mahoney and Cliff C. Bampton, Rockwell International Science Center

---

Bonding Surfaces Containing Oxides

Diffusion bonding can be achieved for materials with adherent surface oxides, but the resultant interface strengths of these materials are considerably less than that measured for the parent material. Aluminum alloys are prime examples of this class of material. Research since 1960 has demonstrated only limited diffusion bond properties. Although interface

strength can be increased for oxide-bearing materials, it requires considerable surface extension of the faying interfaces to create localized plastic flow of the metal and concurrent oxide breakage. This introduces an increased number of locations for metal-to-metal contact via plastic flow around or microextrusion through the broken oxide. In general, the oxide is not removed, but is simply dispersed over a greater surface area in an enclosed environment, in which oxidation cannot recur. Thus, even with significant surface deformation, only a fraction of the interface area contributes to the strength of the bond. The proportion of oxide-free metallic area revealed is dependent on the relative hardness of the metal and its oxide film, as well as on the mechanical properties of the oxide. This type of bonding, although often considered as diffusion bonding, is better described as deformation bonding and does not fit within the strict definition of the low deformation associated with diffusion bonding.

Factors that affect the relative difficulty of diffusion bonding oxide-bearing surfaces include:

- *SURFACE ROUGHNESS PRIOR TO WELDING.* A ROUGHER SURFACE WILL RESULT IN GREATER SHEAR DEFORMATION.
- *MECHANICAL PROPERTIES OF THE OXIDE.* THE MORE BRITTLE THE OXIDE, THE GREATER THE DISPERSION FOR A GIVEN LEVEL OF DEFORMATION.
- *RELATIVE HARDNESS OF THE METAL AND ITS OXIDE FILM.* BECAUSE PLASTIC FLOW CONTROLS THE AMOUNT OF BONDING AREA, LARGE DIFFERENCES IN THEIR HARDNESS SHOULD FACILITATE BONDING.
- *PRESTRAINING OR WORK HARDENING OF THE MATERIAL.* INITIATION OF BONDING WILL OCCUR AT LOWER DEFORMATIONS FOR PRESTRAINED OR WORK-HARDENED MATERIALS, AND THE DEGREE OF SURFACE EXTENSION IN THE CENTRAL REGION OF THE INTERFACE IS CONSIDERABLY GREATER FOR COLD-WORKED MATERIAL. THUS, ANNEALED MATERIAL REQUIRES A LARGER TOTAL DEFORMATION BEFORE BONDING WILL INITIATE.

It is clear that with the appropriate information, sufficient experiments can be performed to determine the diffusion bondability of most materials. Parent metal strength will not always be attained using the DB approach, particularly for materials with adherent oxides, but interface strength can be maximized if the fundamentals of the process are understood.

Fundamentals of Diffusion Bonding

Murray W. Mahoney and Cliff C. Bampton, Rockwell International Science Center

---

Mechanism of Diffusion Bonding

In diffusion bonding, the nature of the joining process is essentially the coalescence of two atomically clean solid surfaces. Complete coalescence comes about through a three-stage metallurgical sequence of events. Each stage, as shown in Fig. 2, is associated with a particular metallurgical mechanism that makes the dominant contribution to the bonding process. Consequently, the stages are not discretely defined, but begin and end gradually, because the metallurgical mechanisms overlap in time. During the first stage, the contact area grows to a large fraction of the joint area by localized deformation of the contacting surface asperities. Factors such as surface roughness, yield strength, work hardening, temperature, and pressure are of primary importance during this stage of bonding. At the completion of this stage, the interface boundary is no longer a planar interface, but consists of voids separated by areas of intimate contact. In these areas of contact, the joint becomes equivalent to a grain boundary between the grains on each surface. The first stage is usually of short duration for the common case of relatively high-pressure diffusion bonding.

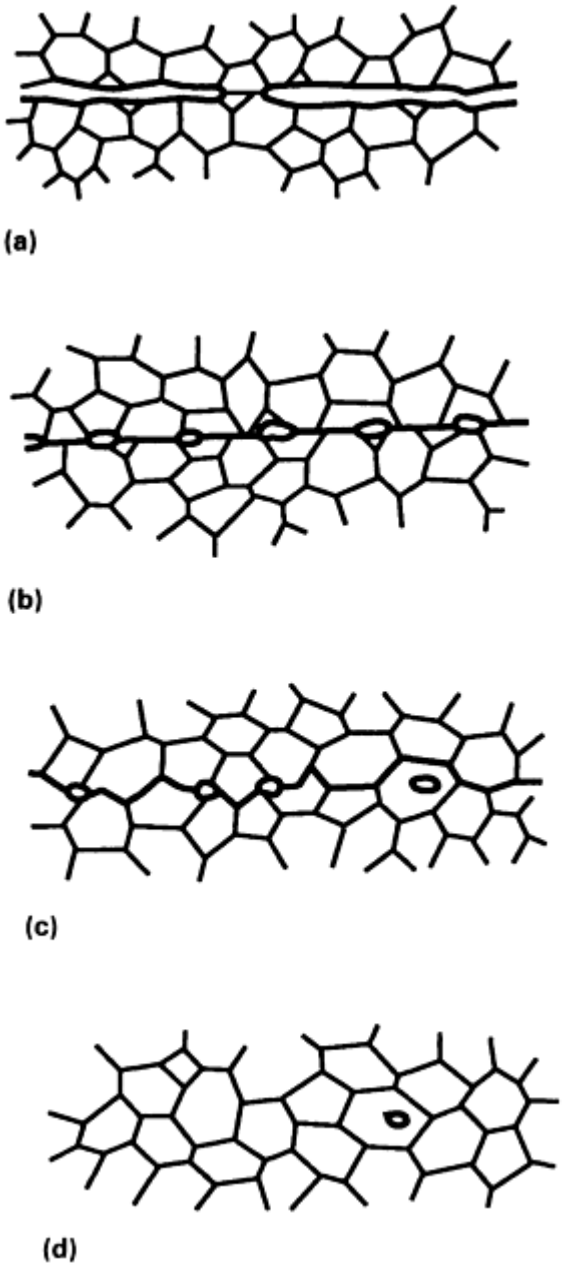

FIG. 2 SEQUENCE OF METALLURGICAL STAGES IN DIFFUSION BONDING PROCESS. (A) INITIAL CONTACT: LIMITED TO A FEW ASPERITIES (ROOM TEMPERATURE). (B) FIRST STAGE: DEFORMATION OF SURFACE ASPERITIES BY PLASTIC FLOW AND CREEP. (C) SECOND STAGE: GRAIN BOUNDARY DIFFUSION OF ATOMS TO THE VOIDS AND GRAIN BOUNDARY MIGRATION. (D) THIRD STAGE: VOLUME DIFFUSION OF ATOMS TO THE VOIDS

During the second stage of joint formation, two changes occur simultaneously. All of the voids in the joints shrink, and most are eliminated. In addition, the interfacial grain boundary migrates out of the plane of the joint to a lower-energy equilibrium. Creep and diffusion mechanisms are important during the second stage of bonding and for most, if not all, practical applications, bonding would be considered essentially complete following this stage. As the boundary moves, any remaining voids are engulfed within grains where they are no longer in contact with a grain boundary. During this third stage of bonding, the voids are very small and very likely have no impact on interface strength. Again, diffusional processes cause the shrinkage and elimination of voids, but the only possible diffusion path is now through the volume of the grains themselves.

Stage I: Microasperity Deformation

The nature of the starting surface is of considerable importance, because of the small macroscopic deformation allowed during diffusion bonding. A real surface is never perfectly clean or perfectly smooth, and the area of metal-to-metal contact between faying surfaces is a very small fraction of the area of joint contact. Contact is limited to a relatively few microasperities. At room temperature and under load, these asperities deform as long as the surface area of contact is such that the yield strength of the material is exceeded. The extent of this deformation is limited at room temperature, and is even more limited for work-hardenable materials. As temperature increases to the diffusion bonding temperature, the flow stress of the material decreases and additional asperity deformation occurs through plastic flow. Again, flow occurs until the area of contact increases to an extent that the yield strength of the material is exceeded. If the temperature is above the recrystalization temperature of the material, then work hardening is no longer a consideration. With time at temperature, creep mechanisms now control the rate of asperity deformation, and the area of contact or bond continues to grow. As the area of contract grows, the stress acting on the surface asperities decreases. Consequently, creep deformation progressively slows and diminishes in significance.

The contributions of temperature and pressure to both plastic and creep deformation during this initial stage of diffusion bonding are synergistic, that is, at higher temperatures, less pressure is required and vice versa. However, for any combination of temperature and pressure, bulk deformation to the part is limited to a small percentage (<2 to 3%). Ideally, at the completion of the first stage, the extent of asperity collapse should result in a planar area of contacting surfaces with individually dispersed voids. It is necessary to achieve this extend of contact in order to complete the final stages of diffusion bonding in a reasonable period of time.

For example, Fig. 3 illustrates the influence of pressure on the bond line morphology for a titanium alloy. At lower pressures, where surface asperity deformation is less during the first stage of bonding, large voids remain at the interface, even after a reasonable time at temperature. Conversely with a higher applied pressure and a correspondingly greater initial interface deformation, the bond interface becomes indistinguishable from the matrix alloy. It should be remembered that, by definition, very little bulk deformation is allowed and that only interface microdeformation contributes to the growth in contact area of the faying surfaces.

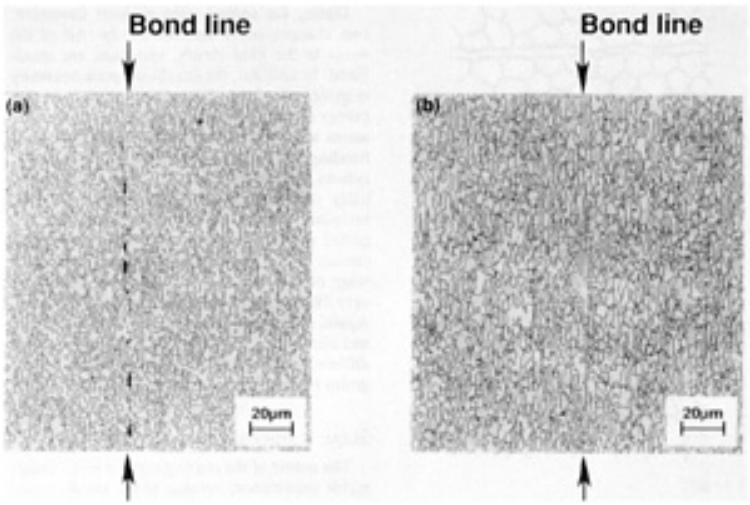

FIG. 3 EFFECT OF PRESSURE ON PRESENCE OF VOIDS AT BAND INTERFACE OF TITANIUM ALLOY DIFFUSION BONDED AT TEMPERATURES OF 980 °C (1795 °F) FOR 2 H. (A) INCOMPLETE BOND AT 7.0 MPA (1.0 KSI). (B) COMPLETE BOND AT 10.0 MPA (1.5 KSI)

Surface Roughness. When considering the sequences in the stages of diffusion bonding, it is clear that the original surface finish plays a significant role in the time dependency for the completion of the different stages. The surfaces that are mated at the bond line are usually rather irregular, as a result of the machining or other surface preparation steps. As shown in Fig. 4, the surface roughness can be viewed as a bimodal distribution of asperities, that is, small, short-wavelength asperities (surface roughness) arrange on larger, long-wavelength asperities (surfaces waviness).

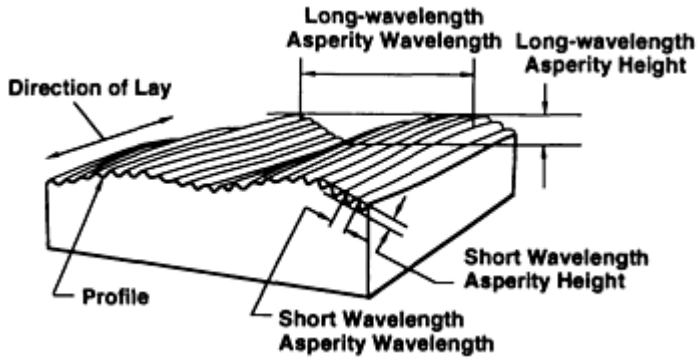

FIG. 4 BIMODAL TOPOGRAPHY OF MECHANICAL SURFACES

It is expected that during the first bonding stage, a more uneven initial surface that is due to either roughness or waviness would produce more large voids than would a smooth initial surface. For example, as load is applied, asperities on rough surfaces will experience higher stresses on the points of contact. Plastic flow will occur at a lower load, and greater interface shear will occur. Although first-stage plastic flow and creep will create more localized interface deformation for a rough surface, fewer but larger voids will remain at the interface (the contact area should approach an equilibrium value independent of the initial surface roughness). In addition to size, the shape and curvature of the voids would be considerably different, with higher aspect ratio voids for the rougher starting surfaces. For the subsequent diffusion-controlled collapse of interface voids during second-stage bonding, an initially rough surface will require a longer time or higher temperatures for the mass-transport processes to shrink and eliminate the voids.

Conversely, because real surfaces are not perfectly clean, some limited degree of interface deformation is necessary for the diffusion bonding of even oxide-free materials. Experimental evidence has demonstrated that even gold is not joined unless some shear displacement occurs as the two faying surfaces come into contact. It seems that the importance of the shear displacement, besides increasing the contact area, is that it destroys the continuity of any adsorbed oxygen layer that can contaminate the oxide-free area because of trapped air at the interface. Procedures as simple as wire brushing have been shown to be a particularly effective surface preparation. This can be partly attributed to the creation of rough layers on the surface.

Stage II: Diffusion-Controlled Mass Transport

The densification or collapse of interface cavities during the second stage of diffusion bonding is attributable to the lowering of the surface free energy by the decrease in surface area. This takes place with the formation of new, but lower-energy, solid-solid interfaces. Because the driving force is the same (reduction of surface energy) for all systems, the considerable differences in behavior in various types of systems are related to the different mechanisms of material transfer.

In diffusion bonding, a number of mass-transport processes are operative simultaneously, including time-dependent plastic flow, diffusion from the interface to the cavity via the lattice and the interface and grain boundaries, and diffusive flow around the surface of the void via the lattice and vapor phase. These different paths of mass transfer are illustrated in Fig. 5 and include:

- PLASTIC YIELDING THAT DEFORMS AN ORIGINAL CONTACTING ASPERITY
- SURFACE DIFFUSION FROM A SURFACE SOURCE TO A NECK
- VOLUME DIFFUSION FROM A SURFACE SOURCE TO A NECK
- EVAPORATION FROM A SURFACE SOURCE TO CONDENSATION AT A NECK
- GRAIN BOUNDARY DIFFUSION FROM AN INTERFACIAL SOURCE TO A NECK
- VOLUME DIFFUSION FROM AN INTERFACIAL SOURCE TO A NECK
- POWER-LAW CREEP

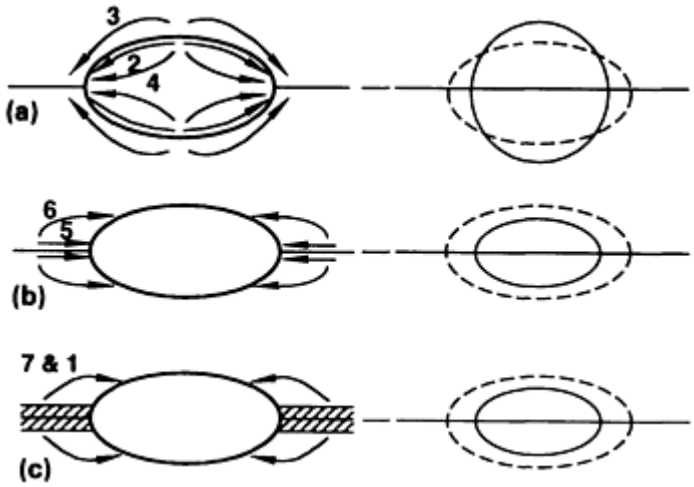

FIG. 5 SCHEMATIC OF NUMEROUS PATHS OF MATERIAL TRANSFER GENERATED DURING DIFFUSION BONDING PROCESS. (A) SURFACE SOURCE MECHANISMS. (B) INTERFACE SOURCE MECHANISMS. (C) BULK DEFORMATION MECHANISMS. SEE TEXT FOR SPECIFIC MECHANISMS INDICATED BY NUMBERS SHOWN IN SCHEMATIC.

Although vapor transport and surface transport of matter change the shape of the void, they do not directly alter the volume. Thus, these transport paths have only a secondary influence on the rate of void collapse indirectly, through a change in void curvature. Only the transfer of matter from the matrix volume or from grain boundaries causes shrinkage and pore elimination. Thus, only the first two mechanisms, plastic flow and interface diffusion, actually reduce the volume of the interfacial voids. The dominance of either of these two processes is dependent on many inseparable factors, including material system, void geometry, microstructure, and bonding parameters.

When considering diffusion, evidence seems to suggest that the most efficient path for atom flow and counterdiffusing vacancies is along the interfacial grain boundary and along grain boundaries that intersect the void when the grain size is less than the pore size. Although the area of a grain boundary is small in comparison to the void surface, this high-diffusivity path has been shown to dominate. For example, bonding has been shown to be enhanced by first blasting the faying surfaces with chilled iron grit. This treatment promoted recrystallization and, thus a finer grain size across the interface, creating additional high-diffusivity paths. In a related process (the sintering of Al_2O_3), porosity was shown to be eliminated next to grain boundaries, with residual porosity remaining at grain centers. Similarly, fine grain size, as exists in superplastic alloys, should create higher rates of void coalescence via grain boundary diffusion. However, because the chemical potential driving force for grain boundary diffusion mechanisms is partly dependent on the angle between the applied pressure and a particular grain boundary, its actual contribution will be dependent on its precise orientation with respect to the applied pressure. The driving force will be maximal when the two are perpendicular and minimal when they are parallel.

Although there is insufficient evidence for generalization, evidence also exists to illustrate that diffusion is, at times, the rate-controlling factor for void coalescence. For example, maintaining temperature while removing pressure following the first bonding stage was shown to not significantly impede the joining process. The rate of void elimination was only slightly slower without the applied pressure. However, this change in rate could be due to either the lost contribution that deformation makes to void coalescence or a reduction in efficiency of the stress-enhanced grain boundary contribution.

Stage III: Interface Migration

During the second stage of diffusion bonding, voids become much smaller and many are eliminated. Their grain boundary pinning influence decreases, so that interfacial grain boundary migrates toward an equilibrium configuration, which is indistinguishable from the other grain boundaries in the microstructure. The driving force for the boundary migration is the reduction in grain boundary area. The initially straight interfacial bond line becomes distorted with local penetrations of a few microns of one material into the other at triple points. As the boundary moves, any remaining voids become enclosed within grains where they are no longer in contact with a grain boundary. Diffusional processes continue to shrink and eliminate these cavities, but the diffusion path is now restricted to volume diffusion through the matrix lattice.

Accordingly, the elimination of this final small volume of porosity would be likely to contribute an inordinate time to the bonding process for any interface strength benefits that might be achieved.

Diffusion Bonding with Interface Aids

Additional layers of material in the form of coatings or foils are often used as bonding aids for a variety of reasons. For example, an intermediate material can be used when joining dissimilar materials where a brittle intermetallic would otherwise form. In this case, the interfacial material would be selected for its compatibility with each of the materials to be joined and for its ability to prevent the creation of a brittle reaction layer. To promote diffusion in materials that contain elements with low diffusivities, the interfacial material should contain an element with a higher mobility than elements found in the joined materials. A common material for such applications is electroless nickel, which contains phosphorus (phosphorus has been shown to have a high diffusivity in other metallic systems). However, caution should be exercised when considering the addition of high-diffusivity elements, because of their potential for accumulation at grain boundaries and their resultant influence on mechanical properties.

Another approach is to add an interfacial material that will scavenge impurity elements at the interface and thus produce clean surfaces *in situ.* Materials with high solubilities for interstitial elements, such as titanium alloys, can be appropriate for this purpose. Because of the importance of localized plastic flow at the interface, a soft material addition can also be of benefit to maximize interfacial contact during the first bonding stage, where deformation mechanisms dominate.

With the addition of interfacial materials, geometric as well as metallurgical considerations become important. The mechanical strength of solid-state metallic bonds achieved with a thin interfacial layer of bonding material goes through a maximum, with decreasing joint thickness. For thick joints, tensile strength is directly related to the bulk properties of the interfacial layer material. As joint thickness decreases, the tensile strength of these joints increases, because of the matrix material restraint on the plastic flow of the interfacial layer. However, for very thin joints, the problems of surface roughness and cleanliness start to diminish the contact area and, thus, effectively reduce the joint tensile strength. experimental studies should be performed for individual materials. In general, thicknesses of approximately 0.025 mm (0.00098 in.) yield maximum interface strengths.

Fundamentals of Diffusion Bonding

Murray W. Mahoney and Cliff C. Bampton, Rockwell International Science Center

Selected References

- B.M. AGERS, THE MECHANISM OF SMALL TOOL PRESSURE WELDING, *BRIT. WELD. J.,* JULY 1964, P 313-319
- N. BREZDS, INVESTIGATION OF THE FACTORS DETERMINING THE TENSILE STRENGTH OF BRAZED JOINTS, *WELD. RES. SUPP.,* NOV 1954, P 545S-563S
- C.L. CLINE, AN ANALYTICAL AND EXPERIMENTAL STUDY OF DIFFUSION BONDING, *WELD. RES. SUPP.,* NOV 1966, P 481S-489S
- R.L. COBLE, DIFFUSION MODELS FOR HOT PRESSING WITH SURFACE ENERGY AND PRESSURE EFFECTS AS DRIVING FORCE, *J. APPL. PHYS.,* VOL 41.12, 1970, P 4798-4807
- B. DERBY AND E.R. WALLACH, THEORETICAL MODEL FOR DIFFUSION BONDING, *MET. SCI.,* VOL 16, JAN 1982, P 49-56
- B. DERBY AND E.R. WALLACH, DIFFUSION BONDING: DEVELOPMENT OF THEORETICAL MODEL, *MET. SCI.,* VOL 18, 1984, P 427-431

- J.W. DINI, USE OF ELECTRODEPOSITION TO PROVIDE COATINGS FOR SOLID STATE BONDING, *WELD. J.*, VOL 61 (NO. 11), NOV 1982, P 33-39
- G. GARMONG, N.E. PATON, AND A.S. ARGON, ATTAINMENT OF FULL INTERFACIAL CONTACT DURING DIFFUSION BONDING, *MET. TRANS. A*, VOL 6A, JUNE 1975, P 1269-1279
- C.H. HAMILTON, PRESSURE REQUIREMENTS FOR DIFFUSION BONDING TITANIUM, *TITANIUM SCIENCE AND TECHNOLOGY*, R.I. JAFFEE AND H.M. BURTE, ED., PLENUM, 1973, P 625-647
- A. HILL AND E.R. WALLACH, MODELING SOLID STATE DIFFUSION BONDING, *ACTA. METALL.*, VOL 37 (NO. 9), SEPT 1989, P 2425-2437
- W.H. KING AND W.A. OWCZARSKI, ADDITIONAL STUDIES ON THE DIFFUSION WELDING OF TITANIUM, *WELD. RES. SUPP.*, OCT 1968, P 444S-450S
- H.A. MOHAMED AND J. WASHBURN, MECHANISM OF SOLID STATE PRESSURE WELDING, *WELD. RES. SUPP.*, SEPT 1975, P 302S-310S
- R. PEARCE, DIFFUSION BONDING, *PROC. INTERNATIONAL CONFERENCE ON DIFFUSION BONDING* (CRANFIELD, SIS), 1987
- J. PILLING, THE KINETICS OF ISOSTATIC DIFFUSION BONDING IN SUPERPLASTIC MATERIALS, *MATER. SCI. ENG.*, VOL 100, APRIL 1988, P 137-144
- E.R. WALLACH, SOLID-STATE DIFFUSION BONDING OF METALS, *TRANS. JWRI*, VOL 17.1, 1988, P 135-148
- D.S. WILKINSON AND M.F. ASHBY, PRESSURE SINTERING BY POWER LAW CREEP, *ACTA. METALL.*, VOL 23, 1975, P 1277-1285

Fundamentals of Explosion Welding

R. Alan Patterson, Los Alamos National Laboratory

Introduction

EXPLOSION WELDING (EXW), also known as explosive bonding, is accomplished by a high-velocity oblique impact between two metals. The impact must have sufficient energy to cause the colliding metal surfaces to flow hydrodynamically when they intimately contact one another in order to promote solid-state bonding. Oblique impact is important because conservation of momentum allows for a reentrant jetting action that is due to hydrodynamic flow of the faying metal surfaces. The jet is ejected outward from the collision apex between the metals and produces a cleaning action by scarfing or effacing the metal surfaces. The resulting virgin metal surfaces are then compressed together under high pressure from the explosion, which promotes atomistic bonding.

This phenomenon was first observed during World War I, when fragments from bombs or shells were often found to be welded to surrounding metal structures (Ref 1). The first publication to recognize the potential for generating metallic welding by using explosively driven plates appeared in 1944 (Ref 2). The first explosive bonding patent associated with the commercial application of the technique was issued in 1962 (Ref 3).

The most beneficial attribute of the technique is that dissimilar metal systems can be bonded even when conventional fusion welding techniques are metallurgically inappropriate, because of the formation of intermetallic compounds. Applications of explosive bonding are diverse and include the production of sandwiched metal for coinage (1965 to 1971), the more-sophisticated use of titanium-to-stainless steel transition joints in the Apollo spacecraft (Ref 4), and the use of aluminum-to-steel transition joints in ships. The most common utilization of explosive bonding is the production of clad metals for the purpose of corrosion resistance and for transition joints that are used to aid dissimilar metal welding. Practical applications of explosive bonding are addressed in greater detail in the article "Explosion Welding" and the Section "Procedure Development and Practice Considerations for Solid-State Welding" in this Volume.

It should be noted that the discussion in this article is restricted to the "parallel gap" explosive bonding technique. Several other bonding geometries that are fundamentally similar to the geometry of the parallel gap technique are utilized in a variety of other techniques. For example, the "preset angle" bonding technique is used to produce flat-plate clads.

Circumferential techniques are used to produce tube-to-tube welds or tubular clads. Spot welding and seam welding techniques, as well as others, are also used in certain situations. All of these techniques require the jet to travel in a straight line between the two metal surfaces (see the section "Flyer Plate Acceleration" in this article).

Several very good reviews of the explosive bonding process have been published (Ref 4, 5, 6, 7, 8). These articles should be used to augment the information presented here. This article attempts to describe the practice of producing an explosive bond/weld and draws on many previous research results in order to explain the mechanisms involved.

References

1. B. CROSSLAND, *EXPLOSIVE WELDING OF METALS AND ITS APPLICATION*, CLARENDON PRESS, 1982
2. L.R. CARL, *MET. PROGR.*, VOL 46, 1944, P 102
3. V. PHILIPCHUK AND F. LEROY BOIS, U.S. PATENT 3,024,526, 1962
4. V.D. LINSE, R.H. WITTMAN, AND R.J. CARLSON, "EXPLOSION BONDING," REPORT X68-10247, BATTELLE MEMORIAL INSTITUTE
5. J.S. RINEHART AND J. PEARSON, *EXPLOSIVE WORKING OF METALS*, PERGAMON PRESS, 1963
6. M.C. NOLAND, H.M. GADBERRY, J.B. LOSER, AND E.C. SNEEGAS, "HIGH VELOCITY METAL-WORKING: A SURVEY," NASA REPORT N67-26560, SP 5062, NASA, 1967
7. A.A. EZRA, *PRINCIPLES AND PRACTICE OF EXPLOSIVE METAL WORKING*, INDUSTRIAL NEWSPAPERS LIMITED, JOHN ADAMS HOUSE, LONDON, 1973
8. T.Z. BLAZYNSKI, *EXPLOSIVE WELDING, FORMING AND COMPACTION*, APPLIED SCIENCE PUBLISHERS, U.K., 1983

Fundamentals of Explosion Welding

R. Alan Patterson, Los Alamos National Laboratory

Bonding Practice

Figure 1 shows the arrangement used in the parallel gap explosive bonding process. The explosive charge is placed in contact with the top plate, hereafter called the flyer plate. The explosive detonation is initiated from one end to generate a linear detonation front, which runs along the flyer plate length. Pressure generated by the expansion of the explosive products accelerates the flyer plate downward at the point where the explosive is reacting and results in the desired impact on the stationary base plate. The principal parameters that affect bond success with this arrangement are:

- DETONATION VELOCITY AND ENERGY, WHICH ARE CHARACTERISTICS OF THE EXPLOSIVE USED AND RESULT IN FLYER PLATE ACCELERATION
- IMPACT ENERGY, WHICH IS A FUNCTION OF THE FLYER PLATE STANDOFF DISTANCE, THE DETONATION ENERGY, AND THE ENERGY TRANSFER CHARACTERISTICS
- DYNAMIC BEND ANGLE AND THE PHYSICAL AND MECHANICAL PROPERTIES OF THE METAL CONSTITUENTS

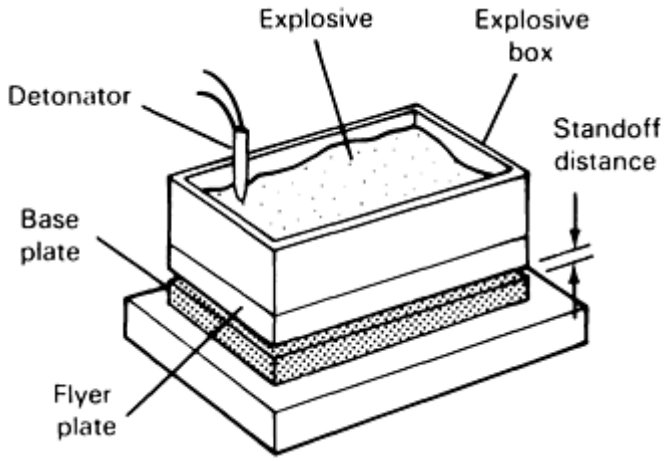

FIG. 1 SCHEMATIC SHOWING KEY COMPONENTS USED IN THE PARALLEL GAP EXPLOSIVE WELDING PROCESS

Flyer Plate Acceleration

Figure 2, an intermediate view of the explosive bonding process, shows an idealization of the metal deformation that results after explosive detonation. Flash radiography performed during the bonding process has been used to develop this pictorial representation (Ref 6, 7). The energy produced by detonating the explosive results from a very rapid expansion of detonation products, which impacts an acceleration to the flyer plate and maintains a high-pressure region in the atmosphere behind the detonation front (Ref 1). Rapid flyer plate acceleration results in a dynamic bending action (Fig. 2). The dynamic bend angle, β, results in an oblique impact between the flyer and base plates, which promotes the hydrodynamic flow of the metal surfaces and a resulting jetting actions.

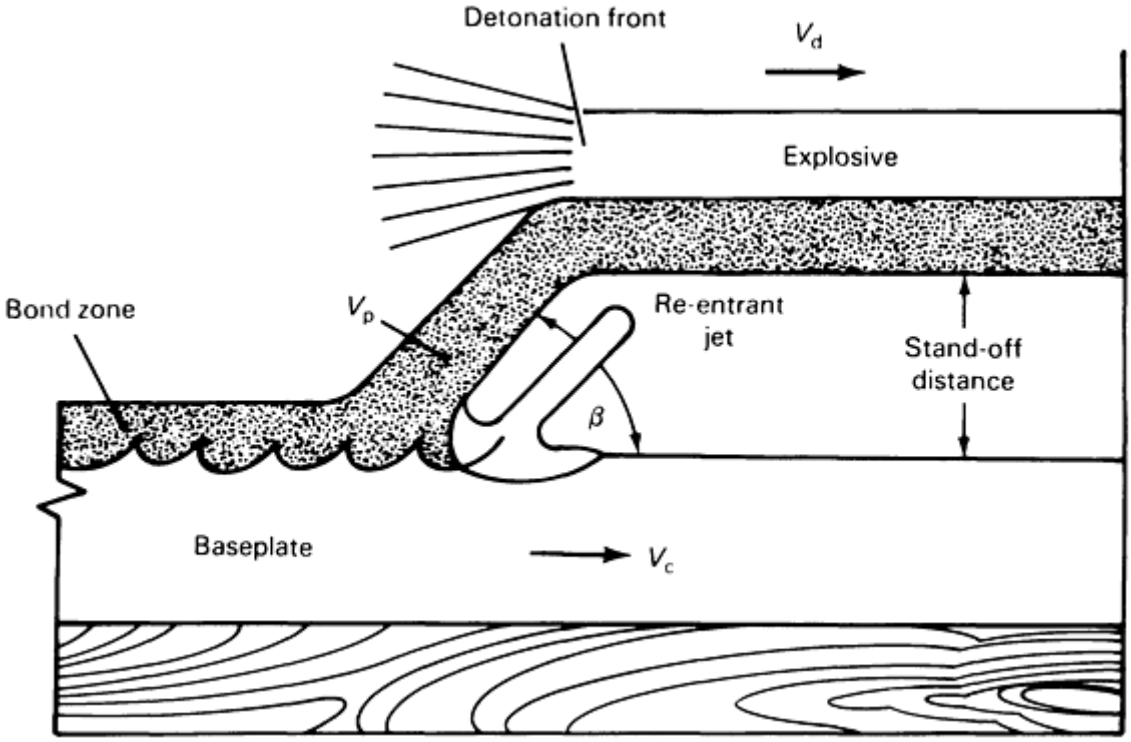

FIG. 2 SCHEMATIC SHOWING AN IDEALIZED VIEW OF THE FLYER PLATE DEFORMATION AND IMPACT RESULTING FROM A MOVING EXPLOSIVE DETONATION FRONT

Conservation of momentum is used to describe the bonding mechanism in which three velocity vectors are of primary importance. The detonation velocity, V_d, is a characteristic of the explosive and is generally directly proportional to the explosive density. From the geometry of the system, it is obvious that the collision point between the impacting metals propagates at the same speed as the explosive detonation front. The collision-point velocity is represented by V_c in Fig. 2. The flyer plate velocity, V_p, can be calculated based on an energy balance and conservation of momentum (Ref 9).

Impact Energy

Impact energy is generally assumed to equal the maximum kinetic energy that is due to the acceleration of the flyer plate. In simpler terms, it is assumed that the flyer plate has been accelerated to the terminal velocity as calculated from models like that proposed by Gurney (Ref 9), and that no deceleration occurs because of atmospheric interference. Furthermore, energy loss that is due to the bending strain energy in the flyer plate has been ignored in much of the earlier literature, because of its complexity. Recent estimates of energy partitioning suggest that only 15 to 20% of the flyer plate energy is used for cladding, whereas 66% is absorbed in flyer plate forming and 15% is dissipated as excess energy in the base plate (Ref 10, 11). The flyer plate standoff distance is therefore a very important factor, because it physically limits the flyer plate acceleration and dynamic bend angle.

Simple determinations of flyer plate standoff distance resulting from empirical testing are often used. Carpenter *et al.* (Ref 10) state that the standoff distance should be small enough to allow continuous acceleration of the flyer plate. Standoff distances that are twice the flyer plate thickness for thin components (up to 6.5 mm, or 0.26 in.) and are equal to the flyer plate thickness for thicker components (up to 13 mm, or 0.5 in.) are generally used (Ref 12). Other studies have indicated that a uniform flyer plate velocity is obtained with a separation distance equal to only a few multiples of the flyer plate thickness (Ref 13, 14, 15). Wolf *et al.* (Ref 16) performed a systematic evaluation of standoff distance and dynamic bend angle, which indicated that:

- A LAMINAR BOND WAS ACHIEVED AT DISTANCES EQUAL TO APPROXIMATELY HALF THE FLYER PLATE THICKNESS
- A STABLE WAVY BOND ZONE WAS PRODUCED AT INTERMEDIATE STANDOFF DISTANCES EQUAL TO 1.0 TO 1.5 TIMES THE FLYER PLATE THICKNESS
- DELAMINATION OCCURRED AT DISTANCES ABOVE TWO TIMES THE FLYER PLATE THICKNESS

Dynamic Bend Angle and Material Properties

Attempts to correlate bonding success to starting material properties have been extremely difficult, because most material property compilations are determined at ambient conditions and do not account for the high strain rates associated with explosive conditions. Rules of thumb often dominate. Carpenter *et al.* (Ref 10) indicated that materials exhibiting tensile ductilities greater than 5% will survive the bending associated with the flyer plate acceleration. It is also generally recognized that the material with the lowest density and tensile yield strength should be used as the flyer plate material. However, brittle materials (for example, refractory metals such as molybdenum and tungsten) have been explosively bonded by elevating the metal temperature above the ductile-to-brittle transition temperature (DBTT) (Ref 17).

Some correlations between initial material properties and the minimum dynamic bend angle, β_{min}, that is required to achieve the desired shear deformation to promote jetting and bonding success have been reported (Ref 18, 19). The suggested relationship between flyer plate hardness, H_v; density, ρ; and the collision-point velocity, V_c, is given by:

$$b_{\min} = k\left(\frac{H_v}{rV^2_c}\right) \qquad \textbf{(EQ 1)}$$

References cited in this section

1. B. CROSSLAND, *EXPLOSIVE WELDING OF METALS AND ITS APPLICATION*, CLARENDON PRESS, 1982
6. M.C. NOLAND, H.M. GADBERRY, J.B. LOSER, AND E.C. SNEEGAS, "HIGH VELOCITY METAL-

WORKING: A SURVEY," NASA REPORT N67-26560, SP 5062, NASA, 1967

7. A.A. EZRA, *PRINCIPLES AND PRACTICE OF EXPLOSIVE METAL WORKING,* INDUSTRIAL NEWSPAPERS LIMITED, JOHN ADAMS HOUSE, LONDON, 1973
9. R.W. GURNEY, "THE INITIAL VELOCITIES OF FRAGMENTS FROM BOMBS, SHELLS, AND GRENADES," REPORT 405, BALLISTIC RESEARCH LABORATORY, 1943
10. S. CARPENTER, R.H. WITTMAN, AND R.J. CARLSON, RELATIONSHIPS OF EXPLOSIVE WELDING PARAMETERS TO MATERIAL PROPERTIES AND GEOMETRY FACTORS, *PROC. FIRST INT. CONF. OF THE CENTER FOR HIGH ENERGY FORMING,* UNIVERSITY OF DENVER, JUNE 1967, P 124
11. B. CROSSLAND AND J.D. WILLIAMS, *METALL. REV.,* NO. 144, 1970
12. H. WOLF, ON THE ENERGY BALANCE OF PLANE AND CYLINDRICAL EXPLOSIVE CLADDING, *PROC. INT. SYMPOSIUM ON INTENSE DYNAMIC LOADING AND ITS EFFECTS,* PERGAMON PRESS, 1988
13. J. GROSCHOPP, V. HEYNE, AND B. HOFFMAN, EXPLOSIVELY CLAD TITANIUM STEEL COMPOSITE, *WELD. INT.,* NO. 9, 1987, P 879-883
14. R.A. PATTERSON, EXPLOSION BONDING: ALUMINUM-MAGNESIUM ALLOYS BONDED TO AUSTENITIC STAINLESS STEEL, *HIGH ENERGY RATE FABRICATION,* M.A. MEYERS AND J.W. SCHROEDER, ED., VOL 70, ASME PRESSURE VESSELS AND PIPING DIV., 1982, P 15-27
15. M.D. CHADWICK, D. HOWD, G. WILDSMITH, AND J.H. CAIRNS, *BR. WELD. J.,* VOL 15, 1968, P 480
16. H. WOLF AND M. KOLBE, EXPERIMENTAL METHODS FOR DETERMINING THE OPTIMUM PROCESS CHARACTERISTICS FOR FLAT EXPLOSIVE CLADDING, *WELD. INT.,* VOL 4 (NO. 7), 1990, P 535-538
17. A.A. POPOFF AND H. CASEY, TECHNICAL PAPER AD 77-36, SME, 1977
18. V.G. PETUSHKOV, THE STRENGTH OF BODIES STRIKING ONE ANOTHER DURING EXPLOSIVE WELDING, *AUTO. WELD.,* VOL 39 (NO. 10), 1986, P 35-38
19. V.M. KUDINOV AND I.D. ZAKHAZENKO, CRITERIA FOR SELECTING THE PARAMETERS OF EXPLOSIVE WELDING, *WELD. PROD.,* VOL 32 (NO. 9), 1985, P 3-6

Fundamentals of Explosion Welding

R. Alan Patterson, Los Alamos National Laboratory

Fundamentals of Bonding

Several important concepts pertaining to the explosive parameters, hydrodynamic flow, jetting, and metal properties were discussed above. The following discussion summarizes the criteria used to model the explosive bonding process.

Explosive Parameters and Shock Effects

Although many different types of explosives have been used for explosive bonding, those that have a broad range of low-detonation velocities are the most appropriate, because fo the deleterious effects of shock rarefaction. Shock fronts are described by a sharp discontinuity in pressure on one side of the transmitting medium where the violent motion that is due to high pressure is separated from a near-quiescent state in the unaffected material (Ref 1). This condition can produce tensile stresses of sufficient magnitude to fracture the explosive bond. Shock waves are not pronounced unless the velocity of the shock front exceeds the sonic velocity of the transmitting medium. Sonic velocity is defined as:

$$U_s = \sqrt{\frac{E'}{r}} \qquad \textbf{(EQ 2)}$$

where U_s is the sonic velocity, E is the appropriate elastic modulus, and ρ is the material density. If the shock wave propagation does not exceed the sonic velocity, then a broadening of the shock front occurs and the magnitude of resultant stress and stress gradients is greatly reduced. Because most metals have a sonic velocity that ranges from 2000 to 6000 m/s (6600 to 20,000 ft/s), it is desirable to use explosives with detonation velocities within this range. Carpenter *et al.* (Ref 10) indicate that explosives with detonation velocities greater than 120% of the sonic velocity of the metal should not be used.

Detonation velocity is a characteristic of the type of explosive and has been shown to be directly proportional to the explosive density. This proportionally is shown in Eq 3, as derived empirically for nitroguanidine explosive (Ref 13):

$$V_D = 1440 + 4020\rho_E \qquad \textbf{(EQ 3)}$$

where V_d equals the detonation velocity and ρ_e is the explosive density. The typical operating range for nitroguanidine is from 2000 to 5000 m/s (6600 to 16,000 ft/s), which corresponds to explosive densities that range from 0.14 to 0.9 g/cm^3 (0.0051 to 0.033 lb/in.^{3}).

The explosive pressure, P, is also proportional to the explosive density, ρ_e, as shown by the Bernoulli equation:

$$P \propto V_d^2 \rho_E \qquad \textbf{(EQ 4)}$$

Flyer plate velocities can be calculated from models like that presented by Gurney (Ref 9), who assumed that the driven metal was accelerated perpendicular to the direction of the detonation propagation and used a specific energy with a characteristic value for each explosive (the Gurney energy). Kennedy (Ref 20) gave a very good explanation of the Gurney model, along with several reconstructions of the Gurney equation, to account for changes in geometry. The equation that is applicable to the parallel gap explosive bonding technique is:

$$V_p^2 = 2E' \frac{3}{\left[1+5+\left(\frac{m}{c}\right)+4\left(\frac{m^2}{c^2}\right)\right]} \qquad \textbf{(EQ 5)}$$

where V_p is the flyer plate velocity, E' is the Gurney energy, m is the flyer plate mass, c is the explosive mass, and m/c is the explosive load factor.

Once the flyer plate and detonation velocities are known, it is a simple matter to define the dynamic nature of the flyer plate bend angle through geometry. The following equation holds for the parallel gap geometry illustrated in Fig. 1 and 2:

$$V_p = 2V_d \sin\left(\frac{b}{2}\right) \qquad \textbf{(EQ 6)}$$

where V_p and V_d are the velocities defined in Eq 5 and 6, respectively, and β is the flyer plate dynamic bend angle.

Equations 1, 2, 3, 4, 5, and 6, as well as an understanding of the metal physical-mechanical properties, are the basis for most models developed for explosive bonding. These models are discussed below in general terms, beginning with a description of jetting phenomena, followed by a description of bonding and the methods used to define explosive parameter boundaries that will produce acceptable bonds.

Jet Formation

During World War II, it was discovered that a hollowed explosive charge lined with metal could be used to produce a high-energy jet to perforate armor plate. Several investigators (Ref 21, 22, 23) have described the limiting conditions for the formation of jets in high-velocity collisions. Walsh *et al.* (Ref 22) indicated that a critical impact angle must be exceeded before jetting will occur. On the other hand, Cowan and Holtzman (Ref 23) indicated that for subsonic collisions, the elastic strength of the metal must be exceeded before jetting will occur. In both cases, jetting is described

by a hydrodynamic flow of the metal surfaces. Walsh *et al.* (Ref 22) presented equations based on this principle and the "equations of state," which enable a calculation of the critical angle for jetting.

Kowalick and Hay (Ref 24) reported an experimental technique to evaluate both the critical angle for jetting and the morphological changes in explosion bonds resulting from changes in collision angle. The experimental setup consisted of the normal flyer plate arrangement used in the parallel gap technique, but with the base plate replaced by a half cylinder. Each bonding trial produced continuously changing flayer plate collision angles that resulted in surface deformation and bond morphology variations. This analysis expands upon the work of previous researchers by evaluating the geometry of fluid flow, jetting, and their effects on bond morphology.

Laminar fluid flow (low collision-point velocity and low Reynolds numbers) was correlated with direct bonding and a very flat bond interface. Turbulent fluid flow was separated into two regimes:

- AT INTERMEDIATE COLLISION-POINT VELOCITIES, THE FLOW WAS DESCRIBED BY VORTICE FORMATION INTO A VON KARMAN VORTEX STREET AND THE PRODUCTION OF A WAVY BOND INTERFACE
- AT HIGH COLLISION-POINT VELOCITIES, THE FLOW WAS DISTURBED BY A DISORDERING OF THE JET WAKE, WHICH LED TO A MOLTEN LAYER BOND INTERFACE.

Selection of Bonding Parameters

The preceding discussion introduced the primary variables used to predict explosive bonding parameters. The following four conditions are used to define a window of acceptable bonding parameters:

- CRITICAL ANGLE FOR JETTING (REF 25)
- CRITICAL FLOW TRANSITION VELOCITY (REF 23, 24)
- MINIMUM FLYER PLATE IMPACT FOR JETTING, BASED ON ANALYSIS OF THE STRESS REQUIRED TO CAUSE FLOW
- MAXIMUM FLYER PLATE IMPACT FOR THE LIMITATION OF WELD DEFECTS, BASED ON JET ENTRAPMENT (REF 23)

The critical angle for jetting is used to define the upper boundary for collision-point velocities. The lower limit in collision velocity is determined by the transition from laminar to turbulent flow, where turbulent flow is preferred (Ref 23). The other two limiting conditions are specified by using the physical and mechanical properties of the material to determine the maximum amount of energy required to either produce hydrodynamic flow (that is, overcome a critical shear stress) or avoid extensive melting. Once the correct set of explosive parameters has been determined by utilizing either predictive models or an empirical approach, the production of explosively welded metal is a relatively simple task.

References cited in this section

1. B. CROSSLAND, *EXPLOSIVE WELDING OF METALS AND ITS APPLICATION,* CLARENDON PRESS, 1982
9. R.W. GURNEY, "THE INITIAL VELOCITIES OF FRAGMENTS FROM BOMBS, SHELLS, AND GRENADES," REPORT 405, BALLISTIC RESEARCH LABORATORY, 1943
10. S. CARPENTER, R.H. WITTMAN, AND R.J. CARLSON, RELATIONSHIPS OF EXPLOSIVE WELDING PARAMETERS TO MATERIAL PROPERTIES AND GEOMETRY FACTORS, *PROC. FIRST INT. CONF. OF THE CENTER FOR HIGH ENERGY FORMING,* UNIVERSITY OF DENVER, JUNE 1967, P 124
13. J. GROSCHOPP, V. HEYNE, AND B. HOFFMAN, EXPLOSIVELY CLAD TITANIUM STEEL COMPOSITE, *WELD. INT.,* NO. 9, 1987, P 879-883
20. J.E. KENNEDY, EXPLOSIVE OUTPUT FOR DRIVING METAL, *PROC. BEHAVIOR AND UTILIZATION OF EXPLOSIVES IN ENGINEERING DESIGN CONF.,* L. DAVIDSON, J.E. KENNEDY,

AND F. COFFEY, ED., ASME (NEW MEXICO SECTION), 1972, P 109
21. G. BIRKOFF, D.P. MACDOUGALL, E.M. PUGH, AND SIR G. TAYLOR, *J. APPL. PHYS.,* VOL 19, 1948, P 563
22. J.M. WALSH, R.G. SHEFFLER, AND F.J. WILLIG, *J. APPL. PHYS.,* VOL 24 (NO. 3), 1953 P 349
23. G.R. COWAN AND A.H. HOLTZMAN, *J. APPL. PHYS.,* VOL 34 (NO. 4), 1963, P 928
24. J.F. KOWALICK AND D.R. HAY, *METALL. TRANS.,* VOL 2, 1971, P 1953
25. R.H. WITTMAN, "AN EXPERIMENTALLY VERIFIED MODEL PREDICTING IMPACT WELDING PARAMETERS," THESIS, UNIVERSITY OF DENVER, 1975

Fundamentals of Explosion Welding

R. Alan Patterson, Los Alamos National Laboratory

Bond Morphology and Properties

In the discussion of the Kowalick and Hay (Ref 24) experiment, reference was made to three types of bond morphologies:

- LAMINAR INTERFACE, OR FLAT BOND
- WAVY INTERFACE
- MOLTEN LAYER INTERFACE

A typical clad trilayer that contains a mixture of wavy interface morphology (with melt pockets decorating each wave crest) and laminar interface (with fairly uniform melt entrapment) is shown in Fig. 3.

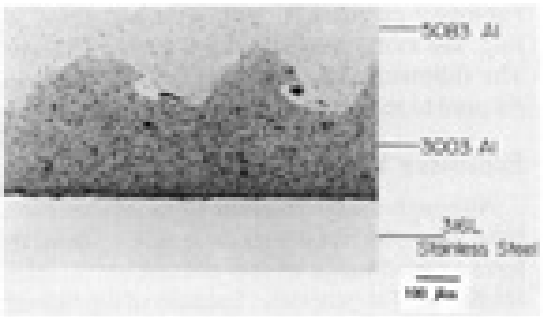

FIG. 3 CROSS-SECTIONAL PHOTOMICROGRAPH OF A 5083 AL-3003 AL-TYPE 316L STAINLESS STEEL CLAD TRI-LAYER TAKEN PARALLEL TO THE BONDING DIRECTION. NOTICE THE WELL-DEVELOPED WAVE MORPHOLOGY AND DARK ETCHING MELT POCKETS IN THE ALUMINUM-TO-ALUMINUM BOND. IN ADDITION, THE LAMINAR ALUMINUM-TO-STAINLESS STEEL BOND INTERFACE INDICATES INTERMITTENT SECOND-PHASE ENTRAPMENT.

Wave Formation. Abrahamson (Ref 26) examined the formation of surface deformations that were caused by a traveling jet using projectiles shot at thin metal targets, resulting in oblique impact. Two primary conclusions drawn from this work were that the target metal deformation was a horizontal shear in the direction of impact and that the resultant wave peaks were deformed in such a pattern that they turned back in the direction opposite to impact. When the angle of impact was varied, two important responses occurred. First, below an impact angle of 5°, no wave formation was observed. Second, as the angle of impact was increased above 5°, the amplitude and wavelength increased.

The proposed mechanism for wave formation in high-velocity oblique impacts was based on subsonic or supersonic metal flow. Good bonding was achieved with low-impact angles, because of a need to prevent jet instabilities.

Baharani *et al.* (Ref 27) and Hunt (Ref 28) drew upon this hypothesis and proposed a physical description of wave formation in explosive bonding, which included the following sequence of events:

- *STEP 1:* IMPACT PRODUCES SHEAR DEFORMATION IN THE STATIONARY BASE PLATE, WHICH RESULTS IN A DEPRESSION
- *STEP 2:* CONSERVATION OF VOLUME CRITERIA PRODUCES AN UPHEAVAL OF METAL (A HUMP) AHEAD OF THE IMPACT APEX
- *STEP 3:* HUMP INTERFERES WITH THE JET FLOW AND PRODUCES AN EDDY IN THE JET, WHICH TRAPS MOLTEN MATERIAL IN THE REAR VORTEX
- *STEP 4:* ALLOWING FOR COLLISION-POINT VELOCITY CAUSES A FORWARD DEFORMATION OF THE HUMP AND FURTHER JET TURBULENCE, WHICH AGAIN CAUSES JET ENTRAPMENT IN THE FRONT VORTEX
- *STEP 5:* PROCESS IS THEN REPEATED, STARTING WITH STEP 1

Lucas *et al.* (Ref 29) reported that when the flyer and base plates of a copper-to-copper explosive bond were electroplated with 1 μm (40 μin.) of nickel, the wave vortices were found to contain free nickel, which was assumed to result from jet entrapment caused by turbulence. Trueb (Ref 30, 31) indicated a similar phenomenon when bonding titanium to steel. The vortices appeared to contain a mix of both metals arranged in an eddy pattern that was "frozen in" by rapid solidification.

Bond Microstructure. Microstructural analysis of explosive bond zones has revealed several interesting results. Numerous metallurgical reactions have been reported:

- EXTENSIVE GRAIN ELONGATION IN THE DIRECTION OF BONDING, WITHIN SEVERAL HUNDREDS OF MICRONS OF THE BOND INTERFACE, AND MEASURED ELONGATIONS OF SEVERAL THOUSAND PERCENT (REF 31)
- RESIDUAL DISLOCATION DENSITIES ON THE ORDER OF $10^{11}/CM^2$ NEAR THE BOND INTERFACE (REF 31)
- MICROTWINNING HAS BEEN OBSERVED (REF 31, 32) IN LOW STACKING FAULT ENERGY METALS (FOR EXAMPLE, COPPER)
- RECRYSTALLIZATION AND RECOVERY HAVE BEEN OBSERVED IN BANDS ON BOTH SIDES OF HIGH-DISLOCATION-DENSITY REGIONS (REF 29)
- VERY LITTLE DIFFUSION OCCURS ACROSS THE BOND INTERFACE (REF 29)

These observations support the hypothesis that says that wave formation is a result of extreme metal deformation and that bonding is a result of solid-state processes with very little diffusion.

However, Hammerschmidt and Kreye (Ref 33) have presented an alternative mechanism for bonding based on the formation of a submicroscopic layer of molten metal, rather than solid-state bonding. Their investigation revealed that in bonds between copper and aluminum, a layer up to 5 μm (200 μin.) wide was obviously molten and resolidified as a fine-grained equiaxed structure. This conclusion raises several questions as to the appropriateness of dissimilar metal systems for explosive bonding, especially when brittle intermetallic compounds can result. Similarly, jet entrapment must be considered deleterious with respect to intermetallic compound formation. Therefore, close attention must be given to the metallurgy of the dissimilar metal couple and bonding parameters when high-strength explosive bonds are required.

The preceding discussion indicates that a very complex combination of metallurgical reactions occur during explosive bonding. These effects have been researched to a limited degree and the general results appear to be understood, but controversy over actual bonding mechanisms still remains.

Oberg *et al.* (Ref 34) used the Miedema model for alloy formation to explain the metallurgical details of explosion bonds. In their analysis, they suggest strong correlations between interfacial bond strength and the formation energies between binary alloy constituents. If the theoretical formation energy, γ_{AB}, is high, then a low bonding success would be predicted, indicating that low formation energies are preferred. Also, if the chemical portion of the interfacial free energy, g_{AB}^{chem},

deviates from theoretical mixing in a negative fashion, then the formation of intermetallic compounds would be favored. Positive deviations indicate the tendency for solid-solution formation and strong bonding.

Explosive bond strength is often negatively affected by the formation of intermetallics and defects that result from rapid quenching of melt regions. Counteracting these effects is the localized hardening and high dislocation densities that occur in a heavily worked structure adjacent to the bond interface. In fact, bonds produced by extreme metal deformations that result in a wavy interface have been reported to be optimum, with respect to strength (Ref 35).

Bond Strength Determination. Bond strength can be measured by a variety of mechanical testing techniques, including the simple bend and shear test identified in the ANSI/ASTM standard specifications A 263, A 264, A 265, and B 432. A special "top hat" tensile test has also been utilized (Fig. 4).

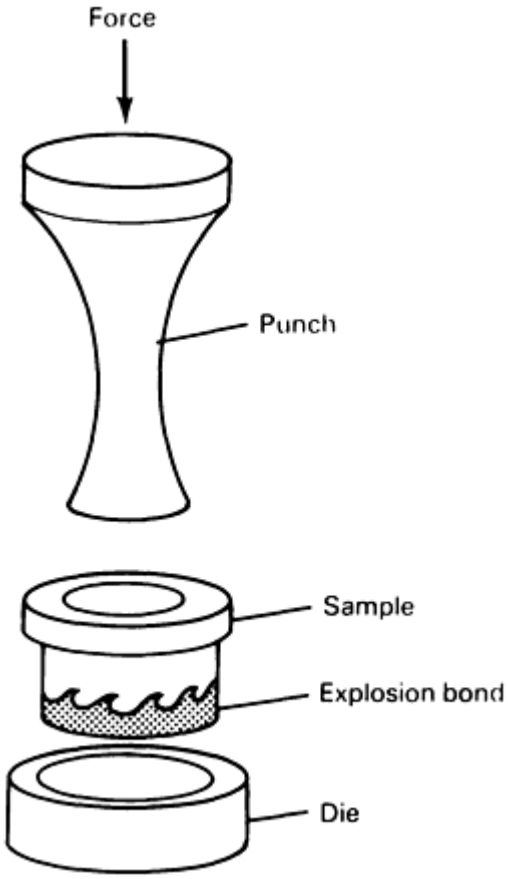

FIG. 4 SCHEMATIC SHOWING TOP-HAT TENSILE TEST APPARATUS AND RELATION OF SAMPLE TO PUNCH-DIE TOOLING COMPONENTS

Figure 5 is a cross-sectional view of a copper-to-stainless steel clad tensile specimen, where failure occurred in the copper base metal (Ref 13). Note the wavy bond interface to the right of the necked fracture zone (Fig. 5a) and the normal dimpled appearance of the copper fracture surface as revealed by the scanning electron microscope (Fig. 5b). This particular sample agrees with accepted bond strength trends, because the well-developed wavy bond performs better than the weaker of the two parent materials.

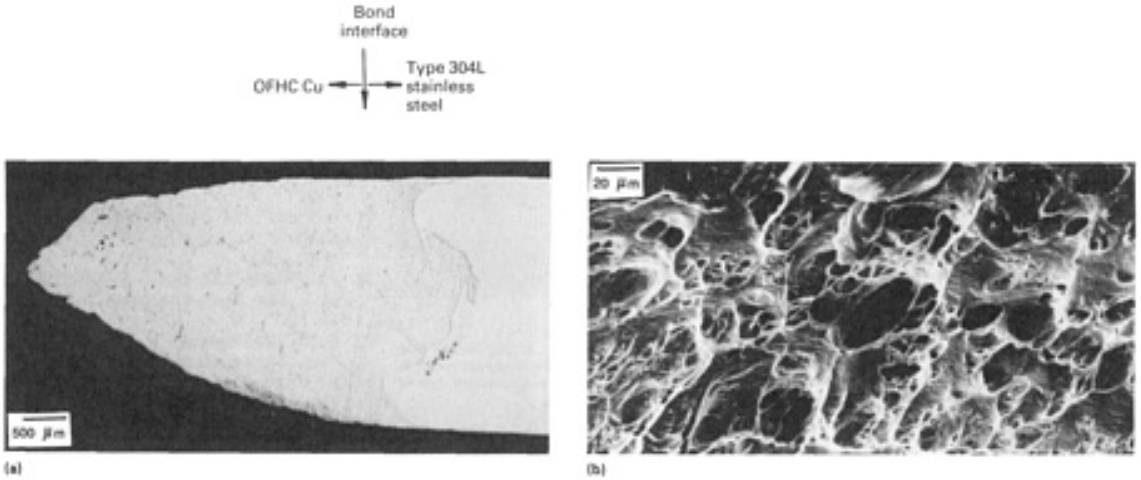

FIG. 5 FAILURE IN COPPER-TO-STAINLESS STEEL TENSILE SPECIMEN THAT WAS EXPLOSION WELDED. (A) PHOTOMICROGRAPH OF FAILED SPECIMEN SHOWING WAVY BOND LINE AND DUCTILE FRACTURE IN PARENT COPPER METAL. 16×. (B) SCANNING ELECTRON FRACTOGRAPH OF COPPER FRACTURE SHOWING DIMPLED APPEARANCE OF TYPICAL DUCTILE TENSILE OVERLOAD FAILURE. 395×

Figure 6, on the other hand, shows scanning electron fractographs of a tensile specimen that failed in the explosive bond interface. This tri-layer specimen (a bond between 5083 A 1-5052 Al-type 304L stainless steel) illustrates one important fact: wavy interface morphologies are not always the strongest (Ref 13). The principal fracture occurred in the wavy interface between the 5083 Al and the 5052 Al layers, whereas the laminar interface between the 5052 Al and the type 304L stainless steel exhibited an incipient fracture appearance with unconnected cracking along the interface. This is a direct contradiction to the previous statements that a wavy bond increases strength and further illustrates the need to evaluate each clad specimen using destructive test methods.

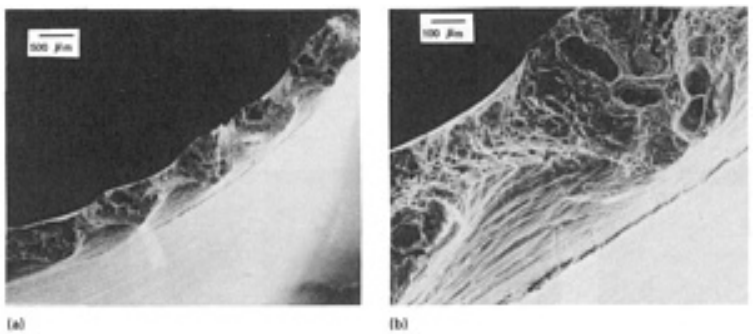

FIG. 6 SCANNING ELECTRON FRACTOGRAPHS OF FRACTURE SPECIMEN FROM CLAD TRILAYER OF 5083 AL-5052 AL-TYPE 304L STAINLESS STEEL. (A) FRACTURE OF 5083 AL-5052 AL BOND INTERFACE, SHOWING DUCTILE TENSILE OVERLOAD CHARACTERISTICS AND INCIPIENT FRACTURE IN THE 5052 AL-TYPE 304L STAINLESS STEEL BOND. 65×. (B) LOW-MAGNIFICATION VIEW OF INTERFACE SHOWING THAT FRACTURE PATH FOLLOWS WAVE MORPHOLOGY. 16×

References cited in this section

13. J. GROSCHOPP, V. HEYNE, AND B. HOFFMAN, EXPLOSIVELY CLAD TITANIUM STEEL COMPOSITE, *WELD. INT.,* NO. 9, 1987, P 879-883

24. J.F. KOWALICK AND D.R. HAY, *METALL. TRANS.,* VOL 2, 1971, P 1953

26. G.R. ABRAHAMSON, *J. APPL. PHYS.*, VOL 34 (NO. 4), 1961, P 519
27. A.S. BAHARANI, T.J. BLACK, AND B. CROSSLAND, *PROC. R. SOC. (LONDON) A*, VOL 296, 1967, P 123
28. J.N. HUNT, *PHILOS. MAG.*, VOL 18, 1968, P 669
29. W. LUCAS, J.D. WILLIAMS, AND B. CROSSLAND, SOME METALLURGICAL OBSERVATIONS ON EXPLOSIVE WELDING, *PROC. SECOND INT. CONF. OF CENTER FOR HIGH ENERGY FORMING*, 1969, P 8.1.1
30. L.F. TRUEB, THE MICROSTRUCTURE OF EXPLOSION-BONDED METALS, *TRANS. AIME*, VOL 242, 1966, P 1057
31. L.F. TRUEB, *J. APPL. PHYS.*, VOL 34 (NO. 4), 1968, P 928
32. M.P. BONDAR AND V.M. OGOLIKHIN, PLASTIC DEFORMATION IN BONDING ZONE UNDER EXPLOSIVE WELDING AND ITS ROLE IN BONDING FORMATION, *J. PHYS.*, C5 (NO. 8-46), 1985, P C5-379 TO C5-384
33. M. HAMMERSCHMIDT AND H. KREYE, MICROSTRUCTURE AND BONDING MECHANISMS IN EXPLOSION WELDING, *SHOCK WAVES AND HIGH-STRAIN RATE PHENOMENA IN METALS*, M.A. MEYERS AND L.E. MURR, ED., PLENUM PRESS, 1981, P 961
34. A. OBERG, N. MARTENSSON, AND J.A. SCHWEITZ, FUNDAMENTAL ASPECTS OF FORMATION AND STABILITY OF EXPLOSIVE WELDS, *METALL. TRANS. A*, VOL 16, MAY 1985, P 841-852
35. H.K. BALAKRISCHMA, V.C. VENTATESH, AND P.K. PHILIP, INFLUENCE OF COLLISION PARAMETERS ON THE MORPHOLOGY OF INTERFACE IN ALUMINUM-STEEL EXPLOSION WELDS, *SHOCK WAVES AND HIGH-STRAIN RATE PHENOMENA IN METALS*, M.A. MEYERS AND L.E. MURR, ED., PLENUM PRESS, 1981, P 975

Future Outlook

In this discussion, brief descriptions of bonding techniques and bonding parameters have been correlated with current experimental results. As shown, attempts to gain a fundamental understanding of explosive bonding involve a large number of highly interactive variables (for example, explosive detonation dynamics, dynamic materials deformation, and solid-state bonding). May of these interactive variables have been defined in this discussion, and the references cited offer additional detail and explanation. However, much of the available knowledge relating to explosive bonding is still based on experimental observation. Models and predictive algorithms have been published, but to a large extent bonding is still considered an art practiced by a rather select group of experienced technologists. Insight into the practice of producing explosive bonds and an introduction to the specific applications is available in the articles "Explosion Welding" and "Procedure Development and Practice Considerations for Explosion Welding," in this Volume.

Fundamentals of Explosion Welding

R. Alan Patterson, Los Alamos National Laboratory

References

1. B. CROSSLAND, *EXPLOSIVE WELDING OF METALS AND ITS APPLICATION*, CLARENDON PRESS, 1982
2. L.R. CARL, *MET. PROGR.*, VOL 46, 1944, P 102
3. V. PHILIPCHUK AND F. LEROY BOIS, U.S. PATENT 3,024,526, 1962

4. V.D. LINSE, R.H. WITTMAN, AND R.J. CARLSON, "EXPLOSION BONDING," REPORT X68-10247, BATTELLE MEMORIAL INSTITUTE
5. J.S. RINEHART AND J. PEARSON, *EXPLOSIVE WORKING OF METALS,* PERGAMON PRESS, 1963
6. M.C. NOLAND, H.M. GADBERRY, J.B. LOSER, AND E.C. SNEEGAS, "HIGH VELOCITY METAL-WORKING: A SURVEY," NASA REPORT N67-26560, SP 5062, NASA, 1967
7. A.A. EZRA, *PRINCIPLES AND PRACTICE OF EXPLOSIVE METAL WORKING,* INDUSTRIAL NEWSPAPERS LIMITED, JOHN ADAMS HOUSE, LONDON, 1973
8. T.Z. BLAZYNSKI, *EXPLOSIVE WELDING, FORMING AND COMPACTION,* APPLIED SCIENCE PUBLISHERS, U.K., 1983
9. R.W. GURNEY, "THE INITIAL VELOCITIES OF FRAGMENTS FROM BOMBS, SHELLS, AND GRENADES," REPORT 405, BALLISTIC RESEARCH LABORATORY, 1943
10. S. CARPENTER, R.H. WITTMAN, AND R.J. CARLSON, RELATIONSHIPS OF EXPLOSIVE WELDING PARAMETERS TO MATERIAL PROPERTIES AND GEOMETRY FACTORS, *PROC. FIRST INT. CONF. OF THE CENTER FOR HIGH ENERGY FORMING,* UNIVERSITY OF DENVER, JUNE 1967, P 124
11. B. CROSSLAND AND J.D. WILLIAMS, *METALL. REV.,* NO. 144, 1970
12. H. WOLF, ON THE ENERGY BALANCE OF PLANE AND CYLINDRICAL EXPLOSIVE CLADDING, *PROC. INT. SYMPOSIUM ON INTENSE DYNAMIC LOADING AND ITS EFFECTS,* PERGAMON PRESS, 1988
13. J. GROSCHOPP, V. HEYNE, AND B. HOFFMAN, EXPLOSIVELY CLAD TITANIUM STEEL COMPOSITE, *WELD. INT.,* NO. 9, 1987, P 879-883
14. R.A. PATTERSON, EXPLOSION BONDING: ALUMINUM-MAGNESIUM ALLOYS BONDED TO AUSTENITIC STAINLESS STEEL, *HIGH ENERGY RATE FABRICATION,* M.A. MEYERS AND J.W. SCHROEDER, ED., VOL 70, ASME PRESSURE VESSELS AND PIPING DIV., 1982, P 15-27
15. M.D. CHADWICK, D. HOWD, G. WILDSMITH, AND J.H. CAIRNS, *BR. WELD. J.,* VOL 15, 1968, P 480
16. H. WOLF AND M. KOLBE, EXPERIMENTAL METHODS FOR DETERMINING THE OPTIMUM PROCESS CHARACTERISTICS FOR FLAT EXPLOSIVE CLADDING, *WELD. INT.,* VOL 4 (NO. 7), 1990, P 535-538
17. A.A. POPOFF AND H. CASEY, TECHNICAL PAPER AD 77-36, SME, 1977
18. V.G. PETUSHKOV, THE STRENGTH OF BODIES STRIKING ONE ANOTHER DURING EXPLOSIVE WELDING, *AUTO. WELD.,* VOL 39 (NO. 10), 1986, P 35-38
19. V.M. KUDINOV AND I.D. ZAKHAZENKO, CRITERIA FOR SELECTING THE PARAMETERS OF EXPLOSIVE WELDING, *WELD. PROD.,* VOL 32 (NO. 9), 1985, P 3-6
20. J.E. KENNEDY, EXPLOSIVE OUTPUT FOR DRIVING METAL, *PROC. BEHAVIOR AND UTILIZATION OF EXPLOSIVES IN ENGINEERING DESIGN CONF.,* L. DAVIDSON, J.E. KENNEDY, AND F. COFFEY, ED., ASME (NEW MEXICO SECTION), 1972, P 109
21. G. BIRKOFF, D.P. MACDOUGALL, E.M. PUGH, AND SIR G. TAYLOR, *J. APPL. PHYS.,* VOL 19, 1948, P 563
22. J.M. WALSH, R.G. SHEFFLER, AND F.J. WILLIG, *J. APPL. PHYS.,* VOL 24 (NO. 3), 1953 P 349
23. G.R. COWAN AND A.H. HOLTZMAN, *J. APPL. PHYS.,* VOL 34 (NO. 4), 1963, P 928
24. J.F. KOWALICK AND D.R. HAY, *METALL. TRANS.,* VOL 2, 1971, P 1953
25. R.H. WITTMAN, "AN EXPERIMENTALLY VERIFIED MODEL PREDICTING IMPACT WELDING PARAMETERS," THESIS, UNIVERSITY OF DENVER, 1975
26. G.R. ABRAHAMSON, *J. APPL. PHYS.,* VOL 34 (NO. 4), 1961, P 519
27. A.S. BAHARANI, T.J. BLACK, AND B. CROSSLAND, *PROC. R. SOC. (LONDON) A,* VOL 296, 1967, P 123
28. J.N. HUNT, *PHILOS. MAG.,* VOL 18, 1968, P 669
29. W. LUCAS, J.D. WILLIAMS, AND B. CROSSLAND, SOME METALLURGICAL OBSERVATIONS

ON EXPLOSIVE WELDING, *PROC. SECOND INT. CONF. OF CENTER FOR HIGH ENERGY FORMING,* 1969, P 8.1.1

30. L.F. TRUEB, THE MICROSTRUCTURE OF EXPLOSION-BONDED METALS, *TRANS. AIME,* VOL 242, 1966, P 1057
31. L.F. TRUEB, *J. APPL. PHYS.,* VOL 34 (NO. 4), 1968, P 928
32. M.P. BONDAR AND V.M. OGOLIKHIN, PLASTIC DEFORMATION IN BONDING ZONE UNDER EXPLOSIVE WELDING AND ITS ROLE IN BONDING FORMATION, *J. PHYS.,* C5 (NO. 8-46), 1985, P C5-379 TO C5-384
33. M. HAMMERSCHMIDT AND H. KREYE, MICROSTRUCTURE AND BONDING MECHANISMS IN EXPLOSION WELDING, *SHOCK WAVES AND HIGH-STRAIN RATE PHENOMENA IN METALS,* M.A. MEYERS AND L.E. MURR, ED., PLENUM PRESS, 1981, P 961
34. A. OBERG, N. MARTENSSON, AND J.A. SCHWEITZ, FUNDAMENTAL ASPECTS OF FORMATION AND STABILITY OF EXPLOSIVE WELDS, *METALL. TRANS. A,* VOL 16, MAY 1985, P 841-852
35. H.K. BALAKRISCHMA, V.C. VENTATESH, AND P.K. PHILIP, INFLUENCE OF COLLISION PARAMETERS ON THE MORPHOLOGY OF INTERFACE IN ALUMINUM-STEEL EXPLOSION WELDS, *SHOCK WAVES AND HIGH-STRAIN RATE PHENOMENA IN METALS,* M.A. MEYERS AND L.E. MURR, ED., PLENUM PRESS, 1981, P 975

Mechanical Properties of Soft-Interlayer Solid-State Welds

R.S. Rosen, Lawrence Livermore National Laboratory; M.E. Kassner, Oregon State University

Introduction

THE UTILIZATION OF METAL INTERLAYERS for solid-state welding can be an appropriate joining method when brittle intermetallic compound formation, differential thermal contraction during cooling, or oxide dissociation and dissolution temperature preclude the use of conventional methods, such as fusion welding, brazing, and direct solid-state welding of the base metals. An interlayer can have the form of a foil (Ref 1, 2, 3, 4, 5, 6, 7, 8), or it can be applied to one or both of the base-metal surfaces by various coating methods, such as electrodeposition (Ref 1, 2, 4, 9), plasma spraying (Ref 2), or vapor-deposition methods.

Methods that utilize coated interlayers require a two-step joining procedure (coating and welding), as opposed to joints fabricated with foil interlayers, which may only require a single solid-state welding step. However, methods that utilize coated interlayers have the advantage of not requiring solid-state welding at the interface of the interlayer and base metal, as necessitated by the use of foil interlayers. The solid-state welding of some foil interlayer and base-metal combinations may require high temperatures and/or pressures, because of the high dissociation temperatures of the surface oxides, which may preclude or restrict their use (Ref 10, 11, 12).

Various base-metal combinations have been solid-state welded using coated silver as the interlayer metal. The principal advantage of silver as an interlayer for solid-state welding is that high-strength joints can be fabricated at relatively low temperature (473 to 673 K) and pressures (100 to 200 MPa, or 15 to 30 ksi), because of the low dissociation temperature (<460 K) for silver oxide. Depending on the strength of the base metals and the method (hydrostatic or uniaxial stress) by which pressure is applied to the silver/silver interface, the joining process may result in variable deformation in the base metals. Because some plasticity in the base metal may be important to assist with intimate atomic contact across the interface, "soft" interlayers are often preferred.

Silver interlayers for solid-state welding are usually applied to one or both of the base metals by deposition using either electrodeposition (Ref 1, 13, 14, 15, 16, 17) or vacuum-coating methods. The vacuum-coating methods have included electron-beam evaporation (Ref 18), hot-hollow cathode (HHC) evaporation (Ref 15, 19, 20, 21, 22, 23, 24, 25, 26), ion-plating using sputtering (Ref 27, 28, 29), and planar-magnetron (PM) sputtering (Ref 30, 31, 32, 33).

Prior to deposition, the surface oxide layer may require removal from the base metal in order to achieve adequate adhesion of the silver. The surface oxide layer is usually removed by chemical- or sputter-etching methods. One

advantage of vacuum coating over electrodeposition is the ability to sputter-etch the base metal *in situ.* This permits silver deposition with minimal recontamination of the oxygen on the base-metal surface (Ref 34).

Soft-interlayer solid-state welds that join stronger base metals have unique mechanical properties that are of fundamental interest and may be of critical importance to designers. These assemblies can be subjected to various applied stress states, such as tensile, where the load is applied perpendicular to the interlayer/base-metal interfaces, or shear, where the applied shear stress lies within the plane of the interlayer. Of course, in application, the interlayer may be subjected to a combination of applied tensile and shear loads. This is important because these types of welds are, mechanically, quite anisotropic. This includes the case where interlayers may be subjected to residual stresses from fabrication. The loading may be continually increasing, as with a conventional tensile test, or static, as with creep tests. Again, these behaviors are quite different.

Additionally, some interlayer/base-metal interfaces have been shown to be susceptible to stress-corrosion cracking when exposed to critical environments (Ref 35). The mechanical properties of soft-interlayer solid-state welds and the implications of these behaviors to service stress states and environments are discussed in this article. It should be noted that although silver interlayers are emphasized, primarily because of their selection by previous researchers and industrial fabricators, the described trends appear to be completely consistent with joints that use other soft-interlayer metals.

References

1. J.T. NIEMANN, R.P. SOPHER, AND P.J. RIEPPEL, DIFFUSION BONDING BELOW 1000 °F, *WELD. J.*, VOL 37, 1958, P 337S-342S
2. I.M. BARTA, LOW TEMPERATURE DIFFUSION BONDING OF ALUMINUM ALLOYS, *WELD. J.*, VOL 43, 1964, P 241S-247S
3. D. HAUSER, P.A. KAMMER, AND J.H. DEDRICK, SOLID-STATE WELDING OF ALUMINUM, *WELD. J.*, VOL 46, 1967, P 11S-22S
4. P.A. KAMMER, R.E. MONROE, AND D.C. MARTIN, FURTHER STUDIES OF DIFFUSION BONDING BELOW 1000 °F, *WELD. J.*, VOL 48, 1969, P 116S-124S
5. Y. IINO AND N. TAGAUCHI, INTERDIFFUSING METALS LAYER TECHNIQUE OF CERAMIC-METAL BONDING, *J. MATER. SCI. LETT.*, VOL 7 (NO. 9), 1988, P 981-982
6. A. URENA, J.M.G.D. SALAZAR, AND J. QUINONES, DIFFUSION BONDING OF ALUMINA TO STEEL USING SOFT COPPER INTERLAYER, *J. MATER. SCI.*, VOL 27, 1992, P 599-606
7. T. YAMADA K, YOKOI, AND A. KOHNO, EFFECT OF RESIDUAL STRESS ON THE STRENGTH OF ALUMINA-STEEL JOINT WITH AL-SI INTERLAYER, *J. MATER. SCI.*, VOL 25, 1990, P 2188-2192
8. M.G. NICHOLAS AND R.M. CRISPIN, DIFFUSION BONDING STAINLESS STEEL TO ALUMINA USING ALUMINUM INTERLAYERS, *J. MATER. SCI.*, VOL 17, 1982, P 3347-3360
9. C.L. CLINE, AN ANALYTICAL AND EXPERIMENTAL STUDY OF DIFFUSION BONDING, *WELD. J.*, VOL 45, 1966, P 481S-489S
10. A.T. D'ANNESSA, THE SOLID-STATE BONDING OF REFRACTORY METALS, *WELD. J.*, VOL 43, 1964, P 232S-240S
11. M.G. NICHOLAS AND R.M. CRISPIN, DIFFUSION BONDING CERAMICS WITH DUCTILE METAL INTERLAYERS, *PROC. INT. DIFFUSION BONDING* (CRANFIELD, U.K.), 1987, P 173-182
12. B. DERBY, ZIRCONIA/METAL DIFFUSION BONDS, *PROC. INT. CONF. DIFFUSION BONDING* (CRANFIELD, U.K.), 1987, P 195-201
13. R.A. MORLEY AND J. CARUSO, THE DIFFUSION WELDING OF 390 ALUMINUM ALLOY HYDRAULIC VALVE BODIES, *WELD. J.*, VOL 59 (NO. 8), 1980, P 29-34
14. C.H. CRANE, D.T. LOVELL, W.A. BAGINSKY, AND M.G. OLSEN, DIFFUSION WELDING OF DISSIMILAR METALS, *WELD. J.*, VOL 46, 1967, P 23S-31S
15. M. O'BRIEN, C.R. RICE, AND D.L. OLSON, HIGH STRENGTH DIFFUSION WELDING OF SILVER COATED BASE METALS, *WELD. J.*, VOL 55 (NO. 1), 1976, P 25-27
16. J.W. DINI, W.K. KELLEY, W.C. COWDEN, AND E.M. LOPEZ, USE OF ELECTRODEPOSITED

SILVER AS AN AID IN DIFFUSION WELDING, *WELD. J.*, VOL 63 (NO. 1), 1983, P 26S-34S

17. R.S. ROSEN, "TIME-DEPENDENT FAILURE OF SILVER INTERLAYER WELDS," PH.D.THESIS, UNIVERSITY OF CALIFORNIA, DAVIS, 1990
18. J.L. KNOWLES AND T.H. HAZLETT, HIGH-STRENGTH LOW-TEMPERATURE BONDING OF BERYLLIUM AND OTHER METALS, *WELD. J.*, VOL 49 (NO. 7), 1970, P 301S-310S
19. P.S. MCLEOD AND G. MAH, THE EFFECT OF SUBSTRATE BIAS VOLTAGE ON THE BONDING OF EVAPORATED SILVER COATINGS, *J. VAC. SCI. TECHNOL.*, VOL 11 (NO. 1), 1974, P 119-121
20. G. MAH, P.S. MCLEOD, AND D.G. WILLIAMS, CHARACTERIZATION OF SILVER COATINGS DEPOSITED FROM A HOLLOW CATHODE SOURCE, *J. VAC. SCI. TECHNOL.*, VOL 11 (NO. 4), 1974, P 663-665
21. D.G. WILLIAMS, VACUUM COATING WITH A HOLLOW CATHODE SOURCE, *J. VAC. SCI. TECHNOL.*, VOL 11 (NO. 1), 1974, P 374-377
22. E.R. NAIMON, D. VIGIL, J.P. VILLEGAS, AND L. WILLIAMS, ADHESION STUDY OF SILVER FILMS DEPOSITED FROM A HOY HOLLOW-CATHODE SOURCE, *J. VAC. SCI TECHNOL.*, VOL 13 (NO. 6), 1976, P 1131-1135
23. E.R. NAIMON, J.H. DOYLE, C.R. RICE, D. VIGIL, AND D.R. WALMSLEY, DIFFUSION WELDING OF ALUMINUM TO STAINLESS STEEL, *WELD. J.*, VOL 60 (NO. 1), 1981, P 17-20
24. D.T. LARSON AND H.L. DRAPER, CHARACTERIZATION OF THE BE-AG INTERFACIAL REGION OF SILVER FILMS DEPOSITED ONTO BERYLLIUM USING A HOT HOLLOW CATHODE DISCHARGE, *THIN SOLID FILMS*, VOL 107, 1983, P 327-334
25. R.S. ROSEN, D.R. WALMSLEY, AND Z.A. MUNIR, THE PROPERTIES OF SILVER-AIDED DIFFUSION WELDS BETWEEN URANIUM AND STAINLESS STEEL, *WELD. J.*, VOL 65 (NO. 4), 1986, P 83S-92S
26. J.W. ELMER, M.E. KASSNER, AND R.S. ROSEN, THE BEHAVIOR OF SILVER-AIDED DIFFUSION-WELDED JOINTS UNDER TENSILE AND TORSIONAL LOADS, *WELD. J.*, VOL 67 (NO. 7), 1988, P 157S-162S
27. J. HARVEY, P.G. PATRIDGE, AND A.M. LURSHEY, FACTORS AFFECTING THE SHEAR STRENGTH OF SOLID STATE DIFFUSION BONDS BETWEEN SILVER-COATED CLAD AL-ZN-MG ALLOY (ALUMINUM ALLOY 70100, *MATER. SCI. ENG.*, VOL 79, 1986, P 191-199
28. P.G. PARTRIDGE AND D.V. DUNFORD, ON THE TESTING OF DIFFUSION-BONDED OVERLAP JOINTS BETWEEN CLAD AL-ZN-MG ALLOY (7010) SHEET, *J. MATER. SCI.* VOL 22, 1987 P 1597-1608
29. D.V. DUNFORD AND P.G. PARTRIDGE, THE PEEL STRENGTHS OF DIFFUSION BONDED. JOINTS BETWEEN CLAD AL-ALLOY SHEETS, *J. MATER. SCI.*, VOL 22, 1987, P 1790-1798
30. R.S. ROSEN AND M.E. KASSNER, DIFFUSION WELDING OF SILVER INTERLAYERS COATED ONTO BASE METALS BY PLANAR-MAGNETRON SPUTTERING, *J. VAC. SCI. TECHNOL. A*, VOL 8 (NO. 1), 1900, P 19-29
31. M.E. KASSNER, R.S. ROSEN, G.A. HENSHALL, AND W.E. KING, DELAYED FAILURE OF SILVER AIDED DIFFUSION WELDS BETWEEN STEEL, *PROC. 2ND INT. CONF. BRAZING, HIGH TEMPERATURE BRAZING, AND DIFFUSION WELDING*, GERMAN WELDING SOCIETY, 1989, P 47-52
32. M.E. KASSNER, R.S. ROSEN, G.A. HENSHALL, AND K.D. CHALLENGER, TIME-DEPENDENT FAILURE OF SILVER-INTERLAYER DIFFUSION WELDS BETWEEN ELASTICALLY-DEFORMING BASE METALS, *SCR. METALL. MATER.*, VOL 24, 1990, P 587-592
33. M.E. KASSNER, R.S. ROSEN, AND G.A. HENSHALL, DELAYED MECHANICAL FAILURE OF SILVER-INTERLAYER DIFFUSION BONDS, *METALL. TRANS. A*, VOL 21, 1990, P 3085-3100
34. P.G. PARTRIDGE AND J. HARVEY, "PROCESS FOR THE DIFFUSION BONDING OF ALUMINUM MATERIALS," U.K. PATENT APPLICATIONS GB 2117691 A, 1983
35. R.S. ROSEN, S. BEITSCHER, AND M.E. KASSNER, STRESS CORROSION CRACKING OF URANIUM-SILVER INTERFACES IN SILVER-AIDED DIFFUSION WELDS, *INT. CONF.*

ENVIRONMENT-INDUCED CRACKING OF METALS, VOL 10, NACE, 1989, P 429-433

Mechanical Properties of Soft-Interlayer Solid-State Welds

R.S. Rosen, Lawrence Livermore National Laboratory; M.E. Kassner, Oregon State University

Microstructure of Interlayer Welds

As-Deposited Coatings. A fine-grained (typically <1 μm, or 40 μin., in diameter) columnar structure commonly forms in coatings that are vacuum deposited onto low-temperature substrates (~0.3 T_m) using a low working-gas pressure (~1 Pa, or 1.5×10^{-4} psi). This type of structure has been reported previously in silver coatings fabricated for interlayer welding by HHC evaporation (Ref 20) and PM sputter deposition (Ref 30). The columns are perpendicular to the base-metal surface, and the axes of the columns are oriented perpendicular to a close-packed crystallographic direction. The columnar grains resulting from the PM sputter-deposition of silver often contain a high density of growth twins that are approximately 15 nm (0.6 μin.) thick (Ref 30).

Solid-State-Welded Interlayers. Figure 1 shows a solid-state-welded silver interlayers that is 150 μm (6 mils) thick between steel base metals after solid-state welding at 673 K (Ref 17). The silver interlayer typically consists of two types of structures: nonrecrystallized silver that has retained the columnar grains and fine microtwins of the as-deposited coating and silver that has recrystallized into large grains (>1 mm, or 0.04 in., in diameter) containing a high density of annealing twins. The solid-state-welded interfaces are generally free of any large voids, or nonbonded regions. In the case of rough base-metal surfaces, large voids can remain along the silver/silver interface.

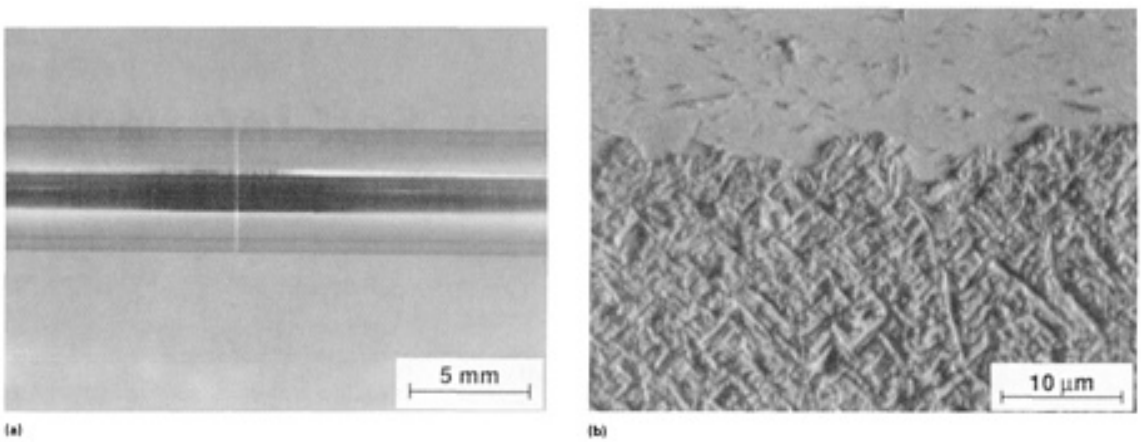

FIG. 1 OPTICAL PHOTOGRAPH SHOWING A 150 μM (6 MIL) THICK SILVER INTERLAYER JOINING BASE METALS (A) AND OPTICAL MICROGRAPH OF THE SOLID-STATE-INTERFACE (B). SOURCE: REF 17

References cited in this section

17. R.S. ROSEN, "TIME-DEPENDENT FAILURE OF SILVER INTERLAYER WELDS," PH.D.THESIS, UNIVERSITY OF CALIFORNIA, DAVIS, 1990
20. G. MAH, P.S. MCLEOD, AND D.G. WILLIAMS, CHARACTERIZATION OF SILVER COATINGS DEPOSITED FROM A HOLLOW CATHODE SOURCE, *J. VAC. SCI. TECHNOL.*, VOL 11 (NO. 4), 1974, P 663-665
30. R.S. ROSEN AND M.E. KASSNER, DIFFUSION WELDING OF SILVER INTERLAYERS COATED ONTO BASE METALS BY PLANAR-MAGNETRON SPUTTERING, *J. VAC. SCI. TECHNOL. A,* VOL 8 (NO. 1), 1900, P 19-29

R.S. Rosen, Lawrence Livermore National Laboratory; M.E. Kassner, Oregon State University

Tensile Loading of Soft-Interlayer Welds

Despite the relatively low strength of the interlayer material, it has long been known that thin (1 μm to 1 mm, or 40 μin. to 0.04 in.) interlayer welds or brazes between stronger base material can have ultimate tensile strengths (UTS) that are much higher than that of the bulk interlayer material (Ref 36, 37). For example, the UTS of silver-interlayer solid-state welds between maraging steel base metals has been reported to be nearly 800 MPa (120 ksi) (Ref 32, 3), whereas the UTS of the bulk silver is only about 250 MPa (35 ksi) (Ref 38). The high tensile strength of the joint is due to the mechanical constraint provided by the stronger base metal, which restricts transverse contraction of the interlayer (Ref 36, 37, 39, 40, 41, 42, 43, 44, 45). The constraint establishes radial (triaxial) stresses that inhibit the development of shear stresses within the joint, thereby decreasing the effective, or von Mises, stress in the interlayer. This inhibits the plastic flow that leads to ductile fracture.

Effect of Interlayer Thickness on Stress. The degree of mechanical constraint in the soft interlayer and the joint strength tend to increase with a decreasing thickness-to-diameter ratio, *t*/*d*, of the interlayer (Ref 36, 37, 39 , 40, 41, 42, 44, 46, 47, 48, 49, 50, 51, 52, 53). Figure 2 summarizes the effect of *t*/*d* on the UTS of solid-state-welded silver interlayers fabricated using PM sputter deposition (Ref 30) and electrodeposition (Ref 15), compared with Ag-4Pd brazed interlayers (no hardening, because of the addition of palladium) (Ref 41). The UTS is shown to increase with a decreasing *t*/*d* ratio to about 0.002, below which only small strength increases can be expected. The higher UTS of sputter-deposited silver interlayer, compared with those utilizing electrodeposition or brazed-silver alloy, are discussed in the section "Effect of Interlayer Fabrication Method" in this article.

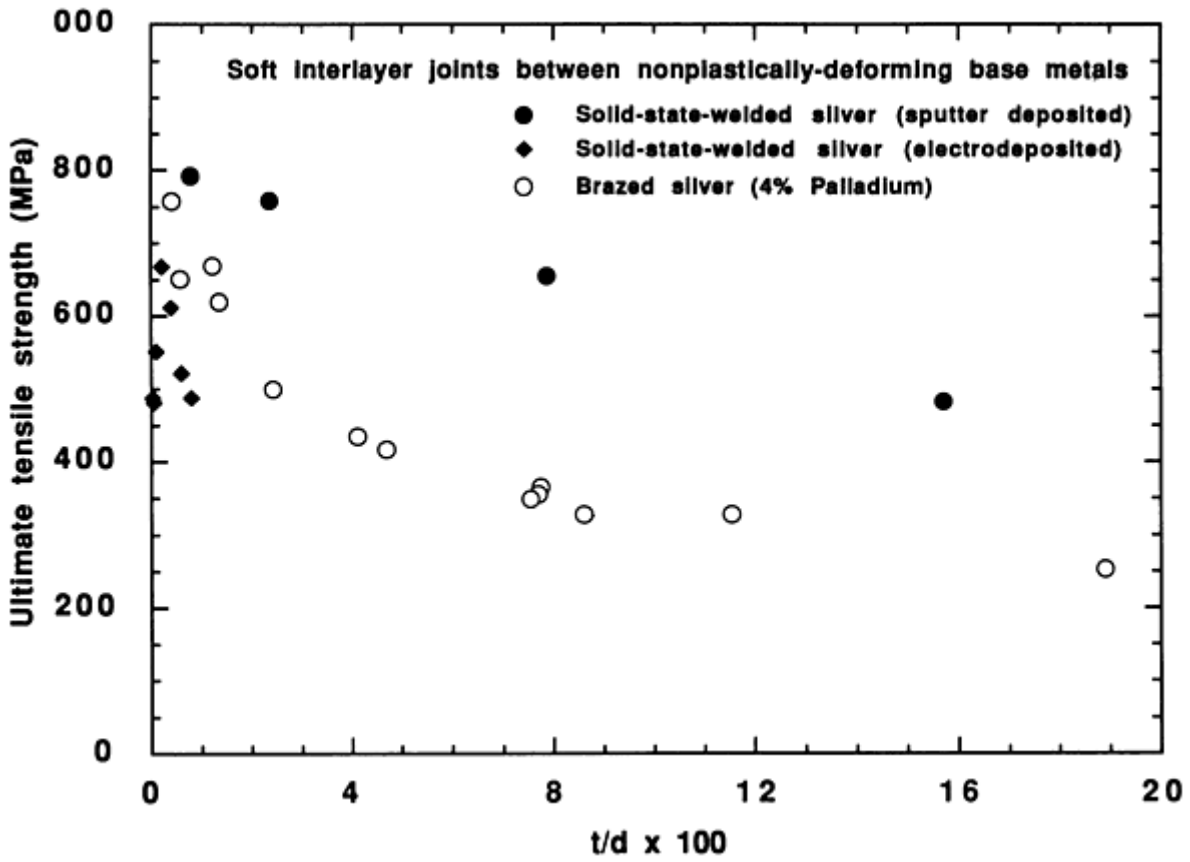

FIG. 2 EFFECT OF INTERLAYER THICKNESS TENSILE STRENGTH OF SOLID-STATE-WELDED SILVER INTERLAYERS FABRICATED USING PM SPUTTER DEPOSITION AND ELECTRODEPOSITION, COMPARED WITH

Although the tensile behavior of interlayer joints has been reasonably well understood qualitatively, particularly for thick interlayers, quantitative prediction has only recently been accomplished with finite-element method (FEM) codes. Orowan (Ref 36, 37) was perhaps the first to derive an analytical expression for the radial (constraining) stress within the interlayer. It was proposed that

$$s_r = \frac{s_y}{t}\left(\frac{d}{2} - r\right) \qquad \textbf{(EQ 1)}$$

where σ_r is the radial stress, t is the thickness, d is the diameter, r is the radius, and σ_y is the yield stress of the interlayer. This equation was originally derived by assuming ideal plastic behavior (that is, no strain hardening) of the interlayer and uniform plastic in the interlayer. Analytical attempts to account for strain hardening within the interlayer have led to modifications of Eq 1 that have, experimentally at least, provided reasonable correlation with upper bounds for UTS of soft-interlayer joints (Ref 41, 43, 48, 49).

More recently, FEM analyses (REf 53, 54) reveal significant deviation from q 1. Figure 3(a) illustrates the effect of *t*/*d* on th radial stress distribution at the center plane for silver interlayer welds between nonplastically deformation base metals at a fixed applied tensile stress. These were determined from a FEM analysis that included the observed strain hardening of the interlayer metal and are plotted along with results predicted by Eq 1. This comparison shows that for large *t*/*d* ratios ("thick" interlayers), Eq 1 predicts qualitatively correct behavior for the radial stress distribution. However, for small *t*/*d* ratios ("thin" interlayers), the FEM results indicate a relatively uniform and substantially lower stress distribution over most of the central portion of the interlayer than predicted by Eq 1. This is partly due to the simplifying assumptions in Eq 1, particularly that of a radially uniform strain state.

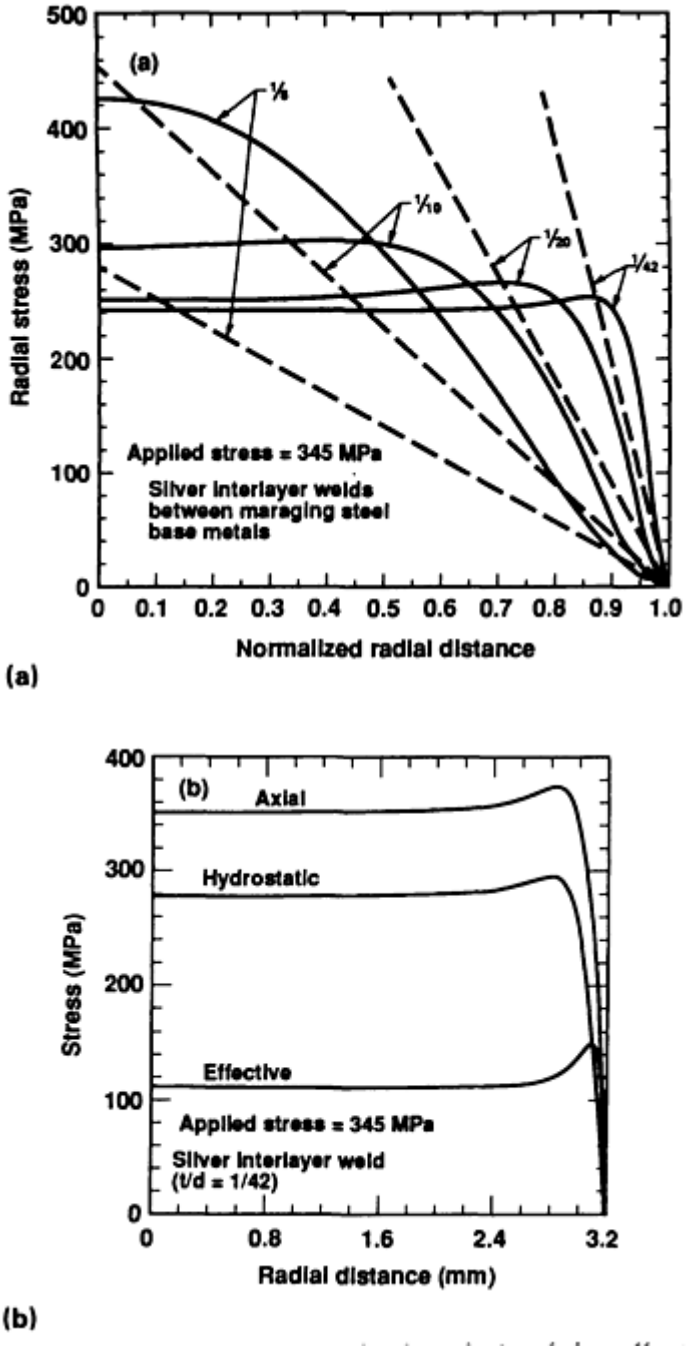

FIG. 3 FINITE-ELEMENT METHOD ANALYSIS OF THE EFFECT OF *T*/*D* ON THE RADIAL STRESS DISTRIBUTION AT THE CENTER PLANE FOR SILVER INTERLAYER WELDS BETWEEN NONPLASTICALLY DEFORMING BASE METALS AT A FIXED APPLIED TENSILE STRESS. (A) PREDICTIONS OF EQ 1 ARE GIVEN BY DASHED LINES. (B) THE STRESS STATE IN A STRAIN-HARDENING SILVER INTERLAYER AT A SMALL FIXED *T*/*D* RATIO

This effect is further illustrated in Fig. 3(b), which shows the stress state in a strain-hardening silver interlayer at a small fixed *t*/*d* ratio. Although it is not shown, the effective (von Mises) stress, which measures the tendency to plastically deform, decreases with decreasing *t*/*d*, down to approximately 0.025. Hence, a decreasing *t*/*d* ratio increases the mechanical constraint in the interlayer such that a larger applied stress is needed to produce a given amount of plastic strain in the interlayer. Interestingly, and in contrast with Eq 1, the effective stress does not appear to substantially changes with decreases in *t*/*d* that are less than approximately 0.025 (Ref 54). This is qualitatively consistent with the extrapolations of the solid-state-welded silver data in Fig. 2 (but not the braze data).

Early investigators (Ref 15, 40, 44, 45, 55) believed that this phenomenon was due only to discontinuities (solidification shrinkage cavities, surface flatness, and such) in very thin brazes and solid-state welds. Recent results (Ref 17, 30) of

solid-state-welded interlayers fabricated using sputter-deposited silver onto lapped base metals (surface roughness of 0.03 μm, or 1.2 μin.) indicate that the modest increase (or plateau) in strength occurs even in the absence of preexisting voids that are common in thin brazes.

Interlayer Strain. Associated with the increased UTS of the constrained interlayers, compared to the UTS of the bulk or unconstrained interlayer metal, is a decreased plastic strain-to-failure, ε_f, of the interlayer. Early results (Ref 42) found that for brazed-silver interlayers joining elastically deforming base metals with a t/d ratio of 0.016, the ε_f is about 0.01. The results from specimens fabricated using solid-state welding of PM sputter-deposited silver interlayers, in which the base metals did not plastically deform, indicated plastic strains of only abut 0.001 for a comparable t/d ratio of 0.024 (Ref 17, 33). The reason for the disparity is not clear. Perhaps the relatively large number of interfaces in the PM sputter-deposited interlayers in the PM sputter-deposited interlayers (Ref 30, 33) led to higher cavity-nucleation rates. Other works do not appear to have made reliable attempts at determining the plastic strain-to-failure value. It should be emphasized that despite the relatively low plastic strain-to-failure, the fracture surface is that of a classic, ductile, microvoid-coalescence type of failure (Ref 33).

Time-Dependent Failure. It has been observed that at stresses substantially less than the UTS, delayed or time-dependent ductile fracture may occur. For at least the case of silver interlayers, decreases in the applied stress are associated with increased times-to-rupture,f as indicated in Fig. 4. This figure shows that decreasing the t/d ratio (to about 0.02) and/or improving the base-metal surface finish (lapping) results in longer tensile creep-rupture times. Time-dependent failure is believed to be a consequence of cavity nucleation and/or growth (Ref 33), as is observed in short-term tensile tests that determine the UTS. For solid-state welds in which two coatings are joined, nucleation occurs principally at the silver/silver welded interface or the base-metal/silver coated interface. The cavities appear to nucleate as a consequence of time-dependent plasticity within the interlayer. The cavities expand in diameter and final interlinkage and failure appears to occur at relatively low "macroscopic" strains within the interlayer (for example, $\varepsilon_f < 10^{-3}$).

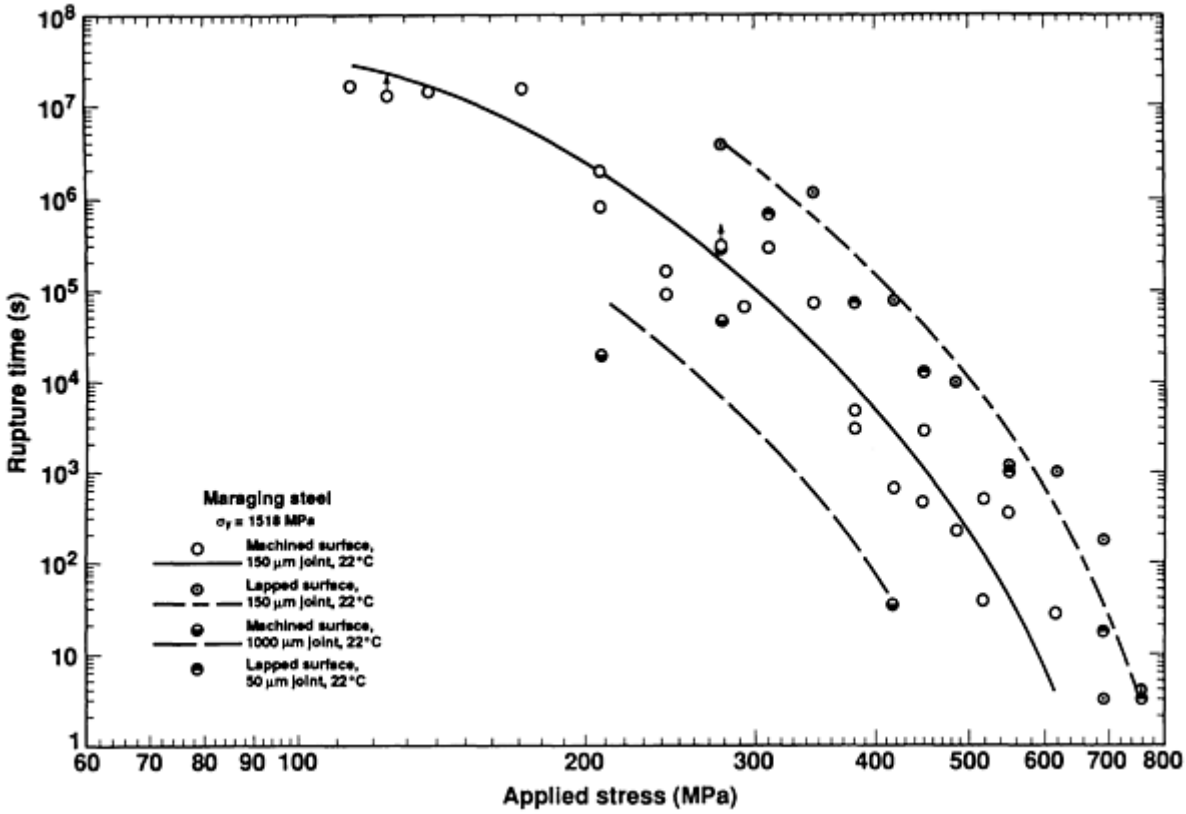

FIG. 4 EFFECT OF INTERLAYER THICKNESS AND BASE-METAL SURFACE FINISH ON CREEP RUPTURE OF SOLID-STATE-WELDED SILVER JOINTS BETWEEN NONPLASTICALLY DEFORMING BASE METALS

Figure 5 shows scanning electron micrographs of a solid-state-welded silver interlayer joining steel base metals, loaded at the relatively low stress level of 207 MPa (30 ksi) (albeit, for a substantial fraction of the expected creep-rupture time).

Some of the larger cavities consist of clusters of smaller (<0.5 μm, or 200 μin., in diameter) microvoids. A typical fracture surface of a creep-rupture specimen is illustrated in Fig. 6. Naturally, the fracture surfaces appear identical to those of the short-term tests in which UTS values were measured. It should be emphasized that, consistent with Fig. 2, as the interlayer metal strength increases, the strength of the weld joint increases. Similarly, as the interlayer metal creep resistance increases, the rupture times of the weld joint should increase. Hence, as reported for gold-nickel high-strength/creep-resistant interlayer brazes (Ref 56), time-dependent failure has not been observed over periods of about 1 y. Also, it appears that for silver brazes (Ref 33), time-dependent failure is observed, but at increasingly longer times at decreasing stresses, perhaps because of differences in substructures, compared with solid-state-welded silver interlayers.

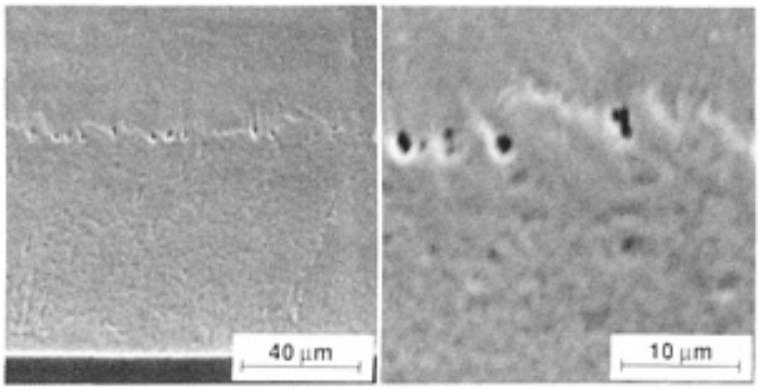

FIG. 5 SCANNING ELECTRON MICROGRAPHS SHOWING SOLID-STATE-WELDED SILVER INTERLAYER JOINING NONPLASTICALLY DEFORMING BASE METALS, LOADED AT 207 MPA (30 KSI) (~$\frac{1}{3}$ ULTIMATE TENSILE STRENGTH) FOR A SUBSTANTIAL FRACTION OF THE EXPECTED CREEP-RUPTURE TIME

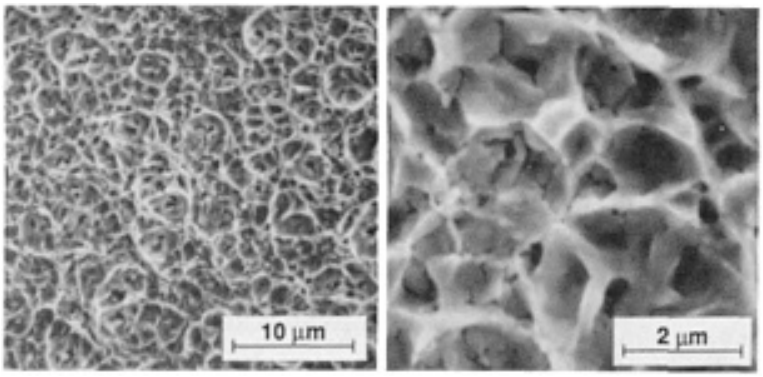

FIG. 6 SOLID-STATE-WELDED SILVER INTERLAYER FRACTURE SURFACE BETWEEN LAPPED MARAGING STEEL BASE METALS

A nucleation-based theory has been proposed to explain the low plastic strain, time-dependent failures of soft-interlayer solid-state welds in which preexisting voids do not exist, and the base metal does not plastically deform (Ref 17, 33, 57). Plastic deformation of the interlayer, acting under the effective stress, causes cavity nucleation by dislocation pile-ups at interfaces. Nucleation continues with further creep of the interlayer, until the concentration of nuclei is sufficiently high to lead to instability in the material between the cavities. Coalescence by interlinkage or by uniform wall expansion ("growth") then occurs. The point of instability between two small nanometer-sized cavities or nuclei separated by a few diameters or so may lead to subsequent rapid nucleation between the cavities, resulting in the formation of a single, larger cavity (as shown in Fig. 5). This process is repeated and eventually leads to the onset of final rupture, and gives the appearance of a classic, ductile, microvoid-coalescence type of fracture.

In contrast with this nucleation-based theory, other investigators (Ref 42) suggest that the macroscopic strain-to-failure is determined by the details of the uniform cavity expansion (growth). Here, once the cavities expand and come in proximity

to other cavities, coalescence and ductile fracture occurs. In a creep experiment, according to the usual cavity-growth models, the rupture time is determined by the cavity growth rate or the speed of the expanding cavity wall. In the absence of vacancy-controlled growth, this speed is controlled by the macroscopic plastic strain rate. Therefore, the static (or creep) and dynamic (or quasi-static) failures of the thin interlayer welds should be, according to cavity-growth-based theories, related to the macroscopic strain in the interlayer. If steady-state plasticity is achieved throughout the silver interlayer material surrounding the cavities, then unstable cavity wall expansion may occur. However, since the macroscopic strains-to-failure are small ($\varepsilon_f < 10^{-3}$, the time or strain up to the onset of final catastrophic failure (where a large ductile-dimple fracture surface begins to form) is not easily explained by a cavity-growth model in a strain-hardening material.

The silver-plasticity concept for rationalizing creep rupture is consistent with the temperature dependence of the time-to-rupture. The activation energy for the creep of silver at ambient and near-ambient temperatures for various substructures falls within the range of 50 to 71 kJ/mole (Ref 38, 58). The activation energy for the creep rupture of the solid-state-welded silver joints of Fig. 2, equal to 65 kJ/mole (Ref 33), falls within the range of activation energies for silver plasticity.

Effect of Base-Metal Properties. Time-dependent tensile fracture can be dramatically accelerated if there is creep, or time-dependent plasticity, of the base materials. Figure 7 shows the creep-rupture behavior of solid-state-welded silver interlayers (t/d = 0.024) joining one of two different strengths of type 304 stainless steel base metals: annealed or cold-worked (Ref 17, 33). Interestingly, these base metals undergo time-dependent plasticity, or creep, at ambient temperatures at stresses that are less than the conventionally yield stress of the metal. Although the accumulated plastic strain in the creeping stainless steel is only about 0.001 to 0.01 at low stress levels, this nonetheless induces concomitant plastic strain within the interlayer that exceeds that which would occur within the interlayer in the absence of base-metal plasticity, resulting in shorter creep-rupture times. This behavior is consistent with previous reported data for creep ruptures of interlayers that join plastically deforming base metals (Ref 25, 26, 59, 60).

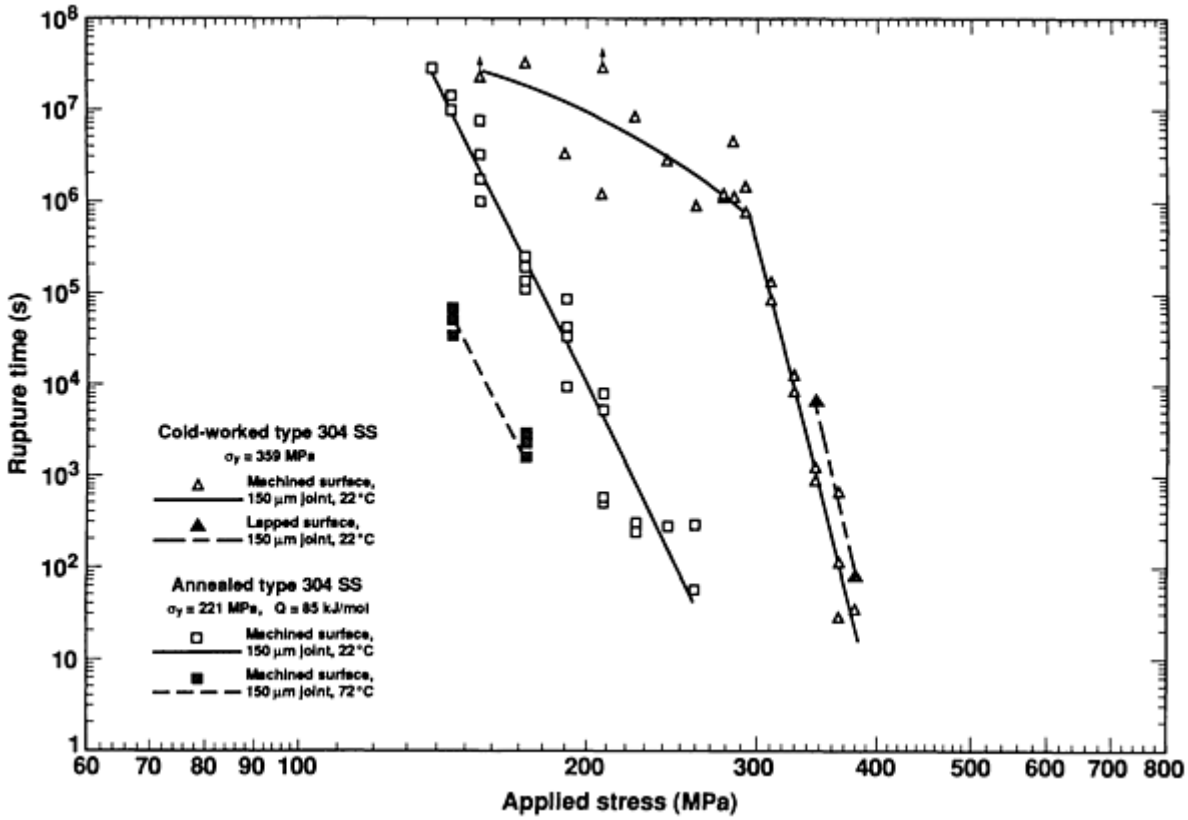

FIG. 7 CREEP-RUPTURE BEHAVIOR OF SOLID-STATE-WELDED SILVER INTERLAYERS (*T/D* = 0.024) JOINING ONE OF TWO DIFFERENT STRENGTHS OF TYPE 304 STAINLESS STEEL BASE METALS (ANNEALED OR COLD-WORKED), BOTH OF WHICH UNDERGO TIME-DEPENDENT PLASTICITY OR CREEP AT AMBIENT TEMPERATURES AT STRESSES LESS THAN THE CONVENTIONAL YIELD STRESS OF THE METAL

Finite-element analyses have confirmed that plasticity in the base metal allows the interlayer to plastically deform to a much greater extent than if the base metal deforms only elastically (Ref 54). This observation is important, because these small levels of time-dependent plasticity (0.001 to 0.01) are often observed, over time, in other structural metals and alloys at ambient temperature at stresses significantly below the conventionally define yield stress. With an increase in test temperature, the stainless steel base-metal creep rate significantly increases and rupture times decrease. The activation energies for the creep rupture of silver interlayers between stainless steel base metals and for plastic flow in stainless steel are comparable, further suggesting that the temperature dependence of creep rupture is determined by creep plasticity in the stainless steel base metal. The transition from base-metal to interlayer-controlled creep rupture occurs at the "knee" of the cold-worked stainless steel data plot, at stress levels below which base-metal creep is negligible.

Figure 7 also shows the effect of base-metal surface finish, which is eventually coated, on the creep-rupture behavior of joints utilizing cold-worked type 304 stainless steel. Lapped cold-worked stainless steel base-metal specimens have longer rupture times than those of machined cold-worked stainless steel, as was the case with the maraging steel specimens. However, the increase in creep-rupture times of specimens utilizing lapped versus machined plastic base metals is only a factor of 5, which is considerably less than the increase of approximately 50 for specimens utilizing lapped versus machined elastic base metals. The difference between the increases in creep-rupture times for lapped plastic versus lapped elastic base-metal specimens may be due to the difference in failure processes. For the case of a plastic base metal, the strain in the silver is externally and uniformly imposed by the deformation of the base metal. For elastic base metals, plasticity is caused by the effective stress within the interlayer. It is believed that the heterogeneities along the solid-state-welded silver interface caused during the joining of the comparatively rough machined surfaces could result in regions that may be more resistant to plasticity than other regions. The heterogeneities at the solid-state-welded silver interface may be less significant in increasing the nucleation and coalescence rate of cavities in specimens utilizing plastic base metals than those utilizing elastic base metals, where the strain is indigenous to the interlayer, rather than being imposed by base-metal deformation.

Effect of Interlayer Fabrication Method. In general, the tensile strengths of PM sputter-deposited silver joints between various base metals have been reported to be equal to or greater than those utilizing other silver-coating methods and similar solid-state-welding parameters. For elastic base metals with lapped surfaces, PM sputter-deposited silver joint tensile strengths (Ref 30) of 758 and 793 MPa (110 and 115 ksi) using interlayers that are 150 and 50 μm (6 and 2 units thick, respectively, are comparable with HHC-deposited silver joints (758 MPa, or 110 ksi, using 10 μm, or 0.4 mil, thick interlayers) and greater than those of electrodeposited silver joints (669 MPa, or 97 ksi, using 25 μm, or 1 mil, thick interlayers) (Ref 15). However, the tensile strength values for silver-interlayer welds fabricated using these other two coating methods are achieved with considerably thinner interlayers, which have the advantage of greater plastic constraint produced by the base metals. For type 304 stainless steel (plastically deforming) base metals with machined surfaces and 150 μm (6 mil) thick joints, PM sputter-deposited silver joint tensile strengths (Ref 30) of 304 MPa (44 ksi) ($\sigma_{y,SS}$ = 221 MPa, or 32 ksi) and 400 MPa (60 ksi) ($\sigma_{y,SS}$ = 359 MPa, or 52 ksi) are comparable with electrodeposited silver joint strengths of 321 to 367 MPa (47 to 53 ksi) ($\sigma_{y,SS}$ = 296 MPa, or 43 ksi) (Ref 16). For uranium (plastic) base metals with machined surface, the PM sputter-deposited silver joint tensile strength of 442 MPa (64 ksi) $\sigma_{y,U}$ =242 MPa, or 35 ksi) (Ref 30) exceed electrodeposited silver joint strengths of approximately 255 MPa (37 ksi) (despite the higher base-metal yield stress; $\sigma_{y,U}$ = 345 MPa, or 50 ksi) and HHC-deposited silver joint strengths of 345 to 373 MPa (50 to 54 ksi) (Ref 16, 61). However, the lower joint strength using HHC-deposited silver (Ref 61) may have resulted from a lower solid-state welding pressure (138 MPa, or 20 ksi) and temperature (589 K) than those using PM sputter-deposited silver. The tensile strength of solid-state-welded silver joints between dissimilar metals, such as uranium (σ_y = 345 MPa, or 50 ksi) and type 304 stainless steel (σ_y = 296 MPa, or 45 ksi) fabricated using HHC deposition has been reported to average 442 MPa (64 ksi) (Ref 25). The tensile strength of electrodeposited silver joints between the same uranium and stainless steel base metals that were solid-state welded at the same pressure (207 MPa, or 30 ksi), temperature (873 K), and time (2 h) averaged only 345 MPa (50 ksi) (Ref 17, 30). Therefore, solid-state-welded silver joints fabricated using electrodeposition appear to be weaker than those fabricated using HHC deposition or PM sputter deposition.

Although there is only a limited amount of published test results of interlayer joint strengths fabricated by low-temperature solid-state welding of foils, it appears that interlayer/base-metal adhesion is difficult to achieve at temperatures below approximately 0.7 T_m of the interlayer. Tensile strengths of silver joints between alumina and type 321 stainless steel were reported to be only 40 MPa (5.8 ksi) when solid-state-welding parameters were 1073 K and 50 MPa (7.3 ksi) for 0.5 h (Ref 11). The investigators reported threshold solid-state-welding temperatures below which no measurable bonding was produced for each of the foils utilized (silver, aluminum, copper, and nickel). The threshold temperature to achieve solid-state welding of silver foils to alumina and type 321 stainless steel was reported to be 873 K (0.7 T_m of the silver), considerably higher than the temperature required to achieve solid-state welding of silver to itself (0.35 T_m) (Ref 18). Joint strengths of the previous interlayer fabrication processes were reported to be comparable (40) to 50 MPa, or 5.8 to 7.3 ksi) to those of silver foils (Ref 11). Tensile tests reported for silver-foil interlayers between type

304L stainless steel and Ti-6Al-4V alloy suggest that higher strengths may be achieved with coated interlayers than with foil interlayers (Ref 62). These joints were fabricated by solid-state welding a 125 μm (5 mil) thick silver foil between the base metals at 1153 K (0.94 T_m). The investigators (Ref 62) reported average joint strengths of 280 MPa (40 ksi). For annealed type 304 stainless steel and 150 μm (6 mil) thick joints fabricated using PM sputter deposition, the reported (Ref 30) tensile strength of 304 MPa (44 ksi) is higher, despite the higher base-metal yield stress of Ti-6Al-4V alloy used in the silver-foil study.

References cited in this section

3. D. HAUSER, P.A. KAMMER, AND J.H. DEDRICK, SOLID-STATE WELDING OF ALUMINUM, *WELD. J.*, VOL 46, 1967, P 11S-22S
11. M.G. NICHOLAS AND R.M. CRISPIN, DIFFUSION BONDING CERAMICS WITH DUCTILE METAL INTERLAYERS, *PROC. INT. DIFFUSION BONDING* (CRANFIELD, U.K.), 1987, P 173-182
15. M. O'BRIEN, C.R. RICE, AND D.L. OLSON, HIGH STRENGTH DIFFUSION WELDING OF SILVER COATED BASE METALS, *WELD. J.*, VOL 55 (NO. 1), 1976, P 25-27
16. J.W. DINI, W.K. KELLEY, W.C. COWDEN, AND E.M. LOPEZ, USE OF ELECTRODEPOSITED SILVER AS AN AID IN DIFFUSION WELDING, *WELD. J.*, VOL 63 (NO. 1), 1983, P 26S-34S
17. R.S. ROSEN, "TIME-DEPENDENT FAILURE OF SILVER INTERLAYER WELDS," PH.D.THESIS, UNIVERSITY OF CALIFORNIA, DAVIS, 1990
18. J.L. KNOWLES AND T.H. HAZLETT, HIGH-STRENGTH LOW-TEMPERATURE BONDING OF BERYLLIUM AND OTHER METALS, *WELD. J.*, VOL 49 (NO. 7), 1970, P 301S-310S
25. R.S. ROSEN, D.R. WALMSLEY, AND Z.A. MUNIR, THE PROPERTIES OF SILVER-AIDED DIFFUSION WELDS BETWEEN URANIUM AND STAINLESS STEEL, *WELD. J.*, VOL 65 (NO. 4), 1986, P 83S-92S
26. J.W. ELMER, M.E. KASSNER, AND R.S. ROSEN, THE BEHAVIOR OF SILVER-AIDED DIFFUSION-WELDED JOINTS UNDER TENSILE AND TORSIONAL LOADS, *WELD. J.*, VOL 67 (NO. 7), 1988, P 157S-162S
30. R.S. ROSEN AND M.E. KASSNER, DIFFUSION WELDING OF SILVER INTERLAYERS COATED ONTO BASE METALS BY PLANAR-MAGNETRON SPUTTERING, *J. VAC. SCI. TECHNOL. A*, VOL 8 (NO. 1), 1900, P 19-29
32. M.E. KASSNER, R.S. ROSEN, G.A. HENSHALL, AND K.D. CHALLENGER, TIME-DEPENDENT FAILURE OF SILVER-INTERLAYER DIFFUSION WELDS BETWEEN ELASTICALLY-DEFORMING BASE METALS, *SCR. METALL. MATER.*, VOL 24, 1990, P 587-592
33. M.E. KASSNER, R.S. ROSEN, AND G.A. HENSHALL, DELAYED MECHANICAL FAILURE OF SILVER-INTERLAYER DIFFUSION BONDS, *METALL. TRANS. A*, VOL 21, 1990, P 3085-3100
36. E. OROWAN, FRACTURE AND STRENGTH OF SOLIDS, *REP. PROG. PHYS.*, VOL 12, 1948, P 185-231
37. E. OROWAN, FUNDAMENTALS OF BRITTLE BEHAVIOR OF METALS, *FATIGUE AND FRACTURE OF METALS*, JOHN WILEY & SONS, 1952
38. M.E. KASSNER, THE RATE DEPENDENCE AND MICROSTRUCTURE OF HIGH-PURITY SILVER DEFORMED TO LARGE STRAINS BETWEEN 0.16 AND 0.30 TM, *METALL. TRANS. A*, VOL 20, 1989, P 2001-2010
39. N. BREDZ, INVESTIGATION OF FACTORS DETERMINING THE TENSILE STRENGTH OF BRAZED JOINTS, *WELD. J.*, VOL 33, 1954, P 545S-563S
40. W.G. MOFFATT AND J. WULFF, TENSILE DEFORMATION AND FRACTURE OF BRAZED JOINTS, *WELD. J.*, VOL 42, 1963, P 115S-125S
41. H.J. SAXTON, A.J. WEST, AND C.R. BARRETT, DEFORMATION AND FAILURE OF BRAZED JOINTS--MACROSCOPIC CONSIDERATIONS, *METALL. TRANS.*, VOL 2, 1971, P 999-1007
42. A.J. WEST, H.J. SAXTON, A.S. TETELMAN, AND C.R. BARRETT, DEFORMATION AND FAILURE OF THIN BRAZED JOINTS--MICROSCOPIC CONSIDERATIONS, *METALL. TRANS.*, VOL 2, 1971, P

1009-1017

43. E.P. LAUTENSCHLAGER, B.C. MARKER, B.K. MOORE, AND R. WILDES, STRENGTH MECHANISMS OF DENTAL SOLDER JOINTS, *J. DENT. RES.*, VOL. 53, 1974, P 1361-1367
44. R.A. MUSIN, V.A. ANTSIVEROV, Y.A. BELIKOV, Y.V. LYAMIN, AND A.N. SOLOKOV, THE EFFECTS ON THE STRENGTH OF THE JOINT OF THE THICKNESS OF THE SOFT INTERLAYER IN DIFFUSION WELDING, *AUTO. WELD.,* VOL 32, 1979, P 38-40
45. R.M. TRIMMER AND A.T. KUHN, THE STRENGTH OF SILVER-BRAZED STEEL JOINTS--A REVIEW, *BRAZING SOLDERING,* VOL 2, 1982 P 6-13
46. N. BREDZ AND H. SCHWARTZBART, TRIAXIAL TENSION TESTING AND THE BRITTLE FRACTURE STRENGTH OF METALS, *WELD. J.,* VOL 53 (NO. 12), 1956, P 610S-615S
47. W.G. MOFFATT AND J. WULFF, STRENGTH OF SILVER BRAZED JOINTS IN MILD STEEL, *TRANS. AIME,* VOL 209 (NO. 4), 1957, P 442-445
48. R.Z. SHRON AND O.A. BAKSHI, THE PROBLEMS OF GAUGING THE STRENGTHS OF WELDED JOINTS IN WHICH THERE IS A SOFT INTERLAYER, *WELD. PROD.,* VOL 9, 1962, P 19-23
49. O.A. BAKSHI AND A.A. SHATOV, THE STRESSED STATE IN WELDED JOINTS WITH HARD AND SOFT INTERLAYERS, *WELD PROD.,* VOL 13, 1966, P 13-19
50. V.S. GOLOVCHENKO AND B.A. GOLOBOV, THE USE OF SILVER AS AN INTERMEDIATE LAYER FOR JOINING TITANIUM TO OTHER METALS, *WELD. PROD.,* VOL 18, 1971, P 55-57
51. G.K. KHARCHENKO AND A.I. IGNATENKO, THE STRENGTH OF JOINTS WITH A THIN SOFT INTERLAYER, *AUTO. WELD.,* VOL 21, 1968, P 33-35
52. W.M. LEHER AND H. SCHWARTZBART, STATIC AND FATIGUE STRENGTHS OF METALS SUBJECTED TO TRIAXIAL STRESSES, VOL 60, 1960, P 610-626
53. E.A. ALMOND, D.K. BROWN, G.J. DAVIES, AND A.M. COTTENDED, THEORETICAL AND EXPERIMENTAL INTERLAYED BUTT JOINTS TESTED IN TENSION, *INT. J. MECH. SCI.,* VOL 25 (NO. 3), 1983, P 175-189
54. G.A. HENSHALL, R.S. ROSEN, M.E. KASSNER, AND R.G. WHIRLEY, FINITE ELEMENT ANALYSIS OF INTERLAYER WELDS LOADED IN TENSION, *WELD. J.,* VOL 69 (NO. 9) 1990, P 337S-345S
55. H.J. SAXTON, A.J. WEST, AND C.R. BARRETT, THE EFFECT OF COOLING RATE ON THE STRENGTH OF BRAZED JOINTS, *METALL. TRANS.,* VOL 2, 1971, P 1019-1028
56. M.C. TOLLE AND M.E. KASSNER, TENSILE PROPERTIES OF THIN AU-NI BRAZES BETWEEN STRONG BASE METALS, *SCR. METALL. MATER.,* VOL 26, 1992, P 1281-1284
57. M.E. KASSNER, M.C. TOLLE. R.S. ROSEN, G.A. HENSHALL, AND J.W. ELMER, RECENT ADVANCES IN UNDERSTANDING THE MECHANICAL BEHAVIOR OF CONSTRAINED THIN METALS IN BRAZES AND SOLID-STATE BONDS, *THE METAL SCIENCE OF JOINING,* M.J. CIESLAK, ED., TMS, 1992, P 223-232
58. R.W. LOGAN, R.G. CASTRO, AND A.K. MUKHERJEE, MECHANICAL PROPERTIES OF SILVER AT LOW TEMPERATURES, *SCR. METALL.,* VOL 17, 1983, P 63-66
59. T.J. MOORE AND K.H. HOLKO, SOLID-STATE WELDING OF TD-NICKEL BAR, *WELD. J.,* VOL 49 (NO. 9), 1970, P 395S-409S
60. R.S. ROSEN, "AN INVESTIGATION OF THE PROPERTIES OF A SILVER-AIDED SOLID-STATE BOND BETWEEN URANIUM AND STAINLESS STEEL," REPORT UCRL-53458, LAWRENCE LIVERMORE NATIONAL LABORATORY, 1983
61. E.R. NAIMON, R.G. KURZ, D. VIGIL, AND L. WILLIAMS, "SILVER FILMS FOR SOLID STATE BONDING,"REPORT RFP-3125, ROCKWELL INTERNATIONAL, 1981
62. Z. NISENHOLTZ, J. MIRONI, AND N. NIR, DIFFUSION BONDING OF STAINLESS STEEL 304L TO TI-6AL-4V ALLOY, *PROC. 3RD INT. CONF. ISOSTATIC PRESSING* (LONDON, U.K.), 1986

Shear Loading

Effect of Microstructure. The base metals provide relatively little mechanical constraint of the interlayer during shear loading (shear stress is parallel to the plane of the interlayer) and, therefore, reveals the mechanical behavior of the interlayer material itself. The behavior of the interlayer to shear can be converted to equivalent uniaxial tensile behavior using the von Mises stress and strain criteria, $\bar{s} = t\sqrt{3}$, and $\bar{e} = \gamma\sqrt{3}$, where t and γ are shear stress and strain, respectively. Effective (von Mises) stress-strain ($\bar{s}$ -ε) behavior for a 150 μm (6 mil) thick (t/d = 0.024) silver joint, fabricated using PM sputter-deposition (between maraging steel) and tested in torsion is shown in Fig. 8 (Ref 33), along with the reported results for bulk polycrystalline (annealed) silver (Ref 38). The yield stress ($\bar{e}_p$ = 0.2%) of the solid-state-welded joint is six times greater than the bulk-silver value, presumably because of the much more refined, twinned substructure. The strain-hardening rate, $d\sigma_{eff}/d\varepsilon_{eff}$, at an effective stress of 100 MPa (15 ksi) is over nine times greater than bulk polycrystalline silver (Ref 38). The maximum interlayer stress is attained after a strain of only 0.3 (99% of the maximum value is attained after a strain of only 0.1). Therefore, although the interlayer silver has a higher yield stress and strain hardens at a higher rate, it reaches essentially the same maximum stress as bulk silver at a substantially lower strain.

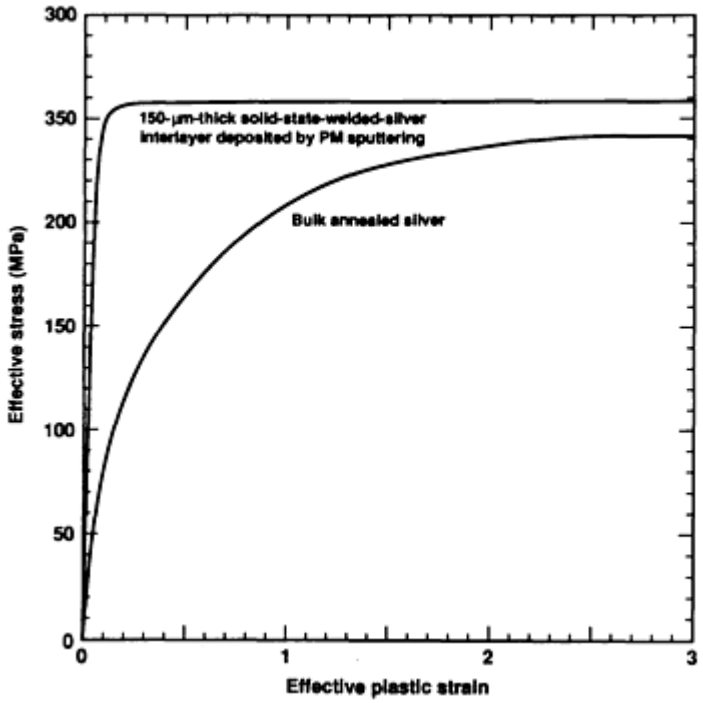

FIG. 8 EFFECTIVE (VON MISES) STRESS-STRAIN BEHAVIOR FOR A 150 μM (6 MIL) THICK SILVER INTERLAYER (*T/D* = 0.024), FABRICATED USING PM SPUTTER DEPOSITION, TESTED IN TORSION, ALONG WITH RESULTS REPORTED FOR BULK POLYCRYSTALLINE (ANNEALED) SILVER

Differences in the maximum (steady-state) stress may result from two factors. First, the interlayer microstructure may not be identical to that of the bulk material. The second explanation is that slip (plasticity) is not isotropic. The plasticity is not isotropic. The plasticity is the result of dislocation activity on limited slip planes with specific Burgers vectors. The shear displacements of individual grains in the interlayer must generally by accommodated by neighboring grains. However, near the base metal, the accommodation is not possible, and additional slip systems may operate in the interlayer grains near the base metal, leading to greater local hardening and higher flow stresses, Torsion tests of solid-state-welded silver interlayers coated by HHC evaporation, using uranium-to-stainless steel base metals (Ref 26), showed similar increases in the yield stress and strain-hardening rates, compared with those of bulk-silver values. However, the steady-state stress of silver joints was approximately 25% higher than that of bulk silver, compared with 105 higher

values for interlayers using PM sputter-deposited silver. One explanation for this difference may be the presence of HHC posits, which may further raise the maximum, or steady-state, stress.

Time-Dependent Failure. Although not shown in Fig. 8, the plastic strain-to-failure in pure shear is very high ($\bar{e}_f$ = 5 to 10) for thin, silver-interlayer specimens, just as for macroscopic, or bulk, silver specimens (Ref 33). This is nearly four orders of magnitude higher than for the case of tension. As previously discussed, cavity nucleation is promoted by the triaxial stress state established with simple uniaxial loading of constrained interlayers. The fact that torque saturates is consistent with the observation that some face-centered cubic (fcc) metals, such as aluminum, copper, and silver (Ref 38), show a saturation in the flow stress. This fact is important because such saturations imply constant torque, or time-dependent, shear-stress failures. Figure 9 shows a comparison between the rupture time versus effective (von Mises) stress behavior in shear (Ref 26) (at torsional stresses less than the maximum of HHC-deposited-silver interlayers), compared with that of tension (Ref 17) (calculated using FEM analyses of PM sputter-deposited silver interlayers). The shear rupture times are longer than tensile rupture times at equivalent uniaxial stresses (calculated using the von Mises relation), consistent with the higher plastic strains-to-failure that are much higher for the torsion specimens ($\bar{e}_f > 5$) than for the tensile specimens ($\varepsilon_f \sim 0.001$). The shorter rupture times for tensile joints are a direct result of the hydrostatic tensile stresses superimposed on the effective stresses caused by the mechanical constraint imposed by the base metal.

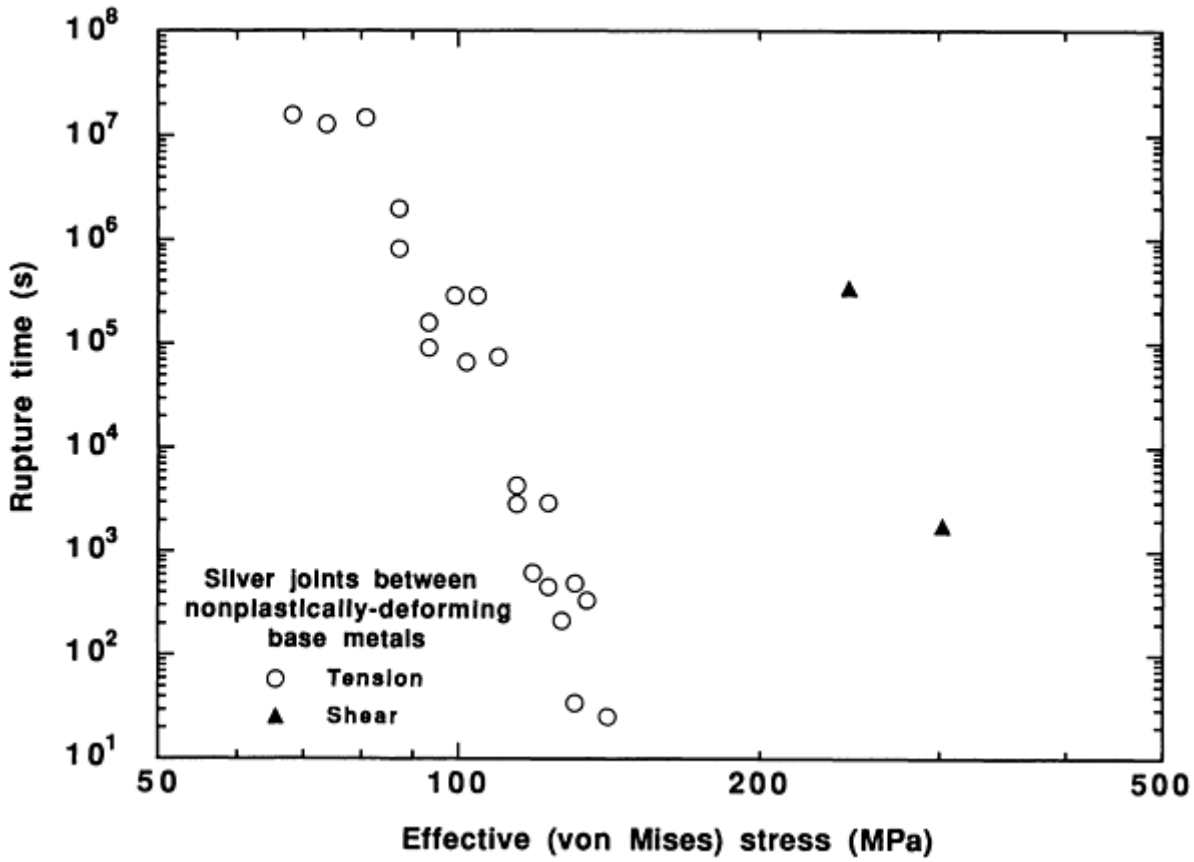

FIG. 9 COMPARISON BETWEEN THE RUPTURE TIME VERSUS EFFECTIVE (VON MISES) STRESS BEHAVIOR IN SHEAR, AT TORSIONAL STRESSES LESS THAN THE MAXIMUM OF HHC-DEPOSITED SILVER INTERLAYERS, COMPARED WITH THAT OF TENSION, CALCULATED USING FEM ANALYSES OF PM SPUTTER-DEPOSITED SILVER INTERLAYERS

The change in steady-state strain-rate (or time-to-rupture, according to the Monkman-Grant relationship) with applied stress is predictable according to the steady-state stress exponent, *n*,

$$n = \left(\frac{\partial \ln e}{\partial \ln s} \right) \qquad \textbf{(EQ 2)}$$

where *n* is about 30 for silver at ambient temperature (Ref 38). Naturally, the steady-state strain rate of the torsional specimens shown in Fig. 9 is less than the constant applied strain rate of the torsional specimens shown in Fig. 8. If the steady-state rate if not achievable in the interlayer metal, then time-dependent failure in shear is not expected to occur.

It is important to realize the consequence of the difference in plastic strains-to-failure between the constant shear-stress case and the constant tensile-stress case. For example, residual shear or tensile stresses may develop during fabrication of interlayer brazes or solid-state welds. This is particularly true in cases where dissimilar base materials are joined, but have substantially different coefficients of thermal expansion. For thin interlayers subjected to residual shear stresses, the dimensions of the base metal and interlayer may be such that the stress is relaxed at strains less than the shear strain-to-failure. However, because the observed tensile strains-to-failure are small, creep rupture by residual tensile stresses is possible, provided a significant stress level exists. If the interlayer metal is resistant to tim-dependent failure, then only the indirect implications of residual stress are important (for example, environmentally induced failure).

References cited in this section

17. R.S. ROSEN, "TIME-DEPENDENT FAILURE OF SILVER INTERLAYER WELDS," PH.D.THESIS, UNIVERSITY OF CALIFORNIA, DAVIS, 1990
26. J.W. ELMER, M.E. KASSNER, AND R.S. ROSEN, THE BEHAVIOR OF SILVER-AIDED DIFFUSION-WELDED JOINTS UNDER TENSILE AND TORSIONAL LOADS, *WELD. J.*, VOL 67 (NO. 7), 1988, P 157S-162S
33. M.E. KASSNER, R.S. ROSEN, AND G.A. HENSHALL, DELAYED MECHANICAL FAILURE OF SILVER-INTERLAYER DIFFUSION BONDS, *METALL. TRANS. A*, VOL 21, 1990, P 3085-3100
38. M.E. KASSNER, THE RATE DEPENDENCE AND MICROSTRUCTURE OF HIGH-PURITY SILVER DEFORMED TO LARGE STRAINS BETWEEN 0.16 AND 0.30 TM, *METALL. TRANS. A*, VOL 20, 1989, P 2001-2010

Multiaxial Loading

As discussed earlier, in tension there is significant mechanical constraint by the base material, which tends to reduce the effective stress. In torsion, where the shear stress is parallel to the plane of the interlayer, there is not constraint, other than, perhaps, the relatively minor constraint associated with plastic strain incompatibilities between the interlayer and the base metal. It was also mentioned earlier that the equivalent uniaxial strain-to-failure for torsional deformation of soft-interlayer joints is roughly four orders of magnitude higher than the values for uniaxial tension, and the (effective) shear stress-to-failure is only about one-half the UTS. This suggests that the interlayers will behave anisotropically to imposed stresses. The mechanical properties of the intermediate cases of biaxial deformation are not readily interpolated between these limits. The authors have preliminary experimental evidence, for example, that low-strain ductile failures in thin interlayers may occur at particularly low stress levels and strains for cases where tensile loads are accompanied by in-plane shear stresses (Ref 63). This implies that some multiaxial residual stress states may render solid-state-welded interlayer joints substantially more vulnerable to failure than simple tensile-stress states, even though the "macroscopic" effective stress may be comparable, when calculated on the basis of the applied stress state in the base material away from the interlayer.

Reference cited in this section

63. M.E. KASSNER, OREGON STATE UNIVERSITY, UNPUBLISHED RESEARCH, 1989

Environmentally Induced Failure of Interlayers

The interlayer/base-metal interfaces of some soft-interlayer welds appear particularly vulnerable to failure when exposed to external (corrosive) environments. For example, it is known that brazed silver interlayers between stainless steel are subject to galvanic corrosion in aqueous NaCl media (Ref 64, 65). When dissimilar base materials are joined, the potential for stress-corrosion cracking (SCC) exists if the joints are exposed simultaneously to some external (corrosive) environments and either shear or tensile stresses. If an interlayer is subjected to stress, then a determination of the vulnerability to SCC is appropriate. It was mentioned earlier that elevated-temperature joining using either solid-state or brazing processes may leave the joint under substantial residual stress, particularly in the case of dissimilar metals for which the coefficients of thermal expansion are significantly different. The authors have reported (Ref 35) that the uranium to type 304 stainless steel solid-state welds, fabricated using HHC-deposited silver interlayers (Ref 25, 26), are very susceptible to SCC. These silver solid-state welds were joined at 873 K, and the difference in thermal expansion coefficients leaves the joints of cylindrical specimens under significant residual shear stresses after cooling to ambient temperature. It was found that these residual stresses led to SCC at the uranium/silver interface in air saturated with water vapor (100% relative humidity) (Ref 35). This cracking resulted in reduced tensile strengths and rupture times, when compared with those specimens tested in laboratory air (~40% relative humidity). Specimens subjected to the same 100% relative humidity in air in an unstressed state exhibited no loss in strength, even after lengthy exposure. This, or course, emphasizes the importance of considering the residual stresses as not only rendering the interlayer joints vulnerable to "pure mechanical" rupture, but also to environmentally induced failures such as SCC, hydrogen embrittlement, and metal-induced embrittlement, if exposed to critical environments.

References cited in this section

25. R.S. ROSEN, D.R. WALMSLEY, AND Z.A. MUNIR, THE PROPERTIES OF SILVER-AIDED DIFFUSION WELDS BETWEEN URANIUM AND STAINLESS STEEL, *WELD. J.*, VOL 65 (NO. 4), 1986, P 83S-92S
26. J.W. ELMER, M.E. KASSNER, AND R.S. ROSEN, THE BEHAVIOR OF SILVER-AIDED DIFFUSION-WELDED JOINTS UNDER TENSILE AND TORSIONAL LOADS, *WELD. J.*, VOL 67 (NO. 7), 1988, P 157S-162S
35. R.S. ROSEN, S. BEITSCHER, AND M.E. KASSNER, STRESS CORROSION CRACKING OF URANIUM-SILVER INTERFACES IN SILVER-AIDED DIFFUSION WELDS, *INT. CONF. ENVIRONMENT-INDUCED CRACKING OF METALS*, VOL 10, NACE, 1989, P 429-433
64. A.T. KUHN AND R.M. TRIMMER, REVIEW OF THE AQUEOUS CORROSION OF STAINLESS STEEL-SILVER BRAZED JOINTS, *BR. CORROS. J.*, VOL 17 (NO. 1), 1982, P 4-8
65. T. TAKEMOTO AND I. OKAMOTO, EFFECT OF COMPOSITION ON THE CORROSION BEHAVIOR OF STAINLESS STEELS BRAZED WITH SILVER-BASE FILLER METALS, *WELD. J.*, VOL 64, 1984, P 300S-307S

Mechanical Properties of Soft-Interlayer Solid-State Welds

R.S. Rosen, Lawrence Livermore National Laboratory; M.E. Kassner, Oregon State University

References

1. J.T. NIEMANN, R.P. SOPHER, AND P.J. RIEPPEL, DIFFUSION BONDING BELOW 1000 °F, *WELD. J.*, VOL 37, 1958, P 337S-342S
2. I.M. BARTA, LOW TEMPERATURE DIFFUSION BONDING OF ALUMINUM ALLOYS, *WELD. J.*, VOL 43, 1964, P 241S-247S

3. D. HAUSER, P.A. KAMMER, AND J.H. DEDRICK, SOLID-STATE WELDING OF ALUMINUM, *WELD. J.*, VOL 46, 1967, P 11S-22S
4. P.A. KAMMER, R.E. MONROE, AND D.C. MARTIN, FURTHER STUDIES OF DIFFUSION BONDING BELOW 1000 °F, *WELD. J.*, VOL 48, 1969, P 116S-124S
5. Y. IINO AND N. TAGAUCHI, INTERDIFFUSING METALS LAYER TECHNIQUE OF CERAMIC-METAL BONDING, *J. MATER. SCI. LETT.*, VOL 7 (NO. 9), 1988, P 981-982
6. A. URENA, J.M.G.D. SALAZAR, AND J. QUINONES, DIFFUSION BONDING OF ALUMINA TO STEEL USING SOFT COPPER INTERLAYER, *J. MATER. SCI.*, VOL 27, 1992, P 599-606
7. T. YAMADA K, YOKOI, AND A. KOHNO, EFFECT OF RESIDUAL STRESS ON THE STRENGTH OF ALUMINA-STEEL JOINT WITH AL-SI INTERLAYER, *J. MATER. SCI.*, VOL 25, 1990, P 2188-2192
8. M.G. NICHOLAS AND R.M. CRISPIN, DIFFUSION BONDING STAINLESS STEEL TO ALUMINA USING ALUMINUM INTERLAYERS, *J. MATER. SCI.*, VOL 17, 1982, P 3347-3360
9. C.L. CLINE, AN ANALYTICAL AND EXPERIMENTAL STUDY OF DIFFUSION BONDING, *WELD. J.*, VOL 45, 1966, P 481S-489S
10. A.T. D'ANNESSA, THE SOLID-STATE BONDING OF REFRACTORY METALS, *WELD. J.*, VOL 43, 1964, P 232S-240S
11. M.G. NICHOLAS AND R.M. CRISPIN, DIFFUSION BONDING CERAMICS WITH DUCTILE METAL INTERLAYERS, *PROC. INT. DIFFUSION BONDING* (CRANFIELD, U.K.), 1987, P 173-182
12. B. DERBY, ZIRCONIA/METAL DIFFUSION BONDS, *PROC. INT. CONF. DIFFUSION BONDING* (CRANFIELD, U.K.), 1987, P 195-201
13. R.A. MORLEY AND J. CARUSO, THE DIFFUSION WELDING OF 390 ALUMINUM ALLOY HYDRAULIC VALVE BODIES, *WELD. J.*, VOL 59 (NO. 8), 1980, P 29-34
14. C.H. CRANE, D.T. LOVELL, W.A. BAGINSKY, AND M.G. OLSEN, DIFFUSION WELDING OF DISSIMILAR METALS, *WELD. J.*, VOL 46, 1967, P 23S-31S
15. M. O'BRIEN, C.R. RICE, AND D.L. OLSON, HIGH STRENGTH DIFFUSION WELDING OF SILVER COATED BASE METALS, *WELD. J.*, VOL 55 (NO. 1), 1976, P 25-27
16. J.W. DINI, W.K. KELLEY, W.C. COWDEN, AND E.M. LOPEZ, USE OF ELECTRODEPOSITED SILVER AS AN AID IN DIFFUSION WELDING, *WELD. J.*, VOL 63 (NO. 1), 1983, P 26S-34S
17. R.S. ROSEN, "TIME-DEPENDENT FAILURE OF SILVER INTERLAYER WELDS," PH.D.THESIS, UNIVERSITY OF CALIFORNIA, DAVIS, 1990
18. J.L. KNOWLES AND T.H. HAZLETT, HIGH-STRENGTH LOW-TEMPERATURE BONDING OF BERYLLIUM AND OTHER METALS, *WELD. J.*, VOL 49 (NO. 7), 1970, P 301S-310S
19. P.S. MCLEOD AND G. MAH, THE EFFECT OF SUBSTRATE BIAS VOLTAGE ON THE BONDING OF EVAPORATED SILVER COATINGS, *J. VAC. SCI. TECHNOL.*, VOL 11 (NO. 1), 1974, P 119-121
20. G. MAH, P.S. MCLEOD, AND D.G. WILLIAMS, CHARACTERIZATION OF SILVER COATINGS DEPOSITED FROM A HOLLOW CATHODE SOURCE, *J. VAC. SCI. TECHNOL.*, VOL 11 (NO. 4), 1974, P 663-665
21. D.G. WILLIAMS, VACUUM COATING WITH A HOLLOW CATHODE SOURCE, *J. VAC. SCI. TECHNOL.*, VOL 11 (NO. 1), 1974, P 374-377
22. E.R. NAIMON, D. VIGIL, J.P. VILLEGAS, AND L. WILLIAMS, ADHESION STUDY OF SILVER FILMS DEPOSITED FROM A HOY HOLLOW-CATHODE SOURCE, *J. VAC. SCI TECHNOL.*, VOL 13 (NO. 6), 1976, P 1131-1135
23. E.R. NAIMON, J.H. DOYLE, C.R. RICE, D. VIGIL, AND D.R. WALMSLEY, DIFFUSION WELDING OF ALUMINUM TO STAINLESS STEEL, *WELD. J.*, VOL 60 (NO. 1), 1981, P 17-20
24. D.T. LARSON AND H.L. DRAPER, CHARACTERIZATION OF THE BE-AG INTERFACIAL REGION OF SILVER FILMS DEPOSITED ONTO BERYLLIUM USING A HOT HOLLOW CATHODE DISCHARGE, *THIN SOLID FILMS*, VOL 107, 1983, P 327-334
25. R.S. ROSEN, D.R. WALMSLEY, AND Z.A. MUNIR, THE PROPERTIES OF SILVER-AIDED

DIFFUSION WELDS BETWEEN URANIUM AND STAINLESS STEEL, *WELD. J.*, VOL 65 (NO. 4), 1986, P 83S-92S

26. J.W. ELMER, M.E. KASSNER, AND R.S. ROSEN, THE BEHAVIOR OF SILVER-AIDED DIFFUSION-WELDED JOINTS UNDER TENSILE AND TORSIONAL LOADS, *WELD. J.*, VOL 67 (NO. 7), 1988, P 157S-162S
27. J. HARVEY, P.G. PATRIDGE, AND A.M. LURSHEY, FACTORS AFFECTING THE SHEAR STRENGTH OF SOLID STATE DIFFUSION BONDS BETWEEN SILVER-COATED CLAD AL-ZN-MG ALLOY (ALUMINUM ALLOY 70100, *MATER. SCI. ENG.*, VOL 79, 1986, P 191-199
28. P.G. PARTRIDGE AND D.V. DUNFORD, ON THE TESTING OF DIFFUSION-BONDED OVERLAP JOINTS BETWEEN CLAD AL-ZN-MG ALLOY (7010) SHEET, *J. MATER. SCI.* VOL 22, 1987 P 1597-1608
29. D.V. DUNFORD AND P.G. PARTRIDGE, THE PEEL STRENGTHS OF DIFFUSION BONDED. JOINTS BETWEEN CLAD AL-ALLOY SHEETS, *J. MATER. SCI.*, VOL 22, 1987, P 1790-1798
30. R.S. ROSEN AND M.E. KASSNER, DIFFUSION WELDING OF SILVER INTERLAYERS COATED ONTO BASE METALS BY PLANAR-MAGNETRON SPUTTERING, *J. VAC. SCI. TECHNOL. A*, VOL 8 (NO. 1), 1900, P 19-29
31. M.E. KASSNER, R.S. ROSEN, G.A. HENSHALL, AND W.E. KING, DELAYED FAILURE OF SILVER AIDED DIFFUSION WELDS BETWEEN STEEL, *PROC. 2ND INT. CONF. BRAZING, HIGH TEMPERATURE BRAZING, AND DIFFUSION WELDING*, GERMAN WELDING SOCIETY, 1989, P 47-52
32. M.E. KASSNER, R.S. ROSEN, G.A. HENSHALL, AND K.D. CHALLENGER, TIME-DEPENDENT FAILURE OF SILVER-INTERLAYER DIFFUSION WELDS BETWEEN ELASTICALLY-DEFORMING BASE METALS, *SCR. METALL. MATER.*, VOL 24, 1990, P 587-592
33. M.E. KASSNER, R.S. ROSEN, AND G.A. HENSHALL, DELAYED MECHANICAL FAILURE OF SILVER-INTERLAYER DIFFUSION BONDS, *METALL. TRANS. A*, VOL 21, 1990, P 3085-3100
34. P.G. PARTRIDGE AND J. HARVEY, "PROCESS FOR THE DIFFUSION BONDING OF ALUMINUM MATERIALS," U.K. PATENT APPLICATIONS GB 2117691 A, 1983
35. R.S. ROSEN, S. BEITSCHER, AND M.E. KASSNER, STRESS CORROSION CRACKING OF URANIUM-SILVER INTERFACES IN SILVER-AIDED DIFFUSION WELDS, *INT. CONF. ENVIRONMENT-INDUCED CRACKING OF METALS*, VOL 10, NACE, 1989, P 429-433
36. E. OROWAN, FRACTURE AND STRENGTH OF SOLIDS, *REP. PROG. PHYS.*, VOL 12, 1948, P 185-231
37. E. OROWAN, FUNDAMENTALS OF BRITTLE BEHAVIOR OF METALS, *FATIGUE AND FRACTURE OF METALS*, JOHN WILEY & SONS, 1952
38. M.E. KASSNER, THE RATE DEPENDENCE AND MICROSTRUCTURE OF HIGH-PURITY SILVER DEFORMED TO LARGE STRAINS BETWEEN 0.16 AND 0.30 TM, *METALL. TRANS. A*, VOL 20, 1989, P 2001-2010
39. N. BREDZ, INVESTIGATION OF FACTORS DETERMINING THE TENSILE STRENGTH OF BRAZED JOINTS, *WELD. J.*, VOL 33, 1954, P 545S-563S
40. W.G. MOFFATT AND J. WULFF, TENSILE DEFORMATION AND FRACTURE OF BRAZED JOINTS, *WELD. J.*, VOL 42, 1963, P 115S-125S
41. H.J. SAXTON, A.J. WEST, AND C.R. BARRETT, DEFORMATION AND FAILURE OF BRAZED JOINTS--MACROSCOPIC CONSIDERATIONS, *METALL. TRANS.*, VOL 2, 1971, P 999-1007
42. A.J. WEST, H.J. SAXTON, A.S. TETELMAN, AND C.R. BARRETT, DEFORMATION AND FAILURE OF THIN BRAZED JOINTS--MICROSCOPIC CONSIDERATIONS, *METALL. TRANS.*, VOL 2, 1971, P 1009-1017
43. E.P. LAUTENSCHLAGER, B.C. MARKER, B.K. MOORE, AND R. WILDES, STRENGTH MECHANISMS OF DENTAL SOLDER JOINTS, *J. DENT. RES.*, VOL. 53, 1974, P 1361-1367
44. R.A. MUSIN, V.A. ANTSIVEROV, Y.A. BELIKOV, Y.V. LYAMIN, AND A.N. SOLOKOV, THE EFFECTS ON THE STRENGTH OF THE JOINT OF THE THICKNESS OF THE SOFT INTERLAYER

IN DIFFUSION WELDING, *AUTO. WELD.,* VOL 32, 1979, P 38-40

45. R.M. TRIMMER AND A.T. KUHN, THE STRENGTH OF SILVER-BRAZED STEEL JOINTS--A REVIEW, *BRAZING SOLDERING,* VOL 2, 1982 P 6-13
46. N. BREDZ AND H. SCHWARTZBART, TRIAXIAL TENSION TESTING AND THE BRITTLE FRACTURE STRENGTH OF METALS, *WELD. J.,* VOL 53 (NO. 12), 1956, P 610S-615S
47. W.G. MOFFATT AND J. WULFF, STRENGTH OF SILVER BRAZED JOINTS IN MILD STEEL, *TRANS. AIME,* VOL 209 (NO. 4), 1957, P 442-445
48. R.Z. SHRON AND O.A. BAKSHI, THE PROBLEMS OF GAUGING THE STRENGTHS OF WELDED JOINTS IN WHICH THERE IS A SOFT INTERLAYER, *WELD. PROD.,* VOL 9, 1962, P 19-23
49. O.A. BAKSHI AND A.A. SHATOV, THE STRESSED STATE IN WELDED JOINTS WITH HARD AND SOFT INTERLAYERS, *WELD PROD.,* VOL 13, 1966, P 13-19
50. V.S. GOLOVCHENKO AND B.A. GOLOBOV, THE USE OF SILVER AS AN INTERMEDIATE LAYER FOR JOINING TITANIUM TO OTHER METALS, *WELD. PROD.,* VOL 18, 1971, P 55-57
51. G.K. KHARCHENKO AND A.I. IGNATENKO, THE STRENGTH OF JOINTS WITH A THIN SOFT INTERLAYER, *AUTO. WELD.,* VOL 21, 1968, P 33-35
52. W.M. LEHER AND H. SCHWARTZBART, STATIC AND FATIGUE STRENGTHS OF METALS SUBJECTED TO TRIAXIAL STRESSES, VOL 60, 1960, P 610-626
53. E.A. ALMOND, D.K. BROWN, G.J. DAVIES, AND A.M. COTTENDED, THEORETICAL AND EXPERIMENTAL INTERLAYED BUTT JOINTS TESTED IN TENSION, *INT. J. MECH. SCI.,* VOL 25 (NO. 3), 1983, P 175-189
54. G.A. HENSHALL, R.S. ROSEN, M.E. KASSNER, AND R.G. WHIRLEY, FINITE ELEMENT ANALYSIS OF INTERLAYER WELDS LOADED IN TENSION, *WELD. J.,* VOL 69 (NO. 9) 1990, P 337S-345S
55. H.J. SAXTON, A.J. WEST, AND C.R. BARRETT, THE EFFECT OF COOLING RATE ON THE STRENGTH OF BRAZED JOINTS, *METALL. TRANS.,* VOL 2, 1971, P 1019-1028
56. M.C. TOLLE AND M.E. KASSNER, TENSILE PROPERTIES OF THIN AU-NI BRAZES BETWEEN STRONG BASE METALS, *SCR. METALL. MATER.,* VOL 26, 1992, P 1281-1284
57. M.E. KASSNER, M.C. TOLLE. R.S. ROSEN, G.A. HENSHALL, AND J.W. ELMER, RECENT ADVANCES IN UNDERSTANDING THE MECHANICAL BEHAVIOR OF CONSTRAINED THIN METALS IN BRAZES AND SOLID-STATE BONDS, *THE METAL SCIENCE OF JOINING,* M.J. CIESLAK, ED., TMS, 1992, P 223-232
58. R.W. LOGAN, R.G. CASTRO, AND A.K. MUKHERJEE, MECHANICAL PROPERTIES OF SILVER AT LOW TEMPERATURES, *SCR. METALL.,* VOL 17, 1983, P 63-66
59. T.J. MOORE AND K.H. HOLKO, SOLID-STATE WELDING OF TD-NICKEL BAR, *WELD. J.,* VOL 49 (NO. 9), 1970, P 395S-409S
60. R.S. ROSEN, "AN INVESTIGATION OF THE PROPERTIES OF A SILVER-AIDED SOLID-STATE BOND BETWEEN URANIUM AND STAINLESS STEEL," REPORT UCRL-53458, LAWRENCE LIVERMORE NATIONAL LABORATORY, 1983
61. E.R. NAIMON, R.G. KURZ, D. VIGIL, AND L. WILLIAMS, "SILVER FILMS FOR SOLID STATE BONDING,"REPORT RFP-3125, ROCKWELL INTERNATIONAL, 1981
62. Z. NISENHOLTZ, J. MIRONI, AND N. NIR, DIFFUSION BONDING OF STAINLESS STEEL 304L TO TI-6AL-4V ALLOY, *PROC. 3RD INT. CONF. ISOSTATIC PRESSING* (LONDON, U.K.), 1986
63. M.E. KASSNER, OREGON STATE UNIVERSITY, UNPUBLISHED RESEARCH, 1989
64. A.T. KUHN AND R.M. TRIMMER, REVIEW OF THE AQUEOUS CORROSION OF STAINLESS STEEL-SILVER BRAZED JOINTS, *BR. CORROS. J.,* VOL 17 (NO. 1), 1982, P 4-8
65. T. TAKEMOTO AND I. OKAMOTO, EFFECT OF COMPOSITION ON THE CORROSION BEHAVIOR OF STAINLESS STEELS BRAZED WITH SILVER-BASE FILLER METALS, *WELD. J.,* VOL 64, 1984, P 300S-307S

Shielded Metal Arc Welding

Raymond H. Juers, Naval Surface Warfare Center

Introduction

SHIELDED METAL ARC WELDING (SMAW), commonly called stick, or covered electrode, welding, is a manual welding process whereby an arc is generated between a flux-covered consumable electrode and the workpiece. The process uses the decomposition of the flux covering to generate a shielding gas and to provide fluxing elements to protect the molten weld-metal droplets and the weld pool.

Shielded Metal Arc Welding

Raymond H. Juers, Naval Surface Warfare Center

The SMAW Process

The important features of the SMAW process are shown in Fig. 1. The arc is initiated by momentarily touching or "scratching" the electrode on the base metal. The resulting arc melts both the base metal and the tip of the welding electrode. The molten electrode metal/flux is transferred across the arc (by arc forces) to the base-metal pool, where it becomes the weld deposit covered by the protective, less-dense slag from the electrode covering.

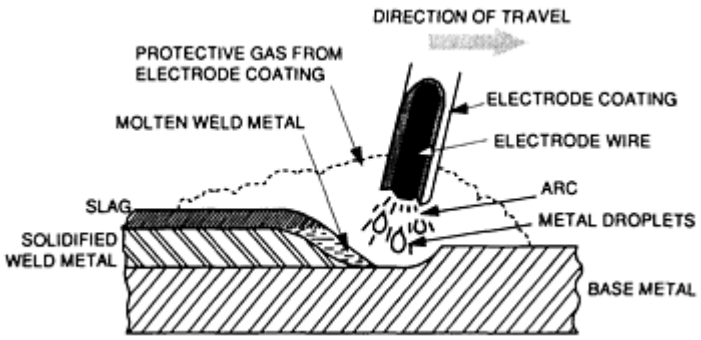

FIG. 1 SMAW PROCESS

Advantages and Limitations. The SMAW process is the most widely used welding process. It is the simplest, in terms of equipment requirements, but it is, perhaps, the most difficult in terms of welder training and skill-level requirements. Although welder skill level is a concern, most welders entering the field start as "stick welders" and develop the necessary skills through training and experience. The equipment investment is relatively small, and welding electrodes (except the very reactive metals, such as titanium, magnesium, and others) are available for virtually all manufacturing, construction, or maintenance applications. Shielded metal arc welding has the greatest flexibility of all the welding processes, because it can be used in all positions (flat, vertical, horizontal, and overhead), with virtually all base-metal thicknesses (1.6 mm, or $\frac{1}{16}$ in., and greater), and in areas of limited accessibility, which is a very important capability.

Because the SMAW process is basically a manual process, the skill level of the welder is of paramount importance in obtaining an acceptable weld. The welder duty cycle is generally low, because of the built-in work break, which occurs after each electrode is consumed and requires replacement. In addition to replacing the electrode when the arc is stopped (broken), the welder may "chip" or remove slag and clean it away from the starting and welding area with a wire brush to allow the proper deposition of the subsequent weld. This electrode replacement and cleaning operation occurs many times during the work day (about every two minutes, or the time it generally takes to consume an electrode). This stopping,

chipping, wire brushing, and electrode replacement prevents the welder from attaining an operator factor, or duty cycle, that is much greater than 25%.

Weld Quality. The quality of the weld depends on the design and accessibility of the joint, as well as on the electrode, the technique, and the skill of the welder. If joint details vary greatly from established design details, then a lower-quality weld can result. Other factors that also reduce quality are improper interbead cleaning, poor location of individual weld beads within the joint, and various problems with individual electrodes, including partially missing flux and core wires that are not centered within the flux covering. Overall, welds of excellent quality can be obtained with the SMAW process, as demonstrated by its use in joining submarine pressure hull sections and high-pressure oil/gas pipe lines.

The base-metal thicknesses. that can be welded using the SMAW process generally range from 1.6 mm ($\frac{1}{16}$ in.) to an unlimited thickness. The thinner materials require a skilled welder, tight fitup, and the proper small-diameter welding electrode. Welding position also is important when determining the minimum plate thicknesses that can be welded. Flat-position butt welds and horizontal fillet welds are generally considered the easiest to weld. Out-of-position welding (vertical, overhead) requires greater skill.

Welding Circuit. The circuit diagram for the SMAW process is shown in Fig. 2. The equipment consists of a power source, electrode holder, and welding cables that connect the power source to the electrode holder and the workpiece. Alternating current (ac), or direct current, electrode negative (DCEN), or direct current, electrode positive (DCEP) can be used, depending on the electrode coating characteristics. The DCEN source is also called dc straight polarity, whereas the DCEP source is also called dc reverse polarity.

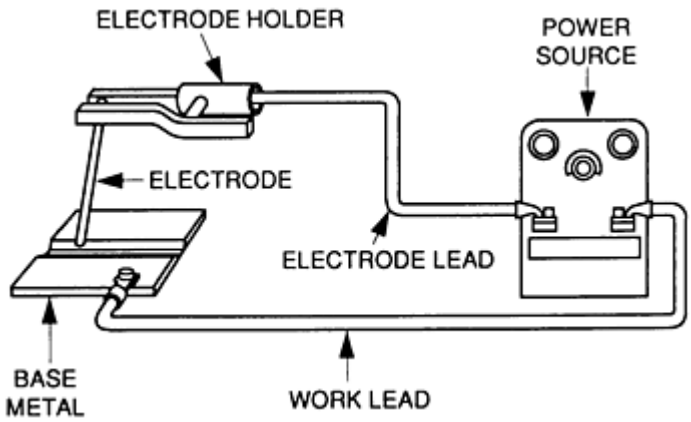

FIG. 2 SHIELDED METAL ARC CIRCUIT DIAGRAM

Equipment. The welding machine, or power source, is the crux of the SMAW process. Its primary purpose is to provide electrical power of the proper current and voltage to maintain a controllable and stable welding arc. Its output characteristics must be of the constant current (CC) type. SMAW electrodes operate within the range from 25 to 500 A. The electrode producer should suggest a narrow optimum range for each size and type of electrode. Operating arc voltage varies between 15 and 35 V.

The electrode holder, which is held by the welder, firmly grips the electrode and transmits the welding current to it. Electrode holders are available in several designs, such as the pincher type and the collet, or twist, type, shown in Fig. 3. Each style has its proponents and the selection is usually a personal preference. Electrode holders are designated by their current capacity. Selection factors, such as the current rating, duty cycle, maximum electrode size, and cable size, are shown in Table 1. The most lightweight holder that will accommodate the required electrode size is usually desired.

TABLE 1 SIZE AND CAPACITY OF ELECTRODE HOLDERS

ELECTRODE HOLDER	RATING	MAXIMUM	MAXIMUM

			ELECTRODE SIZE		CABLE SIZE
	MAXIMUM CURRENT, A	DUTY CYCLE, %	mm	in.	
SMALL	100	50	3.2	$\frac{1}{8}$	1
	200	50	4.0	$\frac{5}{32}$	1/0
MEDIUM	300	60	5.5	$\frac{7}{32}$	2/0
LARGE	400	60	6.4	$\frac{1}{4}$	3/0
EXTRA LARGE	500	75	7.9	$\frac{5}{16}$	4/0
	600	75	9.5	$\frac{3}{8}$	4/0

FIG. 3 SMAW ELECTRODE HOLDERS

All electrode holders should be fully insulated. Because they are used in proximity to the arc and are exposed to high heat, they will deteriorate rapidly. It is extremely important to maintain electrode holders to ensure that they retain their current-carrying efficiency, their insulating qualities, and their electrode gripping action. Manufacturers supply spare parts so that the holders can be rebuilt and maintained for safe and efficient operation.

Certain pieces of auxiliary equipment can be used with the SMAW process, such as low-voltage control circuits, which enable the relatively high open-circuit voltage to be cut off until the electrode touches the workpiece. Other items include remote-control switches for the contactors, remote-control current adjusting devices, and engine idling controllers for engine-driven power sources.

Shielded Metal Arc Welding

Raymond H. Juers, Naval Surface Warfare Center

Applications

Most manufacturing operations that require welding will strive to utilize the mechanized processes that offer greater productivity, higher quality, and, therefore, more cost-effective production. For these reasons, the SMAW process has been replaced where possible. However, the simplicity and ability of the SMAW process to achieve welds in areas of restricted accessibility means that it still finds considerable use in certain situations and applications. Heavy construction, such as shipbuilding, and welding "in the field," away from many support services that would provide shielding gas, cooling water, and other necessities, rely on the SMAW process to a great extent.

Although the SMAW process finds wide application for welding virtually all steels and many of the nonferrous alloys, it is primarily used to join steels. This family of materials includes low-carbon or mild steels, low-alloy steels, high-strength steels, quenched and tempered steels, high-alloy steels, stainless steels, and many of the cast irons. The SMAW process is also used to join nickel and its alloys and, to a lesser degree, copper and its alloys. It can be, but rarely is, used for welding aluminum.

In addition to joining metals, the SMAW process is frequently used for the protective surfacing of base metals. The surfacing deposit can be applied for the purpose of corrosion control or wear resistance (hard surfacing).

Shielded Metal Arc Welding

Raymond H. Juers, Naval Surface Warfare Center

Electrodes

The electrodes used in the SMAW process have many different compositions of core wire and a wide variety of flux-covering types and weights. Standard electrode diameters of the core wire range from 1.6 to 8 mm ($\frac{1}{16}$ to $\frac{5}{16}$ in.). Electrode length usually ranges from 230 to 455 mm (9 to 18 in.); the shorter lengths are associated with the smaller-diameter electrodes. A bare, uncoated end of the electrode (the grip end) is provided for making electrical contact in the electrode holder.

The coating on the electrode has numerous functions. It provides:

- GAS (NORMALLY, CARBON DIOXIDE), FROM THE DECOMPOSITION OF CERTAIN COATING INGREDIENTS TO SHIELD THE ARC AND WELD ZONE FROM THE ATMOSPHERE
- DEOXIDIZERS, FOR SCAVENGING AND PURIFYING THE DEPOSITED WELD METAL
- SLAG FORMERS, TO PROTECT THE DEPOSITED WELD METAL FROM ATMOSPHERIC OXIDATION AND TO HELP SHAPE THE WELD BEAD
- IONIZING ELEMENTS, TO MAKE THE ARC MORE STABLE AND TO OPERATE WITH ALTERNATING CURRENT
- ALLOYING ELEMENTS, TO PROVIDE SPECIAL CHARACTERISTICS TO THE WELD DEPOSIT
- IRON POWDER, IN CERTAIN ELECTRODES, TO INCREASE PRODUCTIVITY FOR WELDING FERROUS METALS

The American Welding Society (AWS) has established a system for identifying and classifying the different types of welding electrodes. All SMAW electrodes have the prefix letter E to indicate welding electrode. The symbols that follow the prefix are based on criteria that best describe the welding capabilities of the electrode metal. These criteria include chemical composition of the deposited weld metal, weld-metal mechanical properties, certain process parameters, or combinations of all factors.

Mild and Low-Alloy Steel-Covered Electrodes. The prefix used to identify these electrodes is followed by a number series that indicates minimum strength level, position capability, and type of covering and welding current. Table 2 explains how the number series is used in AWS A5.1, the specification for carbon steel electrodes for shielded metal arc welding and AWS A5.5, the specification for low-alloy steel electrodes. The first two digits after the E in the E6010 electrode designate a tensile strength of at least 430 MPa (62 ksi) for the deposited metal in the as-welded condition. The third digit indicates the position in which satisfactory welds can be made with the electrode. Thus, the 1 in E6010, for example, means that the electrode is satisfactory for use in all positions (flat, vertical, horizontal, and overhead). The 2 in E6020 indicates that the electrode is suitable for the flat position and horizontal fillets. The last digit or last two digits, taken together, indicate the applicable current type to be used and the type of covering on the electrode.

TABLE 2 CARBON AND LOW-ALLOY STEEL COVERED ELECTRODE IDENTIFICATION SYSTEM

AWS CLASSIFICATION[A]	MINIMUM TENSILE STRENGTH		MINIMUM YIELD STRENGTH		MINIMUM ELONGATION, %
	MPA	KSI	MPA	KSI	

E70XX	480-500	70-72	390-420	57-60	17-25
E80XX	550	80	460-550	67-80	16-24
E90XX	620	90	530-620	77-90	14-24
E100XX	690	100	600	87	13-20
E110XX	760	110	670-760	97-110	15-20
E120XX	830	120	740-830	107-120	14-18

CLASSIFICATION[B]	**FLAT POSITION**	**HORIZONTAL POSITION**	**VERTICAL POSITION**	**OVERHEAD POSITION**
EXXIX	YES	YES	YES	YES
EXX2X	YES	FILLET	NO	NO
EXX4X	YES	YES	DOWN	YES

CLASSIFICATION[C]	**CURRENT**	**ARC**	**PENETRATIONN**	**COVERING/SLAG**	**APPROXIMATE IRON POWDER[D], %**
EXX10	DCEP	DIGGING	DEEP	CELLULOSE/SODIUM	0-10
EXXX1	AC AND DCEP	DIGGING	DEEP	CELLULOSE/POTASSIUM	0
EXXX2	AC AND DCEN	MEDIUM	MEDIUM	RUTILE/SODIUM	0-10
EXXX3	AC AND DC	LIGHT	LIGHT	RUTILE/POTASSIUM	0-10
EXXX4	AC AND DC	LIGHT	LIGHT	RUTILE/IRON POWDER	25-40
EXXX5	DCEP	MEDIUM	MEDIUM	LOW HYDROGEN/SODIUM	0
EXXX6	AC OR DCEP	MEDIUM	MEDIUM	LOW HYDROGEN/POTASSIUM	0
EXXX8	AC OR DCEP	MEDIUM	MEDIUM	LOW HYDROGEN/IRON POWDER	25-40
EXX20	AC OR DC	MEDIUM	MEDIUM	IRON OXIDE/SODIUM	0
EXX24	AC OR DC	LIGHT	LIGHT	RUTILE/IRON POWDER	50
EXX27	AC OR DC	MEDIUM	MEDIUM	IRON OXIDE/IRON POWDER	50
EXX28	AC OR	MEDIUM	MEDIUM	LOW HYDROGEN/IRON	50

(A) FIRST TWO OR THREE DIGITS INDICATE TENSILE STRENGTH IN UNITS OF KSI AND OTHER MECHANICAL PROPERTIES (MECHANICAL PROPERTY REQUIREMENTS VARY WITHIN EACH CLASSIFICATION).

(B) THIRD (OR) FOURTH (SECOND TO LAST) DIGIT INDICATES THE WELDING POSITION THAT CAN BE USED.

(C) LAST DIGIT INDICATES USABILITY OF THE ELECTRODE.

(D) IRON POWDER PERCENTAGE BASED ON WEIGHT OF THE COVERING

Stainless Steel Covered Electrodes. The three-digit number that follows the prefix E indicates the chemical composition. In addition, letters or numbers can be used to indicate composition modifications or position usability. The specification AWS A5.4 identifies and classifies covered corrosion-resisting chromium and chromium-nickel steel welding electrodes.

Nickel and Copper Alloys. The designations for nonferrous product classifications, such as nickel and nickel alloys in AWS A5.11 and copper and copper alloys in AWS A5.6, follow the prefix with a list of chemical element abbreviations that are significant in identifying product composition, such as ENiCu, ENiCrFe, ECuSi, and ECuNi.

Surfacing Welding Electrodes. The designations for these products are contained in specifications AWS A5.13 and A5.21. They are very similar to the system used to identify nonferrous electrodes.

Aluminum and Aluminum Alloys. The specification for aluminum and aluminum alloy arc welding electrodes, AWS A5.3, uses the E prefix to indicate a covered electrode, followed by a series of numbers that identify the chemical composition that is equivalent to Aluminum Association alloy designations (for example, E1100, E3003, and E4043).

Suffix symbols are used in various classifications. The AWS A5.5 specification for low-alloy filler metals uses suffixes such as -A1, -B2, -B2L, and -C1 to indicate chemical compositions. Table 3 identifies the weld deposit chemical composition associated with a number of suffixes found on low-alloy electrodes. The classifications for nonferrous products in the AWS A5.6 specification for copper alloys and in the AWS A5.11 specification for nickel alloys list a letter or number suffix that indicates position in a series of similar alloy groupings. A similar suffix pattern is also used in the AWS A5.13 and AWS A5.21 specifications for surfacing welding electrodes. Covered stainless steel electrodes employ a number, -15 or -16, as a suffix to identify usability. The -15 suffix indicates that the electrode is designed for all-position operation using DCEP electrical current. The -16 suffix indicates all-position operation with either ac or DCEP.

TABLE 3 SUFFIX SYMBOLS AND CORRESPONDING COMPOSITIONS FOR LOW-ALLOY STEEL COVERED ELECTRODES

SUFFIX(A)	COMPOSITION, %						
	C	Mn	Si	Ni	Cr	Mo	V
A1	0.12	0.6-1.0(B)	0.40-0.80(B)	. . .	. . .	0.40-0.65	
B1	0.12	0.90	0.60-0.80(B)	. . .	0.40-0.65	0.40-0.65	. . .
B2L	0.05	0.90	0.8-1.0(B)	. . .	1.00-1.50	0.40-0.65	. . .
B2	0.12	0.90	0.60-0.80(B)	. . .	1.00-1.50	0.40-0.65	. . .
B3L	0.05	0.90	0.8-1.0(B)	. . .	2.00-2.50	0.90-1.20	. . .
B3	0.12	0.90	0.60-0.80(B)	. . .	2.00-2.50	0.90-1.20	. . .
B4L	0.05	0.90	1.00	. . .	1.75-2.25	0.40-0.65	. . .
B5	0.07-0.15	0.40-0.70	0.30-0.60	. . .	0.50-0.60	1.00-1.25	0.05
C1	0.12	1.20	0.6-0.8(B)	1.00-2.75	. . .	. . .	. . .
C2	0.12	1.20	0.6-0.8(B)	3.00-3.75	. . .	. . .	. . .
C3	0.12	0.40-1.25	0.80	0.80-1.10	0.15	0.35	0.05
D1	0.12	1.25-1.75	0.6-0.8(B)	. . .	. . .	0.25-0.45	. . .
D2	0.15	1.65-2.00	0.6-0.8(B)	. . .	. . .	0.25-0.45	. . .
G	. . .	1.0 MIN	0.80 MIN	0.50 MIN	0.30 MIN	0.20 MIN	0.10 MIN
M(C)	0.10	0.6-2.25(B)	0.6-0.8(B)	1.4-2.5(B)	0.15-1.5(B)	0.25-0.55(B)	0.05

(A) THE SUFFIX INDICATES THE CHEMICAL COMPOSITION OF THE WELD-METAL DEPOSIT.

(B) AMOUNT DEPENDS ON ELECTRODE CLASSIFICATION. SINGLE VALUES INDICATE MAXIMUM, CHECK AWS A5.5 FOR THE DIFFERENT ELECTRODE CLASSES.

(C) THERE ARE SEVERAL DIFFERENT M CLASSES; M CLASSIFICATIONS ARE INTENDED TO CONFORM TO MILITARY SPECIFICATIONS.

Deposition Rates. The melting rate of the electrode is directly related to the welding current. The current density in the electrode increases with higher current, which increases the melting rate, which, in turn, increases the deposition rate.

The electrode coating also affects deposition rate. The iron powder types are designed to have higher deposition rates and, therefore, greater productivity. Figure 4 shows the expected deposition rate versus amperage for various electrodes at a 100% duty cycle. (The actual deposition rate will be considerably less. Deposition rate is a function of the duty cycle, which is affected by the time spent changing the electrodes, cleaning slag off of the weld, etc.) Electrode size and, therefore, usable current range are determined by the base-metal thickness, welding position, welder skill level, and joint details.

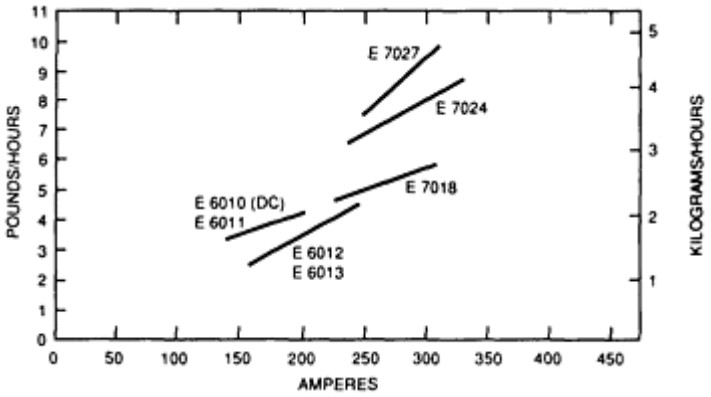

FIG. 4 DEPOSITION RATE VERSUS AMPERES FOR VARIOUS ELECTRODES

Shielded Metal Arc Welding

Raymond H. Juers, Naval Surface Warfare Center

Weld Schedules and Procedures

Welding schedules are tables of operating parameters that will provide high-quality welds under normal conditions. Strict welding schedules are not as important for the manual SMAW process as they are for semiautomatic and automatic welding for several reasons. First, in a manual welding process, the welder controls conditions by arc manipulation, which achieves better control than any of the other arc welding processes. The welder also directly controls the arc voltage and travel speed and, indirectly, the welding current.

Second, meter readings are rarely used in the SMAW process for the duplication of jobs. It is generally considered that the recommended welding current ranges given in Table 4 for the different types of electrodes are sufficient for most operations. The settings provide a good starting point when first welding on a new application, although they are not necessarily the only welding settings that can be used under every condition. For example, for high-production work, the current settings could be increased considerably over those shown. Factors such as weld appearance, welding position, and welder skill also allow variations from the settings.

TABLE 4 TYPICAL AMPERAGE RANGES FOR SELECTED SMAW ELECTRODES

ELECTRODE DIAMETER		E6010 AND E6011	E6012	E6013	E6020	E6022	E6027 AND E7027	E7014	E7015, E7016, AND E7016-1	E7018 AND E7018-1	E7024-1, E7024, AND E7028	E7048
mm	in.											
1.6	1/16	. . .	20-40	20-40	. . .	. . .	. . .	. . .	. . .	. . .	. . .	. . .
2.0	5/64	. . .	25-60	25-60	. . .	. . .	. . .	. . .	. . .	. . .	. . .	. . .
2.4[A]	3/32	40-80	35-85	45-90	. . .	. . .	. . .	80-125	65-110	70-100	100-145	. . .
3.2	1/8	75-125	80-140	80-130	100-150	110-160	125-185	110-160	100-150	115-165	140-190	80-140
4.0	5/32	110-170	110-190	105-180	130-190	140-190	160-240	150-210	140-200	150-220	180-250	150-220
4.8	3/16	140-215	140-240	150-230	175-250	170-400	210-300	200-275	180-255	200-275	230-305	210-270

5.6	7/32	170-250	200-320	210-300	225-310	370-520	250-350	260-340	240-320	260-340	275-365	. . .
6.4	1/4	210-320	250-400	250-350	275-375	. . .	300-420	330-415	300-390	315-400	335-430	. . .
8.0(A)	5/16 (A)	275-425	300-500	320-430	340-450	. . .	375-475	390-500	375-475	375-470	400-525	. . .

(A) THESE DIAMETERS ARE NOT MANUFACTURED IN THE E7028 CLASSIFICATION.

Welder Training. The SMAW process generally requires a high degree of welder skill to consistently produce quality welds. As a result, many training programs emphasize the SMAW process because of the arc manipulation skills developed by the welder. This acquired skill level makes the training on other processes much easier.

The exact content of a training program will vary, depending on the specific application of the process. The complexity of the parts to be welded and the governing codes or specifications involved also dictate the length of the training program. For example, because a pipe welder would need more skill than a tack welder, the length of his training program would be greater.

The job title of arc welder (DOT 810.384-014) describes a person whose responsibility is to weld together many components. This job includes setting up the machine and part to be welded, striking the arc and guiding it along the joint, and performing such duties as chipping, grinding, and slag removal. The welder should be able to:

- WELD IN ALL POSITIONS
- PASS EMPLOYER PERFORMANCE TESTS
- MEET CERTIFICATION STANDARDS OF GOVERNMENTAL AGENCIES OR PROFESSIONAL AND TECHNICAL ASSOCIATIONS

A tack welder (DOT 810.684-010) makes short beads at specific points to hold the parts in place for final welding. The tack welder also performs the duties of fitter helper.

A combination welder (DOT 819-384-010) welds metal parts together to either fabricate or repair assemblies. The combination welder is able to create gas welds and electric arc welds, and to perform flame-cutting operations.

The welder portion of the pipefitter description (DOT 862.381-018) must weld the pipe joint after it has been assembled and tacked in place.

Procedures. There is a definite relationship between the welding current, the size of the welding electrodes, and the welding position. These parameters must be selected to ensure that the welder has the molten weld-metal pool under complete control at all times. If the pool becomes too large, then it becomes unmanageable, perhaps allowing molten metal to run out, particularly during out-of-position welding. The welder should maintain the steady frying and crackling sound that comes with the use of correct procedures. The shape of the molten pool and the movement of the metal at the rear of the pool both serve as guides in checking weld quality. The ripples produced on the bead should be uniform and have good side tie-in with no undercut or excessive reinforcement. The factors described below are essential for maintaining high-quality welding.

Correct Electrode Type. It is important to select the proper electrode for each job. The selection should be based on the type of base metal, expected service, and mechanical properties required.

Correct Electrode Size. The choice of electrode size should depend on the type of electrode, welding position, joint preparation, base-metal thickness, and welder skill.

Correct Current. If the current is too high, then the electrode melts too fast and the molten pool becomes large, irregular, and difficult to control. Current that is too low will not provide enough heat to melt the base metal, causing the molten pool to be sluggish, with a high, irregular, ropey weld bead. It should also be noted that the electrode has inherent

current limits. If the current is too high, then the core wire overheats and the coating cracks. If the current is too low, then there is insufficient heat to maintain the arc and form the protective gas shield.

Correct Arc Length. If an arc is too long, then the metal melts off the electrode in large globules that wobble from side to side, resulting in a wide and irregular weld bead with considerable spatter, and, possibly, porosity and mechanical property degradation. If the arc is too short, then it has insufficient heat to melt the base metal and electrode, which often results in the electrode sticking to the work.

Correct Travel Speed. A speed that is too fast allows the weld pool to freeze before impurities and gases can escape, and the bead will be narrow and inadequate in size. When the speed is too slow, the metal piles up and the bead is larger than required.

Correct Electrode Angle. In fillet welding and deep groove welding, the electrode angle is particularly important. When making a fillet weld, the electrode should be held so that it bisects the angle between the plates and is perpendicular to the line of the weld. When undercut occurs in the vertical member, the angle should be lowered and the arc directed toward the vertical member.

Correct Arc Manipulation. When weaving is used, the width of the weave and the pause at the ends of the weave become important. The welder must pause at each end of the weave to allow adequate fill buildup and fusion to occur. The welder should also quickly move across the center of the weld, because heating is more concentrated in the center than at the edges.

Breaking the Arc. Before an arc is broken, it is important to know whether it will be reestablished with the next electrode and the weld continued or whether it is the end of a weld pass. If welding is to continue, then the crater should remain and the arc quickly broken. If it is the end of a weld pass, then the arc should not be broken until the crater has filled.

Correct Interbead Cleaning. Proper interbead cleaning to remove slag and any spatter is essential to the production of high-quality welds. Proper cleaning prevents slag inclusions, "lack of fusion" defects, and porosity.

Shielded Metal Arc Welding

Raymond H. Juers, Naval Surface Warfare Center

Variations of the SMAW Process

Gravity Welding. Gravity feed is considered to be an automatic method of applying the SMAW process. It utilizes a relatively low-cost mechanism that includes an electrode holder attached to a bracket, which slides down an inclined bar arranged along the line of weld. Special electrodes with a heavy coating are maintained in contact with the workpiece by the weight of the electrode holder and electrode. Once the process is started, it continues automatically until the electrode has burned to a short stub, whereupon the bracket and electrode holder are automatically kicked up to break the arc. One welder can operate several gravity feeders at the same time (Fig. 5). This increases productivity, reduces welder fatigue, and requires less-skilled welders, all of which result in substantial savings in welder labor costs. Table 5 compares the deposition rate, based on pounds per hour, when using one electrode manually versus two, three, four, or five gravity feeders.

TABLE 5 COMPARISON OF DEPOSITION RATES FOR CONVENTIONAL SMAW AND MULTI-ARC GRAVITY-FED WELDING

Data are for making 7.9 mm ($\frac{5}{16}$ in.) fillet welds using E6027 electrodes.

METHOD	DEPOSITION RATE, LB/H
MANUAL, ONE ARC	9
GRAVITY, TWO ARCS	17
GRAVITY, THREE ARCS	26

GRAVITY, FOUR ARCS	34
GRAVITY, FIVE ARCS	43

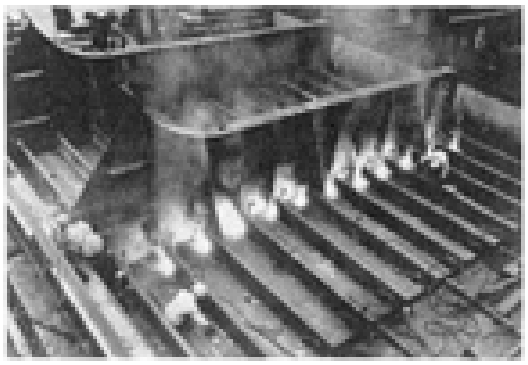

FIG. 5 GRAVITY FEEDERS BEING USED ON SHIP SUBASSEMBLIES

Although gravity-fed SMAW was investigated in the United States, England, and the Scandinavian countries in the late 1940s and early 1950s, credit must be given to the Japanese shipbuilders for perfecting and utilizing the process on a large scale in the early 1960s. The gravity welding process is being used in shipyards, railroad car shops, and barge yards throughout the world. It has reasonable acceptance in applications where large amounts of horizontal fillet welds must be made in a relatively small area.

Firecracker welding is an automatic method by which shielded metal arc welds are made using a long electrode with an electrically nonconductive coating. Human involvement is not required after the arc is initiated. A firecracker weld is generally positioned in the flat position. The welding electrode is placed in the joint and a retaining bar is placed over it. The arc is started by shorting the end of the electrode to the workpiece. The arc length is controlled by the coating thickness. As the arc travels along the stationary electrode, the electrode melts and makes a deposit on the metal immediately underneath. Once the arc is started, the process proceeds to completion automatically. Electrodes that are up to 1 m (39 in.) long and have a core diameter of 5, 6, or 8 mm (0.20, 0.24, or 0.32 in.) have been used. Both alternating and direct current have been applied, and the former may be preferred, because of arc blow problems associated with direct current.

Raymond H. Juers, Naval Surface Warfare Center

Special Applications of the SMAW Process

Underwater welding began during World War I when the British naval force used it to make temporary repairs of leaking rivets on ship hulls. The introduction of covered electrodes enabled succesful underwater welding and the production of welds having approximately 80% of the strength and 40% of the ductility of similar welds made in air. Because of the somewhat diminished weld properties, this SMAW application is generally restricted to salvage operations or underwater repair work.

Underwater welding can be subdivided into two major categories: welding in a wet environment and welding in a dry environment.

Wet Welding. The relatively poor quality of welds made in a wet environment is due primarily to the problem of heat transfer, welder visibility, and the presence of hydrogen in the arc atmosphere during the welding operation. When the base metal and the arc area are surrounded entirely by water, there is no temperature or heat buildup of the base metal at the weld, nor is preheating possible. This creates a weld-metal quench effect, which traps damaging amounts of hydrogen and also produces a weld solidification structure with reduced toughness and ductility. Both conditions contribute to the weld-metal cracking problems experienced when welding steels underwater. Another disadvantage is the restricted visibility, which is due to the equipment and the existing local contaminants in the water, as well as those generated by the welding arc. Under the most ideal conditions, welds produced in wet environments using covered electrodes are

marginal, at best. They can be placed in service for short periods of time under reduced operating conditions, but should be replaced with quality welds as quickly as possible.

The covered electrodes used for wet welding must be waterproofed prior to underwater use. This can be done by wrapping them with waterproof tape or by dipping them in special sodium silicate mixes and allowing them to dry.

Dry Welding. The dry environment enables the production of high-quality welds that meet all code quality requirements. The SMAW process is not very popular for welding in the dry environment, because large amounts of smoke and fumes are produced. An extensive air moving, filtering, and refrigeration system must be employed when the SMAW process is used, because a dry-environment area will quickly fill with the welding fumes, making it impossible for the welder to see that weld area and to function. For this reason, the gas-tungsten arc welding and gas-metal arc welding processes have broader use in dry welding applications.

The article "Underwater Welding" in this Volume explores the topic in greater detail.

Shielded Metal Arc Welding

Raymond H. Juers, Naval Surface Warfare Center

Safety Considerations

The SMAW process, like all open arc welding processes, has a number of potential hazards. To alert welders about these safety concerns, all SMAW electrode containers carry a warning label that identifies the three most common safety hazards in these terms:

- ELECTRIC SHOCK CAN KILLDO NOT PERMIT ELECTRICALLY LIVE PARTS OR ELECTRODES TO CONTACT SKIN . . . OR YOUR CLOTHING OR GLOVES IF THEY ARE WETINSULATE YOURSELF FROM WORK AND GROUND
- FUMES AND GASES CAN BE DANGEROUS TO YOUR HEALTHKEEP FUMES AND GASES FROM YOUR BREATHING ZONE AND GENERAL AREAKEEP YOUR HEAD OUT OF FUMESUSE ENOUGH VENTILATION OR EXHAUST AT THE ARC, OR BOTH
- ARC RAYS CAN INJURE EYES AND BURN SKINWEAR CORRECT EYE, EAR, AND BODY PROTECTION

In addition to the general warnings on the container, further detailed information relating to safety is contained in ANSI/AWS Z49.1, "Safety in Welding and Cutting." The information described below is intended to expand on the general warnings, and should be particularly useful for SMAW welders.

First, the filter plates installed within welding shields must be capable of stopping the harmful levels of infrared, ultraviolet, and visible light rays originating in the arc. Filter plates are now able to absorb 99% or more of the infrared and ultraviolet rays from the arc. The shade of the filter plate suggested for use with SMAW electrodes is given in Table 6.

TABLE 6 RECOMMENDED FILTER LENS SHADES USED IN SHIELDED METAL ARC WELDING

ELECTRODE DIAMETER		LENS SHADE NO.
mm	in.	
1.6	$\frac{1}{16}$	10
2.4	$\frac{3}{32}$	
3.2	$\frac{1}{8}$	

4.0	$\frac{5}{32}$	
4.8	$\frac{3}{16}$	12
5.6	$\frac{7}{32}$	
6.4	$\frac{1}{4}$	
7.9	$\frac{5}{16}$	14
9.5	$\frac{3}{8}$	

Source: ANSI/AWS Z49.1

Second, in addition to protecting himself, the welder must also be aware of others in the area who need protection, which can usually be provided by portable screens. The failure of those working around the arc to use adequate protection can result in eye burn, which is similar to sunburn and is extremely painful for a period of up to 48 h. Usually, eye burn does not permanently injure the eyes, but it can cause intense pain. A physician should be consulted in the case of severe arc burn, regardless of whether it involves the skin or the eyes.

Third, the welding area must be adequately ventilated because of the heavy concentrations of smoke and fumes generated in the SMAW process. If welding is being performed in confined spaces with poor ventilation, such as in a tank, an external air supply in the form of a mask or special helmet may be required. In addition, a second person should be stationed at the tank manhole to provide any necessary assistance. Special ventilation is required when welding stainless steels or metals coated with copper, zinc, lead, or cadmium, because of the toxic nature of these fumes.

Fourth, cables with frayed or cracked insulation and faulty or badly worn connections can cause electrical short circuits and electrical shocks to personnel. When it is necessary to weld in a damp or wet area, the welder should wear rubber boots and stand on a dry, insulated platform.

Shielded Metal Arc Welding

Raymond H. Juers, Naval Surface Warfare Center

Selected References

- H.B. CARY, *MODERN WELDING TECHNOLOGY*, 2ND ED., PRENTICE-HALL, 1989
- "FILLER METAL COMPARISON CHARTS," AWS FMC-89, AMERICAN WELDING SOCIETY
- "SAFETY IN WELDING AND CUTTING," ANSI/AWS Z49.1, AMERICAN WELDING SOCIETY
- "TECHNICAL GUIDE FOR SHIELDED METAL ARC WELDING," HOBART BROTHERS CO.

Gas-Metal Arc Welding

D.B. Holliday, Westinghouse Electric Corporation

Introduction

GAS-METAL ARC WELDING (GMAW) is an arc welding process that joins metals together by heating them with an electric arc that is established between a consumable electrode (wire) and the workpiece. An externally supplied gas or gas mixture acts to shield the arc and molten weld pool.

Although the basic GMAW concept was introduced in the 1920s, it was not commercially available until 1948. At first, it was considered to be fundamentally a high-current-density, small-diameter, bare-metal electrode process using an inert

gas for arc shielding. Its primary application was aluminum welding. As a result, it became known as metal-inert gas (MIG) welding, which is still common nomenclature.

Subsequent process developments included operation at low current densities and pulsed direct current, application to a broader range of materials, and the use of reactive gases (particularly carbon dioxide) and gas mixtures. The latter development, in which both inert and reactive gases are used, led to the formal acceptance of the term gas-metal arc welding.

The GMAW process can be operated in semi-automatic and automatic modes. All commercially important metals, such as carbon steel, high-strength low-alloy steel, stainless steel, aluminum, copper, and nickel alloys can be welded in all positions by this process if appropriate shielding gases, electrodes, and welding parameters are chosen.

Advantages. The applications of the process are dictated by its advantages, the most important of which are:

- ELECTRODE LENGTH DOES NOT FACE THE RESTRICTIONS ENCOUNTERED WITH SHIELDED-METAL ARC WELDING (SMAW).
- WELDING CAN BE ACCOMPLISHED IN ALL POSITIONS, WHEN THE PROPER PARAMETERS ARE USED, A FEATURE NOT FOUND IN SUBMERGED ARC WELDING.
- WELDING SPEEDS ARE HIGHER THAN THOSE OF THE SMAW PROCESS.
- DEPOSITION RATES ARE SIGNIFICANTLY HIGHER THAN THOSE OBTAINED BY THE SMAW PROCESS.
- CONTINUOUS WIRE FEED ENABLES LONG WELDS TO BE DEPOSITED WITHOUT STOPS AND STARTS.
- PENETRATION THAT IS DEEPER THAN THAT OF THE SMAW PROCESS IS POSSIBLE, WHICH MAY PERMIT THE USE OF SMALLER-SIZED FILLET WELDS FOR EQUIVALENT STRENGTHS.
- LESS OPERATOR SKILL IS REQUIRED THAN FOR OTHER CONVENTIONAL PROCESSES, BECAUSE THE ARC LENGTH IS MAINTAINED CONSTANT WITH REASONABLE VARIATIONS IN THE DISTANCE BETWEEN THE CONTACT TIP AND THE WORKPIECE.
- MINIMAL POSTWELD CLEANING IS REQUIRED BECAUSE OF THE ABSENCE OF A HEAVY SLAG.

These advantages make the process particularly well suited to high-production and automated welding applications. With the advent of robotics, gas-metal arc welding has become the predominant process choice.

Limitations. The GMAW process, like any welding process, has certain limitations that restrict its use:

- THE WELDING EQUIPMENT IS MORE COMPLEX, USUALLY MORE COSTLY, AND LESS PORTABLE THAN SMAW EQUIPMENT.
- THE PROCESS IS MORE DIFFICULT TO APPLY IN HARD-TO-REACH PLACES BECAUSE THE WELDING GUN IS LARGER THAN A SMAW HOLDER AND MUST BE HELD CLOSE TO THE JOINT (WITHIN 10 TO 19 MM, OR $\frac{3}{8}$ TO $\frac{3}{4}$ IN.) TO ENSURE THAT THE WELD METAL IS PROPERLY SHIELDED.
- THE WELDING ARC MUST BE PROTECTED AGAINST AIR DRAFTS THAT CAN DISPERSE THE SHIELDING GAS, WHICH LIMITS OUTDOOR APPLICATIONS UNLESS PROTECTIVE SHIELDS ARE PLACED AROUND THE WELDING AREA.
- RELATIVELY HIGH LEVELS OF RADIATED HEAT AND ARC INTENSITY CAN HINDER OPERATOR ACCEPTANCE OF THE PROCESS.

Process Fundamentals

Principles of Operation. In the GMAW process (Fig. 1), an arc is established between a continuously fed electrode of filler metal and the workpiece. After proper settings are made by the operator, the arc length is maintained at the set value, despite the reasonable changes that would be expected in the gun-to-work distance during normal operation. This automatic arc regulation is achieved in one of two ways. The most common method is to utilize a constant-speed (but adjustable) electrode feed unit with a variable-current (constant-voltage) power source. As the gun-to-work relationship changes, which instantaneously alters the arc length, the power source delivers either more current (if the arc length is decreased) or less current (if the arc length is increased). This change in current will cause a corresponding change in the electrode melt-off rate, thus maintaining the desired arc length.

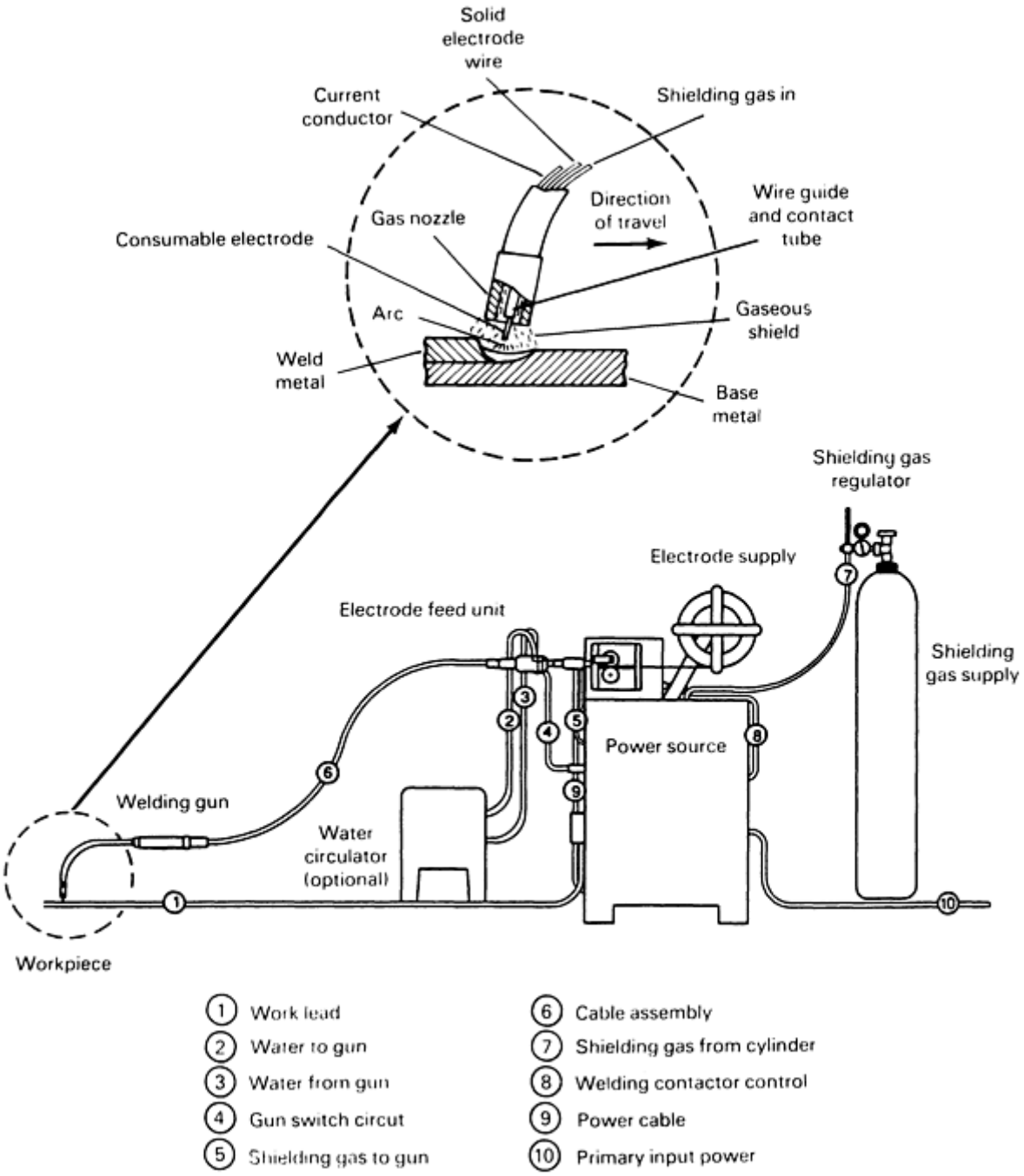

FIG. 1 SCHEMATIC OF GMAW PROCESS

The second method of arc regulation utilizes a constant-current power source and a variable-speed, voltage-sensing electrode feeder. In this case, as the arc length changes, there is a corresponding change in the voltage across the arc. As this voltage change is detected, the speed of the electrode feed unit will change to provide either more or less electrode per unit of time. This method of regulation is usually limited to larger electrodes with lower feed speeds.

Metal Transfer Mechanisms. The characteristics of the GMAW process are best described by reviewing the three basic means by which metal is transferred from the electrode to the work: short-circuiting transfer, globular transfer, or spray transfer. The type of transfer is determined by a number of factors, the most influential of which are:

- MAGNITUDE AND TYPE OF WELDING CURRENT
- ELECTRODE DIAMETER
- ELECTRODE COMPOSITION
- ELECTRODE EXTENSION BEYOND THE CONTACT TIP OR TUBE
- SHIELDING GAS
- POWER SUPPLY OUTPUT

Short-circuiting transfer encompasses the lowest range of welding currents and electrode diameters associated with the GMAW process. This type of transfer produces a small, fast-freezing weld pool that is generally suited for joining thin sections, for out-of-position welding, and for bridging of large root openings. Metal is transferred from the electrode to the workpiece only during a period when the electrode is in contact with the weld pool, and there is no metal transfer across the arc gap (Fig. 2).

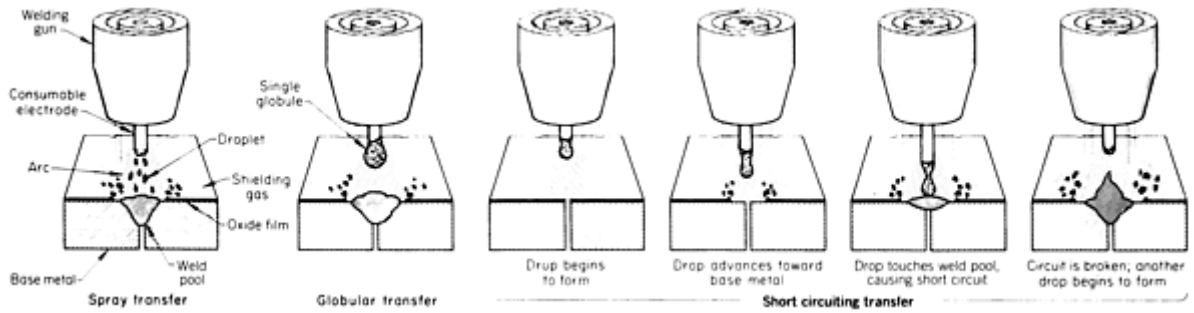

FIG. 2 TRANSFER MODES IN GMAW PROCESS

The electrode contacts the molten weld pool at a steady rate that can range from 20 to over 200 times per second. As the wire touches the weld metal, the current increases and the liquid metal at the wire tip is pinched off, initiating an arc. The rate of current increase must be high enough to heat the electrode and promote metal transfer, yet low enough to minimize spatter caused by violent separation of the molten drop. The rate of current increase is controlled by adjusting the power source inductance. The optimum setting depends on the electrical resistance of the welding circuit and the melting temperature of the electrode. When the arc is initiated, the wire melts at the tip as it is fed forward toward the next short circuit. The open-circuit voltage of the power source must be low enough so that the drop of molten metal cannot transfer until it contacts the weld metal.

Because metal transfer only occurs during short circuiting, the shielding gas has very little effect on the transfer itself. However, the gas does influence the operating characteristics of the arc and the base-metal penetration. The use of carbon dioxide generally produces high spatter levels, when compared with inert gases, but it allows deeper penetration when welding steels. To achieve a good compromise between spatter and penetration, mixtures of carbon dioxide and argon are often used. With nonferrous metals, argon-helium mixtures are used to achieve this compromise.

Globular Transfer. With a positive electrode, globular transfer takes place when the current density is relatively low, regardless of the type of shielding gas. However, the use of carbon dioxide or helium results in this type of transfer at all usable welding currents. Globular transfer is characterized by a drop size with a diameter that is greater than that of the electrode. This large drop is easily acted upon by gravity, which limits successful transfer to the flat position.

At average currents that are slightly higher than those used in short-circuiting transfer, axially directed globular transfer can be achieved in a substantially inert gas shield. However, if the arc length is too short, then the enlarging drop can short to the workpiece, become superheated, and disintegrate, producing considerable spatter. Therefore, the arc length must be long enough to ensure that the drop detaches before it contacts the weld pool. However, when higher voltage values are used, the weld is likely to be unacceptable, because of a lack of fusion, insufficient penetration, and excessive reinforcement. This limits the use of this transfer mode to very few production applications.

Carbon dioxide shielding produces a randomly directed globular transfer when the welding current and voltage values are significantly higher than the range used for short-circuiting transfer. Although severe spatter conditions result when conventional techniques are used, carbon dioxide is still the most commonly used shielding gas for welding mild steel when the quality requirements are not too rigorous. The spatter problem is controlled by "burying" the arc below the weld/base-metal surface. The resulting arc forces are adequate enough to produce a depression that contains the spatter. This technique requires relatively high currents and results in very deep penetration. Good operator setup skills are required. However, poor wetting action can result in an excessive weld reinforcement.

Spray Transfer. A very stable, spatter-free "spray" transfer mode can be produced when argon-rich shielding is used. This type of transfer requires the use of direct current with the electrode positive and a current level that is above a critical value called the "transition current." Below this current level, transfer occurs in the globular mode at the rate of a few drops per second. At values above the transition current, transfer occurs in the form of very small drops that are formed and detached at the rate of hundreds per second and are accelerated axially across the arc gap.

The transition current is proportional to the electrode diameter, and, to a lesser extent, to the electrode extension. It also has a direct relationship to the filler metal melting temperature. Transition currents for various materials and electrode diameters are shown in Table 1.

TABLE 1 GLOBULAR-TO-SPRAY TRANSITION CURRENTS FOR SELECTED ELECTRODES

WIRE ELECTRODE TYPE	SHIELDING GAS	WIRE DIAMETER		SPRAY ARC CURRENT, A
		mm	in.	
LOW-CARBON STEEL	98AR-2O_2	0.58	0.023	135
		0.76	0.030	150
		0.89	0.035	165
		1.14	0.045	220
		1.57	0.062	275
	95AR-5O_2	0.89	0.035	155
		1.14	0.045	200
		1.57	0.062	265
	92AR-8CO_2	0.89	0.035	175
		1.14	0.045	225
		1.57	0.062	290
	85AR-15CO_2	0.89	0.035	180
		1.14	0.045	240
		1.57	0.062	295
	80AR-20CO_2	0.89	0.035	195
		1.14	0.045	255
		1.57	0.062	345
STAINLESS STEEL	99AR-1O_2	0.89	0.035	150
		1.14	0.045	195
		1.57	0.062	265
	AR-HE-CO_2	0.89	0.035	160
		1.14	0.045	205
		1.57	0.062	280
	AR-H_2-CO_2	0.89	0.035	145

		1.14	0.045	185
		1.57	0.062	255
ALUMINUM	ARGON	0.76	0.030	95
		1.19	0.047	135
		1.57	0.062	180
DEOXIDIZED COPPER	ARGON	0.89	0.035	180
		1.14	0.045	210
		1.57	0.062	310
SILICON BRONZE	ARGON	0.89	0.035	165
		1.14	0.045	205
		1.57	0.062	270

Source: Union Carbide Industrial Gases

The spray transfer mode results in a highly directed stream of discrete drops that are accelerated by arc forces to velocities that overcome the effects of gravity. This enables the process to be used in any position, under certain conditions. Because the drops are separated, short circuits do not occur, and the spatter level is negligible, if not totally eliminated.

Another characteristic of spray transfer is the "finger" penetration pattern that it produces directly below the electrode tip. Although the penetration can be deep, it can be affected by magnetic fields that must be controlled to ensure that it is always located at the center of the weld penetration profile. Otherwise, a lack of fusion and an irregular bead surface profile can result.

The spray transfer mode can be used to weld almost any metal or alloy, because of the inert characteristics of the argon shield. Sometimes, thickness can be a factor, because of the relatively high current levels required. The resultant arc forces can cut through, rather than weld, thin sheets. In addition, high deposition rates can result in a weld pool size that cannot be supported by surface tension in the vertical and overhead positions. However, the thickness and position limitations of spray transfer have been largely overcome by specially designed power supplies. These machines produce carefully controlled current outputs that "pulse" the welding current from levels below the transition current to levels above it.

Figure 3 shows the two levels of current provided by these machines. One is a constant, low-background current that sustains the arc without providing enough energy to cause the formation of drops on the wire tip. The other is a superimposed pulsing current with an amplitude that is greater than the transition current necessary for spray transfer. During this pulse, one or more drops are formed and transferred. The frequency and amplitude of the pulses control the energy level of the arc and, therefore, the rate at which the wire melts. By reducing the arc energy and the wire melting rate, it is possible to retain many of the desirable features of spray transfer while joining sheet metals and welding thick metals in all positions.

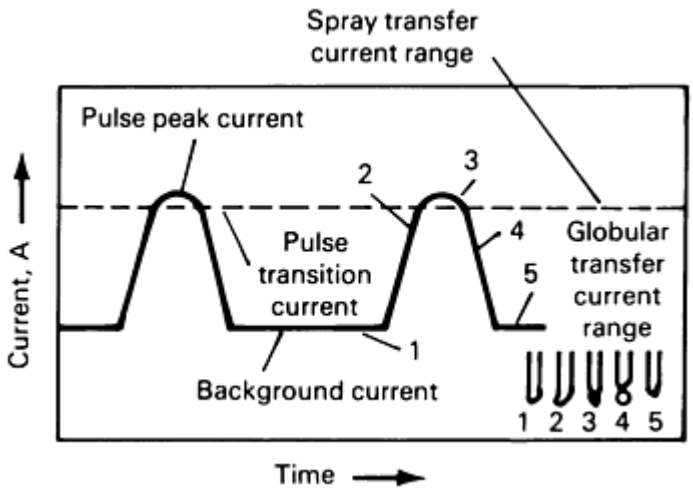

FIG. 3 CHARACTERISTIC CURRENT WAVEFORM FOR A "PULSING" POWER SUPPLY

Many variations of such machines are available. The simplest provide a single frequency of pulsing (60 or 120 pulses/s) and independent control of the background and pulsing current levels. Synergic machines, which are sophisticated, automatically provide the optimum combination of background and pulsing current levels for any given setting of wire feed speed. Normally, these settings are specific to an electrode/shielding gas combination and must be changed or reprogrammed when the combination is changed.

Process Variables. The important variables of the GMAW process that affect weld penetration, bead geometry, and overall weld quality are:

- WELDING CURRENT (ELECTRODE FEED SPEED)
- POLARITY
- ARC VOLTAGE (ARC LENGTH)
- TRAVEL SPEED
- ELECTRODE EXTENSION
- ELECTRODE ORIENTATION (GUN ANGLE)
- ELECTRODE DIAMETER

Knowledge and control of these variables are essential to consistently produce welds of satisfactory quality. Because they are not completely independent of one another, changing one variable generally requires changing one or more of the others to produce the desired results. The effects of these variables on deposit attributes are shown in Table 2.

TABLE 2 EFFECT OF CHANGES IN PROCESS VARIABLES ON WELD ATTRIBUTES

WELDING VARIABLES TO CHANGE	DESIRED CHANGES							
	PENETRATION		DEPOSITION RATE		BEAD SIZE		BEAD WIDTH	
	INCREASE	DECREASE	INCREASE	DECREASE	INCREASE	DECREASE	INCREASE	DECREASE
CURRENT AND WIRE FEED SPEED	INCREASE	DECREASE	INCREASE	DECREASE	INCREASE	DECREASE	LITTLE EFFECT	LITTLE EFFECT
VOLTAGE	NO EFFECT	NO EFFECT	LITTLE EFFECT	LITTLE EFFECT	LITTLE EFFECT	LITTLE EFFECT	INCREASE	DECREASE
TRAVEL SPEED	NO EFFECT	NO EFFECT	LITTLE EFFECT	LITTLE EFFECT	DECREASE	INCREASE	DECREASE	INCREASE
ELECTRODE EXTENSION	DECREASE	INCREASE	INCREASE(A)	DECREASE(A)	INCREASE	DECREASE	DECREASE	INCREASE
WIRE DIAMETER	DECREASE	INCREASE	DECREASE	INCREASE	LITTLE EFFECT	LITTLE EFFECT	LITTLE EFFECT	LITTLE EFFECT
SHIELD GAS %	INCREASE	DECREASE	LITTLE EFFECT	LITTLE EFFECT	LITTLE EFFECT	LITTLE EFFECT	INCREASE	DECREASE
GUN ANGLE	DRAG	PUSH	LITTLE EFFECT	LITTLE EFFECT	LITTLE EFFECT	LITTLE EFFECT	PUSH	DRAG

(A) WILL RESULT IN DESIRED CHANGE IF CURRENT LEVELS ARE MAINTAINED BY ADJUSTMENT OF WIRE FEED SPEED

Considerable skill and experience are necessary to select the optimal combination for each application. This selection is further complicated by the fact that the optimal settings for the variables are also affected by the type of base metal, the electrode composition, the welding position, quality requirements, and the number of completed weldments required. Thus, no single set of parameters provides optimal results in every case.

Welding Current. As the electrode feed speed is varied, the welding current varies in a like manner when a constant-voltage power source is used. This occurs because the current output of the power source varies dramatically with the slight changes in the arc voltage (arc length) that result when changes are made in the electrode feed speed. When all

other variables are held constant, an increase in welding current results in an increase in the depth and width of penetration, deposition rate, and weld bead size.

Polarity is the term used to described the electrical connection of the welding gun in relation to the terminals of a direct-current (dc) power source. When the gun power lead is connected to the positive terminal, the polarity is designated as direct current, electrode positive (DCEP). Alternatively, a connection to the negative terminal is designated as direct current, electrode negative (DCEN). The vast majority of GMAW applications utilize DCEP, because it provides for a stable arc, low spatter, a good weld bead profile, and the greatest depth of penetration.

Arc voltage and arc length are related terms that are often used interchangeably. However, they are different. Arc voltage is an approximate means of stating the physical arc length in electrical terms. The same physical arc length, however, could yield different arc voltage readings, depending on factors such as shielding gas, current, and electrode extension. When all variables are held constant, a reliable relationship exists between the two: an increase in voltage setting will result in longer arc length. Although the arc length is the variable of interest and the one that should be controlled, arc voltage is more easily monitored. Because of this fact, and because the arc voltage is normally required to be specified in welding procedures, it is the term that is more commonly used. From any specific value of arc voltage, an increase tends to flatten the weld bead and increase the width of the fusion zone. Excessively high voltage can cause porosity, spatter, and undercut. A reduction in voltage results in a narrower weld bead with a higher crown.

Travel speed is the linear rate at which the arc is moved along the weld joint. When all other conditions are held constant, weld penetration is a maximum at an intermediate travel speed. When travel speed is decreased, the filler metal deposition per unit length increases. At very slow speeds, the welding arc impinges on the molten weld pool, rather than the base metal, thereby reducing the effective penetration.

As the travel speed is increased, the thermal energy transmitted to the base metal from the arc increases, because the arc acts more directly on the base metal. However, further increases in travel speed impart less thermal energy to the base metal. Thus, melting of the base metal first increases and then decreases with increasing travel speed. As travel speed is increased further, there is a tendency toward undercutting along the edges of the weld bead, because there is insufficient deposition of filler metal to fill the path melted by the arc.

Electrode orientation is described in two ways: by the relationship of the electrode axis with respect to the direction of travel (the travel angle) and by the angle between the electrode axis and the adjacent work surface (work angle). When the electrode points in a direction opposite to the travel direction, it results in a trail angle and is known as the backhand welding technique. When the electrode points in the direction of travel, it results in a lead angle and is called the forehand welding technique.

For all positions, a trailing travel angle that ranges from 5 to 15° (from perpendicular) provides a weld with maximum penetration and a narrow, convex surface configuration. It also provides for maximum shielding of the molten weld pool. However, the common technique utilizes a leading travel angle, which provides better visibility for the operator and a weld with a flatter surface profile. For some materials, such as aluminum, a leading angle is preferred, because it provides a "cleaning action" ahead of the molten weld metal, which promotes wetting and reduces base-material oxidation.

When producing fillet welds in the horizontal position, the work angle should be about 45° to the vertical member.

The electrode extension is the distance between the last point of electrical contact (usually the gun contact tip or tube) and the end of the electrode. An increase in the amount of this extension causes an increase in electrical resistance. This, in turn, generates additional heat in the electrode, which contributes to greater electrode melting rates. Without an increase in arc voltage, the additional metal will be deposited as a narrow, high-crowned weld bead. The optimum electrode extension generally ranges from 6.4 to 13 mm ($\frac{1}{4}$ to $\frac{1}{2}$ in.) for short-circuiting transfer and from 13 to 25 mm ($\frac{1}{2}$ to 1 in.) for spray and globular transfers.

The electrode diameter influences the weld bead configuration. A larger electrode requires a higher minimum current than a smaller electrode does to achieve the same metal transfer characteristics.

Higher currents, in turn, produce additional electrode melting and larger, more-fluid weld deposits. Higher currents also result in higher deposition rates and greater penetration, but may prevent the use of some electrodes in the vertical and overhead positions.

Gas-Metal Arc Welding

D.B. Holliday, Westinghouse Electric Corporation

Equipment

The basic equipment for a typical GMAW installation is shown in Fig. 1. The major components are discussed below.

A welding gun provides electrical current to the electrode, directs it to the workpiece, and provides a vehicle for directing shielding gas to the weld area. Different types of guns have been designed for many varied applications, ranging from heavy-duty guns for high-current, high-volume production to lightweight guns for low-current or out-of-position welding. The most commonly used guns are designed to be cooled by the surrounding air (Fig. 4). However, as amperage requirements increase, a water-cooled gun may be required. Guns are rated based on their current-carrying capacity, generally with a CO_2 shielding gas. If inert gases are used, these gun ratings must be reduced significantly. Guns can also be equipped with their own integral electrode feed units.

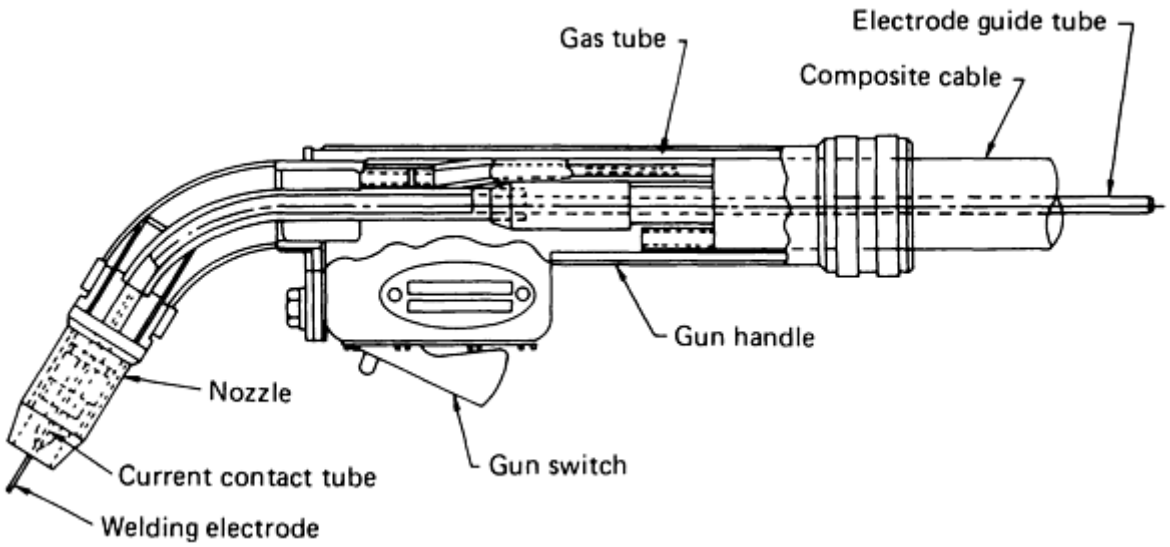

FIG. 4 CROSS SECTION OF AN AIR-COOLED GMAW GUN

The contact tube, usually made of copper or a copper alloy, is used to transmit welding current to the electrode, as well as to direct the electrode toward the work. The contact tube is connected electrically to the welding power supply by the power cable. The inner surface of the contact tube is very important, because the electrode must feed easily through this tube while making a good electrical contact. Generally, the hole in the contact tube would be from 0.13 to 0.25 mm (0.005 to 0.010 in.) larger than the wire being used, although larger sizes may be required for materials such as aluminum. The hole should be checked periodically and replaced if it has become elongated because of excessive wear. If a tip in this condition is used, it can result in poor electrical contact and erratic arc characteristics.

The nozzle directs an even-flowing column of shielding gas into the welding zone. It is extremely important to maintain an even flow in order to adequately protect the molten weld metal from atmospheric contamination. Different-sized nozzles are available and should be chosen according to the application, that is, larger nozzles for high-current work where the puddle is large and smaller nozzles for low-current and short-circuiting welding.

The electrode conduit and liner are connected to a bracket adjacent to the feed rolls on the electrode feed motor. The conduit and liner support both protect and direct the electrode from the feed rolls to the gun and contact tube. Uninterrupted electrode feeding is necessary to ensure good arc stability. A steel liner is recommended when using hard

electrode materials, such as steel and copper, whereas nylon liners should be used for soft electrode materials, such as aluminum and magnesium.

The electrode feed unit, or wire feeder, consists of an electric motor, output shaft, drive rolls, and accessories for maintaining electrode alignment and pressure (Fig. 5). These units can be separate or integrated with the speed control or located remotely from it. The electrode feed motor is usually a direct-current type and provides the mechanical energy for pushing the electrode through the gun and to the work. It has a control circuit that varies the motor speed over a broad range. The feed unit can be an integral component of the gun (Fig. 6) or dual-feed units, one in the gun and one in a separate feeder, can be electrically coupled together to provide a "push-pull" system. The spool-gun and push-pull systems are often used on aluminum, where difficulty can be encountered in trying to push the wire through a conduit to the gun.

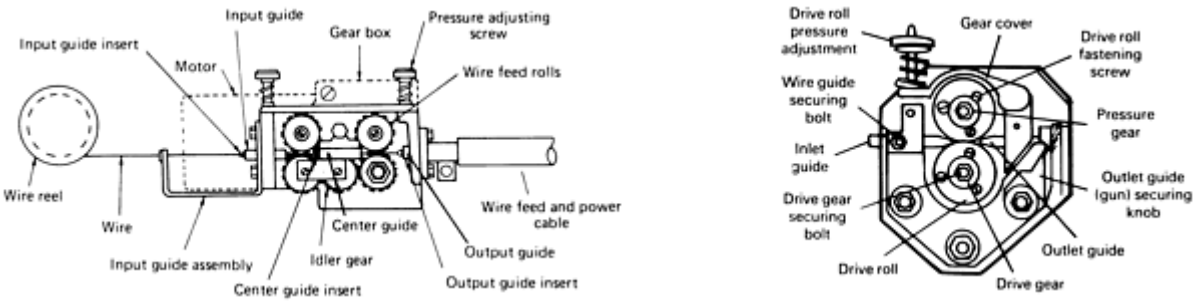

FIG. 5 TYPICAL REMOTE-WIRE FEED UNITS. (A) SCHEMATIC OF A TYPICAL FOUR-ROLL SYSTEM MECHANISM. (B) CLOSE-UP VIEW OF A TYPICAL TWO-ROLL SYSTEM GEARBOX

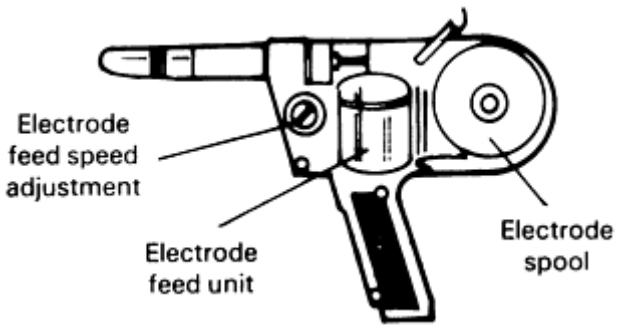

FIG. 6 SPOOL-ON-GUN TYPE TORCH WITH COVER REMOVED TO SHOW SELF-CONTAINED PULL-TYPE FEED-UNIT SYSTEM

The feed motor is connected through a gear reducer to a set of wire feed rolls that transmit mechanical energy to the electrode, pulling it from the source and pushing it through the welding gun. Various types of rolls are available, including knurled, "U" groove, "V" groove, and flat. The knurled design is used for harder wires, such as steel, and allows maximum frictional force to be transmitted to the wire with a minimum of drive roll pressure. These types of rolls are not recommended for soft wires, such as aluminum, because they tend to cause the wire to flake, which can eventually clog the gun or liner. For these softer wires, the "U" groove or "V" groove type will allow the application of uniform pressure around the wire without deforming it. The flat rolls can be used with the smaller-diameter wires and in combination with a "U" or "V" groove.

The welding control mechanism and the electrode feed motor for semiautomatic operation are usually provided in one integrated package. The main function of the welding control mechanism is to regulate the speed of the electrode feed motor, usually through an electronic governor. The control also regulates the starting and stopping of the electrode feed through a signal received from the gun switch.

Normally, shielding gas, water (when used), and welding power are also delivered to the gun through the control mechanism, which requires direct connection to these facilities and the power supply. Gas and water flow are regulated to coincide with the weld start and stop by using solenoid valves. The control mechanism can also sequence gas flow starts and stops and energize the power source contractor. The control mechanism may allow some gas to flow before welding starts (preflow) and after welding stops (postflow) to protect the molten weld puddle. The control mechanism is usually independently powered by 115 V ac.

The welding power source provides suitable electrical power (generally 20 to 80 V) that is delivered to the electrode and workpiece to produce the arc. Because the vast majority of GMAW applications utilize DCEP, the positive lead is connected to the gun and the negative lead, to the workpiece. The power source can be the "static" type in which incoming utility power (120 to 480 V) is reduced to welding voltage by a transformer or solid-state inverter. It could also be the "rotating" type in which the welding power is provided by a rotating generator driven by a motor or internal combustion engine. The static type is normally used in shops where there is an available source of power. It has advantages over the rotating type in that it can respond more rapidly to varying arc conditions. The rotating type is generally used at field sites where external power in unavailable. Both types of power sources can be designed and built to provide either a constant current or constant potential (cp) output, the latter of which is the most common by far. On newer power sources, this cp output can be pulsed at either a constant or variable frequency. With the advent of solid-state electronic power sources, such as inverters, even further control over the pulsing variables (for example, frequency, pulse width, and so on) can be obtained.

When used in conjunction with a constant-speed wire feeder, the constant-voltage power source compensates for the variations in the contact-tip-work-distance that can occur during normal welding operations. It does this by instantaneously increasing or decreasing welding current to increase or decrease the electrode burnoff rate. The initial arc length is established by adjusting the voltage at the power source. Once this is set, no other changes are required during welding. The wire feed speed, which is also the current control, is then set by the operator and adjusted as necessary. In addition to this self-regulating feature of the CP power source, control over slope and inductance is included on those machines intended for short-circuiting transfer. Additional controls are also provided when using power sources that have pulsing capabilities.

Additional information is available in the article "Power Sources" in this Volume.

Electrode Source. The GMAW process uses a continuously fed electrode that is consumed at relatively high speeds. Therefore, the electrode source must provide a large volume of material that can readily be fed to the gun to ensure maximum process efficiency. This source is usually in the form of a spool or coil that can hold from 7 to 27 kg (15 to 60 lb) of wire that has been wound to allow free feeding without kinks or tangles. Larger spools of up to 115 kg (250 lb) are also available, and material can be provided in drums of 340 to 455 kg (750 to 1000 lb). Small spools of 0.45 to 0.9 kg (1 to 2 lb) are used for spool-on-gun equipment.

Regulated Shielding Gas Supply. A system is required to provide constant shielding gas pressure and flow rate during welding. This system consists of a regulator connected to a supply of "welding grade" shielding gas, as well as the necessary hoses or piping. The regulator is a device that reduces the source gas pressure to a constant working pressure, regardless of variations at the source. It can be a single-stage or dual-stage type and may have a built-in flowmeter. The shielding gas source can be a high-pressure cylinder, a liquid-filled cylinder, or a bulk-liquid tank. Gas mixtures are available in a single cylinder. Mixing devices can also be used to obtain the correct proportions when two or more gases or liquids are used. The type and size of the gas storage source depend on economic considerations that are based on the volume of shielding gas consumed per unit of time.

D.B. Holliday, Westinghouse Electric Corporation

Consumables

The two consumable, but essential, elements of the GMAW process are the electrode and the shielding gas, each of which is described below.

The chemical composition of the electrode must be selected to achieve the desired properties in the weld metal. The composition is designed with extra deoxidizers or other scavenging agents to compensate for reactions with the

atmosphere and the base metal. The deoxidizers most commonly used in steel electrodes are silicon and manganese. Silicon can also be added in all transfer modes to increase weld metal fluidity or it can be added when a 300 series stainless steel electrode is used.

The physical characteristics (finish, straightness, and others) of electrodes used in the GMAW process are important to successful welding. The material specifications for these electrodes establish manufacturing requirements to ensure that users receive a uniform product that feeds smoothly through the equipment and has these characteristics, as well:

- UNIFORM WINDING ON THE SPOOL OR COIL WITH NO KINKS OR BENDS
- SMOOTH SURFACE FINISH FREE OF SLIVERS, SCRATCHES, OR SCALE
- PRESCRIBED CAST AND HELIX
- UNIFORM DIAMETER

Cast and helix refer to dimensions of a single coil of wire removed from a spool or coil and layed (that is, cast) on a flat surface. If this coil is too small in diameter (cast) or shows an excessive lift from the flat surface (helix) wire, feeding problems during welding can be anticipated.

Shielding Gas

The primary function of the shielding gas in most of the welding processes is to protect the surrounding atmosphere from contact with molten metal. In the GMAW process, this gas plays an additional role in that it has a pronounced effect on arc characteristics, mode of metal transfer, depth of fusion, weld bead profile, welding speed, and cleaning action.

Inert gases, such as argon and helium, are commonly used, as is the active gas, CO_2. It is also common to use mixtures of these gases and to employ small additions of oxygen.

Information about shielding gas compositions and about which gases to use for specific joining applications is provided in the article "Shielding Gases" in this Volume.

Gas-Metal Arc Welding

D.B. Holliday, Westinghouse Electric Corporation

Safety

The major hazards of concern during GMAW are: the fumes and gases, which can harm health; the high-voltage electricity, which can injure and kill; the arc rays, which can injure eyes and burn skin; and the noise which may be present that can damage hearing.

The type and amount of fumes and gas present during welding depend on the electrode being used, the alloy being welded, and the presence of any coatings on the base metal. To guard against potential hazards, a welder should keep his head out of the fume plume and avoid breathing the fumes and gases caused by the arc. Ventilation is always required.

Electrode shock can result from exposure to the high open-circuit voltages associated with welding power supplies. All electrical equipment and the workpiece must be connected to an approved electrical ground. Cables should be of sufficient size to carry the maximum current required. Insulation should be protected from cuts and abrasion, and the cable should not come into contact with oils, paints, or other fluids which may cause deterioration. Work areas, equipment, and clothing must be kept dry at all times. The welder should be well insulated, wearing dry gloves, rubber-soled shoes, and standing on a dry board or platform while welding.

Radiant energy, especially in the ultraviolet range, is intense during GMAW. To protect the eyes from injury, the proper filter shade for the welding-current level selected should be used. These greater intensities of ultraviolet radiation can cause rapid disintegration of cotton clothing. Leather, wool, and aluminum-coated cloth will better withstand exposure to arc radiation and better protect exposed skin surfaces.

When noise has been determined to be excessive in the work area, ear protection should be used. This can also be used to prevent spatter from entering the ear.

Conventional fire prevention requirements, such as removal of combustibles from the work area, should be followed. Sparks, slag, and spatter can travel long distances, so care must be taken to minimize the start of a fire at locations removed from the welding operation. For further information, see the guidelines set forth in the National Fire Protection Association Standard NFPA No. 51B, "Fire Protection in Use of Cutting and Welding Processes."

Care should be exercised in the handling, storage, and use of cylinders containing high-pressure and liquefied gases. Cylinders should be secured by chains or straps during handling or use. Approved pressure-reducing regulators should be used to provide a constant, controllable working pressure for the equipment in use. Lubricants or pipe fitting compounds should not be used for making any connections, as they can interfere with the regulating equipment, and in the case of oxygen service, they can contribute to a catastrophic fire.

For further safety information, see ANSI/AWS Z49.1, "Safety in Welding and Cutting."

Flux-Cored Arc Welding

David W. Meyer, The Esab Group, Inc.

Introduction

IN THE FLUX-CORED ARC WELDING (FCAW) process, the heat for welding is produced by an electric arc between a continuous filler metal electrode and the workpiece. A tubular, flux-cored electrode makes this welding process unique. The flux contained within the electrode can make the electrode self-shielding. Alternatively, an external shielding gas may be required.

Flux-Cored Arc Welding

David W. Meyer, The Esab Group, Inc.

Process Features

Flux-cored arc welding has two major variations. The gas-shielded FCAW process (Fig. 1) uses an externally supplied gas to assist in shielding the arc from nitrogen and oxygen in the atmosphere. Generally, the core ingredients in gas-shielded electrodes are slag formers, deoxidizers, arc stabilizers, and alloying elements.

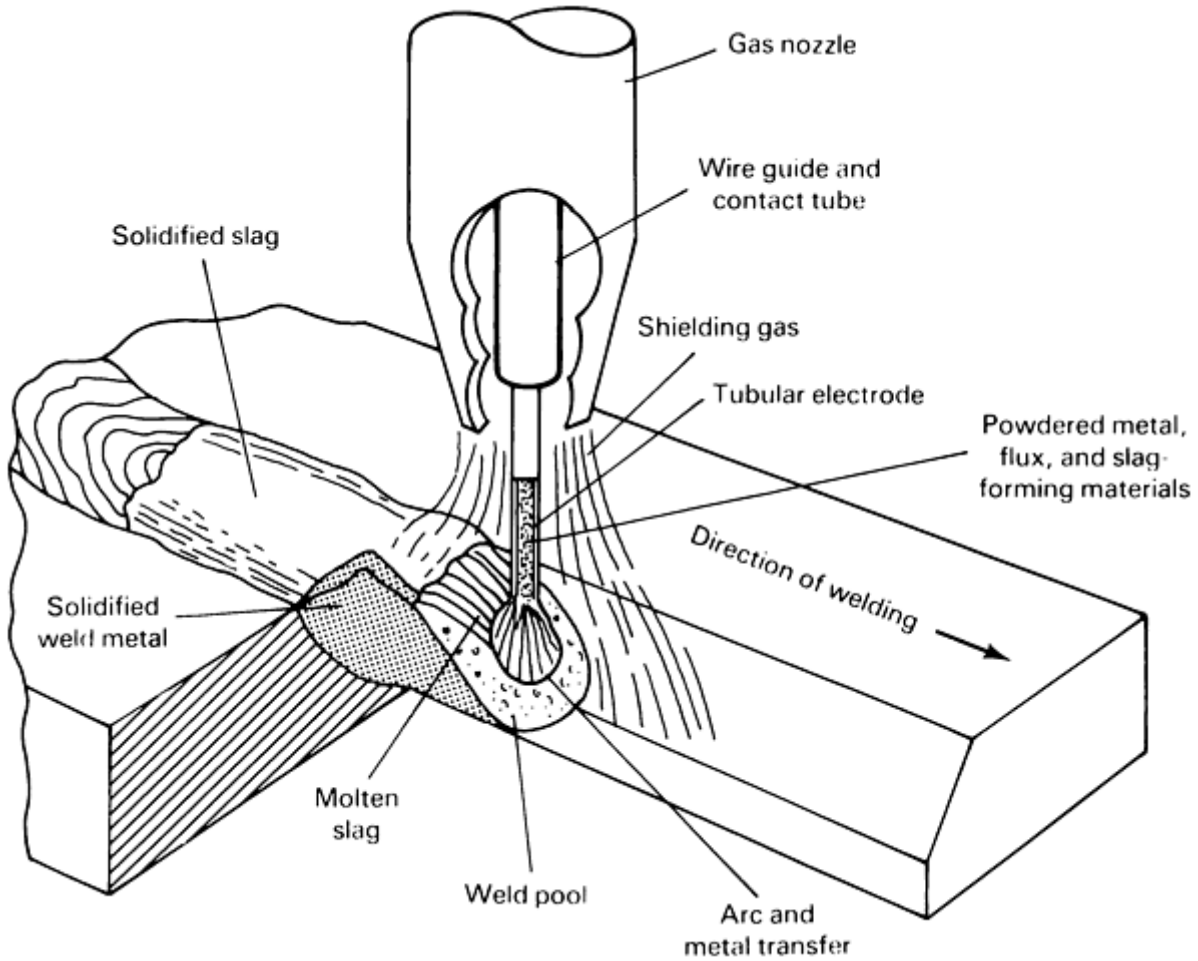

FIG. 1 GAS-SHIELDED FLUX-CORED ARC WELDING. SOURCE: REF 1

In the self-shielded FCAW process, the core ingredients protect the weld metal from the atmosphere without external shielding. Some self-shielded electrodes provide their own shielding gas through the decomposition of core ingredients. Others rely on slag shielding, where the metal drops being transferred across the arc and the molten weld pool are protected from the atmosphere by a slag covering. Many self-shielded electrodes also contain substantial amounts of deoxidizing and denitrifying ingredients to help achieve sound weld metal. Self-shielded electrodes can also contain arc stabilizers and alloying elements.

Advantages. Because it combines the productivity of continuous welding with the benefits of having a flux present, the FCAW process has several advantages relative to other welding processes. These advantages include:

- HIGH DEPOSITION RATES, ESPECIALLY FOR OUT-OF-POSITION WELDING
- LESS OPERATOR SKILL REQUIRED THAN FOR GAS-METAL ARC WELDING (GMAW)
- SIMPLER AND MORE ADAPTABLE THAN SUBMERGED ARC WELDING (SAW)
- DEEPER PENETRATION THAN SHIELDED METAL ARC WELDING (SMAW)
- MORE TOLERANT OF RUST AND MILL SCALE THAN GMAW

Disadvantages of the FCAW process include:

- SLAG MUST BE REMOVED FROM THE WELD AND DISPOSED OF
- MORE SMOKE AND FUME ARE PRODUCED IN FCAW THAN IN THE GMAW AND SAW PROCESSES

- FUME EXTRACTION IS GENERALLY REQUIRED
- EQUIPMENT IS MORE COMPLEX AND MUCH LESS PORTABLE THAN SMAW EQUIPMENT

Reference cited in this section

1. *WELDING HANDBOOK*, 8TH ED., VOL 2, AWS, 1991

Flux-Cored Arc Welding

David W. Meyer, The Esab Group, Inc.

Applications

Flux-cored arc welding enjoys widespread use in many industries. Both the gas-shielded and self-shielded FCAW processes are used to fabricate structures from carbon and low-alloy steels. Both process variants are used for shop fabrication, but the self-shielded FCAW process is preferred for field use. The acceptability of the FCAW process for structural use is illustrated by the fact that prequalified joints are included in the structural welding code of the American Welding Society (AWS).

Gas-shielded flux-cored electrodes are commonly used to weld carbon, low-alloy steel, and stainless steels in the construction of pressure vessels and piping for the chemical processing, petroleum refining, and power-generation industries. In addition, flux-cored electrodes are used to weld some nickel-base alloys.

Flux-cored electrodes are also used in the automotive and heavy-equipment industries in the fabrication of frame members, axle housings, wheel rims, suspension components, and other parts. Small-diameter flux-cored electrodes are used for automotive body repair.

Flux-Cored Arc Welding

David W. Meyer, The Esab Group, Inc.

Equipment

The FCAW process utilizes semiautomatic, mechanized, and fully automatic welding systems. The basic equipment includes a power supply, wire feed system, and welding gun. The required auxiliary equipment, such as shielding gas, depends on the process variant used and the degree of automation. Fume removal equipment must also be considered in most applications of the FCAW process.

Typical semiautomatic equipment is shown in Fig. 2. The equipment used in the gas-shielded FCAW process is typically identical to GMAW equipment.

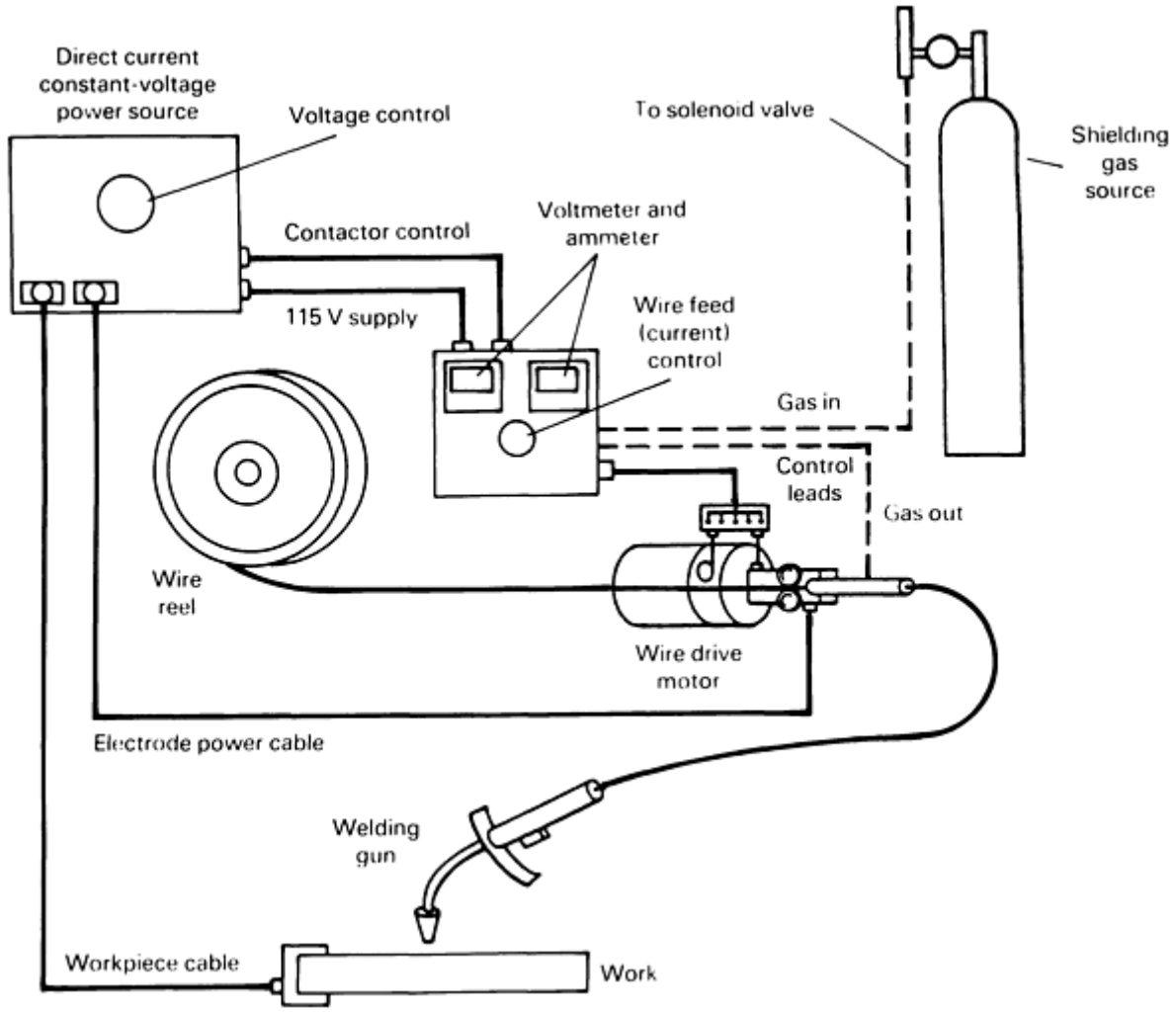

FIG. 2 SEMIAUTOMATIC FCAW EQUIPMENT. SOURCE: REF 1

The recommended power supply for the semi-automatic FCAW process is a constant-voltage direct current (dc) machine. Most power supplies used for semiautomatic FCAW have output ratings of 600 A or less. A power supply rated at 60% or more duty cycle is the best choice for most industrial applications, whereas a duty-cycle rating as low as 20% may be sufficient for maintenance and repair applications.

Constant-current power supplies are used in certain situations, such as field welding applications, where portable constant-current SMAW power supplies are readily available. The addition of a contactor and a voltage-sensing wire feeder makes this an adequate welding system. However, such a system is only recommended when the use of a constant-voltage system is not feasible, because constant-current systems produce an inherently less-stable welding arc than constant-voltage systems.

Wire feeders for constant-voltage FCAW systems are generally simple devices that provide a constant wire feed speed. The power supply provides sufficient current to maintain an arc at the voltage that is preset at the power supply. A change in wire feed speed results in a change in the welding current.

In a constant-current system, the wire feeder is somewhat more complex. The welding current is preset at the power supply. The wire feeder has a voltage-sensing feedback loop that allows it to adjust the wire feed speed to maintain the desired welding voltage. The wire feeder generally contains systems to close the contactor and open the shielding gas solenoid valve (gas-shielded FCAW process only) when welding is started.

Because flux-cored wires are easily deformed by excessive feed roll pressure, knurled feed rolls are generally used in the FCAW process. Some wire feeders use a single drive roll paired with an undriven pressure roll. Others have one or two

pairs of drive rolls. It is generally believed that systems having two pairs of drive rolls require the least drive roll pressure to provide dependable feeding.

Both air-cooled and water-cooled welding guns are used in the semiautomatic FCAW process. Air-cooled guns are generally preferred, because they are simpler to maintain, lighter in weight, and less bulky. Water-cooled guns may be required when welding currents over 500 A are used, especially when the shielding gas is rich in argon.

Air-cooled guns designed for gas-shielded welding should not be used for self-shielded welding, because the gun depends on the flow of shielding gas for proper cooling. Although curved-neck guns are the most common, straight guns are used to a limited extent.

A trigger switch on the welding gun is closed to initiate wire feeding, welding current flow, and shielding gas flow. The electrode is delivered from the wire feeder to the gun through a flexible conduit. Standard conduit lengths are 3, 3.7, 4.6, and 6 m (10, 12, 15, and 20 ft). Other lengths may also be available.

Mechanized and automatic FCAW equipment is not substantially different from that used in the semiautomatic FCAW process. The power supply should be rated for 100% duty cycle. Power supplies capable of outputs up to 1000 A may be required for some applications. Constant-current systems are very seldom used for mechanized and automatic welding.

The wire feed system is separated into a drive motor assembly and a welding control device, the latter of which often has a system to automatically start the travel mechanism when wire feed, current flow, and shielding gas flow are initiated. The welding control device is often equipped with a voltmeter and ammeter, as well.

The welding gun in mechanized and automatic systems is often mounted directly to the drive motor assembly, eliminating the need for a conduit. The gun is usually straight, but curved-neck guns are also used. Both water- and air-cooled guns are used, depending on the welding current level and shielding gas.

Most of the commonly available air-cooled guns can be used at levels up to 500 A with CO_2 shielding gas. When argon-rich shielding gas is used, the same gun may only be suitable for use at levels up to 300 A. Water-cooled guns are generally used at higher current levels.

Various travel mechanisms are used, depending on the applications. These mechanisms include side-beam carriages, tractor-type carriages, and robots.

Fume-Removal Equipment. In many cases, the amount of fumes generated by the FCAW process is sufficient to require fume-removal equipment. Although such equipment can be as simple as exhaust fans in the shop roof, local fume collection is often necessary. These systems can be either collection hoods (located above the welding gun) or fume-extractor guns. These guns are more efficient at collecting fumes, but are heavier and more bulky than standard welding guns. Fume collection hoods must be repositioned each time the welding location is moved in order to be effective.

Reference cited in this section

1. *WELDING HANDBOOK*, 8TH ED., VOL 2, AWS, 1991

Flux-Cored Arc Welding

David W. Meyer, The Esab Group, Inc.

Base Metals

Most weldable carbon and low-alloy steels can be welded by the FCAW process if suitable electrodes are available. Steels for which electrodes are available include:

- MILD STEELS, SUCH AS AISI 1010 TO 1030, ASTM A 36, A 285, A 515, AND A 516

- WEATHERING STRUCTURAL STEELS, SUCH AS ASTM A 588
- HIGH-STRENGTH, LOW-ALLOY STEELS, SUCH AS ASTM A 710
- HIGH-TEMPERATURE CHROMIUM-MOLYBDENUM STEELS, SUCH AS ASTM A 387 GRADES 12 (1CR-0.5MO) AND 22 (2.25CR-1MO)
- NICKEL-BASE STEELS, SUCH AS ASTM A 203
- HIGH-STRENGTH QUENCHED AND TEMPERED STEELS, SUCH AS HY-80 AND ASTM A 514 AND A 517
- MEDIUM-CARBON, HEAT-TREATABLE, LOW-ALLOY STEELS, SUCH AS AISI 4130

Several grades of stainless steel are welded with both gas-shielded and self-shielded flux-cored electrodes. Electrodes designed for welding AISI types 304, 316, 347, and others are available. Also available are electrodes suitable for joining stainless steels to carbon and low-alloy steels.

Electrodes that can be used to weld some nickel-base alloys have also been introduced. Among the nickel-base alloys that have been joined using the FCAW process are alloy 600 (UNS N06600) and alloy 625 (UNS N06625). Some cast irons are also welded using nickel-base flux-cored electrodes designed specifically for this purpose.

Flux-Cored Arc Welding

David W. Meyer, The Esab Group, Inc.

Electrode Manufacture

Flux-cored electrodes are generally manufactured using the process shown in Fig. 3. A flat sheath material is first formed into a "U" shape. The core ingredients are poured into this "U" at the desired rate. The sheath is then closed around the core materials to form a round tube. The diameter of this tube is then reduced, generally by drawing or rolling operations, to compress the core materials and bring the electrodes to a size that is usable for welding. The finished wire is than wound on spools, coils, or other packages. Other manufacturing methods, which are generally considered proprietary, are also used.

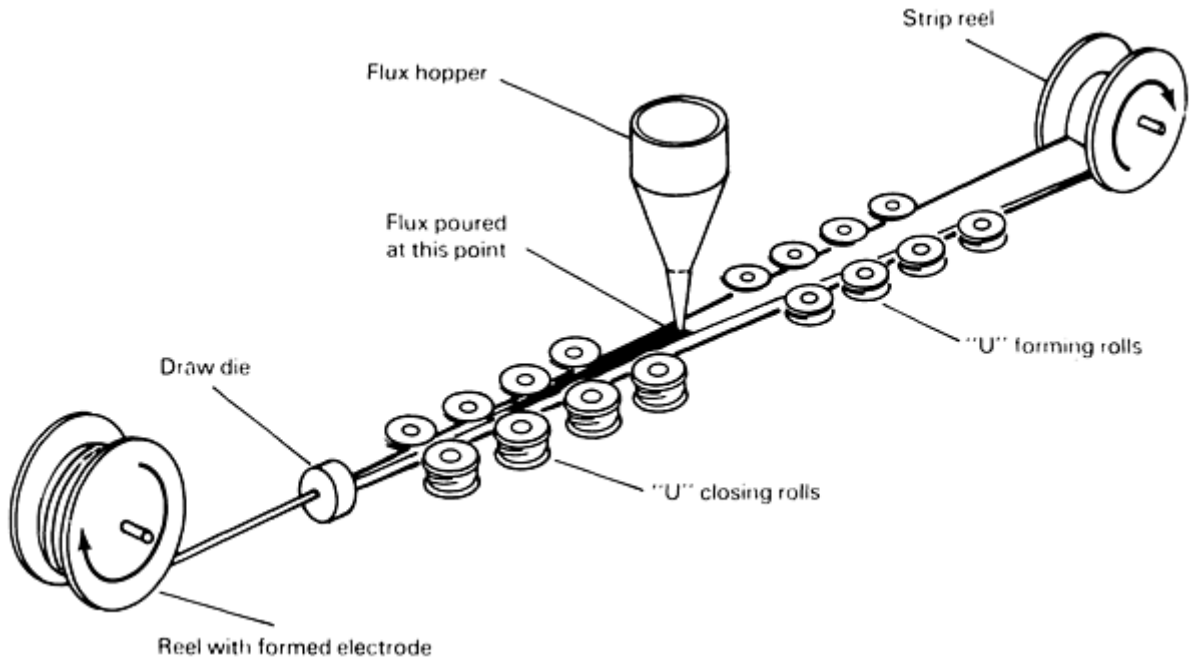

FIG. 3 FLUX-CORED ELECTRODE MANUFACTURING PROCESS. SOURCE: REF 2

The usability of a flux-cored electrode, as well as the properties and chemistry of the weld it deposits, primarily depends on the ingredients in the electrode core. Common core ingredients and their functions are listed in Table 1.

TABLE 1 FUNCTIONS OF COMMON CORE INGREDIENTS IN FCAW ELECTRODES

CORE INGREDIENT	GAS FORMER	DEOXIDIZER	DENITRIFIER	SLAG FORMER	VISCOSITY CONTROL	ARC STABILIZER	ALLOY
RUTILE (TIO_2)				X	X		
FLUORSPAR (CAF_2)				X	X		
LIME ($CACO_3$)	X			X		X	
FELDSPAR				X		X	
SYNTHETIC FRITS				X	X	X	
MANGANESE		X					X
SILICON		X					X
TITANIUM		X	X				
ALUMINUM		X	X				
CHROMIUM, NICKEL, MOLYBDENUM							X

Reference cited in this section

2. C.E. JACKSON, "FLUXES AND SLAGS IN WELDING," WRC BULLETIN 190, WELDING RESEARCH COUNCIL

Flux-Cored Arc Welding

David W. Meyer, The Esab Group, Inc.

Electrode Diameters

Flux-cored electrodes are produced in diameters ranging from 0.8 to 3.2 mm (0.030 to $\frac{1}{8}$ in.). Electrodes for all-position welding may be available in 0.8 mm (0.030 in.), 0.9 mm (0.035 in.), 1.2 mm (0.045 in.), 1.4 mm (0.052 in.), and 1.6 mm ($\frac{1}{16}$ in.) diameters. Electrodes for flat- and horizontal-position welding may be available in 1.6 mm ($\frac{1}{16}$ in.), 2.0 mm ($\frac{5}{64}$ in.), 2.4 mm ($\frac{3}{32}$ in.), 2.8 mm ($\frac{7}{64}$ in.), and 3.2 mm ($\frac{1}{8}$ in.) diameters. Other diameters may be made available by agreement between the manufacturer and the purchaser.

Electrode Classification

Carbon and Low-Alloy Steel Electrodes. Carbon steel flux-cored electrodes are classified by AWS A5.20, "Specification for Carbon Steel Electrodes for Flux Cored Arc Welding." The layout of this classification system is defined in Fig. 4; an "X" indicates a position where a designator would be. For example, the designator indicating minimum tensile strength can be a 6, to denote 62 ksi (430 MPa), or a 7, to denote 72 ksi (495 MPa). The assignment of the final designator depends on the shielding requirements and features of the electrode, as well as the recommended welding polarity. These are described in Table 2. The designations EXXT-G and EXXT-GS are designed to allow the classification of electrodes that are not covered by any of the other classifications.

TABLE 2 USABILITY TYPE DESIGNATORS FOR FLUX-CORED ELECTRODES

TYPE	SHIELDING[A]	SINGLE OR MULTIPASS[B]	TRANSFER	IMPACT TOUGHNESS REQUIREMENT	POLARITY[C]	SPECIAL CHARACTERISTICS
T-1	GAS	MULTIPASS	SPRAY-LIKE	27 J AT -18 °C (20 FT · LBF AT 0 °F)	DCEP	LOW SPATTER, FULL SLAG COVERAGE
T-2	GAS	SINGLE	SPRAY-LIKE	NO REQUIREMENT	DCEP	LOW SPATTER, FULL SLAG COVERAGE, HIGH DEOXIDIZERS
T-3	SELF	SINGLE	SPRAY-LIKE	NO REQUIREMENT	DCEP	HIGH SPEED
T-4	SELF	MULTIPASS	GLOBULAR	NO REQUIREMENT	DCEP	HIGH DEPOSITION, LOW PENETRATION, CRACK RESISTANT
T-5	GAS	MULTIPASS	GLOBULAR	27 J AT -30 °C (20 FT · LBF AT -20 °F)	DCEP[D]	IMPROVED TOUGHNESS, CRACK RESISTANT, THIN SLAG
T-6	SELF	MULTIPASS	SPRAY-LIKE	27 J AT -30 °C (20 FT · LBF AT -20 °F)	DCEP	IMPROVED TOUGHNESS, DEEP PENETRATION
T-7	SELF	MULTIPASS	GLOBULAR	NO REQUIREMENT	DCEN	CRACK RESISTANT, GOOD SLAG REMOVAL
T-8	SELF	MULTIPASS	GLOBULAR	27 J AT -30 °C (20 FT · LBF AT -20 °F)	DCEN	IMPROVED TOUGHNESS, CRACK RESISTANT
T-10	SELF	SINGLE	GLOBULAR	NO REQUIREMENT	DCEN	HIGH SPEED
T-11	SELF	MULTIPASS	SPRAY-LIKE	NO REQUIREMENT	DCEN	GENERAL PURPOSE
T-G	NOT SPECIFIED	MULTIPASS	NOT SPECIFIED	NO REQUIREMENT	NOT SPECIFIED	NOT SPECIFIED
T-GS	NOT SPECIFIED	SINGLE	NOT SPECIFIED	NO REQUIREMENT	NOT SPECIFIED	NOT SPECIFIED

Source: AWS A5.20

(A) GAS-SHIELDED ELECTRODES ARE CLASSIFIED USING CO_2 SHIELDING; HOWEVER, AR-CO_2 MIXTURES ARE COMMONLY USED IN PRACTICE.

(B) MULTIPASS ELECTRODES ARE SUITABLE FOR SINGLE-PASS OR MULTIPASS WELDING; SINGLE-PASS ELECTRODES ARE SUITABLE FOR SINGLE-PASS WELDING ONLY.

(C) DCEP, DIRECT-CURRENT ELECTRODE POSITIVE; DCEN, DIRECT-CURRENT ELECTRODE NEGATIVE.

(D) T-5 ELECTRODES ARE CLASSIFIED USING DCEP; HOWEVER, THEY ARE SOMETIMES USED WITH DCEN IN PRACTICE.

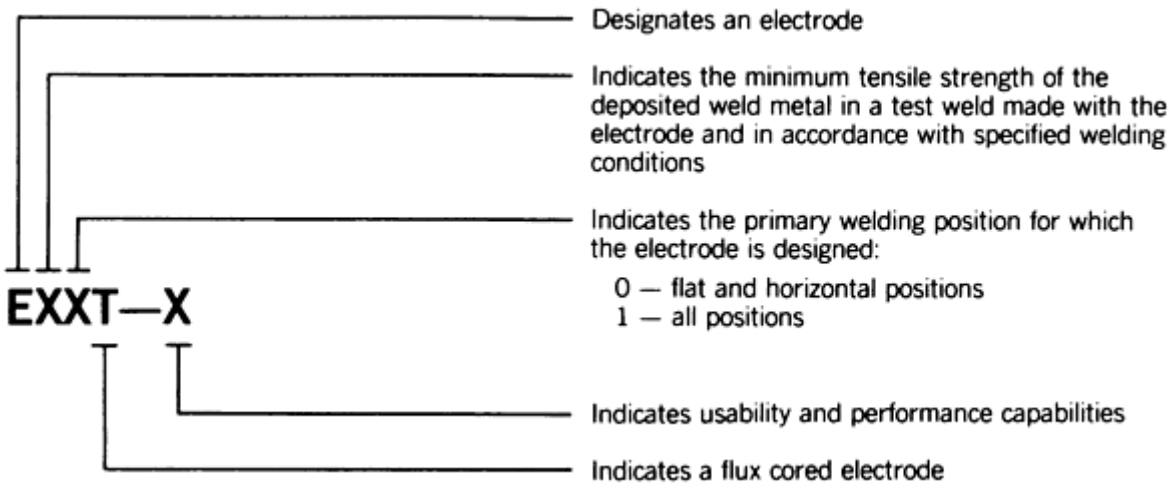

FIG. 4 CLASSIFICATION SYSTEM FOR CARBON STEEL FLUX-CORED ELECTRODES. THE LETTER "X" AS USED IN THIS FIGURE AND IN ELECTRODE CLASSIFICATION DESIGNATIONS IN AWS SPECIFICATION A5.20-79 SUBSTITUTES FOR SPECIFIC DESIGNATIONS INDICATED BY THIS FIGURE. SOURCE: REF 3

It should be noted that the Canadian Standards Association specification W48.5-M1990, "Carbon Steel Electrodes for Flux- and Metal-Cored Arc Welding," includes two additional electrode types that are planned for inclusion in the next revision of the AWS A5.20 specification. These classifications are EXXT-9 and EXXT-12. T-9 electrodes are generally similar to T-1 electrodes, but with improved toughness. T-12 electrodes are generally similar to T-9 electrodes, but with a maximum tensile strength also specified.

Low-alloy steel electrodes are classified under AWS A5.29, "Specification for Low Alloy Steel Electrodes for Flux Cored Arc Welding." This specification uses a classification system very similar to that used in specification AWS A5.20, except that a chemical composition designator is added to the designation. An electrode classified according to this specification will have the form EXXTX-X. All of the positions before the dash have the same meaning as those in specification AWS A5.20. The position behind the dash is the chemical composition designator, which consists of a letter and a number. The letter denotes the alloy type of the electrode as follows:

DESIGNATOR	ALLOY TYPE
A	CARBON-MOLYBDENUM STEEL
B	CHROMIUM-MOLYBDENUM STEEL
NI	NICKEL STEEL
D	MANGANESE-MOLYBDENUM STEEL
W	WEATHERING STEEL
K	OTHER LOW-ALLOY STEELS
G	NOT SPECIFIED

Specification AWS A5.29 classifies only the EXXT1-X, EXXT4-X, EXXT5-X, and EXXT8-X electrode types, and the usability designator has the name meaning as that in specification A5.20. Minimum tensile strengths of up to 830 MPa (120 ksi) are included in specification AWS A5.29. Impact toughness requirements are based on the strength, usability, and chemical composition requirements of the electrode.

Stainless steel electrodes are classified under AWS A5.22, "Specification for Flux Cored Corrosion Resisting Chromium and Chromium-Nickel Steel Electrodes." Classifications to this specification have the form EXXXT-X. The first three positions are the chemical composition designator, which corresponds to the American Iron and Steel Institute (AISI) designations (such as 308, 316, and 410) of steels having a similar composition. The final position is the shielding-type designator. T-1 types are designed for use with CO_2 or Ar-CO_2 shielding gases (classification requires the use of CO_2). T-2 types are designed for use with Ar-$2O_2$ shielding gas. T-3 types are self-shielded. A T-G type is included for electrodes that are not covered by the other shielding-type designators.

Nickel-Base Electrodes. A specification for nickel-base flux-cored electrodes has not yet been published. The manufacturers of these electrodes should be consulted for information on their usability, composition, and properties.

Reference cited in this section

3. "SPECIFICATION FOR CARBON STEEL ELECTRODES FOR FLUX CORED ARC WELDING," AWS A5.20-79, AWS, 1979

Flux-Cored Arc Welding

David W. Meyer, The Esab Group, Inc.

References

1. *WELDING HANDBOOK*, 8TH ED., VOL 2, AWS, 1991
2. C.E. JACKSON, "FLUXES AND SLAGS IN WELDING," WRC BULLETIN 190, WELDING RESEARCH COUNCIL
3. "SPECIFICATION FOR CARBON STEEL ELECTRODES FOR FLUX CORED ARC WELDING," AWS A5.20-79, AWS, 1979

Gas-Tungsten Arc Welding

Grant Ken-Hicken, Sandia National Laboratory

Introduction

GAS-TUNGSTEN ARC WELDING (GTAW), also known as HeliArc, tungsten inert gas (TIG), and tungsten arc welding, was developed in the late 1930s when a need to weld magnesium became apparent. Russell Meredith (Ref 1) developed a welding process using the inert gas helium and a tungsten electrode to fuse magnesium. This joining method replaced riveting as a method of building aircraft with aluminum and magnesium components. The HeliArc welding has continued to this day with many refinements and name changes, but with no change in the fundamentals demonstrated by Meredith (Ref 1).

The melting temperature necessary to weld materials in the GTAW process is obtained by maintaining an arc between a tungsten alloy electrode and the workpiece (Fig. 1). Weld pool temperatures can approach 2500 °C (4530 °F). An inert gas sustains the arc and protects the molten metal from atmospheric contamination. The inert gas is normally argon, helium, or a mixture of helium and argon.

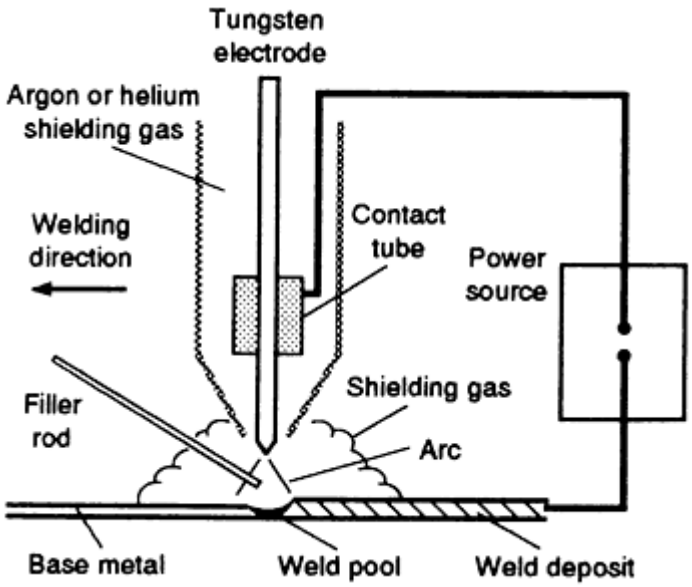

FIG. 1 SCHEMATIC SHOWING KEY COMPONENTS AND PARAMETERS OF THE GTAW PROCESS. SOURCE: REF 2

References

1. R. MEREDITH, U.S. PATENT 2,274,631
2. S. KOU, *WELDING METALLURGY,* JOHN WILEY & SONS, 1987, P 10

Gas-Tungsten Arc Welding

Grant Ken-Hicken, Sandia National Laboratory

Applications

Gas-tungsten arc welding is used extensively for welding stainless steel, aluminum, magnesium, copper, and reactive materials (for example, titanium and tantalum). The process can also be used to join carbon and alloy steels. In carbon steels, it is primarily used for root-pass welding with the application of consumable inserts or open-root techniques on pipe. The materials welded range from a few thousandths of an inch to several inches in thickness.

Advantages and Limitations

Advantages of GTAW include (Ref 3):

- PRODUCES HIGH-QUALITY, LOW-DISTORTION WELDS
- FREE OF THE SPATTER ASSOCIATED WITH OTHER METHODS
- CAN BE USED WITH OR WITHOUT FILLER WIRE
- CAN BE USED WITH A RANGE OF POWER SUPPLIES
- WELDS ALMOST ALL METALS, INCLUDING DISSIMILAR ONES
- GIVES PRECISE CONTROL OF WELDING HEAT

The GTAW process is applicable when the highest weld quality is required. It can be used to weld almost all types of metals. The operator has excellent control of heat input, and vision is not limited by fumes or smoke from the process.

Limitations of GTAW include (Ref 4):

- PRODUCES LOWER DEPOSITION RATES THAN CONSUMABLE ELECTRODE ARC WELDING PROCESSES
- REQUIRES SLIGHTLY MORE DEXTERITY AND WELDER COORDINATION THAN GAS METAL ARC WELDING (GMAW) OR SHIELDED METAL ARC WELDING (SMAW) FOR MANUAL WELDING
- LESS ECONOMICAL THAN CONSUMABLE ELECTRODE ARC WELDING FOR THICK SECTIONS GREATER THAN 9.5 MM ($\frac{3}{8}$ IN.)
- PROBLEMATIC IN DRAFTY ENVIRONMENTS BECAUSE OF DIFFICULTY IN SHIELDING THE WELD ZONE PROPERLY

Additional problems with the process may include:

- TUNGSTEN INCLUSIONS IF THE ELECTRODE IS ALLOWED TO CONTACT THE WELD POOL
- CONTAMINATION OF THE WELD METAL, IF PROPER SHIELDING OF THE FILLER METAL BY THE GAS STREAM IS NOT MAINTAINED
- LOW TOLERANCE FOR CONTAMINANTS ON FILLER OR BASE METALS
- CONTAMINATION OR POROSITY, CAUSED BY COOLANT LEAKAGE FROM WATER-COOLED TORCHES
- ARC BLOW OR ARC DEFLECTION, AS WITH OTHER PROCESSES

Power supplies for GTAW are usually the constant-current type with a drooping (negative) volt-ampere (V-A) curve. Saturable reactors and thyristor-controlled units are the most common. Advances in the electronics industry have readily been accepted in the welding community, resulting in sophisticated, lightweight power supplies. Transistorized direct current (dc) power supplies are becoming common, and the newer rectifier-inverter supplies are very compact and versatile. The inverter power supply consists of three converters:

- 60 HZ PRIMARY ALTERNATING CURRENT (AC) IS RECTIFIED TO DC
- DIRECT CURRENT IS INVERTED TO HIGH-FREQUENCY AC
- ALTERNATING CURRENT IS RECTIFIED TO DC (REF 5)

The inverter supplies can be switched from constant current to constant voltage for GMAW, resulting in a very versatile piece of equipment. The inverter-controlled power supplies are more stable and have faster response times than conventional silicon-controlled rectifier (SCR) power supplies. Figure 2 compares the response of an inverter-controlled arc welding machine and a thyristor-controlled welding machine.

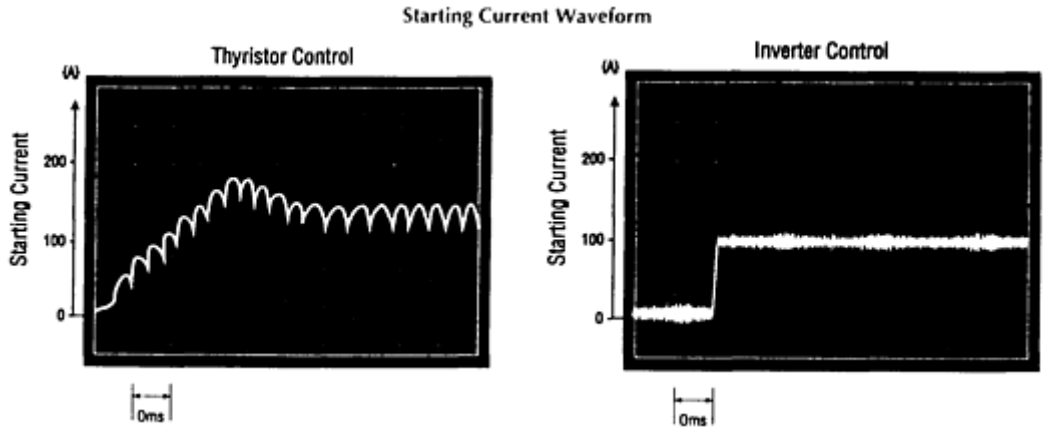

FIG. 2 STARTING CURRENT WAVEFORMS OF TWO POWER SOURCES TO SHOW RELATIVE RESPONSE TIMES OF EACH SOURCE. (A) THYRISTOR-CONTROLLED SOURCE. (B) INVERTER-CONTROLLED SOURCE. FASTER RESPONSE OF INVERTER-CONTROLLED ARC WELDING MACHINE (2 MS TO GO FROM 0 TO 100 A) INDICATES A MORE STABLE ARC.

Torch Construction. The welding torch holds the tungsten electrode that conducts the current to the arc, and it provides a means of shielding the arc and molten metal. The major components of a typical welding torch are shown in Fig. 3.

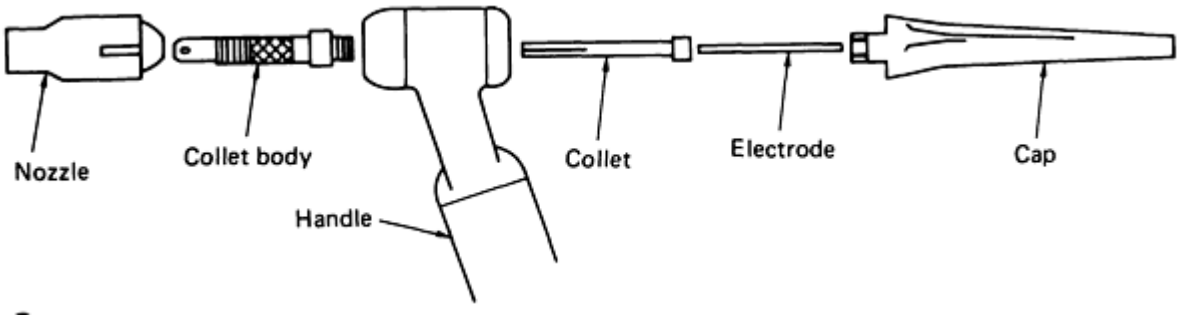

FIG. 3 SCHEMATIC SHOWING EXPLODED VIEW OF KEY COMPONENTS COMPRISING A GTAW MANUAL TORCH

Welding torches rated at less than 200 A are normally gas-cooled (that is, the shielding gas flows around the conductor cable, providing the necessary cooling). Water-cooled torches are used for continuous operation or at higher welding currents and are common for mechanized or automatic welding (see the section "GTAW Process Variations" in this article). The cooling water may be supplied to the torch from a recirculating tank that uses a radiator or chiller to cool the water.

Electrodes. The nonconsumable electrodes used in GTAW are composed of tungsten or alloys of tungsten. The most common electrode is a 2% ThO_2-W alloy (EWTh-2). This material has excellent operating characteristics and good stability. Thoria is radioactive, so care must be taken when sharpening electrodes not to inhale metal dust. The grindings are considered hazardous waste in some states, and disposal may be subject to environmental regulations. Lanthaniated (EWLa-1) and yttriated tungsten electrodes have the best starting characteristics in that an arc can be started and maintained at a lower voltage. Ceriated tungsten (EWCe-2) is only slightly better than the thoriated tungsten with respect to arc starting and melt-off rate. Any of the aforementioned electrodes produce acceptable welds. The easy starting of the lanthaniated electrode is a result of the lower work function (Ref 6) which allows it to emit electrodes readily at a lower voltage.

Pure tungsten is used primarily in ac welding and has the highest consumption rate. Alloys of zirconium are also used. Tungsten electrodes are classified on the basis of their chemical composition (Table 1). Requirements for tungsten

electrodes are given in the latest edition of ANSI/AWS A5.12 ("Specification for Tungsten and Tungsten Alloy Electrodes for Arc Welding and Cutting"). The shape of the electrode tip can affect the resulting weld shape. Electrodes with included angles from 60 to 120° are stable and give good weld penetration depth-to-width ratios (Ref 7). Electrodes with smaller included angles (5 to 30°) are used for grooved weld joints to eliminate arcing to the part side walls.

TABLE 1 CLASSIFICATION OF ALLOYING ELEMENTS IN SELECTED TUNGSTEN ALLOY ELECTRODES FOR GTAW APPLICATIONS

AWS CLASSIFICATION	COLOR[A]	ALLOYING ELEMENT	ALLOYING OXIDE	ALLOYING OXIDE, WT%
EWP	GREEN	. . .	. . .	
EWCE-2	ORANGE	CERIUM	CEO_2	2
EWLA-1	BLACK	LANTHANUM	LA_2O_3	1
EWTH-1	YELLOW	THORIUM	THO_2	1
EWTH-2	RED	THORIUM	THO_2	2
EWZR-1	BROWN	ZIRCONIUM	ZRO_2	0.25
EWG	GRAY	NOT SPECIFIED[B]	. . .	. . .

Source: Ref 4

(A) COLOR MAY BE APPLIED IN THE FORM OF BANDS, DOTS, AND SO ON, AT ANY POINT ON THE SURFACE OF THE ELECTRODE.

(B) MANUFACTURER MUST IDENTIFY THE TYPE AND NOMINAL CONTENT OF THE RARE-EARTH OXIDE ADDITION.

Wire feed systems are made from a number of components and vary from simple to complex. The basic system consists of a means of gripping the wire sufficiently to pull it from the spool and push it through the guide tube to the point of welding. Electronic switches and controls are necessary for the electric drive motor. The wire will be fed into the leading edge for cold wire feeds and into the trailing edge for hot wire feeds.

Cables, hoses, and gas regulators are necessary to deliver the process consumable of electricity, water, and inert gas to the welding torch.

Arc oscillation is used in both manual and mechanized welding (see the section "GTAW Process Variations" in this article). The benefits in manual welding are basic to the control of the weld when adapting to changes in the weld joint and gap. In mechanized welding, the oscillation is typically produced by moving the entire welding torch mechanically or by moving the arc plasma with the aid of an externally applied magnetic field. Oscillation allows the welding heat to be placed at precise locations. This is advantageous when welding irregularly shaped parts. The number of welding passes and total heat input can be decreased when arc oscillation is used, because it reduces the cost as well as the weld shrinkage and upsetting.

Figure 4 shows the effect of magnetic oscillation on distortion. Some alloys need the tempering produced by multipass stringer bead welding techniques, and arc oscillation should not be used. Externally applied magnetic fields can be used to stabilize the arc, minimize arc blow, and displace the arc plasma forward of the welding torch. This results in improved weld appearances and increased welding speeds in tube mills and other high-speed applications (Ref 9).

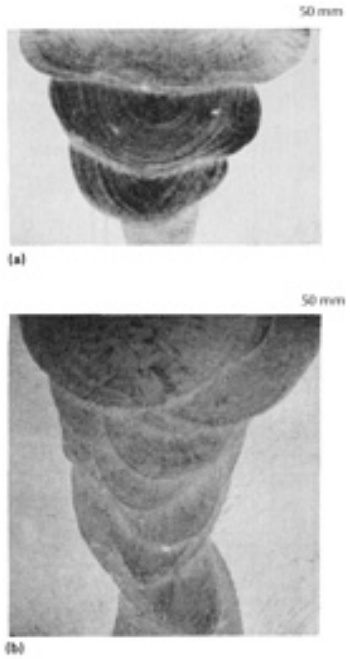

FIG. 4 EFFECT OF MAGNETIC OSCILLATION ON WELD DISTORTION IN 25 MM ($\frac{1}{2}$ IN.) THICK STAINLESS STEEL. (A) WELD PRODUCED WITH ARC OSCILLATION. (B) STRINGER BEADS PRODUCED IN WELD WITHOUT ARC OSCILLATION. NOTE MINIMAL UPSETTING WITH ARC OSCILLATION. SOURCE: REF 8

References cited in this section

3. T. MYERS, WHY THE GROWING INTEREST IN GAS TUNGSTEN ARC WELDING? *THE FABRICATOR*, VOL 22 (NO. 9), NOV 1992, P 38 -39
4. *WELDING HANDBOOK*, 8TH ED., VOL 2, AMERICAN WELDING SOCIETY, 1991, P 74-107
5. T. BYRD, INVERTER POWER SOURCES: AN EFFICIENT ALTERNATIVE, *WELD. J.*, VOL 72 (NO. 1), JAN 1993, P 37-40
6. A.A. SADEK, M. USHIO, AND F. MATSUDA, EFFECTS OF RARE EARTH METAL OXIDE ADDITIONS TO TUNGSTEN ELECTRODES, *METALL. TRANS. A*, VOL 21, 1990, P 3221-3234
7. J.R. KEY, ANODE/CATHODE GEOMETRY AND SHIELDING GAS INTERRELATIONSHIPS IN GTAW, *WELD. J.*, VOL 59 (NO. 12), DEC 1980, P 364-S TO 370-S
8. G.K. HICKEN, N.D. STUCK, AND H.W. RANDAL, APPLICATIONS OF MAGNETICALLY CONTROLLED ARCS, *WELD. J.*, VOL 55 (NO. 4), 1976, P 264-267
9. G.K. HICKEN, C.E. JACKSON, THE EFFECTS OF APPLIED OF MAGNETIC FIELDS ON WELDING ARCS, *WELD. J.*, VOL 45 (NO. 11), NOV 1966, P 515-S TO 524-S

Gas-Tungsten Arc Welding

Grant Ken-Hicken, Sandia National Laboratory

Process Parameters

Welding Current. Current is one of the most important operating conditions to control in any welding operation, because it is related to the depth of penetration, welding speed, deposition rate, and quality of the weld.

Fundamentally, there are but three choices of welding current:

- DIRECT CURRENT ELECTRODE NEGATIVE (DCEN)
- DIRECT CURRENT ELECTRODE POSITIVE (DCEP)
- ALTERNATING CURRENT

Figures 5 and 6 show the effect of dc and ac on weld shape. Table 2 gives the recommended current relative to workpiece material.

TABLE 2 SUITABILITY OF TYPES OF CURRENT FOR GTAW OF SELECTED METALS

METAL WELDED	ALTERNATING CURRENT[A]	DCEN	DCEP
LOW CARBON STEEL:			
0.38-0.76 MM (0.015-0.030 IN.)[A]	G[B]	E	NR
0.76-3.18 MM (0.030-0.125 IN.)	NR	E	NR
HIGH-CARBON STEEL	G[B]	E	NR
CAST IRON	G[B]	E	NR
STAINLESS STEEL	G[B]	E	NR
HEAT-RESISTANT ALLOYS	G[B]	E	NR
REFRACTORY METALS	NR	E	NR
ALUMINUM ALLOYS:			
$\leqslant$0.64 MM (0.025 IN.)	E	NR[C]	G
>0.64 MM (0.025 IN.)	E	NR[C]	NR
CASTINGS	E	NR[C]	NR
BERYLLIUM	G[B]	E	NR
COPPER AND ALLOYS:			
BRASS	G[B]	E	NR
DEOXIDIZED COPPER	NR	E	NR
SILICON BRONZE	NR	E	NR
MAGNESIUM ALLOYS:			
$\leq$ 3.2 MM ($\frac{1}{8}$ IN.)	E	NR[C]	G
>4.8 MM ($\frac{3}{16}$ IN.)	E	NR[C]	NR
CASTINGS	E	NR[C]	NR
SILVER	G[B]	E	NR
TITANIUM ALLOYS	NR	E	NR

Note: E, excellent; G, good; NR, not recommended.

(A) STABILIZED. DO NOT USE ALTERNATING CURRENT ON TIGHTLY JIGGED ASSEMBLIES.

(B) AMPERAGE SHOULD BE ABOUT 25% HIGHER THAN WHEN DCEN IS USED.

(C) UNLESS WORK IS MECHANICALLY OR CHEMICALLY CLEANED IN THE AREAS TO BE WELDED

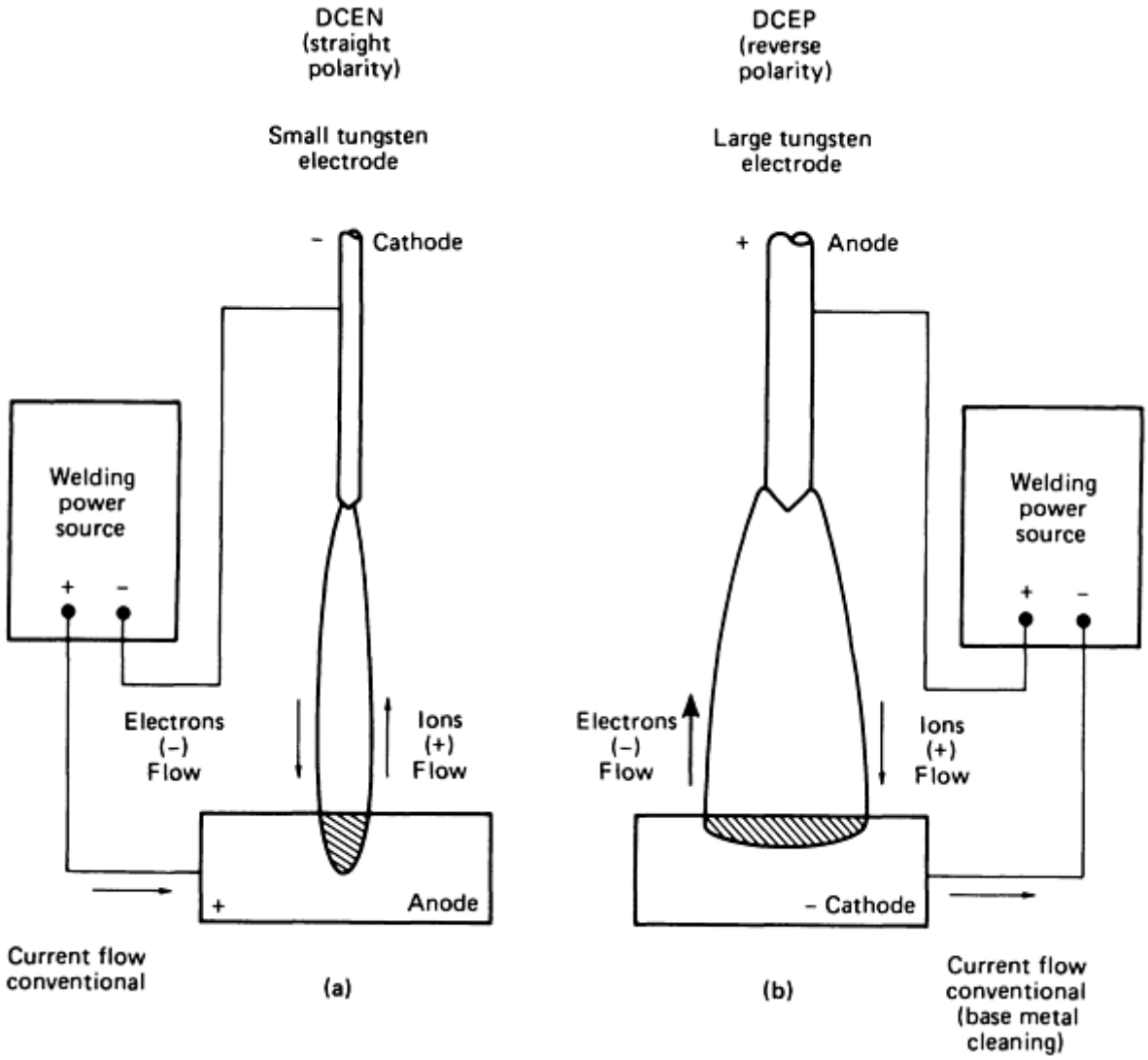

FIG. 5 EFFECT OF POLARITY ON GTAW WELD CONFIGURATION WHEN USING DIRECT CURRENT. (A) DCEN. DEEP PENETRATION, NARROW MELTED AREA, APPROXIMATE 30% HEAT IN ELECTRODE AND 70% HEAT IN BASE METAL. (B) DCEP. SHALLOW PENETRATION, WIDE MELTED AREA, APPROXIMATE 70% HEAT IN ELECTRODE AND 30% HEAT IN BASE METAL

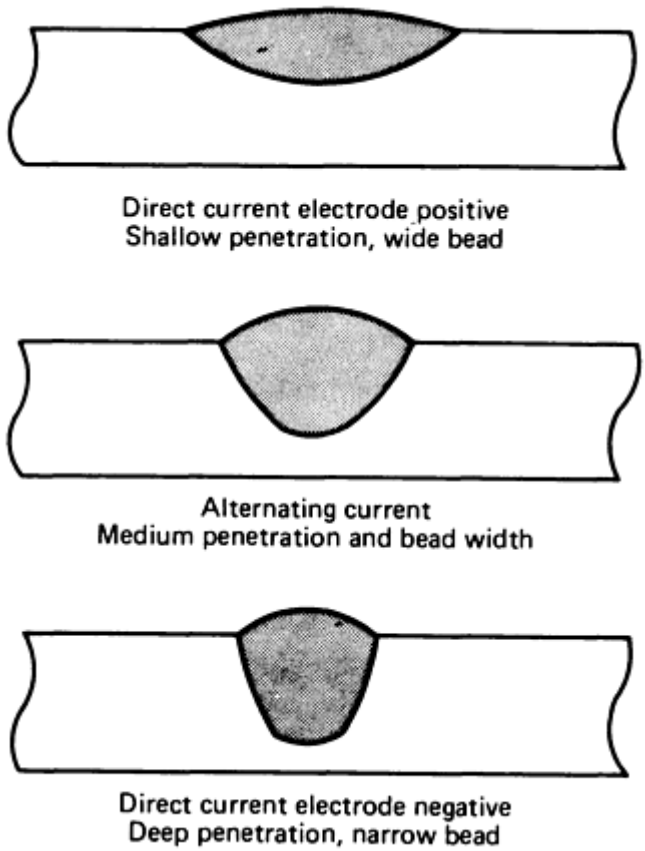

FIG. 6 WELD CONFIGURATION AS A FUNCTION OF TYPE OF CURRENT (AC OR DC) USED

Alternating current is characterized as reversing the polarity of the work and electrode at 60 Hz. The rapidly changing polarity gives a cathodic cleaning action that is beneficial for oxide removal when welding aluminum and magnesium. The alternating currents result in electrode heating during the DCEP portion of each cycle. This necessitates the use of larger-diameter electrodes, normally made of pure tungsten. Variable polarity welding allows the frequency of polarity switching to be preset. This can produce the cleaning effects to ac welding and the high efficiency of dc welding. Direct current electrode negative is most often used in the GTAW process. This results in maximum application of heat to the work and maximum melting of the workpiece.

Pulsed versus Nonpulsed Current. Nonpulsed or continuous current is the standard for GTAW. However, there are several advantages to using pulsed current. Pulsing produces the maximum amount of penetration while minimizing the total heat applied to the part. Pulsing also aids in timing the motion necessary in manual welding and allows the weld pool to cool between pulses.

Microwelding refers to a class of weldments that are made at welding currents from 1 to 20 A. In most cases, the welding is used for electronic applications, bellows, wires, and other components where heat input must be precisely controlled.

Shielding Gases. The original GTAW process used helium as the shielding gas for welding magnesium and aluminum. Today, argon is the predominant shielding gas.

Argon is the least expensive of the inert gases used for shielding gas-tungsten arc welds, which is only partially responsible for its widespread use. Argon has a low ionization potential (2.52×10^{-18} J, or 15.7 eV), making it easier to form an arc plasma than with other shielding gases. Argon is approximately 1.4 times heavier than air, so it displaces air, resulting in excellent shielding of the molten weld pool.

Helium has an ionization potential of 3.92×10^{-18} J (24.5 eV), which results in more difficult arc initiation and operation at a higher arc voltage. The higher arc voltage, *V,* results in a higher heat input, *Q,* for a given arc length and current, *I:*

$$Q = IVT \qquad \textbf{(EQ 1)}$$

where Q is in Joules, I is in amperes; and t is in seconds. This high heat input can be very beneficial when welding copper, aluminum, and other high-conductivity materials. Helium shielding used with DCEN is very effective for welding thick aluminum.

Gas Purity. Most materials can be welded using a welding grade torch gas with a purity of 99.995% or 50 ppm impurities. However, some reactive materials (for example, titanium, molybdenum, and tantalum) require that the contaminant level be less than 50 ppm, which may require certified purity or the use of gas filters and purifiers (Ref 10).

Gas Flow Rates. Helium, because of its low density, must be used at higher flow rates than argon. Typical flow rates for argon are 7 L/min (15 ft^3/h) and 14 L/min (30 ft^3/h) for helium.

Backup Purge. Protecting the molten weld pool from the atmosphere is very important in GTAW. Atmospheric contamination can result in weld cracks, porosity, scaling, and an unacceptable granular appearance. The gas cup on the welding torch is the primary outlet of shielding gas for most GTAW applications. Back side shielding is important because the presence of oxygen can reduce weld metal penetration and result in the effects mentioned above (Ref 11). Balloon and water-soluble paper dams are sometimes used to minimize the volume to be purged. Copper backing bars and ceramics are sometimes used to hold shielding gas against the back surface of the molten weld and support the molten underbead. Reactive materials and special applications may require more elaborate shielding. This can be in the form of a simple trailing device providing the inert shielding gas or may be as elaborate as a special welding chamber equipped with gas purifiers and analyzers. Specially constructed plastic bags have been used successfully to weld large, irregularly shaped components (Fig. 7).

FIG. 7 PLASTIC BAG ENCLOSURE THAT SIMULATES A GLOVE BOX, USED TO PURGE IRREGULARLY SHAPED COMPONENTS IN GTAW OPERATIONS

Filler Metals. The thickness of the part to be welded will determine the need for filler metal additions. Material thinner than 3.2 mm (0.125 in.) can be successfully welded without filler metal additions. Filler metal, when needed, can be added manually in straight length or automatically from a roll or coil. The filler metal is normally added cold; hot wire can be used for automatic applications (Fig. 8). A welding insert is preplaced filler material of several possible configurations to aid in root-pass welding.

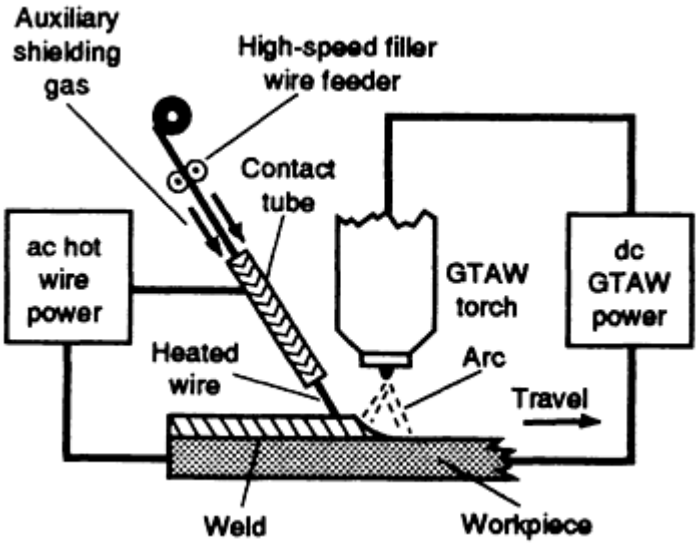

FIG. 8 SCHEMATIC SHOWING KEY COMPONENTS AND PARAMETERS OF A GTAW HOT WIRE SYSTEM. SOURCE: REF 4

Rods. Straight lengths of filler wire, typically 915 mm (36 in.) in length, are used for manual welding. Most straight lengths are round in cross section, but some aluminum fillers are somewhat rectangular.

Cold Wire. Coiled wire may be acquired in small 100 mm (4 in.) spools. Larger 305 mm (12 in.) spools or large coils can weigh over 225 kg (500 lb). The larger coils are normally used with GMAW because it requires larger quantities of filler metal. The filler wire is fed into the leading edge of the weld pool during cold-wire welding.

Hot wire GTAW utilizes a heated filler metal to increase the deposition rate of the process (Fig. 9). The wire is resistance heated to near the melting temperature and fed into the trailing edge of the weld pool. Deposition rates to 29 kg/h (65 lb/h) are achievable. The higher deposition rates obtained with hot wire make the process competitive for welds and overlays and improve productivity. Table 3 lists typical hot wire parameters.

TABLE 3 TYPICAL PARAMETERS FOR AUTOMATIC HOT WIRE GTAW

ARC CURRENT, A	ARC VOLTAGE, V	TORCH TRAVEL SPEED		WIRE FEED RATE[A]		DEPOSITION RATE	
		mm/min	in./min	mm/min	in./min	kg/h	lb/h
300	10-12	100-255	4-10	2790-9400	110-370	1.4-4.5	3-10
400	11-13	150-355	6-14	4700-11300	185-445	2.3-5.4	5-12
500	12-15	205-510	8-20	7490-16900	292-665	3.6-8.2	8-18

Note: Using a 4.0 to 4.8 mm ($\frac{5}{32}$ to $\frac{3}{16}$ in.) diameter 2% Th tungsten electrode with a 75He-25Ar shielding gas.

(A) WIRE DIAMETER: 1.14 MM (0.045 IN.)

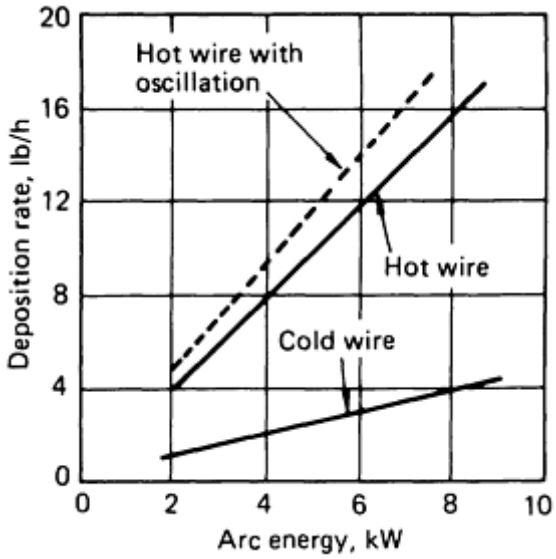

FIG. 9 DEPOSITION RATES FOR GTAW WITH COLD AND HOT FILLER WIRE ON A STEEL WORKPIECE

Welding inserts are used to produce a smooth uniform underbead. The insert is normally a separate piece of material, although integral inserts are sometimes used. Smooth underbead can be produced in a mechanized system or in manual systems when highly skilled welders are available. The insert can be obtained in several different configurations (Fig. 10). The purpose of the insert is to preplace the filler metal at the joint root. Inserts with compositions that differ from that of the base metal can be used to improve the weldability of some materials.

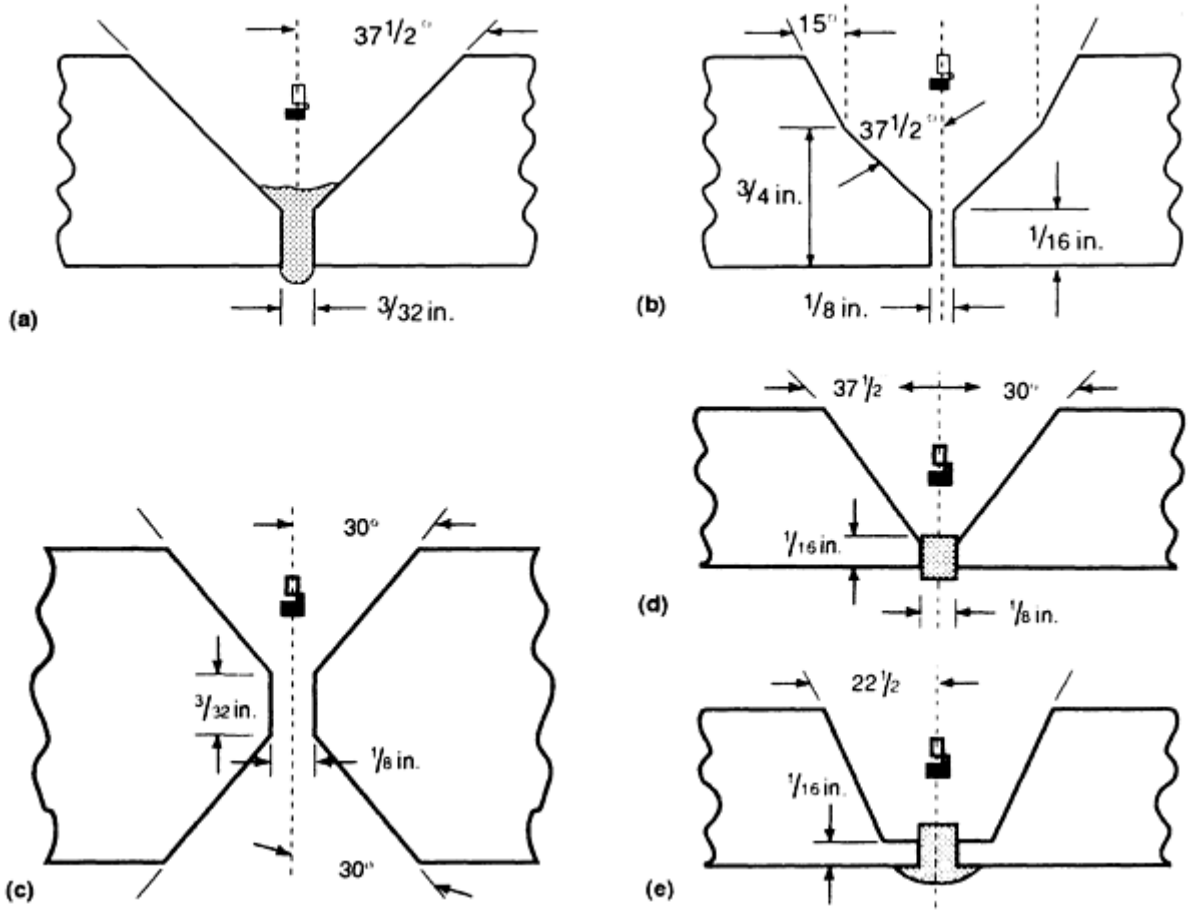

FIG. 10 SELECTED JOINT CONFIGURATIONS AND WELDING INSERTS USED IN GTAW PROCESSES. (A) Y-TYPE INSERT, $\frac{5}{32}$ IN., FOR INDEXING WHEN ACCESSIBILITY IS LIMITED; NO LAND REQUIRED. (B) COMPOUND BEVEL WITH OPEN ROOT, $\frac{1}{8}$ IN. GAP; LAND, $\frac{1}{16}$ IN. THICK. WASHER-TYPE INSERT ($\frac{1}{8}$ × $\frac{5}{32}$ IN.) SHOULD BE USED IF INSERT REQUIRED. (C) INSIDE DIAMETER/OUTSIDE DIAMETER PREPARATION WITH OPEN ROOT, $\frac{1}{8}$ IN. GAP; LAND, $\frac{3}{32}$ IN. THICK. WASHER-TYPE INSERT ($\frac{1}{8}$ × $\frac{5}{32}$ IN.) SHOULD BE USED IF INSERT REQUIRED. (D) WASHER-TYPE INSERT ($\frac{1}{8}$ × $\frac{5}{32}$ IN.); LAND, $\frac{1}{16}$ IN. THICK. (E) J PREP MUSHROOM INSERT; LAND $\frac{1}{16}$ IN. THICK; EXTENDED LAND, $\frac{3}{32}$ IN. LONG

References cited in this section

4. *WELDING HANDBOOK*, 8TH ED., VOL 2, AMERICAN WELDING SOCIETY, 1991, P 74-107
10. K.F. KRYSIAK AND P.M. BHADHA, SHIELDING GAS PURIFICATION IMPROVES WELD QUALITY, *WELD. J.*, NOV 1990, P 47-49
11. H. GIEPL, ORBITAL TIG (GTA) WELDING, *STAINL. STEEL LEUR.*, MAY 1992, P 48-55

Gas-Tungsten Arc Welding

Grant Ken-Hicken, Sandia National Laboratory

GTAW Process Variations

Manual welding refers to the GTAW process in which the welder manipulates the welding torch by hand. If a motorized wire feeder is attached to the torch, the process is classified as semiautomatic welding.

Products generated by skilled manual welders account for a large proportion of GTAW applications. The equipment can be quite inexpensive, and properly trained welders can join a wide variety of materials. Manual welding is used extensively in stainless steel piping as well as for the root pass in carbon steel pipe welds.

Mechanized welding may require adjustment to welding parameters in response to visual observation of the weld. Machine or mechanized welding requires some specialized accessories. The basic system contains a means for holding and moving the welding torch as well as the workpiece. Because arc voltage is an essential variable in GTAW and is proportional to arc length, voltage feedback devices are often used with motorized torch holders to control the arc length.

Narrow groove welding makes use of the GTAW cold wire welding process with a narrowed weld joint. Figure 11 shows a typical weld. Narrow groove welding is limited to mechanized welding applications where precise torch location can be maintained.

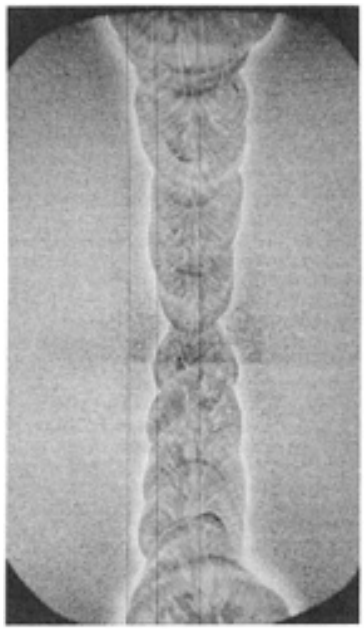

FIG. 11 TYPICAL NARROW GROOVE WELD PRODUCED IN MECHANIZED WELDING APPLICATIONS

Automatic welding does not require manual 0parameter adjustment or observation of the weld during the welding process. The most common application of automatic welding is associated with orbiting weld heads used to weld pipe and tubing. These devices attach to the workpieces and move around the circumference, fusing the metal. Most systems perform an autogenous weld; others have wire feed and oscillation capabilities. These systems are often used in conjunction with a computer to control the welding variables. Automatic controls utilizing microprocessors and computer numerical control servodrives make it possible to use one welding system to weld a variety of materials and shapes. Figure 12 shows 14 different parts welded with an automatic GTAW system.

WELDING SPECIFICATIONS FOR COMPONENTS SHOWN

Welds were made with a 250 A water-cooled GTAW torch that used 1.6 mm (0.062 in.) diameter electrode

	6061 ALUMINUM WORKPIECE[A]			TYPE 304 STAINLESS STEEL WORKPIECE[B]	
	COMPONENT NO. 1	COMPONENT NO. 2	COMPONENT NO. 3	COMPONENT NO. 4	COMPONENT NO. 5
WORKPIECE					
TUBE DIAMETER, MM (IN.)	22.22 (0.875)	28.58 (1.125)	26.82 (1.056)	12.7 (0.5)	19.1 (0.75)
WALL THICKNESS,	1.57 (0.062)	0.88 (0.035)	1.65 (0.065)	0.63 (0.025)	0.63 (0.025)

MM (IN.)					
POWER SUPPLY					
PEAK CURRENT, A	50-100	52-60	70-85	20-45	35-45
BACKGROUND, A	15	15	15	15	15
PULSE RATE, PPS(C)	5	6	6	8	8
WIDTH, %	65	65	65	75	75
TORCH					
WELD TRAVEL SPEED, MM/MIN	405 (16)	405 (16)	405 (16)	380 (15)	380 (15)
WELDING CYCLE TIME, S	8.0	4.5	6.5	6.0	10.0
SHIELDING GAS					
FLOW RATE, L/MIN (FT^3H)	8.5 (18)	8.5 (18)	8.5 (18)	7.1 (15)	7.1 (15)
FILLER METAL					
DIAMETER, MM (IN.)	0.8 (0.03)	0.8 (0.03)	0.8 (0.03)	. . .	. . .
FEED RATE, MM/MIN (IN./MIN)	3810 (150)	3560 (140)	3810 (140)	. . .	. . .
JOINT TYPE	FILLET/BUTT	BUTT	SADDLE	FILLET	FILLET/BUTT

(A) 4043 ALUMINUM FILLER METAL; AC/DC SQUARE WAVE POWER SUPPLY; 2% CERIATED ELECTRODE MATERIAL; 50% HE-50% AR SHIELDING GAS; AC PROCESS

(B) NO FILLER METAL USED; DC PRECISION POWER SUPPLY; 2% THORIATED ELECTRODE MATERIAL; ARGON SHIELDING GAS; DC PROCESS

(C) PULSES PER SECOND

FIG. 12 TYPICAL COMPONENTS PRODUCED BY AUTOMATIC GTAW PROCESS. SOURCE: REF 12

Reference cited in this section

12. K.J. PFAHL, AUTOMATIC CONTOUR WELDING OF TUBE AND PIPE, *TUBE PIPE Q.,* VOL 3 (NO. 4), 1992, P 58-62

Gas-Tungsten Arc Welding

Grant Ken-Hicken, Sandia National Laboratory

References

1. R. MEREDITH, U.S. PATENT 2,274,631
2. S. KOU, *WELDING METALLURGY,* JOHN WILEY & SONS, 1987, P 10
3. T. MYERS, WHY THE GROWING INTEREST IN GAS TUNGSTEN ARC WELDING? *THE FABRICATOR,* VOL 22 (NO. 9), NOV 1992, P 38 -39
4. *WELDING HANDBOOK,* 8TH ED., VOL 2, AMERICAN WELDING SOCIETY, 1991, P 74-107
5. T. BYRD, INVERTER POWER SOURCES: AN EFFICIENT ALTERNATIVE, *WELD. J.,* VOL 72 (NO. 1), JAN 1993, P 37-40
6. A.A. SADEK, M. USHIO, AND F. MATSUDA, EFFECTS OF RARE EARTH METAL OXIDE ADDITIONS TO TUNGSTEN ELECTRODES, *METALL. TRANS. A,* VOL 21, 1990, P 3221-3234

7. J.R. KEY, ANODE/CATHODE GEOMETRY AND SHIELDING GAS INTERRELATIONSHIPS IN GTAW, *WELD. J.*, VOL 59 (NO. 12), DEC 1980, P 364-S TO 370-S
8. G.K. HICKEN, N.D. STUCK, AND H.W. RANDAL, APPLICATIONS OF MAGNETICALLY CONTROLLED ARCS, *WELD. J.*, VOL 55 (NO. 4), 1976, P 264-267
9. G.K. HICKEN, C.E. JACKSON, THE EFFECTS OF APPLIED OF MAGNETIC FIELDS ON WELDING ARCS, *WELD. J.*, VOL 45 (NO. 11), NOV 1966, P 515-S TO 524-S
10. K.F. KRYSIAK AND P.M. BHADHA, SHIELDING GAS PURIFICATION IMPROVES WELD QUALITY, *WELD. J.*, NOV 1990, P 47-49
11. H. GIEPL, ORBITAL TIG (GTA) WELDING, *STAINL. STEEL LEUR.*, MAY 1992, P 48-55
12. K.J. PFAHL, AUTOMATIC CONTOUR WELDING OF TUBE AND PIPE, *TUBE PIPE Q.*, VOL 3 (NO. 4), 1992, P 58-62

Plasma Arc Welding

Ian D. Harris, Edison Welding Institute

Introduction

PLASMA ARC WELDING (PAW) can be defined as a gas-shielded arc welding process where the coalescence of metals is achieved via the heat transferred by an arc that is created between a tungsten electrode and a workpiece. The arc is constricted by a copper alloy nozzle orifice to form a highly collimated arc column (Fig. 1). The plasma is formed through the ionization of a portion of the plasma (orifice) gas. The process can be operated with or without a filler wire addition.

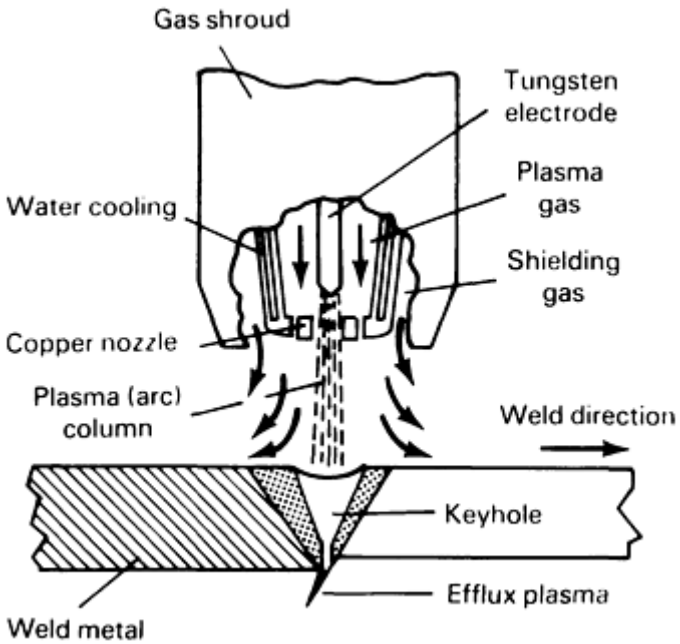

FIG. 1 PLASMA ARC WELDING PROCESS, SHOWING CONSTRICTION OF THE ARC BY A COPPER NOZZLE AND A KEYHOLE THROUGH THE PLATE

Principles of Operation. Once the equipment is set up and the welding sequence is initiated, the plasma and shielding gases are switched on. A pilot arc is then struck between a tungsten alloy electrode and the copper alloy nozzle within the torch (nontransferred arc mode), usually by applying a high-frequency open-circuit voltage. When the torch is brought in close proximity to the workpiece or when the selected welding current is initiated, the arc is transferred from the electrode to the workpiece through the orifice in the copper alloy nozzle (transferred arc mode), at which point a weld pool is formed (Fig. 1).

The PAW process can be used in two distinct operating modes, often described as the melt-in mode and the keyhole mode.

The melt-in-mode refers to a weld pool similar to that which typically forms in the gas-tungsten arc welding (GTAW) process, where a bowl-shaped portion of the workpiece material that is under the arc is melted.

In the keyhole mode, the arc fully penetrates the workpiece material, forming a nominally concentric hole, or keyhole, through the thickness. The molten weld metal flows around the arc and resolidifies behind the keyhole as the torch traverses the workpiece.

Current and Operating Modes. The PAW process uses three current modes: microplasma (melt-in mode), medium-current plasma (melt-in mode), and keyhole plasma (keyhole mode). This categorization is primarily based on the level of welding current. The microplasma mode is usually defined in the current range from 0.1 to 15 A. The medium-current plasma mode ranges from 15 to 100 A. The keyhole plasma mode is above 100 A. There is a certain degree of overlap between these current ranges. For example, keyholing can be achieved at 70 A on a 2 mm (0.08 in.) sheet. Equipment is available for welding currents up to 500 A, although a 300 A maximum is typical. Microplasma and medium-current melt-in modes are used for material up to 3 mm (0.12, or $\frac{1}{8}$, in.) thick, whereas the keyhole plasma mode is used for greater thicknesses and higher travel speeds.

In addition to operating in a continuous and steady direct current electrode negative (DCEN) mode, the PAW process can be carried out using DCEN pulsed current, as well as in the variable polarity mode, which uses both direct current electrode positive (DCEP) and electrode negative polarity switching. The pulsed current mode (both DCEN and DCEN/DCEP) is most often used when current levels (typically, above 100 A) are employed for keyhole plasma welding. Pulsing the current widens the tolerance region of acceptance welding parameters, primarily by further stabilizing the formation of the keyhole itself (Fig. 2).

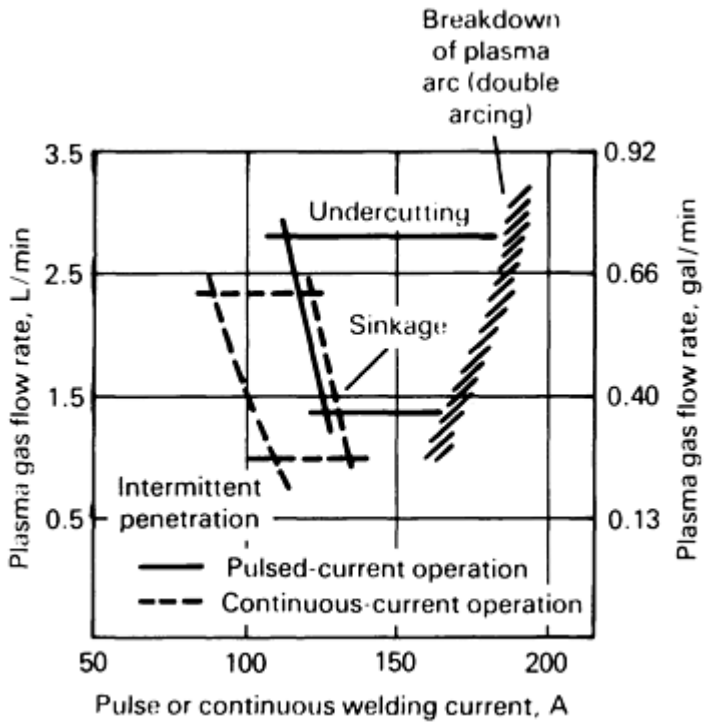

FIG. 2 TOLERANCE TO VARIATION IN WELDING CURRENT AND PLASMA GAS FLOW RATE IN PULSED AND CONTINUOUS CURRENT KEYHOLE WELDING; BOUNDARIES SHOW THE WELDING PARAMETER COMBINATIONS AT WHICH SPECIFIC DEFECTS ARE LIKELY TO OCCUR. WELDING PARAMETERS; NOZZLE BORE, 2.36 MM (0.0929 IN.); ELECTRODE DIAMETER, 4.8 MM (0.19 IN.)

The electrode positive component of the variable polarity plasma arc (VPPA) welding process promotes cathode etching of the tenacious surface oxide film when welding aluminum alloys, allowing good flow characteristics and consistent bead shape. Pulsing times are typically 20 ms for the electrode negative component and 3 ms for the electrode positive polarity. The VPPA welding process is used very effectively in specialized aerospace applications.

The PAW process is generally applied when the high penetration of the keyhole welding mode can be exploited to minimize the number of welding passes and, hence, welding time. The time saved can reduce the direct labor element of the welding operation. At the other end of the scale, the microplasma operating mode is used to weld small, thin-section components (as low as 0.025 mm, or 1 mil, thick), where the high arc constriction and low welding current can be beneficial in controlling heat input and distortion.

Advantages and Disadvantages. The advantages of the PAW process are primarily intrinsic to the keyhole mode of operation, because greater thicknesses of metal can be penetrated in a single pass, compared with other processes, such as GTAW. This greater amount of penetration allows a reduced amount of joint preparation. In some materials, for example, a square-grooved butt joint preparation can be used for thicknesses up to 12 mm (0.5 in.). The process can produce high weld integrity (similar to GTAW) while minimizing weld passes and, hence, welding times and labor costs. The columnar shape of the arc results in a greater tolerance to variations in torch standoff distance, when compared with the conical arc shape of a GTAW arc. The tungsten electrode used in the PAW process is protected from contamination by the constricting nozzle (Fig. 1). The longer arc length allows better viewing of the weld pool, which is important in manual welding.

Disadvantages include the greater capital equipment cost, when compared with its main rival, the GTAW process. Although high arc constriction achieves higher penetration, it also reduces the tolerance of the process to joint gaps and misalignment, when compared with the broader, conical arc of the GTAW process. The greater complexity of the PAW torch design and the greater number of parts requires more scheduled maintenance. The accurate set-back of the electrode tip, with respect to the nozzle orifice, is required to maintain consistent results. However, this task is facilitated by a general-purpose tool designed for nozzle removal and replacement and for electrode set-back adjustment.

Plasma Arc Welding

Ian D. Harris, Edison Welding Institute

Equipment

A basic PAW system consists of a power source, a plasma control console, a water cooler, a welding torch, and a gas supply system for the plasma and shielding gases (Fig. 3).

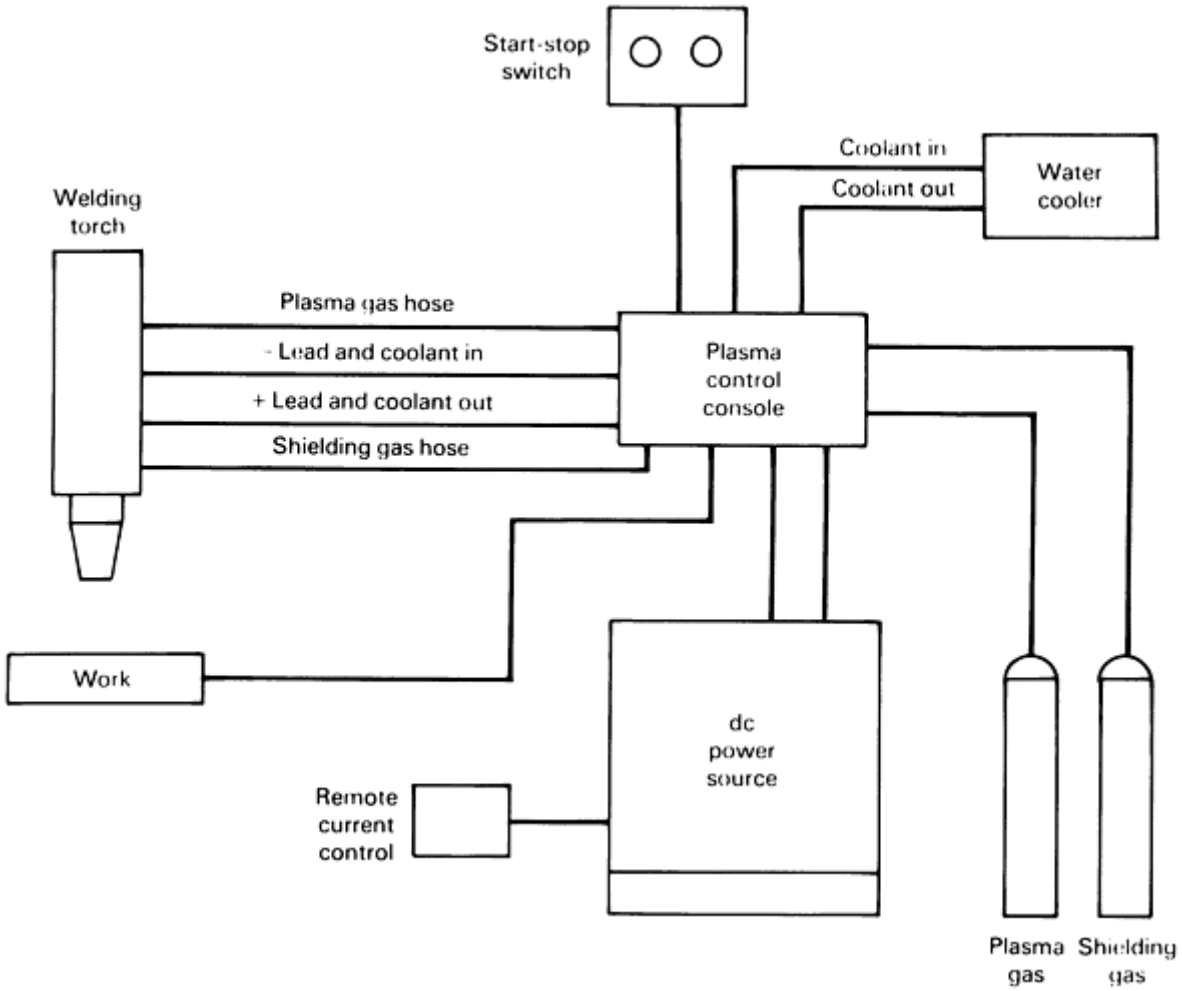

FIG. 3 TYPICAL EQUIPMENT FOR PLASMA ARC WELDING

The power source, which supplies the main power for the welding system, is usually supplemented with a sequence controller and control console. The sequence controller sequences the timing of gas flow, arc initiation, main welding current control, and any up-slope and downslope parameters. In its simplest form, the plasma control console controls the gas flow for plasma and shielding gases from separate flow-meters and incorporates the high-frequency pilot arc initiation circuit. The welding torch can be manual or mechanized and is water cooled to avoid torch overheating and to maximize component life.

In most PAW installations, plasma and shielding gases are supplied from separate gas cylinders, although bulk gas can readily be used. The gas supply is usually routed through the plasma control console, where the individual flow rates are set by the operator.

The power source should be of a constant-current design. Transistorized power sources are most common, although inverter power supplies are also available. It should have a minimum open-circuit voltage of 80 V to ensure the reliable initiation and transfer of the main arc current. The power source can be adjusted for welding current and it should have the capability to adjust the up slope and down slope of the current. It may be equipped with thumbwheels or potentiometers to select the parameters for pulse current operation, that is, peak and background current levels, as well as peak and background times.

Welding Torches. Like those of the other arc welding processes, PAW torches are available in a range of sizes for different power ratings and in manual and mechanized versions. The design principles are the same in each case. A tungsten alloy electrode is held in a collet within the torch body. To avoid one of the most common defects in plasma torches, it is critical to hold concentricity between the tungsten electrode and the orifice in the design and manufacture of the torch. The electrode assembly is set inside a plenum chamber and the plasma gas is supplied to this chamber. A

threaded copper alloy nozzle forms the front of this chamber and contains the nozzle orifice that is used to constrict the plasma arc. A shielding gas nozzle, usually of an insulating ceramic material, is threaded onto the front end of the torch and surrounds the constricting nozzle, creating an annulus through which the shielding gas is supplied. The torch is connected electrically to the power source and the electrode forms the negative pole of the circuit for dc welding. The gas hoses that supply the plasma and shielding gases and the water hoses that supply and remove water from the torch are all connected to the torch body or handle. These hoses are enclosed in a flexible sheath that extends from the torch to the components of the welding system.

Most constricting nozzles have a single orifice in the center. However, multiple-nozzle orifices can be used with higher-power torches to achieve further arc constriction. The most common version of this type of nozzle has a central orifice flanked by a smaller orifice on each side. The common centerline of the three orifices is arranged at 90° to the weld line during operation.

Electrodes. The nonconsummable electrode employed is usually a 2% thoriated tungsten electrode, that is, tungsten with 2% thorium oxide. The electrode specification is covered in AWS A5.12-92. The electrode size is selected according to the welding current level that will be used. The electrode is ground with a tapered point on the end, the angle of which depends on the selected welding current level. Electrode sizes and tip angles for a range of welding current levels are shown in Table 1.

TABLE 1 MAXIMUM CURRENT FOR PLASMA WELDING WITH SELECTED ELECTRODE DIAMETER, VERTEX ANGLE, AND NOZZLE BORE DIAMETER

MAXIMUM CURRENT, A	ELECTRODE DIAM		VERTEX ANGLE, DEGREES	PLASMA[A]				SHIELDING[B]			
				NOZZLE BORE DIAM		FLOW RATE		SHROUD DIAM		FLOW RATE	
	mm	in.		mm	in.	l/min	gal/min	mm	in.	l/min	gal/min
MICROPLASMA											
TORCH RATING, 20 A 5											
5	1.0	0.04	15	0.8	0.03	0.2	0.05	8	0.32	4-7	1-1.8
10				0.8	0.03	0.3	0.08				
20				1.0	0.04	0.5	0.13				
MEDIUM CURRENT											
TORCH RATING, 100 A											
30	2.4	0.10	30	0.79	0.03	0.47	0.12	12	0.48	4-7	1-1.8
50				1.17	0.05	0.71	0.19				
75				1.57	0.06	0.94	0.25				
100				2.06	0.08	1.18	0.31				
TORCH RATING, 200 A											
50	4.8	0.19	30	1.17	0.05	0.71	0.19	17	0.68	4-12	1-3.2
100				1.57	0.06	0.94	0.25				
160				2.36	0.09	1.42	0.38				
200				3.20	0.13	1.65	0.44				
TORCH RATING, 400 A											
180	3.2	0.13	60[C]	2.82	0.11	2.4	0.63	18	0.72	20-35	5.3-9.2
200				2.82[C]	0.11[C]	2.5	0.66				

HIGH CURRENT											
TORCH RATING, 400 A											
250	4.8	0.19	60[C]	3.45[D]	0.14	3.0	0.79	. . .	. . .	20-35	5.3-9.2
300				3.45[D]	0.14[D]	3.5	0.92				
350				3.96[D]	0.16[D]	4.1	1.08				

(A) ARGON PLASMA GAS.

(B) ARGON AND AR-5H_2 SHIELDING GAS.

(C) ELECTRODE TIP BLUNTED TO 1 MM (0.04 IN.) DIAMETER.

(D) MULTIPORT NOZZLE

The new types of tungsten electrodes, which contain oxides of rare-earth elements in place of the thorium oxide, can also be used. These electrodes have been shown to have greater tip life. However, they are more expensive and their usefulness in plasma arc welding may be limited because of the high level of protection provided by the nozzle. In low-current microplasma welding applications, their better emissivity provides easier arc transfer and better overall performance.

If a finer wire is required, to fit the joint or to avoid undercut at the weld toes, then wires suitable for gas-shielded arc welding (for example, those used for GTAW) should be employed. The appropriate AWS specification series is AWS A5.XX.

Plasma (Orifice) and Shielding Gases. The plasma gas is used to generate the arc, whereas the shielding gas is used to provide the weld pool with supplementary shielding from atmospheric contamination while it solidifies and cools. The plasma gas is almost always argon. Gas properties affect both weld shape and quality. Flow rates, particularly of the plasma gas, are also important, because they control the extent of plasma constriction. The flow rate can vary from 0.1 L/min (0.026 gal/min) for microplasma welding up to 10 L/min (2.6 gal/min) for keyhole plasma welding. Considerable care is needed to regulate the gas flow rate if keyhole closure is required, because the flow rate must be sloped out to 1 to 2 L/min (0.26 to 0.52 gal/min) within about 1 s. Gas flow control is best achieved by electronic means.

The design and current rating of welding torches are based on argon plasma gas. Argon provides effective shielding, being heavier than air, and is cheaper than helium. Shielding gas selection is based on the type of base metal (Table 2).

TABLE 2 PLASMA AND SHIELDING GAS COMPOSITIONS

MATERIAL	PLASMA GAS	SHIELDING GAS
MILD STEEL	ARGON	ARGON ARGON-2-5% H_2[A]
LOW-ALLOY STEELS	ARGON	ARGON
AUSTENITIC STAINLESS STEEL	ARGON	ARGON-2-5% H_2 HELIUM[A]
NICKEL AND NICKEL ALLOY	ARGON	ARGON ARGON-2-5% H_2[A]
TITANIUM	ARGON	ARGON 75HE-25AR[A]
ALUMINUM AND ALUMINUM ALLOYS	ARGON	ARGON HELIUM[A]
COPPER AND COPPER ALLOYS	ARGON	ARGON 75HE-25AR[A]

(A) ALSO USED

Helium and argon-helium mixtures can be used as shielding gases to increase the thermal conductivity of the gas and, hence, the heating effect on the weld pool. Helium results in wider weld pools than argon, because it produces a higher arc voltage. Hydrogen additions to argon shielding gas tends to promote slightly narrower weld pools through arc constriction and achieves a very clean weld pool appearance, because it is a reducing gas. Although helium and hydrogen can be added to argon in the shielding gas to give higher heat input, the use of gases with higher heat contents in the plasma gas can result in torch overheating and potential damage.

Ian D. Harris, Edison Welding Institute

Applications

Material Types. The PAW process is commonly used to weld stainless steels in a wide range of thicknesses. The process can also be used with carbon and alloy steels, aluminum alloys, titanium alloys, copper and nickel alloys, and more specialized materials, such as zirconium and tantalum. The thicknesses that can be welded in a single pass range from 0.025 mm (1 mil) for microplasma applications to 12.5 mm (0.5 in.) for the VPPA welding of aluminum. Direct-current pulsing can be used on most materials.

The PAW process is often carried out in an autogenous mode, that is, without filler wire. When edge beveling is used, a filler wire is required to complete the joint. A filler wire can also be used with the keyhole mode of operation to avoid undercut at high welding speeds. Wire composition depends on that of the parent materials in the joint. The same continuous-wound wire that is used in GTAW operations is suitable.

The industries that use the PAW process can be categorized as those that weld thin-section sheet using microplasma or medium-current plasma welding and those that weld plate using keyhole plasma welding.

A wide range of small devices and assemblies made from thin stainless steel sheet, including bellows assemblies and associated fittings, are welded using the microplasma operating mode. The narrow weld bead that can be produced provides sheet-metal fabrications with a good cosmetic appearance. Furthermore, the high welding speed that can be achieved, coupled with the good tolerance to stand-off variations resulting from the columnar nature of the arc, makes the process attractive for high-volume production work.

Microplasma, as well as medium-current plasma modes, can be used to spot weld guide wires and lamp filaments, as well as in other applications that require highly repetitive autogenous welds. This type of application allows a user to limit the number of high-frequency arc starts that would be required with tungsten-inert gas welding.

Keyhole plasma welding is extensively used to weld stainless steel pipe and tankage. The process is applied to individual strakes from plate to make stainless steel vessels in the food and chemical processing industries. Circumferential welding of strakes also can be used to create these products. Longitudinal seam welds in stainless steel pipe with wall thickness of [ges]3 mm ([ges]0.12 in.) are ideally suited to keyhole plasma welding, because joint preparation is minimized and single-pass welding can be consistently achieved without the use of weld-backing devices. Pipes with wall thickness above 5 to 6 mm (0.20 to 0.24 in.) employ the keyhole mode of operation for the root pass. Depending on the material type and wall thickness, melt-mode PAW, GTAW, gas-metal arc welding (GMAW), or submerged arc welding (SAW) are used to complete the joint. High-alloy composition piping is similarly manufactured.

The manufacturing of stainless steel tube from strip was one of the first applications of the PAW process. Because the process can reliably produce full-penetration welds without the use of backing, it is extensively used on tube mills, because a lack of access precludes welding from the inside.

The VPPA welding process has been very effective for welding large space shuttle orbiter sections of aluminum alloys, particularly the external fuel tank. The cathodic cleaning action of the electrode positive portion of the current cycle breaks up tenacious surface oxide film on the aluminum. The process can be used on thicknesses up to 12.5 mm (0.5 in.) with square-grooved butt joints, and it can be used for the root pass on thicker sections with edge beveling. It is anticipated that this technique will be extensively employed in building aluminum alloys structures in a modular space station.

Ian D. Harris, Edison Welding Institute

Typical Components and Joints

The most common joint configuration used with the PAW process is a butt joint. The microplasma mode is used with overlapped butt (micro-lap) joints and with joints that have integral weld metal as a result of flanged, butted edges on very thin metals (Table 3). Corner joints with edge welds are also commonly welded using the microplasma and medium-current modes.

TABLE 3 JOINT CONFIGURATIONS FOR PLASMA WELDING SHEET AND TUBULAR COMPONENTS

Thickness range						
mm	in.	Joint type	Joint configuration	Process variant	No. of runs	Comments
0.5–1.0	0.02–0.04	Micro-lap	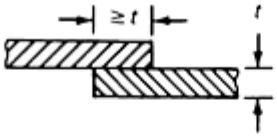	Microplasma	1	Edges fully fused to produce additional weld metal; good clamping essential
0.5–1.5	0.02–0.06	Flanged edge	0.5-1.0 mm 	Microplasma	1	Edges fully fused to produce additional weld metal
3.0–6.0	0.12–0.24	Square butt		Keyhole plasma	1	Grooved backing bar required to prevent disturbance of the efflux plasma. Additional (cosmetic) run using melt mode may be employed
6.0–15	0.24–0.60	Single-V butt	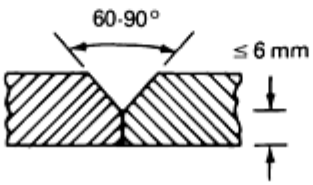	Keyhole plasma	2 or more	Keyhole technique used for root run only. Joint completed with the melt mode plus filler wire

Because the keyhole operating mode fully penetrates the workpiece, it is used exclusively on square-grooved butt joints and single-V joints with a root face (Table 3). For square-grooved butt joint preparation, the thickness that can be welded in a single pass depends on the fluid flow characteristics of the workpiece material for a given heat input from the plasma torch. Thus, alloys of titanium and zirconium can be butt welded with square-grooved preparation at greater thicknesses than steels and stainless steels. Generally, it is an industry-accepted practice to use square-grooved preparation without edge beveling for stainless steels up to 6 mm (0.24 in.) in thickness.

A 4 or 5 mm (0.16 or 0.20 in.) root face and a single-V preparation, usually with a 60° included angle, are used on steels thicker than 6 mm (0.24 in.) (Table 4). The root is welded in the keyhole mode and the rest of the joint is completed with a filler wire addition by melt-mode PAW, GTAW, GMAW, or SAW, depending on the material type, joint volume to be filled, and the mechanical property requirements of the joint.

TABLE 4 KEYHOLE PLASMA WELDING CONDITIONS FOR PIPE PREFABRICATION IN TYPE 304L/316L STAINLESS STEEL

Tube diam		Thickness		Edge preparation	Welding current, A	Welding speed		Gas flow: Plasma gas, argon		Gas flow: Shielding gas, argon + hydrogen		Gas flow: Backing gas		Filler wire feed rate (1.0 mm diam)	
mm	in.	mm	in.			m/min	ft/min	L/min	gal/min	L/min	gal/min	L/min	gal/min	m/min	ft/min
60	2.4	7.5	0.30	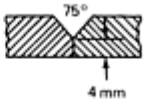	160–100 140–90	0.22 0.22	0.72 0.72	4.5 1.5	0.13 0.40	18 18	4.8 4.8	10 10	2.6 2.6	... 1.10	... 3.6
114(a)	4.6(a)	12	0.48	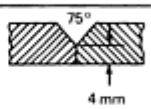	160–100	0.18	0.59	4.5	1.2	18	4.8	10	2.6	1.10	3.6
168(a)	6.7(a)	14	0.56	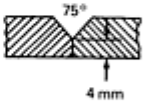	190–120	0.14	0.46	6	1.6	18	4.8	15	4.0	...	...
510 or 710	20.4 or 28.4	6	0.24		180	0.22	0.72	5	1.3	18	4.8	30	6.6	1.10	3.6
1000(b)	40(b)	12	0.48	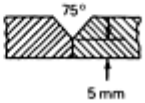	270	0.21	0.69	7	1.8	25	6.6	30	6.6	...	...

(a) Welded thickness, 5 mm (0.20 in.). (b) Welded thickness, 6 mm (0.24 in.)

(a) Welded thickness, 5 mm (0.20 in.). (b) Welded thickness, 6 mm (0.24 in.)

In the PAW process, fixturing for part fit-up is more critical than it is for the GTAW process, primarily because of the narrower, more-constricted arc in PAW. The backing bar design and shielding gas techniques employed for GTAW are appropriate for microplasma and medium-current modes. During keyhole welding, however, the arc passes right through the workpiece, forming an efflux plasma (Fig. 1) that normally extends 10 mm (0.4 in.) below the back face of the joint. This characteristic must be accommodated when designing backing systems. Failure to allow sufficient gap can result in turbulence in the efflux plasma, causing weld pool disturbance and porosity.

When welding longitudinal seams in tube or pipe, the weld can be started and stopped on run-on and run-off tabs, precluding the need for keyhole closure. However, when using the keyhole mode on circumferential seams of vessels or on butt joints in tubes or pipes, the keyhole will overlap the start of the weld to produce a complete joint. Keyhole closure without porosity has been an area of difficulty, particularly when butt welding tubes, and it represented an important concern for more-widespread use of the process. Modern electronic controls for simultaneous reduction in gas flow and current slope-out provide a more reliable method for keyhole closure.

Plasma Arc Welding

Ian D. Harris, Edison Welding Institute

Procedures

Process Operating Procedure. Welding parameters, such as welding current, arc voltage, travel speed (for mechanized/automatic operation), and plasma and shielding gas flow rates, are set by the procedure and implemented by the welder. Torch parameters include the correct electrode vertex angle and set-back distance, as well as the correct orifice diameter for the welding current level.

The operating sequence for the PAW process was described in the section "Principles of Operation" at the beginning of this article. After the weld pool or keyhole is formed, the torch is traversed across the workpiece at the preset welding speed. Welding is terminated by the down slope of the welding current, with simultaneous sloping of the plasma gas flow rate if keyhole welding and keyhole closure are desired. Slope control for the keyhole mode is shown in Fig. 4.

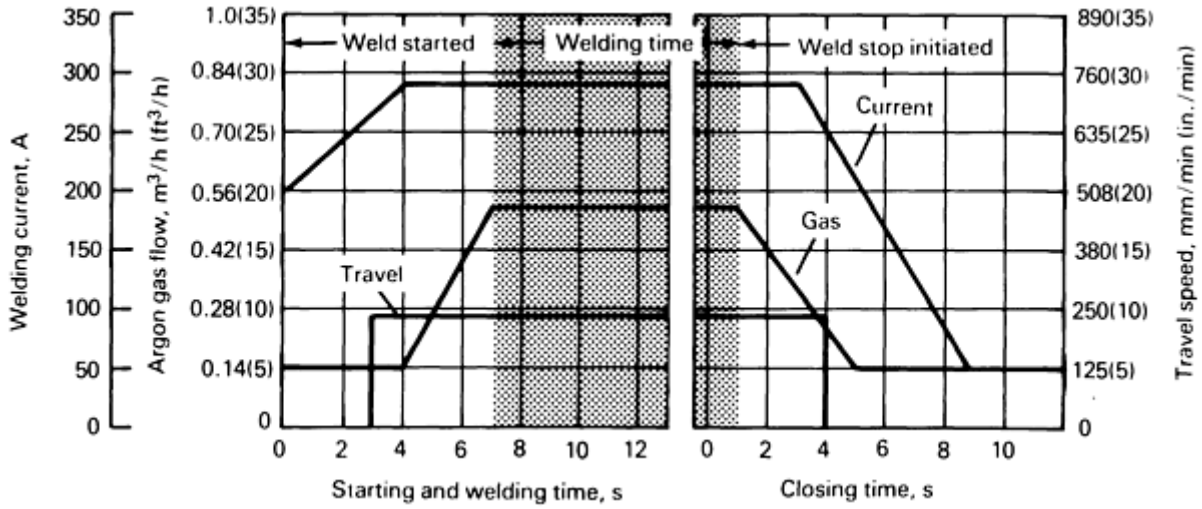

FIG. 4 TYPICAL SLOPE CONTROL PATTERN FOR WELDING CURRENT AND PLASMA GAS FLOW WHEN STARTING AND CLOSING A KEYHOLE; EXAMPLE IS FOR 9.5 MM ($\frac{3}{8}$ IN.) THICK STEEL

Most plasma arc welding is done in a mechanized or automated operation that does not require much operator intervention, except initially to set the parameters and to position the workpiece and torch. When current pulsing and keyhole closure operations are involved, numerous parameters must be set, which requires strict attention to detail, accurate part fit-up, and careful alignment of the torch relative to the joint.

Inspection and Weld Quality Control. All of the common nondestructive evaluation (NDE) techniques are applicable to plasma arc welds. Radiography and ultrasonic inspection are the most common techniques used. The fact that most plasma arc welding is carried out in the keyhole mode means that there is a penetration bead on the root side of the joint. Visual inspection for full penetration, as well as for correct width and profile of both the penetration bead and the weld surface profile, can readily be accomplished. Smooth, even underbeads can be achieved through good procedure development with tolerances improved through current pulsing.

Troubleshooting. When troubleshooting a PAW operation, all of the previously defined basic parameters of the welding schedule should be checked. Welding discontinuities can result from incorrect electrode set-back or from a worn or damaged nozzle orifice. The concentricity of the diameter of the nozzle orifice and the alignment of the electrode and nozzle orifice are very important. Worn nozzles should be replaced. The condition of the tungsten electrode tip should also be checked.

An undercut is one of the most common defects in the PAW process. Depending on material type, thickness, and preset welding parameters, a two-sided undercut can occur above certain threshold welding speeds. This can only be eliminated by increasing welding current. A one-sided undercut can result from misalignment of the torch, the electrode/orifice and multiport nozzles, or from the mismatched fit-up of the workpieces. Correct alignment is essential.

Plasma Arc Welding

Ian D. Harris, Edison Welding Institute

Personnel Requirements

The skill level and training requirements for the PAW process are generally similar to those for the GTAW process. When manual welding, the columnar nature of the plasma arc allows greater variation of the torch-to-workpiece distance without altering the size and shape of the weld pool. The fact that the electrode is protected from contamination by the nozzle means that tungsten contamination and tungsten inclusions in the weld metal are more readily avoided than they are in the GTAW process. From the viewpoint of an operator, disadvantages include the greater complexity of the torch,

in terms of nozzle orifice and electrode set-back considerations, and the correct setting of two gases (plasma and shielding gas).

When mechanized welding is carried out, which is usually the case for the keyhole mode, the operator is required to set a greater number of parameters (compared to GTAW), particularly if current pulsing and keyhole closure operations are required. Specific operator training is required for pulsed keyhole operation, and particularly for VPPA operations, which are usually carried out in the vertical position, welding upward, and thus require a high level of operator competence. Computerization of welding parameter selection is the trend for VPPA welding and other mechanized or automated PAW operations.

The health and safety issues related to the PAW process are very similar to those of other gas-shielded arc welding processes, especially GTAW. These include electrical shock; electromagnetic radiation hazards, particularly ultraviolet radiation; burns from hot metal parts; and welding fumes and gases, including ozone. The volume of welding fumes produced is low and is similar to that produced by the GTAW process. Hexavalent chromium and ozone are concerns when welding stainless steels and aluminum alloys, respectively. Like the GTAW process, the low level of general welding fumes associated with PAW results in a comparatively higher level of ozone. However, the rapid decay of ozone within a short distance of the arc, coupled with the high degree of mechanization and automation typical of the keyhole plasma welding operation, means that operator exposure is generally very low. The microplasma mode, which is more commonly used manually, employs such low current levels that fume and ozone levels are very low.

Carbon Arc Welding

Lance Soisson, Welding Consultants, Inc.

Introduction

CARBON ARC WELDING (CAW) utilizes what is considered to be a nonconsumable electrode, made of carbon or graphite, to establish an arc between itself and either the workpiece or another carbon electrode. However, this electrode erodes fairly quickly and generates carbon monoxide (CO) gas that partially replaces the air around the arc, thereby providing the molten weld with some protection.

The CAW process, which uses either single or twin electrodes, most closely resembles gas-tungsten arc welding (GTAW), where the arc is used only as a source of heat. The single-electrode arrangement usually operates with direct current (dc), electrode negative (straight polarity), using most dc power supplies. The twin-electrode arrangement usually operates with alternating current (ac), generally with small ac power supplies. Figure 1 shows typical configurations for both procedures.

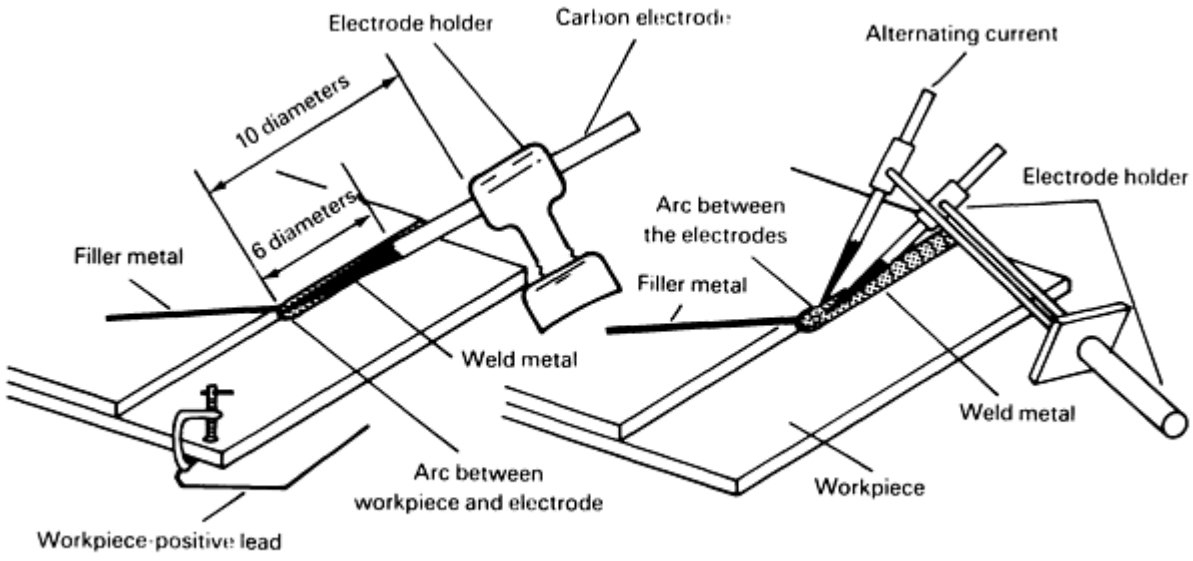

Single-electrode CAW **Twin-electrode CAW**

FIG. 1 TYPICAL ARRANGEMENTS FOR SINGLE-ELECTRODE AND TWIN-ELECTRODE CARBON ARC WELDING

Although the CAW process has been almost completely replaced by the newer processes used in the welding industry, it is still used in certain applications. The process does produce adequate welds in thin-sheet steel, but should be used with caution in any critical application because it provides only limited shielding from the atmosphere.

Carbon Arc Welding

Lance Soisson, Welding Consultants, Inc.

Operation

CAW electrodes can be either carbon or graphite, although baked carbon electrodes are most commonly used because they last longer and are more readily available. Electrode sizes range from 3.2 to 22 mm ($\frac{1}{8}$ to $\frac{7}{8}$ in.). The typical torch is air cooled for the smaller electrodes, but water cooled for the larger ones. The recommended current ranges for both electrode types are given in Table 1.

TABLE 1 RECOMMENDED CURRENT RANGES FOR CARBON AND GRAPHITE ELECTRODES

ELECTRODE DIAMETER		CURRENT, A	
mm	in.	CARBON	GRAPHITE
SINGLE ELECTRODE			
3.2	$\frac{1}{8}$	15-30	15-35
4.8	$\frac{3}{16}$	25-55	25-60
6.4	$\frac{1}{4}$	50-85	50-90
7.9	$\frac{5}{16}$	75-115	80-125
9.5	$\frac{3}{8}$	100-150	110-165
11.1	$\frac{7}{16}$	125-185	140-210
12.7	$\frac{1}{2}$	150-225	170-260
15.9	$\frac{5}{8}$	200-310	230-370
19	$\frac{3}{4}$	250-400	290-490
22.2	$\frac{7}{8}$	300-500	400-750
TWIN ELECTRODES			
6.4	$\frac{1}{4}$	55	. . .
7.9	$\frac{5}{16}$	75	. . .
9.5	$\frac{3}{8}$	95-120	. . .

In the single-electrode operation, the carbon electrode is prepared to a long tapered point that is one half the electrode diameter (see Fig. 1). The arc is established by "scratch starting," that is, by bringing the electrode into contact with the workpiece and immediately withdrawing it to the correct length for welding. The generally accepted arc length is maintained between 6.4 and 9.5 mm ($\frac{1}{4}$ and $\frac{3}{8}$ in.). Holding the length too short can result in carburization of the base metal, creating potentially brittle welds. This is particularly true when welding without filler metal.

When the joint requires filler metal, the same technique that is used in GTAW or oxyfuel gas welding (OFW) should be employed. The welding rod should be fed into the weld pool with one hand while manipulating the arc with the other.

If the arc is broken for any reason, then restart should not occur directly at the hot metal where welding stopped, because a hard spot could result. Rather, a restart should occur in front or to one side of the weld, followed by a quick return to the point where welding stopped. Care should be taken to either incorporate the restart area into the weld or to grind the arc strike after welding is completed. The arc strike areas can be very hard and can cause cracking if they are not fused into the weld or ground out.

In the twin-electrode operation, the workpiece is not part of the electrical circuit. The heat for welding is produced by creating an arc between the two electrodes. The electrode holder has two adjustable arms that grip the carbon electrodes at the proper length to maintain the arc. The operator maintains a constant distance between the carbon electrodes by adjusting them as they are consumed. An experienced welder can make these adjustments while still welding or brazing.

Small ac machines are normally used in the twin-electrode process because the electrodes will wear at an equal rate. Direct current can be used as long as the positive-side electrode is one size larger than the negative electrode. The larger electrode compensates for the faster consumption rate on the positive side of the direct current.

Electrodes range in size from 6.4 to 9.5 mm ($\frac{1}{4}$ to $\frac{3}{8}$ in.) and are copper coated for better current flow. The heat must be maintained so that the copper does not melt more than 13 mm ($\frac{1}{2}$ in.) back from the electrode tip. Only enough heat to cause the filler metal to flow easily should be used (Table 1). High heat causes excessive electrode consumption and could cause carburization of the weld metal.

Carbon Arc Welding

Lance Soisson, Welding Consultants, Inc.

Applications

The single-electrode carbon arc process is primarily used on steel, cast iron, and copper, although it can be used on most ferrous and nonferrous materials. With steels, it is principally applied to make outside corner welds on thinner-gage materials, where no filler metal is used. A good fit-up is required, and a fluxing agent is often used to promote better welds. The resulting welds arc smoother and, frequently, more economical than similar welds created by the shielded metal arc welding (SMAW) process.

Another application is the welding of galvanized steel using a silicon bronze filler metal. In this instance, it is important to maintain a short arc and to direct the heat to the filler metal to minimize damage to the galvanic coating.

Cast iron can be welded using the carbon arc process, but it is more often used in brazing. The casting must be preheated to approximately 650 °C (1200 °F) and then slowly cooled to reduce the possibility of cracking and to produce machinable welds.

The process is also used on copper, because of the high heat capabilities of the larger electrodes. Direct current, electrode negative, should always be used when welding or brazing copper. The workpiece should be preheated to a temperature between 150 and 650 °C (300 and 1200 °F), or at least locally preheated in the weld area. Holding a long arc will allow the carbon to combine with oxygen to form the CO that somewhat shields the weld.

Twin carbon arc welding is used primarily as a maintenance tool in small shops, farms, or homes. It is most commonly applied in brazing or soldering operations, although it can be used to weld, preheat, or postheat smaller parts.

Carbon Arc Welding

Lance Soisson, Welding Consultants, Inc.

Selected References

- H.B. CARY, *MODERN WELDING TECHNOLOGY,* 2ND ED., PRENTICE-HALL, 1989
- *WELDING HANDBOOK,* 8TH ED., VOL 2, *WELDING PROCESSES,* AWS, 1991

Submerged Arc Welding

Jonathan S. Ogborn, The Lincoln Electric Company

Introduction

SUBMERGED ARC WELDING (SAW) is an arc welding process in which the arc is concealed by a blanket of granular and fusible flux (Ref 1, 2, 3). Heat for SAW is generated by an arc between a bare, solid-metal (or cored) consumable-wire or strip electrode and the workpiece. The arc is maintained in a cavity of molten flux or slag, which refines the weld metal and protects it from atmospheric contamination. Alloy ingredients in the flux may be present to enhance the mechanical properties and crack resistance of the weld deposit.

References

1. R.L. O'BRIEN, *WELDING HANDBOOK,* VOL 11, AWS, 1991, P 191-232
2. D.L. OLSON *ET AL.,* SUBMERGED ARC WELDING, VOL 6, 9TH ED., *METALS HANDBOOK,* AMERICAN SOCIETY FOR METALS, 1983, P 114-152
3. *THE PROCEDURE HANDBOOK OF ARC WELDING,* THE LINCOLN ELECTRIC CO., 1973, P 6.3-1 TO 6.3-24

Submerged Arc Welding

Jonathan S. Ogborn, The Lincoln Electric Company

Principles of Operation

Figure 1 shows a typical setup for automatic SAW. A continuous electrode is being fed into the joint by mechanically powered drive rolls. A layer of granular flux, just deep enough to prevent flash through, is being deposited in front of the arc. Electrical current, which produces the arc, is supplied to the electrode through the contact tube. The current can be direct current (dc) with electrode positive (reverse polarity), with electrode negative (straight polarity), or alternating current (ac). Figure 2 shows the melting and solidification sequence of SAW. After welding is completed and the weld metal has solidified, the unfused flux and slag are removed. The unfused flux may be screened and reused. The solidified slag may be collected, crushed, resized, and blended back into new flux. Recrushed slag and blends of recrushed slag with unused (virgin) flux are chemically different from new flux. Blends of recrushed slag may be classified as a welding flux, but cannot be considered the same as the original virgin flux (Ref 4).

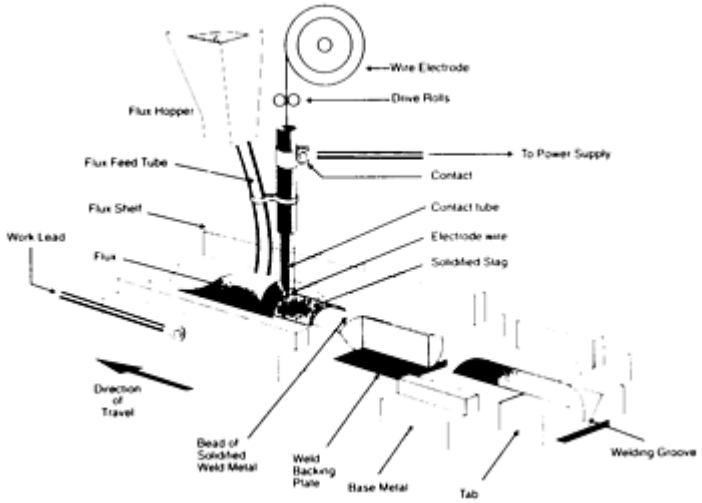

FIG. 1 SCHEMATIC SHOWING KEY COMPONENTS OF AUTOMATIC SUBMERGED ARC WELDING SETUP

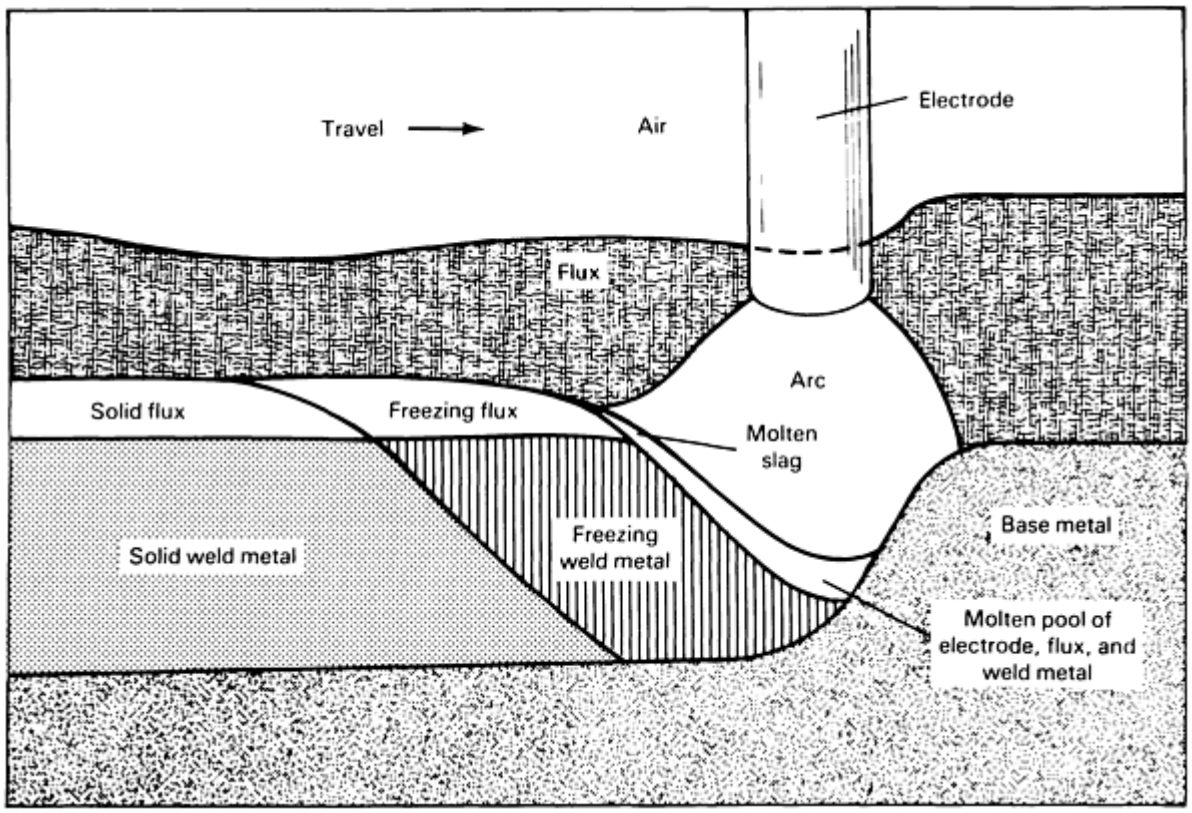

FIG. 2 SCHEMATIC SHOWING TYPICAL WELD POOL DYNAMICS OF A SUBMERGED ARC WELD

Submerged arc welding is adaptable to both semiautomatic and fully automatic operation, although the latter, because of its inherent advantages, is more popular (see the section "Advantages of Submerged Arc Welding" in this article). In semiautomatic welding, the welder controls the travel speed, direction, and placement of the weld. A semiautomatic welding gun is designed to transport the flux and wire to the operator, who welds by dragging the gun along the weld joint. Semiautomatic electrode diameters are usually less than 2.4 mm ($\frac{3}{32}$ in.) to provide sufficient flexibility and feedability in the gun assembly. Manually guiding the gun over the joint requires skill because the joint is obscured from view by the flux layer. In automatic SAW, travel speed and direction are controlled mechanically. Flux may be

automatically deposited in front of the arc, while the unfused flux may be picked by a vacuum recovery system behind the arc.

To increase deposition rate or welding speed, more than one wire can be fed simultaneously into the same weld pool. For example, in the twin arc process, two electrodes are fed into the same weld pool while sharing a common power source and contact tip. In tandem arc SAW, multiple electrodes are arranged with one in front of the other. Each electrode has an independent power supply and contact tip. The spacing, configuration, and electrical nature of the electrodes may be arranged to optimize welding speed and bead shape (Ref 5).

Advantages of submerged arc welding include the following:

- THE ARC IS UNDER A BLANKET OF FLUX, WHICH VIRTUALLY ELIMINATES ARC FLASH, SPATTER, AND FUME (THUS MAKING THE PROCESS ATTRACTIVE FROM AN ENVIRONMENTAL STANDPOINT).
- HIGH CURRENT DENSITIES INCREASE PENETRATION AND DECREASE THE NEED FOR EDGE PREPARATION.
- HIGH DEPOSITION RATES AND WELDING SPEEDS ARE POSSIBLE.
- COST PER UNIT LENGTH OF JOINT IS RELATIVELY LOW.
- THE FLUX ACTS AS A SCAVENGER AND DEOXIDIZER TO REMOVE CONTAMINANTS SUCH AS OXYGEN, NITROGEN, AND SULFUR FROM THE MOLTEN WELD POOL. THIS HELPS TO PRODUCE SOUND WELDS WITH EXCELLENT MECHANICAL PROPERTIES.
- LOW-HYDROGEN WELD DEPOSITS CAN BE PRODUCED.
- THE SHIELDING PROVIDED BY THE FLUX IS SUBSTANTIAL AND IS NOT SENSITIVE TO WIND AS IN SHIELDED METAL ARC WELDING AND GAS METAL ARC WELDING.
- MINIMAL WELDER TRAINING IS REQUIRED (THUS, RELATIVELY UNSKILLED WELDERS CAN BE EMPLOYED).
- THE SLAG CAN BE COLLECTED, REGROUND, AND SIZED FOR MIXING BACK INTO NEW FLUX AS PRESCRIBED BY MANUFACTURERS AND QUALIFIED PROCEDURES.

Limitations of submerged arc welding include the following:

- THE INITIAL COST OF WIRE FEEDER, POWER SUPPLY, CONTROLS, AND FLUX-HANDLING EQUIPMENT IS HIGH.
- THE WELD JOINT NEEDS TO BE PLACED IN THE FLAT OR HORIZONTAL POSITION TO KEEP THE FLUX POSITIONED IN THE JOINT.
- THE SLAG MUST BE REMOVED BEFORE SUBSEQUENT PASSES CAN BE DEPOSITED.
- BECAUSE OF THE HIGH HEAT INPUT, SAW IS MOST COMMONLY USED TO JOIN STEELS MORE THAN 6.4 MM ($\frac{1}{4}$ IN.) THICK.

References cited in this section

4. "SPECIFICATION FOR CARBON STEEL ELECTRODES AND FLUXES FOR SUBMERGED ARC WELDING," A5.17-89, AWS, 1989, P 18
5. *THE PROCEDURE HANDBOOK OF ARC WELDING*, THE LINCOLN ELECTRIC CO., 1973, P 3.2-3, 6.3-21 TO 6.3-22, 6.3-49 TO 6.3-58

Submerged Arc Welding

Jonathan S. Ogborn, The Lincoln Electric Company

Process Applications

If a steel is suitable for welding with gas-metal arc welding, flux-cored arc welding, shielded metal arc welding, or gas-tungsten arc welding, procedures can be developed to weld the steel with SAW (Ref 6). The main limitations of SAW are plate thickness and position. Because SAW is a high heat input and high deposition rate process, it is generally used to weld thicker-section steels. Although the welding of 1.6 mm ($\frac{1}{16}$ in.) thick steel is possible, most SAW is done on plate over 6.4 mm ($\frac{1}{4}$ in.) in thickness.

Types of Metals. Submerged arc welding is most commonly used to join plain carbon steels. Alloy steels can be readily welded with SAW if care is taken to limit the heat input as required to prevent damage to the heat-affected zone (HAZ). Low-heat-input procedures are available for welding alloy steels and heat-treated steels to prevent grain coarsening and cracking in the HAZ. Maintaining proper preheat and interpass temperature is also important when welding alloy steels to prevent weld metal and HAZ cracking and to develop the required mechanical properties in the weld deposit. Submerged arc welding can be used to join stainless steels and nonferrous alloys. It is also commonly used to produce a stainless or nonferrous overlay on top of a base metal.

Joint Configurations. The most common weld deposits made with SAW are groove, fillet, and plug welds, and surfacing deposits. For groove welds, the characteristic deep penetration of SAW plays a role in joint selection. Plate up to 15.9 mm ($\frac{5}{8}$ in.) thick can be completely welded from one side using a square butt joint with a 0.8 mm ($\frac{1}{32}$ in.) root opening. Beveled joints should be used for multiple-pass welds on plate thicknesses greater than 15.9 mm ($\frac{5}{8}$ in.). Backing bars should be used to prevent loss of flux, to prevent melt through, and to ensure full-penetration weldments on one-sided joints. Although groove welds are generally made in the flat position, it is possible to develop special procedures to weld horizontally.

Single-pass fillet welds with throat sizes up to 7.9 mm ($\frac{5}{16}$ in.) thick and multiple-pass fillet welds are usually made in the horizontal position. Single-pass fillet welds over 7.9 mm (5/16 in.) thick are usually made in the flat position. Submerged arc plug welds are made in the flat position by puddling the electrode into the center of the hole until the weld is complete. Surfacing welds are made with both wire and strip electrode. Surfacing is done to rebuild worn parts with a wear-resistant material or to overlay a plain steel part with stainless steel or other alloys (Ref 7, 8, 9).

To prevent porosity, the surface to be welded should be clean and free of grease, oil, paints, moisture, and oxides. All slag from tack welds or previous layers should be removed. Tack welds should be positioned so that the submerged arc weld completely melts out the tack. The workpiece should be firmly clamped to minimize distortion and the need for tack welds.

Industrial Uses for SAW. Because SAW is used to join thick steel sections, it is primarily used for shipbuilding, pipe fabrication, pressure vessels, and structural components for bridges and buildings. Other than joining, SAW is used to build up parts and overlay with stainless or wear-resistant steel (for example, rolls for continuous casting steel, pressure vessels, rail car wheels, and equipment for mining, mineral processing, construction, and agriculture).

References cited in this section

6. *THE PROCEDURE HANDBOOK OF ARC WELDING*, THE LINCOLN ELECTRIC CO., 1973, P 6.3-26 TO 6.3-73
7. R.S. BROWN *ET AL.*, ARC WELDING OF STAINLESS STEELS, VOL 6, 9TH ED., *METALS HANDBOOK*, AMERICAN SOCIETY FOR METALS, 1983, P 327-329
8. K.C. ANTONY *ET AL.*, HARDFACING, VOL 6, 9TH ED., *METALS HANDBOOK*, AMERICAN SOCIETY FOR METALS, 1983, P 784
9. D.R. THOMAS *ET AL.*, WELD OVERLAYS, VOL 6, 9TH ED., *METALS HANDBOOK*, AMERICAN SOCIETY FOR METALS, 1983, P 804-819

Jonathan S. Ogborn, The Lincoln Electric Company

Equipment and Supplies

The power supplied to the contact tip may be direct current or alternating current. In the United States, dc power is most common for welding applications that require less than 1000 A. In Europe and the Far East, however, ac is used extensively, even in applications requiring less than 1000 A. Currents over 1000 A dc tend to create arc blow problems. Alternating current is most commonly used for high-current applications, for applications where arc blow may be a problem, and in multiwire applications. Direct-current power supplies may be either transformer-rectifiers or motor/engine generators that produce either constant voltage or constant-current power. Alternating-current power sources are most commonly transformers.

To produce a submerged arc weld, both flux and electrode are consumed. Each flux and electrode combination, along with the variation of base material and process parameters, will produce a unique weld deposit. Because the integrity of the weld deposit depends on these parameters, specific fluxes and electrodes must be used in combination to optimize the weld metal properties.

Power Sources

A constant-voltage power supply is self-regulating, so it can be used with a constant-speed wire feeder. No voltage or current sensing is required. The current is controlled by the wire diameter, the electrical stickout, and the wire-feed speed, while the voltage is controlled by the power supply. Constant-voltage dc power is the best choice for the high-speed welding of thin steel.

Unlike constant voltage, constant-current power supplies are not self-regulating, so they must be used with voltage-sensing variable-wire-feed speed controls. A constant-current wire feeder monitors arc voltage and adjusts the wire-feed speed in response to changes in the arc voltage. The wire-feed speed control attempts to maintain a constant arc length, while the power supply controls the arc current.

The constant-current output of a conventional ac machine varies with time like a sine wave dropping through zero with each polarity reversal. The voltage associated with the current is approximately a square wave. Because the power output is zero with each polarity change, an open-circuit voltage greater than 80 V may be required to ensure arc initiation. The constant-current ac machine requires voltage-sensing variable-wire-feed speed controls. On newer, solid-state power supplies, the current and voltage output both approximate square waves, with the instantaneous polarity reversal reducing arc initiation problems. The solid-state power supplies have constant-voltage characteristics that may be used with constant-speed wire-feed controls.

Flux Classification

Fluxes can be categorized depending on the method of manufacture, the extent to which they can affect the alloy content of the weld deposit, and the effect on weld deposit properties.

Classification Relative to Production Method. Based on the manufacturing process, there are two different types of fluxes: fused and bonded.

Fused Fluxes. The raw materials for a fused flux are dry mixed and melted in a furnace. The molten mixture is then rapidly solidified, crushed, screened, and packaged. Because of their method of manufacture, fused fluxes typically do not contain ferroalloys and deoxidizers.

Bonded Fluxes. The powdered ingredients of a bonded flux are dry blended, and then mixed with a binder, usually potassium or sodium silicate. After pelletizing, the wet flux is dried in an oven or kiln, sized appropriately, and then packaged. The relatively low baking temperatures allow bonded fluxes to contain deoxidizers and ferroalloys.

Classification Relative to Effect on Alloy Content of Weld Deposit. Independent of manufacturing method, a given flux may be described as an active, neutral, or alloy flux, depending on its ability to change the alloy content of the weld deposit. With all submerged arc fluxes, variations in arc voltage and other welding variables will change the ratio of flux

consumed to electrode or weld metal deposited. This ratio is often referred to as the flux-to-wire ratio. Normal flux-to-wire ratios for SAW are 0.7 to 0.9. An increase in the flux-to-wire ratio may be caused by either an increase in arc voltage or a decrease in the welding current. Likewise, a decrease in the flux-to-wire ratio may be caused by a decrease in arc voltage or an increase in the welding current. How the weld deposit composition changes with voltage (flux-to-wire ratio) provides an additional means of describing a flux.

Active fluxes contain controlled amounts of manganese and/or silicon. These alloys are added as ingredients in the flux to provide improved resistance to porosity and weld cracking caused by contaminants such as oxygen, nitrogen, and sulfur on the plate or in the plate composition itself. Active fluxes are primarily used to make single-pass welds. Because active fluxes contain deoxidizers such as manganese and silicon, the alloy in the weld metal will change with the flux-to-wire ratio. Changes in manganese and silicon content in the weld deposit will affect the strength and impact properties of the weld metal; therefore, the arc voltage must be more tightly controlled when welding with active fluxes than with neutral fluxes.

Neutral fluxes contain little or no deoxidizers, and by definition, will not produce any significant change in the weld metal composition as a result of a large change in arc voltage. Because neutral fluxes contain little or no alloy, they must rely on alloy in the electrode to provide deoxidation. Single-pass welds on oxidized plate may be prone to cracking or porosity due to insufficient alloy content and are usually best welded with active fluxes. Neutral fluxes are primarily used for welding multiple passes on plate exceeding 25 mm (1 in.) in thickness.

To quantify the active/neutral behavior of a flux, the Wall neutrality number (*N*) was developed (Ref 10) and is defined as:

$$N = 100\ [|\Delta\%SI| + |\Delta\%MN|] \qquad \textbf{(EQ 1)}$$

where Δ%Si is the change in the weight percent of silicon, and Δ%Mn is the change in the weight percent of manganese. To determine the Wall neutrality number, two different weld deposit pads must be made. One weld pad is welded with the same parameters as those specified for the weld test plate for the flux and electrode being used. The other weld pad is welded with the same parameters except that the voltage is increased by 8 V. The Δ%Si and Δ%Mn quantities in Eq 1 are then determined by the difference in the amount of silicon and manganese in the two deposits. A flux electrode combination that produces a Wall neutrality number of 40 or less is considered neutral, while a number of 40 indicates an active flux.

Alloy fluxes contain enough alloy as a flux ingredient to produce an alloy weld metal with a carbon steel electrode. They are also used with alloy and stainless steel wire and strip electrodes. Alloy fluxes find application primarily in welding alloy steels and hardfacing. Because the alloy in the weld deposit is a function of arc voltage (flux-to-wire ratio), it is important to follow the manufacturer's recommended procedure for obtaining proper weld deposit composition.

Classification Relative to Basicity Index. Aside from the manufacturing method and the active, neutral, or alloy behavior of flux types, another common method used to describe submerged arc fluxes is the basicity index, *BI*. The basicity index is the ratio of strongly bound metallic oxides to weakly bound metallic oxides (Ref 11). The Boniszewski basicity index is defined by:

$$BI = \frac{\begin{array}{c}CaO + CaF_2 + MgO \\ + K_2O + Na_2O + Li_2O + \\ BaO + SrO + \frac{1}{2}(MnO + FeO)\end{array}}{SiO_2 + \frac{1}{2}(Al_2O_3 + TiO_2 + ZrO_2)} \qquad \textbf{(EQ 2)}$$

The basicity index is an estimate of the oxygen content in the weld metal and is therefore used to predict weld metal properties. Basic fluxes tend to have lower weld metal oxygen content with good weld metal toughness, while acidic fluxes tend to produce higher weld metal oxygen content and coarser microstructure with a lower resistance to cleavage. Fluxes with a basicity index greater than 1.5 are considered basic; fluxes below 1.0 are considered acidic.

Acid fluxes are typically preferred for single-pass welding because of their superior operating and bead-wetting characteristics. In addition, acid fluxes usually have more resistance than basic fluxes to porosity caused by plate contamination by oil, rust, and mill scale.

Basic fluxes tend to have better impact properties than acid fluxes. This advantage is particularly evident on large multiple-pass welds. Highly basic fluxes generally produce weld metal with very good impact properties in large multiple-pass weldments. Basic fluxes tend to exhibit poorer welding characteristics than acid fluxes on single-pass welds. Their use should be limited to large multipass weldments where good weld metal notch toughness is required.

Selection of Electrodes Relative to Steel and Alloy Type

There are three different types of consumable electrodes: solid wire, cored wire, and strip. Electrodes for SAW are available for welding carbon steel, low-alloy steel, stainless steel, and nickel-base alloys. Wire diameters vary from 1.6 to 6.4 mm ($\frac{1}{16}$ to $\frac{1}{4}$ in.). Carbon steel wire usually has a light copper coating, which protects the wire from corrosion and provides good electrical contact in the welding tip.

Cored electrodes were developed to provide a low-cost method of increasing the number of alloys that can be welded with SAW. Cored electrodes typically consist of a mild steel tube with alloying elements in the center. Compositions of cored electrodes vary from mild and low-alloy steels through tool steels to stainless steels and high-alloy austenitic steels.

Strip electrodes are generally used for welding overlays and for hardfacing applications. The advantages of strip are wide weld beads, low penetration, low dilution, and high deposition rates. The equipment is very similar to SAW with wire except that special drive rolls are needed to feed the strip, and sometimes auxiliary magnetic fields are set up to improve bead shape and tie-in. Strip thicknesses vary from 0.5 to 1.0 mm (0.02 to 0.04 in.), and widths vary from about 25 to 100 mm (1 to 4 in.).

Plain Carbon Steels. The requirements for the classification of electrodes and fluxes for welding carbon steels are detailed in Ref 12. Compositional requirements for solid electrodes are given in Table 1. Requirements for composite electrodes are defined in Table 2. Classification of solid electrodes is based on the chemical composition of the electrode. Classification of composite electrodes is based on weld deposit composition. Flux classification is based on the soundness and mechanical properties of the weld metal produced with a particular flux and electrode combination. The classification system used to describe flux-electrode combinations for mild steel welding is defined in Fig. 3. Interpretation of the classification system code is illustrated in the flux-electrode combination examples that follow.

TABLE 1 COMPOSITION OF SOLID-CARBON STEEL ELECTRODES

ELECTRODE		COMPOSITION, WT%[A][B]						
AWS CLASSIFICATION	UNS NO.	C	Mn	Si	S	P	Cu[C]	Ti
LOW-MANGANESE ELECTRODES								
EL8	K01008	0.10	0.25/0.60	0.07	0.030	0.030	0.35	. . .
EL8K	K01009	0.10	0.25/0.60	0.10/0.25	0.030	0.030	0.35	. . .
EL12	K01012	0.04/0.14	0.25/0.60	0.10	0.030	0.030	0.35	. . .
MEDIUM-MANGANESE ELECTRODES								
EM12	K01112	0.06/0.15	0.80/1.25	0.10	0.030	0.030	0.35	. . .
EM12K	K11113	0.05/0.15	0.80/1.25	0.10/0.35	0.030	0.030	0.35	. . .
EM13K	K01313	0.06/0.16	0.90/1.40	0.35/0.75	0.030	0.030	0.35	. . .
EM14K	K01314	0.06/0.19	0.90/1.40	0.35/0.75	0.025	0.025	0.35	0.03-0.17
EM15K	K01515	0.10/0.20	0.80/1.25	0.10/0.35	0.030	0.030	0.35	. . .
HIGH-MANGANESE ELECTRODES								
EH11K	K11140	0.07/0.15	1.40/1.85	0.80/1.15	0.030	0.030	0.35	. . .
EH12K	K01213	0.06/0.15	1.50/2.00	0.25/0.65	0.025	0.025	0.35	. . .
EH14	K11585	0.10/0.20	1.70/2.20	0.10	0.030	0.030	0.35	. . .

Source: Ref 12

(A) THE FILLER METAL SHALL BE ANALYZED FOR THE SPECIFIC ELEMENTS FOR WHICH VALUES ARE SHOWN IN THIS TABLE. IF THE PRESENCE OF OTHER ELEMENTS IS INDICATED, IN THE COURSE OF THIS WORK, THE AMOUNT OF THOSE ELEMENTS SHALL

BE DETERMINED TO ENSURE THAT THEIR TOTAL (EXCLUDING IRON) DOES NOT EXCEED 0.50%.

(B) SINGLE VALUES ARE MAXIMUM.

(C) COPPER LIMIT INCLUDES ANY COPPER COATING THAT MAY BE APPLIED TO THE ELECTRODE.

TABLE 2 COMPOSITION OF CARBON STEEL WELD METAL MADE WITH COMPOSITE ELECTRODE

ELECTRODE AWS CLASSIFICATION	COMPOSITION, WT%[(A)(B)(C)]					
	C	Mn	Si	S	P	Cu
EC1	0.15	1.80	0.90	0.035	0.035	0.35

Source: Ref 12

(A) WELD METAL SHALL BE ANALYZED FOR THE SPECIFIC ELEMENTS FOR WHICH VALUES ARE SHOWN IN THIS TABLE. IF THE PRESENCE OF OTHER ELEMENTS IS INDICATED, IN THE COURSE OF THIS WORK, THE AMOUNT OF THOSE ELEMENTS SHALL BE DETERMINED TO ENSURE THAT THEIR TOTAL (EXCLUDING IRON) DOES NOT EXCEED 0.50%.

(B) SINGLE VALUES ARE MAXIMUM.

(C) A LOW-DILUTION AREA OF A GROOVE WELD OR A FRACTURED TENSION TEST SPECIMEN AS DESCRIBED IN AWS A5.17 (SEE REF 10) MAY BE SUBSTITUTED FOR THE WELD PAD, AND SHALL MEET THE ABOVE REQUIREMENTS. IN CASE OF DISPUTE, THE WELD PAD SHALL BE THE REFEREE METHOD.

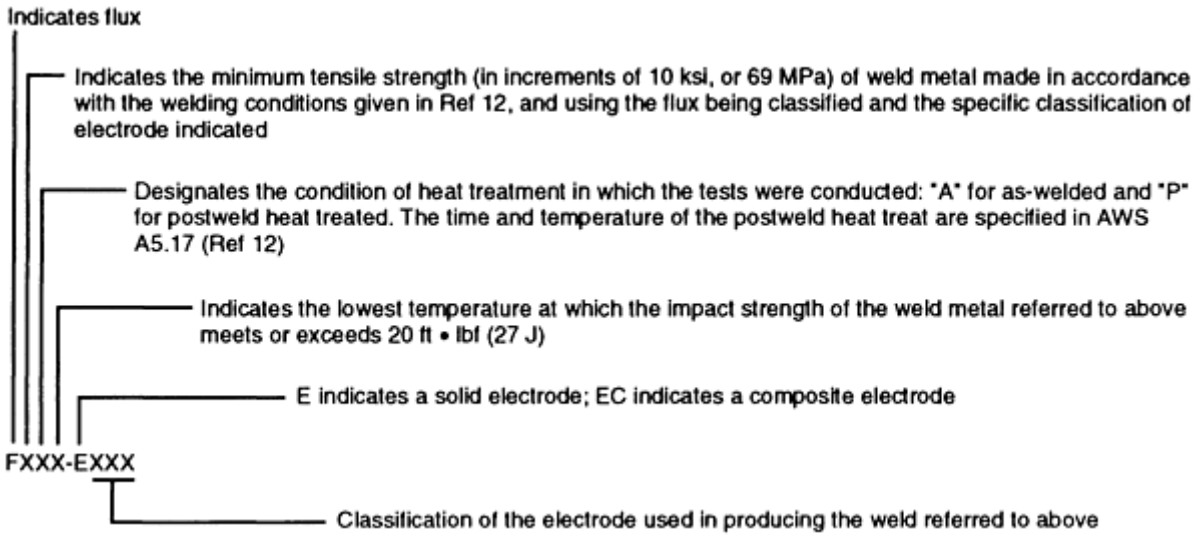

FIG. 3 CLASSIFICATION SYSTEM FOR CARBON STEEL ELECTRODES AND FLUXES USED IN SAW APPLICATIONS. SOURCE: REF 12

F7A6-EM12K is a complete designation. It refers to a flux that will produce weld metal that, in the as-welded condition, will have a tensile strength no lower than 485 MPa (70 ksi) and Charpy V-notch impact strength of at least 27 J (20 ft · lbf) at -51 °C (-60 °F) when produced with an EM12K electrode under the conditions called for in this specification.

F7A4-EC1 is a complete designation for a flux when the trade name of the electrode used in classification is indicated as well. It refers to a flux that will produce weld metal with that electrode, which in the as-welded condition, will have a tensile strength no lower than 485 MPa (70 ksi) and Charpy V-notch energy of at least 27 J (20 ft · lbf) at -40 °C (-40 °F) under the conditions called for in this specification.

Low-Alloy Steels. The requirements for low-alloy steel welding electrodes are detailed in Ref 13. The classification system for flux-electrode combinations of low-alloy steel is shown in Fig. 4. Table 3 shows the AWS electrode classification as determined by the composition of the solid electrode composition, while Table 4 is the flux-electrode classification requirement for the weld deposit composition of both solid and composite flux-electrode combinations. Interpretation of the classification system code is illustrated in the flux-electrode combination examples that follow.

TABLE 3 COMPOSITION OF LOW-ALLOY STEEL SOLID ELECTRODES

ELECTRODE		COMPOSITION, WT%[A][B][C]												
AWS CLASSIFICATION	UNS NO.	C	Mn	Si	S	P	Cr	Ni	Mo	Cu[D]	V	Al	Ti	Zr
EL12[E]	K01012	0.04 - 0.14	0.25 - 0.60	0.10	0.030	0.030	. . .	. . .	. . .	0.35	. . .	. . .	. . .	. . .
EM12K[E]	K01113	0.05 - 0.15	0.80 - 1.25	0.10 - 0.35	0.030	0.030	. . .	. . .	. . .	0.35	. . .	. . .	. . .	. . .
EA1	K11222	0.07 - 0.17	0.65 - 1.00	0.20	0.030	0.025	. . .	. . .	0.45 - 0.65	0.35	. . .	. . .	. . .	. . .
EA2	K11223	0.07 - 0.17	0.95 - 1.35	0.20	0.030	0.025	. . .	. . .	0.45 - 0.65	0.35	. . .	. . .	. . .	. . .
EA3	K11423	0.07 - 0.17	1.65 - 2.20	0.20	0.030	0.025	. . .	. . .	0.45 - 0.65	0.35	. . .	. . .	. . .	. . .
EA3K	K21451	0.07 - 0.12	1.60 - 2.10	0.50 - 0.80	0.025	0.025	. . .	. . .	0.40 - 0.60	0.35	. . .	. . .	. . .	. . .
EA4	K11424	0.07 - 0.17	1.20 - 1.70	0.20	0.030	0.025	. . .	. . .	0.45 - 0.65	0.35	. . .	. . .	. . .	. . .
EB1	K11043	0.10	0.40 - 0.80	0.05 - 0.30	0.025	0.025	0.40 - 0.75	. . .	0.45 - 0.65	0.35	. . .	. . .	. . .	. . .
EB2	K11172	0.07 - 0.15	0.45 - 1.00	0.05 - 0.30	0.030	0.025	1.00 - 1.75	. . .	0.45 - 0.65	0.35	. . .	. . .	. . .	. . .
EB2H	K23016	0.28 - 0.33	0.45 - 0.65	0.55 - 0.75	0.015	0.015	1.00 - 1.50	. . .	0.40 - 0.65	0.30	0.20 - 0.30	. . .	. . .	. . .
EB3	K31115	0.05 - 0.15	0.40 - 0.80	0.05 - 0.30	0.025	0.025	2.25 - 3.00	. . .	0.90 - 1.10	0.35	. . .	. . .	. . .	. . .
EB5	K12187	0.18 - 0.23	0.40 - 0.70	0.40 - 0.60	0.025	0.025	0.45 - 0.65	. . .	0.90 - 1.20	0.30	. . .	. . .	. . .	. . .
EB6[F]	S50280	0.10	0.35 - 0.70	0.05 - 0.50	0.025	0.025	4.50 - 6.50	. . .	0.45 - 0.70	0.35	. . .	. . .	. . .	. . .
EB6H	S50180	0.25 - 0.40	0.75 - 1.00	0.25 - 0.50	0.030	0.025	4.80 - 6.00	. . .	0.45 - 0.65	0.35	. . .	. . .	. . .	. . .

ELECTRODE		COMPOSITION, WT%[A][B][C]												
AWS CLASSIFICATION	UNS NO.	C	Mn	Si	S	P	Cr	Ni	Mo	Cu[d]	V	Al	Ti	Zr
EB8[F]	S50480	0.10	0.30 - 0.65	0.05 - 0.50	0.030	0.040	8.00 - 10.50	. . .	0.80 - 1.20	0.35	. . .	. . .	. . .	. . .
ENI1	K11040	0.12	0.75 - 1.25	0.05 - 0.30	0.020	0.020	0.15	0.75 - 1.25	0.30	0.35	. . .	. . .	. . .	. . .
ENI2	K21010	0.12	0.75 - 1.25	0.05 - 0.30	0.020	0.020	. . .	2.10 - 2.90	. . .	0.35	. . .	. . .	. . .	. . .
ENI3	K31310	0.13	0.60 - 1.20	0.05 - 0.30	0.020	0.020	0.15	3.10 - 3.80	. . .	0.35	. . .	. . .	. . .	. . .
ENI4	K11485	0.12 - 0.19	0.60 - 1.00	0.10 - 0.30	0.020	0.015	. . .	1.60 - 2.10	0.10 - 0.30	0.35	. . .	. . .	. . .	. . .
ENIIK	K11058	0.12	0.80 - 1.40	0.40 - 0.80	0.020	0.020	. . .	0.75 - 1.25	. . .	0.35	. . .	. . .	. . .	. . .
EF1	K11160	0.07 - 0.15	0.90 - 1.70	0.15 - 0.35	0.025	0.025	. . .	0.95 - 1.60	0.25 - 0.55	0.35	. . .	. . .	. . .	. . .
EF2	K21450	0.10 - 0.18	1.70 - 2.40	0.20	0.025	0.025	. . .	0.40 - 0.80	0.40 - 0.65	0.35	. . .	. . .	. . .	. . .
EF3	K21485	0.10 - 0.18	1.70 - 2.40	0.30	0.025	0.025	. . .	0.70 - 1.10	0.40 - 0.65	0.35	. . .	. . .	. . .	. . .
EF4	K12048	0.16 - 0.23	0.60 - 0.90	0.15 - 0.35	0.035	0.025	0.40 -.60	0.40 - 0.80	0.15 - 0.30	0.35	. . .	. . .	. . .	. . .
EF5	K41370	0.10 - 0.17	1.70 - 2.20	0.20	0.010	0.010	0.25 - 0.50	2.30 - 2.80	0.45 - 0.65	0.50	. . .	. . .	. . .	. . .
EF6	K21135	0.07 - 0.15	1.45 - 1.90	0.10 - 0.30	0.015	0.015	0.20 - 0.55	1.75 - 2.25	0.40 - 0.65	0.35	. . .	. . .	. . .	. . .
EM2[G]	K10882	0.10	1.25 - 1.80	0.20 - 0.60	0.010	0.010	0.30	1.40 - 2.10	0.25 - 0.55	0.25	0.05	0.10	0.10	0.10
EM3[G]	K21015	0.10	1.40 - 1.80	0.20 - 0.60	0.010	0.010	0.55	1.90 - 2.60	0.25 - 0.65	0.25	0.04	0.10	0.10	0.10
EM4[G]	K21030	0.10	1.40 - 1.80	0.20 - 0.60	0.010	0.010	0.60	2.00 - 2.80	0.30 - 0.65	0.25	0.03	0.10	0.10	0.10
EW	K11245	0.12	0.35 - 0.65	0.20 - 0.35	0.040	0.030	0.50 - 0.80	0.40 - 0.80	. . .	0.30 - 0.80	. . .	. . .	. . .	. . .
EG	. . .	NOT SPECIFIED												

Source: Ref 13

(A) THE FILLER METAL SHALL BE ANALYZED FOR THE SPECIFIC ELEMENTS FOR WHICH VALUES ARE SHOWN IN THIS TABLE. IF THE PRESENCE OF OTHER ELEMENTS IS INDICATED, IN THE COURSE OF THIS WORK, THE AMOUNT OF THOSE ELEMENTS SHALL BE DETERMINED TO ENSURE THAT THEIR TOTAL (EXCLUDING IRON) DOES NOT EXCEED 0.50 WT%.

(B) SINGLE VALUES ARE MAXIMUM.

(C) THE LETTER "N" AS A SUFFIX TO A CLASSIFICATION INDICATES THAT THE ELECTRODE IS INTENDED FOR WELDS IN THE CORE BELT REGION OF NUCLEAR REACTOR VESSELS. THIS SUFFIX CHANGES THE LIMITS ON THE PHOSPHORUS, VANADIUM, AND COPPER AS FOLLOWS: P = 0.012% MAXIMUM: V = 0.05% MAXIMUM; CU = 0.08% MAXIMUM. "N" ELECTRODES SHALL NOT BE COATED WITH COPPER OR ANY MATERIAL CONTAINING COPPER. THE "EF5" AND "EW" ELECTRODES SHALL NOT BE DESIGNATED AS "N" ELECTRODES.

(D) THE COPPER LIMIT INCLUDES ANY COPPER COATING THAT MAY BE APPLIED TO THE ELECTRODE.

(E) THE EL12 AND EM12K CLASSIFICATIONS ARE IDENTICAL TO THOSE SAME CLASSIFICATIONS IN ANSI/AWS A5.17-89 (REF. 10). THEY ARE INCLUDED IN THIS SPECIFICATION BECAUSE THEY ARE SOMETIMES USED WITH AN ALLOY FLUX TO DEPOSIT SOME OF THE WELD METALS CLASSIFIED IN TABLE 4.

(F) THE EB6 AND EB8 CLASSIFICATIONS ARE SIMILAR, BUT NOT IDENTICAL, TO THE ER502 AND ER505 CLASSIFICATIONS, RESPECTIVELY, IN ANSI/AWS A5.9-80, "SPECIFICATION FOR CORROSION-RESISTING CHROMIUM AND CHROMIUM-NICKEL STEEL BARE AND COMPOSITE METAL CORED AND STRANDED ARC WELDING ELECTRODES AND WELDING RODS." THESE CLASSIFICATIONS WILL BE DROPPED FROM THE NEXT REVISION OF A5.9 (SEE REF 14).

(G) THE COMPOSITION RANGES OF CLASSIFICATIONS WITH THE "EM" PREFIX ARE INTENDED TO CONFORM TO THE RANGES FOR SIMILAR ELECTRODES IN THE MILITARY SPECIFICATIONS.

TABLE 4 COMPOSITION OF LOW-ALLOY STEEL WELD METAL (BOTH SOLID FLUX-ELECTRODE AND COMPOSITE FLUX-ELECTRODE COMBINATIONS)

AWS WELD METAL CLASSIFICATION[E]	UNS NO.		COMPOSITION, WT%[A][B][C][D]											
	SOLID	COMPOSITE	C	Mn	Si	S	P	Cr	Ni	Mo	Cu	V	Ti	Zr
A1	K11222	W17041	0.12	1.00	0.80	0.040	0.030	. . .	. . .	0.40-0.65	0.35	. . .	. . .	. . .
A2	K11223	W17042	0.12	1.40	0.80	0.040	0.030	. . .	. . .	0.40-0.65	0.35	. . .	. . .	. . .
A3	K11423	W17043	0.15	2.10	0.80	0.040	0.030	. . .	. . .	0.40-0.65	0.35	. . .	. . .	. . .
A4	K11424	W17044	0.15	1.60	0.80	0.040	0.030	. . .	. . .	0.40-0.65	0.35	. . .	. . .	. . .

B1	K11043	W51040	0.12	1.60	0.80	0.040	0.030	0.40-0.65	. . .	0.40-0.65	0.35	. . .	. . .	. . .
B2	K11172	W52040	0.15	1.20	0.80	0.040	0.030	1.00-1.50	. . .	0.40-0.65	0.35	. . .	. . .	. . .
B2H	K23016	W52240	0.10-0.25	1.20	0.80	0.040	0.030	1.00-1.50	. . .	0.40-0.65	0.35	0.30	. . .	. . .
B3	K31115	W53040	0.15	1.20	0.80	0.040	0.030	2.00-2.50	. . .	0.90-1.20	0.35	. . .	. . .	. . .
B4	. . .	W53346	0.12	1.20	0.80	0.040	0.030	1.75-2.25	. . .	0.40-0.65	0.35	. . .	. . .	. . .
B5	K12187	W51348	0.18	1.20	0.80	0.040	0.030	0.40-0.65	. . .	0.90-1.20	0.30	. . .	. . .	. . .
B6	S50280	W50240	0.12	1.20	0.80	0.040	0.030	4.50-6.00	. . .	0.40-0.65	0.35	. . .	. . .	. . .
B6H	S50180	W50140	0.10-0.25	1.20	0.80	0.040	0.030	4.50-6.00	. . .	0.40-0.65	0.35	. . .	. . .	. . .
B8	S50180	W50440	0.12	1.20	0.80	0.040	0.030	8.00-10.00	. . .	0.80-1.20	0.35	. . .	. . .	. . .
NIL[F]	K11040	W21048	0.12	1.60	0.80	0.030	0.030	0.15	0.75-1.10	0.35	0.35	. . .	0.05[G]	. . .
NI2[F]	K21010	W22040	0.12	1.60	0.80	0.030	0.030	. . .	2.00-2.90	. . .	0.35	. . .	. . .	. . .
NI3	K31310	W23040	0.12	1.60	0.80	0.030	0.030	0.15	2.80-3.80	. . .	0.35	. . .	. . .	. . .
NI4	K11485	W21250	0.14	1.60	0.80	0.030	0.030	. . .	1.40-2.10	0.35	0.35	. . .	. . .	. . .
F1	K111	W21150	0.1	0.7	0.8	0.04	0.03	0.15	0.9	0.5	0.3	. . .	. . .	.

	60		2	0-1.50	0	0	0		0-1.70	5	5			. . .
F2	K21450	W20240	0.17	1.25-2.25	0.80	0.040	0.030	. . .	0.40-0.80	0.40-0.65	0.35	. . .	. . .	. . .
F3	K21485	W21140	0.17	1.25-2.25	0.80	0.040	0.030	. . .	0.70-1.10	0.40-0.65	0.35	. . .	. . .	. . .
F4	K12048	W20440	0.17	1.60	0.80	0.040	0.030	0.60	0.40-0.80	0.25	0.35	. . .	0.03(G)	. . .
F5	K41370	W22640	0.17	1.20-1.80	0.80	0.030	0.030	0.65	2.00-2.80	0.30-0.80	0.50	. . .	. . .	. . .
F6	K21135	W21040	0.14	0.80-1.85	0.80	0.030	0.030	0.65	1.50-2.25	0.60	0.40	. . .	. . .	. . .
M1	. . .	W21240	0.10	0.60-1.60	0.80	0.040	0.030	0.15	1.25-2.00	0.35	0.30	. . .	0.03(G)	. . .
M2	. . .	W21340	0.10	0.90-1.80	0.80	0.040	0.030	0.35	1.40-2.10	0.25-0.65	0.30	. . .	0.03(G)	. . .
M3	. . .	W22240	0.10	0.90-1.80	0.80	0.030	0.030	0.65	1.80-2.60	0.20-0.70	0.30	. . .	0.03(G)	. . .
M4	. . .	W22440	0.10	1.30-2.25	0.80	0.030	0.030	0.80	2.00-2.80	0.30-0.80	0.30	. . .	0.03(G)	
W	. . .	W21040	0.12	0.50-1.60	0.80	0.040	0.030	0.45-0.70	0.40-0.80	. . .	0.30-0.75	. . .	. . .	. . .
G	NOT SPECIFIED													

Source: Ref 13

(A) THE WELD METAL SHALL BE ANALYZED FOR THE SPECIFIC ELEMENTS FOR WHICH VALUES ARE SHOWN IN THIS TABLE. IF THE PRESENCE OF OTHER ELEMENTS IS INDICATED, IN THE COURSE OF THIS WORK, THE AMOUNT OF THOSE ELEMENTS SHALL BE DETERMINED TO ENSURE THAT THEIR TOTAL (EXCLUDING IRON) DOES NOT EXCEED 0.50%.

(B) SINGLE VALUES ARE MAXIMUM.

(C) THE LETTER "N" AS A SUFFIX TO CLASSIFICATION INDICATES THAT THE WELD METAL IS INTENDED FOR WELDS IN THE CORE BELT REGION OF NUCLEAR REACTOR VESSELS. THIS SUFFIX CHANGES THE LIMITS ON PHOSPHORUS, VANADIUM, AND COPPER AS FOLLOWS: P = 0.012% MAXIMUM; V = 0.05% MAXIMUM; CU = 0.08% MAXIMUM. "N" ELECRODES SHALL NOT BE COATED WITH COPPER OR ANY MATERIAL CONTAINING COPPER. THE F5 AND W CLASSIFICATIONS SHALL NOT BE DESIGNATED AS "N" WELD METALS.

(D) A LOW-DILUTION AREA OF THE GROOVE WELD OR THE REDUCED SECTION OF THE FRACTURED TENSION TEST SPECIMEN MAY BE SUBSTITUTED FOR THE WELD PAD, AND SHALL MEET THE ABOVE REQUIREMENTS. IN CASE OF DISPUTE, THE WELD PAD SHALL BE THE REFEREE METHOD.

(E) THE ELECRODE DESIGNATION FOR COMPOSITE ELECTRODES IS OBTAINED BY PLACING AN "EC" BEFORE THE APPROPRIATE WELD METAL CLASSIFICATION.

(F) MANGANESE IN NI1 AND NI2 CLASSIFICATIONS MAY BE 1.80% MAXIMUM WHEN CARBON IS RESTRICTED TO 0.10% MAXIMUM.

(G) A SINGLE VALUE SPANNING THE COLUMNS FOR VANADIUM, TITANIUM, AND ZIRCONIUM IS THE TOTAL OF THESE ELEMENTS.

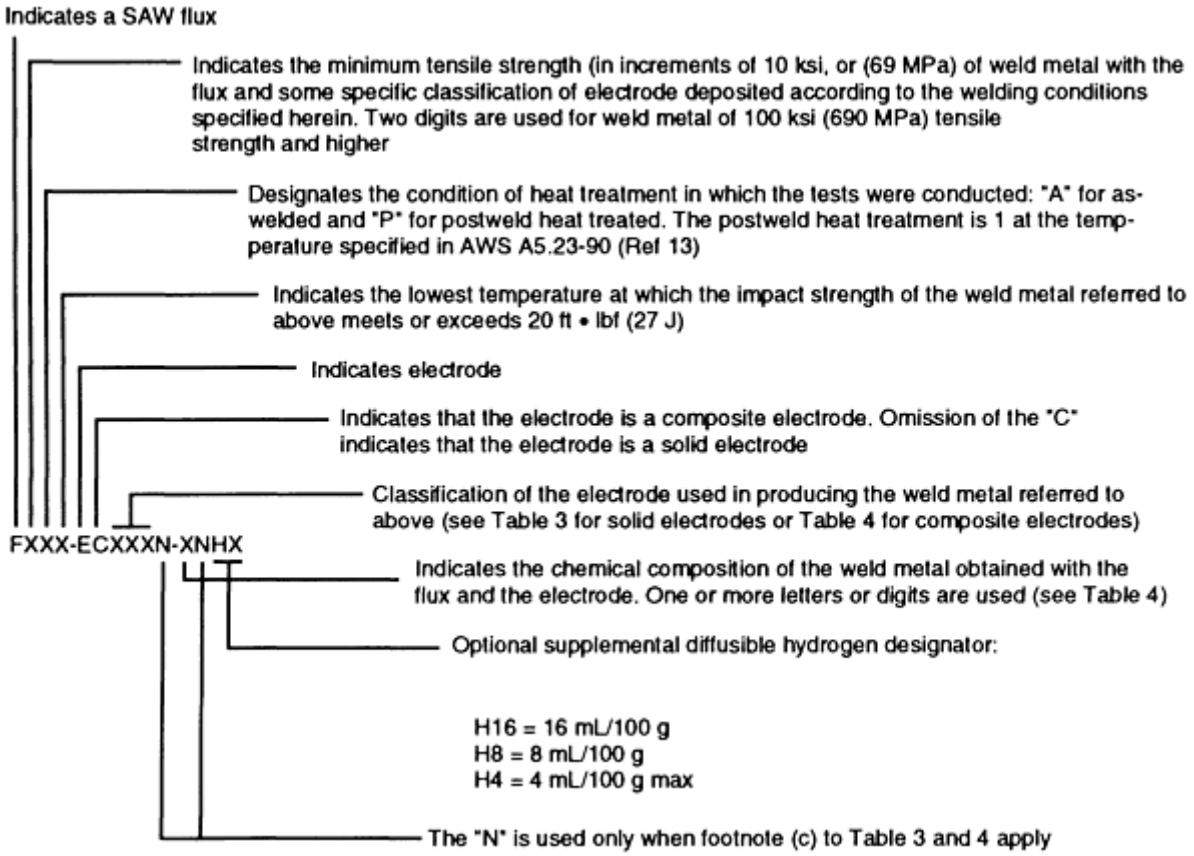

FIG. 4 CLASSIFICATION SYSTEM FOR LOW-ALLOY STEEL ELECTRODES AND FLUXES USED IN SAW APPLICATIONS

F9PO-EB3-B3 is a complete designation for a flux-electrode combination. It refers to a flux that will produce weld metal that, in the postweld heat-treated condition, will have a tensile strength of 620 to 760 MPa (90 to 110 ksi) and Charpy V-notch impact strength of at least 27 J (20 ft · lbf) at - 18 °C (0 °F) when made with an EB3 electrode under the conditions called for in this specification. The composition of the weld metal will be B3 (Table 4).

F9A2-ECM1-M1 is a complete designation for a flux when the trade name of the composite electrode used in the classification tests is indicated as well. The designation refers to a flux that will produce weld metal that, with the M1

electrode, in the as-welded condition, will have a tensile strength of 620 to 760 MPa (90 to 110 ksi) and Charpy V-notch impact strength of at least 27 J (20 ft · lbf) at -29 °C (-20 °F) under the conditions called for in this specification. The composition of the weld metal will be M1 (Table 4).

Stainless and Nickel-Base Alloys. For welding with corrosion-resistant chromium and chromium-nickel bare and composite metal cored and stranded electrodes, the composition of the filler metal is classified according to AWS A5.9 (Table 5). There is no AWS classification of fluxes or of flux-electrode combinations for stainless steel SAW.

TABLE 5 COMPOSITION OF CORROSION-RESISTANT CHROMIUM AND CHROMIUM-NICKEL BARE AND COMPOSITE METAL CORED AND STRANDED ELECTRODES

AWS ELECTRODE CLASSIFICATION	COMPOSITION, WT%[A][B]										
	C	Cr	Ni	Mo	(nb + ta)	Mn	Si	P	S	N	Cu
ER209[D]	0.05	20.5-24.0	9.5-12.0	1.5-3.0	. . .	4.0-7.0	0.90	0.03	0.03	0.10-0.30	0.75
ER218	0.10	16.0-18.0	8.0-9.0	0.75	. . .	7.0-9.0	3.5-4.5	0.03	0.03	0.08-0.18	0.75
ER219	0.05	19.0-21.5	5.5-7.0	0.75	. . .	8.0-10.0	1.00	0.03	0.03	0.10-0.30	0.75
ER240	0.05	17.0-19.0	4.0-6.0	0.75	. . .	10.5-13.5	1.00	0.03	0.03	0.10-0.20	0.75
ER307	0.04-0.14	19.5-22.0	8.0-10.7	0.5-1.5	. . .	3.3-4.75	0.30-0.65	0.03	0.03	. . .	0.75
ER308[C]	0.08	19.5-22.0	9.0-11.0	0.75	. . .	1.0-2.5	0.30-0.65	0.03	0.03	. . .	0.75
ER308H	0.04-0.08	19.5-22.0	9.0-11.0	0.75	. . .	1.0-2.5	0.30-0.65	0.03	0.03	. . .	0.75
ER308L[C]	0.03	19.5-22.0	9.0-11.0	0.75	. . .	1.0-2.5	0.30-0.65	0.03	0.03	. . .	0.75
ER308MO	0.08	18.0-21.0	9.0-12.0	2.0-3.0	. . .	1.0-2.5	0.30-0.65	0.03	0.03	. . .	0.75
ER308MOL	0.04	18.0-21.0	9.0-12.0	2.0-3.0	. . .	1.0-2.5	0.30-0.65	0.03	0.03	. . .	0.75
ER309[D]	0.12	23.0-25.0	12.0-14.0	0.75	. . .	1.0-2.5	0.30-0.65	0.03	0.03	. . .	0.75
ER309L	0.03	23.0-25.0	12.0-14.0	0.75	. . .	1.0-2.5	0.30-0.65	0.03	0.03	. . .	0.75
ER310	0.08-0.15	25.0-28.0	20.0-22.5	0.75	. . .	1.0-2.5	0.30-0.65	0.03	0.03	. . .	0.75
ER312	0.15	28.0-32.0	8.0-10.5	0.75	. . .	1.0-2.5	0.30-065	0.03	0.03	. . .	0.75
ER316[C]	0.08	18.0-20.0	11.0-14.0	2.0-3.0	. . .	1.0-2.5	0.30-0.65	0.03	0.03	. . .	0.75
ER316H	0.04-0.08	18.0-20.0	11.0-14.0	2.0-3.0	. . .	1.0-2.5	0.30-0.65	0.03	0.03	. . .	0.75
ER316L[D]	0.03	18.0-20.0	11.0-14.0	2.0-3.0	. . .	1.0-2.5	0.30-0.65	0.03	0.03	. . .	0.75
ER317	0.08	18.5-20.5	13.0-15.0	3.0-4.0	. . .	1.0-2.5	0.30-0.65	0.03	0.03	. . .	0.75
ER317L	0.03	18.5-20.5	13.0-15.0	3.0-4.0	. . .	1.0-2.5	0.30-0.65	0.03	0.03	. . .	0.75
ER318	0.08	18.0-	11.0-	2.0-	8 × C	1.0-	0.30-	0.03	0.03	. . .	0.75

		20.0	14.0	3.0	MIN TO 1.0 MAX	2.5	0.65				
ER320	0.07	19.0-21.0	32.0-36.0	2.0-3.0	8 × C MIN TO 1.0 MAX	2.5	0.60	0.03	0.03	. . .	3.0-4.0
ER320LR[D]	0.025	19.0-21.0	32.0-36.0	2.0-3.0	8 × C MIN TO 0.40 MAX	1.5-2.0	0.15	0.015	0.020	. . .	3.0-4.0
ER321[E]	0.08	18.5-20.5	9.0-10.5	0.75	. . .	1.0-2.5	0.30-0.65	0.03	0.03	. . .	0.75
ER330	0.18-0.25	15.0-17.0	34.0-37.0	0.75	. . .	1.0-2.5	0.30-0.65	0.03	0.03	. . .	0.75
ER347[C]	0.08	19.0-21.5	9.0-11.0	0.75	10 × C MIN TO 1.0 MAX	1.0-2.5	0.30-0.65	0.03	0.03	. . .	0.75
ER349[F]	0.07-0.13	19.0-21.5	8.0-9.5	0.35-0.65	1.0-1.4	1.0-2.5	0.30-0.65	0.03	0.03	. . .	0.75
ER410	0.12	11.5-13.5	0.6	0.75	. . .	0.6	0.50	0.03	0.03	. . .	0.75
ER410NIMO	0.06	11.0-12.5	4.0-5.0	0.4.-0.7	. . .	0.6	0.50	0.03	0.03	. . .	0.75
ER420	0.25-0.40	12.0-14.0	0.6	0.75	. . .	0.6	0.50	0.03	0.03	. . .	0.75
ER430	0.10	15.5-17.0	0.6	0.75	. . .	0.6	0.50	0.03	0.03	. . .	0.75
ER502	0.10	4.6-6.0	0.6	0.45-0.65	. . .	0.6	0.50	0.03	0.03	. . .	0.75
ER505	0.10	8.0-10.5	0.5	0.8-1.2	. . .	0.6	0.50	0.04	0.03	. . .	0.75
ER630	0.05	16.0-16.75	4.5-5.0	0.75	0.15-0.30	0.25-0.75	0.75	0.04	0.03	. . .	3.25-4.00
ER26-1	0.01	25.0-27.5	[G]	0.75-1.50	. . .	0.40	0.40	0.02	0.02	0.015	0.20[G]
ER16-8-2	0.10	14.5-16.5	7.5-9.5	1.0-2.0	. . .	1.0-2.5	0.30-0.65	0.03	0.03	. . .	0.75

Source: Ref 14

(A) ANALYSIS SHALL BE MADE FOR THE ELEMENTS FOR WHICH SPECIFIC VALUES ARE SHOWN IN THIS TABLE. IF, HOWEVER, THE PRESENCE OF OTHER ELEMENTS IS INDICATED IN THE COURSE OF ROUTINE ANALYSIS, FURTHER ANALYSIS SHALL BE MADE TO DETERMINE THAT THE TOTAL OF THESE OTHER ELEMENTS, EXCEPT IRON, IS NOT PRESENT IN EXCESS OF 0.50 %.

(B) SINGLE VALUES SHOWN ARE MAXIMUM PERCENTAGES EXCEPT WHERE OTHERWISE SPECIFIED.

(C) THESE GRADES ARE AVAILABLE IN HIGH-SILICON CLASSIFICATIONS THAT SHALL HAVE THE SAME CHEMICAL COMPOSITION REQUIREMENTS AS GIVEN BELOW WITH THE EXCEPTION THAT THE SILICON CONTENT SHALL BE 0.65 TO 1.00%. THESE HIGH-SILICON CLASSIFICATIONS SHALL BE DESIGNATED BY THE ADDITION `SI' TO THE STANDARD

CLASSIFICATION DESIGNATIONS INDICATED BELOW. THE FABRICATOR SHOULD CONSIDER CAREFULLY THE USE OF HIGH-SILICON FILLER METALS IN HIGHLY RESTRAINED FULLY AUSTENITIC WELDS. A DISCUSSION OF THE PROBLEM IS PRESENTED IN REF 14.

(D) CARBON SHALL BE REPORTED TO THE NEAREST 0.01% EXCEPT FOR THE CLASSIFICATION E320LR, FOR WHICH CARBON SHALL BE REPORTED TO THE NEAREST 0.005%.

(E) TITANIUM: 9 × C MIN TO 1.0 MAX.

(F) TITANIUM: 0.10 TO 0.30. TUNGSTEN IS 1.25 TO 1.75%.

(G) NICKEL, MAX: 0.5 MINUS THE COPPER CONTENT.

Like stainless steels, nickel and nickel alloys are classified according to the composition of the filler metal only (Ref 15). Classifications of filler metal are shown in Table 6. There is no AWS classification of fluxes or of flux-electrode combinations for nickel alloy SAW.

TABLE 6 COMPOSITION OF NICKEL AND NICKEL-ALLOY BARE ELECTRODES AND RODS

AWS CLASSIFICATION	UNS NO.	COMPOSITION, WT%[A][B]															
		C	MN	FE	P	S	SI	CU	N[C]	CO	AL	TI	CR	(NB + TA)	MO	V	W	OTHER ELEMENTS, TOTAL
ERNI-1	N02061	0.15	1.0	1.0	0.03	0.015	0.75	0.25	93.0 MIN	. . .	1.5	2.0-3.5	. . .	. . .	. . .	. . .	. . .	0.50
ERNICU-7	N04060	0.15	4.0	2.5	0.02	0.015	1.25	BAL	62.0-69.0	. . .	1.25	1.5-3.0	. . .	. . .	. . .	. . .	. . .	0.50
ERNICR-3	N06082	0.10	2.5-3.5	3.0	0.03	0.015	0.50	0.50	67.0 MIN	[D]	. . .	0.75	18.0-22.0	2.0-3.0[E]	. . .	. . .	. . .	0.50
ERNLCRFE-5	N06062	0.08	1.0	6.0-10.0	0.03	0.015	0.35	0.50	70.0 MIN	[D]	. . .	. . .	14.0-17.0	1.5-3.0[E]	. . .	. . .	. . .	0.50
ERNLCRFE-6	N07092	0.08	2.0-2.7	8.0	0.03	0.015	0.35	0.50	67.0 MIN	. . .	. . .	2.0-3.5	14.0-17.0	. . .	. . .	. . .	. . .	0.50
ERNIFECR-1	N08065	0.05	1.0	22.0 MIN	0.03	0.03	0.50	1.50-3.0	38.0-46.0	. . .	0.20	0.60-1.2	19.5 23.5	. . .	2.5-3.5	. . .	. . .	0.50
ERNIFECR-2[F]	N07718	0.08	0.35	BAL	0.015	0.015	0.35	0.30	50.0-55.0	. . .	0.20-0.80	0.65-1.15	17.0-21.0	4.75-5.50	2.80-3.30	. . .	. . .	0.50
ERNIMO-1	N10001	0.08	1.0	4.0-7.0	0.025	0.03	1.0	0.50	BAL	2.5	. . .	. . .	1.0	. . .	26.0-30.0	0.20-0.40	1.0	0.50
ERNIMO-2	N10003	0.04-0.08	1.0	5.0	0.015	0.02	1.0	0.50	BAL	0.20	. . .	. . .	6.0-8.0		15.0-18.0	0.50	0.50	0.50
ERNIMO-3	N10004	0.12	1.0	4.0-7.0	0.04	0.03	1.0	0.50	BAL	2.5	. . .	. . .	4.0-6.0	. . .	23.0-26.0	0.60	1.0	0.50
ERNIMO-7	N1066	0.02	1.0	2.0	0.04	0.03	0.1	0.50	BA	1.0	. . .	. . .	1.0	. . .	26.0	. . .	1.0	0.50

	5						0		L						- 30.0			
ERNICRMO-1	N06007	0.05	1.0-2.0	18.0 - 21.0	0.04	0.03	1.0	1.5-2.5	BAL	2.5	. . .	. . .	21.0 - 23.5	1.75 - 2.50	5.5-7.5	. . .	1.0	0.50
ERNICRMO-2	N06002	0.05-0.15	1.0	17.0 - 20.0	0.04	0.03	1.0	0.50	BAL	0.50 -2.5	. . .	. . .	20.5 - 23.0	. . .	8.0-10.0	. . .	0.20 -1.0	0.50
ERNICRMO-3	N06625	0.10	0.50	5.0	0.02	0.015	0.50	0.50	58.0 MIN	. . .	0.40	0.40	20.0 - 23.0	3.15 - 4.15	8.0-10.0	. . .	. . .	0.50
ERNICRMO-4	N10276	0.02	1.0	4.0-7.0	0.04	0.03	0.08	0.50	BAL	2.5	. . .	. . .	14.5 - 16.5	. . .	15.0 - 17.0	0.35	3.0-4.5	0.50
ERNICRMO-7	N06455	0.015	1.0	3.0	0.04	0.03	0.08	0.50	BAL	2.0	. . .	0.70	14.0 - 18.0	. . .	14.0 - 18.0	. . .	0.50	0.50
ERNICRMO-8	N06975	0.03	1.0	BAL	0.03	0.03	1.0	0.7-1.20	47.0 - 52.0	. . .	. . .	0.70 - 1.50	23.0 - 26.0	. . .	5.0-7.0	. . .	. . .	0.50
ERNICRMO-9	N06985	0.015	1.0	18.0 - 21.0	0.04	0.03	1.0	1.5-2.5	BAL	5.0	. . .	. . .	21.0 - 23.5	0.50	6.0-8.0	. . .	1.5	0.50
ERNICRMO-10	N06022	0.015	0.50	2.0-6.0	0.02	0.010	0.08	0.50	BAL	2.5	. . .	. . .	20.0 - 22.5	. . .	12.5 - 14.5	0.35	2.5-4.5	0.50
ERNICRMO-11	N06030	0.03	1.5	13.0 - 17.0	0.04	0.02	0.80	1.0-2.4	BAL	5.0	. . .	. . .	28.0 - 31.5	0.30 - 1.50	4.0-6.0	. . .	1.5-4.0	0.50
ERNICRCOMO-1	N06617	0.05-0.15	1.0	3.0	0.03	0.015	1.0	0.50	BAL	10.0 - 15.0	0.80 - 1.50	0.60	20.0 - 24.0	. . .	8.0-10.0	. . .	. . .	0.50

Source: Ref 15

(A) THE FILLER METAL SHALL BE ANALYZED FOR THE SPECIFIC ELEMENTS FOR WHICH VALUES AVE SHOWN IN THIS TABLE. IN THE COURSE OF THIS WORK, IF THE PRESENCE OF OTHER ELEMENTS IS INDICATED, THE AMOUNT OF THOSE ELEMENTS SHALL HE DETERMINED TO ENSURE THAT THEIR TOTAL DOES NOT EXCEED THE LIMIT SPECIFIED FOR "OTHER ELEMENTS, TOTAL" IN

THE LAST COLUMN OF THE TABLE.

(B) SINGLE VALUES ARE MAXIMUM, EXCEPT WHERE OTHERWISE SPECIFIED.

(C) INCLUDES INCIDENTAL COBALT.

(D) COBALT: 0.12 MAXIMUM, WHEN SPECIFIED.

(E) TANTALUM: 0.30 MAXIMUM, WHEN SPECIFIED.

(F) BORON IS 0.006% MAXIMUM.

Personnel Considerations

Employee Training. Submerged arc welding is an automatic or semiautomatic process carried out primarily in the flat or horizontal position with the arc obscured from view and does not require a high level of skill. The primary expenditures both in cost and time are consumed in designing jigs and fixtures to hold and position the workpiece so that SAW can be performed. While the actual welding process does not require a high degree of skill, the setup procedure requires skilled personnel with an aptitude for fabricating the fixtures and clamps necessary to position the workpiece in an acceptable position (usually flat).

Health and Safety in the Workplace. The main safety concerns in welding are electric shock, fume inhalation, and burns from both the arc ultraviolet source and the hot-metal infrared source (Ref 16). To reduce the risk of electrical shock, all equipment must be properly grounded and welding cables must be in good condition. The fume is nearly eliminated in SAW. However, certain vaporized elements (for example, chromium, cobalt, manganese, nickel, and vanadium) can be potentially dangerous. To prevent exposure to these elements, the welding area should have adequate ventilation. In SAW, the arcflash and its accompanying spatter are nearly eliminated because of the slag and the depth of the flux pile. However, eye protection should always be worn.

Additional information is available in the article "Safe Practices" in this Volume.

Reference cited in this section

16. *SAFETY IN WELDING AND CUTTING,* AWS, 1988

Submerged Arc Welding

Jonathan S. Ogborn, The Lincoln Electric Company

SAW Parameters

While SAW is the most inexpensive and efficient process for making large, long, and repetitive welds, much time and energy are required to prepare the joint. Care must be taken to line up all joints to have a consistent gap in groove welds and to provide backing plates and flux dams to prevent spillage of flux and molten metal. Once all the pieces are clamped or tacked in place, welding procedures and specifications should be consulted before welding begins.

Procedural Variations and Effect on Weld Bead Characteristics

Procedural variations in SAW include current, voltage, electrical stickout (distance from last electrical contact to plate), travel speed, and flux depth. Variation in any of these parameters will affect the shape and penetration of the weld, as well as the integrity of the weld deposit.

Weld Current. Because the welding current controls such parameters as deposition rate, penetration, and dilution, it is the most important welding variable. An increase in welding current at a constant voltage will decrease the flux-to-wire ratio, while a decrease in current will increase the flux-to-wire ratio. The effect of current variation on weld bead profile is shown in Fig. 5. Welds made at excessively low current will tend to have little penetration and higher width-to-depth ratios. Welds made at an excessively high current will have deep penetration, high dilution, more shrinkage, and excess buildup. Low current will also produce a less stable arc than higher currents.

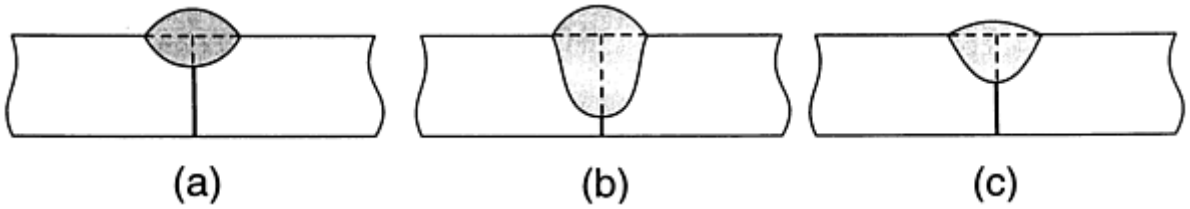

FIG. 5 EFFECT OF VARIATION IN WELDING CURRENT ON WELD BEAD PROFILE. (A) EXCESSIVELY LOW CURRENT. (B) EXCESSIVELY HIGH CURRENT. (C) RECOMMENDED CURRENT

The direction of current flow will also affect the weld bead profile. The current may be direct with the electrode positive (reverse polarity), electrode negative (straight polarity), or alternating. Reverse polarity is most commonly used. For a given set of welding conditions, reverse polarity will produce wider beads with more penetration at a lower deposition rate than straight polarity. Straight-polarity welding will contribute to narrower beads with less penetration and more buildup. Because straight polarity reduces base plate dilution, it is frequently used in surfacing applications. For the same welding current, the deposition rate with straight polarity is higher than with reverse polarity. Straight polarity is preferred for poor fitup. The bead shape, penetration, and deposition rate for alternating current fall between those of straight and reverse polarity. Alternating Current is used when welding current exceeds 1000 A and on multiple-wire applications to reduce arc blow and arc interaction.

In SAW, the current density in the electrode also plays a role in bead shape and penetration. Smaller-diameter electrodes with a high current density will produce narrower beads with deeper penetration than larger-diameter electrodes. Larger-diameter electrodes are able to bridge larger root openings. In cases where a given current can be achieved with two different electrode diameters, the smaller electrode will produce the higher deposition rate.

Weld Voltage. Like current, welding voltage will affect the bead shape and the weld deposit composition. Increasing the arc voltage at a constant current will increase the flux-to-wire electrode ratio, while decreasing the voltage will reduce the flux-to-electrode ratio. The effect of the magnitude of arc voltage on bead shape is shown in Fig. 6. Increasing the arc voltage will produce a longer arc length and a correspondingly wider, flatter bead with less penetration. Higher voltage will increase flux consumption, which could then change deposit composition and properties. Slightly increasing the arc voltage will help the weld to bridge gaps when welding in grooves. Excessively high voltage will produce a hat-shaped concave weld, which has low resistance to cracking and a tendency to undercut. Lower voltages will shorten the arc length and increase penetration. Excessively low voltage will produce an unstable arc and a crowned bead, which has an uneven contour where it meets the plate.

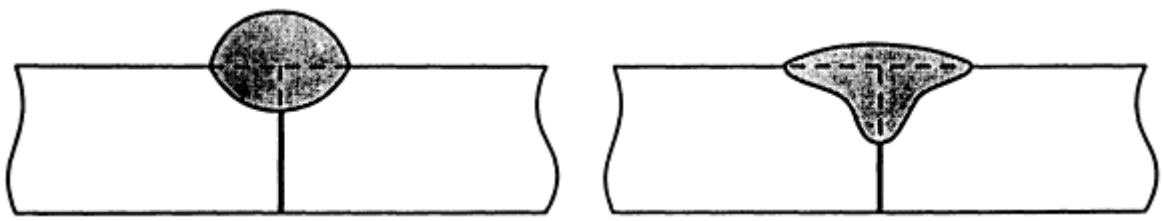

FIG. 6 EFFECT OF VARIATION IN WELDING VOLTAGE AT CONSTANT CURRENT ON WELD BEAD PROFILE. (A) EXCESSIVELY LOW VOLTAGE. (B) EXCESSIVELY HIGH VOLTAGE

Electrical Stickout. In SAW, the current flowing in the electrode between the contact tube and the arc (electrode extension) will cause some I^2R heating, resulting in a voltage drop across that length of electrode. This resistance heating and subsequent voltage drop can be used to obtain higher deposition rates. Normal electrode extension for solid SAW wire is approximately 8 to 12 times the electrode diameter. As this length increases at a constant current, so does the resistance heating and the melt-off rate. To compensate for the voltage drop and the increase in wire-feed speed, the voltage must be increased to obtain a properly shaped bead. Extending the electrode 20 to 40 times the diameter can

increase deposition rates by more than 50% (Ref 17). Although higher deposition rates can be achieved by extending the electrode, keeping the electrode aligned with the joint becomes increasingly difficult as the extension increases.

Travel Speed. Variations in travel speed at a set current and voltage also affect bead shape. As welding speed is decreased, heat input per length of joint increases, and the penetration and bead width increase. The penetration will increase until molten metal begins to flow under the arc and interfere with heat flow at excessively slow speeds. Excessively high travel speeds will promote a crowned bead as well as the tendency for undercut and porosity.

Flux layer depth is another variable that will alter the appearance, penetration, and quality of a submerged arc weld. If the flux layer is too deep, a greater-than-normal amount of flux will be melted, resulting in weld beads that are narrower than normal. Some surface imperfections may also appear because gases may be trapped by the deep flux layer. If the flux layer is too shallow, the arc will flash through, and the bead will have a rough appearance or porosity due to lack of shielding from the atmosphere. The correct depth of flux is just enough to prevent flash through. This will allow welding gases to escape while providing adequate protection.

Sources of Defects in SAW

The fact that SAW is a high heat input process under a protective blanket of flux greatly decreases the chance of weld defects. However, defects such as lack of fusion, slag entrapment, solidification cracking, hydrogen cracking, or porosity occasionally occur.

Insufficient Fusion and Slag Entrapment. Lack-of-fusion defects and slag entrapment are most commonly caused by improper bead placement or procedure. Improper placement can cause the weld metal to roll over and trap slag underneath, or if the weld bead is placed away from the edge to be joined, the liquid metal may not fuse to the base material. A crown-shaped bead caused by low welding voltage may also contribute to slag entrapment and lack of fusion by not allowing the liquid metal to spread out evenly.

Solidification cracking of SAW along the center of the bead is usually due to bead shape, joint design, or incorrect choice of welding consumables. A convex bead shape with a bead width-to-depth ratio greater than one will decrease solidification cracking tendencies. If weld penetration is too deep, the shrinkage stresses may cause centerline cracking. Joint design may also contribute to excessive shrinkage stresses, again increasing the risk of solidification cracking. Because cracking is related to stresses in the weld, high-strength materials will have a greater tendency to crack. Therefore, special care must be taken to generate proper bead shape, preheat temperatures, and interpass temperatures, in addition to correct electrode and flux combinations, when welding these materials.

Hydrogen Cracking. Unlike solidification cracking, which appears immediately after welding, hydrogen cracking is a delayed process and may occur from several hours to several days after welding has been completed. To minimize hydrogen cracking, all possible sources of hydrogen (for example, water, oil, grease, and dirt) present in the flux, electrode, or joint should be eliminated. The flux, electrode, and plate should be clean and dry.

To prevent moisture pickup, fluxes and electrodes should be stored in moisture-resistant containers in dry areas. If a flux or electrode becomes contaminated with moisture, it should be dried according to manufacturer recommendations.

Selection of the consumable, especially when welding high-strength steels that are more susceptible to hydrogen cracking, can also play a role in hydrogen cracking. Special consumables have recently been developed that produce weld deposits that are very low in diffusible hydrogen.

To further reduce hydrogen-related cracking, the joint to be welded should be preheated. Because hydrogen is fairly mobile in steel at temperatures above 95 °C (200 °F), the recommended preheat temperatures should be followed to allow most of the hydrogen to escape and to reduce the risk of hydrogen damage (Ref 18). In thick weldments, maintaining preheat for several hours after welding is completed will also reduce the risk of hydrogen cracking.

Porosity caused by trapped gas is uncommon in SAW because of the protection provided by the flux. When porosity does occur, it may be in the form of internal porosity or as depressions on the weld bead surface. The gas bubbles that cause porosity originate either from a lack of protection from the atmosphere or from contaminants such as water, oil, grease, and dirt. To reduce porosity in SAW, the weld should have sufficient flux coverage, and all water, grease, and dirt should be removed from the plate, electrode, and flux. Another cause of porosity in SAW is excessive travel speed. Travel

at excessively high speeds will not allow the gas bubbles to escape from the weld, and the bubbles may become trapped in the weld metal at the slag-to-metal interface.

References cited in this section

17. *HOW TO MAKE SINGLE ELECTRODE SUBMERGED ARC WELDS,* PUBLICATION S604, THE LINCOLN ELECTRIC CO., 1991, P 11
18. F.R. COE, *WELD. WORLD,* VOL 14 (NO. 1/2), 1976, P 1-7

Submerged Arc Welding

Jonathan S. Ogborn, The Lincoln Electric Company

References

1. R.L. O'BRIEN, *WELDING HANDBOOK,* VOL 11, AWS, 1991, P 191-232
2. D.L. OLSON *ET AL.,* SUBMERGED ARC WELDING, VOL 6, 9TH ED., *METALS HANDBOOK,* AMERICAN SOCIETY FOR METALS, 1983, P 114-152
3. *THE PROCEDURE HANDBOOK OF ARC WELDING,* THE LINCOLN ELECTRIC CO., 1973, P 6.3-1 TO 6.3-24
4. "SPECIFICATION FOR CARBON STEEL ELECTRODES AND FLUXES FOR SUBMERGED ARC WELDING," A5.17-89, AWS, 1989, P 18
5. *THE PROCEDURE HANDBOOK OF ARC WELDING,* THE LINCOLN ELECTRIC CO., 1973, P 3.2-3, 6.3-21 TO 6.3-22, 6.3-49 TO 6.3-58
6. *THE PROCEDURE HANDBOOK OF ARC WELDING,* THE LINCOLN ELECTRIC CO., 1973, P 6.3-26 TO 6.3-73
7. R.S. BROWN *ET AL.,* ARC WELDING OF STAINLESS STEELS, VOL 6, 9TH ED., *METALS HANDBOOK,* AMERICAN SOCIETY FOR METALS, 1983, P 327-329
8. K.C. ANTONY *ET AL.,* HARDFACING, VOL 6, 9TH ED., *METALS HANDBOOK,* AMERICAN SOCIETY FOR METALS, 1983, P 784
9. D.R. THOMAS *ET AL.,* WELD OVERLAYS, VOL 6, 9TH ED., *METALS HANDBOOK,* AMERICAN SOCIETY FOR METALS, 1983, P 804-819
10. "SPECIFICATION FOR CARBON STEEL ELECTRODES AND FLUXES FOR SUBMERGED ARC WELDING," A5.17-89, AWS, 1989, P 17-18
11. S.S. TULIANI, T. BONISZEWSKI, AND N.F. EATON, NOTCH TOUGHNESS OF COMMERCIAL SUBMERGED ARC WELD METAL, *WELD. MET. FABR.,* VOL 8, 1969, P 327-339
12. "SPECIFICATION FOR CARBON STEEL ELECTRODES AND FLUXES FOR SUBMERGED ARC WELDING," A5.17-89, AWS, 1989, P 2-3
13. "SPECIFICATION FOR LOW ALLOY STEEL ELECTRODES AND FLUXES FOR SUBMERGED ARC WELDING," A5.23-90, AWS, 1990, P 2-6
14. "SPECIFICATION FOR CORROSION RESISTING CHROMIUM AND CHROMIUM-NICKEL STEEL BARE AND COMPOSITE METAL CORED AND STRANDED WELDING ELECTRODES AND WELDING RODS," A5.9-81, AWS, 1981, P 3, 4
15. "SPECIFICATION FOR NICKEL AND NICKEL ALLOY BARE WELDING ELECTRODES AND RODS," A5.14-89, AWS, 1989, P 2, 3
16. *SAFETY IN WELDING AND CUTTING,* AWS, 1988
17. *HOW TO MAKE SINGLE ELECTRODE SUBMERGED ARC WELDS,* PUBLICATION S604, THE LINCOLN ELECTRIC CO., 1991, P 11
18. F.R. COE, *WELD. WORLD,* VOL 14 (NO. 1/2), 1976, P 1-7

Stud Arc Welding

Harry A. Chambers, TRW Nelson Stud Welding Division

Introduction

STUD ARC WELDING (SW), also known as arc stud welding, is a commonly used method for joining a metal stud, or fastener, to a metal workpiece. The process has been used as an alternative metal-fastening method since the 1940s. Millions of specially designed and manufactured metal studs are welded by this process every week in such diverse industries as construction, shipbuilding, automotive, and hard goods, as well as in miscellaneous industrial applications.

This article will serve as a basic information source for those interested in accomplishing one-sided, no-hole attachment of metal fasteners. The SW process represents an alternative to other welding processes, and is also a substitute for other fastening procedures, such as drilling and tapping, bolting, and self-tapping screws.

Stud Arc Welding

Harry A. Chambers, TRW Nelson Stud Welding Division

Process Overview

Stud arc welding is similar to many other welding processes, including arc and percussion welding, in that the base (weld end) of a specifically designed stud is joined to a base material by heating both parts with an arc that is drawn between the two. Equipment that is unique to this process regulates the arc length and arc dwell time. After an arc is struck, the stud weld end and the workpiece surface are brought to the proper temperature for joining and, after a controlled period of time, the two heated surfaces are brought together under pressure, creating a metallurgical bond capable of developing the full strength of the stud.

There are two basic types of stud arc welding, which are differentiated by the source of welding power. One type uses direct current (dc) power provided by a transformer/rectifier or a motor generator similar to that used in the shielded metal arc welding (SMAW) process. The second type uses power discharged from a capacitor storage bank. The process based on a dc power source is known as stud arc welding, whereas the process that utilizes capacitors is known as capacitor discharge stud welding (CDSW).

Both the SW and CDSW processes overlap in some areas of application. Generally, the SW process is used in applications that require similar stud and workpiece metals, the workpiece thickness is greater in relation to the stud diameter, and an accommodation must be made for the stud flash (fillet). The term "flash" is preferred to the term "fillet," because the metal that forms the flash during the stud arc welding process is expelled, rather than added, as occurs with other welding processes.

In contrast, the CDSW process is used extensively when welding to thin sheet metal, and is used frequently with dissimilar workpiece and stud alloys. It is also used in cases where marks on the opposite side of the workpiece must be avoided or minimized. With this process, the stud diameter is limited to smaller sizes. The CDSW process is more fully described in the article "Capacitor Discharge Stud Welding" in this Volume. The factors on which process selection should be based are fastener size, base-metal thickness, base-metal composition, and reverse-side marking requirements (Table 1).

TABLE 1 STUD-WELDING PROCESS SELECTION

PARAMETERS	STUD ARC WELDING	CAPACITOR DISCHARGE STUD WELDING	
		GAP AND CONTACT METHODS	DRAWN ARC METHOD
STUD SHAPE			
ROUND	A	A	A
SQUARE	A	A	A

RECTANGULAR	A	A	A
IRREGULAR	A	A	A
STUD DIAMETER OR AREA			
1.6 TO 3.2 MM ($\frac{1}{16}$ TO $\frac{1}{8}$ IN.)	D	A	A
3.2 TO 6.4 MM ($\frac{1}{8}$ TO $\frac{1}{4}$ IN.)	C	A	A
6.4 TO 12.7 MM ($\frac{1}{4}$ TO $\frac{1}{2}$ IN.)	A	B	B
12.7 TO 25.4 MM ($\frac{1}{2}$ TO 1 IN.)	A	D	D
UP TO 32.3 MM^2 (0.05 $IN.^2$)	C	A	A
OVER 32.3 MM^2 (0.05 $IN.^2$)	A	D	D
STUD METAL			
CARBON STEEL	A	A	A
STAINLESS STEEL	A	A	A
ALLOY STEEL	B	C	C
ALUMINUM	B	A	A
BRASS	C	A	D
BASE METAL			
CARBON STEEL	A	A	A
STAINLESS STEEL	A	A	A
ALLOY STEEL	B	A	C
ALUMINUM	B	A	A
BRASS	C	A	D
BASE-METAL THICKNESS			
UNDER 0.4 MM (0.015 IN.)	D	A	B
0.4 TO 1.6 MM (0.015 TO 0.062 IN.)	C	A	A
1.6 TO 3.2 MM (0.062 TO 0.125 IN.)	B	A	A
OVER 3.2 MM (0.125 IN.)	A	A	A
STRENGTH CRITERIA			
HEAT EFFECT ON EXPOSED SURFACES	B	A	A
WELD FILLET CLEARANCE	B	A	A
STRENGTH OF STUD GOVERNS	A	A	A
STRENGTH OF BASE METAL GOVERNS	A	A	A

A. applicable without special procedures or equipment; B. applicable with special techniques or for specific applications that justify preliminary trials or testing to develop welding procedure and technique; C, limited application; D, not recommended-welding methods not developed at this time.

Source: Ref 1

Equipment. As shown in Fig. 1, the basic equipment used for stud arc welding consists of a control system, which regulates the arc time and controls gun movement; a fixed or portable stud-welding gun, which holds the stud in position during the welding process to create the proper arc length and joining pressure; and connecting cables, which must be connected to a separate source of dc power. The other items that are needed to weld the workpiece are the studs themselves and ceramic arc shields, or ferrules. The equipment used for stud welding is comparable, in terms of size, portability, and ease of operation, to the equipment used in the SMAW process. Although the initial cost of stud-welding systems varies with the method selected, stud size, and productivity requirements, it is generally competitive with other fastening methods on an in-place or finished part cost basis.

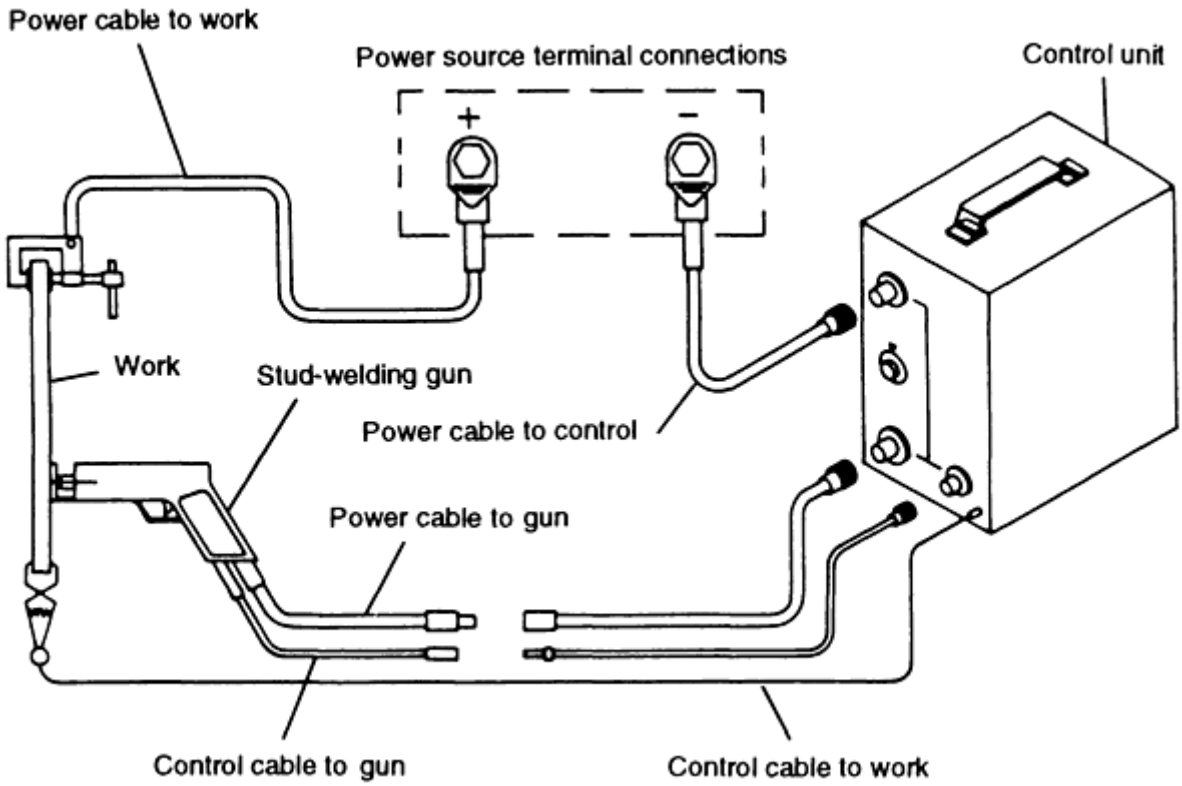

FIG. 1 STUD ARC WELDING CONTROL SYSTEM. THE CONTROL SYSTEM MUST BE CONNECTED TO A DC POWER SOURCE FOR WELDING. IN MOST APPLICATIONS, THE STUD (ELECTRODE) SHOULD BE NEGATIVE.

A stud-welding control system that has been integrated in a transformer/rectifier power source is shown in Fig. 2. This type of equipment, which is the most widely used, is called a power/control system. It can weld studs with diameters up to 28.5 mm ($1\frac{1}{8}$ in.). Either a single gun or dual guns can be used. Although a light-duty control system can weigh 11.3 kg (25 lb), the system shown in Fig. 2 weighs approximately 450 kg (1000 lb) and can be put on a wheeled cart for mobility.

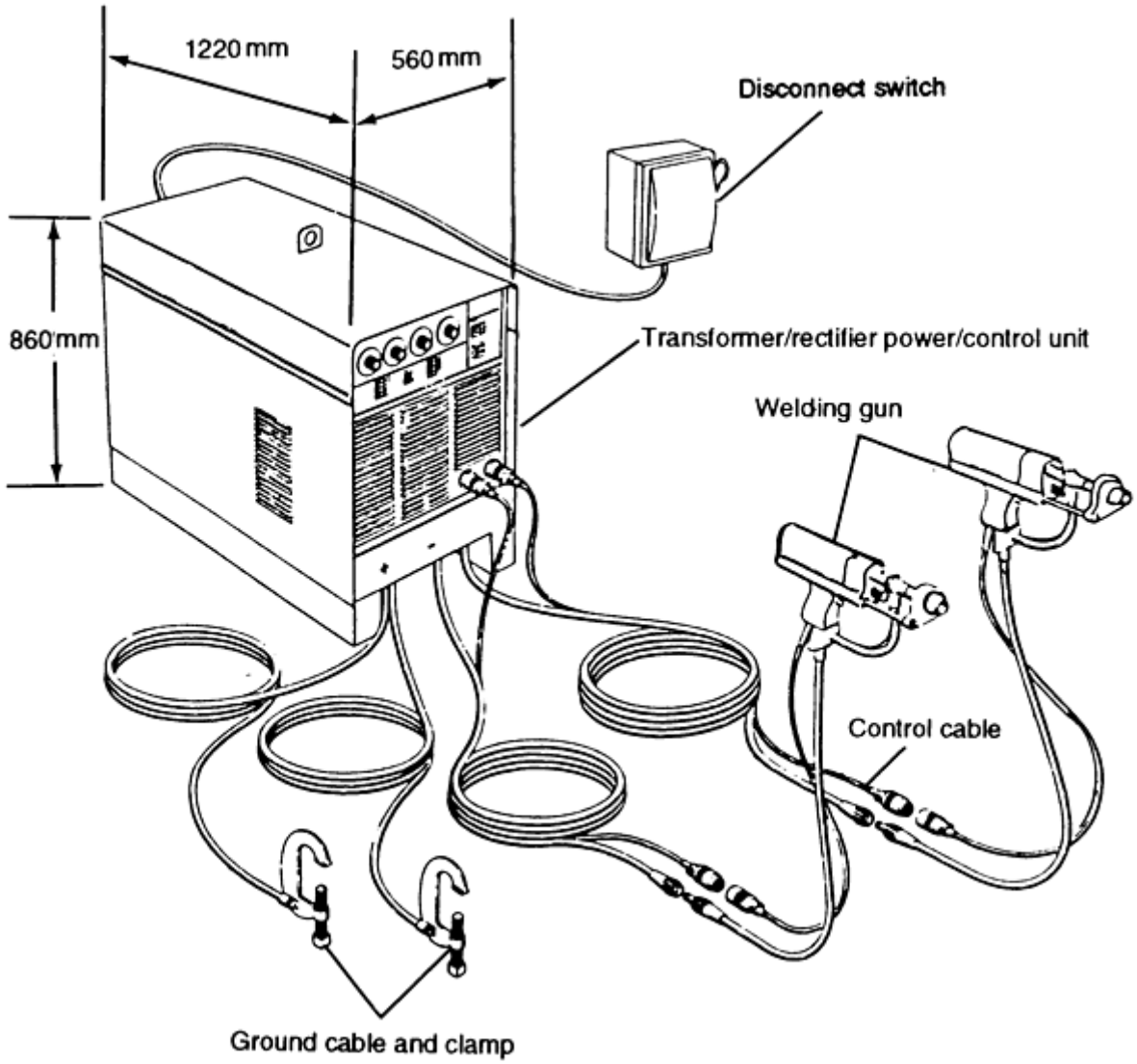

FIG. 2 TYPICAL INTEGRATED POWER/CONTROL SYSTEM FOR STUD ARC WELDING

A typical stud-welding gun (Fig. 3) is usually available in at least two sizes: standard duty, for use with studs up to 16 mm ($\frac{5}{8}$ in.) in diameter, and heavy duty, for use on larger-diameter studs. The weight of the gun can vary from approximately 1.8 kg (4 lb), for a standard-duty gun, to 6.8 kg (15 lb), for heavy-duty models.

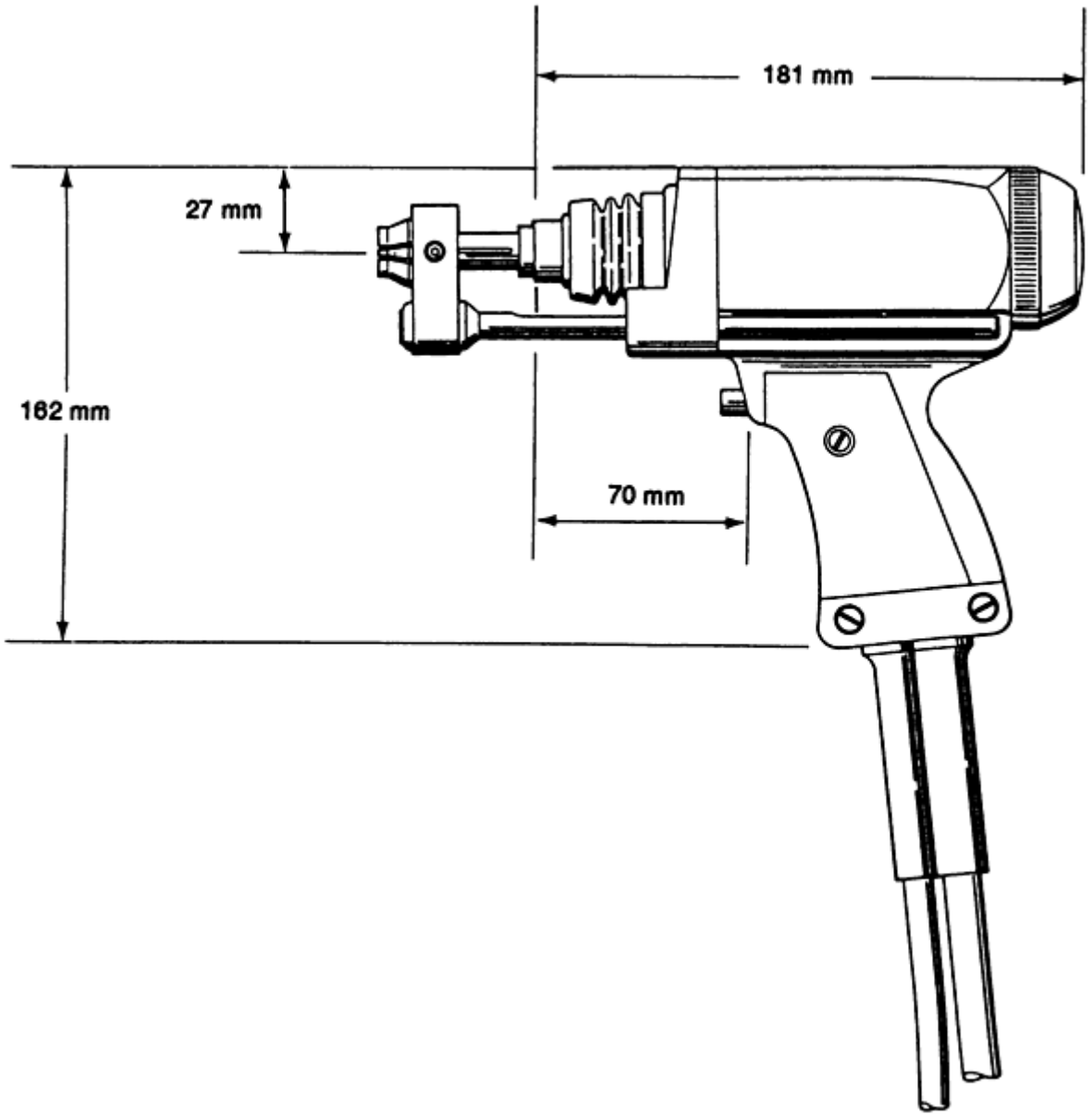

FIG. 3 TYPICAL STANDARD-DUTY GUN FOR STUD ARC WELDING

Operation. The stud arc welding process utilizes the same principles as any other arc welding procedure. First, the stud, which acts as an electrode, is inserted into a chuck on the end of the gun, surrounded by a ceramic ferrule, and positioned against the workpiece (Fig. 4a). Next, the gun trigger is depressed, which starts the automatic weld cycle by energizing a solenoid coil within the gun body that lifts the stud off the work and draws an arc. The arc melts the end of the stud and a portion of the workpiece (Fig. 4b). After a preset arc time (set on the control unit), the welding current is shut off and the solenoid is de-energized (Fig. 4c). A mainspring in the gun forces the stud into the molten pool of metal, producing a full-strength weld, which is shown in Fig. 4(d) after the gun has been lifted off the stud and the ceramic ferrule removed. The result is a full-penetration, full-strength stud-to-workpiece weld, as shown in Fig. 5. This weld is similar to that obtained with other types of arc-welding processes.

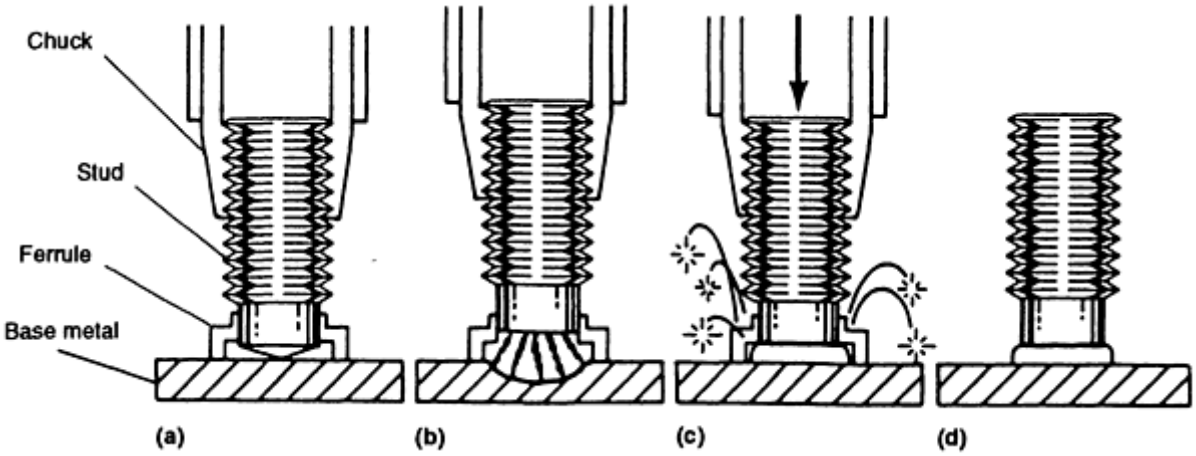

FIG. 4 STUD ARC WELDING PROCESS. (A) GUN IS PROPERLY POSITIONED. (B) TRIGGER IS DEPRESSED AND STUD IS LIFTED, CREATING AN ARC. (C) ARCING PERIOD IS COMPLETED AND STUD IS PLUNGED INTO MOLTEN POOL OF METAL ON BASE MATERIAL. (D) GUN IS WITHDRAWN FROM WELDED STUD AND FERRULE IS REMOVED.

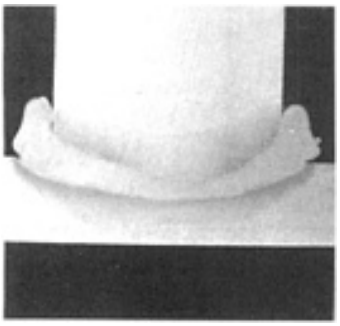

FIG. 5 MACROSECTION OF LOW-CARBON STEEL STUD WELD

Studs and Ferrules. With the exception of special processes, the stud arc welding of steel, stainless steel, and aluminum studs requires the use of a specifically designed weld stud and ceramic ferrule.

Studs. A wide range of studs are made by stud-welding manufacturers for the SW process. They vary in size and weld-base configuration, depending on the application requirements. The typical stud styles that are available include threaded, unthreaded, headed, and rectangular studs (Fig. 6). The steel stud diameters that are commonly welded using the SW process range from 2.7 to 25.4 mm (0.105 to 1.00 in.).

FIG. 6 COMMON STUD CONFIGURATIONS FOR STUD ARC WELDING

Full-strength welds result when using studs made from low-carbon steel that conforms to ASTM A-108 grades C-1010 through C-1020, although other steel grades can be used on a special-application qualified basis (Ref 2). Stainless steel studs are typically made from the austenitic series, including AISI 302, 302 HQ, 304, 305, 308, 309, 310, 316, 321, and 347, in both normal-carbon and low-carbon varieties. Stainless steel 303 is not an acceptable stud alloy. Aluminum studs are usually made from aluminum-magnesium alloys, including 5183, 5356, 5556, 5086, and 5456 (Ref 3).

Steel and stainless steel arc welded studs that are larger than 6.4 mm (0.250 in.) in diameter use a welding flux to stabilize the welding arc and to deoxidize the weld area. The most commonly used flux is commercially pure aluminum, which is installed onto the weld end of the stud by thermal spraying, staking, or pressing a slug into a drilled hole in the end of the stud (Fig. 7). Studs that are 6.4 mm (0.250 in.) and under usually do not require fluxing.

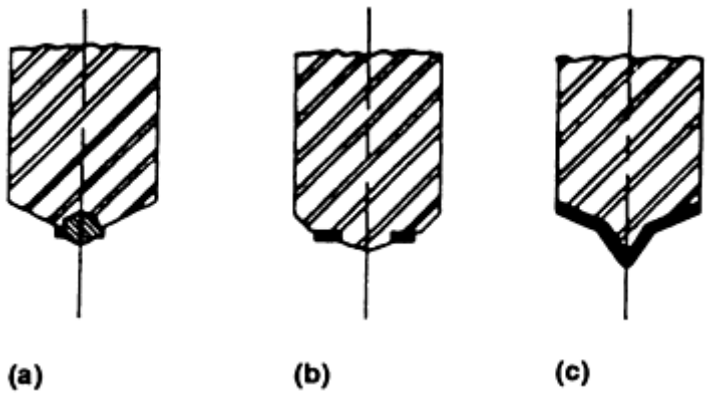

FIG. 7 METHODS OF FLUX LOADING STUDS. (A) PRESSED IN SLUG. (B) STAKED ON WASHER. (C) COATING

Aluminum studs do not have to be flux loaded. Instead, the weld end of the stud has a conical or cylindrical tip that is shaped into the parent metal to help initiate the arc and control the arc length. To prevent the oxidation and embrittlement of the stud/plate weld zone during aluminum stud arc welding, the weld area is purged with an inert gas during the weld cycle. Argon gas is commonly used for this purpose, although helium also can be used. The typical gas flow rates for aluminum studs of various diameters are shown in Table 2.

TABLE 2 GAS FLOW RATES FOR ALUMINUM STUD ARC WELDING

STUD WELD BASE DIAMETER		SHIELDING GAS FLOW[(A)]	
mm	**in.**	**l/min**	**ft^3/h**
6.4	$\frac{1}{4}$	7.1	15
7.9	$\frac{5}{16}$	7.1	15
9.5	$\frac{3}{8}$	9.4	20
11.1	$\frac{7}{16}$	9.4	20
12.7	$\frac{1}{2}$	9.4	20

(A) SHIELDING GAS, 99.95% PURE ARGON

When stud arc welding low-carbon and stainless steel studs, the stud (electrode) should be negative. Aluminum stud arc welding should be set up so that the stud is positive.

Obtaining a full-quality stud arc weld requires a sufficient amount of total energy input to the weld joint in order to produce melting and complete metallurgical bonding of the stud and workpiece. The energy input or weld current that is necessary depends on the stud diameter. Other parameters in the stud arc welding process are: arc voltage, arc time, and plunge. Arc voltage is a function of the arc length, which is set as "lift," or the length the stud is drawn away from the workpiece during weld-cycle initiation. Plunge is the length of stud that extends past the end of the ceramic ferrule and is available for melt off during the weld cycle.

Studs are reduced in length during the weld cycle. Table 3 shows the typical reductions for steel and aluminum studs as a result of welding.

TABLE 3 TYPICAL STUD WELDING SETTINGS

STUD BASE DIAMETER		LENGTH REDUCTION		DOWNHAND WELDING							OVERHEAD WELDING							VERTICAL WELDING						
				CURRENT, A	TIME		LIFT		PLUNGE		CURRENT, A	TIME		LIFT		PLUNGE		CURRENT, A	TIME		LIFT		PLUNGE	
mm	in.	mm	in.		s	cycles	mm	in.	mm	in.		s	cycles	mm	in.	mm	in.		s	cycles	mm	in.	mm	in.
STEEL AND STAINLESS STEEL																								
4.8	0.187	3.2	0.125	300	0.15	8-9	1.6	0.062	3.2	0.125	300	0.15	8-9	1.6	0.062	3.2	0.125	300	0.15	8-9	1.6	0.062	3.2	0.125
6.4	0.250	3.2	0.125	450	0.17	10-12	1.6	0.062	3.2	0.125	450	0.15	10-12	1.6	0.062	3.2	0.125	450	0.17	10-12	1.6	0.062	3.2	0.125
7.9	0.312	3.2	0.125	500	0.25	15	1.6	0.062	3.2	0.125	500	0.25	15	1.6	0.062	3.2	0.125	500	0.25	15	1.6	0.062	3.2	0.125
9.5	0.375	3.2	0.125	550	0.33	20	1.6	0.062	3.2	0.125	550	0.33	20	1.6	0.062	3.2	0.125	600	0.33	20	1.6	0.062	3.2	0.125
11.1	0.437	3.2	0.125	675	0.42	25	1.6	0.062	3.2	0.125	675	0.42	25	1.6	0.062	3.2	0.125	750	0.33	20	1.6	0.062	3.2	0.125
12.7	0.500	4.8	0.125	800	0.55	33	1.6	0.062	3.2	0.125	800	0.55	33	1.6	0.062	3.2	0.125	875	0.47	28	1.6	0.062	3.2	0.125
15.9	0.625	4.8	0.187	1200	0.67	40	2.4	0.093	4.7	0.187	1200	0.67	40	2.4	0.093	4.7	0.187	1275	0.60	36	1.6	0.062	4.7	0.187 (A)
19.1	0.750	4.8	0.187	1500	0.84	50-55	2.4	0.093	4.7	0.187	1500	0.84	50-55	2.4	0.093	4.7	0.187	1700	0.73	50	2.4	0.093	4.7	0.187 (A)
22.2	0.875	4.8	0.187	1700	1.00	60-65	3.2	0.125	6.4	0.250	1700	1.00	65	3.2	0.125	6.4	0.250	NOT RECOMMENDED						
25.4	1.000	6.4	0.250	1900	1.40	85	3.2	0.125	6.4	0.250	2050	1.40	72	3.2	0.125	6.4	0.250	NOT RECOMMENDED						
ALUMINUM (A)																								
4.8	0.187	3.2	0.125	150	0.25	15	2.4	0.093	3.2	0.125	150	0.25	15	2.4	0.093	3.2	0.125	180	0.20	12	2.4	0.093	3.2	0.125
6.4	0.250	3.2	0.125	200	0.40	24	2.4	0.093	3.2	0.125	200	0.40	24	2.4	0.093	3.2	0.125	225	0.30	18	2.4	0.093	3.2	0.125
7.9	0.312	3.2	0.125	250	0.50	30	2.4	0.093	3.2	0.125	250	0.50	30	2.4	0.093	3.2	0.125	275	0.40	24	2.4	0.093	3.2	0.125
9.5	0.375	3.2	0.125	325	0.65	39	3.2	0.125	3.2	0.125	325	0.65	39	2.4	0.093	3.2	0.125	350	0.60	36	3.2	0.125	3.2	0.125

11.1	0.437	3.2	0.125	400	0.80	48	3.2	0.125	3.9	0.156	400	0.80	48	3.9	0.156	3.9	0.156	430	0.70	42	3.2	0.125	3.9	0.156
12.7	0.500	3.2	0.125	460	0.90	54	3.2	0.125	4.7	0.187	460	0.90	54	4.7	0.187	4.7	0.187	475	0.80	48	3.2	0.125	4.7	0.187

(A) STUD ARC WELDED ALUMINUM STUDS REQUIRE INERT GAS SHIELDING: SEE TABLE 2.

There is a range of setting combinations for all stud diameters. The same total energy input can be obtained by varying current input and arc time. For example, a low current input can be compensated for, to some extent, by increasing weld time. Table 3 also shows typical weld settings for various SW stud diameters. The ideal settings in each weld position for a particular stud and workpiece should be established by beginning with typical settings and then varying them within the allowable range to meet the required conditions.

Typical settings are based on good weld conditions, such as a clean workpiece, good ground, and others. Also necessary is a proper dc power source, which should have the following characteristics:

- HIGH OPEN-CIRCUIT VOLTAGE (70 TO 100 V)
- RAPID OUTPUT CURRENT RISE
- DROOPING OUTPUT VOLT-AMPERE CURVE
- HIGH CURRENT OUTPUT OVER A SHORT TIME

Stud arc welding requires a very short weld time (Table 3), but a very high current input, when compared with other types of arc welding. Usually, the duty cycle for this process is much lower than that of other welding processes. Constant-voltage types of dc power sources are not suitable for stud welding. Many of the available dc power sources are acceptable for stud welding, including those supplied as integrated power/control systems by the stud-welding manufacturer. These integrated systems use both three-phase and single-phase incoming alternating current (ac) power. Both standard and special voltage units are available. Single-phase units are relatively low cost, portable systems that are usually suitable for smaller-diameter (≤ 12.7 mm, or $\frac{1}{2}$ in.) stud arc welding. Three-phase units are preferred for larger-diameter studs, because they provide a balanced load on incoming power lines and have smoother arc characteristics. A transformer/rectifier power source, combined with an integral stud-welding control system, is shown in Fig. 2.

Weld cable length and cable size also can affect the total output of a power source. Basically, a larger welding cable size minimizes current loss that is due to cable length, resistance, and heating. Thus, when the distance from the power source to the gun increases significantly, or when the number and size of studs applied per minute are large, larger welding cables should be used. Smaller dc power sources suitable for stud arc welding can be wired in parallel to produce the necessary current range.

Ferrules, or ceramic arc shields, are used in most stud arc weld applications. They are available in a wide variety of sizes and shapes to fit specific stud base designs and applications. For example, there are specific designs for welding studs through metal deck, to the fillet or heel of an angle, to round pipes or bars, or in a vertical position. A ferrule is placed over every stud at the weld end, where it is held in place by a grip on the stud-welding gun. The ferrule is used only once and must be removed from the stud after welding is completed to allow the inspection of the completed weld. Typical ferrule configurations are shown in Fig. 8.

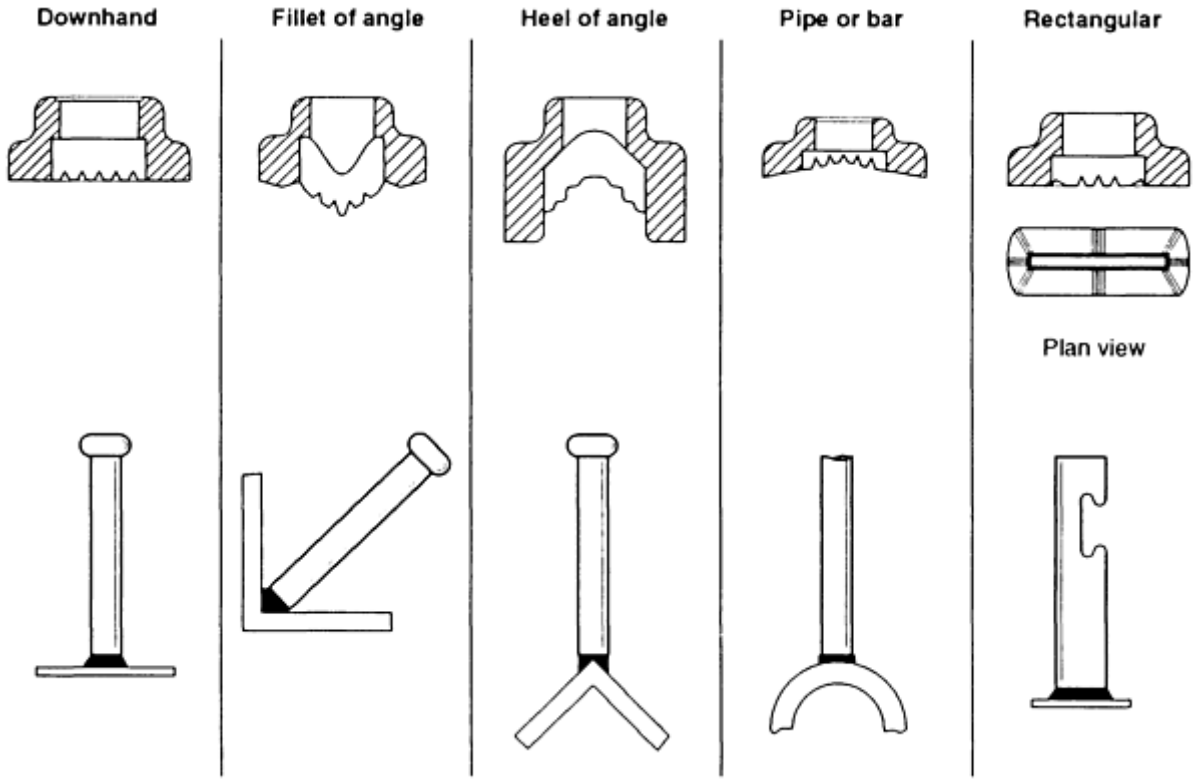

FIG. 8 CROSS SECTIONS OF FERRULES SHOWING SOME OF THE MANY VARIETIES AVAILABLE FOR DIFFERENT STUD BASE GEOMETRIES, WELD POSITIONS, AND APPLICATIONS

Ferrule design is important, because it controls certain functions during welding. For example:

- VENTS ON THE BOTTOM OF THE FERRULE ALLOW WELD GASES TO ESCAPE FROM THE WELD AREA AND RESTRICT THE INFLOW OF AIR TO MINIMIZE WELD POROSITY AND OXIDATION.
- THE INTERNAL CAVITY OF THE FERRULE CONFINES AND SHAPES THE MOLTEN METAL INTO A FLASH (FILLET) AROUND THE STUD PERIPHERY.
- HEAT IN THE WELD AREA IS CONCENTRATED AND CONTAINED.
- FLASH AND WELD SPATTER ARE MINIMIZED.

Although the dimensions of the flash are controlled by the ferrule configuration, the flash diameter and height must be taken into consideration when designing mating parts. Manufacturer specifications on finished stud flash dimensions should be followed, and test welds should be made to establish part fit. Flash dimensions can be accommodated by any of the five methods shown in Fig. 9.

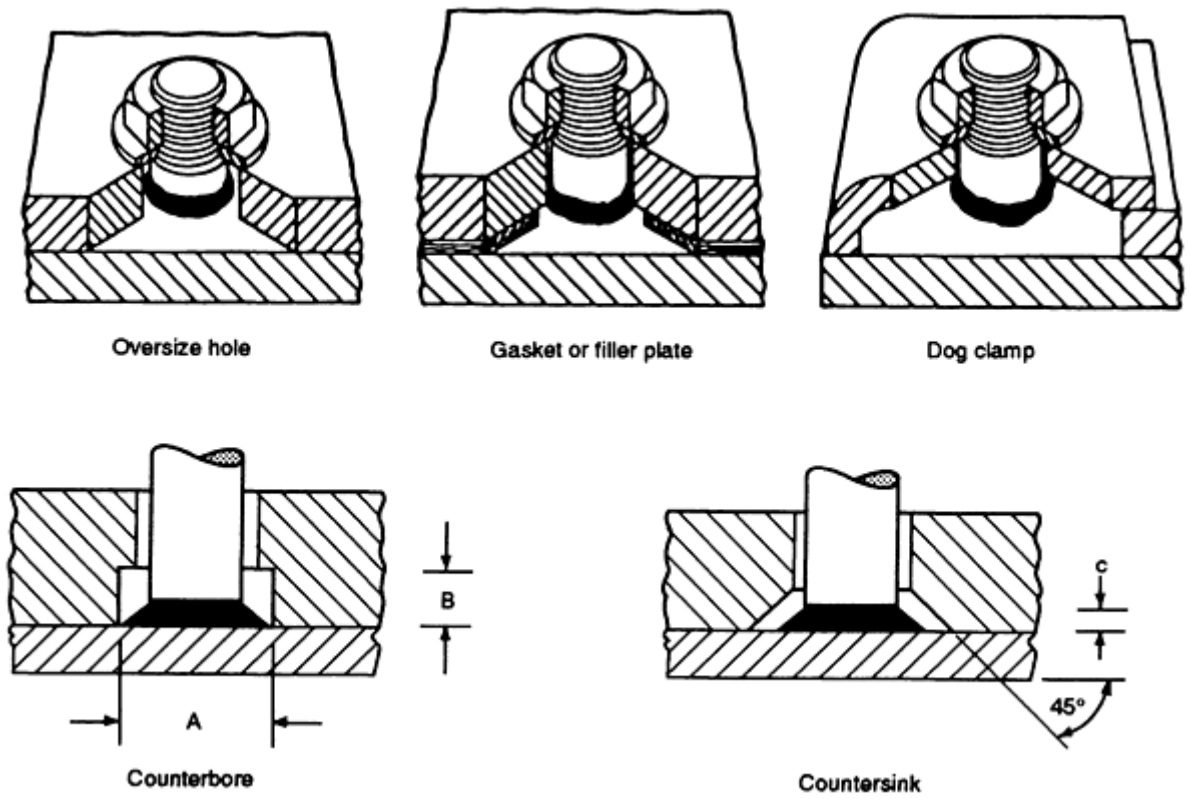

FIG. 9 COMMON METHODS FOR ACCOMMODATING WELD FLASH (FILLET) WITH STUD ARC WELDS. TYPICAL DIMENSIONS FOR A, B, AND C ARE GIVEN IN TABLE 4.

The typical dimensions for flash clearance are shown in Table 4. It should be noted that the flash (fillet) of a stud weld is not the same as the fillet that is produced by conventional welding techniques. It may have areas of nonfusion on its vertical leg or shrink fissures, which have no adverse affect on weld strength or ductility (Ref 4). Consequently, it is not subject to the profile and inspection criteria used for a conventional weld fillet.

TABLE 4 DIMENSIONS FOR COUNTERBORE AND COUNTERSINK WELD FLASH CLEARANCE

A, B, and C are shown in Fig. 9.

STUD BASE DIAMETER		COUNTERBORE				90° COUNTERSINK	
		A		B		C	
mm	in.	mm	in.	mm	in.	mm	in.
6.4	1/4	11.1	0.437	3.2	0.125	3.2	0.125
7.9	5/16	12.7	0.500	3.2	0.125	3.2	0.125
9.5	3/8	15.1	0.593	3.2	0.125	3.2	0.125
11.1	7/16	16.7	0.656	4.7	0.187	3.2	0.125
12.7	1/2	19.1	0.750	4.7	0.187	4.7	0.187
15.9	5/8	22.2	0.875	5.5	0.218	4.7	0.187

19.1	3/4	28.6	1.125	7.9	0.312	4.7	0.187

Note: Dimensions can vary, depending on stud style and ceramic arc shield selected. Consult manufacturer for details.

Base Plate Material and Thickness. To obtain full strength, the stud arc welding of low-carbon steel, stainless steel, or aluminum studs should be made to a base material of sufficient thickness so that the stud fails in tension or torque, rather than by pulling a hole in the base-metal workpiece. In the case of stainless or low-carbon steel studs, the base-metal thickness should be at least one-third that of the stud diameter. For aluminum studs, the aluminum base plate material should be at least half that of the stud diameter. Thinner base plates can be used if strength is not the primary design characteristic that is required. On thinner materials, the studs will pull a hole in the plate at strength levels below their maximum. If the plate is too thin, then the stud will bum a hole through it. The recommended base plate thickness for full-strength development and the minimum thicknesses required to prevent burning through the base plate are given in Table 5.

TABLE 5 RECOMMENDED BASE METAL THICKNESSES FOR STUD ARC WELDING

STUD BASE DIAMETER		STEEL BASE METAL				ALUMINUM BASE METAL			
		FOR FULL STRENGTH[A]		MINIMUM[B]		WITHOUT BACKUP		MINIMUM WITH BACKUP[C]	
mm	in.	mm	in.	mm	in.	mm	in.	mm	in.
4.8	3/16	1.59	0.062	0.91	0.036	3.18	0.125	3.18	0.125
6.4	1/4	3.18	0.125	1.21	0.048	3.18	0.125	3.18	0.125
7.9	5/16	3.18	0.125	1.52	0.060	4.76	0.187	3.18	0.125
9.5	3/8	4.76	0.187	1.90	0.075	4.76	0.187	4.76	0.187
11.1	7/16	4.76	0.187	2.28	0.090	6.35	0.250	4.76	0.187
12.7	1/2	4.76	0.187	3.04	0.120	6.35	0.250	6.35	0.250
15.9	5/8	6.35	0.250	3.68	0.145	. . .	. . .	. . .	. . .
19.1	3/4	7.94	0.318	4.70	0.185	. . .	. . .	. . .	. . .
22.2	7/8	9.53	0.375	6.35	0.250	. . .	. . .	. . .	. . .
25.4	1	9.53	0.375	9.53	0.375	. . .	. . .	. . .	. . .

(A) NEAREST COMMONLY AVAILABLE BASE METAL THICKNESS.

(B) STEEL WITHOUT BACKUP--WILL NOT DEVELOP FULL STUD STRENGTH.

(C) METAL BACKUP REQUIRED TO PREVENT MELT-THROUGH OF BASE METAL

The most widely used combinations of base plate and stud materials are shown in Table 6. With low-carbon steel studs, no preheat or postheat treatments are needed when welding to low-carbon steel or austenitic stainless steel base plate materials. As carbon content in the base plate increases into the medium range, heat treatment for stud welding may be required. Welding to high-carbon base plate is not suggested. When base plate/stud combinations are questionable, an application qualification test is suggested (Ref 5). Details on this procedure are provided in the section "Stud-Welding Quality Control, Qualification, and Inspection" in this article. For best results when welding stainless steel studs to low-carbon steel plate (especially when working stress levels are very high or there are repetitive loading cycles), the studs should either be manufactured from annealed-in-process materials or postmanufacture annealed before use.

TABLE 6 TYPICAL COMBINATIONS OF BASE AND STUD METALS FOR STUD ARC WELDING

BASE METAL	STUD METAL
LOW-CARBON STEEL, AISI 1006 TO 1022[(A)]	LOW-CARBON STEEL, AISI 1006 TO 1020; STAINLESS STEEL, 300 SERIES
STAINLESS STEEL, 300 SERIES[(B)], 405, 410, AND 430	LOW-CARBON STEEL, AISI 1006 TO 1020; STAINLESS STEEL, 300 SERIES
ALUMINUM ALLOYS, 5000 SERIES[(C)]	ALUMINUM ALLOYS, 5000 SERIES[(C)]

Source: Ref 1

(A) REFER TO ANSI/AWS D1.1-92, TABLE 4.1 (GROUPS I AND II) FOR APPROVED STEELS.

(B) EXCEPT FOR THE FREE-MACHINING TYPE 303 STAINLESS STEEL.

(C) REFER TO ANSI/AWS D1.2-89, TABLES 7.1 AND 7.4.

Good welding practice requires that the base plate material at the weld spot be cleaned. Common contaminants that can result in unsatisfactory welds if not removed include paint, heavy mill scale, heavy rust, oxidation, oil or grease, and plating, such as galvanizing and anodizing on aluminum. Removal methods vary according to the contaminant, the base material, and the end use. Wire brushing and grinding may be satisfactory on heavy structural steel but can be destructive to thin-gage metals or anodized aluminum, because they may reduce the thickness to a point where bum through or less-than-full-strength welds result.

Suggested cleaning methods include grinding, wire brushing, or needle scaling on heavy materials; using solvents to clean grease and oil; and using a noncontaminating stainless wire brush or a nonmetallic foam disk to clean aluminum and milling. Because anodizing is difficult to remove from aluminum without reducing the metal thickness, consideration should be given to anodizing the base plate and stud after the welding operation.

Similarly, the weld end of the stud should be free from materials that would contaminate the weld, including paint, rust, galvanizing, and others. Studs cannot be coated with any nonconductive material that would interfere with the flow of welding current. Light copper flashing and nickel or chrome plating usually do not cause welding problems.

Because a high-amperage, short-time current is typical in the stud arc welding process, it is also important that the grounding spot(s) on the base material be clean, that the ground be tight, and that all cables be in good condition and have tight connections.

The position of the ground(s) also can influence stud-welding quality. This depends on the geometry of the base-metal shape and is the result of electromagnetic arc deflection, or arc blow (Ref 6). Occurrences are more common when studs are very near a free edge or are on long and narrow base plates, hollow pipe sections, or irregular peripheries, and can be corrected by moving the ground to a central position or using multiple grounds. Because current flow is usually away from the ground toward the heavier or larger area of the base plate, arc blow is characterized by a lack of flash or fillet on the side of the stud nearer the edge, end, or smaller area.

Stud Strength. Fasteners will develop full material strength when they have been stud arc welded to compatible base plate alloys. Tables 7, 8, and 9 show the tension and torque loads for various threaded stud diameters, based on minimum specified stud strengths (Ref 2, 3, and 6). For unthreaded stud fasteners, the yield strength and tensile or ultimate strength is calculated by:

$$\text{YIELD STRENGTH} = A_S F_Y$$
$$\text{TENSILE STRENGTH} = A_S F_U$$

where A_s is the area of the stud shank (in.^{2}), F_y is the specified stud material yield strength (minimum psi) and F_u is the specified stud material ultimate strength (minimum psi).

TABLE 7 MECHANICAL PROPERTIES OF LOW-CARBON STEEL STUD ARC WELDED FASTENERS

Fasteners have 380 MPa (55 ksi) minimum ultimate strength and 345 MPa (50 ksi) minimum yield strength.

STUD THREAD DIAMETER[A]	MEAN EFFECTIVE THREAD AREA[B]		YIELD TENSILE LOAD[C]		ULTIMATE TENSILE LOAD		YIELD TORQUE[D]		ULTIMATE TORQUE		ULTIMATE SHEAR LOAD[E]	
	mm^2	$in.^2$	kn	lbf	kn	lbf	j	ft · lbf	j	ft · lbf	kn	lbf
10-24 UNC	11	0.017	3.8	850	4.2	935	3.6	32[F]	4.0	35.1[F]	3.1	701
10-32 UNF	13	0.020	4.4	1,000	4.9	1,100	4.3	38[F]	4.7	41.3[F]	3.7	825
$\frac{1}{4}$-20 UNC	21	0.032	7.1	1,600	7.8	1,760	9.1	6.7	9.9	7.3	5.9	1,320
$\frac{1}{4}$-28 UNF	23	0.036	8.0	1,800	8.8	1,980	10.2	7.5	11.3	8.3	6.6	1,485
$\frac{5}{16}$-18 UNC	34	0.052	11.6	2,600	12.7	2,860	18.4	13.6	20.2	14.9	9.5	2,145
$\frac{5}{16}$-24 UNF	37	0.058	12.9	2,900	14.2	3,190	20.5	15.1	22.5	16.6	10.6	2,393
$\frac{3}{8}$-16 UNC	50	0.078	17.3	3,900	19.1	4,290	33.1	24.4	36.3	26.8	14.3	3,218
$\frac{3}{8}$-24 UNF	57	0.088	19.6	4,400	21.5	4,840	37.3	27.5	41.1	30.3	16.1	3,630
$\frac{7}{16}$-14 UNC	68	0.106	23.6	5,300	25.9	5,830	52.3	38.6	57.6	42.5	19.5	4,373
$\frac{7}{16}$-20 UNF	76	0.118	26.2	5,900	28.9	6,490	58.3	43.0	64.1	47.3	21.7	4,868
$\frac{1}{2}$-13 UNC	92	0.142	31.6	7,100	34.7	7,810	80.3	59.2	88.3	65.1	26.0	5,856
$\frac{1}{2}$-20 UNF	103	0.160	35.6	8,000	39.1	8,800	90.4	66.7	99.4	73.3	29.4	6,600
$\frac{5}{8}$-11	146	0.226	50.3	11,300	55.3	12,430	159.6	117.7	175.5	129.5	41.5	9,323

UNC												
$\frac{5}{8}$-18 UNF	165	0.255	56.7	12,750	62.4	14,025	180.1	132.8	198.1	146.1	46.8	10,519
$\frac{3}{4}$-10 UNC	215	0.334	74.3	16,700	81.7	18,370	283.1	208.8	311.3	229.6	61.3	13,778
$\frac{3}{4}$-16 UNF	240	0.372	82.7	18,600	91.0	20,460	315.2	232.5	346.8	255.8	68.3	15,345
$\frac{7}{8}$-9 UNC	298	0.462	102.8	23,100	112.8	25,355	456.8	336.9	501.4	369.8	84.6	19,017
$\frac{7}{8}$-14 UNF	328	0.509	113.2	25,450	124.5	27,995	503.1	371.1	553.6	408.3	93.4	20,996
1-8 UNC	91	0.606	134.8	30,300	148.0	33,275	684.7	505.0	751.9	554.6	111.0	24,956
1-14 UNF	437	0.678	150.8	33,900	165.9	37,290	766.0	565.0	842.6	621.5	124.4	27,967

(A) UNC, UNIFIED COARSE THREAD SERIES; UNF, UNIFIED FINE THREAD SERIES.

(B) MEAN EFFECTIVE THREAD AREA IS BASED ON A MEAN FULL DIAMETER MIDWAY BETWEEN MINOR AND PITCH THREAD DIAMETERS.

(C) IN PRACTICE, A STUD SHOULD NOT BE USED AT OR HIGHER THAN YIELD LOAD. A FACTOR OF SAFETY SHOULD BE APPLIED, AND 60% OF YIELD IS COMMONLY USED, ALTHOUGH OTHER VALUES MAY BE USED AT DISCRETION OF USER.

(D) TORQUE FIGURES ARE BASED ON THE ASSUMPTION THAT EXCESSIVE THREAD DEFORMATION HAS NOT AFFECTED THE PROPORTIONAL RANGE OF TORQUE/TENSION RELATIONSHIP. AN AVERAGE TORQUE COEFFICIENT OF 0.20 WAS USED IN THESE CALCULATIONS.

(E) SHEAR LOAD IS BASED UPON 0.75 TIMES ULTIMATE LOAD. THE USER SHOULD APPLY AN APPROPRIATE SAFETY FACTOR TO THESE FIGURES.

(F) VALUE GIVEN IN IN. · LBF.

TABLE 8 MECHANICAL PROPERTIES OF STAINLESS STEEL STUD ARC WELDED FASTENERS

Fasteners have 520 MPa (75 ksi) minimum ultimate strength and 205 MPa (30 ksi) minimum yield strength.

STUD THREAD DIAMETER(A)	MEAN EFFECTIVE THREAD AREA(B)		YIELD TENSILE LOAD(C)		ULTIMATE TENSILE LOAD		YIELD TORQUE(D)		ULTIMATE TORQUE		ULTIMATE SHEAR LOAD(E)	
	mm^2	$in.^2$	kn	lbf	kn	lbf	j	ft · lbf	j	ft · lbf	kn	lbf
10-24 UNC	11	0.017	2.3	510	5.7	1,275	2.2	19.1(F)	5.4	47.8(F)	4.3	956
10-32 UNF	13	0.020	2.7	600	6.7	1,500	2.5	22.5(F)	6.4	56.3(F)	5.0	1,125
$\frac{1}{4}$-20 UNC	21	0.032	4.3	960	10.7	2,400	5.4	4.0	13.6	10.0	8.0	1,800
$\frac{1}{4}$-28 UNF	23	0.036	4.8	1,080	12.0	2,700	6.1	4.5	15.3	11.3	9.0	2,025
$\frac{5}{16}$-18 UNC	34	0.052	6.9	1,560	17.3	3,900	11.0	8.1	27.5	20.3	13.0	2,925

5/16-24 UNF	37	0.058	7.7	1,740	19.3	4,350	12.3	9.1	30.6	22.6	14.5	3,263
3/8-16 UNC	50	0.078	10.4	2,340	26.0	5,850	19.8	14.6	49.6	36.6	19.5	4,388
3/8-24 UNF	57	0.088	11.7	2,640	29.4	6,600	22.4	16.5	56.0	41.3	22.0	4,950
7/16-14 UNC	68	0.106	14.1	3,180	35.4	7,950	31.5	23.2	78.6	58.0	26.5	5,963
7/16-20 UNF	76	0.118	15.7	3,540	39.4	8,850	35.0	25.8	87.4	64.5	29.5	6,638
1/2-13 UNC	92	0.142	18.9	4,260	47.4	10,650	48.1	35.5	120.4	88.8	35.5	7,988
1/2-20 UNF	103	0.160	21.4	4,800	53.4	12,000	54.2	40.0	135.6	100.0	40.0	9,000
5/8-11 UNC	146	0.226	30.2	6,780	75.4	16,950	95.7	70.6	239.4	176.6	56.5	12,713
5/8-18 UNF	165	0.255	34.0	7,650	85.1	19,125	108.1	79.7	270.1	199.2	63.8	14,344
3/4-10 UNC	215	0.334	44.6	10,020	111.4	25,050	169.9	125.3	424.50	313.1	83.6	18,788
3/4-16 UNF	240	0.372	49.6	11,160	124.1	27,900	189.1	139.5	472.9	348.8	93.1	20,925
7/8-9 UNC	298	0.462	61.7	13,860	154.1	34,650	274.0	202.1	685.1	505.3	115.6	25,988
7/8-14 UNF	328	0.509	67.9	15,270	169.8	38,175	301.9	222.7	754.8	556.7	127.4	28,631
1-8 UNC	391	0.606	80.9	18,180	202.2	45,450	410.8	303.0	1027.0	757.5	151.6	34,088
1-14 UNF	437	0.678	90.5	20,340	226.2	50,850	459.6	339.0	1149.0	847.5	169.6	38,138

(A) UNC, UNIFIED COARSE THREAD SERIES; UNF, UNIFIED FINE THREAD SERIES.

(B) META, MEAN EFFECTIVE THREAD AREA, IS BASED ON A MEAN FULL DIAMETER MIDWAY BETWEEN MINOR AND PITCH THREAD DIAMETERS.

(C) IN PRACTICE, A STUD SHOULD NOT BE USED AT OR HIGHER THAN YIELD LOAD. A FACTOR OF SAFETY SHOULD BE APPLIED, AND 60% OF YIELD IS COMMONLY USED, ALTHOUGH OTHER VALUES MAY BE USED AT THE DISCRETION OF USER.

(D) TORQUE FIGURES ARE BASED ON THE ASSUMPTION THAT EXCESSIVE THREAD DEFORMATION HAS NOT AFFECTED THE PROPORTIONAL RANGE OF TORQUE/TENSION RELATIONSHIP. AN AVERAGE TORQUE COEFFICIENT OF 0.20 WAS USED IN THESE CALCULATIONS.

(E) SHEAR LOAD IS BASED UPON 0.75 TIMES ULTIMATE LOAD. THE USER SHOULD APPLY AN APPROPRIATE SAFETY FACTOR TO THESE FIGURES.

(F) VALUE GIVEN IN IN. · LBF.

TABLE 9 MECHANICAL PROPERTIES OF ALUMINUM STUD ARC WELDED FASTENERS

Fasteners have 290 MPa (42 ksi) minimum ultimate strength and 205 MPa (30 ksi) minimum yield strength.

STUD THREAD DIAMETER[A]	MEAN EFFECTIVE THREAD AREA[B]		YIELD TENSILE LOAD[C]		ULTIMATE TENSILE LOAD		YIELD TORQUE[D]		ULTIMATE TORQUE		ULTIMATE SHEAR LOAD[E]	
	mm^2	$in.^2$	kn	lbf	kn	lbf	j	ft · lbf	j	ft · lbf	kn	lbf
10-24 UNC	11	0.017	2.3	510	3.2	714	2.2	19.1[F]	3.0	26.8[F]	1.9	428
10-32 UNF	13	0.020	2.7	600	3.9	840	2.5	22.5[F]	3.6	31.5[F]	2.2	504
$\frac{1}{4}$-20 UNC	21	0.032	4.3	960	6.0	1344	5.4	4.0	7.6	5.6	3.6	806
$\frac{1}{4}$-28 UNF	23	0.036	4.8	1080	6.7	1512	6.1	4.5	8.5	6.3	4.0	907
$\frac{5}{16}$-18 UNC	34	0.052	6.9	1560	9.7	2184	11.0	8.1	15.5	11.4	5.8	1310
$\frac{5}{16}$-24 UNF	37	0.058	7.7	1740	10.8	2436	12.3	9.1	17.2	12.7	6.5	1462
$\frac{3}{8}$-16 UNC	50	0.078	10.4	2340	14.6	3276	19.8	14.6	27.8	20.5	8.7	1966
$\frac{3}{8}$-24 UNF	57	0.088	11.7	2640	16.4	3696	22.3	16.5	31.3	23.1	9.6	2218
$\frac{7}{16}$-14 UNC	68	0.106	14.1	3180	19.8	4452	31.5	23.2	44.1	32.5	11.9	2671
$\frac{7}{16}$-20 UNF	76	0.118	15.7	3540	22.0	4956	35.0	25.8	48.9	36.1	13.2	2974
$\frac{1}{2}$-13 UNC	92	0.142	18.9	4260	26.5	5964	48.1	35.5	67.4	49.7	15.9	3578
$\frac{1}{2}$-20 UNF	103	0.160	21.4	4800	29.9	6720	54.2	40.0	75.9	56.0	17.9	4032

(A) UNC, UNIFIED COARSE THREAD SERIES; UNF, UNIFIED FINE THREAD SERIES.

(B) MEAN EFFECTIVE THREAD AREA IS BASED ON A MEAN FULL DIAMETER MIDWAY BETWEEN MINOR AND PITCH THREAD DIAMETERS.

(C) IN PRACTICE, A STUD SHOULD NOT BE USED AT OR HIGHER THAN YIELD LOAD. A FACTOR OF SAFETY SHOULD BE APPLIED, AND 60% OF YIELD IS COMMONLY USED, ALTHOUGH OTHER VALUES MAY BE USED AT DISCRETION OF USER.

(D) TORQUE FIGURES ARE BASED ON THE ASSUMPTION THAT EXCESSIVE THREAD DEFORMATION HAS NOT AFFECTED THE PROPORTIONAL RANGE OF TORQUE/TENSION RELATIONSHIP. AN AVERAGE TORQUE COEFFICIENT OF 0.20 WAS USED IN THESE CALCULATIONS.

(E) SHEAR LOAD IS BASED ON 0.60 TIMES ULTIMATE LOAD. THE USER SHOULD APPLY AN APPROPRIATE SAFETY FACTOR TO THESE FIGURES.

(F) VALUE GIVEN IN IN. · LBF.

For threaded studs, the area is based on the mean effective thread area, which is calculated by:

$$A_S = 0.7854\ [D - (0.9743/N)]^2$$

where *D* is the nominal diameter of the stud and *N* is the number of threads per inch.

Process Variations and Special Equipment. There are several specific applications that lend themselves to special variations of the stud arc welding technique. One application is the welding of studs to thin base materials that are less than the minimum thicknesses listed in Table 5. Although full weld base strength is usually not achieved, the resulting strength level is suitable for the application loadings involved. This process variation, which is called short-cycle stud arc welding, does not use a ceramic ferrule. Instead, higher weld current is used with very short times, which minimizes penetration of the stud into the base plate. Normally, this variation is used with stud diameters ≤ 9.5 mm (≤ 0.375 in.) in situations where backside marking is not considered detrimental.

The second special process is gas-shielded arc welding, which also does not use a ceramic ferrule. Instead, the stud-welding area is shielded by an inert gas, usually argon. This process can be used with both steel and aluminum, but is more widely used with the latter material. The welding variables fall into a very narrow range, and conditions for application usually include tight tolerances and a tightly controlled setup. Consequently, the stud arc welding equipment most often consists of a fixed-gun production unit. A typical application is the welding of aluminum studs with special end configurations to aluminum kitchen utensils.

Special equipment is frequently used with the short-cycle and/or gas-shielded arc welding processes, because the application parameters must be tightly controlled and involve large quantities of studs applied in a production environment. Equipment manufacturers assemble many types of special equipment for production-line use. The equipment can be used with automatic stud feed, automatic stud and ferrule feed, computer-programmed indexing, robotic stud-welding guns, and other mechanisms. A typical automated stud arc welding production unit is shown in Fig. 10. A unit can involve simple, column-mounted, single-gun systems or sophisticated, multigun, multiple feed units that cost thousands of dollars.

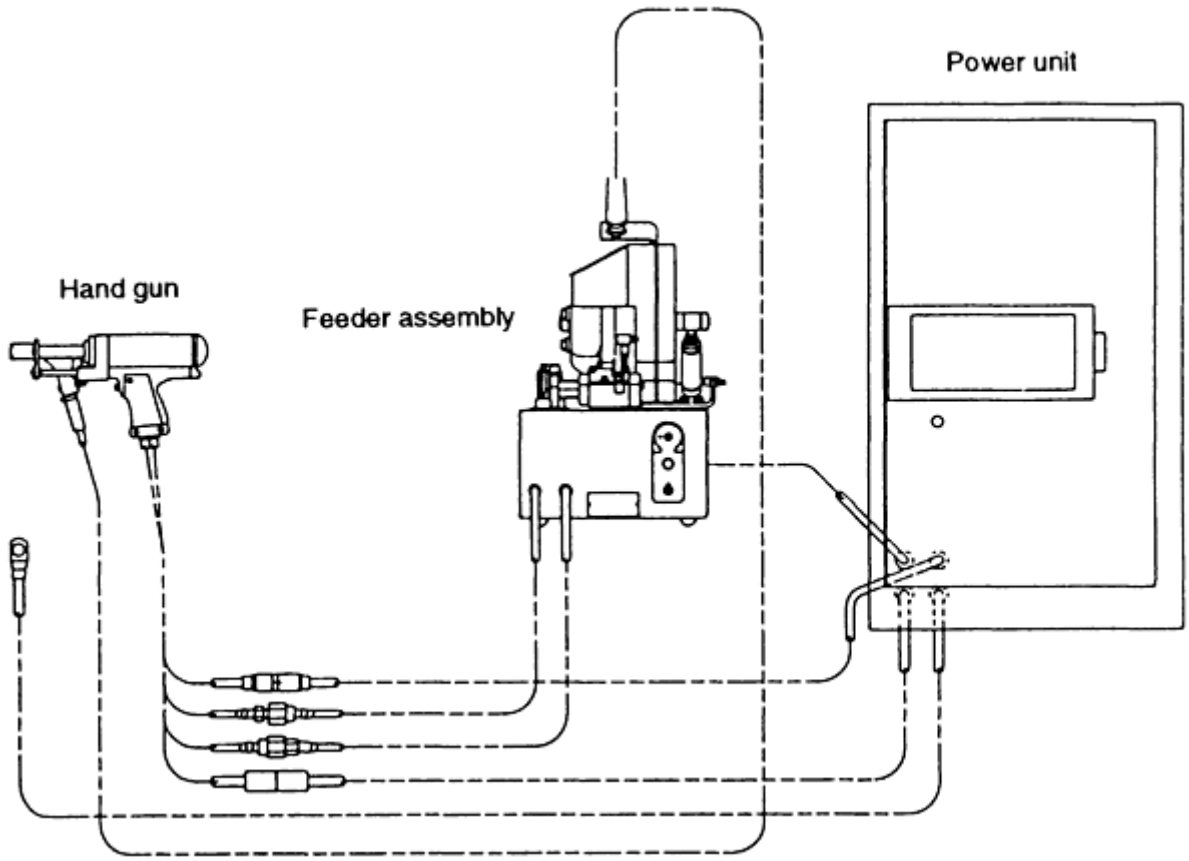

FIG. 10 TYPICAL AUTOMATIC STUD-FEED HAND-GUN SYSTEM FOR PORTABLE OPERATION USING TEMPLATES OR FIXTURES ON THE WORKPIECE

References cited in this section

1. "RECOMMENDED PRACTICES FOR STUD WELDING," ANSI/AWS C5.4, AWS
2. "STRUCTURAL WELDING CODE--STEEL," ANSI/AWS D1.1, SECTION 7, "STUD WELDING," AWS
3. "STRUCTURAL WELDING CODE--ALUMINUM," ANSI/AWS D1.2, AWS
4. "STRUCTURAL WELDING CODE--STEEL," ANSI/AWS D1.1, SECTION 7, "STUD WELDING," FOOTNOTE 27, AWS
5. "STRUCTURAL WELDING CODE--STEEL," ANSI/AWS D1.1, SECTION 7, "STUD WELDING," PARAGRAPH 7.6, AWS
6. W.A. BAESLACK, G. FAYER, S. REAM, AND C.E. JACKSON, QUALITY CONTROL IN ARC STUD WELDING, *WELD. J.*, NOV 1975, P 789-798

Stud Arc Welding

Harry A. Chambers, TRW Nelson Stud Welding Division

Fixturing and Tooling for Stud Arc Welding

Regardless of the stud-welding method employed, certain "expendable" accessories are required. These include such items as a chuck or collet to hold the particular stud being welded, a ferrule grip for the fastener, a foot that holds the ferrule grip, legs that attach to the gun and adjust to accommodate various stud lengths, and other minor items. The operating life of these items is variable, depending on the care and maintenance they receive. For example, a chuck may last for 5000 to 25,000 welds. Legs last indefinitely, whereas ferrule grips and feet usually have a shorter usage life. Accessories are relatively inexpensive items that should be planned for when preparing budgetary estimates on any given project.

The extent and sophistication of tooling for stud welding reflects the required production rate and the total number of studs to be welded. Locating the stud arc welding centers can be as simple as laying out the workpiece and center punching the locations either directly or through a template, as shown in Fig. 11. The studs are then placed in the punch marks, the stud-welding gun is held vertically, and the weld is initiated. Although operator skill is a factor, careful welders can achieve a perpendicularity of ±5° and a location tolerance of approximately 1.2 mm (0.046 in.). Often, the cover plate in a base plate/cover plate assembly can be used as the template for marking.

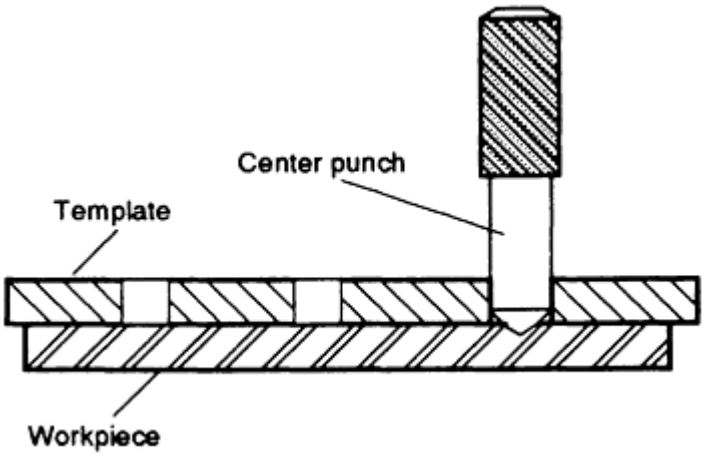

FIG. 11 CENTER PUNCHING BASE MATERIAL THROUGH A TEMPLATE

A permanent template becomes more practical when an increasing number of studs are to be welded on repetitive locations. Stud arc welded fasteners can be welded directly through temperature-resistant material which should be spaced off the work by 1.65 to 6.35 mm (0.065 to 0.250 in.) to allow expelled weld gases and weld spatter to escape without restriction, which could adversely affect weld quality. This type of template arrangement is shown in Fig. 12. Note that the template holes are drilled slightly larger than the outside dimension of the ceramic ferrule. Before the

template is prepared, it is good practice to consult the manufacturer specifications for the ceramic ferrule dimensions to be used with the stud being welded. Location accuracy, in this case, can be as tight as ±0.78 mm (±0.031 in.).

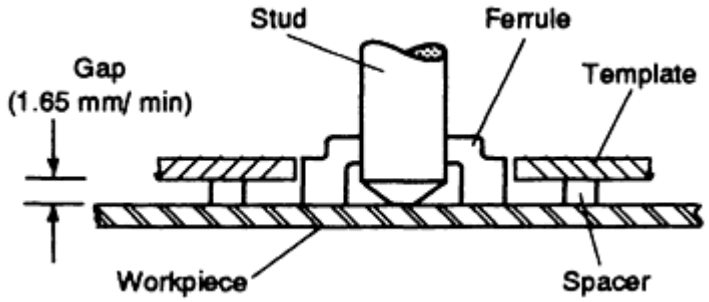

FIG. 12 WELDING THROUGH A TEMPLATE USING A FERRULE WITH STUD ARC WELDING FASTENERS

Even greater accuracy can be obtained, both in the vertical and horizontal directions, by adapting the template hole to fit a drill jig bushing tightly and by inserting the template adapter (or a ferrule tube adapter) through the bushing to the workpiece. The ferrule tube adapter also can be used for welding down into deeply drilled holes or into tight-fit areas (Fig. 13).

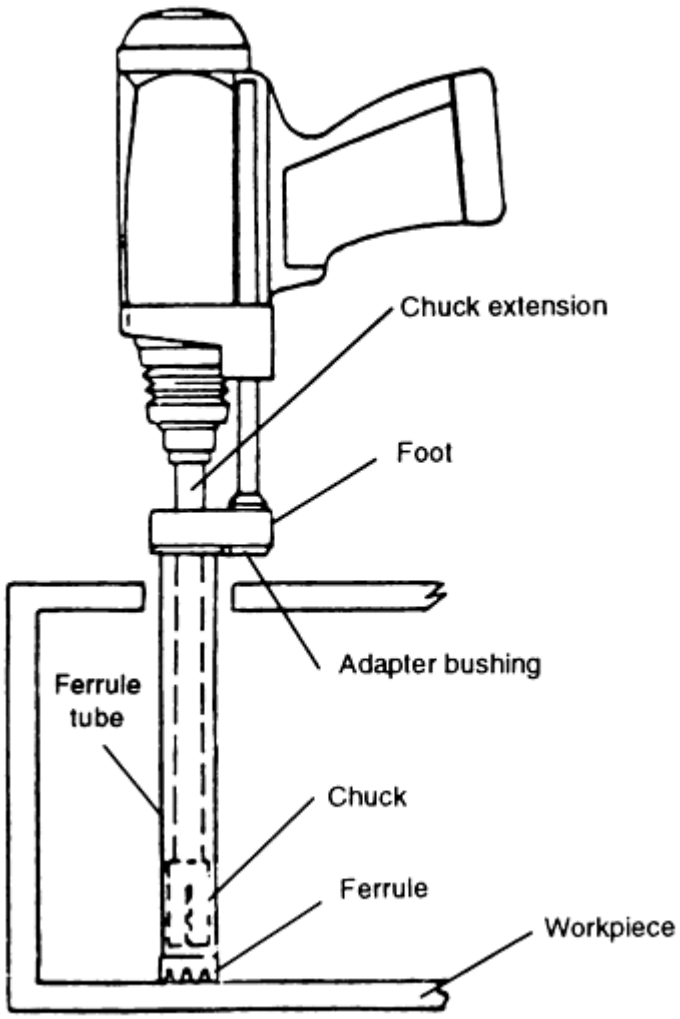

FIG. 13 PORTABLE STUD ARC WELDING GUN EQUIPPED WITH ACCESSORIES FOR WELDING STUDS THROUGH

OR INTO A DRILLED OR FORMED HOLE

With closely spaced studs, the foot grip is sometimes modified so that after welding the initial stud at a center-punched location, the foot can be held against the reference stud to weld the next or adjacent stud on the required spacing.

The verticality of the weld stud can be ensured by several methods. The most accurate is obviously a fixed gun on a slide mechanism of the type used for automatic-feed, high-production work. This type is also the most expensive. A portable gun can be mounted on a machine slide or drill press by fabricating a bracket (Fig. 14) in cases where production quantities do not justify the expense of automatic equipment.

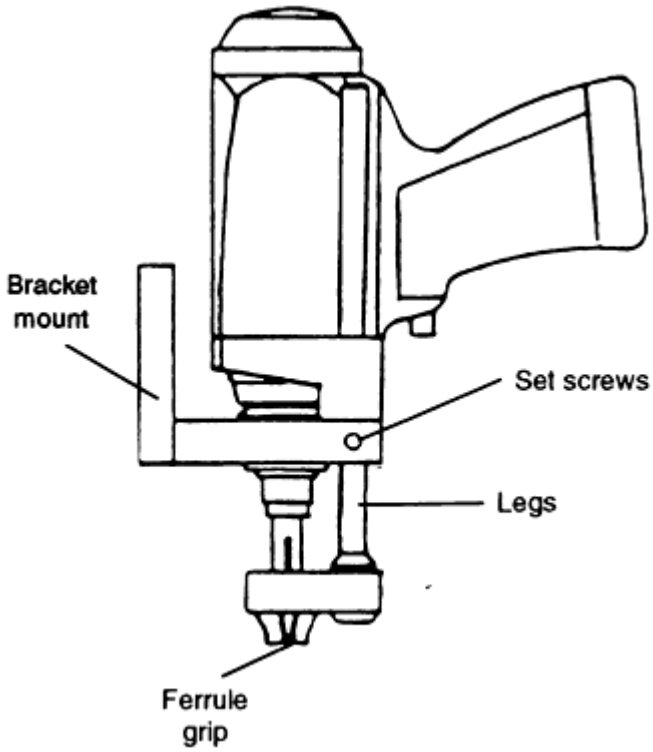

FIG. 14 INEXPENSIVE METHOD OF MOUNTING PORTABLE HAND GUN TO MACHINE SLIDE OR DRILL PRESS TO OBTAIN FIXED-POSITION ACCURACY

Other methods of ensuring verticality are to use a bushing-type template, a bubble level mounted on the rear of the gun, or a bipod foot arrangement, as shown in Fig. 15. With the stud and ferrule acting as one fixed point, the two bipod screws are adjusted to obtain perpendicularity. Vertical variations that are less than ±1° can be achieved with proper accessories and adjustments.

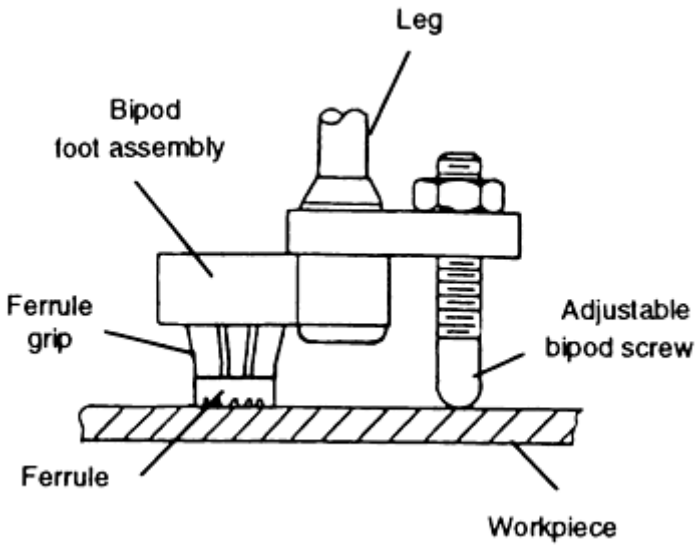

FIG. 15 USE OF AN ADJUSTABLE BIPOD FOOT ASSEMBLY TO PROVIDE THREE-POINT CONTACT, ENSURING PERPENDICULARITY OF STUD TO WORKPIECE

A wide range of accessories is available for welding studs of different lengths or for welding studs into areas with limited access. Two widely used special accessories are shown in Fig. 16 and 17. For unusual situations, the manufacturer should be consulted to suggest or, possibly, design stud-welding accessories.

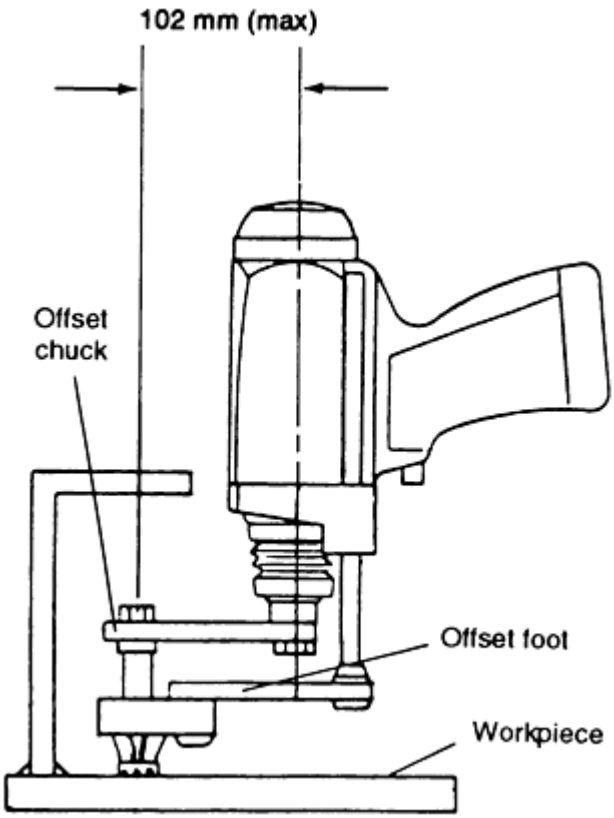

FIG. 16 TYPICAL OFFSET ASSEMBLY USED WHEN STUD ARC WELDED FASTENERS MUST BE WELDED BELOW AN OBSTRUCTION

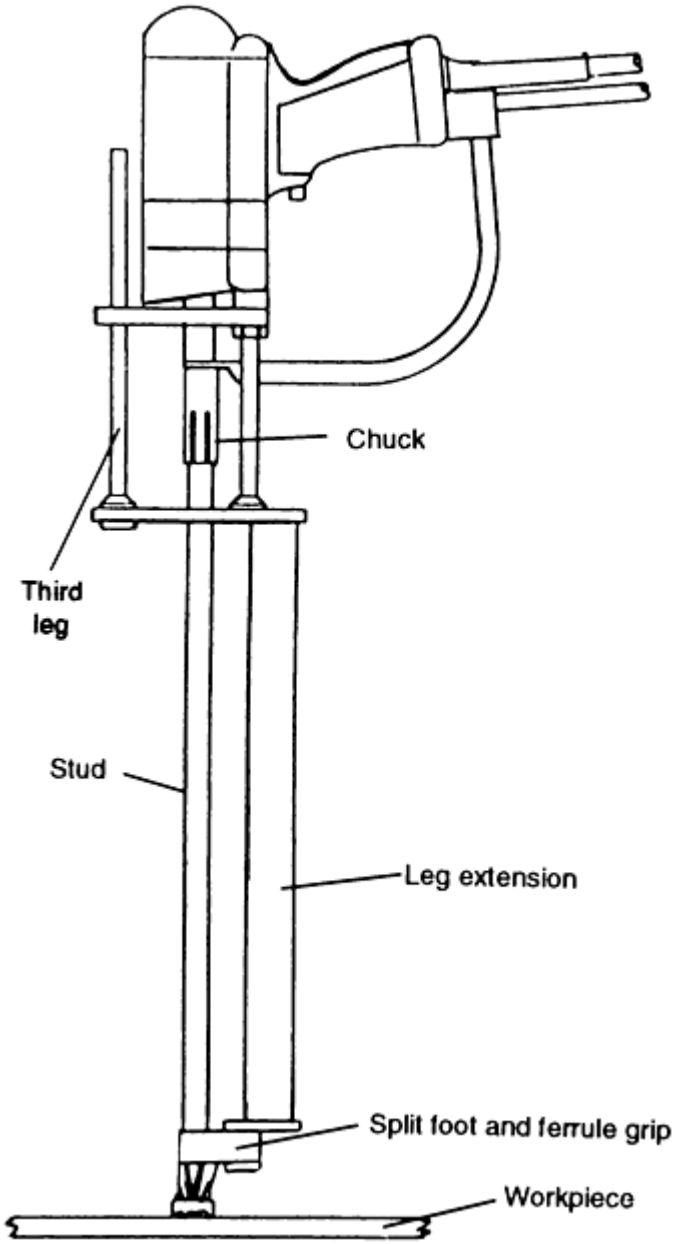

FIG. 17 TYPICAL LEG-EXTENSION ACCESSORY FOR WELDING LONG STUDS (UP TO 1.83 M, OR 6 FT). NOTE THE USE OF A SPLIT FOOT AND FERRULE GRIP; THE GUN DOES NOT HAVE TO BE STRIPPED THE FULL LENGTH OF THE STUD WHEN THE STUD IS WELDED.

Harry A. Chambers, TRW Nelson Stud Welding Division

Stud-Welding Quality Control, Qualification, and Inspection

Because of its broad use for many years and the relative simplicity of its applications, stud welding in the downhand position is considered to be a prequalified procedure, that is, it is only necessary to weld two studs satisfactorily in the downhand position to qualify both the process and the operator. The two qualification studs can be bend tested, torque tested, or tension tested. The physical test is satisfactory if no failure occurs in the weld or the heat-affected zone.

Stud-welding code requirements (for example, Ref 2 and 7) define the necessary tests for prequalified stud welding to the flat or down-hand position, as well as other positions. The limit on the flat position is defined as 0 to 15° slope on the

surface to which the stud is applied. Beyond 15°, a ten-stud test is required. Again, each of the ten studs in the nonflat position must be bend, tensile, or torque tested. Bend testing is 90° from the original axis, whereas torque and tension testing are conducted until failure. Failure must occur in the stud shank or in the workpiece material, not in the weld or the heat-affected zone. All failures require retesting. Satisfactory testing qualifies the welder and the process.

Typical bend, torque, and tensile testing setups are shown in Fig. 18, 19, and 20. Qualification records, including stud drawings, ceramic arc shield drawings (if used), weld settings, and position should be kept.

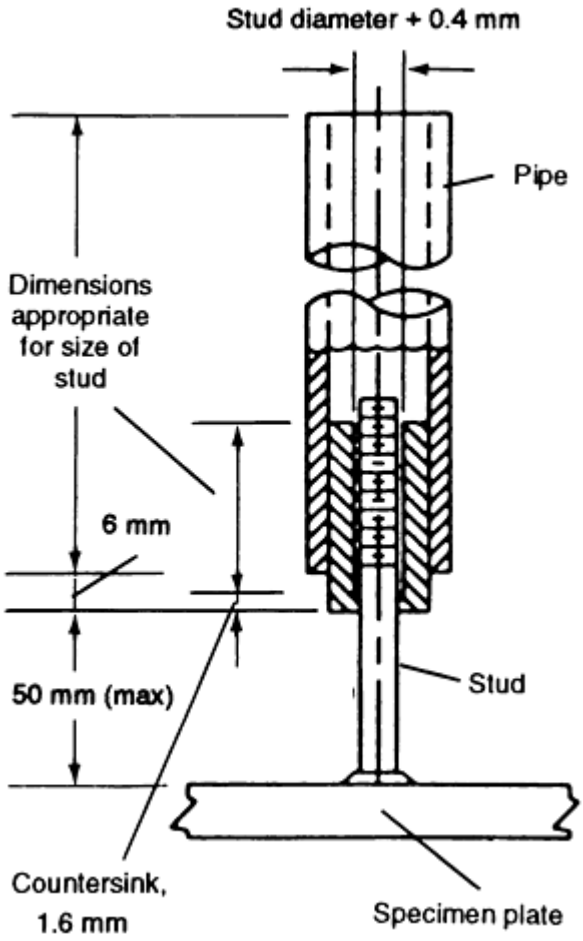

FIG. 18 TYPICAL BEND TESTING SETUP. STUDS THAT MUST UNDERGO APPLICATION QUALIFICATION SHOULD BE BENT 90° WITHOUT WELD FAILURE (15° FOR ALUMINUM STUDS). TESTING FOR PREPRODUCTION OR TESTING DURING PRODUCTION FOR INSPECTION PURPOSES REQUIRES BEND TESTING TO 30° FROM ORIGINAL POSITION (15° FOR ALUMINUM STUDS). FOR THREADED STUDS, TORQUE TESTING PER FIG. 19 SHOULD BE USED. SOURCE: REF 2

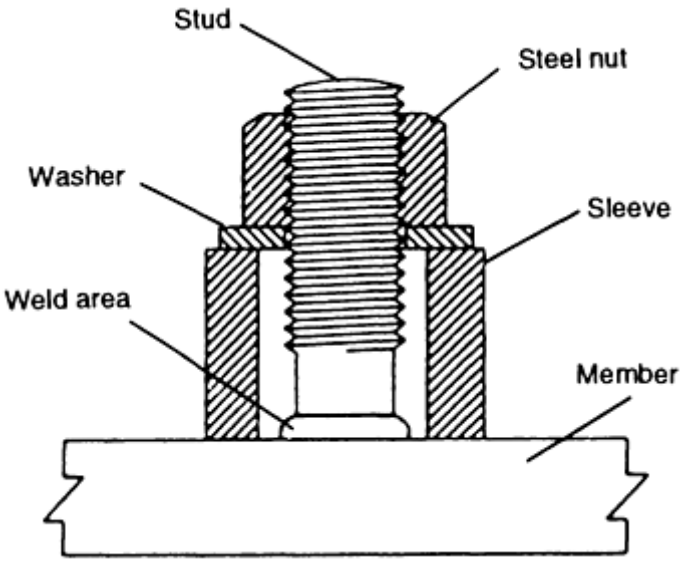

FIG. 19 TYPICAL TORQUE TESTING ARRANGEMENT. STUDS THAT MUST UNDERGO APPLICATION QUALIFICATION OR PREPRODUCTION TESTING SHOULD BE TORQUED TO DESTRUCTION WITHOUT FAILURE IN THE WELD. PROOF TORQUE TESTING DURING INSPECTION OF THREADED STUDS SHOULD BE APPLIED AT 60 TO 66% OF THE YIELD TORQUE LOAD FOR THE STUD SIZE TESTING. REFER TO TABLES 7, 8, AND 9. SOURCE: REF 2

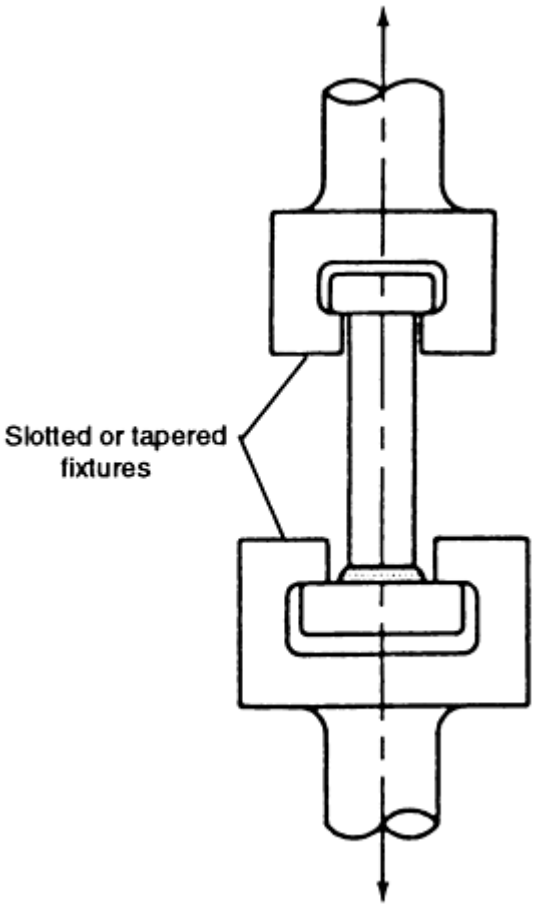

FIG. 20 TYPICAL TENSION TEST FIXTURE. FOR QUALIFICATION OF APPLICATION OR PREPRODUCTION TESTING, EITHER BEND OR TORQUE TESTING CAN BE SUBSTITUTED FOR TENSION TESTING.

Either two-stud or ten-stud testing should be conducted on a production piece or on a separate piece of the same type and thickness (±25%) of material that will be used in the application, in the same position in which the studs will actually be applied.

In addition to physical testing, the studs that are welded for qualification also must be visually inspected, whether there are two or ten. Visual inspection consists of verifying that a full 360 ° weld flash (fillet) is formed around the stud base. There should be no gaps or undercuts in the flash or in the wetted area. As mentioned previously, flash can be irregular in both height and evenness and it can contain shrinkage fissures or cracks. Because flash is expelled, not deposited, metal, it should not be subject to the usual inspection criteria for a weld fillet.

The final visual inspection should be a measurement of the after-weld length. With stud arc welding, the after-weld length of the stud will be shorter by the lengths shown in Table 3. A consistent after-weld length, combined with acceptable visual inspection and physical testing, are assurances of satisfactory welds. Figure 21 shows typical stud arc weld appearances for both acceptable and problematic welds.

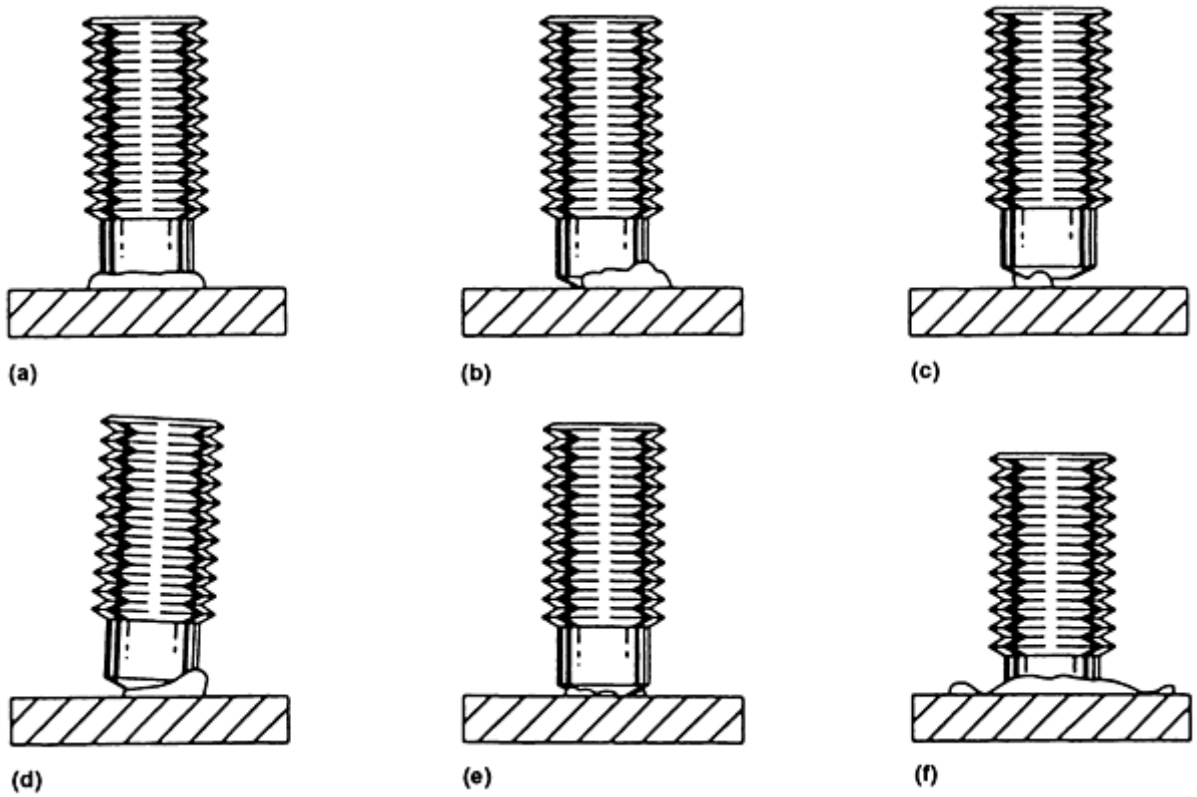

FIG. 21 STUD ARC WELD CHARACTERISTICS FOR SATISFACTORY AND UNSATISFACTORY WELDS. (A) SATISFACTORY; GOOD FLASH FORMATION, WETTING ENTIRE PERIPHERY OF STUD BASE. (B) UNSATISFACTORY; PLUNGE TOO SHORT, NOT ENOUGH MATERIAL ALLOWED FOR BURN-OFF. STUD MUST PROJECT AN ADEQUATE LENGTH BEYOND THE FERRULE. THIS CONDITION CAN ALSO BE CAUSED BY BAD GROUNDING PRACTICE. (C) UNSATISFACTORY; HANG UP CAUSED BY INADEQUATE ARC LENGTH LIFT OR BY MISALIGNMENT OF STUD, RESTRICTING FREE MOVEMENT. (D) UNSATISFACTORY; MISALIGNMENT OF STUD BY POOR GUN POSITION. (E) UNSATISFACTORY; COLD WELD, RESULTING IN NONUNIFORM OR INCOMPLETE FLASH AROUND STUD PERIPHERY. (F) UNSATISFACTORY; HOT WELD, WHERE MOLTEN MATERIAL IS EXPELLED VIOLENTLY FROM WELD, RESULTING IN POOR FLASH FORMATION.

Passing the two-stud preproduction or the ten-stud application qualification test approves the procedure and operator. Production stud welding is then allowed to proceed. However, at the start of each new production period, a two-stud test is again required before production can begin. Similarly, a change in stud diameter, equipment, settings, or operator requires requalification.

During production, welding inspection and testing should be used on a continuous basis to confirm acceptable quality. This can be done on a reasonable number of studs, depending on the welding conditions and stud appearance. After the visual inspection of all stud welds, physical testing of at least one weld per hundred is usually suggested. Any weld that does not show a full 360° flash or wetness should be tested. Welds without a full flash can be repair welded, but repaired welds are also required to be physically tested.

In the case of unthreaded studs, the quality inspection test can be to bend 15°. The studs can be straightened after testing, if required. Threaded studs can be subjected to a torque test to approximately 80% of the yield torque load, rather than a bend test. Failure in the weld or heat-affected zone is cause to reject the weld being tested. Failure also requires that the quantity of studs welded from the previous test to the present test be carefully inspected for weld deficiencies. Additional tests may be necessary to confirm weld quality.

If the quality inspection test studs must be straightened for end use, then they should be returned to the vertical position by using a bending tool. Continuous slow pressure should be applied during the straightening process.

Temperature at the time of stud welding and during stud testing is an influential parameter. Stud welding should not be conducted at temperatures below -18 °C (0 °F). When the temperature is below 0 °C (32 °F), one additional stud per hundred welded should be tested to verify weld quality. Below 10 °C (50 °F), welded studs should be tested using the bending tool, rather than by hammer testing. In colder welding temperature conditions, threaded studs should always be tested by torque, rather than by bending. Impact testing at low temperatures produces brittle failures. This is not a function of weld quality, but of the ambient temperature at the time of welding and testing. Data resulting from extensive tests conducted on studs welded and tested at various temperatures have shown that it is the temperature and manner of testing that influences the failure mode, rather than the temperature at the time of welding (Ref 8).

Another factor, besides temperature, that can affect weld quality is cleanliness of the weld area. Although stud arc welding does provide some cleaning action during welding, it is not sufficient to remove heavy contaminants. Coatings or rust on studs also can cause poor welds. Plating, except for a copper flash, nickel plating, or chromium plating, should be removed from the stud end prior to welding. This includes such materials as paint, zinc, and cadmium. Stud arc welded fasteners are usually capped during plating so that the weld end is left clean.

The plating or contaminant removal methods should be compatible with the base-material thickness and composition. For example, a heavy paint or rust cover on thick structural steel can be removed by grinding, needle scaling, sand blasting, or chipping, and the weld surface will still be acceptable for stud welding. Stainless steel, brass, aluminum, or other polished surfaces should be cleaned with appropriate solvents or other cleaning methods that will not destroy the material finish or contaminate the weld area. For example, a carbon-steel wire wheel or brush should not be used to clean stainless steel or aluminum base material.

Studs and ferrules should be kept clean and dry prior to welding. Although cold conditions will not adversely affect either, they should be protected from exposure to adverse weather conditions, high humidity, marine atmospheres, and other extremes. When ferrules absorb water, the steam generated during the welding process can cause very poor welds and excessive weld spatter. Ferrules exposed to moisture should be oven dried at a temperature between 101 and 120 °C (215 and 250 °F) for 2 h before use.

The condition of weld cables, connections, and ground clamps can affect weld quality. These items should be checked frequently and either repaired or replaced, so that the cables are not frayed, connections are tight and clean, and ground clamps are properly functioning. Ground clamps should be tightly connected to the workpiece or work platen and attached to areas that have been cleaned of all deleterious materials that would prevent good current flow.

References cited in this section

2. "STRUCTURAL WELDING CODE--STEEL," ANSI/AWS D1.1, SECTION 7, "STUD WELDING," AWS
7. "WELDED STEEL CONSTRUCTION (METAL ARC WELDING), STANDARD W59," CANADIAN STANDARDS ASSOCIATION
8. KENNEDY AND D.J. LAURIE, STUD WELDING AT LOW TEMPERATURES, *CAN. J. CIVIL ENG.*, VOL 7, 1980, P 442-455

Harry A. Chambers, TRW Nelson Stud Welding Division

Stud-Welding Safety Precautions

Any welding process can be dangerous if proper safety precautions are not followed. Equipment should be properly installed according to the directions of the manufacturer and maintained in good condition. Operators should be thoroughly trained in the use of the stud-welding process. They also should be familiar with the installation, operation, and maintenance procedures for the equipment being used.

Electrical shock is a potential cause of injury or death. Stud-welding systems should be properly installed and grounded using electrical connections made according to national (Ref 9) and local code guidelines.

Neither operators nor anyone else in the welding area should ever touch live electrical parts, or weld in wet areas, or wear wet gloves or clothing. In addition, all workers should ensure that they are insulated from shock.

All electric cables and connections should be kept in good condition. They should be inspected on a regular basis and frayed sections, broken insulation, or broken connectors should be repaired or replaced at once. Stud welding frequently uses long cable lengths, particularly on construction sites, where the cables are subject to abuse by towmotors, trucks, material storage, or foot traffic. It should be ensured that these conditions do not result in cable damage.

Although weld spatter and arc flash are minimal with the stud-welding process, they do occur and precautions should be taken. All combustible or volatile materials should be removed from the weld area so that sparks or spatter cannot reach them. Gas cylinders should be stored and secured properly and checked to ensure that they do not contact any electrical cables in the welding circuit. Proper protective clothing should be worn, including boots, aprons, and gloves, as necessary. Eye protection is always necessary. Eye glasses with spectacle frames, side shields, and lenses with shade number three absorption filters should be worn by the operator at all times (Ref 10). Helpers or workers within 1.5 m (5 ft) of the weld area also should wear clear safety glasses with side shields. Fire-suppression equipment should be available in or adjacent to the weld area for immediate use in emergencies.

Ventilation of the welding area is necessary. Fumes from welding and cleaning materials, such as solvents, as well as paints, epoxies, and galvanizing or other coatings, can be harmful. Ventilation can be either forced or natural, depending on the job conditions. Material suppliers should provide material safety data sheets on any items being used in the welding area, and proper precautions for potentially dangerous contents should be followed.

Pinch points where fingers or hands can be caught should be avoided during material handling or where moving parts are involved in the welding process.

The instructions of the manufacturer should be followed when maintaining and servicing the stud-welding equipment. If possible, all electric supplies should be disconnected and locked out during maintenance or troubleshooting work.

Finally, certain welding operations produce elevated noise levels during the weld cycle. Operators and other workers near the equipment should use hearing protection that can adequately protect them, in accordance with Ref 11.

References cited in this section

9. "NATIONAL ELECTRICAL CODE" NFPA-70, NATIONAL FIRE PROTECTION ASSOCIATION
10. "SAFE PRACTICE FOR OCCUPATION AND EDUCATIONAL EYE AND FACE PROTECTION," Z87.1, ANSI
11. "WELDING, CUTTING, AND BRAZING," STANDARD 29CFR, PART 1910, OCCUPATIONAL SAFETY AND HEALTH ADMINISTRATION

Harry A. Chambers, TRW Nelson Stud Welding Division

References

1. "RECOMMENDED PRACTICES FOR STUD WELDING," ANSI/AWS C5.4, AWS
2. "STRUCTURAL WELDING CODE--STEEL," ANSI/AWS D1.1, SECTION 7, "STUD WELDING," AWS
3. "STRUCTURAL WELDING CODE--ALUMINUM," ANSI/AWS D1.2, AWS
4. "STRUCTURAL WELDING CODE--STEEL," ANSI/AWS D1.1, SECTION 7, "STUD WELDING," FOOTNOTE 27, AWS
5. "STRUCTURAL WELDING CODE--STEEL," ANSI/AWS D1.1, SECTION 7, "STUD WELDING," PARAGRAPH 7.6, AWS
6. W.A. BAESLACK, G. FAYER, S. REAM, AND C.E. JACKSON, QUALITY CONTROL IN ARC STUD WELDING, *WELD. J.*, NOV 1975, P 789-798
7. "WELDED STEEL CONSTRUCTION (METAL ARC WELDING), STANDARD W59," CANADIAN STANDARDS ASSOCIATION
8. KENNEDY AND D.J. LAURIE, STUD WELDING AT LOW TEMPERATURES, *CAN. J. CIVIL ENG.*, VOL 7, 1980, P 442-455
9. "NATIONAL ELECTRICAL CODE" NFPA-70, NATIONAL FIRE PROTECTION ASSOCIATION
10. "SAFE PRACTICE FOR OCCUPATION AND EDUCATIONAL EYE AND FACE PROTECTION," Z87.1, ANSI
11. "WELDING, CUTTING, AND BRAZING," STANDARD 29CFR, PART 1910, OCCUPATIONAL SAFETY AND HEALTH ADMINISTRATION

Stud Arc Welding

Harry A. Chambers, TRW Nelson Stud Welding Division

Selected References

- "DESIGN AND APPLICATION HAND BOOK FOR LIGHT GAUGE METALWORKING," PUBLICATION CD-92, TRW NELSON STUD WELDING DIVISION, 1992
- "INDUSTRIAL DESIGN DATA--NELSON STUD WELDING PROCESS," PUBLICATION MB-12-86, TRW NELSON STUD WELDING DIVISION
- "SAFETY IN WELDING AND CUTTING," ANSI/AWS Z49.1, AWS
- T.E. SHOUP, "STUD WELDING," BULLETIN 214, WELDING RESEARCH COUNCIL, APRIL 1976
- "TOOLING TECHNIQUES FOR STUD WELDING," TRW NELSON STUD WELDING DIVISION
- STUD WELDING, CHAPTER 9, *WELDING HANDBOOK*, 8TH ED., AWS, 1990

Capacitor Discharge Stud Welding

Richard L. Alley, American Welding Society

Introduction

CAPACITOR DISCHARGE STUD WELDING is a stud arc welding process in which the tip of the stud melts almost instantly when energy stored in capacitors is discharged through it. The three basic modes of capacitor discharge (CD) stud welding are initial-gap welding, initial-contact welding, and drawn-arc welding. Figure 1 shows current-versus-time curves for the three process variations.

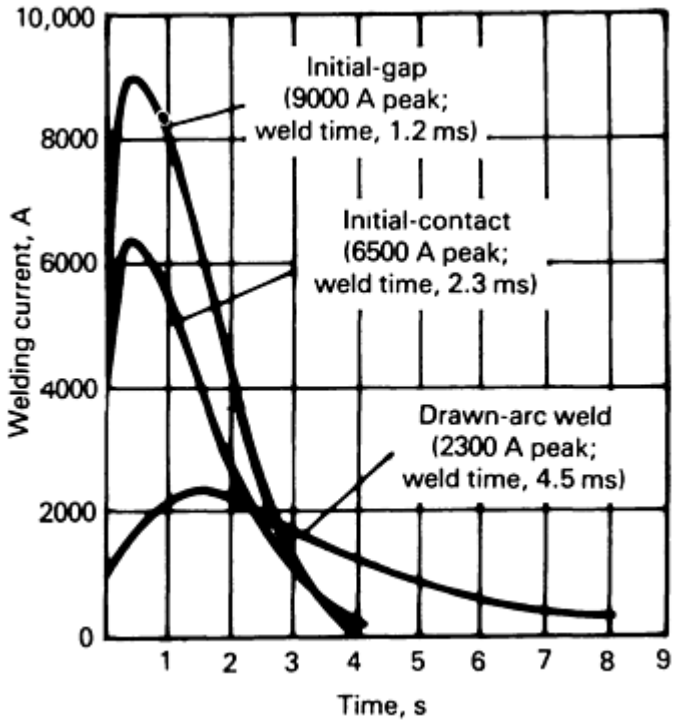

FIG. 1 TYPICAL CURRENT-VERSUS-TIME CURVES FOR THE THREE CD STUD WELDING METHODS. SOURCE: REF 1

The initial-gap mode (Fig. 2) is begun with the stud held away from the work surface by the welding head. At the beginning of the weld cycle, the stud is forced against the work surface, melting the tip, the face of the stud, and the adjoining work surface upon contact with the work surface. The weld is completed using the gun forces (i.e., spring pressure or air pressure) to plunge the stud into the molten materials, forming a strong welded bond between the stud and the work surface. The weld cycle time (Fig. 1) for this process is from 4 to 6 ms, and the penetration of the weld zone into the work surface is normally from 0.10 to 0.15 mm (0.004 to 0.006 in.).

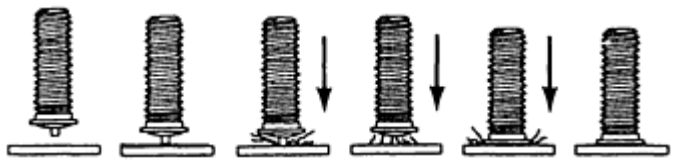

FIG. 2 INITIAL-GAP CD STUD WELDING. SEE TEXT FOR EXPLANATION. SOURCE: REF 1

The initial-contact mode (Fig. 3) begins with the weld stud in contact with the work surface. The weld cycle is initiated with a surge of current that disintegrates the weld tip, thus melting the stud face area and the work surface that it immediately contacts. The stud is forced into the molten material, forming a strong homogeneous weld. This process has a weld cycle time of approximately 6 ms, much like the gap process.

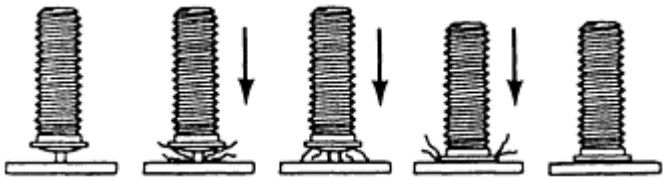

FIG. 3 INITIAL-CONTACT CD STUD WELDING. SEE TEXT FOR EXPLANATION. SOURCE: REF 1

The drawn-arc mode (Fig. 4) begins with the stud in contact with the work surface. When the weld cycle is initiated, a current surge is applied to the weld tip and the stud is retracted from the work surface, drawing an arc that melts the face of the stud and the work surface directly beneath it. The stud is then plunged into the molten pool of material, forming a welded connection. The weld cycle time for this process is longer than for the other two processes, and the heat-affected zone (HAZ) is thicker than it is in the preceding two processes.

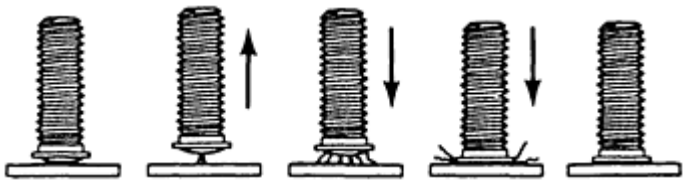

FIG. 4 DRAWN-ARC CD STUD WELDING. SEE TEXT FOR EXPLANATION. SOURCE: REF 1

Advantages and Disadvantages. A major reason for using the CD stud welding process is that it provides a strong welded fastener with either a minimum or no reverse side marking of the work material. Another reason is that it is cost effective, especially for small-diameter fasteners. This process also allows fasteners to be welded to very thin sections of work material, as well as to thick sections (as thick as necessary), with reliable results. Furthermore, the process allows the welding of many dissimilar material combinations, such as aluminum studs to zinc die castings. The disadvantages of using the CD process are the limited stud diameters available and the fact that the work surface must be clean of mill scale, dirt, oxidation products, and oil.

Reference

1. R.L. O'BRIEN, ED., *WELDING HANDBOOK,* 8TH ED., VOL 2, AWS, 1991, P 317-323

Capacitor Discharge Stud Welding

Richard L. Alley, American Welding Society

Applications

The CD process is normally used for fastener sizes of 4-40 through $\frac{1}{4}$-20, with lengths from 6.4 to 38.1 mm ($\frac{1}{4}$ to 1.5 in.). Although there are limited uses of $\frac{5}{16}$-18 and $\frac{3}{8}$-16 diameter studs in special applications, only the more-common

stud diameters will be considered in this article. The work material thickness can typically range from 0.25 mm (0.010 in.) to as thick as the application requires. The determining factors for making successful welds are the stud diameter, the materials being used, the strength required, and the amount of allowable reverse side marking. See Table 1 for guidance on the expected strength parameters.

TABLE 1 STANDARD CAPACITOR DISCHARGE STUD FASTENER LOAD STRENGTHS

STUD MATERIAL	STUD SIZE	MAXIMUM FASTENING TORQUE[(A)]		ULTIMATE TENSILE LOAD		MAXIMUM SHEAR LOAD	
		n · m	lbf · in.	kn	lbf	kn	lbf
LOW-CARBON COPPER-FLASHED STEEL	6-32	0.7	6	2.2	500	1.7	375
	8-32	1.4	12	3.4	765	2.6	575
	10-24	1.6	14	4.3	960	3.2	720
	$\frac{1}{4}$-20	4.9	43	7.8	1750	5.8	1300
	$\frac{5}{16}$-18	8.1	72	12.9	2900	9.8	2200
	$\frac{3}{8}$-16	11.9	106	19.1	4300	14.6	3250
STAINLESS STEEL (TYPE 304)	6-32	1.1	10	3.5	790	2.6	590
	8-32	2.3	20	5.6	1260	4.1	940
	10-24	2.6	23	6.8	1530	5.2	1150
	$\frac{1}{4}$-20	8.5	75	12.8	2880	9.6	2160
	$\frac{5}{16}$-18	14.2	126	16.7	3750	12.5	2800
	$\frac{3}{8}$-16	20.0	186	21.6	4850	16.0	3600
ALUMINUM ALLOY (5000 SERIES)	6-32	0.40	3.5	1.7	375	1.0	235
	8-32	0.85	7.5	2.6	585	1.6	365
	10-24	1.13	10	3.3	735	2.0	460
	$\frac{1}{4}$-20	4.5	40	6.0	1360	3.8	850
	$\frac{5}{16}$-18	7.9	70	10.2	2300	6.2	1400
	$\frac{3}{8}$-16	9.1	81	15.1	3400	9.3	2100
	$\frac{1}{2}$-13	15.8	140	25.0	5500	13.4	3000
BRASS (70-30 AND 65-35)	6-32	0.9	8	2.7	600	1.7	390
	8-32	1.8	16	3.8	860	2.5	560
	10-24	2.09	18.5	4.6	1040	3.0	680
	$\frac{1}{4}$-20	6.9	61	8.7	1950	5.7	1275
	$\frac{5}{16}$-18	11.5	102	14.6	3280	9.5	2140
	$\frac{3}{8}$-16	16.9	150	21.4	4800	14.1	3160

(A) THESE VALUES SHOULD DEVELOP FASTENER TENSION TO SLIGHTLY LESS THAN YIELD POINT AND SHOULD BE USED ONLY AS A GUIDE; BASIC SPECIFICATIONS SHOWN ABOVE COVER TYPICAL MECHANICAL PROPERTY VALUES.

The stud and workpiece materials can be common low-carbon steel, stainless steel, or aluminum. Also used are medium-carbon steel, lead-free brass and copper, Inconel, titanium, René 41, zirconium, gold, silver, and platinum. Table 2 shows

some of the more popular combinations of materials. Various studs and plate materials can be combined, except when aluminum-base material is used.

TABLE 2 WELDING CAPABILITIES OF CAPACITOR DISCHARGE STUD FASTENERS

BASE MATERIAL	STUD MATERIAL			
	MILD STEEL (TYPES 1008, 1010)	STAINLESS STEEL (TYPES 304, 305)	ALUMINUM (5356, 6061)	BRASS (70-30, 65-35)
MILD STEEL (1006 THROUGH 1030)	EXCELLENT	EXCELLENT	. . .	EXCELLENT
MEDIUM-CARBON STEEL (1030 THROUGH 1050)	GOOD(A)	GOOD(A)	. . .	GOOD(A)
GALVANIZED SHEET DUCT OR DECKING	GOOD(A)	GOOD(A)	. . .	. . .
STRUCTURAL STEEL	GOOD(A)	GOOD(A)	. . .	EXCELLENT
STAINLESS STEEL (TYPES 405, 410, 430, AND 300 SERIES, EXCEPT 303)	EXCELLENT	EXCELLENT	. . .	EXCELLENT
LEAD-FREE BRASS, ELECTROLYTIC COPPER, LEAD-FREE ROLLED COPPER	EXCELLENT	EXCELLENT	. . .	EXCELLENT
MOST ALUMINUM ALLOYS OF THE 1000, 3000, 5000, AND 6000 SERIES(B)	. . .	. . .	EXCELLENT	. . .
DIE-CAST ZINC ALLOYS	GOOD(A)	GOOD(A)	EXCELLENT	GOOD(A)

(A) GENERALLY FULL-STRENGTH RESULTS, DEPENDING ON THE COMBINATION OF STUD SIZE AND BASE METAL.

(B) OTHER MATERIALS, SUCH AS 7000 SERIES ALUMINUM, TITANIUM ALLOYS, INCONEL, AND SO ON, CAN BE WELDED UNDER SPECIFIED CONDITIONS.

CD stud welding is used in many industries in a large variety of applications because it is one of the most versatile and reliable processes available. The food processing industry utilizes this process on stainless steel utensils and machinery, aluminum cookware, and appliances. The aerospace industry applies the process to aircraft engines, aircraft parts and instrument areas, and components for outer space vehicles. The appliance industry uses CD welding for its cabinets, trims, and other components. The building industry uses it for doors, facia, subassemblies, and other exposed finished areas. The insulation industry uses it in securing insulation to heating and air conditioning duct work, as well as on apparatus at power plants, schools, and other major buildings. The automotive industry uses the process to secure trim and various components to cars and trucks. The ship-building industry uses it in fabricating components in ship kitchens, in insulation applications aboard ship and in other areas where components and instruments must be secured. The electrical industry uses this process when securing components inside various controllers and equipment, as well as in trim parts for cabinets. The sign industry uses it on both structural and component members of large and small signs.

Capacitor Discharge Stud Welding

Richard L. Alley, American Welding Society

Equipment

The equipment used for CD stud welding can be either portable or stationary production-type units. The portable units consist of the basic controller that utilizes standard 110 V alternating current (ac) power input to charge the capacitors and a lightweight gun-shaped tool used for placing and welding the fasteners. The production-type units typically require

240/480 V ac three-phase incoming power and a compressed air supply. The production units are normally used for higher rates of productivity, close-tolerance work (down to ±0.13 mm, or 0.005 in.), critical reverse side marking requirements, automatic stud feeding, automatic feeding of the part to be welded, automatic location of the stud on the part, and exotic materials.

The production rate of portable equipment normally ranges from 4 to 6 studs/min, depending on the application. Material handling and other factors could cause this rate to be either slower or faster. The production rates for the permanent production equipment can range from 3 to 20 studs/min, depending on the application, special requirements, and tooling.

When the initial-gap or initial-contact modes of stud welding are used, welds are made on all materials without the use of shielding gases or ceramic arc shields. When using the drawn-arc mode while working with aluminum, a shielding gas would be necessary. This mode is also less flexible when working with exotic materials.

Personnel Responsibilities

The CD stud welding process is easy to operate and maintain. The operator must first ensure that his unit is connected to the proper incoming voltage. The operator then determines whether the weld gun is connected to the negative and the ground is connected to the positive. Straight polarity is used for welding in nearly all applications. The operator places a given diameter of fastener into the stud gun. The gun is then placed on the work surface. The operator closes the trigger of the gun and the welding process begins. After the welding process is completed, the operator lifts the gun off the welded stud.

The operator needs to inspect the welds to ensure that the settings were correct. The controller voltage, which is set according to the recommendations of the equipment manufacturer, depends on the material and diameter of the fastener to be welded, as well as on the thickness and type of base material being used.

There are also other parameters that should be considered. If it is desirable to reduce spatter and smoky conditions in the weld area, then wetting the weld area with a wetting agent just prior to making the weld is recommended. If a wetting agent is used, then it is best to add a few drops of liquid hand soap to a pint of plain water and to spray or brush the solution into the weld area. This will produce a clean weld with reduced, if not eliminated, spatter in the weld area. However, the noise of welding increases when a wet weld is made.

Weld inspection is normally done by bending the fastener by applying either a torque or tensile force to it. If a tensile force is applied, then care should be given to the diameter of the hole used to secure the plate material. A hole that is as small as possible should be used to accommodate the flange of the stud. If a large hole is used, the tensile factors may be reduced, because the plate material could yield prematurely. Prior to production welding, it is recommended that sample welds be made on similar materials and tested to destruction. During production, operators should visually inspect the welds periodically. If weld inconsistency occurs, the process should cease, and the cause should be determined and eliminated.

A common occurrence that contributes to inconsistency is movement of the plate material during the short weld cycle. This can occur when working with materials that are less than 3.2 mm (0.125 in.) thick. There should not be a gap between the workpiece and the backup material of the fixture or table being used. Proper fixtures and attention to their clamping system can alleviate this problem.

Reference

1. R.L. O'BRIEN, ED., *WELDING HANDBOOK*, 8TH ED., VOL 2, AWS, 1991, P 317-323

Capacitor Discharge Stud Welding

Richard L. Alley, American Welding Society

Selected References

• *RECOMMENDED PRACTICES FOR STUD WELDING*, C5.4-84, AWS, 1984

Plasma-MIG Welding

Ian D. Harris, Edison Welding Institute

Introduction

PLASMA-MIG WELDING can be defined as a combination of plasma arc welding (PAW) and gas-metal arc welding (GMAW) within a single torch, where a filler wire is fed through the plasma nozzle orifice. The process can be used for both welding and surfacing. The plasma-metal inert gas (MIG) welding process was invented at the Philips Research Laboratories in Eindhoven, Netherlands, around 1969 (Ref 1).

For descriptions of the PAW and GMAW processes, see the articles "Plasma Arc Welding," and "Gas-Metal Arc Welding" in this Section of the Handbook.

The principles of operation, in terms of equipment, are illustrated in Fig. 1. Separate power supplies are used for the PAW and the GMAW elements of the equipment. An arc is struck between the tungsten electrode and the workpiece in a similar fashion to that of a PAW system. The filler wire can be fed to the plasma arc, either with or without the GMAW arc established. Without power supplied to the filler wire, the system can be operated as a PAW system with concentric feed of filler wire. Later versions of the system incorporated an annular electrode to replace the offset tungsten electrode in the welding torch.

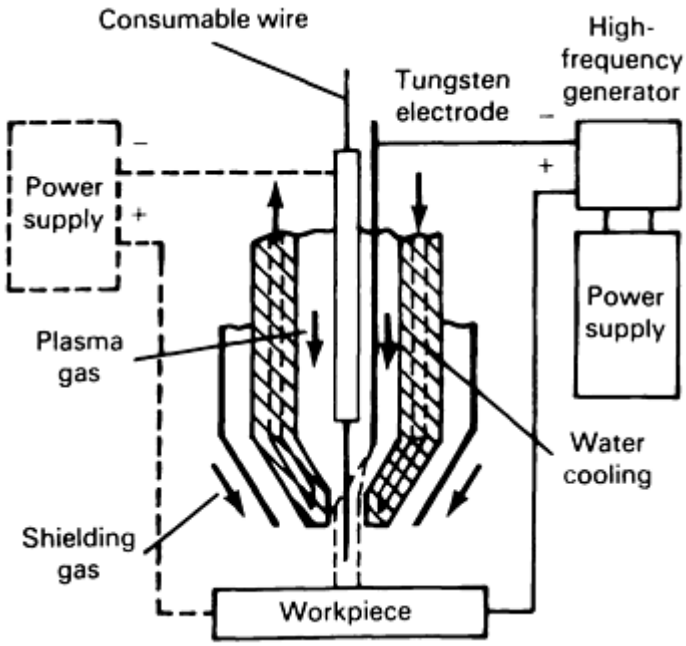

FIG. 1 SCHEMATIC OF PLASMA-MIG WELDING EQUIPMENT. SOURCE: REF 1

Current and Operating Modes. The equipment can be operated either with a single power source, effectively as a PAW system with concentric filler wire feed, or with two power sources, for the plasma-MIG operation.

The polarity of the tungsten electrode is direct current, electrode negative (DCEN), as is that of the GMAW part of the system. The heat of the plasma arc is sufficient to achieve good metal transfer stability for the GMAW element, despite the fact that when this process is used separately, it is almost always used in a direct-current, electrode positive (DCEP) mode. The filler wire is heated by the constricted plasma arc, as well as by the cathode heating of its own arc, and by resistance heating along the wire extension. Therefore, the melting and deposition rates of the wire are higher than the rates achieved by heating with either arc alone.

Metal transfer is governed not only by plasma streaming, but also by arc forces between the wire tip and the workpiece. Because the metal droplets are totally enclosed by the plasma stream, spray transfer takes place even though the GMAW element operates on negative polarity.

Advantages and Disadvantages. The advantages of the plasma-MIG process include deposition rates and joint completion rates that are higher than those of the conventional GMAW process. The independent control of the plasma arc and current to the filler wire leads to more control of metal deposition. This capability can yield improved productivity and good flexibility for controlling heat input and arc characteristics in both welding and surfacing operations. Good control of dilution is achieved by running the system without any power applied to the filler wire. Metal transfer stability is increased, compared to that of the conventional GMAW process, and results in lower spatter levels. The cleaning action of the plasma arc results in lower porosity in aluminum alloys, compared to that of the conventional GMAW process.

Disadvantages include the capital cost of two power sources (although there are systems that are designed to operate with one), the greater complexity of the torch, and the increased maintenance time and cost associated with this complexity. With two power sources, more welding parameters need to be set up, compared to the conventional GMAW process.

Equipment

As noted earlier, the basic equipment includes a power source for the plasma arc and a power source for the GMAW part of the system. A special torch incorporating both a contact tip for the GMAW element and a cathode for the PAW element is required. The initial design incorporated an offset tungsten electrode, as well as a concentric conduit and

contact tip for the delivery of the consumable wire (Fig. 1). A later design incorporated a concentric cathode for the plasma arc (Fig. 2).

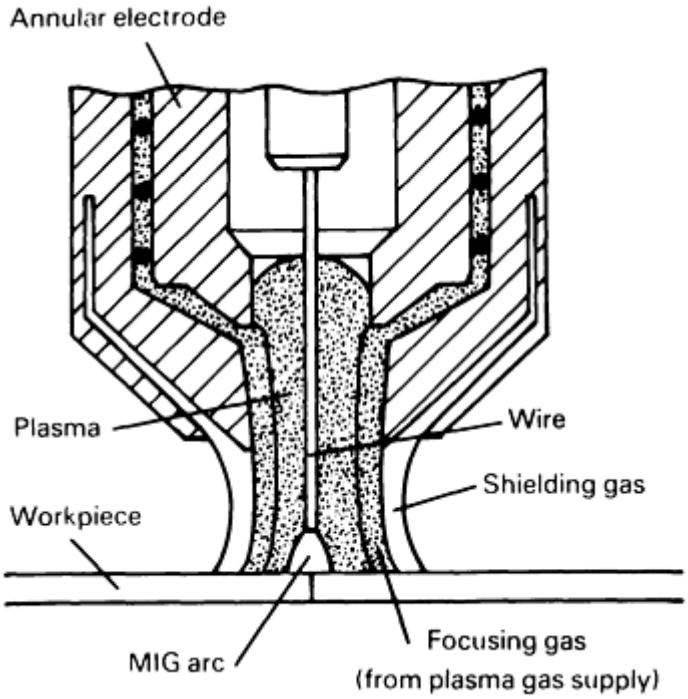

FIG. 2 SCHEMATIC OF MODERN PLASMA-MIG TORCH WITH ANNULAR PAW ELECTRODE AND ADDITIONAL (FOCUSING) GAS STREAM. SOURCE: REF 2

The plasma-MIG torch can be readily fitted to existing welding equipmentsuch as side beams and welding carriages, to replace the GMAW process in mechanized welding operations.

Power Sources. A constant-current power source with a high-frequency circuit to initiate the pilot arc is used for the plasma arc component of the system. The power source for the GMAW component can be used as a constant-voltage or a constant-current rectifier. Power sources have welding currents that typically range from 40 to 200 A for the plasma arc and from 60 to 300 A for the GMAW element at 100% duty cycle. However, equipment with welding currents up to 800 A is available and can be used for surfacing applications.

Welding Torches. A special torch with a concentric cathode for the plasma arc and a concentric conduit and contact tip for the delivery of the consumable wire is required (Fig. 2). A water-cooled copper alloy nozzle is used to constrict the arc and to form a collimated plasma jet that exits the nozzle orifice. A plasma orifice gas and a focusing gas from the same supply are used; the latter is delivered via channels between the plasma welding electrode and the constricting nozzle. The focusing gas results in greater arc constriction and arc stability and prolongs the life of the constricting nozzle by creating a boundary gas layer between the nozzle orifice and the plasma arc. The contact tip, plasma cathode, and the constricting nozzle are all directly water cooled to provide 100% duty cycle at the typical welding currents identified in the preceding section, "Power Sources."

Shielding Gases. Three shielding gases are utilized: one for the plasma (orifice) gas, one to provide additional arc constriction and arc stability, and one for supplementary shielding. The plasma gas and the focusing gas are usually argon, because an inert gas is required to prevent oxidation of the PAW electrode. The supplementary shielding gas can be argon, argon-oxygen, argon-carbon dioxide, or argon-hydrogen, depending on the nature of the workpiece being welded or, in the case of a surfacing operation, on the material being deposited. Argon is used when welding aluminum alloys, whereas argon-oxygen and argon-carbon dioxide are used when welding steels. Argon-hydrogen is used when welding stainless steels or when surfacing with them.

References

1. W.G. ESSERS, A.C.H.G. LIEFKENS, AND G.W. TICHELAAR, PLASMA-MIG WELDING, *PROC. CONF. ADVANCES IN WELDING PROCESSES,* THE WELDING INSTITUTE, 1971, P 216-219
2. J.D. SWART, PLASMA-MIG BOOSTS TANK TRAILER OUTPUT, *WELD. DES. FABR.,* FEB 1983, P 54-55, 59

Plasma-MIG Welding

Ian D. Harris, Edison Welding Institute

Procedure

Process Operating Procedure. The plasma arc is ignited using a pilot arc in a fashion similar to that of a PAW system. The main arc is transferred from the electrode to the workpiece and the plasma jet passes through the nozzle orifice. The system can be operated in this way, with the concentric cold wire being fed through the axis of the torch. A higher melting rate is achieved when power is applied to the wire through the contact tip and when both arcs are run simultaneously. The higher energy imparted to the wire by the plasma arc results in an increased wire deposition rate (Table 1). In this operating mode, deposition rates higher than those typical of the GMAW process can be achieved.

TABLE 1 COMPARISON OF FILLER WIRE MELTING RATES FOR PLASMA-MIG WELDING WITH AND WITHOUT THE GMAW ARC

Mild steel filler wire; plasma gas, argon; shielding gas, 89% Ar + 6% CO_2 + 5% O_2

PLASMA ARC CURRENT, A	PLASMA ARC VOLTAGE, V	FILLER WIRE CURRENT, A	MIG-ARC VOLTAGE, V	DIAMETER OF FILLER WIRE		MELTING RATE OF FILLER WIRE	
				mm	in.	g/min	oz/min
110	29	. . .	. . .	0.9	0.04	22	0.78
135	30	. . .	. . .	0.9	0.04	28	0.99
160	32	. . .	. . .	0.9	0.04	33	1.16
190	34	. . .	. . .	0.9	0.04	40	1.41
190	37	100	31	1.2	0.05	85	3.0
190	38	150	32	1.2	0.05	130	4.6

Source: Ref 1

Inspection and Weld Quality Control. Inspection requirements are similar to those of other arc welding or surfacing operations. Visual, ultrasonic, and radiographic inspection techniques are most appropriate. The dual action of the GMAW and plasma arcs results in weld quality that is sometimes higher than that achieved by the GMAW process alone. This is particularly true for aluminum alloys, because the cleaning action of the plasma arc often results in reduced porosity.

Quality control requires monitoring the welding parameters for both power sources, as well as monitoring the wire feed. In addition, the condition of the nozzle orifice (that is, the wear and concentricity of the orifice) should be monitored.

Troubleshooting. The relatively complex nature of the welding torch involves increased maintenance time. Erosion of the copper alloy nozzle orifice will cause a change in the arc shape and will affect the weld profile. Therefore, the nozzle should be checked periodically.

Reference cited in this section

1. W.G. ESSERS, A.C.H.G. LIEFKENS, AND G.W. TICHELAAR, PLASMA-MIG WELDING, *PROC. CONF. ADVANCES IN WELDING PROCESSES,* THE WELDING INSTITUTE, 1971, P 216-219

Plasma-MIG Welding

Ian D. Harris, Edison Welding Institute

Applications

Material Types. The plasma-MIG process is suitable for welding a wide variety of materials. The high heat energy supplied by the plasma and gas-metal arcs makes the process suitable for high-melting-point materials, such as tungsten and molybdenum. The most common application is welding aluminum sheet and plate. Wear-resistant steels are used with the process in hardfacing applications. Austenitic stainless steels, such as types 308, 309, and 347, as well as nickel alloys, such as alloy 625, are used in cladding applications. Both solid and flux-cored wires (Ref 3) can be employed for welding and surfacing, although most applications involve solid wires.

Industries. The plasma-MIG welding process has been used for the deposition of corrosion-resisting stainless steel and nickel-base alloys in the offshore industry, for the general fabrication of silos and tank trailers made from aluminum alloys (Ref 2), and for hardfacing applications in the excavation equipment industry, as well as the dredging and offshore industries.

Typical Components and Joints. The plasma-MIG process is suitable for welding of joints and for surfacing operations. The wide range of heat inputs available by choosing how to apply current to the consumable electrode provides additional flexibility for surfacing operations, compared to the range of heat inputs available with an external wire feed using the GTAW/PAW or the conventional GMAW process.

Single-V butt joints are commonly used for the plasma-MIG welding of plate. A full-penetration weld can be made in a single pass on a 9.5 mm ($\frac{3}{8}$ in.) thick mild steel plate when operating the plasma and gas-metal arcs simultaneously. This compares to three passes when just the PAW process is used. One would expect the same joint to require two or three passes for the conventional GMAW process.

When butt welding aluminum alloy sheet and plate in thicknesses ranging from 4.6 to 6.1 mm (0.18 to 0.24 in.), single-pass welds can be made at travel speeds that are more than twice as fast as when the GMAW process is used alone (Table 2). Lower porosity levels are achieved with the plasma-MIG process because of the cleaning action of the plasma arc. When using mild steel and stainless steel, the plasma-MIG process can make butt welds comparable to those made with the GMAW process alone at almost twice the travel speed (Table 2).

TABLE 2 COMPARISON OF WELDING SPEEDS FOR GMAW AND PLASMA-MIG WELDING OF ALUMINUM AND STEEL

PARAMETER	MATERIAL				
	ALMG4.5MN			STEEL	
	GMAW	PLASMA-MIG	PLASMA-MIG	GMAW	PLASMA-MIG
SHEET THICKNESS, MM (IN.)	4.6 (0.18)	4.6 (0.18)	5.1 (0.20)	4.1 (0.16)	4.1 (0.16)
WIRE DIAMETER, MM (IN.)	1.6 (0.063)	1.6 (0.063)	1.6 (0.063)	1.2 (0.047)	1.2 (0.047)
GMAW CURRENT, A	280-300	200	280	250	280
PLASMA CURRENT, A	. . .	200	200	. . .	200
WIRE FEED SPEED, M/MIN (IN./MIN)	8.1 (320)	10.9 (430)	10.9 (430)	5.1 (200)	11.4 (450)
WELDING SPEED, M/MIN	0.4 (16)	1.1 (43)	0.97 (38)	0.51 (20)	0.97(38)

(IN./MIN)					

Source: Ref 2

The hardfacing of dredging equipment with martensitic steel was made more productive by using the plasma-MIG process, rather than the conventional GMAW process. Higher deposition rates were achieved, resulting in reduced labor costs for the semiautomatic welding operation. Deposition rates of up to 20 kg/h (44 lb/h) can be achieved by plasma-MIG surfacing of mild steel with stainless steel flux-cored wires (Table 3).

TABLE 3 WELD SURFACING PARAMETERS FOR STAINLESS STEEL DEPOSITS ON MILD STEEL USING PLASMA-MIG WITH FLUX-CORED WIRES

	MIG WELDING CURRENT, A	MIG WELDING VOLTAGE, V	PLASMA WELDING CURRENT, A	PLASMA WELDING VOLTAGE, V	WELDING SPEED		DEPOSITION RATE		INNER WIRE STICK-OUT		DILUTION, %	FERRITE NO.
					mm/mi	in./min	kg/h	lb/h	mm	in.		
UNDILUTED WELD METAL	300	39	150	44	110	4.4	10	22	35	1.4	. . .	15, 12, 13
PZ 6400 (347) SURFACING	200	31	150	40	80	3.2	6.6	14.6	55	2.2	8.6	12
PZ 6410 (308) SURFACING	300	44	150	46	140	5.6	13	28.7	55	2.2	13.8	5.5
PZ 6415 (309) SURFACING	400	50	150	51	190	7.6	20	44	55	2.2	9.7	6.5

Source: Ref 3

References cited in this section

2. J.D. SWART, PLASMA-MIG BOOSTS TANK TRAILER OUTPUT, *WELD. DES. FABR.,* FEB 1983, P 54-55, 59
3. F. EICHHORN AND E. VAN GAEVER, ADVANTAGEOUS SURFACING WITH PLASMA-MIG USING CORED WIRES, *PROC. 1ST INT. CONF. SURFACE ENGINEERING,* THE WELDING INSTITUTE, 1986, P 99-110

Plasma-MIG Welding

Ian D. Harris, Edison Welding Institute

Personnel

Skill Level and Training. The plasma-MIG process can be used for semiautomatic, mechanized, or automated operation. It requires a skill level comparable to that of the conventional GMAW process, although additional parameters

need to be set for the plasma arc. Most welding and surfacing activities are carried out with mechanized equipment. When welding parameters are set, operation is similar to that of the GMAW process.

Health and safety issues are similar to those of other arc welding processes. Electric shock, eye protection, burns, ultraviolet radiation, and fume exposure are typical concerns. The plasma-MIG process generates more radiant heat than the conventional GMAW process.

Plasma-MIG Welding

Ian D. Harris, Edison Welding Institute

References

1. W.G. ESSERS, A.C.H.G. LIEFKENS, AND G.W. TICHELAAR, PLASMA-MIG WELDING, *PROC. CONF. ADVANCES IN WELDING PROCESSES*, THE WELDING INSTITUTE, 1971, P 216-219
2. J.D. SWART, PLASMA-MIG BOOSTS TANK TRAILER OUTPUT, *WELD. DES. FABR.*, FEB 1983, P 54-55, 59
3. F. EICHHORN AND E. VAN GAEVER, ADVANTAGEOUS SURFACING WITH PLASMA-MIG USING CORED WIRES, *PROC. 1ST INT. CONF. SURFACE ENGINEERING*, THE WELDING INSTITUTE, 1986, P 99-110

Resistance Spot Welding

Neville T. Williams, British Steel

Introduction

RESISTANCE SPOT WELDING (RSW) is a process in which faying surfaces are joined in one or more spots by the heat generated by resistance to the flow of electric current through workpieces that are held together under force by electrodes. The contacting surfaces in the region of current concentration are heated by a short-time pulse of low-voltage, high-amperage current to form a fused nugget of weld metal. When the flow of current ceases, the electrode force is maintained while the weld metal rapidly cools and solidifies. The electrodes are retracted after each weld, which usually is completed in a fraction of a second.

Spot welding is the most widely used joining technique for the assembly of sheet metal products such as automotive body-in-white assemblies, domestic appliances, furniture, building products, enclosures and, to a limited extent, aircraft components.

Many assemblies of two or more sheet metal stampings that do not require gas-tight or liquid-tight joints can be more economically joined by high-speed RSW than by mechanical methods. Containers frequently are spot welded. The attachment of braces, brackets, pads, or clips to formed sheet-metal parts such as cases, covers, bases, or trays is another common application of RSW.

Major advantages of spot welding include high operating speeds and suitability for automation or robotization and inclusion in high-production assembly lines together with other fabricating operations. With automatic control of current, timing, and electrode force, sound spot welds can be produced consistently at high production rates and low unit labor costs using semiskilled operators.

Most metals can be resistance spot welded if the appropriate equipment is used coupled with suitable welding conditions. This is particularly true for thin sheet or strip steel products, whether uncoated or coated.

Neville T. Williams, British Steel

Equipment

The equipment needed for RSW can be simple and inexpensive or complex and costly, depending on the degree of automation. Spot welding machines are composed of three principal elements:

- *ELECTRICAL CIRCUIT*, WHICH CONSISTS OF A WELDING TRANSFORMER, TAP SWITCH, AND A SECONDARY CIRCUIT
- *CONTROL CIRCUIT*, WHICH INITIATES AND TIMES THE DURATION OF CURRENT FLOW AND REGULATES THE WELDING CURRENT
- *MECHANICAL SYSTEM*, WHICH CONSISTS OF THE FRAME, FIXTURES, AND OTHER DEVICES THAT HOLD AND CLAMP THE WORKPIECE AND APPLY THE WELDING FORCE

Specifications for resistance welding equipment have been standardized by the Resistance Welder Manufacturers Association (RWMA), and specifications for controls are issued by the National Electrical Manufacturers Association (NEMA).

Resistance Spot Welding

Neville T. Williams, British Steel

Electrical Circuit

The transformer used in a direct energy resistance delivers the power to the workpiece by changing the input high-voltage, low-amperage, alternating current (ac) in the primary winding to a low-voltage, high-amperage current in the secondary winding. This system forms the basis of pedestal, or gun-type, welding machines where the output of the secondary transformer is applied directly to the welding electrodes. More complex secondary circuits are used in multiwelders.

To minimize the size and cost of multiwelders, transformers can be designed with two or more secondary circuits supplied from the same primary circuit. This design is achieved by using transformers in which the primary current is supplied to two or more separate secondary windings. Split or multiple secondary transformers are generally used to produce four or more welds at the same time. One controller is used for control of the timing and current supplied to the electrode, which means that it is not possible, under these circumstances, to achieve individual control or setting of the welding conditions for each pair of welding electrodes. Difficulties can arise in optimizing the necessary welding conditions to maximize the electrode life for each welding station under these conditions. In addition, the possibility exists for developing shunt currents, or an out-of-balance welding current, between each secondary circuit. Multiwelders make large use of single-welding and multiple-welding configurations based on direct, indirect, series, and push-pull secondary circuits (see Fig. 7 of the article "Procedure Development and Practice Considerations for Resistance Welding" in this Volume).

Single-Weld Configurations. Most pedestal and portable gun-welding machines employ direct welding, where the current flows directly through the welding electrodes and the workpiece to produce a single weld. In areas of difficult access, indirect welding may be necessary. Indirect welding is generally used when welding is carried out using either stationary or indexing welding guns and when access to the sheets being welded is limited to one side. In this case, the backing electrode generally consists of a large bar or platen, and the welding current flows from one side of the transformer secondary to the active electrode, through the welded area, and then along the platen/bar electrode or connecting jumper cable to the dummy electrode, which is connected to the other leg of the transformer secondary. Higher welding currents are generally necessary when using dummy welding guns, which can lead to a shorter electrode life. The extent to which larger currents are required depends largely on the distance between the welding electrode and the dummy return electrode. In a multiwelder, this distance can be either fixed or variable, depending on whether a

stationary or indexing head is used. Both types of welding heads can lead to losses due to stray current paths and extensive shunting of the current through jigs and fixtures. These factors need to be considered in any design concept for a multiwelder station.

Two-Weld Configurations. Because of the need to minimize the number of transformers and the overall size and cost of a multiwelder, it is necessary to utilize configurations whereby two welds are made in one stroke of an electrode. Parallel, series, or push-pull welding configurations are used for this purpose.

In parallel welding, two or more direct welds, usually closely spaced, are made simultaneously with all upper electrodes connected to one side of the transformer, and all bottom electrodes connected to the other side of the transformer. Parallel welding has the advantage of lower shunt currents, thereby allowing shorter interweld spacings to be used. However, if two or more circuits are fed from a common transformer secondary winding, the current in each circuit will not be equal unless the impedances of each circuit are identical. This is often difficult to achieve in practice, and the electrode life obtained can, therefore, be different for each of the electrode pairs connected to the same transformer.

Series and Push-Pull Welding. Two simultaneous welds can also be produced by means of series welding in which the secondary circuit is connected to two contoured electrodes that contact the workpiece from the same side, and a current backup bar/platen is used on the reverse side. Push-pull welding is also employed whereby either one or two welds are made, depending on the electrode configuration. In push-pull RSW, two transformers are used to form the circuit between the welding electrodes; such a configuration has advantages, particularly where a deep-throated machine is required. Such machines ordinarily require a large secondary loop because of the need for conducting the welding current around the large working area. Using a push-pull configuration, where the upper set of transformers matches the lower set, eliminates the need for long cable loops to the electrodes, resulting in a lower secondary impedance. A longer electrode life can be obtained in push-pull welding compared to series welding.

It should also be noted that current shunting between the electrodes occurs in both series and push-pull welding configurations, but to a lower extent in the latter. The magnitude of the shunt currents depends on interelectrode distance and the type of material being welded. In all cases, current shunting will lead to a lower electrode life when welding zinc-coated steels due to the need to use higher welding currents to compensate for the shunt currents (this can also lead to additional electrode sticking problems) and to the rapid falloff in weld size that occurs under conditions where current compensation is insufficient or nonexistent. To some extent, the effects of both high secondary circuit impedance and current shunting can be overcome by using a constant-current facility fitted into the welding machine control circuit, but there is a limit to the effectiveness of these controls in a production situation. In addition, direct current (dc) welding systems can be used in which secondary inductance/reactance effects are minimized. However, the effectiveness of using dc depends on the method used to develop the dc waveform and on the extent of the superimposed ac ripple on the dc waveform.

Secondary Impedance. The electrical characteristics of a spot welding machine are best defined in terms of their effect on the impedance of the secondary circuit. The latter is composed of two components:

- *REACTANCE*, WHICH IS DETERMINED PRIMARILY BY THE DEPTH AND HEIGHT OF THE THROAT OF THE MACHINE AND THE AMOUNT OF STEEL IN THE THROAT. ANOTHER CRITICAL FACTOR IS THE FREQUENCY OF THE APPLIED CURRENT.
- *RESISTANCE*, WHICH DEPENDS ON THE LENGTH AND CROSS SECTION OF THE CONDUCTORS. CONDUCTOR MATERIAL AND OPERATING TEMPERATURE NEED ALSO TO BE CONSIDERED.

Cables can be classified into three types: air-cooled jumper cables, water-cooled jumper cables, and kickless cables. In any application, it is necessary to ensure that the type and dimensions of cables are chosen to achieve the best balance between the total circuit resistance and the electrode life to be obtained with a multiple spot welder.

Machine Construction

Welding operations in highly automated production lines are based primarily on multiple spot welders and robotic cells. In addition, manual welding operations can be used to manufacture either subassemblies, which are fed into the main production/assembly lines, or, in many instances, finished products. These differing end uses require welding machines of varying designs and characteristics. RSW machines can be divided into three basic types:

- PEDESTAL-TYPE WELDING MACHINES
- PORTABLE WELDING GUNS
- MULTIPLE SPOT WELDING MACHINES INCORPORATING LIGHTWEIGHT GUN WELDING UNITS

Pedestal-type welding machines form the basis of most resistance spot or projection welding operations. Standard machines are either of the rocker arm type, as determined by the rocker action of the moving upper electrode arm, or stationary, direct-acting machines. The latter outnumber the former because rocker arm machines are difficult to align due to the movement of the electrode in an arc motion. As the electrode wears, various skidding actions can be created between the upper and lower welding electrodes, depending on the extent of the electrode wear. This can change the point at which the electrodes meet relative to the fulcrum point of the moving arm. If the electrodes meet at a point above the fulcrum point, they have a tendency to slide outward from the machine. On the other hand, if the electrodes meet on a line below the fulcrum of the moving arm, the electrodes show a tendency to slide inward toward the machine. These relative movements can be different between the top and bottom electrodes, a consequence of which is a reduction in electrode life, particularly if welding coated steels. Other advantages of direct-acting machines include a lower electrode assembly mass, faster "follow up" during welding, and a degree of rigidity that is impossible to obtain with an ordinary rocker arm machine. Press-type direct-acting machines have an upper electrode and welding head that move vertically in a straight line. The welding head is guided in bearings or guideways of sufficient proportion to withstand the offset loads imposed upon them. All of these factors tend to increase the electrode life obtained in a particular welding cell.

Portable welding guns are used in RSW when it is impractical or inconvenient to transport the work to the machine. The portable welding gun consists of water-cooled electrode holders, an air or hydraulic actuating cylinder, hand grips, and an initiating switch. The gun usually is suspended from an adjustable balancing unit, and the welding force is supplied by an air cylinder. Because of the high secondary losses of portable machines, transformers used in these machines have a secondary voltage two to four times as great as the voltage of transformers used in stationary machines of equal rating.

Welding current is transmitted between the transformer terminals and gun terminals through a secondary cable, usually of the low-impedance or kickless type. The reactance of this type of cable is near zero, which results in a high power factor and reduced kilovolt-ampere (kVA) demand. For safety reasons, the current initiating switch is usually operated at low voltage. Recent developments in encapsulated transformers and high-speed fail-safe devices enable the transformer to be integral with the welding gun. This results in lower secondary losses and is particularly preferred in robotic applications.

Gun welders typical of portable manually operated and robotic welding cells can be classified into two basic types:

- S-TYPE (SCISSORS)
- J-TYPE (DIRECT ACTION OR C/J TYPE)

Two important features that influence the performance of these types of welding guns are the rate of force buildup and the extent to which the arms of the gun deflect under load. These features characterize the welding gun in terms of rigidity and the mechanics involved in their operation. An S-type gun utilizes a lever action to transmit the force applied by the cylinder head to the welding electrodes. However, due to an unbalanced pivot point, the force measured at the electrodes is less than that applied at the cylinder. With J-type welding guns, the force applied by the pneumatic cylinder is transmitted directly to the welding electrode. The rigidity of the framework of the welding gun is characterized by the extent to which the electrode arms deflect on application of the electrode force. This is an important factor in determining weld quality and the amount of skidding that can occur between the two welding electrodes. It should be noted that extensive skidding can lead to elliptical welds and/or decreased electrode life.

Neville T. Williams, British Steel

Welding Electrodes

Materials for RSW electrodes should have sufficiently high thermal and electrical conductivities and sufficiently low contact resistance to prevent burning of the workpiece surface or alloying at the electrode face. In addition, the electrode should have adequate strength to resist deformation at operating pressures and temperatures. Because the part of the electrode that contacts the workpiece becomes heated to high temperatures during welding, hardness and annealing temperatures must also be considered. Electrode materials for RSW have been classified by RWMA and in International Standards Organization (ISO) standard ISO 5182.

When welding two sheets of thickness up to 3 mm ($\frac{1}{8}$ in.) using truncated cone-type electrodes, the electrode tip diameter should be determined from:

$$D_2 = \sqrt{t} \qquad \textbf{(EQ 1)}$$

where d_2 is the initial tip diameter (in mm) and t is the thickness (in mm) of the sheet in contact with the electrode. When using truncated cone electrodes, the initial or set-up weld diameter should be equal to the diameter of the electrode tip:

$$D = D_2 = 5\sqrt{t} \qquad \textbf{(EQ 2)}$$

where d is the weld diameter (in mm). Whenever welding two sheets of dissimilar thicknesses, the electrode dimensions and the required weld size should be specified appropriate to the thinner sheet thickness. In the case of three thicknesses, the second thinnest sheet should be used.

When using domed or pointed electrodes, Eq 1 may not apply and the electrode dimensions will depend on accessibility and flange width. In this case, the electrode tip dimensions and welding conditions should be chosen to give an initial weld diameter as specified in Eq 2. Where a pad or mandrel is used as the second electrode, its surface must be maintained to match the profile of the work.

During normal production, electrodes tend to mushroom leading to an increase in electrode tip size. According to trends in automotive practice and international standards, the diameter of at least one of the electrode tips should not normally be allowed to increase above a value that results in a reduction greater than 30% from the starting weld diameter during a production run. This is equivalent to an increase in the electrode diameter to 1.3*d*. When this diameter has been reached, the electrode should be replaced or redressed to its original size and contour.

Electrode shapes have been standardized by RWMA. Figure 1 shows the six standard face or nose shapes, identified by letters A through F. Electrodes with type A (pointed) tips are used in applications for which full diameter tips are too wide. Type D (eccentric, formerly called offset) faces are used in comers or close to upturned flanges. Special tools are available for dressing the electrode faces, either in or out of the welding machine.

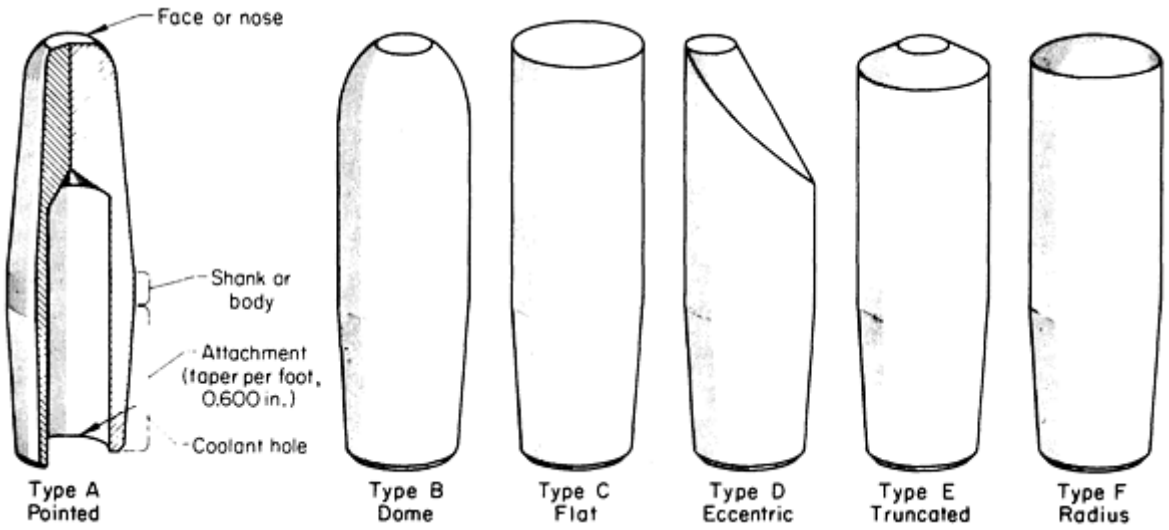

FIG. 1 STANDARD-RESISTANCE SPOT WELDING ELECTRODE FACE AND NOSE CONFIGURATIONS

Electrode Coolant Parameters. Generally, it is recommended that the water flow to the electrodes should be a minimum of 4 L/min (1.1 gal/min) for welding two uncoated steel sheets of thickness up to and including 3.0 mm ($\frac{1}{8}$ in.). Higher flow rates are recommended when welding coated steels. The internal water cooling feed tube should be arranged to ensure that the water impinges onto the back working face of the electrode. The distance between the back and the working face of the electrode should not exceed the values given in the appropriate ISO or RWMA standard. The inlet water temperature should not exceed 20 °C (70 °F), and the outlet temperature should not exceed 30 °C (85 °F). To maintain these temperature levels, the electrode cooling water supply should be independent of transformer and thyristor water cooling circuits. Separate water circuits should be used for both top and bottom electrodes.

Resistance Spot Welding

Neville T. Williams, British Steel

Weldability of Steel

Uncoated Steels. Low-carbon steel can be satisfactorily resistance spot welded using a wide range of time, current, and electrode force parameters. Practices recommended for spot welding SAW 1010 steel have been issued by the RWMA (Ref 1) and the American Welding Society (Ref 2). These data can serve as starting points for the establishment of optimum settings but may require modification, depending on the type of welding machine, the dynamic properties of the welding machine, the pneumatic characteristics, the characteristics of the secondary circuit, the electrode shape, and the material. Sufficient squeeze time should be chosen to enable the electrode force to build up to its preset value. For lightweight gun welders with limited force capability, the electrode force values are reduced up to 30% for sheet thicknesses greater than 1.6 mm ($\frac{1}{16}$ in.). The welding current needs to be adjusted accordingly. When welding sheets of dissimilar thickness, welding conditions may be based on the thinner sheet, or on the second thinnest sheet when welding three thicknesses.

In the case of high-strength low-alloy (HSLA) steels, up to 20% higher electrode force may be necessary. Welding currents may be reduced up to 20%, depending on the type of high-strength steel being welded. Pulse welding schedules may be necessary at the higher carbon equivalent levels and at sheet thicknesses greater than 2.0 mm ($\frac{5}{64}$ in.). The welding conditions required may depend greatly on the analysis of the steel because of differences in the resistivity of the various types of high-strength steel. For example, carbon content has the greatest effect on weldability of steels; weld

hardness increases rapidly with small increases in carbon content. This high hardness causes nugget interfacial tears and nugget deterioration. To obtain acceptable weld performance, carbon content should be kept below 0.10% + 0.3*t*, where *t* is the sheet thickness in inches. For materials above this range, postweld tempering may be necessary.

Low-carbon steels are generally considered to be spot weldable. These steels can be obtained from a number of suppliers with reasonable certainty of only minor variations in weldability. On the other hand, HSLA steels are sold on the basis of strength, with each steelmaker producing its own composition. Therefore, this variation in composition may cause variations in weldability, which the steel user must consider.

Specific alloying elements or combinations of elements can impart desired nugget properties in low-carbon or HSLA steels. The effects of particular elements are discussed below.

Phosphorus and Sulfur. Phosphorus and, to some extent, sulfur, are generally considered to promote nugget interface tearing. When the total content of phosphorus, sulfur, and carbon exceeds a critical value, spot weld interfacial failure is observed. This interfacial tearing during peel testing results in reduced current ranges and minimal lobe curve areas.

Titanium. Data on the effect of titanium on both hot-rolled and cold-rolled steel indicate that the spot weldability of these steels is not as good as that of the HSLA steels containing niobium and/or vanadium. Increasing titanium content generally reduces maximum button diameter, shear and cross-weld tensile strength, and welding current range. Titanium content should not exceed 0.18%, and the use of oversized electrodes and higher force may be required when welding titanium-bearing steels.

Nitrogen. In HSLA steels, nitrogen promotes interfacial nugget failure. Nitrogen appears to be more critical in unkilled cold-rolled steel. However, the sensitivity can be reduced by decreasing the nitrogen content or by combining the nitrogen with aluminum as in aluminum-killed steels.

Zinc-Coated Steels. The present trend in the automotive industry toward the use of larger amounts of zinc-coated steels in automotive assemblies demands that certain strict guidelines regarding the selection of equipment, choice of welding schedules, and maintenance procedures are rigidly followed.

Two basic types of alloy coating are available:

- ZINC-IRON (BOTH HOT-DIP AND ELECTRODEPOSITED)
- ELECTRODEPOSITED ZINC-NICKEL (SUPPLIED WITH OR WITHOUT AN ORGANIC PRIMER TOP COAT)

The available welding ranges for zinc-iron and zinc-nickel coated steels are similar to those for uncoated mild steel although displaced toward slightly higher currents (Fig. 2). When these steels are coated, it is essential that the film thickness not exceed 1 to 1.5 μm (40 to 60 μin.) in order to facilitate breakthrough of the film to enable current flow between the welding electrodes at the low secondary voltages typical of RSW machines.

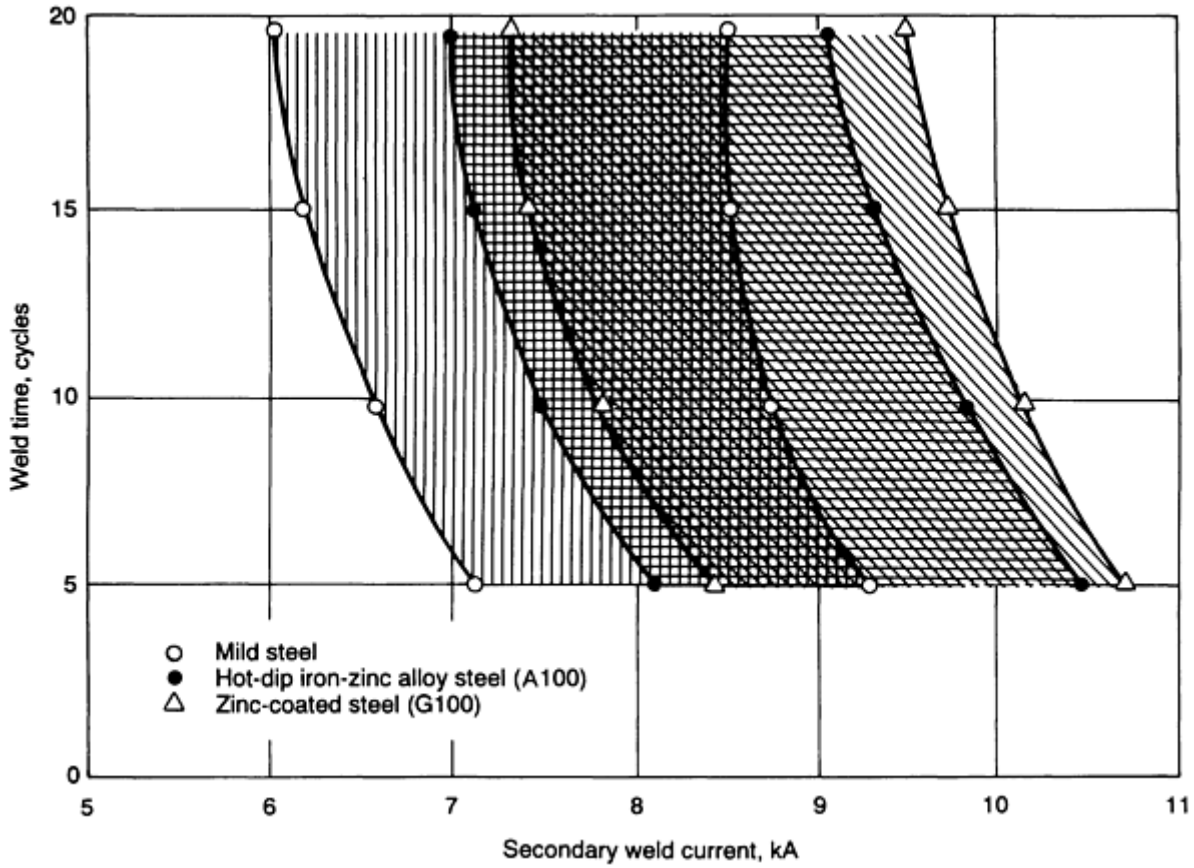

FIG. 2 PLOT OF WELD TIME VERSUS SECONDARY WELD CURRENT TO OBTAIN WELDABILITY LOBES FOR SELECTED 0.8 MM (0.03 IN.) THICK STEELS. ELECTRODE PARAMETERS: FORCE, 1.8 KN (0.20 TONF); TIP DIAMETER, 5.0 MM (0.20 IN.)

Welding conditions can be optimized easily when using pedestal-type welding machines; however, this may not be the case in body-in-white assembly where a combination of multiple spot welders and robotic cells are more commonly used. Such operations are susceptible to poor fit-up of parts, access problems, and electrode configurations that give rise to electrode skidding. Consequently, the welding parameters may need to be adjusted to compensate for such situations. In many instances, one welding gun is called on to weld a range of sheet thickness combinations or even a variety of material combinations in a particular part. Although a multi-program welding control can be used to adjust for the different welding currents necessary for the various combinations, the actual current values may not be optimum because, more often than not, a single compromise electrode force value has to be used.

In these circumstances, the electrode life obtained may be lower than that derived using optimized welding conditions. For example, the electrode life obtained can depend greatly on the type of welding gun used (Fig. 3) or the angle of approach of the electrode. For multiple spot welders, it is essential that all welding stations are balanced electrically and that the same air pressure is supplied to each station. Electrode shape and configuration, water cooling arrangements, and electrode dressing schedules need to be optimized. The last item is most important because satisfactory weld quality can only be provided when the necessary electrode condition and shape are maintained over a production run.

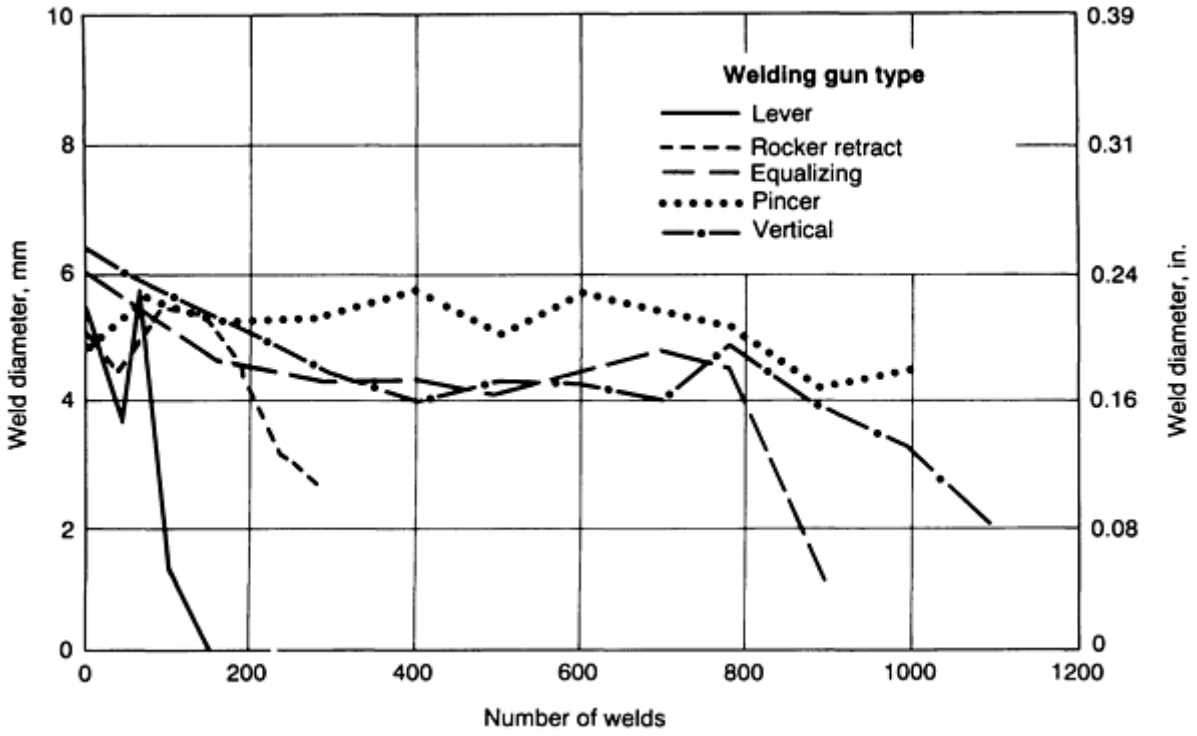

FIG. 3 EFFECT OF RSW ELECTRODE GUN TYPE ON ELECTRODE LIFE FOR SELECTED STEELS AND ALLOYS

References cited in this section

1. *RESISTANCE WELDING MANUAL,* 4TH ED., RESISTANCE WELDER MANUFACTURERS ASSOCIATION, 1989
2. *RECOMMENDED PRACTICES FOR AUTOMOTIVE WELD QUALITY--RESISTANCE SPOT WELDING,* ANSI/AWS D8.7-88, AMERICAN WELDING SOCIETY, 1988

Resistance Spot Welding

Neville T. Williams, British Steel

Weldability of Aluminum Alloys

Most of the commercial aluminum alloys produced in sheet form can be spot welded provided that suitable welding equipment is used. Because of the low electrical resistance of aluminum alloys, considerably higher welding currents are required relative to welding mild steel. In addition, the narrow plastic range between softening and melting means that welding forces, time, and current need to be closely controlled. For consistent weld quality, it is essential that the tenacious surface oxide films are removed by mechanical or chemical techniques prior to welding.

To minimize the likelihood of cracking or porosity in the weld, careful control of the electrode force is necessary. If the force is applied too soon, the welding current may be insufficient due to a premature loss of contact resistance. Thus, correct initiation of the force relative to the current is essential. Dual force schedules are frequently used; therefore, a low-inertia welding head can be beneficial because it allows a more effective buildup of force to its final level.

Because of the higher secondary currents required when welding aluminum alloys, direct current secondary rectified or frequency converter welding machines are favored, particularly if high-quality welds are required (such as in aircraft applications).

Resistance Spot Welding

Neville T. Williams, British Steel

References

1. *RESISTANCE WELDING MANUAL,* 4TH ED., RESISTANCE WELDER MANUFACTURERS ASSOCIATION, 1989
2. *RECOMMENDED PRACTICES FOR AUTOMOTIVE WELD QUALITY--RESISTANCE SPOT WELDING,* ANSI/AWS D8.7-88, AMERICAN WELDING SOCIETY, 1988

Projection Welding

Jerry E. Gould, Edison Welding Institute

Introduction

PROJECTION WELDING (PW) is a variation of resistance welding in which current flow is concentrated at the point of contact with a local geometric extension of one (or both) of the parts being welded. These extensions, or projections, are used to concentrate heat generation at the point of contact. The process typically uses lower currents, lower forces, and shorter welding times than does a similar application without the projections. Projection welding is often used in the most difficult resistance-welding applications because a number of welds can be made at one time, which speeds up the manufacturing process.

PW applications are generally categorized as being either embossed-projection welding or solid-projection welding. These variations are shown in Fig. 1 and 2. Embossed-projection welding is generally a sheet-to-sheet joining process, in which a projection is stamped onto one of the sheets to be joined. Then, resistance welding is conducted on a stack of sheets. Heat initially concentrates at the contact point and in the walls of the projection during resistance welding. Early in the process, the projection itself collapses back into the original sheet. However, the initial heating raises the local resistivity of the joint area, allowing continued resistance heating at this location. Weld development then proceeds in the conventional manner, by forming a fused weld nugget.

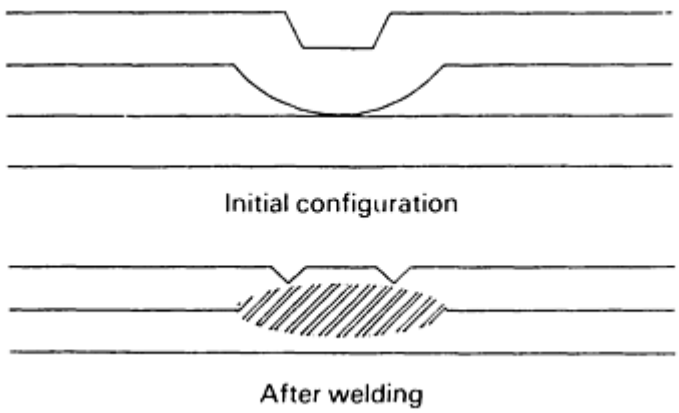

FIG. 1 TYPICAL STACKED CONFIGURATION FOR EMBOSSED-PROJECTION WELDING OF SHEET

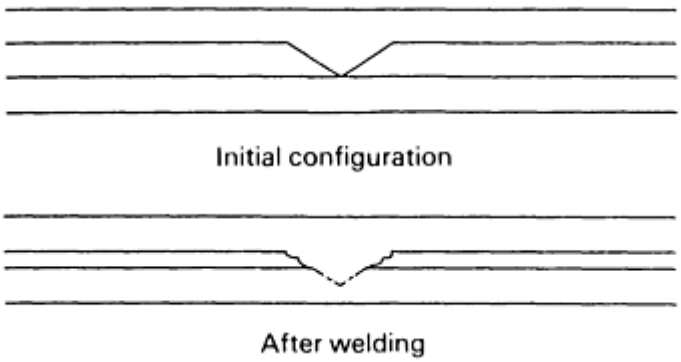

FIG. 2 TYPICAL CONFIGURATION FOR SOLID-PROJECTION WELDING

Solid-projection welding requires that the projection be forged onto one of the two components. Then, during resistance welding, the contact point and the projection itself experience preferential heating. In this case, the projection cannot simply collapse, as it does in embossed-projection welding. Rather, the projection collapses by penetrating the opposing material and by extrusion to the periphery. When compared with embossed-projection welding, the resulting joints are solid-state, rather than fusion, welds. The actual joints are caused by a combination of material forging and diffusion bonding, much like they are in resistance butt and flash butt welding.

Jerry E. Gould, Edison Welding Institute

Applications

Examples of projection welding are shown in Fig. 3. These applications, which range from sheet-to-sheet joints, to cross-wire welds, to annular attachments, to nut welds, to weld screws, include both embossed- and solid-projection types of welding. Specific welding examples, as well as material effects, are described below.

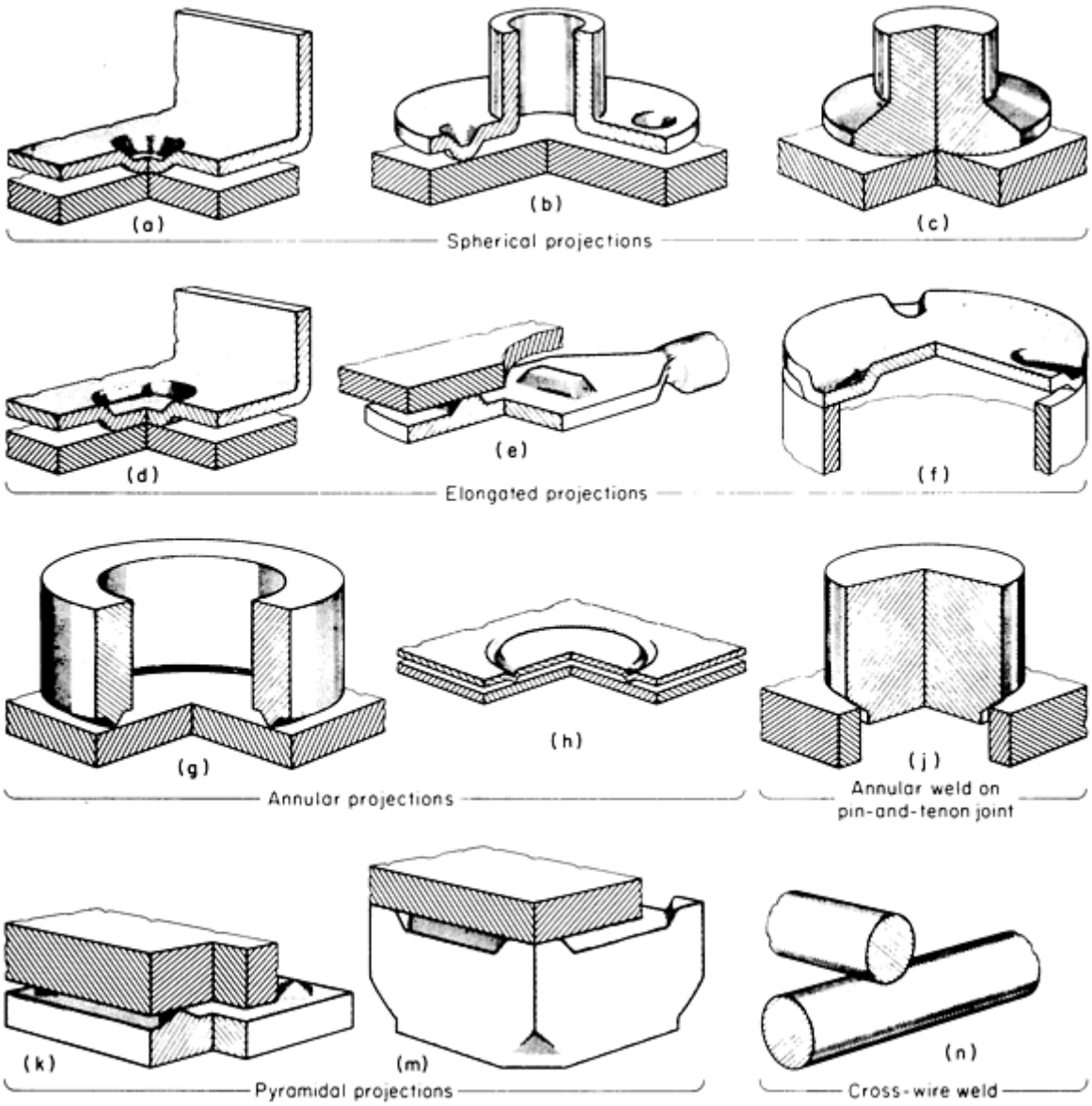

FIG. 3 DIFFERENT PROJECTION-WELDING CONFIGURATIONS

Embossed Projections

Typical embossed-projection weld configurations are shown in Fig. 3(a), (b), (d), and (h). The embossed-projection technique is primarily used for sheet-to-sheet applications. It does involve the additional expense of stamping the projections and ensuring that the electrodes are properly located over the projections. However, the ability of the projection to create highly localized joints allows this technique to extend the applications of resistance welding. Most notably, projection welding widely increases the allowable thickness mismatch associated with resistance welding.

Generally, resistance welding is considered adaptable to thickness variations of less than 3:1. However, with the addition of the projection, there is no limit to the difference in joinable thicknesses. Similarly, embossed-projection welding is highly adaptable to the joining of multiple-sheet stacks. The approach is similar in that the projections are used to localize heat at critical interfaces in the overall joint.

Another more recent use of embossed-projection welding is in applications where external marking must be minimized. This is a concern when a primer has been applied to one side of one of the sheets being joined. Because it is very effective at localizing heat at the interface, and because it uses shorter welding times, the PW process is more adiabatic and there is less residual heat that can damage outside surfaces. However, surface marking still does occur.

Solid Projections

A considerably wider range of solid-projection welding processes is commonly used in production applications. Annular projection welding, like embossed-projection welding, is commonly used to provide a highly localized joint and to minimize thermal damage to other parts of the structure. Common variations of solid-projection welding are described below.

Annular Projection Welds. One of the most common applications of solid-projection welding is to attach either tubular components or members with circular bases to flat or curved substrates. This is commonly accomplished by annular projection welding, in which the projection is machined onto the circular base or tubular section. Then, resistance welding is conducted to set the projection into the substrate. A typical weld geometry is shown in Fig. 3(g). Annular projection welding generally provides high-integrity joints and can be used for leak-tight applications.

Cross-wire welding is a variation of solid-projection welding in which the projection is formed by the contact point of two crossing wires. The geometry for cross-wire welding is shown in Fig. 3(n). Upon resistance welding, heat is maximized at the location of the wire-wire contact, and the parts are subsequently forged together. Depending on the application, either highly localized joints (minimal forging) or heavily forged joints can be made. In some applications, cross-wire welding is conducted at rates up to 30 welds/s.

Weld nuts represent an application of solid-projection welding in which the projections themselves occur as actual extensions of material from the nut. Typically, weld nuts contain 3, 4, or 6 of these projections, or feet, spaced around the nut periphery. During welding, all projections are attached simultaneously. Examples of weld nut geometries are shown in Fig. 3(k) and 3(m).

Edge-to-sheet welds are typically a cross between embossed- and solid-projection welding. They are used to attach the end of a sheet to the flat face of an opposing sheet (Fig. 3f). The projections for welding are generally stamped into the face of the attaching sheet. During welding, the projection does collapse locally back into the base sheet. However, bonding is strictly solid state, similar to that of other solid-projection welding processes.

Material Effects

Solid-projection welds are essentially strain-assisted diffusion bonds. Because the projections typically collapse at very high temperatures (generally, within several hundred °C of the melting point), diffusion bonding can occur within the very limited available time (usually, less than 1 s).

Not surprisingly, some of the material-related factors that affect diffusion bonding also affect solid-projection welding. The most notable of these is the ability of the metal to dissolve its own oxide. As a result, materials that do not energetically favor the solid solubility of oxygen, rather than the formation of the oxide at aluminum forging temperatures, will be relatively difficult to projection weld.

The strength-temperature relationship also affects projection weldability. Materials that maintain their strengths at relatively high temperatures permit substantial heating to occur before projection collapse. This heat then becomes available to promote diffusion after projection collapse. Premature collapse results in lower temperatures in which diffusion can occur and in reduced current density, which prohibits further resistance heating.

Bulk resistivity also plays a role in projection welding, but to a lesser degree. Increased bulk resistivity can reduce the effectiveness of the projection as a current concentrator. With increasing bulk resistivity, the tendency is for delocalized heating and general, rather than local, collapse of the projection. As a result, high-resistivity materials are more difficult to projection weld.

Mild steels and low-alloy, nickel-base alloys are ideal materials for projection welding, because they readily dissolve their own oxides and have adequate strength-temperature and resistivity properties. Stainless steels and higher-alloy nickel-base materials become slightly more difficult to weld, because of the formation of more-stable chromium and aluminum oxides, increased high-temperature properties, and higher resistivities.

Projection welding is commonly applied to copper and copper-base alloys. In many applications, projections are virtually required for resistance welding, because of the high conductivity of these materials.

On the other hand, aluminum and aluminum-base alloys are very difficult to projection weld. The aluminum oxide is so tenacious that solid-projection welding, in particular, is nearly impossible. In addition, it is very difficult to localize heat, because aluminum alloys soften at such low temperatures.

Conventional titanium alloys are also relatively difficult to projection weld. Although titanium readily dissolves its own oxide, its high resistivity and low forging temperature generally cause premature collapse of the projection.

Jerry E. Gould, Edison Welding Institute

Equipment

Resistance projection welding generally utilizes slightly modified resistance-welding equipment. Because the nature of projection welding is to direct current flow to the desired weld locations, there is considerably more flexibility in tooling. A specific example is spot welding that requires electrodes of specific sizes and shapes in order to localize current for welding.

Projection welding is typically done with large, flat electrodes. In most applications, tooling is simply shaped to match the contour of the part in the contacting location. Given the current-locating characteristic of projections, multiple projection welds can be made simultaneously.

Projection welding does require high compliance or the rapid response of the loading system. This is necessary because projection welding requires the collapse of a projection, which, in turn, requires some motion of the welding head. If the follow-up of the welding head is insufficient, then a local loss of force will occur, potentially causing catastrophic overheating of the contacting surfaces. Therefore, PW systems typically utilize "fast follow-up" heads (Fig. 4), which consist of relatively low inertia (mass) head components and mechanisms to maintain a nominally constant force. The head shown in Fig. 4 uses a relatively low volume diaphragm assembly and a spring to maintain this force on the components. Most systems, however, use either these low-volume diaphragm assemblies or springs to accomplish fast follow-up.

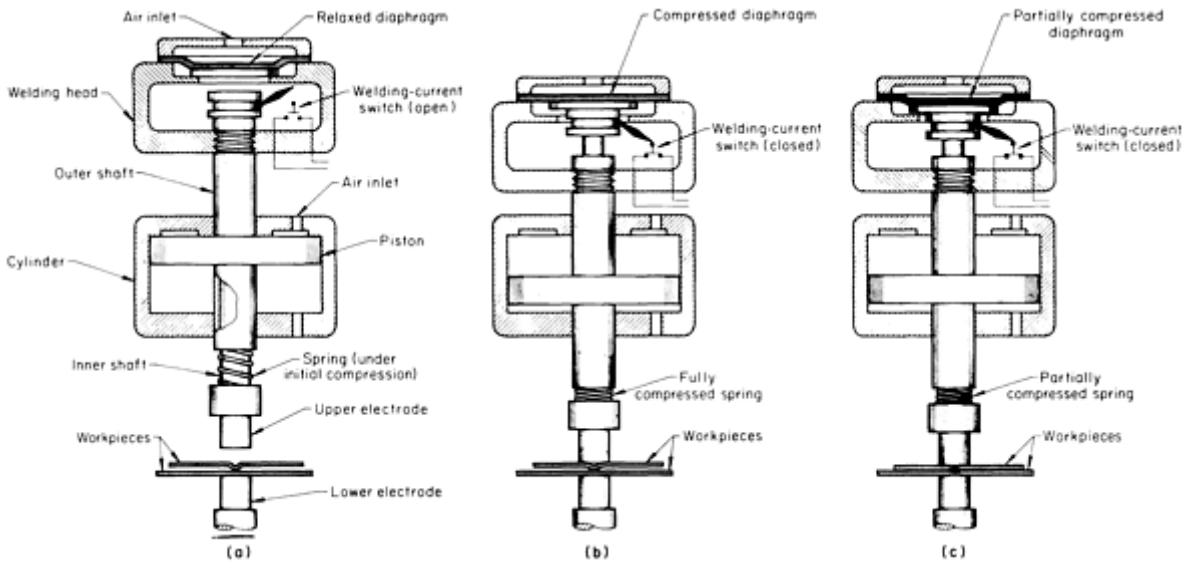

FIG. 4 TYPICAL FAST FOLLOW-UP (LOW INERTIA) HEAD FOR PROJECTION WELDING. (A) IN OPEN POSITION. (B) IN POSITION FOR SQUEEZING AND HEATING THE PROJECTION. (C) AT INSTANT OF PROJECTION COLLAPSE AND START OF NUGGET FORMATION

Personnel

Like all resistance welding processes, PW processes utilize basically automated equipment, which means that the expertise level to operate the equipment is relatively low. Generally, the skill levels and the health and safety issues are identical to those of conventional resistance spot welding. An area in which expertise is beneficial to hardware function and on-stream weld quality is operator attention to detail. Resistance welding is subject to variations in setup conditions, and projection welding may be extraordinarily sensitive to setup variations in situations where the placement of projections is critical.

With limited expertise, operators or supervisory staff can visually inspect the characteristics of the process and the welds themselves to identify improper setups, as well as maintenance needs. These quality assurance efforts, which fall under the auspices of total quality management or total quality joining, can be established with a minimum of on-line training and experience.

Projection Welding

Jerry E. Gould, Edison Welding Institute

Process Requirements

The types of hardware required for projection welding are analogous to those required for other resistance-welding processes.

The embossed-projection welding of heavy-gage, intermediate-gage, and thin-gage sheet, as well as joints of dissimilar thicknesses, is described below.

Heavy-Gage Sheet Steels. The projection welding of heavy-gage steels, which involves an embossed-projection welding process, has many of the characteristics of solid-projection welding particularly in its early stages, because of the thickness of the sheet.

In addition to defining the geometry of the projection, projection designs should provide an annular relief for projection material that is forged to the side during welding. Projection and die geometries for steels that range from 3.12 to 6.22 mm (0.123 to 0.245 in.) are shown in Table 1. The process requirements for forming these welds are given in Table 2. All welding schedules described in this article are single-pulse welding schedules.

TABLE 1 PROJECTION AND DIE GEOMETRIES FOR WELDING A RANGE OF HEAVY-GAGE STEELS

Data are for tool steel hardened to 50-52 HRC.

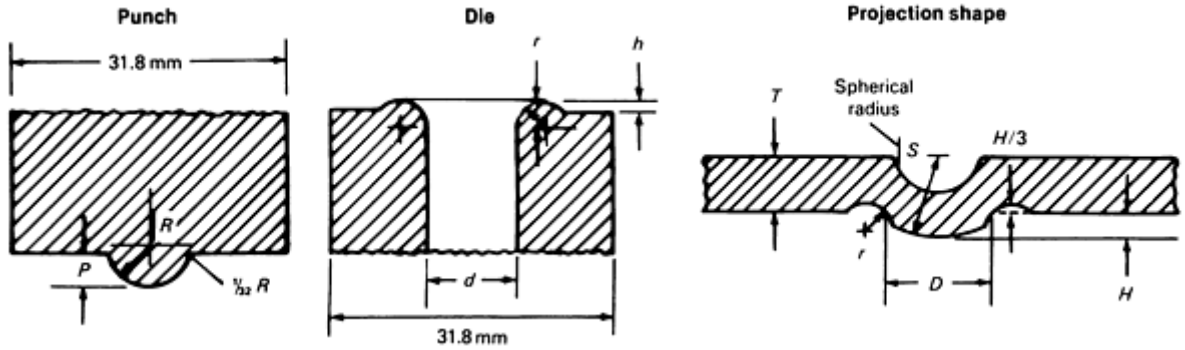

USS GAGE NO.	MATERIAL THICKNESS (*T*)		PROJECTION						PUNCH				DIE					
			HEIGHT (*H*), ±2%		DIAMETER (*D*), ±5%		RADIUS (*S*)		RADIUS (*R*), ±0.1 MM (±0.005 IN.)		HEIGHT (*P*), ±2%		HOLE DIAMETER (*D*), ±0.1 MM (±0.005 IN.)		RECESS RADIUS (*R*), *R* = *S*/3		RECESS HEIGHT (*H*), *H* = *H*/3	
	mm	in.	mm	in.	mm	in.	mm	in.	mm	in.	mm	in.	mm	in.	mm	in.	mm	in.
11	3.12	0.123	1.47	0.058	6.86	0.270	4.98	0.196	2.39	0.094	1.91	0.075	5.61	0.221	1.65	0.065	0.483	0.019
10	3.42	0.135	1.57	0.062	7.62	0.300	5.46	0.215	2.77	0.109	2.06	0.081	6.35	0.250	1.83	0.072	0.508	0.020
9	3.88	0.153	1.63	0.064	8.38	0.330	5.97	0.235	3.18	0.125	2.16	0.085	6.86	0.270	1.98	0.078	0.533	0.021
8	4.17	0.164	1.73	0.068	9.14	0.360	6.30	0.248	3.58	0.141	2.31	0.091	7.54	0.297	2.11	0.083	0.584	0.023
7	4.54	0.179	2.03	0.080	9.90	0.390	6.96	0.274	3.96	0.156	2.64	0.104	8.33	0.328	2.31	0.091	0.686	0.027
6	4.95	0.195	2.13	0.084	10.4	0.410	7.26	0.286	3.96	0.156	2.82	0.111	8.59	0.338	2.41	0.095	0.711	0.028
5	5.33	0.210	2.28	0.090	11.2	0.440	7.75	0.305	4.75	0.187	3.05	0.120	9.09	0.358	2.57	0.101	0.762	0.030
4	5.72	0.225	2.54	0.100	11.9	0.470	8.26	0.325	4.75	0.187	3.35	0.132	9.35	0.368	2.74	0.108	0.838	0.033
3	6.22	0.245	2.84	0.112	13.5	0.530	9.27	0.365	4.75	0.187	3.76	0.146	10.3	0.406	3.07	0.121	0.940	0.037

Source: Ref 1

TABLE 2 PROCESS REQUIREMENTS FOR PROJECTION WELDING OF A RANGE OF HEAVY-GAGE LOW-CARBON STEELS

USS GAGE NO.	THICKNESS [A][B]		PROJECTION SIZE				MINIMUM				ELECTRODE FORCE WELD		ELECTRODE FORCE FORGE		UPSLOPE TIME[D], CYCLES	WELD-TIME[D], CYCLES	WELDING CURRENT[C], A	TENSILE-SHEAR STRENGTH[F]	
			DIAMETER		HEIGHT		MINIMUM SPACING, CENTERLINE TO CENTERLINE		MINIMUM CONTACT OVERLAP										
	mm	in.	mm	in.	mm	in.	mm	in.	mm	in.	mn	lbf	mn	lbf				mpa	ksi
SCHEDULE A: WELDING NORMAL-SIZED WELDS																			
9	3.89	0.153	8.38	0.330	1.57	0.062	44.5	1.75	22.9	0.9	8.9	2000	17.8	4000	15	60	15,400	52	7.5
8	4.17	0.164	8.89	0.350	1.73	0.068	45.7	1.80	24.1	0.95	10.2	2300	20.5	4600	15	70	16,100	56	8.1
7	4.55	0.179	9.91	0.390	2.03	0.080	48.3	1.90	25.4	1.0	11.7	2630	23.4	5260	20	82	17,400	66	9.5
6	4.95	0.195	1.04	0.410	2.13	0.084	50.8	2.00	26.7	1.05	13.0	2930	26.1	5860	20	98	18,800	78	11.3
5	5.33	0.210	1.12	0.440	2.34	0.092	53.3	2.10	29.2	1.15	14.2	3180	28.3	6360	25	112	20,200	86	12.5
4	5.72	0.225	1.19	0.470	2.54	0.100	33.0	1.30	30.5	1.20	16.1	3610	32.1	7220	25	126	21,500	103	15.0
3	6.22	0.245	1.35	0.530	2.84	0.112	63.5	2.50	33.0	1.30	17.4	3900	34.7	7800	30	145	23,300	119	17.3
SCHEDULE B: WELDING SMALL-SIZED WELDS																			
9	3.89	0.153	6.86	0.270	1.47	0.058	40.6	1.60	19.1	0.75	6.2	1400	12.5	2800	15	60	11,100	35	5.1
8	4.17	0.164	7.37	0.290	1.57	0.062	41.9	1.65	20.3	0.80	6.3	1425	12.7	2850	15	70	11,800	38	5.5
7	4.55	0.179	7.87	0.310	1.70	0.067	43.2	1.70	21.6	0.85	6.7	1500	13.4	3000	20	82	12,800	45	6.5
6	4.95	0.195	8.38	0.330	1.83	0.072	44.5	1.75	22.9	0.90	7.1	1600	14.2	3200	20	98	13,900	53	7.7
5	5.33	0.210	8.89	0.350	1.96	0.077	45.7	1.80	24.1	0.95	7.7	1730	15.4	3460	25	112	14,900	59	8.5
4	5.72	0.225	9.40	0.370	2.08	0.082	48.3	1.90	25.4	1.00	8.3	1870	16.6	3740	25	126	16,000	72	10.4
3	6.22	0.245	9.91	0.390	2.24	0.088	53.3	2.10	27.9	1.10	9.3	2100	18.7	4200	30	145	17,300	83	12.0

Source: Ref 1

(A) LOW-CARBON STEEL, SAE 1005-1010, 290-380 MPA (42-55 KSI) ULTIMATE TENSILE STRENGTH.

(B) SURFACE OF STEEL MAY BE OILED LIGHTLY BUT FREE FROM GREASE, SCALE, AND DIRT.

(C) ON SINGLE FORCE WELDS USE ONLY WELD FORCE AS ELECTRODE FORCE. ELECTRODE FORCE CONTAINS NO FACTOR TO FURTHER FORM POORLY MADE PARTS.

(D) BASED ON 60 HZ.

(E) STARTING VALUES SHOWN ARE BASED ON EXPERIENCE OF RWMA MEMBER COMPANIES.

(F) TENSILE-SHEAR STRENGTH PER PROTECTION DEPENDS ON THE JOINT DESIGN.

Slope control is recommended to prevent preflashing of the projection upon initiation of the welding current. Forge forces are also recommended, because weld porosity is often a concern with heavy-gage steel. Electrode or die wear may also be a concern, as it is in the spot welding of heavy-section steels. In such applications, pulsation welding schedules might be recommended.

Intermediate-Gage Sheet Steels. The projection welding of steels ranging in gage from 0.56 to 3.43 mm (0.022 to 0.135 in.), using single-point projections with single-impulse welding schedules, is well established. Projection-stamping die designs are given in Table 3, whereas process requirements are given in Table 4. Lower forces and shorter welding times are required, when compared with the conventional spot welding of these gages.

TABLE 3 PROJECTION AND DIE GEOMETRIES FOR WELDING A RANGE OF INTERMEDIATE-GAGE STEELS TO MAKE SPHERICAL PROJECTIONS

Data are for tool steel hardened to 50-52 HRC.

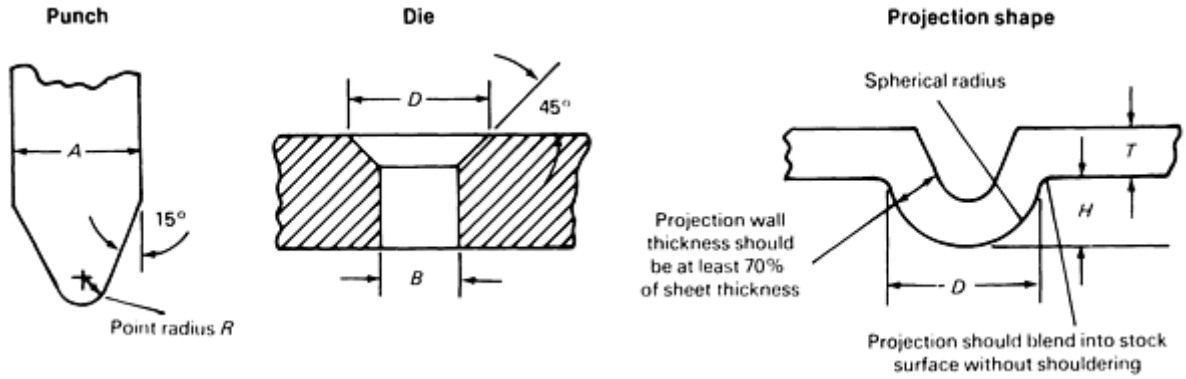

USS GAGE NO.	MATERIAL THICKNESS (*T*)		PROJECTION HEIGHT (*H*), ±2%		PROJECTION DIAMETER (*D*), ±5%		PUNCH DIAMETER (A)		PUNCH POINT RADIUS (*R*), ±0.05 MM (±0.002 IN.)		DIE HOLE DIAMETER (*B*), ±0.1 MM (±0.005 IN.)		DIE CHAMBER DIAMETER (*D*)	
	mm	in.	mm	in.	mm	in.	mm	in.	mm	in.	mm	in.	mm	in.
25-21	0.56-0.86	0.022-0.034	0.64	0.025	2.3	0.090	9.53	0.375	0.79	0.031	1.93	0.076	2.29	0.090
20-19	0.91-1.1	0.036-0.043	0.89	0.035	2.8	0.110	9.53	0.375	1.19	0.047	2.26	0.089	2.79	0.110
18-17	1.2-1.4	0.049-0.054	0.97	0.038	3.6	0.140	9.53	0.375	1.19	0.047	2.64	0.104	3.56	0.140
16-15	1.5-1.7	0.061-0.067	1.1	0.042	3.8	0.150	9.53	0.375	1.57	0.062	3.05	0.120	3.81	0.150
14	1.9	0.077	1.2	0.048	4.6	0.180	9.53	0.375	1.57	0.062	3.66	0.144	4.57	0.180
13	2.3	0.092	1.3	0.050	5.3	0.210	12.7	0.500	1.98	0.078	4.37	0.172	5.33	0.210
12	2.72	0.107	1.4	0.055	6.1	0.240	12.7	0.500	1.98	0.078	4.98	0.196	6.10	0.240
11	3.12	0.123	1.5	0.058	6.9	0.270	12.7	0.500	2.39	0.094	5.61	0.221	6.86	0.270
10	3.43	0.135	1.6	0.062	7.6	0.300	12.7	0.500	2.77	0.109	6.35	0.250	7.62	0.300

Source: Ref 1

TABLE 4 PROCESS REQUIREMENTS FOR PROJECTION WELDING OF A RANGE OF INTERMEDIATE-GAGE LOW-CARBON STEELS

Data are for SAE 1005-1010 steels with ultimate tensile strengths ranging from 290-380 MPa (42-55 ksi). Surface of steel may be oiled lightly but must be free from grease, scale, and dirt.

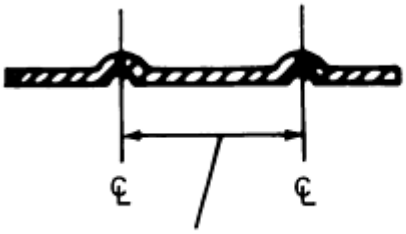

Spacing between projections

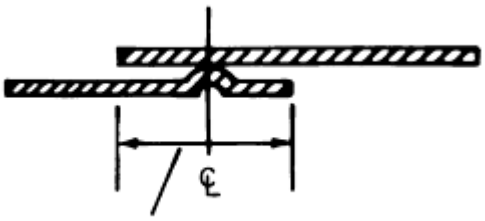

Contacting overlap

CONFIGURATION[A]	USS GAGE NO.	MATERIAL THICKNESS		PROJECTION SIZE				MINIMUM SPACING CENTERLINE TO CENTERLINE		MINIMUM CONTACT OVERLAP	
				DIAMETER		HEIGHT					
		mm	in.	mm	in.	mm	in.	mm	in.	mm	in.
A	25	0.559	0.022	2.29	0.090	0.635	0.025	9.65	0.38	6.35	0.25
B	23	0.711	0.028	2.29	0.090	0.635	0.025	9.65	0.38	6.35	0.25
C	21	0.864	0.034	2.79	0.110	0.889	0.035	12.7	0.50	9.65	0.38
D	19	1.09	0.043	2.79	0.110	0.889	0.035	12.7	0.50	9.65	0.38
E	18	1.24	0.049	3.56	0.140	0.965	0.038	19.1	0.75	12.7	0.50
F	16	1.55	0.061	3.81	0.150	1.07	0.042	19.1	0.75	12.7	0.50
G	14	1.96	0.077	4.57	0.180	1.22	0.048	22.4	0.88	12.7	0.50
H	13	2.34	0.092	5.33	0.210	1.27	0.050	26.9	1.06	15.7	0.62
I	12	2.72	0.107	6.10	0.240	1.40	0.055	31.8	1.25	19.1	0.75
J	11	3.12	0.123	6.86	0.270	1.47	0.058	38.1	1.50	20.6	0.81
K	10	3.43	0.135	7.62	0.300	1.57	0.062	41.4	1.63	22.4	0.88

CONFIGURATION[A]	WELD TIME[B], CYCLES	ELECTRODE FORCE[C]		WELDING CURRENT[D], A	TENSILE-SHEAR STRENGTH[E]	
		kn	lbf		mpa	ksi
WELDING SCHEDULE A (FOR SINGLE PROJECTION)[F]						
A	3	0.67	150	4,400	2.6	0.37
B	3	0.87	195	5,500	3.4	0.50
C	3	1.1	240	6,600	4.8	0.70
D	5	1.5	330	8,000	7.3	1.06
E	8	1.8	400	8,800	9.0	1.30
F	10	2.4	550	10,300	12.4	1.80
G	14	3.6	800	11,850	16.7	2.43
H	16	4.5	1020	13,150	22.4	3.25
I	19	5.6	1250	14,100	26.5	3.85
J	22	6.7	1500	14,850	33.1	4.80
K	24	7.3	1650	15,300	37.9	5.50
WELDING SCHEDULE B (FOR 1-3 PROJECTIONS), EACH PROJECTION[G]						
A	6	0.67	150	3,850	2.3	0.33
B	6	0.67	150	4,450	3.0	0.43
C	6	0.67	150	5,100	3.7	0.53
D	10	0.93	210	6,000	6.1	0.88
E	16	1.2	270	6,500	7.6	1.10
F	20	1.6	365	7,650	11.0	1.58
G	28	2.4	530	8,850	14.8	2.15
H	32	3.0	680	9,750	19.3	2.80
I	38	3.7	830	10,600	23.8	3.45
J	45	4.5	1000	11,300	29.0	4.20
K	48	4.9	1100	11,850	33.4	4.85
WELDING SCHEDULE C (FOR [GES]3 PROJECTIONS), EACH PROJECTION[H]						

B	8	0.45	100	3300	2.3	0.34
C	11	0.56	125	3800	2.9	0.43
D	15	0.71	160	4300	5.0	0.72
E	19	0.98	220	4600	6.1	0.88
F	25	1.5	330	5400	8.5	1.23
G	34	2.1	470	6400	12.1	1.75
H	42	2.7	610	7200	16.0	2.33
I	50	3.3	740	8300	20.0	2.90
J	60	4.0	900	9200	24.8	3.60
K	66	4.5	1000	9900	29.3	4.25

(A) CONFIGURATION DESIGNATIONS ARE FOR THE PURPOSES OF THIS TABLE ONLY.

(B) BASED ON 60 HZ.

(C) ELECTRODE FORCE CONTAINS NO FACTOR TO FURTHER FORM POORLY MADE PARTS.

(D) STARTING VALUES SHOWN ARE BASED ON EXPERIENCE OF RWMA MEMBER COMPANIES.

(E) TENSILE-SHEAR STRENGTH PER PROJECTION DEPENDS ON THE JOINT DESIGN.

(F) SCHEDULE A IS USABLE FOR WELDING MORE THAN ONE PROJECTION IF CURRENT IS DECREASED, BUT EXCESSIVE WELD EXPULSION MAY RESULT AND POWER DEMAND WILL BE GREATER THAN THAT FOR SCHEDULE B OR C.

(G) SCHEDULE B IS USABLE FOR WELDING MORE THAN THREE PROJECTIONS, BUT SOME WELD EXPULSION MAY RESULT, AND POWER DEMAND WILL BE GREATER THAN THAT FOR SCHEDULE C.

(H) SCHEDULE C IS USABLE FOR WELDING LESS THAN THREE PROJECTIONS WITH WELD CURRENT INCREASED APPROXIMATELY 15% AND POSSIBLE OBJECTIONABLE FINAL SHEET SEPARATION.

Thin-Gage Sheet. The projection welding of thin-gage steel sheet (<0.50 mm, or 0.020 in.) differs significantly from the projection welding of intermediate-gage sheet in that single-point projections become mechanically unstable. It also becomes increasingly difficult to use single-point projections to make adequate-sized welds. Therefore, annular projections are typically recommended for thin-gage steel. Table 5 provides the annular projection weld geometry, as well as the required process conditions.

TABLE 5 PROJECTION DESIGNS AND PROCESS REQUIREMENTS FOR ANNULAR PROJECTION WELDING OF THIN-GAGE LOW-CARBON STEEL

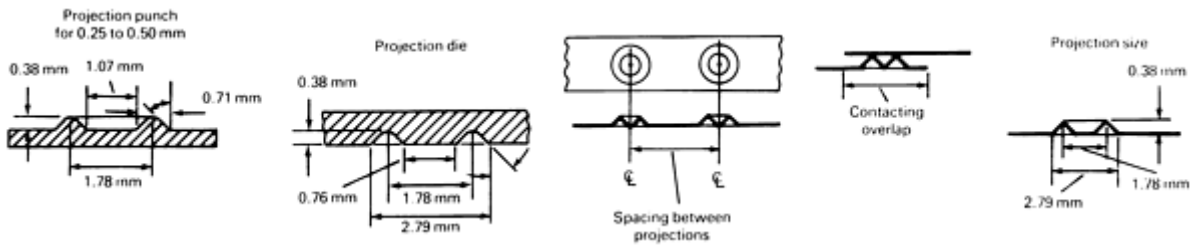

USS GAGE NO.	THICKNESS[A][B]		MINIMUM SPACING CENTERLINE TO CENTERLINE		MINIMUM CONTACT OVERLAP		WELD TIME[C], CYCLES	ELECTRODE FORCE[D]		WELDING CURRENT[E], A	TENSILE-SHEAR STRENGTH EACH PROJECTION[F]			
											ONE		TWO OR MORE	
	mm	in.	mm	in.	mm	in.		n	lbf		mpa	ksi	mpa	ksi

31	0.279	0.011	7.87	0.31	6.35	0.25	6	490	110	5200	1.3	0.19	1.0	0.14
26	0.483	0.019	7.87	0.31	6.35	0.25	6	1000	225	5400	2.8	0.40	1.9	0.28

Source: Ref 1

(A) SAE 1010, LOW-CARBON STEEL, 290-380 MPA (42-55 KSI) ULTIMATE TENSILE STRENGTH.

(B) SURFACE OF STEEL MAY BE OILED LIGHTLY, BUT MUST BE FREE FROM GREASE, SCALE, AND DIRT.

(C) ELECTRODE FORCE CONTAINS NO FACTOR TO FURTHER FORM POORLY MADE PARTS.

(D) BASED ON 60 HZ.

(E) STARTING VALUES SHOWN ARE BASED ON EXPERIENCE OF RWMA MEMBER COMPANIES.

(F) APPROXIMATE STRENGTH PER PROJECTION DEPENDS ON JOINT DESIGN.

Dissimilar Thickness Joints. As previously noted, the PW process is ideally suited for the joining of sheets of widely disparate thickness. When fabricating such joints, the best practice is to place the projection on the thicker sheet, where possible, using the projection design that is appropriate for the thinner sheet. This is done because the projection has the effect of concentrating the heat at the contact surface, regardless of the thicknesses of the sheets being joined. As a result, selecting conditions based on the thinner sheet has the effect of sizing the weld for that (attached) material.

The solid projections that are described below include nut, cross-wire, and annular projection configurations.

Nut Welding. Specific criteria for the design of weld nut projections, as well as appropriate processing conditions, are not well established. However, there is a general consensus that the ideal number of projections on a weld nut is three, because it is assumed that all three will contact the opposing surface when the electrode force is applied, if the projections are of the same height and if the electrodes are aligned properly.

The actual design of the welding projections is not well established, although 90° included angle square pyramidal and hemispherical projections are common. Such projections are nominally scaled according to the opposing sheet. Designs for embossed projections of the appropriate sheet size can be used as a guideline.

Cross-Wire Welding. The process conditions for the cross-wire welding of a range of wire thicknesses are given in Table 6. The conditions are usually specified in terms of requirements to achieve a certain level of compression set-down for the wires. Set-down is defined in Fig. 5. In general, joint strength increases as the degree of set-down increases. The defined process conditions are for mild steels. Higher-strength materials, such as stainless steels or nickel-base alloys, will require higher forces and longer welding times to promote wire collapse and diffusion across the bond line.

TABLE 6 PROCESS REQUIREMENTS FOR CROSS-WIRE WELDING OF HOT- AND COLD-DRAWN STEEL WIRES IN A RANGE OF THICKNESSES

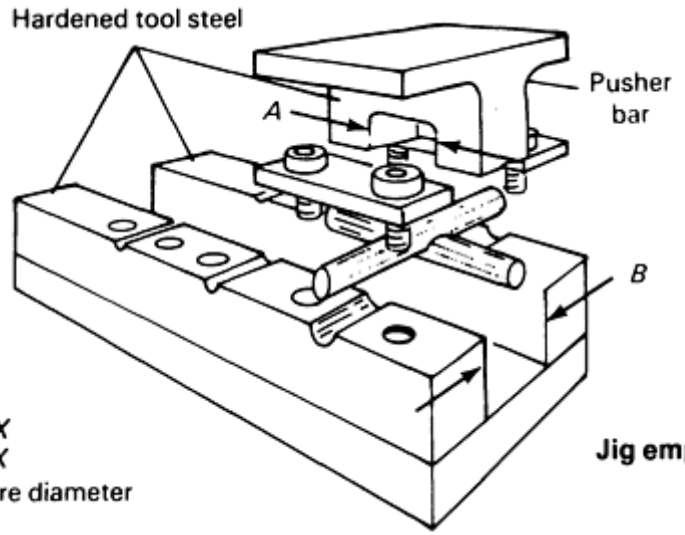

Jig employed in testing crossed-wire welds for strength

COLD-DRAWN WIRE								HOT-DRAWN WIRE					
WIRE DIAMETER		WELD TIME[A], CYCLES	WELD FORCE		WELDING CURRENT[B], A	WELD STRENGTH		WELD TIME[A], CYCLES	WELD FORCE		WELDING CURRENT[B], A	WELD STRENGTH	
mm	in.		kn	lbf		mpa	ksi		kn	lbf		mpa	ksi
15% SETDOWN													
0.63	1/16	5	0.45	100	600	3.1	0.45	5	0.45	100	600	2.4	0.35
3.18	1/8	10	0.56	125	1,800	6.8	0.98	10	0.56	125	1,850	5.2	0.75
4.76	3/16	17	1.60	360	3,300	13.8	2.0	17	1.60	360	3,500	10.3	1.5
6.35	1/4	23	2.58	580	4,500	25.5	3.7	23	2.58	580	4,900	19.3	2.8
7.94	5/16	30	3.67	825	6,200	35.2	5.1	30	3.67	825	6,600	31.7	4.6
9.53	3/8	40	4.90	1,100	7,400	46.2	6.7	40	4.90	1,100	7,700	42.7	6.2
11.1	7/16	50	6.22	1,400	9,300	66.2	9.6	50	6.22	1,400	10,000	60.7	8.8
12.7	1/2	60	7.57	1,700	10,300	84.1	12.2	60	7.57	1,700	11,000	79.3	11.5
30% SETDOWN													
0.63	1/16	5	0.67	150	800	3.4	0.500	5	0.67	150	800	2.8	0.40
3.18	1/8	10	1.16	260	2,650	7.6	1.1	10	1.16	260	2,770	5.9	0.85
4.76	3/16	17	2.67	600	5,000	16.5	2.4	17	2.67	600	5,100	11.7	1.7
6.35	1/4	23	3.78	850	6,700	29.0	4.2	23	3.78	850	7,100	20.7	3.0
7.94	5/16	30	6.45	1,450	9,300	42.1	6.1	30	6.45	1,450	9,600	34.5	5.0
9.53	3/8	40	9.17	2,060	11,300	57.9	8.4	40	9.17	2,060	11,800	46.9	6.8
11.1	7/16	50	12.9	2,900	13,800	77.9	11.3	50	12.9	2,900	14,000	66.2	9.6

12.7	1/2	60	15.1	3,400	15,800	93.8	13.6	60	15.1	3,400	16,500	85.5	12.4
50% SETDOWN													
0.63	1/16	5	0.89	200	1,000	3.8	0.55	5	0.89	200	1,000	3.1	0.45
3.18	1/8	10	1.56	350	3,400	9.0	1.3	10	1.56	350	3,500	6.2	0.90
4.76	3/16	17	3.34	750	6,000	17.2	2.5	17	3.34	750	6,300	12.4	1.8
6.35	1/4	23	5.52	1,240	8,600	30.3	4.4	23	5.52	1,240	9,000	21.4	3.1
7.94	5/16	30	8.90	2,000	11,400	44.8	6.5	30	8.90	2,000	12,000	36.5	5.3
9.53	3/8	40	13.4	3,000	14,400	60.7	8.8	40	13.4	3,000	14,900	49.6	7.2
11.1	7/16	50	19.8	4,450	17,400	82.1	11.9	50	19.8	4,450	18,000	70.3	10.2
12.7	1/2	60	23.6	5,300	21,000	100.7	14.6	60	23.6	5,300	22,000	89.6	13.0

Source: Ref 1

(A) 60 HZ.

(B) STARTING VALUES SHOWN ARE BASED ON EXPERIENCE OF RWMA MEMBER COMPANIES.

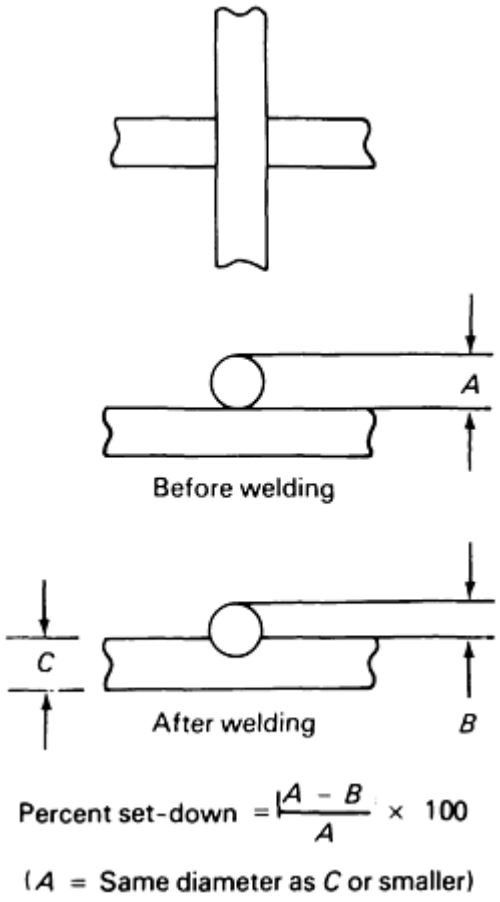

FIG. 5 DEFINITION OF HOW SET-DOWN IS ESTIMATED ON CROSS-WIRE WELDS. SOURCE: REF 1

Annular Projection Welding. Neither specific projection designs nor process conditions for annular projection welding are well established. There is a general consensus on the use of 90 ° included angle triangular cross section projections in sizes that are scaled to the thickness of the opposing sheet. Typical practice includes approximately 4.5 to 8.9 kN (1000 to 2000 lbf) of force per linear inch (or 25 mm) of projection. Weld times for annular projections for diameters ranging from 6.4 to 25 mm (0.25 to 1.0 in.) usually range from a single cycle to about 10 cycles. Typically, longer welding times result in more-robust processing conditions. However, maximum welding times are often limited by concerns over peripheral thermal damage.

The best annular projection design will recess the base diameter of the projection from the outside diameter of the part. Reasons for this are shown in Fig. 6. Projection designs that extend to the outside diameter of the part have the potential for unstable projection collapse, which can result in the formation of an incipient notch at the outside diameter of the part and an increase in the incidence of weld-related failures.

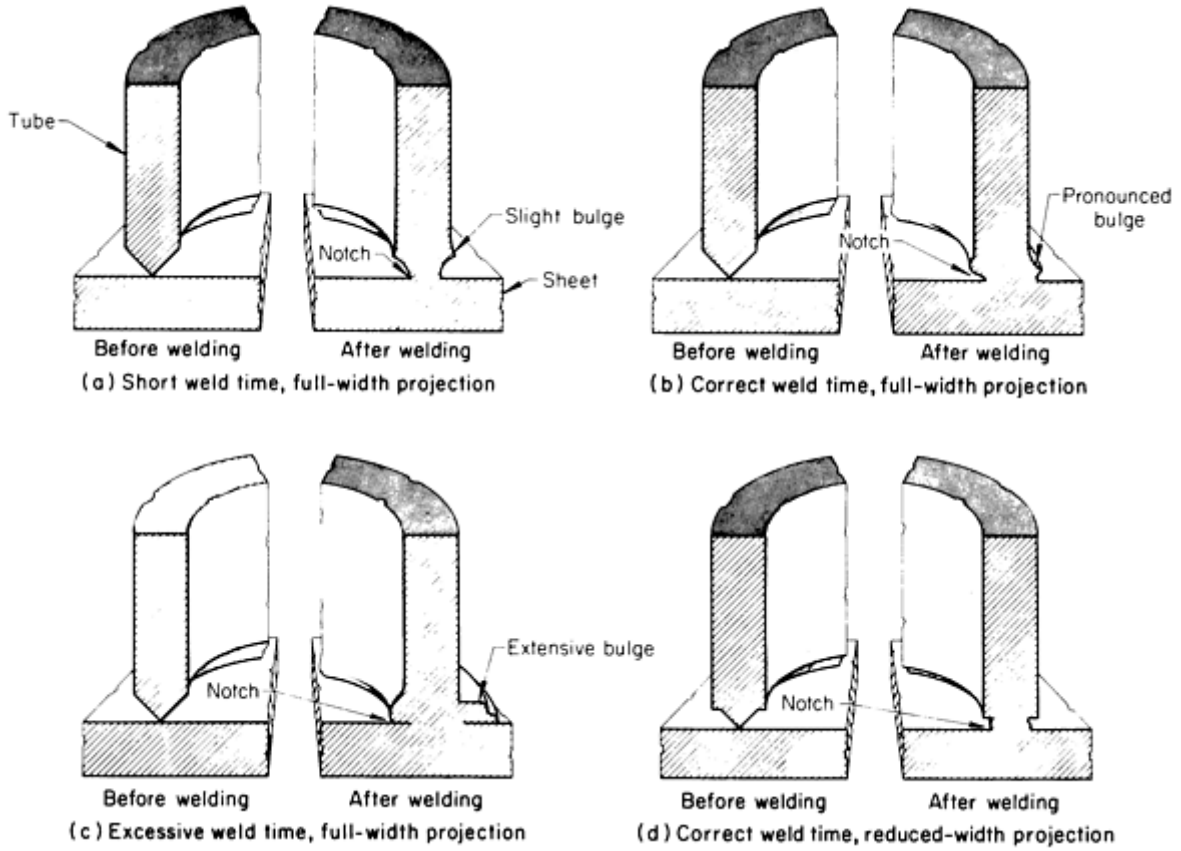

FIG. 6 CHARACTERISTICS OF PROJECTION COLLAPSE DURING ANNULAR PROJECTION WELDING WITH DIFFERENT BASE PROJECTION WIDTHS. (A) SHORT WELD TIME, FULL-WIDTH PROJECTION. (B) CORRECT WELD TIME, FULL-WIDTH PROJECTION. (C) EXCESSIVE WELD TIME, FULL-WIDTH PROJECTION. (D) CORRECT WELD TIME, REDUCED-WIDTH PROJECTION

Larger-diameter annular projection welds do cause a problem in attaining the proper heat balance around the periphery of the projection. Typically, the side of the projection that is toward the throat of the machine will heat preferentially for two reasons. First, the shortest conductive (and highest current flow) path is along the inside of the throat, including the inboard side of the projection. Second, there is an inductive "skin" effect associated with alternating-current machines, which tends to concentrate current along the inside of the welder throat. Intermediate-diameter projections have been successfully welded using direct current, because it minimizes the skin effect and appears to allow better heat balance.

Larger-diameter projections may require dual-throat machines, which have dual transformers located on opposite sides of the workpiece. Each has its own "throat." The effect is to balance the resistive/inductive effects, allowing the welding of very large diameter projections.

Reference cited in this section

1. D. BENETEAU, ED., *RESISTANCE WELDING MANUAL*, 4TH ED., G.H. BUCHANAN CO., 1989

Projection Welding

Jerry E. Gould, Edison Welding Institute

Reference

1. D. BENETEAU, ED., *RESISTANCE WELDING MANUAL*, 4TH ED., G.H. BUCHANAN CO., 1989

Resistance Seam Welding

Michael J. Karagoulis, General Motors Corporation

Introduction

RESISTANCE SEAM WELDING (RSEW) is a process in which heat generated by resistance to the flow of electric current in the work metal is combined with pressure to produce a welded seam. The resulting seam consists of a series of spot welds. The specific seam weld process can be classified as:

- *ROLL SPOT WELDING* (RELATIVELY LARGE UNWELDED GAPS BETWEEN NUGGETS)
- *REINFORCED ROLL SPOT WELDING* (SMALL GAPS BETWEEN NUGGETS)
- *LEAK-TIGHT SEAM WELDING* (NUGGET OVERLAP)

Two rotating circular electrode wheels are often used to apply current, force, and cooling to the work metal. A variety of workpiece/wheel configurations are possible (Fig. 1). When two electrode wheels are used, one or both wheels are driven, either by a direct drive of the wheel axles or by a knurl drive that contacts the peripheral surface of the electrode wheel (Fig. 2). For some applications, the electrode wheels idle while the workpiece is driven.

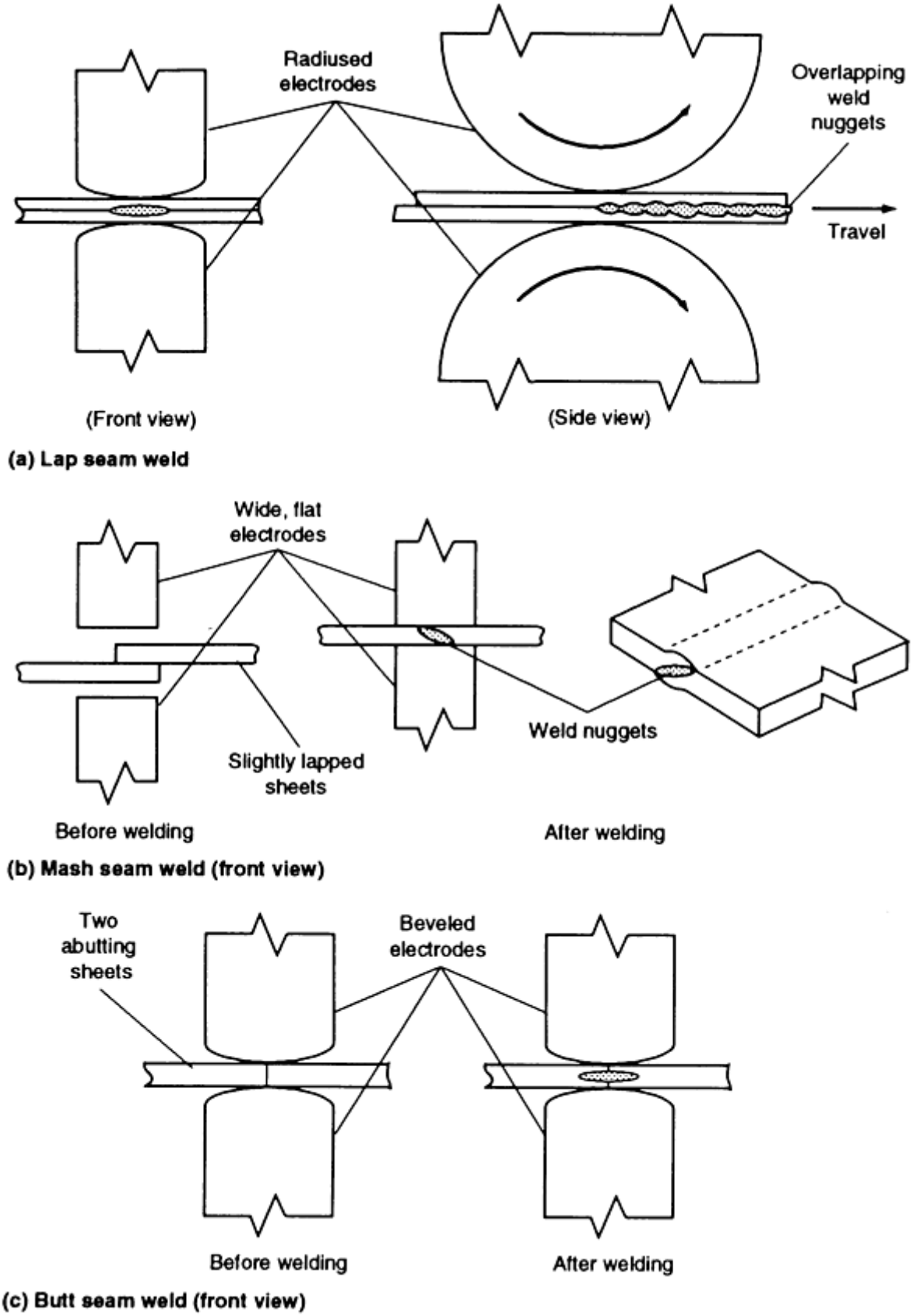

FIG. 1 BASIC CONFIGURATION OF JOINTS AND RESULTANT WELDS FORMED IN RESISTANCE SEAM WELDING. ADAPTED FROM *WELDING HANDBOOK*, 8TH ED., VOL 2, AMERICAN WELDING SOCIETY, 1991, P 554

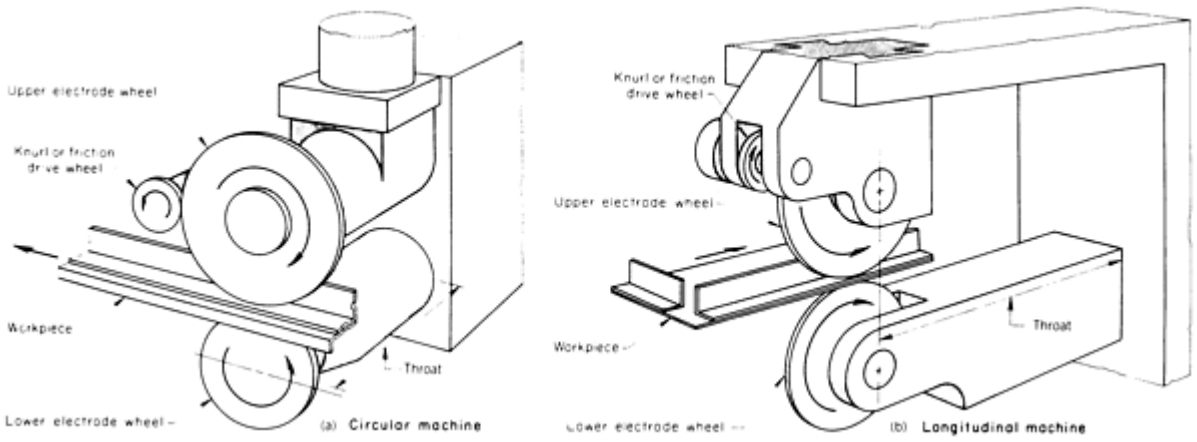

FIG. 2 POSITION OF ELECTRODE WHEELS RELATIVE TO THROAT ON RESISTANCE SEAM WELDING MACHINES

Other electrode systems for seam welding may use one wheel and one flat bar-type electrode (Fig. 3), or a wire-feed system in which a copper wire is fed into a groove on the wheel. This wire-feed process continuously provides a new copper surface for contact with the work metal (Fig. 4).

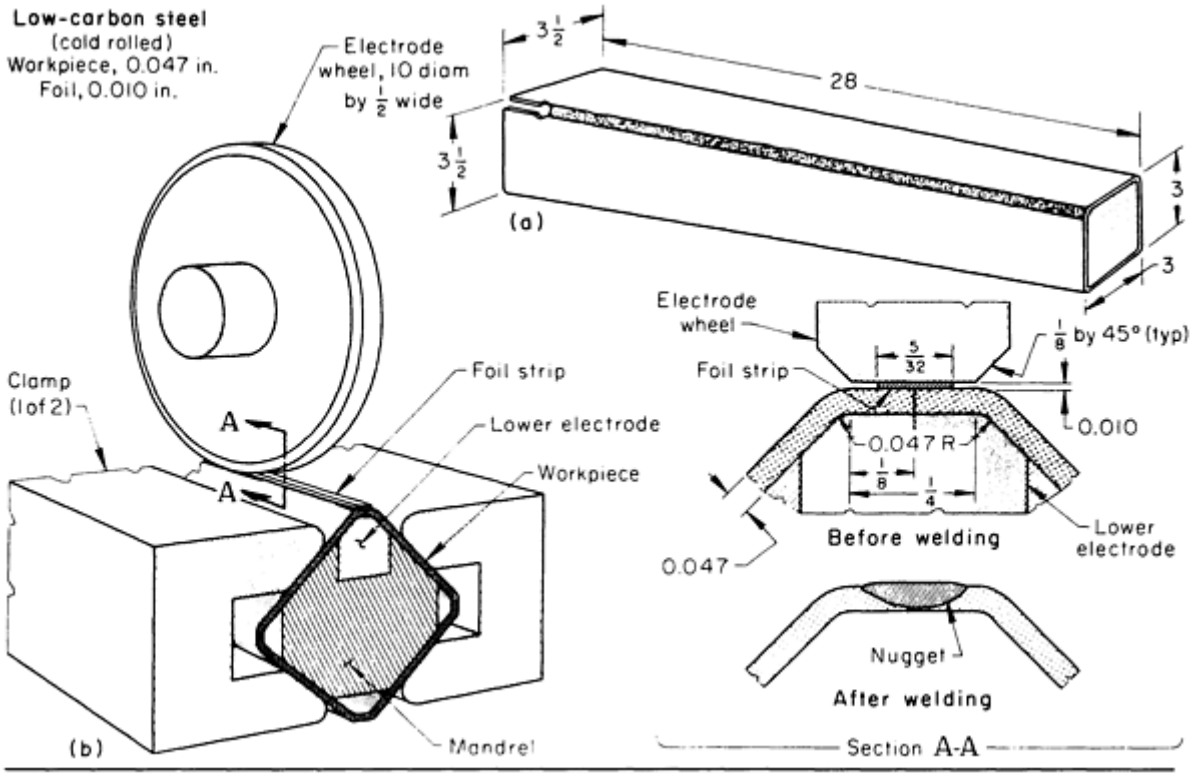

EQUIPMENT SPECIFICATIONS AND WELDING PARAMETERS	
POWER SUPPLY	440 V, SINGLE PHASE
WELDING MACHINE	AUTOMATIC, LONGITUDINAL, WITH MOVABLE CARRIAGE FOR UPPER ELECTRODE
RATING AT 50% DUTY CYCLE	300 KVA

HEAT CONTROL	PHASE SHIFT
ELECTRODE-RAM OPERATION	AIR CYLINDER
ELECTRODE FORCE, MAX	5.4 KN (1200 lbf)
UPPER ELECTRODE	13 MM ($\frac{1}{2}$ in.) WIDE BY 255 MM (10 IN.) DIAM; DOUBLE BEVEL; 6.4 MM ($\frac{1}{4}$ in.) WIDE FIAT FACE
LOWER ELECTRODE	710 mm (28 in.) LONG BAR; DOUBLE BEVEL; 6.4 MM ($\frac{1}{4}$ in.) WIDE FLAT FACE (SEE DRAWING)
ELECTRODE MATERIAL	RWMA CLASS 2
WELDING CURRENT	CONTINUOUS
WELDING SPEED	6 M/MIN (20 FT/MIN)
PRODUCTION RATE	220 LEGS PER HOUR

FIG. 3 SETUP FOR FOIL BUTT SEAM WELDING OF A TABLE LEG MADE OF LOW-CARBON STEEL. DIMENSIONS GIVEN IN INCHES

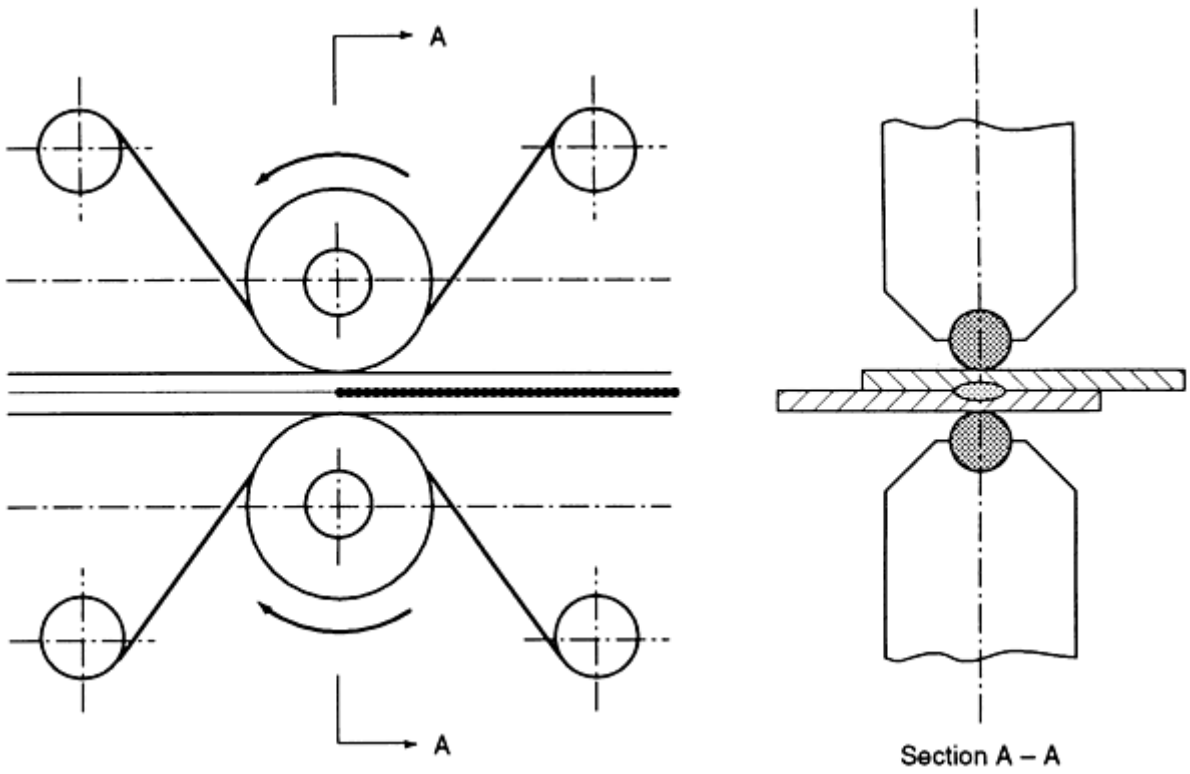

FIG. 4 TYPICAL SETUP FOR AN ELECTRODE WIRE SEAM WELDING PROCESS SHOWING POSITIONS OF WIRE RELATIVE TO GROOVED WHEEL

In seam welding, a series of spot welds is made without retracting the electrode wheels or releasing the electrode force between spots. The electrode wheels may rotate either continuously or intermittently. Weld speed, current magnitude, current waveform, cooling system, and the electrode parameters of force, shape, and diameter are all related and must be carefully selected to optimize the process and produce the highest quality weld.

The principles described in the article "Resistance Spot Welding" in this Volume are also generally applicable to seam welding.

Resistance Seam Welding

Michael J. Karagoulis, General Motors Corporation

RSEW Applications

Lap Seam Weld. A joint in which the workpieces are overlapped sufficiently to prevent the sheet edges from becoming part of the weld is classified as a lap seam weld (Fig. 1a). Lap seams are popular in automotive applications, such as automotive fuel tanks, catalytic converters, mufflers, and roof joints, as well as in nonautomotive applications, such as furnace heat exchangers, water tanks, and certain types of can making (Fig. 5). Lap seam welding of multiple stackups and dissimilar thicknesses is also possible.

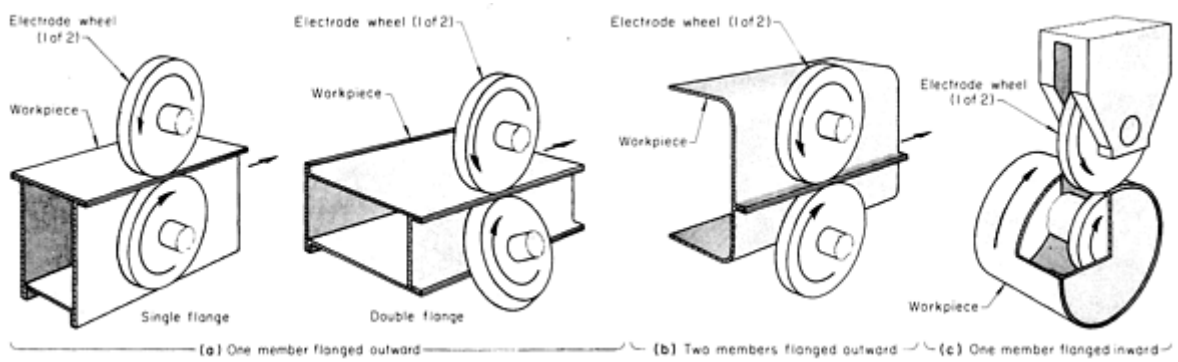

FIG. 5 ARRANGEMENT OF ELECTRODE WHEELS RELATIVE TO WORKPIECE FOR SELECTED FLANGE-JOINT LAP SEAM WELDS

Mash Seam Weld. A joint in which two sheets are overlapped by only one to two times the sheet thickness is classified as a mash seam weld (Fig. 1b). The weld area is forged or mashed down during welding to an overthickness 5 to 25% greater than a single sheet thickness. It is necessary to have some amount of overthickness so the current path can be controlled, because the electrode wheels in mash seam welding are wide and flat-edged. Surface appearance and thickness can be improved through the use of hard steel planishing wheels to cold work the joint before or after welding. Because of the excessive hardening induced by cold work, postweld heat treatment may be necessary (Ref 1).

Typical applications include drums, buckets, vacuum-jacketed bottles, aerosol cans, water tanks, and steel mill coil joining. Sheets of dissimilar thicknesses and/or coatings have been successfully mash seam welded. This development has created a whole new set of applications in tailored blank manufacturing, primarily for automotive use (Ref 2).

Butt Seam Weld. A joint in which two abutting edges are welded is classified as a butt seam joint (Fig. 1c and 3). The thickness of the weld should be approximately the same, or slightly less than, the sheet thickness. Butt seam welding is typically reserved for applications in which other butt welding processes cannot be used (for example, for tube welding and for sheet metal in railroad cars).

References cited in this section

1. K.M. PICKETT, M.F. SHI, K.K. BHATT, AND J. SELVARAJ, STRUCTURE PROPERTY RELATIONSHIPS OF RESISTANCE MASH SEAM WELDED TAILORED BLANKS WITH POST HEAT TREATMENT, *24TH CONF. INT. METALLOGRAPHIC SOC.* (DENVER), AUG 1992

2. Y. ADONYI, J. MILIAN, AND L. ROUDABUSH, WELDED STEEL SHEET PERFORMANCE FOR TAILORED BLANKS, *PROC. SHEET METAL WELDING CONF. V*, PAPER C1, AMERICAN WELDING SOCIETY, OCT 1992

Resistance Seam Welding

Michael J. Karagoulis, General Motors Corporation

Advantages and Limitations

Advantages of seam welding, compared to resistance spot welding, projection welding, and laser welding, are:

- GAS-TIGHT OR LIQUID-TIGHT JOINTS CAN BE PRODUCED (NOT POSSIBLE WITH SPOT WELDING OR PROJECTION WELDING).
- SEAM WIDTH MAY BE LESS THAN THE DIAMETER OF SPOT WELDS, BECAUSE THE ELECTRODE CONTOUR CAN BE CONTINUOUSLY DRESSED AND IS THEREFORE OF A STABLE SHAPE.
- HIGH-SPEED WELDING (ESPECIALLY ON THIN STOCK) IS POSSIBLE.
- TOOLING COST IS GENERALLY FAVORABLE PER INCH OF FLANGE WELDED.
- COATED STEELS ARE GENERALLY MORE WELDABLE USING SEAM WELDING THAN SPOT WELDING, BECAUSE COATING RESIDUE CAN BE CONTINUOUSLY REMOVED FROM THE ELECTRODE WHEELS IF SPECIAL PROVISIONS ARE MADE.
- COATED STEELS ARE GENERALLY MORE WELDABLE USING SEAM WELDING THAN LASER WELDING, BECAUSE COATING VOLATILITY IS MINIMIZED BY THE INTENSE PRESSURE FIELD IN THE WELD ZONE.
- RESISTANCE SEAM WELDING IS NOT PARTICULARLY FITUP-SENSITIVE COMPARED TO LASER WELDING.
- THE HARDNESS OF RESISTANCE SEAM WELDS MADE WITH AIR COOLING IS LESS THAN THAT OF LASER WELDS (120 HV VERSUS 250 HV, RESPECTIVELY, FOR DRAWING-QUALITY BARE STEEL, AND 170 HV VERSUS 300 HV, RESPECTIVELY, FOR ORGANIC COATED DRAWING-QUALITY STEEL) (REF 3).

Limitations of seam welding, apart from those it shares with spot welding and projection welding, are:

- WELDS MUST ORDINARILY PROCEED IN A SINGLE PLANE OR ON A UNIFORMLY CURVED SURFACE. FOR SPECIAL CASES, MULTIPLANE WELDING HAS BEEN ACHIEVED USING A TILTING WELDING HEAD. THE RADIUS OF CURVATURE CONNECTING THE PLANES MUST BE SUFFICIENTLY LARGE.
- OBSTRUCTIONS ALONG THE PATH OF THE ELECTRODE WHEEL MUST BE AVOIDED OR COMPENSATED FOR IN THE DESIGN OF THE WHEEL.
- MATERIAL HANDLING MUST NOT INDUCE EXTRANEOUS FORCES INTO THE FRAGILE, MOLTEN WELD ZONE DURING WELDING.
- THE LENGTH OF SEAMS MADE IN A LONGITUDINAL SEAM WELDING MACHINE IS LIMITED BY THE THROAT DEPTH OF THE MACHINE (FIG. 2B). CURRENT SHUNTING THROUGH THE WELD, OR A CHANGE IN ELECTRICAL IMPEDANCE CAUSED BY THE MOVEMENT OF THE PRODUCT INSIDE THE THROAT OF THE MACHINE, CAN REQUIRE CURRENT COMPENSATION AS WELDING PROCEEDS.
- COMPONENTS USING MULTIPLE CROSSING SEAM WELDS CAN BE QUALITY-SENSITIVE AT THE WELD INTERSECTIONS.
- EXTERNAL WATER COOLING OF THE ELECTRODES AND THE WELD ZONE MAY BE REQUIRED FOR HIGH-SPEED WELDING. (UNDER HIGH-SPEED CONDITIONS THE WELD

NUGGETS ARE STILL MOLTEN AS THEY LEAVE THE PRESSURE FIELD OF THE WHEELS). EXTERNAL COOLING MAY ADD TOOLING COST FOR WATER CONTAINMENT AND WATER REMOVAL FROM THE PARTS AFTER WELDING.

- MATERIALS REQUIRING POSTHEAT AND TEMPER SHOULD NOT BE SEAM WELDED WITHOUT SPECIAL CONSIDERATIONS.
- CHROMATES AND INSULATING LACQUER COATINGS ARE NOT RESISTANCE SEAM WELDABLE.

Reference cited in this section

3. VDI REPORT 818, VEREIN DEUTSCHER INGENIEURE, 1990, P 256 (IN GERMAN)

Resistance Seam Welding

Michael J. Karagoulis, General Motors Corporation

Fundamentals of Lap Seam Welding

Empirical seam welding parameters have been developed over the years and have proven useful under many conditions (Ref 4, 5). However, this discussion is devoted to an alternative approach to process optimization, based on principles of heat transfer in the weld. Hopefully, this approach will shed some light on difficult applications in which traditional methods may fall short of what is necessary to make quality welds.

Weld Time, Speed, and Current Pulsation

Certain concepts from resistance spot welding begin to explain resistance seam welding, because seam welding generally consists of a series of overlapping spot welds.

Spot Weld Analogy. Empirically, the optimum time for the spot welding of low-carbon steel sheet is approximately (Ref 6):

$$T = 0.0292\ S^2 \qquad \textbf{(EQ 1)}$$

where S is the thickness of the total stackup of sheets (in millimeters) and t is the optimum weld time (in seconds).

Applying current for this length of time maximizes the current range from minimum weld diameter through the onset of either cracking, overindentation, or electrode sticking. If weld time is less than this, there will be insufficient time for proper heat flow to occur inside the weld. As such, the weld will begin to exhibit adiabatic character ("thermal runaway"), nugget size instability, and surface expulsion. By the same measure, if weld time is too long, the extra cycles simply heat up the electrodes. Hot electrodes are less capable of keeping the surface of the weld cool to avoid electrode sticking and metallurgical discontinuities on the weld surface. In addition, excessive weld time will also compromise electrode life, waste energy, and could even slow down the production rate of an entire manufacturing line. Thus in any case, for spot welding there seems to be a proper rate of welding, based on material thickness and thermal diffusivity (in the thickness direction).

Application to Seam Welding. For seam welding, the same principle of optimum weld time applies, but weld time refers to how long a given point on the weld will be in contact with the wheel as it passes through the welder. In practice, travel speed and electrode footprint length, L, should be controlled so that the resulting weld time is matched with the $0.0292\ S^2$ rule (see Eq 1, Eq 5, and Fig. 6). The following equations may be used (forward or backward) to fix some variables and calculate the others that result from these assumptions.

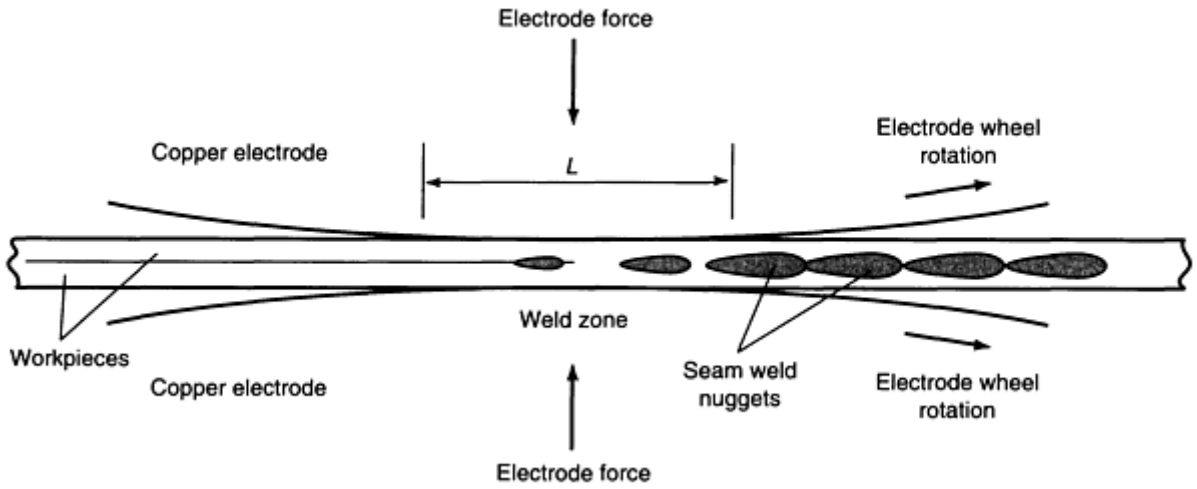

FIG. 6 SCHEMATIC SHOWING LENGTHWISE SECTIONAL VIEW OF PROPER NUGGET DEVELOPMENT IN THE WELD ZONE OF A PULSED LAP SEAM WELD. THE LENGTH OF THE CONTACT FOOTPRINT, *L*, IS SUFFICIENT TO CONTAIN THREE NUGGETS UNDER THE WHEEL (THAT IS, *N* = 3).

For lap seams of low-carbon sheets, Eq 1 becomes:

$$T = N/F = 0.0292\ S^2 \qquad \textbf{(EQ 2)}$$

where *n* is the number of nuggets under development inside the weld zone footprint at any one time (Fig. 6) and *f* is the impulse frequency of the applied current (on-time and off-time).

For process control and leak-tight welds, a good rule for the nugget spacing is:

$$1.7\ S \leq D \leq 2.5\ S \qquad \textbf{(EQ 3)}$$

where *d* is the nugget spacing (in mm).

Welding speed, *v* (in mm/s), is therefore:

$$V = D \cdot F \qquad \textbf{(EQ 4)}$$

However, to predict the optimum welding speed, one must first know *L*, the length of the contact footprint (in mm):

$$L = D \cdot N \qquad \textbf{(EQ 5)}$$

One can calculate the required *L* from *d* and *n*, and then determine the wheel diameter, force, and current needed to achieve *L*.

Substituting Eq 5 and Eq 3 into Eq 4:

$$V = L \cdot F/N \qquad \textbf{(EQ 6)}$$

and

$$L_{MAX} = 2.5\ N \cdot S \qquad \textbf{(EQ 7)}$$

Rearranging Eq 2:

$$N = 0.0292\ F \cdot S^2 \qquad \textbf{(EQ 8)}$$

and:

$$V_{MAX} = L_{MAX} \cdot F/N \qquad \textbf{(EQ 9)}$$

to obtain:

$$V_{MAX} = 85.6\ N/S \qquad \textbf{(EQ 10)}$$

It is important to note that the current range of seam welding is widened by the judicious use of impulsed current to form distinct nuggets. Impulse profiles of 25 to 33% off-times are commonly used. Impulses contain off-time for the electrodes to draw heat away from the weld surface. Therefore, the occurrence of surface discontinuities is lessened. In addition, off-time allows heat to redistribute itself within the weld, away from local hot spots. Hot spots are places within the weld where thermal spikes may be occurring due to either a relatively high local resistance, a nonuniform current density, a multiple stackup, or a stackup of unequal sheets. Hot spots are especially common along the weld interface when welding either thick plates or prepainted sheets. Hot spots on the outside surface of a weld occur naturally with unequal sheet thicknesses (on the thin side), or when welding is faster than permitted by Eq 2. On the other hand, hot spots can also occur within the sheet bulk, if due to erratic time distribution of current during on-time. Bulk hot spots begin to occur when welding near the maximum speed for a material, because current is actually not applied uniformly throughout the on-time, and time is required for the resulting nonuniform heat pattern to redistribute itself (Fig. 7). The ideal impulse shape under high-speed conditions would seem to be a square wave (Fig. 8a). Because typical industrial power sources can only approximate this shape (Fig. 8b), it is worthwhile to accurately record the waveform of the actual secondary current in order to monitor its shape and stability during welding.

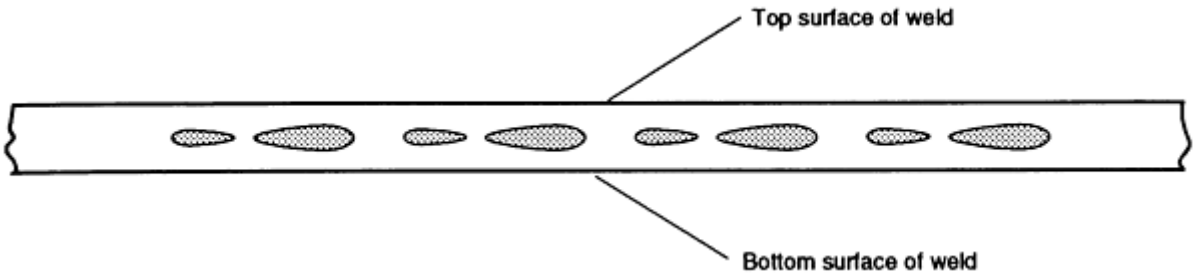

FIG. 7 SCHEMATIC SHOWING LENGTHWISE SECTIONAL VIEW OF THE WELD CENTERLINE OF A LAP SEAM JOINT WITH IRREGULAR NUGGET SHAPES. THE LACK OF UNIFORMITY IN THE SHAPE OF THE NUGGETS IS ATTRIBUTABLE TO AN IRREGULAR PULSE SHAPE THAT DOES NOT PROVIDE SUFFICIENT TIME FOR HEAT FLOW TO BLEND TOGETHER THE DOUBLETS.

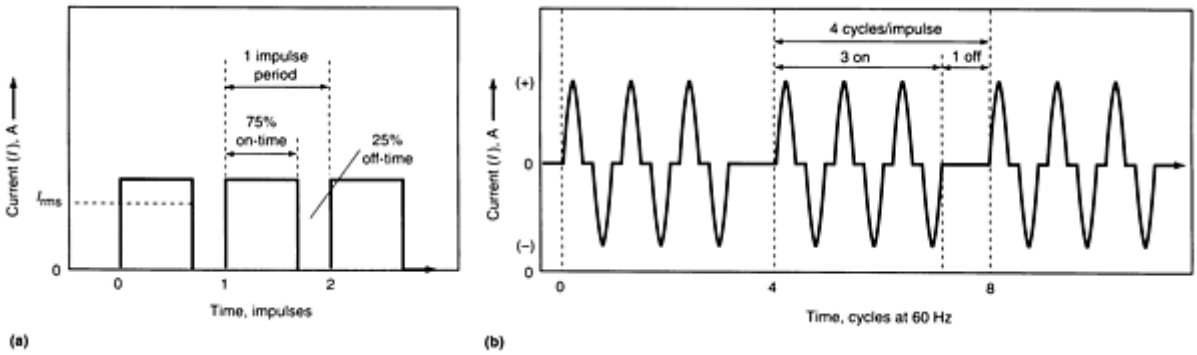

FIG. 8 WELD CURRENT PROFILES FOR SEAM WELDING. (A) IDEAL IMPULSE SHAPE. ON-TIME IS 75% OF IMPULSE PERIOD WHILE OFF-TIME IS 25% OF IMPULSE PERIOD. (B) ACTUAL IMPULSE SHAPE IS TYPICALLY COMPLEX AND NON-IDEAL. IN THIS SPECIFIC CASE, IMPULSES ARE FROM AN AC SINGLE-PHASE (3 ON/1 OFF) CURRENT SOURCE.

Current range is greater in impulse mode than in nonimpulse (continuous current) mode. The extra range seems to provide more robust penetration under difficult welding conditions, such as when intersecting other welds or turning corners with the seam.

One of the disadvantages of seam welding relative to spot welding is that solidification of the weld nugget occurs after the weld metal leaves the pressure field of the electrode wheels. Thus, if there is a large separating force on the weld before it freezes, it can come apart as it leaves the wheels. This postweld separation has been called "unzipping" or "alligatoring." Impulses effectively cure this problem because the off-times create a modulating penetration profile (Fig. 6), providing cool tack joints between the molten spots.

It is desirable from a process control standpoint to select an impulse schedule that will produce nuggets of nearly equal length and width, in conjunction with the other parameters used (speed, wheel diameter, wheel width, and power source).

In Table 1, theoretical parameters from Eq 2, 3, 4, 5, 6, 7, 8, 9, and 10 have been calculated for several commonly available impulse frequencies. The results can be used to predict optimum welding parameters from these basic principles.

TABLE 1 THEORETICAL PARAMETERS FOR LAP SEAM WELDING OF TWO EQUAL SHEETS OF MILD STEEL (PER EQ 2, 3, 4, 5, 6, 7, 8, 9, 10)

IMPULSED CURRENT (I)			UNCOATED[A], ONE SPOT UNDER WHEEL (N = 1)						COATED OR UNCOATED[A]											
									TWO SPOTS UNDER WHEEL (N = 2)						THREE SPOTS UNDER WHEEL (N = 3)					
			STACKUP (S_{MIN})		WELD ZONE LENGTH (L)		TRAVEL SPEED (V)		STACKUP (S_{MIN})		WELD ZONE LENGTH (L)		TRAVEL SPEED (V)		STACKUP (S_{MIN})		WELD ZONE LENGTH (L)		TRAVEL SPEED (V)	
Type	On-time/off-time	Impulse frequency (f), hz	mm	in.	mm	in.	mm/s	in./min	mm	in.	mm	in.	mm/s	in./min	mm	in.	mm	in.	mm/s	in./min
AC	[B]	120	0.53	0.021	1.34	0.053	160	370	0.76	0.030	3.78	0.149	227	535	0.93	0.037	6.94	0.273	278	656
AC	0.33/0.33	90	0.62	0.024	1.54	0.061	139	328	0.87	0.034	4.36	0.172	196	464	1.07	0.042	8.01	0.315	240	568
DC	0.67/0.33	60	0.76	0.030	1.89	0.074	113	268	1.07	0.042	5.34	0.210	160	379	1.31	0.052	9.81	0.386	196	464
AC	1/0.33	45	0.87	0.034	2.18	0.086	98	232	1.23	0.048	6.17	0.243	139	328	1.51	0.059	11.3	0.445	170	402
AC	1/0.67	36	0.98	0.039	2.44	0.096	88	207	1.38	0.054	6.90	0.272	124	293	1.69	0.067	12.7	0.500	152	359
AC	1.33/0.67	30	1.07	0.042	2.67	0.105	80	189	1.51	0.059	7.56	0.298	113	268	1.85	0.073	13.9	0.547	139	328
DC	1/1	30	1.07	0.042	2.67	0.105	80	189	1.51	0.059	7.56	0.298	113	268	1.85	0.073	13.9	0.547	139	328
AC	2/1	20	1.31	0.052	3.27	0.129	65	155	1.85	0.073	9.25	0.364	93	219	2.27	0.089	17.0	0.669	113	268
AC	3/1	15	1.51	0.059	3.78	0.149	57	134	2.14	0.084	10.7	0.421	80	189	2.62	0.103	19.6	0.748	98	232
AC	3/2	12	1.69	0.067	4.22	0.166	51	120	2.39	0.094	11.9	0.468	72	169	2.93	0.115	21.9	0.862	88	207
AC	4/2	10	1.85	0.073	4.63	0.182	46	109	2.62	0.103	13.1	0.516	65	155	3.21	0.126	24.0	0.945	80	189
AC	5/2	8.57	2.00	0.079	5.00	0.197	43	101	2.83	0.111	14.1	0.555	61	143	3.46	0.136	26.0	1.024	74	175
AC	6/2	7.50	2.14	0.084	5.34	0.210	40	95	3.02	0.119	15.1	0.594	57	134	3.70	0.147	27.8	1.094	69	164
AC	6/3	6.67	2.2	0.08	5.6	0.22	38	89	3.2	0.12	16.	0.63	53	126	3.9	0.15	29.	1.15	65	155

			7	9	7	3			0	6	0	0			2	4	4	7		
AC	7/3	6	2.39	0.094	5.97	0.235	36	85	3.38	0.133	16.9	0.665	51	120	4.14	0.163	31.0	1.220	62	147

(A) *N*, NUMBER OF NUGGET SPOTS UNDER THE ELECTRODE WHEEL; *S*, STACKUP, SUM OF BOTH SHEET THICKNESSES; *L*, CONTACT LENGTH OF ELECTRODE ON WORKPIECE.

(B) 60 HZ CONTINUOUS

The optimum weld speed may be identified experimentally as the speed with the widest current range for making good welds. Good welds are nominally free of typical metallurgical discontinuities (for example, surface cracks, gross lack of fusion at the weld interface, or surface melting eruptions).

When welding dissimilar thicknesses, on-time must not be greater than the optimum weld time for the thinnest outer sheet (*TOS*). Mathematically:

$$T = 4(0.0292)\,(TOS)^2 \qquad \textbf{(EQ 11)}$$

where *TOS* is in millimeters.

One way to satisfy the weld time needs of both total stackup, *S* (Eq 1) and *TOS* for thick-thin welding is to raise *n*, the number of nuggets in the weld zone, to 2 or 3. The goal here is to weld for the proper total time dictated by Eq 1, but to do it with pulses of on-time no greater than dictated by Eq 11. To increase *n*, one must carefully consider the electrode wheels as well as the impulse schedule. Even when taking advantage of pulsation, it may become impossible to seam weld extremely dissimilar thicknesses without damaging the thinnest outer sheet. This difficulty should become pronounced for thickness ratios above about 3 to 1.

Wheel Geometry, Weld Force, and Wheel Maintenance

The primary role of wheel geometry and force in seam welding is to control the dimensions of the weld zone or the size of the footprint that the wheel makes on the workpiece while welding.

The length of the footprint, *L*, is an important factor in the weld time equation (see the section "Weld Time, Speed, and Current Pulsation" in this article). The variable *L* is primarily controlled by wheel diameter, force, and current. (As either force or current is increased, the wheel will sink deeper into the work and *L* will increase.) It is worthwhile to measure or estimate *L*. This has been done experimentally using special voltage probes on the electrodes and by an optical silhouette method (Ref 7). A less accurate (but simpler) method is to read the heat pattern at the beginning and end of the weld, in order to estimate *n*, the number of nuggets under the wheel at any one time. For bare steel, *n* can be as low as 1. However, the weldability of coated materials and dissimilar thicknesses improves when *n* is as high as 2 or 3 (see Fig. 6). Keep in mind that the contact length will decrease somewhat as the wheel wears to a smaller diameter. (Normally this change should not be of concern, except possibly when welding beyond the theoretical top speed for a material combination.)

Footprint width is best matched with impulse length, *d*, to produce nearly round nuggets. Width, however, is of secondary importance to impulse length.

A transverse radius on the wheel generally improves the welding range, because under high current conditions it automatically reduces current density by sinking further into the work.

Under given electrode conditions, increasing weld force improves the welding range for speed and helps control cracking.

It is generally true that the current range improves with higher wheel pressure, until longitudinal splits begin to occur at seam starts or stops. On the other hand, at low force, transverse surface cracks may result at the upper end of the current range, especially on coated steels. A good role of thumb is to weld at 80% of the seam-splitting force, or less. In addition, it may be helpful to de-energize the weld force except while welding, so as not to cause undue wheel wear.

For the highest quality joints it may be necessary to lightly machine the wheels as they are used, in order to maintain a constant edge profile. The types of wheel dressing tools are:

- *SCRAPERS* TO REMOVE CONTAMINATION WHEN WELDING COATED MATERIALS
- *WIDTH CUTTERS* TO REMOVE MUSHROOMED COPPER AND CONTROL WHEEL WIDTH
- *KNURLERS* (FIG. 2), TO MAINTAIN THE TRANSVERSE PROFILE ON THE WHEEL AND DRIVE THE WHEELS AS NEEDED

If wheel maintenance on the machine is not feasible, the wheels can be removed and redressed off-line. Alternatively, the wire-electrode seam welding process provides a constant wheel condition and thus eliminates the need for continuous wheel dressing (Fig. 4).

Cooling the Weld

The weld cooling system is very important for process control of seam welding. Its primary role is to minimize thermal damage to the outer surfaces of the weld while the weld interface is being heated above the melting point. The key elements in the success of the weld cooling system are:

- *ELECTRODE MATERIAL* (THERMAL OR ELECTRICAL CONDUCTIVITY)
- *ELECTRODE TRANSVERSE SHAPE* (RADIUS PROFILE IS BEST)
- *ELECTRODE CLEANLINESS* (SHOULD BE DRESSED FREE FROM PICKUP OF NONCONDUCTING COATINGS)
- *ELECTRODE COOLING SYSTEM*
- *COOLING WATER* APPLIED DIRECTLY TO THE WELD (IF APPLICABLE)

Cooling water for seam welding wheels can be either internal or external. Internal cooling systems cool the wheel but not the weld. The key advantage of internal cooling is that the process is dry; the workpiece, the machine, and the operator stay dry. The cost of installing floor drains and water containment facilities is avoided. Neither is it necessary to remove water from inside the workpiece (as in the case of automotive fuel tanks). However, internally cooled wheels may cost more due to additional machining costs. Thus, operating costs for internal cooling may be higher than for external cooling. Some internal systems do not directly cool the wheel, but only the wheel shaft.

On the other hand, with external cooling, spray nozzles are aimed with some precision at the workpiece-wheel separation point. The benefits of external cooling include:

- THERMAL DAMAGE TO THE WELD SURFACE AND ANY COATINGS IS REDUCED, SO THAT WELDABILITY IS IMPROVED.
- WELD DISTORTION IS REDUCED.
- FUME EMISSION IS REDUCED.
- WHEEL CLEANLINESS IMPROVES, BECAUSE WATER IS DIRECTLY APPLIED TO THE HOTTEST POINT ON THE WHEEL, PRODUCING A QUENCH/CLEANING ACTION ON THE WHEEL SURFACE.
- WELD HARDNESS WILL INCREASE, ADDING STRENGTH TO THE WELD UNDER CERTAIN LOADING CONDITIONS SUCH AS CRUSH LOADING. (*CAUTION: SOME QUENCH-SENSITIVE MATERIALS MAY NOT ALLOW EXTERNAL COOLING.*)

In welding bare steel, rust-preventive water solutions are sometimes used, such as 5% borax ($Na_2B_4O_7 \cdot 10H_2O$).

Metals Welded

Most low-carbon, high-carbon, low-alloy, and stainless steels, and many coated steels above approximately 0.15% tend to form areas of hard martensite upon cooling. In critical applications, the welds may require postweld tempering to reduce the hardness and brittleness. In some cases, this can be done in the welding machine. Tempering can also be done in a furnace or by induction heating.

Aluminum and aluminum alloys can be lap seam welded but not mash seam welded, due to their narrow plastic range. Nickel and nickel alloys can also be seam welded, but seam welding is not recommended for copper and high-copper alloys. Compatible combinations of dissimilar metals and alloys also can be seam welded. For additional information on the seam welding of stainless steel, aluminum alloys, and copper alloys, see the article "Procedure Development and Practice Considerations for Resistance Welding" in this Volume.

References cited in this section

4. "RECOMMENDED PRACTICES FOR RESISTANCE WELDING," AWS C1.1, AMERICAN WELDING SOCIETY
5. *RESISTANCE WELDING MANUAL,* 4TH ED., RESISTANCE WELDER MANUFACTURERS ASSOCIATION, 1989
6. T. OKUDA, SPOT WELDING OF THICK PLATES, PART I: THE LAW OF THERMAL SIMILARITY, *YOSETSU GIJUTSI,* VOL 21 (NO. 9), 1973, P 85-88 (IN JAPANESE)
7. T. YAMAMOTO AND T. OKUDA, FUNDAMENTAL STUDY ON WELD FORMATION PHENOMENA OF HIGH SPEED LAP SEAM WELDING, 3RD REPORT: VOLTAGE ACROSS ELECTRODES AND CURRENT FLOW AREA OF PLATE SURFACE, *YOSETSU GAKKAISHI,* VOL 46 (NO. 10), 1977, P 748-753 (IN JAPANESE)

Resistance Seam Welding

Michael J. Karagoulis, General Motors Corporation

Types of Seam Welds

Several types of resistance seam welds can be made:

- *LAP SEAM WELDS* JOINING OVERLAPPING FLAT SHEETS (FIG. 1A)
- *FLANGE-JOINT LAP SEAM WELDS* WITH AT LEAST ONE FLANGE OVERLAPPING THE MATING PIECE (FIG. 5A)
- *FOIL LAP SEAM WELDS,* IN WHICH AN ALLOY METAL FOIL IS PLACED AT THE WELD INTERFACE
- *MASH SEAM WELDS* WITH WORK METAL COMPRESSED AT THE JOINT TO REDUCE JOINT THICKNESS (FIG. 1B)
- *BUTT SEAM WELDS* (FIG. 1C AND 3)

In addition, both low-frequency and high-frequency induction and resistance welding are used for butt welding strip stock into tubes and other shapes.

Lap Seam Welds

The most common type of seam weld is a simple lap seam in which the pieces to be welded are lapped sufficiently to prevent the sheet edges from becoming part of the weld (Fig. 1a). Applications include sealing of cans and tanks in which liquid-tight or gas-tight joints are needed.

Flange-joint lap seam welds are used in joining assemblies having one straight member and one outward-flanged member at the joint to be welded (for example, the duct in Fig. 5a) or assemblies with two outward-ranged members (for example, the automotive gasoline tanks in Fig. 5b). Common applications include containers with out-turned bottoms or tops, and ducts or structural parts with out-turned sides. Unless the workpiece length is less than the usable throat depth of a longitudinal machine, seam welds of this type are made on a circular machine.

Often, container ends are dished for added strength, and one or both electrode wheels must be mounted at an angle to clear the workpiece. Wheel diameter limitations may also necessitate setting a wheel at an angle (Fig. 5a, right view).

Flange-joint seam welds can also be used for welding assemblies in which the flanges face inward at the joint (Fig. 5c). However, to reduce overhang of the arm supporting the lower electrode or to reduce the required throat depth of the

machine, the length of the workpiece should be kept to a minimum. If the lower electrode support is small, too much overhang can result in excessive deflection of the support and thus cause inconsistent weld quality because of force variation.

Mash Seam Welds

Mash seam welds are produced by overlapping two sheets by an amount ranging from one to two times the sheet thickness and applying electrode force and current. The resulting over-thickness is 5 to 25%.

Usually wide, flat edges are used on the electrode wheels. The joint itself acts as a current localizer, as in projection welding, because the overlap is thicker than either sheet by itself. Because the wheels are wide and flat-edged, the transverse position of the joint on the wheels can be oscillated as needed to prevent a groove from forming on the wheels and to increase the period between wheel dressings.

Careful selection of an impulse weld schedule will result in higher penetration and greater joint strength, although the "bumpy" appearance of a weld made with pulsating current may not meet product requirements. Cosmetic mash seam welds can be made with nonpulsed (continuous) current, or by pulsing according to the minimum nugget spacing afforded by Eq 3 (for mash seams use S = thickness after welding).

Because sheet overlap is a critical parameter, workpieces must be rigidly and accurately clamped or tack welded to prevent lateral motion during welding. Clamp distance is highly important and is related to stock thickness. On continuously fed, moving-part setups and thin metal processes (where clamp distance would be too small), clamps may not be feasible. In these cases, a Z-bar and nosepiece tooling arrangement is used to help position the edges to be welded.

In applications in which the mashed surface must be as flat and burr-free as possible after welding to facilitate porcelain enameling and to present a good appearance, a bar-type electrode is used against the surface to be enameled, and an electrode wheel is used against the other surface. The bar-type electrode may require periodic dressing to avoid excessive grooving and subsequent loss of current density. When a premium finish appearance is required, the weld can be ground or roll planished to remove surface imperfections.

In steel coil joining, it is sometimes desirable for the final thickness of the mash seam weld to be similar to the single sheet thickness. To minimize the thickness gain from welding, pre- and/or postweld planishing rolls are used. These rolls are hard steel wheels, typically 100 mm (4 in.) in diameter and 20 mm (0.75 in.) in width. Planishing rolls are typically loaded to 22 kN (5000 lbf) to cold work the weld. In this way the overthickness may be held to as little as 5%. Also, the overlap may be retracted slightly after the preweld planish in order to further limit over-thickness.

The highest quality mash seam welds are made in low-carbon steels and stainless steels. The process is widely used in the manufacture of refrigerators, stoves, laundry equipment, and other products that receive porcelain enamel coatings. Mash seams are gaining popularity in automotive applications for creating tailored blanks that reduce weight and material loss in certain large stampings (for example, body sides and doors), reduce manufacturing complexity, and reduce the number of components and welds required to make finished automotive subassemblies.

Because of their narrow plastic range, nonferrous metals generally cannot be mash seam welded.

Butt Seam Welds

Butt seam welds can be classified as either autogenous or exogenous.

Autogenous (nonfilled) butt seam welds are made by a special seam welding technique in which the two abutting edges are heated and lightly forged together. There is a slight depression where the electrode wheels compress the plastic metal. This type of weld usually has low strength and a reduced cross-sectional area. Resistance tube welding may be a better alternative to this process.

Exogenous (Filled) Butt Seam Welds. The strength of a butt seam weld can be increased by adding filler metal to the outer surface of the weld, against the electrode. Filler metal, in the form of a foil or a shaped wire, is introduced on one or both surfaces adjacent to the joint as the workpiece is passed between conventional seam welding electrodes (Fig. 3). This technique produces a smooth, nonoverlapping seam that is high in strength with good appearance. Highest quality exogenous butt seam welds show nugget penetration to the filler-workpiece interface, complete filler bonding, and

smooth, regular surface contours. The only edge preparation required is to ensure that the sheared edges are clean and straight without excessive burr or gap when they are butted together. The filler acts as a bridge to:

- DISTRIBUTE THE WELDING CURRENT MORE EVENLY TO BOTH SHEETS
- CONCENTRATE THE CURRENT IN THE JOINT
- HELP CONTAIN THE MOLTEN NUGGET AS IT GROWS AND THEN COOLS
- PROVIDE METAL FOR A SLIGHTLY RAISED BEAD, WHICH WILL ADD STRENGTH

The variables having the greatest effect on the tensile strength of filled butt seam welds are current, speed, size of the gap between the edges of the butted workpieces, and work metal thickness. Surface grinding will improve cosmetic appearance but also may reduce weld strength.

For the commonly used thicknesses of low-carbon steel, welding speeds similar to those used in lap seam welding are permissible, providing that the gap is no wider than 0.38 mm (0.015 in.). Either pulsed or continuous current can be used.

Resistance Seam Welding

Michael J. Karagoulis, General Motors Corporation

Processing Equipment

A seam welding machine is similar in construction to a spot welding machine, except that one or two electrode wheels are substituted for the spot welding electrodes.

Seam Welding Machines

In general, seam welding is done in a press-type resistance welding machine. Most seam welding machines are powered by alternating current (ac), either three-phase or single phase; some are designed for use with direct current (dc). Others superimpose a high frequency (16.5 kHz) on the basic power line. Stored-energy seam welding machines have been built, but this type finds little use. Direct current frequency converter power supplies are used to tailor custom pulsation schedules.

Equipment for seam welding must be capable of:

- DELIVERING LOW-VOLTAGE, HIGH-AMPERAGE CURRENT
- SUPPORTING THE ELECTRODES AND WORKPIECE AND APPLYING THE ELECTRODE FORCE
- MOVING THE WORKPIECE AND/OR DRIVING THE ELECTRODES
- REGULATING, TIMING, AND SEQUENCING THE APPLICATION OF THE WELDING CURRENT, FORCE, AND COOLING WATER (IF APPLIED)
- CAREFUL PART HANDLING, SUCH THAT EXTRANEOUS FORCES ARE NOT IMPOSED DURING WELDING

Electrode Force and Support. The upper electrode wheel is mounted to, and insulated from, the operating head. The head, which is actuated by a direct-acting air or hydraulic cylinder, applies the electrode force. The lower electrode is either a wheel, a platen, or a mandrel and is mounted on a supporting arm, table, or knee. This lower support can be made adjustable for applications in which the work metals must be maintained at a constant level above the floor.

Electrode or Workpiece Drives. Workpieces are moved by rotating the electrodes with knurl or friction drive, by direct drive of the wheel shaft, by a driven workpiece and idling wheels, or by clamping the workpieces to a bar electrode and moving the bar electrode (Fig. 3).

Weld travel tends to be continuous on thin steel sheets (less than 1.7 mm, or 0.067 in.), whereas it is intermittent on thick sheets (greater than 3.0 mm, or 0.118 in.). The need for intermittent weld travel arises from the longer weld time requirements of thick steel (Eq 1).

Knurl Drive versus Friction Drive. In a knurl drive or friction drive, one or both of the electrodes are rotated by a knurl or friction wheel on the peripheral surface of the electrode wheel, to provide nearly constant linear speed regardless of the diameter of the electrode wheel. The knurl drive, in which ridges or beads on the drive wheel aid in turning the electrode, minimizes slippage and is more positive than the friction drive, in which the turning surface of the drive wheel is smooth. The knurled wheel also removes some of the pickup from the electrode wheels. A knurl drive is used when welding coated metals, such as galvanized steel and terneplate, in any application in which the electrodes are likely to pick up material from the work metal, and for scaled stock that cannot be precleaned. A knurl drive usually is not employed if good cosmetic appearance of the weld is important. Knurl or friction drives can be used only with electrode wheels large enough in diameter to allow clearance.

Gear drive is used if small-diameter electrode wheels cannot be driven by the use of knurled or friction wheels because of interference, or if the application cannot tolerate an electrode wheel that has been roughened by a knurled drive roll. With gear drive, in which the mounting shaft of the electrode wheel is driven, the speed of welding decreases as the wheel wears down.

In a standard seam welding machine, interference may exist at some minimum distance between electrode wheel centers. If one wheel must be small to clear the workpiece, the other must be correspondingly large. If the ratio of the electrode wheel diameters is greater than 2 to 1, the smaller wheel should be driven, to minimize slippage. Welding speed can be kept constant in spite of wheel wear by a variable-speed gear-driven mechanism.

Movable Carriages. When a mandrel or a platen is used as the lower electrode (Fig. 3), the operating head carrying the upper electrode may be mounted in a carriage. The carriage is moved by an air or hydraulic cylinder, or by a motor-driven screw, and thus the upper electrode is passed over both the workpiece and the lower electrode. The upper electrode is free-wheeling, but it may be equipped with an idling knurl for dressing. Sometimes it is necessary to use a high-slip drive to assist on thin materials, to prevent wrinkling. In some machines, the workpiece is clamped to a bar-type lower electrode and moved under an idling fixed-position upper electrode wheel.

Types of Machines. There are four basic types of resistance seam weld machines: circular, longitudinal, universal, and portable.

Circular. The axis of rotation of the electrode wheels is at right angles to the front of the machine (Fig. 2a). This type of machine is used for circular work, such as for welding the heads on containers and for flat work requiring long seams. Head pivot capability for welding on an inclined plane is optional.

Longitudinal. The axis of rotation of the electrode wheels is parallel to the front of the machine (Fig. 2b), and throat depth is typically 305 to 915 mm (12 to 36 in.). This type of machine is used for welding short longitudinal seams in containers, for attaching pieces to containers, for coil joining, and for similar work. Machines with traveling heads or traveling electrodes, in which a mandrel or a platen is used for the lower electrode, are normally of the longitudinal type.

Universal. A swivel-type head and interchangeable lower arms allow the axis of rotation of the electrode wheels to be set either at right angles or parallel to the front of the machine.

Portable. The workpiece is clamped in a fixture, and a portable welding head is moved over the seam, either manually or by using a robot. This type of machine is used when the workpiece is too bulky to be handled by a regular machine or when it is more efficient to move the welding head rather than the workpiece. This type of machine is sometimes used for joining the roof and body sides on automobiles. The portable welding head is moved by motor-driven wheels, and an air cylinder mechanism provides the electrode force.

Common power sources used for seam welding are similar to those used for spot welding. They usually consist of a welding transformer, with a tap switch in the primary circuit, driven by a silicon-controlled rectifier switching system and a secondary circuit with electrodes for transferring the welding current to the work metal.

Controls for seam welding are generally similar to those for spot welding, except for differences related to the relative motion of the work and the electrodes. Most modern weld timers are capable of generating impulse weld schedules for

seam welding. (Higher impulse frequencies for welding thin stock can be obtained using special high-frequency systems, although complete machine redesign may be necessary due to transformer and throat area limitations that are directed by the frequency.) Tap switches and a phase-shift heat control are used as in spot welding for changing the transformer output current. In theory, direct feedback current regulation would be a desirable feature in seam welding, and some work has been done to develop and improve this. Alternating current is inherently more stable in secondary root-mean-square (rms) current than dc, because in ac there is essentially no current memory from one half-cycle to the next, or from one impulse to the next.

Selection of Electrodes

Alloy type and wheel configuration are the primary factors that determine electrode selection.

Class 1 Copper. Electrode wheels made of Resistance Welder Manufacturers Association (RWMA) class 1 copper (RWMA No. 1.16200) have been used for seam welding of aluminum and magnesium alloys, galvanized steel, and tin-plated steel. The minimum electrical conductivity of class 1 copper is 80% International Annealed Copper Standard (IACS). Recently, this material has been replaced by hot-forged and heat-treated RWMA class 2 copper in the overaged condition (RWMA No. 1.18200). With adequate cooling and proper parameters, the high electrical and thermal conductivities of this material keep the electrode-workpiece interface at a temperature below the point where metallurgical discontinuities are formed near the weld surface.

Class 2 Copper. Seam welding of low-carbon and low-alloy steel is usually done with electrodes made of hot-forged and heat-treated RWMA class 2 copper (RWMA No. 2.18200). Minimum conductivity is 75% IACS. Minimum hardness is typically 65 HRB. Class 2 also works well with all types of coated steel, but the metallurgical optimization of weld parameters and provisions for wheel maintenance are critical to the success of welding coated steels. For longer electrode life, premium class 2 wheels are available in the 20% coldworked form, where a minimum hardness of 75 HRB may be specified. Coldworked wheels show no appreciable loss of conductivity over the forged class 2 material.

Class 20 copper (RWMA No. 20.15760) is also used for electrode wheels, with properties similar to those of class 2 premium wheels. Class 20 wheels are made using a powder metallurgy process that produces a pure copper product, dispersion-strengthened with alumina. The alumina adds hot strength and tends to reduce pickup during welding of coated steels.

Class 3 copper (RWMA No. 3.17510) is sometimes used for seam welding materials with lower electrical conductivities, such as stainless steel, Nichrome, and Monel alloys. However, class 3 is used with special ventilation only because of the health hazard of atmospheric beryllium when welding or machining with class 3 material. (Beryllium-free class 3 alloy RWMA 3.18000 is also available.) Class 3 wheels have lower electrical conductivity (45% IACS), so they tend to run hot.

Sizes and Shapes. Electrode wheels range in diameter from 50 to 610 mm (2 to 24 in.). Popular sizes range from 100 to 305 mm (4 to 12 in.), with widths from 6 to 19 mm ($\frac{1}{4}$ to $\frac{3}{4}$ in.). Edge contours may be flat, radiused, beveled flat, or angled. In lap seam welding, weld quality seems to be easiest to control with a radius edge, as discussed above. The need for nonradius contours is usually a matter of cosmetic appearance, or due to a tool access limitation. Mash seam welders very often use a flat-edge wheel, as in Fig. 1(b).

Resistance Seam Welding

Michael J. Karagoulis, General Motors Corporation

Weld Quality and Process Control

Welding Parameters. It is best to design the entire process around proven weld parameters that have been metallurgically validated on workpieces very similar to actual production parts. Sensitive parts of the weld typically are starts, stops, corners, adjacent shunt paths, intersecting seams, and areas of poor metal fit. On coated metal, parameters should be flexible enough to handle normal coating variations.

To select starting weld parameters, use the guidelines presented in the section "Fundamentals of Lap Seam Welding" in this article and Table 1. For process design, the givens are usually material thickness, available pulsation capability, and wheel diameter. From these three independent variables will spring all of the dependent variables (for example, speed, force, current, and so on) from Eq 2, 3, 4, 5, 6, 7, 8, 9, 10, and 11. At this point, estimates of *S* and *L* would be helpful in order to begin the calculations. Use working values that are not too near the extreme limits of either the material, the weld tool, or the plant facilities. To make leak-tight seams, weld spots should have approximately equal length and width. Ideally, the same welding parameters should be used for the entire length of the weld.

Verify the quality of resulting welds using chisel tests, metallographic sections, pressure tests, or fatigue tests, depending on product requirements. Record target values for speed, force, pulsation, and water cooling (if applicable). Record tap setting and lower and upper rms secondary current limits for acceptable weld quality. Record the actual secondary current waveform to see that it is acceptable (as in Fig. 8) and consistent throughout the weld. Process changes should be made only on the basis of data.

Establish production procedures for maintenance of electrode wheels and cooling sprays (if applicable). Check process parameters against required values frequently, and make adjustments and repairs as needed.

Nondestructive testing (for example, resistivity, ultrasonic testing, dye penetrant, magnetic particle, or eddy current) may be useful in some low-volume testing applications. However, such techniques should come into use only after the optimum parameters are verified metallographically and the process is well understood. In many instances, much can be observed from the external appearance of a lap seam weld, provided the weld surface is not planished or scarfed after welding.

Coated Steels. For a process that has been properly set up and optimized as described in the section "Welding Parameters" in this article, the difference in parameters between coated and uncoated steel lies mainly in weld current. Steels with low-melting metallic coatings require more current than uncoated steels. Organic coated steels require about the same current as uncoated steels (although the current range for making good welds will be smaller for the organic coated steels). Some coatings (for example, zinc and aluminum) are particularly active at the electrode-workpiece interface. For these surface-active coatings, speed, force, and pulsation are selected to keep the surface temperature of the weld below the point where metallurgical discontinuities are developed. Diligent maintenance of the wheel condition and the cooling system cannot be overstated for sensitive applications.

Resistance Seam Welding

Michael J. Karagoulis, General Motors Corporation

References

1. K.M. PICKETT, M.F. SHI, K.K. BHATT, AND J. SELVARAJ, STRUCTURE PROPERTY RELATIONSHIPS OF RESISTANCE MASH SEAM WELDED TAILORED BLANKS WITH POST HEAT TREATMENT, *24TH CONF. INT. METALLOGRAPHIC SOC.* (DENVER), AUG 1992
2. Y. ADONYI, J. MILIAN, AND L. ROUDABUSH, WELDED STEEL SHEET PERFORMANCE FOR TAILORED BLANKS, *PROC. SHEET METAL WELDING CONF. V,* PAPER C1, AMERICAN WELDING SOCIETY, OCT 1992
3. VDI REPORT 818, VEREIN DEUTSCHER INGENIEURE, 1990, P 256 (IN GERMAN)
4. "RECOMMENDED PRACTICES FOR RESISTANCE WELDING," AWS C1.1, AMERICAN WELDING SOCIETY
5. *RESISTANCE WELDING MANUAL,* 4TH ED., RESISTANCE WELDER MANUFACTURERS ASSOCIATION, 1989
6. T. OKUDA, SPOT WELDING OF THICK PLATES, PART I: THE LAW OF THERMAL SIMILARITY, *YOSETSU GIJUTSI,* VOL 21 (NO. 9), 1973, P 85-88 (IN JAPANESE)
7. T. YAMAMOTO AND T. OKUDA, FUNDAMENTAL STUDY ON WELD FORMATION PHENOMENA OF HIGH SPEED LAP SEAM WELDING, 3RD REPORT: VOLTAGE ACROSS ELECTRODES AND

CURRENT FLOW AREA OF PLATE SURFACE, *YOSETSU GAKKAISHI,* VOL 46 (NO. 10), 1977, P 748-753 (IN JAPANESE)

Resistance Seam Welding

Michael J. Karagoulis, General Motors Corporation

Selected References

- Y. ADONYI, RESISTANCE SEAM WELDING OF ENAMELING QUALITY STEEL SHEET, *PROC. PORCELAIN ENAMEL INSTITUTE TECHNICAL FORUM,* VOL 52, 1990, P 729-748
- M.J. KARAGOULIS AND M.A. PUSATERI, SEAM WELDING AND PRE-PAINTED FUEL TANKS AT GENERAL MOTORS, *PROC. SHEET METAL WELDING CONF. II,* AMERICAN WELDING SOCIETY, OCT 1986
- C.A. LEFFEL, "AN INVESTIGATION INTO THE RESISTANCE SEAM WELDABILITY OF COATED STEELS," MASTER'S THESIS, THE OHIO STATE UNIVERSITY, 1990
- A.A. MAZAEV AND G.V. NAZAROV, EFFECT OF THE FORM OF THE WELDING PULSE ON HEATING OF THE WELD ZONE IN ONE-SIDE RESISTANCE SPOT AND SEAM WELDING, *FIZ. KHIM. OBRAB. MATER.,* VOL 17 (NO. 5), 1983, P 125-131 (UDC 621.791.762.5 IS IN ENGLISH)
- A.W. SCHUELER, RESISTANCE SEAM WELDING, *WELD. RES. COUNC.,* BULLETIN 225, APRIL 1977
- SOUDRONIC LTD LITERATURE, 465 NORTH STATE RD., BRIARCLIFF MANOR, NY 10510, USA
- K. TORII, Y. KADANO, AND Y. TAMURA, A STUDY ON THE DEFECTS IN SEAM WELDS OF METAL COATED STEEL SHEETS, *TRANS. JPN. WELD. SOC.,* VOL 2 (NO. 1), 1971, P 77-85
- S.A. WESTGATE, THE HIGH SPEED RESISTANCE SEAM WELDING OF NOMINALLY 1.2 MM LOW CARBON STEEL SHEETS, *BR. WELD. INST.,* DOC 240/1984, 1984
- N.T. WILLIAMS, D.E. THOMAS, AND K. WOOD, HIGH SPEED SEAM WELDING OF TINPLATE CANS, PARTS I AND III, *MET. CONSTR.,* APRIL 1977, P 157-160, MAY 1977, P 406-408

Flash Welding

H.J. Latimer and R.B. Matteson, Taylor-Winfield Corporation

Introduction

FLASH WELDING (FW) is a resistance welding process in which a butt joint weld is produced by a flashing action and by the application of pressure. In basic terms, it is a melting and a forging process. The process is capable of producing welded joints with strengths equal to those of the parent materials. Figure 1 is a schematic representation of a typical flash welding operation.

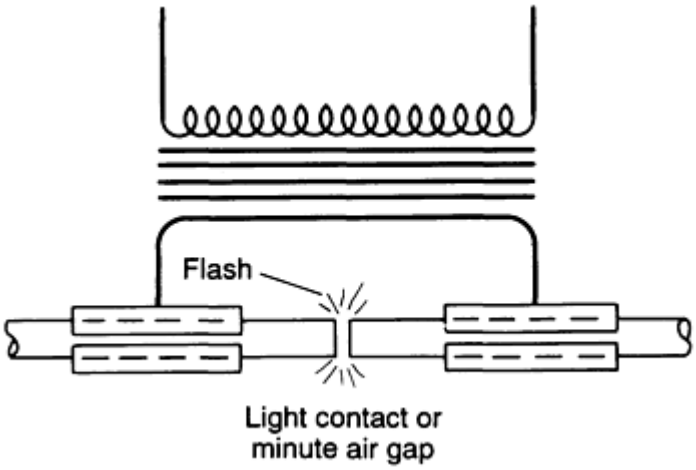

FIG. 1 TYPICAL FLASH-WELDING SETUP SHOWING AIR GAP PRESENT BETWEEN ENDS OF TWO BARS

Flash welding is used to join metallic parts that have similar cross sections, in terms of size and shape. The process lends itself to joining nearly all grades of steel, aluminum, brass, and copper parts, in addition to selected dissimilar materials.

Flash Welding

H.J. Latimer and R.B. Matteson, Taylor-Winfield Corporation

Process Applications

Materials with cross sections ranging from 65 to 13,000 mm^2 (0.1 to 20 $in.^2$) are commonly flash welded. The process is also used to manufacture components of solid and tubular shape, in addition to strips and complex configurations. Flash welding is commonly used to weld rings that range in diameter from a few inches (Fig. 2) to as much as 4.6 m (15 ft) (Fig. 3). The aircraft engine industry uses flash welded rings made from heat-resistant materials in accordance with military specifications for jet aircraft.

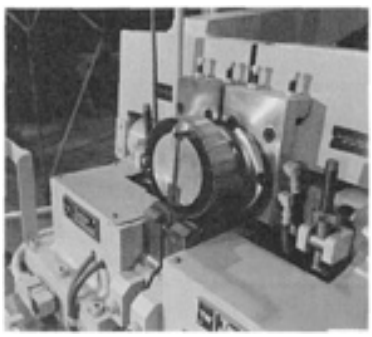

FIG. 2 FLASH-WELDING MACHINE USED TO FABRICATE A COILED STEEL STRIP INTO A SMALL-DIAMETER RING WITH A FLANGE

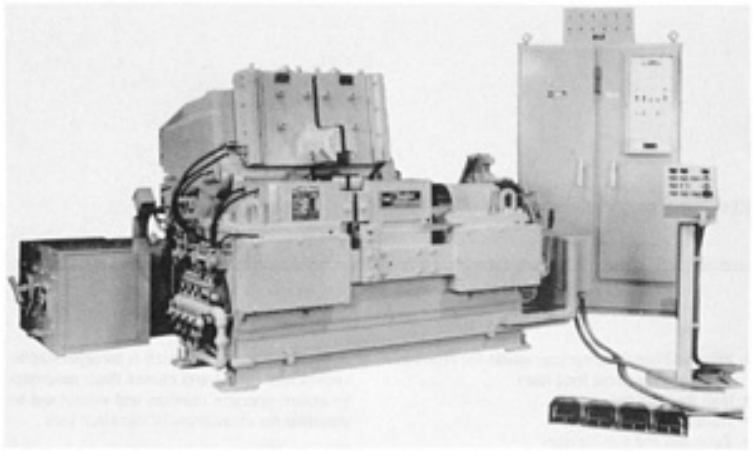

FIG. 3 FLASH-WELDING MACHINE WITH CAPACITY TO WELD RINGS UP TO 4.6 M (15 FT) IN DIAMETER

Other flash-welding applications include:

- CHAIN LINKS
- TRANSMISSION BANDS
- AUTOMOTIVE FLYWHEEL RING GEARS
- STRIPS THAT ARE JOINED FOR CONTINUOUS PROCESSING LINES
- WIRE AND BAR DRAWING OPERATIONS FOR CONTINUOUS STAMPING PRESS FEED LINES
- ROLL FORM LINES
- AIRCRAFT LANDING GEAR
- TUBE AND ROD EYE CLEVISES
- BAND-SAW BLADES (FIG. 4)
- DRILL EXTENSIONS USING TWO DIFFERENT MATERIALS
- MITER JOINTS FOR AUTOMOTIVE AND HOME WINDOW FRAMES
- CRANKSHAFT COUNTER WEIGHTS
- ALUMINUM-TO-COPPER ELECTRICAL TRANSITION FOR POWER TRANSMISSION
- ANODES USED IN ALUMINUM SMELTERS

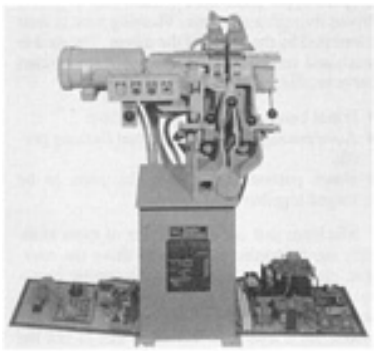

FIG. 4 FLASH-WELDING MACHINE INSTALLATION EQUIPPED TO WELD BAND-SAW BLADES

H.J. Latimer and R.B. Matteson, Taylor-Winfield Corporation

Processing Equipment

A typical flash-welding machine consists of seven major components:

- A MACHINE BED THAT HAS A FIXED PLATEN ATTACHED TO IT, AS WELL AS A SET OF ELECTRICALLY INSULATED WAYS THAT SUPPORT A MOVABLE PLATEN
- A MOVABLE PLATEN, WHICH IS GENERALLY MOUNTED ON THE ELECTRICALLY INSULATED WAYS THAT ARE ATTACHED TO THE MACHINE BED
- TWO CLAMPING ASSEMBLIES, ONE OF WHICH IS RIGIDLY ATTACHED TO EACH PLATEN TO BOTH ALIGN AND HOLD THE PARTS TO BE WELDED IN PLACE
- EQUIPMENT FOR CONTROLLING THE MOTION OF THE MOVABLE PLATEN
- A WELDING TRANSFORMER WITH ADJUSTABLE TAPS
- CONTROLS AND MONITORS FOR MACHINE FUNCTIONS
- A VENT/FLASH CATCHER, WHICH IS INCORPORATED TO COLLECT ANY FUMES AND EXCESS FLASH MATERIALS TO ENSURE OPERATOR COMFORT AND SAFETY AND TO MAINTAIN THE CLEANLINESS OF THE WORK AREA

The movable platen of a flash welder can be driven by a number of different methods. The simplest type often uses a cam that is motor driven through a gear box. Flashing time is then controlled by the speed of the motor. The cam is machined to produce the desired flashing cam curve profile, including the:

- INITIAL BURN-OFF REGION OF LINEAR FLASH
- ACCELERATING CURVE FOR THE ACTUAL FLASHING PROFILE
- UPSET PORTION THAT CAUSES THE PARTS TO BE FORGED TOGETHER AFTER FLASHING

Machines that are either larger or more complex use hydraulic cylinders to drive the movable platen and to incorporate hydraulic servo-systems. Although it is possible to use a servovalve to directly control the position of the platen via a hydraulic cylinder, this is not the preferred method, because contamination by the oil is extremely difficult to prevent. The better approach is to use a hydraulic servoactuator, in which the servovalve operates on its own refined oil system and the oil that circulates through the platen cylinder is derived from another hydraulic source. This approach has been shown to be more reliable and more accurate, and to vastly improve servovalve life.

Controls and Auxiliary Equipment. Electrical controls on flash-welding equipment are designed to sequence the machine, control the weld current, and precisely control the platen position during flashing and upsetting. These controls often comprise programmable controllers, welding current controllers, and either motor or servovalve controllers. Silicon-controlled rectifier (SCR) contactors (solid-state switches) are used as the devices to control the flow of welding current from the power lines to the welding transformer. Older machines used ignitrons for this purpose, but SCRs have fully replaced them in recent years. Preheat and postheat cycles are often required procedures in flash welding operations; timers with phase-shift heat control are used to accomplish these important functions.

Power Sources. The most common source of power for flash welders is single-phase alternating current (ac) power. Flash welding transformers are KVA rated at 50% duty cycle.

Conversions From ac to dc Power. If an extremely large demand current is required and an adequate single-phase ac source is not available, then ac to dc conversion is employed using a three-phase transformer/rectifier. The most frequently used rectifier systems are the three-phase half-wave and three-phase full-wave types. In actual practice, no discernible differences in the weld produced by these two rectifier systems can be detected.

State-of-the Art Welding Unit Components. Devices that monitor and control selected process parameters are commonly incorporated into the latest flash welding units.

A linear ramp preflashing approach rate is usually built into the flashing cam and minimizes any tendency of the weld to freeze at the beginning of flashing. The term "flashing cam" is used regardless of whether the cam is a motor-driven machined cam or if the position curve is generated electronically.

Natural Log Flashing Curves. Numerous technical articles have been published on what constitutes the best flashing curve. Although engineers are divided on this issue, it has been shown that the use of natural log curves results in significantly better welds than are produced using any other curve. The natural log system conforms to the natural heat-transfer characteristics of the metal being welded, thereby creating a flashing progression that parallels the development of heat at the interface with a natural log gradient toward the clamp.

Ramp Turn-On of SCRs. Not to be confused with the linear approach ramp, this control device slowly and progressively turns on the SCRs at the beginning of the flashing cycle. Because the magnetic condition of a weld transformer may be unknown at the end of a previous weld, the ramp turn-on device is used to restore the transformer to a known condition. This greatly extends the life of the transformer itself, in addition to the SCR contactor, because it avoids the high inrush of current that would have occurred when the next weld was initiated.

No Phase Shift During Flashing. This control feature ensures that full voltage will be applied to the dies whenever flashing conditions are present, except during the ramp turn-on interval. A phase shift can reduce the average voltage, but does not reduce the peak voltage. During the phase-delay period of the voltage waveform, the platen continues to travel forward until a peak voltage is suddenly applied, causing violent flashing and deep cratering. Although the pyrotechnics of a phase-shift flashing action can be quite impressive, the resulting weld will be a disaster. The best flashing action is relatively subdued and produces flash particles of significantly lower intensity and size.

The oxygen depletion system used in this process is a patented method of combusting the oxygen that would otherwise exist in the weld interface region. In actual use, the oxygen depletion system does more than remove oxygen. By heating the gases in the interface region, the ionization voltage is reduced and higher flashing currents can be sustained at relatively low flashing voltages.

Upset Welding

W.R. Kanne, Jr., Westinghouse Savannah River Company

Introduction

UPSET WELDING (UW) is a resistance welding process utilizing both heat and deformation to form a weld. The heat is produced by resistance to the flow of electrical current at the interface of the abutting surfaces to be joined. The deformation results from force on the joint in combination with softening from the electrical resistance heat. Upset welding typically results in solid-state welds (no melting at the joint). The deformation at the weld joint provides intimate contact between clean adjoining surfaces, allowing formation of strong metallurgical bonds. If any melting does occur during upset welding, the molten metal is typically extruded out of the weld joint area.

A wide variety of shapes and materials can be joined using upset welding in either a single-pulse or continuous mode. Wire, bar, strip, and tubing can be joined end to end with a single pulse of welding current. Seams on pipe or tubing can be joined using continuous upset welding by feeding a coiled strip into a set of forming rolls, resistance heating the edges with wheel electrodes, and applying a force to upset the edges together.

Equipment for single-pulse upset welding is relatively simple. It consists of a pneumatic or hydraulic system for force application, transformers or a bank of diodes as a source of electrical current, and a standard resistance-welding controller. A data acquisition system usually is employed to record the force, current, voltage, and motion of the weld head during welding. Equivalent welds have been made using both alternating and direct current.

Upset welds have similar characteristics to inertia friction welds, which are also solid-state welds. The amount of deformation is usually less for upset welds, and the deformation can be more precisely controlled using upset welding. For example, a pipe butt weld made using inertia friction welding will have a large upset on both the inside and outside, whereas an upset weld can be controlled, through joint design and welding parameters, to have essentially no internal upset (Fig. 1).

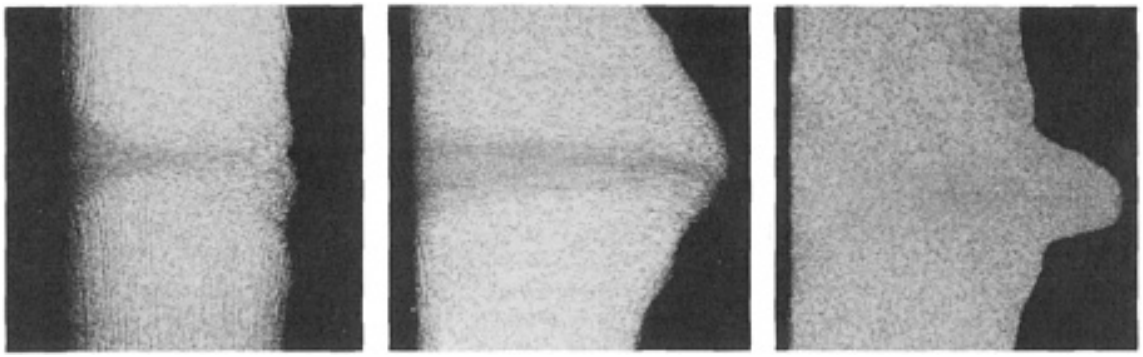

FIG. 1 UPSET WELD CONFIGURATIONS IN BUTT WELDS OF PIPE WITH AN OUTSIDE DIAMETER OF 25 MM (1 IN.) AND A WALL OF 3 MM (0.1 IN.). UPSET HAS BEEN MACHINED FROM THE OUTSIDE SURFACE (ON LEFT). THE INTERNAL UPSET CONFIGURATION WAS CONTROLLED BY ADJUSTING WELD PARAMETERS AND JOINT DESIGN. (A) MINIMUM UPSET. (B) LARGE UPSET. (C) NARROW UPSET AT LOW FORCE. COURTESY OF WESTINGHOUSE SAVANNAH RIVER COMPANY

Upset Welding

W.R. Kanne, Jr., Westinghouse Savannah River Company

Advantages

Solid-state upset welding has advantages compared to typical fusion welding processes. These advantages are due to the simplicity of the welding process and the resulting solid-state weld microstructure. These advantages include:

- *SPEED:* THE UPSET WELDING PROCESS IS FAST (USUALLY LESS THAN 1 S).
- *EASE OF CONTROL:* THE PROCESS HAS ONLY THREE PRIMARY VARIABLES (CURRENT, FORCE, AND TIME).
- *FEWER DEFECTS:* TYPICAL FUSION WELDING DEFECTS SUCH AS POROSITY, MISSED JOINTS, INCOMPLETE FUSION, SPATTER, AND SOLIDIFICATION CRACKING DO NOT OCCUR IN UPSET WELDS.
- *ENHANCED WELD PROPERTIES:* THE METALLURGICAL PROPERTIES OF THE WELD METAL AND HEAT-AFFECTED ZONE IN UPSET WELDS ARE THOSE OF HOT-WORKED MATERIAL. IN OTHER WORDS, THE STRENGTH OF THE WELD ZONE IS NOT REDUCED TO THAT OF AN ANNEALED STRUCTURE, AS IN FUSION WELDS.
- *SIMPLICITY OF EQUIPMENT:* UPSET WELDING EQUIPMENT IS NOT COMPLEX, INVOLVES NO ROTATING PARTS, AND REQUIRES MINIMAL MAINTENANCE.
- *LESS-STRICT COMPOSITION REQUIREMENTS:* MINOR ALLOYING ELEMENTS DO NOT AFFECT UPSET WELD QUALITY, AND THUS ATTENTION TO ALLOY COMPOSITION FOR WELDABILITY CAN BE ELIMINATED.
- *ABILITY TO JOIN DIFFICULT-TO-WELD MATERIALS:* ALLOYS NORMALLY CONSIDERED UNWELDABLE CAN BE JOINED BY UPSET WELDING. FOR EXAMPLE, A VARIETY OF STAINLESS STEELS (INCLUDING A-286), SUPERALLOYS (INCLUDING TD NICKEL), REFRACTORY METALS (INCLUDING TUNGSTEN), GRADE 2 TITANIUM, AND ALUMINUM ALLOYS (INCLUDING 2024) HAVE BEEN SUCCESSFULLY UPSET WELDED.

The effect of welding conditions, other than the basic parameters of force, current, and time, is generally minimal. Surface roughness usually has little effect, because it is overshadowed by the deformation that takes place during welding. Surface

cleanliness and welding atmosphere may or may not be important depending on the amount of deformation that occurs to break up any oxide present before, or formed during, welding.

Limitations

A perceived limitation of the UW process is the lack of a good nondestructive testing technique for determining the quality of solid-state bonds. Normally, control of process variables is sufficient to ensure quality. Nondestructive methods, such as ultrasonics, are being applied to solid-state welds for determination of bond quality. For upset welding of large parts, the peak power drawn from the electrical supply may be a disadvantage.

Upset Welding

W.R. Kanne, Jr., Westinghouse Savannah River Company

Types of Upset Welds

Fixturing of the parts to be joined is usually necessary to achieve alignment of the parts, carry the electrical current to the joint area, and confine deformation to the joint area. In some cases the increased heat at the joint--which is caused by the higher electrical resistivity at the joint--is sufficient to limit deformation to the weld joint area. Electrodes are made from class 2 copper, which may be faced with a harder material such as copper-infiltrated tungsten carbide. Fixturing used to join two cylindrical parts consists of a pair of electrodes confined in an alignment sleeve (Fig. 2). The metallurgical structure of the weld area is that of a hot-worked material with a good diffusion bond across the weld interface, as can be seen in Fig. 1. This microstructure results in higher strength in the weld area than can be achieved for fusion welds (Fig. 3).

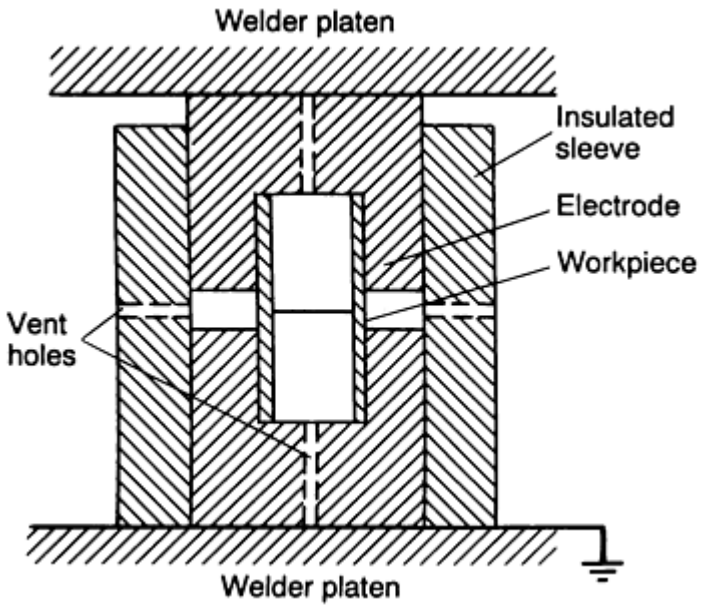

FIG. 2 FIXTURING ARRANGEMENT FOR UPSET WELDING OF CYLINDRICAL PARTS

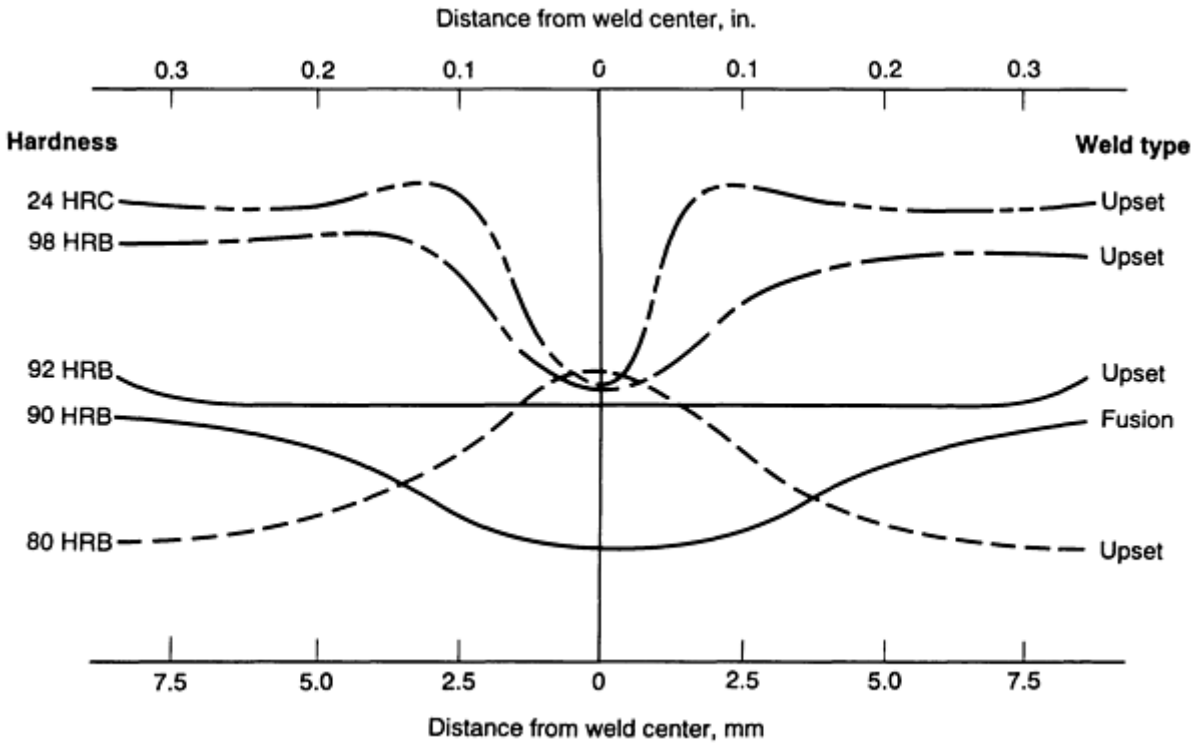

FIG. 3 HARDNESS ACROSS UPSET WELDS AND IN MATERIALS OF VARIOUS STRENGTHS COMPARED TO FUSION WELD HARDNESS. NOTE THAT THE WELD AREA HARDNESS (AND THEREFORE STRENGTH) IS GREATER FOR THE UPSET WELDS THAN FOR THE FUSION WELD.

Plug welds are a type of upset weld that requires little fixturing. Plug welds up to 125 mm (5 in.) in diameter are used to seal the fill holes of canisters employed in the long-term disposal of high-activity nuclear waste. The canisters, which are made from 304L stainless steel, are 610 mm (24 in.) in diameter and 3 m (118 in.) in height. The plug configuration is shown in Fig. 4(a). The considerable upsetting that occurs during the welding process results in a solid-state weld (Fig. 4b). Typically, these welds are made using pressure of 300 kN (75,000 lbf) with 230,000 A current applied for 1.5 s. The resulting welds have the high reliability required for long-term containment of radioactive material.

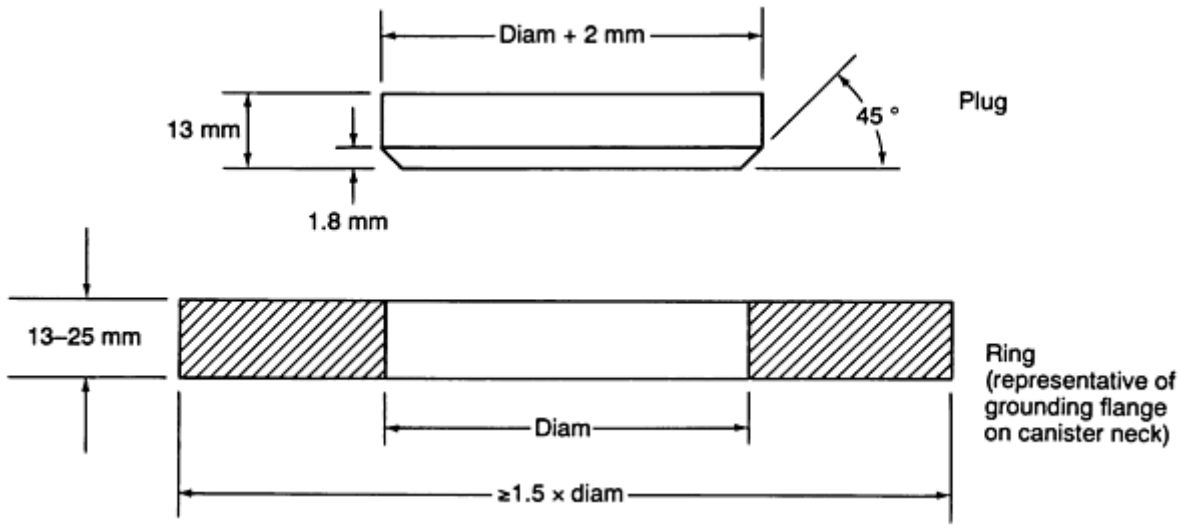

FIG. 4 UPSET PLUG WELD FOR CANISTER CLOSURE. (A) DESIGN OF WELD JOINT. (B) METALLOGRAPHIC SECTION SHOWING SOLID-STATE WELD

Upset Welding

W.R. Kanne, Jr., Westinghouse Savannah River Company

Alternative Energy Supply

A homopolar generator is an alternative method for supplying the electrical current for upset welding. Homopolar generators store energy in a large flywheel and then quickly convert the stored energy to electrical energy. The demand on utility power lines is thus spread over a considerable time period, yet the high peak power required for upset welding large parts can be met over a period of about 1 s. This low demand on the electrical grid is the principal advantage of the homopolar generator, whereas lack of good control of the current waveform and the complexity of the equipment are drawbacks. The application of homopolar generators to resistance upset welding was developed in the late 1970s and has since been applied to welding of pipes up to 168 mm (6.6 in.) in diameter.

Upset Welding

W.R. Kanne, Jr., Westinghouse Savannah River Company

Selected References

- T.A. AANSTOOS AND J.M. WELDON, HOMOPOLAR PULSE UPSET WELDING OF APT X-60 HIGH STRENGTH LINE PIPE, *WELD. J.*, JULY 1984, P 23-28
- B.J. EBERHARD AND J.W. KELKER, JR., HIGH CURRENT RESISTANCE WELDING OF NUCLEAR WASTE CONTAINERS, *WELD. J.*, JUNE 1982, P 15-19
- W.R. KANNE, JR., SOLID-STATE RESISTANCE WELDING OF CYLINDERS AND SPHERES, *WELD. J.*, MAY 1986, P 33-38
- *WELDING HANDBOOK*, 8TH ED., VOL 2, AWS, P 598-602

High-Frequency Welding

Warren Smith and Julian Roberts, Thermatool Corporation

Introduction

HIGH-FREQUENCY WELDING is a welding process in which the heat source used to melt the joining surfaces is obtained from high-frequency (HF) alternating current (ac) resistance heating. High-frequency current has certain characteristics that make it useful for welding. Unlike direct current (dc) or low-frequency alternating current, HF current tends to flow at high densities along surfaces (skin effect) and seeks adjacent parallel surfaces for its return path (proximity effect). This means that the heating and subsequent melting can be efficiently concentrated and focused to the surfaces where it is needed.

In nearly all HF welding processes, the joining surfaces are mechanically squeezed together (upset) after they are melted. This procedure helps produce a high-quality weld by squeezing out residual oxides and molten metal, which are detrimental to weld integrity. The removal of molten metal from the weld zone is beneficial because it eliminates the potentially harmful effects associated with cast structures, such as lower fracture toughness and poorer corrosion resistance. The upset also hot-works the bond plane and subsurface material, which can result in enhanced properties.

The tubemaking incorporates the simplest method of controlling HF currents, that is, the generation of an edge "V." High-frequency currents can be supplied to the welding process or workpiece by using either an induction coil (known as high-frequency induction welding, HFIW) or electrical contacts (known as high-frequency resistance welding, HFRW). The

edge "V" is a series component of the circuit (Fig. 1). Because of proximity and skin effects, current flow is concentrated across the full face width of the strip edges, resulting in controlled surface melting and subsequent welding.

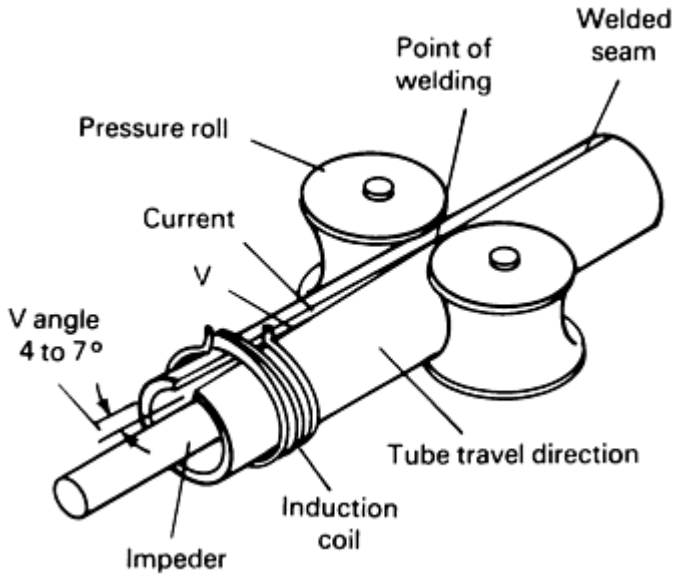

FIG. 1 JOINING A TUBE SEAM BY HIGH-FREQUENCY INDUCTION WELDING

In this process, a coil of strip material is first formed into a longitudinal hollow on a forming mill. The two edges of the strip are then HF welded and squeezed together to form a continuous welded seam.

Materials that can be successfully HF welded into tube and pipe include carbon steels, stainless steels, aluminum, copper, brass, and titanium. Exceptions are materials that are unstable at welding temperatures, have a negligible hot-work capability, or experience property deterioration that cannot be subsequently recovered. Where necessary, a gas shield can be provided for reactive metals. Tube or pipe sizes fabricated by HF welding range in size from 13 to 1220 mm ($\frac{1}{2}$ to 48 in.) in diameter.

The advantages of HF welding are that it is well suited for high-speed welding and can weld a large range of product sizes and materials. Weld quality is not particularly sensitive to the presence of air, and special atmospheres are usually not needed. Weld quality is relatively (but not completely) tolerant of surface oxides and contamination.

The disadvantages of HF welding are that it is not well suited for low welding speeds and small-scale operations where welding is done by hand. HF welding must be done continuously; continuous welds cannot be made in stop/start operations because a discontinuity in the weld will usually occur.

High-Frequency Welding

Warren Smith and Julian Roberts, Thermatool Corporation

Applications

High-frequency welding is most suitable in applications that involve the continuous edge, or butt, joining of metals. The largest single use of HF welding is in the manufacture of tube and pipe. High-frequency welding is useful in the manufacture of certain types of heat-exchanger tube, where the edge of a rectangular strip is continuously welded onto the outside diameter of a tube to form a cooling fin. The fin can be welded around the tube in a spiral configuration (Fig. 2) or it can be straight and parallel to the pipe axis. The greatest volume of heat exchanger tube is made with low-carbon steel for both the tube and fins. However, other alloy combinations are growing in use, such as low-carbon steel fins on both

stainless steel and chromium/molybdenum alloy steel tubes, stainless steel fins on low-carbon steel and stainless steel tubes, and aluminum fins on cupronickel tube.

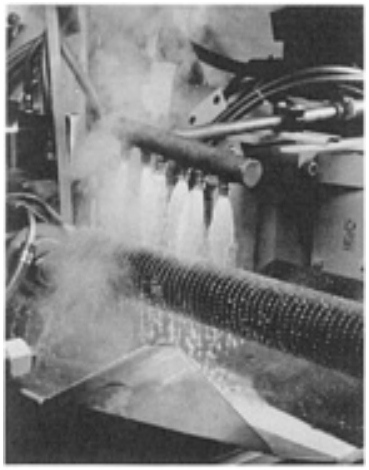

FIG. 2 MANUFACTURING A SPIRAL FIN TUBE USING HIGH-FREQUENCY WELDING

High-frequency welding can also be used for the production of structural shapes, such as T-sections and I- and H-beams. The specific shape is constructed by welding rectangular strips together to produce the desired configuration. A heating "V" is established as the strip materials are brought together.

The end, or butt, welding of metal strip is another application in which HF welding can be used. Single lengths of strip are welded to form a hoop that is subsequently formed into products such as wheel rims. High-frequency butt welding is also used to make long continuous lengths of strip by butt welding together a series of shorter lengths. This is done for certain manufacturing processes that require strip material longer than that which is commercially available.

High-Frequency Welding

Warren Smith and Julian Roberts, Thermatool Corporation

Equipment

Units for producing power for HF welding include vacuum tube oscillators and solid-state inverters. Depending on the application, frequency requirements can vary from 100 to 700 kHz, whereas power requirements vary from 30 to 1000 kW. Solid-state inverters produce frequencies ranging from 100 to 400 kHz. Vacuum-tube oscillators are available in frequencies up to 700 kHz. Because of their improved efficiency, solid-state units are replacing vacuum-tube units when frequency requirements permit.

Water-cooled copper conductors are used to carry the power to the coil or contacts. These conductors must be of minimum length and closely spaced to minimize impedance losses. The use of induction coils or electrical contacts to deliver HF power to the workpiece has specific advantages and disadvantages.

Induction coils are the least-efficient vehicle. They can only be used in applications where the geometry of the workpiece can act as a closed circuit to pick up the induced power (for example, the welding of tube). The advantages of an induction coil are that it is generally more convenient to use and requires less maintenance than contacts. Because the coils do not contact the workpiece, they leave no marks or scratches. Induction coils are usually made from a water-cooled copper conductor that has 1 to 3 turns.

The delivery of HF power through electrical contacts is more efficient than that through the use of coils because the power can be more directly and efficiently distributed to the weld area. The disadvantages of contacts are that they wear

out, require periodic replacement, and can scratch, mar, or leave deposits on the surface of a workpiece, which can be objectionable in some cases.

In the production of tube and pipe, induction coils are usually used to make the smaller diameters (<305 mm, or 12 in.) because their advantages outweigh the loss of efficiency. Contacts are generally used for larger diameters because of their greater efficiency. Contacts are also used in structural shapes and fin heat-exchanger tubes, as well as for end welding, because induction coils cannot induce the current densities necessary for welding.

Impeders are used to improve welding efficiency in tube and pipe production. Impeders that consist of one or more water-cooled cores of ferrite material are placed inside the tube parallel to and under the weld area. The reason for this is the existence of a power-dissipating circuit loop consisting of the inside surface of the tube being welded. The impeder increases the inductive impedance of this path, which bypasses the weld zone.

Inert gases are not needed for HF welding unless certain reactive metals are used. Argon is sometimes employed for the welding of stainless steel, and it is usually necessary for the welding of titanium. Although cleanliness of weld surfaces is not particularly necessary for easily welded materials, a lack of cleanliness is often the cause of problems in more-sensitive metals.

Personnel

A considerable amount of on-the-job training is required for new operators of HF welding equipment, as would be the case in any other mill process. High-frequency welding is a high-speed and, usually, high-volume process that often operates in conjunction with precision forming and handling equipment. The operating speed of tube mills ranges from 30 to 240 m/min (100 to 800 ft/min). A tube must be precisely formed prior to welding. An operator, therefore, must be familiar with both the operation of the welding equipment and the associated mechanical equipment for the forming or handling of the metal. Troubleshooting and repair of the welding equipment generally require specially trained personnel and are often conducted by the manufacturer. Improved and simplified systems for speed and/or power and weld temperature control are reducing the operator dependence of the process.

High-Frequency Welding

Warren Smith and Julian Roberts, Thermatool Corporation

Safety

Serious consideration must be given to the health and safety of welding operators, maintenance personnel, and other workers in the area of the welding operations. Good engineering practice must be followed in the design, construction, installation, operation, and maintenance of equipment, controls, power supplies, and tooling in order to conform to federal, state, and local safety regulations, as well as those of the company using the equipment.

Because HF welding power sources are electrical devices, they require all the usual precautions in handling and repairing such equipment. Voltages, which range from 400 to 25,000 V, can be either low or high frequency and may be lethal. To prevent injury, proper care and safety precautions should be taken while working on high-frequency systems and generators. Modern units are equipped with safety interlocks on access doors, as well as automatic safety grounding devices that prevent unsafe operation of the equipment. The equipment should not be operated when panels or high-voltage covers have been removed or when interlocks and grounding devices have been blocked.

High-frequency, high-voltage leads must be encased in grounded metal ductwork to ensure safety and to minimize electromagnetic radiation. Induction coils and contact systems should always be properly grounded for operator protection. Grounding lines should be kept short to minimize inductive reactance. Injuries from high-frequency power,

especially at the upper range of welding frequencies, tend to produce severe, local, surface tissue damage. Care should be taken that the magnetic field from the output system, particularly the output transformer, does not heat adjacent metallic sections by induction.

Metal or flux fumes should always be vented and the correct safety glasses should be worn in the presence of liquid metal or high-intensity visible radiation.

High-Frequency Welding

Warren Smith and Julian Roberts, Thermatool Corporation

Inspection and Quality Control

Numerous nondestructive and destructive tests can be used to determine weld quality. For example, weld quality can be determined nondestructively by eddy current testing (ASTM E 309 and ASTM A 426), ultrasonic testing (ASTM E 213 and ASTM A 273), flux leakage examination (ASTM E 570), and hydrostatic pressure testing (ASTM 450).

A number of destructive tests that utilize small samples of the product are identified in ASTM A 450. These tests include the flattening test (crush test), reverse flattening test, and the flare test.

Metallographic examination and microhardness testing can also be used to determine weld quality and the character of the adjacent heat-affected zone.

Electron-Beam Welding

Introduction

ELECTRON-BEAM WELDING (EBW) is a high-energy density fusion process that is accomplished by bombarding the joint to be welded with an intense (strongly focused) beam of electrons that have been accelerated up to velocities 0.3 to 0.7 times the speed of light at 25 to 200 kV, respectively. The instantaneous conversion of the kinetic energy of these electrons into thermal energy as they impact and penetrate into the workpiece on which they are impinging causes the weld-seam interface surfaces to melt and produces the weld-joint coalescence desired. Electron-beam welding is used to weld any metal that can be arc welded: weld quality in most metals is equal to or superior to that produced by gas-tungsten arc welding (GTAW).

Because the total kinetic energy of the electrons can be concentrated onto a small area on the workpiece, power densities as high as 10^8 W/cm^2 (10^7 W/in.^{2}) can be obtained (Ref 1). That is higher than is possible with any other known continuous beam, including laser beams. The high-power density plus the extremely small intrinsic penetration of electrons in a solid workpiece results in almost instantaneous local melting and vaporization of the workpiece material. That characteristic distinguishes EBW from other welding methods in which the rate of melting is limited by thermal conduction.

Acknowledgements

This article was adapted from "Electron Beam Welding" in the 9th Edition Volume 6 *Metals Handbook.* Special thanks are due to the committee that prepared the original article.

Reference

1. H.B. CARY, *MODERN WELDING TECHNOLOGY*, 2ND ED., PRENTICE HALL, 1989, P 256

Principles of Operation

Figure 1 shows an electron-beam weld being performed at a weld chamber pressure of approximately 3 Pa (2×10^{-2} torr). The "beam" shown in Fig. 1 is the visible glow that results from the residual (ambient) gas molecules that are excited by the electrons in the actual electron beam.

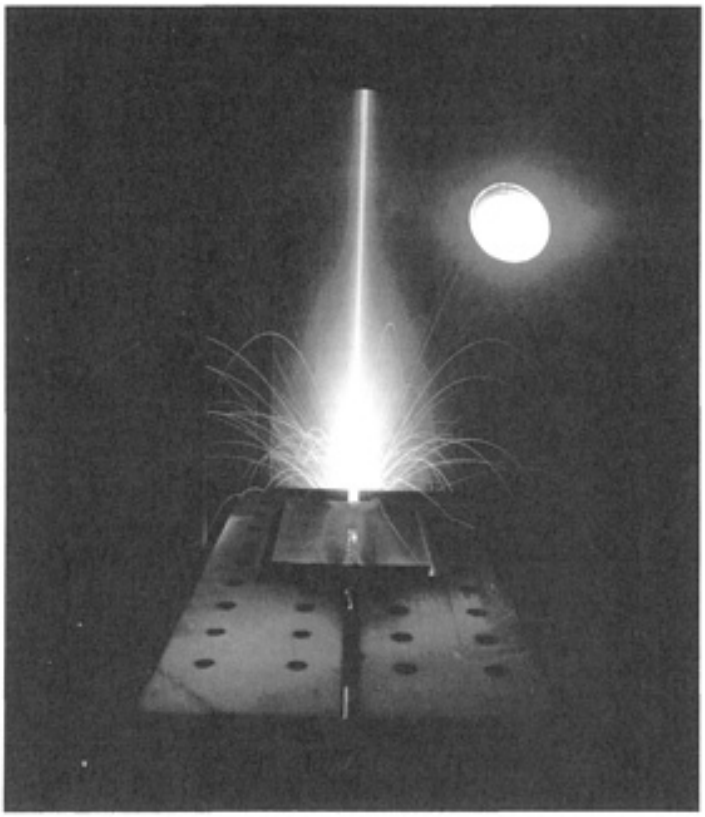

FIG. 1 WELD GENERATED BY AN ELECTRON BEAM OPERATING IN AN ENCLOSED CHAMBER MAINTAINED AT A PRESSURE OF APPROXIMATELY 3 PA (2×10^{-2} TORR)

Basically, the electron beam is formed (under high-vacuum conditions) by employing a triodestyle electron gun consisting of a cathode, a heated source (emitter) of electrons that is maintained at some high negative potential; a grid cup, a specially shaped electrode that can be negatively biased with respect to the hot cathode emitter (filament); and an anode, a ground potential electrode through which the electron flow passes in the form of a collimated beam. The hot cathode emitter (filament) is made from a high-emission material, such as tungsten or tantalum. This emitter material, usually available in wire, ribbon, or sheet form, is fabricated into the desired shape for being either directly or indirectly heated to the required emitting temperature of about 2500 °C (4500 °F).

Electrons emitted from the surface of the filament are accelerated to a high velocity and shaped into a collimated beam by the electrostatic field geometry generated from the cathode/grid/anode configuration employed, thus producing a steady stream of electrons that flows through an aperture in the ground plane anode. By varying the negative potential difference between the grid and cathode, this flow of electrons can be altered easily (i.e., gated "on/off" or ramped up/down to different levels) in a precisely controlled manner.

Diode-style electron guns are also employed, but not to the extent that triode-style electron guns are. In a diode gun, the specially shaped electrode (grid cup) is maintained at the same voltage as the emitter, thus making the diode gun a two-element (cathode and anode) device. With this design, the flow of electrons from a diode gun cannot be adjusted by simply varying a grid voltage, as is done with triode guns, and beam current adjustments are usually accomplished by varying the operating temperature of the cathode emitter instead.

Once the electrons exit the anode, they receive the maximum energy input allowable from the operating voltage being applied to the gun. Electrons then pass down through the electron beam column assembly and into the field of an electromagnetic focusing coil (a magnetic lens). This focusing lens reduces the diameter of the electron beam, as it continues in its passage, and focuses the stream of electrons down to a much smaller beam cross section in the plane of the workpiece. This reduction in beam diameter increases the energy density, producing a very small, high-intensity beam spot at the workpiece. In addition, an electromagnetic deflection coil (positioned below the magnetic lens) can be employed to "bend" the beam, thus providing the flexibility to move the focused beam spot. Figure 2 illustrates the main elements of the electron beam welding head. As described above and shown in Fig. 2, electrons are emitted from the cathode and are accelerated to high speed by the voltage between cathode and anode.

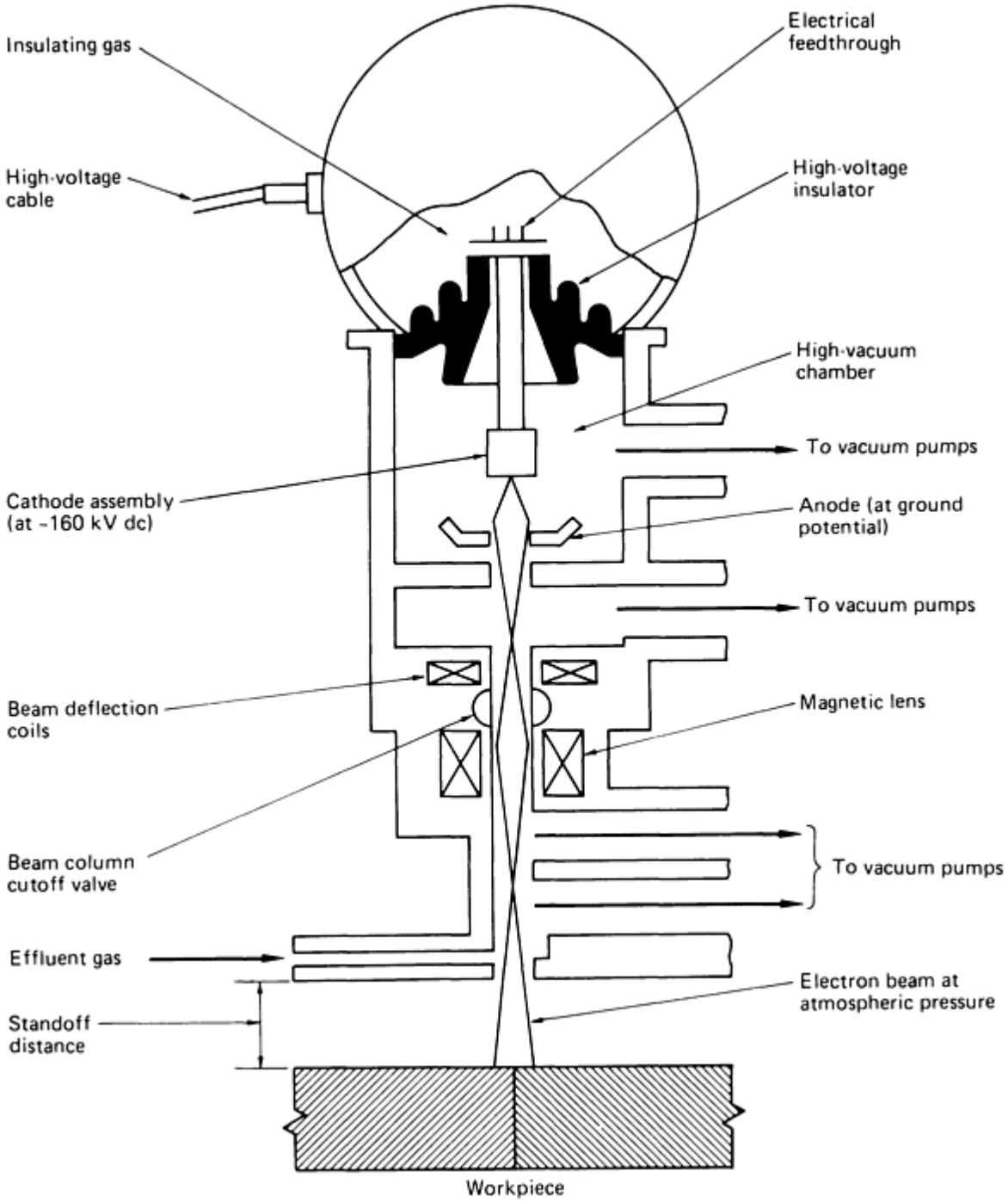

FIG. 2 SCHEMATIC SHOWING PRIMARY COMPONENTS OF AN ELECTRON-BEAM WELDING HEAD

The "gun" portion of an electron gun/column assembly generally is isolated from the welding chamber through the use of valves when desired. The gun may be maintained in a vacuum on the order of 13 mPa (1×10^{-4} torr) when the welding chamber is vented to atmosphere (for access reasons). This level of vacuum in the gun region is needed to maintain gun component cleanliness, prevent filament oxidation, and impede gun arcing (high-pressure short circuiting between electrodes at different voltages). During welding, this same degree of vacuum is required in both the gun column and welding chamber areas to minimize scattering of beam electrons by excitation collisions with residual air molecules as they traverse the distance from the gun to the workpiece. This type of interaction tends to produce a broader beam spot and a resulting decrease in energy density. Generally, electron guns are operated with applied voltages that vary from 30 to 200 kV, and they employ beam currents that range from 0.5 to 1500 mA. Electron-beam welding equipment with power levels up to 30 kW is common, and several units with power levels of up to 200 kW are commercially available.

Typically, high-vacuum EBW beams can be focused down to spot sizes in the range of 0.25 to 1.3 mm (0.010 to 0.050 in.) in diameter, with a power density of about 10^7 W/cm^2 (10^6 W/in.^{2}). This high level of beam spot intensity generates temperatures of approximately 14,000 °C (25,000 °F) and is sufficient to vaporize almost any material, forming a vapor hole that penetrates deep into the workpiece. When this vapor hole is advanced along a weld joint, the weld is produced by three effects that occur simultaneously: (1) the material at the leading edge of the vapor hole melts; (2) this molten material flows around the sides of the vapor hole to the trailing edge; and (3) this continuous flow of molten material fills in the trailing edge of the advancing vapor hole and solidifies as the vapor hole moves forward to produce a continuous weld.

Originally, EBW generally was performed only under high-vacuum ($\leq$13 mPa, or 1×10^{-4} torr) conditions; because an ambient vacuum environment was required to generate the beam, welding the part within the same clean atmosphere was considered beneficial. However, as the demand for greater part production increased, it was found that the weld chamber vacuum level need not be as high as that needed for the gun region; ultimately, the need for any type of vacuum surrounding the workpiece was totally eliminated for some applications. Currently, three distinct modes of EBW are employed:

- HIGH-VACUUM (EBW-HV), WHERE THE WORKPIECE IS IN AN AMBIENT PRESSURE RANGING FROM 0.13 TO 0.30 MPA (10^{-6} TO 10^{-3} TORR)
- MEDIUM-VACUUM (EBW-MV), WHERE THE WORKPIECE MAY BE IN A "SOFT" OR "PARTIAL" VACUUM RANGING FROM 0.13 TO 3300 PA (10^{-3} TO 25 TORR)
- NONVACUUM (EBW-NV), WHICH IS ALSO REFERRED TO AS ATMOSPHERIC EBW, WHERE THE WORKPIECE IS AT ATMOSPHERIC PRESSURE IN AIR OR PROTECTIVE GAS

In all EBW applications, the electron-beam gun region is maintained at a pressure of 13 mPa (10^{-4} torr) or lower.

Advantages

One of the prime advantages of EBW is the ability to make welds that are deeper and narrower than arc welds, with a total heat input that is much lower than that required in arc welding. This ability to achieve a high weld depth-to-width ratio eliminates the need for multiple-pass welds, as is required in arc welding. The lower heat input results in a narrow workpiece heat-affected zone (HAZ) and noticeably fewer thermal effects on the workpiece.

In EBW, a high-purity vacuum environment can be used for welding, which results in freedom from impurities such as oxides and nitrides. The ability to employ higher weld speeds, due to the high melting rates associated with the concentrated heat source, reduces the time required to accomplish welding, thereby resulting in an increased productivity and higher energy efficiency for the process. Total energy conversion efficiency of EBW is approximately 65%, which is slightly higher than so-called conventional welding processes and much higher than other types of high-energy-density welding processes, such as laser-beam welding (EBW). Additional information is available in the article "Laser-Beam Welding" in this Section.

These characteristics (1) minimize distortion and shrinkage during welding; (2) facilitate welding of most hardened or work-strengthened metals, frequently without significant deterioration of mechanical properties in the weld joint; (3) facilitate welding in close proximity to heat-sensitive components or attachments; (4) allow hermetic seal welding of

evacuated enclosures, while retaining a vacuum inside the component; and (5) permit welding of refractory metals, reactive metals, and combinations of many dissimilar metals that are not joinable by arc welding processes. The ability to project the electron beam a distance of over 510 mm (20 in.) under high-vacuum conditions, as well as the low end of medium-vacuum conditions, allows otherwise inaccessible welds to be completed.

Limitations

Equipment costs for EBW generally are higher than those for conventional welding processes. However, when compared to other types of high-energy density welding (such as LBW), production costs are not as high. The cost of joint preparation and tooling is more than that encountered in arc welding processes, because the relatively small electron beam spot size that is used requires precise joint gap and position.

The available vacuum chamber capacities are limited; workpiece size is limited, to some degree, by the size of the vacuum chamber employed. Consequently, the production rate (as well as unit cost) is affected by the need to pump down the chamber for each production load. Because the electron beam is deflected by magnetic fields, nonmagnetic or degaussed metals must be used for tooling and fixturing that are near the beam path.

Although most of the above advantages and disadvantages generally are applicable to all modes of EBW, several do not specifically apply to EBW-NV. Nonvacuum EBW does not offer the advantage of a high-purity environment (unless some form of inert-gas shielding is provided), and it is not subject to vacuum chamber limitations. Because welding is not done within the confines of a vacuum environment, the maximum practical "standoff," the working distance between the bottom of the electron beam column and the top of the workpiece, currently used on EBW-NV systems is limited to approximately 35 mm ($1\frac{3}{8}$ in.). The maximum attainable penetration is currently limited to about 25 to 32 mm (1 to 1.25 in.) for 60-kW, 165 kV machines. These limitations, however, are offset by higher production rates and a lower rate of vacuum-related equipment problems that are typical of EBW-NV systems.

Process Control

Basic variables employed for controlling the results of an electron-beam weld include accelerating (applied gun) voltage, beam current, welding (beam spot travel) speed, focusing current, and standoff (gun column assembly to workpiece) distance. The final beam spot size that is produced in the plane of the workpiece is determined by:

- CHARACTERISTICS OF THE ELECTRON BEAM GUN/COLUMN ASSEMBLY (GUN AND ELECTRON OPTICS)
- FOCUSING CURRENT, WHICH CONTROLS THE FOCAL LENGTH OF THE LENS AND RESULTING BEAM FOCUS LOCATION
- GUN COLUMN ASSEMBLY-TO-WORKPIECE DISTANCE
- ACCELERATING VOLTAGE
- BEAM CURRENT

Each of these variables, separately and jointly, affects final beam spot size.

Increasing the accelerating voltage or beam current increases the depth of penetration; the product of these two variables--the beam power--determines the amount of metal melted for a given exposure time. Increasing welding speed--relative travel motion between beam spot and workpiece--without changing any other process variable, reduces depth of penetration and correspondingly reduces weld width. Changing any of the other basic control variables to increase beam spot size, thereby lowering the beam spot intensity (e.g., reducing the power density), reduces depth of penetration and increases weld width, if welding speed is left unchanged. Beam deflection can be used to change the impact angle of the beam (slightly) or to produce controlled patterns of beam oscillation to create greater beam spot size or other special effects. The beam can also be pulsed to vary the average amount of power inputted per unit of time.

With EBW-NV, the accelerating voltage and focus current are normally preset and held at a fixed value. Beam current may be preset for any application and then turned "on/off" (or programmed to vary in predetermined fashion) with workpiece travel. Workpiece speed and, in certain instances, standoff distance may also be preset to a desired value or varied with workpiece travel. On many of the latest computerized numerical control (CNC) types of EBW-NV systems, beam current, standoff distance, and welding speed are varied simultaneously, as required, throughout the length of the weld. Because of the limited standoff distance involved with EBW-NV, beam deflection normally is not feasible, and beam oscillatory motion generally is not employed.

Operation Sequence and Preparation

Tooling and welding procedures for each EBW application are developed first on experimental workpieces. Details of the welding sequence vary somewhat, depending on equipment differences and application requirements. A typical sequence of operation for welding in vacuum is to:

- ASSEMBLE AND PREPARE WORK AND FIXTURES FOR WELDING. THIS INCLUDES CLEANING AND MAY INCLUDE DEMAGNETIZING, PREHEATING, AND TACK WELDING.
- LOAD FIXTURED WORK ONTO WORKTABLE OR WORK-HOLDING MECHANISM IN WELDING CHAMBER.
- START CHAMBER PUMPDOWN.
- AFTER CHAMBER PRESSURE HAS BEEN REDUCED TO 0.013 TO 13 PA (10^{-4} TO 10^{-1} TORR), FOCUS ON A TARGET BLOCK AND SET BEAM PARAMETERS.
- ALIGN JOINT TO THE BEAM POSITION, USING VERY LOW POWER BEAM SPOT.
- BEGIN WELDING; THIS USUALLY IS PERFORMED AUTOMATICALLY, BUT CAN BE PERFORMED MANUALLY.
- TERMINATE THE WELDING CYCLE.
- ALLOW WORK TO COOL SUFFICIENTLY IF MADE OF REACTIVE MATERIAL, THEN ADMIT AIR TO THE CHAMBER AND REMOVE FIXTURED WORK.

For nonvacuum welding, the electron gun/column assembly is maintained at established pressure levels; work-handling and welding operations for EBW-NV usually are mechanized for high-speed production, and work and fixturing are prepared before a production run is begun, or they are completed as part of the production line operation. Beam parameters, alignment of joint with beam position, and transfer and movement of work for welding are established before a production run. Alignment of the joint with beam position is slightly less critical than for vacuum electron-beam welding, because beam spot size and weld width are slightly larger in nonvacuum welding.

Joint Preparation. A joint for EBW ordinarily has close fitted, abutting, square-groove faces, and filler metal usually is not used. Filler metal can be used if desired, as in EBW of dissimilar metals and alloys. Generally, the faces of the joint are machined to a surface roughness of 3.20 μm (125 μin.) or less.

Surface finish on the weld groove faces may not be critical, depending on part and joint design and the requirements for weld properties. In studies on butt welding of 50 mm (2 in.) thick aluminum alloy 2219 and Ti-6A1-4V specimens that had groove faces with surface roughness values of 1.60, 3.20, 6.3, 12.5, and 25.0 μm (63, 125, 250, 500, and 1000 μin.), respectively, surface finish had no effect on weld quality, as determined by visual examination and x-ray radiography; all welds were sound. Edge surface finish is much less critical on broad welds than on narrow welds. Edge roughness is not critical on lap joints in thin metal, as long as burrs do not separate the surfaces.

Joint Fit-Up. A butt joint is not open, as in arc welding, but has closely fitted, nearly parallel surfaces to enable the narrow electron beam to fuse base metal on both sides of the joint. The members of a joint to be melt-through welded also are closely fitted. Fit-up tolerance depends on work-metal thickness and joint design, but is usually 0.13 mm (0.005 in.) or less. Joint gap is usually smaller for thin work metal and unbacked joints and may be only 0.05 mm (0.002 in.) maximum. Interference fits may be used where shrinkage can cause cracking, as in circular joints on hardenable metals.

Joint gaps of about 0.08 mm (0.003 in.) maximum commonly are used for making narrow vacuum welds, whereas joint gaps of up to 0.8 mm (0.030 in.) are not uncommon in EBW-NV. In making deep welds, poor fit-up or too large a joint

gap can cause excessive shrinkage, underfill, undercut, voids, cold shuts, and missed joints. In most metals, joint gap should not exceed 0.25 mm (0.010 in.) for narrow welds deeper than about 50 mm ($\frac{1}{2}$ in.), although sound welds have been obtained using joint gaps of 0.5 mm (0.020 in.) by increasing the weld width to about 6.4 mm (0.25 in.).

Cleaning. Workpiece surfaces must be properly cleaned for in-vacuum EBW. Inadequate surface cleaning of the weld metal can cause weld flaws and a deterioration of mechanical properties. Inadequate cleaning of weld surfaces also adversely affects pumpdown time and gun operational stability, as well as contributing to the rapid degradation of the oil used in the vacuum pumps.

In EBW-NV, cleanliness of workpiece surfaces is important, but not as critical as with vacuum EBW. Although the effect of workpiece cleanliness on pumpdown time and gun stability is reduced in nonvacuum welding, it still affects final weld quality.

Wire brushing generally is not recommended, because contaminants may become embedded in the metal surface. Acetone is preferred for cleaning electron gun components and workpiece parts. If workpieces are cleaned in chlorine or other halogen-containing compounds, residue from these compounds must be removed by another cleaning method (usually thorough washing in acetone) before welding.

Fixturing Methods. Methods used for fixturing workpieces in EBW are similar to those used for GTAW of precision parts without the use of filler metal, except that clamping force is usually lower and all fixturing and tooling materials should be made of nonmagnetic materials.

Because total heat input to the weld is much less in EBW than for arc welding, and because the heat is highly localized, heavy fixturing, massive heat sinks, or water cooling is not needed. C-clamps are sufficient for many parts. In some applications, clamping may be supplemented or replaced by small tack welds or by a shallow weld pass (sealing pass) over the joint; the penetration weld is completed later at full power.

For EBW-NV, general-purpose welding positioners are satisfactory. Locating and aligning mechanisms are of simpler design than for welding in a vacuum; accessibility and beam widths for nonvacuum welding do not require as much accuracy in tracking of the joint. Maintenance of work-handling equipment for EBW-NV is simplified because of its out-of-chamber location.

Demagnetization. Workpieces and fixtures made of magnetic materials should be demagnetized before welding. Residual magnetism may result from magnetic-particle testing, magnetic chucks, or electrochemical machining. Even a small amount of residual magnetism can cause beam deflection. Workpieces are usually demagnetized by placing them in a 60 cycle inductive field and then slowly removing them. Equipment used for magnetic-particle testing may be used. Before welding, workpieces should be checked with a gauss meter. Acceptable gauss-meter readings vary from 5×10^{-5} T ($\frac{1}{2}$ G) for very narrow (highly critical) welds up to as much as 2×10^{-4} to 4×10^{-4} T (2 to 4 G) for relatively wide welds.

Pumpdown. The time required to pump the work chamber of an in-vacuum EBW unit down to the desired ambient pressure depends on the chamber size used, type of pump employed, and level of vacuum required. Electron-beam welding equipment currently employs either computer or program logic controls, normally providing automatic vacuum sequencing.

For EBW-HV, a pressure of 13 mPa (10^{-4} torr) or less is produced by a mechanical pump (either a simple piston, a rotary vane type, or a combination pump-and-blower package), operating in conjunction with an oil-diffusion pump. The size of these pumps depends mainly on the size of the weld chamber used, as well as on the final operating vacuum level and total pump-down time needed.

Generally, a 1.1 m^3 (40 ft^3) chamber employing a 250 mm (10 in.), 250 m^3/min (8820 ft^3/min) diffusion pump and a 17 m^3/min (600 ft^3/min) mechanical pump package can be expected to reach a welding pressure of less than 40 mPa (3×10^{-4} torr) in approximately 4 min, while an 11 m^3 (400 ft^3) chamber employing a 510 mm (20 in.), 1070 m^3/min (37,800 ft^3/min) diffusion pump and a 37 m^3/min (1300 ft^3/min) mechanical pump package can be expected to pump down to the same pressure in approximately 12 min.

If desired, the pumpdown time of the 11 m^3 (400 ft^3) chamber could be reduced to under 6 min by increasing the size of the pumping system to an 815 mm (32 in.) 3090 m^3/min (109,200 ft^3/min) diffusion pump and a 77.9 m^3/min (2750 ft^3/min) mechanical pump package; however, the higher cost associated with this increased pumping capability would have to be evaluated against the financial benefit of the saving in pumpdown time to determine whether it would be economically feasible. In the examples above, weld chambers are assumed to be clean, dry, and empty. The cleanliness of the work chamber, the amount of water vapor (humidity) in the ambient air, and the workpiece assembly (material and shape of both weldment and fixturing) thus affect the actual pumpdown time obtained in any production application.

For partial-vacuum EBW, where the pressure level required in the weld chamber is approximately 13 Pa (10^{-1} torr) and a pressure level of 13 mPa (10^{-4} torr) is provided only in the electron-beam gun/column regions, diffusion pumps are not needed for the weld chamber, and weld chamber pumping is accomplished strictly by mechanical pumping. For high-production EBW of small parts in a partial vacuum, pumpdown lime ranges from about 20 s for relatively large-volume (general-purpose) partial-vacuum weld chambers of about 0.14 m^3 (5 ft^3) down to less than 5 s for fairly small-volume chambers of 0.014 m^3 (0.5 ft^3), with the use of a mechanical pump rated at 37 m^3/min (1300 ft^3/min).

Preheat and Postheat. Most commonly welded metals can be processed with EBW methods, even in thick sections without preheating, because of the extremely narrow width of the HAZ. Hardenable and difficult-to-weld metals may need to be preheated, especially for thick sections and in applications when the weld is restrained.

High-strength alloy steels and tool steels thicker than about 9.5 mm ($\frac{3}{8}$ in.) ordinarily must be preheated before EBW to prevent cracking. Deep circular welds, especially partial-penetration welds, in thick sections of carbon steel containing more than about 0.35% C usually require preheating. However, welds subject to less restraint, such as circumferential welds on cylindrical shapes, can be made on 13 mm ($\frac{1}{2}$ in.) thick 0.50% C steel without preheating.

Preheating, when required, is usually done before the work is placed in the work chamber. Selection of heating method depends on the size and shape of the work and the preheat temperature; a combination of methods can be used. Torch and furnace heating are widely used; induction and infrared-radiation heating are also used. On small parts or where distortion from localized heating is not a problem and where increased cycle time can be tolerated, heating is sometimes done with a defocused electron beam; this method can also be used to supplement other methods of heating.

When postheating is used on EBW parts, it is accomplished by conventional means (i.e., stress relieving or tempering) after removing the work from the welding chamber.

Operating Conditions. Starting and stopping the weld usually require special consideration to avoid uniformity of the weld at these points and possible melt-through and loss of metal.

One technique that is used to avoid these difficulties is to start the weld at full beam power on a starting tab of the work metal that is tightly fitted against one end of the joint and to conclude the weld on a runoff tab at the other end of the joint. The use of starting and runoff tabs prevents underfill at the ends of the joint, which is caused by the introduction or exit of the beam. Workpieces can also be made oversize to provide extra material for starting and stopping. The tabs or the extra material can be machined off after welding. Starting and runoff tabs are used mainly in low-production operations.

Another technique is to start and stop the weld on the work, raising the current gradually (upslope) at the beginning of the weld and reducing it gradually (downslope) at the end of the weld. Upslope and downslope power may be used at controlled rates and time intervals, as established for a specific application, and can be programmed into the welding procedure. The use of upslope and downslope is of special value where the weld is a closed path, as in welding circular and circumferential joints.

In many applications of closed-path welds, the weld can be started at full power, with downslope at the end providing a sufficiently gradual termination and a suitable distance of overlap. Downslope of current after overlapping the beginning of the weld on circular welds in thick sections of high-hardenability steels is critical to avoid porosity and cracking. Other parameters may also be adjusted to avoid these defects. Upslope is usually rapid; downslope is from a few degrees to a major portion of a revolution.

A "cosmetic pass" is made when needed to smooth or flatten the crown of a weld that is irregular or too high. Such a pass is used to correct undercut or underfill. The beam is usually defocused or reduced in power, or both, in making a cosmetic pass. Filler metal may also be added in making a cosmetic pass intended to correct undercut or underfill.

Weld Geometry

The shape of the parts to be welded and the corresponding joint designs are critical to the successful application of EBW in vacuum or at atmospheric pressures (nonvacuum). While minimum heat input and low thermal distortions are important advantages of EBW, the molten metal still shrinks as it solidifies. Shrinkage stresses may lead to microcracks if parts, due to design restrictions, are unable to shrink at corresponding rates and the joint volume is completely constrained. Additional information is available in the article "Procedure Development and Practice Considerations for Electron-Beam Welding" in this Volume.

Joint Design

Butt, corner, T-, lap, and edge joints can be made by the EBW process using square-groove or seam welds. Fillet welds, which are difficult to make with vacuum EBW, are readily made using EBW-NV. Square-groove welds require fixturing to maintain fit-up and alignment of the joint. They can, however, be self-aligning if a rabbeted joint design is used. Self-alignment is particularly important in batch loading the vacuum chamber for efficient work manipulation. The weld-metal area can be increased using a scarf joint, but fit-up and alignment of the joint are more difficult than with a square-groove weld. Most joints are designed to be welded in a single pass with full penetration or penetration to a specified depth.

Electron-Beam Welding Machines

This brief review is aimed at introducing the potential user to some of the EBW equipment currently available. Further advances in the control and programming of these systems can be expected because of the likelihood of uninterrupted progress in the electronics and computer industries.

As discussed earlier in this article, the EBW process is accomplished at three pressure-dependent lines, referred to as the three modes of EBW. The original mode is the high or "hard" vacuum mode in which welding is carried out in the pressure range of 0.13 to 130 mPa (10^{-6} to 10^{-3} torr). In the second mode, medium vacuum, the pressure ranges from 0.13 to 3300 Pa (10^{-3} to 25 torr). The term "medium vacuum" includes the range of pressure (0.13 to 130 Pa, or 10^{-3} to 1 torr) referred to as the "soft" or partial vacuum. The third mode is called non-vacuum or atmospheric, with welding carried out at atmospheric pressure.

All three modes employ an electron-beam gun/column, a power supply with controls, one or more vacuum pumping systems, and work-handling equipment. Although in nonvacuum welding the workpiece is not placed in an evacuated work chamber, the electron beam gun/column must be in a vacuum environment. The electron gun in all three modes is held at a pressure of 13 mPa (10^{-4} torr) or less; otherwise, the high voltage required for the acceleration of the electrons could not be sustained.

Electron-beam welding equipment comes in two basic designs: (1) the low-voltage system, which uses accelerating voltages in the 15 to 60 kV range; and (2) the high-voltage system, with accelerating voltages in the 100 to 200 kV range. Beam powers up to 100 kW are available with both high-voltage and low-voltage equipment.

The lower-voltage machines operate at a higher current. Typically, 30 to 60 kV machines operate at a 500 mA beam current. The high-voltage machines of 150 kV operate at 40 mA. The higher-voltage machines produce a greater depth-to-width ratio of the weld nugget. This could be the difference between a 12:1 depth-to-width ratio versus a 25:1 depth-to-width ratio. The higher-voltage machines can utilize a longer standoff distance than can low-voltage machines; however, low-voltage machines are simpler in construction and less maintenance is required (Ref 1).

Low-voltage equipment is more suitable for high- and medium-vacuum operations, while nonvacuum welding is carried out at higher voltages (130 to 175 kV minimum). All three modes, however, are operational with high-voltage equipment. The nonvacuum, high-voltage systems generally are used for welding materials less than 25 mm (1 in.) thick. With low-voltage systems, the gun may be fixed in position on the chamber or may be mobile inside the chamber. With high-voltage equipment, the gun is generally fixed in position on the chamber. Figure 3 shows a typical floor plan of a high-voltage, high-vacuum welding facility with a welding chamber size of 1725 by 1725 by 1980 mm (68 by 68 by 78 in.).

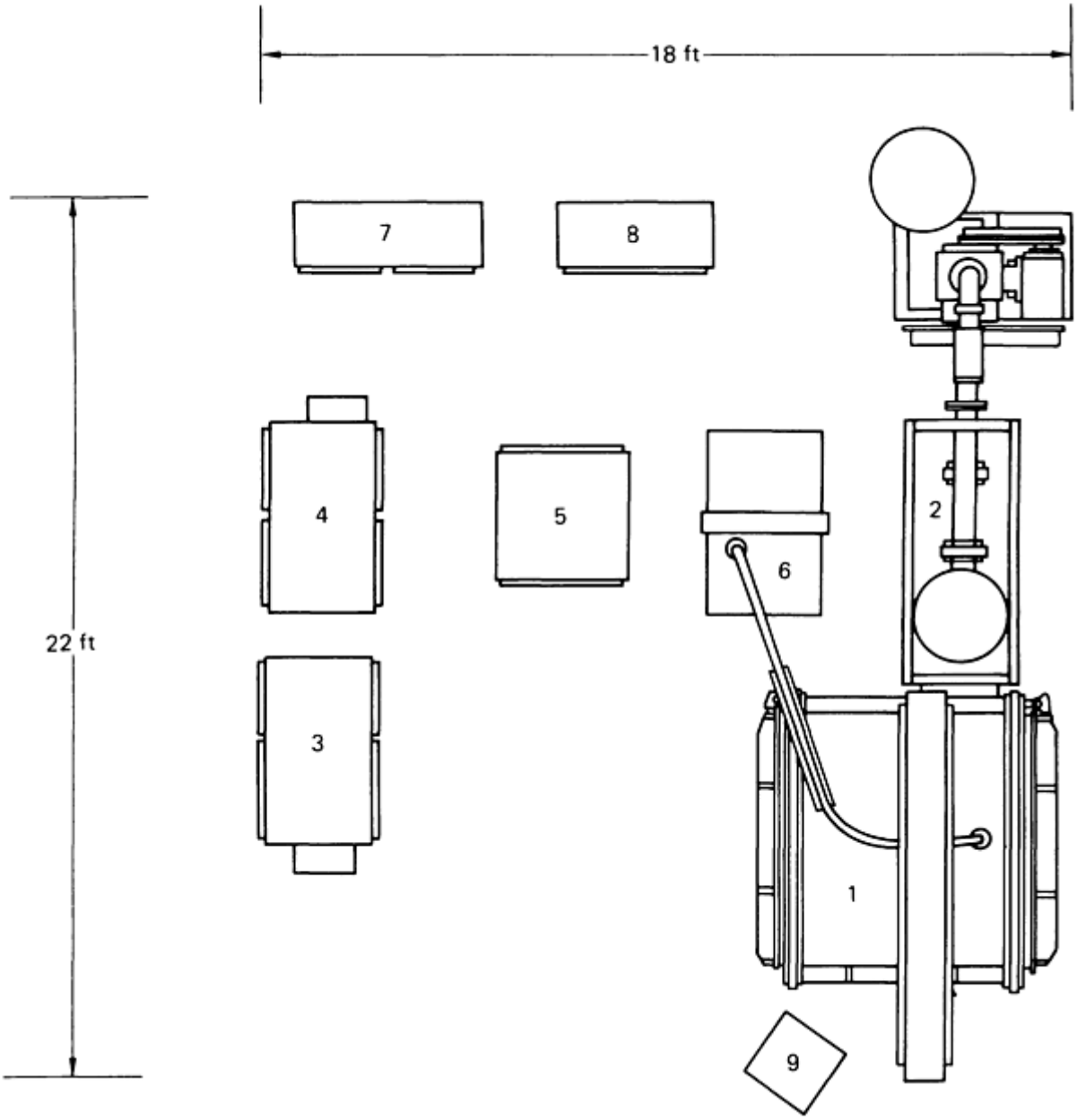

FIG. 3 OVERHEAD VIEW SHOWING TYPICAL FLOOR LAYOUT OF HIGH-VOLTAGE, HIGH-VACUUM EBW SYSTEM. (1) VACUUM CHAMBER AND MANIPULATING MECHANISMS. (2) VACUUM PUMPING SYSTEM. (3) COMPUTER CONTROL CABINET. (4) SERVO CABINET. (5) AUTOMATIC VOLTAGE REGULATOR. (6) HIGH-VOLTAGE POWER SUPPLY. (7) POWER DISTRIBUTION CABINET. (8) PUMPING CONTROL CABINET. (9) OPERATOR CONSOLE

Figure 4 shows a standard high-vacuum machine with a chamber size of 2845 by 1525 by 1830 mm (112 by 60 by 72 in.). This type of unit is available with power ratings of 7.5 kW (150 kV, 50 mA) and 25 kW (150 kV, 267 mA). The gun/column in this unit is fixed, and the work travels under the gun. Work-handling equipment makes processing of workloads of up to 1400 kg (3000 lb) at welding speeds of 3300 mm/min (130 in./min) possible. This system can be obtained with various degrees of automation; most utilize CNC operations. Figure 5 shows a high-vacuum unit with a chamber size of 3505 by 2845 by 2690 mm (138 by 112 by 106 in.). This installation comes with a movable gun. Low-

voltage, high-vacuum systems with movable guns are available with power ratings of 7.5 kW (60 kV, 125 mA) 15 kW (60 kV, 250 mA), 30 kW (60 kV, 125 mA), and 42 kW (60 kV, 700 mA).

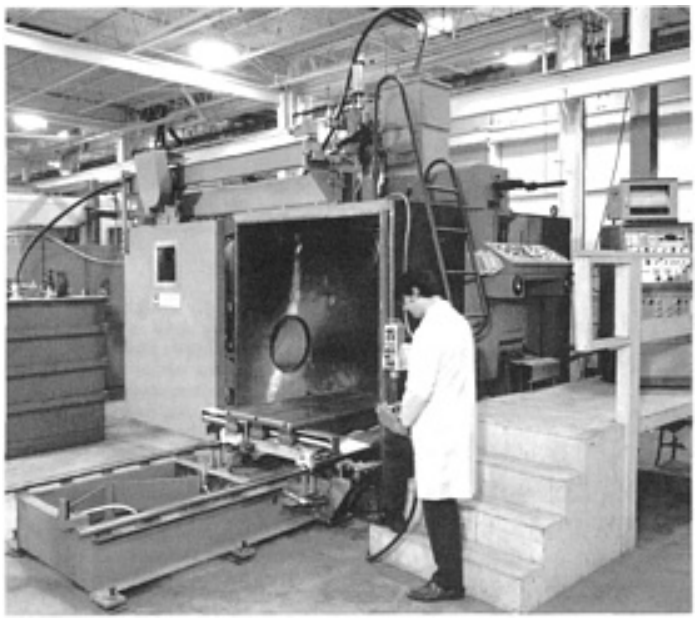

FIG. 4 TYPICAL EBW-HV UNIT WITH A 2845 × 1525 × 1830 MM (112 × 60 × 72 IN.) CHAMBER. COURTESY OF LEYBOLD HERAEUS VACUUM SYSTEMS INC.

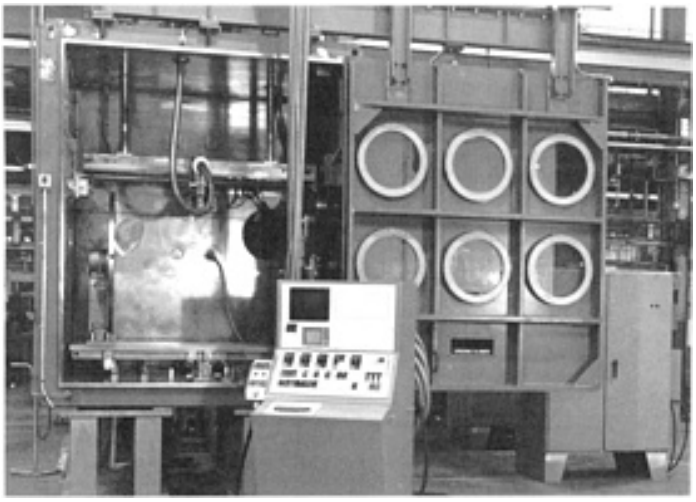

FIG. 5 STANDARD LOW-VOLTAGE EBW-HV UNIT CONSISTING OF A 3505 × 2845 × 2690 MM (138 × 112 × 106 IN.) CHAMBER. COURTESY OF SCIAKY BROS., INC.

Medium-vacuum machines are frequently special-purpose units tooled for particular assemblies. Figure 6 shows a dual-system partial-vacuum welding installation for joining ring gear and counterweight onto flywheels. Dual medium-vacuum systems of this type, which are used for high-production applications, can be readily modified to produce alternate parts by simple changes in the work-handling components and weld programming. As with the system shown in Fig. 4, a wide range of automation and computer control is available.

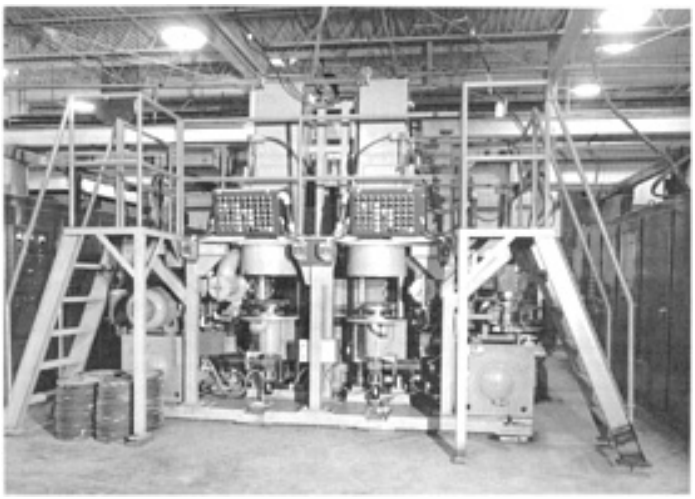

FIG. 6 TWIN EBW-MV INSTALLATION DESIGNED TO WELD A RING GEAR ONTO A FLYWHEEL. COURTESY OF LEYBOLD-HERAEUS VACUUM SYSTEMS INC.

The medium-vacuum mode of EBW was initially employed to increase the production capacity of the process. This mode of application typically involves the use of a chamber custom designed to provide a minimum of weld-zone volume that has to be evacuated during each part cycle (that is, a chamber envelope that is not much bigger in size than the particular workpiece to be welded plus any fixturing it may require). Because only a small volume needs to be evacuated, coupled with the fact that medium-vacuum EBW is normally performed in an ambient vacuum level of nominally 6.5 Pa (5×10^{-2} torr)--which is several orders of magnitude higher in pressure than high-vacuum EBW--the pumpdown times necessary are much less than those required on a high-vacuum EBW system (that is, times of <10 s compared to >3 min). Thus, in order to take advantage of this significant reduction in the time required for evacuating the weld zone, various methods were developed to rapidly transport parts into or out of the weld area on EBW-MV systems. Figure 7 shows one of the conventional methods used for this purpose, employing a dial table arrangement for repeatedly indexing a set of work stations through the weld area. Each individual work station contains whatever fixturing might be required to hold the part. The parts can usually be loaded/unloaded into and out of these work stations either manually or automatically. This particular method for achieving rapid part transfer is capable of being employed both with the drop-bottom (discretely pumped) EBW-MV unit and the sliding-seal (continuously pumped) EBW-MV unit.

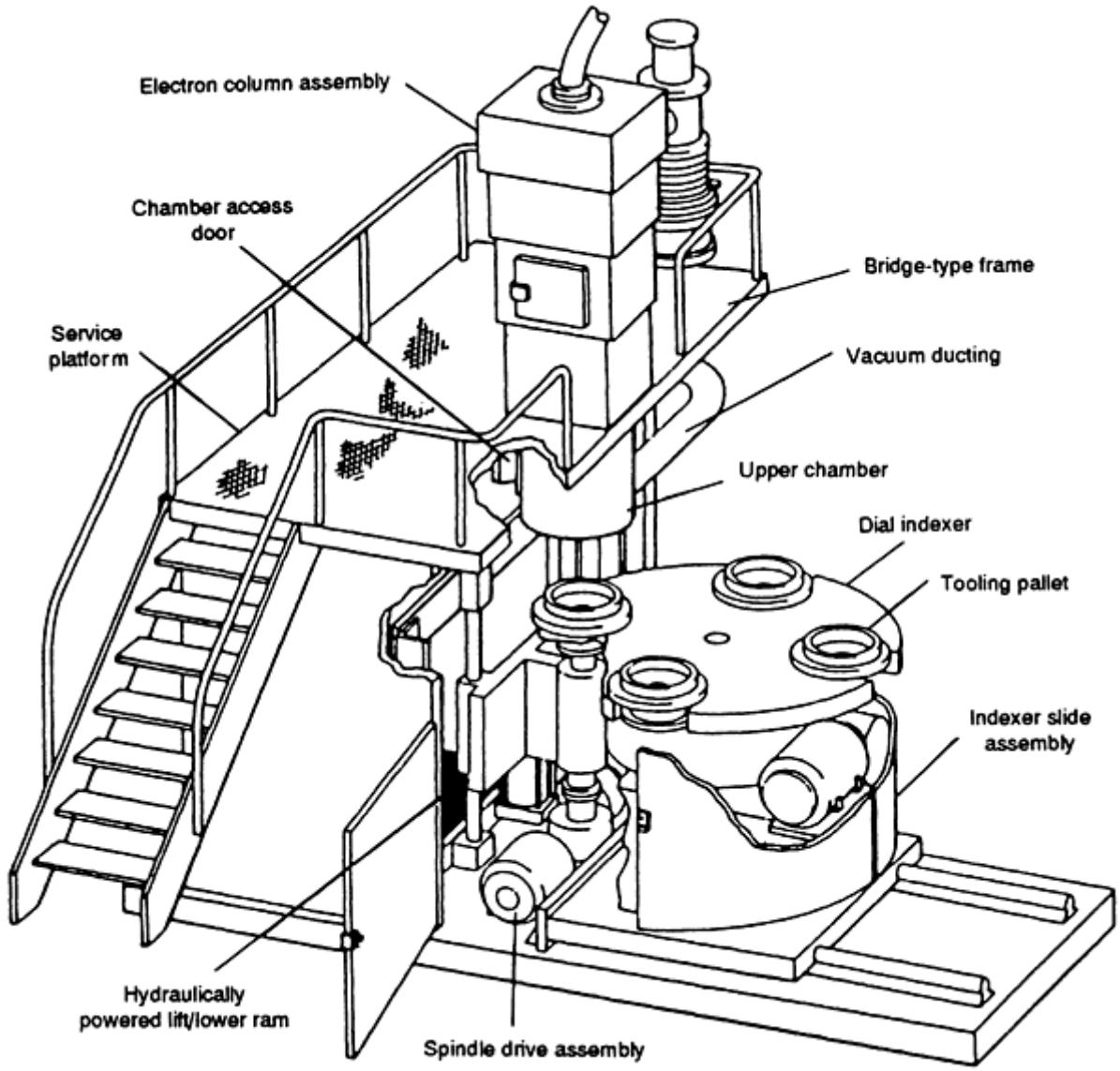

FIG. 7 SCHEMATIC SHOWING A CUTAWAY VIEW OF A DIAL TABLE DEVICE INCORPORATED INTO AN EBW-(MV/PV) SYSTEM TO PROVIDE INDEXING OF WORK STATION INTO WELDING AREA

Figure 8 shows a custom partial-vacuum system, typical of the variety used for high-production automotive parts manufacture. Installations of this type currently are available with power ratings of 100 kW (100 kV, 1 A) for welding heavy cross sections from 50 to 205 mm (2 to 8 in.) thick.

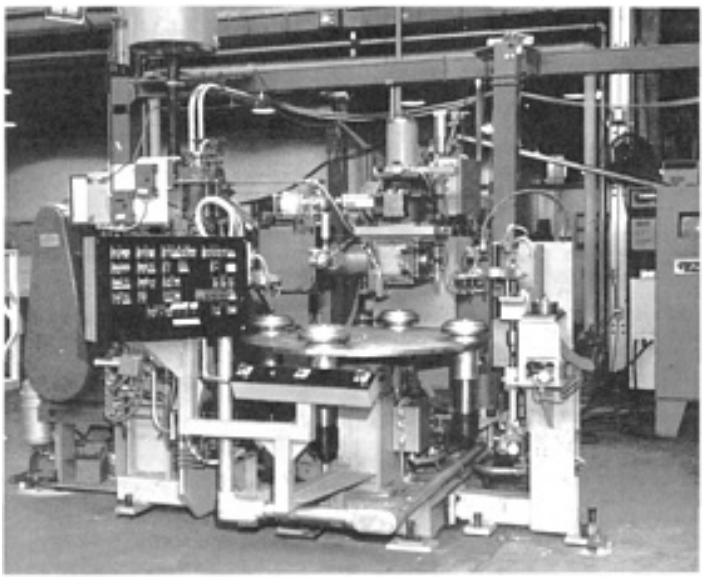

FIG. 8 CUSTOM-DESIGNED EBW-MW SYSTEM USED TO PRODUCE AUTOMOTIVE PARTS. COURTESY OF SCIAKY BROS., INC.

Some smaller units are also available that feature dual-mode operation; they operate in either the high- or medium-vacuum mode, depending on the application. Figure 9 shows a dual-mode portable machine rated at 6 kW (60 kV, 100 mA) with fully automatic and preset pumping and welding cycles. The small weld chamber can be pumped down to 65 mPa (5×10^{-4} torr) in 10 s.

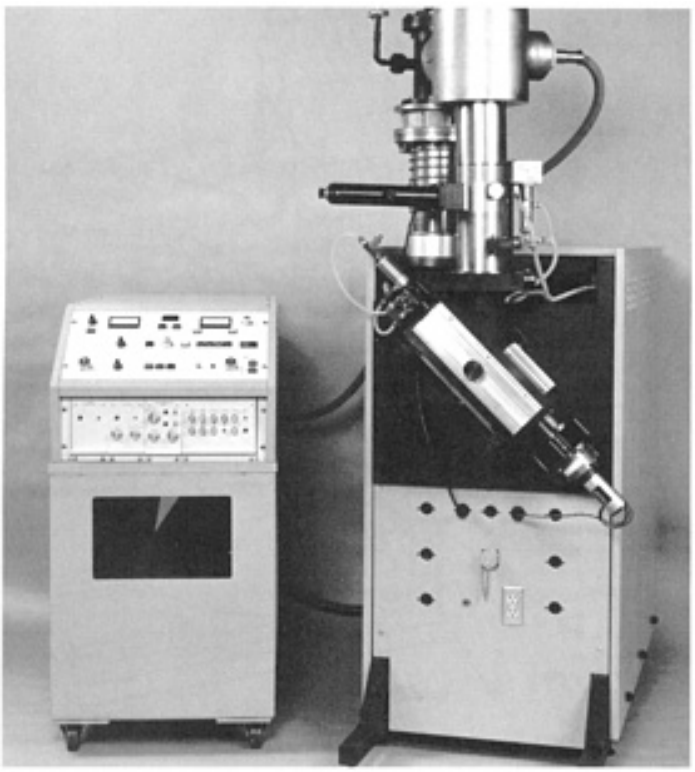

FIG. 9 STANDARD DUAL-MODE PORTABLE EBW SYSTEM. COURTESY OF EBTEC CORP.

The system shown in Fig. 10 is an example of a nonvacuum unit featuring a standard dial index table. Parts are loaded into a fixture nest in the table and are indexed through a small, radiation-tight enclosure in which parts are welded at 100 kPa (1 atm). This nonvacuum unit has power ratings of 17.5 kW (174 kV, 100 mA) or 35 kW (175 kV, 200 mA) and can be used either as a standard system or as a custom-designed special task system.

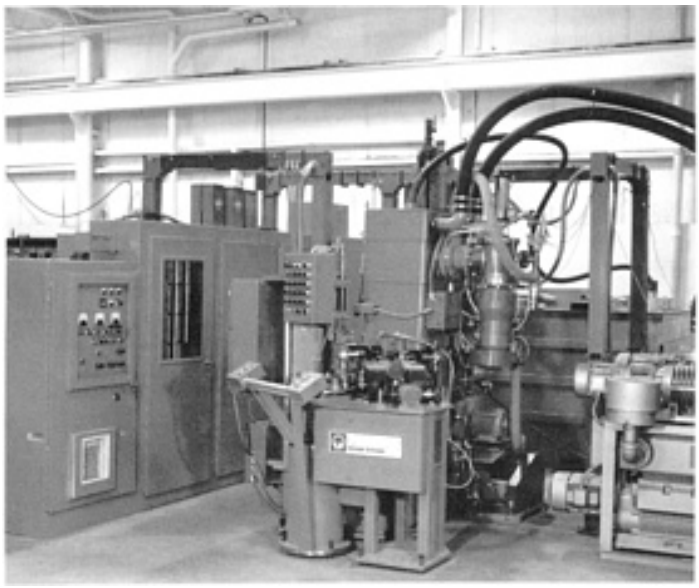

FIG. 10 STANDARD DIAL-INDEX TABLE-TYPE EBW-NV SYSTEM. COURTESY OF LEYBOLD-HERAEUS VACUUM SYSTEMS INC.

Computer control systems available in many EBW units. Control of welding operations can be expanded to include joint locators, five-axis programmable contouring, and several digitizing provisions that can be actuated on the basis of information generated by the seam locator. Many EBW systems can also be adapted for electron-beam heat-treating applications.

Reference cited in this section

1. H.B. CARY, *MODERN WELDING TECHNOLOGY,* 2ND ED., PRENTICE HALL, 1989, P 256

Safety

Protection must be provided by equipment design and arrangement, and by safety precautions in EBW and related operations, against the usual hazards of welding and the special hazards of exposure to (1) the high voltages involved in generating the electron beam, (2) the beam itself (direct viewing of intense radiation emitted by molten weld metal can be harmful to eyesight and thus the beam operation should be viewed only through a filter lens commonly used for arc welding), and (3) radiation of x-rays produced by impingement of the beam on the work or other materials. From a safety standpoint, an accelerating voltage of less than 20 kV produces soft x-rays, while an accelerating voltage of over 20 kV produces hard x-rays (Ref 1). Shielding is more demanding against radiation as the acceleration voltage increases. Suitable precautionary measures are described in AWS F2.1-78, "Recommended Safe Practices for Electron Beam Welding and Cutting," and in AWS/ANSI Z49.1, "Safety in Welding and Cutting."

Reference cited in this section

1. H.B. CARY, *MODERN WELDING TECHNOLOGY*, 2ND ED., PRENTICE HALL, 1989, P 256

Electron-Beam Welding

References

1. H.B. CARY, *MODERN WELDING TECHNOLOGY*, 2ND ED., PRENTICE HALL, 1989, P 256
2. J.F. LOWRY, J.H. FINK, AND B.W. SCHUMACHER, A MAJOR ADVANCE IN HIGH-POWER ELECTRON BEAM WELDING IN AIR, *J. APPL. PHYS.*, VOL 47, 1976, P 95-106

Laser-Beam Welding

Jyoti Mazumder, University of Illinois at Urbana-Champaign

Introduction

LASER-BEAM WELDING (LBW) uses a moving high-density (10^5 to 10^7 W/cm^2, or 6×10^5 to 6×10^7 W/in.^{2}) coherent optical energy source called a laser as the source of heat. "Laser" is an acronym for "light amplification by stimulated emission of radiation." The coherent nature of the laser beam allows it to be focused to a small spot, leading to high energy densities.

Lasers have been promoted as potentially useful welding tools for a variety of applications. Until the 1970s, however, laser welding had been restricted to relatively thin materials and low speeds because of the limited continuous power available. By 1965, a variety of laser systems had been developed for making microwelds in electronic circuit boards, inside vacuum tubes, and in other specialized applications where conventional technology was unable to provide reliable joining. The availability of high-power continuous-wave (CW) carbon dioxide (CO_2) and neodymium-doped yttrium aluminum garnet (Nd:YAG) lasers and the limitations of current welding technology have promoted interest in deep-penetration welding in the past 20 years using these devices.

The ability of the laser to generate a power density greater than 10^6 W/cm^2 (6×10^6 W/in.^{2}) is a primary factor in establishing its potential for welding (Table 1). Numerous experiments have shown that the laser permits precision (that is, high quality) weld joints rivaled only by those made with an electron beam.

TABLE 1 ENERGY CONSUMPTION AND EFFICIENCY OF LBW RELATIVE TO OTHER SELECTED WELDING PROCESSES

WELDING PROCESS	INTENSITY OF ENERGY SOURCE		JOINING EFFICIENCY, MM^2/KJ	FUSION ZONE PROFILE
	w/cm^2	w/in.^{3}		
OXYACETYLENE (OAW)	10^2-10^3	6×10^2-6×10^3	0.2-0.5	SHALLOW FOR SINGLE PASS
ARC WELDING	5×10^2-10^4	3×10^3-6×10^4	0.8-2$^{(A)}$ 2-3$^{(B)}$ 4-10$^{(C)}$	SHALLOW FOR SINGLE PASS
PLASMA ARC (PAW)	10^3-10^6	6×10^3-6×10^6	5-10	SHALLOW AT LOW-ENERGY END DEEP PENETRATION AT HIGH-ENERGY END
LASER BEAM	10^5-10^7	6×10^5-6×10^7	15-25	SHALLOW AT LOW-ENERGY DENSITY RANGE DEEP PENETRATION AT HIGH-ENERGY DENSITY RANGE
ELECTRON BEAM	10^5-10^8	6×10^5-6	20-30	DEEP PENETRATION

		$\times 10^8$		

(A) GAS-TUNGSTEN ARC WELDING (GTAW).

(B) GAS-METAL ARC WELDING (GMAW).

(C) SUBMERGED ARC WELDING (SAW)

Laser-Beam Welding

Jyoti Mazumder, University of Illinois at Urbana-Champaign

Advantages and Limitations of LBW

Laser welding offers the following advantages (Ref 1, 2):

- LIGHT IS INERTIALESS (HENCE, HIGH PROCESSING SPEEDS WITH VERY RAPID STOPPING AND STARTING BECOME POSSIBLE).
- FOCUSED LASER LIGHT PROVIDES HIGH ENERGY DENSITY.
- LASER WELDING CAN BE USED AT ROOM ATMOSPHERE.
- DIFFICULT-TO-WELD MATERIALS (FOR EXAMPLE, TITANIUM, QUARTZ, ETC.) CAN BE JOINED.
- WORKPIECES DO NOT NEED TO BE RIGIDLY HELD.
- NO ELECTRODE OR FILLER MATERIALS ARE REQUIRED.
- NARROW WELDS CAN BE MADE.
- PRECISE WELDS (RELATIVE TO POSITION, DIAMETER, AND PENETRATION) CAN BE OBTAINED.
- WELDS WITH LITTLE OR NO CONTAMINATION CAN BE PRODUCED.
- THE HEAT-AFFECTED ZONE (HAZ) ADJACENT TO THE WELD IS VERY NARROW.
- INTRICATE SHAPES CAN BE CUT OR WELDED AT HIGH SPEED USING AUTOMATICALLY CONTROLLED LIGHT DEFLECTION TECHNIQUES.
- THE LASER BEAM CAN ALSO BE TIME SHARED.

Precise part fit-up and alignment are much more critical in laser welding than in ordinary arc welding. The typical focal spot diameter for a laser beam ranges from 100 to 1000 μm (0.004 to 0.040 in.). In addition, capital cost for laser welding devices is almost 10 times more expensive than comparable power arc welding systems. On the other hand, laser welding can provide much higher throughput relative to conventional arc welding. When the capital cost of laser-beam welding is compared to electron-beam welding (EBW), laser-beam welding becomes the more cost-effective of the two processes because no vacuum enclosure is necessary for laser-beam welding.

The penetration depth obtained in laser welding is less than that observed in electron-beam welding. The maximum thickness of type 304 stainless steel plate that can be welded using a 77 kW (105 hp) CO_2 laser is 50 mm (2 in.) (Ref 3), whereas EBW can produce welds in type 304 stainless steel up to several inches in thickness. However, the penetration depth of EBW extends only a relatively short distance under atmospheric pressure. Welding under a vacuum is required to obtain optimum efficiency in EBW. A laser beam, however, can be transmitted an appreciable distance through the atmosphere without serious attenuation or optical degradation because of its coherent nature. Laser-beam welding thus offers an easily maneuverable, chemically clean, high intensity, atmospheric welding process with narrow HAZ and subsequent low distortion. Peak penetration, p_{max}, for LBW is defined by:

$$P_{MAX} \propto P^{0.7} \qquad \textbf{(EQ 1)}$$

where P is the power (in watts). In terms of weld width (w) and depth (d), both conduction-mode welding (w/d [ges] 1) and deep-penetration welding ($w/d < 1$) can be obtained with lasers.

References cited in this section

1. I.J. SPALDING, LASER SYSTEM DEVELOPMENTS, *PHYS. BULL.*, JULY 1971, P 402
2. Y.S. ARATA AND J. MIYAMOTO, *TECHNOCRAT*, VOL 11 (NO. 5), 1978, P 33
3. C.M. BANAS, "LASER WELDING TO 100 KW," REPORT NO. R76-912260-2, UNITED TECHNOLOGIES, FEB 1977

Laser-Beam Welding

Jyoti Mazumder, University of Illinois at Urbana-Champaign

Process Applications

A large variety of metals and alloys have been welded with pulsed or CW lasers. Until the first reported demonstration of deep-penetration laser-beam welding by Brown and Banas (Ref 4), most laser welds were made with pulsed lasers.

The localized heating obtained with laser sources was soon realized to be an important advantage. Anderson and Jackson (Ref 5) reported an interesting comparison between heating effects produced with a conventional arc source and those occurring with a pulsed laser for an iron substrate. They show that not only is the laser-produced HAZ small, but also that the laser source is more efficient because it requires only 37.8 J/cm^2 (0.229 Btu/in.^{2}) to produce melting to the required depth, while the arc source must deliver 246 J/cm^2 (1.49 Btu/in.^{2}) to the workpiece. Localized heating makes the laser ideal for welding electronic components on a printed circuit board (PCB) where high average temperatures in even small volumes surrounding the weld region cannot be tolerated (Ref 6).

Microwelding with Pulsed Lasers. Microwelding with pulsed ruby lasers and pulsed Nd:YAG lasers is credited with some of the earliest successful applications of laser welding, including laser welding of thermocouple gages in the Apollo lunar probes in the late 1960s (Ref 7). Table 2 shows the various lasers available for welding and the maximum thicknesses that can be welded with these lasers.

TABLE 2 PARAMETERS FOR SELECTED PULSED AND CONTINUOUS WAVE LASERS USED FOR LBW APPLICATIONS

LASER	PULSE LENGTH, MS	PULSE ENERGY, J	PEAK POWER, KW	MAXIMUM WELD THICKNESS[(A)]		WELDING SPEED	
				mm	in.	mm/s	in./min
PULSED							
RUBY	3-10	20-50	1-5	0.13-0.50	0.005-0.020	1.2	3.0
ND:GLASS	3-10	20-50	1-5	0.13-0.50	0.005-0.020	0.63	1.5
ND:YAG	3-10	10-100	1-10	0.13-0.60	0.005-0.025	2.1	5.0
CO_2	5-20	0.1-10	1-5	0.13	0.005	1.2	3.0
CONTINUOUS WAVE							
ND:YAG	. . .	. . .	1.8	5.56	0.022	5.8	14.0
CO_2 (DC EXCITED)	. . .	. . .	1	0.60	0.025	12.7	30.0
CO_2 GAS DYNAMIC	. . .	. . .	20	19.0	0.750	21.2	50.0
CO_2 GAS DYNAMIC	. . .	. . .	77	50.8	2.00	26.7	63.0

CO_2 (RF EXCITED)[B]	. . .	. . .	5	10.0	0.4	10.8	25.6

Source: Ref 3, 8, 9, 10

(A) DATA ARE FOR TYPE 304 STAINLESS STEEL.

(B) DATA PROVIDED BY TRUMPF INDUSTRIAL LASER.

Microwelding with pulsed solid-state lasers is now used to:

- SEAL BATTERIES FOR DIGITAL WATCHES AND PACEMAKERS
- SEAL INK CARTRIDGES FOR FOUNTAIN PENS
- WELD WIRES TO TERMINALS ON SHUNT PLATES
- WELD TELEPHONE SWITCHING DEVICES
- ATTACH BATTERY TERMINALS IN DISK CAMERAS
- JOIN LAMP TERMINAL FEED-THROUGHS
- ASSEMBLE GYROSCOPE BEAMING DEVICES
- CONSTRUCT TANTALUM DIAPHRAGMS
- WELD REPAIR INCONEL 718 CASTINGS

Laser microwelding has found its way into almost all types of manufacturing industries including aerospace, automotive, electronics, and consumer durables (Ref 11). Figure 1 shows the approximate penetration possible for high-quality welds using Nd:YAG lasers. It should be noted that for the same average power, pulsed Nd:YAG lasers provide much higher penetration levels than continuous-wave Nd:YAG lasers.

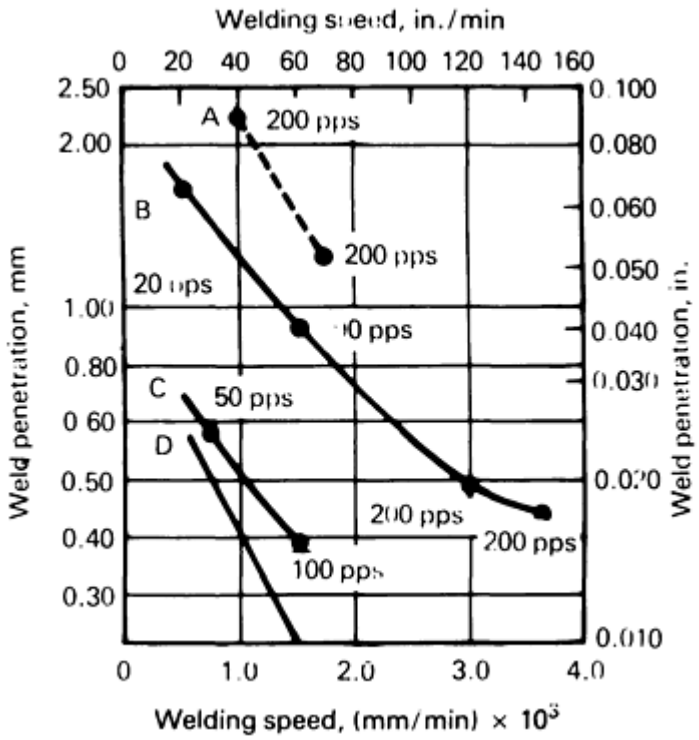

CURVE	WELDING MODE	AVERAGE OUTPUT, W	
		PULSED	CONTINUOUS WAVE

A	PENETRATION	400	. . .
B	CONDUCTION	400	. . .
C	CONDUCTION	150	. . .
D	CONDUCTION	. . .	400

FIG. 1 PLOT OF WELD PENETRATION VERSUS WELDING SPEED AS A FUNCTION OF WELDING MODE, MODE OF OPERATION, AND AVERAGE OUTPUT FOR ND:YAG LASERS AT A WAVELENGTH OF 1.06 μM (41.7 μIN.). SOURCE: REF 12

Penetration Welding. The scope of technically and commercially feasible LBW applications has increased greatly since the demonstration of penetration welding using a multikilowatt CW CO_2 laser by Brown and Banas (Ref 4). Numerous experiments have shown that the laser produces precision weld joints of high quality in ferrous alloys, nickel alloys, and titanium alloys that is rivaled only by those made by EBW. Data describing the plate thickness of different laser-welded materials are given in Table 3.

TABLE 3 PARAMETERS FOR HIGH-POWER LBW RELATIVE TO ALLOY TYPE FOR BEAD-ON-PLATE JOINTS

MATERIAL	TYPE OF JOINT	THICKNESS		LASER POWER, KW
		mm	in.	
SHIP STEEL, GRADES A, B, C	BUTT	28.6	1.125	12.8
	BUTT	25.4	1.0	12.0
	BUTT	19.0	0.75	12.0
	BUTT	15.9	0.625	12.0
	BUTT	12.7	0.50	12.0
	BUTT	9.5	0.375	10.8
	TEE	9.5-12.7	0.375 TO 0.5	11.9
LOW-ALLOY CARBON STEEL	TEE	9.5-12.7	0.375 TO 0.5	7.5
AISI 1010	BEAM PLATE	4	0.157	1.8[A]
AISI 4130	BUTT	15.2	0.60	14
LOW-ALLOY HIGH-STRENGTH STEEL, 300M	BUTT	19.0	0.75	14
ARCTIC PIPELINE STEEL X-80	BUTT	13.2	0.52	12
D-6AC STEEL	BUTT	6.4	0.25	15
HY-80	. . .	12.5	0.49	10.6
HY-130 STEEL	BUTT	6.4	0.25	5.5
HY-180 STEEL (HP9-4-20)	BUTT	1.6	0.062	5.5
	. . .	1.6	0.062	10.5
	. . .	16.3	0.64	5.5
NICKEL-BASE ALLOY, INCONEL 718	BUTT	14.5	0.57	14
STAINLESS STEEL				
AISI TYPE 304	. . .	6	0.24	17
	. . .	12.5	0.49	17
	. . .	17	0.67	17
	. . .	16.5	0.65	17
	. . .	3.8	0.15	11.5
	. . .	5.6	0.22	11.5[B]

				1.8[C]
	. . .	8.9	0.35	8
	. . .	20.3	0.8	20
	. . .	12.7	0.5	20
	. . .	50.8	2.0	77
AISI TYPE 321	BUTT	14.5	0.57	14
ALUMINUM ALLOY:				
2219	BUTT	12.7	0.50	13
2219	BUTT	6.4	0.25	5
2219	BUTT	6.4	0.25	16
5083	BUTT	6.4	0.25	7
5456	BUTT	3.2	0.125	5.5
5456	BUTT	12.5	0.187	8
5456	BUTT	12.5	0.49	. . .
TITANIUM ALLOY, TI-6AL-4V	BUTT	15.2	0.60	13.5
	. . .	3.2, 6.4	0.125, 0.25	5.5
	. . .	3	0.12	4.7
	. . .	12.5	0.49	11

Source: Ref 10, 13

(A) ND:YAG LASER.

(B) CO_2 LASER.

(C) CONTINUOUS WAVE ND:YAG LASER.

Aluminum and its alloys have recently generated lots of interest in the laser welding community because of their potential application in the auto industry for their weight reduction properties (Ref 14, 15, 16, 17, 18, 19). During the 1970s and 1980s, aluminum alloys were reported to be rather difficult to weld due to the high initial surface reflections of 10.6 μm (417 μin.) radiation emitted by CO_2 lasers (Ref 20, 21, 22, 23, 24, 25, 26, 27). Surface coating often reduces this problem. Low melting point and relevant fluidity sometimes lead to "drop through" problems, and thus energy input is a critical parameter for laser welding. Another critical factor involving laser welding is the vaporization of alloying elements such as magnesium. Suppression of the plasma with a properly designed shielded gas nozzle can be used to avoid the loss of alloying elements (Ref 25). The other alternative is to use filler metal (Ref 17). Although the welding of aluminum is difficult with LBW, it has already been demonstrated that, with proper precautions, welds having tensile strength equivalent to the parent materials can be obtained.

Steels. A great deal of laser welding research has been conducted on ferrous alloys. Most of the initial parametric studies were carried out on stainless steel (Ref 4, 27, 28). Stainless steel was investigated (Ref 28, 29) because of its importance in the power plant and chemical industries. Laser welding of rimmed steel sheet was evaluated for automotive applications by Baardsen *et al.* (Ref 30). High-speed LBW of tin plate and tin-free steel for container industries was reported by Mazumder and Steen (Ref 31). Results in HY-alloy steels were evaluated and reported by Banas (Ref 32) and by Metzbower and Moon (Ref 21). Laser-beam welding of modified 4340 alloy was reported by Seaman and Hella (Ref 33). Several other ferrous alloys that have been studied for the applicability of laser welding include X-80 Arctic pipeline steel (Ref 34), tanker construction steels (Ref 35), D-6ac low-alloy ultrahigh-strength steel (Ref 36), and high-strength low-alloy grade steels (Ref 36).

One of the earliest applications of LBW was for the welding of planetary gear assemblies for the automotive industry. Welding was carried out at 10 m/min (400 in./min) using a 5 kW (7 hp) laser. Subsequently, LBW was applied to produce automobile powertrain components. A most recent mass production application is in the production of the "body-in-white" tailored blank shown in Fig. 2. An LBW process developed by Fraunhofer Institute at Aachen that uses a polarized beam was applied by Krupps Steel to produce steel pipe (Ref 38).

FIG. 2 SEQUENCE OF OPERATIONS REQUIRED TO PRODUCE "BODY-IN-WHITE" TAILORED BLANK AUTOMOTIVE BODIES USING LASER-BEAM WELDING. (A) ARRANGEMENT AND WELDING OF DIVIDED-TYPE BODY PANELS BEFORE FORMING. (B) TAILORED BLANK OBTAINED AFTER STRUCTURAL COMPONENTS HAVE BEEN FORMED IN A PRESS. SOURCE: REF 37

Titanium and Titanium Alloys. Until recently, the EBW technique has been the most popular method used to weld Ti-6Al-4V, which is the most widely used titanium material in the aerospace industry due to its remarkable strength-to-weight ratio. However, the deep penetration of EBW can be obtained only up to a short distance under nonvacuum conditions. For optimum efficiency, electron beam welding must be carried out in an evacuated chamber (Ref 24). In contrast, CO_2 laser beams can be transmitted for appreciable distances through the atmosphere without serious attenuation or optical degradation.

The application of the laser technique to a metal such as a titanium alloy, which is normally difficult to weld, is not only of direct interest to the aerospace and chemical industries, but also is of interest to those who need to weld chemically sensitive metals with complex temperature-dependent structures. The need for better joining methods for titanium and its alloys resulted in several investigations of LBW techniques over various power ranges (maximum 16 kW, or 21 hp). A detailed review is available in Ref 13. Welding speeds in excess of 15 m/min (49 ft/min) were used to weld 1 mm (0.04 in.) thick Ti-6Al-4V with a 4.7 kW (6.3 hp) CO_2 laser, and materials up to 12.5 mm (0.492 in.) thick were joined using an 11 kW (15 hp) CO_2 laser.

References cited in this section

3. C.M. BANAS, "LASER WELDING TO 100 KW," REPORT NO. R76-912260-2, UNITED TECHNOLOGIES, FEB 1977
4. C.O. BROWN AND C.M. BANAS, "DEEP PENETRATION LASER WELDING," AWS ANNUAL MEETING (SAN FRANCISCO), APRIL 1971
5. J.E. ANDERSON AND J.E. JACKSON, *WELD. J.*, VOL 44, 1965, P 1018
6. W.W. DULEY, *CO_2 LASERS: EFFECTS AND APPLICATIONS,* ACADEMIC PRESS, 1976
7. A.J. MOOREHEAD AND P.N. TURNER, *WELD. J.*, VOL 49, 1970, P 15
8. M.A. ACHAREKAR, LASERS, *WELD. ENG.*, DEC 1974, P 9-11
9. T. WEBER, HOBART LASER PRODUCTS, INC., LIVERMORE, CA, 1992, PRIVATE COMMUNICATION
10. M.M. SCHWARTZ, *METAL JOINING MANUAL,* MCGRAW-HILL, 1979
11. S.R. BOLIN, ND-YAG LASER APPLICATION SURVEY, CHAPTER 8, *LASER MATERIALS PROCESSING,* M. BASS, ED., NORTH HOLLAND PUBLISHING CO., AMSTERDAM, 1983
12. H.L. MARSHALL, *PROC. OF THE SPIE,* VOL 86, 1976
13. J. MAZUMDER, LASER WELDING, CHAPTER 3, *LASER MATERIALS PROCESSING,* M. BASS, ED., NORTH HOLLAND PUBLISHING CO., AMSTERDAM, 1983
14. L. RAPP, C. GLUMANN, F. DOUSINGER, AND H. HÜGEL, *LASER TREATMENT OF MATERIALS,* B.L. MORDIKE, ED., DGM INFORMATIONSGESELLSCHAFT MBH, GERMANY, 1992, P 99-104
15. A.S. BRANDSON AND T. ENDERS, *LASER TREATMENT OF MATERIALS,* B.L. MORDIKE, ED., DGM INFORMATIONSGESELLSCHAFT MBH, GERMANY, 1992, P 117-124

16. H. SAKAMOTO, K. SHIBATA, AND F. DAUSINGER, *LASER TREATMENT OF MATERIALS,* B.L. MORDIKE, ED., DGM INFORMATIONSGESELLSCHAFT MBH, GERMANY, 1992, P 125-130
17. J. BERKMANN, S.K. BEHLER, AND E. BEYER, *LASER TREATMENT OF MATERIALS,* B.L. MORDIKE, ED., DGM INFORMATIONSGESELLSCHAFT MBH, GERMANY, 1992, P 151-156
18. A. LANG AND H.W. BERGMAN, *LASER TREATMENT OF MATERIALS,* B.L. MORDIKE, ED., DGM INFORMATIONSGESELLSCHAFT MBH, GERMANY, 1992, P 163-170
19. L.C. MALLORY, R.F. ORR, AND W. WELLS, *LASER MATERIALS PROCESSING III,* J. MAZUMDER AND K. MUKHERJEE, ED., MINERALS, METALS, AND MATERIALS SOCIETY, 1989, P 123-134
20. R.C. CRAFER, *WELD. INST. RES. BULL.,* APRIL 1976, P 17
21. E.A. METZBOWER AND D.W. MOON, MECHANICAL PROPERTIES, FRACTURE TOUGHNESS, AND MICROSTRUCTURES OF LASER WELDS OF HIGH STRENGTH ALLOYS, *PROC. CONF. ON APPLICATIONS OF LASERS IN MATERIALS PROCESSING* (WASHINGTON, DC), 18-20 APRIL 1979
22. D.B. SNOW AND E.M. BREINAN, "EVALUATION OF BASIC WELDING CAPABILITIES," UNITED TECHNOLOGIES RESEARCH CENTER, JULY 1978
23. E.M. BREINAN, C.M. BANAS, AND M.A. GREENFIELD, LASER WELDING--THE PRESENT STATE OF THE ART, DOC IV-181-75, *11TH ANNUAL MEETING OF THE WELDING INSTITUTE* (TEL AVIV), 6-12 JULY 1975, P 1-53
24. M.M. SCHWARTZ, *METAL JOINING MANUAL,* MCGRAW-HILL, 1979
25. A. BLAKE AND J. MAZUMDER, *ASME J. ENG. IND.,* VOL 107 (NO. 3), AUG 1985, P 275-280
26. D.W. MOON AND E. METZBOWER, *WELD. J.,* 1983, P 535-585
27. E.V. LOCKE AND R.A. HELLA, *IEEE J. QUANTUM ELECTRONICS,* VOL QE-10 (NO. 2), FEB 1974, P 179-185
28. R.C. CRAFER, ADVANCES IN WELDING PROCESSES, PAPER NO. 46, *PROC. 4TH LNT. CONF.* (HARROGATE, YORKS, ENGLAND), 9-11 MAY 1978, P 267-278
29. R.A. WILLGOSS, J.H.P.C. MEGAW, AND J.N. CLARK, *WELD. MET. FABR.,* MARCH 1979, P 117-126
30. E.L. BEARDSON, D.J. SCHMATZ, AND R.E. BISARO, *WELD. J.,* VOL 52, APRIL 1973, P 227-229
31. J. MAZUMDER AND W.M. STEEN, LASER WELDING OF STEELS USED IN CAN MAKING, *WELD. J.,* VOL 60 (NO. 6), JUNE 1981, P 19-25
32. C.M. BANAS, "LASER WELDING DEVELOPMENTS," PROC. CEGB INT. CONF. ON WELDING RES. RELATED TO POWER PLANTS (SOUTHAMPTON, ENGLAND), 17-21 SEPT 1972
33. F.D. SEAMAN AND R.A. HELLA, "ESTABLISHMENT OF A CONTINUOUS WAVE LASER WELDING PROCESS," IR-809-3 (1-10), REPORT IN CONFERENCE PROCEEDINGS AFML CONTRACT F336 15-73-C5004, OCT 1976
34. E.M. BREINAN AND C.M. BANAS, PRELIMINARY EVALUATION OF LASER WELDING OF X-80 ARCTIC PIPELINE STEEL, *WRC BULL.,* DEC 1971, P 201
35. C.M. BANAS AND G.T. PETERS, "STUDY OF THE FEASIBILITY OF LASER WELDING IN MERCHANT SHIP CONSTRUCTION," CONTRACT NO. 2-36214, U.S. DEPT. OF COMMERCE, FINAL REPORT TO BETHLEHEM STEEL CORP., AUG 1974
36. M. YESSIK AND D.J. SCHMATZ, "LASER PROCESSING IN THE AUTOMOTIVE INDUSTRY," PAPER MR74-962, SME, 1974
37. F.A. DIPIETRO, *LASER SYSTEM APPLICATION IN INDUSTRY,* ATA-ASSOCIAZIONE TECNIER DELL' AUTOMOBILE, TORINO, ITALY, 1990, P 103-120
38. E. BEYER, FRAUNHOFER INSTITUTE, AACHEN, GERMANY, PRIVATE COMMUNICATION, 1992

Jyoti Mazumder, University of Illinois at Urbana-Champaign

Fundamentals of Laser Welding

Lasers are capable of both conduction-mode welding and deep-penetration welding.

Conduction-Mode Welding. Momentum transfer or convection dominates conduction-mode welding. High-power density (10^5 to 10^7 W/cm^2, or 6×10^5 to 6×10^7 W/in.^{2}) in laser welding produces a temperature gradient of the order of 10^6 K/cm (5×10^6 °F/in.) and this in turn leads to surface-tension-driven thermocapillary flow (Marangoni convection) with surface velocities of the order of 1 m/s (Ref 39). Convection is the single most important factor affecting the geometry of the laser melt pool (that is, pool shape, aspect ratio, and surface ripples) and can result in defects such as variable penetration, porosity, and lack of fusion. Convection is also responsible for mixing and therefore affects the composition of the melt pool during laser welds because pool configuration in conduction-mode laser welding is a function of the Prandtl number (kinematic viscosity/molecular diffusivity), Pr_m, of the materials (Ref 40). In materials with low Prandtl numbers (for example, aluminum, with $Pr_m = 0.02$), the pool shape is more spherical and is dominated by conduction heat transfer when compared to high Prandtl number material (for example, steel, with $Pr_m = 0.1$), where pool shape is shallow and wide because it is dominated by the surface-tension-driven flow (Ref 40). Free surface deformation leading to defects such as undercuts is also influenced by convection. A small amount of surface reactant elements (for example, sulfur) can change the convection direction. For most metals, thermocapillary flow drives the hot metal to the cold side (Fig. 3), but the addition of sulfur changes the sign of the temperature dependence function of the surface tension and drives the liquid metal to the center of the pool.

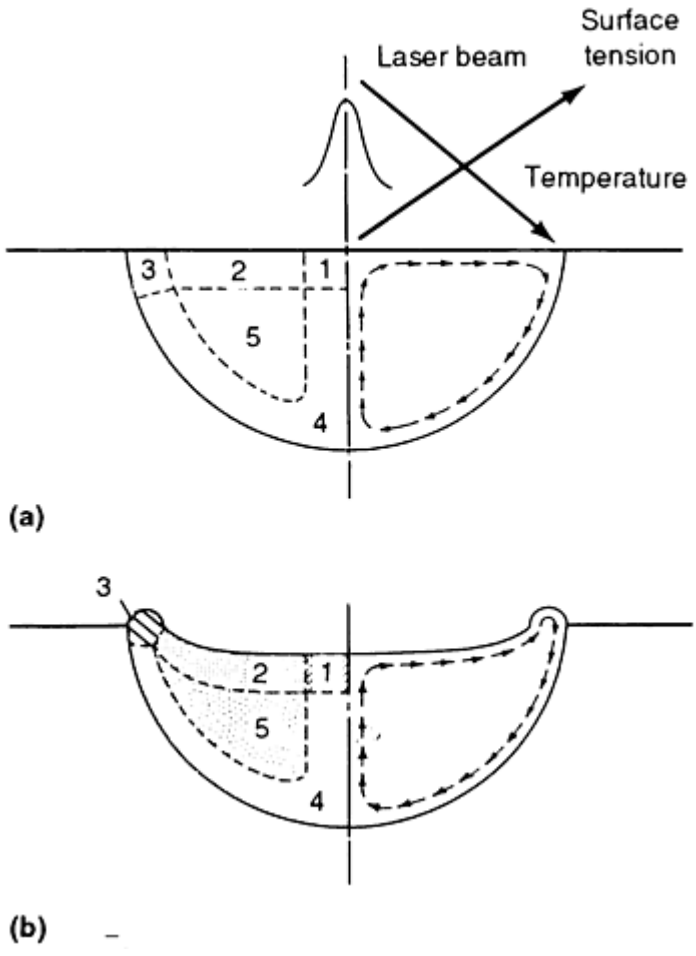

FIG. 3 SCHEMATIC SHOWING EFFECT OF CONVECTION ON LBW MELT POOL CONFIGURATION. (A) SPHERICAL SHAPE WITH FLAT SURFACE TYPICAL OF LOW PR_M MATERIALS. (B) SHALLOW AND UNDERCUT FREE SURFACE CHARACTERISTICS OF HIGH PR_M MATERIALS. NUMBERS IN FIGURE IDENTIFY SPECIFIC REGIONS: (1) STAGNATION FLOW REGION; (2) FREE SURFACE BOUNDARY LAYER REGION; (3) COOLED CORNER REGION; (4) SOLID-LIQUID INTERFACE BOUNDARY LAYER REGION; AND (5) ISOTHERMAL INVISCID CORE. SOURCE: REF 39

Deep-Penetration-Mode Welding. The mechanism of deep-penetration welding by a laser beam is very similar to that encountered with an electron beam (that is, energy transfer is via "keyhole" formation) (Ref 41, 42, 43). This keyhole may be produced when a beam of sufficiently high power density causes vaporization of the substrate and the pressure produced by the vapor in the crater causes displacement of the molten metal upward along the walls of the hole. This hole acts as a blackbody, aiding the absorption of the laser beam as well as distributing the heat deep in the material. The energy in most conventional welding processes is deposited at the surface of the workpiece and brought into the interior by conduction.

The conditions of energy and material flow during beam welding were investigated theoretically by Klemens (Ref 44). According to Klemens, the keyhole or cavity is formed only if the beam has sufficient power density. The keyhole is filled with gas or vapor created by continuous vaporization of wall material by the beam. This cavity is surrounded by liquid that, in turn, is surrounded by solid.

The flow of the liquid and the surface tension tends to obliterate the cavity while the vapor, which is continuously generated, tends to maintain the cavity. There is a continuous flow of material out of the cavity at the point where the beam enters. For a moving beam, this "keyhole" achieves a steady state (that is, the cavity and the beam associated with the molten zone move forward at the speed set by the advance of the beam). The material lost by vaporization shows up as a depression in the solidified melt as porosity, as an inward deformation of the workpiece, or possibly as a combination of these effects. The requirement that sufficient vapor be produced to maintain a steady state leads to a minimum advance speed for a steady state. While the cavity moves through the solid and liquid material at a speed determined by the motion of the beam, material must be moved continuously from the region ahead of the cavity to the region behind it. This is confirmed by the experimental work of Sickman and Morijn (Ref 45, 46) and Arata *et al.* (Ref 47).

An interesting experiment on the mechanism of deep-penetration welding with a CW CO_2 laser has been reported by Sickman and Morijn (Ref 45, 46). It was conducted on transparent fused quartz so that the formation of the weld as a function of time could be photographed. The tip of the hole appears to bend toward the direction in which the workpiece is moving. This process is caused by the reflection of laser light from the leading edge of the hole. Material evaporated at this surface is effectively trapped by the cooler trailing edge. Thus, material is transported across the laser beam from the hot leading edge to the cooler trailing edge without significant ejection of material back out toward the beam. For welding speeds in the range of 10 to 45 mm/min (0.4 to 1.8 in./min), the depth of penetration was linearly related to welding speed. As expected, the minimum penetration was obtained at maximum welding speed.

Fluid flow during penetration welding was also studied by Arata *et al.* (Ref 47), using laser beam irradiation of low-viscosity glass at high temperature. High-speed photography of the phenomenon, taken at 8000 frames per second (fps), clearly shows melt flow and the motion of the cavity. Molten fluid, which forms at the front wall of the cavity, accelerates at an angle along the wall as it is driven by the forces of the turbulence generated by laser vaporization. In this process, a large vortex is formed behind the cavity near the weld surface. This vortex is considered to be the cause of the so-called "wine-glass" beads that are produced by the process.

The transport of material is mainly due to flow in the liquid. However, part of the material is transported in the vapor phase, and this vapor transport generates the excess pressure that drives the liquid flow.

Laser Welding Parameters. The major independent process variables for laser welding include:

- INCIDENT LASER BEAM POWER
- INCIDENT LASER BEAM DIAMETER
- ABSORPTIVITY
- TRAVERSE SPEED OF THE LASER BEAM ACROSS THE SUBSTRATE SURFACE

Parameters such as weld design, shielding gas, gap size for butt welds, and depth of focus with respect to the substrate also play important roles. These parameters are discussed in the article "Procedure Development and Practice Considerations for Laser-Beam Welding" in this Volume.

The dependent variables are considered to be:

- DEPTH OF PENETRATION

- MICROSTRUCTURE AND METALLURGICAL PROPERTIES OF THE LASER-WELDED JOINTS

The effects of some of the important variables are briefly discussed below.

Laser-Beam Power. The depth of penetration with laser welding is directly related to the power density of the laser beam and is a function of incident beam power and beam diameter. For a constant beam diameter, penetration typically increases as the beam power is increased. Locke *et al.* (Ref 27) and Baardsen *et al.* (Ref 30) report that penetration increases almost linearly with incident laser power. It is generally observed that for LBW of a particular thickness, a minimum threshold power is required.

Laser-Beam Diameter. This parameter is one of the most important because it determines the power density. However, it is very difficult to measure for high-power laser beams. This difficulty is due partly to the nature of the beam diameter and partly to the definition of what is to be measured. A Gaussian beam diameter, d_G, can be defined as the diameter where the power has dropped to $1/e^2$ or $1/e$ of the central value:

$$\frac{1}{e^2} < P_{dG} < \frac{1}{e} \qquad \textbf{(EQ 2)}$$

The beam diameter defined on the basis of $1/e^2$ of the central value contains more than 80% of the total power, whereas the power contained for $1/e$ beam definition is slightly over 60% (Ref 49). Therefore, the $1/e^2$ beam diameter is recommended.

Many techniques have been used to measure the beam diameter, but most are unsatisfactory in some respect. Single isotherm contouring techniques (for example, charting paper and drilling acrylic or metal plates) suffer because the particular isotherm they plot depends both on power and on exposure time. These techniques are also highly unlikely to coincide with either the $1/e$ or $1/e^2$ diameters. Multiple isotherm contouring techniques overcome these difficulties but are tedious to interpret. However, several commercial systems are now available (see the article "Procedure Development and Practice Considerations for Laser-Beam Welding" in this Volume).

Absorptivity. The efficiency of LBW depends on the absorption of light energy by the workpiece. Any heat transfer calculation for laser processing is based on the energy absorbed by the workpiece.

The infrared absorption of metals largely depends on the conductive absorption by free electrons. Therefore, absorptivity is a function of the electrical resistivity of the substrate material. Arata and Miyamoto (Ref 50) and McCay *et al.* (Ref 51) measured the absorptivity of polished surfaces of various materials and concluded that absorptivity is proportional to the square root of the electrical resistivity. This agrees closely with:

$$A = 112.2\sqrt{r_r} \qquad \textbf{(EQ 3)}$$

where A is the absorptivity and ρ_r is the electrical resistivity. A temperature-dependent relationship between the electrical resistivity and emissivity of the metal was derived by Bramson (Ref 52). Bramson's formula can be used for theoretical calculation of the absorptivity from the electrical resistivity because absorptivity equals emissivity. However, Eq 4 will be valid only for metals without surface oxide layers that are heated in a vacuum. The presence of an oxide layer will increase the absorptivity. The relationship between the emissivity and the electrical resistivity of a substrate for the perpendicular incidence of radiation of long wavelength derived by Bramson is:

$$e_l(T) = 0.365\left[\frac{r_r(T)}{l}\right]^{1/2} - 0.667\left[\frac{r_r(T)}{l}\right] + 0.006\left[\frac{r_r(T)}{l}\right]^{3/2} \qquad \textbf{(EQ 4)}$$

where $\rho_r(T)$ is the electrical resistivity at absolute temperature, T, expressed in Ohm-centimeter ($\Omega \cdot$ cm), and $\varepsilon\lambda(T)$ is the emissivity of the substrate at temperature T (in °C) for radiation having a wavelength, λ.

The estimated absorptivity for Ti-6Al-4V at 300 °C (572 °F) using Bramson's formula is approximately 15%. Experimental data published by Arata and Miyamoto (Ref 50) and Bramson (Ref 52) indicate that the absorptivities of aluminum, silver, and copper are between 2 to 3% and those of stainless steel (type 304), iron, and zirconium are below 15% even in the molten state. Reflection losses of this magnitude are significant. Therefore, when a sheet metal product form is welded, measures must be taken to avoid reflection losses. Applying an absorbent powder to the surface or forming an anodized film on the surface are two techniques that are considered to be very effective (Ref 51).

Absorptivity can also be increased by the use of reactive gases. Jørgensen (Ref 53) reported that the addition of 10% O_2 to an argon shielding gas gives an increase of up to 100% in welding depth. Jørgensen also found that gas flow had no significant effect on weld depth. However, an increase in depth was associated with a decrease in reflectivity, which was obtained by the addition of a small amount of oxygen.

Although metals are poor absorbers of infrared energy at room temperature, above a certain threshold (approximately 10^6 to 10^7 W/cm^2, or 6×10^6 to 6×10^7 W/in.^{2}) energy transfer via the keyhole leads to much higher effective absorptivity. Once a keyhole has formed, absorptivity increases rapidly. Multiple internal reflections inside a keyhole are responsible for the deep-penetration welding by the laser despite the large convergence angles for laser beams relative to electron beams (Ref 51). However, the threshold energy required for keyhole formation in laser welding is higher than that required for an electron beam (1.5×10^5 W/cm^2, or 9.5×10^5 W/in.^{2}) because of the poor absorptivity. Nevertheless, energy transfer by this keyhole mechanism permits the laser to provide efficient welding of even highly reflective materials (for example, aluminum) (Ref 25).

Traverse Speed. The correlation of penetration depth relative to welding speed with both LBW and EBW processes was studied by Duley (Ref 41) and Locke and Hella (Ref 27). The penetration in the laser weld is consistently less than that obtained with an electron beam, but the relative difference between the two penetration depths diminishes as the welding speed is increased. However, Duley (Ref 41) found this somewhat surprising because as pointed out by Baardsen *et al.* (Ref 48), the time to form a void or keyhole depends on the illumination time for a particular area on the surface of the workpiece as the welding speed is increased. When this occurs, the average power dissipated in the sheet is expected to drop because the keyhole is no longer a completely effective trap for the incident laser radiation. For an electron beam, absorptivity of the material is independent of the shape and extent of the keyhole. Hence, the total power dissipated in the workpiece is less dependent on the welding speed. However, Crafer (Ref 54) reports that the keyhole penetration threshold for laser beams or electron beams of radius 0.1 mm (0.004 in.) incident on a steel surface of thermal diffusivity 10 mm^2/s (0.4 ft^2/h) is achieved in 1 ms. This could be regarded as instantaneous. Again, for very low welding speeds, the penetration depth of laser welds becomes significantly less than that attainable with the electron beam. According to Locke *et al.* (Ref 28), this can be attributed to the formation of a plasma cloud, which attenuates the incident beam.

References cited in this section

25. A. BLAKE AND J. MAZUMDER, *ASME J. ENG. IND.*, VOL 107 (NO. 3), AUG 1985, P 275-280
27. E.V. LOCKE AND R.A. HELLA, *IEEE J. QUANTUM ELECTRONICS*, VOL QE-10 (NO. 2), FEB 1974, P 179-185
28. R.C. CRAFER, ADVANCES IN WELDING PROCESSES, PAPER NO. 46, *PROC. 4TH LNT. CONF.* (HARROGATE, YORKS, ENGLAND), 9-11 MAY 1978, P 267-278
30. E.L. BEARDSON, D.J. SCHMATZ, AND R.E. BISARO, *WELD. J.*, VOL 52, APRIL 1973, P 227-229
39. J. MAZUMDER, *OPT. ENG.*, VOL 30 (NO. 8), 1991, P 1208-1219
40. C.L. CHAN, J. MAZUMDER, AND M.M. CHAN, *METALL. TRANS.* A, VOL 15, 1982, P 2175
41. W.W. DULEY, *CO_2 LASERS: EFFECTS AND APPLICATIONS*, ACADEMIC PRESS, 1976, P 241
42. A.M. MALEKA, ED., *ELECTRON BEAM WELDING PRINCIPLES AND PRACTICE*, WELDING INSTITUTE, MCGRAW-HILL, 1971, P 95-96
43. D.T. SWIFTHOOK AND E.E.F. GICK, *WELD. J.*, 1973, P 492S-499S
44. P.G. KLEMENS, *J. APPL. PHYSICS*, VOL 47, 1976, P 2165-2174
45. J.G. SICKMAN AND R. MORIJN, *PHILLIPS RES. REP.*, VOL 23, 1968, P 376
46. J.G. SICKMAN AND R. MORIJN, *PHILLIPS RES. REP.*, VOL 23, 1968, P 375
47. Y. ARATA, H. MARUO, I. MIYAMOTO, AND Y. INOUE, "DYNAMIC BEHAVIOR OF LASER

WELDING," IIW DOC IV/222/77, INTERNATIONAL INSTITUTE OF WELDING, 1977
48. E.L. BAARDSEN, D.J. SCHMATZ, AND R.E. BISARO, *WELD. J.*, VOL 52, APRIL 1973, P 227-229
49. J.E. HARRY, *INDUSTRIAL APPLICATION OF LASERS*, MCGRAW-HILL, 1974
50. Y. ARATA AND I. MIYAMOTO, *LASER FOCUS*, VOL 3, 1977
51. M.H. MCCAY, T.D. MCCAY, A. SEDGHINA-SAB, AND D.R. KEEFER, *LASER MATERIALS PROCESSING III*, J. MAZUMDER AND K. MUKHERJEE, ED., MINERALS, METALS, AND MATERIALS SOCIETY, 1989
52. M.A. BRAMSON, *INFRARED RADIATION: A HANDBOOK FOR APPLICATION*, PLENUM PRESS, 1968
53. M. JØRGENSEN, *MET. CONSTR.*, VOL 12 (NO. 2), FEB 1980, P 88
54. R.C. CRAFER, *WELD. INST. RES. BULL.*, VOL 17, FEB 1976

Laser-Beam Welding

Jyoti Mazumder, University of Illinois at Urbana-Champaign

Processing Equipment

Solid-State Optically Pumped Lasers. The majority of pulsed ruby and Nd:YAG solid-state lasers are used for microwelding applications. Continuous wave CO_2 (commercially available up to 25 kW, or 34 hp) and Nd:YAG (commercially available up to 2.4 kW, or 3.2 hp) versions are primarily used for deep-penetration welding. Table 2 gives the capabilities of lasers used for welding. Typical specifications of commercially available Nd:YAG lasers feature:

- UP TO 400 TO 600 W (0.5 TO 0.8 HP) AVERAGE POWER WITH PEAK POWER OF UP TO 8 TO 10 KW (11 TO 13 HP)
- PULSING WIDTH OF 250 MS
- PULSING RATE OF 400 PULSES PER SECOND (PPS)

Nd:YAG rods used as the active medium are pumped by a xenon flash lamp arranged in an elliptical cavity (Fig. 4). Typically, the cavity is coated with gold to maximize reflection of the flash lamp and subsequently to maximize the absorption in the rod. Recently, diode lasers have been explored as the pumping source to replace the flash lamp as the energy source. This improves the pumping efficiency and minimizes the thermal distortion of the medium.

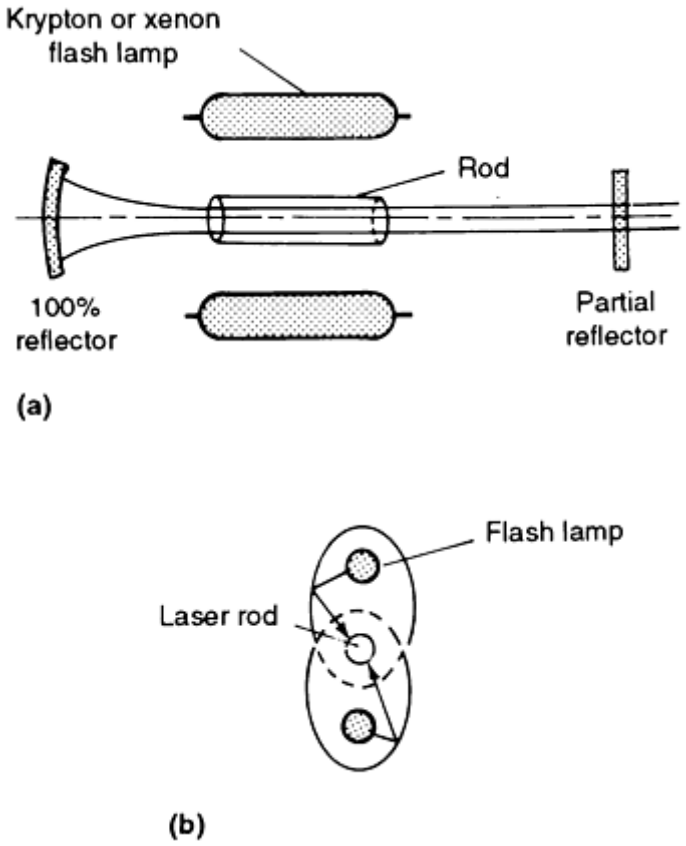

FIG. 4 TYPICAL CONSTRUCTION OF A PULSED OPTICALLY PUMPED ND: YAG SOLID-STATE LASER. (A) TOP VIEW. (B) END VIEW, SHOWING ELLIPTICAL CROSS SECTION OF REFLECTOR CAVITY HAVING THE ROD AT ONE FOCUS OF THE ELLIPSE AND THE FLASH LAMP AT THE OTHER FOCUS

Another new development in the Nd:YAG laser field is the face-pumped Nd:YAG laser (Fig. 5). The crystal slab provides much better beam quality because the temperature fluctuation across the active medium is much less for the slab configuration than the rod configuration. The "rod" geometry is at a disadvantage because only the surface of the rod is used as the active medium to produce a temperature gradient between the center and the surface. In the slab geometry, however, almost the entire crystal serves as the active medium, thus minimizing temperature gradient, which in turn reduces the thermal lensing effect. Although these solidstate optical systems have been used internally by General Electric for a long time, only recently, after the patent expired, did commercial systems become available. Beam generation in most rod systems is pulsed, whereas in most slab systems it is continuous wave.

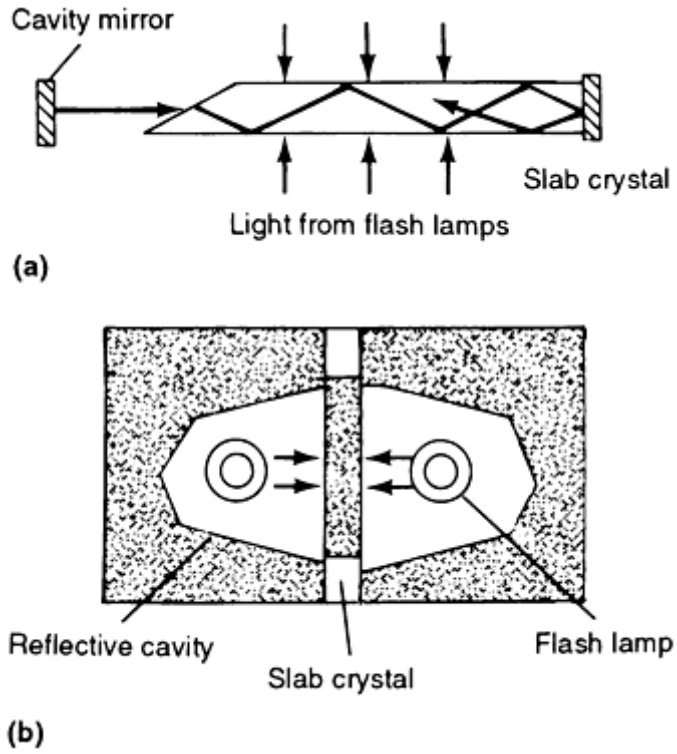

FIG. 5 KEY COMPONENTS OF A FACE-PUMPED ND:YAG SOLID-STATE LASER INCORPORATING A SLAB CRYSTAL. (A) FRONT VIEW. (B) END VIEW (CROSS SECTION)

The emergence of commercial multikilowatt (up to 2.4 kW, or 3.2 hp) CW Nd:YAG lasers is a recent development that has generated considerable interest with the laser industry because the energy can be transmitted through fiber optics. The maneuverability of the beam provided by fiber optics opens many complicated manufacturing operations previously closed to LBW processing.

Gas Lasers. Continuous wave CO_2 lasers are generally chosen for penetration welding applications. Figure 6 shows different types of pumping designs for CO_2 lasers. The primary components of a fast-axial-flow (FAF) CO_2 laser are shown in Fig. 7. Table 4 gives the four major types of CO_2 lasers commercially available.

TABLE 4 TYPICAL OUTPUT POWER OF COMMERCIALLY AVAILABLE CW CO_2 LASERS

DESIGNATION		ELECTRIC EXCITATION DISCHARGE(A)	OUTPUT POWER PER CAVITY LENGTH	
FLOW CONFIGURATION	TYPE		w/m	w/ft
AXIAL	SLOW	DC	60	18
	FAST	DC	600	180
		RF	750	230
TRANSVERSE	. . .	. . .	7000	2100

(A) DC. DIRECT CURRENT; RF, RADIO FREQUENCY

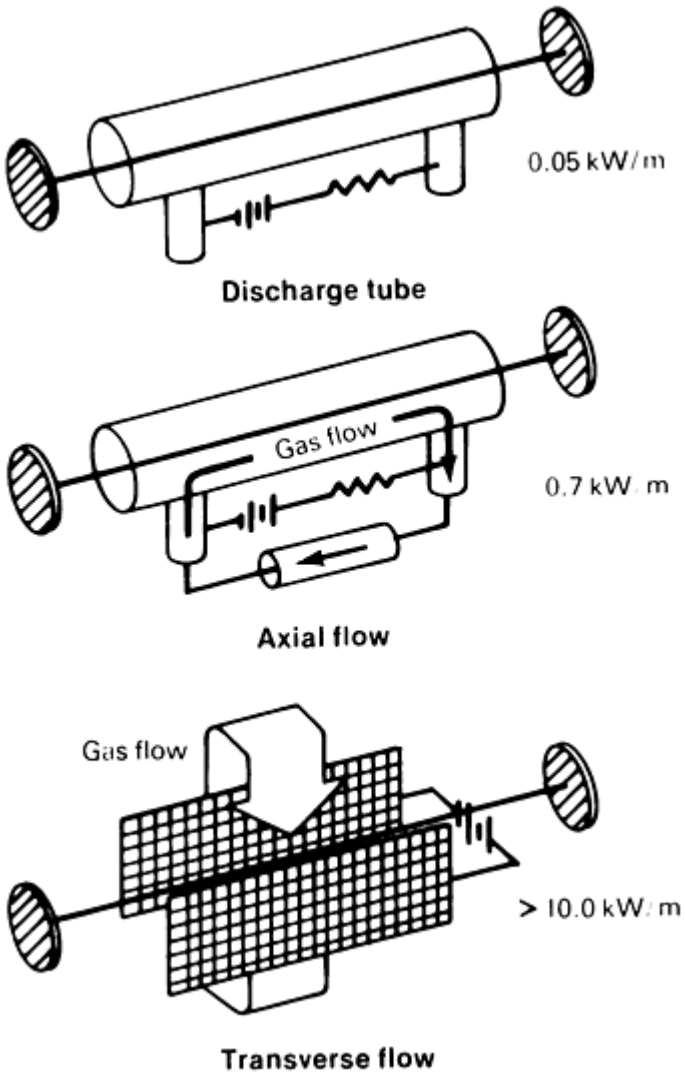

FIG. 6 TYPES OF ELECTRIC EXCITATION DISCHARGE GAS LASERS AND THE PRACTICAL LIMITS OF THE OUTPUT POWER PER CAVITY LENGTH. COURTESY OF TRUMPF LASER

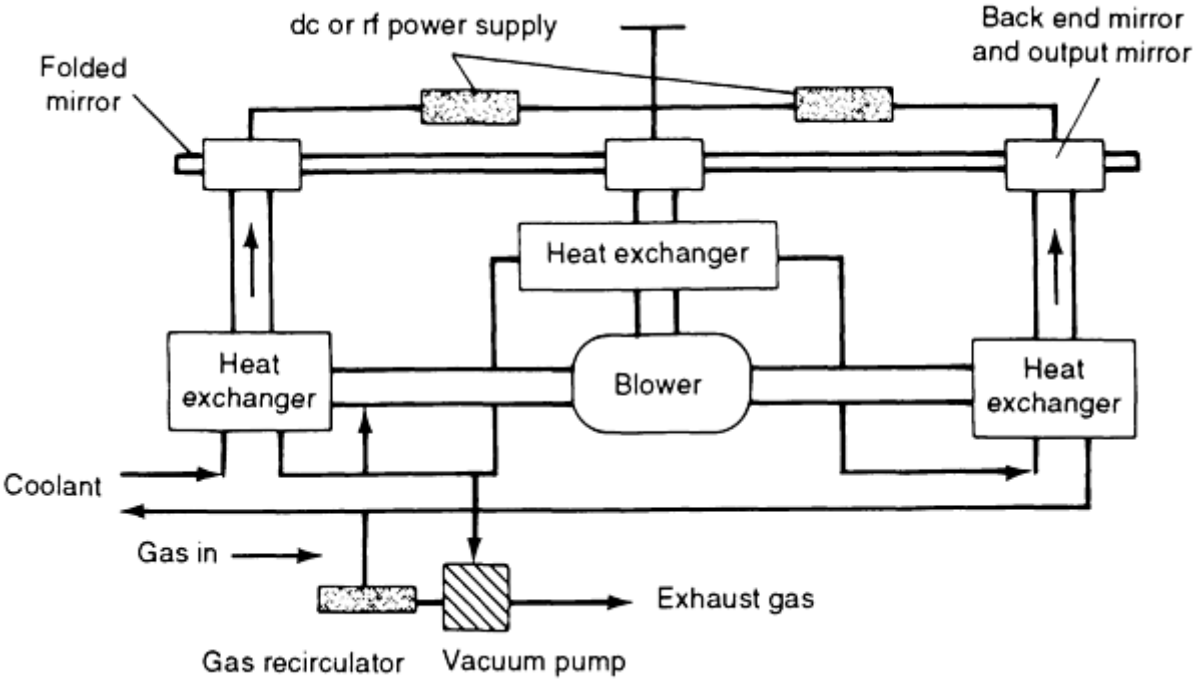

FIG. 7 FLOWCHART SHOWING HEAT EXTRACTION DEVICES USED TO COOL A FAST AXIAL-FLOW LASER. SOURCE: REF 55

Robotics. Robotic equipment is now available that can be integrated with lasers to provide beam delivery to the workpiece. In addition, almost any multiaxis or single-axis workstation can be integrated with lasers to steer the beam to the workpiece.

Ergonomics. Proper use of the laser as a machine tool requires a basic knowledge of optics. Knowledge of optical properties such as beam spatial distribution, depth of focus, and wavelength is critical to LBW processing. Textbooks should be consulted to make operators familiar with the fundamentals of laser physics and optics.

Reference cited in this section

55. W.M. STEEN, *LASER MATERIALS PROCESSING,* SPRINGER-VERLAG, 1991

Laser-Beam Welding

Jyoti Mazumder, University of Illinois at Urbana-Champaign

Health and Safety

Laser-beam welding hazards differ substantively from hazards encountered in other welding techniques. The hazards are not readily apparent, and inexperienced personnel may suffer permanent injury before the existence of hazardous conditions is recognized. For this reason, the American National Standards Institute specification ANSI Z136.1, "Safe Use of Lasers" (latest edition), requires that each facility using lasers designates an individual as "laser safety officer." This individual should be familiar with laser safety and ANSI Z136.1. The officer should monitor the use of lasers to ensure adherence to safe laser practice and the ANSI requirements. Because of the complexity of laser safety, this approach is strongly endorsed. The following brief review of laser safety by itself is not sufficient to ensure personnel safety.

Electrical Hazards. All lasers used for welding employ high voltages capable of inflicting lethal electric shocks. Therefore, maintenance should be performed by personnel familiar with high-voltage safety procedures.

Power supplies for high-power lasers contain capacitors capable of lethal shock even after initial discharge due to a phenomenon known as charge buildup. To facilitate safe maintenance access, the following provisions should be included:

- AN AUTOMATIC DISCHARGE AND GROUNDING CIRCUIT THAT IS ACTUATED WHEN THE LASER IS TURNED OFF
- DISCHARGE AND GROUNDING INTERLOCKS ON ALL ACCESS PANELS
- GROUNDING RODS FOR MANUAL VERIFICATION OF COMPLETE DISCHARGE. SAFETY GLASSES SHOULD BE USED, BECAUSE EXPLOSION-LIKE DISCHARGES ARE POSSIBLE ON PARTLY CHARGED CAPACITORS
- GROUNDING STRAPS TO SHORT OUT CAPACITORS TO PREVENT CHARGE BUILD-UP

In addition, all capacitors should be discharged and grounded before any work is performed on or near high-voltage components.

Control of laser performance usually requires switching of capacitors. Insulated switches that do not expose personnel to electric conductors are preferred. If switching requires work on bus bars, the procedure listed above should be followed, and the use of insulated tools should be considered. Cooling water leaks are not acceptable, especially when electrical and cooling lines share the same umbilical.

Eye Hazards. Any laser beam capable of welding metals is also capable of causing serious eye damage. Personnel exposure to the beam and any specularly reflected beam must therefore be prevented at all times. Certain lasers, however, are also capable of producing diffuse reflections that can cause permanent eye damage. Hence, viewing of the impact area of the laser beam or reflected beams also must be prevented. The preferred method for this is by complete enclosure.

Enclosures can range from a simple sleeve between the laser optic and the part to be welded to fully automatic operations in enclosed rooms. The following are general guidelines:

- THE ENCLOSURE MUST BE OPAQUE TO THE LASER WAVELENGTH. METAL ENCLOSURES ARE GENERALLY SUITABLE, BUT PLASTICS ALSO ARE A POSSIBLE SELECTION. INFRARED LASERS, FOR EXAMPLE, CAN BE ENCLOSED IN CLEAR POLY METHYLMETHACRYLATE. THE REQUIRED THICKNESS CAN BE CALCULATED USING ANSI Z136.1 AND THE TRANSMITTANCE PROPERTIES OF THE MATERIAL.
- THE ENCLOSURE MUST BE INTERLOCKED TO PREVENT FIRING OF THE LASER BEAM WHEN PERSONNEL COULD BE EXPOSED. WHEN THE PIECE TO BE WELDED IS A PART OF THE ENCLOSURE, THE INTERLOCKS SHOULD ALSO PREVENT FIRING, UNLESS THE PIECE IS IN PLACE. IN THE CASE OF PULSED LASERS, BREAKING OF THE INTERLOCKS SHOULD ALSO DISCHARGE THE STORED ENERGY INTO A DUMMY LOAD.
- SIGNS ARE REQUIRED AT ACCESS POINTS TO THE ENCLOSURES; SEE ANSI Z136.1.
- VIEWING OF THE WELD AREA CAN BE ACCOMPLISHED IN SEVERAL WAYS. MOST COMMON ARE VIEWING PORTS WITH FILTERS AND TELEVISION MONITORS. FOR MICROWELDING, MICROSCOPES SHOULD HAVE FILTERED VIEWING OPTICS OR FLIP MIRRORS THAT PERMIT EITHER WELDING OR VIEWING.
- ALIGNMENT OF LASER WELDING SYSTEMS SHOULD BE ACCOMPLISHED USING LOW-POWER LASERS.

Laser welding can also be performed with personnel in attendance. When done in this manner, the hazard must be evaluated for each welding process using the ANSI standard. General requirements include:

- THE LASER WELDING AREA MUST BE COMPLETELY ENCLOSED AND ACCESS MUST BE

RESTRICTED.

- IN MOST CASES, LASER EYE PROTECTION IS REQUIRED FOR ALL PERSONNEL IN THE AREA. THE OPTICAL DENSITY OF THE EYE PROTECTION MUST BE CALCULATED TO REDUCE THE POTENTIAL EYE EXPOSURE TO LESS THAN THE MAXIMUM PERMISSIBLE EXPOSURE (MPE) LEVEL.
- THE WELDING BEAM MUST BE CAREFULLY CONTROLLED AND SHOULD STILL BE ENCLOSED TO THE GREATEST EXTENT POSSIBLE. EYE PROTECTION IS LIKELY TO FAIL ON EXPOSURE TO THE PRIMARY BEAM.
- COMPLIANCE WITH PERSONNEL TRAINING REQUIREMENTS IS EXCEEDINGLY IMPORTANT.

Skin Exposure. Skin exposure to the primary beam obviously can result in thermal burns and must be prevented by complete enclosure and operator training. Even in attended operations where the operator is permitted to view the welding process, provision of partial enclosures to prevent personnel from placing any part of the body into the beam path is desirable.

The ANSI standard also prescribes MPE values for skin exposure. In the visible and near infrared regions, these are much greater than the MPE values for the eyes; hence, a problem from excessive exposure due to diffuse reflections at these wavelengths rarely occurs. Excessive skin exposures in the ultraviolet and far infrared regions are possible, however. Typically, ultraviolet exposures can be controlled with clothing of tightly woven material and barrier creams applied to exposed skin. Harmful levels of ultraviolet light can also be generated by flash lamps; hence, covers should be kept in place.

Chemical Hazards. Laser welding generates metal fumes similar to other welding processes, and the hazard is largely dependent on the composition of the welded metals. Ventilation is required to meet OSHA standards and American Conference of Governmental and Industrial Hygienists (ACGIH) threshold limit values. In high-power welding applications, fumes can be generated in sufficient quantities to make local exhaust ventilation, in addition to general room ventilation, both necessary and economical.

Harmful fumes or vapors can also be generated when laser energy is deposited in unwanted materials, such as breakdown of plastic enclosure materials due to laser exposure and failure of exotic lens materials due to thermal runaway. These conditions are best controlled by careful material selection and monitoring of welder performance. Finally, laser optics cleaning agents may be toxic and flammable and should be handled accordingly.

Training, Medical Examinations, and Documentation. ANSI Z136.1 requires that training in the potential hazards and control measures be provided to operators, engineers, technicians, and maintenance and service personnel. Special training on subjects such as potential hazards (including biological effects), control measures, and applicable standards is required for the laser safety officer. A model safety and training program is outlined in Appendix D of the standard.

Routine medical surveillance of laser users is no longer mandated by the standard. However, an employer may wish to provide such for medical/legal reasons (that is, to document what eye damage existed prior to commencement of laser work and that no additional damage has occurred).

Good documentation includes:

- LISTING OF LASERS, DURATION OF USE
- RESULTS OF HAZARD SURVEYS AND CALCULATIONS OF ACCESSIBLE LASER RADIATION
- INTERLOCK TESTS
- LASER USE PROCEDURES
- EMPLOYEES WORKING IN LASER AREA
- DATE AND EXTENT OF EMPLOYEE TRAINING
- DATES AND RESULTS OF MEDICAL EXAMINATIONS (IF ANY)
- TRAINING AND QUALIFICATIONS OF LASER SAFETY OFFICER

References

1. I.J. SPALDING, LASER SYSTEM DEVELOPMENTS, *PHYS. BULL.*, JULY 1971, P 402
2. Y.S. ARATA AND J. MIYAMOTO, *TECHNOCRAT*, VOL 11 (NO. 5), 1978, P 33
3. C.M. BANAS, "LASER WELDING TO 100 KW," REPORT NO. R76-912260-2, UNITED TECHNOLOGIES, FEB 1977
4. C.O. BROWN AND C.M. BANAS, "DEEP PENETRATION LASER WELDING," AWS ANNUAL MEETING (SAN FRANCISCO), APRIL 1971
5. J.E. ANDERSON AND J.E. JACKSON, *WELD. J.*, VOL 44, 1965, P 1018
6. W.W. DULEY, *CO_2 LASERS: EFFECTS AND APPLICATIONS*, ACADEMIC PRESS, 1976
7. A.J. MOOREHEAD AND P.N. TURNER, *WELD. J.*, VOL 49, 1970, P 15
8. M.A. ACHAREKAR, LASERS, *WELD. ENG.*, DEC 1974, P 9-11
9. T. WEBER, HOBART LASER PRODUCTS, INC., LIVERMORE, CA, 1992, PRIVATE COMMUNICATION
10. M.M. SCHWARTZ, *METAL JOINING MANUAL*, MCGRAW-HILL, 1979
11. S.R. BOLIN, ND-YAG LASER APPLICATION SURVEY, CHAPTER 8, *LASER MATERIALS PROCESSING*, M. BASS, ED., NORTH HOLLAND PUBLISHING CO., AMSTERDAM, 1983
12. H.L. MARSHALL, *PROC. OF THE SPIE*, VOL 86, 1976
13. J. MAZUMDER, LASER WELDING, CHAPTER 3, *LASER MATERIALS PROCESSING*, M. BASS, ED., NORTH HOLLAND PUBLISHING CO., AMSTERDAM, 1983
14. L. RAPP, C. GLUMANN, F. DOUSINGER, AND H. HÜGEL, *LASER TREATMENT OF MATERIALS*, B.L. MORDIKE, ED., DGM INFORMATIONSGESELLSCHAFT MBH, GERMANY, 1992, P 99-104
15. A.S. BRANDSON AND T. ENDERS, *LASER TREATMENT OF MATERIALS*, B.L. MORDIKE, ED., DGM INFORMATIONSGESELLSCHAFT MBH, GERMANY, 1992, P 117-124
16. H. SAKAMOTO, K. SHIBATA, AND F. DAUSINGER, *LASER TREATMENT OF MATERIALS*, B.L. MORDIKE, ED., DGM INFORMATIONSGESELLSCHAFT MBH, GERMANY, 1992, P 125-130
17. J. BERKMANN, S.K. BEHLER, AND E. BEYER, *LASER TREATMENT OF MATERIALS*, B.L. MORDIKE, ED., DGM INFORMATIONSGESELLSCHAFT MBH, GERMANY, 1992, P 151-156
18. A. LANG AND H.W. BERGMAN, *LASER TREATMENT OF MATERIALS*, B.L. MORDIKE, ED., DGM INFORMATIONSGESELLSCHAFT MBH, GERMANY, 1992, P 163-170
19. L.C. MALLORY, R.F. ORR, AND W. WELLS, *LASER MATERIALS PROCESSING III*, J. MAZUMDER AND K. MUKHERJEE, ED., MINERALS, METALS, AND MATERIALS SOCIETY, 1989, P 123-134
20. R.C. CRAFER, *WELD. INST. RES. BULL.*, APRIL 1976, P 17
21. E.A. METZBOWER AND D.W. MOON, MECHANICAL PROPERTIES, FRACTURE TOUGHNESS, AND MICROSTRUCTURES OF LASER WELDS OF HIGH STRENGTH ALLOYS, *PROC. CONF. ON APPLICATIONS OF LASERS IN MATERIALS PROCESSING* (WASHINGTON, DC), 18-20 APRIL 1979
22. D.B. SNOW AND E.M. BREINAN, "EVALUATION OF BASIC WELDING CAPABILITIES," UNITED TECHNOLOGIES RESEARCH CENTER, JULY 1978
23. E.M. BREINAN, C.M. BANAS, AND M.A. GREENFIELD, LASER WELDING--THE PRESENT STATE OF THE ART, DOC IV-181-75, *11TH ANNUAL MEETING OF THE WELDING INSTITUTE* (TEL AVIV), 6-12 JULY 1975, P 1-53
24. M.M. SCHWARTZ, *METAL JOINING MANUAL*, MCGRAW-HILL, 1979
25. A. BLAKE AND J. MAZUMDER, *ASME J. ENG. IND.*, VOL 107 (NO. 3), AUG 1985, P 275-280

26. D.W. MOON AND E. METZBOWER, *WELD. J.*, 1983, P 535-585
27. E.V. LOCKE AND R.A. HELLA, *IEEE J. QUANTUM ELECTRONICS*, VOL QE-10 (NO. 2), FEB 1974, P 179-185
28. R.C. CRAFER, ADVANCES IN WELDING PROCESSES, PAPER NO. 46, *PROC. 4TH LNT. CONF.* (HARROGATE, YORKS, ENGLAND), 9-11 MAY 1978, P 267-278
29. R.A. WILLGOSS, J.H.P.C. MEGAW, AND J.N. CLARK, *WELD. MET. FABR.*, MARCH 1979, P 117-126
30. E.L. BEARDSON, D.J. SCHMATZ, AND R.E. BISARO, *WELD. J.*, VOL 52, APRIL 1973, P 227-229
31. J. MAZUMDER AND W.M. STEEN, LASER WELDING OF STEELS USED IN CAN MAKING, *WELD. J.*, VOL 60 (NO. 6), JUNE 1981, P 19-25
32. C.M. BANAS, "LASER WELDING DEVELOPMENTS," PROC. CEGB INT. CONF. ON WELDING RES. RELATED TO POWER PLANTS (SOUTHAMPTON, ENGLAND), 17-21 SEPT 1972
33. F.D. SEAMAN AND R.A. HELLA, "ESTABLISHMENT OF A CONTINUOUS WAVE LASER WELDING PROCESS," IR-809-3 (1-10), REPORT IN CONFERENCE PROCEEDINGS AFML CONTRACT F336 15-73-C5004, OCT 1976
34. E.M. BREINAN AND C.M. BANAS, PRELIMINARY EVALUATION OF LASER WELDING OF X-80 ARCTIC PIPELINE STEEL, *WRC BULL.*, DEC 1971, P 201
35. C.M. BANAS AND G.T. PETERS, "STUDY OF THE FEASIBILITY OF LASER WELDING IN MERCHANT SHIP CONSTRUCTION," CONTRACT NO. 2-36214, U.S. DEPT. OF COMMERCE, FINAL REPORT TO BETHLEHEM STEEL CORP., AUG 1974
36. M. YESSIK AND D.J. SCHMATZ, "LASER PROCESSING IN THE AUTOMOTIVE INDUSTRY," PAPER MR74-962, SME, 1974
37. F.A. DIPIETRO, *LASER SYSTEM APPLICATION IN INDUSTRY*, ATA-ASSOCIAZIONE TECNIER DELL' AUTOMOBILE, TORINO, ITALY, 1990, P 103-120
38. E. BEYER, FRAUNHOFER INSTITUTE, AACHEN, GERMANY, PRIVATE COMMUNICATION, 1992
39. J. MAZUMDER, *OPT. ENG.*, VOL 30 (NO. 8), 1991, P 1208-1219
40. C.L. CHAN, J. MAZUMDER, AND M.M. CHAN, *METALL. TRANS.* A, VOL 15, 1982, P 2175
41. W.W. DULEY, *CO_2 LASERS: EFFECTS AND APPLICATIONS*, ACADEMIC PRESS, 1976, P 241
42. A.M. MALEKA, ED., *ELECTRON BEAM WELDING PRINCIPLES AND PRACTICE*, WELDING INSTITUTE, MCGRAW-HILL, 1971, P 95-96
43. D.T. SWIFTHOOK AND E.E.F. GICK, *WELD. J.*, 1973, P 492S-499S
44. P.G. KLEMENS, *J. APPL. PHYSICS*, VOL 47, 1976, P 2165-2174
45. J.G. SICKMAN AND R. MORIJN, *PHILLIPS RES. REP.*, VOL 23, 1968, P 376
46. J.G. SICKMAN AND R. MORIJN, *PHILLIPS RES. REP.*, VOL 23, 1968, P 375
47. Y. ARATA, H. MARUO, I. MIYAMOTO, AND Y. INOUE, "DYNAMIC BEHAVIOR OF LASER WELDING," IIW DOC IV/222/77, INTERNATIONAL INSTITUTE OF WELDING, 1977
48. E.L. BAARDSEN, D.J. SCHMATZ, AND R.E. BISARO, *WELD. J.*, VOL 52, APRIL 1973, P 227-229
49. J.E. HARRY, *INDUSTRIAL APPLICATION OF LASERS*, MCGRAW-HILL, 1974
50. Y. ARATA AND I. MIYAMOTO, *LASER FOCUS*, VOL 3, 1977
51. M.H. MCCAY, T.D. MCCAY, A. SEDGHINA-SAB, AND D.R. KEEFER, *LASER MATERIALS PROCESSING III*, J. MAZUMDER AND K. MUKHERJEE, ED., MINERALS, METALS, AND MATERIALS SOCIETY, 1989
52. M.A. BRAMSON, *INFRARED RADIATION: A HANDBOOK FOR APPLICATION*, PLENUM PRESS, 1968
53. M. JØRGENSEN, *MET. CONSTR.*, VOL 12 (NO. 2), FEB 1980, P 88
54. R.C. CRAFER, *WELD. INST. RES. BULL.*, VOL 17, FEB 1976
55. W.M. STEEN, *LASER MATERIALS PROCESSING*, SPRINGER-VERLAG, 1991

Jyoti Mazumder, University of Illinois at Urbana-Champaign

Selected References

- M. BORN AND E. WOLF, *PRINCIPLES OF OPTICS,* PERGAMON PRESS, 1987
- O. SVELTO, *PRINCIPLES OF LASERS,* PLENUM PRESS, 1982
- J. VERDEYEN, *LASER ELECTRONICS,* PRENTICE-HALL, 1989

Electroslag and Electrogas Welding*

S. Liu, Colorado School of Mines; S.D. Brandi, Escola de Politecnica da USP; R.D. Thomas, Jr., R.D. Thomas and Company

Introduction

ELECTROSLAG WELDING AND ELECTROGAS WELDING are two related procedures that are presently used to weld thick-section materials in the vertical or near-vertical position between retaining shoes. Primarily applied for joining steels of thicknesses over 50 mm (2 in.), electroslag welding (ESW) involves high energy input relative to other welding processes, resulting in generally inferior mechanical properties, specifically lower toughness of the heat-affected zone (HAZ). However, the high deposition rate and relatively low cost of the process make it attractive for heavy structural fabrication. The as-welded properties of electrogas welding (EGW), usually applied to steels under 50 mm (2 in.), are generally superior to those of electroslag welds, and the process is commonly applied to the field erection of storage vessels and other less critical structures.

Electroslag welding is a vertical welding process producing coalescence with molten slag which melts the filler metal and the surface of the work to be welded. Confined by cooling shoes, the molten weld pool is shielded by the molten slag, which moves along the full cross section of the joint as welding progresses. The conductive slag is maintained in a molten condition by its resistance to electric current passing between the electrode and the work (Ref 1). ESW can be considered a progressive melting and casting process in which the heat of a bath of molten flux is used to melt the filler metal and the edges of the plates to be welded. Electric arc occurs only at the beginning of the process, and once a molten bath is achieved, the arc is extinguished. During the process, flux is added periodically or continuously to maintain an adequate slag covering over the pool of molten metal. Two or more retaining shoes hold the molten metal in place until it has solidified. In normal operation with a constant potential power source, the electrode melts off while dipping only partly through the flux bath and gathers in the molten metal puddle. In the case of low-carbon steel, the temperature of the bath is reported to be in the vicinity of 1925 °C (3500 °F), while the surface temperature is approximately 1650 °C (3000 °F) (Ref 2). The major process variables are welding current and voltage. Welding current is directly responsible for the electrode melt rate, while voltage influences the base metal penetration and weld bead width. Both variables are sensitive to the physical properties of the welding flux, such as electrical resistivity and fluidity.

Electrogas welding is a method of gas-metal arc welding (if a solid wire is used) or flux-cored arc welding (if a tubular wire is used), wherein an external gas is supplied to shield the arc and molding shoes are used to confine the molten weld metal for vertical position welding (Ref 2). Electrogas welding may or may not use an added flux. In the solid wire process, CO_2 shielding gas is commonly used and no flux is added. With the flux-cored process, the core ingredients provide a small amount of flux to form a thin deposit of slag between the weld and the shoes. Self-shielding electrodes eliminate the need for external shielding gas. A major difference between ESW and EGW is that the former relies on slag conduction to carry the welding current and the latter uses arc conduction. Despite the differences, similarities between ESW and EGW in terms of equipment, joint preparation, and welding procedures are such that they can be grouped into one category and described as allied processes.

References

1. ELECTROSLAG AND ELECTROGAS WELDING, *AWS WELDING HANDBOOK*, VOL 2 (NO. 7), AWS, 1978, P 226-260
2. H.C. CAMPBELL, ELECTROSLAG, ELECTROGAS, AND RELATED WELDING PROCESSES, *WRC BULL.*, VOL 154, 1970

Note

* ADAPTED FROM R.D. THOMAS, JR., AND S. LIU, INTERPRETIVE REPORT ON ELECTROSLAG, ELECTROGAS, AND RELATED PROCESSES, *WELDING RESEARCH COUNCIL BULLETIN*, NO. 338, NOVEMBER 1988. USED WITH PERMISSION OF THE WELDING RESEARCH COUNCIL.

Electroslag and Electrogas Welding*

S. Liu, Colorado School of Mines; S.D. Brandi, Escola de Politecnica da USP; R.D. Thomas, Jr., R.D. Thomas and Company

Fundamentals of the Electroslag Process

Heat Flow Conditions. Electroslag welding is quite similar to *in situ* casting, with large volumes of molten metal and high heat content. When compared with other arc welding processes, electroslag welds have a long thermal cycle with very slow cooling rate. Electroslag welding generally consumes hundreds of kilo-joules per inch, as compared to 10 to 40 kJ/mm (250 to 1000 kJ/in.) found in most arc welding. Figure 1 shows a typical thermal cycle of an electroslag weld compared with that of an arc welded weld. As a consequence of the thermal experience, weld metal solidification is extremely slow, resulting in a coarse primary solidification structure. The heat absorbed into the base metal also creates an extremely large HAZ (Fig. 2).

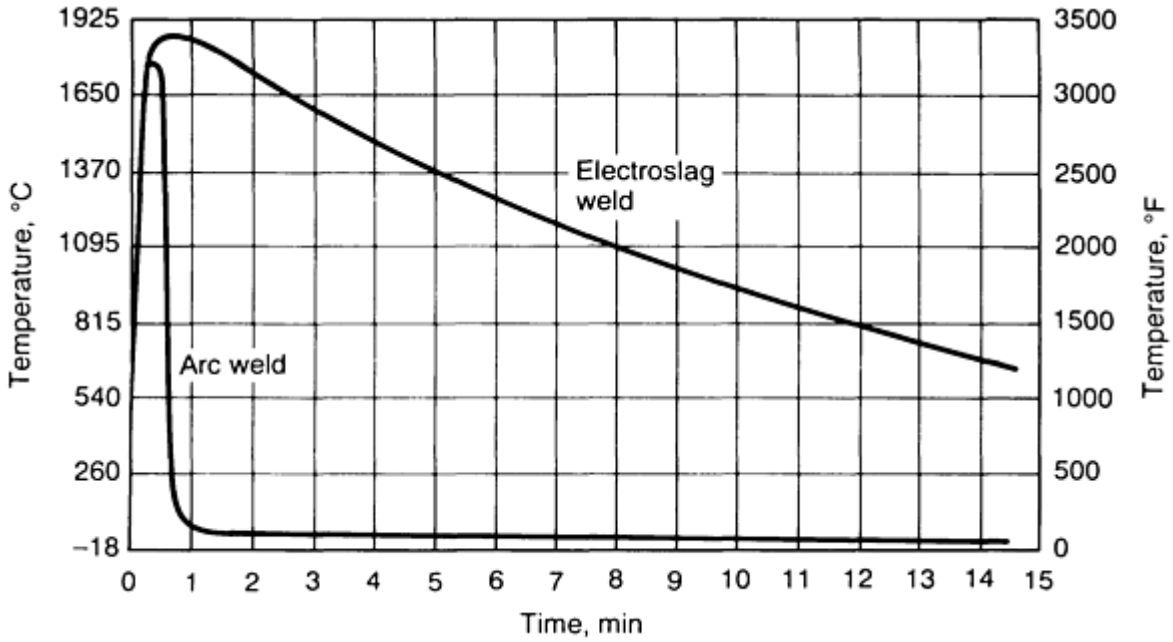

FIG. 1 TYPICAL THERMAL CYCLE OF AN ELECTROSLAG WELD RELATIVE TO THAT OF AN ARC WELDED WELD

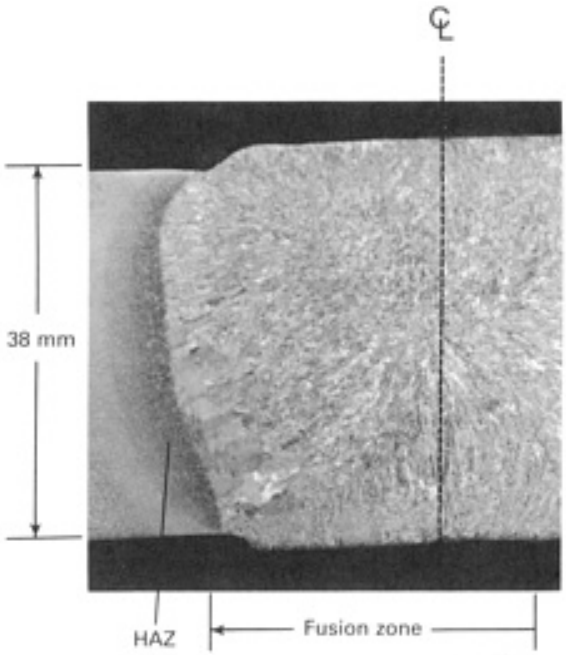

FIG. 2 MACROGRAPH SHOWING FUSION ZONE AND HEAT-AFFECTED ZONE IN AN ELECTROSLAG WELDMENT

A heat balance diagram of a typical electroslag weld (Fig. 3) illustrates that approximately 60% of the heat is absorbed by the workpart, close to 25% of the total heat is expended in the melting of the electrode, and around 10% of the heat is used to superheat the molten metal (Ref 3). The amount of heat extracted by the cooling shoes varies, depending on the thickness of the plate and on the welding conditions. In the welding of steel plates 90 mm (3 $\frac{1}{2}$ in.) thick, less than 10% of the heat of the molten slag and metal pool is transferred to the cooling shoes. In thinner plates, however, the cooling shoes play a more significant role in the heat balance.

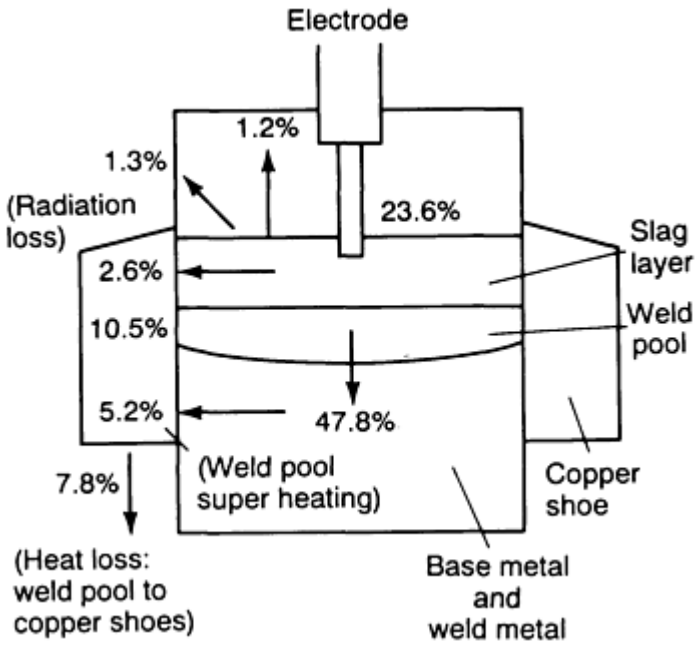

FIG. 3 HEAT BALANCE DIAGRAM OF A TYPICAL ELECTROSLAG WELDMENT. SOURCE: REF 3

Mathematical models are used to estimate the three-dimensional temperature field in the slag, metal pool, and base metal regions in an electroslag weldment, and to predict HAZ size and grain growth in the HAZ. Figure 4 shows an example of the calculated temperature distribution for a base plate 25.4 mm (1 in.) thick, 470 mm (18.5 in.) long, and 610 mm (24 in.) wide, at the time that corresponds to half the total time required for completion of the weld (Ref 4). The maximum temperatures reached in the slag and weld pool were 2230 K (3555 °F) and 1900 K (2960 °F), respectively. The temperature distribution in a weldment along planes parallel and normal to the parent plate surface can also be represented in the form of isometric temperature plots (Fig. 5).

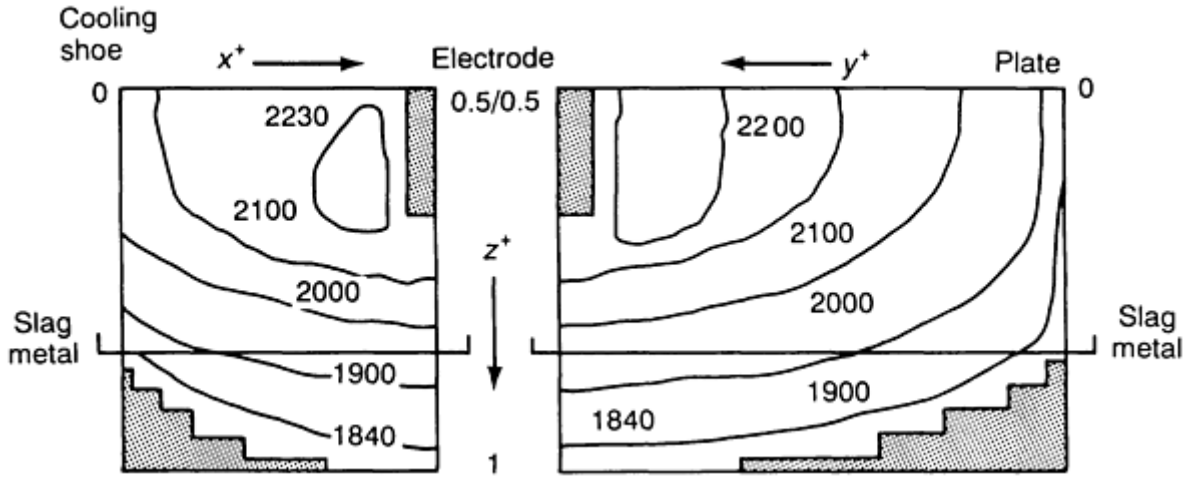

FIG. 4 CALCULATED TEMPERATURE DISTRIBUTION OF AN ELECTROSLAG WELDMENT SHOWING THREE-DIMENSIONAL TEMPERATURE FIELD IN THE SLAG, METAL POOL, AND BASE METAL. ALL TEMPERATURES SHOWN ARE IN KELVIN. SOURCE: REF 4

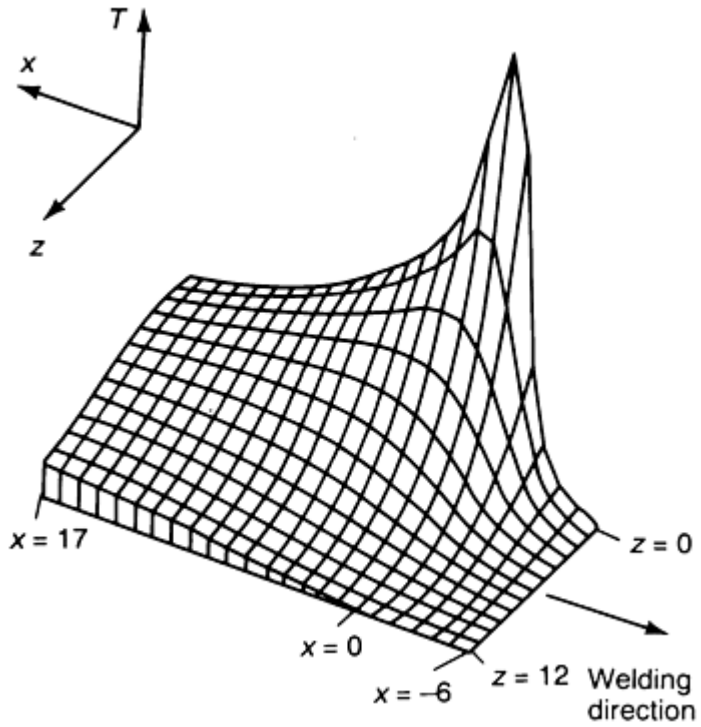

FIG. 5 ISOMETRIC THREE-DIMENSIONAL TEMPERATURE DISTRIBUTION IN AN ELECTROSLAG WELDMENT ALLOWING IMPROVED VISUALIZATION OF THE TEMPERATURE PROFILE. SOURCE: REF 5

The energy balance in the slag phase is summarized in Table 1. A major portion of the heat generated in the slag layer was transferred to the cooling shoes (36.1%). Approximately 22 and 15% of the heat was used in base metal heating and electrode melting, respectively. The heat-generating patterns are highly sensitive to the geometric location of the electrode in the slag. With careful control of the process variables (such as gap distance and convective flow suppression) by external application of electromagnetic field, reductions of two or three times the usual heat input could be practical.

TABLE 1 ENERGY BALANCE IN THE SLAG PHASE OF ELECTROSLAG WELDING

PARAMETER[(A)]	ENERGY DISSIPATED, %
HEAT TRANSFER FROM SLAG:	
TO COPPER SHOE	36.10
TO BASE PLATES	20.22
TO LIQUID METAL	8.71
HEAT USED TO HEAT THE ELECTRODE TO ITS MELTING POINT	15.26
HEAT REQUIRED:	
TO MELT THE ELECTRODE	4.07
TO HEAT FLUX COOLING ON THE CONSUMABLE GUIDE	1.84
HEAT CARRIED BY LIQUID METAL DROPS	2.04
RADIATION LOSS FROM THE SLAG SURFACE	1.75
ELECTROCHEMICAL LOSS	10.00

Source: Ref 5

(A) ACTUAL WIDTH OF THE SLAG POOL 0.044 MM (0.0017 IN.); CURRENT 534 A; OTHER CONDITIONS ARE THE SAME AS THOSE PRESENTED IN TABLE 2.

To distribute the energy uniformly across the thickness of the weldment, empirical rules have been developed (Table 2) to determine the preferred number of electrodes, the wire spacing, and the traverse (oscillation) distance (Fig. 6). Oscillation speeds depend on the plate thickness, usually allowing a traverse time of 3 to 5 s; a dwell time at the end of each traverse ensures adequate penetration at the plate edges.

TABLE 2 EFFECT OF JOINT GEOMETRY ON MULTIPLE-WIRE BUTT ELECTROSLAG WELDING

STEEL PLATE THICKNESS		NUMBER OF WIRES	OSCILLATION	SQUARE BUTT GAP OPENING	
mm	in.			mm	in.
19-75	$\frac{3}{4}$ -3	1	NO	22-32	$\frac{7}{8}$ -1 $\frac{1}{4}$
25-130	1-5	1	YES	32-35	1 $\frac{1}{4}$ -1 $\frac{3}{8}$
75-150	3-6	2	NO	32-35	1 $\frac{1}{4}$ -1 $\frac{3}{8}$
75-280	3-11	2	YES	32-35	1 $\frac{1}{4}$ -1 $\frac{3}{8}$
130-535	5-21	3	YES	35	1 $\frac{3}{8}$

Source: Ref 6

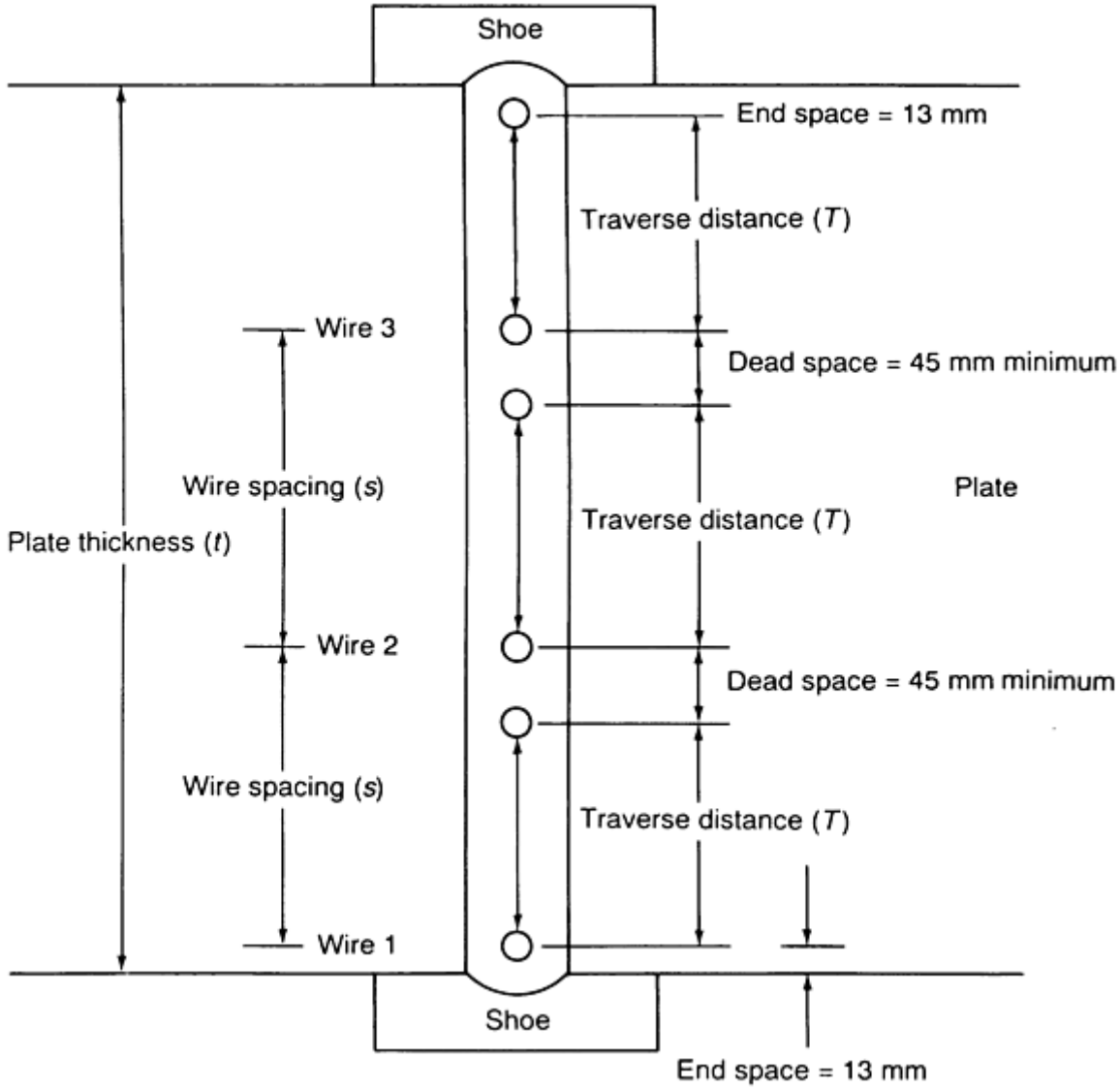

FIG. 6 WIRE SPACING DIAGRAM FOR MULTIPLE-ELECTRODE ELECTROSLAG WELDING INCORPORATING OSCILLATION FOR BETTER ENERGY DISTRIBUTION ACROSS THE THICKNESS OF THE WELDMENT. SOURCE: REF 6

Metal Transfer and Weld Pool Morphology. The droplet transfer rate and the length of time each droplet is in contact with the slag layer profoundly affect the chemical composition and the metallurgical properties of the weld pool.

Droplet Formation. In steady-state operation, the molten filler metal transfers into the weld pool in a globular mode. Current and voltage oscillograms indicate that despite the droplet size decrease observed with increasing voltage, welding current has no significant effect on the size of the droplets. Rather, the length of time that a droplet is in contact with the slag layer decreases considerably with increasing current. On the other hand, the length of time a droplet is in contact with the layer of slag increases with voltage, because the electrode tip is further away from the molten metal pool. The extent of interaction between a metal droplet and the slag layer determines the chemical composition of the weld pool.

Weld Pool Morphology. In an electroslag weldment, solidification begins at the fusion line, surfaces adjacent to the retaining shoes, and progresses toward the center of the weld. Because the process is continuous in a vertical or near vertical-up position, solidification also progresses from the bottom toward the top part of the joint. The angles at which the columnar grains meet at the center of the weld depend on the shape of the weld pool, which can be described by the weld pool form factor. Form factor is defined as the ratio between the width, *W*, and the maximum depth, *h*, of the pool (Fig. 7). Welds having a high form factor (>2.0) will have grains meeting at an acute angle at the center line, while welds with a low form factor (<1.0) will solidify with grains meeting at an obtuse angle. Low form factor is highly undesirable

because of the potential accumulation of residual elements at the center of the weld joint. High welding current usually results in a low form factor, while low welding current usually results in a high form factor and shallow metal pool. High voltage promotes shallow pools and low voltage. Figure 7 shows two examples of different pool morphologies and form factors as a function of the welding current and voltage.

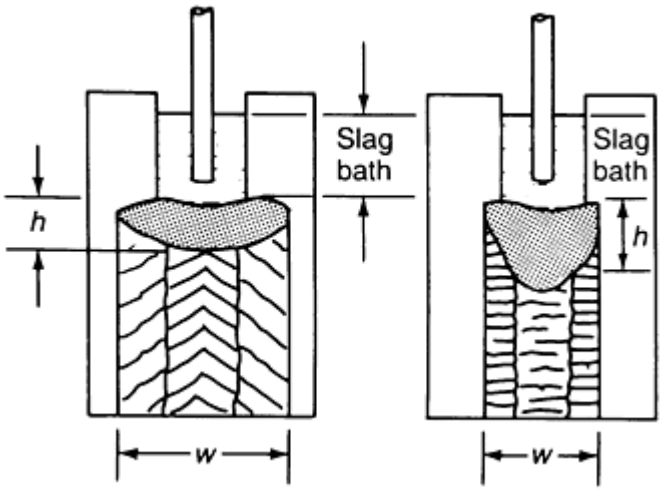

EFFECT OF WELDING PARAMETERS ON WELD METAL POOL SHAPE

PARAMETER	EFFECT OF PARAMETER INCREASE ON WELD-METAL POOL DIMENSION[A]		
	POOL WIDTH (*W*)	POOL DEPTH (*H*)	FORM FACTOR (*F* = *W*/*H*)
CURRENT OR WIRE-FEED SPEED:			
LOW VALUES	A	A	B
HIGH VALUES	D	A	D
VOLTAGE	A	B	A
SLAG POOL DEPTH	D	B	D
ROOT OPENING	A	C	A

FIG. 7 EFFECT OF INCREASE IN WELDING PARAMETERS ON WELD POOL FORM FACTOR. (A) OPTIMUM WELD POOL DIMENSIONS (SHALLOW WELD POOL, HIGH FORM FACTOR, ACUTE ANGLE BETWEEN GRAINS). (B) UNDESIRABLE WELD POOL DIMENSIONS (DEEP WELD POOL, LOW FORM FACTOR, OBTUSE ANGLE BETWEEN GRAINS). SOURCE: REF 6

An additional factor controlling the weld puddle morphology is the welding flux conductivity. Actually, the bulk of the electrical energy is converted into thermal energy in a thin layer of the slag contiguous to the electrode tip, which acts as the heat source in ESW (Ref 3). High conductivity fluxes generate less heat and result in less base metal penetration and shallower weld pools.

Out-of-Position (Nonvertical) ESW. Electroslag welding has been successfully done in joints that are inclined from the vertical position. The stability of the process and the quality of the weld joint are both functions of the angle of inclination. Weld morphology, including penetration, HAZ, and weld metal microstructure, is sensitive to the welding parameters. Preferential radiative heating of the upper weld surface is considered the cause of asymmetric penetration and HAZ geometry (Ref 7).

Weld Pool Penetration and Magnetic Field Coupling. Magnetic field is not generally applied in ESW. For electroslag overlays, however, some use of magnetic field to promote fluid flow and to drive the molten slag layer from the hotter region to the colder region to eliminate undercutting has been reported (Ref 8). However, the effect of magnetic stirring, which induced convective fluid motion in the weld pool and disrupted the solidification and growth of the columnar dendrites, can be seen in Fig. 8 (Ref 9, 10). Mechanical vibration on electroslag weld pools generally does not cause significant microstructural modification. However, some refinement of the as-deposited grains can result when the slag-molten metal interface is disturbed. The use of a quartz-shielded electrode guide tube as an extended stirrer has been reported to form a deeper weld pool, with the form factor decreasing from 3 to 1.5 (Ref 11, 12). Other techniques for refining weld metal microstructures include ultrasonic cavitation and the use of chemical inoculators.

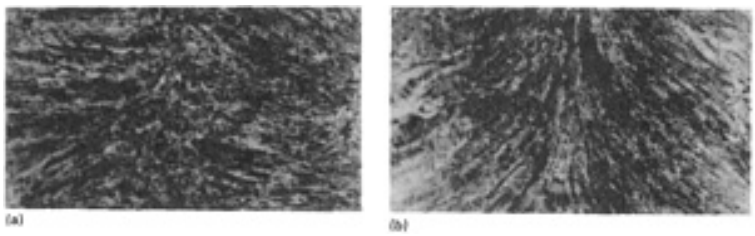

FIG. 8 MACROGRAPH SHOWING EFFECT OF SUPERIMPOSED MAGNETIC FIELD ON ELECTROSLAG WELDMENTS. (A) FIELD PRESENT. (B) FIELD ABSENT. BOTH 1.6×. SOURCE: REF 9

References cited in this section

3. B. PATON, *ELECTROSLAG WELDING,* AWS, 1962
4. T. DEBROY, J. SZEKELY, AND T. EAGER, HEAT GENERATION PATTERNS AND TEMPERATURE PROFILES IN ELECTROSLAG WELDING, *METALL. TRANS. B,* VOL 11, 1980, P 593-605
5. R.H. FROST, J.E. JONES, AND D.L. OLSON, ELECTROSLAG WELDING OF PRESSURE VESSEL STEELS, *ELECTROSLAG WELDING FOR MARINE APPLICATIONS,* PAPER 2, U.S. NAVY ACADEMY, MARCH 1985
6. "ELECTROSLAG ELECTROGAS TIPS & TECHNIQUES," BULLETIN OF ELECTROTHERM CORP., 1973
7. J.E. JONES, D.L. OLSON, AND G.P. MARTINAS, METALLURGICAL AND THERMAL CHARACTERISTICS OF NON-VERTICAL ELECTROSLAG WELDING, *WELD. J.,* VOL 59 (NO. 9), 1980, P 245S-254S
8. S. NAKANO, N. NISHIYAMA, T. HIRO, AND J. TSUBOI, MAGLAY PROCESS--ELECTROMAGNETIC CONTROLLED OVERLAY WELDING PROCESS WITH ESW, *KAWASAKI STEEL TECH. REP.,* VOL 2, 1981, P 31-42
9. S. LIU AND C.T. SU, GRAIN REFINEMENT IN ELECTROSLAG WELDMENTS BY METAL POWDER ADDITION, *WELD. J.,* VOL 68 (NO. 4), 1989, P 132S-144S
10. C.T. SU, "HIGH SPEED ELECTROSLAG WELDING," M.S. THESIS, PENNSYLVANIA STATE UNIV., 1987
11. S. VENKATARAMAN, J.H. DEVLETIAN, W.E. WOOD, AND D.G. ATTERIDGE, GRAIN REFINEMENT DEPENDENCE ON SOLIDIFICATION AND SOLID STATE REACTIONS IN ELECTROSLAG WELDS, *GRAIN REFINEMENT IN CASTINGS AND WELDS,* AIME, 1982, P 275-288
12. D.G. ATTERIDGE, S. VENKATARAMAN, AND W.E. WOOD, "IMPROVING THE RELIABILITY AND INTEGRITY OF CONSUMABLE GUIDE ELECTROSLAG WELDMENTS IN BRIDGE STRUCTURES," RESEARCH REPORT, OREGON GRADUATE CENTER, 1982

S. Liu, Colorado School of Mines; S.D. Brandi, Escola de Politecnica da USP; R.D. Thomas, Jr., R.D. Thomas and Company

Constitutive Equations for Welding Current, Voltage, and Travel Rate

The power input per unit length of a weld is the primary variable that influences the degree of base metal melting, the amount of filler metal deposition, and the thermal history of the weldment. In ESW, current and travel speed are not independent variables, as in the other arc welding processes. For a constant voltage power supply, the current and power are both functions of the resistance of the slag pool. Hence, they are functions of the electrode feed rate, the mechanics of electrode melting, and the nature of the electrical and thermal transport at the electrodeslag interface. To control the welding process, a constitutive equation has been proposed (Ref 13):

$$I = B\,W^{1/2}V^{1/3} \qquad \textbf{(EQ 1)}$$

where I is the welding current, W is the electrode feed rate, V is the welding voltage, and B is a proportionality constant. Equation 1 expresses the functional relationship between the various process variables and has the primary objective of selecting a voltage and current range that provides sufficient energy input for base plate penetration without excessive overheating of the HAZ. The relation can be empirically determined from Fig. 9. The total energy input per unit area of weld surface, E, can also be determined:

$$E = B\frac{L_g}{2p\,r^2(L+g)}\cdot\frac{V^{5/3}}{I} \qquad \textbf{(EQ 2)}$$

where L is the width of the base plate, g is the root gap opening, and r is the radius of the welding electrode. Note also that this equation takes into consideration the electrode-to-joint geometry, which is related to the electrical and thermal transport in the process.

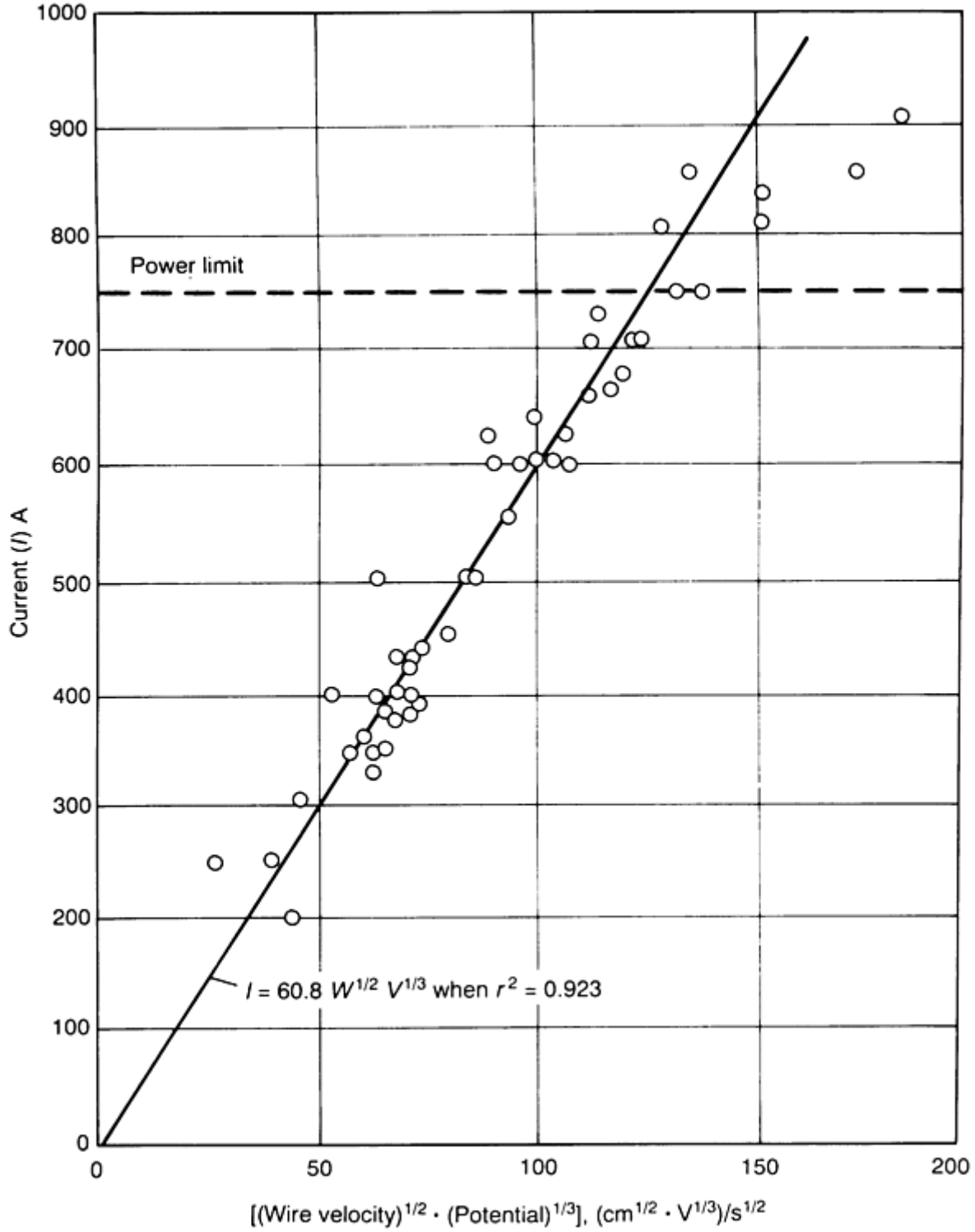

FIG. 9 FUNCTIONAL RELATION AMONG WELDING CURRENT (*I*), POTENTIAL (*V*), AND WIRE-FEED RATE (*W*) FOR ELECTROSLAG WELDING OF 2 $\frac{1}{4}$ CR-1MO STEEL. LINE INDICATES VALUE OF $I = BW^{1/2}V^{1/3}$ FOR $B = 60.8$ AND $R = 0.923$. SOURCE: REF 14

Unlike arc welding processes, in which an increase in current results in greater energy input and deeper penetration, the reverse occurs in ESW. An increase in current requires an increase in electrode burn-off rate, which increases the welding speed and decreases the energy input per unit area of weld. An excessive increase in the current at constant voltage, however, can shift the process from penetration to nonpenetration of the base plate. The process control boundaries for ESW can be easily developed (Fig. 10). Boundaries A through D enclose an operating space that exhibits good process

stability and base metal melting. Outside the indicated boundary, the process often appears to operate well but with inadequate base metal penetration (Ref 13).

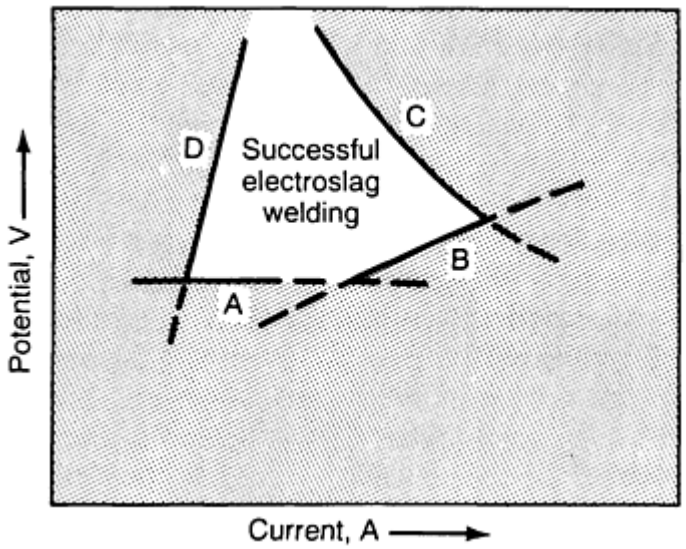

FIG. 10 OPERATING PARAMETER WINDOW FOR ELECTROSLAG WELDING. BOUNDARY A REPRESENTS THE VOLTAGE THRESHOLD FOR PARENT PLATE FUSION AT LOW-POWER INPUTS. BOUNDARY B REPRESENTS THE CONSTITUTIVE EQUATION FOR ADEQUATE PENETRATION AT HIGH POWER LEVELS. BOUNDARY C REPRESENTS THE MAXIMUM POWER OUTPUT OF THE WELDING POWER SUPPLY. BOUNDARY D REPRESENTS THE LIMIT OF ELECTRODE FEED RATE AT WHICH THE WIRE ELECTRODE MELTS BY OHMIC HEATING. SOURCE: REF 14

A change in electrode geometry and nature (cored) may result in a different constitutive equation (Ref 9, 15):

$$I = B' W^{0.35} V^{1.63} \qquad \textbf{(EQ 3)}$$

where B' is the proportionality constant. The total energy input, E, is:

$$E = B' \frac{L_g - 2w_g t_g}{[L + (g + 2t_g)][w_c t_c d_c]} \cdot \frac{V^4}{I^2} \qquad \textbf{(EQ 4)}$$

where w_g is width of the consumable plate guide; t_g is the thickness of the consumable plate guide; w_e is the width of the consumable electrode; and t_e is the thickness of the consumable electrode.

References cited in this section

9. S. LIU AND C.T. SU, GRAIN REFINEMENT IN ELECTROSLAG WELDMENTS BY METAL POWDER ADDITION, *WELD. J.*, VOL 68 (NO. 4), 1989, P 132S-144S
13. R.H. FROST, G.R. EDWARDS, AND M.D. RHEINLANDER, A CONSTITUTIVE EQUATION FOR THE CRITICAL ENERGY INPUT DURING ELECTROSLAG WELDING, *WELD. J.*, VOL 60 (NO. 1), 1981, P 12-62
14. S. LIU AND C.T. SU, PERFORMANCE EVALUATION OF A METAL POWDER CORED STRIP ELECTRODE IN HIGH SPEED ELECTROSLAG WELDING, *ADVANCES IN WELDING SCIENCE AND TECHNOLOGY*, ASM INTERNATIONAL, 1986, P 401-412
15. R.D. THOMAS, JR., CORROSION RESISTANT WELD OVERLAYS BY THE DUAL STRIP PROCESS, *BRIT. WELD. J.*, MAY 1966

S. Liu, Colorado School of Mines; S.D. Brandi, Escola de Politecnica da USP; R.D. Thomas, Jr., R.D. Thomas and Company

ESW Consumables

ESW Fluxes. Similar to the fluxes used in other welding processes, ESW fluxes are formulated to refine the weld metal, to coat the surface of the retaining shoes and the completed weld metal, and to protect the molten metal from oxidation. However, several physical and chemical properties distinguish ESW fluxes from the others used in arc welding. Electroslag welding fluxes are invariably fused, rather than agglomerated. Compared with the arc welding fluxes, fluxes for ESW are higher in resistivity, because the arc is extinguished soon after the process becomes stable. Sometimes, an agglomerated starting flux with high conductivity is used to initiate the process and form the weld pool. After that, a running flux of high resistivity is added to generate heat for melting the filler metal and to maintain steady welding operation. In fact, for high-current welding the use of starting flux is often omitted.

A typical running flux for low-carbon steels has the following composition (Ref 11):

CONSTITUENT	CONTENT, WT%
SIO_2	25
MNO	10
CAF_2	15
AL_2O_3	25
CAO	15
MGO	10

Electrical Resistivity. A flux of high resistance (or low conductivity) will draw less current, resulting in a colder weld pool and lower base metal penetration. It will also allow the wire to drive deeper into the pool. On the other hand, a flux of low resistance may draw excessive current, raising the temperature of the bath until the process stabilizes with a shorter electrode extension. However, if resistance is too low, then arcing may occur between the electrode and the slag bath surface, especially at higher voltages. This condition is aggravated in fluxes that show steeply increasing conductivity with rising temperature. In terms of process conditions, lower slag resistivity may result in operation at lower voltage.

Fluidity. In addition to its heat-generating ability, the molten slag must also have sufficient fluidity to cause rapid convection and good circulation, needed to distribute heat throughout the weld joint. Fluidity of a slag depends mainly on its chemical composition and operating temperature. The melting point of a flux must be below that of the base metal for weld pool refining, and its boiling temperature must be higher than the operating temperature to avoid loss by vaporization. Any preferential loss (of one or more ingredients) will alter the bath composition, which may greatly change the slag fluidity and electrical conductivity, resulting in improper shielding. If the composition of the fluxes is altered during operation, the change in energy imparted to the slag may cause an increase in temperature and in conductivity during welding of long seams, which may give rise to arcing on the top surface of the slag bath.

Low fluidity will tend to trap slag inclusions in the weld metal; excessive fluidity will cause leakage through the small space between the work and the retaining shoes. For joining thin plates, higher fluidity fluxes are desirable to obtain good circulation in the relatively small bath.

Metallurgical Compatibility. Finally, the slag should be metallurgically compatible with the alloy being welded. For steel welding, the fluxes are generally mixed oxides of silicon, manganese, titanium, calcium, magnesium, and aluminum (Ref 1). These oxide components play an important role in the shielding and refining of the weld pool. Calcium fluoride (CaF_2) is added to basic oxides or silicate systems to achieve the proper resistivity and fluidity. Increasing CaF_2 decreases viscosity, melting point, and resistivity. Additions of TiO_2 also decrease resistivity, while Al_2O_3 increases it. However, TiO_2 also increases slag viscosity (Ref 2, 3). Special applications, such as inclusion control or sulfur removal, may require the addition of rare-earth compounds (Ref 16).

Slag detachability after weld metal solidification is not a major problem in ESW. The addition of large quantities of TiO_2, however, will often result in difficult slag removal. Fluoride additions generally improve slag detachability.

ESW Electrodes. Various ESW techniques are available, depending on the type of electrodes and the feeding mechanism. The electrodes can be solid wires, tubular flux-cored wires, large-section solid electrodes, and large-section cored electrodes. The guides or nozzles can be consumable or nonconsumable. The conventional method uses nonconsumable guides (also known as snorkels), which are maintained approximately 50 to 75 mm (2.0 to 3.0 in.) above the molten flux. In this case, a mobile feeding head is used and is raised vertically to match the weld pool travel speed. If the electrode feeding mechanism is stationary, then the nozzle will be "consumed," becoming part of the weld metal when it is reached by the slag pool. Accordingly, the materials used in consumable guides generally match the chemical composition of the electrode or base metal. A consumable guide can either be a thin-wall tube or an assembly of plates or rods with conduits to feed the electrode wire. Fin-shape guide tubes are prepared by welding webs to circular-section guide tubes to obtain more uniform weld pool heating (Ref 1, 3, 6). Among the different types of electrodes, only the wire type and the large-section cored electrodes require the use of nozzles for delivering the electrode into the root gap. Bare guides sometimes need insulation along their lateral surfaces if they cannot be precisely aligned within the weld joint. One solution is to insert insulating plugs at critical locations in the assembly. Flux-coated consumable nozzles are available to minimize the problem of insulating the electrode assembly. Figure 11 shows several shapes of electrodes and guides used in ESW.

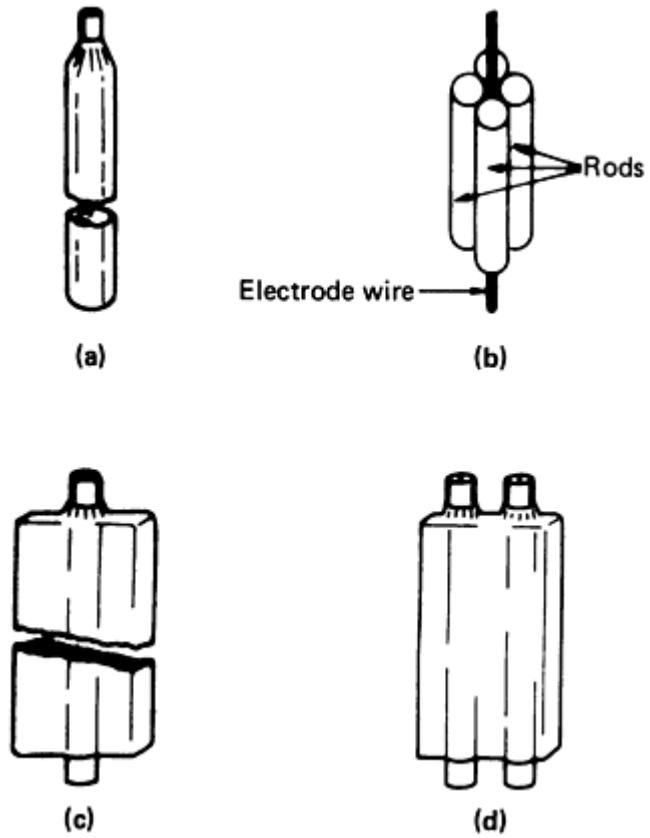

FIG. 11 SELECTED ELECTRODES AND GUIDES (NOZZLES) USED IN ELECTROSLAG WELDING. (A) SINGLE FLUX-COVERED TUBE. (B) CLUSTER OF RODS TAPED TOGETHER. (C) FLUX-COVERED WING NOZZLE. (D) FLUX-COVERED WING OR WEB NOZZLE WITH TWO TUBES

References cited in this section

1. ELECTROSLAG AND ELECTROGAS WELDING, *AWS WELDING HANDBOOK,* VOL 2 (NO. 7), AWS, 1978, P 226-260
2. H.C. CAMPBELL, ELECTROSLAG, ELECTROGAS, AND RELATED WELDING PROCESSES, *WRC*

BULL., VOL 154, 1970

3. B. PATON, *ELECTROSLAG WELDING*, AWS, 1962
6. "ELECTROSLAG ELECTROGAS TIPS & TECHNIQUES," BULLETIN OF ELECTROTHERM CORP., 1973
11. S. VENKATARAMAN, J.H. DEVLETIAN, W.E. WOOD, AND D.G. ATTERIDGE, GRAIN REFINEMENT DEPENDENCE ON SOLIDIFICATION AND SOLID STATE REACTIONS IN ELECTROSLAG WELDS, *GRAIN REFINEMENT IN CASTINGS AND WELDS*, AIME, 1982, P 275-288
16. A. MITCHELL AND G. BEYNON, ELECTROCHEMICAL REACTIONS IN THE ELECTROSLAG WELDING OF THICK WALLED STRUCTURES, *AVTOM. SVARKA*, VOL 6, 1965, P 32-37

Electroslag and Electrogas Welding*

S. Liu, Colorado School of Mines; S.D. Brandi, Escola de Politecnica da USP; R.D. Thomas, Jr., R.D. Thomas and Company

ESW Consumables

ESW Fluxes. Similar to the fluxes used in other welding processes, ESW fluxes are formulated to refine the weld metal, to coat the surface of the retaining shoes and the completed weld metal, and to protect the molten metal from oxidation. However, several physical and chemical properties distinguish ESW fluxes from the others used in arc welding. Electroslag welding fluxes are invariably fused, rather than agglomerated. Compared with the arc welding fluxes, fluxes for ESW are higher in resistivity, because the arc is extinguished soon after the process becomes stable. Sometimes, an agglomerated starting flux with high conductivity is used to initiate the process and form the weld pool. After that, a running flux of high resistivity is added to generate heat for melting the filler metal and to maintain steady welding operation. In fact, for high-current welding the use of starting flux is often omitted.

A typical running flux for low-carbon steels has the following composition (Ref 11):

CONSTITUENT	CONTENT, WT%
SIO_2	25
MNO	10
CAF_2	15
AL_2O_3	25
CAO	15
MGO	10

Electrical Resistivity. A flux of high resistance (or low conductivity) will draw less current, resulting in a colder weld pool and lower base metal penetration. It will also allow the wire to drive deeper into the pool. On the other hand, a flux of low resistance may draw excessive current, raising the temperature of the bath until the process stabilizes with a shorter electrode extension. However, if resistance is too low, then arcing may occur between the electrode and the slag bath surface, especially at higher voltages. This condition is aggravated in fluxes that show steeply increasing conductivity with rising temperature. In terms of process conditions, lower slag resistivity may result in operation at lower voltage.

Fluidity. In addition to its heat-generating ability, the molten slag must also have sufficient fluidity to cause rapid convection and good circulation, needed to distribute heat throughout the weld joint. Fluidity of a slag depends mainly on its chemical composition and operating temperature. The melting point of a flux must be below that of the base metal for weld pool refining, and its boiling temperature must be higher than the operating temperature to avoid loss by vaporization. Any preferential loss (of one or more ingredients) will alter the bath composition, which may greatly change the slag fluidity and electrical conductivity, resulting in improper shielding. If the composition of the fluxes is altered during operation, the change in energy imparted to the slag may cause an increase in temperature and in conductivity during welding of long seams, which may give rise to arcing on the top surface of the slag bath.

Low fluidity will tend to trap slag inclusions in the weld metal; excessive fluidity will cause leakage through the small space between the work and the retaining shoes. For joining thin plates, higher fluidity fluxes are desirable to obtain good circulation in the relatively small bath.

Metallurgical Compatibility. Finally, the slag should be metallurgically compatible with the alloy being welded. For steel welding, the fluxes are generally mixed oxides of silicon, manganese, titanium, calcium, magnesium, and aluminum (Ref 1). These oxide components play an important role in the shielding and refining of the weld pool. Calcium fluoride (CaF_2) is added to basic oxides or silicate systems to achieve the proper resistivity and fluidity. Increasing CaF_2 decreases viscosity, melting point, and resistivity. Additions of TiO_2 also decrease resistivity, while Al_2O_3 increases it. However, TiO_2 also increases slag viscosity (Ref 2, 3). Special applications, such as inclusion control or sulfur removal, may require the addition of rare-earth compounds (Ref 16).

Slag detachability after weld metal solidification is not a major problem in ESW. The addition of large quantities of TiO_2, however, will often result in difficult slag removal. Fluoride additions generally improve slag detachability.

ESW Electrodes. Various ESW techniques are available, depending on the type of electrodes and the feeding mechanism. The electrodes can be solid wires, tubular flux-cored wires, large-section solid electrodes, and large-section cored electrodes. The guides or nozzles can be consumable or nonconsumable. The conventional method uses nonconsumable guides (also known as snorkels), which are maintained approximately 50 to 75 mm (2.0 to 3.0 in.) above the molten flux. In this case, a mobile feeding head is used and is raised vertically to match the weld pool travel speed. If the electrode feeding mechanism is stationary, then the nozzle will be "consumed," becoming part of the weld metal when it is reached by the slag pool. Accordingly, the materials used in consumable guides generally match the chemical composition of the electrode or base metal. A consumable guide can either be a thin-wall tube or an assembly of plates or rods with conduits to feed the electrode wire. Fin-shape guide tubes are prepared by welding webs to circular-section guide tubes to obtain more uniform weld pool heating (Ref 1, 3, 6). Among the different types of electrodes, only the wire type and the large-section cored electrodes require the use of nozzles for delivering the electrode into the root gap. Bare guides sometimes need insulation along their lateral surfaces if they cannot be precisely aligned within the weld joint. One solution is to insert insulating plugs at critical locations in the assembly. Flux-coated consumable nozzles are available to minimize the problem of insulating the electrode assembly. Figure 11 shows several shapes of electrodes and guides used in ESW.

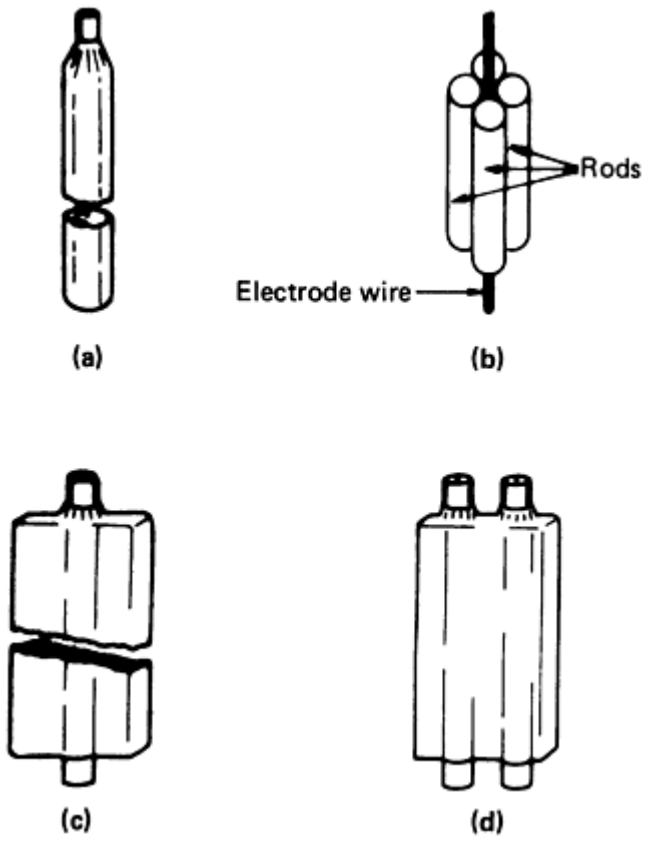

FIG. 11 SELECTED ELECTRODES AND GUIDES (NOZZLES) USED IN ELECTROSLAG WELDING. (A) SINGLE FLUX-COVERED TUBE. (B) CLUSTER OF RODS TAPED TOGETHER. (C) FLUX-COVERED WING NOZZLE. (D) FLUX-COVERED WING OR WEB NOZZLE WITH TWO TUBES

References cited in this section

1. ELECTROSLAG AND ELECTROGAS WELDING, *AWS WELDING HANDBOOK*, VOL 2 (NO. 7), AWS, 1978, P 226-260
2. H.C. CAMPBELL, ELECTROSLAG, ELECTROGAS, AND RELATED WELDING PROCESSES, *WRC BULL.*, VOL 154, 1970
3. B. PATON, *ELECTROSLAG WELDING*, AWS, 1962
6. "ELECTROSLAG ELECTROGAS TIPS & TECHNIQUES," BULLETIN OF ELECTROTHERM CORP., 1973
11. S. VENKATARAMAN, J.H. DEVLETIAN, W.E. WOOD, AND D.G. ATTERIDGE, GRAIN REFINEMENT DEPENDENCE ON SOLIDIFICATION AND SOLID STATE REACTIONS IN ELECTROSLAG WELDS, *GRAIN REFINEMENT IN CASTINGS AND WELDS*, AIME, 1982, P 275-288
16. A. MITCHELL AND G. BEYNON, ELECTROCHEMICAL REACTIONS IN THE ELECTROSLAG WELDING OF THICK WALLED STRUCTURES, *AVTOM. SVARKA*, VOL 6, 1965, P 32-37

Electroslag and Electrogas Welding*

S. Liu, Colorado School of Mines; S.D. Brandi, Escola de Politecnica da USP; R.D. Thomas, Jr., R.D. Thomas and Company

Metallurgical and Chemical Reactions

Fusion Zone Compositional Effects. In ESW of carbon and low-alloy steels, the major reactions involve manganese, silicon, carbon, and impurities such as oxygen, sulfur, and phosphorus. In the welding of high-alloy steels, reactions involving chromium, titanium, aluminum, and other elements are important. The extent and control of reactions are determined mainly by the concentrations of the elements in the liquid metal and by the concentrations of their oxides in the slag. The temperature in the reaction zone, the metal droplet-slag surface area, and the duration of contact between the molten metal and slag are other factors that affect the final weld metal composition. The concentration of elements in the metal and slag is determined by the electrode wire and flux compositions and by the renewal of the slag pool (that is, the frequency with which the make-up flux is added to the pool).

Thermochemistry. In the case of slags containing high MnO and SiO_2, the reactions between the metal and slag can be described:

$$[FE] + (MNO) \rightarrow [MN] + (FEO) \quad \textbf{(EQ 5)}$$

$$2[FE] + (SIO_2) \rightarrow [SI] + 2(FEO) \quad \textbf{(EQ 6)}$$

In Eq 5 and 6, [*M*] and (*N*O) represent the activities of the metal *M* in the weld pool and of the oxide of element *N* in the slag layer. However, for all practical purposes, concentrations of the metallic element and oxide can be used instead of their activities in thermodynamic calculations. When electrodes containing high silicon are used, the reduction of manganese oxide by silicon must also be taken into account:

$$[SI] + 2(MNO) \rightarrow 2[MN] + (SIO_2) \quad \textbf{(EQ 7)}$$

The lower the temperature, the more intense will be the reaction between manganese oxide and silicon. Changes in welding conditions, such as power input and temperature distribution, will have a definite effect on the recovery of alloying elements.

Like silicon, aluminum is often employed as a deoxidizer for steels and, to a lesser degree, as a microalloying element. The deoxidation reaction is:

$$2[AL] + 3(FEO) \rightarrow 3[FE] + (AL_2O_3) \qquad \textbf{(EQ 8)}$$

The reaction of aluminum with nitrogen is also important because it has a strong affinity for dissolved nitrogen in the weld pool and because aluminum nitride is responsible for the pinning of grain boundaries and grain growth control.

Titanium is widely used to alloy and modify steels. In welding, it is oxidized by the slag:

$$[TI] + 2(FEO) \rightarrow 2[FE] + (TIO_2) \qquad \textbf{(EQ 9)}$$

Similar to aluminum, titanium also reacts with carbon, nitrogen, and oxygen to form TiN, TiC, Ti(C,N), TiO, and TiO_2 particles that may remain trapped in the weld metal, moderating excessive grain growth.

The oxidation of carbon may take place as a result of carbon reacting with dissolved oxygen and metal oxides in the liquid metal:

$$[C] + [O] \rightarrow CO \qquad \textbf{(EQ 10)}$$

$$[C] + (MnO) \rightarrow CO + [Mn] \qquad \textbf{(EQ 11)}$$

$$2[C] + (SiO_2) \rightarrow 2CO + [Si] \qquad \textbf{(EQ 12)}$$

$$[C] + (FeO) \rightarrow CO + [Fe] \qquad \textbf{(EQ 13)}$$

Other minor constituents, such as vanadium and niobium, are oxidized by the slag at the expense of FeO to form a series of oxides, such as VO, V_2O_5, NbO, and Nb_2O_5.

When ESW is used to surface machine parts, metal-cored tubular wire electrodes are often used to provide high contents of alloy elements, such as chromium, molybdenum, vanadium, or titanium, in the deposited metal. When silicate fluxes are used, the oxidation of chromium takes place according to the following main reactions:

$$[Cr] + (MnO) = (CrO) + [Mn] \qquad \textbf{(EQ 14)}$$

$$[CR] + (FeO) \rightarrow (CrO) + [Fe] \qquad \textbf{(EQ 15)}$$

The welding consumables (fluxes and welding electrodes) and base metal are the major contributors of tramp elements, such as sulfur and phosphorus, to the weld pool. In addition, the temperature and welding conditions in ESW are not optimal for dephosphorization. As a result, increased migration of phosphorus from the slag to the weld pool occurs not only at the initiation of the weld but also at points where the electroslag process is resumed after an interruption. Sulfur in carbon steel welds is considerably more dangerous than phosphorus because it is the main cause of hot cracking. More recently, desulfurization slags with approximately 60 to 85 wt% CaF_2, and 15 to 40 wt% CaO have been adopted in ESW. Substantial desulfurization can also be achieved when carbon is added to a lime-fluorspar system.

There is also indication that in ESW the slag bath receives oxygen continuously from the surrounding atmosphere. With higher oxygen potential, the slag will also tend to oxidize the weld metal. Therefore, some modified electroslag processes include an inert gas cover on top of the slag layer to ensure a more deoxidized weld pool.

Electrochemistry. In addition to the thermochemistry of the process, electrochemistry plays an important role in ESW (Ref 17, 18). Because the anode and cathode reactions all occur in one pool, the weight of electrode melted is

approximately equal to the weight recovered in the weld pool. Current efficiency can then be expressed as a function of electrode melted and element concentration change. Anodic current efficiency data show that the bulk of the current at the anode is carried by the oxidation reactions of iron, chromium, manganese, and silicon (Ref 19), which also indicates that electrochemical reactions account for a large fraction of the charges transferred. The major charge-carrying reactions at the cathode are the reductions of iron, aluminum, chromium, manganese, and silicon cations from the flux. Furthermore, the current efficiencies for electrochemical reactions involving chromium, manganese, silicon, molybdenum, oxygen, and aluminum increase with increasing current density. The concentration changes are directly proportional to the welding current and to the current efficiency for the reactions, and they are inversely proportional to the electrode melt rate.

Weld Metal Inclusions. Due to the almost "equilibrium" operating conditions of ESW as compared with other arc welding processes, inclusion separation is expected to be more complete. The larger volume of molten metal, less turbulent weld pool, slower cooling, and slower solidification rate in ESW contribute to a cleaner weld metal with relatively few submicron-size inclusions.

Solidification Structure. The morphology of steel electroslag weld deposits was first characterized and summarized by Paton (Fig. 12). Yu, Ann, Devletian, and Wood (Ref 20) further characterized the solidification substructure of low-carbon structural steel electroslag weldments and related them to the weld pool form factor:

- *GROUP 1:* TRANSITION FROM CELLULAR TO COLUMNAR DENDRITES OCCURS AT A SHORT DISTANCE FROM THE FUSION LINE. WELDS FROM THIS GROUP SHOW SHALLOW MOLTEN METAL POOLS WITH HIGH FORM FACTOR.
- *GROUP 2:* CELLULAR TO COLUMNAR DENDRITE TRANSITION OCCURS FURTHER AWAY FROM THE FUSION LINE, WITH A FINE COLUMNAR GRAIN ZONE AT THE CENTER OF THE WELD.
- *GROUP 3:* CHARACTERIZED BY A SHALLOW ANGLE OF INCLINATION (APPROXIMATELY 10°) BETWEEN THE COLUMNAR GRAINS AND THE FUSION LINE. THE TRANSITION FROM DENDRITIC TO COLUMNAR DENDRITES OCCURS CLOSE TO THE CENTER LINE OF THE WELD. THE GRAINS MEET AT THE CENTER AT AN OBTUSE ANGLE.
- *GROUP 4:* DENDRITIC TO COLUMNAR DENDRITE TRANSITION OCCURS CLOSE TO THE CENTER LINE, WITH EQUIAXED GRAINS AT THE CENTER OF THE WELD.

The deep pools and low form factor generally found in group 3 and group 4 welds are also responsible for the high sensitivity to centerline cracking and radial hot cracking of these welds.

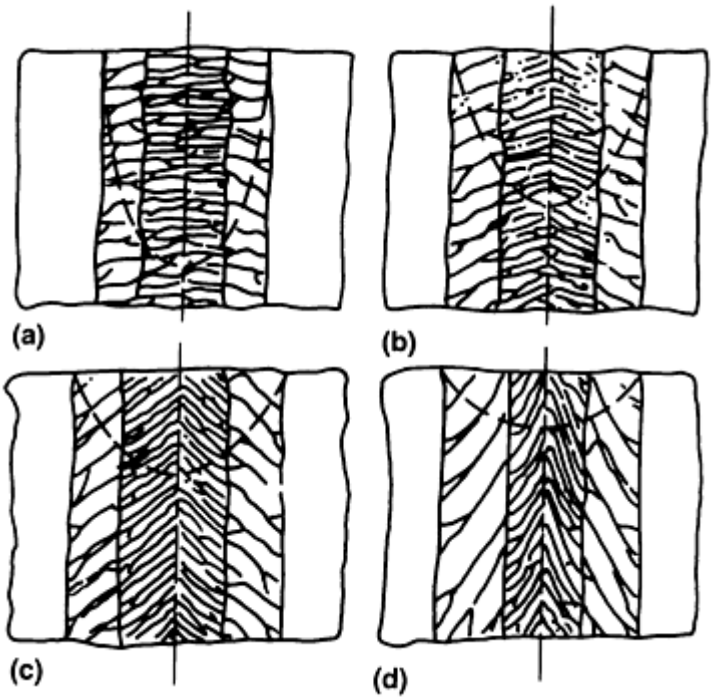

FIG. 12 ELECTROSLAG WELD METAL SOLIDIFICATION STRUCTURE ACCORDING TO THE VARIATION OF THE ORIENTATION AND THE THICKNESS OF THE COLUMNAR GRAINS ZONE. (A) GROUP 1. (B) GROUP 2. (C) GROUP 3. (D) GROUP 4. SEE TEXT FOR DETAILS. SOURCE: REF 3

Solid-State Transformations. The cooling rate of an electroslag weld metal is so much slower than those of other welding processes that reasonably coarse microstructures are found. During the austenite-to-ferrite transformation, primary ferrite and grain boundary ferrite are the principal constituents, along with carbides, mostly in the form of pearlite. In low-alloy steels, acicular ferrite, martensite, bainite, and retained austenite can be found only in those welds that have considerable amounts of alloying ingredients.

References cited in this section

3. B. PATON, *ELECTROSLAG WELDING*, AWS, 1962
17. A. MITCHELL AND G. BEYNON, ELECTROCHEMICAL REACTIONS IN THE ELECTROSLAG PROCESS, CH. 2, *BUR. MINES BULL.*, 1976, P 669
18. M.E. PEOVER, ELECTROSLAG REMELTING, A REVIEW OF ELECTRICAL AND ELECTROCHEMICAL ASPECTS, *J. INST. MET.*, VOL 100, 1972, P 97
19. R.H. FROST, D.L. OLSON, AND G.R. EDWARDS, "THE INFLUENCE OF ELECTROCHEMICAL REACTIONS ON THE CHEMISTRY OF THE ELECTROSLAG WELDING PROCESS, *MODELING OF CASTING AND WELDING PROCESSES II*, AIME, 1983, P 279-294
20. D. YU, H. ANN, J.H. DEVLETIAN, AND W.E. WOOD, SOLIDIFICATION STUDY OF NARROW-GAP ELECTROSLAG WELDING, *WELDING RESEARCH: THE STATE OF THE ART*, E. NIPPES AND D. BALL, ED., ASM, 1985, P 21-32

Electroslag Process Development

High-Productivity Electroslag Processes. Responding to the technological challenge of the need for a large volume of deposited metal and low heat input, many high-speed ESW techniques have been developed (Ref 9, 10, 11, 12, 15, 21, 23, 24, 25, 26). There have been essentially two approaches:

- NARROWING THE GAP TO DECREASE THE VOLUME OF METAL DEPOSIT (THEREBY SHORTENING THE TIME NEEDED TO FORM THE WELD JOINT)
- INCREASING THE WELDING SPEED

With either approach, the productivity is increased and the heat can be distributed throughout a longer section of the weld.

With respect to the narrow-gap approach, the extent of gap cross-sectional area reductions is limited by the stability of the process and the size of the electrode and guide tube. Too narrow a gap may cause arcing between the electrode and the base metal. Solid flux blocks may be inserted at regular intervals to avoid arcing between a solid strip electrode in a thin-channel consumable guide and the base metal. Gaps as small as 12 mm ($\frac{1}{2}$ in.) have been reported (Ref 22). Narrow-gap welding, however, can result in higher base metal dilution.

The use of powdered filler metal has been reported to increase the deposition rate in ESW (to over 24 kg/h, or 53 lb/h) with reduction in the specific heat input and to refine the weld metal and HAZ microstructure. The supply of metal powder (ferrous, mainly) to the weld metal can be obtained by a flow of argon gas (Fig. 13). Welding speed as high as 230 mm (9 in.) per minute has been reported. Notch impact testing results measured with samples taken 1 to 2 mm (0.04 to 0.08 in.) from the fusion line showed good Charpy impact toughness.

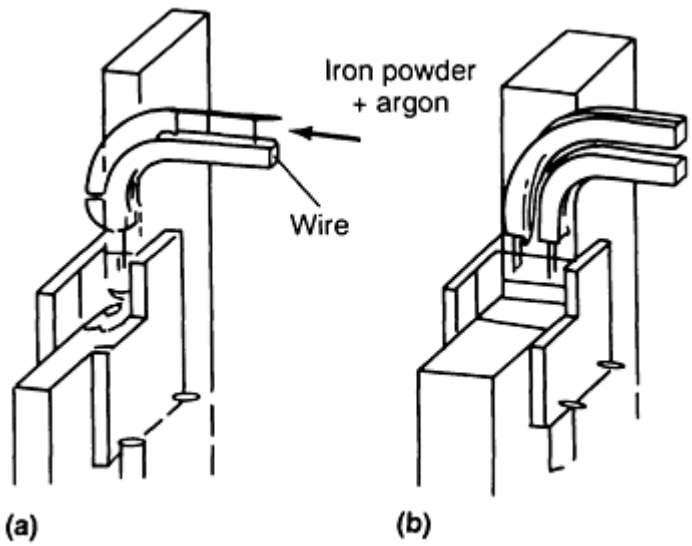

FIG. 13 EQUIPMENT SETUP FOR SQUARE-GROOVED HIGH-SPEED WELDING WITH METAL POWDER ADDITION. (A) PLATE THICKNESS OF 10 TO 40 MM ($\frac{3}{8}$ TO 1 $\frac{9}{16}$ IN.). (B) PLATE THICKNESS OF 40 TO 100 MM (1 $\frac{9}{16}$ TO 4 IN.). SOURCE: REF 25

Metal powder cored strip electrode for consumable guide ESW has also been used (Ref 9, 17). The average weld deposition rate is approximately two to three times higher than the solid wire process, over 38 kg/h (85 lb/h). The specific

heat input of these welds was lower, at 0.8 kJ/mm^2 (520 kJ/in.^{2}). Rather than add metal powder to increase the deposition rate and absorb the excess thermal energy in the molten metal bath, a separate filler wire can be used (Ref 27). This is shown in Fig. 14. This setup resembles the feeding of a cold wire into plasma arc welding or gas-tungsten arc welding processes. Not only is the productivity of the process increased, but the HAZ width is also reduced.

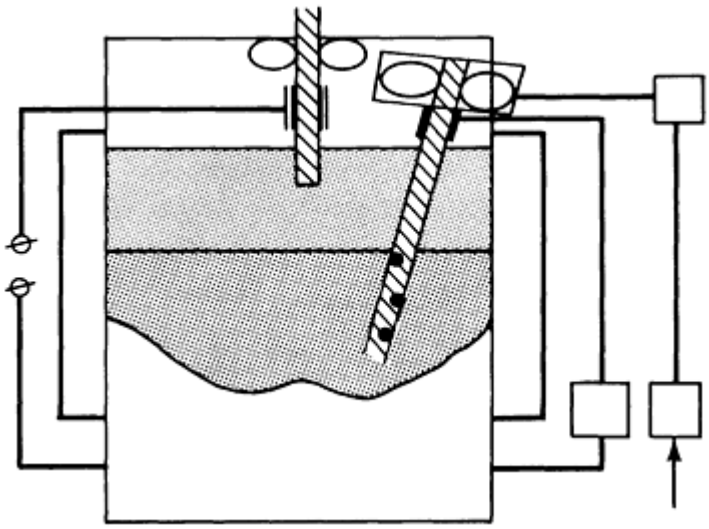

FIG. 14 SCHEMATIC OF ELECTROSLAG WELDING PROCESS USING SEPARATE FILLER WIRE TO INCREASE DEPOSITION RATE AND ABSORB EXCESS THERMAL ENERGY IN MOLTEN METAL BATH. SOURCE: REF 28

Electroslag Surfacing. Surfacing by means of weld overlays has a long history. Electroslag surfacing can be done in either the vertical or flat position. Where the area to be surfaced is small relative to the base metal, vertical electroslag surfacing is usually used. Adapting the vertical orientation of ESW to produce composite metallic structures involves replacing one of the parent metal plates with a water-cooled mold. An interesting application is tool steel ingots that are given a soft steel electroslag welded deposit on each end to facilitate the rolling operation.

For large areas, such as plates for tube sheets or cylindrical pressure vessels, electroslag surfacing is conducted in the flat position. Excellent process stability is one of the characteristics of the process. Even with electrodes as wide as 150 mm (6 in.), the quality of the surface weld is still comparable to that of welds produced by other processes. To minimize the undercutting problem and improve bead smoothness, Kawasaki Steel (Ref 6) developed the Maglay process, which utilizes an external magnetic field to control the flow of molten slag and metal. Dilution can also be controlled, to less than 10%. Forsberg (Ref 28) reports the development of a similar process, which uses strips of 60 to 90 mm (2.4 to 3.5 in.) width and emphasizes the higher deposition rate and lower dilution ratio.

References cited in this section

6. "ELECTROSLAG ELECTROGAS TIPS & TECHNIQUES," BULLETIN OF ELECTROTHERM CORP., 1973
9. S. LIU AND C.T. SU, GRAIN REFINEMENT IN ELECTROSLAG WELDMENTS BY METAL POWDER ADDITION, *WELD. J.*, VOL 68 (NO. 4), 1989, P 132S-144S
10. C.T. SU, "HIGH SPEED ELECTROSLAG WELDING," M.S. THESIS, PENNSYLVANIA STATE UNIV., 1987
11. S. VENKATARAMAN, J.H. DEVLETIAN, W.E. WOOD, AND D.G. ATTERIDGE, GRAIN REFINEMENT DEPENDENCE ON SOLIDIFICATION AND SOLID STATE REACTIONS IN ELECTROSLAG WELDS, *GRAIN REFINEMENT IN CASTINGS AND WELDS*, AIME, 1982, P 275-288
12. D.G. ATTERIDGE, S. VENKATARAMAN, AND W.E. WOOD, "IMPROVING THE RELIABILITY AND INTEGRITY OF CONSUMABLE GUIDE ELECTROSLAG WELDMENTS IN BRIDGE

STRUCTURES," RESEARCH REPORT, OREGON GRADUATE CENTER, 1982

15. R.D. THOMAS, JR., CORROSION RESISTANT WELD OVERLAYS BY THE DUAL STRIP PROCESS, *BRIT. WELD. J.*, MAY 1966

17. A. MITCHELL AND G. BEYNON, ELECTROCHEMICAL REACTIONS IN THE ELECTROSLAG PROCESS, CH. 2, *BUR. MINES BULL.*, 1976, P 669

21. V.I. AVRAMENKO, B.F. LEBEDEV, AND V.I. BOZHKO, SOME WAYS OF INCREASING THE PRODUCTIVITY OF ELECTROSLAG WELDING, *SVAR. PROIZVOD.*, VOL 10, 1973, P 16

22. K. WATANABE, I. SEJIMA, S. KOKURA, G. TAKI, AND H. MIYAKE, PROBLEMS AND IMPROVEMENT OF LARGE HEAT INPUT ELECTROSLAG WELDING, *J. JPN. WELD. SOC.*, 1975, P 519

23. S.A. SMIRNOV AND L.A. EFIMENKO, SPECIAL STRUCTURAL FEATURES AND MECHANICAL PROPERTIES OF ELECTROSLAG WELDED JOINTS MADE USING POWDERED FILLER METAL, *SVT. SVARKA*, VOL 9, 1973, P 46

24. F. EICHHORN AND J. REMMEL, SITUATION OF RESEARCH IN ELECTROSLAG WELDING--A TENDENCY OF FURTHER DEVELOPMENT, *IND. WELD. J.*, VOL 4, 1983, P 37

25. F. EICHHORN, J. REMMEL, AND B. WUBBELS, HIGH SPEED ELECTROSLAG WELDING, *WELD. J.*, VOL 62 (NO. 1), 1984, P 37

26. F. EICHHORN AND J. REMMEL, EFFICIENT FILLET WELDING IN THE VERTICAL WELDING POSITION WITH ELECTROGAS AND ELECTROSLAG WELDING METHODS, DOC. XII-908-85, IIW, 1985

27. B.F. YAKUSHIN *ET AL.*, IMPROVING THE CAPACITY OF ELECTROSLAG WELDED JOINTS FOR RESISTING HOT CRACKING, *WELD. RES. ABROAD*, JUNE/JULY 1984 (TRANSLATION FROM RUSSIAN BY AUTOMATIC WELDING, OCT 1982)

28. S. FORSBERG, RESISTANCE ELECTROSLAG (RES) SURFACING, *WELD. J.*, VOL 63 (NO. 8), 1985, P 41-48

Electroslag and Electrogas Welding*

S. Liu, Colorado School of Mines; S.D. Brandi, Escola de Politecnica da USP; R.D. Thomas, Jr., R.D. Thomas and Company

Electrogas Welding

Electrogas welding (EGW) can be classified as a gas-metal arc welding process. It was introduced in the early 1960s to perform single-pass welding of relatively thin plates in the vertical position. As shown in Fig. 15, the process is very similar to ESW, with the exception of the presence of an arc and the weld pool shielding mechanism (Ref 6). In most cases, shielding gas is used together with a bare or flux-cored wire to provide a shielding gas on top of the molten pool of slag and weld metal. Self-shielded flux-cored wires are often used without a separate gas shield. The production rate can be as high as 34 kg/h (75 lb/h), depending on the joint configuration and plate size. Special flux-cored wires that contain fewer slagging ingredients must be formulated for EGW, because slag buildup on the molten weld metal surface can affect arc stability and cause slag entrapment. The thicker the plate being welded, the less flux needed. When bare wire is used, small amounts of granular flux are usually added at the start. The slag needed for protection is produced from the deoxidizers in the electrode wire. For steel welding, the most common shielding gas is carbon dioxide. Additions of argon (75 to 80 vol%) to carbon dioxide seem to improve the arc stability and weld metal properties. Flow rates are usually of the order of 14 to 19 L/min (30 to 40 ft^3/h).

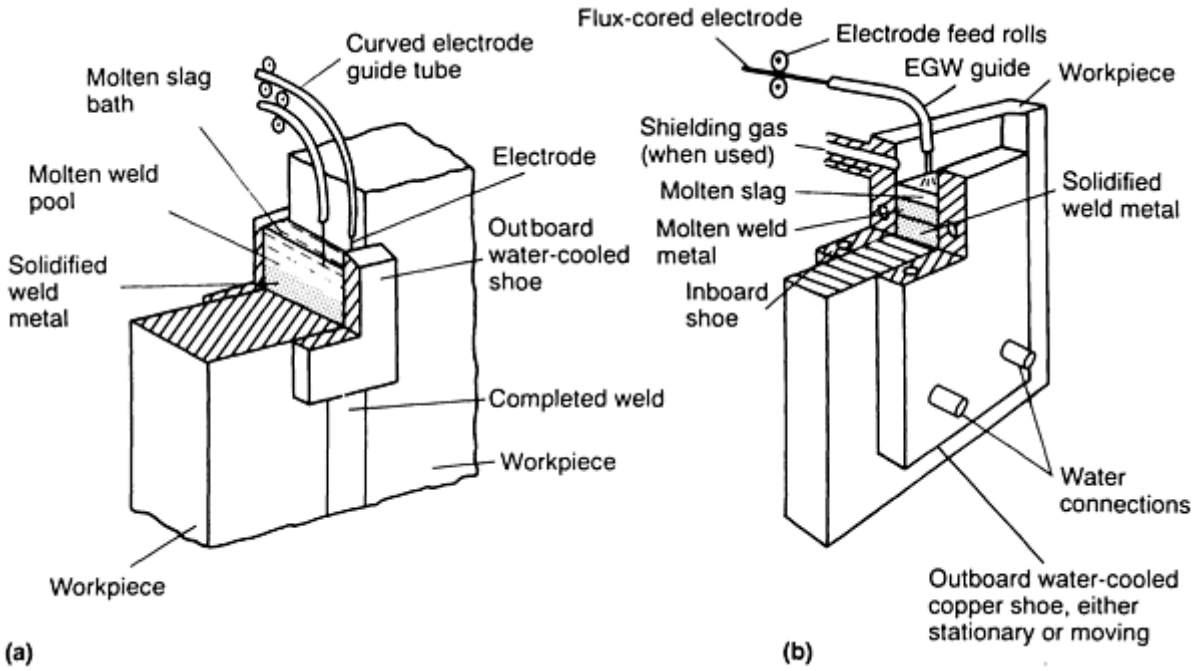

FIG. 15 SCHEMATICS COMPARING PRIMARY COMPONENTS OF TWO VERTICAL WELDING PROCESSES IN WHICH MOLTEN WELD POOLS ARE CONFINED BY COOLING SHOES. (A) ELECTROSLAG WELDING. (B) ELECTROGAS WELDING

Heavy aluminum weldments are produced by EGW using argon-helium gas shielding with flow rates of 28 to 38 L/min (60 to 80 ft^3/h).

In addition to its higher deposition rate, EGW presents the advantages of lower heat input, more refined microstructure, and improved HAZ properties. Consequently, postweld heat treatment is not mandatory in many EGW applications. The process also offers easy restarting if the weld is interrupted (complicated in ESW). However, as the thickness of a plate increases, the shielding gas often fails to cover the entire joint area, leading to unacceptable porosity. Thick plates favor the choice of ESW because electroslag welds exhibit fewer inclusions and defects.

Multipass ESW and EGW. The metallurgical problems encountered in single-pass electroslag and electrogas processes can be largely overcome by multipass welding. An example is a thick steel square-butt electroslag weld joint with a fixed copper chill bar or water-cooled copper tube inserted at midwall, and a weld being produced with a moving shoe on one side. The copper chill is then removed, and the opposite side is welded. In practice, however, several problems may appear. One is related to the removal of the copper chill, gripped by the shrinkage that occurs during the first weld pass. Another is the problem of ensuring penetration by the second pass into the first pass. Unless the plate edges are machined and carefully fitted up, slag leakage may also occur.

Reference 29 reports the use of a copper chill bar that penetrated to the root of one side of a double V-joint preparation while EGW proceeded from the opposite side. An alternative method is to manually deposit the root pass, to avoid the problem of close fit-up tolerances needed for complete penetration. Where welding can only be approached from one side, conventional backing bars are used, and the copper shoe protrudes into the joint to mold the initial pass, followed by the surface pass deposited in the conventional manner. This technique is satisfactory for EGW, but slag retention in the cavity formed by the protruding shoe and the base plates is a challenge in the electroslag process.

The consumable nozzle electroslag process can be used to make a multipass electroslag weld with a pass from each side. A tightly fitted spacer bar is placed at midwall. The electroslag weld pass from the first side partially penetrates the spacer bar, and the second pass from the opposite side consumes the remaining spacer and penetrates the first pass.

These process modifications do not solve the problem of the wide HAZ on the surface of the plates being welded, because toughness and fatigue properties at or near the outer surface of a weld are essential for the integrity and performance of the structure.

References cited in this section

6. "ELECTROSLAG ELECTROGAS TIPS & TECHNIQUES," BULLETIN OF ELECTROTHERM CORP., 1973

29. P.C. ARNOLD AND D.C. BERTOSSA, MULTIPLE PASS AUTOMATIC VERTICAL WELDING, *WELD. J.*, VOL 45 (NO. 8), 1966, P 651-660

Electroslag and Electrogas Welding*

S. Liu, Colorado School of Mines; S.D. Brandi, Escola de Politecnica da USP; R.D. Thomas, Jr., R.D. Thomas and Company

Electroslag and Electrogas Process Applications

Carbon and Low-Alloy Steels. The joining of heavy-section steels is the most common application of both ESW and EGW. As previously stated, ESW is commonly done on plates of thickness 50 mm (2 in.) and greater. In fact, economy is greatly increased if the section thickness is greater than 100 mm (4 in.). The range of application of EGW is between 9.5 mm ($\frac{3}{8}$ in.) and 75 mm (3 in.). When compared with arc welding processes, minimum distortion, vertical position, and minimum joint penetration are the major advantages. Typical applications include fabrication of pressure vessels, nuclear components, power generation equipment, rolling mills, heavy presses, bridges, ships, and oil drilling rigs (Ref 30). Other structural applications reported are blast furnace shells (carbon steel) and a wind tunnel structure (HY-100 steel) (Ref 31, 32).

Structural Steels. A considerable number of highway bridges were fabricated using ESW prior to its ban in bridge construction. Some failures have been attributed to defects such as hydrogen cracking, lack of fusion, low HAZ fatigue properties, and so on. However, properly made welds were found to meet the radiographic standards required for impact and fatigue loading of structural members (Ref 33). In the case of low-alloy steels for structural applications, austenitizing postweld heat treatments have been considered necessary for electroslag welds. However, when proper attention is given to consumable (flux and electrode) selection, a stress-relieving heat treatment is generally sufficient to obtain good impact properties (Ref 34).

Shipbuilding. Electroslag and electrogas welding can be used for the welding of components and for on-ship welding. One application is the propeller shaft bracket assembly for natural gas and oil tankers. Stem frame parts, heavy rudderstock plates, longitudinal and vertical hull stiffeners, and shaft struts are often electroslag welded (Ref 35).

Pressure Vessels. Thick-wall pressure vessels used in the chemical, power generating, petroleum, and marine industries are manufactured using ESW. Plates are rolled to form the shell of the pressure vessel, and the longitudinal seam created is then welded. Lifting lugs on the vessels, nozzles, and branch pipes are also electroslag welded to thick-walled vessels. Due to the high heat input, the welding practice must be critically controlled. Where code requirements are specified, a normalizing heat treatment is also performed.

Penetrating members, such as nozzles and pipe fittings, are often costly to weld into thick-wall pressure vessels by conventional processes. A unique method employing both welding and casting techniques has been proposed by Norcross (Ref 36). A cylindrical water-cooled mold is tightly affixed to the outside surface of the vessel, and weld metal is cast in place. The hole of the nozzle is then machined to provide an opening into the vessel, at the end of which pipes or other attachments can be easily welded (Fig. 16). Even large-diameter penetrating members can be made by this method, by casting hollow cylinders after first tapering the vessel wall to allow the starting zone of the electroslag weld to be machined away (Ref 38, 39).

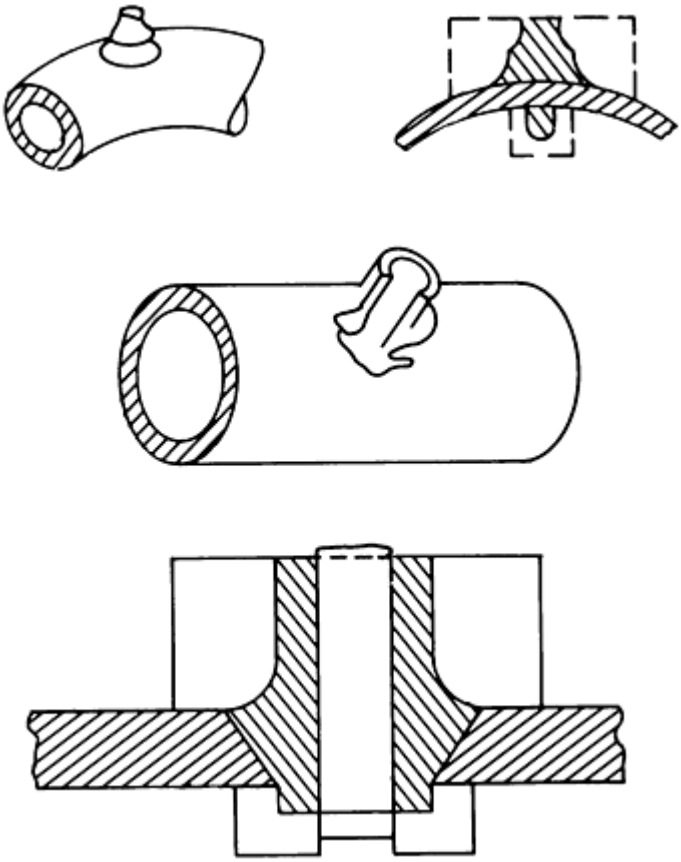

FIG. 16 APPLICATION OF ELECTROSLAG WELDING TO INCORPORATE PENETRATING MEMBERS SUCH AS NOZZLES ONTO THICK-WALL PRESSURE VESSELS. SOURCE: REF 39

Heavy Machinery. Large presses and machine tools are often manufactured from plates that are larger than the mills can produce, so ESW is used to join large plates together. Motor frames, press frames, gear blanks, turbine rings, crane rails, and crusher bodies are some of the common applications. In the transmission pipeline industries, ball valves and stop-gate valves are often electroslag welded.

Dissimilar Metal Joining. Electroslag remelting has been used to develop transition pieces for heavy-wall steam piping where low-alloy chromium-molybdenum steel pipe is to be joined to austenitic stainless steel pipe. Two round ingots, one of the ferritic alloy and one of the austenitic stainless steel, are welded together to form the electrode for electroslag remelting. As the electrode is melted in the molten slag bath, the composition gradually changes from one to the other, depositing a graded alloy billet which is later pierced and formed into a transition piece (Ref 37, 39, 40).

Joining and Repairing of Castings. Electroslag welding is also used to weld cast components. Instead of producing a large casting, many small castings of lower cost and simpler fabrication are produced and welded together. One such application is described by Brosholen, Skaug, and Vesser (Ref 41) to construct a cast steel propeller shaft bracket. Cast iron has been electroslag welded using a cored wire containing either white or gray cast iron powders and a graphite nozzle (Ref 42). Defective thick sections of cast steels can be repaired by ESW, by drilling a series of connecting holes into the defect zone. A close-fitting water-cooled copper mold is inserted in one of the drilled holes while welding proceeds in the adjacent hole. On completion of that weld, the mold is moved to the next hole before the molten slag has cooled, which allows ESW to start in the vacated hole (Ref 43, 44).

Tool and Die Surfacing and Welding. The slow thermal cycles involved in ESW are favorable for depositing hardenable alloys. For large forging hammers and forming dies, hard wear-resisting alloys can be spilled to the surface of a carbon steel backing using multiple electrodes and current pulsing techniques (Ref 45, 46, 47).

Stainless Steel and Nickel-Base Alloys. Two halves of large 38 tonne (42 ton) cast stainless steel pumps for nuclear electric power facilities have been successfully joined by circumferential welding of their equatorial surfaces and have

been qualified to rigid nuclear code requirements. As-welded electroslag welds in austenitic stainless steels were found to be insensitive to knife-line attack after sensitization for 1 to 5000 h at temperatures ranging from 450 to 750 °C (842 to 1382 °F) in tests (Ref 48). It has also been demonstrated that ESW is suitable for welding 25 mm (1 in.) thick alloy 600 plates and 25 mm (1 in.) and 114 mm ($4\frac{1}{2}$ in.) thick plates of alloy 800. Matching filler metals and Inconel filler-metal 82 produced sound welds with excellent elevated-temperature strength and stress-rupture results. Because stainless steels and nickel-base alloys do not undergo allotropic transformations, electroslag welds do not require a high-temperature postweld heat treatment.

Aluminum. Both ESW and EGW have been used to join thick sections of aluminum. One such application is to join 240 mm (9.5 in.) thick electrical conductors (busbars). Instead of the typical copper shoes, graphite shoes are used to obtain satisfactory weld surfaces and edge penetration (Ref 49). Gagan *et al.* (Ref 50) reported erratic penetration encountered in ESW of thick-section aluminum due to the magnetic fields generated by the welding process, which required special shielding screens around the weld zone. The high conductivity of aluminum and the prompt formation of a refractive oxide are also of concern. High-fluoride-content fluxes and an inert gas shield in EGW typically produce good results in welding thick-section aluminum. For ESW of aluminum containing 4.5 wt% Mg, the following flux has been suggested (Ref 51):

CONSTITUENT	CONTENT, WT%
MGF_2	1-30
$MGCL_2$	5-60
LIF	5-60
KCL	5-6

As welding progresses, additions are made to the flux containing 30 wt% each of KCl, LiF, and $MgCl_2$, and 10 wt% MgF_2. This flux is reported to work well for ESW of aluminum with copper shoes (Ref 51).

Titanium. The reactivity of titanium requires that residual elements such as hydrogen, oxygen, and nitrogen be minimized in ESW. A slag bath high in halides and containing virtually no oxides, and an inert gas (argon) shield over the bath, are required. Plate electrodes seem to produce better results (Ref 3, 52). Commonly, fluxes are halide compounds based on CaF_2 with ram-earth additions to produce welds low in oxygen, nitrogen, and hydrogen. Devletian (Ref 53) reported that because the high resistivity of titanium promotes rapid ohmic heating of the titanium consumables, stable welding operation generally requires large-diameter electrodes for nonconsumable guide welding, and nozzles or guide plates for consumable guide welding.

References cited in this section

3. B. PATON, *ELECTROSLAG WELDING,* AWS, 1962
30. D.J. ELLIS AND A.F. GIFFORD, APPLICATION OF ELECTRO-SLAG AND CONSUMABLE GUIDE WELDING--PARTS 1-6, *MET. FABR.*, APRIL-NOV 1973
31. H. PASS, THE ELECTRO-SLAG WELDING OF A BLAST FURNACE HEARTH JACKET, *WELD. MET. FABR.*, JAN/FEB 1976
32. ELECTROSLAG WELDING HELPS TO RESTORE WIND TUNNEL, *MET. PROGR.*, MARCH 1976
33. J.S. NOEL AND A.A. TOPRAC, STATIC, FATIGUE, AND IMPACT STRENGTH OF ELECTROSLAG WELDMENTS, RESEARCH REPORT 157-1F, RESEARCH PROJECT 3-5-71-157, CENTER FOR HIGHWAY RESEARCH, UNIV. OF TEXAS, 1971
34. A.M. MAKARA *ET AL.*, ELECTROSLAG WELDING OF STRUCTURAL STEELS WITHOUT NORMALIZING, *AVTOM. SVARKA*, VOL 7, 1974, P 511-514
35. B. HOWSER, APPLICATION AND TRENDS IN ELECTROSLAG WELDING IN THE UNITED STATES, *ELECTROSLAG WELDING FOR MARINE APPLICATIONS*, U.S. NAVAL ACADEMY,

MARCH 1985, P 4-1

36. J.E. NORCROSS, ELECTROSLAG DEVELOPMENTS, *FWP J.*, VOL 18 (NO. 2), 1978, P 41-58
37. D. YAPP AND A.P. BENNETT, DEVELOPMENT OF ELECTROSLAG-MELTED GRADED TRANSITION JOINTS, *WELDING RESEARCH RELATED TO POWER PLANT*, PAPER 34, CENTRAL ELECTRICITY GENERATING BOARD, SOUTHAMPTON, ENGLAND, SEPT 1972, P 464-481
38. J.E. NORCROSS, ELECTROSLAG BOSS AND PROCESS, U.S. PATENT 4,130,931, DEC 1978
39. ELECTROSLAG CASTING AND WELDING, BRITISH PATENT 1,390,674, APRIL 1975
40. A.P. BENNETT, AN ELECTRICAL ANALOGUE OF AN ELECTROSLAG REMELTING OPERATION USED AS A GUIDE TO IMPROVED CONTROL OF THE PROCESS, *MET. MATER.*, APRIL 1972, P 146-149
41. A. BROSHOLEN, E. SKAUD, AND J.J. VESSER, ELECTROSLAG WELDING OF LARGE CASTINGS FOR SHIP CONSTRUCTION, *WELD. J.*, VOL 56 (NO. 8), 1977, P 26-30
42. Y. ISHII, ELECTROSLAG WELDING OF CAST IRON, *TRANS. JAP. WELD. SOC.*, NO. 2, SEPT 1970, P 241-252
43. V.F. YAKOVLEV, P.I. KOVALKIN, N.I. EVDOKIMOV, M.G. KOZULIN, AND I.I. SUSHCHUCK-SLYUSARENKO, ELECTROSLAG WELDING OF STEEL CASTING DEFECTS, *AVTOM. SVARKA*, VOL 2, 1970, P 72
44. V.G. SVYNYUK, ELECTROSLAG WELDING FOR RECTIFYING DEFECTS IN CAST CENTRIFUGAL PUMP WHEELS, *AUTOM. WELD.*, VOL 28 (NO. 7), 1975, P 57-58
45. V.T. ARSENKIN, V.G. RADCHENKO, AND D.M. LIKHOHSHERSTOV, THE ELECTROSLAG DEPOSITION OF DIE STEEL ON CARBON STEEL, *AVTOM. SVARKA*, VOL 3, 1976, P 46-49
46. M.P. IVANAN, *ET AL.*, ELECTROSLAG HARDFACING OF BEATERS OF HAMMER CRUSHERS, *SVAR. PROIZVOD.*, VOL 7, 1974, P 48
47. Y.I. GORBACHEV, E.A. KOVALEVSKII, AND A.V. MATELEV, ELECTROSLAG WELDING OF DIE STEEL, *SVAR. PROIZVOD.*, VOL 11, 1984, P 12-13
48. N. LEHKA, PROBLEMS ASSOCIATED WITH THE CORROSION OF THE PROPERTIES OF ELECTROSLAG WELDED JOINTS IN AUSTENITIC STEELS OF INCREASED STRENGTH, *ZVRACSKE SPRAVY/WELDING NEWS*, VOL 26 (NO. 3), 1976, P 61-68
49. P.M. BARTLE, DEVELOPMENT OF AN ELECTROGAS TECHNIQUE FOR WELDING THICK ALUMINUM, *WELD. INST. RES. BULL.*, VOL 12 (NO. 3), 1971, P 67-71
50. Y.G. GAGEN, *ET AL.*, ELECTROSLAG WELDING OF ALUMINUM BUS-BARS LOCATED IN THE ZONE OF A STRONG MAGNETIC FIELD, *SVAR. PROIZVOD.*, VOL 12, 1972, P 19-21
51. ELECTROSLAG OR SUBMERGED ARC WELDING OF ALUMINIUM OR ITS ALLOYS OR ELECTROSLAG REMELTING ALUMINUM, BRITISH PATENT 1,544,248, APRIL 1979
52. V.Y. MALIN, ELECTROSLAG WELDING OF TITANIUM AND ITS ALLOYS, *WELD. J.*, VOL 64, FEB 1985, P 42-49
53. J.H. DEVLETIAN, ELECTROSLAG WELDING OF NON-FERROUS METALS--A REVIEW, *ELECTROSLAG WELDING FOR MARINE APPLICATIONS*, U.S. NAVAL ACADEMY, 1985, P 3-1 TO 3-32

Electroslag and Electrogas Welding*

S. Liu, Colorado School of Mines; S.D. Brandi, Escola de Politecnica da USP; R.D. Thomas, Jr., R.D. Thomas and Company

---

Problems and Quality Control

Fusion Zone. As discussed earlier in the section "Solidification Structure" of this article, both cellular and columnar dendrites are observed in the solidification structure of an electroslag weldment. Particularly in the cases of welds with low form factor, in which the transition from cellular to columnar dendrites occurs close to the centerline of the weld and

the grains meet at an obtuse angle, centerline cracking and radial hot cracking are more frequently observed. These defects can be attributed to the combined effects of temperature gradient, solidification rate, degree of restraint in fit-up of the weld, high welding speed, and low form factor. In general, a long, straight-sided columnar grain structure (the result of high welding speed) tends to be weaker under load than the more equiaxed and finer grain structure of a slow-speed weld. At the same time, the cellular structure may be coarser and higher in segregation for the case of low welding speed. Figure 17 shows a proposed mechanism of solidification cracking.

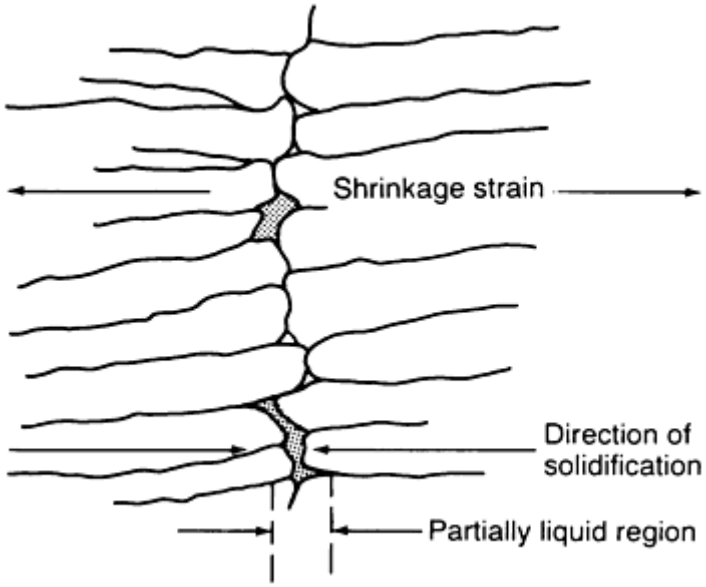

FIG. 17 SCHEMATIC INDICATING PROJECTED MECHANISM OF SOLIDIFICATION CRACKING IN AN ELECTROSLAG WELDMENT. SOURCE: REF 54, 55

Partially Melted Zone. Liquation cracking is associated with the melting of heavily segregated grain boundaries near the fusion line region. Carbon and manganese are the most common alloying elements involved in the formation of compounds such as (Mn,Fe)S that lower the melting temperature of the grain boundaries. Phosphorus, nitrogen, and boron are some of the other embrittling agents found in ferrous alloys. During cooling, residual stresses may build up and rupture these weakened boundaries. Under the slow heating and cooling conditions experienced by an electroslag weld, the susceptibility of a ferrous alloy to liquation cracking is increased. It has been reported that liquation cracks can be eliminated in heavy electroslag welds by microalloying the steels with cerium, titanium, and other elements to combine with sulfur and form small high-melting-point inclusions (Ref 56).

Temper Embrittlement. Thick-section $2\frac{1}{4}$ Cr-1Mo steel plates used in pressure vessels for petroleum and chemical service at elevated temperatures are susceptible to temper embrittlement in service. The problem has been attributed to the presence of residual elements such as phosphorus and antimony. Bruscato (Ref 55) established an *X* factor to describe the effect of the residual elements:

$$X = \frac{10P + Sb + 4Sn + As}{100} \qquad \textbf{(EQ 16)}$$

where *X* is in parts per million. Acceptable weld metal ductility can be obtained if the manganese and silicon contents and the *X* factor are low. Reduction of these elements can be achieved using basic fluxes. Another indicator, the Watanabe number, *J*, shows that welds and base metal are not susceptible to temper embrittlement if *J* is less than 200 (Ref 57):

$$J = (\mathrm{SI} + \mathrm{MN})\,(\mathrm{P} + \mathrm{SN}) \times 10^4 \qquad \textbf{(EQ 17)}$$

Hydrogen Cracking. Generally speaking, ESW is performed under perfect slag shielding conditions, and the rate of cooling of the weld metal is low. Therefore, the occurrence of hydrogen-induced cracking is minimal. However, under circumstances that require the use of a moist argillaceous material to prevent the slag from leaking out of the joint region, an atmosphere high in water vapor is present. Microcracks, and sometimes blowholes, may result in the weld metal. Grain boundary separation, observed in some electroslag welds, can be completely eliminated by postweld heat treating at 300 °C (570 °F) immediately after welding, which indicates that by allowing hydrogen to diffuse out of the specimen, the integrity of the welds can be maintained. This effect is further evidenced by the higher cracking incidence at the bottom part of an electroslag weld. In addition, diffusible hydrogen content is high at a region close to the weld start, decreasing to a relatively constant value at short distances from the starting point. By increasing the depth of the pool, the cooling rate is reduced, and hydrogen escapes by diffusion before it causes damage (Ref 58).

Weld Distortion. When compared with welds produced using other processes, electroslag slag welds do not present significant distortion problems. Measurements show that both transverse and angular distortion are present and that the gap distance changes as welding progresses. However, the distortion is only of the order of 1 to 2%. Angular distortion occurs because of the rapid cooling of the welded portion of the joint, which tends to draw the parts together, reducing the gap distance. Material ahead of the weld is separated by a gap, so heating has no effect. Material in the weld is either liquid or so hot that it is soft. Neither can support much of a load. As the weld progresses, the very bottom of the weld (coldest metal) resists motion. A contraction of 3 mm ($\frac{1}{8}$ in.) at the top of a weld 1.3 m (4.3 ft) long is normal. This separation must be allowed during joint setup to avoid jamming the guides and disrupting the normal progress of welding. Parts to be joined must be fitted up so that the gap is wider at the top of the joint. For improved dimensional accuracy, welding must be done at the maximum travel speed attainable.

Postweld Heat Treatment. As discussed in the previous section "Solidification Structure" of this article, most of the as-welded electroslag weldments have very coarse as-cast structure in the weld metal and coarse grains in the HAZ. As a result, such electroslag weldments may not qualify for many critical applications. For example, in the case of ferritic steels, normalizing is generally required to refine the weld metal and HAZ structure. In the case of electroslag welded nuclear transport flasks, normalizing is frequently followed by tempering (Ref 59). In some low-alloy steels, subcritical postweld heat treatments (for example, stress relief) may not be useful because they can be either detrimental or harmful to mechanical properties, particularly notch toughness. As an example, stress relief 2 $\frac{1}{4}$ Cr-1Mo steel weldments at 760 °C (1400 °F) significantly increased the fusion zone and HAZ toughness, but they coarsened the carbides in the base metal, reducing its toughness (Ref 60). Quenched and tempered material, when joined by ESW, must be heat-treated after welding to obtain adequate mechanical strength in the weld and HAZ. Kapadia (Ref 61) examined the need for stress-relieving components that will be exposed to fatigue loading and determined that in butt welds in the as-welded condition the outside surfaces cool and contract before the center, and thus compressive residual stresses are present, which improves fatigue life. Stress-relief heat treatments actually reduce this beneficial effect.

References cited in this section

54. K. EASTERLING, *INTRODUCTION TO THE PHYSICAL METALLURGY OF WELDING,* BUTTERWORTHS, 1983
55. R. BRUSCATO, TEMPER EMBRITTLEMENT AND CREEP EMBRITTLEMENT OF 2-1/4CR 1MO SHIELDED METAL ARC WELD DEPOSITS, *WELD. J.,* VOL 9 (NO. 4), 1970, P 148S-156S
56. A.M. MAKARA, Y.Y. KOKALEV, AND I.V. NOVIKOV, LIQUIDATION CRACKS IN THE HAZ IN STRUCTURAL STEELS DURING ELECTROSLAG WELDING, *AVTOM. SVARKA,* VOL 5, 1972, P 1-5
57. Y. MURAKAMI, T. NAMURA, AND J. WATANABE, HEAVY SECTION 2-1/4CR-1MO STEEL FOR HYDROGENATION REACTORS, STP 755, ASTM, 1982, P 383-417
58. T. KUNIHIRO AND H. NAKAJIMA, MICRO-CRACKING IN CONSUMABLE-NOZZLE ELECTROSLAG WELD METAL, *SIGNIFICANCE OF DEFECTS IN WELDED STRUCTURES,* UNIV. TOKYO PRESS, 1973, P 105-109
59. S.S. TULIANI, K.S. PROBERT, AND A.H. BRISCOE, FABRICATION OF ELECTROSLAG WELDED MAGNOX FUEL TRANSPORT FLASKS, *WELDING AND FABRICATION IN THE NUCLEAR INDUSTRY,* 1979, P 327-333

60. O. SERRANO, G.E. EDWARDS, AND R.H. FROST, A COMPARISON OF AS-WELDED AND STRESS-RELIEVED 2-1/4CR-1MO STEEL ELECTROSLAG WELDMENTS: MICROSTRUCTURAL AND PROPERTIES, *THE APPLICATION OF 2-1/4CR-1MO STEEL FOR THICK WALL PRESSURE VESSELS,* ASTM, 1980
61. B.M. KAPADIA, INFLUENCE OF RESIDUAL STRESS ON FATIGUE CRACK PROPAGATION IN ELECTROSLAG WELDS, *FATIGUE TESTING OF WELDMENTS,* STP 648, ASTM, 1977, P 244-260

Electroslag and Electrogas Welding*

S. Liu, Colorado School of Mines; S.D. Brandi, Escola de Politecnica da USP; R.D. Thomas, Jr., R.D. Thomas and Company

References

1. ELECTROSLAG AND ELECTROGAS WELDING, *AWS WELDING HANDBOOK,* VOL 2 (NO. 7), AWS, 1978, P 226-260
2. H.C. CAMPBELL, ELECTROSLAG, ELECTROGAS, AND RELATED WELDING PROCESSES, *WRC BULL.,* VOL 154, 1970
3. B. PATON, *ELECTROSLAG WELDING,* AWS, 1962
4. T. DEBROY, J. SZEKELY, AND T. EAGER, HEAT GENERATION PATTERNS AND TEMPERATURE PROFILES IN ELECTROSLAG WELDING, *METALL. TRANS. B,* VOL 11, 1980, P 593-605
5. R.H. FROST, J.E. JONES, AND D.L. OLSON, ELECTROSLAG WELDING OF PRESSURE VESSEL STEELS, *ELECTROSLAG WELDING FOR MARINE APPLICATIONS,* PAPER 2, U.S. NAVY ACADEMY, MARCH 1985
6. "ELECTROSLAG ELECTROGAS TIPS & TECHNIQUES," BULLETIN OF ELECTROTHERM CORP., 1973
7. J.E. JONES, D.L. OLSON, AND G.P. MARTINAS, METALLURGICAL AND THERMAL CHARACTERISTICS OF NON-VERTICAL ELECTROSLAG WELDING, *WELD. J.,* VOL 59 (NO. 9), 1980, P 245S-254S
8. S. NAKANO, N. NISHIYAMA, T. HIRO, AND J. TSUBOI, MAGLAY PROCESS--ELECTROMAGNETIC CONTROLLED OVERLAY WELDING PROCESS WITH ESW, *KAWASAKI STEEL TECH. REP.,* VOL 2, 1981, P 31-42
9. S. LIU AND C.T. SU, GRAIN REFINEMENT IN ELECTROSLAG WELDMENTS BY METAL POWDER ADDITION, *WELD. J.,* VOL 68 (NO. 4), 1989, P 132S-144S
10. C.T. SU, "HIGH SPEED ELECTROSLAG WELDING," M.S. THESIS, PENNSYLVANIA STATE UNIV., 1987
11. S. VENKATARAMAN, J.H. DEVLETIAN, W.E. WOOD, AND D.G. ATTERIDGE, GRAIN REFINEMENT DEPENDENCE ON SOLIDIFICATION AND SOLID STATE REACTIONS IN ELECTROSLAG WELDS, *GRAIN REFINEMENT IN CASTINGS AND WELDS,* AIME, 1982, P 275-288
12. D.G. ATTERIDGE, S. VENKATARAMAN, AND W.E. WOOD, "IMPROVING THE RELIABILITY AND INTEGRITY OF CONSUMABLE GUIDE ELECTROSLAG WELDMENTS IN BRIDGE STRUCTURES," RESEARCH REPORT, OREGON GRADUATE CENTER, 1982
13. R.H. FROST, G.R. EDWARDS, AND M.D. RHEINLANDER, A CONSTITUTIVE EQUATION FOR THE CRITICAL ENERGY INPUT DURING ELECTROSLAG WELDING, *WELD. J.,* VOL 60 (NO. 1), 1981, P 12-62
14. S. LIU AND C.T. SU, PERFORMANCE EVALUATION OF A METAL POWDER CORED STRIP ELECTRODE IN HIGH SPEED ELECTROSLAG WELDING, *ADVANCES IN WELDING SCIENCE AND TECHNOLOGY,* ASM INTERNATIONAL, 1986, P 401-412
15. R.D. THOMAS, JR., CORROSION RESISTANT WELD OVERLAYS BY THE DUAL STRIP

PROCESS, *BRIT. WELD. J.*, MAY 1966

16. A. MITCHELL AND G. BEYNON, ELECTROCHEMICAL REACTIONS IN THE ELECTROSLAG WELDING OF THICK WALLED STRUCTURES, *AVTOM. SVARKA*, VOL 6, 1965, P 32-37
17. A. MITCHELL AND G. BEYNON, ELECTROCHEMICAL REACTIONS IN THE ELECTROSLAG PROCESS, CH. 2, *BUR. MINES BULL.*, 1976, P 669
18. M.E. PEOVER, ELECTROSLAG REMELTING, A REVIEW OF ELECTRICAL AND ELECTROCHEMICAL ASPECTS, *J. INST. MET.*, VOL 100, 1972, P 97
19. R.H. FROST, D.L. OLSON, AND G.R. EDWARDS, "THE INFLUENCE OF ELECTROCHEMICAL REACTIONS ON THE CHEMISTRY OF THE ELECTROSLAG WELDING PROCESS, *MODELING OF CASTING AND WELDING PROCESSES II*, AIME, 1983, P 279-294
20. D. YU, H. ANN, J.H. DEVLETIAN, AND W.E. WOOD, SOLIDIFICATION STUDY OF NARROW-GAP ELECTROSLAG WELDING, *WELDING RESEARCH: THE STATE OF THE ART*, E. NIPPES AND D. BALL, ED., ASM, 1985, P 21-32
21. V.I. AVRAMENKO, B.F. LEBEDEV, AND V.I. BOZHKO, SOME WAYS OF INCREASING THE PRODUCTIVITY OF ELECTROSLAG WELDING, *SVAR. PROIZVOD.*, VOL 10, 1973, P 16
22. K. WATANABE, I. SEJIMA, S. KOKURA, G. TAKI, AND H. MIYAKE, PROBLEMS AND IMPROVEMENT OF LARGE HEAT INPUT ELECTROSLAG WELDING, *J. JPN. WELD. SOC.*, 1975, P 519
23. S.A. SMIRNOV AND L.A. EFIMENKO, SPECIAL STRUCTURAL FEATURES AND MECHANICAL PROPERTIES OF ELECTROSLAG WELDED JOINTS MADE USING POWDERED FILLER METAL, *SVT. SVARKA*, VOL 9, 1973, P 46
24. F. EICHHORN AND J. REMMEL, SITUATION OF RESEARCH IN ELECTROSLAG WELDING--A TENDENCY OF FURTHER DEVELOPMENT, *IND. WELD. J.*, VOL 4, 1983, P 37
25. F. EICHHORN, J. REMMEL, AND B. WUBBELS, HIGH SPEED ELECTROSLAG WELDING, *WELD. J.*, VOL 62 (NO. 1), 1984, P 37
26. F. EICHHORN AND J. REMMEL, EFFICIENT FILLET WELDING IN THE VERTICAL WELDING POSITION WITH ELECTROGAS AND ELECTROSLAG WELDING METHODS, DOC. XII-908-85, IIW, 1985
27. B.F. YAKUSHIN *ET AL.*, IMPROVING THE CAPACITY OF ELECTROSLAG WELDED JOINTS FOR RESISTING HOT CRACKING, *WELD. RES. ABROAD*, JUNE/JULY 1984 (TRANSLATION FROM RUSSIAN BY AUTOMATIC WELDING, OCT 1982)
28. S. FORSBERG, RESISTANCE ELECTROSLAG (RES) SURFACING, *WELD. J.*, VOL 63 (NO. 8), 1985, P 41-48
29. P.C. ARNOLD AND D.C. BERTOSSA, MULTIPLE PASS AUTOMATIC VERTICAL WELDING, *WELD. J.*, VOL 45 (NO. 8), 1966, P 651-660
30. D.J. ELLIS AND A.F. GIFFORD, APPLICATION OF ELECTRO-SLAG AND CONSUMABLE GUIDE WELDING--PARTS 1-6, *MET. FABR.*, APRIL-NOV 1973
31. H. PASS, THE ELECTRO-SLAG WELDING OF A BLAST FURNACE HEARTH JACKET, *WELD. MET. FABR.*, JAN/FEB 1976
32. ELECTROSLAG WELDING HELPS TO RESTORE WIND TUNNEL, *MET. PROGR.*, MARCH 1976
33. J.S. NOEL AND A.A. TOPRAC, STATIC, FATIGUE, AND IMPACT STRENGTH OF ELECTROSLAG WELDMENTS, RESEARCH REPORT 157-1F, RESEARCH PROJECT 3-5-71-157, CENTER FOR HIGHWAY RESEARCH, UNIV. OF TEXAS, 1971
34. A.M. MAKARA *ET AL.*, ELECTROSLAG WELDING OF STRUCTURAL STEELS WITHOUT NORMALIZING, *AVTOM. SVARKA*, VOL 7, 1974, P 511-514
35. B. HOWSER, APPLICATION AND TRENDS IN ELECTROSLAG WELDING IN THE UNITED STATES, *ELECTROSLAG WELDING FOR MARINE APPLICATIONS*, U.S. NAVAL ACADEMY, MARCH 1985, P 4-1
36. J.E. NORCROSS, ELECTROSLAG DEVELOPMENTS, *FWP J.*, VOL 18 (NO. 2), 1978, P 41-58

37. D. YAPP AND A.P. BENNETT, DEVELOPMENT OF ELECTROSLAG-MELTED GRADED TRANSITION JOINTS, *WELDING RESEARCH RELATED TO POWER PLANT*, PAPER 34, CENTRAL ELECTRICITY GENERATING BOARD, SOUTHAMPTON, ENGLAND, SEPT 1972, P 464-481
38. J.E. NORCROSS, ELECTROSLAG BOSS AND PROCESS, U.S. PATENT 4,130,931, DEC 1978
39. ELECTROSLAG CASTING AND WELDING, BRITISH PATENT 1,390,674, APRIL 1975
40. A.P. BENNETT, AN ELECTRICAL ANALOGUE OF AN ELECTROSLAG REMELTING OPERATION USED AS A GUIDE TO IMPROVED CONTROL OF THE PROCESS, *MET. MATER.,* APRIL 1972, P 146-149
41. A. BROSHOLEN, E. SKAUD, AND J.J. VESSER, ELECTROSLAG WELDING OF LARGE CASTINGS FOR SHIP CONSTRUCTION, *WELD. J.,* VOL 56 (NO. 8), 1977, P 26-30
42. Y. ISHII, ELECTROSLAG WELDING OF CAST IRON, *TRANS. JAP. WELD. SOC.,* NO. 2, SEPT 1970, P 241-252
43. V.F. YAKOVLEV, P.I. KOVALKIN, N.I. EVDOKIMOV, M.G. KOZULIN, AND I.I. SUSHCHUCK-SLYUSARENKO, ELECTROSLAG WELDING OF STEEL CASTING DEFECTS, *AVTOM. SVARKA,* VOL 2, 1970, P 72
44. V.G. SVYNYUK, ELECTROSLAG WELDING FOR RECTIFYING DEFECTS IN CAST CENTRIFUGAL PUMP WHEELS, *AUTOM. WELD.,* VOL 28 (NO. 7), 1975, P 57-58
45. V.T. ARSENKIN, V.G. RADCHENKO, AND D.M. LIKHOHSHERSTOV, THE ELECTROSLAG DEPOSITION OF DIE STEEL ON CARBON STEEL, *AVTOM. SVARKA,* VOL 3, 1976, P 46-49
46. M.P. IVANAN, *ET AL.,* ELECTROSLAG HARDFACING OF BEATERS OF HAMMER CRUSHERS, *SVAR. PROIZVOD.,* VOL 7, 1974, P 48
47. Y.I. GORBACHEV, E.A. KOVALEVSKII, AND A.V. MATELEV, ELECTROSLAG WELDING OF DIE STEEL, *SVAR. PROIZVOD.,* VOL 11, 1984, P 12-13
48. N. LEHKA, PROBLEMS ASSOCIATED WITH THE CORROSION OF THE PROPERTIES OF ELECTROSLAG WELDED JOINTS IN AUSTENITIC STEELS OF INCREASED STRENGTH, *ZVRACSKE SPRAVY/WELDING NEWS,* VOL 26 (NO. 3), 1976, P 61-68
49. P.M. BARTLE, DEVELOPMENT OF AN ELECTROGAS TECHNIQUE FOR WELDING THICK ALUMINUM, *WELD. INST. RES. BULL.,* VOL 12 (NO. 3), 1971, P 67-71
50. Y.G. GAGEN, *ET AL.,* ELECTROSLAG WELDING OF ALUMINUM BUS-BARS LOCATED IN THE ZONE OF A STRONG MAGNETIC FIELD, *SVAR. PROIZVOD.,* VOL 12, 1972, P 19-21
51. ELECTROSLAG OR SUBMERGED ARC WELDING OF ALUMINIUM OR ITS ALLOYS OR ELECTROSLAG REMELTING ALUMINUM, BRITISH PATENT 1,544,248, APRIL 1979
52. V.Y. MALIN, ELECTROSLAG WELDING OF TITANIUM AND ITS ALLOYS, *WELD. J.,* VOL 64, FEB 1985, P 42-49
53. J.H. DEVLETIAN, ELECTROSLAG WELDING OF NON-FERROUS METALS--A REVIEW, *ELECTROSLAG WELDING FOR MARINE APPLICATIONS,* U.S. NAVAL ACADEMY, 1985, P 3-1 TO 3-32
54. K. EASTERLING, *INTRODUCTION TO THE PHYSICAL METALLURGY OF WELDING,* BUTTERWORTHS, 1983
55. R. BRUSCATO, TEMPER EMBRITTLEMENT AND CREEP EMBRITTLEMENT OF 2-1/4CR 1MO SHIELDED METAL ARC WELD DEPOSITS, *WELD. J.,* VOL 9 (NO. 4), 1970, P 148S-156S
56. A.M. MAKARA, Y.Y. KOKALEV, AND I.V. NOVIKOV, LIQUIDATION CRACKS IN THE HAZ IN STRUCTURAL STEELS DURING ELECTROSLAG WELDING, *AVTOM. SVARKA,* VOL 5, 1972, P 1-5
57. Y. MURAKAMI, T. NAMURA, AND J. WATANABE, HEAVY SECTION 2-1/4CR-1MO STEEL FOR HYDROGENATION REACTORS, STP 755, ASTM, 1982, P 383-417
58. T. KUNIHIRO AND H. NAKAJIMA, MICRO-CRACKING IN CONSUMABLE-NOZZLE ELECTROSLAG WELD METAL, *SIGNIFICANCE OF DEFECTS IN WELDED STRUCTURES,* UNIV. TOKYO PRESS, 1973, P 105-109
59. S.S. TULIANI, K.S. PROBERT, AND A.H. BRISCOE, FABRICATION OF ELECTROSLAG WELDED

MAGNOX FUEL TRANSPORT FLASKS, *WELDING AND FABRICATION IN THE NUCLEAR INDUSTRY,* 1979, P 327-333

60. O. SERRANO, G.E. EDWARDS, AND R.H. FROST, A COMPARISON OF AS-WELDED AND STRESS-RELIEVED 2-1/4CR-1MO STEEL ELECTROSLAG WELDMENTS: MICROSTRUCTURAL AND PROPERTIES, *THE APPLICATION OF 2-1/4CR-1MO STEEL FOR THICK WALL PRESSURE VESSELS,* ASTM, 1980
61. B.M. KAPADIA, INFLUENCE OF RESIDUAL STRESS ON FATIGUE CRACK PROPAGATION IN ELECTROSLAG WELDS, *FATIGUE TESTING OF WELDMENTS,* STP 648, ASTM, 1977, P 244-260

Introduction

OXYFUEL GAS WELDING (OFW) is a manual process in which the metal surfaces to be joined are melted progressively by heat from a gas flame, with or without filler metal, and are caused to flow together and solidify without the application of pressure to the parts being joined. The most important source of heat for OFW is the oxyacetylene welding (OAW) torch.

The simplest and most frequently used OFW system consists of compressed gas cylinders, gas pressure regulators, hoses, and a welding torch. Oxygen and fuel are stored in separate cylinders. The gas regulator attached to each cylinder, whether fuel gas or oxygen, controls the pressure at which the gas flows to the welding torch. At the torch, the gas passes through an inlet control valve and into the torch body, through a tube or tubes within the handle, through the torch head, and into the mixing chamber of the welding nozzle or other device attached to the welding torch. The mixed gases then pass through the welding tip and produce the flame at the exit end of the tip. This equipment can be mounted on and operated from a cylinder cart, or it can be a stationary installation. Filler metal, when needed, is provided by a welding rod that is melted progressively along with the surfaces to be joined.

Acknowledgements

This article was revised from "Oxyfuel Gas Welding Processes and Their Application to Steel" in Volume 6 of the 9th Edition of *Metals Handbook.* Special thanks are due to the authors of that article: Gene Meyer, Victor Equipment; Joseph E. McQuillen, Air Products and Chemicals, Inc.; and Clarence E. Vaughn, Chicago Bridge & Iron Company.

Oxyfuel Gas Welding

Revised by William Ballis, Columbia Gas of Ohio

Capabilities, Advantages, and Limitations

In OFW, the welder has considerable control over the temperature of the metal in the weld zone. When the rate of heat input from the flame is properly coordinated with the speed of welding, the size, viscosity, and surface tension of the welding pool can be controlled, permitting the pressure of the flame to be used to aid in positioning and shaping the weld. The welder has control over filler-metal deposition rates because the sources of heat and filler metal are separate. Heat can be applied preferentially to the base metal or the filler metal without removing either from the flame envelope. With these capabilities, OFW can be used for joining thin sheet metal, thin-walled tube, small pipe, and assemblies with poor fit-up, as well as for smoothing or repairing rough arc welds.

The equipment is versatile, low-cost, self-sufficient, and usually portable. It can be used for preheating, postheating, welding, braze welding, and torch brazing, and it is readily converted into oxygen cutting. The process can be adapted to short production runs, field work, repairs, and alterations.

Metals That Can Be Oxyfuel Gas Welded. Most ferrous and nonferrous metals can be oxyfuel gas welded. Oxyacetylene supplies the heat intensity and flame atmosphere necessary for welding carbon steel, cast iron, and other ferrous, copper, and nickel alloys (Table 1). Aluminum and zinc alloys can also be welded by the oxyacetylene process. Oxyfuel gas welding of steel is done almost exclusively with an oxyacetylene flame. Hydrogen, natural gas, propane, and several proprietary gases are used as fuel gases in welding metals with lower melting temperatures, such as aluminum, magnesium, zinc, lead, and some precious metals. Metals unsuited to OFW are the refractory metals, such as niobium, tantalum, molybdenum, and tungsten, as well as the reactive metals, such as titanium and zirconium.

TABLE 1 FERROUS AND NONFERROUS METALS THAT CAN BE WELDED BY OXYACETYLENE WELDING

Base metal	Filler-metal type	Flame type	Flux type
Aluminums	(a)	Slightly reducing	Aluminum
Brasses	Navy brass	Slightly oxidizing	Borax
Bronzes	Copper tin	Slightly oxidizing	Borax
Copper	Copper	Neutral	(b)
Copper nickel	Copper nickel	Reducing	(b)
Inconel	(a)	Slightly reducing	Fluoride
Iron, cast	Cast iron	Neutral	Borax
Iron, wrought	Steel	Neutral	(b)
Lead	Lead	Slightly reducing	(b)
Monel	(a)	Slightly reducing	Monel
Nickel	Nickel	Slightly reducing	(b)
Nickel silver	Nickel silver	Reducing	(b)
Low-alloy steel	Steel	Slightly reducing	(b)
High-carbon steel	Steel	Reducing	(b)
Low-carbon steel	Steel	Neutral	(b)
Medium-carbon steel	Steel	Slightly reducing	(b)
Stainless steel	(a)	Slightly reducing	Stainless steel

Source: Ref 1

(A) MATCH BASE METAL.

(B) NO FLUX REQUIRED.

Fluxes. Except for lead, zinc, and some precious metals, OFW of nonferrous metals, cast irons, and stainless steels generally requires a flux. In welding carbon steel, the gas flame shields the weld adequately, and no flux is required. Adjustment for correct flame atmosphere is important, but the absence of flux results in one less variable to control.

Major Applications. Oxyfuel gas welding can be used to join thin carbon steel sheet and carbon steel tube and pipe. The advantages of OFW include the ability to control heat input, bridge large gaps, avoid melt-through, and clearly view the weld pool. Carbon steel sheet, formed in a variety of shapes, can often be welded more economically by OFW than by other processes. Oxyfuel gas welding is capable of joining small-diameter carbon steel pipe (up to about 75 mm, or 3 in., in diameter) with resulting weld quality equal to competitive processes and often with greater economy. Pipe with wall thickness up to 4.8 mm ($\frac{3}{16}$ in.) can be welded in a single pass.

Welder Skill. Oxyfuel gas welding requires skill in manipulating the welding rod and the torch flame. In depositing a weld, the welder uses both hands to melt base metal and filler metal, control the weld pool, and obtain progressive solidification of weld metal in the correct bead shape.

Reference cited in this section

1. H.B. CARY, *MODERN WELDING TECHNOLOGY*, PRENTICE-HALL, 1989, P 211

Oxyfuel Gas Welding

Revised by William Ballis, Columbia Gas of Ohio

Gases

Oxygen and acetylene are the principal gases used in OFW. Oxygen supports combustion of the fuel gases. Acetylene supplies both the heat intensity and the atmosphere needed to weld steel. Hydrogen, natural gas, propane, and proprietary gases are used only to a limited extent in oxyfuel gas welding or brazing of metals with a low melting temperature.

Oxygen. Only by burning selected fuel gases with high-purity oxygen in a high-velocity flame can the high heat transfer intensity required in OFW be obtained. Oxygen is supplied for oxyfuel gas welding and cutting at a purity of 99.5% and higher, because small percentages of contaminants have a noticeable effect on combustion efficiency.

When the consumption requirement is relatively small, the oxygen is supplied and stored as a compressed gas in a standard steel cylinder under an initial pressure of up to 180 MPa (26 ksi). The most frequently used cylinder (Fig. 1) has a capacity of 6.91 m^3 (244 scf).* The gas is distributed for use under reduced pressure. When consumption of oxygen is somewhat greater, banks of cylinders are joined through a manifold to permanent pipeline systems that terminate at various stations of use.

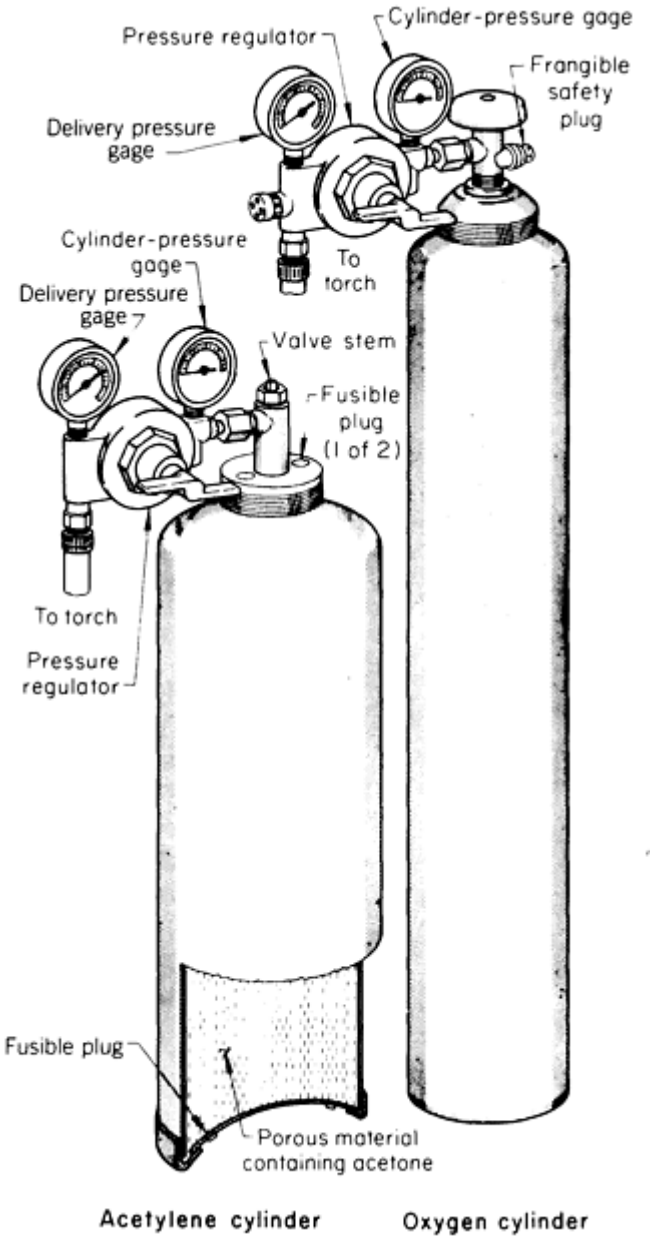

FIG. 1 GAS CYLINDERS AND REGULATORS USED IN OXYFUEL GAS WELDING. THE ACETYLENE CYLINDER SHOWN IS 1029 MM (40.5 IN.) HIGH, 314 MM (12.35 IN.) IN DIAMETER, AND HAS A WALL THICKNESS OF 4.4 MM (0.175 IN.). THE OXYGEN CYLINDER IS 1295 MM (51 IN.) HIGH, 229 MM (9 IN.) IN DIAMETER, AND HAS A WALL THICKNESS OF 6.3 MM (0.25 IN.).

When oxygen consumption exceeds approximately 6.91 m^3 (244 scf) cylinders per week, it may be more economical to obtain and store oxygen in liquid form. Liquid oxygen can be supplied in portable cryogenic cylinders of 130 m^3 (4500 scf) capacity, or it can be delivered in bulk to an on-site cryogenic storage tank. The gas is then piped to points of use. The distribution and use of oxygen are covered by laws and safety regulations designed to help prevent injury to persons and damage to property.

Acetylene is a hydrocarbon gas with the chemical formula C_2H_2. When under pressure of 203 kPa (29.4 psi) and above, acetylene is unstable, and a slight shock can cause it to explode, even in the absence of oxygen or air. Safety rules for the use of acetylene and the handling of acetylene equipment are extremely important.

Acetylene should not be used at pressure greater than 105 kPa (15 psi). Acetylene generators for on-site gas production are constructed so that the gas is not given off at pressures much greater than 105 kPa (15 psi). Commercially supplied portable cylinders are specially constructed (Fig. 1) to store acetylene under high pressure. By dissolving acetylene in

liquid acetone, a cylinder such as that shown in Fig. 1 can be used to store about 7.79 m^3 (275 scf) of acetylene under a pressure of 1.7 MPa (250 psi). This pressure must be reduced to 105 kPa (15 psi) or less by the regulator (Fig. 1) before the gas enters the hose or distribution line.

Acetylene cylinders must not be subjected to sudden shock and should be stored well away from any source of heat or sparks. The cylinders must be stored in an upright position to keep the acetone from escaping during use. Under normal sustained use, withdrawal rate from an acetylene cylinder should not exceed one-seventh of the cylinder capacity per hour.

Hydrogen is used chiefly for welding lower-melting-temperature metals, such as aluminum, magnesium, and lead. It cannot be used to weld common thicknesses of steel sheet, because it results in a flame temperature that is too low to produce good fusion. Hydrogen has, however, been used in welding thin sheet, where its lower combustion intensity (about 60% of that of acetylene) can be an advantage. It is used for brazing and, to some extent, for braze welding. Hydrogen is available in compressed-gas cylinders of various sizes.

Natural gas, propane, and proprietary gases can be used with oxygen to weld some lower-melting-temperature metals. Special welding rods may be required depending on the gas, base metal, and quality of metal desired. These gas mixtures cannot usually be applied to the welding of steel because when they are burned at temperatures high enough for welding, their flame atmospheres are excessively oxidizing. When ratios of oxygen to fuel gas are reduced to a carburizing condition, flame temperatures are too low. Therefore, these gases are usually limited to brazing, braze welding, heating, and related processes.

Note cited in this section

* * A STANDARD CUBIC FOOT (SCF) OF GAS IS DEFINED AS EQUIVALENT TO 0.028 M^3 (1 FT^3) OF GAS AT 20 °C (70 °F) AND 100 KPA (1 ATM, OR 14.7 PSI) PRESSURE. THIS DEFINITION, WHICH IS USED IN THE GAS INDUSTRY AND SOME ENGINEERING PRACTICE, DIFFERS FROM THE STANDARD TEMPERATURE AND PRESSURE OF 0 °C (32 °F) AND 100 KPA (1 ATM) USED IN SCIENTIFIC WORK.

Oxyfuel Gas Welding

Revised by William Ballis, Columbia Gas of Ohio

Equipment

The principal function of OFW equipment is to supply the oxyfuel gas mixture to the welding tip at the correct rate of flow, exit velocity, and mixture ratio. The rate of gas flow affects the quantity of metal melted; the pressure and velocity affect the manipulation of the weld pool and the rate of heating; and the ratio of oxygen to fuel gas determines the flame temperature and the atmosphere, which must be chemically suited to the metal being welded. Important elements in an OFW system include gas storage facilities, pressure regulators, hoses, torches, related safety devices, and accessories.

Gas Storage Equipment. Compressed-gas cylinders and storage tanks are used as on-site supply sources for gases. They are constructed under regulations of the Department of Transportation and are regulated to some extent by federal, state, and local laws. Cylinders are designed for specific gases and are not generally interchangeable. Sizes and threading of cylinder connections for oxygen, for example, differ from those for acetylene, hydrogen, and other gases. Only the appropriate fittings can be used for delivery of compressed gas. Users should not tamper with valves or safety devices on cylinders.

When portable equipment is not required and gas consumption is large enough, permanent installations are constructed. Gases can be supplied from a variety of bulk-storage vessels, manifolded gas cylinders, or gas generators. The gases are then separately piped, at suitable pressure, to terminal stations, where they are drawn off through station regulators and used as in a portable setup (Ref 2).

Pressure regulators reduce the supply gas pressure to a desired delivery pressure. They are designed for specific gases and are not generally interchangeable. In Fig. 1, oxygen and acetylene pressure regulators used in OFW are shown attached to their respective cylinders and hoses. In operation, gas enters the inlet side of the regulator at cylinder pressure and emerges from the outlet side at the desired delivery pressure.

Regulators are made for various ranges of inlet and outlet pressure. They can be adjusted within their delivery pressure range by turning an adjusting screw. Although some regulators do not have gages and are preset to deliver at a specific and constant pressure, most are equipped with two pressure gages. The one on the outlet side permits the operator to read the adjusted delivery pressure; the one on the inlet side indicates the pressure in the cylinder.

Two basic types of regulators are used in OFW: single-stage and two-stage. Both are available with either direct or inverse actuation of the valve mechanism. Regulators with direct actuation are known also as positive or nozzle regulators; those with inverse actuation, as negative or stem regulators. All single-stage regulators reduce cylinder pressure in one step. Pipeline regulators, made for lower pressures, must not be used on cylinders (the higher cylinder pressure can blow apart a pipeline regulator).

When adjusted for a desired delivery pressure, regulators continue to deliver gas at the pressure shown on the outlet gage within a fairly narrow range of deviation, as the cylinder pressure drops. The amount and direction of the deviations depend on the design of the regulator. The variation in delivery pressure as cylinder pressure decreases is shown in Fig. 2 for three types of regulators. Both types of single-stage regulators may require occasional adjustment as cylinder pressure drops. The more costly two-stage regulator supplies a more constant working pressure until cylinder pressure nearly equals delivery pressure. On full oxygen cylinders exposed to low outdoor temperatures in winter, two-stage regulators are more reliable than single-stage regulators. The temperature drop of expanding gas is less severe because pressure is reduced in two steps. Less chance exists for ice to form and clog regulator passages if water vapor is present.

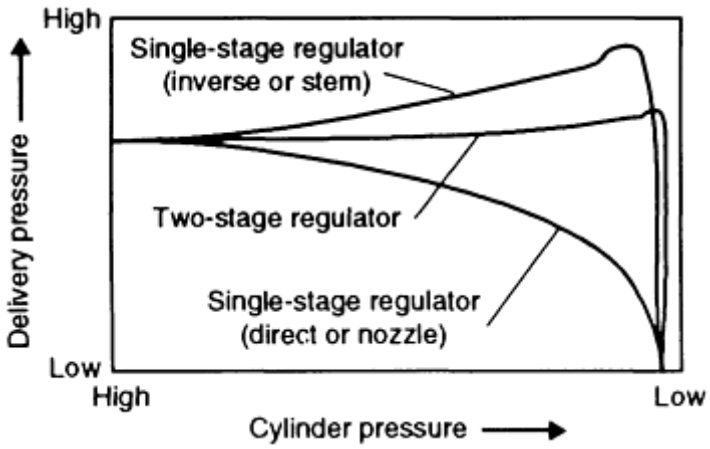

FIG. 2 DELIVERY PRESSURE FOR SELECTED TYPES OF PRESSURE REGULATORS

Hoses. Flexible hoses permit gas cylinders and regulators to be kept at a safe distance from the working area and also allow the welder freedom of movement. Hoses usually range from 3.2 to 13 mm ($\frac{1}{8}$ to $\frac{1}{2}$ in.) in inside diameter, with larger sizes available for special applications, and are usually available in 7.6 m (25 ft) lengths. If hoses are longer than 7.6 m (25 ft), either the next larger size hose or a length of larger diameter hose with a short length of the usual size hose should be used to connect to the welding torch. This facilitates ease of movement. To ensure that oxygen and fuel gas hoses are used with the proper gas and correct fittings, oxygen hoses are generally green, with right-hand threaded fittings; acetylene and other fuel gas hoses are generally red, with left-hand threaded fittings. Left-hand threaded fittings are grooved on the outside so they can be readily identified.

Welding torches control the operating characteristics of the welding flame and enable the flame to be manipulated during welding. The choice of torch size and style depends on the work to be performed. Aircraft welding torches, for example, are small and light to permit ease of handling. Most torch styles permit one of several sizes of welding tips or a cutting attachment to be added.

The general construction of an OFW torch is shown schematically in Fig. 3. The principal operating parts are inlet valves, rear body, handle, and head. A mixing chamber with a welding tip, heating nozzle, or cutting attachment is added to the head. By unscrewing the sleeve nut (Fig. 3), the welding tip and mixing-chamber assembly can be removed and replaced by units with different capacity.

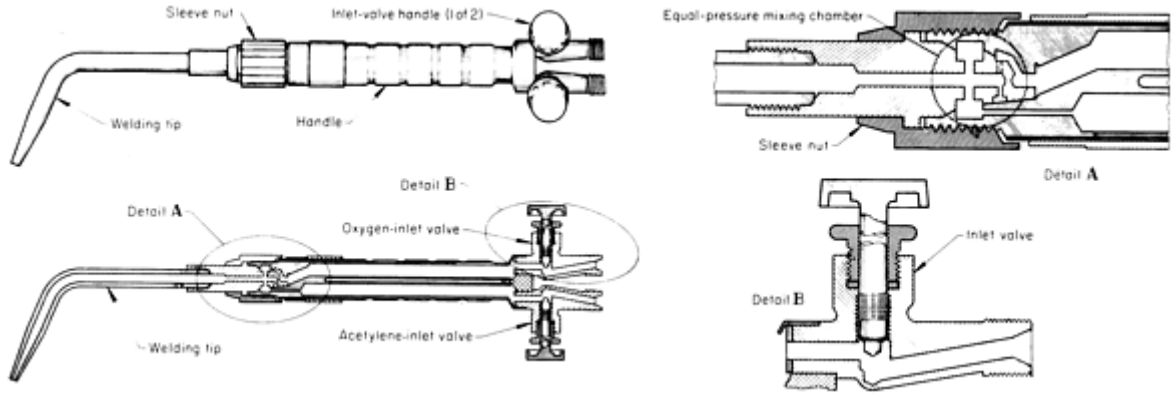

FIG. 3 SCHEMATIC SHOWING CROSS-SECTIONAL VIEWS OF GAS PASSAGES IN A TYPICAL OXYFUEL GAS WELDING TORCH

Torch inlet valves provide the welder with two important controls. First, the gas pressure, velocity, and flow rate can be adjusted within the limits set by the pressure regulators and the practical requirements of the welding flame. Second, the ratio of oxygen to fuel gas can be varied. The ability of the oxyfuel flame to produce the combustion intensity needed for welding, while providing a suitable protective atmosphere for the weld metal, is largely a property of the fuel gas, but correct torch settings must be used.

Mixing Chambers. In Fig. 3, the mixing chamber is shown as part of an assembly with the welding tip. Two general mixing chambers are available: equal-pressure (also called positive-pressure and medium-pressure) and injector. In an equal-pressure mixing chamber, gases are at approximately the same pressure and are mixed by directing the fuel gas into the oxygen stream. Detail A in Fig. 3 shows an equal-pressure mixing chamber assembled in position. Figure 4 is a spiral equal-pressure mixer.

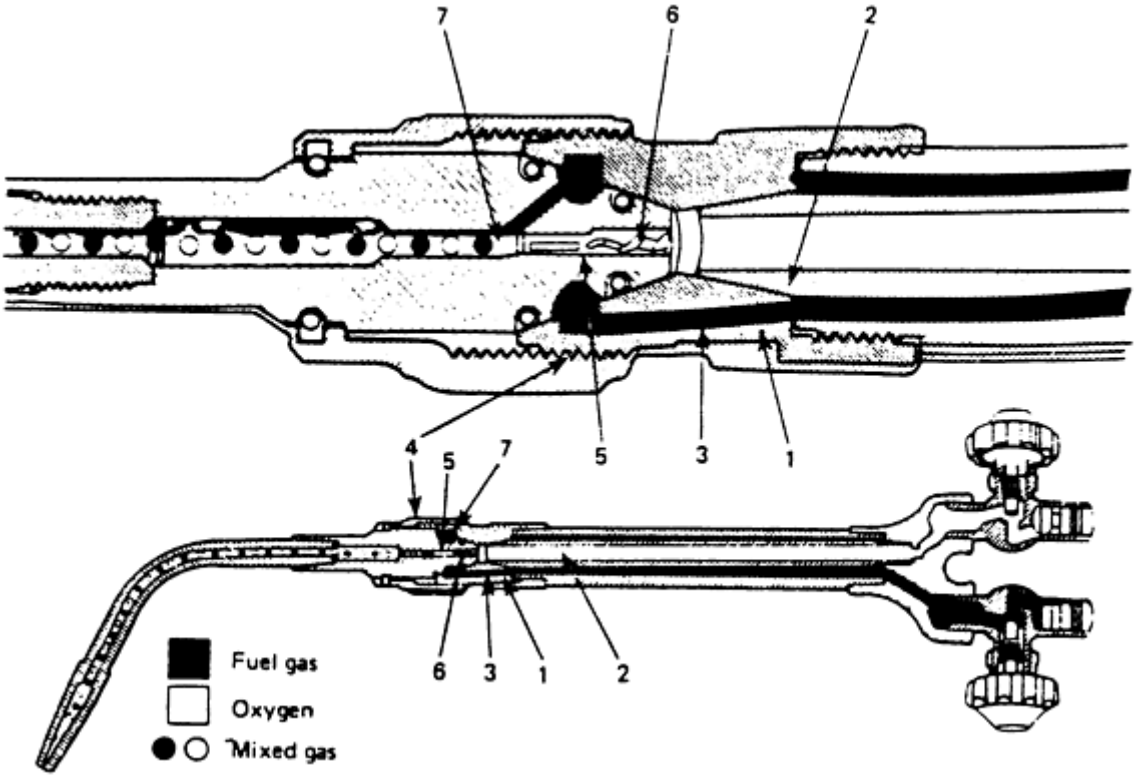

FIG. 4 SCHEMATIC SHOWING CROSS-SECTIONAL VIEW OF A SPIRAL EQUAL-PRESSURE MIXER. (1) WELDING TORCH HEAD. (2) OXYGEN TUBE FROM TORCH HEAD. (3) ACETYLENE (FUEL GAS) PASSAGES FROM TORCH HEAD. (4) NOZZLE NUT. (5) WELDING NOZZLE CONE END. (6) SPIRAL IN WELDING NOZZLE. (7) MIXER ORIFICE AND MIXING CHAMBER

In the injector mixing chamber, low-pressure fuel gas is aspirated by directing it into a high-velocity stream of oxygen. A nozzle system based on the flow principles of the venturi tube is used. Injector torches are useful when fuel gases are supplied at pressures too low to produce a flame of adequate combustion intensity. Supplying oxygen at desired pressure is not usually difficult. By varying the design of the injector nozzle, different degrees of aspiration can be obtained, and designs for injector mixing chambers differ considerably in detail.

Welding tips are replaceable nozzles that control gas flow through the diameter of the exit orifice. Tips of various orifice diameter are usually available for any welding torch. Orifice diameters are identified by drill-size number, decimal size in inches, or manufacturer's code number. Because code numbers of different manufacturers do not necessarily correspond, drill sizes or decimals are needed to compare the orifice size of different makes of tips. The performance of tips of equal size at equal pressure-regulator settings may differ, however, because of differences in torch and mixing-chamber designs.

Small-diameter tips produce small flames for welding thin sections; large-diameter tips are required for heavier work. Welding tips are made with a smooth bore at the exit end to ensure laminar flow and a uniform flame. The influence of bore shape on the shape of the flame is shown in Fig. 5. When foreign matter, such as carbon, dirt, or weld spatter, enters the welding-tip orifice, it must be carefully removed. Specially designed dressing tools (known as tip cleaners) are available for this purpose.

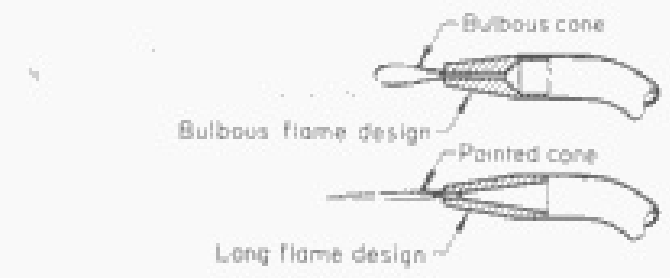

FIG. 5 VARIATION IN THE SHAPE OF THE INNER CONE OF AN OXYACETYLENE WELDING FLAME PRODUCED BY WELDING TIPS WITH TWO DIFFERENT BORE SHAPES. VARYING THE TRANSITION TAPER PRODUCES CONE SHAPES INTERMEDIATE BETWEEN THOSE SHOWN.

Accessories essential to OFW include a friction lighter for igniting the torch; welder's goggles, gloves, and protective clothing; and related safety devices.

Welder's goggles are covered by ANSI standard Z49.1 (Ref 3), which suggests the following lens shade numbers for use in OFW of steel:

STEEL THICKNESS		SHADE NUMBER
MM	IN.	
≤ 3.2	≤ $\frac{1}{8}$	4 OR 5
3.2-13	$\frac{1}{8}$ - $\frac{1}{2}$	5 OR 6
>13	> $\frac{1}{2}$	6 TO 8

For general OFW, goggles must have side shields.

References cited in this section

2. "OXYGEN-FUEL GAS SYSTEMS FOR WELDING AND CUTTING," BULLETIN NO. 51, NATIONAL FIRE PROTECTION ASSOCIATION, 1977
3. "SAFETY IN WELDING AND CUTTING," ANSI/AWS ZA9.1, AMERICAN WELDING SOCIETY, 1983

Oxyfuel Gas Welding

Revised by William Ballis, Columbia Gas of Ohio

Selection of Tip-Orifice Size and Gas Pressure

Torch manufacturers provide charts that give tip-orifice sizes to be used for welding different thicknesses of metal. Table 2 presents the data from a chart showing these relationships. Tip size number and drill size are not precise means of comparing tips because significant differences exist between tips of the same dimensions when operated under positive pressure and when operated under injector pressure. The only valid basis of comparison is the volume of fuel passing

through the tip in a unit of time. Most tips operate within a range, usually recorded as cubic feet of fuel per hour. The manufacturer's recommendations should always be followed for optimum performance and safety.

TABLE 2 TYPICAL TIP-ORIFICE SIZES AND ACETYLENE CONSUMPTION FOR OXYFUEL GAS WELDING OF 0.25 TO 6.4 MM (0.010 TO $\frac{1}{4}$ IN.) THICK STEEL

THICKNESS OF STEEL		**TIP-ORIFICE SIZE**			ACETYLENE CONSUMPTION	
		DIAMETER		**DRILL NO.**		
MM	**IN.**	**MM**	**IN.**		**M^3/H**	FT^3/H
0.25	0.010	0.571	0.0225	74	≤ 0.028	≤ **1**
0.41	0.016	0.711	0.0280	70	≤ 0.028	≤ **1**
0.48	0.019	0.711	0.0280	70	≤ 0.028	≤ **1**
0.8	$\frac{1}{32}$	0.889	0.0350	65	0.014-0.057	$\frac{1}{2}$ **-2**
1.6	$\frac{1}{16}$	1.12	0.0465	56	0.028-0.11	**1-4**
2.4	$\frac{3}{32}$	1.12-1.40	0.0465-0.0550	56-54	0.11-0.17	**4-6**
3.2	$\frac{1}{8}$	1.40-1.51	0.0550-0.0595	54-53	0.17-0.28	**6-10**
4.8	$\frac{3}{16}$	1.51-1.78	0.0595-0.0700	53-50	0.28-0.48	**10-17**
6.4	$\frac{1}{4}$	**1.78-2.06**	**0.0700-0.0810**	**50-46**	**0.48-0.85**	**17-30**

Oxyfuel Gas Welding

Revised by William Ballis, Columbia Gas of Ohio

Flame Adjustment

Different welding atmospheres and flame temperatures can be produced by varying the relative amounts of oxygen and fuel gas in the gas flowing to the tip of the torch. Usually, a welder makes the appropriate adjustments in gas flow based on the appearance of the flame. This is not true for oxyhydrogen welding, however. The sequence for setting up a positive-pressure welding outfit is:

- CHECK ALL PARTS OF THE APPARATUS, MAKING SURE THEY ARE FREE OF DIRT, OIL, OR GREASE AND IN PROPER WORKING CONDITION.
- CRACK EACH CYLINDER VALVE INDIVIDUALLY TO BLOW OUT FOREIGN MATTER. MAKE SURE VENTED GASES ARE SAFELY DISPERSED. WIPE OUT THE CYLINDER-VALVE OUTLET WITH A CLEAN, LINT-FREE CLOTH.
- ATTACH THE OXYGEN REGULATOR TO THE OXYGEN CYLINDER OR MANIFOLD.
- ATTACH THE ACETYLENE (OR FUEL GAS) REGULATOR TO THE FUEL CYLINDER OR SOURCE.
- CONNECT THE WELDING HOSE TO THE REGULATORS AND THE WELDING TORCH.
- OPEN THE CYLINDER VALVE SLOWLY AND CAREFULLY. THE OPERATOR SHOULD NEVER STAND IN FRONT OF THE REGULATOR WHEN OPENING THE CYLINDER VALVE.
- PURGE THE OXYGEN LINE WHILE THE ACETYLENE LINE IS CLOSED AND THE ACETYLENE LINE WHILE THE OXYGEN LINE IS CLOSED. VENT GASES SAFELY.
- SET THE OXYGEN AND FUEL GAS REGULATORS TO THE RECOMMENDED WORKING

PRESSURE WITH APPROPRIATE TORCH VALVE OPEN.

- OPEN THE ACETYLENE (OR FUEL GAS) INLET VALVE AND LIGHT THE WELDING TORCH, USING A SPARK LIGHTER.
- OPEN THE OXYGEN INLET VALVE AND ADJUST THE FLAME, USING BOTH INLET VALVES.

For injector equipment, the sequence and method of setting up differ because high-pressure oxygen aspirates low-pressure acetylene into the torch. The differences among brands make it essential to always follow the manufacturer's directions for setting up.

Oxyfuel Gas Welding

Revised by William Ballis, Columbia Gas of Ohio

Oxyacetylene Combustion

As the acetylene/oxygen mixture burns from the tip of the welding torch, it displays several clearly recognizable zones of combustion. The overall chemical equation for the complete combustion of acetylene is:

$$2C_2H_2 + 5O_2 \rightarrow 4CO_2 + 2H_2O \qquad \textbf{(EQ 1)}$$

Combustion takes place in two stages. The first stage:

$$2C_2H_2 + 2O_2 \rightarrow 4CO + 2\,H_2 \qquad \textbf{(EQ 2)}$$

uses the oxygen supplied from the cylinder and available in the oxyacetylene mixture. The reaction can be seen as the small inner cone of the flame. The highest temperature is at the point of this cone. The second stage:

$$4CO + 2H_2 + 3O_2 \rightarrow 4CO_2 + 2H_2O \qquad \textbf{(EQ 3)}$$

uses the oxygen supplied from the air surrounding the flame. This combustion zone constitutes the outer envelope of the flame.

About two-fifths of the oxygen necessary for the complete combustion of acetylene comes from the oxygen cylinder; the remainder comes from the air. Because of the need for supplemental oxygen from the atmosphere, the acetylene/oxygen flame cannot be used inside tubes of structures subject to oxygen depletion from OFW. By varying the relative amounts of acetylene and oxygen in the gas mixture in the torch, a welder can produce different flame atmospheres and temperatures.

The second equation shows that in the first stage, when equal amounts of oxygen and acetylene are burning, neither excess acetylene nor excess oxygen is present at the high-temperature tip of the inner cone. For this reason, the flame is called neutral, and the gas mixture is often described as an acetylene-to-oxygen ratio of 1 to 1, or an equal ratio. The condition of the flame is important because the inner cone is held close to, but not touching, the work metal. If excess oxygen is present, the molten metal foams and sparks, and brittle oxides may form in the weld metal. If acetylene is present in sufficient excess, indicated by an acetylene feather greater than about one-half the length of the inner cone, carbon can enter the metal. Some of the carbon forms carbides and some burns, causing gas and porosity in the solidified weld metal. In austenitic stainless steels, carbides formed in this manner aggravate susceptibility to intergranular corrosion. In welding steel, the flame should be as nearly neutral as possible, but a perfectly neutral flame is difficult to recognize, and a flame containing a slight excess of acetylene is often used.

A neutral flame is obtained by observing the size and color of the combustion zones in the flame as the oxygen-to-acetylene ratio is changed by adjusting the torch inlet valves. Figure 6 shows five typical flame conditions that appear as

oxygen flow is increased from zero to excess oxygen, as well as a separated flame condition that results from excessive gas pressure.

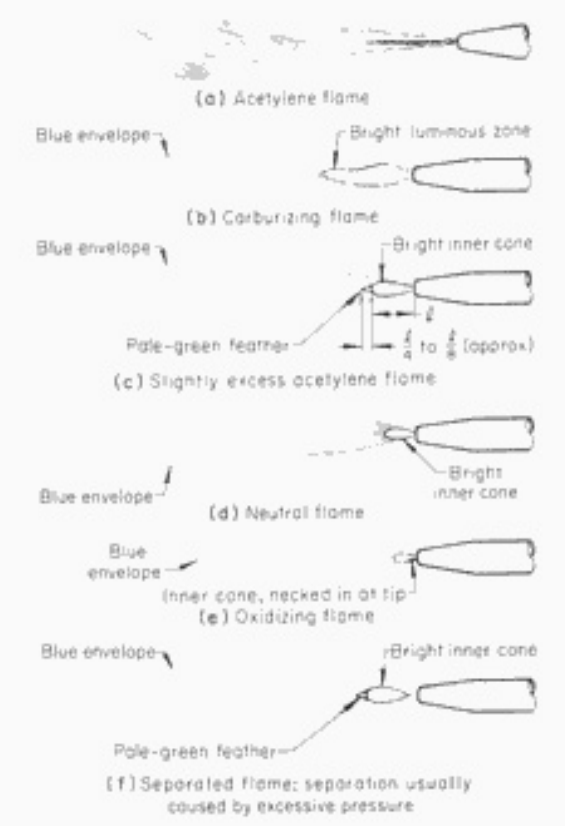

FIG. 6 FLAME CONDITIONS OBTAINED AS OXYGEN FLOW RATE INCREASES FROM ZERO TO AN EXCESS OF OXYGEN IN AN OXYACETYLENE WELDING TORCH

Acetylene Flame. When acetylene alone is burned in air, it produces a flame that varies in color from yellow near the torch tip to orange-red at the outer extremity. If soot particles are present at the end of the flame, the volume of gas should be increased until the flame burns clear (Fig. 6a).

Carburizing Flame. As the oxygen valve in the torch is progressively opened and the ratio of oxygen to acetylene increases, the flame becomes generally luminous. Then, the luminous portion contracts toward the welding tip, forming a distinct bright zone within a blue outer envelope (Fig. 6b). This is a carburizing flame because it has a large excess of acetylene; it is sometimes described as a soft flame because it has very little force. It has a relatively low temperature and is used in silver brazing and soldering, as well as in the welding of lead.

Reducing Flame. As more oxygen is introduced, the bright zone of the flame contracts farther and is seen to consist of two parts: a bright inner cone and a pale-green streamer, or feather, trailing off its end into the blue envelope. The streamer or feather is caused by a slight excess of acetylene. It disappears as the oxygen-to-acetylene ratio approaches 1 to 1. In Fig. 6(c), the feather is shown adjusted to about one-quarter the length of the inner cone. For welding steel, the length of the feather should be about one-eighth to one-quarter, but never more than one-half, the length of the inner cone. The flame is properly described as a slightly excess acetylene or reducing flame. It should not be called a carburizing flame because it does not carburize the metal, but it does ensure the absence of the oxidizing condition. It is frequently used for welding with low-alloy steel rods. The flame temperature at the tip of the inner cone is about 2930 to 3040 °C (5300 to 5500 °F).

Neutral Flame. In the neutral flame shown in Fig. 6(d), the oxygen-to-acetylene ratio is 1 to 1 (more accurately, 1.1 to 1), and the temperature at the tip of the inner cone is probably above 3040 °C (5500 °F) (Fig. 7). As pointed out earlier, making the precise adjustment of the inlet valves that results in a neutral flame is difficult, particularly in sunlight, because the oxidizing flame is of similar appearance. The neutral flame is ideal for the welding of steel, and it is also

needed when the presence of carbon must be strictly avoided. When the oxidizing condition is unacceptable, as in welding stainless steel, the use of a neutral flame is essential for good results.

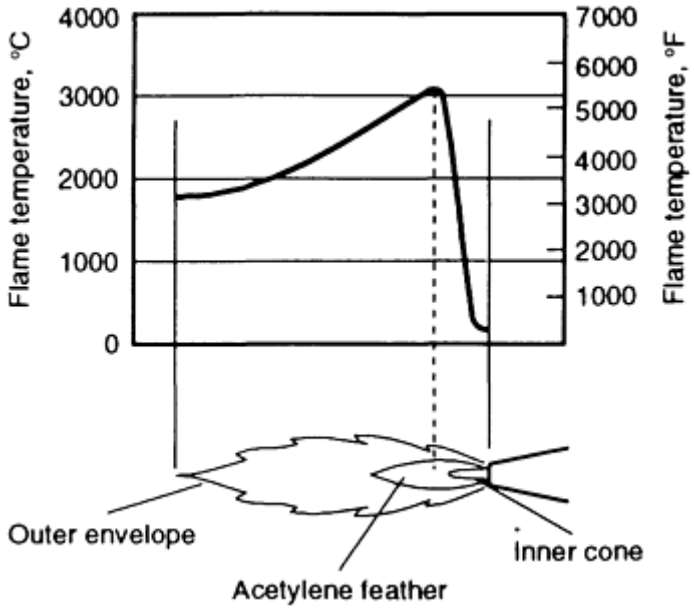

FIG. 7 FLAME TEMPERATURE AS A FUNCTION OF RELATIVE DISTANCE FROM THE TORCH TIP FOR A NEUTRAL (1:1 RATIO OF ACETYLENE TO OXYGEN) OXYACETYLENE FLAME. SOURCE: REF 4

Oxidizing Flame. An oxidizing flame is shown in Fig. 6(e). The adjustment of the inlet valves for this flame is difficult because it cannot be made on the basis of luminosity. When the flame tends to neck in at the juncture of the inner cone and the tip of the torch, this best indicates an oxidizing condition. When the flame is adjusted to be extremely oxidizing, it may also produce a hissing sound. An oxidizing flame should never be used in welding steel. It is used only in welding copper and certain copper-base alloys, and the flame should be sufficiently rich in oxygen to ensure that a film of oxide slag forms over the weld to provide shielding for the weld pool. With oxygen-to-acetylene ratios of about $1\frac{3}{4}$ to 1, flame temperature can approach 3315 °C (6000 °F).

Separated Flame. When gas pressure is too high for the size of the tip used, the flame can separate from the tip (Fig. 6f) and may even blow out. This is an unusable flame condition and must be avoided. Another cause of this condition is a clogged tip orifice.

Shape of Flame Cone. The design of the welding tip largely determines the shape of the inner cone of the oxyacetylene flame (Fig. 5); however, as the amount of oxygen used in the gas mixture is increased, the shape of the cone becomes more pointed. Both bulbous and pointed cones produce sound welds. The flame with the bulbous inner cone is preferred for welding in deep grooves in heavy sections. The flame with the long, pointed inner cone is softer and is generally preferred for welding thin sheet and aircraft assemblies.

Reference cited in this section

4. H.B. CARY, *MODERN WELDING TECHNOLOGY,* PRENTICE-HALL, 1989, P 210

Revised by William Ballis, Columbia Gas of Ohio

Oxyhydrogen Combustion

Complete combustion of hydrogen requires an oxygen-to-hydrogen ratio of 1 to 2, as can be seen from the following equation:

$$2H_2 + O_2 \rightarrow 2H_2O \qquad \textbf{(EQ 4)}$$

This gas mixture produces a strongly oxidizing flame having a temperature of about 2760 °C (5000 °F).

It is impossible to obtain a neutral oxyhydrogen flame by the visual methods of flame adjustment described for the oxyacetylene flame. The oxyhydrogen flame itself is scarcely visible, and no combustion zones, typical of the hydrocarbon gases, can be determined. To avoid an oxidizing flame, the pressure regulators must be set to ensure an excess of hydrogen. The flame is then reducing, but not carburizing. It has no carbon, and the temperature is several hundred degrees lower than that of the neutral flame. Metering flow regulators permit establishing the desired ratio of hydrogen to oxygen, usually 4 to 1. The oxyhydrogen flame is useful for welding and brazing aluminum alloys and lead.

Combustion of Natural Gas and Propane

Complete combustion of natural gas (methane) and propane is shown, respectively, by the following equations:

$$CH_4 + 2O_2 \rightarrow CO_2 + 2H_2O \qquad \textbf{(EQ 5)}$$

$$C_3H_8 + 5O_2 \rightarrow 3CO_2 + 4H_2O \qquad \textbf{(EQ 6)}$$

When the flame temperature is high enough to weld steel, the flame atmosphere is excessively oxidizing, but when the ratio of oxygen to fuel gas is decreased to produce a carburizing condition, flame temperature is too low for welding steel.

Welding Rods

Filler metal for OFW of low-carbon steel is available in the form of cold-drawn steel rods 915 mm (36 in.) long and 1.6 to 4.0 mm ($\frac{1}{16}$ to $\frac{5}{32}$ in.) in diameter. Welding rods for OFW of other metals are supplied in various lengths, depending on whether they are wrought or cast.

Specifications. Steel welding rods have been standardized in the American Welding Society (AWS) specification A5.2, "Iron and Steel Gas Welding Rods." This specification shows three classifications of welding rods based on the minimum tensile strength of all-weld-metal and transverse weld test specimens:

AWS	**MINIMUM TENSILE**	MINIMUM

CLASSIFICATION	STRENGTH[A]		ELONGATION IN $4D$[B], %
	MPA	KSI	
RG65	460	67	**16**
RG60	415	60	**20**
RG45	**310**	**45**	**. . .**

(A) ALL-WELD-METAL TEST SPECIMENS, 6.40 ± 0.13 MM (0.252 ± 0.005 IN.) IN DIAMETER.
(B) ELONGATION IN APPROXIMATELY 25 MM (1 IN.)

The mechanical properties specified for the RG65, RG60, and RG45 rods are obtained by welding in a neutral to slightly excess acetylene atmosphere.

The specification covers the chemical composition of the welding rods only to the extent of limiting sulfur and phosphorus to 0.040% maximum, and aluminum, if present, to 0.02% maximum. Therefore, welding rods of different manufacturers may vary appreciably in chemical composition.

Rods for OFW of steel have no flux covering. In the absence of flux coverings, weld-metal properties depend on chemical composition of the welding rod, control of the welding atmosphere, and techniques used to provide for mixing of base metal and filler metal.

Weld-Metal Strengthening. The ability to control the properties of the weld by mixing base metal and filler metal in the weld pool means that the choice of welding rod can influence weld strength to a considerable extent. Fully reinforced welds in thin-walled tubes of 4130 welded with RG45 rod consistently showed tensile strengths of 620 to 690 MPa (90 to 100 ksi). When the welds were made with RG60 rods, the strengths increased to 690 to 860 MPa (100 to 125 ksi), and with RG65 rods, strengths as high as 1000 MPa (145 ksi) were attained when the joint was heat treated after welding.

Class RG65 welding rods have a low-alloy steel composition and are used for OFW of carbon and low-alloy steels that have strengths of 450 to 515 MPa (65 to 75 ksi). They are used on sheet, plate, tube, and pipe. These rods give the highest strengths in welding 4130, 4340, and 8630 alloy steels when base metal and filler metal are mixed properly. The end use has a marked effect on selection of filler metal. If the base metal was selected to meet a specific corrosion- or heat-resistant application, the filler metal should be of similar composition. However, if a room-temperature mechanical property is the primary requirement, the strength and ductility of the filler metal should be the basis of selection.

Class RG60 welding rods are probably used most widely. They are generally made of low-alloy steel and are preferred for OFW of carbon and low-alloy steels in the tensile-strength range of 345 to 450 MPa (50 to 65 ksi). Class RG60 rods are most commonly used for welding carbon steel pipes for power plants.

Class RG45 welding rods have a simple low-carbon steel composition. These rods can be used for OFW of carbon and low-alloy steels.

Oxyfuel Gas Welding

Revised by William Ballis, Columbia Gas of Ohio

Welding Techniques

Most OFW is done with the one-pass forehand technique, particularly on thinner materials. A two-pass weld, using the backhand technique for the first pass and the forehand technique for the second pass, is preferred for thicker material (maximum thickness of 4.8 mm, or $\frac{3}{16}$ in.).

Forehand Welding. In forehand welding (Fig. 8), the flame is pointed away from the completed weld in the direction of welding. The torch is held at about 90° to the workpiece. The welding rod is held at an angle of about 30° to the workpiece, and the flame is between the tip of the rod and the weld. The inner cone of the flame is held close to the work

without actually touching it. The torch is moved from side to side or oscillated so that the flame heats the welding rod, the edges to be welded, and the weld metal ahead of the flame. The rod may be oscillated in a direction counter to the side-to-side movement of the torch. Both the welding rod-tip and the weld pool should be kept under the shielding influence of the flame. The forehand technique utilizes a zero work angle for both the torch and the welding rod.

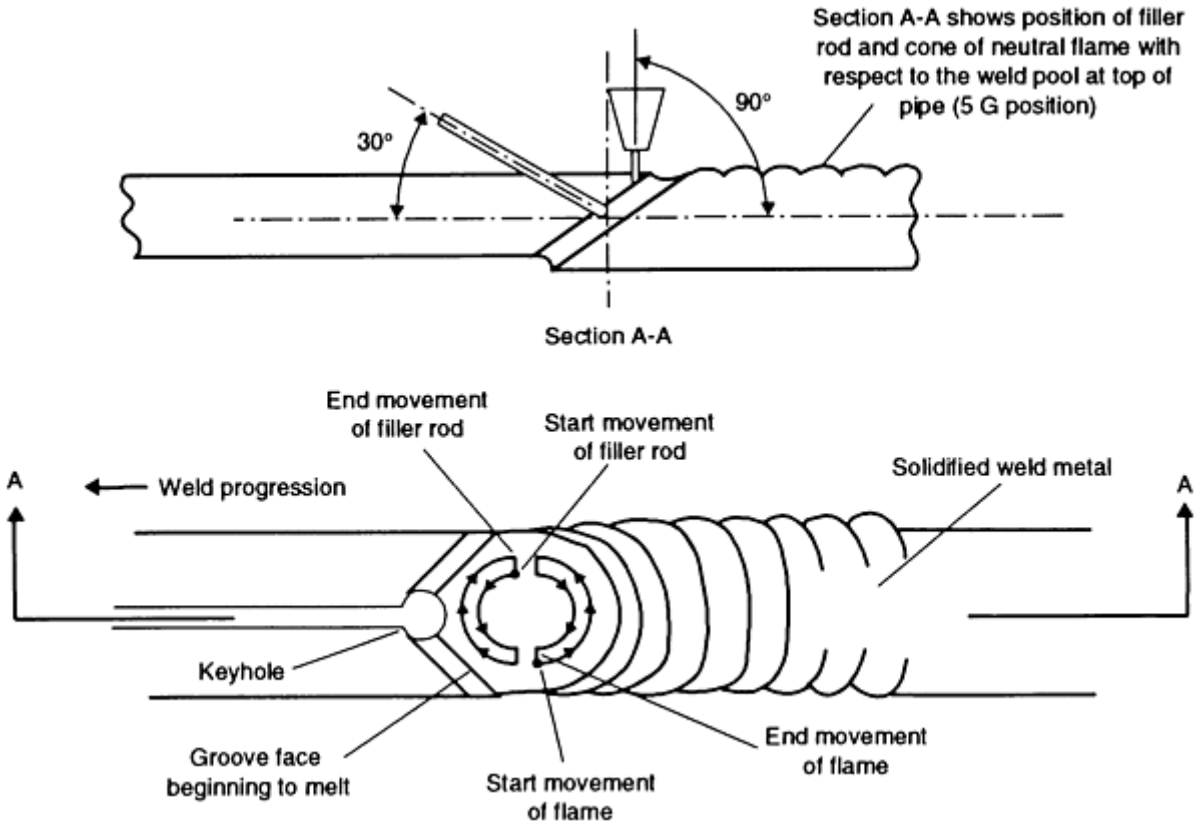

FIG. 8 ORIENTATION AND MOTION OF TORCH RELATIVE TO WORKPIECE IN ONE-PASS FOREHAND OXYACETYLENE WELDING. THE CONE OF FLAME SHOULD BE KEPT CLOSE TO, BUT SHOULD NEVER TOUCH, THE WELD POOL OR PIPE GROOVE FACE. SOURCE: REF 5

Backhand Welding. In backhand welding (Fig. 9), the flame is pointed toward the completed weld. The tip of the welding rod is held between the flame and the weld at an angle of about 30° to the workpiece, and the torch is held at an angle of about 30° to the workpiece. Rod and torch are usually oscillated as shown in Fig. 9. Because of less side-to-side movement of the flame and less melting of the joint edges, a backhand weld is more likely to retain the properties of filler metal unaltered by the base metal. The weld pool receives less agitation, and the weld metal is better protected by the flame.

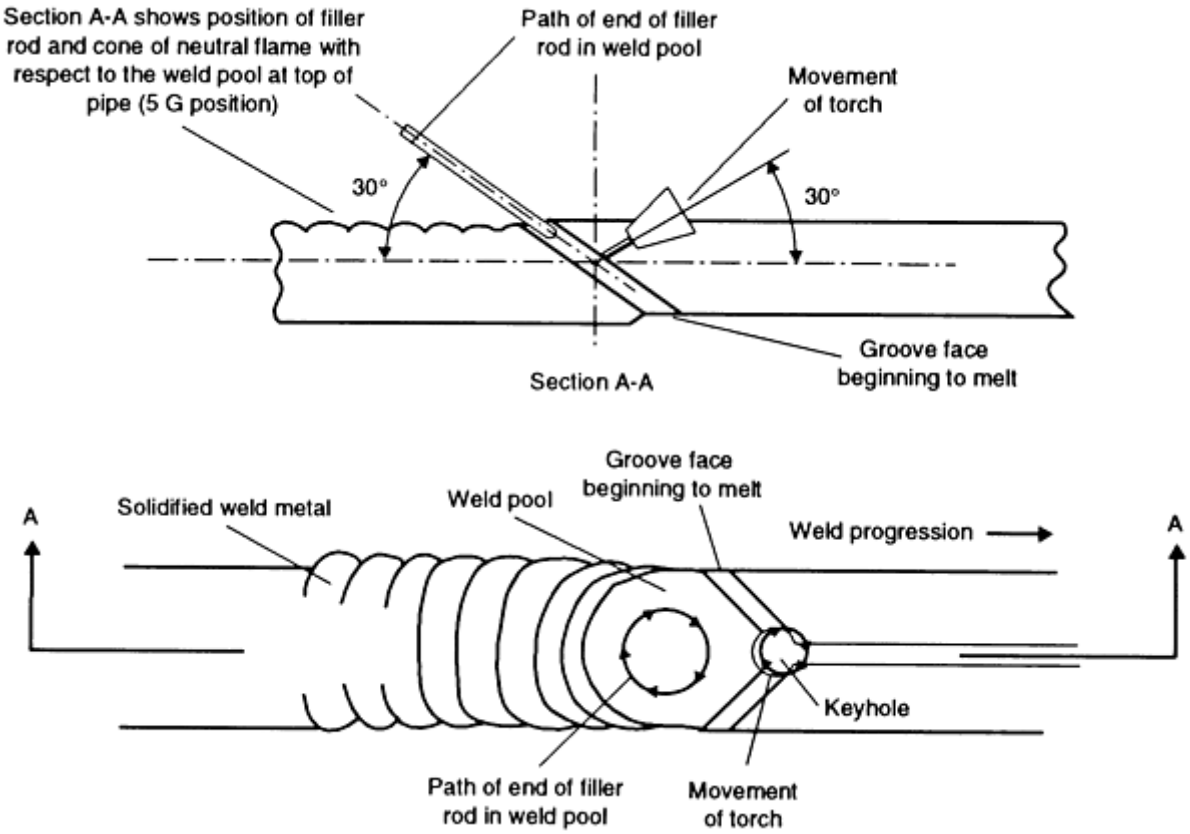

FIG. 9 ORIENTATION AND MOTION OF TORCH RELATIVE TO WORKPIECE IN ONE-PASS BACKHAND OXYACETYLENE WELDING. THE CONE OF FLAME SHOULD BE KEPT CLOSE TO, BUT SHOULD NEVER TOUCH, THE WELD POOL OR PIPE GROOVE FACE. SOURCE: REF 5

Backhand welding is often preferred for joints in the 2G fixed position. Smaller grooves can be used with this method because the flame does not need to be moved around the rod to melt the edges of the groove. Proponents of this technique believe that it saves time, filler metal, and gas. When working with a weld fillet, the flame should be directed primarily at the heavier and continuous section of base metal.

Reference cited in this section

5. "RECOMMENDED PRACTICES AND PROCEDURES FOR WELDING LOW CARBON STEEL PIPE," ANSI/AWS D10.12, AMERICAN WELDING SOCIETY, 1989

Oxyfuel Gas Welding

Revised by William Ballis, Columbia Gas of Ohio

Joint Design and Edge Preparation

Joints used in OFW are butt, lap, edge, T-, and comer joints. Either fillet or groove welds are used, depending on workpiece and strength requirements.

Sheet. Five joints used for single-pass OFW of low-carbon steel sheet are shown in Fig. 10. For OFW, beveling of joint edges is not needed in sheet up to 3.2 mm ($\frac{1}{8}$ in.) thick, and if proper shearing practice has been followed in trimming sheets to size, no special edge preparation is required. However, edges must be free of rust, dirt, oil, and grease.

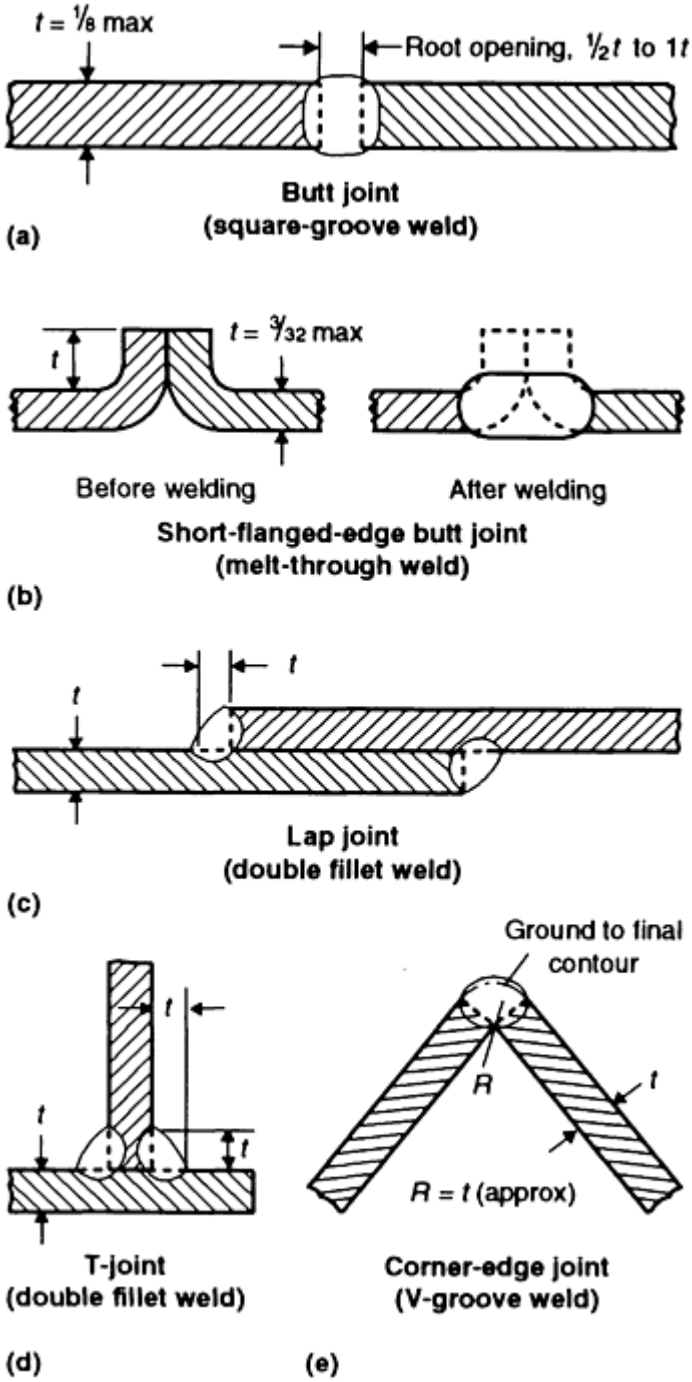

FIG. 10 TYPES OF JOINTS AND RESULTING SINGLE-PASS WELDS OBTAINED WITH OXYFUEL GAS WELDING OF THIN SHEET MATERIAL. MEASUREMENTS IN INCHES

Square-groove butt joints (Fig. 10a) can be single-pass welded from one side in sheet up to approximately 3.2 mm ($\frac{1}{8}$ in.) thick. Complete-penetration welds, properly made, develop the same or greater strength in low-carbon steel as the members joined.

Short-Flanged-Edge Butt Joints. For making butt joints in sheet up to about 2.4 mm ($\frac{3}{32}$ in.) thick, a short flanged edge (Fig. 10b) is beneficial. The weld is called a melt-through weld, because the flanges are melted down to form the butt joint. Filler metal is not required. The oscillating technique for melting down the flanges is shown in Fig. 11. The flanges keep the sheet in flat alignment.

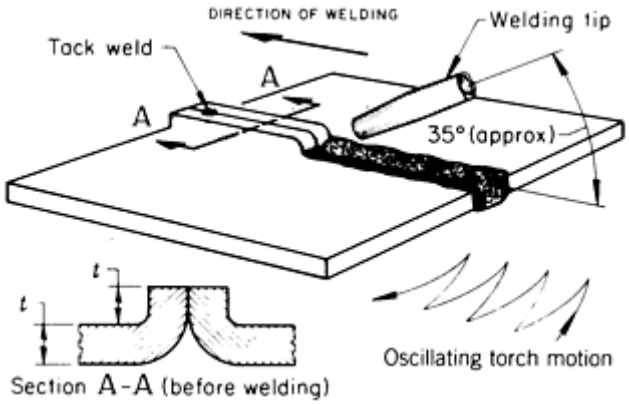

FIG. 11 OXYFUEL GAS WELDING PRACTICE USED TO PRODUCE A SHORT-FLANGED-EDGE BUTT JOINT IN THIN SHEET MATERIAL ($\leq$ 2.4 MM, OR $\frac{3}{32}$ IN., THICK)

Although the sheet has to undergo a special flanging operation, this joint is practical for long production runs when filler-metal deposition and melt-through are difficult to control. High welding speeds can be attained. Sheet thicknesses are limited to approximately 0.8 mm ($\frac{1}{32}$ in.) because short flanges are difficult to bend in heavier material. In other flanged-edge joints, the weld is deposited on the edges, and the flanges retain their structural identity.

Without support from adjacent sheet, long sections of thin material cannot be welded without buckling and distortion. The amount of distortion resulting from expansion during welding and contraction during cooling of the welded sheet-metal section or structure is proportional to the amount of heat applied to the metal as well as to its inherent stiffness and rigidity. Jigs and fixtures are essential to counteract the adverse effects of welding heat. Figure 12(a) shows the elements of a jig used for making butt or flange welds in thin sheet.

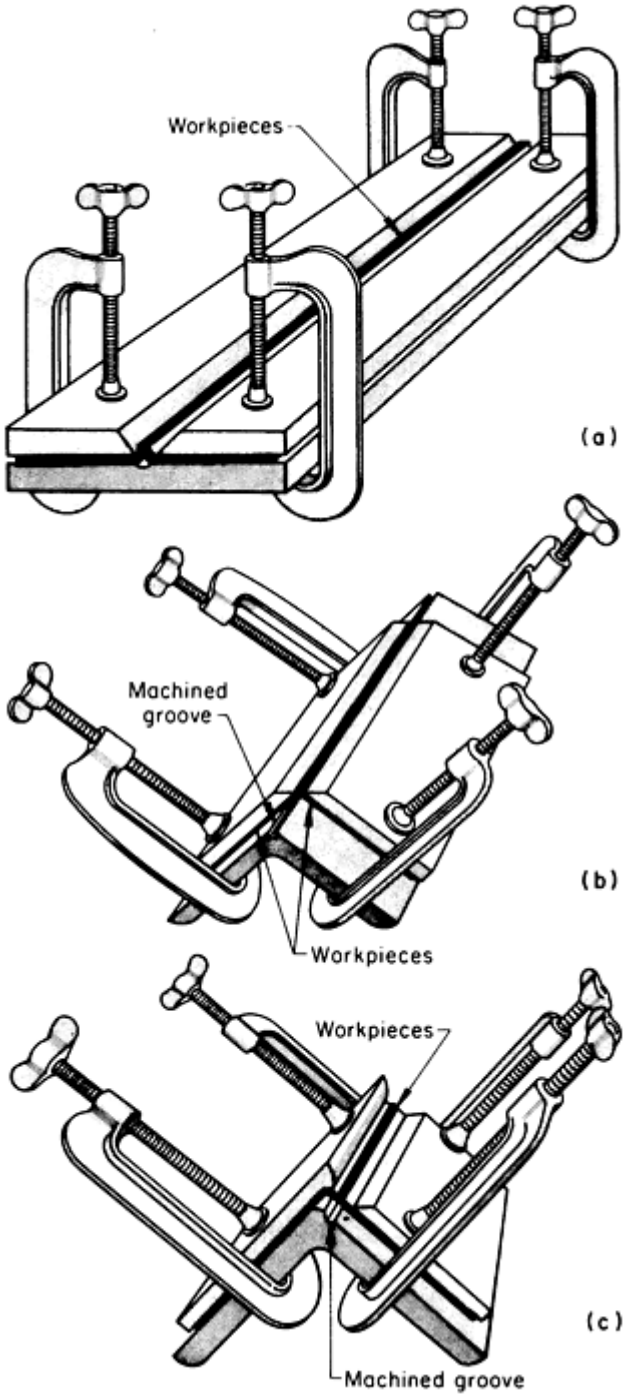

FIG. 12 APPLICATION OF JIGS TO MAINTAIN FLATNESS AND TO MINIMIZE DISTORTION WHEN WELDING THIN SHEET MATERIAL

Lap and T-joints, shown in Fig. 10(c) and 10(d), are single or double fillet welded, depending on strength requirements. A single fillet weld should not be used if the joint is likely to open under service loads. The amount of overlap in lap joints varies with design requirements and sheet thickness. For double-welded lap joints, a minimum overlap of approximately 25 mm (1 in.) is usually adequate for sheet.

The size of fillet weld, with size defined as the length of the shortest side of the fillet, is generally equal to the thickness of the sheet, because this size weld is easily produced in a single pass and has a good appearance.

Both lap and T-joints are somewhat more difficult to weld in thin sections than in thick sections. Danger of melt-through exists when a welder attempts to penetrate to the root of the joint.

Corner-edge joints (Fig. 10e) are used in thin material, mainly because of their simplicity and low cost. In addition, skillful OFW can produce a weld of good external appearance in a single pass.

To improve internal appearance and to provide added strength, an internal pass or removable ceramic backing is needed. Square comer joints in thin material can be made with good appearance and strength and with little or no distortion by using a jig as shown in Fig. 12(b). A recess is machined or ground in the corner of the backing plate to provide for root reinforcement of the V-groove weld.

When parts with rounded corner joints are designed in thin sheet, corners should be bent rather than joined. Joints next to corners can be made by butt welding in a jig constructed as shown in Fig. 12(c). Note the use of a recess in the backing member to provide for root reinforcement of the weld.

Plate. Butt, lap, T-, and corner joints are oxyfuel gas welded in steel plate up to 4.8 mm ($\frac{3}{16}$ in.) thick.

Butt joints welded from one side only require beveled edges in thicknesses 3.2 mm ($\frac{1}{8}$ in.) and over.

Fillet Welds. When compared to groove welds, fillet welds have advantages and limitations. No edge preparation such as chamfering or beveling of joint edges is required. If the weld serves mainly to hold structural members together, or if forces transmitted by the weld are low, fillet welds can be relatively small and economical.

Groove welds are used in butt joints and can be used in lap, T-, and corner joints as an alternative to fillet welds. In low-carbon steel, properly made complete-penetration groove welds develop strength equal to the strength of the members joined.

Typical grooves used for OFW of butt, T-, and corner joints in steel plate with thicknesses of 4.8 mm ($\frac{3}{16}$ in.) or less are shown in Fig. 13. Grooves for OFW are the same as those for arc welding, except that the root opening is larger.

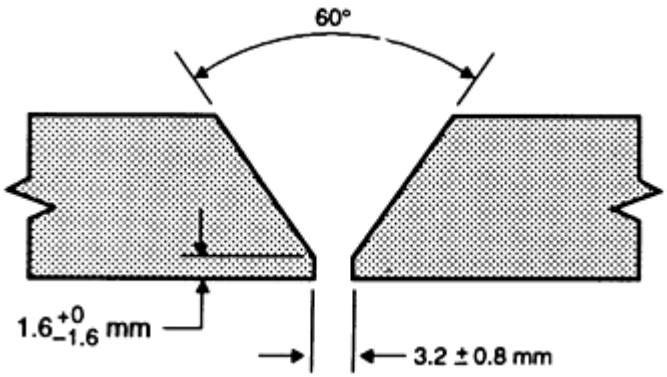

FIG. 13 USE OF GROOVES TO FACILITATE OXYFUEL GAS WELDING OF ≤ 4.8 MM (≤ $\frac{3}{16}$ IN.) THICK PLATES

Pipe. All OFW of low-carbon steel pipe is done with the oxyacetylene process. The techniques used are the one-pass forehand technique, the one-pass backhand technique, or the two-pass technique using a backhand first pass with a forehand second pass. Most production oxyacetylene welding (OAW) in the horizontal fixed (5G) or rolled position (1G) is done using the two-pass technique. When the pipe is fixed in the vertical position (2G), most welders use the one-pass

backhand technique. Oxyacetylene welding is cost effective for pipe with diameters of 150 mm (6 in.) and less and with wall thicknesses of 4.8 mm ($\frac{3}{16}$ in.) or less.

Most OAW of low-carbon steel pipe is done using a neutral flame and a work angle of 0°. The travel angles for the torch and welding rod vary with position (Ref 3).

Full-Penetration Welds. If a full penetration weld is desired, a keyhole must be maintained at all times. The torch and rod movements are shown in Fig. 8 for the one-pass forehand method and in Fig. 9 for the one-pass backhand method.

Tack welds should be small and have the general appearance shown in Fig. 14. Both ends of the tack should have a keyhole. The start end of the tack is reheated to form the start keyhole in order to obtain completed fusion when the first pass is connected with the tack weld.

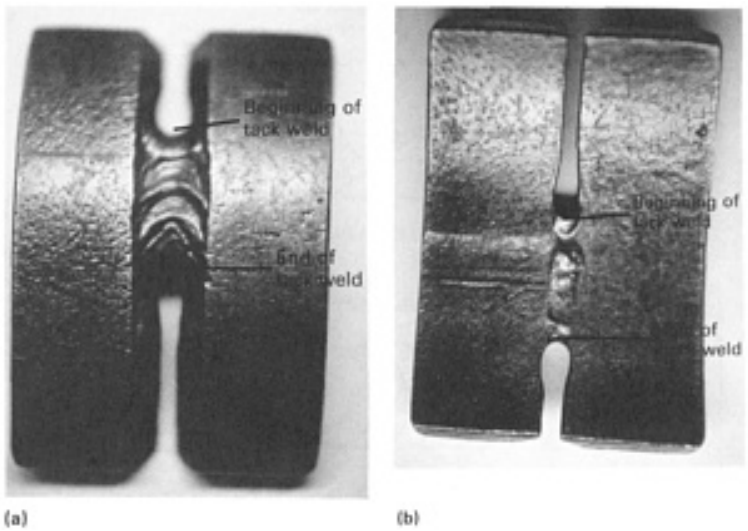

FIG. 14 TACK WELD IN API 5L STEEL PIPE. PIPE DIAMETER, 150 MM (6 IN.) WALL THICKNESS, 7 MM (0.28 IN.). (A) OUTSIDE DIAMETER VIEW. (B) INSIDE DIAMETER VIEW

The 1G, 2G, and 5G positions for welding pipe are shown in Fig. 15.

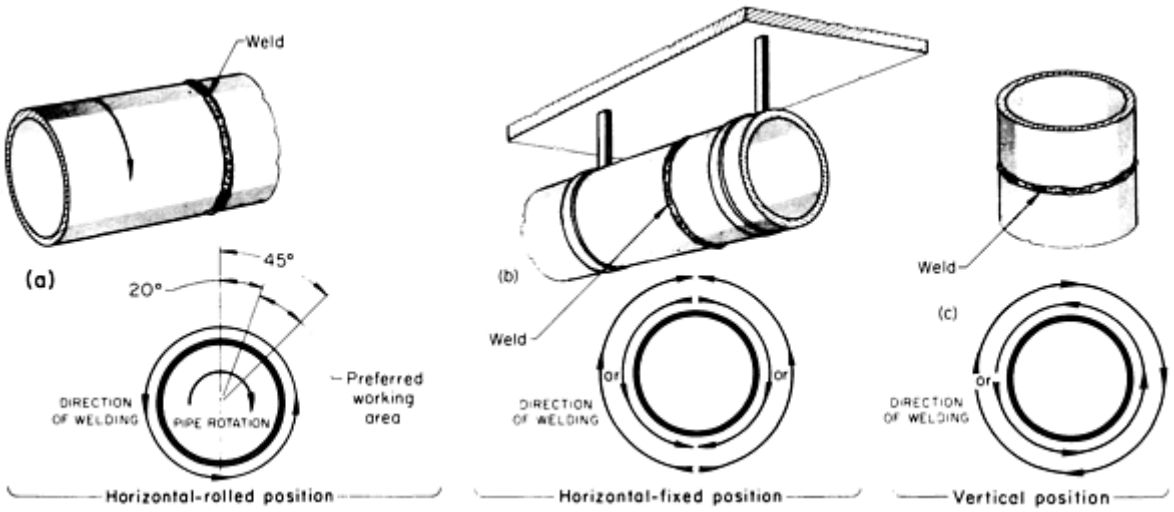

FIG. 15 TYPICAL WELDING POSITIONS FOR OXYFUEL GAS WELDING OF PIPE

Applications. The oxyacetylene process can be used to join low-carbon steel pipe having a maximum diameter of 150 mm (6 in.) and a maximum wall thickness of 4.8 mm ($\frac{3}{16}$ in.). Because of the slow travel speed and close adjustment of welding heat that characterize OAW, small-diameter steel pipe can be oxyacetylene welded faster and with better quality than can be obtained by using most other welding processes.

One of the reasons that the oxyacetylene process is seldom used today is that it is becoming a lost art. There are very few welders that are knowledgeable in the techniques used to oxyacetylene weld steel pipe. Good sources of information on oxyacetylene welding practices are manufacturers of oxyacetylene torch equipment, the American Welding Society, and welding textbooks.

Thin Sheet. Techniques used in OFW of thin sheet depend on joint design and welding position, as well as on the style used by the welder. Although forehand and backhand techniques can be used for OFW of thin sheet, forehand welding is often preferred because the flame points away from the completed weld. This results in less heat buildup and less risk of distortion and melt-through. Proponents of the forehand technique also believe that thin sections can be forehand welded faster using flat or horizontal positions because the flame forces the weld metal to flow in the direction of welding. Figure 11 shows forehand welding of a short-flanged-edge butt joint.

Assemblies of steel sheet less than 3.2 mm ($\frac{1}{8}$ in.) thick are often made by OFW. Because of the relatively long welding time involved, OFW does not permit critical control over total heat input, and distortion can occur when long, continuous welds are made in large, flat thin sheets. For this reason, OFW of thin sections should be done on small parts, where welds can be short, or on sections that have been strengthened by forming. Welding fixtures are often used to prevent distortion and to maintain alignment of joint edges.

The problems arising from difficulties in heat control in joining thin sections by OFW are sometimes solved by using other metal-joining processes:

- SHORT CIRCUITING GAS METAL ARC WELDING
- PULSED ARC WELDING
- GAS TUNGSTEN ARC WELDING
- PLASMA ARC WELDING
- ELECTRON-BEAM WELDING
- ULTRASONIC WELDING
- RESISTANCE WELDING
- BRAZING
- BRAZE WELDING

Products made by OFW of thin sheet use materials ranging in thickness from 0.607 mm (0.0239 in., or 24 gage) to 3.038 mm (0.1196 in., or 11 gage). Typical items include truck bodies, furniture, office equipment, utensils, enclosures, and refrigeration equipment.

Reference cited in this section

3. "SAFETY IN WELDING AND CUTTING," ANSI/AWS ZA9.1, AMERICAN WELDING SOCIETY, 1983

Revised by William Ballis, Columbia Gas of Ohio

Repairs and Alterations

Oxyfuel gas welding is frequently used for repairs and alterations because the equipment is portable, welding can be done in all positions, and acetylene and oxygen are readily available. Also, gas cutting, braze welding, brazing, or flame heating is often needed, and the same personnel, equipment, and gases required for these operations can be used for OFW.

Repair Welding. Edge preparation for repair welding generally involves cutting a V-groove to expose clean metal down to the root of the joint. The groove must be large enough to allow room for manipulation of the torch and welding rod.

On many repair welding jobs, sections that must be rebuilt to specific contours or dimensions require backing to support the weld metal. Carbon paste, which can be molded, or carbon plate, which can be easily machined, can be used for backing (Fig. 16). To avoid carbon pickup, copper or a thick steel plate can be used. Welding of the backing to the part should be prevented.

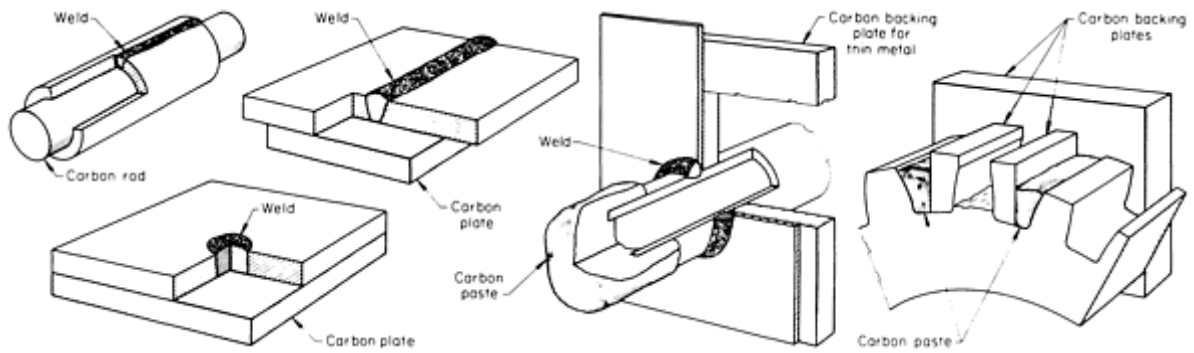

FIG. 16 USE OF CARBON BACKING TO PROVIDE SUPPORT WHEN REPAIR WELDING SURFACES AND CONTOURS

In weld repairing of parts that have cracked, the crack should be fully dressed out. Metal can be removed by chipping, grinding, machining, arc air gouging, or oxyfuel gouging. For OFW, oxyfuel gouging is convenient, because a cutting torch is generally available and only a special gouging tip is needed.

When using oxyfuel gouging for dressing cracks, the crack remains visible until it is completely removed. Grinding may result in a fine crack being smeared over, and chipping is also likely to cover the crack. The disadvantage in using oxyfuel gouging is that the heat input may cause the crack to propagate through differential expansion in the workpiece. The risk is especially great if some of the stresses that caused the crack are still present. Drilling a 6.4 to 13 mm ($\frac{1}{4}$ to $\frac{1}{2}$ in.) hole at the end of the crack may prevent the crack from propagating. Cleanliness of the joint is also a prerequisite for OFW. Rust, scale, dirt, grease, oil, paint, and slag must be removed from the joint areas. The soundness of the weld metal depends in large part on the care used in cleaning. To ensure complete crack removal, liquid-penetrant or magnetic-particle testing can be used.

Workpiece Alterations. When OFW is used to correct production parts that would be rejected because of a small error or defect in manufacture, it must be determined if the salvaged part, after welding, is as good as a new part for the required service. Some fabricating codes identify the defects that may be rectified by welding and define the standards for repair. Rectification may include correction of defects, building up of undersize parts, and filling in of drilled holes.

Preheating and Postheating

Preweld and postweld heat treatments are not usually required to reduce the hardness of low-carbon steel, but either or both treatments are beneficial and can be effective in avoiding or reducing distortion. Most steels that are oxyacetylene gas welded fall within the low-carbon range.

Oxyacetylene gas welding distributes a large amount of heat over a wide area. This results in relatively slow cooling rates and relatively low stress gradients, which, in turn, reduce the degree of hardening and the magnitude of residual stresses that are usually associated with welding heat cycles.

Example 1. Use of Oxyacetylene Welding to Eliminate Postweld Tempering. Aircraft landing gear side stay assemblies made of 1330 steel (Fig. 17) were joined in the form of a trapezoid. The assembly was originally welded by the shielded metal arc welding process; E7016 electrodes were used. Several assemblies cracked in a tube adjacent to a weld after a short time in service. Examination revealed high hardness (50 HRC) in the heat-affected zone (HAZ) was caused by the chilling effect of the large mass of metal in the end fittings. A postweld tempering treatment at 650 °C (1200 °F) to reduce the high hardness could not be used because the tubes became distorted.

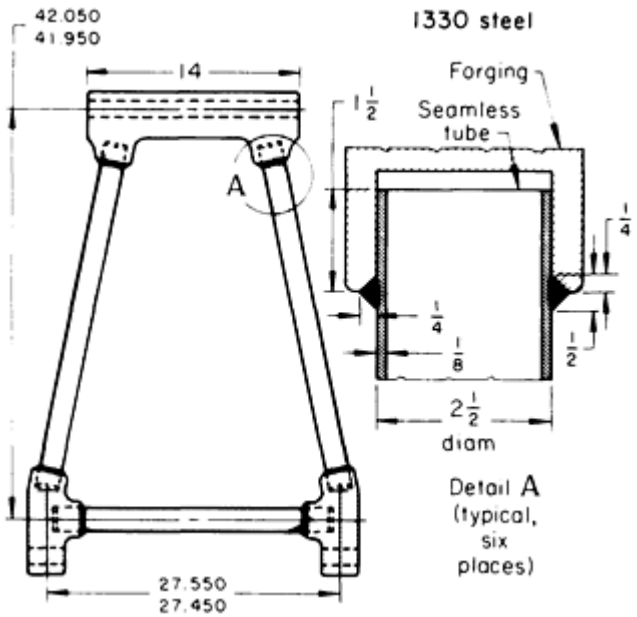

FIG. 17 OXYACETYLENE WELDING OF AIRCRAFT LANDING GEAR SUPPORT. USE OF OAW REDUCED HAZ HARDNESS AND ELIMINATED NEED FOR POSTWELD TEMPERING. MEASUREMENTS SHOWN IN SCHEMATIC ARE IN INCHES.

Local stress relief of the welded joint with a gas torch was successful but laborious, and it was finally decided to oxyacetylene gas weld the assembly. Hardness tests in the area of the welded joint showed that the maximum hardness in the HAZ was 285 HB (29 HRC). This was only moderately higher than the hardness of the end fittings and tubes, which had a hardness of 223 HB (98 HRB). The improvement was believed to result from the wider area heated during OAW, which produced a lower temperature gradient.

Bridging Gaps in Poor Fit-Ups

The ability to control the flow of molten weld metal in OFW provides a high degree of versatility in bridging large gaps caused by a poor fitup. By manipulating the gas torch, weld-metal temperature can be held to the minimum, and the pressure of the gas flame can be used to help support the weld pool in any position, including overhead.

Oxyfuel Gas Welding

Revised by William Ballis, Columbia Gas of Ohio

Safety

The gases used in OFW can form explosive mixtures if improperly handled, and burning of these gases must be controlled within recommended limits for the safety of the welder and surrounding property. Workers must be familiar with safe welding practices and should be aware that any deviation from recognized safety standards can result in damage to apparatus or in personal injury. Workers in charge of welding operations should be instructed and judged competent by their employers.

Rules and instructions covering safety, operation, and maintenance procedures are readily available. Federal, state, and local governments, in addition to equipment manufacturers, gas suppliers, and regulatory agencies, have cooperated in publishing documents on safe welding practices.

Additional safety guidelines and reference sources for further information are provided in the article "Safe Practices" in this Volume.

Oxyfuel Gas Welding

Revised by William Ballis, Columbia Gas of Ohio

References

1. H.B. CARY, *MODERN WELDING TECHNOLOGY*, PRENTICE-HALL, 1989, P 211
2. "OXYGEN-FUEL GAS SYSTEMS FOR WELDING AND CUTTING," BULLETIN NO. 51, NATIONAL

FIRE PROTECTION ASSOCIATION, 1977
3. "SAFETY IN WELDING AND CUTTING," ANSI/AWS ZA9.1, AMERICAN WELDING SOCIETY, 1983
4. H.B. CARY, *MODERN WELDING TECHNOLOGY*, PRENTICE-HALL, 1989, P 210
5. "RECOMMENDED PRACTICES AND PROCEDURES FOR WELDING LOW CARBON STEEL PIPE," ANSI/AWS D10.12, AMERICAN WELDING SOCIETY, 1989

Thermite Welding

Bernard Schwartz, Norfolk Southern Railway Company

Introduction

THERMITE WELDING (TW) is a fusion welding process in which two metals become bonded after being heated by superheated metal that has experienced an aluminothermic reaction. The liquid metal that results from the reaction between a metal oxide and aluminum acts as the filler metal. This exothermic process was discovered in 1898, in Germany, by Dr. Hans Goldschmidt of Goldschmidt AG.

In the United States, this process was used in the early 1920s to join trolley car track. In 1933, thermite welding was used on the Delaware and Hudson Railroad at Albany, NY to produce long rail sections. In 1938, a researcher at the Electric Railway Improvement Company invented a copper-base aluminothermic process for welding copper conductors to steel rails. Currently, thermite welding is widely used in the field welding of track, where its portability and versatility are strong assets.

It should be noted that the standard term for this process is often listed as "thermit" welding. However, Thermit is a registered trademark of Th. Goldschmidt AG of Essen, Germany. Therefore, this Volume uses the generic term, "thermite."

Thermite Welding

Bernard Schwartz, Norfolk Southern Railway Company

Thermite Welding Principles

The aluminothermic reaction that occurs in thermite welding follows the general formula:

$$\textit{metal}\ \text{oxide} + \underset{\text{(reducing agent)}}{\text{Aluminum}} \rightarrow \underset{\text{oxide+metal+heat}}{\text{Aluminum}}$$

whereas the typical reaction that occurs in the thermite welding of rails is:

$$FE_2O_3 + 2AL \rightarrow 2FE + AL_2O_3\ (HEAT \rightarrow 850\ KJ)$$

and the typical reaction that occurs in the welding of copper conductors to steel rails is:

$$3CU_2O + 2AL \rightarrow 6CU + AL_2O_3\ (HEAT \rightarrow 1060\ KJ)$$

This exothermic reaction is extremely violent if only the metal oxide and aluminum reducing agent are used. Pellets of ferroalloy are added to cool this reaction from a typical temperature of 3090 °C (5600 °F) to 2480 °C (4500 °F). These additions also are used to produce the desired chemistry. The amount of added alloy is very critical, because larger

amounts will cool the reaction to temperatures below 2040 °C (3700 °F), at which point the slag/metal separation could be incomplete.

Thermite Welding Metallurgy

Metallurgical structures that are present in thermite welds depend on the chemical composition of the weld metal and on the cooling rate of the joint after pouring is completed.

Figure 1 shows a typical macrostructure of a carbon steel rail thermite weld and the microstructure of the fusion zone, the fusion line, the end of the heat-affected zone (HAZ), and the unaffected rail. Typically, the weld is 100% pearlite with varying degrees of coarseness. This is due to the slow cooling rate that completes transformation before reaching the martensite start temperature and the formation of untempered martensite.

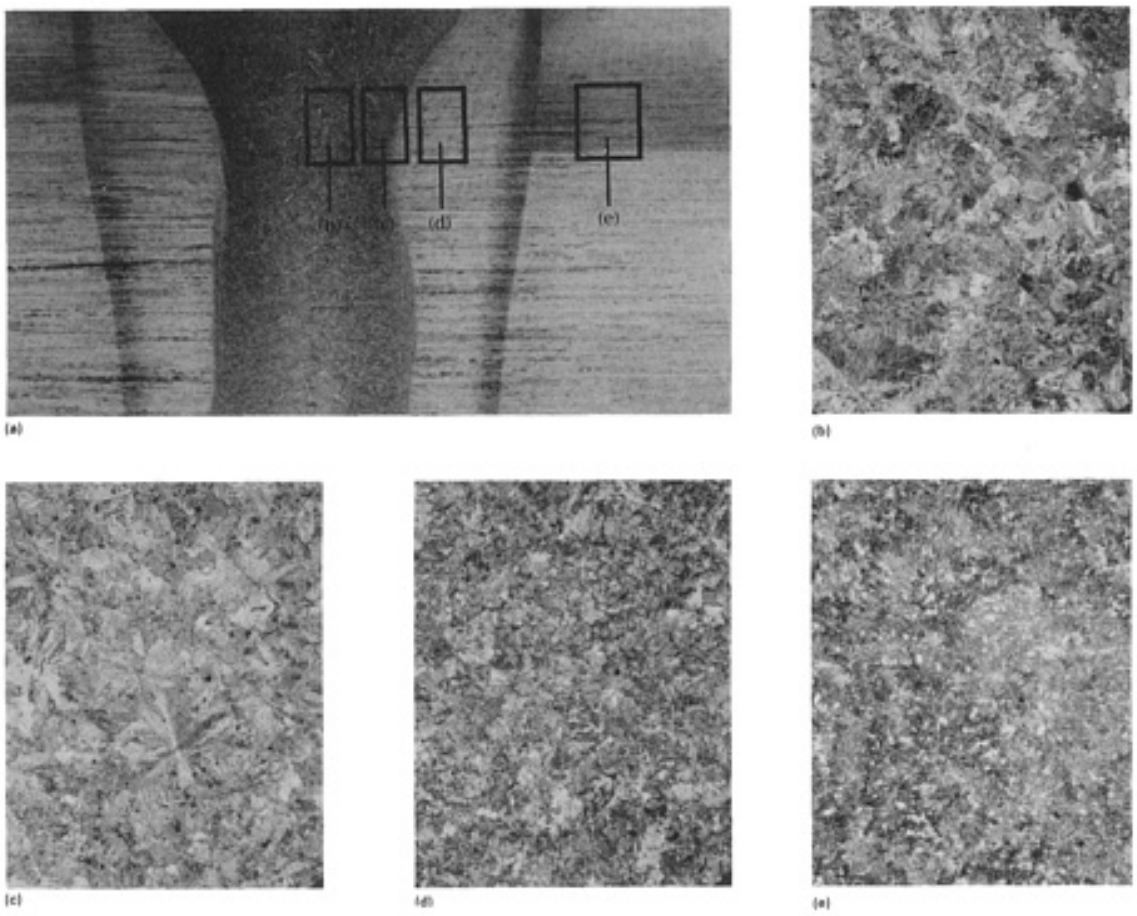

FIG. 1 CARBON STEEL RAIL THERMITE WELD. (A) MACROSTRUCTURE. (B) WELD MATERIAL. 65×. (C) FUSION LINE AREA. 65×. (D) HEAT-AFFECTED ZONE. 65×. (E) UNAFFECTED RAIL AREA. 65×

Thermite Welding

Bernard Schwartz, Norfolk Southern Railway Company

Applications for Thermite Welding

Rail welding is the most widely used application of the thermite welding process. The use of that process, as well as the electric flash butt welding process, has eliminated joint bars (mechanical fasteners) and greatly lessened track maintenance. Long sections of continuous welded rail (CWR) (typically, 440 m, or 1440 ft) that are welded by the flash butt welding process are transported to the track site and set into place. Then, the CWR sections are joined by thermite welding. A short preheating process is typically used in the thermite welding of rail.

The thermite process is also utilized to replace rail defects, to weld insulated joint assemblies into track, and to make electrical bonding connections using copper conductors between rails that will not be welded together.

Process Description. The thermite welding of rails, including a short preheat, involves the following basic operations:

- CUT OR SPACE THE RAILS TO BE WELDED SO THAT THE GAP SPECIFIED BY THE MANUFACTURER IS ACHIEVED
- REMOVE SLAG, MOISTURE, FOREIGN MATTER, AND SUCH FROM THE AREA TO BE WELDED
- ALIGN THE RAIL ENDS, BOTH VERTICALLY AND HORIZONTALLY
- CENTER THE THERMITE MOLDS OVER THE RAIL GAP AND SEAL THE GAPS WITH LUTING MATERIAL
- SITUATE THE PREHEATING EQUIPMENT, MOLD CLAMPS, AND THERMITE CRUCIBLE IN POSITION ABOVE THE JOINT GAP AND THE MOLD OPENING (FIG. 2)
- ADJUST THE PREHEATING EQUIPMENT TO ACHIEVE THE MOST UNIFORM HEATING OF THE RAIL ENDS FROM ONE SIDE TO THE OTHER AND FROM TOP TO BOTTOM
- IGNITE THE THERMITE CHARGE AND ALLOW IT TO TAP INTO THE MOLD, THE TIMING OF WHICH IS USUALLY CONTROLLED BY A SELF-TAPPING THIMBLE. THE LIQUID METAL FLOWS ONTO A DIVERTER PLUG TO REDIRECT THE FLOW OF LIQUID METAL INTO THE SIDE SPRUES SO THAT THE CASTING IS PRODUCED FROM THE BOTTOM UPWARD
- ALLOW THE PROPER SOLIDIFICATION TIME, AS RECOMMENDED BY THE MANUFACTURER
- REMOVE THE MOLD MATERIAL AND FINISH-GRIND THE WELD TO RAILROAD SPECIFICATIONS
- CONDUCT A FINAL INSPECTION OF THE WELD, BOTH VISUALLY AND WITH THE AID OF ULTRASONIC EQUIPMENT

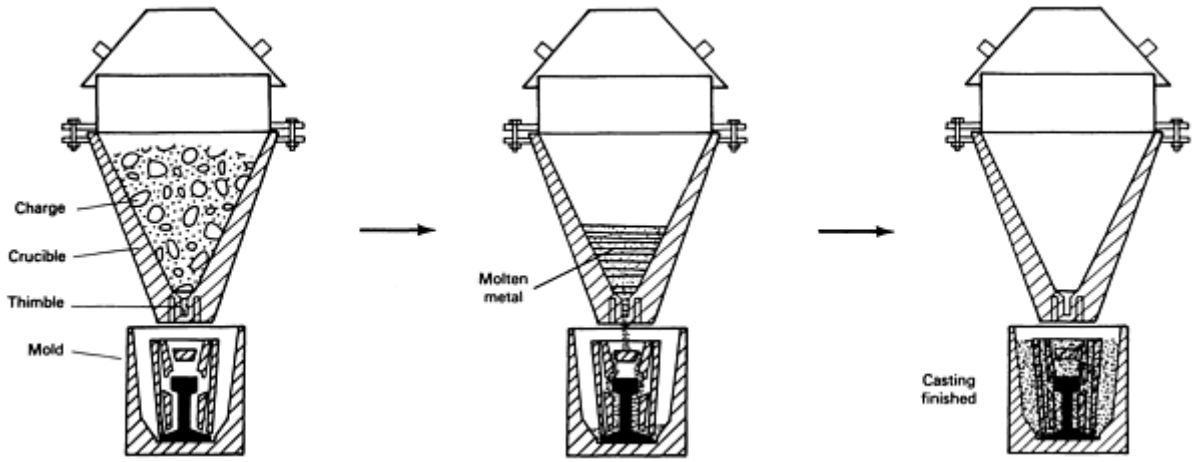

FIG. 2 TYPICAL CRUCIBLE-MOLD SETUP FOR RAIL THERMITE WELDING

Electrical Connections. The thermite welding process also is used to weld electrical conducting joints, particularly to provide electrical continuity for railroad signal systems. A copper oxide powder is reduced by aluminum to form a

metallurgical bond between the steel rail and the copper conductor. The resulting joint has an excellent current-carrying capacity and the ability to withstand corrosion, when compared with a mechanical bond.

Repair Welding. Large-diameter rolls, shafts, ingot molds, and heavy mill housings can be successfully repaired by using the thermite welding process. The metallurgical aspects of the process, when used to make repair welds, are similar to those of rail welding, except for the large volume of the weld. The primary difference is that a customized mold, which is usually manufactured on-site, is used. A wax pattern is built around the weld cavity, and a collar is shaped in wax to overlap the base metal. Sand is hand rammed around the pattern within a mold box. Then, sufficient gates and risers are incorporated into the system.

New Railroad Applications. Recent developments include:

- HIGHER-STRENGTH THERMITE MIXTURES THAT MORE CLOSELY MATCH THE HARDNESS OF CURRENT HIGH-STRENGTH RAILS (RAIL HARDNESS HAS STEADILY INCREASED TO 300 HB, MINIMUM, FOR STANDARD CARBON RAILS AND TO 360 HB, MINIMUM, FOR PREMIUM RAILS)
- ONE-USE CRUCIBLES THAT REDUCE OR ELIMINATE WELD-METAL CONTAMINATION BY THE RESIDUAL ELEMENTS AND IMPURITIES THAT REMAIN IN CONVENTIONAL REUSABLE CRUCIBLES
- POSTWELD HEAT TREATMENT THAT REFINES THE GRAINS IN OLDER WELDS AND IMPROVES THE STRUCTURAL PROPERTIES OF THE THERMITE WELD TO THE LEVEL OF THOSE OF ELECTRIC FLASH BUTT WELDS
- A HEAD WASH REPAIR WELD THAT CAN REPAIR DISCONTINUITIES ON THE RUNNING SURFACE OF THE RAIL HEAD. (IN THE HEAD WASH REPAIR, RAIL SURFACE DEFECTS OR DISCONTINUITIES ARE TORCH WASHED AWAY DOWN TO THE SOUND METAL. THIS OCCURS OVER A VERY SHORT TIME SPAN. THE TORCH WASH AREA IS CLEARED, A THERMITE MOLD IS APPLIED, AND THE AREA IS PREHEATED AND THEN THERMITE WELDED TO PRODUCE A COMPLETE RAIL HEAD OF SOUND METAL.)
- WIDE-GAP REPAIR WELDS (50 AND 75 MM, OR 2 AND 3 IN.) THAT CAN BE UTILIZED TO WELD WIDER GAPS AND TO ELIMINATE SPECIFIC RAIL DEFECTS, WITHOUT REQUIRING THE INSTALLATION OF A PLUG RAIL
- NEW MOLD CONFIGURATIONS (REPOSITIONED RISERS, METAL GUSSETS, AND SO ON) THAT MAY INCREASE THE MECHANICAL PROPERTIES OF RAIL THERMITE WELDS
- A ZIRCON-BASE MOLD WASH COATING FOR THERMITE WELD MOLDS THAT IMPROVES THE SURFACE CONDITION OF RAIL THERMITE WELDS, THEREBY IMPROVING FATIGUE LIFE

Thermite Welding

Bernard Schwartz, Norfolk Southern Railway Company

Thermite Welding Safety

As already noted, the thermite welding process produces a violent reaction and a large release of heat. The presence of moisture in the charge, crucible, molds, or tooling should be avoided in order to prevent the rapid release of steam and the resulting ejection of molten metal from the crucible. The thermite charge and molds must be stored in a dry location. Tooling should be preheated prior to use, and the surrounding work area should be dry and free of combustible materials.

Appropriate protective clothing, safety boots, gloves, safety glasses, or a full face shield with filter lenses should be worn by all personnel in the immediate vicinity.

Thermite Welding

Bernard Schwartz, Norfolk Southern Railway Company

Selected References

- *METALS HANDBOOK,* 9TH ED., VOL 6, *WELDING, BRAZING, AND SOLDERING,* AMERICAN SOCIETY FOR METALS, 1983, P 692-704
- RAIL, CHAPTER 4, *AREA MANUAL,* AMERICAN RAILWAY ENGINEERING ASSOCIATION, 1980, P 4-2-6.7 TO 4-2-7
- *WELDING HANDBOOK,* 8TH ED., VOL 2, *WELDING PROCESSES,* AMERICAN WELDING SOCIETY, 1991, P 892-900

High-Temperature Solid-State Welding

W. Lehrheuer, Forschungszentrum Jülich GmbH

Introduction

HIGH-TEMPERATURE SOLID-STATE WELDING is used to join members of similar or dissimilar materials by compressing and heating the surfaces to be joined in a suitable atmosphere and by maintaining pressure and temperature until the parts are joined.

The processes that occur on the surfaces to be joined can be categorized by three stages.

Primary Bonding. In this first stage, the surface layers of the pieces being welded are prepared to accept the initial bond. The deformation of rough points will crack brittle surface layers and, thus, will achieve limited local bonding of metallic surfaces, leading to reactions between the atoms of the pieces being welded.

Bond-Surface Extension. In this second stage, the bond surface is enlarged by virtue of plastic flow processes, which are determined by surface loading, and the mechanical properties of the pieces being welded. An expansion of the weld surface area occurs because of diffusion along the surfaces being bonded. The metallic bond becomes improved as a result of the removal of surface films and impurities by dissolution and diffusion into the base material. The diffusion process actually reorients surface atoms, thereby providing a configuration that is more suitable for bonding. Finally, the reaction processes that occur between the atoms (and their electrons) of the enlarged bond surfaces of the pieces being welded result in good adhesion between the components.

Elimination of the Original Joining Surface. In this third stage, the joined zone experiences recrystallization, grain growth, and diffusion that are beyond the characteristics of the original weld interface. The formation of a largely homogeneous weld with normal metallic cohesion is achieved by reactions that occur between the materials being joined.

Because diffusion processes have a significant role in this type of welding, the operation is frequently called "diffusion welding" or "diffusion bonding."

High-Temperature Solid-State Welding

W. Lehrheuer, Forschungszentrum Jülich GmbH

Process Advantages and Disadvantages

The major advantages of the process are that:

- IT ALLOWS THE PREPARATION OF STRESS-RELIEVED AND, IN MANY CASES, PRIMARILY HOMOGENEOUS 0JOINTS ON VERY DIFFERENT MATERIALS.
- IT ALLOWS THE WELDING OF MATERIAL COMBINATIONS THAT CANNOT BE JOINED BY FUSION WELDING. THIS APPLIES TO MATERIALS THAT FORM BRITTLE INTERMETALLIC PHASES AND TO METALS THAT ARE JOINED TO NONMETALS.
- IT ENABLES THE JOINING OF COMPONENTS WITH VERY DIFFERENT JOINING SURFACE GEOMETRIES THAT ARE NOT SUBJECT TO ANY PARTICULAR REQUIREMENTS. HOWEVER, THE PRESSURE APPLICATION METHOD CAN BE A LIMITING FACTOR. MATERIALS ARE JOINED IN THE SOLID STATE. METALLURGICAL CONDITIONS ARE GENERALLY FAVORABLE AND EASY TO INFLUENCE, BECAUSE THERE IS LESS SHRINKAGE AND FEWER STRESSES.
- COMPONENT DEFORMATION IS KEPT WITHIN RELATIVELY CLOSE LIMITS, THEREBY OMITTING THE NEED FOR REWORKING, IN MANY CASES.
- THE PROCESS MAY BE ALMOST FULLY AUTOMATED. THEREFORE, HIGHLY QUALIFIED TECHNICIANS ARE NOT REQUIRED FOR PRODUCTION TASKS.

The disadvantages of the process are:

- HIGH EQUIPMENT COST
- HIGH DEMANDS IN TERMS OF SURFACE CLEANLINESS AND PRECISION, AS WELL AS WELDING ATMOSPHERE
- CONSIDERABLE TIME REQUIREMENTS FOR EXECUTING THE JOINT, EXCEEDING BY FAR THE REQUIREMENTS OF MOST OTHER PROCESSES
- INCREASED CAPITAL COSTS WITH INCREASING COMPONENT SIZE, BECAUSE A WELDING CHAMBER BECOMES NECESSARY
- VERIFICATION OF PROPER JOINT EXECUTION BY NON-DESTRUCTIVE TESTING IS SIGNIFICANTLY IMPAIRED, IN MANY CASES

Although these disadvantages and process features prevent large-scale technical applications that replace welding, the possibilities for using this process to solve special problems are impressive.

High-Temperature Solid-State Welding

W. Lehrheuer, Forschungszentrum Jülich GmbH

Equipment

Mass production is not possible when this process is used. The type of equipment, process temperatures, atmospheres, materials, component sizes, and numbers of workpieces can differ in each application and can result in entirely different systems and devices. The process is frequently conducted in facilities designed for other purposes, such as hot presses, hot isostatic pressing facilities, and vacuum or inert-atmosphere furnaces (with dead-weight loading). The configuration shown in Fig. 1 represents a typical equipment design.

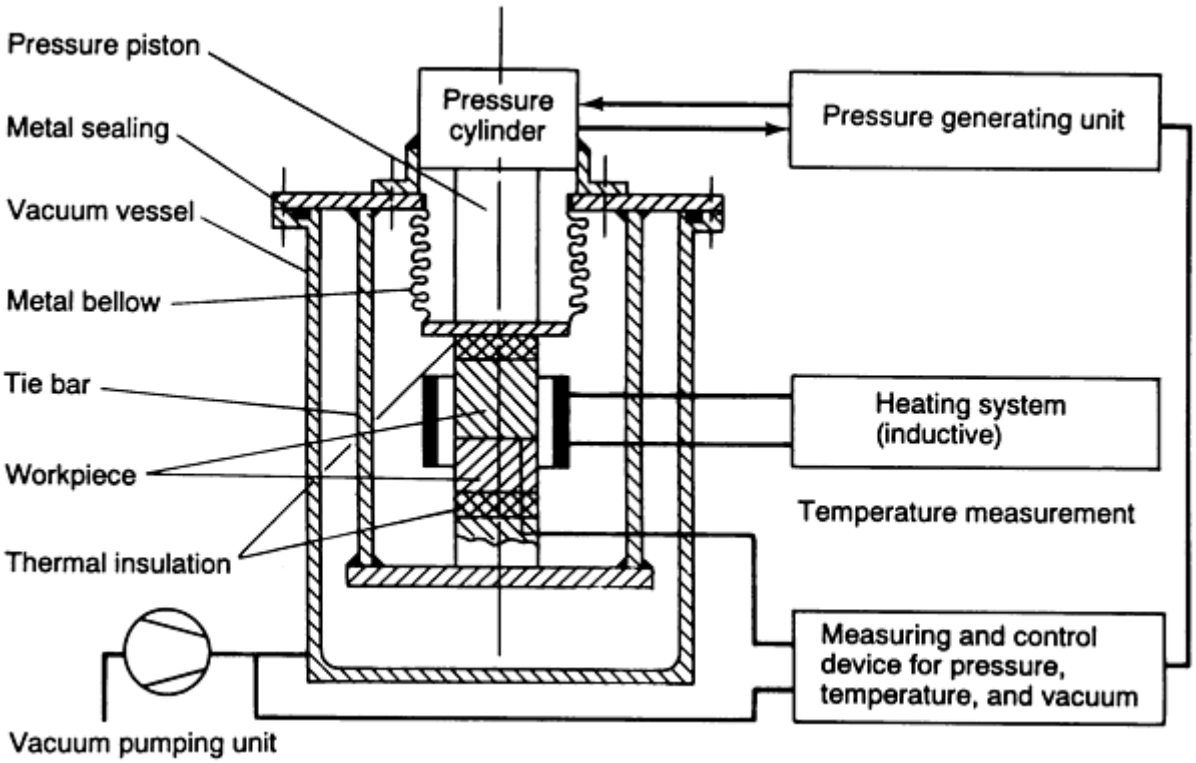

FIG. 1 PRINCIPLE OF OPERATION OF TYPICAL HIGH-TEMPERATURE SOLID-STATE WELDING EQUIPMENT

High-Temperature Solid-State Welding

W. Lehrheuer, Forschungszentrum Jülich GmbH

Procedures for High-Temperature Solid-State Welding

The procedures used to make this type of weld can be described in simple terms. Clean surfaces are pressed together in an atmosphere that is suited for the materials being joined and then heated to welding temperatures. The temperature is maintained until welding is completed. The component is then cooled.

The most important process parameters are temperature, pressure, welding time, and welding atmosphere. Figure 2 shows the dependence of the strength of a diffusion weld on temperature, pressure, and time. It should be noted that these three parameters are not independent of one another. Within certain limits, higher temperature can shorten the time required for welding and reduce the pressure, and vice versa.

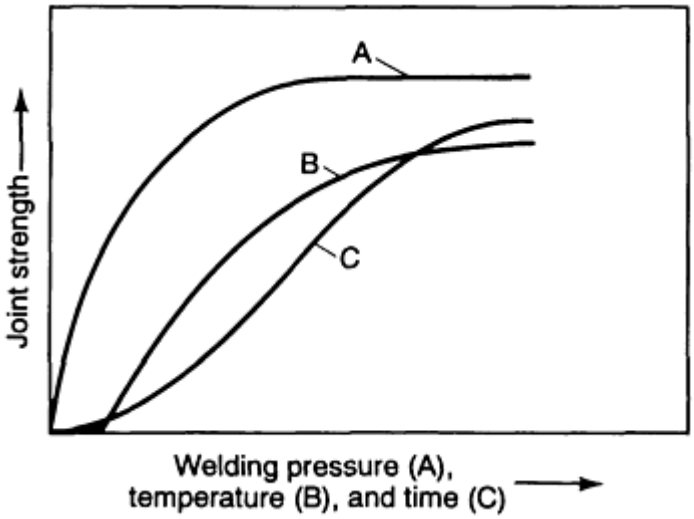

FIG. 2 INFLUENCE OF WELDING PRESSURE, TEMPERATURE, AND TIME ON JOINT STRENGTH

Temperature is the most important welding parameter. The requisite temperature depends on the material or the combination of materials. It must be sufficiently high to ensure plastic flow and intimate contact of the surfaces at the selected surface pressure, as well as adequate diffusion within a reasonable time. As a general rule, a welding temperature ranging from 0.5 to 0.7 T_s is advisable, where T_s is the melting temperature, in K, of the lower-melting-point material or component.

Pressure is required in order to achieve a large contact area at the welding temperature. The pressure level depends on the mechanical properties of the materials being joined. Its upper limit is determined by the admissible degree of deformation. A pressure increase beyond a certain level does not improve strength any further. As a general rule, a surface pressure that ranges from 1 to 20 MPa (0.15 to 2.9 ksi) can be considered adequate for the execution of high-temperature solid-state welds. The deformation at the joint interface, as a result of surface pressure, also has a positive influence on the joint. Surface impurity layers, such as oxides, are cracked, surface roughness is removed, and the atoms in the joint surfaces are brought close together. Plastic deformation facilitates the approach of the metallic atoms by fragmentation and dispersion of surface oxide and impurity barriers. Therefore, it is often better to match a surface of elevated roughness by deformation in the surface region than it is to bond, for example, highly polished surfaces with minor deformation. A precondition, however, is good surface cleaning and the removal of impurity surface layers prior to welding.

The welding time required for the preparation of a proper joint can range from a few minutes to several hours, depending on the material or material combination, as well as on the selected welding temperature.

The welding atmosphere used in most welding systems is a vacuum. In most cases, a vacuum of 0.01 Pa (1.4×10^{-6} psi) is sufficient. The use of high-purity shielding gases, such as argon or helium, is possible for many materials, but generally does not present any technical or economic advantages. Materials that are relatively insensitive to oxygen, such as structural steels, have been successfully welded in air. Welding has also been performed in liquids, such as molten salt.

Prior to welding, it is important to clean the surfaces to be joined and to remove any surface layers, especially oxide films. Although it is not possible to prevent the formation of new layers in air, these newly formed layers are very thin and hardly impair the welding process. Higher welding temperatures and greater deformation on the surfaces reduce the influence of such layers. Surface cleaning can be accomplished by chemical or mechanical methods. Proven techniques are degreasing with a suitable agent or removing the layers with wire brushes immediately prior to welding.

The most metallurgically simple type of weld results when similar materials are joined without using an interlayer material. In this case, the properties of only one material determine the process parameters. Two materials are involved in the rarely practiced joining of similar materials using an interlayer of softer material, which may facilitate surface matching or improve diffusion. An interlayer is more frequently used in the joining of dissimilar materials. When interlayers are used, the welding process involves a metallurgically complicated multicomponent system, even in the case

of pure metals. The interlayers primarily serve to bridge different melting points and different coefficients of thermal expansion, improve the diffusion properties, and form favorable structures in the joining zones. Practically any metal combination can he joined using suitable interlayers. Even extreme combinations, such as molybdenum and lead or tungsten and lead, can be processed by selecting several suitable interlayers, although several welding operations at different temperatures would be required.

In addition to welding metals to each other, diffusion welding permits the joining of metals to nonmetals. However, the problems encountered in this case are even more complex, because the chemical and physical properties of the components being welded differ significantly from each other. Nevertheless, welds between metals and glasses, as well as between metals and ceramics, have been successfully produced. The main problems arise from differences in the coefficients of thermal expansion and in the brittleness of the nonmetallic members.

High-Temperature Solid-State Welding

W. Lehrheuer, Forschungszentrum Jülich GmbH

Practical Applications

The high-temperature solid-state welding process has been primarily used on an industrial scale in the fields of aerospace and nuclear engineering. A typical application is the fabrication of complicated hollow structures. Figure 3 shows a cross section of a rotating-anode x-ray tube. The body consists of austenitic stainless steel, whereas the outer welded ring is made of aluminum. Both parts form several cooling channels.

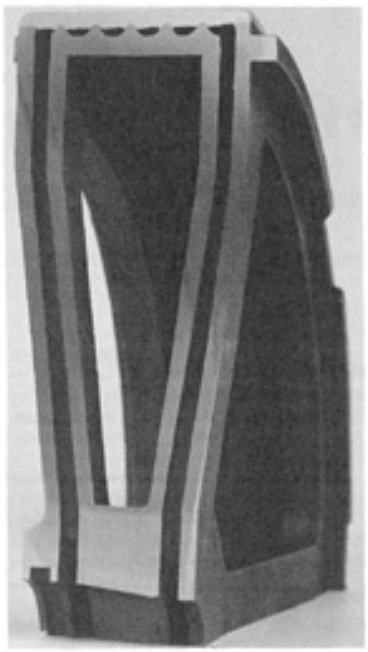

FIG. 3 ROTATING X-RAY ANODE WITH OUTER ALUMINUM RING DIFFUSION WELDED TO STAINLESS STEEL BODY

Another important application is the joining of dissimilar materials. Of particular significance to nuclear engineering applications are joints made of aluminum and stainless steel. Figure 4 shows welds of these materials in different joint geometries. An economical use of this process for mass production frequently is not possible, because of the long welding times and expensive equipment involved. Therefore, applications will probably continue to be limited to special complicated geometries, expensive materials and dissimilar material combinations. In recent years, the combined use of this process with a heat-treatment step has been increasing. Economic efficiency is much easier to achieve with such a process combination. The process is undoubtedly of great significance for joining very dissimilar materials, including

metals and ceramics, and the newly developed high-temperature materials, anisotropic materials, and fiber-reinforced materials.

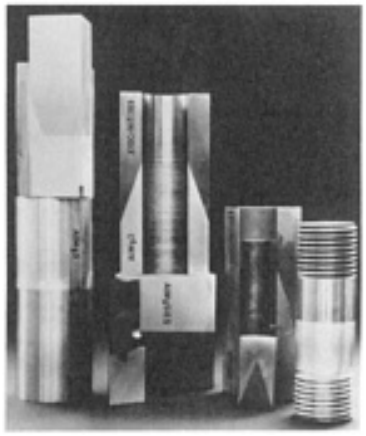

FIG. 4 ALUMINUM-STAINLESS STEEL JOINTS

High-Temperature Solid-State Welding

W. Lehrheuer, Forschungszentrum Jülich GmbH

Selected References

- V.A. BACHIN AND K.E. TSIOLKOVSKY, "DIFFUSION WELDING METALS VERSUS NON-METALS," DVS REPORT 148, DVS-VERLAG, DÜSSELDORF, 1992
- W.D. LUDEMAN, "A FUNDAMENTAL STUDY OF THE PRESSURE WELDING OF DISSIMILAR METALS THROUGH OXIDE LAYERS," UCRL-50744, LAWRENCE RADIATION LABORATORY, UNIVERSITY OF CALIFORNIA, OCT 1969
- N.F. KAZAKOV, VACUUM DIFFUSION WELDING OF METALS AND NON-METALS, *WELD. PROD.*, VOL 11 (NO. 63), 1967, P 83-86
- Y.N. KOPYLOV AND N.F. KAZAKOV, DIFFUSION WELDING OF QUARTZ GLASS TO METALS, *AUT. WELD.*, VOL 6 (NO. 73), 1968, P 77-78
- A.Y. MAKARKIN, M.A. PAVLOVA, AND I.I. METELKIN, WELDING TOGETHER CERAMIC AND METALS, *WELD. PROD.*, VOL 6, 1967, P 17-22
- M.M. SCHWARTZ, "DIFFUSION WELDING," MARTIN MARIETTA CORPORATION, MARCH 1970
- J.K. SOLBERG AND L.K. RUDSRUD, "DIFFUSION BONDING OF 253 MA AUSTENITIC STAINLESS STEEL," DVS REPORT 148, DVS-VERLAG, DÜSSELDORF, 1992
- V.T. SLEPUKHA, FORMATION OF SURFACES FREE FROM OXIDE FILMS IN VACUUM DIFFUSION WELDING, *SVAR. PROIZ.*, VOL 5, 1965, P 38-40
- R.F. TYLECOTE, *THE SOLID-PHASE WELDING OF METALS*, ST. MARTINS PRESS, 1968

Low-Temperature Solid-State Welding

R.S. Rosen, Lawrence Livermore National Laboratory

Introduction

SOLID-STATE WELDING is the joining of base metals (metals, alloys, ceramics, etc.) by chemical bond formation without heating the base metals above their respective melting points. The advantages of solid-state welding processes include the ability to join parts to a finished size or shape without additional machining, and the ability to join multiple interfaces during a single welding cycle. The disadvantages of solid-state welding processes compared with conventional fusion welding or brazing include generally longer welding cycles, and more restrictive size limitations for the parts to be joined. In this article, low-temperature solid-state welding processes are described in relation to the interlayer fabrication method, welding method, and welding parameters. These findings are discussed relative to the mechanical properties of the joints.

Low-Temperature Solid-State Welding

R.S. Rosen, Lawrence Livermore National Laboratory

Applications

The utilization of soft-metal interlayers for solid-state welding may be an appropriate joining method when brittle intermetallic formation, differential thermal contraction during cooling, or oxide dissociation and dissolution temperatures preclude conventional methods such as fusion welding, brazing, and direct solid-state welding of the base metals. An interlayer can be in the form of a foil, or it can be applied to one or both of the base-metal surfaces by various coating methods (e.g., electrodeposition, plasma spraying, or vapor-deposition methods). Methods utilizing coated interlayers require a two-step joining procedure (coating and welding) as opposed to joints fabricated with foil interlayers, which may only require a single solid-state welding step. However, methods utilizing coated interlayers have the advantage over foil interlayers in not requiring solid-state welding at the interlayer/base-metal interface. Solid-state welding of some interlayer/base-metal combinations may require high temperatures and/or pressures, due to the high dissociation temperatures of the surface oxides, which may preclude or restrict the use of foil interlayers.

Interlayer Materials. Silver is the predominant material utilized as a low-temperature interlayer because high-strength joints can be fabricated at relatively low temperatures (473 to 673 K, or 392 to 752 °F) and pressures (100 to 200 MPa, or 15 to 30 ksi) due to the low dissociation temperature (<460 K, or 370 °F) of silver oxide. Other interlayer materials utilized--such as copper (Ref 1), aluminum (Ref 2), and aluminum-silicon alloys (Ref 3)--require higher welding temperatures (873 to 1273 K, or 1110 to 1832 °F) to achieve joint strengths comparable to those of silver. Gold, thought to be a promising interlayer material for low-temperature applications due to the absence of a surface oxide layer at room temperature, has not been utilized as much. This may be due to its propensity to form brittle intermetallics at relatively low temperatures with a number of base metals (Ref 4). Low-temperature (616 K, or 525 °F) solid-state welding of dissimilar (electroplated) interlayer materials, such as gold-to-silver and gold-to-copper, has been achieved at a pressure of 50 MPa (7 ksi) for 3 h using various base metals (Ref 5).

Joint Geometry. Soft interlayer welds between stronger base materials may have ultimate tensile strengths much higher than those of the bulk interlayer materials. For example, the tensile strength of silver interlayer solid-state welds between maraging steel base metals has been reported to be nearly 800 MPa (115 ksi) (Ref 6), while the ultimate tensile strength of the bulk silver is only about 250 MPa (35 ksi) (Ref 7). The high tensile strength of the joint is due to the mechanical constraint provided by the stronger base metal, which restricts transverse contraction of the interlayer. The constraint establishes radial (triaxial) stresses that inhibit the development of shear stresses within the joint, thereby decreasing the effective stress in the interlayer. This reduction in stress inhibits the plastic flow that leads to the ductile fracture. The base metals provide relatively little mechanical constraint of the interlayer during shear loading because the shear stress is parallel to the plane of the interlayer. Therefore, soft interlayer welds between stronger base metals are capable of higher loads in tension (loading perpendicular to the plane of the interlayer, such as in a butt joint) than in shear (loading parallel to the plane of the interlayer, such as in a lap joint).

In general, joint strengths of soft interlayer solid-state welds increase with decreasing interlayer thickness and increasing welding temperature and pressure. However, increasing welding times do not necessarily result in increased joint strength. For example, resultant joint strengths of silver solid-state welds have been reported to be independent of welding times from 1 to 240 min (Ref 4). In addition, decreasing interlayer thickness-to-diameter ratios to less than 0.025 does not result in higher joint strengths and may actually result in a lowering of tensile strength (Ref 8, 9).

References cited in this section

1. A. URENA, J.M.G.D. SALAZAR, AND J. QUINONES, DIFFUSION BONDING OF ALUMINA TO STEEL USING A SOFT COPPER INTERLAYER, *J. MATER. SCI.,* VOL 27, 1992, P 599-606
2. M.G. NICHOLAS AND R.M. CRISPIN, DIFFUSION BONDING STAINLESS STEEL TO ALUMINA USING ALUMINUM INTERLAYERS, *J. MATER. SCI.,* VOL 17, 1982, P 3347-3360
3. T. YAMADA, K. YOKOI, AND A. KOHNO, EFFECT OF RESIDUAL STRESS ON THE STRENGTH OF ALUMINA-STEEL JOINT WITH AL-SI INTERLAYER, *J. MATER. SCI.,* VOL 25, 1990, P 2188-2192
4. J.L. KNOWLES AND T.H. HAZLETT, HIGH-STRENGTH LOW-TEMPERATURE BONDING OF BERYLLIUM AND OTHER METALS, *WELD. J.,* VOL 49 (NO. 7). 1970, P 301S-310S
5. J.T. NIEMANN, R.P. SOPHER, AND P.J. RIEPPEL, DIFFUSION BONDING BELOW 1000 °F, *WELD. J.,* VOL 37, 1958, P 337S-342S
6. M.E. KASSNER, R.S. ROSEN, AND G.A. HENSHALL, DELAYED MECHANICAL FAILURE OF SILVER-INTERLAYER DIFFUSION BONDS, *METALL. TRANS. A,* VOL 21, 1990, P 3085-3100
7. M.E. KASSNER, THE RATE DEPENDENCE AND MICROSTRUCTURE OF HIGH-PURITY SILVER DEFORMED TO LARGE STRAINS BETWEEN 0.16 AND 0.30 TM, *METALL. TRANS. A,* VOL 20, 1989, P 2001-2010
8. R.S. ROSEN AND M.E. KASSNER, DIFFUSION WELDING OF SILVER INTERLAYERS COATED ONTO BASE METALS BY PLANAR-MAGNETRON SPUTTERING, *J. VAC. SCI. TECHNOL. A,* VOL 8 (NO. 1), 1990, P 19-29
9. R.A. MUSIN, V.A. ANTSIVEROV, Y.A. BELIKOV, Y.V. LYAMIN, AND A.N. SOLOKOV, THE EFFECTS ON THE STRENGTH OF THE JOINT OF THE THICKNESS OF THE SOFT INTERLAYER IN DIFFUSION WELDING, *AUTO. WELD.,* VOL 32, 1979, P 38-40

Low-Temperature Solid-State Welding

R.S. Rosen, Lawrence Livermore National Laboratory

Surface Preparation

Surface Cleaning. Prior to coating and/or welding, machined base-metal surfaces are usually degreased by a multiple-step procedure. The following method (Ref 8) has been used to clean a variety of base metals (for example, type 304 stainless steel, maraging steel, uranium, beryllium, and aluminum) before they undergo subsequent ion-sputter etching and silver interlayer deposition in vacuum:

1. WASH WITH ABRASIVE DETERGENT FOLLOWED BY A HOT-WATER RINSE
2. RINSE IN DEIONIZED WATER
3. ULTRASONICALLY CLEAN IN ETHYL ALCOHOL
4. BLOW DRY USING INERT GAS

For other fabrication methods, such as electrodeposited interlayers or foils, the base metal surfaces are degreased prior to plating or joining to remove organic surface films that would otherwise degrade the metallic bonding at the interlayer/base-metal interfaces.

Surface Finish. Joint strength generally increases with decreasing base-metal surface roughness and flatness. This is true for foil interlayers and for coated interlayers, where the surface roughness of the coating generally replicates that of the underlying base-metal surface. Table 1 shows the increases in tensile strengths of silver interlayer welds utilizing lapped base-metal surfaces (0.15 μm, or 6 μin., flatness, 0.03 μm, or 1.2 μin., arithmetic average surface roughness, R_a) over those of machined surfaces (2 μm, or 80 μin., flatness, 0.1 μm, or 4 μin., R_a) (Ref 8, 10). The increase in strength achieved

through use of smoother base-metal surfaces is generally attributed to more complete welding from the increased contact area of the laying surfaces.

TABLE 1 EFFECT OF BASE-METAL SURFACE FINISH ON THE TENSILE STRENGTH OF JOINTS SOLID-STATE WELDED USING SILVER INTERLAYERS

BASE METAL	SURFACE FINISH (TO BE COATED)	TENSILE STRENGTH		PLASTIC STRAIN IN BASE METAL AT FRACTURE, %	INTERLAYER THICKNESS, $T/D \times 100$
		MPA	KSI		
MARAGING STEEL	MACHINED	656	95	0	**2.4**
MARAGING STEEL(A)	LAPPED	758	110	0	**2.4**
TYPE 304 STAINLESS STEEL(A)	MACHINED	400	58	2.2	**2.4**
TYPE 304 STAINLESS STEEL(A)	LAPPED	414	60	2.8	**2.4**
BERYLLIUM(B)	MACHINED	235	34	~0.2	**0.1**
BERYLLIUM(B)	**LAPPED**	**280**	**41**	**~1**	**0.1**

(A) SOURCE: REF 8.

(B) SOURCE: REF 9

References cited in this section

8. R.S. ROSEN AND M.E. KASSNER, DIFFUSION WELDING OF SILVER INTERLAYERS COATED ONTO BASE METALS BY PLANAR-MAGNETRON SPUTTERING, *J. VAC. SCI. TECHNOL. A,* VOL 8 (NO. 1), 1990, P 19-29
9. R.A. MUSIN, V.A. ANTSIVEROV, Y.A. BELIKOV, Y.V. LYAMIN, AND A.N. SOLOKOV, THE EFFECTS ON THE STRENGTH OF THE JOINT OF THE THICKNESS OF THE SOFT INTERLAYER IN DIFFUSION WELDING, *AUTO. WELD.,* VOL 32, 1979, P 38-40
10. E.R. NAIMON, R.G. KURZ, D. VIGIL, AND L. WILLIAMS, "SILVER FILMS FOR SOLID STATE BONDING," REPORT RFP-312S, ROCKWELL INTERNATIONAL, 1981

Low-Temperature Solid-State Welding

R.S. Rosen, Lawrence Livermore National Laboratory

Interlayer Fabrication Method

Vacuum Coated Interlayers. Specimens to be coated are usually mounted in a fixture (which may be water-cooled) inside the vacuum chamber, with the base-metal surfaces facing the evaporation or sputtering source. The chamber is evacuated using a roughing pump is conjunction with an ultrahigh vacuum turbomolecular or cryogenic pump. After achieving the desired chamber base pressure (typically 10 μPa, or 0.075 μtorr), argon gas is then introduced into the vacuum chamber and maintained at a pressure of about 5 Pa (38 mtorr) for sputtering. A glow-discharge power supply is then used to initiate a plasma at 1 to 2 kV with reference to the base-metal specimens. Depending on the base metals utilized, specimens are usually sputter-etched for 5 to 45 min, resulting in 0.1 to 1 μm (4 to 40 μin.) etched from the surfaces. Figure 1 shows a schematic of a typical vacuum chamber and the two-stage etching and sputter-coated procedure. The shutter is shown placed between the target surface during the etching phase. The coating phase is accomplished (after evacuating the argon gas from the chamber) by evaporation of the interlayer material, or by using a high-rate sputter-target source such as a planar magnetron. Deposition of interlayer metal onto the specimens is usually started after reducing the chamber pressure to 1 t 2 Pa (8 to 15 mtorr). Typical deposition rates at the specimen surfaces are 5 to 20 nm/s (50 to 200 Å/s). Some interlayer/base-metal combinations are capable of achieving high interfacial

strengths without having to sputter-etch the native oxide layer prior to deposition. Adhesion of the deposited material is enhanced by preheating the base metals prior to deposition. For the case of beryllium base metal, high-strength joints result when silver is vacuum coated onto the beryllium surfaces at base-metal temperatures exceeding 773 K (932 °F).

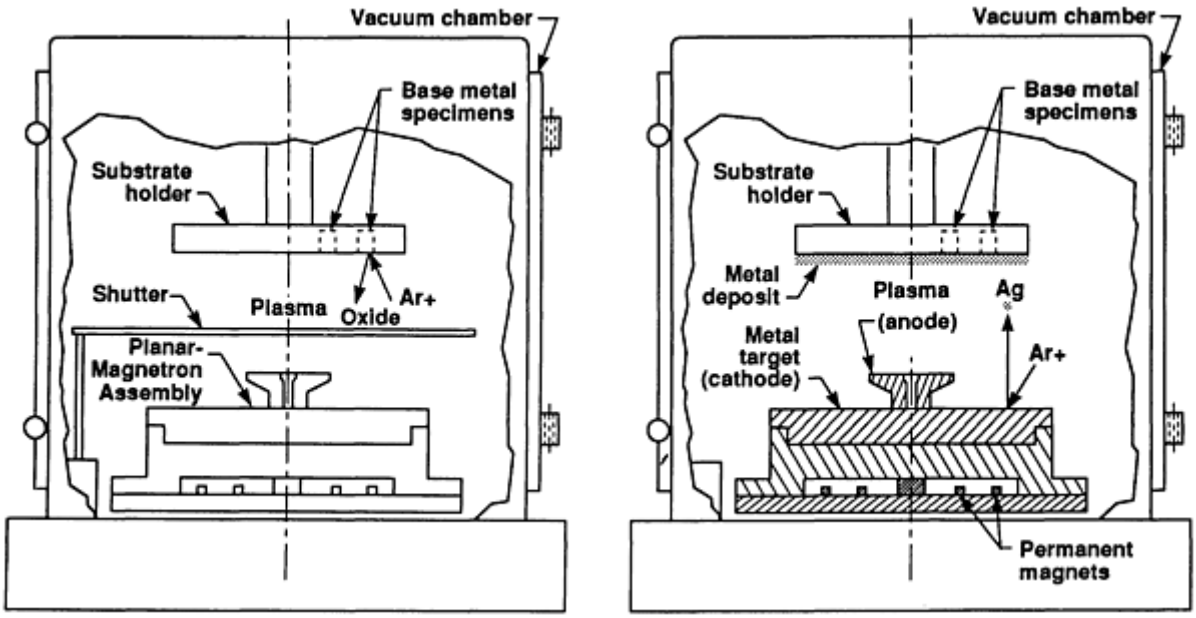

FIG. 1 SCHEMATIC OF VACUUM COATING CHAMBER AND ASSOCIATED HARDWARE SHOWING (A) ION-ETCHING AND (B) INTERLAYER METAL DEPOSITION PHASES. AN EVAPORATION SOURCE MAY BE USED INSTEAD OF THE SPUTTERING SOURCE TO DEPOSIT THE INTERLAYER MATERIAL.

Electrodeposited Interlayers. Prior to plating of the interlayer metal onto the base-metal surfaces, the specimens are generally masked to restrict the deposition to the surfaces to be joined. The specimens are usually degreased and then chemically or electrochemically etched in an appropriate solution to remove surface oxide layers. The initial plated layer (~1 to 5 μm, or 40 to 200 μin.) may be deposited at higher current densities (>200 A/m^2, or 20 A/ft^2) to improve the adhesive strength, followed by plating of the remaining interlayer thickness (~10 to 100 μm, or 400 to 4000 μin.) at lower current densities (~40 A/m^2, or 4 A/ft^2). It should be noted that electrodeposited interlayer metals are usually not as pure as vapor-deposited metals due to the presence of impurities in the plating solutions.

Foil Interlayers. Use of foils requires the same cleaning considerations for surface oxides and contaminants as that of deposited interlayers. The base metal as well as the foil material may be etched to remove the oxide layer prior to welding. Foils are usually cut to the desired shape prior to placing between the base metal surfaces to be joined.

Low-Temperature Solid-State Welding

R.S. Rosen, Lawrence Livermore National Laboratory

Welding Methods

The mechanism of solid-state welding is believed to consist of:

- PLASTIC DEFORMATION OF THE CONTACTING SURFACE ASPERITIES DURING INITIAL APPLICATION OF THE LOAD
- OXIDE DISSOLUTION AND DIFFUSION AWAY FROM THE FORMING INTERFACE
- TIME-DEPENDENT PLASTICITY (CREEP) AND/OR DIFFUSION OF METALS TO THE

In addition to these processes, recrystallization and grain growth of the (formed) interface may occur.

Uniaxial Compression. Solid-state welding by uniaxial compression is usually accomplished in a vacuum furnace; for the case of silver at temperatures above about 473 K (392 °F), welding may be accomplished directly in air. Pairs of specimens to be joined are usually loaded with a hydraulic ram. If a vacuum furnace is used, the chamber is evacuated to a gas pressure below about 100 μPa (0.75 μtorr) prior to applying the peak welding pressure (~70 to 210 MPa, or 10 to 30 ksi) to the coated surfaces in contact. The specimen temperature is then elevated to peak temperature (~473 to 873 K, or 392 to 1110 °F) and maintained for 10 to 240 min. The furnace is usually cooled to below 323 K (122 °F) before the pressure is relieved.

Figure 2 shows a schematic of a typical vacuum furnace used for brazing. The constraining fixture shown surrounding the specimen is used to prevent excessive deformation from base-metal yielding during applied loading. This is often the case when dissimilar metals such as aluminum and stainless steels are joined at temperatures and pressures exceeding 473 K (392 °F) and 100 MPa (15 ksi), respectively, using silver as the interlayer material.

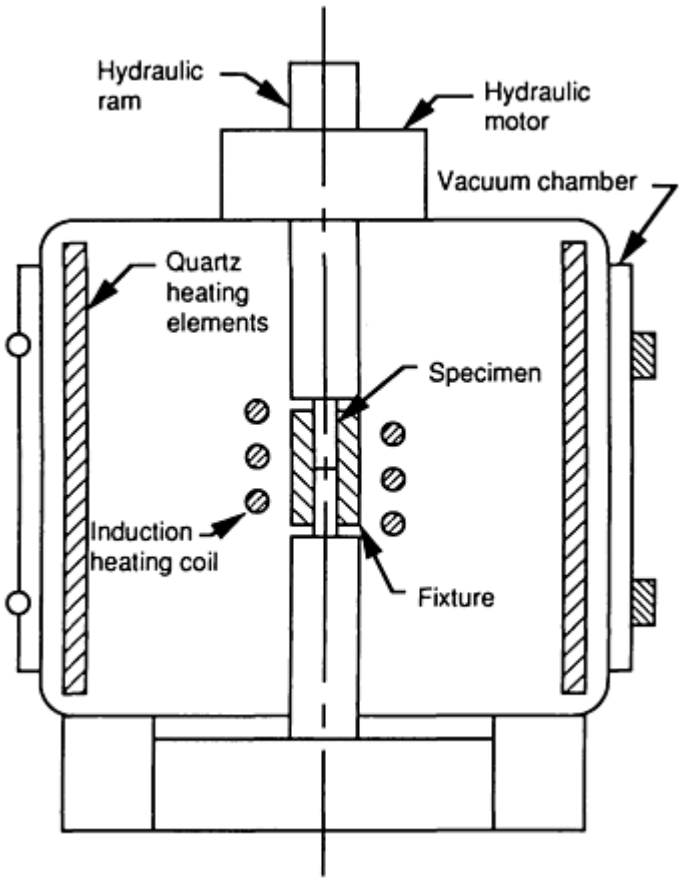

FIG. 2 SCHEMATIC OF A TYPICAL VACUUM FURNACE USED FOR SOLID-STATE WELDING BY UNIAXIAL COMPRESSION. HEATING WOULD BE BY EITHER AN INDUCTION COIL OR RADIANT ELEMENTS AS SHOWN. THE CONSTRAINING FIXTURE SURROUNDING THE SPECIMEN IS USED TO PREVENT EXCESSIVE DEFORMATION FROM BASE-METAL YIELDING DURING APPLIED LOADING.

Isostatic Pressure. Solid-state welding by hot isostatic pressing is accomplished in an autoclave. Parts to be joined are placed with the coated surfaces in contact and then encapsulated with a thin (0.25 to 1 mm, or 0.01 to 0.04 in.) stainless steel membrane, or "can." The cans are sealed using a suitable fusion welding method such as electron-beam or gas-tungsten arc welding. The sealed assemblies are usually evacuated through a small tube welded on one end of the can using a vacuum pump. The evacuated assemblies are placed in an autoclave and isostatically compressed with gas or

liquid to a pressure of about 100 MPa (15 ksi). The temperature is then raised to the peak value of 473 to 873 K (392 to 1110 °F) while the gas pressure is increased to the desired peak value (~70 to 350 MPa, or 10 to 50 ksi). Peak temperature and pressure are maintained for 1 to 2 h. The autoclave is usually cooled to below 373 K (212 °F) before the gas is vented.

Final Machining of Welded Parts

After welding, the parts may be finish machined if desired. For the case of dissimilar base metals where one material is considerably stiffer than the other, some allowances may have to be made for single-point cutting-type operations where the tool passes over the joint. For example, machining by lathe turning has resulted in a step remaining at the joint between the base metals due to the differences in elasticity of the base metals. Additionally, lathe cutting with a single-point tool may result in a smearing of the harder base metals across surfaces of the softer interlayer material. These problems can be avoided by utilizing surface grinding as the final machining operation.

Low-Temperature Solid-State Welding

R.S. Rosen, Lawrence Livermore National Laboratory

References

1. A. URENA, J.M.G.D. SALAZAR, AND J. QUINONES, DIFFUSION BONDING OF ALUMINA TO STEEL USING A SOFT COPPER INTERLAYER, *J. MATER. SCI.*, VOL 27, 1992, P 599-606
2. M.G. NICHOLAS AND R.M. CRISPIN, DIFFUSION BONDING STAINLESS STEEL TO ALUMINA USING ALUMINUM INTERLAYERS, *J. MATER. SCI.*, VOL 17, 1982, P 3347-3360
3. T. YAMADA, K. YOKOI, AND A. KOHNO, EFFECT OF RESIDUAL STRESS ON THE STRENGTH OF ALUMINA-STEEL JOINT WITH AL-SI INTERLAYER, *J. MATER. SCI.*, VOL 25, 1990, P 2188-2192
4. J.L. KNOWLES AND T.H. HAZLETT, HIGH-STRENGTH LOW-TEMPERATURE BONDING OF BERYLLIUM AND OTHER METALS, *WELD. J.*, VOL 49 (NO. 7). 1970, P 301S-310S
5. J.T. NIEMANN, R.P. SOPHER, AND P.J. RIEPPEL, DIFFUSION BONDING BELOW 1000 °F, *WELD. J.*, VOL 37, 1958, P 337S-342S
6. M.E. KASSNER, R.S. ROSEN, AND G.A. HENSHALL, DELAYED MECHANICAL FAILURE OF SILVER-INTERLAYER DIFFUSION BONDS, *METALL. TRANS. A*, VOL 21, 1990, P 3085-3100
7. M.E. KASSNER, THE RATE DEPENDENCE AND MICROSTRUCTURE OF HIGH-PURITY SILVER DEFORMED TO LARGE STRAINS BETWEEN 0.16 AND 0.30 TM, *METALL. TRANS. A*, VOL 20, 1989, P 2001-2010
8. R.S. ROSEN AND M.E. KASSNER, DIFFUSION WELDING OF SILVER INTERLAYERS COATED ONTO BASE METALS BY PLANAR-MAGNETRON SPUTTERING, *J. VAC. SCI. TECHNOL. A*, VOL 8 (NO. 1), 1990, P 19-29
9. R.A. MUSIN, V.A. ANTSIVEROV, Y.A. BELIKOV, Y.V. LYAMIN, AND A.N. SOLOKOV, THE EFFECTS ON THE STRENGTH OF THE JOINT OF THE THICKNESS OF THE SOFT INTERLAYER IN DIFFUSION WELDING, *AUTO. WELD.*, VOL 32, 1979, P 38-40
10. E.R. NAIMON, R.G. KURZ, D. VIGIL, AND L. WILLIAMS, "SILVER FILMS FOR SOLID STATE BONDING," REPORT RFP-312S, ROCKWELL INTERNATIONAL, 1981

Explosion Welding

John G. Banker and Edward G. Reineke, Explosive Fabricators, Inc.

Introduction

EXPLOSION WELDING (EXW) is a solid-state metal-joining process that uses explosive force to create an electron-sharing metallurgical bond between two metal components. Although the explosive detonation generates considerable heat, there is not time for heat transfer to the component metals; therefore, there is no appreciable temperature increase in the metals. The physics of the process are discussed in the article "Fundamentals of Explosion Welding" in this Volume.

Explosion Welding

John G. Banker and Edward G. Reineke, Explosive Fabricators, Inc.

EXW Process Attributes

Metallurgical Attributes. Because of the absence of heating, EXW products do not exhibit many of the metallurgical characteristics of fusion-welded, brazed, or hot-rolled/forged products. Unlike those processes, in EXW (Ref 1, 2, 3, 4):

- THE COMPONENT METALS REMAIN IN THEIR WROUGHT STATES; CONTINUOUS CASE STRUCTURES ARE NOT CREATED.
- THE MICROSTRUCTURES, MECHANICAL PROPERTIES, AND CORROSION PROPERTIES OF THE WROUGHT PARENT COMPONENTS ARE NOT ALTERED FROM APPLICABLE PREBONDING SPECIFICATION REQUIREMENTS.
- THERE ARE NO HEAT-AFFECTED ZONES.
- THERE ARE NO CONTINUOUS-MELT BANDS EXHIBITING MIXED CHEMISTRY.
- THERE IS ALMOST NO DIFFUSION OF ALLOYING ELEMENTS BETWEEN COMPONENTS.

Metals Combinations. Explosion welding is an effective joining method for virtually any combination of metals. The only metallurgical limitation is sufficient ductility and fracture toughness to undergo the rapid deformation of the process without fracture. Generally accepted limits are 10% and 30 J (22 ft · lbf) minimum, respectively.

Explosion welding is suitable for joining metals of the same type--for example, steel to steel--as well as metals with substantially different densities, melting points, and/or yield strengths--for example, tantalum to alloy titanium. The process is commonly used to join corrosion-resistant alloys to carbon or alloy steels.

Size Limitations. Explosion welding is appropriate for use over a broad range of sizes. It has been used for joining electronic components of widths less than 0.5 mm (0.020 in.) and for cladding plates up to 5 × 13 m (16 × 40 ft). Cladding metal thicknesses can range from 0.025 to 100 mm (0.001 to 4 in.), and base metal thickness can range from 0.025 mm (0.001 in.) to over 1 m (40 in.). The size limits are generally mandated by component metal manufacturability and transport requirements.

Configuration Limitations. Explosion welding is limited to the bonding of flat surfaces or coaxial cylindrical surfaces. It is ideally suited for bonding large, flat areas, as in clad plate manufacture.

Bond Zone Morphology. Explosion welding is traditionally known for its wavy bond zone morphology. The physics of the wave formation process and its relation to process variables are discussed in the article "Fundamentals of Explosion Welding" in this Volume. The EXW bond zone morphology is flat at the low end of the bonding velocity range and transitions to wavy as the velocity is increased. Through proper selection of EXW parameters, the bond zone morphology

can be tailored to satisfy product performance requirements. Although a low-velocity wavy bond zone is preferred for most needs (Fig. 1), certain applications are better served by flat or turbulent-wavy interfaces (Ref 5).

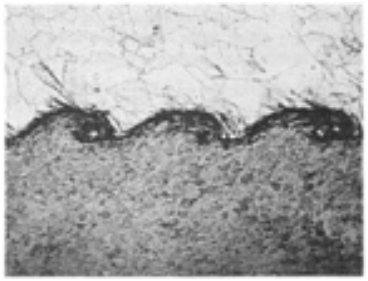

FIG. 1 BOND ZONE PATTERN TYPICAL OF EXPLOSION CLAD METALS. MATERIALS ARE TYPE 304L STAINLESS STEEL AND MEDIUM-CARBON STEEL. 20×

Interlayers. The physical and mechanical performance requirements of the EXW bond zone are determined by the product application. With some combinations of metals, the required bond zone performance characteristics are best achieved with an interlayer between the two primary metals. For example, a titanium interlayer can be used to increase the performance temperature of an aluminum/copper weld, and a silver interlayer can be used to improve the leak tightness of an aluminum/stainless steel weld.

References cited in this section

1. R.E. SAVIDGE, *MECHANICAL PROPERTIES OF EXPLOSION CLAD BONDS OF HIGH NICKEL ALLOYS ON LOW ALLOY STEELS AND THE EFFECT OF EXPLOSION CLADDING ON THE FRACTURE PROPERTIES OF THE STEEL,* THIRD INTERNATIONAL CONFERENCE ON HIGH ENERGY RATE FABRICATION, 1971, P 3.3.1
2. W. LUCAS, J.D. WILLIAMS, AND B. CROSSLAND, *SOME METALLURGICAL OBSERVATIONS ON EXPLOSION WELDING,* SECOND INTERNATIONAL CONFERENCE OF THE CENTRE FOR HIGH ENERGY FORMING, 1969, P 8.1.2
3. S.H. CARPENTER AND M. NAGARKAR, *THE EFFECTS OF EXPLOSIVE WELDING ON THE KINETICS OF METALLURGICAL REACTIONS,* THIRD INTERNATIONAL CONFERENCE OF THE CENTRE FOR HIGH ENERGY FORMING, 1971, P 3.4.1
4. L.F. TRUEB, MICROSTRUCTURAL EFFECTS OF HEAT TREATMENT ON THE BOND INTERFACE OF EXPLOSIVELY WELDED METALS, *METALL. TRANS.,* VOL 2, JAN 1971, P 145
5. A. SZECKET, O.T. INAL, AND J. ROCCO, EXPLOSIVE WELDING OF ALUMINUM TO STEEL; A WAVY VERSUS A STRAIGHT INTERFACE, *HIGH ENERGY RATE FABRICATION,* 1984, P 153

Explosion Welding

John G. Banker and Edward G. Reineke, Explosive Fabricators, Inc.

EXW Products and Applications

Common Industrial Applications. Because of the unique safety and noise-vibration considerations, EXW is generally performed in relatively isolated facilities by companies specializing in explosives operations. The major products are large clad plates, which are used in pressure vessel, heat exchanger, and electrochemical process applications (Fig. 2). The dissimilar-metal welding features of EXW are made available to a broader industrial base through the concept of welding transition joints (Fig. 3).

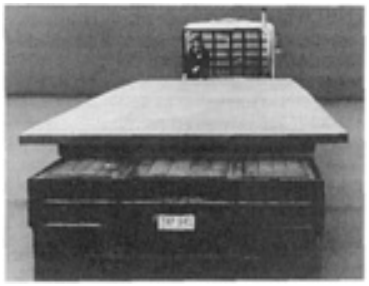

FIG. 2 TITANIUM/STEEL EXPLOSION-BONDED CLAD PLATE

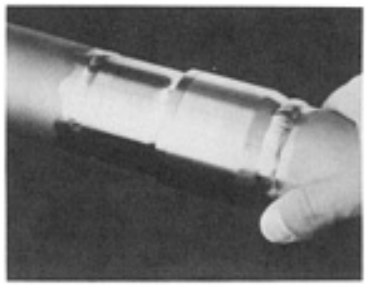

FIG. 3 ALUMINUM-TO-STAINLESS WELD ACCOMPLISHED WITH AN EXPLOSION-BONDED TUBULAR TRANSITION JOINT. ALUMINUM AND STAINLESS STEEL ARE WELDED TO THE RESPECTIVE ENDS USING CONVENTIONAL FUSION-WELDING PROCESSES.

Transition joint components are produced by explosion welders at their production facilities and then provided in the form of blocks, strips, or tubular couplings to equipment fabricators for use in the conventional welding of dissimilar metals. Common applications are aluminum/steel (Ref 6, 7), aluminum/titanium, and aluminum/copper-nickel for shipboard construction (Fig. 4); aluminum/copper and aluminum/steel for electrical contacts and buss systems; aluminum/stainless steel for cryogenic pipe couplings; titanium/stainless steel for aerospace and aircraft applications (Fig. 5); and Kovar/copper and Kovar/aluminum for electronic packaging (Ref 8).

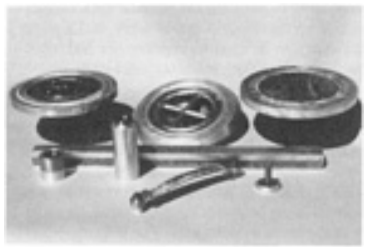

FIG. 4 TRANSITION JOINT MATERIALS FOR JOINING DISSIMILAR METALS IN SHIPBOARD AND MARINE EQUIPMENT CONSTRUCTION

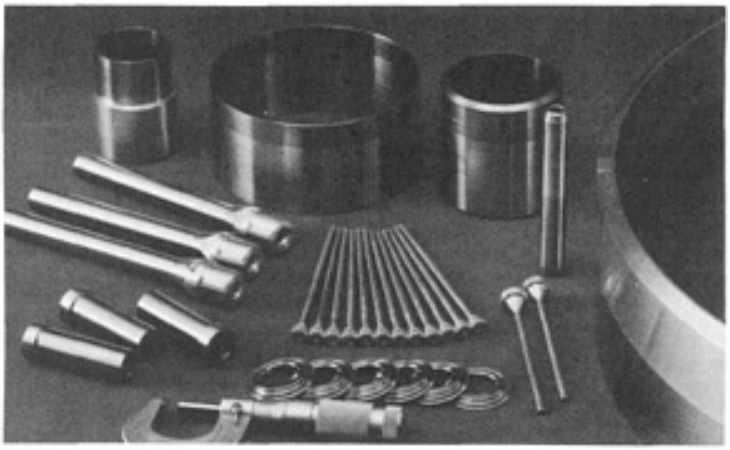

FIG. 5 TUBULAR WELDING TRANSITION JOINTS FOR HERMETIC WELDS BETWEEN TITANIUM, ALUMINUM, AND ZIRCONIUM AND STAINLESS STEEL

Shop Welding Applications. Small, specialty EXW devices have been developed for a few unique shop applications. Explosion welding is used in heat exchanger shops for joining tubes to tubesheets and tube plugging. Explosion spot welding devices have also been used in limited commercial applications (Ref 9).

References cited in this section

6. C.R. MCKENNEY AND J.G. BANKER, *EXPLOSION-BONDED METALS FOR MARINE STRUCTURAL APPLICATIONS,* THE SOCIETY OF NAVAL ARCHITECTS AND MARINE ENGINEERS, NOV 1970, P 285-292
7. E. GAINES AND J. BANKER, *SHIPYARD ALUMINUM/STEEL WELDED TRANSITION JOINTS,* 1991 SHIP PRODUCTION SYMPOSIUM, SEPT 1991
8. H. MANSELL, HYBRID METAL PACKAGES BY EXPLOSION BONDING, *HYBRID CIRCUIT TECHNOL.,* SEPT 1990, P 67
9. L.G. LAZARI, EXPLOSIVE WELDING AND ITS PRACTICAL APPLICATIONS, *WELD. REV.,* MAY 1988, P 74

Explosion Welding

John G. Banker and Edward G. Reineke, Explosive Fabricators, Inc.

EXW Manufacturing Process and Practice

Safety and Regulations. Safety is of critical importance in the practice of EXW. Guidelines and regulations for the safe handling and transport of explosives are provided by the U.S. Bureau of Alcohol, Tobacco, and Fire Arms (Ref 10), the U.S. Department of Transportation in its Federal Motor Carrier Safety Regulations (Ref 11), and the Institute of Makers of Explosives Safety Library Publications (Ref 12). Licensing and regulations for the purchase, transport, manufacture, and use of explosives may vary significantly among states and municipalities. Depending on the types of explosives used, the detonation by-products may be subject to environmental regulation. Potential practitioners of explosion-bonding operations should understand the safety standards and regulations before proceeding (Ref 13).

Noise and Vibration Abatement. The sound and ground vibration generated during EXW can be considerable. Common methods for noise abatement include performing the operation in a highly remote geographic location, in a mine

or bunker, or in a specially designed blast chamber or vacuum chamber. Safety considerations vary among these options. Precautions must be taken to ensure that personnel are protected from shrapnel and facility deterioration.

Process Geometry. Two basic geometric configurations of the EXW process are commonly used: angle bonding and parallel-plate bonding. Angle bonding is normally used for bonding sheet components and tubes, where the required bond width does not exceed 20 times the flyer plate thickness. The more commonly used parallel-plate geometry (Fig. 6) is applicable for welding larger flat areas and concentric cylinders (Ref 14).

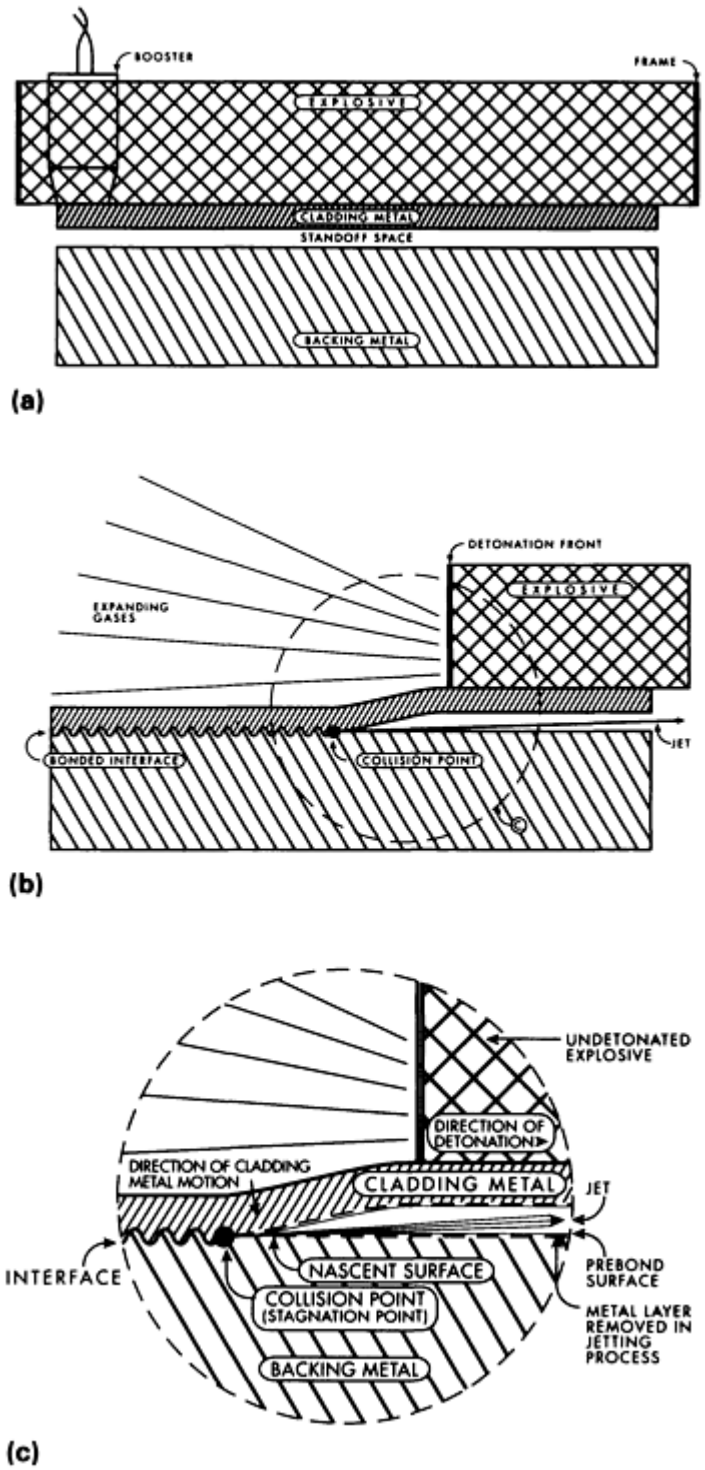

FIG. 6 PARALLEL-PLATE EXPLOSION WELDING PROCESS. (A) EXPLOSION-CLADDING ASSEMBLY BEFORE DETONATION. (B) EXPLOSION-CLADDING ASSEMBLY DURING DETONATION. (C) CLOSE-UP OF (B) SHOWING MECHANISM FOR JETTING AWAY THE SURFACE LAYER FROM THE PARENT LAYER

Basic parameters of EXW are flyer plate velocity, collision point velocity, and collision angle. The process variables that affect these parameters are explosive detonation rate, explosive mass, flyer plate mass, standoff distance, and/or preset angle. These process variables are normally controlled to provide:

- A FLYER PLATE VELOCITY OF 250 TO 500 M/S (820 TO 1600 FT/S)
- A COLLISION POINT VELOCITY OF 1500 TO 3500 M/S (4900 TO 11,000 FT/S) BUT LESS THAN 120% OF THE SONIC VELOCITY OF THE COMPONENT METALS
- A COLLISION ANGLE OF 5 TO 20°

Selecting the specific parameters is discussed in the Section "Procedure Development and Practice Considerations for Solid-State Welding" in this Volume.

Sizing Considerations. It is common practice to provision materials that are wider, longer, and thicker than required in the finished product to compensate for thinning and edge effects. In most situations, metals cannot be reliably bonded fully to the edges. Typically, edge nonbond allowances are four to eight times flyer plate thickness, depending on the combination of metals. Additionally, an area of nonbond is typical near the explosive initiator.

The thickness of the component metals is reduced during surface preparation and bonding. Surface conditioning removes up to 0.75 mm (0.030 in.) from the thickness. During the bonding operation, the force vector parallel to the detonation causes a 1 to 2% increase in plate lateral dimensions; this is accomplished by a corresponding reduction in thickness. The jetting of the metal surfaces during the bonding process causes only a thin layer to be removed, usually less than 0.05 mm (0.002 in.).

References cited in this section

10. *ATF--EXPLOSIVES LAW AND REGULATIONS,* BUREAU OF ALCOHOL, TOBACCO, AND FIREARMS, DEPARTMENT OF THE TREASURY, JUNE 1990
11. *FEDERAL MOTOR CARRIER SAFETY REGULATIONS,* U.S. DEPARTMENT OF TRANSPORTATION; FEDERAL HIGHWAY ADMINISTRATION, FEB 1991
12. *SUGGESTED CODE OF REGULATIONS FOR THE MANUFACTURE, TRANSPORTATION, STORAGE, SALES, POSSESSION AND USE OF EXPLOSIVE MATERIALS,* INSTITUTE OF MAKERS OF EXPLOSIVES, JAN 1985
13. SALES DEVELOPMENT SECTION OF THE EXPLOSIVES DEPARTMENT OF E.I. DU PONT DE NEMOURS & CO., INC., *BLASTERS' HANDBOOK*
14. W. SHARP, THE EXPLOSION CLADDING PROCESS, *ENG. DES.,* SEPT/OCT 1979

Explosion Welding

John G. Banker and Edward G. Reineke, Explosive Fabricators, Inc.

Typical EXW Process Sequence (Parallel-Plate Bonding)

Surface Preparation. The faying surfaces of the components are ground to achieve a smooth, pitfree finish of 1 to 3 μm (50 to 100 μin.).

Assembly. The plates are fixtured parallel while separated by a standoff gap. Methods for determining the standoff gap are presented in the article "Introduction to Solid-State Welding" and the Section "Procedure Development and Practice Considerations for Solid-State Welding" in this Volume. Small standoff devices are required to bear the weight of the flyer plate and the explosive. Edge standoff devices are easily ejected from the system during bonding; therefore, material of construction is rarely critical. Internal standoff devices must be of sufficiently low mass to be removed by the jet, or must be located in trim regions. Commonly used internal standoff materials are thin metal ribbons and foam blocks.

Explosive Loading. The explosive is placed on top of the flyers metal surface. The most commonly used explosives are granular or liquid and are typically contained within a simple box structure fabricated around the perimeter of the flyer plate. Initiating explosives are positioned in a suitable location on the plate surface.

The required detonation range of EXW is below that of most commercially manufactured explosives. Consequently, most practitioners of EXW use proprietary explosive blends. Appropriate detonation characteristics can be achieved by specialized blending of commercial explosives such as Amatol, Dynamite, or NCN.

Bonding. The primer is electrically initiated, causing a progressive detonation of the explosive, which creates the actions shown in Fig. 6 and welds the plates together.

Flattening. The energy of bonding typically creates sufficient deformation that flattening or straightening is required prior to further processing. Flattening is performed with equipment of the same design used in plate and sheet manufacture.

Testing and inspection are performed as mandated by the product specifications. Ultrasonic inspection, using standard procedures such as ASTM A 578, is the most commonly accepted method for inspecting the bond continuity. Bond shear strength is normally measured using the test defined in ASTM A 265. The tensile strength of the bond is normally measured using a Ram Tensile Procedure; the standard design is presented in MIL-J-24445.

Preparation of the Required Product. Because of the process edge effects, it is common practice to cut the product from a larger plate after bonding. The process options vary with the metal combinations and include oxyfuel gas cutting, plasma cutting, waterjet cutting, sawing, and machining.

Heat Treatment. Most metal systems do not require postbond heat treatment; however, some combinations provide superior properties if they are given a stress relief after bonding. For example, titanium/steel and zirconium/steel exhibit improved bond toughness after stress relief, and ferritic stainless steels exhibit an improvement in ductile-to-brittle transition temperature after stress relief.

Specifications

There are no universal ASTM, ASME, or military standard specifications for EXW products. Specific combinations of metals are covered in ASTM A 263, A 264, A 265, and B 432 (and their ASME equivalents) and in MIL-J-24445. The International Explosion Metalworking Association (IEMA) has established IEMA Guide Note 100, which provides recommended specification content.

Explosion Welding

John G. Banker and Edward G. Reineke, Explosive Fabricators, Inc.

Process Variations

The preceding discussion describes the process for welding a two-component flat plate product. Essentially the same approach can be used for producing multilayer products or cylindrical shapes:

- MULTIPLE LAYERS CAN BE BONDED SEQUENTIALLY IN A SINGLE BONDING OPERATION; AS MANY AS 50 INDIVIDUAL THIN LAYERS HAVE BEEN IN A SINGLE ASSEMBLY.
- TWO-SIDED CLAD PLATES, WITH A HEAVY CORE METAL, CAN BE PRODUCED BY

SIMULTANEOUSLY BONDING BOTH SIDES USING A VERTICAL ASSEMBLY.

- TWO OR MORE CYLINDERS CAN BE BONDED CONCENTRICALLY. THE EXPLOSIVE IS PLACED EITHER INSIDE OF THE CYLINDER OR OUTSIDE OF THE OUTER CYLINDER, DEPENDING ON DIAMETER AND WALL THICKNESS.

Explosion Welding

John G. Banker and Edward G. Reineke, Explosive Fabricators, Inc.

References

1. R.E. SAVIDGE, *MECHANICAL PROPERTIES OF EXPLOSION CLAD BONDS OF HIGH NICKEL ALLOYS ON LOW ALLOY STEELS AND THE EFFECT OF EXPLOSION CLADDING ON THE FRACTURE PROPERTIES OF THE STEEL,* THIRD INTERNATIONAL CONFERENCE ON HIGH ENERGY RATE FABRICATION, 1971, P 3.3.1
2. W. LUCAS, J.D. WILLIAMS, AND B. CROSSLAND, *SOME METALLURGICAL OBSERVATIONS ON EXPLOSION WELDING,* SECOND INTERNATIONAL CONFERENCE OF THE CENTRE FOR HIGH ENERGY FORMING, 1969, P 8.1.2
3. S.H. CARPENTER AND M. NAGARKAR, *THE EFFECTS OF EXPLOSIVE WELDING ON THE KINETICS OF METALLURGICAL REACTIONS,* THIRD INTERNATIONAL CONFERENCE OF THE CENTRE FOR HIGH ENERGY FORMING, 1971, P 3.4.1
4. L.F. TRUEB, MICROSTRUCTURAL EFFECTS OF HEAT TREATMENT ON THE BOND INTERFACE OF EXPLOSIVELY WELDED METALS, *METALL. TRANS.,* VOL 2, JAN 1971, P 145
5. A. SZECKET, O.T. INAL, AND J. ROCCO, EXPLOSIVE WELDING OF ALUMINUM TO STEEL; A WAVY VERSUS A STRAIGHT INTERFACE, *HIGH ENERGY RATE FABRICATION,* 1984, P 153
6. C.R. MCKENNEY AND J.G. BANKER, *EXPLOSION-BONDED METALS FOR MARINE STRUCTURAL APPLICATIONS,* THE SOCIETY OF NAVAL ARCHITECTS AND MARINE ENGINEERS, NOV 1970, P 285-292
7. E. GAINES AND J. BANKER, *SHIPYARD ALUMINUM/STEEL WELDED TRANSITION JOINTS,* 1991 SHIP PRODUCTION SYMPOSIUM, SEPT 1991
8. H. MANSELL, HYBRID METAL PACKAGES BY EXPLOSION BONDING, *HYBRID CIRCUIT TECHNOL.,* SEPT 1990, P 67
9. L.G. LAZARI, EXPLOSIVE WELDING AND ITS PRACTICAL APPLICATIONS, *WELD. REV.,* MAY 1988, P 74
10. *ATF--EXPLOSIVES LAW AND REGULATIONS,* BUREAU OF ALCOHOL, TOBACCO, AND FIREARMS, DEPARTMENT OF THE TREASURY, JUNE 1990
11. *FEDERAL MOTOR CARRIER SAFETY REGULATIONS,* U.S. DEPARTMENT OF TRANSPORTATION; FEDERAL HIGHWAY ADMINISTRATION, FEB 1991
12. *SUGGESTED CODE OF REGULATIONS FOR THE MANUFACTURE, TRANSPORTATION, STORAGE, SALES, POSSESSION AND USE OF EXPLOSIVE MATERIALS,* INSTITUTE OF MAKERS OF EXPLOSIVES, JAN 1985
13. SALES DEVELOPMENT SECTION OF THE EXPLOSIVES DEPARTMENT OF E.I. DU PONT DE NEMOURS & CO., INC., *BLASTERS' HANDBOOK*
14. W. SHARP, THE EXPLOSION CLADDING PROCESS, *ENG. DES.,* SEPT/OCT 1979

Forge Welding

FORGE WELDING (FOW) is a solid-state process in which the workpieces are heated to the welding temperature and then applied with blows sufficient to cause permanent deformation at the faying surfaces. It is most commonly applied to the butt welding of steels. As contrasted with hot pressure (thermocompression) welding of ductile face-centered cubic (fcc) metals, which is normally performed at temperatures of less than one-half the melting temperature (T_m), forge welding is typically conducted at temperatures in the 0.8 to 0.9 T_m range. The forge welding temperature is generally selected to be as high as possible with due consideration to avoiding such metallurgical problems as hot shortness, embrittlement, sensitization, and excessive grain coarsening. This implies an understanding of the unique metallurgical problems of the alloy to be welded.

Forge welding requires the application of pressure by means of either a hammer (hammer welding), rolls (roll welding), or dies (die welding). Joint configurations differ depending on whether the joints are to be produced manually or using automatic equipment. Typical joint designs used in manual forge welding operations are shown in Fig. 1. The joint surfaces in Fig. 1 are slightly rounded or crowned to ensure that the centerline region of the components joined will be welded first to force any contaminants (for example, slag, dirt, or oxide) present on the surfaces out of the joint. Typical joint configurations used for automatic forge welding operations are shown in Fig. 2 (Ref 1).

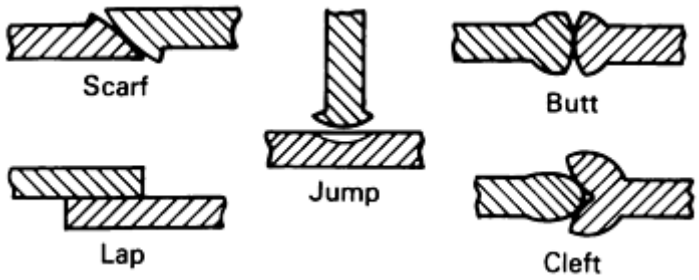

FIG. 1 TYPICAL JOINT CONFIGURATIONS USED FOR MANUAL FORGE WELDING APPLICATIONS. SOURCE: REF 1

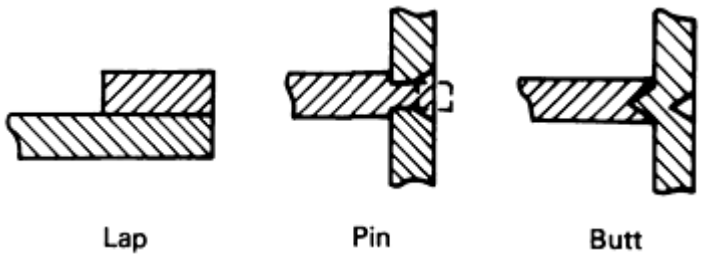

FIG. 2 RECOMMENDED JOINT CONFIGURATIONS USED IN AUTOMATIC FORGE WELDING APPLICATIONS. SOURCE: REF 1

Hydraulic presses are typically employed to apply pressure. Presses are often highly automated, featuring microprocessor control of pressure and temperature cycles. Heat is applied locally to the joint area by multiple-tip oxyacetylene torches, resistance heating, or induction heating. Often the oxyacetylene torches are oscillated to ensure uniformity of heating. In a closely related process, magnetically induced arc butt welding, the surfaces to be welded are heated by a rapidly rotating arc plasma. Generally, the process is conducted in the open air, with oxygen partially occluded from the joint area by the initial contact of the faying surfaces. When employing oxyacetylene torches, a slightly reducing flame affords some atmospheric protection. Vacuum, inert, and reducing atmospheres have been used.

The normal welding sequence is to (1) apply sufficient pressure to firmly seat the faying surfaces against one another, (2) heat the joint to welding temperature, and (3) rapidly apply additional pressure to upset the weld zone. Typical weld durations are 1 to 2 min. A less common procedure is to initially apply high pressure and permit deformation to occur during the heating cycle. Most forge welding employs sufficient pressure to upset the surface until the increase in the

surface area is 125% or more. However, such high deformation tend to cause flow lines to bend toward the surface during upsetting. Consequently, alloys that contain significant stringers and inclusions may exhibit poor impact or fatigue properties when welded with high amounts of upset. This effect may be minimized by reducing the upset, which normally requires increasing welding temperature and/or time to ensure complete elimination of voids and surface oxide.

Forge welding is most commonly applied to carbon and low-alloy steels, with typical welding temperatures of about 1125 °C (2060 °F). Low-carbon steels can be used in the as-welded condition, but medium-carbon steels and low-alloy steels normally are given full heat treatments following welding. In those cases where full heat treatment is impractical, but hardening due to rapid cooling has occurred, induction heating may be used to temper the weld zone. Other metals welded by forge welding include high-alloy steels, nickel-base alloys, cobalt-base alloys, aluminum alloys, titanium alloys, and tungsten. Applications of this process include welding rods, bars, tubes, rails, aircraft landing gear, chains, and cans. The forge welding process is competitive with flash welding (see the article "Flash Welding" in this Volume) and friction welding (see the article "Friction Welding" in this Volume).

Flux must be added when forge welding certain meals to prevent the formation of oxide scale. The flux and the oxides present combine to form a protective coating on the heated surfaces of the metal that prevents the formation of additional oxide and lowers the melting point of the existing oxide.

Silica sand and borax are two fluxes commonly used on steels. Silica sand can be used as a flux in the forge welding of low-carbon steel. The oxides of very low-carbon steels (ingot irons) and wrought irons do not require fluxes because their oxides have low melting points. Borax, sprinkled on the workpiece while it is in the process of being heated, is commonly used in the forge welding of high-carbon steels because of its low fusion point (Ref 1).

Weld durations for resistance welding are very short (seconds) compared to those for forge welding where gas torches are employed. This is because heat is generated internally in resistance welding, but externally with gas torches. Terms that are sometimes used synonymously with forge welding include pressure welding, upset welding, and solid-state resistance welding.

Reference

1. R.L. O'BRIEN, ED., *WELDING HANDBOOK,* VOL 2, 8TH ED., AWS, 1991, P 917-918

Forge Welding

Reference

1. R.L. O'BRIEN, ED., *WELDING HANDBOOK,* VOL 2, 8TH ED., AWS, 1991, P 917-918

Cold Welding

Karl Thomas, Technische Universität Braunschweig; Manfred Petri, Gerhard Petri GmbH + Co. KG

Introduction

COLD WELDING (also known as cold pressure welding) in normal ambient conditions involves the destruction of the surface (that is, oxide) layers of the metallic materials in the weld area. This exposes areas of clean metal surface on the two components to be welded, which must be brought into contact with each other to generate the interatomic forces needed to form a weld. Examinations of butt-welded joints of aluminum using transmission electron microscopy (TEM) have shown that the common deformation of the material in the weld zone leads to the destruction of the surface (that is, oxide and contaminant). TEM showed these surface layers in the form of numerous minute particles in the joint. The largest of these particles had a diameter of 12 nm (120 Å).

The actual interface between two dissimilar materials is a phase boundary, the same as a grain boundary between similar materials. Thermally induced processes such as recrystallization or diffusion are not required for welding to take place (Ref 1, 2). This makes cold-formable materials with a brittle cover layer especially suitable for cold pressure welding. The technique is frequently used with nonferrous metals (primarily copper and aluminum) (Fig. 1).

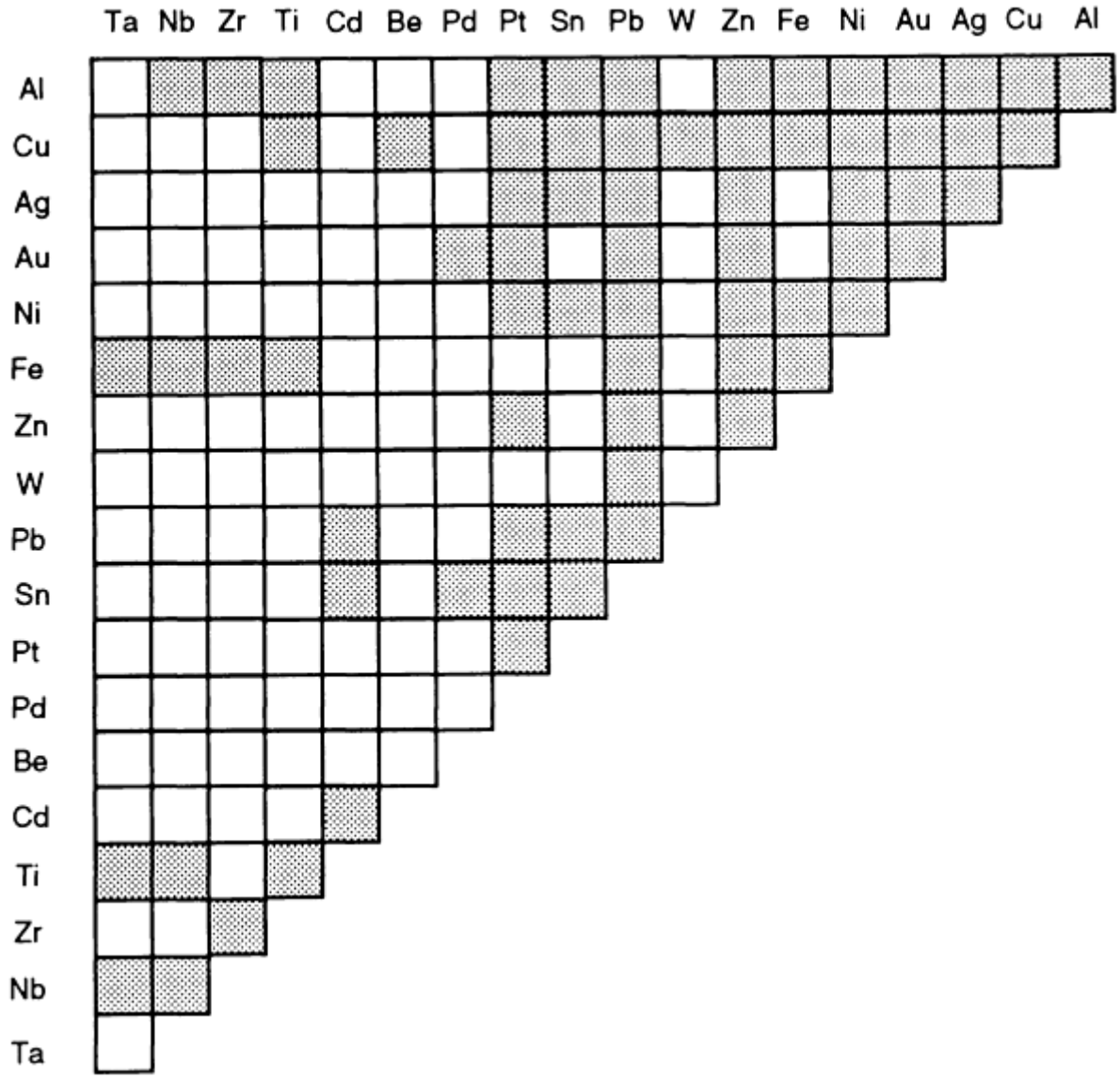

FIG. 1 CHART SHOWING COMBINATIONS OF METALS THAT CAN BE SUCCESSFULLY COLD WELDED (INDICATED BY SHADED BOX). SOURCE: ADAPTED FROM REF 3

In general, welds are examined by destructive techniques. As with other pressure welded joints, nondestructive testing methods fail to generate reliable results. It is expedient, therefore, to prepare the parts to be joined with great care and to control the parameters of the welding process as closely as the equipment tolerance specifications allow.

References

1. H. KREYE AND K. THOMAS, ELECTRON-MICROSCOPICAL TESTS AND THE BONDING MECHANISM OF COLD PRESSURE WELDING, *WELD. CUTTING,* VOL 29, 1977, P 249-252
2. H. PRIES, TESTS ON THE BONDING MECHANISM OF WELDING METALS TO NON-METALS IN ULTRA-HIGH VACUUM, *VDI PROGRESS REPORTS,* SERIES 5, *PRIMARY AND MANUFACTURING*

MATERIALS, NO. 89, VDI, 1985.
3. N. BAY, COLD WELDING: CHARACTERISTICS, BONDING MECHANISMS, BOND STRENGTH (PART 1), *MET. CONSTR.*, VOL 18 (NO. 8), JUNE 1986, P 369-372

Cold Welding

Karl Thomas, Technische Universität Braunschweig; Manfred Petri, Gerhard Petri GmbH + Co. KG

Variations of Cold Pressure Welding

Because welding lends itself to numerous techniques of forming, there are many variants of the cold pressure welding process. Cold pressure welding can be accomplished by deforming in a lap or butt configuration, drawing, extrusion, and rolling. The following discussion deals with only the first three variants.

Cold Pressure Lap Welding. The geometry of the cold pressure lap welding method (Fig. 2) is similar to the geometry of resistance spot welding. Two sheets of metal are joined in such a way that the direction of material flow is perpendicular to the direction of pressure. After a material-dependent reduction of the sheet thickness, the joint is formed. A high-quality joint will not be formed unless all superfluous oil has been removed and the contact surfaces have been mechanically cleaned (for example, by scratch-brushing with a rotating steel brush). Cleaning should be performed immediately before welding. Depending on the material, sheet thicknesses between 0.1 to 15 mm (0.004 to $\frac{19}{32}$ in.) can be welded.

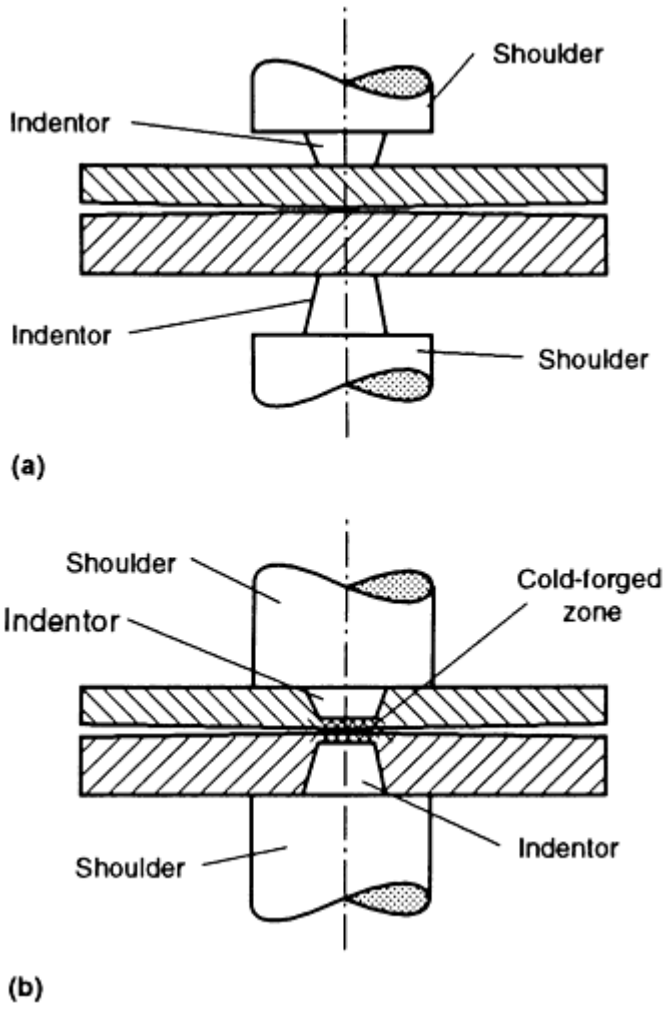

FIG. 2 SCHEMATIC SHOWING TWO DIES BEING USED FOR COLD PRESSURE LAP WELDING OF TWO METALLIC SHEETS. (A) DIE POSITION BEFORE WELDING. (B) DIE POSITION AFTER WELDING

The welds are produced by annular, point, or line-shaped pressure dies in mechanical or hydraulic presses or pneumatic clamps. The reduction in thickness produced by the dies must be limited by a solid stop or deformation measurement method. The bending distortion of the sheets is small when several spots or adjacent narrow areas are welded at the same time. Dies that generate a ring-shaped area of pressure produce welds superior to dies that generate a circular area of pressure. For line welds, dies with relatively long and narrow pressure areas should be used. The width of the pressure area and its distance to an adjacent pressure area will be greater with increasing thickness of the plate. For example, coils of aluminum and copper for electric machines were welded to each other and to connecting pieces. The joints consisted of two aluminum parts having cross-sections measuring 7 by 1.6 mm (0.3 by 0.063 in.) and welds between aluminum measuring 7 by 1.6 mm (0.3 by 0.063 in.) and copper measuring 7 by 1 mm (0.3 by 0.039 in.) cross section (Ref 4). It is possible to produce cold pressure lap welds with very large cross sections if the proper tooling and required pressure forces are available.

Cold pressure butt welding implies that the ends of two bars of similar or dissimilar metals are jointly upset. The two bars are placed in a device or machine having suitable clamping shoes (Fig. 3). The compressive force applied along the axis of the bars causes an expansion of the contact surfaces and forms a bulb. Both bar ends will weld together when the contact surfaces have reached a certain size, which depends on both the material and the condition of the contact surface. The strength of the joint increases as the contact surface expands until it reaches the strength of the softer of the two materials used. The strength of the softer material is thus enhanced by cold work hardening.

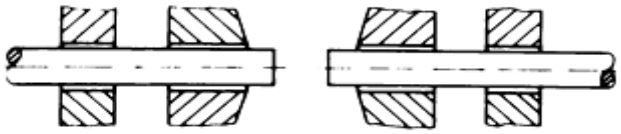

Bars clamped in dies

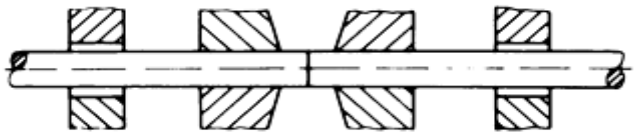

Beginning of first upsetting operation

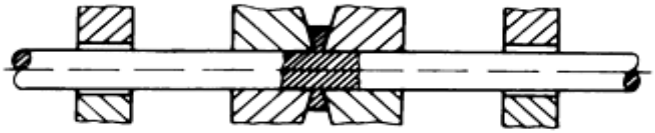

End of first upsetting operation

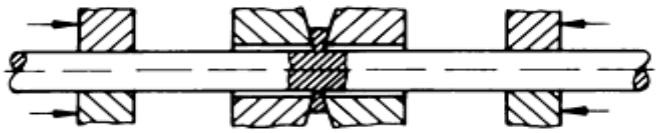

Initial loading by auxiliary clamp jaws along the bar; removal of main clamp jaws

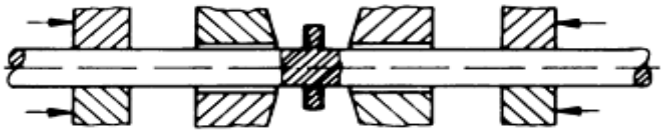

Movement of main clamp jaws

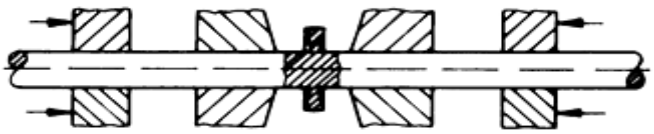

Main clamp jaws grip ends of each bar

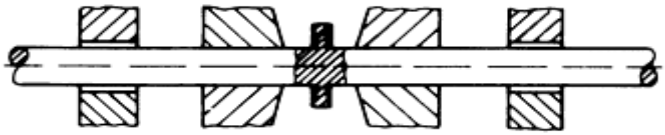

Beginning of second upsetting sequence

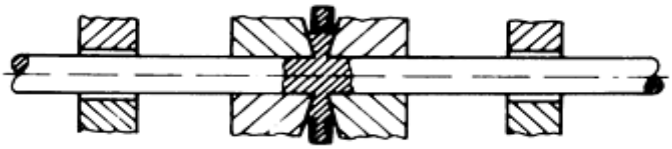

End of second upsetting sequence

FIG. 3 COLD PRESSURE BUTT WELDING OF TWO BARS USING MULTIPLE-STEP UPSETTING METHOD

Cold pressure butt welding may require one or more steps of upsetting. The parameter characterizing the weld is the surface extension parameter, V_o:

$$Vo = \left(\frac{A_s}{A_o} \right) - 1 \qquad \textbf{(EQ 1)}$$

where A_s is the size of the contact surface after welding and A_o is the original surface area. The extension of the surface area can be particularly large when several steps of upsetting are used on materials that are easily cold-formed. When single-step upsetting and a rather simple upsetting device are used, the material ends that project from the clamping shoes may buckle. This limits the surface expansion that can be obtained.

When single-step upsetting is applied on machines made for this purpose and in multiple-step upsetting, buckling is not a consideration, because only very short rod ends will project from the clamping shoes. Because the clamping shoes with an initial loading are transposed in multiple-step upsetting, no cracks can form in the weld during transposition (Fig. 3). No gases from the ambient atmosphere can contact the exposed surface and, hence, no new oxides form.

Many devices have been developed for cold pressure butt welding. There are hand-held tongs for wires in diameters up to 1 mm (0.04 in.) and even an oil-hydraulically powered welding machine with a programmable device to interface with a multiple-step upsetting system. The largest known system applies upsetting forces as high as 1.2 MN (135 tonf), which permits the joining of aluminum up to 1500 mm^2 (2.3 $in.^2$) in cross-sectional area and of copper up to 1000 mm^2 (1.55 $in.^2$) in cross-sectional area (Ref 4). A system capable of butt welding of plastic-coated aluminum ribbons of 0.1 to 0.2 mm (0.004 to 0.008 in.) thickness and up to 50 mm (2 in.) wide has been constructed. This system can complete as many as 99 upsetting steps to produce a weld (Ref 5).

Figure 4 is a schematic of the mechanical part of a servohydraulic, computer-aided cold pressure welding machine. The base, which consists of a base plate and two vertical side plates, houses two horizontally arranged structural members. These structural members support two traverses, one of which can be moved by two hydraulic actuators that operate in unison. The second traverse is held by several binder plugs that have to be loosened only for changeover to a new welding job. Bolted to the traverse are two dies that support the blanks to be welded. The dies, in turn, are attached to two fixtures to which the piston rods of the hydraulic actuators are bolted. Each hydraulic actuator has a sensor to monitor the inductive force acting on the piston rod and to record the inductive displacement. Software is available to produce butt-welded joints by two methods. In cold pressure butt welding with continuous thrust, the piston rods of the 630 kN cylinders are displaced by the same amount. The 250 kN cylinders maintain their positions as set by the computer program. They determine the thickness of the upset. Three bladelike cutters are arranged on the spot faces on the dies. They produce notches in the forming flash that cause the flash to rupture under circumferential tension. While weld material is flowing, the flash is automatically sheared off. The surface extensions obtained are very large. Because of the high tool load, this method should be used only with materials of low tensile strength and moderate work-hardening properties.

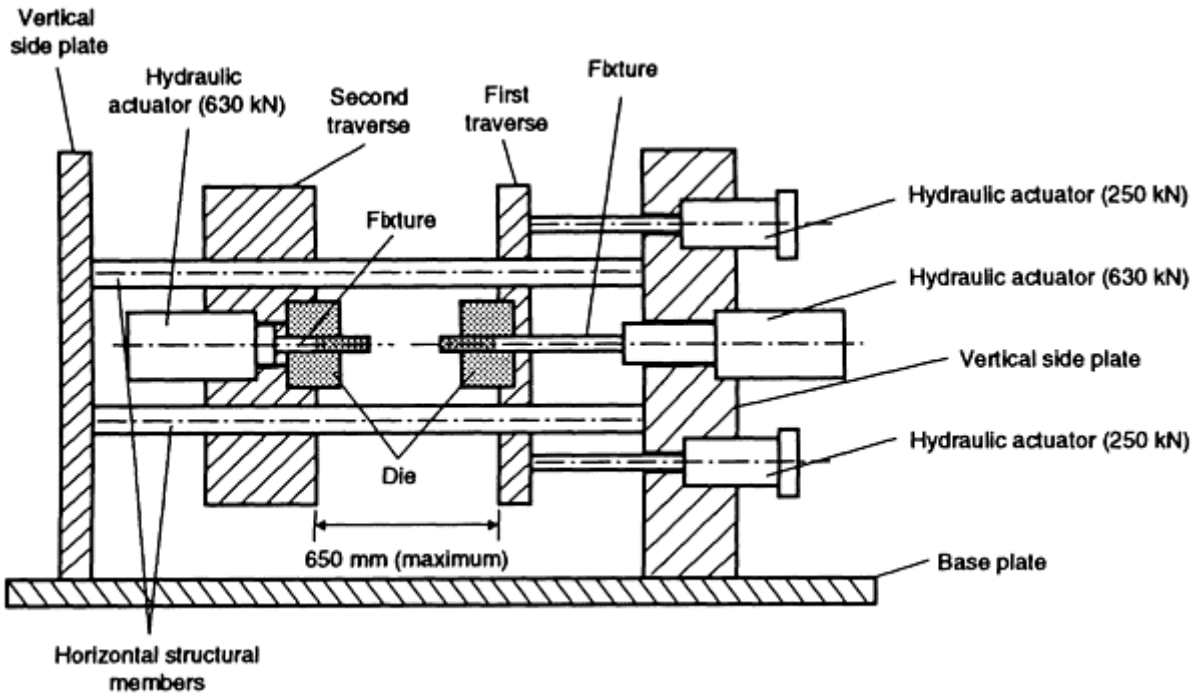

FIG. 4 SCHEMATIC SHOWING SERVOHYDRAULIC, COMPUTER-AIDED COLD PRESSURE WELDING MACHINE CONSISTING OF TWO 250 KN (28 TONF) ACTUATORS AND TWO 630 KN (71 TONF) ACTUATORS

In the second method, multiple-step upsetting, the computer controls a sequence of operations that corresponds to the schematic in Fig. 3. Large surface extensions are obtained with this method, but the tool load is lower than in the continuous thrust method. Figure 5 illustrates two copper-aluminum joints produced by the two methods in which the upset metal was not removed automatically (Ref 6).

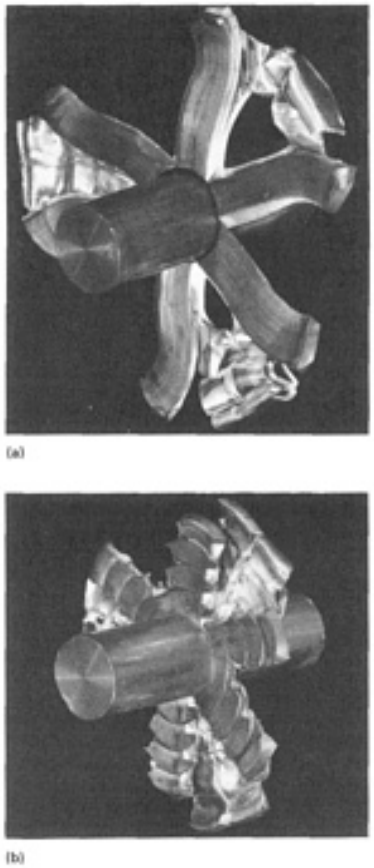

FIG. 5 COPPER-ALUMINUM JOINT OBTAINED BY BUTT WELDING OF TWO 20 MM ($\frac{25}{32}$ IN.) COMPONENTS USING TWO DIFFERENT TECHNIQUES. (A) CONTINUOUS THRUST METHOD. (B) MULTIPLE-STEP UPSETTING METHOD

An example of multiple-step upsetting is the production of interlocking connections of copper and aluminum components for installation in national power grids. The connecting pieces are welded by the single-step upsetting method from 12 to 45 mm ($\frac{15}{32}$ to $1\frac{3}{4}$ in.) diameter blanks. Before welding, the contact surfaces on the blanks are machined with a dry milling tool. The milling tool is periodically cleaned with a solvent. In a manual operation, the blanks are inserted in the upsetting die of a power press without touching the contact surfaces. They are welded together and ejected, and the flash is immediately removed by subsequent machining. Before the mechanical operation is finished, a connecting plate is attached to the copper side of the component by deformation and a hole with a cross-section formed by backward extrusion is made in the aluminum. By deforming the copper closely adjacent to the seam, the quality of the joint can be safely assessed because welds of insufficient strength would rupture along the seam (Ref 7).

Cold Pressure Welding in Drawing Processes. By common deformation in the drawing tool of a drawing bench, multilayer tubes or solid multilayer (clad) bars can be made that have numerous inside and outside layers that consist of different materials (Fig. 6). In this variant also, the contact surfaces must be thoroughly cleaned before welding. This need for cleanliness limits the initial tube length to 800 mm (32 in.). High-intensity compressive stresses exist between the commonly deformed contact surfaces during the drawing operation. The extension of the contact surfaces along the longitudinal axis of the bar is the essential characteristic of the weld. Shear strength values of about 50 MPa (7 ksi) have been reported for copper-aluminum joints after a surface extension of 300% (Ref 8).

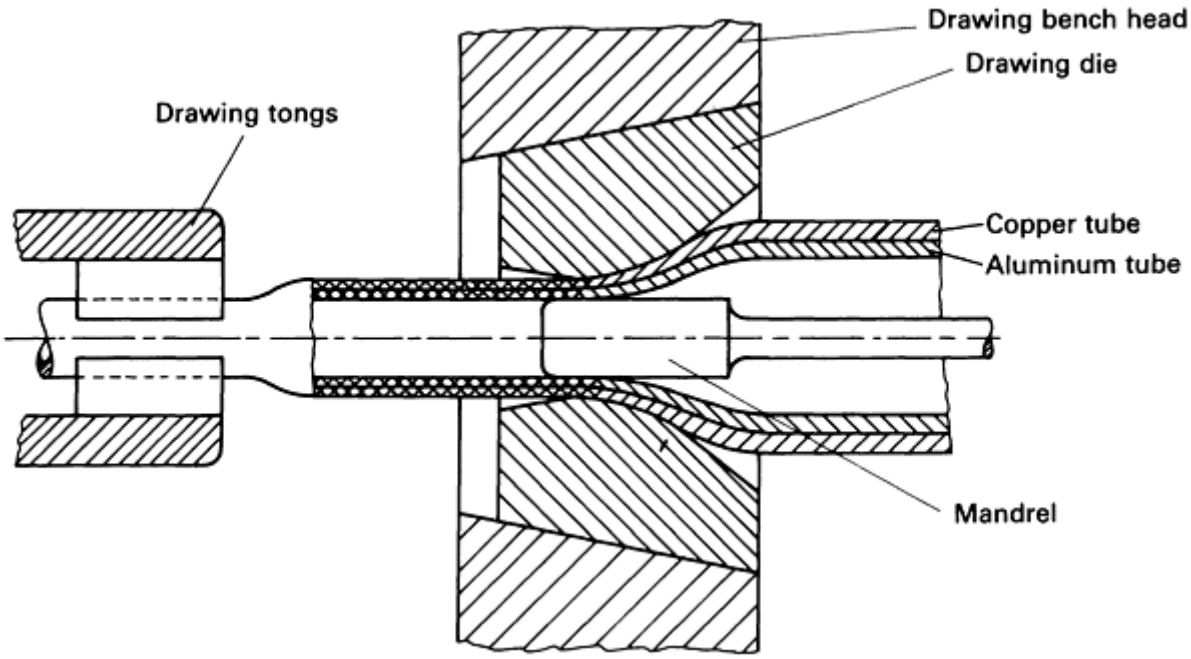

FIG. 6 APPLICATION OF DRAWING TO COLD PRESSURE WELD MULTILAYER TUBES INCORPORATING COPPER ON THE OUTSIDE DIAMETER AND ALUMINUM ON THE INSIDE DIAMETER

References cited in this section

4. A. STEFANESCU AND T. ZRNA, SVAROVÁNÍ TLAKEM ZA STUDENA, SNTL--NAKLADATATELSTVÍ TECHNICKÉ LITERATURY, 1975
5. J. RUGE, SOLID STATE WELDING, COLD PRESSURE WELDING, DIFFUSION WELDING, SPIN WELDING, *DVS REPORTS,* NO. 65, 1980, P 41-46
6. K. THOMAS, APPLICATION OF PROCESS CONTROL COMPUTERS IN SPIN WELDING AND COLD PRESSURE WELDING, *DVS REPORTS,* NO. 120, 1989, P 167-185
7. J. RUGE, H. PRIES, AND K. THOMAS, SURVEY ON THE ACTUAL STAGE AND DEVELOPMENT TRENDS IN COLD PRESSURE WELDING, *DVS REPORTS,* NO. 139, 1991, P 25-32
8. J. RUGE, *MANUAL OF WELDING TECHNICS,* VOL II, 2ND ED., SPRINGER-VERLAG, 1980

Karl Thomas, Technische Universität Braunschweig; Manfred Petri, Gerhard Petri GmbH + Co. KG

References

1. H. KREYE AND K. THOMAS, ELECTRON-MICROSCOPICAL TESTS AND THE BONDING MECHANISM OF COLD PRESSURE WELDING, *WELD. CUTTING,* VOL 29, 1977, P 249-252
2. H. PRIES, TESTS ON THE BONDING MECHANISM OF WELDING METALS TO NON-METALS IN ULTRA-HIGH VACUUM, *VDI PROGRESS REPORTS,* SERIES 5, *PRIMARY AND MANUFACTURING MATERIALS,* NO. 89, VDI, 1985.
3. N. BAY, COLD WELDING: CHARACTERISTICS, BONDING MECHANISMS, BOND STRENGTH (PART 1), *MET. CONSTR.,* VOL 18 (NO. 8), JUNE 1986, P 369-372
4. A. STEFANESCU AND T. ZRNA, SVAROVÁNÍ TLAKEM ZA STUDENA, SNTL--

NAKLADATATELSTVÍ TECHNICKÉ LITERATURY, 1975

5. J. RUGE, SOLID STATE WELDING, COLD PRESSURE WELDING, DIFFUSION WELDING, SPIN WELDING, *DVS REPORTS,* NO. 65, 1980, P 41-46
6. K. THOMAS, APPLICATION OF PROCESS CONTROL COMPUTERS IN SPIN WELDING AND COLD PRESSURE WELDING, *DVS REPORTS,* NO. 120, 1989, P 167-185
7. J. RUGE, H. PRIES, AND K. THOMAS, SURVEY ON THE ACTUAL STAGE AND DEVELOPMENT TRENDS IN COLD PRESSURE WELDING, *DVS REPORTS,* NO. 139, 1991, P 25-32
8. J. RUGE, *MANUAL OF WELDING TECHNICS,* VOL II, 2ND ED., SPRINGER-VERLAG, 1980

Coextrusion Welding

Introduction

COEXTRUSION WELDING (CEW) is a solid-state process that produces a weld by heating two or more workpieces to the welding temperature and forcing them through an extrusion die. The process typically is conducted at elevated temperatures not only to improve welding but also to lower extrusion pressures. Some cold coextrusion welding of aluminum and copper has been performed. For hot coextrusion, the parts to be welded are often assembled in a can or retort that is designed with the appropriate leading taper and wall thickness to promote initiation of extrusion. For reactive metals, such as zirconium, titanium, and tantalum, the retort may be evacuated and sealed. Both forward and back coextrusion have been employed, but forward coextrusion is the usual mode. A principal advantage of coextrusion welding is that the high isostatic pressures associated with the process are favorable to the deformation welding of low-ductility alloys.

In a similar process, extrusion welding has been used to butt weld tubes. The ends of the tubes are prepared for extrusion by beveling at a 45 to 60° angle to produce an overlapping joint (Fig. 1). The leading tube contains the female portion of the beveled joint and is the stronger of the two metals in dissimilar metal joints. Extrusion press die angles of 30 to 35° are common. An advantage of extrusion welding over other methods of deformation butt welding of tubes is that there is no flash or upset to remove following extrusion.

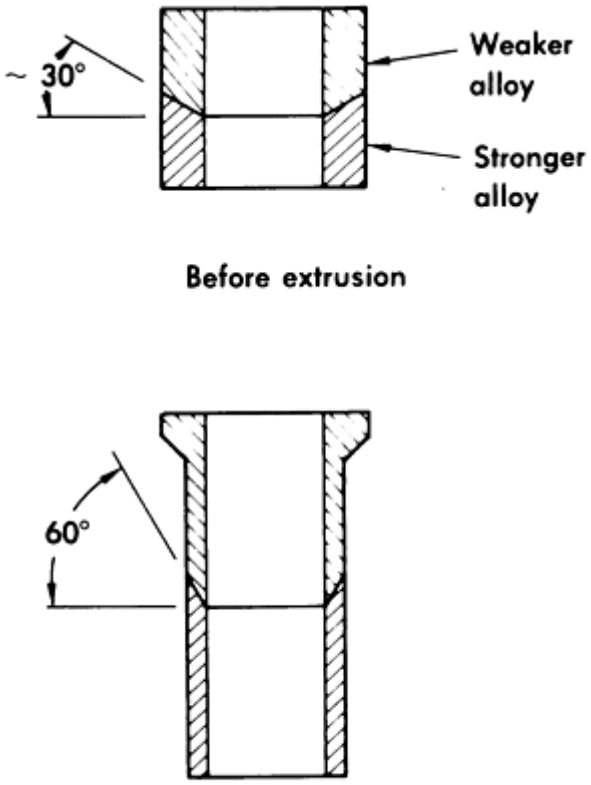

FIG. 1 DESIGN FOR BUTT WELDING OF TUBES BY EXTRUSION

Coextrusion Welding

Common Metals Welded

The most common metals welded by the coextrusion process include low-carbon steel, aluminum, aluminum alloys, copper, and copper alloys. Additional applicable materials include nickel, nickel-base alloys, zirconium, titanium, tantalum, and niobium.

Roll Welding

Introduction

ROLL WELDING (ROW) is a process in which two or more sheets or plates are stacked together and then passed through rolls until sufficient deformation has occurred to produce solid-state welds.

Roll Welding

Process Description

Two modes of roll welding are common. In the first, the parts to be welded are merely stacked and passed through the rolls. The second method, usually termed pack rolling, involves sealing the parts to be rolled in a pack or sheath and then roll welding the pack assembly.

The first method is more generally employed in the cold welding of ductile metals and alloys. Sometimes the stack to be welded is first tack welded at several locations to ensure alignment during rolling. Also, when using this method, the

deformation during the first rolling pass must exceed the threshold for welding (typically greater than 60% for cold rolling) to keep the parts together. The required first pass reduction can be reduced by hot rolling, if the metals to be rolled can tolerate preheating without excessive oxidation. Once the first pass has been accomplished, the reduction per pass can be decreased, as is often desirable because roll-separating forces increase as the parts to be rolled become thinner. However, the nonuniform stress distribution that builds up during a sequence of very light passes can cause the weld to open up or "alligator." Therefore, the reduction for subsequent passes is generally a compromise between applying excessive separating forces and "alligatoring."

In pack roll welding, the parts to be welded are completely enclosed in a pack that is sealed (typically by fusion welding) and often evacuated to provide a vacuum atmosphere. This may be accomplished by a frame that surrounds the parts to be welded, which is sandwiched by two lids, or may simply consist of two covers formed to encapsulate the parts to be welded (Fig. 1). Semikilled or killed low-carbon steel is a common material for the pack, but is not suitable for all alloy and temperature combinations. Although the preparation costs of pack roll welding are significant, the process has the advantages of (1) providing atmospheric protection, which may be particularly important for reactive alloys such as those of titanium, zirconium, niobium, and tantalum; and (2) permitting welding of complex assemblies involving several layers of parts. A significant limitation of the process is that packs become difficult to process when their length exceeds several feet.

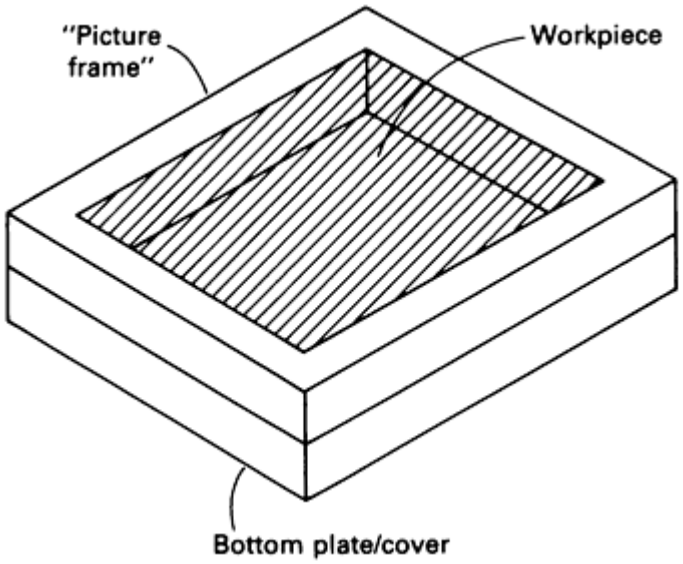

FIG. 1 PACK USED FOR ROLL WELDING. THE TOP COVER, WHICH WOULD BE WELDED IN PLACE BEFORE ROLLING, IS NOT SHOWN.

Titanium and titanium alloys are considerably more difficult to pack roll than are either steels or copper and aluminum alloys because most titanium alloys have very narrow working temperature ranges. To overcome this problem, titanium alloys that are pack rolled are sometimes encased in a steel envelope, or can. The can is evacuated to minimize oxidation of the work metal, and also serves to minimize heat loss to the relatively cold rolls upon deformation. The narrow working temperature range of titanium alloys makes the rolling of these materials labor intensive. Rolling passes are done by hand on relatively small pieces, and many intermediate reheating steps are required. Some β titanium alloys, however, are being continuously rolled on hot and cold strip mills.

Nonpack rolling, of course, can employ continuous strip rolling. A seldom used hybrid version of roll welding is to seal the edges of the parts to be welded by fusion welding prior to rolling. This method does not provide atmospheric protection to the outer surfaces, as in pack roll welding, but does occlude air from the more critical inner surfaces.

In roll welding, successful welding depends not only on the total amount of deformation but also on the pressure during rolling. A high isostatic pressure component during rolling is promoted by large reductions per pass, large roll diameters, and rough roll surfaces. A nonuniform distribution of normal stresses, referred to as pressure hill effects, is caused by frictional and mechanical restraint and results in lower pressure near the outer edges of the parts being rolled. Therefore, rolling conditions must be such to ensure sufficient pressure near the edges to avoid weak welds in these regions.

Copper, aluminum, and their alloys are often cold roll welded. Hot rolling is applicable to a wide spectrum of alloys. Typically, hot rolling is performed above recrystallization temperatures. In practice, weldability is often improved by raising the temperature to the region where oxygen mobility becomes significant to promote oxide assimilation by diffusion. Also, welded assemblies are often postheat treated to cause recrystallization (in cold rolling), oxygen diffusion, and/or sintering. In welding dissimilar metals, selection of temperatures for rolling and postheating must take into consideration the possibility of intermetallic compound formation, eutectic melting, and/or porosity due to Kirkendall diffusion. The most common metals that are roll welded are low-carbon steels, aluminum and aluminum alloys, copper and copper alloys, and nickel. Low-alloy steels, high-alloy steels, nickel-base alloys, and titanium and titanium alloys have also been roll welded.

Applications

One of the more important applications of roll welding is the fabrication of heat exchangers. A patented roll welding process is described in the section "Roll Welding Heat Exchangers" in this article. This process is used to fabricate flat solar collectors. In another method of heat-exchanger fabrication, three plates are stacked, with the middle plate containing the flow channels. The stacked plates are initially held together by tack fusion welds or resistance spot welds. This approach has been employed for both aluminum and steel heat exchangers. A second important application of this process is in the cladding of sheet metal products.

Roll Welded Heat Exchangers. A principal application of roll welding is the production of heat-exchanger panels with flow tubes as an integral part of the composite. Millions of refrigerator evaporator plates have been formed by this process. A cross section of a similar application, solar collector panels, is illustrated in Fig. 2. Roll welded heat-exchanger panels are most often made of aluminum, although copper and stainless steel panels have also been produced commercially.

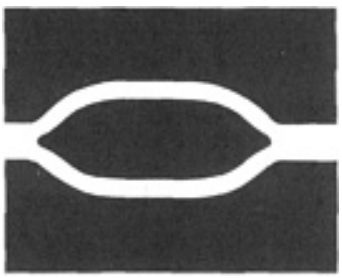

FIG. 2 CROSS SECTION OF AN ALUMINUM SOLAR COLLECTOR PANEL PRODUCED BY THE ROLL WELDING PROCESS

The first major step in the production of roll welded heat exchangers is to thoroughly clean the surfaces of the sheets to be joined by combinations of solvent cleaning, chemical cleaning, and wire brushing. Next, a stop-weld pattern is reproduced on one of the sheets that will later form the passageways in the heat exchanger. This is accomplished by transferring ink onto the surface by silkscreen processing. These stop-off inks contain materials such as graphite or titanium oxide.

The prepared plates are placed together and temporarily joined by spot welding to form a sandwich that is then roll welded, with at least partial welding occurring during the first rolling pass. The sandwich sometimes is heated prior to this first rolling pass. Whether hot rolling or cold rolling is employed, the major reduction takes place in this first pass (50 to 80%). Subsequently, cold rolling may be employed to reduce the panel to final gage. Also, panels are generally given a postweld heat treatment. This heat treatment results in an annealed part and, particularly in the case of cold rolled panels, may improve the weld quality through recrystallization and diffusion. Finally, the passageways are formed by inflating them with air pressure while the sandwich is held between platens. The panel is then ready for trimming, additional forming, and painting, as required for the application.

The process has been used to produce heat exchangers for refrigerators, solar panels, poultry incubators, electronic equipment temperature controllers, industrial heat exchangers, and special applications such as thermal control of spacecraft. Modifications of the process permit as many as six sheets to be welded at one time and inclusion of passageways oriented along different principal directions at the different layers. Also, it is possible to produce panels where the passageways are expanded on one side only.

Cladding of Metals by Strip Roll Welding. The common early application of strip roll welding was the fabrication of bimetallic strips for thermostats. This remains an important application, with thermostats taking many complex forms and finding use in furnaces, color televisions, cars, and numerous industrial controls.

A key cladding application is the production of coins by the U.S. Mint. Silver shortages in the 1960s and 1970s resulted in the introduction of coins made from new materials. These coins required a unique set of properties for acceptance by the general public and use in automatic vending machines. Copper clad with cupro-nickel was found to meet these requirements (Fig. 3). The cladding process is relatively simple, although stringent in its requirement for surface preparation. Cladded strips are produced by continuous rolling with the surfaces prepared just prior to rolling by processes such as wire brushing. Welding typically is accomplished in a single rolling pass. Subsequent heat treatments may be employed to improve the weld quality by processes such as sintering, diffusion, and recrystallization.

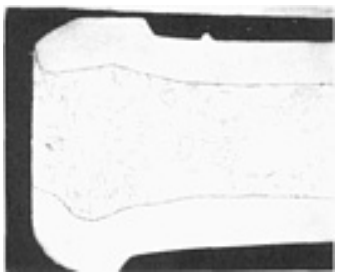

FIG. 3 METALLOGRAPHIC CROSS SECTION OF THE EDGE OF A CUPRONICKEL-CLAD COPPER COIN

The starting material for the U.S. quarter is two outer layers of 75Cu-25Ni, each 1.2 mm (0.048 in.) thick, with an inner layer of pure copper that is 5.1 mm (0.20 in.) thick. To obtain good bond strength, the surfaces are chemically cleaned and wire brushed. The strips are then roll welded to a combined thickness of 2.29 mm (0.090 in.) (Fig. 4). A second rolling operation reduces the final thickness 1.36 mm (0.0535 in.). The strips thus undergo a total reduction of 82% (Ref 1).

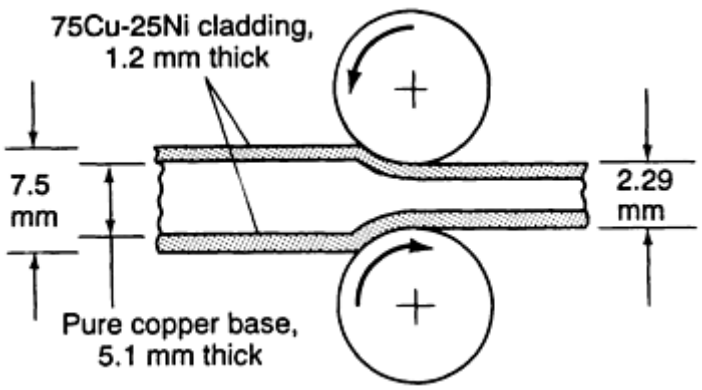

FIG. 4 SCHEMATIC SHOWING 70% REDUCTION IN CROSS SECTION OF A U.S. MINT QUARTER COIN (COMPOSED OF AN INSIDE LAYER OF PURE COPPER SANDWICHED BETWEEN TWO THIN LAYERS OF CUPRONICKEL MATERIAL) AS IT UNDERGOES AN INITIAL ROLL WELDING OPERATION. A SECOND ROLLING OPERATION FURTHER REDUCES THE MATERIAL TO A FINAL THICKNESS OF 1.36 MM (0.0535 IN.) FOR A TOTAL REDUCTION OF 82%. SOURCE: REF 1

Similar processing is applied to many new products, including electrical contacts, conductive springs, automotive windshield wiper sockets, automotive trim, clad cookware, wrap for underground cable, and electromagnetic shielding (Table 1).

TABLE 1 TYPICAL PROPERTIES OF COMMON ROLL WELDED CLAD LAMINATES

MATERIALS SYSTEM	COMPOSITE RATIO, %	THICKNESS		WIDTH		TENSILE STRENGTH		YIELD STRENGTH		ELONGATION, %	APPLICATIONS
		MM	IN.	MM	IN.	MPA	KSI	MPA	KSI		
COPPER 10300/LOW-CARBON STEEL	50:50	0.25-2.54	0.010-0.100	12.7-50	0.5-2	260[A]	38[A]	215[A]	31[A]	40[A]	**TYPICALLY USED FOR COMMUTATORS IN ELECTRIC MOTORS, REPLACING COPPER 10400. THE LOWER CONDUCTIVITY OF STEEL CAUSES LESS HEAT LOSS DURING WELDING, RESULTING IN FASTER, BETTER QUALITY WELDS. THE ADDED STRENGTH OF STEEL ALLOWS THICKNESS REDUCTION.**
DEOXIDIZED COPPER/CARBON STEEL/DEOXIDIZED COPPER	5:90:5, 10:80:10, 15:70:15	0.25-2.54	0.010-0.100	≤ 610	≤ 24	420[B]	61[B]	250[B]	36[B]	35[B]	**USED IN HEAT EXCHANGERS, REPLACING BRAZING SHIM MATERIAL. ONE-PIECE MANUFACTURING ELIMINATES SEPARATE SHIMS AND REDUCES ASSEMBLY COST. BECAUSE NO FERROUS SURFACES ARE EXPOSED, NO FLUX IS NEEDED.**
TYPE 434 STAINLESS/5052 ALUMINUM	40:60	0.56-0.76	0.022-0.030	≤ 610	≤ 24	395	57	360	52	12	**WIDELY USED FOR AUTOMOTIVE BODY MOLDINGS, DRIP RAILS, ROCKER PANELS, AND OTHER TRIM COMPONENTS, OFTEN REPLACING SOLID STAINLESS STEEL OR ALUMINUM. STAINLESS STEEL PROVIDES BRIGHT APPEARANCE; THE HIDDEN ALUMINUM BASE PROVIDES CATHODIC PROTECTION, CORRODING SACRIFICIALLY TO THE BODY STEEL.**
COPPER 11000/1100 ALUMINUM	50:50	0.51-2.54	0.020-0.100	50-510	2-20	180[C]	26[C]	12[C]	1.7	35[C]	**DEVELOPED SPECIFICALLY FOR TRANSITION JOINTS BETWEEN COPPER AND ALUMINUM IN REFRIGERATION EQUIPMENT. USUALLY USED IN THE FORM OF DEEP-DRAWN TUBING.**
C1008 STEEL/TYPE 347 STAINLESS STEEL/ C1008 STEEL	43:10:45	0.36	0.014	305	12	393	57	195	28	35	**USED IN HYDRAULIC TUBING IN VEHICLES, REPLACING TERNE-COATED CARBON STEEL TUBING. THE OUTER LAYER OF CARBON STEEL CATHODICALLY PROTECTS THE STAINLESS CORE OF THE TUBE, EXTENDING ITS LIFE SIGNIFICANTLY.**

NICKEL 201/TYPE 304 STAINLESS STEEL/NICKEL 201	7.5:85:7.5	0.20-2.41	0.008-0.095	25-64	1-2.5	. . .	. . .	310	45	40	**USED IN FORMED CANS FOR TRANSISTOR AND BUTTON CELL BATTERIES, REPLACING SOLID NICKEL AT A LOWER COST.**
COPPER 10300/TYPE 430 STAINLESS STEEL/ COPPER 10300	17:66:17, 20:60:20, 33:34:33	0.10-0.15	0.004-0.006	12.7-150	0.5-6	415[D]	60[D]	275	40	20[D]	**REPLACES HEAVIER GAPES OF COPPER AND BRONZE IN BURIED COMMUNICATIONS CABLE. THE STAINLESS STEEL PROVIDES RESISTANCE TO GNAWING BY RODENTS, WHICH IS A SERIOUS PROBLEM IN UNDERGROUND INSTALLATIONS.**
PHOSPHOR BRONZE 51000/CARBON STEEL/COPPER	**10:85:5**	**0.38-1.52**	**0.015-0.060**	**≤ 610**	**≤ 24**	**455[E]**	**66[E]**	**435**	**63**	**16[E]**	**USED IN AUTOMOTIVE APPLICATIONS, SUCH AS WINDSHIELD-WIPER BEARINGS. THE BRONZE PROVIDES THE BEARING QUALITIES, THE STEEL PROVIDES STRENGTH, AND THE COPPER AIDS TOOLING LIFE AND PROVIDES CORROSION RESISTANCE IN SERVICE.**

Source: Ref 2

(A) IN EIGHTH-HARD TEMPER.

(B) 10:80:10 MATERIAL.

(C) IN THREE-QUARTER-HARD TEMPER.

(D) 20:60:20 MATERIAL.

(E) IN QUARTER-HARD TEMPER.

Essentially all combinations of ductile metals and alloys can be clad by roll welding, although the oxides of some metals may make welding difficult and other combinations may suffer from intermetallic compound formation on heating. Most engineering metals and alloys can be processed into clad-laminate form, but some cannot (Table 2). One characteristic that makes some metals difficult or impossible to combine by deformation is low ductility. Such metals cannot be co-reduced to the extent necessary to achieve a metallurgical bond. Another characteristic that can cause problems is the tendency of some metals to form a tenacious oxide film that inhibits weld formation. Finally, some metals are thermally unstable; they form brittle intermetallic compounds when heated above a certain temperature. Those metals that are readily processed into clad laminates have opposite characteristics. They are ductile and easily cleaned of oxides, and they form no intermetallic compounds. In most cases, when a metal is named, alloys of that metal also apply.

TABLE 2 RELATIVE WELDABILITY OF SELECTED DISSIMILAR METALS AND ALLOYS ROLL WELDED INTO CLAD-LAMINATE FORM

BASE METAL NO. 1	BASE METAL NO. 2																	
	Ag	**Al**	**Al alloys**	**Au**	**Carbon Steel**	**Co**	**Cu**	**Mn**	**Mn-Ni**	**Nb**	**Ni**	**Pt**	**Stainless Steel**	**Steel**	**Sn**	**Ta**	**Ti**	**U**	Zr
AG	. . .	. . .	. . .	. . .	. . .	. . .	A	B	. . .	. . .	. . .	. . .	. . .	B	. . .	. . .	. . .	. . .	**. . .**
AL	. . .	. . .	A	C	B	C	B	. . .	. . .	. . .	B	. . .	B	. . .	. . .	. . .	. . .	. . .	**C**
ALFESIL	D	D	D	D	D	D	D	D	D	D	D	D	D	D	D	D	D	D	**D**
BE	D	D	D	D	D	D	D	D	D	D	D	D	D	D	D	D	D	D	**D**
CARBON STEEL	. . .	B	. . .	. . .	. . .	. . .	. . .	. . .	. . .	. . .	. . .	. . .	B	. . .	. . .	. . .	B	. . .	**. . .**
CU	A	B	. . .	A	. . .	. . .	. . .	B	B	B	A	B	B	A	A	B	B	. . .	**B**
MN	B	. . .	. . .	. . .	. . .	. . .	B	. . .	. . .	. . .	A	B	. . .	. . .	. . .	. . .	. . .	. . .	**. . .**
NI	. . .	B	. . .	A	. . .	. . .	A	. . .	. . .	. . .	. . .	B	. . .	B	A	. . .	. . .	. . .	**. . .**
NB	. . .	. . .	. . .	. . .	. . .	. . .	B	. . .	. . .	. . .	. . .	. . .	. . .	. . .	. . .	B	. . .	. . .	**. . .**
STAINLESS STEEL	. . .	B	. . .	. . .	B	. . .	B	. . .	. . .	. . .	. . .	. . .	. . .	. . .	. . .	. . .	B	. . .	**B**
STEEL	B	. . .	. . .	. . .	. . .	. . .	A	. . .	. . .	. . .	B	. . .	. . .	. . .	. . .	. . .	. . .	. . .	**B**
U	**. . .**	**. . .**	**. . .**	**. . .**	**. . .**	**. . .**	**. . .**	**. . .**	**. . .**	**. . .**	**. . .**	**. . .**	**. . .**	**. . .**	**. . .**	**. . .**	**. . .**	**. . .**	**B**

A, easy to weld; B, difficult but possible to weld; C, impractical to weld; D, impossible to weld.

Source: Ref 2

References cited in this section

1. S. KALPAKJIAN, *MANUFACTURING PROCESSES FOR ENGINEERING MATERIALS,* ADDISON-WESLEY, 1984, P 703-704
2. R.G. DELAGI, "DESIGNING WITH CLAD METALS," METALLURGICAL MATERIALS DIVISION OF TEXAS INSTRUMENTS, INC.

Roll Welding

References

1. S. KALPAKJIAN, *MANUFACTURING PROCESSES FOR ENGINEERING MATERIALS,* ADDISON-WESLEY, 1984, P 703-704
2. R.G. DELAGI, "DESIGNING WITH CLAD METALS," METALLURGICAL MATERIALS DIVISION OF TEXAS INSTRUMENTS, INC.

Friction Welding

Schillings Tsang, EG&G Rocky Flats

Introduction

FRICTION WELDING (FRW), in its simplest form, involves two axially aligned parts. While one part is rotated, the other stationary part is advanced to make pressure contact. Axial force then increases to generate the frictional heat necessary for welding at the abutting surfaces in order to form a solid-state joint. Friction welding can be divided into two major process variations, depending on the manner by which rotational energy is converted into frictional heat. The first process, direct-drive, or continuous-drive, FRW, has been used commercially since the 1940s. It requires constant energy from a source for any desired duration. The second process, inertia-drive FRW, which was developed in the early 1960s, uses the kinetic energy stored in a rotating flywheel.

Friction Welding

Schillings Tsang, EG&G Rocky Flats

Direct-Drive Friction Welding

Figure 1 shows the layout of a direct-drive FRW system. The spindle is first driven to a predetermined constant speed, and the two parts are brought together under a preset axial force. Both rotation and force are maintained for a specific period determined either by a time or a distance, so that the frictional heat will raise temperatures at the abutting surfaces enough to render the material plastic and suitable for welding. (However, direct-drive friction welds are almost never made using a single level of axial load. The vast majority of welds are made using a minimum of two axial force levels. The second axial load is basically added to the beginning of the weld cycle to yield a preheating phase. In fact, direct-drive friction welds using three axial loads are more commonly applied than those using a single load.) The spindle is then disengaged from the driving unit, and a brake is applied to bring the spindle to rest. At the same time, axial force either remains unchanged or is raised to complete the weld.

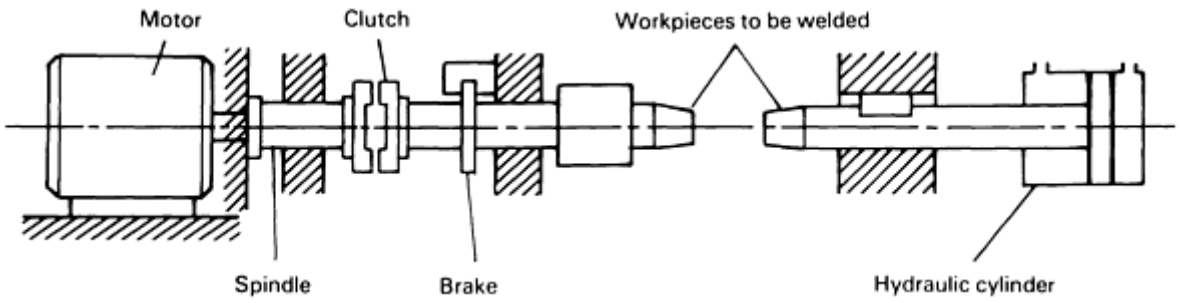

FIG. 1 SCHEMATIC SHOWING RELATION OF WORKPIECES TO KEY COMPONENTS OF A DIRECT-DRIVE FRW SYSTEM. SOURCE: REF 1

Reference cited in this section

1. INERTIA WELDING: SIMPLE IN PRINCIPLE AND APPLICATION, *WELD. MET. FABRIC.*, VOL 47 (NO. 8), 1979, P 585

Schillings Tsang, EG&G Rocky Flats

Inertia-Drive Friction Welding

In inertia-drive FRW (Fig. 2), a flywheel and the rotating part are mounted in a spindle, which is driven to the desired speed. The drive source is then disengaged, and the two parts make contact under a preset axial force. The free-rotating flywheel decelerates under either the same applied force or later under a larger force. Meanwhile, kinetic energy stored in the flywheel and spindle is converted to frictional heat at the abutting surfaces. The weld is complete when the flywheel comes to a stop. A subsequent higher forging force may be used after the flywheel has stopped.

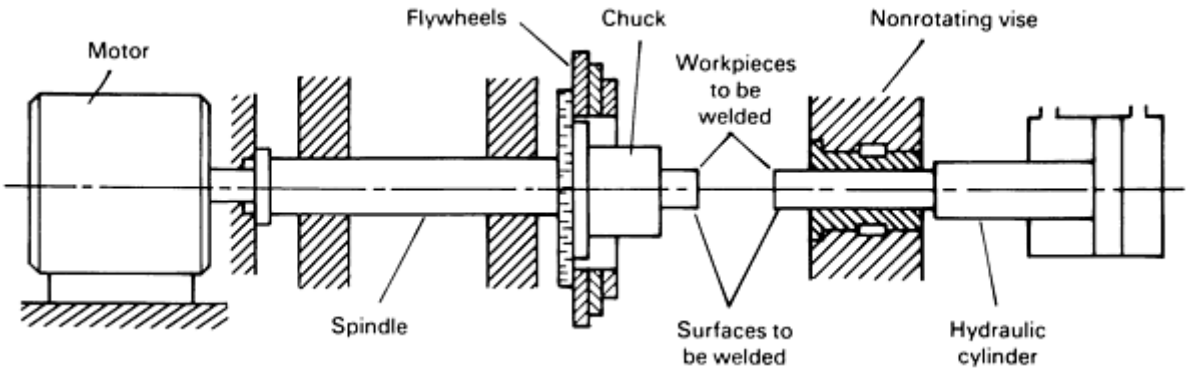

FIG. 2 SCHEMATIC SHOWING RELATION OF WORKPIECES TO KEY COMPONENTS OF AN INERTIA-DRIVE FRW SYSTEM. SOURCE: REF 1

Reference cited in this section

1. INERTIA WELDING: SIMPLE IN PRINCIPLE AND APPLICATION, *WELD. MET. FABRIC.*, VOL 47

(NO. 8), 1979, P 585

Friction Welding

Schillings Tsang, EG&G Rocky Flats

Welding Parameters

Direct-Drive FRW Variables. Three parameters control the character of a weld in direct-drive FRW: rotational speed, duration of rotation, and axial force. During welding, there is not only an axial shortening of the part length, often called axial displacement or upset, but also a resisting torque of friction to rotation, which also undergoes change. Figure 3 shows the change in various events occurring throughout the whole process. Based on the shape of the friction torque curve, it is convenient to divide direct-drive FRW into three phases:

- *PHASE 1:* INITIAL FRICTION (THAT IS, BREAK-IN OR FIRST FRICTION) PHASE
- *PHASE 2:* HEATING (THAT IS, FRICTION) PHASE
- *PHASE 3:* FORGING (THAT IS, UPSETTING) PHASE

In phase 1, the torque rises rapidly after the start of the process. It then peaks and drops before leveling off when phase 1 ends. The rapid rise and gradual fall of torque is associated with the interlocking and breaking of asperities and subsequent softening of the material at the faying surfaces by frictional heating.

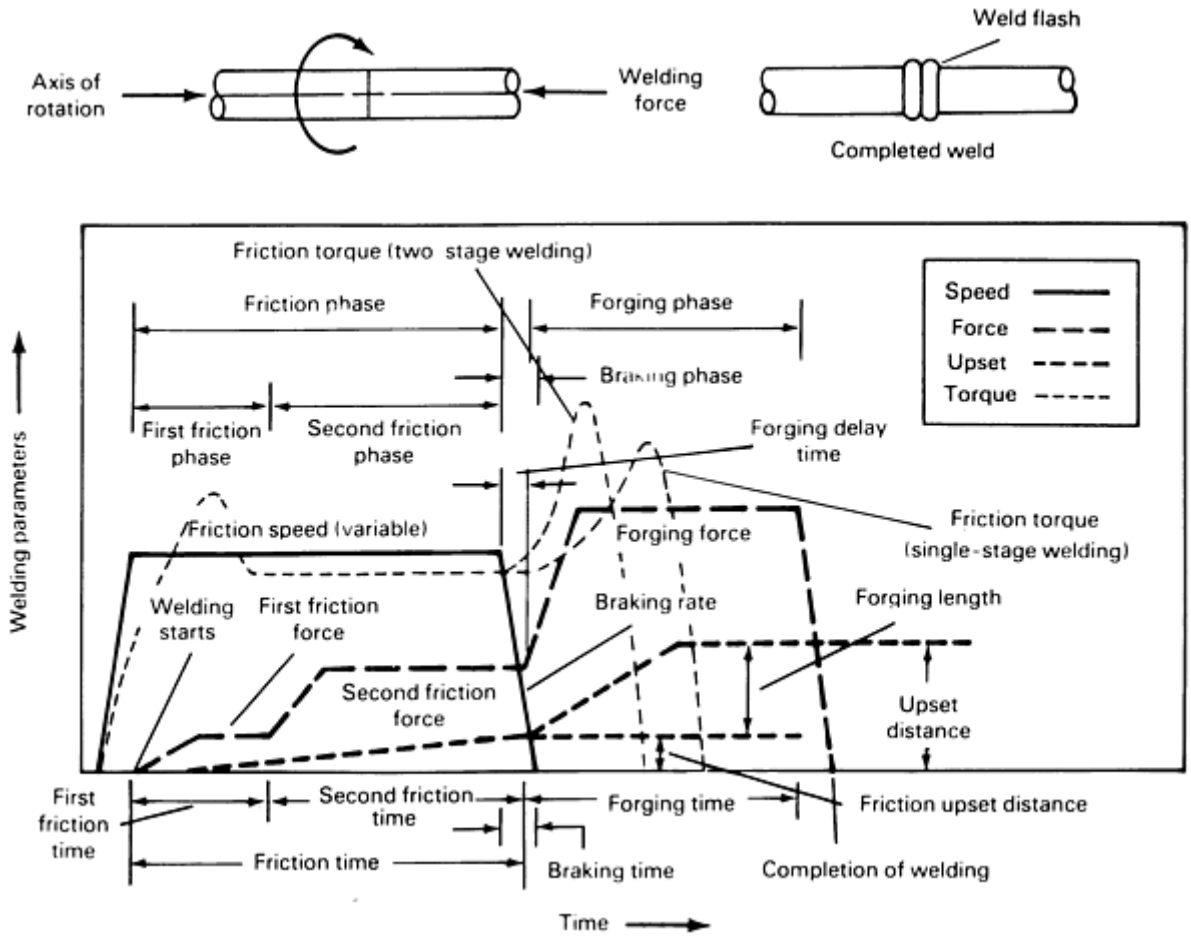

FIG. 3 PLOT OF WELDING PARAMETERS VERSUS TIME FOR A DIRECT-DRIVE FRW SYSTEM. COURTESY OF D.L.

Friction torque remains somewhat constant in phase 2, indicating that the process reaches a balance of effects between strain hardening and thermal softening. Both the faying surfaces and material immediately behind are by then sufficiently heated to permit the two parts to be forged together.

Forging takes place in phase 3, which starts at the time of declutching and braking. Spindle rotation is immediately retarded, and the deceleration depends on braking time. Because the brake force itself can be set, braking time can also be a variable. Deceleration varies in the welding of different materials. However, the torque may not rise at all but drops abruptly at the onset of phase 3 if braking is sudden. This brings the rotating spindle to rest almost instantly, and the larger force is applied after spindle rotation stops. In this case, there is no torsional forge, and forging is brought about by upsetting.

Axial force in phase 3 is usually increased to effect forging. The friction torque again rises after the onset of this phase, reaching another peak before sharply falling off to zero. This peak varies with deceleration and applied axial force. Under some circumstances, this final peak can be omitted by delaying the onset of the forging force.

This is done only at or after the stoppage of spindle rotation by braking. In this case, forging is carried out by upsetting without torsional forging. Although two-stage welding is applied more frequently in direct-drive friction welding, one-stage welding is sometimes used, especially in research work (Ref 2).

When the axial force remains unchanged, slower deceleration (longer braking time by reduced braking) leads to higher peak. If the axial force is increased in phase 3, braking time is shortened, but the peak still rises because of the larger applied force. Rising friction torque in phase 3, characteristic of FRW, contributes to torsional forge, which is more effective than conventional forge by upsetting. Phase 3 ends shortly after spindle rotation stops. This period of forging or upsetting time can also be considered a fourth welding parameter.

Inertia-Drive FRW Variables. There are three welding parameters in inertia-drive FRW: flywheel mass (expressed by moment of inertia), rotational speed, and axial force. The events described for direct-drive FRW also occur in inertia-drive FRW. Except for rotational speed, the curves shown in Fig. 4 are similar to those shown in Fig. 3. The process can also be divided into three phases based on the shape of the friction-torque curve. Unlike direct-drive FRW, duration of rotation and forging time in phase 3 are not predetermined but controlled by the three welding parameters.

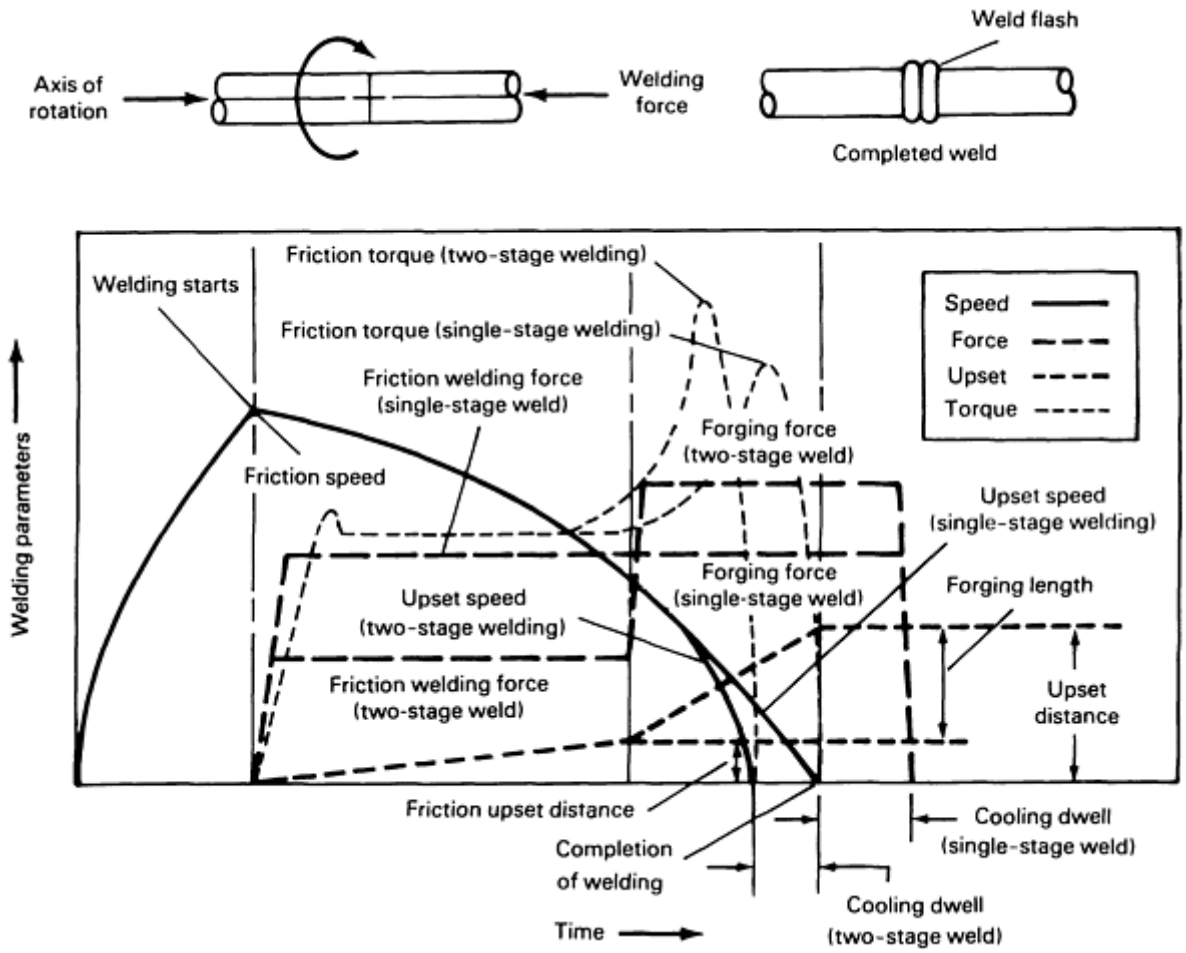

FIG. 4 PLOT OF WELDING PARAMETERS VERSUS TIME FOR AN INERTIA-DRIVE FRW SYSTEM. COURTESY OF D.L. KURUZAR, MANUFACTURING TECHNOLOGY, INC.

If axial force differs in phases 2 and 3, the process is called two-stage welding, and the forces, called heating force and forging force, respectively, are both included as a welding parameter of axial force. On the other hand, when the force remains constant throughout the process, it is called one-stage welding. The second friction-torque peak in two-stage welding is generally higher than that in one-stage welding because of the larger axial force applied in phase 3. As stated in the section "Direct-Drive FRW Variables" in this article, the peak in one-stage welding depends on braking time: It rises with longer braking time.

In two-stage welding, the larger axial forging force is applied when the flywheel rotational speed decreases to a fraction of the initial value--for example, 0.1 to 0.5. Friction torque again rises to a second peak, which as in direct-drive FRW, is higher than in one-stage welding. This phase is prolonged beyond cessation of the flywheel rotation. This extra time, called dwell time, is used for cooling of the joint to avoid debonding by the release of stored strain energy. Although dwell times can range from 0 to 30 s, 1 to 2 s is typical.

The kinetic energy used for inertia-drive FRW depends on the product of the flywheel moment of inertia and the square of rotational speed. The frictional heat generated at the faying surfaces, however, is determined by the rate of change of this energy (or the energy delivery rate), which is influenced by the moment of inertia of the flywheel and the axial force. For a given kinetic energy input and a given axial force, a smaller flywheel (with smaller moment of inertia) delivers the energy at the faying surfaces faster than a larger flywheel (with larger moment of inertia). For a given energy input using the same flywheel, a larger axial force increases flywheel deceleration rates, intensifies heat generation, and raises temperatures at the faying surfaces. A rapid energy input and a high rate of heat generation, typical of inertia-drive FRW, result in very short weld cycles. There is little time for heat to dissipate in the axial direction, so the heat-affected zone (HAZ) remains narrow.

Direct-Drive Versus Inertia-Drive FRW. Lower rotational speed and smaller axial force are generally used in direct-drive FRW. Direct-drive FRW also offers greater latitude in process variables, because heating time in phases 1 and 2 is preset as duration of rotation or upset distance, which is a welding parameter, and because forging phase can be controlled by braking time, axial force, and forging time. Nevertheless, both processes do produce welds of equal quality when proper welding parameters are implemented. Torsional forging is required when forging by upsetting with inertia-drive friction welding; it is not required when forging by upsetting with direct-drive friction welding. A comparison of the two processes is presented in Table 1.

TABLE 1 PROCESS PARAMETERS OF DIRECT-DRIVE FRW SYSTEMS RELATIVE TO INERTIA-DRIVE FRW SYSTEMS

It is assumed that similar or dissimilar metals of the same size are being joined.

PROCESS PARAMETER	**DIRECT-DRIVE FRW**	INERTIA-DRIVE FRW
WELDING PARAMETERS	ROTATIONAL SPEED	**FLYWHEEL MOMENT OF INERTIA**
	DURATION OF ROTATION OR FRICTION BURNOFF DISTANCE	**ROTATIONAL SPEED**
	AXIAL FORCE	**AXIAL FORCE**
CONVERSION OF ENERGY TO FRICTIONAL HEAT	CONSTANT ENERGY IN A PRESET DURATION OF ROTATION	**FIXED ENERGY IN FLYWHEEL; DURATION OF ROTATION DETERMINED BY WELDING PARAMETERS**
ENERGY INPUT	LOW	**HIGH**
HEAT GENERATION RATE	LOW	**HIGH**
CYCLE TIME	SIMILAR	**SIMILAR**
HAZ WIDTH	WIDE	**NARROW**
MACHINE SYSTEM SPINDLE RIGIDITY	**LESS RIGIDITY**	**GREATER RIGIDITY AND MORE POWERFUL CLAMPING FORCES REQUIRED**

Reference cited in this section

2. C.R.G. ELLIS, CONTINUOUS DRIVE FRICTION WELDING OF MILD STEEL, *WELD. J.*, VOL 51 (NO. 4), 1972, P 183-185

Schillings Tsang, EG&G Rocky Flats

Weld Quality and Product Evaluation

At present, there is no satisfactory nondestructive method for detecting a friction weld of poor strength. (X-rays are used to identify defects that can cause welds of poor quality.) Weld quality control and product evaluation must rely on the control of the process and the machine that is used to produce the welds.

In direct-drive FRW, both rotational speed and axial force affect axial shortening or upset in addition to the mechanical properties of the weld produced. There can be a correlation between the upset and the quality of the weld. Further, upset in phase 2 increases almost linearly with time. The upset of this phase, often called friction burn off, and its rate, the friction burn off rate, have been believed to control weld quality. Indeed, some researchers use burn off instead of duration of rotation as a welding parameter. In inertia-drive FRW, because duration of rotation is not preset but controlled by the three welding parameters, the total upset, instead of friction burn off, is supposed to indicate weld quality. This presumes that the same amount of kineticenergy and axial force will produce the same amount of upset at the end of the process (given the same materials and cross sections).

The welding parameters of either direct-drive or inertia-drive FRW are set using a particular machine. So once this machine is properly calibrated, the process becomes almost entirely machine-dependent. Regardless of the process used to evaluate the product of friction welding under a given set of parameters, once variations in machine components and

dimensional tolerances for a particular weld are determined, an acceptable tolerance band of the total upset can be established as a standard. A monitor will compare the upset of each weld relative to this reference. The machine will automatically stop to indicate a defective weld when its upset falls outside the proven band of the standard.

Advantages and Limitations

Advantages of FRW. Friction welding has a number of advantages over other joining processes (such as fusion welding, brazing, and diffusion bonding):

- SPECIAL ATTENTION TO SURFACE CLEANLINESS IS NOT NECESSARY, BECAUSE FRW TENDS TO DISRUPT, DISPLACE, AND FINALLY REMOVE SURFACE FILMS IN WELD FLASH (THIS DOES NOT APPLY TO HEAVY MILL OR HEAT-TREAT SCALES, WHICH CAN INTERFERE WITH FRICTIONAL HEATING).
- FILLER METAL, FLUX, AND SHIELDING GAS ARE NOT REQUIRED. UNLIKE FUSION WELDING, FRICTION WELDING IS NOT HAZARDOUS TO OPERATOR HEALTH AND IS SAFER, BECAUSE THERE IS NO METAL SPATTER, RADIATION, FUME, OR ELECTRIC HAZARD INVOLVING HIGH VOLTAGE, ARCS, AND SPARKS.
- DEFECTS ASSOCIATED WITH MELTING-SOLIDIFICATION PHENOMENA ARE NOT PRESENT IN FRW, BECAUSE IT IS A SOLID-STATE PROCESS.
- IT IS POSSIBLE TO MAKE TRANSITION JOINTS OF DISSIMILAR METALS THAT ARE DIFFICULT OR EVEN IMPOSSIBLE TO WELD BY OTHER PROCESSES (FOR EXAMPLE, REFRACTORY AND EXOTIC METALS).
- LOWER LABOR COSTS, SIMPLE PART DESIGN, SIMPLER WELD FIXTURES, LOWER ENERGY REQUIREMENTS, AND A SHORT WELD CYCLE (A MATTER OF SECONDS) MAKE THE PROCESS COST EFFECTIVE FOR PRODUCING COMPONENTS NORMALLY MADE BY OTHER PROCESSES.

Limitations of FRW include the following:

- THE WELDING AREA OF AT LEAST ONE PART MUST BE ROTATIONALLY SYMMETRICAL, SO THAT THE PART CAN ROTATE ABOUT THE AXIS OF THE WELDING PLANE. TYPICAL PART GEOMETRIES THAT CAN BE FRICTION WELDED ARE: BAR TO BAR, BAR TO TUBE, BAR TO PLATE, TUBE TO TUBE, AND TUBE TO PLATE.
- THIS PROCESS IS NORMALLY LIMITED TO MAKING FLAT AND ANGULAR (OR CONICAL) BUTT JOINTS.
- THE MATERIAL OF AT LEAST ONE COMPONENT MUST BE PLASTICALLY DEFORMABLE UNDER THE GIVEN WELDING CONDITIONS. FOR EXAMPLE, ALUMINA CAN BE JOINED TO ALUMINUM, BUT ALUMINA CANNOT BE JOINED TO ALUMINA. ANOTHER EXAMPLE IS THE JOINING OF POLYMERS (THAT IS, PLASTICS). THERMOPLASTICS, UNLIKE THERMOSETTING PLASTICS, CAN BE FRICTION WELDED BECAUSE THERMOPLASTICS ARE SOFTENED BY FRICTIONAL HEAT BUT THERMOSETTING PLASTICS DECOMPOSE.

Process Applications

The applications of FRW fall into two categories:

- *BATCH AND JOBBING WORK:* USED WHEN A RELATIVELY LOW VOLUME OF PARTS IS REQUIRED, ESPECIALLY WHEN EXPENSIVE DIES MUST BE USED BUT CANNOT BE JUSTIFIED
- *MASS PRODUCTION:* APPLICATIONS THAT SPAN A WIDE RANGE OF INDUSTRIES (AGRICULTURAL, AIRCRAFT ENGINE, AUTOMOTIVE, EARTHMOVING, ELECTRICAL, PETROLEUM, AND SO ON) PRODUCING COMPONENTS RANGING FROM SIMPLE BUTT JOINTS OF DRIVE SHAFTS AND OIL DRILLING PIPES TO COMPLICATED OR CRITICAL AIRCRAFT ENGINE COMPONENTS

Friction Welding

Schillings Tsang, EG&G Rocky Flats

References

1. INERTIA WELDING: SIMPLE IN PRINCIPLE AND APPLICATION, *WELD. MET. FABRIC.*, VOL 47 (NO. 8), 1979, P 585
2. C.R.G. ELLIS, CONTINUOUS DRIVE FRICTION WELDING OF MILD STEEL, *WELD. J.*, VOL 51 (NO. 4), 1972, P 183-185

Radial Friction Welding

E.D. Nicholas, The Welding Institute

Introduction

THE CONVENTIONAL FRICTION-WELDING PROCEDURE of rotating one component against another while an axial thrust is being applied is well known. Autogenous welds in the solid state are made in one operation. The procedure is an accepted production joining method because it provides excellent weld quality and good productivity, it allows the use of unskilled labor, and it enables a wide range of similar and dissimilar metal combinations to be joined. However, continuous-drive and stored-energy (inertia) friction-welding systems have not been as successfully exploited for the joining of long, hollow sections, where restrictions in the bore cannot be tolerated.

The difficulties involved in rotating an intermediate length of hollow section, and in applying uniform and consistent welding forces to both weld interfaces, represent some of the problems that face the machine designer. Furthermore, because two internal upset metal collars are formed, additional machining of the bore is necessary in order to avoid restriction. In 1975, a new approach, called radial friction welding (Ref 1), attempted to provide a means for overcoming these limitations.

Method. The radial friction-welding process adopts the principle of rotating and compressing a solid ring around two stationary pipe ends (Fig. 1a). The pipes to be welded are bevelled to provide a "V" groove when they are butted together. They are then securely clamped to prevent axial and rotational movement. A solid, internally bevelled ring of compatible material with a bevelled angle that is less than that of the pipes is positioned around the pipe ends.

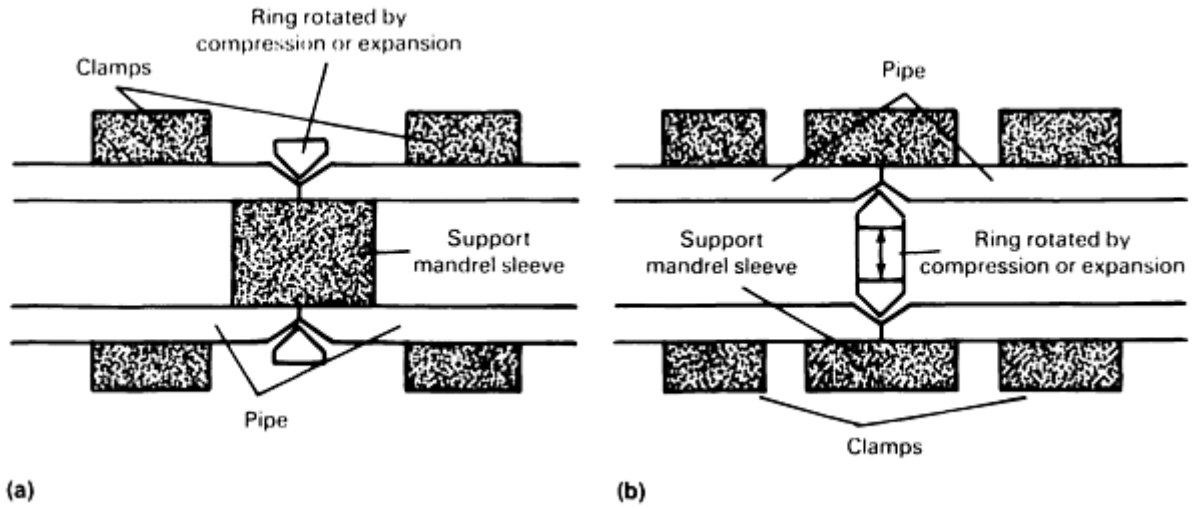

FIG. 1 RADIAL FRICTION WELDING. (A) USING COMPRESSION. (B) USING EXPANSION

The "V" groove for the 108 mm ($4\frac{1}{4}$ in.) outside diameter by 9.5 mm ($\frac{3}{8}$ in.) wall thickness pipe is typically 100°, while the internal bevel of the ring is 80°. It is important for the latter angle to be less than that of the groove in order to limit the initial peak torque and also to promote metal flow from the bottom of the groove in an outward direction toward the outside diameter. Optimum angles for selected sizes of tubes and pipes are determined experimentally.

A support mandrel is located in the bore at the weld position, in order to prevent both the flow of metal into the bore and the collapse of the pipe ends. The ring is then rotated and subjected to radial compressive loading in order to obtain the frictional interaction between the rubbing surfaces, which, in turn, will generate the thermomechanical conditions necessary for weld formation. After a predetermined heating duration, the ring rotation is terminated. The level of compressive load is then either maintained or increased to consolidate the bond. Alternatively, it is also feasible to change the direction of deformation (Fig. 1b). Thus, by providing an expansion load to the ring, the ring can be deformed radially outwards to make the weld.

The included, or bevelled, angle of the solid-compression ring (Fig. 1a) or the expansion ring (Fig. 1b) can have a pronounced effect on weld integrity. The joining of the abutted area is effected and promoted by metal flow from the bore to the outer surface of the pipe. There can be little or no penetration at the pipe root. If the included angle is too narrow, the result will be a weak bond area at the weld root, leading to poor weld strength and a short fatigue life.

Process Development. It was first necessary to prove that the concept of both rotating and compressing/expanding solid rings was feasible. Consequently, conventional friction-welding machines that could provide both rotary motion and axial force were used in the initial development trials. Various bolt-on units were designed, built, and then fitted to these machines.

The results of these initial experiments are summarized in Fig. 2. Although the units were relatively simple, the concept was able to produce sound, solid-state welds with a variety of material combinations. One important outcome of this development effort was that nickel-base alloys were identified as being necessary for the internal mandrel, because they provided good resistance to radial compression loads and wear at the elevated temperatures that were attained during welding. Additional information is available in the section "Prototype/Production Machine" in this article.

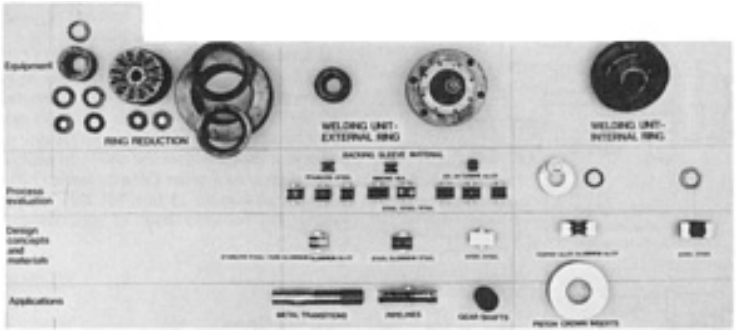

FIG. 2 PROCESS EVOLUTION OF RADIAL FRICTION WELDING

Reference

1. "FRICTION WELDING METHODS AND APPARATUS," U.K. PATENT 1,505,832, 30 MAR 1978

Radial Friction Welding

E.D. Nicholas, The Welding Institute

Equipment

When a prototype radial friction welder was built in the mid-1970s, the primary emphasis was directed toward the application of pipe joining. From the early experimental trials, it was recognized that the shortcomings of using this process in production would be:

- THE NEED FOR AXIAL MOVEMENT OF THE RING THROUGH A TAPER HOUSING
- THE ADDITIONAL MACHINING OF DRIVE GROOVES IN THE RING
- THE RELATIVELY COMPLEX RING GEOMETRY, WHICH WOULD INCLUDE A TAPER SURFACE ON ITS PERIPHERY

Consequently, the idea of using circumferentially located individual jaws (similar to multijaw collet chucks) to provide radial compression and rotation of simple rings was considered. An evaluation program using the arrangement (Ref 2) proved to be successful and, thus, provided the impetus to design and construct a prototype machine based on the multijaw rotation/compression arrangement.

Research Machine. A unique friction-welding facility was developed in order to join pipe of maximum dimensions, that is, 51 mm (2 in.) in outside diameter (OD), by 6 mm (0.24 in.) in wall thickness. The resulting machine is shown in Fig. 3 and its major features are described below.

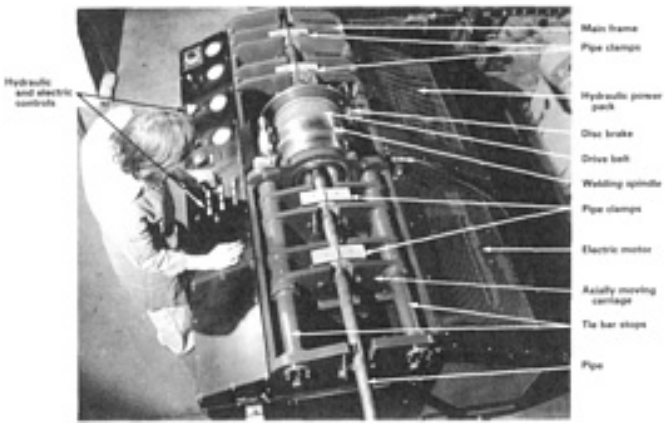

FIG. 3 RADIAL FRICTION-WELDING MACHINE WITH A 51 MM (2 IN.) DIAMETER

Welding Spindle. It was imperative that the ring rotation/compression unit, or welding spindle, be capable of exerting a grip on the ring that was adequate for the transmission of welding power during rotation and of delivering a radial compressive force to reduce the ring into the weld groove. The welding spindle was supposed to incorporate a multijaw arrangement. The heavy steel body of the welding spindle, which needed to contain the radial compressive forces, was supported at each end by simple bearings, and was rotated through a "V"-drive pulley on its outside surface. The spindle was fixed in the machine frame using two simple yoke clamps. A hydraulic caliper disk brake unit was incorporated, when necessary, to assist ring deceleration.

An electric motor rated at 56 kW (75 hp) provided rotation to the welding spindle via a clutch and transmission. The latter enables the setting of rotation speeds ranging from 700 to 2000 rev/min, after a suitable selection of pulley ratios. The clutch and final belt drive were located in line with the welding spindle. The inside of the welding spindle housed an annular piston, which moved in an axial direction, when actuated by hydraulic means, to operate the 12 ring compression jaws via wedges. A maximum axial load of 350 kN (7.8×10^4 lbf) could be generated when oil was supplied to the piston through a rotary oil distributor, at a pressure of 3.4 MPa (0.5 ksi).

The welding spindle had a 340 mm (13.4 in.) OD and was 595 mm (23.4 in.) in length. Consequently, the pipe that passed through it had to be supported close to the weld area by a manually operated collet assembly at the center of the welding spindle.

Pipe Clamping. In order to react to both the axial and torsional forces generated on the pipes, four clamps (two for each pipe) were housed in the top bed of the machine (Fig. 3). The clamps opened and closed by the vertical movement of hydraulic rams that forced wedges between the pivoted jaws. These rams are capable of exerting a maximum thrust of 200 kN (4.5×10^4 lbf).

The machine framework was manufactured as two main assemblies. The machine bed was a heavy-section box-type fabrication that housed the welding spindle and pipe clamps. In contrast, the support framework was of a lighter construction in order to accommodate the motor drive, transmission, and other auxiliary equipment.

Hydraulic Services. The hydraulic circuit had a conventional layout, in that all services were supplied from a dual pump. A gear pump that operated at a pressure of 13.8 MPa (2 ksi) supplied the clutch, bore support mandrel, and moving carriage, whereas a high-volume vane pump that was set to provide a maximum pressure of 3.4 MPa (0.5 ksi) fed only the welding head through a flow-control valve, in order to operate the axially moving annular piston. The latter pump was used to developed the radial compressive forces on the ring. The flow-control valve could be set to provide different rates of piston movement and, thus, varying radial displacement rates to the ring.

Electrical Services. The electrical circuit utilized standard machine controls with relays and timers to sequence the operation of the initial ring preload pressure, the weld heating cycle, the disk brake, the application of forge force, the compression jaws, the mandrel, and the retraction of the moving carriage.

Internal Support Mandrel. The ideal arrangement for a support mandrel should include materials that possess good wear resistance at elevated temperatures and the capability to expand and contract from the pipe bore. The ability of the mandrel to expand proved to be useful to both round and size the pipe ends prior to welding. However, problems were anticipated during the development effort because of the limited working area available for the 50 mm (2 in.) OD pipe (that is, the 38 mm, or 1.5 in., bore), and because of the requirement to eliminate longitudinal gaps in the mandrel.

An expanding mandrel that closed 1 mm (0.039 in.) below the minimum bore diameter was devised. It was operated by a hydraulic cylinder through a draw bar. The mandrel consisted of six segments machined from a nickel-base superalloy (Nimocast PK24). Earlier trials had proved the suitability of this material. Three of the segments were used as wedges, and all segments were operated by the tapered cone on the draw bar, with the wedge segments being removed by the extraction cone first, upon release of the mandrel.

The operating sequence to produce a weld was determined to consist of the steps described below. First, both pipes and ring were machined to provide the necessary weld groove and bevel, respectively. Then, the 16 mm (0.630 in.) wide ring was located in the reduction jaws and held under a light preload pressure.

Next, one pipe was positioned in the welding spindle and clamped, while the collet-steadying device was locked. (The collet-steadying device is of tubular construction and located around that portion of the pipe positioned inside the radial compression. When activated, it provides additional support to the pipe.) Then, the second pipe was fitted with the bore support mandrel, loaded into the machine, and clamped so that it butted against the other pipe.

After setting the rotation speed, as well as the friction welding force timing device that controlled heating duration and the flow-control valve that provided a fixed rate of piston movement (compression rate), the weld sequence was initiated. Upon completion of the weld cycle, the reduction jaws were retracted and the mandrel was sequenced to be extracted after 5 s. To remove the welded pipe, the collet-steadying device was released, along with both pairs of clamps.

Subsequent trials with this research machine demonstrated that the radial friction-welding process could produce welds of acceptable mechanical and metallurgical properties (Ref 3), and that the process could operate in the field, either on land or offshore.

Prototype/Production Machine. During the 1980s, a Norwegian company continued with the development of the process. Its efforts culminated in the design, manufacture, and subsequent commissioning of a prototype/production machine that could weld pipes ranging in size from 89 to 170 mm (3.5 to 6.625 in.) (Ref 4). This machine, which was constructed by another firm based in Oslo Norway, was designed on a twin tie-bar arrangement, upon which the welding head and pipe clamps were mounted (Fig. 4). The welding head, which consists of the drive spindle for rotating the ring, is driven by a 370 kW (500 hp) direct-current motor. The pipe clamps operate hydraulically, as does the ring compression. Additional pipe support and alignment are provided by collets located near and inside the welding head. Although it is not yet fitted as such, the machine has space for a machining station to allow the removal of excess ring/flash metal soon after welding.

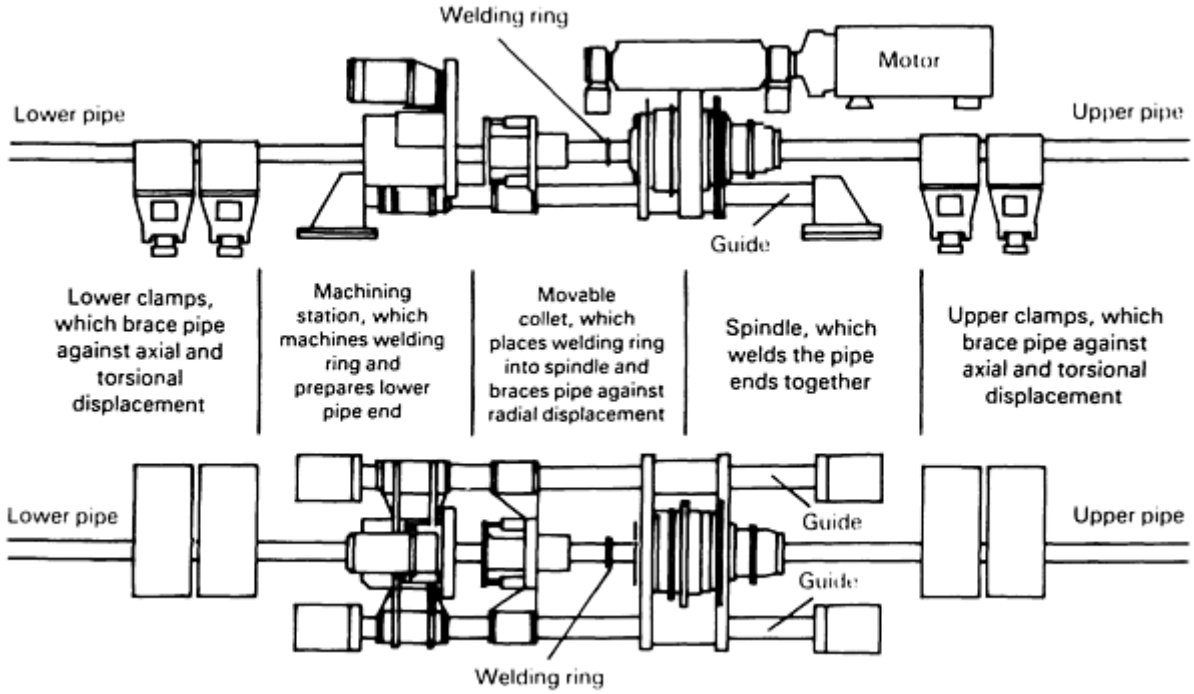

FIG. 4 SCHEMATIC OF THE PROTOTYPE RADIAL FRICTION-WELDING MACHINE

In a parallel effort to the development of this machine, special compression rigs for radial friction welding were manufactured to interface with 1000 to 1800 kN (110 to 200 tonf) axial thrust friction welders. These units provide experimental facilities with the ability to evaluate the process over a wider OD size range (100 to 273 mm, or 4 to 10.75 in.), not only for pipe joining, but for other areas of application, as well.

References cited in this section

2. E.D. NICHOLAS AND R.H. LILLY, RADIAL FRICTION WELDING, *PROC. CONF. ADVANCES IN WELDING PROCESSES* (HARROGATE, U.K.), 1978, P 48
3. E.D. NICHOLAS, RADIAL FRICTION WELDING, *WELD. J.*, VOL 62 (NO. 7), 1983, P 17
4. S.B. DUNKERTON, A. JOHANSEN, AND S. FRICH, RADIAL FRICTION WELDING FOR OFFSHORE PIPELINES, *WELD. J.*, VOL 66 (NO. 7), 1987, P 40

Radial Friction Welding

E.D. Nicholas, The Welding Institute

Applications

The applications that would be suitable for radial friction welding are:

- ATTACHMENT OF COLLARS TO SHAFTS
- WELDING OF ROTATING DRIVING BANDS TO ARTILLERY SHELLS
- ATTACHMENT OF WEAR/SUPPORT RINGS ONTO CYLINDRICAL BODIES
- PIPE JOINING AT BOTH LAND AND OFFSHORE SITES
- FABRICATION OF SHAFTS OR PIPEWORK SYSTEMS WITH CORRECT ALIGNMENT OF

PARTS

- REPAIR OF PIPELINES, BOTH ABOVE WATER AND UNDERWATER
- MANUFACTURE OF BIMETAL TRANSITIONS USING A COMPATIBLE INTERMEDIATE MATERIAL
- INSERTION OF NONMAGNETIC CENTER PIECES
- INSERTION OF BETTER HEAT- OR WEAR-RESISTANT MATERIALS INTO DIESEL PISTON COMBUSTION BOWLS

Radial Friction Welding

E.D. Nicholas, The Welding Institute

References

1. "FRICTION WELDING METHODS AND APPARATUS," U.K. PATENT 1,505,832, 30 MAR 1978
2. E.D. NICHOLAS AND R.H. LILLY, RADIAL FRICTION WELDING, *PROC. CONF. ADVANCES IN WELDING PROCESSES* (HARROGATE, U.K.), 1978, P 48
3. E.D. NICHOLAS, RADIAL FRICTION WELDING, *WELD. J.*, VOL 62 (NO. 7), 1983, P 17
4. S.B. DUNKERTON, A. JOHANSEN, AND S. FRICH, RADIAL FRICTION WELDING FOR OFFSHORE PIPELINES, *WELD. J.*, VOL 66 (NO. 7), 1987, P 40

Friction Surfacing

E.D. Nicholas, The Welding Institute

Introduction

FRICTION WELDING, a solid-state (non-melting) joining process, relies on the presence of relative motion between the parts while they are being pressed together under an applied axial force to generate the thermomechanical conditions for welding. The process, in its simplest form, makes use of rotary motion. A modification of conventional friction welding makes it possible to deposit layers of metal onto a substrate, a metal-transfer method that is called "friction surfacing."

Although surfacing by friction can be regarded as novel, the original concept was reported, and a patent application filed, in 1941 (Ref 1). The technology was dormant until the late 1950s, when the process was rediscovered by Russian workers (Ref 2). A review of the literature has identified a wide variety of applications that utilized the process at that time:

- SHAFT RECLAMATION (REF 3)
- HARDFACING OF AGRICULTURAL PARTS (REF 4)
- RECONDITIONING BUSHINGS OF SLIDING FRICTION BEARINGS AND ROLL TRUNNIONS (REF 5, 6, 7, 8, 9)
- HARDFACING (REF 10) AND IMPROVING WEAR RESISTANCE IN GAS AND OIL EQUIPMENT (REF 11)

References

1. H. KLOPSTOCK AND A.R. NEELANDS, "AN IMPROVED METHOD OF JOINING AND WELDING METALS," BRITISH PATENT SPECIFICATION 572789, APPLICATION DATE, OCT 1941
2. E. BISHOP, FRICTION WELDING IN THE SOVIET UNION, *WELD. MET. FABR.*, OCT 1960, P 408-410
3. KH.A. TYAYAR, FRICTION WELDING IN THE RECONDITIONING OF WORN COMPONENTS, *SVAR. PROIZVOD.*, VOL 1 (NO. 10), 1959, P 3-24
4. R.I. ZAKSON AND F.G. TURUKIN, FRICTION WELDING AND HARDFACING OF AGRICULTURAL MACHINE PARTS, *AVESTA SVARKA*, VOL 3, 1965, P 48-50
5. V.YA. KERSHENBAUM AND B.A. AVERBUKH, SPECIAL FEATURES IN THE FRICTION DEPOSITION OF BRONZE ON STEEL, *AVESTA SVARKA*, VOL 3, 1964, P 19-22
6. G.K. SCHREIBER, V.YA. KERSHENBAUM, AND S.G. TKACHENKO, INFLUENCE OF FRICTION SURFACING CONDITIONS ON TRANSITION LAYER PROPERTIES IN CLAD METALS, *SVAR, PROIZVOD.*, VOL 9, 1971, P 32-33
7. V.YA. KERSHENBAUM *ET AL.*, PERFORMANCE OF STEEL BRONZE BIMETAL PRODUCED BY FRICTION SURFACING, *SVAR. PROIZVOD.*, VOL 7, 1972, P 29-30
8. V.YA KERSHENBAUM AND B.A. AVERBUKH, OPTIMUM DIMENSIONS OF FRICTION SURFACED COMPONENTS, *AVESTA SVARKA*, VOL 5, 1972, P 64-66
9. B.A. AVERBUKH AND A.L. VELINSKII, THERMAL EFFECTS IN FRICTION SURFACING, *AVESTA SVARKA*, VOL 11, 1975, P 29-31
10. E.I. PLUZHIKOVA, E.L. DEMINA, V.YA. KERSHENBAUM, AND G.K. SCHREIBER, FRICTION FACING OF CAST IRON ON STEEL, TRANSLATED FROM *METALLOVED. TERM. OBRAB. MET.*, VOL 11, 1971, P 46-47
11. M.V. NOGIK *ET AL.*, FRICTION HARDFACING STEEL WITH STELLITE V3K, *SVAR. PROIZVOD.*, VOL 8, 1970, P 16-17

Friction Surfacing

E.D. Nicholas, The Welding Institute

Process

In the friction-surfacing process, a rotating consumable is brought into contact with a moving substrate, which results in a deposited layer on the substrate (Fig. 1). First, the consumable rod is rotated to the desired speed. Next, it is brought into contact, under an axial force, with the stationary substrate. An initial rubbing period is required to allow the generation of a plasticized layer in the consumable. Several seconds are required before this condition is achieved. Then, the substrate is traversed across the consumable, leaving a layer of deposited material. The deposit is characterized by a fine hot-worked microstructure, zero dilution, and a very strong bond with the substrate.

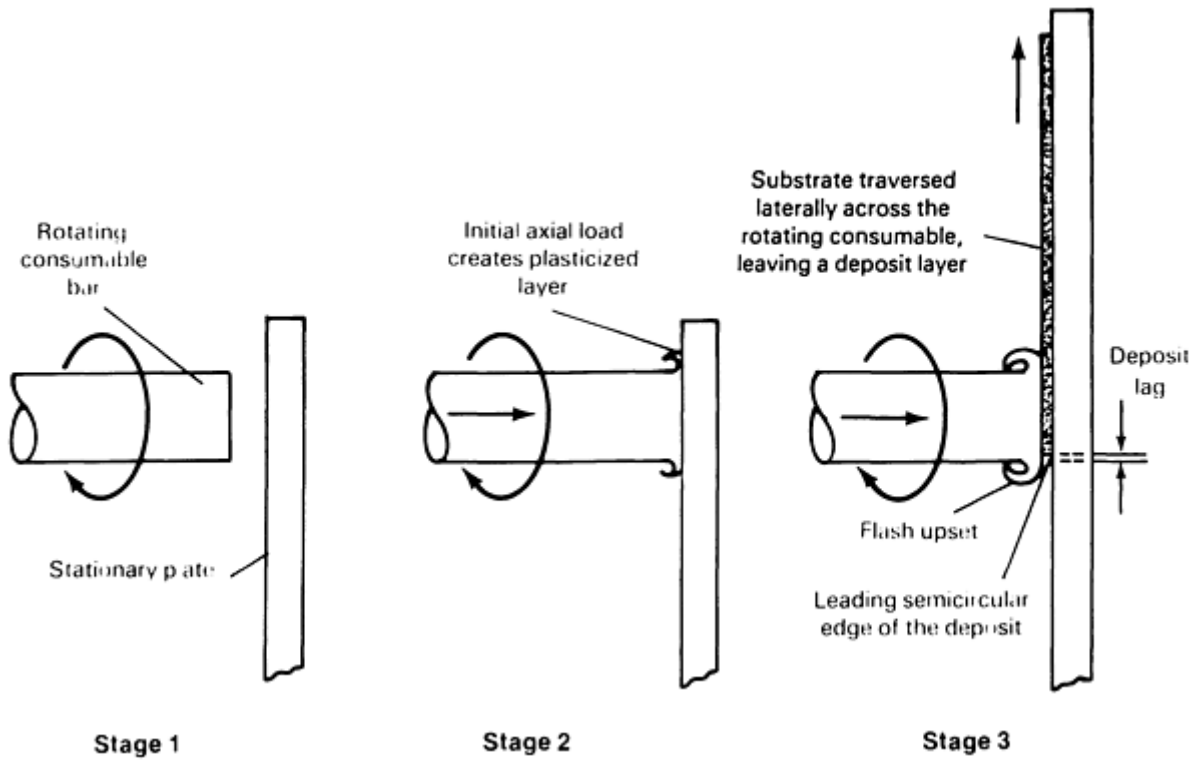

FIG. 1 BASIC TECHNIQUE FOR FRICTION SURFACING

The process utilizes equipment that is similar to a machine tool, for which the surfacing conditions are preset. Therefore, the process can provide good reproducibility, and is not dependent on operator skill.

The width and thickness of the deposited layer is influenced by the primary surfacing variables of rotational speed, axial force, substrate traverse rate, consumable diameter, and type of material. Generally, the fully bonded width of the deposit is approximately 1 to 3 mm (0.04 to 0.12 in.) less than the diameter of the consumable, with the extreme angles of the deposit being characterized by lack of bond. It is thought that this lack of bond is associated with nonuniform pressure distribution across the consumable; lack of restraint to the highly plasticized flowing material; and the reduced time in action seen at the outer edges as compared to the center of the consumable.

The deposit thickness in a single pass is considerably influenced by the type of consumable material. Materials that have good resistance to plastic deformation at elevated temperatures, such as the nickel-base alloys and the Stellite alloys, will only yield thicknesses of the order of 0.5 to 1 mm (0.02 to 0.04 in.). When austenitic stainless steel and carbon steels are used, the thickness increases to approximately 3 mm (0.12 in.). For materials with low strength at elevated temperature, such as aluminum and its alloys, thicknesses can approach 5 to 6 mm (0.20 to 0.24 in.).

Representative variables associated with friction surfacing conditions are shown in Table 1. A typical deposit of austenitic stainless steel from a 25 mm (1 in.) diameter rod that has been laid down on mild steel by the friction surfacing process is shown in Fig. 2(a). The layer is characterized by a uniformly rippled surface of consistent width and thickness. A transverse section reveals lack of bond at the edges and sound bond formation between the deposit and substrate, above the narrow, crescent-shaped, heat-affected zone (HAZ) in the latter (Fig. 2b). Figure 2(c) shows the microstructural features at the bond interface. It is important to remember that a uniform and smooth mushroom-shaped upset is continuously formed on the consumable rod during the surfacing operation.

TABLE 1 FRICTION-SURFACING PARAMETERS FOR SELECTED MATERIAL COMBINATIONS

COMBINATION	CONSUMABLE DIAMETER		ROTATION SPEED, REV/MIN	APPLIED FORCE		TRAVERSE RATE	
	mm	in.		kn	10^3 lbf	mm/s	in./s
AUSTENITIC STAINLESS STEEL TO MILD STEEL	25	1.0	550	50	11.3	5	0.20
STELLITE 6 TO AUSTENITIC STAINLESS STEEL	20	0.8	330	50	11.3	2.5	0.10
AL-4CU TO AL-4CU	25	1.0	780	17	3.8	4	0.16

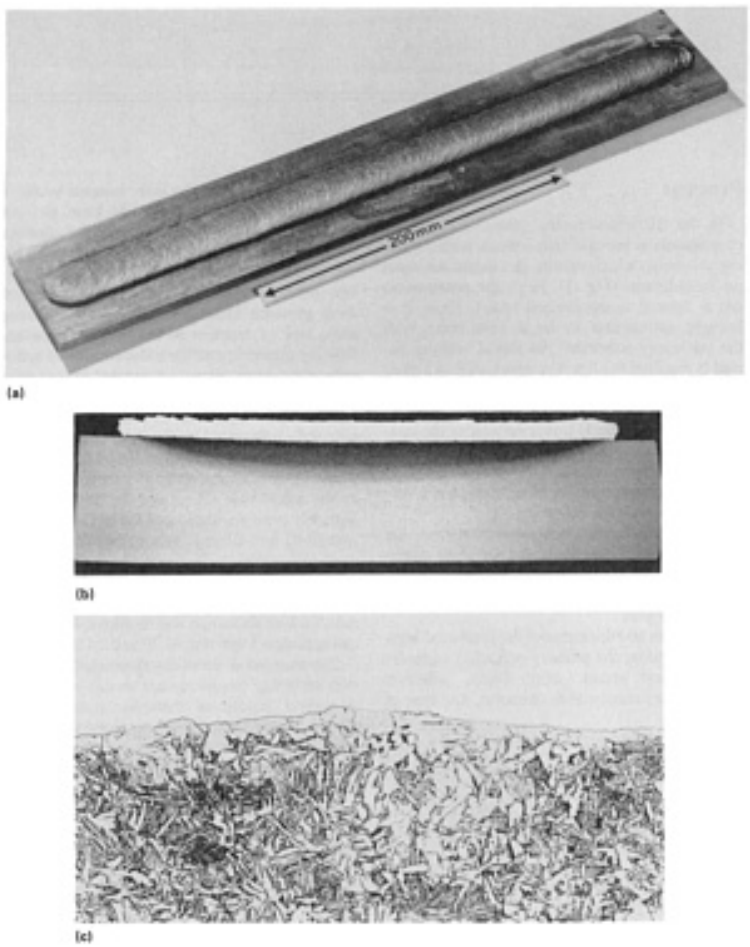

FIG. 2 THREE VIEWS OF 500 MM (20 IN.) FRICTION-SURFACED DEPOSIT OF AUSTENITIC STAINLESS STEEL ON MILD STEEL. (A) VIEW SHOWING ENTIRE SECTION. (B) TRANSVERSE SECTION OF DEPOSIT. (C) MICROSTRUCTURE AT THE DEPOSIT SUBSTRATE WELD INTERFACE. 550×

If it is necessary to clad larger surface areas, then multiple side-by-side layers can be laid down. If thicker deposits are needed, then layers one on top of another can be used. If both approaches are called for, then interpass machining may be required to ensure sound adhesion properties.

Friction Surfacing

E.D. Nicholas, The Welding Institute

Equipment

The earliest feasibility studies were conducted on a modified, continuous-drive, friction-welding machine (Ref 12). However, further practical investigations necessitated an increased surfacing capacity. Therefore, a milling machine (Ref 13) designed for the heaviest class of milling was used for longer deposition runs and larger-diameter components.

Ample power for the steady rotation of 64 spindle speeds between 12 and 540 rev/min is provided by the two-speed reversing motor, which develops 22 kW at 1430 rev/min and 15 kW at 960 rev/min. The robust machine frame minimizes deflection during friction surfacing, and the table, which moves longitudinally and transversely, also is designed to withstand large loads. The table is driven by a 2.2 kW variable-speed motor for 1575 mm (65 in.) of longitudinal travel and 724 mm (30 in.) of transverse travel at a lateral rate between 0.5 and 17 mm/s (0.02 and 0.68 in./s).

A rotary manipulator is used for circumferential deposition onto curved surfaces that are up to 480 mm (20 in.) in diameter. This manipulator is designed to handle the desired radial compressive loads while providing the required peripheral velocity. Similarly, by using a 610 mm (24 in.) diameter rotary table, annular deposits can be applied to the contact face of disks and flanges. Modifications have included fitting a direct-current variable-speed 2.2 kW motor to allow the feed rate of the consumable bar to be varied independently of the table traverse. Changes include a control system that allows consumable feed rates to be changed during the process, in these ways:

- TOUCH DOWN (SLOW FEED RATE, WITH NO LATERAL MOVEMENT)
- RAMP-UP (GRADUAL INCREASE IN THE FEED RATE TO THE SET VALUE)
- CONSTANT FEED RATE DURING LATERAL MOVEMENT
- PAUSE (IN LATERAL MOVEMENT) AT END OF RUN
- WITHDRAWAL OF THE CONSUMABLE (WHILE STILL ROTATING)
- STOP

The ability to use converted machine tools offers a low-cost option in the technology of friction surfacing. A certain manufacturer has recently designed and built a machine dedicated to this surfacing method (Fig. 3). The machine, which is particularly suited for longitudinal deposition, can:

- PUT DOWN RUNS OF 3 M (10 FT)
- USE CONSUMABLES UP TO 70 MM (3 IN.) IN DIAMETER
- PROVIDE A RANGE OF ROTATION SPEEDS FROM 250 TO 1800 REV/MIN
- DEVELOP AXIAL FORCES UP TO A MAXIMUM OF 180 KN (40.5×10^3 LBF)

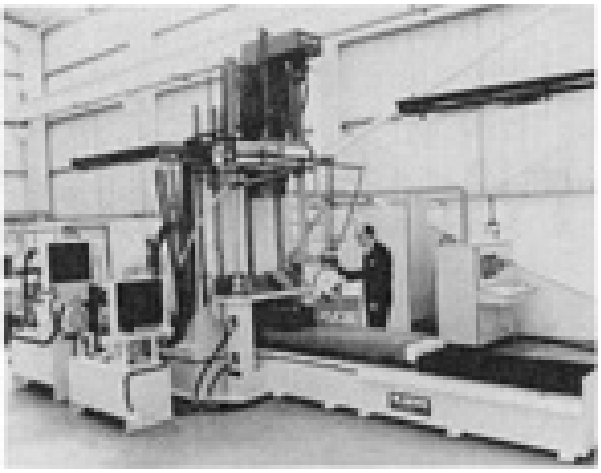

FIG. 3 COMMERCIAL FRICTION-SURFACING MACHINE. COURTESY OF BLACKS EQUIPMENT LTD.

References cited in this section

12. W.M. THOMAS, E.D. NICHOLAS, AND S.B. DUNKERTON, "FEASIBILITY STUDIES INTO SURFACING BY FRICTION WELDING," TWI RESEARCH REPORT 236, THE WELDING INSTITUTE, APRIL 1984
13. W.M. THOMAS, SOLID PHASE CLADDING BY FRICTION SURFACING, *PROC. TWI INTERNATIONAL SYMPOSIUM 18,* APRIL 1988, P 18

Friction Surfacing

E.D. Nicholas, The Welding Institute

Applications

The available methods, in terms of surfacing and surface-treatment technology, are far from complete. The development of friction surfacing provides an alternative (in some cases, complementary) technique. The process may increasingly accompany other solid-state, large-overlay techniques, especially with respect to localized repair and the reclamation of explosively clad and roll-bonded composite materials.

Hardfacing applications on cutting edges and agricultural tools have been reported to be successful (Ref 11). Other workers (Ref 14, 15) suggest that thin-clad sheet can be produced from heavily cold-rolled friction-surfaced deposits. They believe that another promising application is the hermetic sealing of containers with heat-sensitive contents. Friction surfacing also will undoubtedly be applied to the reclamation of worn parts. The reconditioning of worn shafts, in which good-quality deposits were achieved, has been described (Ref 13).

Initially, potential applications for this solidstate technique are in the cladding of localized areas. Typical examples include the anticorrosion surfacing of slide valve plates, the surfacing of the annular contact face of composite pipe flanges, the inlay cladding by suitable strategic materials in positions that suit bearings and seal-contact areas on shafts, and the cladding of the exposed regions of shafts that are used in pernicious environments.

Various substrate geometries that have interesting potential for friction cladding are shown in Fig. 4. Shell banding may be another application, where suitably soft material is friction surfaced to the bodies of artillery shells (Ref 16). Other possibilities include the manufacture of specialized wear tiles (for sinter plant and quarrying equipment) and the in-situ reclamation of worn railway points. Turbine blades, guillotine and shear blades, disk brakes, machine-tipped tools, and press tool dies are also considered to be potential friction-surfacing applications.

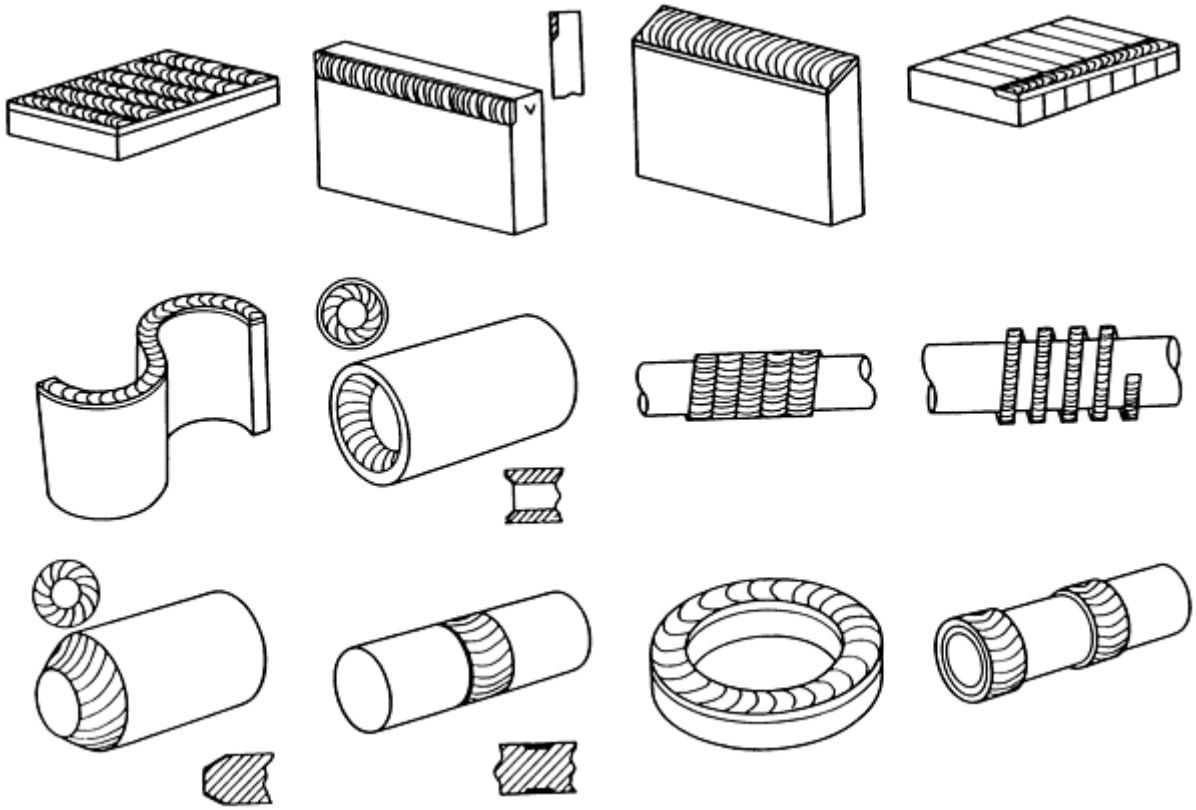

FIG. 4 GEOMETRIC ARRANGEMENTS FOR FRICTION SURFACING

Monolithic Structures. Friction surfacing has now been applied to a wide range of monolithic deposit/substrate combinations. There has been considerable success in producing high-strength bonding, fine-grained forged microstructures, and full homogeneity. A lack of porosity has also been attained, as have desirable surface properties, such as corrosion and wear characteristics that either equal or surpass the bar stock from which the deposit originated. Combinations include:

- INCO 625 TO AUSTENITIC STAINLESS STEEL
- AUSTENITIC STAINLESS STEEL TO CARBON STEEL
- STELLITE 6 AND 12 TO AUSTENITIC STAINLESS STEEL
- HASTELLOY TO AUSTENITIC STAINLESS STEEL
- TI-6AL-4V ALLOY TO TI-6AL-4V ALLOY
- AL-4CU ALLOY TO AL-4CU ALLOY
- HARDFACING STEELS, SUCH AS D2 AND H13, TO MEDIUM-CARBON STEELS

These and other applications are evidence that the process is coming of age and should be given serious consideration in the high-technology industries.

Metal-matrix composites. (MMC) offer considerable potential in high-temperature and wear-resistant applications. During 1988, friction surfacing with a MMC was accomplished using a consumable rod (matrix) that had a predrilled hole filled with alumina powder. Success was achieved, particularly when the matrix metal was 6063 aluminum alloy. It was equally possible to deposit a ferrous-based MMC (5 to 7 vol% of alumina in 4130 steel) from a proprietary MMC consumable rod produced by the Osprey process. The MMC deposited most easily onto a carbon steel, providing a hard, fine-grained martensitic matrix with uniformly distributed particulates of alumina. Further work was done to increase the volume fraction and distribution of the particulate in the matrix for the inclusion of zirconia and alumina by introducing changes in hole geometry and position in the consumable rod (Ref 17). An encouraging volume fraction of approximately 14% was obtained, although the particulate distribution needed to be improved.

References cited in this section

11. M.V. NOGIK *ET AL.,* FRICTION HARDFACING STEEL WITH STELLITE V3K, *SVAR. PROIZVOD.,* VOL 8, 1970, P 16-17
13. W.M. THOMAS, SOLID PHASE CLADDING BY FRICTION SURFACING, *PROC. TWI INTERNATIONAL SYMPOSIUM 18,* APRIL 1988, P 18
14. G.M. BEDFORD AND P.J. RICHARDS, "RECENT DEVELOPMENTS OF FRICTION COATING REPAIR AND RECLAMATION," THE ROYAL SOCIETY (LONDON, U.K.), 24-25 SEPT 1984
15. G.M. BEDFORD AND P.J. RICHARDS, "THE ABSENCE OF DILUTION IN FRICTION SURFACING AND LATERAL FRICTION WELDING," PAPER NO. 70, THE 1ST INTERNATIONAL CONFERENCE ON SURFACE ENGINEERING (BRIGHTON, U.K.), 25-28 JUNE 1985
16. E.D. NICHOLAS AND W.M. THOMAS, METAL DEPOSITION BY FRICTION WELDING, *WELD J.,* VOL 65 (NO. 8), AUG 1986, P 17-27
17. P.L. THREADGILL AND W.M. THOMAS, MANUFACTURE OF METAL MATRIX COMPOSITE CLAD LAYERS DURING FRICTION SURFACING: PRELIMINARY STUDIES, *PROC. EUROJOIN 1 CONF.* (STRASBOURG), NOV 1992, P 433-440

Friction Surfacing

E.D. Nicholas, The Welding Institute

References

1. H. KLOPSTOCK AND A.R. NEELANDS, "AN IMPROVED METHOD OF JOINING AND WELDING METALS," BRITISH PATENT SPECIFICATION 572789, APPLICATION DATE, OCT 1941
2. E. BISHOP, FRICTION WELDING IN THE SOVIET UNION, *WELD. MET. FABR.,* OCT 1960, P 408-410
3. KH.A. TYAYAR, FRICTION WELDING IN THE RECONDITIONING OF WORN COMPONENTS, *SVAR. PROIZVOD.,* VOL 1 (NO. 10), 1959, P 3-24
4. R.I. ZAKSON AND F.G. TURUKIN, FRICTION WELDING AND HARDFACING OF AGRICULTURAL MACHINE PARTS, *AVESTA SVARKA,* VOL 3, 1965, P 48-50
5. V.YA. KERSHENBAUM AND B.A. AVERBUKH, SPECIAL FEATURES IN THE FRICTION DEPOSITION OF BRONZE ON STEEL, *AVESTA SVARKA,* VOL 3, 1964, P 19-22
6. G.K. SCHREIBER, V.YA. KERSHENBAUM, AND S.G. TKACHENKO, INFLUENCE OF FRICTION SURFACING CONDITIONS ON TRANSITION LAYER PROPERTIES IN CLAD METALS, *SVAR, PROIZVOD.,* VOL 9, 1971, P 32-33
7. V.YA. KERSHENBAUM *ET AL.,* PERFORMANCE OF STEEL BRONZE BIMETAL PRODUCED BY FRICTION SURFACING, *SVAR. PROIZVOD.,* VOL 7, 1972, P 29-30
8. V.YA KERSHENBAUM AND B.A. AVERBUKH, OPTIMUM DIMENSIONS OF FRICTION SURFACED COMPONENTS, *AVESTA SVARKA,* VOL 5, 1972, P 64-66
9. B.A. AVERBUKH AND A.L. VELINSKII, THERMAL EFFECTS IN FRICTION SURFACING, *AVESTA SVARKA,* VOL 11, 1975, P 29-31
10. E.I. PLUZHIKOVA, E.L. DEMINA, V.YA. KERSHENBAUM, AND G.K. SCHREIBER, FRICTION FACING OF CAST IRON ON STEEL, TRANSLATED FROM *METALLOVED. TERM. OBRAB. MET.,* VOL 11, 1971, P 46-47
11. M.V. NOGIK *ET AL.,* FRICTION HARDFACING STEEL WITH STELLITE V3K, *SVAR. PROIZVOD.,* VOL 8, 1970, P 16-17
12. W.M. THOMAS, E.D. NICHOLAS, AND S.B. DUNKERTON, "FEASIBILITY STUDIES INTO SURFACING BY FRICTION WELDING," TWI RESEARCH REPORT 236, THE WELDING INSTITUTE, APRIL 1984

13. W.M. THOMAS, SOLID PHASE CLADDING BY FRICTION SURFACING, *PROC. TWI INTERNATIONAL SYMPOSIUM 18,* APRIL 1988, P 18
14. G.M. BEDFORD AND P.J. RICHARDS, "RECENT DEVELOPMENTS OF FRICTION COATING REPAIR AND RECLAMATION," THE ROYAL SOCIETY (LONDON, U.K.), 24-25 SEPT 1984
15. G.M. BEDFORD AND P.J. RICHARDS, "THE ABSENCE OF DILUTION IN FRICTION SURFACING AND LATERAL FRICTION WELDING," PAPER NO. 70, THE 1ST INTERNATIONAL CONFERENCE ON SURFACE ENGINEERING (BRIGHTON, U.K.), 25-28 JUNE 1985
16. E.D. NICHOLAS AND W.M. THOMAS, METAL DEPOSITION BY FRICTION WELDING, *WELD J.*, VOL 65 (NO. 8), AUG 1986, P 17-27
17. P.L. THREADGILL AND W.M. THOMAS, MANUFACTURE OF METAL MATRIX COMPOSITE CLAD LAYERS DURING FRICTION SURFACING: PRELIMINARY STUDIES, *PROC. EUROJOIN 1 CONF*. (STRASBOURG), NOV 1992, P 433-440

Ultrasonic Welding

Janet Devine, Sonobond Ultrasonics

Introduction

ULTRASONIC WELDING (USW) is a quasi-solid-state process that produces a weld by introducing high-frequency vibration to the weldment as it is held under moderately high clamping forces. The weld is produced without significant melting of the base materials.

In some respects, ultrasonic welding is an infant process that still awaits thorough exploration. A greater understanding is needed of the processes that occur at the bond interface. Specifically, the interaction of the process parameters, as well as their role in bond development, needs to be better understood.

The advantages of ultrasonic welding are that it:

- PERMITS JOINING OF THIN MATERIALS TO THICK MATERIALS
- PERMITS DISSIMILAR METAL JOINTS
- PROVIDES JOINTS WITH GOOD THERMAL AND ELECTRICAL CONDUCTIVITY
- JOINS METALS WITHOUT THE HEAT OF FUSION
- PROVIDES EFFICIENT ENERGY USE
- TYPICALLY REQUIRES NO FILLER MATERIAL, FLUX, OR SPECIAL ATMOSPHERE
- TYPICALLY REQUIRES NO SPECIAL CLEANING PROCESSES
- WELDS THROUGH MOST OXIDES

Applications. Commercially successful applications generally have certain characteristics. First, joints must be lap joints, not butt joints. Second, thin sections are required adjacent to the welding tip. Third, better results are obtained with nonferrous alloys.

Production applications include electrical wire harnesses for the appliance and automotive industry; buss bars; fuses; circuit breakers; contacts; ignition modules; starter motors; aluminum and copper foil; battery foils; capacitors; encapsulation of explosives; microelectronic wires; heating, ventilation, and air conditioning (HVAC) tubing; and many others. Military applications in the aircraft industry are described in MIL-STD 1947, issued May 15, 1985.

Ultrasonic Welding

Janet Devine, Sonobond Ultrasonics

Equipment and Process Parameters

An ultrasonic welding system requires a power supply that converts line power to the high frequency and high voltage needed by the transducer. The transducer transforms high-frequency electrical energy to vibratory energy and is incorporated into the welding head, which also provides the means (that is, either pneumatic, hydraulic, or mechanical) to clamp the workpieces. The transducer assembly also incorporates components or waveguides to transmit the energy to the desired weld area.

Process Mechanism. Ultrasonic welding products a weld by oscillating shear forces at the interface between the two metals being joined while they are held together under moderate static clamping force. The resulting internal stresses result in elastoplastic deformation at the interface.

Highly localized interfacial slip at the interface tends to break up oxides and surface films, permitting metal-to-metal contact at many points. As continued oscillation breaks down the points and the contact area grows, diffusion occurs across the interface to produce a structure similar to that of a diffusion weld.

Ultrasonic welding produces a localized temperature rise from the combined effects of elastic hysteresis, interfacial slip, and plastic deformation. The welding process is completed without having fully melted metal at the interface when the correct combination of force, power, and time parameters are used.

Interface temperature rise is greater for metals with low thermal conductivity (for example, steel) than it is for metals of high conductivity (for example, aluminum or copper). Ultrasonic welding of such high-conductivity materials consumes substantially less energy than does resistance welding.

In the case of alloys that have a broad melting temperature range, it is likely that as the low end of the range is reached, a slushing condition that facilitates plasticity in the weld interface is produced.

Process Variations and Limitations. Variations of the USW process produce different weld geometries. There are spot, line, continuous seam, and ring welding machines. Two other versions of spot welding machines are used to join microelectronic components.

Spot welds can be circular, elliptical, or rectangular, and solid or ringlike in geometry. They are formed when the material is clamped between a shaped tip (sometimes called a sonotrode) and an anvil (Fig. 1). The tip vibrates as ultrasonic energy is momentarily introduced in a plane parallel to the interface and perpendicular to the clamping force. Although weld time varies according to the thickness and composition of the material to be joined and the power of the welding machine, most spot welds can be produced in less than 1.5 s (Fig. 2).

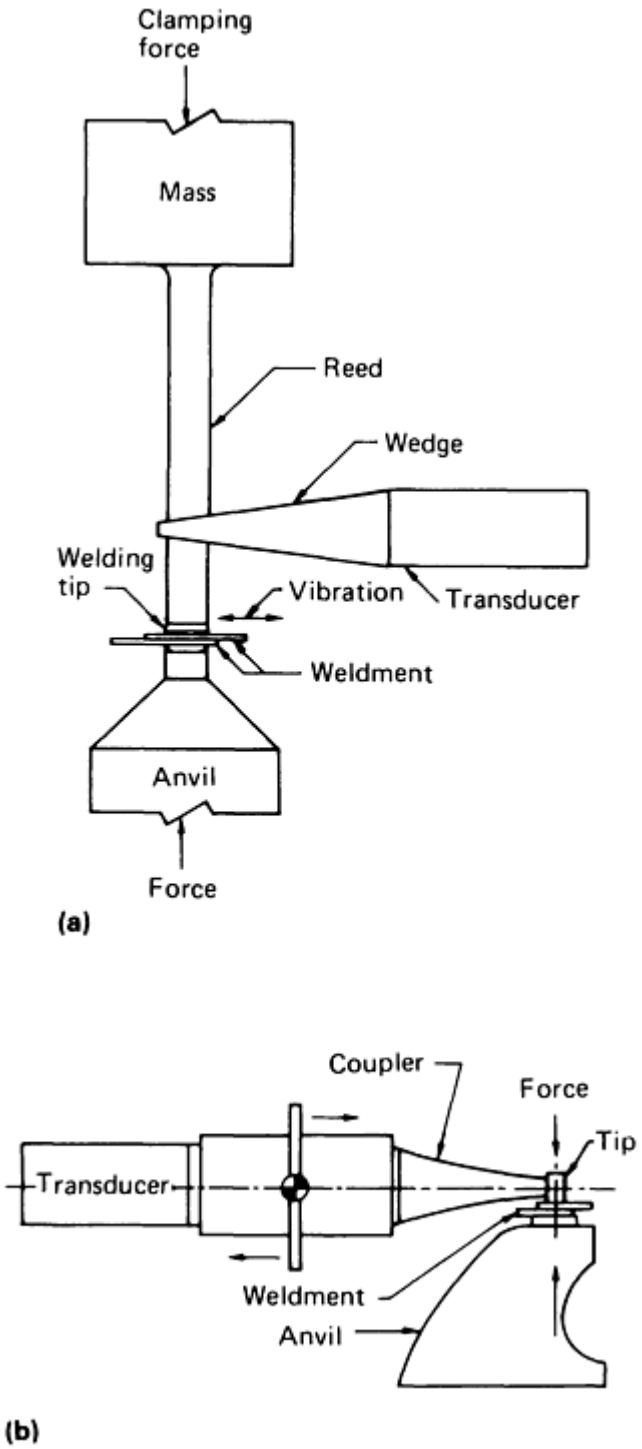

FIG. 1 TWO VERSIONS OF AN ULTRASONIC WELDING SYSTEM USED FOR SPOT WELDING APPLICATIONS. (A) WEDGE-REED SYSTEM. (B) LATERAL DRIVE SYSTEM

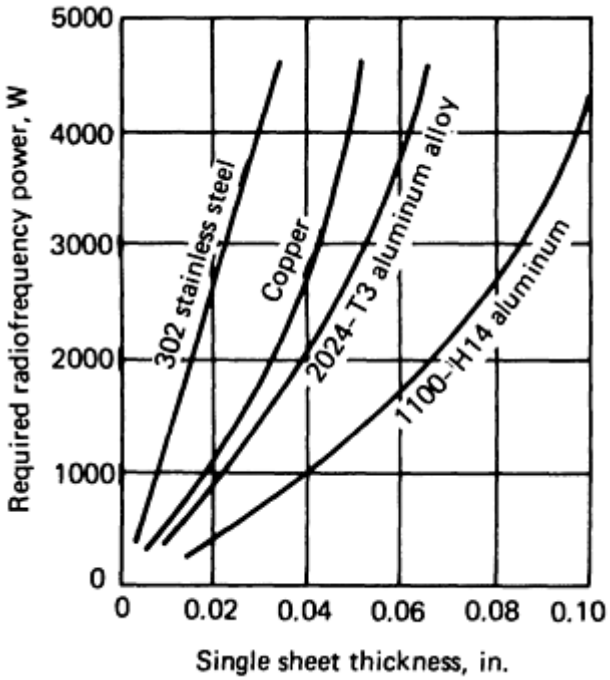

FIG. 2 PLOT OF WELDING MACHINE POWER CONSUMPTION VERSUS MATERIAL THICKNESS FOR SELECTED METALS JOINED BY ULTRASONIC WELDING

Welds can be made adjacent to or overlapping previous welds to form a continuous welded joint. A product clamp may be necessary to prevent the dispersion of ultrasonic energy into adjacent areas of the workpiece. The product clamp is usually concentric with the welding tip and has a slightly larger diameter than the tip.

Line welds are produced by a variation of spot welding in which the weld geometry is elongated by using a linear sonotrode tip and anvil. Custom multiple transducer heads have been used to produce line welds that are several inches long, but most commercially available equipment is limited to lines of 38 mm (1.5 in.) or less in length. Adjacent welds can produce a longer line. Typically, the longer welds are attainable only in thin materials (that is, less than 0.25 mm, or 0.010 in., thick). Single line welds up to 50 mm (2 in.) long have been made to join expanded nickel foil to solid foil for a lithium battery application.

Line welding is also used to seal copper tubes in HVAC applications (Fig. 3). This technique can replace seals normally produced by crimping and brazing.

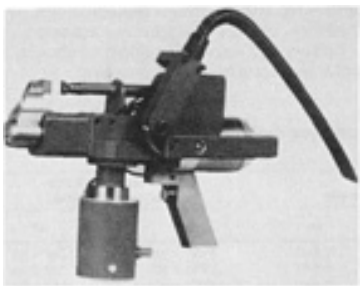

FIG. 3 TYPICAL ULTRASONIC LINE WELDER USED FOR METAL TUBE CLOSURE APPLICATIONS

Continuous seam welds are produced when a disk-shaped ultrasonically vibrating roller is rotated and traversed over a workpiece that is supported on a fixed anvil. Typical uses include joining foil ends in aluminum and copper foil mills. Commercial equipment is available to weld sheet thicknesses up to about 0.15 mm (0.006 in.). High-frequency systems

(typically, 50 kHz) permit excellent welds in even the thinnest of foils, such as 0.0043 mm (0.00017 in.), without tearing or puckering. This technique is also used to join 0.038 mm (0.0015 in.) aluminum interconnects to foil in photovoltaic panels.

Ring Welds. A circular tip used on a spot welder can be used to form a ring weld. Systems designed especially for ring welding often use the torsional or circular motion of an annular-shaped tip instead of a forward and backward motion. Such a system utilizes two transducers, one of each side of a hollow reed. Each transducer produces motion 180° out of phase with the other, thus causing a torsional motion at the interface of the weldment.

Ring welds with diameters up to about 50 mm (2 in.) and an annular weld track of about 1.25 mm (0.050 in.) have been produced in thin aluminum or copper foils. Typical applications include the encapsulation of liquid and powder propellant or explosive materials by welding a thin foil cover on a container. Foils are usually 0.2 mm (0.008 in.) or less. The weld process does not produce much heat, which makes it suitable for use with heat-sensitive materials. Many small, high-frequency (28 kHz) systems are in operation to hermetically seal small explosive initiators or fuses for armaments.

Microelectronic Welds. fine wire bonding represents the earliest widely used USW application and still accounts for a large volume of industrial activity. Millions of wire bonds are performed daily. Figure 4 shows an ultrasonic wire welding apparatus.

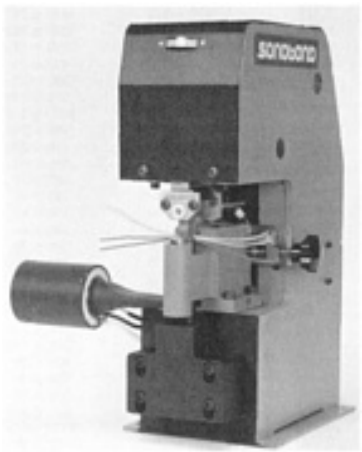

FIG. 4 ULTRASONIC WIRE WELDER USED TO BOND WIRES FOR MICROELECTRONIC APPLICATIONS

Wire diameters range from less than 0.025 to 0.5 mm (0.001 to 0.020 in.), and the highest volume occurs in the 0.025 to 0.050 mm (0.001 to 0.002 in.) diameter range. Vibratory action at high frequency (typically, 60 kHz) removes surface contaminants, induces material flow, and permits a solid-state weld between the wire and either the metallized bond pad or the leads on the semiconductor package.

A combination of ultrasonic and thermocompression bonding techniques, known as thermosonic bonding, is now a popular wire bonding method. The technique involves ultrasonic welding with heated substrates, typically with interface temperatures that range from 100 to 200 °C (210 to 390 °F).

Ultrasonic Welding

Janet Devine, Sonobond Ultrasonics

Personnel

Operators of the USW process do not need elaborate or extensive training. Once the process parameters have been determined by a process engineer, the operator is required only to load the parts into a nest of supporting/locating anvil

assembly, to press the palm buttons or other starting device, and then to unload the finished part. In-process monitoring can be performed either electronically, using a microprocessor, or visually by the operator, which usually requires the operator to look at a power indication gage. The process engineer needs to work closely with the equipment manufacturer for guidance regarding tooling design and the selection of process parameters.

No arc, spark, or molten filler material is associated with ultrasonic welding, and no electrical current passes through the weldment. Because the welder is usually configured in a press form with moderately high forces, the normal precautions need to be observed to ensure operator safety, that is, the use of anti-tie-down palm buttons or a similar provision to protect the hands of the operator. Another common consideration involves the high-frequency noise level produced by the ultrasonic vibration. In some instances, especially with the higher power level equipment, the noise exceeds the Occupational Safety and Health Administration (OSHA) approved levels and sound-deadening barriers or enclosures must be provided. Even where the noise level meets the approved requirements, the operator may find it necessary to wear ear protection.

Ultrasonic Welding

Janet Devine, Sonobond Ultrasonics

USW Procedures

The USW process requires the overlapping of the materials to be welded. Generally, the materials need only be presented to the welder in proper orientation. Correct orientation is usually achieved by using a nest or anvil fixture, which supports the parts while they are being welded. When joining stranded wires to other solid or stranded wires or to a terminal, a "gathering" fixture must be used to pull the wires together and to exert a slight pressure while welding to prevent the wires from escaping from the intended weld area. This type of fixture is usually supplied by the manufacturer with machines intended for use with wires and can be adjusted to accommodate a wide range of sizes and combinations.

Special considerations described below include the condition of the surface, the use of an interlayer, and the control of resonance.

Surface Condition. Most of the readily weldable materials, such as aluminum, copper, or brass, can be welded as received from the mill or must be degreased with a common solvent or detergent to remove surface lubricants. Oxide coatings will disperse during the process, unless they are very thick. Heavy surface scale should be removed by mechanical abrading or chemical etching before welding. The time lapse between cleaning and welding is generally not critical, unless the atmosphere is corrosive. Some types of coatings and insulations (for example, low-temperature magnet-wire coating) may be penetrated during the welding process, whereas other types must be mechanically removed. Fairly consistent surface cleanliness and quality must be maintained to ensure uniform weld quality.

Use of an Interlayer. A useful technique for improving the weld quality of some weldments involves placing a thin foil, usually aluminum or copper, between the metals to be bonded. This is particularly useful when materials of varying hardness are to be bonded. This interlayer is sometime more convenient and cost effective than plating the materials with a more weldable material (for example, copper or gold).

In a technique known as weld bonding, a layer of adhesive is placed between the panels to be ultrasonically welded. This technique not only provides a watertight seal, but also increases the weld strength beyond that obtained by either adhesive bonding or ultrasonic welding alone. Either a paste adhesive or a fabric-supported adhesive can be used in the ultrasonic bonding process.

Control of Resonance. Complex workpieces, especially those with multiple parts or thin wall sections, may be induced to vibrate by the ultrasonic welding system, which can produce fractures in the workpiece itself and in previously made welds or can cause inconsistent weld quality. This resonance can be either eliminated or minimized by applying pressure to the vibrating section. For example, in the ultrasonic welding of aluminum foil layers to the studs of capacitor caps, the stud must be clamped tightly or else the vibration will not only prevent the formation of a good joint, but can even melt the plastic cap that surrounds the stud.

Another option is to clamp the vibrating part to a comparatively large fixture or anvil. Significant pressure is required, and some machines come equipped with a product clamp for this purpose. Because resonance in the tooling can also occur, fixtures should be rugged and should not contain multiple small devices, such as springs or pins. It is best to avoid using light materials (for example, aluminum) for part fixtures, anvils, or supports. Steel is the preferred material for these components.

Tooling, Tips, and Anvils. The welding tip (or sonotrode) that contacts the weldment is usually made of the high-quality heat-treated tool steel. A precision fit between the tip and the waveguides is necessary to ensure efficient transmission of the vibratory energy. A locking (Morse) taper is frequently used, and the fit should cover 75% of the contacting surface area between the tip and its matching receptacle. In lower-power systems, the tip and the waveguide (horn) can be integral and can sometimes have several surfaces for welding. Rotation of the horn provides a new welding surface. A welding tip with a taper lock fit is less expensive to replace and easier to resurface, when necessary, than an integral horn-tip combination.

Certain alloys, especially the very soft aluminum alloys, may stick to the tip when welded. A mechanical stripper may be needed to pull the part free. Sometimes, a low-power, ultrasonic pulse may be sufficient to remove the stuck part from the tip. If a nugget remains on the tip, a weld pulse, with the tip clamped against a thick piece of brass, can remove the sticking nugget easier than mechanical abrasion methods.

Tips composed of exotic alloys have been used to prevent particularly tenacious sticking conditions, but with limited success. A steel shim with an oxidized surface was found to be particularly effective in preventing both sticking and deformation when bonding high-strength aluminum and titanium alloys, which are extensively used by the aircraft industry.

The anvil tip is subject to the same problems of wear and tip sticking that plague the sonotrode tip. The same high-strength heat-treated tool steel (typically, M2 heat treated to 58 to 60 HRC hardness) is recommended.

Welding tip and anvil tip surfaces with serrated or crosshatched patterns are useful in preventing slip between the tip and the weldment. Slip can result in a weld location between the metal and the tools, instead of at the required interface. A typical crosshatched pattern would be 0.5 mm (0.02 in.) peak-to-peak and about 0.2 mm (0.008 in.) deep.

Special Atmospheres. Although ultrasonic welding does not require a special atmosphere, it may be applicable under certain conditions. For example, use of an inert gas can reduce or prevent oxidation when bonding a metal such as lithium. Ultrasonic welding is not adversely affected by the presence of an inert atmosphere.

Weld quality is described below in terms of influencing factors, surface appearance and deformation, and metallographic examination.

Influencing Factors. The quality of ultrasonic welds is affected by these parameters:

- COMPOSITION AND GEOMETRY OF THE WELDMENT
- HARDNESS OF THE WORKPIECE
- CLEANLINESS OF THE WELDMENT
- SELECTION OF WELDING CONDITIONS, SUCH AS POWER, CLAMPING FORCE, AND WELD TIME
- CAPACITY OF THE TOOLING TO PROPERLY SUPPORT AND CLAMP THE PARTS TO PREVENT UNWANTED VIBRATION

Surfaces to be welded should be reasonably flat the parallel. This is especially critical for ring welding where a high degree of hermeticity is required. Some materials may be weldable in the as-received condition. However, a change in lubricants or other surface condition can require an adjustment in machine settings to maintain quality. Therefore, it is sometimes advisable to degrease or to abrade surfaces before welding to maintain a certain level of consistency.

Surface Appearance and Deformation. Depending on the material and the tip geometry, the surface of an ultrasonic weld can leave a slight scuff mark or a significant depression. This thickness deformation is more visible in soft, ductile

materials, such as soft aluminum. The actual weld interface is usually smaller than the surface impression. Harder materials generally have a shallower and smaller surface depression than soft, ductile materials.

A tip surface that has serrations or a cross-hatched pattern will replicate this pattern in the surface of the weldment. A spherical radius on the tip will generally produce a deeper, bowl-shaped depression than a flat tip of the same diameter.

Stranded or braided wires can be welded to form a solid cross section, if required. Slightly lower power, time, or force can give a compressed, but not solid, cross section.

Judicious radiusing and angling of tools is recommended to avoid sharp transitions in areas that can lead to early failure of an assembly.

The metallographic examination of ultrasonic welds in a wide variety of metals reveals phenomena that occur in the microstructure, such as surface film and oxide disruption, plastic flow and extrusion, recrystallization, phase transformation, and diffusion. Photomicrographs of selected ultrasonically welded materials are shown in the Section "Procedure Development and Practice Considerations for Solid-State Welding" in this Volume.

A heat-affected zone is significant in certain alloys, such as aluminum and nickel. Phase transformation, recrystallization, and precipitation may occur.

Diffusion across the interface is usually shallow, because of the relatively short weld times required, although significant penetration across the interface can take place. Alloying may occur then welding certain dissimilar metals, and the possibility of galvanic corrosion should be considered.

Ultrasonic Welding

Janet Devine, Sonobond Ultrasonics

Mechanical Properties

Tensile shear tests conducted on single-weld lap joints indicated that failure was caused by a fracture in the base metal itself or by a tear out of the weld button, rather than shear in the actual weld. Typical spot weld strengths in a variety of metals are summarized in Tables 1 and 2. These data were published as the result of a government-sponsored research program undertaken in the 1970s. With more modern equipment and practices, improved results can be obtained.

TABLE 1 TYPICAL SHEAR STRENGTHS OF ULTRASONIC SPOT-TYPE WELDS IN SELECTED PURE METALS AND ALLOYS

METAL	ALLOY OR PRODUCT TYPE	SHEET THICKNESS		MEAN STRENGTH WITH 90% CONFIDENCE INTERVAL[(A)]	
		mm	in.	n	lbf
ALUMINUM	X2020-T6	1.02	0.040	5520 ± 220	1240 ± 50
COPPER	ELECTROLYTIC	1.02	0.040	3470 ± 90	780 ± 20
		1.14	0.045	3780 ± 90	850 ± 20
BRASS	70-30 (HARD)	0.74	0.029	2400 ± 135	540 ± 30
STEEL	1020	0.64	0.025	2220 ± 90	500 ± 20
	AISI TYPE 301	0.20	0.008	2220 ± 45	500 ± 10
		0.36	0.014	3910 ± 180	880 ± 40
		0.41	0.016	6000 ± 710	1350 ± 160
	AISI TYPE 302	0.33	0.013	1820 ± 90	410 ± 20
		0.46	0.018	2800 ± 135	630 ± 30
		0.64	0.025	4630 ± 310	1040 ± 70

		0.81	0.032	5780 ± 900	1300 ± 200
	AISI TYPE 316	0.30	0.012	1020 ± 180	230 ± 40
		0.46	0.018	1960 ± 220	440 ± 50
	17-7 PH	0.20	0.008	1420 ± 90	320 ± 20
		0.51	0.020	440 ± 440	990 ± 100
		1.02	0.040	6230 ± 440	1400 ± 100
	PH 15-7 MO	0.20	0.008	1200 ± 45	270 ± 10
	AM350	0.20	0.008	1380 ± 90	310 ± 20
	AM335	0.20	0.008	1690 ± 180	380 ± 40
	A-286	0.38	0.015	3020 ± 310	680 ± 70
MOLYBDENUM	ARC-CAST	0.38	0.015	1070 ± 180	240 ± 40
		0.51	0.020	1470 ± 180	330 ± 40
		0.64	0.025	1600 ± 180	360 ± 40
	SINTERED	0.38	0.015	1510 ± 310	340 ± 70
		0.51	0.020	1690 ± 335	380 ± 80
		0.64	0.025	1910 ± 220	430 ± 50
TANTALUM	. . .	0.25	0.010	1110 ± 135	250 ± 30
TITANIUM ALLOY	TI-5AL-2.5SN	0.71	0.028	8670 ± 535	1950 ± 120
	TI-8MN	0.81	0.032	7690 ± 890	1730 ± 200
	TI-6AL-4V	1.02	0.040	10005 ± 800	2260 ± 180
ZIRCALOY-2	. . .	0.51	0.020	2760 ± 90	620 ± 20
NICKEL ALLOY	J-1500	0.33	0.013	3690 ± 735	830 ± 30
	INCONEL	0.25	0.010	755 ± 310	170 ± 70
		0.51	0.020	980 ± 445	220 ± 100
	INCONEL X	0.81	0.032	6760 ± 445	1520 ± 100
	K-MONEL	0.51	0.020	3025 ± 355	680 ± 80
		0.81	0.032	4000 ± 645	900 ± 60

(A) 90% CONFIDENCE INTERVAL INDICATES STATISTICAL PROBABILITY THAT STRENGTHS OF 90% OF THE WELDS WILL FALL WITHIN THE RANGE INDICATED.

TABLE 2 TENSION-TO-SHEAR RATIOS FOR SELECTED ULTRASONICALLY WELDED MATERIALS

METAL	TYPE	CONDITION	THICKNESS		CROSS-TENSION STRENGTH		TENSILE-SHEAR STRENGTH		TENSION-TO-SHEAR RATIO
			mm	in.	n	lbf	n	lbf	
ALUMINUM	2014-T6	. . .	0.81	0.032	1025	230	3115	700	0.33
			1.02	0.040	1380	310	3290	740	0.42
			1.27	0.050	1245	280	4005	900	0.31
	2024-T3	BARE	1.02	0.040	1070	240	3780	850	0.28
	2024-T3	ALUMINUM CLAD	1.27	0.050	1200	270	4715	1090	0.25
	7075-T6	ALUMINUM CLAD	1.27	0.050	1110	250	4890	1100	0.23
TITANIUM	TI-6AL-4V	. . .	0.64	0.025	1155	260	5425	1220	0.21
	TI-8MN	. . .	0.81	0.032	1955	440	7785	1750	0.25
MOLYBDENUM	SINTERED	. . .	0.13-0.25	0.005-0.010	110	25	425	95	0.26
TANTALUM	SINTERED	. . .	0.13-0.25	0.005-0.010	135	30	380	85	0.35
STAINLESS STEEL	17-7 PH	ANNEALED	0.51	0.020	845	190	2400	540	0.35
		HEAT-	0.30	0.012	490	110	1600	360	0.31

		TREATED							
		HEAT-TREATED AND AGED	0.13	0.005	290	65	690	155	0.42

Consistency is generally good, with one standard deviation, σ, typically less than 5% of the average strength value. Consistency of results in the manufacturing environment will follow from control of vital parameters (for example, part temperature, tooling temperature, machine and tooling stability, and surface condition of the parts).

Welds tested after thermal cycling, exposure to salt baths, and other corrosive environments maintain a relatively high tensile strength level.

Fatigue strength of ultrasonically welded metals often exceeds that of fusion-welded metals, because the ultrasonic bonding does not leave the cast button structure that is typical of melted and resolidified metal.

For relatively thin foils, the ductility of the ultrasonic bond permits the reforming of parts after welding without cracking the welded joint.

Ultrasonic Welding

Janet Devine, Sonobond Ultrasonics

Selected References

- J. DEVINE, ULTRASONIC BONDING FOR MOTOR MANUFACTURE, *PROC. ICWA CONF.* (BOSTON), 1979, P 1-5
- J. DEVINE, ULTRASONIC WELDING, *WELDING HANDBOOK,* 8TH ED., VOL 2, CHAPTER 25, 1991, P 784-812
- J. DEVINE, JOINING ELECTRICAL CONTACTS?, *WELD. DES. FABR.,* VOL 53 (NO. 3), 1980, P 112-115
- J. DEVINE, ULTRASONIC WELDING HELPS LIGHTEN AIRCRAFT, *WELD. DES. FABR.,* VOL 51 (NO. 8), 1978, P 74-76
- J. DEVINE AND R.G. VOLLMER, ULTRASONIC BONDING ARRIVES, *U.S. ARMY MAN. TECH. J.,* VOL 3 (NO. 1), 1978, P 11-14
- J. DEVINE, G.K. DINGLE, AND R.G. VOLLMER, ULTRASONIC BONDING, PANACEA OR PIE IN THE SKY, *PROC. ULTRASONIC INDUSTRIES ASSOCIATION* (NEW YORK), 1977, P 1-15
- T.J. KELLY, ULTRASONIC WELDING OF CUNI TO STEEL, *WELD. J.,* VOL 60 (NO. 4), 1981, P 29-31
- F.R. MEYER, ULTRASONIC WELDING PROCESS FOR DETONATABLE MATERIALS, *NATL. DEF.,* VOL 70 (NO. 334), 1976, P 291-293
- F.R. MEYER, ULTRASONICS PRODUCES STRONG OXIDE-FREE WELDS, *ASS. ENG.,* VOL 20 (NO. 5), 1977, P 26-29
- T. RENSHAW, J. CURATOLA, AND A. SARRANTONIO, DEVELOPMENTS IN ULTRASONIC WELDING FOR AIRCRAFT, *PROC. 11TH NATL. SAMPE TECHNICAL CONF.* (BOSTON). 1979, P 681-693
- T. RENSHAW AND A. SARRANTONIO, "PROPERTIES OF LARGE MULTISPOT ULTRASONICALLY WELDED JOINTS," AIAA STRUCTURES AND MATERIALS CONFERENCE (SEATTLE), 12-14 MAY 1980
- T. RENSHAW, K. WONGWIWAT, AND A. SARRANTONIO, A COMPARISON OF PROPERTIES OF SINGLE OVERLAP TENSION JOINTS PREPARED BY ULTRASONIC WELDING AND OTHER MEANS, *PROC. AIAA/ASME/ASCE 23RD CONF.* (NEW ORLEANS), 1983, P 1-8

• T. RENSHAW, AIRCRAFT SERVICE TESTING OF ULTRASONICALLY WELDED PANELS, *PROC. 16TH NATIONAL SAMPE TECHNICAL CONF*. (ALBUQUERQUE), 1984
• "ULTRASONIC WELDING OF ALUMINUM AND ALUMINUM ALLOY MATERIALS," MIL-STD 1947, 15 MAY 1985
• WELDING ALUMINUM THEORY AND PRACTICE, *ULTRASONIC WELDING,* THE ALUMINUM ASSOCIATION, 1989, P 14.3, 14.4

Introduction

TORCH BRAZING (TB) utilizes a fuel gas flame as the heat source for the brazing process. The fuel gas is mixed with either air or oxygen to produce a flame, which is applied to the workpiece until the assembly reaches the proper brazing temperature. Then, preplaced filler metal will be melted or hand-fed wire can be introduced.

Torch Brazing

Charles E. Fuerstenau, Lucas-Milhaupt, Inc.

Advantages and Limitations

Torch brazing is used with various base metals and on many different sizes of assemblies. The process offers many advantages, including:

- FLEXIBILITY, IN THAT ONE TORCH WITH MULTIPLE TIPS CAN BE USED TO BRAZE A VARIETY OF ASSEMBLIES
- LOW CAPITAL EQUIPMENT COST (MANUAL TORCH BRAZING)
- ENTIRE ASSEMBLY DOES NOT HAVE TO BE HEATED; SMALL JOINTS ON LARGE ASSEMBLIES CAN BE HEATED LOCALLY
- AUTOMATION IS POSSIBLE IN MANY CASES
- MOST BASE METALS AND COMBINATIONS OF BASE METALS CAN BE TORCH BRAZED IF A SUITABLE FLUX IS AVAILABLE

Although the process provides versatile, low-cost heating for brazing, its limitations include:

- OXIDATION/DISCOLORATION CAN OCCUR ON SURFACES OF THE ASSEMBLY NOT COVERED WITH FLUX, BECAUSE PROCESS IS CONDUCTED IN AIR
- FLUX RESIDUES NEED TO BE REMOVED AFTER BRAZING
- HIGHLY REACTIVE MATERIALS, SUCH AS TITANIUM AND ZIRCONIUM, CANNOT BE TORCH BRAZED, BECAUSE NO FLUX IS AVAILABLE
- LARGE ASSEMBLIES CAN BE DIFFICULT TO HEAT, BECAUSE OF THE LOCALIZED NATURE OF FLAME HEATING

Applications

Torch brazing is commonly used on copper, brass, and other copper alloys, as well as steel, stainless steel, aluminum, carbides, and various heat-resistant materials. Most combinations of these materials can also be torch brazed. It is necessary to use flux with these materials, except when a phosphorus brazing alloy is used to braze pure copper parts. In this case, the phosphorus acts as the flux. The low-temperature silver-base and silver/copper/phosphorus filler metals are commonly used with torch brazing. Various other copper-base and gold-base filler metals can also be used with this process.

Torch brazing is often used to join copper and Bundy steel tube assemblies for the heating, air conditioning, and refrigeration industries. The process is also commonly used when brazing heat exchangers, bicycles, furniture, carbide tools, plumbing components, automotive subassemblies, medical instruments, and many other workpiece types. A wide range of components can be torch brazed, including small joints for jewelry parts, large-diameter (75 mm, or 5 in.) tubes, and fitting joints. The process provides strong, leak-tight joints on a wide variety of base materials.

Torch Brazing

Charles E. Fuerstenau, Lucas-Milhaupt, Inc.

Equipment

The equipment for torch brazing has several components. Single torches are typically used for hand brazing, whereas multiple torches can be used in an automated system. The gas-oxygen is mixed in the torch body and is adjusted using the needle valves on the torch. Gas-air combinations can be mixed at the torch or, alternatively, a central mixing system can be used to supply many torches, particularly in automated applications.

The typical fuel gases used in torch brazing are acetylene, propane, and methane (natural gas). Various flame temperatures and heat contents are given in Table 1.

TABLE 1 COMMON FUEL GASES USED IN TORCH BRAZING

FUEL GAS	FORMULA	OXYGEN-TO-FUEL GAS RATIO(A)	FLAME TEMPERATURE FOR OXYGEN		HEAT CONTENT	
			°c	°f	mj/m^3	btu/ft^3
ACETYLENE	C_2H_2	2.5	3087	5589	55	1470
PROPANE	C_3H_8	5.0	2526	4579	104	2498
METHANE	CH_4	2.0	2538	4600	37	1000

(A) THE VOLUME UNITS OF OXYGEN REQUIRED TO COMPLETELY BURN A UNIT VOLUME OF FUEL GAS; A PORTION OF THE OXYGEN IS OBTAINED FROM THE ATMOSPHERE.

An automated brazing system that can braze up to 40,000 heat-exchanger return bend joints per hour is shown in Fig. 1. Multiple torches are used to provide the necessary heat.

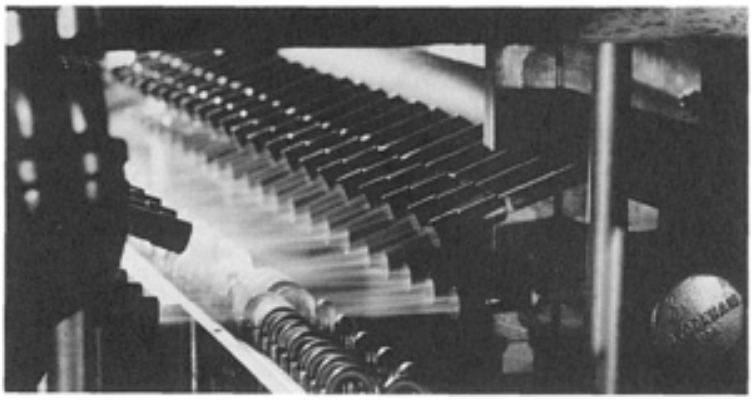

FIG. 1 AUTOMATED TORCH BRAZING SYSTEM

Torch brazing gases are normally supplied from bulk sources. An individual gas cylinder may supply one torch, whereas large bulk tanks are used to supply many torches or an automated system utilizing many burners. In all torch brazing systems, regulators are used to safely control the gas distribution. Individual regulators are used on the gas and oxygen lines. Standard safety precautions should be utilized when handling the equipment, and operators should be thoroughly trained in safety practices related to the use of compressed and combustible gases.

Torch Brazing

Charles E. Fuerstenau, Lucas-Milhaupt, Inc.

Techniques

The key to torch brazing, as in all methods of heating, is to heat evenly the components to be brazed. This may require directing the torch primarily on a large, rather than small, component. Because the filler metal will flow to the hottest portion of an assembly, the flame should be applied in such a way as to flow the filler metal in the required direction.

When preplaced (preform or paste) filler metal is used in torch brazing, the operator need only know where and how much heat to apply. When the operator is also responsible for the filler metal, he must not apply it until the assembly has reached brazing temperatures. This may require practice and experience. Torch brazing is a skill that can be attained relatively quickly with the proper training.

Torch Brazing

Charles E. Fuerstenau, Lucas-Milhaupt, Inc.

Selected References

- *BRAZING HANDBOOK*, 4TH ED., AMERICAN WELDING SOCIETY, 1991
- *THE BRAZING BOOK*, HANDY & HARMAN/LUCAS-MILHAUPT, INC., 1991

Furnace Brazing

Toshi Oyama and Howard Mizuhara, WESGO, Inc.

Introduction

FURNACE BRAZING is a mass production process for joining the components of small assemblies with a metallurgical bond, using a nonferrous filler metal as the bonding material and a furnace as the heat source (Fig. 1). Furnace brazing technology was initiated in the 1920s and was first used commercially circa 1930, primarily to provide a brazing process that did not require a chemical flux, thereby eliminating the flux entrapment problem. Currently, furnace brazing is widely applied in a variety of industries. The essentially automatic nature of the process and its use of unskilled labor account for its popularity.

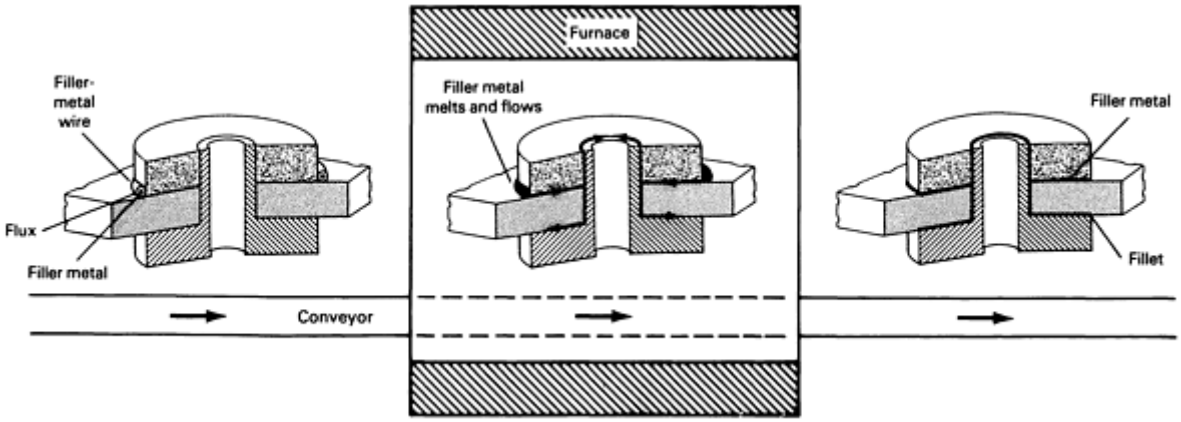

FIG. 1 CROSS-SECTIONAL VIEW OF THREE-PART ASSEMBLY AS IT PROCEEDS THROUGH FURNACE BRAZING OPERATION. FILLER-METAL WIRE (FILLER METAL ENCIRCLED BY FLUX) GRADUALLY MELTS AND FLOWS INTO VOIDS BETWEEN THE THREE SECTIONS AND THEN COOLS TO FORM A SINGLE-UNIT WORKPIECE AS IT IS CONVEYED THROUGH THE FURNACE.

In the furnace brazing process, cleaned parts and brazing filler metal are assembled, placed in a furnace, and heated to the brazing temperature. Furnace brazing is only practical if the filler metal can be placed on the joint before brazing and retained in position during brazing. Heating rate, brazing temperature and time, and cooling rate are controlled. Furthermore, in most cases, the brazing is carried out in a controlled atmosphere, which may be either reducing, inert, or vacuum. The advantages and limitations of furnace brazing are identified below.

Process Advantages. There are at least five advantages to using the furnace brazing process:

- IT IS A METHOD IN WHICH MANY VARIABLES CAN BE EASILY CONTROLLED TO ENSURE REPEATABILITY OF THE PROCESS AND GUARANTEE A HIGH-QUALITY JOINT. BRAZING TEMPERATURE AND PROCESS DURATION, AS WELL AS HEATING AND COOLING RATES, CAN BE CONTROLLED AND MONITORED. IN ADDITION, THE BRAZING ATMOSPHERE CAN BE EASILY REGULATED.
- WHEN ALL THE BRAZING PROCEDURES ARE WELL ESTABLISHED, RELATIVELY UNSKILLED OPERATORS CAN CARRY OUT EVERYDAY MANUFACTURING OPERATIONS.
- THE ABSENCE OF FLUX ENTRAPMENT ALLOWS MORE FLEXIBILITY IN JOINT DESIGN. THE POSTBRAZE CLEANING OF THE BRAZED PART AND THE FURNACE ARE UNNECESSARY.
- BECAUSE A WHOLE ASSEMBLY IS HEATED, DISTORTION OF THE PARTS CAN BE MINIMIZED OR ELIMINATED. IN SOME CASES, HEAT TREATMENT OF THE PART CAN BE INCORPORATED INTO THE BRAZING CYCLE.
- MORE THAN ONE JOINT PER WORKPIECE CAN BE BRAZED IN A BRAZING CYCLE. SEVERAL DIFFERENT ASSEMBLIES REQUIRING THE SAME BRAZING CONDITIONS CAN ALSO BE BRAZED SIMULTANEOUSLY.

Process limitations include:

- THE INITIAL INVESTMENT IN FURNACE BRAZING EQUIPMENT IS RELATIVELY HIGH. FURTHERMORE, THE MAINTENANCE OF THE EQUIPMENT IS CRITICAL AND CAN BE MORE EXPENSIVE THAN OTHER BRAZING TECHNIQUES. THE COST OF A SPECIAL ATMOSPHERE MUST ALSO BE CONSIDERED.
- BECAUSE THE WHOLE ASSEMBLY IS HEATED, THE COST OF HEATING EXCEEDS THAT OF OTHER BRAZING OPERATIONS. IN ADDITION, MICROSTRUCTURAL CHANGES IN THE BASE MATERIAL CAN OCCUR, DEPENDING ON THE MATERIAL BEING BRAZED AND THE BRAZING TEMPERATURE.
- BECAUSE BRAZING IS PERFORMED INSIDE THE FURNACE, JOINT DESIGN IS IMPORTANT. THE FIXTURES FOR HOLDING A BRAZED ASSEMBLY REQUIRE EXTRA HEAT MASS, WHICH INCREASES THE MANUFACTURING COST. PROPER JOINT DESIGN CAN MINIMIZE OR EVEN ELIMINATE FIXTURE COMPLEXITY.

Furnace Brazing

Toshi Oyama and Howard Mizuhara, WESGO, Inc.

Furnaces and Control Instrumentation

Brazing furnaces can be either oxyfuel fire or electrically heated. Whether they furnish heat directly or indirectly, all furnaces must provide a uniform work-load temperature. For example, the brazing of high-temperature nickel-base alloys at 1095 °C (2000 °F) and higher generally requires a hot-zone uniformity of ±8 °C (±15 °F). When brazing aluminum alloys, the temperature uniformity must be ±3 °C (±5 °F). Thus it is vital that each work load be closely monitored with a minimum of two thermocouples attached to or embedded in the parts to be brazed.

There are basically three types of furnaces: continuous, semicontinuous, and batch. Proper furnace selection primarily depends on the application. An example of the continuous-type furnace is a belt-conveyor furnace (Fig. 2). The brazing conditions are controlled by the speed of the conveyor and the set temperature. Because initial start-up involves several days to heat and to prepare the furnace for operation, these parameters are constantly maintained. The furnaces are seldom shut down and, when idling, are usually run at a temperature that is approximately several hundred degrees below the operating temperature. Therefore, the cost of furnace operation is very high if the equipment is not fully utilized. The furnace is used for mass production applications (that is, production rates of a few thousand parts per hour). Typically, a reducing gas is introduced into the brazing chamber. When the furnace is fully utilized, the cost per unit part becomes cost effective.

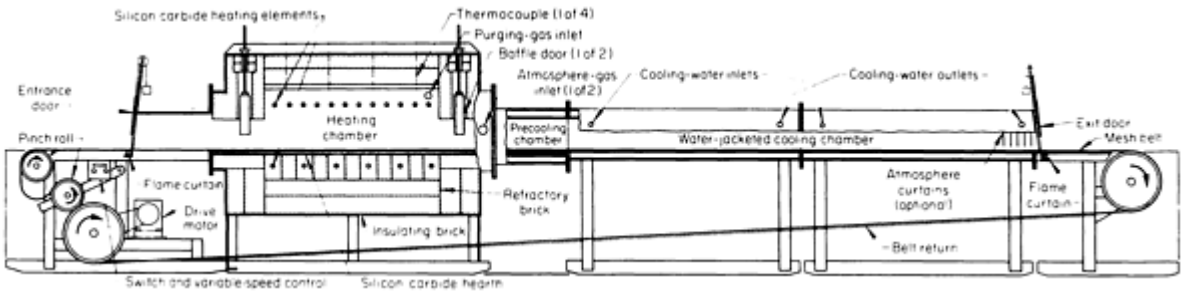

FIG. 2 MESH-BELT CONVEYOR BRAZING FURNACE THAT UTILIZES A WATER-JACKETED COOLING CHAMBER

Retort (or bell-type) furnaces are often used as semicontinuous furnaces (Fig. 3). In this type of furnace, brazing assemblies are encapsulated in the retort and a special gas is introduced. Then, the retort is placed in a furnace for brazing.

In the semicontinuous operation, two or more retorts are used in the production process. While one retort is in a brazing cycle, another retort is cooled, unloaded, and reloaded. Such furnace systems are typically equipped with microprocessors to control the furnace cycle.

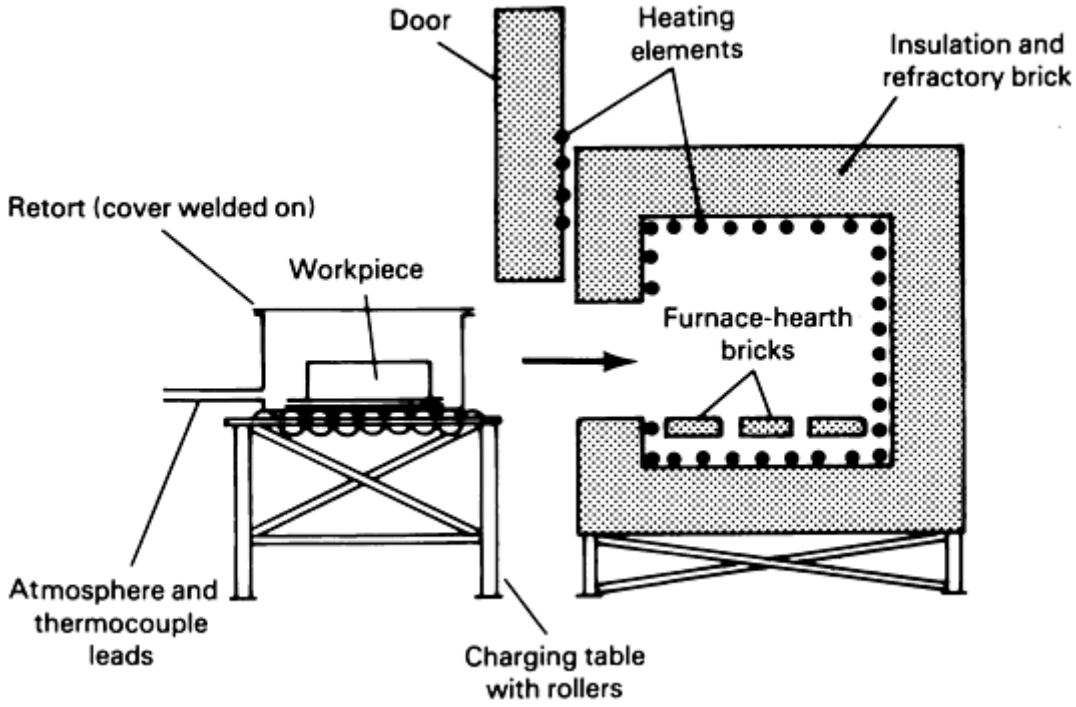

FIG. 3 SEALED RETORT ABOUT TO BE LOADED INTO ELECTRIC-FIRED BOX FURNACE IN ORDER TO BRAZE A WORKPIECE IN A CONTROLLED ATMOSPHERE

The vacuum furnace is typically used for batch processing (Fig. 4), although a semicontinuous vacuum furnace version is also available. The vacuum brazing furnace is typically interfaced with a microprocessor (Fig. 5). The programmable microprocessor controls all of the brazing parameters: heating rate, brazing temperature and time, cooling rate, and back-filled gas. Because several different brazing cycles can be stored in the microprocessor memory, the vacuum furnaces are quite versatile. Furthermore, an alarm system can be installed in the microprocessor to detect any operational abnormality that has the potential to terminate the brazing operation.

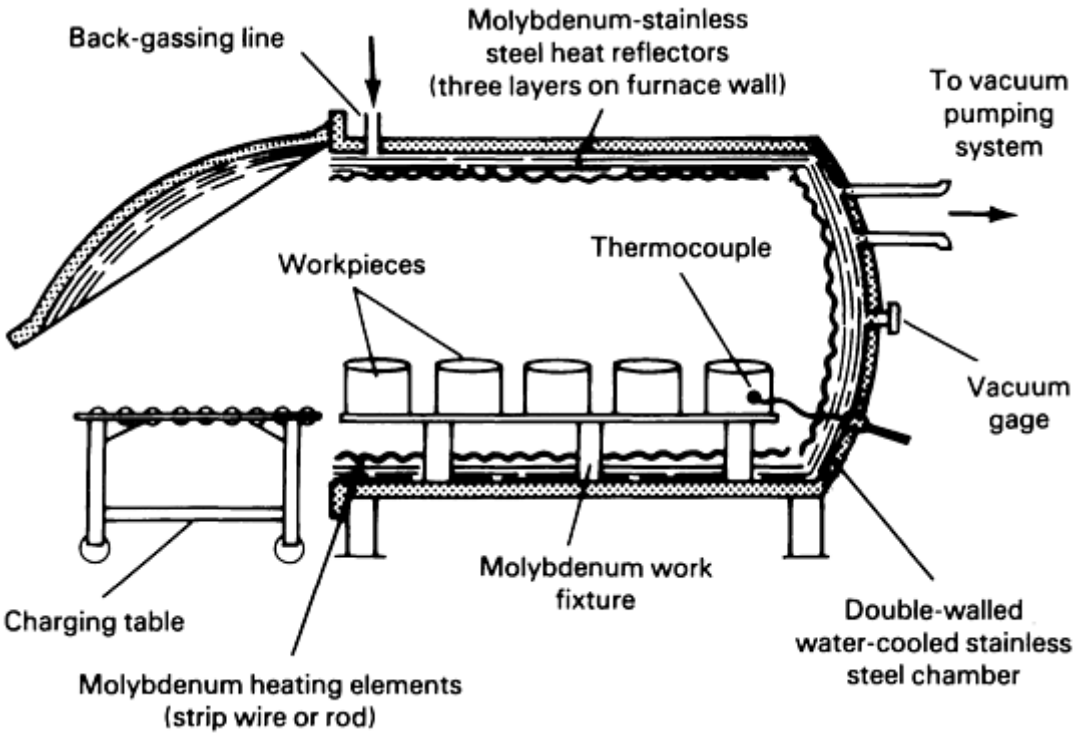

FIG. 4 TYPICAL CONSTRUCTION OF HORIZONTAL SIDE-LOADED COLD-WALL VACUUM FURNACE, WHICH IS IDEAL FOR BRAZING OF SMALL ASSEMBLIES THAT CAN BE PLACED IN STACKED BASKETS OR ON TIERS OF WORK GRIDS

FIG. 5 BRAZING FURNACE INSTALLATION SHOWING RELATIVE SIZE OF BRAZING CHAMBER OF THE UNIT TO THE MICROPROCESSOR-BASED CONTROL MODULE. COURTESY OF CENTORR/VACUUM INDUSTRIES

Furnace Brazing

Toshi Oyama and Howard Mizuhara, WESGO, Inc.

Industrial Applications

The furnace brazing process is employed in many industries because of its high quality and reproducibility. The vacuum device, jet engine, and automotive industries represent three examples. In the vacuum device industry, a vacuum tube with an envelope of alumina ceramic is used, the nature of which requires that the whole assembly be heated. The control of heating and cooling rates is very important to the prevention of alumina ceramic cracking.

Other applications of furnace brazing can be found in the jet engine industry, where the quality of the brazed joint and the dimensional control of the brazed assembly are critical. Vacuum furnace brazing is the most common system used in the production of jet engine components.

The automotive industry makes extensive use of the continuous belt furnace because it is easily automated and is a cost-effective, high-production joining process for components made of carbon steel, stainless steel, and aluminum.

Furnace Brazing

Toshi Oyama and Howard Mizuhara, WESGO, Inc.

Health and Safety Guidelines

Although everyday production is relatively simple and trouble-free, the furnace operator should be instructed on the proper use of the equipment, the hazards of the gases and atmospheres used, and the importance of proper operating procedures. An alarm system should be installed to monitor furnace parameters and to alert operators of any potential equipment breakdowns or hazardous working conditions. Routine maintenance of the furnace and auxiliary equipment is vital if accidents are to be prevented.

Furnace Brazing

Toshi Oyama and Howard Mizuhara, WESGO, Inc.

Selected References

• M.M. SCHWARTZ, *BRAZING,* ASM INTERNATIONAL, 1987
• *BRAZING HANDBOOK,* AWS, 1991
• *MANUFACTURING TECHNIQUES IN BRAZING,* YOUSETSU SHINBUN SHA, 1982 (IN JAPANESE)
• "SAFETY IN WELDING AND CUTTING," STANDARD ZA9.1, ANSI/AWS

Induction Brazing

J.F. Libsch, Lepel Corporation

Introduction

INDUCTION BRAZING (IB) is a process that joins metal components to form an assembly by selectively heating the joint area to the brazing temperature with electrical energy transmitted from an inductor that has been energized by a heating generator. It is classified as a brazing process because joints are made at elevated temperatures (540 °C, or 1000 °F, or above), using copper alloys that often contain silver (Ref 1).

Heating results from resistance to the flow of induced current (I^2R losses) in the assembly components. It occurs when the electrically conductive components are placed in the electromagnetic field created by rapidly alternating current flow in the inductor (Fig. 1). With proper coil design, heating occurs rapidly at the joint area, providing localized brazing temperatures. Response to the electromagnetic field depends on the frequency of the alternating current and the nature of the materials being heated, as well as on the shape of the component parts and coil design. Nonmagnetic materials with low electrical resistance such as copper and brass take longer to heat than magnetic, higher resistivity, ferrous materials such as steel.

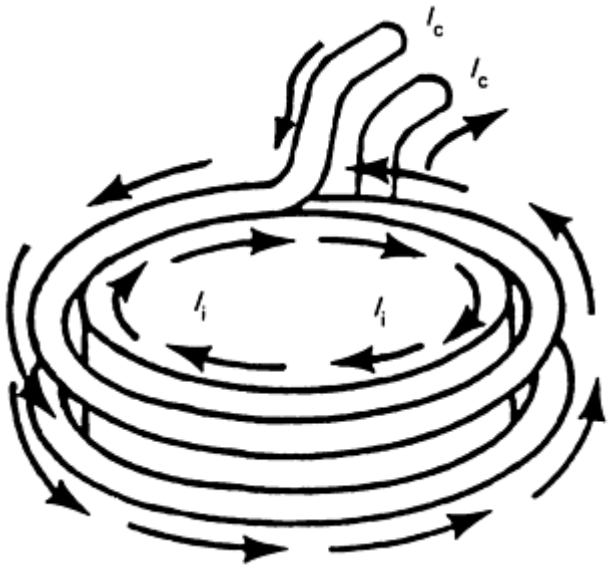

FIG. 1 RELATION OF COIL CURRENT, I_C, TO INDUCED CURRENT IN THE WORKPIECE, I_I, GENERATED BY ELECTROMAGNETIC FIELD IN THE INDUCTION COIL

While a strong electromagnetic field and high power density (2×10^{-3} kW/mm^2, or 1 kW/in.^{2}) can create highly localized temperatures, most brazing applications use relatively low power densities of 1×10^{-3} kW/mm^2 (0.5 kW/in.^{2}) to ensure that the joint area comes to brazing temperature uniformly. Heat conduction plays an important role.

Because a multitude of joint configurations are encountered, proper inductor or coil design is essential to ensure uniform joint temperature and to permit handling of components onto the coil for processing. Some typical coils that are fabricated from copper tubing and that use water cooling are shown in Fig. 2. Inductors made from solid copper bar for single- or multiple-joint heating and that employ both internal and external water cooling are used for some applications.

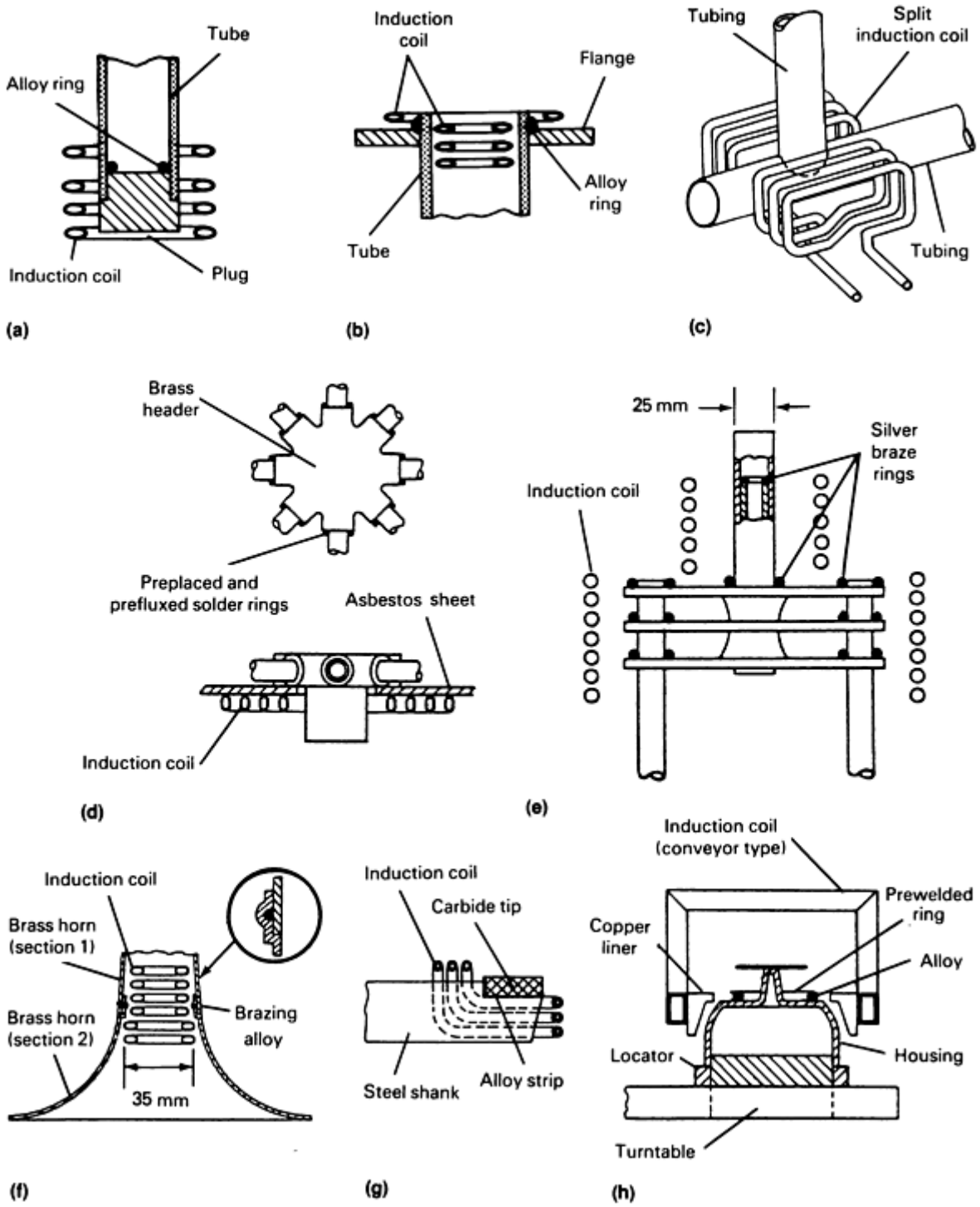

FIG. 2 TYPICAL COIL AND JOINT CONFIGURATIONS USED IN INDUCTION BRAZING. (A) SOLENOID COIL FOR PLUG-TO-TUBE JOINT (NOTE LOCATION OF BRAZING ALLOY RING). (B) INTERNAL-EXTERNAL COIL FOR FLANGE-TO-TUBE JOINT (FLANGE CHAMFERED TO ASSIST PREPLACED ALLOY RING. (C) SPLIT SOLENOID COIL FOR TUBE-TO-TUBE T-JOINT (BRAZE RING PREPLACED INTERNALLY TO PROVIDE UNIFORM FILLET). (D) PANCAKE OR PIE WOUND COIL FOR HEATING BRASS HEADER TO PERMIT SIMULTANEOUS BRAZING OF EIGHT COPPER TUBES TO HEADER. (E) EXTERNAL COILS FOR SIMULTANEOUS PRODUCTION OF A NUMBER OF BRAZED JOINTS. (F) FORMED INTERNAL COIL TO JOIN TWO SECTIONS OF MUSICAL HORN (SPECIAL JOINT DESIGN FOR PREPLACEMENT OF BRAZING ALLOY MAINTAINS SMOOTH JOINT ON OUTSIDE OF INSTRUMENT. (G) OPEN-END COIL FOR BRAZING CARBIDE TIPS TO SHANKS (ALLOY STRIP PREPLACED AS SHOWN). (H) CONVEYOR TYPE COIL FOR CONTINUOUSLY BRAZING FUSE ASSEMBLIES ON A ROTARY FIXTURE

Reference

1. "SPECIFICATION FOR FILLER METALS FOR BRAZING," A.58-89, AMERICAN WELDING SOCIETY, 1989

Induction Brazing

J.F. Libsch, Lepel Corporation

Process Applications

Induction brazing is used where relatively high-strength heat-resistant joints are required between components parts. The strength of the joint depends on the joint design, the brazing alloy, the strength of the components being joined, and the clearance between the components. A clearance of 0.038 to 0.050 mm (0.0015 to 0.002 in.) is recommended. Induction brazing has been used extensively in the production of consumer and industrial products, structural assemblies, electric and electronic products, mining equipment, machine and hand tools, military and ordnance equipment, and aerospace components.

Advantages. Induction brazing features rapid heating that produces joints in seconds because each joint area is exposed to the electromagnetic field of the specific coil involved. Uniform and reliable joints can be produced piece after piece with smooth joint fillets, eliminating the need for finishing operations. Because a suitable induction coil can provide heat simultaneously at several locations in an assembly, a number of joints can be made in a single heating operation. Induction brazing provides control of the heat pattern and rapid heating, which serve to localize the heated zone, thereby preventing or minimizing deterioration of properties in previously heat-treated or cold-worked materials, and, if desired, permitting sequential brazing of nearby joints using alloys with decreasing melting temperatures.

Induction brazing uses predetermined amounts of brazing alloys in the form of rings, strip, or powder; thus, the possibility of excessive material use is avoided, lowering joining alloy costs. Rapid heating minimizes oxidation and discoloration in most instances, even without the use of a controlled atmosphere.

Limitations of induction brazing include:

- DIFFICULTY IN HEATING OF COMPLEX ASSEMBLIES
- NEED FOR RELATIVELY UNIFORM CLEARANCE BETWEEN COMPONENTS
- INITIAL COST OF EQUIPMENT
- NEED FOR SPECIALIZED KNOWLEDGE FOR SYSTEM DESIGN

For complex assemblies involving several brazed joints and special geometry, induction brazing fixturing may be difficult, and furnace brazing may be a more practical process choice.

Induction Brazing

J.F. Libsch, Lepel Corporation

Brazing Equipment and Fixturing

Major changes have been made in the design of generators and temperature control equipment in recent years. Most significant perhaps has been the development of solid-state generators to complement or replace motor generators and vacuum tube generators. Solid-state generators of intermediate power levels that operate at frequencies of 50 to 200 kHz or 50 to 350 kHz have become available, providing an alternate to tube generators that operate at nominal frequencies of 450 kHz. Improvements have been made in generator control design, permitting precise and instantaneous response to changes transmitted by a suitable sensor element.

The proper size generator required for a given operation is best determined by an actual trial in the laboratory. However, a preliminary estimate can be made by considering the power absorbed by the pieces to be joined, the amount of radiation lost from the heated piece, and the required production rate. (The accuracy of this estimate depends on good coil design and electrical matching between the generator and the work load.) The curves in Fig. 3 represent the approximate heat content or heat energy required to heat 1 kg (2.2 lb) of material to the temperatures indicated from 20 °C (68 °F); these curves reflect the variation in specific heat with temperature for each metal.

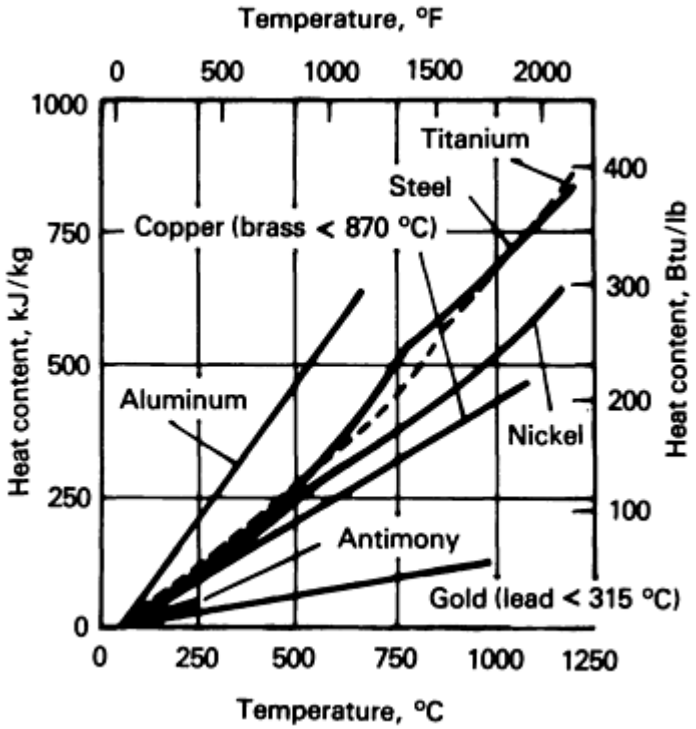

FIG. 3 PLOT OF HEAT CONTENT (MASS BASIS) VERSUS TEMPERATURE FOR SELECTED METALS AND ALLOYS. SOURCE: REF 3

Precise determination of the weight being heated in most brazing applications is difficult because heat is conducted away from the joint area, thus creating a temperature gradient for some distance beyond the induction-heated joint and adding to the amount of energy required. Furthermore, Fig. 3 does not account for the energy required to compensate for radiation losses. Fortunately, the temperatures most often used in induction brazing are relatively low (620 to 815 °C, or 1150 to 1500 °F); thus, radiation losses are small and can generally be neglected in the preliminary estimate. While rapid heating rates using high power may increase production, they are a frequent source of difficulty in induction brazing; very rapid heating exaggerates the effects of electrical resistivity and thermal conduction. Slower heating rates minimize the effects of thermal conduction when dissimilar metal joints, such as steel to copper, are involved. In some situations, slower heating rates can help compensate for considerable differences in the mass of the components being brazed.

The most common frequencies currently used for brazing applications are 10 kHz, 25 to 50 kHz, 50 to 200 kHz, and 50 to 350 kHz with solid-state generators, and 250 to 450 kHz with tube equipment. The lower frequencies heat more deeply and may provide more uniform heating of the matching surfaces if one of the components to be brazed has a large mass. Higher operating frequencies, such as 450 kHz, may be suitable for brazing of nonferrous metals, or for brazing of steel to a nonferrous metal or to a nonmagnetic (austenitic) steel. High frequency may also provide more efficient heating of parts; in fact, tube equipment operating at 2.5 to 8 MHz may be necessary for very thin components. As a general. rule, cost in dollars per kilowatt is lower with lower frequency generators.

Figure 4 shows a system for induction brazing components for refrigeration and air conditioning using a 7.5 kW solid-state unit operating at a frequency of 100 kHz.

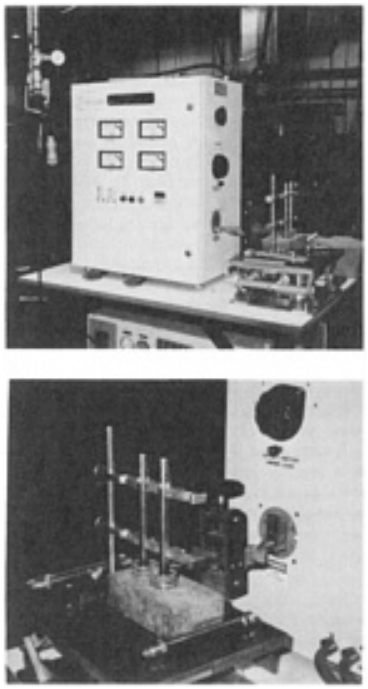

FIG. 4 INDUCTION BRAZING INSTALLATION THAT USES A 7.5 KW SOLID-STATE INDUCTION GENERATOR OPERATING AT 100 KHZ TO JOIN BRASS AND STAINLESS STEEL COMPONENTS FOR HEAVY-DUTY VEHICLE REFRIGERATION AND AIR CONDITIONING SYSTEMS. COURTESY OF RED DOT CORPORATION AND LEPEL CORPORATION

An inert or reducing atmosphere surrounding the brazed joint area is desirable in some applications. Appropriate fixturing and/or bell-jar arrangements (Ref 4) are used in such applications.

References cited in this section

3. C.A. TUDBURY, *BASICS OF INDUCTION HEATING*, VOL 1
4. P.F. GERBOSI AND J.F. LIBSCH, CONTROLLED-ATMOSPHERE BRAZING WITH INDUCTION HEATING, *WELD. J.*, OCT 1989, P 32-37

Induction Brazing

J.F. Libsch, Lepel Corporation

Joint Design

Figure 2 illustrates several basic joint designs for induction brazing as well as typical coils and some frequent applications (Ref 5). The schematics show the placement of brazing alloy preforms and coil-part arrangements.

Joint Parameters (Ref 2). The following joint parameters for parts to be brazed by induction heating require special attention:

- HEATING PATTERN
- METHOD OF PREPLACING THE JOINING ALLOY
- CLEARANCES BETWEEN MATING PARTS

- THERMAL CONDUCTIVITY AND EXPANSION CHARACTERISTICS OF THE MATERIALS TO BE JOINED

Effect of Thermal Expansion on Stress (Ref 2). Stress concentration and high residual stresses in the joint become critical factors when the joint members are stronger than the brazing filler metal, or when differential contraction takes place with dissimilar materials. The marked difference in the thermal expansion between tungsten carbide (5.9×10^{-6}/K, or 3.3×10^{-6}/°F) and carbon steel (12.1×10^{-6}/K, or 6.7×10^{-6}/°F) may be particularly troublesome when the carbide is placed in tension. This frequently results in cracked carbide. A "sandwich" braze utilizing a clad brazing strip (that is, copper clad with silver brazing filler metal on both sides) can overcome this problem. In a sandwich braze, stresses are minimized as a result of plastic deformation in the low-yield-strength copper layer.

References cited in this section

2. *BRAZING HANDBOOK,* 4TH ED., AMERICAN WELDING SOCIETY, 1989, P 214-218
5. J.F. LIBSCH AND P. CAPOLONGO, HIGH FREQUENCY INDUCTION BRAZING AND SOLDERING, *LEPEL REV.*, VOL 1 (NO. 5)

Induction Brazing

J.F. Libsch, Lepel Corporation

Human Factors Engineering Ergonomics

In induction brazing, the heating function is essentially independent of the operator once the generator, coil, and heating program have been set up. The amount of handling of the component parts, the brazing alloy preforms, and flux depend upon the degree to which the application is automated. In fully automated systems, the operator oversees the operations and ensures the supply of the various joint elements from feed mechanisms, including mechanisms that provide automatic placement of brazing alloy preforms and fluxing. In semiautomatic systems, the operator loads the component parts on a fixture, preplaces the preform, and fluxes the joint region at a workstation on a continuously moving conveyor, rotary, or indexing device. In these systems, the operator serves primarily as an unskilled machine operator. Specialized complex assemblies (for example, electron tubes) that are brazed in controlled atmospheres may require skilled personnel with specialized training in induction heating processing.

Good joint design provides for simple inspection of the assembly, which involves simply noting alloy flow from the joint area to the edges of the joint. The presence of smooth continuous fillets also indicates a successful joint. Complex inspection methods such as radiography or ultrasonic inspection may be specified in critical applications.

Induction Brazing

J.F. Libsch, Lepel Corporation

References

1. "SPECIFICATION FOR FILLER METALS FOR BRAZING," A.58-89, AMERICAN WELDING SOCIETY, 1989
2. *BRAZING HANDBOOK,* 4TH ED., AMERICAN WELDING SOCIETY, 1989, P 214-218
3. C.A. TUDBURY, *BASICS OF INDUCTION HEATING*, VOL 1
4. P.F. GERBOSI AND J.F. LIBSCH, CONTROLLED-ATMOSPHERE BRAZING WITH INDUCTION

HEATING, *WELD. J.*, OCT 1989, P 32-37
5. J.F. LIBSCH AND P. CAPOLONGO, HIGH FREQUENCY INDUCTION BRAZING AND SOLDERING, *LEPEL REV.*, VOL 1 (NO. 5)

Induction Brazing

J.F. Libsch, Lepel Corporation

Selected References

- M.M. SCHWARTZ, *BRAZING*, ASM INTERNATIONAL, 1987

Dip Brazing

Daryl D. Peter, Daryl D. Peter and Associates

Introduction

DIP BRAZING (DB) is one of the oldest brazing processes. The materials to be joined are immersed in a hot liquid, which is either a molten flux or a molten filler metal that usually contains a layer of flux to prevent oxidation. Dip brazing is primarily used because of its ability to uniformly heat parts that have a wide range of thicknesses. The process is simple when compared with modem, complex brazing equipment and processes. The drawback of the process is that it coats everything with flux or braze alloy; flux can be corrosive to fixtures and surrounding metal structures and equipment. Even when compared with more modern heating methods, the speed of immersion heating is hard to match and dip brazing, therefore, continues to be a common process.

Dip Brazing

Daryl D. Peter, Daryl D. Peter and Associates

Furnace Construction

Dip brazing systems can be described by the type of pot vessel, heating method, and heating media that is used. Vessel construction can be ceramic, fired brick, or, possibly, cast (Fig. 1). A metal tank of a suitable alloy can also be used. Heating is facilitated by either gas or electric current. Flux baths favor electric heating, because of their higher resistivity when molten.

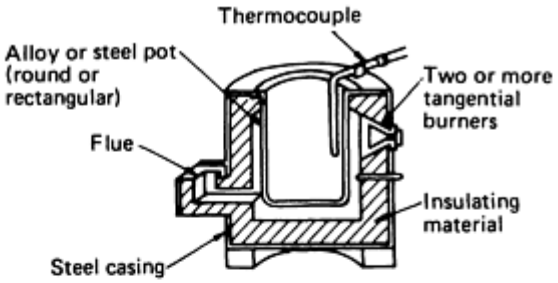

(a) Gas fired or oil fired

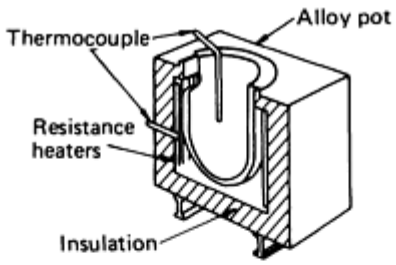

(b) Resistance heated

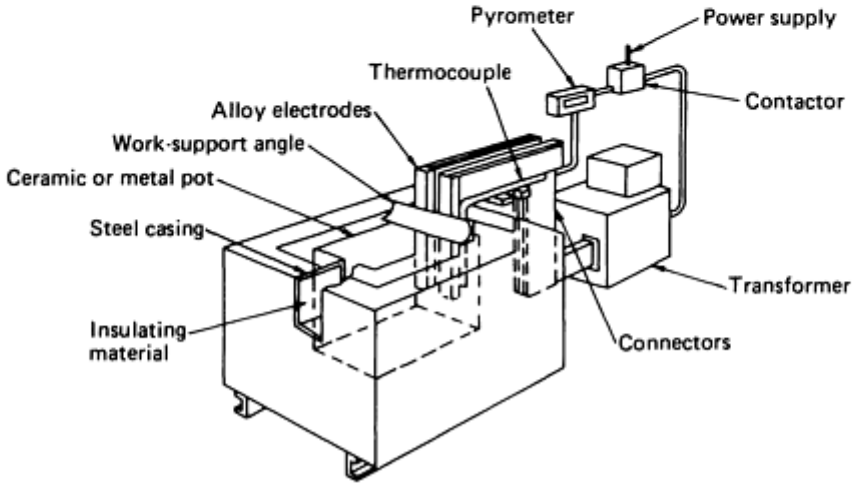

(c) Immersed electrodes

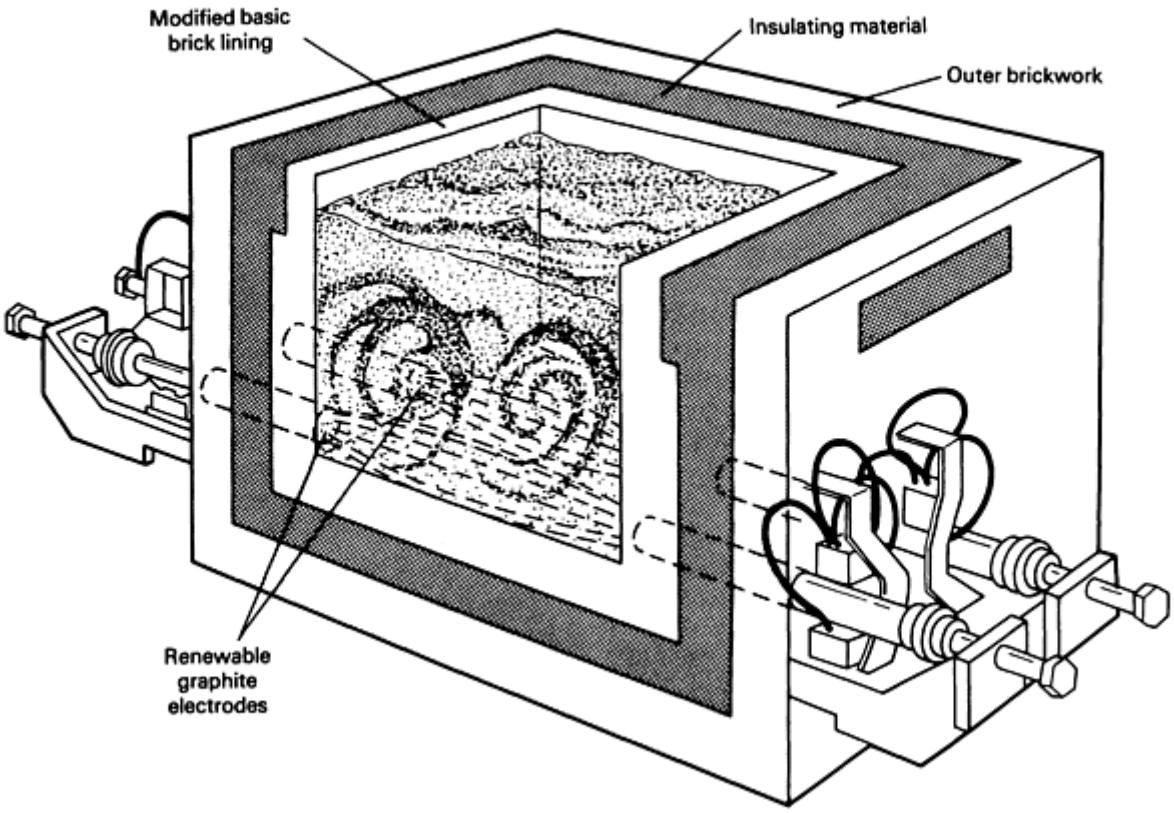

(d) Electrically heated (submerged electrodes)

FIG. 1 PRINCIPAL TYPES OF FURNACES USED FOR MOLTEN-SALT-BATH DIP-BRAZING APPLICATIONS. (A) AND (B) EXTERNALLY HEATED; (C) AND (D) INTERNALLY HEATED

Figure 2 shows a typical furnace used for flux brazing applications. Electricity is conducted into the bath by either carbon or nickel electrodes that penetrate the furnace wall. Ultrasonic generators can also be incorporated into the molten metal processes to provide a scrubbing action.

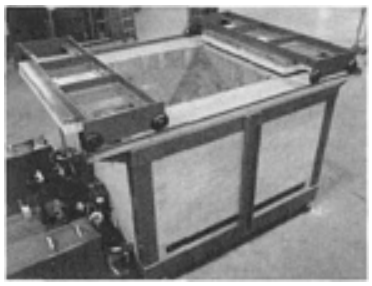

FIG. 2 SUBMERGED-ELECTRODE FURNACE INSTALLATION INCORPORATING A TOP-LOADING DOOR MECHANISM WITH RAIL TRAVERSE

Dip Brazing

Daryl D. Peter, Daryl D. Peter and Associates

Process Details

The process for brazing in molten flux is straightforward. To prepare for brazing, the operator must perform the following steps:

- CLEAN THE WORKPIECE
- MAINTAIN FLUX ACTIVITY
- ASSEMBLE THE PARTS AND POSITION THE FILLER METAL
- FIXTURE TO MAINTAIN CONTACT WITH PARTS
- HEAT UNIFORMLY TO MINIMIZE DISTORTION

The fixtured parts are then placed into a preheated furnace and heated to a temperature that is both above the liquidus of the flux in the immersion bath and below any temperature detrimental to the fixtured parts. Next, the parts are transferred to the bath and immersed for a period of time that is sufficient to reach brazing temperatures. They are then removed and allowed to drain and cool enough to set the brazing alloy, before being transferred to a cooling area. When the parts have cooled to a temperature at which distortion is no longer a factor, they are then quenched in hot water. The flux is then removed and the brazements are cleaned.

The process technician must work closely with the designer to ensure that the part design will not trap flux or air during brazing. In addition, the process technician is typically responsible for the choice of materials used in fixturing (ensuring that they are compatible with the material in the bath, immersion angles to prevent trapped air, and speed through the liquid to control erosion). Fluxes can be very damaging to most metals. Stainless steel that is satisfactory for torch or induction brazing applications may not be suitable for dip brazing. High-nickel content alloys are therefore more commonly used, because of their superior corrosion-resistant properties.

Equipment Maintenance

Preventive maintenance is critical to the process and can be divided into three categories:

- TEMPERATURE CONTROL
- CONTROL OF THE LIQUID
- MAINTENANCE OF THE VESSEL

A daily satisfactory braze sample tends to verify that all is well. Once every 30 days, an inspection of the operating electronics for accuracy and a survey of the bath temperature are recommended. The composition of the bath tends to change slowly. However, the time interval between tests will be determined by how the bath is used and by the nature of the bath. This test frequency interval can range from one week to one month in duration.

Care of the vessel is usually the most neglected part of the preventive maintenance system. Besides looking unkempt, it is totally inhospitable, because of the heated liquid. As the repository of the molten material, the vessel also holds some form of solid residues (for example, oxides, salts, and organics) from all items that have been dipped since its last thorough cleaning. It is also likely to contain parts of fixtures, parts that fell off the rack, dripped braze alloy, and other substances.

For the most efficient performance, it is necessary to clean the pot daily. The material (that is, sludge) that collects on the vessel bottom stays soft for a short time and should be removed on a regular basis. Chipping and hammering to remove hardened sludge material on cemented fire brick can shorten the life of the pot. Common techniques for removing sludge before hardening include scraping and scooping. Scooping tools should be ventilated to allow the liquid to drain back into the pot. Disposal of the sludge should conform to environmental regulations. Sludge buildup causes problems with both bath chemistry and heating. If allowed to remain, the buildup will eventually either produce poor-quality brazements or cause damage to the pot.

Dip Brazing

Daryl D. Peter, Daryl D. Peter and Associates

Applications

The use of dip brazing in a molten filler metal bath is limited to the brazing of wire, small components, and aluminum return bends, whereas dip brazing in a molten-salt (flux) bath is used extensively for the brazing of aluminum, copper, and ferrous alloys (Table 1).

TABLE 1 PARAMETERS FOR MOLTEN-SALT DIP BRAZING OF SELECTED ALLOY ASSEMBLIES

WORKPIECE ALLOY(S)	TEMPERATURE		FILTER METAL	SALT
	°C	°F		
ALUMINUM	540-615	1000-1140	[A]	FLUORIDE-CHLORIDE-BASE
COPPER	815-870	1500-1600	BCUP[B]	CHLORIDE-BASE
FERROUS	915-955	1675-	RBCUZN	CHLORIDE-BASE +

		1750		BORAX[C]
	980-1205	1800-2200	BNI	CYANIDE-BASE
	1120	2050	BCU	CHLORIDE-BASE
FERROUS AND NONFERROUS	675-1010	1250-1850	BAG[D]	CHLORIDE-BASE

Source: Ref 1

(A) SALT ACTS AS BOTH FILLER METAL AND HEATING MEDIUM.

(B) SELF-FLUXING.

(C) NO DEZINCIFICATION TAKES PLACE.

(D) SEPARATE FLUX REQUIRED.

Dip-brazed parts are ideally suited for limited as well as high-production runs. The method of applying the process can be either manual or automatic. The process is used to braze small to very large assemblies with multiple or hidden joints. It is appropriate for all metals that can be brazed and is particularly suited for aluminum and other alloys that have melting points very close to the brazing temperature. The brazing operation can also simultaneously serve as a source for heat treating, carburizing, or cyaniding.

Reference cited in this section

1. *BRAZING HANDBOOK,* 4TH ED., AWS, 1991, P 223

Dip Brazing

Daryl D. Peter, Daryl D. Peter and Associates

Carbon and Low-Alloy Steels

The types of salts used in the dip brazing of carbon and low-alloy steels are neutral chloride salts, neutral chloride salts plus a fluxing agent such as borax or cryolite, and carburizing and cyaniding salts, which are also fluxing types of salts. Specific types and compositions of brazing salts and temperatures used for brazing of carbon and low-alloy steels with various filler metals are given in Table 2.

TABLE 2 TYPICAL SALTS USED FOR MOLTEN-SALT DIP BRAZING OF CARBON AND LOW-ALLOY STEELS WITH SELECTED FILLER METALS

FILLER METAL	TYPE OF SALT	NOMINAL COMPOSITION, %	BRAZING TEMPERATURE RANGE[A]	
			°C	°F
BAG-1 THROUGH BAG-8, AND BAG-18	NEUTRAL	55 $BACL_2$, 25 NACL, 20 KCL	620-870	1150-1600
	CYANIDING-FLUXING	20-30 NA_2CO_3, 20-30 KCL, 30-40 NACN	650-870	1200-1600
	NEUTRAL	50 NACL, 50 KCL	730-870	1350-1600
RBCUZN-A	NEUTRAL	80 $BACL_2$, 20 NACL	915-940	1675-1725

	FLUXING	79 $BACL_2$, 20 NACL, 1 BORAX	915-940	1675-1725
	CARBURIZING-FLUXING (WATER SOLUBLE)	30 NACL, 30 KCL, 20 CARBONATE, 15-20 NACN, ACTIVATOR (PROPRIETARY)	915-940	1675-1725
	CARBURIZING AND SELF-FLUXING	50 CARBONATE, 50 CHLORIDE WITH GRAPHITE ADDITION(B)	815-925	1500-1700
RBCUZN-D	NEUTRAL	90 $BACL_2$, 10 NACL	1040-1050	1900-1925
BCU-1 AND 1A	NEUTRAL	95 $BACL_2$, 5 NACL	1095-1150	2000-2100
	NEUTRAL	100 $BACL_2$	1095-1150	2000-2100

(A) TEMPERATURES SHOWN ARE THOSE OF THE SALT BATH.

(B) USED WITH MECHANICAL AGITATION

Neutral salts, so called because normally they do not add or subtract anything from the surface of the steel being treated, protect the surface from attack by oxygen in the air. Oxide on the workpiece, however, cannot be reduced by the salt, and a flux must generally be provided.

The neutral salts are mildly oxidizing to steel when they are used at recommended austenitizing temperatures. The oxides produced by heating steel in molten salt are largely soluble; hence, the steel is scale-free after heating. The accumulation of oxide in the molten salt, however, progressively makes the salt more decarburizing, and for this reason baths may require periodic rectification.

Flux that is applied to the surface of the assembly and dried before the assembly is immersed in the neutral salt will be quickly dissipated by dissolving in the salt or escaping from the surface of the bath as a volatilized salt or gas. For this reason, there is generally no difficulty in removing flux from an assembly that has been brazed in a salt bath.

Fluxing agents, such as borax and cryolite, are added to neutral chloride salts to produce a fluxing environment in the bath. When these fluxing agents are used with silver alloy or copper-zinc filler metals, periodic flux additions are required to maintain the fluxing potential of the bath. Above 650 °C (1200 °F), the fluxing potential can decrease rapidly because of oxidation from contact with air or the parts being brazed; therefore, the fluxing agent must be replenished more frequently.

Carburizing and cyaniding salts provide their own fluxing action. In addition, they supply carbon or carbon and nitrogen to the surface of the steel assembly as it is being brazed. Although silver brazing alloys have been used successfully, RBCuZn-A filler metal is generally preferred. A case depth of up to 0.30 mm (0.012 in.) can be obtained without adversely affecting the quality of a joint brazed with this copper-zinc filler metal.

Fluxes. An adequate fluxing environment is needed to ensure good flow and penetration of the brazing alloy in molten-salt-bath dip brazing. When brazing is done in a neutral flux chloride salt bath, an active flux is usually applied to the assemblies before brazing. Generally, the application of additional flux to the assembly isnot necessary when using a cyanide bath or another active fluxing bath.

Flux can be applied by brushing, dipping, or spraying the parts to be brazed before, during, or after assembly. After flux application, if any moisture is present, the assemblies must be preheated to dry them before immersion in the salt bath. Typical fluxes employed for prefluxing carbon steels and low-alloy steels that are to be brazed in a salt bath are American Welding Society (AWS) types 3A and 3B.

A temporary insulating cocoon of frozen salt forms instantly around a piece of cold metal when it is immersed in a molten-salt bath, and externally located filler metal can reach the melting temperature range before the workpiece has reached a temperature high enough for proper wetting to take place. When this occurs, the molten filler metal flows away from the joint with no brazing. This can be avoided either by preheating the assembly to a temperature above the melting range of the flux or by relocating the filler metal inside the joint in grooves, recesses, or drilled holes.

Filler Metals. The brazing filler metals shown in Table are the most widely used for molten-salt-bath dip brazing of carbon and low-alloy steels. Although silver alloys BAg-13 and 13A (not shown in Table 2) can be used for brazing in a molten-salt bath, they have been supplanted in most applications by copper-zinc alloys, which are less costly and have similar brazing temperature ranges. The rapid heating rate and nonoxidizing environment in a salt bath minimize dezincification of copper-zinc alloys, thereby facilitating the use of these alloys.

The brazing filler metal must be in contact with the joint. Filler metals in the form of wire, strip, powder, paste, and cladding are available. Special preform rings or other shapes can be obtained for specific joint requirements.

For additional information, see the article "Brazing of Carbon Steel and Cast Iron" in this Volume.

Stainless Steels

The brazing of stainless steel by immersing all or a portion of the assembly in molten salt offers essentially the same advantages that would apply to brazing similar assemblies made of carbon steel. The same limitations are also applicable. See the article "Brazing of Stainless Steels" in this Volume for more information.

Cast Irons

One of the more-common applications for the dip brazing of cast iron is the joining of steel tubing to headers, special fittings, and stanchions. Various mechanical assemblies are brazed to cast iron because different metal properties are needed in different parts of the assembly or, more often, because the fitting portion of such an assembly can be made most economically from cast iron.

Assemblies containing malleable iron castings are water quenched to remove the brazing salt--a practice that is common with steel assemblies. To avoid warpage and cracking, however, brazed assemblies containing gray and ductile iron castings should never be water quenched from the brazing temperature. Instead, the assemblies should be cooled slowly to about 150 °C (300 °F) and then immersed in water to remove the salt.

For additional information, see the article "Brazing of Carbon Steel and Cast Iron" in this Volume.

Aluminum Alloys

The best method of heating and fluxing aluminum joints simultaneously is to immerse the entire assembly in a bath of molten flux. Because of the low specific heat of flux, assemblies usually are heated to about 540 °C (1000 °F) prior to flux immersion. Dip brazing has been used successfully in the manufacture of complex, multiple-joint heat exchangers.

Immersing the entire assembly into molten flux has many advantages. Heat is applied to all parts simultaneously and uniformly, and air is replaced by a buoyant and surface-active environment, promoting brazing filler metal flow. In addition, the uniform temperature permits production assembly of parts with dimensional tolerances as low as ±0.05 mm (±0.002 in.) or even less.

Heat-transfer units assembled from alternate corrugated and flat aluminum brazing sheets or from various crimped and formed pieces are examples of the type of work that dip brazing can handle advantageously. Units weighing up to 9 Mg (20,000 lb) have been joined by dip brazing. Certain designs have to withstand a service pressure of 8 MPa (1150 psi). Brazing sheet is essential to this type of work, reducing assembly and brazing costs. The rapid and even heating and flux buoyancy minimize distortion.

For assemblies designed with components in close proximity, flux removal can be tedious and expensive. For instance, when components such as those of a heat-exchanger matrix are spaced closer than 3.2 mm ($\frac{1}{8}$ in.), the flux holds to the surfaces by surface tension and capillary action; it will not drain from the components freely. This is not as great a problem with spacings greater than 3.2 mm ($\frac{1}{8}$ in.) between components of normal length; wider spacing of long components is desirable.

For additional information, see the article "Brazing of Aluminum Alloys" in this Volume.

Dip Brazing

Daryl D. Peter, Daryl D. Peter and Associates

Safety Precautions

When dip-brazing furnaces contain flux, corrosion of the surroundings is a problem. Ventilation is critical, and protection of all metal exposed to the fumes is mandatory. Scrubbers are often required for the air removed from above the liquid.

Safety equipment, such as full-face protection, heat suits, heat shields, and gloves, should be required when working around molten flux or metal. Clothing of synthetic fibers should be prohibited. In addition, nothing wet or even damp should be immersed, because the resulting burst of steam may blow the molten material over anyone standing near the flux furnace installation.

Dip Brazing

Daryl D. Peter, Daryl D. Peter and Associates

Reference

1. *BRAZING HANDBOOK*, 4TH ED., AWS, 1991, P 223

Resistance Brazing

Allen Cedilote, Industrial Testing Laboratory Services

Introduction

RESISTANCE BRAZING (RB) is a resistance joining process. The workpieces are heated locally, and the filler metal that is preplaced between the workpieces is melted by the heat generated from resistance to the flow of electric current through the electrodes and the work. In the usual application of RB, the heating current is passed through the joint itself. Equipment is the same as that used for resistance welding, and the pressure needed for establishing electrical contact across the joint is ordinarily applied through the electrodes (Fig. 1). The electrode pressure is also the usual means for providing the tight fit needed for capillary behavior in the joint. The heat for resistance brazing can be generated mainly in the workpieces themselves, in the electrodes, or in both, depending on the electrical resistivity and dimensions.

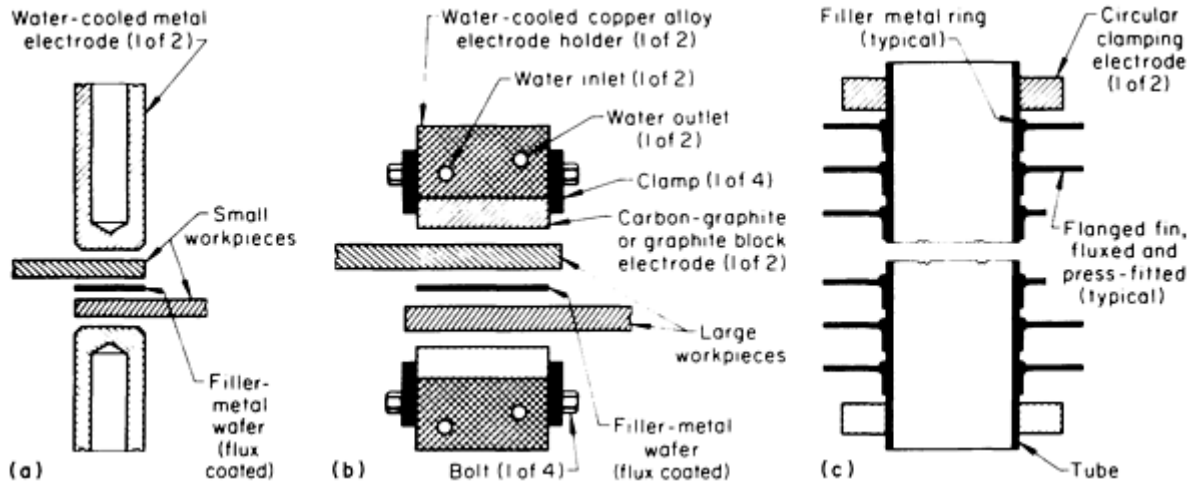

FIG. 1 TYPICAL SETUPS FOR RESISTANCE BRAZING. (A) FOR SMALL PARTS OR SMALL FLAT PORTIONS OF LARGER COMPONENTS, USING OPPOSED WATER-COOLED METAL ELECTRODES OF THE CONVENTIONAL RESISTANCE WELDING TYPE. (B) FOR LARGE FLAT PARTS, TYPICALLY OF A HIGHLY CONDUCTIVE METAL (FOR EXAMPLE, COPPER), USING OPPOSED CARBON BLOCK ELECTRODES ATTACHED TO WATER-COOLED COPPER ALLOY ELECTRODE HOLDERS. (C) FOR JOINING FLANGED FINS TO A TUBE, USING CIRCULAR CLAMPING ELECTRODES

Resistance brazing is used for many applications involving small workpieces, for small joints that are part of very large equipment, or for low-volume production runs because it provides:

- VERY RAPID AND HIGHLY LOCALIZED HEATING
- FLAMELESS, CLEAN OPERATION
- PRECISE BRAZING THAT IS EASY TO CONTROL
- HIGH-QUALITY JOINTS WITHOUT EXTENSIVE OPERATOR TRAINING
- EQUIPMENT COST SAVINGS (ONE TRANSFORMER AND A PAIR OF ELECTRODES CAN BE USED FOR A WIDE VARIETY OF JOINT DESIGNS)
- EASY PORTABILITY IN SOME OF ITS EQUIPMENT (FIG. 2)

However, RB is impractical for:

- JOINT AREAS THAT EXCEED APPROXIMATELY 1300 MM^2 (2 $IN.^2$)
- WORKPIECES THAT ARE LARGE OR HEAVY
- WORKPIECES THAT HAVE VARIABLE THICKNESS OR COMPLEX CONTOURS

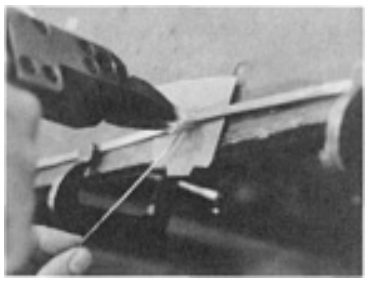

FIG. 2 PORTABLE ELECTRICAL RB ELECTRODES USED TO JOIN A WIRE TO A PLATE. COURTESY OF ROBIN

GROSS GOURLEY, WESTINGHOUSE ELECTRIC CORPORATION

Resistance Brazing

Allen Cedilote, Industrial Testing Laboratory Services

Process Parameters

Workpiece material, workpiece size and shape, and joint design are the major factors that must be considered in developing a detailed RB procedure. The workpiece material is of primary importance because it has the greatest influence on the choice of electrode material and on the type of filler metal selected (see the Sections "Brazeability and Solderability of Engineering Materials" and "Procedure Development and Practical Considerations for Brazing and Soldering" in this Volume).

High-resistance workpieces should be brazed with low-resistance electrodes; conversely, high-conductivity (that is, low-resistance) workpieces must be brazed with low-conductivity electrodes. If at least one workpiece is made of a high-resistance material and if that workpiece is of sufficient mass, then the electrodes can be a high-conductivity material, such as a chromium-copper alloy (UNS C18200). When such an RB electrical circuit (which includes not only the transformer and electrodes but also at least one workpiece) is energized, heat will be generated within the high resistance circuit component of the circuit (that is, the workpiece). Conversely, if all workpieces have low electrical resistance, then the brazing current flowing through them will not generate enough heat to melt the filler metal. In this case, the electrodes must supply the necessary heat by virtue of their electrical resistance. Consequently, in resistance brazing high-conductivity workpieces, graphite (and in some cases, tungsten or molybdenum) electrodes are used. The heat generated in the electrodes flows into the workpieces by conduction or convection through the electrode-to-workpiece contact areas.

Assuming that the brazing procedure is fundamentally correct and capable of yielding properly bonded workpieces, there are a number of factors that strongly affect the quality of an RB joint. In descending order of priority, the factors that contribute to high quality in an RB joint are:

- CLEANLINESS OF THE WORKPIECES AND FILLER METAL SURFACES
- PROPER FIT BETWEEN THE WORKPIECES
- UNIFORMITY OF HEATING TO BRAZING TEMPERATURE
- MAINTAINING UNIFORM TEMPERATURE DURING BRAZING
- AVOIDING OVERHEATING
- MAINTAINING THE BRAZING TEMPERATURE FOR NO LONGER THAN SPECIFIED
- KEEPING THE PROPER LEVEL OF PRESSURE ON THE WORKPIECES DURING BRAZING

Each of these vital factors is influenced by the joint/workpiece design and the brazer's skill, experience, and ability to focus on the dynamic details of the process.

Workpiece and braze filler metal cleanliness is an absolute requirement for all types of brazing. In particular, cleanliness is of utmost importance in RB because in torch, furnace, and induction brazing the gaseous atmosphere around the workpieces can be controlled relatively easily to decompose surface oxides. Almost all common contaminants (grease, oil, perspiration, dust, abrasive particles, and oxides) are effective barriers to braze metal flow. At brazing temperature, most of these contaminants either vaporize or outgas, and because gases expand when heated, they can prevent bonding over a large area when confined within the braze joint.

Regardless of the electrical conductivity of the electrodes or workpieces, it is important to position and maintain the electrodes so as to sustain maximum electrode-to-workpiece contact through the entire brazing cycle. In addition, although it is preferable for the electrode-to-workpiece contact area to equal that of the braze joint in order to achieve even heating, the contact area should be no less than half the area of the braze joint.

For high-conductivity electrodes, maximum contact area is an optimum condition because:

- ELECTRODE-TO-WORKPIECE INTERFACE RESISTANCE IS MINIMIZED, THEREBY PROLONGING ELECTRODE LIFE AND ELIMINATING LOCALIZED HOTSPOTS ON THE WORKPIECE
- CURRENT FLOW INTO THE WORKPIECE WILL BE MORE EVENLY DISTRIBUTED, THUS HEATING THE WORKPIECE MORE UNIFORMLY

For low-conductivity electrodes, maximum contact area is even more critical because the workpieces are heated only by conduction from the electrode surfaces.

Because molten braze filler metal tends to flow to the hottest region in the joint, uniform heating is vitally important in achieving a uniform brazed joint. Therefore, it is necessary that the shape of the electrodes conform closely to the contour of the workpieces.

Pressure on the workpieces must be controlled carefully in order to achieve a properly bonded joint. Thermal expansion (and, commonly, differential thermal expansion in dissimilar joints) of the workpieces and electrodes must be allowed for. On one hand, too much pressure can squeeze molten filler metal out of the joint. Excessive pressure can cause the formation of a complete fillet around the joint perimeter while little or no bonding exists within. On the other hand, insufficient pressure can allow an unacceptably thick layer of filler metal to remain in the joint, which can result in a low-strength brazement that could fail prematurely in service.

Resistance Brazing

Allen Cedilote, Industrial Testing Laboratory Services

Equipment and System Selection

Resistance brazing may be classified as either manual or automatic, with manual resistance brazing being by far the most widely used.

In both manual and automatic RB, the kinds and models of transformers that provide the power are the same as those used for resistance welding. In many cases that involve high-resistance workpieces, the electrodes are also the same as those used in resistance welding applications. Welding transformers for RB can be purchased with automatic current/voltage controls, timers, electrode motion and pressure controls, and even automatic parts-handling devices, presuming that the production run is sufficient to warrant the added investment and a complexity of process optimization.

For manual RB, electrodes are usually incorporated into tongs made of chromium-copper, silver-tungsten, or copper-tungsten (for high-resistivity workpieces), and graphite, molybdenum, or tungsten (for low-resistivity workpieces). Graphite is the most common material for high-resistance electrodes because of its low cost and easy machinability. In addition, because it is not wetted by molten braze filler metals, there is no danger that graphite electrodes will be brazed to the workpieces. However, hot graphite is attacked by atmospheric oxygen during the brazing process. Thus, graphite electrodes must be inspected often and dressed as needed in order to maintain good workpiece contact. Special oxidation-resistant grades are available from graphite suppliers.

There is no standard design for manual RB tongs. Most RB organizations design and fabricate their own. As a result, there is an enormous variety of manual RB tongs and electrodes. However, the various types do contain some common elements; for example:

- WATER-COOLED, QUICK-RELEASE ELECTRODE CLAMPS (USUALLY MADE OF COPPER OR COPPER-CHROMIUM)
- WATER-COOLED CABLES FROM THE TRANSFORMER TO THE TONGS
- NONCONDUCTIVE HANDLES
- INSULATION OF THE ELECTRODES FROM EACH OTHER
- GROUND-FAULT INTERRUPTER PROTECTION

- INSULATING SHIELDS TO PREVENT INADVERTENT CONTACT WITH HOT OR ELECTRICALLY ENERGIZED AREAS

Resistance Brazing

Allen Cedilote, Industrial Testing Laboratory Services

Metal Electrodes

Selection of electrode material for RB depends on the electrical conductivity of the workpieces to be joined, the design and dimensions of the joint, appearance requirements for the brazed product, susceptibility of the workpieces to damage or marking, pressure needed on the work, production quantity of brazed joints, and cost of reconditioning or replacing an electrode.

The materials used most frequently in RB are RWMA class 2 (chromium-copper), RWMA class 14 (molybdenum), and various grades of carbon-graphite and graphite. Other standard and special electrode materials are sometimes used for special applications.

Class 2 (chromium-copper), a general-purpose resistance welding electrode material with a minimum electrical conductivity of about 75% IACS, is usually used to make electrode holders and shanks of faced electrodes for RB.

Refractory metal electrodes include class 14 (molybdenum), which is intermediate in mechanical and electrical properties in that classification, having a nominal electrical conductivity of 30% IACS. This material and RWMA class 13 (tungsten), because of resistance to high temperatures and nonsticking characteristics, are the only common electrode materials that have long life in resistance brazing of copper and other highly conductive nonferrous metals (i.e., aluminum and precious metals). They are about equal in electrical conductivity.

Class 14 (molybdenum) is generally preferred because class 13 (tungsten) is harder to machine and is likely to develop radial cracks in service. For reasons of economy, common practice is to use facings, buttons, or inserts of the refractory metal instead of making the entire electrode of the refractory metal.

Special electrode materials are sometimes needed to meet the unusual requirements of specific RB applications. An electrode made of 60% Pt and 40% Rh provides long life in the high-speed mass-production RB of insulated copper wires to copper terminal pads clad with BCuP-5. This electrode can withstand the heating used to melt the polyurethane insulation on the copper wire, the contact with molten BCuP-5 filler metal, and the heating in air used for burning off insulation residues after each brazed connection is made. This electrode material can be used at temperatures approaching 925 °C (1700 °F).

Carbon Electrodes

Ordinarily, two general types of carbon electrodes are used in RB: carbon-graphite and electrographite (artificial graphite). These electrode materials are made by simultaneously heating and blending the finely divided raw materials with coal tar pitch, which serves as a binder.

The stock from which RB electrodes are made comprises a few of the many grades of carbon stock that are manufactured primarily for use in melting ferrous and nonferrous metals. Composition and properties of the commercial carbon electrode materials vary; no generally accepted industry standards and terminology exist. The properties of five grades that are generally typical of the materials used in carbon electrodes for resistance brazing are given in Table 1.

TABLE 1 PROPERTIES OF FIVE CARBON ELECTRODE MATERIALS USED IN RESISTANCE BRAZING

GRADE	ELECTRODE MATERIAL	ELECTRICAL RESISTIVITY		SCLEROSCOPE HARDNESS	FLEXURAL STRENGTH (MINIMUM)		APPARENT DENSITY	
		μΩ· mm	Ω· in.		mpa	ksi	g/cm^3	$lb/in.^3$
1	CARBON-GRAPHITE, HARD(A)	20	0.00080	70	24	3.5	1.74	0.0629
2	CARBON-GRAPHITE, HARD, OXIDATION RESISTANT(B)	20	0.00080	70	24	3.5	1.75	0.0632
3	CARBON-GRAPHITE, SOFT	19	0.00075	40	16.5	2.4	1.57	0.0567
4	ELECTROGRAPHITE(A)	11	0.00042	50	17.2	2.5	1.73	0.0625
5	ELECTROGRAPHITE, OXIDATION RESISTANT(B)	11	0.00042	50	17.2	2.5	1.75	0.0632

(A) THIS TYPE OF CARBON ELECTRODE MATERIAL IS ALSO FREQUENTLY USED IN AIR CARBON ARC CUTTING.

(B) SIMILAR TO THE ELECTRODE MATERIAL LISTED IMMEDIATELY ABOVE, BUT IMPREGNATED WITH A SMALL PERCENTAGE OF AN OXIDATION RETARDANT, USUALLY AN INORGANIC COMPOUND CONTAINING BORON OR PHOSPHORUS, FOR LONGER LIFE

Carbon-Graphite. The first three types of electrode materials listed in Table 1 are called carbon-graphite. They are made from mixtures of finely ground petroleum coke (carbon) and natural or artificial (electro) graphite with coal tar pitch. These electrode materials are extruded in suitable shapes and heated in an electric furnace at about 815 °C (1500 °F) to develop the desired properties shown in Table 1. The heating converts about half of the pitch to carbon; the remainder is driven off as gases.

The final properties can be varied from those shown by changing the proportions of the raw materials, the particle size, and the time and temperature of heating. Increasing the ratio of graphite to carbon in the mixture, prolonging the heating time, or increasing the temperature lowers resistivity, hardness, and strength. Density is influenced chiefly by particle size.

Oxidation resistance for some grades of carbon-graphite is improved, for longer electrode life, by impregnating the cured material with a small percentage of an oxidation retardant, usually an inorganic compound that contains boron or phosphorus. In Table 1, oxidation-resistant grades 2 and 5 are the same as grades 1 and 4, respectively, except for the presence of an additive of this type.

Electrographite Electrode Material. Carbon-graphite grades and electrographite materials are produced in the same way except that the extruded mixture of raw materials is heated in "beehive" furnaces at about 2480 to 2705 °C (4500 to 4900 °F) for approximately four weeks, thus converting the mixture to graphite (called artificial graphite or electrographite). Properties of a representative material of this type and of an oxidation-resistant or long-life impregnated form of the same material are given in Table 1. Resistivity, hardness, and flexural strength of electrographite electrode materials are substantially lower than for the hard carbon-graphite electrode materials.

Selection of Carbon Electrode Material. The general types of carbon electrode material shown in Table 1 (carbon, graphite, and electrographite) have almost completely replaced the formerly used straight-carbon types, which are made by heating finely ground petroleum coke and a binder at about 815 °C (1500 °F). The straight-carbon grades typically have an electrical resistivity of about 51.2 μΩ· mm (0.0020 Ω· in.) and a Scleroscope hardness of about 100. Machining of these materials is much more difficult and costly than that of carbon-graphite and electrographite.

The hard carbon-graphite types are general-purpose materials and are preferred for most RB with carbon electrodes because brazing temperatures can be reached with less current than when the less-resistive electrographite types are used. Electrographite is preferred for RB of metals that have a high surface resistance, particularly when one of the metals being joined is steel or another iron-base alloy. Soft carbon-graphite material combines high heating capacity with a low tendency to produce local hot spots on the workpieces, but has comparatively low wear resistance. The first and fourth grades in Table l are the same types of material ordinarily used in air-carbon arc cutting.

In RB with carbon electrodes, nonuniform current flow and resultant local overheating of the electrodes can shorten electrode life excessively. To prevent this, carbon electrodes must be tightly fitted into matching tapered adapters or clamped securely to the electrode holder making contact with the holder over as large an area as possible. Provision also must be made for adequate flow of cooling water in the electrode holder. In addition, some carbon brazing electrodes are electroplated or sprayed with a copper coating about 0.05 mm (0.002 in.) in thickness to reduce contact resistance against the electrode holder and to minimize internal temperature buildup in the carbon electrode.

Design of Electrodes

Commercially available resistance seam welding electrodes are used where the design and dimensions of workpiece and joint permit. The electrode tip is machined, where necessary, to provide a tip shape and face dimensions suitable for the work. Carbon electrodes, depending on the size and design of the work, are in the shape of either standard metallic electrodes or flat blocks that may be several inches in length and width (size is usually limited by ability to obtain uniform heating and water cooling or by the current capacity of the power source).

When a high-resistance or long-wearing electrode is required, it is often used in the form of facings, inserts, or buttons that are attached to electrode shanks or bodies made of a less-expensive material. Electrode design is developed to work with workpiece and joint design in eliminating the need for holding and locating fixtures or clamps wherever possible and in permitting rapid and easy loading and unloading of workpieces, filler metal, and flux. Provision for water cooling of electrode holders and electrodes generally is the same as in resistance welding.

Filler Metals

Of the large number of filler metals available, only a few are used extensively in RB (Table 2). Selection of filler metal for RB is similar to that for other brazing processes and is discussed in the Section "Procedure Development and Practice Considerations for Brazing and Soldering" in this Volume.

TABLE 2 COMPOSITION AND THERMAL PROPERTIES OF SELECTED FILLER METALS USED FOR RESISTANCE BRAZING OPERATIONS

AWS CLASS	UNS NUMBER	COMPOSITION, WT%						LIQUIDUS		SOLIDUS	
		Ag	Cu	Zn	Cd	P	Sn	°C	°F	°C	°F
BAG-1	P07450	45	15	16	24	. . .	. . .	620	1145	605	1125
BAG-1A	P07500	50	15.5	16.5	18	. . .	. . .	635	1175	625	1160
BAG-2	P07350	35	26	21	18	. . .	. . .	700	1295	605	1125
BAG-7	P07563	56	22	17	. . .	. . .	5	650	1205	620	1145
BAG-8	P07720	72	28	. . .	. . .		. . .	780	1435	780	1435
BAG-18	P07600	60	30	. . .	. . .	. . .	10	720	1325	600	1115
BCUP-1	C55180	. . .	95	. . .	. . .	5	. . .	925	1695	710	1310
BCUP-2	C55181	. . .	97	. . .	. . .	3	. . .	795	1460	710	1310
BCUP-5	C55284	15	80	. . .	. . .	5	. . .	800	1475	645	1190

Source: Ref 1

More attention is given in RB to selecting compatible filler metals having the lowest brazing temperature, because in RB, the maximum local temperature reached by the work must be kept as low as possible, while providing uniform heating of the faying surfaces and the filler metal. Fluidity of the filler metal is not critical in most RB, because the filler metal is

usually preplaced and the bond area is relatively large. The general types of filler metal usually selected for resistance brazing various classes of work metals are:

WORKPIECE METAL	FILLER METAL ALLOYS
STEEL, STAINLESS STEEL, HEAT-RESISTANT ALLOYS, COPPER, COPPER ALLOYS, NICKEL ALLOYS	SILVER (BAG TYPE)
ALUMINUM ALLOYS	AL-SI
COPPER AND COPPER ALLOYS	CU-P

These types of filler metal all have relatively low brazing temperatures (Table 3).

TABLE 3 SOLIDUS, LIQUIDUS, AND BRAZING TEMPERATURES FOR SELECTED RESISTANCE BRAZING FILLER METALS

FILLER METAL	SOLIDUS		LIQUIDUS		BRAZING TEMPERATURE	
	°C	°F	°C	°F	°C	°F
BCUP-2	710	1310	795	1460	730-845	1350-1550
BCUP-5	645	1190	800	1475	705-815	1300-1500
BAG-1A	625	1160	635	1175	635-760	1175-1400

Silver Alloys. Of the silver alloy (BAg type) group of filler metals, the two most often used are BAg-1 and BAg-1A, which are free-flowing alloys that permit the use of low brazing temperatures. In addition, their narrow melting ranges (-7 and -9 °C, or 20 and 15 °F, respectively) prevent liquation, making them insensitive to variations in the rate of heating or cooling. Their narrow melting ranges are also advantageous in step brazing. For making corrosion-resistantbrazed joints in stainless steel, BAg-3 and BAg-18 are preferred.

Aluminum-Silicon Alloys. Aluminum-silicon alloys (BAlSi type) are used in the RB of aluminum alloys. These low-melting alloys are available in sheet or wire form; BAlSi-2 and BAlSi-5 are also available as cladding on aluminum brazing sheet. Temperature must be controlled with special care in brazing of the lower melting brazeable aluminum alloys, such as wrought alloy 6151 (UNS A96151) and cast alloys 443.0 (UNS A04430) and 356.0 (UNS A03560), because the melting range of these filler metals approaches closely or overlaps the melting range of the work metal.

Copper-Phosphorus Alloys. Filler metals of copper-phosphorus alloys (BCuP type) are widely used for resistance brazing of copper and copper alloys. They are low-cost, general-purpose filler metals and have the special advantage of being self-fluxing on copper (by virtue of their phosphorus content), although flux is ordinarily needed when using them on copper alloys because phosphorus does not reduce metallic oxides other than those of copper. BCuP-5 is by far the most frequently used of the group.

In some applications on copper or copper alloys, the wider melting range, higher working temperature, and lower ductility of the BCuP filler metals make them less suitable than the BAg types. For example, in applications requiring higher ductility and corrosion resistance, silver brazing alloys are sometimes preferred to the BCuP filler metals for brazing of copper, despite the resulting need for fluxing. The difficulty in restricting flow of BCuP filler metals to joint surfaces may be a disadvantage.

Reference cited in this section

1. *BRAZING HANDBOOK,* 4TH ED., AMERICAN WELDING SOCIETY, 1991, P 239

Allen Cedilote, Industrial Testing Laboratory Services

Reference

1. *BRAZING HANDBOOK*, 4TH ED., AMERICAN WELDING SOCIETY, 1991, P 239

Diffusion Brazing

W. Daniel Kay, Wall Colmonoy Corporation

Introduction

DIFFUSION BRAZING (DFB) is a process that coalesces, or joins, metals by heating them to a suitable brazing temperature at which either a preplaced filler metal will melt and flow by capillary attraction or a liquid phase will form *in situ* between one faying surface and another. In either case, the filler metal diffuses into the base metal until the physical and mechanical properties of the joint become almost identical to those of the base metal. Pressure may or may not be applied to accomplish this.

"Diffusion bonding," a term that can refer to either diffusion brazing or diffusion welding, is now considered to be a nonstandard term. Where diffusion brazing is required, it should be clearly specified, However, in the aerospace industry, diffusion brazing is still commonly referred to by such tradenames as Activated Diffusion Bonding (ADB), Activated Diffusion Healing (ADH), and Transient Liquid-Phase Bonding (TLP). In each case, the process is actually diffusion brazing.

Two critical aspects of DFB are:

- A *LIQUID* FILLER METAL MUST BE FORMED AND BECOME ACTIVE IN THE JOINT AREA.
- EXTENSIVE DIFFUSION OF FILLER METAL ELEMENTS INTO THE BASE METAL MUST OCCUR.

This diffusion process often results in the total loss of identity of the original brazed joint (Fig. 1).

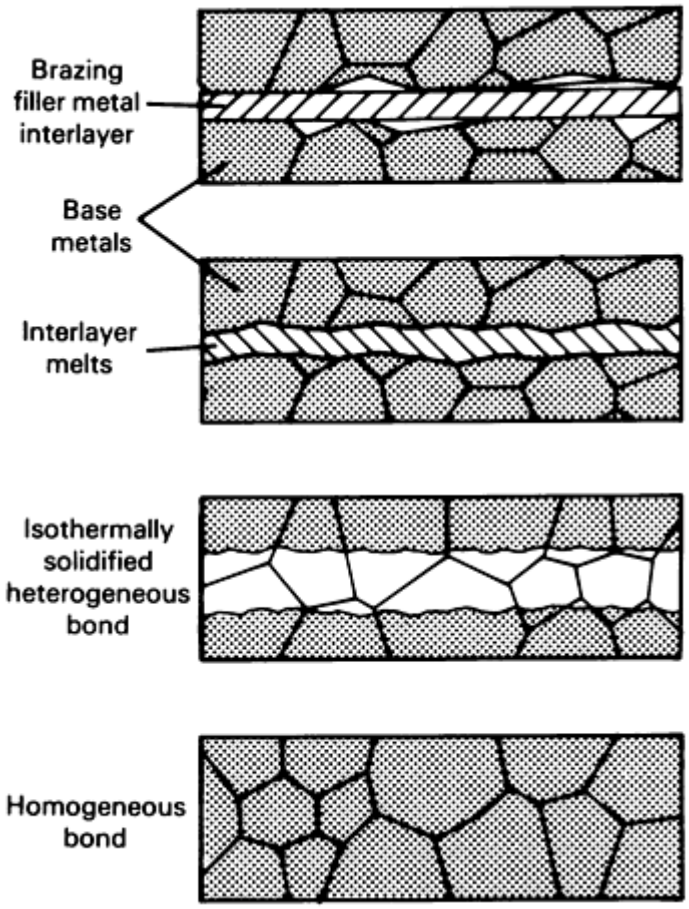

FIG. 1 DIFFUSION PROCESS RESULTING IN LOSS OF IDENTITY OF ORIGINAL BRAZED JOINT

Diffusion Brazing

W. Daniel Kay, Wall Colmonoy Corporation

Diffusion Brazing Processes

The most advanced diffusion brazing processes are used in the aerospace industry, particularly for brazements involving titanium, nickel, cobalt, and aluminum alloys. However, many similar and dissimilar metal combinations can be diffusion brazed, because diffusion is involved in all brazing processes, to a lesser or greater extent.

Although diffusion brazing is commonly performed in furnaces specifically set aside for brazing or heat treating, it is also possible to initially braze two components together by induction heating or by torch brazing, and then place the brazement into a furnace for the extended diffusion cycle. This cycle can range from 30 min to 80 h, or even longer.

As an example of a typical DFB process, a round bar of 304L stainless steel was diffusion brazed (end-to-end) to a round bar of pure copper in a furnace at 930 °C (1700 °F) for 60 min at temperature, using pure dry hydrogen as the atmosphere. The laying surface of the stainless steel was electrolytically plated with about 0.13 mm (0.005 in.) of pure silver. As this assembly was heated (without external pressure), the silver and copper diffused together to form a liquid eutectic filler metal alloy (72Ag-28Cu) in the butt joint at 780 °C (1435 °F), which metallurgically bonded the stainless steel and copper bars together permanently. When the brazement was subsequently heated in another furnace at 1040 °C (1900 °F), with a weight attached to the copper side of the part (in an effort to remelt the braze joint and take the brazement apart), it was found that the copper elongated until the pure copper portion of the part, rather than the brazed joint, failed. Diffusion had been complete enough that the remelt temperature of the brazement approached that of pure copper.

This example shows that, once the liquid has been distributed throughout the joint area, the assembly should be held at the brazing temperature long enough for one or more of the filler metal elements to adequately diffuse into the base metals (and vice versa). In this way, the mechanical properties of the brazed joint area become essentially identical to those of either or both of the base metals.

The amount of diffusion that occurs will be a function of:

- THE BRAZING TEMPERATURE
- THE LENGTH OF TIME THE PART IS HELD AT TEMPERATURE
- THE QUANTITY OF FILLER METAL AVAILABLE FOR DIFFUSION
- THE MUTUAL SOLUBILITY OF FILLER METAL AND THE BASE METALS

A fully diffused joint will lose all joint identity because of base-metal grain growth across the entire joint (Fig. 2).

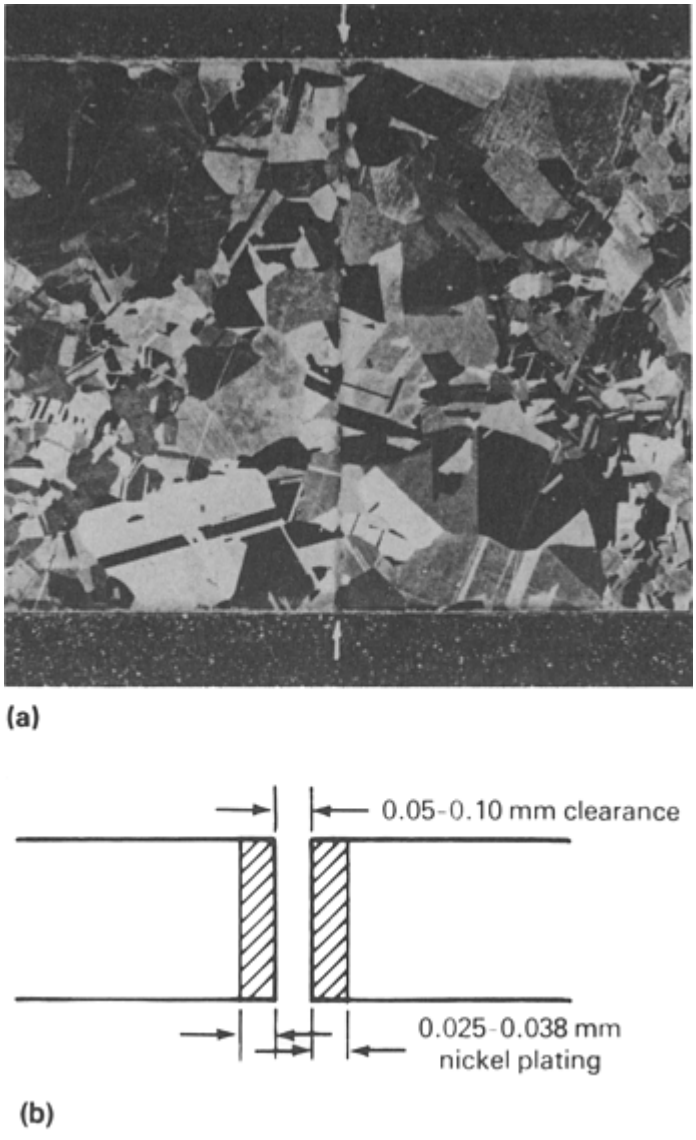

FIG. 2 DFB JOINT ILLUSTRATING HOW THE BRAZING FILLER METAL AND NICKEL PLATE DIFFUSED INTO THE BASE METAL, ALMOST OBLITERATING THE JOINT. SPECIMEN: NICKEL-PLATED NIMONIC 80A 6.4 MM (0.252 IN.) TENSILE TEST BAR MACHINED FROM RECTANGULAR BRAZED BLOCKS. BRAZING PROCEDURE: 30 MIN AT 1175 °C (2150 °F); NICROBRAZ 125 BRAZING FILLER METAL; AGED AFTER BRAZING. (A) MACROSTRUCTURE OF JOINT. 8×. (B) SCHEMATIC OF JOINT

When a brazement is to be made using either a preplaced sheet of filler metal or a layer of filler metal powder, it is wise to apply pressure to the assembly so that, when filler metal becomes molten, the gap between the two base metals is reduced. As an example of this process, a cobalt-base alloy was diffusion brazed at 1120 °C (2050 °F) in a vacuum furnace using a nickel-chromium-boron filler material in sheet form. The assembly was held at temperature for 8 h. Even though the solidus of the filler metal was only 970 °C (1780 °F), the braze joint completely lost its identity through diffusion, and the resulting remelt temperature was above 1370 °C (2500 °F). In this case, pressure was applied using simple weights on top of the part. Because the filler metal contained boron as a melting-point depressant, the diffusion of the boron out of the filler metal into the base metal caused the remelt temperature of the filler metal to rise. Because boron is also a very small atom, it very readily diffuses (as an interstitial atom) away from the joint as the temperature of the base metal rises.

Diffusion brazing is very advantageous for the effective joining of aerospace components that are intended for elevated-temperature service, such as jet engine hot-section parts. It is critical that they be able to perform well and safely at operating temperatures from 1040 to 1150 °C (1900 to 2100 °F). These objectives can be readily achieved when diffusion brazing is properly understood and used.

Diffusion Brazing

W. Daniel Kay, Wall Colmonoy Corporation

Selected References

- I.M. BARTA, LOW TEMPERATURE DIFFUSION BONDING OF ALUMINUM ALLOYS, *WELD. J.*, VOL 43 (NO. 6), JUNE 1964, P 241S-247S
- P.M. BARTLE, DIFFUSION BONDING: A LOOK AT THE FUTURE, *WELD. J.*, VOL 54 (NO. 11), NOV 1975, P 799-804
- G.F. BLANK, A PRACTICAL GUIDE TO DIFFUSION BONDING, *MATER. DES. ENG.*, OCT 1966, P 76-79
- C.L. CLINE, AN ANALYTICAL AND EXPERIMENTAL STUDY OF DIFFUSION BONDING, *WELD. J.*, VOL 45 (NO. 11), NOV 1966, P 481S-489S
- W.A. DEMO AND S.J. FERRIGNO, BRAZING METHOD HELPS REPAIR AIRCRAFT GAS-TURBINE NOZZLES, *ADV. MATER. PROCESS.*, MARCH 1992, P 43-45
- D.S. DUVALL, W.A. OWCZARSKI, AND D.F. PANIONIS, TLP BONDING: A NEW METHOD FOR JOINING HEAT RESISTANT ALLOYS, *WELD. J.*, VOL 53 (NO. 4), APRIL 1974, P 203-214
- A.H. FREEDMAN, BASIC PROPERTIES OF THIN-FILMED DIFFUSION BRAZED JOINTS IN TI-6AL-4V, *WELD. J.*, VOL 50 (NO. 8), AUG 1971, P 343S-356S
- G.S. HOPPIN III AND T.F. BERRY, ACTIVATED DIFFUSION BONDING, *WELD. J.*, VOL 49 (NO.11), NOV 1970, P 505S-509S
- S. LIU, D.L. OLSON, G.P. MARTINS, AND G.R. EDWARDS, THE USE OF COATING AND INTERLAYER TECHNOLOGY IN BRAZING, *WELD. J.*, VOL 70 (NO. 8), AUG 1991, P 207S-215S
- J.T. NIEMANN, R.P. SOPHER, AND P.J. RIEPPEL, DIFFUSION BONDING BELOW 1000 °F, *WELD. J.*, VOL 37 (NO. 8), AUG 1958, P 337S-342S
- R.L. PEASLEE, DIFFUSION BRAZING, *WELD. J.*, VOL 55 (NO. 8), AUG 1976, P 695-696
- J.E. RAMIREZ AND S. LIU, DIFFUSION BRAZING IN THE NICKEL-BORON SYSTEM, *WELD. J.*, VOL 71 (NO. 10), OCT 1992, P 365S-375S
- M.M. SCHWARTZ, DIFFUSION BRAZING TITANIUM SANDWICH STRUCTURES, *WELD. J.*, VOL 57 (NO.9), SEPT 1978, P 35-38
- R.F. SEKERKA, ON THE MODELING OF DIFFUSION BONDING, *PROC. PHYSICAL METALLURGY*, TMS-AIME, 1980
- R.R. WELLS, MICROSTRUCTURAL CONTROL OF THIN-FILM DIFFUSION-BRAZED TITANIUM,

WELD. J., VOL 55 (NO. 1), JAN 1976, P 20S-28S

Exothermic Brazing

Donald W. Bucholz, IBM Federal Systems Corporation

Introduction

EXOTHERMIC BRAZING (EXB) is a process that utilizes the heat produced in a solid-state chemical reaction to melt a conventional filler metal or to produce molten filler metal as a product of the reaction.

When used to melt a conventional filler metal, exothermic brazing is similar to thermite welding (see the article "Thermite Welding" in this Volume) in that the heat required is derived from the chemical reaction, but it is different from thermite welding because only the heat is used. The brazing filler metal is not a component of the exothermic heat source and therefore does not include contaminants from the reaction.

When the EXB process is used to produce molten filler metal as a product of the reaction, an exothermic reaction occurs between two or more melting-point-depressant elements, which react to form a compound with a higher melting point. The result is an intermetallic compound that forms a heterogeneous filler metal. During this type of reaction, surface oxides are either displaced or disintegrated, which can eliminate the need for protective atmospheres or fluxes (Ref 1).

Reference

1. N. BREDSZ *ET AL.*, U.S. PATENT 3,415,697, 10 DEC 1968

Exothermic Brazing

Donald W. Bucholz, IBM Federal Systems Corporation

Process Advantages and Disadvantages

Exothermic brazing is most frequently used to make brazed joints in remote locations, inaccessible areas, physically complex structures, or situations that require the application of localized heat for a brief period of time. The basic advantages of this process are:

- RAPID CYCLE TIME (20 TO 30 S)
- LOCALIZED APPLICATION OF HEAT
- SIMPLICITY AND PORTABILITY OF EQUIPMENT
- PREPLACEMENT OF FILLER METAL

Some disadvantages of the EXB process are:

- DIFFERING JOINT DESIGNS REQUIRE EXPERIMENTATION PRIOR TO ACTUAL PRODUCTION IN ORDER TO EFFECTIVELY BRAZE EXOTHERMICALLY
- SAFETY ISSUES THAT CONCERN HANDLING AND APPLICATION MUST BE THOROUGHLY EVALUATED WHEN USING IGNITABLE, HIGH-HEAT-PRODUCING MATERIALS
- FILLER METAL SELECTION IS LIMITED BY THE THERMODYNAMIC BEHAVIOR OF THE EXOTHERMIC MATERIAL

Types of Compounds

Exothermic compounds that generate enough heat to melt conventional filler metals have been developed for iron alloys, copper alloys, and refractory metals. Aluminum compounds that react and produce a heterogeneous filler metal can be used to join aluminum alloys.

The aerospace industry has utilized exothermic brazing to replace hydraulic fittings in corrosion-resistant steel tubing (AM-350 CRT). An example of this application using a commercial filler metal and an exothermic compound to braze a 25.4 mm (1 in.) outside diameter stainless steel tube with a 1 mm (0.04 in.) wall thickness has shown that a satisfactory braze joint can be made (Ref 2, 3). The exothermic compound in that example consisted of 30 g (1 oz) of 19.90% Mg, 51.84% NiO, 18.24% MnO, 4.24% Al, and 5.36% MnO_2.

Refractory metals exothermically brazed at approximately 1760 °C (3200 °F) with conventional filler metals, using either 24.9% B and 75.1% V_2O_5 or 19.8% B, 60.2% V_2O_5, 16.5% Ta_2O_5, and 6.8% Al as the exothermic compound, have shown minimal base metal recrystallization and braze filler metal/base metal interdiffusion (Ref 4).

Aluminum alloys have been brazed utilizing an exothermic compound consisting of powdered mixtures of: 3.5 g (0.12 oz) of 50% Al and 50% Mg; 10.0 g (0.35 oz) of 88% Al and 12% Si; and 13.5 g (0.48 oz) Al. The resulting intermetallic compound that forms the filler metal is composed of 27 g (0.95 oz) of 89.1% Al, 10.2% Mg_2Si, and 0.7% Si. More than a dozen of these types of exothermic brazing filler metals used with aluminum alloys are described in Ref 1 and 5.

References cited in this section

1. N. BREDSZ *ET AL.*, U.S. PATENT 3,415,697, 10 DEC 1968
2. R.A. LONG, EXOTHERMICALLY BRAZED HYDRAULIC FITTINGS FOR AIRCRAFT, *PROC. AWS NATIONAL FALL MEETING*, AWS, OCT 1966, P 28-38
3. R.A. LONG *ET AL.*, U.S. PATENT 3,308,532, 14 MARCH 1967
4. R.A. LONG, EXOTHERMIC BRAZING OF REFRACTORY METALS, *PROC. METALL. SOC. CONF.*, AIME, 1966, P 249-258,
5. W.V. KNOPP *ET AL.*, U.S. PATENT 3,899,306, 12 AUG 1975

Exothermic Brazing

Donald W. Bucholz, IBM Federal Systems Corporation

Equipment

The type of equipment used for exothermic brazing is shown in Fig. 1. The principal components are the joint itself, the brazing filler metal (if it is not a component of the exothermic compound), the exothermic compound, the igniter, the tubing sleeve insulation, and the container. Variations that utilize different joint designs, shielding gases, and external sources for preheating can also be used.

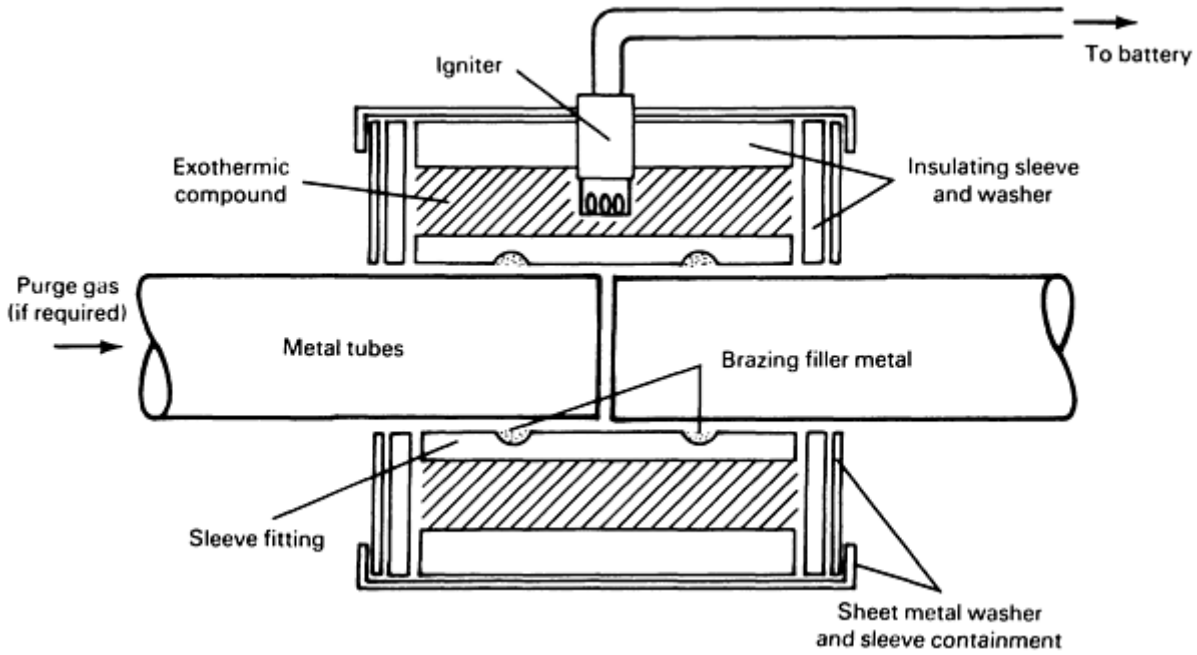

FIG. 1 TYPICAL ARRANGEMENT FOR EXOTHERMIC BRAZING OF TUBE. SOURCE: REF 2

A moderate amount of technical skill and knowledge of the fundamental principles, as well as empirical experience for the particular joining situation, are needed in order to make high-quality brazed joints. In addition to typical joint inspection methods and braze filler metal quality control requirements, exothermic brazing also can require lot control for exothermic compounds to ensure uniformity of performance.

Reference cited in this section

2. R.A. LONG, EXOTHERMICALLY BRAZED HYDRAULIC FITTINGS FOR AIRCRAFT, *PROC. AWS NATIONAL FALL MEETING*, AWS, OCT 1966, P 28-38

Exothermic Brazing

Donald W. Bucholz, IBM Federal Systems Corporation

Procedure

When performing exothermic brazing, the standard steps that are followed in any other brazing process apply, such as joint design, alloy selection, and surface preparation. However, additional parameters must be considered: selection of exothermic compound, required quantity of exothermic compound, and brazing assembly configuration.

The typical effects of joint mass on the heat-up time and the mass of exothermic material that is required to achieve a specific temperature are shown in Fig. 2 and 3, respectively. The exothermic material is usually placed around or over the joint to be made, and an electric igniter is embedded in the exothermic compound. The assembly is typically insulated with ceramic or ceramic fiber and then covered and held in place with metal sheet or foil. The electrical leads of the igniter should be connected to a low-voltage battery. Once the assembly has been prepared, the battery and igniter circuit is closed, and the process runs to completion.

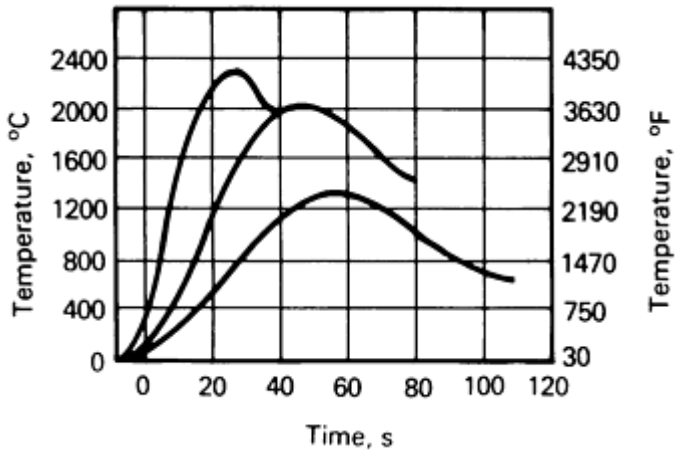

FIG. 2 HEATING VERSUS TIME CHARACTERISTICS FOR EXOTHERMIC BRAZING. LARGER MASSES REQUIRE LONGER TIMES TO HEAT UP AND ACHIEVE LOWER MAXIMUM TEMPERATURES FOR A FIXED AMOUNT OF EXOTHERMIC COMPOUND. SOURCE: REF 2, 6

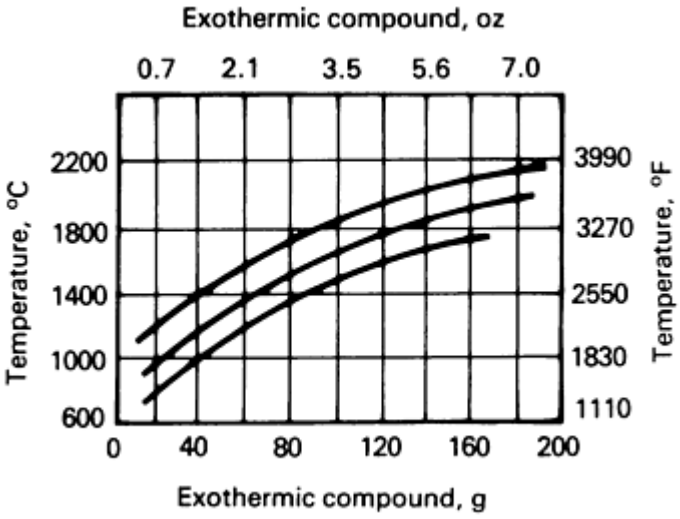

FIG. 3 MAXIMUM TEMPERATURE VERSUS MASS OF EXOTHERMIC COMPOUND (CHARACTERISTIC CURVE). A PARTICULAR EXOTHERMIC COMPOUND WILL PRODUCE A SINGLE CHARACTERISTIC CURVE FOR A GIVEN JOINT MASS AND CONFIGURATION. SOURCE: REF 6

References cited in this section

2. R.A. LONG, EXOTHERMICALLY BRAZED HYDRAULIC FITTINGS FOR AIRCRAFT, *PROC. AWS NATIONAL FALL MEETING*, AWS, OCT 1966, P 28-38
6. I.P. CHEKUNOV *ET AL.*, EXOTHERMAL BRAZING OF STEEL PIPING WITH HIGH TEMPERATURE BRAZING ALLOYS, *WELD. PROD.* (ENGLISH TRANSLATION OF *SVAR. PROIZVOD.*), NOV 1972, P 39-42

Exothermic Brazing

Donald W. Bucholz, IBM Federal Systems Corporation

References

1. N. BREDSZ *ET AL.*, U.S. PATENT 3,415,697, 10 DEC 1968
2. R.A. LONG, EXOTHERMICALLY BRAZED HYDRAULIC FITTINGS FOR AIRCRAFT, *PROC. AWS NATIONAL FALL MEETING*, AWS, OCT 1966, P 28-38
3. R.A. LONG *ET AL.*, U.S. PATENT 3,308,532, 14 MARCH 1967
4. R.A. LONG, EXOTHERMIC BRAZING OF REFRACTORY METALS, *PROC. METALL. SOC. CONF.*, AIME, 1966, P 249-258,
5. W.V. KNOPP *ET AL.*, U.S. PATENT 3,899,306, 12 AUG 1975
6. I.P. CHEKUNOV *ET AL.*, EXOTHERMAL BRAZING OF STEEL PIPING WITH HIGH TEMPERATURE BRAZING ALLOYS, *WELD. PROD.* (ENGLISH TRANSLATION OF *SVAR. PROIZVOD.*), NOV 1972, P 39-42

Exothermic Brazing

Donald W. Bucholz, IBM Federal Systems Corporation

Selected References

- R. BECK *ET AL.*, "ASSESSMENT OF THE RESULTS OF THE SKYLAB SPACE PROCESSING EXPERIMENTS WITH RESPECT TO THEIR SCIENTIFIC-TECHNICAL SIGNIFICANCE," FINAL REPORT NO. ESA-CR(P)-623, EUROPEAN SPACE RESEARCH ORGANISATION, OCT 1974
- "EXOTHERMIC BRAZING SPECIMENS", FINAL REPORT NO. NASA-CR-103169, WHITAKER CORPORATION, SAN DIEGO RESEARCH AND DEVELOPMENT DIVISION, DEC 1970
- R.W. HEINE *ET AL.*, "FLIGHT/GROUND SAMPLE COMPARISON RELATING TO FLIGHT EXPERIMENT M552, EXOTHERMIC BRAZING," REPORT NO. NASA-CR-12059, UNIVERSITY OF WISCONSIN, DEPARTMENT OF METALLURGY AND MINERAL ENGINEERING, PREPARED FOR GEORGE C. MARSHALL SPACE FLIGHT CENTER, DEC 1973
- R.A. LONG, U.S. PATENT 3,358,356, 19 DEC 1967
- R.A. LONG, U.S. PATENT 3,287,190, 22 NOV 1966
- H.E. PATTEE AND R.E. MONROE, "PHASE B REPORT ON MATERIALS PROCESSING IN SPACE M512," REPORT NO. NASA-CR-120266, BATTELLE COLUMBUS LABS, PREPARED FOR GEORGE C. MARSHALL SPACE FLIGHT CENTER, JULY 1973
- H.E. PATTEE AND R.E. MONROE, "CHARACTERIZATION OF EXOTHERMIC BRAZING COMPONENTS, SKYLAB EXPERIMENT M552," REPORT NO. NASA-CR-120518, BATTELLE COLUMBUS LABS, PREPARED FOR GEORGE C. MARSHALL SPACE FLIGHT CENTER, DEC 1973

Exothermic Brazing

Donald W. Bucholz, IBM Federal Systems Corporation

Selected References

- R. BECK *ET AL.*, "ASSESSMENT OF THE RESULTS OF THE SKYLAB SPACE PROCESSING EXPERIMENTS WITH RESPECT TO THEIR SCIENTIFIC-TECHNICAL SIGNIFICANCE," FINAL REPORT NO. ESA-CR(P)-623, EUROPEAN SPACE RESEARCH ORGANISATION, OCT 1974
- "EXOTHERMIC BRAZING SPECIMENS", FINAL REPORT NO. NASA-CR-103169, WHITAKER

CORPORATION, SAN DIEGO RESEARCH AND DEVELOPMENT DIVISION, DEC 1970
- R.W. HEINE *ET AL.*, "FLIGHT/GROUND SAMPLE COMPARISON RELATING TO FLIGHT EXPERIMENT M552, EXOTHERMIC BRAZING," REPORT NO. NASA-CR-12059, UNIVERSITY OF WISCONSIN, DEPARTMENT OF METALLURGY AND MINERAL ENGINEERING, PREPARED FOR GEORGE C. MARSHALL SPACE FLIGHT CENTER, DEC 1973
- R.A. LONG, U.S. PATENT 3,358,356, 19 DEC 1967
- R.A. LONG, U.S. PATENT 3,287,190, 22 NOV 1966
- H.E. PATTEE AND R.E. MONROE, "PHASE B REPORT ON MATERIALS PROCESSING IN SPACE M512," REPORT NO. NASA-CR-120266, BATTELLE COLUMBUS LABS, PREPARED FOR GEORGE C. MARSHALL SPACE FLIGHT CENTER, JULY 1973
- H.E. PATTEE AND R.E. MONROE, "CHARACTERIZATION OF EXOTHERMIC BRAZING COMPONENTS, SKYLAB EXPERIMENT M552," REPORT NO. NASA-CR-120518, BATTELLE COLUMBUS LABS, PREPARED FOR GEORGE C. MARSHALL SPACE FLIGHT CENTER, DEC 1973

Brazing With Clad Brazing Materials

Sunil Jha, Michael Karavolis, Kevin Dunn, and James Forster, Texas Instruments, Inc.

Introduction

BRAZING is the preferred method for manufacturing complex assemblies such as heat exchangers, which contain a large number of joints (Ref 1). In the conventional plate-and-fin type of heat exchanger, the fins are brazed to the plates. Often, the brazing filler metal, which can be in the form of a foil, a paste, or a powder that has been consolidated into a sheet using a polymer carrier, is inserted between the plate and fin, and a multiple stack of plate, brazing foil, and fin is fixtured for brazing in a furnace. This complex assembly requires the precise fit of multiple components and the use of a flux, which allows the filler metal to "wet" the surfaces to be joined. To reduce part count and thereby simplify the assembly operation, the brazing filler metal can be clad to the plate material by a roll bonding technique.

This article focuses on clad brazing material, which is defined as any base material or alloy that is clad with an appropriate lower-melting-point brazing filler metal. The most common example is the aluminum-braze clad sheet that is used in the fabrication of aluminum heat exchangers (Ref 2). In these sheets, the aluminum brazing filler alloy (BAlSi series) is clad to the aluminum-base alloy by hot roll bonding. The aluminum-clad brazing sheets can be brazed in a variety of atmospheres, and are used in numerous applications.

Another commercial example of a clad brazing material is copper-clad stainless steel sheet, which is used in the fabrication of heat exchangers for automotive, electronic, and other applications. The copper layer acts as the brazing filler material. The clad brazing material can be formed by drawing, bending, stamping, or other metalworking processes. The formed parts can be assembled and brazed without using any additional filler metal in the joint. Clad brazing materials are frequently used as one member of an assembly, in which the mating piece is made from a brazeable alloy, so that the clad filler metal flows by capillarity to the joint area.

On a more limited scale, aluminum-clad titanium strips have been used to fabricate titanium heat exchangers for electronics applications. In addition, silver brazing alloy (BAg3) that is clad on copper is often used in the brazing of carbide tools (Ref 3). The copper core remains in the joint area and acts as a ductile member that plastically deforms during cooling of the brazed joint.

References

1. T. PROFUGHI, BRAZING: THE SOLUTION FOR MANY COMPLEX ASSEMBLY PROBLEMS, *HEAT TREAT.*, OCT 1990, P 16-17
2. *BRAZING MANUAL*, 3RD ED., AWS, 1984, P 150

3. *BRAZING MANUAL*, 3RD ED., AWS, 1984, P 236

Brazing With Clad Brazing Materials

Sunil Jha, Michael Karavolis, Kevin Dunn, and James Forster, Texas Instruments, Inc.

Cladding Materials

Clad brazing materials are produced as strips, using the roll bonding technique. The strips comprise a base metal that is clad with a brazing filler metal on either one or both sides. These products are used primarily in high-volume manufacturing operations, such as the production of heat exchangers, brazed bellows, and honeycomb structures. The use of a self-brazing sheet reduces the total part count, simplifies the assembly operation (because the brazing filler metal is always present on the core material), and reduces assembly time and, therefore, cost. In addition, there is no need for the application of flux, nor for its subsequent removal. This not only saves the initial purchase cost of the flux, but the waste-management cost that is associated with the disposal of the spent material.

Aluminum-braze clad products, copper-clad steel, and copper-clad stainless steel are the most commonly used clad brazing materials. Table 1 lists the typical clad brazing strip products that are used in the fabrication of compact heat exchangers for the automotive, truck, and aircraft industries.

TABLE 1 TYPICAL CLAD BRAZING STRIP PRODUCTS

MATERIAL	CLAD LAYER RATIOS	THICKNESS		TEMPER	TENSILE STRENGTH		0.2% YIELD STRENGTH		ELONGATION, %
		mm	in.		mpa	ksi	mpa	ksi	
C12200 COPPER CLAD TO 409 STAINLESS STEEL	10/80/10 5/80/15	0.51-0.76	0.020-0.030	ANNEALED	400	58	230	33	37
C12200 COPPER CLAD TO 304 L STAINLESS STEEL	13.5/86.5	0.51-0.30	0.020-0.012	ANNEALED	635	92	290	42	56
	10/80/10			ANNEALED	620	90	275	40	55
C12200 COPPER CLAD TO 1008 STEEL	10/80/10	0.38	0.015	NO. 4 TEMPER	380	55	290	42	35
C52400 PHOSPHOROUS BRONZE CLAD TO C10200	10/80/10	0.51	0.020	ANNEALED	275	40	97	14	48

The thickness of the brazing filler metal used in a clad brazing material can range from 0.050 to 2.54 mm (0.002 to 0.100 in.) and will represent 5 to 20% of the total strip thickness. This range of strip thickness covers the majority of applications in the heat-exchanger industry. Figure 1 shows a typical clad brazing strip of copper-clad stainless steel.

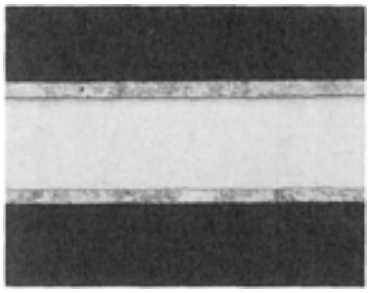

FIG. 1 PHOTOMICROGRAPH OF TYPICAL CLAD BRAZING MATERIAL, C12200 COPPER CLAD TO 304 L STAINLESS STEEL

Figure 2 compares the steps in using brazing preforms to fabricate a brazed assembly with the steps involved in using clad brazing materials. The latter is shown to be more efficient.

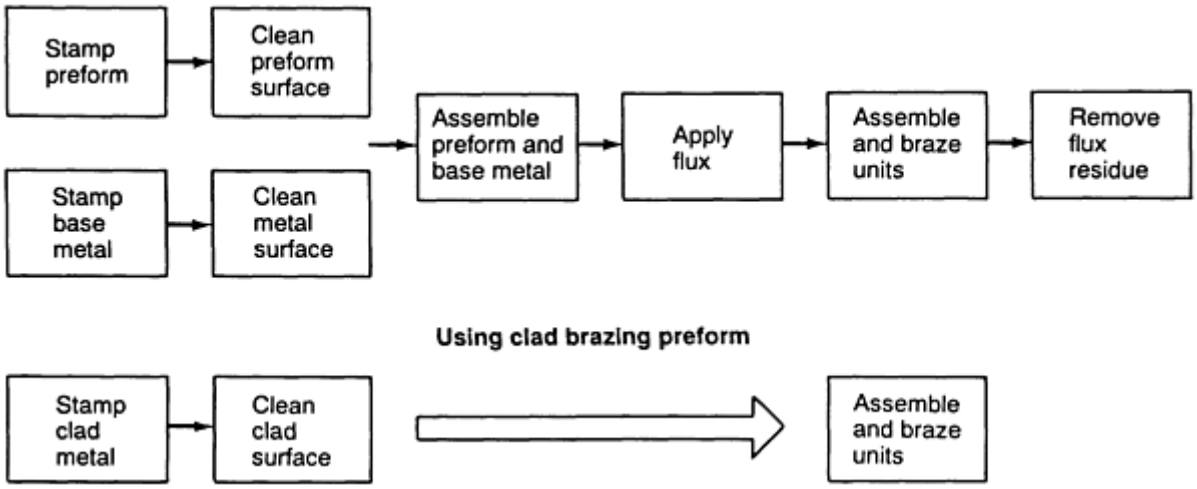

FIG. 2 COMPARISON OF BRAZING PROCESS USING BRAZING PREFORM VERSUS PROCESS USING CLAD BRAZING SHEET

Figure 3 depicts an automotive transmission fluid cooler that was assembled using clad brazing materials. A turbulator is brazed to a copper-clad stainless steel base and cover. The base and cover are formed from a stainless steel strip containing copper braze on one side. After brazing, the dimensional changes in this part are minimal, which is important when making a hermetically sealed heat exchanger.

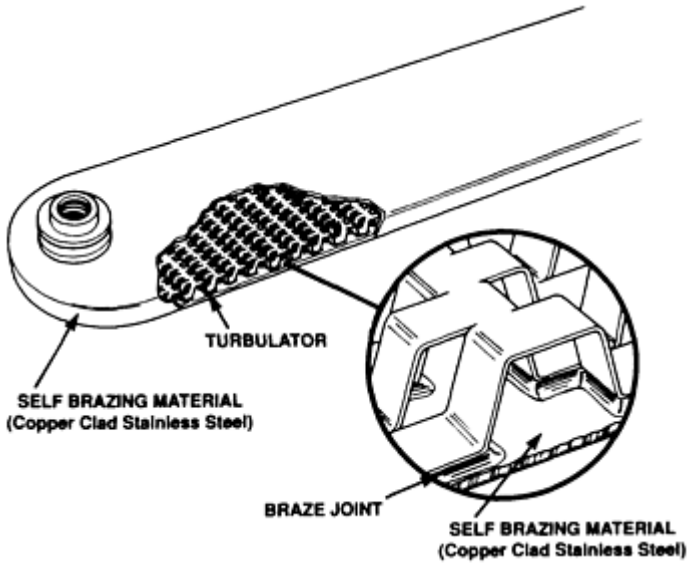

FIG. 3 HEAT EXCHANGER FABRICATED USING CLAD BRAZING ("SELF-BRAZING") MATERIALS

To fabricate clad brazing materials, the brazing filler metal must be ductile enough to be roll bonded to the base metal. The roll bonding technique is described in the article "Roll Welding" in this Volume and in Ref 4 and 5. A nickel brazing alloy that contains high levels of boron and silicon as melting-point depressants, such as the BNi-W series, is not available in thin-strip form, because these materials are brittle. Therefore, it cannot be roll bonded or processed by conventional metalworking methods.

The advantages of using clad brazing materials are that they:

- REDUCE THE TOTAL NUMBER OF PARTS THAT NEED TO BE ASSEMBLED
- ELIMINATE THE STAMPING AND ASSEMBLY COSTS ASSOCIATED WITH THE PRODUCTION OF A BRAZING FILLER METAL PREFORM
- ELIMINATE THE USE OF FLUXES AND REDUCING OR SURFACE-ACTIVATING ATMOSPHERES, BECAUSE ROLL BONDING ALLOWS THE BRAZING FILLER METAL TO METALLURGICALLY BOND TO THE SURFACES TO BE JOINED
- IMPROVE THE MANUFACTURING YIELD, BECAUSE PRECISE POSITIONING OF THE FILLER METAL IN THE JOINT AREA IS POSSIBLE
- ENHANCE DESIGN FLEXIBILITY, BECAUSE THE BRAZING FILLER METAL IS INTEGRAL WITH THE STRUCTURAL COMPONENTS THROUGH ALL MANUFACTURING STEPS, WHICH PERMITS THE DESIGN OF COMPACT, MORE COMPLEX, AND COST-EFFECTIVE ASSEMBLIES
- IMPROVE PROCESS REPEATABILITY, BECAUSE OF THE UNIFORMITY OF BRAZING FILLER METAL AND TIGHTER DESIGN TOLERANCES
- ELIMINATE HANDLING PROBLEMS WITH THIN AND WEAK FILLER METAL SHIMS, FOILS, OR PASTES

References cited in this section

4. G. DURST, A NEW DEVELOPMENT IN METAL CLADDING, *J. MET.*, MARCH 1956
5. R.G. DELAGI, DESIGNING WITH CLAD METALS, *MACH. DES.*, NOV 1980

Sunil Jha, Michael Karavolis, Kevin Dunn, and James Forster, Texas Instruments, Inc.

Brazing With Clad Brazing Materials

The design and manufacturing considerations associated with obtaining a good joint when using a clad brazing material are similar to those associated with producing joints when using conventional brazing techniques (Ref 6). Because the brazing filler metal is metallurgically bonded to the base metal, it acts as a protective (oxide-inhibiting) layer. This somewhat reduces the requirement for cleaning and fixturing before brazing, because the total part count is reduced. Similarly, the use of clad brazing materials often imposes a less-stringent requirement on the furnace atmosphere.

In the case of copper-clad stainless steel, the copper protects the surface of the stainless steel during heating. At the brazing temperature, it readily melts and flows to form the braze joint. Therefore, self-brazing materials often eliminate the need for pretreatments and fluxes to ensure adequate flow and wetting.

Clad brazing materials should not be used solely as a substitute material or as a joining method in an existing design that is based on conventional assembly techniques and placement of the filler metal. The greatest benefits of clad brazing materials are obtained when their use is comprehended in the basic design of the assembly and in the manufacturing process. The decision to use clad brazing material in the design stage of a heat exchanger allows greater design flexibility, tighter tolerances, and a more-robust process, because the design engineer does not need to allow spaces for wires or shims, or to specify the application method and handling procedure for the brazing filler metal. During the high-volume production of brazed assemblies that utilize clad brazing materials, the same amount of brazing filler metal is located at any given location every time.

Reference cited in this section

6. *THE BRAZING BOOK*, HANDY AND HARMAN, 1985

Brazing With Clad Brazing Materials

Sunil Jha, Michael Karavolis, Kevin Dunn, and James Forster, Texas Instruments, Inc.

References

1. T. PROFUGHI, BRAZING: THE SOLUTION FOR MANY COMPLEX ASSEMBLY PROBLEMS, *HEAT TREAT.*, OCT 1990, P 16-17
2. *BRAZING MANUAL*, 3RD ED., AWS, 1984, P 150
3. *BRAZING MANUAL*, 3RD ED., AWS, 1984, P 236
4. G. DURST, A NEW DEVELOPMENT IN METAL CLADDING, *J. MET.*, MARCH 1956
5. R.G. DELAGI, DESIGNING WITH CLAD METALS, *MACH. DES.*, NOV 1980
6. *THE BRAZING BOOK*, HANDY AND HARMAN, 1985

Iron Soldering

Mark Cowell, Metcal, Inc.

Equipment

Hand soldering equipment can be broadly classified by its temperature control method. There are constant-voltage, variable temperature, and tip-temperature-controlled soldering iron types, each of which is described below.

Constant-voltage soldering irons are temperature-limited, but do not incorporate a temperature sensor. Temperature calibration of the tip is not possible, because these irons depend on the increasing resistance of the heating element to limit tip temperature. Line voltage fluctuations and ambient temperatures greatly affect the temperature of the soldering tip. A constant-voltage soldering iron is the least-expensive hand soldering tool. However, this type of soldering iron requires highly skilled operators to create reliable joints.

Variable-temperature soldering irons incorporate a temperature control device in the soldering handle. A control knob on the power source provides a means for the user to vary the tip temperature. When the soldering tip achieves the prescribed temperature, current to the heater is turned off. The tip cools to the lower temperature setpoint of the controller, and current to the heater is turned back on. Tip temperature calibration is possible with variable-temperature soldering irons. This type of iron can be adjusted so that its temperature is balanced with the thermal requirements of the joint. However, one of its drawbacks is that an unskilled or inattentive operator may leave the temperature at the highest setting, in an attempt to solder more quickly, damaging heat-sensitive components or printed circuit boards. Damage can also occur when the heat is too low and an operator stays on the termination too long while adding pressure.

Temperature-controlled irons incorporate a temperature sensor in the soldering tip. These soldering irons operate at a manufacturer's preselected temperature, and tip temperature calibration is not required. Tips are selected for their shape, as well as their operating temperatures. At the preselected temperature, either the resistance of the heating element changes or the current supplied to the heating element is turned off. The resulting reduction in heat generation stabilizes the tip temperature at its setpoint. Temperature-controlled soldering tips help ensure that the proper tip is used in a production environment, thus eliminating costly damage to printed circuit boards and components. This tool requires the least amount of operator training.

Iron Soldering

Mark Cowell, Metcal, Inc.

Soldering Iron Selection

When selecting a soldering iron, potential damage to the printed circuit board and its components must be considered. Damage can result from excessive joint temperatures or electrical overstress. Thermal damage can result from an iron that is not temperature controlled or is operated at too high a temperature, whereas electrical overstress results from the flow of electrical energy (leakage or electrostatic) when the iron is placed in contact with the component, which damages or weakens an electrical component. Military soldering standard MIL-STD-2000A and industry soldering standard IPC-S-815B cover the minimum soldering requirements in detail.

Figure 2 illustrates a typical soldering iron tip and joint thermal profile for repetitive joints. When an iron and tip have been properly selected, the tip temperature will decrease when the tip is placed in contact with the joint and solder is applied. When the temperature of the joint is from 28 to 55 °C (50 to 100 °F) greater than the solder liquidus temperature, the tip is removed from the joint. The tip temperature recovers (increases) to its setpoint as the solder joint cools.

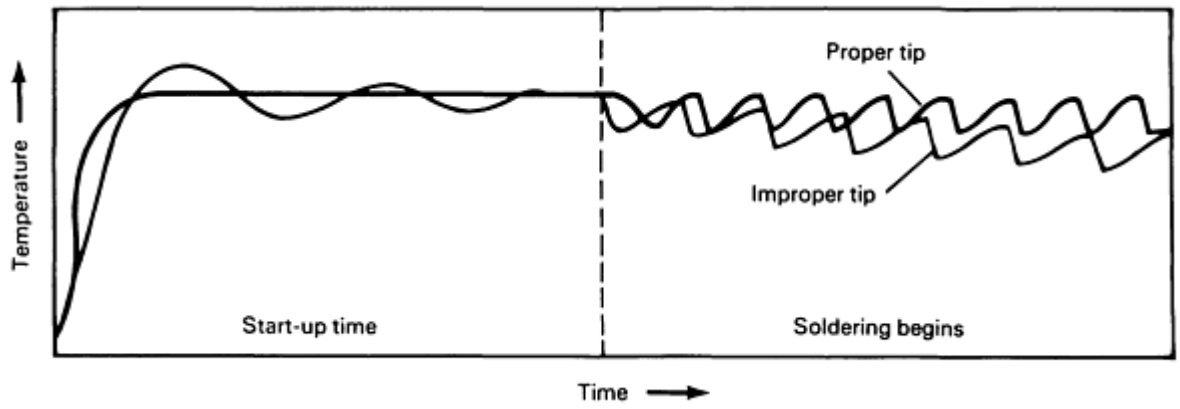

FIG. 2 TYPICAL SOLDERING IRON TIP AND JOINT THERMAL PROFILE

When a soldering iron is improperly selected, each successive joint connection decreases the working temperature of the tip. After several solder joints have been completed, the tool may be unable to form reliable joints. A properly selected soldering iron will stabilize the tip at a temperature that does not damage components, while providing a working temperature sufficient for soldering successive joints reliably.

Iron Soldering

Mark Cowell, Metcal, Inc.

Selected References

- M. FREDERICKSON, *CONDUCTIVE POINT-TO-POINT SOLDERING*, ELECTRONICS MANUFACTURING PRODUCTIVITY FACILITY (NAVIRSA-DET.), 1989
- L. LAMBERT, *SOLDERING FOR ELECTRONIC ASSEMBLIES*, MARCEL DEKKER, 1988
- H. MANKO, *SOLDERS AND SOLDERING*, MCGRAWHILL, 1964, P 225-250
- R. SKIPP, *SOLDERING HANDBOOK*, BSP PROFESSIONAL BOOKS, 1988, P 28-47

Torch Soldering

Charles E. Fuerstenau, Lucas-Milhaupt, Inc.

Introduction

TORCH SOLDERING (TS) utilizes a fuel gas flame as the heat source in the soldering process. The fuel gas is mixed with either air or oxygen to produce the flame, which is applied to the materials to be soldered until the assembly reaches the proper soldering temperature. Solder filler metal, which melts at temperatures below 450 °C (840 °F), is added to the assembly to bond it. Successful torch soldering is accomplished when parts are clean and fit together closely, and when oxides are not excessive.

Torch soldering is used in numerous industries that utilize a variety of base metals. It is most often used to produce a leak-tight assembly with some degree of mechanical strength. This process does have several advantages when compared with other metal-joining methods.

These advantages include:

- RELATIVELY LOW TEMPERATURES, WHICH RESULT IN MINIMAL DISTORTION AND HEAT DISCOLORATION OF THE SOLDERED ASSEMBLY
- FLEXIBILITY, SUCH THAT ONE TORCH CAN BE USED TO SOLDER A VARIETY OF ASSEMBLIES
- RELATIVELY INEXPENSIVE CAPITAL EQUIPMENT COST
- ABILITY TO SOLDER MOST BASE METALS AND BASEMETAL COMBINATIONS WITH AN APPROPRIATE FLUX
- LOCAL HEATING OF SMALL JOINTS ON LARGE ASSEMBLIES, WHICH PRECLUDES THE NEED TO HEAT THE ENTIRE ASSEMBLY
- PROCESS AUTOMATION, IN MANY CASES

The limitations of the process are that:

- A FLUX IS NEEDED BECAUSE THE PROCESS IS ACCOMPLISHED IN AIR, AND THIS FLUX OFTEN MUST BE REMOVED IN ORDER TO PREVENT PART CORROSION
- HIGHLY REACTIVE MATERIALS, SUCH AS TITANIUM AND MANY REFRACTORY METALS, CANNOT BE SOLDERED, BECAUSE NO SUITABLE FLUXES ARE AVAILABLE
- SOLDERED JOINTS DO NOT NORMALLY EXCEED THE STRENGTH OF THE PARTS BEING SOLDERED, THAT IS, THE PROCESS PRODUCES RELATIVELY WEAK JOINTS, WHEN COMPARED WITH BRAZED AND WELDED ASSEMBLIES

Torch Soldering

Charles E. Fuerstenau, Lucas-Milhaupt, Inc.

Applications

Materials. Torch soldering is used extensively on copper, brass, and other copper alloys. Steel, stainless steel, aluminum, gold, and other metals, as well as many combinations of these, also can be soldered by this process.

Industries. The plumbing industry utilizes this process extensively on residential copper tubing for water lines, primarily because of its flexibility and ease of use. Soldered copper water lines provide leak-tight joints with the requisite strength. Torch heating is also used for liquid and gas conduit in industrial processing applications.

This process is also used by many other industries in assembly processes, such as the soldering of jewelry, aluminum heat exchangers, radiators, and pressure-sensing devices. Tube-to-fitting types of assemblies also are commonly torch soldered, as are butt and lap joints.

Torch Soldering

Charles E. Fuerstenau, Lucas-Milhaupt, Inc.

Equipment

Torch. Typically, the equipment required for torch soldering is simple. Single torches are often used for hand soldering, whereas multiple torches can be used together on automated systems.

Gases. Fuel gas and air systems are frequently used for torch soldering because of the low heat requirements. The plumbing industry often utilizes a simple hand-held propane/air torch that is attached to the top of a small, rechargeable cylinder. Surrounding air is mixed with the propane from the cylinder in the appropriate ratio.

Gas/oxygen systems can also be used for torch soldering, although they produce more heat than gas/air systems. This amount of heat is not normally required for torch soldering.

A reducing flame--that is, a flame where excess fuel is present and surrounding air is used to complete combustion--is typically used when soldering. A reducing flame helps keep the assembly clean by reducing surface oxides.

Filler Metals. Many different filler metals are used in the torch soldering process. Tin-lead, tin-silver, and tin-antimony filler metals are commonly used on copper alloys, steel, and stainless steels. Zinc-aluminum is used exclusively on aluminum-base metals. The solders that are commonly used as filler metals are shown in Table 1.

TABLE 1 COMMON SOLDERS FOR TORCH SOLDERING

COMPOSITION	SOLIDUS TEMPERATURE		LIQUIDUS TEMPERATURE		COMMENTS
	°C	°F	°C	°F	
63SN-37PB	183	361	183	361	EUTECTIC COMPOSITION; MOST FLUID OF THE SNPB ALLOYS
40SN-60PB	183	361	238	460	LONG MELTING RANGE; GOOD FOR FILLING GAPS
96.5SN-3.5AG	221	430	221	430	FLUID SOLDER; STRONGEST OF LOW-TEMPERATURE SOLDERS
95SN-5SB	233	452	240	464	FOR COPPER- AND IRON-BASE ALLOYS; NOT FOR USE ON ZINC-BEARING ALLOYS, SUCH AS BRASS
98ZN-2AL	376	710	385	725	FOR SOLDERING OF ALUMINUM; USED EXTENSIVELY ON HEAT EXCHANGERS

Torch Soldering

Charles E. Fuerstenau, Lucas-Milhaupt, Inc.

Basic Heating Techniques

The key to torch soldering, as in all methods of heating, is to equally heat the components that need to be soldered. This may require directing the torch to a larger mass component of an assembly. Because the filler metal will flow to the hottest portion of an assembly, the flame should be applied so that the filler metal will flow in the intended direction. Also, movement of the torch is required to avoid overheating or burning the assembly.

Figure 1 shows the appropriate wire and torch placement for the soldering of tubing. Proper heating will result in the flow of filler metal through the joint, resulting in a fillet both inside and outside the joint. This ensures that a leak-tight joint has been produced.

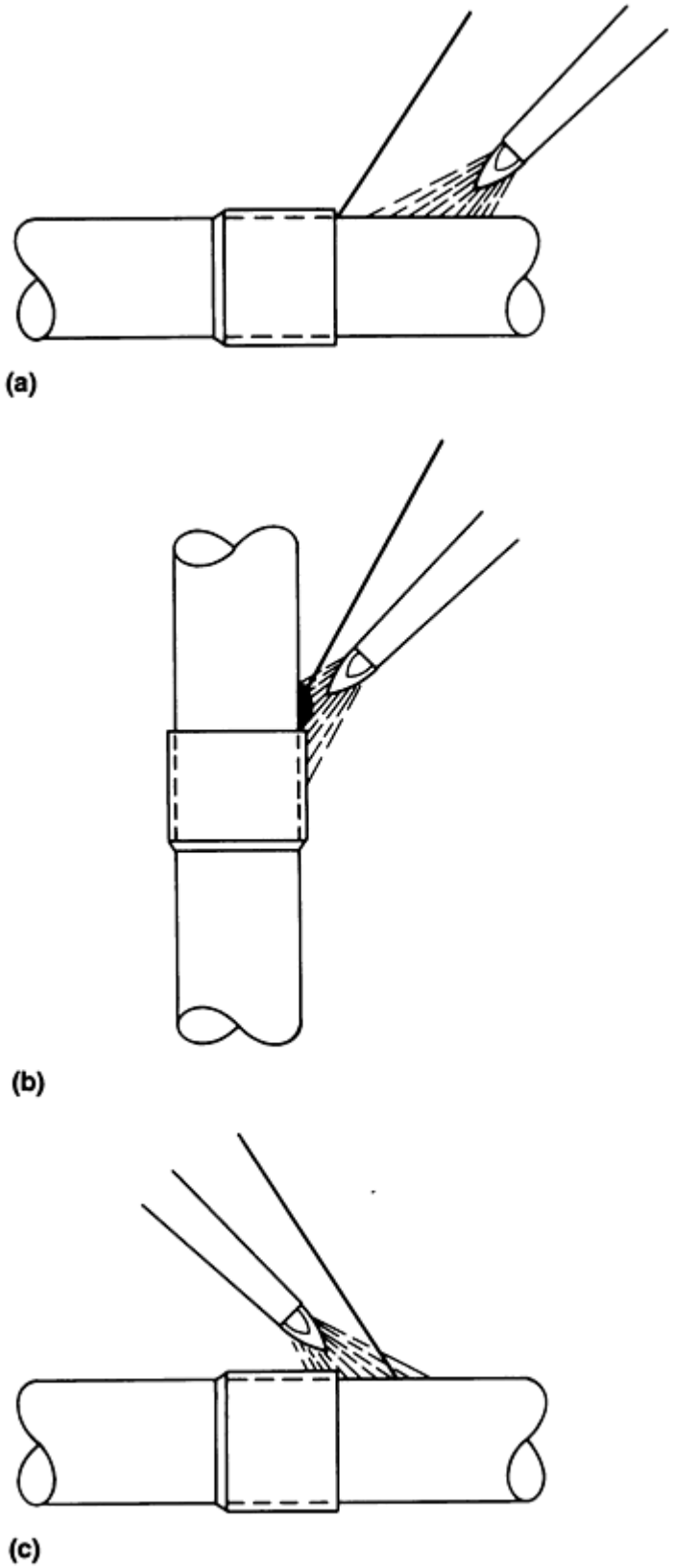

FIG. 1 EXAMPLES OF PLACEMENT OF FILLER-METAL WIRE AND FLAME. (A) AND (B) PROPER PLACEMENT. (C) POOR PLACEMENT

Torch soldering techniques are easy to learn when proper training and experience are provided.

Charles E. Fuerstenau, Lucas-Milhaupt, Inc.

Selected References

- *FILLER METAL SELECTION GUIDE,* HANDY AND HARMAN/LUCAS-MILHAUPT, 1992
- *THE BRAZING BOOK,* HANDY AND HARMAN/LUCAS-MILHAUPT, 1991

Furnace and Infrared Soldering

Phil Zarrow, Synergistek Associates

Introduction

FURNACE SOLDERING (FS) encompasses a group of reflow soldering techniques in which the parts to be joined and preplaced filler metal are put in a furnace and then heated to the soldering temperature. Five reflow technologies are currently certified for use in surface-mount technology (SMT) applications:

- TYPE A: VAPOR PHASE
- TYPE B: AREA CONDUCTION (THAT IS, LINEAR CONDUCTION)
- TYPE C: HOT BAR
- TYPE D: CONVECTION AND CONVECTION/INFRARED (IR)
- TYPE E: LASER

Of these five methods, three are considered to be mass reflow techniques (Types A, B, and D), because all of the solderable interconnections on the surface of a printed wiring board (PWB) assembly are brought through the reflow heating cycle simultaneously.

Vapor-phase reflow, or condensation heating, had early prominence as an SMT reflow soldering method. A fluid that has a boiling point higher than the solder melting point is heated and the vapor is contained in a chamber, through which the PWB assembly is passed. Heat transfer is achieved through the heat of vaporization released by the fluid as it condenses on the PWB surface. The fluids are compatible with most substrate and device packaging materials. The process is relatively insusceptible to variances in component distribution and assembly densities. Additional information can be found in the article "Vapor-Phase Soldering" in this Volume.

Area conduction comprises multiple "hot-plates" with a substrate conveyance system. This method can also be combined with other energy-transfer techniques, including convection and infrared, when appropriate for specific applications.

Infrared heating technology has also been very successfully adapted to SMT reflow soldering. Area IR emitters, that is, radiant panels, and lamp radiant emitters that are arranged in arrays with reflectors are incorporated in a conveyorized oven to provide the source of heat. By using mid- to far-infrared emissions and presenting a large heated surface area to heat the resident atmosphere in the oven, the dual heat transfer technologies (that is, IR heat provided by the direct lamp heat and conduction-generated heat provided by the indirect heating of the atmosphere) can achieve a very controlled rate of heating, which is ideal for SMT reflow soldering.

IR reflow has continued to evolve. Emphasis has been placed on enhancing heat transfer through forced convection (class 3), also known as convection-dominant reflow soldering (Fig. 1 and 2). Convection evens out the "hot" and "cold" spots caused by different surface adsorptivity. The intent is to approach the beneficial near-equilibrium aspects of vapor-phase reflow, but with the multizone profile control that has been traditionally offered by the convection/IR method. This objective is driven by the more-complex soldering applications, in terms of assembly mass and surface geometries.

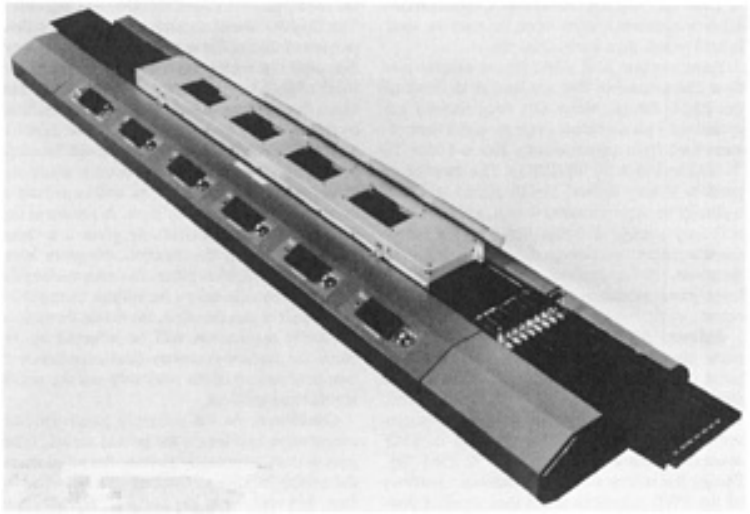

FIG. 1 CONDUCTION REFLOW SOLDERING OVEN WITH FORCED CONVECTION ENHANCEMENT. COURTESY OF SIKAMA INTERNATIONAL

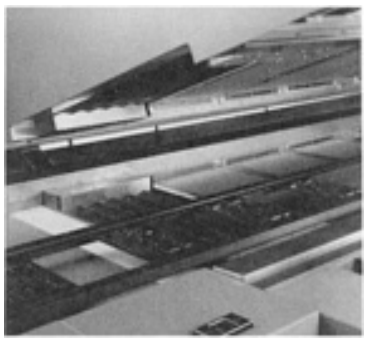

FIG. 2 FORCED CONVECTION REFLOW SOLDERING OVEN USED TO SOLDER PWB COMPONENTS. COURTESY OF VITRONICS CORPORATION

Furnace and Infrared Soldering

Phil Zarrow, Synergistek Associates

Reflow Profile

The heating cycle of the PWB assembly should be precisely controlled. The reflow profile is composed of four regions (Fig. 3):

- PREHEAT (PREBAKE)
- PREFLOW (SOAK)
- REFLOW
- COOLDOWN

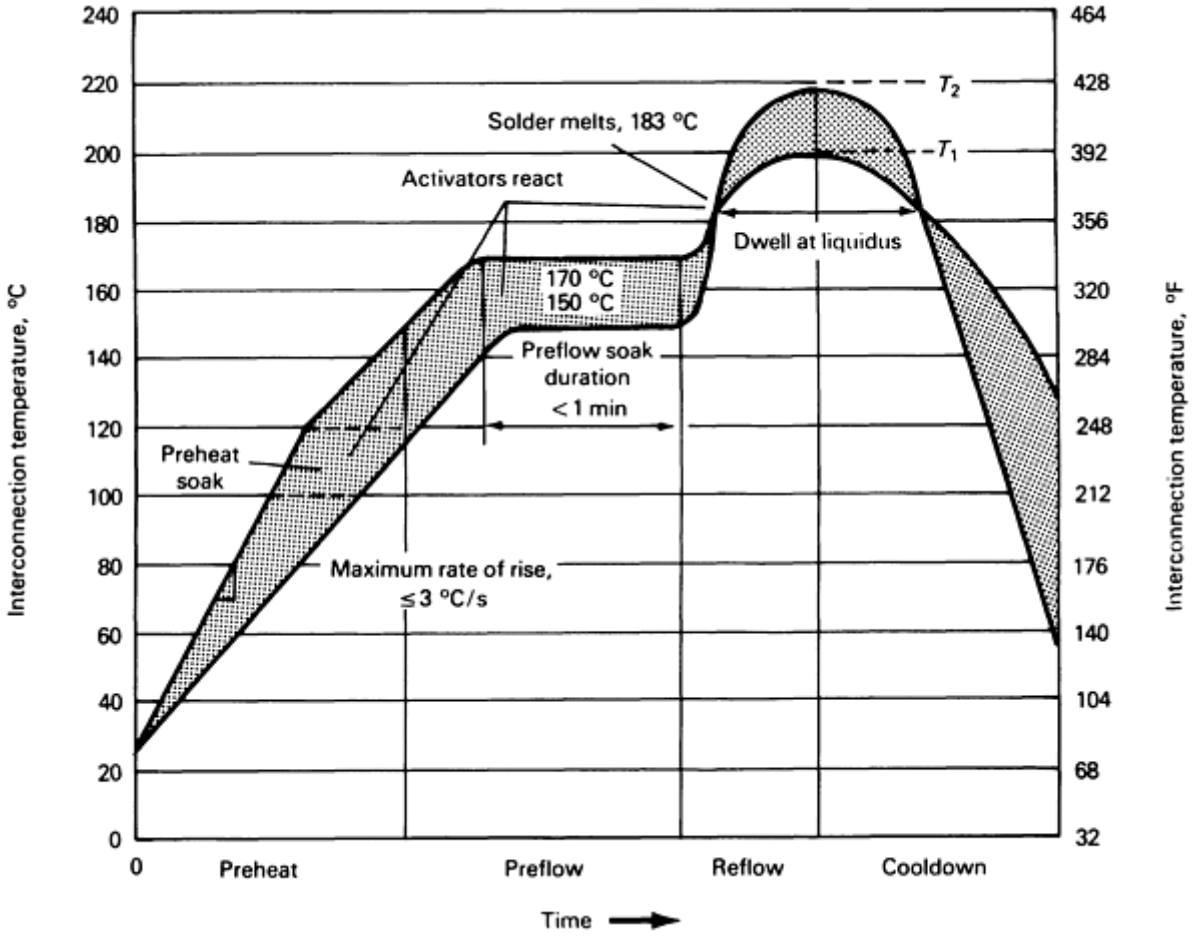

FIG. 3 PLOT OF INTERCONNECTION TEMPERATURE VERSUS ELAPSED TIME SHOWING FOUR REGIONS THAT CONSTITUTE REFLOW PROFILE. TOTAL ELAPSED TIME FROM PREHEAT TO COOLDOWN VARIES FROM 3 TO 6 MIN.

Preheat. As the PWB assembly enters the oven tunnel (at ambient temperature) and energy is introduced to the assembly, the heat transfer process begins. The interconnection temperature is brought up to approximately 100 to 120 °C (212 to 250 °F) to reduce the risk of thermal shock to the components and PWB delamination. The control of the rate of heating is most critical in the preheat portion of the profile. Many component manufacturers, particularly suppliers of ceramic capacitors, recommend a preheat rate of heating that is less than 4 °C/s (7 °F/s). The rate of heating should be based on the application, and the component complement should be considered.

Throughout the preheat stage, activators commence "scrubbing" and some solvents begin to evaporate. In certain solder paste formulations, some of the flux activators may begin oxide reduction at this stage.

Preflow. Before it attains reflow temperatures, the assembly is allowed to "soak" for a period of time. Those PWB assemblies that have polymer-base substrates require time to allow the transfer of heat throughout the assembly, in order to reduce thermal gradients. The remainder of the noncontributing solvents contained in the solder paste are driven off. As the temperature of the solderable interconnections are brought to just below the solder melting point, flux activators react with the surface to clean component and pad interfacing surfaces.

The temperature range and duration of this stage varies among flux types and the solder paste formulations that different manufacturers produce. Generally, rosin mildly activated (RMA) fluxes become fully activated in a preflow soak at temperatures between 150 and 170 °C (300 and 340 °F). Some RMA formulations achieve optimum results when the preflow soak is held to less than 1 rain (Fig. 3).

Some organic acid (OA) fluxes exhibit preflow characteristics that are similar to those of the RMA fluxes. Many OA formulations are optimized with a gradual slope in which temperature rises from approximately 100 to 170 ± 15 °C (212

to 340 ± 30 °F) (Ref 1). The duration of preflow is very critical to OA fluxes and will typically be approximately 1 min, although this will vary among different formulations (some manufacturers recommend minimizing the duration). If the preflow time interval is too long, paste oxidation and flux degradation can occur.

Reflow. As the temperature of the solder paste on the interconnect passes the melting point of the solder alloy and enters a molten state, the reflow portion of the process begins. With 63Sn-37Pb, a eutectic solder that represents the most commonly used alloy in SMT assembly, reflow occurs at 183 °C (361 °F). During the reflow stage, all solderable portions of the PWB assembly reach their desired peak temperatures. Most solder manufacturers recommend bringing the interconnect temperature to approximately 15 to 30 °C (27 to 54 °F) above the alloy melting point to ensure complete melting, as well as good solder flow, and to aid fillet formation. This is designated T_1 in Fig. 3. The supplier should be consulted to provide the actual temperature for a particular formulation.

The duration of time at which a solderable interconnect resides above the melting point of the solder paste is called the "dwell at liquidus." The liquidus dwell extends through the reflow portion of the profile and into the cooldown portion until the solder reaches solidus. This is the most critical portion of the reflow profile. Because these are the highest temperatures endured by the assembly during the process, the duration at these elevated temperatures should be minimized. Intermetallic growth occurs while the solder is in the molten state, as well as a result of diffusion over a period of time. A sustained liquidus dwell period essentially gives it a "head start." The longer the duration, the more intermetallic growth takes place. Because cooling the interconnection to below the solidus temperature is also part of this duration, the actual dwell for a particular application will be affected by the mass and surface geometry (and expediency of heat dissipation) of the assembly and the resulting thermal gradient.

Cooldown. As the assembly passes its peak temperature and leaves the heated tunnel, it begins to cool, eventually passing the point where the solder solidifies. Cooling can be aided by fans, blowers, inert gas curtains, refrigeration, normal exposure to ambient air, or a combination of several of these mechanisms. To avoid thermal shock to components, it is currently recommended that the rate of cooling not exceed -4 °C/s (-7 °F/s). However, rapid cooling does promote a finer grain growth in the joint and contributes to a stronger interconnect.

The actual time and temperature duration range for each zone not only varies among the different types of fluxes used in SMT soldering, but also among similar flux designation formulations of different manufacturers. The user should consult his supplier to obtain the actual time and temperature durations that are recommended for the specific solder paste being used. It is important to note that most fluxes have a fairly substantial "envelope" in terms of temperatures at the different stages. In some cases, however, actual duration can be more stringent.

Reference cited in this section

1. J.S. HWANG, *SOLDER PASTE IN ELECTRONIC PACKAGING*, VAN NOSTRAND REINHOLD, 1989, P 38

Furnace and Infrared Soldering

Phil Zarrow, Synergistek Associates

Reflow Schedule

A reflow specification should be required for any facility that uses mass reflow techniques. This procedure should mandate the temperatures that the PWB assembly will be exposed to at the peak of the reflow cycle. The full peak liquidus temperature, T_1, is the minimum peak temperature that any solder and interconnection must be exposed to for proper joint formation and is a parameter of the reflow schedule. It is affected by factors such as solder paste alloy, metal content, particle size, flux, surface tension, and fluidity of the solder. As noted earlier, this value will vary among different formulations and should be specified by the solder paste manufacturer (see the section "Reflow Profile" in this article).

The most vulnerable component (MVC) maximum peak temperature is represented by the value T_2. It identifies the component that has the lowest thermal threshold and is most likely to be thermally damaged. The MVC might be an inserted component with a low material melting point (that is, an electrolytic capacitor), a plastic connector, a switch, a label, or some other heat-sensitive part or material. The lowest common denominator within the assembly will determine the highest temperature to which any part should be exposed. A buffer of -5 °C (-9 °F) should be taken from that threshold to establish the MVC temperature used in the specification.

In some applications, the MVC temperature might be determined by the internal heat sensitivity of an active device. Hence, the internal temperature tolerances should also be taken into consideration.

Processing in Inert Atmosphere

Reflow soldering in an inert atmosphere can, in some instances, be beneficial to improved wettability. However, implementing nitrogen in the reflow oven is being driven by two specific factors: "no-clean" fluxes and the bare copper assembly process.

No-clean (or low-residue) fluxes represent one solution to the search for alternatives to cleaning PWB assemblies with environmentally damaging chlorofluorocarbon (CFC) solvents. The result is the development of solder formulations that do not require cleaning.

A number of factors will ultimately affect feasibility for a given application. Besides external cosmetic appearance requirements, both solder joint quality and testability (in light of remaining residue) will be dictated by other user standards and requirements. Although some low-residue solder paste formulations that work well in ambient (oxygen-laden) atmosphere are available, many very low residue no-clean solder pastes require that reflow take place in an inert (N_2) atmosphere. Some no-clean solder paste formulations have been successfully tested at approximately 300 ppm of O_2, but the higher the concentration of inert atmosphere, the wider the process window. Optimum results, in terms of very low residue, have been attained with nitrogen atmosphere of less than 20 ppm O_2.

The bare copper assembly process has been prompted by the need for coplanarity on the PWB substrate when placing fine- pitch devices. Hot-air leveling of solder during PWB fabrication has not attained adequate levels of coplanarity when components of 0.51 mm (0.020 in.) pitch or finer are being attached. In the bare copper assembly process, the PWB is fabricated in the usual manner, except that the tin-lead solder coating is omitted. Instead, the substrate is coated with a sealant (that is, inhibitor) that prevents the copper from oxidizing. In assembly, solder paste deposition (screened or stencilled) and component placement are accomplished "as usual." During reflow, the sealant vaporizes between 100 and 120 °C (212 and 250 °F) (during the preheat stage), which exposes the copper to the solder paste. Because the copper is exposed, the furnace must contain an inert atmosphere to prevent excessive oxidation of the lands. Just how oxygen-free the oven atmosphere needs to be varies among users. Some obtain successful results in atmospheres composed of approximately 500 to 700 ppm O_2. The most stringent specification requires a nitrogen atmosphere with less than 50 ppm O_2 at any point in the process where the PWB assembly becomes elevated above 150 °C (300 °F).

Reference

1. J.S. HWANG, *SOLDER PASTE IN ELECTRONIC PACKAGING,* VAN NOSTRAND REINHOLD, 1989, P 38

Phil Zarrow, Synergistek Associates

Selected References

- C.L. HUTCHINS, SOLDERING SURFACE MOUNT ASSEMBLIES, *ELECTRON. PACK. PROD.,* AUG 1992
- N. SOCOLOWSKI, SOLDER PASTE-KEY PARAMETERS TO FINE PITCH COMPONENT ASSEMBLIES, *NEPCON WEST PROC.,* MARCH 1990
- P. ZARROW, MAJOR FACTORS FOR SUCCESS IN SMT REFLOW SOLDERING, *ELECTRON. PACK. PROD.,* JUNE 1992
- P. ZARROW, "SMT REFLOW SOLDERING WORK-BOOK," SYNERGISTEK ASSOCIATES, 1992

Dip Soldering

Roy E. Beal, Amalgamated Technologies, Inc.

Introduction

DIP SOLDERING (DS) is accomplished by submerging parts to be joined into a molten solder bath. The molten bath can be any suitable filler metal, but the selection is usually confined to the lower melting point elements. The most common dip soldering operations use zinc-aluminum and tin-lead solders.

The molten bath can be heated by electricity or gas. The bath container is made from ceramic materials or a metal that is nonreactive to the filler metal used for dipping. The dip baths, which can range in size from very small to large, are used in a wide range of industries.

The process of dip soldering is simple to carry out. The joint areas are cleaned and then coated with an appropriate flux. The parts are then lowered into the molten filler metal and joining takes place by capillary attraction into the joints. The solder does not wet surfaces that are not coated with flux. Jigs and fixtures are normally essential to hold components at proper clearances for joining purposes and to maintain overall dimensions of the finished product. They should not be wetted by the solder. Furthermore, any substrates that must be submerged should be able to tolerate the solder temperature.

The molten bath supplies both the heat for raising the temperature of the part and the filler metal to make the joints. It is therefore important that the dip soldering pot capacity be large enough to allow heating of the part and joining without significantly reducing the temperature of the molten filler metal. For some applications, soldering pots are designed for specific production rates.

An advantage of the dip soldering process is the wide range of part sizes, shapes, and thicknesses that can be accommodated by the same apparatus and still result in satisfactory joints. Larger parts require a preheating operation in order to reduce thermal shock when the part enters the dip pot. The preheat also allows quicker attainment of equilibrium between the molten metal in the pot and the part being joined. Atmosphere protection of the dip soldering pot is necessary when the filler metal has oxidation tendencies. Surface oxides on the workpieces must be removed prior to dip soldering, because they can interfere with a proper joining operation.

Dip Soldering

Roy E. Beal, Amalgamated Technologies, Inc.

Applications

Dip soldering is used in job shops, as well as high-rate production situations. Therefore, the parts joined by dip soldering vary from individually designed products to mass-produced items. Dip soldering is ideal for the production of prototype engineered products, which are often made for test purposes. The process also can be used to join limited-production items for the automotive, aircraft, consumer, electronic, and other industries. High-production products are typically heat exchangers for automotive use, high-volume telecommunications equipment, and appliances.

Joints produced by dip soldering techniques are usually sleeve, lap, or T-joints that fill by capillary attraction. The parts to be joined are assembled with gaps appropriate to the particular filler metal surface tension and viscosity characteristics. The joint/fixture design must accommodate thermal expansion that is due to heating the entire substrate or part. Joint gaps also depend on the reactions of the molten filler metal with the material to be joined. For example, aluminum filler metals (or those with zinc, tin-zinc, or zinc-aluminum alloys) react more quickly with aluminum than a tin-lead solder will with copper and therefore require larger gaps for joining.

Equipment

Dip soldering equipment is very basic, comprising a bath made of metal or ceramic to hold the molten filler metal and a means to heat and control the molten filler metal temperature. In the radiator industry, job shops use gas heating with their pots for the sake of economy. Much equipment is made to operate electrically, either because of space considerations or because the pots are used in conjunction with other equipment on a production line that might be affected by a gas heating system. Some systems include a metal pump that raises the level of the liquid metal in areas smaller than the overall pot in order to ensure that no surface oxides are present during the dip operation. This type of equipment is used in automotive radiator manufacture. A typical installation is illustrated in Fig. 1.

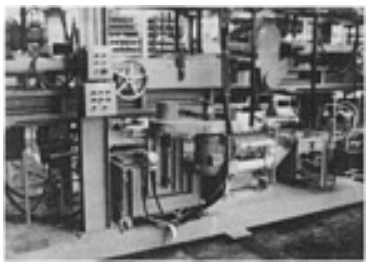

FIG. 1 DIP SOLDERING POT IN A RADIATOR PRODUCTION LINE

Dip Soldering

Roy E. Beal, Amalgamated Technologies, Inc.

Personnel

Solder pots are generally run by production personnel who should be trained to handle and care for equipment that contains molten metals. A substrate that has been raised to the soldering temperature represents a high-temperature hazard. Parts must be dry upon entering the dip solder pot to avoid splashes or explosions. Suitable protective wear (with guards, where possible) is necessary. Good ventilation is important, because of flux and, possibly, metal fumes. Generally, operators of tin-lead solder dip pots are now checked for lead content in the blood, because of possible health hazards.

Introduction

RESISTANCE SOLDERING (RS) is a soldering process in which the heat needed to melt the solder is developed by the resistance of the material when a large electrical current is supplied. Resistance soldering can be applied to electrically conductive materials that allow the passage of electric current. The process can be used for selective spot soldering of small components, for the soldering of closely placed parts on an assembly, or for heat restriction when necessary. It is similar in many ways to resistance brazing (see the article "Resistance Brazing" in this Volume).

When the current is applied, rapid local heating occurs, melting the solder. This molten solder wets the surface. As a result, the resistance in the material falls and the current increases, tripping a control. The heat rapidly dissipates into the surrounding area, and the solder quickly solidifies.

Resistance Soldering

Karl Lazar

Process Applications

The RS process can be used in all soldering operations and with all solderable metals. The only limitations are the thickness and the design of the parts to be soldered. Resistance soldering is used to join steels (for example, carbon, low alloy, and stainless) and nonferrous alloys (for example, aluminum and aluminum alloys, nickel and nickel alloys, and copper and copper alloys) up to 3.2 mm ($\frac{1}{8}$ in.) in thickness (Ref 1).

The RS process is suitable where:

- AN OPEN FLAME CONSTITUTES A POTENTIAL HAZARD IN THE WORKPLACE.
- THE HEAT NEEDED FOR SOLDERING MUST BE CONFINED TO A SPECIFIC AREA.
- THE OXIDATION ATTRIBUTED TO HEATING OF THE SOLDER MUST BE MINIMIZED.
- THE COMPONENTS TO BE JOINED ARE INACCESSIBLE WITH A CONVENTIONAL SOLDERING IRON.
- THE BEAD PRODUCED CAN BE ADAPTED TO AUTOMATED PROCESSING/MASS PRODUCTION METHODS.

Reference cited in this section

1. H.E. BOYER AND T.L. GALL, ED., *METALS HANDBOOK DESK EDITION*, AMERICAN SOCIETY FOR METALS, 1985, P 30-8 TO 30-9

Resistance Soldering

Karl Lazar

Equipment

Resistance soldering equipment typically consists of two electrodes that have been modified for use with a specific part configuration. These electrodes are made of a high-resistance electrical conductor (for example, carbon, graphite, or tungsten). The geometry of the electrode can assume any one or a combination of the following forms (Fig. 1):

- PENCIL
- TWIN-PENCIL
- ROLLER
- CLAMP
- PLIER-TYPE

The electrodes are connected to the transformer by oversized current-carrying conductors. The heart of the system is a heavy-duty, variable, step-down transformer designed to develop an output of 2 to 25 V_{ac} and a current of 5 to 500 A (Fig. 2). A footswitch, a timer, or an adjustable-resistance bridging device across the electrodes can be used to provide a method for the parts to reach the desired solder temperature and shutdown. This allows the solder to solidify and the parts to return to ambient temperature in a 4 to 6 s cycle.

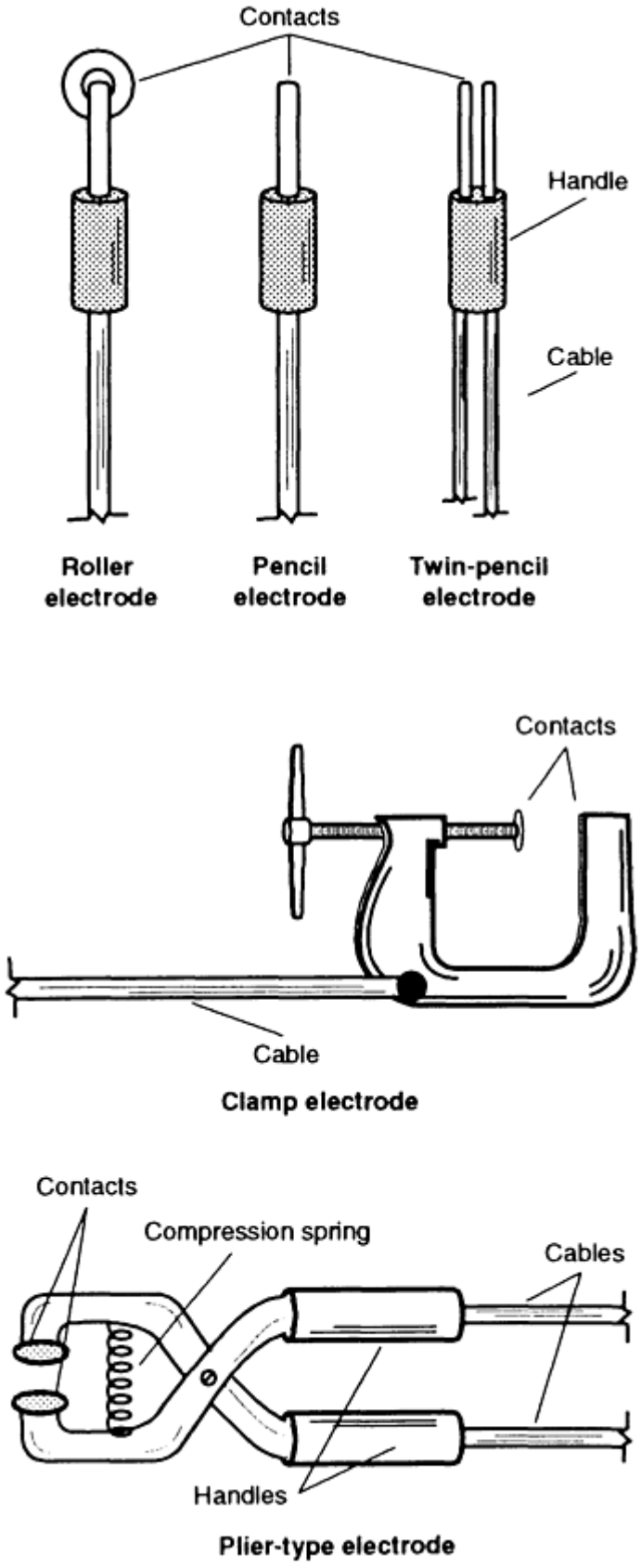

FIG. 1 TYPICAL ELECTRODE CONFIGURATIONS USED IN RESISTANCE SOLDERING APPLICATIONS

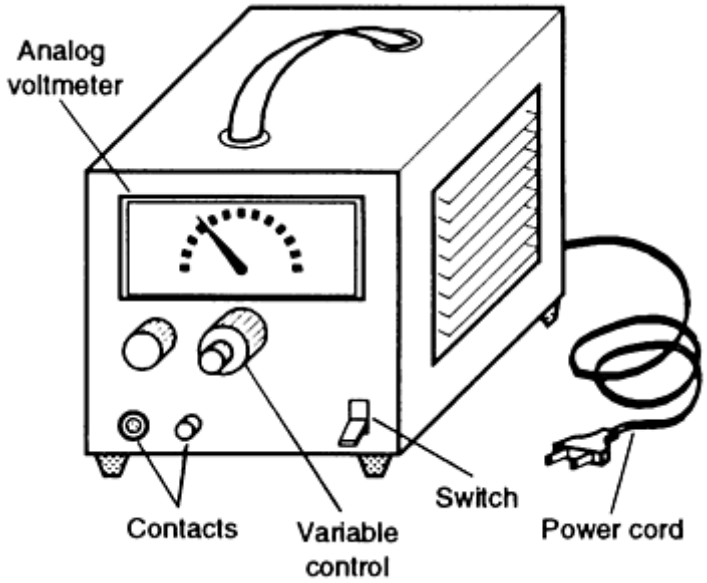

FIG. 2 TYPICAL VARIABLE STEP-DOWN TRANSFORMER WITH 2 TO 25 V OUTPUT (AT 5 TO 500 A CURRENT) USED IN RESISTANCE SOLDERING PROCESSING

Personnel Training

Soldering personnel with a strong basic training will need some additional special training to operate an RS system. The operator's function is to load and unload the parts and to maintain or replace the electrode heads when required. General soldering health and safety rules should be observed to avoid electrical shock and the potential for overheating solder to cause spatter. Typically, the engineer who originally designs the electrode heads is responsible for the equipment's initial start-up.

Resistance Soldering

Karl Lazar

Resistance Soldering Practice

The RS process requires preassembly of the workpiece components. Because the workpiece and the solder are integral parts of the current loop, care must be taken to ensure that the current path is not blocked by any foreign or nonmetallic substance. Hence, the preassembled workpiece requires a clean, deburred surface and the proper solder alloys (preform or in paste form). The use of wire solder and flux is not recommended because of the rapidity of heating and the potential hazard of electrical shock.

The preassembled workpieces are positioned in a grounded jig or clamp, and the movable electrode is brought in contact with the workpiece to complete the circuit. When the power is turned on, the operator waits for signs that the solder is starting to flow and then immediately turns the power off. When using automatic soldering equipment, the duration of the current flow is monitored by sensors that determine the length of the "on" cycle. As the workpiece cools, the solder

solidifies, and the workpiece is removed from the jig. The next assembly can then be placed in the jig. A properly designed movable electrode head allows multiple solder connections to be produced in a single operation.

Resistance Soldering

Karl Lazar

Reference

1. H.E. BOYER AND T.L. GALL, ED., *METALS HANDBOOK DESK EDITION*, AMERICAN SOCIETY FOR METALS, 1985, P 30-8 TO 30-9

Laser Soldering

Riccardo Vanzetti, Vanzetti Systems, Inc.

Introduction

INDUSTRIAL LASERS are able to deliver large amounts of heat with great precision and without contact, making them ideal for applications that have either a destructive nature, such as cutting or drilling, or a constructive nature, such as soldering or annealing.

The use of focused energy generated by either a CO_2 or a neodymium-doped yttrium-aluminum-garnet (Nd:YAG) laser continues to gain acceptance as a process for a number of operations requiring high-temperature injection with speed and precision. For example, in the electronics field, component soldering can be carried out one joint at a time with highly reliable results. Laser soldering uses the well-focused, highly controlled beam to deliver energy to a desired location for a precisely measured length of time.

Advantages of laser soldering are that it is a noncontact procedure; it avoids thermal stress by localizing heat input and confining it to the solder joint area; it reduces intermetallic compound formation, due to rapid joint formation which results in a more ductile joint; and it involves a fine grain size (due to rapid cooling), resulting in better fatigue properties. Disadvantages include low output rates, high power requirements, and high capital requirements.

This discussion focuses on two types of laser soldering operations, blind laser soldering and intelligent laser soldering, and the conditions under which their application is suitable. Key attributes of each system, relative to other types of soldering operations, are also identified.

Laser Soldering

Riccardo Vanzetti, Vanzetti Systems, Inc.

Blind Laser Soldering

The early configurations of production lasers were of the "blind" (no feedback) type. The system included a laser programmed for power, as well as length of heat injection time. The focal spot of the laser beam was brought to impinge on the target by moving either the target itself or the laser beam, or a combination of the two.

Among the vast array of currently available lasers, the preferred systems for industrial soldering applications are the CO_2 laser, which emits at a wavelength of 10.6 μm, and the Nd:YAG laser, which emits at a wavelength of 1.06 μm. The total energy emitted by these lasers (or by any laser, in fact) is in part absorbed by the target, in part reflected by the target, and the balance causes an instantaneous emission of highly energized atomic and subatomic particles from the target's

uppermost surface layer. The ratio of these three parts is a function of laser wavelength and of surface emissivity of the target. The latter, in turn, is a function of chemical composition, crystal structure, and degree of smoothness.

For all practical purposes, certain solder alloys are known to reflect about 74% of the energy from a CO_2 laser, but just 21% of the energy from a Nd:YAG laser. These figures are approximate, because the presence of fluxes and activators reduces the reflection factor. However, the Nd:YAG laser, when used for soldering, is more efficient.

In a blind system, the coordinates of the target, the power of the laser, the diameter of the beam at its focal point, the duration of the incident heat pulse, and other parameters must be preprogrammed and cannot be changed during the operation. Without a feedback mechanism, the quality of the work done by the laser can only be assessed after the operation has been completed.

This approach is adequate for highly repeatable production situations in which the targets are nearly identical to one another. Once the optimum settings for all variables have been established, uniformly good results can be expected. Care must be taken to avoid any process variations, such as changes in surface emissivity of the target or its contamination by a host of other factors, including solderability degradation from oxidation and handling.

However, blind laser soldering is less suitable in electronics applications, where components and the printed circuit pose a serious problem, because no two joints are identical. Although they might visually appear to be identical, their heat requirements can vary substantially. This is due to hidden differences in their heat-sinking efficiency, which is a function of the thermal mass of the subsurface elements connected to the joint. Especially critical is the diameter of the laser beam at the focal spot, because it must cover proportional areas of the elements to be joined, plus some of the solder material. This is why blind laser soldering seldom finds practical applications in the field of electronics. The most difficult applications involve fine pitch technology (FPT) and tape automated bonding (TAB), where the very small dimensions of the joints make the use of conventional soldering systems critical.

Key attributes of blind laser soldering are:

- *REPEATABILITY:* GOOD FOR LARGE PRODUCTION RUNS OF IDENTICAL PARTS, BUT POOR FOR PROCESSES THAT INVOLVE A NUMBER OF NONCONTROLLABLE ITEMS
- *SPEED:* FAST, WHEN COMPARED WITH ANY SOLDERING APPROACH IN WHICH JOINTS ARE MADE ONE AT A TIME
- *QUALITY:* GOOD, WHEN OPTIMIZED FOR LARGE PRODUCTION RUNS OF IDENTICAL CONDUCTORS AND PARTS
- *COST:* EXPENSIVE, WHEN COMPARED WITH MOST OTHER SOLDERING TECHNOLOGIES
- *SAFETY:* CRITICAL, BECAUSE SERIOUS BURNS AND EYE DAMAGE CAN RESULT IF SPECIAL PRECAUTIONS ARE NOT TAKEN
- *FLEXIBILITY:* POOR, BECAUSE ANY DRIFT OF THE MANY PROCESS VARIABLES WILL CAUSE DEFECTS, UNLESS THE PROGRAM IS MODIFIED ACCORDINGLY

Laser Soldering

Riccardo Vanzetti, Vanzetti Systems, Inc.

Intelligent Laser Soldering

Because solder joints can differ from one another in terms of thermal mass, emissivity, contamination, presence of internal thermal barriers, and heat-sinking efficiency, an infrared (IR) detector was added to create an "intelligent" laser soldering system. This system enables the precise control of heat input to the joint, because the IR "eye," constantly focused on the joint being heated, monitors its thermal radiation, and turns off the laser beam right after lead and pad substrates have been thermally soaked by the molten solder. The resulting solder joints are neither overexposed nor underexposed.

Figure 1, which depicts an intelligent system, shows two lasers with coaxial beams: a He-Ne 0.5 mW visible beam and a Nd:YAG 50 W "heating" beam emitting at a 1.06 μm wavelength. After traveling through an optical fiber, these two beams are focused on the solder joint to be formed. At the same time, the IR (thermal) radiation emitted by the heated solder joint is focused on the IR detector, which does not register the wavelength of the laser beams and therefore is not disturbed by their reflections. The visible image of the solder joint is picked up by a closed-circuit television camera and displayed on a television screen. These three optical signals are separated by dichroic mirrors in the optical head while the solder joints are brought, one at a time, under the focal spot of the system. The preprogrammed sequence is based on the *x* and *y* coordinates of each joint.

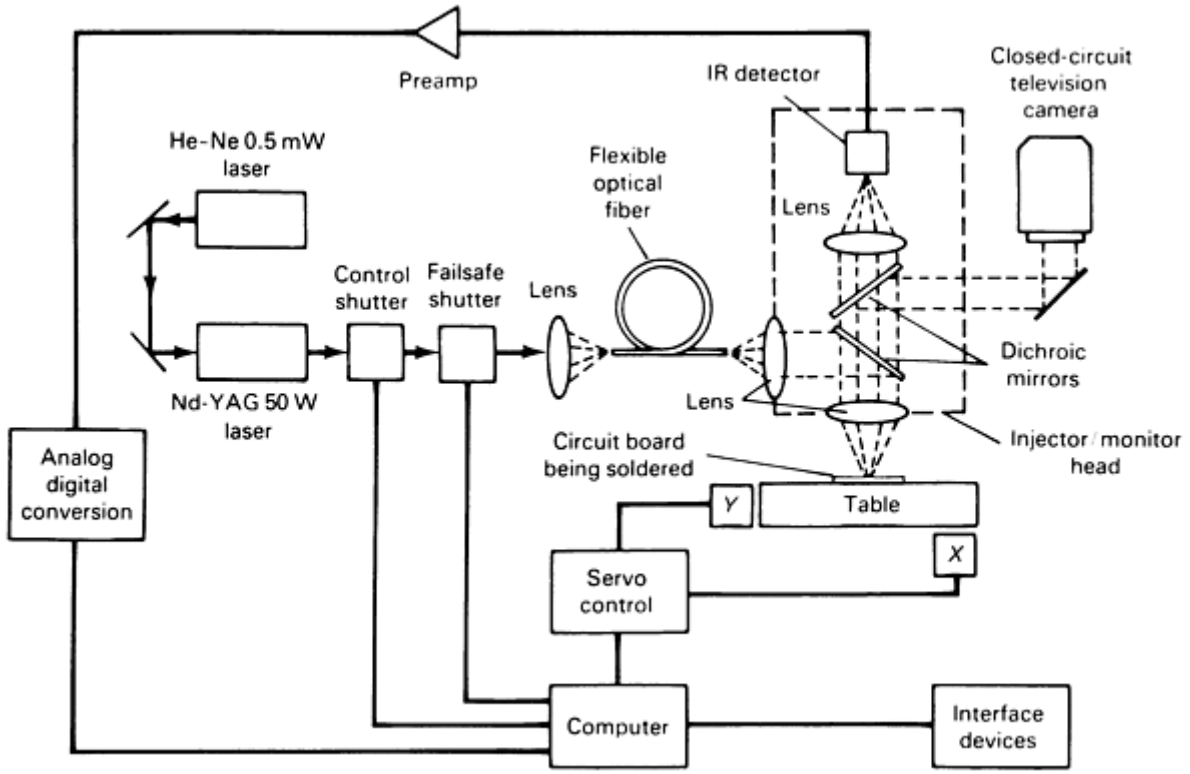

FIG. 1 SCHEMATIC OF INTELLIGENT LASER SOLDERING SYSTEM

The output of the IR detector is an analog signal that depicts, in real time, the radiation history of a spot on the surface of the solder joint during fabrication. This signal, called the "infrared signature" of the joint, is unique for every joint. The amplitude of the signal records the thermal radiation of the joint as it first rises during the heat injection by the laser and then as it decays after the laser is shut off. After the IR signature is turned into digital form, it is forwarded to the computer, which watches for the dip in the amplitude of the signal radiated by the joint, which pinpoints the transition from a solid to a liquid phase. At this point, the computer decreases the power of the laser for several milliseconds (the "dwell" phase) to allow adequate thermal soaking of the substrate. The laser is then turned off to allow the joint to quickly cool down to ambient temperature.

Figure 2 shows the theoretical signature of a typical good joint. The top curve is the radiation signal, as seen by the detector, and the lower curve is the temperature of the joint at each corresponding point in time. The sharp peak of the upper curve signals, with unequivocable precision, the instant when melting begins, so that the computer can initiate the laser control sequence, thus making it impossible to either overheat or underheat the joint. The resulting joint is free from defects such as excess intermetallics, nonreflowed solder, voids, cracks, or substrate damage.

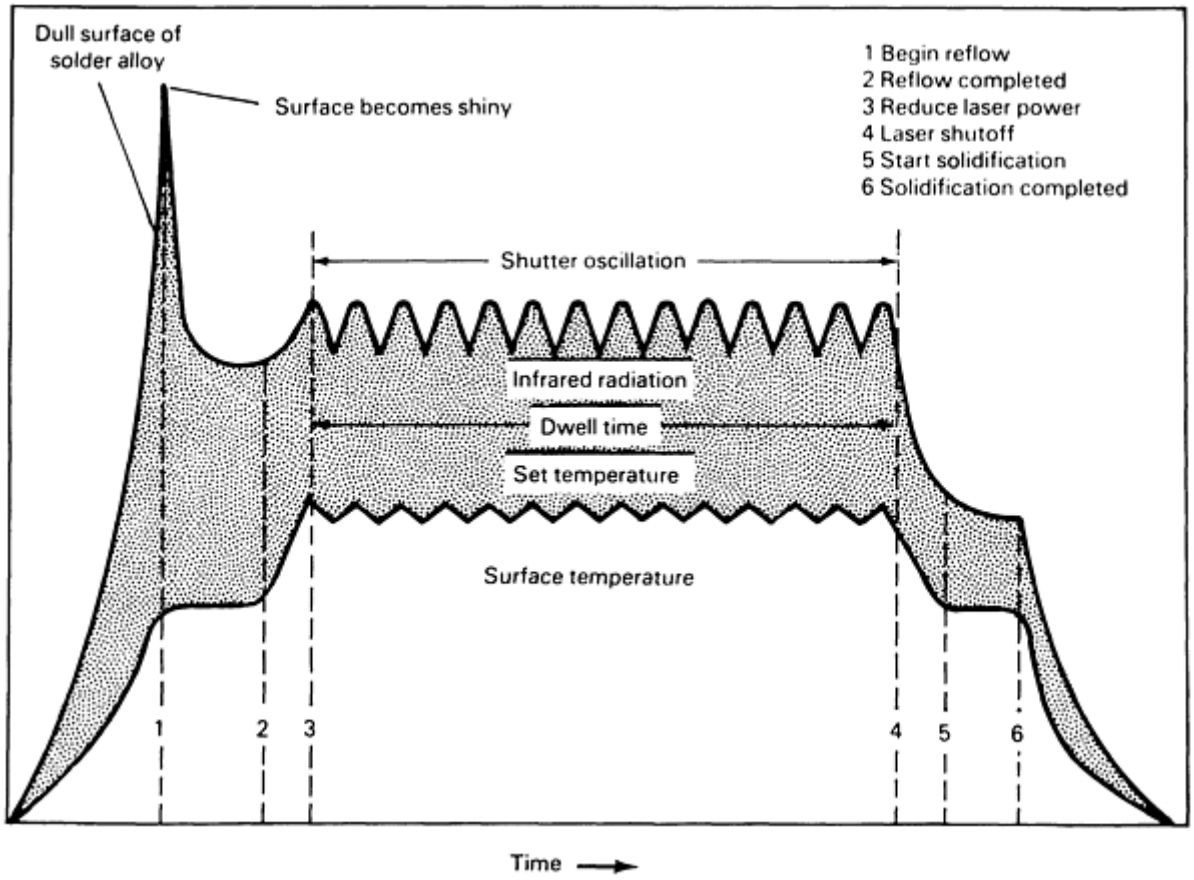

FIG. 2 THEORETICAL SIGNATURE OF A TYPICAL GOOD SOLDER JOINT

Key attributes of intelligent laser soldering are:

- *REPEATABILITY:* GOOD FOR ANY TARGET
- *SPEED:* FAST, WHEN COMPARED WITH ANY OTHER SOLDERING AND INSPECTION SYSTEM, BECAUSE THE IR SIGNATURE IS THE INSPECTION CERTIFICATE, AND IS AVAILABLE SIMULTANEOUSLY WITH THE COMPLETION OF THE JOINT
- *QUALITY:* GOOD FOR ANY TARGET
- *COST:* INEXPENSIVE, WHEN COMPARED WITH THE COST OF THE TWO SYSTEMS IT REPLACES, THAT IS, SOLDERING AND INSPECTION
- *SAFETY:* CRITICAL, BECAUSE SERIOUS BURNS AND EYE DAMAGE CAN RESULT UNLESS SPECIAL PRECAUTIONS ARE USED
- *FLEXIBILITY:* EXCELLENT, BECAUSE NO MATTER HOW DIFFERENT THE JOINTS ARE FROM ONE ANOTHER, EACH RECEIVES A CUSTOM DOSE OF THE LASER HEAT NECESSARY FOR OPTIMUM RESULTS

Hot Gas Soldering

Michael D. Frederickson, Electronics Manufacturing Productivity Facility

Introduction

HOT GAS SOLDERING is a process that is commonly used in applications where the workpiece thermal mass is small and the melting temperature of the solder is relatively low. The efficiency of heating large-mass substrates with hot gas is low, when compared with radiative or conductive methods of heating. The electronics industry utilizes hot gas soldering to reflow or melt solder in localized areas on circuit assemblies. A common application is the reworking or removal of electronic components.

Michael D. Frederickson, Electronics Manufacturing Productivity Facility

Process Characteristics

Characteristics of hot gas heating that are critical to its effectiveness in soldering are:

- FOCUS OF GAS FLOW
- GAS FLOW RATES (VELOCITY AND VOLUME)
- TEMPERATURE CONTROL
- GAS MEDIA OR CONSTITUENT

The focus of gas flow defines the area of localized heating, determines the efficiency rate of heating a defined area, and controls the excessive heating of adjacent areas. In most electronic applications, because the areas that need to reach the solder melting temperature are relatively small, confining thermal energy to a small area is critical. The focus of gas flow is usually controlled via nozzle design or the use of baffle plates. The nozzle collimates the gas stream to optimize the gas impingement across one or more solder interconnects, whereas the baffle plates attempt to block the gas from impinging on adjacent areas or on a component body directly. Common nozzle materials are stainless steel or quartz glass.

Gas flow rates primarily determine heat transfer efficiency (that is, the temperature and heating rate of the workpiece) and may affect the total area being heated. Insufficient gas flow will reduce the efficiency of thermal energy transfer, whereas excessive gas flow will disperse heat across the assembly, which may result in the overheating of adjacent areas. On some hot gas soldering systems, the flow rates are adjustable in both volume and velocity and can be used to establish the most appropriate heating profile for soldering. The selection of optimum flow rates usually depends on the gas temperature selected for the soldering process and on the size of the openings in the nozzle, as well as the configuration of the workpiece or circuit board.

The gas temperature also affects the heat transfer efficiency and ultimately the time required to form the solder interconnect. Typically, the gas is heated by passing it through a set of resistive heating elements. The usual temperature of interest for soldering process control is the temperature at the exit aperture of the nozzle. Because air is a poor heat conductor, the gas temperature will fall off rapidly as the distance from the nozzle to the solder interconnect increases. In electronics applications, the component body tends to heat more rapidly than the actual interconnect; therefore, excessive nozzle-exit temperatures with a high flow rate may thermally damage components or circuit boards.

Typical gas media used in hot gas soldering are air, nitrogen, and a nitrogen-hydrogen mix ($75N_2$-$25H_2$). Air is the most common gas used because of its ready availability and low cost. Nitrogen is sometimes used to minimize the oxidation of the component and board metallizations and to potentially improve solder wetting performance and interconnect reliability. In some cases, a nitrogen-hydrogen mixture is used to capitalize on its lower density relative to air. The lighter gases allow for the same heat transfer performance and inert nature, while reducing the force of the gas against the area being soldered. This reduction in the force of the gas decreases the dispersive effects upon impingement. In addition, some no-clean flux materials perform better in an inert atmosphere, such as nitrogen, during the soldering process.

Hot Gas Soldering

Michael D. Frederickson, Electronics Manufacturing Productivity Facility

Process Parameters

Heating profiles are established in hot gas soldering by using a combination of gas flow rates, gas temperatures, and time. Some systems use lower flow rates and higher temperatures, whereas others use higher flow rates and lower temperatures. The actual selection of flow rates and temperatures depends on the physical and dimensional characteristics of the item being soldered, as well as component mounting density. Figure 1 illustrates a thermal profile of a component being soldered and the temperature across adjacent components.

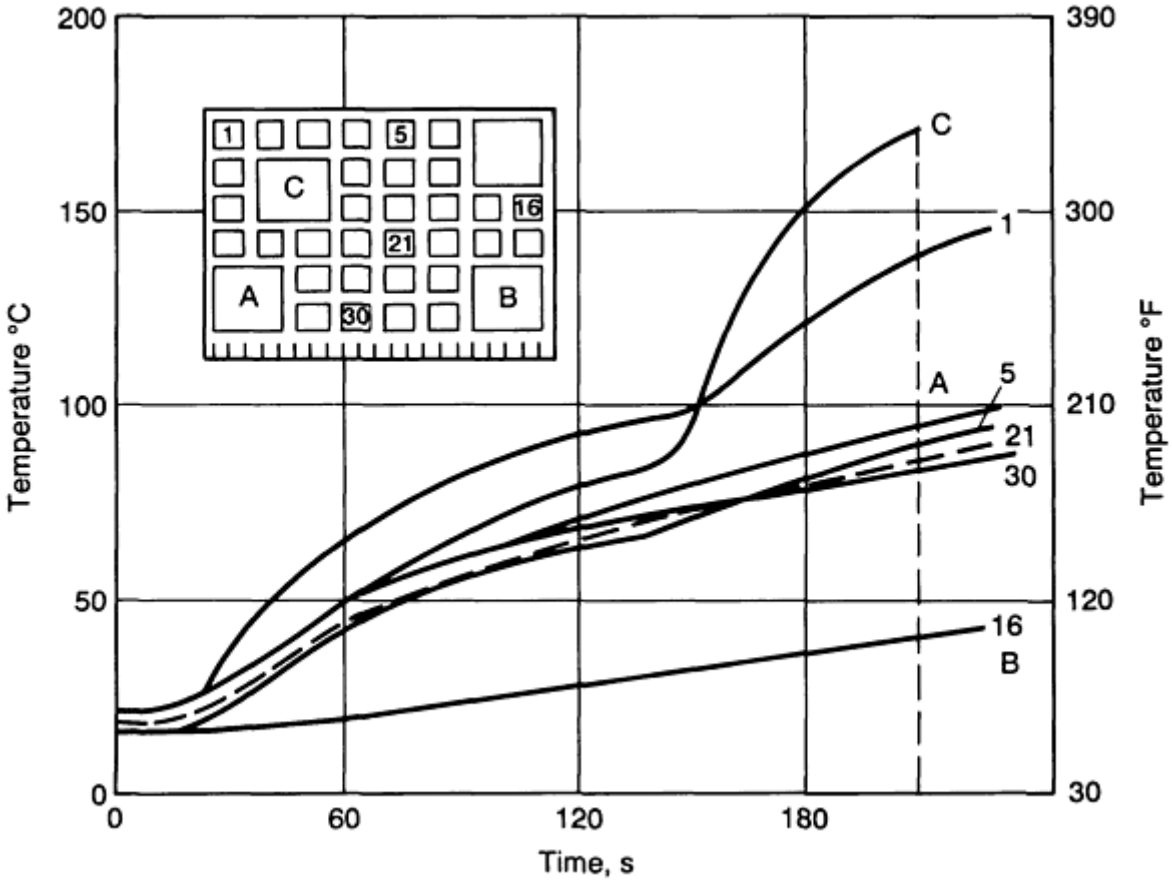

FIG. 1 TIME-TEMPERATURE RELATIONSHIP OF COMPONENT BEING SOLDERED (LINE C) AND ADJACENT COMPONENTS (LINES A AND B). LOCATIONS OF SPECIFIC SENSOR COMPONENTS ARE SHOWN IN INSET DIAGRAM.

Reliability concerns do exist when hot gas soldering techniques are used in electronics assembly. There is a potential for solder joint fracture when melting or reflowing a portion of a multi-leaded component. Fractures in solder joints occur when the joints are thermally cycled in use because of the induced stress caused by partially reflowing the component. If the hot gas process excessively heats adjacent components, causing a percentage of the interconnects on a component to reflow, then a residual stress may be established, which can significantly reduce the overall fatigue life of the solder interconnects. Therefore, gas flow rates and focus are critical to the overall reliability of the solder interconnects. The use of properly maintained equipment and trained operators should minimize these concerns.

Processing concerns also exist when using hot gas soldering in electronics assembly. Because this technique has inefficiencies relative to conductive and radiative methods, it is difficult to reflow solder joints that have large heat sinks. Therefore, an additional heating process may be needed to reduce the total hot gas heat energy required to reflow the solder interconnects. There are four methods of preheating the assemblies: oven bake, diffused hot gas, radiant, and conduction (edge rail or hot plate) heating. All methods are effective. However, the working time of assemblies preheated in an oven is very short. The selection of the preheating technique depends on the physical characteristics of the assembly being soldered and on the process equipment.

Hot Gas Soldering

Michael D. Frederickson, Electronics Manufacturing Productivity Facility

Selected References

- C. LEA, *A SCIENTIFIC GUIDE TO SURFACE MOUNT TECHNOLOGY,* ELECTROCHEMICAL PUBLICATIONS LIMITED, 1988
- "SURFACE MOUNT REPAIR STUDY," TECHNICAL REPORT TP60-07073, NAVAL SURFACE WARFARE CENTER, 1991
- R.S. WASSINK, *SOLDERING IN ELECTRONICS,* ELECTROCHEMICAL PUBLICATIONS LIMITED, 1989

Induction Soldering

Paul T. Vianco, Sandia National Laboratories

Introduction

INDUCTION OR (RADIO FREQUENCY) HEATING is a versatile means of providing heat to the joint area. Heating is caused by electrical resistance to eddy currents induced in the workpiece. These currents are induced by the rapidly changing magnetic field generated by a coil supplied with an alternating current. The eddy currents are generated at the surface of the workpiece (skin effect) and diminish toward the interior. The depth of direct heating by eddy currents depends on the electromagnetic properties of the workpiece material, the frequency of the alternating current (higher frequency results in shallower penetration depth), and the power level of the magnetic field (i.e., the current in the coil).

The advantages of induction heating include the ability to supply heat uniformly over the entire joint area while maintaining a localized temperature rise so heat sensitive materials or devices neighboring the joint are not damaged. Induction heating is a compromise between global heating processes such as furnaces, which warm the entire part, and more concentrated heat sources, such as torches or soldering irons, which warm only a very localized area. A second advantage of induction heating is that the temperature rise can be very rapid, thereby limiting heat loss into the workpiece, oxidation of the substrate, and thermal degradation of the flux. Limitations that must be considered with the application of induction heating are the cost of the equipment and the need for specially trained personnel. These personnel are needed to ensure proper equipment setup so that efficient transfer (coupling) of energy between the coil and the workpiece take place.

In the induction process, heat energy is not delivered to the workpiece; instead, it is generated within the material by electromagnetic field coupling between the workpiece and the alternating current in the coil (i.e., the workpiece and the coil form an inductance-capacitance-resistance circuit with the power supply).

Acknowledgement

This work was performed at Sandia National Laboratories and supported by the U.S. Department of Energy under contract DE-AC04-76DP00789.

Induction Soldering

Paul T. Vianco, Sandia National Laboratories

Coupling Efficiency

The coupling efficiency is optimized over a narrow range of operating parameters (frequency, coil turns, coil proximity, etc.) per the given workpiece parameters (electromagnetic properties and part geometry). The first consideration regarding the use of induction heating in a soldering operation is the electrical and magnetic properties of the materials to be joined. First, the energy coupling is more efficient in ferromagnetic materials, that is, materials with large magnetic permeability values (e.g., iron, low-carbon steels, nickel, etc.). Permeability being the same, materials with higher electrical resistivity heat more efficiently than low-resistivity materials. Therefore, heating efficiency is optimized by joints having metals with large permeability and high electrical resistance as opposed to low-permeability, low-resistance metals (e.g., copper, brass, or aluminum). Figure 1 illustrates the energy input required to bring several ferrous and nonferrous materials to 188 °C (370 °F) (Ref 1). These differences become especially critical when joining dissimilar materials, where one part may heat up more quickly than the other.

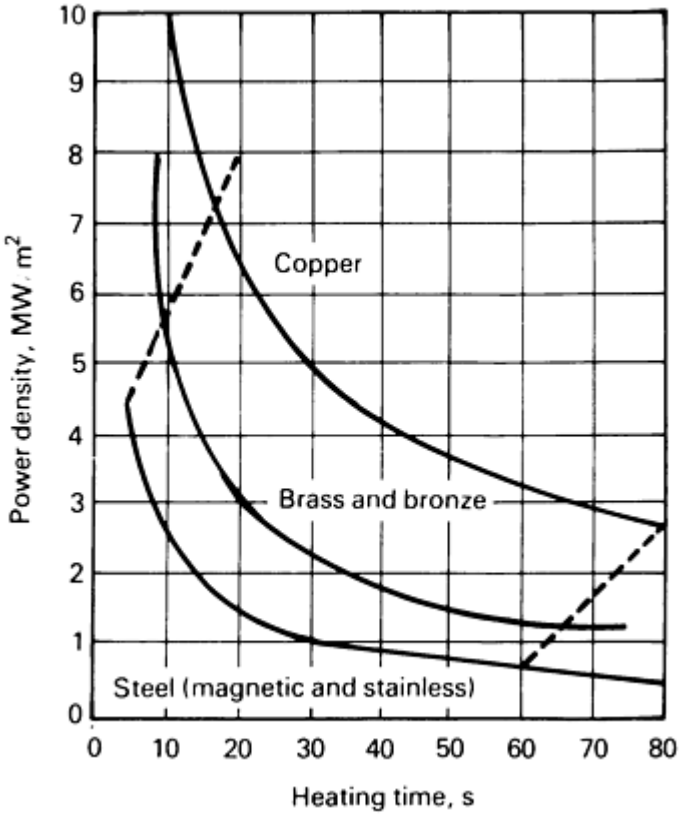

FIG. 1 POWER INPUTS AND HEATING TIMES FOR SELECTED FERROUS AND NONFERROUS MATERIALS. SOURCE: REF 1

Resistivity Effects. The coupling efficiency changes as the material warms up due to the temperature dependence of the electrical and/or magnetic properties. Resistivity increases with temperature for most metals and is the most important concern in nonmagnetic materials. Table 1 shows the resistivity changes in materials over the typical range of soldering temperatures. Unfortunately, changes to the overall coupling efficiency (and therefore heating rate) caused by resistance changes are not easily predicted because part geometry and penetration depth of the electromagnetic field have a synergistic effect.

TABLE 1 RELATIONSHIP OF TEMPERATURE TO ELECTRICAL RESISTIVITY, THE PRODUCT OF SPECIFIC HEAT AND MATERIAL DENSITY, AND THERMAL CONDUCTIVITY FOR SELECTED MATERIALS

TEMPERATURE		ELECTRICAL RESISTIVITY (ρ), 10^{-6} Ω· M	PRODUCT OF SPECIFIC HEAT AND MATERIAL DENSITY ($C\gamma$), 10^{6} W · S/M^3 · K	THERMAL CONDUCTIVITY (K), W/M · K
°C	°F			
MILD STEEL (0.23% C)				
20	68	0.160	3.65	52.0
100	212	0.220	3.85	51.0
200	392	0.290	4.10	49.0
300	572	0.380	4.40	46.0
400	752	0.483	4.77	43.0
500	932	0.610	5.19	39.3
STAINLESS STEEL (19.11% CR, 8.14% NI, 0.60% W)				
20	68	0.695	4.04	15.9
100	212	0.776	4.15	16.3
200	392	0.850	4.24	17.2
300	572	0.915	4.36	18.0
400	752	0.976	4.51	19.7
500	932	1.030	4.83	21.4
COPPER				
20	68	0.017	3.39	395
100	212	0.022	3.48	387
200	392	0.033	3.57	380
300	572	0.037	3.65	373
400	752	0.044	3.72	366
500	932	0.052	3.77	360
ALUMINUM				
20	68	0.027	2.52	211
100	212	0.0364	2.59	219
200	392	0.0478	2.65	224
300	572	0.0599	2.71	223
400	752	0.073	2.78	216
500	932	0.087	2.84	209

Source: Ref 1

Curie Temperature Effects. In magnetic materials, a significant reduction in coupling efficiency occurs when the material passes through its Curie temperature upon heating (i.e., changes from ferromagnetic to paramagnetic). Curie points for iron and nickel are 770 °C (1418 °F) and 358 °C (676 °F), respectively (Ref 2). Clearly, only nickel would be of concern at soldering temperatures. The magnitude of the coupling loss depends strongly on the geometry of the part and the coil configuration. Lost coupling efficiency due to resistance or magnetic property variations can be regained by changes to the power supply frequency during the soldering procedure. However, in the case of the Curie transition, the exceptional heating rate of ferromagnetic materials can never be wholly recovered.

Temperature rise in the workpiece is also affected by the thermal mass of the part(s) as reflected by thermal conductivity, specific heat, and size of the part. Heat loss from the joint area due to thermal conductivity as well as excessive part size can lengthen heating times, making it difficult to uniformly heat joints containing dissimilar metals. Thermal mass is often expressed quantitatively by the product of the specific heat (c) and the material density (γ). Values of $c\,\gamma$ are given in Table 1.

References cited in this section

1. P. SIMPSON, *INDUCTION HEATING*, MCGRAW-HILL, 1960
2. F. LOBKOWICZ AND A. MELISSINOS, *PHYSICS FOR SCIENTISTS AND ENGINEERS*, SAUNDERS CO., 1975, P 355

Induction Soldering

Paul T. Vianco, Sandia National Laboratories

Workpiece Geometry

Induction heating is more efficient and more easily practiced on workpieces with simple, axis-symmetric geometries because they, in turn, require simple coil geometries. Electromagnetic energy is more easily coupled into the part due to closer proximity to the workpiece and the generation of a more uniform magnetic field. Uniformity, as well as field strength, improves as the number of turns in the coil is increased. A larger coil also provides a more uniform field but at the expense of delocalizing the heating area. Some sample coil configurations for typical part geometries are shown in Fig. 2. Finally, uniform heating of the workpiece can be achieved in relatively nonuniform magnetic fields by rotating the part within the coil.

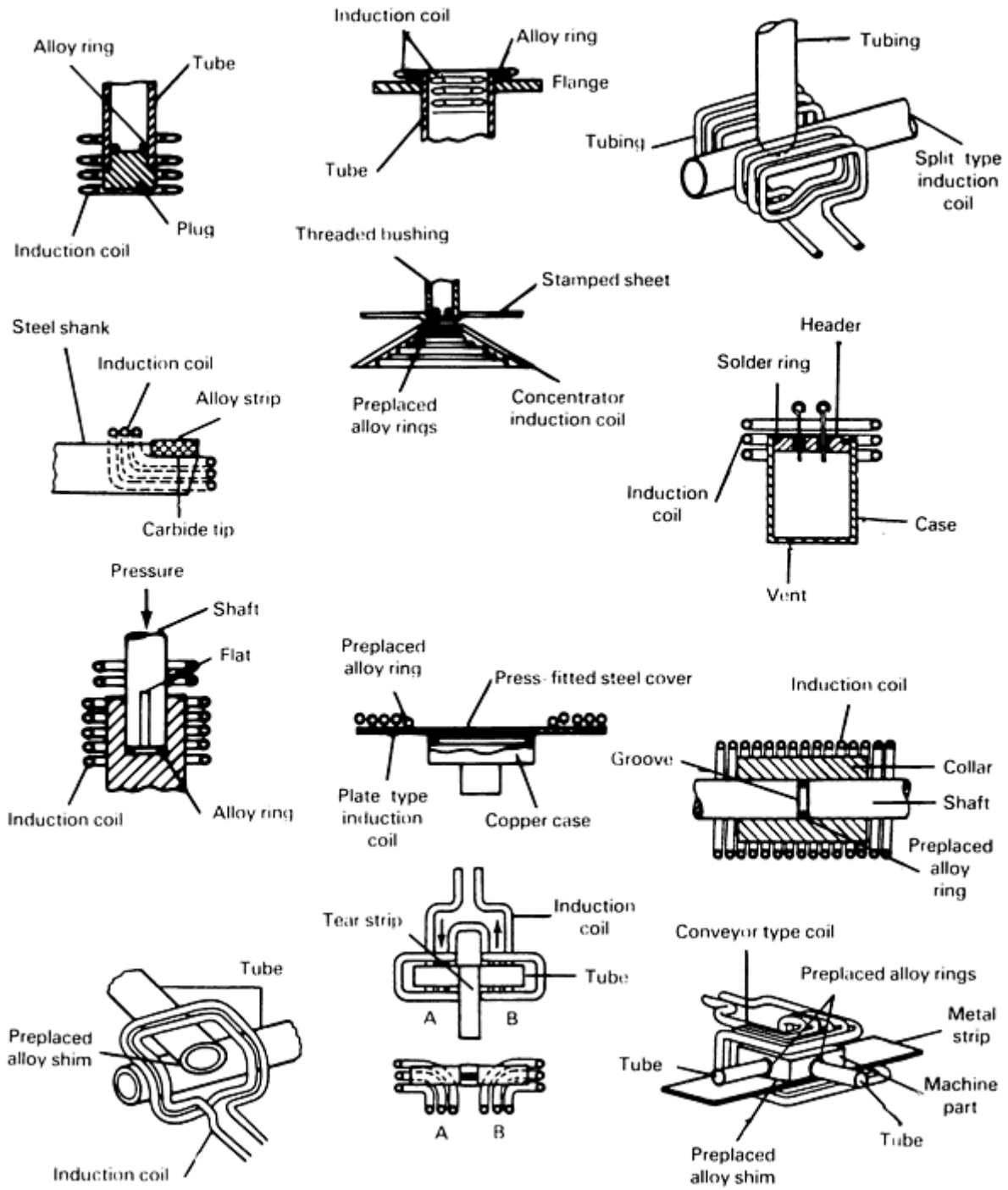

FIG. 2 COIL CONFIGURATIONS FOR TYPICAL JOINT SHAPES. SOURCE: REF 1

Use of induction heating becomes more limited as the workpiece geometry becomes complex. First, the placement of the coils about or near the joint area becomes more difficult. Secondly, corners and protrusive shapes in the magnetic field may develop hot spots caused by proximity to the coil or low thermal mass, thereby possibly damaging the material at those locations. To accommodate complex part configurations, coil shapes can be altered to vary the local magnetic field strength and hence change the localized heating of the part. For example, the overheating of a corner or protrusion can be reduced by locally decreasing the number of coil turns in that area or by positioning the coil farther from the workpiece. The opposite actions apply to part configurations with large thermal mass that require additional power input to prevent heat-sinking effects.

In addition to surrounding the part with the coil to maximize coupling, coils can be used as proximity sources for localized heating. In this technique, a coil (typically smaller than the part) is located next to the joint area to be heated. As

expected, the limited magnetic field intensity causes this technique to have very low coupling. The heating area can be extended by manually scanning the coil over a larger area (such as is done in torch heating).

Reference cited in this section

1. P. SIMPSON, *INDUCTION HEATING,* MCGRAW-HILL, 1960

Preplaced Solder

Soldering by induction heating necessarily implies joints designed for the use of solder preforms or paste; these items are introduced into the joint area prior to applying heat. The amount of solder is much less than the mass of the parts, so the effect of the preform on the induction heating process is typically negligible. Space restraints, as well as the danger of electrical shock and severe burns, prohibit manual interaction with the workpiece during heating. Therefore, certain practices associated with the use of preplaced solder must be followed:

- AN ADEQUATE SUPPLY OF SOLDER ALLOY MUST BE PRESENT TO COMPLETELY FILL THE GAP.
- PROVISION MUST BE MADE FOR SOLDER FLOW THROUGH THE JOINT AND THE ESCAPE OF FLUX VOLATILES FROM THE JOINT.
- DESIGN CONSIDERATIONS MUST ALLOW FOR AN INCREASED PROPENSITY OF VOID FORMATION DUE TO LIMITED CAPILLARY FILL WITH PREPLACED SOLDER.
- FIXTURING THAT SECURES THE WORKPIECE DURING SOLDERING MUST MAINTAIN SUBSTRATE ALIGNMENT AND THE JOINT GAP SPECIFIED FOR THE FINAL PRODUCT.

Wetting of the parts can be enhanced by hot solder dipping or by electroplating a coating of tin-lead solder on the joint surfaces prior to final assembly. Although typically performed in air, induction soldering can also be practiced in inert atmospheres or in vacuum (e.g., localized cover gas blankets or more sophisticated equipment such as glove boxes and large chambers). Induction heating is well suited for robotic automation, including bench-top systems as well as larger-scale factory production lines. Monitoring the workpiece temperature by optical pyrometry can provide a feedback signal for real-time control of the induction power source, thereby improving reproducibility of the heating schedule parameters.

Induction Soldering

Paul T. Vianco, Sandia National Laboratories

Setup Parameters

The heating requirements of some simple workpiece geometries (and accompanying simple coil geometries) have been calculated, and performance parameters have been tabulated in charts (Ref 1). However, maximizing the energy coupled into a particular workpiece is more often the result of trial-and-error experiments with coil configurations, power supply frequency, and voltage. Nonoptimum coupling causes greater current to be drawn from the power supply to achieve the desired heating of the part, possibly exceeding the power capacity of the generator. Joints between dissimilar metals further lessen optimum coupling and diminish efficiency.

Although induction heating may require some trial-and-error efforts to optimize the process for a given product, some preliminary calculations can provide approximate design criteria from which to begin process development.

The first parameter required to set up an induction system is the power required to heat the workpiece(s). For localized heating, heat is lost to the remaining mass of the part as well as through radiation, conduction, and convection with the atmosphere. For a first-order approximation, ambient heat loss can be neglected, particularly with the relatively low temperatures necessary for soldering processes. However, conduction into the solid away from the joint area can be significant; moreover, the calculations to quantify the effect may be very complex. An estimate of the power, ***P***, required to heat a section of material can be determined from:

$$P = \frac{g\,c\Delta TV}{t} \qquad \textbf{(EQ 1)}$$

where V is the volume to be heated, c is the specific heat of the material, ΔT is the temperature rise, γ is the density of the material, and t is the time for the temperature increase to take place. Of course, the power rating of the induction heating equipment must be higher than that calculated in Eq 1 to account for coupling inefficiencies and the heat loss mechanisms noted above. The overall efficiency of induction heating nonferrous metals is 50 to 75%. Values are approximately 75% for magnetic metals that are below the Curie temperature (i.e., in the ferromagnetic state).

Selection of a power frequency depends on the type of soldering material and the size of the workpiece. Table 2 gives typical frequencies for the through-heating of nonferrous metals. The representative geometry is that of round bar. A similar range of values can also be used for magnetic materials below the Curie temperature. Heating the material above the Curie point requires a frequency increase to maintain reasonable power coupling, particularly as the part size increases (power input to the workpiece is proportional to the square root of the frequency). Frequency values at temperatures exceeding the Curie point are 3 to 10 kHz for part sizes of 5 to 40 mm (0.20 to 1.6 in.) diameter and 1 to 3 kHz for diameters of 40 to 150 mm (1.6 to 5.9 in.).

TABLE 2 FREQUENCIES FOR THE THROUGH-HEATING OF NONFERROUS METAL ROUND BARS

BAR DIAMETER		FREQUENCY, KHZ
mm	in.	
0-12	0-$\frac{1}{2}$	450
12-25	$\frac{1}{2}$-1	10 AND 3
25-75	1-3	1
>75	>3	50

A parameter of particular interest to induction heating is the penetration depth of heating (also called the skin depth), and this is denoted by the symbol δ. The skin depth is defined as the position in the solid away from the surface at which the magnitude of the magnetic field falls to approximately 37% of its value at the part surface. The skin depth is given by:

$$d = \frac{r}{pm\,f} \qquad \textbf{(EQ 2)}$$

where ρ is the resistivity of the part, $\rho$is the absolute magnetic permeability, and f is the frequency. The absolute permeability is equal to the product $\mu_r\mu_0$, where μ_r is the relative permeability of the material (e.g., pure iron = 18,000 and nonmagnetic copper = 1) and μ_0 is the permeability of "free space," which equals 1.257×10^{-6} V · s/m · A (a universal constant). Skin depth increases as the material resistivity increases and as the frequency decreases. For magnetic materials at temperatures below the Curie point, the value of μ_r is not a constant; it is dependent on the magnetic field intensity, H_0. For example, the value of μ_r for a low-carbon 1044 steel is $734{,}000/H_0^{0.92}$.

Reference cited in this section

1. P. SIMPSON, *INDUCTION HEATING*, MCGRAW-HILL, 1960

Reference cited in this section

1. P. SIMPSON, *INDUCTION HEATING*, MCGRAW-HILL, 1960

Induction Soldering

Paul T. Vianco, Sandia National Laboratories

Safety Concerns

The safety hazards accompanying the use of induction heating include electrical shock from contact with the coils as well as burns caused by the heated workpiece. A third hazard is the danger of steam explosion caused by arcing between the coil and the part. Typically, the heating coils are hollow copper tubing; they are cooled by the internal flow of water or a water-base coolant. The vapor cloud accompanying the spatter of flux during soldering can cause an electric arc that may puncture the copper tubing if the induction coil is close to the workpiece. Arcing can also be caused by movement of the coil windings through forces generated by the magnetic field. Water contacting the hot part produces an immediate, violent steam explosion. To prevent this occurrence, adequate clearance should be maintained between the coil and the part (typical minimum spacing is 6.4 to 13 mm, or 0.25 to 0.50 in.). Moreover, trial heating runs, in which the current is slowly increased to assess coil movement and part-to-coil shorting, should be performed prior to product assembly.

Induction Soldering

Paul T. Vianco, Sandia National Laboratories

References

1. P. SIMPSON, *INDUCTION HEATING*, MCGRAW-HILL, 1960
2. F. LOBKOWICZ AND A. MELISSINOS, *PHYSICS FOR SCIENTISTS AND ENGINEERS*, SAUNDERS CO., 1975, P 355

Wave Soldering

Paul T. Vianco, Sandia National Laboratories

Introduction

WAVE SOLDERING is one of the primary techniques for mass assembly of printed wiring boards involving through holes, surface mount devices, or a combination of these two technologies. A schematic of the wave soldering process is shown in Fig. 1. A solder "fountain" or "wave" is created by a pump located at the bottom of the solder pot; suitable baffles are mounted in the pot to direct the flow of solder into the desired configuration. The printed wiring board is placed onto a conveyor, which brings it into contact with the wave surface. Note from Fig. 1 that the circuit boards travel along the surface of the solder; molten alloy does not flow on top of the board. As the printed circuit board passes on the wave, the solder wets the surface-mount package leads, terminations, and exposed metal surfaces in the circuit board, and also fills plated through holes. This technique can produce several thousand solder joints in a matter of minutes.

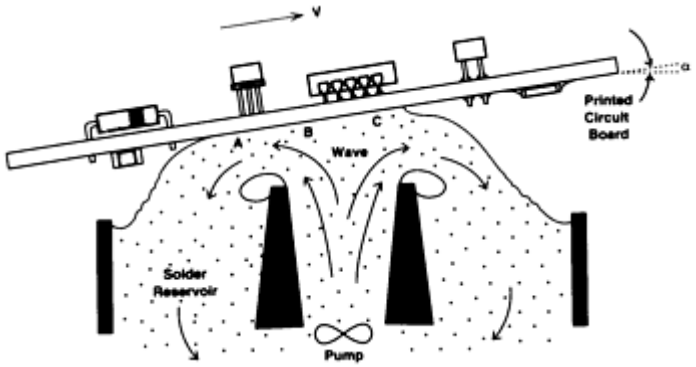

FIG. 1 SCHEMATIC OF THE WAVE SOLDERING PROCESS. THE THREE IMPORTANT PROCESS CONTROL REGIONS ARE THE ENTRY (A), THE INTERIOR (B), AND THE PEEL-BACK REGION (C).

The implementation of wave soldering for surface-mount technology requires that the devices be glued to the substrate prior to wave soldering. Moreover, the entire surface-mount package must be able to withstand contact with the flux and temperatures of the molten solder without a loss of reliability. Small-outline transistors and discrete components (chip resistors, capacitors, etc.) are readily attached by wave soldering; larger packages (e.g., leaded or leadless chip carriers) may be damaged by exposure to the harsh environments (flux and molten solder) as well as be more prone to solder defects (Ref 1).

The wave soldering technique encompasses a sequence of processes, all of which are typically contained in the same apparatus. First, the substrate receives a coating of flux. Flux application methods include:

- A WAVE TECHNIQUE SIMILAR TO THAT SHOWN IN FIG. 1
- COATING THE CIRCUIT BOARD BY A FLUX FOAM CREATED BY PASSING AIR OR NITROGEN THROUGH A FLUX BATH TO GENERATE THE FOAM (OR FROTH) ON THE BATH SURFACE
- DIRECTLY SPRAYING THE FLUX ONTO THE BOARD SURFACE

After flux is applied, the substrate is passed through a preheating stage. Warming the board promotes activation of the flux, accelerates the evaporation of volatiles from the flux (which can cause voids and solder balls by spattering upon contact with the hot solder bath), and reduces thermal shock to the substrate and devices when it passes onto the solder wave. Then, the circuit board contacts the solder wave for the formation of the joints. After passing the wave, the board cools through natural heat loss or, more quickly, by the use of forced air.

Acknowledgement

This work was performed at Sandia National Laboratories and supported by the U.S. Department of Energy under contract DE-AC04-76DP00789.

Reference

1. R. PRASAD, *SURFACE MOUNT TECHNOLOGY: PRINCIPLES AND PRACTICES*, VAN NOSTRAND-RHEINHOLD, 1989, P 426-428

Paul T. Vianco, Sandia National Laboratories

Design Considerations and Process Parameters

The successful assembly of a printed circuit board by the wave soldering technique relies on the proper process parameters and the layout of the board for the respective technology (through-hole, surface-mount, or mixed). The hole or via size (diameter) must permit adequate capillary filling by the molten solder and form the joint or to interconnect within the short time period (5 to 7 s) that the board contacts the wave. Holes with small diameters (<0.076 mm, or 0.003 in.) and long length joints with very thin gaps restrict the elimination of flux volatiles, causing voids and insufficient solder quantity. Excessively large holes (>1.0 mm, or 0.039 in.) and gaps (>0.40 mm, or 0.016 in.) decrease the capillary driving force of the solder to fill the volume and create the joint; in some cases, the solder simply drains from the hole under its own weight.

In addition to insufficient solder in holes and vias, other defects in wave-soldered products include bridges, icicles, and skips. Bridges are defects in which a quantity of solder forms a short across two conductors (leads, lands, or traces). A piece of solder that does not short two conductors, but rather hangs from one surface, is an icicle. Skips refer to the failure of solder in the wave to reach the metal surface and form the joint.

Design Considerations

Design considerations, such as the orientation of through-hole leads and surface-mount devices with respect to the direction of travel past the wave, as well as the proximity of packages to 0one another, can dramatically affect yields (Ref 1, 2). Figure 2 is a diagram showing the preferred orientation of through-hole and surface-mount packages.

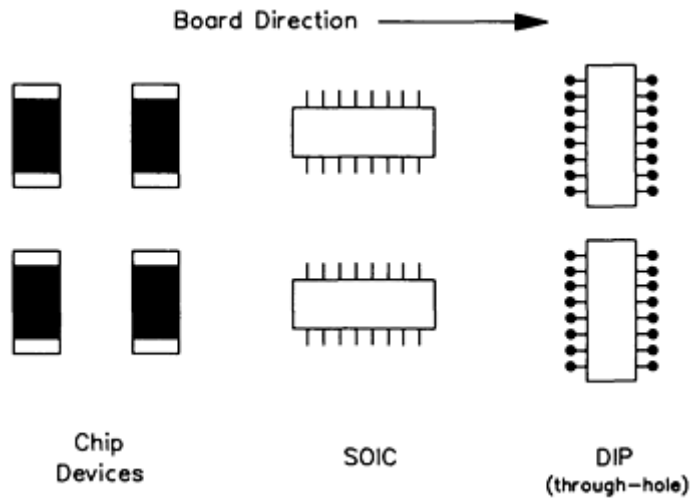

FIG. 2 SCHEMATIC OF PREFERRED DEVICE ORIENTATION FOR WAVE-SOLDERED ASSEMBLIES. SOIC, SMALL-OUT-LINE INTEGRATED CIRCUIT (SURFACE-MOUNT); DIP, DUAL-INLINE PACKAGE (THROUGH-HOLE)

Through-Hole Technology. In the case of through-hole assemblies, the leads on the side of a through-hole 16-pin dual-in-line package (DIP) should be oriented perpendicular to the travel direction of the conveyor to prevent bridging between them. Moreover, the bridging of leaded packages can be limited by maintaining the lead extension beneath the circuit board at less than 1.0 mm (0.039 in.). Leads that are too close to each other also increase the chances of solder bridges. Solder skips are less frequently observed on through-hole products (assuming adequate wettability of the metal surfaces) because the device package body is on the top surface, and therefore does not shadow joints from the wave.

Surface-Mount Technology. The circumstances of solder defect function are different for surface-mount technology because the entire package passes through the wave. Solder joint skips are more common because the package body can shadow nearby leads or terminations from contact with the wave, causing an inadequate supply of solder at the joint. Therefore, the joint areas of the package should be fully exposed to the wave, as suggested by Fig. 2. Packages with leads or terminations on all four sides experience an increased propensity for defects on the leads in the nonpreferred orientation. Also, the greater density of devices on surface-mount circuit boards increases the frequency of solder skips due to the closer proximity of the packages. Finally, the finer lead pitch used on surface-mount leaded and leadless (chip carrier) packages limits or prohibits their assembly on boards by wave soldering.

Process Parameters

The second factor critical to successful implantation of wave soldering of printed circuit boards is the process parameters. Process parameters can be divided into three groups: the fluxing operation, the solder wave properties, and the process schedule.

The fluxing operation not only includes the particular parameters (wave or foam height, spraying pressure, etc.) needed to ensure adequate flux supply to the board for solder wetting, but also the condition of the flux. In-line fluxing techniques (wave or foam) frequently use the same quantity of flux to process a large number of boards. Deterioration of the flux due to board contaminants, as well as loss of the flux vehicle, must be monitored to minimize defects in the final product. Specific gravity is used to indicate flux condition.

Low-solids fluxes are gaining popularity as a "no-clean" alternative to rosin-base fluxes, including their use in wave soldering. The low-solids contents (typically less than 5%) make these fluxes difficult to foam, so spray or wave applications are preferred (Ref 3). Tighter control of the flux chemistry, reduced solder pot temperatures (by 10 to 15 °C, or 18 to 27 °F), shorter solder dwell times (by 1 to 2 s), and the use of inert or reducing atmospheres (Ref 4) can reduce the number of defects.

Solder Wave Properties. The second process factor is the solder wave properties. The simple wave geometry (also called the T-wave) is shown in Fig. 1. Three regions of the wave are identified. The entry region (on the left with the board moving to the right) should be sufficiently turbulent to supply solder to all of the exposed metal surfaces and should permit the escape of flux volatiles that may cause voids in the joint. In the case of surface-mount assemblies, fluid motion must be sufficiently active to force solder close to the packages for adequate wetting of terminations and leads, thereby avoiding solder skips. The interior region of the wave acts as the heat source and solder supply to promote wetting of the substrate features. The exit or peelback region is the point at which the board leaves the wave and is critical in preventing solder bridge and icicle defects on the circuit board. For example, defects are reduced by having a smooth wave that separates very slowly from the board. This effect is achieved by matching the solder flow velocity with the speed of the circuit board (Ref 5) as well as by making adjustments to the wave configuration. Hot air knives positioned after the wave have been used to remove solder bridges and icicles prior to solidification of the solder.

Figure 3 shows several equipment modifications used to produce different wave geometries. The extended T-wave and lambda-wave modifications to the standard T-wave cause a smooth surface at the exit region to limit bridges, icicles, and the formation of excessive dross. The dual-wave configuration provides separate turbulent and smooth (laminar) waves to effect the desired solder joint qualities. Note that these modifications generally require that the circuit board laminate and devices withstand a longer period of contact with the molten solder.

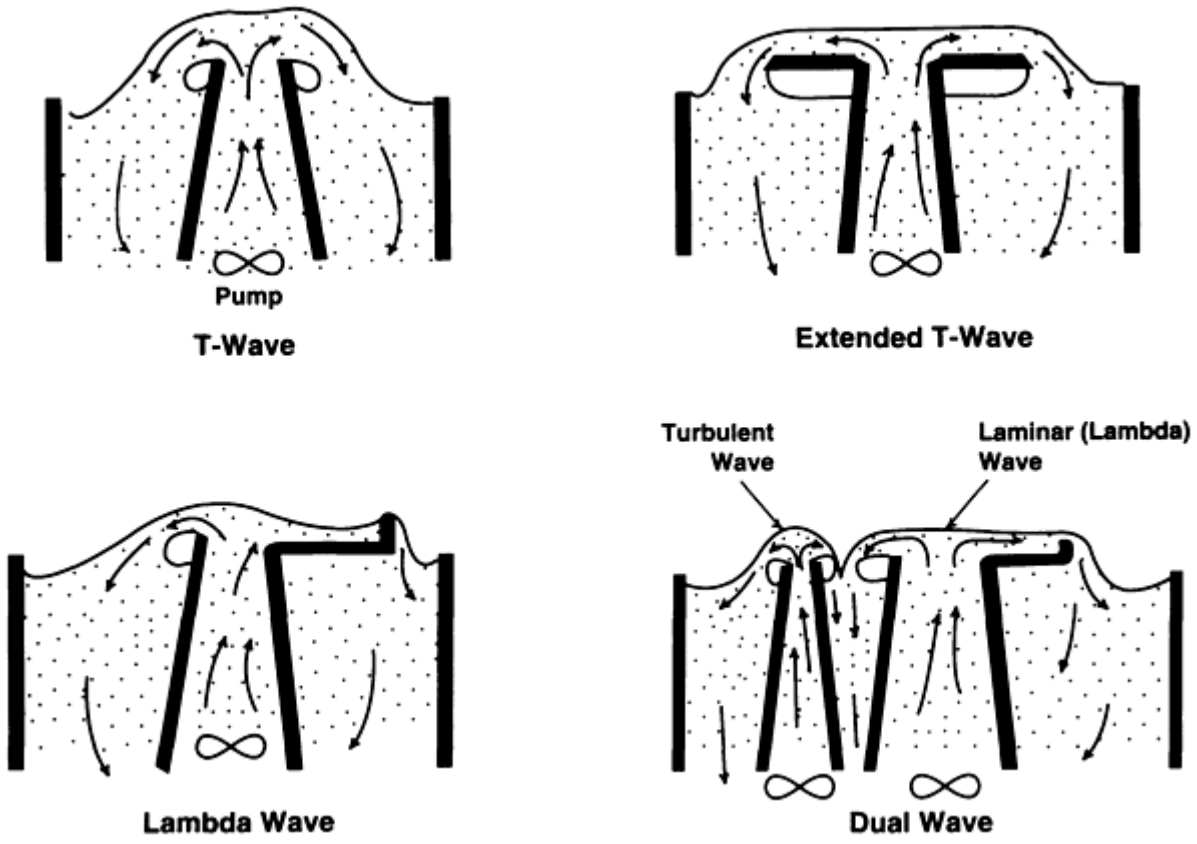

FIG. 3 EQUIPMENT MODIFICATIONS USED TO PRODUCE DIFFERENT WAVE GEOMETRIES. THE NOMENCLATURE DESCRIBES THE PROFILE GEOMETRY OF THE WAVE.

Dross formation tends to be high in wave soldering due to the large surface areas of solder exposed to the atmosphere (which is further aggravated by the turbulent flow of the solder in the pot). Dross particles can become embedded in the solder joints as well as disturb the peel back of the solder upon exiting the board. The use of inert atmospheres, reduced solder temperatures, and oils to cover the solder surface limit the formation of dross.

Solder temperatures are typically higher than those used in reflow processes. The higher temperatures are required to provide sufficient heat transfer to the substrate for adequate wetting as well as to reduce the solder surface tension to limit defects at the peel-back region. Solder pot temperatures are typically 50 to 80 °C (90 to 145 °F) above the liquidus temperature of the alloy; higher values are required for thicker substrates (e.g., multilayer or controlled-expansion substrates). The potential for damage to the laminate, including warpage and distortion as well as delamination of the conductor, increases with higher solder temperatures. Continuous processing with wave soldering equipment can cause a build-up of contaminants in the solder pot (e.g., nickel, copper, and gold from circuit board and lead finishes). See the article "Soldering in Electronic Applications" in this Volume for guidelines on acceptability limits for solder pot contamination.

In addition to the traditional tin-lead alloys, wave soldering has been adapted to other solders, including the eutectic tin-bismuth solder and the tin-lead-bismuth alloys (Ref 6).

Process Schedule. The third factor in the wave soldering technique is the process schedule, which includes the preheat zone temperature profile, the solder wave temperature, the conveyor tilt angle (α in Fig. 1, which affects the exit geometry of the board), and the conveyor speed. The conveyor speed determines the dwell time of the circuit board in the preheat zone and solder wave. Although specific settings depend on the type of equipment and the product being assembled, some general guidelines can be applied. First, the preheat stage should bring the board temperature to the range of 100 to 150 °C (210 to 300 °F). These temperatures provide suitable activation of the flux and lessen thermal shock to the circuit board (and devices) upon contact with the solder wave. The dwell time in the molten solder wave should be limited to 3 to 5 s. Dwell times at the molten solder temperature can reach 5 to 10 s for dual-wave systems. Time-temperature exposure limits for soldering processes are typically specified for devices and the laminate; manufacturer recommendations should

always be followed. Also, dwell times should be minimized to limit the leaching of conductor or lead finishes (e.g., copper, nickel, or gold) into the solder.

References cited in this section

1. R. PRASAD, *SURFACE MOUNT TECHNOLOGY: PRINCIPLES AND PRACTICES,* VAN NOSTRAND-RHEINHOLD, 1989, P 426-428
2. R. GENGLER AND J. HABIB, MINIMIZING DEFECTS IN THE MASS SOLDERING OF PRINTED WIRING ASSEMBLIES, *WESTERN ELECTRIC ENGINEER,* 1983
3. D. KOCKA, NO-CLEAN FLUXES ARE A VIABLE ALTERNATIVE TO CFC CLEANING,*ELECT. PACK. PROD.,* JUNE 1990, P 95
4. P. FODOR AND P. LENSCH, COVER GAS SOLDERING LEAVES NOTHING TO CLEAN OFF PCB ASSEMBLY, *ELECT. PACK. PROD.,* APRIL 1990, P 64
5. R. BOTHAM, C. LOWELL, AND J. STERRITT, WAVE SOLDERING MIXED TECHNOLOGY BOARDS, *ELECT. PACK. PROD.,* NOV 1990, P 28
6. M. NYLEN, K. JOSEFSON, AND H. STEEN, USE OF TIN-LEAD-BISMUTH ALLOY AS A SUBSTITUTE FOR EUTECTIC TIN-LEAD IN WAVE SOLDERING, *BRAZING AND SOLDERING,* SPRING 1988, P 38

Wave Soldering

Paul T. Vianco, Sandia National Laboratories

Defects

Certain defect trends can be identified with particular process conditions (Ref 7). For example, voids and blowholes are more frequent at fast conveyor speeds and higher solder temperatures. These process conditions generate an excessively fast heating rate, which causes the rapid volatilization of the flux components and subsequent void formation. Rapid conveyor speed can be responsible for several other defects:

- AN INCREASED PROPENSITY FOR POOR FILLING OF HOLES AND VIAS CAUSED BY INSUFFICIENT DWELL TIME IN THE SOLDER WAVE. AS A RESULT, THE WETTING KINETICS MAY NOT FILL THE VOLUME (THIS IS FURTHER EXAGGERATED BY LOW SOLDER TEMPERATURES)
- THE PRESENCE OF SOLDER BRIDGES AND ICICLES DUE TO POOR MATCHING OF THE SUBSTRATE SPEED AND FLOW OF THE SOLDER WAVE AT THE PEEL-BACK REGION UPON BOARD EXIT
- CRACKING OF SURFACE-MOUNT CERAMIC CHIP CAPACITORS CAUSED BY THERMAL SHOCK

High solder pot temperatures and slow conveyor speeds (i.e., long dwell times) can create difficult-to-remove flux residues. Also, excessive warpage or distortion of the board results from inadequate support of the substrate by the conveyor system; this is particularly acute with thinner laminates, higher soldering temperatures, or longer dwell times (e.g., dual-wave systems). Thicker circuit boards (backplanes) may also warp due to the large thermal gradients through the thickness of the laminate due to inadequate preheating of the board.

Clearly, the various process parameters can interact to produce certain defects. Therefore, optimization experiments and statistical process control are required to obtain and maintain acceptable product yields. The qualitative guidelines cited above provide a first measure of correlating defects to process conditions for subsequent improvement to the assembly procedure.

Reference cited in this section

7. C. LEA, *A SCIENTIFIC GUIDE TO SURFACE MOUNT TECHNOLOGY,* ELECTROCHEMICAL PUBLISHERS, LTD., 1988, P 148-153

Wave Soldering

Paul T. Vianco, Sandia National Laboratories

References

1. R. PRASAD, *SURFACE MOUNT TECHNOLOGY: PRINCIPLES AND PRACTICES,* VAN NOSTRAND-RHEINHOLD, 1989, P 426-428
2. R. GENGLER AND J. HABIB, MINIMIZING DEFECTS IN THE MASS SOLDERING OF PRINTED WIRING ASSEMBLIES, *WESTERN ELECTRIC ENGINEER,* 1983
3. D. KOCKA, NO-CLEAN FLUXES ARE A VIABLE ALTERNATIVE TO CFC CLEANING,*ELECT. PACK. PROD.,* JUNE 1990, P 95
4. P. FODOR AND P. LENSCH, COVER GAS SOLDERING LEAVES NOTHING TO CLEAN OFF PCB ASSEMBLY, *ELECT. PACK. PROD.,* APRIL 1990, P 64
5. R. BOTHAM, C. LOWELL, AND J. STERRITT, WAVE SOLDERING MIXED TECHNOLOGY BOARDS, *ELECT. PACK. PROD.,* NOV 1990, P 28
6. M. NYLEN, K. JOSEFSON, AND H. STEEN, USE OF TIN-LEAD-BISMUTH ALLOY AS A SUBSTITUTE FOR EUTECTIC TIN-LEAD IN WAVE SOLDERING, *BRAZING AND SOLDERING,* SPRING 1988, P 38
7. C. LEA, *A SCIENTIFIC GUIDE TO SURFACE MOUNT TECHNOLOGY,* ELECTROCHEMICAL PUBLISHERS, LTD., 1988, P 148-153

Vapor-Phase Soldering

Dale L. Linman, Centech Corporation

Introduction

VAPOR-PHASE SOLDERING is a process of condensation heating, in which a product prepared for soldering is passed through or into a layer of saturated vapor. The vapor condenses on the relatively cool part, which transfers the latent heat of vaporization to the part and heats it rapidly and uniformly. The process reaches thermal equilibrium in a few seconds at a temperature that is only limited by the boiling point of the fluid used in the process. Typically, newer equipment utilizes a single perfluorocarbon fluid vapor layer, which does not contain chlorine or bromine and is environmentally safe. This fluid is also chemically inert, thermally stable, and has very low solvent action.

Although the process is used in a variety of heating applications, such as curing epoxies and polymers or stress relieving various platings, it is primarily useful when soldering surface-mounted components to various substrate materials. Because of the precise temperature control that this process offers (by virtue of a fixed boiling point), multilevel soldering is possible using up to three solder compositions with three different melting temperatures. Fluid temperatures that range from 100 to 265 °C (212 to 510 °F) are available. The most common fluid used boils at 215 °C (420 °F) and is used for 63-37 type solder, which melts at 183 °C (360 °F). A 30 °C (55 °F) differential is typical, to enable the heating process to proceed rapidly. Temperature precision also prevents the assembly from overheating.

Typical Materials

The typical materials that are joined by this process are solder-coated substrates made from various ceramic materials and G10 or FR4 epoxy laminates mated with surface-mounted components. Solder paste is typically applied to the substrate by screening, stenciling, or using *X-Y* dot placement. Components are then placed in the correct position in the solder paste, which temporarily holds them until they are soldered. The assembly is then passed through the vapor-phase setup, where the solder is melted, joining the components to the substrate. Typical surface-mount lead density is 1.25 mm (0.050 in.) on centers. Fine-pitch components as small as 0.38 mm (0.015 in.) on centers can also be processed. There is no inherent lead-pitch limitation in the vapor-phase process, because it is essentially an oxygen-free soldering process. Because of its uniformity, rapid heating, precise temperature control, and oxygen-free environment, the process is preferred for high-value assemblies. Also, because of the thermal capacity, ease of profiling, and forgiving nature of the process, it is also used when high throughput is required from limited floor space or when a large number of different types of boards need to be run in a given time period.

Equipment is normally configured for either batch or in-line operations (Fig. 1 and 2). The majority of machines available are of single-vapor design (Fig. 3). Earlier models had vertical access and used less-expensive fluid as a cover layer. These machines also lacked a preheating capability, which was found to be necessary in order to reduce the temperature differential at the point of solder melting. This measure prevents wicking and other undesirable characteristics that can develop when one part of a solder joint heats faster than the other. Both a preheating capability, typically provided by infrared panels, and a cooldown stage have been incorporated in newer models. The cooldown stage brings the solder joint through the liquidus phase more quickly (Fig. 4). This procedure reduces the time that the joint can form undesirable intermetallic layers and simultaneously improves the grain structure of the joint, thus improving its capability to withstand thermal cycling.

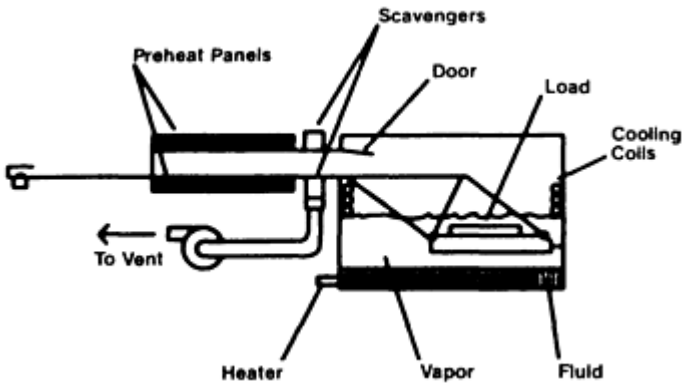

FIG. 1 PELLETIZED VAPOR-PHASE BATCH SYSTEM

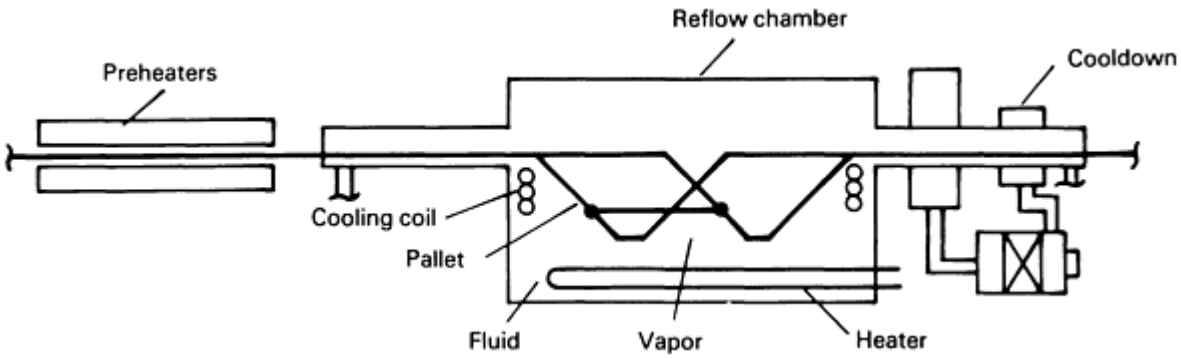

FIG. 2 THIRD-GENERATION VAPOR-PHASE REFLOW SYSTEM

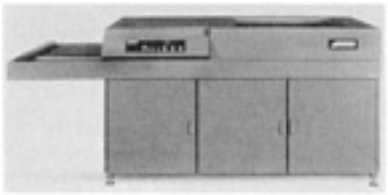

FIG. 3 SINGLE-VAPOR BATCH-TYPE EQUIPMENT

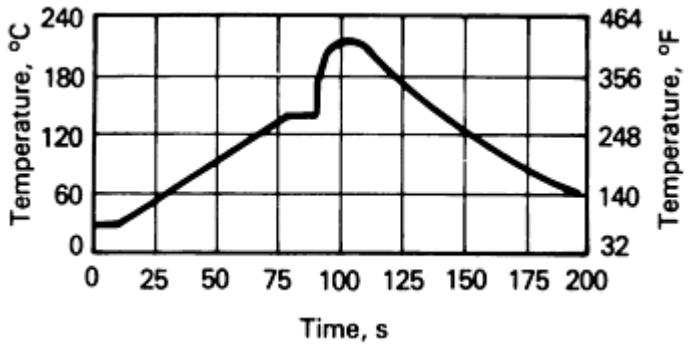

FIG. 4 THERMAL PROFILE

The stability of the vapor-phase process and its ease of profiling means that machine operators require little training. If the overall process is established correctly, then there are few elements that require adjustments. A smooth, vibration-free conveying mechanism enables defect-free soldering and assembly.

The proper setup procedure is to attach a thermocouple to a strategic location on the printed board, such as a sensitive component or a solder joint. Then, the board is processed to reach a preheat temperature of between 125 and 150 °C (255 and 300 °F) in 50 to 60 s. A desirable heating rate is approximately a 2 °C/s (4 °F/s) rise to within 100 °C (180 °F) of the reflow temperature. Major parameters are dwell time (batch machines), conveyor speed (in-line machines), and preheat panel temperature. Reflow time is established by observing the solder melt through the window in the chamber. In the batch machine, the dwell times can be set from those obtained and the process replicated. With in-line machines, the reflow time is established by the conveyor speed and the preheat temperature is adjusted with the panel temperature. Similar board assemblies can be processed using very similar profiles, which minimizes lost machine time due to the complex repetitive profiling that is common with other reflow methods.

Because vapor-phase soldering depends on the series of processes that precede it, every parameter leading to the actual soldering process must be carefully controlled to ensure a high yield. For example, thickness, viscosity, and location accuracy are just some of the parameters involved in solder paste application. Pad design and board layout are equally important to the process, as is the accurate placement of components. With proper controls, it becomes possible to solder with defect rates under 50 ppm using the vapor-phase process. Information on guidelines for parameter control can be obtained by contacting the Institute for Interconnecting and Packaging Electronic Circuits.

Material Requirements for Service Conditions

ASM Committee on Material Requirements for Service Conditions*

Introduction

THE SELECTION of materials for welded construction applications involves a number of considerations, including design codes and specifications where they exist. Mobile structures, such as automobiles and aerospace vehicles, have quite different materials requirements for weight, durability, and safety than stationary structures, such as buildings and bridges, which are built to last for many years. In every design situation, economics--choosing the correct material for the life cycle of the part and its cost of fabrication--are of great importance. Design codes or experience frequently offers an adequate basis for material selection; for new or specialized applications, however, the engineer encounters problems of an unusual nature and thus must rely on basic properties of the material, such as strength, corrosion or erosion resistance, ductility, and toughness. The properties of the various metallurgical structures associated with the thermal cycles encountered in the welding operation must also be included in the design process. The various subsections in this article offer guidance for material selection applications involving bridges and buildings, pressure vessels and piping, shipbuilding and offshore structures, aerospace systems, machinery and equipment, automobiles, railroad systems, and sheet metal. Material properties and welding processes that may be significant in meeting design goals are described.

Note

* R. DAVID THOMAS, JR., *CHAIRMAN*, R.D. THOMAS & COMPANY; BRUNO L. ALIA; WILLIAM R. APBLETT. AMET ENGINEERING; ROBERT G. BARTIFAY, ALUMINUM COMPANY OF AMERICA; STEPHEN A. COUGHLIN, ACF INDUSTRIES, INC.; GREGORY MELEKIAN, GENERAL MOTORS CORPORATION; ANTHONY R. MELLINI, ST., MELLINI AND ASSOCIATES, INC.; LARRY PERKINS, WRIGHT LABORATORY; JAMES E. ROTH, JAMES E. ROTH, INC.; WILLIAM J. RUPRECHT, GENERAL ELECTRIC COMPANY; BERNARD E. SCHALTENBRAND, ALUMINUM COMPANY OF AMERICA; ROBERT E. SOMERS, SOMERS CONSULTANTS; ROGER K. STEELE, AAR TECHNICAL CENTER

Material Requirements for Service Conditions

ASM Committee on Material Requirements for Service Conditions*

Overview

Principles of Material Selection

Structural Integrity. Before a structure is initially placed in service, the properties of its materials of construction must be adequate to ensure that the structure will perform as intended. Its components must be strong enough to bear the loads that will be imposed. It must be capable of meeting various inspection and qualification tests required by the end user to measure base material and weld soundness, ductility, toughness, and strength.

Length of Service. The service environment is often the largest influence on material selection. Materials of construction rarely last indefinitely. One of the principal selection considerations is the intended length of service for the structure. The designer needs to choose materials that will meet the conditions imposed initially and that can adapt to possible changes in conditions during the life of the structure.

The length of service is often dictated by obsolescence. Military hardware fabricated during wartime is an example of structures with relatively high obsolescence and short service life. Rocket cases for the propulsion of space vehicles need

to last one launching. At the other end of the spectrum, hydroelectric projects have expected lifetimes of a century or longer.

Materials or components rarely reach the end of their useful lives at the same time. Although a hydroelectric project is designed to last 100 years, some components may reach the end of their expected lives in less time, either by obsolescence due to improved technology or by unavoidable wear. At the outset of the material selection process, the length-of-service criterion must take into consideration the following: inspectability for potential failure, ease of maintenance of areas subject to deterioration, and ease of replacement of obsolete or life-exhausted components.

Joining Process. The suitability of the materials for the fabrication process to be employed must be considered early in the selection process. Weldability is the property of a material that dictates its ease of joining. The term most often applies to various types of steels joined by arc welding processes. This property often determines whether preheat is needed for successful welding and whether some type of postweld heat treatment is required to restore properties degraded by the welding operation.

Although weldability usually relates to the joining of relatively thick plates, the choice of materials for sheet metal applications must also take the welding process into account. The thinner the metal, the more difficult it is to arc weld. Brazing, soldering, or resistance welding is often used to join thin sheet materials. Resistance welding is frequently employed in the assembly of automobile bodies, for example; however, this process may not perform as reliably on coated steels as it does on uncoated steels.

Design Codes. Material selection is often dictated by the codes by which the design is governed, but there is still frequently a choice of materials. For example, pressure vessel codes offer a choice of steels, depending on the service temperature. Structural codes for buildings and bridges allow the use of both plain carbon and low-alloy steels. However, the codes tend to narrow the choice of materials.

Economics. An overriding selection criterion is often cost. In the broadest sense, this can be determined by the price of the material. However, a designer must assess not only the unit cost of the selected material, but also the costs imposed by fabrication. Compared with unalloyed steel, a low-alloy steel may allow a structure to be built using 25% less steel at a nominal 15% increase in unit price, but the cost of fabrication, such as the need for preheat and postweld heat treatment, may outweigh the material saving. A more costly steel that does not require painting or other protection from atmospheric corrosion may be a more economical choice, if not for initial construction, then for the life of the structure.

Material Requirements for Service Conditions

ASM Committee on Material Requirements for Service Conditions*

Service Conditions

The service environment is a principal determinant in the selection of materials for welded construction applications. The physical, mechanical, and corrosion properties of a material must be considered (Table 1).

TABLE 1 PRINCIPAL ATTRIBUTES OF A MATERIAL

PHYSICAL PROPERTIES

- DENSITY
- MELTING POINT
- THERMAL EXPANSION
- ELECTRICAL CONDUCTIVITY
- FERROMAGNETISM

MECHANICAL PROPERTIES

- TENSILE STRENGTH
- IMPACT STRENGTH
- FATIGUE STRENGTH
- CREEP STRENGTH
- DUCTILITY
- HARDNESS
- FRACTURE TOUGHNESS
- ELASTIC LIMIT

CORROSION PROPERTIES

- GENERAL CORROSION
- PITTING ATTACK
- STRESS CORROSION
- EROSION
- CAVITATION
- OXIDATION

Ambient Temperatures and Pressures. Most welded structures are designed to work in normal atmospheric conditions. The properties of common materials are well known for such conditions, and ample data are available to assist the designer in material selection.

Elevated Temperatures. The chemical industry has many processes that operate at temperatures of 1000 °C (1830 °F) and higher. Fossil fuel electric power generation makes use of steam temperatures from 500 to 600 °C (930 to 1110 °F). At such temperatures, most steels will exhibit creep--that is, a gradual deformation in the direction of the principal stresses--and thus the creep strength of a material becomes the controlling property. Creep strength determines the unit stress allowed to minimize the rate of creep and hence the permanent distortion and ultimate failure of a component.

Materials operating at high temperatures are frequently exposed to corrosive, erosive, or oxidizing environments, which may determine the life span of a structure. The resistance of proposed materials of construction to these types of environments should be examined during the selection process.

In processes where heat transfer occurs, the thermal conductivity of a material becomes an important consideration. Allowance must be made in the design for the expansion and contraction of components during heating and cooling--phenomena related to the coefficient of thermal expansion of a material.

Low Temperatures. Most ferritic metals become brittle at low temperatures, losing their ability to deform plastically to adjust to localized stresses and to accept a sudden shock. Thus, materials for use at low temperatures must have good toughness, a property usually measured by the Charpy V-notch impact test. For low-temperature applications, as for elevated-temperature service, the physical properties of thermal conductivity and coefficient of expansion become important.

High Pressures. Structures intended to contain high pressures are usually weldments and are designed according to American Society of Mechanical Engineers (ASME) codes for pressure vessels and piping. Strength properties are of primary importance. The codes specify the unit stress allowed for pressure-containing components. In cylindrical vessels, the maximum stress is in the tangential (i.e., hoop) direction, and the axial stress is half the hoop stress. In its simplest form, hoop stress is determined by:

$$S = \frac{PD}{2T}$$

where S is unit stress, P is pressure, D is the diameter of the cylinder, and T is wall thickness.

The tensile strength of a material determines the allowable stress and is specified in the ASME codes. The codes for steels allow a stress in excess of two-thirds of the minimum yield strength but less than 90% of the minimum yield strength. The minimum wall thickness, T_m, is then determined by:

$$T_m = \frac{PD}{2S + P_v} + A$$

where the extra thickness allowance, *A*, provides for anticipated corrosion or wear, and the coefficient *y* is specified by the code and varies with the temperature of operation and the wall thickness relative to the diameter.

Vacuum Conditions. Materials that are selected for very-low-pressure applications are primarily concerned with the tightness of the joints to prevent leakage from the exterior higher (or ambient) pressures into the vacuum chamber. For welded containers, the properties of the weld metal are critical to ensure lack of defects, such as porosity, cracks, and microfissures.

Vacuum conditions exist in outer space. In such applications, the vacuum condition is on the exterior of the vessel, and design for pressure containment is similar to that described for high pressures. Material selection also requires consideration of dynamic loads experienced during launches (hence, toughness), density for light weight (as in aircraft and aerospace applications), and corrosive and erosive effects, especially for reentry into the atmosphere.

Underwater Applications. A wide variety of material properties are involved in the application of weldments under water. Corrosion resistance is frequently a major concern, especially in seawater. Ships and offshore drilling platforms are notable examples.

For ships and for piping operating in biologically active waters, microbiologic organisms pose an unusual problem in material selection. Barnacles that attach themselves to the hulls of ships greatly increase the resistance to propulsion. The use of copper cladding or paints containing copper-bearing compounds is one means of discouraging barnacle formation. In turbid waters, piping is sometimes attacked by microorganisms that form surface pits, causing cracks in areas of local tension stresses. Because high tensile stresses frequently occur in or adjacent to welds, failures of weldments in these conditions can be attributed to these organisms, even in materials that otherwise are considered corrosion resistant to such environments.

Corrosion, Erosion, and Oxidation. Corrosion generally refers to surface attack by aqueous solutions or organic chemicals in either the liquid or vapor phase. Erosion implies the mechanical removal of metal from the surface, sometimes by high-pressure impingement of a fluid, in which case it is termed cavitation. Oxidation commonly occurs in metals at elevated temperatures and results in the removal of metal in the form of oxides.

Data on the resistance of materials to deterioration in many of these environments are frequently available from handbooks and material suppliers. In the case of weldments, the performance depends largely on experience gained in a variety of applications. The weld metal has a structure distinctly different from that of the parent metal, and sometimes a different composition as well. An electrochemical potential may exist between the weld and parent metal structures, causing attack on one or the other (frequently the weld metal because of its lower surface area).

Corrosive attack in weldments often is attributed to stress-corrosion cracking (SCC). In the presence of chloride ions (even at levels of parts per million), high tensile stress zones in or adjacent to welds can cause failure in materials whose corrosion life in the absence of stress is more than adequate for a particular application.

The welds in components carrying fluids at high velocity may erode during service. Under such conditions, hardness is the critical property. Localized areas of components, such as valve seats and turbine blades, may be protected from erosion by applying a hard weld metal, known as hard surfacing. For more information, see the article "Hardfacing, Weld Cladding, and Dissimilar Metal Joining" in this Volume.

In high-temperature service, allowance must be made for the thinning of metal sections due to progressive oxidation. In some applications the initial oxide layer protects the underlying metal, and progress is arrested. Adjacent to welds, oxidation can form preferentially in the highly stressed zones adjacent to welds and progress through the wall, causing weakness and possible failure.

Fatigue. In weldments subjected to fluctuating stresses, the fatigue strength of a metal may be the primary consideration in material selection and design loads. In the absence of flaws, the fatigue strength of most metals used for dynamically loaded structures is considerably higher than that of the welds. Designs for such structures must take into consideration both service experience and laboratory experiments dealing with various types of welds.

Weld metal cracks (even fine microfissures), lack of penetration or lack of fusion at the interface, and geometric discontinuities on the surface (such as overlaps and undercuts) are the major causes of poor performance in fatigue tests of welds. In the absence of such flaws, the fatigue properties of the weld metal itself or of the weld heat-affected zone (HAZ) rarely need to be considered, even though these zones may be inferior compared with the wrought parent metals. Design allowances for fatigue of weldments primarily take into account potentially damaging flaws.

Effect of Weld Thermal Cycles

Thermal Excursions During Welding. The thermal cycles encountered during the welding operation must be considered when selecting material for weldments. To make a weld requires that temperatures in the fusion zone reach above the melting point of the metal. Zones adjacent to the fusion region reach varying peak temperatures, depending on their distance from the fusion zone. Each of these thermal cycles causes metallurgical changes that affect the properties of the metal.

In the weld metal itself, the dendritic structure formed during solidification in a single thermal cycle is similar to that of a casting. In multipass welding, which is common when arc welding thicknesses greater than 6.4 mm ($\frac{1}{4}$ in.), the weld metal will undergo several thermal cycles, a process that refines the dendritic structure and alters the weld properties.

Similarly, in the HAZs immediately adjacent to the weld, one or more heat cycles will be experienced, causing changes in properties. When selecting materials for welded construction, the properties of these HAZs must be considered.

Cooling from the peak temperatures causes residual stresses, most often of a magnitude matching the yield strength of the material. Residual stresses may add to the service stresses. In cases where residual stresses may influence the integrity of the structure during its life expectancy, the designer may specify a postweld heat treatment.

Postweld Heat Treatments. Many weldments are placed in service in the as-welded condition. Under certain circumstances, postweld heat treatments may be required, thereby changing the properties of the selected metal.

Stress relieving is a thermal cycle that takes a weldment up to a high temperature where its yield strength is substantially reduced, allowing localized plastic deformation of the highly stressed regions. In ferritic steels, most stresses are relieved by heating to a temperature of less than 720 °C (1330 °F) for carbon steels (note that alloy steel values are higher). This is below the temperature transformation of ferrite to austenite, known as the critical temperature. This softens the structures that have been hardened by fast cooling from above the austenite-forming temperatures. Such subcritical heat treatments are said to "temper" the steel.

To cause the structures to become more similar to that of the parent metal, a supercritical heat treatment is sometimes specified. The properties of such welds are then likely to be comparable to those of the parent metal, provided that the compositions are similar.

Bridges and Buildings

This section deals with large welded structures built of plain carbon steels--the tonnage items in the construction industry. These structures generally conform to established codes.

Material Requirements for Service Conditions

ASM Committee on Material Requirements for Service Conditions*

Material Selection

The four code-writing organizations listed in Table 2 specify the chemical compositions, tensile properties, and other pertinent characteristics of steels used for large welded structures. Most employ the steel specifications of ASTM.

TABLE 2 CODES FOR STEEL STRUCTURES

ORGANIZATION	TITLE	SPECIFICATION NO.
AMERICAN WELDING SOCIETY (AWS)	"STRUCTURAL WELDING CODE--STEEL"	D1.1
	"BRIDGE WELDING CODE"	D1.5
AMERICAN INSTITUTE OF STEEL CONSTRUCTION (AISC)	"DESIGN, FABRICATION, AND ERECTION OF STRUCTURAL STEEL FOR BUILDINGS"	. . .
AMERICAN ASSOCIATION OF STATE HIGHWAY AND TRANSPORTATION OFFICIALS (AASHTO)	"STANDARD SPECIFICATION FOR WELDING STRUCTURAL STEEL HIGHWAY BRIDGES"	. . .
AMERICAN RAILWAY ENGINEERS ASSOCIATION (AREA)	"MANUAL FOR RAILWAY ENGINEERING"	. . .

The "Structural Welding Code--Steel" (AWS D1.1) considers three classes of structures:

- STATICALLY LOADED (BUILDINGS)
- DYNAMICALLY LOADED (BRIDGES)
- TUBULAR (OFFSHORE AND ARCHITECTURAL)

Fifteen ASTM specifications are applicable to buildings, 13 to bridges, and 34 to tubular structures, including four of the American Petroleum Institute (API) and two of the American Bureau of Shipping (ABS). The six most commonly used ASTM specifications, applicable to all three classes, are:

NO.	TITLE
A 36	"SPECIFICATION FOR STRUCTURAL STEEL"
A 500	"SPECIFICATION FOR COLD-FORMED WELDED AND SEAMLESS CARBON STEEL STRUCTURAL TUBING"
A 501	"SPECIFICATION FOR HOT-FORMED WELDED AND SEAMLESS CARBON STEEL STRUCTURAL TUBING"
A 514	"SPECIFICATION FOR HIGH-YIELD STRENGTH, QUENCHED AND TEMPERED ALLOY STEEL PLATE, SUITABLE FOR WELDING"
A 572	"SPECIFICATION FOR HIGH-STRENGTH LOW-ALLOY COLUMBIUM-VANADIUM STEELS OF STRUCTURAL QUALITY"

A 588	"SPECIFICATION FOR HIGH-STRENGTH LOW-ALLOY STRUCTURAL STEEL WITH 50 KSI (345 MPA) MINIMUM YIELD POINT TO 4 IN. THICK"
A 852	"STANDARD SPECIFICATION FOR QUENCHED AND TEMPERED LOW-ALLOY STRUCTURAL STEEL PLATE WITH 70 KSI YIELD STRENGTH TO 4 IN. THICK"

These specifications vary considerably in properties important to notch sensitivity (toughness) and weldability. The summary in Table 3 provides a guide as to what to look for in these and other specifications referred to in the structural codes. The supplementary requirements in some of these specifications are useful to the designer and fabricator when evaluating the need for additional acceptance tests for unusual applications.

TABLE 3 PROPERTIES RELATING TO SELECTION FOR SERVICE OF ASTM STEELS APPROVED IN AWS D1.1-92

Includes only the seven steels approved for all three AWS structural classes: (1) statically loaded, (2) dynamically loaded, and (3) tubular designs.

ASTM NO.	MAXIMUM CARBON CONTENT, %	TENSILE TEST REQUIREMENTS[(A)]	DEOXIDATION	SUPPLEMENTARY REQUIREMENTS
A 36	0.25-0.29 (FOR PLATE THICKER THAN 4 IN., OR 100 MM)	400-550 MPA (55-80 KSI); 250 MPA (36 KSI) MIN YP	NO RIMMED OR CAPPED STEEL FOR PLATE THICKER THAN 13 MM ($\frac{1}{2}$ IN.)	CHARPY V-NOTCH TESTING; SILICON KILLED, FINE-GRAIN PRACTICE
A 500	0.23-0.30	MIN TENSILE, THREE GRADES; 230, 290, 320 MPA (33, 42, 46 KSI) MIN YP	. . .	. . .
A 501	0.26-0.30	400 MPA (58 KSI) MIN TENSILE; 250 MPA (36 KSI) MIN YP	. . .	. . .
A 514	0.10-0.21 (15 PROPRIETARY COMPOSITIONS)	760-900 MPA (110-130 KSI) TO 65 MM (2.5 IN.) THICK; 690 MPA (100 KSI) MIN YP	FULLY KILLED, FINE-GRAIN PRACTICE	CLOSER THAN STANDARD FLATNESS
A 516	0.18-0.27	PLATES THICKER THAN 38 MM (1.5 IN.) NORMALIZED	KILLED, FINE-GRAIN PRACTICE	VACUUM TREATMENT; CHARPY V-NOTCH TEST; DROP-WEIGHT TEST[(B)]
A 572	0.21-0.26	MIN TENSILE, FOUR GRADES; 290-450 MPA (42-65 KSI) MIN YP	. . .	MAX TENSILE
A 588	0.15-0.20 (WEATHERING STEELS)	MIN TENSILE	FINE-GRAIN PRACTICE	MAX TENSILE; CHARPY V-NOTCH TEST; DROP-WEIGHT TEST(B); ULTRASONIC TEST

(A) YP, YIELD POINT.

(B) SEE ASTM E 208.

In general, the lower the carbon content and the finer the grain size of a steel, the better its notch toughness and weldability. The methods for achieving superior properties add to the unit price of the steel, so a designer striving for a low-cost structure tries to reduce steel cost, which is usually the most expensive single item in a job. This is especially true of static structures.

Material Requirements for Service Conditions

ASM Committee on Material Requirements for Service Conditions*

Environment

Low Temperatures. In the design of bridges, certain components merit special-toughness steel. Such components, termed fracture critical tension members (FCMs), would allow the bridge to collapse should they fail. The steel selection criteria are based on the minimum Charpy V-notch energy at a given temperature. For bridges financed in part by the Federal Highway Administration (FHA), the minimum winter temperature is the criterion used for the required Charpy V-notch energy at that temperature. A bridge located in the northern United States requires FCMs made with steel that exhibits the required minimum Charpy V-notch energy at a lower temperature than the same bridge constructed in the southern U.S.

The same FCM concept also applies for railroad bridges constructed under the codes established by AREA. The Charpy V-notch requirements for the three temperature zones defined by AREA codes are shown in Table 4. The required temperatures for measuring the Charpy V-notch energy are 21 °C (70 °F) for zone 1, 4 °C (40 °F) for zone 2, and -23 °C (-10 °F) for zone 3. Higher minimum Charpy V-notch values are required for weathering steels in heavier thicknesses. These values have been selected on the basis of extensive studies of steel structures, especially those of the Liberty ship failures during World War II.

TABLE 4 CHARPY IMPACT TEST REQUIREMENTS FOR WELDED STRUCTURAL STEEL: FRACTURE CRITICAL MEMBERS

ASTM	THICKNESS	MINIMUM AVERAGE ENERGY AND TEST TEMPERATURE		
		ZONE 1	ZONE 2	ZONE 3
A 36 OR A 709, GRADE 36	≤38 MM (≤1.5 IN.)	34 J (25 FT · LBF) AT 21 °C (70 °F)	34 J (25 FT · LBF) AT -12 °C (10 °F)	34 J (25 FT · LBF) AT 4 °C (40 °F)
	>38 TO ≤100 MM (>1.5 TO ≤4 IN.)	34 J (25 FT · LBF) AT -1 °C (30 °F)	34 J (25 FT · LBF) AT -7 °C (20 °F)	34 J (25 FT · LBF) AT -23 °C (-10 °F)
A 572, GRADE 50	≤38 MM (≤1.5 IN.)	34 J (25 FT · LBF) AT 21 °C (70 °F)	34 J (25 FT · LBF) AT -12 °C (10 °F)	34 J (25 FT · LBF) AT 4 °C (40 °F)
A 709, GRADE 50	>38 TO ≤50 MM (>1.5 TO ≤2 IN.)	34 J (25 FT · LBF) AT -1 °C (30 °F)	34 J (25 FT · LBF) AT -7 °C (20 °F)	34 J (25 FT · LBF) AT -23 °C (-10 °F)
A 588 A 709, GRADE 50 W	>38 TO ≤100 MM (>1.5 TO ≤4 IN.)	41 J (30 FT · LBF) AT -1 °C (30 °F)	41 J (30 FT · LBF) AT -7 °C (20 °F)	41 J (30 FT · LBF) AT -23 °C (-10 °F)
MINIMUM SERVICE TEMPERATURE		-18 °C (0 °F)	-34 °C (-30 °F)	-51 °C (-60 °F)

Source: Adapted from "Manual for Railway Engineering," Table 1.14.7. American Railway Engineers Association

Earthquakes. Structures for locations subject to earthquakes should be designed to withstand the impact of such events. This is a constantly evolving technology. For up-to-date information, contact the Earthquake Engineering Research Center (EERC) at the University of California at Berkeley.

Atmospheric Corrosion. Steel structures that are to remain exposed to the atmosphere without painting or other surface protection can be constructed of a steel that forms an adherent oxide. Such steel is known as weathering steel and is covered by ASTM specification A 588. Corrosion resistance is provided by additions of approximately 0.35% Cu in most grades and/or small amounts of chromium or nickel in other grades. Weathering steels are suitable for resisting corrosion in air, but are not significantly better than other structural steels under water. In highway bridges where salt is used to control icing conditions, progressive corrosion is encountered, especially at expansion joints. A matching filler metal should be used to weld these steels, such as those with the designation "W" in the AWS specifications (e.g., E7018W in A5.5 or EW in A5.23).

Material Requirements for Service Conditions

ASM Committee on Material Requirements for Service Conditions*

Fitness for Service

No structure is entirely free from flaws. Fitness for service is a term applied to an evaluation of the flaws found on inspection. The codes define the allowance for defects considered acceptable for the intended service.

Workmanship. Prior to assembly, the base metals are inspected for evidence of surface flaws that could impair the integrity of the structure. Before welding, the prepared edges are examined for discontinuities longer than 25 mm (1 in.). Such flaws must be removed and weld repaired before final assembly.

Distortion and shrinkage result from the welding operation. Permissible variations in the dimensions, straightness, and camber of structural members are defined in the codes. Peening of intermediate layers of multi-pass welds can be used to control distortion, but should be avoided on the weld surfaces.

Acceptable weld profiles are also defined as part of the workmanship standards of the codes for buildings and bridges. Unacceptable profiles, cracks, undercuts, overlaps, and other deficiencies are generally repaired by grinding the objectionable flaw and, if necessary, rewelding.

Inspection. Visual inspection is relied on for assessing workmanship criteria. In the construction of large structures, the general contract defines the extent of nondestructive testing of welds that may be required. Methods of nondestructive testing include radiography, ultrasonic testing, magnetic-particle inspection, and dye-penetrant inspection. For more information, see the article "Inspection of Welded Joints" in this Volume.

Radiography and ultrasonic testing allow examination of the full cross section of a weld. Flaws larger than 1% of the thickness, including cracks, lack of fusion, inclusions, and porosity can be detected by these techniques. X-ray analysis will detect only cracks substantially parallel to the impinging x-ray beam. Ultrasonic pulses can be introduced at an angle of 30 or 45° from the perpendicular to the plate surface, which permits a more complete inspection coverage of a weld.

Magnetic-particle and dye-penetrant methods are limited to the detection of defects on or near the surface. Dye penetrants can detect surface flaws only, whereas magnetic-particle testing can detect flaws slightly below the surface.

Flaw Assessment. The integrity and performance of welded structures depend heavily on the assessment of the significance of flaws identified during inspection. The discipline of fracture mechanics allows judgments to be made as to the likelihood of a flaw to cause a failure.

For static structures, the acceptance of a flaw of a given size that is found during inspection makes use of the material property evaluated by the crack-opening displacement (COD) test. Acceptance is based on the principle illustrated in Fig. 1. An example of the application of the COD test to flaw assessment is shown in Fig. 2.

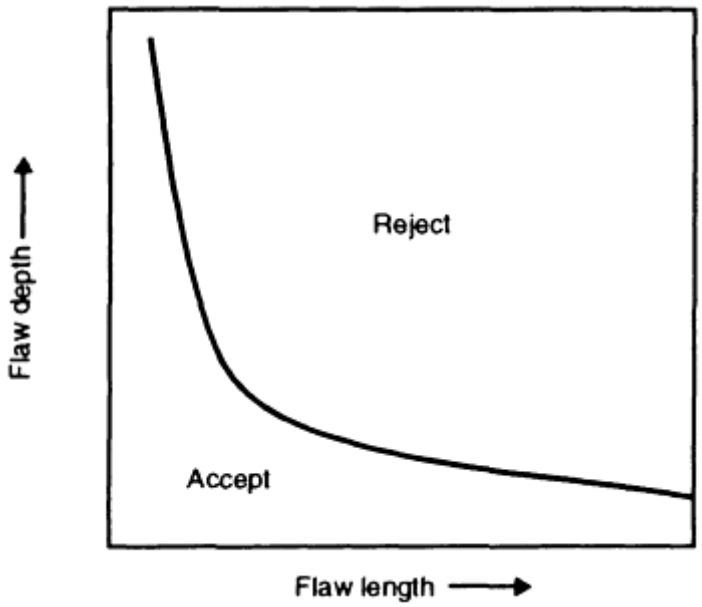

FIG. 1 SCHEMATIC OF AN ALLOWABLE FLAW-SIZE CURVE

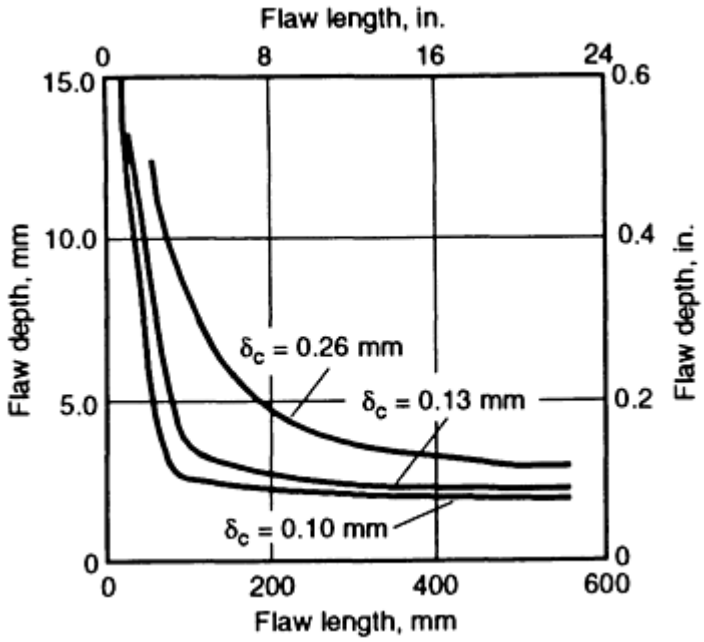

FIG. 2 ALLOWABLE FLAW SIZES DETERMINED FOR GIRTH WELDS IN PIPELINES CONSTRUCTED FROM API X70 STEEL, ASSUMING A COD VARYING FROM 0.1 TO 0.25 MM (0.004 TO 0.010 IN.), A FLOW STRESS OF 520 MPA (75 SKI), AND AN APPLIED STRESS OF 435 MPA (63 KSI). SOURCE: REF 1

Tolerance for Flaws. The inherent material properties of steels and welds that allow them to withstand the existence of flaws are measured by tensile testing (ductility), Charpy impact testing (toughness), and COD testing. For welds in FCMs, values of these measurements should be well above the minimum specification requirements. These tests are conducted on the welded joints prepared according to the specified qualification test procedures. An evaluation of ductility, toughness, and crack-opening displacement should be obtained on the weld metal, the HAZ, and the unaffected base metal.

Reference cited in this section

1. R.P. REED, M.B. KASEN, H.I. MCHENRY, C.M. FORTUNKO, AND D.T. REED, *FITNESS FOR SERVICE CRITERIA FOR PIPELINE GIRTH WELD QUALITY*, BULL. 296, WELDING RESEARCH COUNCIL, JULY 1984

Pressure Vessels and Piping

Codes and Specifications

The primary users of pressure vessels and piping are the chemical, petroleum, and electric power industries. While there are numerous codes, standards, and specifications that govern the selection of materials for pressure vessels and piping, the manufacture of boilers and pressure vessels in the United States falls under the general specification issued by ASME titled "Boiler and Pressure Vessel Code." This code is published in several parts. The rules governing the design of boilers are included in section I, "Power Boilers." The design rules for pressure vessels are included in section VIII, divisions 1 and 2, "Rules for Construction of Pressure Vessels." The materials requirements are included in section II, "Materials Specifications":

- PART A: FERROUS
- PART B: NONFERROUS
- PART C: WELDING RODS, ELECTRODES, AND FILLER METALS
- PART D: PROPERTIES

The ferrous (SA) and nonferrous (SB) ASME materials specifications were originally developed by ASTM and in most cases are identical. Thus, ASME specifications designated SA 204 and SB 467 may also be found as ASTM specifications A 204 and B 467, respectively.

In the United States, the AWS filler metal specifications are the primary guidelines used by the pressure vessel and piping industry. Here again, the ASME specifications (part C) are identical. The ASME specifications carry the initial designation SFA to correspond to the AWS specification designations starting with A; for example, SFA 5.5 is identical to AWS A 5.5. The AWS specifications are written to provide the specific chemical analysis of the filler material and the mechanical properties (minimum tensile and yield strengths) of the deposited weld metal.

Standards for pressure piping are covered by the American National Standards Institute (ANSI) document B31.1, "Code for Pressure Piping." This standard also applies to industrial pipelines and piping. Material selection is primarily from the ASTM and ASME materials specifications, although the API does provide a number of pipe specifications for material with yield strengths ranging from 170 to 760 MPa (25 to 110 ksi) and tensile strengths ranging from 275 to 860 MPa (40 to 125 ksi). The intended service temperatures, corrosion resistance, and fabricability are the primary considerations in the selection of materials for pressure vessels and piping.

Environment

Ordinary-Temperature Service (-30 to 345 °C, or -20 to 650 °F). The ASME, recognizing the fact that the ultimate strength of steels remains relatively constant over the temperature range from -30 to 345 °C (-20 to 650 °F), elected to set a safe maximum design stress of 25% of the ultimate tensile strength at temperatures over this temperature range. Consequently, the plain carbon steels are the most economical, with the popular grades being SA 515 ("Pressure

Vessel Plates, Carbon Steel, for Intermediate- and Higher-Temperature Service") and SA 516 ("Pressure Vessel Plates, Carbon Steel, for Moderate- and Lower-Temperature Service"). SA 516, a fine-grain, silicon-aluminum killed steel, is often preferred to SA 515, a coarse-grain, silicon killed steel, because of its better notch toughness characteristics.

A steam drum for an electric utility boiler fabricated from SA 515 grade 70 material is shown in Fig. 3. Where reduction in weight is important and operating pressures are high, the higher strength weldable steels are used, such as SA 302 ("Pressure Vessel Plates, Alloy Steel Manganese-Molybdenum and Manganese-Molybdenum-Nickel"). The quenched and tempered version of this steel, SA 533 (grade B, class 1), is used extensively in nuclear reactor vessels. Pertinent data for these materials are listed in Table 5. The specifications listed in Table 5 (and also Tables 6 and 7, to be discussed later) are for plate material. Similar ASME specifications exist for forgings, pipe, tube, and cast material.

TABLE 5 PRESSURE VESSEL STEELS FOR ORDINARY-TEMPERATURE SERVICE

ASME NO.	ALLOY AND NOMINAL COMPOSITION	MINIMUM SPECIFIED TENSILE STRENGTH		ALLOWABLE DESIGN STRESS	
		mpa	ksi	mpa	ksi
SA 515	PLAIN-CARBON; COARSE-GRAIN PRACTICE				
SA 516	PLAIN-CARBON; FINE-GRAIN PRACTICE; IMPROVED TOUGHNESS				
GRADE 55	0.26% C MAX; 0.60-0.90% MN	380	55	95	13.75
GRADE 60	0.27% C MAX; 0.60-0.90% MN	415	60	103	15.00
GRADE 65	0.29% C MAX; 0.85-1.20% MN	450	65	112	16.25
GRADE 70	0.31% C MAX; 0.85-1.20% MN	485	70	121	17.50
SA 302					
SA 302 GRADE A	MN-MO	515	75	130	18.8
GRADE B	MN-MO	550	80	138	20
GRADE C	MN-MO-NI	550	80	138	20
GRADE D	MN-MO-NI	550	80	138	20
SA 202					
GRADE A	CR-MN-SI	515	75	130	18.8
GRADE B	CR-MN-SI	585	85	147	21.3
SA 537					
CLASS 1	C-MN-SI; NORMALIZED; 63.5 MM (2.5 IN.) MAX THICKNESS	485	70	121	17.5
CLASS 2	C-MN-SI: QUENCHED AND TEMPERED; 63.5 MM (2.5 IN.) MAX THICKNESS	550	80	138	20

TABLE 6 PRESSURE VESSEL STEELS FOR LOW-TEMPERATURE SERVICE

ASME NO.	ALLOY AND NOMINAL COMPOSITION	MINIMUM SPECIFIED TENSILE STRENGTH		ALLOWABLE DESIGN STRESS		LOWEST TEST TEMPERATURE FOR CHARPY V-NOTCH TEST	
		MPa	ksi	MPa	ksi	°C	°F
SA 516	PLAIN-CARBON; FINE-GRAIN						

	PRACTICE						
GRADE 60	0.27% C MAX; 0.60-0.90% MN	415	60	103	15.0	-46	-50
GRADE 65	0.29% C MAX; 0.85-1.20% MN	450	65	112	16.25	-46	-50
GRADE 70	0.31% C MAX; 0.85-1.20% MN	485	70	121	17.5	-46	-50
SA 537	FINE-GRAIN PRACTICE						
CLASS 1	NORMALIZED; 0.24% C MAX; 0.70-1.35% MN	485	70	. . .	. . .	-62	-80
CLASS 2	QUENCHED AND TEMPERED; 0.24% C MAX; 0.70-1.35 MN	550	80	. . .	. . .	-60	-76
SA 203							
GRADE A	2.4% NI	450	65	112	16.25	-60	-75
GRADE B	2.4% NI	485	70	121	17.5	-60	-75
GRADE D	3.5% NI	450	65	112	16.25	-100	-150
GRADE E	3.5% NI	485	70	121	17.5	-100	-150
SA 645	5.0% NI	655	95	164	23.75	-170	-275
SA 553							
TYPE II	8.0% NI	690	100	172	25.0	-170	-175
TYPE I	9.0% NI	690	100	172	25.0	-195	-320

TABLE 7 PRESSURE VESSEL STEELS FOR HIGH-TEMPERATURE SERVICE

ASME NO.	ALLOY AND NOMINAL COMPOSITION	NORMAL TEMPERATURE RANGE OF USAGE		ALLOWABLE STRESS AT LOW END OF USAGE TEMPERATURE		ALLOWABLE STRESS AT HIGH END OF USAGE TEMPERATURE	
		°C	°F	Mpa	Ksi	Mpa	Ksi
SA 204, GRADE C	0.28% C MAX; 0.45-0.60% MO	430-510	800-950	130	18.8	57	8.2
SA 302, GRADE B	0.25% C MAX; 1.15-1.50% MN; 0.45-0.60% MO	430-510	800-950	130	18.8	57	8.2
SA 387, GRADE 12							
CLASS 1	1.0CR-0.5MO	455-565	850-1050	92	13.4	30	43
CLASS 2	1.0CR-0.5MO	345-480	650-900	112	16.3	104	15.1
SA 387, GRADE 112							
CLASS 1	1.25CR-0.5MO	455-565	850-1050	101	14.6	32	4.6
CLASS 2	1.25CR-0.5MO	345-480	650-900	130	18.8	110	15.9
SA 387, GRADE 22							
CLASS 1	2.25CR-1.0MO	455-	850-	99	14.4	40	5.8

		595	1100				
CLASS 2	2.25CR-1.0MO	370-480	700-900	119	17.2	109	15.8
SA 387, GRADE 5							
CLASS 1	5.0CR-0.5MO	480-620	900-1150	83	12.1	29	4.2
CLASS 2	5.0CR-0.5MO						
SA 387, GRADE 9	9.0CR-1.0MO	510-595	950-1100	73	10.6	22	3.3
SA 387, GRADE 91	9.0CR-1.0MO + NI, V, NB, N, AL	540-650	1000-1200	99	14.3	28	4.3
SA 240	AUSTENITIC STAINLESS STEELS						
GRADE 304H	18CR-8NI	595-815	1100-1500	61	8.9	9.7	1.4
GRADE 316H	16CR-12NI-2MO	595-815	1100-1500	71	10.3	8.3	1.2
GRADE 321H	18CR-10NI-TI	595-815	1100-1500	48	6.9	2	0.3
GRADE 347H	18CR-10NI-NB	595-815	1100-1500	90	13.0	9	1.3

FIG. 3 STEAM DRUM FOR AN SA 515 STEEL ELECTRIC UTILITY BOILER

Low-Temperature Service (-30 to -195 °C, or -20 to -320 °F). The commonly measured mechanical properties of steels, such as ultimate strength, yield strength, and elongation, do not always ensure freedom from failure at low temperatures, even when the design load is not exceeded. To ensure safe performance, the steel must be resistant to the initiation and propagation of a crack under all service conditions. Resistance to brittle crack initiation and propagation is commonly referred to as notch toughness or notch ductility. Factors that adversely affect notch toughness include cold working, strain aging, large grain size, increasing section thickness, and increasing the compositional contents of carbon, sulfur, phosphorus, nitrogen, and silicon. Beneficial factors include fine grain size, deoxidation, heat treatment, increasing the manganese and nickel contents, and decreasing the sulfur content. The notch toughness of a steel is also dependent on fabrication procedures, workmanship, and design details. Even the best design will contain some notch effects, and there will also be some imperfections in the highest level of workmanship. In the presence of these notches, the breaking strength of a pressure vessel and, more importantly, its failure mode (ductile or brittle) depend largely on the capacity of the steel at the root of some critical notch to yield plastically as the stress increases.

In thick sections, plain carbon steels produced according to fine-grain practice and normalized or quenched and tempered are used for service to -45 °C (-50 °F). Low-carbon high-nickel (e.g., 9% Ni) alloy steels are used for service down to -195 °C (-320 °F). Ferritic steels covered by ASME specifications are shown in Table 6. Austenitic chromium-nickel steels, aluminum, and special copper and aluminum-base alloys have been found to be particularly suitable for applications close to absolute zero. Because austenitic steels have a face-centered cubic (fcc) crystal structure, they retain their toughness to very low temperatures.

High-Temperature Service (345 to 815 °C, or 650 to 1500 °F). In the design of pressure vessels and piping, engineers and designers are confronted with the problem of selecting materials for a wide range of high-temperature service conditions. The chromium-molybdenum ferritic steels and austenitic stainless steels are generally used for design temperatures above 425 °C (800 °F). In addition to service temperature, corrosion resistance, and fabricability, the following conditions should be considered in high-temperature applications:

- POSSIBLE MAXIMUM TEMPERATURE
- TYPE AND SIZE OF LOAD
- EXPECTED LIFE OF THE STRUCTURE
- COST

Service experience and laboratory test data have established the normal temperature range of usage shown in Table 7 for the materials commonly used for high-temperature service. The allowable stresses in the ASME code, section VIII, division 1, for the low and high ends of the usage temperature ranges are also given in Table 7.

The following material properties must be taken into account in addition to the aforementioned service conditions:

- CREEP STRENGTH
- STRESS-RUPTURE LIFE
- DUCTILITY
- SHORT-TERM TENSILE PROPERTIES
- SURFACE STABILITY
- STRUCTURAL STABILITY
- THERMAL CONDUCTIVITY
- THERMAL FATIGUE
- THERMAL EXPANSION
- WELDABILITY
- HOT AND COLD WORKABILITY

All of these factors are important in arriving at the most suitable alloy for a given application.

Corrosion. Because of the many chemical compounds that may be encountered in pressure vessel and piping service, a discussion of corrosion is outside the scope of this section. However, there are two areas of concern in both the petrochemical field and the electric power industry: the effect of hydrogen absorption on materials properties and the possible metal loss due to steam/air oxidation.

High-Pressure, High-Temperature Hydrogen Service. Pressure vessels and piping exposed to hot high-pressure hydrogen may embrittle, crack, and ultimately fail without visible thinning of the metal or a superficially observable change in appearance of the exposed surfaces. A tool known as the Nelson diagram (Ref 3) is generally used to predict the behavior of alloy material in high-pressure, high-temperature hydrogen (Fig. 4). The Nelson diagram is based on actual service experience and indicates the temperature-pressure limits below which a material has not failed to date. Allowance must be made for temperature and pressure excursions that may occur over the design life of the component. Hydrogen can affect the mechanical properties of steel in two ways. Absorbed hydrogen causes a reduction in yield strength and impairs material toughness. More advanced attack, as manifested by fissuring and decarburization, is reflected in severely reduced tensile strength, ductility, and toughness.

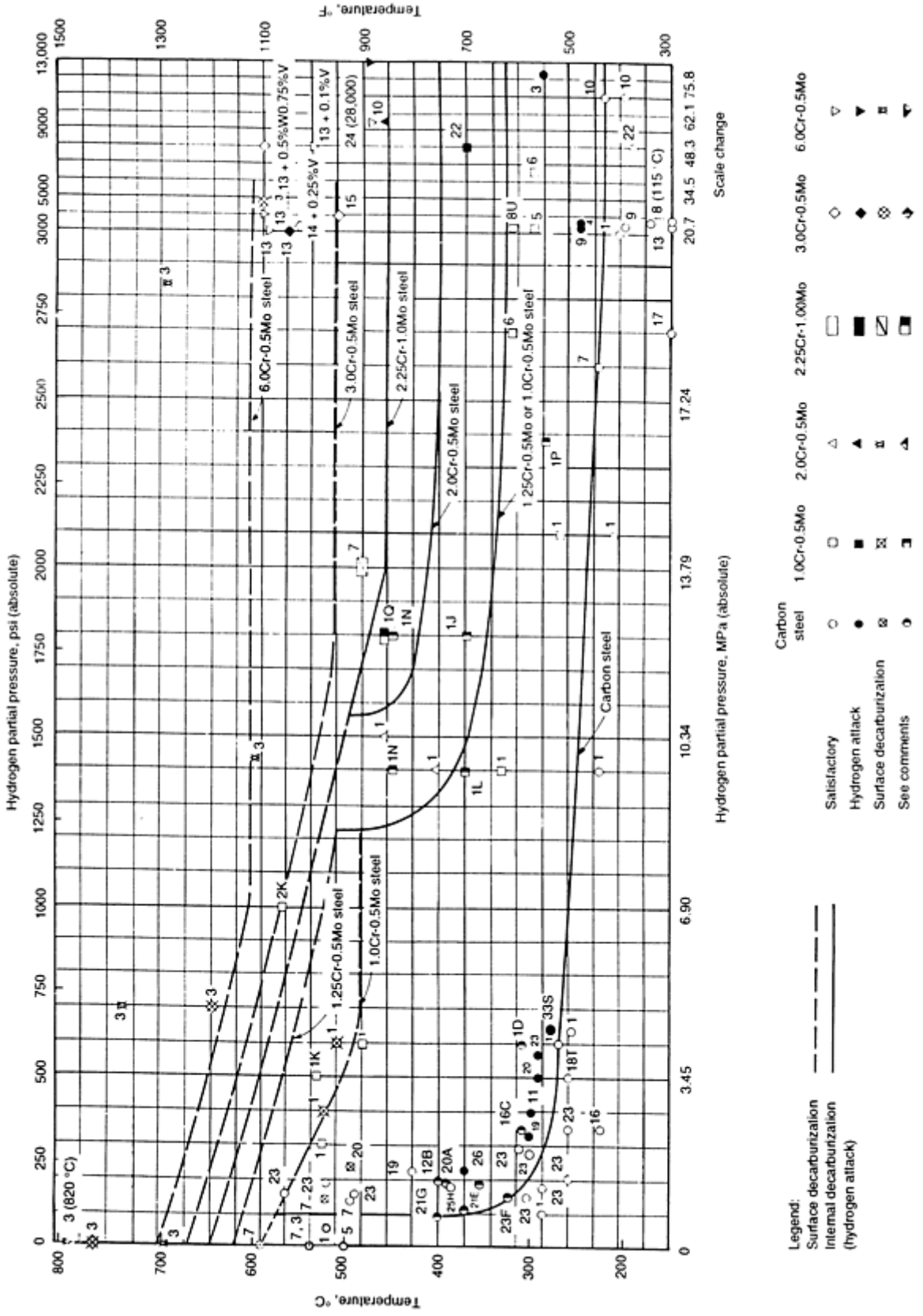

FIG. 4 NELSON DIAGRAM. 1, THE LIMITS DESCRIBED BY THESE CURVES ARE BASED ON ACTUAL SERVICE EXPERIENCE AND ON INFORMATION GATHERED BY API (REF 3). 2, AUTENITIC STAINLESS STEELS ARE GENERALLY NOT DECARBURIZED IN HYDROGEN AT ANY TEMPERATURE OR HYDROGEN PRESSURE. 3, THE LIMITS DESCRIBED BY THESE CURVES ARE BASED ON EXPERIENCE WITH CAST STEEL AS WELL AS ANNEALED AND NORMALIZED STEELS AT STRESS LEVELS DEFINED BY THE ASME CODE, SECTION VIII, DIVISION I. LINES REPRESENT THE UPPER LIMIT OF CONDITIONS FOR ACCEPTABLE USE OF THE ALLOY STEEL. SOURCE:

The recent trend in low-alloy steels for hydrogen service has been in the direction of steels of the chromium-molybdenum-vanadium type, such as 3Cr-1Mo-0.25V or 2.25Cr-1Mo-0.25V. For the most severe corrosive conditions, particularly those involving hydrogen sulfide (H_2S) in addition to hydrogen, austenitic steels of the 18Cr-8Ni type are used.

The National Association of Corrosion Engineers (NACE) standard MR-01-75 is the accepted reference in terms of materials and fabrication requirements for H_2S service. This standard specifies the materials and fabrication that are considered to provide satisfactory resistance to H_2S attack. Carbon steels for use in wet H_2S service are usually evaluated in accordance with NACE TM-01-77 (test solution) and TM-02084 (test method).

The relatively high cost of the austenitic steels frequently dictates the use of carbon or low-alloy steel vessels with applied corrosion-resistant cladding. In general, three methods of attaching the cladding to the backing plate are utilized: integral cladding, strip lining, and weld overlay cladding. Integrally clad plate is fabricated by hot rolling in a steel mill or by explosive cladding. Strip lining is applied by using long, narrow alloy sheet attached to the vessel by a continuous weld around the edges. Weld overlay cladding produces a continuous bonded layer of corrosion-resistant alloy on the base metal. Weld overlay cladding can be applied on irregular shapes, such as nozzles, thus avoiding dissimilar-alloy welds in the main pressure boundary.

Oxidation in Steam Service. In choosing a steel for service at elevated temperature, consideration must be given not only to its resistance to applied stress at temperature but also to its resistance to scaling, both of which decrease rapidly with increasing temperature above about 600 °C (1110 °F). Chromium, alone or in combination with silicon or molybdenum, contributes to increased resistance. For plain carbon steels, Fe_3O_4 is the only oxidation product and is stable until a temperature of 570 °C (1060 °F) is reached. Above 570 °C (1060 °F), FeO is the stable oxide phase and contributes to more rapid metal loss. The addition of chromium raises the temperature at which the Fe_3O_4/FeO transition occurs (see Table 8). Metal loss due to oxidation is of relatively little importance in heavy-wall pressure vessels; however, it deserves consideration in thinner-wall piping and in thinner low-pressure vessels.

TABLE 8 FE_3O_4/FEO TRANSITION TEMPERATURES

ALLOY	TEMPERATURE	
	°C	°F
0.5CR-0.5MO	590	1095
1CR-0.5MO	600	1110
1.25CR-0.5MO	605	1120
2.25CR-1MO	615	1140
5CR-0.5MO	625	1155

Other Factors Causing Degradation of Materials (Ref 4). Specific service conditions may degrade materials to an extent that requires replacement or retirement of components in the system. One of the more common failure modes in pressure vessels is SCC, which can be characterized as either intergranular (IGSCC) or transgranular (TGSCC), depending on the environment. Hydrogen-induced cracking (HIC) is another failure mechanism, again influenced by the localized stress condition.

Low-alloy steels in service at temperatures above 450 °C (850 °F) will suffer a loss in ductility due to temper embrittlement unless the composition is rigidly controlled. Phosphorus, tin, arsenic, and antimony are the principal elements that contribute to temper embrittlement.

The ductility of steels operating in the creep temperature range (generally above 480 °C, or 900 °F) suffers from a condition known as creep embrittlement. The loss in ductility is caused by the formation of small cavities in grain boundaries. In the presence of relatively low stress, the number of cavities grow and eventually link together to form microcracks, thus preventing the plastic deformation that is characteristic of ductile behavior. Sulfur is one of the elements that contribute to cavity formation and loss in ductility in creep service.

References cited in this section

3. *STEELS FOR HYDROGEN SERVICE AT ELEVATED TEMPERATURES AND PRESSURES IN PETROLEUM REFINERIES AND PETROCHEMICAL PLANTS*, 4TH ED., API PUBL. 941, AMERICAN PETROLEUM INSTITUTE, APRIL 1990
4. S. YUKAWA, *GUIDELINE FOR PRESSURE VESSEL SAFETY ASSESSMENT*, NIST SPEC. PUBL. 780, NATIONAL INSTITUTE FOR STANDARDS AND TECHNOLOGY, P 14-22

ASM Committee on Material Requirements for Service Conditions*

Fabricability

Fabrication operations can affect the performance of pressure vessels and piping in several ways: (1) cold forming operations may lead to strain aging, with a loss in toughness and ductility; (2) hot forming, unless carefully controlled, may produce undesirable changes in microstructure; (3) welding operations may produce an HAZ with reduced toughness and high hardness, and may also produce high tensile residual stresses that could lead to stress-rupture cracking (reheat cracking) during postweld heat treatment of susceptible materials.

Welding Process Selection. Considerations which govern the selection of a welding process are those that define the end use of a vessel, such as toughness, tensile properties, creep properties, and corrosion. There are also practical considerations, such as weldment size, equipment limitations, welding position, and access to the weldment area.

Two welding processes are primarily used: shielded metal arc welding (SMAW) and submerged arc welding (SAW). Other processes, such as electroslag welding, gas-tungsten arc welding, and gas-metal arc welding, are also used, but historically SMAW (see the article "Shielded Metal Arc Welding" in this Volume) and SAW (see the article "Submerged Arc Welding" in this Volume) have been dominant in vessel manufacture. A characteristic of both the SMAW and SAW processes is that they rely on the use of a flux to produce a slag over the molten weld pool, protecting it from atmospheric contamination. These fluxes vary significantly in formulation and operating characteristics and can modify the chemical composition, inclusion content, and microstructure of the final weld metal.

Weldability. Steels for pressure vessel fabrications are often classified as weldable based on composition, thickness, and need for preheat (see the article "Weldability Testing" in this Volume). Carbon and low-alloy steels are the most frequently used materials for pressure vessels; consequently, their weldability has received the greatest attention.

Preheating is utilized to prevent cracking, to permit diffusion of hydrogen from the weld and HAZ during and following welding, to reduce distortion, and to prevent loss of toughness and ductility. Preheating is also used to ensure that all traces of moisture have been removed from the surface of the material. Of the various schemes proposed for predicting preheating requirements, most are based on the carbon equivalent (C_{eq}). A variety of equations have been developed by various researchers for determining the C_{eq}, one of which has demonstrated that prevention of cracking due to hydrogen can be correlated with chemical composition in terms of a carbon equivalent formula of the form:

$$C_{eq} = C + \frac{Mn}{6} + \frac{Si}{24} + \frac{Ni}{40} + \frac{Cr}{5} + \frac{Mo}{4}$$

This formula was developed by Winn (Ref 5). A plot of carbon equivalents for a series of steel compositions used by Winn against preheat temperature is shown in Fig. 5. A linear relationship exists between the steel chemical composition, expressed by the carbon equivalent formula, and the minimum preheat temperature to avoid HAZ cracking.

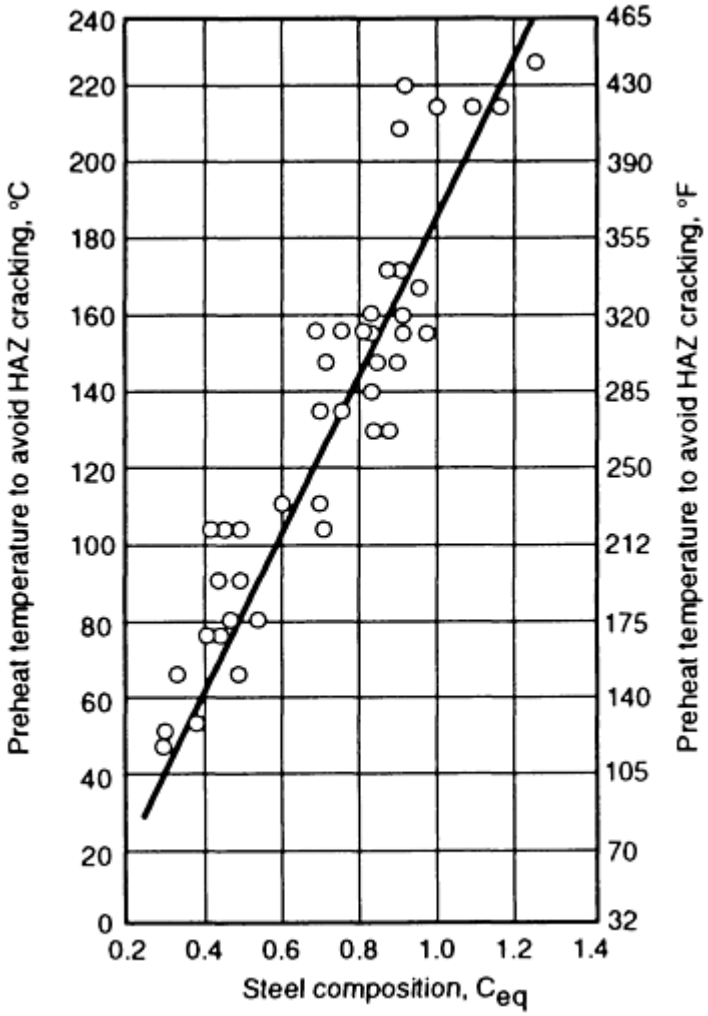

FIG. 5 CARBON EQUIVALENT VERSUS MINIMUM PREHEAT TEMPERATURE. THE BEST-FIT LINE SHOWN MAY BE REPRESENTED APPROXIMATELY BY: $T = 210(C_{EQ}) - 25$, WHERE T IS THE PREHEAT TEMPERATURE (°C).

The formula used by the International Institute of Welding (IIW) for judging the risk of underbead cracking and the resultant need for preheat is as follows:

$$C_{eq} = C + \frac{Mn}{6} + \frac{Cr + Mo + V}{5} + \frac{Ni + Cu}{15}$$

Regardless of the formula used, the C_{eq} values must be considered as approximations, because all factors affecting hardenability (e.g., section thickness, mass, restraint, grain size, and environmental effects) are not included.

Weld Zones. Based on work published by Savage, Nippes, and Szekeres (Ref 6), a typical weld consists of the composite zone, the unmixed zone, the weld interface, the partially melted zone, the HAZ, and the unaffected base metal (Fig. 6). All of these zones possess different mechanical properties, which are determined by the chemical compositions of the weld metal and the base metal. The preheat used, the weld energy input, and whether or not postweld heat treatment is specified also affect the resultant mechanical properties of the weldment.

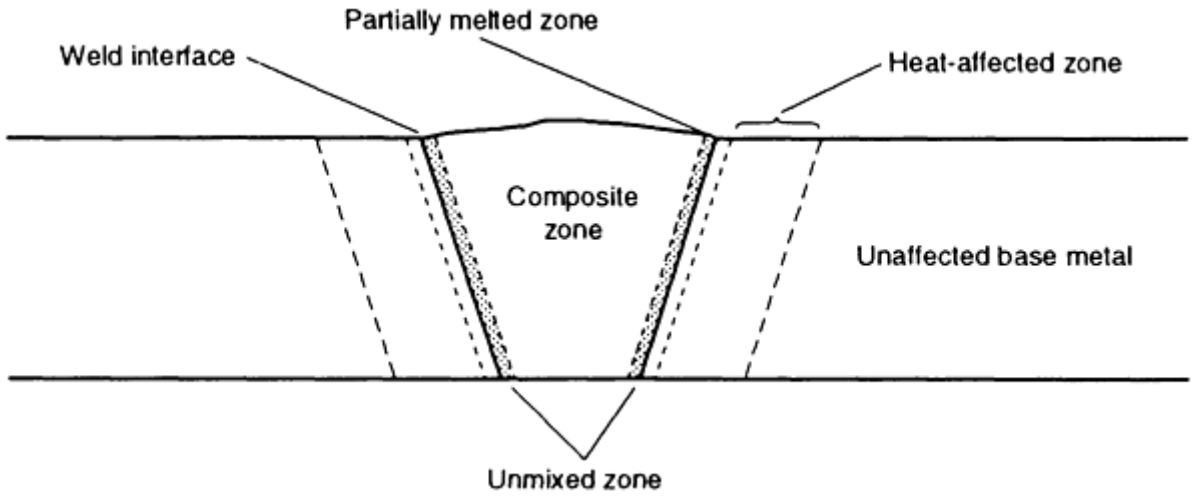

FIG. 6 TYPICAL ZONES ASSOCIATED WITH FUSION WELDS. SOURCE: REF 6

Postweld Heat Treatment. The circumstances under which the postweld heat treatment of pressure vessels is required are set forth in the ASME pressure vessel codes. They are determined primarily by the steel composition, thickness, specific fabrication operations, and intended service.

The principal beneficial effects of postweld heat treatment are the relief of residual stresses and the tempering action on the microstructures produced by the welding thermal cycles. Undesirable metallurgical phenomena may also be produced, such as temper embrittlement or cracking due to stress-rupture failures at grain boundaries.

References cited in this section

5. W.H. WINN, WELDABILITY OF LOW ALLOY STEELS, *BR. WELD. J.*, VOL 11 (NO. 8), AUG 1964
6. W.F. SAVAGE, E.F. NIPPES, AND E.S. SZEKERES, A STUDY OF WELD INTERFACE PHENOMENA IN A LOW ALLOY STEEL, *WELD. J.*, SEPT 1976, P 260S-268S

Material Requirements for Service Conditions

ASM Committee on Material Requirements for Service Conditions*

Mechanical Properties of Weldments

Design Considerations. Some designers have tacitly assumed that a pressure vessel behaves as if it were manufactured from an isotropic material with the same properties throughout the vessel. Because of the presence of welded seams and welded attachments, however, no actual vessel fulfills this simple concept. Welds produce regions where the mechanical properties are considerably different from those of the base material. The stress-rupture life and the ductility at rupture may also be significantly different.

Weld Metal Strength. There is a tendency for weld metal to overmatch the parent metal in strength at ambient and low temperatures. While a slight overmatch is not harmful, excessive hardness in welds can cause greater susceptibility to weld cracking.

Creep of Welds in High-Temperature Service. Recent developments suggest that welded joints in some chromium-molybdenum steels are a potential source of weakness in creep. Vessels that have performed satisfactorily in service thus far may have safety factors lower than those suggested by present design rules. This arises from the mismatch of creep

properties in the different weld zones, especially in thick sections. In recognition of this fact, section III of the ASME code, "Nuclear Power Plant Components," has assigned stress-reduction factors to weldments operating in the creep range of temperatures.

Material Requirements for Service Conditions

ASM Committee on Material Requirements for Service Conditions*

Shipbuilding and Offshore Structures

The materials used for ships and offshore structures encounter a broad range of service conditions and must be capable of withstanding the rigors of weather and sea. With the advent of sophisticated communications systems, ships can often avoid heavy weather, whereas site-dependent offshore structures must be built to withstand any service condition that arises.

Material Requirements for Service Conditions

ASM Committee on Material Requirements for Service Conditions*

Ships

Steel ship structures are comprised of shell plating and shapes joined by welding. The structures vary considerably among various ship types, including small boats 10 to 25 m (30 to 80 ft) long to supertankers with lengths ranging from 100 to 400 m (330 to 1300 ft) or more. In between are container ships, liquefied natural gas (LNG) and liquefied petroleum gas (LPG) carriers, passenger ships, ore carriers, and others. Requirements for ordinary- and higher-strength steels according to the rules of the American Bureau of Shipping Rules (ABS) are given in Tables 9 and 10, respectively.

TABLE 9 ABS REQUIREMENTS FOR ORDINARY-STRENGTH HULL STRUCTURAL STEEL (≤50 MM, OR 2 IN., THICK)

GRADE	DEOXIDATION	CHEMICAL COMPOSITION[A], %				
		C	Mn	P	S	Si
A	SEMIKILLED OR KILLED FOR MATERIAL THICKER THAN 12.5 MM (0.5 IN.)	0.23 MAX[B]	2.5 × C MIN FOR PLATE THICKER THAN 12.5 MM (0.5 IN.)	0.04 MAX	0.04 MAX	. . .
B	SEMIKILLED OR KILLED	0.21 MAX	0.08-1.10; 0.60 MIN FOR FULLY KILLED OR COLD FLANGING	0.04 MAX	0.04 MAX	0.35 MAX
D	FULLY KILLED; FINE-GRAIN PRACTICE[C]	0.21 MAX	0.70-1.35; 0.60 MIN FOR THICKNESS ≤25 MM (1 IN.)	0.04 MAX	0.04 MAX	0.10-0.35
E	FULLY KILLED; FINE-GRAIN PRACTICE	0.18 MAX	0.70-1.35	0.04 MAX	0.04 MAX	0.10-0.35

TENSILE STRENGTH		YIELD POINT (MIN)		ELONGATION (MIN)
Mpa	Ksi	Mpa	Ksi	
FOR ALL GRADES:		FOR ALL GRADES:		FOR ALL GRADES:
400-490	58-71	235	34	21% IN 200 MM (8 IN.) OR 24% IN 50 MM (2 IN.)
FOR GRADE A SHAPES		FOR GRADE A THICKER THAN		FOR COLD FLANGING QUALITY:

AND BARS:		25 MM (1 IN.)		
400-550	58-80	220	32	23% MIN IN 200 MM (8 IN.)
FOR COLD FLANGING QUALITY:		FOR COLD FLANGING:		
380-450	55-65	205	30	

GRADE	CHARPY V-NOTCH IMPACT TEMPERATURE		ENERGY AVERAGE (MIN), J (FT · LBF)		HEAT TREATMENT	MARKING
	°C	°F	LONGITUDINAL SPECIMENS	TRANSVERSE SPECIMENS		
A	. . .	. . .	. . .	. . .	. . .	AB/A
B	0	32	27 (20)	20 (14)	. . .	AB/B
D	-10	14	27 (20)[D]	20 (14)[D]	NORMALIZED FOR MATERIAL THICKER THAN 35 MM (1.4 IN.)[E]	AB/D[F]
E	-40	-40	27 (20)	20 (14)	NORMALIZED[G]	AB/E

(A) FOR ALL GRADES EXCLUSIVE OF GRADE A SHAPES AND BARS, THE SUM OF CARBON CONTENT AND ONE-SIXTH OF THE MANGANESE CONTENT IS NOT TO EXCEED 0.40%. THE UPPER LIMIT OF MANGANESE MAY BE EXCEEDED UP TO A MAXIMUM OF 1.65%, PROVIDED THAT THIS CONDITION IS SATISFIED. THE CONTENTS OF NICKEL, CHROMIUM, MOLYBDENUM, AND COPPER ARE TO BE DETERMINED AND REPORTED, AND WHEN THE AMOUNT PRESENT IS LESS THAN 0.02%, THESE ELEMENTS MAY BE REPORTED AS 0.02%.

(B) A MAXIMUM CARBON CONTENT OF 0.26% IS ACCEPTABLE FOR GRADE A PLATES $\leqslant$12.5 MM (0.5 IN.) AND ALL THICKNESSES OF GRADE A SHAPES AND BARS.

(C) GRADE D MAY BE FURNISHED SEMIKILLED IN THICKNESSES UP TO 35 MM (1.4 IN.), PROVIDED THAT STEEL >25 MM (1 IN.) THICK IS NORMALIZED. IN THIS CASE THE REQUIREMENTS RELATIVE TO MINIMUM SILICON AND ALUMINUM CONTENTS AND FINE-GRAIN PRACTICE DO NOT APPLY.

(D) IMPACT TESTS ARE NOT REQUIRED FOR NORMALIZED GRADE D STEEL WHEN FURNISHED FULLY KILLED, FINE-GRAIN PRACTICE.

(E) CONTROLLED ROLLING OR THERMOMECHANICAL CONTROLLED ROLLING OF GRADE D STEEL MAY BE CONSIDERED AS A SUBSTITUTE FOR NORMALIZING.

(F) GRADE D HULL STEEL THAT IS NORMALIZED, THERMOMECHANICAL CONTROLLED ROLLED, OR CONTROLLED ROLLED IN ACCORDANCE WITH [E] IS TO BE MARKED AB/DN.

(G) CONTROLLED ROLLING OR THERMOMECHANICAL CONTROLLED ROLLING OF GRADE E SHAPES AND THERMOMECHANICAL CONTROLLED ROLLING OF GRADE E PLATES MAY BE CONSIDERED AS A SUBSTITUTE FOR NORMALIZING.

TABLE 10 ABS REQUIREMENTS FOR HIGHER-STRENGTH HULL STRUCTURAL STEEL ($\leq$50 MM, OR 2 IN., THICK)

GRADE[A]	DEOXIDATION	TENSILE STRENGTH		YIELD POINT (MIN)		ELONGATION (MIN)	CHARPY V-NOTCH IMPACT TEMPERATURE		ENERGY AVERAGE (MIN), J (FT · LBF)		HEAT TREATMENT	MARKING
		Mpa	Ksi	Mpa	Ksi		°C	°F	LONGITUDINAL SPECIMENS	TRANSVERSE SPECIMENS		
AH32	SEMIKILLED	470-	68-	315	45.5		0	32	34 (25)[B]	24 (17)[B]	. . .	AB/AH32

	OR KILLED	585	85									
AH36		490-620	71-90	355	51							AB/AH36
DH32	KILLED; FINE-GRAIN PRACTICE[C]	470-585	68-85	315	45.5	FOR ALL GRADES: 19% IN 200 MM (8 IN.) OR 22% IN 50 MM (2 IN.)	-20	-4	34 25[B]	24 (17)[B]	NORMALIZED[D] FOR MATERIAL >12.5 MM (0.5 IN.) THICK[E]	AB/DH32[F]
DH36		490-620	71-90	355	51							AB/DH36[F]
EH32	KILLED; FINE-GRAIN PRACTICE [C]	470-585	68-85	315	45.5		-40	-40	34 (25)	24 (17)	NORMALIZED[G]	AB/EH32
EH36		490-620	71-90	355	51							AB/EH36

(A) THE NUMBERS FOLLOWING THE GRADE DESIGNATION INDICATE THE YIELD POINT OR YIELD STRENGTH TO WHICH THE STEEL IS ORDERED AND PRODUCED IN KGF/MM^2. THE CHEMICAL COMPOSITION FOR ALL GRADES IS: 0.18% MAX C; 0.90-1.60% MN (GRADE AH THAT IS ≤12.5 MM, OR 0.5 IN., THICK MAY HAVE A MINIMUM MANGANESE CONTENT OF 0.70%); 0.04% MAX P; 0.04.% MAX S; 0.10-0.50% SI (GRADE AH PLATE THAT IS ≤12.5 MM, OR 0.5 IN., THICK AND ALL THICKNESSES OF AH SHAPES MAY BE SEMIKILLED, IN WHICH CASE THE 0.10% MIN SI DOES NOT APPLY; UNLESS OTHERWISE SPECIALLY APPROVED, AH PLATE >12.5 MM, OR 0.5 IN., THICK ARE TO BE KILLED WITH 0.10-0.50% SI); 0.40% MAX NI; 0.25% MAX CR; 0.08% MAX MO: 0.35% MAX CU; 0.05% MAX NB; 0.10 MAX V. NICKEL, CHROMIUM, AND MOLYBDENUM MAY BE REPORTED AS 0.02% WHEN THE AMOUNT PRESENT IS LESS THAN 0.02%. NIOBIUM AND VANADIUM NEED NOT BE REPORTED ON THE MILL SHEET UNLESS INTENTIONALLY ADDED.

(B) IMPACT TESTS ARE NOT REQUIRED FOR AH THAT IS ≤12.5 MM (0.5 IN.) THICK OR FOR ALUMINUM TREATED GRADE AH THAT IS ≤35 MM (1.4 IN.) THICK, NOR FOR FULLY KILLED FINE-GRAIN NORMALIZED GRADES AH OR DH THAT IS ≤50 MM (2 IN.) THICK.

(C) GRADES DH AND EH ARE TO CONTAIN AT LEAST ONE OF THE GRAIN-REFINING ELEMENTS IN SUFFICIENT AMOUNT TO MEET THE FINE-GRAIN PRACTICE REQUIREMENT.

(D) CONTROLLED ROLLING OR THERMOMECHANICAL CONTROLLED ROLLING OF GRADE D STEEL MAY BE CONSIDERED AS A SUBSTITUTE FOR NORMALIZING.

(E) CONTROLLED ROLLING OR THERMOMECHANICAL CONTROLLED ROLLING OF GRADE EH SHAPES AND THERMOMECHANICAL CONTROLLED ROLLING OF GRADE EH PLATES MAY BE CONSIDERED AS A SUBSTITUTE FOR NORMALIZING.

(F) THE MARKING AB/DHN IS TO BE USED TO DENOTE GRADE DH PLATES WHICH HAVE EITHER BEEN NORMALIZED, THERMOMECHANICAL CONTROLLED ROLLED, OR CONTROL ROLLED IN ACCORDANCE WITH APPROVED PROCEDURE.

(G) FOR DH TREATED WITH NIOBIUM OR VANADIUM, OR WHEN USED IN COMBINATION WITH ALUMINUM OR EACH OTHER. DH TREATED ONLY WITH ALUMINUM IS TO BE

NORMALIZED WHEN >25 MM (1 IN.) THICK.

Tankers and Container Ships. Large ocean-going tankers have been built with both single and double hulls, with the latter type becoming more popular due to environmental considerations and the belief that oil spills are more readily prevented by double-hull construction. However, most tankers in service today have single hulls. In the design of typical ships, 0 °C (32 °F) is normally assumed to be the lowest service temperature.

Material selection for single-hull tankers for a particular steel strength level is based on stress level, location, thickness, and toughness. A typical cross section of the shell and longitudinal bulkheads for a large tanker is shown in Fig. 7. Plating for various parts of the ship can be categorized as secondary, intermediary, and special application. The four corners of a ship and the deck and bottom plating in the way of the longitudinal bulkheads are usually highly stressed and are made from "special" steels with improved toughness properties. The side shell and areas close to the neutral axis of the ship are the least stressed, and thus the toughness of the steels employed is of "secondary" importance. The remaining deck and bottom of a tanker are moderately stressed and are constructed of intermediate-toughness steels.

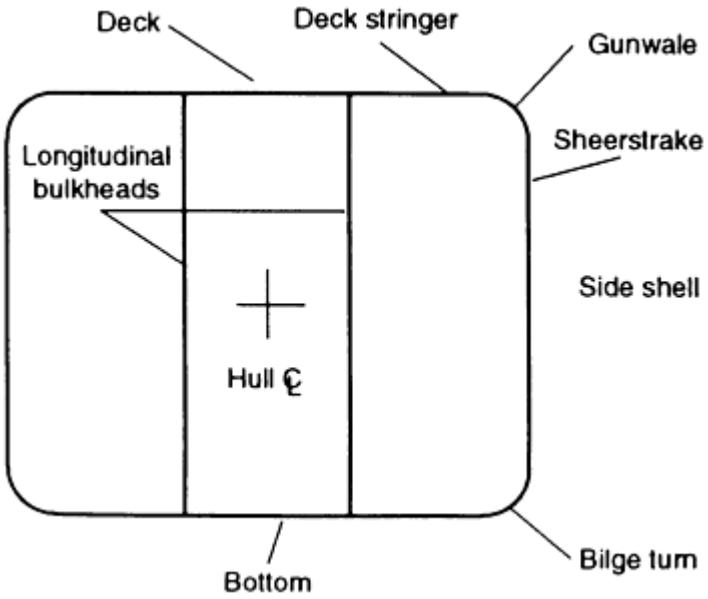

FIG. 7 MIDSHIP CROSS SECTION OF A LARGE TANKER, INDICATING SHELL PLATING AND LONGITUDINAL BULKHEADS.

The design considerations for tankers can also apply to container ships. However, because of the large cutouts on the deck that allow access for loading and unloading, the most critical structural area of a container ship is the box girder that connects the side shell to the deck. Major stresses are transmitted through this member, and thus the steels selected for these areas must have improved notch toughness.

Liquefied Natural Gas/Liquefied Petroleum Gas Ships. The minimum service temperature for most ships is approximately 0 °C (32 °F), and hull steels are selected and applied on this basis. Where temperatures below 0 °C (32 °F) are expected, application adjustments or selection of materials with superior low-temperature notch toughness must be considered. In the marine industry, low-temperature service is a significant factor in the design of ships carrying liquefied gases in bulk and of structures operating for prolonged periods in cold weather. Liquefied gases--both petroleum and natural--are transported in bulk by ship at temperatures ranging from -50 to -165 °C (-58 to -265 °F).

Steels for ship hulls are brittle at cryogenic temperatures. Thus, for safety reasons, it is essential to prevent the liquefied gas from contacting the steel hull and to minimize excessive conduction cooling of the hull. The primary requisite for the cargo tank material is high notch toughness at low temperature. Also, because shipboard tanks are subjected to dynamic loads resulting from ship motions, fatigue is another consideration.

Fracture mechanics concepts, which require knowledge of fracture toughness and fatigue crack-growth rate properties at low temperature, are frequently used in design. One design concept applied is "leak before failure," combined with a small-leak protection system. Utilizing this concept, a ship will be able to journey to an unloading and repair site before a detected flaw grows to critical size. Other systems are provided with large secondary containment barriers that can contain major leaks while permitting the ship to proceed to an unloading facility. All designs incorporate insulation to prevent excessive conduction cooling of the hull structure. For LNG containment systems, designed for cargo temperatures of -65 °C (-265 °F), external insulations of balsa, pearlite, polyurethane foam, and polyvinyl chloride foam have been used. For higher-temperature liquefied gases, such as LPG transported at a temperature of about -50 °C (-60 °F), some tanks have been internally insulated, which permits the use of less expensive tank structure materials than would be necessary with external insulation.

The worldwide adoption of International Maritime Organization (IMO) requirements for the carriage of liquefied gases by sea has unified material requirements for ships carrying cryogenic cargos in bulk. For the primary containment of such cryogenic cargos as LNG (methane) at a temperature of -165 °C (-265 °F), the most commonly selected materials have hexagonal close-packed (hcp) crystal structures; these include alloys such as 5083 aluminum, austenitic stainless steels, and 36% Ni steels, selected because of their superior low-temperature toughness properties. Nickel-bearing body-centered cubic (bcc) alloys, such as 9% Ni steels, have also been used, although less extensively.

The most important characteristic of the low-temperature mechanical behavior of ferritic steels is the ductile-to-brittle fracture transition. The transition occurs over a narrow temperature range for sharply notched specimens, and at temperatures below the transition, failure occurs by the brittle cleavage mode. This low-temperature embrittlement severely restricts the use of ferritic materials in cryogenic systems. Structural applications of ferritic materials are generally limited to environments where the service temperature remains above the ductile-to-brittle transition. The ferritic steels that are used for low-temperature applications usually contain nickel to improve low-temperature toughness. At the lower end of the cargo temperature range, austenitic alloys and 5083 aluminum are commonly used.

Table 11 indicates the service temperature specified in the ABS rules for each material. Austenitic stainless steel and 36% Ni steel are used for nonpressurized membrane tank designs. These alloys are provided in thin 0.5 to 1.5 mm (0.02 to 0.06 in.) sheets, usually corrugated to provide stiffness and allow for thermal expansion.

TABLE 11 MATERIALS FOR CRYOGENIC APPLICATIONS

MATERIAL	ASTM NO.	SERVICE TEMPERATURE	
		°C	°F
2% NI STEEL	A 203, GRADE A	-62	-80
	A 203, GRADE B	-59	-75
3% NI STEEL	A 203, GRADE D	-90	-130
	A 203, GRADE E	-79	-1L0
5% NI STEEL	A 645	-105(A)	-155(A)
9% NI STEEL	A 353	-196	-320
9% NI STEEL	A 553	-196	-320
AUSTENITIC STAINLESS STEEL	A 240	-196	-320
36% NI ALLOY	A 658	-196(B)	320(B)
ALUMINUM ALLOY	E 209, ALLOY 5083	-196	-320

(A) 5% NI STEEL MAY BE USED DOWN TO -165 °C (-265 °F) PROVIDED THAT IMPACT TESTS ARE CONDUCTED AT -196 °C (-320 °F).

(B) CHEMISTRY WILL BE SPECIALLY CONSIDERED FOR LOWERING THE COEFFICIENT OF EXPANSION.

For spherical pressurized tanks, 5083 aluminum alloy at a thickness of 40 to 60 mm (1.6 to 2.4 in.) is used to form tanks up to 35 m (115 ft) in diameter. The aluminum tank is attached to the steel hull by means of an explosion-bonded aluminum-to-steel plate; the tank connects to the aluminum side, and the steel side connects to the hull. This type of explosion-bonded plate is also used for connecting aluminum superstructures to steel decks.

ASM Committee on Material Requirements for Service Conditions*

Offshore Structures

Several important characteristics and operations of many offshore drilling units dictate the use of materials different from those used for ships, or restrictions on the application of similar materials. Much offshore exploration by mobile drilling or fixed units is carried out in areas where ambient air temperatures remain below 0 °C (32 °F) for long periods, such as in the Arctic. Toughness for these applications must be considered on the basis of the lowest expected steel temperature, because ferritic steels undergo a ductile-to-brittle fracture transition. The lowest steel temperature expected in service is estimated from meteorological data representing the coldest region in which the structure is designed to operate.

Toughness Versus Structural Application. In general, toughness testing of structural steel for offshore structures is conducted at a temperature below the minimum expected service temperature, the extent of the temperature increment being based on certain design criteria, such as anticipated stresses, stress concentrations, and redundancy of the structural member. For example, the ABS defines three structural categories to which different levels of toughness are assigned (see Table 12). The three categories are assigned to structural components based on consideration of the following: consequence of failure; redundancy of component; service experience with similar design; stress level, including stress concentration and restraint; fatigue; loading rate; and capability of inspection and repair in service.

TABLE 12 TEST TEMPERATURE FOR STEELS WITH A YIELD STRENGTH OF LESS THAN 415 MPA (60 KSI)

STRUCTURAL CATEGORY	DESCRIPTION	CHARPY V-NOTCH TEST TEMPERATURE
SECONDARY	LEAST CRITICAL: REDUNDANT	AT SERVICE TEMPERATURE
PRIMARY	MAIN STRUCTURAL MEMBERS THAT SUSTAIN PRIMARY TENSILE STRESS AND WHOSE FAILURE WOULD JEOPARDIZE THE SAFETY OF THE STRUCTURE	10 °C (18 °F) BELOW SERVICE TEMPERATURE
SPECIAL	MOST CRITICAL: FRACTURE CRITICAL MEMBERS THAT COULD EXPERIENCE RAPID LOADING AT POINTS OF STRESS CONCENTRATION	30 °C (55 °F) BELOW SERVICE TEMPERATURE

Absorbed energy obtained by a Charpy V-notch test is the most commonly used criterion for grading steels according to toughness. This criterion cannot be related directly to design, but is used as an expression of a toughness quality level.

Structural steel elements for offshore structures are often fabricated from cold-formed sections. As most structural steels are strain-age sensitive, it is important to evaluate the extent to which a given steel loses toughness after being cold strained. Outer fiber strains of less than 3% usually do not reduce toughness significantly. In general, at above 3% strain the material is either heat treated to restore the toughness or tested to determine that the poststrain toughness has not degraded below minimum acceptable values.

Quenched and Tempered Steels. Certain offshore drilling unit designs, especially the self-elevating type, make weight savings in the upper structure and the legs an important consideration in order to reduce the size and power requirements for lifting equipment and to aid stability. Therefore, high-strength quenched and tempered martensitic steels with yield strengths of approximately 700 MPa (100 ksi) find wider application in offshore structures than in ships. Areas subject to concentrated loads, such as openings for leg structures, cantilever overhangs for drilling booms, helicopter decks, and crane pedestals, are other locations on offshore drilling structures in which high-strength steels are commonly used.

Welding Process Selection

Welding has exclusively replaced riveting for joining structural steels in the fabrication of ships and offshore structures. In shipbuilding, welding permits large subassemblies to be built quickly and efficiently; these subassemblies are then welded together to form ship hulls.

Manual Welding. Shielded metal arc welding with stick electrodes, semiautomatic gas metal arc welding (GMAW), and flux-cored arc welding (FCAW) are all used in shipbuilding. These processes offer a high degree of versatility because of the portability of equipment and are commonly used for short weld runs and for erection welds.

Gravity-feed welding is used in the assembly of ships and offshore structures. It is carried out using contact or drag-type electrodes with tripod-type holding mechanisms, which allow welding to be done semiautomatically. An operator places the electrode in the holder and positions the holding mechanism, and welding progresses unrestricted until the electrode is consumed. Long electrodes enable welds more than 750 mm (30 in.) in length to be made with one electrode. Specific electrode diameters with proper current and voltage settings control the size of the deposited weld. One operator can handle two to six gravity-type devices at the same time.

This process has been largely employed for attaching stiffeners to plating by fillet welding. It is particularly attractive when the weld lengths are less than 3 m (10 ft), in which case the use of a fully automatic process may not be justified due to setup time, portability, and other considerations. Applications include internal stiffening of drilling-rig support columns and braces, as well as stiffening of decks.

Mechanized Welding. Submerged arc welding is used for making long, continuous butt welds to join plate panels or for joining stiffeners to plating by fillet welding. Modern shipyards that build large ships, especially tankers, where a considerable amount of flat panel work is required, have invested heavily in panel lines to further mechanize or automate the SAW process. Such panel lines are capable of making panel subassemblies up to about 20 m^2 (200 ft^2) in size.

One-side welding using SAW was introduced and perfected in Japan during the 1960s and early 1970s in connection with a massive tanker-building program for very large and ultralarge crude-oil carriers. In one-side welding, weld backing on the underside is provided by copper bars, ceramic forms, solid flux systems, or powdered flux held in place by various troughing systems.

Electroslag welding (ESW) and electrogas welding (EGW) have been used to make relatively long (more than 10 m, or 30 ft) continuous vertical erection welds in the side shells of large ships. These processes offer higher deposition and production rates than more conventional welding processes. The minimum plating thickness is about 19 to 25 mm ($\frac{3}{4}$ to 1 in.).

Consumable-nozzle ESW, a variation of the basic electroslag process, is used for making vertical butt welds in deck and bottom longitudinals and in heavy face plates of girders.

Oxyfuel Gas (OFG) and Plasma Arc Cutting. Oxyfuel gas cutting is used predominantly for cutting panels and stiffeners and for handfitting miscellaneous members. Plasma arc cutting has been used for mechanized cutting of plating up to about 12 to 20 mm (0.5 to 0.8 in.) thick. It offers the advantage of faster cutting speeds and less heat distortion as compared with gas cutting for thin plating. Because the significant tonnages of plating and shaping that must be cut or beveled for welding large ships, a high degree of mechanization has been introduced. Numerical control cutting permits panels up to about 2.5 by 15 m (8 by 50 ft) to be completely cut to size with appropriate cutouts, as well as edge beveling for welding to make large subassemblies.

Weld Considerations

The materials used for ship construction are generally ordinary-strength or higher-strength steels with a maximum yield strength of 355 MPa (52 ksi) (see Tables 9 and 10). For offshore drilling units and platforms, a variety of high-strength quenched and tempered steels with yield strengths up to 700 MPa (100 ksi) are also used. Weld filler metals should approximate the tensile and toughness properties of the base material; where materials of two different strengths or toughnesses are to be joined, the lower-strength or lower-toughness weld metal can be used.

Weld metal toughness is an important parameter in shipbuilding. Quantitative measurements of toughness are based on Charpy V-notch properties, and values comparable to those of the base materials are specified for weld metal. For offshore structures such as fixed platforms or drilling units, which must stay on station and encounter severe storms, winds, waves, and temperature fluctuations, toughness is also an important consideration. Materials and weld metals with yield strengths of up to 700 MPa (100 ksi) are commonly offered for tubular leg chord sections, braces, and rack material. The racks that form part of the leg chord are often 100 to 150 mm (4 to 6 in.) thick.

Hydrogen Cracking. When joining thick high-strength quenched and tempered steels, appropriate preheat and interpass temperatures are necessary to avoid HIC (see the article "Cracking Phenomena Associated with Welding" in this Volume). This condition is generally more prevalent in HSLA steels than in ordinary-strength steels, and its occurrence is generally proportional to the hardenability and tensile strength of the base material. Hydrogen cracks are usually found in the HAZ and can occur in both fillet- and butt-welded connections. Hydrogen cracking is often referred to as cold or delayed cracking because of the tendency for these cracks to occur and propagate after the weld has cooled to ambient temperatures. It is not uncommon for such cracks to be revealed hours or even days after welding, depending on the restraint conditions within the structure. For this reason, it is common practice to postpone the final nondestructive testing until several days after completing a weld.

Hydrogen sources in and around the arc atmosphere include moisture in the electrode coating, flux, gas, and base material and the presence of hydrocarbons, such as grease, paint, or oil. Moisture requirements for electrode coatings, along with storage and conditioning recommendations, are included in specifications and become more severe as strength levels increase. In SAW, where the flux is a common source of moisture, storage should be controlled to avoid moisture contamination from the atmosphere. Inadequate protection from hydrogen must be provided, especially in final erection or field welding applications, where hydrogen sources are more prevalent and where accessibility to the welded joint is less than ideal.

Lamellar tearing is the separation of steel plate underneath a weld in a plane generally parallel to the plate surface. It usually results from high through-thickness strains induced by weld shrinkage. These strains cause nonmetallic inclusions present in the steel to decohere. The resulting tears or cracks are planar in appear- ance, with some steplike characteristics. Welded connections joining two or more tubular sections are common in offshore structures. On several occasions, lamellar tearing has been observed in diaphragm plates used between two tubulars to simplify construction. Improvement in through-thickness properties is possible by using steels with fewer impurities or nonmetallic inclusions, lowering the permitted sulfur contents (typically 0.010% maximum), and treating the molten steel with rare earth elements, which combine with sulfur to form refractory sulfides that resist deformation at hot rolling temperatures. Another approach to eliminate lamellar tearing, and to simplify fabrication, is to use steel castings for the node connections. Centrifugally cast straight tubulars have also been proposed for offshore structural applications.

Lamellar tearing has been reported in sheer-strake-to-deck connections in ships. This problem can be eliminated by the use of gunwale connections. Lamellar tearing or cracking at welded connections is best avoided by the selection of a design that reduces the tendency for stressing through the thickness of the structural members.

In the construction of offshore drilling units and platforms, lamellar tearing presents a more acute problem because of the complexity of welded joints and connections. Sometimes joints may be unavoidably susceptible to lamellar tearing; in such cases, carefully planned welding sequences should be employed. It is common practice to use other than full-penetration welds; for instance, double-bevel partial-penetration T-welds are often used. Steel exhibiting the equivalent of 20% (minimum) reduction of area in a through-thickness tensile specimen (as per ASTM A 770) is considered to be less susceptible to lamellar tearing. Commonly used structural steels, including ABS hull steels, that meet the A 770 specification are available from some producers. Such steels have additional restrictions on chemistry and are produced using special melting practices.

Undermatching Weld Metal Strength. In some cases, weld metal that undermatches the base plates may be used in the fabrication and repair of high-strength steels, primarily for fillet welding and local repairs. The use of the lower-strength weld metal minimizes cracking tendency by providing a weld with reduced residual stresses and somewhat higher ductility. Such lower-strength filler metals are permitted when the strength level of the particular weld fulfills design requirements. When lower-strength covered electrodes are used to weld higher-strength materials, special precautions associated with welding the higher-strength materials are still required to prevent hydrogen cracking. When E80*xx* or E90*xx* electrodes are used to weld 700 MPa (100 ksi) yield strength material, such as ASTM A 514, the electrodes should be subjected to appropriate baking to reduce electrode-covering moisture to 0.15% maximum. This precaution should also be taken in the more common case where E7018-type electrodes are used to join high-strength steels (e.g., 700 MPa, or 100 ksi, yield strength) to lower-strength steels.

To summarize, in the following circumstances, the use of undermatching electrodes should be considered:

- *FILLET WELDING:* USE OF E9018 OR EVEN E8018 ELECTRODES FOR FILLET WELDING OF STEELS WITH A YIELD STRENGTH OF 700 MPA (100 KSI) IS A CONVENIENT WAY OF MINIMIZING CRACKING TENDENCY IN THE WELD METAL AND HAZ. ELECTRODES SHOULD BE BAKED TO A 0.15% MAXIMUM MOISTURE CONTENT.
- *REPAIR WELDING:* THE LOWER STRENGTH AND LOWER RESIDUAL STRESS ASSOCIATED WITH THE E9018 ELECTRODE MAKE IT THE ELECTRODE OF CHOICE FOR ISOLATED REPAIRS IN BUTT OR FILLET WELDS IN THE HIGHER-STRENGTH STEELS (700 MPA, OR 100 KSI, YIELD STRENGTH), PROVIDED THAT THE OVERALL STRENGTH OF THE STRUCTURE IS MAINTAINED TO MEET DESIGN REQUIREMENTS.

Material Requirements for Service Conditions

ASM Committee on Material Requirements for Service Conditions*

Aerospace

Aerospace systems push materials to the limits of their physical and mechanical properties. Therefore, it is important to optimize designs, which often involves consideration of nonmechanical fastening methods. Welding, brazing, soldering, and/or adhesive bonding are the only options in many aerospace structures. Whether the driving force is weight, leakproof seals, continuous load paths, or any number of other requirements, nonmechanical joining of materials is essential in the manufacture of aerospace systems. The list of materials used in the construction of such systems is quite large. This section will present an overview of mechanical and physical property considerations as they relate to joining.

Material Requirements for Service Conditions

ASM Committee on Material Requirements for Service Conditions*

Material Selection Criteria

Properties. Modern aerospace systems employ metals, ceramics, composites, and polymers. Important mechanical and physical properties for aerospace applications are listed in Table 13 (Ref 7).

TABLE 13 MATERIAL PROPERTIES OF IMPORTANCE IN AEROSPACE APPLICATIONS

PHYSICAL PROPERTIES

CRYSTAL STRUCTURE
DENSITY
MELTING POINT
VAPOR PRESSURE
VISCOSITY
POROSITY
PERMEABILITY
REFLECTIVITY
TRANSPARENCY
OTHER OPTICAL PROPERTIES
DIMENSIONAL STABILITY
ELECTRICAL/MAGNETIC PROPERTIES
CONDUCTIVITY
DIELECTRIC CONSTANT
COERCIVE FORCE
HYSTERESIS
SUSCEPTIBILITY
PERMEABILITY
REMANENCE
MECHANICAL PROPERTIES
HARDNESS
MODULUS OF ELASTICITY TENSION
COMPRESSION
POISSON'S RATIO
STRESS-STRAIN CURVE
YIELD STRENGTH TENSION
COMPRESSION
SHEAR
ULTIMATE STRENGTH TENSION
SHEAR
BEARING
FATIGUE PROPERTIES SMOOTH
NOTCHED
CORROSION FATIGUE
ROLLING CONTACT
FRETTING
CHARPY TRANSITION TEMPERATURE
FRACTURE TOUGHNESS (K_{IC})
HIGH-TEMPERATURE PROPERTIES CREEP
STRESS RUPTURE
DAMPING PROPERTIES
WEAR PROPERTIES GALLING
ABRASION
EROSION
CAVITATION

SPALLING
BALLISTIC IMPACT
THERMAL PROPERTIES
CONDUCTIVITY
SPECIFIC HEAT
COEFFICIENT OF EXPANSION
EMISSIVITY
ABSORPTIVITY
ABLATION RATE
FIRE RESISTANCE
MAXIMUM/MINIMUM OPERATING TEMPERATURE
CHEMICAL PROPERTIES
POSITION IN ELECTROMOTIVE SERIES
CORROSION AND DEGRADATION
ATMOSPHERIC
SALT WATER
ACIDS
HOT GASES
ULTRAVIOLET
OXIDATION
THERMAL STABILITY
BIOLOGICAL STABILITY
STRESS CORROSION
HYDROGEN EMBRITTLEMENT
HYDRAULIC PERMEABILITY
FABRICATION PROPERTIES
CASTABILITY
HEAT TREATABILITY
HARDENABILITY
FORMABILITY
MACHINABILITY
WELDABILITY

Source: Ref 7

Applications. The service requirements for a particular application will order the material properties. As shown in Fig. 8, material selection is based on a number of interrelated factors, including material properties, manufacturability, repairability, and availability (Ref 8). Because compromise is required to ensure optimal material selection, both the service requirements and the materials characterization must be thorough and complete. Design also plays an important role. For example, if a material is selected for a design using mechanical fastening, and nonmechanical joining is substituted as the manufacturing technique, the material and the design must be reevaluated. A design requiring mechanical fastening generally is not optimal for nonmechanical joining.

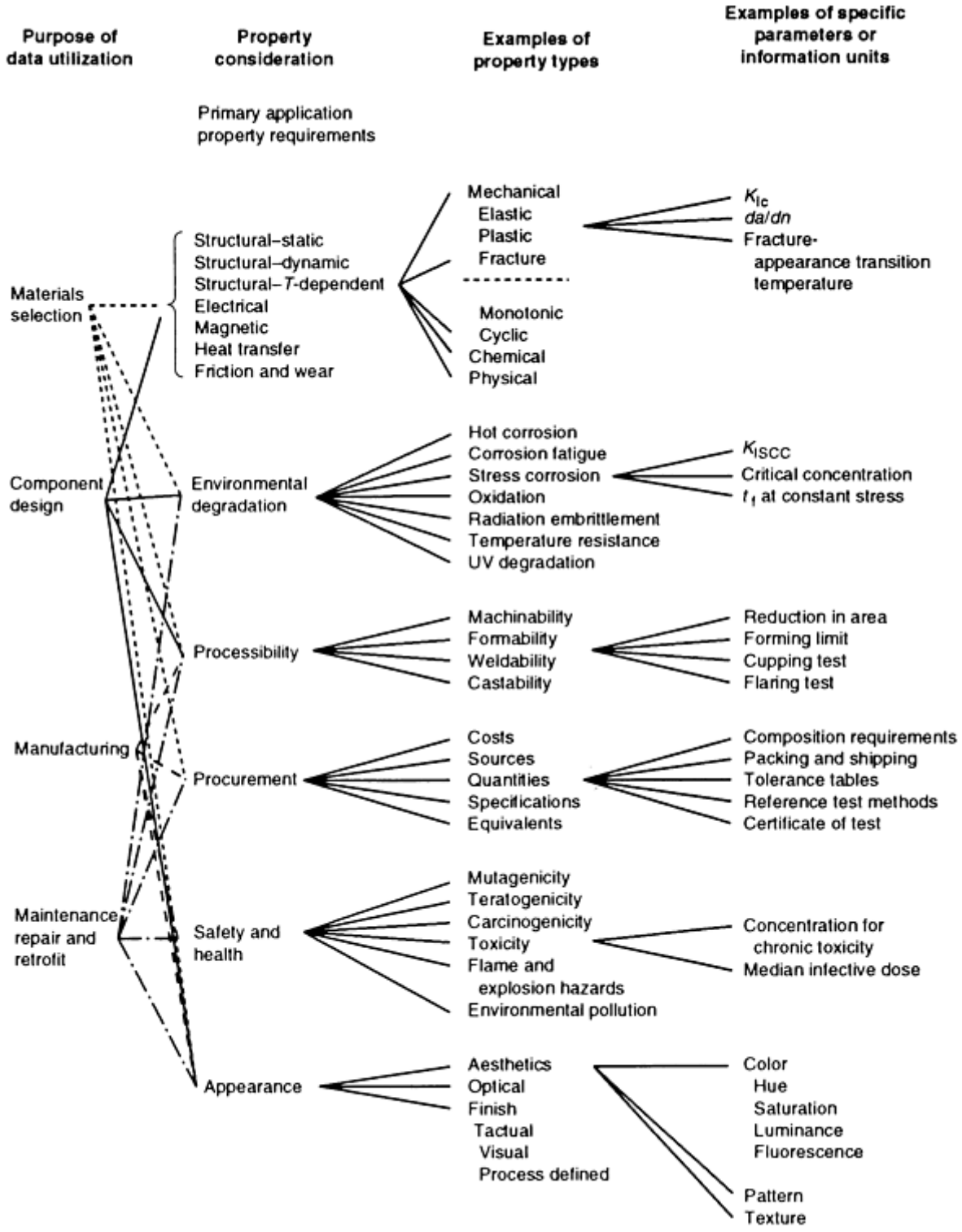

FIG. 8 INTERRELATIONSHIPS AMONG AEROSPACE DESIGN, MANUFACTURE, MAINTENANCE AND REPAIR, AND MATERIAL SELECTION. SOURCE: REF 8

Thermal Stability. A clear understanding of the material properties of importance for a given application is crucial to optimal material selection. For example, thermal stability, both metallurgical and physical, is a very important factor in elevated-temperature applications. Over time, microstructural thermal instability may alter mechanical properties, such as toughness, creep, or crack growth. The thermal stability of a material may be affected by a thermal joining process. Precipitation of unstable phases in the fusion zones of structural alloys, such as advanced titanium alloys, can be difficult to evaluate. Also, the tensile strength of high-strength aluminum alloys can be adversely affected during high-temperature

curing of adhesives if the aging temperature is exceeded for a sufficient length of time (Ref 9). Thermal stability can be maintained by ensuring proper material chemistry, heat treatment, joining process, joining consumable, and/or postjoining thermal treatments. Thermal instability may manifest itself as creep, cracking, buckling, and/or a reduction in corrosion resistance (Ref 4, 10, 11, 12). The corrosion properties of stainless steels may be severely impaired by elevated-temperature exposure, such as welding and brazing. The degradation referred to as sensitization can also reduce fatigue performance. Thermal stability has been used here as an example. A similar discussion could be presented for each property listed in Table 13.

Weight is an overriding concern in aerospace applications because of its adverse effect on performance and operational costs. Many decisions are based on the specific property of a material, such as those shown in Fig. 9. Specific properties are defined as the mechanical or physical property of the material divided by its density:

$$\frac{\textit{Material}\ \text{property}}{\text{Material density}} = \textit{specific}\ \text{property}$$

When using specific properties, one must be careful to fully characterize anisotropic materials. When considering a material for a nonmechanical joining application, an understanding of the effect of joining on these properties is essential. Joinability often is ignored during the development of aerospace materials (and materials in general) and can considerably inhibit their versatility during construction. Because compromise is the standard when selecting materials for a specific application, the effect of joining on properties must be considered.

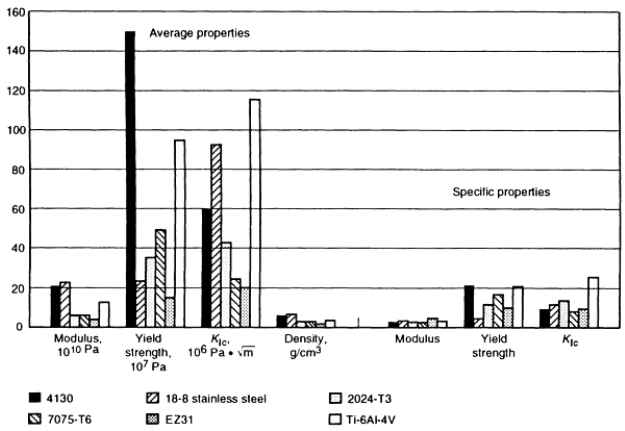

FIG. 9 AVERAGE VERSUS SPECIFIC PROPERTIES

Specifications. Aerospace materials are most often purchased to a military (MIL) or Aerospace Materials Specification (AMS). Some materials, such as A286, are available in standard and weldable grades. The weldable grade is formulated to reduce the tendency for microcracking. Filler metal specifications are provided by AWS or by the Society of Automotive Engineers (SAE) as Aerospace Materials Specifications.

Economics. Cost is another important material consideration. The cost of the raw materials is usually a small percentage of the cost of the end product in applications such as aerospace airframes and engine components, structures, and assemblies. The costs of some common materials as a function of volume production are presented in Fig. 10. However, material selection can have a significant cost impact in the areas of manufacturability and life-cycle costs (repairability and maintainability). The designation of materials must be as specific as possible to ensure maintenance of quality for joining applications (Ref 10, 11, 13). If multiple welds are to be performed on a given structure, the requirement for intermediate heat treatments or other processing steps must be considered. In large structures where full heat treatments are difficult because of distortion, the reduction in properties may require increased joint thickness, thereby increasing weight and complicating the manufacturing process.

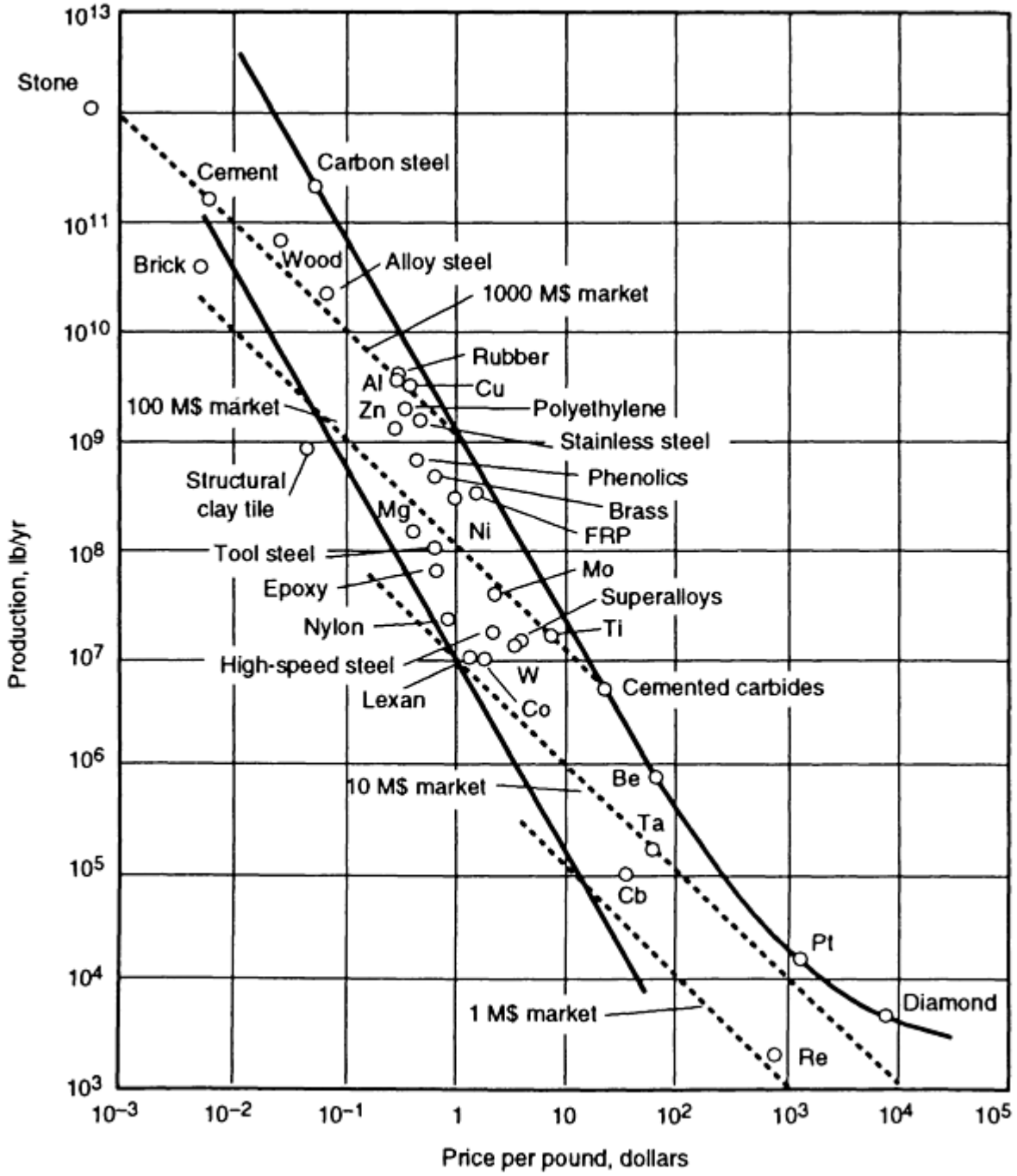

FIG. 10 COST VERSUS PRODUCTION FOR SEVERAL COMMON AEROSPACE MATERIALS. SOURCE: REF 8

Joining process selection and practice are influenced by material selection. For example, titanium requires vacuum or complete inert shielding (chambers with glove ports) to produce high-quality joints when elevated-temperature joining processes are used, which increases production costs in comparison with some other materials.

Finally, the environmental ramifications of joining must be considered when selecting a material. Toxic materials, such as beryllium, are sometimes used in aerospace structures because of their very high specific properties. However, when joining these materials, especially by welding, health and safety issues may drive manufacturing costs very high.

References cited in this section

4. S. YUKAWA, *GUIDELINE FOR PRESSURE VESSEL SAFETY ASSESSMENT,* NIST SPEC. PUBL. 780, NATIONAL INSTITUTE FOR STANDARDS AND TECHNOLOGY, P 14-22
7. G.E. DIETER, *ENGINEERING DESIGN,* MCGRAW-HILL, 1983
8. B.D. TAPLEY, *ESCHBACK'S HANDBOOK OF ENGINEERING FUNDAMENTALS,* JOHN WILEY & SONS, 1990
9. *AEROSPACE STRUCTURAL MATERIALS HANDBOOK,* VOL III, 1984
10. SIMS AND HAGEL, *THE SUPERALLOYS,* JOHN WILEY & SONS, 1972
11. CASTRO AND DECADENT, *WELDING METALLURGY OF STAINLESS AND HEAT RESISTING STEELS,* CAMBRIDGE PRESS, 1968
12. EVANS AND WILSHIRE, *CREEP IN METALS AND ALLOYS,* DOTESIOS PRINTERS, U.K., 1985
13. *AEROSPACE STRUCTURAL MATERIALS HANDBOOK,* VOL IV, 1984

Material Requirements for Service Conditions

ASM Committee on Material Requirements for Service Conditions*

Joinability

Material Characteristics Related to Joining. Materials for aerospace use can be divided into two major categories: structural and engine, the latter being materials for elevated temperatures. There is considerable overlap, but it is instructive to examine materials from these points of view. Although the practice of welding of critical structural members in modern aircraft is small, but growing, the use of welding in missiles and space hardware has always been extensive. The joinability of aerospace materials takes on various definitions. Joint efficiency, cracking resistance, welding characteristics (such as flow), maintenance of corrosion resistance, and long-term metallurgical stability are all measures of joinability. Design, process, and consumable selection affect the joining characteristics of materials.

Dissimilar-materials joining muddies these definitions even further. For example, the welding of titanium to stainless steel is not recommended, but brazing these two materials together is possible. The usefulness of the hybrid braze would be determined by the service requirements. Joinability is often determined by standardized tests or by the ability of a material to meet certain mechanical or inspection requirements.

When evaluating joinability, it is important to consider the range of conditions to be experienced n production. For example, most material specifications allow a range of compositions. Because joinability may vary considerably as a function of chemistry, addressing these concerns prior to production will avoid costly rework.

The joinability of a material is influenced by the condition of the material when joined. For example, nickel-base superalloys should always be stress relieved prior to brazing to prevent stress cracking (Ref 14). Heat-treatable aluminum alloys are sometimes welded in the T4 condition and then postweld aged to the T6 condition to achieve more uniform properties in the weldment. Alpha-beta titanium alloys are sensitive to preweld heat treatment.

The thermal history can become very important during repair operations. If a material has been exposed to elevated temperatures or high loading in service, its joinability may be altered. In such instances, specialized testing may be required to ensure adequate joinability for repair operation.

The joinability of a material may be contingent on the postjoining operations, such as heat treatments. Many as-joined materials do not have the properties required for a particular application, but can be brought to an acceptable condition by a postjoining process. Postjoining thermal treatments can consist of full heat treatments (solution, intermediate, age), stress relief, or stabilization treatments (age). These can be localized or can be applied to the entire part. Other postjoining treatments include shot peening, machining, vibration stress relief, and sizing.

Base Materials. When characterizing the joinability of a material, it is important to consider the effect of joining on the base material as well as on the nexus (the actual joint; i.e., the fusion zone in welding). Nonthermal joining operations, such as room-temperature-cured adhesive bonding, may have no effect on the base material. In contrast, thermal

processes, such as brazing, soldering, and welding, can radically change material properties, especially near the nexus. Characterization of the affected base material can be difficult because of its size and makeup. For example, the HAZ in an electron beam weld in thick-section titanium may be as little as half the fusion-zone width. If the weld is on the order of 2.5 mm (0.10 in.) in width, the HAZ is only 1.25 mm (0.05 in.) in width. Locating a notch in the HAZ to evaluate fatigue or fracture toughness can be challenging. Moreover, if the HAZ is small enough, its effect on the service performance of the joint may be negligible, which signals a caution when service life is evaluated by using "simulated" HAZ microstructure. Joints of the same configuration as the production parts should be used whenever possible.

Filler Materials. The selection of filler materials is a critical factor that sometimes receives less than proper attention when joining aerospace materials (Ref 15). Filler materials are most often selected on the basis of chemistry match. However, other considerations sometimes take precedence, such as ferrite control in the welding of stainless steels, distortion/residual stress control for high-strength steels, optimization of elevated-temperature properties for nickel-base superalloys, and strength optimization in aluminum welding or optimization of environmental resistance in brazing and adhesive bonding.

Selection of filler materials for dissimilar-material joining requires careful consideration. Some brazing alloys contain melting-point depressants to allow brazing at temperatures lower than the operating environment (diffusion brazing). The effect of the formation of detrimental phases in the base materials is a factor when these alloys are used. Special corrosion or wear requirements will sometimes direct the use of a particular joining consumable.

Joining Techniques Other Than Fusion Welding. Process is another consideration in the joinability of aerospace materials. Alloys that are nonfusion weldable may be readily joined by other methods, such as friction, explosion, diffusion, brazing, or soldering.

Service Considerations. The joinability of materials is influenced by service requirements. A titanium weldment used for a missile fuselage or a wing support must have high strength, low fatigue crack-growth rates, and high toughness. Good corrosion resistance and thermal stability are also desirable. The properties of the weldments made from such material must reflect the base material requirements. On the other hand, an Inconel 626 weld used to build up a turbine blade tip may not have the same requirements as the turbine blade. Ease of welding and adequate elevated-temperature oxidation resistance are overriding concerns in this case. Because the tip buildup is not "structural" in nature and the consequences of failure not as severe as for the wing support, weldability is based on different criteria. Therefore, the joinability of a given material can vary depending on the end service requirements.

References cited in this section

14. *BRAZING HANDBOOK,* AMERICAN WELDING SOCIETY, 1976
15. D. HARVEY, FILLER METAL SELECTIONS FOR CRITICAL AEROSPACE FABRICATION, *WELD. DESIGN FABR.*, VOL 60 (NO. 2), MARCH 1991, P 765-80

Material Requirements for Service Conditions

ASM Committee on Material Requirements for Service Conditions*

Damage Tolerance

Existence of Flaws. Damage tolerance is a design methodology often used for aerospace systems. The basic premise is that all structures contain inherent flaws. The effect of these flaws on flight safety depends on their geometry, growth rate at the service conditions, and critical size, and on the inspectability of the structure and the consequence of failure (Ref 16).

In the design of damage-tolerant structures, it is imperative that the relevant material properties, such as fatigue crack-growth rates, fracture toughness, and SCC, be well characterized. When applying damage-tolerant methodologies to structures joined by other methods than mechanical, unique considerations include:

- RESIDUAL STRESS EFFECTS
- PROPERTY GRADIENTS ACROSS THE JOINT
- INHERENT FLAWS, SUCH AS MICROFISSURES AND POROSITY
- LONG-TERM STABILITY
- CORROSION
- STRESS CONCENTRATIONS

These concerns are not well characterized for many of the materials and joining processes used in aerospace.

Finally, because the properties of the base metal may be altered nonuniformly during thermal joining, specialized testing may be required. For example, the crack-growth rate may be improved in the fusion zone of a weld, but the fracture toughness and SCC resistance may be reduced in the HAZ. All of these factors are important to the damage-tolerance analysis, and thus full characterization is required.

Inspection Criteria. For complex structures, the limiting factor may well be the inspectability of the joint. As a result, many welding specifications used for aerospace production, such as MIL-STD-2219 and AMS 2680, include defect allowable tables. When contractually requiring one of these standards, it is important to review the defect allowables to ensure that they are realistic for the application. Many unnecessary repairs are performed on welded structures because of improper defect criteria. As a result of the additional thermal cycles, the repairs may be more detrimental than the flaw in many materials. For many joining processes and materials combinations used in aerospace, the information necessary to perform a damage-tolerance analysis is not available; therefore, the defect criteria in the welding specifications are used, as this procedure is less expensive than developing the required data. Also, the effect of residual stress on fracture toughness and fatigue crack growth is difficult to evaluate with current damage-tolerance methodologies. Much work needs to be accomplished in this area.

Nondestructive examination (NDE) concerns require consideration of both the process and design limitations. Many times joints are designed without adequate attention to inspection requirements, often making effective NDE impossible due to inaccessibility.

Reference cited in this section

16. *USAF DAMAGE TOLERANT DESIGN HANDBOOK: GUIDELINES FOR ANALYSIS AND DESIGN OF DAMAGE TOLERANT AIRCRAFT,* U.S. AIR FORCE, 1984

Material Requirements for Service Conditions

ASM Committee on Material Requirements for Service Conditions*

Advanced Materials

Some materials used for aerospace systems present special problems in relation to joining. Among these materials are composites and intermetallics. Composite materials, including metal matrix and organic matrix, are used because of their increased stiffness, damping properties, and high specific properties. Composites present challenges when joined by any method, and much work is currently underway to establish their joinability. Maintenance of properties when using nonmechanical joining is difficult. Metal-matrix composites have been successfully joined by brazing, diffusion, and high-energy density welding. During the development of these materials, joinability was not a high priority and is thus limited.

The bond integrity between the fibers and the matrix of a composite greatly affects material properties. Special coatings are applied to the fibers to ensure adequate bonding. The stability of these coatings to a large degree determines joinability when using elevated-temperature processes. Coating schemes that optimize joinability should be addressed during materials development. A further challenge involves the attainment of material properties across the joint.

Intermetallics, such as Ti_3Al_2, offer very promising elevated-temperature properties. Limited studies to date concerning the fusion weldability of these materials indicate that tight control of base-metal chemistry, accurate regulation of heat input and cooling rate, and joint design to minimize residual stress are required to produce sound joints (Ref 17). Brazing offers some advantages, but may be limited by operating temperature unless suitable diffusion-bonding fillers can be developed. The joinability of these types of emerging materials will to a large degree determine their long-term usefulness in aerospace systems.

Reference cited in this section

17. PATTERSON *ET AL.* TITANIUM ALUMINIDE: ELECTRON BEAM WELDABILITY," *WELD. J.*, JAN 1990, P 39S-44S

Material Requirements for Service Conditions

ASM Committee on Material Requirements for Service Conditions*

Machinery and Equipment

Welding plays an important role in the wide variety of structures broadly characterized as machinery and equipment. This section will discuss three categories: stationary equipment, such as presses, rolling mills, and machine tools; mobile equipment, such as cranes, earthmoving, and other construction equipment; and rotating components of machines. In all of these categories, the materials requirements for serviceability are distinctly different for the structural machine support parts and for those involving the machine-moving and working parts.

Material Requirements for Service Conditions

ASM Committee on Material Requirements for Service Conditions*

Applications

Stationary Equipment. The working parts of machine tools require stability. Massive cast iron or cast steel bases are used to provide a damping capacity, thus ensuring that cutting tools do not vibrate or chatter. In applications that use weldments, thick steel components are specified.

The principal design requirement for metalworking presses is adequate strength to counter the forces imposed during press operation. Weldments of various sections using both wrought and cast carbon steels offer adequate strength and rigidity. The elastic deflections of the components created by work forces affect the design, which must take into account the cyclical nature of the stress and hence the fatigue properties of the materials and welded joints.

Mobile Equipment. In the design of components for earthmoving and other construction equipment, static and dynamic loads are important factors, as are erosion, wear, weight, and ease of maintenance. The materials for each working part of such equipment must be considered separately.

As an example, booms used in mobile industrial cranes must be light in weight, yet rigid under load. Wear resistance is another important factor in this application.

Rotating Elements. Materials specified for the rotating parts of pumps, fans, compressors, and similar machinery have a wide variety of properties. For large rotating components, weldments are commonly required, sometimes employing different metals for improved performance in specific environments. Erosion, corrosion, and cavitation are often the

mechanisms that limit the lives of such machine elements. Critical surfaces are frequently weld surfaced with corrosion-resistant materials.

Material Requirements for Service Conditions

ASM Committee on Material Requirements for Service Conditions*

Design Considerations

Welds and members of weldments are sized to withstand the working stress and stress range induced by static and fluctuating loads. The magnitude of the fluctuation between maximum and minimum working stress is termed the working stress range. The magnitude of the static and fluctuating stresses is influenced by such factors as dead load, live load, type of operating mechanism, machine geometry, component size, shock or impact, accidental overloads, corrosion, wear misalignment, stress concentration, and weld joint design. The allowable stress and stress range must be greater than the expected working stress and stress range. The relationships among the various stresses, stress ranges, strengths, and loads are shown graphically in Fig. 11.

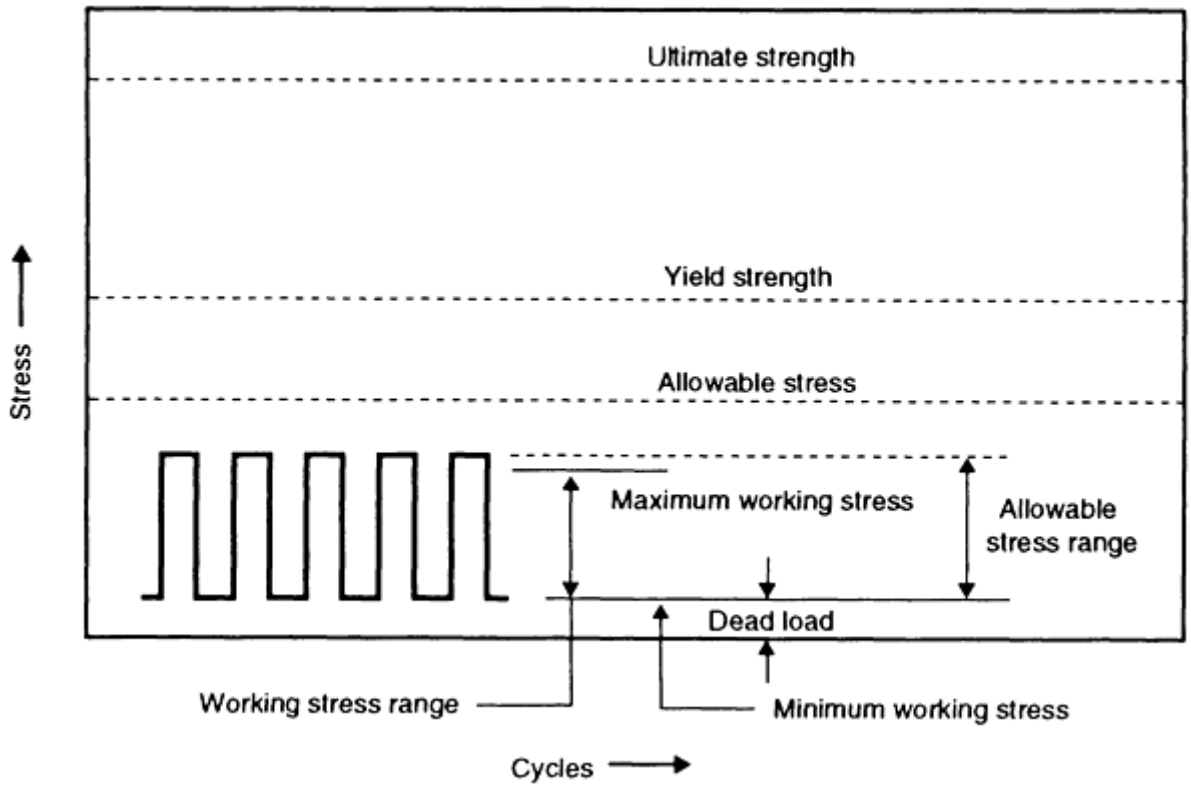

FIG. 11 STRESS RELATIONSHIPS RESULTING FROM STATIC AND FLUCTUATING LOADS

Allowable stresses in weld and base metals are usually specified by an applicable code or standard based on a history of satisfactory operating performance. In the absence of an industry standard, as in the case of most machinery and equipment, the determination of an allowable stress value is left to the discretion of the manufacturer or designer. In such case, the allowable stress (SA) is calculated by dividing the ultimate tensile strength (UTS) or yield strength (YS) by an appropriate factor of safety (FS) selected by the designer:

$$SA = \frac{UTS}{\text{FS}} \text{ or } \frac{\text{YS}}{\text{FS}}$$

The selection of an appropriate factor of safety to prevent failure from unpredictable causes is empirical and depends on industry data and the experience and judgment of the designer. Table 14 provides guidance in selecting a factor of safety, based on the ultimate tensile strength of the material. The assigned factors in Table 14 may be increased as warranted by safety, cost, plant utilization, and engineering judgment. Also, the assigned factors may be reduced if detailed analysis increases confidence in design factors, such as loading, material properties, and fabrication controls.

TABLE 14 FACTOR OF SAFETY SELECTION CRITERIA

CONDITION	ASSIGNED FACTOR OF SAFETY(A)
EXCEPTIONALLY RELIABLE MATERIALS USED UNDER CONTROLLABLE CONDITIONS AND SUBJECTED TO LOADS AND STRESSES THAT CAN BE DETERMINED WITH CERTAINTY. USED ALMOST INVARIABLY WHERE LOW WEIGHT IS A PARTICULARLY IMPORTANT CONSIDERATION	2.5-3
WELL-KNOWN MATERIALS, UNDER REASONABLY CONSTANT ENVIRONMENTAL CONDITIONS, SUBJECTED TO LOADS AND STRESSES THAT CAN BE DETERMINED	4-5
LESS TRIED OR BRITTLE MATERIALS UNDER AVERAGE CONDITIONS OF ENVIRONMENT, LOAD, AND STRESS	5-6
KNOWN MATERIALS THAT ARE TO BE USED IN UNCERTAIN ENVIRONMENTS OR SUBJECTED TO UNCERTAIN STRESSES	6-8

(A) FOR REPEATED LOADS, THE FACTORS SHOULD BE DOUBLED. FOR IMPACT LOADS. THE FACTORS SHOULD BE INCREASED AS WARRANTED.

When a design is analyzed using a mathematical model, it must be understood that subsequent calculations only approximate the working stress. With all models, various assumptions, limitations, and simplifications used to fit equations to the component model influence the accuracy of the calculations. (This is true even when using finite-element methods.) The calculated stress values that result from applying "good" theory to a "good" model are, at best, ballpark figures that give the design engineer a rational basis for making design decisions. For the most part, the allowable stress ranges specified in current standards for welded joints subjected to fatigue loading are based on testing of representative full-size welded joints in actual or mockup structures.

Static Loads. Nearly every machine is subjected to static and fluctuating loads; few useful machine structures have only static loads applied. Structures subjected to slowly applied loads, few cycles (less than 20,000) of loading, or nearly steady loads are considered statically loaded and are designed using rules that apply to static structures. These rules assume that localized areas of high stress due to stress concentrations are relieved by yielding of the highly stressed material to redistribute internal stresses.

Steels commonly used for welded construction of machinery and equipment have yield strengths of less than 700 MPa (100 ksi) and are listed in Table 15. Class I materials have the highest weldability, and class V have the lowest. Carbon and carbon-manganese steels--those class I and class II steels designated by the American Iron and Steel Institute (AISI), SAE, and ASTM--are the most commonly used materials for welded machinery and equipment. These steels do not require preheat unless the thickness is greater than 150 mm ($1\frac{1}{2}$ in.). High-strength low-alloy steels (classes III, IV, and V) allow the thickness and hence the weight of a machine structure subjected to high static loads to be reduced.

TABLE 15 WELDABILITY CLASSES OF STEELS USED IN MACHINERY AND EQUIPMENT

STEEL	TYPICAL MINIMUM YIELD	CARBON EQUIVALENT (C_{EQ})	SPECIFICATION

	STRENGTH		(MAX)[A]			
	MPA	KSI		AISI-SAE	ASTM	API
STRUCTURAL CARBON						
CLASS I	200-400	30-60	0.38	1005, 1006, 1008, 1010, 1012, 1015, 1016, 1017, 1018, 1020, 1021	. . .	. . .
CLASS II	240-380	35-55	0.48	. . .	A 36, A 38 (GRADE Y35), A 53 (GRADE B), A 106, A 131, A 139, A 374, A 500, A 501, A 516, A 524, A 529, A 570 (GRADES D, E), A 573	52 (GRADE B)
HSLA						
CLASS III	275-380	40-55	0.63	. . .	A 242, A 441, A 537 (GRADES A, E), A 572 (GRADES 42, 45, 50), A 588, A 618	5LX (GRADE 42)
CLASS IV	410-450	60-65	NOT SPECIFIED	. . .	A 572 (GRADES 60, 65)	. . .
QUENCHED AND TEMPERED						
CLASS V	620-700	90-100	0.74	. . .	A 514, A 517	. . .

(A) CARBON EQUIVALENT IS A MEASURE OF WELDABILITY. FOR UNALLOYED (STRUCTURAL) STEELS. C_{EQ} = %C + (MN/4) + (SI/4). FOR LOW-ALLOY STEELS, C_{EQ} = %C + (MN/6) + (NI/20) + (CR/10) + (MO/40) + (V/10).

The AISI and SAE carbon-manganese steels have carbon contents of less than 0.25% and manganese contents of less than 0.90% and are supplied to meet composition specifications that do not include mechanical properties. Unless verified by mechanical tests, an ultimate tensile strength of 380 MPa (55 ksi) and a yield strength of 190 MPa (27.5 ksi) should be used for design purposes. These steels have the highest weldability rating shown in the machinery welding specifications that classify steels according to weldability.

ASTM material specifications include mechanical property requirements that demand higher strength than the AISI and SAE carbon-manganese steels, and thus offer the opportunity to reduce thickness and weight for statically loaded conditions. The weldability of these higher-strength steels is lower, and they usually require higher preheat and low-hydrogen welding processes.

Allowable stress for statically loaded steel base metals can be determined from the equation given above after selecting a factor of safety. Allowable stress levels for statically loaded weld metal are presented in Table 16.

TABLE 16 ALLOWABLE STRESSES IN WELD METAL

TYPE OF WELD	STRESS IN WELD	ALLOWABLE STRESS	REQUIRED WELD STRENGTH LEVEL[A]
GROOVE WELDS WITH COMPLETE JOINT PENETRATION	TENSION NORMAL TO EFFECTIVE AREA	SAME AS BASE METAL	MATCHING WELD METAL SHALL BE USED.
	COMPRESSION NORMAL TO	SAME AS BASE METAL	WELD METAL WITH A STRENGTH LEVEL EQUAL

	EFFECTIVE AREA		TO OR ONE CLASSIFICATION (69 MPA, OR 10 KSI) LESS THAN MATCHING WELD METAL MAY BE USED.
	TENSION OR COMPRESSION PARALLEL TO WELD AXIS	SAME AS BASE METAL	WELD METAL WITH A STRENGTH LEVEL EQUAL TO OR LESS THAN MATCHING WELD METAL MAY BE USED.
	SHEAR ON EFFECTIVE AREA	0.27 × NOMINAL TENSILE STRENGTH OF WELD METAL, EXCEPT SHEAR STRESS ON BASE METAL SHALL NOT EXCEED 0.40 × YIELD STRENGTH OF BASE METAL.	
GROOVE WELDS WITH PARTIAL JOINT PENETRATION	COMPRESSION NORMAL TO EFFECTIVE AREA: JOINT NOT DESIGNED TO BEAR	0.45 × NOMINAL TENSILE STRENGTH OF WELD METAL, EXCEPT STRESS ON BASE METAL SHALL NOT EXCEED 0.55 × YIELD STRENGTH OF BASE METAL.	WELD METAL WITH A STRENGTH LEVEL EQUAL TO OR LESS THAN MATCHING WELD METAL MAY BE USED.
	COMPRESSION NORMAL TO EFFECTIVE AREA; JOINT DESIGNED TO BEAR	SAME AS BASE METAL	
	TENSION OR COMPRESSION PARALLEL TO WELD AXIS[B]	SAME AS BASE METAL	
	SHEAR PARALLEL TO WELD AXIS	0.27 × NOMINAL TENSILE STRENGTH OF WELD METAL. EXCEPT SHEAR STRESS ON BASE METAL SHALL NOT EXCEED 0.36 × YIELD STRENGTH OF BASE METAL.	
	TENSION NORMAL TO EFFECTIVE AREA	0.27 × NOMINAL TENSILE STRENGTH OF WELD METAL, EXCEPT SHEAR STRESS ON BASE METAL SHALL NOT EXCEED 0.55 × YIELD STRENGTH OF BASE METAL.	
FILLET WELDS	SHEAR ON EFFECTIVE AREA	0.27 × NOMINAL TENSILE STRENGTH OF WELD METAL	WELD METAL WITH A STRENGTH LEVEL EQUAL TO OR LESS THAN

	TENSION OR COMPRESSION PARALLEL TO WELD AXIS[B]	SAME AS BASE METAL	MATCHING WELD METAL MAY BE USED
PLUG AND SLOT WELDS	SHEAR PARALLEL TO FAYING SURFACES (ON EFFECTIVE AREA)	0.27 × NOMINAL TENSILE STRENGTH OF WELD METAL, EXCEPT SHEAR STRESS ON BASE METAL SHALL NOT EXCEED 0.36 × YIELD STRENGTH OF BASE METAL.	WELD METAL WITH A STRENGTH LEVEL EQUAL TO OR LESS THAN MATCHING WELD METAL MAY BE USED.

(A) FOR MATCHING WELD METAL, SEE TABLE 20.

(B) FILLET WELDS AND GROOVE WELDS WITH PARTIAL JOINT PENETRATION JOINING THE COMPONENT ELEMENTS OF BUILT-UP MEMBERS, SUCH AS FLANGE-TO-WEB CONNECTIONS, MAY BE DESIGNED WITHOUT REGARD TO THE TENSILE OR COMPRESSIVE STRESS IN THESE ELEMENTS PARALLEL TO THE AXIS OF THE WELDS.

Fluctuating Loads. Fatigue is the process of progressive localized damage that may result in cracks or complete fracture after a sufficient number of working stress fluctuations. Fatigue life is the number of stress fluctuations sustained to failure.

The fatigue design of welded joints is different from the "modified Goodman diagram" method used for plain (unwelded) machine and structural members. The fatigue life of plain base metal is a function of its tensile strength. Welded joints introduce stress concentrations in a structure, which reduces fatigue life. Examples of stress concentrations include weld ripple, undercut, crowned reinforcement, lack of penetration, slag inclusions, microcracks, and craters. The fatigue life of a steel welded joint is independent of base metal tensile strength. An ASTM A 36 steel weld joint has the same fatigue strength as a joint made from ASTM A 514 steel. The fatigue life of a steel weld joint is indirectly proportional to working stress range; that is, as the magnitude of working stress range increases, fatigue life decreases (see Table 17). The fatigue life of a steel weld joint is a function of the weld joint category, which in turn is a function of joint geometry, type of weld, direction of load application, and weld quality assurance (see Table 18 and Fig. 12).

TABLE 17 ALLOWABLE STRESS RANGES

STRESS CATEGORY (SEE TABLE 18)	**NOMINAL NUMBER OF LOADING CYCLES**							
	20,000-100,000		**100,000-500,000**		**500,000-2,000,000**		**>2,000,000**	
	MPA	**KSI**	**MPA**	**KSI**	**MPA**	**KSI**	**MPA**	**KSI**
A	434	63	255	37	165	24	165	24
B	338	49	200	29	124	18	110	16
B'	269	39	159	23	103	15	83	12
C	241	35	145	21	90	13	69[A]	10[A]
D	193	28	110	16	69	10	48	7
E	152	22	90	13	55	8	31	4.5
E'	110	16	63	9.2	40	5.8	18	2.6
F	103	15	83	12	62	9	55	8

(A) FLEXURAL STRESS RANGE OF 83 MPA (12 KSI) PERMITTED AT TOE OF STIFFENER WELDS OR FLANGES

TABLE 18 STRESS CATEGORY CLASSIFICATIONS

GENERAL CONDITION	SITUATION	TYPES OF STRESS[A]	STRESS CATEGORY (SEE TABLE 17)	ILLUSTRATIVE EXAMPLE NOS. (SEE FIG. 12)[B]
PLAIN MATERIAL	BASE METAL WITH ROLLED OR CLEANED SURFACE. FLAME-CUT EDGES WITH ANSI SMOOTHNESS OF 1000 OR LESS	T OR REV	A	1, 2
BUILT-UP MEMBERS	BASE METAL IN MEMBERS WITHOUT ATTACHMENTS, BUILT-UP PLATES, OR SHAPES CONNECTED BY CONTINUOUS FULL-PENETRATION GROOVE WELDS OR BY CONTINUOUS FILLET WELDS PARALLEL TO THE DIRECTION OF APPLIED STRESS	T OR REV	B	3-6
	BASE METAL IN MEMBERS WITHOUT ATTACHMENTS, BUILD-UP PLATES, OR SHAPES CONNECTED BY FULL-PENETRATION GROOVE WELDS WITH BACKING BARS NOT REMOVED, OR BY PARTIAL-PENETRATION GROOVE WELDS PARALLEL TO THE DIRECTION OF APPLIED STRESS	T OR REV	B'	3-6
	BASE METAL AT TOE WELDS ON GIRDER WEBS OR FLANGES ADJACENT TO WELDED TRANSVERSE STIFFENERS	T OR REV	C	7
	BASE METAL AT ENDS OF PARTIAL-LENGTH WELDED COVER PLATES NARROWER THAN THE FLANGE, HAVING SQUARE OR TAPERED ENDS, WITH OR WITHOUT WELDS ACROSS THE ENDS OR WIDER THAN FLANGE WITH WELDS ACROSS THE ENDS			
	FLANGE THICKNESS ≤20 MM (0.8 IN.)	T OR REV	E	5
	FLANGE THICKNESS >20 MM (0.8 IN.)	T OR REV	E'	5
	BASE METAL AT END OF PARTIAL-LENGTH WELDED COVER PLATES WIDER THAN THE FLANGE WITHOUT WELDS ACROSS THE ENDS		E'	5
GROOVE WELDS	BASE METAL AND WELD METAL AT FULL-PENETRATION GROOVE WELDED SPLICES OF PARTS OF SIMILAR CROSS SECTION GROUND FLUSH, WITH GRINDING IN THE DIRECTION OF APPLIED STRESS AND WITH WELD SOUNDNESS ESTABLISHED BY RADIOGRAPHIC OR ULTRASONIC INSPECTION IN	T OR REV	B	10, 11

	ACCORDANCE WITH THE REQUIREMENTS OF 9.25.2 OR 9.25.3 OF AWS D1. I			
	BASE METAL AND WELD METAL AT FULL-PENETRATION GROOVE WELDED SPLICES AT TRANSITIONS IN WIDTH OR THICKNESS; WITH WELDS GROUND TO PROVIDE SLOPES NO STEEPER THAN 1 TO $2\frac{1}{2}$, WITH GRINDING IN THE DIRECTION OF APPLIED STRESS AND WITH WELD SOUNDNESS ESTABLISHED BY RADIOGRAPHIC OR ULTRASONIC INSPECTION IN ACCORDANCE WITH THE REQUIREMENTS OF 9.25.2 OR 9.25.3 OF AWS D1. 1			
	A 514 BASE METAL	T OR REV	B'	12, 13
	OTHER BASE METALS	T OR REV	B	12, 13
	BASE METAL AND WELD METAL AT FULL-PENETRATION GROOVE WELDED SPLICES, WITH OR WITHOUT TRANSITIONS HAVING SLOPES NO GREATER THAN 1 TO $2\frac{1}{2}$ WHEN REINFORCEMENT IS NOT REMOVED BUT WELD SOUNDNESS IS ESTABLISHED BY RADIOGRAPHIC OR ULTRASONIC INSPECTION IN ACCORDANCE WITH THE REQUIREMENTS OF 9.25.2 OR 9.25.3 OF AWS D1.1	T OR REV	C	10-13
PARTIAL-PENETRATION GROOVE WELDS	WELD METAL OF PARTIAL-PENETRATION TRANSVERSE GROOVE WELDS, BASED ON EFFECTIVE THROAT AREA OF THE WELD OR WELDS	T OR REV	F[C]	16
FILLET-WELDED CONNECTIONS	BASE METAL AT INTERMITTENT FILLET WELDS	T OR REV	E	. . .
	BASE METAL AT JUNCTION OF AXIALLY LOADED MEMBERS WITH FILLET-WELDED END CONNECTIONS. WELDS SHALL BE DISPOSED ABOUT THE AXIS OF THE MEMBER SO AS TO BALANCE WELD STRESSES.			
	B ≤25 MM (1 IN.)	T OR REV	E	17, 18
	B >25 MM (1 IN.)	T OR REV	E'	17, 18
	BASE METAL AT MEMBERS			

	CONNECTED WITH TRANSVERSE FILLET WELDS			
	B ≤ 13 MM (0.5 IN.)	T OR REV	C[(C)]	20, 21
	B > 13 MM (0.5 IN.)			
FILLET WELDS	WELD METAL OF CONTINUOUS OR INTERMITTENT LONGITUDINAL OR TRANSVERSE FILLET WELDS	S	F[(C)]	15, 17, 18, 20, 21
PLUG OR SLOT WELDS	BASE METAL AT PLUG OR SLOT WELDS	T OR REV	E	27
	SHEAR ON PLUG OR SLOT WELDS	S	F	27
MECHANICALLY FASTENED CONNECTIONS	BASE METAL AT GROSS SECTION OF HIGH-STRENGTH BOLTED SLIP-CRITICAL CONNECTIONS, EXCEPT AXIALLY LOADED JOINTS THAT INDUCE OUT-OF-PLANE BENDING IN CONNECTED MATERIAL	T OR REV	B	8
	BASE METAL AT NET SECTION OF OTHER MECHANICALLY FASTENED JOINTS	T OR REV	D	8, 9
	BASE METAL AT NET SECTION OF FULLY TENSIONED HIGH-STRENGTH, BOLTED-BEARING CONNECTIONS	T OR REV	B	8, 9
ATTACHMENTS	BASE METAL AT DETAILS ATTACHED BY FULL-PENETRATION GROOVE WELDS SUBJECT TO LONGITUDINAL AND/OR TRANSVERSE LOADING WHEN THE DETAIL EMBODIES A TRANSITION RADIUS, *R*, WITH THE WELD TERMINATION GROUND SMOOTH AND FOR TRANSVERSE LOADING, THE WELD SOUNDNESS ESTABLISHED BY RADIOGRAPHIC OR ULTRASONIC INSPECTION IN ACCORDANCE WITH 9.25.2 OR 9.25.3 OF AWS D1.1			
	LONGITUDINAL LOADING			
	R > 600 MM (24 IN.)	T OR REV	B	14
	600 MM (24 IN.) > *R* > 150 MM (6 IN.)	T OR REV	C	14
	150 MM (6 IN.) > *R* > 50 MM (2 IN.)	T OR REV	D	14
	50 MM (2 IN.) > *R*	T OR REV	E	14
	DETAIL BASE METAL FOR TRANSVERSE LOADING: EQUAL THICKNESS AND REINFORCEMENT REMOVED			
	R > 600 MM (24 IN.)	T OR REV	B	14

	600 MM (24 IN.) > *R* > 150 MM (6 IN.)	T OR REV	C	14
	150 MM (6 IN.) > *R* > 50 MM (2 IN.)	T OR REV	D	14
	50 MM (2 IN.) > *R*	T OR REV	E	14, 15
	DETAIL BASE METAL FOR TRANSVERSE LOADING; EQUAL THICKNESS AND REINFORCEMENT NOT REMOVED			
	R > 600 MM (24 IN.)	T OR REV	C	14
	600 MM (24 IN.) > *R* > 150 MM (6 IN.)	T OR REV	C	14
	150 MM (6 IN.) > *R* > 50 MM (2 IN.)	T OR REV	D	14
	50 MM (2 IN.) > *R*	T OR REV	E	14, 15
	DETAIL BASE METAL FOR TRANSVERSE LOADING: UNEQUAL THICKNESS AND REINFORCEMENT REMOVED			
	R > 50 MM (2 IN.)	T OR REV	D	14
	50 MM (2 IN.) > *R*		E	14, 15
	DETAIL BASE METAL FOR TRANSVERSE LOADING; UNEQUAL THICKNESS AND REINFORCEMENT NOT REMOVED			
	ALL *R*	T OR REV	E	14, 15
	DETAIL BASE METAL FOR TRANSVERSE LOADING			
	R > 150 MM (6 IN.)	T OR REV	C	19
	150 MM (6 IN.) > *R* > 50 MM (2 IN.)	T OR REV	D	19
	50 MM (2 IN.) > *R*	T OR REV	E	19
	BASE METAL AT DETAIL ATTACHED BY FULL-PENETRATION GROOVE WELDS SUBJECT TO LONGITUDINAL LOADING			
	50 MM (2 IN.) < *A* < 12*B* OR 100 MM (4 IN.)	T OR REV	D	15
	A > 12*B* OR 100 MM (4 IN.) WHEN *B* ≤ 25 MM (1 IN.)	T OR REV	E	15
	A > 12*B* OR 100 MM (4 IN.) WHEN *B* > 25 MM (1 IN.)	T OR REV	E'	15
	BASE METAL AT DETAIL ATTACHED BY FILLET WELDS OR PARTIAL-PENETRATION GROOVE WELDS			

	SUBJECT TO LONGITUDINAL LOADING			
	A < 50 MM (2 IN.)	T OR REV	C	15, 23-26
	50 MM (2 IN.) < *A* < 12*B* OR 100 MM (4 IN.)	T OR REV	D	15, 23, 24, 26
	A > 12*B* OR 100 MM (4 IN.) WHEN *B* ≤25 MM (1 IN.)	T OR REV	E	15, 23, 24, 26
	A > 12*B* OR 100 MM (4 IN.), WHEN *B* > 25 MM (1 IN.)	T OR REV	E'	15, 23, 24, 26
	BASE METAL ATTACHED BY FILLET WELDS OR PARTIAL-PENETRATION GROOVE WELDS SUBJECTED TO LONGITUDINAL LOADING WHEN THE WELD TERMINATION EMBODIES A TRANSITION RADIUS WITH THE WELD TERMINATION GROUND SMOOTH			
	R > 50 MM (2 IN.)	T OR REV	D	19
	R ≤50 MM (2 IN.)	T OR REV	E	19
	FILLET-WELDED ATTACHMENTS WHERE THE WELD TERMINATION EMBODIES A TRANSITION RADIUS, WELD TERMINATION GROUND SMOOTH, AND MAIN MATERIAL SUBJECT TO LONGITUDINAL LOADING			
	DETAIL BASE METAL FOR TRANSVERSE LOADING:			
	R > 50 MM (2 IN.)	T OR REV	D	19
	R < 50 MM (2 IN.)	T OR REV	E	19
	BASE METAL AT STUD-TYPE SHEAR CONNECTOR ATTACHED BY FILLET WELD OR AUTOMATIC END WELD	T OR REV	C	22
	SHEAR STRESS ON NOMINAL AREA OF STUD-TYPE SHEAR CONNECTORS	S	F	. . .

(A) T, RANGE IN TENSILE STRESS ONLY; REV, RANGE INVOLVING REVERSAL OF TENSILE OR COMPRESSIVE STRESS; S, RANGE IN SHEAR, INCLUDING SHEAR-STRESS REVERSAL.

(B) THESE EXAMPLES ARE PROVIDED AS GUIDELINES AND ARE NOT INTENDED TO EXCLUDE OTHER REASONABLY SIMILAR SITUATIONS.

(C) ALLOWABLE FATIGUE STRESS RANGE FOR TRANSVERSE PARTIAL-PENETRATION AND TRANSVERSE FILLET WELDS IS A FUNCTION OF THE EFFECTIVE THROAT, DEPTH OF PENETRATION, AND PLATE THICKNESS.

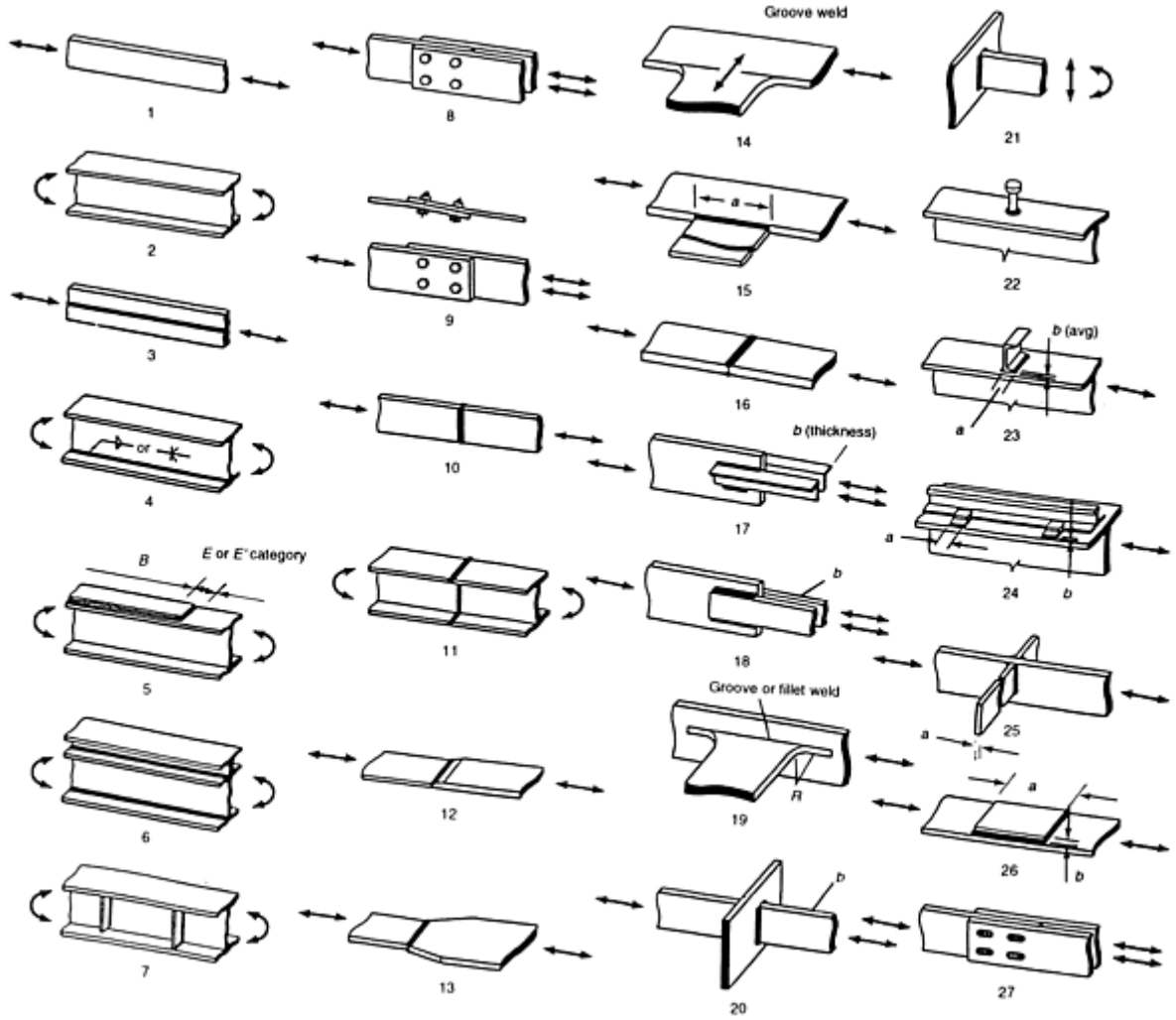

FIG. 12 ILLUSTRATIVE EXAMPLES OF THE STRESS CATEGORIES IN TABLE 18

The primary design requirement for some machine members can be rigidity. Such members, even when subjected to both static and fluctuating loads, are treated as statically loaded structures. Deflection under load is very small and the working stress is only 14 to 28 MPa (2 to 4 ksi). In this case, the weld need not be sized to carry the full load capacity of the member.

Loads are considered cyclic if the stress range exceeds 10% of the allowable stress range or if the total life cycles exceed 20,000. Care must be taken when selecting higher-strength materials, because the allowable stress range of welded joints is independent of material strength. The maximum allowable stress is higher for higher-strength steels, but the allowable stress range is the same. The use of higher-strength steels in cyclic load applications is beneficial only when the part is not welded or when the part is in a tensile prestress condition.

The materials listed in Table 15 are commonly used steels that are considered prequalified. Other steels, such as AISI 4340 and 4140, are also commonly used in machinery components, but are not prequalified. Weld procedure qualifications must be developed as required by the appropriate machinery weld specifications. Preheats for these high-hardenable steels must be above the martensitic start (M_s) temperature of 290 °C (550 °F) for AISI 4340 and 4140 to allow the formation of the more ductile bainitic structure and thus avoid brittleness and HAZ cracks. A low-hydrogen welding process is mandatory. The postheat temperature must be no higher than 28 °C (50 °F) below the hardening temper temperature incurred when the part was prehardened.

A table of welding practices applicable to most steels for machinery and equipment is available in Ref 18. Related AWS specifications are listed in Table 19.

TABLE 19 AWS SPECIFICATIONS RELATING TO MACHINERY AND EQUIPMENT

AWS NO.	TITLE
D14.1	"WELDING INDUSTRIAL AND MILL CRANES AND OTHER MATERIAL HANDLING EQUIPMENT"
D14.2	"METAL CUTTING MACHINE TOOL WELDMENTS"
D14.3	"WELDING EARTHMOVING AND CONSTRUCTION EQUIPMENT"
D14.4	"CLASSIFICATION AND APPLICATION OF WELDED JOINTS FOR MACHINERY AND EQUIPMENT"
D14.5	"WELDING OF PRESSES AND PRESS COMPONENTS"
D14.6	"WELDING ROTATING ELEMENTS OF EQUIPMENT"

Service Life. Material selection for machine tools, presses, and heavy rolling and forging equipment is usually governed by an indefinite life expectancy. The working parts (e.g., tools, hammers, forming or punching dies, and mill rolls) and the moving parts (e.g., motors, gears, and clutches) are subject to wear and may need to be either replaced or rebuilt. The basic equipment, however, should be constructed from materials that will last until the machine is retired due to obsolescence.

Obsolescence is also a design consideration in material selection for mobile equipment. Because of weight restrictions, however, material election must make use of the maximum load-carrying capacity of the principal components. The life of wear surfaces, especially in earth-moving equipment, is often enhanced by careful selection of weld surfacing materials.

Maintenance and repair of components must also factor into the material selection process. If it is known that parts will need replacement, access for this type of maintenance should be part of the design. If welds must be removed to provide access, necessitating rewelding, the weldability of the steel used for that part is important. A design that seems perfectly feasible during the initial fabrication of a component may present difficult, or even insoluble, problems during disassembly and reassembly for replacement or repair of a worn part.

Safety. Construction equipment is used in a variety of applications, some of which may endanger the operator or other workers at the site. The designer is responsible for ensuring that the material selected is appropriate for the intended use, making allowances for improper uses that cause stress higher than the rated load stress. Material selection should therefore be based on conservative estimates for components whose failure might jeopardize operators and others.

Economics. Machinery and equipment involve the same economic principles with regard to material choice as other types of welded structures. In most applications the unit cost of the material is a small percentage of the overall cost of the fabricated component or machine. Too often the driving force for low initial cost fails to consider the life-cycle cost of a machine. The cost of maintenance, repair, or replacement of components subject to failure or wear can in many cases justify the selection of more costly materials with longer life cycles. Pumps that handle corrosive liquids and dredges that handle erosive slurries are useful examples. Impellers and casings made of materials resistant to corrosion and erosion can add enormously to the utility of a pump over its anticipated life in comparison with materials that may require frequent replacement or rebuilding. In some cases, maintaining the efficiency of a machine component during its life by selecting materials with greater resistance to the environment will offset its cost. Life-cycle cost assessments should be applied to the choice of materials for machinery and equipment during the design phase.

Reference cited in this section

18. R.D. STOUT, *WELDABILITY OF STEELS,* 4TH ED., WELDING RESEARCH COUNCIL, 1987, P 338-437

Material Properties of Weldments

Assessment of the performance of welded components must include the ability of the various metallurgical structures to perform the tasks specified by the designer. These structures are broadly defined as the fusion zone and the heat-affected zone. The thermal excursions that occur during welding invariably result in residual stresses, which in some instances may add considerably to the service stresses encountered by a weldment. The effect of welds on the service-ability of weldments for machinery and equipment may influence material selection.

Heat-Affected Zone. In unalloyed steels, the properties of a region that has experienced one or more thermal excursions during welding are quite similar to those of the unaffected base metal. In low-alloy steels, especially those in weldability classes IV and V (Table 15), the HAZ becomes considerably stronger, harder, and less ductile. This impairs the ability of the metal to adjust to the strains imposed by static loads; moreover, the fatigue properties are degraded, lowering resistance to cyclic loads. When low-alloy steels are used for critical weldments in machinery, postweld heat treatments are employed to overcome most of these adverse effects. Preheat is necessary to permit these hardenable steels to overcome the effect of hydrogen, which can cause cracks in the HAZ during arc welding operations.

Fusion Zone. In an arc weld, the fusion zone comprises the amount of base metal that has been melted in addition to the filler metal that is fused by the arc. This is a cast structure distinctly different from the base material--which in wrought materials is usually a polycrystalline structure of more or less uniform size. The welding filler metals normally used for unalloyed carbon steels produce welds whose yield strength is generally higher in the as-deposited condition than that of the base metal. In most machinery applications, this higher strength is considered advantageous. Failures in static loading will therefore depend on the strength of the base metal, which the designer has chosen based on its known properties. Weld failures in statically loaded full-strength welds are thus unlikely, assuming that the welds meet specified workmanship standards.

Low-alloy steel welds of matching weld-metal composition are considerably stronger than the base metal. In these applications, it is often preferable to choose a filler metal of lower alloy content (especially carbon) to match, or even undermatch, the strength of the base metal. As long as the yield strength of the weld metal is not less than that of the base metal, static loads will not cause significant plastic deformation in the welds. Because filler metals are traditionally classified on the basis of the ultimate tensile strength of the welds that they produce, it is possible to use filler metal that is one classification lower in ultimate strength than the base metal. Generally, the yield strength of the lower-strength weld metal will more nearly match that of the base metal. Table 20 lists matching filler metal specifications.

TABLE 20 MATCHING FILLER METAL SPECIFICATIONS

BASE METAL[B]	WELDING PROCESS[A]			
	SMAW	SAW	GMAW	FCAW
CLASSES I AND II	AWS A5.1 OR A5.5 E60*XX* OR E70*XX*	AWS A5.17 F6*X* OR F7*X*-E*XXXX*	AWS A5.18 E70S-*X*	AWS A5.20 E60T-*X* OR E70T-1 (EXCEPT E*XX*T-2 AND E*XX*T-3)[C]
CLASS III	AWS A5.1 OR A5.5 E70*XX*[D]	AWS A5.17 F7*X*-E*XXXX*	AWS A5.18 E70S-*X*	AWS A5.20 E70T-*X* (EXCEPT E70T-2 AND E70-T3)[C]
CLASS IV[E]	AWS A5.5 E80*XX*[D]	AWS A5.23 F8*X*-E*XXX*	GRADE E80S[F]	GRADE E80T[F]
CLASS V	AWS A5.5 E110*XX*[D]	AWS A5.23 F11*X*-E*XXX*	GRADE E110S[F]	GRADE E110T[F]

Note: The use of the same type of filler metal having the next higher mechanical properties as listed in AWS specification is permitted.

(A) A FILLER METAL OF A LOWER STRENGTH MAY BE USED WHERE THE DESIGN ENGINEER HAS STIPULATED LESS THAN 100% JOINT EFFICIENCY.

(B) IN JOINTS INVOLVING BASE METALS OF DIFFERENT YIELD POINTS OR STRENGTHS, FILLER METALS APPLICABLE TO THE LOWER-STRENGTH BASE METAL MAY BE USED.

(C) IF TYPE 2 FILLER METALS ARE USED ON SUCCESSFULLY TESTED PROTOTYPE VEHICLES, THIS QUALIFIES THE USE OF TYPE 2 FILLER METALS FOR PRODUCTION.

(D) LOW-HYDROGEN CLASSIFICATION.

(E) WHEN WELDS ARE TO BE THERMALLY STRESS RELIEVED, THE DEPOSITED WELD METAL SHALL NOT EXCEED 0.05% V.

(F) FOR WELD METAL HAVING A MINIMUM SPECIFIED YIELD STRENGTH GREATER THAN 415 MPA (60 KSI), THE USER SHALL DEMONSTRATE THAT EACH COMBINATION OF ELECTRODE AND SHIELDING PROPOSED FOR USE WILL PRODUCE LOW-ALLOY WELD METAL HAVING THE MECHANICAL PROPERTIES LISTED. THE MECHANICAL PROPERTIES SHALL BE DETERMINED FROM A MULTIPLE-PASS WELD MADE IN ACCORDANCE WITH THE TEST REQUIREMENTS OF THE LATEST EDITION OF AWS A5.18 ("SPECIFICATION FOR MILD STEEL ELECTRODES FOR GAS METAL ARC WELDING") OR A5.20 ("SPECIFICATION FOR MILD STEEL ELECTRODES FOR FLUX CORED ARC WELDING"), AS APPLICABLE. WHEN AN APPLICABLE AWS FILLER METAL SPECIFICATION IS ISSUED, IT WILL TAKE PRECEDENCE OVER ALL OTHERS, AND TESTING BY THE USER WILL NOT BE REQUIRED. THE MECHANICAL PROPERTY TESTS REQUIRED FOR GRADES E110S. E100T, AND E110T SHALL BE MADE USING ASTM A 514 BASE METAL. WHEN REQUESTED, THE ELECTRODE MANUFACTURER SHALL FURNISH CERTIFICATION THAT THE ELECTRODE WILL MEET THE REQUIREMENTS OF CLASSIFICATION OR GRADE.

As-Welded Versus Postweld Heat-Treated Welds. Most welds used for machinery and equipment, including HSLA steels, are placed in service in the as-welded condition. Postweld heat treatment is usually specified to reduce residual stress and to attain dimensional stability when the weldment is to be machined after welding and the machining dimensional tolerances are small. Postweld heat treatment is sometimes specified to improve corrosion resistance in the welded area. The allowable stresses in specifications for components to be postweld heat treated are based on experience or on laboratory tests of the various types of weld joints.

High residual stresses remain in welds that have not undergone postweld heat treatment. In some cases, service loads added to the residual stresses in the weld area will cause sufficient distortion to present problems of dimensional misalignment. A stress-relief thermal treatment may be needed to overcome problems caused by residual stresses. Additional information is available in the article "Residual Stresses and Distortion" in this Volume.

Material Requirements for Service Conditions

ASM Committee on Material Requirements for Service Conditions*

Automobiles

Since its inception nearly a century ago, the automobile industry has relied heavily on joining technologies. Improvements in those technologies over the years have enabled improvements in automotive design--a constantly changing field driven by the ever-increasing demands of customers and governmental agencies. Customers want vehicles to meet criteria ranging from performance and function to appearance and styling; governmental agencies dictate that vehicles meet stringent safety and environmental standards. Producing automotive designs under such demands and constraints can often create difficulties in joining operations.

Service Conditions. The automotive design engineer must consider numerous types of service conditions. Structurally, a vehicle must be capable of withstanding on- and/or offroad service, must be crashworthy in order to meet Federal Motor Vehicle Safety Standards (FMVSS), and yet must possess an economy in terms of overall weight to meet Corporate Average Fuel Economy (CAFE) regulations. A vehicle must be able to withstand diverse environmental conditions,

ranging from the external environment (weather, electrolyte exposure, acid rain, etc.) to the internal environment (engine heat, fuels, lubricants, sealers, etc.), and must be watertight and airtight as well. Finally, all of this must be accomplished within the boundaries of cost-effective and manufacturable processes, including joining.

Welding Processes. The automobile industry utilizes a wide array of welding processes, materials, coatings, and designs. Given the many possible combinations of these factors, difficulties in the manufacturing process are inevitable. However, many problems can be avoided by exercising care in the initial design phase. By taking into account structural requirements (strength, crashworthiness, and fatigue resistance) as well as appearance requirements (corrosion resistance and finish), the design engineer can determine the most effective combination of materials and joining processes to fit the intended design and maximize performance.

Joining processes commonly used in the automotive industry include, but are not limited to, the following:

- RESISTANCE SPOT WELDING
- GAS-METAL ARC WELDING
- GAS-TUNGSTEN ARC WELDING
- FLUX-CORED ARC WELDING
- RESISTANCE PROJECTION WELDING
- STUD ARC WELDING
- LASER BEAM WELDING
- RESISTANCE SEAM WELDING
- BRAZING
- SOLDERING
- PLASTIC WELDING

These processes are applied and controlled either by the automotive industry itself or by suppliers within the industry. In either case, each joining technique should be governed by a reliable set of standards to ensure that the technique is properly defined and applied. The sections that follow will describe how the more commonly used joining techniques listed above are affected by the various material and mechanical factors encountered in the automotive industry.

Material Requirements for Service Conditions

ASM Committee on Material Requirements for Service Conditions*

Resistance Spot Welding

Resistance spot welding is the primary joining process used in automobile production. Its widespread use can be attributed to its many advantages. Specifically, the method is easy, cost effective, and, when properly applied, can produce structures with greater integrity than the sum of the individual welds. Therefore, RSW lends itself to the extremely high production volumes common in the automotive industry. Despite the obvious advantages of the spot welding process, adequate results cannot be achieved without special consideration of a number of factors that can ultimately affect the welded structure, including raw material coatings, processing fluids, raw material chemistry, joint design, joint sealers, and joint adhesives.

Steel Composition. Raw material chemistry is of primary importance in the design of a spot-welded structure. Most automotive applications use SAE 1008-1010 steel. This material has a low carbon equivalent, which makes it readily formable and weldable and relatively inexpensive and abundantly produced. However, low-carbon material is not used exclusively. Automobile manufacturers must reduce weight while retaining structural integrity. This has resulted in increasing use of high-strength steels, such as bake-hardenable, dual-phase, precipitation-hardenable, and martensitic steels. These materials are inherently more difficult to weld because of the residual elements added for solid-solution strengthening, but weldable grades are available. As a rule, welding of these materials requires increased heat input compared with low-carbon steel material.

Steel Thickness. In the design of a spot-welded joint, a critical factor is the combination of materials to be joined, along with their thicknesses. As the number of sheets to be welded increases, the difficulty of the welding operation also increases. Similarly, welding becomes more difficult as the ratio of material thicknesses between sheets becomes overly large. Flange size is another important factor. Flanges must be large enough to accommodate weld equipment constraints and required weld sizes. Too often, designers fail to consider these important yet simple manufacturing requirements.

Coated Steels. Due to consumer demand, the automobile industry has been striving in recent years to produce vehicles with greater corrosion resistance. For the most part, this demand has been met by the use of steels coated by galvanizing, aluminizing, prepainting, or laminating. Such coatings greatly enhance the corrosion resistance of the base material, but reduce its weldability. In general, spot welding of coated materials generally requires an increase in weld current and hold time. Greater electrode wear is also exhibited, which can ultimately affect the resultant welds.

Joint Sealers. Passenger comfort is always an overriding concern in the design of a vehicle; therefore, much attention is paid to the reduction of wind noise, fume intrusion, and water leakage. Body sealers, particularly weld-through sealers, are used to control these factors. Welding problems associated with the use of the sealers include reduced conductivity at the faying surface and increased fuming as the sealer is burned away at the weld. Solutions to these problems include increasing heat input to ensure proper welding and providing for adequate ventilation to remove fumes generated (although minimal) by the vaporized sealer.

Joint adhesives are used to enhance joint integrity. They are commonly used in conjunction with the spot welding process to improve joint shear strength. Similar to joint sealers, adhesives can cause problems in welding, which can be overcome by the methods described above.

Material Requirements for Service Conditions

ASM Committee on Material Requirements for Service Conditions*

Gas Metal Arc Welding

The GMAW process is widely used in the automotive industry to weld frames, brackets, body panels, and many other structural components. This method is easily applied (automated and manually) and lends itself well to high productivity at a relatively low cost; in addition, it allows most metals to be joined to themselves. Disadvantages include the fact that GMAW is sensitive to material chemistry, surface coatings, and joint design. When these factors are not considered in the initial design, weld quality problems, such as cracks, porosity, lack of fusion, and burnthrough, often result, which may affect the structural integrity of an assembly.

Steel Properties. In the automotive industry, a wide variety of steel chemistries are used to meet strength and durability requirements, ranging from low-strength plain carbon steels to high-strength alloys. To avoid GMAW problems associated with chemistry, the designer must take into account the compatibility of the materials to be joined as well as their individual chemistries. Both plain carbon and alloy steels with carbon equivalents of approximately 0.30 are generally considered to be weldable. Once the material chemistries have been established, the appropriate solid filler material must be chosen to produce a weld with characteristics similar to those of the base materials being joined. By taking these initial design steps, problems such as underbead cracking and weld-metal embrittlement can be avoided.

Surface Condition. The GMAW process is sensitive to surface impurities on the base material, such as corrosion, dirt, and oil. Surface coatings can also adversely affect the resultant weld. When improperly prepared surfaces are welded by this method, quality problems (typically porosity and cracking) are often observed. The solution involves simply removing the surface contaminants. Surface coatings are not dealt with as easily, for either the coating must be selectively removed from the weld joint or the welding parameters must be adjusted to reduce the effects of the off-gassing material. This is sometimes done through a trial-and-error process, but can be refined to produce sound welds. In addition, if the coatings are removed in the weld area, provisions must be made to reapply corrosion protection where necessary.

Joint Preparation. Joint designs for GMAW are quite important in the automotive industry. Joints must be designed in such a way as to minimize the amount of joint preparation necessary, yet produce a weld that will serve the intended purpose. Joint preparation is a time-consuming process, which is not desirable for high-volume vehicle production.

Therefore, naturally occurring joints that result from strategic part placement are preferred to prepared joints, such as groove welds, which often require extra processing steps.

Gas Tungsten Arc Welding and Flux-Cored Arc Welding

The GTAW process is well suited to handle thin-section welding with or without filler materials. The FCAW process can handle the same types of welding conditions as the GMAW process, despite the filler material differences (flux-filled wires versus solid wires, respectively). In terms of automotive applications, both processes involve considerations similar to those listed for the GMAW process.

Fasteners: Resistance Projection Welding and Stud Welding

The intricate assembly of an automobile requires that parts be securely fastened, yet the ease of manufacturing must not be compromised. In order to accomplish this task, projection-welded screws, nuts, and studs are often used. These fasteners must possess welds that can withstand the rigors of a production environment as well as endure the torquing operations in assembly. Types of service conditions that can affect the welding and subsequent use of these parts include:

- BASE METAL/FASTENER CHEMISTRY
- BASE METAL/FASTENER STRENGTH CHARACTERISTICS
- BASE METAL/FASTENER COATINGS
- BASE METAL CLEANLINESS PRIOR TO WELDING

Materials Properties. Selection of the correct base metal and fastener chemistries is extremely important to ensure compatibility at the weld interface and HAZs. In order to avoid exotic weld schedules, materials with carbon equivalents of approximately 0.30 are ordinarily used, as they are readily weldable. It should be noted that these types of welds result in a similar type of weld metal/HAZ transition as other joining processes; this fact must be recognized in the design of such weldments.

Base-metal strength and fastener strength characteristics can affect the ultimate mechanical joint integrity. Designs must reflect conditions where the base-metal strength is compatible with that of the fastener; otherwise, premature failures or insufficient mechanical joints may result. The different strength characteristics may be a result of chemistry, heat treatment, cold working, or simply section thickness.

Surface Condition. Projection-welded fasteners may also be affected by coatings present on the base material or the fastener. As described previously, the automotive industry utilizes different corrosion-resistant coatings on many areas of vehicles. Such coatings can affect projection or stud welds in several ways. If the base material is zinc coated or the fastener is coated with a corrosion-resistant plating, the arc characteristics of the welding process are much different than for bare materials. In either case, provisions must be made in welding schedules. Lastly, use of an antispatter/antifriction coating, such as Teflon, can also affect the welding process. Such coatings are being used increasingly to prevent production problems associated with weld spatter and expulsions generated by other processes.

Laser Beam Welding

Laser beam welding is an emerging technology that has shown promise for use in the automotive industry. Basically, the technique utilizes a high-power laser beam capable of penetrating deep into the weld joint. Laser welding offers high speed, precision, and flexibility to automotive applications. The resultant welds exhibit very small HAZs and are easily formed to final part configuration without weld degradation.

The diverse capabilities of the laser welding technique enable the user to produce parts with properties unattainable with common methods, such as resistance spot welding or GMAW. Laser welding is most often used to make lap and butt joints. It allows blanks to be fabricated through the welding of different-gage materials as well as materials with dissimilar coatings. After the welding operation, the parts can be formed to their final shape. This allows heavier-gage materials to be used in place of reinforced areas, thereby eliminating parts. Similarly, coated parts can be strategically placed in corrosion-prone areas, which eliminates the need to coat the entire assembly.

Despite the obvious advantages of laser welding, application of the technique requires care, especially with the types of materials used in automotive applications. Coated steels complicate the laser welding process, because the off-gassing of the lower-boiling-point material interferes with the maintenance of the weld keyhole. Once this keyhole is broken, the weld must be restarted, resulting in inferior quality. Joint edges and part alignment/fit-up are also common production problems when laser welding. They affect the continuity of the welding process by disrupting the laser beam or by deflecting the beam from the joint.

Material Requirements for Service Conditions

ASM Committee on Material Requirements for Service Conditions*

Other Joining Processes

Many other joining techniques are commonly used in the automotive industry, but to a lesser extent than those discussed above. Some of these processes include resistance seam welding, soldering, brazing, and plastic welding, each of which requires due care in its application to ensure the production of sound joints.

Material Requirements for Service Conditions

ASM Committee on Material Requirements for Service Conditions*

Railroad Equipment

The transporting of freight and passengers by railroads in the United States involves over 200,000 miles of track, 1,200,000 freight cars, 19,000 locomotives, and thousands of passenger vehicles (Ref 19). Welding is the major process used in the fabrication of railroad facilities and structures, as well as in their repair and maintenance. Practically all known welding processes are being used or have been applied to components used by the industry. This section will deal with freight cars, locomotives, and track.

Reference cited in this section

19. *RAILROAD FACTS,* ASSOCIATION OF AMERICAN RAILROADS, 1990

ASM Committee on Material Requirements for Service Conditions*

Freight Cars

Freight car requirements vary considerably, depending on the type of load being carried. A variety of products are transported by rail, including various liquid and solid commodities. Some commodities must be kept at low temperatures and some at high pressures, and some are classified as hazardous. Public safety is always a key issue.

Many freight cars are in "interchange service," which means that they may be handled by any railroad. It also means that repair work may be done by a variety of shops throughout North America. Ease of repair welding is therefore a critical consideration in material selection.

It is not unusual to expect a freight car to last 40 years. Cars for interchange are designed for required service conditions, which for high-utilization cars may be up to 3 million miles of service. Freight cars must be able to sustain 4.5 MN (10^6 lbf) of squeeze and single-end impacts of 5.6 MN (1.25×10^6 lbf). Designs must include buff and draft forces of up to 3.5 MN (630,000 lbf) without exceeding the yield strength of the materials.

Freight cars are subject to a variety of cyclic stresses due to train action, track irregularities, and track hunting. Most failures are caused by fatigue crack propagation, with a lesser number caused by a single overspeed impact.

Types of freight cars in common use include tank, flat, gondola, box, hopper, and covered hopper cars. Of these, only tank and covered hopper cars have seen a net increase in number over the last 21 years (Ref 20). The largest increase has been in the use of covered hopper cars, which handle a variety of dry commodities that must be kept clean.

Tank cars consist of a tank, which is basically a pressure vessel, and an underframe, which provides connection to other cars and to the "trucks." Underframes may be continuous or may consist of attachments to the ends of the tank, with the tank being a structural member. Tank cars and covered hopper cars are often lined with epoxy, rubber, or other protective materials to prevent car body corrosion and/or contamination of the commodity being carried.

Specifications. Freight car construction is regulated by the Association of American Railroads (AAR). Tank car welding is covered by the AAR "Tank Car Specification." For other types of freight car welding, the AAR references the AWS "Railroad Welding Specification" (D15.1).

Design Considerations and Materials of Construction. With the type of welded construction employed on freight cars, the use of higher-strength materials does not improve fatigue resistance. Where fatigue is a significant factor, structural designs incorporating welding are based on carbon steel and HSLA steels with moderate strengths (usually 345 MPa, or 50 ksi, yield strength or less). For applications requiring high static strength and moderate fatigue resistance, quenched and tempered steels with yield strengths of 690 MPa (100 ksi) and high-strength controlled rolled steels with yield strengths of 550 MPa (80 ksi) have been used.

The most common steels used in the production of modern tank cars are ASTM A 516 grade 70 and AAR TC128 grade B (similar to ASTM A 612 grade B). For all pressure tank cars and for some nonpressure cars, these steels are used in the normalized condition. For general-purpose nonpressure cars, hot-rolled steel is used.

Certain components are exposed to severe wear conditions, including "truck" components as well as couplers and related wear plates. Wear materials used include plain high-carbon steel, quenched and tempered alloy steel, and austenitic manganese steel, which are attached by welding or by mechanical fasteners.

Some commodities warrant the use of stainless steel tanks or covered hopper cars, which are generally fabricated of AISI type 304 or 316 stainless steel. However, this constitutes a small percentage of the freight car business.

The empty car weight, or tare weight, is an important factor in determining the hauling capacity of a car. The tare weight is deducted from the total allowed weight (i.e., gross rail load) to determine the weight of commodity that can be loaded (i.e., load capacity). The energy used to haul the tare weight around is wasted fuel. For this reason, the use of aluminum

car bodies has recently become more popular, especially in coal-hauling service. The corrosion resistance of aluminum alloys is an added benefit. In some designs, the aluminum is mechanically fastened to the welded steel underframe, and little or no welding of the aluminum is required.

Freight cars generally consist of six components: tracks, brakes, underframes, draft components, safety appliances, and bodies. Figure 13 shows a side view of a general-purpose boxcar. A high percentage of the welding operation is performed in the underframes and the car bodies. Underframe components typically are from 6.4 to 25 mm ($\frac{1}{4}$ to 1 in.) thick, but may be thicker for heavy-duty cars. Bodies vary from 3.2 to 7.8 mm ($\frac{1}{8}$ to $\frac{5}{16}$ in.) in thickness. Tank car tanks range from 11 mm ($\frac{7}{16}$ in.) to slightly more than 25 mm (1 in.) in thickness.

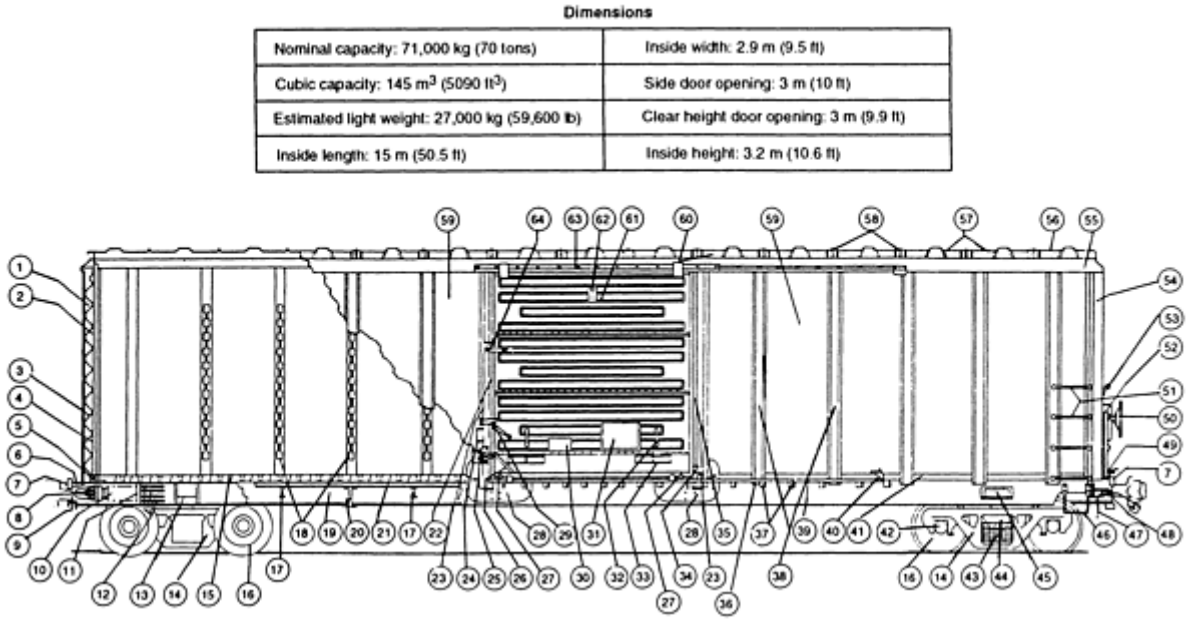

FIG. 13 SIDE VIEW OF A GENERAL-PURPOSE BOXCAR. 1, END SHEET (TOP); 2, END LINING (TOP); 3, END SHEET (BOTTOM); 4, END LINING (BOTTOM); 5, END SILL; 6, STRIKER FACE RIB; 7, STRIKER FACE; 8, KEY SLOT LINER AND FRONT DRAFT LUG; 9, COUPLER CARRIER; 10, DRAFT GEAR; 11, FRONT DRAFT GEAR STOP; 12, REAR DRAFT LUG RIBS; 13, COMBINATION CENTER FILLER/CENTER PLATE; 14, TRUCK FRAME; 15, NAILABLE STEEL FLOORING; 16, WHEEL; 17, FLOOR BEAM; 18, LADING STRAP ANCHOR; 19, CENTER SILL; 20, CROSSBEARER; 21, FLOOR STRINGER; 22, DOOR FRONT STOP; 23, DOOR POST; 24, DOOR LOCK BRACKET; 25, DOOR LOCK; 26, DOOR LOCK REINFORCING GUSSET; 27, DOOR ROLLERS; 28, DOOR POST AND SIDE SILL GUSSET; 29, STARTER AND CLOSURE LEVER; 30, ROUTING BOARD; 31, PLACARD BOARD; 32, DOOR HANDLE; 33, FORKLIFT PUSHER BLOCK; 34, DOOR CATCH; 35, SPARK STRIP; 36, SIDE SILL REINFORCEMENT; 37, DOOR TRACK BRACKET; 38, SIDE POST; 39, DOOR TRACK (BOTTOM); 40, DOOR CATCH ASSEMBLY; 41, SIDE SILL; 42, AXLE; 43, TRUCK SPRINGS; 44, TRUCK BOLSTER; 45, JACKING PAD; 46, SILL STEP; 47, UNCOUPLING ROD; 48, KEY SLOT; 49, CROSSOVER STEP; 50, HAND BRAKE WHEEL; 51, LADDER GRAB; 52, LADDER STILE; 53, GRAB; 54, CORNER POST; 55, SIDE PLATE; 56, ROOF SHEET (END); 57, ROOF SHEET (INTERMEDIATE); 58, SEAM CAP; 59, SIDE SHEET (PLAIN); 60, DOOR SAFETY HANGER; 61, SLIDING DOOR; 62, LIFTING LUG; 63, DOOR TOP RETAINER; 64, ANTIPILFERAGE LOCK. COPYRIGHT SIMMONS-BOARDMAN PUBLISHING COMPANY/THE RAILWAY EDUCATIONAL BUREAU. REPRODUCED WITH PERMISSION

Welding Processes. The most common welding processes used in the manufacture of freight cars are FCAW, GMAW, and SAW. SMAW has been largely displaced by semiautomatic, mechanized, or automatic welding procedures. Seams in tank car tanks are produced primarily by SAW. Except for carbon and low-alloy steel tank car tanks, which are stress relieved, most freight car components are used in the as-welded condition.

Reference cited in this section

Material Requirements for Service Conditions

ASM Committee on Material Requirements for Service Conditions*

Locomotives

Modern locomotives are diesel-electric, ranging from 0.75 to 3.3 MW (1000 to 4500 hp) in power and weighing as much as 181,000 kg (400,000 lb). The life of a locomotive is expected to be 20 years and with rebuild can be extended to as long as 40 years. Locomotives are generally owned by a railroad and remain within its control. Maintenance is normally done by the owners, but major overhauls and rebuilds are performed by remanufacturing specialists.

Design Considerations and Materials of Construction. The modern diesel-electric locomotive consists of welded components fabricated using the full range of welding processes. The basic components are the underframe, cab structures, engine, generator, tracks, traction motors, electrical cabinets, fuel tank, air compressor, and brake equipment. Components are fabricated from rolled plate, sheet metal, forgings, castings, and various shapes.

Locomotives must be able to withstand forces similar to those experienced by freight cars, including 4.5 MN (10^6 lbf) of squeeze. Buff and draft forces are transmitted through a self-supporting rigid underframe consisting of a fabricated draft gear pocket, "T" or "I" sills, and a bottom plate.

Materials used for fabrication of the main components of a locomotive are typically selected on the basis of good weldability in order to facilitate original construction and subsequent maintenance and rebuild. The underframe, fuel tank, traction motor frame, generator frame, and other structural steel components are fabricated from low-carbon steel containing less than 0.26% C, with and without added alloying. Typical tensile and yield strengths are 415 and 275 MPa (60 and 40 ksi), respectively. Weld filler metals used for these components include E70*xx*, ER70S-X, and E70T-X-type electrodes. Although higher-strength base materials do not improve high-cycle fatigue life, quenched and tempered steels with a tensile strength of 690 MPa (100 ksi) and normalized carbon-manganese steels with a tensile strength of 550 MPa (80 ksi) may be used when high static strength or weight reduction is an issue.

Diesel locomotive track frames are made of cast steel. Except for the application of wear plates, welding on cast steel truck frames is accomplished using E70-type electrodes. Wear plates made of medium-carbon, high-carbon, or austenitic manganese steels are welded using austenitic stainless steel electrodes.

With the exception of certain critical subassemblies (bolsters, center plates, and traction motor frames), which are stress relieved, most diesel locomotive structural fabrications are used in the as-welded condition.

Material Requirements for Service Conditions

ASM Committee on Material Requirements for Service Conditions*

Track

Rails are designed for strength and wear resistance. Locomotives and freight cars weighing up to 181,000 kg (400,000 lb) and riding on steel wheels create high bearing stresses, requiring very-high-strength rail material. Bearing stresses may be up to 2750 MPa (400 ksi).

Rail life averages 70 years. Replacement of rail is extremely expensive. Maintenance of high wear areas, such as switch points and rail ends, requires that repairs be made economically in the field. The desire for long, continuous rails necessitates the use of materials that allow butt welds to be made in the rail that have properties matching the unwelded rail.

Design Considerations and Materials of Construction. There are two categories of rail materials. The largest category by far is T-rail, typically of near-eutectoid composition (~0.8% C), which makes up the thousands of miles of railroad track. The much smaller category is austenitic manganese steel, which is used extensively in cast frogs. The welding practices for each type of material are very different. This section will address the metallurgical reasons for these differences. Welding is applied to T-rail for joining and repair purposes, and is applied to austenitic manganese steel solely for repair purposes.

The controlling feature for welding of near-eutectoid T-rail is hardenability--that is, its tendency to form transformation products such as martensite and bainite, rather than the preferred pearlite. Untempered martensite is unacceptable because of its possible embrittling effect on rail steel; near-eutectoid composition bainite and tempered martensite are avoided because of their poor wear resistance compared with pearlite of the same hardness.

Historically, rail steels have had carbon contents near 0.7 to 0.75%, with manganese contents of 0.85 to 0.95% and silicon levels of up to 0.5% maximum. The as-hot-rolled hardness generally has been near 240 to 270 HB. More modern conventional carbon rail steel has a slightly higher maximum manganese content (1.25%) and allows up to 0.25% Cr to be added to ensure as-hot-rolled hardness near 300 HB.

Metallurgical Characterization. The time-temperature-transformation (TTT) characteristics of steel control the type of transformation product that results from the welding process. A typical continuous cooling curve diagram for the older grades of conventional carbon rail steel is illustrated at the left in Fig. 14. In an effort to ensure that the transformation product resulting from welding is pearlitic, the maximum cooling rate through the transformation region generally must not exceed approximately 4 °C/s (7 °F/s). For rates up to this maximum level, transformation will take place entirely between the pearlite start and finish boundaries. However, should the cooling rates exceed approximately 4 °C/s (7 °F/s), it is possible that the cooling path will miss the nose of the pearlite finish boundary such that untransformed austenite will be available for transformation to bainite or untempered martensite at temperatures below 540 °C (1000 °F).

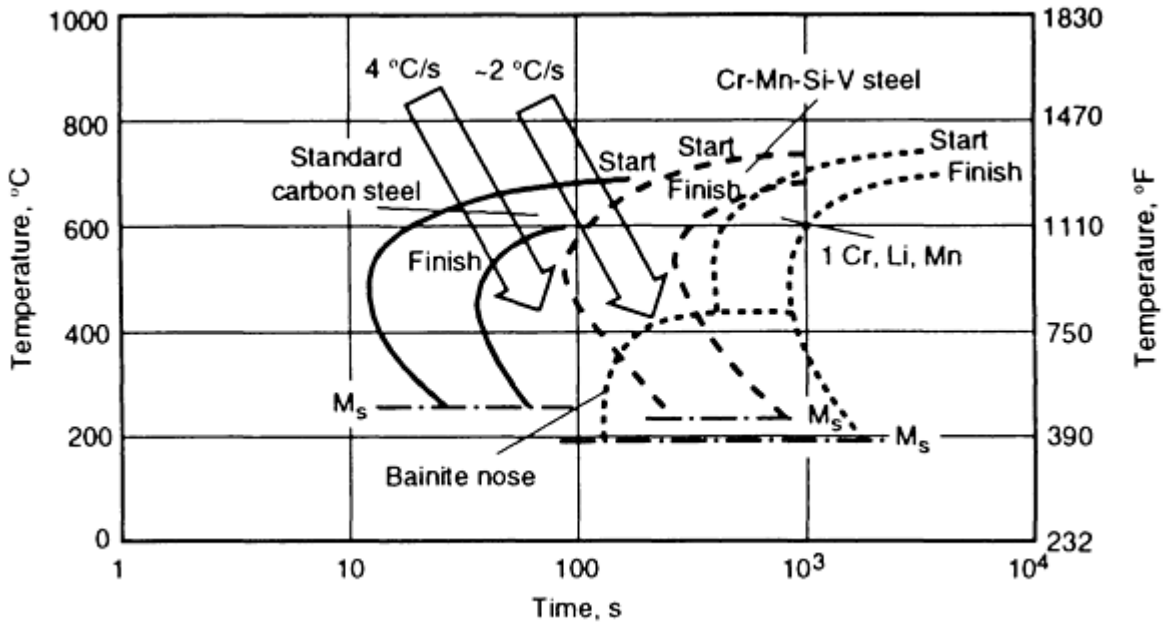

FIG. 14 TTT CHARACTERISTICS OF RAIL STEELS

Alloying additions are sometimes made to near-eutectoid rail steels in an effort to produce pearlite having a smaller spacing between the Fe_3C platelets during cooling following hot rolling; this yields superior hardness and greater wear resistance. The alloying additions most commonly used are the carbide formers: chromium, molybdenum, and vanadium. If added in sufficient amounts (1% Cr; 0.6 to 0.8% Cr and 0.20% Mo; or 1% Cr and 0.08% V), these types of alloy additions tend to increase hardenability significantly and in so doing shift the diagram to longer times. In fact, a specific bainite nose can be obtained (see Fig. 14).

Welding Thermal Cycles. One of the limitations of the alloy approach to strengthening is that a welding practice resulting in a cooling rate near 2 °C/s (3.6 °F/s) (which would be perfectly satisfactory for conventional carbon steel rail) would now lead to the formation of undesirable bainite or untempered martensite. Welding practices must be modified to slow the cooling rate to less than 2 °C/s (3.6 °F/s).

By and large, most rail welding is done to join rails into strings up to 440 m (1440 ft) in length. The most common practice for that purpose is flash butt welding utilizing either ac or dc current. This practice generally involves the use of a number of preheating cycles to heat the rail ends and control the subsequent cooling rate. When the rail ends have been sufficiently preheated, a flashing phase is initiated that removes oxidized metal and establishes a metal ion plasma in which forge welding of the rail ends can be accomplished. The forging operation ideally expels all liquid metal from the bond interface, such that the weld is in reality a solid-state bond.

Postweld Heating and Cooling Cycles. For significantly alloyed rail steels, adjustment of the preheat practice may not be sufficient to limit the final cooling rate. To this end, postheat cycles are applied after the forging cycle. The added expense of postheating has caused railroads to prefer the use of heat-treated carbon steel rails--both those achieving full section hardening and those in which only the head is hardened. These rails generally require no modification of the electric flash butt welding practice. However, a consequence of welding most heat-treated rails (except those classified as slack quenched) is the loss of the heat-treat strengthening in the weldment. This loss can lead to severe batter of the weldment under heavy wheel loads. Thus, some railroads have introduced a postweld air quench to refine the pearlite in weldments.

An alternative approach to air quenching is the use of head-hardened rails having their composition adjusted slightly to achieve slack quenching during the normal cooling after flash butt welding. Typically, such modified compositions will include increased silicon (up to 0.8%) and chromium (up to 0.5%) levels. After normal cooling, the hardness of the weldment will have returned to about the same level (~350 HB) as that of the head-hardened region of the rail. Although this approach works very well, the cost of the rail may be notably higher than that of conventional head-hardened rail. Neither air quenching nor slack quenching prevents the softening that occurs in the outer boundaries of the HAZs.

Other Welding Processes. Rails are also joined together in track by thermite welding--a metal casting process based on the reaction between aluminum powder and iron oxide (see the article "Thermite Welding" in this Volume). The resulting cast structure has low ductility and toughness compared with the hot-worked structure of a flash butt weld. The cooling rates typical of thermite welding are low in comparison with those of the flash butt process, so there generally is no need to alter standard welding practices for use with alloy rail.

Welding also is applied to near-eutectoid rail steels to repair battered and chipped rail ends, wheel burns, and worn and chipped switch points and frogs. Both arc welding and oxyfuel gas welding processes are possible, although arc welding is preferred. Either coated electrodes or flux-cored wire can be used. Electrodes may contain high nickel and manganese contents, and deposits are generally austenitic. Both longitudinal and transverse lay-down patterns have been employed.

Austenitic Manganese Steels. The nominal chemical composition range for austenitic manganese steel is 10 to 14% Mn and 1.0 to 1.4% C. The presence of such high levels of manganese stabilizes the high-temperature fcc austenite phase so that, with rapid cooling, the austenite is retained to room temperatures. The austenite has a relatively low yield strength that is not strongly influenced by carbon or manganese levels. However, its ultimate tensile strength, which is influenced by carbon or manganese levels, can be quite high in comparison with yield strength. This wide separation imbues the steel with a much higher work-hardening capacity than pearlitic rail steels. It is this high work-hardening capacity that makes manganese steels effective in resisting impact loads such as those occurring at railroad frogs. Although the high manganese content can delay the transformation of the high-temperature austenite phase to the room-temperature equilibrium phases (ferrite and carbides), it cannot completely suppress the transformation. If temperatures are elevated to 315 °C (600 °F) for very long periods or to temperatures 480 to 540 °C (900 to 1000 °F) for much shorter periods (a few minutes), the steel can become embrittled. The mechanism of embrittlement is the precipitation of carbides, usually along austenite grain boundaries. For this reason, repair welding must cease when the casting temperature reaches 315 to 370 °C (600 to 700 °F), and the parts must be allowed to cool to a more suitable range.

Sheet Metals

This section deals with a wide variety of sheet metal fabrications, excluding those discussed in previous sections of this article. Ductwork of many types, small and large appliances, containers, pharmaceutical and food processing vessels, and industrial and domestic kitchen equipment are examples of sheet metal applications.

Service conditions are the principal consideration in material selection for such applications. The material attributes listed in Table 1 are a useful starting point. If an application requires cold forming or deep drawing, the ductility of the material will be of primary importance. Corrosion properties are paramount in applications where the weldment will not be protected by some type of coating following fabrication. Mechanical properties figure prominently in designs for structural applications. Density becomes important in many applications for products where shipping weight is a factor. Fracture toughness, conductivity, and magnetic properties are rarely significant in sheet metal fabrications.

Weldability is extremely important in the material selection process, particularly when an application involves very thin sheet materials. The choice of welding process will be determined by the ability to weld thin materials without burnthrough. When dealing with sheet metals, the ability to make sound welds without burnthrough is often synonymous with weldability.

The weldability of sheet metals is vitally affected by the welding process selected, the manner of welding (manual, semiautomatic, or automatic), and the number of parts to be fabricated in a given manufacturing operation. This section will deal with material selection criteria as determined by the joining process to be employed.

Welding process selection is greatly influenced by the need to control distortion. Thinner material is inherently more difficult to weld because of the thermal cycles encountered in welded joints. Distortion is minimized by rigid fixturing and by use of high-energy rapid-travel-rate welding processes. Brazing or soldering allows lower peak temperatures to be used for joining, which is advantageous in distortion control. Materials with low heat conductivity, such as stainless steels, aggravate distortion problems. Warpage of materials during joining is one of the principal problems encountered in the fabrication of sheet metal by any of the joining processes that involve fusion of metal.

Material Requirements for Service Conditions

ASM Committee on Material Requirements for Service Conditions*

Joining Processes

Resistance Welding. Spot, seam, and projection welding are commonly used in sheet metal fabrications. The most commonly used material joined by these processes is low-carbon steel, although low-alloy steels, stainless steels, nickel, and copper-base alloys are also readily joined.

When an unalloyed carbon steel is suitable for an application, the carbon content is generally limited to 0.20% maximum. For products that are to be enameled after welding, the carbon content is usually kept below 0.04% to avoid blistering of the enamel. The designer can then take advantage of the enamel thickness in assessing the strength properties of the part, which will offset the relatively low strength of the very-low-carbon steel.

Spot welding and projection welding are advantageous for control of distortion, but are unsatisfactory for containment of fluids or for elimination of crevices. Seam welding can be suitable for fluid containment, but distortion is a greater problem and crevices continue to be present. As described in the section titled "Automobiles" in this article, joint sealants and adhesives can be used with the resistance welding processes, offering the possibility of fluid containment and crevice elimination.

Arc Welding. Developments over the past 20 years have greatly increased the application of arc welding in the fabrication of sheet metals. All of the arc welding processes are employed, although some are more suitable than others.

The simplest arc welding process is SMAW. For nonrepetitive parts, it is the preferred process and is suitable for thicknesses of most steels down to about 2 mm (0.080 in.). Covered electrodes down to 1.6 mm ($\frac{1}{16}$ in.) in diameter are available in most types of low-carbon, low-alloy, and stainless steels. Burnthrough is a problem with the thinner sheet metals, more so with stainless steel than with carbon steels because of its low thermal conductivity. The SMAW process is commonly used in job shops and for repairs. Fixturing for prevention of distortion and warpage is needed in cases where large, flat surfaces must be kept flat.

Manual welding with the gas-shielded arc welding processes (GMAW, FCAW, and GTAW) offers improved control of the arc energy, especially when using more sophisticated power sources with pulsed current controls. However, travel rate in manual welding is generally slow, so the distortion problem is similar to that encountered with SMAW. Automation of the process offers increased welding speed, use of fixtures with heat sinks for more rapid cooling, and higher productivity and quality.

High-energy-beam welding processes, such as electron and laser beam, offer even higher welding speed and lower distortion. Materials sensitive to atmospheric effects during welding, such as titanium and zirconium, are especially suited to electron beam welding in vacuum chambers or with an inert gas trailing shield. Laser welding is being increasingly used for unalloyed carbon steel sheet fabrication, because the process requires no protection from the atmosphere during welding and because relatively low-power laser equipment of nominal cost is adaptable for thin metal sections. Fully automatic welding systems are generally required for high-energy-beam welding processes.

Brazing and soldering are suitable joining methods for many sheet metal materials. The metal surfaces must be compatible with the liquid-phase joining material. For successful joining, both brazing and soldering depend on capillary action between the mating surfaces to cause flow of the liquid joining material. Oxides on the metal surface must be mechanically or chemically removed in many instances for the liquid metal to flow freely. Fluxes are frequently used to assist this flow process.

These joining processes are easily adaptable to manual low-volume fabrication using oxyfuel torches for the heat source. Job shops customarily use these methods for fabrication or repair. The lower joining temperature is a distinct advantage in that fusion of the base metals does not take place, minimizing distortion.

Soldering is commonly used to join galvanized steel and tin plate. The surface zinc or tin becomes alloyed with the solder during the fusion process and assists in establishing an adherent bond with the underlying steel. The coated surface adjacent to the joint is unaffected and is thus resistant to the service environment.

Brazing requires much higher temperatures and offers many more types of filler metals than soldering. A filler metal must be chosen not only for its ability to flow at the brazing temperature, but also for its compatibility with the service environment. The filler metal is distinctly different from the base metal and may set up electrochemical cells, causing localized corrosion adjacent to the joint.

Brazing and soldering are superior to resistance welding for producing crevice-free joints, but are usually less satisfactory than the arc welding processes for joints that require mechanical and corrosion-resistance properties comparable to those of the base metals.

Nonfusion Joining Processes. Bonding of metal surfaces can be accomplished in many metal systems without fusion. Diffusion bonding, ultrasonic welding, and similar techniques can be used to join very thin metals. These processes are particularly appropriate for the precious metals--for example, in making contacts to foils in electronic circuitry. They are economically unsuitable for continuous seams in liquid or gas containers.

Materials and Properties

Steels. Low-carbon steels are characterized by their considerable ductility at ambient temperatures, which becomes even higher at elevated temperatures. During the welding thermal cycle, plastic deformation occurs in the HAZ. Unless restrained by clamping devices or by the inherent shape of the piece, unwanted distortion in the weld area will result. The thinner the steel, the greater the distortion problem.

Fusion welds have greater strength and lower ductility than the base metal. If a sheet metal is to be cold formed after joining, this strength mismatch may need to be addressed in the design. Although the ductility of the weld is less than that of the base metal, it is usually adequate for most cold-forming operations. Distortion that forms during the welding operation can sometimes be ignored if the component is subsequently cold formed.

In corrosive or high-temperature environments, carbon steel weldments will perform in a manner generally comparable to that of the unaffected base metal. The cast structure of the weld is often less resistant to some environments than the wrought structure of the unaffected steel. Also, the welding process usually results in fine oxide inclusions in the weld, which are often less resistant to corrosion.

The higher strength of low-alloy steels does not offer the same advantages to sheet metal welding applications that it does to structural steel applications. Thinner sections might be possible by using the higher-strength steels, but distortion and weldability considerations usually make such choices uneconomical unless weight savings are critical.

Table 21 lists the principal ASTM specifications for weldable carbon and low-alloy sheet steels.

TABLE 21 PRINCIPAL ASTM SPECIFICATIONS FOR WELDABLE CARBON AND LOW-ALLOY SHEET STEELS

TYPE OF STEEL	PURPOSE	ASTM NO.	
		COLD ROLLED	HOT ROLLED
LOW CARBON	COMMERCIAL QUALITY	A 366	A 569
		A 794	A 659
	STRUCTURAL	A 611	A 570
	ENAMELING	A 424	A 424
	DEEP DRAWING	A 619	A 621
		A 620	A 622
CARBON-MANGANESE	ATMOSPHERIC CORROSION	A 606	A 606
	PRESSURE VESSELS	. . .	A 414
LOW ALLOY	HIGH STRENGTH	. . .	A 715
	NIOBIUM OR VANADIUM ADDED	A 607	A 607

Aluminum and aluminum alloy specifications for sheet metal are included in ASTM B 209. The low density of aluminum when compared with most metals makes aluminum sheet metal desirable for fabrications where weight savings are important. It is also useful for its adherent oxide, which makes it resistant to many environments at ambient temperatures.

The refractory oxide on the surface of aluminum becomes increasingly important as the thickness of the sheet is reduced. Gas-shielded arc welding processes, especially those using ac power, are essential to break down this adherent refractory aluminum oxide in order to make successful welds. Manual welding with covered electrodes is employed occasionally; oxyfuel welding is not suitable. Brazing and soldering are possible only with chemically active fluxes that dissolve the oxide layer.

The high thermal conductivity of aluminum can cause distortion. Gas-shielded arc welding processes overcome this problem by concentrating the arc energy sufficiently to cause fusion to occur. Electron beam welding is also suitable.

Aluminum alloys offer higher strength, which is especially important in applications where weight saving is a factor. Furthermore, their thermal conductivity is lower than that of pure aluminum, making fusion welding easier.

Distortion control is usually provided by rigid fixturing and backups. The metallic backup of the fixtures offers the advantage of heat sinks and backside weld contour control. Adding an inert backing gas often prevents oxidation of the molten weld pool.

Stainless Steel. The corrosion resistance of stainless steel is provided by chromium in an amount of at least 12%. When the content of nickel is greater than 8%, the austenitic form of iron becomes stable at ambient temperatures. The most frequently employed stainless steels for sheet metal fabrication contain 18% Cr and 8% Ni and are known as austenitic stainless steels. ASTM specifications normally used in stainless steel sheet metal applications are listed in Table 22.

TABLE 22 PRINCIPAL ASTM SPECIFICATIONS FOR WELDABLE STAINLESS STEEL SHEET

TYPE OF STEEL	PURPOSE	ASTM NO.
AUSTENITIC CHROMIUM-NICKEL	GENERAL REQUIREMENTS	A 480
	GENERAL PURPOSES	A 167
		A 240
	ARCHITECTURAL	A 666
	ROLL CLAD	A 264
DUPLEX CHROMIUM-NICKEL	GENERAL PURPOSES	A 240
FERRITIC CHROMIUM	GENERAL REQUIREMENTS	A 480
	GENERAL PURPOSES	A 240
		A 276
	ROLL CLAD	A 263

The austenitic stainless steels are extremely ductile and easily welded. The weld strengths, both yield and ultimate tensile, are generally higher than those of the base metal, but ductility remains high, permitting subsequent cold forming or straightening if necessary.

The thermal conductivity of stainless steels is about 30% less than that of carbon steels. The thermal cycles during welding cause plastic deformation to occur in the widely heated zones adjacent to the weld. Moreover, the coefficient of thermal expansion for stainless steels is about 30% greater than that of carbon steels. These two properties account for the even greater distortion problems encountered in the austenitic stainless steels compared with carbon steels. Therefore, rigid fixturing and heat sinks are essential when welding these alloys.

Stainless steels are principally used for their resistance to aqueous corrosion and for their strength and oxidation resistance at elevated temperatures. With regard to certain corrosive media, it is important to recognize that the thermal cycles during welding cause carbide precipitation to occur in the HAZ, with severe loss in corrosion resistance. This can be overcome by the use of low-carbon types (0.03% maximum) or those stabilized with titanium or niobium. The stabilized stainless steels are also stronger at elevated temperatures. The fluidity of the very-low-carbon stainless steels often affects the attainment of the desired weld profiles. This is particularly troublesome in autogenous GTAW when sulfur is unusually low (<0.010%).

Because many applications require avoidance of crevices at weld joints, arc welding is the preferred joining method. Shielding from the atmosphere during welding is essential, and while manual arc welding with covered electrodes is suitable for many applications, gas-shielded processes, especially those using inert gases, are useful in minimizing the oxidation of chromium and other essential alloying ingredients.

Butt joints in sheet metals are welded in a single pass. If the backside of the weld will be exposed in the finished weldment, it should have a suitable contour. Purging of the backside of the joint with an inert or inactive gas, usually

argon or helium, but sometimes nitrogen, is useful in producing the desired finish. Gas purging is often built into the distortion-control fixturing.

Austenitic stainless steel welds are almost invariably put into service in the as-deposited condition. The residual stresses associated with the welding operation can give rise to SCC in certain service environments. This situation can be substantially overcome by selecting one of the duplex stainless steels, which have structures of roughly half austenite and half ferrite. These steels contain less nickel than the austenitic stainless steels and provide corrosion resistance by the addition of molybdenum. Filler metals with matching compositions are available for the duplex stainless steels; more commonly, welds are made using an austenitic stainless steel filler metal, provided that the type is suitable for the service environment.

The ferritic stainless steels that contain little or no nickel are less suitable for sheet metal fabrications. Although they do not present the problems of the austenitic stainless steels in terms of low thermal conductivity and high coefficient of expansion, their metallurgical weldability is troublesome, forming constituents that have low ductility in the HAZs. Postweld heat treatments are required to restore ductility, which in practice complicate the distortion problem.

Other Metals and Alloys. ASTM specifications for weldable nonferrous sheet metals are listed in Table 23. Like the stainless steels, nickel-base alloys are commonly used in sheet metal weldments. The welding processes and controls are similar to those described for the austenitic stainless steels, although corrosion impairment due to carbide precipitation is not a concern. Unalloyed nickel, nickel-chromium alloys, and nickel-copper alloys are readily weldable, although their physical properties can affect distortion and burnthrough.

TABLE 23 PRINCIPAL ASTM SPECIFICATIONS FOR WELDABLE NONFERROUS SHEET METALS

TYPE	PRINCIPAL ALLOYING ELEMENTS	ASTM NO.
NICKEL ALLOYS	NONE	B 162
	CU	B 127
	CR-FC	B 168
	MO	B 333
	FE-CR	B 409
	FE-CR-MO-CU	B 424
	MO-CR-FE	B 434
	CR-MO-FE	B 435
	CR-MO-NB	B 443
	CR-FE-MO-CU-NB	B 463
	FE-CR-SI	B 536
	MO-CR	B 575
	CR-FE-MO-CU	B 582
	FE-CR-MO-NB	B 599
	FE-CR-MO	B 620
	FE-CR-MO-CU	B 625
COPPER ALLOYS	NONE	B 152
	SI	B 96, B 97
	SN	B 103
	AL	B 169
	NI	B 402, B 422
TITANIUM AND ITS ALLOYS	. . .	B 265
ZIRCONIUM AND ITS ALLOYS	. . .	B 352, B 551
NIOBIUM AND ITS ALLOYS	. . .	B 393
MOLYBDENUM AND ITS ALLOYS	. . .	B 386

Copper and its alloys in sheet metal form are somewhat more difficult to weld. Unalloyed copper has a very high thermal conductivity. The tin-alloyed bronzes are much more easily welded, whereas suitable fusion welds are virtually impossible in the zinc-alloyed brasses. Copper-nickel alloys (both 10% and 30% Ni), on the other hand, are easily welded with many of the processes and controls cited for stainless steels.

Titanium is used in sheet metal fabrications for its superior corrosion-resistance properties in many environments. Gas shielding or vacuum environments are needed during the welding operation to protect against contamination of the weld zone by oxygen and nitrogen from the air. Gas-shielded arc welding processes are almost invariably used, because smooth contour welds free from crevices are usually demanded. These can be fabricated without resorting to vacuum chambers, provided that both sides of the weld at the welding arc and in the trailing solidifying weld regions are protected from the atmosphere.

Zirconium, niobium, and molybdenum and their alloys are occasionally produced in sheet metal form and are welded using the gas-shielded processes.

High-energy-beam welding processes are also adaptable to exotic metals and alloys. Electron beam welding in vacuum chambers is especially suited to joining these metals, the unit cost of which is high. The added equipment and fixturing costs can be justified by the reliable welds that are produced.

Coated Metals. Among the most commonly used coated sheet metals are galvanized steel and tin plate. As described above, soldering is a useful technique for joining these metals. Arc welding is possible, but it destroys the coating adjacent to the weld, thus negating the corrosion resistance for which the coated steel was specified. If arc welding is used on galvanized steel, good ventilation must be provided to protect the operator from zinc fumes.

In applications where the corrosion resistance offered by austenitic stainless steels is needed on only one side of a vessel, roll-clad steels are often an economical choice, especially for heavier-gage thicknesses. Distortion during welding is much less of a problem than with solid stainless steel because of the physical properties of the steel backing and its greater thickness. The welding of clad steels in thin sections is usually accomplished in a single pass using a higher-alloyed filler metal (e.g., type 309 for joining type 304 clad steel) to offset the effect of dilution with the unalloyed steel backing.

Painted sheet steels are commonly encountered in repair welding applications. Paints or other surface contaminants should be removed before welding to ensure sound joints.

Material Requirements for Service Conditions

ASM Committee on Material Requirements for Service Conditions*

Surface Finishing

Protective Coatings. Sheet metal weldments fabricated from unalloyed carbon steel are often more vulnerable to failure by corrosion or other environmental deterioration because of their relatively thin sections. Moreover, the welds themselves are frequently anodic to the base metal, causing corrosion failure in those regions. Suitable protective coatings, such as enamels, are often mandated for sheet steel weldments.

Postweld Finishing. Sheet metal fabrications frequently remain in the as-deposited condition, with only slag removal considered essential. This places a premium on smooth contours and good workmanship standards for meeting appearance criteria.

Appearance demands sometimes require the removal of all evidence of the weld. Grinding of the weld surface to blend with the base metal is often performed for appearance reasons or to remove notches for fatigue service applications. The amount of grinding can be substantially reduced if the welding process is intelligently selected and if the controls are carefully set forth in the fabrication specifications. Sheet metal fabrications in which the welds are to be ground smooth are more economically produced when the amount of weld reinforcement is kept to a minimum by appropriate welding process selection and controls.

Stainless steel sheet fabrications often require polishing to match the finish of the base metal. Polishing of the welds can be done either on the as-deposited finish or, if necessary, on the ground and blended finish.

Material Requirements for Service Conditions

ASM Committee on Material Requirements for Service Conditions*

Fabrication Codes and Specifications

Most of the requirements for sheet metal fabrications are set forth in user specifications or contractual documents. Aside from those considered in the preceding sections, few industry-wide codes are available. The American Welding Society publishes a specification titled "Structural Welding Code--Sheet Steel" (AWS D9.1) that covers the welding of low-carbon hot-rolled and cold-rolled sheet and strip steel with and without zinc coatings (galvanized steel). Qualification of welding procedures and welding operators is set forth in this specification.

Material Requirements for Service Conditions

ASM Committee on Material Requirements for Service Conditions*

References

1. R.P. REED, M.B. KASEN, H.I. MCHENRY, C.M. FORTUNKO, AND D.T. REED, *FITNESS FOR SERVICE CRITERIA FOR PIPELINE GIRTH WELD QUALITY,* BULL. 296, WELDING RESEARCH COUNCIL, JULY 1984
2. "BOILER AND PRESSURE VESSEL CODE," SECTION II, AMERICAN SOCIETY OF MECHANICAL ENGINEERS
3. *STEELS FOR HYDROGEN SERVICE AT ELEVATED TEMPERATURES AND PRESSURES IN PETROLEUM REFINERIES AND PETROCHEMICAL PLANTS,* 4TH ED., API PUBL. 941, AMERICAN PETROLEUM INSTITUTE, APRIL 1990
4. S. YUKAWA, *GUIDELINE FOR PRESSURE VESSEL SAFETY ASSESSMENT,* NIST SPEC. PUBL. 780, NATIONAL INSTITUTE FOR STANDARDS AND TECHNOLOGY, P 14-22
5. W.H. WINN, WELDABILITY OF LOW ALLOY STEELS, *BR. WELD. J.,* VOL 11 (NO. 8), AUG 1964
6. W.F. SAVAGE, E.F. NIPPES, AND E.S. SZEKERES, A STUDY OF WELD INTERFACE PHENOMENA IN A LOW ALLOY STEEL, *WELD. J.,* SEPT 1976, P 260S-268S
7. G.E. DIETER, *ENGINEERING DESIGN,* MCGRAW-HILL, 1983
8. B.D. TAPLEY, *ESCHBACK'S HANDBOOK OF ENGINEERING FUNDAMENTALS,* JOHN WILEY & SONS, 1990
9. *AEROSPACE STRUCTURAL MATERIALS HANDBOOK,* VOL III, 1984
10. SIMS AND HAGEL, *THE SUPERALLOYS,* JOHN WILEY & SONS, 1972
11. CASTRO AND DECADENT, *WELDING METALLURGY OF STAINLESS AND HEAT RESISTING STEELS,* CAMBRIDGE PRESS, 1968
12. EVANS AND WILSHIRE, *CREEP IN METALS AND ALLOYS,* DOTESIOS PRINTERS, U.K., 1985
13. *AEROSPACE STRUCTURAL MATERIALS HANDBOOK,* VOL IV, 1984
14. *BRAZING HANDBOOK,* AMERICAN WELDING SOCIETY, 1976
15. D. HARVEY, FILLER METAL SELECTIONS FOR CRITICAL AEROSPACE FABRICATION, *WELD. DESIGN FABR.,* VOL 60 (NO. 2), MARCH 1991, P 765-80
16. *USAF DAMAGE TOLERANT DESIGN HANDBOOK: GUIDELINES FOR ANALYSIS AND DESIGN OF DAMAGE TOLERANT AIRCRAFT,* U.S. AIR FORCE, 1984

17. PATTERSON *ET AL.* TITANIUM ALUMINIDE: ELECTRON BEAM WELDABILITY," *WELD. J.*, JAN 1990, P 39S-44S
18. R.D. STOUT, *WELDABILITY OF STEELS,* 4TH ED., WELDING RESEARCH COUNCIL, 1987, P 338-437
19. *RAILROAD FACTS,* ASSOCIATION OF AMERICAN RAILROADS, 1990
20. FREIGHT CARS 1992: THE QUALITY PROCESS AT WORK, *PROGRESS. RAILROAD.,* APRIL 1992

Material Requirements for Service Conditions

ASM Committee on Material Requirements for Service Conditions*

Selected References

- "RECOMMENDED PRACTICE FOR RESISTANCE WELDING," AWS C1.1-66, AMERICAN WELDING SOCIETY, 1966
- "RECOMMENDED PRACTICE FOR RESISTANCE WELDING COATED LOW CARBON STEELS," AWS C1.3-70, AMERICAN WELDING SOCIETY, 1970
- "AUTOMOTIVE RESISTANCE SPOTWELDING," ENGINEERING STANDARD GM4488M, GENERAL MOTORS CORP., AUG 1990
- G.E. LINNERT, *WELDING METALLURGY,* VOL II, AMERICAN WELDING SOCIETY, 1967
- NATIONAL RESEARCH COUNCIL, *MATERIALS SCIENCE AND ENGINEERING FOR THE 1990'S: MAINTAINING COMPETITIVENESS IN THE AGE OF MATERIALS,* NATIONAL ACADEMY PRESS, 1989
- K. MASUBUCHI, *ANALYSIS OF WELDED STRUCTURES,* PERGAMON PRESS, 1980
- RUSSELL *ET AL.,* "CONSIDERATIONS OF METAL JOINING PROCESSES FOR SPACE FABRICATION, CONSTRUCTION AND REPAIR," PAPER PRESENTED AT 23RD INT. SAMPE TECH. CONF., 21-24 OCT 1991

Introduction to the Selection of Carbon and Low-Alloy Steels

Bruce R. Somers, Lehigh University

Introduction

CARBON AND LOW-ALLOY STEELS are welded more frequently than any other materials because of their widespread applications and good weldability. This versatility is principally due to the metallurgical characteristics of the iron-base system. The characteristics include the ability to undergo allotropic (that is, microstructural) transformations that allow the opportunity for hardening and strengthening through martensitic and bainitic transformations or precipitation mechanisms in addition to the ability to be readily alloyed with a wide variety of elements.

This Section of the Handbook will provide the reader with information about the suitability of these materials for particular types of assemblies. This Section will also provide in-depth metallurgical information about the response of these materials to welding conditions and microstructural evolution in the weld heat-affected zone (HAZ).

Introduction to the Selection of Carbon and Low-Alloy Steels

Bruce R. Somers, Lehigh University

Weldability

The articles in this Section focus on the weldability of carbon and low-alloy steels. The user should consider weldability as being divided into two general classes: (1) fabrication weldability and (2) service weldability.

Fabrication weldability addresses the question, "Can one join these materials by welding without introducing detrimental discontinuities?" The acceptability of these discontinuities depends on the application requirements for the particular weldment. The fabrication weldability of a steel may be adequate for a noncritical application. However, this same steel may not be recommended for a critical application, or special precautions, such as preheat, may be required when welding. Fabrication weldability deals primarily with discontinuities such as hydrogen-assisted cold cracks, hot cracks, reheat cracks, lamellar tearing, and porosity.

Service weldability addresses the question, "Will the finished weldment have properties adequate to serve the intended function?" An important aspect of service weldability is the comparison of HAZ properties with those of the unaffected base metal. Again, the acceptability of the service weldability depends on the intended application. The service weldability of a particular steel may be acceptable for an application where corrosion is of prime importance and toughness is secondary. However, the same steel may be unacceptable for an application where toughness is most important.

Service weldability involves the effect of the welding thermal cycle on the properties in the HAZ. Service weldability often determines the range of heat inputs allowable for a particular steel. Low heat inputs may introduce unacceptable low-toughness microstructures, as well as fabrication-weldability problems associated with cold cracking. High heat inputs can introduce coarse microstructures with both low toughness and low strength. The heat input alone does not control the resulting microstructure and HAZ properties, but the induced thermal cycle controls the microstructure and properties. Therefore, both heat input and thickness should be considered.

Introduction to the Selection of Carbon and Low-Alloy Steels

Bruce R. Somers, Lehigh University

Classification of Steels

The carbon and low-alloy steels discussed in this Section cover a wide variety of compositions and properties. Steels are most often classified according to their carbon and/or alloy content. The various classifications have become known under assorted designations, such as plain-carbon steel, carbon-manganese steel, medium-carbon steel, low-alloy steel, high-strength low-alloy steel, and microalloyed steel. Recently, a new classification of steel has introduced the steel-processing technique as a categorization factor. These steels, known by various designations, are most often described as thermal-mechanical-controlled processing (TMCP) steels. The boundaries between all the above classes are often diffuse, they frequently overlap, and they are sometimes arbitrary (Table 1).

TABLE 1 CARBON STEELS CLASSIFIED ACCORDING TO CARBON CONTENT

REF	CARBON, %			
	LOW-CARBON STEEL	MILD STEEL	MEDIUM-CARBON STEEL	HIGH-CARBON STEEL
1	≤0.15	0.15-0.30	0.30-0.50	0.50-1.00
2	≤0.15	0.15-0.35	0.35-0.60	0.60-1.0
3	<0.30	. . .	0.30-0.60	>0.6
4	≤0.30	≤0.25	0.30-0.60	0.60-1.00

The steels covered in this Section have been grouped into six general classes according to composition or processing:

- LOW-CARBON STEELS
- HIGH-STRENGTH LOW-ALLOY STEELS
- QUENCHED-AND-TEMPERED STEELS

- HEAT-TREATABLE LOW-ALLOY STEELS
- THERMAL-MECHANICAL-CONTROLLED PROCESSING STEELS
- CHROMIUM-MOLYBDENUM STEELS

There will be some overlap between these classifications because fabricators often use some steels in more than one heat-treated condition. Typical steel compositions in these classifications are given in Table 2.

TABLE 2 COMPOSITION AND CARBON EQUIVALENT OF SELECTED CARBON AND LOW-ALLOY STEELS

STEEL DESIGNATIONS			COMPOSITION, WT%										CARBON EQUIVALENT, %
AISI	ASTM	MIL-STD	C	Mn	P	S	Si	Ni	Cr	Mo	V	Nb	
LOW-CARBON STEELS													
1010, 1020, 1030	A 36	. . .	0.10-0.30	0.50-1.0	<0.04	<0.05	0.10-0.25	. . .	. . .	. . .	. . .	. . .	0.20-0.50
HIGH-STRENGTH LOW-ALLOY STEELS													
. . .	A 242, A 572, A 588	. . .	0.10-0.25	0.50-1.5	<0.04	<0.05	0.20-0.35	0-0.75	0-0.75	0-0.25	0-0.05	0-0.04	0.25-0.75
QUENCHED-AND-TEMPERED STEELS													
. . .	A 508, A 517	S-16216 (HY-80)	0.10-0.30	0.20-1.5	<0.04	<0.05	0.20-0.35	0-3.4	0-1.5	0-0.5	0-0.05	0-0.04	0.35-1.10
HIGH-TREATABLE LOW-ALLOY STEELS													
4140, 4340	. . .	. . .	0.30-0.50	0.50-1.0	<0.04	<0.05	0.15-0.30	0-3.0	0.50-1.0	0.15-0.25	. . .	. . .	0.55-1.20
THERMAL-MECHANICAL-CONTROLLED PROCESSING STEELS													
. . .	A 841		0.04-0.15	0.70-1.5	<0.03	<0.03	0.20-0.35	. . .	0-0.25	0-0.05	0-0.05	0-0.03	0.20-0.50
CHROMIUM-MOLYBDENUM STEELS													
. . .	A 217, A 387	. . .	0.10-0.20	0.50-0.70	<0.035	<0.04	0.15-0.50	. . .	0.50-9.0	0.50-1.0	. . .	. . .	0.38-2.0

Low-carbon steels contain up to approximately 0.30 wt% C and up to about 1.65 wt% Mn. Most as-rolled steel used for welded applications consists of low-carbon steel. This group encompasses steels that can have wide variations in weldability. For example, it is possible to weld low-carbon steels with less than 0.15% C by most welding processes. It is also possible to weld low-carbon steels containing 0.15 to 0.30% C (sometimes termed mild steels) in thicknesses up to

25 mm (1 in.). However, thicker sections of these steels may require additional measures in order to produce successful welds.

High-strength low-alloy (HSLA) steels are designed to provide better mechanical properties than those of conventional carbon steels. These steels generally have yield strengths of 290 to 550 MPa (42 to 80 ksi). They are also generally of the carbon-manganese type, with very small additions of niobium and vanadium to ensure both grain refinement and precipitation hardening. The term microalloyed steels is often used in reference to these materials. Fabricators usually weld these steels in the as-rolled or the normalized condition. The weldability of most HSLA steels is similar to that of mild steel.

Recently, a new family of steels has been appearing in the literature under the designation HSLA steels. These are the low-carbon, copper-bearing age-hardening steels, also frequently referred to by their ASTM designations, A 710 or A 736 (Table 3); or by their military specification grade designation, HSLA 80 or HSLA 100 (MIL-S-24645). These steels are not truly low-alloy, because the copper, nickel, and chromium contents are all usually near 1%. However, the weldability of these materials is very good, mainly because of their low carbon contents (less than 0.06% C). These steels are usually used in the quenched-and-aged condition. Because of these two conditions, it is probably more appropriate to group these materials with the thermal-mechanical-controlled processing steels.

TABLE 3 HEAT ANALYSIS COMPOSITIONS OF SELECTED LOW-CARBON COPPER-BEARING AGE-HARDENING STEELS

SPECIFICATION	GRADE	COMPOSITION, %									
		C (max)	Mn	P (max)	S (max)	Si (max)	Cr	Ni	Mo	Cu	Nb (min)
A710/A710M	A	0.07	0.40-0.70	0.025	0.025	0.40	0.60-0.90	0.70-1.00	0.15-0.25	1.00-1.30	0.02
	B	0.06	0.40-0.65	0.025	0.025	0.15-0.40	. . .	1.20-1.50	. . .	1.00-1.30	0.02
	C	0.07	1.30-1.65	0.025	0.025	0.40	. . .	0.70-1.00	0.15-0.25	1.00-1.30	0.02
A736/A736M	A	0.07	0.40-0.70	0.025	0.025	0.40	0.60-0.90	0.70-1.00	0.15-0.25	1.00-1.30	0.02
	C	0.07	1.30-1.65	0.025	0.025	0.40	. . .	0.70-1.00	0.15-0.25	1.00-1.30	0.02

Source: Ref 5

Quenched-and-tempered steels are heat treated to provide yield strengths of 345 to 1035 MPa (50 to 150 ksi). ASTM A 514 and A 517 are well-known examples of this category of steel. Other examples include the HY-80, HY-100, and HY-130 nickel-chromium-molybdenum steels covered by military specifications. Weldments fabricated from these materials generally do not need further heat treatment except for a postweld heat treatment (stress relief) in some special applications. For example, HY-100 and HY-130 require controls on the filler-metal carbon content, preheat/interpass minimums and maximums, heat input, and postweld soaks to achieve the desired military mechanical properties.

Advantages of HSLA Steels Over Selected Quenched-and-Tempered Steels. In certain situations, the U.S. Navy substitutes HSLA-80 for HY-80, and HSLA-100 for HY-100. One significant advantage of this substitution is the reduced welding preheat required for the copper age-hardening HSLA versus the HY steels. It should also be noted that HSLA-100 steel does not weld like a mild steel.

Heat-treatable low-alloy (HTLA) steels are usually reaustenitized, then quenched and tempered after welding. These are relatively hardenable steels that in their quenched-and-tempered condition develop yield strengths well above 965 MPa (140 ksi). Weld metals usually cannot develop acceptable combinations of strength and toughness at these levels in the as-welded or stress-relieved condition. Therefore, it is necessary to reaustenitize and then quench and temper the entire weldment after welding. These steels are often referred to by their AISI designations (for example, AISI 4140 and AISI 4340).

Thermal-mechanical-controlled processing (TMCP) steels are a relatively recent addition to the family of steels. These steels are generally produced with a combination of controlled rolling followed by accelerated cooling or in-line direct quenching. This processing allows the steelmaker to develop a combination of high strength and high toughness while maintaining good weldability. The weldability is good because the alloy content of these steels can be kept very lean, with carbon contents generally below 0.06 wt%. Yield strength levels as high as 700 MPa (100 ksi) and above are possible with these steels. Generally, they can be welded without preheat. However, at the high strength levels, preheat may be required in order to prevent cracking in the weld metal.

Chromium-molybdenum steels are extensively used for elevated-temperature applications in the power and petroleum refinery industries. The chromium content of these steels varies from 0.5 to 9%, and the molybdenum content from 0.5 to 1.0%. Typical compositional ranges for chromium-molybdenum steels are given in Table 2. They are usually supplied in the normalized-and-tempered or the quenched-and-tempered condition.

Because these materials have reasonable hardenability, adequate precautions must be taken to avoid hydrogen-assisted cold cracking. The service application frequently imposes additional requirements on the welding of these steels. For example, in the power industry, these materials are required for their creep resistance, and the weld metal and HAZ must provide adequate creep properties. The corrosion environment in refineries requires that the maximum HAZ hardness be limited to avoid corrosion cracking.

References cited in this section

1. *WELDING HANDBOOK*, VOL 4, 7TH ED., AWS, 1982, P 9
2. G. LINNERT, *WELDING METALLURGY*, VOL 1, 3RD ED., P 45
3. S. KALPAKJIAN, *MANUFACTURING PROCESSES FOR ENGINEERING MATERIALS*, ADDISON-WESLEY, 1984, P 146
4. *PROPERTIES AND SELECTION: IRONS, STEELS, AND HIGH-PERFORMANCE ALLOYS*, VOL 1, *ASM HANDBOOK*, ASM INTERNATIONAL, 1990, P 147-148, 390
5. *1989 ANNUAL BOOK OF ASTM STANDARDS*, VOL 1.04, *STEEL*: *STRUCTURAL*, *REINFORCING*, *PRESSURE VESSEL*, RAILWAY ASTM, 1989, P 494, 523

Bruce R. Somers, Lehigh University

Relative Susceptibility of Steels to Hydrogen-Assisted Cold Cracking

Figure 1 illustrates where these classes of steel are located on a Graville diagram. Graville has suggested that the susceptibility to hydrogen-assisted cold cracking can be evaluated by calculating the carbon equivalent (CE) and comparing it to the carbon content (Fig. 1). Zone I steels have low carbon and low hardenability and are not very susceptible to cracking. Zone III steels have both high carbon and high hardenability, and all welding conditions will produce crack-sensitive microstructures. Therefore, to avoid hydrogen-assisted cold cracking in Zone III steels, the user must apply low-hydrogen procedures, including preheat and postweld heat treatment. Zone II steels have higher carbon levels with lower hardenability. Thus, it is possible to avoid crack-sensitive microstructures by restricting HAZ cooling rates. This can be accomplished through control of heat input and, to a minor extent, with preheat.

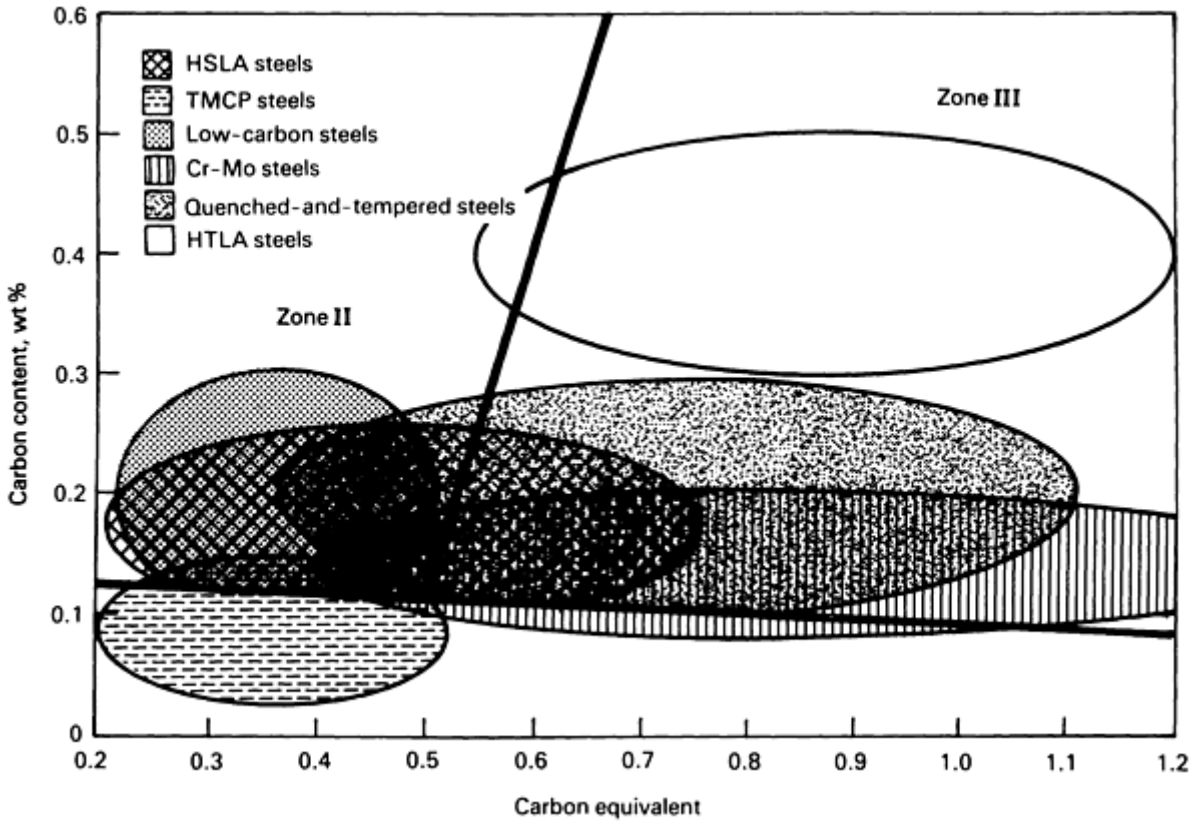

FIG. 1 GRAVILLE DIAGRAM SHOWING SUSCEPTIBILITY OF STEELS TO HYDROGEN-ASSISTED COLD CRACKING RELATIVE TO CARBON CONTENT AND CARBON EQUIVALENT (CE), WHERE CE = %C + (%MN + %SI)/6 + (%NI + %CU)/15 + (%CR + %MO + %V)/5. SUSCEPTIBILITY TO COLD CRACKING PROGRESSIVELY INCREASES AS STEELS MIGRATE FROM ZONES I TO II, TO III. SEE TEXT FOR EXPLANATION. SOURCE: REF 6

Figure 1 also shows that heat-treatable alloy steels, squarely in Zone III, require special considerations for welding. Chromium-molybdenum and quenched-and-tempered steels also require attention, as will some HSLA steels. As mentioned in the section "Low-Carbon Steels" of this article, low-carbon steels are readily welded except in thick sections, for which some precautions may be necessary. The TMCP steels have been specifically developed to lie in Zone I, and so their weldability is excellent. Although Fig. 1 represents only one aspect of weldability and there are many other considerations, the desired preference with regard to hydrogen-assisted cold cracking is to use steels that push the compositional envelope toward the lower-left corner of the Graville diagram.

Reference cited in this section

6. B.A. GRAVILLE, COLD CRACKING IN WELDS IN HSLA STEELS, *WELDING OF HSLA (MICROALLOYED) STRUCTURAL STEELS*, PROC. INT. CONF., AMERICAN SOCIETY FOR METALS, NOV 1976

Introduction to the Selection of Carbon and Low-Alloy Steels

Bruce R. Somers, Lehigh University

References

1. *WELDING HANDBOOK*, VOL 4, 7TH ED., AWS, 1982, P 9
2. G. LINNERT, *WELDING METALLURGY*, VOL 1, 3RD ED., P 45
3. S. KALPAKJIAN, *MANUFACTURING PROCESSES FOR ENGINEERING MATERIALS*, ADDISON-WESLEY, 1984, P 146
4. *PROPERTIES AND SELECTION: IRONS, STEELS, AND HIGH-PERFORMANCE ALLOYS*, VOL 1, *ASM HANDBOOK*, ASM INTERNATIONAL, 1990, P 147-148, 390
5. *1989 ANNUAL BOOK OF ASTM STANDARDS*, VOL 1.04, *STEEL*: *STRUCTURAL*, *REINFORCING*, *PRESSURE VESSEL*, RAILWAY ASTM, 1989, P 494, 523
6. B.A. GRAVILLE, COLD CRACKING IN WELDS IN HSLA STEELS, *WELDING OF HSLA (MICROALLOYED) STRUCTURAL STEELS*, PROC. INT. CONF., AMERICAN SOCIETY FOR METALS, NOV 1976

Introduction

ARC WELDING is a process by which metals are joined by coalescence. In most cases, the process uses a compatible filler metal. Before a well-bonded joint can be produced, the joint surfaces must be heated above their melting temperatures in order to completely fuse with the weld metal. Although the metallurgical reactions that involve melting, solidification, and solid-state transformations may not be unusual, the temperatures and cooling rates observed are severe. Active gases also are present and can dissolve in the fused metal. Fluxes are introduced to alloy with and protect the weld metal.

Generally, joints are rigid and will restrain dimensional changes caused by shrinkage and solid-state transformations, producing residual stresses of yield-strength magnitude. Because the metallurgical changes do not occur under equilibrium conditions, and because the stresses are high, many of the reactions can take place in either or both the weld metal and the heat-affected zone (HAZ) of the plate and can produce defects that impair their soundness.

The intent of this article is to point out those defects. However, because of the tremendous variability of the welding processes, it is impossible to provide much detail about the exact mechanisms involved or the corrections that can be made. Furthermore, many corrective measures are self-evident once most defects are explained. One problem, which relates to hydrogen, is not so simple. Because this problem is becoming more relevant as more high-strength, low-alloy (HSLA) steels are being welded, the subject of hydrogen-induced cracking will be emphasized.

Influence of Welding on Steel Weldment Soundness

A. Lesnewich

Common Defects Associated with Arc Welds

Porosity is caused by the entrapment of small pockets of gas, particularly nitrogen and hydrogen, which typically have a higher solubility in molten, rather than solid, iron. During solidification, gases attempt to leave the weld metal. However, because of high solidification rates, some gas may become trapped. This entrapment depends both on the rate of gas dissolution and on the rate of weld-metal solidification. If the dissolution rate is high, gas bubbles have a chance to develop and escape before the metal solidifies. If the rate is very low the gas may remain in solution, which avoids porosity but allows other problems such as hydrogen-induced cracking or poor toughness. At intermediate rates, the gas can nucleate and, depending on the amount of gas dissolved in the weld metal and the weld-solidification rates, develop bubbles that become trapped. A very severe form of porosity, called worm holes, occurs when the rates of gas evolution and solidification are similar, causing elongated gas pockets to develop instead of essentially spherical bubbles.

Among the possible sources of hydrogen are moisture in fluxes, hydrocarbons in either wiredrawing lubricants or surface contaminants in the joint to be welded, and water leaks in gas-metal arc welding (GMAW) equipment. Nitrogen is gleaned from air that enters the arc regions as a result of poor shielding of the arc. With GMAW, this can happen when the gas flow rates are either so low that crossdraf ts displace the shielding or so high that the surrounding atmosphere is aspirated into the shielding gas. With the shielded metal arc welding (SMAW) process, this can happen because welders are not sufficiently skilled or use improper procedures that cause the arc length to be excessive.

Incomplete fusion can take a number of forms, such as inadequate joint penetration (Fig. 1), absence of root fusion, or lack of side-wall fusion (Fig. 2). These defects can be caused by: inadequate energy input to the weld, particularly insufficient current; excessive travel speed, which allows weld metal to flow ahead of the arc; or improper electrode angles or work positions.

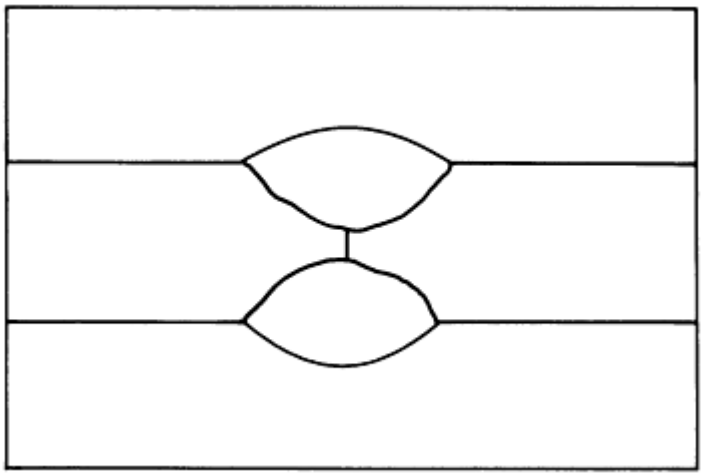

FIG. 1 INCOMPLETE PENETRATION OF WELD INTO BUTT JOINT

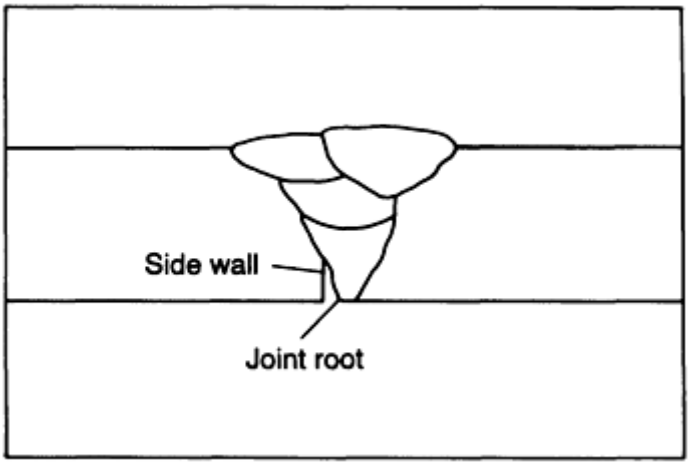

FIG. 2 INCOMPLETE FUSION OF WELD METAL TO SIDE WALL AND TO JOINT ROOT

Problems with joint penetration and root fusion commonly are due to the use of a joint design that is not proper for the welding process being used or to a disregard for the procedures that are intended to provide adequate penetration of the arc. In most cases, this would mean that the welding current is too low. However, in the case of the gas-shielded welding processes, it could mean that the wrong shield gas is being used. For example, with argon-rich gas mixtures, the penetration pattern is relatively shallow, with the exception of a fairly deep central "finger," which is shown in Fig. 3. Unfortunately, this finger generally is not positioned centrally and, therefore, cannot be relied upon. However, shield gas mixtures that are rich in helium or carbon dioxide are capable of a more uniform and deeper useful penetration pattern.

Poor root fusion that occurs when welding from one side requires either a modification in the joint design to allow better penetration or a change to welding from both sides of the plate.

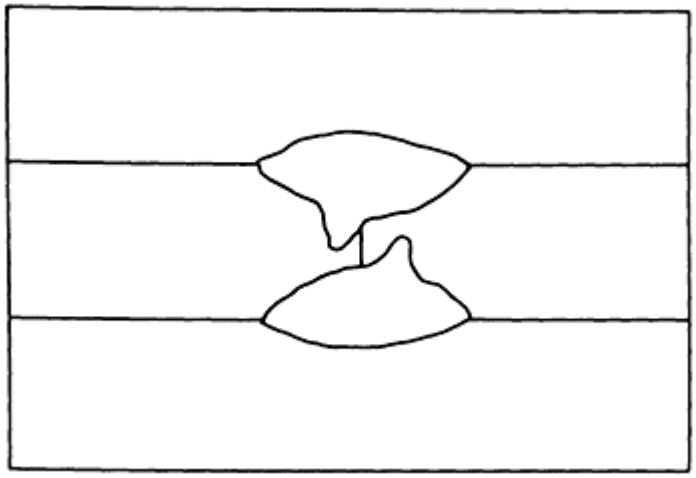

FIG. 3 OFF-CENTER PENETRATION OF CENTRAL CORE OF WELD USING ARGON SHIELD

In most cases, the lack of side-wall fusion between the weld metal and the joint occurs when proper procedures or manipulative techniques are not being used by welders. With the GMAW process, it can be due to using inappropriate variations, such as short-circuiting transfer, when welding heavy sections. Short-circuiting transfer is effective only at low energy levels, which makes it very suitable for welding sheet or thin plate in all positions. This is because the process is designed to provide little penetration and to quickly freeze weld metal. For that reason, the weld metal may not fuse the side walls of joints from which heat is extracted rapidly, that is, those thicker than 6 mm ($\frac{1}{4}$ in.). Both a spray arc with argon and a buried arc with carbon dioxide shielding will deposit welds that are too massive and fluid to be supported in the vertical or overhead positions. However, these processes are very effective for making welds in the flat or horizontal positions. On the other hand, the pulsed-arc variation with argon-rich shielding is very effective in all positions, offering both adequate penetration and control of the weld pool to prevent defects caused by poor side-wall fusion.

Hot cracks, also called centerline or solidification cracks (Fig. 4), are caused by the rejection of low-melting constituents along the centerline of restrained welds. They are called hot cracks because they develop immediately after welds are completed and, sometimes, while the welds are being made. If the welds are broken to expose these cracks, they are found to be blued, or heat tinted. These defects, which are often caused by sulfur and phosphorus, are more likely to occur in higher-carbon alloys. Nearly always, the base plate is their source. The susceptibility to cracking, based on weld composition, has been compared with empirical equations, such as:

$$UCS = 230\,C + 190\,S + 75\,P + 45\,NB - 12.3\,SI - 5.4\,MN - 1 \quad \textbf{(EQ 1)}$$

where the elemental values are given in percent. If the *UCS* value is less than 10, then the susceptibility to cracking is low, whereas a value higher than 30 means that this susceptibility is high, and a value between 10 and 30 means that the welding procedures become controlling.

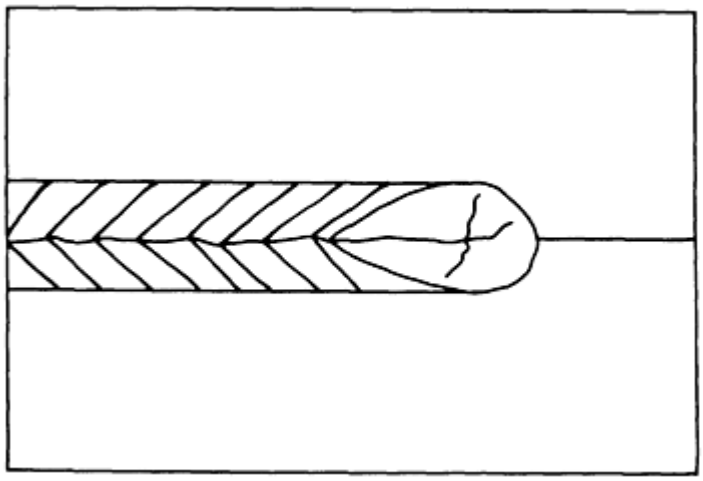

FIG. 4 HOT CRACK AND CRATER CRACKS IN WELD BEAD

Such defects are more likely to occur with welding processes or procedures that produce high dilution (that is, deep penetration). Another factor that contributes to centerline cracking is a sharp tear-drop profile of the weld crater, which is characteristic of high welding speeds. In these situations, the weld crater often develops shrinkage cracks, called crater cracks. Both the teardrop crater and deep penetration are produced with the submerged arc welding (SAW) process and the GMAW process using carbon dioxide shielding. The problem also may occur in fillet welds that are very concave, because their cross section might not be sufficient to tolerate the transverse stresses that are due to weld shrinkage.

In most cases, the problem can be prevented by keeping the combined phosphorus and sulfur levels below 0.06%. However, when welding highly restrained joints using high-strength steels, a combined level below 0.03% might be necessary. When the steels to be welded contain excessive amounts of sulfur or phosphorus, hot cracks can be avoided by:

- USING WELDING PROCESSES OR PROCEDURES THAT ARE NOT DEEPLY PENETRATING
- SELECTING TRAVEL SPEEDS THAT ARE SUFFICIENTLY SLOW TO PREVENT THE FORMATION OF TEAR-DROP CRATERS
- PROVIDING CONVEX BEAD PROFILES
- FILLING THE CRATERS AT THE END OF EACH BEAD

Lamellar tearing occurs in the base plate when stressed through its thickness and generally is found just below the HAZ (Fig. 5). It is associated with banded steels that contain thin layers of inclusions located beneath the plate surfaces. If the dirty steels must be used, the problem can be prevented by changing the joint design to minimize strain through the thickness of the plate at the weld.

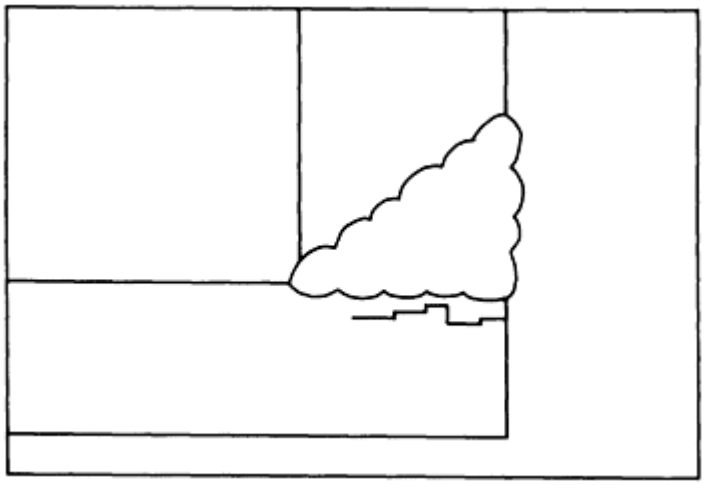

FIG. 5 LAMELLAR TEARING

An undercut is an irregular gouge that is generally found in the upper toe of a horizontal fillet weld. The base plate in that section of the weld shown on the left side of Fig. 6 had been melted by the arc, but not refilled by the weld metal. Most often, this defect is caused by improperly selected welding conditions such as the electrode angle, travel speed, and welding current. It is more likely to occur when attempting to make fillet welds with legs that are more than 8 mm (0.3 in.) in length. With the GMAW process, it also can occur when using an argon shield containing less than 2% oxygen. Undercut also can be found in welds made in the vertical position, where it is generally attributed to excessive weaving.

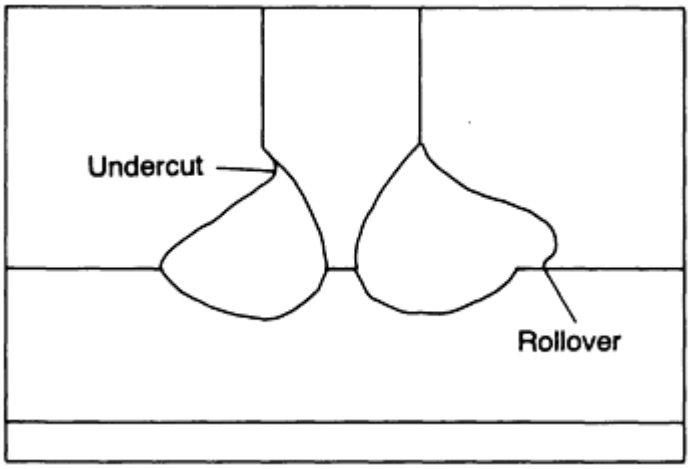

FIG. 6 UNDERCUT IN VERTICAL LEG OF FILLET WELD AND ROLLER IN HORIZONTAL FILLET WELD

A rollover, also called an overlap (Fig. 6), generally is associated with fillet welds and can be found when either the welding current is too low to properly fuse the base plate or the travel speed is too low to accept the amount of metal being deposited. Poor manipulation of the electrode during the SMAW process also can be a factor.

Inclusions are produced by slag that is trapped between weld passes. They originate as pieces of unfused fluxes that may be trapped in a joint, or as slag that is allowed to flow ahead of the arc and is covered by the weld, or as solidified slag that has not been removed between weld passes, or as heavy mill scale that has not been removed from a joint prior to welding. The problem is most common with the SMAW process because it can be aggravated by poor manipulative techniques on the part of the welder. The presence of inclusions can be anticipated when welding over highly crowned or rough welds because their edges are difficult to clean between passes or to penetrate during welding.

Prevention is possible by:

- TRAINING WELDERS TO DEPOSIT WELDS THAT HAVE PROPERLY FLAT PROFILES
- POSITIONING WELDS TO ALLOW HIGHER ENERGY AND MORE FLUID DEPOSITS TO BE MADE
- PREVENTING THE DEVELOPMENT OF RUST BETWEEN PASSES
- ENSURING THAT THE WELDS ARE PROPERLY CONDITIONED BETWEEN PASSES BY EITHER CLEANING OR GRINDING

Hydrogen-Induced Cracking

Hydrogen-induced cracking (HIC) is a phenomenon primarily associated with welds in low-alloy steels. Figure 7 depicts a typical crack, which was taken from the HAZ of a weld. The factors that contribute to HIC are the presence of hydrogen, high tensile stress, susceptible microstructures, temperatures between approximately 200 and -100 °C (400 and -150 °F), and time. At lower strength levels (approximately 485 MPa, or 70 ksi) HIC is most often observed as longitudinal cracks in the HAZ of the base metal, often called underbead cracking. At higher strength levels (approximately 830 MPa, or 120 ksi, and higher), transverse cracks can occur in the weld metal as well.

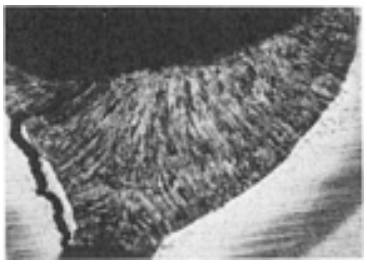

FIG. 7 PHOTOMICROGRAPH OF HYDROGEN-INDUCED CRACK IN HAZ OF WELD. 5×

The commonly used expression "hydrogen embrittlement" suggests that hydrogen impairs the toughness of welds, but that designation is a misnomer. Impact tests on material removed from the area between cracks show that the material exhibits levels of toughness equivalent to welds made in the absence of hydrogen and, of course, cracks. However, tensile ductility can be reduced because HIC can occur while the tensile test is in progress, which reduces the cross-sectional area of the test specimens. The resulting defects in the fractured surfaces are called "fisheyes."

Cold cracking is another expression that has been used to differentiate these cracks from the hot cracks that are found in weld metal and are produced by low-melting constituents that segregate during solidification. Delayed cracking is another term that has been used. It is descriptive because HIC might not occur for days or weeks. When HIC is anticipated, welds often are not radiographed for a week or more in order to allow the cracks to develop.

Mechanism. Hydrogen is a ubiquitous contaminant in all arc welding processes. It exists in the water that is unavoidable in fluxes, in the organic lubricants on the surfaces of filler wires, in the debris that collects in weld joints, and in the moisture in air that can be aspirated into the arc stream. Hydrogen has a much higher solubility in molten iron than it does in solid iron, and its solubility decreases with temperature in the solid state as well. The hydrogen solubility in iron as a function of temperature is shown in Fig. 8. The solubility above the liquidus at 1500 °C (2730 °F) is about 30 ppm by weight, but about 8 ppm in the solid state. At 400 °C (750 °F), its solubility drops to less than 1 ppm. The rates of weld-metal solidification are very high and, as a result, the hydrogen that has dissolved in the fused weld metal is retained.

Although that which does escape as gas often is trapped in the form of small bubbles or weld-metal porosity, a substantial amount does remain in the solidified weld metal as supersaturated hydrogen. The residue might appear to be insignificant, but it should be recognized that as little as 1 ppm of hydrogen can cause cracking problems in high-strength steels.

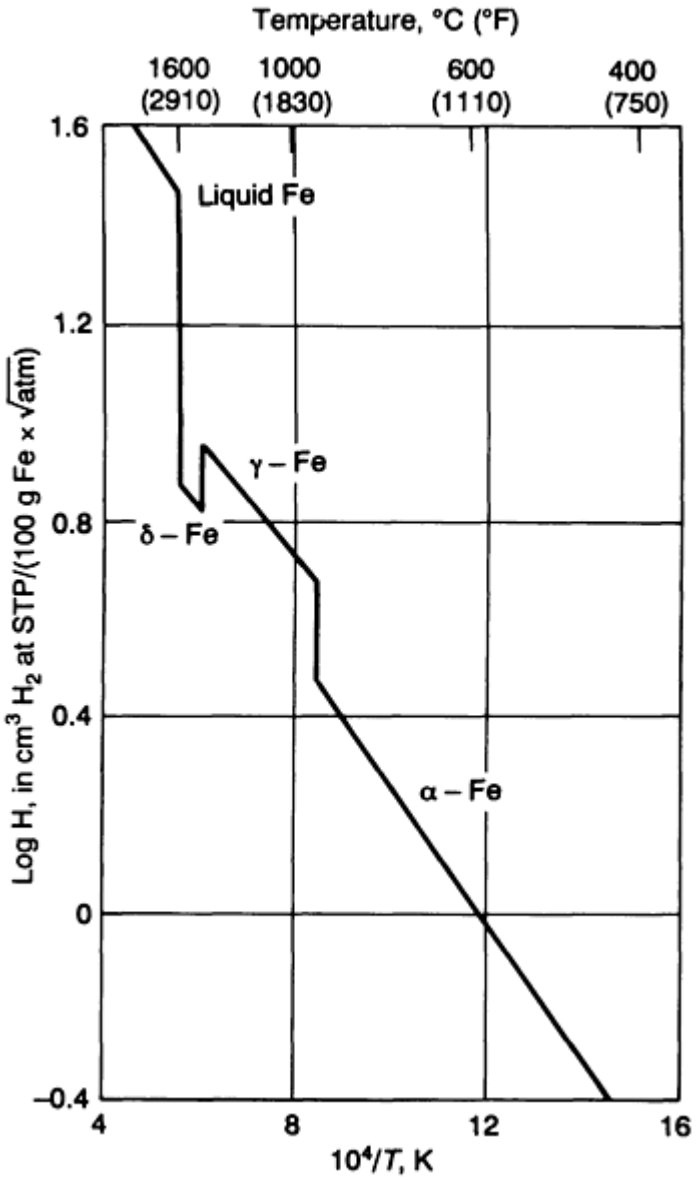

FIG. 8 EFFECT OF TEMPERATURE ON THE SOLUBILITY OF HYDROGEN IN IRON

During the cooling interval, the atomic hydrogen diffuses rapidly, with some going into the weld HAZ, some escaping to the air, and the rest remaining within the weld metal. Given the right conditions, these highly mobile atoms seek rifts and discontinuities in the metal lattice and concentrate at those points. In concert with the residual stresses in the lattice that are due to external restraint and volume changes caused by solidification and solid-state transformation, the hydrogen enlarges the discontinuities to form microcracks. The localized stresses are relieved abruptly as the atoms penetrate the fissures and become trapped as molecules. The resulting microcracks, which have sharp tips, also are associated with high stress concentrations at which additional atoms collect. Those stresses build up until they, too, are relieved as the crack is extended. This process of stress build up and relief by cracking continues until:

- THE CROSS-SECTIONAL AREA IS REDUCED SUFFICIENTLY TO CAUSE FAILURE.
- HYDROGEN ESCAPES IN A SUFFICIENT AMOUNT TO LOWER ITS CONCENTRATION BELOW THAT WHICH IS NEEDED FOR CRACKING TO PROCEED.

- UNDERBEAD CRACKS HAVE REDUCED THE RESIDUAL STRESSES IN THE WELD BELOW THAT LEVEL NEEDED FOR CRACKING TO PROCEED.

HIC does not occur spontaneously, but as discrete steps. The stepwise progression can be observed acoustically. In small specimens, its progression also can be monitored by measuring changes in resistance, as shown in Fig. 9. The lower portion of this illustration depicts the changes in resistance that occur after the process of HIC begins, as well as the way in which HIC progresses a step at a time until failure. The upper portion of Fig. 9 illustrates the sensitivity of HIC to the level of external stress. Failure occurs quickly when the stress on a specimen exceeds its tensile strength, whether or not hydrogen is present. However, when enough hydrogen is present, damage that is caused by HIC can be initiated with stresses well below the tensile strength. Given enough hydrogen and time, HIC can cause failure. Note that the time needed for initiating the cracks and leading to failure increases as the stress is reduced.

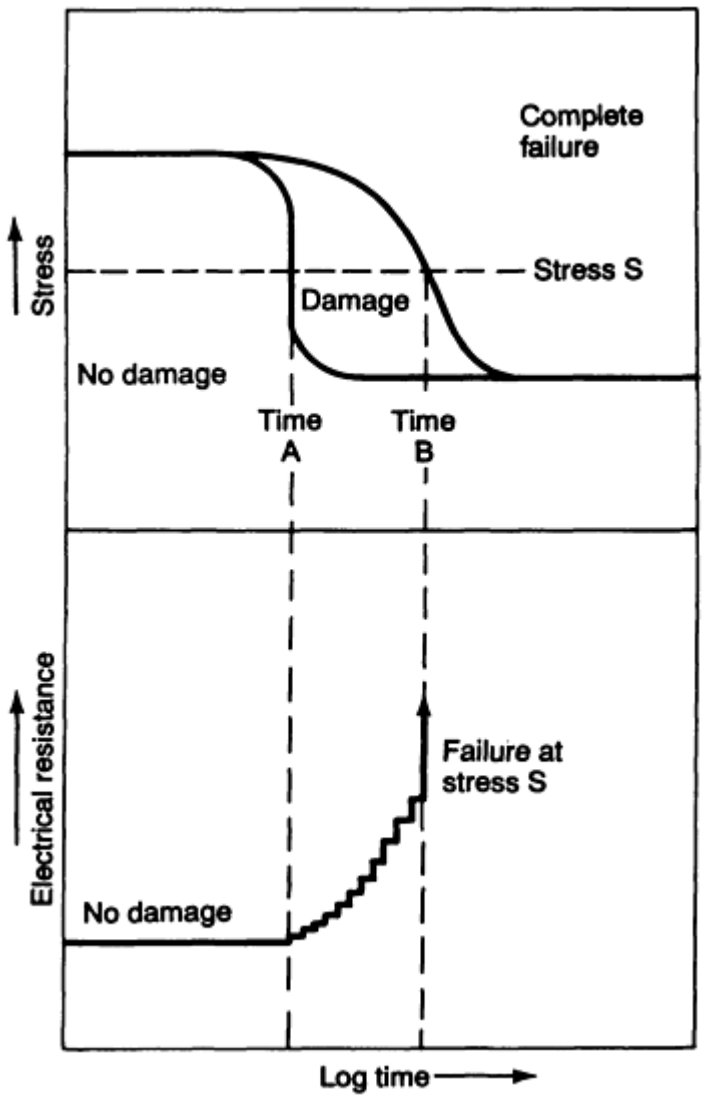

FIG. 9 DAMAGE CAUSED BY HIC, AS AFFECTED BY APPLIED STRESS. IN SMALL SPECIMENS, ELECTRICAL RESISTANCE INCREASES AS HYDROGEN-INDUCED CRACKS GROW.

Most important is the observation that HIC does not occur below a critical stress. In addition to the applied stress, the amount of hydrogen dissolved in the steel also plays an important role. With increasing hydrogen, less stress is needed to initiate HIC, and the times required for its initiation are reduced, as well. The interaction of these two variables, stress and hydrogen, on HIC is shown in Fig. 10. Note that both the time to initiate HIC and the critical stress below which failure will not occur are inversely proportional to the amount of hydrogen present in the steel.

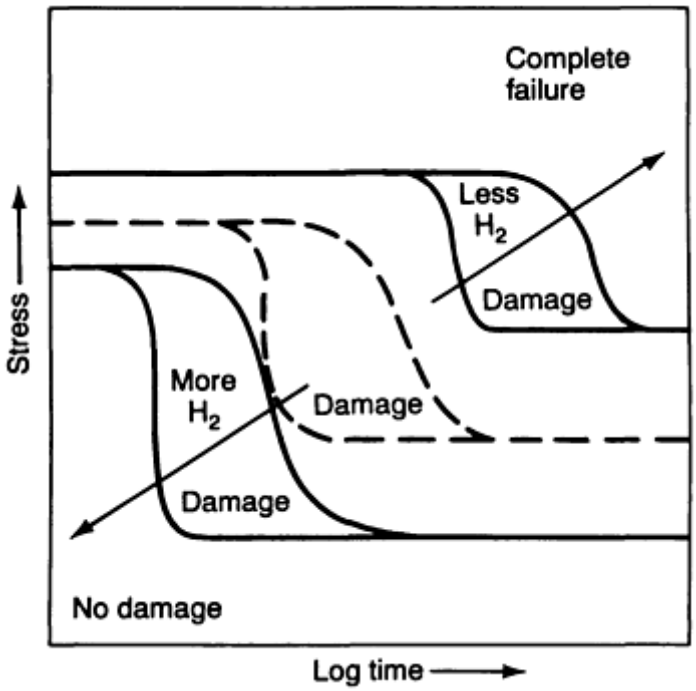

FIG. 10 EFFECT OF HYDROGEN AND STRESS ON DAMAGE CAUSED BY HIC. AS HYDROGEN INCREASES, LESS STRESS IS NEEDED TO CAUSE DAMAGE BY HYDROGEN-INDUCED CRACKS.

The third variable that affects HIC is the microstructure of the steel (either the weld metal or the HAZ). Twinned martensites, which occur in higher-carbon-content steels (above approximately 0.3% C), are the most troublesome, although the problem can occur with all acicular microstructures, including the bainites. This hypothesis might be flawed because the acicular microstructures are typical of those associated with high-strength steels, and higher stresses, in themselves, are an aggravating factor with HIC. However, as shown in Fig. 11, a steel with a relatively tolerant microstructure can exhibit a higher critical stress than a stronger steel with a sensitive microstructure. Note that the stronger steel is more sensitive to hydrogen with regard to both an earlier initiation time for HIC and a lower critical stress. Such behavioral differences have been observed between high-strength martensitic and weaker bainitic steels.

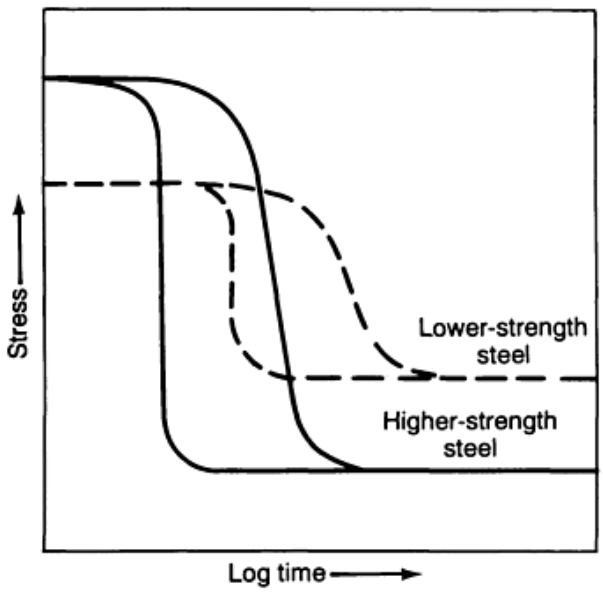

FIG. 11 EFFECT OF STEEL STRENGTH ON SUSCEPTIBILITY TO HIC DAMAGE. STRONGER STEELS CAN BE MORE SENSITIVE TO HYDROGEN, RESULTING IN LOWER CRITICAL STRESSES THAN THOSE EXHIBITED BY WEAKER

STEELS, WHICH ARE MORE TOLERANT.

Inclusions also are important. The toughness of HSLA steels is impaired by contaminants, particularly when in the form of inclusions. However, because inclusions can serve as sinks for hydrogen atoms, they also can have a beneficial effect. For this reason, some very high-purity steels have been shown to be surprisingly sensitive to HIC.

One should not conclude that welds need to be stressed externally in order to develop HIC. The differential shrinkage associated with fusion welding always produces residual stresses in weldments, and, with rare exceptions, those stresses are at least equivalent to the yield strength of the weakest component of the joint. Because most weld metals are stronger than the base metal, the residual stresses are close to the yield strength of the base plate. Often, it is possible to minimize the development of HIC in critical structures by selecting a weaker, or undermatching, weld metal to keep the residual stresses as low as possible. With some applications, such as those involving fatigue, a weaker but sound structure could be more suitable than one that contains HIC. However, given a sensitive microstructure and enough hydrogen, the critical stress can be very low, that is, substantially less than typical residual stresses. Therefore, if HIC is a problem, it will develop, in most cases, before a welded structure leaves the fabrication shop.

Another important observation that needs to be noted is that the mechanism of hydrogen-induced cracking is affected by temperature. The chances for HIC are minimal when temperatures exceed about 205 °C (400 °F). At higher temperatures, the hydrogen diffusion rates are too high to allow the atoms to concentrate at lattice defects or other sharp discontinuities in the weld. Because the mobility of hydrogen is essentially nil, HIC is unlikely to occur in welds cooled below -130 °C (-200 °F). The relevance of the different behaviors at temperatures above 205 °C (400 °F) will be discussed later.

Control of Hydrogen-Induced Cracks. In reviewing the metallurgical requirements for HIC, it is evident that a number of approaches might be taken to prevent its occurrence. They include reducing the residual stresses associated with a weldment; either avoiding acicular microstructures in the weld metal and HAZ or at least selecting those that are bainitic, rather than martensitic; reducing the amount of hydrogen dissolved in the weld metal during the welding operation; or allowing hydrogen to escape before it can cause damage. The most appropriate of these options will depend on the size of the component to be welded, the mechanical properties required, the service anticipated, the welding process to be used, and any cost constraints. In most cases, compromises have to be made and a combination of these approaches probably will prove to be most cost effective.

As mentioned earlier, the residual stresses in welds are generally equivalent to the yield strength of the weakest material in the joint. In joint configurations that introduce high triaxial stresses, the residual stresses can be significantly higher than the yield strengths. Although designers rarely use weaker materials just to reduce residual stresses, they should recognize that HIC can have a significant effect on the fatigue life of a structure. To accommodate weaker steels, a more-acceptable compromise might be to redesign the weldment to incorporate thicker sections. However, other approaches can be taken to gain full advantage of the strengths available in low-alloy steels without incurring HIC.

For the reasons mentioned earlier, the possibility of changing the microstructure of the weld metal or the HAZ is remote, unless given the option of selecting different alloys. In that case, the alloy that is most forgiving of HIC should be chosen.

Another method for reducing the residual stresses in welds is by using a postweld heat treatment at temperatures below the critical temperature. Because steels are weaker at higher temperatures, a significant reduction of residual stresses is possible by heating welds to a temperature at which plastic yielding can occur. For a steel with a tempered martensite structure, the most suitable choice for this heat treatment would be at or just below its original tempering temperature, which is generally close to 620 °C (1150 °F). This treatment is called stress relief annealing (SRA). For this treatment to be effective, the weldment must be placed in a suitably large furnace before its temperature drops below 205 °C (400 °F) and then, to prevent difficulties associated with distortion, heated and cooled slowly. Considering the temperatures and times needed for the SRA treatment, it is obvious that all of the diffusible hydrogen in the weld will escape. However, unless the stresses in a weld must be relieved for reasons other than the avoidance of HIC, SRA can prove to be a very expensive option.

Postheating does have a place in the scheme of preventing HIC. It is not necessary to reheat weldments to temperatures that are much higher than 205 °C (400 °F) in order to accelerate the escape of hydrogen and still avoid the temperature range within which HIC is likely. Such thermal treatments are excellent candidates for welded components that are small enough to be preheated in a furnace prior to welding and returned to the furnace immediately after welding for a period of

time that allows all of the hydrogen to escape. This approach is particularly important for very high strength alloys, such as SAE 4340, that are very sensitive to cracking problems associated with hydrogen.

Similar results are possible by slowing the rates at which welds are allowed to cool after welding. This provides more time for hydrogen to escape before temperatures drop below 205 °C (400 °F). Retarding the cooling rate also allows the transformation of austenite to softer microstructures that are less sensitive to HIC.

The cooling rates of arc welds are affected primarily by three factors: the temperature of the joint before welding begins, the arc energy input during welding, and the joint thickness. The initial temperature can be that of the shop in which the steel had been stored, or the temperature to which the weldment had been heated as the result of a previous weld by external methods (the interpass temperature), or the temperature to which the joint had been heated (the preheat temperature). As preheat temperatures are increased, the cooling rates decrease. The arc energy input is defined by the electrical energy dissipated by the arc and the speed at which the arc is moved along the joint. Higher arc energy inputs retard the cooling rate.

The joint thickness also affects cooling rates because much of the heat entering the joint is extracted by conduction into the body of the weldmerit. Conduction is at a maximum with three-dimensional cooling. This occurs when the joint is thicker than about 25 mm (1 in.). Conduction is less effective in thinner sections, that is, the weld cooling rate is inversely proportional to thickness. Although the cooling rates of thin sections are also influenced by radiation and convection, the effect is much less pronounced than that of conduction.

The variables described above can be incorporated into a single equation that allows calculations to be made of the rate at which welds cool at a specific temperature:

$$CR_T = C\frac{(T - T_0)^2}{E} \qquad \textbf{(EQ 2)}$$

where CR_T is the cooling rate at temperature T, C is a constant of proportionality (including an adjustment for plate thickness, if it is thinner than 25 mm, or 1 in.), T_o is the preheat or interpass temperature, E is the arc energy input, which is calculated as:

$$E = \frac{VI}{S} \qquad \textbf{(EQ 3)}$$

where V is the arc voltage, I is the welding current, and S is the arc travel speed. By combining the above two equations, a general expression for cooling rate is obtained:

$$CR_T = C\frac{(T - T_0)^2 S}{VI} \qquad \textbf{(EQ 4)}$$

This equation was developed for the purpose of predicting weld and HAZ microstructures in conjunction with continuous-cooling transformation diagrams. These diagrams allow the determination of the cooling rates above which strong martensites or bainites are ensured or below which they can be avoided. The same equation can be used to calculate the cooling rates at temperatures critical to the evolution of hydrogen and the avoidance of HIC.

The adjustment of welding procedures is accomplished by varying the current or the travel speed. Voltage is a strongly dependent variable that is determined by the welding process; the characteristics of the electrodes, fluxes, or shielding gases; and the current. It should not be viewed as a variable with which to control weld cooling rates.

The other method of retarding cooling rates, which is probably the most common method, is to control the preheat or interpass temperature of the joint prior to welding. Relatively small changes in those temperatures can exert strong effects on cooling rates at temperatures around 205 °C (400 °F), which is critical with regard to the onset of HIC. For example, by increasing the preheat temperature from 20 to 95 °C (70 to 200 °F), the cooling rate at 205 °C (400 °F) is reduced by approximately one third. By preheating to 150 °C (300 °F), the cooling rate is reduced by a factor of approximately ten, which is a very significant amount when fabricating high-strength steels that have little tolerance to HIC.

Unfortunately, preheating is expensive, it can affect the weld microstructures, and it can make working conditions unbearable for welders. Nevertheless, as Fig. 12 shows, a preheat is important for reducing HIC. The data plotted in Fig. 12 clearly show how a preheat affects the lower critical stress in the HAZ of HY-80 steel when welded with an E11018-M covered electrode. The ultimate tensile stress of this heat of HY-80 is approximately 760 MPa (110 ksi). However, with a 25 °C (78 °F) preheat, that is, room temperature, failure was caused by HIC in less than 10 min, at a stress level of only 480 MPa (70 ksi). The lower critical stress below which failure did not occur was only 415 MPa (60 ksi). By preheating to a temperature of 120 °C (250 °F), the critical stress was increased to 620 MPa (90 ksi), which is approximately the yield strength of the HY-80 steel, but still considered unsafe. To avoid HIC entirely, under the conditions used to produce the welds shown, the preheat temperature would need to exceed 150 °C (300 °F).

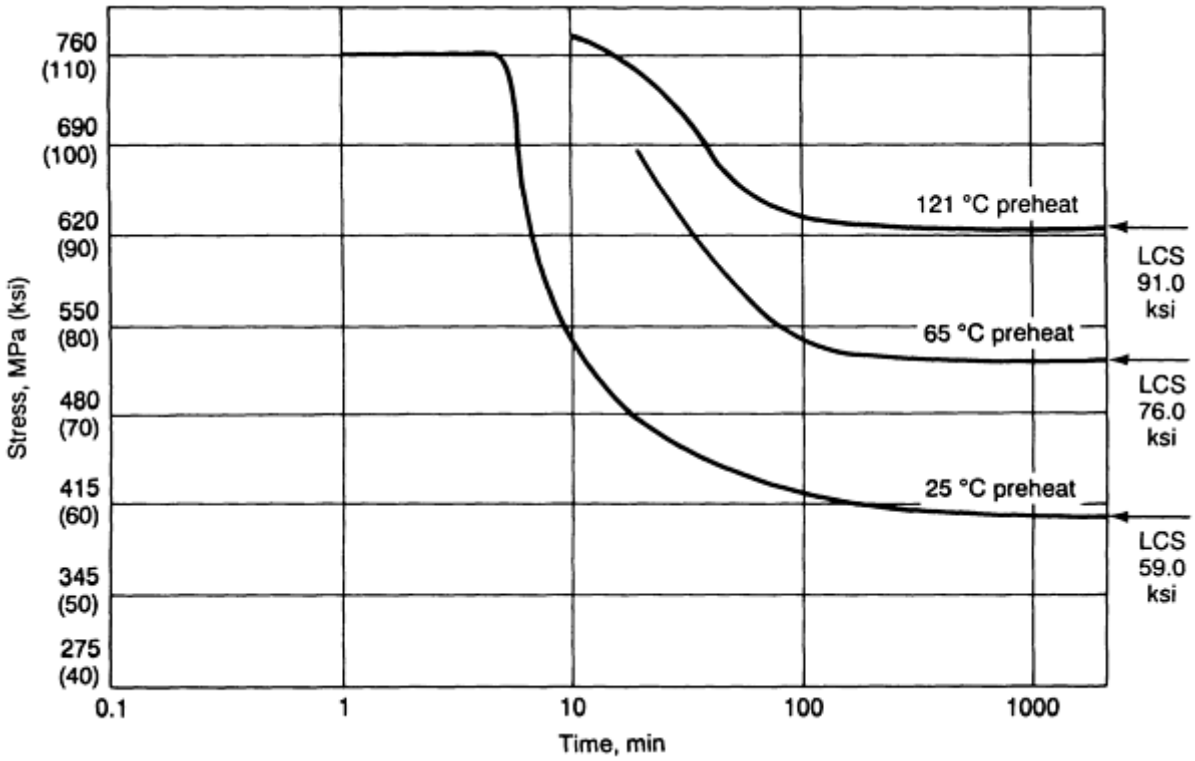

FIG. 12 EFFECT OF PREHEAT ON HIC SUSCEPTIBILITY. PREHEAT INCREASES CRITICAL STRESS NEEDED TO CAUSE HIC. LCS, LOWER CRITICAL STRESS

A number of approaches can be used to select the most appropriate temperature for preheating a steel to avoid HIC. Some approaches rely on empirically derived tables that list the steels and recommended welding procedures, including those for preheat and postheat. Another relates cracking tendencies quantitatively to the hardenability of the alloy steel, calculating it on the basis of the carbon equivalence. One such formula for carbon equivalence is given as:

$$CE = C + \frac{Mn}{6} + \frac{Si}{24} + \frac{Ni}{40} + \frac{Cr}{5} + \frac{Mo}{4} \qquad \textbf{(EQ 5)}$$

For applications that involve welds made with covered electrodes, the recommended preheat temperatures for steels having different carbon equivalencies are plotted in Fig. 13. Although considerable scatter is seen, the overall trend demonstrates a linear relationship between the carbon equivalence and the preheat temperature. For a quick approximation of the required preheat, the following relationship can be used:

$$T_O = 200\ CE \qquad \textbf{(EQ 6)}$$

where T_o is in °C.

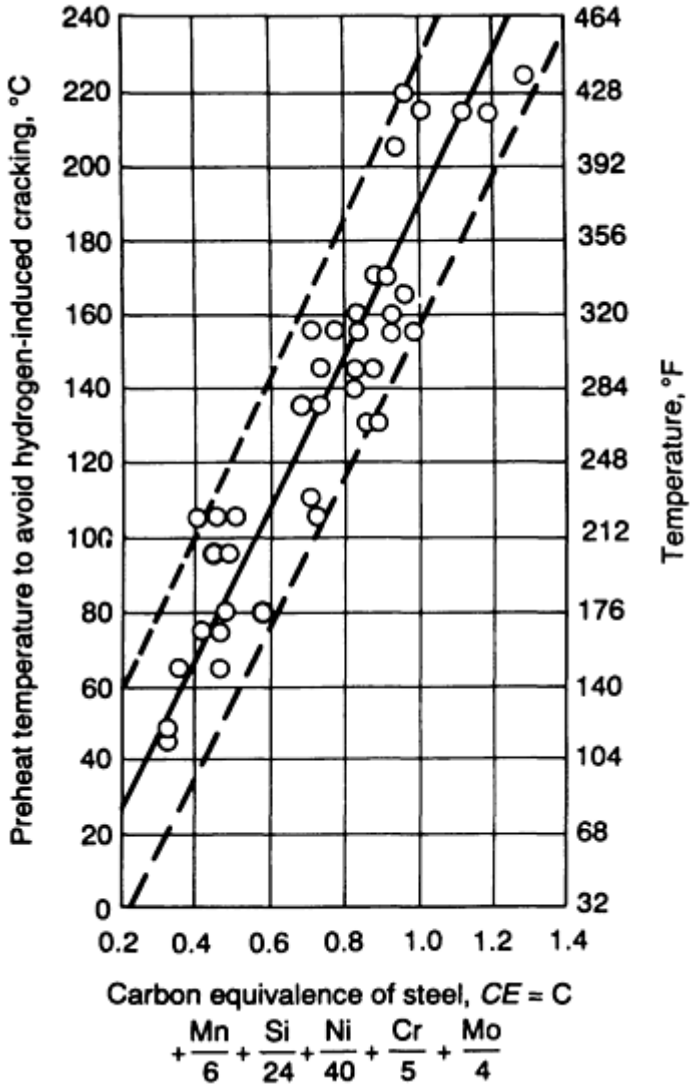

FIG. 13 EFFECT OF CARBON EQUIVALENT ON PREHEAT REQUIREMENTS. AMOUNT OF PREHEAT NEEDED TO PREVENT HIC IS PROPORTIONAL TO THE CARBON EQUIVALENT OF THE STEEL BEING WELDED

To include the scatter band that incorporates all of the data points, a more-precise interaction between the carbon equivalence and the preheat temperature can be shown as:

$$T_O = 210\ CE + 15/-45 \qquad \textbf{(EQ 7)}$$

The scatter band of 60 °C (108 °F) is quite large, which suggests that the upper portion be used for selecting suitable preheat temperatures with which to avoid potential problems. However, if metallurgical softening needs to be avoided, then the most appropriate course of action would be to rely on laboratory trials for determining the minimum effective level of preheat. Of course, such a determination would require that the energy input, the thickness of the joint, and the welding process also be considered.

Measurement of Hydrogen. Direct measurements of hydrogen in weld metal are difficult. Unless great care is taken to stop its escape from a weld before an analysis can be made, the amount found will not be representative of that which might have caused a crack to develop. This means that specimens must be designed to be analyzed quickly or supercooled in liquid nitrogen to stop the diffusion of hydrogen while awaiting analysis. The procedure recommended by the American Welding Society (AWS A4.386) measures the volume of hydrogen gas that escapes from a test weld approximately 75 mm (3 in.) in length. It is collected in either a eudiometer tube (in a mercury or glycerine bath) or in the isolation chamber of a gas chromatograph.

Indirect methods also have been used by measuring the sources of the hydrogen. For wires used in the GMAW and SAW processes, this can be done by measuring the hydrocarbons on their surface. Mass spectrometry can be used for the analysis. For the SMAW and SAW processes, the moisture adsorbed in the fluxes can be determined. Often, this is done by measuring weight loss after drying at high temperatures of approximately 400 to 425 °C (750 to 800 °F). The problem with indirect measurements is that the efficiency of transfer of the hydrogen to the weld from the wires or fluxes is difficult to predict. It can be very dependent on the welding procedures. Therefore, empirical results are used to relate the amount of hydrogen present in the welding materials to the HIC in the weldment. For this reason, a comparison among processes becomes very difficult. However, even the measurements of gas evolution can be faulted, because only the diffusible hydrogen is measured. Some remains in solution and some is trapped within weld defects or inclusions.

Importance of Welding Processes. The arc welding processes require a source of filler metal and methods for protecting and controlling the arc and the deposited metal. In almost all cases, the filler metals are provided in the form of rods, continuous wires, or continuous tubes. The surfaces of all of these materials are contaminated with residues of hydrogen-rich drawing lubricants. In the GMAW process, a shield gas is used for protection. For cored wires, a combination of shield gases and fluxes are used. The submerged-arc and covered-electrode methods involve only fluxes. All of the fluxes are sources of chemically combined or adsorbed water. The quantity of hydrogen dissolved in weld metal can vary, not only between but within processes. Some indication of the variability to be expected is shown in Table 1.

TABLE 1 EFFECT OF WELDING PROCESSES AND ELECTRODES ON HYDROGEN LEVELS IN WELDS

TYPE OF ELECTRODE	DIFFUSIBLE H_2, ML/100 G
GMAW SOLID WIRE	0-10
BASIC SMAW ELECTRODE	3-20
ACID SMAW ELECTRODE	20-40
SAW SOLID WIRE AND FLUX	4-20
GMAW CORED WIRE	3-30

Of all of the arc welding processes using consumable electrodes, the GMAW process is associated with the lowest hydrogen levels, the primary source being residual drawing lubricants on the wire surface. Totally dry wire is unacceptable, because it is difficult to feed. The amount of residual lubricant generally is not a problem with steels having yield strengths below 520 MPa (75 ksi). However, as the yield strengths approach 620 MPa (90 ksi), the residual lubricants become a potentially important factor if HIC is to be avoided, unless relatively high preheat temperatures can be used. When the yield strengths exceed 830 MPa (120 ksi), the residual lubricants must be kept as low as possible.

The importance of such residues is shown in Fig. 14, which summarizes the effects of hydrogen on HIC in welds that have a yield strength of 930 MPa (135 ksi) and shows how it can be minimized by controlling cooling rates. In this case, the cooling rates indicated were determined at 540 °C (1000 °F), a temperature close to that at which the weld metal transforms from austenite to martensite. The closed circles indicate the presence of HIC in the welds, whereas the open circles indicate sound welds. At the relatively rapid cooling rates of 28 °C/s (50 °F/s), 4 ppm of hydrogen on the wire surface is shown to have caused HIC. To be securely free of HIC, the hydrogen had to be maintained at levels below 3 ppm. By adjusting the welding procedures, preheat temperatures, or both, in order to retard the cooling rate at 540 °C (1000 °F) to less than 20 °C/s (35 °F/s), the tolerance for hydrogen on the wire was increased to 5 ppm.

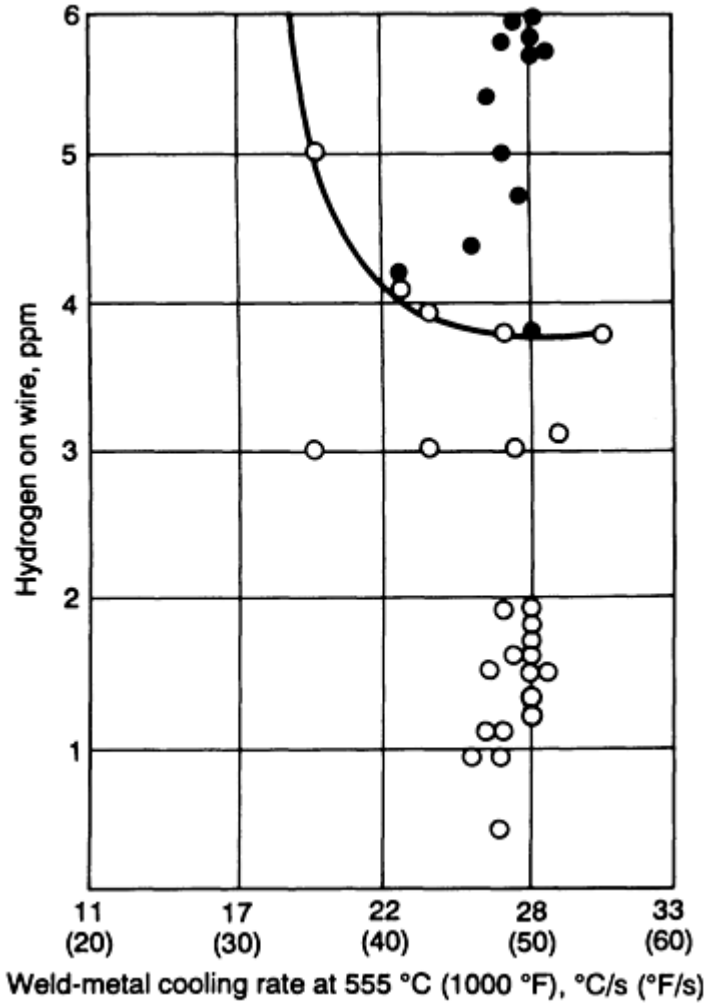

FIG. 14 INFLUENCE OF HYDROGEN PRESENT ON A WIRE SURFACE AND WELD-METAL COOLING RATE ON HIC. DATA ARE BASED ON GMAW WELD METAL WITH YIELD STRENGTH OF 930 MPA (135 KSI).

As mentioned earlier in the discussion of hydrogen measurements, it is difficult to predict the amount of hydrogen that will transfer to a weld from surface contaminants that are decomposed in the arc (or before reaching the arc), particularly when the levels are measured in single-digit parts per million. These levels are so low as to preclude the use of gas-evolution techniques to measure the hydrogen.

The higher tolerance for wire surface contaminants at lower cooling rates may be due as much to softer microstructures as it is to the escape of hydrogen. The effect of cooling rate on the tensile yield strength of these alloys is illustrated in Fig. 15. To retain high strengths, the higher cooling rates are essential. In this example, a very abrupt drop in strength is shown as the cooling rate drops below 10 °C/s (20 °F/s). Obviously, to obtain the strongest possible welds without encountering HIC, it is necessary to minimize the presence of any contaminants that contain hydrogen.

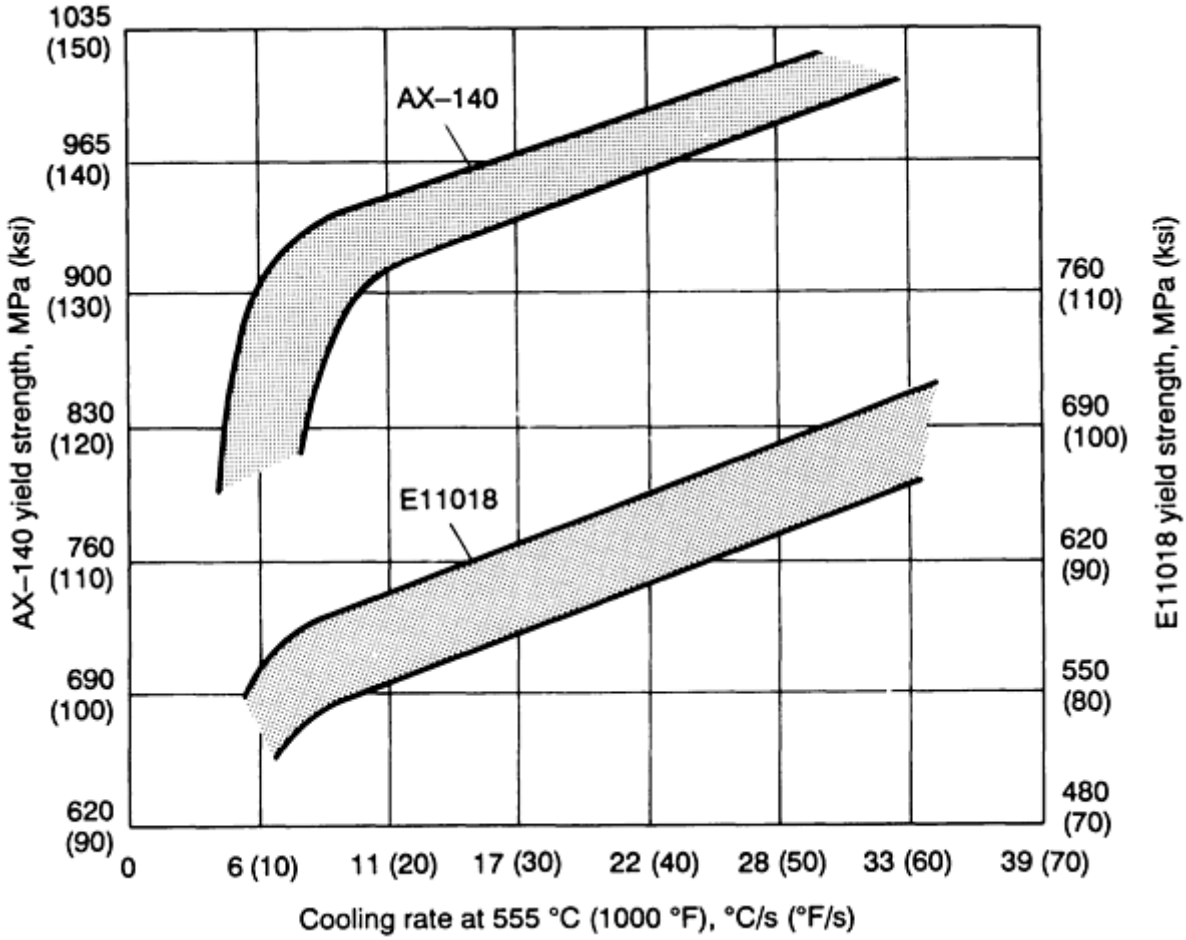

FIG. 15 EFFECT OF COOLING RATE ON STRENGTH OF HSLA STEEL WELD METAL. TENSILE YIELD STRENGTH OF HSLA STEEL WELD METAL IS AFFECTED BY THE COOLING RATE AT WHICH IT TRANSFORMS. DATA ARE BASED ON AX-140 GMAW AND E11018 SMAW FILLER METALS.

The attainment of such low levels of hydrogen is not possible with any of the other arc welding processes, because they require fluxes instead of shield gases for protection. Fluxes can absorb water. The data in Fig. 16 summarize the importance of moisture in a submerged arc flux on the cracking sensitivity of a Soviet weld metal that has a yield strength of 830 MPa (120 ksi). It demonstrates that diffusible hydrogen levels as low as 7 mL/100 g can drop the critical strength to 105 MPa (15 ksi). (Note that a hydrogen content of 1 ppm is equivalent to 1.11 mL/100 g). Even baking the flux to reduce the weld-diffusible hydrogen below 2 mL/100 g did not eliminate HIC. The critical stress remained below 415 MPa (60 ksi). It is evident that the welding conditions used for these submerged arc welds were not acceptable. Either this steel is unusually sensitive to hydrogen or the flux used is not capable of being dried sufficiently to reduce hydrogen contamination.

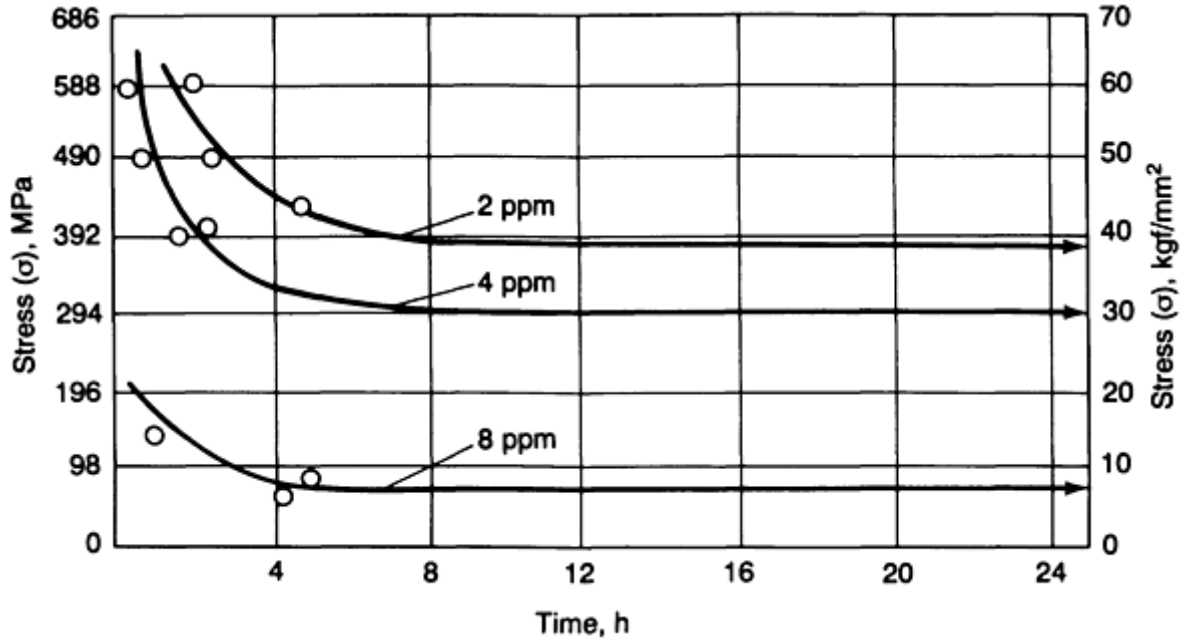

FIG. 16 EFFECT OF HYDROGEN ASSOCIATED WITH SUBMERGED ARC WELDS ON THE LOWER CRITICAL STRESS AND THE TIME NEEDED FOR HIC. FLUX AS RECEIVED, 4 PPM; FLUX BAKED, 2 PPM; FLUX MOISTENED, 8 PPM. DATA ARE BASED ON 30KH2N2M SOVIET STEEL WITH A YIELD STRENGTH OF 930 MPA (135 KSI).

Similar HIC problems are encountered in the SMAW process when weld strengths exceed 480 MPa (70 ksi). For this reason, low-hydrogen electrodes were developed specifically to minimize, if not prevent, these problems. Low-hydrogen electrode coatings are formulated without any organic materials, such as the cellulose that characterizes the EXX10 classes. These low-hydrogen coatings are baked at temperatures exceeding 425 °C (800 °F) to reduce residual moisture to a level of approximately 0.1 wt%. This is nearly the lowest practicable level, because the absence of moisture in a coating tends to make it brittle. The effect of baking on the residual moisture during initial manufacture is shown in Fig. 17. Even with careful control of formulations and baking, the moisture level of covered-electrode coatings cannot be reduced to levels sufficiently low to prevent HIC in steels having yield strengths higher than 830 MPa (120 ksi).

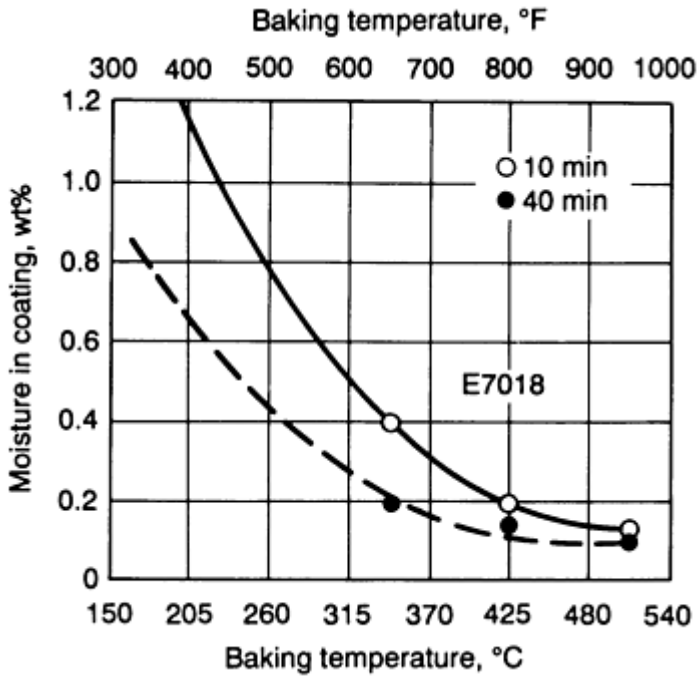

FIG. 17 EFFECT OF BAKING TIME AND TEMPERATURE ON MOISTURE IN E-7018 COVERED ELECTRODES

The moisture in low-hydrogen electrodes generally is specified as 0.2% max. This moisture level is what is expected to be found in coatings of commercial low-hydrogen electrodes, immediately after being removed from hermetically sealed containers. However, if exposed to humid, warm air, these electrode coatings will reabsorb moisture, as shown in Fig. 18. The rate of moisture pickup depends on the constituents in the coating. In some cases, reabsorbed moisture can reach levels exceeding 1%. For this reason, electrodes must be stored in heated ovens on hot and humid days and exposed to shop environments for only short times.

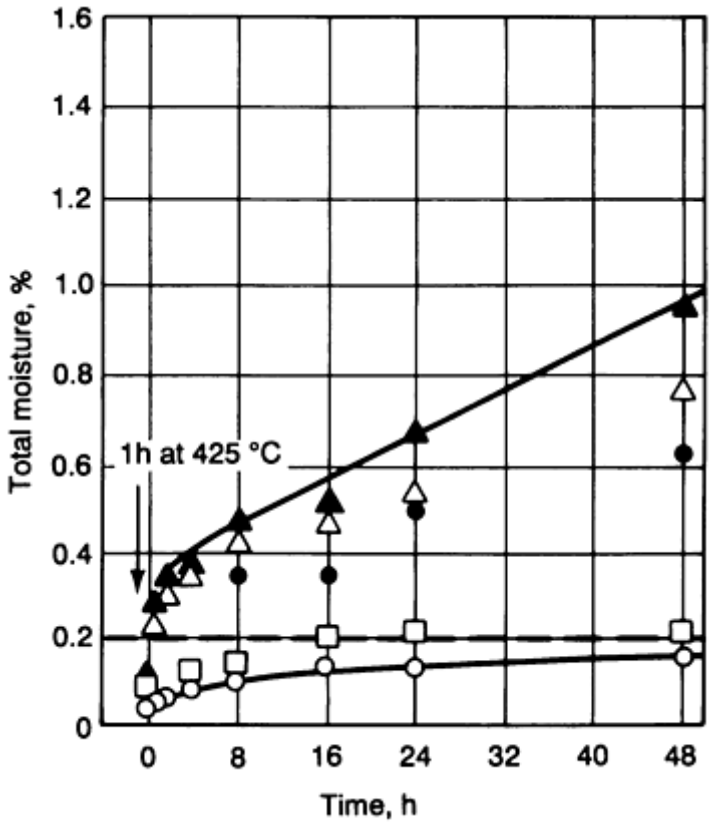

FIG. 18 MOISTURE ABSORPTION IN COVERED-ELECTRODE COATINGS WHEN EXPOSED TO MOIST, HUMID ENVIRONMENTS. THE AMOUNT ABSORBED DEPENDS ON THE ELECTRODE AND INCREASES WITH TIME. TEMPERATURE, 21 ± 3 °C (70 ± 5 °F); RELATIVE HUMIDITY, 65 ± 5%

Moisture-resistant coatings have been developed to counter the reabsorption problem. Their rates of reabsorption are typical of the lower curve shown in Fig. 13. Although they are quite safe when exposed to the relatively cool and moderately humid environment indicated, extra precautions are essential when welding in tropical conditions.

It is possible to salvage electrodes that have become "wet" by rebaking them at temperatures that approach those used during their manufacture. Typical results are shown in Fig. 19. Drying times of about 1 h are needed to recondition typical electrodes at approximately 400 to 425 °C (750 to 800 °F). Although rebaking can salvage electrodes that are inadvertently exposed to moist conditions, it should not be repeated. Covered electrodes are alloyed with metal powders that can be oxidized during rebaking operations. Therefore, the resulting alloys are leaner and weaker, as seen in Table 2.

TABLE 2 EFFECT OF REBAKING ON COMPOSITION AND STRENGTH

NUMBER OF	COMPOSITION, WT%	YIELD STRENGTH

BAKE CYCLES	C	MN	SI	MPA	KSI
1	0.069	1.54	0.39	723.3	104.9
2	0.064	1.46	0.37	714.3	103.6
3	0.066	1.45	0.37	688.8	99.9

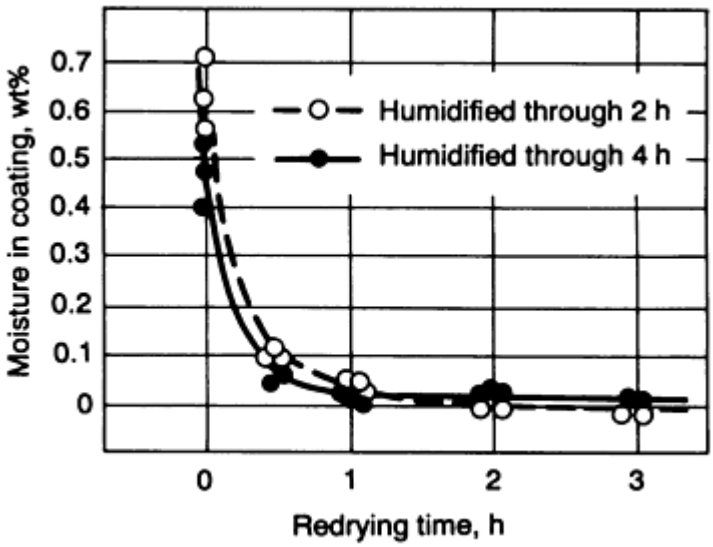

FIG. 19 EFFECT OF DRYING TIME ON MOISTURE ABSORBED BY COVERED ELECTRODES AFTER EXPOSURE TO MOIST ENVIRONMENTS. E11016 LOW-HYDROGEN TYPE ELECTRODE, 4 MM (0.16 IN.); REDRYING TEMPERATURE, 400 °C (750 °F)

Rebaking caused a loss in both manganese and silicon in the weld metal, resulting in a drop in the weld yield strength. These data were obtained after very controlled rebaking. Unfortunately, the same care is not always taken in shop environments. Significantly greater losses in the manganese and silicon contents, as well as mechanical properties, can be expected.

Influence of Welding on Steel Weldment Properties

C.C. Chen and Abe Pollack, Microalloying International, Inc.

Introduction

THE FUNDAMENTAL AND THE SPECIFIC FACTORS that control the properties of steel weldments in both the weld metal and heat-affected zone (HAZ) of carbon and low-alloy steels are described in this article. The influence of welding processes, welding consumables, and welding parameters on the weldment properties also will be discussed. The service properties of weldments in corrosive environments and subjected to cyclic loading will be considered, as well.

Influence of Welding on Steel Weldment Properties

C.C. Chen and Abe Pollack, Microalloying International, Inc.

Heat-Affected Zone

In terms of materials selection, the service characteristics of the HAZ should be emphasized more than those of the weld metal. This is because the metallurgical and mechanical properties of the HAZ are directly related to the selected base metal, even though they can be modified by welding parameters and postweld heat treatment (PWHT). It is also true that

any metallurgical and/or weldability problems associated with the HAZ characteristics will be more difficult to handle than those associated with the weld metal. Welding problems that occur in the weld metal can often be overcome by changing the welding electrode and/or other welding consumables. In contrast, problems with the HAZ sometimes can only be resolved by changing the base metal, which is often an excessively costly measure, or by changing the heat input.

Various empirical carbon equivalents have been developed and utilized to evaluate the weldability (hydrogen-induced cold-cracking tendency) of the base materials. In the United States and European countries, the International Institute of Welding (IIW) equation is most common:

$$CE(IIW) = C + \frac{Mn}{6} + \frac{Cu + Ni}{15} + \frac{Cr + Mo + V}{5} \qquad \textbf{(EQ 1)}$$

In Japan, the Ito-Bessyo (Ref 1) composition-characterizing parameter, P_{cm}, is more widely used. This carbon equivalent is considered to allow a more realistic assessment of the weldability of low-carbon steels, when compared with the IIW equation:

$$P_{cm} = C + \frac{Si}{30} + \frac{Mn + Cu + Cr}{20} + \frac{Ni}{60} + \frac{Mo}{15} + \frac{V}{10} + 5B \qquad \textbf{(EQ 2)}$$

Yurioka *et al.* (Ref 2) have also developed another carbon-equivalent number, CEN, which incorporates both the IIW carbon equivalent and the P_{cm}. The CEN is similar to the P_{cm} for steels with carbon levels that are less than 0.17%, and it follows the IIW formula at high carbon levels.

$$CEN = C + A(C)\left(\frac{Si}{24} + \frac{Mn}{6} + \frac{Cu}{15} + \frac{Ni}{20} + \frac{Cr + Mo + Nb + V}{5} + 5B\right) \qquad \textbf{(EQ 3)}$$

where A(C) equals 0.75 plus 0.25 tan*h* [20(C - 0.12)].

Although these carbon-equivalent expressions were initially developed to characterize the hydrogen cracking tendency for steel plates, they also have been utilized to assess the hardenability of steels based on their chemistry. Figure 1 illustrates the correlation between carbon equivalent, P_{cm}, and the martensite volume in both the coarse-grained region and the grain-refined region (Ref 3). As the P_{cm} increases, the martensite volume and hardness in both regions increase.

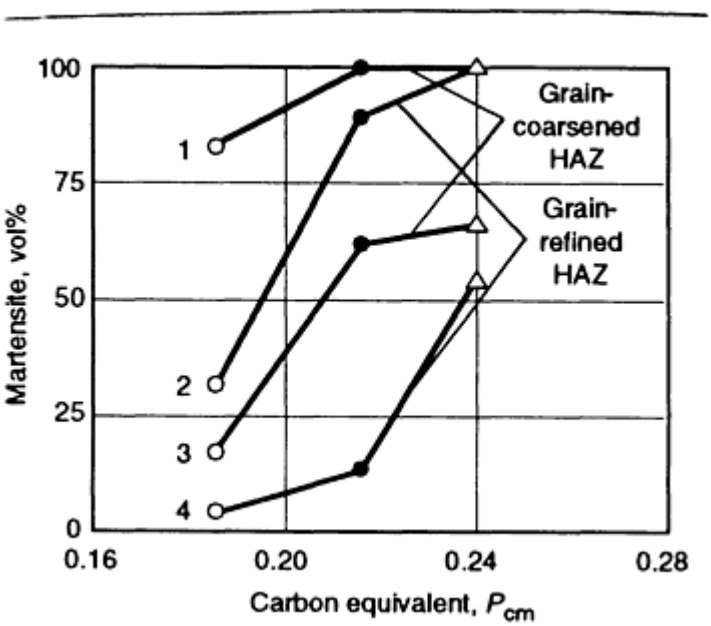

FIG. 1 RELATIONSHIP BETWEEN HAZ VOLUME FRACTION OF MARTENSITE AND THE P_{CM} CARBON EQUIVALENT

OF THERMALLY CYCLED SPECIMENS. FOUR THERMAL PROGRAMS ARE INCLUDED: (1) PEAK TEMPERATURE (T_P) ≈ 1350 °C (2460 °F), COOLING TIME FROM 800 TO 500 °C ($\Delta T_{8/5}$) = 3 S; (2) T_P ≈ 1000 °C (1830 °F), $\Delta T_{8/5}$ = 3 S; (3) T_P ≈ 1350 °C (2460 °F), $\Delta T_{8/5}$ = 13 S; (4) T_P ≈ 1000 °C (1830 °F), $\Delta T_{8/5}$ = 13 S. SOURCE: REF 3

Various regions in the HAZ of ferritic steels have been defined and characterized using a specific peak temperature of the HAZ weld thermal cycle in conjunction with an iron-carbon equilibrium phase diagram (Ref 4). These regions are the coarse-grained, grain-refined, intercritical, subcritical, and partly molten regions. However, the metallurgical behavior in the HAZ that undergoes rapid heating and cooling is a nonequilibrium process. Consequently, a continuous cooling transformation (CCT) diagram is more appropriately used to predict the microstructures in the HAZ.

The cooling rate is closely related to plate thickness, joint geometry, and welding heat input. The cooling rate that is often most critical in welding applications is that which falls between 800 and 500 °C (1470 to 930 °F). As the welding heat input is increased or the plate thickness is reduced, the cooling rate between these temperatures is reduced. (The effects of welding parameters on the HAZ cooling rate will be discussed in detail later in this article.)

The effects of major alloying elements in carbon and low-alloy steels on HAZ microstructure and toughness is summarized below (Ref 3).

Carbon has a tremendously important role in the overall hardness of welded steels. This can be clearly seen by its role in the carbon-equivalent and P_{cm}, equations. An increase in carbon level promotes the formation of lower-temperature transformation products, such as bainite and martensite, and leads to a significant reduction in HAZ cleavage resistance.

Manganese. In addition to solid-solution hardening, manganese can lower the transformation temperature of austenite to ferrite while providing strengthening effects by grain refinement. However, the level of manganese should be limited to minimize solidification segregation and microstructural banding.

Chromium is a solid-solution strengthener and carbide former. It increases the hardenability of steels and improves oxidation and corrosion resistance. The addition of chromium can be favorable in cases where the precipitation of chromium carbides suppresses the formation of ferrite side plates through a pinning effect.

Nickel is considered to have a beneficial effect on steel transformation, similar to that of manganese, by lowering the austenite transformation temperature. The addition of nickel also can improve toughness, as well as provide a solid-solution hardening effect.

Vanadium and niobium are added in small quantities in low-alloy steels to obtain the desired mechanical properties. By forming V(C,N) and Nb(C,N), the vanadium and niobium can retard the recrystallization and grain growth of austenite during rolling and normalizing. During fusion welding, especially with high heat input, V(C,N) and Nb(C,N) dissolve in the HAZ with peak temperatures greater than 1100 °C (2012 °F) and reprecipitate during slower cooling. The reprecipitation of V(C,N) and Nb(C,N) impairs the toughness of the HAZ.

Titanium, in the form of stable titanium nitride, has been found to prevent coarsening of the prior austenite grain in regions adjacent to the weld fusion boundary.

References cited in this section

1. Y. ITO AND K. BESSYO, "WELDABILITY OF HIGH STRENGTH STEELS RELATED TO HEAT AFFECTED ZONE CRACKING," DOCUMENT IX-567-68, IIW, 1968
2. N. YURIOKA, H. SUZUKI, AND S. OHSHITA, *WELD. J.*, VOL 62, 1983, P 1475-1535
3. O. GRONG AND O.M. AKSELSEN, HAZ TOUGHNESS OF MICROALLOYED STEELS FOR OFFSHORE, *MET. CONSTR.*, SEPT 1986, P 557
4. K.E. EASTERLIN, *INTRODUCTION TO THE PHYSICAL METALLURGY OF WELDING*, BUTTERWORTHS, 1983

Weld Metal

The use of a filler metal is very common in many fusion-welding processes. When selecting the proper filler metal/electrode, the primary considerations are whether or not the weld metal can be produced defect-free and whether or not the weld metals are compatible with the base metal and can provide satisfactory properties. These characteristics are determined by the:

- CHEMISTRY OF THE ELECTRODES
- DILUTION OF THE BASE METAL
- FLUX SYSTEM OR SHIELDING GAS
- WELD-POOL SOLIDIFICATION AND SUBSEQUENT COOLING AND TRANSFORMATION

The selection of the proper filler metal is not based on matching the chemistry of the base metal. Rather, it is based on matching the weld metal and base metal service properties. Using a filler metal with a chemistry identical to that of the base metal may not provide the desired results, because the microstructures of the weld metal are entirely different from those of the base metal. For most carbon and low-alloy steels, the solidification and rapid cooling rate involved in fusion welding will result in a weld metal that has higher strength and lower toughness properties than the base metal when they are of the same chemistry. Consequently, the filler metal often contains a lower carbon level than the base metal. The strength of the weld metal is not improved by increasing the carbon content, but by adding the alloying elements that provide solid-solution or precipitation strengthening and modification of the microstructures (Ref 5).

The weld-metal microstructure in carbon and low-alloy steels contains a variety of constituents, ranging from blocky ferrite, to acicular ferrite, to bainite, to martensite. The effects of alloying elements and cooling on the weld-metal microstructure can be expressed in a schematic CCT diagram (Fig. 2), whereas the effects of alloying elements on the hardness and notch toughness of weld metal are illustrated in Fig. 3.

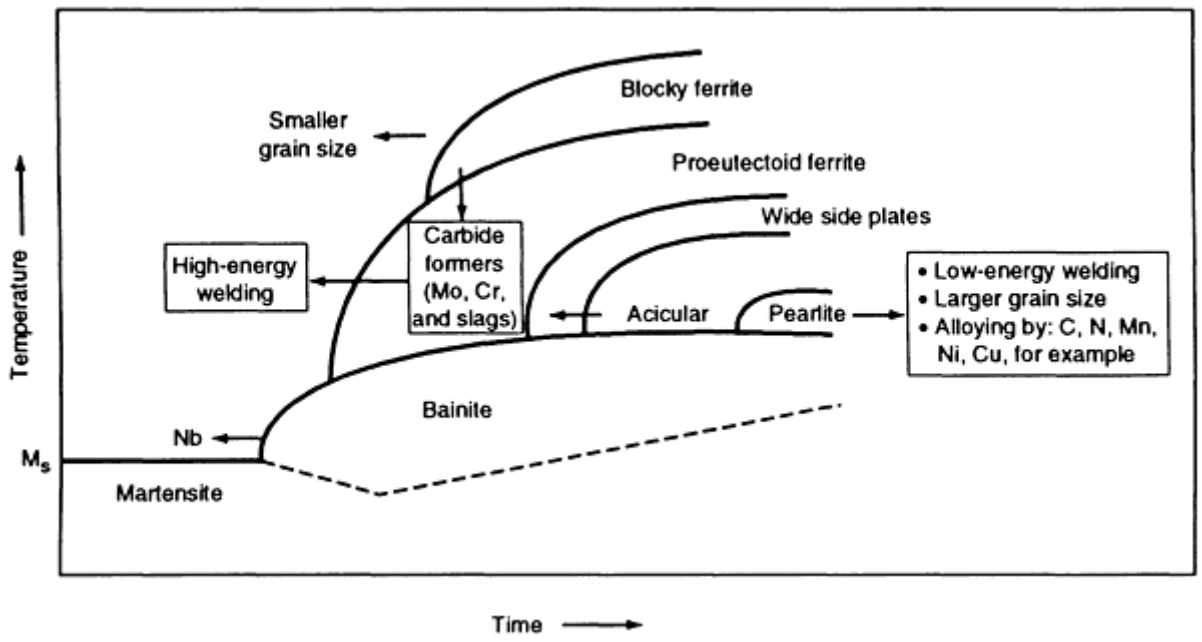

FIG. 2 SCHEMATIC CCT DIAGRAM FOR STEEL WELD METAL, SUMMARIZING THE POSSIBLE EFFECT OF MICROSTRUCTURE AND ALLOYING ON THE TRANSFORMATION PRODUCT FOR A GIVEN WELD COOLING TIME. SOURCE: REF 4

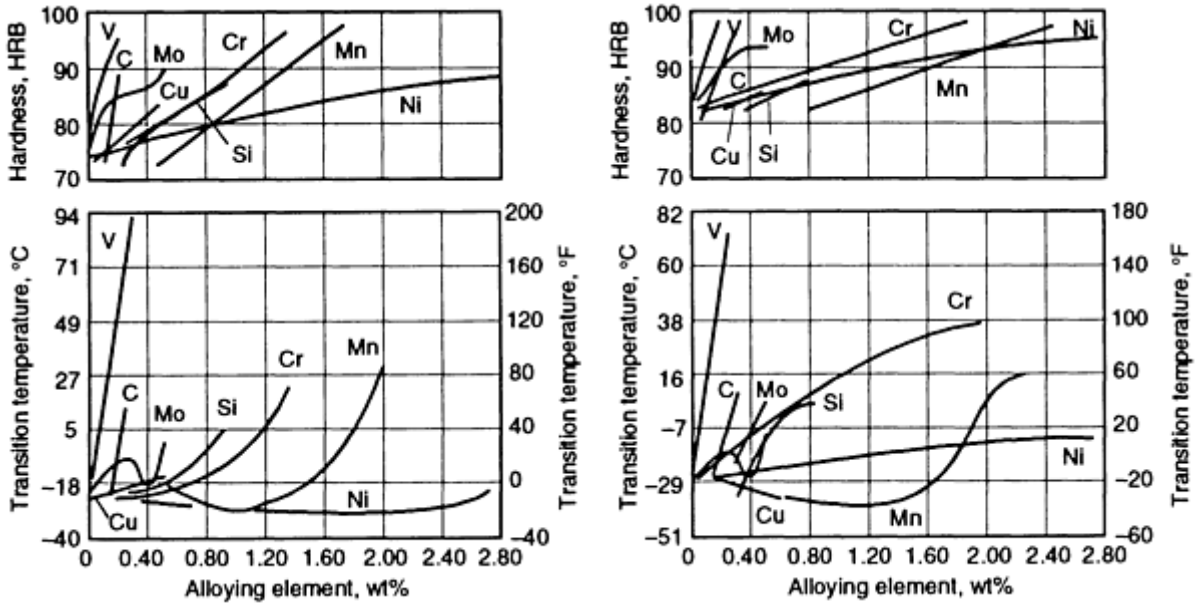

FIG. 3 EFFECTS OF ALLOY ADDITIONS ON HARDNESS AND NOTCH-TOUGHNESS OF WELD METAL. TRANSITION TEMPERATURE MEASURED AT 20 J (15 FT · LBF). (A) SUBMERGED ARC WELD METAL. (B) GAS-METAL ARC WELD METAL. SOURCE: REF 6

Dilution. The melting of base metal and the subsequent mixing with filler metal causes the final chemistry of the weld deposit to be between that of the base and filler metals. When a filler metal has the same chemistry as the base metal, the final weld-metal chemistry remains the same, theoretically. Depending on the amount of base metal that is melted and the amount of filler metal that is added, the final chemistry of the weld deposit can be approximated using the dilution equation:

$$Dilution, \% = \left(\frac{Weight \text{ of parent metal melted}}{\text{Total weight of used metal}} \right) 100 \qquad \textbf{(EQ 4)}$$

Figure 4 shows how factors such as joint configuration and edge preparation influence dilution. Welding processes and parameters that increase penetration can also increase dilution (Ref 7).

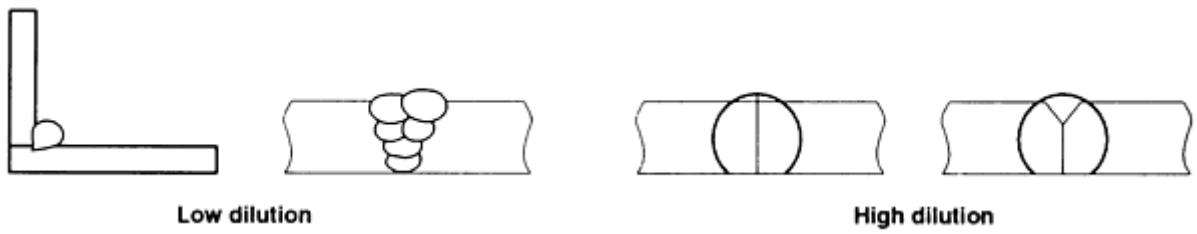

FIG. 4 DILUTION OF WELD DEPOSIT. SOURCE: REF 7

In a single-pass weld, certain element contents in the weld metal can be approximated using this formula: Specific element in weld metal equals (that element in the base metal multiplied by the dilution) plus (that element in the filler metal multiplied by [1 - dilution]).

In certain cases, greater dilution is favorable, considering the less-drastic change in mechanical and other properties across the fusion boundary. However, in applications involving weld cladding or weld surfacing, it is more desirable to

minimize the dilution. This is because filler metal contains more-expensive alloying elements tailored to impart specific weld-metal properties. When there are concerns that the base metal may introduce undesired impurities and/or alloying elements, then welding practices that lower the dilution are recommended. This also includes considerations for phosphorus and sulfur and for higher carbon and silicon contents, which adversely affect the properties of weld metal.

References cited in this section

4. K.E. EASTERLIN, *INTRODUCTION TO THE PHYSICAL METALLURGY OF WELDING*, BUTTERWORTHS, 1983
5. C.F. CHOU, *THEORY AND TECHNOLOGY OF METAL WELDING*, VOL 2, MECHANICAL INDUSTRY PUBLISHER, 1981 (IN CHINESE)
6. R.D. STOUT AND W.D. DOTY, *WELDABILITY OF STEELS*, 3RD ED., S. EPSTEIN AND R.E. SOMERS, ED., WELDING RESEARCH COUNCIL, NEW YORK, 1978
7. J.F. LANCASTER, *METALLURGY OF WELDING*, GEORGE ALLEN & UNWIN, 1980

C.C. Chen and Abe Pollack, Microalloying International, Inc.

Single-Pass versus Multipass Welding

In terms of mechanical properties, especially toughness, multipass weld metal is usually better than single-pass weld metal for these reasons:

- THE REHEAT THERMAL CYCLE OF EACH SUBSEQUENT WELDING PASS NORMALIZES AND REFINES PORTIONS OF THE MICROSTRUCTURE IN THE PREVIOUS WELD METAL.
- SUBSEQUENT WELD RUNS TEMPER THE PREVIOUS WELD METAL AND REDUCE RESIDUAL STRESSES FROM PREVIOUS RUNS.
- THE TOTAL ENERGY INPUT PER PASS IS REDUCED, WHICH IS HELPFUL FOR LIMITING THE AMOUNT OF GRAIN GROWTH.
- PREVIOUS WELD PASSES PROVIDE A CERTAIN PRE-HEAT THAT SLOWS DOWN THE COOLING RATE OF THE SUBSEQUENT PASS.

Figure 5 shows that the weld-metal ductility (cross-sectional area) increases as the total grain-refined areas are increased (Ref 8).

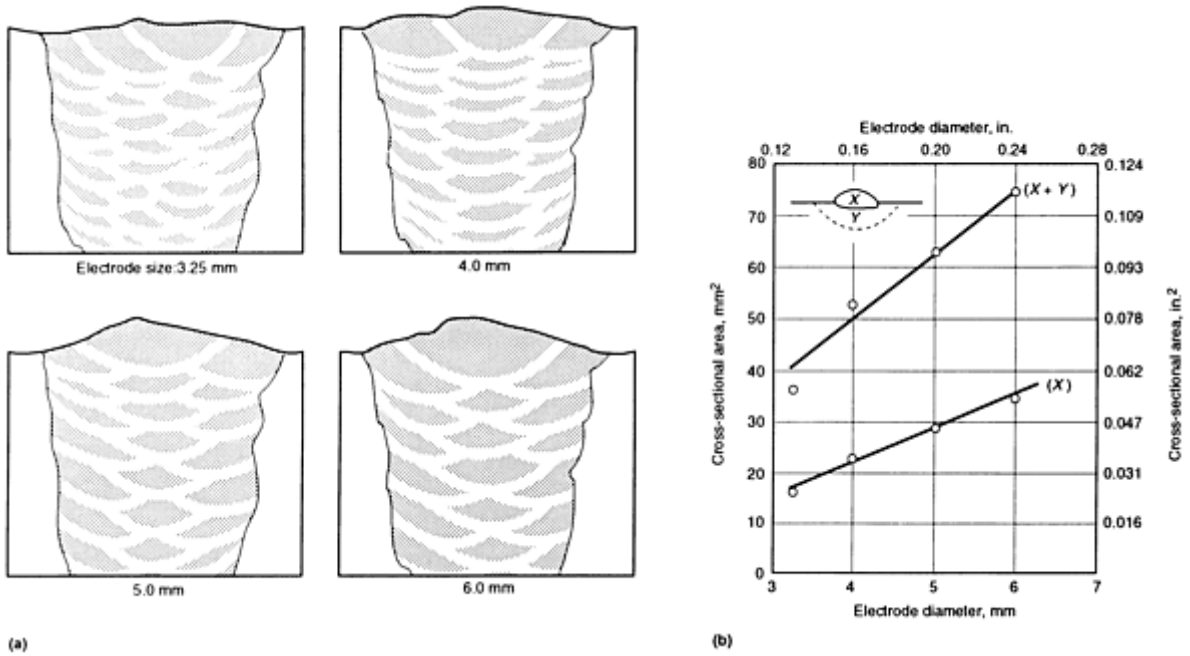

FIG. 5 EFFECT OF ELECTRODE SIZE ON AMOUNT OF RECRYSTALLIZED WELD METAL IN MULTIRUN WELDING. (A) CROSS SECTIONS AS A FUNCTION OF ELECTRODE DIAMETER; WHITE AREAS REPRESENT RECRYSTALLIZED WELD METAL. (B) GRAPHICAL REPRESENTATION. SOURCE: BASED ON REF 8

In contrast, when an active flux is used in submerged arc welding, the number of weld passes to be applied in a joint is limited. This is because there is a tendency for alloying elements (such as silicon and manganese) to build up during multipass welding, which impairs the fracture toughness values in the final weld pass.

Reference cited in this section

8. G.M. EVANS, FACTOR AFFECTING THE MICROSTRUCTURES AND PROPERTIES OF C-MN ALL-WELD METAL DEPOSITS, *WELD. REV.*, VOL 4, MAY 1982

Influence of Welding on Steel Weldment Properties

C.C. Chen and Abe Pollack, Microalloying International, Inc.

Steel Types and Weldability

The high-strength, low-alloy (HSLA) steels were designed to have improved mechanical properties and weldability, when compared with conventional carbon steels. These improvements are obtained through the addition of small amounts of alloying elements, such as niobium, vanadium, titanium, nitrogen, and carbon, which strengthen the ferrite, increase the hardenability, and control the grain size. Most of these steels are provided in the as-rolled, normalized condition, and some are provided in the precipitation-treated condition, as well. The finer grain size and greater amount of pearlite account for the greater strength and toughness of this group of steels. In addition, the lower carbon content (0.22% max) leads to good weldability. Figure 6 shows the CCT diagram for a titanium-boron HSLA steel (Ref 9).

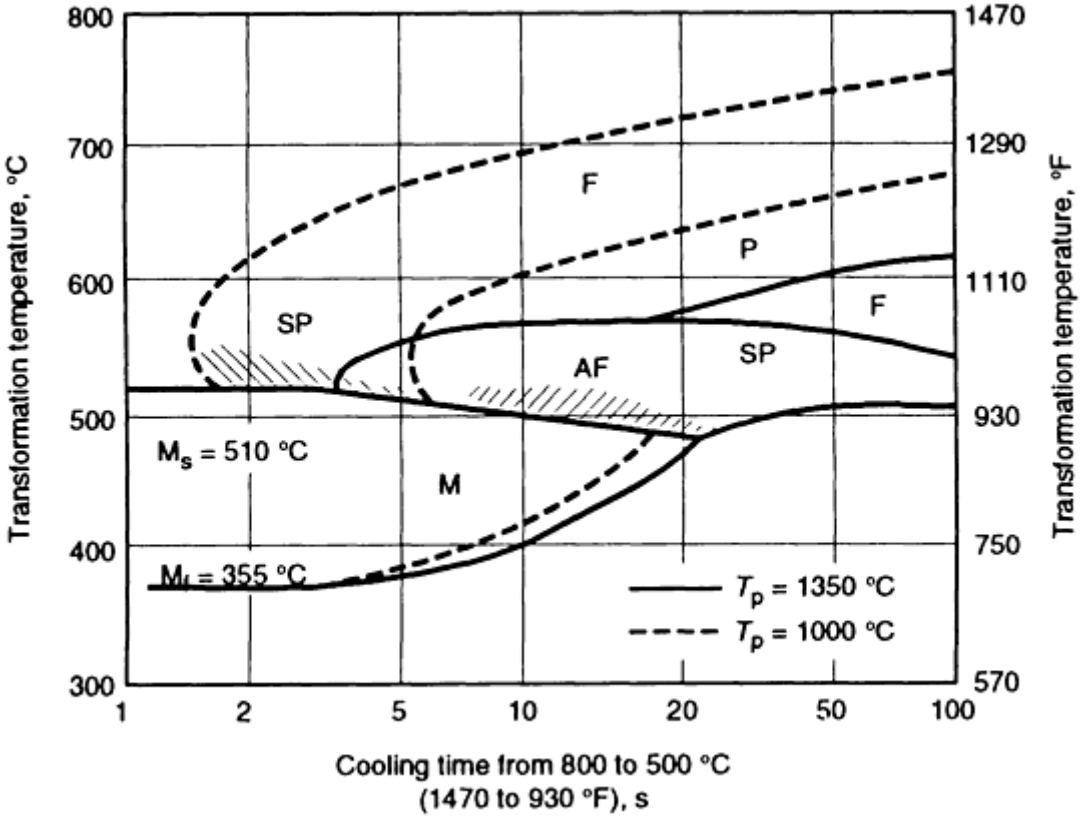

FIG. 6 CCT DIAGRAM FOR A TITANIUM-BORON MICROALLOYED STEEL. T_P, PEAK TEMPERATURE. SOURCE: REF 9

Generally, the weldability of HSLA steels is similar to that of mild steels (Ref 10). Although HSLA steels have good weldability, the consideration of preheating and controlling hydrogen in the welding process is still necessary to ensure a successful weldment. The embrittlement in the coarse-grained HAZ is one of the concerns during the welding of HSLA steels. This embrittlement is attributed to the slow cooling rate leading to the formation of undesirable microstructures, such as coarse ferrite side plates (Widmanstätten ferrite and upper bainite) and grain-boundary ferrite (Ref 3), especially at high-energy input levels.

For HSLA steels that contain niobium and vanadium, the weld metal and the HAZ will exhibit low notch toughness at high heat inputs, such as those used in the electroslag and submerged arc welding processes. This is because the high heat input increases the extent of coarse-grained HAZ. The associated low cooling rate in the HAZ reduces the scope for grain refinement and increases the likelihood of the precipitation of niobium and vanadium carbides, leading to embrittlement of the coarse-grained HAZ. The high heat input and the resulting greater dilution also brings the precipitation-hardening problem of niobium and vanadium carbides to the weld metal.

The use of steels with small additions of titanium (up to 0.04%) and nitrogen has been found to effectively minimize the grain growth in the coarse-grained HAZ (Ref 11). This is due to the greater stability of titanium nitride at the peak temperature experienced in coarse-grained regions (>1100 °C, or 2012 °F), where niobium and vanadium carbides are turned back into solution.

Low-carbon steels comprise two classes of steels, namely, low-carbon steels with a carbon content of less than 0.15% and mild steels with a carbon content between 0.15 and 0.30%.

For these low-carbon steels in the annealed condition, the major microstructure is relatively soft ferrite with scattered small carbide particles, whereas low-carbon steel in the hot-rolled or normalized condition has islands of pearlite. During fusion welding, the HAZ will undergo transformation from ferrite to austenite upon heating, and from austenite back to ferrite during cooling. At this carbon level, the hardening involved in the HAZ is approximately 10 HRC or less. However, when the weldment undergoes a cold-forming operation, it is recommended that the carbon content be limited

to 0.06%. The HAZ of steels with higher carbon contents may not have good ductility to accommodate the strain involved in cold forming (Ref 10).

When low-carbon steels are furnished as rimmed steels, their central core regions tend to contain concentrations of elements such as carbon monoxide and carbon dioxide, as well as elements such as sulfur and phosphorus, as a result of segregation during the rimming action. In addition, the gaseous species that result from the reaction between dissolved oxygen and carbon are also trapped in the central core region. During the welding operation, certain amounts of base metal will melt and mix with filler metal because of dilution. The high-temperature, molten weld pool provides conditions that allow the incomplete oxygen-carbon reaction to resume and trapped carbon monoxide and carbon dioxide to evolve. When the weld-pool solidification rate is too rapid for gaseous species to escape, their entrapment will lead to pores in the weld metal. Consequently, sufficient weld-pool deoxidation is the practical way of avoiding porosity problems when welding rimmed steels (Ref 10).

When low-carbon steels are furnished as killed steels, weld-metal porosity is no longer a problem during fusion welding. Instead, a viscous refractory slag sometimes forms on the weld-pool surface of the killed steels, which makes the flow of molten metal sluggish and weld-pool manipulation difficult. The slag becomes viscous when deoxidizers, such as the aluminum, titanium, and zirconium used in the steel-ingot killing practice, form oxides with relatively high melting temperatures. This problem with slag is more intensified for oxyacetylene welding, because of the low temperatures involved in that process. The common remedy is to select a filler metal that contains a sufficient amount of manganese and silicon to reduce the melting point and improve the flow of the slag (Ref 10).

Mild steels are also considered to be very weldable, and cold cracking is usually not a problem when the carbon content is less than 0.2% and the manganese content is less than 1.0%. Preheat, interpass temperature control, PWHT, or special welding procedures are usually not necessary when welding plate with thicknesses of 25 mm (1 in.) or less. The carbon content is usually higher in thicker plates in order to provide the required strength. In addition, the related HAZ cooling rate during the fusion welding of a thicker plate is higher. Consequently, when welding plate that is thicker than 25 mm (1 in.), or when the carbon and manganese contents are beyond 0.3 and 1.4%, respectively, proper caution and the use of low-hydrogen electrodes/fluxes is required to prevent hydrogen cracking (Ref 10).

A useful guideline in selecting carbon-manganese and microalloyed carbon-manganese steels with optimum weldability and toughness, as established by Dolby (Ref 4, 12), is provided below.

For carbon-manganese and microalloyed carbon-manganese steels with more than 0.1% C, use steel base materials with both a low-carbon content and a low-carbon equivalent, but high toughness properties. Select steels that are aluminum-treated to restrict the width of the coarse-grained region in the HAZ and minimize the free-nitrogen level (aluminum-nitride precipitates are relatively stable). The selected steels should be clean. The aluminum-treated or vacuum degassed steels will have lower sulfur levels. The calcium treatment for sulfide shape control will improve the mechanical properties in the through-thickness direction and reduce the lamellar tearing associated with liquidation cracking problems.

When using welding processes with high-energy input for the same base-metal carbon-manganese compositions, the addition of niobium and vanadium will lower HAZ toughness, because of the niobium and vanadium precipitations that occur during cooling and reheating.

Microalloyed steels with less than 0.1% C should have higher toughness and a reduced tendency for hydrogen cracking in the HAZ. Clean aluminum-treated steels with high toughness values should be selected for the reasons described above for carbon-manganese steels. The same precaution regarding welding processes with high-energy inputs, as mentioned above, also applies.

Low-alloy steels that have a low-carbon level should be selected. A high cleavage resistance can be obtained when the hardenability of the steels is sufficient to develop low-carbon martensite for the welding conditions used. Caution should be used in the PWHT of steels that have significant amounts of secondary precipitation-hardening alloying elements, such as vanadium and niobium. Care also should be given to the PWHT of steels that contain high amounts of residual elements such as antimony, phosphorus, arsenic, and tin.

Clean, aluminum-treated steels with high toughness values should be selected for the reasons described above for carbon-manganese steels. The same precaution regarding welding processes with high-energy inputs, as mentioned above, also applies.

Thermomechanically controlled process (TMCP) steels are recently developed steels that exhibit significantly improved strength and toughness properties and weldability. The new technology of using accelerated cooling makes it possible to achieve the same strength level as conventional controlled rolled steels at a lower carbon content (<0.06%). Instead of strengthening by increasing the carbon content, TMCP steels derive their strength and toughness from the very fine ferrite and second-phase microstructure (finely dispersed pearlite or bainite) that occur during the accelerated cooling of the manufacturing process. As a result of the reduction in carbon content and carbon equivalent, these steels significantly improve their resistance to hydrogen-induced cold cracking. Therefore, the concern with preheat, interpass temperature control, and PWHT during welding fabrication is not critical.

However, HAZ softening, especially at high heat inputs, is a concern, because the favorable microstructure of the TMCP steel is reverted during the slow cooling in the HAZ at high heat input levels. Figure 7 shows the hardness profiles in the HAZ of a TMCP steel welded using various heat inputs (Ref 13).

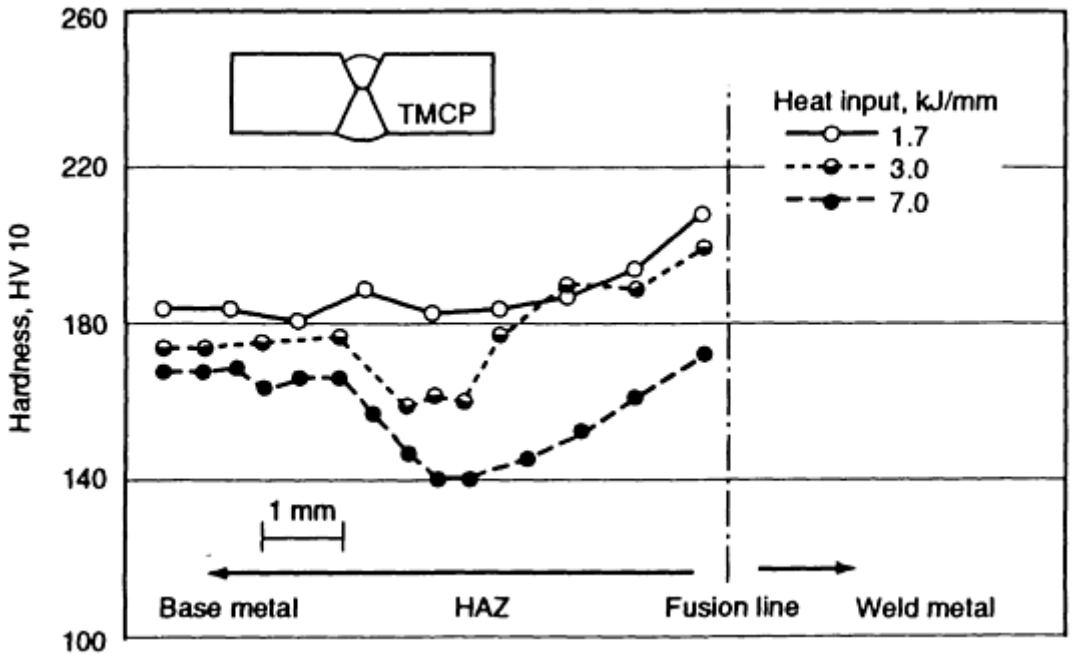

FIG. 7 VARIATION OF HARDNESS PROFILES IN HAZ OF TMCP STEEL WELDED WITH HEAT INPUT OF 1.7, 3.0, AND 7.0 KJ/MM (43, 76, AND 178 KJ/IN.). CARBON, 0.06%; SILICON, 0.14%; MANGANESE, 1.33%; PHOSPHORUS, 0.010%; SULFUR, 0.001%; COPPER, 0.31%; NICKEL, 0.31%; CHROMIUM, 0.05%; NIOBIUM, 0.15%; AND ALUMINUM, 0.034%. SOURCE: REF 13

Chromium-molybdenum steels are relatively inexpensive materials, when compared with high-alloy steels used in the power and petrochemical industries, because of their oxidation resistance, elevated-temperature creep resistance, and sulfide corrosion resistance. The chromium content provides oxidation corrosion resistance, whereas the molybdenum content increases elevated-temperature strength. The presence of finely distributed stable carbide enhances the creep resistance. Because of the alloying element content and approximate 0.15% C level, these steels are air hardenable. Most of these steels are supplied in normalized and tempered or quenched and tempered condition.

The weldability of chromium-molybdenum steels is very similar to that of quenched and tempered and hardenable low-alloy steels. The major problem in the HAZ is cracking in the hardened coarse-grained region, as well as HAZ softening between Ac_1 and Ac_3. Reheat cracking during PWHT and long-term exposure in elevated-temperature service conditions also can cause severe problems. The appropriate preheat and interpass temperature should be selected, and low-hydrogen practice should be used. The recommended practice for welding these steels is provided in ANSI/AWS D 10.8-86.

Although a PWHT is not required for chromium-molybdenum steels with lower chromium contents and thinner gages, it is often conducted immediately after welding as part of the welding procedure. The PWHT of a chromium-molybdenum weldment is also referred to as a stress-relief heat treatment. Such a heat treatment is designed to relieve the residual stresses by a creep-relaxation process and to temper the as-welded hardened microstructures to improve the fracture

toughness of the HAZ and the weld metal. Additional beneficial effects of a PWHT are to allow for more dissipation of hydrogen in the weld region and to further reduce the likelihood of hydrogen-induced cold cracking.

Although a stress-relief treatment or PWHT is often used in chromium-molybdenum steel weldments, this type of steel is susceptible to either stress-relief cracking in the HAZ during such a treatment or reheat cracking during postweld reheating processes, including short-term exposure to elevated-temperature service environments. The temperature range for the occurrence of stress-relief/reheat cracking is between 500 and 700 °C (932 and 1292 °F). Although it is not clear, the cracking mechanism is believed to be related to the strengthening of the grain interior as a result of precipitation. Cracking occurs during reheating when the relatively soft grain boundaries that are free of precipitates cannot accommodate the plastic deformation during creep relaxation. A parameter known as the P_{SR} has been developed (Ref 14) to correlate the susceptibility of chromium-molybdenum steels to reheat cracking when the steels contain $\leq$1.5% Cr, $\leq$1.0% Cu, $\leq$2.0% Mo, and $\leq$0.15% V, Nb, and Ti:

$$P_{SR} = CR + CU + 2MO + 10V + 7NB + 5TI - 2 \qquad \textbf{(EQ 5)}$$

When P_{SR} is less than zero, the material is considered sensitive to reheat cracking. However, when there is more than 2% Cr, the tendency for cracking is eliminated.

Another parameter that takes into account the tramp elements that lead to grain-boundary embrittlement and increase the tendency for reheat cracking is the metal composition factor (MCF) (Ref 15):

$$MCF = SI + 2CU + 2P + 10AS + 15SN + 20SB \qquad \textbf{(EQ 6)}$$

A greater MCF also increases the susceptibility of chromium-molybdenum steels to reheat cracking.

The common welding practices that are used to reduce the likelihood for reheat cracking can be summarized as (Ref 5):

- REDUCE THE STRESS RISERS IN WELDMENT DESIGN.
- USE WELDING PRACTICES THAT MINIMIZE RESIDUAL STRESS, SUCH AS INCREASING THE PREHEAT TEMPERATURE AND REDUCING RESTRAINT.
- WHEN APPLICABLE AND NECESSARY, REDUCE WELD-METAL STRENGTH TO ACCOMMODATE THE PLASTIC DEFORMATION IN THE WELD METAL, AND REDUCE THE STRESS CONCENTRATION IN THE COARSE-GRAINED REGION.

Quenched and tempered steels (Q&T) steels are normally furnished in heat-treated conditions that involve austenitizing and/or quenching and tempering to obtain high-strength properties. The hardenability of Q&T steels is such that the HAZ consists of microstructures of low-carbon martensite and bainite. This type of as-welded HAZ microstructure has desirable mechanical properties that are close to those of the base metal. Consequently, these materials generally do not require a PWHT or stress-relief treatment, except in certain special situations.

Unlike other hardenable low-alloy steels in which high-energy input has to be used to avoid the formation of martensite in the HAZ, the use of Q&T steels requires that welding conditions include a cooling rate in the HAZ that is rapid enough to ensure the reformation of martensite and bainite microstructures. This is necessary because a HAZ cooling rate is too slow will cause the austenitized HAZ to transform into ferrite and a mixture of bainite and martensite. When proetectoid ferrite is undergoing transformation from austenite, the untransformed austenite will become enriched in carbon and will subsequently transform into hard and brittle bainite and martensite. This mixed microstructure of ferrite, bainite, and martensite leads to embrittlement of the coarse-grained HAZ. The slower the cooling rate, the greater the extent of embrittlement in the HAZ. When welding less-hardenable or thinner material, an even faster critical cooling rate (less heat input) is required to avoid transformation of brittle mixed microstructures (Ref 10).

Another concern with welding Q&T steels is the strict maintenance of low-hydrogen welding practice in order to prevent underbead cold cracking. A preheat is one of the most effective ways of reducing the tendency for cold cracking. However, a preheat also significantly reduces the cooling rate in the HAZ. Consequently, it should be applied in such a manner that a satisfactorily fast cooling rate can be achieved in the HAZ.

When welding Q&T steels with a higher strength level, the tendency for hydrogen cracking to occur in the weld metal increases. Consequently, the allowable moisture content in the electrode coating and flux, as well as the handling of these materials, become much more critical. For Q&T steels with a yield strength level under 483 MPa (70 ksi), a 0.4 wt% moisture content is the allowable limit in covered electrode, whereas for steels with a strength level above 690 MPa (100 ksi), the limit is 0.1 wt% (Ref 10). The use of a temper bead technique, as shown in Fig. 8, also can help avoid undesirable regions of high hardness and low toughness in the HAZ.

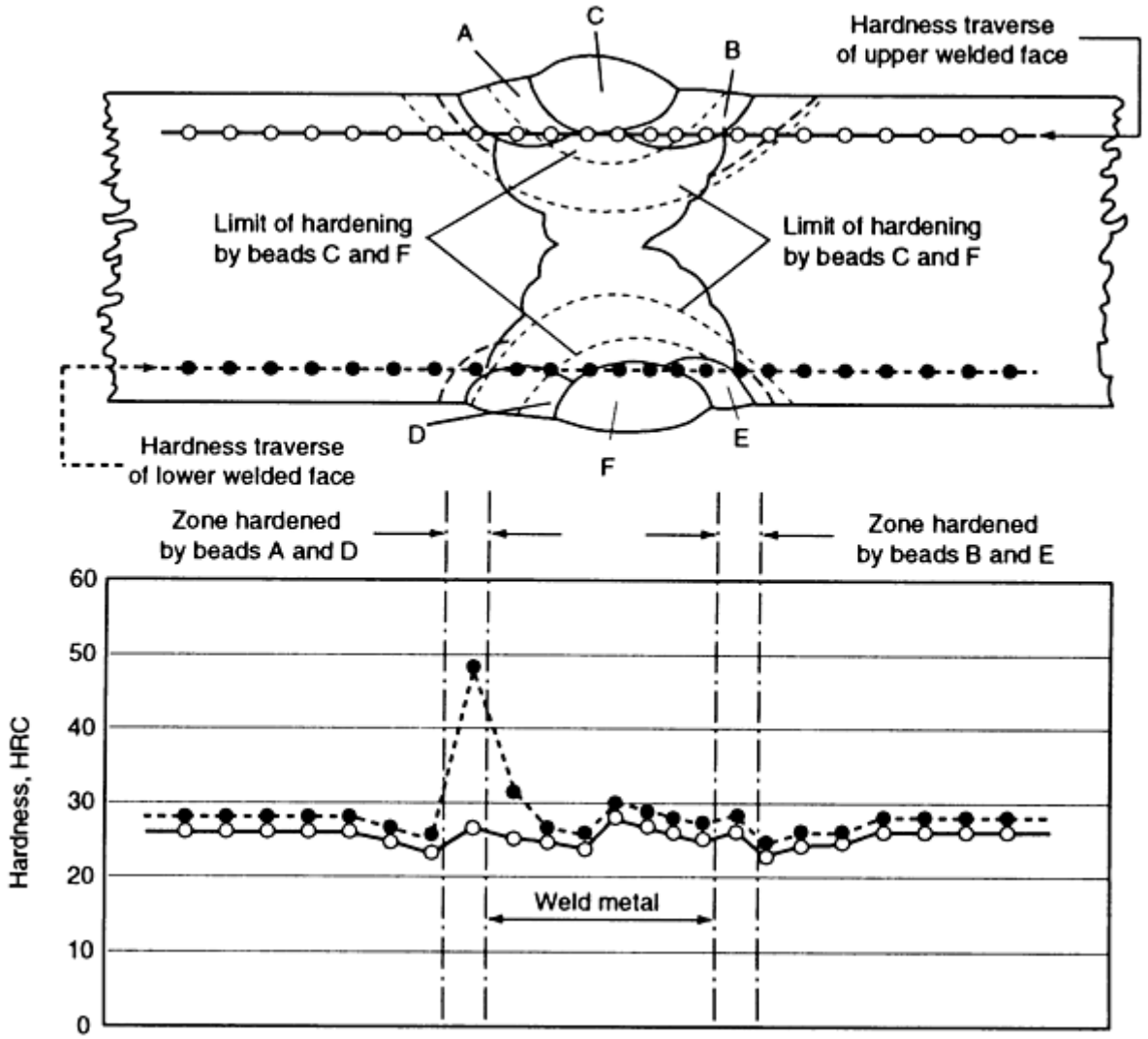

FIG. 8 TEMPERING BEAD TECHNIQUE FOR MULTIPASS WELDING OF A BUTT JOINT IN A Q&T ALLOY STEEL. HARDNESS VALUES FOUND BY UPPER AND LOWER TRAVERSES. DISTRIBUTION OF HARDNESS IS ALMOST IDENTICAL, EXCEPT FOR UNTEMPERED ZONE OF BEAD D, AT LEFT. SOURCE: REF 16

Multipass welding is a good practice when welding Q&T steels. In addition to the refining and tempering effects on the weld metal of the previous weld pass, the smaller heat input of multipass welding, compared to that of single-pass welding, can help achieve a fast cooling rate. When hydrogen cracking in weld metal is a concern, it is recommended that thin-layer multipass welding be used, along with soaking at the interpass temperature for a predetermined time before depositing the subsequent pass (Ref 17). Although this practice helps dissipate the hydrogen in the weld metal in each weld pass, productivity is decreased.

In Q&T steels, there is a softening region in the HAZ that is caused by a HAZ thermal cycle with a peak temperature between A_{c1} and A_{c3} (intercritical region). At temperatures below A_{c3} during heating, the carbides do not completely dissolve in the austenite. Therefore, the carbon level in the austenite is a lower concentration. During cooling, the unsaturated austenite transforms at high temperature and results in a microstructure with lower strength.

References cited in this section

3. O. GRONG AND O.M. AKSELSEN, HAZ TOUGHNESS OF MICROALLOYED STEELS FOR OFFSHORE, *MET. CONSTR.,* SEPT 1986, P 557
4. K.E. EASTERLIN, *INTRODUCTION TO THE PHYSICAL METALLURGY OF WELDING,* BUTTERWORTHS, 1983
5. C.F. CHOU, *THEORY AND TECHNOLOGY OF METAL WELDING,* VOL 2, MECHANICAL INDUSTRY PUBLISHER, 1981 (IN CHINESE)
9. O.M. AKSELSEN, "MICROSTRUCTURE AND TOUGHNESS IN HAZ OF BORON CONTAINING STEELS," REPORT STF A84065, THE WELDING CENTER (SINTEF), TRONDHEIM, NORWAY, 1984
10. W.H. KEARNS, *WELDING HANDBOOK,* VOL 4, AWS, 1984
11. M. GRAY, WELDABILITY OF NIOBIUM CONTAINING HIGH STRENGTH LOW ALLOY STEEL, *WELD. RES. COUNC. BULL.,* NO. 213, FEB 1976
12. R.E. DOLBY, "FACTORS CONTROLLING WELD TOUGHNESS--THE PRESENT POSITION," REPORT NO. 14, THE WELDING INSTITUTE, 1976
13. H.J. KIM AND J.G. YOUN, CHARACTERISTICS OF TMCP STEEL AND ITS SOFTENING, *WELDING METALLURGY OF STRUCTURAL STEEL,* J.Y. KOO, ED., AIME, 1987
14. Y. ITO AND M. NAKANISH, STUDY ON STRESS RELIEF CRACKING IN WELDING LOW ALLOY STEELS, *SUMITOMO SEARCH,* NO. 7, MAY 1972, P 27-36
15. C.J. MCMAHON, JR., R.J. DOBBS, AND D.H. GENTUER, STRESS RELIEF CRACKING IN MN, MO, NI, AND MN-MO-NI-CR PRESSURE VESSEL STEELS, *MATER. SCI. ENG.,* VOL 37, 1979, P 179-186
16. G.E. LINERT, *WELDING METALLURGY,* AWS
17. D.N. SHACKLETON, *WELDING HY-100 AND HY-130 STEELS,* THE WELDING INSTITUTE, 1973

Influence of Welding on Steel Weldment Properties

C.C. Chen and Abe Pollack, Microalloying International, Inc.

Weldment Considerations

Corrosion. Carbon and low-alloy steels used for structural applications are not commonly utilized in severe corrosion environments. However, they are used in moderate corrosive service conditions, such as those in oil refinery facilities and sour gas/oil pipelines. The presence of a weld often leads to a reduction in corrosion resistance because of these circumstances (Ref 6):

- COMPOSITIONAL VARIATIONS IN THE BASE METAL, HAZ, AND WELD METAL THAT RESULT IN A CONDITION FAVORING GALVANIC CORROSION
- PRESENCE OF WELDING RESIDUAL STRESSES THAT LEAD TO STRESS-CORROSION CRACKING
- PRESENCE OF WELD DISCONTINUITIES, SUCH AS SURFACE FLAWS, WHICH ACT AS PREFERENTIAL SITES FOR LOCAL CORROSION ATTACK

In a corrosive environment, the prevention of hydrogen-induced cracking (HIC) and sulfide stress-corrosion cracking (SCC) is of great importance.

Hydrogen-induced cracking, which has been observed in both high- and low-strength steels, even under nonstressed conditions, occurs primarily in the low-strength steels that are exposed to a hydrogen-containing environment. Because of

its rapid cooling and solidification, weld metal forms a structure of rendrites and has oxide inclusions dispersed in the form of fine globules. It has been confirmed that weld metals, even when used without a filler metal of special chemistry, do not develop HIC up to a maximum hardness of 280 HV. In comparison, HIC has been observed primarily in the base metal and HAZ (Ref 18, 19).

Stress-corrosion cracking is defined as a cracking phenomenon that occurs under sulfide-corrosive conditions when steel materials are subjected to stress. Steels that are to be used in environments containing hydrogen sulfide can be selected per Ref 20. According to this standard, a value of 22 HRC (248 Hv) is recommended as the hardness limit for steel line pipe used in sour-gas service.

In the case of a weldment, the HAZ generally becomes harder than the base metal, and, consequently, is more susceptible to SCC. In addition to the more susceptible microstructure, other factors that contribute adversely to SCC are weld residual stresses and the presence of the entrant angle of the weld cap as a stress raiser in the welded region.

When the welded joints are quenched and tempered or normalized, the HAZ disappears and the tendency for the previous HAZ to develop SCC is altered (Ref 18, 19). The SCC susceptibility is greater in the as-welded condition than in the Q&T (PWHT) condition.

Fatigue Strength of Weld Joints. Fatigue cracks in a welded structure under cyclic loading are often observed to develop at weld toe regions. This is because the weld toes are regions of stress concentration. The toes are the point at which the base metal and weld metal meet and where changes are greatest in both sections. More importantly, slag intrusions that result from a welding operation are often present at the weld toe regions.

Various methods have been utilized to improve the fatigue strength of welded structures by reducing the stress concentration in the regions of weld toes and weld reinforcements. These methods are (Ref 21, 22):

- REMOVING THE WELD REINFORCEMENT ON BOTH SIDES OF A BUTT JOINT BY MACHINING THE WELD TO THE LEVEL OF THE BASE METAL
- INCREASING THE RADIUS AND ENTRANT ANGLE OF WELD TOES BY MECHANICALLY GRINDING THE INTERSECTING REGIONS BETWEEN THE WELD AND THE BASE METAL
- CHANGING THE STATE OF THE SURFACE-WELD RESIDUAL STRESS BY THE MECHANICAL COLD WORKING OF THE WELD SURFACE AND THE BASE METAL AT THE WELD TOE REGIONS
- COATING AND/OR PAINTING THE WELDS AND BASE METAL TO PREVENT CORROSION IN THE REGION OF STRESS CONCENTRATION
- INCREASING THE TOE RADIUS AND WELD ENTRANT ANGLE BY ADDING A WELD BEAD ON BOTH SIDES OF THE REINFORCEMENTS USING A FILLER METAL WITH HIGH FLUIDITY
- USING WELDING CONDITIONS THAT WILL RESULT IN A GREATER WELD TOE RADIUS AND ENTRANT ANGLE
- REMELTING THE SURFACE IN THE WELD TOE REGIONS FOR FLATTENING AND SMOOTHING WELD PROFILES USING THE GAS-TUNGSTEN ARC WELDING PROCESS

References cited in this section

6. R.D. STOUT AND W.D. DOTY, *WELDABILITY OF STEELS,* 3RD ED., S. EPSTEIN AND R.E. SOMERS, ED., WELDING RESEARCH COUNCIL, NEW YORK, 1978
18. T. TAIRA *ET AL.*, "SULFIDE CORROSION CRACKING OF GIRTH-WELDED JOINT OF LINE PIPE FOR SOUR GAS SERVICE," CORROSION '79, T-1F SYMPOSIUM (ATLANTA, GA), NACE, MARCH 1979
19. M. ITOH *ET AL.*, "HYDROGEN SULFIDE CORROSION CRACKING OF LARGE DIAMETER LINE PIPE UP TO GRADE X-65," MIDDLE EAST CORROSION CONFERENCE (BAHRAIN), NACE, APRIL 1979
20. "SULFIDE STRESS CRACKING RESISTANT METALLIC MATERIALS FOR OIL FIELD

EQUIPMENT," STANDARD MATERIAL REQUIREMENTS DOCUMENT MR0175-91, NACE
21. Z. ZACZEK, IMPROVEMENT IN THE FATIGUE STRENGTH OF BUTT WELDED JOINTS BY TIG REMELTING OF WELDING REINFORCEMENTS, *MET. CONSTR.*, JULY 1986
22. G.S. BOOTH, IMPROVING THE FATIGUE STRENGTH OF WELDED JOINT BY GRINDING--TECHNIQUES AND BENEFITS, *MET. CONSTR.*, JULY 1986

Influence of Welding on Steel Weldment Properties

C.C. Chen and Abe Pollack, Microalloying International, Inc.

Effect of Welding Procedure on Steel-Weldment Properties

The American Welding Society defines a welding procedure as the detailed methods and practices that include all joint welding procedures involved in the production of a weldment (Ref 23). In a comprehensive review of the relationship between procedures and weldment properties, the conclusions described below were made (Ref 23).

First, for any welding process/steel combination, welding procedures have a predominant role, along with the electrode (if a filler metal is used), in determining the quality and mechanical properties of the weldment. However, these two variables (welding procedures and mechanical properties) do not have a direct cause-effect relationship.

Second, the mechanical properties of any metal are attributable only to its soundness, microstructure, and chemical composition, and to whether or not it is base plate, weld metal, vapor-deposited metal, electrodeposited metal, or any other type. The response of a metal to mechanical forces depends on its current state and not on the manner in which this state was created.

Third, metallurgical research has established relationships between mechanical properties and microstructure, such as the inverse relationship between grain size and strength, the difference in strength between pearlite and martensite, the embrittling effect of grain-boundary films, the deleterious effect of inclusions, and others. Conversely, there is no direct relationship between the current setting of a welding machine and the final properties of the weldment. Rather, the true cause and effect relationship is that:

- INCREASED CURRENT INTRODUCES MORE HEAT INTO THE ALLOY
- INCREASED HEAT AFFECTS THE STRUCTURE OF BOTH THE WELD METAL AND THE HAZ IN A PARTICULAR MANNER, DEPENDING ON THE ALLOY CHEMISTRY, PHASES THAT ARE PRESENT, AND OTHER FACTORS
- DIFFERENCES IN STRUCTURE PRODUCE DIFFERENT MECHANICAL PROPERTIES

Described below are the specific welding procedure factors that affect weldment properties.

Preheat Temperature

Preheating is the application of heat to the base metal immediately before welding, brazing, soldering, or cutting (Ref 24). The preheat temperature depends on many factors, such as the composition and mass of the base metal, the ambient temperature, and the welding procedure.

Preheating is used to:

- REDUCE SHRINKAGE STRESSES IN THE WELD AND ADJACENT BASE METAL, WHICH IS ESPECIALLY IMPORTANT WITH HIGHLY RESTRAINED JOINTS
- PROVIDE A SLOWER RATE OF COOLING THROUGH THE CRITICAL TEMPERATURE RANGE (APPROXIMATELY 879 TO 720 °C, OR 1600 TO 1330 °F), WHICH PREVENTS EXCESSIVE HARDENING AND LOWERS THE DUCTILITY OF BOTH THE WELD AND HEAT-

AFFECTED AREA OF THE BASE PLATE

- PROVIDE A SLOWER RATE OF COOLING DOWN TO 205 °C (400 °F), ALLOWING MORE TIME FOR ANY HYDROGEN THAT IS PRESENT TO DIFFUSE AWAY FROM THE WELD AND ADJACENT PLATE IN ORDER TO AVOID UNDERBEAD CRACKING

Gas torches, gas burners, heat-treating furnaces, electric-resistance heaters, low-frequency induction heating, and temporary furnaces are some of the preheating methods that are used. The selection of the method depends on several factors, such as the preheat temperature, the length of preheating time, the size and shape of the parts, and whether it is a one-of-a-kind or a continuous production type of operation.

For critical applications, the preheat temperature must be precisely controlled. In these cases, controllable heating systems are used, and thermocouples are attached directly to the part being heated. The thermocouple measures the exact temperature of the part and provides a signal to a controller, which regulates the fuel or electrical power required for heating. By accurately regulating the fuel or power, the temperature of the part being heated can be held to close limits. Most code work requires precise heat-temperature control. Preheat and interpass temperature requirements are described in the article "Welding of Carbon Steels" in this Volume and in ANSI/AWS D1.1-92.

The effect of preheat is illustrated by the data in Table 1. The analysis indicates that the extent to which the ductility and fracture-transition temperature are affected depends on the chemical composition of the steel. Changes in preheat temperature for the steel with 0.24% C were effective only above 120 °C (250 °F), whereas for the steel with 0.18% C, the changes were effective over the entire range from -12 to 260 °C (10 to 500 °F).

TABLE 1 EFFECT OF PREHEAT AND STRESS-RELIEF TREATMENT ON TRANSITION TEMPERATURE OF WELDED STEELS

CONDITION OF PLATE	19 MM ($\frac{3}{4}$ IN.) 0.18% C, SEMIKILLED STEEL				19 MM ($\frac{3}{4}$ IN.) 0.24% C, SEMIKILLED STEEL			
	DUCTILITY-TRANSITION TEMPERATURE		FRACTURE-TRANSITION TEMPERATURE		DUCTILITY-TRANSITION TEMPERATURE		FRACTURE-TRANSITION TEMPERATURE	
	°C	°F	°C	°F	°C	°F	°C	°F
AS-ROLLED PLATE	-79	-110	-1	30	-40	-40	66	150
WELDED AT 5 °C (10 °F)	-8	18	10	50	14	58	60	140
WELDED AT 21 °C (70 °F)	-18	0	-9	15	17	62	68	155
WELDED AT 65 °C (150 °F)	-42	-44	-9	15	19	67	66	150
WELDED AT 120 °C (250 °F)	-57	-70	-18	0	18	65	54	130
WELDED AT 250 °C (400 °F)	-36	-32	-18	0	-1	30	49	120
WELDED AT 260 °C (500 °F)	-50	-58	-46	-50	-18	0	82	180
WELDED AT 21 °C (70 °F) AND STRESS RELIEVED AT 620 °C (1150 °F)	-51	-60	-18	0	-18	0	60	140
WELDED AT 38 °C (100 °F) AND STRESS RELIEVED AT 620 °C (1150 °F)	-58	-73	-7	+20	. . .	. . .	. . .	. . .

Note: Ductility-transition temperature selected at 1% lateral contraction; fracture-transition temperature selected at 50% shear.

Source: Ref 6

Interpass Temperature

The interpass temperature, which is involved in multipass welds, is represented by the minimum and maximum temperatures of the deposited weld metal and adjacent base metal before the next pass is started.

Usually, a steel that requires preheating to a specified temperature also must be kept at this temperature between weld passes. With many weldments, the heat input during welding is adequate to maintain the interpass temperature. On a massive weldment, it is not likely that the heat input of the welding process will be sufficient to maintain the required interpass temperature. If this is the case, then torch heating between passes may be required.

Once an assembly has been preheated and the welding begun, it is desirable to finish welding as soon as possible, in order to avoid the need for interpass heating.

Because the purpose of preheating is to reduce the cooling rate, it logically follows that the same slow cooling should be accorded all passes. This can only be accomplished by maintaining an interpass temperature that is at least equal to the preheat temperature. If this is not done, then each individual bead will be subjected to the same high quench rate as the first bead of a nonpreheated assembly.

The required minimum temperatures, based on specific steel, welding process, and plate thickness, should be heeded. When heat buildup becomes excessive, the weldment must be allowed to cool, but not below the minimum interpass temperature. The temperature of the welding area must be maintained within minimum and maximum interpass temperatures.

Postweld Heat Treatment

A PWHT is generally considered necessary for welds in thicker-section steels, in order to reduce the high as-welded residual stress levels and improve the toughness and defect tolerance of the joint. Many fabrication codes offer guidance on the duration and temperature of the PWHT, although some discrepancies between various codes exist. In assessing the time and temperature required to provide a suitable PWHT, it is necessary to know how such parameters will respond to various heat-treatment schedules.

In all heat treatments, with the possible exception of fusion, the heating rate and time can be specified. The maximum temperature is related to the composition of the steel, the holding time (at the maximum temperature) is related to the material thickness, and the cooling rate is related to the particular treatment and to the code. The rate of heating usually ranges from 149 to 177 °C (300 to 350 °F) per hour. The holding temperature is usually 2.4 min/mm (1 h/in.) of maximum thickness in order to provide uniform heating throughout. The cooling rate also ranges from 149 to 177 °C (300 to 350 °F) per hour, down to a specific temperature. In some cases, the cooling rate can be increased when the part has cooled to a temperature from 260 to 316 °C (500 to 600 °F). These rates of heating, holding, and cooling are usually part of the specification and must be followed explicitly.

Example 1: Effects of PWHT on the HAZ Properties of Welds in a Carbon-Manganese Grade Steel.

An investigation (Ref 25) of the effects of PWHT has reported the variation in HAZ properties (strength, hardness, and toughness) with different PWHT parameters. The tests were carried out on a 50 mm (2 in.) BS1501-225-490B-LT50 steel manufactured by the British Steel Corporation. The steel was a carbon-manganese grade that had been silicon killed and treated with aluminum and niobium. This grade was chosen because it is increasingly being used in pressure-vessel applications and is also similar to BS4360 grade 50E, a steel that is used in many off-shore fabrications and other structures. The submerged arc welding process was used with a heat input of approximately 3.4 kJ/mm (89 kJ/in.) of the fill passes. In addition, the effects of multiple PWHT cycles, which are often encountered in pressure-vessel fabrication or in cases where repairs have been made, have been investigated in the same manner.

Longitudinal tensile tests of the HAZ were conducted, and the data are plotted in Fig. 9(a). No significant effect that was due to multiple stress-relief cycles was noted in the HAZ regions. The values observed exceeded the plate minimum requirements. Adequate ductility and elongation values were observed at 600 °C (1112 °F). Figure 9(b) indicates no significant effect of PWHT time on the HAZ yield-stress tensile strength or ductility at this temperature. The data plotted in Fig. 9(c) indicated that only a minor reduction in yield stress and tensile strength were observed with increasing PWHT temperature. No significant effects on ductility were observed.

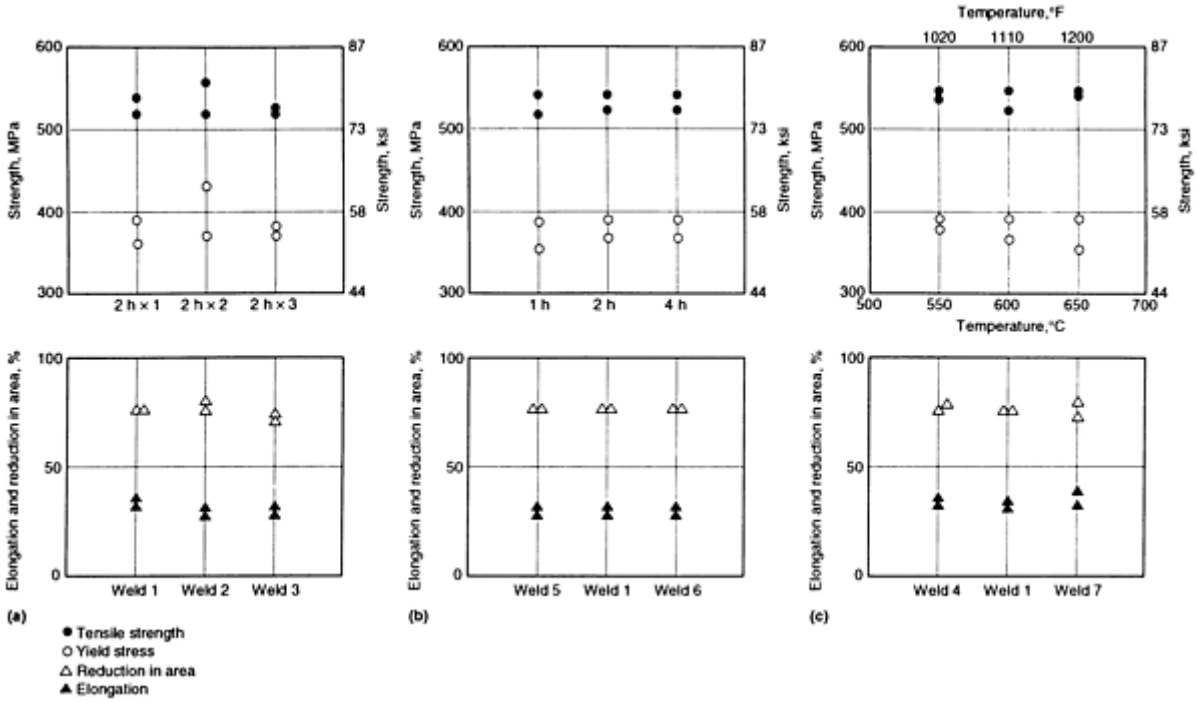

FIG. 9 EFFECT OF PWHT ON THE HAZ TENSILE PROPERTIES OF A CARBON-MANGANESE GRADE STEEL. (A) EFFECT OF MULTIPLE PWHT AT 600 °C (1112 °F), (B) EFFECT OF PWHT TIME. (C) EFFECT OF PWHT TEMPERATURE. SOURCE: REF 25

Charpy Tests. Five testing temperatures were chosen and three specimens were tested at each of the temperatures, which were -80 °C (-112 °F), -60 °C (-76 °F), -40 °C (-40 °F), -20 °C (-4 °F), and 0 °C (32 °F). For the welds, one specimen was taken from the first side of the HAZ, one from the second side of the HAZ, and one from the HAZ at the plate midthickness, which was associated with second-side welds. The data in Fig. 10 show that multiple PWHT cycles had only a marginal effect, in that a slight increase in the number of low values at low temperatures was observed at two and three cycles, particularly from specimens machined from the plate midthickness.

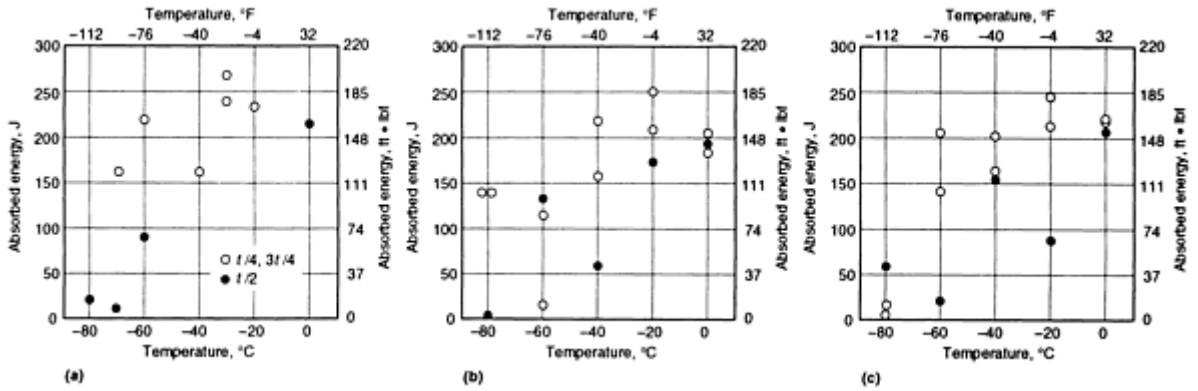

FIG. 10 EFFECT OF MULTIPLE PWHT CYCLES ON THE HAZ CHARPY V-NOTCH PROPERTIES OF A CARBON-MANGANESE GRADE STEEL. (A) WELD 1; PWHT, 1 × 2H. (B) WELD 2; PWHT, 2 × 2 H. (C) WELD 3; PWHT, 3 × 2 H. SOURCE:REF 25

Although extended PWHT has not led to an appreciable variation in HAZ Charpy properties from the $(\frac{1}{4})t$ and $(\frac{3}{4})t$ locations, a pronounced drop in absorbed energy levels has been observed after 4 h in specimens machined from the plate

midthickness. This is clearly shown in Fig. 11, from which the toughness at the plate midthickness appears to fall off with time, although this does not happen at the $(\frac{1}{4})t$ locations.

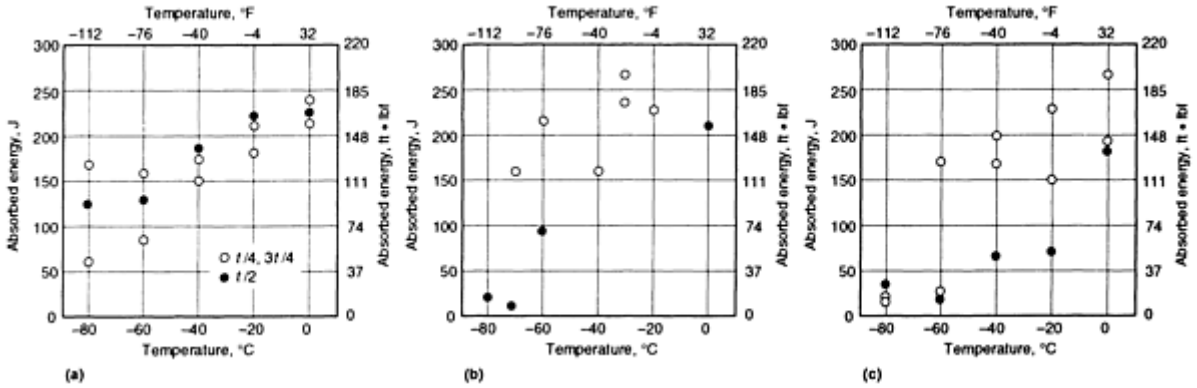

FIG. 11 EFFECT OF PWHT TIME AT 600 °C (1112 °F) ON THE HAZ CHARPY V-NOTCH PROPERTIES OF A CARBON-MANGANESE GRADE STEEL. (A) WELD 5; PWHT TIME, 1 H. (B) WELD 1; PWHT TIME, 2 H. (C) WELD 6; PWHT TIME, 4 H. SOURCE:REF 25

The effects of increasing the PWHT temperature are shown in Fig. 12, from which it is clear that no pronounced effect of temperature on toughness exists, except at the plate midthickness. Here, there seems to be a trend of increasing transition temperature with increasing PWHT temperature.

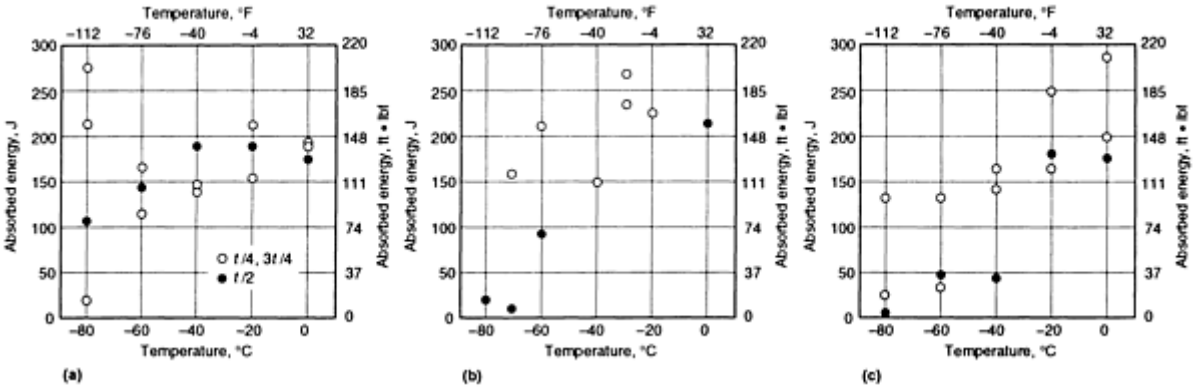

FIG. 12 EFFECT OF PWHT TEMPERATURE ON THE HAZ CHARPY V-NOTCH PROPERTIES OF A CARBON-MANGANESE GRADE STEEL. (A) WELD 4, 550 °C (1020 °F). (B) WELD 1, 600 °C (1110 °F). (C) WELD 7, 650 °C (1200 °F). SOURCE:REF 25

Hardness Survey. Hardness traverses were conducted in the macrosection from each weld after PWHT, reaching from the parent plate that was unaffected by the welding processes into the weld metal. Similar traverses were made on welds 1 and 2 in the as-welded condition. On each macrosection, three traverses were made at these locations: 3 mm (0.12 in.) below the surface of the first side; at the plate midthickness; and 3 mm (0.12 in.) below the surface of the second side. In all cases, a 98 N (10 kgf) load was used on a Vickers hardness machine.

The as-welded hardness data from welds 1 and 2 are shown in Fig. 13. Plate values were approximately 170 to 180 HV 10, and weld-metal values were 200 to 220 HV 10. Peak HAZ hardness was below 240 HV 10.

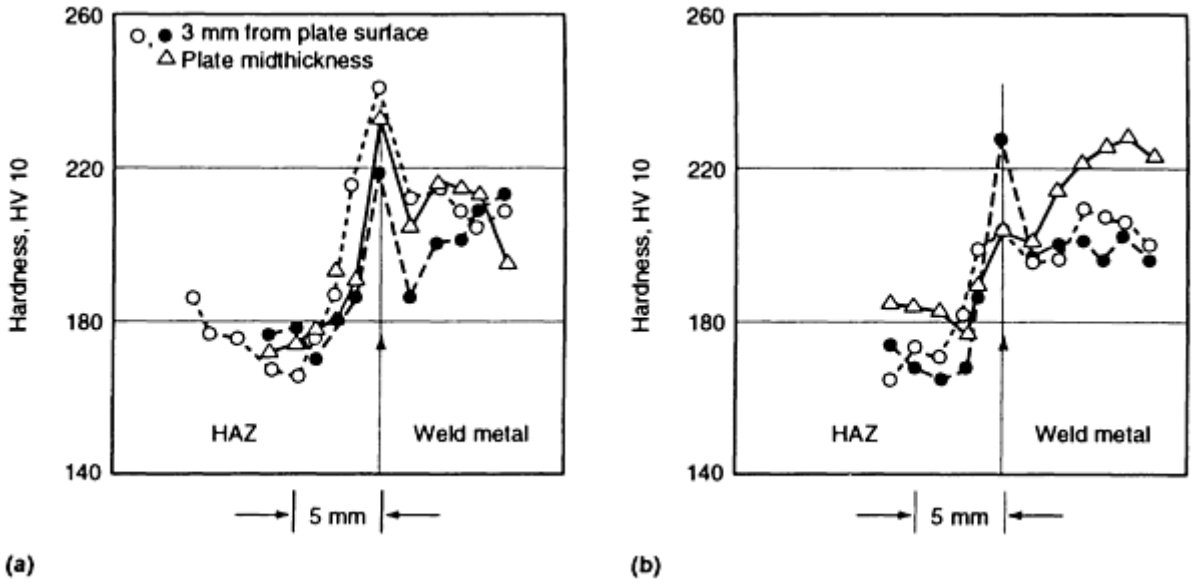

FIG. 13 AS-WELDED HARDNESS DATA FOR TWO WELDS IN A CARBON-MANGANESE GRADE STEEL. (A) WELD 1. (B) WELD 2. SOURCE: REF 25

The effect of multiple PWHT cycles is shown in Fig. 14. Multiple PWHTs had little influence on HAZ or plate hardness, where peak HAZ values of less than 240 HV were obtained and plate values were approximately 140 to 160 HV 10. In all welds, the hardness at the plate midthickness was slightly higher than it was at the surfaces, because of the presence of a segregated band, as is frequently observed in continuously cast steel.

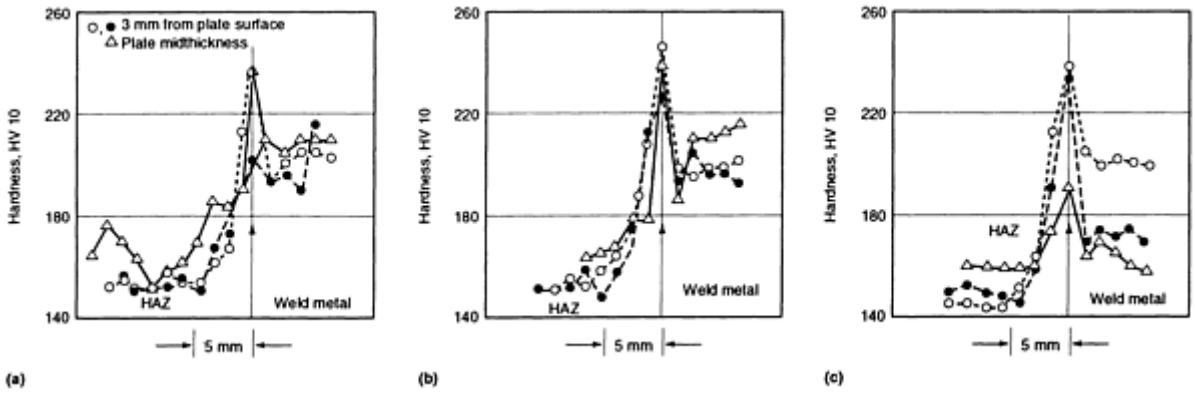

FIG. 14 EFFECT OF MULTIPLE PWHT CYCLES ON THE HARDNESS OF WELDS IN A CARBON-MANGANESE GRADE STEEL. (A) WELD 1; PWHT, 1 × 2 H. (B) WELD 2; PWHT, 2 × 2 H. (C) WELD 3; PWHT, 3 × 2 H. SOURCE: REF 25

Weld-metal hardness shows a more noticeable effect when exposed to multiple stress-relief cycles. Welds 1 and 2 had a fairly uniform hardness of approximately 200 HV, but after the third PWHT cycle, the weld-metal hardness levels dropped to 160 to 220 HV, with the lowest values appearing at the weld midthickness.

The values in Fig. 15 show only a slight reduction in HAZ hardness as PWHT time increases. Plate values are unaffected. The weld metal behaves in a nonsystematic manner. Values between approximately 190 and 210 HV 10 were observed after 1 h, increasing to approximately 200 to 220 HV 10 after 2 h, and decreasing to approximately 160 to 195 HV 10 after 4 h.

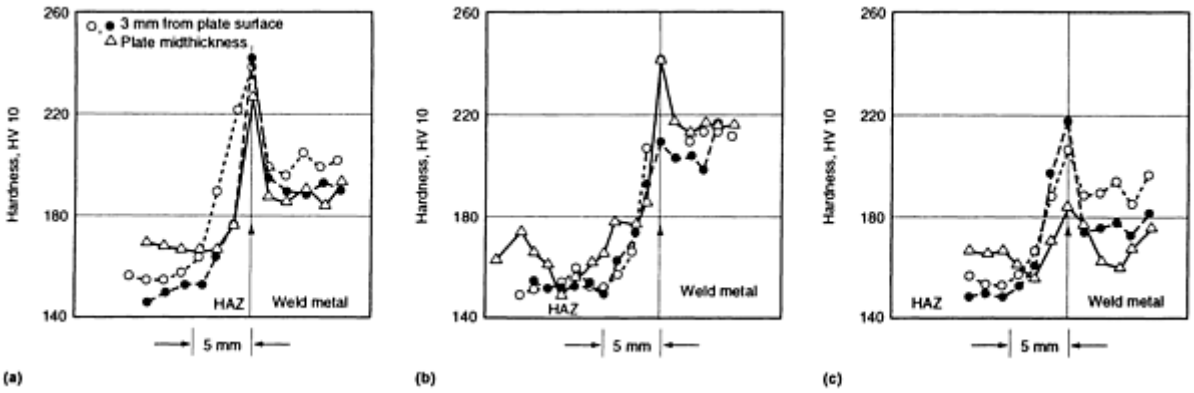

FIG. 15 EFFECT OF PWHT TIME AT 600 °C (1112 °F) ON THE HARDNESS OF WELDS IN A CARBON-MANGANESE GRADE STEEL. (A)WELD 5, 1 H. (B)WELD 1, 2 H. (C) WELD 6, 4 H. SOURCE: REF 25

Figure 16 shows that plate and HAZ hardness levels appear to be fairly insensitive to PWHT temperature. No obvious trends in the variation of hardness with temperature are apparent. However, a slight drop in plate hardness has been observed. Weld-metal hardness appears to decline after a 650 °C (1202 °F) PWHT, where values of approximately 180 to 190 HV 10 have been recorded. This compared with values of approximately 190 to 210 HV 10, which were recorded at 550 and 600 °C (1022 and 1112 °F).

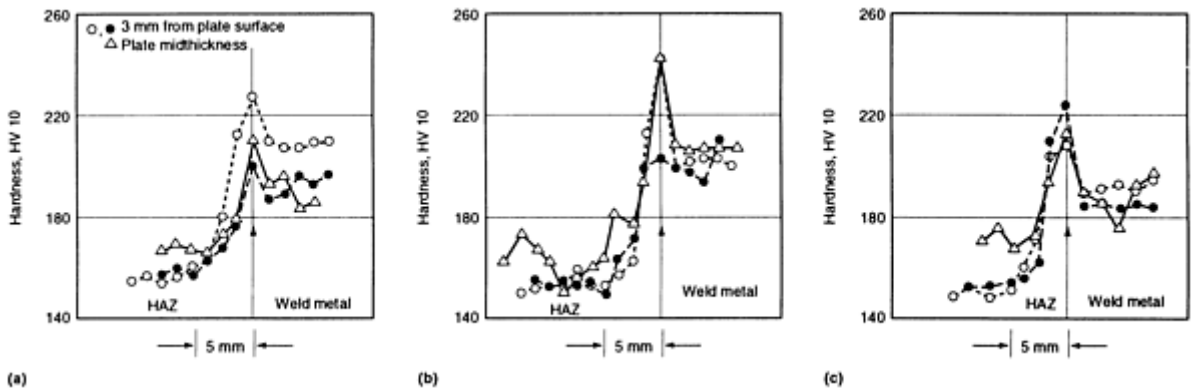

FIG. 16 EFFECT OF PWHT TEMPERATURE ON THE HARDNESS OF WELDS IN A CARBON-MANGANESE GRADE STEEL. (A) WELD 4, 550 °C (1020 °F). (B) WELD 1, 600 °C (1110 °F). (C) WELD 7, 650 °C (1200 °F). SOURCE: REF 25

It was concluded that increasing the PWHT time at 600 °C (1112 °F), whether by prolonging single treatments or by using multiple treatments, had little effect on the mechanized properties. In addition, increasing the PWHT temperature from 550 to 650 °C (1022 to 1202 °F) resulted in no significant drop in HAZ strength or hardness. However, evidence for a drop in the HAZ Charpy V notch-toughness at the plate midthickness with increasing temperature was found.

Heat Input

The welding process and procedure both influence the energy input used to made a weld. The greater the energy input, the slower the cooling rate. Heat input is a function of welding current, arc voltage, and travel speed. To increase the heat input, either the welding current should be increased or the travel speed should be reduced. Welding current is related to the process and the electrode size. Heat input is calculated by using the following formula:

$$HE = EI\frac{60}{S} \qquad \textbf{(EQ 7)}$$

where *HE* is the energy input in joules per linear measure of weld, *E* is the arc voltage in volts, *I* is the welding current in amperes, and *S* is the travel speed (linear measure) per minute.

By increasing the amperage or voltage, heat input increases, but by increasing the travel speed, heat input decreases. The voltage has a minor effect, because it varies only slightly, when compared with the other factors. The general higher input reduces the cooling rate. This must be used with caution, because with Q&T steels, too high a heat input will tend to soften the HAZ, and its strength level will be reduced.

In relatively low hardenability steels, it is possible to produce an unhardened HAZ by increasing the heat input. In higher-hardenability steels, the tendency toward cracking and the maximum hardness will be reduced by a slower cooling rate.

There are limits to the amount of heat input that can be used. In this case, preheating is used in order to reduce cooling rates.

Effect of Welding Process. Each welding process has a different thermal cycle. Figure 17 shows the time-temperature relationship of base metal taken immediately adjacent to welds made by two welding processes (Ref 26). The rate of heat rise, the maximum temperature, the time at high temperature, and the rate at which the metal cools are quite different for the shielded metal arc and the electroslag welding processes. Those processes with the highest concentration of heat will cause the temperature to both rise and fall much more rapidly. The curve shown for the shielded metal arc weld rises almost instantaneously, and the cooling rate of the base metal is a very steep slope, which indicates quick cooling. The curve for electroslag welding rises more slowly, is held at a high temperature for a fairly long time, and then decreases slowly. The temperature changes that occur during an arc welding operation are much quicker and more abrupt than for most metallurgical processes. The metallurgical reactions from the heat of welding do not follow the normal heat-treating relationships. The temperature changes with electroslag welding are more similar to those encountered in foundry metallurgy.

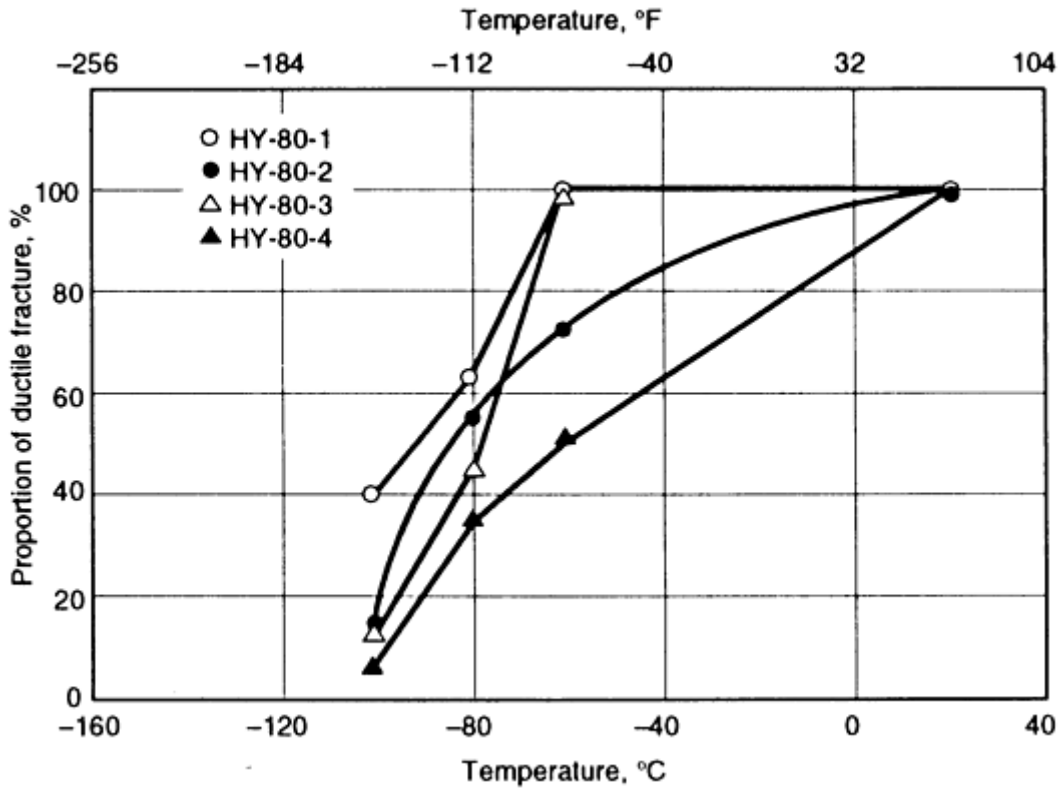

FIG. 17 PERCENT DUCTILE FRACTURE VERSUS TEST TEMPERATURE FOR THE SUBMERGED ARC BEND-IN-

Example 2: Effect of Heat Input on Properties of HY-80 and HSLA-80 Weld Metals.

Because the low-alloy Q&T steels are already in a heat-treated condition, any heating beyond a certain temperature will destroy the properties developed in them by the manufacturing process. A study (Ref 27) was conducted to assess the influence of composition and energy input on the structure and properties of single-pass submerged arc bead-in-groove welds produced on HY-80 and HSLA-80 steels.

Table 2 and 3 gives the chemical composition of the high-strength steels and the welding electrodes used in the study; Table 3 lists the welding conditions. The single-pass welds were produced at energy input levels of 1, 2, 3, and 4 kJ/mm (25, 51, 76, and 101 kJ/in.). The size of the machined grooves was increased to accommodate the increase in energy input, while maintaining the same level of dilution (50%) from the base plate.

TABLE 2 CHEMICAL COMPOSITIONS OF HIGH-STRENGTH STEELS AND WELDING ELECTRODES FROM EXAMPLE 2

MATERIAL	COMPOSITION, WT%									
	C	Mn	Si	S	P	Ni	Cr	Mo	Cu	Nb
HY-80	0.17	0.30	0.19	0.014	0.007	2.59	1.53	0.42	0.03	0.005
HSLA-80	0.06	0.50	0.27	0.004	0.007	0.92	0.66	0.25	1.02	0.044
100S-1	0.07	1.57	0.52	0.004	0.004	1.86	0.03	0.28	0.06	
HY-80(A)	0.12-0.18	0.10-0.40	0.15-0.35	0.002-0.020	0.020	2.00-3.25	1.00-1.80	0.20-0.60	0.25	
HSLA-80(B)	0.06	0.40-0.70	0.40	0.006	0.020	0.70-1.00	0.60-0.90	0.15-0.25	1.00-1.30	0.02-0.06
100S-1(C)	0.08	1.25-1.80	0.20-0.55	0.01	0.01	1.40-2.10	0.30	0.25-0.55	0.30	

Source: Ref 27

(A) MILITARY SPECIFICATION MLL-S-16216J.

(B) MILITARY SPECIFICATION MIL-S-24645A.

(C) MILITARY SPECIFICATIONS MIL-E-23765/2C.

TABLE 3 WELDING CONDITIONS FOR THE SUBMERGED ARC BEAD-IN-GROOVE WELDS FROM EXAMPLE 2

ENERGY INPUT		CURRENT, A	TRAVEL SPEED	
kj/mm	kj/in.		mm/s	in./s
1	25	400	12.5	0.50
2	50	450	7.8	0.31
3	75	500	5.9	0.24
4	100	570	5.1	0.20

Note: Voltage, 35 V; electrode extension, 35 mm; and preheat temperature, 93 °C (199 °F).

Source: Ref 27

Effect on HY-80 Tensile Properties. The weld-metal tensile results noted in Table 4 exhibited yield strengths that were greater than the targeted level of 56 MPa (81.9 ksi) with HY-80-1 weld deposited at 1 kJ/mm (25 k J/in.), which displayed very high yield strength and lower ductility. Upon increasing the energy input from 1 to 4 kJ/mm (25 to 101 kJ/in.), there was a pronounced decrease in yield strength (209 MPa, or 30 ksi) for the HY-80 welds.

TABLE 4 TENSILE PROPERTIES OF SUBMERGED ARC BEAD-IN-GROOVE WELDS DEPOSITED IN HY-80 STEEL FROM EXAMPLE 2

WELD NO.	ENERGY INPUT		YIELD STRENGTH		ULTIMATE STRENGTH		ELONGATION, %	REDUCTION IN AREA, %
	KJ/MM	KJ/IN.	MPA	KSI	MPA	KSI		
HY-80-1	1	25	875	127	1124	163	18	54
HY-80-2	2	50	745	108	930	135	24	59
HY-80-3	3	75	680	99	858	124	25	64
HY-80-4	4	100	666	97	867	126	25	63

Source: Ref 27

Effect on HY-80 Charpy Properties. Charpy impact transition curves for HY-80 welds based on 5 × 10 mm (0.2 × 0.4 in.) subsized specimens and plots of the percentage of ductile fracture versus test temperature are shown in Fig. 12. The investigators noted that, for HY-80 welds, the lowest energy input weld displayed the lowest toughness values, despite ductile behavior at temperatures above -80 °C (-112 °F). Figure 12 shows the variation in proportion of ductile fracture for the series of HY-80 welds. For 2 and 4 kJ/mm (5 and 10 kJ/in.) welds, ductile fracture occurred at temperatures above -50 °C (-58 °F), with the transition to brittle cleavage fracture occurring below -50 °C (-58 °F). The 1 and 3 kJ/mm (25 and 75 kJ/in.) welds displayed fully ductile fracture at temperatures above -80 °C (-112 °F).

Effect on HSLA-80 Tensile Properties. Tensile property results (Table 5) show that the HSLA-80 welds displayed lower strengths and better ductilities than the HY-80 welds. A slight decrease (45 MPa, or 6.5 ksi) was observed for the HSLA-80 welds, compared with the pronounced decreased in yield strength (209 MPa, or 30 ksi) for the HY-80 welds.

TABLE 5 PROPERTIES OF SUBMERGED ARC BEAD-IN-GROOVE WELDS DEPOSITED IN HSLA-80 STEEL FROM EXAMPLE 2

WELD NO.	ENERGY INPUT		YIELD STRENGTH		ULTIMATE STRENGTH		ELONGATION, %	REDUCTION IN AREA, %
	kj/mm	kj/in.	MPa	ksi	MPa	ksi		
HSLA-80-1	1	25	640	93	806	117	25	64
HSLA-80-2	2	50	618	90	756	110	28	66
HSLA-80-3	3	75	607	88	720	105	27	65
HSLA-80-4	4	100	595	86	710	103	28	65

Source: Ref 27

Effect on HSLA-80 Charpy Properties. In the case of the HSLA-80 welds, only slight variations in notch toughness were observed, as plotted in Fig. 18. The weld metals deposited at energy inputs of ≤3 kJ/mm (75 kJ/in.) displayed ductile behavior down to -80 °C (-112 °F). The transition to cleavage fracture occurred at temperatures between -80 and -150 °C (-112 and -238 °F), as shown in Fig. 18. The superior toughness of the HSLA-80 weld metals was generally attributed to the combined effect of the acicular ferrite microstructure and the lower yield strength.

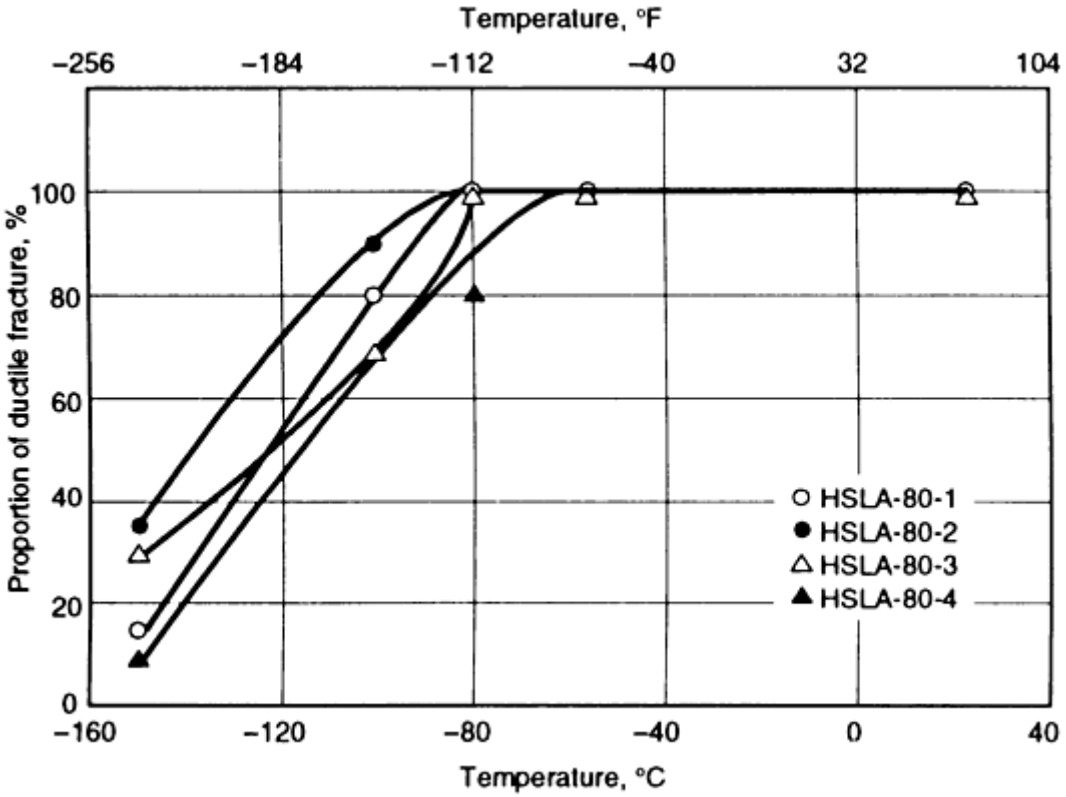

FIG. 18 PERCENT DUCTILE FRACTURE VERSUS TEST TEMPERATURE FOR THE SUBMERGED ARC BEAD-IN-GROOVE WELDS DEPOSITED IN HSLA STEEL. SOURCE: REF 27

With regard to the effect of heat input on weldment properties, the investigators concluded that:

- A PRONOUNCED DECREASE IN WELD-METAL YIELD STRENGTH AND REDUCTION IN HARDNESS WERE ALSO OBSERVED FOR THE HY-80 WELDS WITH INCREASING ENERGY INPUT. POOR LOW-TEMPERATURE NOTCH TOUGHNESS WAS DISPLAYED BY BOTH THE LOW- AND HIGH-ENERGY INPUT WELDS, WHEREAS CONSIDERABLE IMPROVEMENTS OCCURRED FOR THE 2 AND 3 KJ/MM (50 AND 75 K J/IN.) WELDS.
- THE NOTCH TOUGHNESS WAS RELATED TO THE PACKET SIZE AND THE RELATIVE STRENGTH OF THE MICROSTRUCTURES. THE EXCESSIVELY HIGH YIELD STRENGTH OF THE HY-80-1 WELD RESULTED IN LOW RESISTANCE TO BOTH DUCTILE AND CLEAVAGE FRACTURE, DESPITE FINE CLEAVAGE FACETS, WHICH CORRESPONDED CLOSELY TO THE MARTENSITIC PACKET SIZES (≤ 5 μM, OR 0.2 MIL). AT A HIGH-ENERGY INPUT, POOR TOUGHNESS OCCURRED, BECAUSE OF AN INCREASE IN THE PACKET SIZE FOR THE FULLY BAINITIC MICROSTRUCTURE.
- SUPERIOR NOTCH TOUGHNESS PROPERTIES WERE OBSERVED TO BE INDEPENDENT OF THE ENERGY INPUT FOR THE HSLA-80 WELDS AS A RESULT OF THE TRANSFORMATION TO A HIGH PROPORTION OF ACICULAR FERRITE WITH THE LOWER YIELD STRENGTHS.

References cited in this section

6. R.D. STOUT AND W.D. DOTY, *WELDABILITY OF STEELS*, 3RD ED., S. EPSTEIN AND R.E. SOMERS, ED., WELDING RESEARCH COUNCIL, NEW YORK, 1978

23. "STANDARD WELDING TERMS AND DEFINITIONS," ANSI/AWS A3.0-85, AWS

24. H.B. CARY, *MODERN WELDING TECHNOLOGY*, PRENTICE HALL, 1979

25. P.L. THREADGITT AND R.H. LEGGOTT, EFFECTS OF POSTWELD HEAT TREATMENT ON MECHANICAL PROPERTIES AND RESIDUAL STRESS LEVELS OF SUBMERGED ARC WELDING IN A C-MN-NB-AL STEEL, NOV 1984
26. I. HRIVNAK, THE THEORY OF MILD STEEL AND MICRO ALLOY STEEL WELDABILITY, 1969
27. J.A. GIANETOO, N.S. SMITH, J.T. MCGRATH, AND J.T. BOWKER, EFFECT OF COMPOSITION AND ENERGY INPUT ON STRUCTURAL AND PROPERTIES OF HIGH-STRENGTH WELD METALS, *WELD. J. RES. SUPP.,* NOV 1992

Influence of Welding on Steel Weldment Properties

C.C. Chen and Abe Pollack, Microalloying International, Inc.

References

1. Y. ITO AND K. BESSYO, "WELDABILITY OF HIGH STRENGTH STEELS RELATED TO HEAT AFFECTED ZONE CRACKING," DOCUMENT IX-567-68, IIW, 1968
2. N. YURIOKA, H. SUZUKI, AND S. OHSHITA, *WELD. J.,* VOL 62, 1983, P 1475-1535
3. O. GRONG AND O.M. AKSELSEN, HAZ TOUGHNESS OF MICROALLOYED STEELS FOR OFFSHORE, *MET. CONSTR.,* SEPT 1986, P 557
4. K.E. EASTERLIN, *INTRODUCTION TO THE PHYSICAL METALLURGY OF WELDING,* BUTTERWORTHS, 1983
5. C.F. CHOU, *THEORY AND TECHNOLOGY OF METAL WELDING,* VOL 2, MECHANICAL INDUSTRY PUBLISHER, 1981 (IN CHINESE)
6. R.D. STOUT AND W.D. DOTY, *WELDABILITY OF STEELS,* 3RD ED., S. EPSTEIN AND R.E. SOMERS, ED., WELDING RESEARCH COUNCIL, NEW YORK, 1978
7. J.F. LANCASTER, *METALLURGY OF WELDING,* GEORGE ALLEN & UNWIN, 1980
8. G.M. EVANS, FACTOR AFFECTING THE MICROSTRUCTURES AND PROPERTIES OF C-MN ALL-WELD METAL DEPOSITS, *WELD. REV.,* VOL 4, MAY 1982
9. O.M. AKSELSEN, "MICROSTRUCTURE AND TOUGHNESS IN HAZ OF BORON CONTAINING STEELS," REPORT STF A84065, THE WELDING CENTER (SINTEF), TRONDHEIM, NORWAY, 1984
10. W.H. KEARNS, *WELDING HANDBOOK,* VOL 4, AWS, 1984
11. M. GRAY, WELDABILITY OF NIOBIUM CONTAINING HIGH STRENGTH LOW ALLOY STEEL, *WELD. RES. COUNC. BULL.,* NO. 213, FEB 1976
12. R.E. DOLBY, "FACTORS CONTROLLING WELD TOUGHNESS--THE PRESENT POSITION," REPORT NO. 14, THE WELDING INSTITUTE, 1976
13. H.J. KIM AND J.G. YOUN, CHARACTERISTICS OF TMCP STEEL AND ITS SOFTENING, *WELDING METALLURGY OF STRUCTURAL STEEL,* J.Y. KOO, ED., AIME, 1987
14. Y. ITO AND M. NAKANISH, STUDY ON STRESS RELIEF CRACKING IN WELDING LOW ALLOY STEELS, *SUMITOMO SEARCH,* NO. 7, MAY 1972, P 27-36
15. C.J. MCMAHON, JR., R.J. DOBBS, AND D.H. GENTUER, STRESS RELIEF CRACKING IN MN, MO, NI, AND MN-MO-NI-CR PRESSURE VESSEL STEELS, *MATER. SCI. ENG.,* VOL 37, 1979, P 179-186
16. G.E. LINERT, *WELDING METALLURGY,* AWS
17. D.N. SHACKLETON, *WELDING HY-100 AND HY-130 STEELS,* THE WELDING INSTITUTE, 1973
18. T. TAIRA *ET AL.,* "SULFIDE CORROSION CRACKING OF GIRTH-WELDED JOINT OF LINE PIPE FOR SOUR GAS SERVICE," CORROSION '79, T-1F SYMPOSIUM (ATLANTA, GA), NACE, MARCH 1979
19. M. ITOH *ET AL.,* "HYDROGEN SULFIDE CORROSION CRACKING OF LARGE DIAMETER LINE

PIPE UP TO GRADE X-65," MIDDLE EAST CORROSION CONFERENCE (BAHRAIN), NACE, APRIL 1979

20. "SULFIDE STRESS CRACKING RESISTANT METALLIC MATERIALS FOR OIL FIELD EQUIPMENT," STANDARD MATERIAL REQUIREMENTS DOCUMENT MR0175-91, NACE
21. Z. ZACZEK, IMPROVEMENT IN THE FATIGUE STRENGTH OF BUTT WELDED JOINTS BY TIG REMELTING OF WELDING REINFORCEMENTS, *MET. CONSTR.*, JULY 1986
22. G.S. BOOTH, IMPROVING THE FATIGUE STRENGTH OF WELDED JOINT BY GRINDING--TECHNIQUES AND BENEFITS, *MET. CONSTR.*, JULY 1986
23. "STANDARD WELDING TERMS AND DEFINITIONS," ANSI/AWS A3.0-85, AWS
24. H.B. CARY, *MODERN WELDING TECHNOLOGY*, PRENTICE HALL, 1979
25. P.L. THREADGITT AND R.H. LEGGOTT, EFFECTS OF POSTWELD HEAT TREATMENT ON MECHANICAL PROPERTIES AND RESIDUAL STRESS LEVELS OF SUBMERGED ARC WELDING IN A C-MN-NB-AL STEEL, NOV 1984
26. I. HRIVNAK, THE THEORY OF MILD STEEL AND MICRO ALLOY STEEL WELDABILITY, 1969
27. J.A. GIANETOO, N.S. SMITH, J.T. MCGRATH, AND J.T. BOWKER, EFFECT OF COMPOSITION AND ENERGY INPUT ON STRUCTURAL AND PROPERTIES OF HIGH-STRENGTH WELD METALS, *WELD. J. RES. SUPP.*, NOV 1992

Introduction to the Selection of Stainless Steels

John C. Lippold, Edison Welding Institute

Introduction

STAINLESS STEELS are an important class of engineering alloys used in both wrought and cast form for a wide range of applications and in many environments. Stainless steels are used extensively in the power generation, pulp and paper, and chemical processing industries, but are also chosen for use in many everyday household and commercial products. The widespread use of stainless steels and their importance in critical industrial technologies has led to considerable investigation of the weldability and service integrity of these steels. The purpose of the articles in this Section of the Handbook is to aid the reader in the selection of stainless steels based on these criteria.

Introduction to the Selection of Stainless Steels

John C. Lippold, Edison Welding Institute

Selection of Stainless Steels

Fundamentally, stainless steels are based on the iron-chromium, iron-chromium-carbon, and iron-chromium-nickel systems, but may contain a number of other alloying additions that alter their microstructures and/or properties. The "stainless" nature of these steels arises primarily from the addition of chromium in quantities greater than 12 wt%. This level of chromium ensures that a continuous layer of protective chromium-rich oxide forms on the surface. In practice, however, stainless steels may contain as little as 9 wt% Cr and be subject to general corrosion ("rusting") at ambient temperatures. Few stainless steels contain more than 30 wt% Cr or less than 50 wt% Fe.

Historically, stainless steels have been classified by microstructure and are described as ferritic, martensitic, austenitic, or duplex (austenitic and ferritic). In addition, a number of precipitation-hardenable (PH) martensitic and austenitic stainless steels exist and are normally classified separately as PH stainless steels. Cast versions of all of the microstructural variants exist, but their welding behavior is often unique relative to the corresponding wrought alloys. The articles in this Section are organized according to the categories of stainless steels described above.

In order to control microstructure and properties, a number of alloying elements are added to the basic iron-chromium, iron-chromium-carbon, and iron-chromium-nickel systems; these alloying elements include manganese, silicon, molybdenum, niobium, titanium, and nitrogen. In order to broadly describe the effect of composition on microstructure in a wide range of stainless steels, the concept of chromium and nickel equivalents was developed to normalize the effect of these alloying additions on microstructural evolution, relative to chromium and nickel. Plotting the chromium and nickel equivalents on opposing axes provides a graphic depiction of the relationship between composition and microstructure for stainless steel welds. The Schaeffler diagram (Fig. 1) has become known as the "roadmap" of stainless steels. The compositional ranges of the ferritic, martensitic, austenitic, and duplex alloys have been superimposed on this diagram.

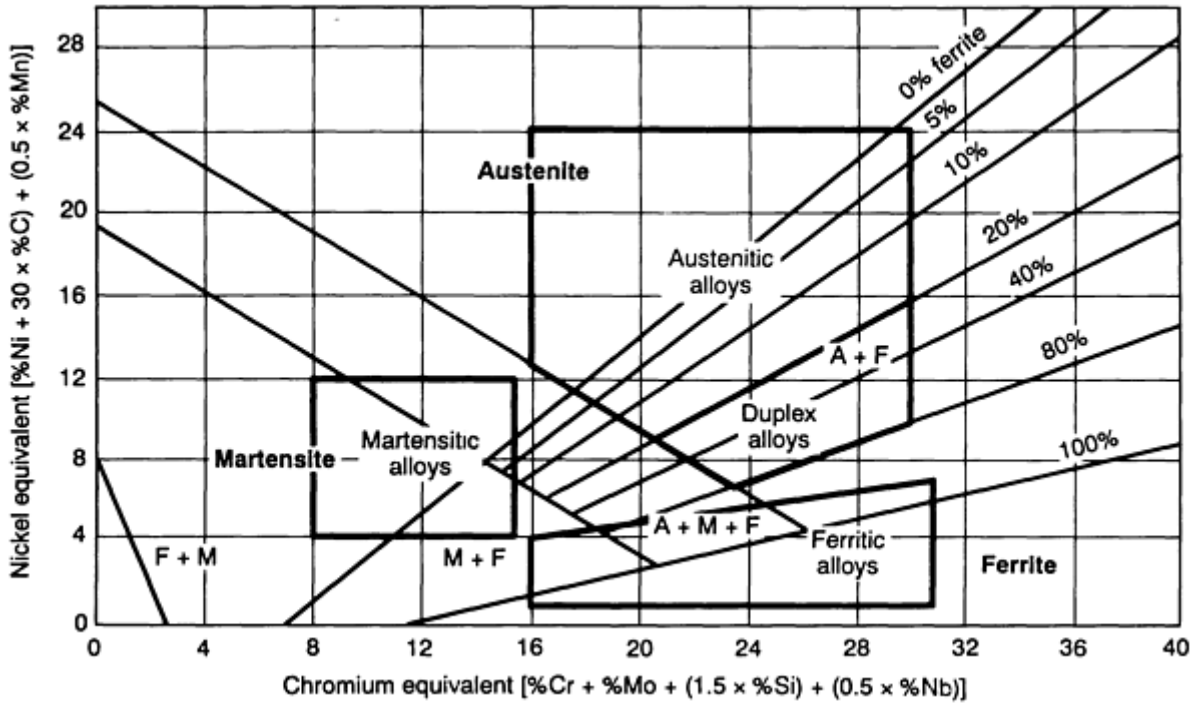

FIG. 1 SCHAEFFLER CONSTITUTION DIAGRAM FOR STAINLESS STEELS

The following articles describe the metallurgical aspects of welded stainless steels to be considered when selecting these materials for particular engineering applications and service conditions. Each article describes the microstructural evolution of the weld metal and the heat-affected zone, susceptibility to defect formation during welding, mechanical and corrosion properties, and weld process tolerance. In addition, each article lists the compositions and base metal properties for commercially available alloys. Information regarding filler metal selection and detailed process applications related to the joining of stainless steels can be found in the articles "Welding of Stainless Steels," "Brazing of Stainless Steels," and "General Soldering" in this Volume.

Selection of Wrought Martensitic Stainless Steels

J.R. Davis, Davis & Associates

Introduction

MARTENSITIC STAINLESS STEELS are essentially alloys of chromium and carbon that possess a body-centered cubic (bcc) or body-centered tetragonal (bct) crystal (martensitic) structure in the hardened condition. They are ferromagnetic and hardenable by heat treatments. They generally resist relatively mild corrosive environments.

The chromium content of these materials generally ranges from 11.5 to 18 wt%, and their carbon content can be as high as 1.2 wt%. The chromium and carbon contents are balanced to ensure a martensitic structure after hardening. Tables 1 and 2 list the chemical compositions for standard and nonstandard grades, respectively.

TABLE 1 CHEMICAL COMPOSITIONS OF STANDARD WROUGHT MARTENSITIC STAINLESS STEELS

TYPE	UNS NO.	COMPOSITION, %[A]							
		C	Mn	Si	Cr	Ni	P	S	Other
403	S40300	0.15	1.00	0.50	11.5-	. . .	0.04	0.03	. . .

					13.0				
410	S41000	0.15	1.00	1.00	11.5-13.5	. . .	0.04	0.03	. . .
414	S41400	0.15	1.00	1.00	11.5-13.5	1.25-2.50	0.04	0.03	. . .
416	S41600	0.15	1.25	1.00	12.0-14.0	. . .	0.06	0.15 MIN	0.6 MO[B]
416SE	S41623	0.15	1.25	1.00	12.0-14.0	. . .	0.06	0.06	0.15 MIN SE
420	S42000	0.15 MIN	1.00	1.00	12.0-14.0	. . .	0.04	0.03	. . .
420F	S42020	0.15 MIN	1.25	1.00	12.0-14.0	. . .	0.06	0.15 MIN	0.6 MO[B]
422	S42200	0.20-0.25	1.00	0.75	11.5-13.5	0.5-1.0	0.04	0.03	0.75-1.25 MO; 0.75-1.25 W; 0.15-0.3 V
431	S43100	0.20	1.00	1.00	15.0-17.0	1.25-2.50	0.04	0.03	. . .
440A	S44002	0.60-0.75	1.00	1.00	16.0-18.0	. . .	0.04	0.03	0.75 MO
440B	S44003	0.75-0.95	1.00	1.00	16.0-18.0	. . .	0.04	0.03	0.75 MO
440C	S44004	0.95-1.20	1.00	1.00	16.0-18.0	. . .	0.04	0.03	0.75 MO

(A) SINGLE VALUES ARE MAXIMUM VALUES UNLESS OTHERWISE INDICATED.

(B) OPTIONAL

TABLE 2 CHEMICAL COMPOSITIONS OF NONSTANDARD WROUGHT MARTENSITIC STAINLESS STEELS

DESIGNATION[A]	**UNS NO.**	**COMPOSITION, %[B]**							
		C	**Mn**	**Si**	**Cr**	**Ni**	**P**	**S**	**Other**
TYPE 410S	S41008	0.08	1.00	1.00	11.5-13.5	0.60	0.040	0.030	. . .
TYPE 410 CB (XM-30)	S41040	0.15	1.00	1.00	11.5-13.5	. . .	0.040	0.030	0.05-0.20 NB
HT9	DIN 1.4935[C]	0.17-0.23	0.30-0.80	0.10-0.50	11.0-12.5	0.30-0.80	0.035	0.035	0.80-1.20 MO; 0.25-0.35 V; 0.4-0.6 W
416 PLUX X (XM-6)	S41610	0.15	1.5-2.5	1.00	12.0-14.0	. . .	0.060	0.15 MIN	0.6 MO
TYPE 418 (GREEK ASCOLLOY)	S41800	0.15-0.20	0.50	0.50	12.0-14.0	1.8-2.2	0.040	0.030	2.5-3.5 W
TRIMRITE	S42010	0.15-0.30	1.00	1.00	13.5-15.0	0.25-1.00	0.040	0.030	0.40-1.00 MO
TYPE 429 F SE	S42023	0.3-0.4	1.25	1.00	12.0-14.0	. . .	0.060	0.060	0.15 MIN SE; 0.6 ZR; 0.6 CU
LAPELLOY	S42300	0.27-0.32	0.95-1.35	0.50	11.0-12.0	0.50	0.025	0.025	2.5-3.0 MO; 0.2-0.3 V
TYPE 440 F	S44020	0.95-1.20	1.25	1.00	16.0-18.0	0.75	0.040	0.10-0.35	0.08 N

TYPE 440 F SE	S44023	0.95-1.20	1.25	1.00	16.0-18.0	0.75	0.040	0.030	0.15 MIN SE; 0.60 MO

(A) XM DESIGNATIONS IN THIS COLUMN ARE ASTM DESIGNATIONS FOR THE LISTED ALLOY.
(B) SINGLE VALUES ARE MAXIMUM VALUES UNLESS OTHERWISE INDICATED.
(C) GERMAN (DIN) SPECIFICATION

The most commonly used alloy within this stainless steel family is type 410, which contains about 12 wt% Cr and 0.1 wt% C to provide strength. The carbon level and, consequently, strength, increase in the 420, 440A, 440B, and 440C alloy series. The latter three alloys, in particular, have an increased chromium level in order to maintain corrosion resistance.

Molybdenum can be added to improve mechanical properties or corrosion resistance, as it is in type 422 stainless steel. Nickel can be added for the same reasons, as it is in types 414 and 431. When higher chromium levels are used to improve corrosion resistance, nickel also serves to maintain the desired microstructure and to prevent excessive free ferrite. The limitations on the alloy content required to maintain the desired fully martensitic structure restrict the obtainable corrosion resistance to moderate levels.

In the annealed condition, martensitic stainless steels have a tensile yield strength of approximately 275 MPa (40 ksi) and can be moderately hardened by cold working. However, martensitic alloys are typically heat treated by both hardening and tempering in order to yield strength levels up to 1900 MPa (275 ksi), depending on carbon level, primarily. These alloys have good ductility and toughness properties, which decrease as strength increases. Depending on the heat treatment, hardness values range from approximately 150 HB (80 HRB) for materials in the annealed condition to levels greater than 600 HB (58 HRC) for fully hardened materials (Fig. 1). Basic room-temperature properties of the martensitic types are given in Table 3. Typical physical properties of annealed martensitic stainless steels are listed in Table 4.

TABLE 3 MINIMUM MECHANICAL PROPERTIES OF MARTENSITIC STAINLESS STEELS

PRODUCT FORM[A]	CONDITION	TENSILE STRENGTH		0.2% YIELD STRENGTH		ELONGATION, %	REDUCTION IN AREA, %	ROCKWELL HARDNESS	ASTM SPECIFICATION
		MPA	KSI	MPA	KSI				
TYPE 403 (UNS S40300)									
B, F	ANNEALED, HOT FINISHED	485	70	275	40	20	45	. . .	A 276, A 473, A 479
B	ANNEALED, COLD FINISHED	485	70	275	40	16	45	. . .	A 276
B	INTERMEDIATE TEMPER, HOT FINISHED	690	100	550	80	15	45	. . .	A 276
B	INTERMEDIATE TEMPER, COLD FINISHED	690	100	550	80	12	40	. . .	A 276
B	HARD TEMPER, HOT OR COLD FINISHED	825	120	620	90	12	40	. . .	A 276
W	ANNEALED	485	70	275	40	20	45	. . .	A 580
W	ANNEALED, COLD FINISHED	485	70	275	40	16	45	. . .	A 580
W	INTERMEDIATE TEMPER, COLD FINISHED	690	100	550	80	12	40	. . .	A 580
W	HARD TEMPER, COLD FINISHED	825	120	620	90	12	40	. . .	A 580
P, SH, ST	ANNEALED	485	70	205	30	25[B]	. . .	88 HRB MAX	A 176
TYPE 410 (UNS S41000)									
B, F	ANNEALED, HOT FINISHED	485	70	275	40	20	45	. . .	A 276, A 473, A 479
B	ANNEALED, COLD FINISHED	485	70	275	40	16	45	. . .	A 276
B	INTERMEDIATE TEMPER, HOT FINISHED	690	100	550	80	15	45	. . .	A 276
B	INTERMEDIATE TEMPER, COLD FINISHED	690	100	550	80	12	40	. . .	A 276
B	HARD TEMPER, HOT OR COLD FINISHED	825	120	620	90	12	40	. . .	A 276
W	ANNEALED	485	70	275	40	20	45	. . .	A 580
W	ANNEALED, COLD FINISHED	485	70	275	40	16	45	. . .	A 580
W	INTERMEDIATE TEMPER, COLD FINISHED	690	100	550	80	12	40	. . .	A 580

W	HARD TEMPER, COLD FINISHED	825	120	620	90	12	40	. . .	A 580
P, SH, ST	ANNEALED	450	65	205	30	22[B]	. . .	95 HRB MAX	A 176
P, SH, ST	ANNEALED	450	65	205	30	20	. . .	95 HRB MAX	A 240
TYPE 410S (UNS S41008)									
F	ANNEALED	450	65	240	35	22	45	. . .	A 473
P, SH, ST	ANNEALED	415	60	205	30	22[B]	. . .	88 HRB MAX	A 176, A 240
TYPE 410CB (UNS S41040)									
B	ANNEALED, HOT FINISHED	485	70	275	40	13	45	. . .	A 276, A 479
B	ANNEALED, COLD FINISHED	485	70	275	40	12	35	. . .	A 276, A 479
B	INTERMEDIATE TEMPER, HOT FINISHED	860	125	690	100	13	45	. . .	A 276, A 479
B	INTERMEDIATE TEMPER, COLD FINISHED	860	125	690	100	12	35	. . .	A 276, A 479
E-4 (UNS S41050)									
P, SH, ST	ANNEALED	415	60	205	30	22	. . .	88 HRB MAX	A 276, A 240
TYPE 414 (UNS S41400)									
B	INTERMEDIATE TEMPER, COLD OR HOT FINISHED	795	115	620	90	15	45	. . .	A 276, A 479
W	ANNEALED, COLD FINISHED	1030 MAX	150 MAX	. . .	. . .	. . .	. . .	. . .	A 580
CA6NM (UNS S41500)									
P, SH, ST	TEMPERED	795	115	620	90	15	. . .	32 HRC MAX	A 176, A 240
B, F	TEMPERED	795	115	620	90	15	45	. . .	A 276, A 473, A 479
TYPES 416 (UNS S41600) AND 416SE (UNS S41623)									
F	ANNEALED	485	70	275	40	20	45	. . .	A 473
W	ANNEALED	585-860	85-125	. . .	. . .	. . .	. . .	. . .	A 581
W	INTERMEDIATE TEMPER	795-1000	115-145	. . .	. . .	. . .	. . .	. . .	A 581
W	HARD TEMPER	965-1210	140-175	. . .	. . .	. . .	. . .	. . .	A 581

TYPE 416 PLUS X (UNS S41610)									
W	ANNEALED	585-860	85-125	. . .	. . .	. . .	. . .	. . .	A 581
W	INTERMEDIATE TEMPER	795-1000	115-145	. . .	. . .	. . .	. . .	. . .	A 581
W	HARD TEMPER	965-1210	140-175	. . .	. . .	. . .	. . .	. . .	A 581
TYPE 418 (UNS S41800)									
B, F	TEMPERED AT 620 °C (1150 °F)	965	140	760	110	15	45	. . .	A 565
TYPE 420 (UNS S42000)									
B	TEMPERED AT 204 °C (400 °F)	1720	250	1480[C]	215[C]	8[C]	25[C]	52 HRC[C]	. . .
W	ANNEALED, COLD FINISHED	860 MAX	125 MAX	. . .	. . .	. . .	. . .	. . .	A 580
P, SH, ST	ANNEALED	690	100	. . .	. . .	15	. . .	96 HRB MAX	A 176
TRIMRITE (UNS S42010)									
W	ANNEALED	690 MAX	100 MAX	. . .	. . .	. . .	. . .	. . .	A 493
W	LIGHTLY DRAFTED	725 MAX	105 MAX	. . .	. . .	. . .	. . .	. . .	A 493
TYPE 422 (UNS S42200)									
B, F	TEMPERED AT 675 °C (1250 °F)	825	120	585	85	17[D]	35	. . .	A 565
B, F	TEMPERED AT 620 °C (1150 °F)	965	140	760	110	13	30	. . .	A 565
LAPELLOY (UNS S42300)									
B, F	TEMPERED AT 620 °C (1150 °F)	965	140	760	110	8	20	. . .	A 565
TYPE 431 (UNS S43100)									
F	INTERMEDIATE TEMPER	795	115	620	90	15	. . .	. . .	A 473
F	HARD TEMPER	1210	175	930	135	13	. . .	. . .	A 473
W	ANNEALED, COLD FINISHED	965 MAX	140 MAX	. . .	. . .	. . .	. . .	. . .	A 580
W	ANNEALED	760	110	. . .	. . .	. . .	. . .	. . .	A 493
W	LIGHTLY DRAFTED	795	115	. . .	. . .	. . .	. . .	. . .	A 493
TYPE 440A (UNS S44002)									
B	ANNEALED	725[C]	105[C]	415[C]	60[C]	20[C]	. . .	95 HRB[C]	. . .

B	TEMPERED AT 135 °C (600 °F)	1790[C]	260[C]	1650[C]	240[C]	5[C]	20[C]	51 HRC[C]	. . .
W	ANNEALED, COLD FINISHED	965 MAX	140 MAX	. . .	. . .	. . .	. . .	. . .	A 580
TYPE 440B (UNS S44003)									
B	ANNEALED	740[C]	107[C]	425[C]	62[C]	18[C]	. . .	96 HRB[C]	. . .
B	TEMPERED AT 315 °C (600 °F)	1930[C]	280[C]	1860[C]	270[C]	3[C]	15[C]	55 HRC[C]	. . .
W	ANNEALED, COLD FINISHED	965 MAX	140 MAX	. . .	. . .	. . .	. . .	. . .	A 580
TYPE 440C (UNS S44004)									
B	ANNEALED	760[C]	110[C]	450[C]	65[C]	14[C]	. . .	97 HRB[C]	. . .
B	TEMPERED AT 315 °C (600 °F)	1970[C]	285[C]	1900[C]	275[C]	2[C]	10[C]	57 HRC[C]	. . .
W	ANNEALED, COLD FINISHED	965 MAX	140 MAX	. . .	. . .	. . .	. . .	. . .	A 580

(A) B, BAR; F, FORGINGS; P, PLATE; SH, SHEET; ST, STRIP; W, WIRE.

(B) 20% ELONGATION FOR 1.3 MM (0.050 IN.) AND UNDER IN THICKNESS.

(C) TYPICAL VALUES.

(D) MINIMUM ELONGATION OF 15% FOR FORGINGS

TABLE 4 TYPICAL PHYSICAL PROPERTIES OF WROUGHT MARTENSITIC STAINLESS STEELS IN THE ANNEALED CONDITION

TYPE	UNS NO.	DENSITY, G/CM^3	ELASTIC MODULUS		MEAN CTE FROM 0 °C (32 °F) TO:			THERMAL CONDUCTIVITY				SPECIFIC HEAT[A]		ELECTRICAL RESISTIVITY, NΩ · M	MAGNETIC PERMEABILITY[B]	MELTING RANGE	
								AT 100 °C (212 °F)		AT 500 °C (932 °F)							
			GPA	10^6 PSI	100 °C (212 °F), 10^{-6}/K	315 °C (600 °F), 10^{-6}/K	538 °C (1000 °F), 10^{-6}/K	W/M · K	BTU/FT · H · °F	W/M · K	BTU/FT · H · °F	J/KG · K	BTU/LB · H · °F			°C	°F
410	S41000	7.8	200	29.0	9.9	11.4	11.6	24.9	14.4	28.7	16.6	460	0.11	570	700-1000	1480-1530	2700-2790
414	S41400	7.8	200	29.0	10.4	11.0	12.1	24.9	14.4	28.7	16.6	460	0.11	700	. . .	1425-1480	2600-2700
416	S41600	7.8	200	29.0	9.9	11.0	11.6	24.9	14.4	28.7	16.6	460	0.11	570	700-1000	1480-1530	2700-2790
420	S42000	7.8	200	29.0	10.3	10.8	11.7	24.9	14.4	. . .	. . .	460	0.11	550	. . .	1450-1510	2650-2750
422	S42200	7.8	. . .	. . .	11.2	11.4	11.9	23.9	13.8	27.3	15.8	460	0.11	. . .	. . .	1470-	2675-

																1480	2700
431	S43100	7.8	200	29.0	10.2	12.1	. . .	20.2	11.7	. . .	. . .	460	0.11	720	. . .	. . .	. . .
440A	S44002	7.8	200	29.0	10.2	. . .	. . .	24.2	14.0	. . .	. . .	460	0.11	600	. . .	1370-1480	2500-2700
440C	S44004	7.8	200	29.0	10.2	. . .	. . .	24.2	14.0	. . .	. . .	460	0.11	600	. . .	1370-1480	2500-2700

CTE, coefficient of thermal expansion.

(A) AT 0 TO 100 °C (932 TO 212 °F).

(B) APPROXIMATE VALUES

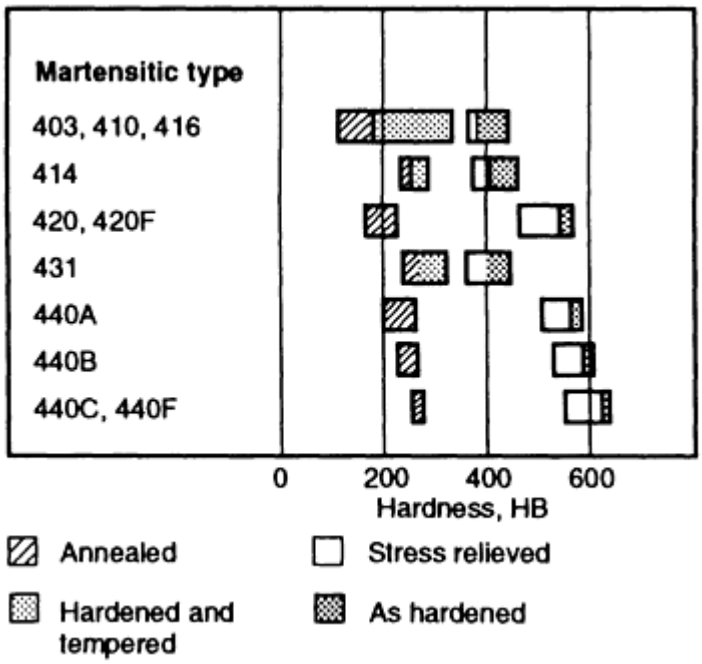

FIG. 1 RANGE OF HARDNESS IN VARIOUS MARTENSITIC STAINLESS STEELS

Martensitic stainless steels are specified when the application requires good tensile strength, creep, and fatigue strength properties, in combination with moderate corrosion resistance and heat resistance up to approximately 650 °C (1200 °F). In the United States, low- and medium-carbon martensitic steels (for example, type 410 and modified versions of this alloy) have been used primarily in steam turbines, jet engines, and gas turbines. Martensitic stainless steels are also used in petroleum and petrochemical equipment. Other applications for higher-carbon-level grades (type 440 grades) include cutlery, surgical and dental instruments, scissors, springs, valves, gears, shafts, cams, and ball bearings.

In Europe, these alloys have been used in similar applications. In addition, certain alloys, particularly 12Cr-1Mo-0.3V (HT9), have been widely used in elevated-temperature pressure-containment applications, including steam piping and steam generator reheater and superheater tubing used in fossil fuel power plants. The 12Cr-1Mo-0.3V alloy also has been investigated as a candidate material for the first wall of fusion reactors in both Europe and the United States (Ref 1, 2, 3, 4).

References

1. T. LECHTENBERG, WELDING AND FABRICATION CONSIDERATIONS FOR A 12CR-1MO MARTENSITIC STEEL FOR FUSION ENERGY SYSTEMS, *FERRITIC STEELS FOR HIGH-TEMPERATURE APPLICATIONS*, AMERICAN SOCIETY FOR METALS, 1983, P 163-177
2. J.C. LIPPOLD, TRANSFORMATION AND TEMPERING BEHAVIOR OF 12CR-1MO-0.3V MARTENSITIC STAINLESS STEEL WELDMENTS, *J. NUCL. MATER.*, VOL 103 AND 104, 1981, P 1127-1132
3. J.C. LIPPOLD, "MICROSTRUCTURAL CHARACTERIZATION OF AUTOGENOUS GTA WELDS IN A 12CR-1MO-0.3V STEEL," DOCUMENT NO. SAND80-8236, SANDIA NATIONAL LABORATORIES, OCT 1980
4. J.C. LIPPOLD, THE EFFECT OF POSTWELD HEAT TREATMENT ON THE MICROSTRUCTURE AND PROPERTIES OF THE HEAT-AFFECTED ZONE IN 12CR-1MO-0.3V (HT9) WELDMENTS, *PROC. TOPICAL CONFERENCE ON FERRITIC ALLOYS FOR USE IN NUCLEAR ENERGY TECHNOLOGIES*, TMS, 1984, P 497-506

General Welding Characteristics

As mentioned above, the compositions of martensitic stainless steels are specifically formulated to render them amenable to a quench-and-temper heat treatment in order to produce high levels of strength and hardness. The response of martensitic stainless steels to the heattreat process is essentially the same as that of plain carbon or low-alloy steels, where maximum strength and hardness primarily depend on carbon content. Although the chromium level of approximately 11 to 18 wt% in martensitic grades is the same as in ferritic stainless steels, the higher carbon content of the martensitic grades results in a complete transformation from delta (δ) ferrite to austenite at high temperature (~980 °C, or 1800 °F), followed by a subsequent change to the hard martensite phase upon rapid cooling. The thermal cycle of heating and rapid cooling, which occurs within the confined heat-affected zone (HAZ) during welding, is equivalent to a quenching cycle.

The high-carbon martensitic structure that is produced is extremely brittle in the untempered condition. Cracking can occur when the heated weldment and the surrounding martensitic HAZ are unable to contract to the same degree and at the same rate as the weld metal. Preheat and postweld cooling rates are important vehicles for controlling these shrinkage stresses and will be further discussed later in this article. Because of their response to welding thermal cycles, martensitic stainless steels are considered to be the most difficult of the five stainless steel families to weld.

The extent to which HAZ hardening is present depends on the carbon content of the base metal. Higher carbon contents (>0.15%) will produce greater hardness and, therefore, an increased susceptibility to cracking. Thus, type 440A, B, and C stainless steels are not usually considered for applications that require welding, and filler metals are not readily available in type 440 compositions.

In addition to the problems that result from localized stresses associated with the volume change upon martensitic transformation, the risk of cracking will increase when hydrogen from various sources is present in the weld metal. Therefore, the use of low-hydrogen consumables is mandatory. Hydrogen-induced cold cracking in martensitic stainless steel weldments is also discussed in more detail later in this article.

Selection of Wrought Martensitic Stainless Steels

J.R. Davis, Davis & Associates

Weld Microstructure (Ref 2, 3, 4)

Detailed studies have been made on the transformation, tempering behavior, and resulting microstructures of martensitic stainless steel weldments. These studies were spurred by an interest in using 12Cr-1Mo-0.3V (HT9) martensitic stainless steel as a candidate material for the first wall/blanket of fusion-containment devices (Tokamaks), because of its improved resistance to swelling, low coefficient of thermal expansion (CTE), and high thermal conductivity relative to austenitic stainless steel (Ref 2).

During the welding of martensitic stainless steels, the fusion zone and that portion of the HAZ that is heated to a temperature higher than the austenitization temperature is transformed to a brittle, untempered martensite upon cooling to room temperature (Ref 4). Because the ductility, or fracture toughness, of the untempered martensite is inferior to that of the surrounding quenched-and-tempered microstructure, the material is unfit for service in the as-welded condition. Consequently, a postweld heat treatment (PWHT) must be employed to reduce the hardness and increase the toughness of the weld region. Recommended PWHT practices for martensitic stainless steels, including HT9, are described in the section "Specific Welding Recommendations" in this article.

The as-welded properties of the weld fusion zone and its response to PWHT can often be controlled by the appropriate choice of weld filler metal (Ref 4). However, the properties of the HAZ can be controlled only by the judicious selection of the welding process and process parameters, and by the use of a PWHT. As a result, the utilization of martensitic

stainless steels depends, to a large extent, on the ability of the user to understand and control the properties of the weld HAZ.

An extensive review of the microstructure and properties of the HAZ in martensitic HT9 weldments is provided by Lippold (Ref 2, 3, 4). In his studies, a variety of autogenous bead-on-plate gas-tungsten arc welds were evaluated using both light optical microscopy and microhardness techniques. Prior to welding, the base-metal plates were austenitized for 30 min at 1040 °C (1900 °F), followed by an air cool. Tempering was performed at 760 °C (1400 °F) for 1 h. The base-metal microstructure consisted of a mixture of tempered lath martensite and alloy carbides, as shown in Fig. 2.

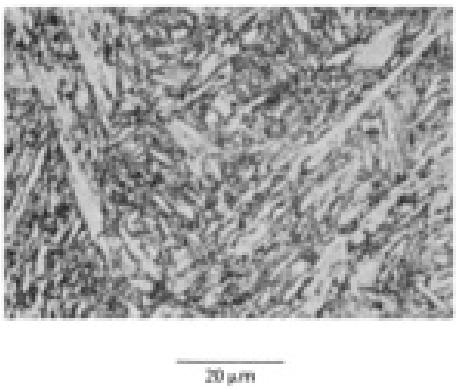

FIG. 2 QUENCHED-AND-TEMPERED BASE METAL (HT9) MICROSTRUCTURE, 22 TO 25 HRC. SOURCE: REF 2

The welding parameters used in these studies are listed in Table 5. The welding current was varied in the range from 100 to 225 A in order to produce weld heat inputs ranging from 0.71 to 2.13 kJ/mm (18 to 54 kJ/in.). The plates were clamped in a copper fixture during welding in order to stimulate the structural restraint experienced by actual components during fabrication.

TABLE 5 PARAMETERS FOR GAS-TUNGSTEN ARC WELDING OF HT9 MARTENSITIC STAINLESS STEEL

VOLTAGE, V	12-16
ARC CURRENT, A	100-225
TRAVEL SPEED, MM/S (IN./MIN)	1.69 (4)
ELECTRODE/WORK DISTANCE, MM (IN.)	2.38 (0.094)
ELECTRODE DIAMETER, MM (IN.)	3.18 (0.125)
ELECTRODE MATERIAL	W-2THO$_2$
SHIELDING GAS (ARGON), MM^3/S (FT^3/H)	365 (30)
PREHEAT	NONE

Source: Ref 2, 3

As shown in Fig. 3, the weld area consisted of the base metal (described above and shown in Fig. 2), the HAZ, and the fusion zone. Prior to tempering, the fusion zone microstructure comprised a mixture of untempered martensite and δ ferrite, as shown in Fig. 4.

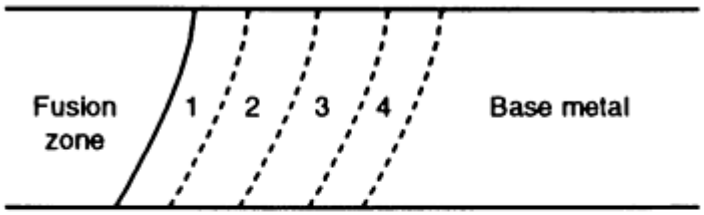

Four HAZ regions:

1 γ + ferrite ⟶ martensite + ferrite
2 Coarse-grained γ ⟶ martensite
3 Fine-grained γ ⟶ martensite
4 Overtempered base metal

FIG. 3 FOUR HAZ REGIONS OBSERVED IN HT9 WELDMENTS. γ REPRESENTS AUSTENITE. SOURCE: REF 3

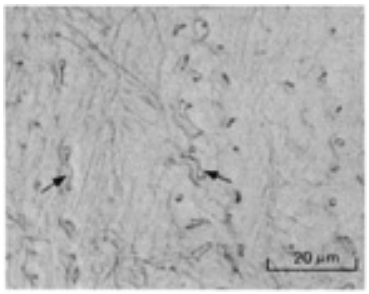

FIG. 4 AS-WELDED GAS-TUNGSTEN ARC FUSION ZONE MICROSTRUCTURE IN HT9 WELDMENTS. ARROWS INDICATE METASTABLE δFERRITE, WHICH CONSTITUTES APPROXIMATELY 2 TO 3 VOL% OF THE STRUCTURE. 1000×. SOURCE: REF 2

Four distinct regions were identified within the HAZ. These regions can be related to the phase fields on the iron-chromium-carbon equilibrium diagram shown in Fig. 5. The microstructures associated with these four regions are (Ref 4):

- *REGION 1,* WHICH IS A TWO-PHASE REGION ADJACENT TO THE FUSION LINE THAT CONSISTS OF UNTEMPERED MARTENSITE AND FERRITE. THE FERRITE FORMS ALONG PRIOR AUSTENITE GRAIN BOUNDARIES AS THIS REGION IS HEATED INTO THE AUSTENITE-PLUS-FERRITE PHASE FIELD (DESIGNATED 1 IN FIG. 3 AND 5).
- *REGION 2,* WHICH CONSISTS ENTIRELY OF UNTEMPERED MARTENSITE. AS THIS PORTION OF THE HAZ IS HEATED INTO THE HIGH-TEMPERATURE REGIME OF THE AUSTENITE PHASE FIELD, ALLOY CARBIDES FROM THE ORIGINAL BASE-METAL MICROSTRUCTURE COMPLETELY DISSOLVE, RESULTING IN A CARBIDE-FREE UNTEMPERED MARTENSITE THAT EXHIBITS A LARGE PRIOR AUSTENITE GRAIN.
- *REGION 3,* WHICH CONTAINS UNTEMPERED MARTENSITE INTERSPERSED WITH UNDISSOLVED ALLOY CARBIDES. BECAUSE THIS REGION EXPERIENCES A TEMPERATURE EXCURSION INTO THE LOWER REGIME OF THE AUSTENITE PHASE FIELD, CARBIDE DISSOLUTION IS INCOMPLETE AND THE PRIOR AUSTENITE GRAIN SIZE IS SMALLER RELATIVE TO REGION 2.
- *REGION 4,* WHICH CONSISTS OF TEMPERED MARTENSITE AND OVERAGED CARBIDES. IT APPEARS TO BE VIRTUALLY IDENTICAL TO THE BASE-METAL MICROSTRUCTURE.

Representative microstructures of these four regions are shown in Fig. 6.

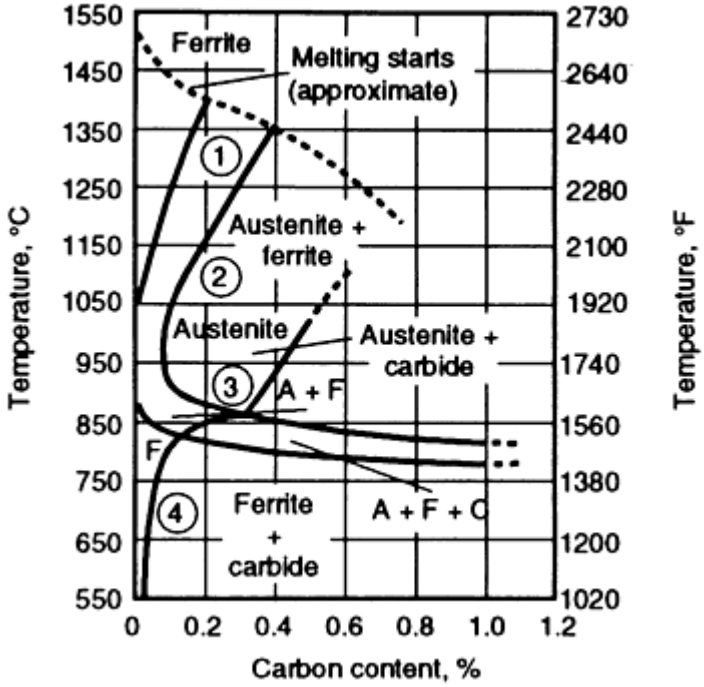

FIG. 5 IRON-CHROMIUM-CARBON PSEUDO-BINARY PHASE DIAGRAM FOR 12 WT% CR STEEL. CIRCLED NUMBERS REPRESENT THE FOUR HAZ REGIONS SHOWN IN FIG. 3 AND 6. SOURCE: ADAPTED FROM REF 5

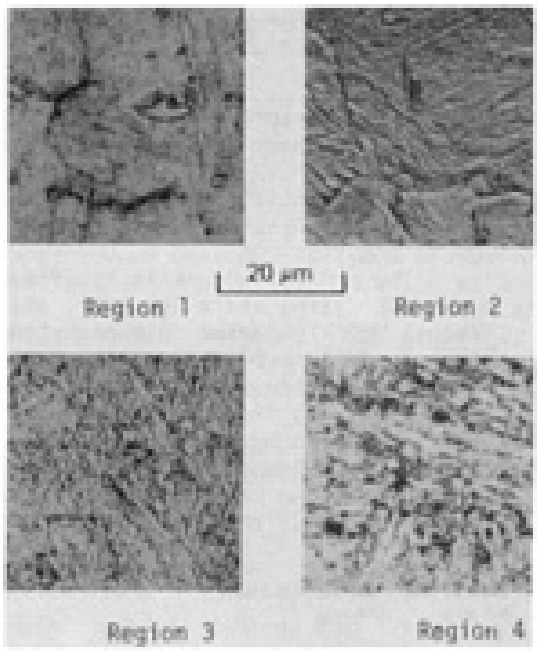

FIG. 6 GAS-TUNGSTEN ARC WELDED HAZ MICROSTRUCTURES IN HT9 WELDMENTS. SOURCE: REF 2

The microstructures in the HAZ can also be differentiated by means of a microhardness traverse, as shown in Fig. 7. The drop in hardness in Region 1 results from the presence of the softer ferrite phase situated at prior austenite grain boundaries within the untempered martensite matrix. The highest hardness in the HAZ occurs in the region where carbide dissolution is nearly complete. Because the hardness of the martensite is almost entirely a function of the carbon content of the prior austentite, Region 2 exhibits the peak HAZ hardness. Within Region 3, the carbon content of the austenite is

less, because of the incomplete dissolution of the carbides at lower austenitization temperatures. Therefore, the resultant microstructure, which consists of untempered martensite and residual carbides, is softer than the adjacent untempered microstructure (Region 2). The hardness decrease in Region 4 results from overtempering the base-metal microstructure at a temperature just below Ac_1 (the temperature at which austenite begins to form during heating), which is approximately 840 °C (1545 °F).

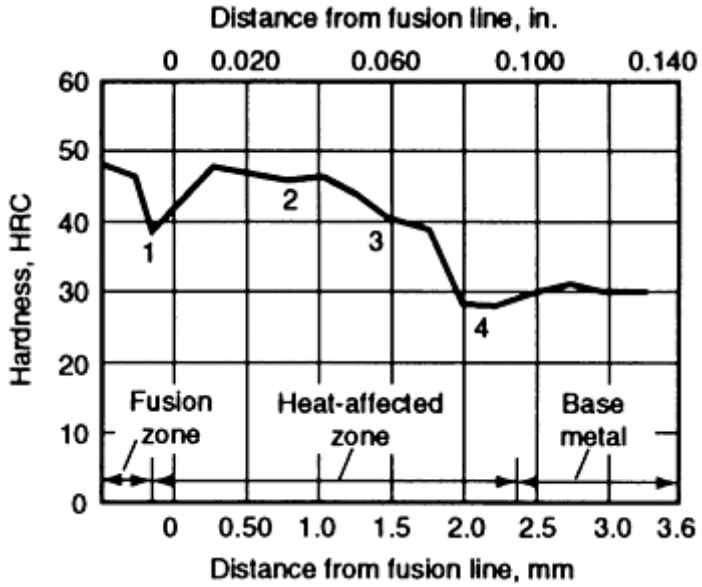

FIG. 7 MICROHARDNESS TRAVERSE ACROSS A GAS-TUNGSTEN ARC WELD IN HT9 STAINLESS STEEL (NO PREHEAT OR POSTHEAT TREATMENT). SOURCE: REF 3

Figures 8 and 9 demonstrate the effect of PWHT on the hardness and toughness, respectively, of the four HAZ regions described above. As shown in these figures, a PWHT of 760 °C (1400 °F) for 1 h produced superior results.

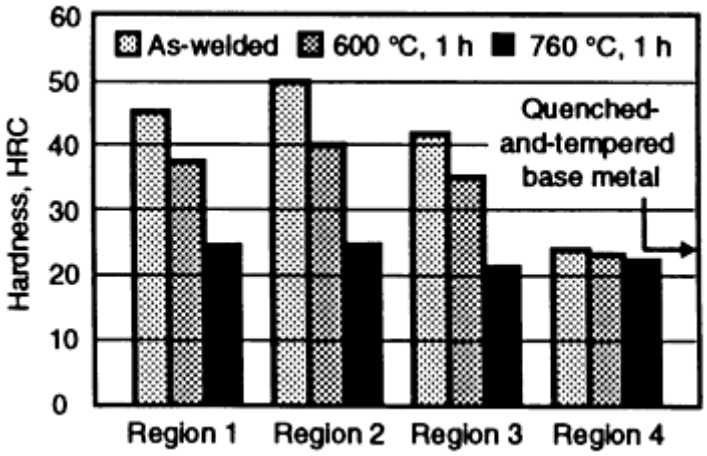

FIG. 8 HARDNESS AS A FUNCTION OF PWHT TEMPERATURE IN THE FOUR HAZ REGIONS OF HT9 WELDMENTS. SOURCE: REF 4

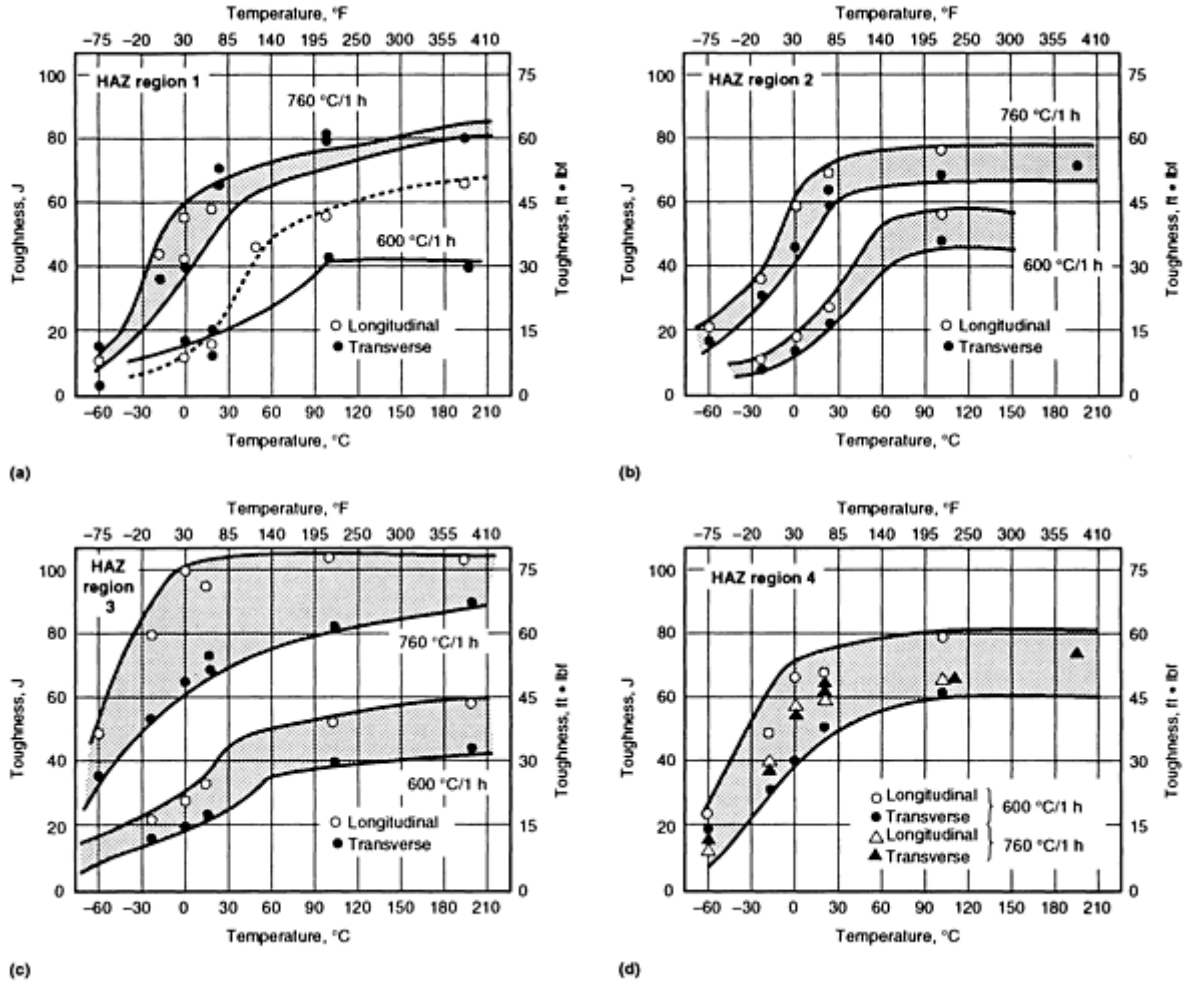

FIG. 9 EFFECT OF ORIENTATION AND PWHT ON THE TOUGHNESS OF HT9 WELDMENTS. (A) REGION 1. (B) REGION 2. (C) REGION 3. (D) REGION 4. SEE ALSO FIG. 3 AND 6. SOURCE: REF 4

Similar studies on HT9 have been carried out by Fenn and Jordan, with particular attention being given to δ ferrite formation (Ref 6). Maintaining a δ ferrite content that is as low as possible (< 10 vol%) is important, because a homogeneous martensitic structure that is free of δ ferrite islands results in a tougher weld. The investigations of these workers covered a variety of welding processes and a wide range of welding heat inputs, and involved real and simulated HAZ material.

References cited in this section

2. J.C. LIPPOLD, TRANSFORMATION AND TEMPERING BEHAVIOR OF 12CR-1MO-0.3V MARTENSITIC STAINLESS STEEL WELDMENTS, *J. NUCL. MATER.*, VOL 103 AND 104, 1981, P 1127-1132
3. J.C. LIPPOLD, "MICROSTRUCTURAL CHARACTERIZATION OF AUTOGENOUS GTA WELDS IN A 12CR-1MO-0.3V STEEL," DOCUMENT NO. SAND80-8236, SANDIA NATIONAL LABORATORIES, OCT 1980
4. J.C. LIPPOLD, THE EFFECT OF POSTWELD HEAT TREATMENT ON THE MICROSTRUCTURE AND PROPERTIES OF THE HEAT-AFFECTED ZONE IN 12CR-1MO-0.3V (HT9) WELDMENTS, *PROC. TOPICAL CONFERENCE ON FERRITIC ALLOYS FOR USE IN NUCLEAR ENERGY TECHNOLOGIES*, TMS, 1984, P 497-506
5. J.Z. BRIGGS AND T.D. PARKER, *THE SUPER 12% CR STEELS*, CLIMAX MOLYBDENUM

COMPANY, 1965
6. R. FENN AND M.F. JORDAN, MICROSTRUCTURE OF WELD HEAT-AFFECTED ZONE IN 12CR-1MO STEEL, *MET. TECHNOL.*, VOL 9 (NO. 8), 1982, P 327-337

Selection of Wrought Martensitic Stainless Steels

J.R. Davis, Davis & Associates

Weldability

Martensitic stainless steels can be welded in the annealed, hardened, and hardened-and-tempered conditions. Regardless of the prior condition of the steel, welding produces a hardened martensitic zone adjacent to the weld. In other words, the high-temperature HAZ will be in the "as-quenched" condition after welding, regardless of the prior condition of the material. In addition, the HAZ hardness is very much independent of the cooling rate over the temperature range experienced in common arc welding practices. This is evident from the isothermal transformation diagram shown in Fig. 10. Because such high hardness values render the material prone to cracking during fabrication, the selection of appropriate preheating levels and welding procedures is critical to the success of the welding process.

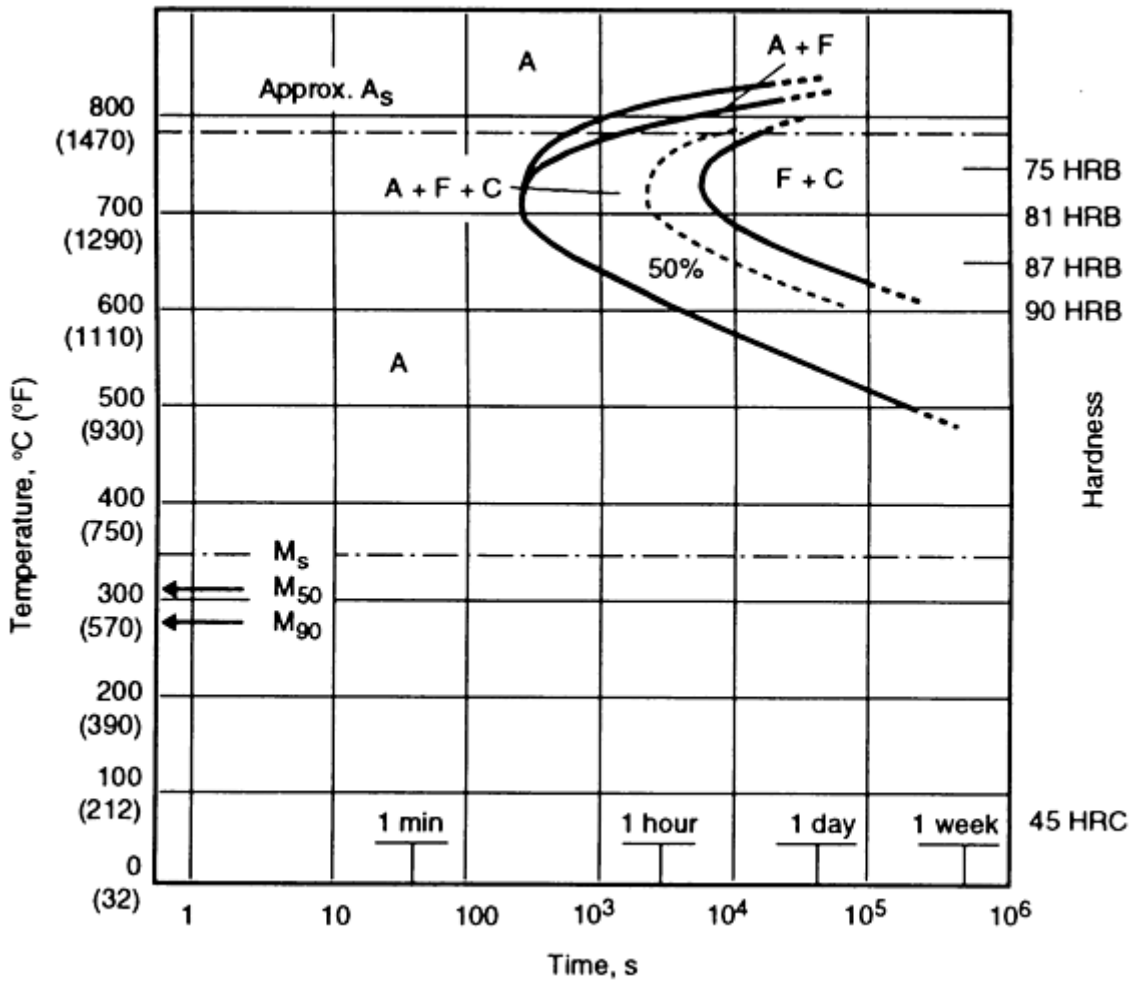

FIG. 10 ISOTHERMAL TRANSFORMATION DIAGRAM FOR TYPE 410 STAINLESS STEEL

Hydrogen-Induced Cold Cracking. Weld-area cracking in martensitic stainless steels is primarily due to the presence of hydrogen in the hardened structure (Ref 7). Hydrogen-induced cold cracks form in welds when the weldment is at or

near room temperature (typically, less than 150 °C, or 300 °F). Cracking may occur almost immediately or hours after cooling. In steel, cold cracks depend on the presence of a tensile stress, a susceptible microstructure, and sufficient hydrogen in the weld. Elimination of one or more of these factors greatly reduces crack susceptibility. The stress may arise from restraint by other components of a weldment or from the simple thermal stresses created by welding in a butt, groove, or "T" joint.

The susceptibility of the microstructure to cold cracking relates to the solubility of hydrogen and the possibility of supersaturation. Austenite, in which hydrogen is highly soluble, is least susceptible to cold cracking, and martensite, in which the solubility is lower, is most susceptible, because the rapid cooling necessary for the austenite-to-martensite transformation traps the hydrogen in a state of supersaturation in the martensite. Because the solubility of hydrogen in bcc martensite is low and diffusivity is high, austenitic filler metals are often selected to weld martensitic stainless steels. The discussion on filler metal selection later in this article provides more details.

The presence of hydrogen in a weld is generally due to moisture that is introduced in the shielding gas (or the electrode coating or flux), dissociated by the arc to form elemental hydrogen, and dissolved by the molten weld pool and by the adjacent region in the HAZ. In the supersaturated state, the hydrogen diffuses to regions of high stress, where it can initiate a crack. Continued diffusion of the hydrogen to the region of stress concentration at the crack tip extends the crack. This behavior means that hydrogen-induced cold cracking is time dependent--that is, time is needed for hydrogen diffusion--and the appearance of detectable cracks can be delayed until long after the weld has passed inspection. Additional information on the mechanisms of hydrogen cracking of weldments can be found in Ref 8 and 9.

For most commercial steels, the avoidance of hydrogen-induced cold cracking is based on the control of hydrogen (Ref 7). The sources of hydrogen (water, oils, greases, waxes, and rust that contains hydrogen or hydrates) should be eliminated. The hydrogen potential also can be minimized by using low-hydrogen, inert-gas welding processes, such as gas-tungsten arc welding (GTAW) or gas-metal arc welding (GMAW), or by paying stringent attention to consumable drying and baking for flux-shielded welding processes, such as shielded metal arc welding (SMAW) or flux-cored arc welding (FCAW). In addition, preheating must be applied to slow the rate of cooling. This allows more time for hydrogen to diffuse away from the weld area during cooling within the austenite range and, especially, following transformation to martensite.

Preheating is generally carried out in the temperature range from 200 to 300 °C (400 to 600 °F). In multipass welds, interpass temperatures must be maintained at the same level, and it is frequently beneficial to hold this temperature for some time after arc extinction to permit further hydrogen diffusion out of the joint. Postweld tempering is carried out to improve weld-area toughness. For higher-carbon steels (>0.2 wt% C), this process should be applied as soon as possible after welding to avoid the possibility of hydrogen-induced cracking from atmospheric corrosion. The weld must be cooled to a sufficiently low temperature to induce the austenite-to-martensite transformation (in principle, below the martensite completion point, M_f, as described below) prior to PWHT.

Material Composition and Selection of Preheat Temperature (Ref 10). The temperature at which austenite transforms to martensite upon cooling in martensitic stainless steels depends on material composition, particularly the carbon, manganese, nickel, chromium, and molybdenum contents. The martensitic start temperature, M_s, for such steels can be calculated using the following equation developed by The Welding Institute (Ref 11):

$$M_S = 540 - (497 \times \%C + 6.3 \times \%MN + 36.3 \times \%NI + 10.8 \times \%CR + 46.6 \times \%MO)\ ^\circ C \quad \textbf{(EQ 1)}$$

It should be noted that all of the elements listed above lower the M_s temperature.

Using Eq 1 for a type 410 stainless steel of the composition listed in Table 1, the M_s temperature is approximately 350 °C (660 °F). The temperature at which the transformation to martensite is complete, denoted by M_f, is approximately 100 °C (180 °F) below the M_s, that is, 256 °C (493 °F) for type 410. The preheat level should be below the M_f wherever possible, for example, 250 °C (480 °F) for type 410. However, if the M_f is less than about 150 °C (300 °F), as is the case with high-carbon (>0.2 wt% C) steels, it is not advisable to select a lower preheat level, because the embrittling effect of hydrogen can be significant at this temperature.

In most cases, the reason for choosing a preheat temperature below the M_f is to ensure that maximum transformation to martensite occurs. If this has not happened, then subsequent PWHT immediately after welding may be ineffective for two

reasons. First, the partially austenitic structure will retain hydrogen, which can lead to hydrogen cracking problems upon eventual cooling to room temperature, where untempered martensite with a high hydrogen concentration could form. Second, an isothermal transformation of the weld can take place during heat treatment, and the martensite that forms upon cooling to room temperature will be untempered and hard.

The major compositional factor influencing hydrogen-induced cold cracking is the material carbon content, because it determines the hardness of the transformed structure and its sensitivity to hydrogen embrittlement (Ref 7). Below levels of approximately 0.1 wt% C, and at least in thin sections (<5 mm, or 0.2 in.) it may be possible to weld without a preheat, if hydrogen levels are low. For materials with high carbon levels (above 0.2 wt% C), both a preheat and a PWHT are essential. Such materials are particularly difficult to weld, because the M_f temperature may be well below 150 °C (300 °F). In such cases, alloys are frequently welded with a preheat of 250 °C (480 °F), but are allowed to cool to an intermediate temperature of approximately 150 °C (300 °F) prior to a hydrogen release treatment or a full PWHT or both. For both low- and high-carbon martensitic stainless steels, it should be stressed that the weld should not be allowed to cool to room temperature after welding before either a full PWHT or a hydrogen release treatment is conducted.

Conventional martensitic stainless steels containing 12 wt% Cr and 0.15 wt% C have been successfully welded for many years, but a number of developments have reduced the risk of hydrogen-induced cold cracking. In terms of composition, this is best achieved by lowering the carbon content, except that this also reduces the hardenability of the material. Consequently, alloys that contain nickel have been produced in order to attain higher hardenability. The most common of these grades, particularly in Europe, is the 13Cr-4Ni-0.05C steels (Ref 12). Although the additional alloying reduces the M_s temperature, HAZ hydrogen-induced cold cracking resistance is substantially improved.

References cited in this section

7. R.A. WALKER AND T.G. GOOCH, ARC WELDABILITY OF STAINLESS STEELS, *MET. MATER.,* VOL 2 (NO. 1), 1986, P 18-24
8. J.H. DEVLETIAN AND W.E. WOOD, PRINCIPLES OF JOINING METALLURGY, *METALS HANDBOOK,* 9TH ED., VOL 6, AMERICAN SOCIETY FOR METALS, 1983, P 21-49
9. R.D. STOUT *ET AL., WELDABILITY OF STEELS,* 3RD ED., WELDING RESEARCH COUNCIL, 1978
10. D.N. NOBLE, "REVIEW OF PRACTICES FOR WELDING TYPE 410 STAINLESS STEEL," EDISON WELDING INSTITUTE
11. T.G. GOOCH, WELDING MARTENSITIC STAINLESS STEELS, *THE WELDING INSTITUTE RESEARCH BULLETIN,* VOL 18, DEC 1977
12. E. FOLKHARD, WELDING METALLURGY OF LOW CARBON CHROMIUM-NICKEL MARTENSITIC STAINLESS STEELS, *WELDING METALLURGY OF STAINLESS STEELS,* SPRINGER-VERLAG, 1984, P 179-184

Selection of Wrought Martensitic Stainless Steels

J.R. Davis, Davis & Associates

Heat Treatment

Preheating is one of the most effective means of avoiding weld cracking in martensitic stainless steels. The preheating temperature usually ranges from 200 to 300 °C (400 to 600 °F). As discussed previously, the material composition (particularly the carbon content) affects the preheat temperature. The use of the M_s equation (Eq 1) is helpful in determining an acceptable preheat temperature.

Another consideration that influences preheating requirements is material thickness. As described above, the restraint imposed by material thickness is also one of the factors controlling hydrogen-induced cold cracking in any welded joint (Ref 10). If the weld metal or HAZ has been embrittled by the presence of hydrogen, then the level of restraint in the joint may determine whether cracking occurs. The general rule for joint thickness is that the thicker the material, the greater the

restraint, that is, the more material that is present, the greater the force opposing the dimensional changes in the weld area that is brought about through thermal and transformation stresses. In a repair weld situation that involves a groove, the restraint will be very high and a conservative approach is recommended. However, for a simple butt joint involving very thin material, for example, 3 mm (0.12 in.) or less, a preheat is generally considered unnecessary. This is particularly true with low-carbon (<0.10 wt% C) base metals. However, a preheating step is typically carried out.

Postweld Heat Treatment. The functions of a PWHT are to temper the martensite in the weld metal and HAZ, in order to reduce the hardness and increase the toughness, and to decrease residual stresses associated with welding. Postweld heat treatments used for martensitic stainless steels usually take one of two forms. The most common form involves tempering the weldment by heating it below the austenite-start temperature, A_s (Fig. 10). This is generally carried out at temperatures ranging from 650 to 750 °C (1200 to 1400 °F). The weldment should be held at temperature for a minimum of 1 h per inch of weld thickness (Ref 10). Another form of PWHT involves heating the weldment above the austenite-finish temperature, A_f, to austenitize the entire mass, and then cooling it back to just above room temperature, followed by a second heat treatment at a temperature below the A_s, in order to temper the metal to the desired properties. The latter PWHT is utilized only when matching filler metals are used and maximum joint toughness must be achieved.

In addition, a low-temperature PWHT is sometimes carried out to facilitate the diffusion of hydrogen from the joint and decrease the likelihood of hydrogen-induced cold cracking (Ref 10). This type of PWHT is carried out at, or slightly above, the preheat temperature range of, for example, 300 to 400 °C (550 to 750 °F). The 450 to 500 °C (840 to 930 °F) range should be avoided because it can compromise weld toughness.

Except for very small weldments or very-low-carbon base metals, martensitic stainless steels are not typically used in the as-welded condition. If a weldment of martensitic stainless steel must be used in the as-welded condition, then it is recommended that both autogenous welds and welds with matching filler metal be avoided.

Correlations of Heat Treatment and Carbon Content. The following correlations of preheating and PWHT practice with carbon contents and welding characteristics of martensitic stainless steels can be used:

- *CARBON CONTENT BELOW 0.10%:* NEITHER PREHEATING NOR PWHT IS REQUIRED EXCEPT FOR VERY HEAVY SECTIONS; MARTENSITIC STAINLESS STEELS WITH CARBON CONTENTS THIS LOW ARE NOT STANDARD
- *CARBON CONTENT 0.10 TO 0.20%:* PREHEAT TO 260 °C (500 °F); WELD AT THIS TEMPERATURE; SLOW COOL BELOW 65 °C (150 °F); TEMPER
- *CARBON CONTENT 0.20 TO 0.50%:* PREHEAT TO 260 °C (500 °F); WELD AT THIS TEMPERATURE; SLOW COOL BELOW 65 °C (150 °F); AUSTENITIZE AND TEMPER
- *CARBON CONTENT OVER 0.50%:* PREHEAT TO 260 °C (500 °F); WELD WITH HIGH HEAT INPUT; ANNEAL WITHOUT LETTING THE WELDMENT COOL BELOW 260 °C (500 °F); AUSTENITIZE AND TEMPER

Reference cited in this section

10. D.N. NOBLE, "REVIEW OF PRACTICES FOR WELDING TYPE 410 STAINLESS STEEL," EDISON WELDING INSTITUTE

Selection of Wrought Martensitic Stainless Steels

J.R. Davis, Davis & Associates

Filler-Metal Selection

On the basis of hydrogen-cracking risk, the use of austenitic filler metals is preferable to the use of martensitic consumables of "matching" composition, because the solubility of hydrogen in a bcc structure (martensite) is low and diffusivity is high, as noted earlier. This contrasts with the situation in fcc materials, such as austenite, where the

solubility is high and diffusivity is low (Ref 10). It follows that if a matching martensitic filler metal is employed, then the hydrogen introduced via the welding consumable (which occurs in every case, regardless of cleanliness) will diffuse into the adjacent HAZ, where it has the opportunity to embrittle the steel. However, if an austenitic filler metal is used, then the majority of hydrogen introduced through welding will remain in the austenitic weld metal, where its solubility is high. A high hydrogen concentration in the austenitic weld metal is unlikely to cause weld-metal hydrogen-induced cracking, because the embrittling effect of hydrogen is considerably less in a predominantly austenitic weld structure than it is in a martensitic one. Suitable austenitic filler metals used for welding martensitic stainless steels include AWS E/ER308, 309, and 310, or a duplex austenitic-ferritic filler metal, such as 312.

Matching filler metals are used when the strength of the weld metal must be similar to that of the base metal or when maximum weld toughness is specified. The availability of matching filler metals is a problem for some martensitic stainless steels. Only AWS E410 and 410NiMo types are available in covered-electrode form. These compositions, as well as AWS ER420, are available as solid wires. Chemical compositions of martensitic stainless steel filler metals are given in Table 6.

TABLE 6 ALL-WELD-METAL CHEMICAL COMPOSITIONS FOR MARTENSITIC STAINLESS STEEL FILLER METALS

AWS CLASSIFICATION	COMPOSITION, %								
	C	Cr	Ni	Mo	Mn	Si	P	S	Cu
SMAW (PER AWS 5.4)									
E410	0.12	11.0-13.5	0.60	0.75	1.0	0.90	0.04	0.03	0.75
E410NIMO	0.06	11.0-12.5	4.0-5.0	0.40-7.0	1.0	0.90	0.04	0.03	0.75
GMAW, GTAW, AND SAW (PER AWS 5.9)									
ER410	0.12	11.5-13.5	0.6	0.75	0.6	0.50	0.03	0.03	0.75
ER410NIMO	0.06	11.0-12.5	4.0-5.0	0.4-0.7	0.6	0.50	0.03	0.03	0.75
ER420	0.15-0.40	12.0-14.0	0.6	0.75	0.6	0.50	0.03	0.03	0.75

Electrodes and welding rods that are suitable for use as filler metals in the welding of martensitic stainless steels are listed in Table 7. More detailed information on filler-metal selection, including case histories that review the steps necessary during the filler-metal selection process, can be found in the article "Welding of Stainless Steels" in the Section "Consumable Selection, Procedure Development, and Practice Considerations for Welding" in this Volume.

TABLE 7 FILLER METALS FOR USE IN ARC WELDING OF SELECTED MARTENSITIC STAINLESS STEELS

TYPE OF STEEL	ELECTRODE OR WELDING ROD[(A)]
403	410, 410NIMO, 309
410	410, 308, 309
414	410NIMO, 410, 309
416	312
420	420, 308, 309
431	410, 310
440A	312

Source: Carpenter Technology Corporation, Stoody Company, and *Metals Handbook,* 9th ed., Vol 6

(A) PREFIX E OR ER OMITTED.

Reference cited in this section

10. D.N. NOBLE, "REVIEW OF PRACTICES FOR WELDING TYPE 410 STAINLESS STEEL," EDISON WELDING INSTITUTE

Specific Welding Recommendations

This section provides specific arc welding procedural recommendations for the more commonly welded martensitic stainless steels. The free-machining grades (types 416, 416Se, 420F, 440F, and 440FSe) are not included, because these enhanced-machining alloys are not recommended for welding. Weld data related to the welding of martensitic stainless steels are available from both alloy producers and manufacturers of welding equipment and consumables. For example, some of the data listed below were obtained from Carpenter Technology Corporation and from Sandvik. Such companies should be consulted prior to welding martensitic stainless steels.

Type 403 can be satisfactorily welded using AWS E/ER309 austenitic filler metal. If a martensitic consumable must be used, then either AWS E/ER410 or 410NiMo are acceptable. Parts should be preheated to at least 200 to 250 °C (400 to 450 °F) before welding to prevent cracking. Following welding, a PWHT of 650 to 750 °C (1200 to 1400 °F) should be conducted.

Because of the considerable cracking that can occur when welding thick sections (greater than 25 mm, or 1 in.) of type 403, a program designed to select the optimal filler metal to produce crack-free welds was conducted by Westinghouse Electric Corporation (Ref 13). This study compared the mechanical properties of AWS ER410 and 410NiMo gas-metal arc welds in 25 mm (1 in.) thick type 403 stainless steel (normalized and tempered to 585 MPa, or 85 ksi; 0.2% yield strength). Table 8 lists the welding parameters that were used in this study.

TABLE 8 PARAMETERS FOR GMAW OF TYPE 403 MARTENSITIC STAINLESS STEEL

	ELECTRODE	
	ER410NIMO	**ER410**
VOLTAGE, V	30.5	28.0
ARC CURRENT, A	460	420
TRAVEL SPEED, MM/S (IN./MIN)	3.8 (9)	5.0 (12)
ELECTRODE DIAMETER, MM (IN.)	2.38 ($\frac{3}{32}$)	2.38 ($\frac{3}{32}$)
SHIELDING GAS (ARGON), MM^3/S (FT^3/H)	600 (50)	600 (50)
PREHEAT, °C (°F)	NONE	200 TO 250 (400 TO 450)

Source: Ref 13

Weldments were tested using U-bend, tensile, stress-rupture, and Charpy V-notch tests. Results indicated that AWS ER410NiMo weldments exhibited superior tensile and impact properties (Fig. 11 and 12), but had lower stress-rupture values (Fig. 13).

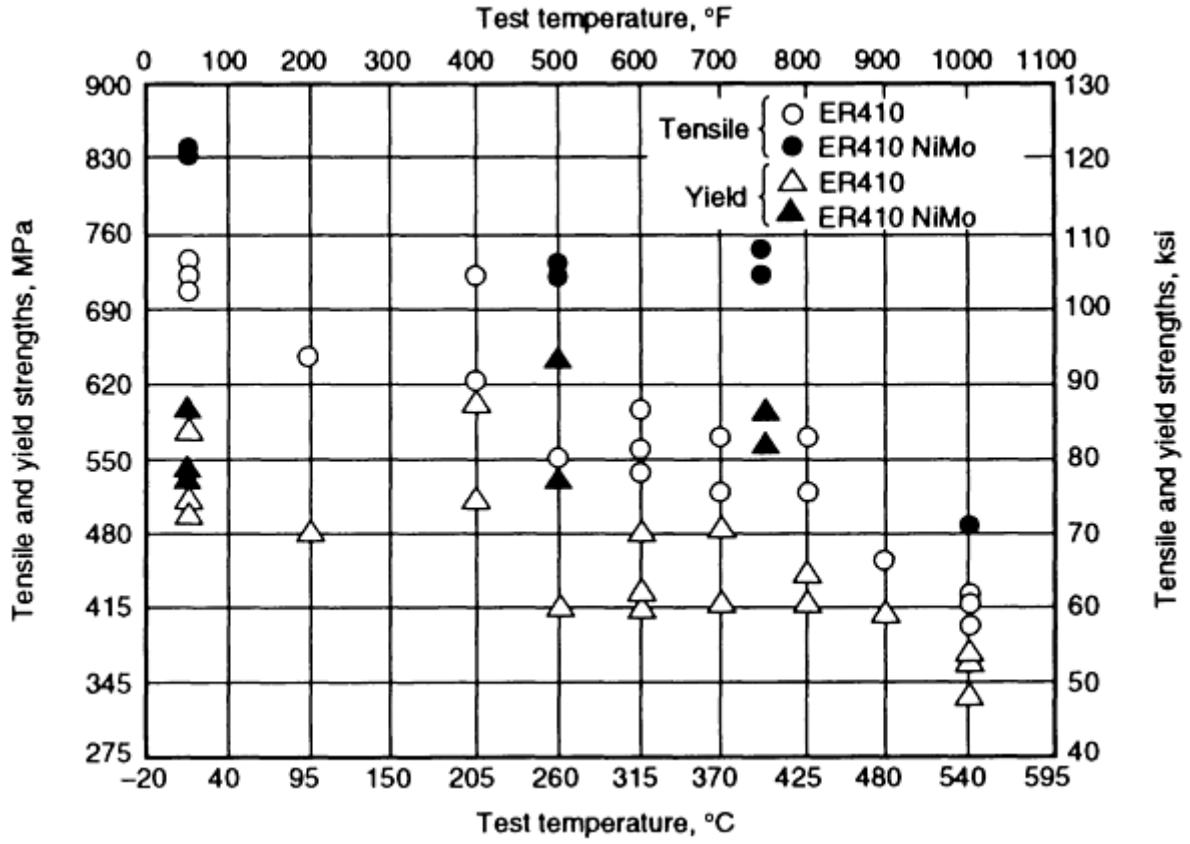

FIG. 11 STRENGTH VERSUS TEST TEMPERATURE FOR TWO MARTENSITIC STAINLESS FILLER METALS. SOURCE: REF 13

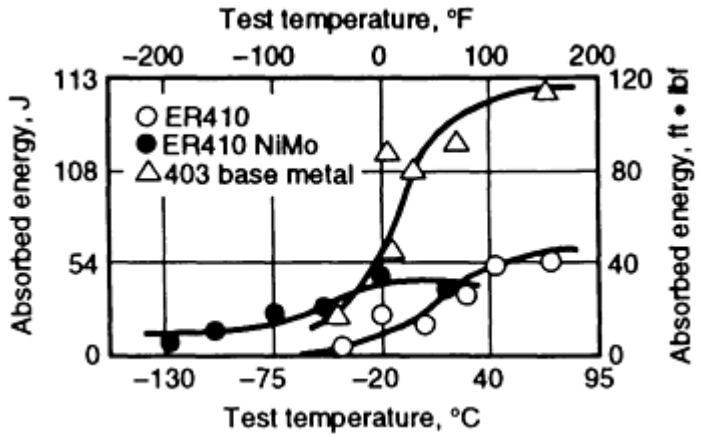

FIG. 12 CHARPY V-NOTCH VALUES VERSUS TEST TEMPERATURE FOR TWO MARTENSITIC STAINLESS STEEL FILLER METALS. SOURCE: REF 13

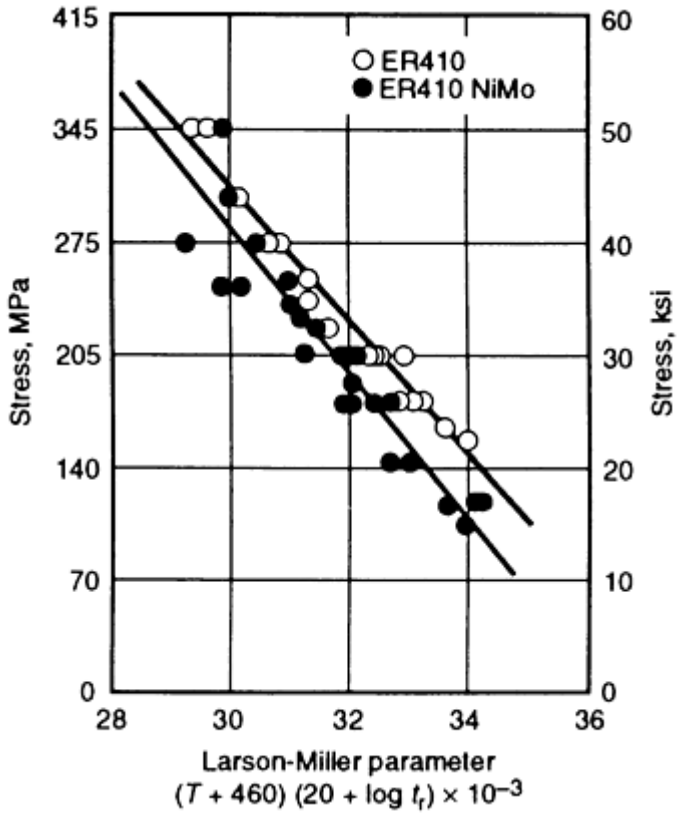

FIG. 13 RUPTURE STRESS AS A FUNCTION OF THE LARSON-MILLER PARAMETER FOR TWO MARTENSITIC STAINLESS STEEL FILLER METALS. SOURCE: REF 13

Type 410. The following recommendations for the arc welding of type 410 stainless steel are taken from Ref 10:

- PREHEAT TO 250 °C (480 °F) AND MAINTAIN THIS TEMPERATURE DURING WELDING. USE AN AUSTENITIC CONSUMABLE SUCH AS AWS E/ER308 OR 309. IF A STRONGER WELD IS DESIRED, AWS E/ER410 SHOULD BE USED.
- AFTER WELDING, ALLOW THE JOINT TO COOL TO THE PREHEAT TEMPERATURE, THAT IS, 250 °C (480 °F).
- BEFORE ALLOWING THE JOINT TO COOL TO ROOM TEMPERATURE, CONDUCT A TEMPERING OPERATION AT 720 °C (1330 °F) AND ALLOW APPROXIMATELY 1 H PER INCH OF THICKNESS, WITH A MINIMUM OF 1 H.
- COOL TO ROOM TEMPERATURE.

Type 414 can be welded using a filler metal of similar composition (AWS E/ER410 or 410NiMo) or an austenitic consumable (AWS E/ER309). Cracking is best prevented by preheating the part to at least 200 °C (400 °F) and maintaining that as a minimum interpass temperature. In addition, a PWHT that is in the range from 650 to 700 °C (1200 to 1300 °F) should be conducted.

Type 420. Satisfactory welds have been obtained in type 420 by preheating to a minimum of 200 °C (400 °F) before welding, followed by a PWHT of 675 to 750 °C (1250 to 1400 °F) (Ref 14). If a filler metal is required, then AWS ER420 should be considered when the mechanical properties of the weld are important. If the mechanical properties of the weld do not have to match those of the base metal, then AWS E/ER309 should be considered.

HT9 (12Cr-1Mo-0.3V) martensitic stainless steel can be welded using shielded-metal arc, gas-tungsten arc, or gas-metal arc welding processes (Ref 1). The joint should be preheated to a temperature between 200 and 400 °C (400 and 600 °F). In the case of multipass welds, an interpass temperature of 250 °C (480 °F) is specified to prevent the transformation to

untempered martensite that occurs upon cooling to room temperature. Finally, a PWHT in the temperature range from 740 to 780 °C (1365 to 1470 °F), for a period ranging from 30 min to 2 h, is required immediately following welding. If a filler metal is used, then consumables of matching composition should be selected.

Type 431 can be welded satisfactorily with most of the arc welding processes. If a filler metal is required, then one of a similar composition, such as AWS E/ER410, should be considered. An austenitic filler metal, such as AWS E/ER310, can also be used if the mechanical properties of the weld and the response to heat treatment are not required to be similar to those of the base metal. To prevent cracking of the weldment, it is necessary to preheat the base metal to a temperature between 200 and 300 °C (400 and 600 °F) and maintain a minimum interpass temperature of 200 °C (400 °F). After welding, the weldment should receive a PWHT at 650 °C (1200 °F).

Types 440A, B, and C. Because of their high carbon contents (0.6 to 1.2 wt% C, as listed in Table 1), these alloys are not generally considered to be weldable. However, successful welds using austenitic filler metals (AWS E312) have been made in type 440A stainless steel, which has the lowest carbon content of this group (0.60 to 0.75 wt% C). A case history outlining the proper gas-metal arc welding of type 440A stainless steel is given in the article "Welding of Stainless Steels" in this Volume.

References cited in this section

1. T. LECHTENBERG, WELDING AND FABRICATION CONSIDERATIONS FOR A 12CR-1MO MARTENSITIC STEEL FOR FUSION ENERGY SYSTEMS, *FERRITIC STEELS FOR HIGH-TEMPERATURE APPLICATIONS*, AMERICAN SOCIETY FOR METALS, 1983, P 163-177

10. D.N. NOBLE, "REVIEW OF PRACTICES FOR WELDING TYPE 410 STAINLESS STEEL," EDISON WELDING INSTITUTE

13. R.E. CLARK AND L.E. WAGNER, COMPARISON OF ER410 AND ER410NIMO GAS METAL ARC WELD METAL, *CAST METALS FOR STRUCTURAL AND PRESSURE CONTAINMENT APPLICATIONS*, AMERICAN SOCIETY OF MECHANICAL ENGINEERS, 1979, P 153-169

14. *WELDING HANDBOOK*, 7TH ED., VOL 4, AMERICAN WELDING SOCIETY, 1982, P 87-93

Selection of Wrought Martensitic Stainless Steels

J.R. Davis, Davis & Associates

Non-Arc Welding Processes

Although arc welding processes (particularly GMAW, GTAW, and SMAW) are commonly used to join martensitic stainless steels, a variety of other joining methods also can be employed, such as laser- and electron-beam welding, resistance welding, flash welding, and friction welding. However, regardless of the method selected, a hard (untempered) weld microstructure results from the welding process, and the same PWHTs as those discussed above must be carried out.

Laser-Beam Welding. Although the lower heat input that is typical of laser welds results in faster cooling rates and steeper temperature gradients in the weld HAZ, the problems of high hardness and low toughness in the weld area persist. Lippold has studied the microstructure of laser-beam welded martensitic stainless steels (Ref 2). The microstructure along the fusion boundary consists almost entirely of untempered martensite. The HAZ consists of two distinct microstructural regions. The first region immediately adjacent to the fusion line consists entirely of untempered martensite and extends less than 0.25 mm (0.01 in.) from the fusion line. The microstructure that is more remote from the fusion line consists of untempered martensite and carbides. The as-welded hardness of both the fusion zone and HAZ range from 52 to 56 HRC. As a result, a postweld tempering treatment is necessary. Lippold has shown that the tempering response of martensitic stainless steel laser welds is similar to that of arc welded specimens. As shown in Fig. 14, tempering for 1 h at 800 °C (1470 °F) reduced the as-welded hardness of laser welds.

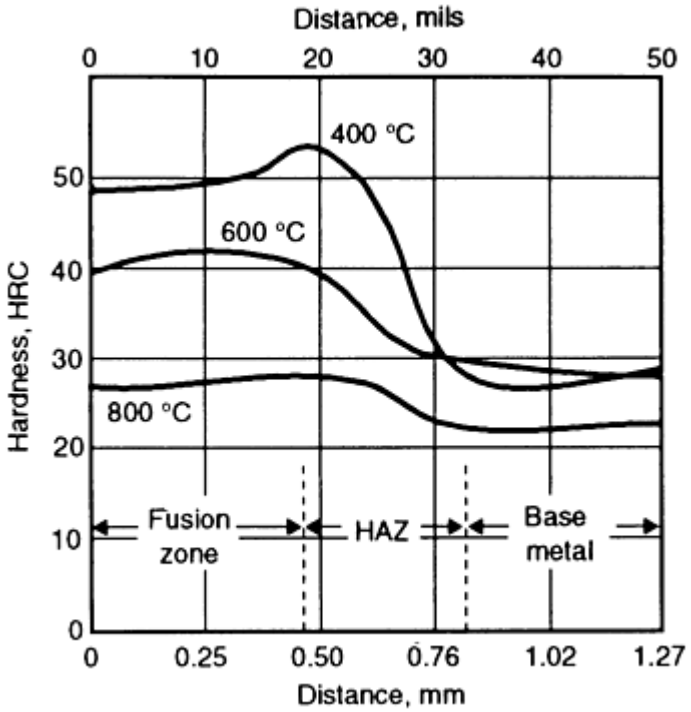

FIG. 14 TEMPERING BEHAVIOR OF HT9 LASER WELDS. SOURCE: REF 2

Lippold has also studied the effects of welding parameters on the quality of laser welds in HT9 martensitic steels (Ref 15). Laser welds were made in 6.35 mm (0.25 in.) thick HT9 plate using a variety of travel speed/focal length combinations at a constant power level of 6 kW. Welds made using low travel speed (1.27 mm/s, or 30 in./min), high heat input (0.47 kJ/mm, or 12 kJ/in.), and sharp focus produced sound welds. Welds performed at sharp focus with travel speeds ranging from 1.69 to 4.23 mm/s (40 to 100 in./min) and heat inputs decreasing from 0.35 to 0.14 kJ/mm (12 to 3.6 kJ/in.) exhibited scattered porosity and occasional centerline cracking that occurred during the final stages of solidification. Defocusing the laser beam relative to the plate resulted in welds containing severe porosity and centerline cracks. Microstructural and microhardness evaluation of the welds indicated that the region of highest hardness occurred in the HAZ immediately adjacent to the fusion line.

Laser-beam welds can be autogenous, or, alternatively, filler metals can be used. Martensitic stainless steels can be joined to each other or to dissimilar materials. For example, successful welds have been made between type 403 stainless steel and Inconel 600 using AWS A5.14 Class ENiCr-3 (Ni-20Cr-2.5Mn-2.25Nb) filler wire (Ref 16).

Electron-beam (EB) welding has been successfully conducted on modified 12 wt% Cr steels used for high-pressure, high-temperature components in power plants and in the chemical industry. In one study, EB welds were made to join 21 mm (0.83 in.) thick Fe-12Cr-1Mo plates (Ref 17). After tempering at 740 °C (1365 °F) for 2 h, the welds were investigated by Charpy V-notch and tensile tests at temperatures up to 550 °C (1020 °F). Impact properties of the EB welded joint were superior to those of submerged arc welded joints in the same alloy (Fig. 15) and exceeded those of the base metal. As is the case with laser-beam welds, the HAZ of the EB welds consisted of untempered martensite. A microhardness traverse across the weld revealed that the hardness in the fusion zone and HAZ region ranged from 300 to nearly 600 HV (30 to 55 HRC) (Fig. 16). Tempering subsequently lowered the hardness to below 300 HV.

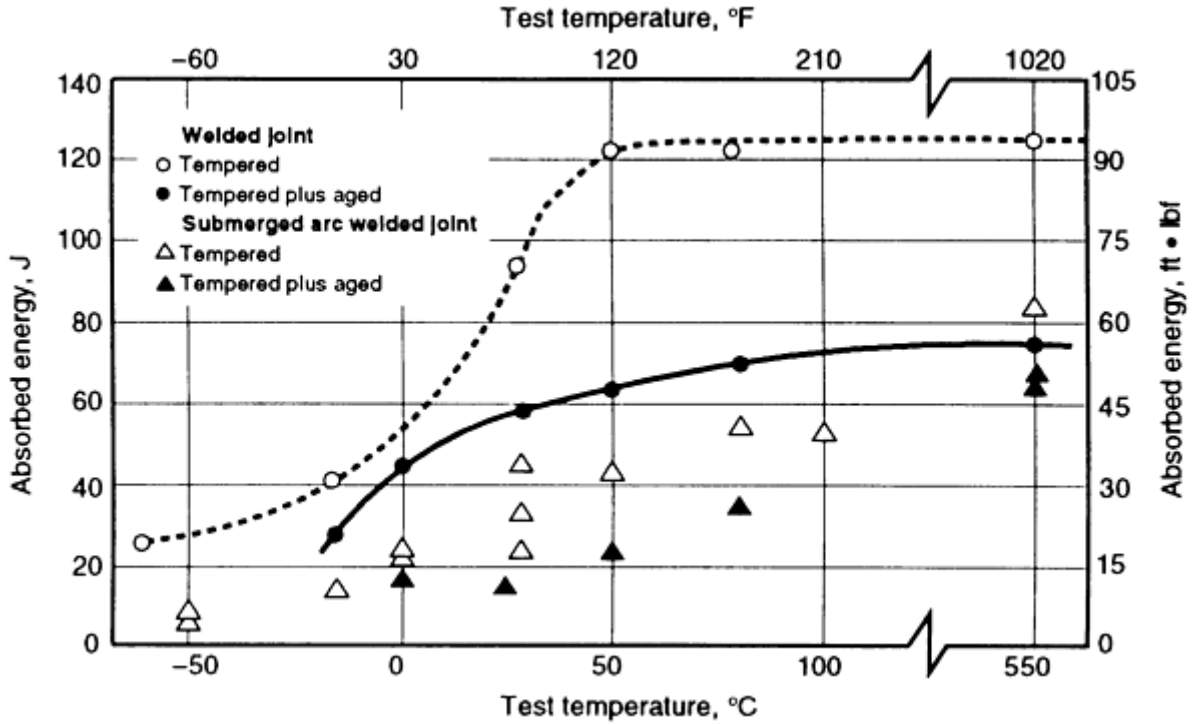

FIG. 15 CHARPY V-NOTCH DATA FOR WELD JOINTS OF EB WELDED ALLOY FE-0.2C-12CR-1MO PLATES, COMPARED WITH IMPACT DATA FOR SUBMERGED ARC WELDED JOINT USING A FILLER METAL SIMILAR TO FE-0.2C-12CR-1MO. CONDITIONS: TEMPERED AT 740 °C (1365 °F) AND TEMPERED PLUS AGED AT 550 °C (1020 °F) FOR 5000 H. SPECIMEN ORIENTATION: TRANSVERSE TO WELD. SOURCE: REF 17

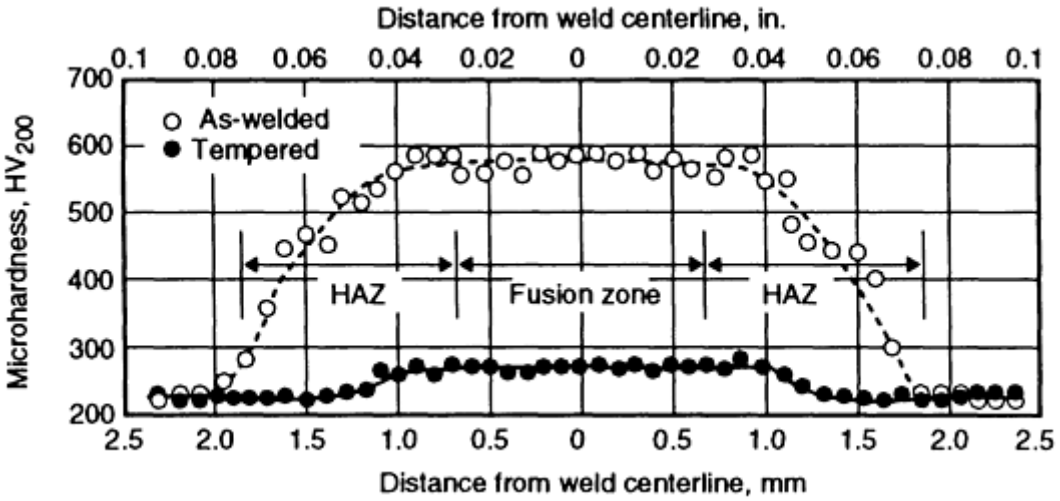

FIG. 16 MICROHARDNESS TRAVERSE ACROSS THE WELD IN TRANSVERSE CROSS SECTIONS OF EB WELDED ALLOY FE-0.2C-12CR-1MO PLATE AT THE CENTER OF PLATE THICKNESS; AS-WELDED AND CONDITIONED AND TEMPERED FOR 2 H AT 740 °C (1365 °F). SOURCE: REF 17

Friction welding can be used to join martensitic stainless steels to themselves, as well as to other steels. As is the case with other welding processes, changes in hardness at and near the weld interface can be expected (Ref 18). Figure 17 shows changes in hardness of a welded joint made of JIS S45C (0.45 wt% C) carbon steel and type 440C stainless steel.

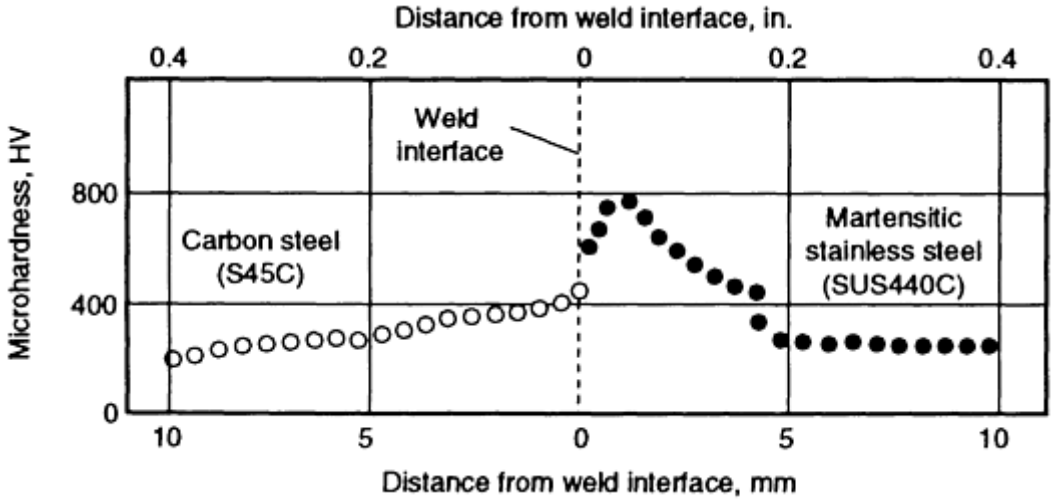

FIG. 17 CHANGES IN HARDNESS AT AND NEAR A FRICTION WELD INTERFACE. SOURCE: REF 18

Resistance Welding. Martensitic stainless steels can be spot welded in the annealed, hardened, or quenched-and-tempered conditions. Regardless of the initial base-metal hardness and the welding schedule, the HAZ adjacent to the weld nugget quenches to martensite. The hardness of the weld nugget and HAZ primarily depends on the carbon content of the steel, although it can be controlled somewhat with preheat, postheat, and tempering during the spot-welding cycle. The likelihood of cracking in the HAZ increases with the carbon content of the steel.

Flash Welding. As is the case with resistance spot welding, a hard HAZ is formed during the flash welding of martensitic stainless steels. This hard HAZ can be softened somewhat by a tempering cycle in the welding machine. A PWHT will produce welds with properties approximately equal to those of the base metal (Ref 19).

References cited in this section

2. J.C. LIPPOLD, TRANSFORMATION AND TEMPERING BEHAVIOR OF 12CR-1MO-0.3V MARTENSITIC STAINLESS STEEL WELDMENTS, *J. NUCL. MATER.*, VOL 103 AND 104, 1981, P 1127-1132
15. J.C. LIPPOLD, ANALYSIS OF WELDS IN HT9, *ALLOY DEVELOPMENT FOR IRRADIATION PERFORMANCE*, DOCUMENT DOE/ER 0045-4, U.S. DEPARTMENT OF ENERGY, 1981, P 126-139
16. G.J. BRUCK, DILUTION CONTROL IN HORIZONTAL LASER BEAM WELDING OF DISSIMILAR METALS, *THE CHANGING FRONTIERS OF LASER MATERIALS PROCESSING*, IFS PUBLICATIONS, 1987, P 149-159
17. K. KUSSMAUL *ET AL.*, MECHANICAL PROPERTIES AND STRUCTURE OF ELECTRON BEAM WELDS IN ALLOY FE-0.2%C-12%CR-1%MO, *WELD J.*, VOL 63 (NO. 9), SEPT 1984, P 267S-272S
18. A. ISHIBASHI *ET AL.*, STUDIES ON FRICTION WELDING OF CARBON AND ALLOY STEELS (3RD REPORT: ADEQUATE WELDING CONDITIONS FOR HIGH ALLOY STEELS AND DISTRIBUTIONS OF ALLOY ELEMENTS NEAR WELD INTERFACE), PAPER NO. 216, *BULL. JPN. SOC. MECH. ENG.*, VOL 26, JUNE 1983, P 1080-1087
19. L.W. WELLER AND R.H. FOXALL, FLASH WELDING, *METALS HANDBOOK*, 9TH ED., VOL 6, AMERICAN SOCIETY FOR METALS, 1984, P 557-580

References

1. T. LECHTENBERG, WELDING AND FABRICATION CONSIDERATIONS FOR A 12CR-1MO MARTENSITIC STEEL FOR FUSION ENERGY SYSTEMS, *FERRITIC STEELS FOR HIGH-TEMPERATURE APPLICATIONS,* AMERICAN SOCIETY FOR METALS, 1983, P 163-177
2. J.C. LIPPOLD, TRANSFORMATION AND TEMPERING BEHAVIOR OF 12CR-1MO-0.3V MARTENSITIC STAINLESS STEEL WELDMENTS, *J. NUCL. MATER.,* VOL 103 AND 104, 1981, P 1127-1132
3. J.C. LIPPOLD, "MICROSTRUCTURAL CHARACTERIZATION OF AUTOGENOUS GTA WELDS IN A 12CR-1MO-0.3V STEEL," DOCUMENT NO. SAND80-8236, SANDIA NATIONAL LABORATORIES, OCT 1980
4. J.C. LIPPOLD, THE EFFECT OF POSTWELD HEAT TREATMENT ON THE MICROSTRUCTURE AND PROPERTIES OF THE HEAT-AFFECTED ZONE IN 12CR-1MO-0.3V (HT9) WELDMENTS, *PROC. TOPICAL CONFERENCE ON FERRITIC ALLOYS FOR USE IN NUCLEAR ENERGY TECHNOLOGIES,* TMS, 1984, P 497-506
5. J.Z. BRIGGS AND T.D. PARKER, *THE SUPER 12% CR STEELS,* CLIMAX MOLYBDENUM COMPANY, 1965
6. R. FENN AND M.F. JORDAN, MICROSTRUCTURE OF WELD HEAT-AFFECTED ZONE IN 12CR-1MO STEEL, *MET. TECHNOL.,* VOL 9 (NO. 8), 1982, P 327-337
7. R.A. WALKER AND T.G. GOOCH, ARC WELDABILITY OF STAINLESS STEELS, *MET. MATER.,* VOL 2 (NO. 1), 1986, P 18-24
8. J.H. DEVLETIAN AND W.E. WOOD, PRINCIPLES OF JOINING METALLURGY, *METALS HANDBOOK,* 9TH ED., VOL 6, AMERICAN SOCIETY FOR METALS, 1983, P 21-49
9. R.D. STOUT *ET AL., WELDABILITY OF STEELS,* 3RD ED., WELDING RESEARCH COUNCIL, 1978
10. D.N. NOBLE, "REVIEW OF PRACTICES FOR WELDING TYPE 410 STAINLESS STEEL," EDISON WELDING INSTITUTE
11. T.G. GOOCH, WELDING MARTENSITIC STAINLESS STEELS, *THE WELDING INSTITUTE RESEARCH BULLETIN,* VOL 18, DEC 1977
12. E. FOLKHARD, WELDING METALLURGY OF LOW CARBON CHROMIUM-NICKEL MARTENSITIC STAINLESS STEELS, *WELDING METALLURGY OF STAINLESS STEELS,* SPRINGER-VERLAG, 1984, P 179-184
13. R.E. CLARK AND L.E. WAGNER, COMPARISON OF ER410 AND ER410NIMO GAS METAL ARC WELD METAL, *CAST METALS FOR STRUCTURAL AND PRESSURE CONTAINMENT APPLICATIONS,* AMERICAN SOCIETY OF MECHANICAL ENGINEERS, 1979, P 153-169
14. *WELDING HANDBOOK,* 7TH ED., VOL 4, AMERICAN WELDING SOCIETY, 1982, P 87-93
15. J.C. LIPPOLD, ANALYSIS OF WELDS IN HT9, *ALLOY DEVELOPMENT FOR IRRADIATION PERFORMANCE,* DOCUMENT DOE/ER 0045-4, U.S. DEPARTMENT OF ENERGY, 1981, P 126-139
16. G.J. BRUCK, DILUTION CONTROL IN HORIZONTAL LASER BEAM WELDING OF DISSIMILAR METALS, *THE CHANGING FRONTIERS OF LASER MATERIALS PROCESSING,* IFS PUBLICATIONS, 1987, P 149-159
17. K. KUSSMAUL *ET AL.,* MECHANICAL PROPERTIES AND STRUCTURE OF ELECTRON BEAM WELDS IN ALLOY FE-0.2%C-12%CR-1%MO, *WELD J.,* VOL 63 (NO. 9), SEPT 1984, P 267S-272S
18. A. ISHIBASHI *ET AL.,* STUDIES ON FRICTION WELDING OF CARBON AND ALLOY STEELS (3RD REPORT: ADEQUATE WELDING CONDITIONS FOR HIGH ALLOY STEELS AND DISTRIBUTIONS OF ALLOY ELEMENTS NEAR WELD INTERFACE), PAPER NO. 216, *BULL. JPN.*

SOC. MECH. ENG., VOL 26, JUNE 1983, P 1080-1087

19. L.W. WELLER AND R.H. FOXALL, FLASH WELDING, *METALS HANDBOOK*, 9TH ED., VOL 6, AMERICAN SOCIETY FOR METALS, 1984, P 557-580

Selection of Wrought Ferritic Stainless Steels

K.F. Krysiak, Hercules, Inc.; J.F. Grubb, Allegheny Ludlum Corporation; B. Pollard; R.D. Campbell, Joining Services, Inc.

Introduction

FERRITIC STAINLESS STEELS comprise approximately one-half of the SAE-AISI-type 400-series stainless steels. These steels contain from 10.5 to 30% Cr along with other alloying elements, notably molybdenum. Ferritic stainless steels are noted for their excellent stress-corrosion cracking (SCC) resistance and good resistance to pitting and crevice corrosion in chloride environments.

Following a discussion on how ferritic stainless steels can be classified, this article will review the metallurgical characteristics of various ferritic grades as well as the factors that influence their weldability. Emphasis will be placed on arc welding processes. Additional information on ferritic stainless steels can be found in the companion article "Welding of Stainless Steels" in this Volume.

Selection of Wrought Ferritic Stainless Steels

K.F. Krysiak, Hercules, Inc.; J.F. Grubb, Allegheny Ludlum Corporation; B. Pollard; R.D. Campbell, Joining Services, Inc.

Classification of Ferritic Stainless Steels

The ferritic stainless steels can be classified into three groups. These include: Group I alloys, which are the standard ferritic stainless steels; Group II alloys, which are modified versions of the standard alloys; and Group III alloys, which contain very low interstitial element (carbon, nitrogen, and oxygen) contents or stabilizing elements for improved corrosion resistance and ductility in the as-welded condition.

Group I Alloys. Ferritic stainless steels of the 400-series Group I variety have been available for many years and are used primarily for their resistance to corrosion and scaling at elevated temperatures. Table 1 lists chemical compositions of standard-grade Group I ferritic stainless steels. While these alloys have useful properties in the wrought condition, welding is known to reduce toughness and ductility and corrosion resistance because of grain coarsening and formation of martensite (Ref 1). Welding these commercial grades usually requires preheat and postweld heat treatment. For these reasons, the application of the 400-series Group I ferritic stainless steels is not as extensive as it might otherwise be, compared with the 300-series austenitic stainless steels, which enjoy ease of weldability.

TABLE 1 NOMINAL CHEMICAL COMPOSITION OF REPRESENTATIVE GROUP I STANDARD-GRADE 400-SERIES FERRITIC STAINLESS STEELS

UNS NO.	TYPE	COMPOSITION[(A)], WT%			
		C	Cr	Mo	OTHER
S42900	429	0.12	14.0-16.0	. . .	. . .
S43000	430	0.12	16.0-18.0	. . .	. . .
S43020	430F	0.12	16.0-18.0	0.6	0.06 P; 0.15 MIN S
S43023	430FSE	0.12	16.0-18.0	. . .	0.15 MIN SE
S43400	434	0.12	16.0-18.0	0.75-1.25	. . .

S43600	436	0.12	16.0-18.0	0.75-1.25	NB + TA = 5 × %C MIN
S44200	442	0.20	18.0-23.0	. . .	. . .
S44600	446	0.20	23.0-27.0	. . .	. . .

(A) SINGLE VALUES ARE MAXIMUM UNLESS OTHERWISE INDICATED

Group II Alloys. To overcome some of the difficulties and to improve weldability, several of the standard grade ferritics have been modified. These Group II ferritic stainless steels which contain lower levels of chromium and carbon, along with additions of ferrite stabilizers, are listed in Table 2. Applications of these alloys involve exposure to high temperatures, such as for quenching racks and annealing boxes, and also for tanks for agricultural sprays, transformer cases, and automotive applications.

TABLE 2 CHEMICAL COMPOSITIONS OF GROUP II FERRITIC STAINLESS STEELS

UNS NO.	ALLOY DESIGNATION	COMPOSITION[A], WT%				
		C	Cr	Mo	Ni	Other
S40500	405	0.08	11.5-14.5			0.10-0.30 AL
S40900	409	0.08	10.5-11.75	. . .	0.5	TI = 6 × C MIN TO 0.75 MAX
. . .	409CB	0.02[B]	12.5[B]	. . .	0.2[B]	0.4 NB[B]
S44100	441	0.02[B]	18.0[B]	. . .	0.3[B]	0.7 NB[B], 0.3 TI[B]
. . .	AL433	0.02[B]	19.0[B]	. . .	0.3[B]	0.4 NB[B], 0.5 SI[B], 0.4 CU[B]
. . .	AL446	0.01[B]	11.5[B]	. . .	0.2[B]	0.2 NB[B], 0.1 TI[B]
. . .	AL468	0.01[B]	18.2[B]	. . .	0.2[B]	0.2 NB[B], 0.1 TI[B]
. . .	YUS436S	0.01[B]	17.4[B]	1.2[B]	. . .	0.2 TI[B]
S43035	439	0.07	17.00-19.00	. . .	0.5	TI = 0.20 + 4 (C + N) MIN TO 1.0 MAX
. . .	12SR	0.2	12.0	. . .	. . .	1.2 AL: 0.3 TI
. . .	18SR	0.04	18.0	. . .	. . .	2.0 AL; 0.4 TI
K41970	406	0.06	12.0-14.0	. . .	0.5	2.75-4.25 AL; 0.6 TI

(A) SINGLE VALUES ARE MAXIMUM UNLESS OTHERWISE INDICATED.

(B) TYPICAL VALUE

For example, type 405, containing nominally 12% Cr, is made with lower carbon and a small aluminum addition of 0.20% to restrict the formation of austenite at high temperature so that hardening is reduced during welding. For maximum ductility and corrosion resistance, however, postweld annealing is necessary (Ref 2). Recommendations for welding include either a 430- or a 309-type filler metal, the latter being used when increased weld ductility is desired.

Type 409 is one of the most widely used ferritic stainless steels. This alloy, which has a titanium addition, is used extensively in automotive exhaust systems and is often welded using the resistance welding processes.

Group III Alloys. In the late 1960s and early 1970s, researchers recognized that highly alloyed (higher chromium and molybdenum contents) ferritic stainless steels possessed a desirable combination of resistance to general corrosion, pitting, and SCC (Ref 3, 4, 5, 6, 7, 8, 9, 10). These properties made them attractive alternatives to the 300-series austenitic stainless steels that are commonly plagued by failure as a result of chloride SCC. It was reasoned that by controlling the interstitial element content (carbon, C, nitrogen, N, and oxygen, O) of these new ferritic alloys, either by ultrahigh purity processing methods or by stabilization, the formation of martensite could be eliminated, as well as the need for preheat and postweld heat treatment, so that welds would be corrosion resistant, tough, and ductile in the as-welded condition. To achieve these results, electron-beam vacuum refining, vacuum and argon-oxygen decarburization (AOD), and vacuum induction melting processes were used. From this beginning, two basic ferritic stainless alloy systems evolved.

Ultrahigh-Purity Group III Alloys. Ferritic alloys that have an interstitial element (C + N) content less than 150 ppm are termed ultrahigh purity. Examples of these alloys, shown in Table 3, are available commercially. These alloys are produced by either electron beam vacuum refining, vacuum induction melting (VIM), or vacuum oxygen decarburization

(VOD). Plate is available up to 13 mm ($\frac{1}{2}$ in.) in thickness. Purity is especially important with the higher-chromium alloys because of the effect on ductility, toughness, and weldability. Although not mentioned in the chemistry specification for these alloys, oxygen and hydrogen are particularly harmful, and their levels must also be carefully restricted. A modest amount of niobium (columbium) is added to some of these alloys to preserve corrosion resistance in the welded condition.

TABLE 3 NOMINAL CHEMICAL COMPOSITIONS OF GROUP III ULTRAHIGH-PURITY FERRITIC STAINLESS STEELS

UNS NO.	ALLOY DESIGNATION	COMPOSITION[A], WT%						
		C	N	Cr	Mo	Ni	Nb	Other
S44726	E-BRITE 26-1 (XM-27)	0.010	0.015	25-27	0.75-1.5	0.30	0.05-0.20	0.4 MN
S44800	AL 29-4-2	0.010	0.020	28-30	3.5-4.2	2.0-2.5	. . .	. . .
S44700	AL 29-4	0.010	0.020	28-30	3.5-4.2	0.15	. . .	0.3 MN
. . .	SHOMAC 30-2	0.003[B]	0.007[B]	30[B]	2[B]	0.2[B]	. . .	0.3 MN
S44400	YUS 190L	0.004[B]	0.0085[B]	18[B]	2[B]	0.4[B]	. . .	. . .

(A) SINGLE VALUES ARE MAXIMUM UNLESS OTHERWISE STATED.

(B) TYPICAL VALUE

Intermediate-Purity Group III Alloys. When the (C + N) interstitial element content exceeds 150 ppm (but is less than 800 ppm), ferritic alloys are considered to be of intermediate purity. Alloys listed in Table 4 are available commercially and are produced typically by the AOD process. Because these steels have higher carbon and nitrogen contents, their ductility and toughness are inferior to those of the ultrahigh-purity alloys. For this reason, metal thickness is limited to a maximum of approximately 3 mm ($\frac{1}{8}$ in.) where toughness is adequate. In order to maintain acceptable corrosion resistance in the as-welded condition, titanium and/or niobium are added to tie up the carbon and nitrogen that otherwise would combine with the chromium to form chromium carbides and nitrides, which can lead to preferential intergranular attack in many environments. This form of attack is most readily observed in the weld heat-affected zone (HAZ). Although niobium and titanium are both stabilizers, they are not equivalent. Autogenous welds in titanium-containing alloys typically exhibit an equiaxed grain region near the weld centerline. Alloys stabilized only with niobium typically show a columnar weld structure with a sharply defined centerline and a propensity for weld cracking. To avoid this, one must: (1) keep the carbon content below 0.01%, (2) keep the niobium content below 0.1%, and (3) add titanium in amounts greater than 0.1%.

TABLE 4 NOMINAL CHEMICAL COMPOSITIONS OF GROUP III INTERMEDIATE-PURITY FERRITIC STAINLESS STEELS

UNS NO.	ALLOY DESIGNATION	COMPOSITION[A], WT%					
		C	N	Cr	Mo	Ni	Ti
S44626	26-1 TI	0.02[B]	0.025[B]	26[B]	1[B]	0.25[B]	0.5[B]
S44400	AISI 444	0.02[B]	0.02[B]	18[B]	2[B]	0.4[B]	0.5[B]
S44660	SEA-CURE	0.025	0.035	25-27	2.5-3.5	1.5-3.5	$[0.20 + 4\,(C + N)] \le (NB + TI) \le 0.80$
S44635	NU MONIT	0.025	0.035	24.5-26	3.5-4.5	3.5-4.5	$[0.20 + 4\,(C + N)] \le (NB + TI) \le 0.80$
S44735	AL 29-4C	0.030	0.045	28-30	3.6-4.2	1.0	$6\,(C + N) \le (NB + TI) \le 1.0$

(A) SINGLE VALUES ARE MAXIMUM VALUES UNLESS OTHERWISE STATED.

(B) TYPICAL VALUE

Although it was claimed that the ultrahigh-purity alloys were costly to produce, many users found that the cost differential of similar alloys produced by the AOD melting practice was not economical enough to warrant purchase of these alloys in preference to similar alloys of ultrahigh purity, especially considering the inferior ductility and toughness of welded AOD-refined materials.

References cited in this section

1. *METALS HANDBOOK*, VOL 6, 8TH ED., *WELDING AND BRAZING*, AMERICAN SOCIETY FOR METALS, 1971, P 248
2. WORKING DATA, CARPENTER STAINLESS STEELS, 1971
3. W.A. MATEJKA AND R.J. KNOTH, E-BRITE 26-1, THE HIGH-PURITY APPROACH TO HIGH CHROMIUM FERRITIC STAINLESS STEELS, *ASM SYMPOSIUM*, BAL HARBOUR, FLORIDA, ASTM, 6 DEC 1973
4. R.N. WRIGHT, MECHANICAL BEHAVIOR AND WELDABILITY OF HIGH-CHROMIUM FERRITIC STAINLESS STEELS AS A FUNCTION OF PURITY, *WELD. J.*, OCT 1971, P 434S-440S
5. I.A. FRANSON, MECHANICAL PROPERTIES OF HIGH-PURITY FE-26CR-1MO FERRITIC STAINLESS STEEL, *METALL. TRANS.*, VOL 5, NOV 1974, P 2257-2264
6. J.J. DEMO, WELDABLE AND CORROSION-RESISTANT FERRITIC STAINLESS STEELS, *METALL. TRANS.*, VOL 5, NO. 11, NOV 1974, P 2253-2256
7. K.E. PINNOW, J.P. BRASSANELLI, AND A. MOSKOWITZ, A NEW HIGH-CHROMIUM FERRITIC STAINLESS STEEL, *MET. ENG. QUART.*, AUG 1975, P 32-41
8. R.F. STEIGERWALD, LOW INTERSTITIAL FE-CR-MO FERRITIC STAINLESS, *SOVIET-AMERICAN SYMPOSIUM ON NEW DEVELOPMENTS IN THE FIELD OF MOLYBDENUM-ALLOYED CAST IRON AND STEEL*, MOSCOW, JAN 1973
9. A.P. BOND, *TRANS. TMS-AIME*, VOL 245, 1969, P 2127
10. M.A. STREICHER, DEVELOPMENT OF PITTING-RESISTANT FE-CR-MO ALLOYS, *CORROSION*, VOL 30 (NO. 3), 1974, P 77-91

Selection of Wrought Ferritic Stainless Steels

K.F. Krysiak, Hercules, Inc.; J.F. Grubb, Allegheny Ludlum Corporation; B. Pollard; R.D. Campbell, Joining Services, Inc.

Metallurgical Characteristics

All of the ferritic stainless steels ideally possess the body-centered cubic (bcc) crystal structure known as ferrite at all temperatures below their melting temperatures (Fig. 1). Many of these alloys are subject to the precipitation of undesirable intermetallic phases when exposed to certain temperature ranges. The higher-chromium alloys can be embrittled by precipitation of the tetragonal sigma (σ) phase, which is based on the compound FeCr. Sigma phase has a lower temperature limit of formation (about 440 °C, or 825 °F). The σ solvus for the E-Brite alloy (see Table 3) is relatively low, probably less than 675 °C (1250 °F), and σ formation at low temperatures is sluggish. As a result, σ precipitation is rarely an issue for the E-Brite alloy during welding. The presence of increased chromium and molybdenum contents in other ultrahigh-purity ferritic stainless steels raises their σ solvus temperatures to approximately 1000 °C (1830 °F). Molybdenum also promotes formation of the complex cubic chi (χ) phase, which has a nominal composition of $Fe_{36}Cr_{12}Mo_{10}$. Sigma and χ phases are also stabilized by titanium. In the alloys other than E-Brite, these intermetallic phases form most rapidly at about 850 °C (1560 °F) and these alloys must consequently be cooled rapidly after annealing. Service exposure of welded ferritic alloys containing high levels of chromium and molybdenum should avoid these temperature ranges.

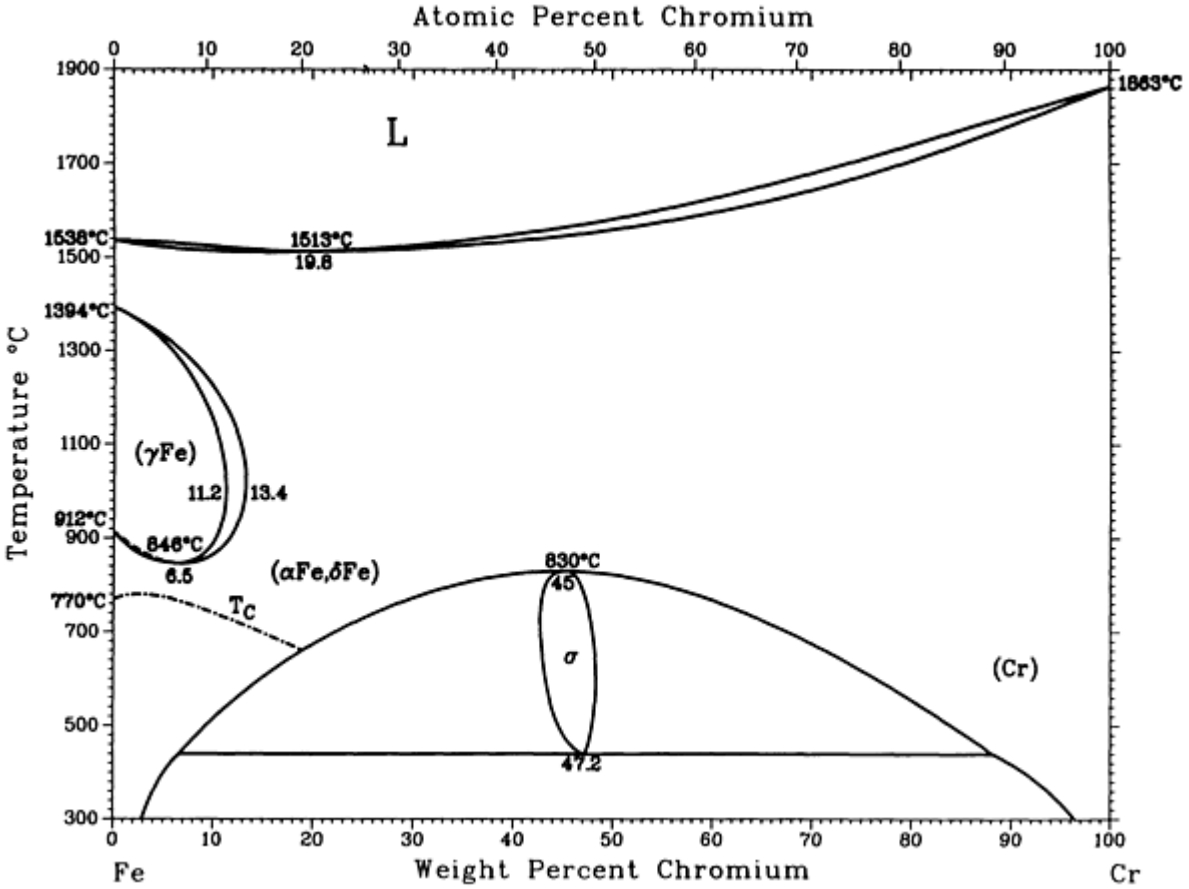

FIG. 1 THE IRON-CHROMIUM PHASE DIAGRAM. SOURCE: ASM/NIST PHASE DIAGRAM PROJECT

All of the ferritic stainless steels with chromium contents higher than 12% are also subject to embrittlement when exposed in the 370 to 550 °C (700 to 1200 °F) range. This embrittlement is most rapid at about 475 °C (885 °F) and is usually called "885 °F (475 °C) embrittlement." The rate of 475 °C (885 °F) embrittlement increases with increasing chromium plus molybdenum contents. It is generally agreed that the severe embrittlement which occurs upon long-term exposure at these temperatures is due to the decomposition of the iron-chromium ferrite phase into a mixture of iron-rich alpha (α) and chromium-rich alpha-prime (α') phases. This embrittlement is thus often called "alpha-prime embrittlement." Additional reactions such as chromium carbide and nitride precipitation may play a significant role in the more rapid, early stages of 475 °C (885 °F) embrittlement. Short-term heat treatments at 620 to 650 °C (1120 to 1210 °F) can often alleviate 885 °F embrittlement, and 885 °F embrittlement can always be cured by a full anneal heat treatment followed by rapid cooling.

The ferritic stainless steels have higher yield strengths and lower ductilities than austenitic stainless steels. Like carbon steels, and unlike austenitic stainless steels, the ferritic stainless alloys exhibit a transition from ductile-to-brittle behavior (Fig. 2) as the temperature is reduced, especially in notched impact tests. The ductile-to-brittle transition temperature (DBTT) for the ultrahigh-purity ferritic stainless steels is lower than that for type 430 and similar standard ferritic stainless steels. It is typically well below room temperature. The DBTT for the intermediate-purity stabilized ferritic stainless steels is similar to that for type 430 stainless steel. Since the DBTF decreases as metal thickness decreases, the stabilized alloys are available commercially only as sheet, strip, and light-wall tubing. The high-purity grades, because of their superior toughness, are available in thicker gages up to at least 6 mm ($\frac{1}{4}$ in.) plate. Nickel additions lower the DBTT and somewhat increase the thicknesses compatible with high toughness; nonetheless, with or without nickel, the ferritic stainless steels are not suitable for heavy-section applications.

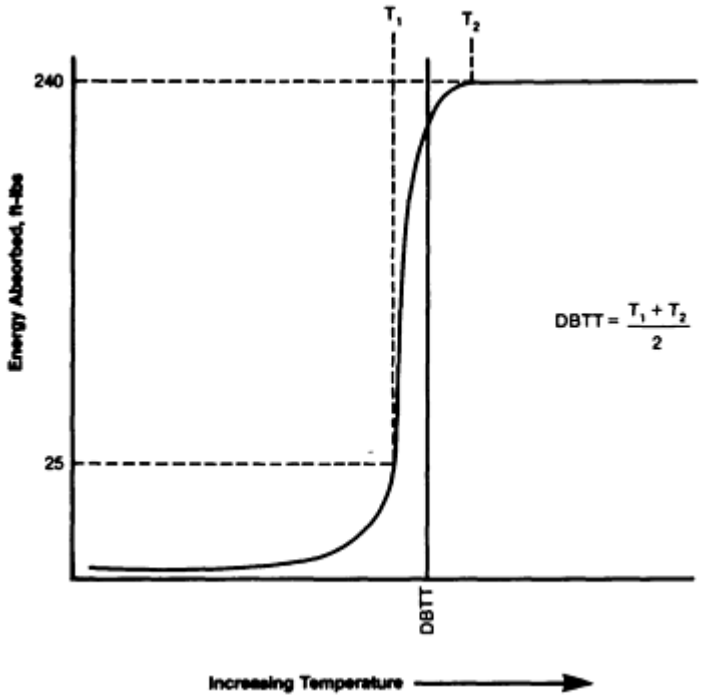

FIG. 2 SCHEMATIC OF THE DUCTILE-TO-BRITTLE IMPACT TOUGHNESS BEHAVIOR IN FERRITIC STAINLESS STEELS

In addition to the significant influence of section size (that is, thickness or mass) on the impact toughness of ferritic stainless steels, these alloys are cooling-rate sensitive (Ref 3). This effect is illustrated in Fig. 3. Depending on the cooling rate, precipitates of carbides and nitrides will tend to align along the grain boundaries or be randomly distributed in the matrix. Thus, grain size is an important factor relative to ductility and toughness. The finer the grain size, the higher the impact energy, just as in carbon or low-alloy steels.

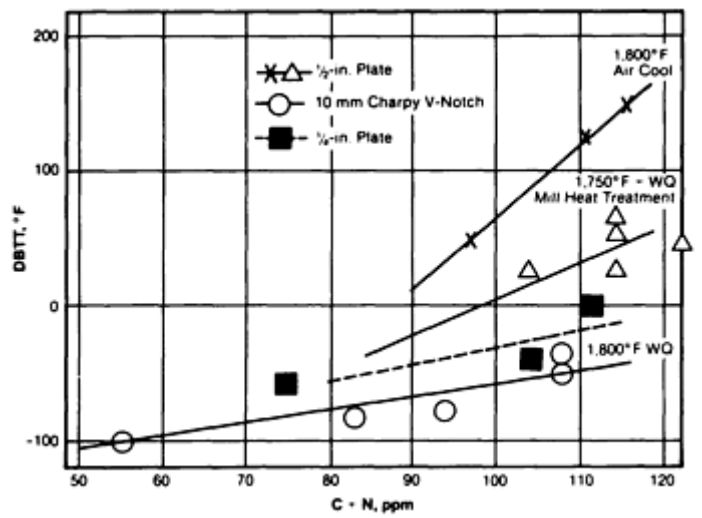

FIG. 3 THE DUCTILE-TO-BRITTLE TRANSITION TEMPERATURE (DBTT) AS A FUNCTION OF (C + N) CONTENT AND THERMAL TREATMENT. WC, WATER COOLED

Hunter and Eagar (Ref 11) investigated the mechanism of ductility loss in type 444 ferritic stainless steel (UNS S44400) welds stabilized with niobium and, in particular, titanium. It was found that stabilizing TiN or Nb(C,N) precipitates are

dissolved during the autogenous gas-tungsten arc welding process resulting in a finer distribution of precipitates in the weld metal during solidification than in the base metal. The fracture appearance transition temperature (FATT) was studied using an Olsen cup test and was found to increase by almost 200 °C (360 °F) leading to decreased room-temperature ductility. Such an increase in FATT was not explainable solely in terms of grain growth. It was proposed that these finer precipitates were likely to contain chromium as well as titanium and niobium. The combination of chromium with the nitrogen releases more free titanium, which may have an embrittling effect.

Earlier, Pollard (Ref 12) studied the ductility of ferritic stainless steel weld metal in the 26 to 35% Cr range. He concluded that the most practical methods for maximizing the ductility of welds in ferritic stainless steels in gage thicknesses of at least 6 mm ($\frac{1}{4}$ in.) are:

- KEEP THE LEVEL OF BOTH SUBSTITUTIONAL AND INTERSTITIAL ALLOYING ELEMENTS AS LOW AS POSSIBLE
- MAKE ADDITIONS OF STRONG CARBONITRIDE-FORMING ELEMENTS (LOGICALLY AS LOW AS POSSIBLE)

References cited in this section

3. W.A. MATEJKA AND R.J. KNOTH, E-BRITE 26-1, THE HIGH-PURITY APPROACH TO HIGH CHROMIUM FERRITIC STAINLESS STEELS, *ASM SYMPOSIUM*, BAL HARBOUR, FLORIDA, ASTM, 6 DEC 1973
11. G.B. HUNTER AND T.W. EAGAR, DUCTILITY OF STABILIZED FERRITIC STAINLESS STEELS WELDS
12. B. POLLARD, DUCTILITY OF FERRITIC STAINLESS WELD METAL, *WELD. J.*, APR 1972, P 222S-230S

Selection of Wrought Ferritic Stainless Steels

K.F. Krysiak, Hercules, Inc.; J.F. Grubb, Allegheny Ludlum Corporation; B. Pollard; R.D. Campbell, Joining Services, Inc.

Weldability

The term "weldability" is defined here as meaning the ease with which sound welds can be made and the suitability of these welds to perform satisfactorily in service. It is necessary, therefore, that weldability include both the mechanical aspects, such as strength, ductility, and Charpy V-notch (CVN) impact toughness, and the corrosion aspects, such as resistance to intergranular attack (IGA), SCC, and general overall corrosion resistance.

The relative performance and weldability of ferritic alloys can best be determined by comparing the impact fracture behavior of these steels. Furthermore, impact testing of the HAZ as well as the weld should be included when qualifying both the welding procedure specification(s) and the welder for these materials. In addition to the CVN impact energy (which includes examination of the DBTT), the lateral expansion and percent shear fracture of CVN specimens also should be a part of a thorough analysis of weldability.

Over the years, two schools of thought have existed on how to weld the Group III ferritic stainless steels. One school recommends welding these alloys as one would the austenitics (this is not acceptable), and the other endorses using extra care and special techniques somewhat like those used to weld titanium. Extra care and special techniques are mandatory for Group III alloys. While the Group I alloys also require care, the welding of the Group II alloys is rather routine.

During the early to mid-1970s, a reluctance developed on the part of many users and fabricators to follow recommended procedures (Ref 13). As a result, many welds were produced that had inferior corrosion resistance, ductility, and impact

toughness. Because of these problems, the weldability of the new ferritics was explored by many (Ref 14, 15, 16, 17, 18, 19, 20).

The unique as-welded properties of the Group III ferritics have been made possible by obtaining either very low levels of impurities, including carbon, nitrogen, and oxygen (ultrahigh-purity Grade III alloys), and a careful balance of niobium and/or titanium to match the carbon, nitrogen, and oxygen contents (intermediate-purity Group III alloys). For these reasons, every precaution must be taken and welding procedures must be selected that optimize gas shielding and cleanliness to avoid pickup of carbon, nitrogen, oxygen, and hydrogen.

Autogenous welds in ferritic stainless steels exhibit relatively simple microstructures. The grain size gradually increases from the edge of the heat-affected zone (HAZ) to the fusion boundary. In unstabilized or niobium-stabilized welds, columnar grains extend from the fusion boundary to meet at well-defined centerline (Fig. 4). In titanium-stabilized or dual-stabilized welds (niobium and titanium), there is typically a transition from columnar grains near the fusion boundary to equiaxed grains near the weld centerline (Ref 23, 24). The former structure shows a greater tendency for hot cracking (Ref 47).

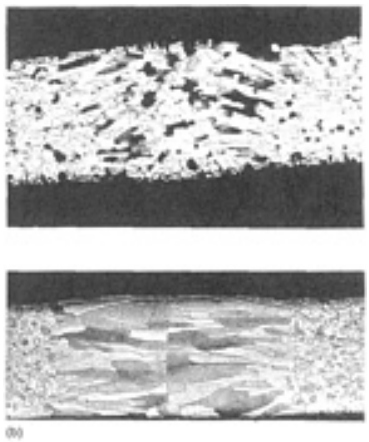

FIG. 4 PHOTOMICROGRAPH SHOWING CROSS SECTIONS OF WELDS IN 1.4 MM (0.06 IN.) SHEET. (A) 18CR-2MO-TI STEEL. (B) 18CR-2MO-NB STEEL. ETCHANT USED WAS X20 (HYDROCHLORIC-NITRIC-GLYCEROL SOLUTION). SOURCE: REF 21, 22

With lower chromium or high-carbon-content ferritic stainless alloys, such as types 409, 430, 434, 442, and 446, martensite formation during welding can occur as illustrated in Fig. 5. In the as-welded condition, the DBTT will easily be above room temperature with increased susceptibility to weld cracking during and after cooling from the molten state. Caution is advised when making welds under high restraint or in heavier section sizes. Preheat can be used under these conditions to slow the cooling rate and minimize stresses that can lead to cracking.

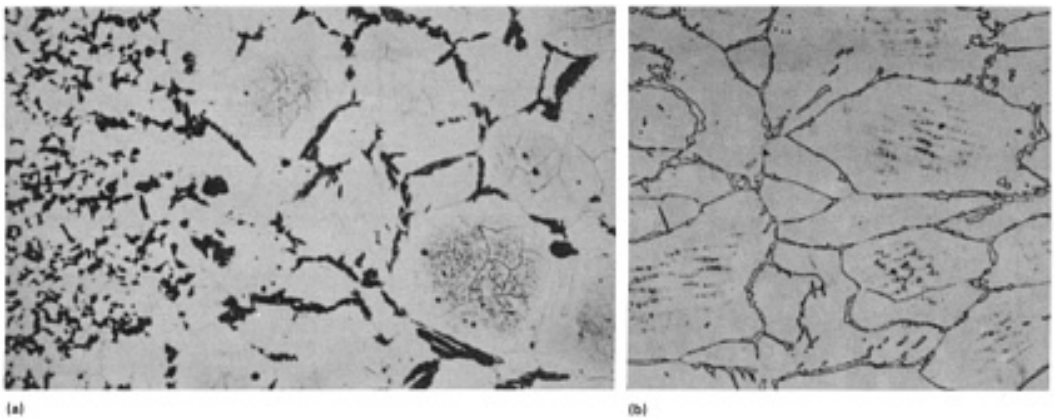

FIG. 5 GRAIN BOUNDARY MARTENSITE FORMATION IN A TYPE 430 FERRITIC STAINLESS STEEL GAS-TUNGSTEN ARC WELD. (A) FUSION ZONE. 100×. (B) HEAT-AFFECTED ZONE. 150×. SOURCE: REF 47, 48

A further word of caution is advised regarding selection of preheat and welding parameters. One must not forget that while higher heat inputs and preheats can reduce weld cracking in some ferritic stainless steels, grain growth in the weld HAZ can occur. Figure 6 shows grain growth in an ultrahigh-purity Fe-28Cr-2Mo alloy in the base metal and HAZ. Excessive grain growth can produce loss in fracture toughness, ductility, and corrosion resistance.

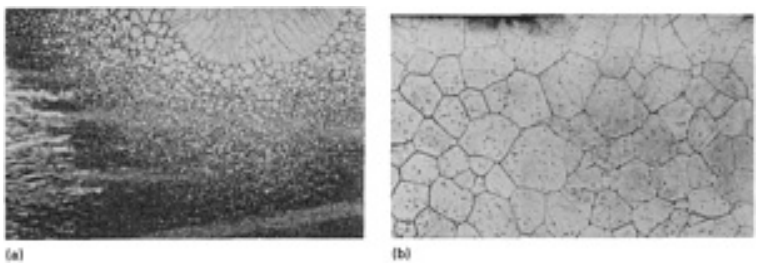

FIG. 6 CROSS SECTIONS OF PARTIAL PENETRATION GAS-TUNGSTEN ARC WELDS IN HIGH-PURITY FE-28CR-5MO FERRITIC STAINLESS STEEL. (A) WELD IN WARM-ROLLED SHEET. (B) WELD IN SHEET WHICH WAS PREWELD ANNEALED AT 1040 °C (1900 °F) FOR 60 MIN. ETCHED IN 40% NITRIC ACID ELECTROETCH. 11×

Under some conditions, annealing after welding can be performed to eliminate martensite, however the ferrite grains that have coarsened may grow even more. Generally annealing after welding is costly, can cause distortion, and usually is not practical in the field. Annealing of tubular products at the steel mill is the exception and is performed as standard procedure. This tube annealing is performed at high rates and is followed by quenching.

Regardless of which welding process is used, joint preparation and thorough solvent degreasing (using a solvent that does not leave a residue) on both sides of the joint (inside and outside) are of paramount importance.

Welding Processes

Gas-Tungsten Arc Welding (GTAW). When welding with the GTAW process, direct current electrode negative (DCEN), or straight polarity should be used. A tungsten-2% thoria electrode (AWS classification EWTh-2) with a tapered tip is recommended. Oxidation of the electrode tip or filler metal pickup are not acceptable as they reduce arc stability. When this occurs, welding must be stopped and the electrode redressed. To optimize weld quality, a gas lens collet body and the largest size ceramic nozzle should be used. With higher speed automatic processes, a trailing gas shield is recommended to prevent excessive oxidation of the weld bead.

Argon, helium, or mixtures of the two can be used for shielding. Only high-purity gas should be used. Standard welding grade gas may not be adequate because of cylinder contamination, and standard grade cylinders are not certified as to purity level. On full penetration welds or when welding thinner gages where oxidation of the back-side can occur, back gas shielding with a high-quality gas is mandatory. When welding the austenitic grades of stainless alloys, it is common to use nitrogen backing gas (usually to reduce costs, or enhance corrosion performance with these alloys). Nitrogen backing gas *must never be used* when welding ferritics because nitrogen pickup will cause severe embrittlement (loss of toughness and ductility) and loss of corrosion resistance. Inert backing gas should be used for at least two layers of deposited weld metal (3 mm, or $\frac{1}{8}$ in., minimum). Another common technique that is used when welding austenitics is to butt two pieces of metal together, weld from one side, then back grind the backside to sound metal and complete the joint. This procedure must *never* be attempted when welding ferritics because all of the contaminated metal may not be completely removed. The result is a defective, crack-sensitive ferritic weld.

To enhance weld quality and performance, especially for the Group III alloys, the following are recommended:

- THOROUGHLY DEGREASE THE WELD JOINT AND ADJACENT SURFACES BACK AT LEAST 50 MM (2 IN.) ON BOTH SIDES OF EACH JOINT MEMBER. THIS MUST ALSO INCLUDE THE WELD FILLER WIRE. WELDING SHOULD ONLY BE PERFORMED WITH CLEAN GLOVES. DIRTY AND SWEATY (DAMP) WELDING GLOVES MUST NEVER BE USED.
- KEEP THE WELDING TORCH AT RIGHT ANGLES TO THE WORK SURFACE WITHIN 15° OF VERTICAL TO PREVENT AIR ASPIRATION INTO THE INERT GAS SHIELD.
- GAS LENS SCREENS THAT BECOME CONTAMINATED WITH A DROP OR MORE OF WELD SPATTER MUST BE CHANGED IMMEDIATELY BECAUSE THE DISRUPTION OF GAS FLOW FROM THE TORCH NOZZLE CAUSES AIR ASPIRATION INTO THE MOLTEN WELD POOL. REMOVAL OF CONTAMINATED WELD METAL IS ADVISED. USUALLY, THE LENS MUST BE CHANGED.
- WEAVING THE ELECTRODE IS NOT PERMITTED, EXCEPT FOR A SMALL AMOUNT TO ALLOW GOOD SIDE-WALL FUSION AND TIE-IN. IT SHOULD BE NOTED THAT EXCESSIVE WEAVING CAUSES CONTAMINATION OF THE WELD POOL WITH A SUBSEQUENT LOSS IN FRACTURE TOUGHNESS, DUCTILITY, AND CORROSION RESISTANCE.
- WHEN WELDING, KEEP THE TIP OF THE FILLER WIRE WITHIN THE SHIELDING GAS ENVELOPE--ANOTHER REASON TO USE A GAS LENS AND AS LARGE A GAS CUP AS POSSIBLE. IF THE FILLER WIRE TIP BECOMES CONTAMINATED, EITHER BECAUSE IT TOUCHED THE TUNGSTEN ELECTRODE OR WAS WITHDRAWN OUTSIDE THE INERT GAS ENVELOPE, WELDING MUST STOP, THE TIP OF THE CONTAMINATED WIRE CUT BACK TO SOUND METAL, AND THE CONTAMINATED WELD, IF ANY, GROUND OUT, AND REPAIRED.
- ALL HOSE CONNECTIONS MUST BE OF GOOD QUALITY AND BE TIGHT TO PREVENT AIR INGESTION. CHECK ALL WATER SEALS IN THE TORCH. AIR DRAFTS IN THE WELDING AREA ARE TO BE AVOIDED TO PREVENT LOSS OF THE INERT GAS SHIELD. VERIFY THE INTEGRITY OF THE GAS SYSTEM WITH A WELD BUTTON TEST. THIS IS DONE BY STRIKING AN ARC ON A TEST PIECE OF E-BRITE PLATE OR OTHER HIGH-PURITY FERRITIC, ESTABLISHING A SMALL CIRCULAR POOL OF MOLTEN METAL APPROXIMATELY 13 MM ($\frac{1}{2}$ IN.) IN DIAMETER, EXTINGUISHING THE ARC, AND POSTPURGING AT LEAST SIX SECONDS OR MORE. THE WELD BUTTON MUST BE BRIGHT AND SHINY AND FREE OF ANY HEAT TINT. IF NOT, THE SOURCE OF CONTAMINATION MUST BE FOUND AND CORRECTED.
- PREPURGE THE TORCH BEFORE WELDING TO REMOVE AIR AND/OR MOISTURE WHICH HAS INFILTRATED INTO THE SYSTEM. POSTPURGE ALL WELD STOPS TO PREVENT CONTAMINATION. THE POSTPURGE TIME SHOULD BE SUFFICIENT SUCH THAT THE WELD STOP IS BRIGHT AND SHINY AND FREE OF ANY OXIDE HEAT TINT OR DISCOLORATION.
- A REMOTE CONTROL SHOULD BE USED TO ALLOW GRADUAL INCREASE AND DECREASE OF CURRENT WHEN INITIATING OR EXTINGUISHING THE ARC.
- AVOID OVERHEATING AND EMBRITTLING THE WELD BY MINIMIZING HEAT INPUT, AND IN MULTIPASS WELDS, BY KEEPING THE INTERPASS TEMPERATURE BELOW 95 °C (200 °F).
- WHEN HIGH-SPEED AUTOMATIC WELDING IS PERFORMED, A TRAILING GAS SHIELD IS RECOMMENDED.

Gas-Metal Arc Welding (GMAW). With the GMAW process, direct current electrode positive (DCEP), or reverse polarity, is used. The following methods of metal transfer across the welding arc are possible with GMAW:

- *SPRAY TRANSFER* IS CHARACTERIZED BY HIGH HEAT INPUT AND A FLUID WELD POOL. EXCESSIVE GRAIN GROWTH IS LIKELY IN THE WELD AND HAZ. SPRAY TRANSFER IS NOT USUALLY RECOMMENDED WHEN WELDING FERRITIC STAINLESS STEELS,

ALTHOUGH SOME STABILIZED GRADES APPEAR TO BE LESS SENSITIVE TO HEAT INPUT. HEAT INPUT CAN BE REDUCED WITH THE PULSED GMAW PROCESS, THUS OFFERING OUT-OF-POSITION WELDING.

- *GLOBULAR TRANSFER* IS CHARACTERIZED BY LOWER HEAT INPUT, BUT IS NOT NORMALLY USED BECAUSE OF EXCESSIVE SPATTER. SPATTER CAN BE MINIMIZED WITH PROPER CHOICE OF HIGH-PURITY SHIELDING GAS AND THE PROPER CHOICE OF POWER SUPPLY (FOR EXAMPLE, RAPID ARC POWER SUPPLIES THAT FEATURE CAPACITIVE DISCHARGE ELECTRONICS).
- *SHORT-CIRCUITING TRANSFER* FEATURES THE LOWEST HEAT INPUT OF ALL THE GMAW PROCESSES. HOWEVER, LACK OF FUSION DEFECTS ARE COMMON WITH SHORT-CIRCUITING TRANSFER IF PROPER TECHNIQUES ARE NOT FOLLOWED.

While grain growth can be controlled to some degree with higher weld travel speeds, lower interpass temperatures, and heat sinks, care must be taken to avoid weld defects such as lack of fusion and insufficient penetration. In some situations, the use of an austenitic filler metal can overcome the problem of weld grain growth because of the formation of a two-phase grain structure. However, the HAZ grain growth must not be forgotten when using one of these filler metals.

When welding ferritic and austenitic stainless steels with the GMAW process using one of the standard power supplies, pure argon shielding gas is usually not used because of arc instability which causes air to be aspirated into the arc. As a result, the weld pool becomes enriched in nitrogen and oxygen. In the DCEP mode, the arc wanders, seeking spots which are emissive in character, usually oxides. This erratic arc behavior causes a disruption of the laminar flow of the inert gas, resulting in air being aspirated into the gas envelope.

One way to solve the arc wander problem has been to add an oxidizing element to the inert gas. Argon with 2% oxygen (O_2) or with 2% carbon dioxide (CO_2) typically used to weld plain carbon steel, low-alloy steel, and austenitic stainless steel, has been recommended for ferritic stainless steels as well. While this seems to be satisfactory for the stabilized ferritics in Group II where the bulk of the applications are for automobile exhaust systems (type 409), these active, oxidizing shielding gases should *never* be used for the Group III higher-purity ferritics, stabilized or not, because of the dramatic effect on degrading toughness and ductility.

Still other investigators have shown that the arc wander problems associated with the GMAW process can be resolved by using an argon-helium mix, typically 75Ar-25He, and by ensuring that the inert gas is purified and free of contaminants such as air, moisture, and hydrocarbons. To further enhance operability and weld quality, a device covered in a U.S. patent (No. 5,081,334, Improved Gas Shielding," 14 Jan 1992) enables air and moisture to be excluded from entering the welding arc. By taking the high-purity inert gas system approach rather than using a gas mixture containing reactive gases (O_2 and CO_2), critical reactive alloying elements such as titanium, niobium, aluminum, and chromium are not removed by oxidation. In this way, arc wander is virtually eliminated and wetting action is enhanced. With this new technology stable GMAW has been attained with pure argon. This patent also has possible application in any welding process that uses a wire feed system.

Flux-cored arc welding (FCAW) functions essentially the same as GMAW, except that instead of the filler wire being solid, it is fabricated from a carbon steel, stainless steel, or nickel sheath that surrounds a core of alloying additions formulated to the desired weld deposit chemistry. Some FCAW consumables contain active fluxing ingredients while others do not. In some instances, suppliers recommend the use of a supplementary gas shield, and sometimes the consumable is self-shielding. It is important to know the operating characteristics of the wire and when to use supplementary shielding gas which usually gives better results. The advantages of using shielding gas purification as discussed for GMAW may apply here as well.

The FCAW process is not recommended for the Group III ferritic stainless steels because of the difficulty of maintaining alloy purity and because of the pickup of carbon, nitrogen, and oxygen. Flux-cored arc weld deposits are never as clean as those produced by solid wire, inert gas welding processes. For less critical applications, or where an austenitic filler metal can usually be used, FCAW may be possible.

Because FCAW operates in the spray arc mode, higher heat inputs will result, making grain growth a potential problem. Although higher travel speeds can be employed with lower interpass temperature and heat sinks, care must be used to avoid lack-of-fusion defects.

Shielded Metal Arc Welding (SMAW). When welding with the SMAW process, DCEP (reverse polarity) is typically used. Shielded metal arc weld deposits made with covered electrodes are never as tough as welds made with an inert gas shielded process. For this reason, covered electrodes with matching composition are not available for the Group III ferritic stainless steels. Basically, the problem is one of purity, because carbon, nitrogen, and oxygen are difficult to suppress without seriously hampering welding electrode operability.

Where covered electrodes are available, proper storage is essential to avoid any pickup of moisture. Improper storage of SMAW consumables resulting in moisture pickup usually leads to weld porosity, and in some cases hydrogen cracking.

For some ferritic stainless steels that must be used in the as-welded condition, and where postweld annealing is not practical or cost effective, a dissimilar welding electrode can be used. The choice varies from the high-chromium austenitic grades such as a type E310 or E310 ELC (which are fully austenitic) to a high-nickel alloy such as an ENiCrFe-2. Type E309 coated electrode (welds contain ferrite for resistance to hot cracking) and its low-carbon and higher-silicon variations have been used to advantage.

High-alloy austenitic weld metals do not flow as readily as the ferritic stainless steels. High-nickel alloy weld metal is particularly sluggish with shallow penetration. This behavior requires that the welder make adjustments in technique. This means the welder must use arc force and electrode manipulation to physically move the molten weld pool against the sides of the joint. Ferritic stainless steels have significantly higher melting temperatures than do the austenitic stainless steels or corrosion-resistant nickel-base alloys. When using austenitic filler metals to join ferritic stainless steel base metals, care must be exercised to ensure that sufficient heat has been applied to fuse the ferritic stainless steel base metal. Failure to follow these recommendations usually results in lack-of-fusion defects.

Depending on weld bead profile, slag entrapment can be a problem with some covered electrodes. If the slag does not chip out readily, grinding will be necessary. Trying to float out residual slag with successive molten weld passes is rarely successful. The net result is slag entrapment which readily shows up on radiographic inspection. It should be remembered that grinding, if it becomes excessive, can result in more heat input via additional weld passes and ultimately will cause grain growth. The net result could be a loss in HAZ toughness and ductility.

When welding ferritic stainless steels with the SMAW process, the following techniques are recommended:

- AS WITH ALL OTHER WELDING PROCESSES, WELD JOINT SURFACES SHOULD BE CAREFULLY CLEANED WITH SOLVENT (BOTH SIDES OF EACH JOINT MEMBER) TO REMOVE ANY CONTAMINANT SUCH AS OIL, GREASE, OR DIRT WHICH WOULD DEGRADE WELD PROPERTIES AND CORROSION RESISTANCE.
- THE ARC SHOULD BE STRUCK IN THE BEVEL OF THE WELD JOINT, AND NOT ON THE ADJACENT BASE METAL.
- A SHORT ARC SHOULD BE MAINTAINED TO AVOID THE FORMATION OF POROSITY AND TO MINIMIZE OXIDATION EFFECTS AND PICKUP OF OXYGEN AND NITROGEN.
- AVOID EXCESSIVE INCLINATION OF THE ELECTRODE (A MAXIMUM INCLINE OF 20° FROM THE VERTICAL IS GENERALLY SATISFACTORY).
- A SLIGHT WEAVE FOR TIE-IN AND FUSION IS ALLOWED PROVIDED IT IS NOT WIDER THAN THREE TIMES THE DIAMETER OF THE ELECTRODE CORE WIRE.
- CRATER CRACKS AT WELD STOPS MUST BE GROUND OUT TO SOUND METAL BEFORE PROCEEDING. DYE PENETRANT INSPECTION IS THE BEST WAY TO BE SURE ALL CRACKED MATERIAL HAS BEEN REMOVED.

Plasma arc welding (PAW) of ferritic stainless steels is very similar to GTAW and the same precautions and recommendations apply. Concern has been voiced about the use of hydrogen gas with PAW because of the possibility of weld metal cracking caused by the interaction of hydrogen in the weld metal and in high stress conditions. Gas-tungsten arc welding experience with type 409 indicates that hydrogen additions will cause embrittlement immediately after welding but most of the hydrogen diffuses out of the weld metal within 48 h and ductility is restored. The situation, however, is more critical with higher-chromium alloys.

An advantage of the PAW process is that the unique high-intensity arc produces a weld bead characterized by deep penetration and a HAZ narrower than that produced by the GTAW process. The net result is that less HAZ grain growth is possible with PAW than with GTAW.

Resistance Welding. Spot welding, seam welding, and flash welding processes can be used provided the loss in toughness can be tolerated. Seam welding has been used to fabricate panel coil-type heat exchanger surfaces. Whenever possible argon inert gas should be used to protect the weld joint or seam (back side included) to minimize oxidation and the pickup of nitrogen. Titanium-stabilized alloys appear to be more resistant to the effects of nitrogen pickup due to poor shielding than are the high-purity alloys. This is apparently due to the formation of a protective TiN film which covers the weld pool (Ref 26).

Other Welding Processes. Ferritic stainless steels can be readily welded using the electron beam process with hard vacuum. Friction welding and laser welding are also possible. Where practical, the molten zone should be protected with an inert gas shield.

Submerged arc welding (SAW) can be used to join some of the ferritic stainless grades; however, the high heat input with the process becomes troublesome because of undesirable grain growth in the weld HAZ. Choice of fluxes and control of residues become critical. Dilution can exceed 50%. Submerged arc welding is not suitable for the Group III alloys and generally would also not be suitable for most of the other alloys.

Selection of Welding Consumables

Welds in ferritic stainless steel base metals can be produced several ways: (1) autogenously (that is, without the addition of filler metal) (Ref 27), (2) with a matching filler metal composition, (3) with an austenitic stainless steel filler metal (Ref 25), or (4) using a high-nickel filler alloy (Ref 17). Table 5 lists some base metal-filler metal combinations for several ferritic stainless steels.

TABLE 5 TYPICAL FERRITIC BASE METAL-FILLER METAL COMBINATIONS

BASE METAL	COVERED ELECTRODE, BARE ROD, OR FILLER WIRE	APPLICATION
405	405 NB	AS-WELDED
	430	ANNEALED
	308(L), 309(L), 310(ELC)	AS-WELDED
409	430	ANNEALED
	308(L), 409, 409NB, 309LSI	AS-WELDED
429	208(L), 309(L), 310(ELC)	AS-WELDED
430	430	ANNEALED
	308(L), 309(L), 310(ELC)	ANNEALED OR AS-WELDED
439	430, 430TI	ANNEALED OR AS-WELDED
442	442	ANNEALED
	308(L), 309(L), 310(ELC)	AS-WELDED
446	446	ANNEALED
	308(L), 309(L), 310(ELC)	AS-WELDED
E-BRITE 26-1	ER26-1	AS-WELDED
	INCONEL 112, HASTELOY C-276, OR HASTELOY C-22	AS-WELDED
AL 29-4C	AL 29-4-2	AS-WELDED
AL 29-4	AL 29-4-2	AS-WELDED
AL-29-4-2	AL 29-4-2	AS-WELDED

Before selecting a welding consumable, consideration must be given not only to mechanical property requirements, especially weld ductility and toughness (including the weld HAZ), but also to the level of corrosion resistance required for the application. Autogenous welding may be considered for some of the high-purity Group III alloys such as E-Brite 26-1. The mill annealed product will have good mechanical properties and corrosion resistance, but if the interstitial levels of carbon, oxygen, and nitrogen are on the high side of the specification limits, the autogenous weld will not only exhibit poor ductility and toughness, but also poor corrosion resistance. To avoid this kind of a problem, material should be purchased with interstitial element levels on the low side of the specification range.

Filler metals of matching composition for the more common grades of Groups I and II ferritic stainless steels, such as types 409 and 430, are available as solid wire, metal cored, or fluxcored wire (both gas shielded and self-shielded), covered electrodes, and bare rod. Because of the reactivity of titanium and aluminum and poor transfer of these elements across the arc, the availability of consumables containing these elements is usually limited to bare wire or rod.

When nonstandard grade ferritic filler metals are not available, or because poor wire drawing characteristics make production prohibitive, metal-cored or flux-cored filler metals offer a solution. Weld metal properties should be qualified before purchase.

Welding consumables for the Group III alloys are available as matching composition in bare wire or rod form. Because Group III weldments are usually always used in the as-welded condition, it is strongly recommended that these filler metals be purchased having interstitials at the very low end of the alloy specification. For best ductility, toughness and corrosion performance, the (C + N + O) content should not exceed 120 ppm for the ultrahigh-purity grades (such as E-Brite 26-1, 29-4, and 29-4-2).

Because the Group III ferritics of intermediate purity rely on stabilization with titanium or titanium and niobium, welds have such poor toughness that welding with these filler metals is limited to very thin section sizes such as thin-walled pipe, tubing, or sheet. When better toughness is required of stabilized grades with a ferritic consumable, welding should be performed with an ultrahigh-purity filler metal containing very low levels of (C + N + O). It should be noted that ultrahigh-purity welding consumables require careful handling and processing to keep interstitials at these very low levels. Keeping them clean at the job site is also mandatory.

Austenitic stainless steel welding consumables are often used to join ferritic stainless steels to overcome poor weld ductility and toughness deficiencies and they do not display a DBTT like ferritics. Although weld metal grain growth is usually not a problem (because a two-phase mixture of austenite and ferrite forms), grain growth in the weld HAZ of the ferritic base metal must not be overlooked. Sometimes the application of an austenitic filler can be a problem because of the rather large discrepancy in thermal expansion between the two alloys. In this regard, problems can range from (1) cracking due to thermal stress, (2) sensitization and loss of corrosion resistance if the austenitic filler metal is not a low-carbon grade or stabilized with titanium or niobium (corrosion can also result because of the heat from multipass welds or some subsequent thermal treatment after welding), or (3) stress relief which may not be fully effective because of the thermal expansion differences.

High-nickel alloy welding consumables have also been used successfully to join ferritics, especially the Group III alloys to themselves as well as to carbon steel, 300-series stainless steels, duplex stainless steels, superaustenitic stainless steels, and nickel-base alloys. Examples of nickel-base filler metals that have been used successfully are ENiCrFe-2, ENiCrMo-3, ERNiCrMo-1, and ERNiCrMo-3. In addition to their outstanding corrosion resistance, these high-nickel filler metals have coefficients of thermal expansion that are similar to the ferritics they are joining. While they have worked well with E-Brite alloy, attempts to use them with the 3 to 4% Mo grades of ultrahigh-purity ferritics have occasionally been less successful (Ref 28). Formation of brittle intermetallic compounds at the fusion boundary has been encountered in some cases, but good welds can be produced (Fig. 7). Sound welds have been produced using duplex stainless steel filler metal, but corrosion resistance of such joints may not be adequate in some applications.

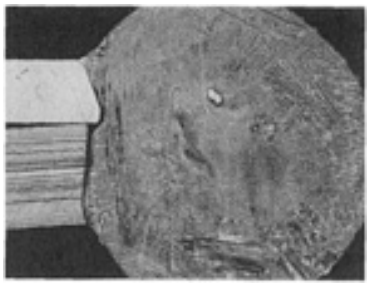

FIG. 7 WELD JOINING UNS S43735 SUPERFERRITIC STAINLESS STEEL (TOP) TO N08367 SUPERAUSTENITIC ALLOY (BOTTOM) USING N06625 NICKEL ALLOY FILLER METAL. NOTE DIFFERENCE BETWEEN MELT-BACK OF SUPERFERRITIC AND SUPERAUSTENITIC MATERIALS AND ISLAND OF UNMELTED SUPERFERRITIC STAINLESS STEEL NEAR CENTER OF WELD DEPOSIT. BOTH CONDITIONS INDICATE THE HIGH MELTING TEMPERATURE OF SUPERFERRITIC STAINLESS STEELS RELATIVE TO AUSTENITIC STAINLESS STEELS OR NICKEL ALLOYS. ETCHED WITH MIXED NITRIC/HYDROCHLORIC/ACETIC ACID SOLUTION. 14×

Welding Procedures and Weld Properties

Effect of Shielding Gas Purity on Weld Toughness (Ref 29, 30, 31, 32, 33, 34). The primary reasons for using shielding and backing gas are to protect the molten filler wire tip, the nonconsumable electrode (when used), the weld pool, and the solidified weld bead from atmospheric contamination. Researchers have shown that gas contaminants can cause cracking, varying degrees of weld bead oxidation, arc instability, and degradation of mechanical and corrosion properties. A particular gas or gas mixture might be used for enhanced arc stability, a particular mode of weld metal transfer, enhanced penetration or bead profile, its availability, or easier arc ignition.

Certainly, there is no question that quality welds require quality shielding. What is essential is that clean gas be maintained and delivered to the point of use. From a practical standpoint, some factors that have been identified as relating to "bad gas" and welding problems are:

- CONTAMINATED GAS CYLINDERS (BY MOISTURE/AIR)
- CONTAMINATED AND/OR LEAKING GAS MANIFOLD SYSTEMS
- DAMAGED, DEFECTIVE, OR LOOSE SHIELDING/BACKING GAS LINE FITTINGS
- INTRUSION OF CONTAMINANTS WHEN MIXING GASES

Achieving gas quality at the point of use can be elusive. Welding problems can show up with a single cylinder of gas or a series of cylinders. A manifold system can be particularly difficult to deal with because of its long length and numerous welding stations. As a result of poor gas quality, defects are produced which require repair, job completion can be delayed, and job quality may be compromised. What is needed is a portable, cost-effective system that will remove contaminants from the shielding gas and backing gas, not only when working in the shop, but also in the field.

Because ferritic stainless steels are sensitive to interstitial element contaminants, it is important that these elements be removed so as not to degrade properties such as ductility, toughness, and corrosion resistance. Impurities commonly found in gas cylinder or manifold systems are moisture, oxygen, hydrocarbons (such as oils from compressors), and carbon dioxide (when not intentionally added). Moisture in CO_2 gas is also a common problem.

While there are systems on the market that can eliminate gas contaminants to levels below one part per million (ppm), they have to rely on multicomponent, energy-intensive gettering. These systems are heavy, flow rates are usually restrictive, and they are not very portable. Another system relies on a resin that is a single rechargeable compound that can provide effective removal of a variety of impurities to less than 10 parts per billion (ppb), operates at room temperature, and is light and portable. The effects of using such a system on the impact properties of 6 mm ($\frac{1}{4}$ in.) thick E-Brite 26-1 alloy plate are shown in Fig. 8.

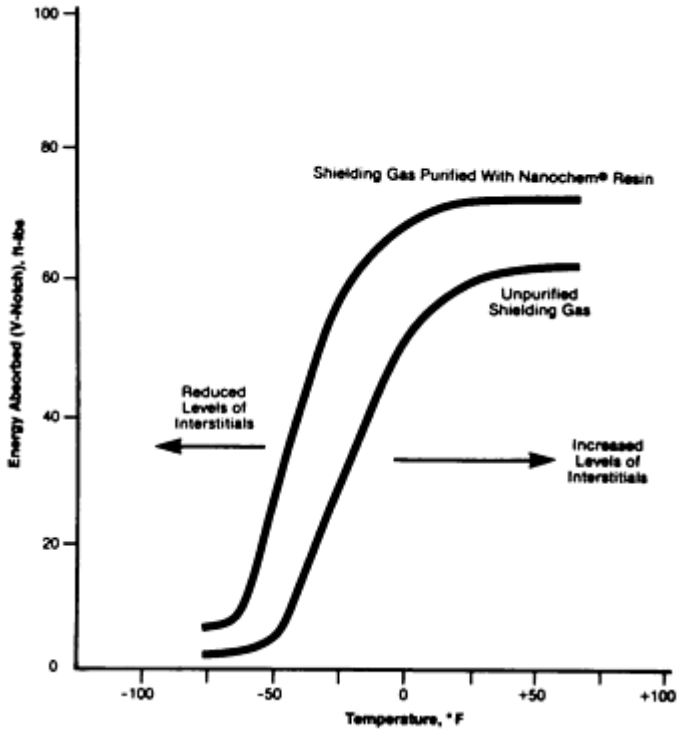

FIG. 8 CHARPY V-NOTCH IMPACT TEST RESULTS FROM GAS-TUNGSTEN ARC WELDED E-BRITE 26-1 PLATE. WELD CONDITIONS: PLATE THICKNESS, 6 MM ($\frac{1}{4}$ IN.); SHIELDING/BACKING GAS, ARGON; SHIELDING/BACKING GAS IMPURITY LEVELS, H_2O 40 PPM AND O_2 20 PPM; SHIELDING GAS FLOW RATE, 28 L/MIN (60 FT^3/H); VOLTAGE, 14V; CURRENT (DCEN), 150 A; TRAVEL SPEED, 1.5 TO 2.5 MM/S (3.5 TO 6 IN./MIN). NANOCHEM IS A REGISTERED TRADEMARK OF HERCULES INC. SOURCE: REF 35

Hydrogen Embrittlement. Like other ferritic materials, the ferritic stainless steels are susceptible to hydrogen embrittlement. For this reason, the use of hydrogen-containing shielding gas should be avoided. Hydrogen can also be created from water, water vapor, or oils, and these should be rigorously excluded from the weld region. The presence of hydrogen in the weld can lead to cracking of the weld bead shortly after welding. It can also reduce ductility in uncracked welds. Hydrogen is often spontaneously outgassed from these alloys at room temperature and is readily lost during low-temperature (90 to 200 °C, or 200 to 400 °F) heat treatments (Ref 36). Hydrogen outgassing at room temperature, if it will occur, requires a few days to a few weeks. Surface films of oxides and/or nitrides can inhibit hydrogen outgassing, and it may be necessary to remove such films to facilitate hydrogen outgassing and restoration of ductility. Sensitivity to hydrogen is a function of alloy composition, microstructure, and strength. In general, the stabilized, high-chromium plus molybdenum materials, such as AL 29-4C alloy, are more sensitive than the high-purity, lower-chromium plus molybdenum materials, such as the E-Brite alloy.

Preheating. One of the main reasons for preheating is to reduce the temperature gradient between the weld area and the unaffected base metal. Any austenite which forms in nominally ferritic stainless steels will air harden to martensite even in heavy (>300 mm, or 12 in., diam) sections. Preheating light-gage sheet will not prevent the formation of martensite. It is also unlikely that enough preheat could be applied to produce any significant post-transformation tempering. Hydrogen may be a factor in situations involving high stress and restraint. When additional preheat time is allowed, the hydrogen can diffuse out safely. Ferritic stainless steels that would benefit from preheat would be the Group I types (430, 434, 442, and 446).

When required, a preheat in the range of 150 to 230 °C (300 to 450 °F) is usually sufficient. Section sizes of $\leq$6 mm ($\leq \frac{1}{4}$ in.) generally do not need preheat, but such parameters as joint design, restraint, welding process, cooling rate, and dissimilar metal combinations (different coefficients of thermal expansion), and base metal composition should be reviewed before making a final decision.

Preheat should not be used on the Group III alloys, especially the ultra-high purity steels. These alloys do not form martensite when welded, so no preheat is necessary. Furthermore, because these alloys have such low levels of impurities, excessive grain growth would occur, compared with the Group I and Group II alloys.

Postweld annealing is normally performed on the Group I ferritic stainless steels. The purpose is to transform any martensite that may have formed during welding into a wholly ferritic structure (usually containing some spheroidized carbides), or to remove effects of high-temperature embrittlement and improve corrosion resistance. Annealing under these conditions does not refine coarsened ferrite grains (some form of metal working is needed to achieve recrystallization and grain refinement).

When postweld annealing is required, the recommended temperature range is 790 to 850 °C (1450 to 1550 °F). At these temperatures consideration must be given to oxidation of the metal surface and distortion effects. Fixturing to prevent metal deformation may be required. Sigma, σ, and chi, χ, formation is typically not a problem with the Group I alloys.

Cooling from the annealing temperature must be done carefully. Furnace cooling to 600 °C (1100 °F) is usually specified to minimize distortion from handling. Rapid cooling through the temperature range of 565 to 400 °C (1050 to 750 °F) is necessary to avoid 475 °C (885 °F) embrittlement. Depending on section thickness, forced air cooling or water spray quenching is usually performed.

Group III ferritic stainless steels (ultralow interstitials and the stabilized grades), particularly the high-chromium, high-molybdenum alloys, are typically not annealed after welding because of the danger of precipitation of σ and χ phases in the temperature range of 550 to 900 °C (1020 to 1650 °F) unless the anneal is followed by a rapid quench. However, postweld annealing of welded tubes is common.

Corrosion Resistance. Investigators have determined that the loss of corrosion resistance of ferritic stainless steels after welding is caused by chromium depletion upon cooling from exposure to temperatures of 925 °C (1700 °F) (Ref 37, 38, 39, 40, 41, 42). Sensitization* due to chromium depletion occurs by holding or cooling through the temperature range of 425 to 700 °C (800 to 1300 °F). In the temperature range from 700 to 925 °C (1300 to 1700 °F), rapid diffusion of chromium in ferrite occurs, replenishing the chromium-depleted zones. For this reason, weldments which are annealed at 790 to 850 °C (1450 to 1550 °F) show good intergranular corrosion resistance despite the presence of intergranular precipitates of chromium-rich carbides and nitrides. Below 700 °C (1300 °F), little chromium diffusion occurs and corrosion resistance is not completely restored.

Conventional (Group I) 400-series ferritic stainless steels such as types 430, 434, and 446 are susceptible to intergranular corrosion and to embrittlement in the as-welded condition. Corrosion in the weld area generally encompasses both the weld metal and weld HAZ. Early attempts to avoid some of these problems involved the use of austenitic stainless steel filler metals; however, failure by corrosion of the HAZ usually occurred even when exposure was to rather mild media for relatively short periods of time.

Figure 9 shows an example of a saturator tank used to manufacture carbonated water at room temperature that failed by leakage through the weld HAZ of the type 430 base metal after being in service for only 2 months. This vessel, fabricated by welding with a type 308 stainless steel welding electrode, was placed in service in the as-welded condition. Figure 10 shows a photomicrograph of the weld/base metal interface at the outside surface of the vessel; corrosion initiated at the inside surface. Postweld annealing--at 785 °C (1450 °F) for 4 h in the case of type 430 stainless steel--restores weld area ductility and resistance to corrosion to that of the unwelded base metal.

FIG. 9 AS-WELDED TYPE 430 STAINLESS STEEL SATURATOR TANK USED IN THE MANUFACTURE OF CARBONATED WATER THAT FAILED AFTER 2 MONTHS OF SERVICE. THE TANK WAS SHIELDED METAL ARC WELDED USING TYPE E308 FILLER METAL. SOURCE: REF 34

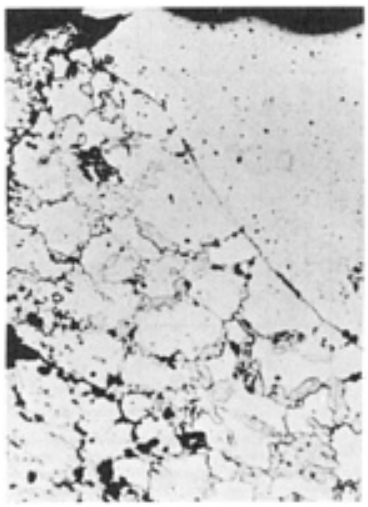

FIG. 10 PHOTOMICROGRAPH OF THE OUTSIDE SURFACE OF THE SATURATOR TANK SHOWN IN FIG. 9 SHOWING CORROSION AT THE FUSION LINE. SOURCE: REF 34

To overcome some of these earlier difficulties and to improve weldability, several of the standard grade ferritic stainless steels were modified. For example, type 405, containing nominally 12% Cr, is made with lower carbon and a small aluminum addition of 0.20% to restrict the formation of austenite at high temperature so that hardening is reduced during welding. For maximum ductility and corrosion resistance, however, postweld annealing is necessary. Recommendations for welding include either a 430- or a 309-type filler metal, the latter being used when increased weld ductility is desired.

As mentioned earlier in this article, researchers recognized that the high-chromium, high-molybdenum ferritic stainless steels possessed a desirable combination of good mechanical properties and resistance to corrosion. These properties made them attractive alternatives to the austenitic stainless steels, which often failed due to chloride SCC.

Reducing the total interstitial element levels in ferritic stainless steels improves weldability and corrosion resistance. Figure 11 shows the relationship of chromium content and (C + N) content on the combined properties of as-welded corrosion resistance and ductility. Table 6 lists this relationship separately for each property. As chromium content increases, the amount of (C + N) that can be tolerated for intergranular corrosion resistance increases. Conversely, for aswelded ductility, the amount of tolerable (C + N) is drastically reduced. Thus, at low chromium levels, as-welded corrosion resistance is the controlling factor; at high chromium levels, as-welded ductility is the factor that limits the use of high-chromium stainless steels.

TABLE 6 LIMITS OF INTERSTITIAL ELEMENT (C + N) CONTENT FOR ACCEPTABLE AS-WELDED INTERGRANULAR CORROSION RESISTANCE AND AS-WELDED DUCTILITY

Sample thickness: 2.5 mm (0.1 in.)

CHROMIUM CONTENT, WT%	INTERGRANULAR CORROSION RESISTANCE[(A)], PPM (C + N)	DUCTILITY[(B)], PPM (C + N)
19	60-80	>700
26	100-130	200-500
30	130-200	80-100
35	<250	<20

(A) INTERGRANULAR CORROSION RESISTANCE IN BOILING 50% FERRIC SULFATE-50% SULFURIC ACID SOLUTION.

(B) NO CRACKING AS DETERMINED BY SLOW BENDING AROUND A 5 MM (0.2 IN.) MANDREL

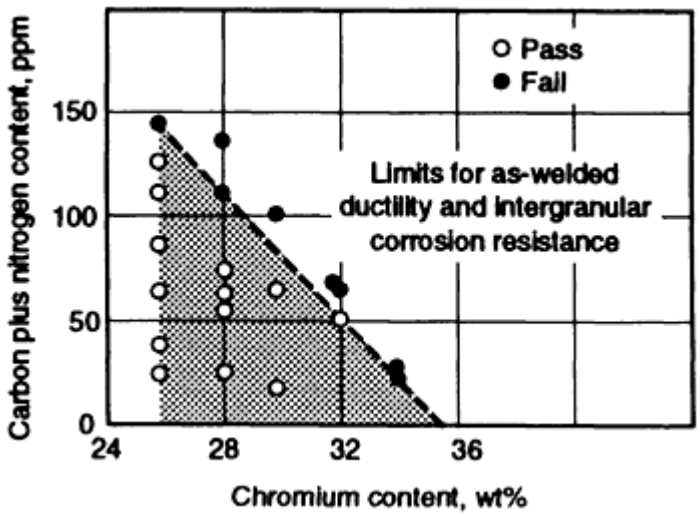

FIG. 11 THE EFFECT OF INTERSTITIAL LEVELS AND CHROMIUM CONTENT ON AS-WELDED DUCTILITY AND INTERGRANULAR CORROSION RESISTANCE. SOURCE: REF 43

To improve the corrosion resistance of ferritic stainless steels, two practical methods have been applied:

- *LOWER INTERSTITIAL LEVELS.* BECAUSE THE SOLUBILITY OF INTERSTITIAL ELEMENTS IS LOW IN FERRITE, NEW MELTING AND REFINING PRACTICES HAVE BEEN UTILIZED TO PRODUCE ULTRAHIGH-PURITY FERRITIC (GROUP III) STAINLESS ALLOYS LIKE THOSE SHOWN IN TABLE 3. WITH THESE LOW LEVELS OF CARBON AND NITROGEN, CHROMIUM CARBIDE AND NITRIDE PRECIPITATION CANNOT OCCUR TO A HARMFUL DEGREE, THUS AS-WELDED DUCTILITY AND CORROSION RESISTANCE ARE MAINTAINED

- *STABILIZATION OF CARBON AND NITROGEN.* THIS IS ACHIEVED BY THE ADDITION OF CARBIDE- AND NITRIDE-FORMING ELEMENTS WHICH ARE MORE STABLE THAN CHROMIUM CARBIDES AND CHROMIUM NITRIDES. TITANIUM AND/OR NIOBIUM ARE USED TO TIE UP THE CARBON AND NITROGEN IN THE MATRIX. STABILIZATION HAS PROVEN EFFECTIVE IN PREVENTING SENSITIZATION OF FERRITIC ALLOYS SUCH AS 18CR-2MO AND 26CR-1MO, AS WELL AS THE HIGHER CHROMIUM-MOLYBDENUM GRADES (REF 44). INVESTIGATORS HAVE SHOWN, HOWEVER, THAT IF EXCESSIVE AMOUNTS OF STABILIZER ARE USED BEYOND WHAT IS REQUIRED FOR CORROSION RESISTANCE, DUCTILITY AND ROOM-TEMPERATURE IMPACT PROPERTIES ARE DEGRADED (REF 15, 44, 45, 46).

It should also be pointed out that corrosion resistance can also be improved by following proper welding procedures and recommendations. As described previously, preheating (except to remove moisture) or postweld heat treating should not be performed. Postweld heat treatment is used only with the conventional ferritic stainless alloys. The following example illustrates the results of not following proper procedures.

Example 1. Leaking Welds in a Ferritic Stainless Steel Wastewater Vaporizer. A nozzle in a wastewater vaporizer began leaking after approximately 3 years of service with acetic and formic acid wastewaters at 105 °C (225 °F) and 414 kPa (60 psig).

Investigation. The shell of the vessel was gas-tungsten arc welded in 1972 from 6.5 mm ($\frac{1}{4}$ in.) E-Brite stainless steel plate. The shell measured 1.5 m (58 in.) in diameter and 8.5 m (28 ft) in length. Nondestructive examination included 100% radiography, dye-penetrant inspection, and hydrostatic testing of all E-Brite welds.

An internal inspection of the vessel revealed that portions of the circumferential and longitudinal seam welds, in addition to the leaking nozzle weld, displayed intergranular corrosion. At the point of leakage, there was a small intergranular crack. Figure 12 shows a typical example of the corroded weld. A transverse cross section through this weld characteristically displays intergranular corrosion with grains dropping out (Fig. 13). The HAZ next to the weld fusion line also experiences intergranular corrosion a couple of grains deep as a result of sensitization (Fig. 14).

FIG. 12 TOP VIEW OF A LONGITUDINAL WELD IN 6 MM ($\frac{1}{4}$ IN.) THICK E-BRITE STAINLESS STEEL PLATE SHOWING INTERGRANULAR CORROSION. THE WELD WAS MADE WITH MATCHING FILLER METAL. ABOUT 4×. SOURCE: REF 47

FIG. 13 INTERGRANULAR CORROSION OF A CONTAMINATED E-BRITE STAINLESS STEEL WELD. ELECTROLYTICALLY ETCHED WITH 10% OXALIC ACID. 200×. SOURCE: REF 47

FIG. 14 INTERGRANULAR CORROSION OF THE INSIDE SURFACE HAZ OF E-BRITE STAINLESS STEEL ADJACENT TO THE WELD FUSION LINE. ELECTROLYTICALLY ETCHED WITH 10% OXALIC ACID. 100×. SOURCE: REF 47

The evidence indicated weldment contamination; therefore, effort was directed at finding levels of carbon, nitrogen, and oxygen in the various components present before and after welding. The following are the average results:

ELEMENT	**CONTENT, PPM**
E-BRITE BASE PLATE	
C	6
N	108 (C + N = 114)
O	57
CORRODED LONGITUDINAL WELD	

C	133
N	328 (C + N = 461)
O	262
CORRODED CIRCUMFERENTIAL WELD	
C	34
N	169 (C + N = 203)
O	225
E-BRITE WELD WIRE	
C	3
N	53 (C + N = 56)
O	55
SOUND LONGITUDINAL WELD	
C	10
N	124 (C + N = 134)
O	188
SOUND CIRCUMFERENTIAL WELD	
C	20
N	106 (C + N = 126)
O	85

These results confirmed suspicions that failure was due to excessive amounts of nitrogen, carbon, and oxygen. To characterize the condition of the vessel further, subsize CVN impact tests were run on the unaffected base metal, the HAZ, and the uncorroded (sound) weld metal. These tests showed the following ductile-to-brittle transition temperatures:

SPECIMEN	**DUCTILE-TO-BRITTLE TRANSITION TEMPERATURE**	
	°C	**°F**
BASE METAL	40 ± 3	105 ± 5
HAZ	85 ± 3	180 ± 5
WELD	5 ± 3	40 ± 5

Comparison of the interstitial levels of the corroded welds, sound welds, base metal, and filler wire suggested that insufficient joint cleaning and faulty gas shielding were probably the main contributing factors that caused this weld corrosion failure. Discussions with the vendor uncovered two discrepancies. First, the welder was using a large, 19 mm ($\frac{3}{4}$ in.) inside diameter ceramic nozzle with a gas lens, but was flowing only 19 L/min (40 ft^3/h) of argon; this was the flow rate previously used with a 13 mm ($\frac{1}{2}$ in.) inside diameter gas lens nozzle. Second, a manifold system, found to be contaminated, was used to distribute pure argon welding gas from a large liquid argon tank to various satellite welding stations in the welding shop. The exact cause for the carbon pickup was not determined.

Conclusions. Failure of the nozzle weld was the result of intergranular corrosion caused by the pickup of interstitial elements and subsequent precipitation (sensitization) of chromium carbides and nitrides. Carbon pickup was believed to have been caused by inadequate joint cleaning prior to welding. The increase in the weld nitrogen level was a direct result of inadequate argon gas shielding of the molten weld puddle. Two areas of inadequate shielding were identified:

- IMPROPER GAS FLOW RATE FOR A 19 MM ($\frac{3}{4}$ IN.) DIAM GAS LENS NOZZLE
- CONTAMINATION OF THE MANIFOLD GAS SYSTEM (LEAKS)

In order to preserve the structural integrity and corrosion performance of the new Group III ferritic stainless steels, it is important to avoid the pickup of the interstitial elements carbon, nitrogen, oxygen, and hydrogen. In this particular case, the vendor used a flow rate of 23 to 28 L/min (50 to 60 ft^3/h) of argon for a 19 mm ($\frac{3}{4}$ in.) gas lens nozzle. As was mentioned previously in this article, the gas lens collet body is an important and necessary part of the torch used to weld these alloys. Failure to use a gas lens will result in a flow condition that is turbulent enough to aspirate air into the gas stream, thus contaminating the weld and destroying its mechanical and corrosion properties.

The manifold gas system also contributed to this failure. When a system such as this is first used, it is necessary to purge the contents of the manifold of any air to avoid oxidation and contamination. When that is done, the system functions satisfactorily; however, when it is shut down overnight or for repairs, air infiltrates back in, and a source of contamination is reestablished. Manifold systems are never fully purged, and leaks are common.

The contaminated welds were removed, and the vessels were rewelded and put back into service. Some rework involved the use of covered electrodes of dissimilar composition. No problems have been reported to date.

Recommendations. First, to ensure proper joint cleaning, solvent washing and wiping with a lint-free cloth should be performed immediately before welding. Also, a word of caution: Solvents are generally flammable and can be toxic. Ventilation should be adequate. Cleaning should continue until cloths are free of any residues.

Second, when GTAW, a 19 mm ($\frac{3}{4}$ in.) diameter ceramic nozzle with gas lens collet body is recommended. An argon gas flow rate of 28 L/min (60 ft^3/h) is optimum. Smaller nozzles are not recommended. Argon back gas shielding is mandatory at a slight positive pressure to avoid disrupting the flow of the welding torch.

Third, the tip of the filler wire should be kept within the torch shielding gas envelope to avoid contamination and pickup of nitrogen and oxygen (they embrittle the weld). If the tip becomes contaminated, welding should be stopped, the contaminated weld area ground out, and the tip of the filler wire that has been oxidized should be snipped off before proceeding with welding.

Fourth, a manifold gas system can be a problem when supplying shielding and backing gas. Individual argon gas cylinders (or individual liquid dewars) were found to provide good performance. A weld button spot test should be performed to confirm the integrity of the argon cylinder and all hose connections. In this test, the weld button sample must be absolutely bright and shiny. Any cloudiness is an indication of contamination. It is then necessary to check for leaks or to replace the cylinder. The best insurance is to purify the gas.

Fifth, it is important to remember that corrosion resistance is not the only criterion when evaluating these new ferritic stainless steels. Welds must also be tough and ductile, and these factors must be considered when making welds.

Lastly, dissimilar weld filler metals can be successfully used. To avoid premature failure, the dissimilar combination should be corrosion tested to ensure suitability for the intended service.

Weld toughness is an important property, and of great interest to the design engineer as well as the end user because of the influence of weld defects or notches on the performance of the material such as in a piping system or pressure vessel, especially under high strain rate conditions. Because ferritic stainless steels undergo a transition from ductile-to-brittle behavior as the temperature decreases (Fig. 2), researchers have been able to show rather good correlation between the DBTT and weldability. The common method used to measure DBTT is the CVN test.

Section size and thickness have a significant effect on the impact toughness of ferritic stainless steels (and all ferritic alloys). The effect of section size on DBTT is shown in Fig. 15. The thinner the material, the lower the DBTT.

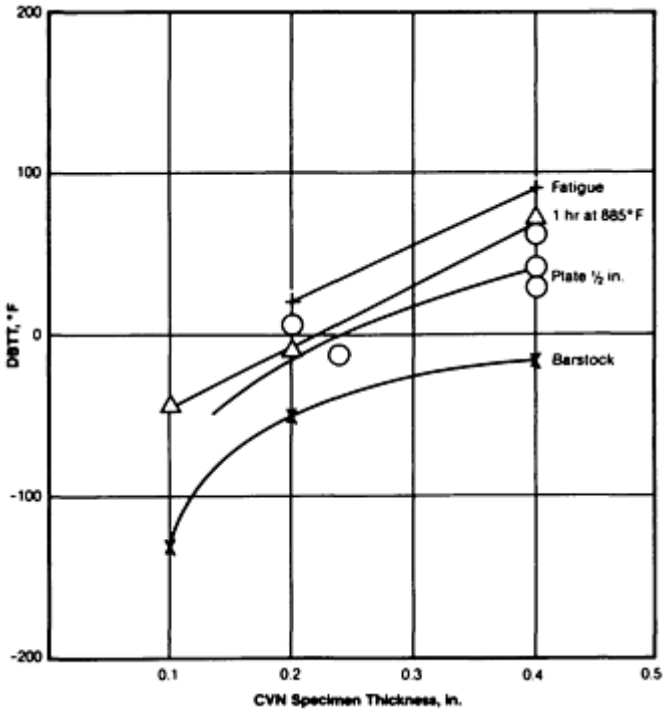

FIG. 15 IMPACT PROPERTIES AS A FUNCTION OF SECTION THICKNESS FOR XM-27 FERRITIC STAINLESS STEEL. SOURCE: REF 3

The cooling rate from peak welding temperatures is very important because toughness appears to be strongly related to the precipitation and morphology of carbides and nitrides. Even in ultrahigh-purity E-Brite 26-1, chromium nitrides have been observed (Ref 3). Depending on cooling rate, these precipitates will align along the grain boundaries or intragranularly within the matrix. For this reason, grain size is important. The finer the grain size, the more uniform the properties and the tougher the material.

Figure 16 illustrates the effect of carbon, nitrogen, and stabilizing elements on 26Cr-1Mo alloys. As shown in this figure, low interstitial levels correspond to lower DBTT values. Similar results are reported in Ref 4, 6, 44, 46, 48, and 49. It was further observed that notch brittleness was the result of the total interstitial element content (C + N), rather than the absolute value of each. Reducing the total interstitial element levels in ferritic stainless steels improves weldability and notch toughness. Another comparison is shown in Fig. 17. Here, the higher the purity of a 26Cr-1Mo alloy, the better the notch toughness and the lower the DBTT when compared to a 26Cr-1Mo alloy stabilized with titanium. Although the titanium-stabilized alloy was 3 mm ($\frac{1}{8}$ in.) thick compared to the 6 mm ($\frac{1}{4}$ in.) thick E-Brite plate, the ultrahigh-purity alloy had decidedly superior notch toughness (DBTT = -40 °C, or -40 °F, for E-Brite versus DBTT = +80 °C, or +175 °F, for 26-1 with titanium).

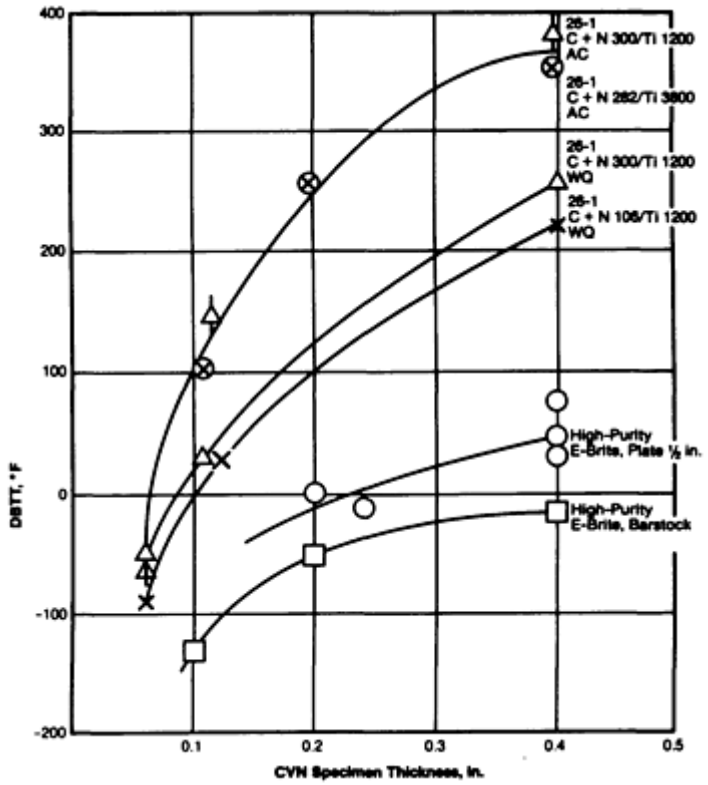

FIG. 16 EFFECT OF ALLOY PURITY (INTERSTITIAL ELEMENT CONTENT) AND STABILIZER CONTENT (VALUES GIVEN IN PARTS PER MILLION) ON THE DBTT OF FERRITIC STAINLESS STEELS. AC, AIR COOL; WQ, WATER QUENCHED. SOURCE: REF 3

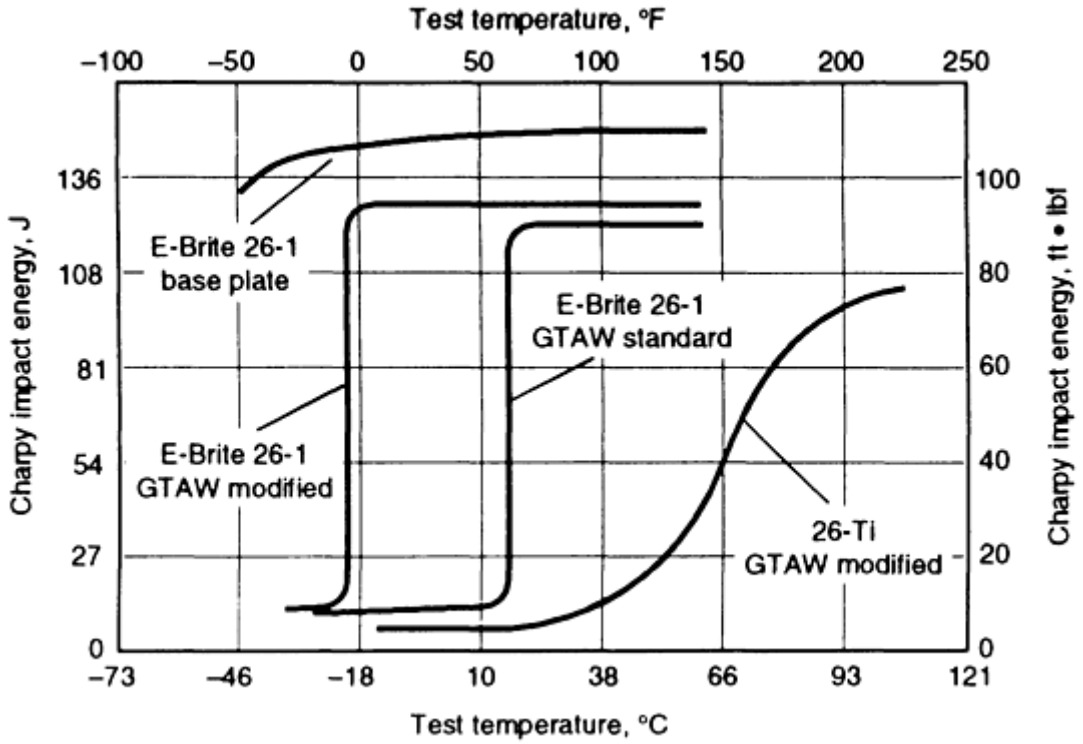

FIG. 17 NOTCH TOUGHNESS OF A GAS-TUNGSTEN ARC WELDED HIGH-PURITY FERRITIC STAINLESS STEEL (6 MM, OR $\frac{1}{4}$ IN., THICK E-BRITE 26-1 PLATE) VERSUS A TITANIUM-STABILIZED ALLOY (3 MM, OR $\frac{1}{8}$ IN., THICK

26-1 TI PLATE). SOURCE: REF 17

If the alloy thickness is reduced below 3 mm ($\frac{1}{8}$ in.), the stabilized grades start to display somewhat improved toughness. Because of the difficulty of measuring CVN impact toughness in those thin gages, weld ductility as measured by a bend test (see Table 6) or bend angle, was determined to be an acceptable method of measuring weldability. Under these conditions, stabilized ferritic stainless steels have excellent aswelded ductility when stabilizers are present in the minimum amounts necessary for stabilization, but the room-temperature impact properties suffer. When excessive stabilizing element(s) are present, weld ductility decreases as excess stabilizer content increases (Ref 50). If welding techniques are poor and shielding gas is contaminated, the amounts of stabilizer added to prevent sensitization and embrittlement may be insufficient to combine with all of the carbon and nitrogen. Oxygen pickup can also be detrimental. The result is loss of ductility, toughness, and corrosion resistance. Shielding gas purity must not be overlooked.

Dissimilar austenitic filler metals can be used to overcome the difficulties of higher than desired weld metal DBTT. Typical CVN toughness data are shown in Fig. 18.

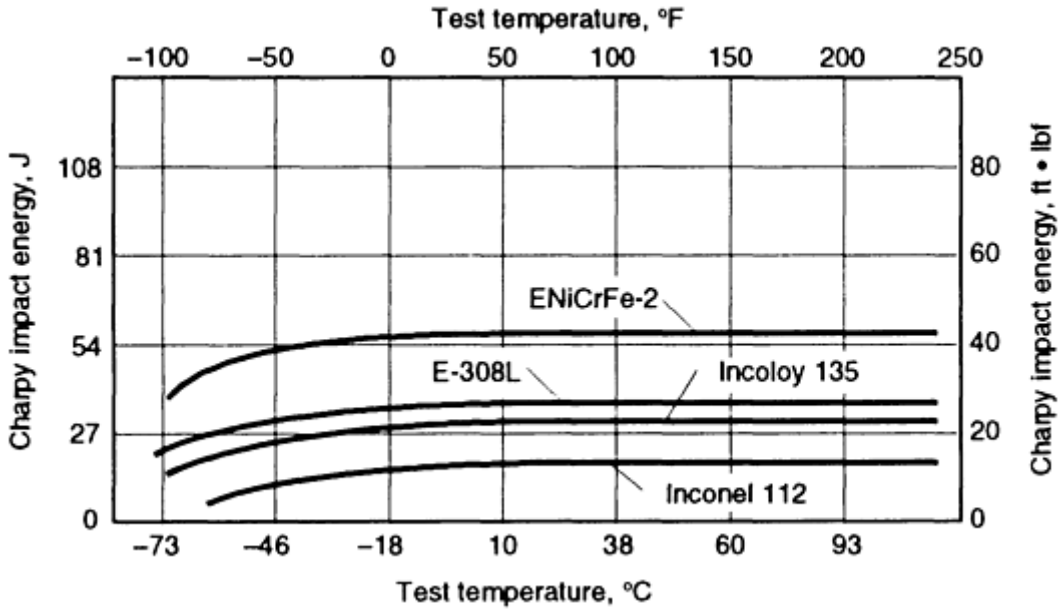

FIG. 18 CHARPY V-NOTCH TOUGHNESS OF SHIELDED METAL ARC WELDS MADE IN 6 MM ($\frac{1}{4}$ IN.) THICK E-BRITE 26-1 PLATE WITH DIFFERENT FILLER METALS. SOURCE: REF 17

Hot Cracking. Weld and HAZ hot cracking in the ferritic stainless steels is not as common a problem as with austenitic stainless steels. This is a result of the lower coefficient of thermal expansion of the ferritic stainless steels, as well as the greater solubility of sulfur and phosphorus in ferrite. However, excessive amounts of stabilizing elements have been shown to cause hot cracking as well as reduced ductility (Ref 25). Figure 19 shows hot cracks in the top surfaces of autogenous gas-tungsten arc welds in two type 444 ferritic stainless steel subscale varestraint test specimens. The stabilized alloys were found to be more susceptible to hot cracking than an alloy of similar composition with ultralow levels of impurities.

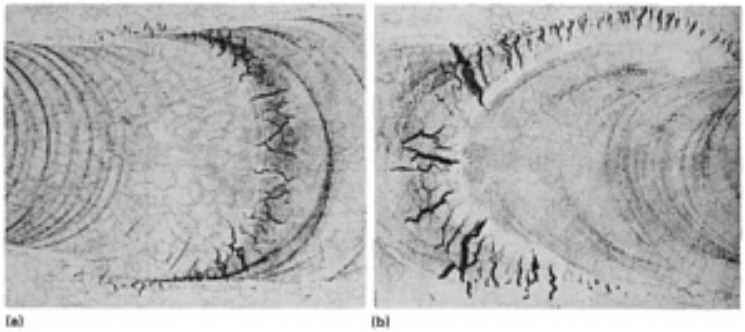

FIG. 19 TOP SURFACES OF SUBSCALE VARESTRAINT TEST GAS-TUNGSTEN WELDS IN TYPE 444 STAINLESS STEELS. (A) TITANIUM-STABILIZED (0.333% TI) TYPE 444 ALLOY. (B) NIOBIUM-STABILIZED (0.401% NB) TYPE 444 ALLOY. SOURCE: REF 25

The alloy which contained 0.40% Nb as a stabilizing element cracked more severely than the alloy which contained 0.333% Ti, but the worst cracking occurred in an alloy which contained both niobium (0.394%) and titanium (0.171%). The high-purity alloy which contained a total (C + N) content of 47 ppm (and no stabilizing elements), produced no hot cracks when tested under the same conditions. Although sulfur and phosphorus can also cause hot cracking in the ferritic stainless steels, the excess levels of niobium and titanium (above that necessary to tie up the carbon and nitrogen) are a more common cause of hot cracking. Thus, the stabilizing elements must be kept to the minimum practical levels to avoid hot cracking and reduced ductility.

Along with hot cracking, which is not often a problem for ferritic stainless steel welds, autogenous welds in alloys stabilized only with niobium often suffer from low ductility and poor toughness. In highly restrained situations, cracks may propagate in the weld along its length. For this reason, ferritic stainless steels of high or intermediate interstitial content stabilized only with niobium are rarely welded. (Titanium-free, stabilized ferritic stainless steels do, however, provide better brazeability and may be selected for brazed rather than welded applications.) Reduction of total interstitial element content to below approximately 0.02% largely eliminates this problem (Ref 51). Thus, the Group III ultra high purity alloys that contain niobium additions can be welded without fear of cracking. Addition of approximately 0.05% or greater titanium causes equiaxed grains to form near the weld centerline and yields improved weld properties (Ref 22). Thus, dual stabilized, intermediate purity Group III ferritic stainless steels are used to provide toughness in both the base metal and the weld regions.

References cited in this section

3. W.A. MATEJKA AND R.J. KNOTH, E-BRITE 26-1, THE HIGH-PURITY APPROACH TO HIGH CHROMIUM FERRITIC STAINLESS STEELS, *ASM SYMPOSIUM*, BAL HARBOUR, FLORIDA, ASTM, 6 DEC 1973
4. R.N. WRIGHT, MECHANICAL BEHAVIOR AND WELDABILITY OF HIGH-CHROMIUM FERRITIC STAINLESS STEELS AS A FUNCTION OF PURITY, *WELD. J.*, OCT 1971, P 434S-440S
6. J.J. DEMO, WELDABLE AND CORROSION-RESISTANT FERRITIC STAINLESS STEELS, *METALL. TRANS.*, VOL 5, NO. 11, NOV 1974, P 2253-2256
13. G. ROTHSCHILD, WELDING OF E-BRITE 26-1, PROCEDURE NO. W-2, WELDING SEMINAR HELD IN HOUSTON, TEXAS, 13 SEPT 1973
14. K.E. DORSCHU, WELDABILITY OF A NEW FERRITIC STAINLESS STEEL, *WELD. J.*, SEPT 1971
15. R.N. WRIGHT, "THE TOUGHNESS OF FERRITIC STAINLESS STEELS," MATERIALS ENGINEERING DEPARTMENT, RENSSELAER POLYTECHNIC INSTITUTE, TROY, NY, 1979
16. D.H. KAH AND D.W. DICKINSON, WELDABILITY OF FERRITIC STAINLESS STEEL, *WELD. J.*, AUG 1981, P 135S-142S
17. K.F. KRYSIAK, WELDABILITY OF THE NEW GENERATION OF FERRITIC STAINLESS STEELS--

PART I, PAPER NO. 92 PRESENTED AT THE NATIONAL ASSOCIATION OF CORROSION ENGINEERS CONFERENCE (TORONTO, CANADA), 14-18 APRIL 1975

18. K.F. KRYSIAK, WELDABILITY OF THE NEW GENERATION OF FERRITIC STAINLESS STEELS--UPDATE, *SYMPOSIUM ON FERRITIC STAINLESS STEELS* (SAN FRANCISCO, CA), 23-24 MAY 1979
19. R. LOWRIE, WELDING E-BRITE 26-1 TO OTHER ALLOYS, *WELD. J.*, NOV 1973, P 500S-506S
20. Y. OKAZAKI, R. TODOROKI, T. SAKAMOTO, AND T. ZAIZEN, ON THE PROPERTIES OF HIGH-PURITY 19 CR-2 MO FERRITIC STAINLESS STEEL WELDS, PAPER NO. 118, PRESENTED AT THE NATIONAL ASSOCIATION OF CORROSION ENGINEERS CONFERENCE (TORONTO, CANADA), 6-10 APRIL 1981
21. J.M. SAWHILL, JR. AND A.P. BOND, DUCTILITY AND TOUGHNESS OF STAINLESS STEEL WELDS, *WELD. J.*, VOL 55 (NO. 10), 1976, P 33S-41S
22. J.F. GRUBB AND S.D. WASHKO, THE EFFECT OF NIOBIUM AND TITANIUM DUAL STABILIZATION ON THE WELDABILITY OF 11% CHROMIUM FERRITIC STAINLESS STEELS, *PROC. INT. CONF. STAINLESS STEELS* (CHIBA, JAPAN), 10-13 JUNE 1991, ISIJ, P 1062-1068
23. J.C. VILLAFUERTE AND H.W. KERR, ELECTROMAGNETIC STIRRING AND GRAIN REFINEMENT IN STAINLESS STEEL GTA WELDS, *WELD. J.*, VOL 69 (NO. 1), 1990, P 1S-13S
24. J.C. VILLAFUERTE, E. PARDO, AND H.W. KERR, THE EFFECT OF ALLOY COMPOSITION AND WELDING COMPOSITIONS ON COLUMNAR-EQUIAXED TRANSITIONS IN FERRITIC STAINLESS STEEL GAS-TUNGSTEN ARC WELDS, *METALL. TRANS. A*, VOL 21 (NO. 7), JULY 1990, P 2009-2019
25. R.D. CAMPBELL, FERRITIC STAINLESS STEEL WELDING METALLURGY, *KEY ENGINEERING MATERIALS*, VOL 69 & 70, TRANS TECH PUBLICATIONS, SWITZERLAND, 1992, P 167-216
26. J.D. GATES AND R.A. JAGO, ABSORPTION OF GASEOUS CONTAMINANTS BY WELDS AND WELD SIMULATIONS IN FERRITIC STAINLESS STEELS, *MATER. SCI. TECHNOL.*, VOL 3, MAY 1987, P 386-393
27. J.M. SAWHILL, "DUCTILITY AND TOUGHNESS OF AUTOGENOUS GAS TUNGSTEN-ARC WELDS IN 18CR-2MO STEELS," RP-33-73-21, CLIMAX MOLYBDENUM CO. OF MICHIGAN, 24 FEB 1975
28. J.F. GRUBB, HYDROGEN EMBRITTLEMENT OF SUPERFERRITIC STAINLESS STEELS, *NEW DEVELOPMENTS IN STAINLESS STEEL TECHNOLOGY*, R.A. LULA, ED., AMERICAN SOCIETY FOR METALS, 1985, P 175-187
29. K.F. KRYSIAK *ET AL.*, CORROSION OF WELDMENTS, *METALS HANDBOOK*, VOL 13, 9TH ED., *CORROSION*, ASM INTERNATIONAL, 1987, P 344-368
30. E.J. MORGAN-WARREN, ATMOSPHERE CONTROL CRITERIA FOR WELDING TITANIUM, *ADVANCES IN WELDING PROCESS*, VOL 1, THE WELDING INSTITUTE, ABINGTON HALL, ABINGTON, CAMBRIDGE, 1978
31. G.G. PSARES, THE EFFECTS OF MOISTURE CONTENTS OF SHIELDING GASES ON THE FORMATION OF PORES WHEN ALUMINUM IS WELDED, *AUTOMAT. WELD.*, VOL 32 (NO. 10), P 6-8
32. D. NORTHCOTE, THE GAS TUNGSTEN ARC WELDING PROCESSES--ELECTRODES AND SHIELDING GASES--CRITERIA FOR OPTIMUM WELD QUALITY, *AUST. WELD. J.*, VOL 29 (NO. 1), AUTUMN 1984, P 18-20
33. K.F. KRYSIAK AND P.M. BHADHA, SHIELDING GAS PURIFICATION IMPROVES WELD QUALITY, *WELD. J.*, VOL 69 (NO. 11), NOV 1990, P 47-49
34. R.H. ESPY, HOW CORROSION AND WELDING CONDITIONS AFFECT CORROSION RESISTANCE OF WELDMENTS IN TYPE 430 STAINLESS STEEL, PAPER NO. 22, PRESENTED AT *CORROSION 68* (HOUSTON, TX), NATIONAL ASSOCIATION OF CORROSION ENGINEERS, 1968
35. K.F. KRYSIAK, WELDABILITY OF FERRITIC STAINLESS STEELS--AN OVERVIEW, *WELD. J.*, APRIL 1986
36. L. BERMUDEZ DE HELGUERO, WELDING OF HIGHLY ALLOYED DISSIMILAR STAINLESS

STEELS (USING STABILIZED AUSTENITIC OR FERRITIC STAINLESS STEEL FILLERS), *SIDERURGIA*, VOL 48, DEC 1988, P 55-60

37. J.J. DEMO, *CORROSION*, VOL 27 (NO. 3), 1971, P 531
38. R.H. HODGES, *CORROSION*, VOL 27 (NO. 3), 1971, P 119
39. R.H. HODGES, *CORROSION*, VOL 27 (NO. 3), 1971, P 164
40. E. BAERLECKEN, W.A. FISCHER, AND K. LORENZ, UNTERSUCHUNGEN ÜBER DAS UMWANDLUNGSVERHALTEN, DIE KERBSCHLAGZÄHIGKEIT UND DIE NEIGUNG ZUR INTERKRISTALLINEN KORROSION VON EISEN-CHROM-LEGIERUNGEN MIT CHROMGEHALTEN BIS 30% [INQUIRY INTO THE TRANSFORMATION, NOTCHED IMPACT TOUGHNESS, AND THE SUSCEPTIBILITY TOWARD INTERCRYSTALLINE CORROSION OF IRON-CHROMIUM ALLOYS WITH CHROMIUM CONTENTS UP TO 30%], *STAHL EISEN*, VOL 81 (NO. 12), JUNE 1961, P 768-778
41. G. HERBSLEB AND W. SCHEWENK, *WERKST. KORROS.*, VOL 19, 1968, P 103
42. J.J. DEMO AND A.P. BOND, INTERGRANULAR CORROSION AND EMBRITTLEMENT OF FERRITIC STAINLESS STEELS, VOL 31 (NO. 1), JAN 1975, P 21-22
43. J.J. DEMO, *METALL. TRANS.*, VOL 5 (NO. 11), NOV 1974, P 2253
44. M. SEMCHYSHEN, A.P. BOND, AND J.H. DUNDAS, *PROC. SYMP. TOWARD IMPROVING DUCTILITY AND TOUGHNESS* (KYOTO, JAPAN), 1971, P 239
45. B. POLLARD, *MET. TECHNOL.*, VOL 1, PART 1, JAN 1974, P 31
46. J. HOCHMANN, "THE INFLUENCE OF VACUUM FUSION ON THE PROPERTIES OF 25% CR FERRITIC STEELS," PH.D. THESIS, PARIS, FRANCE, 1950
47. *METALS HANDBOOK*, 9TH ED., VOL 13, *CORROSION*, ASM INTERNATIONAL, 1987, P 355-358
48. J.F. GRUBB, PH.D. THESIS, RENSSELAER POLYTECHNIC INSTITUTE, TROY, NY, MAY 1982
49. W.O. BINDER AND H.R. SPINDELOW, *TRANS. ASM*, VOL 43, 1951, P 759
50. J.F. GRUBB, STABILIZATION OF HIGH-CHROMIUM, FERRITIC STAINLESS STEELS, *PROC. INT. CONF. STAINLESS STEELS* (CHIBA, JAPAN), 10-13 JUNE 1991, ISIJ, P 541-548
51. K.E. PINNOW AND J.P. BRESSANELLI, "WELDED FERRITIC STAINLESS STEEL ARTICLES," U.S. PATENT 4,119,765, 10 OCT 1978

Note cited in this section

* * SENSITIZATION OF FERRITIC STAINLESS STEELS DIFFERS FROM THAT OF AUSTENITIC STAINLESS STEELS BECAUSE OF THE LOWER SOLUBILITY OF (C + N) IN FERRITE AND THE MUCH GREATER (APPROXIMATELY 10^3 TIMES) DIFFUSION RATE OF (C + N) AND CHROMIUM IN FERRITE THAN IN AUSTENITE.

Selection of Wrought Ferritic Stainless Steels

K.F. Krysiak, Hercules, Inc.; J.F. Grubb, Allegheny Ludlum Corporation; B. Pollard; R.D. Campbell, Joining Services, Inc.

References

1. *METALS HANDBOOK*, VOL 6, 8TH ED., *WELDING AND BRAZING*, AMERICAN SOCIETY FOR METALS, 1971, P 248
2. WORKING DATA, CARPENTER STAINLESS STEELS, 1971
3. W.A. MATEJKA AND R.J. KNOTH, E-BRITE 26-1, THE HIGH-PURITY APPROACH TO HIGH CHROMIUM FERRITIC STAINLESS STEELS, *ASM SYMPOSIUM*, BAL HARBOUR, FLORIDA, ASTM, 6 DEC 1973

4. R.N. WRIGHT, MECHANICAL BEHAVIOR AND WELDABILITY OF HIGH-CHROMIUM FERRITIC STAINLESS STEELS AS A FUNCTION OF PURITY, *WELD. J.*, OCT 1971, P 434S-440S
5. I.A. FRANSON, MECHANICAL PROPERTIES OF HIGH-PURITY FE-26CR-1MO FERRITIC STAINLESS STEEL, *METALL. TRANS.*, VOL 5, NOV 1974, P 2257-2264
6. J.J. DEMO, WELDABLE AND CORROSION-RESISTANT FERRITIC STAINLESS STEELS, *METALL. TRANS.*, VOL 5, NO. 11, NOV 1974, P 2253-2256
7. K.E. PINNOW, J.P. BRASSANELLI, AND A. MOSKOWITZ, A NEW HIGH-CHROMIUM FERRITIC STAINLESS STEEL, *MET. ENG. QUART.*, AUG 1975, P 32-41
8. R.F. STEIGERWALD, LOW INTERSTITIAL FE-CR-MO FERRITIC STAINLESS, *SOVIET-AMERICAN SYMPOSIUM ON NEW DEVELOPMENTS IN THE FIELD OF MOLYBDENUM-ALLOYED CAST IRON AND STEEL*, MOSCOW, JAN 1973
9. A.P. BOND, *TRANS. TMS-AIME*, VOL 245, 1969, P 2127
10. M.A. STREICHER, DEVELOPMENT OF PITTING-RESISTANT FE-CR-MO ALLOYS, *CORROSION*, VOL 30 (NO. 3), 1974, P 77-91
11. G.B. HUNTER AND T.W. EAGAR, DUCTILITY OF STABILIZED FERRITIC STAINLESS STEELS WELDS
12. B. POLLARD, DUCTILITY OF FERRITIC STAINLESS WELD METAL, *WELD. J.*, APR 1972, P 222S-230S
13. G. ROTHSCHILD, WELDING OF E-BRITE 26-1, PROCEDURE NO. W-2, WELDING SEMINAR HELD IN HOUSTON, TEXAS, 13 SEPT 1973
14. K.E. DORSCHU, WELDABILITY OF A NEW FERRITIC STAINLESS STEEL, *WELD. J.*, SEPT 1971
15. R.N. WRIGHT, "THE TOUGHNESS OF FERRITIC STAINLESS STEELS," MATERIALS ENGINEERING DEPARTMENT, RENSSELAER POLYTECHNIC INSTITUTE, TROY, NY, 1979
16. D.H. KAH AND D.W. DICKINSON, WELDABILITY OF FERRITIC STAINLESS STEEL, *WELD. J.*, AUG 1981, P 135S-142S
17. K.F. KRYSIAK, WELDABILITY OF THE NEW GENERATION OF FERRITIC STAINLESS STEELS--PART I, PAPER NO. 92 PRESENTED AT THE NATIONAL ASSOCIATION OF CORROSION ENGINEERS CONFERENCE (TORONTO, CANADA), 14-18 APRIL 1975
18. K.F. KRYSIAK, WELDABILITY OF THE NEW GENERATION OF FERRITIC STAINLESS STEELS--UPDATE, *SYMPOSIUM ON FERRITIC STAINLESS STEELS* (SAN FRANCISCO, CA), 23-24 MAY 1979
19. R. LOWRIE, WELDING E-BRITE 26-1 TO OTHER ALLOYS, *WELD. J.*, NOV 1973, P 500S-506S
20. Y. OKAZAKI, R. TODOROKI, T. SAKAMOTO, AND T. ZAIZEN, ON THE PROPERTIES OF HIGH-PURITY 19 CR-2 MO FERRITIC STAINLESS STEEL WELDS, PAPER NO. 118, PRESENTED AT THE NATIONAL ASSOCIATION OF CORROSION ENGINEERS CONFERENCE (TORONTO, CANADA), 6-10 APRIL 1981
21. J.M. SAWHILL, JR. AND A.P. BOND, DUCTILITY AND TOUGHNESS OF STAINLESS STEEL WELDS, *WELD. J.*, VOL 55 (NO. 10), 1976, P 33S-41S
22. J.F. GRUBB AND S.D. WASHKO, THE EFFECT OF NIOBIUM AND TITANIUM DUAL STABILIZATION ON THE WELDABILITY OF 11% CHROMIUM FERRITIC STAINLESS STEELS, *PROC. INT. CONF. STAINLESS STEELS* (CHIBA, JAPAN), 10-13 JUNE 1991, ISIJ, P 1062-1068
23. J.C. VILLAFUERTE AND H.W. KERR, ELECTROMAGNETIC STIRRING AND GRAIN REFINEMENT IN STAINLESS STEEL GTA WELDS, *WELD. J.*, VOL 69 (NO. 1), 1990, P 1S-13S
24. J.C. VILLAFUERTE, E. PARDO, AND H.W. KERR, THE EFFECT OF ALLOY COMPOSITION AND WELDING COMPOSITIONS ON COLUMNAR-EQUIAXED TRANSITIONS IN FERRITIC STAINLESS STEEL GAS-TUNGSTEN ARC WELDS, *METALL. TRANS. A*, VOL 21 (NO. 7), JULY 1990, P 2009-2019
25. R.D. CAMPBELL, FERRITIC STAINLESS STEEL WELDING METALLURGY, *KEY ENGINEERING MATERIALS*, VOL 69 & 70, TRANS TECH PUBLICATIONS, SWITZERLAND, 1992, P 167-216
26. J.D. GATES AND R.A. JAGO, ABSORPTION OF GASEOUS CONTAMINANTS BY WELDS AND

WELD SIMULATIONS IN FERRITIC STAINLESS STEELS, *MATER. SCI. TECHNOL.,* VOL 3, MAY 1987, P 386-393

27. J.M. SAWHILL, "DUCTILITY AND TOUGHNESS OF AUTOGENOUS GAS TUNGSTEN-ARC WELDS IN 18CR-2MO STEELS," RP-33-73-21, CLIMAX MOLYBDENUM CO. OF MICHIGAN, 24 FEB 1975
28. J.F. GRUBB, HYDROGEN EMBRITTLEMENT OF SUPERFERRITIC STAINLESS STEELS, *NEW DEVELOPMENTS IN STAINLESS STEEL TECHNOLOGY,* R.A. LULA, ED., AMERICAN SOCIETY FOR METALS, 1985, P 175-187
29. K.F. KRYSIAK *ET AL.,* CORROSION OF WELDMENTS, *METALS HANDBOOK,* VOL 13, 9TH ED., *CORROSION,* ASM INTERNATIONAL, 1987, P 344-368
30. E.J. MORGAN-WARREN, ATMOSPHERE CONTROL CRITERIA FOR WELDING TITANIUM, *ADVANCES IN WELDING PROCESS,* VOL 1, THE WELDING INSTITUTE, ABINGTON HALL, ABINGTON, CAMBRIDGE, 1978
31. G.G. PSARES, THE EFFECTS OF MOISTURE CONTENTS OF SHIELDING GASES ON THE FORMATION OF PORES WHEN ALUMINUM IS WELDED, *AUTOMAT. WELD.,* VOL 32 (NO. 10), P 6-8
32. D. NORTHCOTE, THE GAS TUNGSTEN ARC WELDING PROCESSES--ELECTRODES AND SHIELDING GASES--CRITERIA FOR OPTIMUM WELD QUALITY, *AUST. WELD. J.,* VOL 29 (NO. 1), AUTUMN 1984, P 18-20
33. K.F. KRYSIAK AND P.M. BHADHA, SHIELDING GAS PURIFICATION IMPROVES WELD QUALITY, *WELD. J.,* VOL 69 (NO. 11), NOV 1990, P 47-49
34. R.H. ESPY, HOW CORROSION AND WELDING CONDITIONS AFFECT CORROSION RESISTANCE OF WELDMENTS IN TYPE 430 STAINLESS STEEL, PAPER NO. 22, PRESENTED AT *CORROSION 68* (HOUSTON, TX), NATIONAL ASSOCIATION OF CORROSION ENGINEERS, 1968
35. K.F. KRYSIAK, WELDABILITY OF FERRITIC STAINLESS STEELS--AN OVERVIEW, *WELD. J.,* APRIL 1986
36. L. BERMUDEZ DE HELGUERO, WELDING OF HIGHLY ALLOYED DISSIMILAR STAINLESS STEELS (USING STABILIZED AUSTENITIC OR FERRITIC STAINLESS STEEL FILLERS), *SIDERURGIA,* VOL 48, DEC 1988, P 55-60
37. J.J. DEMO, *CORROSION,* VOL 27 (NO. 3), 1971, P 531
38. R.H. HODGES, *CORROSION,* VOL 27 (NO. 3), 1971, P 119
39. R.H. HODGES, *CORROSION,* VOL 27 (NO. 3), 1971, P 164
40. E. BAERLECKEN, W.A. FISCHER, AND K. LORENZ, UNTERSUCHUNGEN ÜBER DAS UMWANDLUNGSVERHALTEN, DIE KERBSCHLAGZÄHIGKEIT UND DIE NEIGUNG ZUR INTERKRISTALLINEN KORROSION VON EISEN-CHROM-LEGIERUNGEN MIT CHROMGEHALTEN BIS 30% [INQUIRY INTO THE TRANSFORMATION, NOTCHED IMPACT TOUGHNESS, AND THE SUSCEPTIBILITY TOWARD INTERCRYSTALLINE CORROSION OF IRON-CHROMIUM ALLOYS WITH CHROMIUM CONTENTS UP TO 30%], *STAHL EISEN,* VOL 81 (NO. 12), JUNE 1961, P 768-778
41. G. HERBSLEB AND W. SCHEWENK, *WERKST. KORROS.,* VOL 19, 1968, P 103
42. J.J. DEMO AND A.P. BOND, INTERGRANULAR CORROSION AND EMBRITTLEMENT OF FERRITIC STAINLESS STEELS, VOL 31 (NO. 1), JAN 1975, P 21-22
43. J.J. DEMO, *METALL. TRANS.,* VOL 5 (NO. 11), NOV 1974, P 2253
44. M. SEMCHYSHEN, A.P. BOND, AND J.H. DUNDAS, *PROC. SYMP. TOWARD IMPROVING DUCTILITY AND TOUGHNESS* (KYOTO, JAPAN), 1971, P 239
45. B. POLLARD, *MET. TECHNOL.,* VOL 1, PART 1, JAN 1974, P 31
46. J. HOCHMANN, "THE INFLUENCE OF VACUUM FUSION ON THE PROPERTIES OF 25% CR FERRITIC STEELS," PH.D. THESIS, PARIS, FRANCE, 1950
47. *METALS HANDBOOK,* 9TH ED., VOL 13, *CORROSION,* ASM INTERNATIONAL, 1987, P 355-358

48. J.F. GRUBB, PH.D. THESIS, RENSSELAER POLYTECHNIC INSTITUTE, TROY, NY, MAY 1982
49. W.O. BINDER AND H.R. SPINDELOW, *TRANS. ASM*, VOL 43, 1951, P 759
50. J.F. GRUBB, STABILIZATION OF HIGH-CHROMIUM, FERRITIC STAINLESS STEELS, *PROC. INT. CONF. STAINLESS STEELS* (CHIBA, JAPAN), 10-13 JUNE 1991, ISIJ, P 541-548
51. K.E. PINNOW AND J.P. BRESSANELLI, "WELDED FERRITIC STAINLESS STEEL ARTICLES," U.S. PATENT 4,119,765, 10 OCT 1978

Selection of Wrought Austenitic Stainless Steels

John A. Brooks, Sandia National Laboratories; John C. Lippold, Edison Welding Institute

Introduction

AUSTENITIC STAINLESS STEELS exhibit a single-phase, face-centered cubic (fcc) structure that is maintained over a wide range of temperatures. This structure results from a balance of alloying additions that stabilize the austenite phase from elevated to cryogenic temperatures. Because these alloys are predominantly single phase, they can only be strengthened by solid-solution alloying or by work hardening. The exceptions are the precipitation-strengthened austenitic stainless steels that are discussed in the article "Selection of Wrought Precipitation-Hardening Stainless Steels" in this Section of the Volume.

The austenitic stainless steels were developed for use in both mild and severe corrosive conditions. They are also used at temperatures that range from cryogenic temperatures, where they exhibit high toughness, to elevated temperatures of nearly 600 °C (1110 °F), where they exhibit good oxidation resistance. Because the austenitic materials are nonmagnetic, they are sometimes used in applications where magnetic materials are not acceptable.

The most common types of austenitic stainless steels are the UNS S20000 and S30000 alloys (AISI 200 and 300 series). Within these two grades, the alloying additions, which are chosen to provide the desired properties at reasonable cost, can be considerably different. Furthermore, alloying additions and specific alloy composition can have a major effect on weldability and the as-welded microstructure. The AISI 300 series of alloys typically contain from 8 to 20% Ni and from 16 to 25% Cr. Minor alloying additions are approximately 1% Si (maximum), which is used as a deoxidizer; 0.02 to 0.08% C, which is used as an austenite stabilizer; and approximately 1.5% Mn, which is used both as an austenite stabilizer and as a sulfur and silicon compound former. A more-complete compositional range of common AISI 200- and 300-series alloys is shown in Table 1. The less common alloys, including some of the superaustenitic stainless steels, are identified in Table 2.

TABLE 1 COMPOSITIONS OF STANDARD AUSTENITIC STAINLESS STEELS

TYPE	UNS NO.	COMPOSITION, %[A]							
		C	Mn	Si	Cr	Ni	P	S	Other
201	S20100	0.15	5.5-7.5	1.00	16.0-18.0	3.5-5.5	0.06	0.03	0.25 N
202	S20200	0.15	7.5-10.0	1.00	17.0-19.0	4.0-6.0	0.06	0.03	0.25 N
205	S20500	0.12-0.25	14.0-15.5	1.00	16.5-18.0	1.0-1.75	0.06	0.03	0.32-0.40 N
301	S30100	0.15	2.0	1.00	16.0-18.0	6.0-8.0	0.045	0.03	. . .
302	S30200	0.15	2.0	1.00	17.0-19.0	8.0-10.0	0.045	0.03	. . .
302B	S30215	0.15	2.0	2.0-3.0	17.0-19.0	8.0-10.0	0.045	0.03	. . .

303	S30300	0.15	2.0	1.00	17.0-19.0	8.0-10.0	0.20	0.15 MIN	0.6 MO[B]
303SE	S30323	0.15	2.0	1.00	17.0-19.0	8.0-10.0	0.20	0.06	0.15 MIN SE
304	S30400	0.08	2.0	1.00	18.0-20.0	8.0-10.5	0.045	0.03	. . .
304H	S30409	0.04-0.10	2.0	1.00	18.0-20.0	8.0-10.5	0.045	0.03	. . .
304L	S30403	0.03	2.0	1.00	18.0-20.0	8.0-12.0	0.045	0.03	. . .
304LN	S30453	0.03	2.0	1.00	18.0-20.0	8.0-12.0	0.045	0.03	0.10-0.16 N
302CU	S30430	0.08	2.0	1.00	17.0-19.0	8.0-10.0	0.045	0.03	3.0-4.0 CU
304N	S30451	0.08	2.0	1.00	18.0-20.0	8.0-10.5	0.045	0.03	0.10-0.16 N
305	S30500	0.12	2.0	1.00	17.0-19.0	10.5-13.0	0.045	0.03	. . .
308	S30800	0.08	2.0	1.00	19.0-21.0	10.0-12.0	0.045	0.03	. . .
309	S30900	0.20	2.0	1.00	22.0-24.0	12.0-15.0	0.045	0.03	. . .
309S	S30908	0.08	2.0	1.00	22.0-24.0	12.0-15.0	0.045	0.03	. . .
310	S31000	0.25	2.0	1.50	24.0-26.0	19.0-22.0	0.045	0.03	. . .
310S	S31008	0.08	2.0	1.50	24.0-26.0	19.0-22.0	0.045	0.03	. . .
314	S31400	0.25	2.0	1.5-3.0	23.0-26.0	19.0-22.0	0.045	0.03	. . .
316	S31600	0.08	2.0	1.00	16.0-18.0	10.0-14.0	0.045	0.03	2.0-3.0 MO
316F	S31620	0.08	2.0	1.00	16.0-18.0	10.0-14.0	0.20	0.10 MIN	1.75-2.5 MO
316H	S31609	0.04-0.10	2.0	1.00	16.0-18.0	10.0-14.0	0.045	0.03	2.0-3.0 MO
316L	S31603	0.03	2.0	1.00	16.0-18.0	10.0-14.0	0.045	0.03	2.0-3.0 MO
316LN	S31653	0.03	2.0	1.00	16.0-18.0	10.0-14.0	0.045	0.03	2.0-3.0 MO; 0.10-0.16 N
316N	S31651	0.08	2.0	1.00	16.0-18.0	10.0-14.0	0.045	0.03	2.0-3.0 MO; 0.10-0.16 N
317	S31700	0.08	2.0	1.00	18.0-20.0	11.0-15.0	0.045	0.03	3.0-4.0 MO
317L	S31703	0.03	2.0	1.00	18.0-20.0	11.0-15.0	0.045	0.03	3.0-4.0 MO
321	S32100	0.08	2.0	1.00	17.0-19.0	9.0-12.0	0.045	0.03	5 × %C MIN TI
321H	S32109	0.04-0.10	2.0	1.00	17.0-19.0	9.0-12.0	0.045	0.03	5 × %C MIN TI
330	N08330	0.08	2.0	0.75-1.5	17.0-20.0	34.0-37.0	0.04	0.03	. . .
347	S34700	0.08	2.0	1.00	17.0-	9.0-	0.045	0.03	10 × %C MIN NB

					19.0	13.0			
347H	S34709	0.04-0.10	2.0	1.00	17.0-19.0	9.0-13.0	0.045	0.03	8 × %C MIN - 1.0 MAX NB
348	S34800	0.08	2.0	1.00	17.0-19.0	9.0-13.0	0.045	0.03	0.2 CO; 10 × %C MIN NB; 0.10 TA
348H	S34809	0.04-0.10	2.0	1.00	17.0-19.0	9.0-13.0	0.045	0.03	0.2 CO; 10 × %C MIN - 1.0 MAX NB; 0.10 TA
384	S38400	0.08	2.0	1.00	15.0-17.0	17.0-19.0	0.045	0.03	. . .

(A) SINGLE VALUES ARE MAXIMUM VALUES UNLESS OTHERWISE INDICATED.

(B) OPTIONAL

TABLE 2 COMPOSITIONS OF NONSTANDARD AUSTENITIC STAINLESS STEELS

DESIGNATION[A]	**UNS NO.**	**COMPOSITION, %[B]**							
		C	**Mn**	**Si**	**Cr**	**Ni**	**P**	**S**	**Other**
GALL-TOUGH	S20161	0.15	4.00-6.00	3.00-4.00	15.0-18.0	4.00-6.00	0.040	0.040	0.08-0.20 N
203 EZ (XM-I)	S20300	0.08	5.0-6.5	1.00	16.0-18.0	5.0-6.5	0.040	0.18-0.35	0.5 MO; 1.75-2.25 CU
NITRONIC 50 (XM-19)	S20910	0.06	4.0-6.0	1.00	20.5-23.5	11.5-13.5	0.040	0.030	1.5-3.0 MO; 0.2-0.4 N; 0.1-0.3 NB; 0.1-0.3 V
TENELON (XM-31)	S21400	0.12	14.5-16.0	0.3-1.0	17.0-18.5	0.75	0.045	0.030	0.35 N
CRYOGENIC TENELON (XM-14)	S21460	0.12	14.0-16.0	1.00	17.0-19.0	5.0-6.0	0.060	0.030	0.35-0.50 N
ESSHETE 1250	S21500	0.15	5.5-7.0	1.20	14.0-16.0	9.0-11.0	0.040	0.030	0.003-0.009 B; 0.75-1.25 NB; 0.15-0.40 V
TYPE 216 (XM-17)	S21600	0.08	7.5-9.0	1.00	17.5-22.0	5.0-7.0	0.045	0.030	2.0-3.0 MO; 0.25-0.50 N
TYPE 216 L (XM-18)	S21603	0.03	7.5-9.0	1.00	17.5-22.0	7.5-9.0	0.045	0.030	2.0-3.0 MO; 0.25-0.50 N
NITRONIC 60	S21800	0.10	7.0-9.0	3.5-4.5	16.0-18.0	8.0-9.0	0.040	0.030	0.08-0.18 N
NITRONIC 40 (XM-10)	S21900	0.08	8.0-10.0	1.00	19.0-21.5	5.5-7.5	0.060	0.030	0.15-0.40 N
21-6-9 LC	S21904	0.04	8.00-10.00	1.00	19.00-21.50	5.50-7.50	0.060	0.030	0.15-0.40 N
NITRONIC 33 (18-3 MN)	S24000	0.08	11.50-14.50	1.00	17.00-19.00	2.50-3.75	0.060	0.030	0.20-0.40 N
NITRONIC 32 (18-2 MN)	S24100	0.15	11.00-14.00	1.00	16.50-19.50	0.50-2.50	0.060	0.030	0.20-0.40 N
18-18 PLUS	S28200	0.15	17.0-19.0	1.00	17.5-19.5	. . .	0.045	0.030	0.5-1.5 MO; 0.5-1.5 CU; 0.4-0.6 N
303 PLUS X (XM-5)	S30310	0.15	2.5-4.5	1.00	17.0-19.0	7.0-10.0	0.020	0.25 MIN	0.6 MO
MVMA[C]	S30415	0.05	0.60	1.30	18.5	9.50	. . .	. . .	0.15 N; 0.04

									CE
304BI[D]	S30424	0.08	2.00	0.75	18.00-20.00	12.00-15.00	0.045	0.030	0.10 N; 1.00-1.25 B
304 HN (XM-21)	S30452	0.04-0.10	2.00	1.00	18.0-20.0	8.0-10.5	0.045	0.030	0.16-0.30 N
CRONIFER 1815 LCSI	S30600	0.018	2.00	3.73-4.3	17.0-18.5	14.0-15.5	0.020	0.020	0.2 MO
RA 85 H[C]	S30615	0.20	0.80	3.50	18.5	14.50	. . .	. . .	1.0 AL
253 MA	S30815	0.05-0.10	0.80	1.4-2.0	20.0-22.0	10.0-12.0	0.040	0.030	0.14-0.20 N; 0.03-0.08 CE; 1.0 AL
TYPE 309 S CB	S30940	0.08	2.00	1.00	22.0-24.0	12.0-15.0	0.045	0.030	10 × %C MIN TO 1.10 MAX NB
TYPE 310 CB	S31040	0.08	2.00	1.50	24.0-26.0	19.0-22.0	0.045	0.030	10 × %C MIN TO 1.10 MAX NB + TA
254 SMO	S31254	0.20	1.00	0.80	19.50-20.50	17.50-18.50	0.030	0.010	6.00-6.50 MO; 0.50-1.00 CU; 0.180-0.220 N
TYPE 316 TI	S31635	0.08	2.00	1.00	16.0-18.0	10.0-14.0	0.045	0.030	5 × %(C + N) MIN TO 0.70 MAX TI; 2.0-3.0 MO; 0.10 N
TYPE 316 CB	S31640	0.08	2.00	1.00	16.0-18.0	10.0-14.0	0.045	0.030	10 × %C MIN TO 1.10 MAX NB + TA; 2.0-3.0 MO; 0.10 N
TYPE 316 HQ	. . .	0.030	2.00	1.00	16.00-18.25	10.00-14.00	0.030	0.015	3.00-4.00 CU; 2.00-3.00 MO
TYPE 317 LM	S31725	0.03	2.00	1.00	18.0-20.0	13.5-17.5	0.045	0.030	4.0-5.0 MO; 0.10 N
17-14-4 LN	S31726	0.03	2.00	0.75	17.0-20.0	13.5-17.5	0.045	0.030	4.0-5.0 MO; 0.10-0.20 N
TYPE 317 LN	S31753	0.03	2.00	1.00	18.0-21.0	11.0-15.0	0.030	0.030	0.10-0.22 N
TYPE 370	S37000	0.03-0.05	1.65-2.35	0.5-1.0	12.5-14.5	14.5-16.5	0.040	0.010	1.5-2.5 MO; 0.1-0.4 TI; 0.005 N; 0.05 CO
18-18-2 (XM-15)	S38100	0.08	2.00	1.5-2.5	17.0-19.0	17.5-18.5	0.030	0.030	. . .
19-9 DL	S63198	0.28-0.35	0.75-1.50	0.03-0.8	18.0-21.0	8.0-11.0	0.040	0.030	1.0-1.75 MO; 0.1-0.35 TI; 1.0-1.75 W; 0.25-0.60 NB
20CB-3	N08020	0.07	2.00	1.00	19.0-	32.0-	0.045	0.035	2.0-3.0 MO;

					21.0	38.0			3.0-4.0 CU; 8 × %C MIN TO 1.00 MAX NB
20MO-4	N08024	0.03	1.00	0.50	22.5-25.0	35.0-40.0	0.035	0.035	3.50-5.00 MO; 0.50-1.50 CU; 0.15-0.35 NB
20MO-6	N08026	0.03	1.00	0.50	22.00-26.00	33.00-37.20	0.03	0.03	5.00-6.70 MO; 2.00-4.00 CU
SANICRO 28	N08028	0.02	2.00	1.00	26.0-28.0	29.5-32.5	0.020	0.015	3.0-4.0 MO; 0.6-1.4 CU
AL-6X	N08366	0.035	2.00	1.00	20.0-22.0	23.5-25.5	0.030	0.030	6.0-7.0 MO
AL-6XN	N08367	0.030	2.00	1.00	20.0-22.0	23.50-25.50	0.040	0.030	6.0-7.0 MO; 0.18-0.25 N
JS-700	N08700	0.04	2.00	1.00	19.0-23.0	24.0-26.0	0.040	0.030	4.3-5.0 MO; 8 × %C MIN TO 0.5 MAX NB; 0.5 CU; 0.005 PB; 0.035 S
TYPE 332	N08800	0.01	1.50	1.00	19.0-23.0	30.0-35.0	0.045	0.015	0.15-0.60 TI; 0.15-0.60 AL
904L	N08904	0.02	2.00	1.00	19.0-23.0	23.0-28.0	0.045	0.035	4.0-5.0 MO; 1.0-2.0 CU
CRONIFER 1925 HMO	N08925	0.02	1.00	0.50	24.0-26.0	19.0-21.0	0.045	0.030	6.0-7.0 MO; 0.8-1.5 CU; 0.10-0.20 N
CRONIFER 2328	. . .	0.04	0.75	0.75	22.0-24.0	26.0-28.0	0.030	0.015	2.5-3.5 CU; 0.4-0.7 TI; 2.5-3.0 MO

(A) XM DESIGNATIONS IN THIS COLUMN ARE ASTM DESIGNATIONS FOR THE LISTED ALLOY.

(B) SINGLE VALUES ARE MAXIMUM VALUES UNLESS OTHERWISE INDICATED.

(C) NOMINAL COMPOSITIONS.

(D) UNS DESIGNATION HAS NOT BEEN SPECIFIED; THIS DESIGNATION APPEARS IN ASTM A 887 AND MERELY INDICATES THE FORM TO BE USED.

Depending on alloy composition, the austenitic stainless steels may solidify with a microstructure containing some retained ferrite at room temperature, as a result of welding. Weld cracking, of which the most common form is solidification cracking, can be another consequence of welding. Cracks can occur in various regions of the weld with different orientations, such as centerline cracks, transverse cracks, and microcracks in the underlying weld metal or adjacent heat-affected zone (HAZ). These cracks are due, primarily, to low-melting liquid phases, which allow boundaries to separate under the thermal and shrinkage stresses resulting from weld solidification and cooling. Other possible metallurgical consequences of welding are:

- THE PRECIPITATION OF INTERGRANULAR, CHROMIUM-RICH $M_{23}C_6$ CHROMIUM CARBIDES IN THE WELD HAZ, WHICH CAN LEAVE THESE REGIONS SENSITIVE TO CORROSION
- THE TRANSFORMATION OF WELD FERRITE TO SIGMA PHASE DURING ELEVATED-

TEMPERATURE SERVICE, WHICH CAN REDUCE DUCTILITY AND TOUGHNESS

These phenomena can be either minimized or eliminated through alloy selection, process optimization, or postweld heat treatment. In general, these alloys are very weldable. With an understanding of the evolution of the weld microstructure and the ability to control it, one can produce welds to meet a wide variety of service requirements.

Alloy Types. One of the most important decisions of engineering design is the selection of the appropriate stainless steel type for the desired application and service. The factors for selection are covered more thoroughly in *Properties and Selection: Irons, Steels, and High-Performance Alloys,* Volume 1 of the *ASM Handbook.* However, when the engineering design includes welding as a fabrication process, then alloy selection must consider weldability and weld performance.

An important criterion for alloy selection in welding applications may be to use low-carbon grades to prevent chromium carbide precipitation and sensitization to intergranular corrosion. On the other hand, additions of sulfur or selenium may be used to improve machinability, although these elements can result in severe weld hot-cracking problems and, thus, may not be suitable when welding is required.

In reviewing the composition of the alloys listed in Tables 1 and 2, one can see that a wide range of alloy additions exists, as well as a fairly wide range in composition within the specification of individual alloy types. These two factors can have major effects on the welding behavior of the different alloy types, in addition to heat-to-heat variations in weldability. One goal of this article is to provide an understanding of the effects of composition on welding behavior, and another is to provide guidance in the selection and welding of these materials.

General Welding Characteristics. The austenitic stainless steels are generally considered the most weldable of the stainless steels. Because of their physical properties, their welding behavior may be considerably different than those of the ferritic, martensitic, and duplex stainless steels. For example, the thermal conductivity of typical austenitic alloys is only approximately half that of the ferritic steels. Therefore, the weld heat input that is required to achieve the same penetration is considerably reduced. In contrast, the coefficient of thermal expansion (CTE) of austenite is 30 to 40% greater than that of ferrite, which can result in increases in both distortion and residual stress, because of welding. The molten weld pool of the austenitic stainless steels also tends to be more viscous, or "sluggish," than ferritic and martensitic grades. This impedes the metal flow and wettability of welds in these materials, which may promote lack-of-fusion defects.

A major concern, when welding the austenitic stainless steels, is the susceptibility to solidification and liquation cracking. As discussed below, these materials can be very resistant to these forms of high-temperature cracking, if the material is compositionally balanced such that the solidification behavior and microstructure is controlled to ensure that the weld metal contains more than 3 vol% ferrite.

In cases where fully austenitic welds are required, such as when the weld must be nonmagnetic or when it is placed in corrosive environments that selectively attack the ferrite phase, the welds will solidify as austenite and the propensity for weld cracking will increase. In some alloys, such as AISI 310 and the superaustenitic grades, all the allowable compositions within the specification range solidify as austenite when welded. To minimize cracking in these welds, it is generally advisable to weld with low heat input and under low constraint conditions.

Welds that are made at slower speeds and produce elliptical-, rather than teardrop-, shaped pools are also generally less susceptible to cracking. This effect is particularly pronounced when welding thin sheet, as in the production of thin-walled tubing. Residual elements, which form low-melting liquid phases that promote cracking, should be kept to a minimum. These elements include phosphorus, sulfur, boron, selenium, niobium, silicon and titanium. Small additions of oxygen and nitrogen are somewhat beneficial and are thought to affect the wetting characteristics of the liquid phases. However, high concentrations of these elements may promote porosity. Manganese also can reduce cracking susceptibility, primarily by tying up sulfur and silicon that would otherwise be available to form low-melting phases.

Microstructural Development

Although austenitic stainless steels are predominantly austenitic, they often contain small amounts of body-centered cubic (bcc) ferrite, particularly in the weld metal. This ferrite is often described as "delta" ferrite, because it forms at elevated temperatures and is distinguished from "alpha" ferrite, which is the low-temperature form in iron-base alloys. In this article, the term ferrite will refer to high-temperature delta ferrite, unless noted otherwise. These alloys also may contain martensite, although the presence of this phase is unusual and limited to special composition and temperature ranges, forming only as a result of plastic deformation (Ref 1).

The solidification behavior and microstructural development of the weld metal of these alloys are quite complex, and, until recently, were not well understood. In this class of alloys, weldability and subsequent weld performance are often directly related to weld microstructure. Thus, when welding these alloys, a general understanding of the welding metallurgy can be very beneficial in optimizing weld performance. Because chemical composition has the greatest influence on weld microstructure, a number of empirical relationships and constitution diagrams have been developed to predict microstructure based on actual or approximated composition. In all cases, the concept of chromium equivalence (Cr_{eq}) and nickel equivalence (Ni_{eq}) has been used to normalize the effect of various alloying additions on the ferrite-forming and austenite-forming potency, respectively. Considerable disagreement still exists regarding these equivalency relationships (Table 3) for austenitic stainless steels.

TABLE 3 CHROMIUM- AND NICKEL-EQUIVALENCY RELATIONSHIPS FOR AUSTENITIC STAINLESS STEELS

AUTHOR	YEAR	CHROMIUM EQUIVALENT, WT%	NICKEL EQUIVALENT, WT%
SCHAEFFLER	1949	CR + MO + 1.5SI + 0.5NB	NI + 0.5MN + 30C
DELONG *ET AL.*	1956	CR + MO + 1.5SI + 0.5NB	NI + 0.5MN + 30C +30N
HULL	1973	CR + 1.21MO + 0.48SI + 0.14NB + 2.27V + 0.72W + 2.20TI + 0.21TA + 2.48AL	NI +(0.11MN - 0.0086MN^2) + 24.5C + 14.2N + 0.41CO + 0.44CU
HAMMAR AND SVENNSON	1979	CR + 1.37MO + 1.5SI + 2NB + 3TI	NI + 0.31MN + 22C + 14.2N + CU
SIEWERT *ET AL.*	1992	CR + MO + 0.7NB	NI + 35C + 20N + 0.25CU

The Schaeffier diagram (Ref 2) was developed in the late 1940s in an attempt to predict weld microstructure for a wide range of stainless steels. This diagram was refined as the DeLong diagram (Ref 3), which pertained to the range of compositions associated with 300-series stainless steels and filler metals. In 1988, the Welding Research Council introduced a further improvement, when compared with the DeLong diagram, which was called the WRC-1988 diagram (Ref 4). This diagram was further modified in 1992 by adding copper to the Ni_{eq} formula. The WRC-1992 diagram (Fig. 1) allows the amount of weld-metal ferrite to be predicted using newly developed Cr_{eq} and Ni_{eq} formulas. The use of this diagram will be described later.

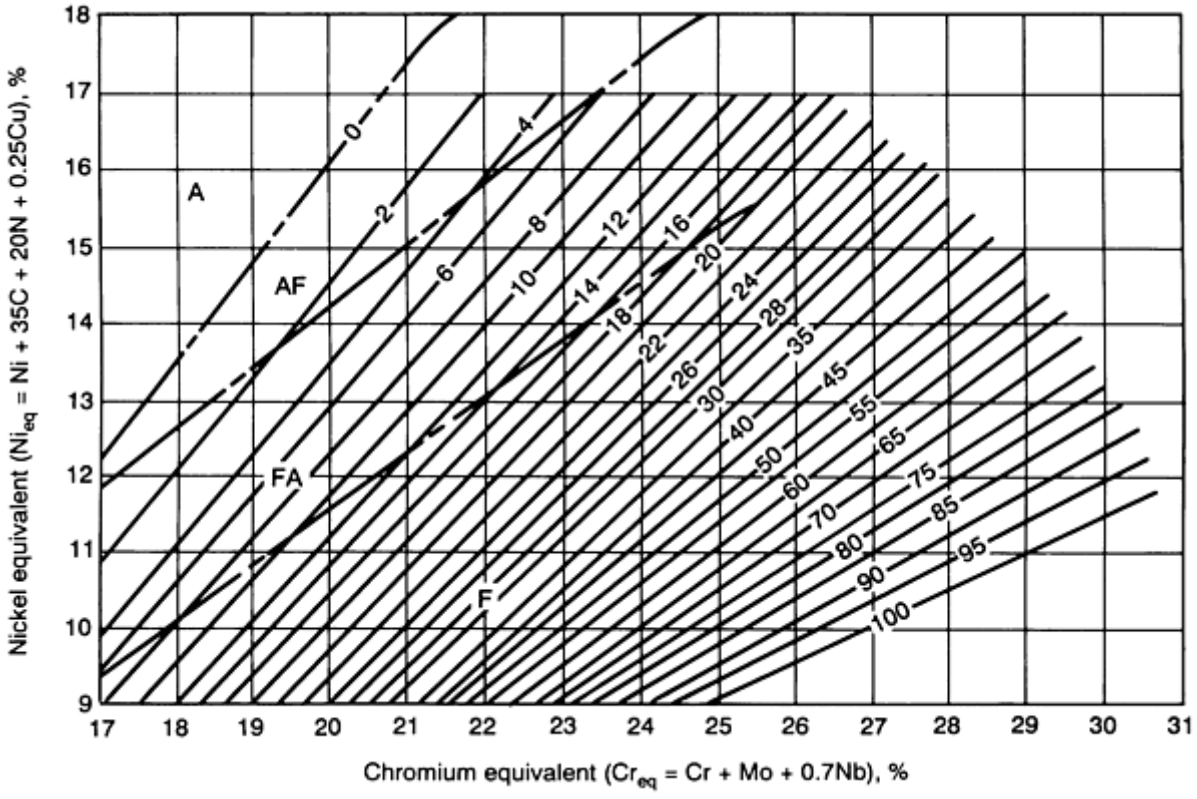

FIG. 1 WRC-1992 DIAGRAM FOR PREDICTING WELD FERRITE CONTENT AND SOLIDIFICATION MODE. SOURCE: REF 4

The following sections in this article summarize the important aspects of solidification behavior and microstructural evolution that dictate weld-metal ferrite content and morphology. An understanding of microstructural evolution and its ramifications in austenitic stainless steel welds is crucial, because it will dictate base- and filler-metal selection, as well as welding conditions.

References cited in this section

1. J.C. LIPPOLD, M.C. JUHAS, AND E.N.C. DALDER, *METALL. TRANS. A,* VOL 16, 1985, P 1835-1848
2. A.L. SCHAEFFLER, *MET. PROG.,* VOL 26, 1949, P 680
3. C.J. LONG AND W.T. DELONG, *WELD. J.,* VOL 52, 1973, P 281-S TO 297-S
4. D. KOTECKI AND T.A. SIEWERT, *WELD. J.,* VOL 71, 1992, P 171S-179S

Selection of Wrought Austenitic Stainless Steels

John A. Brooks, Sandia National Laboratories; John C. Lippold, Edison Welding Institute

Solidification Behavior

In austenitic stainless steels, the primary phase of solidification may be either austenite or ferrite. This is dictated predominantly by composition. It has been well documented (Ref 5, 6, 7) that welds that solidify as primary austenite are inherently more susceptible to weld solidification cracking than welds that solidify as primary ferrite. Thus, control of weld solidification behavior is critical to ensuring crack-free welds.

The iron-nickel-chromium ternary diagram assembled by Speich (Ref 8) can be used to discuss, in general terms, the solidification process. Figure 2 shows both liquidus and solidus surfaces. A eutectic trough extends to the ternary eutectic

composition of roughly 49Cr-43Ni-8Fe. A peritectic trough at Fe-4Ni extends into the diagram to about 75% iron, at which location the liquidus crosses the nickel-rich solidus, changing from peritectic to eutectic behavior (Ref 9).

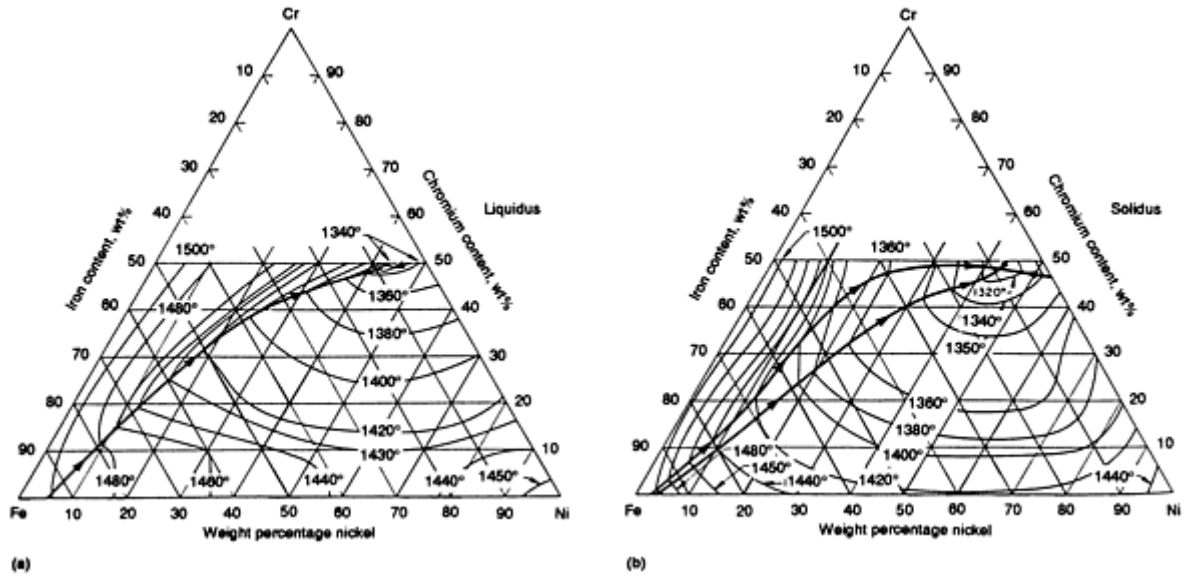

FIG. 2 PROJECTIONS OF (A) LIQUIDUS AND (B) SOLIDUS SURFACES, AS ISOTHERMAL CONTOURS ON IRON-NICKEL-CHROMIUM TERNARY DIAGRAM. TEMPERATURES SHOWN ARE IN °F. SOURCE: REF 8

In Fig. 2, it can be seen that for approximately 60 to 70% Fe, which is the iron content of many of the austenitic stainless steels, the liquidus lies along the chromium/nickel ratio of approximately 1.5. Compositions on the nickel-rich side of the liquidus will solidify as primary austenite, sometimes referred to as A-type solidification. Depending on composition, it may solidify with a small fraction of eutectic ferrite (AF-type solidification). Alloys on the chromium-rich side of the liquidus will solidify as primary ferrite with the peritectic or eutectic solidification of austenite (FA-type solidification). However, the solidification boundary between ferrite and austenite can be shifted, because of the nonequilibrium solidification conditions of welding. For compositions that are further from the peritectic/eutectic liquidus, the welds solidify completely as ferrite at higher chromium/nickel ratios (F-type solidification). The chromium/nickel ratio for single-phase ferrite solidification is often reported to range from 1.9 to 2.0.

A number of diagrams can be used to predict the primary phase of solidification based on the weld-metal composition. The WRC-1992 diagram (Fig. 1) can be used to predict solidification behavior, in addition to ferrite content. Note that this diagram contains four solidification regimes, designated as A, AF, FA, and F. The austenite-ferrite microstructural morphologies associated with these regimes are described below.

References cited in this section

5. H. THIER, *DVS-BER.*, VOL 41, 1976, P 100-104
6. I. MATSUMOTO, K. TAMAKI, AND M. MATSUMA, *J. JPN. WELD. SOC.*, VOL 41 (NO. 11), 1972, P 1306-1314
7. J.C. LIPPOLD AND W.F. SAVAGE, *WELD. J.*, VOL 61, 1982, P 388S-396S
8. G.R. SPEICH, *METALS HANDBOOK*, 8TH ED., VOL 8, AMERICAN SOCIETY FOR METALS, 1973, P 424
9. S.E. SCHURMANN AND I. BRAUCKMANN, *ARCH. EISENHUTTEN.*, VOL 48, 1977, P 3-8

John A. Brooks, Sandia National Laboratories; John C. Lippold, Edison Welding Institute

Solid-State Transformations and Ferrite Morphologies

The final weld microstructure is controlled by both the solidification behavior and the subsequent solid-state transformations. A number of schematics have been published (Ref 10, 11, 12, 13), such as the one by Brooks *et al.* (Ref 11) shown in Fig. 3, which depicts some of the general characteristics of microstructural development. However, a much wider variety of microstructures exists in actual welds. The vertical sections of the iron-nickel-chromium ternary diagram for 70% and 60% Fe (Fig. 4) are useful in discussing the solid-state transformations. As indicated by these diagrams, during the cooling of primary austenite welds (AF-type), some of the eutectic ferrite may transform to austenite. The primary ferrite-solidified welds that exhibit peritectic/eutectic behavior during the final stages of solidification (FA-type) typically solidify with a large fraction of ferrite (Fig. 3). During cooling through the $\delta + \gamma$ two-phase field, much of the ferrite transforms to austenite, with chromium partitioning to the ferrite and nickel partitioning to the austenite, leaving ferrite only within the very cores of the original dendrites. When only several percent of the original ferrite is retained, which is often referred to as skeletal, or vermicular, ferrite, it may be difficult to distinguish between it and the eutectic ferrite that results from primary austenite solidification, unless good metallographic techniques are used (Fig. 3a and b). However, the location of the ferrite is different. It resides within the core of the dendrites, in the case of FA-type solidification, rather than at the dendrite boundaries, in the case of AF-type solidification.

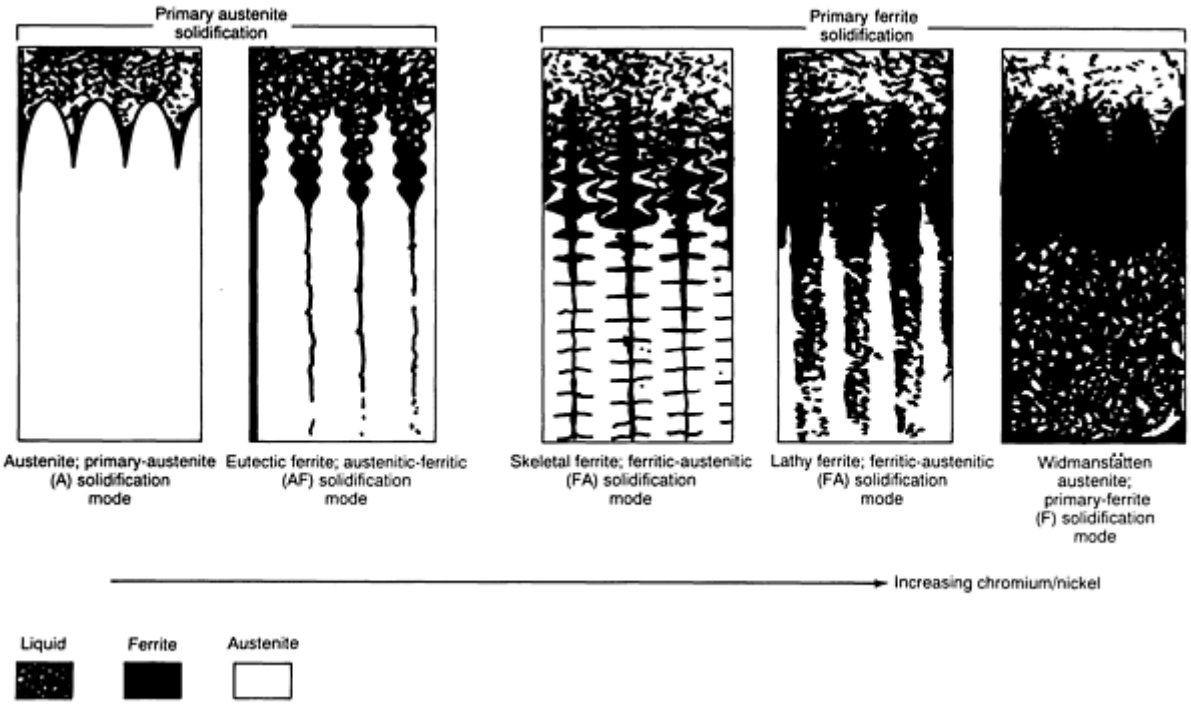

FIG. 3 SCHEMATICS SHOWING SOLIDIFICATION AND SOLID-STATE TRANSFORMATION BEHAVIOR OF WELDS WITH INCREASING CR_{EQ}/NI_{EQ} RATIOS. SOURCE: REF 11

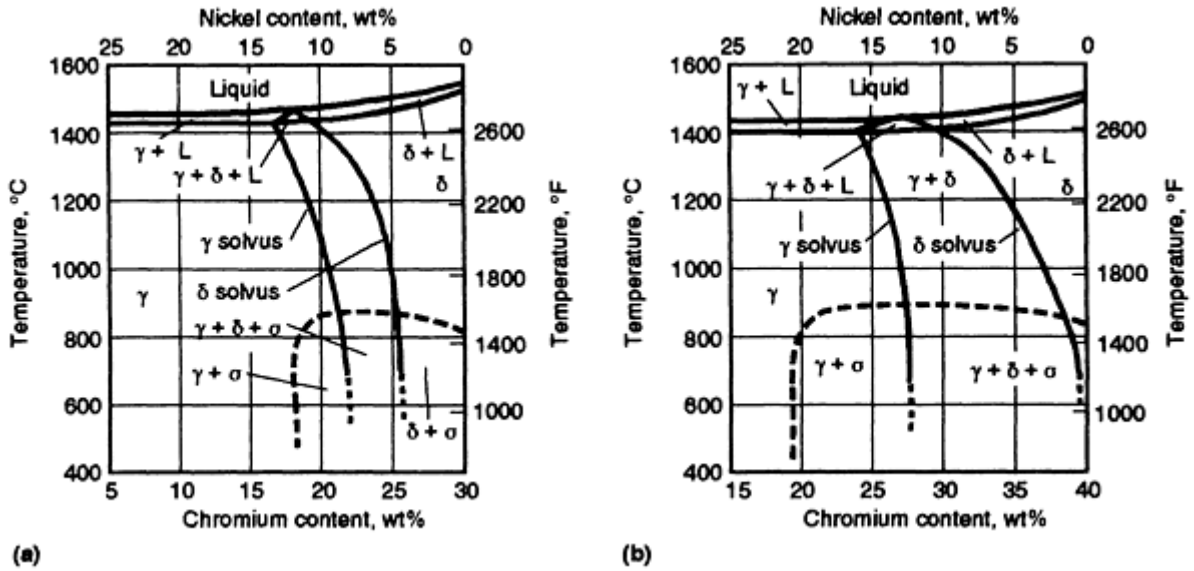

FIG. 4 VERTICAL SECTIONS OF IRON-NICKEL-CHROMIUM TERNARY DIAGRAM, AT CONSTANT IRON CONTENT. (A) 70% FE. (B) 60% FE. SOURCE: REF 14

At higher chromium/nickel ratios, other ferrite morphologies are often observed, such as the lathy structure shown in Fig. 5(c). It is generally reported that the skeletal and lathy ferrite morphologies are indicative of primary ferrite with the secondary solidification of austenite, but these ferrite morphologies can also exist in welds that solidify as single-phase ferrite, as shown in Fig. 3(c) and (d). At higher chromium/ nickel ratios, a Widmanstätten austenite structure can also form in welds that solidify as single-phase ferrite. It should be noted that the solidification and transformation behavior shown in Fig. 3 is dependent not only on composition, but also on cooling rate. Extremely high solidification and cooling rates, such as those encountered during electron-beam or laser-beam welding, may significantly alter the microstructure relative to that predicted using the WRC-1992 diagram. This behavior is described in the section "Solidification Behavior and Microstructure of High-Energy-Density Welds."

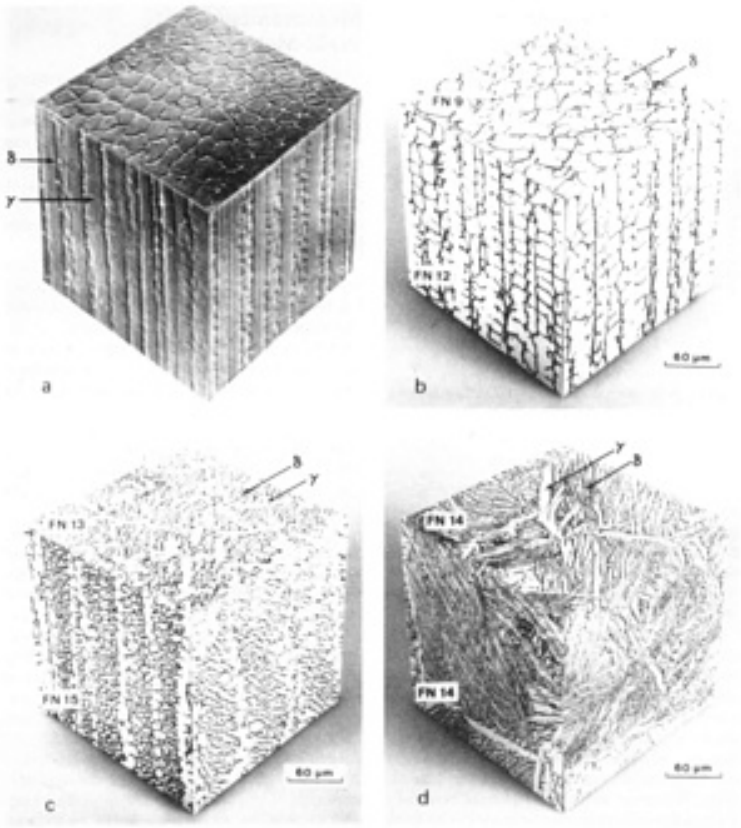

FIG. 5 THREE-DIMENSIONAL VIEWS OF TYPICAL AUSTENITIC STAINLESS STEEL WELD MORPHOLOGIES; SOLIDIFICATION DIRECTION, VERTICAL. IN EACH PHOTOGRAPH, FERRITE IS DARKER PHASE. (A) CELLULAR PRIMARY AUSTENITE SOLIDIFICATION STRUCTURE WITH INTERCELLULAR EUTECTIC FERRITE IN AISI 310. (B) SKELETAL FERRITE, 9-12 FN, IN AISI 308. (C) LATHY OR LACY FERRITE, 13-15 FN IN AISI 308 MULTIPASS WELD. (D) ACICULAR OR WIDMANSTÄTTEN AUSTENITE, 14 FN, IN UPPER PORTION OF AISI 308 WELD. WELDS IN (B)-(D) SOLIDIFIED AS PRIMARY FERRITE. SOURCE: REF 15

Micrographs of the three-dimensional structure of several weld ferrite morphologies compiled by David (Ref 15) are shown in Fig. 5. Small amounts of ferrite along solidification cell boundaries of a primary austenite structure are shown in Fig. 5(a). This very cellular-appearing solidification structure is characteristic of welds that solidify as austenite and results primarily from the microsegregation of chromium and, to a lesser extent, nickel, along the solidification cell boundaries. Depending on alloy composition and welding conditions, final solidification may occur as a eutectic of ferrite and austenite. Figure 5(b) and (c) show ferrite along cell cores of primary ferrite structures, whereas Fig. 5(d) shows acicular ferrite or Widmanstätten austenite in a structure that solidified completely as ferrite. Additional details on solidification behavior and microstructural development are provided in Ref 11 and 16.

Alloying Effects on Solidification Behavior, Weld Microstructure, and Cracking Susceptibility. The relationship between solidification behavior and a composition factor, in terms of Cr_{eq}/Ni_{eq}, was established by Suutala and Moisio (Ref 17) using coefficients of: $Ni_{eq} = Ni + 0.3Mn + 22C + 14.2N + Cu$; and $Cr_{eq} = Cr + 1.37Mo + 1.5Si + 2Nb + 3Ti$ (see Table 3). A diagram (Fig. 6) was developed that delineates the four solidification types, A, AF, FA, and F, as described previously. Using their data, the demarcation between single-phase austenite solidification (A) and austenite solidification with the eutectic solidification of ferrite (FA) occurs at a Cr_{eq}/Ni_{eq} ratio of approximately 1.35. The transition to solidification as primary ferrite with the eutectic/peritectic solidification of austenite (FA) occurs at a Cr_{eq}/Ni_{eq} of approximately 1.5. This value has been found to be valid for most conventional 300-series alloys welded under normal arc-welding conditions. This ratio increases with increasing solidification velocity. At the lower bounds of primary ferrite, some regions may solidify as ferrite and others as austenite (Ref 18). In this case, the region where primary austenite is most commonly located is along the weld centerline, where the solidification velocity is maximum. This transition between primary austenite and primary ferrite is especially important, because of the strong relationship between solidification behavior and solidification-cracking susceptibility.

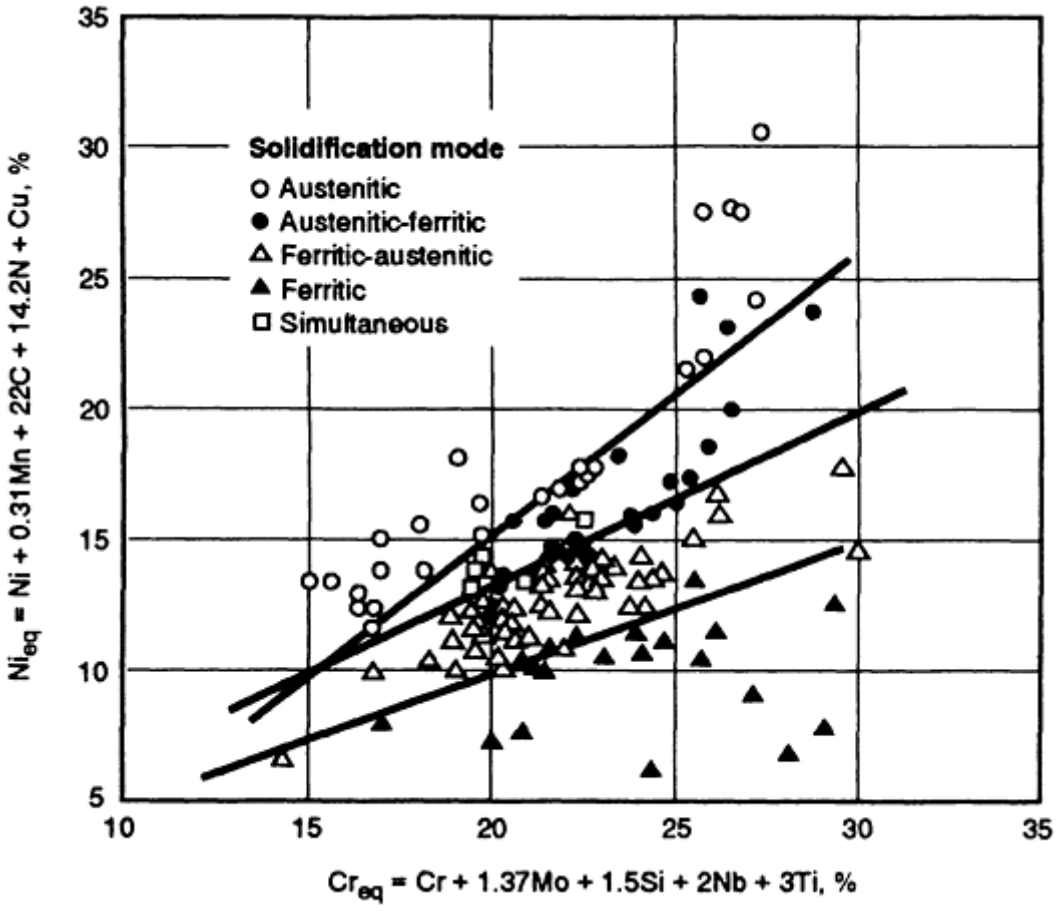

FIG. 6 SOLIDIFICATION MODE (EXPERIMENTAL) FOR VARIETY OF COMPOSITIONS, COMPARED ON BASIS OF CR_{EQ}/NI_{EQ} RATIO. SOURCE: REF 17

As indicated in Fig. 6, above a Cr_{eq}/Ni_{eq} ratio of approximately 1.95, solidification occurs as single-phase ferrite. However, other studies (Ref 13) indicate that single-phase ferrite solidification occurs at considerably lower Cr_{eq}/Ni_{eq} ratios, and that the ratio of approximately 1.95 may more closely correlate to microstructures containing Widmanstätten austenite.

Note that the Cr_{eq}/Ni_{eq} ratios defined above are valid only when using the Suutala and Moisio equivalency relationships. Corresponding ratios for delineating the solidification behavior by using the WRC-1992 equivalencies are somewhat different. However, discrepancies between the two diagrams exist, as is apparent for lean alloys or pure iron-nickel-chromium ternaries. For example, the transition from primary austenite to primary ferrite is reported to occur at a Cr_{eq}/Ni_{eq} ratio of 1.5 by Suutala and Moisio (Ref 17), versus 1.4 in the WRC diagram.

Takalo, Suutala, and Moisio (Ref 18) also described the solidification-cracking susceptibility of austenitic stainless steels by plotting their Cr_{eq}/Ni_{eq} ratios versus impurity content in terms of sulfur plus phosphorus. Their results are shown in Fig. 7. Note that a dramatic transition in cracking susceptibility occurs at a value of approximately 1.5. This transition represents the shift in solidification behavior from primary austenite to primary ferrite, as described above, and reinforces the importance of controlling solidification behavior in order to avoid weld solidification cracking.

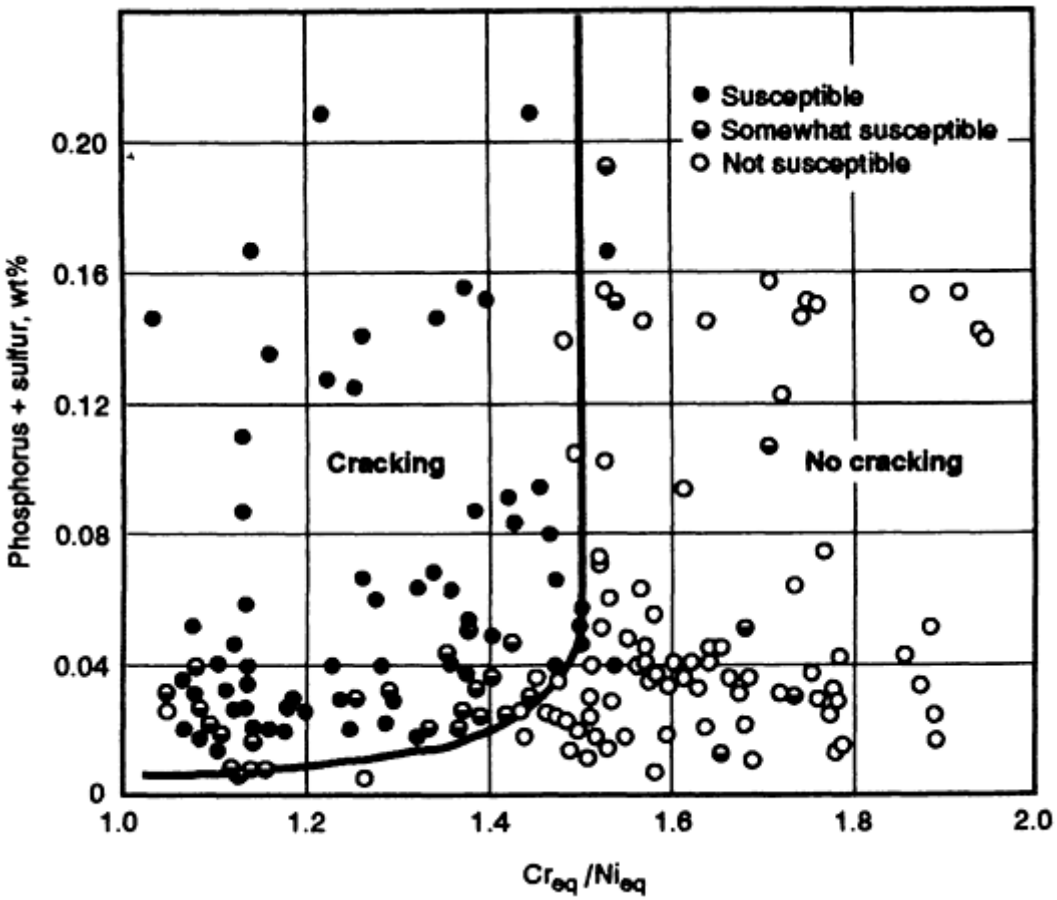

FIG. 7 RELATIONSHIP BETWEEN SOLIDIFICATION CRACKING SUSCEPTIBILITY AND CR_{EQ}/NI_{EQ} RATIO. BOUNDARY BETWEEN CRACKING AND NO CRACKING AT CR_{EQ}/NI_{EQ} = 1.5 CORRESPONDS TO CHANGE IN SOLIDIFICATION MODE FROM PRIMARY AUSTENITE BELOW 1.5 TO PRIMARY FERRITE ABOVE 1.5. SOURCE: REF 18

As noted previously, Schaeffler developed one of the first diagrams for predicting weld microstructures. This diagram is especially useful for predicting microstructures between dissimilar alloys using a tie line between the two alloy compositions and the appropriate alloy dilution. The diagram was developed using the shielded metal arc welding (SMAW) process, where the nominal nitrogen level was about 0.06 wt% and, as such, was not shown as an alloying addition. This diagram described the behavior of most of the alloys in use at that time, and is relatively accurate for most 300-series alloys when using conventional welding processes. The use of this diagram is discussed in more detail in the article "Welding of Stainless Steels." Other diagrams that have been developed, often using limited alloy compositional ranges, are reviewed in detail in Ref 19.

The WRC-1992 diagram, developed primarily with data from welds made by SMAW, is the most accurate diagram and is preferred in terms of the composition ranges for which it was established. In this diagram, the alloying elements have been limited to nickel, carbon, nitrogen, and copper in the Ni_{eq}, and to chromium, molybdenum, and niobium in the Cr_{eq}. However, the diagram is applicable for manganese contents up to 10%, molybdenum contents up to 3%, nitrogen contents up to 0.2%, and silicon contents up to 1%.

When the diagram is used for alloy systems containing significant amounts of alloying elements that have not been included in the diagram, predictions may be inaccurate. As discussed above, boundaries between the different solidification modes are also included on the diagram, although some disagreement exists with the boundaries established by other investigators. However, the most important boundary by far is the one separating primary ferrite from primary austenite solidification, in which some discrepancy still exists. The diagram does predict that the maximum amount of eutectic ferrite will not exceed a few percent, which is consistent with that observed in practice.

When using these diagrams to predict weld behavior, one must be aware that uncertainties in compositional analysis, as well as welding process and parameters, can affect predicted solidification behavior and ferrite content. One common occurrence in the welding of stainless steels is the possibility of nitrogen adsorption during welding when inadequate shielding is used. It is not uncommon that nitrogen levels of approximately 0.02% in the base material can be increased to values as high as 0.1%. This will significantly decrease ferrite content and may also result in a change in solidification mode from primary ferrite to primary austenite, which can have a drastic effect on weld solidification-cracking susceptibility. Thus, the nitrogen content of the deposited weld material must be used in making the predictions. However, with the use of the diagrams, magnetic measurements of ferrite number, and an understanding of weld microstructural evolution, one can reasonably predict the nature of the weld microstructure.

References cited in this section

10. N. SUUTALA, T. TAKALO, AND T. MOISIO, *METALL. TRANS. A*, VOL 10, 1979, P 512-514
11. J.A. BROOKS, J.C. WILLIAMS, AND A.W. THOMPSON, IN *TRENDS IN WELDING RESEARCH*, S.A. DAVID, ED., AMERICAN SOCIETY FOR METALS, 1982, P 331-355
12. S. KATAYAMA AND A. MATSUNAWA, *PROC. INT. CONF. ON ADVANCED LASER ELECTRO-OPTICS (ICALEO)* (SAN FRANCISCO), 1985
13. J.A. BROOKS, N.C.Y. YANG, AND J.S. KRAFCIK, ON THE ORIGIN OF FERRITE MORPHOLOGIES OF PRIMARY FERRITE SOLIDIFIED STAINLESS STEEL WELDS, *TRENDS IN WELDING RESEARCH*, ASM INTERNATIONAL, 1993
14. J.W. PUGH AND J.D. NISBET, *TRANS. TMS-AIME*, VOL 188, 1950, P 268-276
15. S.A. DAVID, *WELD. J.*, VOL 60, 1981, P 63-S TO 71-S
16. J.A. BROOKS AND A.W. THOMPSON, *LNT. MATER. REV.*, VOL 36 (NO. 1), 1991, P 16-44
17. N. SUUTALA AND T. MOISIO, THE USE OF CHROMIUM AND NICKEL EQUIVALENTS IN CONSIDERING SOLIDIFICATION PHENOMENA IN AUSTENITIC STAINLESS STEELS, *SOLIDIFICATION TECHNOLOGY IN THE FOUNDRY AND CASTHOUSE*, THE METALS SOCIETY PREPRINT, LONDON, 1980
18. T. TAKALO, N. SUUTALA, AND T. MOISIO, *METALL. TRANS. A* , VOL 10, 1979, P 1173-1181
19. D.L. OLSON, *WELD. J.*, VOL 64, 1985, P 281S-295S

Selection of Wrought Austenitic Stainless Steels

John A. Brooks, Sandia National Laboratories; John C. Lippold, Edison Welding Institute

Measurement of Weld-Metal Ferrite

As described previously, weld-metal ferrite content significantly influences both the weldability and service performance of austenitic stainless steels. Weld-metal ferrite content can either be predicted using constitution diagrams, such as the WRC-1992 diagram (Fig. 1), or measured using instruments that take advantage of the ferromagnetic characteristics of the ferrite phase.

The term *Ferrite Number*, designated FN, has been adopted as a relative measure for quantifying ferrite content using standardized magnetic techniques (Ref 20). The FN approach was developed in order to reduce the large variation in ferrite levels determined on a given specimen when measured using different techniques by different laboratories. FN approximates the "volume percent ferrite" at levels below 8 FN. Above this level, deviation occurs, where the FN value exceeds the actual volume percent ferrite. For example, a weld metal with 16 FN contains approximately 13.8 vol%.

A number of instruments are commercially available for determining the ferrite content of welds, including the Magne gage, Severn gage, and ferrite scope (Ref 20). The Severn gage and ferrite scope are particularly applicable for use in the field or on the production floor. The ferrite scope is also useful in measuring ferrite on welds of small cross section, as is often the case with electron-beam welds. Calibration procedures for magnetic measurement techniques have been

recommended by the American Welding Society in AWS A4.2 (Ref 20). These procedures use either the thickness standards of the National Institute of Standards and Technology (NIST) or actual weld-metal standards that include certified levels of weldmetal ferrite.

However, it is important to understand that it is impossible to accurately determine the absolute ferrite content of austenitic stainless steel weld metals. Even on undiluted weld pads, ferrite variations from pad to pad must be expected, because of slight changes in welding and measuring variables. On a large group of pads made from one heat or lot, using a standard pad welding and preparation procedure, two sigma values indicate that 95% of the tests are expected to be within a range of approximately ±2.2 FN at about 8 FN. If different pad welding and preparation procedures are used, then these variations will increase. Variations are also introduced based on the composition of the ferrite. The magnetic attraction of the ferrite may vary significantly with chemical composition. Thus, for the same volume percent ferrite, the FN determined by magnetic instruments may vary for weld pads made using different filler materials.

Even larger variations in ferrite content may be encountered if the welding technique allows excessive nitrogen pickup, in which case the ferrite can be much lower than otherwise expected. A nitrogen pickup of 0.10% typically will decrease the FN by about 8.

Austenitic stainless steel base materials are intentionally balanced compositionally to produce inherently lower ferrite content than matching weld metals. This is done, in part, to facilitate the hot workability of the material during forging, extrusion, and rolling operations. For this reason, special attention is required when making autogenous welds if primary ferrite solidification is desired to prevent solidification cracking. In general, weld metal diluted with base metal will also be somewhat lower in ferrite than the undiluted weld metal. For example, this effect is commonly observed when welding types 304 or 304L base metals with ER308 or ER309 filler materials.

The agreement between the predicted and measured weld-metal ferrite content is also strongly dependent on the accuracy of the chemical analysis. Variations in the results of the chemical analyses encountered from laboratory to laboratory can have significant effects on the predicted ferrite level, particularly if these variations occur in the detection of carbon and nitrogen. It is not uncommon for predicted and measured ferrite levels to differ by as much as 4 to 8 FN.

Nitrogen-Strengthened Stainless Steels. The addition of nitrogen to austenitic stainless steels significantly improves the strength and pitting resistance of the alloy, and may also improve cryogenic toughness. These alloys may contain relatively high levels of manganese, because manganese increases the solubility of nitrogen in the austenite matrix, in addition to substituting for nickel as an austenite stabilizer.

In general, the weldability of these alloys is similar to the 300-series materials. The presence of ferrite in the as-deposited weld microstructure reduces weld-cracking susceptibility for the same reasons described previously. The prediction of weld-metal ferrite content in these alloys has historically been problematic, because the DeLong diagram did not adequately account for large concentrations of nitrogen and manganese. Both Espy and Hull developed equivalency relationships and predictive diagrams that better coped with high levels of nitrogen. The Espy diagram (Ref 21) represented a modification of the DeLong diagram and accounted for higher nitrogen and manganese levels. Hull (Ref 22) developed equivalencies (see Table 3) to predict ferrite levels in high-nitrogen, high-manganese stainless steels. The Ni_{eq} of 14.2 developed by Hull for nitrogen is significantly lower than the value of 20.0 used in the WRC-1992 diagram. However, the omission of manganese in the diagram is in agreement with the small Ni_{eq} assigned by Hull. Limited data suggest that the Hull and WRC-1992 diagrams are in fair agreement when predicting weld ferrite contents in these alloys with nitrogen contents as high as approximately 0.25%. At the higher nitrogen contents, one may expect that the WRC-1992 diagram would predict higher ferrite contents than that of the Hull diagram. From Table 3, it can be seen that Hammer and Svennson (Ref 23) used the same nickel equivalent developed by Hull.

Because of the high nitrogen contents of these steels, weld porosity may sometimes be encountered. The critical level of nitrogen, in terms of porosity problems, is lower for electron-beam welds made in vacuum (approximately 0.25%) than it is for welds made by gas-tungsten arc welding (GTAW), where porosity problems are usually not encountered at nitrogen levels less than approximately 0.35%.

References cited in this section

20. "STANDARD PROCEDURES FOR CALIBRATING MAGNETIC INSTRUMENTS TO MEASURE THE DELTA FERRITE CONTENT OF AUSTENITIC AND DUPLEX AUSTENITIC-FERRITIC STEEL

WELD METAL," AWS 4.2-91, AWS, 1991
21. R.H. ESPY, *WELD. J.*, VOL 61, 1982, P 1492-156S
22. F.C. HULL, *WELD. J.*, VOL 46, 1967, P 399-S TO 409-S
23. O. HAMMER AND U. SVENNSON, *SOLIDIFICATION AND CASTING OF METALS*, THE METALS SOCIETY, LONDON, 1979, P 401-410

Solidification Behavior and Microstructure of High-Energy-Density Welds

Differences exist between the solidification behavior and microstructures of high-energy-density welds, such as electron-beam and laser-beam welds, and more-conventional welds, such as shielded metal arc and gas-tungsten arc welds (Ref 12, 16, 24). These differences have been attributed to the rapid solidification velocities and cooling rates of the high-energy-density welds and, if not recognized, can have a drastic effect on weld quality and performance.

One characteristic of the high cooling rates during high-energy-density welding is a fine solidification cell size. However, changes in solidification behavior and solid-state transformation, compared with the behavior and transformation observed in gas-tungsten arc welds of the same alloy composition, can also occur. One of the most important effects of the rapid solidification rates of high-energy-density welds is a shift in the solidification transition from primary austenite to primary ferrite to higher Cr_{eq}/Ni_{eq} ratios than those encountered in conventional arc welds. A change in solidification mode from primary ferrite to primary austenite, which resulted in centerline cracking of an electron-beam weld in type 304L, is shown in Fig. 8. It must be recognized that similar changes in solidification mode from primary ferrite to primary austenite can occur along the centerline of welds made with the more-conventional welding processes, such as the GTAW process (Ref 25). This is especially common at higher welding speeds in materials with Cr_{eq}/Ni_{eq} ratios (Suutala and Moisio equivalents) slightly above 1.5.

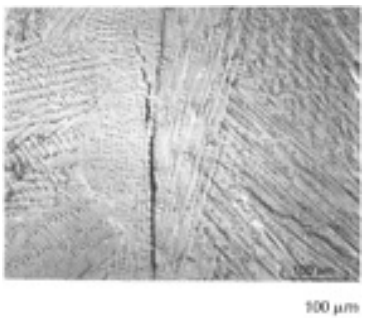

FIG. 8 SOLIDIFICATION CRACK IN ELECTRON-BEAM WELD ALONG WELD CENTER IN REGION WHERE SOLIDIFICATION OCCURRED AS PRIMARY AUSTENITE AS A RESULT OF HIGHER SOLIDIFICATION AND COOLING RATES

Several microstructures can also exist in high-energy-density welds that have not been reported in welds of more-moderate cooling rates. Basically, these microstructures consist of a single phase of either ferrite or austenite. An example of the single-phase austenite structure is shown on the right side of Fig. 9(a), where a carbon dioxide laser-beam weld was made over a gas-tungsten arc weld in an alloy of 23Cr-12Ni-balance Fe with a Cr_{eq}/Ni_{eq} ratio of 1.9 (Ref 26). These welds solidify as single-phase ferrite, but subsequently transform to approximately 100% austenite during cooling via a massive transformation. The gas-tungsten arc weld of this composition, shown to the left in Fig. 9(a), exhibits a typical two-phase microstructure with a FN of approximately 21.

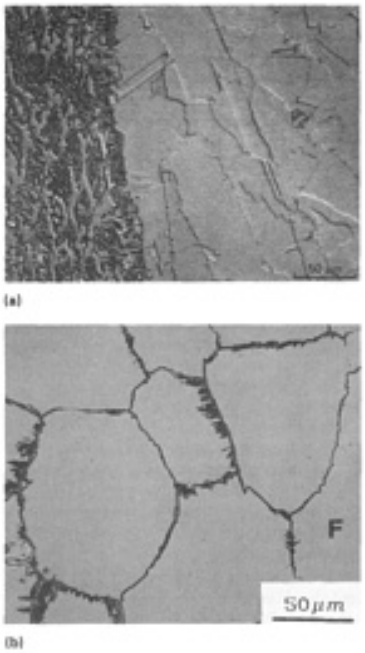

FIG. 9 MICROSTRUCTURES OF LASER-BEAM-WELDED AUSTENITIC STAINLESS STEELS. (A) GAS-TUNGSTEN ARC WELD SHOWN ON LEFT, WITH CO_2 LASER-BEAM WELD SHOWN ON RIGHT, IN ALLOY OF CR_{EQ}/NI_{EQ} = 1.8. LASER-BEAM WELD ON RIGHT IS SINGLE-PHASE AUSTENITE FORMED AS A PRODUCT OF MASSIVE TRANSFORMATION. (B) FERRITIC STRUCTURE FORMED IN LASER-BEAM WELD OF CR_{EQ}/NI_{EQ} = 2.0. SOURCE: REF 26, 27

Characteristics of the massively transformed austenitic structure are fairly small-faceted-appearing grain boundaries and little or no evidence of the cellular solidification that would result from microsegregation. This apparent lack of microsegregation may be due to the higher solute diffusivities in ferrite, as compared with austenite, which results in homogenization occurring during solidification and cooling and/or by reduced alloy partitioning occurring at the rapid solidification velocities (Ref 26, 27).

At high Cr_{eq}/Ni_{eq} ratios, high-energy-density welds can solidify completely as ferrite. However, because of suppression of the solid-state transformation of ferrite to austenite during the rapid cooling, a large fraction of the ferrite is retained at room temperature. This behavior has been reported in laser-beam welds of AISI 312. Microsegregation is also minimal in these welds, and the grain boundary region sometimes exhibits Widmanstätten austenites rather than the faceted grain structure of the massively transformed austenite. An example of this microstructure is shown in Fig. 9(b). In some applications, such as the containment of high-pressure hydrogen, for which the austenitics are highly suited, a weld that completely comprises ferrite would be unacceptable. With the massively transformed ferrite and the retention of ferrite at high Cr_{eq}/Ni_{eq} ratios, the composition range in which two-phase $\delta+\gamma$ microstructures exists in the high-energy-density welds is greatly reduced.

The shift from primary ferrite to primary austenite solidification at high solidification rates often leads to problems with weld cracking, as shown in the electron-beam weld in Fig. 8. Alloy selection based on solidification behavior predicted by the WRC-1992 diagram or that of Moisio and coworkers (Ref 17) may not be valid.

For example, a pulsed Nd:YAG laser-beam weld in a 316L alloy with a Cr_{eq}/Ni_{eq} (Suutala and Moisio equivalents) of approximately 1.6 is shown in Fig. 10. Solidification of this weld has occurred as primary austenite, with resultant solidification cracking. Reference to the Suutala and WRC-1992 diagrams indicate that solidification would occur as primary ferrite with conventional gas-tungsten arc welds and that the weld should contain approximately 6 FN.

FIG. 10 PULSED ND:YAG LASER-BEAM WELD EXHIBITING SEVERE SOLIDIFICATION CRACKING AS A CONSEQUENCE OF PRIMARY AUSTENITE SOLIDIFICATION, CR_{EQ}/NI_{EQ} = 1.6. SOURCE: REF 28

A modified Suutala diagram developed by Pacary *et al.* (Ref 28) (Fig. 11) shows the shift in solidification mode and associated cracking behavior of pulsed laser-beam welds. The critical cracking/no cracking demarcation shifts from the Cr_{eq}/Ni_{eq} ratio of approximately 1.48 (Suutala and Moisio equivalents) for conventional arc welding to approximately 1.7 for the pulsed laser-beam welds.

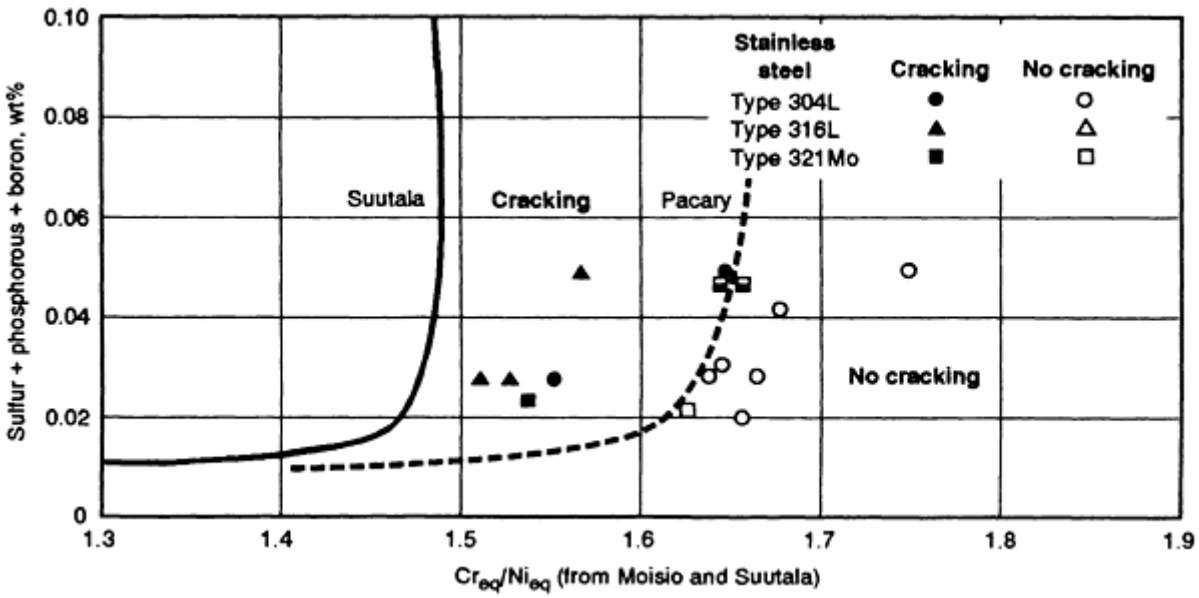

FIG. 11 DIAGRAM FOR PREDICTING WELD SOLIDIFICATION CRACKING SUSCEPTIBILITY OF PULSED LASER WELDS IN AUSTENITIC STAINLESS STEELS. NOTE WRC EQUIVALENTS ARE USED. SOURCE: REF 28

Katayama and Matsunawa (Ref 12) established the change in solidification using Schaeffler equivalents to also occur at the value of 1.7. These values are dependent on the welding process (for example, electron-beam and pulsed-Nd:YAG and carbon dioxide laser-beam welds), as well as on weld parameters (Ref 27). Because the pulsed-YAG technique produces the most rapid solidification interface velocities and cooling rates, the transition for this process should occur at the highest ratio. Thus, the selection of alloy compositions above the Cr_{eq}/Ni_{eq} ratio of approximately 1.7 (Suutala and Moisio equivalents) ensures solidification as primary ferrite and significantly reduces the risk of cracking, although higher accompanying ferrite content in the base material must also be expected.

References cited in this section

12. S. KATAYAMA AND A. MATSUNAWA, *PROC. INT. CONF. ON ADVANCED LASER ELECTRO-OPTICS (ICALEO)* (SAN FRANCISCO), 1985
16. J.A. BROOKS AND A.W. THOMPSON, *LNT. MATER. REV.,* VOL 36 (NO. 1), 1991, P 16-44
17. N. SUUTALA AND T. MOISIO, THE USE OF CHROMIUM AND NICKEL EQUIVALENTS IN CONSIDERING SOLIDIFICATION PHENOMENA IN AUSTENITIC STAINLESS STEELS, *SOLIDIFICATION TECHNOLOGY IN THE FOUNDRY AND CASTHOUSE,* THE METALS SOCIETY PREPRINT, LONDON, 1980
24. S.A. DAVID, J.M. VITEK, AND T.L. HEBBLE, *WELD. J.*, VOL 66 (NO. 10), 1987, P 289S-300S
25. N. SUUTALA, EFFECT OF SOLIDIFICATION CONDITIONS ON THE SOLIDIFICATION MODE IN AUSTENITIC STAINLESS STEELS, *TECHNOLOGY IN THE FOUNDRY AND CASTHOUSE*, THE METALS SOCIETY PREPRINT, LONDON, 1980
26. J.A. BROOKS, M.I. BASKES, AND F.A. GREULICH, *METALL. TRANS. A*, VOL 22A, 1991, P 915-925
27. J.W. ELMER, S.M. ALLEN, AND T.W. EAGAR, *METALL. TRANS. A*, VOL 20A, 1989, P 2117-2131
28. G. PACARY, M. MOLINE, AND J.C. LIPPOLD, EWI RESEARCH BRIEF NO. B9008, EDISON WELDING INSTITUTE, 1990

John A. Brooks, Sandia National Laboratories; John C. Lippold, Edison Welding Institute

Weld Defect Formation

Solidification cracking, which results from the formation of low-melting liquid films along grain boundaries during the last stages of solidification, is probably of greater concern to the welding engineer than is any other metallurgical defect in austenitic stainless steel welds. As discussed above, welds that solidify as primary austenite may be very susceptible to solidification cracking. This susceptibility is increased by elements that promote the formation of liquid phases. These elements include phosphorus and sulfur, which are often present as impurities, and silicon, niobium, titanium, and boron, which are sometimes present as minor alloying additions. In these welds, high manganese levels may be beneficial in reducing cracking, for example, by tying up sulfur and silicon. Several percent of eutectic ferrite may be somewhat beneficial in counteracting the detrimental effect of phosphorus and sulfur. However, because the amount of eutectic ferrite is alloy dependent and seldom exceeds several percent (see Fig. 1), it is not a practical solution for improving cracking resistance.

Cracking susceptibility is drastically reduced in welds that solidify as primary ferrite with the peritectic/eutectic solidification of austenite (FA-type), even at high levels of phosphorus and sulfur, as shown in Fig. 7. Welding electrodes such as 308L are specifically designed to produce a desired range of ferrite, and thus promote this solidification mode. In applications where no such filler metal is used and cracking is a concern, it may be necessary to limit composition ranges or to select heats of material that solidify in this mode. However, at the higher Cr_{eq}/Ni_{eq} ratios, where welds solidify completely as ferrite, and when the transformation of ferrite to austenite occurs at lower temperatures, cracking susceptibility again increases, but not to the extent of welds solidifying as austenite. The solidification-cracking behavior can thus be directly related to the structures shown in Fig. 3 and 5. The welds that solidify as ferrite and exhibit skeletal and lathy morphologies are very resistant to cracking, whereas cracking increases in welds that exhibit microstructures of Widmanstätten austenite.

Many rationales have been proposed to explain the cracking behavior of the austenitic stainless steel welds. The two that seem to be most consistent in explaining this behavior are related to the nature of the weld microstructure during solidification and the early stages of cooling.

During single-phase solidification, the fairly planar ferrite/ferrite or austenite/austenite grain boundaries that form are easily wet by low-melting liquids, often involving eutectics with phosphides and sulfides. If sufficient stresses and strains

are developed before these liquids are solidified, then solidification cracks can easily form and propagate. However, when solidification occurs as primary ferrite with the secondary solidification of austenite (FA-type), or if austenite is nucleated at the grain boundaries near the solidus temperature of welds solidifying completely as ferrite (F-type), then very irregular grain-boundary structures are formed. These ferrite/austenite boundaries that become potential crack paths are of lower energy than the grain boundaries of either of the single-phase structures. The resulting tortuous crack paths and/or the low-energy boundary configurations not readily wetted by the low-melting liquids are very resistant to the nucleation and propagation of cracks (Ref 29).

Thus, it can be seen that understanding and being able to identify solidification behavior are important in preventing solidification-cracking problems. Because increased solidification velocities and cooling rates shift the transition between primary austenite and primary ferrite to higher Cr_{eq}/Ni_{eq} ratios, this effect on weld cracking must be considered, as discussed in the section "Solidification Behavior and Microstructure of High-Energy-Density Welds." .

Heat-affected zone liquation cracking is occasionally observed in austenitic stainless steels, particularly in the stabilized grades (containing titanium and/or niobium). This cracking occurs as a result of the constitutional liquation of carbides, such as niobium carbide, in AISI type 347 alloy, resulting in grain-boundary liquation. HAZ cracking can also occur in other alloy types as a result of impurity segregation along HAZ grain boundaries. This form of cracking is always intergranular and located immediately adjacent to the weld fusion boundary. Occasionally, cracking is continuous across the fusion boundary into the weld metal.

Analogous to weld solidification cracking, alloys with a ferrite potential (predicted FN) above approximately 2 to 3 FN are generally resistant to HAZ liquation cracking (Ref 30). This results from the formation of ferrite along HAZ grain boundaries. HAZ cracking that is due to grain-boundary liquation also can be limited by minimizing heat input. Lower weld heat inputs result in steeper HAZ thermal gradients, thereby limiting the spatial extent over which cracking is possible.

Weld-metal liquation cracking is defined as HAZ cracking that occurs in weld metal. By definition, this form of cracking is associated with multipass welds. The cracking that occurs is sometimes referred to as "microfissuring," or underbead cracking, because the cracks are typically small and located adjacent to the interpass fusion boundary in the previously deposited weld metal. These defects are almost always associated with fully austenitic weld metal and are located along solidification grain boundaries or migrated grain boundaries.

Analogous to weld solidification cracking, weld-metal liquation cracking can generally be avoided by reducing the impurity levels in fully austenitic microstructures or by selecting filler metals that produce weld deposits containing more than approximately 3 FN.

Copper contamination cracking adjacent to austenitic stainless steel welds can also occur as a result of contact with copper or copper-bearing alloys, such as brass. This type of cracking is a form of liquid-metal embrittlement, whereby molten copper embrittles austenitic grain boundaries. Because copper melts at 1083 °C (1981 °F), this type of cracking caused by pure copper is only observed in regions of the weld (typically, the HAZ) that are heated near or above this temperature. Cracking is always intergranular and, normally, traces of copper or copper-rich material can be observed along the grain boundary.

This contamination can often be traced to copper weld fixturing, contact tips, or fabrication tools. The use of alternate fixturing, often incorporating chromium plating, and the prevention of copper abrasion normally eliminates the problem.

Ductility dip cracking occurs in the solid state and is typically associated with the HAZ or weld metal in highly constrained welds or thick sections. Such cracking occurs as a result of strain-induced grain-boundary precipitation, which limits mid-temperature ductility, but is much more common in precipitation-strengthened nickel-base alloys. However, this type of cracking has been observed in type 347 alloy, resulting from strain-induced precipitation of niobium carbides.

Weld porosity can result either from alloying additions (especially in the high-nitrogen alloys) or by contamination. In the Nitronic alloys, for example, nitrogen levels near the upper limit of 0.4% can result in porosity in gas-tungsten arc weld deposits, whereas lower levels (above approximately 0.25%) can result in excessive porosity in electron-beam welds (Ref 31). Porosity can also occur as a result of surface contamination, such as by oil and greases or undetected leaks in water-cooled welding torches or weld fixtures. Thus, surfaces should be thoroughly cleaned prior to welding. If wire

brushing is used, then the brushes should be made of stainless steel and dedicated to stainless usage, rather than made of steel, which can result in iron deposition and in-service corrosion.

References cited in this section

29. J.A. BROOKS, A.W. THOMPSON, AND J.C. WILLIAMS, *WELD. J.*, VOL 63, 1984, P 71-S TO 83-S
30. J.C. LIPPOLD, I. VAROL, AND W.A. BAESLACK III, *WELD. J.*, VOL 71, 1992, P 1S-14S
31. J.A. BROOKS, *WELD. J.*, VOL 54, 1975, P 189S-195S

Selection of Wrought Austenitic Stainless Steels

John A. Brooks, Sandia National Laboratories; John C. Lippold, Edison Welding Institute

Sigma-Phase Embrittlement

Sigma is a hard, brittle phase that can form in stainless steels when they are held in the temperature range from approximately 600 to 800 °C (1110 to 1470 °F). The sigma-phase compositional range shown in the vertical sections of Fig. 4 reveals that sigma can form over a wide range of compositions. The tendency for sigma-phase formation increases with increasing amounts of chromium, molybdenum, and silicon, and is reduced somewhat by nitrogen, nickel, and carbon. As a consequence of alloy partitioning during both solidification and the solid-state transformation of ferrite to austenite, ferrite is enriched in the alloying elements, which promotes the sigma phase, and depleted in the elements that retard its formation. Thus, ferrite in austenitic stainless welds is especially susceptible to sigma-phase formation. The sigma phase has been observed to nucleate preferentially at the ferrite-austenite interface in weld metal.

The transformation kinetics of ferrite to sigma has been studied by Vitek and David (Ref 32) in type 308 gas-tungsten arc welds (Fig. 12). They found that sigma started to form after approximately 15 h at 725 °C (1335 °F), and all the ferrite had transformed to sigma and $M_{23}C_6$ after approximately 3000 h.

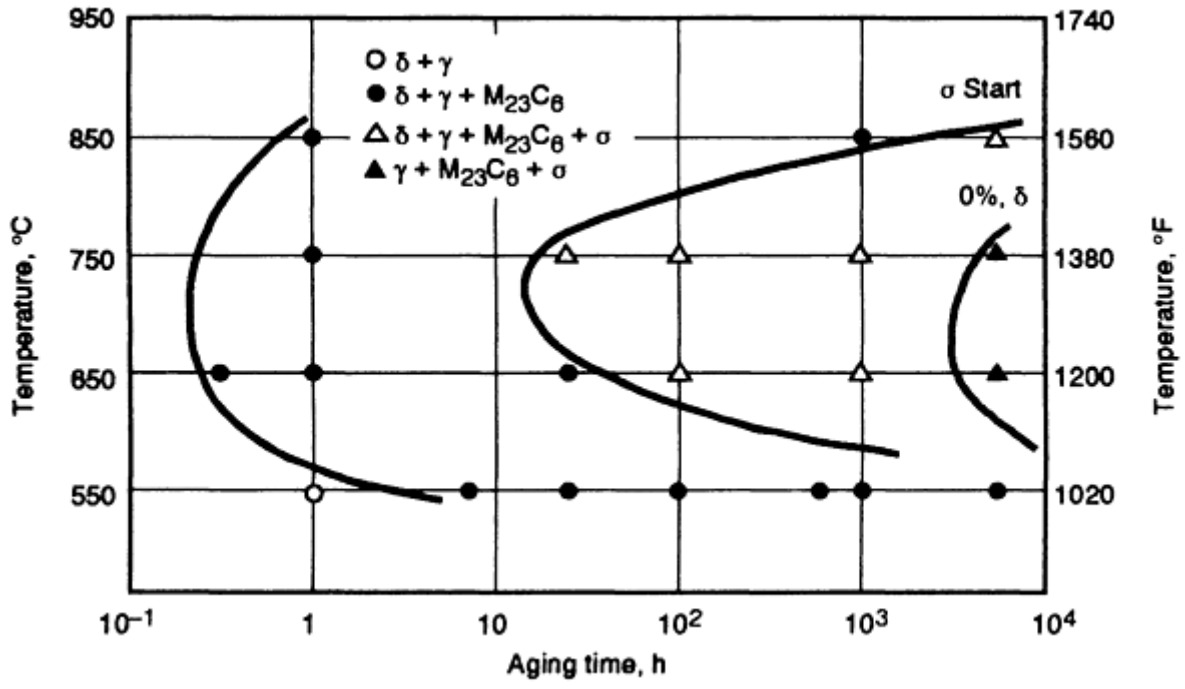

FIG. 12 TIME-TEMPERATURE TRANSFORMATION DIAGRAM FOR WELDED AND AGED TYPE 308L ALLOY GAS-

TUNGSTEN ARC WELDS. SOURCE: REF 32

The notorious effect of sigma phase is a decrease in ductility and toughness. When materials are to be used in elevated-temperature service, the effects of sigma formation must be considered. The sigma phase can be minimized by using filler materials that produce fully austenitic structures. However, even in these compositions, sigma formation can still occur, initiating in chromium-enriched interdendritic boundaries.

In cases where solidification cracking is a concern, some ferrite in the weld deposit is required. Weld-metal ferrite content should be controlled in the range from 3 to 8 FN to prevent the formation of a continuous network of ferrite. Because the chromium content of sigma is nearly double that of the weld ferrite, the potential maximum level of the sigma phase is always less than that of the original weld-metal ferrite.

Reference cited in this section

32. J.M. VITEK AND S.A. DAVID, *WELD. J.*, VOL 63, 1984, P 246S-253S

Selection of Wrought Austenitic Stainless Steels

John A. Brooks, Sandia National Laboratories; John C. Lippold, Edison Welding Institute

Corrosion Behavior

Austenitic stainless steel weldments are often subject to corrosive attack. The nature of this attack is a function of weld thermal history, service temperature and environment, and stress level (both residual and applied). Four general types of corrosive attack have been reported:

- INTERGRANULAR ATTACK
- STRESS-CORROSION CRACKING
- PITTING AND CREVICE CORROSION
- MICROBIOLOGICALLY INFLUENCED CORROSION

Each phenomena and its effect on service integrity is discussed below.

Carbide Precipitation and Intergranular Corrosion. Austenitic stainless steel weldments have often been subject to intergranular attack (IGA). This behavior is particularly prevalent in chloride-beating aqueous environments, and it is usually typified by accelerated attack in the HAZ. The basis for this attack is related to a phenomenon known as sensitization, whereby exposure or slow cooling in the temperature range from 400 to 850 °C (750 to 1550 °F) promotes the formation of chromium-rich carbides ($M_{23}C_6$) along the austenite grain boundaries. This temperature range is commonly described as the "sensitization" temperature range, because exposure within it makes austenitic stainless steels particularly sensitive to IGA. An example of intergranular corrosion in the HAZ of a weld in type 316L NaOH reactor vessel is shown in Fig. 13.

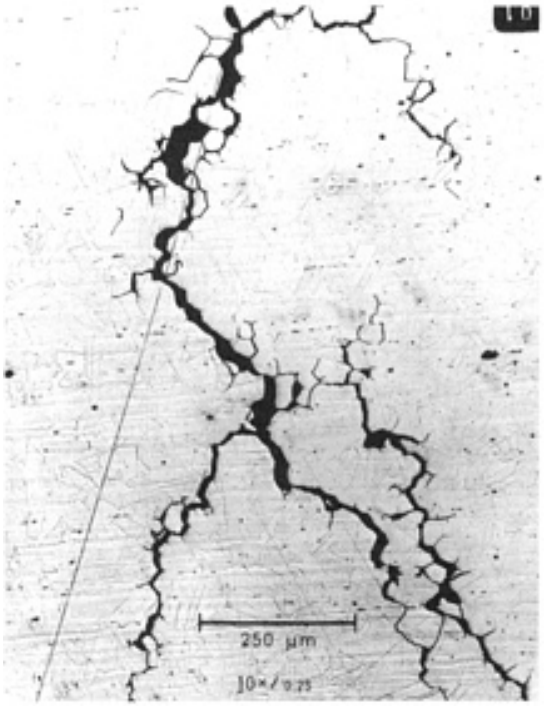

FIG. 13 CAUSTIC SCC IN THE HAZ OF A TYPE 316L STAINLESS STEEL NAOH REACTOR VESSEL. CRACKS ARE BRANCHING AND INTERGRANULAR.

Mechanistically, localized attack occurs immediately adjacent to the grain boundary, because of precipitation of the chromium-rich carbides in the boundary. Carbide formation depletes the adjacent matrix in chromium to a level generally estimated to be less than 12 wt% Cr. The severity of attack depends on the corrosive media, the time and temperature of exposure, and the composition and metallurgical condition of the steel.

Unfortunately, sensitization can be a by-product of the fusion-welding process. During welding, the weld HAZ experiences peak temperatures, ranging from the melting point to the ambient base-metal temperature, depending on the distance from the weld fusion boundary. Because heating and cooling in the weld HAZ is relatively rapid, regions of the HAZ that are heated to peak temperatures below about 650 °C (1200 °F) are immune to sensitization.

In addition, the HAZ region immediately adjacent to the fusion boundary is also resistant to sensitization, because carbon solubility is high at the peak temperatures achieved and cooling through the sensitization range is generally rapid enough to suppress carbide precipitation. This leaves a narrow region in the HAZ, somewhat removed from the fusion boundary, that will be heated into the sensitization temperature range. If the time within this temperature range is sufficient, then intergranular carbides will nucleate along austenite grain boundaries.

For a given thermal history, the level of precipitation and the associated degree of sensitization are approximately proportional to the carbon content of the austenitic stainless steel. Conventional austenitic stainless steels can retain a maximum of about 0.02 wt% C in solid solution over their service temperature range (up to 600 °C, or 1110 °F). Thus, as carbon content increases above this level, the driving force for carbide precipitation increases.

This can be illustrated by the time-temperature-precipitation (TTP) curves shown in Fig. 14 for an 18Cr-9Ni alloy. Because of this, low-carbon grades of stainless steel (the so-called L-grades) are preferred for corrosive service where weldments must be used in the as-welded condition. The use of "stabilized" alloys, such as types 321 and 347, which contain additions of titanium and niobium, respectively, are also effective in reducing susceptibility to IGA. Both titanium and niobium form stable carbides in the base metal that resist dissolution in the weld HAZ and/or at service temperatures in the sensitization range.

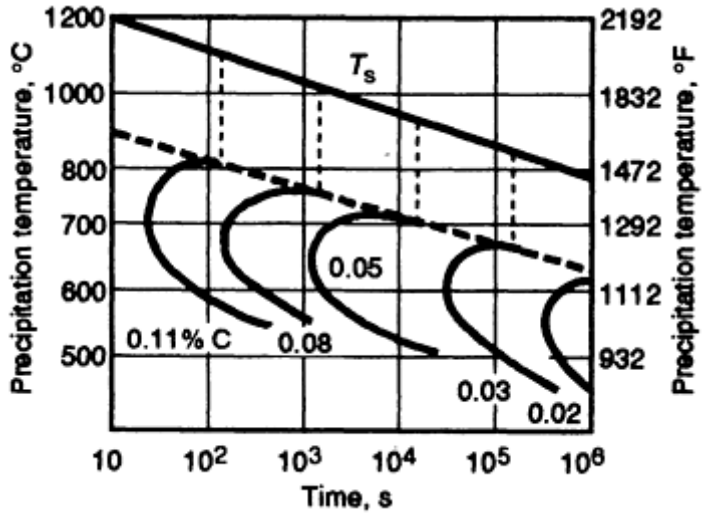

FIG. 14 TIME-TEMPERATURE PRECIPITATION CURVES FOR AN 18CR-9NI ALLOY WITH VARIOUS CARBON CONTENTS. SOURCE: REF 33

A phenomenon known as "knifeline" attack has been observed in the stabilized grades. However, its occurrence is associated with localized HAZ attack adjacent to the weld fusion boundary (Ref 34). Where temperatures exceed 1300 °C (2370 °F), niobium carbide and titanium carbide precipitates may dissolve and, upon reheating into the sensitization temperature range, chromium carbide ($M_{23}C_6$-type) precipitation occurs preferentially to the reformation of either niobium carbide or titanium carbide. Subsequent exposure to a corrosive medium may result in IGA that is extremely localized. In severe cases, it may often appear as if the weld has been cut out by a knife.

Weld metals containing even small amounts of delta ferrite are not generally susceptible to such severe sensitization as wrought material of similar composition. In ferrite-containing weld metal, carbide precipitation occurs more uniformly throughout the structure at the austenite-ferrite interphase boundaries. Because the ferrite phase has a relatively high chromium content (on the order of 25 wt% in a 18Cr-8Ni alloy), chromium depletion caused by carbide formation is not so significant. Consequently, weld metal is not generally susceptible to intergranular corrosion. However, fully austenitic weld metals may be susceptible to IGA when exposed to severely corrosive environments.

In general, it is possible to either minimize or eliminate IGA in austenitic stainless steel weldments by using one or more of these methods:

- USE A LOW-CARBON-CONTENT ALLOY, SUCH AS "L-GRADE" ALLOYS WITH CARBON CONTENTS ON THE ORDER OF 0.03 WT%.
- USE ALLOYS THAT ARE STABILIZED BY ADDITIONS OF NIOBIUM AND TITANIUM (SUCH AS TYPES 347 AND 321).
- ANNEAL THE MATERIAL PRIOR TO WELDING TO REMOVE ANY PRIOR COLD WORK (COLD WORK ACCELERATES CARBIDE PRECIPITATION).
- USE LOW WELD HEAT INPUTS AND LOW INTERPASS TEMPERATURES TO INCREASE WELD COOLING RATES, THEREBY MINIMIZING THE TIME IN THE SENSITIZATION TEMPERATURE RANGE.
- IN PIPE WELDING, WATER COOL THE INSIDE DIAMETER AFTER THE ROOT PASS, WHICH WILL ELIMINATE SENSITIZATION OF THE INSIDE DIAMETER CAUSED BY SUBSEQUENT PASSES.
- SOLUTION HEAT TREAT AFTER WELDING. HEATING THE STRUCTURE INTO THE TEMPERATURE RANGE FROM 900 TO 1100 °C (1650 TO 2010 °F) DISSOLVES ANY CARBIDES THAT MAY HAVE FORMED ALONG GRAIN BOUNDARIES IN THE HAZ. FOR LARGE STRUCTURES, THIS APPROACH IS USUALLY IMPRACTICAL.

The IGA of the weld HAZ has also been observed at service temperatures well below the classic sensitization temperature range. This behavior, often called low-temperature sensitization (LTS), typically occurs after years of service exposure at temperatures below 400 °C (750 °F), even in low-carbon grades. Mechanistically, it is proposed (Ref 35) that carbide embryos form along grain boundaries in the weld HAZ and then grow to form chromium-rich carbides in service. Corrosive attack occurs via the chromium-depletion mechanism described previously. In order to combat LTS, either stabilized alloys or alloys containing higher nitrogen contents (such as type 316LN) are substituted for conventional or L-grade materials.

The stress-corrosion cracking (SCC) of austenitic stainless steels may occur when an alloy is subjected simultaneously to a tensile stress and a specific corrosive medium. The important variables affecting SCC are temperature, environment, material composition, stress level, and microstructure. Crack propagation may be either transgranular or intergranular, depending on the interaction of these variables. Intergranular stress-corrosion cracking (IGSCC) can occur even though the alloy is insensitive to intergranular corrosion. The presence of residual tensile stresses in the HAZ may accelerate corrosion attack and cracking, particularly along sensitized grain boundaries.

Transgranular SCC is also observed in austenitic stainless steels. This form of cracking is usually indigenous to chloride environments (seawater), but may also occur in caustic media. The ions of the halogen family (fluorine, chlorine, bromine, and iodine) are largely responsible for promoting transgranular SCC. Of the halides, the chloride ion causes the greatest number of failures. Figure 15 shows an example of transgranular SCC in type 316 stainless steel. Note that cracking has initiated at the toe of the weld, probably because of the high residual stress level at that location.

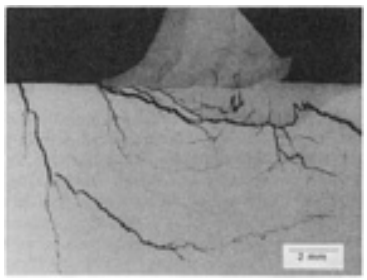

FIG. 15 TRANSGRANULAR SCC THAT HAS INITIATED NEAR THE TOE OF A WELD IN TYPE 316L ALLOY

Methods for controlling SCC include:

- A STRESS-RELIEVING OR ANNEALING HEAT TREATMENT TO REDUCE WELD RESIDUAL STRESSES
- SUBSTITUTION OF MORE-RESISTANT HIGH-NICKEL ALLOYS, HIGH-CHROMIUM FERRITIC STAINLESS STEELS, OR DUPLEX STAINLESS STEELS, THE LATTER OF WHICH HAVE BEEN DESIGNED SPECIFICALLY TO MINIMIZE SCC
- REDUCTION OF CHLORIDE AND OXYGEN CONTENTS FROM THE ENVIRONMENT, BECAUSE THESE TWO ELEMENTS, IN COMBINATION, ARE RESPONSIBLE FOR MOST SCC FAILURES IN AUSTENITIC STAINLESS STEELS

Pitting, Crevice Corrosion, and Microbiologically Influenced Corrosion. Localized attack in the weld metal or HAZ may occur in the form of pitting or crevice corrosion, particularly in aqueous, chlorine-bearing environments.

Microbiologically influenced corrosion (MIC) often occurs preferentially in the weld metal of austenitic stainless steels (Ref 36, 37). This curious form of attack is restricted to aqueous environments containing microbes that attach to the surface of the weld. In pipe welds, pitting from MIC often initiates at the weld fusion line and proceeds into the weld metal. Sensitized HAZs also are common regions of attack, although the most preferred site of attack seems to be the weld metal. Attack is a strong function of pitting resistance of the material and is thus more common in type 304 alloy, than in type 316.

The surface condition seems to have a large effect on MIC. Machining and grinding conducted on the inside of piping is thought to increase susceptibility to MIC by introducing rough surfaces for easy attachment by microbes and residual stresses, as well as localized metallurgical changes and corrosion pitting.

References cited in this section

33. V. CIHAL, *PROT. MET.* (RUSSIA), VOL 4 (NO. 6), 1968, P 653
34. C.J. NOVAK, SENSITIZATION, *HANDBOOK OF STAINLESS STEELS,* D. PECKHER AND I.M. BERNSTEIN, ED., MCGRAW-HILL, 1977, P 4-35 TO 4-53
35. M.C. JUHAS AND B.E. WILDE, *CORROSION,* VOL 46, 1990, P 812-822
36. D.H. POPE, "MICROBIOLOGICAL ASPECTS OF C INFLUENCED CORROSION," ER-6345, ELECTRIC POWER RESEARCH INSTITUTE, 1988
37. S.W. BORENSTEIN, MICROBIOLOGICALLY INDUCED CORROSION OF AUSTENITIC STAINLESS STEEL WELDMENTS, *MATER. PERFORM.,* VOL 1, 1991, P 52-54

Selection of Wrought Austenitic Stainless Steels

John A. Brooks, Sandia National Laboratories; John C. Lippold, Edison Welding Institute

Superaustenitic Stainless Steels

The superaustenitic stainless steels represent a special class of austenitic stainless steels that contain high levels of nickel, molybdenum, and, in some cases, nitrogen. These alloys are designed for severely corrosive environments. They provide improved resistance to SCC, pitting, and crevice corrosion, relative to the standard 300 series of austenitic alloys. Higher nickel contents improve chloride SCC resistance, whereas molybdenum and nitrogen provide improved pitting and crevice corrosion resistance. In general, these alloys are compositionally balanced to ensure fully austenitic microstructures. The compositions of selected commercially available superaustenitic alloys are shown in Table 2.

The weldability of most of these alloys is similar to that of fully austenitic grades of conventional stainless steel. Because these welds solidify as austenite and exhibit fully austenitic (no ferrite) microstructures, solidification cracking may be a problem in highly restrained joints. Typically, these alloys contain extremely low impurity levels, thus minimizing the likelihood of cracking.

The segregation of molybdenum in 6% Mo alloys during weld solidification has been reported to reduce corrosion resistance (Ref 38), particularly in severe pitting environments. The cell or dendrite cores in these alloys may exhibit molybdenum contents as low as 4.2 wt%, resulting in localized pitting attack at these sites. As a result, autogenous welding or the use of matching filler materials is normally avoided when severe service environments are anticipated. The use of molybdenum-containing, nickel-base filler materials, such as alloy 625 (AWS ERNi-CrMo-3), alloy C-276 (AWS ERNiCrMo-4), or alloy C-22 (AWS ERNiCrMo-10), is often recommended in order to avoid pitting. Precautions must be taken to prevent the formation of an unmixed zone adjacent to these overalloyed weld metals, because this region may have the same susceptibility to corrosive attack as autogenous weld metal does. Much more detail is provided in Ref 39.

References cited in this section

38. T.G. GOOCH, *PROC. CORROSION '92* (NASHVILLE), PAPER 296, NACE, 1992
39. CORROSION OF AUSTENITIC STAINLESS WELDMENTS, *CORROSION,* VOL 13, *ASM HANDBOOK,* ASM INTERNATIONAL, 1987, P 347-361

John A. Brooks, Sandia National Laboratories; John C. Lippold, Edison Welding Institute

Mechanical Properties

Austenitic stainless steels exhibit moderate strength and excellent toughness and ductility. Because of these properties, austenitic filler materials are often used in dissimilar combinations with carbon steels and ferritic and martensitic stainless steels. The weld properties of austenitic stainless steels are essentially similar to those of the annealed base material. Typical base-metal properties for austenitic stainless steels are listed in Table 4. Weld-metal properties are described in the article "Welding of Stainless Steels" in this Volume.

TABLE 4 MINIMUM ROOM-TEMPERATURE MECHANICAL PROPERTIES OF SELECTED AUSTENITIC STAINLESS STEELS

DESIGNATION	PRODUCT FORM	CONDITION	TENSILE STRENGTH		0.2% YIELD STRENGTH		ELONGATION, %	REDUCTION IN AREA, %	HARDNESS, HRB	ASTM SPECIFICATION
			MPA	KSI	MPA	KSI				
TYPE 301 (UNS S30100)	BAR	ANNEALED	620	90	205	30	40	. . .	95 MAX	A 666
TYPE 302 (UNS S30200)	BAR, FORGINGS	HOT FINISHED AND ANNEALED	515	75	205	30	40	50	. . .	A 276, A 473
TYPES 303 (UNS S30300) AND 303SE (UNS S30323)	FORGINGS	ANNEALED	515	75	205	30	40	50	. . .	A 473
TYPE 304 (UNS S30400)	BAR, FORGINGS[(A)]	HOT FINISHED AND ANNEALED	515	75	205	30	40	50	. . .	A 276, A 473
TYPE 304L (UNS S30403)	BAR	HOT FINISHED AND ANNEALED	480	70	170	25	40	50	. . .	A 276
TYPE 305 (UNS S30500)	BAR, FORGINGS	HOT FINISHED AND ANNEALED	515	75	205	30	40	50	. . .	A 276, A 473
TYPE 308 (UNS S30800)	BAR, FORGINGS	HOT FINISHED AND ANNEALED	515	75	205	30	40	50	. . .	A 276, A 473
TYPE 309 (UNS S30900), 309S (UNS S30908), 310 (UNS S31000) AND 310S (UNS S31008)	BAR, FORGINGS	HOT FINISHED AND ANNEALED	515	75	205	30	40	50	. . .	A 276, A 473
310CB (UNS S31040)	BAR, SHAPES	HOT FINISHED	515	75	205	30	40	50	. . .	A 276

		AND ANNEALED								
TYPE 316 (UNS S31600)	BAR, FORGINGS[A]	HOT FINISHED AND ANNEALED	515	75	205	30	40	50	. . .	A 276, A 473
TYPE 316L (UNS S31603)	BAR	HOT FINISHED AND ANNEALED	480	70	170	25	40	50	. . .	A 276
TYPE 317 (UNS S31700)	BAR, FORGINGS	HOT FINISHED AND ANNEALED	515	75	205	30	40	50	. . .	A 276, A 473
TYPE 317L (UNS S31703)	PLATE, SHEET, STRIP	ANNEALED	515	75	205	30	40	. . .	95 MAX	A 167
TYPES 321 (UNS S32100) AND 321H (UNS 32109)	BAR, FORGINGS	HOT FINISHED AND ANNEALED	515	75	205	30	40	50	. . .	A 276, A 473
TYPES 347 (UNS S34700) AND 348 (UNS S34800)	BAR, FORGINGS	HOT FINISHED AND ANNEALED	515	75	205	30	40	50	. . .	A 276, A 473
20CB-3 (UNS N08020), 20MO-4 (UNS N08024), AND 20MO-6 (UNS N08026)	BAR, WIRE	ANNEALED	550	80	240	35	30	50	. . .	B 473
TYPE 330 (UNS N08330)	BAR	ANNEALED	485	70	210	30	30	. . .	. . .	B 511
AL-6X (UNS N08366)	BAR, WIRE	ANNEALED	515	75	210	30	30	. . .	. . .	B 691
TYPE 332 (UNS N08800)	PIPE, TUBE	ANNEALED	515	75	210	30	30	. . .	. . .	B 163, B 407, B 514, B 515
TYPE 904L (UNS N08904)	BAR	ANNEALED	490	71	220	31	35	. . .	. . .	B 649

(A) FOR FORGED SECTIONS 127 MM (5 IN.) AND OVER, THE TENSILE STRENGTH SHALL BE 485 MPA (70 KSI).

Weld geometry and alloy composition also affect weld properties. Most weld tensile properties are determined using specimens transverse to the weld direction. Because failure often occurs outside the weld metal, only minimum tensile strength values can be determined and no weld-metal ductility data are generated. Impact toughness data are much more accurate, because a notch can be placed in the weld metal. HAZ mechanical property data are essentially nonexistent. Because the HAZ undergoes high temperatures during welding where carbide dissolution and grain growth can occur, it would be expected that this region may exhibit slightly lower strength than the annealed base metal.

In welds containing ferrite, the ferrite provides second-phase strengthening with a concomitant decrease in ductility. Thus, for an autogenous weld, the actual properties may vary somewhat from heat to heat in the same manner as the ferrite content. Typically, the tensile strength of welds is fractionally higher than the annealed wrought properties of similar compositions. However, the elongation and impact properties are reduced on the order of 30%. In multipass welds of thicker sections, warm working that results from the large strains encountered during cooling of subsequent passes can also result in significant increases in yield strengths and variations in strength from the top to the bottom of the weld deposit.

Nitrogen is a strong solid-solution strengthener and, thus, its increase or decrease in the welding process may also affect weld properties. In wrought materials, each addition of approximately 0.01% N results in an approximate increase of 5.5 to 7 MPa (0.8 to 1 ksi) in yield strength. Thus, from a conservative standpoint, weld strength is often considered to be the same as that of the annealed base material.

Weld properties may be significantly influenced by service temperature. At elevated temperatures, carbide, nitride, and intermetallic formation may reduce mechanical and corrosion properties. At cryogenic temperatures, the strain-induced martensite transformation from austenite can result in reduced toughness and ductility, relative to those properties in the homogeneous single-phase base material. In cases where filler metal is added, ASTM specifications provide minimum requirements. The reader is referred to the article "Welding for Cryogenic Service" in this Volume to obtain information on mechanical properties at cryogenic temperatures.

Weld penetration characteristics of austenitic stainless steels are generally poor, relative to ferritic and martensitic grades, because of the low thermal conductivity of the austenite. In addition, large heat-to-heat variations in weld penetration can occur when welding austenitic stainless, especially in autogenous welds or the root pass of multiple-pass gas-tungsten arc welds. These penetration variations have been attributed primarily to minor elements affecting the surface-tension-driven fluid flow within the weld pool (known as the Marongoni effect) (Ref 40).

The elements that influence penetration tend to be surface active and include sulfur, selenium, and oxygen. When present in sufficient quantity, these elements tend to increase weld penetration. However, other elements can have synergistic effects. Aluminum combined with oxygen can mitigate the effect of oxygen. Thus, high levels of aluminum can decrease penetration. For example, heats of type 304L alloy with low sulfur contents (0.001 to 0.003 wt%) may have a weld depth-to-width ratio of only 0.25, whereas the same material, but with a sulfur content of 0.01 wt%, welded under identical conditions, will exhibit a depth-to-width ratio higher than 0.5. Increased surface-oxygen content that results from wire brushing may also result in increased depth-to-width ratios in materials that otherwise have low penetration characteristics. However, this method is not often practiced, because of problems with reproducibility.

In autogenous welds, penetration control is best achieved by the proper selection of base materials. The addition of hydrogen and helium to argon shielding gas may help to compensate for poor penetration. For example, 98Ar-2H_2 and Ar-5H_2 are commonly used in the manufacture of welded tubing to increase penetration at high travel speeds. Trimixes of argon, helium, and H_2 may also be used to increase weld penetration.

Reference cited in this section

40. C.R. HEIPLE AND J.R. ROPER, *WELD. J.*, VOL 61, 1982, P 97S

John A. Brooks, Sandia National Laboratories; John C. Lippold, Edison Welding Institute

Weld Thermal Treatments

Preheat and Interpass Heat Treatments. Because the austenitic stainless steels do not experience a martensitic transformation upon cooling, there is generally no benefit derived from the use of preheat or interpass temperature control during multipass welding. In fact, these thermal treatments may actually increase the degree of sensitization by reducing cooling rates and allowing more time for carbide precipitation. Preheat and interpass heating can also increase distortion and cracking susceptibility.

Postweld heat treatment (PWHT) is often required to relieve residual stresses in austenitic stainless steel weldments, particularly in thick sections. Because the CTE value and the elevated-temperature yield and creep strengths of austenitic materials are significantly greater than for ferritic materials, the magnitude of residual stresses is generally larger. Although the effect of residual stresses from welding is typically not as severe as when less-ductile materials are used, they may still affect mechanical properties and corrosion behavior. PWHT is particularly critical when machining must be performed after welding, because significant distortion may occur.

Perhaps of greatest concern, however, is the influence of residual stress on SCC resistance. As described in the section "Corrosion Behavior" in this article, high levels of residual stress associated with the weld may severely reduce SCC resistance in chlorine-beating and caustic environments.

Stress relieving can be performed over a wide range of temperatures, depending on the amount of stress relaxation required. Time at temperature ranges from about 1 h per inch of section thickness at temperatures above 650 °C (1200 °F) to 4 h per inch of thickness at temperatures below 650 °C (1200 °F). Because of the high CTE value and low thermal conductivity of austenitic stainless steels, cooling from the stress-relieving temperature must be slow. Because the stress-relieving temperature range overlaps the sensitization temperature range, the stress-relieving temperature must be compatible with the extent of acceptable carbide precipitation and with the required amount of corrosion resistance. Nonstabilized stainless steels cannot be stress relieved in the sensitizing range without sacrificing corrosion resistance. Extra-low-carbon grades are affected much less, because sensitization is more sluggish. Stabilized grades exhibit minimal chromium carbide precipitation tendencies.

Higher stress-relief temperatures can be used for fully austenitic weld metals. For weld metals that contain ferrite, stress-relief temperatures above 650 °C (1200 °F) may result in weld embrittlement via sigma formation.

For austenitic stainless steels, the estimated percentages of residual stresses relieved at various temperatures at the times previously noted are 85% stress relief at 845 to 900 °C (1550 to 1650 °F) and 35% stress relief at 540 to 650 °C (1000 to 1200 °F). The data compiled by Cole and Jones (Ref 41) in Table 5 show specific time-temperature combinations that represent a compromise between the degree of stress relieving and carbide precipitation, which can lead to reduced corrosion resistance and ductility.

TABLE 5 EFFECT OF STRESS-RELIEF TREATMENTS ON AUSTENITIC STAINLESS STEELS

STAINLESS STEEL	CONDITION[A]	STRESS-RELIEF HEAT TREATMENT[B]			
		200-400 °C (392-752 °F), ~40% PEAK	550-650 °C (1022-1202 °F), ~35%	850-900 °C (1562-1652 °F), ~85%	950-1050 °C (1742-1922 °F), ~95%
TYPE 304	SHT, SA[C]	NME	IGP	IGP	IGP[D]
	WELDMENTS[C]	NME	IGP AND SIP	IGP AND SIP	IGP[D] AND SIP[E]
TYPE 321	SHT, SA	NME	NME	NME	NME
	WELDMENTS		SIP	SIP	SIP[E]
TYPE 304L	SHT, SA, AND WELDMENTS	NME	NME	NME	NME
TYPE 316	SHT, SA[C], AND WELDMENTS[C]	NME	IGP	IGP	IGP[D]
TYPE 316 + TI	SHT, SA, AND WELDMENTS	NME	NME	NME	NME
TYPE 316L	SHT, SA, AND WELDMENTS	NME	NME	NME	NME

(A) SHT, SOLUTION HEAT TREATMENT, RAPIDLY COOLED FROM ~1050 °C (1922 °F); SA, SOLUTION ANNEALED, SLOWLY COOLED FROM ~1050 °C (1922 °F).

(B) IGP, INTERGRANULAR PRECIPITATION OF CHROMIUM CARBIDE (SENSITIZATION); NME, NO METALLURGICAL EFFECT; SIP, STRAIN-INDUCED PRECIPITATION OF CARBIDES, IN WELDMENTS OVER 19 MM (0.75 IN.).

(C) LIKELY TO BE SENSITIZED PRIOR TO STRESS RELIEF, UNLESS OF SMALL SECTION SIZE AND/OR LOW CARBON CONTENT.

(D) DURING COOLING (ASSUMED ALWAYS TO BE SLOW).

(E) DURING HEATING

Reference cited in this section

41. C.L. COLE AND J.D. JONES, PUBLICATION 117, IRON AND STEEL INSTITUTE, LONDON, 1969, P 74

Selection of Wrought Austenitic Stainless Steels

John A. Brooks, Sandia National Laboratories; John C. Lippold, Edison Welding Institute

References

1. J.C. LIPPOLD, M.C. JUHAS, AND E.N.C. DALDER, *METALL. TRANS. A*, VOL 16, 1985, P 1835-1848
2. A.L. SCHAEFFLER, *MET. PROG.*, VOL 26, 1949, P 680
3. C.J. LONG AND W.T. DELONG, *WELD. J.*, VOL 52, 1973, P 281-S TO 297-S
4. D. KOTECKI AND T.A. SIEWERT, *WELD. J.*, VOL 71, 1992, P 171S-179S
5. H. THIER, *DVS-BER.*, VOL 41, 1976, P 100-104
6. I. MATSUMOTO, K. TAMAKI, AND M. MATSUMA, *J. JPN. WELD. SOC.*, VOL 41 (NO. 11), 1972, P 1306-1314
7. J.C. LIPPOLD AND W.F. SAVAGE, *WELD. J.*, VOL 61, 1982, P 388S-396S
8. G.R. SPEICH, *METALS HANDBOOK*, 8TH ED., VOL 8, AMERICAN SOCIETY FOR METALS, 1973, P 424
9. S.E. SCHURMANN AND I. BRAUCKMANN, *ARCH. EISENHUTTEN.*, VOL 48, 1977, P 3-8
10. N. SUUTALA, T. TAKALO, AND T. MOISIO, *METALL. TRANS. A*, VOL 10, 1979, P 512-514
11. J.A. BROOKS, J.C. WILLIAMS, AND A.W. THOMPSON, IN *TRENDS IN WELDING RESEARCH*, S.A. DAVID, ED., AMERICAN SOCIETY FOR METALS, 1982, P 331-355
12. S. KATAYAMA AND A. MATSUNAWA, *PROC. INT. CONF. ON ADVANCED LASER ELECTRO-OPTICS (ICALEO)* (SAN FRANCISCO), 1985
13. J.A. BROOKS, N.C.Y. YANG, AND J.S. KRAFCIK, ON THE ORIGIN OF FERRITE MORPHOLOGIES OF PRIMARY FERRITE SOLIDIFIED STAINLESS STEEL WELDS, *TRENDS IN WELDING RESEARCH*, ASM INTERNATIONAL, 1993
14. J.W. PUGH AND J.D. NISBET, *TRANS. TMS-AIME*, VOL 188, 1950, P 268-276
15. S.A. DAVID, *WELD. J.*, VOL 60, 1981, P 63-S TO 71-S
16. J.A. BROOKS AND A.W. THOMPSON, *LNT. MATER. REV.*, VOL 36 (NO. 1), 1991, P 16-44
17. N. SUUTALA AND T. MOISIO, THE USE OF CHROMIUM AND NICKEL EQUIVALENTS IN CONSIDERING SOLIDIFICATION PHENOMENA IN AUSTENITIC STAINLESS STEELS, *SOLIDIFICATION TECHNOLOGY IN THE FOUNDRY AND CASTHOUSE*, THE METALS SOCIETY PREPRINT, LONDON, 1980
18. T. TAKALO, N. SUUTALA, AND T. MOISIO, *METALL. TRANS. A* , VOL 10, 1979, P 1173-1181
19. D.L. OLSON, *WELD. J.*, VOL 64, 1985, P 281S-295S
20. "STANDARD PROCEDURES FOR CALIBRATING MAGNETIC INSTRUMENTS TO MEASURE THE DELTA FERRITE CONTENT OF AUSTENITIC AND DUPLEX AUSTENITIC-FERRITIC STEEL WELD METAL," AWS 4.2-91, AWS, 1991
21. R.H. ESPY, *WELD. J.*, VOL 61, 1982, P 1492-156S
22. F.C. HULL, *WELD. J.*, VOL 46, 1967, P 399-S TO 409-S
23. O. HAMMER AND U. SVENNSON, *SOLIDIFICATION AND CASTING OF METALS*, THE METALS SOCIETY, LONDON, 1979, P 401-410

24. S.A. DAVID, J.M. VITEK, AND T.L. HEBBLE, *WELD. J.*, VOL 66 (NO. 10), 1987, P 289S-300S
25. N. SUUTALA, EFFECT OF SOLIDIFICATION CONDITIONS ON THE SOLIDIFICATION MODE IN AUSTENITIC STAINLESS STEELS, *TECHNOLOGY IN THE FOUNDRY AND CASTHOUSE*, THE METALS SOCIETY PREPRINT, LONDON, 1980
26. J.A. BROOKS, M.I. BASKES, AND F.A. GREULICH, *METALL. TRANS. A*, VOL 22A, 1991, P 915-925
27. J.W. ELMER, S.M. ALLEN, AND T.W. EAGAR, *METALL. TRANS. A*, VOL 20A, 1989, P 2117-2131
28. G. PACARY, M. MOLINE, AND J.C. LIPPOLD, EWI RESEARCH BRIEF NO. B9008, EDISON WELDING INSTITUTE, 1990
29. J.A. BROOKS, A.W. THOMPSON, AND J.C. WILLIAMS, *WELD. J.*, VOL 63, 1984, P 71-S TO 83-S
30. J.C. LIPPOLD, I. VAROL, AND W.A. BAESLACK III, *WELD. J.*, VOL 71, 1992, P 1S-14S
31. J.A. BROOKS, *WELD. J.*, VOL 54, 1975, P 189S-195S
32. J.M. VITEK AND S.A. DAVID, *WELD. J.*, VOL 63, 1984, P 246S-253S
33. V. CIHAL, *PROT. MET.* (RUSSIA), VOL 4 (NO. 6), 1968, P 653
34. C.J. NOVAK, SENSITIZATION, *HANDBOOK OF STAINLESS STEELS*, D. PECKHER AND I.M. BERNSTEIN, ED., MCGRAW-HILL, 1977, P 4-35 TO 4-53
35. M.C. JUHAS AND B.E. WILDE, *CORROSION*, VOL 46, 1990, P 812-822
36. D.H. POPE, "MICROBIOLOGICAL ASPECTS OF C INFLUENCED CORROSION," ER-6345, ELECTRIC POWER RESEARCH INSTITUTE, 1988
37. S.W. BORENSTEIN, MICROBIOLOGICALLY INDUCED CORROSION OF AUSTENITIC STAINLESS STEEL WELDMENTS, *MATER. PERFORM.*, VOL 1, 1991, P 52-54
38. T.G. GOOCH, *PROC. CORROSION '92* (NASHVILLE), PAPER 296, NACE, 1992
39. CORROSION OF AUSTENITIC STAINLESS WELDMENTS, *CORROSION*, VOL 13, *ASM HANDBOOK*, ASM INTERNATIONAL, 1987, P 347-361
40. C.R. HEIPLE AND J.R. ROPER, *WELD. J.*, VOL 61, 1982, P 97S
41. C.L. COLE AND J.D. JONES, PUBLICATION 117, IRON AND STEEL INSTITUTE, LONDON, 1969, P 74

Selection of Wrought Duplex Stainless Steels

David N. Noble, ARCO Alaska, Inc.

Introduction

WROUGHT DUPLEX STAINLESS STEELS (DSS) are two-phase alloys based on the iron-chromium-nickel system. These materials typically comprise approximately equal proportions of the body-centered cubic (bcc) ferrite and face-centered cubic (fcc) austenite phases in their microstructure and are characterized by their low carbon content (<0.03 wt%) and additions of molybdenum, nitrogen, tungsten, and copper (Ref 1). Typical chromium and nickel contents are 20 to 30% and 5 to 10%, respectively. The specific advantages offered by DSS over conventional 300 series stainless steels are strength (about twice that of austenitic stainless steels), chloride stress-corrosion cracking (Cl SCC) resistance, and pitting corrosion resistance (Ref 2). These materials are used in the intermediate temperature range (about -60 to 300 °C, or -75 to 570 °F) where resistance to acids and aqueous chlorides is required. The weldability and welding characteristics of DSS are somewhat better than those of ferritic stainless steels, but generally not as good as austenitic materials.

Wrought DSS development in the 1970s and 1980s was particularly rapid, although the steels had been available in a number of compositions for several decades, particularly in the form of castings (Ref 3). Early grades were alloyed with approximately 18% Cr, about 4 to 6% Ni, and sometimes with molybdenum. Current commercial grades contain between 22 and 26% Cr, 4 to 7% Ni, up to 4.5% Mo, and 0.7% Cu and W, and are alloyed with 0.08 to 0.35% N (Ref 4). Continual modifications to the alloy compositions have been made to improve corrosion resistance, workability, and weldability. In particular, nitrogen additions have been effective in improving pitting corrosion resistance and weldability.

The current commercial DSS can be loosely divided into four generic types. With increasing corrosion resistance these alloy groups are:

- FE-23CR-4NI-0.1N
- FE-22CR-5.5NI-3MO-0.15N
- FE-25CR-5NI-2.5MO-0.17N-CU
- FE-25CR-7NI-3.5MO-0.25N-W-CU

As with 18-8 austenitic stainless steels, DSS are also frequently referred to by their chromium and nickel contents to describe the alloy class. The alloys listed above are then described as 2304, 2205, 25% Cr, and 2507, respectively. The last alloy class is also frequently termed "super" duplex stainless steel.

The performance of DSS can be significantly affected by welding. Due to the importance of maintaining a balanced microstructure and avoiding the formation of undesirable metallurgical phases, the welding parameters and filler metals employed must be accurately specified and closely monitored. The balanced microstructure of the base material (that is, equal proportions of austenite and ferrite) will be affected by the welding thermal cycle. If the balance is significantly altered and the two phases are no longer in similar proportions, the loss of material properties can be acute. Because the steels derive properties from both austenitic and ferritic portions of the structure, many of the single-phase base material characteristics are also evident in duplex materials. Austenitic stainless steels have excellent weldability and low-temperature toughness, whereas their Cl SCC resistance and strength are comparatively poor. Ferritic stainless steels have high resistance to Cl SCC but have poor toughness, especially in the welded condition. A duplex microstructure with high ferrite content can therefore have poor low-temperature notch toughness, whereas a structure with high austenite content can possess low strength and reduced resistance to Cl SCC (Ref 5). The high alloy content of DSS also renders them susceptible to formation of intermetallic phases from extended exposure to high temperatures. Extensive intermetallic precipitation may lead to a loss of corrosion resistance and sometimes to a loss of toughness (Ref 6).

References

1. H.D. SOLOMON AND T.M. DEVINE, JR., DUPLEX STAINLESS STEELS--A TALE OF TWO PHASES, *DUPLEX STAINLESS STEELS CONF. PROC.*, AMERICAN SOCIETY FOR METALS, 1983
2. B. LARSSON AND B. LUNDQVIST, FABRICATING FERRITIC-AUSTENITIC STAINLESS STEELS, SANDVIK STEEL TRADE LITERATURE, PAMPHLET S-51-33-ENG, OCT 1987
3. S. BERNHARDSSON, THE CORROSION RESISTANCE OF DUPLEX STAINLESS STEELS, *DUPLEX STAINLESS STEELS CONF. PROC.*, LES EDITIONS DE PHYSIQUE, LES ULIS CEDEX, FRANCE, OCT 1991, P 185-210
4. L. VAN NASSAU, H. MEELKER, AND J. HILKES, WELDING DUPLEX AND SUPER-DUPLEX STAINLESS STEELS--A GUIDE FOR INDUSTRY, DOCUMENT 01463, LINCOLN NORWELD, JULY 1992
5. T.G. GOOCH, WELDABILITY OF DUPLEX FERRITIC-AUSTENITIC STAINLESS STEELS, *DUPLEX STAINLESS STEELS CONF. PROC.*, AMERICAN SOCIETY FOR METALS, 1983, P 573-602
6. J. CHARLES, SUPER DUPLEX STAINLESS STEEL: STRUCTURE AND PROPERTIES, *DUPLEX STAINLESS STEELS CONF. PROC.*, VOL 1, LES EDITIONS DE PHYSIQUE, LES ULIS CEDEX, FRANCE, OCT 1991, P 3-48

Selection of Wrought Duplex Stainless Steels

David N. Noble, ARCO Alaska, Inc.

Base Material Properties

Microstructure. Duplex stainless steel parent materials have approximately equal proportions of austenite and ferrite, with ferrite comprising the matrix. Representative base material microstructures are shown in Fig. 1 and 2. Both exhibit a ferritic matrix with austenite islands of various morphologies. The wrought structure in Fig. 1 (a) parallel to the rolling direction has a pronounced orientation. The transverse view in Fig 1 (b) shows the austenite islands "end-on." The plan view in Fig 1 (c) also has some directionality but it is not as pronounced as in Fig. 1(a). A cast microstructure (Fig. 2) is coarser and displays a different morphology of austenite than that observed in the wrought plate.

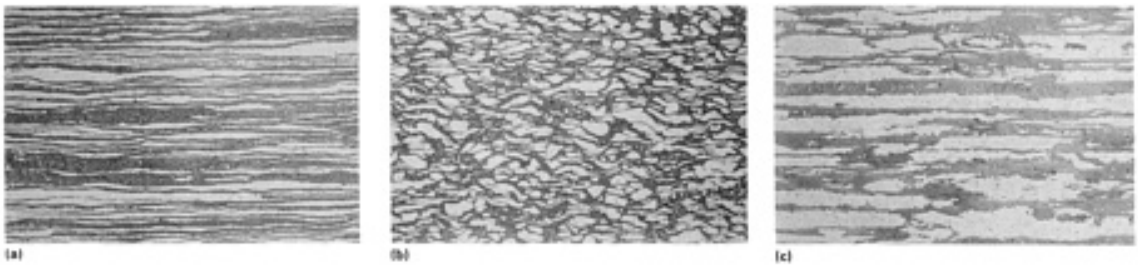

FIG. 1 EFFECT OF ORIENTATION PLANE ON THE MICROSTRUCTURE OF FE-22CR-5.5NI-3MO-0.15N WROUGHT DUPLEX STAINLESS STEEL BASE MATERIAL ELECTROLYTICALLY ETCHED IN 40% NAOH. (A) PARALLEL TO ROLLING DIRECTION. (B) TRANSVERSE TO ROLLING DIRECTION. (C) PLAN VIEW. 100X. COURTESY OF THE WELDING INSTITUTE

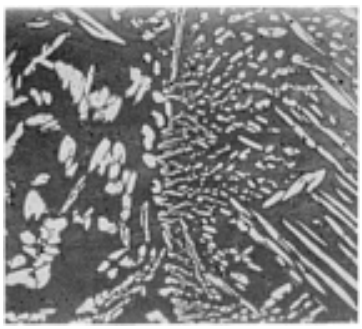

FIG. 2 MICROSTRUCTURE OF CAST FE-22CR-5.5NI-3MO-0.15N DUPLEX STAINLESS STEEL ETCHED ELECTROLYTICALLY IN 40% NAOH. 25×. COURTESY OF THE WELDING INSTITUTE

Alloy Grades. There are several types of DSS that have slightly different chemical compositions to cover the range of possible applications. The effects of chromium, nickel, molybdenum, and nitrogen on corrosion resistance are well understood and apply to most grades of stainless steels. The additional requirement of the alloying elements in the DSS base metal is to ensure that a balanced microstructure at room temperature is developed.

The DSS alloying additions are either austenite or ferrite formers. As the names suggest, certain elements will favor a higher proportion of austenite and others will favor ferrite. This is achieved by extending the temperature range over which the phase is stable. Among the major alloying elements in DSS, chromium and molybdenum are ferrite formers, whereas nickel, carbon, nitrogen, and copper are austenite formers (Ref 7, 8). The balance of austenite and ferrite formers will dictate the base material microstructure. Constitutional diagrams, such as the WRC-1992 diagram (Fig. 3) can be used for estimating the weld metal ferrite content in welds and developing appropriate base material compositions (Ref 8).

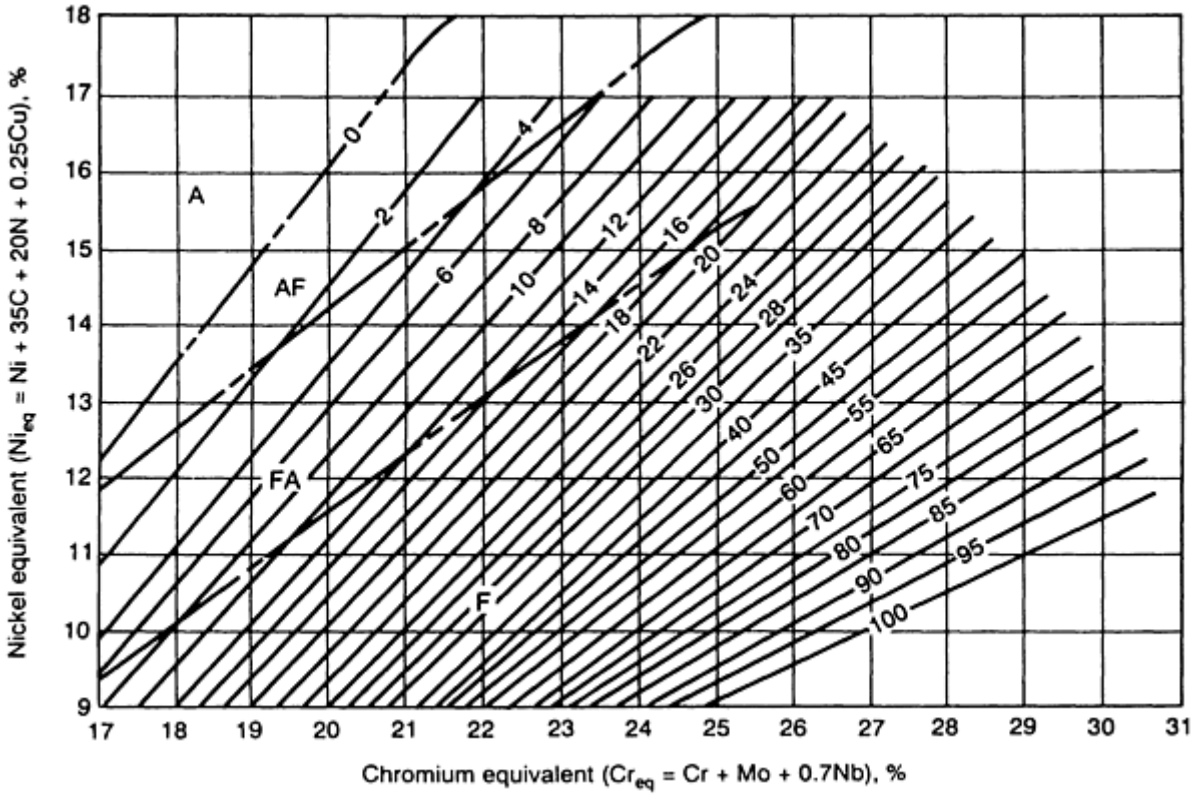

FIG. 3 WRC-1992 DIAGRAM FOR PREDICTING FERRITE CONTENT IN STAINLESS STEELS. FERRITE CONTENT IS GIVEN BY THE FERRITE NUMBER (FN), WHERE 100 FN IS APPROXIMATELY EQUAL TO 65 VOL% FERRITE. BOUNDARIES DENOTING A CHANGE IN SOLIDIFICATION MODE (A, PRIMARY AUSTENITE; AF, AUSTENITIC-FERRITIC; FA, FERRITIC-AUSTENITIC; F, PRIMARY FERRITE) ARE ALSO SHOWN (INDICATED BY DOTTED LINES). SOURCE: REF 8

Composition also plays a major role in the corrosion resistance of DSS. Pitting corrosion resistance is most easily affected. To determine the extent of pitting corrosion resistance offered by the material, the pitting resistance equivalent (PRE) is commonly used. This concept was proposed in the 1970s to characterize alloy resistance to pitting in chloride solutions (Ref 9). The PRE is calculated by adding the weight percentages of elements that affect pitting corrosion resistance, namely chromium, molybdenum, and nitrogen, then normalizing them with respect to the effect of 1% Cr. There are several formulas, which principally vary in the coefficient used for nitrogen, from 13 to 30. The PRE may also include negative coefficients for sulfur and phosphorus (Ref 10, 11). The most commonly used formula for pitting resistance equivalent is:

$$PRE = \%CR + 3.3(\%MO) + 16(\%N) \qquad \textbf{(EQ 1)}$$

The four types of DSS can also be classified by their PRE values. These range from 24 for the Fe-23Cr-4Ni-0.1N steel without molybdenum to over 40 for the Fe-25Cr-7Ni-3.5Mo-0.25N-Cu-W "super" grades. A minimum PRE value of 40 is often used to define the "super" DSS grades.

The chemical composition ranges of wrought DSS are given in Table 1, with the corresponding UNS numbers and PRE range for each. ASTM product specifications, in which the UNS numbers are referenced, are reported in Table 2. Some commercial grades of DSS, relevant composition ranges, and closest UNS numbers are given in Table 3.

TABLE 1 COMPOSITION AND PITTING RESISTANCE EQUIVALENT (PRE) VALUES OF SELECTED WROUGHT DUPLEX STAINLESS STEELS

UNS	COMPOSITION, %[A]

NUMBER	C	Mn	S	P	Si	Cr	Ni	Mo	N_2	OTHER	PRE RANGE[B]
S31200	0.03	2.00	0.03	0.045	1.00	24.0-26.0	5.5-6.5	1.2-2.0	0.14-0.20	. . .	30.2-35.8
S31260	0.03	1.00	0.030	0.030	0.75	24.0-26.0	5.5-7.5	2.5-3.5	0.10-0.30	0.10-0.50 W, 0.20-0.80 CU	33.9-42.4
S31500	0.03	1.2-2.0	0.03	0.03	1.4-2.0	18.0-19.0	4.25-5.25	2.5-3.0	0.05-0.10	. . .	27.1-30.5
S31803	0.03	2.00	0.02	0.03	1.00	21.0-23.0	4.5-6.5	2.5-3.5	0.08-0.20	. . .	30.5-37.8
S32304	0.03	2.5	0.04	0.04	1.0	21.5-24.5	3.0-5.5	0.05-0.60	0.05-0.20	0.05-0.60 CU	22.5-29.7
S32550	0.03	1.5	0.03	0.04	1.0	24.0-27.0	4.5-6.5	2.9-3.9	0.10-0.25	1.5-2.5 CU	35.2-43.9
S32750	0.03	1.2	0.02	0.035	1.0	24.0-26.0	6.0-8.0	3.0-5.0	0.24-0.32	0.5 CU	37.7-47.6
S32760	0.03	1.0	0.01	0.03	1.0	24.0-26.0	6.0-8.0	3.0-4.0	0.30	0.5-1.0 CU, 0.5-1.0 W	40[C]
S32900	0.06	1.00	0.03	0.04	0.75	23.0-28.0	2.5-5.0	1.0-2.0	[D]	. . .	26.3-34.6
S32950	0.03	2.00	0.01	0.035	0.60	26.0-29.0	3.5-5.2	1.0-2.5	0.15-0.35	. . .	. . .

(A) SINGLE VALUES ARE MAXIMUM.

(B) PRE = %CR + 3.3(%MO) + 16(%N).

(C) MINIMUM VALUE.

(D) NOT SPECIFIED

TABLE 2 ASTM STANDARDS INCORPORATING WROUGHT DUPLEX STAINLESS STEELS OR THEIR EQUIVALENTS

ASTM STANDARD	PRODUCT APPLICATION	UNS NUMBERS INCLUDED
A 790/A 790M-91	SEAMLESS AND WELDED FERRITIC/AUSTENITIC STAINLESS STEEL PIPE	S31803, S31500, S32550, S31200, S31260, S32304, S32750, S32900, S32950
A 240-91A	HEAT-RESISTING CHROMIUM AND CHROMIUM-NICKEL STAINLESS STEEL PLATE, SHEET, AND STRIP FOR PRESSURE VESSELS	S31200, S31260, S31803, S32304, S32550, S32750, S32900, S32950
A 182/A 182-90B	FORGED OR ROLLED ALLOY-STEEL PIPE FLANGES, FORGED FITTINGS, AND VALVES AND PARTS FOR HIGH-TEMPERATURE SERVICE	S31200, S31803
A 789/A 789M-90	SEAMLESS AND WELDED FERRITIC/AUSTENITIC STAINLESS STEEL TUBING FOR GENERAL SERVICE	S31803, S31500, S32550, S31200, S31260, S32304, S32750, S32900, S32950
A 276-91	STAINLESS AND HEAT-RESISTING STEEL BARS AND SHAPES	S31803

TABLE 3 COMPOSITION AND PITTING RESISTANCE EQUIVALENT (PRE) VALUES FOR SELECTED COMMERCIAL DUPLEX STAINLESS STEELS

STEEL PRODUCER	GRADE	COMPOSITION, %							
		Cr	Ni	Mo	N	Cu	OTHER	TYPICAL PRE VALUE	APPLICABLE UNS NO.
FE-23CR-4NI-0.1N									
AVESTA	2304	23	4	. . .	0.10	. . .	. . .	25	S32304
CLI	UR 35 N	23	4	. . .	0.12	. . .	. . .	25	S32304
SANDVIK	SAF 2304	23	4	. . .	0.10	. . .	. . .	25	S32304
FE-22CR-5.5NI-3MO-0.15N									
ALLEGHENY LUDLUM	AL 2205	22	5.5	3.0	0.16	. . .	. . .	33-35	S31803
AVESTA	2205	22	5.5	3.0	0.16	. . .	. . .	33-35	S31803
BOHLER	A 903	22	5.5	3.0	0.16	. . .	. . .	33-35	S31803
CLI	UR 45 N	22	5.5	3.0	0.16	. . .	. . .	33-35	S31803
KRUPP	FALC 223	22	5.5	3.0	0.16	. . .	. . .	33-35	S31803
MANNESMANN	AF22	22	5.5	3.0	0.16	. . .	. . .	33-35	S31803
NIPPON KOKAN	NKCR22	22	5.5	3.0	0.16	. . .	. . .	33-35	S31803
SANDVIK	SAF 2205	22	5.5	3.0	0.16	. . .	. . .	33-35	S31803
SUMITOMO	SM22CR	22	5.5	3.0	0.16	. . .	. . .	33-35	S31803
THYSSEN	REMANIT 4462	22	5.5	3.0	0.16	. . .	. . .	33-35	S31803
VALOUREC	VS22	22	5.5	3.0	0.16	. . .	. . .	33-35	S31803
BRITISH STEEL	HYRESIST 22/5	22	5.5	3.0	0.16	. . .	. . .	33-35	S31803
FE-25CR-5NI-2.5MO-0.17N-CU									
BOHLER	A 905	25.5	3.7	2.3	0.37	. . .	5.8 MN	39	. . .
CARPENTER	7-MO PLUS	27.5	4.5	1.5	0.25	. . .	. . .	37	. . .
CLI	UR 47N	25	7	3.0	0.16	0.2	. . .	38	S31260
CLI	UR 52N	25	7	3.0	0.16	1.5	. . .	38	S32550
LANGLEY ALLOYS	FERRALIUM 255	26	5.5	3.3	0.17	2.0	. . .	39	S32550
MATHER AND PLATT	ZERON 25	25	4	2.5	0.15	. . .	. . .	36	. . .
SUMITOMO	DP-3	25	6.5	3.0	0.2	0.5	0.3 W	38	. . .
FE-25CR-7NI-3.5MO-0.25N-CU-W									
KRUPP-VDM	FALC 100	25	7	3.5	0.25	0.7	0.7 W	41	S32760
AVESTA	2507	25	7	4	0.28	. . .	. . .	43	S32750
SANDVIK	SAF 2507	25	7	4	0.28	. . .	. . .	43	S32750
WEIR MATERIALS LTD.	ZERON 100	25	6.5	3.7	0.25	0.7	0.7 W	41	S32760
CLI	UR 52N +	25	6.5	3.7	0.24	1.6	. . .	41	S32550

Mechanical and Physical Properties. The high yield strength of DSS offers designers the use of thin-wall material with adequate pressure-containing and load-bearing capacity. This can lead to major reductions in weight and welding time. The yield strength of the Fe-22Cr-5.5Ni- 3Mo-0.15N grade is 450 MPa (65 ksi) minimum, which is double that of austenitic stainless steels and significantly higher than that of ferritic stainless steels. Base material hardness varies dependent upon processing route and extent of cold working, but it generally averages about 260 HV 10 (25 HRC) for the Fe-22Cr-5.5Ni-3Mo-0.15N grade (Ref 2). Details of room-temperature tensile properties and hardnesses for each grade are given in Table 4, and the physical properties are reported in Table 5.

TABLE 4 ROOM-TEMPERATURE MECHANICAL PROPERTIES OF SELECTED DUPLEX STAINLESS

STEELS PER ASTM A 790

UNS NO.	MINIMUM YIELD STRENGTH		MINIMUM TENSILE STRENGTH		ELONGATION (MINIMUM), %	HARDNESS	
	MPA	KSI	MPA	KSI		HB	HRC
S31200	450	65	690	100	25	280	. . .
S31500	440	64	630	92	30	290	30.5
S31803	450	65	620	90	25	290	30.5
S32304	400	58	600	87	25	290	30.5
S32550	550	80	760	110	15	297	31.5
S32750	550	80	800	116	15	310	32
S32760(A)	550	80	750	109	25	200-270	. . .
S32900	485	70	620	90	20	271	28
S32950	480	70	690	100	20	290	30.5

(A) NOT LISTED IN ASTM A 790

TABLE 5 TYPICAL PHYSICAL PROPERTIES OF SELECTED DUPLEX STAINLESS STEELS

PROPERTY(A)	GRADE		
	UNS S32750	UNS S32550	UNS S31803
DENSITY, G/CM^3 (LB/IN.^{3})	7.8 (0.28)	7.8 (0.28)	7.8 (0.28)
THERMAL CONDUCTIVITY, W/M · K (BTU/FT · H · °F)			
AT 20 °C (70 °F)	16 (9.2)	17 (9.8)	. . .
AT 100 °C (210 °F)	17 (9.8)	18 (10.4)	. . .
AT 200 °C (390 °F)	19 (11.0)	19 (11.0)	. . .
AT 300 °C (570 °F)	20 (11.6)	. . .	. . .
AT 400 °C (750 °F)	21 (12.1)	. . .	. . .
THERMAL EXPANSION, 10^{-6}/K (10^{-6}/°F)			
AT 20-100 °C (70-210 °F)	13 (7.2)	. . .	. . .
AT 20-200 °C (70-390 °F)	13.5 (7.5)	. . .	. . .
AT 20-300 °C (70-570 °F)	14.0 (7.8)	. . .	. . .
AT 20-400 °C (70-750 °F)	14.5 (8.1)	. . .	. . .
YOUNG'S MODULUS, GPA (10^6 PSI)			
AT 20 °C (70 °F)	200 (29.0)	. . .	. . .
AT 100 °C (210 °F)	190 (27.6)	. . .	. . .
AT 200 °C (390 °F)	180 (26.1)	. . .	. . .
AT 300 °C (570 °F)	170 (24.7)	. . .	. . .
AT 400 °C (750 °F)	160 (23.2)	. . .	. . .
SPECIFIC HEAT CAPACITY AT 20 °C (70 °F), J/KG · K (BTU/LB · °F)	470 (112)	475 (113)	450 (107)

(A) UNLIKELY TO CHANGE SIGNIFICANTLY RELATIVE TO GRADE

The parent metal toughness down to approximately -100 °C (-150 °F) is good, but the weld metal and heat-affected zone (HAZ) are commonly much less tough and are frequently the limiting factor in DSS application. The parent metal will undergo a slight ductile-to-brittle transition (Fig. 4) but the change is not as marked as in other steels with bcc matrices. These alloys are not suitable for cryogenic applications.

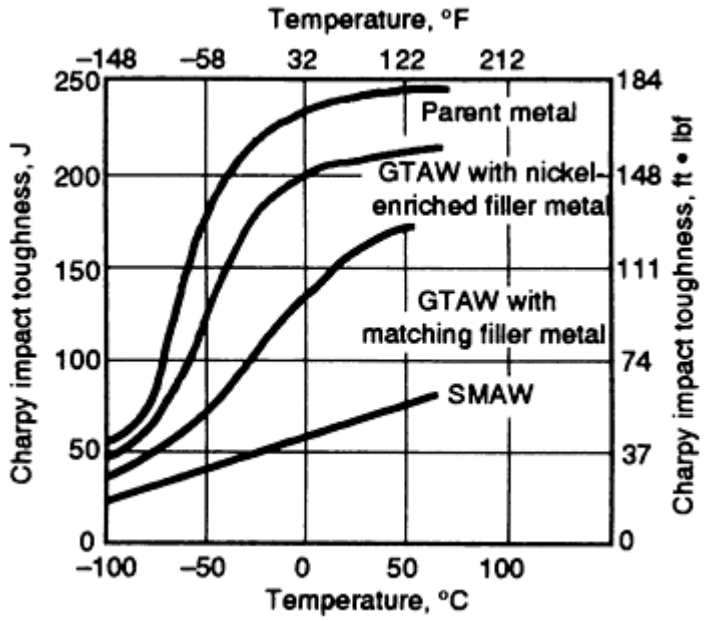

FIG. 4 PLOT OF CHARPY IMPACT TOUGHNESS VERSUS TEMPERATURE FOR FE-22CR-5.5NI-3MO-0.15N DSS BASE METAL AND WELDS PRODUCED WITH GAS-TUNGSTEN ARC WELDING (GTAW) AND SHIELDED METAL ARC WELDING (SMAW) PROCESSES. SOURCE: REF 2

The high alloy content and the presence of a ferritic matrix render DSS susceptible to embrittlement and loss of mechanical properties, particularly toughness, through prolonged exposure to elevated temperatures. This is caused by the precipitation of intermetallic phases, principally σ phase, χ phase, and η phase (Laves phase) (Ref 6). For this reason, the upper temperature of application is typically approximately 280 °C (535 °F) for parent material and 250 °C (480 °F) for welded structures (Ref 4). The more highly alloyed steels (for example, the Fe-25Cr-5Ni-2.5Mo-0.17N-Cu and Fe-25Cr-7Ni-3.5Mo-0.25N-Cu-W grades) are the most susceptible to the formation of these detrimental phases. Figure 5 shows the phases that can be formed in DSS, the approximate temperature range over which they will develop, and the effects of alloying elements on the transformation kinetics.

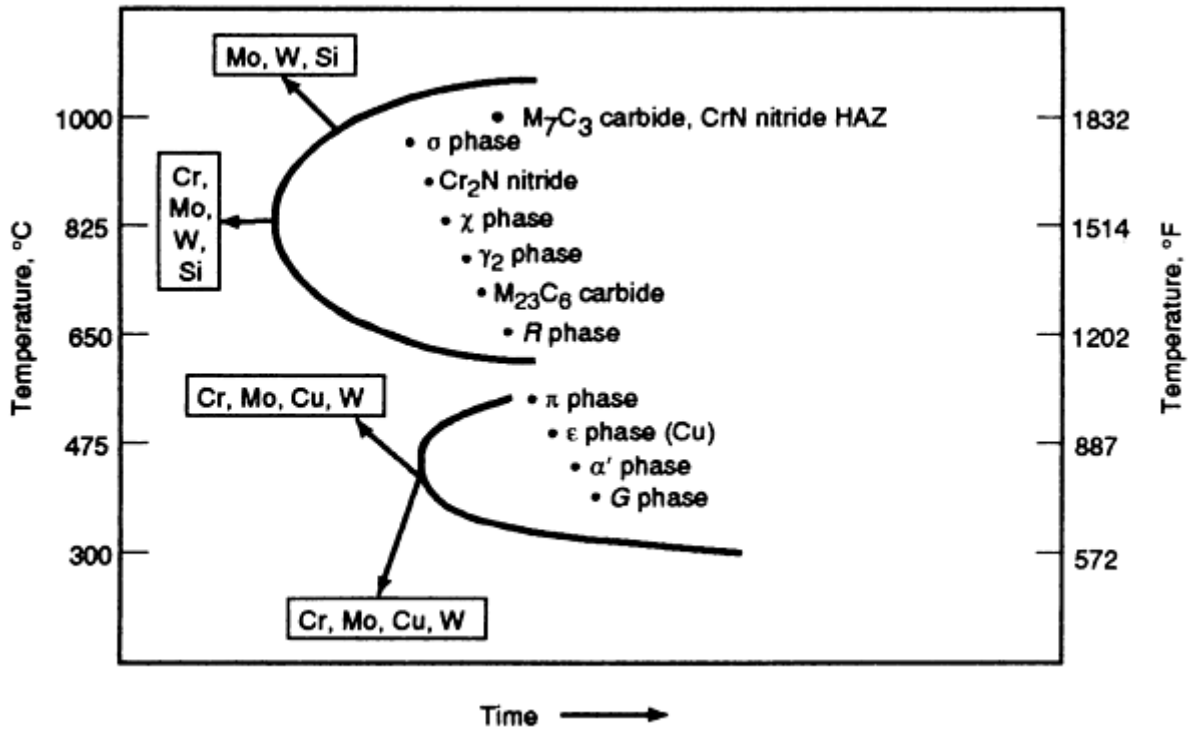

FIG. 5 TIME-TEMPERATURE TRANSFORMATION DIAGRAM SHOWING EFFECT OF ALLOYING ELEMENTS ON PRECIPITATION REACTIONS. SOURCE: REF 6

Corrosion Resistance. Duplex stainless steels were principally developed for their improved resistance to Cl SCC. Compared with conventional austenitic grades, they are clearly superior (Fig. 6). The more highly alloyed DSS are more resistant to Cl SCC than those with lower alloy contents.

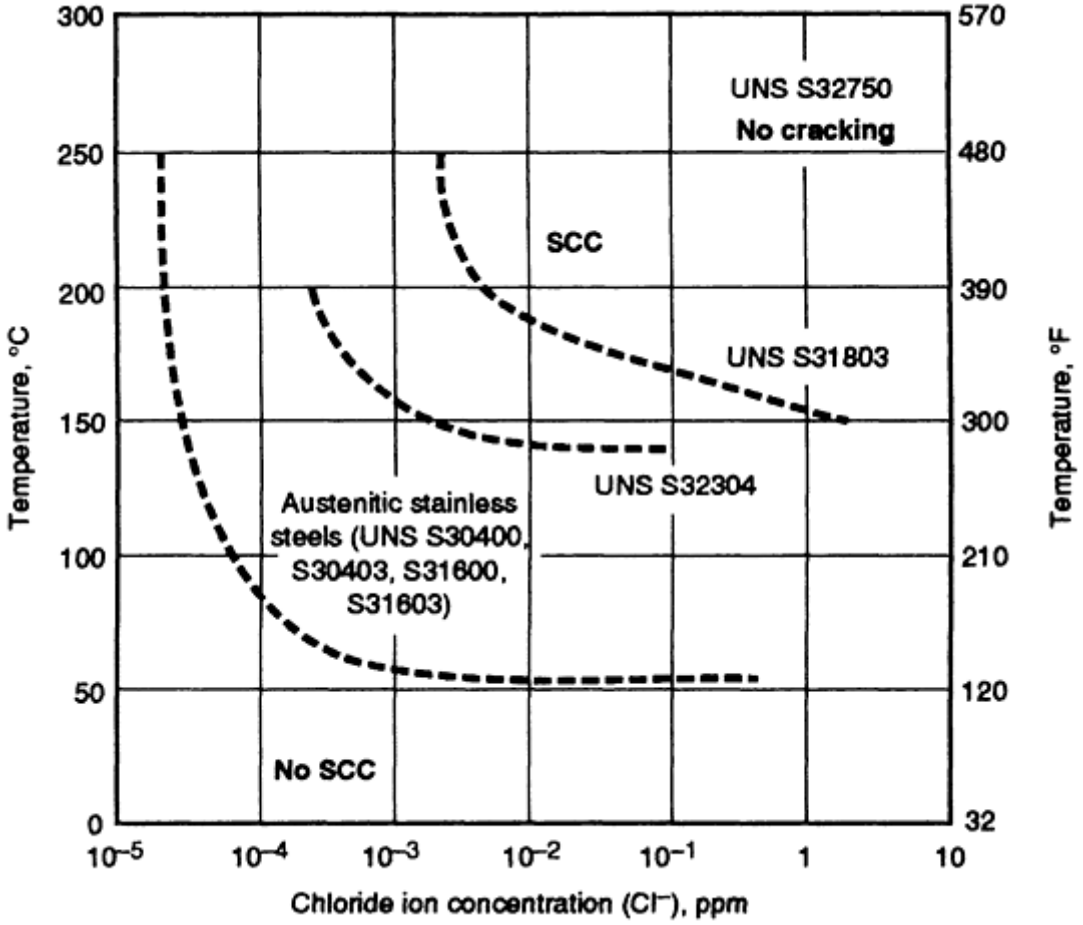

FIG. 6 STRESS-CORROSION CRACKING RESISTANCE OF SELECTED DUPLEX STAINLESS STEELS (S31803, S32304, AND S32750) RELATIVE TO AUSTENITIC STAINLESS STEELS (S30400, S30403, S31600, AND S31603) AS A FUNCTION OF TEMPERATURE AND CHLORIDE CONCENTRATION IN NEUTRAL O_2-BEARING SOLUTIONS (APPROXIMATELY 8 PPM). TEST DURATION WAS 1000 H. APPLIED STRESS WAS EQUAL TO YIELD STRENGTH. SOURCE: REF 2

Pitting corrosion resistance and general corrosion in acids are also generally acceptable (Fig. 7, 8) but these materials are susceptible to cracking in H_2S/Cl^- environments (Ref 12, 13, 14, 15). The tolerable H_2S limit for each grade depends on additional environmental factors (such as pH, temperature, chloride ion concentration, and so on) and is therefore not easily identified. Nevertheless, H_2S partial pressures of typically from 3.5 to 10 kPa (0.5 to 1.5 psi), dependent upon grade, have been reported as maxima for sour (H_2S-containing) service limits (Ref 16, 17). Regardless of H_2S partial pressure and chloride ion concentration, resistance to H_2S/Cl cracking appears to reach a minimum at about 60 to 100 °C (140 to 212 °F) (Ref 18).

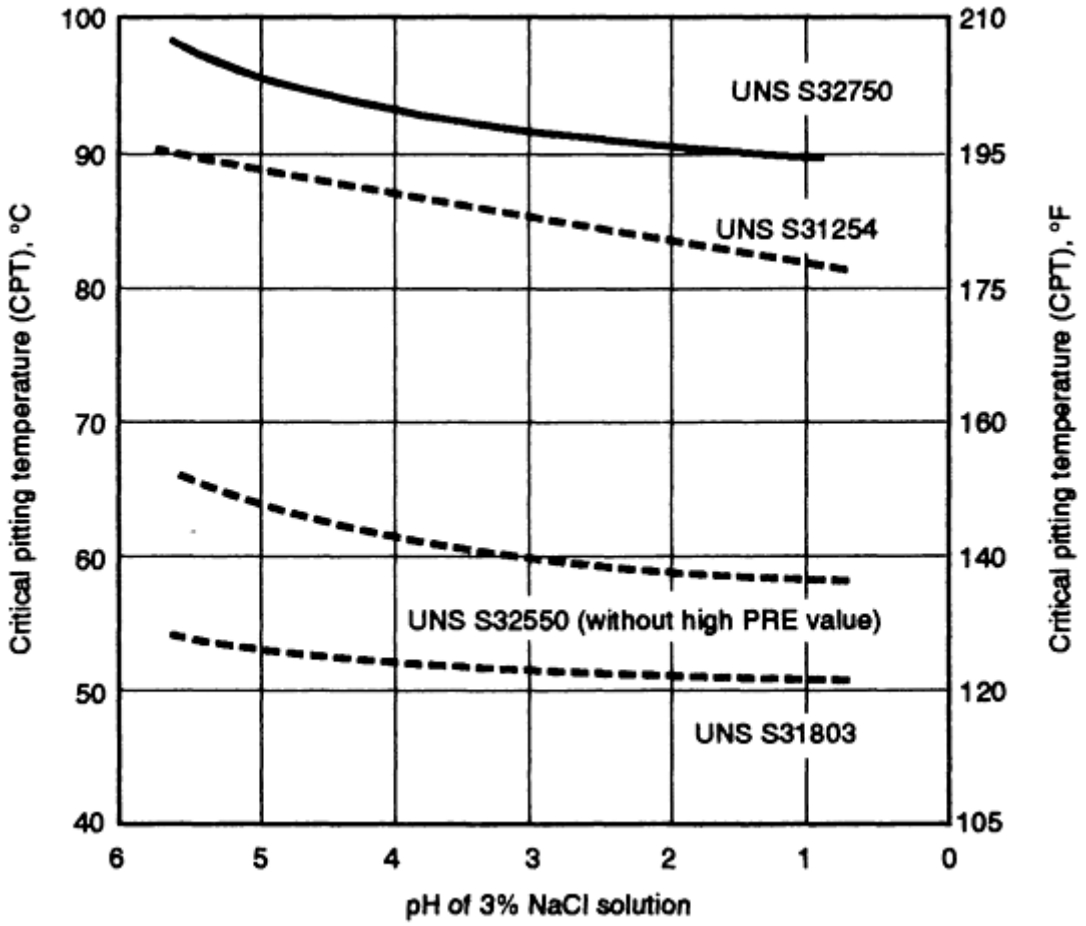

FIG. 7 CRITICAL PITTING TEMPERATURES FOR SELECTED DUPLEX STAINLESS STEELS (S31803, S32750, AND S32550) RELATIVE TO AUSTENITIC STAINLESS STEEL (S31254) IN 3% NACL SOLUTION WITH VARYING PH HELD AT AN ANODIC POTENTIAL OF +600 MV SATURATED CALOMEL ELECTRODE (SCE). SPECIMENS WERE SURFACE GROUND TO 600 GRIT. SOURCE: REF 2

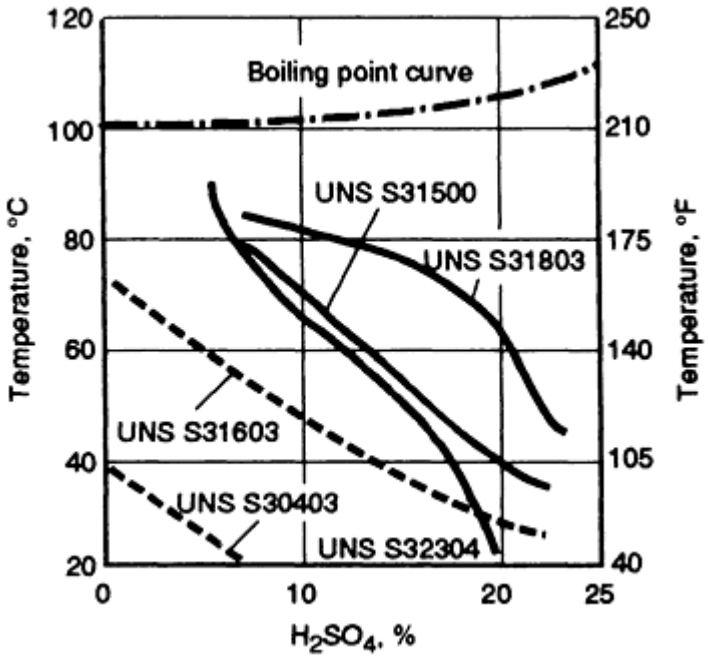

FIG. 8 ISOCORROSION DIAGRAM FOR SELECTED DUPLEX STAINLESS STEELS (S31803, S32304, AND S31500)

RELATIVE TO AUSTENITIC STAINLESS STEELS (S30403 AND S31603) IN STAGNANT SULFURIC ACID. CURVES REPRESENT CORROSION RATE OF 0.1 MM/YR (4 MILS/YR). SOURCE: REF 2

When considering corrosion performance, the effect of alloy partitioning within the microstructure is important. Even in base material that has undergone a soaking heat treatment at over 1000 °C (1830 °F), the austenite and ferrite phases will contain different amounts of the alloying elements. The ferrite will generally be highest in chromium and molybdenum, whereas the austenite will be richer in nickel and nitrogen (Ref 19). This imbalance in composition between the phases may translate into a difference in corrosion behavior, particularly pitting resistance. Significant differences in the PRE values have been reported between the ferrite and austenite phases in base material (Ref 19).

References cited in this section

2. B. LARSSON AND B. LUNDQVIST, FABRICATING FERRITIC-AUSTENITIC STAINLESS STEELS, SANDVIK STEEL TRADE LITERATURE, PAMPHLET S-51-33-ENG, OCT 1987
4. L. VAN NASSAU, H. MEELKER, AND J. HILKES, WELDING DUPLEX AND SUPER-DUPLEX STAINLESS STEELS--A GUIDE FOR INDUSTRY, DOCUMENT 01463, LINCOLN NORWELD, JULY 1992
6. J. CHARLES, SUPER DUPLEX STAINLESS STEEL: STRUCTURE AND PROPERTIES, *DUPLEX STAINLESS STEELS CONF. PROC.,* VOL 1, LES EDITIONS DE PHYSIQUE, LES ULIS CEDEX, FRANCE, OCT 1991, P 3-48
7. R. CASTRO AND J.J. DE CADENET, *WELDING METALLURGY OF STAINLESS AND HEAT-RESISTING STEELS,* CAMBRIDGE UNIVERSITY PRESS, 1974
8. D.J. KOTECKI AND T.A. SIEWERT, WRC-1992 CONSTITUTIONAL DIAGRAM FOR STAINLESS STEEL WELD METALS: A MODIFICATION OF THE WRC 1988 DIAGRAM, *WELD. J.,* MAY 1992, P 171S-178S
9. R.J. BRIGHAM AND E.W. TOZER, EFFECT OF ALLOYING ADDITIONS ON THE PITTING RESISTANCE OF 18% CR AUSTENITIC STAINLESS STEEL, *CORROSION,* VOL 30 (NO. 5), MAY 1974, P 161-166
10. N. SUUTALA AND M. KURKELA, *STAINLESS STEELS CONF. PROC.,* THE INSTITUTE OF METALS, 1985, P 240-247
11. R. DOLLING, V. NEUBERT, AND P. KNOLL, THE CORROSION BEHAVIOUR OF SUPER DUPLEX STEEL CAST ALLOYS WITH A PREN>41, *DUPLEX STAINLESS STEELS CONF. PROC.,* VOL 2, LES EDITIONS DE PHYSIQUE, LES ULIS CEDEX, FRANCE, OCT 1991, P 1341-1351
12. H. ERIKSSON AND S. BERNHARDSSON, THE APPLICABILITY OF DUPLEX STAINLESS STEELS IN SOUR ENVIRONMENTS, *CORROSION,* VOL 47 (NO. 8), SEPT 1991, P 719-727
13. A. MLYASAKA AND H. OGAWA, CRITICAL STRESS FOR SCC OF CORROSION RESISTANT ALLOY IN SOUR ENVIRONMENTS, PAPER 5, *CORROSION '89,* NATIONAL ASSOCIATION OF CORROSION ENGINEERS, 1989
14. S. BERNHARDSSON, THE CORROSION RESISTANCE OF DUPLEX STAINLESS STEELS, *DUPLEX STAINLESS STEELS CONF. PROC.,* AMERICAN SOCIETY FOR METALS, 1983, P 185-210
15. S. AZUMA, H. TSUGE, T. KUDO, AND T. MOROISHI, CREVICE CORROSION OF DUPLEX STAINLESS STEELS IN SIMULATED SOUR GAS ENVIRONMENTS, PAPER 306, *CORROSION '87,* NATIONAL ASSOCIATION OF CORROSION ENGINEERS, 1987
16. "SULFIDE STRESS CRACKING RESISTANT METALLIC MATERIALS FOR OILFIELD EQUIPMENT," MR-01-75-93, NATIONAL ASSOCIATION OF CORROSION ENGINEERS
17. L. SMITH, CORROSION RESISTANT ALLOYS OFFER PIPELINE ALTERNATIVES, *STAINL. STEEL EUR.,* JAN/FEB 1993, P 32-42
18. M.J. SCHOFIELD, AND R.D. KANE, DEFINING SAFE USE LIMITS FOR DUPLEX STAINLESS STEELS, *DUPLEX STAINLESS STEEL CONF. PROC.,* LES EDITIONS DE PHYSIQUE, LES ULIS CEDEX, FRANCE, OCT 1991, P 241-255

19. T. OGAWA AND T. KOSEKI, EFFECT OF COMPOSITION PROFILES ON METALLURGY AND CORROSION BEHAVIOUR OF DUPLEX STAINLESS STEEL WELD METALS, *WELD. J.*, VOL 88 (NO. 5), MAY 1989, P 181S-191S

David N. Noble, ARCO Alaska, Inc.

Applications

Duplex stainless steels have found widespread use in a range of industries, particularly the oil and gas, petrochemical, pulp and paper, and pollution control industries. They are commonly used in aqueous, chloride-containing environments and as replacements for austenitic stainless steels that have suffered from either Cl SCC or pitting during service (Ref 20). The more highly alloyed grades (that is, the "super" DSS) are resistant to oxygenated or chlorinated sea water (Ref 21). The leaner alloy materials are not resistant to live sea water and will suffer from pitting. Several grades have been used for transportation of wet, CO_2-containing gas where carbon would have suffered general corrosion (Ref 22). Table 6 gives a list of DSS grades and typical applications.

TABLE 6 TYPICAL APPLICATIONS OF DUPLEX STAINLESS STEELS

GRADE(S)	APPLICATION
S31803, S32760, S32750, S32550	TUBING FOR HEAT EXCHANGERS IN REFINERIES, CHEMICAL INDUSTRIES, PROCESS INDUSTRIES, AND OTHER INDUSTRIES USING WATER AS A COOLANT; KRAFT PAPER DIGESTERS
ALL	HEAT EXCHANGERS, CHEMICAL TANKERS, CHEMICAL REACTOR VESSELS, FLUE GAS FILTERS, ACETIC AND PHOSPHORIC ACID HANDLING SYSTEMS, OIL AND GAS INDUSTRY EQUIPMENT (MULTIPHASE FLOW LINES, DOWNHOLE PRODUCTION TUBULARS, COMMONLY COLD WORKED)
S32304	DOMESTIC WATER HEATERS AND WHERE PITTING RESISTANCE IS NOT OF OVERRIDING IMPORTANCE
S32750, S32760, S32550	PIPE FOR SEAWATER HANDLING AND FIREFIGHTING SYSTEMS, OIL AND GAS SEPARATORS, SALT EVAPORATION EQUIPMENT, DESALINATION PLANTS, GEOTHERMAL WELL HEAT EXCHANGERS, HUMAN BODY IMPLANTS (S32550 MAY SUFFER SLIGHT PITTING AND CREVICE CORROSION IN SEAWATER SERVICE)

References cited in this section

20. D. FRUYTIER, INDUSTRIAL EXPERIENCES WITH DUPLEX STAINLESS STEEL, *STAINL. STEEL EUR.*, VOL 3 (NO. 13), DEC 1991
21. B. WALLEN AND S. HENRIKSON, EFFECT OF CHLORINATION ON STAINLESS STEELS IN SEAWATER, PAPER 403, *CORROSION '86,* NATIONAL ASSOCIATION OF CORROSION ENGINEERS, 1986
22. J. HARSTON, E. HUTCHINS, AND S. SWEENEY, THE DEVELOPMENT AND CONSTRUCTION OF DUPLEX STAINLESS STEEL PIPELINES FOR USE OFFSHORE IN THE SOUTHERN NORTH SEA, *PROC. 3RD LNT. CONF. WELDING AND PERFORMANCE OF PIPELINES,* THE WELDING INSTITUTE, 1986

David N. Noble, ARCO Alaska, Inc.

Microstructural Development

Factors Controlling Microstructure. By assuming a duplex stainless steel contains 68% Fe and 32% alloying elements (comprising nickel and chromium, but representing austenite and ferrite formers, respectively), the 68% Fe pseudo-binary phase diagram can be used to explain the microstructural transformations that occur during heating and cooling (Fig. 9).

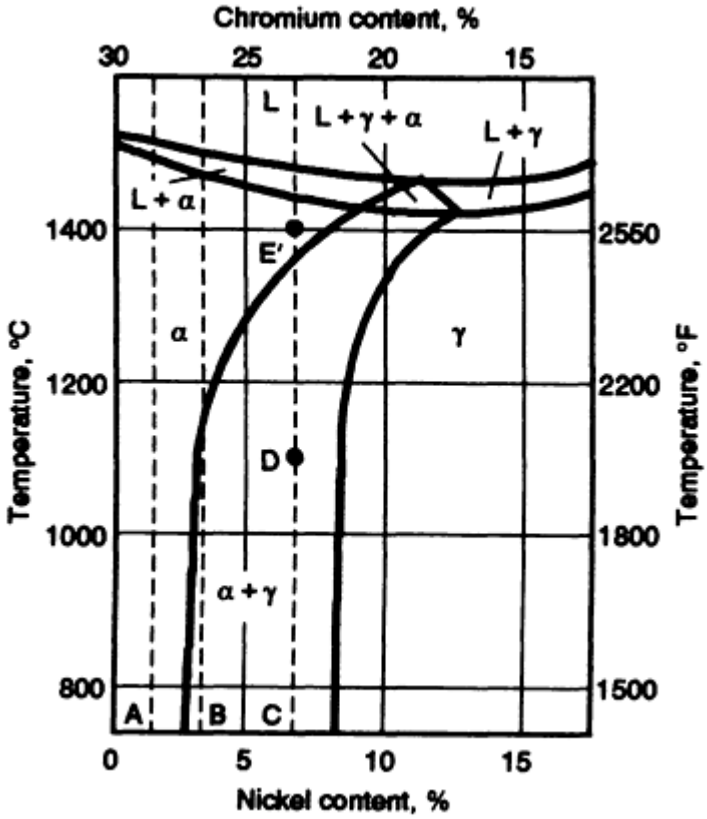

FIG. 9 PSEUDO-BINARY DIAGRAM AT CONSTANT IRON SECTION (68 WT% FE) OF THE FE/CR/NI TERNARY SYSTEM. SEE TEXT FOR DEFINITION OF LINES A, B, AND C AND POINTS D AND E. SOURCE: REF 9

Composition. With approximately 30% Cr and 2% Ni (composition indicated by line A), the steel will solidify completely to ferrite and remain ferritic down to room temperature. As the chromium content decreases and the nickel content increases, an alloy containing 28% Cr and 4% Ni, indicated by line B, will solidify as ferrite, remain fully ferritic until about 1200 to 1300 °C (2190 to 2370 °F), and then enter the dual-phase field (denoted by $\alpha + \gamma$). A two-phase microstructure will be developed and maintained down to room temperature. Because the composition of alloy B lies to the far left of the dual-phase field, a microstructure rich in ferrite would be anticipated. Current commercial DSS with 25% Cr are more likely to contain about 7% Ni, indicated by line C, which upon cooling enters the dual-phase field at a much higher temperature, thereby allowing more time for the diffusion-driven solid-state transformation from ferrite to austenite. An alloy with composition C will solidify as ferrite and be fully ferritic for a narrow temperature range prior to entering the dual-phase field. It should be noted that alloys A, B, and C will solidify primarily as ferrite and will have ferritic matrices.

Heat Treatment. The sequence of phase transformation in DSS upon cooling is (Fig. 9):

$$\text{LIQUID} \rightarrow \text{LIQUID} + \text{FERRITE} \rightarrow \text{FERRITE} \rightarrow \text{FERRITE} + \text{AUSTENITE} \qquad \textbf{(EQ 2)}$$

The solid-state transformation from ferrite to austenite is considered to be diffusional (Ref 23) and therefore affected by time and temperature. Very rapid cooling from a temperature at which the steel is fully ferritic will result in suppression

of the ferrite-to-austenite transformation and retention of a predominantly ferritic structure. The temperature range over which the transformation from ferrite to austenite occurs is highly dependent upon composition and grade (Fig. 9), but is typically from 1200 to 800 °C (2190 to 1470 °F). For this reason, a $\Delta T_{12\text{-}8}$ cooling rate term has been used when characterizing a DSS thermal cycle (Ref 24, 25). A longer $\Delta T_{12\text{-}8}$ will result in more transformation from ferrite to austenite. In a weld of given thickness, longer $\Delta T_{12\text{-}8}$ values can be achieved by a higher heat input weld. The $\Delta T_{12\text{-}8}$ term has been employed in an effort to identify critical cooling rates necessary to develop acceptable austenite content in weld heat-affected zones to achieve the desired mechanical and corrosion resistance properties. The critical $\Delta T_{12\text{-}8}$ for phase transformation is independent of material thickness, unlike heat input, but is highly dependent on alloy composition.

Low-temperature thermal cycles will not affect the austenite/ferrite balance, but they will control the extent of intermetallic phase precipitation. These steels should undergo rapid cooling (that is, water quenching) through the precipitation temperature range to develop optimum properties. For welds, water quenching is usually not necessary or practical, but some means of forced cooling may be beneficial for productivity and quality reasons, particularly for multipass welds in the high-alloy grades (Ref 26, 27).

To produce the necessary base material microstructure, an isothermal heat treatment is carried out at a temperature at which the steel is dual phase, approximately 1050 to 1100 °C (1920 to 2010 °F), or point D in Fig. 9 (Ref 28). To avoid the formation of intermetallic phases during cooling, water quenching from the soaking temperature is necessary.

Morphology. Wrought DSS base material microstructures have a pronounced orientation of austenite islands in the ferritic matrix, parallel and transverse to the rolling direction, as a result of the hot and cold working following casting (Fig. 1). The cast microstructure (Fig. 2) is very different, and more similar to that observed in weld metal and the HAZ.

During the weld thermal cycle, the HAZ adjacent to the fusion line will become fully ferritic at temperatures above the austenite-to-ferrite transition temperature (point E in Fig. 9). Grain growth will occur and, regardless of the extent of austenite transformation that occurs during subsequent cooling, the coarse prior ferrite grain boundaries will still be apparent (Fig. 10). Very rapid cooling from the fully ferritic phase field will retard austenite reformation in the HAZ, and result in a predominantly ferritic structure, also shown in Fig. 10. When cooled more slowly, the austenite will form initially on the ferrite grain boundaries and then within the ferrite grains along preferred crystallographic planes in a manner similar to the cast material.

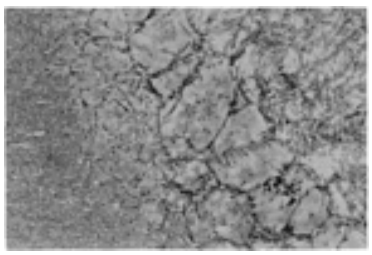

FIG. 10 PHOTOMICROGRAPH OF A FE-22CR-5.5NI-3MO-0.15N DSS WELD AREA SHOWING ELONGATED PARENT PLATE MORPHOLOGY, A COARSE GRAIN HEAT-AFFECTED ZONE HIGH IN FERRITE, AND COLUMNAR WELD METAL GRAINS. SPECIMEN ELECTROLYTICALLY ETCHED IN 40% NAOH. 30×. COURTESY OF THE WELDING INSTITUTE

The HAZ in Fig. 10 is relatively wide and has a high ferrite content. Such a structure may lead to poor low-temperature notch toughness and reduced corrosion resistance. Nitrogen levels in the base steel are being steadily increased to improve weldability and to avoid the formation of structures similar to that shown in Fig. 10; some DSS contain as much as 0.35 wt% N (Ref 4). A higher nitrogen level will increase the temperature at which ferrite begins to transform to austenite on cooling (Ref 6). This reduces the width of the transformed HAZ by limiting to a narrow temperature range the extent of the fully ferritic phase field. It also encourages more austenite reformation by starting the transformation at a much higher temperature. The recent grades of DSS, which typically have minimum 0.20 wt% N, develop a very narrow HAZ in which the transformed region is often difficult to distinguish.

The sequence of transformation reactions in the weld metal is the same as for the HAZ, but due to the solidification pattern, the macroappearance is different and columnar grains are more typical (this can be seen on the top left of Fig.

10). Duplex weld metal grain growth is epitaxial, with the large prior ferrite grains in the HAZ dictating weld metal grain size and orientation. Austenite again forms preferentially on the grain boundaries, and intragranular austenite forms along preferred crystallographic planes as the weld metal continues to cool (Fig. 11).

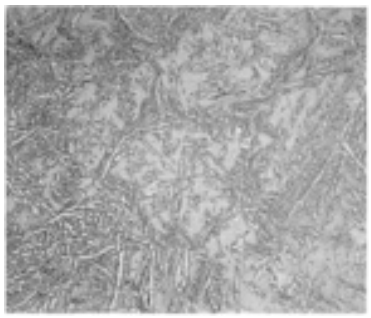

FIG. 11 PHOTOMICROGRAPH OF DSS WELD METAL WITH AUSTENITE LATHS (WHITE) AT PRIOR FERRITE GRAIN BOUNDARIES AND ALONG PREFERRED CRYSTALLOGRAPHIC PLANES IN A FERRITIC MATRIX. SAMPLE ELECTROLYTICALLY ETCHED IN 40% NAOH. 100×. COURTESY OF THE WELDING INSTITUTE

Precipitates are often difficult to observe and require precise etching techniques and experience with the type of microstructure. Due to its highly detrimental effect on corrosion resistance and toughness and relative ease of formation, the most commonly investigated precipitate in DSS is σ phase, an Fe(Cr,Mo) intermetallic. Sigma will initially precipitate at phase boundaries in the ferrite phase and will then grow into the ferrite phase, which is richer in chromium and molybdenum. Only a small amount of σ precipitation is required to reduce mechanical and corrosion properties.

References cited in this section

4. L. VAN NASSAU, H. MEELKER, AND J. HILKES, WELDING DUPLEX AND SUPER-DUPLEX STAINLESS STEELS--A GUIDE FOR INDUSTRY, DOCUMENT 01463, LINCOLN NORWELD, JULY 1992
6. J. CHARLES, SUPER DUPLEX STAINLESS STEEL: STRUCTURE AND PROPERTIES, *DUPLEX STAINLESS STEELS CONF. PROC.*, VOL 1, LES EDITIONS DE PHYSIQUE, LES ULIS CEDEX, FRANCE, OCT 1991, P 3-48
9. R.J. BRIGHAM AND E.W. TOZER, EFFECT OF ALLOYING ADDITIONS ON THE PITTING RESISTANCE OF 18% CR AUSTENITIC STAINLESS STEEL, *CORROSION*, VOL 30 (NO. 5), MAY 1974, P 161-166
23. J.E. LIPPOLD AND W.A. BAESLACK, *MET. CONSTR.*, VOL 20 (NO. L), 1988, P 21
24. H. HOFFMEISTER AND R. MUNDT, *ARCH. EISENHUTT.*, VOL 52 (NO. 4), P 159-164
25. D.N. NOBLE AND T.G. GOOCH, THE EFFECTS OF HEAT INPUT AND CHEMICAL COMPOSITION ON MICROSTRUCTURE IN ARC WELDED UNS S31803 TYPE DUPLEX STAINLESS STEELS, *ASM MATERIALS WEEK '87*, ASM INTERNATIONAL, OCT 1987
26. B. JOSEFSSON, J.-O. NILSSON, AND A. WILSON, PHASE TRANSFORMATION IN DUPLEX STEELS AND THE RELATION BETWEEN CONTINUOUS COOLING AND ISOTHERMAL HEAT TREATMENTS, *DUPLEX STAINLESS STEELS CONF. PROC.*, AMERICAN SOCIETY FOR METALS, 1983
27. L. ITRURGOYEN, J. ALCALA, AND M. ANGLADA, THE INFLUENCE OF AGEING AT 475 C ON THE FRACTURE RESISTANCE OF A DUPLEX STAINLESS STEEL, *CORROSION*, VOL 47 (NO. 8), SEPT 1991, P 757-764
28. "SANDVIK SAF 2507--A HIGH PERFORMANCE DUPLEX STAINLESS STEEL," SANDVIK STEEL TRADE LITERATURE, PAMPHLET S-1875-ENG, SEPT 1987

David N. Noble, ARCO Alaska, Inc.

Welding and Weldability

Duplex stainless steel weldability is generally good, although it are not as forgiving as austenitic stainless steels or as prone to degradation of properties as fully ferritic stainless steels. The current commercial grades are low in carbon (less than 0.03 wt%), thereby essentially eliminating the risk of sensitization and intergranular corrosion from carbide precipitation. The base material and filler metals also have low sulfur and phosphorus levels (less than 0.03 wt%), which in combination with the ferritic solidification reduce the likelihood of solidification cracking (hot cracking). Hydrogen cracking (cold cracking) resistance is also good due to the high hydrogen solubility in the austenite (Ref 29) and the high percentage of austenite in the matrix. Nevertheless, solidification cracking and hydrogen cracking can occur in duplex alloys, and some precautions are necessary.

Preheat is generally not recommended for DSS, but may sometimes be specified in low-nitrogen grades, because thick sections and low heat input welding processes may, in combination, develop highly ferritic heat-affected zones (Ref 30). For the more highly alloyed DSS, a preheat can be highly detrimental and reduce corrosion resistance and mechanical properties.

Postweld heat treatment (PWHT) is not commonly used except in autogenous welds or welds with a filler metal composition that exactly matches the base steel. Although not always necessary, particularly if a nickel-enriched filler metal is used, it is common to postweld heat treat DSS welded pipe after longitudinal seam welding. The PWHT will largely be for the purpose of restoring the correct phase balance and redissolving unwanted precipitates. Postweld heat treatment temperatures of about 1050 to 1100 °C (1920 to 2010 °F) are used, depending on grade, followed by the same heat treatment applied to the base material during solution annealing--usually water quenching (Ref 31). The heat treatments commonly used for structural steels (for example, 550 to 600 °C, or 1020 to 1110 °F) (Ref 32) are totally inappropriate for duplex alloys and should never be considered.

Interpass Temperature Control. The need for interpass temperature control depends on alloy grade and composition. The more highly alloyed grades should have tighter interpass control. For the Fe-22Cr-5.5Ni-3Mo-0.15N steels, interpass temperatures of 150 to 200 °C (300 to 390 °F) are typical, whereas for the Fe-25Cr-7Ni-3.5Mo-0.25N-(Cu-W) steels, temperatures as low as 70 °C (160 °F) have been recommended (Ref 33).

Welding practices employed for austenitic stainless steels (for example, cleanliness, use of a backing gas, avoidance of contamination with carbon steel, and so on) should also be adopted for DSS. The backing gas most commonly used is pure argon. However, the use of a backing gas without nitrogen can lead to nitrogen loss from the molten weld nugget (Ref 34) with probable loss in corrosion performance and toughness. Because of this, argon/nitrogen mixed gases for shielding and backing have been explored (Ref 35), and generally the corrosion resistance of welds produced with these gases has been superior to that of welds made with nitrogen-free gases. Pure nitrogen may also be used as a backing gas (Ref 2), but a concern exists that too much nitrogen may be picked up, thereby significantly affecting the phase balance locally by promoting the formation of austenite.

Open root gaps are commonly used in manual DSS welding to limit the extent of dilution from the base material, because extensive base metal dilution will negate the effect of the nickel over-alloying in the filler metal. To control the problems of too little austenite and intermetallic phase formation, associated with too-low and too-high heat inputs, respectively, DSS welding procedures typically specify a "window" of allowable heat inputs. For the highly alloyed and heat-sensitive super DSS, stringer beads are commonly specified, particularly in the hot pass (that is, weld pass immediately following the root), and in some cases in split hot passes (that is, two hot passes side by side). The technique of using a low heat input hot pass has led to the use of the term "cold" pass (Ref 33).

Welding procedure qualification generally follows the mechanical property test requirements of a major code, for example, ASME Section IX (Ref 36) or API 1104 (Ref 37). There are also several tests (specifically phase balance assessment, microstructural examination, and a pitting corrosion test) used for DSS weldment evaluation that are not typically employed for other stainless steels.

Phase-Balance Assessment. The phase balance test measures the amount of austenite and ferrite present in the microstructure and is similar to tests used to measure ferrite in austenitic weld metals. However, the testing requirements are usually more exhaustive for duplex alloys and will typically call for assessment of the ferrite content in the HAZ and weld metal. and possibly at several through-thickness locations (Ref 38). The amount of ferrite in a duplex structure can be specified and measured in two ways. Percentage ferrite is measured by manual point counting or image analysis. These methods measure the area fraction of ferrite and austenite exposed on the surface of a sample under examination. The values are reported as a volume fraction, thereby linking the surface area measurement on one plane to the overall volume fraction in the sample. Percentage ferrite requirements are typically 35 to 65% and are applied to weld metal and the HAZ.

The alternative method uses the ferromagnetic properties of the ferrite to measure its proportion in the matrix. The Ferrite Number (FN) system used for austenitic stainless steel weld metals (where the ferrite content is measured by attraction of a spring-loaded magnet) was not originally developed for high ferrite levels, such as those in duplex alloys, and was only calibrated to about 28 FN (Ref 39). Furthermore, the variations in iron content between the various duplex grades affected the magnetic attraction for a given phase balance (Ref 40). Because no reliable magnetic attraction system had been fully developed and proven at the time duplex alloys were seeing widespread industrial application, most specifications required ferrite percentage measurements. However, changes to the FN measuring system have now been made so that all ferrite levels in duplex alloys can be recorded, and the system has been shown to be more reliable. To achieve the extended range, counterweights were added to the spring-loaded magnet (Ref 40). Specification requirements for weld metals are typically 50 to 90 FN. A rule-of-thumb conversion from FN to percentage is:

$$0.70(\text{FN}) = \%\ \text{FERRITE} \qquad \textbf{(EQ 3)}$$

Measurement of ferrite content in DSS, however, is seldom currently performed with a magnetic measuring technique and is more commonly referred to in terms of percentage.

There are also some limitations to the application of the FN measuring system in certain regions of the weld. The measurement tool applies well to large areas of finely dispersed ferrite, such as in the weld metal, but it cannot accurately measure small areas that may have locally high ferrite levels (for example, the weld HAZ). It also may provide inaccurate readings in base material measurements due to the effect of magnet deflection toward the relatively coarse base material ferritic matrix.

Microstructural Examination. Optical microstructural examination is included to determine whether extensive phase precipitation has occurred (for example, σ-phase, carbides, nitrides, and so on), and specifications frequently call for the absence of any deleterious phases. However, the interpretation of DSS microstructures is so difficult that one cannot make a definitive assessment, especially without experience in studying similar structures. Detecting small proportions of precipitates by optical means is also relatively difficult.

Pitting Corrosion Test. The pitting corrosion test most commonly used for qualifying DSS is a modification of the ASTM G 48 Practice A ferric chloride test (Ref 41). Other tests are available (for example, potentiostatic critical pitting temperature tests in 3 or 15% NaCl, and others involving the use of CO_2), but the ASTM G 48 test has been shown to detect material with substandard properties and is preferred to most other common test techniques (Ref 42). The test solution is not representative of most service conditions in that it is highly acidic, oxidizing, and has a high chloride concentration, but the test is relatively easy to perform and can distinguish between good and bad welds. As used on DSS, the test involves the immersion of a welded coupon into a 10% $FeCl_3 \cdot 6H_2O$ solution for a duration of between 24 and 72 h at a temperature from 15 to 70 °C (60 to 160 °F), depending on material grade and specification requirements. Test assessment can be by direct weight loss, visual observation of pitting, weight loss per unit of exposed area, or corrosion rate. The procedure as laid out by ASTM was not designed for DSS weldment testing, and although it has been adapted in a number of ways, its interpretation still presents difficulties (Ref 43).

Filler Metal Requirements. For most DSS grades there are two types of filler metals:

- MATCHING COMPOSITION FILLER METALS
- FILLER METALS THAT ARE SLIGHTLY OVERALLOYED, PRINCIPALLY WITH RESPECT TO NICKEL

The matching filler metal is used where a PWHT is performed, whereas welds made with the filler metal enriched with nickel are used in the as-welded condition. The weld metal microstructure from a composition exactly matching that of the parent steel will contain a high ferrite content. The increase in nickel is made to improve the as-welded phase balance and increase austenite content. The ferrite content of a weld made with a nickel-enriched consumable would decrease significantly if it underwent a PWHT. It may suffer from slightly reduced weld metal strength and could also be more susceptible to σ phase formation during heat treatment (Ref 44). The nickel level in the enriched weld metal will be approximately 2.5 to 3.5% greater than in the base material (for example, for the Fe-22Cr-5.5Ni-3Mo-0.15N DSS base material containing 5.5% Ni, the filler metal will comprise 8.0 to 9.0% Ni, depending on consumable manufacturer and form). Nominal filler metal compositions for the Fe-22Cr-5.5Ni-3Mo-0.15N grade of DSS, proprietary names, and the American Welding Society classifications, where appropriate, are reported in Table 7.

TABLE 7 TYPICAL COMPOSITION OF SELECTED COMMERCIAL NICKEL-OVERALLOYED WELDING CONSUMABLES AND AWS SPECIFICATIONS FOR FE-22CR-5.5NI-3MO-0.15N DUPLEX STAINLESS STEEL

MANUFACTURER	TRADE NAME	COMPOSITION, %				
		C	Cr	Ni	Mo	N
COVERED ELECTRODES						
METRODE	SUPERMET 2205	0.02	25	9.5	3.5	0.17
SANDVIK	22.9.3.L	0.03	22	9.5	3.0	0.15
AVESTA	2205-PW	0.025	22	9.5	3.0	0.13
LINCOLN NORWELD	AROSTA 4462	0.025	22.0	9.0	3.0	0.14
THYSSEN	THERMANIT 22/09	<0.04	22.5	9.0	3.0	. . .
AWS A5.4	E2209	0.04(A)	21.0-24.0	8.0-10.0	2.5-4.0	0.08-0.20
BARE WIRE						
SANDVIK	22.8.3.L	<0.02	22.5	8.0	3.0	0.14
METRODE	ER329N	0.015	22.3	8.3	3.0	0.15
THYSSEN	22/09/SG	<0.025	23.0	9.0	3.0	. . .
LINCOLN NORWELD	LNT/LNM 4462	0.015	22.5	8.5	3.0	0.15
AWS A5.9(B)	ER 2209	0.04(A)	21.0-24.0	8.0-10.0	2.5-4.0	0.084-0.20

(A) MAXIMUM.

(B) PENDING

The higher alloy filler metals are sometimes used for welding a less alloyed base material (for example, a DSS filler metal with 25% Cr could be used for the root run in a Fe-22Cr-5.5Ni-3Mo-0.15N base metal). This is usually done to improve root weld metal corrosion resistance and thereby pass the qualification test requirements. In most cases, this does not lead to loss of mechanical properties; indeed, the more highly alloyed filler metal in the case above is likely to have greater strength.

To avoid all the requirements for weld metal phase balance and microstructural control necessary with duplex filler metals, nickel-base consumables (for example, AWS A 5.14 ERNi-CrMo-3) have been used. The yield strength, however, is slightly below that of the more highly alloyed grades, and the lack of nitrogen and the presence of niobium in the filler metal may contribute to unfavorable metallurgical reactions and the formation of intermetallic precipitates and areas of high ferrite content in the HAZ (Ref 45, 46).

Cracking Behavior. Duplex stainless steels can suffer from weld metal hydrogen cracking and solidification cracking (Ref 47, 48), but HAZ cracking has not been reported in practice and is considered highly unlikely to develop. Hydrogen cracking from welding and in-service hydrogen pickup has been observed (Ref 49). The duplex microstructure provides a combination of a ferritic matrix, where hydrogen diffusion can be fairly rapid, with intergranular and intragranular austenite, where the hydrogen diffusion is significantly slower, thereby acting as a barrier to hydrogen diffusion. The net effect appears to be that hydrogen can be "trapped" within ferrite grains by the surrounding austenite, particularly where it decorates the prior ferrite grain boundaries. Due to these characteristics, low-temperature hydrogen release treatments are not effective, and the hydrogen is likely to remain in the structure for a long period (Ref 49). Whether cracking actually develops will depend upon a number of factors, including the total amount of trapped hydrogen, the applied strain, and

the amount of ferrite and austenite in the structure. Weld metal hydrogen content from covered electrodes can be relatively high, and levels up to 25 ppm have been reported (Ref 50).

The problem of weld metal hydrogen cracking in practice must not be overstated. The reported incidences of hydrogen cracking in DSS have been restricted to cases in which the alloy has been heavily cold worked or weld metals have seen high levels of restraint or possessed very high ferrite contents in combination with very high hydrogen levels as a result of poor control of covered electrodes or the use of hydrogen-containing shielding gas. Indeed, other studies have shown how resistant DSS weld metals are to hydrogen cracking, even with consumables intentionally humidified (Ref 51), and that hydrogen-containing backing gases can be employed without producing cracking (Ref 2). There is no doubt an effect of hydrogen on the ductility of DSS, and to avoid fabrication-related cracking problems, high-hydrogen-potential welding processes, such as shielded metal arc welding, should be controlled by careful storage and use of electrodes, and by ensuring that the weld metal phase balance is within acceptable limits.

Solidification cracking in DSS has not been reported as a commercial problem, but it has been witnessed in laboratory-made high heat input submerged arc welds (Ref 48). Cracking occurs at the solidification grain boundaries and has the appearance of running through the austenite phase. This is due to the subsequent solid-state transformation that occurs, in which the austenite forms predominantly on the prior ferrite grain boundaries. The solidification cracking susceptibility is not great, however, and weldability cracking tests have shown that the performance of DSS is similar to that of austenitic stainless materials with approximately 3 to 5 FN (Ref 52). Resistance to HAZ liquation cracking is also reportedly similar to type 304 stainless steel (Ref 53) and unlikely to develop in practical welding situations.

Loss of Properties. The weld is usually the part of a system with reduced corrosion resistance and low-temperature toughness, and therefore in many cases it is the limiting factor in material application. Welding primarily affects pitting corrosion, stress corrosion, and Charpy toughness.

Pitting corrosion resistance can be affected by many features of the welding operation, including:

- LOCALIZED SEGREGATION OF ALLOYING ELEMENTS TO THE DIFFERENT CONSTITUENT PHASES IN THE MICROSTRUCTURE, PRODUCING AREAS LEAN IN MOLYBDENUM AND CHROMIUM
- INCORRECT FERRITE/AUSTENITE PHASE BALANCE
- FORMATION OF NITRIDES OR INTERMETALLIC PHASES
- LOSS OF NITROGEN FROM THE ROOT PASS
- PRESENCE OF AN OXIDIZED SURFACE ON THE UNDERSIDE OF THE ROOT BEAD

The extent to which the reduction occurs depends on which of these factors are active and to what degree. Partitioning of alloying elements between the austenite and ferrite occurs in the weld metal, with chromium, molybdenum, and silicon partitioning to the ferrite and carbon, nickel, and nitrogen to the austenite (Ref 19, 54). The effect is not so apparent in as-deposited weld metals, but it becomes more significant as a result of reheating a previously deposited weld pass. The effect is also exacerbated by higher welding heat inputs (Ref 4, 54).

Weld metal and HAZ microstructures with very high ferrite contents are also less resistant to pitting attack than am balanced structures. This is largely because predominantly ferritic structures are more prone to chromium nitride precipitation, which locally denudes the chromium concentration and lowers resistance to pitting attack.

Nitrogen loss in the root pass may reduce weld metal corrosion resistance. Up to 20% loss of nitrogen has been reported for gas-tungsten arc welds (Ref 34), and nitrogen-bearing backing gases have been explored and used in limited applications (Ref 35).

Cleanliness of the root side purge gas may also affect pitting resistance. Figure 12 shows the effect of reducing oxygen content in an otherwise pure argon purge gas and its beneficial effect on pitting resistance. Also shown is the apparent benefit of using a reducing gas (NH_{10}), which would significantly reduce the tendency for oxide formation and leave the underbead appearance very shiny (Ref 55).

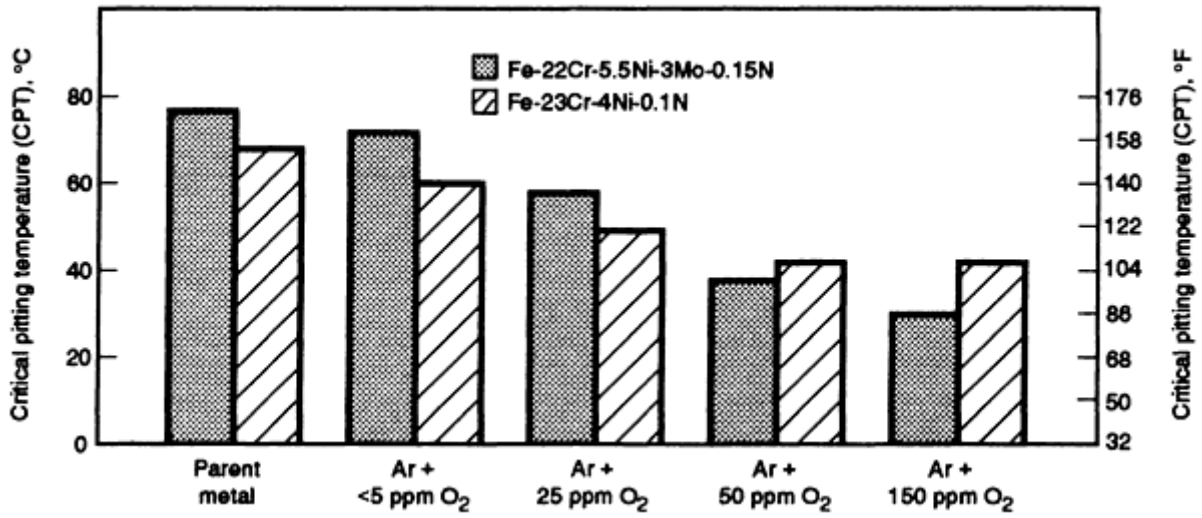

FIG. 12 PLOT OF PITTING TEMPERATURE VERSUS OXYGEN CONTENT OF BACKING GAS FOR FE-22CR-5.5NI-3MO-0.15N AND FE-23CR-4NI-0.1N DUPLEX STAINLESS STEELS TESTED IN 3% NACL AND 0.1% NACI SOLUTIONS, RESPECTIVELY, BOTH AT ANODIC POTENTIAL OF + 300 MV. SOURCE: REF 55

The net effect on pitting corrosion resistance may be observed by applying the ASTM G 48 pitting corrosion test to welds and base material with the same PRE value, then assessing the reduction in critical pitting temperature (that is, the temperature at which pitting in the ferric chloride solution is first observed). The difference is approximately 20 °C (35 °F), as reported in Fig. 13, thereby quantifying the effect of reduced weld metal properties. Figure 13 also shows that the use of a super DSS filler metal with a PRE value of about 40 on a Fe-22Cr-5.5Ni-3Mo-0.15N parent steel (which typically has a PRE value of about 33 to 35) will improve the weld metal pitting corrosion resistance, as assessed by the ASTM G 48 test, to approximately match that of the base material.

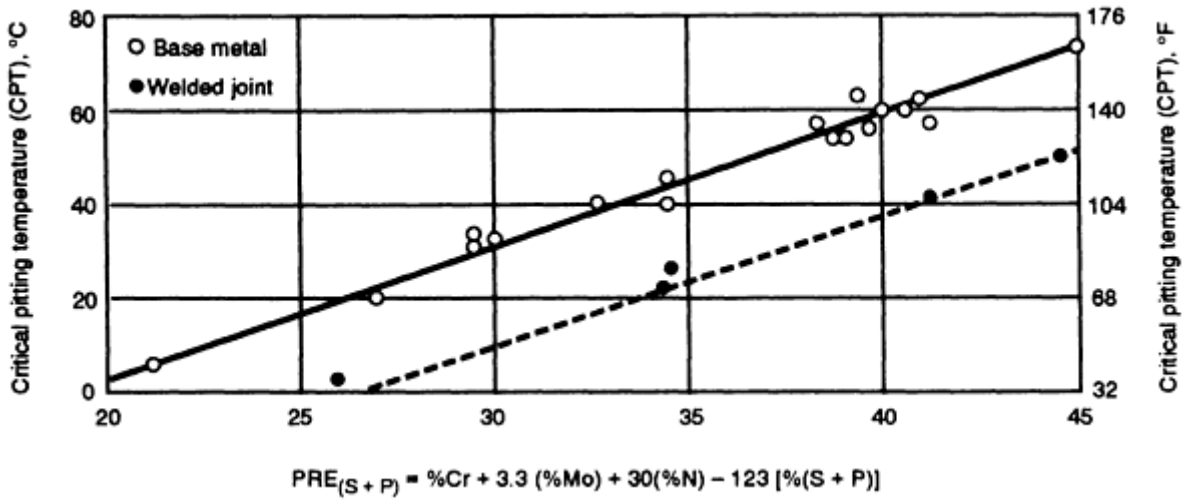

FIG. 13 PITTING CORROSION RESISTANCE OF BASE METAL RELATIVE TO WELD METAL PLACED IN 6 WT% $FECI_3$ SOLUTION FOR 24 H DURATION PER ASTM 6 48 (METHOD A). SOURCE: REF 11

Resistance to CI SCC does not appear to be affected significantly by welding per se (Ref 56). Nevertheless, welds are likely regions of attack for CI SCC due to the presence of high stresses and the structural inhomogeneity present at the weld. If localized pitting is a necessary precursor for CI SCC, the effects described above will also ultimately affect Cl SCC resistance.

There are three main causes of poor weld metal toughness:

- VERY HIGH FERRITE CONTENT
- PRESENCE OF INTERMETALLIC PHASES OR NITRIDES
- HIGH WELD METAL OXYGEN CONCENTRATION

Predominantly ferritic microstructures with a coarse grain size, as may be developed in a weld HAZ, have poor low-temperature notch toughness. Their performance is similar to that of ferritic stainless steels, and they may undergo low energy cleavage fracture. The Fe-25Cr-5Ni-2.5Mo-0.17N-Cu and super DSS are more susceptible to embrittlement through intermetallic phase precipitation, due to their increased kinetics of formation (Ref 57), and heat input and interpass temperature control are advised. Welding processes that produce high weld metal oxygen contents also produce welds with lower toughness, mainly due to the size and distribution of nonmetallic inclusions. Gas-shielded processes have the least oxygen potential and generally exhibit superior Charpy toughness properties (Fig. 14).

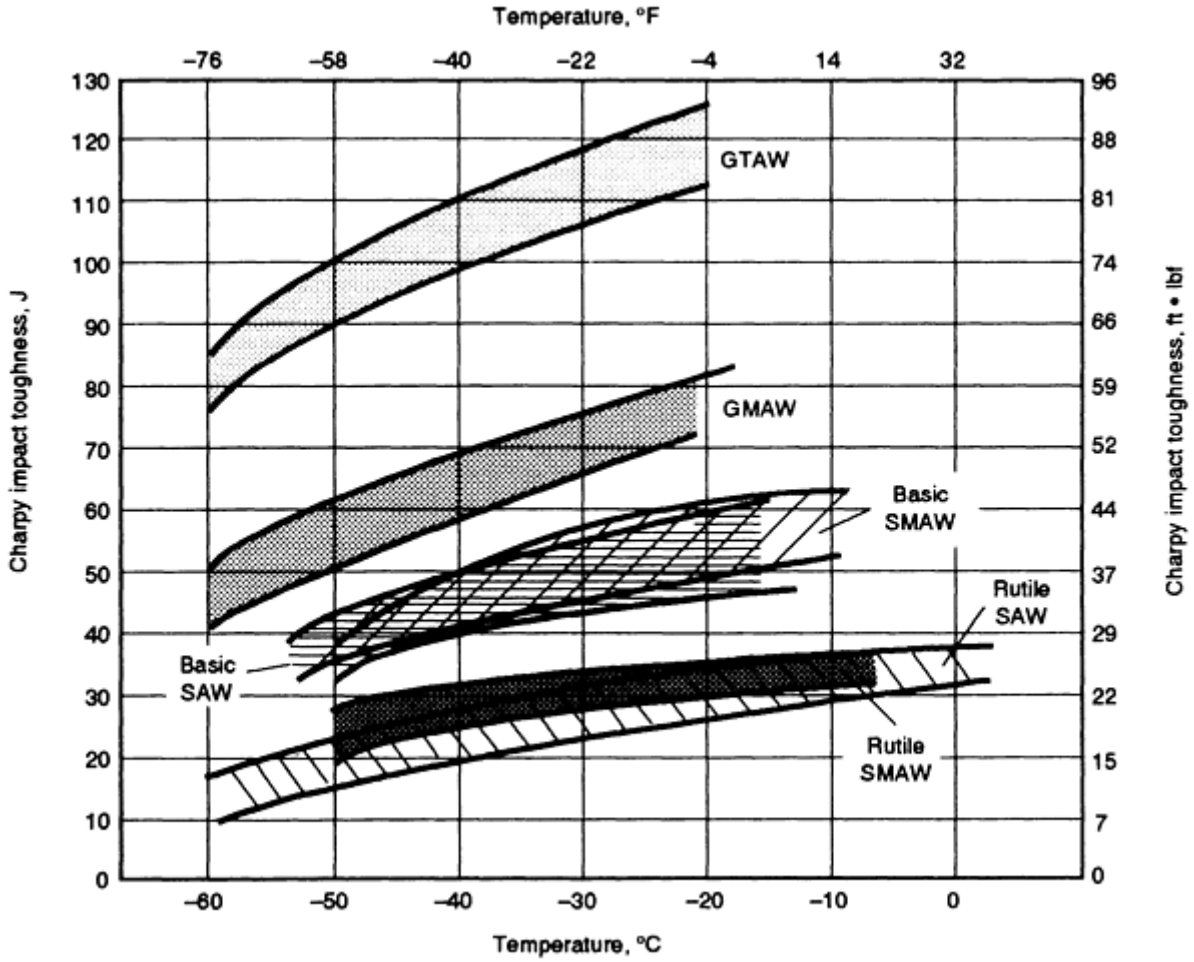

FIG. 14 PLOT OF CHARPY V-NOTCH TOUGHNESS VERSUS TEMPERATURE AS A FUNCTION OF WELDING PROCESS FOR UNS S32760 ALLOY. THE TERMS "BASIC" AND "RUTILE" REFER TO LIME-BASED AND TITANIA-BASED ELECTRODE COATINGS USED WITH SAW AND SMAW. SOURCE: REF 58

References cited in this section

2. B. LARSSON AND B. LUNDQVIST, FABRICATING FERRITIC-AUSTENITIC STAINLESS STEELS, SANDVIK STEEL TRADE LITERATURE, PAMPHLET S-51-33-ENG, OCT 1987
4. L. VAN NASSAU, H. MEELKER, AND J. HILKES, WELDING DUPLEX AND SUPER-DUPLEX

STAINLESS STEELS--A GUIDE FOR INDUSTRY, DOCUMENT 01463, LINCOLN NORWELD, JULY 1992

11. R. DOLLING, V. NEUBERT, AND P. KNOLL, THE CORROSION BEHAVIOUR OF SUPER DUPLEX STEEL CAST ALLOYS WITH A PREN>41, *DUPLEX STAINLESS STEELS CONF. PROC.,* VOL 2, LES EDITIONS DE PHYSIQUE, LES ULIS CEDEX, FRANCE, OCT 1991, P 1341-1351
19. T. OGAWA AND T. KOSEKI, EFFECT OF COMPOSITION PROFILES ON METALLURGY AND CORROSION BEHAVIOUR OF DUPLEX STAINLESS STEEL WELD METALS, *WELD. J.,* VOL 88 (NO. 5), MAY 1989, P 181S-191S
29. F.R. COE, *WELDING STEELS WITHOUT HYDROGEN CRACKING,* TWI PUBLICATIONS, 1978
30. "HOW TO WELD 2205," AVESTA WELDING TRADE LITERATURE
31. "SEAMLESS AND WELDED FERRITIC/AUSTENITIC STAINLESS STEEL PIPE," ASTM A 790-91
32. "CHEMICAL PLANT AND PETROLEUM REFINERY PIPING," ASME CODE B31.3, P 66-67
33. A.W. STEPHENSON, P.C. GOUGH, AND J.C.M. FARRAR, "THE WELDABILITY OF SUPER DUPLEX ALLOYS--WELDING CONSUMABLES AND PROCEDURE DEVELOPMENT FOR ZERON 100, *PROC. LNT. INST. WELDING ANNUAL ASSEMBLY CONFERENCE,* JULY 1991
34. T.G. GOOCH, CORROSION RESISTANCE OF WELDS IN DUPLEX STAINLESS STEELS, *DUPLEX STAINLESS STEELS CONF. PROC.,* AMERICAN SOCIETY FOR METALS, 1983, P 325-346
35. O. JONSSON, M. LILJAS, AND P. STENVALL, THE ROLE OF NITROGEN IN LONGITUDINAL WELDING OF TUBING IN DUPLEX STAINLESS STEELS, *DUPLEX STAINLESS STEELS CONF. PROC.,* AMERICAN SOCIETY FOR METALS, 1983, P 461-468
36. "WELDING AND BRAZING QUALIFICATIONS," ASME 1989 BOILER AND PRESSURE VESSEL CODE SECTION IX
37. "WELDING OF PIPELINES AND RELATED FACILITIES," STANDARD 1104, AMERICAN PETROLEUM INSTITUTE
38. "SPECIFICATION FOR CRA LINEPIPE," STANDARD 5LC, AMERICAN PETROLEUM INSTITUTE
39. "STANDARD PROCEDURES FOR CALIBRATING MAGNETIC INSTRUMENTS TO MEASURE THE DELTA FERRITE CONTENT OF AUSTENITIC STAINLESS STEEL WELD METALS," AWS A4.2-74, AMERICAN WELDING SOCIETY
40. D.J. KOTECKI, EXTENSION OF THE WRC FERRITE NUMBER SYSTEM, *WELD. J.,* NOV 1982, P 352S-361S
41. "TESTING FOR PITTING AND CREVICE CORROSION RESISTANCE OF STAINLESS STEELS AND RELATED ALLOYS BY THE USE OF FERRIC CHLORIDE SOLUTION," G 48 PRACTICE A, ASTM
42. R.M. DAVISON AND J.D. REDMOND, DEVELOPMENT OF QUALIFICATION TESTS FOR DUPLEX STAINLESS STEEL MILL PRODUCTS, PAPER 302, *CORROSION '91,* NATIONAL ASSOCIATION OF CORROSION ENGINEERS, 1991
43. R.A. CORBETT, PROBLEMS IN UTILIZING ASTM G 48 TO EVALUATE HIGH ALLOY STAINLESS STEELS, PAPER 298, *CORROSION '92,* NATIONAL ASSOCIATION OF CORROSION ENGINEERS, 1992
44. D.J. KOTECKI, HEAT TREATMENT OF DUPLEX STAINLESS STEEL WELD METALS, *WELD. J.,* NOV 1989, P 431S-441S
45. L. ODEGARG AND S.-A. FAGER, CHOICE OF RIGHT FILLER METAL FOR JOINING SANDVIK SAF 2507 TO A SUPER AUSTENITIC STAINLESS 6 MO STEEL, *ASM MATERIALS WEEK '87,* ASM INTERNATIONAL, OCT 1987, P 441-449
46. R.N. GUNN, THE INFLUENCE OF COMPOSITION AND MICROSTRUCTURE ON THE CORROSION BEHAVIOUR OF COMMERCIAL DUPLEX ALLOYS, *RECENT DEVELOPMENTS IN THE JOINING OF STAINLESS STEELS AND HIGH ALLOYS,* EDISON WELDING INSTITUTE, COLUMBUS, OHIO, OCT 1992
47. G.A. CLARK AND P. GUHA, *BR. WELD. J.,* VOL 13 (NO. 5), MAY 1981, P 269-273

48. J. HONEYCOMBE AND T.G. GOOCH, *WELD. J.,* VOL 56 (NO. 11), NOV 1977, P 339S-353S
49. P. SENTANCE, THE BRAE FIELD, *STAINL. STEEL EUR.,* VOL 4 (NO. 20), SEPT 1992, P 38-41
50. C.D. LUNDIN, K. KIKUCHI, AND K.K. KAHN, PHASE 1 REPORT; "MEASUREMENT OF DIFFUSIBLE HYDROGEN CONTENT AND HYDROGEN EFFECTS ON THE CRACKING POTENTIAL OF DUPLEX STAINLESS STEEL WELDMENTS," THE WELDING RESEARCH COUNCIL, MARCH 1991
51. R.A. WALKER AND T.G. GOOCH, HYDROGEN CRACKING OF WELDS IN DUPLEX STAINLESS STEEL, *CORROSION,* VOL 47 (NO. 8), SEPT 1991, P 1053-1063
52. I. VAROL, W.A. BAESLACK, AND J.C. LIPPOLD, *METALLOGRAPHY,* VOL 23 (NO. 1), 1989
53. J.C. LIPPOLD, W.A. BAESLACK, AND I. VAROL, WELDING OF DUPLEX STAINLESS STEELS, *WELD. J.,* IN PRESS
54. R.A. WALKER AND T.G. GOOCH, PITTING RESISTANCE OF WELD METAL FOR 22CR-5NI FERRITIC-AUSTENITIC STAINLESS STEEL, *BR. CORROS. J.,* VOL 26 (NO. 1), 1991, P 51-59
55. L. ODEGARD AND S.-A. FAGER, THE ROOT SIDE PITTING CORROSION RESISTANCE OF STAINLESS STEEL WELDS, *SANDVIK STEEL WELD. REP.,* NO. 1, 1990
56. T.G. GOOCH, *WELDING IN THE WORLD,* VOL 24 (NO. 7/8), 1986, P 148-167
57. J. CHARLES, SUPER DUPLEX STAINLESS STEEL: STRUCTURE AND PROPERTIES, *DUPLEX STAINLESS STEELS CONF. PROC.,* AMERICAN SOCIETY FOR METALS, 1983, P 151-168
58. P.C. GOUGH AND J.C.M. FARRAR, FACTORS AFFECTING WELD ROOT RUN CORROSION PERFORMANCE IN DUPLEX AND SUPER DUPLEX PIPEWORK, *ASM MATERIALS WEEK '87,* ASM INTERNATIONAL, OCT 1987, P 1009-1025

Selection of Wrought Duplex Stainless Steels

David N. Noble, ARCO Alaska, Inc.

Applicable Welding Processes

Fusion Welding. Nearly all of the arc welding processes that are employed for other stainless steels can be used with duplex alloys, except where the process characteristic is to weld autogenously, such as electron-beam welding and laser-beam welding. In such circumstances a PWHT is nearly always necessary to restore the correct phase balance to the weld metal and remove any undesirable precipitates. There are few reported differences in corrosion resistance between welding processes, but the nonmetallic inclusion distribution would be anticipated to have an effect. In most instances of pipe welding, where access is from one side only, gastungsten arc welding is almost exclusively employed for the root pass (Ref 22). This provides a controllable, high-quality root bead that dictates the final corrosion performance of the weld. The inert gas on the backside of the weld can also be more closely controlled with this process. Aside from this preference, process selection will probably be dictated more by the availability of consumable form and economic and logistic considerations than by desired properties for the particular welding process. Welds in DSS have been made by all the major fusion welding processes and have performed satisfactorily. However, in a very few cases, the final application may necessitate the stipulation of a particular welding process. Where exceptional low-temperature toughness is required, gasshielded processes may be specified because they produce higher weld metal toughness properties than flux-shielded processes (Fig. 14). Some consumable forms have not yet been fully developed for all grades of DSS. Nevertheless, gas-tungsten arc welding, shielded metal arc welding, submerged arc welding, flux-cored arc welding, and gas-metal arc welding are commonly used with success for most alloy classes.

Additional information is available in the article "Welding of Stainless Steels" in this Volume.

Solid-State Welding Processes. Few studies have been made of the solid-state welding characteristics of DSS. Explosive welding has been applied to overlaying of tube sheets and similar items (Ref 2). Corrosion and mechanical properties are presumed to be similar to parent material. Friction welding of DSS has shown that the corrosion resistance of a friction weld zone can be significantly better than that of a corresponding arc weld in the same material (Ref 34). This is attributed to the absence of fusion and the related effects that can result (that is, segregation and nitrogen loss).

The bond line will, however, experience high temperatures, and some degree of transformation of the austenite to ferrite would be anticipated. Very rapid cooling will then probably suppress reformation of austenite, and a structure high in ferrite could result. There is ongoing effort to establish whether solid-state welding processes offer significant advantages over fusion processes. The lack of a fused zone is potentially attractive to the welding of alloys that are prone to localized segregation effects.

References cited in this section

2. B. LARSSON AND B. LUNDQVIST, FABRICATING FERRITIC-AUSTENITIC STAINLESS STEELS, SANDVIK STEEL TRADE LITERATURE, PAMPHLET S-51-33-ENG, OCT 1987
22. J. HARSTON, E. HUTCHINS, AND S. SWEENEY, THE DEVELOPMENT AND CONSTRUCTION OF DUPLEX STAINLESS STEEL PIPELINES FOR USE OFFSHORE IN THE SOUTHERN NORTH SEA, *PROC. 3RD LNT. CONF. WELDING AND PERFORMANCE OF PIPELINES,* THE WELDING INSTITUTE, 1986
34. T.G. GOOCH, CORROSION RESISTANCE OF WELDS IN DUPLEX STAINLESS STEELS, *DUPLEX STAINLESS STEELS CONF. PROC.,* AMERICAN SOCIETY FOR METALS, 1983, P 325-346

Selection of Wrought Duplex Stainless Steels

David N. Noble, ARCO Alaska, Inc.

References

1. H.D. SOLOMON AND T.M. DEVINE, JR., DUPLEX STAINLESS STEELS--A TALE OF TWO PHASES, *DUPLEX STAINLESS STEELS CONF. PROC.,* AMERICAN SOCIETY FOR METALS, 1983
2. B. LARSSON AND B. LUNDQVIST, FABRICATING FERRITIC-AUSTENITIC STAINLESS STEELS, SANDVIK STEEL TRADE LITERATURE, PAMPHLET S-51-33-ENG, OCT 1987
3. S. BERNHARDSSON, THE CORROSION RESISTANCE OF DUPLEX STAINLESS STEELS, *DUPLEX STAINLESS STEELS CONF. PROC.,* LES EDITIONS DE PHYSIQUE, LES ULIS CEDEX, FRANCE, OCT 1991, P 185-210
4. L. VAN NASSAU, H. MEELKER, AND J. HILKES, WELDING DUPLEX AND SUPER-DUPLEX STAINLESS STEELS--A GUIDE FOR INDUSTRY, DOCUMENT 01463, LINCOLN NORWELD, JULY 1992
5. T.G. GOOCH, WELDABILITY OF DUPLEX FERRITIC-AUSTENITIC STAINLESS STEELS, *DUPLEX STAINLESS STEELS CONF. PROC.,* AMERICAN SOCIETY FOR METALS, 1983, P 573-602
6. J. CHARLES, SUPER DUPLEX STAINLESS STEEL: STRUCTURE AND PROPERTIES, *DUPLEX STAINLESS STEELS CONF. PROC.,* VOL 1, LES EDITIONS DE PHYSIQUE, LES ULIS CEDEX, FRANCE, OCT 1991, P 3-48
7. R. CASTRO AND J.J. DE CADENET, *WELDING METALLURGY OF STAINLESS AND HEAT-RESISTING STEELS,* CAMBRIDGE UNIVERSITY PRESS, 1974
8. D.J. KOTECKI AND T.A. SIEWERT, WRC-1992 CONSTITUTIONAL DIAGRAM FOR STAINLESS STEEL WELD METALS: A MODIFICATION OF THE WRC 1988 DIAGRAM, *WELD. J.,* MAY 1992, P 171S-178S
9. R.J. BRIGHAM AND E.W. TOZER, EFFECT OF ALLOYING ADDITIONS ON THE PITTING RESISTANCE OF 18% CR AUSTENITIC STAINLESS STEEL, *CORROSION,* VOL 30 (NO. 5), MAY 1974, P 161-166
10. N. SUUTALA AND M. KURKELA, *STAINLESS STEELS CONF. PROC.,* THE INSTITUTE OF METALS, 1985, P 240-247
11. R. DOLLING, V. NEUBERT, AND P. KNOLL, THE CORROSION BEHAVIOUR OF SUPER DUPLEX

STEEL CAST ALLOYS WITH A PREN>41, *DUPLEX STAINLESS STEELS CONF. PROC.,* VOL 2, LES EDITIONS DE PHYSIQUE, LES ULIS CEDEX, FRANCE, OCT 1991, P 1341-1351

12. H. ERIKSSON AND S. BERNHARDSSON, THE APPLICABILITY OF DUPLEX STAINLESS STEELS IN SOUR ENVIRONMENTS, *CORROSION,* VOL 47 (NO. 8), SEPT 1991, P 719-727
13. A. MLYASAKA AND H. OGAWA, CRITICAL STRESS FOR SCC OF CORROSION RESISTANT ALLOY IN SOUR ENVIRONMENTS, PAPER 5, *CORROSION '89,* NATIONAL ASSOCIATION OF CORROSION ENGINEERS, 1989
14. S. BERNHARDSSON, THE CORROSION RESISTANCE OF DUPLEX STAINLESS STEELS, *DUPLEX STAINLESS STEELS CONF. PROC.,* AMERICAN SOCIETY FOR METALS, 1983, P 185-210
15. S. AZUMA, H. TSUGE, T. KUDO, AND T. MOROISHI, CREVICE CORROSION OF DUPLEX STAINLESS STEELS IN SIMULATED SOUR GAS ENVIRONMENTS, PAPER 306, *CORROSION '87,* NATIONAL ASSOCIATION OF CORROSION ENGINEERS, 1987
16. "SULFIDE STRESS CRACKING RESISTANT METALLIC MATERIALS FOR OILFIELD EQUIPMENT," MR-01-75-93, NATIONAL ASSOCIATION OF CORROSION ENGINEERS
17. L. SMITH, CORROSION RESISTANT ALLOYS OFFER PIPELINE ALTERNATIVES, *STAINL. STEEL EUR.,* JAN/FEB 1993, P 32-42
18. M.J. SCHOFIELD, AND R.D. KANE, DEFINING SAFE USE LIMITS FOR DUPLEX STAINLESS STEELS, *DUPLEX STAINLESS STEEL CONF. PROC.,* LES EDITIONS DE PHYSIQUE, LES ULIS CEDEX, FRANCE, OCT 1991, P 241-255
19. T. OGAWA AND T. KOSEKI, EFFECT OF COMPOSITION PROFILES ON METALLURGY AND CORROSION BEHAVIOUR OF DUPLEX STAINLESS STEEL WELD METALS, *WELD. J.,* VOL 88 (NO. 5), MAY 1989, P 181S-191S
20. D. FRUYTIER, INDUSTRIAL EXPERIENCES WITH DUPLEX STAINLESS STEEL, *STAINL. STEEL EUR.,* VOL 3 (NO. 13), DEC 1991
21. B. WALLEN AND S. HENRIKSON, EFFECT OF CHLORINATION ON STAINLESS STEELS IN SEAWATER, PAPER 403, *CORROSION '86,* NATIONAL ASSOCIATION OF CORROSION ENGINEERS, 1986
22. J. HARSTON, E. HUTCHINS, AND S. SWEENEY, THE DEVELOPMENT AND CONSTRUCTION OF DUPLEX STAINLESS STEEL PIPELINES FOR USE OFFSHORE IN THE SOUTHERN NORTH SEA, *PROC. 3RD LNT. CONF. WELDING AND PERFORMANCE OF PIPELINES,* THE WELDING INSTITUTE, 1986
23. J.E. LIPPOLD AND W.A. BAESLACK, *MET. CONSTR.,* VOL 20 (NO. L), 1988, P 21
24. H. HOFFMEISTER AND R. MUNDT, *ARCH. EISENHUTT.,* VOL 52 (NO. 4), P 159-164
25. D.N. NOBLE AND T.G. GOOCH, THE EFFECTS OF HEAT INPUT AND CHEMICAL COMPOSITION ON MICROSTRUCTURE IN ARC WELDED UNS S31803 TYPE DUPLEX STAINLESS STEELS, *ASM MATERIALS WEEK '87,* ASM INTERNATIONAL, OCT 1987
26. B. JOSEFSSON, J.-O. NILSSON, AND A. WILSON, PHASE TRANSFORMATION IN DUPLEX STEELS AND THE RELATION BETWEEN CONTINUOUS COOLING AND ISOTHERMAL HEAT TREATMENTS, *DUPLEX STAINLESS STEELS CONF. PROC.,* AMERICAN SOCIETY FOR METALS, 1983
27. L. ITRURGOYEN, J. ALCALA, AND M. ANGLADA, THE INFLUENCE OF AGEING AT 475 C ON THE FRACTURE RESISTANCE OF A DUPLEX STAINLESS STEEL, *CORROSION,* VOL 47 (NO. 8), SEPT 1991, P 757-764
28. "SANDVIK SAF 2507--A HIGH PERFORMANCE DUPLEX STAINLESS STEEL," SANDVIK STEEL TRADE LITERATURE, PAMPHLET S-1875-ENG, SEPT 1987
29. F.R. COE, *WELDING STEELS WITHOUT HYDROGEN CRACKING,* TWI PUBLICATIONS, 1978
30. "HOW TO WELD 2205," AVESTA WELDING TRADE LITERATURE
31. "SEAMLESS AND WELDED FERRITIC/AUSTENITIC STAINLESS STEEL PIPE," ASTM A 790-91
32. "CHEMICAL PLANT AND PETROLEUM REFINERY PIPING," ASME CODE B31.3, P 66-67

33. A.W. STEPHENSON, P.C. GOUGH, AND J.C.M. FARRAR, "THE WELDABILITY OF SUPER DUPLEX ALLOYS--WELDING CONSUMABLES AND PROCEDURE DEVELOPMENT FOR ZERON 100, *PROC. LNT. INST. WELDING ANNUAL ASSEMBLY CONFERENCE,* JULY 1991
34. T.G. GOOCH, CORROSION RESISTANCE OF WELDS IN DUPLEX STAINLESS STEELS, *DUPLEX STAINLESS STEELS CONF. PROC.,* AMERICAN SOCIETY FOR METALS, 1983, P 325-346
35. O. JONSSON, M. LILJAS, AND P. STENVALL, THE ROLE OF NITROGEN IN LONGITUDINAL WELDING OF TUBING IN DUPLEX STAINLESS STEELS, *DUPLEX STAINLESS STEELS CONF. PROC.,* AMERICAN SOCIETY FOR METALS, 1983, P 461-468
36. "WELDING AND BRAZING QUALIFICATIONS," ASME 1989 BOILER AND PRESSURE VESSEL CODE SECTION IX
37. "WELDING OF PIPELINES AND RELATED FACILITIES," STANDARD 1104, AMERICAN PETROLEUM INSTITUTE
38. "SPECIFICATION FOR CRA LINEPIPE," STANDARD 5LC, AMERICAN PETROLEUM INSTITUTE
39. "STANDARD PROCEDURES FOR CALIBRATING MAGNETIC INSTRUMENTS TO MEASURE THE DELTA FERRITE CONTENT OF AUSTENITIC STAINLESS STEEL WELD METALS," AWS A4.2-74, AMERICAN WELDING SOCIETY
40. D.J. KOTECKI, EXTENSION OF THE WRC FERRITE NUMBER SYSTEM, *WELD. J.,* NOV 1982, P 352S-361S
41. "TESTING FOR PITTING AND CREVICE CORROSION RESISTANCE OF STAINLESS STEELS AND RELATED ALLOYS BY THE USE OF FERRIC CHLORIDE SOLUTION," G 48 PRACTICE A, ASTM
42. R.M. DAVISON AND J.D. REDMOND, DEVELOPMENT OF QUALIFICATION TESTS FOR DUPLEX STAINLESS STEEL MILL PRODUCTS, PAPER 302, *CORROSION '91,* NATIONAL ASSOCIATION OF CORROSION ENGINEERS, 1991
43. R.A. CORBETT, PROBLEMS IN UTILIZING ASTM G 48 TO EVALUATE HIGH ALLOY STAINLESS STEELS, PAPER 298, *CORROSION '92,* NATIONAL ASSOCIATION OF CORROSION ENGINEERS, 1992
44. D.J. KOTECKI, HEAT TREATMENT OF DUPLEX STAINLESS STEEL WELD METALS, *WELD. J.,* NOV 1989, P 431S-441S
45. L. ODEGARG AND S.-A. FAGER, CHOICE OF RIGHT FILLER METAL FOR JOINING SANDVIK SAF 2507 TO A SUPER AUSTENITIC STAINLESS 6 MO STEEL, *ASM MATERIALS WEEK '87,* ASM INTERNATIONAL, OCT 1987, P 441-449
46. R.N. GUNN, THE INFLUENCE OF COMPOSITION AND MICROSTRUCTURE ON THE CORROSION BEHAVIOUR OF COMMERCIAL DUPLEX ALLOYS, *RECENT DEVELOPMENTS IN THE JOINING OF STAINLESS STEELS AND HIGH ALLOYS,* EDISON WELDING INSTITUTE, COLUMBUS, OHIO, OCT 1992
47. G.A. CLARK AND P. GUHA, *BR. WELD. J.,* VOL 13 (NO. 5), MAY 1981, P 269-273
48. J. HONEYCOMBE AND T.G. GOOCH, *WELD. J.,* VOL 56 (NO. 11), NOV 1977, P 339S-353S
49. P. SENTANCE, THE BRAE FIELD, *STAINL. STEEL EUR.,* VOL 4 (NO. 20), SEPT 1992, P 38-41
50. C.D. LUNDIN, K. KIKUCHI, AND K.K. KAHN, PHASE 1 REPORT; "MEASUREMENT OF DIFFUSIBLE HYDROGEN CONTENT AND HYDROGEN EFFECTS ON THE CRACKING POTENTIAL OF DUPLEX STAINLESS STEEL WELDMENTS," THE WELDING RESEARCH COUNCIL, MARCH 1991
51. R.A. WALKER AND T.G. GOOCH, HYDROGEN CRACKING OF WELDS IN DUPLEX STAINLESS STEEL, *CORROSION,* VOL 47 (NO. 8), SEPT 1991, P 1053-1063
52. I. VAROL, W.A. BAESLACK, AND J.C. LIPPOLD, *METALLOGRAPHY,* VOL 23 (NO. 1), 1989
53. J.C. LIPPOLD, W.A. BAESLACK, AND I. VAROL, WELDING OF DUPLEX STAINLESS STEELS, *WELD. J.,* IN PRESS
54. R.A. WALKER AND T.G. GOOCH, PITTING RESISTANCE OF WELD METAL FOR 22CR-5NI FERRITIC-AUSTENITIC STAINLESS STEEL, *BR. CORROS. J.,* VOL 26 (NO. 1), 1991, P 51-59

55. L. ODEGARD AND S.-A. FAGER, THE ROOT SIDE PITTING CORROSION RESISTANCE OF STAINLESS STEEL WELDS, *SANDVIK STEEL WELD. REP.*, NO. 1, 1990

56. T.G. GOOCH, *WELDING IN THE WORLD*, VOL 24 (NO. 7/8), 1986, P 148-167

57. J. CHARLES, SUPER DUPLEX STAINLESS STEEL: STRUCTURE AND PROPERTIES, *DUPLEX STAINLESS STEELS CONF. PROC.*, AMERICAN SOCIETY FOR METALS, 1983, P 151-168

58. P.C. GOUGH AND J.C.M. FARRAR, FACTORS AFFECTING WELD ROOT RUN CORROSION PERFORMANCE IN DUPLEX AND SUPER DUPLEX PIPEWORK, *ASM MATERIALS WEEK '87*, ASM INTERNATIONAL, OCT 1987, P 1009-1025

Selection of Wrought Precipitation-Hardening Stainless Steels

B. Pollard

Introduction

PRECIPITATION-HARDENING (PH) STAINLESS STEELS are iron-chromium-nickel alloys with corrosion resistance superior to that of the hardenable 400 series stainless steels and yield strengths of 585 to 1795 MPa (85 to 260 ksi). These high strengths are obtained by precipitation hardening a martensitic or austenitic matrix with one or more of the following elements: copper, aluminum, titanium, niobium (columbium), and molybdenum. Precipitation-hardening steels can be grouped into three types--martensitic, semiaustenitic, and austenitic--based on their martensite start and finish (M_s and M_f) temperatures and resultant behavior upon cooling from a suitable solution treatment temperature.

The martensitic PH steels, such as 17-4PH, have M_f temperatures just above room temperature so that they transform completely to martensite upon air cooling from the solution treatment temperature and thus are martensitic in the annealed condition. Hardening is accomplished by a single aging treatment of 1 to 4 h at 480 to 620 °C (900 to 1150 °F).

The semiaustenitic PH steels, such as 17-7PH, have compositions that are balanced so that their M_s temperatures are well below room temperature. Therefore, they are predominantly austenitic upon cooling from the solution treatment temperature and are highly ductile and readily formed in that condition. After forming, transformation to martensite is accomplished by a conditioning treatment, which raises their M_s and M_f temperatures by precipitating carbon and alloying elements from solution. If a low conditioning temperature is used (730 to 760 °C, or 1350 to 1400 °F), the M_f temperature is raised to the vicinity of room temperature and transformation to martensite is complete upon cooling. If a high conditioning temperature (930 to 955 °C, or 1710 to 1750 °F) is used, less carbon is precipitated, the M_f temperature remains below zero, and refrigeration is required to accomplish transformation to martensite. However, since the martensite produced in this manner contains more carbon, it is of higher strength than that produced by transformation at lower temperatures. Transformation may also be accomplished by cold working. In all cases, the martensite structure is then hardened by aging at a temperature in the range of 455 to 565 °C (850 to 1050 °F) for 1 to 3 h.

The austenitic PH steels, such as A-286, have M_s temperatures so low that they cannot be transformed to martensite. Strengthening is obtained by the precipitation of intermetallic compounds in an austenitic matrix.

The chemical compositions of the PH steels presently produced in North America are presented in Table 1. A detailed treatment of aging in PH stainless steels is beyond the scope of this article because many different precipitation hardening phases are involved. Table 2, which was compiled from Ref 1, 2, 3, 4, 5, 6, 7, 8, 9, 10, 11, 12, 13, 14, and 15, lists the phases produced in martensitic, semiaustenitic, and austenitic PH grades. However, certain aging characteristics are common to most PH stainless steels. For martensitic and semiaustenitic types, maximum strengthening is obtained by aging at 455 to 510 °C (850 to 950 °F). Higher temperatures increase ductility and toughness but reduce both the maximum strength level and the time required to attain it. Typical aging curves for selected martensitic and semiaustenitic PH steels aged at 480 °C (900 °F) and 510 °C (950 °F) are shown in Fig. 1(a) and 1(b), respectively (Ref 16 17, 18, 19, 20).

TABLE 1 COMPOSITIONS OF PRECIPITATION-HARDENING STAINLESS STEELS

ALLOY	UNS NO.	COMPOSITION, %[(A)]								
		C	Mn	Si	Cr	Ni	Mo	P	S	OTHER
MARTENSITIC TYPES										
PH13-8 MO	S13800	0.05	0.10	0.10	12.25-13.25	7.5-8.5	2.0-2.5	0.01	0.008	0.90-1.35 AL; 0.01 N
15-5PH	S15500	0.07	1.00	1.00	14.0-15.5	3.5-5.5	. . .	0.04	0.03	2.5-4.5 CU; 0.15-0.45 NB
17-4PH	S17400	0.07	1.00	1.00	15.0-17.5	3.0-5.0	. . .	0.04	0.03	3.0-5.0 CU; 0.15-0.45 NB

CUSTOM 450	S45000	0.05	1.00	1.00	14.0-16.0	5.0-7.0	0.5-1.0	0.03	0.03	1.25-1.75 CU; 8 × %C MIN NB
CUSTOM 455	S45500	0.05	0.50	0.50	11.0-12.5	7.5-9.5	0.50	0.04	0.03	1.5-2.5 CU; 0.8-1.4 TI; 0.1-0.5 NB
SEMIAUSTENITIC TYPES										
PH15-7 MO	S15700	0.09	1.00	1.00	14.0-16.0	6.50-7.75	2.0-3.0	0.04	0.04	0.75-1.50 AL
17-7PH	SI7700	0.09	1.00	1.00	16.0-18.0	6.50-7.75	. . .	0.04	0.04	0.75-1.50 AL
AM-350	S35000	0.07-0.11	0.50-1.25	0.50	16.0-17.0	4.0-5.0	2.50-3.25	0.04	0.03	0.07-0.13 N
AM-355	S35500	0.10-0.15	0.50-1.25	0.50	15.0-16.0	4.0-5.0	2.50-3.25	0.04	0.03	0.07-0.13 N
AUSTENITIC TYPES										
A-286	S66286	0.08	2.00	1.00	13.5-16.0	24.0-27.0	1.0-1.5	0.025	0.025	1.90-2.35 TI; 0.35 MAX AL; 0.10-0.50 V; 0.0030-0.0100 B
JBK-75[B]	. . .	0.015	0.05	0.02	14.5	29.5	1.25	0.006	0.002	2.15 TI; 0.25 AL; 0.27 V; 0.0015 B

(A) SINGLE VALUES ARE MAXIMUM VALUES UNLESS OTHERWISE INDICATED.

(B) TYPICAL VALUES

TABLE 2 PRECIPITATION-HARDENING PHASES IN PH STEELS

ALLOY	PRECIPITATION-HARDENING PHASE	REF
MARTENSITIC TYPES		
PH13-8 MO	COHERENT NIAL + FINE γ PARTICLES	1
15-5PH	FACE-CENTERED CUBIC CU-RICH PHASE[A]	
17-4PH	FACE-CENTERED CUBIC CU-RICH PHASE	2, 3
CUSTOM 450	LAVES-TYPE PHASE CONTAINING FE, NB, MO	4, 5
CUSTOM 455	HEXAGONAL CLOSE-PACKED ORDERED COHERENT NI_3TI	6
SEMIAUSTENITIC TYPES		
17-7PH	ORDERED BODY-CENTERED CUBIC	7, 8, AND 9
PH15-7 MO	β-NIAL + NI_3AL	10, 11
AM-350	CR_2N	12
AM-355	CR_2N	12
AUSTENITIC TYPES		
A-286	NI_3 (AL,TI)	13, 14
JBK-75	NI_3 (AL,TI)	15

(A) ASSUMED TO BE THE SAME PRECIPITATE AS FORMED IN 17-4PH

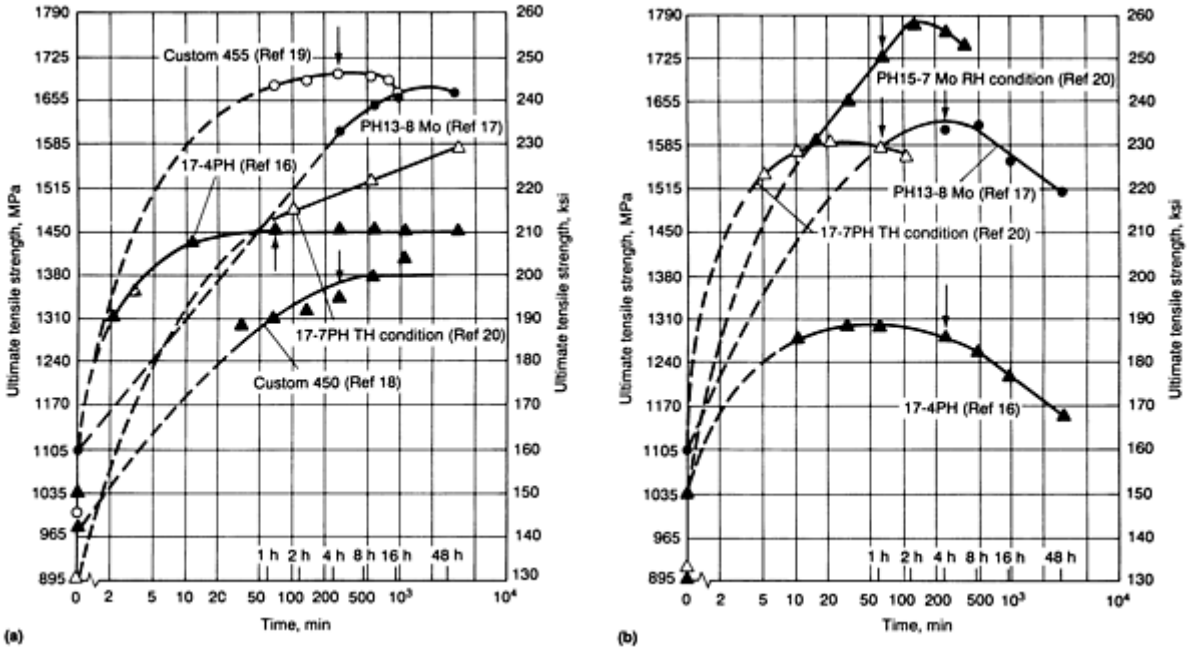

FIG. 1 AGING CURVES FOR SELECTED PH STAINLESS STEELS. (A) AGED AT 480 °C (900 °F). (B) AGED AT 510 °C (950 °F). ARROWS INDICATE STANDARD AGING TIME FOR EACH STEEL

For any alloy, a wide range of properties can be obtained by varying the heat treatment practice. However, certain standard heat treatments for which mechanical property data are available am generally used. These are summarized in Table 3. The corresponding mechanical properties are presented in Table 4.

TABLE 3 HEAT TREATMENT OF PRECIPITATION-HARDENING STAINLESS STEELS

ALLOY	CONDITION CODE	SOLUTION ANNEAL	CONDITIONING AND HARDENING TREATMENT	AGING AND/OR TEMPERING TREATMENT
MARTENSITIC TYPES				
PH13-8 MO	A	925 °C (1700 °F) FOR 15-30 MIN; OIL OR AIR COOL (AC) BELOW 15 °C (60 °F)	. . .	. . .
	RH950	925 °C (1700 °F) FOR 15-30 MIN; OIL OR AC BELOW 15 °C (60 °F)	REFRIGERATE AT -75 °C (-100 °F) FOR 8 H	AGE 510 °C (950 °F) FOR 4 H; AC
	H950	925 °C (1700 °F) FOR 15-30 MIN; OIL OR AC BELOW 15 °C (60 °F)	. . .	AGE 510 °C (950 °F) FOR 4 H; AC
	H1000	925 °C (1700 °F) FOR 15-30 MIN; OIL OR AC BELOW 15 °C (60 °F)	. . .	AGE 535 °C (1000 °F) FOR 4 H; AC
	H1050	925 °C (1700 °F) FOR 15-30 MIN; OIL OR AC BELOW 15 °C (60 °F)	. . .	AGE 565 °C (1050 °F) FOR 4 H; AC
	H1100	925 °C (1700 °F) FOR 15-30 MIN; OIL OR AC BELOW 15 °C (60 °F)	. . .	AGE 595 °C (1100 °F) FOR 4 H; AC
	H1150	925 °C (1700 °F) FOR 15-30 RAIN; OIL OR AC BELOW 15 °C (60 °F)	. . .	AGE 620 °C (1150 °F) FOR 4 H; AC
15-5PH	A	1035 °C (1900 °F) FOR 30	. . .	. . .

		MIN; OIL OR AC BELOW 30 °C (90 °F)		
	H900	1035 °C (1900 °F) FOR 30 MIN; OIL OR AC BELOW 30 °C (90 °F)	. . .	AGE 480 °C (900 °F) FOR 1 H; AC
	H925	1035 °C (1900 °F) FOR 30 MIN; OIL OR AC BELOW 30 °C (90 °F)	. . .	AGE 495 °C (925 °F) FOR 4 H; AC
	H1025	1035 °C (1900 °F) FOR 30 MIN; OIL OR AC BELOW 30 °C (90 °F)	. . .	AGE 550 °C (1025 °F) FOR 4 H; AC
	H1075	1035 °C (1900 °F) FOR 30 MIN; OIL OR AC BELOW 30 °C (90 °F)	. . .	AGE 580 °C (1075 °F) FOR 4 H; AC
	H1150	1035 °C (1900 °F) FOR 30 MIN; OIL OR AC BELOW 30 °C (90 °F)	. . .	AGE 620 °C (1150 °F) FOR 4 H; AC
17-4PH	A	1035 °C (1900 °F) FOR 30 MIN; OIL OR AC BELOW 30 °C (90 °F)	. . .	. . .
	H900	1035 °C (1900 °F) FOR 30 MIN; OIL OR AC BELOW 30 °C (90 °F)	. . .	AGE 480 °C (900 °F) FOR 1 H; AC
	H925	1035 °C (1900 °F) FOR 30 MIN; OIL OR AC BELOW 30 °C (90 °F)	. . .	AGE 495 °C (925 °F) FOR 4 H; AC
	H1025	1035 °C (1900 °F) FOR 30 RAIN; OIL OR AC BELOW 30 °C (90 °F)	. . .	AGE 550 °C (1025 °F) FOR 4 H; AC
	H1075	1035 °C (1900 °F) FOR 30 RAIN; OIL OR AC BELOW 30 °C (90 °F)	. . .	AGE 580 °C (1075 °F) FOR 4 H; AC
	H1100	1035 °C (1900 °F) FOR 30 MIN; OIL OR AC BELOW 30 °C (90 °F)	. . .	AGE 595 °C (1100 °F) FOR 4 H; AC
	H1150	1035 °C (1900 °F) FOR 30 MIN; OIL OR AC BELOW 30 °C (90 °F)	. . .	AGE 620 °C (1150 °F) FOR 4 H; AC
CUSTOM 450	A	1035 °C (1900 °F) FOR 1 H; WATER QUENCH	. . .	. . .
	H900	1035 °C (1900 °F) FOR 1 H; WATER QUENCH	. . .	AGE 480 °C (900 °F) FOR 4 H; AC
	H1000	1035 °C (1900 °F) FOR 1 H; WATER QUENCH	. . .	AGE 535 °C (1000 °F) FOR 4 H; AC
	H1150	1035 °C (1900 °F) FOR 1 H; WATER QUENCH	. . .	AGE 620 °C (1150 °F) FOR 4 H; AC
CUSTOM 455	A	830 °C (1525 °F) FOR 1 H; WATER QUENCH	. . .	. . .
	H900	830 °C (1525 °F) FOR 1 H; WATER QUENCH	. . .	AGE 480 °C (900 °F) FOR 4 H; AC
	H950	830 °C (1525 °F) FOR 1 H; WATER QUENCH	. . .	AGE 510 °C (950 °F) FOR 4 H; AC
	H1000	830 °C (1525 °F) FOR 1 H; WATER QUENCH	. . .	AGE 535 °C (1000 °F) FOR 4 H; AC
SEMIAUSTENITIC TYPES				
17-7PH AND PH15-7 MO	A	1065 °C (1950 °F) FOR 30 MIN/25 MM (1 IN.) OF THICKNESS; AC	. . .	. . .
	T	1065 °C (1950 °F) FOR 30 MIN/25 MM (1 IN.) OF THICKNESS; AC	760 °C (1400 °F) $1\frac{1}{2}$ H; AC TO 15 °C (60 °F) FOR 30 MIN	. . .
	TH1050	1065 °C (1950 °F) FOR 30 MIN/25 MM (1 IN.) OF	760 °C (1400 °F) $1\frac{1}{2}$ H; AC TO 15 °C (60	AGE 565 °C (1050

		THICKNESS; AC	°F) FOR 30 MIN	°F) FOR $1\frac{1}{2}$ H; AC
	A1750	1065 °C (1950 °F) FOR 30 MIN/25 MM (1 IN.) OF THICKNESS; AC	955 °C (1750 °F) FOR 10 MIN; AC	. . .
	R100	1065 °C (1950 °F) FOR 30 MIN/25 MM (1 IN.) OF THICKNESS; AC	955 °C (1750 °F) FOR 10 MIN; AC; REFRIGERATE AT -75 °C (-100 °F) FOR 8 H	. . .
	RH950	1065 °C (1950 °F) FOR 30 MIN/25 MM (1 IN.) OF THICKNESS; AC	955 °C (1750 °F) FOR 10 MIN; AC; REFRIGERATE AT -75 °C (-100 °F) FOR 8 H	AGE 510 °C (950 °F) FOR 1 H; AC
	C	1065 °C (1950 °F) FOR 30 MIN/25 MM (1 IN.) OF THICKNESS; AC	COLD REDUCE	. . .
	CH900	1065 °C (1950 °F) FOR 30 MIN/25 MM (1 IN.) OF THICKNESS; AC	COLD REDUCE	AGE 480 °C (900 °F) FOR 1 H; AC
AM-350	H	1065 °C (1950 °F) FOR 90 MIN/25 MM (1 IN.) OF THICKNESS; RAPID COOL	. . .	. . .
	L	1065 °C (1950 °F) FOR 90 MIN/25 MM (1 IN.) OF THICKNESS; RAPID COOL	930 °C (1710 °F) FOR 90 MIN/25 MM (1 IN.) OF THICKNESS; AC	. . .
	SCT850	1065 °C (1950 °F) FOR 90 MIN/25 MM (1 IN.) OF THICKNESS; RAPID COOL	930 °C (1710 °F) FOR 90 MIN/25 MM (1 IN.) OF THICKNESS; AC; REFRIGERATE AT -75 °C (-100 °F) FOR 3 H	TEMPER 455 °C (850 °F) FOR 3 H; AC
	SCT1000	1065 °C (1950 °F) FOR 90 MIN/25 MM (1 IN.) OF THICKNESS; RAPID COOL	930 °C (1710 °F) FOR 90 MIN/25 MM (1 IN.) OF THICKNESS; AC; REFRIGERATE AT -75 °C (-100 °F) FOR 3 H	TEMPER 535 °C (1000 °F) FOR 3 H; AC
AM-355	H	1025 °C (1875 °F) FOR 90 MIN/25 MM (1 IN.) OF THICKNESS; RAPID COOL	. . .	. . .
	L	1025 °C (1875 °F) FOR 90 MIN/25 MM (1 IN.) OF THICKNESS; RAPID COOL	(1710 °F) FOR 90 MIN/25 MM (1 IN.) OF THICKNESS; AC[(A)]	. . .
	SCT850	1025 °C (1875 °F) FOR 90 MIN/25 MM (1 IN.) OF THICKNESS; RAPID COOL	REFRIGERATE AT -75 °C (-100 °F); 930 °C (1710 °F) FOR 90 MIN/25 MM (1 IN.) OF THICKNESS; AC; REFRIGERATE AT -75 °C (-100 °F) FOR 3 H	TEMPER 455 °C (850 °F) FOR 3 H; AC
	SCT1000	1025 °C (1875 °F) FOR 90 MIN/25 MM (1 IN.) OF THICKNESS; RAPID COOL	REFRIGERATE AT -75 °C (-100 °F); 930 °C (1710 °F) FOR 90 MIN/25 MM (1 IN.) OF THICKNESS; AC; REFRIGERATE AT -75 °C (-100 °F) FOR 3 H	TEMPER 535 °C (1000 °F) FOR 3 H; AC
AUSTENITIC TYPE				
A-286	ST1650	900 °C (1650 °F) FOR 2 H; OIL OR WATER QUENCH	. . .	. . .
	ST1650A	900 °C (1650 °F) FOR 2 H; OIL OR WATER QUENCH	. . .	AGE 730 °C (1350 °F) FOR 16 H; AC
	ST1800	980 °C (1800 °F) FOR 1 H; OIL OR WATER QUENCH	. . .	. . .
	ST1800A	980 °C (1800 °F) FOR 1 H; OIL OR WATER QUENCH	. . .	AGE 730 °C (1350 °F) FOR 16 H; AC

(A) FOR BARS AND FORGING BILLETS, EMPLOY AN EQUALIZING TREATMENT OF 3 H AT 745-800 °C (1375-1475 °F) + 3 H AT 535-620 °C (1000-1150 °F) (CONDITION E + OT) BEFORE THE RESOLUTION TREATMENT AT 930 °C (1710 °F).

TABLE 4 MINIMUM MECHANICAL PROPERTIES OF PRECIPITATION-HARDENING STAINLESS STEELS PER SPECIFICATION NOTED

ALLOY AND PRODUCT FORM[A]	CONDITION	TENSILE STRENGTH		YIELD STRENGTH		ELONGATION, %	REDUCTION IN AREA, %	HARDNESS, HRC		ASTM SPECIFICATION
		MPA	KSI	MPA	KSI			MIN	MAX	
MARTENSITIC TYPES										
PH13-8 MO (UNS S13800)										
B, F	H950	1520	220	1410	205	10	45; 35[B]	45	. . .	A 564, A 705
B, F	H1000	1410	205	1310	190	10	50; 40[B]	43	. . .	A 564, A 705
B, F	H1025	1275	185	1210	175	11	50; 45[B]	41	. . .	A 564, A 705
B, F	H1050	1210	175	1140	165	12	50; 45[B]	40	. . .	A 564, A 705
B, F	H1100	1030	150	930	135	14	50	34	. . .	A 564, A 705
B, F	H1150	930	135	620	90	14	50	30	. . .	A 564, A 705
B, F	H1150M	860	125	585	85	16	55	26	. . .	A 564, A 705
P, SH, ST	H950	1520	220	1410	205	6-10[C]	. . .	45	. . .	A 693
P, SH, ST	H1000	1380	200	1310	190	6-10[C]	. . .	43	. . .	A 693
15-5PH (UNS S15500)										
B, F	H900	1310	190	1170	170	10; 6[B]	35; 15[B]	40	. . .	A 564, A 705
B, F	H925	1170	170	1070	155	10; 7[B]	38; 20[B]	38	. . .	A 564, A 705
B, F	H1025	1070	155	1000	145	12; 8[B]	45; 27[B]	35	. . .	A 564, A 705
B, F	H1075	1000	145	860	125	13; 9[B]	45; 28[B]	32	. . .	A 564, A 705
B, F	H1100	965	140	795	115	14; 10[B]	45; 29[B]	31	. . .	A 564, A 705
B, F	H1150	930	135	725	105	16; 11[B]	50; 30[B]	28	. . .	A 564, A 705
B, F	H1150M	795	115	515	75	18; 14[B]	55; 35[B]	24	. . .	A 564, A 705
P, SH, ST	H900	1310	190	1170	170	5-10[C]	. . .	40	48	A 693
P, SH, ST	H1100	965	140	790	115	5-14[C]	. . .	29	40	A 693
17-4PH (UNS S17400)										
B, F	H900[D]	1310	190	1170	170	10	40; 35[E]	40	. . .	A 564, A 705
B, F	H925[D]	1170	170	1070	155	10	44; 38[E]	38	. . .	A 564, A 705
B, F	H1025[D]	1070	155	1000	145	12	45	35	. . .	A 564, A 705
B, F	H1075[D]	1000	145	860	125	13	45	32	. . .	A 564, A 705
B, F	H1100[D]	965	140	795	115	14	45	31	. . .	A 564, A 705
B, F	H1150[D]	930	135	725	105	16	50	28	. . .	A 564, A 705
B, F	H1150M[D]	795	115	515	75	18	55	24	. . .	A 564, A 705
P, SH, ST	H900	1310	190	1170	170	5-10[C]	. . .	40	48	A 693
P, SH, ST	H1100	965	140	790	115	5-14[C]	. . .	29	40	A 693

CUSTOM 450 (UNS S45000)										
B, SHAPES	ANNEALED	895[F]	130[F]	655	95	10	40	. . .	32	A 564[F]
F, SHAPES	ANNEALED	860[F]	125[F]	655	95	10	40	. . .	33	A 705[F]
B, F, SHAPES	H900	1240[G]	180[G]	1170	170	6; 10[B]	20; 40[B]	39	. . .	A 564[G], A 705[G]
B, F, SHAPES	H950	1170[G]	170[G]	1100	160	7; 10[B]	22; 40[B]	37	. . .	A 564[G], A 705[G]
B, F, SHAPES	H1000	1100	160[G]	1030	150	8; 12[B]	27; 45[B]	36	. . .	A 564[G], A 705
B, F, SHAPES	H1025	1030[G]	150[G]	965	140	12	45	34	. . .	A 564[G], A 705
B, F, SHAPES	H1050	1000[G]	145[G]	930	135	9; 12[B]	30; 45[B]	34	. . .	A 564[G], A 705
B, F, SHAPES	H1100	895[G]	130[G]	725	105	11; 16[B]	30; 50[B]	30	. . .	A 564[G], A 705
B, F, SHAPES	H1150	860[G]	125[G]	515	75	12-18[H]	35-55[H]	26	. . .	A 564[G], A 705
P, SH, ST	ANNEALED	895-1205	130-165	620-1035	90-150	4 MIN	. . .	25	33	A 693
P, SH, ST	H900	1240	180	1170	170	3-5[C]	. . .	40	. . .	A 693
P, SH, ST	H1000	1105	160	1035	150	5-7[C]	. . .	36	. . .	A 693
P, SH, ST	H1150	860	125	515	75	8-10[C]	. . .	26	. . .	A 693
MARTENSITIC TYPES										
CUSTOM 455 (UNS S45500)										
B, F, SHAPES	H900[I]	1620	235	1520	220	8	30	47	. . .	A 564[G], A 705[G]
B, F, SHAPES	H950[I]	1520	220	1410	205	10	40	44	. . .	A 564[G], A 705[G]
B, F, SHAPES	H1000[I]	1410	205	1280	185	10	40	40	. . .	A 564[G], A 705[G]
P, SH, ST	H950	1530	222	1410	205	≤4	. . .	44		A 693
SEMIAUSTENITIC TYPES										
PH15-7 MO (UNS S15700)										
B, F	RH950	1380	200	1210	175	7	25	. . .	. . .	A 564, A 705
B, F	TH1050	1240	180	1100	160	8	25	. . .	. . .	A 564, A 705

P, SH, ST	ANNEALED	1035 MAX	150 MAX	450 MAX	65 MAX	25 MIN	. . .	. . .	. . .	A 693
P, SH, ST	RH950[D]	1550	225	1380	200	1-4[C]	. . .	45-46	. . .	A 693
P, SH, ST	TH1050[D]	1310	190	1170	170	2-5[C]	. . .	40	. . .	A 693
P, SH, ST	COLD ROLLED CONDITION C	1380	200	1210	175	1	. . .	41	. . .	A 693
P, SH, ST	CH900	1650	240	1590	230	1	. . .	46	. . .	A 693
17-7PH (UNS S17700)										
B, F	RH950[D]	1275	185	1030	150	6	10	41	. . .	A 564, A 705
B, F	TH1050[D]	1170	170	965	140	6	25	38	. . .	A 564, A 705
P, SH, ST	RH950	1450[C]	210[C]	1310[C]	190[C]	1-6[C]	. . .	43[C]	44[C]	A 693
P, SH, ST	TH1050	1240[C]	180[C]	1030[C]	150[C]	3-7[C]	. . .	38	. . .	A 693
P, SH, ST	COLD ROLLED CONDITION C	1380	200	1210	175	1	. . .	41	. . .	A 693
P, SH, ST	CH900	1650	240	1590	230	1	. . .	46	. . .	A 693
W	COLD DRAWN CONDITION C	1400-2035[C]	203-295[C]	. . .	. . .	. . .	. . .	. . .	. . .	A 313
W	CH900	1585-2515[C]	230-365[C]	. . .	. . .	. . .	. . .	. . .	. . .	A 313
AM-350 (UNS S35000)										
P, SH, ST	ANNEALED	1380 MAX	200 MAX	585-620 MAX[C]	85-90 MAX[C]	8-12[C]	. . .	. . .	30	A 693
P, SH, ST	SCT850	1275	185	1030	150	2-8[C]	. . .	42	. . .	A 693
P, SH, ST	SCT1000	1140	165	1000	145	2-8[C]	. . .	36	. . .	A 693
AM-355 (UNS 35500)										
F	SCT1000	1170	170	1070	155	12	25	37	. . .	A 705
P, SH, ST	SCT850	1310	190	1140	165	10	. . .	. . .	. . .	A 693
P, SH, ST	SCT1000	1170	170	1030	150	12	. . .	37	. . .	A 693
AUSTENITIC TYPE										
A-286 (UNS S66286)										
B, F	ST 1650	724 MAX	105 MAX	. . .	. . .	. . .	. . .	. . .	201 HB	AMS NO. 5734, 5737
B, F	ST 1650A	965	140	655	95	12	15	277 HB	363 HB	AMS NO. 5734, 5737
B, F	ST 1800	724 MAX	105 MAX	. . .	. . .	. . .	. . .	. . .	201 HB	AMS NO. 5731, 5732
B, F	ST 1800A	895	130	585	85	15	20	248	341	AMS NO. 5731,

								HB	HB	5732
P, SH, ST	ST 1800	724 MAX	105 MAX	. . .	. . .	10-25	. . .	. . .	90 HRB	AMS NO. 5525, 5858
P, SH, ST	ST 1800A	862-965	125-140	655	95	4-15	. . .	24	35	AMS NO. 5525, 5858

(A) B, BAR; F, FORGINGS, P, PLATE; SH, SHEET; ST, STRIP; W, WIRE.

(B) HIGHER VALUE IS LONGITUDINAL; LOWER VALUE IS TRANSVERSE.

(C) VALUES VARY WITH THICKNESS OR DIAMETER.

(D) LONGITUDINAL PROPERTIES ONLY.

(E) HIGHER VALUES ARE FOR SIZES UP TO AND INCLUDING 75 MM (3 IN.); LOWER VALUES ARE FOR SIZES OVER 75 MM (3 IN.) UP TO AND INCLUDING 200 MM (8 IN.).

(F) TENSILE STRENGTHS OF 860 TO 140 MPA (125 TO 165 KSI) FOR SIZES UP TO 13 MM ($\frac{1}{2}$ IN.).

(G) TENSILE STRENGTH ONLY APPLICABLE UP TO SIZES OF 13 MM ($\frac{1}{2}$ IN.).

(H) VARIES WITH SECTION SIZE AND TEST DIRECTION.

(I) UP TO AND INCLUDING 150 MM (6 IN.)

The standard aging times used for aging temperatures of 480 and 510 °C (900 and 950 °F) are such that most steels so heat treated are in the fully aged or slightly overaged condition, whichever gives the best combination of strength and ductility. PH 15-7 Mo stainless steel is unusual in that it has the best combination of strength and ductility when slightly underaged. Material aged at temperatures above 510 °C (950 °F) and, therefore, in a significantly overaged condition, is used when greater ductility or toughness is required. Precipitation in austenitic PH steels is markedly slower than in martensitic or semiaustenitic PH steels. For example, 16 h at 720 °C (1325 °F) is required to produce near-maximum hardening in A-286.

The problems likely to be encountered in welding PH steels are different for each group, but similar for different steels within a group. Therefore, the weldability of the steels within each group can be best understood by first considering the welding of a typical steel from that group, which is invariably also the steel for which the most welding data are available. The weldability of other steels within the same group can then be understood by comparison with the "typical" steel.

References

1. V. SEETHARAMAN ET AL., PRECIPITATION HARDENING IN A PH13-8 MO STAINLESS STEEL, *MATER. SCI. ENG.*, VOL 47, JAN 1981, P 1-11
2. H.J. RACK AND D. KALISH, THE STRENGTH, FRACTURE TOUGHNESS AND LOW CYCLE FATIGUE BEHAVIOR OF 17-4PH STAINLESS STEEL, *METALL. TRANS. A*, VOL 5, JULY 1974, P 1595-1605
3. K.C. ANTHONY, AGING REACTIONS IN PRECIPITATION HARDENABLE STAINLESS STEEL, *J. MET.*, VOL 15, DEC 1963, P 922-927
4. M. HENTHORNE, T.A. DEBOLD, AND R.J. YINGER, "CUSTOM 450-A NEW HIGHER STRENGTH STAINLESS STEEL," PAPER NO. 53, CORROSION '72, NATIONAL ASSOCIATION OF CORROSION ENGINEERS CONFERENCE, 1972
5. J.E. MCBRIDE, JR., AND G.N. MANIAR, *METALLOGRAPHY AS A QUALITY CONTROL TOOL*, PLENUM PUBLISHING, 1980, P 279
6. S. WIDGE, "A STUDY OF THE EFFECTS OF VARYING SOLUTION TREATMENT ON THE TOUGHNESS OF A STAINLESS MARAGING ALLOY," PH.D. DISSERTATION, LEHIGH UNIVERSITY, 1984
7. E.E. UNDERWOOD, A.E. AUSTIN, AND G.K. MANNING, THE MECHANISM OF HARDENING IN 17-7 NI-CR PRECIPITATION-HARDENING STAINLESS STEEL, *JISI*, VOL 200, AUG 1962, P 644-651
8. H.C. BURNETT, R.H. DUFF, AND H.C. VACHER, IDENTIFICATION OF METALLURGICAL REACTIONS AND THEIR EFFECT ON MECHANICAL PROPERTIES OF 17-7PH STEEL, *J. RES. NATL. BUR. STAND.--ENG. INSTRUMENTATION*, VOL 66C, 1962, P 113-119
9. E.G. FEL'DGANDLER AND M.V. PRIDANTSEV, PHASE TRANSFORMATION IN KH 17 N7 YU STAINLESS STEEL, *METALLOVED. TERM. OBRAB. MET.*, NOV 1960, P 2-7
10. J.C. WILKENS AND R.E. PENCE, A STUDY OF THE MICROSTRUCTURE OF PRECIPITATION HARDENING STAINLESS STEEL SHEET, *ADVANCES IN ELECTRON METALLOGRAPHY AND ELECTRON PROBE MICROANALYSIS*, STP 317, ASTM, 1962, P 140-149
11. J.C. WILKENS, PRIVATE COMMUNICATION, IN PRECIPITATION FROM IRON-BASE ALLOYS, PROCEEDINGS OF AN AIME SYMPOSIUM, CLEVELAND, OH, 21 OCT 1963, P 98
12. G. AGGEN, "PHASE TRANSFORMATIONS AND HEAT TREATMENT STUDIES OF A CONTROLLED TRANSFORMATION STAINLESS STEEL ALLOY," DR. ENG. SC. THESIS, RENSSELAER POLYTECHNIC INSTITUTE, AUG 1963
13. D.R. MUZYKA, *THE METALLURGY OF NICKEL-IRON ALLOYS, THE SUPERALLOYS*, C.T. SIMS AND W.C. HAGEL, ED., JOHN WILEY & SONS, 1972, P 113-143
14. A.W. THOMPSON AND J.A. BROOKS, THE MECHANISM OF PRECIPITATION STRENGTHENING IN AN IRON-BASE SUPERALLOY, *ACTA METALL.*, VOL 30, DEC 1982, P 2197-2203
15. T.J. HEADLEY, M.M. KAMOUSKY, AND W.R. SORENSON, EFFECT OF COMPOSITION AND

HIGH ENERGY RATE FORGING ON THE ONSET OF PRECIPITATION IN AN IRON-BASE SUPERALLOY, *METALL. TRANS. A*, VOL 13, MARCH 1982, P 345-353

16. "ARMCO 17-4PH STAINLESS STEEL BAR AND WIRE," PRODUCT DATA BULLETIN NO. S-24, ARMCO, INC., MIDDLETOWN, OH, SEPT 1966
17. "ARMCO PH 13-8MO STAINLESS STEEL," PRODUCT DATA BULLETIN NO. S-24, ARMCO, INC., MIDDLETOWN, OH, OCT 1986
18. "CARPENTER CUSTOM 450," PRODUCT DATA BULLETIN, CARPENTER TECHNOLOGY CORP., READING, PA, 1971
19. "CARPENTER CUSTOM 455," PRODUCT DATA BULLETIN, CARPENTER TECHNOLOGY CORP., READING, PA, 1971
20. "ARMCO 17-7PH AND PH15-7MO STAINLESS STEEL SHEET AND STRIP," PRODUCT DATA BULLETIN, ARMCO, INC., MIDDLETOWN, OH, JAN 1975

Selection of Wrought Precipitation-Hardening Stainless Steels

B. Pollard

Welding Martensitic PH Steels

Following a brief description of the solidification characteristics and microstructures of martensitic PH stainless steels, this section reviews welding parameters for types 17-4PH, 15-5PH, PH13-8 Mo, Custom 450, and Custom 455. Tables 1, 2, 3, and 4 list properties and heat treatment recommendations for these materials. Additional information can be found in the article "Welding of Stainless Steels" in this Volume.

Microstructural Evolution

There have been no systematic studies of the solidification of welds in PH stainless steels, but since the mechanisms involved are the same as for the standard austenitic stainless steels, the primary solidification mode can be predicted for a specific composition by using equations that were originally developed by Suutala and have since been modified by the addition of an aluminum term and higher values for the carbon and nitrogen equivalents. These equations are (Ref 21):

$$CR_{EQ} = \%Cr + 1.4(\%Mo) + 1.5(\%Si) + 2(\%Nb) + 2.5(\%A1) + 3(\%Ti)$$

$$NI_{EQ} = \%Ni + 0.3(\%Mn) + 35(\%C) + 20(\%N) + \%Cu$$

Calculated values of the Cr_{eq}/Ni_{eq} ratios for typical PH steels are given in Table 5. According to Suutala, a Cr_{eq}/Ni_{eq} greater than 1.55 is required for primary ferrite solidification (Ref 22). Therefore, the calculated values for the Cr_{eq}/Ni_{eq} ratio indicate that all the martensitic PH stainless steels except Custom 455 solidify as primary δ-ferrite. Upon cooling, nearly all this ferrite first undergoes a transformation to austenite, which subsequently transforms to martensite at temperatures close to ambient. Custom 455 solidifies as primary austenite, which transforms to martensite upon cooling to ambient temperature. Although the as-welded fusion zone microstructures of welds in martensitic PH steels made without filler metal or with a matching filler metal are predominantly martensitic, they may also contain a few percent of δ-ferrite in the untempered martensitic matrix (Fig. 2a). The morphology of this δ-ferrite is summarized in Table 5. The δ-ferrite in welds made with moderate-to-high heat inputs may be intercellular or vermicular. Intercellular ferrite is formed as part of a divorced δ-γ eutectic, which is a result of segregation during the last stages of primary austenite solidification, while vermicular ferrite constitutes the untransformed cores of the primary ferrite dendrites. Very high cooling rates, such as may be experienced by welds made at high speeds in sheet material, suppress the transformation of δ-ferrite to austenite and promote the formation of acicular austenitic-ferritic structures, the austenite content of which subsequently transforms to martensite.

TABLE 5 EFFECT OF COMPOSITION ON THE PRIMARY SOLIDIFICATION MODE AND FINAL AS-WELDED MICROSTRUCTURE OF WELDS IN PH STEELS

ALLOY	CR_{EQ}/NI_{EQ} (A)	OBSERVED WELD-METAL δ-FERRITE, %	PREDICTED PRIMARY SOLIDIFICATION MODE (B)	FINAL AS-WELDED MICROSTRUCTURE
AUSTENITIC TYPES				
JBK-75	0.77	0	A	100% AUSTENITE
A-286	0.88	0	A	100% AUSTENITE
MARTENSITIC TYPES				
CUSTOM 455	1.33	~0	A	~100% MARTENSITE
15-5PH	1.60	0-5	F	MARTENSITE + INTERCELLULAR OR VERMICULAR **δ** -FERRITE
17-4PH	1.74	3-8	F	MARTENSITE + VERMICULAR **δ** -FERRITE OR ACICULAR STRUCTURE
CUSTOM 450	1.82	0-5	F	MARTENSITE + VERMICULAR **δ** -FERRITE OR ACICULAR STRUCTURE
PH13-8 MO	1.98	0	F	100% MARTENSITE
SEMIAUSTENITIC TYPES				
AM-355	1.77	~5	F	AUSTENITE + VERMICULAR **δ** -FERRITE OR ACICULAR STRUCTURE
17-7PH	1.92	~25	F	WIDMANSTÄTTEN AUSTENITE IN FERRITIC MATRIX
PH15-7 MO	2.01	25-40	F	WIDMANSTÄTTEN AUSTENITE IN FERRITIC MATRIX
AM-350	2.22	>15	F	WIDMANSTÄTTEN AUSTENITE IN FERRITIC MATRIX

(A) CR_{EQ} = %CR + 1.4(%MO) + 1.5(%SI) + 2(%NB) + 2.5(%AL) + 3(%TI); NI_{EQ} = %NI + 0.3(%MN) + 35(%C) + 20(%N) + %CU. VALUES ARE FOR TYPICAL COMPOSITIONS.

(B) A, AUSTENITIC; F, DELTA FERRITIC

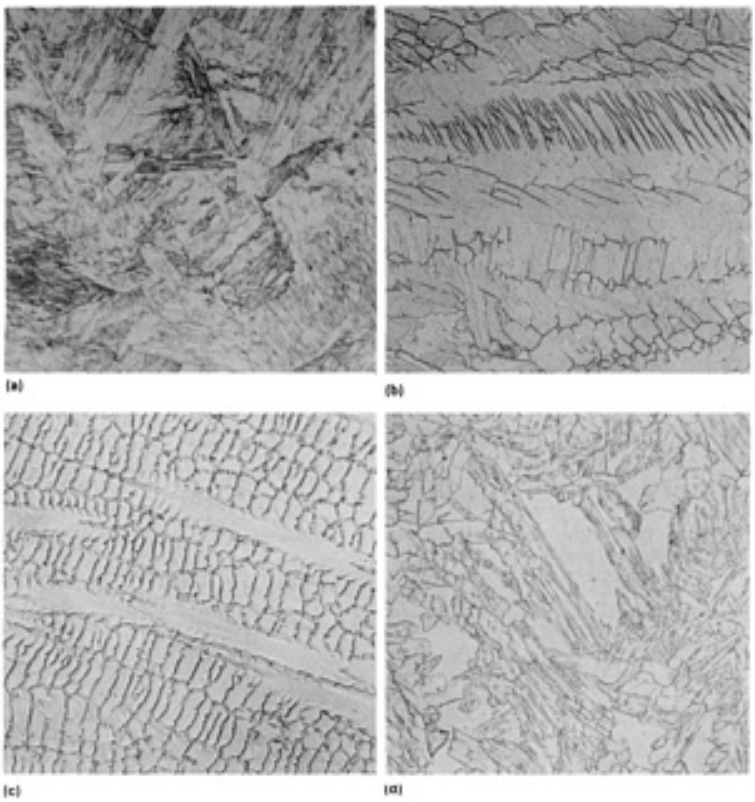

FIG. 2 MICROSTRUCTURES OF AUTOGENOUS GTA WELD METAL IN THE AS-WELDED CONDITION. (A) 17-4PH, δ -FERRITE IN A MATRIX OF UNTEMPERED MARTENSITE. ETCHANT: FRY'S REAGENT. 440×. (B) PH13-8 MO, UNTEMPERED MARTENSITE. ETCHANT: VILELLA'S REAGENT. 440×. (C) 17-7PH, AUSTENITE PLUS ABOUT 20% δ -FERRITE. ETCHANT: ELECTROLYTIC NITRIC ACID-ACETIC ACID FOLLOWED BY ELECTROLYTIC OXALIC ACID. 440×. (D) A-286, FULLY AUSTENITIC STRUCTURE. ETCHANT: 90 ML HYDROCHLORIC ACID, 5 ML NITRIC ACID, 5 ML SULFURIC ACID, 1 ML HYDROFLUORIC ACID. 440×

In the as-welded condition, the heat-affected zones of welds in martensitic PH steels are distinguishable from the base metal by grain growth and an increased amount of ferrite in the high-temperature region close to the fusion line.

Postweld solution treatments reduce the residual δ-ferrite content and refine the prior-austenite grain size of both the fusion and heat-affected zones (HAZ). Aging, likewise, simultaneously tempers the martensite and precipitates the age-hardening particles in the fusion zone, HAZ, and base metal. However, these particles are too small to observe by optical microscopy. Aging may also reform up to 10% austenite at temperatures of 540 to 620 °C (1000 to 1150 °F), the amount increasing with aging temperature.

17-4PH Stainless Steel

Weldability. 17-4PH stainless steel is typical of the martensitic PH stainless steels. Its weldability is superior to that of the standard austenitic stainless steels because, due to its low carbon content, it does not require preheat to prevent cracking in thicknesses up to 100 mm (4.0 in.) (Ref 23 , 24, 25). The welding conditions used for arc welding 17-4PH stainless steel are essentially the same as those used for joining the standard austenitic stainless steels. However, neither welds nor base metal have the high ductility of the austenitic stainless steels, so care must be taken to avoid the presence of stress raisers (Ref 23 24, 25). One common form of stress raiser is the built-in notch at the root of a partial penetration weld. If design requirements dictate partial-penetration welds, the initiation of cracks at the root of the weld can be avoided by making the root pass with a ductile, low-strength filler metal such as type 308L, and then completing the balance of the weld with a matching high-strength heat-treatable filler metal.

Arc Welding. Gas-tungsten arc, gas-metal arc, and shielded metal arc welding processes have all been used extensively for joining 17-4PH stainless steel (Ref 23, 24, 25). Typical mechanical properties of arc welds in 17-4PH are presented in Table 6. The choice of welding process has little effect on the strength of welds after postweld heat treatment (PWHT),

but does affect the weld metal cleanliness and resultant ductility and toughness (Ref 23). Gas-tungsten arc welds have the highest and shielded metal arc welds the lowest quality. However, shielded metal arc welds are generally satisfactory for all but the most critical applications.

TABLE 6 MECHANICAL PROPERTIES OF 17-4PH ARC WELDS

THICKNESS		POSTWELD HEAT TREATMENT[B]	TENSILE STRENGTH		0.2% YIELD STRENGTH		ELONGATION, %			REDUCTION IN AREA, %	FAILURE LOCATION[C]	IZOD IMPACT ENERGY[D]	
MM	IN.		mpa	ksi	mpa	ksi	in 13 mm (0.5 in.)	in 25 mm (1 in.)	in 50 mm (2 in.)			J	FT · LBF
GTA WELDS[A]													
1.3	0.050	AGED 480 °C (900 °F), 1 H	1340	194	1295	188	7	. . .	3.0	. . .	FL	. . .	. . .
1.3	0.050	AGED 540 °C (1000 °F), 4 H	1235	179	1170	170	. . .	. . .	5.0	. . .	BM	. . .	. . .
1.3	0.050	AGED 595 °C (1100 °F), 4 H	1140	165	1105	160	14	. . .	5.5	. . .	FL	. . .	. . .
2.3	0.090	AGED 480 °C (900 °F), 1 H	1395	202	1290	187	16	. . .	5.0	. . .	FL	. . .	. . .
2.3	0.090	AGED 540 °C (1000 °F), 4 H	1240	180	1160	168	17	. . .	7.0	. . .	WM	. . .	. . .
2.3	0.090	AGED 595 °C (1100 °F). 4 H	1125	163	1060	154	. . .	. . .	9.0	. . .	BM	. . .	. . .
4.8	0.188	ST + AGED 480 °C (900 °F), 1 H	1370	199	1260	183	. . .	17.0	9.0	35	WM	. . .	. . .
4.8	0.188	ST + AGED 510 °C (950 °F), 1 H	1345	195	1255	182	. . .	18.0	9.0	42	WM	. . .	. . .
4.8	0.188	ST + AGED 550 °C (1025 °F), 1 H	1215	176	1145	166	. . .	17.0	9,2	45	WM	. . .	. . .
GMA WELDS[A]													
4.8	0.188	ST + AGED 480 °C (900 °F), 1 H	1400	203	1250	181	. . .	14.0	7.0	. . .	WM	. . .	. . .
4.8	0.188	ST + AGED 510 °C (950 °F), 1 H	1275	185	1200	174	. . .	14.0	7.5	. . .	WM	. . .	. . .
4.8	0.188	ST + AGED 550 °C (1025 °F), 1 H	1195	173	1125	163	. . .	15.0	7.5	. . .	WM	. . .	. . .
25	1.00	ST + AGED 480 °C (900 °F), 1 H	1305	189	1150	167	. . .	. . .	7.3	21	WM	15	11
SMA WELDS[A]													
4.8	0.188	ST + AGED 480 °C (900 °F), 1 H	1380	200	1275	185	. . .	13.0	6.5	29	. . .	. . .	. . .
4.8	0.188	ST + AGED 510 °C (950 °F), 1 H	1280	186	1205	175	. . .	12.0	6.0	30	. . .	. . .	. . .
4.8	0.188	ST + AGED 550 °C (1025 °F), 1 H	1195	173	1115	162	. . .	12.0	6.0	32	. . .	. . .	. . .
9.5	0.375	AGED 480 °C (900 °F), 1 H	1225	178	1060	154	. . .	10.0	. . .	32	BM	. . .	. . .
9.5	0.375	ST + AGED 480 °C (900 °F), 1 H	1290	187	1185	172	. . .	11.0	. . .	48	WM	. . .	. . .
9.5	0.375	AGED 540 °C (1000 °F), 1 H	1105	160	940	136	. . .	11.0	. . .	29	WM	. . .	. . .
9.5	0.375	ST + AGED 540 °C (1000 °F), 1 H	1170	170	1110	161	. . .	12.0	. . .	48	WM	. . .	. . .
9.5	0.375	AGED 595 °C (1100 °F), 1 H	1095	159	770	112	. . .	13.5	. . .	50	BM	. . .	. . .
9.5	0.375	ST + AGED 595 °C (1100 °F), 1 H	1090	158	925	134	. . .	12.0	. . .	54	WM	. . .	. . .
25	1.00	AGED 480 °C, (900 °F), 1 H	1090	158	815	118	. . .	. . .	8.0	21	WM	38	28
25	1.00	ST + AGED 480 °C (900 °F), 1 H	1280	186	1125	163	. . .	. . .	9.5	36	WM	8	6
25	1.00	AGED 540 °C (1000 °F), 1 H	1070	155	745	108	. . .	. . .	9.5	27	WM	46	34
25	1.00	ST + AGED 540 °C (1000 °F), 1 H	1150	167	1005	146	. . .	. . .	9.5	39	WM	23	17

25	1.00	AGED 595 °C (1100 °F), 1 H	1090	158	765	111	. . .	. . .	7.5	18	WM	12	9
25	1.00	ST + AGED 595 °C (1100 °F), 1 H	1090	158	890	129	. . .	. . .	11.0	38	WM	30	22

Source: Ref 25

(A) ALL WELDS MADE IN CONDITION A WITH A 17-4PH COATED ELECTRODE OR FILLER WIRE.

(B) ST = SOLUTION TREATED AT 1035 °C (1900 °F) FOR 30 MIN; AIR COOLED TO 15 °C (60 °F) AND HELD FOR 1 H.

(C) WM, WELD METAL; FL, FUSION LINE; BM, BASE METAL.

(D) NOTCH IN TRANSVERSE FACE OF WELD METAL.

Base-Metal Condition for Welding. Depending on the thickness and level of restraint, 17-4PH stainless steel can be welded in the annealed (A) or overaged (H1100 or H1150) conditions. The welding of material in conditions H900 through H1075 is generally not recommended. Material up to 25 mm (1.0 in.) thick can usually be welded in condition A provided that the weld is not very heavily restrained. Highly restrained welds or welds in heavier sections are best welded in conditions H1100 or H1150.

Filler Metals. Type 630 covered electrodes and filler wires, which deposit weld metal that closely matches 17-4PH base metal in composition and heat treatment response, are used when high-strength welds are required. Austenitic filler metals, such as type 308L, can be used for joining 17-4PH when high strength is not required in the joint. Welds made with austenitic filler metals are less susceptible to hydrogen embrittlement than those made with martensitic filler metals and may be used in the as-welded condition.

Postweld Heat Treatment. In the as-welded condition, the weld metal and the high-temperature regions of the HAZs of welds in 17-4PH stainless steel have structures consisting primarily of untempered martensite plus a small amount of ferrite (Fig. 2a). Weldments exhibit an aging peak in the HAZ and a weld metal hardness that is only slightly less than that of the base metal in condition A (Fig. 3a). Weldments in 17-4PH stainless steel are not usually put into service in the as-welded condition except for repair welds where PWHT is impractical. In order to obtain weld properties approximating those of the base metal, PWHT is necessary. For single-pass welds made with the base metal in condition A, a simple aging treatment of 1 to 4 h at 480 to 620 °C (900 to 1150 °F) is usually sufficient. It simultaneously hardens the weld metal, HAZ, and base metal and lowers the residual stresses associated with the weld. Because only slight overaging occurs in the portion of the HAZ that is heated into the aging temperature range during welding (Fig. 3a), joint efficiencies of 97 to 100% are obtained (Ref 25).

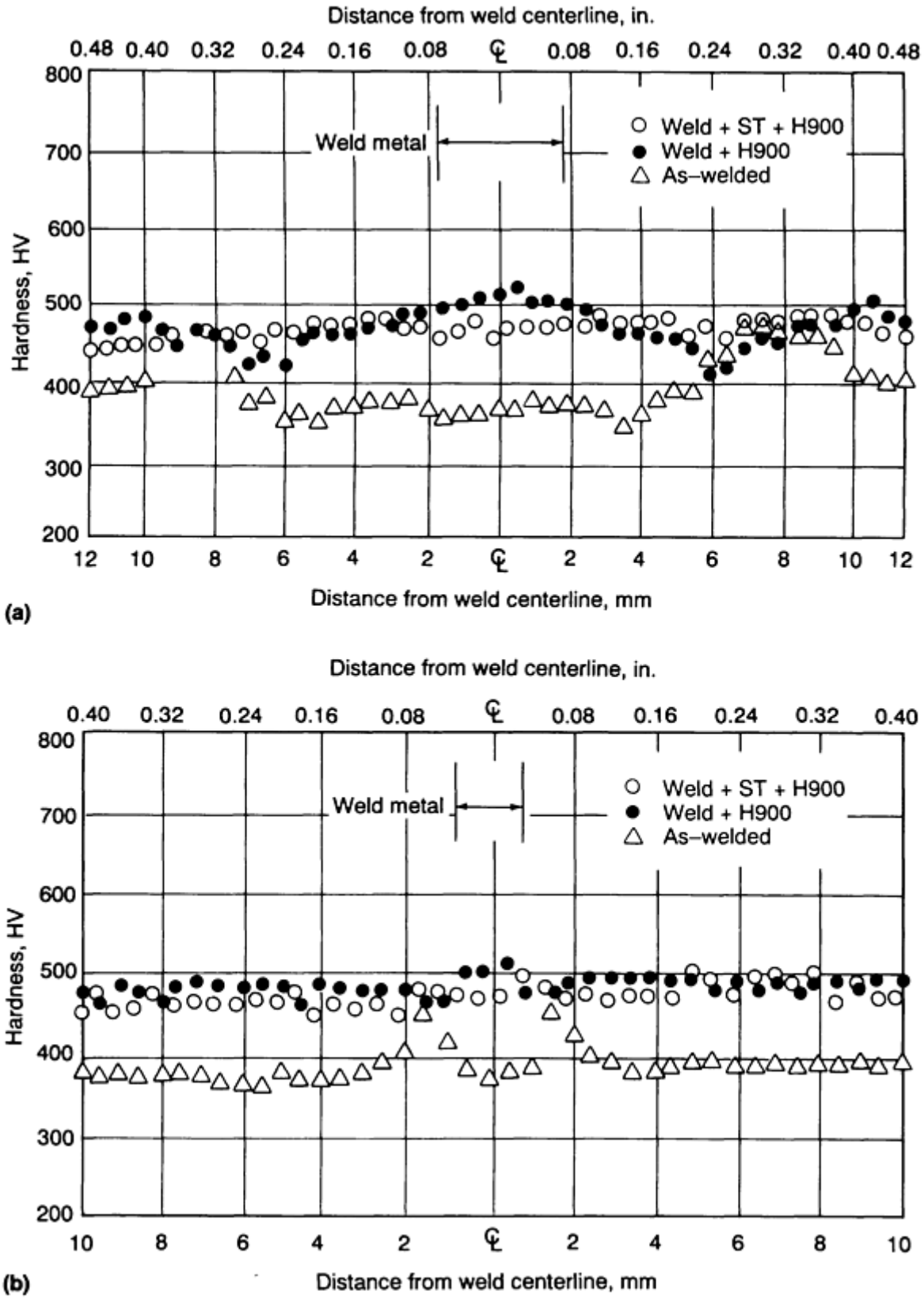

FIG. 3 MICROHARDNESS PROFILES OF AS-WELDED AND POSTWELD HEAT-TREATED WELDS IN 17-4PH MADE WITH (A) PAW AND (B) EBW PROCESSES. SOURCE: REF 26

In multipass welds, the repeated heating from the deposition of successive beads may leave a variation in structure from bead to bead that will result in nonuniform response to the aging treatment. Consequently, in the aged condition, weld

yield and ultimate tensile strengths are only about 65% and 80 to 90%, respectively, of the base-metal values (Ref 25). Solution treating the weld before hardening reduces the weld metal and HAZ ferrite contents and improves weld metal uniformity and response to heat treatment. As a result, weld strength increases to 80 to 90% and 90 to 95%, respectively, of the base-metal yield and ultimate tensile strengths. For welds made with the base metal in the overaged condition, solution treatment is required if it is desired to heat treat the weldment to a higher strength level. In general, if the weld deposit is less than 13 mm (0.5 in.) in thickness, fairly good tensile properties can be obtained even if the solution treatment is omitted prior to aging. However, the toughness of the weld metal decreases with aging temperature above 540 °C (1000 °F), probably due to an unfavorable carbide morphology. Therefore, if weld deposits are 13 mm (0.5 in.) or greater in thickness and a postweld solution treatment is not feasible, an age-hardening temperature of 550 °C (1025 °F) or lower is suggested (Ref 25).

Electron-beam (EB) welding is used for joining 17-4PH stainless steel when precision welds with maximum strength and minimum distortion are required. Welding parameters are similar to those used for welding the standard austenitic stainless steels and the same considerations as in arc welding apply to the choice of base-metal condition for welding. The most important characteristic of an EB weld is the total heat input, which is only about 20% of that of a comparable arc weld (Ref 26). As a result, the HAZ is much narrower (Fig. 3b) and the weld metal is finer grained and has a lower ferrite content. Furthermore, since an EB weld is usually a single-pass weld, the weld-metal structure does not exhibit the inhomogeneities of a multipass arc weld. Consequently, the mechanical properties of EB welds are generally superior to those of arc welds, particularly in regard to fracture toughness (Ref 27). Typical mechanical properties of EB welds in 17-4PH are presented in Table 7. Postweld aging alone results in joint efficiencies of 95 to 100% (Ref 26, 28) and total elongation values only slightly lower than those of the base metal; however, the toughness of welds in the H900 condition is low (Ref 26). Re-solution treating before aging has little effect on weld strength but markedly increases the toughness of welds aged at 480 °C (900 °F). However, it produces only a small increase in toughness for welds aged at higher temperatures.

TABLE 7 MECHANICAL PROPERTIES OF ELECTRON-BEAM WELDS IN MARTENSITIC PH STEELS

THICKNESS		PREWELD CONDITION	POSTWELD HEAT TREATMENT[A]	TENSILE STRENGTH		0.2% YIELD STRENGTH		ELONGATION IN 50 MM (2 IN.), %	FAILURE LOCATION[B]	CVN IMPACT ENERGY		FRACTURE TOUGHNESS		REF
mm	in.			mpa	ksi	mpa	ksi			j	ft · lbf	mpa $\sqrt{m}$	ksi $\sqrt{in}$	
17-4 PH														
3.2	0.125	A	AGED 480 °C (900 °F), 1 H	1435	208	1365	198	11.0	BM	2.4	1.8	. . .	. . .	26
3.2	0.125	A	ST + AGED 480 °C (900 °F), 1 H	1400	203	1270	184	12.2	BM	14.0	10.3	. . .	. . .	26
3.2	0.125	A	AGED 550 °C (1025 °F), 4 H	1165	169	1125	163	12.0	BM	15.6	11.5	. . .	. . .	26
3.2	0.125	A	ST + AGED 550 °C (1025 °F), 4 H	1140	165	1090	158	12.0	BM	18.3	13.5	. . .	. . .	26
3.2	0.125	A	AGED 620 °C (1150 °F), 4 H	1025	149	985	143	15.4	BM	17.6	13.0	. . .	. . .	26
3.2	0.125	A	ST + AGED 620 °C (1150 °F), 4 H	1020	148	985	143	14.6	BM	19.4	14.3	. . .	. . .	26
3.2	0.125	A	AGED 760 °C (1400 °F), 2 H + 620 °C (1150 °F), 4 H	965	140	745	108	16.4	BM	20.6	15.2	. . .	. . .	26
9.5	0.375	A	AGED 480 °C (900 °F), 1 H	1315	191	1235	179	12.6[C]	. . .	. . .	. . .	. . .	. . .	28
(E)	(E)	H1150	NONE	885	128	705	102	11[D] TO 22	WM/BM	. . .	. . .	. . .	. . .	27
(E)	(E)	H1150	ST + AGED 595 °C (1 100 °F), 4 H	1055	153	. . .	. . .	. . .	. . .	. . .	. . .	K_Q = 187	K_Q = 170	27
15-5PH														
(E)	(E)	1150	ST + AGED 565 °C (1050 °F), 4 H	. . .	. . .	1125	163	. . .	. . .	. . .	. . .	K_Q = 194	K_Q = 176	27
(E)	(E)	1150	ST + AGED 595 °C (1100 °F), 4 H	. . .	. . .	1020	148	. . .	. . .	. . .	. . .	K_{IC} = 262	K_{IC} = 238	27
PH13-8 MO														
(E)	(E)	H1150M	ST + AGED 540 °C (1000 °F), 4 H	. . .	. . .	1415	205	. . .	. . .	. . .	. . .	K_{IC} = 110	K_{IC} = 100	31

(A) ST = SOLUTION TREATED: 17-4PH AND 15-5PH AT 1035 °C (1900 °F), PH 13-8 MO AT 925 °C (1700 °F) FOR 30 MIN; AIR COOL.

(B) WM, WELD METAL; BM, BASE METAL.

(C) IN 25 MM (1 IN.).

(D) LOW VALUE IS FOR FAILURE IN THE WELD METAL.

(E) EXACT VALUE NOT REPORTED. IN RANGE OF 23 TO 60 MM (0.90 TO 2.37 IN.)

15-5PH Stainless Steel

15-5PH stainless steel differs from 17-4PH in that its composition is balanced so that its structure is ferrite-free and material for bar and forging billets is vacuum arc remelted. As a result, the transverse ductility and toughness of 15-5PH stainless steel are superior to those of 17-4PH. However, its weldability is essentially the same as that of 17-4PH and the same welding processes and procedures are used. A matching 15-5PH filler wire (AMS 5826) is available for critical applications but it is most often welded with type 630 (17-4PH) covered electrodes or filler wire. Postweld heat treatment and weld mechanical properties are essentially identical to those for 17-4PH.

Autogenous welds in 15-5PH stainless steel contain less δ-ferrite than those in 17-4PH. Sufficient δ-ferrite is normally formed to prevent weld solidification cracking in GTA welds. However, the rapid cooling rates that are characteristic of EB and laser welding can produce welds with little or no δ-ferrite, which are susceptible to weld solidification cracking if welded with excessively high welding speeds (Ref 29). The strengths of defect-free EB welds in 15-5PH are similar to those in 17-4PH, but the fracture toughness is higher (Table 7).

PH13-8 Mo Stainless Steel

PH13-8 Mo stainless steel is vacuum induction melted plus vacuum arc remelted. It is ferrite-free and is used where high fracture toughness is required in heavy sections. Weldability is similar to 17-4PH stainless steel and the same procedures are used. It can be welded with the same processes, although covered electrodes for SMA welding are not available. Gas-tungsten arc and GMA welds can be made using a matching filler wire (AMS 5840). Although the final weld metal microstructure is ferrite-free (Fig. 2b), PH13-8 Mo has excellent resistance to weld solidification cracking because it solidifies as δ-ferrite and has low sulfur and phosphorus contents (Ref 30). After postweld solution treating and aging, the yield strengths and Charpy V-notch (CVN) impact energies of multipass GTA welds in PH13-8 Mo stainless steel are 96 to 100% and 50 to 100%, respectively, of the base-metal values (Fig. 4a), the difference between weld- and base-metal properties being greatest for aging temperatures above 540 °C (1000 °F). In heavy sections, PH13-8 Mo stainless steel is often joined by EB welding. After PWHT, EB welds have joint efficiencies of virtually 100% and their fracture toughness is approximately the same as that of the base metal (Ref 31).

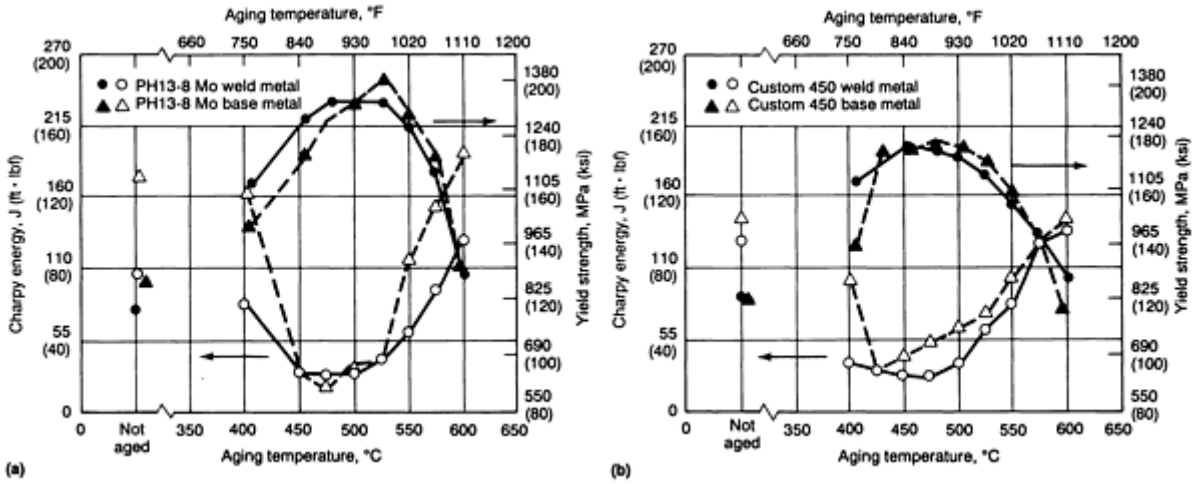

FIG. 4 EFFECT OF AGING TEMPERATURE ON THE YIELD STRENGTH AND CHARPY V-NOTCH IMPACT ENERGY OF (A) PH13-8 MO AND (B) CUSTOM 450 BASE METAL AND WELD METAL. GTA WELDS MADE IN 13 MM (0.50 IN.) THICK PLATE (CONDITION A) WITH MATCHING FILLER METALS. CLOSED SYMBOLS REPRESENT YIELD STRENGTH VALUES; OPEN SYMBOLS REPRESENT IMPACT VALUES. SOURCE: REF 30

Custom 450 Stainless Steel

The composition of Custom 450 stainless steel is balanced so that base metal, HAZ, and weld metal are essentially fully martensitic. In most respects, its weldability is similar to that of 17-4PH, and it can be joined using the same welding processes and procedures (Ref 32). A matching filler wire (AMS 5763) is usually used for GTA and GMA welding Custom 450 and is essential if the weldment is to be used without PWHT. A type 630 (17-4PH) filler wire or coated electrode can be used for joining Custom 450 if the weldment is postweld aged or solution treated and aged.

Custom 450 stainless steel is often used in condition A when only moderate strength is required. Material welded in this condition has acceptable weld properties in the as-welded condition, but CVN impact energy is substantially increased by a postweld solution anneal at 1040 °C (1900 °F) (Ref 32). Higher strength levels are obtained by postweld aging or solution treating and aging. After postweld solution treating and aging, the yield strengths of multipass GTA welds in Custom 450 are 98 to 100% of the base-metal values. Weld metal CVN impact energy increases with aging temperature from about 50% of the base-metal value for welds aged at 480 °C (900 °F) to 100% for welds aged at 565 °C (1050 °F) as shown in Fig. 4(b).

Custom 455 Stainless Steel

Custom 455 stainless steel is vacuum induction melted plus vacuum arc remelted and is completely martensitic. It is joined primarily by GTA welding and a Custom 455 filler metal is available for multipass welds. Procedures are similar to those used for 17-4PH, but a lower postweld solution treatment temperature (815 to 845 °C, or 1500 to 1550 °F) is used. In small sections, joint efficiencies of 80% are obtained by postweld aging only and 100% by solution treating and aging the weldment (Ref 33, 34). In large sections, joint efficiencies in excess of 85% are possible (Ref 19).

References cited in this section

19. "CARPENTER CUSTOM 455," PRODUCT DATA BULLETIN, CARPENTER TECHNOLOGY CORP., READING, PA, 1971
21. B. POLLARD, UNPUBLISHED WORK
22. N. SUUTALA, EFFECT OF SOLIDIFICATION CONDITIONS ON THE SOLIDIFICATION MODE IN STAINLESS STEELS, *METALL. TRANS. A*, VOL 14, FEB 1983, P 191-197
23. G.E. LINNERT, WELDING PRECIPITATION-HARDENING STAINLESS STEELS, *WELD. J.*, VOL 36, JAN 1957, P 9-27
24. F.J. HAWKINS, WELDING OF AGE-HARDENABLE STAINLESS STEELS, *WELD. RES. COUNC. BULL.*, NO. 103, FEB 1965
25. "ARMCO FABRICATING DATA," BULLETIN SF-2, ARMCO, INC., MIDDLETOWN, OH, FEB 1966
26. C. CHEN AND J.S. YEH, ELECTRON BEAM AND PLASMA ARC WELDING OF 17-4PH STAINLESS STEEL, *PROC. CONF. POWER BEAM PROCESSING: ELECTRON, LASER, PLASMA ARC* (SAN DIEGO, CA), ASM INTERNATIONAL, 1988, P 45-54
27. A.J. TURNER, ELECTRON BEAM WELDING THICK SECTION PRECIPITATION-HARDENING STEEL, *WELD. J.*, VOL 60, JAN 1981, P 18-26
28. M.U. ISLAM, G. CAMPBELL, AND R. HSU, FATIGUE AND TENSILE PROPERTIES OF EB WELDED 17-4PH STEEL, *WELD. J.*, VOL 68, SEPT 1989, P 45-50
29. S. MATSUI *ET AL.*, ELECTRON BEAM WELDING OF THE PRECIPITATION HARDENING STAINLESS STEEL, *REVUE DE LA SOUDURE-LASTIJDSCRIFT*, VOL 46, JAN 1990, P 52-57
30. W.R. CIESLAK, J.A. BROOKS, AND W.M. GARRISON, JR., THE WELDABILITY, MICROSTRUCTURE AND PROPERTIES OF PRECIPITATION STRENGTHENED MARTENSITIC STAINLESS STEELS, *PROC. CONF. ADVANCES IN WELDING SCIENCE AND TECHNOLOGY* (GATLINBURG, TN), ASM INTERNATIONAL, 1986
31. A.J. TURNER, ELECTRON BEAM WELDING OF HIGH VOLUME AIRCRAFT COMPONENTS, *PROC. CONF. FUNDAMENTAL AND PRACTICAL APPROACHES TO THE RELIABILITY OF WELDED STRUCTURES* (OSAKA, JAPAN), VOL 1, JAPAN WELDING SOCIETY, 1982, P 139-144
32. "WELDING CARPENTER CUSTOM 450 MULTIPLE-STRENGTH STAINLESS STEEL," PRODUCT DATA BULLETIN, CARPENTER TECHNOLOGY CORP., READING, PA, JAN 1973
33. *ALLOY DIG.*, FILING CODE SS-193, APRIL 1967
34. R. KALTENHAUSER, WELDABILITY OF PRECIPITATION HARDENING STEELS, *MET. ENG. QUART.*, VOL 9 (NO. 1), FEB 1969, P 44-57

B. Pollard

Welding Semiaustenitic PH Steels

As shown in Tables 1, 2, 3, and 4, semiaustenitic PH stainless steels include types 17-7PH, PH15-7 Mo, AM-350, and AM-355. As with the previous section on martensitic PH stainless steels, both microstructural evolution and weld parameters associated with semiaustenitic PH steels are described. The article "Welding of Stainless Steels" in this Volume should also be consulted.

Microstructural Evolution

The semiaustenitic PH steels have a primary δ-ferritic solidification mode and, on cooling, the δ-ferrite partially transforms to austenite by a Widmanstätten reaction. This austenite is stable down to ambient temperature so the as-welded structure of the fusion zone consists of austenite in a ferrite matrix (Fig. 2c). With the exception of AM-355, the percentage of retained ferrite in semiaustenitic PH welds is substantially higher than for welds in martensitic PH steels.

Postweld conditioning treatments destabilize the austenite so that it transforms to martensite at ambient or subzero temperatures. Subsequent aging simultaneously tempers the martensite and precipitates the strengthening particles, which are not visible by optical microscopy. The final fusion zone microstructure, therefore, consists of areas of retained ferrite in a tempered martensitic matrix. If a low conditioning temperature is used, carbide particles may also be observed at the ferrite-martensite interfaces.

In the as-welded and, to a lesser degree, the postweld heat-treated conditions, the HAZ is distinguishable from the base metal by an increase in grain size and ferrite content in the high-temperature region close to the fusion line.

17-7PH and PH15-7 Mo Stainless Steels

Weldability. 17-7PH and PH15-7 Mo stainless steels are typical of the semiaustenitic PH steels. As-deposited welds made without filler metal have weld metal and HAZ structures that are predominantly austenitic (Fig. 2c). This ductile structure is not susceptible to cold cracking, so 17-7PH and PH15-7 Mo are readily welded in any condition without preheat and without the need for critical control of interpass temperature or cooling rate (Ref 24, 35). However, autogenous 17-7PH weld metal is not fully austenitic, but rather contains about 25% δ-ferrite versus 10 to 15% in the base metal. Likewise, autogenous PH15-7 Mo weld metal may contain up to 40% δ-ferrite versus 15% in the base metal. The δ-ferrite content of the weld metal is determined primarily by composition, but high values are also promoted to a lesser degree by thicker weld beads, higher welding currents, and higher welding speeds. A large volume fraction of δ-ferrite can make the weld metal susceptible to hot cracking and reduce the ductility of the weld metal in the heat-treated condition. If necessary, the δ-ferrite content of the weld metal can be reduced by the addition of an appropriate filler metal.

Filler Metals. Filler wires are available for 17-7PH (AMS 5824) and PH15-7 Mo (AMS 5812) stainless steels. The compositions of these wires have been adjusted so as to produce deposits with lower δ-ferrite contents than would be produced by the base-metal compositions while still responding correctly to the age-hardening treatment (Ref 24, 35). Covered electrodes are not available for 17-7PH and PH15-7 Mo stainless steels because excessive oxidation of aluminum would occur in the arc. However, type 630 (17-4PH) covered electrodes have been used successfully for joining 17-7PH. To obtain adequate heat treat response with this filler metal, welding conditions that produce high dilution and a compromise PWHT practice are required (Ref 24). A heat treatment of 870 °C (1600 °F) for 90 min is used to simultaneously solution treat the type 630 weld metal and condition the 17-7PH base metal (Ref 35). The weld is then refrigerated at -75 °C (-100 °F) for 8 h and aged at 510 to 595 °C (950 to 1050 °F) for 1 h, depending on the properties required. Standard iron-chromium-nickel filler metals, such as types 308, 308L, 309, and 347, can also be used for joining 17-7PH and PH15-7 Mo, but the weld metal will not respond to heat treatment in the same manner as the base metal. Response to heat treatment will depend on the ratio of austenite-to-ferrite-forming elements in the filler metal and the amount of dilution by the base metal. In most instances, weld strength will be much lower than that obtained with a matching filler metal, but ductility and toughness will be higher.

Gas-Tungsten Arc Welding. Because 17-7PH and PH15-7 Mo stainless steels are used primarily as sheet and strip, they are most frequently joined by GTA welding. Preheating and postheating are not required to prevent cracking, but the

selection of welding conditions requires more care than for the standard austenitic stainless steels. Helium gas is preferred over argon for shielding the arc because helium minimizes the formation of a continuous aluminum oxide film on the surface of the weld pool (Ref 23). Particular care should be taken to provide efficient shielding of the weld pool in order to minimize loss of aluminum. Inert gas shielding should also be used on the underside of full penetration welds to protect the weld root. Welding speeds typically are of the order of 5 mm/s (12 in./min) (Ref 35). Higher welding speeds can cause porosity at the fusion line. Welding currents and weld-pass sequence should be selected to minimize the weld cross-sectional area.

Gas-metal arc welding is used for joining 17-7PH and PH15-7 Mo in heavy sheet and plate thicknesses. A mixture of 75He-25Ar is the most widely used shielding gas. Welding conditions are otherwise similar to those used for the standard austenitic stainless steels.

Postweld Heat Treatment. As-deposited welds in 17-7PH and PH15-7 Mo steels have a structure of austenite plus ferrite that is of much lower strength than the hardened base metal. A PWHT is, therefore, essential if a weld strength similar to the base-metal strength is required. The effects of PWHT on the tensile properties of GTA welds in 17-7PH and PH15-7 Mo steels are presented in Table 8; corresponding welding conditions are given in Table 9. The joint efficiencies of welds postweld hardened to the RH950 or TH1050 conditions without reannealing are 100% with weld reinforcement and 95 to 98% without it. Postweld reannealing before hardening has negligible effect on weld strength but increases weld ductility.

TABLE 8 TENSILE PROPERTIES OF GTA WELDS IN 1.6 MM (0.062 IN.) THICK 17-7PH AND PH15-7 MO STEELS

See also Table 9

ALLOY	PREWELD CONDITION[A]	POSTWELD HEAT TREATMENT[A]	REINFORCEMENT	TENSILE STRENGTH		0.2% YIELD STRENGTH		ELONGATION, %		FAILURE LOCATION[B]
				MPA	KSI	MPA	KSI	IN 13 MM (0.5 IN.)	IN 50 MM (2 IN.)	
HARDENED AND TESTED AS-WELDED										
PH15-7 MO	TH1050	NONE	OFF	840	122	605	88	25.0	7.0	WM
PH15-7 MO	R950	NONE	OFF	795	115	600	87	22.0	6.0	WM
WELDED AND HARDENED										
17-7PH	A	TH1050	ON	1415	205	1345	195	6.0	1.5	BM
17-7PH	A	RH950	ON	1515	220	1415	205	6.0	2.0	BM
PH15-7 MO	A	TH1050	ON	1450	210	1415	205	. . .	5.0	BM
PH15-7 MO	A	TH1050	OFF	1415	205	1345	195	8.0	2.0	WM
PH15-7 MO	A	RH950	ON	1655	240	1550	225	. . .	5.0	BM
PH15-7 MO	A	RH950	OFF	1585	230	1480	215	5.0	2.0	WM
WELDED, REANNEALED, AND HARDENED										
17-7PH	A	A + TH1050	ON	1435	208	1345	195	8.0	2.5	BM
PH15-7 MO	A	A + TH1050	ON	1450	210	1415	205	. . .	5.0	BM
PH15-7 MO	A	A + TH1050	OFF	1380	200	1345	195	10.0	2.5	WM
PH15-7 MO	A	A + RH950	ON	1620	235	1480	215	. . .	4.0	BM
PH15-7 MO	A	A + RH950	OFF	1585	230	1450	210	7.0	2.0	WM
PH15-7 MO	A	R + A + RH950	OFF	1660	241	1505	218	9.0	3.5	WM

(A) PREWELD AND POSTWELD HEAT TREATING CONDITIONS. A (CONDITION A): ANNEAL AT 1065 °C (1950 °F) FOR 10 MIN. AIR COOL. R (REFRIGERATION TREATMENT FOR TRANSFORMATION): -75 °C (-100 °F) FOR 8 H. TH1050: 760 °C (1400 °F) FOR 90 MIN, AIR COOL + 565 °C (1050 °F) FOR 90 MIN, AIR COOL. RH950: 955 °C (1750 °F) FOR 10 MIN; AIR COOL + -75 °C (-100 °F) FOR 8 H + 510 °C (950 °F) FOR 60 MIN; AIR COOL.

(B) WM, WELD METAL; BM, BASE METAL

TABLE 9 WELDING CONDITIONS FOR GTA WELDS DESCRIBED IN TABLE 8

WELDING CONDITION	ALLOY	
	17-7PH	**PH15-7 MO**
THICKNESS, MM (IN.)	1.59 (0.0625)	1.57 (0.062)
SHIELDING GAS	HELIUM	HELIUM
GAS FLOW RATE, L/RAIN (FT3/H)	28 (60)	24 (50)
WELDING SPEED, MM/S (IN./MIN)	6.3 (15)	5.1 (12)
CURRENT	AS REQUIRED FOR FULL PENETRATION IN A SINGLE PASS	AS REQUIRED FOR FULL PENETRATION IN A SINGLE PASS
FILLER WIRE	1.6 MM (0.062 IN.) DIAM W17-7PH	1.6 MM (0.062 IN.) DIAM WPH15-7MO
WIRE FEED RATE, MM/S (IN./MIN)	12 (28)	1 TO 1

Resistance Welding. Spot and seam welding have been used extensively for joining 17-7PH and PH15-7 Mo steels. For good results, particular attention should be given to the surface cleanliness of the steel. Surfaces to be joined should be free of oil, grease, dirt, and heat treating scale. Welding schedules should use longer weld times, lower weld currents, and electrode forces 10 to 20% higher than those normally used for the standard austenitic stainless steels (Ref 24). The best mechanical properties are obtained by welding just before or after final hardening. This practice produces weld nuggets with a tough austenitic microstructure. The tensile strength normal to the weld interface is a maximum for this condition, and the shear strength is not significantly lower than for nuggets in the hardened condition (Ref 35).

Sound flash butt welds can be produced in 17-7PH and PH15-7 Mo stainless steels, but ductility may be low as a result of ferrite stringers in the base metal being bent parallel to the weld interface (Ref 35).

AM-350 and AM-355 Stainless Steels

Weldability. AM-350 and AM-355 differ from 17-7PH and PH15-7 Mo stainless steels in that they do not contain aluminum. Martensitic transformation provides their major strengthening mechanism with an additional but smaller contribution from the precipitation of Cr_2N or an isostructurally similar phase during tempering (Ref 12). The absence of any reactive elements makes the weldability of AM-350 and AM-355 as good as that of the standard austenitic stainless steels and superior to that of 17-7PH. Although these steels are most often joined by GTA and GMA welding, they can be joined by any of the processes used for the standard austenitic stainless steels, including submerged arc, electron-beam, laser-beam, and resistance welding (Ref 34, 36, 37). Like 17-7PH and PH15-7 Mo, these steels may be welded in the annealed or hardened conditions and neither preheat nor special precautions with regard to interpass temperature or cooling rate are necessary. However, PWHT must be used if maximum weld strength is required.

Annealed AM-350 base metal contains 10 to 15% δ-ferrite, and welding produces even higher levels in autogeneous weld metal and the high-temperature portion of the HAZ. In the subzero cooled and tempered (SCT) condition, the final structure consists of islands of ferrite surrounded by carbides in a tempered martensitic matrix. In contrast, the composition of AM-355 is balanced so that the base metal contains less than 5% δ-ferrite in condition H (solution treated at 1065 °C, or 1950 °F) and 0% ferrite in the equalized plus overaged and tempered (EOT+) condition, and welding does not increase the ferrite content to any significant extent.

Filler Metals. An AM-355 filler wire (AMS 5780) with a composition identical to that of the base metal is available for joining AM-355. Likewise, a matching AM-350 filler wire (AMS 4774) is available for welding AM-350, but the AM-355 filler wire is usually preferred for this material because it gives slightly higher weld strengths after PWHT (Ref 36). The AM-355 filler wire can also be used with a proprietary flux for submerged arc welding. AM-355 covered electrodes have been developed for SMA welding but may not be readily available.

Postweld Heat Treatment. Joint efficiencies of 90 to 100% can be obtained by PWHT of AM-350 and AM-355 welds (Ref 36). The PWHT for welds in AM-350 consists of annealing at 930 °C (1710 °F) (condition L) and cooling rapidly to

room temperature, followed by subzero cooling to -75 °C (-100 °F) and tempering at 455 or 540 °C (850 or 1000 °F) (condition SCT).

Unlike AM-350, AM-355 must have a suitably prepared microstructure prior to the condition L treatment in order to minimize intergranular precipitation during this treatment. The required microstructure is produced by a prior heat treatment which involves carbide solution annealing for 1 to 3 h at 1040 °C (1900 °F), cooling rapidly enough to room temperature to avoid intergranular carbide precipitation in the temperature range 870 to 650 °C (1600 to 1200 °F), and subzero cooling to -75 °C (-100 °F). The subzero cooling causes a partial transformation to martensite and, during subsequent heat treatments in the carbide precipitation range, carbides precipitate in the former martensitic areas in preference to the grain boundaries. After this treatment, AM-355 weldments are annealed at 915 to 970 °C (1675 to 1775 °F), subzero cooled to -75 °C (-100 °F), and tempered at 455 or 540 °C (850 or 1000 °F) (condition SCT).

Resistance Welding. AM-350 and AM-355 can be spot welded either before or after the hardening treatment using similar conditions as for standard austenitic stainless steels. Postweld heat treatments (for example, condition SCT) produce a moderate increase in tensile shear strength, but also a corresponding decrease in cross-tension strength. Consequently, the best combination of tensile shear and cross-tension strength is obtained by welding in the hardened condition and not postweld heat treating (Ref 24, 37).

References cited in this section

12. G. AGGEN, "PHASE TRANSFORMATIONS AND HEAT TREATMENT STUDIES OF A CONTROLLED TRANSFORMATION STAINLESS STEEL ALLOY," DR. ENG. SC. THESIS, RENSSELAER POLYTECHNIC INSTITUTE, AUG 1963
23. G.E. LINNERT, WELDING PRECIPITATION-HARDENING STAINLESS STEELS, *WELD. J.*, VOL 36, JAN 1957, P 9-27
24. F.J. HAWKINS, WELDING OF AGE-HARDENABLE STAINLESS STEELS, *WELD. RES. COUNC. BULL.*, NO. 103, FEB 1965
34. R. KALTENHAUSER, WELDABILITY OF PRECIPITATION HARDENING STEELS, *MET. ENG. QUART.*, VOL 9 (NO. 1), FEB 1969, P 44-57
35. "ARMCO FABRICATING DATA," BULLETIN SF-5, ARMCO, INC., MIDDLETOWN, OH, DEC 1967
36. "AM-350/AM-355 PRECIPITATION HARDENING STAINLESS STEELS," PRODUCT DATA BULLETIN, ALLEGHENY LUDLUM CORP., PITTSBURGH, PA, 1963
37. H.W. MISHLER, R.E. MONROE, AND P.J. RIEPPEL, "WELDING OF HIGH STRENGTH STEELS FOR AIRCRAFT AND MISSILE APPLICATIONS," DMIC REPORT 118, DEFENSE METALS INFORMATION CENTER, COLUMBUS, OH, 12 OCT 1959

Selection of Wrought Precipitation-Hardening Stainless Steels

B. Pollard

Welding Austenitic PH Steels

Weldability and welding recommendations for A-286 and JBK-75 austenitic PH stainless steels are discussed below. Tables 1, 2, 3, and 4 list properties and heat treatments for these steels. As noted previously, additional information can be found in the article "Welding of Stainless Steels" in this Volume.

A-286 Stainless Steel

Weldability. A-286 stainless steel is highly alloyed and since welds solidify entirely as austenite (Fig. 2d), they are susceptible to hot cracking in both the fusion zone and HAZ (Ref 38, 39, 40, 41, 42). Solidification cracking in the fusion zone results from the formation of a low-melting-point Laves-phase eutectic at the grain boundaries, which is produced by the segregation of titanium and other solutes during the last stages of solidification (Ref 40, 42). This phase is enriched

in titanium, nickel, silicon, and molybdenum and depleted in iron and chromium (Ref 40). The same phase is also responsible for HAZ cracking (Ref 39, 40, 41, 42). However, in the HAZ, the Laves-phase eutectic is formed by the constitutional liquation of (Ti,Mo)(C,N) inclusions (Ref 41, 42). Constitutional liquation is a result of the rapid, nonequilibrium heating conditions typical of arc welding, which cause the carbonitrides to decompose more rapidly than their constituent elements can diffuse into the matrix. The result is the formation of solute-rich zones of eutectic composition (and hence low melting point) around the decomposing carbonitrides. This liquid then wets the grain boundaries, and the grains are pulled apart by shrinkage stresses as the weld cools. Of the residual elements normally present in A-286, silicon and boron have been found to have the greatest effect on hot cracking in both the fusion zone and HAZ (Ref 40, 41, 42).

The ease with which crack-free arc welds can be produced in A-286 depends on the grade of material, weld-section thickness, amount of restraint, the welding process used, the welding procedure, and the choice of filler metal. Both regular and welding grades of A-286 are produced. The welding grades (AMS 5858 and AMS 5895) have lower limits on manganese, silicon, sulfur, and phosphorus than the regular grades and exhibit greater resistance to hot cracking. Whenever possible, they should be specified in preference to the regular grades for applications that involve welding. Although A-286 is classified as a difficult-to-weld material, it can be joined successfully by GTA, EB, and resistance welding if the correct procedures are used.

Gas-Tungsten Arc Welding. When GTA welding A-286, the best results are obtained with the base metal in the solution treated condition, low-heat inputs, and minimum restraint (Ref 24, 34). Autogenous crack-free GTA welds can be produced in thin sheet, but welds in thick sheet and plate require filler metal. A stringer bead technique should be used for multipass welds in heavy sections.

The choice of filler metal depends on the application. The regular A-286 filler wires (AMS 5804) have lower limits on sulfur and phosphorus contents but are otherwise similar in composition to the base metal. Deposits made with these wires are the most prone to hot cracking, so they have been used primarily for single-pass welds (Ref 34). Premium quality A-286 filler wires (AMS 5805) with lower carbon, manganese, silicon, phosphorus, and boron contents and limits on oxygen, nitrogen, and hydrogen levels are also available. These wires are produced from vacuum induction melted material by wire rolling instead of drawing (Ref 43, 44). They produce high-purity deposits that are less susceptible to hot cracking than those made using the regular filler wires and are used for critical applications such as jet engine repairs.

Dissimilar metal filler wires are the usual choice for multipass welds if a matching filler metal is not essential because they exhibit greater resistance to hot cracking than A-286 weld metal. Hastelloy W has been used extensively for joining A-286 (Ref 24, 43). It has excellent resistance to hot cracking, but its stress-rupture strength is substantially lower than that of A-286 weld metal and it is not suitable for many high-temperature environments. Type 310 filler metal has been used for joining A-286 plate (Ref 24). It has very good corrosion resistance in many media but is nonhardening. AMS 5675 (AWS A5.14 Class ERNiCrFe-6) filler metal is significantly less crack sensitive than A-286 and is age hardenable, but it does not quite match the strength of A-286.

Postweld Heat Treatment. Typical tensile properties of welds in A-286 are presented in Table 10. A-286 weld metal does not age harden as rapidly or to the same extent as the base metal. A PWHT of 725 °C (1335 °F) for 48 h is required to increase the yield and ultimate tensile strengths to 93% and 89%, respectively, of the base-metal values (Ref 45). However, aging is much more rapid if the weld is first solution treated (Ref 46). For example, solution treating at 1080 °C (1975 °F) for 2 h and aging at 725 °C (1335 °F) for 16 h increases the yield and ultimate tensile strengths to 94% and 97%, respectively, of the base-metal values. If a high-temperature solution treatment is not feasible, weld strength can be increased by using a low-temperature multistep heat treatment consisting of 725 °C (1335 °F), 4 h plus 650 °C (1202 °F), 5 h plus 725 °C (1335 °F), 44 h (Ref 45). This heat treatment raises the yield and ultimate tensile strengths to 99% and 93%, respectively, of the base-metal values.

TABLE 10 TENSILE PROPERTIES OF WELDS IN AUSTENITIC PH STEELS

THICKNESS		FILLER METAL	PREWELD CONDITION[A]	SPECIMEN[B]	POSTWELD HEAT TREATMENT	TENSILE STRENGTH		0.2% YIELD STRENGTH		ELONGATION, %		REDUCTION IN AREA, %	COMMENTS	REF
mm	in.					mpa	ksi	mpa	ksi	in 25 mm (1 in.)	in 50 mm (2 in.)			
A-286 GTA WELDS														
3.0	0.118	NONE	ST	BM	AGED 725 °C (1335 °F), 48 H	952	138	710	103	16	. . .	29	. . .	45
3.0	0.118	NONE	ST	W	AGED 725 °C (1335 °F), 48 H	850	123	659	96	8	. . .	35	NO CRACKING	45
3.0	0.118	NONE	ST	BM	AGED 725 °C (1335 °F), 4 H + 650 °C (1200 °F), 5 H + 725 °C 1335 °F, 44 H	1020	148	777	113	20	. . .	28	. . .	45
3.0	0.118	NONE	ST	W	AGED 725 °C (1335 °F), 4 H + 650 °C (1200 °F), 5 H + 725 °C (1335 °F), 44	952	138	769	112	. . .	. . .	45	NO CRACKING	45
35	1.38	A-286	ST	BM	ST 980 °C (1795 °F), 2 H + AGED 725 °C (1335 °F), 16 H	1069	155	708	103	30	. . .	43	. . .	46
35	1.38	A-286	ST	W	NONE	724	105	611	89	15	. . .	34	. . .	46
35	1.38	A-286	ST	W	ST 980 °C (1795 °F), 2 H + AGED 725 °C (1335 °F), 16 H	1033	150	665	96	31	. . .	48	SCATTERED MICROFISSURES IN WELD METAL	46
A-286 EB WELDS														
3.2	0.125	NONE	ST	BM	AGED 730 °C (1350 °F), 16 H	1047	152	793	115	. . .	23.0	. . .	. . .	47
3.2	0.125	NONE	ST	W	AGED 730 °C (1350 °F), 16 H	919	133	775	112	. . .	5.6	. . .	MICROFISSURES IN HAZ	47
3.2	0.125	NONE	ST + AGED	W	REAGED 730 °C (1350 °F),	889	130	. . .	. . .	. . .	9.4	. . .	MICROFISSURES IN HAZ	47

					16 H									
JBK-75 GTA WELDS														
3.2	0.125	NONE	ST	BM	AGED 725 °C (1335 °F), 24 H	L130[(C)]	164[(C)]	. . .	. . .	. . .	. . .	. . .	. . .	52
3.2	0.125	NONE	ST	W	AGED 725 °C (1335 °F), 24 H	800[(C)]	116[(C)]	. . .	. . .	. . .	. . .	. . .	NO CRACKING	52
3.2	0.125	NONE	ST	BM	AGED 725 °C (1335 °F), 24 H + 650 °C (1200 °F), 24 H	1215	176	965	140	17	. . .	41	. . .	52
3.2	0.125	NONE	ST	W	AGED 725 °C (1335 °F), 24 H + 650 °C (1200 °F), 24 H	945	137	841	122	4	. . .	26	NO CRACKING	52
3.2	0.125	NONE	ST	BM	ST 950 °C (1740 °F), 24 H + 725 °C (1335 °F), 24 H	980[(C)]	142[(C)]	. . .	. . .	. . .	. . .	. . .	. . .	52
3.2	0.125	NONE	ST	W	ST 950 °C (1335 °F), 24 H + 650 °C (1200 °F), 24 H	980[(C)]	142[(C)]	. . .	. . .	. . .	. . .	. . .	NO CRACKING	52

(A) ST = SOLUTION TREATED.

(B) TRANSVERSE TENSILE SPECIMENS: BM. BASE METAL; W, WELDMENT.

(C) ESTIMATED FROM HARDNESS

Electron-Beam Welding. Although EB welding is a low-heat input process compared to arc welding, the use of EB welding does not guarantee freedom from hot cracking. However, crack-free EB welds can be made in A-286 if heat input, welding speed, and restraint are low. A-286 can be EB welded in both the solution treated and hardened conditions. However, resistance to hot cracking is greater in the solution treated condition. EB welds in A-286 are usually made without filler metal. In the as-welded condition, weld strength is about the same as for GTA welds in the same condition, but postweld aging is more effective in increasing weld strength than for GTA welds in A-286. For example, the yield and ultimate tensile strengths of EB welds made in 3.2 mm (0.128 in.) thick A-286 in the solution treated condition has yield and ultimate tensile strengths of 98% and 88%, respectively, of the base-metal values after aging at 720 °C (1330 °F) for 16 h (Ref 47).

Resistance Welding. A-286 stainless steel can be joined by resistance spot and seam welding in both the soft and hardened conditions, but the welds, as with those made by other fusion welding processes, are susceptible to hot cracking. However, some hot cracking can be tolerated in spot and seam welds since cracking of up to 5 vol% of the weld nugget has little effect on static or cyclic weld strength if it is concentrated at the center of the weld nugget (Ref 48). Hot cracking can be reduced or eliminated by using electrode forces significantly higher than those used for the standard austenitic stainless steels (Ref 24, 48). Welding conditions that slow down the cooling rate (for example, downsloping the weld current) have also been recommended as a means of eliminating cracking (Ref 48). Limited data suggest that longer weld times and lower weld currents than those used for standard austenitic stainless steels may also be beneficial.

Spot welds made in hardened material without PWHT have the best combination of shear and cross-tension strengths (Ref 37).

Seam welds in A-286 are also susceptible to hot cracking. Limited data indicate that the best results are obtained with a lower wheel speed, lower weld current and longer (on plus off) time than are generally used for the standard austenitic stainless steels. Increased electrode force and continuous (rather than interrupted) weld current may also be used to prevent cracking (Ref 49).

Little information is available on welding conditions for flash butt welding A-286 because these conditions vary from machine to machine and application to application. However, A-286 is routinely joined by flash butt welding with excellent results. After postweld aging at 720 °C (1325 °F), weld properties are virtually equal to those of the base metal (Ref 50).

JBK-75 Stainless Steel

JBK-75 is a modification of A-286 with the low carbon, manganese, silicon, and boron contents of welding grade A-286 plus a higher nickel content. The beneficial effect of the higher nickel content is explained by the concept of shrinkage brittleness (Ref 51). According to this concept, during the last stages of solidification, a minimum amount of eutectic liquid is required to fill all the dendritic fissures formed by the eutectic films. If a critical, subminimum amount of eutectic forms, severe cracking occurs. On the other hand, if only a very small amount of eutectic forms, no cracking occurs because enough solid boundaries are present to withstand the shrinkage stresses. Therefore, the beneficial effect of the high nickel content of JBK-75 is due to it increasing the amount of eutectic formed so that any microfissures which nucleate are self-healing. Consequently, JBK-75 has greater resistance to hot cracking than A-286 and can be GTA welded in heavier sections without cracking.

Mechanical properties of GTA welds in JBK-75 are presented in Table 10. Hardness measurements indicate that the weld ultimate tensile strength (UTS) is only about 70% of the base-metal value after postweld aging at 725 °C (1335 °F) for 24 h (Ref 52). Higher weld- and base-metal strengths and a joint efficiency, based on the UTS, of about 78% are obtained by a double aging treatment consisting of 725 °C (1335 °F), 24 h plus 650 °C (1200 °F), for 24 h. Homogenizing at 950 °C (1740 °F) before aging also increases weld-metal strength but simultaneously reduces the strength of the base metal. For example, a heat treatment consisting of 950 °C (1740 °F) for 24 h plus 725 °C (1335 °F) for 24 h produces a hardness of 30 HRC, which is equivalent to a UTS of about 965 MPa (140 ksi) in both the weld and base metal.

References cited in this section

24. F.J. HAWKINS, WELDING OF AGE-HARDENABLE STAINLESS STEELS, *WELD. RES. COUNC. BULL.*, NO. 103, FEB 1965

34. R. KALTENHAUSER, WELDABILITY OF PRECIPITATION HARDENING STEELS, *MET. ENG. QUART.*, VOL 9 (NO. 1), FEB 1969, P 44-57
37. H.W. MISHLER, R.E. MONROE, AND P.J. RIEPPEL, "WELDING OF HIGH STRENGTH STEELS FOR AIRCRAFT AND MISSILE APPLICATIONS," DMIC REPORT 118, DEFENSE METALS INFORMATION CENTER, COLUMBUS, OH, 12 OCT 1959
38. J.J. VAGI AND D.C. MARTIN, WELDING OF HIGH-STRENGTH STAINLESS STEELS FOR ELEVATED TEMPERATURE USE, *WELD. J.*, VOL 35, MARCH 1956, P 137S-144S
39. B.S. BLUM AND R.H. WITT, HEAT AFFECTED ZONE CRACKING IN A-286 WELDMENTS, *WELD. J.*, VOL 42, AUG 1963, P 365S-370S
40. J.A. BROOKS AND R.W. KRENZER, PROGRESS TOWARD A MORE WELDABLE A-286, *WELD. J.*, VOL 53, JUNE 1974, P 242S-245S
41. J.A. BROOKS, EFFECT OF ALLOY MODIFICATIONS ON HAZ CRACKING OF A-286 STAINLESS STEEL, *WELD. J.*, VOL 53, NOV 1974, P 517S-523S
42. J.A. BROOKS, A.W. THOMPSON, AND J.C. WILLIAMS, WELD CRACKING OF AUSTENITIC STAINLESS STEELS--EFFECTS OF IMPURITIES AND MINOR ELEMENTS, *PROC. CONF. PHYS. METALLURGY OF METAL JOINING* (ST. LOUIS, MO), TMS/AIME, 1980, P 117-136
43. W.H. SIMON, S. BANERJEE, AND R.S. CREMISIO, METALLURGICALLY CONTROLLED WELDING FILLER WIRE--TRACE ELEMENT CONTROLLED TO PRODUCE CONSISTENTLY SOUND WELDS, *PROC. INT. CONF.: THE EFFECTS OF RESIDUAL IMPURITY AND MICRO-ALLOYING ELEMENTS ON WELDABILITY AND WELD PROPERTIES* (LONDON, ENGLAND), WELDING INSTITUTE, PAPER 14, 1983
44. D.W. HARVEY, METALLURGICALLY CONTROLLED WELDING FILLER WIRE, *WELD. REV.*, MAY 1988, P 80, 82, 122, 123
45. L.T. SUMMERS, "EFFECT OF CHEMICAL SEGREGATION ON THE MICROSTRUCTURE AND PROPERTIES OF A-286 WELDMENTS," PH.D. DISSERTATION, UNIVERSITY OF CALIFORNIA, BERKELEY, 1984
46. A. INOUE *ET AL.*, FATIGUE STRENGTH OF ALLOY A-286 AT CRYOGENIC TEMPERATURE, *PROC. CONF. FATIGUE '87*, VOL 1 (CHARLOTTESVILLE, VA), ENGINEERING MATERIALS ADVISORY SERVICES, LTD., 1987, P 547-555
47. R.E. ROTH AND N.F. BRATKOVICH, CHARACTERISTICS AND STRENGTH DATA OF ELECTRON BEAM WELDS IN FOUR REPRESENTATIVE MATERIALS, *WELD. J.*, VOL 41, MAY 1962, P 229S-240S
48. I.F. SQUIRES, DETERMINATION OF RESISTANCE SPOT WELDING CONDITIONS FOR SOME HEAT-RESISTING STAINLESS STEELS, BR. *WELD. J.*, VOL 9, MARCH 1962, P 149-157
49. P.M. KNOWLSON, DETERMINATION OF RESISTANCE SEAM WELDING CONDITIONS FOR SOME HEAT RESISTING STEELS, *BR. WELD. J.*, VOL 9, 1962, P 436-445
50. J.J. VAGI, R.M. EVANS, AND D.C. MARTIN, "WELDING PRECIPITATION-HARDENING STAINLESS STEELS," NASA TECHNICAL MEMORANDUM X-53582, 28 FEB 1967
51. B.I. MEDOVAR, ON THE NATURE OF WELD HOT CRACKING, TRANSLATED FROM *AVTOM. SVARKA*, VOL 7 (NO. 4), 1954, P 12-28
52. M.J. STRUM, L.T. SUMMERS, AND J.W. MORRIS, JR., THE AGING RESPONSE OF A WELDED IRON-BASED SUPERALLOY, *WELD. J.*, VOL 62, SEPT 1983, P 235S-242S

Selection of Wrought Precipitation-Hardening Stainless Steels

B. Pollard

References

1. V. SEETHARAMAN ET AL., PRECIPITATION HARDENING IN A PH13-8 MO STAINLESS STEEL, *MATER. SCI. ENG.*, VOL 47, JAN 1981, P 1-11
2. H.J. RACK AND D. KALISH, THE STRENGTH, FRACTURE TOUGHNESS AND LOW CYCLE FATIGUE BEHAVIOR OF 17-4PH STAINLESS STEEL, *METALL. TRANS. A*, VOL 5, JULY 1974, P 1595-1605
3. K.C. ANTHONY, AGING REACTIONS IN PRECIPITATION HARDENABLE STAINLESS STEEL, *J. MET.*, VOL 15, DEC 1963, P 922-927
4. M. HENTHORNE, T.A. DEBOLD, AND R.J. YINGER, "CUSTOM 450-A NEW HIGHER STRENGTH STAINLESS STEEL," PAPER NO. 53, CORROSION '72, NATIONAL ASSOCIATION OF CORROSION ENGINEERS CONFERENCE, 1972
5. J.E. MCBRIDE, JR., AND G.N. MANIAR, *METALLOGRAPHY AS A QUALITY CONTROL TOOL*, PLENUM PUBLISHING, 1980, P 279
6. S. WIDGE, "A STUDY OF THE EFFECTS OF VARYING SOLUTION TREATMENT ON THE TOUGHNESS OF A STAINLESS MARAGING ALLOY," PH.D. DISSERTATION, LEHIGH UNIVERSITY, 1984
7. E.E. UNDERWOOD, A.E. AUSTIN, AND G.K. MANNING, THE MECHANISM OF HARDENING IN 17-7 NI-CR PRECIPITATION-HARDENING STAINLESS STEEL, *JISI*, VOL 200, AUG 1962, P 644-651
8. H.C. BURNETT, R.H. DUFF, AND H.C. VACHER, IDENTIFICATION OF METALLURGICAL REACTIONS AND THEIR EFFECT ON MECHANICAL PROPERTIES OF 17-7PH STEEL, *J. RES. NATL. BUR. STAND.--ENG. INSTRUMENTATION*, VOL 66C, 1962, P 113-119
9. E.G. FEL'DGANDLER AND M.V. PRIDANTSEV, PHASE TRANSFORMATION IN KH 17 N7 YU STAINLESS STEEL, *METALLOVED. TERM. OBRAB. MET.*, NOV 1960, P 2-7
10. J.C. WILKENS AND R.E. PENCE, A STUDY OF THE MICROSTRUCTURE OF PRECIPITATION HARDENING STAINLESS STEEL SHEET, *ADVANCES IN ELECTRON METALLOGRAPHY AND ELECTRON PROBE MICROANALYSIS*, STP 317, ASTM, 1962, P 140-149
11. J.C. WILKENS, PRIVATE COMMUNICATION, IN PRECIPITATION FROM IRON-BASE ALLOYS, PROCEEDINGS OF AN AIME SYMPOSIUM, CLEVELAND, OH, 21 OCT 1963, P 98
12. G. AGGEN, "PHASE TRANSFORMATIONS AND HEAT TREATMENT STUDIES OF A CONTROLLED TRANSFORMATION STAINLESS STEEL ALLOY," DR. ENG. SC. THESIS, RENSSELAER POLYTECHNIC INSTITUTE, AUG 1963
13. D.R. MUZYKA, *THE METALLURGY OF NICKEL-IRON ALLOYS, THE SUPERALLOYS*, C.T. SIMS AND W.C. HAGEL, ED., JOHN WILEY & SONS, 1972, P 113-143
14. A.W. THOMPSON AND J.A. BROOKS, THE MECHANISM OF PRECIPITATION STRENGTHENING IN AN IRON-BASE SUPERALLOY, *ACTA METALL.*, VOL 30, DEC 1982, P 2197-2203
15. T.J. HEADLEY, M.M. KAMOUSKY, AND W.R. SORENSON, EFFECT OF COMPOSITION AND HIGH ENERGY RATE FORGING ON THE ONSET OF PRECIPITATION IN AN IRON-BASE SUPERALLOY, *METALL. TRANS. A*, VOL 13, MARCH 1982, P 345-353
16. "ARMCO 17-4PH STAINLESS STEEL BAR AND WIRE," PRODUCT DATA BULLETIN NO. S-24, ARMCO, INC., MIDDLETOWN, OH, SEPT 1966
17. "ARMCO PH 13-8MO STAINLESS STEEL," PRODUCT DATA BULLETIN NO. S-24, ARMCO, INC., MIDDLETOWN, OH, OCT 1986
18. "CARPENTER CUSTOM 450," PRODUCT DATA BULLETIN, CARPENTER TECHNOLOGY CORP., READING, PA, 1971
19. "CARPENTER CUSTOM 455," PRODUCT DATA BULLETIN, CARPENTER TECHNOLOGY CORP., READING, PA, 1971
20. "ARMCO 17-7PH AND PH15-7MO STAINLESS STEEL SHEET AND STRIP," PRODUCT DATA BULLETIN, ARMCO, INC., MIDDLETOWN, OH, JAN 1975
21. B. POLLARD, UNPUBLISHED WORK
22. N. SUUTALA, EFFECT OF SOLIDIFICATION CONDITIONS ON THE SOLIDIFICATION MODE IN

STAINLESS STEELS, *METALL. TRANS. A,* VOL 14, FEB 1983, P 191-197

23. G.E. LINNERT, WELDING PRECIPITATION-HARDENING STAINLESS STEELS, *WELD. J.,* VOL 36, JAN 1957, P 9-27
24. F.J. HAWKINS, WELDING OF AGE-HARDENABLE STAINLESS STEELS, *WELD. RES. COUNC. BULL.,* NO. 103, FEB 1965
25. "ARMCO FABRICATING DATA," BULLETIN SF-2, ARMCO, INC., MIDDLETOWN, OH, FEB 1966
26. C. CHEN AND J.S. YEH, ELECTRON BEAM AND PLASMA ARC WELDING OF 17-4PH STAINLESS STEEL, *PROC. CONF. POWER BEAM PROCESSING: ELECTRON, LASER, PLASMA ARC* (SAN DIEGO, CA), ASM INTERNATIONAL, 1988, P 45-54
27. A.J. TURNER, ELECTRON BEAM WELDING THICK SECTION PRECIPITATION-HARDENING STEEL, *WELD. J.,* VOL 60, JAN 1981, P 18-26
28. M.U. ISLAM, G. CAMPBELL, AND R. HSU, FATIGUE AND TENSILE PROPERTIES OF EB WELDED 17-4PH STEEL, *WELD. J.,* VOL 68, SEPT 1989, P 45-50
29. S. MATSUI *ET AL.,* ELECTRON BEAM WELDING OF THE PRECIPITATION HARDENING STAINLESS STEEL, *REVUE DE LA SOUDURE-LASTIJDSCRIFT,* VOL 46, JAN 1990, P 52-57
30. W.R. CIESLAK, J.A. BROOKS, AND W.M. GARRISON, JR., THE WELDABILITY, MICROSTRUCTURE AND PROPERTIES OF PRECIPITATION STRENGTHENED MARTENSITIC STAINLESS STEELS, *PROC. CONF. ADVANCES IN WELDING SCIENCE AND TECHNOLOGY* (GATLINBURG, TN), ASM INTERNATIONAL, 1986
31. A.J. TURNER, ELECTRON BEAM WELDING OF HIGH VOLUME AIRCRAFT COMPONENTS, *PROC. CONF. FUNDAMENTAL AND PRACTICAL APPROACHES TO THE RELIABILITY OF WELDED STRUCTURES* (OSAKA, JAPAN), VOL 1, JAPAN WELDING SOCIETY, 1982, P 139-144
32. "WELDING CARPENTER CUSTOM 450 MULTIPLE-STRENGTH STAINLESS STEEL," PRODUCT DATA BULLETIN, CARPENTER TECHNOLOGY CORP., READING, PA, JAN 1973
33. *ALLOY DIG.,* FILING CODE SS-193, APRIL 1967
34. R. KALTENHAUSER, WELDABILITY OF PRECIPITATION HARDENING STEELS, *MET. ENG. QUART.,* VOL 9 (NO. 1), FEB 1969, P 44-57
35. "ARMCO FABRICATING DATA," BULLETIN SF-5, ARMCO, INC., MIDDLETOWN, OH, DEC 1967
36. "AM-350/AM-355 PRECIPITATION HARDENING STAINLESS STEELS," PRODUCT DATA BULLETIN, ALLEGHENY LUDLUM CORP., PITTSBURGH, PA, 1963
37. H.W. MISHLER, R.E. MONROE, AND P.J. RIEPPEL, "WELDING OF HIGH STRENGTH STEELS FOR AIRCRAFT AND MISSILE APPLICATIONS," DMIC REPORT 118, DEFENSE METALS INFORMATION CENTER, COLUMBUS, OH, 12 OCT 1959
38. J.J. VAGI AND D.C. MARTIN, WELDING OF HIGH-STRENGTH STAINLESS STEELS FOR ELEVATED TEMPERATURE USE, *WELD. J.,* VOL 35, MARCH 1956, P 137S-144S
39. B.S. BLUM AND R.H. WITT, HEAT AFFECTED ZONE CRACKING IN A-286 WELDMENTS, *WELD. J.,* VOL 42, AUG 1963, P 365S-370S
40. J.A. BROOKS AND R.W. KRENZER, PROGRESS TOWARD A MORE WELDABLE A-286, *WELD. J.,* VOL 53, JUNE 1974, P 242S-245S
41. J.A. BROOKS, EFFECT OF ALLOY MODIFICATIONS ON HAZ CRACKING OF A-286 STAINLESS STEEL, *WELD. J.,* VOL 53, NOV 1974, P 517S-523S
42. J.A. BROOKS, A.W. THOMPSON, AND J.C. WILLIAMS, WELD CRACKING OF AUSTENITIC STAINLESS STEELS--EFFECTS OF IMPURITIES AND MINOR ELEMENTS, *PROC. CONF. PHYS. METALLURGY OF METAL JOINING* (ST. LOUIS, MO), TMS/AIME, 1980, P 117-136
43. W.H. SIMON, S. BANERJEE, AND R.S. CREMISIO, METALLURGICALLY CONTROLLED WELDING FILLER WIRE--TRACE ELEMENT CONTROLLED TO PRODUCE CONSISTENTLY SOUND WELDS, *PROC. INT. CONF.: THE EFFECTS OF RESIDUAL IMPURITY AND MICRO-ALLOYING ELEMENTS ON WELDABILITY AND WELD PROPERTIES* (LONDON, ENGLAND), WELDING INSTITUTE, PAPER 14, 1983

44. D.W. HARVEY, METALLURGICALLY CONTROLLED WELDING FILLER WIRE, *WELD. REV.*, MAY 1988, P 80, 82, 122, 123
45. L.T. SUMMERS, "EFFECT OF CHEMICAL SEGREGATION ON THE MICROSTRUCTURE AND PROPERTIES OF A-286 WELDMENTS," PH.D. DISSERTATION, UNIVERSITY OF CALIFORNIA, BERKELEY, 1984
46. A. INOUE *ET AL.*, FATIGUE STRENGTH OF ALLOY A-286 AT CRYOGENIC TEMPERATURE, *PROC. CONF. FATIGUE '87*, VOL 1 (CHARLOTTESVILLE, VA), ENGINEERING MATERIALS ADVISORY SERVICES, LTD., 1987, P 547-555
47. R.E. ROTH AND N.F. BRATKOVICH, CHARACTERISTICS AND STRENGTH DATA OF ELECTRON BEAM WELDS IN FOUR REPRESENTATIVE MATERIALS, *WELD. J.*, VOL 41, MAY 1962, P 229S-240S
48. I.F. SQUIRES, DETERMINATION OF RESISTANCE SPOT WELDING CONDITIONS FOR SOME HEAT-RESISTING STAINLESS STEELS, BR. *WELD. J.*, VOL 9, MARCH 1962, P 149-157
49. P.M. KNOWLSON, DETERMINATION OF RESISTANCE SEAM WELDING CONDITIONS FOR SOME HEAT RESISTING STEELS, *BR. WELD. J.*, VOL 9, 1962, P 436-445
50. J.J. VAGI, R.M. EVANS, AND D.C. MARTIN, "WELDING PRECIPITATION-HARDENING STAINLESS STEELS," NASA TECHNICAL MEMORANDUM X-53582, 28 FEB 1967
51. B.I. MEDOVAR, ON THE NATURE OF WELD HOT CRACKING, TRANSLATED FROM *AVTOM. SVARKA*, VOL 7 (NO. 4), 1954, P 12-28
52. M.J. STRUM, L.T. SUMMERS, AND J.W. MORRIS, JR., THE AGING RESPONSE OF A WELDED IRON-BASED SUPERALLOY, *WELD. J.*, VOL 62, SEPT 1983, P 235S-242S

Selection of Cast Stainless Steels

Michael J. Cieslak, Sandia National Laboratories

Introduction

THE DEVELOPMENT OF CASTING TECHNOLOGY has been driven by two distinct engineering perspectives. The first involves the potential economy of cast hardware relative to totally machined wrought parts. Complex, nearnet shapes can be produced by a variety of casting processes, including sand casting, investment casting, and centrifugal casting (used almost exclusively for making tubular products). Casting also can be an extremely effective way of producing very large parts.

The second perspective is associated with metallurgical realities. Many alloys have been developed for which there are no true wrought counterparts. The chemical composition and microstructure of these alloys is such that deformation processing of large ingots into wrought product forms would be problematic. In addition, the very nature of the cast microstructure, which in general is composed of large grains, can provide benefits in high-temperature creep applications.

Some common examples of stainless steel castings include valve and pump bodies, compressor wheels, propellers, turbine impellers, large pipe elbows, heat treating fixtures, and food, paper, and chemical processing equipment. Extensive reviews on the properties and applications of cast stainless steels can be found in Ref 1, 2, 3, and 4.

Acknowledgement

This work was performed at Sandia National Laboratories, supported by the U.S. Department of Energy under contract number DE-AC04-76DP00789.

References

1. J.M. SVOBODA, HIGH-ALLOY STEELS, *CASTING*, 9TH ED., VOL 15, *METALS HANDBOOK*, ASM INTERNATIONAL, 1988, P 722-735
2. M. BLAIR, CAST STAINLESS STEELS, *PROPERTIES AND SELECTION: IRONS, STEELS, AND HIGH-PERFORMANCE ALLOYS*, VOL 1, *ASM HANDBOOK*, ASM INTERNATIONAL, 1990, P 908-929
3. R.W. MONROE AND S.J. PAWEL, CORROSION OF CAST STEELS, *CORROSION*, 9TH ED., VOL 13, *METALS HANDBOOK*, ASM INTERNATIONAL, 1987, P 573-582
4. P.R. WEISER, *ED.*, *STEEL CASTINGS HANDBOOK*, 5TH ED., STEEL FOUNDERS' SOCIETY OF AMERICA, 1980

Selection of Cast Stainless Steels

Michael J. Cieslak, Sandia National Laboratories

Stainless Steel Casting Alloys

Categories. Unlike the case of wrought alloy designators, cast stainless steels are not grouped according to microstructural types, but by the intended service environment. The general classification of stainless steel castings places these alloys in one of two categories: corrosion-resistant alloys and heat-resistant alloys. The corrosion-resistant alloys have been designed primarily for service environments involving aqueous or liquid-vapor corrosives at temperatures generally less than 315 °C (600 °F). Use at extended temperatures up to 650 °C (1200 °F) in selected environments may also be considered.

The heat-resistant alloys have been designed for use in service environments exceeding 650 °C (1200 °F) where aqueous corrosives do not exist. At these elevated temperatures, oxidation, sulfidation, and carburization/decarburization are the environmental effects of consequence. High-temperature mechanical strength, creep and stress-rupture resistance, and microstructural stability are the engineering requirements for these alloys. The high-temperature alloys are most readily distinguished from the corrosion-resistant alloys on the basis of carbon content (although other alloying elements may also vary considerably in response to service needs) with the high-temperature alloys containing 0.20 to 0.70 wt% C and the corrosion-resistant alloys generally containing less than 0.20 wt% C.

Nomenclature. Cast stainless steels are most often specified on the basis of composition using the designation system of the High Alloy Product Group of the Steel Founders' Society of America. (The High Alloy Product Group has replaced the Alloy Casting Institute, or ACI, which formerly administered these designations.) The first letter of the designation indicates whether the alloy is intended primarily for liquid corrosion service (C) or high-temperature service (H). The second letter in either group of alloys indicates an approximate ratio of nickel-to-chromium with the ratio increasing in alphabetical order. (As the nickel content increases, the second letter of the designation progresses through the alphabet from A to Z.) The number immediately following the hyphen indicates the carbon content of the alloy in hundredths of a weight percent (also known as "points" of carbon). For the corrosion-resistant alloys, the carbon content indicated is the maximum allowable for the alloy. For the heat-resistant alloys, the carbon content identified is the midpoint with an allowable range of ± 0.05 wt%. Finally, if further alloying elements are present, these are indicated by the addition of one or more letters as a suffix. Thus, the designation of CF-8M refers to an alloy for corrosion-resistant service (C) of the 19Cr-9Ni type with a maximum carbon content of 0.08% that contains molybdenum (M). Figure 1 graphically shows the range of nickel and chromium contents in several grades of corrosion-resistant and heat-resistant alloys identified by the aforementioned designation system. Tables 1 and 2 list the chemical compositions of the common corrosion-resistant and heat-resistant alloys, respectively.

TABLE 1 COMPOSITIONS AND TYPICAL MICROSTRUCTURES OF CORROSION-RESISTANT STAINLESS STEEL CASTING ALLOYS

ALLOY DESIGNATION	WROUGHT ALLOY TYPE[A]	ASTM SPECIFICATIONS	MOST COMMON END-USE MICROSTRUCTURE	COMPOSITIONS, %[B]					
				C	Mn	Si	Cr	Ni	OTHERS[C]
CHROMIUM STEELS									
CA-15	410	A 743, A 217, A 487	MARTENSITE	0.15	1.00	1.50	11.5-14.0	1.0	0.50 MO[D]
CA-15M	. . .	A 743	MARTENSITE	0.15	1.00	0.65	11.5-14.0	1.0	0.15-1.00 MO
CA-40	420	A 743	MARTENSITE	0.40	1.00	1.50	11.5-14.0	1.0	0.5 MO[D]
CA-40F	. . .	A 743	MARTENSITE	0.2-0.4	1.00	1.50	11.5-14.0	1.0	. . .
CB-30	431, 442	A 743	FERRITE AND CARBIDES	0.30	1.00	1.50	18.0-22.0	2.0	. . .
CC-50	446	A 743	FERRITE AND CARBIDES	0.30	1.00	1.50	26.0-30.0	4.0	. . .
CHROMIUM-NICKEL STEELS									
CA-6N	. . .	A 743	MARTENSITE	0.06	0.50	1.00	1.0-12.5	6.0-8.0	. . .
CA-6NM	. . .	A 743, A 487	MARTENSITE	0.06	1.00	1.00	11.5-14.0	3.5-4.5	0.4-1.0 MO
CA-28MWV	. . .	A 743	MARTENSITE	0.20-0.28	0.50-1.00	1.00	11.0-12.5	0.50-1.00	0.9-1.25 MO; 0.9-1.25 W; 0.2-0.3 V
CB-7CU-1	. . .	A 747	MARTENSITE, AGE HARDENABLE	0.07	0.70	1.00	15.5-17.7	3.6-4.6	2.5-3.2 CU; 0.20-0.35 NB; 0.05 N MAX
CB-7CU-2	. . .	A 747	MARTENSITE, AGE HARDENABLE	0.07	0.70	1.00	14.0-15.5	4.5-5.5	2.5-3.2 CU; 0.20-0.35 NB; 0.05 N MAX
CD-4MCU	. . .	A 351, A 743, A 744, A 890	AUSTENITE IN FERRITE, AGE HARDENABLE	0.04	1.00	1.00	25.0-26.5	4.75-6.0	1.75-2.25 MO; 2.75-3.25 CU
CE-30	312	A 743	FERRITE IN AUSTENITE	0.30	1.50	2.00	26.0-30.0	8.0-11.0	. . .
CF-3[E]	304L	A 351, A 743, A 744	FERRITE IN AUSTENITE	0.03	1.50	2.00	17.0-	8.0-	. . .

							21.0	12.0	
CF-3M[E]	316L	A 351, A 743, A 744	FERRITE IN AUSTENITE	0.03	1.50	2.00	17.0-21.0	8.0-12.0	2.0-3.0 MO
CF-3MN	. . .	A 743	FERRITE TN AUSTENITE	0.03	1.50	1.50	17.0-21.0	9.0-13.0	2.0-3.0 MO; 0.10-0.20 N
CF-8[E]	304	A 351, A 743, A 744	FERRITE IN AUSTENITE	0.08	1.50	2.00	18.0-21.0	8.0-11.0	. . .
CF-8C	347	A 351, A 743, A 744	FERRITE IN AUSTENITE	0.08	1.50	2.00	18.0-21.0	9.0-12.0	NB[F]
CF-8M	316	A 351, A 743, A 744	FERRITE IN AUSTENITE	0.08	1.50	2.00	18.0-21.0	9.0-12.0	2.0-3.0 MO
CF-10	. . .	A 351	FERRITE IN AUSTENITE	0.04-0.10	1.50	2.00	18.0-21.0	8.0-11.0	. . .
CF-10M	. . .	A 351	FERRITE IN AUSTENITE	0.04-0.10	1.50	1.50	18.0-21.0	9.0-12.0	2.0-3.0 MO
CF-10MC	. . .	A 351	FERRITE IN AUSTENITE	0.10	1.50	1.50	15.0-18.0	13.0-16.0	1.75-2.25 MO
CF-10SMNN	. . .	A 351, A 743	FERRITE IN AUSTENITE	0.10	7.00-9.00	3.50-4.50	16.0-18.0	8.0-9.0	0.08-0.18 N
CF-12M	316	. . .	FERRITE IN AUSTENITE OR AUSTENITE	0.12	1.50	2.00	18.0-21.0	9.0-12.0	2.0-3.0 MO
CF-16F	303	A 743	AUSTENITE	0.16	1.50	2.00	18.0-21.0	9.0-12.0	1.50 MO MAX; 0.20-0.35 SE
CF-20	302	A 743	AUSTENITE	0.20	1.50	2.00	18.0-21.0	8.0-11.0	. . .
CG-6MMN	. . .	A 351, A 743	FERRITE IN AUSTENITE	0.06	4.00-6.00	1.00	20.5-23.5	11.5-13.5	1.50-3.00 MO; 0.10-0.30 NB; 0.10-30 V; 0.20-40 N
CG-8M	317	A 351, A 743, A 744	FERRITE IN AUSTENITE	0.08	1.50	1.50	18.0-21.0	9.0-13.0	3.0-4.0 MO
CG-12	. . .	A 743	FERRITE IN AUSTENITE	0.12	1.50	2.00	20.0-23.0	10.0-13.0	. . .
CH-8	. . .	A 351	FERRITE IN AUSTENITE	0.08	1.50	1.50	22.0-26.0	12.0-15.0	. . .
CH-10	. . .	A 351	FERRITE IN AUSTENITE	0.04-0.10	1.50	2.00	22.0-26.0	12.0-15.0	. . .

CH-20	309	A 351, A 743	AUSTENITE	0.20	1.50	2.00	22.0-26.0	12.0-15.0	. . .
CK-3MCUN	. . .	A 351, A 743, A 744	FERRITE IN AUSTENITE	0.025	1.20	1.00	19.5-20.5	17.5-19.5	6.0-7.0 V; 0.18-0.24 N; 0.50-1.00 CU
CK-20	310	A 743	AUSTENITE	0.20	2.00	2.00	23.0-27.0	19.0-22.0	. . .
NICKEL-CHROMIUM STEEL									
CN-3M	. . .	A 743	AUSTENITE	0.03	2.00	1.00	20.0-22.0	23.0-27.0	4.5-5.5 MO
CN-7M	. . .	A 351, A 743, A 744	AUSTENITE	0.07	1.50	1.50	19.0-22.0	27.5-30.5	2.0-3.0 MO; 3.0-4.0 CU
CN-7MS	. . .	A 743, A 744	AUSTENITE	0.07	1.50	3.50(G)	18.0-20.0	22.0-25.0	2.5-3.0 MO; 1.5-2.0 CU
CT-15C	. . .	A 351	AUSTENITE	0.05-0.15	0.15-1.50	0.50-1.50	19.0-21.0	31.0-34.0	0.5-1.5 V

(A) TYPE NUMBERS OF WROUGHT ALLOYS ARE LISTED ONLY FOR NOMINAL IDENTIFICATION OF CORRESPONDING WROUGHT AND CAST GRADES. COMPOSITION RANGES OF CAST ALLOYS ARE NOT THE SAME AS FOR CORRESPONDING WROUGHT ALLOYS; CAST ALLOY DESIGNATIONS SHOULD BE USED FOR CASTINGS ONLY.

(B) MAXIMUM UNLESS A RANGE IS GIVEN. THE BALANCE OF ALL COMPOSITIONS IS IRON.

(C) SULFUR CONTENT IS 0.04% IN ALL GRADES EXCEPT: CG-6MMN, 0.030% S (MAX); CF-10SMNN, 0.03% S (MAX); CT-15C, 0.03% S (MAX); CK-3MCUN, 0.010% S (MAX); CN-3M 0.030% S (MAX), CA-6N, 0.020% S (MAX); CA-28MWV, 0.030% S (MAX); CA-40F, 0.20-0.40% S; CB-7CU-1 AND -2, 0.03% S (MAX). PHOSPHORUS CONTENT IS 0.04% (MAX) IN ALL GRADES EXCEPT; CF-16F, 0.17% P (MAX); CF-10SMNN, 0.060% P (MAX); CT-15C, 0.030% P (MAX); CK-3MCUN, 0.045% P (MAX); CN-3M, 0.030% P (MAX); CA-6N, 0.020% P (MAX); CA-28MWV, 0.030% P (MAX); CB-7CU-1 AND -2, 0.035% P (MAX).

(D) MOLYBDENUM NOT INTENTIONALLY ADDED.

(E) CF-3A, CF-3MA, AND CF-8A HAVE THE SAME COMPOSITION RANGES AS CF-3, CF-3M, AND CF-8, RESPECTIVELY, BUT HAVE BALANCED COMPOSITIONS SO THAT FERRITE CONTENTS ARE AT LEVELS THAT PERMIT HIGHER MECHANICAL PROPERTY SPECIFICATIONS THAN THOSE FOR RELATED GRADES. THEY ARE COVERED BY ASTM A 351.

(F) NB, 8 × %C MIN (1.0% MAX); OR NB + TA × %C (1.1% MAX).

(G) FOR CN-7MS, SILICON RANGES FROM 2.50 TO 3.50%.

TABLE 2 COMPOSITIONS OF HEAT-RESISTANT STAINLESS STEEL CASTING ALLOYS

ALLOY	UNS	ASTM SPECIFICATIONS(A)	COMPOSITION, %(B)

DESIGNATION	NO.		C	Cr	Ni	Si (max)
HA	. . .	A217	0.20 MAX	8-10	. . .	1.00
HC	J92605	A 297, A 608	0.50 MAX	26-30	4 MAX	2.00
HD	J93005	A 297, A 608	0.50 MAX	26-30	4-7	2.00
HE	J93403	A 297, A 608	0.20-0.50	26-30	8-11	2.00
HF	J92603	A 297, A 608	0.20-0.40	19-23	9-12	2.00
HH	J93503	A 297, A 608, A 447	0.20-0.50	24-28	11-14	2.00
HI	J94003	A 297, A 567, A 608	0.20-0.50	26-30	14-18	2.00
HK	J94224	A 297, A 351, A 567, A 608	0.20-0.60	24-28	18-22	2.00
HK30	. . .	A 351	0.25-0.35	23.0-27.0	19.0-22.0	1.75
HK40	. . .	A 351	0.35-0.45	23.0-27.0	19.0-22.0	1.75
HL	J94604	A 297, A 608	0.20-0.60	28-32	18-22	2.00
HN	J94213	A 297, A 608	0.20-0.50	19-23	23-27	2.00
HP	. . .	A 297	0.35-0.75	24-28	33-37	2.00
HP-50WZ(C)	. . .	. . .	0.45-0.55	24-28	33-37	2.50
HT	J94605	A 297, A 351, A 567, A 608	0.35-0.75	13-17	33-37	2.50
HT30	. . .	A 351	0.25-0.35	13.0-17.0	33.0-37.0	2.50
HU	. . .	A 297, A 608	0.35-0.75	17-21	37-41	2.50
HW	. . .	A 297, A 608	0.35-0.75	10-14	58-62	2.50
HX	. . .	A 297, A 608	0.35-0.75	15-19	64-68	2.50

(A) ASTM DESIGNATIONS ARE THE SAME AS ACI DESIGNATIONS.

(B) BALANCE IRON IN ALL COMPOSITIONS. MANGANESE CONTENT: 0.35 TO 0.65% FOR HA. 1% FOR HC. 1.5% FOR HD AND 2% FOR THE OTHER ALLOYS. PHOSPHORUS AND SULFUR CONTENTS: 0.04% (MAX) FOR ALL BUT HP-50WZ. MOLYBDENUM IS INTENTIONALLY ADDED ONLY TO HA, WHICH HAS 0.90 TO 1.20% MO; MAXIMUM FOR OTHER ALLOYS IS SET AT 0.5% MO. HH ALSO CONTAINS 0.2% N (MAX).

(C) ALSO CONTAINS 4 TO 6% W, 0.1 TO 1.0% ZR, AND 0.035% S (MAX) AND P (MAX)

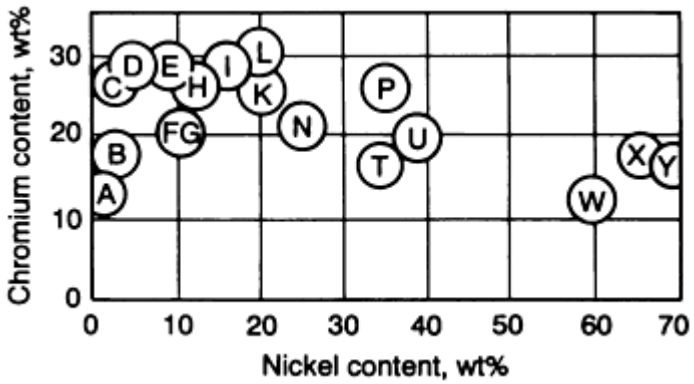

FIG. 1 SCHEMATIC OF THE CHROMIUM AND NICKEL CONTENT RANGES FOR CORROSION-RESISTANT AND HEAT-RESISTANT STAINLESS STEEL ALLOYS. THE LETTERS IN CIRCLES REPRESENT THE SECOND LETTER IN THE ALLOY DESIGNATION SYSTEM. SOURCE: REF 4

Reference cited in this section

4. P.R. WEISER, *ED., STEEL CASTINGS HANDBOOK,* 5TH ED., STEEL FOUNDERS' SOCIETY OF AMERICA, 1980

Michael J. Cieslak, Sandia National Laboratories

Welding and Weldability of Cast Stainless Steels

Welding and Welding Processes. In general terms, there are two situations in which welding of stainless steel castings is required. One of these occurs before the casting ever leaves the foundry. Casting defects, such as hot tears, shrinkage cavities, and cold shuts, are often observed in stainless steel castings. Certain specifications preclude the acceptance of these castings for service use without repair. Fusion welding is an appropriate method for repair of these casting defects. The defects, identified through one of several possible procedures (for example, dye penetrant, radiography, or ultrasonic inspection), are removed by machining or grinding, leaving a clean joint surface onto which weld filler metal is added to produce a sound final product. For small, near-surface defects, autogenous welds (that is, no filler metal added) may be sufficient to eliminate the defects. A special case of repair welding is known by the term "upgrading." An "upgraded" casting is one that has been selectively welded in order to achieve a higher level of product specification acceptance.

The second situation requiring welding involves joining of the casting to other hardware, cast or wrought, as part of an engineering design. In this circumstance, the design rules for welding are similar to those for wrought alloys, as discussed in the articles on wrought stainless steels that appear in this Section of the Handbook. Any of the fusion welding processes can be successfully employed in the welding of castings. Most common are the arc welding processes, especially autogenous and filler-metal-added gas-tungsten arc welding, shielded metal arc welding, and gas-metal arc welding. Fabrication involving the use of extremely large castings may employ electroslag welding as the only reasonable economic choice. Other processes, such as electron-beam welding, laser-beam welding, and plasma arc welding, are also appropriate choices in many instances. A wide range of filler metals exists for joining of the various casting alloys. The choice depends on the specifics of the situation and whether the weld will be to a similar or dissimilar alloy. The use of matching filler metal is generally suggested when welding like alloys. Where a matching consumable is not available, common choices are 308L and 316L for the low-nickel-content corrosion-resistant austenitic alloys. For the higher-nickel-content corrosion-resistant and heat-resistant alloys, appropriate choices may be consumables (bare electrodes for gas-tungsten arc welding and gas-metal arc welding) such as 20Cb-3 (AWS ER320/ER320LR) and nickel alloys such as C-276 (AWS ERNiCrMo-4), Alloy 625 (ERNiCrMo-3), and Inconel alloys 82 (AWS ERNiCr-3), 92 (AWS ERNiCrFe-6), and 182 (AWS ERNiCrFe-3).

Metallurgical Considerations. Castings are metallurgically more complex than wrought alloys. Segregation during dendritic solidification can lead to local variations in both chemical composition and microstructure. The vast majority of the heat-resistant alloys will terminate solidification with the formation of a eutectic-like carbide constituent that remains upon cooling of the casting to room temperature. This microstructural constituent helps to augment the creep resistance of this group of alloys. Subsequent heat treatment of these alloys is not common.

Many of the lower-nickel-content corrosion-resistant alloys (for example, CF-3, CF-8M, and CB-7Cu) will have a duplex microstructure consisting of ferrite islands in a matrix of either austenite or martensite. Postcasting solution heat treatments used to prepare corrosion-resistant alloys for service are insufficient to homogenize the microstructure. The inhomogeneous microstructure of both groups of alloys will tend to promote relatively wide areas of partial melting adjacent to the fusion zone when compared with similar wrought alloys.

Martensitic Stainless Steel Castings. Special considerations exist for the welding of martensitic stainless steel castings (CA-6NM, CA-15, CA40, and CB-7Cu-1, and CB-7Cu-2). Quench cracking and a marked reduction in mechanical properties (especially ductility and impact toughness) may result from the welding of these alloys. Corrosion resistance may also be detrimentally affected by the thermal cycle that the material undergoes in the fusion zone and heat-affected-zone (HAZ) of welds.

Suggested welding practice often calls for the preheating and postheating of most of the martensitic alloys. Alloys CA-15 and CA-40 require preheating temperatures in the range of 200 to 315 °C (390 to 600 °F) and a postweld heat treatment (PWHT) temperature range of 610 to 760 °C (1130 to 1400 °F). Alloy CA-6NM requires a preheat temperature range of 100 to 150 °C (210 to 300 °F) and a PWHT temperature range of 590 to 620 °C (1095 to 1150 °F). The higher preheating temperatures should be used when welding thicker sections and higher carbon compositions of these alloys.

The PWHT for these alloys is a tempering operation intended to restore ductility and toughness at the expense of strength and hardness. Because of the broad range of potential tempering temperatures, a wide range of PWHT properties are possible.

Alloy CB-7Cu (1 and 2) has no suggested preheat temperature, but a range (480 to 590 °C, or 895 to 1095 °F) of PWHT temperatures is recommended. In the case of this alloy, the PWHT is an aging operation. In order to recover properties in the welded product, a full solution anneal (1040 °C, or 1095 °F, oil quench), followed by aging, is required. Direct aging without solution annealing will not fully restore preweld properties. The higher aging temperatures result in the lowest strength but also provide the highest ductility and toughness.

Welding Defects. The two most serious problems encountered in the welding of stainless steel castings, either during the repair of casting defects or for subsequent attachment to other structures, are solidification hot cracking and heat-affected zone (HAZ) hot cracking. Figure 2 shows a prototypical hot crack extending both into the fusion zone and the HAZ of a casting alloy. Both of these phenomena involve separation of grain boundaries due to the presence of a wetting liquid phase and sufficient mechanical imposition.

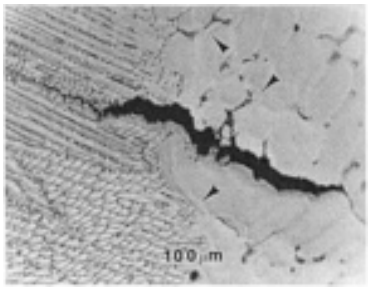

FIG. 2 OPTICAL MICROGRAPH OF THE FUSION LINE REGION IN A CAST CORROSION-RESISTANT AUSTENITIC STAINLESS STEEL. NOTE THE HOT CRACK EXTENDING BOTH INTO THE FUSION ZONE (LEFT) AND BACK INTO THE PARTIALLY MELTED REGION OF THE HAZ. ARROWS INDICATE REGIONS OF PARTIAL MELTING.

Studies (Ref 5, 6, 7, 8, 9) have indicated that wholly austenitic stainless steel casting alloys are more susceptible to the formation of these types of defects than are duplex ferrite plus austenite alloys. In particular, Cieslak (Ref 7, 8) and Cadden (Ref 9) have shown that CF-8M alloys (being prototypic of a wide range of low-nickel corrosion-resistant casting alloys) having welds that solidify with ferrite as the primary solidification phase are much more resistant to hot cracking than are alloys that solidify with austenite as the primary solidification phase.

Table 3 lists the chemical compositions and ferrite content of a series of CF-8M castings used in a study of weldability (Ref 8). Figure 3 shows the fusion zone hot cracking susceptibility of these alloys determined using the Varestraint test at $\frac{1}{2}$ % applied strain. The alloys that solidified as primary austenite (γ) were more susceptible to cracking than those which solidified as primary ferrite (δ). With the exception of heat number 7, the primary ferrite alloys did not experience any cracking under this set of experimental conditions. The high level of sulfur (0.032 wt%) and phosphorus (0.046 wt%) were identified as being responsible for the greater cracking sensitivity in heat number 7. This particular observation was important for establishing that ferrite content alone was not a sufficient criterion to preclude the possibility of hot cracking in duplex alloys.

TABLE 3 COMPOSITIONS OF ALLOYS IN CF-8M WELDABILITY STUDY

HEAT NO.	COMPOSITION, WT%[A]									FERRITE, VOL%
	C	Mn	Si	Cr	Ni	Mo	S	P	N	
1	0.08	0.60	1.05	18.32	13.20	2.26	0.016	0.035	0.041	0.17
2	0.06	0.44	1.08	21.10	9.55	2.52	0.008	0.021	0.048	22.8
3	0.05	0.26	0.83	17.65	12.03	2.05	0.017	0.021	0.06	1.48
4	0.06	1.17	0.60	18.18	12.08	2.48	0.016	0.027	0.05	4.16

5	0.07	0.57	0.99	18.21	9.57	2.39	0.019	0.024	0.06	7.60
6	0.04	0.21	0.38	19.55	15.38	2.88	0.025	0.036	0.04	2.00
7	0.10	0.30	0.69	21.31	10.62	2.34	0.032	0.046	0.05	14.24

Source: Ref 8

(A) THE BALANCE IS IRON.

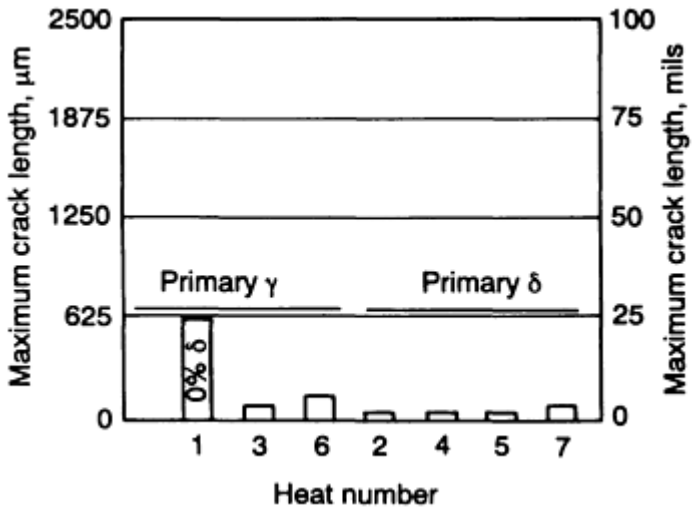

FIG. 3 VARESTRAINT TEST RESULTS ON SEVERAL HEATS OF CF-8M CORROSION-RESISTANT ALLOY. TESTS WERE RUN AT $\frac{1}{2}$ % AUGMENTED STRAIN USING AN ENERGY INPUT OF APPROXIMATELY 2.7 KJ/MM (69 KJ/IN.). SEE TABLE 3 FOR HEAT NUMBER CHEMICAL COMPOSITIONS.

In the same investigation, the hot cracking sensitivity of the heat-resistant alloy HK-40 was also examined. This alloy solidifies as primary austenite and terminates solidification with a eutectic-like Cr_7C_3 carbide constituent. This is prototypical solidification behavior of a wide range of heat-resistant stainless steel casting alloys. It was found that cracking was exacerbated by low carbon content (0.38 wt%), and high levels of combined sulfur and phosphorus (>0.026 wt%). Silicon addition also had a detrimental effect on cracking susceptibility when either carbon content was low or sulfur or phosphorus was high. It was observed that hot cracks could be "healed" by the carbide eutecticlike constituent, suggesting that higher carbon contents in alloys of this type could be helpful in minimizing this type of defect. Similar results have been found for 16Cr-35Ni (HT type) (Ref 10) and high-carbon-content alloys such as 25Cr-20Ni (the cast equivalent of wrought type 310 containing up to 0.2 wt% C) (Ref 11).

A study of the weldability of alloy CN-7M identified sulfur, phosphorus, and silicon as being detrimental to the hot cracking resistance of this high-nickel-content (29 wt% Ni) corrosion-resistant alloy (Ref 12). Specifically, silicon was found to promote the formation of an M_6C carbide eutecticlike constituent associated with intergranular hot cracked regions. For a discussion of the hot cracking susceptibility of a wide range of corrosion-resistant and heat-resistant casting alloys, along with microstructural analysis of the cracking behavior, a review of the work of Cadden (Ref 9) is suggested.

In many studies examining both the fusion zone and HAZ hot cracking behavior of stainless steel casting alloys, the presence of sulfur and phosphorus has universally been identified with increased cracking susceptibility. To a somewhat lesser extent, so have silicon and niobium. Carbon can also be detrimental, although not all studies have reached the same conclusion. It can be said that if there is sufficient carbon present to result in the formation of terminal-stage, eutectic-like constituents, then the hot cracking susceptibility will increase up to the point where the level of carbon promotes eutectic healing. Eutectic healing may eliminate the hot cracking problem, but the reduction in ductility with increasing carbon content can limit the utility of the weld joint for an engineering application (Ref 10).

Each of these elements appears to increase cracking susceptibility in two possible ways. The first is by promoting the formation of low-melting-point constituents, and the second is by acting as a surfactant which promotes wetting of solidifying grain boundaries. As discussed elsewhere in this Volume (see, for example, the articles in this Section of the

Handbook that describe wrought stainless steels), either phenomenon will promote an increased tendency toward fusion zone or HAZ hot cracking.

A specific concern in the welding of corrosion-resistant stainless steel castings is the production of a sensitized microstructure. Sensitization occurs in stainless steel alloys when chromium-rich phases--$M_{23}C_6$ carbides, sigma (σ), chi (χ), and Laves phases--precipitate during exposure to temperatures between 400 and 900 °C (750 and 1650 °F). The precipitation of these constituents can result in a local depletion of chromium (and also molybdenum), lowering the corrosion resistance to a point where corrosion-induced failure of the casting can result. Primary among the phases of concern is the $M_{23}C_6$ carbide (with M being primarily chromium). Precipitation of carbides at grain boundaries can occur during the fusion welding cycle at sites in both the HAZ and the fusion zone. Because the kinetics of precipitation are proportional to the carbon concentration, low-carbon grades (such as CF-3 or CF-3M) have been developed that can experience welding without producing a sensitized microstructure.

A final metallurgical consideration involves the welding of castings that have seen extended service at relatively high temperatures. For a variety of reasons, castings may have to be rewelded sometime during their service lifetime. This can pose a difficult problem if the temperature environment has modified the alloy microstructure so that additional constituents are present that adversely affect alloy ductility. It is always preferable to heat treat the casting to remove these unwanted microstructural features. This process may require solutionizing at temperatures above 1000 °C (1830 °F) and may be impractical for large castings. If solution heat treatment is not an option, then special care must be taken to ensure that the new weld joint design will have the lowest possible level of inherent restraint.

Weld Parameters. From an understanding of the metallurgical behavior of stainless steel casting alloys given above, general rules for fusion welding can be inferred. Low-heat-input processes are almost universally suggested. For alloys that are far from homogeneous, a high-heat-input process would produce flatter thermal gradients outside of the fusion zone, creating a wider zone of partial melting and a greater microstructural sensitivity to HAZ hot cracking. The greater total shrinkage strain associated with the solidification of a large (high-energy-input) weld can create a restraint situation more likely to result in fusion zone solidification cracking. The flatter thermal gradients of higher-energy-input welds reduce the cooling rates through the carbide precipitation temperature range, resulting in a higher likelihood of a sensitized structure in the corrosion-resistant alloys.

For the same reasons, low interpass temperatures are generally employed in the welding of these alloys. Interpass temperatures below 200 °C (400 °F) are common. For critical applications (especially among corrosion-resistant alloys), interpass temperatures of less than 150 °C (300 °F) are often specified. Spraying castings with water between passes is not uncommon for the austenitic corrosion-resistant alloys (Ref 4).

Preheating of castings prior to welding is almost never required and generally not suggested, at least for the corrosion-resistant alloys, because the sensitization impact of such processing is similar to the use of high-energy-input welding parameters. In the case of heat-resistant alloy castings, preheating can be used to reduce the magnitude of thermal shrinkage strains, but again this benefit comes at the expense of a wider zone of partial melting. There is no known formula for preheating temperature and welding parameters for a given alloy that can ensure the preclusion of welding defects. Because of this technological limitation, the use of preheating prior to welding of these alloys is questionable.

Postweld solutionizing of corrosion-resistant alloys is always recommended. For the heat treatable alloys (for example, CB-7Cu), a complete solutionizing and aging heat treatment is recommended to reestablish baseline properties. Where PWHT is not possible, it is even more important to weld using low-heat-input parameters.

Where direct fusion welding is not appropriate, as in the case of an extremely hot-crack-sensitive casting, other approaches might prove useful. One option is to "butter" the area of the crack-sensitive casting to be joined, using a consumable of a less crack-sensitive material. This "buttering" involves surfacing the casting locally with a consumable before fabricating the actual weld joint. With no joint present during the buttering operation, the restraint on the solidifying surface pass and the underlying HAZ of the casting can be quite small and defects (fusion zone and HAZ hot cracks) may be avoided. This surfaced area can be built up slowly to a thickness where it can then be prepared as a joint for subsequent welded attachment. Additional information on buttering can be found in the article "Hardfacing, Weld Cladding, and Dissimilar Metal Joining" in this Volume. As another option, an insert of a less hot-crack-sensitive alloy can be inertia or friction welded onto the mating surface of the hot-crack-sensitive casting. This insert could then be prepared for subsequent fusion welding to the required structure. These options are contingent upon the availability of consumable materials that are acceptable in the service environment.

References cited in this section

4. P.R. WEISER, *ED., STEEL CASTINGS HANDBOOK,* 5TH ED., STEEL FOUNDERS' SOCIETY OF AMERICA, 1980
5. H.S. AVERY, CAST HEAT-RESISTANT ALLOYS FOR HIGH-TEMPERATURE SERVICE, *WELD. RES. COUNC. BULL.,* NO. 143, AUG 1969
6. "THE WELDING OF CAST AUSTENITIC STEELS," WELDING INSTITUTE REPORT SERIES, THE WELDING INSTITUTE, SEPT 1970, PHASES 1-4
7. M.J. CIESLAK AND W.F. SAVAGE, *WELD. J.,* MAY 1980, P 136-S TO 146-S
8. M.J. CIESLAK AND W.F. SAVAGE, "WELDABILITY AND SOLIDIFICATION PHENOMENA OF CAST HIGH ALLOY HEAT RESISTANT ALLOY HK-40 AND CORROSION RESISTANT 19CR-9NI-2.5MO STEELS," REPORT A-69, STEEL FOUNDERS' SOCIETY OF AMERICA, 1980
9. C.H. CADDEN, "WELDABILITY OF HIGH ALLOY CASTINGS," M.S. THESIS, RENSSELAER POLYTECHNIC INSTITUTE, TROY, NEW YORK, MAY 1981
10. D. ROZET, H.C. CAMPBELL, AND R.D. THOMAS, *WELD. J.,* OCT 1949, P 481-S TO 491-S
11. Y. ARATA, F. MATSUDA, AND S. KATAYAMA, *TRANS. JWRI,* JUNE 1977, P 105-116
12. M.J. CIESLAK AND W.F. SAVAGE, *WELD. J.,* MAY 1985, P 119-S TO 126-S

Selection of Cast Stainless Steels

Michael J. Cieslak, Sandia National Laboratories

References

1. J.M. SVOBODA, HIGH-ALLOY STEELS, *CASTING,* 9TH ED., VOL 15, *METALS HANDBOOK,* ASM INTERNATIONAL, 1988, P 722-735
2. M. BLAIR, CAST STAINLESS STEELS, *PROPERTIES AND SELECTION: IRONS, STEELS, AND HIGH-PERFORMANCE ALLOYS,* VOL 1, *ASM HANDBOOK,* ASM INTERNATIONAL, 1990, P 908-929
3. R.W. MONROE AND S.J. PAWEL, CORROSION OF CAST STEELS, *CORROSION,* 9TH ED., VOL 13, *METALS HANDBOOK,* ASM INTERNATIONAL, 1987, P 573-582
4. P.R. WEISER, *ED., STEEL CASTINGS HANDBOOK,* 5TH ED., STEEL FOUNDERS' SOCIETY OF AMERICA, 1980
5. H.S. AVERY, CAST HEAT-RESISTANT ALLOYS FOR HIGH-TEMPERATURE SERVICE, *WELD. RES. COUNC. BULL.,* NO. 143, AUG 1969
6. "THE WELDING OF CAST AUSTENITIC STEELS," WELDING INSTITUTE REPORT SERIES, THE WELDING INSTITUTE, SEPT 1970, PHASES 1-4
7. M.J. CIESLAK AND W.F. SAVAGE, *WELD. J.,* MAY 1980, P 136-S TO 146-S
8. M.J. CIESLAK AND W.F. SAVAGE, "WELDABILITY AND SOLIDIFICATION PHENOMENA OF CAST HIGH ALLOY HEAT RESISTANT ALLOY HK-40 AND CORROSION RESISTANT 19CR-9NI-2.5MO STEELS," REPORT A-69, STEEL FOUNDERS' SOCIETY OF AMERICA, 1980
9. C.H. CADDEN, "WELDABILITY OF HIGH ALLOY CASTINGS," M.S. THESIS, RENSSELAER POLYTECHNIC INSTITUTE, TROY, NEW YORK, MAY 1981
10. D. ROZET, H.C. CAMPBELL, AND R.D. THOMAS, *WELD. J.,* OCT 1949, P 481-S TO 491-S
11. Y. ARATA, F. MATSUDA, AND S. KATAYAMA, *TRANS. JWRI,* JUNE 1977, P 105-116
12. M.J. CIESLAK AND W.F. SAVAGE, *WELD. J.,* MAY 1985, P 119-S TO 126-S

Dissimilar Welds With Stainless Steels

Joel G. Feldstein, Foster Wheeler Energy Corporation

Introduction

THE WELDING OF DISSIMILAR AUSTENITIC STAINLESS STEELS to each other is fairly common practice. When suitable welding procedures and filler metals are employed, most austenitic stainless steels can also be welded satisfactorily to several other classes of weldable steel, including ferritic and precipitation-hardening stainless steels, carbon steels, and low-alloy steels.

As a general rule, the weld metal should be at least equal in strength and corrosion properties to the poorest component in the joint. Additionally, there should be no intermetallic compounds or other phases to degrade the properties of the weld metal. Further, the microstructure must be resistant to cracking. An austenitic microstructure with a Ferrite Number (FN) of 5 to 10 has been shown to be highly resistant to cracking. If a fully austenitic weld metal occurs, satisfactory resistance to cracking can be achieved in certain applications by using a filler metal of high manganese content or a nickel-base alloy.

Dissimilar Welds With Stainless Steels

Joel G. Feldstein, Foster Wheeler Energy Corporation

Welding Dissimilar Austenitic Stainless Steels

In general, the deposited weld metal composition should nearly match the base metal composition when welding different austenitic stainless steels to themselves. However, it is not uncommon to weld different austenitic stainless steels, such as types 304 and 347, to each other or to a nickel-base alloy using a filler metal that differs in chemical composition from both base metals provided the weld metal will have suitable corrosion resistance or mechanical properties (or both) for the required service. Generally, the alternate filler metal should be more highly alloyed than the base metal, but the ferrite content of the resulting weld metal should be considered for corrosion or high-temperature service. Some filler metals may give too high a ferrite content, particularly the high-chromium, low-nickel types, such as type 312. Recommended filler metals for welding dissimilar austenitic stainless steels are given in Table 1. Additional information on stainless steel filler metals can be found in the article "Welding of Stainless Steels" in this Volume.

TABLE 1 STAINLESS STEEL FILLER METALS FOR WELDING SIMILAR AND DISSIMILAR AUSTENITIC STAINLESS STEELS

BASE METALS	**FILLER METALS**									
	201, 202, 301, 302, 302B, 303, 304, 305, 308	**304L**	**309 309S**	**310 310S, 314**	**316**	**316L**	**317**	**317L**	**321, 347, 348**	**330**
201,202, 301,302, 302B, 303,304, 305,308	E308[A]	E308[A]	E308[A]	E308[A]	E308[A]	E308[A]	E308[A]	E308[A]	E308[A]	E309
340L		E308L	E308[A]	E308[A]	E308[A]	E308[A]	E308[A]	E308[A]	E308[A]	309
309, 309S			E309	E309	E309	E309	E309	E309	E309	E309
310, 310S, 314				310	E316[B]	E316[B]	E317	E317	E308[A]	310
316					E316[B]	E316[B]	E316[B]	E316[B]	E308[A]	E309MO
316L						E316L	E316[B]	E316L	E316L	E309MO
317							E317	E317	E308[A]	E309MO
317L								E417L	308L	E309MO
321,347,348									E347[A]	E309
330										E330

(A) FOR SERVICE TEMPERATURE OF <370 °C (700 °F), E308L CAN BE USED.

(B) FOR SERVICE TEMPERATURE OF <370 °C (700 °F), E316L CAN BE USED.

Dissimilar Welds With Stainless Steels

Joel G. Feldstein, Foster Wheeler Energy Corporation

Welding Austenitic Stainless Steels to Carbon or Low-Alloy Steels

In joining austenitic stainless steel to carbon or low-alloy steel for service applications involving exposure to temperatures not exceeding 370 °C (700 °F), it is good practice to use a stainless steel filler metal with a total alloy content high enough to prevent the formation of martensite in the weld after dilution by the base metal and to preserve residual amounts of ferrite to minimize the possibility of hot cracking resulting from welding under severe restraint. Dilution is the change in chemical composition of a welding filler metal caused by the admixture of the base metal or previously deposited weld metal in the deposited weld bead. It is normally measured by the percentage of base metal or previously deposited weld metal in the weld bead. Dilution control, which is of primary concern when joining dissimilar metal combinations, is described in detail in the article "Hardfacing, Weld Cladding, and Dissimilar Metal Joining" in this Volume.

The Schaeffler diagram is particularly useful when examining what filler metal is suitable for joining dissimilar metals. The example in Fig. 1 shows the joining of a carbon steel (point A) to a type 304 austenitic stainless steel (point B) using type 309 as the filler metal (point D). Point C shows what the composition of the weld metal would be if these items were joined without a filler metal. If we assume that each base metal is fused to the same extent, point C will lie halfway between A and B. Because the welding is done using type 309 filler metal, the composition of the weld metal will lie along the line CD, depending on the degree of dilution. At point E a suitable weld metal composition is obtained, that is, an austenitic structure with 8 to 9% ferrite (Ferrite Number). This weld metal will be crack resistant, in contrast to that obtained at point C, which is very sensitive to cracking because of martensite formation. Types 309 and 309L (25Cr-12Ni) filler metals are most widely used for joining carbon or low-alloy steel to austenitic stainless steel; they normally contains about 8 to 15 FN. Types 304Cb, 309Mo, 309MoL, and 312 (29Cr-9Ni) are progressively more strongly ferritic. Satisfactory welds are also obtained with nickel-chromium-iron filler metal and these filler metals allow the service temperature to exceed 370 °C (700 °F) and minimize some stress relieving problems.

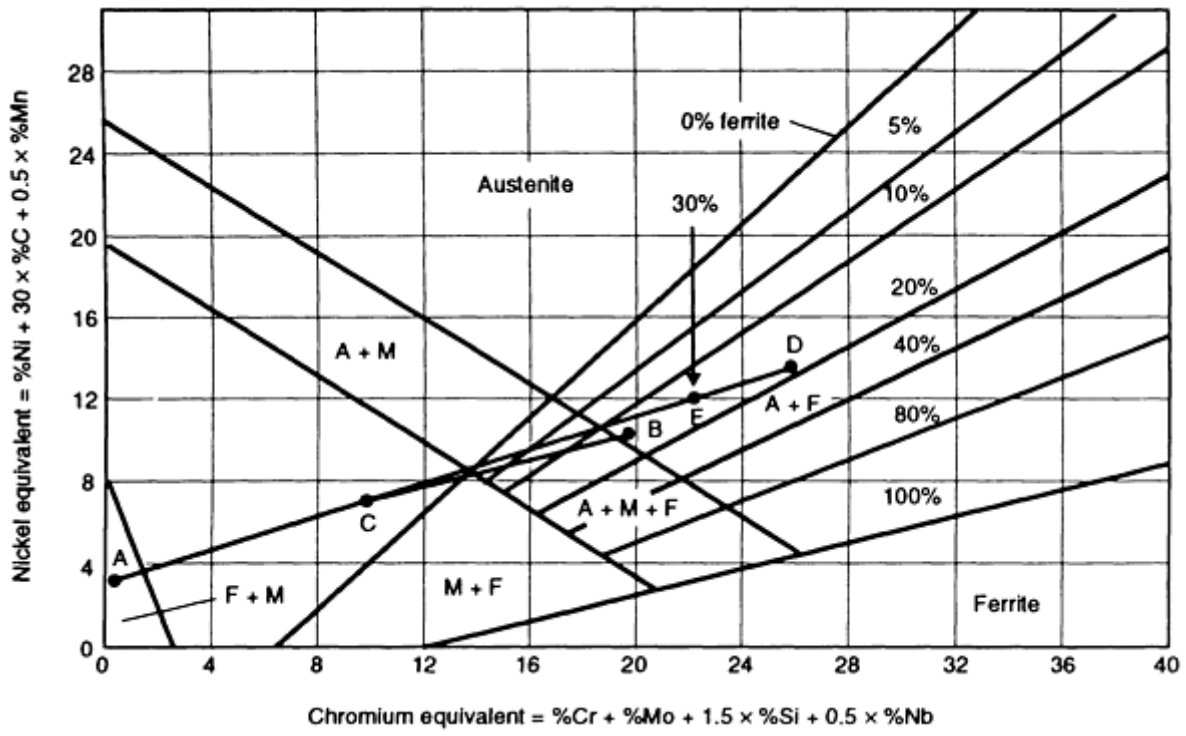

FIG. 1 THE SCHAEFFLER DIAGRAM USED FOR PREDICTING WELD MICROSTRUCTURE USING TYPE 309 TO JOIN

TYPE 304 STAINLESS STEEL TO CARBON STEEL. SEE TEXT FOR DETAILS.

Although the Schaeffler diagram is still widely used to predict the ferrite content of dissimilar metal weld deposits, more recently developed diagrams have increased the scope and accuracy of FN prediction in stainless steel weld metal and related dissimilar metal joints. These include the DeLong diagram, which is described later in this article, and the Welding Research Council 1988 and 1992 diagrams (WRC-1988 and WRC-1992). A review of each of the aforementioned diagrams can be found in the article "Hardfacing, Weld Cladding, and Dissimilar Metal Joining" in this Volume.

Specific Welding Practices. In joining austenitic stainless steel to carbon steel, it is good practice to first surface, or "butter," the carbon steel with a layer of type 309 or other suitable stainless steel weld metal, so that the portion of the weld (on the carbon steel member) where difficulties are most likely to occur is deposited with stainless steel filler metal while there is little restraint on the weld metal. Thus, following deposition and inspection of the buttered surface, the joint between the stainless steel member and the surfaced layer becomes a stainless-to-stainless joint that can be welded using a conventional stainless steel filler metal. The deposition of carbon steel or low-alloy steel filler metal on austenitic stainless steel should be avoided whenever possible because it can result in hard, brittle weld deposits.

A procedure for joining stainless steel to carbon steel or stainless steel to stainless-clad carbon steel is shown in Fig. 2. This procedure is widely used in the welding of stainless steel pipe to carbon steel, low-alloy steel, and stainless-clad carbon steel. Weld cladding procedures are described later in this article.

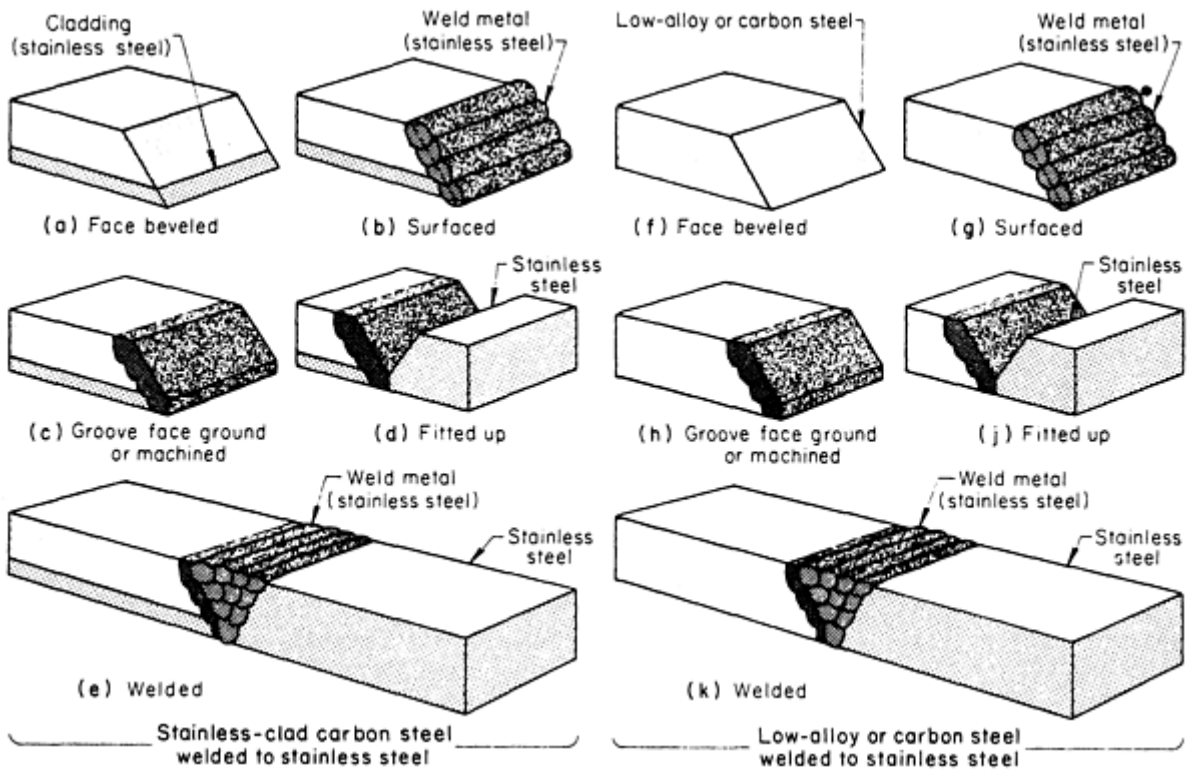

FIG. 2 PROCEDURES FOR JOINING AUSTENITIC STAINLESS STEEL TO STAINLESS-CLAD CARBON STEEL, CARBON STEEL, AND LOW-ALLOY STEEL. STAINLESS-CLAD, LOW-ALLOY, OR CARBON STEEL EDGES ARE BEVELED FOR WELDING (A AND F). AN OVERLAY (OR "BUTTERING" LAYER) OF STAINLESS STEEL FILLER METAL IS APPLIED TO THE BEVELED EDGE (B AND G). THE LAYER IS MACHINED OR GROUND TO REQUIRED DIMENSIONS AND STRESS RELIEVED, IF REQUIRED (C AND H). THE COMPONENTS ARE FITTED UP FOR WELDING (D AND J). THE WELD IS COMPLETED, USING THE FILLER METAL NORMALLY USED FOR WELDING THE STAINLESS STEEL MEMBER OR THAT USED FOR THE SURFACING PASS ON STAINLESS-CLAD LOW-ALLOY OR CARBON STEEL (E AND K).

In depositing the surface layer, dilution of the stainless steel weld metal by carbon steel, which can cause cracking of the weld, can be minimized with the following practices. If the cladding on stainless-clad steel is type 304 stainless steel, types 309 and 309L should be used for the surfacing layer. After depositing the surfacing layer, the component is stress relieved, if necessary. The final weld between the solid stainless steel and the surfaced stainless-clad steel or carbon steel can be made either with the filler metal normally employed for welding the solid stainless steel member or with the one that was used for the overlay.

In another method, a short stainless steel transition member is welded to the carbon steel or stainless-clad carbon steel member prior to stress relieving and final welding. This method ensures protection of the carbon steel base metal from the effect of final welding, and stress relieving can be done while there is little restraint on the joint. This method, however, is more costly than the procedure for producing a surfacing layer.

In a third method, the workpiece interface (stainless steel and carbon steel or stainless steel and stainless-clad carbon steel) is beveled and fitted, leaving a root opening at the joint that is then welded with a filler metal of sufficiently high alloy content to prevent cracking of the weld after dilution by the carbon steel. The welding procedure should be controlled to hold penetration to a minimum. A disadvantage of this method is that the joint is under restraint both during welding and local stress relieving. Although often used, this method is the least desirable of the three.

Dissimilar Welds With Stainless Steels

Joel G. Feldstein, Foster Wheeler Energy Corporation

Welding of Ferritic and Martensitic Stainless Steels to Carbon and Low-Alloy Steels

When welding ferritic or martensitic stainless steel to carbon or low-alloy steel for general service (not high-temperature service), the use of austenitic stainless steel or nickel-base (NiCrFe) filler metal can produce welds of suitable quality if correct welding procedures are followed. (If an austenitic stainless steel or NiCrFe filler metal cannot be used, a filler metal similar to the stainless steel base metal is usually specified.) Two methods are commonly employed. The first involves surfacing both members of the joint, using suitable preheat and postheat treatments as required, and then making a weld between the buttered surfaces without preheat or postheat. Filler metals (such as type 309) that are sufficiently high in alloy content to minimize the effects of dilution by carbon steel, or straight-chromium grades of stainless steel (400 series) are widely used with this method. Penetration into the base metal should be kept to a minimum. The second method involves depositing the filler metal directly on the surfaces of the two members of the joint without using a separate surfacing layer. Dilution of the weld metal by both base metals must be kept under close control while the restrained joint is being welded.

Dissimilar Welds With Stainless Steels

Joel G. Feldstein, Foster Wheeler Energy Corporation

Welding Austenitic-Stainless-Clad Carbon or Low-Alloy Steels

To preserve its desirable properties, stainless-clad plate can be welded by either of the two following methods, depending on plate thickness and service conditions.

- THE UNCLAD SIDES OF THE PLATE SECTIONS ARE BEVELED AND WELDED WITH CARBON OR LOW-ALLOY STEEL FILLER METAL. A PORTION OF THE STAINLESS STEEL CLADDING IS REMOVED FROM THE BACK OF THE JOINT AND STAINLESS STEEL FILLER METAL IS DEPOSITED.
- THE ENTIRE THICKNESS OF THE STAINLESS-CLAD PLATE IS WELDED WITH STAINLESS STEEL FILLER METAL.

When the non-stainless portion of the plate is comparatively thick, as in most pressure vessel applications, it is more economical to use the first method. When the non-stainless portion of the plate is thin, the second method is often preferred. When welding components for applications involving elevated or cyclic temperatures, the differences in the coefficients of thermal expansion of the base plate and the weld should be taken into consideration.

All stainless steel deposits on carbon steel should be made with filler metal of sufficiently high alloy content to ensure that normal amounts of dilution by carbon steel will not result in a brittle weld. In general, filler metals of type 308, 316, or 347 should not be deposited directly on carbon or low-alloy steel. Deposits of types 309, 309L, 309Cb, 309Mo, 310, or 312 are usually acceptable, although type 310 is fully austenitic and is susceptible to hot cracking when there is high restraint in a welded joint. Thus, welds made with type 310 filler metal should be carefully inspected. Welds made with types 309 and 312 filler metals are partially ferritic and therefore are highly resistant to hot cracking.

The procedure most commonly used for making welded joints in stainless-clad carbon or low-alloy steel plate is shown in Fig. 3. Stainless steel filler metal is deposited only in that portion of the weld where the stainless steel cladding has been removed, and carbon or low-alloy steel filler metal is used for the remainder. The backgouged portion of the stainless steel cladding should be filled with a minimum of two layers of stainless steel filler metal (Fig. 3e); an additional layer is recommended if a high weld reinforcement at the cladding surface can be tolerated.

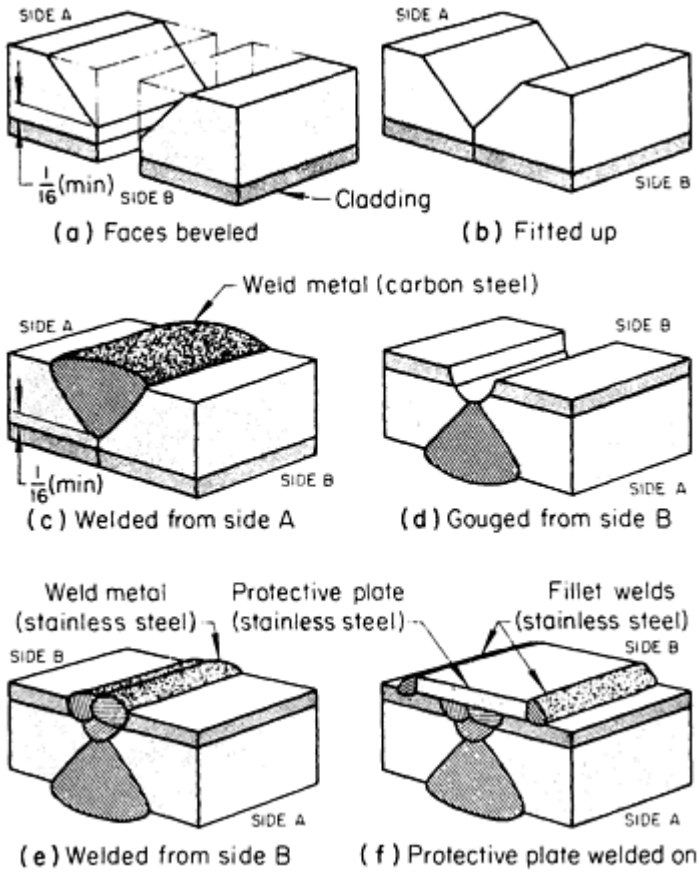

FIG. 3 PROCEDURE FOR WELDING STAINLESS-CLAD CARBON AND LOW-ALLOY STEEL, USING STAINLESS STEEL FILLER METAL ONLY IN PORTION OF JOINT FROM WHICH CLADDING WAS REMOVED. (A) AND (B) THE CLAD PLATES ARE MACHINED FOR A TIGHT FIT-UP, WITH THE BOTTOM OF THE WELD GROOVE NOT LESS THAN 1.6 MM ($\frac{1}{16}$ IN.) ABOVE THE STAINLESS STEEL CLADDING. (C) CARBON STEEL FILLER METAL IS DEPOSITED FROM SIDE A (A LOW-HYDROGEN FILLER METAL IS USED FOR THE FIRST PASS), TAKING CARE NOT TO PENETRATE CLOSER THAN 1.6 MM ($\frac{1}{16}$ IN.) TO THE CLADDING. (D) STAINLESS STEEL CLADDING ON SIDE B IS BACKGOUGED UNTIL SOUND CARBON STEEL WELD METAL IS REACHED. (E) THE BACKGOUGED GROOVE IS FILLED WITH STAINLESS STEEL WELD METAL IN A MINIMUM OF TWO LAYERS. (F) WHEN REQUIRED FOR SEVERELY CORROSIVE SERVICE, A PROTECTIVE STRIP OF STAINLESS STEEL PLATE MAY BE

FILLET WELDED TO THE CLADDING TO COVER THE WELD ZONE.

If the cladding is of type 304 stainless steel, the first layer of stainless steel weld metal should be of type 309 or 312. Subsequent layers of weld metal can be of type 308. If the cladding is of type 316, the first layer is deposited with type 309 Mo filler metal and the subsequent layers with type 316. When the cladding is of type 304L or type 347, the welding procedure must be carefully controlled to obtain the desired weld metal composition in the outer layers of the weld. Chemical analysis of sample welds should be made before joining of clad plates intended for use under severely corrosive conditions.

In some applications, a narrow protective plate of wrought stainless steel of the same composition as the cladding is welded over the completed weld (Fig. 3f) to ensure uniformity of corrosion resistance. The fillet welds joining the protective plate to the cladding should be carefully inspected after deposition. These welds, of course, are made with stainless steel filler metal.

Figure 4 illustrates an alternative method (method A) of welding clad plate in which a carbon or low-alloy steel weld joins the carbon steel portion of the plate and the use of stainless steel filler metal is limited to replacement of the cladding that was removed prior to making the carbon or low-alloy steel weld. This method is more expensive than the method described in Fig. 3 because of the cost of removing a larger portion of the cladding and depositing more stainless steel filler metal. Because there is no danger of alloy contamination from the cladding layer, method A in Fig. 4 permits the use of faster welding processes, such as submerged arc welding in depositing the carbon steel weld.

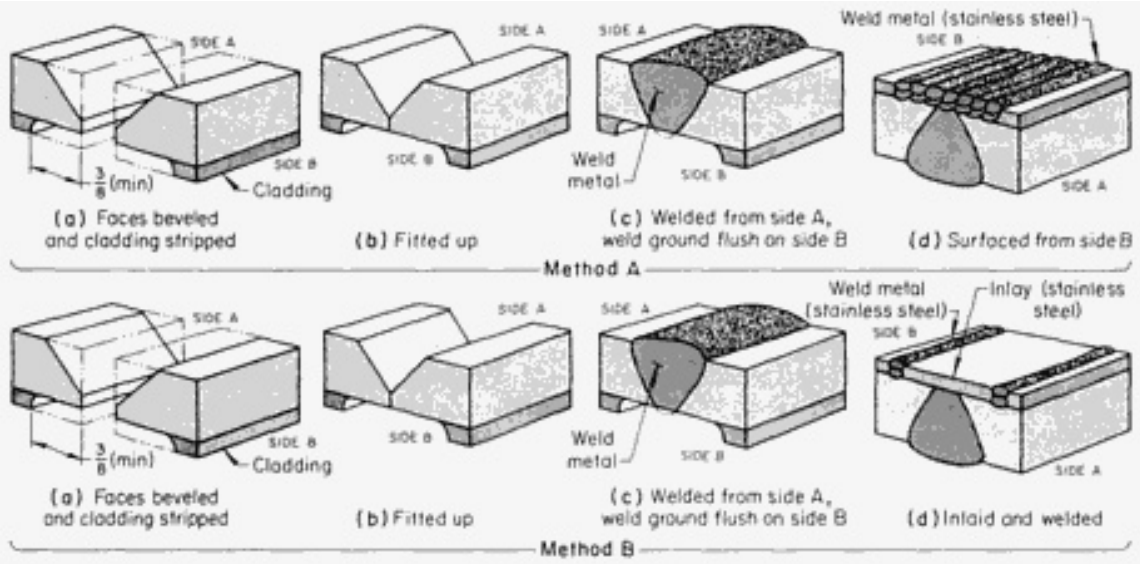

FIG. 4 ALTERNATIVE PROCEDURES FOR JOINING STAINLESS-CLAD CARBON AND LOW-ALLOY STEEL PLATE INVOLVING DIFFERENT TECHNIQUES FOR REPLACING PORTIONS OF THE STAINLESS STEEL CLADDING REMOVED BEFORE WELDING THE CARBON OR LOW-ALLOY STEEL SIDE. THE JOINT IS PREPARED BY BEVELING SIDE A AND REMOVING A PORTION OF THE STAINLESS STEEL CLADDING FROM SIDE B TO A MINIMUM WIDTH OF 9.5 MM ($\frac{3}{8}$ IN.) FROM EACH SIDE OF THE JOINT, AND THE JOINT IS FITTED UP IN POSITION FOR WELDING. USE OF A ROOT GAP (NOT SHOWN) IS PERMISSIBLE (A AND B, METHODS A AND B). CARBON STEEL FILLER METAL IS DEPOSITED AND THE ROOT OF THE WELD IS GROUND FLUSH WITH THE UNDERSIDE OF THE CARBON STEEL PLATE (C, METHODS A AND B). THE AREA FROM WHICH CLADDING WAS REMOVED IS SURFACED WITH AT LEAST TWO LAYERS OF STAINLESS STEEL WELD METAL (D, METHOD A), OR AN INLAY OF WROUGHT STAINLESS STEEL CAN BE WELDED IN PLACE (D, METHOD B).

In depositing the stainless steel weld metal, the first layer must be sufficiently high in alloy content to avoid cracking as a result of normal dilution by the carbon steel base metal. A stringer bead technique should be employed; penetration must be held to a minimum. If the proper weld metal composition is not achieved after the second layer has been deposited, a portion of the second layer should be ground off and additional filler metal should be deposited to obtain the desired

composition. Figure 4(d) of method B shows an alternative procedure in which the exposed carbon steel weld on side B is covered by welding an inlay of wrought stainless steel to the edges of the cladding.

The most common method of joining stainless steel-clad carbon or low-alloy steel plate with a weld that consists entirely of stainless steel is shown in Fig. 5. This method is most frequently used for joining thin sections of stainless-clad plate. The same basic welding procedure is followed for both the butt and comer joints shown in Fig. 5. After the plate has been beveled and fitted up for welding, a stainless steel weld is deposited from the carbon steel side, using a filler metal sufficiently high in alloy content to minimize difficulties (such as cracking) resulting from weld dilution and joint restraint. Types 309 and 312 filler metals are suitable for this application.

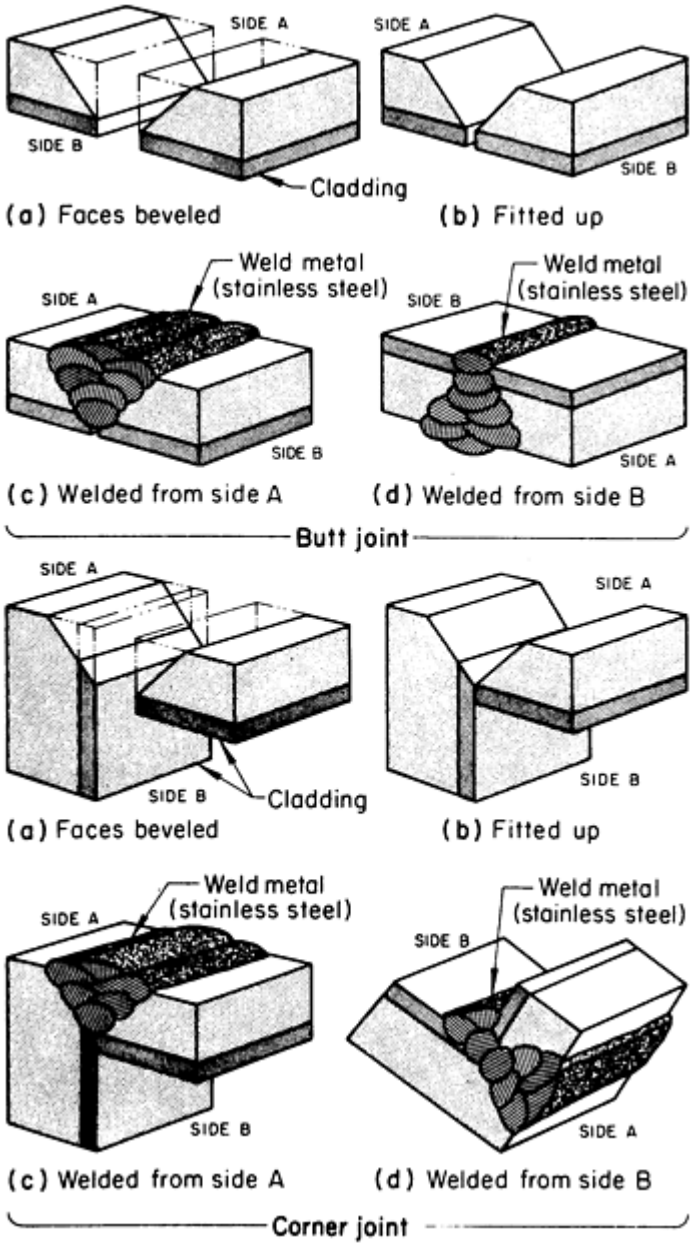

FIG. 5 PROCEDURES FOR WELDING V-GROOVE BUTT AND CORNER JOINTS IN STAINLESS-CLAD CARBON OR LOW-ALLOY STEEL PLATE, USING STAINLESS STEEL FILLER METAL EXCLUSIVELY. THE CLAD PLATES ARE BEVELED AND FITTED UP (A AND B, BUTT AND CORNER JOINTS). THE ROOT OF THE WELD IS CLEANED AND GOUGED, IF NECESSARY, BEFORE DEPOSITING STAINLESS WELD METAL FROM THE STAINLESS STEEL SIDE (D, BUTT AND CORNER JOINTS).

After the stainless steel weld has been deposited from the carbon steel side (Fig. 5c), the root of the weld is cleaned by brushing, chipping, or grinding, as required, and one or more layers of stainless steel filler metal are deposited (Fig. 5d).

The filler metal composition should correspond to that normally employed to weld the type of stainless steel used for the cladding. If the cladding is type 304, the final layer of weld metal should be type 308. If the cladding is type 316, it may be necessary to backgouge before deposition of the final weld metal layers to ensure that the proper weld metal composition is obtained at the surface of the weld.

Joel G. Feldstein, Foster Wheeler Energy Corporation

Cladding Austenitic Stainless Steel to Carbon or Low-Alloy Steels

Weld cladding involves the deposition of a relatively thick layer of weld metal by an arc welding process to impart a corrosion- or oxidation-resistant surface (see the article "Hardfacing, Weld Cladding, and Dissimilar Metal Joining" in this Volume). Materials of interest for cladding carbon or low-alloy steels include types 308, 309, 310, 316, 320, and 347. The exact chemical composition of a weld overlay depends on the composition of the cladding metal (determined from undiluted weld metals), the composition of the base metal, and dilution, and can be calculated if these variables are known. The chromium-nickel austenitic stainless steels, however, often contain more than one phase in the as-deposited structure. These materials are primarily austenitic with varying amounts of ferrite, martensite, and σ phases determined by the composition and cladding conditions.

The amounts of ferrite and martensite present in the austenitic structures can be estimated from a DeLong constitutional diagram similar to the one shown in Fig. 6. Chromium (ferrite formers) and nickel (austenite formers) equivalents are calculated from the following equations:

CHROMIUM
EQUIVALENT = %CR + %MO + 1.5(%SI) + 0.5(%NB)
NICKEL
EQUIVALENT = %NI + 30(%C) + 0.5(%MN) + 30(%N)

These values are then plotted and the percentages of phases present are read directly from the diagram. Care should be taken in this technique, however, because the as-clad microstructure also depends on cooling rate. Cooling rates can vary significantly, depending on cladding conditions. Another method of quickly determining the phases present is by using magnetic measuring devices. Austenite is nonmagnetic, whereas ferrite and martensite are ferromagnetic. When properly calibrated in accordance with AWS A4.2, these instruments can quickly give an indication of the amount of magnetic phase present. However, one should be aware that excessive dilution can result in martensite in the cladding, which will give a false high FN value when using a magnetic instrument.

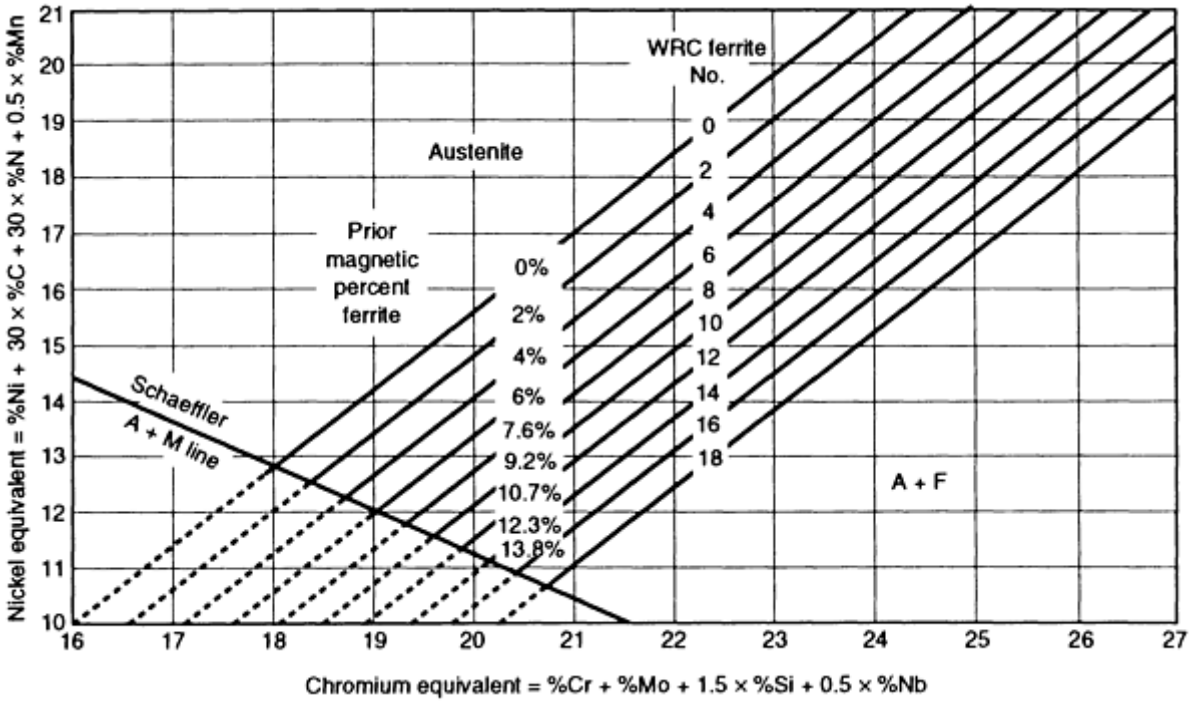

FIG. 6 THE DELONG DIAGRAM USED FOR PREDICTING WELD MICROSTRUCTURE. SEE TEXT FOR DETAILS.

Sigma phase is not common in as-clad structures but can occur where high-heat-input processes are used. It forms most readily from ferrite phase, but can also form from austenite in high-chromium areas. The transformation to σ phase occurs in the temperature range 500 to 900 °C (930 to 1650 °F), with longer times at these temperatures producing larger amounts of σ phase. The percentage of σ phase can be determined only by metallographic techniques.

Fully austenitic overlays are generally susceptible to hot cracking, which can occur upon solidification or reheating by a subsequent overlay pass (microfissures). Solidification cracks are generally very large and can be found by visual or dye-penetrant examination. However, microfissures are often subsurface and difficult to detect by conventional nondestructive examination techniques. For the austenitic stainless steels, the tendency for hot cracking is greatly reduced by the presence of a small amount of δ-ferrite in the structure. The amount of ferrite required to eliminate hot cracking varies from material to material, but it is generally recognized that a 4 or 5 FN minimum in the as-clad structure is sufficient for most austenitic stainless steel cladding alloys.

Finally, stainless steel cladding materials are susceptible to sensitization (precipitation of chromium carbides in grain boundaries that leaves chromium-depleted adjacent areas). Sensitization can occur when unstabilized stainless steels are heated in the range of 430 to 820 °C (800 to 1500 °F) either during stress relief or in service. The best way to inhibit these problems is to use low-carbon grades (such as type 308L or 309L) or stabilized grades (such as type 347) of austenitic stainless steels that are not readily sensitized. Also, finer microstructures produced by the lower-heat-input processes improve corrosion resistance for all grades. Additional material on weld sensitization can be found in the article "Corrosion of Weldments" in this Volume as well as in *Corrosion,* Volume 13 of the *ASM Handbook.*

Dissimilar Welds With Stainless Steels

Joel G. Feldstein, Foster Wheeler Energy Corporation

Selected References

- W.T. DELONG, FERRITE IN AUSTENITIC STAINLESS STEEL WELD METAL, *WELD. J.,* VOL 53 (NO. 7), 1974, P 273S-286S
- D.L. OLSON, PREDICTION OF AUSTENITIC WELD METAL MICROSTRUCTURES AND

PROPERTIES, *WELD. J.* VOL 64 (NO. 10), 1985, P 281S-295S

- A.L. SCHAEFFLER, CONSTITUTION DIAGRAM FOR STAINLESS STEEL WELD METAL, *MET. PROG.,* VOL 56 (NO. 11), 1949, P 680-688

Selection and Weldability of Conventional Titanium Alloys

W.A. Baeslack III, The Ohio State University; J.R. Davis, Davis and Associates; C.E. Cross, Martin Marietta Astronautics Group

Introduction

TITANIUM is a low-density element (approximately 60% of the density of steel) that can be highly modified by alloying and deformation processing. Titanium is nonmagnetic and has good heat transfer properties. Its coefficient of thermal expansion is somewhat lower than that of steels and less than half that of aluminum. Titanium and its alloys have melting points higher than those of steels, but maximum useful temperatures for structural applications generally range from 425 to 540 °C (800 to 1000 °F). More recently developed alloys such as IMI-834 or Ti-1100 have temperature limits approaching 600 °C (1100 °F). Titanium has the ability to passivate, and thereby exhibits a high degree of immunity to attack by most mineral acids and chlorides. Titanium is nontoxic and generally biologically compatible with human tissues and bones. The combination of high strength, stiffness, good toughness, low density, and good corrosion resistance provided by various titanium alloys at very low to moderately elevated temperatures allows weight savings in aerospace structures and other high-performance applications. The excellent corrosion resistance and biocompatibility coupled with good strengths make titanium and its alloys useful in chemical and petrochemical applications, marine environments, and biomaterials applications.

Titanium and its alloys are used primarily in two areas of application where the unique characteristics of these metals justify their selection: corrosion-resistant service and specific strength-efficient structures. For these two diverse areas, selection criteria differ markedly. Corrosion applications normally utilize low-strength unalloyed titanium mill products fabricated into tanks, heat exchangers, or reactor vessels for chemical-processing, desalination, or power-generation plants. In contrast, high-performance applications typically utilize high-strength titanium alloys in a very selective manner that depends on factors such as thermal environment, loading parameters, available product forms, fabrication characteristics, and inspection and/or reliability requirements. As a result of their specialized usage, alloys for high-performance applications normally are processed to more stringent and costly requirements than unalloyed titanium for corrosion service.

Historically, titanium alloys have been used instead of iron or nickel alloys in aerospace applications because titanium saves weight in highly loaded components that operate at low to moderately elevated temperatures. Many titanium alloys have been custom designed to have optimum tensile, compressive, and/or creep strength at selected temperatures and, at the same time, to have sufficient workability to be fabricated into mill products suitable for specific applications. During the past four decades, various compositions have had transient usage, but one alloy, Ti-6Al-4V, has been consistently responsible for about 50% of industry application. Ti-6Al-4V is unique in that it combines attractive properties with inherent workability (which allows it to be produced in all types of mill products, in both large and small sizes), good weldability (which allows the mill products to be made into complex hardware), and the production experience and commercial availability that lead to reliable and economic usage. Thus Ti-6Al-4V has become the standard alloy against which other alloys must be compared when selecting a titanium alloy for a specific application.

Strength, fatigue-crack growth rate, and fracture toughness, plus manufacturing considerations such as welding and forming requirements, normally provide the criteria that determine the alloy composition, structure (alpha, near-alpha, alpha-beta, or metastable beta), heat treatment (some variant of either annealing or solution treating and aging), and level of process control selected or prescribed for structural titanium alloy applications. Detailed information on the selection and properties of wrought, cast, and powder metallurgy titanium alloys can be found in *Properties and Selection: Nonferrous Alloys and Special-Purpose Materials*, Volume 2 of the *ASM Handbook.*

In the present article, emphasis will be placed on the physical metallurgy of titanium and titanium alloys and their microstructural response to fusion welding conditions. A companion article, which immediately follows in this Section of the Handbook, describes welding characteristics of advanced high-temperature and high fracture toughness alloys, titanium-matrix composites, and ordered intermetallic (titanium aluminides) alloys. Additional information on filler metal and shielding gas selection can be found in the article "Welding of Titanium Alloys" in this Volume.

Selection and Weldability of Conventional Titanium Alloys

W.A. Baeslack III, The Ohio State University; J.R. Davis, Davis and Associates; C.E. Cross, Martin Marietta Astronautics Group

Physical Metallurgy (Ref 1)

Titanium undergoes an allotropic phase transformation at about 885 °C (1625 °F), changing from a close-packed hexagonal crystal structure (alpha phase) to a body-centered cubic crystal structure (beta phase). The transformation temperature (beta transus, or the completion of transformation to beta on heating) is strongly influenced by the interstitial elements oxygen, nitrogen, and carbon (alpha stabilizers), which raise the transformation temperature; by hydrogen (beta stabilizer), which lowers the transformation temperature; and by metallic impurity or alloying elements, which may either raise or lower the transformation temperature.

Depending on their microstructure, titanium alloys fall into one of four classes: alpha, near-alpha, alpha-beta, or metastable beta. These classes, which are described below, denote the general type of microstructure after processing. An alpha alloy will contain only trace amounts of beta phase. A near-alpha alloy will contain limited beta phase and may appear microstructurally similar to an alpha alloy. An alpha-beta alloy will consist of alpha and retained or transformed beta. A metastable beta alloy will tend to retain the beta phase on initial cooling to room temperature but will precipitate fine alpha phase during heat treatment.

Effects of Alloying Elements. The role of the interstitial elements oxygen, nitrogen, and carbon was described above. The principal effect of an alloying element in titanium alloys is its effect on the alpha-to-beta transformation temperature and the resulting microstructure and properties (Fig. 1).

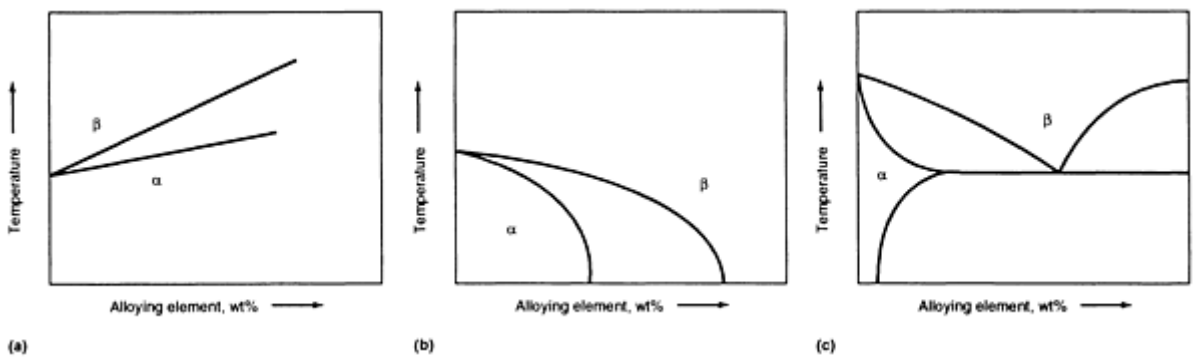

FIG. 1 EFFECT OF ALLOYING ELEMENTS ON TITANIUM MICROSTRUCTURE. (A) ALPHA STABILIZER (FOR EXAMPLE, ALUMINUM AND OXYGEN). (B) BETA STABILIZER (FOR EXAMPLE, VANADIUM AND NIOBIUM). (C) BETA STABILIZER PLUS ($\alpha + \beta$) STRENGTHENER (FOR EXAMPLE, COPPER AND IRON)

Tantalum, vanadium, niobium, and molybdenum are beta isomorphous with body-centered cubic titanium. Titanium does not form intermetallic compounds with the beta isomorphous elements. Eutectoid systems are formed with chromium, iron, copper, nickel, palladium, cobalt, manganese, and certain other transition metals. These elements have low solubility in alpha titanium and decrease the transformation temperature. They usually are added to alloys in combination with one or more of the beta isomorphous elements to stabilize the beta phase and prevent or minimize formation of intermetallic compounds, which might occur during service at elevated temperature.

Zirconium and hafnium are unique in that they are isomorphous with both the alpha and beta phases of titanium. Tin and aluminum have significant solubility in both alpha and beta phases. Aluminum increases the transformation temperature significantly, whereas tin lowers it slightly. Aluminum, tin, and zirconium are commonly used together in alpha and near-alpha alloys. In alpha-beta alloys, these elements are distributed approximately equally between the alpha and beta phases. Almost all commercial titanium alloys contain one or more of these three elements because they are soluble in both alpha and beta phases, and particularly because they improve creep strength of the alpha phase. Many more elements are soluble in beta titanium than in alpha. Beta isomorphous alloying elements are preferred as additions because they do

not form intermetallic compounds. However, iron, chromium, manganese, and other compound formers sometimes are used in beta-rich alpha-beta alloys or in metastable beta alloys, because they are strong beta stabilizers and improve hardenability and response to heat treatment. Nickel, molybdenum, and palladium improve corrosion resistance of unalloyed titanium in certain media. The approximate chemical composition ranges and effects of some alloying elements used in titanium can be summarized as follows (Ref 2):

ALLOYING ELEMENT	CONTENT, WT%	EFFECT ON STRUCTURE
ALUMINUM	2-7	α STABILIZER
TIN	2-6	α STABILIZER
VANADIUM	2-15	β STABILIZER
MOLYBDENUM	2- 13	β STABILIZER
CHROMIUM	2-12	β STABILIZER
COPPER	-3	β STABILIZER (α AND β STRENGTHENER)
ZIRCONIUM	2-8	IMPROVES CREEP STRENGTH
SILICON	0.05-1	IMPROVES CREEP STRENGTH

Secondary Phases and Martensitic Transformations. The basis for microstructural manipulation during elevated-temperature processing of titanium alloys centers around the beta-to-alpha transformation that occurs in these alloys during cooling. This transformation can occur by nucleation and growth, or it can occur martensitically, depending on the alloy composition and the cooling rate. The martensitic product is usually hexagonal close-packed and is designated alpha prime (α'). There also is an orthorhombic martensite, designated alpha double-prime (α"), which forms in alloys that contain higher concentrations of refractory elements such as molybdenum, tantalum, or niobium. Essentially all thermomechanical processing is conducted above the M_s temperature for either alpha prime or alpha double-prime. Alloys that contain enough beta-stabilizing elements to depress the M_s temperature below room temperature can be rapidly cooled to retain the metastable beta phase. More detailed information on the physical metallurgy and phase transformations associated with titanium alloys can be found in Ref 3.

A graphic illustration of the microstructural transformations that can occur in an alpha-beta alloy (Ti-6Al-4V) is shown in Fig. 2. As can be seen, the morphology (shape/location) of the phase changes with prior treatments. The alpha phase may remain relatively globular (equiaxed), but the transformed beta (martensites or alpha) may be very acicular or elongated. The amount of equiaxed alpha and the coarseness or fineness of the transformed beta products will affect alloy properties. For example, the fine, predominantly alpha-prime structures in rapidly cooled near-alpha and alpha-beta alloy weldments exhibit high strength levels that can become even higher after low-temperature postweld heat treatment. However, as the microstructure coarsens due to a reduced weld cooling rate or increased postweld heat treatment temperature, yield and ultimate tensile strengths decrease. See the section "Effect of Postweld Heat Treatment" in this article for additional information on the effects of PWHT on structure-property relationships.

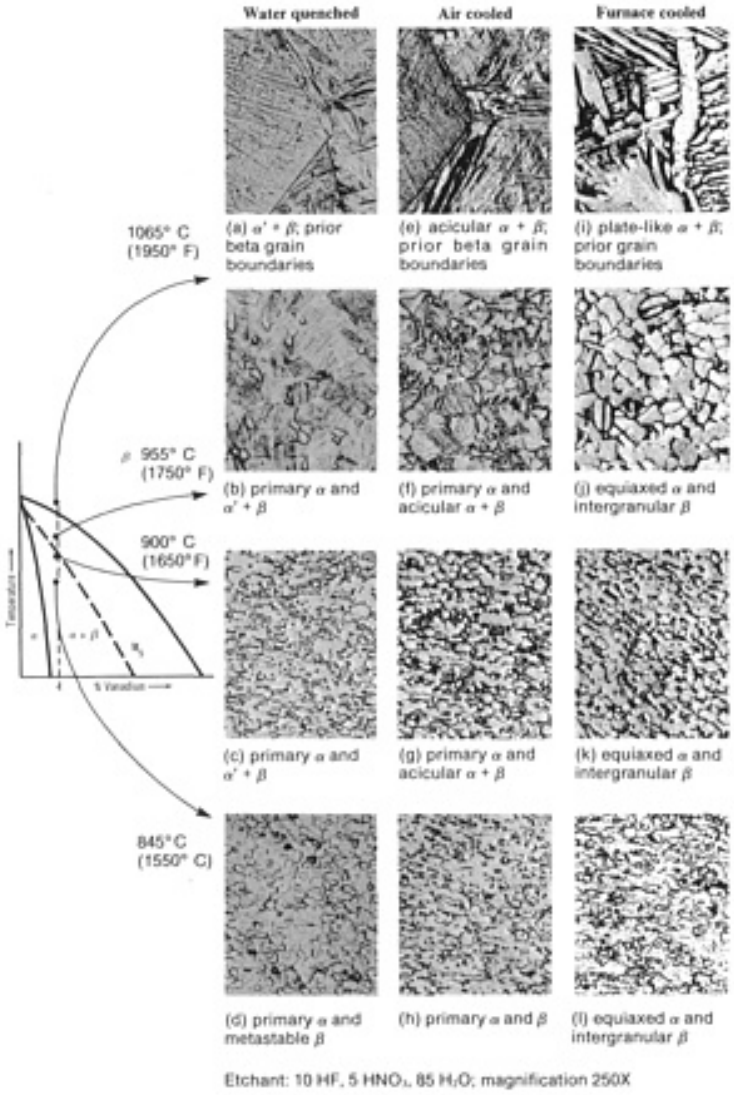

FIG. 2 MICROSTRUCTURAL TRANSFORMATIONS THAT OCCUR IN TI-6AL-4V ON COOLING

References cited in this section

1. M.J. DONACHIE, JR., TITANIUM, *METALS HANDBOOK DESK EDITION,* AMERICAN SOCIETY FOR METALS, 1985, P 9-1 TO 9-3
2. S. LAMPMAN, WROUGHT TITANIUM AND TITANIUM ALLOYS, *PROPERTIES AND SELECTION: NONFERROUS ALLOYS AND SPECIAL-PURPOSE MATERIALS,* VOL 2, *ASM HANDBOOK,* ASM INTERNATIONAL, 1990, P 592-633
3. E.W. COLLINGS, *THE PHYSICAL METALLURGY OF TITANIUM ALLOYS,* AMERICAN SOCIETY FOR METALS, 1984

Selection and Weldability of Conventional Titanium Alloys

W.A. Baeslack III, The Ohio State University; J.R. Davis, Davis and Associates; C.E. Cross, Martin Marietta Astronautics Group

Classification of Titanium Alloys

When classifying unalloyed and alloyed titanium, it is common to group the materials as:

- UNALLOYED, OR COMMERCIALLY PURE (CP) TITANIUM
- ALPHA AND NEAR-ALPHA ALLOYS
- ALPHA-BETA ALLOYS
- METASTABLE BETA ALLOYS

Table 1 lists compositions and tensile properties of some of the more common grades. Of the alloys listed in Table 1, Ti-6Al-4V is the most widely used titanium alloy, accounting for about 50% of total titanium production. Unalloyed grades comprise about 25% of production, and all other alloys combined comprise the remaining 25%.

TABLE 1 PROPERTIES AND COMPOSITIONS OF TITANIUM AND TITANIUM ALLOYS

DESIGNATION	TENSILE STRENGTH (MIN)		0.2% YIELD STRENGTH (MIN)		IMPURITY LIMITS (MAX), WT%					NOMINAL COMPOSITION, WT%				
	MPA	KSI	MPA	KSI	N	C	H	Fe	O	Al	Sn	Zr	Mo	OTHERS
UNALLOYED GRADES														
ASTM GRADE 1	240	35	170	25	0.03	0.10	0.015	0.20	0.18	. . .	. . .	. . .	. . .	. . .
ASTM GRADE 2	340	50	280	40	0.03	0.10	0.015	0.30	0.25	. . .	. . .	. . .	. . .	. . .
ASTM GRADE 3	450	65	380	55	0.05	0.10	0.015	0.30	0.35	. . .	. . .	. . .	. . .	. . .
ASTM GRADE 4	550	80	480	70	0.05	0.10	0.015	0.50	0.40	. . .	. . .	. . .	. . .	. . .
ASTM GRADE 7	340	50	280	40	0.03	0.10	0.015	0.30	0.25	. . .	. . .	. . .	. . .	0.2 PD
ASTM GRADE 11	240	35	170	25	0.03	0.10	0.015	0.20	0.18	. . .	. . .	. . .	. . .	0.12-0.25 PD
ASTM GRADE 12	480	70	380	55	0.03	0.10	0.015	0.30	0.25	. . .	. . .	. . .	0.3	0.6-0.9 NI
ALPHA AND NEAR-ALPHA ALLOYS														
TI-0.3MO-0.8NI	480	70	380	55	0.03	0.10	0.015	0.30	0.25	. . .	. . .	. . .	0.3	0.8 NI
TI-5AL-2.5SN	790	115	760	110	0.05	0.08	0.02	0.50	0.20	5	2.5	. . .	. . .	. . .
TI-5AL-2.5SN-ELI	690	1130	620	90	0.07	0.08	0.0125	0.25	0.12	5	2.5	. . .	. . .	. . .
TI-8AL-1MO-1V	900	130	830	120	0.05	0.08	0.015	0.30	0.12	8	. . .	. . .	1	1 V
TI-6AL-2SN-4ZR-2MO	900	130	830	120	0.05	0.05	0.0125	0.25	0.15	6	2	4	2	. . .
TI-6AL-2NB-1TA-0.8MO	790	115	690	100	0.02	0.03	0.0125	0.12	0.10	6	. . .	. . .	1	2 NB, 1 TA
TI-2.25AL-11SN-5ZR-1MO	1000	145	900	130	0.04	0.04	0.008	0.12	0.17	2.25	11.0	5.0	1.0	0.2 SI
TI-5AL-5SN-2ZR-2MO[A]	900	130	830	120	0.03	0.05	0.0125	0.15	0.13	5	5	2	2	0.25 SI
ALPHA-BETA ALLOYS														
TI-6AL-4V[B]	900	130	83	120	0.05	0.10	0.0125	0.30	0.20	6.0	. . .	. . .	. . .	4.0 V
TI-6AL-4V-ELI[B]	830	120	760	110	0.05	0.08	0.0125	0.25	0.13	6.0	. . .	. . .	. . .	4.0 V
TI-6AL-6V-2SN[B]	1030	150	970	140	0.04	0.05	0.015	1.0	0.20	6.0	2.0	. . .	. . .	0.75 CU, 6.0 V
TI-8MN[B]	860	125	760	110	0.05	0.08	0.015	0.50	0.20	. . .	. . .	. . .	. . .	8.0 MN
TI-7AL-4MO[B]	1030	150	970	140	0.05	0.10	0.013	0.30	0.20	7.0	. . .	. . .	4.0	. . .
TI-6AL-2SN-4ZR-6MO[C]	1170	170	1100	160	0.04	0.04	0.0125	0.15	0.15	6.0	2.0	4.0	6.0	. . .
TI-5AL-2SN-2ZR-4MO-4CR[A][C]	1125	163	1055	153	0.04	0.05	0.0125	0.30	0.13	5.0	2.0	2.0	4.0	4.0 CR
TI-6AL-2SN-2ZR-2MO-2CR[A][B]	1030	150	970	140	0.03	0.05	0.0125	0.25	0.14	5.7	2.0	2.0	2.0	2.0 CR, 0.25 SI
TI-3AL-2.5V[D]	620	90	520	75	0.015	0.05	0.015	0.30	0.12	3.0	. . .	. . .	. . .	2.5 V
TI-1100	1000	145	900	130	. . .	. . .	. . .	0.02	0.07	6.0	2.75	4.0	0.4	0.45 SI

TI-4.5AL-5MO-1.5CR (CORONA 5)	900	130	830	120	. . .	. . .	. . .	. . .	. . .	4.5	. . .	. . .	5.0	1.5 CR
METASTABLE BETA ALLOYS														
TI-10V-2FE-3AL[(A)(C)]	1170	170	1100	160	0.05	0.05	0.015	2.5	0.16	3.0	. . .	. . .	. . .	10.0 V
TI-13V-11CR-3AL[(C)]	1170	170	1100	160	0.05	0.05	0.025	0.35	0.17	3.0	. . .	. . .	. . .	11.0 CR, 13.0 V
TI-8MO-8V-2FE-3AL[(A)(C)]	1170	170	1100	160	0.05	0.05	0.015	2.5	0.17	3.0	. . .	. . .	8.0	8.0 V
TI-3AL-8V-6CR-4MO-4ZR[(A)(B)]	900	130	830	120	0.03	0.05	0.020	0.25	0.12	3.0	. . .	4.0	4.0	6.0 CR, 8.0 V
TI-11.5MO-6ZR-4.5SN (BETA III)[(B)]	690	100	620	90	0.05	0.10	0.020	0.35	0.18	. . .	4.5	6.0	11.5	. . .
TI-15V-3AL-3SN-3CR	790	115	775	115	0.03	0.03	0.015	0.30	0.13	3.0	3.0	. . .	. . .	15.0 V, 3.0 CR
TI-15MO-2.7NB-3AL-0.2SI (BETA 21S)[(C)]	1100	160	1030	150	. . .	. . .	. . .	. . .	. . .	3.0	. . .	. . .	15.0	2.7 NB, 0.2 SI

(A) SEMICOMMERCIAL ALLOY; MECHANICAL PROPERTIES AND COMPOSITION LIMITS SUBJECT TO NEGOTIATION WITH SUPPLIERS.

(B) MECHANICAL PROPERTIES GIVEN FOR ANNEALED CONDITION; MAY BE SOLUTION TREATED AND AGED TO INCREASE STRENGTH.

(C) MECHANICAL PROPERTIES GIVEN FOR SOLUTION TREATED AND AGED CONDITION; ALLOY NOT NORMALLY APPLIED IN ANNEALED CONDITION. PROPERTIES MAY BE SENSITIVE TO SECTION SIZE AND PROCESSING.

(D) PRIMARILY A TUBING ALLOY; MAY BE COLD DRAWN TO INCREASE STRENGTH.

Unalloyed titanium products, which have minimum titanium contents ranging from about 98 to 99.5 wt%, are usually selected for their excellent corrosion resistance, especially in applications where high strength is not required. These materials are also used because they are highly formable and weldable. Yield strengths of unalloyed (commercially pure) grades (see Table 1) vary from 170 MPa (25 ksi) to 480 MPa (70 ksi) simply as a result of variations in the interstitial and impurity levels. Oxygen and iron are the primary variants in these grades; strength increases with increasing oxygen and iron contents. If the iron content is above about 0.05%, preferential corrosive attack of weld metal can occur in nitric acid solutions (Ref 4). Welds are particularly vulnerable because of the acicular nature of any retained beta phase that is stabilized by the iron. Galvanic cells between the beta and the contiguous alpha phase initiate corrosion of the weld metal. This behavior is not true for the base metal, where retained beta is finely divided and discontinuous, and corrosive attack is slight. Filler metal with low iron content should be used, and all sources of iron contamination during preparation and welding should be avoided.

Alpha and Near-Alpha Alloys. Alpha alloys that contain aluminum, tin, and/or zirconium are preferred for high-temperature as well as cryogenic applications. Alpha-rich alloys generally are more resistant to creep at high temperature than alpha-beta or metastable beta alloys. The extra-low-interstitial alpha alloys (ELI grades) retain ductility and toughness at cryogenic temperatures, and Ti-5Al-2.5Sn-ELI has been used extensively in such applications.

Unlike alpha-beta and metastable beta alloys, alpha alloys cannot be strengthened by heat treatment. Generally, alpha alloys are annealed or recrystallized to remove residual stresses induced by cold working. Alpha alloys have good weldability because they are insensitive to heat treatment. They generally have poorer forgeability and narrower forging-temperature ranges than alpha-beta or metastable beta alloys, particularly at temperatures below the beta transus. This poorer forgeability is manifested by a greater tendency for center bursts or surface cracks to occur, which means that small reduction steps and frequent reheats must be incorporated in forging schedules.

Alpha alloys that contain small additions of beta stabilizers (Ti-8Al-1Mo-1V or Ti-6Al-2Nb-1Ta-0.8Mo, for example) sometimes have been classed as "super-alpha" or "near-alpha" alloys. Although they contain some retained beta phase, these alloys consist primarily of alpha and behave more like conventional alpha alloys than alpha-beta alloys.

The alpha and near-alpha alloys have good weldability because of their good ductility (Ref 4). Welding operations have little effect on the mechanical properties of annealed material in the heat-affected zone. However, the strength of cold-worked material in the weld heat-affected zone is decreased as a result of heating. Therefore, these alloys are normally welded in the annealed condition. Stress relieving of weldments is commonly recommended.

Alpha-beta alloys contain one or more alpha stabilizers or alpha-soluble elements plus one or more beta stabilizers. These alloys retain more beta phase after solution treatment than do near-alpha alloys, the specific amount depending on the quantity of beta stabilizers present and on the heat treatment.

Alpha-beta alloys can be strengthened by solution treating and aging. Solution treating usually is done at a temperature high in the two-phase alpha-beta field, and is followed by quenching in water, oil, or other suitable quenchant. As a result of quenching, the beta phase present at the solution treating temperature may be retained or may be partly transformed during cooling by either martensitic transformation or nucleation and growth. The specific response depends on alloy composition, solution treating temperature (beta-phase composition at the solution temperature), cooling rate, and section size. Solution treatment is followed by aging, normally at 480 to 600 °C (900 to 1100 °F) to precipitate alpha and produce a fine mixture of alpha in the retained or transformed beta phase. Transformation kinetics, transformation products, and specific response of a given alloy can be quite complex; a detailed review is provided in Ref 3.

Solution treating and aging can increase the strength of alpha-beta alloys 30 to 50%, or more, over the annealed or over-aged condition. Response to solution treating and aging depends on section size; alloys relatively low in beta stabilizers (Ti-6Al-4V, for example) have poor hardenability and must be quenched rapidly to achieve significant strengthening. For Ti-6Al-4V, the cooling rate of a water quench is not rapid enough to significantly harden sections thicker than about 25 mm (1 in.). As the content of beta stabilizers increases, hardenability increases. For some alloys of intermediate beta-stabilizer content, the surface of a relatively thick section can be strengthened, but the core may be 10 to 20% lower in hardness and strength. The strength that can be achieved by heat treatment is also a function of the volume fraction of beta phase present at the solution treating temperature. Alloy composition, solution temperature, and aging conditions must be carefully selected and balanced to produce the desired mechanical properties in the final product. Table 2 summarizes typical heat treatments for alpha-beta alloys.

TABLE 2 SUMMARY OF HEAT TREATMENTS FOR ALPHA-BETA TITANIUM ALLOYS

HEAT TREATMENT DESIGNATION	HEAT TREATMENT CYCLE[(A)]	MICROSTRUCTURE
DUPLEX ANNEAL	SOLUTION TREAT AT 50-75 °C (90-135 °F) BELOW T β, AIR COOL AND AGE FOR 2-8 H AT 540-675 °C (1000-1250 °F)	PRIMARY α, PLUS WIDMANSTÄTTEN α - β REGIONS
SOLUTION TREAT AND AGE	SOLUTION TREAT AT ~40 °C (70 °F) BELOW T β, WATER QUENCH AND AGE FOR 2-8 H AT 535-675 °C (995-1250 °F)	PRIMARY α, PLUS TEMPERED α ' OR A β - α MIXTURE
BETA ANNEAL	SOLUTION TREAT AT ~15 °C (30 °F) ABOVE T β, AIR COOL STABILIZE AT 650-760 °C (1200-1400 °F) FOR 2 H	WIDMANSTÄTTEN α - β COLONY MIXTURE
BETA QUENCH	SOLUTION TREAT AT ~15 °C (30 °F) T β, WATER QUENCH AND TEMPER AT 650-760 °C (1200-1400 °F) FOR 2 H	TEMPERED α '
RECRYSTALLIZATION-ANNEAL	925 °C (1700 °F) FOR 4 H, COOL AT 50 °C/H (90 °F/H) TO 760 °C (1400 °F), AIR COOL	EQUIAXED α WITH β AT GRAIN-BOUNDARY TRIPLE JOINTS
MILL ANNEAL	α - β HOT WORK PLUS ANNEAL AT 705 °C (1300 °F) FOR 30 MIN TO SEVERAL HOURS AND AIR COOL	INCOMPLETELY RECRYSTALLIZED α WITH A SMALL VOLUME FRACTION OF SMALL β PARTICLE

(A) T β IS THE β TRANSUS TEMPERATURE FOR THE PARTICULAR ALLOY IN QUESTION. IN MORE HEAVILY β -STABILIZED ALLOYS SUCH AS TI-6AL-2SN-4ZR-6MO OR TI-6AL-6V-2SN, SOLUTION TREATMENT IS FOLLOWED BY AIR COOLING. SUBSEQUENT AGING CAUSES PRECIPITATION OF α PHASE TO FORM AN α - β MIXTURE.

Welding alpha-beta alloys may significantly change their strength, ductility, and toughness characteristics as a result of the thermal cycle to which the alloy is exposed (Ref 4). The low ductility of most alpha-beta alloy welds is caused by phase transformations in the weld metal or the heat-affected zone, or both (see the section "Weld Microstructure" below). Alpha-beta alloys can be welded with unalloyed titanium or alpha-titanium alloy filler metal to produce a weld metal that is low in beta phase. This improves weld ductility. However, this procedure does not overcome the low ductility of the heat-affected zone in alloys that contain large amounts of beta stabilizers.

Ti-6Al-4V has the best weldability of the alpha-beta alloys. This weldability can be attributed to two principal factors. First, the alpha-prime martensite which forms in Ti-6Al-4V is not as hard and brittle as that exhibited by more heavily beta-stabilized alloys, such as Ti-6Al-6V-2Sn. Secondly, Ti-6Al-4V exhibits a relatively low hardenability, which allows the formation of higher proportions of the more desirable Widmanstätten alpha plus retained beta microstructure even at relatively high weld cooling rates.

Due to its single-phase mode of solidification (i.e., absence of low-melting-point eutectics), Ti-6Al-4V is also highly resistant to solidification- and liquation-related cracking. However, the occurrence of solid-state cracking and the formation of porosity can be encountered during welding. Fortunately, these defects are not metallurgically inherent in Ti-6Al-4V, but rather originate from readily correctable deficiencies in preweld cleaning of the workpieces and shielding of the weld zone from atmospheric contamination.

Alpha-beta alloys that are highly beta stabilized, such as Ti-6Al-2Sn-4Zr-6Mo and Ti-6Al-6V-2Sn, have limited weldability. They tend to crack when welded under high restraint or when minor defects are present in the weld zone (Ref

4). The resistance to cracking may be improved by preheating in the range of 150 to 175 °C (300 to 350 °F) and then stress-relieving immediately after welding.

Metastable beta alloys are sufficiently rich in beta stabilizers (and lean in alpha stabilizers) that the beta phase can be completely retained with appropriate cooling rates. These alloys are metestable, and precipitation of alpha phase in the metestable beta is a method used to strengthen the alloys. Metestable beta alloys contain small amounts of alpha-stabilizing elements as strengthening agents.

As a class, metestable beta alloys offer increased fracture toughness over alpha-beta alloys at a given strength level (Ref 2). However, metastable beta and beta alloys require close control of processing and fabrication steps to achieve optimal properties. In the past, metestable beta alloys had rather limited applications, such as springs and fasteners, where very high strength was required.

In recent years, however, metestable beta alloys have received closer attention because their fracture toughness characteristics respond to the increased need for damage tolerance in aerospace structures. In addition, some metastable beta alloys containing molybdenum have good corrosion characteristics. Metastable beta alloys also exhibit:

- BETTER ROOM-TEMPERATURE FORMING AND SHAPING CHARACTERISTICS THAN ALPHA-BETA ALLOYS
- HIGHER STRENGTH THAN ALPHA-BETA ALLOYS AT TEMPERATURES WHERE YIELD STRENGTH (INSTEAD OF CREEP STRENGTH) IS THE APPLICABLE CRITERION
- BETTER RESPONSE TO HEAT TREATMENT (SOLUTION TREATMENT, QUENCHING, AND AGING) IN HEAVIER SECTIONS THAN THE ALPHA-BETA ALLOYS

Most metastable beta alloys are weldable in either the annealed or the heat-treated condition (Ref 4). These alloys include Ti-13V-11Cr-3Al, Ti-8Mo-8V-3A1-2Fe, and Ti-15V-3Al-3Cr-3Sn alloys. Welded joints have good ductility but relatively low strength in the as-welded condition. They are used most often in this condition because the welded joint can respond differently to heat treatment than the base metal and have low ductility after aging. Aging can take place if the welds are exposed to elevated temperatures in service.

References cited in this section

2. S. LAMPMAN, WROUGHT TITANIUM AND TITANIUM ALLOYS, *PROPERTIES AND SELECTION: NONFERROUS ALLOYS AND SPECIAL-PURPOSE MATERIALS,* VOL 2, *ASM HANDBOOK,* ASM INTERNATIONAL, 1990, P 592-633
3. E.W. COLLINGS, *THE PHYSICAL METALLURGY OF TITANIUM ALLOYS,* AMERICAN SOCIETY FOR METALS, 1984
4. TITANIUM, ZIRCONIUM, HAFNIUM, TANTALUM, AND COLUMBIUM, *WELDING HANDBOOK,* 7TH ED., VOL 4, AMERICAN WELDING SOCIETY, 1982, P 434-470

Selection and Weldability of Conventional Titanium Alloys

W.A. Baeslack III, The Ohio State University; J.R. Davis, Davis and Associates; C.E. Cross, Martin Marietta Astronautics Group

General Welding Considerations (Ref 5)

Titanium has a strong chemical affinity for oxygen, and a stable, tenacious oxide layer forms rapidly on a clean surface, even at room temperature. This behavior leads to a natural passivity that provides a high degree of corrosion resistance (Ref 6). The strong affinity of titanium for oxygen increases with temperature, and the surface oxide layer increases in thickness at elevated temperatures (Fig. 3). At temperatures exceeding 500 °C (930 °F), its oxidation resistance decreases rapidly, and the metal becomes highly susceptible to embrittlement by oxygen, nitrogen, and hydrogen, which dissolve

interstitially in titanium. Therefore, the melting, solidification, and solid-state cooling associated with fusion welding must be conducted in completely inert or vacuum environments. The fusion welding processes most widely used for joining titanium are gas-tungsten arc welding (GTAW), gas-metal arc welding (GMAW), plasma arc welding (PAW), laser-beam welding (LBW), and electron-beam welding (EBW); each of these processes are discussed later in this article. With the arc and laser welding processes, protection of the weld zone can be provided by localized inert-gas shielding. Complete enclosure in a protective chamber of the high vacuum environment associated with the electron-beam welding process inherently provides better atmospheric protection. In addition to proper shielding, welded component cleanliness (including filler metals) is necessary to avoid weld contamination.

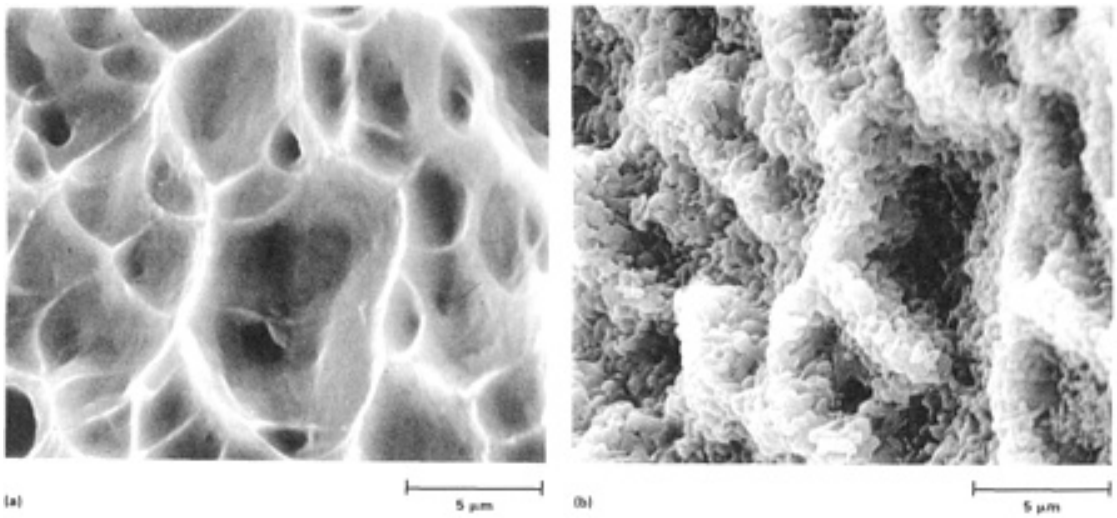

FIG. 3 EFFECT OF A 15 MIN 800 °C (1470 °F) AIR EXPOSURE ON A FRACTURE SURFACE OF AN ANNEALED TI-6AL-6V-2SN ALLOY. (A) FRACTURE APPEARANCE BEFORE EXPOSURE. (B) THE IDENTICAL FRACTURE SURFACE AFTER EXPOSURE; THE OXIDE BUILDUP IS SO GREAT THAT IT IS IMPOSSIBLE TO IDENTIFY THE FRACTURE MODE. COURTESY OF V. KERLINS, MCDONNELL DOUGLAS ASTRONAUTICS COMPANY

The welding of thin-to-moderate section thicknesses in titanium alloys can be accomplished using all of the aforementioned processes. The GTAW process offers the greatest flexibility for both manual and automatic application at minimum capital investment. If production volume is large, the high capital investment required for LBW and EBW systems can be acceptable, based on higher welding rates and improved productivity. For titanium plate thickness exceeding about 5 mm (0.20 in.), the high-energy density processes are the most efficient. Plasma are welding, for producing welds up to about 15 mm (0.6 in.) thick, and EBW, which can readily generate single-pass welds in plates over 50 mm (2 in.) thick, are used in current aerospace practice. In addition to thickness requirements, complex geometries may require manual welding or the use of extensive fixturing. The automatic welding of extremely large components may also prove difficult, particularly with the EBW process.

Residual stresses in titanium welds can greatly influence the performance of a fabricated aerospace component by degrading fatigue properties, while distortion can cause difficulties in the final assembly and operation of high-tolerance aerospace systems. Thus, the use of high-energy-density welding processes to produce full-penetration, single-pass autogenous welds, rather than multipass conventional arc welding, is desirable to minimize these difficulties.

Several important and interrelated aspects of welding phenomena contribute to the overall understanding of titanium alloy welding metallurgy. These factors include melting and solidification effects on weld microstructure, postweld heat treatment effects, and structure/mechanical property/fracture relationships. Each of these are described below as well as in several excellent review articles (Ref 5, 7, 8, 9).

References cited in this section

5. W.A. BAESLACK III, D.W. BECKER, AND F.H. FROES, ADVANCES IN TITANIUM ALLOY WELDING METALLURGY, *J. MET.*, MAY 1984, P 46-58

6. R.W. SCHUTZ AND D.E. THOMAS, CORROSION OF TITANIUM AND TITANIUM ALLOYS, *CORROSION,* VOL 13, *ASM HANDBOOK,* ASM INTERNATIONAL, 1987, P 669-706
7. D.W. BECKER, W.A. BAESLACK III, AND R.W. MESSLER, JR., TITANIUM WELDING, *TITANIUM '80 SCIENCE AND TECHNOLOGY,* VOL 1, H. KIMURA AND O. IZUMI, ED., THE METALLURGICAL SOCIETY OF AIME, 1980, P 255-275
8. D.F. HASSON, "A REVIEW OF TITANIUM WELDING PROCESSES," U.S. NAVY REPORT, ANNAPOLIS, MD, 1985
9. J.R. HARTMAN AND W.A. BAESLACK III, ADVANCES IN ARC WELDING OF TITANIUM ALLOYS, *WELDABILITY OF MATERIALS,* R.A. PATTERSON AND K.W. MAHIN, ED., ASM INTERNATIONAL, 1990, P 319-330

Selection and Weldability of Conventional Titanium Alloys

W.A. Baeslack III, The Ohio State University; J.R. Davis, Davis and Associates; C.E. Cross, Martin Marietta Astronautics Group

Weld Microstructure

The microstructure of the weldment and the extent to which it differs from the thermomechanically processed base material is strongly influenced by the thermal cycle of welding. Two characteristics that are vitally important are the size and shape of the prior-beta grains and the phase transformations that take place during weld cooling. These characteristics are described for both alpha-beta (Ti-6Al-4V) and metastable beta alloys in this section. Also described are weld defects (macrosegregation, microsegregation, and solidification defect formation) and the effects of postweld heat treatment on welded titanium structures.

Alpha-Beta Alloys

Prior-Beta Grain Size. Mechanical properties of composite weld structures in titanium alloys depend on structural characteristics of each weld region, which in turn depend on the specific thermal cycle(s) imposed during welding and on subsequent postweld heat treatment. As the weld macrographs in Fig. 4, 5, 6, and 7 illustrate, the weld fusion zone in titanium alloys is characterized by coarse, columnar prior-beta grains that originate during weld solidification. The size and morphology of these grains depend on the nature of the heat flow that occurs during weld solidification.

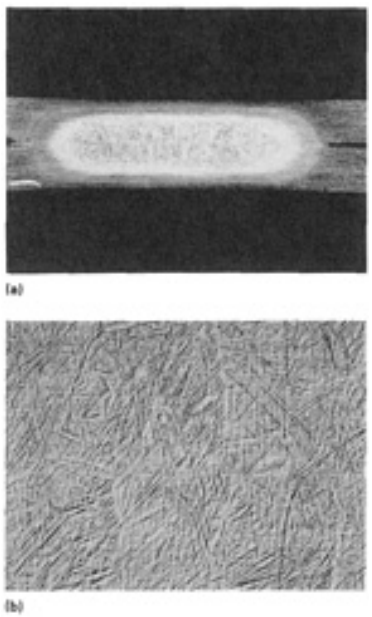

FIG. 4 COLUMNAR BETA GRAINS IN A TI-6AL-4V SPOT WELD. (A) 10×. (B) 240×. COURTESY OF THE

WELDING INSTITUTE

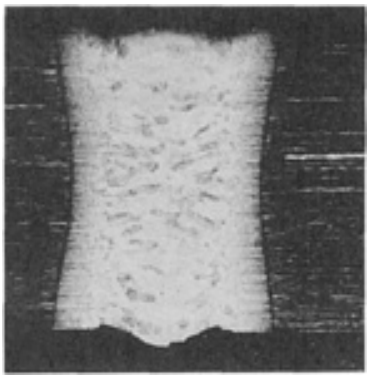

FIG. 5 MACROGRAPH SHOWING COLUMNAR BETA GRAINS IN A TI-6AL-4V LASER-BEAM WELD. 13×. COURTESY OF THE WELDING INSTITUTE

FIG. 6 MACROGRAPH SHOWING COARSE PRIOR-BETA GRAIN SIZE IN AN ELECTRON-BEAM WELDED TI-6AL-4V FORGING. COURTESY OF THE WELDING INSTITUTE

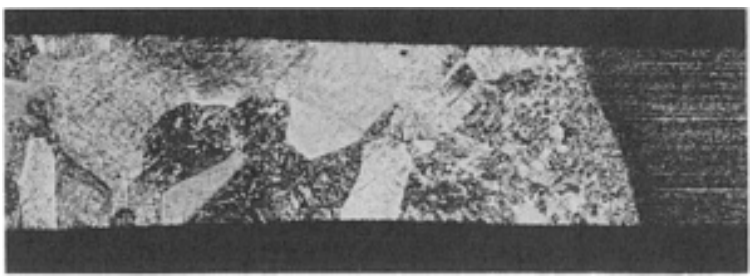

FIG. 7 MACROGRAPH SHOWING MULTIDIRECTIONAL BETA GRAIN MORPHOLOGY IN A TI-6AL-4V GAS-TUNGSTEN ARC WELD. 30×. COURTESY OF THE WELDING INSTITUTE

Under simple, uniaxial heat flow, such as occurs in a spot weld, the beta grains nucleate epitaxially on beta grains in the base-metal substrates and solidify preferentially in a direction parallel to the maximum temperature gradient (i.e., parallel to the welding electrodes) until they impinge at a horizontal weld centerline (Fig. 4). Under two-dimensional heat-flow conditions characteristic of full-penetration plasma-arc, laser-beam, and electron-beam welds, the columnar beta grains solidify inward from the base metal in a direction nearly parallel to the sheet or plate surface, ultimately impinging to form a vertical grain boundary at the weld centerline (Fig. 5 and 6). Three-dimensional or mixed two-dimensional/three-dimensional heat-flow conditions, such as those present in single-pass and multipass gas-tungsten arc and gas-metal arc weldments, promote the formation of more complex, multidirectional beta grain morphologies (Fig. 7).

The fusion-zone beta grain size depends primarily on the weld energy input, with a higher energy input promoting a larger grain size. Due to epitaxial grain growth, the fusion-zone beta grain size may also depend on the beta grain size in the near heat-affected zone (HAZ) directly adjacent to the fusion line. This latter effect of base metal grain size is most significant in the welding of extremely coarse-grained cast or beta-annealed alloys, as shown in Fig. 6 for an electron-beam weld produced in a coarse-grained forging. Because weld mechanical properties, particularly ductility, can be degraded by a coarse prior-beta grain size, it is important to maintain as fine a grain structure as possible by minimizing the weld energy input.

As indicated above, appreciable beta grain growth occurs in the near HAZ directly adjacent to the weld fusion line, where peak temperatures range from between the alloy solidus down to the beta transus (approximately 995 °C, or 1825 °F, for Ti-6Al-4V). As in the fusion zone, the extent of this growth increases with energy input into the weld zone. Consequently, this region can vary markedly in width, being almost unresolvable in electron-beam and laser-beam welds and yet being several beta grains wide in gas-tungsten arc welds (Fig. 5 and 7). Further from the fusion line, temperatures below the beta transus are encountered, which promote transformation of alpha phase in the mill-annealed microstructure to various proportions of the high-temperature beta phase. The presence of even small quantities of alpha phase at peak temperatures in the weld thermal cycle is sufficient to prevent beta grain growth, thereby contributing to the improved ductility of this region as compared with the coarser-grained fusion zone and near HAZ.

During the past two decades, numerous investigators in the former Soviet Union and in the United States have evaluated methodologies for promoting beta grain refinement in titanium alloy fusion welds. This work, which has recently been reviewed (Ref 10), utilized principally electromagnetic stirring techniques and inoculation with rare-earth (RE) elements and titanium "microcooler" particles to promote nonepitaxial heterogenous nucleation of beta grains during solidification and thereby provide a refined fusion zone grain structure. Several of these approaches have been effective in refining the beta grain structure, and correspondingly improving fusion zone mechanical properties. Figure 8 shows the equiaxed prior-beta grain structure in the fusion zone of a gas-tungsten arc weld produced in a Ti-6Al-4V joint using titanium powder microcooler additions. Despite the success of these techniques, particularly in thin sheet materials, their commercial application has been extremely limited, particularly in the United States.

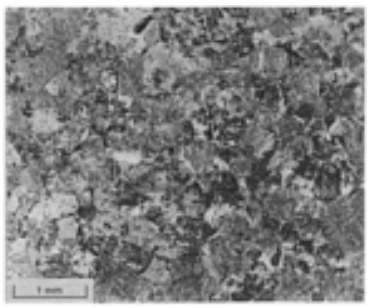

FIG. 8 PHOTOMICROGRAPH SHOWING EQUIAXED PRIOR-BETA MICROSTRUCTURE IN THE FUSION ZONE OF A TI-6AL-4V WELD JOINT. GTAW PROCESS UTILIZED TITANIUM MICROCOOLER ADDITIONS. 12×

Phase Transformations. In addition to prior-beta grain size, weld zone mechanical properties in Ti-6Al-4V are significantly influenced by the manner in which the high-temperature, body-centered-cubic beta phase transforms on cooling to the low-temperature, hexagonal-close-packed phase. Characteristics of this "transformed-beta" microstructure depend principally on the cooling rate from above the beta transus temperature, which is correspondingly influenced by the welding process, process parameters, and other welding conditions (such as workpiece geometry and fixturing). In the near-HAZ regions, high cooling rates associated with low-energy-input welding processes such as laser-beam, electron-beam, and resistance welding (100 to 10,000 °C/s, or 180 to 18,000 °F/s), promote transformation of beta to alpha-prime martensite. This extremely fine, acicular transformation product exhibits high strength and hardness but relatively low ductility and toughness. At the lower cooling rates associated with gas-tungsten arc or plasma-arc welding (10 to 100 °C/s, or 18 to 180 °F/s), a coarser structure of Widmanstätten alpha plus retained beta, or a mixture of this structure and alpha-prime, is produced, which exhibits yield and tensile strengths superior to those of the mill-annealed base metal and a ductility and toughness greater than those of an entirely martensitic microstructure. In the far HAZ, microstructures are comprised of primary alpha phase originating from the base-metal microstructure in a matrix of transformed beta.

The weld microstructure and mechanical properties may also be influenced by postweld heat treatment, with specific postweld heat treatment effects depending on the heat treatment time and temperature and on the as-welded microstructure. See the section on the "Effect of Postweld Heat Treatment" in this article.

Metastable-Beta Alloys

The weld HAZ and fusion zone beta grain macrostructures in metastable-beta titanium alloys are essentially identical to those observed in alpha-beta alloys. Due to the appreciable beta-stabilizer content in metastable-beta titanium alloys, and the relatively slow diffusivity of these elements, the high-temperature beta phase is retained on weld cooling to room temperature (although athermal transformation to omega phase may occur in certain alloys) (Ref 11, 12). Subsequent postweld aging heat treatment at temperatures ranging from about 450 to 650 °C (840 to 1200 °F) promotes the precipitation of fine alpha phase both intragranularly and along prior-beta grain boundaries. Through proper control of the aging temperature and time, a wide range of base metal and weld zone strength/ductility combinations can be achieved. The relatively uniform precipitation of extremely fine alpha phase during low-temperature aging (482 °C, or 900 °F, for 24 h), as shown in Fig. 9(a) and (b) for gas-tungsten arc weld fusion zone in Beta C, promotes high fusion zone hardness and strength (UTS, ultimate tensile strength, of 1382 MPa, or 200 ksi) and low ductility (2.5% elongation). An increased aging temperature promotes coarser alpha precipitation, softening (UTS of 1121 MPa, or 163 ksi), and an increase in ductility (8.0% elongation), as shown in Fig. 9(c) and 9(d) for the gas-tungsten arc weld fusion zone in Beta C aged at 593 °C (1100 °F) for 8 h. It should be noted that in contrast to alpha-beta alloys, residual microsegregation from weld solidification can influence alpha precipitation on aging, particularly for low-temperature aging heat treatments (Fig. 9).

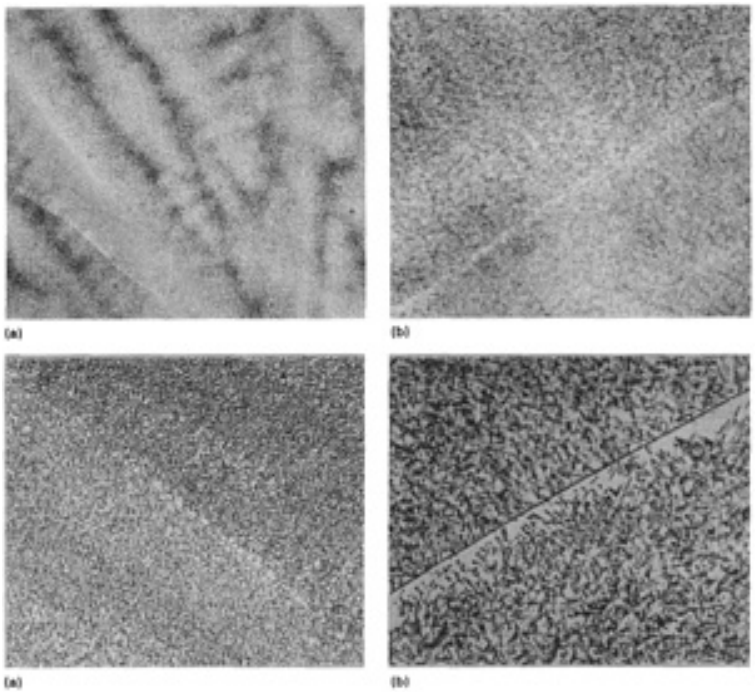

FIG. 9 POSTWELD HEAT TREATED GAS-TUNGSTEN ARC WELD FUSION ZONE IN BETA-C SHEET. (A) AGED AT 482 °C (900 °F) FOR 24 H; 275×. (B) SAME HEAT TREATMENT AS (A); 690×. (C) AGED AT 593 °C (1100 °F) FOR 8 H; 275×. (D) SAME HEAT TREATMENT AS (C); 690×. SOURCE: REF 12

Welding Defects

In many alloy systems, weldability is determined by the capability of the alloy to produce a weld that is free of discontinuities or defects. Defects that may be encountered when welding titanium alloys include:

- SOLIDIFICATION SEGREGATION (MACROSEGREGATION AND MICROSEGREGATION)
- SOLIDIFICATION CRACKING
- CONTAMINATION CRACKING
- HYDROGEN EMBRITTLEMENT

- SUBSOLIDUS (DUCTILITY DIP) CRACKING
- POROSITY

Macrosegregation in weldments is defined as segregation that extends over distances of several grain diameters. In titanium alloy fusion weldments, macrosegregation occurs primarily in the form of transverse solute banding (Ref 5). These solute-enriched or solute-depleted bands normally appear as curvilinear contours on the polished and etched weldment surface and are attributed to thermal variations in the weld pool, which periodically change the solid-liquid interface velocity. Transverse solute banding has occurred using both arc and high-energy welding processes. Studies on solute redistribution in Ti-6Al-4V gas-tungsten arc welds found distinct metallographic evidence of transverse solute banding. Electron microprobe analysis determined the bands resulted from vanadium and aluminum segregation (Ref 13).

The effect of macrosegregation on subsequent beta phase decomposition during cooling depends on the extent of segregation residual at the transformation temperature and the local alloy chemistry. Solute diffusion that occurs after solidification and prior to solid-state phase transformations reduces the magnitude of macrosegregation. In near-alpha and alpha-beta alloys, little effect of macrosegregation has been reported. However, in the more heavily beta-stabilized alloys, strong macrosegregation effects have been observed (Ref 14). This effect is shown in Fig. 10 for a gas-tungsten arc weld fusion zone produced between the alpha-beta alloy Ti-6Al-4V and the metastable-beta alloy Ti-15V-3Cr-3Al-3Sn. Transverse solute bands in the weld fusion zone, which were found to be depleted in the beta stabilizers vanadium and chromium, transformed to martensite while the remaining more heavily beta-stabilized regions were retained as beta phase during weld cooling. A similar effect of macrosegregation due to transverse-solute banding and incomplete mixing was recently observed for dissimilar-alloy laser welds produced between Ti-6Al-4V and the metastable-beta alloys Beta-C and Beta-21S (Ref 15, 16).

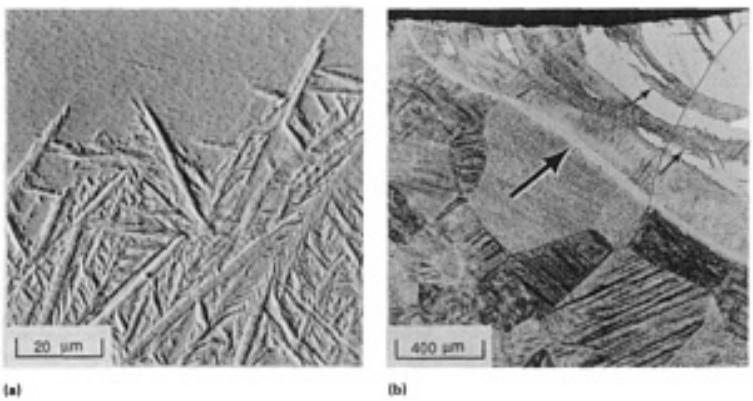

FIG. 10 LIGHT (A) AND SCANNING ELECTRON (B) MICROGRAPHS SHOWING MARTENSITICALLY-TRANSFORMED TRANSVERSE-SOLUTE BANDS (SMALL ARROWS) IN DISSIMILAR ALLOY GAS-TUNGSTEN ARC WELD BETWEEN TI-6AL-4V AND TI-15V-3AL-3CR-3SN SHEETS. LARGE ARROW IN (A) INDICATES FUSION LINE.

It should be pointed out, however, that the degradation of weld integrity, structure, or properties due to macro- and/or microsegregation is generally not significant in titanium alloys due to the limited extent of segregation of common alloying elements and the appreciable diffusional homogenization of alloying elements during weld cooling through the beta-phase field. This significant effect of alloying element homogenization on cooling through the beta-phase field has been recently demonstrated by lnoue and Ogawa (Ref 17) for gas-tungsten arc welds in Ti-6Al-4V using liquid tin quenching experiments that allowed analysis of the "as-solidified" fusion zone solidification structure. They observed in gas-tungsten arc welds produced in Ti-6Al-4V that the segregation of vanadium and iron to dendrite interstices disappeared at a very early stage of weld cooling following the completion of weld solidification due to their high diffusivity in the beta phase at high temperatures.

Microsegregation. The nonequilibrium solidification conditions experienced during fusion welding result in a breakdown of the advancing solid-liquid interface into cellular, cellular-dendritic, and dendritic substructures (Ref 5). This interface breakdown in commercial titanium alloy welds is associated with the segregation of alloying elements on

an intercellular or interdendritic scale. Microsegregation is much more evident in metastable-beta titanium alloy weldments than in alpha-beta weldments. This behavior is due primarily to the appreciably higher alloying levels (and therefore higher absolute compositional differences in segregated regions) and the absence of a transformed structure in the completely retained-beta fusion zone. As indicated earlier, local variations in beta-stabilizer content due to microsegregation can affect the alpha-phase precipitation response during subsequent postweld heat treatment.

Microsegregation effects have also become significant in the joining of advanced, elevated-temperature titanium alloys that contain rare earth elements for dispersoid strengthening (Ref 17). Figure 11 shows the fusion zone of a laser weld in a rapidly-solidified, powder metallurgy Ti-8Al-2.8Sn-5.4Hf-3.6Ta-1Y-0.2Si (wt%) alloy. The segregation of yttrium to dendrite interstices during weld solidification promotes the nucleation and growth of yttrium-enriched dispersoids in these regions both during the final states of solidification and possibly in the solid-state during cooling. Similar segregation of yttrium and dispersoid formation would be expected in gas-tungsten arc welds, but with a coarser grain and dispersoid size.

FIG. 11 TRANSMISSION ELECTRON MICROGRAPH OF LASER WELD FUSION ZONE IN RAPIDLY-SOLIDIFIED/POWDER METALLURGY TI-8AL-2.8SN-5.4HF-3.6TA-1Y-0.2SI ALLOY SHOWING YTTRIUM-ENRICHED DISPERSOIDS (INDICATED BY ARROWS) LOCATED ALONG SOLIDIFICATION SUBSTRUCTURE BOUNDARIES. SOURCE: REF 17

Solidification Cracking (Ref 9). Relative to many other structural alloys, such as aluminum alloys and many austenitic stainless steels, titanium alloys are generally not considered susceptible to fusion zone solidification cracking. Studies have demonstrated, however, that under severe conditions of restraint, solidification cracking along columnar beta grain boundaries can occur (Ref 18). Centerline cracking in a gas-tungsten arc welded alpha-beta alloy Ti-6Al-6V-2Sn is shown in Fig. 12. Recent work by Prokhorov *et al.* (Ref 19) has further evaluated the solidification cracking of Ti-6Al-4V using a weldability test in which a gas-tungsten arc weld is strained during the welding operation. They reported the formation of solidification cracks oriented along the welding direction and a quantitative susceptibility comparable to some steels, and concluded that solidification cracking must be considered when designing joints in Ti-6Al-4V structural components. However, this observation generally conflicts with the well-known excellent cracking resistance of this alloy, and suggests that their test imposed an excessive strain condition not representative of that experienced during conventional arc welding.

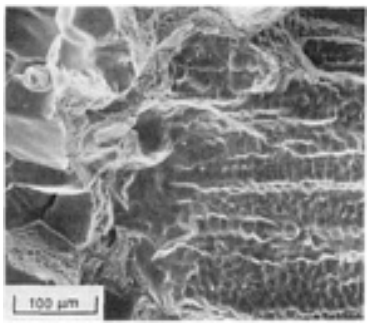

FIG. 12 SEM FRACTOGRAPH SHOWING SURFACE OF FUSION ZONE SOLIDIFICATION CRACK IN GAS-

Due to an absence of second-phase dispersoids or precipitate particles, or impurities at grain boundaries, conventional titanium alloys are also generally very resistant to HAZ or weld metal liquation cracking. However, recent welding trials on selected rare earth dispersion-strengthened titanium alloys have indicated that the liquation of these particles in the weld HAZ can occur, with this liquid subsequently wetting adjacent beta grain boundaries. Although cracking along these boundaries has not been observed, it may be expected in the arc welding of these alloys under conditions of high weld restraint.

Contamination Cracking. When titanium is exposed to air, moisture, or hydrocarbons at temperatures exceeding 500 °C (930 °F), it will readily pick up oxygen, nitrogen, carbon, and hydrogen. These small atoms of the interstitial elements will enter the crystal lattice in monatomic form and will migrate to interstitial sites (sites located between titanium atoms). The presence of these interstitial elements serves to inhibit plastic deformation and increase strength, but with a substantial loss in ductility. If contamination levels exceed a certain amount, cracking may ensue from the stresses generated during welding. Levels of oxygen on the order of 3000 ppm in the weld have been known to result in transverse cracking (Ref 20). The alpha phase is particularly susceptible to contamination cracking. The hexagonal crystal lattice of alpha-titanium is distorted by the presence of interstitial atoms. In particular, the *c*/*a* ratio is increased (Fig. 13), which results in a reduced number of active slip planes from three (prism, pyramidal, and basal) down to one (prism or pyramidal) (Ref 21). Slip planes are crystallographic planes upon which dislocations move to achieve plastic deformation.

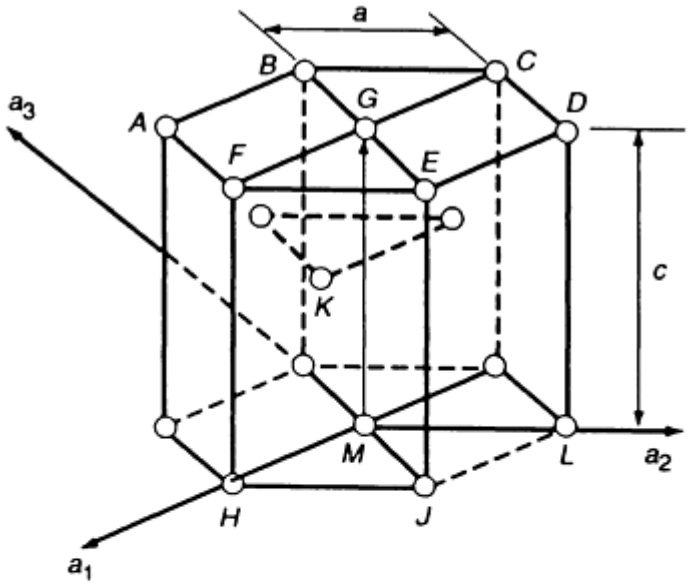

Basal plane (0001) – *ABCDEF*
Prism plane (10$\bar{1}$0) – *FEJH*
Pyramidal planes
Type I, order 1 (10$\bar{1}$1) – *GHJ*
Type I, order 2 (10$\bar{1}$2) – *KJH*
Type II, order 1 (11$\bar{2}$1) – *GHL*
Type II, order 2 (11$\bar{2}$2) – *KHL*
Diagonal axis [11$\bar{2}$0] – *FGC*

FIG. 13 DIAGRAM OF THE UNIT CELL FOR A HEXAGONAL CLOSE-PACKED CRYSTAL SHOWING BASAL, PRISM, AND PYRAMIDAL PLANES. THE *C/A* RATIO OF THE UNIT CELL FOR ALPHA-TITANIUM IS AFFECTED BY THE PRESENCE OF INTERSTITIAL ATOMS.

Contamination cracking can be avoided by minimizing exposure of the molten weld pool and the heated weld region to interstitial elements. This practice is accomplished by:

- THOROUGHLY DEGREASING THE JOINT PRIOR TO WELDING
- PROVIDING SUFFICIENT INERT GAS SHIELDING TO THE TORCH, TRAILING SHOE, AND BACK SIDE OF THE JOINT
- USING SHIELDING GAS WITH A SUFFICIENTLY LOW DEW POINT

When titanium is oxidized, it assumes different colors depending on alloy content and the degree of oxidation. These colors range from silver to straw, to blue, to white (severe oxidation). While the presence of a blue or white oxide serves as a good indicator that unacceptable contamination has occurred, its absence is no guarantee that the weld is interstitial free.

Hydrogen Embrittlement. While hydrogen can play a role in contamination cracking as discussed above, it can also lead to a more insidious type of defect known as hydrogen embrittlement, or hydrogen delayed cracking. One mechanism proposed for this problem involves the precipitation of titanium hydrides in the vicinity of cracks (Ref 22). If it is assumed that a microcrack is present in the weldment, it follows that hydrogen atoms will diffuse to the crack tip, where a triaxial stress state produces large interstitial sites (holes) in the lattice. These large interstitial sites can more easily accommodate the hydrogen atoms.

Once a critical concentration of hydrogen is reached, titanium hydrides will precipitate ahead of the crack tip (Fig. 14). Hydrogen may also diffuse to the crack to form diatomic gas, increasing pressure within the crack and increasing the load at the crack tip. Eventually the hydrides will rupture, allowing the crack to advance. Upon rupture, the hydrides will redissolve and hydrogen will diffuse to the new crack tip, thus reinitiating the sequence. This cycle may repeat many times, each cycle resulting in a small advancement of the crack.

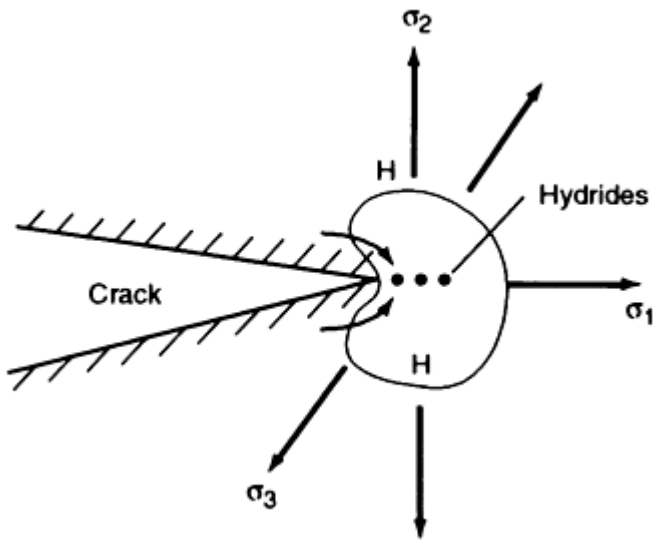

FIG. 14 SCHEMATIC DIAGRAM SHOWING HOW HYDROGEN ATOMS MAY DIFFUSE TO A CRACK TIP IN A TITANIUM WELDMENT TO FORM TITANIUM HYDRIDES

Because the hydrogen embrittlement sequence requires diffusion of hydrogen, the rate of crack advancement depends on time and temperature. Hours, days, or months may pass following welding before significant cracking is observed. This problem can be avoided by minimizing exposure of the weld to hydrogen (hydrocarbons and moisture). Hydrogen concentrations on the order of 200 ppm are known to cause cracking problems (Ref 15), although the combined presence of other interstitials (for example, oxygen or nitrogen) may lower this tolerance limit. The inert shielding gas should have a dew point of at least -50 °C (-60 °F) (34 ppm H_20). Welding-grade argon or helium gas (grade 4.5 with 50 ppm impurities) may not always satisfy this requirement. Also, the use of postweld heat treatment is beneficial because it relieves residual stress, thus reducing the driving force for crack advancement.

Subsolidus Cracking. Certain alloy compositions and microstructures have been found to be susceptible to a severe ductility loss (ductility dip) in a temperature range from about 750 to 850 °C (1380 to 1560 °F) on cooling from temperatures above the beta transus. In particular, alpha-beta alloys that contain niobium rather than vanadium as a beta-stabilizing element are more susceptible to this form of cracking. Microstructures having alpha films at prior-beta grain boundaries, with coarse Widmanstätten alpha colonies, are also more prone to subsolidus cracking.

Lewis *et al.* (Ref 23) utilized a Gleeble system and a typical gas-tungsten arc weld thermal cycle to evaluate the sensitivity of several near-alpha and alpha-beta titanium alloys to this phenomenon. The results of their analysis indicate that Ti-6211 (Ti-6Al-2Nb-1Ta-0.8Mo) exhibits the largest ductility dip and will be the most likely to crack during weld cool down, provided that the welding stresses are high enough (Fig. 15). Ductility dip cracks are intergranular, but show signs of microplasticity (ductile dimples) when examined at high magnification. They are believed to occur due to volumetric differences as a result of the beta-to-alpha transformation. It has been proposed that when the prior-beta grains transform to alpha, the grain boundaries are loaded in tension, causing rupture within grain boundary alpha films (Ref 24).

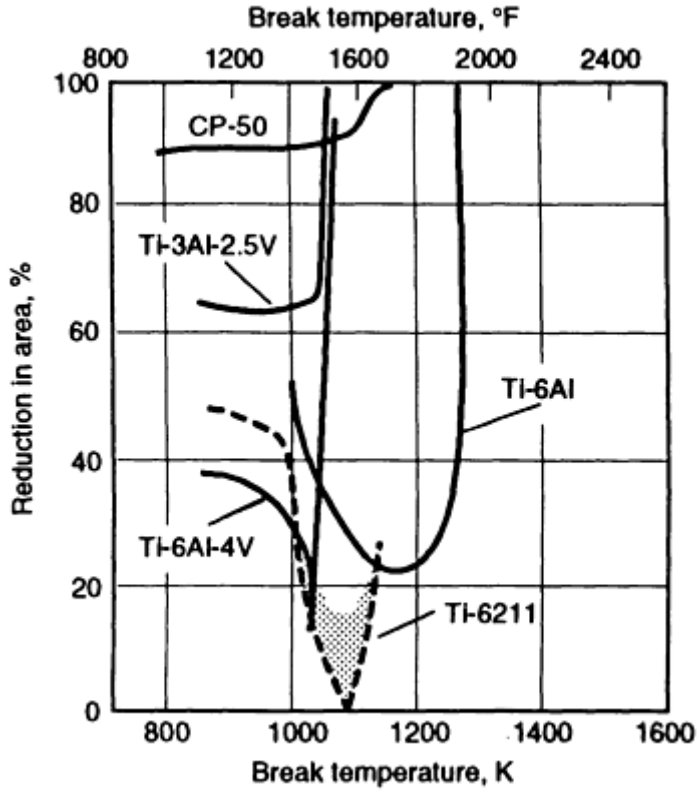

FIG. 15 DUCTILITY VERSUS TEMPERATURE FOR FIVE TITANIUM ALLOYS WITH VARYING ALUMINUM CONTENTS. SHADED AREAS INDICATE EXCESSIVE DATA SCATTER. SOURCE: REF 23

Considerable additional work has been performed in order to understand the origin of ductility-dip weld cracking in titanium alloys (Ref 25, 26, 27, 28). It is important to note, however, that difficulties with the occurrence of such defects in actual welds have not been reported in the literature, and therefore the potential for their formation is quite limited and may be encountered only under conditions of extreme restraint and for certain cooling rates.

Weld metal porosity originates at the trailing edge of the weld pool, where interstitial elements (oxygen or hydrogen) are partitioned between dendrites during solidification (Fig. 16). Partitioning occurs because of the large drop in oxygen (or hydrogen) solubility when transforming from liquid to solid.

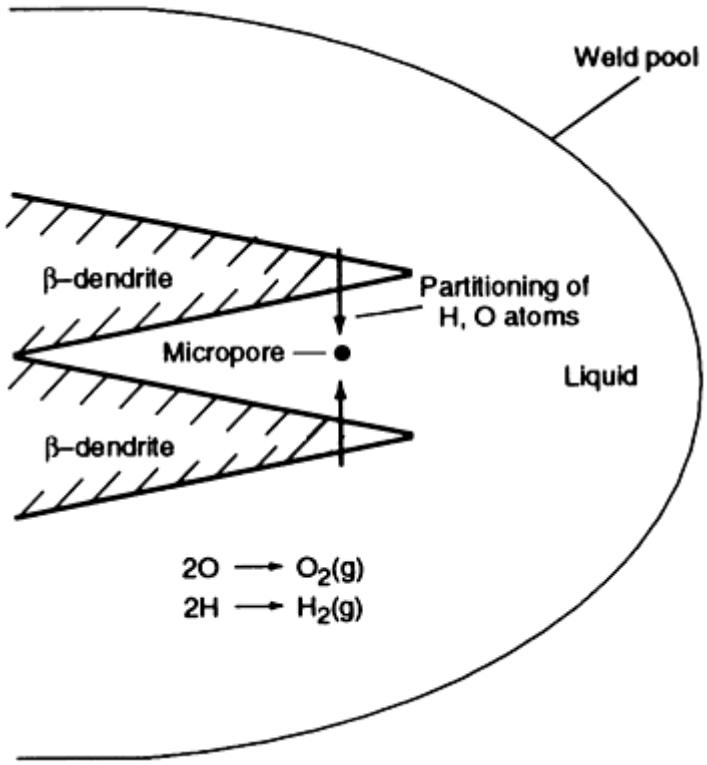

FIG. 16 SCHEMATIC DIAGRAM SHOWING HOW MICRO-PORES ARE NUCLEATED BETWEEN BETA-TITANIUM DENDRITES DURING WELD SOLIDIFICATION

As the concentration of monatomic oxygen (or hydrogen) in the interdendritic liquid reaches a critical concentration, micropores (~1 μm diam) of diatomic gas are nucleated. In order to nucleate, these micropores must overcome atmospheric pressure, liquid head pressure, and liquid/gas surface tension (Ref 29). Once nucleated, these micropores will either become entrapped interdendritically or will coalesce into larger pores (up to 3 mm, or 0.12 in., diam). These macropores will either become enveloped by the advancing solid/liquid interface or they will work their way to the weld pool surface and escape under buoyancy forces.

Avoiding porosity requires that the molten weld pool be protected from exposure to oxygen or hydrogen during welding. This means that the joint must be thoroughly degreased prior to welding and that adequate inert gas shielding with a low dew point must be provided. Porosity can occur at lower impurity levels than is required for contamination cracking, although the existence of porosity implies the possibility of contamination or hydrogen cracking. Porosity is also affected by process parameters and welding position. Welding at slow travel speeds favors the escape of gas pores, as does welding in the flat or vertical-up position.

Effect of Postweld Heat Treatment

Titanium alloy weldments are postweld heat treated for (Ref 5):

- RELIEF OF RESIDUAL STRESSES IMPARTED DURING THE WELDING OPERATION
- MODIFICATION OF THE METASTABLE WELD ZONE MICROSTRUCTURE
- COMPLETION OF THE SECOND STEP IN A TWO-STEP BASE METAL HEAT TREATMENT
- STABILIZATION OF THE MICROSTRUCTURE FOR WELD STRUCTURE APPLICATIONS AT ELEVATED TEMPERATURES

Numerous investigators have studied the influence of postweld heat treatment on the structure and properties of titanium alloy welds (Ref 30, 31, 32, 33, 34, 35). The structures commonly encountered include: alpha and hexagonal martensite in

near-alpha and linear alpha-beta alloys, alpha and orthorhombic martensite in heavily beta-stabilized alpha-beta alloys, and retained beta in metastable-beta alloys.

Alpha and Alpha-Beta Alloys. Heat treatment of rapidly cooled welds in near-alpha and alpha-beta alloys at relatively low temperatures (between about 450 and 600 °C, or 840 and 1110 °F), which are commonly employed for stress relief, age the martensitic structure and can further increase its strength and decrease its ductility and toughness. At higher postweld heat treatment temperatures, which are limited to about 760 °C (1400 °F) for large fabricated structures, tempering of the martensite and subsequent coarsening of the resultant alpha phase promote softening of the fusion zone with concurrent increases in ductility and toughness. Microstructures comprised of Widmanstätten alpha plus retained beta, which are produced at slower weld cooling rates, are influenced to a lesser extent by postweld heat treatment at these low-to-moderate temperatures. However, welds exhibiting these microstructures are still normally postweld treated to relieve residual stresses.

Metastable Beta Alloys. In contrast to near-alpha and alpha-beta alloys, metastable-beta alloys can undergo appreciable structural changes at the lower temperatures. In the as-welded condition, the alloy exhibits a retained beta microstructure that contains athermal omega, an extremely fine phase that is unresolvable with light microscopy. On aging isothermally at 480 °C (900 °F), extremely fine alpha forms intergranularly and in a continuous manner at beta grain boundaries. As the heat treatment temperature is increased to 565 °C (1050 °F) and to 650 °C (1200 °F), both alpha structures coarsen appreciably. From a practical standpoint, the post-weld heat treatment of welded structures is difficult and expensive because inert shielding is required at temperatures above about 500 °C (930 °F). Additionally, the loss of strength at temperatures approaching the beta transus limits the capability to maintain weld tolerances unless complex fixturing is employed.

Table 3 lists the temperature ranges used for stress-relieving titanium alloy weldments. Postweld heat treatments that employ high temperatures (exceeding 800 °C, or 1470 °F) with water quenching followed by an aging treatment between 350 to 500 °C (660 to 930 °F) have also been developed for near-alpha and alpha-beta alloys (Ref 36). Tensile properties of postweld heat-treated titanium weldments are given in Table 4.

TABLE 3 RECOMMENDED STRESS-RELIEF TREATMENTS FOR TITANIUM AND TITANIUM ALLOYS

Parts can be cooled from stress relief by either air cooling or slow cooling.

ALLOY	TEMPERATURE		TIME, H
	°C	°F	
COMMERCIALLY PURE TITANIUM (ALL GRADES)	480-595	900-1100	$\frac{1}{4}$ -4
α OR NEAR- α TITANIUM ALLOYS			
TI-5AL-2.5SN	540-650	1000-1200	$\frac{1}{4}$ -4
TI-8AL-1MO-1V	595-705	1100-1300	$\frac{1}{4}$ -4
TI-2.5CU (IMI 230)	400-600	750-1110	0.5-24
TI-6AL-2SN-4ZR-2MO	595-705	1100-1300	$\frac{1}{4}$ -4
TI-6AL-5ZR-0.5MO-0.2SI (IMI 685)	530-570	980-1050	24-48
TI-5.5AL-3.5SN-3ZR-1NB-0.3MO-0.3SI (IMI 829)	610-640	1130-1190	1-3
TI-5.8AL-4SN-3.5ZR-0.7NB-0.5MO-0.3SI (IMI 834)	625-750	1160-1380	1-3
TI-6AL-2CB-1TA-0.8MO	595-650	1100-1200	$\frac{1}{4}$ -2
TI-0.3MO-0.8NI (TI CODE 12)	480-595	900-1100	$\frac{1}{4}$ -4
α -β TITANIUM ALLOYS			
TI-6AL-4V	480-650	900-1200	1-4
TI-6AL-7NB (IMI 367)	500-600	930-1110	1-4
TI-6AL-6V-2SN (CU + FE)	480-650	900-1200	1-4

TI-3AL-2.5V	540-650	1000-1200	$\frac{1}{2}$ -2
TI-6AL-2SN-4ZR-6MO	595-705	1100-1300	$\frac{1}{4}$ -4
TI-4AL-4MO-2SN-0.5SI (IMI 550)	600-700	1110-1290	2-4
TI-4AL-4MO-4SN-0.5SI (IMI 551)	600-700	1110-1290	2-4
TI-5AL-2SN-4MO-2ZR-4CR (TI-17)	480-650	900-1200	1-4
TI-7AL-4MO	480-705	900-1300	1-8
TI-6AL-2SN-2ZR-2MO-2CR-0.25SI	480-650	900-1200	1-4
TI-8MN	480-595	900-1100	$\frac{1}{4}$-2
β OR NEAR- β TITANIUM ALLOYS			
TI-13V-11CR-3AL	705-730	1300-1350	$\frac{1}{12}$ - $\frac{1}{4}$
TI-11.5MO-6ZR-4.5SN (BETA III)	720-730	1325-1350	$\frac{1}{12}$ - $\frac{1}{4}$
TI-3AL-8V-6CR-4ZR-4MO (BETA C)	705-760	1300-1400	$\frac{1}{6}$ - $\frac{1}{2}$
TI-10V-2FE-3AL	675-705	1250-1300	$\frac{1}{2}$ -2
TI-15V-3AL-3CR-3SN	790-815	1450-1500	$\frac{1}{12}$ - $\frac{1}{4}$

TABLE 4 FUSION ZONE TENSILE PROPERTIES OF GAS-TUNGSTEN ARC-WELDED TITANIUM ALLOYS

ALLOY	CONDITION[(A)]	YIELD STRENGTH		ULTIMATE TENSILE STRENGTH		ELONGATION, %
		MPA	KSI	MPA	KSI	
TI-6AL-2SN-4ZR-2MO-0.1SI	BASE METAL (ANNEALED)	915	133	1020	148	13
	AS-WELDED	1050	152	1185	172	3
	PWHT: 595 °C (1100 °F)/6 H AC	1104	160	1254	182	2
	PWHT: 705 °C (1300 °F)/6 H AC	1116	162	1171	170	2
	PWHT: 900 °C (1650 °F)/ $\frac{1}{2}$ H AC + 650 C (1200 °F)/6 H AC	930	135	1020	148	6
CORONA 5	BASE METAL (ANNEALED)	1048	152	1158	168	16
	AS-WELDED	1262	183	1268	184	1
	PWHT: 650 °C (1250 °F)/4 H AC	1179	171	1220	177	1-2
	PWHT: 705 °C (1300 °F)/4 H AC	1144	166	1165	179	2-3
	PWHT: 775 °C (1425 °F)/ $\frac{1}{2}$ H AC + 650 °C (1200 °F)/4 H AC	1048	152	1082	157	5
	PWHT: 725 °C (1695 °F)/ $\frac{1}{2}$ H AC + 650 °C (1200 °F)/4 H AC	1027	149	1055	153	7
TI-15V-3CR-3AL-3SN	BASE METAL (SOLUTION ANNEALED)	730	106	760	110	24

	AS-WELDED	725	105	750	109	20
	PWHT: 565 °C (1050 °F)/4 H AC	1007	146	1063	154	8
	PWHT: 620 °C (1150 °F)/4 H AC	896	130	985	143	9
	PWHT: 675 °C (1250 °F)/4 H AC	794	115	854	124	18

Weld cooling rate, ~100 °C/s (180 °F/s).

Source: Ref 9

(A) PWHT, POSTWELD HEAT TREATMENT; AC, AIR COOLED.

References cited in this section

5. W.A. BAESLACK III, D.W. BECKER, AND F.H. FROES, ADVANCES IN TITANIUM ALLOY WELDING METALLURGY, *J. MET.*, MAY 1984, P 46-58
9. J.R. HARTMAN AND W.A. BAESLACK III, ADVANCES IN ARC WELDING OF TITANIUM ALLOYS, *WELDABILITY OF MATERIALS*, R.A. PATTERSON AND K.W. MAHIN, ED., ASM INTERNATIONAL, 1990, P 319-330
10. W.A. BAESLACK III AND D.L. HALLUM, NATURE OF GRAIN REFINEMENT IN TITANIUM ALLOY WELDS BY MICROCOOLER INOCULATION, *WELD. J. RES. SUPPL.*, VOL 69 (NO. 12), DEC 1990, P 326S-336S
11. D.W. BECKER AND W.A. BAESLACK III, PROPERTY-MICROSTRUCTURE RELATIONSHIPS IN METASTABLE-BETA TITANIUM ALLOY WELDMENTS, *WELD. J. RES. SUPPL.*, VOL 59, 1980, P 85S-92S
12. W.A. BAESLACK III, P.S. LIU, D.P. BARBIS, J.R. SCHLEY, AND J.R. WOOD, POSTWELD HEAT TREATMENT OF GTA WELDS IN A HIGH-STRENGTH, METASTABLE-BETA TITANIUM ALLOY--BETA-C, *PROC. OF 1992 INT. CONF. ON TITANIUM ALLOYS* (SAN DIEGO), 1992
13. A.T. D'ANNESSA, REDISTRIBUTION OF SOLUTE IN FUSION WELDING, *WELD. J.*, VOL 45, 1966, P 569S-576S
14. W.A. BAESLACK III, EFFECT OF SOLUTE BANDING ON TRANSFORMATIONS IN DISSIMILAR TITANIUM ALLOY WELDMENTS, *J. MAT. SCI. LET.*, VOL 1, 1982, P 229-231
15. P.S. LIU, W.A. BAESLACK III, AND J. HURLEY, DISSIMILAR ALLOY LASER WELDING OF TITANIUM: TI-6AL-4V TO BETA-C, *WELD. J. RES. SUPPL.*, IN PRESS
16. P.S. LIU, W.A. BAESLACK III, AND J. HURLEY, LASER WELDING OF TI-6AL-4V TO BETA-21S, *PROC. OF TMS CONF. ON BETA TITANIUM ALLOYS* (DENVER, CO), TMS, 1993
17. W.A. BAESLACK III, S. CHIANG, AND C.A. ALBRIGHT, *J. MAT. SCI. LET*, VOL 9, 1990, P 698-702
18. W.A. BAESLACK ILL, *METALLOGRAPHY*, VOL 13, 1980, P 277-281
19. N.N. PROKHOROV, *WELD. PROD.*, VOL 9, 1986, P 30-32
20. P.W. HOLSBERG, "CRACKING AND POROSITY IN TITANIUM ALLOY WELDMENTS," U.S. NAVY DTNSRDC REPORT, 1979
21. F.D. ROSI, D.A. DUBE, AND B.H. ALEXANDER, *TRANS. AIME*, VOL 197, 1953, P 257
22. N.E. PATON AND J.C. WILLIAMS, THE EFFECT OF HYDROGEN ON TITANIUM AND ITS ALLOYS, *HYDROGEN IN METALS*, AMERICAN SOCIETY FOR METALS, 1974, P 409-431
23. R.E. LEWIS, I.L. CAPLAN, AND W.C. COONS, THE ELEVATED TEMPERATURE DUCTILITY DIP PHENOMENON IN ALPHA, NEAR-ALPHA AND ALPHA-BETA TITANIUM ALLOYS, *TITANIUM SCIENCE AND TECHNOLOGY*, VOL 2, G. LÜTJERING, U. ZWICKER, AND W. BUNK, ED., DEUTSCHE GESELLSCHAFT FÜR METALLKUNDE E.V., WEST GERMANY, 1985
24. B.K. DAMKROGER, G.R. EDWARDS, AND B.B. RATH, A MODEL FOR HIGH TEMPERATURE

DUCTILITY LOSS IN ALPHA-BETA TITANIUM ALLOYS, *METALL. TRANS. A,* VOL 18, 1987, P 483-485

25. D.M. BOWDEN AND E.A. STARKE, JR., HOT CRACKING SUSCEPTIBILITY OF TITANIUM 6211, *TITANIUM SCIENCE AND TECHNOLOGY,* VOL 2, G. LÜTJERING, U. ZWICKER, AND W. BUNK, ED., DEUTSCHE GESELLSCHAFT FÜR METALLKUNDE E.V., WEST GERMANY, 1985, P 853
26. D.M. BOWDEN AND E.A. STARKE, JR., *METALL. TRANS. A,* VOL 15, 1984, P 1687-1698
27. D. HAYDUK, B.K. DAMKROGER, G.R. EDWARDS, AND D.L. OLSON, *WELD. J.,* VOL 65, 1986, P 251S-260S
28. B.K. DAMKROGER, G.R. EDWARDS, AND B.B. RATH, *WELD. J.,* VOL 68, 1989, P 290S-302S
29. R.E. TREVISAN, D.D. SCHWEMMER, AND D.L. OLSON, THE FUNDAMENTALS OF WELD PORE FORMATION, *WELDING: THEORY AND PRACTICE,* ELSEVIER, 1990, P 79-115
30. K. BORGGREEN AND I. WILSON, USE OF POSTWELD HEAT TREATMENTS TO IMPROVE DUCTILITY IN THIN SHEETS OF TI-6AL-4V, *WELD. J.,* VOL 59, 1980, P 1S-8S
31. S.L. BOSTON AND W.A. BAESLACK III, "MICROSTRUCTURE/MECHANICAL PROPERTY RELATIONSHIPS IN GTA WELDED TI-10V-2FE-3AL," AFML-TM-LL-80-1, WRIGHT PATTERSON AIR FORCE BASE, DAYTON, OH, 1980
32. M.A. GREENFIELD AND C.M. PIERCE, POSTWELD AGING OF A METASTABLE BETA TITANIUM ALLOY, *WELD. J.,* VOL 52, 1973, P 524S-527S
33. W.A. BAESLACK III, EVALUATION OF TRIPLEX HEAT TREATMENTS FOR TITANIUM ALLOYS, *WELD. J.,* VOL 61, 1982, P 193S-199S
34. D.W. BECKER AND W.A. BAESLACK III, PROPERTY/MICROSTRUCTURE RELATIONSHIPS IN METASTABLE-BETA TITANIUM ALLOY WELDMENTS, *WELD. J.,* VOL 59, 1980, P 850-920
35. W.A. BAESLACK III AND F.D. MULLINS, RELATIONSHIP OF MICROSTRUCTURE, MECHANICAL PROPERTIES AND FRACTOGRAPHIC FEATURES IN WELDED HIGH TOUGHNESS TITANIUM ALLOYS, *TRENDS IN WELDING RESEARCH,* S.A. DAVID, ED., AMERICAN SOCIETY FOR METALS, 1982, P 541
36. V.N. ZAMKOV *ET AL.,* WAYS OF PROVIDING THE HIGH SERVICEABILITY OF HEAT-HARDENED WELDED JOINTS OF ALPHA + BETA TITANIUM ALLOYS, *TITANIUM SCIENCE AND TECHNOLOGY,* VOL 2, G. LÜTJERING, U. ZWICKER, AND W. BUNK, ED., DEUTSCHE GESELLSCHAFT FÜR METALLKUNDE, E.V., WEST GERMANY, 1985, P 877

Selection and Weldability of Conventional Titanium Alloys

W.A. Baeslack III, The Ohio State University; J.R. Davis, Davis and Associates; C.E. Cross, Martin Marietta Astronautics Group

Titanium Weldment Structure/Property Relationships (Ref 5, 9)

Macro- and microstructural characteristics of weldments in titanium alloys, as influenced by weld solidification, cooling rate, and postweld heat treatment, significantly influence weldment mechanical properties. In the welding of thin sheet materials for aerospace applications, the principal properties of interest are room- and elevated-temperature tensile properties and *S-N* fatigue characteristics. For welds produced in plate materials for either aerospace or marine applications, fracture toughness and fatigue-crack growth rate properties also become important.

Tensile Properties. The strength across an arc weld is determined by the strength of the weakest link in the composite weld region, which consists of the fusion zone, the near HAZ (where the peak temperature exceeded the beta transus temperature), and the far HAZ (where peak temperatures were below the beta transus). In the United States, sheet products of near-alpha or alpha-beta titanium alloys are most commonly welded in a mill-annealed condition (Table 2). In all but extremely slowly cooled manual arc welds, the fine alpha or alpha-prime martensite structures produced in the weld fusion zone and near-HAZ regions exhibit hardnesses and strengths above that of the affected base metal, and transverse weld failures consequently occur in the base metal (Table 4). Although these welds exhibit 100% joint efficiency, the ductility of the weld zone as measured by longitudinal-weld-oriented bend or all-weld-metal tensile tests

may be unacceptably low, particularly in rapidly cooled arc welds in the more heavily beta-stabilized alloys (for example, Ti-6Al-6V-2Sn, CORONA 5, and Ti-6Al-2Sn-4Zr-6Mo), which contain hard martensitic microstructures within a coarse prior-beta grain macrostructure. As shown in Table 4 for gas-tungsten arc welds in the near-alpha alloy Ti-6Al-2Sn-4Zr-2Mo-0.1Si and the alpha-beta alloy CORONA 5, the tempering of martensite in the weld zone and ultimate coarsening of the alpha + beta microstructure result in a decrease in strength but an increase in ductility with increasing heat treatment temperature.

Arc welds produced on near-alpha and alpha-beta base metals that have been solution heat treated and aged to high strength may exhibit weld zones exhibiting strengths below that of the base metal; consequently, transverse tensile fracture would occur preferentially in these regions. For example, the strength and ductility of weldments produced in Ti-6Al-4V that has been solution heat treated and aged to high strength levels are highly dependent on the weld zone structure. The completely martensitic microstructures exhibited in electron-beam and laser-beam welds having high depth-to-width ratios are sufficiently strong to promote base-metal fracture in the solution heat treated and aged base metal. However, the softer Widmanstätten plus retained-beta microstructures exhibited by the more slowly cooled gas-tungsten arc and plasma arc welds may promote preferential fracture in the weld zone at low macroscopic elongation.

As expected, the tensile properties of weldments in metastable-beta titanium alloys differ considerably from those of near-alpha and alpha-beta alloys. If arc welds are produced in solution-annealed base material, joints commonly fracture in the base metal because of a slightly higher strength in the weld metal due to oxygen pickup or the initiation of second-phase precipitation if cooling rates are sufficiently slow. Following postweld heat treatment, the presence of a coarse beta grain structure in the fusion zone combined with the formation of alpha preferentially along these grain boundaries (in addition to precipitation homogeneously within the beta grains) can promote fracture in the fusion zone at lower ductilities. As shown in Table 4 for the metastable-beta titanium alloy Ti-15V-3Al-3Sn-3Cr, postweld heat treatment significantly increases the fusion zone strength versus the as-welded condition. As indicated, this strength is maximum for low aging temperatures and decreases with an increase in aging temperature.

Figure 17 plots longitudinal weld tensile data for a variety of alloys. The most desirable weldment characteristic is the highest strength level that exhibits adequate ductility. Therefore, alloys and welding conditions would be selected that offer properties near the upper boundary of the scatter band shown in Fig. 17. Within the high-strength regions shown on such diagrams, the metastable beta and richer alpha-beta alloys show the most promise (Ref 7).

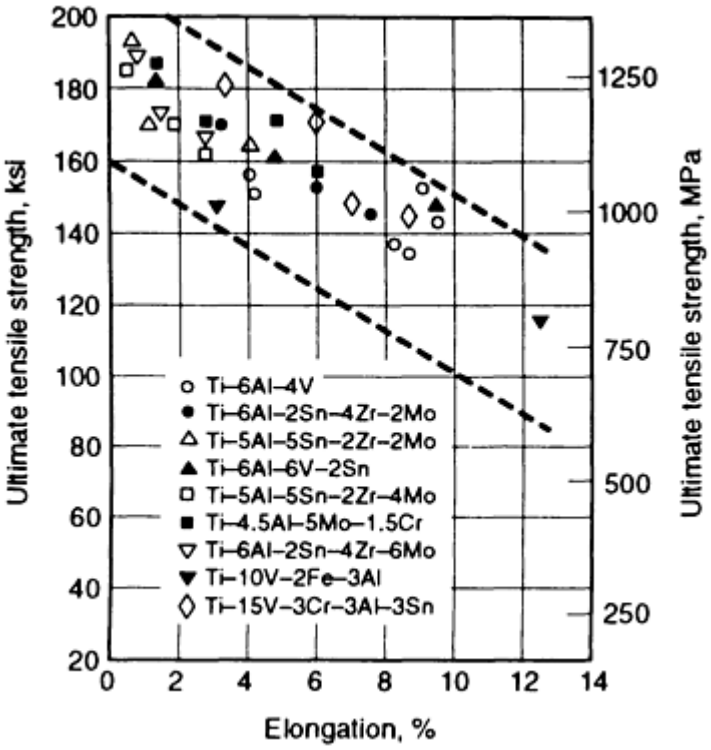

FIG. 17 LONGITUDINAL WELDMENT TENSILE DATA FOR COMMERCIAL TITANIUM ALLOYS. SOURCE: REF 7

The fracture toughness of suitably heat-treated titanium alloy weldments is generally equivalent or superior to that of the alpha-beta processed base material. The good fracture toughness of the fine Widmanstätten plus grain-boundary alpha microstructure in the weld fusion zone and HAZ is consistent with the good toughness of microstructurally similar beta-processed titanium alloy microstructures. Figure 18 shows fracture toughness versus ultimate-tensile strength for heat-treated electron-beam and plasma arc welds in wrought CORONA 5 base plate. Note that the values fall well within the scatterband of data for base-metal alloys exhibiting a lenticular alpha morphology (Ref 37).

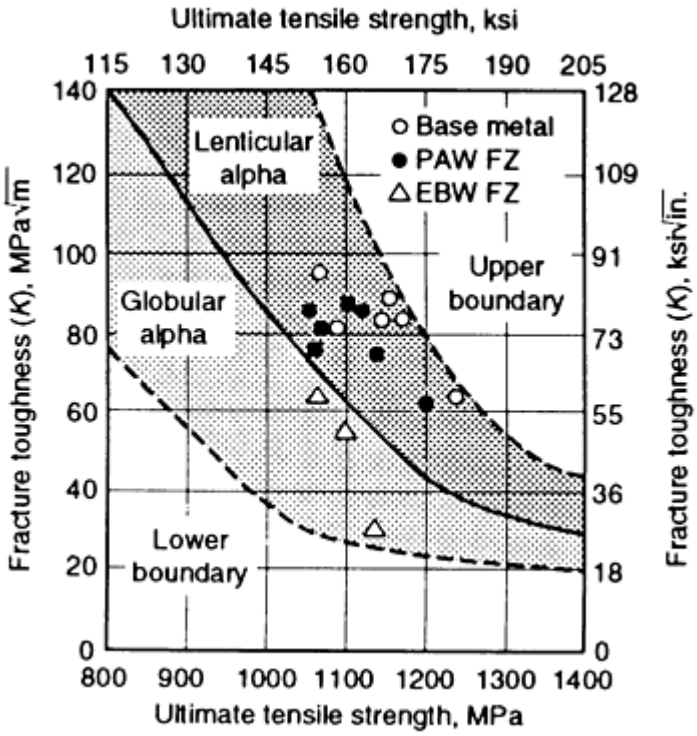

FIG. 18 FRACTURE TOUGHNESS VERSUS ULTIMATE TENSILE STRENGTH FOR CORONA 5 BASE METAL AND POSTWELD HEAT TREATED ELECTRON-BEAM AND PLASMA-ARC WELD FUSION ZONE REGIONS. SOURCE: REF 37

Fracture toughness is also markedly influenced by the interstitial content of the weld metal. When selecting a titanium alloy for a fracture-toughness-critical application, the use of extra-low interstitial (ELI) grades of base metal and consumable are recommended.

Lewis *et al.* (Ref 38) investigated the influence of boron on the dynamic tear toughness of gas-tungsten arc weldments in Ti-6Al-2Nb-1Ta-1Mo and found that welds containing a high boron content of 0.005 wt% exhibited toughness levels 40% below those containing 0.001 wt% B (boron can be introduced as an impurity in master alloys or during processing of welding wire). They attributed this difference to the occurrence of a beta + TiB to alpha peritectoid reaction during weld cooling in the alloy with a high boron content, which provided nucleation sites for alpha platelets. The absence of this transformation in low-boron weldments allowed greater undercooling of the beta phase and transformation to a martensitic structure.

Fatigue Properties. Generally, *S-N* fatigue properties of weld structures in the alpha-beta alloys such as Ti-6Al-4V and Ti-6Al-6V-2Sn are similar to that of the base material if the weld zones are free of defects such as porosity and undercut. Failure in transverse-oriented specimens occurs in the base metal remote from the weld zone. This greater resistance to crack initiation of these composite weld structures relates to the higher strength levels of the weld regions because the large prior-beta grain/transformed beta microstructures, which characterize these regions, generally exhibit reduced resistance to cyclic crack initiation compared to equiaxed-alpha type base metal structures. Studies of *S-N* fatigue properties of electron-beam-welded ELI CORONA 5 indicated that fatigue properties of all-fusion-zone specimens and transverse-weld specimens are comparable to those of the base metal over a range of stresses, even when fracture was initiated by weld porosity (Ref 35). Results from these studies are shown in Fig. 19.

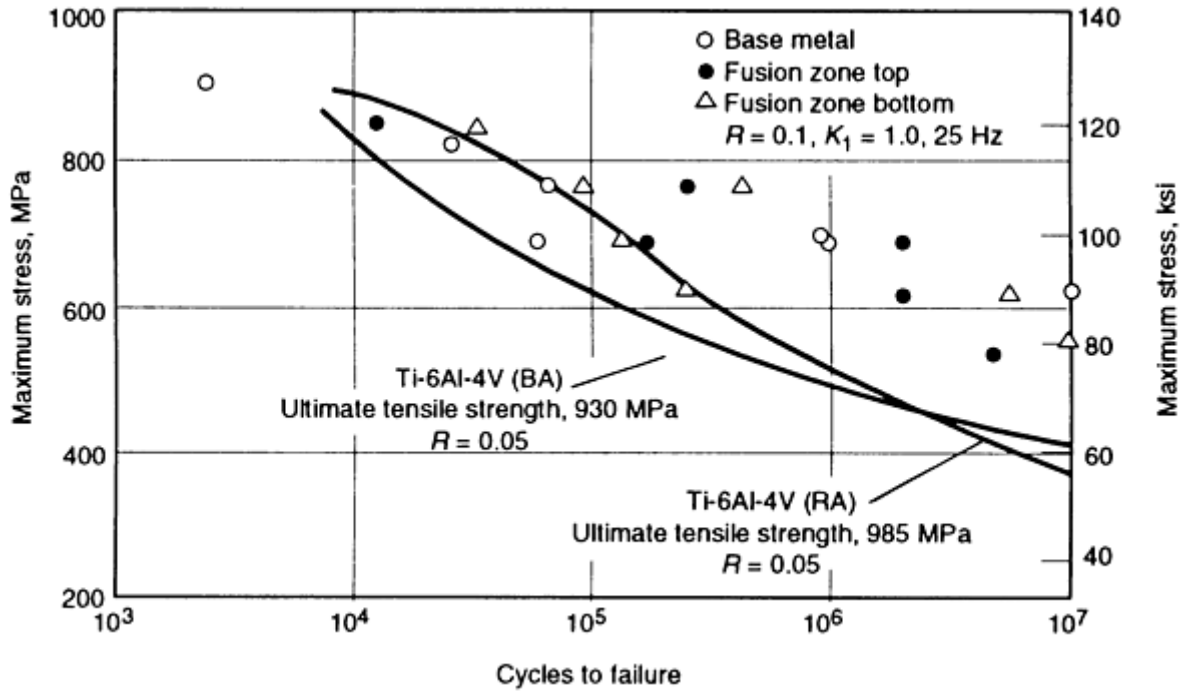

FIG. 19 AXIAL TENSION FATIGUE DATA FOR POSTWELD HEAT TREATED ELI CORONA 5 BASE METAL AND ELECTRON-BEAM-WELDED SPECIMENS COMPARED TO BETA-ANNEALED (BA) AND RECRYSTALLIZED ANNEALED (RA) TI-6AL-4V. SOURCE: REF 35

Although, as indicated above, equivalent weld zone and base-metal fatigue properties can be obtained, lower weld zone axial fatigue properties are commonly observed in actual practice. This is particularly true with high-energy-density welding processes (Fig. 20). This behavior is attributed to the presence of fine porosity, often unresolvable by radiography, and of other defects such as undercuts or underfills in fusion welds, or lack of bonding regions at the weld interface in solid-state diffusion or friction welds. As with tensile properties, the axial fatigue behavior of welds produced in solution heat treated and aged base metals depends on both the weld integrity and the strength of the weld zone.

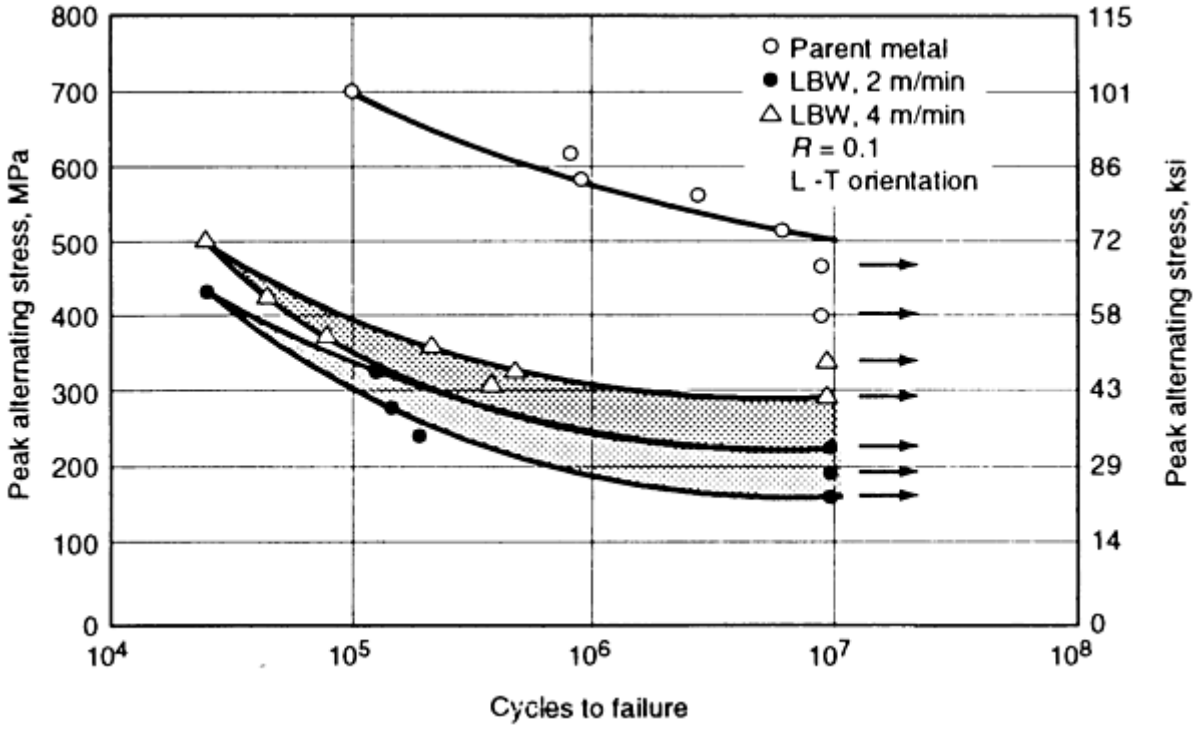

FIG. 20 *S/N* FATIGUE CURVES FOR LASER-BEAM WELDS IN 4 MM (0.16 IN.) TI-6AL-4V SHEET PRODUCED AT 2 AND 4 M/MIN (0.6 AND 1.2 FT/MIN). TESTED IN AS-WELDED CONDITION. FRACTURE INITIATED AT WELD UNDERCUT. BASE METAL PROPERTIES ARE PROVIDED FOR COMPARATIVE PURPOSES. SOURCE: REF 39

It should be noted that poor axial fatigue properties also can limit the application of lap joints produced in titanium using resistance, diffusion, and ultrasonic welding. In the case of resistance welds, the mechanical notch at the perimeter of the weld nugget, the presence of a brittle martensitic microstructure, and residual stresses can promote early fatigue crack initiation and low fatigue life. Although the metallurgical structure and residual stresses can be modified through process control, the presence of a notch is inherent to a lap joint and subject to less modification.

With the increased application of damage-tolerant design criteria, fatigue crack growth rate data for weldments are of increased importance. A comparison of fatigue-crack propagation rates between gas-tungsten arc, laser-beam, and electron-beam welds in Ti-6Al-4V and Ti-15V-3Al-3Cr-3Sn was made by Pao *et al.* (Ref 40). Their results indicated that the average fatigue crack growth rates through the postweld heat treated weld zones did not differ appreciably with the welding process (Fig. 21), although the scatter bands were narrower for the high-energy density versus the arc welding processes (Fig. 22). For Ti-6Al-4V, they found the average crack growth rates to be lower than that in the base metal, while in Ti-15V-3Al-3Cr-3Sn they found nearly equivalent base metal and weld metal crack growth rates (Fig. 21).

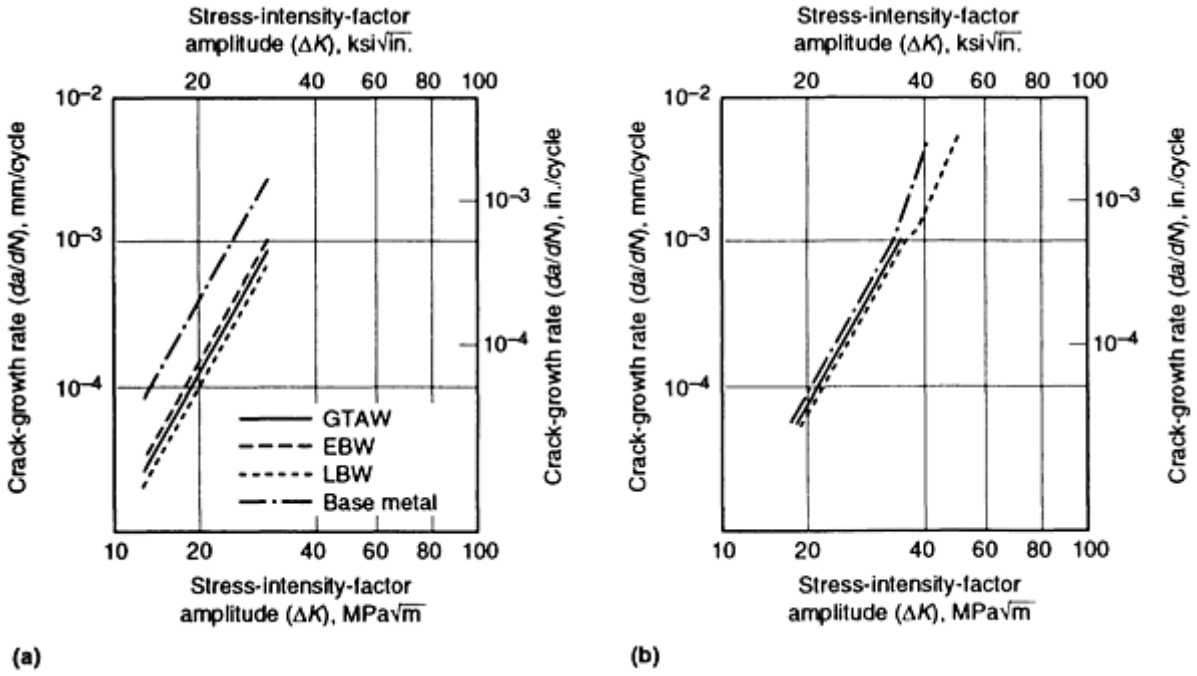

FIG. 21 EFFECT OF WELDING PROCESSES ON THE FATIGUE-CRACK-GROWTH RATE OF LONGITUDINALLY ORIENTED (A) TI-6AL-4V AND (B)TI-15V-3CR-3AL-3SN. SOURCE: REF 40

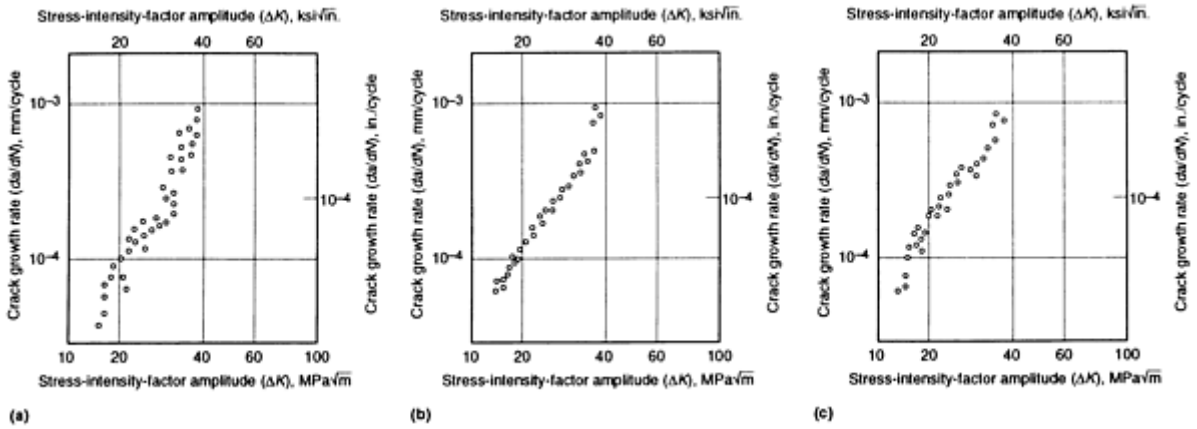

FIG. 22 EFFECT OF WELDING PROCESS ON THE FATIGUE-CRACK-GROWTH RATE SCATTERING IN TI-6AL-4V. (A) GAS-TUNGSTEN ARC WELDING. (B) ELECTRON-BEAM WELDING. (C) LASER-BEAM WELDING. SOURCE: REF 40

References cited in this section

5. W.A. BAESLACK III, D.W. BECKER, AND F.H. FROES, ADVANCES IN TITANIUM ALLOY WELDING METALLURGY, *J. MET.,* MAY 1984, P 46-58
7. D.W. BECKER, W.A. BAESLACK III, AND R.W. MESSLER, JR., TITANIUM WELDING, *TITANIUM '80 SCIENCE AND TECHNOLOGY,* VOL 1, H. KIMURA AND O. IZUMI, ED., THE METALLURGICAL SOCIETY OF AIME, 1980, P 255-275
9. J.R. HARTMAN AND W.A. BAESLACK III, ADVANCES IN ARC WELDING OF TITANIUM ALLOYS, *WELDABILITY OF MATERIALS,* R.A. PATTERSON AND K.W. MAHIN, ED., ASM INTERNATIONAL, 1990, P 319-330

35. W.A. BAESLACK III AND F.D. MULLINS, RELATIONSHIP OF MICROSTRUCTURE, MECHANICAL PROPERTIES AND FRACTOGRAPHIC FEATURES IN WELDED HIGH TOUGHNESS TITANIUM ALLOYS, *TRENDS IN WELDING RESEARCH,* S.A. DAVID, ED., AMERICAN SOCIETY FOR METALS, 1982, P 541
37. W.A. BAESLACK III, D.W. BECKER, AND F.H. FROES, WELDABILITY OF A HIGH TOUGHNESS TITANIUM ALLOY, A METALLURGICAL EVALUATION, *TITANIUM '80 SCIENCE AND TECHNOLOGY,* VOL 2, H. KIMURA AND O. IZUMI, ED., THE METALLURGICAL SOCIETY OF AIME, 1980, P 2369
38. R.E. LEWIS *ET AL.,* THE EFFECT OF BORON ON WELDMENT MICROSTRUCTURES IN TI-6AL-2NB-1TA-1MO ALLOY, *TITANIUM SCIENCE AND TECHNOLOGY,* VOL 2, G. LÜTJERING, U. ZWICKER, AND W. BUNK, ED., DEUTSCHE GESELLSCHAFT FÜR METALLKUNDE E.V., WEST GERMANY, 1985, P 799
39. T.S. PARKER AND P.G. PARTRRIDGE, FATIGUE PROPERTIES OF 4 MM THICK LASER WELDED TI-6AL-4V SHEET, *FATIGUE '84,* C.J. BEEVERS, ED., ENGINEERING MATERIALS ADVISORY SERVICES LTD., LONDON, 1984
40. P.S. PAO, T.C. PENG, AND J.E. O'NEAL, FATIGUE CRACK PROPAGATION THROUGH TITANIUM WELDS, *TITANIUM SCIENCE AND TECHNOLOGY,* VOL 2, G. LÜTJERING, U. ZWICKER, AND W. BUNK, ED., DEUTSCHE GESELLSCHAFT FÜR METALLKUNDE, E.V., WEST GERMANY, 1985, P 887

Selection and Weldability of Conventional Titanium Alloys

W.A. Baeslack III, The Ohio State University; J.R. Davis, Davis and Associates; C.E. Cross, Martin Marietta Astronautics Group

Welding Process Application

Titanium and its alloys can be welded by a wide variety of conventional fusion and solid-state processes, although titanium's chemical reactivity typically requires special procedures and precautions. In the United States, fusion welding of titanium is performed principally by inert gas-shielded arc welding and high-energy-beam welding processes. To date, the commercial joining of titanium alloys using flux-based processes (for example, submerged arc welding, flux-cored arc welding, and electroslag welding) has not been shown to be competitive due to requirements for costly high-purity fluoride-base fluxes. However, recent studies on submerged arc welding of 25 mm (1 in.) thick titanium alloy plate indicate that it is possible to weld heavy sections using a flux composed of 85% calcium fluoride, 10% strontium chloride, and 3% lithium chloride (Ref 41). Tensile and corrosion properties of the weld were equal to that of the base plate material; however, the coarser weld grain structure did not provide adequate toughness.

Additional information on the welding processes described below can be found in the Section "Joining Processes" in this Volume.

Gas-tungsten arc welding (GTAW), in which the heat of welding is provided by an arc maintained between a nonconsumable tungsten electrode and the workpiece, is the most widely used process for joining titanium sheet. In general, gas-tungsten arc welds can be produced manually (in complex joint geometries or for weld repair) and automatically in sheet up to about 3 mm (0.125 in.) in thickness without joint preparation or filler metal additions. For welding of greater thicknesses, suitable joint preparation and the cold or hot-wire addition of a filler metal are required. Although conventional GTAW equipment can be used for welding of titanium alloys, the heated metal in the weld zone must be shielded from the atmosphere to prevent pickup of oxygen and nitrogen, which can be deleterious to weld mechanical properties. Such protection is best provided by welding within a rigid or collapsible plastic chamber that has been evacuated and purged with argon, although local shielding is also suitable for many welding operations. Typical parameters for welding of Ti-6Al-4V by GTAW are shown in Table 5.

TABLE 5 WELDING PARAMETERS FOR GAS-TUNGSTEN ARC WELDING OF TI-6AL-4V

MATERIAL THICKNESS[A]		TUNGSTEN ELECTRODE DIAMETER		FILLER ROD DIAMETER		NOZZLE SIZE ID		SHIELDING GAS FLOW		WELDING CURRENT[B]	NUMBER OF PASSES	TRAVEL SPEED[C]	
mm	in.	mm	in.	mm	in.	mm	in.	m^3/h	ft^3/h			mm/min	in./min
SQUARE-GROOVE AND FILLET WELDS													
0.61	0.024	1.6	1/16	. . .	. . .	9.5	3/8	0.51	18	20-35	1	150	6
1.60	0.063	1.6	1/16	. . .	. . .	16	5/8	0.51	18	85-140	1	150	6
2.36	0.093	2.4	3/32	1.6	1/16	16	5/8	0.71	25	170-215	1	205	8
3.18	0.125	2.4	3/32	1.6	1/16	16	5/8	0.71	25	190-235	1	205	8
4.78	0.188	2.4	3/32	3.2	1/8	16	5/8	0.71	25	220-280	2	205	8
V-GROOVE AND FILLET WELDS													
6.35	0.25	3.2	1/8	3.2	1/8	16	5/8	0.76	30	275-320	2	205	8
9.52	0.375	3.2	1/8	3.2	1/8	19	3/4	0.99	35	300-350	2	150	6
12.7	0.50	3.2	1/8	4.0	5/32	19	3/4	1.13	40	325-425	3	150	6

Note: Tungsten used for the electrode; first choice 2% thoriated EWTh2, second choice 1% thoriated EWTh1. Use filler metal one or two grades lower in strength than the base metal. Adequate gas shielding is essential not only for the arc, but for heated material also. Backing gas is recommended at all times. A trailing gas shield is also recommended. Argon is preferred. For higher heat input, on thicker material use argon-helium mixture. Without backing or chill bar, decrease current 20%.

(A) OR FILLET SIZE.

(B) DIRECT CURRENT ELECTRODE NEGATIVE.

(C) PER PASS

Gas-metal arc welding (GMAW), in which the heat of welding is provided by an arc maintained between a consumable electrode and the workpiece, is more cost-effective than GTAW for the welding of titanium plate over 13 mm (0.5 in.) in thickness. However, the application of GMAW to titanium has been restricted by poor arc stability, which promotes appreciable spatter during welding, thereby reducing weld quality and overall process efficiency. Typical welding parameters for welding of Ti-6Al-4V by GMAW are given in Table 6.

TABLE 6 TYPICAL PARAMETERS FOR GAS-METAL ARC WELDING OF TITANIUM ALLOY PLATE

THICKNESS		WELDING POSITION[A]	SHIELDING GAS	ELECTRODE					ARC VOLTAGE, V	WELDING CURRENT			TRAVEL SPEED	
				TYPE OF TRANSFER[B]	DIAMETER		FEED							
mm	in.				mm	in.	m/min	in./min		A[C]	BACKGROUND	MEAN PULSE	mm/min.	in./min.
3.18	0.125	F	75AR-25HE	S	0.16	0.062	5.1-5.7	200-225	20	250-260	. . .	. . .	380	15
6.35	0.250	F	75AR-25HE	S	0.16	0.062	7.6-8.1	300-320	30	300-320	. . .	. . .	380	15
9.53	0.375	F	85HE-15AR	S	0.11	0.045	22.0	865	33	350-360	. . .	. . .	640	25
12.7	0.500	F	75AR-25HE	S	0.16	0.062	9.5-10.2	375-400	40	340-360	. . .	. . .	380	15
15.9	0.625	F	75AR-25HE	S	0.16	0.062	10.2-10.8	400-425	45	350-370	. . .	. . .	380	15
25.4	1.00	F	AR	S	0.16	0.062	9.7	380	36-37	320-350	. . .	. . .	510-585	20-23
		F	AR	S	0.16	0.062	14.0	550	31-33	315-340	. . .	. . .	330	13
		F	75AR-25HE	PS	0.16	0.062	4.3	170	22-24	. . .	75	80	100	4
		V-UP	75AR-25HE	PS	0.16	0.062	3.8	150	21-23	. . .	35	100	64	2.5
		F	75AR-25HE	SC[D]	0.08	0.030	16.5	650	17-21	140-185	. . .	. . .	180	7
		V-UP	75AR-25HE	SC[D]	0.08	0.030	14.0	550	15-16	100-135	. . .	. . .	46	1.8

Source: Ref 4

(A) F, FLAT; V-UP, VERTICAL UP.

(B) S, SPRAY (ELECTRODE POSITIVE); PS, PULSED SPRAY (ELECTRODE POSITIVE); SC, SHORT-CIRCUITING (ELECTRODE NEGATIVE).

(C) DIRECT CURRENT.

(D) FOR GROOVE WELDS, THE GROOVE ANGLE AND ROOT OPENING SHOULD BE LARGER THAN THOSE USED WITH SPRAY TRANSFER TO PROVIDE GOOD ACCESSIBILITY TO THE ROOT AND FACES OF THE JOINT.

Plasma arc welding (PAW) is an extension of the GTAW process in which the arc plasma is constricted by a nozzle, thereby increasing its temperature and energy density as compared with the more diffuse GTAW arc. This higher energy density provides greater penetration capabilities, allowing the production of full-penetration, keyhole square-butt welds in thicknesses up to 13 mm (0.5 in.). Typical welding parameters for PAW of Ti-6Al-4V are given in Table 7.

TABLE 7 TYPICAL OPERATING CONDITIONS FOR PLASMA ARC WELDING OF TI-6AL-4V

Backing gas and trailing shield required; keyhole technique used with orifice-to-work distance of 4.8 ($\frac{3}{16}$ in.)

THICKNESS		TRAVEL SPEED		CURRENT (DCEN), A	ARC VOLTAGE, V	GAS	ORIFICE GAS		SHIELDING GAS		JOINT TYPE
mm	in.	mm/min	in./min				m^3/h	ft^3/h	m^3/h	ft^3/h	
3.18	0.125	510	20	185	21	ARGON	0.23	8	1.7	60	SQUARE BUTT
4.74	0.187	330	13	175	25	ARGON	0.51	18	1.7	60	SQUARE BUTT
9.91	0.390	255	10	225	38	75HE-25AR	0.91	32	1.7	60	SQUARE BUTT
12.7	0.500	255	10	270	36	50HE-50AR	0.76	27	1.7	60	SQUARE BUTT
15.2	0.600	180	7	250	39	50HE-50AR	0.85	30	1.7	60	V-GROOVE[A]

(A) 30° INCLUDED ANGLE; 9.5 MM ($\frac{3}{8}$ IN.) ROOT FACE

Electron-beam welding (EBW) involves melting of the base metals to be joined by the impingement of a focused beam of high-energy electrons. This process has been widely used in the aerospace industry for producing high-quality welds in titanium plate ranging from 6 to more than 75 mm (0.25 to more than 3 in.) in thickness. Advantages of EBW welding include high depth-of-penetration, minimum joint preparation, a narrow weld HAZ, low distortion, and excellent weld cleanliness as welding is performed in a high vacuum. Disadvantages of the EBW process include high capital equipment cost and high weld cooling rates, the latter of which promote formation of undesirable martensite in the weld zone. Table 8 lists typical welding parameters used in the EBW of Ti-6Al-4V. Tensile and fracture toughness data for Ti-6Al-4V are shown in Table 9.

TABLE 8 TYPICAL OPERATING PARAMETERS FOR ELECTRON-BEAM WELDING OF TI-6AL-4V

MATERIAL THICKNESS		ACCELERATING VOLTAGE, KV	BEAM CURRENT, MA	TRAVEL RATE	
mm	in.			mm/min	in./min
3.18	0.125	20	95	760	30
5.08	0.20	28	170	2490	98
16.0	0.63	30	260	1525	60
25.4	1.0	36.5	375	1120	44
50.8	2.0	45	450	660	26
88.9	3.5	90.0	500	510	20

TABLE 9 PROPERTIES OF ELECTRON-BEAM-WELDED TI-6AL-4V

CONDITION[A]	0.2% OFFSET YIELD STRENGTH		ULTIMATE TENSILE STRENGTH		ELONGATION, %	REDUCTION IN AREA, %	FRACTURE TOUGHNESS (K_Q)	
	MPA	KSI	MPA	KSI			MPA $\sqrt{m}$	KSI $\sqrt{in}$
WELDED + 700 °C	944	137	1032	150	12	32[B]	63.7	58.0

(1290 °F)/1 H AC								
WELDED + 500 °C (930 °F)/6 H AC	965	140	1055	153	12	37[B]	58.7	53.5
AS-WELDED	935	136	1030	149	12	34[B]	67.2	61.2
BASE METAL	927	134	991	144	12	39	44.5	40.5

Source: Ref 41

(A) AC. AIR COOLED.

(B) FRACTURE IN BASE METAL.

Laser-Beam Welding (LBW). During the past decade, LBW has become increasingly competitive as a joining process for titanium sheet and thin plate. In LBW, melting of the workpieces is produced by the impingement of a high-intensity, coherent beam of light. Because the laser beam can be readily transmitted through air, the LBW process offers significant practical advantages over conventional EBW, which requires welding in a high vacuum. However, the LBW process is more limited than EBW from the standpoint of joining thick titanium plate, with 15 kW required to produce a full-penetration weld in 13 mm (0.5 in.) thick Ti-6Al-4V. As expected, considering similarities in the heat sources, the metallurgical and mechanical properties of laser-beam and electron-beam welds are quite similar. Table 10 presents typical parameters for LBW of Ti-6Al-4V. Weld properties of laser-beam welded Ti-6Al-4V are given in Table 11.

TABLE 10 DIMENSIONS AND PROCESS VARIABLES FOR SUCCESSFUL LASER WELDS IN TI-6AL-4V

POWER, W	WELDING SPEED		THICKNESS		MELT WIDTH AT SURFACE		WIDTH OF HAZ AT SURFACE		MELT WIDTH AT BOTTOM		WIDTH OF HAZ AT BOTTOM		NUGGET AREA		HAZ AREA		MELTING EFFICIENCY	JOINING, AREA MM^2/KJ
	mm/s	in./s	mm	in.	mm	in.	mm	in.	mm	in.	mm	in.	mm^2	$in.^2 \times 10^{-3}$	mm^3	$in.^2 \times 10^{-3}$		
1000	23	0.91	1.00	0.039	1.85	0.073	3.75	0.148	0.90	0.035	2.50	0.098	1.38	2.14	1.75	2.71	21.37	23
1000	34	1.34	1.00	0.039	1.65	0.065	3.30	0.130	0.80	0.031	2.50	0.098	1.22	1.89	1.67	2.59	28.14	34
1000	15	0.59	1.00	0.039	2.15	0.085	4.70	0.185	1.60	0.063	3.40	0.134	1.88	2.91	2.17	3.36	19.00	15
1000	11	0.43	1.00	0.039	2.65	0.104	6.40	0.252	2.00	0.078	4.60	0.181	2.33	3.61	3.17	4.91	17.28	11
1480	60	2.36	0.89	0.035	1.00	0.039	2.20	0.087	0.60	0.024	1.50	0.059	0.71	1.10	0.93	1.44	19.50	36
1480	50	1.97	0.89	0.035	1.35	0.053	3.00	0.118	0.90	0.035	2.00	0.079	1.00	1.55	1.22	1.89	22.86	30
1480	23	0.91	0.89	0.035	1.60	0.063	3.10	0.122	1.35	0.053	2.75	0.108	1.31	2.03	1.29	2.00	13.78	13.83
1500	60	2.36	0.81	0.032	1.00	0.039	2.00	0.079	0.90	0.035	1.50	0.059	0.77	1.19	0.65	1.01	20.80	32.4
1500	50	1.96	0.81	0.032	1.20	0.047	2.20	0.087	0.90	0.035	1.75	0.069	0.85	1.32	0.75	1.16	19.16	27
1500	23	0.91	0.81	0.032	1.35	0.053	5.60	0.220	1.25	0.049	4.00	0.157	1.05	1.63	2.82	4.37	10.91	12.42
1500	7	0.28	2.03	0.080	4.30	0.169	10.00	0.394	3.00	0.118	5.50	0.217	7.41	11.48	8.32	12.90	25.03	10.15
1500	9	0.35	2.03	0.080	3.85	0.152	8.35	0.329	2.15	0.085	4.00	0.157	6.09	9.44	6.45	10.00	26.06	12.86
1500	13	0.51	2.03	0.080	3.25	0.128	6.25	0.246	2.00	0.079	4.00	0.157	5.33	8.26	5.08	7.87	31.20	17.6
1110	6	0.24	2.03	0.080	3.75	0.148	8.25	0.324	0.75	0.030	8.25	0.324	4.57	7.08	12.18	18.88	16.68	10.97
1500	23	0.91	1.00	0.039	1.75	0.069	3.00	0. 118	1.45	0.057	2.75	0.108	1.60	2.48	1.27	1.97	16.58	15.33
1540	50	1.96	1.00	0.039	1.45	0.057	2.50	0.098	0.95	0.037	2.45	0.096	1.20	1.86	1.27	1.97	26.32	32.47
1540	60	2.36	1.00	0.039	1.15	0.045	2.25	0.089	0.85	0.033	2.00	0.079	1.00	1.55	1.12	1.74	26.32	38.96

Source: Ref 42

TABLE 11 TYPICAL MECHANICAL PROPERTIES OF LASER-BEAM-WELDED TITANIUM ALLOYS

MATERIAL	ULTIMATE TENSILE STRENGTH		0.2% PROOF STRESS		ELONGATION, %
	MPA	KSI	MPA	KSI	
TI-6AL-4V					
AS-WELDED	~860-923	~125-134	~800-860	~116-125	11-14

BASE MATERIAL	895-1004	130-146	834-895	121-130	10-15
COMMERCIALLY PURE TITANIUM					
AS-WELDED	~530-573	~77-83	460-503	~67-73	~27
BASE MATERIAL	>494	>72	>416	>60	27-28

Ref 42

Resistance welding is a process in which heat is produced by resistance to the flow of high electrical currents (5 to 10 kA) across the interface between two contacting surfaces. At sufficiently high current levels, melting is induced at the interface and a weld fusion zone (i.e., weld nugget) is created. At lower current levels, welding of the faying surfaces occurs entirely by a solid-state deformation or diffusion welding mechanism. Resistance welding is most commonly used to join sheet and can produce either discrete, individual spot welds or continuous, overlapping seam welds. The resistance welding parameters employed for titanium are generally comparable to those used for austenitic stainless steels, due to similarities in thermal conductivity between the two materials. As expected, the production of high-quality resistance welds requires careful cleaning of the sheet surfaces prior to welding. However, the rapid thermal cycles employed and the self-contained nature of the weld zone generally preclude the necessity for inert-gas shielding during welding. Table 12 presents typical parameters for resistance spot welding of Ti-6Al-4V.

TABLE 12 TYPICAL OPERATING CONDITIONS FOR RESISTANCE SPOT WELDING OF TI-6AL-4V

MATERIAL THICKNESS		WELDING CURRENT, KA	ELECTRODE FORCE[(A)]		WELD TIME, CYCLES (60 HZ)	NUGGET DIAMETER	
mm	in.		kn	lbf		mm	in.
0.89	0.035	5.5	2.7	600	7	6.35	0.25
1.57	0.062	10.6	6.7	1500	10	9.15	0.36
2.36	0.093	12.5	10.7	2400	16	10.9	0.43

Source: Ref 4

(A) RWMA CLASS 2 COPPER ALLOY ELECTRODES, 75 MM (3 IN.) FACE RADIUS.

Diffusion welding is a solid-state joining process that is finding increased application for the fabrication of complex titanium alloy components. Diffusion welding (or bonding) of titanium involves four basic steps: (1) development of intimate physical contact between the faying surfaces through deformation of asperity peaks (surface roughness) by yielding and creep at low pressures and high temperatures, (2) formation of a metallic bond, (3) diffusion across the faying surface, and (4) grain growth across the original weld interface. Prerequisites for accomplishing these steps include a clean and smooth surface combined with a low applied pressure to promote steps 1 and 2, and moderate-to-high temperatures to promote steps 3 and 4. Titanium alloys are ideal for diffusion welding because titanium exhibits a high solubility for oxygen, which promotes dissolution of surface oxides at elevated temperatures. In addition, the yield and creep strengths of titanium are low at welding temperatures, thereby enhancing stages 1 and 2 of the diffusion welding process. Diffusion welding of Ti-6Al-4V is generally performed at temperatures ranging from about 900 to 950 °C (1650 to 1740 °F), at pressures ranging from 1.3 to 13.8 MPa (200 to 2000 psi), and for times ranging from about 1 to 6 h. In combination with superplastic forming, diffusion welding has been utilized to produce a wide variety of complex Ti-6Al-4V shapes, such as honeycomb panels for aerospace applications.

Other Weld Processes. A wide variety of more specialized welding processes have been used to join titanium, including flash-butt welding, continuous-drive and inertia friction welding, ultrasonic welding, and explosive welding. In general, these processes have been effective, producing defect-free joints with properties that depend principally on the cooling rates from high temperatures and the characteristics of the resulting transformed-beta microstructure.

Special Welding Precautions and Requirements. Production of high-quality welds in titanium and titanium alloys requires meticulous preweld cleaning of the workpiece and consumables and adequate gas shielding to prevent atmospheric contamination. Mill-annealed titanium sheet and plate are generally supplied in a condition that requires only

the removal of surface grease, oil, and dirt. Such cleaning is normally accomplished by wiping with or dipping in a nonchlorinated solvent such as acetone or methyl-ethyl-ketone (MEK). Materials that exhibit a light oxide scale as a result of heat treatment below about 600 °C (1110 °F) or that contain entrapped oil from machining operations should be pickled for 5 to 10 min in a solution of 30 to 40% nitric acid and 4 to 5% hydrofluoric acid in water at a temperature between 20 and 70 °C (68 and 160 °F). Heavier oxide scales resulting from high-temperature heat treatment or thermomechanical processing may require cleaning in a molten salt bath or mechanical removal, followed by pickling. Pickled pieces should be rinsed in water, dried, and either directly welded or wrapped in clean plastic. All handling should be performed with clean white gloves. Weld contamination can also result from filler metal that has become dirty due to inadequate storage or careless handling prior to or during the welding operation. Degreasing the filler rod or wire is generally sufficient to eliminate contamination problems originating from these sources.

Effective shielding of the weld zone from the atmosphere during welding is extremely important in ensuring maximum weld ductility and toughness and in reducing the potential for solid-state weld cracking. Optimum shielding conditions are provided by welding within a permanent or collapsible clear plastic enclosure that has been evacuated and purged with argon (dew point, -24 °C, or -11 °F). Alternatively, localized trailing and backing shields can be used, particularly for automatic welding of simple joint geometries (for example, automatic butt welding of sheet). Use of localized shielding for manual welding of complex parts, although feasible, requires specially designed shielding fixtures and generally is not recommended. Fortunately, evidence of titanium weld contamination is readily apparent by discoloration of the weld surface, with a change from bright silver to straw, to magenta, to blue, with a gradual increase in the level of contamination. Severe contamination is associated with a white or gray powdery-appearing weld surface, and is often accompanied by solid-state cracking in the weld metal. In many high-performance applications, a bright silver color is required, although a light straw color may be accepted in less-critical applications.

Because titanium alloy welds are commonly used in fatigue-critical applications, a stress relief operation is generally required following welding. Specific stress-relief temperatures and times depend on the base-metal microstructure (Table 3). In order to prevent property degradation, stress relieving should be performed on components free of surface contamination and in an inert or vacuum environment.

Weld Design Criteria and Limitations. Designers of titanium welded structures must consider both welding process applicability and the physical characteristics and mechanical properties of the welds. From a welding process stand-point, an efficient design will utilize a welding process optimally suited to a particular material thickness and joint configuration. Such process suitability is also based on component size and shape (for example, whether the component will fit in an available EBW chamber, or whether the entire part can be suitably protected from the atmosphere during GTAW or PAW), the cost of producing the weld (including both capital equipment and operating costs), and postweld processing requirements.

The design of titanium welded structures is also influenced by the characteristics and mechanical properties of a joint produced by a particular welding process. Physical characteristics of the weld, including undercut or underfill in fusion welds, upset in solid-state welds, and weld distortion are important considerations, because these characteristics affect not only the physical dimensions of the component but also joint mechanical properties. Obviously, the mechanical properties of the joint, as influenced by the integrity and metallurgical structure of the weld zone, are the principal considerations in weld design. As indicated above, low fusion zone ductility and toughness in rapidly cooled welds, and poor axial fatigue behavior in welds containing defects, are important characteristics of welds that may influence the design of the welded component.

Welding Specifications. The American Welding Society has published two specifications related to welding of titanium. AWS Specification 5.16, "Specification for Titanium and Titanium Alloy Bare Welding Rods and Electrodes," provides requirements for titanium and titanium-alloy welding rods for use with GTAW and GMAW processes (see the article "Welding of Titanium Alloys" in this Volume for filler metal compositions). Although the basic specification principally covers filler metal chemical composition requirements, a rather lengthy appendix presents additional general information on welding of titanium, including toughness data for alpha-beta titanium alloy welds. AWS Specification D10.6, "Recommended Practices for Gas Tungsten-Arc Welding of Titanium Pipe and Tubing," is specific to single-phase alpha alloys.

Numerous additional specifications developed by the government and by industry discuss the procedural aspects of the welding of titanium and set forth minimum weld quality and mechanical property requirements. These specifications may be quite general or very specific, describing in detail the fabrication or weld repair of an individual component.

References cited in this section

4. TITANIUM, ZIRCONIUM, HAFNIUM, TANTALUM, AND COLUMBIUM, *WELDING HANDBOOK*, 7TH ED., VOL 4, AMERICAN WELDING SOCIETY, 1982, P 434-470
41. R.F. VAUGHAN, PROPERTIES OF WELDED TITANIUM ALLOYS AND THEIR APPLICATION IN THE AEROSPACE INDUSTRY, *TITANIUM '80 SCIENCE AND TECHNOLOGY*, VOL 4, H. KIMURA AND O. IZUMI, ED., THE METALLURGICAL SOCIETY OF AIME, 1983, P 2423
42. J. MAZUMDER AND W.M. STEEN, MICROSTRUCTURE AND MECHANICAL PROPERTIES OF LASER WELDED TI-6AL-4V, *METALL. TRANS. A*, VOL 13, 1982, P 865-871

Selection and Weldability of Conventional Titanium Alloys

W.A. Baeslack III, The Ohio State University; J.R. Davis, Davis and Associates; C.E. Cross, Martin Marietta Astronautics Group

References

1. M.J. DONACHIE, JR., TITANIUM, *METALS HANDBOOK DESK EDITION*, AMERICAN SOCIETY FOR METALS, 1985, P 9-1 TO 9-3
2. S. LAMPMAN, WROUGHT TITANIUM AND TITANIUM ALLOYS, *PROPERTIES AND SELECTION: NONFERROUS ALLOYS AND SPECIAL-PURPOSE MATERIALS*, VOL 2, *ASM HANDBOOK*, ASM INTERNATIONAL, 1990, P 592-633
3. E.W. COLLINGS, *THE PHYSICAL METALLURGY OF TITANIUM ALLOYS*, AMERICAN SOCIETY FOR METALS, 1984
4. TITANIUM, ZIRCONIUM, HAFNIUM, TANTALUM, AND COLUMBIUM, *WELDING HANDBOOK*, 7TH ED., VOL 4, AMERICAN WELDING SOCIETY, 1982, P 434-470
5. W.A. BAESLACK III, D.W. BECKER, AND F.H. FROES, ADVANCES IN TITANIUM ALLOY WELDING METALLURGY, *J. MET.*, MAY 1984, P 46-58
6. R.W. SCHUTZ AND D.E. THOMAS, CORROSION OF TITANIUM AND TITANIUM ALLOYS, *CORROSION*, VOL 13, *ASM HANDBOOK*, ASM INTERNATIONAL, 1987, P 669-706
7. D.W. BECKER, W.A. BAESLACK III, AND R.W. MESSLER, JR., TITANIUM WELDING, *TITANIUM '80 SCIENCE AND TECHNOLOGY*, VOL 1, H. KIMURA AND O. IZUMI, ED., THE METALLURGICAL SOCIETY OF AIME, 1980, P 255-275
8. D.F. HASSON, "A REVIEW OF TITANIUM WELDING PROCESSES," U.S. NAVY REPORT, ANNAPOLIS, MD, 1985
9. J.R. HARTMAN AND W.A. BAESLACK III, ADVANCES IN ARC WELDING OF TITANIUM ALLOYS, *WELDABILITY OF MATERIALS*, R.A. PATTERSON AND K.W. MAHIN, ED., ASM INTERNATIONAL, 1990, P 319-330
10. W.A. BAESLACK III AND D.L. HALLUM, NATURE OF GRAIN REFINEMENT IN TITANIUM ALLOY WELDS BY MICROCOOLER INOCULATION, *WELD. J. RES. SUPPL.*, VOL 69 (NO. 12), DEC 1990, P 326S-336S
11. D.W. BECKER AND W.A. BAESLACK III, PROPERTY-MICROSTRUCTURE RELATIONSHIPS IN METASTABLE-BETA TITANIUM ALLOY WELDMENTS, *WELD. J. RES. SUPPL.*, VOL 59, 1980, P 85S-92S
12. W.A. BAESLACK III, P.S. LIU, D.P. BARBIS, J.R. SCHLEY, AND J.R. WOOD, POSTWELD HEAT TREATMENT OF GTA WELDS IN A HIGH-STRENGTH, METASTABLE-BETA TITANIUM ALLOY--BETA-C, *PROC. OF 1992 INT. CONF. ON TITANIUM ALLOYS* (SAN DIEGO), 1992
13. A.T. D'ANNESSA, REDISTRIBUTION OF SOLUTE IN FUSION WELDING, *WELD. J.*, VOL 45, 1966, P 569S-576S
14. W.A. BAESLACK III, EFFECT OF SOLUTE BANDING ON TRANSFORMATIONS IN DISSIMILAR

TITANIUM ALLOY WELDMENTS, *J. MAT. SCI. LET.*, VOL 1, 1982, P 229-231

15. P.S. LIU, W.A. BAESLACK III, AND J. HURLEY, DISSIMILAR ALLOY LASER WELDING OF TITANIUM: TI-6AL-4V TO BETA-C, *WELD. J. RES. SUPPL.*, IN PRESS
16. P.S. LIU, W.A. BAESLACK III, AND J. HURLEY, LASER WELDING OF TI-6AL-4V TO BETA-21S, *PROC. OF TMS CONF. ON BETA TITANIUM ALLOYS* (DENVER, CO), TMS, 1993
17. W.A. BAESLACK III, S. CHIANG, AND C.A. ALBRIGHT, *J. MAT. SCI. LET,* VOL 9, 1990, P 698-702
18. W.A. BAESLACK ILL, *METALLOGRAPHY,* VOL 13, 1980, P 277-281
19. N.N. PROKHOROV, *WELD. PROD.,* VOL 9, 1986, P 30-32
20. P.W. HOLSBERG, "CRACKING AND POROSITY IN TITANIUM ALLOY WELDMENTS," U.S. NAVY DTNSRDC REPORT, 1979
21. F.D. ROSI, D.A. DUBE, AND B.H. ALEXANDER, *TRANS. AIME,* VOL 197, 1953, P 257
22. N.E. PATON AND J.C. WILLIAMS, THE EFFECT OF HYDROGEN ON TITANIUM AND ITS ALLOYS, *HYDROGEN IN METALS,* AMERICAN SOCIETY FOR METALS, 1974, P 409-431
23. R.E. LEWIS, I.L. CAPLAN, AND W.C. COONS, THE ELEVATED TEMPERATURE DUCTILITY DIP PHENOMENON IN ALPHA, NEAR-ALPHA AND ALPHA-BETA TITANIUM ALLOYS, *TITANIUM SCIENCE AND TECHNOLOGY,* VOL 2, G. LÜTJERING, U. ZWICKER, AND W. BUNK, ED., DEUTSCHE GESELLSCHAFT FÜR METALLKUNDE E.V., WEST GERMANY, 1985
24. B.K. DAMKROGER, G.R. EDWARDS, AND B.B. RATH, A MODEL FOR HIGH TEMPERATURE DUCTILITY LOSS IN ALPHA-BETA TITANIUM ALLOYS, *METALL. TRANS. A,* VOL 18, 1987, P 483-485
25. D.M. BOWDEN AND E.A. STARKE, JR., HOT CRACKING SUSCEPTIBILITY OF TITANIUM 6211, *TITANIUM SCIENCE AND TECHNOLOGY,* VOL 2, G. LÜTJERING, U. ZWICKER, AND W. BUNK, ED., DEUTSCHE GESELLSCHAFT FÜR METALLKUNDE E.V., WEST GERMANY, 1985, P 853
26. D.M. BOWDEN AND E.A. STARKE, JR., *METALL. TRANS. A,* VOL 15, 1984, P 1687-1698
27. D. HAYDUK, B.K. DAMKROGER, G.R. EDWARDS, AND D.L. OLSON, *WELD. J.,* VOL 65, 1986, P 251S-260S
28. B.K. DAMKROGER, G.R. EDWARDS, AND B.B. RATH, *WELD. J.,* VOL 68, 1989, P 290S-302S
29. R.E. TREVISAN, D.D. SCHWEMMER, AND D.L. OLSON, THE FUNDAMENTALS OF WELD PORE FORMATION, *WELDING: THEORY AND PRACTICE,* ELSEVIER, 1990, P 79-115
30. K. BORGGREEN AND I. WILSON, USE OF POSTWELD HEAT TREATMENTS TO IMPROVE DUCTILITY IN THIN SHEETS OF TI-6AL-4V, *WELD. J.,* VOL 59, 1980, P 1S-8S
31. S.L. BOSTON AND W.A. BAESLACK III, "MICROSTRUCTURE/MECHANICAL PROPERTY RELATIONSHIPS IN GTA WELDED TI-10V-2FE-3AL," AFML-TM-LL-80-1, WRIGHT PATTERSON AIR FORCE BASE, DAYTON, OH, 1980
32. M.A. GREENFIELD AND C.M. PIERCE, POSTWELD AGING OF A METASTABLE BETA TITANIUM ALLOY, *WELD. J.,* VOL 52, 1973, P 524S-527S
33. W.A. BAESLACK III, EVALUATION OF TRIPLEX HEAT TREATMENTS FOR TITANIUM ALLOYS, *WELD. J.,* VOL 61, 1982, P 193S-199S
34. D.W. BECKER AND W.A. BAESLACK III, PROPERTY/MICROSTRUCTURE RELATIONSHIPS IN METASTABLE-BETA TITANIUM ALLOY WELDMENTS, *WELD. J.,* VOL 59, 1980, P 850-920
35. W.A. BAESLACK III AND F.D. MULLINS, RELATIONSHIP OF MICROSTRUCTURE, MECHANICAL PROPERTIES AND FRACTOGRAPHIC FEATURES IN WELDED HIGH TOUGHNESS TITANIUM ALLOYS, *TRENDS IN WELDING RESEARCH,* S.A. DAVID, ED., AMERICAN SOCIETY FOR METALS, 1982, P 541
36. V.N. ZAMKOV *ET AL.,* WAYS OF PROVIDING THE HIGH SERVICEABILITY OF HEAT-HARDENED WELDED JOINTS OF ALPHA + BETA TITANIUM ALLOYS, *TITANIUM SCIENCE AND TECHNOLOGY,* VOL 2, G. LÜTJERING, U. ZWICKER, AND W. BUNK, ED., DEUTSCHE GESELLSCHAFT FÜR METALLKUNDE, E.V., WEST GERMANY, 1985, P 877
37. W.A. BAESLACK III, D.W. BECKER, AND F.H. FROES, WELDABILITY OF A HIGH TOUGHNESS

TITANIUM ALLOY, A METALLURGICAL EVALUATION, *TITANIUM '80 SCIENCE AND TECHNOLOGY*, VOL 2, H. KIMURA AND O. IZUMI, ED., THE METALLURGICAL SOCIETY OF AIME, 1980, P 2369

38. R.E. LEWIS *ET AL.*, THE EFFECT OF BORON ON WELDMENT MICROSTRUCTURES IN TI-6AL-2NB-1TA-1MO ALLOY, *TITANIUM SCIENCE AND TECHNOLOGY*, VOL 2, G. LÜTJERING, U. ZWICKER, AND W. BUNK, ED., DEUTSCHE GESELLSCHAFT FÜR METALLKUNDE E.V., WEST GERMANY, 1985, P 799
39. T.S. PARKER AND P.G. PARTRRIDGE, FATIGUE PROPERTIES OF 4 MM THICK LASER WELDED TI-6AL-4V SHEET, *FATIGUE '84*, C.J. BEEVERS, ED., ENGINEERING MATERIALS ADVISORY SERVICES LTD., LONDON, 1984
40. P.S. PAO, T.C. PENG, AND J.E. O'NEAL, FATIGUE CRACK PROPAGATION THROUGH TITANIUM WELDS, *TITANIUM SCIENCE AND TECHNOLOGY*, VOL 2, G. LÜTJERING, U. ZWICKER, AND W. BUNK, ED., DEUTSCHE GESELLSCHAFT FÜR METALLKUNDE, E.V., WEST GERMANY, 1985, P 887
41. R.F. VAUGHAN, PROPERTIES OF WELDED TITANIUM ALLOYS AND THEIR APPLICATION IN THE AEROSPACE INDUSTRY, *TITANIUM '80 SCIENCE AND TECHNOLOGY*, VOL 4, H. KIMURA AND O. IZUMI, ED., THE METALLURGICAL SOCIETY OF AIME, 1983, P 2423
42. J. MAZUMDER AND W.M. STEEN, MICROSTRUCTURE AND MECHANICAL PROPERTIES OF LASER WELDED TI-6AL-4V, *METALL. TRANS. A*, VOL 13, 1982, P 865-871

Selection and Weldability of Advanced Titanium-Base Alloys

David H. Phillips, Edison Welding Institute

Introduction

ADVANCED TITANIUM-BASE ALLOYS can generally be categorized as having conventional (terminal phase), intermetallic, or titanium-matrix composite structures. Conventional alloys can be further subdivided, on the basis of the amount of beta phase that is present, into four families: near-alpha, alpha-beta, near-beta, or metastable-beta (Table 1). Intermetallics that are based on titanium most commonly include alpha-2, gamma, and orthorhombic systems. Although the phrase titanium-matrix composite covers a potentially wide range of matrix materials and either continuous or discontinuous reinforcements, the most common composite used is continuous silicon-carbide-reinforced Ti-6Al-4V. This article will describe the physical metallurgy of each alloy category and its families, followed by a brief discussion on the weldability of each.

TABLE 1 ADVANCED TITANIUM ALLOY FAMILIES

CONVENTIONAL ALLOYS
NEAR-ALPHA: TI-1100; IMI-834 ALPHA-BETA: CORONA 5 NEAR-BETA: TI-10V-2FE-3AL METASTABLE-BETA: BETA 215; BETA C
INTERMETALLIC ALLOYS
ALPHA-2: TI24AL-11NB; TI25AL-10NB-3V-1MO GAMMA: TI-AL-NB-CR ORTHORHOMBIC: TI-AL-NB
TITANIUM-MATRIX COMPOSITES
TI-6AL-4V WITH SIC CONTINUOUS FIBERS

David H. Phillips, Edison Welding Institute

Physical Metallurgy

Conventional alloys can usually be described by one of the four families shown in Table 1. The compositions and maximum use temperatures of selected alloys from these families are shown in Table 2, whereas basic mechanical properties are shown in Table 3.

TABLE 2 MAXIMUM USEFUL TEMPERATURES AND CHEMICAL COMPOSITIONS OF SELECTED HIGH-TEMPERATURE TITANIUM ALLOYS

ALLOY DESIGNATION	MAXIMUM USEFUL TEMPERATURE		COMPOSITION, WT%								
	°C	°F	Al	Sn	Zr	Mo	Nb	V	Si	Cr	C
TI-1100	595	1100	6	2.75	4	0.4	. . .	. . .	0.45	. . .	. . .
IMI-834	595	1100	5.5	4	4	0.3	1	. . .	0.5	. . .	0.06
CORONA 5	. . .	. . .	4.5	. . .	. . .	5	. . .	. . .	. . .	1.5	. . .
TI-10V-2FE-3AL	315	600	3	. . .	. . .	. . .	. . .	10	. . .	. . .	. . .
BETA 21S	. . .	. . .	3	. . .	. . .	15	2.7	. . .	0.2	. . .	. . .
BETA C	. . .	. . .	3	. . .	4	4	. . .	8	. . .	6	. . .

TABLE 3 BASIC MECHANICAL PROPERTIES OF ADVANCED TITANIUM-BASE ALLOYS

COMMON NAME	ULTIMATE TENSILE STRENGTH		YIELD STRENGTH		REDUCTION IN AREA, %	ELONGATION, %	FRACTURE TOUGHNESS	
	MPa	Ksi	MPa	Ksi			MPa $\sqrt{m}$	Ksi $\sqrt{in}$
TI-1100	1010	145	910	130	21	. . .	67	61
IMI 834	1050	150	950	140	24	. . .	44	40
CORONA 5	1200	175	1170	170	22	. . .	. . .	. . .
TI-10V-2FE-3AL	1000	145	1000	140	50	. . .	55	50
BETA 21S	1100	160	1000	140	. . .	9	. . .	. . .
BETA C	1300	190	1200	175	. . .	9	88	80
ALPHA-2	690	100	590	85	4	. . .	22	20
GAMMA	480	70	340	50	2	. . .	16	15
ORTHORHOMBIC	1100	160	1030	150	5	. . .	22	20

The physical metallurgies of selected alloys from each family are described below.

Near-Alpha Alloys. The alloy Ti-1100 was developed in response to a requirement for higher creep properties in Ti-6242S. It was determined that, by adjusting the tin and molybdenum compositions and adding silicon, significant improvements to the creep properties could be realized (Ref 1). Because it was developed for a maximum use temperature of 595 °C (1100 °F), it was named Ti-1100. The processing of this alloy usually involves a final beta forge, followed by an 8-h stabilization at 600 °C (1110 °F). This results in a fully transformed acicular structure, which is the proper microstructure for most applications.

The near-alpha alloy IMI-834 was developed for applications requiring a better balance of creep and fatigue properties. Because fully transformed microstructures are not ideal, in terms of fatigue, IMI-834 was developed to facilitate processing into a duplex microstructure. This was achieved by adding carbon, which stabilizes the alpha phase, thus

increasing the size of the alpha-beta phase field. As a result, although careful control is required, a duplex microstructure can be achieved through subsequent alpha-beta processing (Ref 2). The microstructure typically contains 15% primary alpha. Niobium was added to increase oxidation resistance during high-temperature exposures, and silicon was added to improve strength and creep resistance.

Alpha-Beta Alloys. The need for titanium alloys with higher levels of toughness led to the development of Corona 5. This alpha-beta titanium alloy has intermediate strength and exceptionally high fracture toughness. In order to achieve the latter property, this alloy is typically processed high in the alpha-beta phase field, which results in an alpha and beta microstructure containing moderately high aspect ratio primary alpha particles. One of the principal attractions of this alloy is that its strength level can easily be adjusted by modifying the dispersion of the fine alpha (transformed beta) phase (Ref 3).

Near-Beta Alloys. Ti-10V-2Fe-3Al, which is considered to be a relatively high-strength near-beta alloy, can be processed for either high strength and medium toughness or moderate strength and high toughness. It is typically solution treated and aged, which results in a mostly transformed alpha and beta microstructure.

Metastable-Beta Alloys. The Beta 21S alloy was developed primarily as a material that had acceptable high-temperature properties and oxidation resistance, could be readily cold rolled, and was age hardenable. These features (primarily the cold rollability) make it an excellent candidate as a matrix material for titanium-matrix composites. Base-metal processing usually involves the hot and cold working of the ingot to form billet or strip product, followed by solution annealing, cold forming to near-net shape, resolution annealing, and then aging. The fine alpha platelets that precipitate during the aging process provide increased strength in the alloy. The resultant microstructure contains the fine alpha platelets in a beta-phase matrix.

Beta C is a metastable-beta alloy that can be processed and heat treated to provide an excellent combination of yield and tensile strengths, ductility, fracture toughness, and fatigue strength (Ref 4). The alloy contains the beta-isomorphous elements molybdenum and vanadium, as well as the sluggish beta-eutectoid element chromium at levels that depress the beta transus temperature to approximately 750 °C (1380 °F) and promote retention of the high-temperature beta phase down to room temperature upon air cooling. A solution heat treatment, followed by aging, promotes the precipitation of a fine distribution of alpha phase in the beta-phase matrix.

Intermetallics. Titanium intermetallics consist primarily of the titanium aluminides alpha-2 and gamma, as well as the orthorhombic plus beta types of alloys. The aluminides, as shown on the titanium-aluminum phase diagram of Fig. 1, consist of two alloy families: alpha-2, which is based on the Ti_3Al intermetallic, and gamma, which is based on the titanium-aluminum intermetallic. These alloys offer greater stiffness and improved specific creep resistance, and they are capable of extending the use temperature range of conventional titanium alloys. The orthorhombic alloys contain large amounts of niobium, which promotes formation of the orthorhombic phase, Ti_2AlNb.

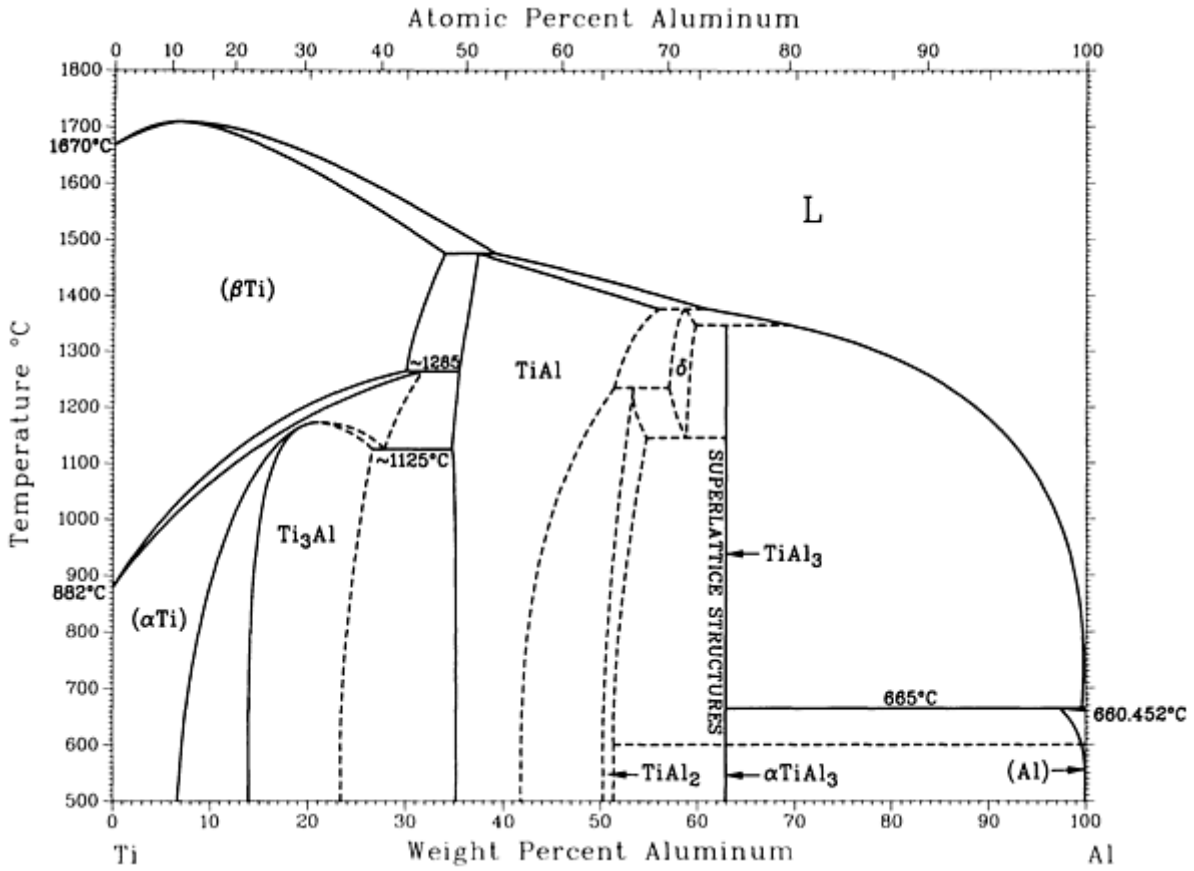

FIG. 1 TITANIUM-ALUMINUM PHASE DIAGRAM. SOURCE: REF 5

Alpha-2 alloys represent a growing family of intermetallics that contain from 14 to 25 at.% aluminum, which places them in the Ti_3Al phase field of Fig. 1. They usually contain beta-stabilizing elements, such as niobium and molybdenum, to promote beta-phase retention and ductility. These alloys are typically alpha-beta processed, resulting in a microstructure similar to that of conventional alloys, which consists of islands of equiaxed primary alpha-2 in a matrix of transformed beta. When compared with conventional titanium alloys, alpha-2 alloys offer higher temperature capabilities (from 100 to 150 °C, or 180 to 270 °F, higher), but have reduced room-temperature toughness and ductility properties (3 to 6% elongation).

The gamma alloy family, which is growing even more rapidly than the alpha-2 alloy family, typically contains from 45 to 52 at.% aluminum, which places these alloys primarily in the gamma phase field, with some overlap in the gamma/alpha-2 phase field. This results in a range of alloy microstructures, including single-phase gamma (TiAl) and duplex structures containing varying amounts of alpha-2 phase (Ti_3Al). Duplex microstructures are generally preferred, because of their higher ductility. Alloying elements such as niobium, chromium, vanadium, tantalum, manganese, and molybdenum are added in small amounts (generally from 2 to 4 at.%) to improve properties such as room-temperature ductility and oxidation resistance. The gamma alloys are more difficult to thermomechanically process than are the alpha-2 alloys, primarily because of their very high strengths at elevated temperatures. Accordingly, compared to alpha-2 alloys, the gamma alloys offer temperature capabilities that are from 100 to 150 °C (180 to 270 °F) higher. They also are known to suffer from low fracture toughness and ductility, although aggressive alloy development programs are currently attempting to improve these properties.

Orthorhombic alloys represent a new class of alloys based on the orthorhombic and beta phases. These alloys offer temperature capabilities similar to those of the alpha-2 alloys, but with higher ductilities and toughness at low temperatures. Although these alloys are similar to alpha-2 alloys, a higher niobium content results in an orthorhombic extension of the hexagonal lattice. The large amounts of niobium also result in a highly stabilized beta phase, compared with alpha-2 alloys. Processing is similar to that used with other titanium alloys. Forging is typically conducted below the beta transus temperature, resulting in a two-phase orthorhombic plus transformed-beta microstructure. A direct age then can be subsequently applied to develop properties.

Titanium-Matrix Composites. Although many titanium matrix/fiber combinations are currently being evaluated by aerospace companies and titanium producers, the most popular composite consists of a conventional Ti-6Al-4V or Ti-6242 matrix with layers of continuous silicon-carbide fibers. The layers can be either unidirectional or cross-ply. Two manufacturing techniques can be used: a foil/fiber/foil approach, in which layers of monolithic foil and fiber sets are either vacuum hot pressed or hot isostatically pressed to form the composite, or a plasma-spray approach, in which the composite is built up by sequentially winding individual layers of fibers and then spraying the monolithic layers, followed by consolidation using either vacuum hot pressing or hot isostatic pressing.

References cited in this section

1. P. BANIA, NEXT GENERATION TITANIUM ALLOYS FOR ELEVATED TEMPERATURE SERVICE, *ISIJ INT.*, VOL 31, 1991, P 840-847
2. OPTIMIZATION OF CREEP AND FATIGUE RESISTANCE IN HIGH TEMPERATURE TI ALLOYS IMI 829 AND IMI 834, *PROC. 5TH INT. CONFERENCE ON TITANIUM* (MUNICH, GERMANY), 1984, P 2419
3. D.W. BECKER, W.A. BAESLACK, AND F.H. FROES, POWDER METALLURGY OF TITANIUM ALLOYS, *PROC. CONF. AIME,* AIME, 1980
4. W.A. BAESLACK, P.S. LIU, D.B. BARBIS, J.R. SCHLEY, AND J.R. WOOD, POSTWELD HEAT TREATMENT OF GTA WELDS IN A HIGH-STRENGTH METASTABLE-BETA TITANIUM ALLOY--BETA-C, INTERNATIONAL TITANIUM CONFERENCE (SAN DIEGO), 1992
5. T.B. MASSALSKI, ED., *BINARY ALLOY PHASE DIAGRAMS,* 2ND ED., VOL 1, ASM INTERNATIONAL, 1990, P 226

Selection and Weldability of Advanced Titanium-Base Alloys

David H. Phillips, Edison Welding Institute

Weldability

There are many weldability (fusion welding) concerns associated with advanced titanium alloys. These differ appreciably from the weldability concerns that are characteristic of steels, such as hydrogen cracking, or of superalloys, such as strain age or liquation cracking. The weldability problems associated with advanced titanium alloys are related to their microstructural sensitivity to high heat input and rapid cooling rates. These thermal excursions, which are characteristic of many welding processes, can result in excessive beta grain growth and the formation of undesirable solid-state transformation products. The affected microstructures typically suffer from poor ductility and toughness. Such effects can be minimized, however, through proper welding practices, such as those discussed below.

Conventional Alloys. Each of the four families previously identified are described below in terms of weldability.

The near-alpha alloy Ti-1100 is generally considered to be a very weldable alloy, because of its high ductility. However, the excellent creep resistance of this alloy also means that high residual stresses will be developed when welding, especially with thick sections. These stresses may have to be relieved by a postweld heat treatment following welding, in order to avoid cracking.

The near-alpha alloy IMI 834 is also considered to be weldable, but the weld fusion zone and heat-affected zone (HAZ) may be void in primary alpha phase. These regions may not retain a good balance of creep and fatigue properties, for which IMI 834 is designed.

Alpha-Beta Alloys. The Corona 5 high-toughness alloy can be successfully welded, but it requires carefully controlled cooling rates, as well as postweld heat-treatment conditions. Excessively high cooling rates can result in the formation of orthorhombic martensite, a structure that exhibits inferior strength and fracture toughness. The aging of this martensite at low and intermediate postweld heat-treatment temperatures results in high strength, but low ductility and fracture

toughness. However, through proper cooling and postweld heat treating, a fine alpha-beta fusion zone and HAZ microstructure that exhibits good mechanical properties can be created.

Near-Beta Alloys. The Ti-10V-2Fe-3Al alloy is very weldable in the heat-treated condition. Tensile and fracture toughness values that are near those of the base metal can be achieved with as-welded Ti-10V-2Fe-3Al.

Metastable-Beta Alloys. Although metastable-beta titanium alloys, such as Beta 21S, are generally considered to be weldable, cooling rates should be kept relatively high, and the weld fusion zone size should be minimized to avoid the formation of coarse columnar beta fusion zone grains and large beta HAZ grains, both of which can degrade ductility (Ref 6). If a relatively fine as-welded grain structure can be achieved, then moderate weld strength and high ductility can be achieved. Postweld heat treating to precipitate the alpha phase can significantly increase weld tensile strengths, but at the expense of ductility. Higher postweld aging temperatures may result in the formation of significant amounts of alpha phase along the beta grain boundaries, which changes the fracture mode, but does not necessarily degrade the properties.

Like Beta 21S, the Beta C alloy is considered to be highly weldable, but the fusion zone and HAZ beta grain size should be minimized (Ref 4). As-welded structures are characterized by low strength and high ductility. Relatively low postweld aging treatments can significantly increase strength levels, but ductility levels will be reduced, compared with those of the base metal, because of the large beta grain size and fine alpha phase distribution. Figure 2 shows a Beta C gas-tungsten arc weld microstructure, which reveals the large beta grain size. Higher postweld aging cycles coarsen the alpha phase, which reduces the strength but increases the ductility. As with Beta 21S, the higher aging temperatures can result in significant grain boundary alpha formation, which changes the fracture mode, but does not necessarily degrade the properties.

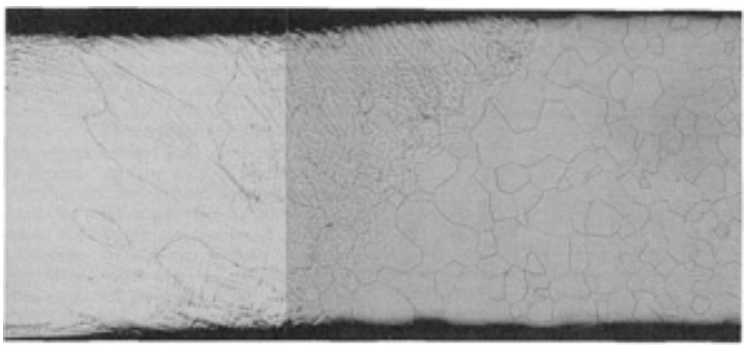

FIG. 2 MICROSTRUCTURE OF AS-WELDED GAS-TUNGSTEN ARC WELD IN BETA C SHEET

The intermetallic alloys are currently in the early stages of development. As a result, only limited weldability studies have been conducted to date. However, cursory fundamental studies have provided some indication of their weld sensitivities, and are discussed below.

Alpha-2 alloys form a similar weld and HAZ to many conventional alpha-beta titanium alloys. However, because of limited ductility and notch sensitivity, alpha-2 alloys are susceptible to solid-state fusion zone and HAZ cracking. Preheating to reduce residual stress and promote a more-ductile fusion zone and HAZ microstructure may be required in order to eliminate cracking. Weldability can also be improved by minimizing the size of the weld fusion zone and maximizing the cooling rate through the use of high-energy-density welding processes, such as laser-beam or electron-beam welding. Although this has the effect of retaining the metastable-beta phase, which can then be postweld heat treated, cracking may also occur during the heat treatment. Figure 3 shows cracking in the root of an alpha-2 electron-beam weld.

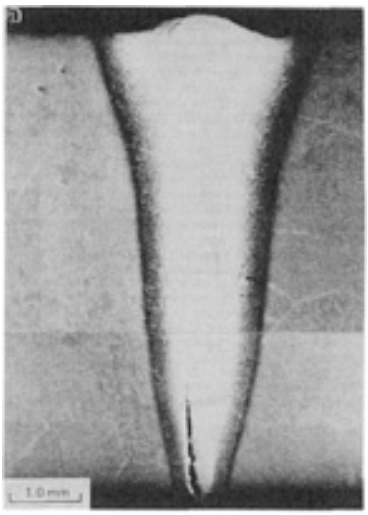

FIG. 3 CRACKING IN ALPHA-2 ELECTRON-BEAM WELD

Gamma Alloys. The gamma fusion zone and weld HAZ microstructures are significantly different from those of other titanium alloys. Depending on the weld process and metallographic technique used, the HAZ adjacent to the fusion zone can be nearly indistinguishable from the base-metal microstructure. Excessive grain growth does not appear to be an issue with gamma weldments. Because of low ductility and a high modulus, gamma alloys are very susceptible to weld fusion zone and HAZ cracking, resulting in the requirement for a weld preheat or controlled cooling.

Orthorhombic alloys are more ductile than the alpha-2 and gamma alloys, and are therefore easier to weld. Because of high beta-phase stabilities, a large retained-beta-phase HAZ will result from welding. Postweld heat treatments may be required to achieve an optimum combination of properties.

Titanium-Matrix Composites. The weldability issues relative to the monolithic titanium alloys also apply to titanium-matrix composites, with the additional complication of fiber/matrix interaction. Although some fiber damage from the welding process should not significantly degrade the properties, the damage should, of course, be minimized, where possible. Joint design is especially critical with titanium-matrix composites. The selection of a joining process is also critical, where processes such as brazing, solid-state diffusion welding, or transient liquid phase bonding may be required to minimize fiber damage. These processes eliminate or minimize base-metal melting that would damage the fibers.

References cited in this section

4. W.A. BAESLACK, P.S. LIU, D.B. BARBIS, J.R. SCHLEY, AND J.R. WOOD, POSTWELD HEAT TREATMENT OF GTA WELDS IN A HIGH-STRENGTH METASTABLE-BETA TITANIUM ALLOY--BETA-C, INTERNATIONAL TITANIUM CONFERENCE (SAN DIEGO), 1992
6. P.S. LIU, K.H. HOU, J. HURLEY, AND W.A. BAESLACK, LASER WELDING OF AN OXIDATION RESISTANT METASTABLE-BETA TITANIUM ALLOY--BETA-215, INTERNATIONAL TITANIUM CONFERENCE (SAN DIEGO), 1992

Selection and Weldability of Advanced Titanium-Base Alloys

David H. Phillips, Edison Welding Institute

References

1. P. BANIA, NEXT GENERATION TITANIUM ALLOYS FOR ELEVATED TEMPERATURE SERVICE, *ISIJ INT.,* VOL 31, 1991, P 840-847
2. OPTIMIZATION OF CREEP AND FATIGUE RESISTANCE IN HIGH TEMPERATURE TI ALLOYS IMI 829 AND IMI 834, *PROC. 5TH INT. CONFERENCE ON TITANIUM* (MUNICH, GERMANY), 1984, P 2419
3. D.W. BECKER, W.A. BAESLACK, AND F.H. FROES, POWDER METALLURGY OF TITANIUM ALLOYS, *PROC. CONF. AIME,* AIME, 1980
4. W.A. BAESLACK, P.S. LIU, D.B. BARBIS, J.R. SCHLEY, AND J.R. WOOD, POSTWELD HEAT TREATMENT OF GTA WELDS IN A HIGH-STRENGTH METASTABLE-BETA TITANIUM ALLOY--BETA-C, INTERNATIONAL TITANIUM CONFERENCE (SAN DIEGO), 1992
5. T.B. MASSALSKI, ED., *BINARY ALLOY PHASE DIAGRAMS,* 2ND ED., VOL 1, ASM INTERNATIONAL, 1990, P 226
6. P.S. LIU, K.H. HOU, J. HURLEY, AND W.A. BAESLACK, LASER WELDING OF AN OXIDATION RESISTANT METASTABLE-BETA TITANIUM ALLOY--BETA-215, INTERNATIONAL TITANIUM CONFERENCE (SAN DIEGO), 1992

Selection and Weldability of Heat-Treatable Aluminum Alloys

Richard P. Martukanitz, Applied Research Laboratory, Pennsylvania State University

Introduction

THE HEAT-TREATABLE ALUMINUM ALLOYS provide good strength and toughness in engineering applications while maintaining the low density and corrosion resistance of aluminum. These attributes allow the heat-treatable alloys to be used in a wide variety of applications, which include the aerospace, transportation, shipbuilding, tankage, piping, and appliance industries. The majority of these alloys are easily welded by the conventional arc welding processes (gas-metal arc and gas-tungsten arc welding), resistance spot and seam welding processes, as well as the high-energy processes (laser-beam and electron-beam welding).

However, these alloys also possess certain characteristics inherent to all aluminum alloys that must be considered during welding (Ref 1). Aluminum possesses a tenacious oxide that not only prevents corrosion, but may also impair welding if not minimized. This is achieved by mechanically or chemically removing heavy oxides prior to welding and using cathodic cleaning during direct current electrode positive (DCEP) gas-metal arc welding (GMAW) or alternating current gas-tungsten arc welding (GTAW). The high thermal conductivity of aluminum alloys requires the use of higher heat input for welding when compared to ferrous alloys. This requires greater welding current during arc welding of aluminum alloys. The high coefficient of thermal expansion of aluminum may also result in greater distortion when compared to ferrous alloys. Hence, aluminum is typically arc welded using high currents and high travel speeds. When in the liquid state, aluminum alloys possess a high solubility for hydrogen and very low solubility after solidification. Hence, proper cleaning and shielding must be utilized to ensure the production of welds free of gas porosity. Finally, aluminum alloys, and particularly the heat-treatable alloys, are sensitive to weld cracking. This condition is most easily avoided by proper filler and base alloy selection and adequate filler metal dilution. Anticipation of these characteristics and general knowledge of these materials allow the heat-treatable aluminum alloys to be readily welded.

Reference

1. P.B. DICKERSON AND B. IRVING, WELDING ALUMINUM: IT'S NOT AS DIFFICULT AS IT SOUNDS, *WELD. J.,* VOL 71 (NO. 4), 1992, P 45

Selection and Weldability of Heat-Treatable Aluminum Alloys

Richard P. Martukanitz, Applied Research Laboratory, Pennsylvania State University

Description of Heat-Treatable Aluminum Alloys

Designation Systems. The mechanical, physical, and chemical properties of aluminum alloys depend upon composition and microstructure. The addition of selected elements to pure aluminum greatly enhances its properties and usefulness. Because of this, most applications for aluminum utilize alloys having one or more elemental additions. The major alloying additions used with aluminum are copper, manganese, silicon, magnesium, and zinc. The total amount of these elements can constitute up to 10% of the alloy's composition (all percentages given in weight percent unless otherwise noted). Impurity elements are also present, but their total percentage is usually less than 0.15% in aluminum alloys. The two most commonly used methods of increasing the strength of aluminum alloys are to disperse alloying elements in solid solution and cold work the alloy, or to dissolve the alloying elements into solid solution and precipitate them throughout the alloy's matrix as strengthening particles (Ref 2). Alloys in which the first method applies are referred to as the work-hardenable alloys, and the latter method describes the precipitation-hardenable or heat-treatable alloys.

The designations used throughout North America for wrought aluminum alloys involve four digits, with the first digit indicating the major alloying additions, such as 6061 alloy representing the 6*xxx* alloy series. Aluminum casting alloy designations also involve four digits and may be proceeded by a letter to distinguish impurity levels or modifications of an original classification, such as A356.0 casting alloy. It should be pointed out that the fourth digit, which is separated from the others by a decimal point, indicates the product form (ingot or casting). The designations representing the heat-treatable wrought aluminum alloys are the 2*xxx* series (A1-Cu), the 6*xxx* series (Al-Mg-Si), and the 7*xxx* series (Al-Zn). The various combinations of alloying additions and strengthening mechanisms used for wrought aluminum alloys are shown in Table 1. The 8*xxx* aluminum alloy series denotes "other" major alloying constituents and may be found in both the work-hardenable and precipitation-hardenable classes of alloys. Table 2 provides the nominal composition of some of the common heat-treatable aluminum alloys (Ref 3). Included in Table 2 are compositions of selected heat-treatable casting alloys (Ref 4) and the recently commercialized aluminum-lithium alloys (Ref 5). Welding characteristics of aluminum-lithium alloys are described in the article "Selection and Weldability of Aluminum-Lithium Alloys" in this Volume.

TABLE 1 ALLOY DESIGNATIONS OF WROUGHT ALUMINUM ALLOYS

ALLOY SYSTEM	ALUMINUM SERIES
WORK-HARDENABLE ALLOYS	
PURE AL	1*XXX*
AL-MN	3*XXX*
AI-SI	4*XXX*
AL-MG	5*XXX*
AL-FE	8*XXX*
AL-FE-NI	8*XXX*
PRECIPITATION-HARDENABLE ALLOYS	
AL-CU	2*XXX*
AL-CU-MG	2*XXX*
AL-CU-LI	2*XXX*
AL-MG-SI	6*XXX*
AL-ZN	7*XXX*
AL-ZN-MG	7*XXX*
AL-ZN-MG-CU	7*XXX*
AL-LI-CU-MG	8*XXX*

TABLE 2 NOMINAL COMPOSITION OF SELECTED COMMON HEAT-TREATABLE ALUMINUM

ALLOYS

ALLOY	COMPOSITION, WT%						
	Si	Cu	Mn	Mg	Cr	Zn	OTHER
WROUGHT ALLOYS							
2014	0.8	4.4	0.8	0.5	. . .		
2024	. . .	4.4	0.6	1.5	. . .	. . .	. . .
2090	. . .	2.7	. . .	0.2	. . .	. . .	2.3 LI, 0.12 ZR
2095	. . .	4.0	. . .	0.4	. . .	. . .	1.0 LI, 0.4 AG
2219	. . .	6.3	0.3	. . .	. . .	. . .	0.06 TI, 0.18 ZR
2519	. . .	5.8	0.3	0.2	. . .	0.06	0.06 TI, 0.17 ZR
6005	0.8	. . .	. . .	0.5	. . .	. . .	. . .
6009	0.8	0.4	0.5	0.6	0.1	0.25	. . .
6010	1.0	0.4	0.5	0.8	0.1	0.25	. . .
6013	0.8	0.9	0.4	1.0	. . .	. . .	. . .
6061	0.6	0.3	. . .	1.0	0.2	. . .	. . .
6063	0.4	. . .	. . .	0.7	. . .	. . .	. . .
6262	0.6	0.3	. . .	1.0	0.1	. . .	0.6 PB, 0.6 BI
7005	. . .	. . .	0.5	1.4	0.1	4.5	0.04 TI, 0.14 ZR
7039	. . .	. . .	0.3	2.8	0.2	4.0	. . .
7050	. . .	2.3	. . .	2.2	. . .	6.2	0.12 ZR
7075	. . .	1.6	. . .	2.5	0.2	5.6	. . .
7178	. . .	2.0	. . .	2.8	0.2	6.8	. . .
8090	. . .	1.0	. . .	1.0	. . .	. . .	2.5 LI, 0.10 ZR
CASTING ALLOYS							
242.0	. . .	4.0	. . .	1.5	. . .	. . .	2.0 NI
319.0	6.0	3.5	. . .	. . .	. . .	. . .	. . .
355.0	5.0	1.2	. . .	0.5	. . .	. . .	. . .
356.0	7.0	. . .	. . .	0.4	. . .	. . .	. . .
357.0	7.0	. . .	. . .	0.6	. . .	. . .	. . .

Source: Ref 3, 4, 5

In commercial product forms, such as aluminum sheet, plate, extrusions, and forgings, these alloys have also undergone varying degrees of mechanical working at ambient and elevated temperatures. It is the combination of alloying additions and thermal-mechanical processing that imparts the desired characteristics to the product. Common considerations in designing alloy compositions and processing practices are strength, toughness, and resistance to corrosion.

The temper designation, which follows the alloy designation, is used to describe the thermal and mechanical processing history of the material. The common temper designations for aluminum alloys utilize an H to denote work-hardening, a T to describe various heat-treatment sequences, or an O to represent annealed material. The most common product forms of the heat-treatable alloys dictate the use of either the T or O tempers, such as 6061-T6 or 6061-O. One or more numbers may follow the T to indicate the specific sequence of thermal treatments. Table 3 summarizes the numerical designations used to describe the specific heat-treating sequences of the T-tempers (Ref 6). Additional information on systems for designating aluminum and aluminum alloys can be found in the article "Alloy and Temper Designation Systems for Aluminum and Aluminum Alloys" in Volume 2 of the *ASM Handbook.*

TABLE 3 NUMERICAL DESIGNATIONS FOR THE HEAT-TREATED TEMPERS OF ALUMINUM ALLOYS

TEMPER	DESCRIPTION
T1	COOLED FROM AN ELEVATED-TEMPERATURE SHAPING PROCESS AND NATURALLY AGED TO A SUBSTANTIALLY STABLE CONDITION

T2	COOLED FROM AN ELEVATED-TEMPERATURE SHAPING PROCESS, COLD WORKED, AND NATURALLY AGED TO A SUBSTANTIALLY STABLE CONDITION
T3	SOLUTION HEAT TREATED, COLD WORKED, AND NATURALLY AGED TO A SUBSTANTIALLY STABLE CONDITION
T4	SOLUTION HEAT TREATED AND NATURALLY AGED TO A SUBSTANTIALLY STABLE CONDITION
T5	COOLED FROM AN ELEVATED-TEMPERATURE SHAPING PROCESS AND THEN ARTIFICIALLY AGED
T6	SOLUTION HEAT TREATED AND THEN ARTIFICIALLY AGED
T7	SOLUTION HEAT TREATED AND OVERAGED/STABILIZED
T8	SOLUTION HEAT TREATED, COLD WORKED, AND THEN ARTIFICIALLY AGED
T9	SOLUTION HEAT TREATED, ARTIFICIALLY AGED, AND THEN COLD WORKED
T10	COOLED FROM AN ELEVATED-TEMPERATURE SHAPING PROCESS, COLD WORKED, AND THEN ARTIFICIALLY AGED

Source: Ref 6

Metallurgy. Wrought alloys that constitute heat-treatable (precipitation-hardenable) aluminum alloys include the 2*xxx*, 6*xxx*, 7*xxx*, and some of the 8*xxx* series alloys. They develop their maximum strength from appropriate solution, quenching, and precipitation treatments. The precipitation mechanism requires alloying elements with appreciable solid solubility in aluminum at elevated temperatures, but with limited solubility at lower temperatures. The solution heat treating operation, which involves heating the alloy to an elevated temperature, allows the alloyed elements to form a solid solution with aluminum. The temperature is then quickly reduced by quenching the material in water to create a supersaturated solid solution. A lower-temperature precipitation process, also referred to as artificial aging, is then used to precipitate strengthening phases throughout the metal in a controlled fashion. The driving force for precipitation is the supersaturation present after quenching.

This procedure is illustrated using the partial phase diagram for the aluminum-copper system in Fig. 1. Superimposed on the phase diagram are the temperature ranges used for solution heat treating and precipitation heat treating for a composition representing an aluminum alloy containing 4.0% Cu. Increasing the temperature of the 4.0% Cu alloy to 525 °C (980 °F) causes the copper to form a solid solution. When quenched to room temperature, the solid solution becomes supersaturated. If allowed to become stable, this condition is referred to as a T4 temper. Aging the alloy at a temperature of 175 °C (350 °F) causes nucleation and growth of strengthening precipitate. After solution heat treating and aging, the alloy condition is described as being in the T6 temper.

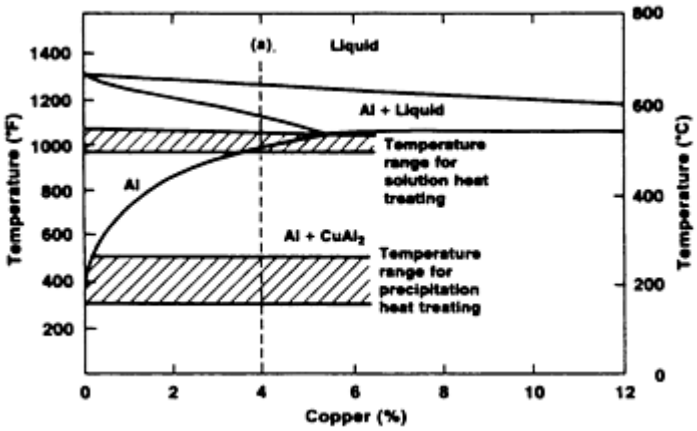

FIG. 1 PARTIAL PHASE DIAGRAM FOR THE ALUMINUM-COPPER SYSTEM SHOWING TEMPERATURE RANGES FOR SOLUTION AND PRECIPITATION HEAT TREATING

Many times these strengthening precipitates are not the equilibrium phases, such as $CuAl_2$ for the case of the 4.0% Cu alloy, but metastable phases. The metastable precipitates that form are determined by the time and temperature of the precipitation heat treating practice. The precipitation sequence for the aluminum-copper system is shown below:

$$\text{SOLID SOLUTION} \rightarrow \text{GP1} \rightarrow \text{GP2} + \theta'' \rightarrow \theta' \rightarrow \theta \quad (CuAl_2) \qquad \textbf{(EQ 1)}$$

In this system, strengthening is due to the formation of localized concentrations of copper atoms forming Guinier-Preston zones (GP1 and GP2) that are structurally coherent with the aluminum matrix. At longer aging times and higher aging temperatures the number of Guinier-Preston zones increase and lead to increased strength; the maximum strength is regarded as the peakaged condition. At still higher temperatures or longer times the Guinier-Preston zones are replaced by the noncoherent, metastable precipitates (θ" and θ'). The decrease in the amount of Guinier-Preston zones formed and the loss of particle coherency result in a subsequent reduction of strength, termed the overaged condition. Figure 2 shows the relationship between strength and precipitate formation during aging of an aluminum 4.0% Cu alloy at 190 °C (375 °F) and 130 °C (265 °F) (Ref 7).

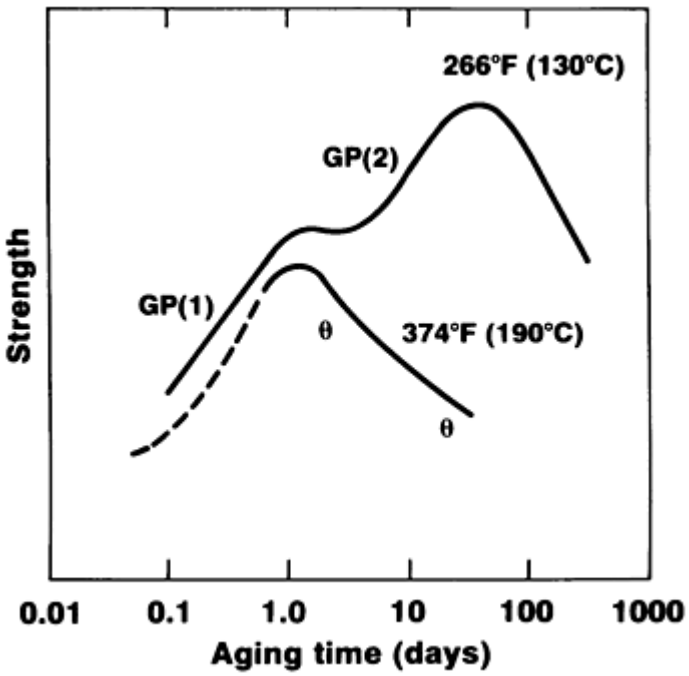

FIG. 2 RELATIONSHIP BETWEEN STRENGTH AND PRECIPITATE FORMATION DURING AGING OF AN AL-4CU ALLOY. SOURCE: REF 7

Characteristics and Applications. Alloying additions and subsequent thermal and mechanical processing dictate characteristics such as strength, toughness, and corrosion resistance of the heat-treatable aluminum alloys. However, it is usually the combination of these properties, that is, strength versus toughness, that is controlled, depending on application requirements. The utility of the heat-treatable aluminum alloys is greatly enhanced by the wide variety of product forms available. This includes sheet, plate, rod, bar, extruded shapes, forgings, and castings.

The 2*xxx* series alloys, having copper as the primary alloying addition, possess high strength but somewhat lower corrosion resistance than most other aluminum alloys. Many of these alloys also possess relatively good elevated-temperature strength. Magnesium is also added to the 2*xxx* series alloys for increased strength but results in greater weld crack sensitivity. Alloy 2024 is one of the highest strength 2*xxx* alloys and is used extensively in the aircraft industry; however, the 1.5% nominal Cu content of 2024 hinders its weldability due to increased weld crack sensitivity. Alloys having controlled levels of magnesium, such as 2014, 2219, and 2519, are utilized for applications requiring good weldability. Generally, these alloys provide good machinability, but less formability, than other heat-treatable aluminum

alloys. Some applications of the 2*xxx* alloys are aircraft skin sheet, automotive panels, ballistic armor, and forged and machined components.

The 6*xxx* series alloys containing magnesium and silicon provide moderate strengths and good corrosion resistance in relation to other heat-treatable aluminum alloys. Because they are easily extruded, they are available in a wide range of structural shapes, as well as sheet and plate products. The versatility of these alloys is represented in 6061, which is one of the most commonly used aluminum alloys. Typically, the 6*xxx* alloys have good formability and good weldability. The 6*xxx* series alloys are used in autobody sheet, structural members, architectural panels, piping, marine applications, screw machine stock, and many other applications.

The 7*xxx* series provides the highest strength of all aluminum alloys, although this claim is being challenged by the recently developed aluminum-lithium alloys. High strength in the 7*xxx* alloys is achieved by alloying additions of zinc, magnesium, and often copper, combined with controlled thermal and mechanical processing. Copper, in combination with zinc and magnesium in the 7*xxx* series alloys, increases strength but hampers weldability due to increased susceptibility to weld cracking. Alloy 7075, containing nominally 5.6% Zn, 2.5% Mg, and 1.6% Cu, is a common alloy of this system having a propensity for weld cracking. Alloys 7004, 7005, and 7039 were designed for applications requiring high strength and good weldability. These alloys have limited amounts of copper that reduce the sensitivity to weld cracking. One important characteristic of the 7*xxx* series is the ability of the heat-affected zone (HAZ) in these alloys to naturally age, or become precipitation-strengthened at room temperature, after welding. Because of this, weld properties continue to improve for up to 30 days after welding. These alloys typically provide good machinability and adequate formability. Applications for the 7*xxx* alloys include aircraft construction, truck trailers, railcars, and armor plate.

References cited in this section

2. *ALUMINUM: PROPERTIES AND PHYSICAL METALLURGY,* J.E. HATCH, ED., AMERICAN SOCIETY FOR METALS, 1984, P 222
3. *ALUMINUM STANDARDS AND DATA,* THE ALUMINUM ASSOCIATION, INC., 1988, P 15
4. *ALUMINUM: PROPERTIES AND PHYSICAL METALLURGY,* J.E. HATCH, ED., AMERICAN SOCIETY FOR METALS, 1984, P 320
5. R.S. JAMES, ALUMINUM-LITHIUM ALLOYS, VOL 2, *ASM HANDBOOK,* ASM INTERNATIONAL, 1990, P 178-199
6. *ALUMINUM STANDARDS AND DATA,* THE ALUMINUM ASSOCIATION, INC., 1988, P 11
7. J.M. SILCOCK, T.J. HEAL, AND H.K. HARDY, STRUCTURAL AGEING CHARACTERISTICS OF BINARY ALUMINUM-COPPER ALLOYS, *J. INST. MET.,* VOL 82, 1953-1954, P 239

Selection and Weldability of Heat-Treatable Aluminum Alloys

Richard P. Martukanitz, Applied Research Laboratory, Pennsylvania State University

Welding of Heat-Treatable Aluminum Alloys

As stated earlier, the heat-treatable aluminum alloys possess characteristics inherent to all aluminum alloys that must be considered before successful welding can be employed. These characteristics include a tenacious oxide, high thermal conductivity, high coefficient of thermal expansion, solidification shrinkage almost twice that of ferrous alloys, relatively wide solidification-temperature ranges, and high solubility of hydrogen when in the molten state. The first two items may be addressed by weld pretreatment and processing conditions--proper weld pretreating to minimize the oxide and welding at high currents and high travel speeds to ensure that adequate penetration is utilized. However, the remaining characteristics, if not carefully considered, may result in the production of welds of unacceptable quality. The high coefficient of thermal expansion and solidification shrinkage, combined with the relatively wide solidification-temperature range, makes these alloys susceptible to weld cracking. The high solubility of hydrogen in molten aluminum can result in gas porosity unless proper precautions are heeded. In addition, the degree of degradation of the HAZ for these alloys may differ markedly, depending upon weld processing conditions. An understanding of these aspects yields welds in the heat-treatable aluminum alloys having excellent joint properties.

Crack Sensitivity during Welding

Weld cracking in aluminum alloys is of concern due to aluminum's relatively high thermal expansion, large change in volume upon solidification, and wide solidification-temperature range. The weld crack sensitivity of heat-treatable aluminum alloys is especially of concern due to the greater amounts of alloying additions used for these alloys. Because of the detrimental effect of weld cracks on joint properties, the weldability of aluminum alloys is defined as its resistance to weld cracking. Weld cracking in aluminum alloys may be classified into two primary categories based on the mechanism responsible for cracking and crack location. Solidification cracking takes place within the weld fusion zone and typically appears along the center of the weld or at termination craters. Liquation cracks occur adjacent to the fusion zone and may or may not be readily apparent.

Solidification cracking, or hot tearing, occurs when high levels of thermal stress and solidification shrinkage are present while the weld pool is undergoing various degrees of solidification. The hot tearing sensitivity of any given aluminum alloy is influenced by a combination of mechanical, thermal, and metallurgical factors (Ref 8). The degree of restraint of welded assemblies plays a significant role in crack sensitivity by increasing the stress on the solidifying weld. Hot tearing occurs within the weld fusion zone and is affected by weld-metal composition and welding parameters. High heat inputs, such as high currents and slow welding speeds, are believed to contribute to weld solidification cracking (Ref 9). It follows that processes that result in minimal heat input, such as electron-beam welding, reduce weld crack sensitivity. The primary method for eliminating cracking in aluminum welds is to control weld-metal composition through filler alloy additions. Crack sensitivity, determined experimentally as a function of weld composition, is shown in Fig. 3 for various binary aluminum systems (Al-Li, Al-Si, Al-Cu, Al-Mg, and the quasibinary Al-Mg_2Si) (Ref 10, 11, 12, 13, 14, 15).

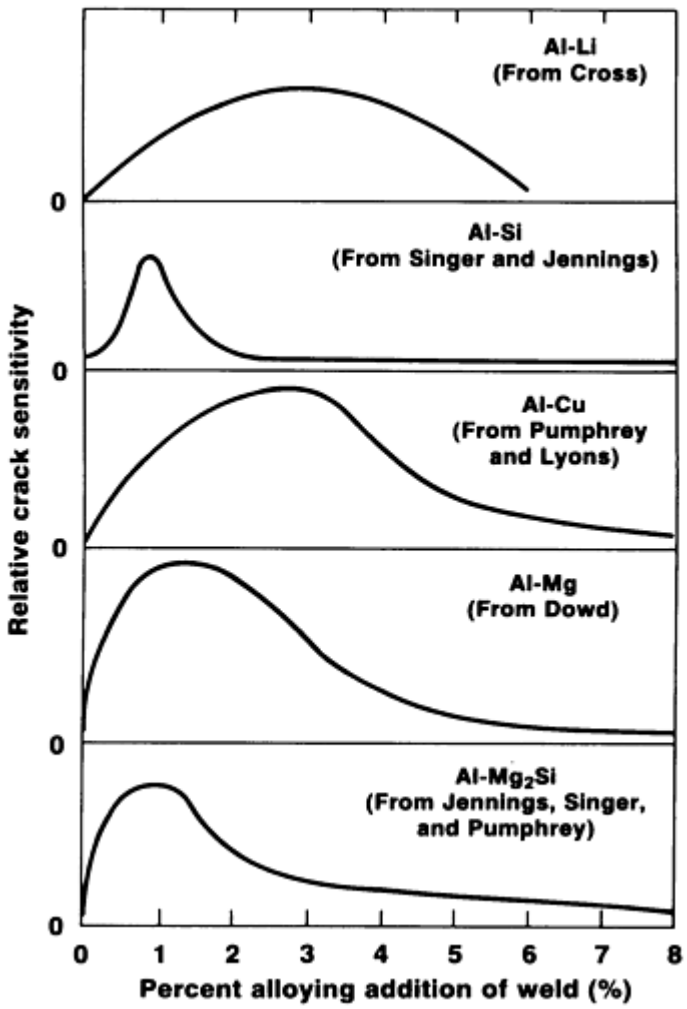

FIG. 3 RELATIVE CRACK SENSITIVITY VERSUS WELD COMPOSITION FOR VARIOUS BINARY ALUMINUM SYSTEMS. SOURCE: REF 10, 11, 12, 13, 14, 15

Although most commercial aluminum alloys are not strictly binary systems, crack-sensitivity curves based on binary systems are still useful in selecting a filler alloy to minimize weld crack sensitivity. In complex alloy systems, minor alloying additions may impact crack sensitivity by widening the temperature range in which a coherent solidifying structure is formed. This effect is shown in Fig. 4, which describes the weld crack sensitivity of two commercial quaternary aluminum systems (Al-Zn-Mg-Cu and Al-Mg-Si-Cu) and a ternary system (Al-Cu-Mg) (Ref 16, 17, 18). In all cases, the curves show the dramatic effect of minor alloying additions, such as copper or magnesium, on weld crack sensitivity. Several high-strength, precipitation-hardenable aluminum alloys rely on complex alloying additions to develop properties; however, these additions dramatically increase weld crack sensitivity. The most notable examples are alloys 2024 (Al-4.4Cu-1.5Mg) and 7075 (Al-5.6Zn-2.5Mg-1.6Cu). Increased weld crack sensitivity may also result when welding dissimilar aluminum alloys to produce weld compositions that widen the coherency temperature range, such as welding 2*xxx* series to 5*xxx* series alloys (Al-Cu alloys to Al-Mg alloys).

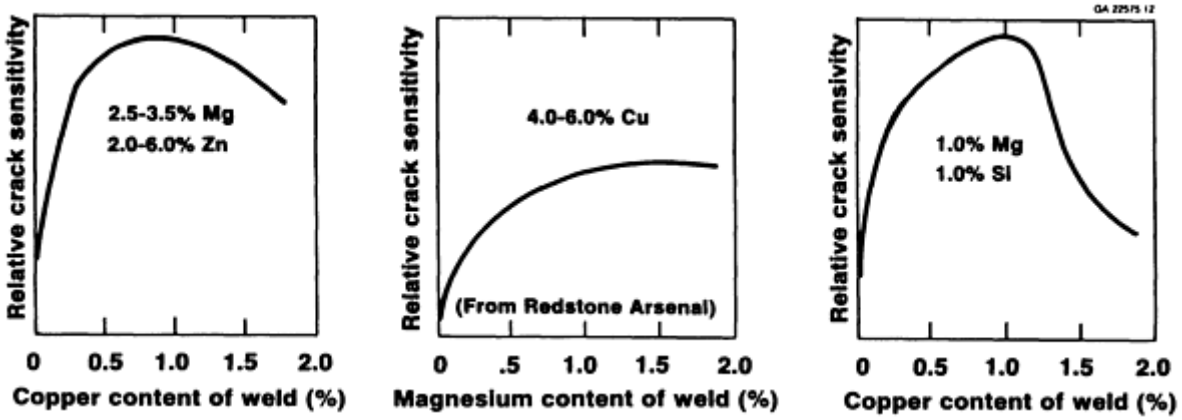

FIG. 4 WELD CRACK SENSITIVITY OF TWO COMMON QUATERNARY ALUMINUM ALLOY SYSTEMS (AL-MG-ZN-CU AND AL-MG-SI-CU) AND A COMMON TERNARY SYSTEM (AL-CU-MG). SOURCE: REF 16, 17, 18

Liquation Cracking. An important element of the HAZ for precipitation-hardenable alloys is the thin boundary layer adjacent to the fusion zone that is referred to as the partially melted region. This region is produced when eutectic phases or constituents that have low melting points (melting points below the melting point of the bulk material) liquate, or melt, at grain boundaries during welding (Ref 19). It occurs in precipitation-hardenable alloys because of the relatively large amount of alloying additions available to form eutectic phases. During welding, these phases liquate and, if sufficient stress is present, may be accompanied by tears. Under extreme conditions, continuous cracks may form along the fusion zone interface. As expected, higher heat input widens the partially melted region and makes it more prone to cracking. An example of cracks formed in this region for alloy 6013-T6 welded with 5356 filler alloy is shown in Fig. 5 (Ref 20). Filler alloy composition greatly affects whether cracks form in this liquated region (Ref 21 and 22). Filler alloys that have low-solidification temperatures provide less susceptibility to liquation cracks, since the solidification shrinkage strains occur at lower temperatures. This allows healing, or solidification, of the partially melted region to occur prior to solidification shrinkage strains.

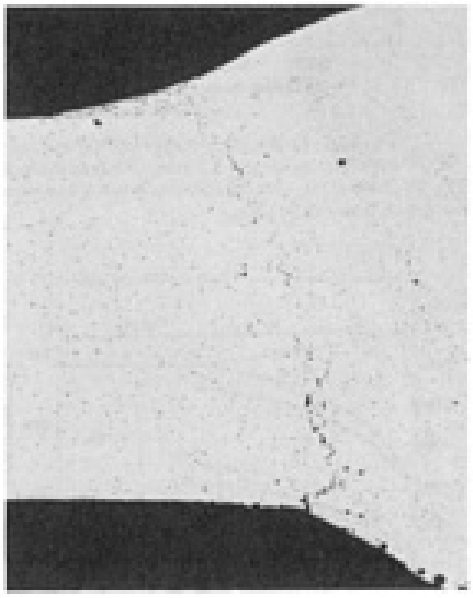

FIG. 5 MICROGRAPH OF A GAS-TUNGSTEN ARC WELD ON 2.0 MM (0.080 IN.) THICK 6013-T6 BASE METAL WITH 5356 FILLER ALLOY SHOWING CRACKS IN THE PARTIALLY MELTED REGION. SOURCE: REF 20

Porosity during Welding

Porosity in aluminum weldments occurs when hydrogen gas is entrapped during solidification (Ref 23 and 24). Hydrogen has an appreciable solubility in molten aluminum and a low solubility in the solid. Figure 6 shows the solubility of hydrogen in pure aluminum at temperatures representing the solid and liquid states (Ref 25).

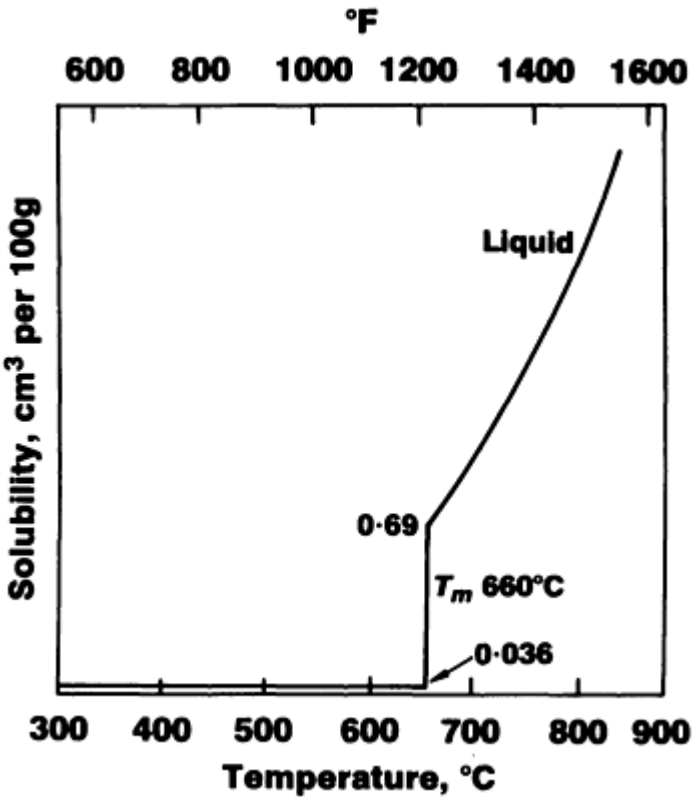

FIG. 6 HYDROGEN SOLUBILITY IN PURE ALUMINUM. SOURCE: REF 25

Hydrogen is absorbed into the molten pool during welding because of its high solubility, and it forms gas pores upon solidification due to the decrease in solubility. It is this difference in solubility that is the driving force for porosity formation (Ref 26). Once a gas bubble forms, it may be expelled from the weld by natural buoyancy or forced convection within the molten pool. Redistribution of hydrogen during solidification may also act to push pores ahead of the solidifying front. Therefore, the welding position and weld parameters may dramatically alter the amount of porosity found in solidified welds.

The expulsion of hydrogen pores may be described by the pore's buoyancy velocity and welding speed. If the solidification front is moving at a lower velocity than the pore's buoyancy velocity, gas pores may escape (Ref 27). Lower welding speeds create slower solidification fronts and favor expulsion of gas pores. Welding position may either help or hinder the expulsion of pores. In general, vertical-up welding of aluminum produces the least porosity because the solidifying pool provides easy escape of gas pores. Converse]y, overhead welding produces the greatest amount of porosity because float direction and pool convection patterns cause pores to be entrapped in the weld root during solidification.

The sources of hydrogen present in the welding system depend on the particular welding process. In arc welding these sources are: (1) hydrogen from the base metal, (2) hydrogen from the filler metal, and (3) hydrogen within the shielding gas (Ref 28). This is illustrated in Fig. 7 for GMAW. Hydrogen from the base metal may be attributed to the surface in the form of hydrocarbons (lubricants) and hydrated oxides, or it may be internal, as with castings and aluminum powder-metallurgy (PM) parts. Filler metal hydrogen is in the form of hydrocarbons (lubricants) or hydrated oxides on the surface of the filler. Hydrogen in the shielding gas is due to moisture contamination within the gas or aspiration of moist air into the gas system due to defective gas lines and couplings. A dew-point determination of the shielding gas may provide an indication of moisture contamination. Normally, a dew-point measurement of -50 °C (-60 °F) or below, measured at the gas cylinder outlet, is considered sufficient gas quality (Ref 29).

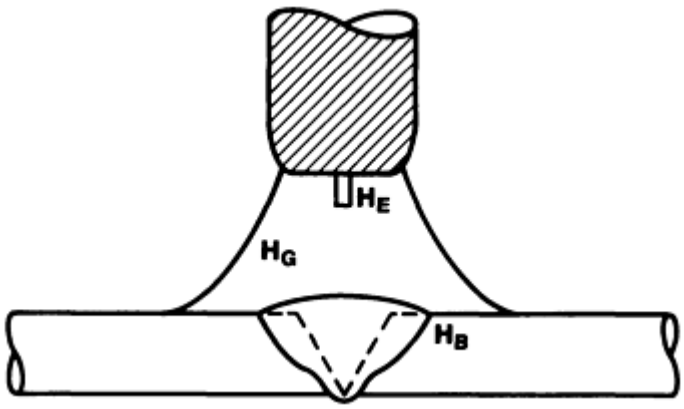

FIG. 7 SOURCES OF HYDROGEN IN GAS-METAL ARC WELDING. H_G, HYDROGEN FROM SHIELDING GAS; H_E, HYDROGEN FROM ELECTRODE; H_B, HYDROGEN FROM BASE METAL. SOURCE: REF 28

In the case of GMAW of aluminum wrought products, the filler electrode, shielding gas, and base-metal surface contaminants may contribute to gas porosity. In the case of welding aluminum castings or PM parts, internal hydrogen of the base metal typically governs pore formation (Ref 30). Because porosity in aluminum welds is attributed to a source of hydrogen contamination within the welding system, preventative measures may be taken to ensure sound welds. This begins with proper precleaning of the parts to be welded. Mill and machining lubricant must be removed by solvent degreasing before welding. Stainless steel wire brushing of the joint to remove thick mill oxides is recommended just prior to welding. During GTAW of aluminum, alternating current with sufficient electrode-positive polarity provides excellent arc cleaning action to remove surface oxides. For GMAW, procurement of quality electrodes and proper electrode storage are necessary to minimize porosity. In all cases, maintenance of gas hoses, regulators, and auxiliary equipment is required to produce porosity-free welds.

HAZ Degradation

A HAZ is created adjacent to the fusion zone and results in a degradation of base-metal properties. This degradation is caused by microstructural modifications associated with elevated temperatures experienced in this zone. For heat-treatable aluminum alloys, the HAZ is distinguished by dissolution or growth of precipitates. The response in the HAZ of 2*xxx* aluminum alloys follows dissolution, whereas the primary modification for the 6*xxx* alloys is growth of precipitates (Ref 31, 32, 33). Although the nature of these HAZs may differ, they are all diffusion-controlled and thermally dependent (Ref 34). A common method of determining the width and extent of the HAZ is by measuring the hardness across this zone. Hardness profiles for gas-tungsten arc welds of two common heat-treatable alloys, 2219-T87 and 6061-T6, are shown in Fig. 8 (Ref 35). A hardness profile for the work-hardenable alloy 5456-H116 is also shown in Fig. 8 for comparison.

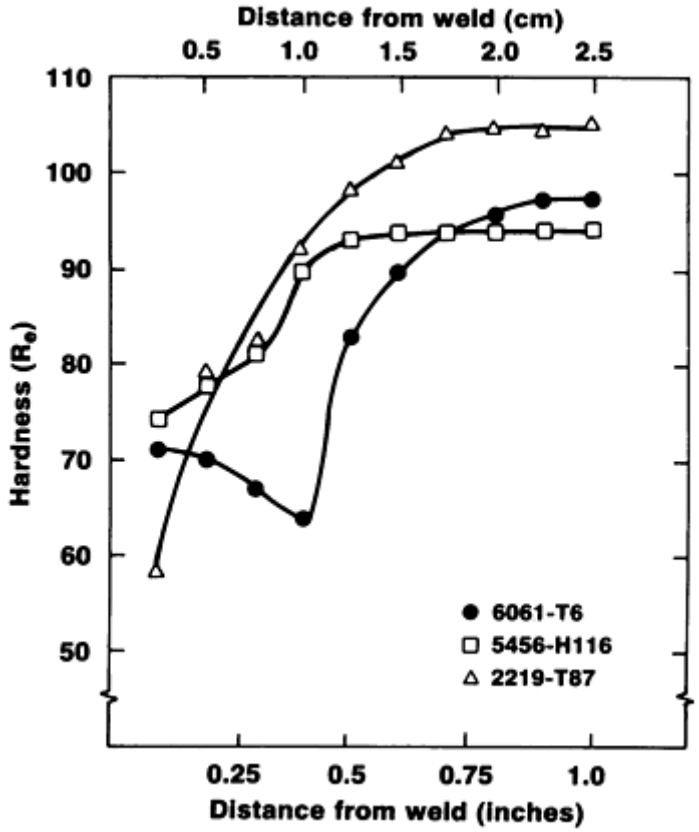

FIG. 8 HARDNESS PROFILES ACROSS THE HAZ OF GAS-TUNGSTEN ARC WELDS ON 3.2 MM (0.125 IN.) THICK 2219-T87, 5456-H116, AND 6061-T6 MADE USING CONSTANT HEAT INPUT. SOURCE: REF 35

The hardness profile for 2219-T87 exhibits dissolution of precipitates. The strengthening particles for these alloys are Guinier-Preston zones, which are metastable precipitates. The solvus curves for these phases are superimposed on the partial aluminum-copper phase diagram in Fig. 9 (Ref 31). When the temperatures in the HAZ exceed the various solvi, the respective phases are dissolved. At positions close to the fusion zone, higher temperatures are experienced and greater dissolution of strengthening phases occurs. This results in a continual decrease in strength in the HAZ of aluminum-copper alloys and is illustrated in Fig. 8 for 2219-T87 alloy.

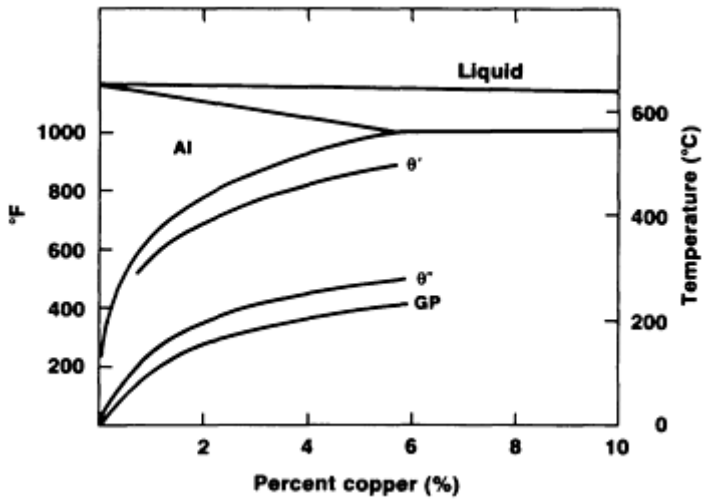

FIG. 9 PARTIAL PHASE DIAGRAM FOR THE ALUMINUM-COPPER SYSTEM SHOWING METASTABLE PHASE SOLVI. SOURCE: REF 31

The hardness profile for the HAZ of 6061-T6 is representative of the 6*xxx* series alloys and is governed by a growthlike transformation of precipitate. This system also exhibits a precipitation sequence of metastable precipitates, with the principal strengthening phases occurring early in the sequence in the form of Guinier-Preston zones. The transformation of these precipitates at elevated temperatures occurs in a smooth, continuous fashion and is closely akin to growth (Ref 31). The result is the formation of nonstrengthening phases. Due to the competing nature of the diffusion rate and supersaturation with increasing temperatures, the transformation proceeds at the greatest rate when temperatures are between 290 and 425 °C (550 and 800 °F) (Ref 36, 37, 38). The minimum hardness value for 6061-T6 in Fig. 8 represents the position in the HAZ that experiences temperatures within this range. This minimum has also been referred to as the overaged zone for these alloys. At higher temperatures, indicative of positions close to the fusion zone, particles are dissolved into solid solution and upon cooling may precipitate as strengthening phases. This contributes to the slight increase in hardness that typically occurs near the fusion zone for the 6*xxx* series alloys.

Effect of Heat Input on the HAZ. Because the metallurgical transformations of the HAZ of aluminum alloys are thermally dependent, the welding process and parameters determine the extent of base-metal degradation. High heat input and preheating increase both the degree and width of the HAZ. This is especially true for the precipitation-hardenable aluminum alloys and is illustrated for 6061-T6 welds made using various heat inputs in Fig. 10 (Ref 39). Thus, the HAZ degradation of the heat-treatable alloys can be reduced by employment of multipass welding, close control of interpass temperature, and elimination of preheating. The highest weld strengths for these alloys are achieved when interpass temperatures do not exceed 65 °C (150 °F) and welding heat input is minimized.

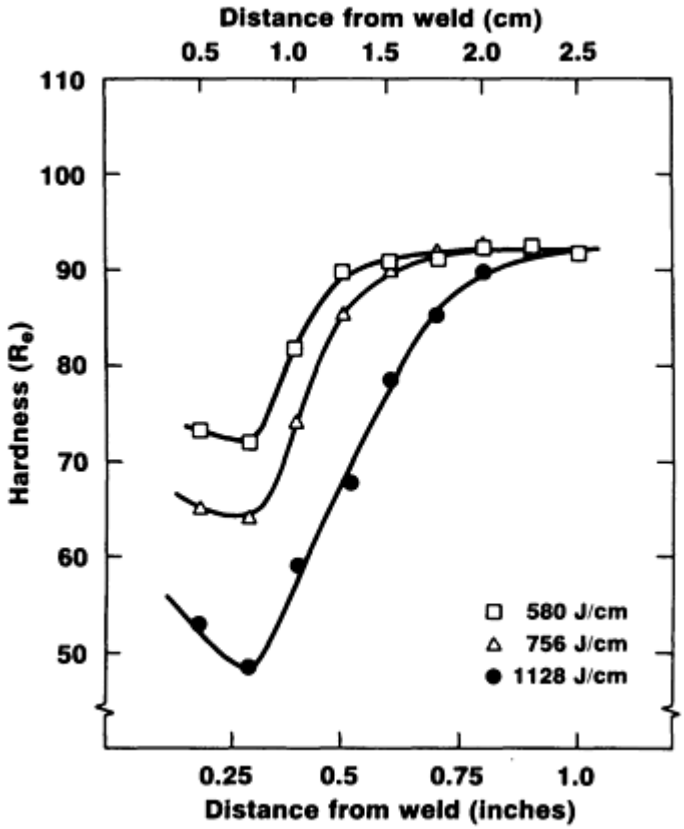

FIG. 10 HARDNESS PROFILES OF THE HAZ OF GAS-TUNGSTEN ARC WELDS ON 6061-T6 USING VARIOUS HEAT INPUTS. SOURCE: REF 39

Postweld Heat Treatment and the HAZ Postweld thermal heat treatments can also be used to improve the strength of the HAZ for heat-treatable alloys. This may involve complete postweld solution heat treating and aging or postweld aging only. Although the recovery of strength in the HAZ after postweld aging is less than postweld solution heat treating and aging, there are advantages to postweld aging only. Temperatures used for postweld aging are much lower than postweld solution heat treating, and postweld aging does not involve water quenching that imposes residual stresses and distortion to welded assemblies. However, great strides have been made in the development and application of polymer quenchants that reduce the amount of distortion observed after quenching and may complement the use of postweld solution heat treating and aging.

Figure 11 depicts hardness profiles of the HAZ for 6061-T4 and 6061-T6 starting material in the as-welded and postweld aged conditions (Ref 40). A dramatic recovery of strength in the HAZ is observed when welding 6061-T4 and postweld aging. Postweld thermal treatments may be used to recover strength in the HAZ of the heat-treatable alloys; however, when 6061-T6 is postweld aged, strength in the HAZ is increased while strength in the unaffected base metal is decreased. This is due to overaging of the 6061-T6 base metal; therefore, T4 or T3 material should be utilized when postweld aging the precipitation-hardenable alloys. The 7*xxx* series alloys possess the ability to naturally age (age at room temperature) in the HAZ. The recovery of strength is similar to postweld artificial aging, but because of the relatively low-temperature aging, the time is substantial. Usually, a period of 14 days is required for improving the HAZ strength of the 7*xxx* series alloys by natural aging.

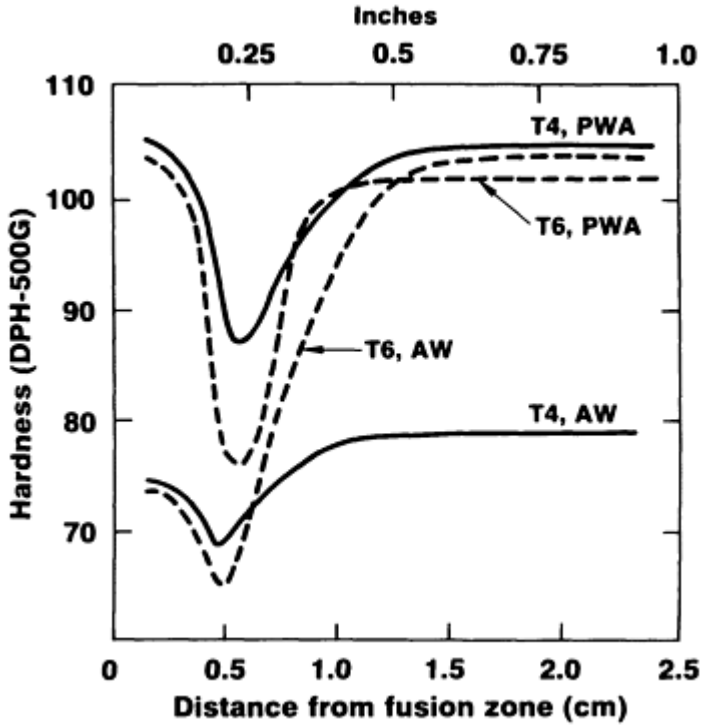

FIG. 11 HARDNESS PROFILES OF THE HAZ FOR 6061-T4 AND T6 STARTING MATERIALS IN THE AS-WELDED (AW) AND POSTWELD AGED (PWA) CONDITIONS. SOURCE: REF 40

References cited in this section

8. C.E. CROSS, W.T. TACK, L.W. LOECHEL, AND L.S. KRAMER, ALUMINUM WELDABILITY AND HOT TEARING THEORY, *WELDABILITY OF MATERIALS,* ASM INTERNATIONAL, 1990, P 275
9. R.A. CHIHOSKI, THE CHARACTER OF STRESS FIELDS AROUND A WELD ARC MOVING ON ALUMINUM SHEET, *WELD J.*, VOL 51 (NO. 1), 1972, P 9-S
10. C.L. CROSS, "WELDABILITY OF ALUMINUM-LITHIUM ALLOYS: AN INVESTIGATION OF HOT TEARING MECHANISMS," PH.D. THESIS, COLORADO SCHOOL OF MINES, GOLDEN, CO, 1986, P 144
11. A.R.E. SINGER AND P.H. JENNINGS, HOT SHORTNESS OF THE ALUMINUM SILICON ALLOYS OF COMMERCIAL PURITY, *J. INST. MET.*, VOL 73, 1947, P 197
12. W.I. PUMPHREY AND J.V. LYONS, CRACKING DURING THE CASTING AND WELDING OF THE MORE COMMON BINARY ALUMINUM ALLOYS, *J. INST. MET.*, VOL 74, 1948, P 439
13. J.D. DOWD, WELD CRACKING OF ALUMINUM ALLOYS, *WELD. J.*, VOL 31 (NO. 10), 1952, P 448-S
14. P.H. JENNINGS, A.R.E. SINGER, AND W.I. PUMPHREY, HOT-SHORTNESS OF SOME HIGH-PURITY ALLOYS IN THE SYSTEMS ALUMINUM-COPPER-SILICON AND ALUMINUM-MAGNESIUM-SILICON, *J. INST. MET.*, 1948, P 227
15. J.H. DUDAS AND F.R. COLLINS, PREVENTING CRACKS IN HIGH-STRENGTH ALUMINUM ALLOYS, *WELD. J.*, VOL 45 (NO. 6), 1966, P 241-S
16. W.I. PUMPHREY AND D.C. MOORE, CRACKING DURING AND AFTER SOLIDIFICATION IN SOME ALUMINUM-COPPER-MAGNESIUM ALLOYS OF HIGH PURITY, *J. INST. MET.*, VOL 74, 1948, P 425
17. J.K. DAWSON, WELD CRACK SENSITIVITY OF ALUMINUM ALLOYS, *MET. PROG.*, VOL 76 (NO. 1), 1959, P 116

18. R.P. MEISTER AND D.C. MARTIN, "WELDING OF ALUMINUM AND ALUMINUM ALLOYS," DEFENSE METALS INFORMATION CENTER, BATTELLE MEMORIAL INSTITUTE, 1967, P 51
19. S. KOU, *WELDING METALLURGY,* JOHN WILEY & SONS, 1987, P 239
20. R.P. MARTUKANITZ, ALCOA LABORATORIES, UNPUBLISHED RESEARCH, 1985
21. N.F. GITTOS AND M.H. SCOTT, HEAT AFFECTED ZONE CRACKING OF AL-MG-SI ALLOYS, *WELD. J.*, VOL 60 (NO. 6), 1981, P 95-S
22. H.W. KERR AND M. KATOH, INVESTIGATION OF HEAT-AFFECTED ZONE CRACKING OF GMA WELDS OF AL-MG-SI ALLOYS USING THE VARESTRAINT TEST, *WELD. J.*, VOL 66 (NO. 9), 1987, P 251-S
23. D.G. HOWDEN AND D.R. MILNER, *BRIT. WELD. J.*, VOL 10, 1963, P 304
24. Z.P. SAPERSTEIN, G.R. PRESCOTT, AND E.W. MONROE, POROSITY IN ALUMINUM WELDS, *WELD. J.*, VOL 43 (NO. 10), 1964, P 443-S
25. C. RANSLEY AND J. NEUFELD, *J. INST. MET.*, VOL 74, 1948, P 617
26. M. UDA AND S. OHNO, *TRANS. NATL. RES. INST. MET.* (JPN), VOL 16, 1974, P 2
27. R.P. MARTUKANITZ, ALCOA LABORATORIES, UNPUBLISHED RESEARCH, 1986
28. R.P. MARTUKANITZ AND P.R. MICHNUK, SOURCES OF POROSITY IN GAS METAL ARC WELDING OF ALUMINUM, *ALUMINIUM,* VOL 58 (NO. 5), 1982, P 276
29. P.B. DICKERSON, ALCOA LABORATORIES, PRIVATE COMMUNICATION, 1987
30. A.N. O'SHANSKII AND V.V. D'YACHENCHO, EVALUATION OF THE SUSCEPTIBILITY OF ALLOYS TO THE FORMATION OF PORES IN WELDING, *WELD. PROD.*, VOL 24 (NO. 7), 1977, P 52
31. S.D. DUMOLT, "METALLURGICAL TRANSACTIONS IN THE HEAT AFFECTED ZONE OF ALUMINUM ALLOYS BY TRANSMISSION ELECTRON MICROSCOPY," PH.D. THESIS, CARNEGIE-MELLON UNIVERSITY, PITTSBURGH, PA, 1983
32. T. ENGO AND T. KURODA, MICROSTRUCTURE IN WELD HEAT-AFFECTED ZONE OF AL-MG-SI ALLOYS, *TRANS. JPN. WELD. RES. INST.,* VOL 11 (NO. 1), 1982, P 61
33. R.P. MARTUKANITZ, "MODELING THE HEAT AFFECTED ZONES OF ALUMINUM ARC WELDS, *ADVANCES IN WELDING SCIENCE AND TECHNOLOGY,* S.A. DAVID, ED., ASM INTERNATIONAL, 1986, P 193
34. S. KOU, WELDING METALLURGY AND WELDABILITY OF HIGH STRENGTH ALUMINUM ALLOYS, *WELD. RES. COUNC. BULL.*, NO. 320, WELDING RESEARCH COUNCIL, 1986
35. R.P. MARTUKANITZ, ALCOA LABORATORIES, UNPUBLISHED RESEARCH, 1985
36. S.D. DUMOLT, PH.D. THESIS, CARNEGIE-MELLON UNIVERSITY, PITTSBURGH, PA, 1983
37. W.L. BURCH, THE EFFECT OF WELDING SPEED ON STRENGTH OF 6061-T4 ALUMINUM JOINTS, *WELD. J.*, VOL 37 (NO. 7), 1958, P 361-S
38. R.P. MARTUKANITZ, "MODELING THE HEAT AFFECTED ZONES OF ALUMINUM ARC WELDS, ADVANCES IN WELDING SCIENCE AND TECHNOLOGY, S.A. DAVID, ED., ASM INTERNATIONAL, 1986, P 195
39. R.J. BRUNGRABER AND F.G. NELSON, EFFECT OF WELDING VARIABLES ON ALUMINUM ALLOY WELDMENTS, *WELD. J.*, VOL 52 (NO. 3), 1973, P 97-S
40. G.E. METZGER, SOME MECHANICAL PROPERTIES OF WELDS IN 6061 ALUMINUM ALLOY SHEET, *WELD. J.*, VOL 56 (NO. 10), 1967, P 457-S

Selection and Weldability of Heat-Treatable Aluminum Alloys

Richard P. Martukanitz, Applied Research Laboratory, Pennsylvania State University

---

Filler Alloy Selection and Properties of Welds

Although the selected base alloy and welding process greatly influence the characteristics of aluminum joints, the filler alloy plays a significant role in establishing a number of important weld properties for hem-treatable aluminum alloys. Of foremost concern is the weldability of a particular base alloy and filler alloy combination, which is defined as its susceptibility to weld cracking. Shear strength of a fillet weld, response to postweld heat treatments, and color match after anodizing are other attributes that are highly governed by the filler alloy used to produce the weld in heat-treatable aluminum alloys. Properties such as joint strength, ductility, toughness, and corrosion resistance across the weld are also dictated by the base alloy and filler alloy combination selected. The filler alloy selection chart in the article "Welding of Aluminum Alloys" in this Volume (see Table 14 in that article) provides a comprehensive guide for selecting the proper filler metal. Recently a knowledge-based system using computer software has also been constructed to allow greater interaction in selecting aluminum base metal and filler metal alloys for welding (Ref 41).

Filler Alloy Selection and Weld Crack Sensitivity

Weld crack sensitivity is most easily controlled by influencing the composition of the weld. This is achieved by selecting the proper filler alloy and ensuring adequate dilution of the filler alloy to the weld. Generally, joint designs that increase filler metal dilution (for example, square groove with gap as opposed to no gap) are beneficial in reducing the tendency for cracking. The principal filler alloys for welding aluminum are the 1*xxx* (1100), 2*xxx* (2319), 4*xxx* (4043, 4047, 4145, and 4643), and 5*xxx* (5154, 5183, 5356, 5554, 5556, and 5654) series. Nominal compositions of aluminum filler alloys are shown in Table 4 (Ref 42). Most of these alloys are high in solute to reduce crack sensitivity. Because of their narrow solidification temperature range, the 4*xxx* series filler alloys provide excellent insensitivity to weld cracking but are not applicable for welding all aluminum-base alloys. Because of the formation of large amounts of brittle magnesium-silicide (Mg_2Si), the 4*xxx* series filler alloys are not applicable for welding the 7*xxx* series alloys containing appreciable amounts of magnesium. Table 5 shows the filler alloys recommended for welding various base alloys to minimize sensitivity to weld cracking.

TABLE 4 NOMINAL COMPOSITION OF ALUMINUM FILLER METAL ALLOYS

ALLOY	COMPOSITION, WT%						
	Si	Cu	Mn	Mg	Cr	Ti	OTHER
1100	. . .	0.12	. . .	. . .	. . .	. . .	99.00 AL MIN
1188	. . .	. . .	. . .	. . .	. . .	. . .	99.88 AL MIN
2319	. . .	6.3	0.30	. . .	. . .	0.15	0.17 ZR, 0.10 V
4043	5.2	. . .	. . .	. . .	. . .	. . .	. . .
4047	12.0	. . .	. . .	. . .	. . .	. . .	. . .
4145	10.0	4.0	. . .	. . .	. . .	. . .	. . .
4643	4.1	. . .	. . .	0.2	. . .	. . .	. . .
5183	. . .	. . .	0.75	4.7	0.15	. . .	. . .
5356	. . .	. . .	0.12	5.0	0.12	0.13	. . .
5554	. . .	. . .	0.75	2.7	0.12	0.12	. . .
5556	. . .	. . .	0.75	5.1	0.12	0.12	. . .
5654	. . .	. . .	. . .	3.5	0.25	0.10	. . .
C355.0	5.0	1.25	. . .	0.5	. . .	. . .	. . .
A356.0	7.0	. . .	. . .	0.4	. . .	. . .	. . .
357.0	7.0	. . .	. . .	0.5	. . .	. . .	. . .
A357.0	7.0	. . .	. . .	0.6	. . .	0.12	. . .

Source: Ref 42

TABLE 5 FILLER ALLOYS RECOMMENDED FOR WELDING SELECTED ALUMINUM-BASE ALLOYS TO MINIMIZE SENSITIVITY TO WELD CRACKING

BASE METAL	319.0, 333.0, 354.0, 355.0, C355.0, 380.0	356.0, A356.0, A357.0, 359.0, 413.0, A444,0, 443.0	511.0, 512.0, 513.0, 514.0	7005[A], 7039, 710.0, 711.0, 712.0	6070	6061, 6463, 6101, 6201, 6151, 6351, 6951	5456	5454	5154, 5254[B]	5086	5083	5052, 5652[B]	5005 5050	3004 ALCLAD 3004	2219, 2519	2014, 2036	1100, 1060, 3004, ALCLAD 3003	1060 1070, 1080, 1350
1060, 1070, 1080, 1350	4145[C][D]	4043[D][C]	4043[D] [F]	4043[D]	4043[D]	4043[D]	5356[C]	4043[D]	4043[D] [F]	5356[C]	5356[C]	4043[D]	1100[C]	4043	4145	4145	1100[C]	1188[G]
1100, 3003, ALCLAD 3003	4145[C][D]	4043[D][E]	4043[D] [F]	4043[D]	4043[D]	4043[D]	5356[C]	4043[D] [F]	4043[D] [F]	5356[C]	5356[C]	4043[D][F]	4043[F]	4043[F]	4145	4145	1100[C]	. . .
2014, 2036	4145[H]	4145	. . .	. . .	4145	4145	. . .	. . .	. . .	. . .	. . .	. . .	. . .	. . .	4145[H]	4145[H]	. . .	. . .
2219, 2519	4145[C][D] [H]	4145[C][D]	4043[D]	4043[D]	4043[D] [E]	4043[D] [E]	4043	4043[D]	4043[D]	4043	4043	4043[D]	4043	4043	2319[C][D] [E]	. . .	. . .	. . .
3004, ALCLAD 3004	4043[D]	4043[D]	5654[I]	5356[F]	4043[F]	4043[I]	5356[F]	5654[I]	5654[I]	5356[F]	5356[F]	4043[D][F]	4043[F]	4043[F]	. . .	. . .	. . .	. . .
5005, 5050	4043[D]	4043[D]	5654[I]	5356[F]	4043[F]	4043[I]	5356[F]	5654[I]	5654[I]	5356[F]	5356[F]	4043[D][F]	4043[F] [J]	. . .	. . .	. . .	. . .	. . .
5052, 5652[B]	4043[D]	4043[D][I]	5654[I]	5356[F]	5356[C][I]	5356[C][I]	5356[I]	5654[I]	5654[I]	5356[F]	5356[F]	5654[B][C][I]	. . .	. . .	. . .	. . .	. . .	. . .
5083		5356[C][D] [F]	5356[F]	5183[F]	5356[F]	5356[F]	5183[F]	5356[F]	5356[F]	5356[F]	5183[F]	. . .	. . .	. . .	. . .	. . .	. . .	. . .
5086		5356[C][D] [F]	5356[F]	5356[F]	5356[F]	5356[F]	5356[F]	5356[I]	5356[I]	5356[F]	. . .	. . .	. . .	. . .	. . .	. . .	. . .	. . .
5154, 5254[B]		043[D][I]	5654[I]	5356[I]	5356[C][I]	5356[C][I]	5356[I]	5654[I]	5354[B] [I]	. . .	. . .	. . .	. . .	. . .	. . .	. . .	. . .	. . .
5454	4043[D]	4043[D][I]	5654[I]	5356[I]	5356[C][I]	5356[C][I]	5356[I]	5554[C] [F]	. . .	. . .	. . .	. . .	. . .	. . .	. . .	. . .	. . .	. . .
5456		4043[D][I]	5356[F]	5556[F]	5356[F]	5356[F]	5556[F]	. . .	. . .	. . .	. . .	. . .	. . .	. . .	. . .	. . .	. . .	. . .
6061,6063, 6351, 6101, 6201, 6151, 6951	4145[C][D]	5356[C][D] [F]	5356[C] [I]	5356[C][D] [I]	4043[D] [I]	4043[D] [I]	. . .	. . .	. . .	. . .	. . .	. . .	. . .	. . .	. . .	. . .	. . .	. . .
6070	4145[C][D]	4043[D][F]	5356[C]	5356[C][D]	4043[D]	. . .	. . .	. . .	. . .	. . .	. . .	. . .	. . .	. . .	. . .	. . .	. . .	. . .

			(F)	(F)	(F)													
7005[A], 7039, 710.0, 711.0, 712.0	4043[D]	4043[D][I]	5356[I]	5356[F]	. . .	. . .	. . .	. . .	. . .	. . .	. . .	. . .	. . .	. . .	. . .	. . .	. . .	. . .
511.0, 512.0, 513.0, 514.0		4043[D][I]	5654[I][J]	. . .	. . .	. . .	. . .	. . .	. . .	. . .	. . .	. . .	. . .	. . .	. . .	. . .	. . .	. . .
356.0, A356.0, A357.0, 359.0, 413.0, A444.0, 443.0	4145[C][D]	4043[D][J]	. . .	. . .	. . .	. . .	. . .	. . .	. . .	. . .	. . .	. . .	. . .	. . .	. . .	. . .	. . .	. . .
319.0, 333.0, 354.0, 355.0, C355.0 380.0	4145[C][D][J]	. . .	. . .	. . .	. . .	. . .	. . .	. . .	. . .	. . .	. . .	. . .	. . .	. . .	. . .	. . .	. . .	. . .

Notes: (1) Service conditions such as immersion in fresh or salt water, exposure to specific chemicals, or a sustained high temperature (higher than 65 °C, or 150 °F) may limit choice of filler metals Filler alloys 5356, 5183, 5556, and 5654 are not recommended for sustained elevated-temperature service. (2) Recommendations in this table apply to gas-shielded arc welding processes. For gas welding, only 1100, 1188, and 4043 filler metals are ordinarily used. (3) All filler metals are listed in AWS specification A5.10. (4) Where no filler metal is listed, the base metal combination is not recommended for welding.

Source: Ref 43

(A) REFERS TO 7005 EXTRUSIONS ONLY (X-PREFIX STILL APPLIES TO SHEET AND PLATE).

(B) BASE METAL ALLOYS 5652 AND 5654 ARE USED FOR HYDROGEN PEROXIDE SERVICE. 5654 FILLER METAL IS USED FOR WELDING BETH ALLOYS FOR LOW-TEMPERATURE SERVICE (65 °C, OR 150 °F, OR BELOW).

(C) 4043 MAY BE USED FOR SOME APPLICATIONS.

(D) 4047 MAY BE USED FOR SOME APPLICATIONS.

(E) 4145 MAY BE USED FOR SOME APPLICATIONS.

(F) 5183, 5356, OR 5556 MAY BE USED.

(G) 1100 MAY BE USED FOR SOME APPLICATIONS.

(H) 2319 MAY BE USED FOR SOME APPLICATIONS.

(I) 5183, 5356, 5554, 5556. OR 5654 MAY BE USED. IN SOME CASES THEY PROVIDE IMPROVED COLOR MATCH AFTER ANODIZING TREATMENT, HIGHEST WELD QUALITY, AND HIGHER WELD STRENGTH 5554 IS SUITABLE FOR ELEVATED TEMPERATURE SERVICE.

(J) FILLER METAL WITH THE SAME ANALYSIS AS THE BASE METAL IS SOMETIMES USED.

Weld Strength and Ductility

The strength and ductility of welds in aluminum alloys are determined by a number of parameters. These may include base alloy and temper, filler alloy, welding process and parameters, use of postweld heat treatments, joint type, principal loading condition, and the presence of weld defects. As described earlier, metallurgical transformations in the HAZ of heat-treatable aluminum alloys result in a degradation of strength in this region. The degree of degradation may be related to heat input used to produce the weld. Processes that provide higher travel speeds minimize the degradation in the HAZ and typically result in higher weld strength. Postweld heat treatments may be used to recover the loss of strength in the HAZ. Postweld solution heat treating and aging provides the greatest improvement in joint strength; however, this practice requires the use of a cold-water quench that may impart unacceptable part distortion. Postweld aging, which is a lower-temperature treatment, results in a moderate improvement in joint strength and does not require water quenching. It is also appropriate to comment on the effects of loading that distinguish the properties of welded joints. The transverse tensile strength of a butt weld provides a relative indication of joint strength in service, although butt welds may also undergo multiaxial loading that hinders direct comparison to tabular data representing uniaxial behavior. In the case of fillet welds, the transverse or longitudinal shear strength (depending on the principal loading condition) obtained from shear test specimens may be used to ascertain joint performance. The strength and ductility of groove welds in the as-welded condition, the postweld aged only condition, and the solution heat treated and aged (artificially and naturally aged) condition are described in the article "Welding of Aluminum Alloys" in this Volume. Transverse and longitudinal shear strengths of fillet welds are also listed in the aforementioned article. Additional information on properties of aluminum weldments can be found in Ref 44 and 45.

Figure 12 displays strength profiles across gas-tungsten arc welds of 2219-T87 and 6061-T6 alloys. The 2219-T87 alloy was welded with 2319 filler alloy and the 6061-T6 was welded with 4043 alloy. The strength profile of the work-hardenable alloy 5456-H116 welded with filler alloy 5356 is also shown in the figure for comparison. The strength values in Fig. 12 are approximations obtained by converting hardness measurements using the empirically derived relationship for aluminum alloys (Ref 46):

$$UTS = 10,66 - 19,42 \ln\left(1 - \frac{HRE}{109}\right) \qquad \textbf{(EQ 2)}$$

where UTS is the ultimate tensile strength in ksi, and HRE is the Rockwell hardness using the E-scale.

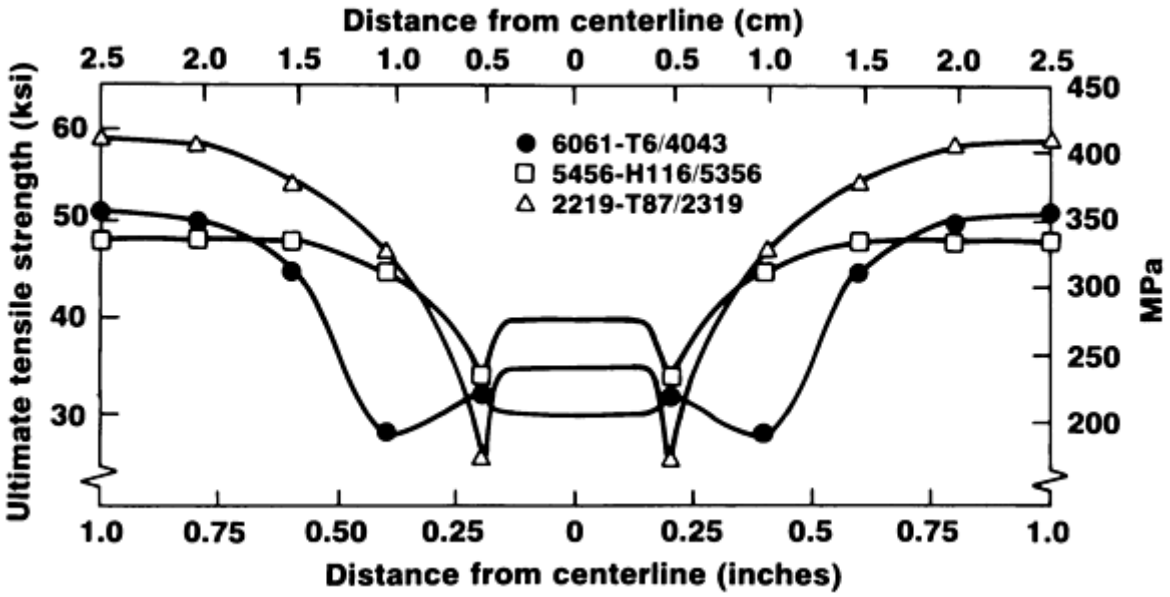

FIG. 12 STRENGTH PROFILES ACROSS ALTERNATING CURRENT GAS-TUNGSTEN ARC WELDS ON 3.2 MM (0.125 IN.) THICK 2219-T87 USING 2319 FILLER ALLOY, 6061-T6 USING 4043 FILLER ALLOY, AND 5456-H116 USING 5356 FILLER ALLOY. SOURCE: REF 35

It is evident from Fig. 12 that the degradation of strength associated with the HAZ usually dictates the strength of the joint for aluminum alloys. This is not true when weldments have been postweld heat treated, because the fusion zone may not respond to these treatments to the same degree as the HAZ.

The 2*xxx* series alloys exhibit the lowest ductility of the precipitation-hardenable alloys. This is due to the formation of brittle, copper-bearing eutectic phases at grain boundaries near the fusion zone interface. The 6*xxx* and 7*xxx* series alloys display good weld ductility. Postweld solution heat treating and aging of the heat-treat-able alloys or postweld aging only, usually decreases weld ductility.

Corrosion Resistance of Welds

Many of the heat-treatable aluminum alloys can be welded without reducing the resistance of the assembly to corrosion. However, because welding generates residual tensile stresses and modifies the parent metal structure, some alloys may have their resistance to corrosion lowered by welding. Corrosion of aluminum weldments is usually localized or preferential in nature and depends on the base alloy, filler alloy, and HAZ structure. The corrosion potential variations determined by electrode potential measurements across 2219 and 7039 weldments are shown in Fig. 13. The corrosion potential variations across the weld of the work-hardenable alloy 5456 are also shown in Fig. 13. The corrosion potentials of various base and filler alloys are also described in the article "Welding of Aluminum Alloys" in this Volume.

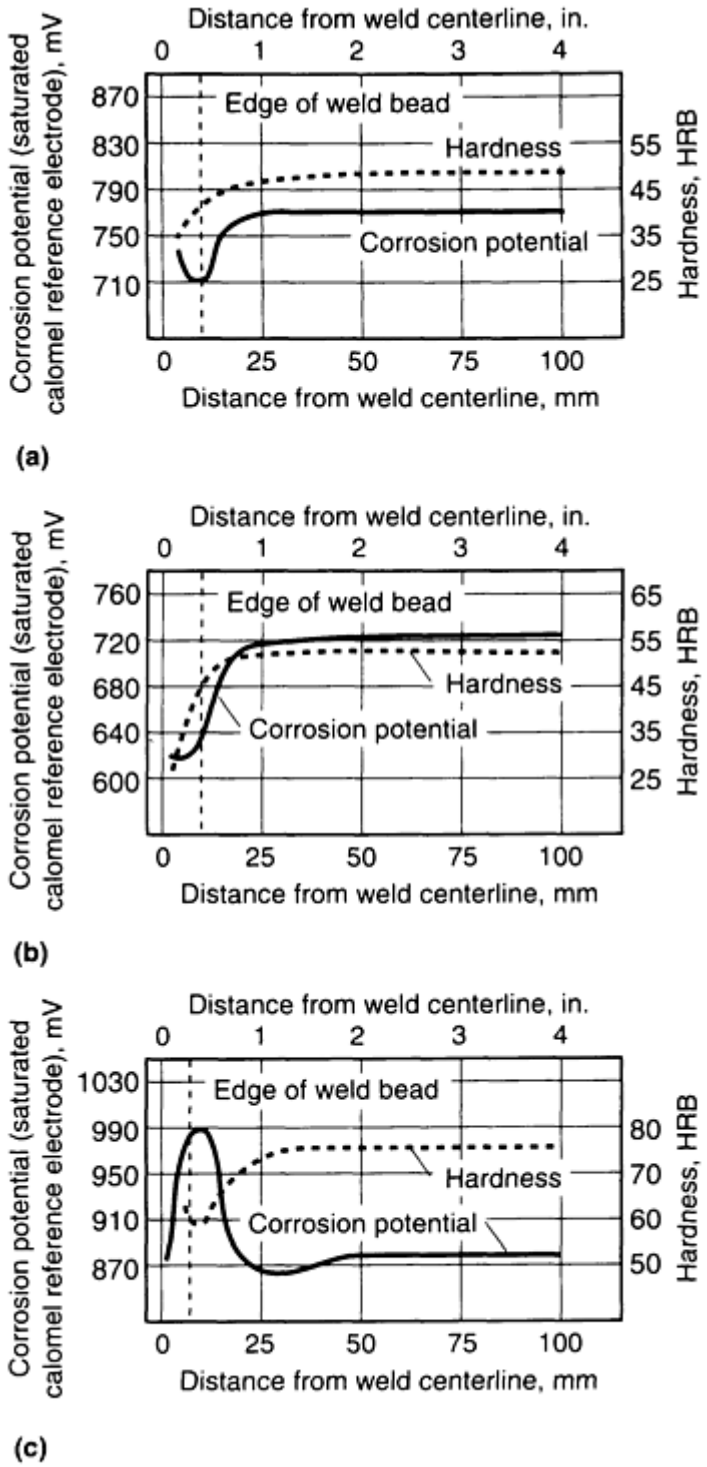

FIG. 13 PLOT OF CORROSION POTENTIAL AND HARDNESS LEVELS VERSUS DISTANCE FROM WELD CENTERLINE FOR SELECTED ALUMINUM ALLOYS. (A) ALLOY 5456-H321 (5556 FILLER METAL; DCRP-MIG WELD PRODUCED IN THREE PASSES). (B) 2219-T87 (2319 FILLER METAL; DCSP-TIG WELD PRODUCED IN TWO PASSES). (C) 7039-T651 (5183 FILLER METAL; DCRP-TIG WELD PRODUCED IN TWO PASSES). DCRP, DIRECT CURRENT REVERSE POLARITY; DCSP, DIRECT CURRENT STRAIGHT POLARITY. COURTESY OF ALCOA LABORATORIES

The 6*xxx* series alloys are highly resistant to localized corrosion after welding. The weldable alloy 2219 of the 2*xxx* series also exhibits good corrosion resistance after welding. The corrosion potential for 2219-T87 weldments produced using 2319 filler metal is shown in Fig. 13 and depicts a lower corrosion potential in the weld area as compared to the unaffected base metal. The weldable 7*xxx* series alloys produce greater sensitivity to corrosion after welding (Ref 47). In this case, the structural transformation of the HAZ due to the heat of welding makes the HAZ anodic to either the 5*xxx*

weld metal or the unaffected base metal. This mechanism is also shown in Fig. 13 for 7089-T651 welded with 5183 filler metal. The highly anodic, small area of the HAZ will pit and corrode in the presence of an electrolyte to protect both the weld metal and the much larger unaffected base metal. Postweld solution heat treating and aging of the 7*xxx* series alloys will improve their corrosion resistance; however, aluminum-magnesium filler alloys containing more than 3.5% Mg should not be used when postweld heat treating because the fusion zone can be sensitized to stress-corrosion cracking (Ref 48).

Wrought alloys usually have greater resistance to stress-corrosion cracking in the longitudinal orientation (direction of working) than in the transverse orientation or in the short-transverse orientation (through the thickness). Because of this, welding of the 7*xxx* series alloys near a base-metal edge may result in a tensile stress in the short-transverse direction sufficient to cause stress-corrosion cracking in the exposed edge. "Buttering" the edge with weld metal provides compressive stress at the edge and overcomes the stress-corrosion cracking problem. Finally, paint protection or metallizing with selected aluminum alloys can be used to reduce the general corrosion sensitivity of heat-treated aluminum weldments.

Other Joint Characteristics

Other joint characteristics may be of importance, depending upon the service requirements of the welded assembly. These may include characteristics that can affect the structural performance of the assembly, such as strength and toughness at the service temperature, as well as aesthetic qualities, such as joint color match after anodizing. Aluminum alloys are compatible with all known cryogenics; base-metal strength and weld strength generally increase at cryogenic temperatures (Ref 49 and 50). The 2*xxx* series heat-treatable alloys, as well as the work-hardenable 5*xxx* series alloys, display a good combination of strength and ductility at low temperatures. Alloy 2219 is used extensively for cryogenic applications requiring high strength and good weldability. Toughness of welds in aluminum alloys is defined as the ability of the joint to absorb energy by deformation rather than fracture catastrophically. Fracture toughness in aluminum alloy welds is typically not determined by Charpy impact tests but may be reasonably obtained by tear or tension tests involving notched specimens (Ref 51, 52, 53). Based on results of these tests, welds of 2219 and 7039 possess good notch toughness, although it must also be mentioned that welds representing the work-hardenable alloys of the 5*xxx* series also exhibit good toughness.

Although the weld and base-metal strengths of the heat-treatable aluminum alloys, particularly the 2*xxx* series, fare well at elevated temperatures up to 150 °C (300 °F), caution must be observed when selecting filler alloys for welded assemblies functioning at these temperatures. Elevated-temperature service for aluminum welds is usually defined as service at sustained temperatures above 65 °C (150 °F). Sustained elevated-temperature service of welds containing high amounts of magnesium may result in increased sensitivity to stress-corrosion cracking due to the formation of Mg_2Al_3 at grain boundaries. Therefore, most welded applications involving sustained elevated-temperature service dictate the use of filler alloys that do not contain magnesium. An exception is the use of filler alloy 5554 (containing approximately 2.7% Mg) when welds of 6*xxx* series alloys at sustained elevated temperatures also require good color match after anodizing. Typically, 2319 filler alloy is used in welds on 2*xxx* series base alloys that require good color match after anodizing. When good color match after anodizing is desired for welds in the 6*xxx* or 7*xxx* series base alloys, filler alloys of the 5*xxx* series containing magnesium are utilized. High levels of silicon in the weld when using the 4*xxx* series filler alloys result in darkening of the fusion zone in comparison to the base metal after anodizing.

References cited in this section

35. R.P. MARTUKANITZ, ALCOA LABORATORIES, UNPUBLISHED RESEARCH, 1985
41. R.J. NAPOLITANO, H. KULLUK, M.L. NAGURKA, R.P. MARTUKANITZ, AND P.B. DICKERSON, DEVELOPMENT OF KNOWLEDGE-BASED SYSTEMS FOR ALUMINUM WELDING, *WELD. J.*, VOL 71 (NO. 12), 1992, P 43
42. P.B. DICKERSON AND B. IRVING, WELDING ALUMINUM: IT'S NOT AS DIFFICULT AS IT SOUNDS, *WELD. J.*, VOL 71 (NO. 4), 1992, P 47
43. *WELDING ALUMINUM: THEORY AND PRACTICE*, H.L. SAUNDERS, ED., THE ALUMINUM ASSOCIATION, 1991, P 3.8
44. *WELDING ALUMINUM*, AMERICAN WELDING SOCIETY, 1972, P 69.94-69.106
45. F.G. NELSON AND R.L. ROLF, SHEAR STRENGTH OF AL ALLOY FILLET WELDS, *WELD. J.*,

VOL 45 (NO. 2), 1966, P 82-S

46. B.S. SHABEL AND R.F. YOUNG, *PROC. CONF. NONDESTRUCTIVE CHARACTERIZATION OF MATERIALS II,* J.F. BUSSIERE, J.P. MONCHALIN, C.O. RUUD, AND R.E. GREEN, JR., ED., PLENUM, 1987, P 335
47. R.P. MEISTER AND D.C. MARTIN, "WELDING OF ALUMINUM AND ALUMINUM ALLOYS," DMIC REPORT 236, DEFENSE METALS INFORMATION CENTER, 1967, P 65
48. "ALCOA ALUMINUM ALLOY 7005 GREEN LETTER," ALUMINUM COMPANY OF AMERICA, 1974
49. R.P. MEISTER AND D.C. MARTIN, "WELDING OF ALUMINUM AND ALUMINUM ALLOYS," DMIC REPORT 236, DEFENSE METALS INFORMATION CENTER, 1967, P 55
50. J.F. CAMPBELL, ALUMINUM ALLOYS FOR CRYOGENIC SERVICE, *MATER. RES. STAND.,* VOL 4 (NO. 10), 1964, P 540
51. F.G. NELSON AND J.G. KAUFMAN, FRACTURE CHARACTERISTICS OF WELDS IN ALUMINUM ALLOYS, *WELD. J.,* VOL 45 (NO. 7), 1966, P 321-S
52. ALUMINUM FOR CRYOGENIC ENVIRONMENT, PART I: GENERAL CONSIDERATIONS, *CRYOG. ENG. NEWS,* BUSINESS COMMUNICATIONS PUBLISHERS, MARCH 1966
53. ALUMINUM FOR CRYOGENIC ENVIRONMENT, PART II: ALLOY GROUPS, *CRYOG. ENG. NEWS,* BUSINESS COMMUNICATIONS PUBLISHERS, APRIL 1966

Selection and Weldability of Heat-Treatable Aluminum Alloys

Richard P. Martukanitz, Applied Research Laboratory, Pennsylvania State University

---

References

1. P.B. DICKERSON AND B. IRVING, WELDING ALUMINUM: IT'S NOT AS DIFFICULT AS IT SOUNDS, *WELD. J.,* VOL 71 (NO. 4), 1992, P 45
2. *ALUMINUM: PROPERTIES AND PHYSICAL METALLURGY,* J.E. HATCH, ED., AMERICAN SOCIETY FOR METALS, 1984, P 222
3. *ALUMINUM STANDARDS AND DATA,* THE ALUMINUM ASSOCIATION, INC., 1988, P 15
4. *ALUMINUM: PROPERTIES AND PHYSICAL METALLURGY,* J.E. HATCH, ED., AMERICAN SOCIETY FOR METALS, 1984, P 320
5. R.S. JAMES, ALUMINUM-LITHIUM ALLOYS, VOL 2, *ASM HANDBOOK,* ASM INTERNATIONAL, 1990, P 178-199
6. *ALUMINUM STANDARDS AND DATA,* THE ALUMINUM ASSOCIATION, INC., 1988, P 11
7. J.M. SILCOCK, T.J. HEAL, AND H.K. HARDY, STRUCTURAL AGEING CHARACTERISTICS OF BINARY ALUMINUM-COPPER ALLOYS, *J. INST. MET.,* VOL 82, 1953-1954, P 239
8. C.E. CROSS, W.T. TACK, L.W. LOECHEL, AND L.S. KRAMER, ALUMINUM WELDABILITY AND HOT TEARING THEORY, *WELDABILITY OF MATERIALS,* ASM INTERNATIONAL, 1990, P 275
9. R.A. CHIHOSKI, THE CHARACTER OF STRESS FIELDS AROUND A WELD ARC MOVING ON ALUMINUM SHEET, *WELD J.,* VOL 51 (NO. 1), 1972, P 9-S
10. C.L. CROSS, "WELDABILITY OF ALUMINUM-LITHIUM ALLOYS: AN INVESTIGATION OF HOT TEARING MECHANISMS," PH.D. THESIS, COLORADO SCHOOL OF MINES, GOLDEN, CO, 1986, P 144
11. A.R.E. SINGER AND P.H. JENNINGS, HOT SHORTNESS OF THE ALUMINUM SILICON ALLOYS OF COMMERCIAL PURITY, *J. INST. MET.,* VOL 73, 1947, P 197
12. W.I. PUMPHREY AND J.V. LYONS, CRACKING DURING THE CASTING AND WELDING OF THE MORE COMMON BINARY ALUMINUM ALLOYS, *J. INST. MET.,* VOL 74, 1948, P 439

13. J.D. DOWD, WELD CRACKING OF ALUMINUM ALLOYS, *WELD. J.,* VOL 31 (NO. 10), 1952, P 448-S
14. P.H. JENNINGS, A.R.E. SINGER, AND W.I. PUMPHREY, HOT-SHORTNESS OF SOME HIGH-PURITY ALLOYS IN THE SYSTEMS ALUMINUM-COPPER-SILICON AND ALUMINUM-MAGNESIUM-SILICON, *J. INST. MET.,* 1948, P 227
15. J.H. DUDAS AND F.R. COLLINS, PREVENTING CRACKS IN HIGH-STRENGTH ALUMINUM ALLOYS, *WELD. J.,* VOL 45 (NO. 6), 1966, P 241-S
16. W.I. PUMPHREY AND D.C. MOORE, CRACKING DURING AND AFTER SOLIDIFICATION IN SOME ALUMINUM-COPPER-MAGNESIUM ALLOYS OF HIGH PURITY, *J. INST. MET.,* VOL 74, 1948, P 425
17. J.K. DAWSON, WELD CRACK SENSITIVITY OF ALUMINUM ALLOYS, *MET. PROG.,* VOL 76 (NO. 1), 1959, P 116
18. R.P. MEISTER AND D.C. MARTIN, "WELDING OF ALUMINUM AND ALUMINUM ALLOYS," DEFENSE METALS INFORMATION CENTER, BATTELLE MEMORIAL INSTITUTE, 1967, P 51
19. S. KOU, *WELDING METALLURGY,* JOHN WILEY & SONS, 1987, P 239
20. R.P. MARTUKANITZ, ALCOA LABORATORIES, UNPUBLISHED RESEARCH, 1985
21. N.F. GITTOS AND M.H. SCOTT, HEAT AFFECTED ZONE CRACKING OF AL-MG-SI ALLOYS, *WELD. J.,* VOL 60 (NO. 6), 1981, P 95-S
22. H.W. KERR AND M. KATOH, INVESTIGATION OF HEAT-AFFECTED ZONE CRACKING OF GMA WELDS OF AL-MG-SI ALLOYS USING THE VARESTRAINT TEST, *WELD. J.,* VOL 66 (NO. 9), 1987, P 251-S
23. D.G. HOWDEN AND D.R. MILNER, *BRIT. WELD. J.,* VOL 10, 1963, P 304
24. Z.P. SAPERSTEIN, G.R. PRESCOTT, AND E.W. MONROE, POROSITY IN ALUMINUM WELDS, *WELD. J.,* VOL 43 (NO. 10), 1964, P 443-S
25. C. RANSLEY AND J. NEUFELD, *J. INST. MET.,* VOL 74, 1948, P 617
26. M. UDA AND S. OHNO, *TRANS. NATL. RES. INST. MET.* (JPN), VOL 16, 1974, P 2
27. R.P. MARTUKANITZ, ALCOA LABORATORIES, UNPUBLISHED RESEARCH, 1986
28. R.P. MARTUKANITZ AND P.R. MICHNUK, SOURCES OF POROSITY IN GAS METAL ARC WELDING OF ALUMINUM, *ALUMINIUM,* VOL 58 (NO. 5), 1982, P 276
29. P.B. DICKERSON, ALCOA LABORATORIES, PRIVATE COMMUNICATION, 1987
30. A.N. O'SHANSKII AND V.V. D'YACHENCHO, EVALUATION OF THE SUSCEPTIBILITY OF ALLOYS TO THE FORMATION OF PORES IN WELDING, *WELD. PROD.,* VOL 24 (NO. 7), 1977, P 52
31. S.D. DUMOLT, "METALLURGICAL TRANSACTIONS IN THE HEAT AFFECTED ZONE OF ALUMINUM ALLOYS BY TRANSMISSION ELECTRON MICROSCOPY," PH.D. THESIS, CARNEGIE-MELLON UNIVERSITY, PITTSBURGH, PA, 1983
32. T. ENGO AND T. KURODA, MICROSTRUCTURE IN WELD HEAT-AFFECTED ZONE OF AL-MG-SI ALLOYS, *TRANS. JPN. WELD. RES. INST.,* VOL 11 (NO. 1), 1982, P 61
33. R.P. MARTUKANITZ, "MODELING THE HEAT AFFECTED ZONES OF ALUMINUM ARC WELDS, *ADVANCES IN WELDING SCIENCE AND TECHNOLOGY,* S.A. DAVID, ED., ASM INTERNATIONAL, 1986, P 193
34. S. KOU, WELDING METALLURGY AND WELDABILITY OF HIGH STRENGTH ALUMINUM ALLOYS, *WELD. RES. COUNC. BULL.,* NO. 320, WELDING RESEARCH COUNCIL, 1986
35. R.P. MARTUKANITZ, ALCOA LABORATORIES, UNPUBLISHED RESEARCH, 1985
36. S.D. DUMOLT, PH.D. THESIS, CARNEGIE-MELLON UNIVERSITY, PITTSBURGH, PA, 1983
37. W.L. BURCH, THE EFFECT OF WELDING SPEED ON STRENGTH OF 6061-T4 ALUMINUM JOINTS, *WELD. J.,* VOL 37 (NO. 7), 1958, P 361-S
38. R.P. MARTUKANITZ, "MODELING THE HEAT AFFECTED ZONES OF ALUMINUM ARC WELDS, ADVANCES IN WELDING SCIENCE AND TECHNOLOGY, S.A. DAVID, ED., ASM

INTERNATIONAL, 1986, P 195

39. R.J. BRUNGRABER AND F.G. NELSON, EFFECT OF WELDING VARIABLES ON ALUMINUM ALLOY WELDMENTS, *WELD. J.*, VOL 52 (NO. 3), 1973, P 97-S
40. G.E. METZGER, SOME MECHANICAL PROPERTIES OF WELDS IN 6061 ALUMINUM ALLOY SHEET, *WELD. J.*, VOL 56 (NO. 10), 1967, P 457-S
41. R.J. NAPOLITANO, H. KULLUK, M.L. NAGURKA, R.P. MARTUKANITZ, AND P.B. DICKERSON, DEVELOPMENT OF KNOWLEDGE-BASED SYSTEMS FOR ALUMINUM WELDING, *WELD. J.*, VOL 71 (NO. 12), 1992, P 43
42. P.B. DICKERSON AND B. IRVING, WELDING ALUMINUM: IT'S NOT AS DIFFICULT AS IT SOUNDS, *WELD. J.*, VOL 71 (NO. 4), 1992, P 47
43. *WELDING ALUMINUM: THEORY AND PRACTICE*, H.L. SAUNDERS, ED., THE ALUMINUM ASSOCIATION, 1991, P 3.8
44. *WELDING ALUMINUM*, AMERICAN WELDING SOCIETY, 1972, P 69.94-69.106
45. F.G. NELSON AND R.L. ROLF, SHEAR STRENGTH OF AL ALLOY FILLET WELDS, *WELD. J.*, VOL 45 (NO. 2), 1966, P 82-S
46. B.S. SHABEL AND R.F. YOUNG, *PROC. CONF. NONDESTRUCTIVE CHARACTERIZATION OF MATERIALS II*, J.F. BUSSIERE, J.P. MONCHALIN, C.O. RUUD, AND R.E. GREEN, JR., ED., PLENUM, 1987, P 335
47. R.P. MEISTER AND D.C. MARTIN, "WELDING OF ALUMINUM AND ALUMINUM ALLOYS," DMIC REPORT 236, DEFENSE METALS INFORMATION CENTER, 1967, P 65
48. "ALCOA ALUMINUM ALLOY 7005 GREEN LETTER," ALUMINUM COMPANY OF AMERICA, 1974
49. R.P. MEISTER AND D.C. MARTIN, "WELDING OF ALUMINUM AND ALUMINUM ALLOYS," DMIC REPORT 236, DEFENSE METALS INFORMATION CENTER, 1967, P 55
50. J.F. CAMPBELL, ALUMINUM ALLOYS FOR CRYOGENIC SERVICE, *MATER. RES. STAND.*, VOL 4 (NO. 10), 1964, P 540
51. F.G. NELSON AND J.G. KAUFMAN, FRACTURE CHARACTERISTICS OF WELDS IN ALUMINUM ALLOYS, *WELD. J.*, VOL 45 (NO. 7), 1966, P 321-S
52. ALUMINUM FOR CRYOGENIC ENVIRONMENT, PART I: GENERAL CONSIDERATIONS, *CRYOG. ENG. NEWS*, BUSINESS COMMUNICATIONS PUBLISHERS, MARCH 1966
53. ALUMINUM FOR CRYOGENIC ENVIRONMENT, PART II: ALLOY GROUPS, *CRYOG. ENG. NEWS*, BUSINESS COMMUNICATIONS PUBLISHERS, APRIL 1966

Selection and Weldability of Non-Heat-Treatable Aluminum Alloys

C.E. Cross, Martin Marietta Astronautics Group; M.L. Kohn, FMC Corporation

Introduction

NON-HEAT-TREATABLE ALUMINUM ALLOYS constitute a group of alloys that rely solely upon cold work and solid solution strengthening for their strength properties. They differ from heat-treatable alloys in that they are incapable of forming second-phase precipitates for improved strength (see the article "Selection and Weldability of Heat-Treatable Aluminum Alloys" in this Volume). As such, the non-heat-treatable alloys cannot achieve the high strengths characteristic of precipitation-hardened alloys. For example, the yield strength of precipitation-hardened alloy 7075-T6 (505 MPa, or 73 ksi) is significantly greater than that of cold-worked and solution-strengthened alloy 5083-H32 (230 MPa, or 33 ksi).

The absence of precipitate-forming elements in these low- to moderate-strength non-heat-treatable alloys becomes a positive attribute when considering weldability, because many of the alloy additions needed for precipitation hardening (for example, copper plus magnesium, or magnesium plus silicon) can lead to liquation or hot cracking during welding. In addition, joint efficiencies are higher in non-heat-treatable alloys because the heat-affected zone (HAZ) is not compromised by the coarsening or dissolution of precipitates. This obviates the need for thick joint lands or postweld heat treatment and favors the use of welded structures in the as-welded condition.

Selection and Weldability of Non-Heat-Treatable Aluminum Alloys

C.E. Cross, Martin Marietta Astronautics Group; M.L. Kohn, FMC Corporation

Alloy Classification and Typical Applications

Non-heat-treatable wrought aluminum alloys can be placed into one of three groups using standard Aluminum Association designations:

ALLOY NUMBER	ALLOY ADDITION
1*XXX*	AL (99% MINIMUM PURITY)
3*XXX*	AL-MN
4*XXX*	AL-SI
5*XXX*	AL-MG

Nominal compositions for common non-heat-treatable alloys are given in Table 1.

TABLE 1 COMPOSITION OF WROUGHT NON-HEAT-TREATABLE ALUMINUM ALLOYS

ALLOY DESIGNATION	COMPOSITION, WT%[A]											
	Si	Fe	Cu	Mn	Mg	Cr	Ni	Zn	Ti	OTHERS		AL MIN.[D]
										EACH[B]	TOTAL[C]	
1050	0.25	0.40	0.05	0.05	0.05	. . .	. . .	0.05	0.03	0.03[E]	. . .	**99.50**
1060	0.25	0.35	0.05	0.03	0.03	. . .	. . .	0.05	0.03	0.03[E]	. . .	**99.60**

1100	0.95 (SI + FE)		0.05-0.20	0.05	. . .	. . .	. . .	0.10	. . .	0.05[F]	0.15	**99.00**
1145[G]	0.55 (SI + FE)		0.05	0.05	0.05	. . .	. . .	0.05	0.03	0.03[E]	. . .	**99.45**
1175[H]	0.15 (SI + FE)		0.10	0.02	0.02	. . .	. . .	0.04	0.02	0.02[I]	. . .	**99.75**
1188	0.00	0.06	0.005	0.01	0.01	. . .	. . .	0.03	0.01	. . .	. . .	**99.88**
1200	1.00 (SI + FE)		0.05	0.05	. . .	. . .	. . .	0.10	0.05	0.05	0.15	**99.00**
1230[H]	0.70 (SI + FE)		0.10	0.05	0.05	. . .	. . .	0.10	0.03	0.03[E]	. . .	**99.30**
1235	0.65 (SI + FE)		0.05	0.05	0.05	. . .	. . .	0.10	0.06	0.03[E]	. . .	**99.35**
1345	0.03	0.40	0.10	0.05	0.05	. . .	. . .	0.05	0.03	0.03[E]	. . .	**99.45**
1350[J]	0.10	0.40	0.05	0.01	. . .	0.01	. . .	0.05	. . .	0.03[K]	0.10	**99.50**
3003	0.6	0.7	0.05-0.20	1.0-1.5	. . .	. . .	. . .	0.10	. . .	0.05	0.15	**BAL**
3004	0.30	0.7	0.25	1.0-1.5	0.8-1.3	. . .	. . .	0.25	. . .	0.05	0.15	**BAL**
3005	0.6	0.7	0.30	1.0-1.5	0.20-0.6	0.10	. . .	0.25	0.10	0.05	0.15	**BAL**
3105	0.6	0.7	0.30	0.03-0.8	0.20-0.8	0.20	. . .	0.40	0.10	0.05	0.15	**BAL**
4032	11.0-13.5	1.0	0.50-1.3	. . .	0.8-1.3	0.10	0.50-1.3	0.25	. . .	0.05	0.15	**BAL**
4043	4.5-6.0	0.8	0.30	0.05	0.05	. . .	. . .	0.10	0.20	0.05[F]	0.15	**BAL**
4045[L]	9.0-11.0	0.8	0.30	0.05	0.05	. . .	. . .	0.10	0.20	0.05	0.15	**BAL**
4047[L]	11.0-13.0	0.8	0.30	0.15	0.10	. . .	. . .	0.20	. . .	0.05[F]	0.15	**BAL**
4145[L]	9.3-10.7	0.8	3.3-4.7	0.15	0.15	0.15	. . .	0.20	. . .	0.05[F]	0.15	**BAL**
4343[L]	6.8-8.2	0.8	0.25	0.10	. . .	. . .	. . .	0.20	. . .	0.05[F]	0.15	**BAL**
4643	3.6-4.6	0.8	0.10	0.05	0.10-0.30	. . .	. . .	0.10	0.15	0.05[F]	0.15	**BAL**
5005	0.30	0.7	0.20	0.20	0.50-1.1	0.10	. . .	0.25	. . .	0.05	0.15	**BAL**
5050	0.40	0.7	0.20	0.10	1.1-1.8	0.10	. . .	0.25	. . .	0.05	0.15	**BAL**
5052	0.25	0.40	0.10	0.10	2.2-2.8	0.15-0.35	. . .	0.10	. . .	0.05	0.15	**BAL**
5056	0.30	0.40	0.10	0.05-0.20	4.5-5.6	0.05-0.20	. . .	0.10	. . .	0.05	0.15	**BAL**

5083	0.40	0.40	0.10	0.40-1.0	4.0-4.9	0.05-0.25	. . .	0.25	0.15	0.05	0.15	**BAL**
5086	0.40	0.50	0.10	0.20-0.7	3.5-4.5	0.05-0.25	. . .	0.25	0.15	0.05	0.15	**BAL**
5154	0.25	0.40	0.10	0.10	3.1-3.9	0.15-0.35	. . .	0.20	0.20	0.05	0.15	**BAL**
5183	0.40	0.40	0.10	0.50-1.0	4.3-5.2	0.05-0.25	. . .	0.25	0.15	0.05(F)	0.15	**BAL**
5252	0.08	0.10	0.10	0.10	2.2-2.8	. . .	. . .	0.05	. . .	0.03(E)	0.10	**BAL**
5254	0.45 (SI + FE)		0.05	0.01	3.1-3.9	0.15-0.35	. . .	0.20	0.05	0.05	0.15	**BAL**
5356	0.25	0.40	0.10	0.05-0.20	4.5-5.5	0.05-0.20	. . .	0.10	0.06-0.20	0.05(F)	0.15	**BAL**
5454	0.25	0.40	0.10	0.50-1.0	2.4-3.0	0.05-0.20	. . .	0.25	0.20	0.05	0.15	**BAL**
5456	0.25	0.40	0.10	0.50-1.0	4.7-5.5	0.05-0.20	. . .	0.25	0.20	0.05	0.15	**BAL**
5457	0.08	0.10	0.20	0.15-0.45	0.8-1.2	. . .	. . .	0.05	. . .	0.03(E)	0.10	**BAL**
5554	0.25	0.40	0.10	0.50-1.0	2.4-3.0	0.05-0.20	. . .	0.25	0.05-0.20	0.05(F)	0.15	**BAL**
5556	0.25	0.40	0.10	0.50-1.0	4.7-5.5	0.05-0.20	. . .	0.25	0.05-0.20	0.05(F)	0.15	**BAL**
5652	0.40 (SI + FE)		0.04	0.01	2.2-2.8	0.15-0.35	. . .	0.10	. . .	0.05	0.15	**BAL**
5654	0.45 (SI + FE)		0.05	0.01	3.1-3.9	0.15-0.35	. . .	0.20	0.05-0.15	0.05(F)	0.15	**BAL**
5657	**0.08**	**0.10**	**0.10**	**0.03**	**0.6-1.0**	**. . .**	**. . .**	**0.05**	**. . .**	**0.02(I)**	**0.05**	**BAL**

Source: Ref 1

(A) COMPOSITION IN MAXIMUM WT% UNLESS SHOWN AS A RANGE OR A MINIMUM.

(B) A 0.0008 WT% BE MAXIMUM IS APPLICABLE TO ANY ALLOY TO BE USED AS WELDING ELECTRODE OR WELDING ROD.

(C) THE SUM OF THOSE "OTHERS" METALLIC ELEMENTS 0.010% OR MORE EACH, EXPRESSED TO THE SECOND DECIMAL BEFORE DETERMINING THE SUM.

(D) THE ALUMINUM CONTENT FOR UNALLOYED ALUMINUM NOT MADE BY A REFINING PROCESS IS THE DIFFERENCE BETWEEN 100.00% AND THE SUM OF ALL OTHER METALLIC

ELEMENTS PRESENT IN AMOUNTS OF 0.010% OR MORE EACH, EXPRESSED TO THE SECOND DECIMAL BEFORE DETERMINING THE SUM.

(E) 0.05% V MAXIMUM.

(F) 0.0008% BE MAX FOR WELDING ELECTRODE AND WELDING ROD ONLY.

(G) FOIL.

(H) CLADDING ALLOY.

(I) 0.03% GA MAXIMUM; 0.05% V MAXIMUM.

(J) ELECTRIC CONDUCTOR (EC).

(K) 0.02% (V + TI) MAXIMUM; 0.05% B MAX; 0.03% GA MAXIMUM.

(L) BRAZING ALLOY.

1*xxx* Alloys. The 1*xxx*-series alloys are of commercial purity (>99% Al) and are used where thermal/electrical conduction or corrosion resistance becomes paramount over strength in design considerations (for example, alloy 1100 is used for sheet metal work, fin stock and chemical equipment). Alloys with purity levels greater than 99.5% are used for electrical conductors (for example, alloy 1350).

3*xxx* Alloys. The 3*xxx*-series alloys are used in applications where added additional strength and formability are needed, in addition to maintaining excellent corrosion resistance (for example, alloy 3004 is used for sheet metal work, storage tanks, and beverage containers). Typical applications include cooking utensils, pressure vessels, and building products (siding, gutters, and so on). These alloys get their strength from cold work and fine $(Mn,Fe)Al_6$ dispersoids that pin grain and subgrain boundaries. There is also a small degree of solid solution strengthening from both manganese and magnesium.

4*xxx* Alloys. Apart from their use as welding filler material (see the section "Filler Alloy Selection" in this article), the 4*xxx*-series alloys have limited industrial application in wrought form.

5*xxx* Alloys. The 5*xxx*-series alloys are used in cases where still higher strengths are required; this strength is achieved from large quantities of magnesium in solid solution. More importantly, magnesium promotes work hardening by lowering the stacking fault energy, thus reducing the tendency for dynamic recovery. Applications for 5*xxx*-series alloys include automobile and appliance trim, pressure vessels, armor plate, and components for marine and cryogenic service. The ballistic analysis of alloy 5083 is given in the section "Weld Properties" of this article.

While these alloys normally exhibit good corrosion resistance, care must be taken during processing to avoid formation of continuous β-Mg_3Al_2 precipitates at grain boundaries, which can lead to intergranular corrosion. This can occur in heavily cold-worked, high-magnesium alloys exposed to temperatures from 120 to 200 °C (250 to 390 °F). Alloy 5454 possesses the highest magnesium content suitable for sustained elevated temperatures and has become the standard alloy used for truck bodies for hot oil or asphalt applications, and storage tanks for heated products.

Temper Designations. Appropriate heat treatments and temper designations for non-heat-treatable alloys include a solution anneal (O temper) and a cold-worked condition (H1 temper). When the cold work achieved during processing is more than desired, a partial anneal can be used to reduce strength (H2 temper). When dealing with 5*xxx*-series alloys, it is common to use a low-temperature heat treatment (H3 temper) to stabilize the microstructure and prevent intergranular corrosion. This treatment involves heating to 120 °C (250 °F), resulting in partial recovery and making properties less susceptible to change with time.

When working with H-type tempers, a second digit is used to indicate the degree of cold work:

RELATIVE HARDNESS	TEMPER DESIGNATION
FULL HARD	**H18**
$\frac{3}{4}$ HARD	**H16**

$\frac{1}{2}$HARD	**H14**
$\frac{1}{4}$**HARD**	**H12**

A more thorough and complete description of non-heat-treatable alloys and tempers is given in Volume 2 of the *ASM Handbook* (Ref 2).

References cited in this section

1. *ALUMINUM STANDARDS AND DATA*, ALUMINUM ASSOCIATION, 1984, P 93
2. PROPERTIES AND SELECTION NONFERROUS ALLOYS AND SPECIAL-PURPOSE MATERIALS, VOL 2, *ASM HANDBOOK*, ASM INTERNATIONAL, 1990, P 15-28

Selection and Weldability of Non-Heat-Treatable Aluminum Alloys

C.E. Cross, Martin Marietta Astronautics Group; M.L. Kohn, FMC Corporation

Filler Alloy Selection

Filler alloys used to join non-heat-treatable alloys can be selected from one of three alloy groups:

ALLOY NUMBER	ALLOY ADDITION
1*XXX*	**AL (99% MINIMUM PURITY)**
4*XXX*	**A1-SI**
5*XXX*	**AL-MG**

Commonly used filler alloys include 1100, 1188, 4043, 4047, 5554, 5654, 5183, 5356, and 5556. Nominal compositions for selected filler alloys are included in Table 1. Selecting the best filler alloy for a given application depends on the desired performance relative to weldability, strength, ductility, and corrosion resistance. In general, the filler alloy selected should be similar in composition to the base metal alloy. Thus, a 1*xxx* filler alloy is recommended for joining 1*xxx*- or 3*xxx*-series base metal alloys. Similarly, 5*xxx* filler alloys are used to join 5*xxx*-series base metal alloys. An exception to this rule is encountered when weldability becomes an issue. Weldability of non-heat-treatable aluminum alloys can be measured in terms of resistance to hot cracking and porosity.

Hot Cracking. Problems with hot cracking are encountered when welding under highly constrained conditions or when welding certain alloys that are highly susceptible to cracking. Such is the case when welding 5*xxx* alloys that have a low-range magnesium content ($\frac{1}{2}$ to $2\frac{1}{2}$ wt% Mg) where, according to the crack susceptibility curve (Fig. 1), a peak in susceptibility occurs. To avoid cracking, use of a high-magnesium filler alloy is recommended.

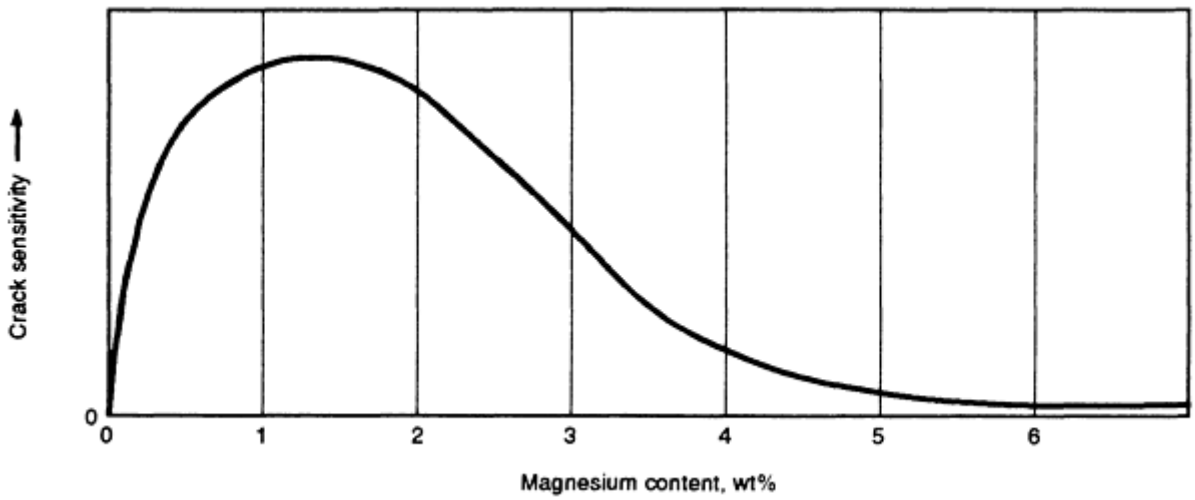

FIG. 1 PLOT OF HOT CRACKING SENSITIVITY VERSUS MAGNESIUM CONTENT TO SHOW PEAK IN SUSCEPTIBILITY OBTAINED FOR ALUMINUM-MAGNESIUM (5*XXX*) ALLOYS. SOURCE: REF 3

Similar problems may be encountered when 1*xxx* fillers are used to join 5*xxx* alloys (or vice versa), or when welding dissimilar metal alloys such as alloys 1100 and 5083, where mutual dilution may result in low magnesium levels. Electron-beam welding or laser-beam welding can also result in cracking when magnesium, a high-vapor-pressure alloying element, is boiled off. The problem is aggravated when welding in a vacuum environment. An example of a center-line hot crack produced when electron-beam welding alloy 5083 is shown in Fig. 2, where magnesium levels were measured to be approximately 3 wt% in the vicinity of the crack, based on microprobe analysis. This was an autogenous weld made in a hard vacuum (0.13 mPa, or 10^{-6} torr).

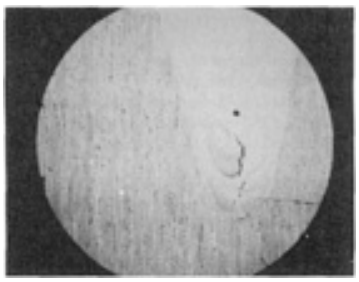

FIG. 2 CENTERLINE HOT CRACK PRODUCED IN AUTOGENOUS ELECTRON-BEAM WELDED ALLOY 5083

Another approach to be taken when hot cracking persists is to use 4*xxx* fillers. These aluminum-silicon alloys have exceptional resistance to cracking, due in part to their abundance of liquid eutectic available for back-filling (Ref 4). However, their use should be avoided when welding high-magnesium alloys (>3 wt%) because of embrittlement from excessive Mg_2Si precipitation. Other drawbacks include low joint ductility and nonmatching color when anodized. Weldability will improve with increased silicon content (for example, alloy 4047 versus alloy 4043), but the disadvantages discussed above will likewise become more predominant.

Porosity. Non-heat-treatable aluminum alloys are susceptible to hydrogen-induced weld metal porosity, as are all aluminum alloys in general. This porosity forms during solidification due to the abrupt drop in hydrogen solubility when going from liquid to solid. Porosity can best be avoided by minimizing hydrogen pickup during welding. This can be accomplished through proper joint preparation (that is, removal of hydrocarbons), use of high-grade (low-dew-point) shielding gas, and careful storage of filler wire (that is, protection from exposure to moisture and oil). It has been determined that welding filler wire is often the primary source of hydrogen contamination. The 5*xxx*-series filler alloys, in particular, are susceptible to the hydration of surface oxides, which can result in porosity (Ref 5).

In summary, guidelines for filler alloy selection when welding non-heat-treatable alloys are:

BASE METAL	FILLER METAL
1*XXX*	**1*XXX*, 4*XXX***
3*XXX*	**1*XXX*, 4*XXX***
5*XXX* (LOW MAGNESIUM)	**5*XXX*, 4*XXX***
5*XXX* (HIGH MAGNESIUM)	**5*XXX***

References cited in this section

3. J.H. DUDAS AND F.R. COLLINS, PREVENTING WELD CRACKS IN HIGH-STRENGTH ALUMINUM ALLOYS, *WELD. J.*, VOL 45, 1966, P 241S-249S
4. C.E. CROSS, L.S. KRAMER, W.T. TACK, AND L.W. LOECHEL, ALUMINUM WELDABILITY AND HOT TEARING THEORY, *WELDABILITY OF MATERIALS*, ASM INTERNATIONAL, 1990, P 275-282
5. R.P. MARTUKANITZ AND P.R. MICHNUK, SOURCES OF POROSITY IN GAS METAL ARC WELDING OF ALUMINUM, *TRENDS IN WELDING RESEARCH*, ASM INTERNATIONAL, 1982, P 315-330

Selection and Weldability of Non-Heat-Treatable Aluminum Alloys

C.E. Cross, Martin Marietta Astronautics Group; M.L. Kohn, FMC Corporation

Weld Properties

When non-heat-treatable alloys are welded, microstructural damage is incurred in the HAZ. Unlike the case of heat-treatable alloys, whose strengthening precipitates may dissolve or coarsen, the HAZ damage in non-heat-treatable alloys is limited to recovery, recrystallization, and grain growth. Thus, loss in strength in the HAZ is not nearly as severe as that experienced in heat-treatable alloys. (An example of this is shown in the hardness traverses of Fig. 8 in the article "Selection and Weldability of Heat-Treatable Aluminum Alloys" in this Volume, where alloy 5456 is compared against alloys 6061 and 2219.) For this reason, 5*xxx*-series alloys are popular for use in welded pressure vessels where reasonable joint strengths can be obtained in the as-welded condition without the need for post-weld heat treatment.

The weld metal of non-heat-treatable aluminum alloys is typically the weakest part of the joint and is the location of failure when the joint is loaded in tension. This is in contrast to most heat-treatable aluminum alloys, where the heat-affected zone often is the weakest link. The weld metal microstructure of the non-heat-treatable alloys consists of columnar, epitaxial grains with a cellular or columnar-dendritic substructure that has interdendritic eutectic constituents-primarily $(Fe,Mn)Al_6$ for 1*xxx* and 3*xxx* alloys; Si for 4*xxx* alloys; and Mg_3Al_2 for 5*xxx* alloys.

Joint efficiencies for several non-heat-treatable alloys are compared in Table 2. It should be noted that joint efficiency is highest for annealed plate (approaching 100%) and decreases continuously with the degree of cold working. Also shown in Table 2 is the effect of composition and cold work on plate properties. The two 5*xxx*-series alloys shown exhibit significant improvement in strength over 1*xxx*- and 3*xxx*-series alloys, a reflection on the strengthening ability of magnesium. Likewise, 5*xxx*-series alloys with higher magnesium content have higher strength (for example, alloy 5083 versus alloy 5050). This same trend is observed for weld metal strength. For example, a weld made on high-magnesium alloy 5083 (4% Mg) is much stronger than a similar weld made on alloy 5050 (1% Mg).

TABLE 2 EFFECT OF VARIATIONS IN TEMPER AND FILLER ALLOY ON NON-HEAT-TREATABLE ALUMINUM GAS-METAL ARC WELDMENT PROPERTIES

BASE ALLOY AND TEMPER	PLATE PROPERTIES					FILLER ALLOY	WELD PROPERTIES					JOINT EFFICIENCY, %[A]
	YIELD STRENGTH		ULTIMATE TENSILE STRENGTH		ELONGATION IN 50 MM (2 IN.), %		YIELD STRENGTH		ULTIMATE TENSILE STRENGTH		ELONGATION IN 50 MM (2 IN.), %	
	MPA	KSI	MPA	KSI			MPA	KSI	MPA	KSI		
1100-O	34	5	90	13	35	1100	41	6	93	13.5	23	**100**
						4043	41	6	90	13	21	**100**
3003-O	41	6	110	16	30	1100	41	6	90	13	20	**81**
						4043	48	7	91	13.2	17	**83**
3003-H18	186	27	200	29	4	1100	59	8.5	110	16	15	**55**
5050-O	55	8	145	21	24	5356	55	8	145	21	20	**100**
5050-H32	145	21	172	25	9	5356	97	14	159	23	14.5	**92**
						4043	90	13	152	22	15	**88**
5050-H38	200	29	221	32	6	5356	97	14	162	23.5	14.5	**73**
5083-O	145	21	290	42	22	5356	145	21	283	41	17	**98**
5083-H32	228	33	317	46	16	5356	145	21	276	40	16	**87**
						5183	**152**	**22**	**300**	**43.5**	**12**	**95**

Source: Ref 6

(A) JOINT EFFICIENCY = (UTS OF WELD)/(UTS OF PLATE), WHERE UTS STANDS FOR ULTIMATE TENSILE STRENGTH.

The correspondence between plate and joint strength does not apply to temper. For the high-magnesium alloy 5083 plate, no increase in joint strength is observed when welding an annealed versus a cold-worked temper (see Table 2). Likewise, filler metal selection has little effect on joint strength, as shown in Table 2. However, it is clear that use of a 4*xxx* filler does result in ductility loss. Also, filler alloys high in iron, silicon, or manganese (for example, filler alloy 5183) will have greater amounts of eutectic constituents, which will result in lower weld ductility. Even so, non-heat-treatable alloy welds exhibit significantly better ductility in comparison to similar heat-treatable welds.

Example 1: Use of Welded Alloy 5083 in Ballistic Applications.

An important application for heavy-gage alloy 5083 is the construction of tactical military vehicles. The hulls and turrets of Army vehicles such as the M113 armored personnel carrier, the M2/M3 infantry and cavalry fighting vehicles, the M109 self-propelled howitzer, and the Marine Corps AAV7A amphibians all consist of welded 5083 aluminum structures. There are also a myriad of brackets, clips, and so on, welded to the hulls and turrets, although not normally fabricated to ballistic requirements.

Aluminum alloys considered for use as armor include alloys 5083, 7039, and 2519. Alloys 7039 and 2519 are weldable and heat-treatable, capable of yield strengths exceeding 330 MPa (48 ksi). However, alloy 2519 weldments have failed rigorous ballistic shock tests (MIL-STD-1946, discussed below), even though the base material exhibits excellent ballistic and mechanical properties. Alloy 7039 possesses superior ballistic properties compared to alloy 5083, but it suffers from a tendency to delaminate and to exhibit stress-corrosion cracking. Alloy 5083 weldments have passed ballistic weld tests, and they possess the necessary resistance to corrosion.

In the MIL-STD-1946 ballistic test, a weldment is subjected to impact by a blunt-nose 75 mm (3 in.) aluminum projectile, fired at a velocity specified according to material thickness and alloy composition. Butt-welded specimens are struck no more than 13 mm ($\frac{1}{2}$ in.) from the weld centerline. Corner joints are struck so that the center of the impact projectile is

within 50 ± 13 mm (2 ± $\frac{1}{2}$ in.) from the weld toe on its back side. Welds are considered acceptable when the total length of cracking generated is less than 305 mm (12 in.).

An offset double-V configuration of the butt joint is commonly used in ballistic applications (Fig. 3). This results in solid metal backing for both welds and allows for a slip fit between adjoining plates, thereby simplifying the fit-up of large, heavy plates.

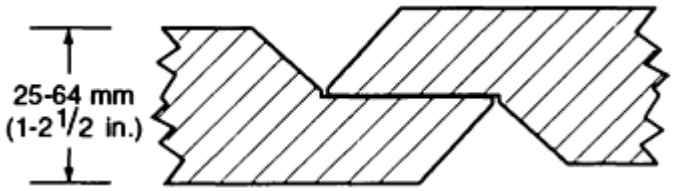

FIG. 3 OFFSET DOUBLE-V JOINT CONFIGURATION USED TO WELD THICK SECTION ALUMINUM ARMOR PLATE

Reference cited in this section

6. "WELDING KAISER ALUMINUM," KAISER ALUMINUM & SALES, INC., OAKLAND, CA, 1978, P 3.25-3.26

Selection and Weldability of Non-Heat-Treatable Aluminum Alloys

C.E. Cross, Martin Marietta Astronautics Group; M.L. Kohn, FMC Corporation

References

1. *ALUMINUM STANDARDS AND DATA*, ALUMINUM ASSOCIATION, 1984, P 93
2. PROPERTIES AND SELECTION NONFERROUS ALLOYS AND SPECIAL-PURPOSE MATERIALS, VOL 2, *ASM HANDBOOK*, ASM INTERNATIONAL, 1990, P 15-28
3. J.H. DUDAS AND F.R. COLLINS, PREVENTING WELD CRACKS IN HIGH-STRENGTH ALUMINUM ALLOYS, *WELD. J.*, VOL 45, 1966, P 241S-249S
4. C.E. CROSS, L.S. KRAMER, W.T. TACK, AND L.W. LOECHEL, ALUMINUM WELDABILITY AND HOT TEARING THEORY, *WELDABILITY OF MATERIALS*, ASM INTERNATIONAL, 1990, P 275-282
5. R.P. MARTUKANITZ AND P.R. MICHNUK, SOURCES OF POROSITY IN GAS METAL ARC WELDING OF ALUMINUM, *TRENDS IN WELDING RESEARCH*, ASM INTERNATIONAL, 1982, P 315-330
6. "WELDING KAISER ALUMINUM," KAISER ALUMINUM & SALES, INC., OAKLAND, CA, 1978, P 3.25-3.26

Selection and Weldability of Dispersion-Strengthened Aluminum Alloys

K. Sampath, Concurrent Technologies Corporation; W.A. Baeslack III, The Ohio State University

Introduction

CONVENTIONAL HIGH-STRENGTH ALUMINUM ALLOYS produced via ingot metallurgy (I/M) processing contain precipitate particles that interact with moving dislocations, thus providing high strength at room temperature. However, when these alloys are exposed to elevated temperatures, the precipitate particles undergo dissolution and/or coarsening,

thereby reducing the strength of the base alloy. This behavior precludes the use of these alloys for elevated-temperature applications. In recent years, advances in two broad powder metallurgy (P/M) technologies--rapid solidification (RS) and mechanical alloying (mechanical attrition)--have enabled the development of a new family of high-strength aluminum alloys for elevated-temperature applications (Ref 1).

These new high-strength P/M aluminum alloys depend primarily on dispersion strengthening. Unlike the precipitate particles in I/M aluminum alloys, the dispersoid particles resist dissolution and/or coarsening when the alloys are exposed to elevated temperatures. In addition to high strength, these dispersion-strengthened aluminum alloys exhibit light weight, appreciable ductility, excellent fracture toughness, and resistance to stress-corrosion cracking (Ref 2). These alloys also exhibit coefficients of thermal expansion and galvanic properties comparable to those of conventional structural aluminum alloys (Ref 2). In view of the above properties, these dispersion-strengthened aluminum alloys are considered candidate materials to replace conventional high-strength aluminum alloys and titanium alloys used in the manufacture of selected aerospace components such as fan and compressor cases; vanes and blades in gas turbine engines; and fins, winglets, and rocket motor cases of missiles (Ref 3). Use of these alloys is expected to increase the thrust-to-weight ratio of gas turbine engines and allow significant improvements in the performance characteristics of advanced aircraft and weapons systems.

High-strength aluminum alloys produced via RS-P/M technology am primarily based on hypereutectic aluminum-iron compositions, although other alloys based on aluminum-chromium-zirconium, aluminum-manganese, aluminum-titanium, and aluminum-beryllium systems are also under various stages of development and/or evaluation (Ref 1). The dispersion-strengthened aluminum alloys produced via mechanical alloying contain a fine distribution of oxides, oxynitrides, and/or carbides in a fine-grain α-aluminum matrix. The α-aluminum matrix may additionally be strengthened by solid-solution strengthening or work hardening (Ref 1). Although many dispersion-strengthened aluminum alloys produced via mechanical alloying do not exhibit strength comparable to that of the conventional high-strength I/M aluminum alloys at room temperature, these alloys exhibit a minimal decrease in strength with increasing temperature (Ref 1).

The twofold purpose of this article is: (1) to guide users in the selection and application of welding processes and conditions for the joining of dispersion-strengthened aluminum alloys, based primarily on an understanding of the weldability of the material; and (2) to provide specific examples of material responses to welding conditions, chiefly by highlighting the microstructural development in the weld zone. In view of the limited number of publications available on the weldability and metallurgical response of this broad class of alloys, this article refers exclusively to the metallurgy and weldability of alloys based on the aluminum-iron system that are produced using various RS-P/M processing techniques.

References

1. J.R. PICKENS, HIGH STRENGTH ALUMINUM P/M ALLOYS, 10TH ED., VOL 2, *METALS HANDBOOK, PROPERTIES AND SELECTION: NON FERROUS ALLOYS AND SPECIAL-PURPOSE MATERIALS,* ASM INTERNATIONAL, 1990, P 200-215
2. S.K. DAS AND L.A. DAVIES, HIGH PERFORMANCE AEROSPACE ALLOYS VIA RAPID SOLIDIFICATION PROCESSING, *MATER. SCI. ENG.,* VOL 98, 1988, P 1-12
3. C.M. ADAM, RAPID SOLIDIFICATION PROCESSING METHODS, *MECHANICAL BEHAVIOR OF RAPIDLY SOLIDIFIED MATERIALS,* S.M.L. SASTRY AND B.A. MACDONALD, ED., THE METALLURGICAL SOCIETY OF AIME, 1985, P 21-39

Selection and Weldability of Dispersion-Strengthened Aluminum Alloys

K. Sampath, Concurrent Technologies Corporation; W.A. Baeslack III, The Ohio State University

Metallurgy of RS-P/M Aluminum-Iron-Base Alloys

Table 1 shows a list of selected dispersion-strengthened aluminum-iron-base alloys produced via RS-P/M processing. These alloys contain ternary and quaternary additions of transition and rare earth metals such as molybdenum, nickel,

cerium, vanadium, and silicon. These alloy additions exhibit low solid-solubility and low solid-state diffusivity in α aluminum (Ref 4), and consequently they tend to form thermally stable dispersoid particles. However, these alloy compositions are characterized by a wider freezing range (typically in excess of 300 °C, or 540 °F) than most aluminum alloys. Conventional I/M processing of these compositions produces equilibrium or near-equilibrium microstructures containing coarse Al_3Fe-type primary intermetallic particles in a coarse α-aluminum matrix. Such microstructures exhibit poor ductility and cannot be used for structural engineering applications. In contrast, RS processing of these novel chemistries suppresses the formation of Al_3Fe-type primary intermetallic particles. It instead produces particulates exhibiting refined metastable microstructures, such as an Al-Al_6Fe-type microeutectic and/or a solute-supersaturated dendritic aluminum. In other words, RS processing conditions produce refined hypoeutectic-type microstructures from hypereutectic melts. The occurrence of these metastable hypoeutectic-type microstructures is attributed to the following two characteristics of RS processing techniques: (1) subdivision of the melt into particulates isolates potential nucleants and produces nucleant-free particulates that undergo nonequilibrium solidification (Ref 5); and (2) the rapid cooling rate does not provide sufficient reaction time for a potential nucleant to produce the equilibrium microstructure (Ref 6).

TABLE 1 CHEMICAL COMPOSITIONS OF DISPERSION-STRENGTHENED ALUMINUM-BASE ALLOYS PRODUCED BY RS-P/M

NOMINAL CHEMICAL COMPOSITION, WT%	MANUFACTURER
AL-8FE-1.7NI	**ALCOA**
AL-8.4FE-3.7CE	**ALCOA**
AL-9FE-4CE (AA8019 ALLOY)	**ALCOA**
AL-9FE-7CE	**ALCOA**
AL-10FE-5CE	**ALCOA**
AL-8.5FE-1.3V-1.7SI (AA8009 ALLOY)	**ALLIEDSIGNAL INC.**
AL-11.7FE-1.2V-2.4SI (FVS 1212 ALLOY)	**ALLIEDSIGNAL INC.**
AL-8FE-2.3MO	**PRATT & WHITNEY**
AL-8.7FE-2.8MO-1V	**PRATT & WHITNEY**

Subsequent thermomechanical processing of the rapidly solidified particulates produces a consolidated product with a unique "engineered" microstructure consisting of submicron-size dispersoid particles in an extremely fine-grain (<1 μm) α-aluminum matrix. During thermomechanical processing, the as-solidified hypoeutectic-type microstructures undergo solid-state phase transformations and produce fine dispersoid particles in an α-aluminum matrix. These particles result from the low-equilibrium solid-solubility limit of the alloy addition, and they consist of both the stable, "non-shearable," incoherent θ(Al_3Fe-type) dispersoid particles and metastable, "shearable," partially coherent θ' (Al_3Fe-type) dispersoid particles. The ternary and quaternary alloy additions promote the formation of complex metastable and stable dispersoid particles, and they reduce the surface free energy or the lattice misfit between the dispersoid particles and the α-aluminum matrix (Ref 2, 4, 7, 8). The partially coherent particles exhibit a spherical morphology and provide excellent resistance to fracture or crack initiation. These microstructural features provide excellent thermal stability and superior mechanical properties, including high strength and ductility, both at room temperature and at elevated temperatures up to 345 °C (650 °F). Because RS-P/M processing results in microstructures finer than the resolution limit of light microscopy, transmission electron microscopy (TEM) is often required to resolve the distribution and morphology of the microstructural constituents. Figures 1(a) and 1(b) compare a light micrograph of alloy AA8009 with a TEM micrograph. Figures 1(c) and 1(d) show the TEM micrographs of Al-8Fe-4Ce and Al-9Fe-3Mo-1V alloys. The volume fraction of the dispersoid particles in these representative alloys typically ranges from 15 to 35%.

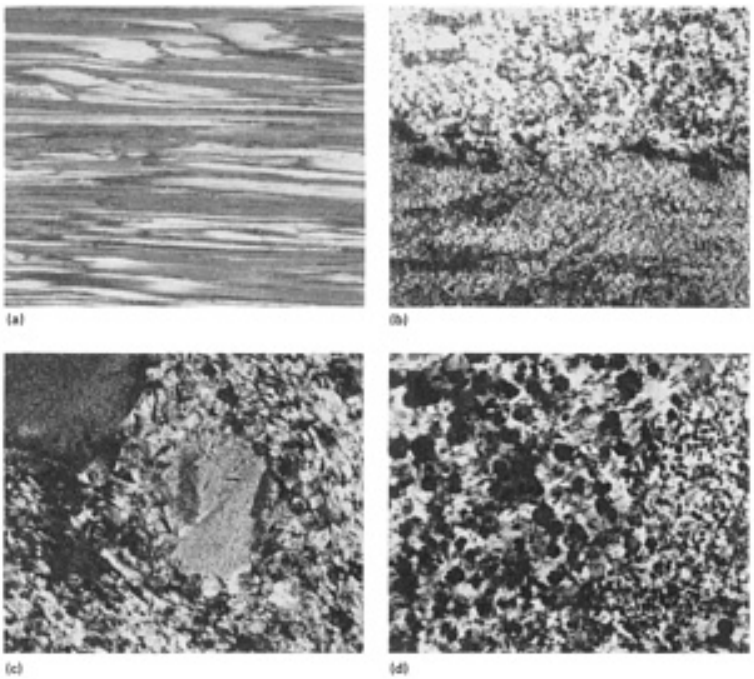

FIG. 1 MICROSTRUCTURE OF THREE REPRESENTATIVE RS-P/M ALUMINUM-IRON-BASE ALLOYS. (A) LIGHT MICROGRAPH OF AA8009 ALLOY. (B) TEM MICROGRAPH OF AA8009 ALLOY. SOURCE: REF 9. (C) AL-8.4FE-3.7CE ALLOY. SOURCE: REF 10. (D) AL-9FE-3MO-1V ALLOY. SOURCE: REF 11

References cited in this section

2. S.K. DAS AND L.A. DAVIES, HIGH PERFORMANCE AEROSPACE ALLOYS VIA RAPID SOLIDIFICATION PROCESSING, *MATER. SCI. ENG.*, VOL 98, 1988, P 1-12
4. C.M. ADAM AND R.G. BOURDEAU, TRANSITION AND REFRACTORY ELEMENT ADDITIONS TO RAPIDLY SOLIDIFIED ALUMINUM ALLOYS, *RAPID SOLIDIFICATION PROCESSING: PRINCIPLES AND TECHNOLOGIES II*,R. MEHRABIAN, B.H. KEAR, AND M. COHEN, ED., CLAITORS PUBLISHING, 1980, P 246-259
5. I.E. ANDERSON AND M.P. KEMPAINEN, UNDERCOOLING EFFECTS IN GAS-ATOMIZED POWDERS, *UNDERCOOLED ALLOY PHASES,* E.W. COLLINGS AND C.C. KOCH, ED., THE METALLURGICAL SOCIETY OF AIME, 1988, P 269-285
6. C.M. ADAM, RAPID SOLIDIFICATION TECHNOLOGY: THE POTENTIAL FOR INNOVATIVE ALLOY PROPERTIES, *SCIENCE AND TECHNOLOGY OF UNDERCOOLED MELTS,* P.R. SAHM, H. JONES, AND C.M. ADAMS, ED., NATO-ASI SERIES, MARTINUS-NIJHOFF PUBLISHERS, 1986, P 186-209
7. C.M. ADAM, STRUCTURE/PROPERTY RELATIONSHIPS AND APPLICATIONS OF RAPIDLY SOLIDIFIED ALUMINUM ALLOYS, *RAPIDLY SOLIDIFIED AMORPHOUS AND CRYSTALLINE ALLOYS*, VOL 8, B.H. KEAR, B.C. GIESSEN, AND M. COHEN, ED., ELSEVIER SCIENCE PUBLISHING CO., 1982, P 411-422
8. S.L. LANGENBECK, W.M. GRIFFITH, G.J. HILDEMAN, AND J.W. SIMON, DEVELOPMENT OF DISPERSION-STRENGTHENED ALUMINUM ALLOYS, *RAPIDLY SOLIDIFIED ALUMINUM ALLOYS*, STP 890, M.E. FINE AND E.A. STARKE, JR., ED., ASTM, 1986, P 410-422
9. H.H. KOO, S. KRISHNASWAMY, AND W.A. BAESLACK III, CHARACTERIZATION OF AN INERTIA-FRICTION WELD IN A HIGH-TEMPERATURE RS/PM AI-FE-V-SI ALLOY-AA8009, *MATER. CHARACT.*, VOL 26 (NO. 3), 1991, P 123-136
10. W.A. BAESLACK III, K.H. HOU, AND J.H. DEVLETIAN, ELECTRON MICROSCOPY OF RAPIDLY SOLIDIFIED WELDMENTS IN A POWDER METALLURGY AL-FE-CE ALLOY, *J. MATER. SCI.*

LETT., VOL 8 (NO. 6), 1989, P 716-720

11. H.H. KOO, K. SAMPATH, AND W.A. BAESLACK III, CHARACTERIZATION OF INERTIA-FRICTION WELDS BETWEEN A RAPIDLY-SOLIDIFIED AL-FE-MO-V ALLOY AND IM 2024-T351, *J. MATER. SCI.*, VOL 27, 1992, P 3266-3280

Selection and Weldability of Dispersion-Strengthened Aluminum Alloys

K. Sampath, Concurrent Technologies Corporation; W.A. Baeslack III, The Ohio State University

Weldability Issues

Although a variety of fusion welding and solid-state welding processes and techniques are available to join the conventional I/M aluminum alloys (Ref 12), several weldability issues, including the absence of compatible filler metals, preclude the application of many conventional welding processes and methodologies to the joining of dispersion-strengthened aluminum alloys. In particular, weldability issues related to weld solidification behavior, formation of hydrogen-induced porosity in the weld zone, and high-temperature deformation behavior of these alloys affect the selection and application of both fusion and solid-state welding processes.

Weld Solidification Behavior

The application of high-strength dispersion-strengthened aluminum alloys in the manufacture of specific aerospace structural components, where weight savings are critical for mission range and performance, will require the application of welding processes and procedures that optimize weld joint efficiency and minimize weld reinforcement. Because the high strength of the base alloy is due to the unique engineered microstructure obtained through RS-P/M processing, welding processes and procedures must re-create high-performance microstructures similar to the base alloy microstructures, and/or retain the superior base alloy microstructure in the weld zone. Since the wide freezing range of these alloys will tend to promote hypereutectic solidification and equilibrium or near-equilibrium microstructures, fusion welding conditions that promote RS or hypoeutectic-type solidification within the fusion zone will be required to re-create high-performance microstructures in the fusion zone. Welding conditions such as high energy density and minimum energy input, that increase the temperature gradients in both the fusion zone and the heat-affected zone (HAZ) and increase the overall weld cooling rate, will be required to minimize the widths of the partially melted region and the HAZ. Such welding conditions can be expected to facilitate the occurrence of plane front solidification, promote microstructural refining in the fusion zone, and minimize the extent of microstructural coarsening in the HAZ.

Alternatively, fusion welding conditions that provide minimum energy density and a shallow temperature gradient in the fusion zone can be expected to produce a wider HAZ and a wider partially melted region near the fusion boundary with the base metal. Depending on the local solidification conditions, this partially melted region can solidify to an equilibrium or near-equilibrium structure containing coarse intermetallic particles in a coarse-grain α-aluminum matrix. Coarse intermetallic particles can be expected to localize stress concentrations, thereby reducing the ductility and fracture toughness of the weldment. A distribution of coarse intermetallic particles can also be expected to be less effective at strengthening the matrix, especially at elevated temperatures.

Hydrogen-Induced Fusion Zone Porosity

The weldability of the dispersion-strengthened aluminum alloys is also limited by the hydrogen content of the base alloy. Hydrogen content in excess of 1 mL/100 g of aluminum is believed to produce excessive fusion zone porosity. Porosity in the fusion zone often reduces weld static strength and fatigue properties. Porosity occurs in aluminum alloy fusion welds mainly due to the rejection of hydrogen during weld solidification. It is related to the presence of hydrogen in the base alloy, filler metal, and the atmosphere and to the high ratio of solubility of hydrogen absorbed in the weld to the solubility limit of hydrogen at the melting point. The dispersion-strengthened aluminum alloys produced via RS-P/M processing often exhibit a residual hydrogen content in excess of 1 to 5 mL/100 g of aluminum and therefore show an increased tendency to form fusion zone porosity. Depending on the specific RS processing technique employed to produce the dispersion-strengthened aluminum alloy, the surface of the rapidly solidified particulates forms oxide layers to varying degrees (Ref 4, 7). During subsequent consolidation and handling, these surface oxides tend to hydrate. Decomposition of these hydrated oxides during fusion welding produces porosity in the weld fusion zone. Additionally, these oxides may

serve as heterogeneous nucleation sites during fusion zone solidification, thereby limiting the extent of undercooling and promoting hypereutectic solidification conditions and the formation of equilibrium microstructures.

Controlling the Hydrogen Content. Three approaches are available to control the residual hydrogen content in RS-P/M aluminum alloys:

- USE VACUUM OR OTHER COMPLETELY INERT PROCESSING STEPS DURING RS PROCESSING AND CONSOLIDATION.
- DEGAS THE RAPIDLY SOLIDIFIED PARTICULATES PRIOR TO CONSOLIDATION, EITHER IN VACUUM OR IN OTHER INERT CARRIER GASES (DEPURITIVE TREATMENTS).
- DEGAS THE CONSOLIDATED PRODUCT (DIFFUSION CONSIDERATIONS NORMALLY RESTRICT THIS TREATMENT TO SHEETS AND PLATES) PRIOR TO FUSION WELDING.

The use of vacuum or other complete inert processing steps during RS processing and consolidation will minimize the formation of surface oxides and thereby control consequent hydrate formation. Degassing of either the rapidly solidified particulates or the consolidated products is aimed at removing or reducing the residual hydrogen to an acceptable level, preferably below 1 mL/100 g of aluminum. The critical factors that contribute to effective degassing are temperature, time, environment, and the product size and shape. Degassing treatments are effective only at temperatures in excess of 530 to 550 °C (990 to 1020 °F). Unfortunately, the use of such high temperatures often decomposes the metastable base alloy microstructure and/or promotes microstructural coarsening, thereby irreversibly degrading the mechanical properties of the base material (Ref 13).

Alternatively, despite a higher hydrogen content in the RS-P/M aluminum-base alloy, the occurrence of fusion zone porosity can be minimized by using welding techniques that increase the total pressure during welding. Since the equilibrium solubility of hydrogen in molten aluminum is governed by Sievert's law, the solubility of hydrogen in aluminum near the boiling point of aluminum can be decreased by reducing the partial pressure of hydrogen (that is, by increasing the total pressure). Depending on the specific characteristics of the fusion welding process, welding techniques that provide increased total pressure will reduce the partial pressure of hydrogen in the welding atmosphere and thereby reduce the level of fusion zone porosity. Increased total pressure is also believed to minimize the nucleation of hydrogen bubbles (Ref 14). However, such welds will contain excessive hydrogen, either in solution or as fine-size pores not detectable using conventional nondestructive evaluation techniques.

Applicable Welding Processes. The above weldability considerations show that RS-P/M aluminum-base alloys characterized by a low residual hydrogen content (<1 mL/100 g of aluminum) can be joined using fusion welding methods. As mentioned before, the absence of compatible fillers restricts the choice to essentially autogenous welding processes, while a need to recreate high-performance microstructures further limits that choice to high-energy-density welding methods such as capacitor-discharge welding, electron-beam welding, and laser welding. In fact, considering the effects of laser wavelength on the weldability of aluminum alloys, the application of the pulsed Nd:YAG laser welding process is preferred because this process provides 1.06 μm wavelength radiation, which is more efficiently absorbed by the base alloys than the 10.6 μm wavelength CO_2 laser radiation.

Fusion welding of base alloys with higher residual hydrogen will require the use of weld pretreatment or other special techniques to control hydrogen content in the weld atmosphere. In fact, one company that manufactures high-strength aluminum alloys containing iron, vanadium, and silicon additions has developed material pretreatments that can enhance joining and provide acceptable welding procedures (with minimal porosity) for resistance spot welding, gas-tungsten arc welding (GTAW), laser-beam welding, and vacuum brazing of these alloys (Ref 15).

The RS-P/M aluminum-base alloys characterized by a higher residual hydrogen content (>1 mL/100 g of aluminum) will require the use of solid-state welding methods such as conventional friction welding, inertia friction welding, or linear friction welding. These solid-state welding processes employ relative motion of the parts to be joined under an axial force to generate frictional heat at the weld interface. During the initial stages of welding, the interface becomes plastic (softened) due to frictional heating. When adequate heating (softening) of the interface is obtained, the relative motion is slowed down and a forging force is applied to produce the weld joint. The forging force produces localized plastic deformation and expels the heated material from the interface (as a flash around the weld joint), thereby enabling the formation of a weld joint between nearly unaffected base metals. In this regard, the weldability of the dispersion-strengthened aluminum alloys is influenced by the effects of welding process conditions and parameters on the high-temperature deformation characteristics, and subsequent microstructural development in the weld zone of these alloys.

Since these solid-state welding processes preclude melting and solidification, these welds tolerate higher levels of residual hydrogen. Further, the absence of melting at the faying surfaces during these processes prevents solidification-related discontinuities, such as cracking, and enables joining with dissimilar materials. However, despite the inherent ability of solid-state welding processes to produce high-integrity weld joints, such processes are only selectively applicable in view of specific limitations on component size, cross-sectional shape, weld joint design, and difficulties in evaluating the weld joint integrity using conventional nondestructive evaluation techniques. Application of joining processes such as brazing or diffusion welding using interlayers may potentially circumvent the aforementioned weldability issues related to the dispersion-strengthened aluminum alloys.

References cited in this section

4. C.M. ADAM AND R.G. BOURDEAU, TRANSITION AND REFRACTORY ELEMENT ADDITIONS TO RAPIDLY SOLIDIFIED ALUMINUM ALLOYS, *RAPID SOLIDIFICATION PROCESSING: PRINCIPLES AND TECHNOLOGIES II*,R. MEHRABIAN, B.H. KEAR, AND M. COHEN, ED., CLAITORS PUBLISHING, 1980, P 246-259
7. C.M. ADAM, STRUCTURE/PROPERTY RELATIONSHIPS AND APPLICATIONS OF RAPIDLY SOLIDIFIED ALUMINUM ALLOYS, *RAPIDLY SOLIDIFIED AMORPHOUS AND CRYSTALLINE ALLOYS*, VOL 8, B.H. KEAR, B.C. GIESSEN, AND M. COHEN, ED., ELSEVIER SCIENCE PUBLISHING CO., 1982, P 411-422
12. *SOURCE BOOK ON SELECTION AND FABRICATION OF ALUMINUM ALLOYS*, AMERICAN SOCIETY FOR METALS, 1978, P 233-263
13. G.E. METZGER, GAS TUNGSTEN ARC WELDING OF A POWDER METALLURGY ALUMINUM ALLOY, *WELD. J.*, VOL 71 (NO. 8), 1992, P 297S-304S
14. M.C. FLEMINGS, *SOLIDIFICATION PROCESSING*, MCGRAW-HILL INC., 1974, P 207-208
15. P.S. GILMAN, ALLIED-SIGNAL INC., PRIVATE COMMUNICATION, 2 FEB 1993

Selection and Weldability of Dispersion-Strengthened Aluminum Alloys

K. Sampath, Concurrent Technologies Corporation; W.A. Baeslack III, The Ohio State University

Fusion Welding

Fusion welding studies on dispersion-strengthened aluminum alloys have focused on the use of GTAW, with and without the addition of filler wire; resistance spot welding; and autogenous welding using capacitor-discharge, electron-beam (EB), and pulsed Nd:YAG laser welding processes. These studies have related welding conditions to their effects on weld microstructure and mechanical properties.

Gas-Tungsten Arc Welding. Autogenous butt welding of 1.6 mm (0.06 in.) thick Al-10Fe-5Ce alloy sheets using the GTAW process has resulted in excessive porosity in the fusion zone (Ref 13). However, vacuum pretreating the base alloy sheets for 20 h at 400 °C (750 °F) prior to GTAW using direct current electrode negative and helium gas shielding conditions reduced the level of porosity in the weld zone significantly. Unfortunately, this pretreatment also resulted in an 8% decrease in the tensile strength of the base alloy due to microstructural coarsening.

The same investigation evaluated the application of three conventional, unmatched filler wire additions--ER4043 (Al-5Si), ER4047 (Al-12Si), and ER5356 (Al-5Mg)--to the gas-tungsten arc weld pool. The results indicated that the ER5356 filler metal provided virtually porosity-free weld deposits following the vacuum pretreatment of the base alloy. Transverse weld tensile testing of the gas-tungsten arc welds produced using the ER5356 filler wire additions and vacuum pretreatment showed the joint efficiency to increase from 55% at room temperature to about 81% at 315 °C (600 °F). Despite an acceptable weld joint efficiency at elevated temperature, the transverse weld tensile testing revealed low (1%) ductility. Weld microstructure characterization showed that the minimal ductility was related to the presence of brittle, acicular intermetallics near the fusion boundary with the base metal. The formation of these brittle intermetallics is evidently related to the occurrence of near-equilibrium weld solidification conditions.

Capacitor-Discharge Welding. Compared to the gas-tungsten arc weld in the Al-10Fe-5Ce alloy, the microstructural characterization of autogenous capacitor-discharge welds produced in 6.4 mm (0.25 in.) cylindrical specimens of an Al-8Fe-4Ce alloy showed that the extremely rapid heating and cooling rates obtainable in this process can allow the generation of rapidly solidified, size-refined fusion zone microstructures (Ref 10, 16). In addition, this investigation revealed that increasing the forge pressure during the final bonding stage minimized fusion zone porosity. Transmission electron microscopy characterization of a moderately cooled capacitor-discharged weld in Al-8Fe-4Ce alloy showed fine-size acicular intermetallic particles in an extremely fine dendritic α-aluminum matrix, along with a minimal distribution of spherical intermetallic particles (Fig. 2). Although the microstructural features of the weld zone were similar to those of the RS-P/M base alloy microstructure, the relatively fine weld zone microstructures showed a higher hardness than the base alloy.

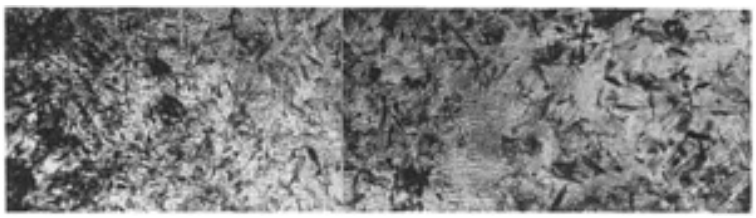

FIG. 2 A TEM MICROSTRUCTURE TRAVERSE ACROSS A MODERATELY COOLED CAPACITOR-DISCHARGE WELD IN AL-8FE-4CE ALLOY. SOURCE: REF 10

Electron-Beam and Laser-Beam Welding. Table 2 shows the weld parameters and weldment characteristics of autogenous EB and pulsed Nd:YAG laser welds produced in a low-hydrogen (<1 mL/100 g of aluminum) Al-8Fe-2Mo alloy. These welds showed only occasional evidence of fusion zone porosity (Ref 17, 18, 19). Evaluation of room-temperature weld mechanical properties of the EB welds produced in 1.27 mm (0.05 in.) thick Al-8Fe-2Mo alloy sheet showed a high weld joint efficiency of 73%, corresponding to 19.3 J/mm (490 J/in.) weld energy input, and preferential failure along the weld interface with the base material at minimal weld ductility. In comparison, transverse weld tensile testing of the EB weld, produced in 0.65 mm (0.026 in.) thick Al-8Fe-2Mo alloy sheet using 4.5 J/mm (114 J/in.) energy input determined 88% weld joint efficiency, appreciable weld ductility, and preferential failure in the weld HAZ. These observations indicate that reducing the energy input shifted the area most susceptible to failure from the fusion boundary region to the base metal. In fact, scanning electron microscopy examination of the fracture surfaces showed that the preferential failure along the weld interface was invariably related to the presence of acicular intermetallic particles in the fusion boundary region (Fig. 3).

TABLE 2 WELDING PARAMETERS AND WELDMENT CHARACTERISTICS OF AL-8FE-2.3MO ALLOY WELDS

WELDMENT NO.	TRAVEL SPEED		ENERGY INPUT		THRESHOLD BENDING STRAIN, %	TRANSVERSE WELD TENSILE TEST RESULTS				
						ULTIMATE TENSILE STRENGTH		ELONGATION, %	FAILURE LOCATION[A]	JOINT EFFICIENCY, %[B]
	MM/S	IN./MIN	J/MM	J/IN.		MPA	KSI			
ELECTRON-BEAM WELDING OF 1.27 MM (0.05 IN.) SHEET (REF 17)										
1[C]	16.9	41	23.6	599	4.0	330	47.8	1.6	FBR	**65**
2[C]	23.3	56	19.3	490	4.0	370	53.6	5.6	FBR	**73**
ELECTRON-BEAM WELDING OF 0.65 MM (0.026 IN.) SHEET (REF 18)										
3[D]	27.5	66	4.5	114	14.0	360	52.2	1.6	HAZ	**85**
PULSED ND:YAG LASER WELDING OF 1.27 MM (0.05 IN.) SHEET (REF 1)										
4[E]	**2.5**	**6**	**41.3[F]**	**1049[F]**	**11.0**	**374**	**54.2**	**11**	**UBM**	**100**

(A) FBR, FUSION BOUNDARY REGION; HAZ, HEAT AFFECTED ZONE; UBM, UNAFFECTED BASE METAL.

(B) JOINT EFFICIENCY IS A RATIO OF WELD STRENGTH TO BASE METAL STRENGTH IN THE SAME ORIENTATION.

(C) WELD PARAMETERS: ACCELERATION VOLTAGE 100 KV; CURRENT 3.5 MA.

(D) WELD PARAMETERS: ACCELERATION VOLTAGE 100 KV; CURRENT 1.25 MA.

(E) WELD PARAMETERS: 10 HZ PULSE RATE; 5.0 MS PULSE DURATION; 105 W PULSE POWER (10.5 J/PULSE); 2.1 KW PEAK POWER; 102 MM (4 IN.) FOCAL LENGTH; 10^6 W/MM^2 POWER DENSITY; 16.5 L/MIN (35 FT^3/H) ARGON SHIELDING GAS FLOW RATE.

(F) AVERAGE ENERGY INPUT

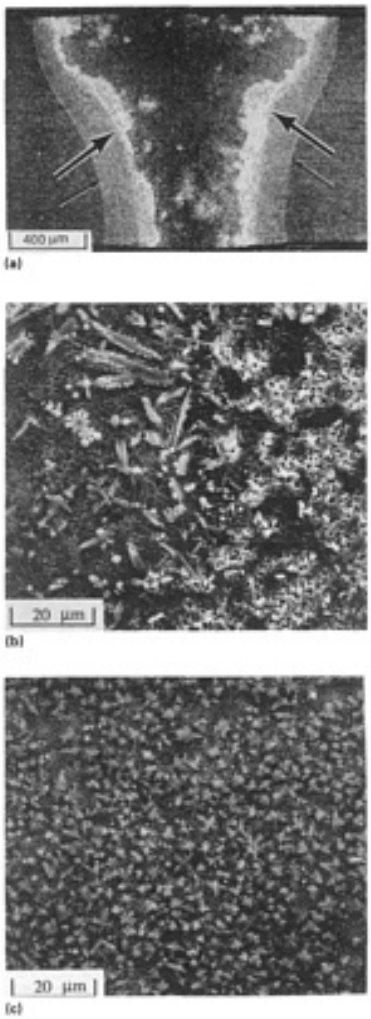

FIG. 3 ELECTRON-BEAM WELD (ENERGY INPUT 15 J/MM, OR 38 J/IN.) IN 1.27 MM (0.05 IN.) THICK AL-8FE-2MO SHEET. (A) WELD MACROSTRUCTURE (LARGE ARROWS INDICATE FUSION BOUNDARY; SMALL ARROWS INDICATE HAZ BOUNDING FUSION ZONE). (B) SEM MICROSTRUCTURE NEAR THE FUSION BOUNDARY. (C) SEM MICROSTRUCTURE NEAR WELD CENTER. SOURCE: REF 17

Microscopic examination of the low-energy-input EB weld showed that reducing the weld energy input minimized or eliminated the occurrence of acicular intermetallic particles within the fusion zone and produced refined α-aluminum dendrites (Ref 18). Coincident with the elimination of the acicular intermetallic particles near the fusion boundary, a relatively light-etching region was observed within the weld zone. Transmission electron microscopy examination of these regions revealed α-aluminum growth structures around coarse-size intermetallic particles (Fig. 4). In fact, TEM examination of a keyhole-type EB weld produced in a 2.5 mm (0.10 in.) thick RS-P/M Al-8Fe-1.7Ni alloy showed a similar microstructure at the weld center, one that contained primary Al_3Fe-type intermetallic particles nucleating an α-aluminum sheath around the primary particles (Ref 21). The α-aluminum sheath structure changed to a lamellar eutectic structure. In contrast to this structure, the fusion boundary region of this weld showed an epitaxially grown, extremely fine Al/Al_6Fe-type coupled-eutectic structure.

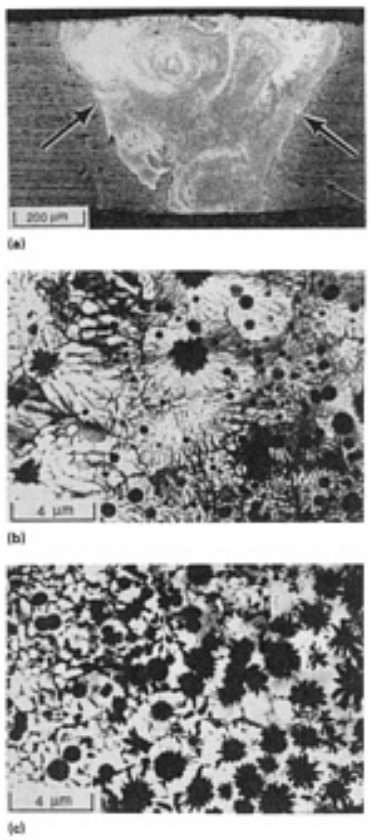

FIG. 4 ELECTRON-BEAM WELD (ENERGY INPUT 4.5 J/MM, OR 114 J/IN.) IN 0.65 MM (0.026 IN.) THICK AL-8FE-2MO SHEET. (A) WELD MACROSTRUCTURE (LARGE ARROWS INDICATE FUSION BOUNDARY, SMALL ARROWS INDICATE HAZ BOUNDING FUSION ZONE). (B) TEM MICROSTRUCTURE OF THE LIGHT-ETCHING REGIONS. (C) TEM MICROSTRUCTURE OF THE DARK-ETCHING REGIONS NEAR WELD CENTER. SOURCE: REF 20

Compared with the EB welds, autogenous pulsed Nd:YAG laser welding studies on 1.27 mm (0.05 in.) thick Al-8Fe-2Mo alloy sheet using a higher-energy-density (power density $>10^6$ W/mm^2) welding condition showed that the transverse weld joint efficiency could be improved to 100% (Ref 19). The longitudinal weld bend ductility was also comparable with that of the RS-P/M base alloy. Transmission electron microscopy examination of the fusion boundary region showed that the pulsed Nd:YAG laser welding conditions produced a matrix consisting of a columnar-dendritic α-aluminum structure with a uniform distribution of fine Al_6Fe-type spherical intermetallic particles and solute-rich particles at the dendrite interstices (Fig. 5). The pulse overlap region of the weld zone showed microstructures very similar to those observed in the EB welds, albeit on a structurally finer scale. The low overall weld energy input resulted in a narrow HAZ with the base metal and only minimal structural coarsening (Ref 21, 22).

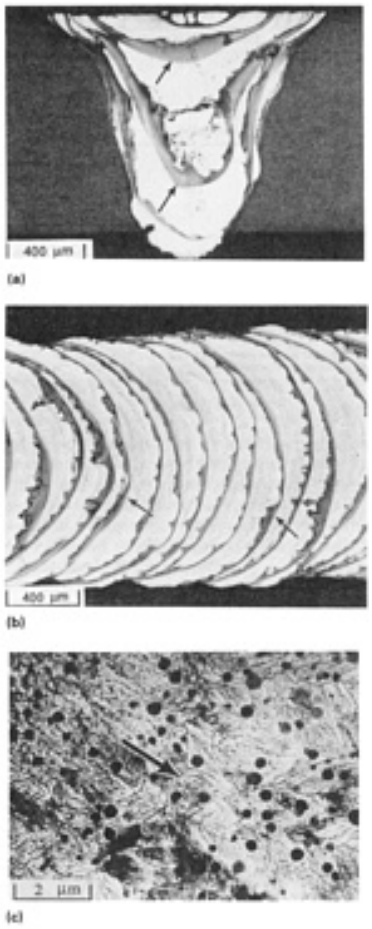

FIG. 5 PULSED ND:YAG LASER WELD IN AL-8FE-2MO SHEET. (A) TRANSVERSE SECTION. (B) PLAN VIEW. (C) TEM MICROSTRUCTURE OF THE LIGHT-ETCHING REGIONS NEAR THE FUSION BOUNDARY WITH BASE ALLOY. ARROWS IN (A) AND (B) INDICATE CURVILINEAR BANDS BOUNDING SUCCESSIVE MELT ZONES. ARROW IN (C) INDICATES COLUMNAR-DENDRITIC GROWTH DIRECTION. SOURCE: REF 19

Development of Weld Microstructure. The occurrence of different types of weld zone microstructures and significant differences in weld mechanical properties underscore the effects of welding process conditions and parameters on weld microstructure development. Specifically, distinct variations in the morphology and population density of the intermetallic particles within the weld zone occur as the weld energy input is decreased and/or as the energy density (power density) is increased. An analysis based on peak temperature distribution during fusion welding indicated that despite the use of high-energy-density welding processes, these welds likely contained undissolved base metal dispersoid particles within the bulk fusion zone (Ref 20). A weld solidification analysis based on this premise showed that the subsequent microstructure development within the fusion zone occurs as one of the following three different types, depending on local thermal conditions--principally cooling rate and temperature gradient--that depend on welding process condition and parameters:

- *TYPE A:* AL_3FE-TYPE INTERMETALLIC PARTICLES IN A MATRIX OF DENDRITIC A ALUMINUM WITH INTERDENDRITIC LAMELLAR OR DIVORCED EUTECTIC
- *TYPE B:* AL_3FE-TYPE INTERMETALLIC PARTICLES THAT ACT AS GROWTH CENTERS FOR DENDRITIC α ALUMINUM WITH INTERDENDRITIC LAMELLAR OR DIVORCED EUTECTIC
- *TYPE C:* AL_6FE-TYPE INTERMETALLIC PARTICLES ENTRAPPED IN A MATRIX OF DENDRITIC α ALUMINUM WITH INTERDENDRITIC DIVORCED EUTECTIC

Depending on local weld solidification conditions, the above three types of microstructures can be observed at different regions within the same weld.

Figures 6, 7, and 8 show Al-Al_3Fe pseudobinary phase diagrams to illustrate possible solidification events that promote the formation of type A, type B, and type C microstructures, respectively. In these diagrams, C_O represents the nominal composition of the alloy, and C_O' represents the effective composition of the melt (containing undissolved base metal dispersoid particles) prior to the onset of weld solidification, T_E is the equilibrium (Al-Al_3Fe) eutectic temperature and T'_E is the metastable (Al-Al_3Fe) eutectic temperature. In Fig. 6 and 7, C''_O represents the composition of the melt at which the solidification mode changes from hypereutectic to hypoeutectic with respect to the metastable eutectic composition.

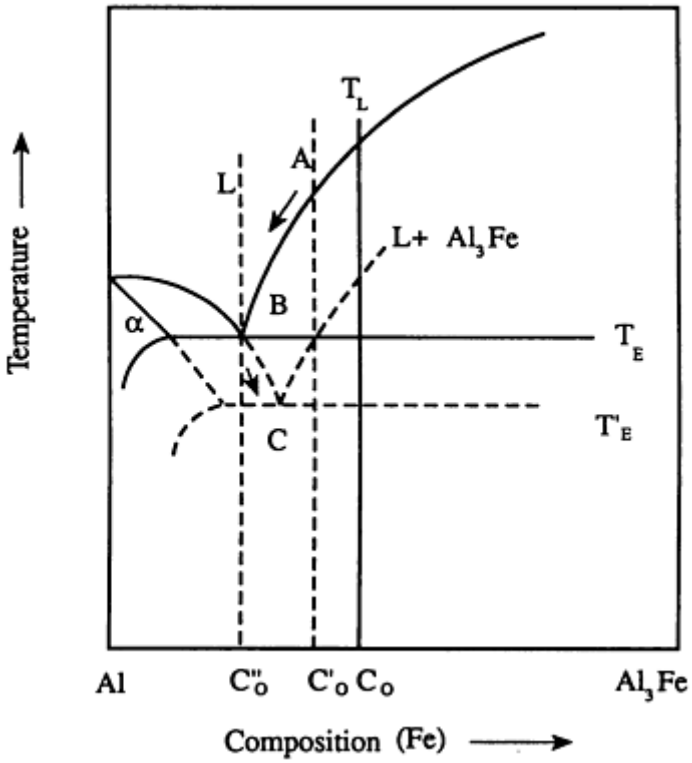

FIG. 6 AL-AL_3FE PSEUDOBINARY PHASE DIAGRAM ILLUSTRATING THE SEQUENCE OF SOLIDIFICATION EVENTS LEADING TO THE FORMATION OF TYPE A MICROSTRUCTURE. SOURCE: REF 20

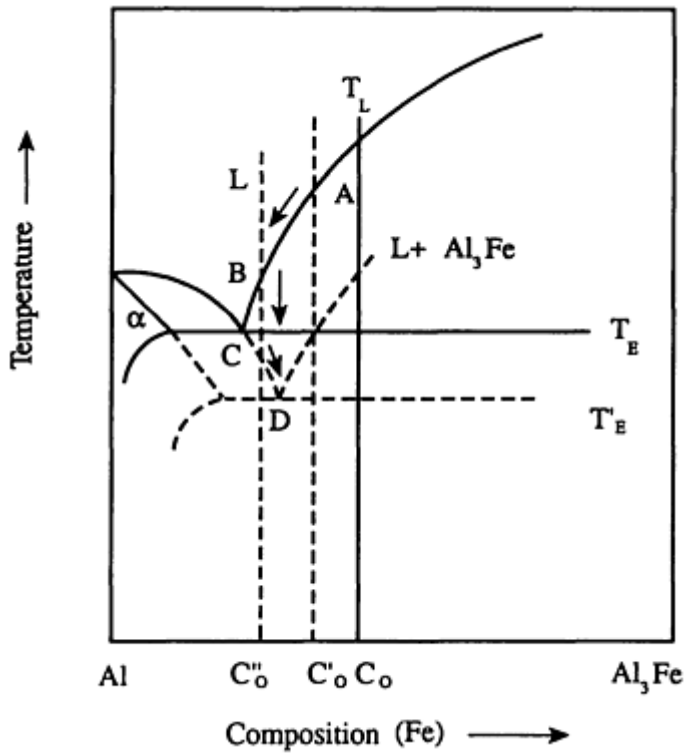

FIG. 7 AL-AL_3FE PSEUDOBINARY PHASE DIAGRAM ILLUSTRATING THE SEQUENCE OF SOLIDIFICATION EVENTS LEADING TO THE FORMATION OF TYPE B MICROSTRUCTURE. SOURCE: REF 20

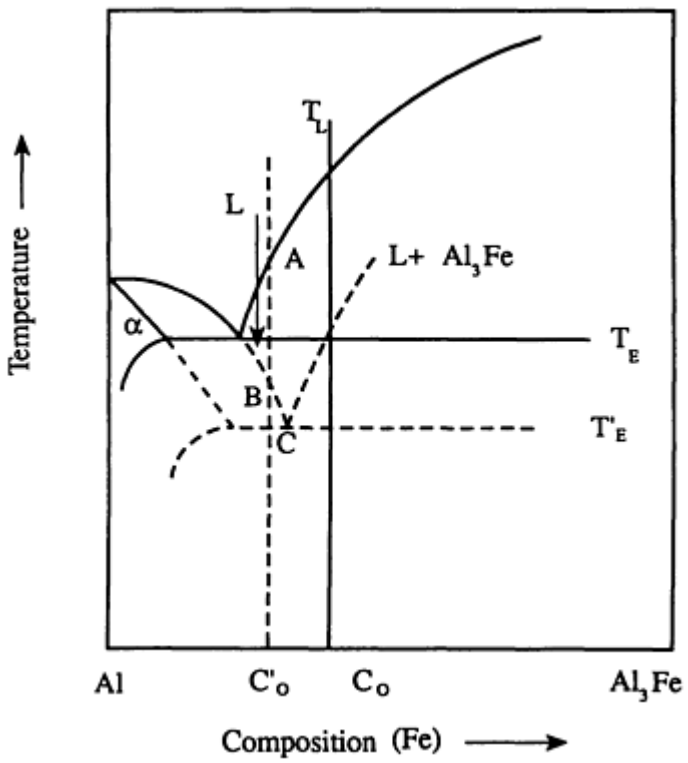

FIG. 8 AL-AL_3FE PSEUDOBINARY PHASE DIAGRAM ILLUSTRATING THE SEQUENCE OF SOLIDIFICATION EVENTS LEADING TO THE FORMATION OF TYPE C MICROSTRUCTURE. SOURCE: REF 20

The Type A Microstructure is a near-equilibrium microstructure and occurs within the fusion boundary region of high-energy-input welds. As shown in Fig. 6, the type A microstructure appears to occur in three stages. Initially, the undissolved base metal dispersoid particles grow in a relatively stagnant liquid region into randomly oriented, primary intermetallic particles and promote solute depletion in the remaining melt (from A to B). Since the primary intermetallic particles have a poor nucleation potency for α aluminum, solute depletion in the melt promotes the epitaxial growth of columnar-dendritic α aluminum from base metal α(from B to C). Further, since the α-aluminum solidification initiates from the fusion boundary at relatively low solidification velocities, the local solidification conditions promote appreciable structural coarsening and produce relatively coarse α-aluminum dendrites. Solute partitioning accompanying the α-aluminum growth promotes a solute-rich melt at the interdendritic regions, which undergoes terminal solidification to a metastable Al/Al_6Fe-type lamellar eutectic at the α-aluminum dendrite interstices (at C). These types of microstructures are commonly observed throughout the fusion zone in gas-tungsten arc weldments produced in these alloy types (Ref 13).

The Type B Microstructure contains both stable and metastable microstructural constituents. This structure is associated with high-energy-input welding conditions and is commonly observed within the central weld zone. As shown in Fig. 7, this microstructure appears to form with the growth of Al_3Fe-type intermetallic particles (from A to B). Due to high weld cooling rates, considerable undercooling occurs (from B to C) subsequent to the initial growth of the primary intermetallic particles, which allows the growth of supersaturated α-aluminum dendrites (from C to D). The occurrence of a metastable α-aluminum growth structure also indicates that the composition of the melt surrounding the equiaxed intermetallic particles was essentially hypoeutectic relative to the metastable eutectic composition. With the growth of the α-aluminum, the composition of the remaining melt in the dendrite interstices is enriched with solute elements. It ultimately reaches the metastable eutectic composition and undergoes terminal (metastable) eutectic solidification (at D). In view of the fine size of the interdendritic region, solute-rich particles are formed in this region instead of a regular lamellar eutectic (Ref 23).

The formation of the metastable α-aluminum growth structure around the primary intermetallic particles is attributed to catalytic nucleation. Catalytic nucleation of α aluminum occurs when the lattice disregistry between the potential nucleant and αaluminum is reduced below 10% (Ref 24). Since the supersaturation of solute elements in aluminum shows a negative deviation from Vegard's law and reduces the lattice parameter of α aluminum (Ref 25), improved lattice registry between the primary intermetallic particles and the metastable α aluminum, along with shallow temperature gradients in the central fusion zone, is considered responsible for the occurrence of the equiaxed-dendritic α-aluminum growth structure.

The Type C Microstructure is essentially a metastable growth structure and is associated with the extremely high-energy-density, low-energy-input welding conditions. Similar to the type A near-equilibrium microstructure, the type C metastable microstructure starts from the fusion boundary region with the base metal, by epitaxial solidification of α(or coupled eutectic) from base metal α in the fusion boundary. As shown in Fig. 8, the epitaxial growth of the α-aluminum grains appears to occur at significantly high undercoolings, possibly at temperatures slightly above the metastable eutectic temperature. Evidently, the coupled eutectic growth structures occur when the undercooling is below the metastable eutectic temperature.

The epitaxially grown α-aluminum grains entrap the undissolved dispersoid particles as solidification proceeds along a relatively steep temperature gradient across the advancing solid-liquid interface. The spherical morphology of the intermetallic particles is attributed to the high fusion zone cooling rate (in excess of 10^5 °C/s, or 1.8×10^5 °F/s), which does not provide adequate time for the growth of the undissolved base metal dispersoid particles. The steep temperature gradients in this region promote solidification of the melt to a columnar-dendritic substructure with fine intermetallics or solute-rich particles partitioning to the dendrite interstices. Coincident with the growth of the metastable α aluminum, the remaining melt is enriched with solute elements, which undergo final solidification to fine particles due to the relatively fine size of the interdendritic regions (Ref 23).

Epitaxial solidification generally indicates local wetting of the fusion boundary and minimal melt undercooling. However, epitaxially grown type C microstructures in the fusion boundary suggest that despite a readily wettable substrate, metastable growth structures in the weld fusion zone can likely occur from the combined effects of a minimal nucleation barrier for the metastable phase, a steep temperature gradient that restricts the growth of the stable phase, and perhaps a minimal difference in the level of undercooling required to allow the growth of metastable structures. In fact, although the nucleation of Al_3Fe occurs at less than 8 °C (14 °F) undercooling in aluminum-iron melts, the nucle tion of Al_6Fe is favored at undercoolings in excess of 10 °C (18 °F) (Ref 26).

References cited in this section

1. J.R. PICKENS, HIGH STRENGTH ALUMINUM P/M ALLOYS, 10TH ED., VOL 2, *METALS HANDBOOK, PROPERTIES AND SELECTION: NON FERROUS ALLOYS AND SPECIAL-PURPOSE MATERIALS,* ASM INTERNATIONAL, 1990, P 200-215

10. W.A. BAESLACK III, K.H. HOU, AND J.H. DEVLETIAN, ELECTRON MICROSCOPY OF RAPIDLY SOLIDIFIED WELDMENTS IN A POWDER METALLURGY AL-FE-CE ALLOY, *J. MATER. SCI. LETT.,* VOL 8 (NO. 6), 1989, P 716-720

13. G.E. METZGER, GAS TUNGSTEN ARC WELDING OF A POWDER METALLURGY ALUMINUM ALLOY, *WELD. J.,* VOL 71 (NO. 8), 1992, P 297S-304S

16. W.A. BAESLACK III, K.H. HOU, AND J.H. DEVLETIAN, RAPID SOLIDIFICATION JOINING OF A POWDER METALLURGY AL-FE-CE ALLOY, *J. MATER. SCI. LETT.,* VOL 7 (NO. 9), 1988, P 944-948

17. W.A. BAESLACK III AND S. KRISHNASWAMY, ELECTRON BEAM WELDABILITY OF A RAPIDLY SOLIDIFIED ALUMINUM ALLOY, *ADVANCES IN WELDING SCIENCE & TECHNOLOGY,* S.A. DAVID, ED., ASM INTERNATIONAL, 1986, P 357-362

18. S. KRISHNASWAMY AND W.A. BAESLACK III, STRUCTURE, PROPERTIES AND FRACTURE OF EB WELDS IN AL-8FE-2MO, *MATER. SCI. ENG.,* VOL 98, 1988, P 137-141

19. S. KRISHNASWAMY AND W.A. BAESLACK III, ND:YAG LASER WELDABILITY OF RS/PM AL-8FE-2MO SHEET, *RECENT TRENDS IN WELDING SCIENCE & TECHNOLOGY,* S.A. DAVID AND J.M. VITEK, ED., ASM INTERNATIONAL, 1990, P 631-636

20. S. KRISHNASWAMY, WELDABILITY OF A RAPID SOLIDIFICATION POWDER METALLURGY AL-8FE-2MO ALLOY, PH.D. DISSERTATION, THE OHIO STATE UNIVERSITY, MARCH 1989

21. W.A. BAESLACK III, MICROSTRUCTURAL TRANSITIONS IN A WELDED POWDER METALLURGY AL-8FE-1.7NI ALLOY, *METALLOGRAPHY,* VOL 18, 1985, P 73-82

22. S. KRISHNASWAMY AND W.A. BAESLACK III, METALLOGRAPHY OF A PULSED ND:YAG LASER WELD IN A RS/PM AL-8FE-2MO SHEET, *MATER. CHARACT.,* VOL 24 (NO. 4), 1990, P 331-353

23. H. JONES, *RAPID SOLIDIFICATION OF METALS AND ALLOYS,* MONOGRAPH 8, INSTITUTION OF METALLURGISTS, LONDON, 1982, P 45

24. J.H. PEREPEZKO AND S.E. LEBEAU, NUCLEATION OF AL DURING SOLIDIFICATION, *ALUMINUM TRANSFORMATION TECHNOLOGY AND APPLICATIONS--1981,* C.A. PAMPILLO, H. BILONI, L.F. MONDOLFO, AND F. SACCHI, ED., AMERICAN SOCIETY FOR METALS, 1982, P 309-346

25. H. JONES, OBSERVATIONS ON A STRUCTURAL TRANSITION IN ALUMINUM ALLOYS HARDENED BY RAPID SOLIDIFICATION, *MATER. SCI. ENG.,* 1969-70, P 1-18

26. L.F. MONDOLFO, ALUMINUM-IRON SYSTEM, *ALUMINUM ALLOYS: STRUCTURE AND PROPERTIES,* BUTTERWORTHS, LONDON, 1976, P 283-289

Solid-State Welding

The solid-state welding studies on RS-P/M aluminum-iron-base alloys are mostly limited to the application of conventional friction welding, inertia friction welding, or linear friction welding methods to produce similar or dissimilar metal welds in cylindrical specimens. In general, these studies evaluated the effects of weld axial force on the structure, mechanical properties, and fracture behavior of the friction welds. These studies include similar welds between Al-9Fe-4Ce and Al-9Fe-7Ce alloys, dissimilar welds between Al-9Fe-4Ce and I/M 2024-T351 (Ref 27), similar welds between AA8009 alloy (Ref 9), similar welds between FVS1212 alloy (Ref 28), dissimilar welds between FVS1212 alloy and I/M

2024-T351 (Ref 29), similar welds between Al-9Fe-3Mo-1V alloys (Ref 30), and dissimilar welds between Al-9Fe-3Mo-1V alloy and I/M 2024-T351 (Ref 11). The similar welds exhibit a uniform flash around the weld joint, the amount of the flash increasing with the weld axial force. The dissimilar welds, however, show a nonuniform flash around the weld joint. The alloy with the higher strength at elevated temperatures (RS-P/M base alloy) forms a minimal flash compared to the alloy with a higher strength at room temperature (I/M 2024-T351 alloy).

Light and analytical electron microscopy examinations of the interface region (weld center) in inertia friction welds have shown extensive high-temperature plastic deformation in the heat-and-deformation zone. This plastic deformation was generally beneficial in effectively homogenizing the base metal microstructure. The plastic deformation often promoted the fracture of coarse, acicular dispersoid particles present in selected base alloys (Ref 11, 30). However, the fine spherical dispersoid particles commonly observed in AA8009 alloy were relatively unaffected by the level of plastic deformation occurring in the weld zone and usually did not show any evidence of coarsening or fracture (Ref 9). Further, in welds produced using a low axial force, nonuniform deformation at the weld outer periphery resulted in the formation of dispersoid-lean, coarse-grain regions with a hardness appreciably lower than that of the base alloy. The application of a sufficiently higher axial force extruded out this softened region as weld flash, thereby preventing the hardness degradation across the weld zone (Fig. 9). Results of transverse weld tensile testing were generally consistent with the microstructural observations, showing that weld joint efficiency up to 95% of the base metal tensile strength can be obtained in welds produced using high axial force.

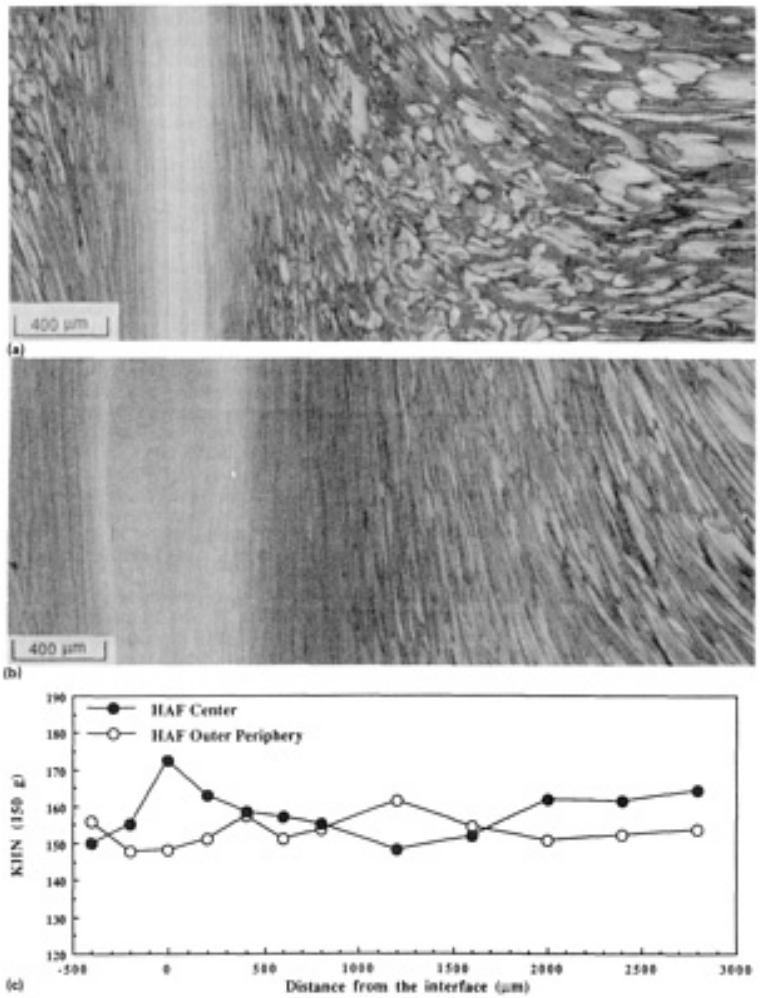

FIG. 9 LIGHT MICROGRAPHS OF AN INERTIA-FRICTION WELD IN AA8009 ALLOY PRODUCED USING HIGH AXIAL FORCE. (A) CENTER. (B) OUTER PERIPHERY. (C) CORRESPONDING KNOOP HARDNESS TRAVERSE. SOURCE: REF 9

Unlike the microstructure of the inertia friction welds, linear friction welds (produced in similar welds between FVS1212 alloy and dissimilar welds between FVS1212 alloy and I/M 2024-T351) showed appreciable coarsening of the α-

aluminum grains and the base metal dispersoid particles resulting from a somewhat slower weld thermal cycle and less forging force (Ref 29). Appropriate optimization of welding parameters to provide rapid weld thermal cycles is expected to minimize the microstructural coarsening in the weld zone.

References cited in this section

9. H.H. KOO, S. KRISHNASWAMY, AND W.A. BAESLACK III, CHARACTERIZATION OF AN INERTIA-FRICTION WELD IN A HIGH-TEMPERATURE RS/PM AI-FE-V-SI ALLOY-AA8009, *MATER. CHARACT.*, VOL 26 (NO. 3), 1991, P 123-136
11. H.H. KOO, K. SAMPATH, AND W.A. BAESLACK III, CHARACTERIZATION OF INERTIA-FRICTION WELDS BETWEEN A RAPIDLY-SOLIDIFIED AL-FE-MO-V ALLOY AND IM 2024-T351, *J. MATER. SCI.*, VOL 27, 1992, P 3266-3280
27. W.A. BAESLACK III AND K. HAGEY, INERTIA FRICTION WELDING OF RAPIDLY SOLIDIFIED POWDER METALLURGY ALUMINUM, *WELD. J.*, VOL 67 (NO. 8), 1988, P 139S-149S
28. H.H. KOO, S. KRISHNASWAMY, AND W.A. BAESLACK III, SOLID-PHASE WELDING OF A DISPERSION-STRENGTHENED AL-FE-V-SI ALLOY-FVS1212, *LOW DENSITY, HIGH STRENGTH POWDER METALLURGY ALLOYS*, W.E. FRAZIER, M.J. KOCZAK, AND P.W. LEE, ED., THE METALLURGICAL SOCIETY OF AIME, 1991, P 183-196
29. H.H. KOO AND W.A. BAESLACK III, FRICTION WELDING OF A RAPIDLY SOLIDIFIED AL-FE-V-SI ALLOY, *WELD. J.*, VOL 71 (NO. 5), 1992, P 147S-169S
30. K.H. HOU AND W.A. BAESLACK III, ELECTRON MICROSCOPY OF INERTIA-FRICTION WELDMENTS IN A RAPIDLY SOLIDIFIED AL-FE-MO-V ALLOY, *J. MATER. SCI.*, VOL 25, 1990, P 2642-2653

Diffusion Welding

Diffusion welding of RS-P/M aluminum-iron-cerium alloy was investigated using electroplated silver interlayers (Ref 31). Temperature-time and temperature-pressure diffusion welding parameter zones were developed for an A1-9Fe-4Ce alloy and showed that it was possible to perform diffusion welding operations at temperatures up to 600 °C (1110 °F) without structural support. Although poor joint efficiencies were obtained for welds produced at low pressures, an increase in pressure and the promotion of deformation at the weld interface promoted joint efficiencies of up to 70%. The weld interface regions were characterized by the presence of a silver-aluminum intermetallic and occasional Kirkendall porosity.

Reference cited in this section

31. V. ANANTHANARAYANAN, "DIFFUSION WELDING OF AN RS/PM ALUMINUM ALLOY," PH.D. DISSERTATION, THE OHIO STATE UNIVERSITY, 1988

References

1. J.R. PICKENS, HIGH STRENGTH ALUMINUM P/M ALLOYS, 10TH ED., VOL 2, *METALS HANDBOOK, PROPERTIES AND SELECTION: NON FERROUS ALLOYS AND SPECIAL-PURPOSE MATERIALS,* ASM INTERNATIONAL, 1990, P 200-215
2. S.K. DAS AND L.A. DAVIES, HIGH PERFORMANCE AEROSPACE ALLOYS VIA RAPID SOLIDIFICATION PROCESSING, *MATER. SCI. ENG.,* VOL 98, 1988, P 1-12
3. C.M. ADAM, RAPID SOLIDIFICATION PROCESSING METHODS, *MECHANICAL BEHAVIOR OF RAPIDLY SOLIDIFIED MATERIALS,* S.M.L. SASTRY AND B.A. MACDONALD, ED., THE METALLURGICAL SOCIETY OF AIME, 1985, P 21-39
4. C.M. ADAM AND R.G. BOURDEAU, TRANSITION AND REFRACTORY ELEMENT ADDITIONS TO RAPIDLY SOLIDIFIED ALUMINUM ALLOYS, *RAPID SOLIDIFICATION PROCESSING: PRINCIPLES AND TECHNOLOGIES II,*R. MEHRABIAN, B.H. KEAR, AND M. COHEN, ED., CLAITORS PUBLISHING, 1980, P 246-259
5. I.E. ANDERSON AND M.P. KEMPAINEN, UNDERCOOLING EFFECTS IN GAS-ATOMIZED POWDERS, *UNDERCOOLED ALLOY PHASES,* E.W. COLLINGS AND C.C. KOCH, ED., THE METALLURGICAL SOCIETY OF AIME, 1988, P 269-285
6. C.M. ADAM, RAPID SOLIDIFICATION TECHNOLOGY: THE POTENTIAL FOR INNOVATIVE ALLOY PROPERTIES, *SCIENCE AND TECHNOLOGY OF UNDERCOOLED MELTS,* P.R. SAHM, H. JONES, AND C.M. ADAMS, ED., NATO-ASI SERIES, MARTINUS-NIJHOFF PUBLISHERS, 1986, P 186-209
7. C.M. ADAM, STRUCTURE/PROPERTY RELATIONSHIPS AND APPLICATIONS OF RAPIDLY SOLIDIFIED ALUMINUM ALLOYS, *RAPIDLY SOLIDIFIED AMORPHOUS AND CRYSTALLINE ALLOYS,* VOL 8, B.H. KEAR, B.C. GIESSEN, AND M. COHEN, ED., ELSEVIER SCIENCE PUBLISHING CO., 1982, P 411-422
8. S.L. LANGENBECK, W.M. GRIFFITH, G.J. HILDEMAN, AND J.W. SIMON, DEVELOPMENT OF DISPERSION-STRENGTHENED ALUMINUM ALLOYS, *RAPIDLY SOLIDIFIED ALUMINUM ALLOYS,* STP 890, M.E. FINE AND E.A. STARKE, JR., ED., ASTM, 1986, P 410-422
9. H.H. KOO, S. KRISHNASWAMY, AND W.A. BAESLACK III, CHARACTERIZATION OF AN INERTIA-FRICTION WELD IN A HIGH-TEMPERATURE RS/PM AI-FE-V-SI ALLOY-AA8009, *MATER. CHARACT.,* VOL 26 (NO. 3), 1991, P 123-136
10. W.A. BAESLACK III, K.H. HOU, AND J.H. DEVLETIAN, ELECTRON MICROSCOPY OF RAPIDLY SOLIDIFIED WELDMENTS IN A POWDER METALLURGY AL-FE-CE ALLOY, *J. MATER. SCI. LETT.,* VOL 8 (NO. 6), 1989, P 716-720
11. H.H. KOO, K. SAMPATH, AND W.A. BAESLACK III, CHARACTERIZATION OF INERTIA-FRICTION WELDS BETWEEN A RAPIDLY-SOLIDIFIED AL-FE-MO-V ALLOY AND IM 2024-T351, *J. MATER. SCI.,* VOL 27, 1992, P 3266-3280
12. *SOURCE BOOK ON SELECTION AND FABRICATION OF ALUMINUM ALLOYS,* AMERICAN SOCIETY FOR METALS, 1978, P 233-263
13. G.E. METZGER, GAS TUNGSTEN ARC WELDING OF A POWDER METALLURGY ALUMINUM ALLOY, *WELD. J.,* VOL 71 (NO. 8), 1992, P 297S-304S
14. M.C. FLEMINGS, *SOLIDIFICATION PROCESSING,* MCGRAW-HILL INC., 1974, P 207-208
15. P.S. GILMAN, ALLIED-SIGNAL INC., PRIVATE COMMUNICATION, 2 FEB 1993
16. W.A. BAESLACK III, K.H. HOU, AND J.H. DEVLETIAN, RAPID SOLIDIFICATION JOINING OF A POWDER METALLURGY AL-FE-CE ALLOY, *J. MATER. SCI. LETT.,* VOL 7 (NO. 9), 1988, P 944-948
17. W.A. BAESLACK III AND S. KRISHNASWAMY, ELECTRON BEAM WELDABILITY OF A RAPIDLY SOLIDIFIED ALUMINUM ALLOY, *ADVANCES IN WELDING SCIENCE & TECHNOLOGY,* S.A. DAVID, ED., ASM INTERNATIONAL, 1986, P 357-362
18. S. KRISHNASWAMY AND W.A. BAESLACK III, STRUCTURE, PROPERTIES AND FRACTURE OF EB WELDS IN AL-8FE-2MO, *MATER. SCI. ENG.,* VOL 98, 1988, P 137-141
19. S. KRISHNASWAMY AND W.A. BAESLACK III, ND:YAG LASER WELDABILITY OF RS/PM AL-8FE-2MO SHEET, *RECENT TRENDS IN WELDING SCIENCE & TECHNOLOGY,* S.A. DAVID AND

J.M. VITEK, ED., ASM INTERNATIONAL, 1990, P 631-636

20. S. KRISHNASWAMY, WELDABILITY OF A RAPID SOLIDIFICATION POWDER METALLURGY AL-8FE-2MO ALLOY, PH.D. DISSERTATION, THE OHIO STATE UNIVERSITY, MARCH 1989
21. W.A. BAESLACK III, MICROSTRUCTURAL TRANSITIONS IN A WELDED POWDER METALLURGY AL-8FE-1.7NI ALLOY, *METALLOGRAPHY,* VOL 18, 1985, P 73-82
22. S. KRISHNASWAMY AND W.A. BAESLACK III, METALLOGRAPHY OF A PULSED ND:YAG LASER WELD IN A RS/PM AL-8FE-2MO SHEET, *MATER. CHARACT.,* VOL 24 (NO. 4), 1990, P 331-353
23. H. JONES, *RAPID SOLIDIFICATION OF METALS AND ALLOYS,* MONOGRAPH 8, INSTITUTION OF METALLURGISTS, LONDON, 1982, P 45
24. J.H. PEREPEZKO AND S.E. LEBEAU, NUCLEATION OF AL DURING SOLIDIFICATION, *ALUMINUM TRANSFORMATION TECHNOLOGY AND APPLICATIONS--1981,* C.A. PAMPILLO, H. BILONI, L.F. MONDOLFO, AND F. SACCHI, ED., AMERICAN SOCIETY FOR METALS, 1982, P 309-346
25. H. JONES, OBSERVATIONS ON A STRUCTURAL TRANSITION IN ALUMINUM ALLOYS HARDENED BY RAPID SOLIDIFICATION, *MATER. SCI. ENG.,* 1969-70, P 1-18
26. L.F. MONDOLFO, ALUMINUM-IRON SYSTEM, *ALUMINUM ALLOYS: STRUCTURE AND PROPERTIES,* BUTTERWORTHS, LONDON, 1976, P 283-289
27. W.A. BAESLACK III AND K. HAGEY, INERTIA FRICTION WELDING OF RAPIDLY SOLIDIFIED POWDER METALLURGY ALUMINUM, *WELD. J.,* VOL 67 (NO. 8), 1988, P 139S-149S
28. H.H. KOO, S. KRISHNASWAMY, AND W.A. BAESLACK III, SOLID-PHASE WELDING OF A DISPERSION-STRENGTHENED AL-FE-V-SI ALLOY-FVS1212, *LOW DENSITY, HIGH STRENGTH POWDER METALLURGY ALLOYS,* W.E. FRAZIER, M.J. KOCZAK, AND P.W. LEE, ED., THE METALLURGICAL SOCIETY OF AIME, 1991, P 183-196
29. H.H. KOO AND W.A. BAESLACK III, FRICTION WELDING OF A RAPIDLY SOLIDIFIED AL-FE-V-SI ALLOY, *WELD. J.,* VOL 71 (NO. 5), 1992, P 147S-169S
30. K.H. HOU AND W.A. BAESLACK III, ELECTRON MICROSCOPY OF INERTIA-FRICTION WELDMENTS IN A RAPIDLY SOLIDIFIED AL-FE-MO-V ALLOY, *J. MATER. SCI.,* VOL 25, 1990, P 2642-2653
31. V. ANANTHANARAYANAN, "DIFFUSION WELDING OF AN RS/PM ALUMINUM ALLOY," PH.D. DISSERTATION, THE OHIO STATE UNIVERSITY, 1988

Selection and Weldability of Aluminum-Lithium Alloys

C.E. Cross and W.T. Tack, Martin Marietta Astronautics Group

Introduction

ALUMINUM-LITHIUM alloys constitute the most recently developed group of high-performance wrought aluminum alloys intended for use primarily in aircraft and aerospace structures. Because aluminum alloys account for a large portion of the structural weight of most aerospace structures, designers can use the higher elastic modulus, lower density, and, in some cases, higher strength and fracture toughness of aluminum-lithium alloys to reduce structural weight. Another benefit is that the use of aluminum-lithium alloys does not require changes in manufacturing equipment, design methods, or fabrication techniques. In particular, aluminum-lithium alloys have been found to be readily weldable, a characteristic that is uncommon with other high-strength aluminum alloys such as 7075 and 2024.

The purpose of this article is to provide a guide to the welding of aluminum-lithium alloys that are now available commercially. Tabular data are provided for alloy composition, density, and modulus; tensile properties of plate; and tensile properties of weldments. There is limited information in the open literature regarding many of the newer alloys; therefore, some of these tables are incomplete. Weld properties are also characterized in terms of aging response, microstructure, and corrosion resistance.

A detailed and more thorough discussion of aluminum-lithium alloy weldability can be found in two review articles by Pickens (Ref 1, 2). An attempt is made here to give a very concise overview of the subject, including pertinent information from more recent conference proceedings not available for publication in previous reviews. With the fast-accumulating bank of information regarding aluminum-lithium weldments, design engineers can now begin to select and utilize aluminum-lithium alloys based on well-established behavior and property data.

References

1. J.R. PICKENS, THE WELDABILITY OF LITHIUM-CONTAINING ALUMINUM ALLOYS, *J. MATER. SCI.*, VOL 20, 1985, P 4247-4258
2. J.R. PICKENS, RECENT DEVELOPMENTS IN THE WELDABILITY OF LITHIUM-CONTAINING ALUMINUM ALLOYS, *J. MATER. SCI.*, VOL 25, 1990, P 3035-3047

Selection and Weldability of Aluminum-Lithium Alloys

C.E. Cross and W.T. Tack, Martin Marietta Astronautics Group

Commercial Alloys

Classification. Aluminum-lithium alloys can be divided into two groups: aluminum-lithium-magnesium ternary and aluminum-lithium-copper-magnesium quaternary alloy systems. These alloy groups are shown schematically in Fig. 1 with accompanying alloy designations and primary strengthening phases associated with each alloy. In addition to the solid-solution strengthening effects of alloying additions, the important strengthening phases δ' (Al_3Li), S' (Al_2CuMg), and T_1 (Al_2CuLi) are formed upon aging and are dependent on alloy composition (Ref 3, 4).

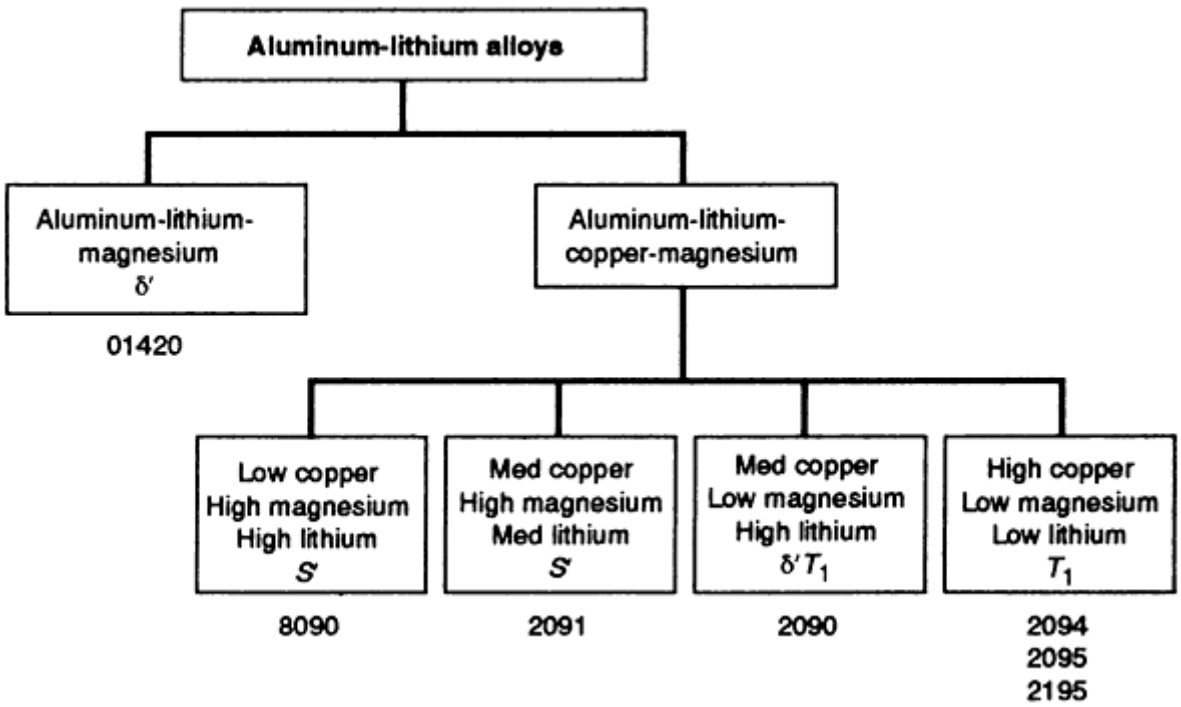

FIG. 1 SCHEMATIC OF TERNARY AND QUATERNARY ALUMINUM-LITHIUM ALLOY SYSTEMS SHOWING PRIMARY STRENGTHENING PHASES AND CORRESPONDING COMMERCIAL ALLOY DESIGNATIONS

Properties. Of the specific alloy compositions shown in Table 1, the high copper/magnesium ratio of alloy 2090 and the Weldalite 049 family of alloys (2094, 2095, 2195) results in the precipitation of T_1, which is the most potent strengthening phase in this alloy system (Ref 4, 5, 6). Accordingly, these alloys possess higher yield strengths than other aluminum-lithium alloys (Table 2). At lower copper/magnesium ratios, the *S*' phase is favored, and lower strengths are achieved (e.g., alloys 8090 and 2091). In the absence of copper, the δ' phase becomes predominant, resulting in even lower strength (e.g., Soviet alloy 01420). Density increases with copper content and decreases with lithium and magnesium contents; thus, alloy 01420 has the lowest density and the Weldalite 049 alloys have the highest densities. The elastic modulus tends to increase with lithium content; alloys 8090 and 2090 have the highest moduli in the aluminum-lithium-copper-magnesium alloy group.

TABLE 1 NOMINAL COMPOSITIONS AND SELECTED PROPERTIES OF ALUMINUM-LITHIUM ALLOYS

ALLOY	COMPOSITION, WT%[(A)]					DENSITY		MODULUS OF ELASTICITY		SPECIFIC MODULUS, GPA · CM^3/G
	Li	Cu	Mg	Zr	Other	gr/cm^3	lb/in^3	gpa	10^6 psi	
01420	2.0	. . .	5.3	. . .	0.5 MN	2.47	0.089	73.8	10.7	**29.9**
8090	2.5	1.0	1.0	0.10	. . .	2.54	0.091	79.3	11.5	**31.2**
2091	2.0	2.2	1.5	0.10	. . .	2.58	0.093	77.9	11.3	**30.2**
2090	2.3	2.7	0.2	0.12	. . .	2.57	0.093	78.6	11.4	**30.6**
2094	1.3	4.7	0.4	0.14	0.4 AG	2.71	0.098	77.9	11.3	**28.7**
2095	1.3	4.3	0.4	0.14	0.4 AG	. . .	. . .	. . .	. . .	**. . .**
2195	**1.0**	**4.0**	**0.4**	**0.14**	**0.4 AG**	**. . .**	**. . .**	**. . .**	**. . .**	**. . .**

Source: Ref 3, 4, 5

(A) BALANCE ALUMINUM.

TABLE 2 LONGITUDINAL TENSILE PROPERTIES OF ALUMINUM-LITHIUM ALLOY PLATE

ALLOY AND TEMPER	YIELD STRENGTH		ULTIMATE STRENGTH		REF
	mpa	ksi	mpa	ksi	
01420-T6	280	41	460	67	**7**
8090-T6	429	62	504	73	**8**
2091-T8	440	64	480	70	**9**
2090-T8	518	75	559	81	**10**
2195-T8	**585**	**86**	**612**	**90**	**11**

Zirconium is added to most aluminum-lithium alloys to form β'-Al_3Zr or α'-Al_3(Zr,Li) dispersoids; these dispersoids serve to inhibit recrystallization and nucleate the δ' phase giving improved strength and toughness (Ref 3, 12, 13). However, the presence of these dispersoids also leads to an inherent tendency toward texturing and subsequent anisotropic behavior (Ref 14). The β' phase may also act to promote grain refinement during solidification in both ingots and welds (Ref 15). Silver is added to the Weldalite 049 alloys to assist in precipitate nucleation (Ref 2).

Applications. Because of their good weldability, high strength, and accompanying high fracture toughness, the Weldalite 049 alloys have been considered as candidates to replace alloy 2219 in welded propellant tank applications, for example, the Space Shuttle external tank (Ref 14, 16). In this case, the weight savings gained from using a high-strength alloy (enabling the use of thinner sections) allows for a larger launch payload, which, in turn, offsets any additional cost in material. Weight savings can also be achieved by taking advantage of the high specific modulus of aluminum-lithium alloys (8090 and 2090 in particular) for use in stiffened or compression-loaded structures. Alloy 8090 has been successfully used in a welded tubular structure constructed with over 400 manual welds (Ref 17). Future applications may include welded skirt assemblies for space launch vehicles and other compression-loaded structures.

References cited in this section

2. J.R. PICKENS, RECENT DEVELOPMENTS IN THE WELDABILITY OF LITHIUM-CONTAINING ALUMINUM ALLOYS, *J. MATER. SCI.*, VOL 25, 1990, P 3035-3047
3. W.E. QUIST AND G.H. NARAYANAN, ALUMINUM-LITHIUM ALLOYS, *TREATISE MATER. SCI. TECH.*, VOL 31, MATERIALS AND COMPONENTS ENGINEERING PUBLISHING, LTD., 1989, P 219-254
4. T.J. LANGAN AND J.R. PICKENS, IDENTIFICATION OF STRENGTHENING PHASES IN THE AL-CU-LI ALLOY WELDALITE™ 049, *PROC. 5TH INT. AL-LI CONF.*, 1989, P 691-700
5. REGISTRATION RECORD OF ALUMINUM ASSOCIATION DESIGNATIONS AND CHEMICAL COMPOSITION LIMITS FOR WROUGHT ALUMINUM ALLOYS, ALUMINUM ASSOCIATION, WASHINGTON, D.C., 1993
6. J.C. HUANG AND A.J. ARDELL, MICROSTRUCTURAL EVOLUTION IN TWO AL-LI-CU ALLOYS, *PROC. 3RD INT. AL-LI CONF.*, INSTITUTE OF METALS, 1986, P 455-469
7. I.N. FRIDLYANDER, AL-LI WELDABLE ALLOY 1420, *PROC. 5TH INT. AL-LI CONF.*, 1989, P 1359-1364
8. M.R. EDWARDS AND V.E. STONEHAM, THE FUSION WELDING OF AL-LI-CU-MG (8090) ALLOY, *J. PHYS.*, VOL 48, 1987, P 293-299
9. J. GLAZER AND J.W. MORRIS, THE STRENGTH-TOUGHNESS RELATIONSHIP AT CRYOGENIC TEMPERATURES IN AL-LI PLATE, *PROC. 5TH INT. AL-LI CONF.*, MATERIALS AND COMPONENTS ENGINEERING PUBLISHING, LTD., 1989, P 1471-1480
10. J.R. KERR AND R.E. MERINO, CRYOGENIC PROPERTIES OF VPPA WELDED AL-LI ALLOYS, *PROC. 5TH INT. AL-LI CONF.*, 1989, P 1491-1500
11. ALLOY 2195 DATA SHEET, REYNOLDS METALS CO., RICHMOND, VA, 1993
12. F.W. GAYLE AND J.B. VANDERSANDE, AL_3(LI,ZR) OR α' PHASE IN AL-LI-ZR SYSTEM, *PROC. 5TH INT. AL-LI CONF.*, INSTITUTE OF METALS, 1986, P 375-385
13. T.H. SANDERS AND E.A. STARKE, THE PHYSICAL METALLURGY OF ALUMINUM-LITHIUM ALLOYS--A REVIEW, *PROC. 5TH INT. AL-LI CONF.*, MATERIALS AND COMPONENTS ENGINEERING PUBLISHING, LTD., 1989, P 1-37
14. W.T. TACK AND L.W. LOECHEL, WELDALITE™ 049: APPLICATION OF A NEW HIGH STRENGTH WELDABLE AL-LI-CU ALLOY, *PROC. 5TH INT. AL-LI CONF.*, MATERIALS AND COMPONENTS ENGINEERING PUBLISHING, LTD., 1989, P 1457-1467
15. L.F. MONDOLFO, GRAIN REFINEMENT IN THE CASTING OF NON-FERROUS ALLOYS, *PROC. CONF. GRAIN REFINEMENT IN CASTINGS AND WELDS*, TMS-AIME, 1982, P 3-50
16. W.T. TACK AND L.W. LOECHEL, USE OF APPLIED FRACTURE MECHANICS PRINCIPLES TO EVALUATE THE CRYOGENIC FRACTURE TOUGHNESS OF ALLOY 2090, *PROC. 5TH INT. AL-LI CONF.*, DEUTSCHE GESELLSCHAFT FUR MATERIALKUNDE, 1991, P 415-420
17. E. WILLNER AND D.L. YANEY, LOCKHEED MISSILES & SPACE CO., PRIVATE COMMUNICATION, 1993

Selection and Weldability of Aluminum-Lithium Alloys

C.E. Cross and W.T. Tack, Martin Marietta Astronautics Group

Weldability

Porosity. Weld metal porosity can form in aluminum alloys when monatomic hydrogen is partitioned interdendritically during solidification. A sufficient amount of hydrogen must be partitioned so that the interdendritic liquid becomes supersaturated, thus increasing the drive for pore nucleation. In order for diatomic gas pores to form, pore nuclei must overcome atmospheric pressure, surface tension, and liquid head pressure (Ref 18). Lithium-containing aluminum alloys exhibit a higher than normal propensity for weld metal porosity, although this does not appear to be due to any inherent

thermodynamic property. Lithium has been shown to increase the solubility of hydrogen in aluminum for both solid and liquid phases such that less hydrogen is partitioned during solidification in comparison with other aluminum alloys (Ref 19). The observed tendency to form porosity in aluminum-lithium alloys may, however, be due to higher initial amounts of hydrogen in the weld pool, making it easier to reach the threshold concentration needed for pore nucleation.

Hydrogen can enter the weld pool from the base plate, from hydrated oxides or hydrocarbons on the plate surface, and from moisture in the shielding gas. Similar in behavior to aluminum-magnesium alloys, aluminum-lithium alloys are particularly susceptible to the formation of hydrated oxides (Ref 20). Thus, preweld joint preparation requires special attention to avoid porosity. A thorough removal of mill scale at the weld joint, by means of dry machining or chemical milling, is required. In a review of Soviet literature (Ref 1), it was reported that a marked drop in porosity in alloy 01420 weldments could be achieved by removing 0.05 mm (0.002 in.) from the joint surface prior to welding. It has become common practice in the welding of all aluminum-lithium alloys to dry machine approximately 0.25 mm (0.01 in.) off abutting surfaces as well as top and bottom plate surfaces, 25 to 50 mm (1 to 2 in.) from the centerline, on both sides of the joint. It is also considered good practice to weld within a few hours of machining and to degrease immediately prior to welding.

Another factor affecting weld quality and porosity entrapment is the weld cover gas, which is typically argon, helium, or a mixture of the two. It has been determined that low levels of oxygen impurity (less than 300 ppm) must be maintained to produce acceptable welds in alloy 2090 (Ref 21). In this same study, normal welding-grade bottled gas was found to vary from between 100 and 300 ppm O. Thus, in-line gas purifiers (getter or sieve type) or oxygen sensors at the welding torch may be necessary if shielding gas of consistently high quality cannot be supplied. Also, when making through-thickness welds, as in a keyhole welding process, backside shielding must be used to prevent excessive oxidation and the occurrence of porosity.

Hot cracking occurs when low-melting, eutectic liquid films are torn apart at the trailing edge of the weld pool during solidification. The hot cracking susceptibility of any aluminum-lithium alloy, or any aluminum alloy in general, appears to be related to its copper and magnesium contents and may involve an aluminum-copper-magnesium eutectic (Ref 22). Alloys with high copper and low magnesium (e.g., alloy 2219) are weldable, as are alloys with low copper and high magnesium (e.g., alloy 5083). It is alloys containing large amounts of both copper and magnesium--for example, conventional high-strength aerospace alloys such as 2024 and 7075--that encounter problems with weldability. With aluminum-lithium alloys, the formation of strengthening precipitates such as T_1 does not require large quantities of both copper and magnesium, and thus weldability can be maintained without compromising strength.

The relationship between copper and magnesium contents and weldability is demonstrated in the weldability index of Fig. 2. This index was obtained by superimposing modern alloy compositions on an existing crack susceptibility (castability) diagram generated by Pumphrey and Moore in 1948 for aluminum-copper-magnesium ternary alloys (Ref 23). In Fig. 2, it is predicted that aluminum-lithium alloys with high copper and low magnesium contents (e.g., alloys 2094 and 2090) should have good weldability. On the other hand, alloy 2091, an aluminum-lithium alloy with intermediate amounts of both copper and magnesium, is predicted to be less weldable. Weldability predictions made using this index do not account for the effect lithium has on copper or magnesium solubility, nor do they account for the use of filler alloys to modify weld metal composition. Nevertheless, this index has proven useful in aluminum-lithium base metal and filler alloy development by predicting trends in weldability behavior with variations in alloy composition.

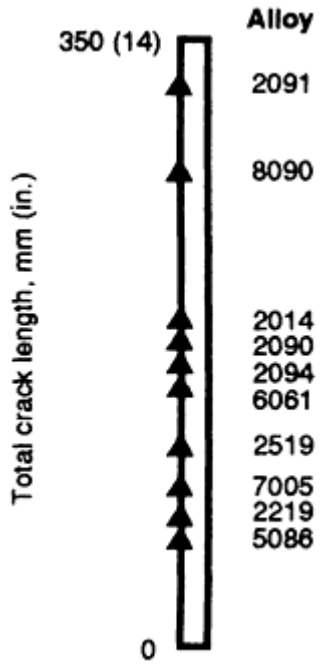

FIG. 2 PUMPHREY-MOORE CRACKING INDEX BASED ON CASTABILITY DATA OBTAINED FROM ALUMINUM-COPPER-MAGNESIUM ALLOYS. SOURCE: REF 25

Filler Metal Selection. Filler metal alloys used to join aluminum-lithium alloys are selected to give acceptable weldability and, at the same time, to optimize mechanical properties. Alloy 2319 has typically been used to join the high-copper alloys (e.g., alloys 2090, 2094, 2095, and 2195). Low-copper, high-magnesium alloys (e.g., alloy 8090) call for the use of a high-magnesium filler metal such as alloy 5356. Alloys that are difficult to weld (e.g., alloy 2091) require the use of an aluminum-silicon filler metal such as alloy 4043. Aluminum-silicon filler metal alloys provide excellent weldability, but are not normally used due to their characteristic low toughness and low ductility and their inability to respond to aging. Experimental aluminum-lithium filler metal alloys have been developed and show promise for future applications where high filler metal dilutions are required (Ref 24).

In a recent weldability study, a trans-Varestraint test was used to compare aluminum-lithium alloys with conventional aluminum alloys (Ref 25). Tests were performed using an applied strain of 0.5%, appropriate filler metal alloys at 30% filler dilution, and a gas-tungsten arc welding process operated at welding currents selected to achieve constant penetration for each alloy tested. Results of this study are shown in Fig. 3; alloy 2219 appears to be the most weldable and alloys 2090 and 2094 the least weldable of those alloys investigated. However, extensive weld development programs (Ref 10, 14, 26) have demonstrated that these aluminum-lithium alloys can be easily welded in practice with little concern for cracking. Weldability tests can provide a relative rating among alloys; they cannot be used to predict real-world behavior.

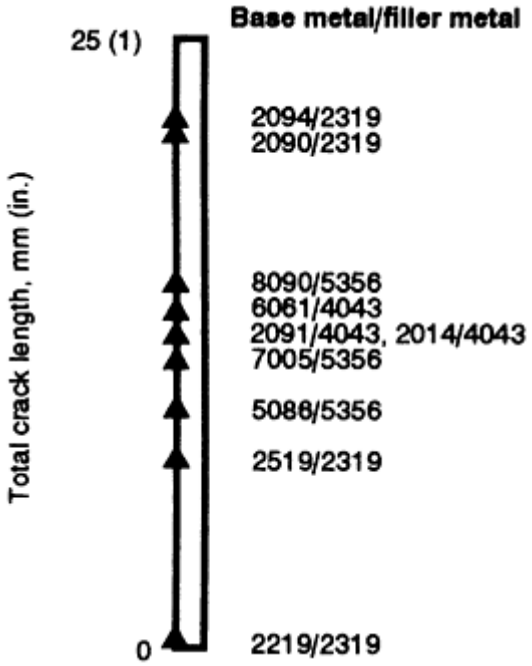

FIG. 3 TRANS-VARESTRAINT WELDABILITY DATA FOR ALUMINUM ALLOYS. SOURCE: REF 25

As shown in Fig. 4, the weldability of alloys 2090 and 2094 can be improved using high-silicon filler metal alloys (e.g., alloy 4047), although this is not normally deemed necessary or desirable (Ref 25, 27). Figure 4(b) shows that the use of a 2319 filler metal results in less cracking than a 4043 filler metal when welding alloy 2090. The same is not true when welding alloy 2094 (Fig. 4a). Alloy 2090 is much leaner in copper than alloy 2094, and thus it responds more to the use of a high-copper filler metal alloy. It should be noted that results from two different weldability tests are displayed in Fig. 4, and the magnitude of cracking is different for each test.

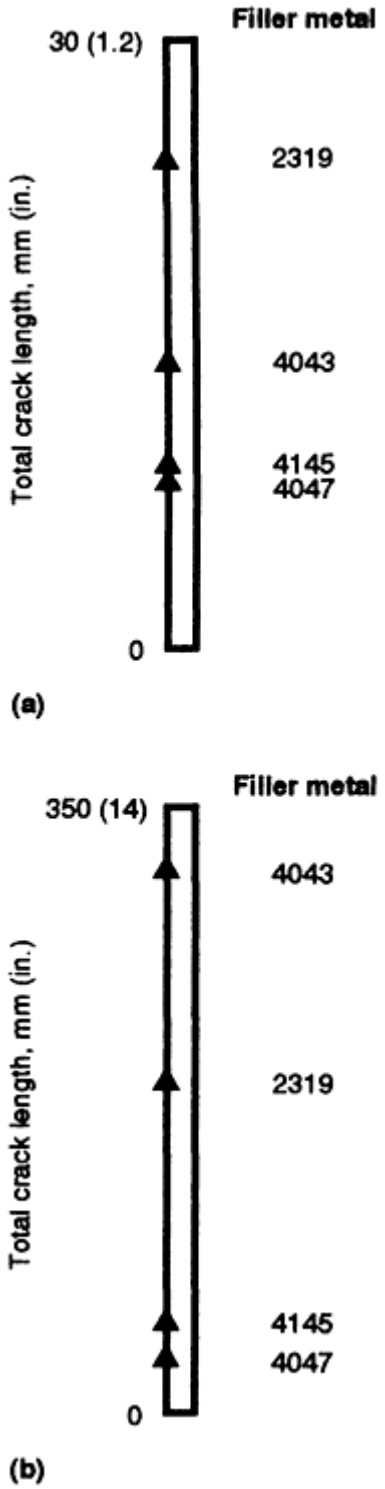

FIG. 4 WELDABILITY DATA SHOWING THE IMPROVED RESISTANCE TO HOT CRACKING OBTAINED WHEN USING AN ALUMINUM-SILICON FILLER ALLOY. (A) TRANS-VARESTRAINT TEST DATA FOR ALLOY 2094 WELDMENTS. SOURCE: REF 25. (B) INVERTED-TEE TEST DATA FOR ALLOY 2090 WELDMENTS. SOURCE: REF 27

References cited in this section

1. J.R. PICKENS, THE WELDABILITY OF LITHIUM-CONTAINING ALUMINUM ALLOYS, *J. MATER. SCI.*, VOL 20, 1985, P 4247-4258

10. J.R. KERR AND R.E. MERINO, CRYOGENIC PROPERTIES OF VPPA WELDED AL-LI ALLOYS, *PROC. 5TH INT. AL-LI CONF.*, 1989, P 1491-1500
14. W.T. TACK AND L.W. LOECHEL, WELDALITE™ 049: APPLICATION OF A NEW HIGH STRENGTH WELDABLE AL-LI-CU ALLOY, *PROC. 5TH INT. AL-LI CONF.*, MATERIALS AND COMPONENTS ENGINEERING PUBLISHING, LTD., 1989, P 1457-1467
18. R.E. TREVISAN, D.D. SCHWEMMER, AND D.L. OLSON, THE FUNDAMENTALS OF WELD METAL PORE FORMATION, *WELDING*: *THEORY AND PRACTICE*, ELSEVIER, 1990
19. D.E.J. TALBOT, INFLUENCES OF HYDROGEN ON QUALITY OF ALUMINUM AND ALUMINUM ALLOY INGOTS, *PROC. 3RD INT.* SOLIDIFICATION PROCESSING CONF., INSTITUTE OF METALS, 1987, P 29-31
20. D.J. FIELD, OXIDATION OF ALUMINUM AND ITS ALLOYS, *TREATISE MATER. SCI. TECH.*, VOL 31, 1989, P 523-537
21. L.F. MARINEZ, J.C. MCCLURE, AND A.C. NUNES, THE EFFECT OF GAS CONTAMINATION DURING WELDING OF ALUMINUM-LITHIUM ALLOYS, *PROD. ENG. DES.* ASME, VOL 51, 1991, P 235-243
22. C.E. CROSS, L.S. KRAMER, W.T. TACK, AND L.W. LOECHEL, ALUMINUM WELDABILITY AND HOT TEARING THEORY, *WELDABILITY OF MATERIALS*, ASM INTERNATIONAL, 1990, P 275-282
23. W.I. PUMPHREY AND D.C. MOORE, CRACKING DURING AND AFTER SOLIDIFICATION IN SOME ALUMINUM-COPPER-MAGNESIUM ALLOYS OF HIGH PURITY, *J. INST. MET.*, VOL 73, 1948, P 425-438
24. L.S. KRAMER, C.E. CROSS, AND J.R. PICKENS, THE EFFECT OF COMPOSITION ON THE WELDABILITY OF AL-CU-LI-AG-MG ALLOYS IN THE HIGH CU:LI REGIME, *PROC. 6TH INT. AL-LI CONF.*, DEUTSCHE GESELLSCHAFT FUR MATERIALKUNDE, 1991, P 1197-1202
25. C.E. CROSS AND W.T. TACK, "FACTORS AFFECTING THE WELDABILITY EVALUATION OF ALUMINUM ALLOYS," PRESENTED AT THE 73RD AMERICAN WELDING SOCIETY CONVENTION (CHICAGO), 1992
26. E.F. SCHOLZ, L.W. LOECHEL, AND M.O. ROBERTS, ADVANCED CRYOGENIC PROPELLENT TANK DEVELOPMENT STATUS, *PROC. 28TH AIAA PROPULSION CONF.*, 1992, P 1-11
27. R.P. MARTUKANITZ, C.A. NATALIE, AND J.O. KNOEFEL, THE WELDABILITY OF AN AL-LI-CU ALLOY, *J. MET.*, VOL 39, 1987, P 38-42

Selection and Weldability of Aluminum-Lithium Alloys

C.E. Cross and W.T. Tack, Martin Marietta Astronautics Group

Weld Characterization

Joint Strength. Although the tensile properties of many wrought aluminum-lithium alloys are exceptionally high, the strength of the welded joints in these alloys is limited by the strength of the solidified weld metal. Even though joint strengths are higher than those found in conventional aluminum alloys, joint efficiencies on the order of 50% are to be expected for the high-strength aluminum-lithium alloys.

A comparison of gas-tungsten arc, variable polarity plasma arc, and gas-metal arc weldment properties for aluminum-lithium alloys, taken from numerous sources, is given in Table 3. Alloy 2094 is found to have the highest joint strength (372 MPa, or 54 ksi, ultimate strength), which corresponds to a 38% improvement over alloy 2219 weldments (269 MPa, or 39 ksi, ultimate strength) (Ref 10). Alloy 01420 is found to have the lowest weld strength (241 MPa, or 35 ksi, ultimate strength).

TABLE 3 TRANSVERSE TENSILE PROPERTIES FOR ARC WELDED ALUMINUM-LITHIUM WELDMENTS

IN THE AS-WELDED CONDITION

ALLOY AND TEMPER	WELDING PROCESS[(A)]	FILLER METAL	YIELD STRENGTH		ULTIMATE STRENGTH		REF
			MPA	KSI	MPA	KSI	
01420-T6	GTAW	5356	103	15	241	35	**28**
2090-T8	GTAW	2319	165	24	248	36	**29**
	VPPAW	2319	165	24	283	41	**10**
	GMAW	2319	207	30	234	34	**27**
8090-T8	GTAW	5356	179	26	310	45	**29**
	VPPAW	5356	193	28	296	43	**29**
	GMAW	5356	186	27	276	40	**30**
2094-T8	GTAW	2319	. . .	. . .	352	51	**31**
	VPPAW	2319	269	39	372	54	**32**
	GMAW	**2319**	**. . .**	**. . .**	**283**	**41**	**31**

(A) GTAW, GAS-TUNGSTEN ARC WELDING; VPPAW, VARIABLE-POLARITY PLASMA ARC WELDING; GMAW, GAS-METAL ARC WELDING

High-energy-density welding processes have also been used successfully to join aluminum-lithium alloys. Electron-beam welding has been used to join alloys 8090, 2090, and 2094; tensile strength results for electron-beam weldments are given in Table 4. Typically, a slight improvement in strength above arc welding properties is to be expected because of a finer microstructure, narrower fusion zone, and better response to natural aging. Similarly, good results for laser-beam-welded alloy 2090 have been reported (Ref 34, 35).

TABLE 4 TRANSVERSE TENSILE PROPERTIES FOR ELECTRON-BEAM-WELDED ALUMINUM-LITHIUM ALLOYS IN THE AS-WELDED CONDITION

ALLOY AND TEMPER	ULTIMATE STRENGTH		REF
	MPA	KSI	
8090-T6	317	46	**33**
2090-T8	324	47	**27**
2094-T8	**434**	**63**	**2**

Postweld Aging. The Weldalite 049 alloys have been observed to naturally age in both the weld metal and the heat-affected zone (HAZ). It is important to wait a sufficient time (typically 30 days) between welding and proof or tensile testing to allow for precipitate stabilization, thereby ensuring accurate characterization of joint properties. In addition, postweld solution heat treatment and artificial aging, although not practical for large structures, have been found to significantly increase the strength of high-copper alloy gas-tungsten arc weldments; by using these postweld treatments, an ultimate tensile strength of 400 MPa (58 ksi) has been obtained with alloy 2090 (Ref 36) and 510 MPa (73 ksi) with alloy 2094 (Ref 37).

Ductility and Toughness. If the weld metal is significantly lower in strength than the base metal, when the weldment is plastically deformed, most of the strain will be concentrated in the weld metal. Such is the case for high-strength aluminum-lithium alloys, where hardness traverses for both alloy 2090 and 2094 have confirmed a steep gradient in strength in the HAZ between weld metal and base metal (Ref 31, 38). Typically, joint ductility measured over a 50 mm (2 in.) gage length will be 2 to 4% even though the actual weld metal ductility approaches 10 to 12%.

Fracture toughness is an important criterion in the design of welded tanks for aerospace applications. Also, an increase in toughness with decreasing temperature is particularly desirable for cryogenic tanks because it allows proof testing to be performed at room temperature, a much more feasible and economical procedure. Weld toughness values have been measured for alloy 2090 gas-tungsten arc (dual torch, variable polarity) weldments using a surface crack tension test. K_{Ie} values increasing from 30 MPa/ $\sqrt{m}$ at room temperature to 34 MPa/ $\sqrt{m}$ at 73 K have been reported, which is an improvement over similar measurements for alloy 2219 (19 to 24 MPa/ $\sqrt{m}$) (Ref 31). It should be noted that these are not plane-strain toughness values, and their magnitude is sensitive to precrack geometry.

Fatigue. Initial results from an ongoing study involving alloy 2095 weldments (Ref 39) have shown that fatigue growth resistance is higher in both the weld metal and HAZ when compared with the base metal. For precracks placed in the HAZ, there is a tendency for cracks to grow to the fusion line, where the fatigue crack growth rate is greater. In both the weld metal and HAZ (unconstrained condition), the general tendency is for the fatigue crack growth rate to increase with increasing stress ratio ($\sigma_{min}/\sigma_{max}$).

Microstructure. The high strength of aluminum-lithium weld metal is due to a combination of fine grain size and precipitate formation. This unexplained tendency for fine grains, as small as 10 μm in diameter (equiaxed), has been noted elsewhere (Ref 40). Constitutional undercooling by lithium has been ruled out as a possible cause (Ref 41). The tensile fracture of alloy 2094 weldments has been found to be intergranular, associated with a band of fine grains located along the fusion line (Ref 31, 42). Based onphase equilibria, two eutectic constituents are likely present in aluminum-lithium-copper weld metal: θ(Al_2Cu) and T_B ($Al_{15}Cu_8Li_2$) (Ref 43). Weld metal precipitates δ' and β' have been identified in alloy 2090 in the as-welded condition, and platelike precipitates, believed to be T_1, have been observed upon aging (Ref 36).

Corrosion. A study involving corrosion potential measurements taken across weldments (through base metal, HAZ, and weld metal) has identified certain aluminum-lithium alloy compositions as being susceptible to galvanic attack in a saline environment (Ref 44). In particular, two experimental alloys with high lithium content (2.9 wt% Li and 3.0 wt% Cu), welded with either 2319 or 4043 fillers, displayed a narrow region within the HAZ that was highly anodic to both base metal and weld metal. This behavior was attributed to the formation of the equilibrium δ(AlLi) phase and resulted in severe pitting in the HAZ. In contrast, a 2090-type alloy showed a continuously increasing (cathodic) potential when going from base metal to weld metal and was resistant to pitting attack. This behavior was attributed to the absence of the δ phase due to a higher copper-lithium ratio.

References cited in this section

2. J.R. PICKENS, RECENT DEVELOPMENTS IN THE WELDABILITY OF LITHIUM-CONTAINING ALUMINUM ALLOYS, *J. MATER. SCI.*, VOL 25, 1990, P 3035-3047
10. J.R. KERR AND R.E. MERINO, CRYOGENIC PROPERTIES OF VPPA WELDED AL-LI ALLOYS, *PROC. 5TH INT. AL-LI CONF.*, 1989, P 1491-1500
27. R.P. MARTUKANITZ, C.A. NATALIE, AND J.O. KNOEFEL, THE WELDABILITY OF AN AL-LI-CU ALLOY, *J. MET.*, VOL 39, 1987, P 38-42
28. J.R. PICKENS, T.J. LANGAN, AND E. BARTA, THE WELDABILITY OF AL-5MG-2LI-0.1ZR ALLOY 01420, *PROC. 5TH INT. AL-LI CONF.*, INSTITUTE OF METALS, 1985, P 137-147
29. C.C. GRIFFEE, G.A. JENSEN, AND T.L. REINHART, FACTORS INFLUENCING THE QUALITY AND PROPERTIES OF AL-LI ALLOY WELDS, *PROC. 5TH INT. AL-LI CONF.*, MATERIALS AND COMPONENTS ENGINEERING PUBLISHING LTD., 1989, P 1425-1434
30. M.H. SKILLINGBERG, FUSION WELDING OF AL-LI-CU-(MG)-ZR PLATE, PROC. CONF. ALUMINUM TECHNOLOGY, INSTITUTE OF METALS, 1986, P 509-515
31. C.E. CROSS, L.W. LOECHEL, AND G.F. BRAUN, WELDALITE™ 049 WELD DEVELOPMENT FOR AEROSPACE TANKAGE, *PROC. 5TH INT. AL-LI CONF.*, DEUTSCHE GESELLSCHAFT FUR MATERIALKUNDE, 1991, P 1165-1170
32. M.O. ROBERTS AND L.W. LOECHEL, "WELDING PROCESS PROCEDURE DEVELOPMENT AND OPTIMIZATION USING DESIGN OF EXPERIMENTS," PRESENTED AT THE AMERICAN WELDING SOCIETY CONVENTION (HOUSTON), 1993
33. P. LE POAC, A.M. NOMINE, AND D. MIANNAY, MECHANICAL PROPERTIES OF BEAM ELECTRON WELDINGS IN 8090 ALLOY, *J. PHYS.*, VOL 48, 1987, P 301-306
34. P.A. MOLIAN AND T.S. STRIVATSAN, WELDABILITY OF AI-LI-CU ALLOY 2090, USING LASER WELDING, *PROC. 5TH INT. AL-LI CONF.*, MATERIALS AND COMPONENTS ENGINEERING PUBLISHING LTD., 1989, P 1435-1445
35. T.A. MARSICO AND R. KOSSOWSKY, PHYSICAL PROPERTIES OF LASER WELDED AL-LI ALLOY 2090, *PROC. 5TH INT. AL-LI CONF.*, 1989, P 1447-1456

36. A.J. SUNWOO, "WELDMENT MECHANICAL PROPERTIES OF AL-LI-CU ALLOY 2090 AT AMBIENT AND CRYOGENIC TEMPERATURES," PH.D. THESIS, UNIVERSITY OF CALIFORNIA-BERKELEY, 1990
37. L.S. KRAMER AND J.R. PICKENS, MICROSTRUCTURE AND PROPERTIES OF A WELDED AL-CU-LI ALLOY, *WELD. J.*, VOL 71, 1992, P 115S-121S
38. R.P. MARTUKANITZ, R.H. STEVENS, AND L.R. JOHNSTON, MICROSTRUCTURAL AND MICROHARDNESS CHARACTERIZATIONS OF A GAS METAL ARC WELDED ALUMINUM-LITHIUM ALLOY, *MICROSTRUCT. SCI.*, VOL 14, 1985, P 53-64
39. G.O. RADING, "FATIGUE CRACK GROWTH IN WELDED AL-LI ALLOY 2095 (WELDALITE™ 049)," PH.D. THESIS PROGRESS REPORT, UNIVERSITY OF ALABAMA, 1992
40. C.E. CROSS, D.L. OLSON, G.R. EDWARDS, AND J.F. CAPES, WELDABILITY OF ALUMINUM-LITHIUM ALLOYS, *PROC. 2ND INT. AL-LI CONF.*, TMS-AIME, 1983, P 676-682
41. C.E. CROSS, G.R. EDWARDS, D.L. OLSON, AND R.H. FROST, INTRINSIC NUCLEATION OF WELD METAL GRAINS, *PROC. 3RD INT.* CONF. SOLIDIFICATION PROCESSING, INSTITUTE OF METALS, 1987, P 388-391
42. S.R. SHAH, J.E. WITTIG, AND G.T. HAHN, MICROSTRUCTURE ANALYSIS OF A HIGH STRENGTH AL-CU-LI (WELDALITE™ 049) ALLOY WELD, *PROC. 3RD INT.* CONF. TRENDS IN WELDING RESEARCH, ASM INTERNATIONAL, 1992, P 281-285
43. K.A. MONTOYA, F.H. HEUBAUM, K.S. KUMAR, AND J.R. PICKENS, COMPOSITIONAL EFFECTS ON THE SOLIDUS TEMPERATURE OF AN AL-CU-LI-AG-MG ALLOY, *SCR. MET.*, VOL 25, 1991, P 1489-1494
44. G. BEVERINI, "INVESTIGATIONS OF THE CORROSION CHARACTERISTICS OF AL-LI AND AL-LI-CU WELDMENTS IN A 3.5% NACL SOLUTION," M.SC. THESIS T-3508, COLORADO SCHOOL OF MINES, 1988

Selection and Weldability of Aluminum-Lithium Alloys

C.E. Cross and W.T. Tack, Martin Marietta Astronautics Group

References

1. J.R. PICKENS, THE WELDABILITY OF LITHIUM-CONTAINING ALUMINUM ALLOYS, *J. MATER. SCI.*, VOL 20, 1985, P 4247-4258
2. J.R. PICKENS, RECENT DEVELOPMENTS IN THE WELDABILITY OF LITHIUM-CONTAINING ALUMINUM ALLOYS, *J. MATER. SCI.*, VOL 25, 1990, P 3035-3047
3. W.E. QUIST AND G.H. NARAYANAN, ALUMINUM-LITHIUM ALLOYS, *TREATISE MATER. SCI. TECH.*, VOL 31, MATERIALS AND COMPONENTS ENGINEERING PUBLISHING, LTD., 1989, P 219-254
4. T.J. LANGAN AND J.R. PICKENS, IDENTIFICATION OF STRENGTHENING PHASES IN THE AL-CU-LI ALLOY WELDALITE™ 049, *PROC. 5TH INT. AL-LI CONF.*, 1989, P 691-700
5. REGISTRATION RECORD OF ALUMINUM ASSOCIATION DESIGNATIONS AND CHEMICAL COMPOSITION LIMITS FOR WROUGHT ALUMINUM ALLOYS, ALUMINUM ASSOCIATION, WASHINGTON, D.C., 1993
6. J.C. HUANG AND A.J. ARDELL, MICROSTRUCTURAL EVOLUTION IN TWO AL-LI-CU ALLOYS, *PROC. 3RD INT. AL-LI CONF.*, INSTITUTE OF METALS, 1986, P 455-469
7. I.N. FRIDLYANDER, AL-LI WELDABLE ALLOY 1420, *PROC. 5TH INT. AL-LI CONF.*, 1989, P 1359-1364
8. M.R. EDWARDS AND V.E. STONEHAM, THE FUSION WELDING OF AL-LI-CU-MG (8090) ALLOY, *J. PHYS.*, VOL 48, 1987, P 293-299

9. J. GLAZER AND J.W. MORRIS, THE STRENGTH-TOUGHNESS RELATIONSHIP AT CRYOGENIC TEMPERATURES IN AL-LI PLATE, *PROC. 5TH INT. AL-LI CONF.*, MATERIALS AND COMPONENTS ENGINEERING PUBLISHING, LTD., 1989, P 1471-1480
10. J.R. KERR AND R.E. MERINO, CRYOGENIC PROPERTIES OF VPPA WELDED AL-LI ALLOYS, *PROC. 5TH INT. AL-LI CONF.*, 1989, P 1491-1500
11. ALLOY 2195 DATA SHEET, REYNOLDS METALS CO., RICHMOND, VA, 1993
12. F.W. GAYLE AND J.B. VANDERSANDE, AL_3(LI,ZR) OR α' PHASE IN AL-LI-ZR SYSTEM, *PROC. 5TH INT. AL-LI CONF.*, INSTITUTE OF METALS, 1986, P 375-385
13. T.H. SANDERS AND E.A. STARKE, THE PHYSICAL METALLURGY OF ALUMINUM-LITHIUM ALLOYS--A REVIEW, *PROC. 5TH INT. AL-LI CONF.*, MATERIALS AND COMPONENTS ENGINEERING PUBLISHING, LTD., 1989, P 1-37
14. W.T. TACK AND L.W. LOECHEL, WELDALITE^{TM} 049: APPLICATION OF A NEW HIGH STRENGTH WELDABLE AL-LI-CU ALLOY, *PROC. 5TH INT. AL-LI CONF.*, MATERIALS AND COMPONENTS ENGINEERING PUBLISHING, LTD., 1989, P 1457-1467
15. L.F. MONDOLFO, GRAIN REFINEMENT IN THE CASTING OF NON-FERROUS ALLOYS, *PROC. CONF. GRAIN REFINEMENT IN CASTINGS AND WELDS*, TMS-AIME, 1982, P 3-50
16. W.T. TACK AND L.W. LOECHEL, USE OF APPLIED FRACTURE MECHANICS PRINCIPLES TO EVALUATE THE CRYOGENIC FRACTURE TOUGHNESS OF ALLOY 2090, *PROC. 5TH INT. AL-LI CONF.*, DEUTSCHE GESELLSCHAFT FUR MATERIALKUNDE, 1991, P 415-420
17. E. WILLNER AND D.L. YANEY, LOCKHEED MISSILES & SPACE CO., PRIVATE COMMUNICATION, 1993
18. R.E. TREVISAN, D.D. SCHWEMMER, AND D.L. OLSON, THE FUNDAMENTALS OF WELD METAL PORE FORMATION, *WELDING*: *THEORY AND PRACTICE*, ELSEVIER, 1990
19. D.E.J. TALBOT, INFLUENCES OF HYDROGEN ON QUALITY OF ALUMINUM AND ALUMINUM ALLOY INGOTS, *PROC. 3RD INT.* SOLIDIFICATION PROCESSING CONF., INSTITUTE OF METALS, 1987, P 29-31
20. D.J. FIELD, OXIDATION OF ALUMINUM AND ITS ALLOYS, *TREATISE MATER. SCI. TECH.*, VOL 31, 1989, P 523-537
21. L.F. MARINEZ, J.C. MCCLURE, AND A.C. NUNES, THE EFFECT OF GAS CONTAMINATION DURING WELDING OF ALUMINUM-LITHIUM ALLOYS, *PROD. ENG. DES.* ASME, VOL 51, 1991, P 235-243
22. C.E. CROSS, L.S. KRAMER, W.T. TACK, AND L.W. LOECHEL, ALUMINUM WELDABILITY AND HOT TEARING THEORY, *WELDABILITY OF MATERIALS*, ASM INTERNATIONAL, 1990, P 275-282
23. W.I. PUMPHREY AND D.C. MOORE, CRACKING DURING AND AFTER SOLIDIFICATION IN SOME ALUMINUM-COPPER-MAGNESIUM ALLOYS OF HIGH PURITY, *J. INST. MET.*, VOL 73, 1948, P 425-438
24. L.S. KRAMER, C.E. CROSS, AND J.R. PICKENS, THE EFFECT OF COMPOSITION ON THE WELDABILITY OF AL-CU-LI-AG-MG ALLOYS IN THE HIGH CU:LI REGIME, *PROC. 6TH INT. AL-LI CONF.*, DEUTSCHE GESELLSCHAFT FUR MATERIALKUNDE, 1991, P 1197-1202
25. C.E. CROSS AND W.T. TACK, "FACTORS AFFECTING THE WELDABILITY EVALUATION OF ALUMINUM ALLOYS," PRESENTED AT THE 73RD AMERICAN WELDING SOCIETY CONVENTION (CHICAGO), 1992
26. E.F. SCHOLZ, L.W. LOECHEL, AND M.O. ROBERTS, ADVANCED CRYOGENIC PROPELLENT TANK DEVELOPMENT STATUS, *PROC. 28TH AIAA PROPULSION CONF.*, 1992, P 1-11
27. R.P. MARTUKANITZ, C.A. NATALIE, AND J.O. KNOEFEL, THE WELDABILITY OF AN AL-LI-CU ALLOY, *J. MET.*, VOL 39, 1987, P 38-42
28. J.R. PICKENS, T.J. LANGAN, AND E. BARTA, THE WELDABILITY OF AL-5MG-2LI-0.1ZR ALLOY 01420, *PROC. 5TH INT. AL-LI CONF.*, INSTITUTE OF METALS, 1985, P 137-147
29. C.C. GRIFFEE, G.A. JENSEN, AND T.L. REINHART, FACTORS INFLUENCING THE QUALITY AND PROPERTIES OF AL-LI ALLOY WELDS, *PROC. 5TH INT. AL-LI CONF.*, MATERIALS AND

COMPONENTS ENGINEERING PUBLISHING LTD., 1989, P 1425-1434

30. M.H. SKILLINGBERG, FUSION WELDING OF AL-LI-CU-(MG)-ZR PLATE, PROC. CONF. ALUMINUM TECHNOLOGY, INSTITUTE OF METALS, 1986, P 509-515
31. C.E. CROSS, L.W. LOECHEL, AND G.F. BRAUN, WELDALITE™ 049 WELD DEVELOPMENT FOR AEROSPACE TANKAGE, *PROC. 5TH INT. AL-LI CONF.*, DEUTSCHE GESELLSCHAFT FUR MATERIALKUNDE, 1991, P 1165-1170
32. M.O. ROBERTS AND L.W. LOECHEL, "WELDING PROCESS PROCEDURE DEVELOPMENT AND OPTIMIZATION USING DESIGN OF EXPERIMENTS," PRESENTED AT THE AMERICAN WELDING SOCIETY CONVENTION (HOUSTON), 1993
33. P. LE POAC, A.M. NOMINE, AND D. MIANNAY, MECHANICAL PROPERTIES OF BEAM ELECTRON WELDINGS IN 8090 ALLOY, *J. PHYS.*, VOL 48, 1987, P 301-306
34. P.A. MOLIAN AND T.S. STRIVATSAN, WELDABILITY OF AI-LI-CU ALLOY 2090, USING LASER WELDING, *PROC. 5TH INT. AL-LI CONF.*, MATERIALS AND COMPONENTS ENGINEERING PUBLISHING LTD., 1989, P 1435-1445
35. T.A. MARSICO AND R. KOSSOWSKY, PHYSICAL PROPERTIES OF LASER WELDED AL-LI ALLOY 2090, *PROC. 5TH INT. AL-LI CONF.*, 1989, P 1447-1456
36. A.J. SUNWOO, "WELDMENT MECHANICAL PROPERTIES OF AL-LI-CU ALLOY 2090 AT AMBIENT AND CRYOGENIC TEMPERATURES," PH.D. THESIS, UNIVERSITY OF CALIFORNIA-BERKELEY, 1990
37. L.S. KRAMER AND J.R. PICKENS, MICROSTRUCTURE AND PROPERTIES OF A WELDED AL-CU-LI ALLOY, *WELD. J.*, VOL 71, 1992, P 115S-121S
38. R.P. MARTUKANITZ, R.H. STEVENS, AND L.R. JOHNSTON, MICROSTRUCTURAL AND MICROHARDNESS CHARACTERIZATIONS OF A GAS METAL ARC WELDED ALUMINUM-LITHIUM ALLOY, *MICROSTRUCT. SCI.*, VOL 14, 1985, P 53-64
39. G.O. RADING, "FATIGUE CRACK GROWTH IN WELDED AL-LI ALLOY 2095 (WELDALITE™ 049)," PH.D. THESIS PROGRESS REPORT, UNIVERSITY OF ALABAMA, 1992
40. C.E. CROSS, D.L. OLSON, G.R. EDWARDS, AND J.F. CAPES, WELDABILITY OF ALUMINUM-LITHIUM ALLOYS, *PROC. 2ND INT. AL-LI CONF.*, TMS-AIME, 1983, P 676-682
41. C.E. CROSS, G.R. EDWARDS, D.L. OLSON, AND R.H. FROST, INTRINSIC NUCLEATION OF WELD METAL GRAINS, *PROC. 3RD INT.* CONF. SOLIDIFICATION PROCESSING, INSTITUTE OF METALS, 1987, P 388-391
42. S.R. SHAH, J.E. WITTIG, AND G.T. HAHN, MICROSTRUCTURE ANALYSIS OF A HIGH STRENGTH AL-CU-LI (WELDALITE™ 049) ALLOY WELD, *PROC. 3RD INT.* CONF. TRENDS IN WELDING RESEARCH, ASM INTERNATIONAL, 1992, P 281-285
43. K.A. MONTOYA, F.H. HEUBAUM, K.S. KUMAR, AND J.R. PICKENS, COMPOSITIONAL EFFECTS ON THE SOLIDUS TEMPERATURE OF AN AL-CU-LI-AG-MG ALLOY, *SCR. MET.*, VOL 25, 1991, P 1489-1494
44. G. BEVERINI, "INVESTIGATIONS OF THE CORROSION CHARACTERISTICS OF AL-LI AND AL-LI-CU WELDMENTS IN A 3.5% NACL SOLUTION," M.SC. THESIS T-3508, COLORADO SCHOOL OF MINES, 1988

Selection and Weldability of Aluminum Metal-Matrix Composites

Thomas J. Lienert, The Ohio State University; Charles T. Lane, Duralcan USA; Jerry E. Gould, Edison Welding Institute

---

Introduction

THE PURPOSE of this article is to review the current understanding of the joinability of aluminum metal-matrix composites (Al-MMCs).* Unfortunately, the joining of Al-MMCs is not a mature technology, and many important details

are not well understood. Relatively little work has been directed toward furthering the understanding of Al-MMC joining. Much of the work has been either proprietary or protected for national security reasons and is not available in the open literature.

Although much of the early work on Al-MMCs, including that on joining, concentrated on continuous fiber types, most of the present work is focused on discontinuously reinforced (particle or whisker) Al-MMCs, because of their greater ease of manufacture, lower production costs, and relatively isotropic properties. The most commonly used reinforcement materials in discontinuously reinforced aluminum (DRA) composites are silicon carbide (SiC) and aluminum oxide (Al_2O_3). Consequently, this article focuses on composites that incorporate these specific materials. A review of Al-MMC joining technology up to 1975 is provided in Ref 1.

Reference

1. G.E. METZGER, JOINING OF METAL-MATRIX FIBER-REINFORCED COMPOSITE MATERIALS, *WELD. RES. COUNC. BULL.*, NO. 207, 1975

Note

* * AL-MMCS ARE NORMALLY SPECIFIED ACCORDING TO A NOMENCLATURE DEVELOPED BY THE ALUMINUM ASSOCIATION (AA) AND LATER ADOPTED BY THE AMERICAN NATIONAL STANDARD INSTITUTE (ANSI 35.5-1992). IN THIS SPECIFICATION, THE MATRIX ALLOY IS LISTED FIRST, FOLLOWED BY THE REINFORCEMENT MATERIAL, AND THEN THE VOLUME PERCENT AND SHAPE OF REINFORCEMENT, EACH SEPARATED BY A SLASH. THE HEAT TREATMENT DESIGNATION, IF USED, IS PLACED AFTER THE ENTRY FOR PERCENT AND SHAPE OF REINFORCEMENT. FOR EXAMPLE, $6061/AL_2O_3/15_P$-T6 REFERS TO AN AL-MMC WITH A 6061 AL ALLOY MATRIX THAT HAS BEEN HEAT-TREATED TO THE T6 CONDITION AND IS REINFORCED WITH 15 VOL% AL_2O_3 PARTICLES. A 15_W DESIGNATION WOULD INDICATE REINFORCEMENT IN WHISKER (W) FORM. THIS NOMENCLATURE WILL BE USED THROUGHOUT THE ARTICLE.

Selection and Weldability of Aluminum Metal-Matrix Composites

Thomas J. Lienert, The Ohio State University; Charles T. Lane, Duralcan USA; Jerry E. Gould, Edison Welding Institute

General Joining Considerations

The effective integration of Al-MMCs into useful structures and devices often requires that they be joined to similar and dissimilar materials. As a result, the ultimate utility of Al-MMCs hinges on the ability to effectively join them within reasonable economic constraints. As with all aluminum products, appropriate cleaning before joining and proper shielding during joining are necessary to avoid hydrogen contamination and the subsequent formation of porosity. However, the weldability of Al-MMCs differs markedly from that of monolithic aluminum alloys, because of the presence of the reinforcement. The addition of reinforcement to the aluminum matrix acts to modify several physical and chemical properties, which in turn greatly affect the weldability of Al-MMCs. Thus, an understanding of the weldability of Al-MMCs must include a thorough knowledge of the effects of the various interactions between matrix and reinforcement.

Viscosity Effects. The welding of Al-MMCs differs from the welding of monolithic aluminum alloys in that the weld pool of the composite contains a solid phase, because the reinforcement does not necessarily melt at welding temperatures. Thus, in the strictest sense, the composite weld pool is actually a partially melted zone. The most obvious effect of the presence of the reinforcement is the increased viscosity of the Al-MMC weld pool (Ref 2). This weld pool does not flow and wet as readily as that of monolithic aluminum alloys. Mass transfer is limited, because of the viscous nature of the MMC weld pool. Therefore, heat flow by convection in the weld pool is believed to be less effective than it is in aluminum alloys. Consequently, conductive heat flow through the aluminum alloy matrix is thought to play a larger than normal role in determining the temperature distributions and cooling rates in and around the weld pool of Al-MMCs.

The differences in heat flow in the MMC, relative to monolithic aluminum alloys, can affect the resulting microstructures and the stress distributions in the MMC weld.

Chemical Reactions. From a thermodynamic standpoint, Al-MMCs are nonequilibrium materials. Because a chemical potential difference exists between the matrix and the reinforcement, chemical reactions may occur. The contact between liquid aluminum and the reinforcement during joining can lead to the formation of unplanned or undesirable phases. The new phases may form at the matrix-reinforcement interface or they may entirely consume the original reinforcement.

For example, Al_4C_3 will spontaneously form when joining silicon carbide- or graphite-reinforced Al-MMCs by one of the following reactions:

$$3SIC(S) + 4AL(L) \leftrightarrow AL_4C_3(S) + 3SI_{AL} \quad \textbf{(EQ 1)}$$

$$3C(S) + 4AL(L) \leftrightarrow AL_4C_3(S) \quad \textbf{(EQ 2)}$$

where (*s*) and (*l*) represent solid and liquid, respectively.

Studies of the thermodynamics of Eq 1 and 2 show that the standard free energy, $\Delta G°$, of the reaction becomes increasingly negative (that is, the reaction proceeds further to the right) with increasing temperature and that the addition of silicon to the aluminum alloy matrix, which increases the activity of the silicon, aids in limiting the formation of Al_4C_3 during joining (Ref 3). The formation of Al_4C_3 creates concern for two reasons. First, its presence (in a very coarse or clustered form) is associated with a decrease in the mechanical properties of Al-MMCs. Second, it will readily dissolve in aqueous environments, resulting in formation of porosity and a loss of integrity to the weld.

Some control of the Al_4C_3 microstructure and, thus, the joint properties of silicon carbide- or graphite-reinforced Al MMCs can be achieved by tailoring the joining process. For these two types of composites, the integrated time at temperature above the matrix liquidus experienced by the composite during joining should be minimized, in order to limit the formation of Al_4C_3. Thus, joining should be performed using either a solid-state joining process or a fusion-welding process that can provide rapid thermal cycles with low heat inputs. Alternatively, a matrix alloy (or filler metal) with a high silicon content should be chosen, if possible, for the MMC.

A second type of chemical reaction occurs in aluminum-magnesium composites reinforced with Al_2O_3, where a magnesium spinel ($MgAl_2O_4$) is formed by the following reaction:

$$3MG + 4AL_2O_3 \leftrightarrow 3MGAL_2O_4 + 2AL \quad \textbf{(EQ 3)}$$

The formation of copper spinel ($CuAl_2O_4$) by similar reactions has also been reported in aluminum-copper alloy composites reinforced with Al_2O_3. The formation of these spinels is known to enhance wetting of the reinforcement by the aluminum, which limits or mitigates the agglomeration of the aluminum oxide into large clusters. The presence of the spinels at the interface does not appear to markedly change the mechanical properties of the weld.

Effects on Solidification. The third type of matrix-reinforcement interaction occurs during the solidification of discontinuously reinforced aluminum composites (Ref 4). Below a certain critical solidification rate, the reinforcement is pushed ahead of the solidification front. Because the reinforcement is pushed to the last areas to solidify, the uniformity of its distribution is governed by solidification conditions. The collection of reinforcement in front of the interface locally hinders heat flow and mass transport and causes a decrease in the extent of microsegregation, which diminishes the amount of terminal solidification phase(s) that forms. Furthermore, the modification of the amount and distribution of the terminal solidification phase(s) appears to improve the resistance of at least some Al-MMCs to solidification cracking. Modifications to microsegregation can also occur in continuous fiber reinforced Al-MMCs when solidification occurs along the small capillaries formed between the fibers. Both the pushing of reinforcement and the decrease in microsegregation can have an effect on the final microstructure and the properties of Al-MMC welds.

Weld Preparation. The standard methods of weld preparation are generally suitable for Al-MMCs, although a few modifications should be adopted. Because of their ceramic reinforcement, most MMCs are very wear resistant. Thus, standard steel-cutting tools and saw blades are ineffective for preparing the joint. Solid carbide (speed <100 m/min, or 330 ft/min) or diamond-tipped and diamond-plated tools (speed >400 m/min, or 1310 ft/min) are recommended for all

beveling and back gouging. Feeds that are greater than 0.3 mm/tooth (0.012 in./tooth) should be used for cutting tools, whereas constant, medium-heavy pressures should be used for saws.

Although the lower coefficient of thermal expansion (CTE) of the MMC will reduce the tendency of the joint to close ahead of the arc, the root gap and included angle of the joint should still be increased slightly to allow for the reduced fluidity of the composite weld pool.

The welding processes used for Al-MMCs can be characterized by the state of the matrix during welding. Several fusion-welding processes have been used to join these composites, including gas-tungsten arc welding (GTAW), gas-metal arc welding (GWAW), laser-beam welding (LBW), electron-beam welding (EBW), and resistance welding (RW). In addition, friction welding (FRW), transient liquid phase (TLP) bonding, and capacitor discharge welding (CDW) also have been used. Details on each process are provided below.

References cited in this section

2. B. ALTSHULLER, W. CHRISTY, AND B. WISKEL, GMA WELDING OF AL-AL_2O_3 METAL MATRIX COMPOSITE, *WELDABILITY OF MATERIALS, PROC. MATERIALS WELDABILITY SYMP.,* ASM INTERNATIONAL, 1990, P 305-309
3. T. ISEKI, T. KAMEDA, AND T. MARUYAMA, INTERFACIAL REACTIONS BETWEEN SIC AND ALUMINUM DURING JOINING, *J. MATER. SCI.,* VOL 19, 1984, P 1692-1698
4. P.K. ROHATGI, R. ASTHANA, AND S. DAS, SOLIDIFICATION, STRUCTURES, AND PROPERTIES OF CAST METAL-CERAMIC PARTICLE COMPOSITES, *INT. MET. REV.,* VOL 31 (NO. 3), 1986, P 115-139

Thomas J. Lienert, The Ohio State University; Charles T. Lane, Duralcan USA; Jerry E. Gould, Edison Welding Institute

Fusion-Welding Processes

Arc Welding. The metallurgy of arc welding, more so than other joining processes, is akin to a casting process. Aluminum is melted, undergoes mixing, and then resolidifies. The microstructure of the weld, including its defects, is not dissimilar to that of an aluminum casting. Unfortunately, this "recasting" process can significantly degrade the microstructure and properties of most MMCs.

In terms of equipment and consumables, the arc-welding practice for Al-MMCs is substantially similar to that for aluminum alloys. When one considers that from 75 to 90 vol% of the MMC is aluminum, it becomes apparent that the basic rules for equipment and filler-metal selection still apply. The constant-current power supply is still recommended for most welding, although constant voltage is preferred for some automated welding. Argon is generally the preferred shielding gas, except in the usual cases where it is either mixed with or replaced by helium. Filler metals are usually matched to the matrix alloy of the composite and the service requirements of the weld.

For example, the alloy 6061 is typically welded with ER4043 or ER5356. These filler metals would be appropriate for a composite that has 6061 as its matrix. In the case of $6061/Al_2O_3/10_p$, the ER5356 is used for its ability to keep the reinforcement wetted. In the case of $6061/SiC/15_w$, the ER4043 would be preferred for its assistance in suppressing the Al_4C_3 reaction. The extra silicon in ER4045 or ER4047 may be even more effective in this regard. However, the near-eutectic composition of the resulting weld metal is unsuitable for postweld solution heat treatments because of the coarsening of the silicon phase (Ref 5).

Primary silicon will precipitate in significant amounts only if the silicon content of the melt is greater than 12.6%, or the cooling rate is sufficiently high at a lower silicon level to prevent eutectic formation. Although 4047 contains 11 to 13% Si, the weld pool contains less, owing to dilution by the base material being welded (6061 has only 4% Si). Arc welds do

not cool rapidly enough to precipitate primary silicon from a hypoeutectic aluminum-silicon solution. Finally, primary silicon *enhances* properties if it is small and well-refined versus large and coarse.

The GTAW process is the original inert-gas arc-welding process developed for aluminum. Its low, controlled heat input is ideal for thin sections and complex shapes. The control of heat input is especially important for welding silicon carbide-reinforced wrought alloys. For most applications, the GTAW process is used with alternating current (ac), and the arc balance is adjusted to favor either cleaning or penetration. A cleaning arc can help minimize reactions between the reinforcement and matrix by reducing heat input. However, dilution of the composite into the weld pool is also decreased. Thus, some welds do not have homogeneous microstructures and do not reflect the properties of the parent material.

An arc set for cleaning is capable of breaking up the thin surface oxides that exist on the surface of a typical aluminum weld pool. However, in the case of a metal-matrix composite, the skin is stabilized by the ceramic particles (diluted from the base material), which are held at the pool surface by buoyancy forces and surface tension. A cleaning arc does not register properly on this "shielded" surface and tends to "skitter" along the joint. Formation and advancement of the weld pool is difficult, and some surface melting adjacent to the weld bead may occur.

For most Al-MMCs, a balanced, or penetrating, arc is preferred, because it is more focused and forces heat into the weld pool and joint, rather than melting the adjacent base material. The increased specific heat makes feeding the filler wire significantly easier and results in an improved bead profile. The degree of penetrating balance will depend on the geometry of the joint and the preferred technique of the welder.

Another effect of the particle-stabilized oxide skin is the dull appearance of the weld-pool surface. In fact, the initial formation of the weld pool is difficult to discern, and welders may overmelt the area while waiting for a bright pool to form. This is further complicated by the fact that the work area is not as well illuminated, because of the reduction in reflected light from the arc. Welders should watch the area under the arc for a "slumping" of the surface or another indication that subsurface melting is present. Feeding the filler rod into the weld pool early will accelerate pool formation, increase its fluidity, and partially dissipate the oxide skin. However, the pool will not become bright, like an unreinforced aluminum weld pool does, and the welder should begin advancing the weld as soon as he can feed in the filler.

An example of this procedure is a single-pass butt weld on 6.35 mm (0.25 in.) thick plate of Al-MMC. A series of different Al-MMC extrusions was prepared with a 30° edge bevel (60° included angle) and a 1.6 mm (0.06 in.) root land. After degreasing and scrubbing with a clean stainless steel brush, the plates were fixtured to a grooved stainless steel backing bar using a 1.6 mm (0.06 in.) root gap. The power supply was set for 22 V and 325 A, maximum, with the ac balance towards penetration (a setting of 5, where 3 equals balance for a range of 0 to 10). A 2.4 mm (0.094 in.) filler rod of ER5356 was fed into the weld at 23.3 mm/s (0.917 in./s) as the automatic cold-wire feed traveled at 25.8 mm/s (1.02 in./s). The shielding gas of 100% argon was metered at 16.5 L/min (35 ft^3/h).

The resulting welds passed the bead appearance, radiography, and tensile requirements for 6061, as described in AWS D1.2-90. Typical as-welded properties are listed in Table 1, and a cross section of a representative weld is shown in Fig. 1. Note the smooth bead contour, minimal porosity, and even distribution of particles in the weld.

TABLE 1 PROPERTIES OF SELECTED ALUMINUM ALLOYS AND MMCS JOINED USING THE GAS-TUNGSTEN ARC WELDING PROCESS

BASE MATERIAL (T6 TEMPER)	0.2% YIELD STRENGTH		ULTIMATE TENSILE STRENGTH		ELONGATION, %	FAILURE LOCATION
	mpa	ksi	mpa	ksi		
6061[(A)]	131	19	207	30	11	. . .
6061/AL_2O_3/10P	145	21	218	32	9.8	**HEAT-AFFECTED ZONE**
6061/AL_2O_3/20P	160	23	221	32	5.2	**HEAT-AFFECTED ZONE**
7005/AL_2O_3/10P	190	28	283	41	7.3	**WELD**
7005[(B)]	**207**	**30**	**317**	**46**	**10**	**. . .**

(A) TYPICAL HANDBOOK VALUES FOR ER5356 FILLER (REF 6).

(B) TYPICAL HANDBOOK VALUES FOR ER5556 FILLER (REF 6)

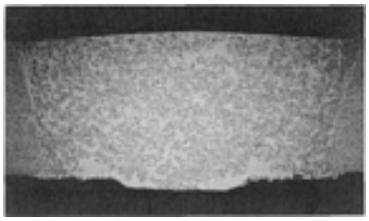

FIG. 1 MICROSTRUCTURE OF GAS-TUNGSTEN ARC WELDED 6061/AL_2O_3/10_P (6.35 MM, OR 0.25 IN., PLATE)

The GMAW process is preferred for most production welding, because of its high deposition rate and ease of automation. A root gap of 1 to 2 mm (0.04 to 0.08 in.), in conjunction with a temporary grooved backing bar, is recommended for single-sided welds, because of the lower fluidity and reduced penetration of the composite weld pool. A root gap is also preferred for double-sided welds; the root should be thoroughly back gouged before welding the second side. Joint openings range from 60° for single-V to 90° for double-V butt welds with root lands of 10 to 20% of the plate thickness. For multipass welds, it is recommended that the weld be vigorously scrubbed with a clean stainless steel wire brush between passes to remove any dewetted reinforcing phase, condensed magnesium oxide (a black, powdery residue), or other contaminants.

This procedure is illustrated by a multipass butt weld on a 19 mm (0.75 in.) plate of 6061/Al_2O_3/20_p-T6 (Ref 7). The extrusion was prepared with a 30° edge bevel (60° included angle) and a 3.2 mm (0.16 in.) root land. After degreasing and scrubbing with a clean stainless steel brush, the plates were fixtured to a grooved, stainless steel backing bar using a 1.6 mm (0.06 in.) root gap. A constant-current, dc, inverter-type power supply was set for 305 A and 26 V_{dc}, electrode positive (DCEP). The four passes were made at different travel speeds. The root pass was made at 384 mm/min (15 in./min) to keep the arc at the leading edge of the weld pool and ensure good root penetration. The speed was slowed to 252 mm/min (10 in./min) during the second pass to ensure good side-wall fusion. Capping passes (third and fourth) were made at 354 mm/min (14 in./min). A 1.6 mm (0.06 in.) filler wire of ER5356 was used with 100% argon shielding metered at 23.6 L/min (50 ft^3/h).

Typical as-welded properties are listed in Table 2, and a representative microstructure from the fusion zone is shown in Fig. 2. In this figure, the base material is to the right and the weld is on the left. There are no visible reaction products at the particle interface, and the dilution of the particles from the base material is relatively even, with minimal agglomeration.

TABLE 2 PROPERTIES OF ALUMINUM ALLOY 6061 AND ALUMINUM MMC 6061/AL_2O_3/20_P JOINED USING THE GAS-METAL ARC WELDING PROCESS

BASE MATERIAL	0.2% YIELD STRENGTH		ULTIMATE TENSILE STRENGTH		ELONGATION, %	FAILURE LOCATION
	Mpa	Ksi	Mpa	Ksi		
6061, AS-WELDED(A)	131	19	207	30	11	. . .
6061-T6(B)	276	40	304	44	5	. . .
6061/AL_2O_3/20_P, AS-WELDED	132	19	228	33	6.6	**HEAT-AFFECTED ZONE**
6061/AL_2O_3/20_P-T6	**189**	**27**	**283**	**41**	**3.9**	**WELD**

(A) TYPICAL HANDBOOK VALUES FOR ER5356 FILLER (REF 6).

(B) TYPICAL HANDBOOK VALUES FOR ER4043 FILLER; NO DATA AVAILABLE FOR ER5356 (REF 6)

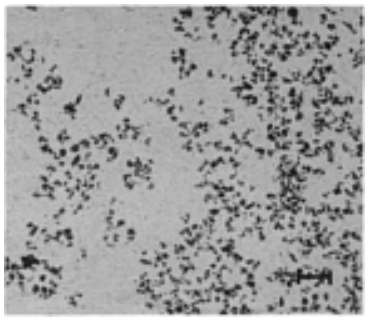

FIG. 2 MICROSTRUCTURE OF GAS-METAL ARC WELDED 6061/AL_2O_3/20_P

Laser-Beam Welding of Silicon Carbide-Reinforced Al-MMCs. Several researchers have attempted to limit the formation of aluminum carbide during fusion welding by employing welding processes, such as LBW, that can produce very rapid thermal cycles. Fully dense, crack-free welds have been produced with both continuous wave (CW) and pulsed carbon dioxide LBW processes, as well as the pulsed Nd:YAG process. The rapid thermal cycles made possible by these processes result in uniform distribution of reinforcement and a very fine grain size.

In one study, CW carbon dioxide laser-beam welds were produced on cast A356 (Al-7Si-0.3Mg)/SiC/15_p discontinuously reinforced aluminum at 1.0 and 1.5 kW and travel speeds ranging from 2.3 to 5.8 m/min (90 to 230 in./min) (Ref 8). These conditions resulted in heat inputs of 15.7 to 39.4 kJ/m (400 to 1000 J/in.). Pulsed Nd:YAG laser-beam welds were made on the same composite at an average power of 200 W with pulse energies that varied from 5 to 20 J. All welds were autogenous bead-on-plate welds.

The fusion zone of the CO_2 laser-beam welds made in this study exhibited three distinct regions (Fig. 3). The upper central region (region 1) contained large amounts of Al_4C_3 and silicon in the aluminum alloy matrix, with little remaining SiC. This region was spike-shape and encompassed less than 25% of the weld cross section. The Al_4C_3 in this region was not continuous with any silicon carbide, and it was relatively long (up to 45 μm, or 1.8 mil). The width of region 1 did not change with variations in heat input, and it was shown to be approximately the same size as the focused beam diameter. This suggests that region I is associated with the high temperatures of the weld keyhole, where the beam and material interact.

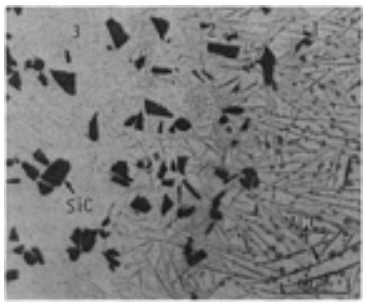

FIG. 3 MICROSTRUCTURE OF CO_2 LASER-BEAM WELD ON A356/SIC/15_P (UNETCHED)

The central region of the CO_2 laser-beam welds was surrounded by a very narrow region (region 2) in which the SiC had partially reacted to form Al_4C_3 and silicon, in accordance with Eq 1. The nucleation and growth of tiny needles of Al_4C_3 from the SiC in the partially reacted zone are evident. These needles, which are straight and relatively short, show an orientation relation with the silicon carbide.

Surrounding the partially reacted zone was a large region (region 3) in which the SiC appeared to be unreacted. This unreacted zone constituted approximately 70% of the total weld volume. Similar phenomena were also observed in the pulsed Nd:YAG laser-beam welds.

Other experiments showed that the extent of aluminum carbide formation in pulsed carbon dioxide laser-beam welds on a cast A356/SiC/15_p composite could be modified by changes in welding parameters. In one study, the size and quantity of Al_4C_3 was observed to increase proportionally with laser specific energy (Ref 9). In another experiment, measurements were made of the strength and ductility of pulsed carbon dioxide laser-beam welds made at a peak power of 3.2 kW and at duty cycles ranging from 50 to 91% (Ref 10). The laser processing resulted in increased strength in most of the welds, relative to the coarse-grained base material, despite the formation of a large amount of Al_4C_3. The presence of other phases, such as $Al_4Si_2C_5$ and MC-type carbides, in the pulsed CO_2 laser-beam welds was also reported.

Whereas LBW experiments have shown that the Al_4C_3 microstructure can be modified by varying process parameters, it appears that LBW is incapable of producing welds that are free of Al_4C_3. Experimental observations and physical data suggest that the laser energy is preferentially absorbed by the SiC, because of its greater absorptivity, relative to aluminum, at the laser wavelengths. The increased energy absorption results in local superheating of the SiC and surrounding areas and promotes Al_4C_3 formation. In summation, it appears that the LBW processes may have limited potential in joining silicon carbide-reinforced Al-MMCs.

Laser-Beam Welding of Aluminum Oxide-Reinforced Al-MMCs. Few LBW studies on aluminum oxide-reinforced Al-MMCs have been reported. It appears that the Al_2O_3 reinforcement also preferentially absorbs the impinging laser energy. The carbon dioxide LBW process was used on a 6061/Al_2O_3/20_p composite produced by powder metallurgy (Ref 11). Initial attempts at welding resulted in cutting of the samples. However, acceptable welds were ultimately produced when the shims of 5083 and 4047 filler wire were placed in the joints.

Similar problems were reported by other researchers on a 6061/aluminum oxide/20_p composite produced via ingot metallurgy (Ref 12). They attributed the difficulty to an unstable plasma above the weld pool and attempted to improve weldability with plasma control. Sound welds with a uniform distribution of reinforcement were produced by placing a small gas nozzle close to the weld area to blow away the plasma material. The quality of the welds was found to strikingly depend on the direction of the suppression gas flow, relative to the welding direction, and on nozzle positioning. Optimum welding conditions were realized when the flow was opposite to the welding direction and the end of the nozzle was inclined upward by 5° to the horizontal. The gas pressures at the nozzle ranged from 70 to 275 kPa (10 to 40 psi). Based on this study, LBW offers some potential for joining aluminum oxide-reinforced Al-MMCs.

Electron-Beam Welding of Silicon Carbide-Reinforced Al-MMCs. The EBW process appears to have potential for joining at least some silicon carbide-reinforced Al-MMCs. A follow-up study to the LBW work described in Ref 6 determined that EBW can be used successfully to join the same cast discontinuously reinforced aluminum (A356/SiC/15_p) without the formation of large amounts of Al_4C_3 (Ref 13). Like LBW, the EBW process is capable of producing rapid thermal cycles. However, the physics of beam-material interaction differs for the two processes. Heating during LBW results from the absorption of photons by the substrate, whereas heating during EBW occurs by the transfer of kinetic energy to the atoms of the substrate via collisions with the high-energy electrons of the beam. In this study, CO_2 laser-beam and electron-beam welds were produced at identical energy inputs, travel speeds, and focused beam diameters. The use of EBW resulted in sound welds with a uniform distribution of reinforcement and a fine grain size. The electron-beam welds exhibited orders of magnitude less Al_4C_3 than the laser-beam welds made using the same parameters. The electron-beam welds made at 85 mm/s (200 in./min) with sharp beam focus contained almost no Al_4C_3. Electron-beam welds made at slower speeds and/or with defocused beams contained somewhat more Al_4C_3.

The different mechanisms of energy transfer in EBW and LBW appear to affect the final weld microstructures of silicon carbide-reinforced Al-MMCs and, thus, the weld properties, despite the fact that both welding processes allow for rapid thermal cycles with low overall heat input.

Unfortunately, EBW cannot be successfully applied to all silicon carbide-reinforced Al-MMCs. For example, attempts at EBW on a wrought 2014/SiC/15_p MMC resulted in cutting of the sample. It is not known whether the problem resulted from the manufacturing process (powder metallurgy) or was inherent to the material.

Transient liquid-phase (TLP) bonding has proven fairly successful in joining Al-MMCs. The process employs a filler material or interlayer to produce a transient liquid layer at the interface to be joined. Solidification of the joint occurs isothermally, by diffusion. The advantage of TLP bonding of Al-MMCs involves the lower peak-processing temperatures, compared with the temperatures used in other fusion-welding processes. The lower processing temperatures result in less damage to the engineering properties of the composite in and around the joint. However, there is a concern for damage to the properties of the composite base material during processing, because the thermal cycles for TLP bonding hold the entire assembly at temperatures near the solidus for a longer time, relative to the other fusion-welding processes.

Transient liquid-phase bonding processes for Al-MMCs are controlled by several parameters, including surface finish, type and thickness of interlayer or filler metal, processing time and temperature, and clamping pressure on the joint. The surface aluminum oxides must be removed from the samples to facilitate wetting of the substrate by the interlayer. The choice of the correct combination of processing parameters is critical in avoiding such problems as reinforcement enriched or depleted zones and Kirkendall porosity. In general, the thinnest interlayer possible should be used to allow for the shortest processing times and a narrow liquid zone. Additionally, the lowest possible temperatures should be used to limit damage to the material properties of the composite. Although the application of pressure can aid in improving interlayer-substrate contact, excess pressure can lead to expulsion of the liquid zone, which results in reinforcement-rich areas at the joint line.

Silicon Carbide-Reinforced Al-MMCs. Transient liquid-phase bonding with gold and aluminum-silicon-magnesium interlayers has been used to join two 6061/SiC/25_p composite sheets (Ref 14). Based on thermomechanical simulation studies, a process window of time-temperature combinations that would not produce damage to the properties of the base material was developed. The window ranged from 30 min at 565 °C (1050 °F) to 10 min at 580 °C (1075 °F). A 0.025 mm (0.001 in.) gold interlayer was shown to produce better results than the aluminum-silicon-magnesium material. Optimum conditions of 30 min at 567 to 580 °C (1053 to 1075 °F) were reported for the gold interlayer. Three distinct zones were observed in the vicinity of the bond interface: a particle-enriched zone, a diffuse flow zone that showed a pattern of material flow, and the undisturbed base material. No mention was made of the formation of Al_4C_3 for these conditions. Low tensile joint efficiencies (<30%) were attributed to voids at the joint interface.

Aluminum Oxide-Reinforced Al-MMCs. The joining of a 6061/Al_2O_3/15_p Al-MMC using TLP bonding also has been reported (Ref 15). Three types of interlayers demonstrated an ability to join the material: gold, copper, and Al-12Si. The bonding experiments were performed in vacuum (1.3×10^{-8} Pa, or 10^{-10} torr) on mechanically cleaned samples using a clamping pressure of less than 70 kPa (10 psi). Joining with a 25 μm (1 mil) thick interlayer of gold at 580 °C (1075 °F) for 130 min produced the strongest bonds. The joints had a 323 MPa (47 ksi) yield strength and a 341 MPa (49 ksi) ultimate tensile strength with a joint efficiency of 95%. Joining with a 125 μm (0.005 in.) thick layer of Al-12Si at 585 °C for 20 min yielded bonds with nearly identical properties; however, the bond line contained residual filler material, as well as voids. A 25 μm (0.001 in.) thick layer of copper produced bonds with much lower strengths. An increase in volume fraction of the reinforcement was observed near the bond lines of joints made with gold and copper. Increased loading of reinforcement was not observed for bonds made with the Al-12Si.

The brazing of a 6061 MMC reinforced with 5, 10, and 15 vol% short Al_2O_3 fibers using aluminum-silicon and aluminum-manganese interlayers has been studied (Ref 16). However, the reported bonding temperature range of 580 to 610 °C (1075 to 1130 °F) suggests that TLP bonding may have actually occurred. A 150 μm (0.006 in.) thick sheet of Al-10Si was used for joining, as well as a 140 μm (0.0056 in.) thick sheet of Al-1.5Mn clad with 20 μm (800 μin.) of Al-10Si on each side. The bonding time for each test was 10 min at a vacuum of 6.7 mPa (5×10^{-5} torr). Bonding the composite to itself proved easier than joining the composite to a monolithic 6061 alloy. The tensile strengths for the similar material bonds of 5% aluminum oxide fiber material exceeded 230 MPa (33 ksi). The joint efficiencies of these bonds were not reported.

References cited in this section

5. S.H. LO, S. DIONNE, M. POPESCU, S. GEDEON, AND C.T. LANE, EFFECTS OF PRIOR- AND POST-WELD HEAT TREATMENTS ON THE PROPERTIES OF SIC/AL-SI COMPOSITE GAS METAL ARC WELDED JOINTS, *PROC. ADVANCES IN PRODUCTION AND FABRICATION OF LIGHT METALS AND MMCS,* M. AVEDESIAN, L. LAROUCHE, AND J. MASOUNAVE, ED., CANADIAN INSTITUTE OF MINING, METALLURGY AND PETROLEUM, 1992, P 575-588
6. J.E. HATCH, *ALUMINUM--PROPERTIES AND PHYSICAL METALLURGY,* AMERICAN SOCIETY FOR METALS, 1984, P 359
7. KAISER ALUMINUM, *WELDING,* 1978, P 3-24 TO 3-31
8. M.J. COLA, T.J. LIENERT, J.E. GOULD, AND J.P. HURLEY, LASER WELDING OF A SIC PARTICULATE REINFORCED ALUMINUM METAL MATRIX COMPOSITE, *WELDABILITY OF MATERIALS, PROC. MATERIALS WELDABILITY SYMP.,* ASM INTERNATIONAL, 1990, P 297-303
9. N.B. DAHOTRE, T.D. MCCAY, AND M.H. MCCAY, LASER PROCESSING OF A SIC/AL-ALLOY METAL MATRIX COMPOSITE, *J. APPL. PHYS.,* VOL 65 (NO. 12), 1989, P 5072-5077

10. N.B. DAHOTRE, M.H. MCCAY, T.D. MCCAY, AND S. GOPINATHAN, PULSE LASER PROCESSING OF A SIC/AL-ALLOY METAL MATRIX COMPOSITE, *J. MATER. RES.*, VOL 6 (NO. 3), 1991, P 514-529
11. R.P. MARTUKANITZ AND R.B. BHAGAT, LASER PROCESSING OF DISCONTINUOUSLY REINFORCED, ALUMINUM MATRIX COMPOSITES, *THE METAL SCIENCE OF JOINING,* ASM INTERNATIONAL, 1992, P 241-247
12. S.M. KAWALI, G.L. VIEGELAHN, AND R. SCHEUERMAN, LASER WELDING OF ALUMINA REINFORCED 6061 ALUMINUM ALLOY COMPOSITE, *PROC. LASER MATERIALS PROCESSING SYMPOSIUM,* ICALEO '91, LASER INSTITUTE OF AMERICA, 1991, P 156-167
13. T.J. LIENERT, E.D. BRANDON, AND J.C. LIPPOLD, LASER AND ELECTRON BEAM WELDING OF SIC_P REINFORCED ALUMINUM A356 METAL MATRIX COMPOSITE, *SCR. METALL. MATER.,* VOL 28, JUNE 1993, P 1341-1346
14. K. SUDHAKAR, "JOINING OF ALUMINUM BASED PARTICULATE-REINFORCED METAL-MATRIX COMPOSITES," DISSERTATION, THE OHIO STATE UNIVERSITY, 1990
15. R. KLEHN, "JOINING OF 6061 ALUMINUM MATRIX CERAMIC PARTICLE REINFORCED COMPOSITES," M.S. THESIS, MASSACHUSETTS INSTITUTE OF TECHNOLOGY, SEPT 1991
16. K. SUGANUMA, T. OKAMOTO, AND N. SUZUKI, JOINING OF ALUMINA SHORT-FIBRE REINFORCED AA6061 ALLOY TO AA6061 ALLOY AND TO ITSELF, *J. MATER. SCI.*, 1987, P 1580-1584

Resistance Welding and Forge Welding

Both resistance welding and forge welding are quite adaptable to a range of discontinuously reinforced aluminum composites. As described previously, problems associated with welding these materials typically have two causes. For the silicon carbide-reinforced Al-MMCs, the high temperatures and relatively long times at temperatures permit dissolution of the carbides and subsequent precipitation of detrimental phases (Al_4C_3). For the aluminum oxide-reinforced Al-MMCs, similar conditions allow the individual reinforcing particles to agglomerate, which reduces material performance. Both resistance and forge welding processes have rapid thermal cycles that may limit these problems. Particular aspects of these processes are described separately below.

Resistance Welding. Virtually all available work concerning the resistance welding of MMCs has been done using the resistance spot welding technique. An example of a cross section of a spot weld made on an A359 (Al-9Si-0.3Mg)/SiC/10_p is shown in Fig. 4. Aluminum MMCs are generally spot welded using conditions similar to those for conventional aluminum alloys. However, these materials typically require substantially less current (about half) for welding. This is likely due to an increase in bulk resistivity associated with the addition of the particles. The spot weld in Fig. 4, which shows a full-size nugget, does not show any of the Al_4C_3 plates seen in the fusion zones of the laser welds. Rather, a uniform distribution of the SiC particles is noted.

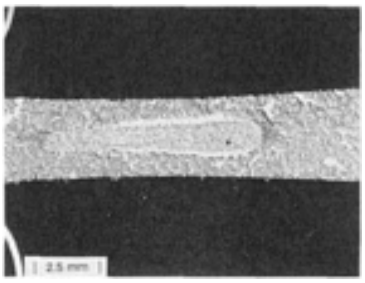

FIG. 4 RESISTANCE SPOT WELD ON A359/SIC/10$_p$

It is believed that the minimal reaction of the SiC to form Al_4C_3 is due to two factors. First, in resistance welds, the temperature of the liquid nugget only barely exceeds the melting point of the material (Ref 17), providing little, if any, driving force for the reaction. Second, temperature excursions above the liquidus are relatively short, typically less than 0.1 s, which minimizes any potential reaction.

Spot welds on discontinuously reinforced aluminum composites do show some redistribution of the reinforcement in the fusion zone (Fig. 4). Typically, the fusion zone is relatively free of the reinforcement near the fusion line, with an increased density of the reinforcement near the center of the weld. It is possible that this redistribution of the composite is the result of macroscopic liquid flow during solidification, but the effect is still under study. The effect of this reinforcement-free zone on the mechanical performance of the weld is not known.

Friction Welding. Both silicon carbide- and aluminum oxide-reinforced Al-MMCs have been friction welded using continuous-drive and inertia machines (Ref 18, 19). Friction welding is a solid-state process and does not require melting. Thus, it is not hampered by the melting and solidification concerns described previously. An examination of friction welds on these materials typically shows a distribution of reinforcement particles similar to that in the base material. There is, however, concern with the development of high in-process torques associated with these processes. High torques, particularly during stopping, can cause debonding of the matrix and the reinforcement, resulting in cracking near the bond line. In addition, stringers, if present in the material, can "open up" under the influence of these resultant torques.

Compared to conventional aluminum alloys, discontinuously reinforced aluminum composites require about double the applied force. This is because the reinforcement particles substantially increase the flow stress of the composite, even at high temperatures, preventing metal flow.

Inertia friction welding studies on an A356/SiC/20$_p$ and an A359/SiC/20$_p$ have been performed (Ref 18). Both similar and dissimilar material welds to a monolithic 6061-T651 aluminum alloy were produced over a range of flywheel speeds and axial pressures. High joint efficiencies (greater than 70%) were realized when high flywheel speeds and high axial pressures, relative to those used for monolithic aluminum alloys, were employed for the similar material welds. The joint efficiencies of the dissimilar welds were less than 70%, relative to the composite base material.

Flash-butt welding, another nominally solid-state process, has also been found to be effective for joining these materials (Ref 20). The flash welding of conventional aluminum alloys is typically characterized by very fast flashing rates and upset velocities. Similar approaches are recommended for the flash welding of Al-MMCs. Other process features that contribute to weld quality are the use of shielding gases during flashing (minimizing bond-line oxidation) and dc power for flashing. The dc power appears to provide a finer flash, resulting in higher thermal gradients in the workpiece.

Capacitor discharge welding is a generic term relating to all resistance-welding processes that supply energy to the workpiece by the discharge of charged capacitors. Variations on this process range from spot welding to small-scale butt welding. Generally, capacitive discharge welding processes are characterized by extremely rapid discharge rates (on the order of 5 to 25 ms) and subsequent rapid thermal cycles. In terms of suppressing chemical reactions in silicon carbide-reinforced Al-MMCs, the capacitive discharge processes offer considerable potential.

Work on the capacitive discharge welding of Al-MMCs has been reported (Ref 21). The capacitive system used in this work was basically a forge-butt welding process. Specifically, the system used oriented parts in a butt configuration, with the ends separated by a projection on one of the surfaces. A force was then applied to the workpieces and the energy from the discharging capacitors introduced. The result was surface melting, followed by impact and forging of the components. This work has shown that Al_4C_3 formation can be precluded on several types of silicon carbide-reinforced Al-MMCs. Consistent with the other resistance-welding processes, the short exposure times and rapid cooling rates (approximately 10^6 °C/s, or 2×10^6 °F/s) were responsible for the retention of the SiC.

References cited in this section

17. J.E. GOULD, AN EXAMINATION OF NUGGET DEVELOPMENTS DURING RESISTANCE SPOT

WELDING USING EXPERIMENTAL AND ANALYTICAL TECHNIQUES, *WELD. J. RES. SUPP.*, VOL 68 (NO. 1), 1987, P 1S-10S

18. M.J. COLA, "INERTIA-FRICTION WELDING OF PARTICULATE-REINFORCED ALUMINUM MATRIX COMPOSITES," THESIS, THE OHIO STATE UNIVERSITY, 1992
19. M.J. COLA, G.S. MARTIN, AND C.E. ALBRIGHT, "INERTIA-FRICTION WELDING OF A 6061-T6/AL_2O_3/15_P METAL-MATRIX COMPOSITE," RESEARCH REPORT MR9108, EDISON WELDING INSTITUTE, JUNE 1991
20. D.S. SCHWARTZ, J.H. DEVLETIAN, S.J. CHEN, AND J.E. GOULD, CAPACITOR DISCHARGE AND FLASH WELDING OF SIC-REINFORCED HIGH TEMPERATURE AL ALLOYS, JOINING AND ADHESION OF INORGANIC MATERIALS, PROCEEDINGS OF MATERIALS RESEARCH SOCIETY SPRING 1993 MEETING, VOL 314
21. J.H. DEVLETIAN, SIC/AL METAL MATRIX COMPOSITE WELDING BY A CAPACITOR DISCHARGE PROCESS, *WELD. J.*, 1987, P 33-39

Selection and Weldability of Aluminum Metal-Matrix Composites

Thomas J. Lienert, The Ohio State University; Charles T. Lane, Duralcan USA; Jerry E. Gould, Edison Welding Institute

---

References

1. G.E. METZGER, JOINING OF METAL-MATRIX FIBER-REINFORCED COMPOSITE MATERIALS, *WELD. RES. COUNC. BULL.*, NO. 207, 1975
2. B. ALTSHULLER, W. CHRISTY, AND B. WISKEL, GMA WELDING OF AL-AL_2O_3 METAL MATRIX COMPOSITE, *WELDABILITY OF MATERIALS, PROC. MATERIALS WELDABILITY SYMP.*, ASM INTERNATIONAL, 1990, P 305-309
3. T. ISEKI, T. KAMEDA, AND T. MARUYAMA, INTERFACIAL REACTIONS BETWEEN SIC AND ALUMINUM DURING JOINING, *J. MATER. SCI.*, VOL 19, 1984, P 1692-1698
4. P.K. ROHATGI, R. ASTHANA, AND S. DAS, SOLIDIFICATION, STRUCTURES, AND PROPERTIES OF CAST METAL-CERAMIC PARTICLE COMPOSITES, *INT. MET. REV.*, VOL 31 (NO. 3), 1986, P 115-139
5. S.H. LO, S. DIONNE, M. POPESCU, S. GEDEON, AND C.T. LANE, EFFECTS OF PRIOR- AND POST-WELD HEAT TREATMENTS ON THE PROPERTIES OF SIC/AL-SI COMPOSITE GAS METAL ARC WELDED JOINTS, *PROC. ADVANCES IN PRODUCTION AND FABRICATION OF LIGHT METALS AND MMCS*, M. AVEDESIAN, L. LAROUCHE, AND J. MASOUNAVE, ED., CANADIAN INSTITUTE OF MINING, METALLURGY AND PETROLEUM, 1992, P 575-588
6. J.E. HATCH, *ALUMINUM--PROPERTIES AND PHYSICAL METALLURGY*, AMERICAN SOCIETY FOR METALS, 1984, P 359
7. KAISER ALUMINUM, *WELDING*, 1978, P 3-24 TO 3-31
8. M.J. COLA, T.J. LIENERT, J.E. GOULD, AND J.P. HURLEY, LASER WELDING OF A SIC PARTICULATE REINFORCED ALUMINUM METAL MATRIX COMPOSITE, *WELDABILITY OF MATERIALS, PROC. MATERIALS WELDABILITY SYMP.*, ASM INTERNATIONAL, 1990, P 297-303
9. N.B. DAHOTRE, T.D. MCCAY, AND M.H. MCCAY, LASER PROCESSING OF A SIC/AL-ALLOY METAL MATRIX COMPOSITE, *J. APPL. PHYS.*, VOL 65 (NO. 12), 1989, P 5072-5077
10. N.B. DAHOTRE, M.H. MCCAY, T.D. MCCAY, AND S. GOPINATHAN, PULSE LASER PROCESSING OF A SIC/AL-ALLOY METAL MATRIX COMPOSITE, *J. MATER. RES.*, VOL 6 (NO. 3), 1991, P 514-529
11. R.P. MARTUKANITZ AND R.B. BHAGAT, LASER PROCESSING OF DISCONTINUOUSLY REINFORCED, ALUMINUM MATRIX COMPOSITES, *THE METAL SCIENCE OF JOINING*, ASM INTERNATIONAL, 1992, P 241-247

12. S.M. KAWALI, G.L. VIEGELAHN, AND R. SCHEUERMAN, LASER WELDING OF ALUMINA REINFORCED 6061 ALUMINUM ALLOY COMPOSITE, *PROC. LASER MATERIALS PROCESSING SYMPOSIUM*, ICALEO '91, LASER INSTITUTE OF AMERICA, 1991, P 156-167
13. T.J. LIENERT, E.D. BRANDON, AND J.C. LIPPOLD, LASER AND ELECTRON BEAM WELDING OF SIC_P REINFORCED ALUMINUM A356 METAL MATRIX COMPOSITE, *SCR. METALL. MATER.*, VOL 28, JUNE 1993, P 1341-1346
14. K. SUDHAKAR, "JOINING OF ALUMINUM BASED PARTICULATE-REINFORCED METAL-MATRIX COMPOSITES," DISSERTATION, THE OHIO STATE UNIVERSITY, 1990
15. R. KLEHN, "JOINING OF 6061 ALUMINUM MATRIX CERAMIC PARTICLE REINFORCED COMPOSITES," M.S. THESIS, MASSACHUSETTS INSTITUTE OF TECHNOLOGY, SEPT 1991
16. K. SUGANUMA, T. OKAMOTO, AND N. SUZUKI, JOINING OF ALUMINA SHORT-FIBRE REINFORCED AA6061 ALLOY TO AA6061 ALLOY AND TO ITSELF, *J. MATER. SCI.*, 1987, P 1580-1584
17. J.E. GOULD, AN EXAMINATION OF NUGGET DEVELOPMENTS DURING RESISTANCE SPOT WELDING USING EXPERIMENTAL AND ANALYTICAL TECHNIQUES, *WELD. J. RES. SUPP.*, VOL 68 (NO. 1), 1987, P 1S-10S
18. M.J. COLA, "INERTIA-FRICTION WELDING OF PARTICULATE-REINFORCED ALUMINUM MATRIX COMPOSITES," THESIS, THE OHIO STATE UNIVERSITY, 1992
19. M.J. COLA, G.S. MARTIN, AND C.E. ALBRIGHT, "INERTIA-FRICTION WELDING OF A 6061-T6/AL_2O_3/15_P METAL-MATRIX COMPOSITE," RESEARCH REPORT MR9108, EDISON WELDING INSTITUTE, JUNE 1991
20. D.S. SCHWARTZ, J.H. DEVLETIAN, S.J. CHEN, AND J.E. GOULD, CAPACITOR DISCHARGE AND FLASH WELDING OF SIC-REINFORCED HIGH TEMPERATURE AL ALLOYS, JOINING AND ADHESION OF INORGANIC MATERIALS, PROCEEDINGS OF MATERIALS RESEARCH SOCIETY SPRING 1993 MEETING, VOL 314
21. J.H. DEVLETIAN, SIC/AL METAL MATRIX COMPOSITE WELDING BY A CAPACITOR DISCHARGE PROCESS, *WELD. J.*, 1987, P 33-39

General Welding Characteristics of High-Temperature Materials

A.C. Lingenfelter, Lawrence Livermore National Laboratory

Introduction

HIGH-TEMPERATURE ALLOYS are generally recognized as being those alloys that are used at temperatures of 540 °C (1000 °F) and above. These alloys exhibit some combination of high strength at temperature; resistance to environmental attack (including nitridation, carbonization, oxidation, and sulfidation), excellent creep resistance, creep rupture strength, toughness, and metallurgical stability; useful thermal expansion characteristics; and resistance to thermal fatigue and corrosion. This article addresses the general welding characteristics common to both solid-solution-strengthened and precipitation-hardened nickel-, iron-, and cobalt alloys. The remaining articles in this Section focus on characteristics of nonferrous high-temperature materials.

Table 1 is a reasonably inclusive list of the alloys that have found application as high-temperature materials and that have demonstrated some degree of weldability. (It should be noted that the refractory metals and alloys that are applied at high temperature are not listed in Table 1; information about these materials can be found in the article "Special Metallurgical Welding Considerations for Refractory Metals" in this Section of the Handbook.) Many of the alloys listed in Table 1 are general-purpose materials that find application in a full temperature range, from cryogenic temperatures on up. In addition, certain of these alloys may be used for their corrosion resistance or some other property not associated with high-temperature application. These considerations make it difficult to precisely estimate the amount of material used specifically for high-temperature applications, although a rough estimate would be of the order of 30,000 tons/year (27,000 tonnes/year). Most of the alloys listed are produced as wrought products; however, some cast materials appear on the list, and cast versions of many of the wrought alloys are produced.

TABLE 1 NOMINAL COMPOSITIONS OF HIGH-TEMPERATURE ALLOYS

ALLOY	COMPOSITION, %										
	Ni	**Cr**	**Co**	**Fe**	**Mo**	**Ti**	**W**	**Nb**	**Al**	**C**	OTHER
SOLID-SOLUTION NICKEL-BASE ALLOYS											
HASTELLOY N	72.0	7.0	. . .	5.0 MAX	16.0	0.5 MAX	. . .	. . .	. . .	0.06	**. . .**
HASTELLOY S	67.0	15.5	. . .	1.0	15.5	. . .	. . .	. . .	0.2	0.02 MAX	**0.02 LA**
HASTELLOY X	49.0	22.0	1.5 MAX	18.5	9.0	. . .	0.6	. . .	2.0	0.15	**. . .**
HAYNES 230	BAL	22	0-5	0-3	2	. . .	14	. . .	0.3	0.1	**0.5 MN, 0.4 SI, 0.02 LA, 0.005 B**
INCONEL 600	76.0	15.5	. . .	8.0	. . .	. . .	. . .	. . .	. . .	0.08	**0.25 CU MAX**
INCONEL 601	60.5	23.0	. . .	14.1	. . .	. . .	. . .	. . .	1.35	0.05	**0.5 CU MAX**
INCONEL 617	55.0	22.0	12.5	. . .	9.0	. . .	. . .	. . .	1.0	0.07	**. . .**
INCONEL 625	61.0	21.5	. . .	2.5	9.0	0.2	. . .	3.6	0.2	0.05	**. . .**
PRECIPITATION-HARDENABLE NICKEL-BASE ALLOYS											
GMR-235	63.0	15.5	. . .	10.0	5.25	2.0	. . .	. . .	3.0	0.15	**0.06 B**
INCONEL 702	79.5	15.5	. . .	0.4	. . .	0.7	. . .	. . .	3.4	0.04	**. . .**
INCONEL 706	41.5	16.0	. . .	37.5	. . .	1.75	. . .	2.9[A]	0.2	0.03	**. . .**
IN-713C	74.0	12.5	. . .	. . .	4.2	0.8	. . .	2.0	6.0	0.12	**0.012 B, 0.10 ZR**
INCONEL 718	52.5	19.0	. . .	18.5	3.0	0.9	. . .	5.0	0.5	0.08 MAX	**0.15 CU MAX**
INCONEL 722	75.0	15.5	. . .	7.0	. . .	2.5	. . .	. . .	0.7	0.04	**. . .**
INCONEL X-750	73.0	15.5	. . .	7.0	. . .	2.5	. . .	1.0	0.7	0.04	**0.25 CU MAX**
INCOLOY 901	42.5	12.5	. . .	36.2	6.0	2.7	. . .	. . .	. . .	0.10 MAX	**. . .**
M-252	56.5	19.0	10.0	<0.75	10.0	2.6	. . .	. . .	1.0	0.15	**0.005B**
RENÉ	55.0	19.0	11.0	<0.3	10.0	3.1	. . .	. . .	1.5	0.09	**0.01 B**
UDIMET 700	53.0	15.0	18.5	<1.0	5.0	3.4	. . .	. . .	4.3	0.07	**0.03 B**
WASPALOY	57.0	19.5	13.5	2.0 MAX	4.3	3.0	. . .	. . .	1.4	0.07	**0.006 B, 0.09 ZR**
SOLID-SOLUTION IRON-BASE ALLOYS											
16-25-6	25.0	16.0	. . .	50.7	6.0	. . .	. . .	. . .	. . .	0.06	**1.35 MN, 0.70 SI**
17-14 CUMO	14.0	16.0	. . .	62.4	2.5	0.3	. . .	0.4	. . .	0.12	**0.75 MN, 0.50 SI, 3.0 CU**
19-9 DL	9.0	19.0	. . .	66.8	1.25	0.3	1.25	0.4	. . .	0.30	**1.10 MN, 0.60 SI**
INCOLOY 800	32.5	21.0	. . .	45.7	. . .	0.38	. . .	. . .	0.38	0.05	**. . .**
INCOLOY 800H	33.0	21.0	. . .	45.8	. . .	. . .	. . .	. . .	. . .	0.08	**. . .**
INCOLOY 800HT	32.5	21	. . .	46	. . .	0.4	. . .	. . .	0.4	0.08	**0.8 MN, 0.008 S, 0.5**

											SI, 0.4 CU
INCOLOY 801	32.0	20.5	. . .	46.3	. . .	1.13	. . .	. . .	. . .	0.05	**. . .**
INCOLOY 802	32.5	21.0	. . .	44.8	. . .	0.75	. . .	. . .	0.58	0.35	**. . .**
MULTIMET (N-155)	20.0	21.0	20.0	32.2	3.0	. . .	2.5	1.0	. . .	0.15	**0.15 N, 0.02 LA, 0.02 ZR**
RA 330	36.0	19.0	. . .	45.1	. . .	. . .	. . .	. . .	. . .	0.05	**. . .**
PRECIPITATION-HARDENABLE IRON-BASE ALLOYS											
A-286	26.0	15.0	. . .	55.2	1.25	2.0	. . .	. . .	0.2	0.04	**0.005 B, 0.3 V**
DISCOLOY	26.0	14.0	. . .	55.0	3.0	1.7	. . .	. . .	0.25	0.06	**. . .**
HAYNES 556	21.0	22.0	20.0	29.0	3.0	. . .	2.5	0.1	0.3	0.10	**0.50 TA, 0.02 LA**
INCOLOY 903	0.1 MAX	38.0	15.0	41.0	0.1	1.4	. . .	3.0	0.7	0.04	**. . .**
INCOLOY 909	38	. . .	13	42	. . .	1.5	. . .	4.7	0.03	0.01	**0.4 SI**
INCOLOY 925	44	21	. . .	28	3	2.1	. . .	. . .	0.3	0.01	**1.8 CU**
SOLID-SOLUTION COBALT-BASE ALLOYS											
HAYNES 25 (-605)	10.0	20.0	50.0	3.0	. . .	. . .	15.0	. . .	. . .	0.10	**1.5 MN**
HAYNES 188	22.0	22.0	37.0	3.0 MAX	. . .	. . .	14.5	. . .	. . .	0.10	**0.04 LA**
S-816	20.0	20.0	42.0	4.0	4.0	. . .	4.0	4.0	. . .	0.38	**. . .**
STELLITE 6B	1.0	30.0	61.5	1.0	. . .	. . .	4.5	. . .	. . .	1.0	**. . .**
UMCO-50	. . .	28.0	49.0	21.0	. . .	. . .	. . .	. . .	. . .	0.12 MAX	**. . .**
PRECIPITATION-HARDENABLE COBALT-BASE ALLOYS											
AR-213	0.5 MAX	19.0	65.0	0.5 MAX	. . .	. . .	4.5	. . .	3.5	0.17	**6.5 TA, 0.15 ZR, 0.1 Y**
MP-35N	35.0	20.0	35.0	. . .	10.0	. . .	. . .	. . .	. . .	. . .	**. . .**
MP-159	**25.0**	**19.0**	**36.0**	**9.0**	**7.0**	**3.0**	**. . .**	**0.6**	**0.2**	**. . .**	**. . .**

(A) NB + TA

Applications of these materials include:

- HEAT TREATMENT FIXTURES AND FURNACE PARTS
- HEATING ELEMENTS USED FOR DOMESTIC OR INDUSTRIAL APPLICATIONS
- NUCLEAR AND FOSSIL FUEL POWER PLANT COMPONENTS (BOTH ROTATING PARTS AND STRUCTURAL COMPONENTS SUCH AS PIPING AND PUMP HARDWARE)
- GAS TURBINE ENGINE COMPONENTS (AGAIN, BOTH ROTATING PARTS AND THE STATIC STRUCTURAL MEMBERS)
- PYROCHEMICAL AND PYROMETALLURGICAL PROCESSING EQUIPMENT, PARTICULARLY WHERE HIGH TEMPERATURE IS COMBINED WITH HIGH STRESS AND/OR AN AGGRESSIVE ENVIRONMENT
- ENVIRONMENTAL REMEDIATION EQUIPMENT SUCH AS THAT USED TO PROCESS STACK GASES, RECUPERATORS USED TO RECOVER WASTE HEAT, AND INCINERATORS OR OTHER HARDWARE USED FOR HIGH-TEMPERATURE DESTRUCTION OF WASTE

A.C. Lingenfelter, Lawrence Livermore National Laboratory

General Welding Characteristics of High-Temperature Alloys

As with all materials, successful welding of high-temperature alloys requires a thorough understanding of the metallurgy of the individual alloys involved. Strengthening of these alloys is achieved by the precipitation of a finely dispersed age-hardening constituent in the matrix of the alloy and/or by the addition of solid-solution-strengthening alloy additions in the matrix. In addition, the strength of these materials can be significantly increased by careful control of their thermomechanical history. Hot-working finishing temperatures can be lowered below the recrystallization temperature of the alloy, resulting in the retention of the hot/cold work introduced in the final hot-working operations. This retained strain energy significantly increases the strength of the material, particularly when combined with subsequent aging heat treatments. Yield strengths in excess of 1380 MPa (200 ksi) are possible with at least a few of these alloys.

Effect of Welding on Performance and Properties. The thermal cycle(s) introduced by the welding process can significantly alter the physical properties of the base material in the region of the weld. The heat of welding can result in the solutioning of age-hardening constituents on other precipitates such as delta phase or carbides, which define the strength, ductility, corrosion resistance, grain size, or other properties of the material. Temperatures immediately adjacent to the weld will reach and exceed the recrystallization temperature, resulting in grain growth and elimination of the retained strain energy from thermomechanical processing. These effects can significantly alter the properties of the weld heat-affected zone (HAZ).

The interaction of the alloy with the welding process can introduce micro- and, in some cases, macrofissuring in the base metal, either in the as-welded condition or as a result of subsequent heat treatment. Variables such as grain size, chemical composition, and level of restraint have been linked to the sensitivity of materials to base metal fissuring.

Applications that require good creep strength and resistance to creep rupture frequently require that the material be in a grain-coarsened condition. Applying a high-energy-input welding process to a coarse-grain material can frequently result in HAZ micro- or macrofissures. The addition of elements such as boron and zirconium to enhance stress rupture life and ductility has been shown to increase fissuring sensitivity. Fortunately, many of these materials have inherently good ductility, and the micro- or macrofissures, although undesirable, may not detract from the useful service of the material. Each case needs to be evaluated on the basis of the fitness-for-service requirements of the particular application.

Heat Treatment. Postweld heat treatment is required for most age-hardenable materials so that they can develop their full strength and physical property potential. Yield-strength-level residual stresses are introduced by the welding thermal cycle. Direct age hardening of some of these alloys after welding can result in strain age cracking; this is particularly a problem with the aluminum/titanium-hardened alloys, which exhibit a very rapid age-hardening response. Because of the relaxation resistance of these alloys, the yield-strength-level stresses can result in short-time stress rupture failures. Preweld heat treatments, which put the material in a condition that promotes stress relaxation (generally an overaged condition), as well as postweld heat treatment cycles, which stress relieve the structure prior to the age-hardening treatment, can serve to minimize or eliminate the strain age cracking problem.

Alloys with very high hardener contents, such as cast IN-713C, were once considered unweldable because of their susceptibility to strain age cracking. However, IN-713C has been successfully repair welded by preheating the material into or slightly above the age-hardening temperature range before welding and by applying the appropriate postweld heat treatment to avoid cracking.

The sluggish aging response of the niobium-hardened alloys, such as Inconel 718, helps them avoid the strain age cracking problem. Direct aging of such alloys, while possible in most instances, needs to be evaluated where highly restrained conditions are imposed.

In some cases, non-age-hardenable solution-strengthened materials exposed to high postweld temperatures--whether from a postweld heat treatment or the application environment--experienced base metal macrofissuring. These instances generally occurred with highly restrained heavy-section weldments made in grain-coarsened base materials. Again, the apparent cause is the inability of the base metal to relax the yield-strength-level residual stress prior to suffering a short-time stress rupture failure.

For additional information about the heat treatment response of high-temperature materials, see the article "Postweld Heat Treatment of Nonferrous High-Temperature Materials" in this Section of the Handbook.

Effect of Contaminants on Weld Soundness. High-temperature alloys must be clean and free of machining oils and other contaminants if welds free of defects are to be achieved. Introducing contaminants to the fusion zone can lead to fissuring and porosity.

The presence of low-melting elements and alloys in the HAZ can lead to fissuring. This problem has been noted with the presence of copper, brass, and lead, to name a few. The low-melting material becomes liquid in the HAZ as the arc passes and the liquid penetrates the grain boundary. This grain boundary penetration reduces the strength of the boundary and, coupled with yield-strength-level stress, leads to microfissuring. Care must be taken when using copper chills and tooling not to deposit the copper on the surface of the base material. Lead can cause weld metal fissuring if introduced even in minute quantities to the fusion zone. Unfortunately, lead/brass/copper hammers are commonly used in shops to "adjust" the position of metal parts in the tooling. Instances have been noted where this practice resulted in weld heat-affected zone and/or weld fusion zone fissuring.

Most of the high-temperature alloys have excellent oxidation resistance because they develop a tightly adhering refractory oxide on the surface of the material. This is a highly useful property from an application standpoint, but it can lead to problems such as trapped oxide in the weld metal and lack-of-fusion defects at the weld metal/parent metal interface if the surface of the material to be welded is not free of oxide. The oxide cannot be removed by simple wire brushing; the metal surface may appear to be clean after brushing, but the oxide has only been polished. An aggressive abrasive grinding operation is needed to positively remove the oxide. Less-than-ideal inert gas protection can allow the formation of an oxide film on the surface of the deposited weld metal. Care needs to be taken to remove this oxide before multipass welding to avoid the problems of entrapped oxide and lack-of-fusion defects.

Welding Metallurgy of Nonferrous High-Temperature Materials

R.G. Thompson, University of Alabama at Birmingham

Introduction

THE PHYSICAL METALLURGY of nonferrous high-temperature materials that affects weldability centers on the precipitates used for age hardening (γ' and γ'') and those associated with solidification and solidification segregation (primarily, Laves and carbides). Age hardening creates problems associated with strain-age (that is, reheat) cracking, while carbides and Laves phases can initiate melting and cause cracking of heat-affected zone (HAZ) grain boundaries. The weldability of these alloys generally affects both the fabricator, who must weld complicated assemblies, and the foundry, which must make repair welds to salvage expensive castings. Thus, weldability problems are not solved by designating some alloys weldable and others unweldable. Weldability solutions are often needed for both weldable and unweldable alloys.

Welding Metallurgy of Nonferrous High-Temperature Materials

R.G. Thompson, University of Alabama at Birmingham

Strain-Age Cracking

Cracking is sometimes found in age-hardenable alloys that are slowly cooled or reheated through the hardening temperature range in the presence of residual or applied stress in a constrained condition. The rate of hardening is of primary importance relative to the heating or cooling rate through the hardening temperature range. For cracking to occur, the thermal cycle must allow sufficient hardening for the imposed stress to cause cracking. Of equal importance is the

imposed stress, which must be sufficient in magnitude to initiate cracking. When these two phenomena occur simultaneously, they can result in severe cracking.

The root of the strain-age cracking problem from the metallurgical viewpoint is γ' precipitation. The nominal composition of γ' is Ni_3Al. However, the precise composition is even more complex. A typical γ' precipitate in alloy 731 is:

$$(NI_{0.884}CO_{0.070}CR_{0.032}MO_{0.008}\ V_{0.003})_3(AL_{0.632}TI_{0.347}\ V_{0.013}CR_{0.006}MO_{0.002})$$

A typical range of heat treatments for hardening nickel superalloys is given in Table 1.

TABLE 1 TYPICAL HEAT TREATMENT PARAMETERS FOR HARDENING NICKEL-BASE SUPERALLOYS

TREATMENT	**TEMPERATURE**		TIME, H
	°C	**°F**	
HOMOGENIZE AND HOT ISOSTATIC PRESSING	NEAR SOLIDUS		**1-20**
SOLUTION ANNEAL	925-1150	1700-2100	**1-5**
UPPER AGE HARDENING	815-980	1500-1800	**10-25**
LOWER AGE HARDENING	**650-815**	**1200-1500**	**10-20**

After welding, the residual stress is relieved, and the maximum strength is obtained by a solution anneal and aging heat treatment. Problems arise when the welded structure is heated through the aging temperature range on its way to the solution temperature. Strain-age weldability is dependent on both the rate and the magnitude of γ' precipitation (Ref 1). Figure 1 shows a plot of weldability as a function of the (Ti + Al) content. Titanium and aluminum are the γ' strengtheners in many superalloys. When the (Al + Ti) level exceeds some critical value, strain-age cracking becomes a significant problem. The base metal can be effectively protected against strain-age cracking by welding in the overaged condition. This prevents aging during reheating.

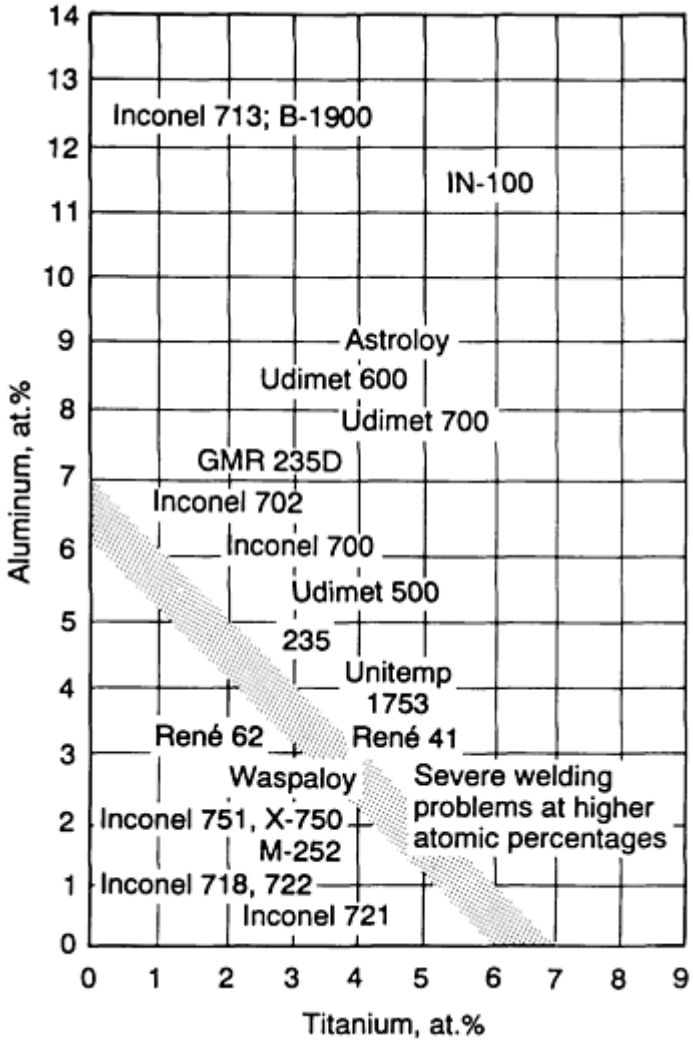

FIG. 1 PLOT OF ALUMINUM CONTENT VERSUS TITANIUM CONTENT TO INDICATE COMMERCIAL NICKEL-BASE ALLOYS THAT PRESENT WELDABILITY PROBLEMS WHEN (AL + TI) CONTENT EXCEEDS 6%. SOURCE: REF 1

Unfortunately, the HAZ cannot be protected in a similar manner. The welding process invariably produces a HAZ thermal cycle, which puts some of the age-hardening constituents into solution. During slow cooling or reheating these constituents can reprecipitate, age harden, and produce a crack-susceptible condition in the HAZ. This will be the case regardless of the preweld heat treatment.

Alloy 718 does not undergo strain-age cracking (Ref 2). The age hardening develops around a Ni_3Nb, γ", precipitate. The γ" precipitates at a much slower rate than the γ'. This allows alloys to be heated into the solution temperature range without suffering aging and the resultant strain-age cracking. Figure 2 compares the aging rates of several γ' alloys with those of alloy 718, which is strengthened with the γ" precipitate. Hardening is retarded in the γ" alloys, and they offer great latitude in methods for heating and cooling parts.

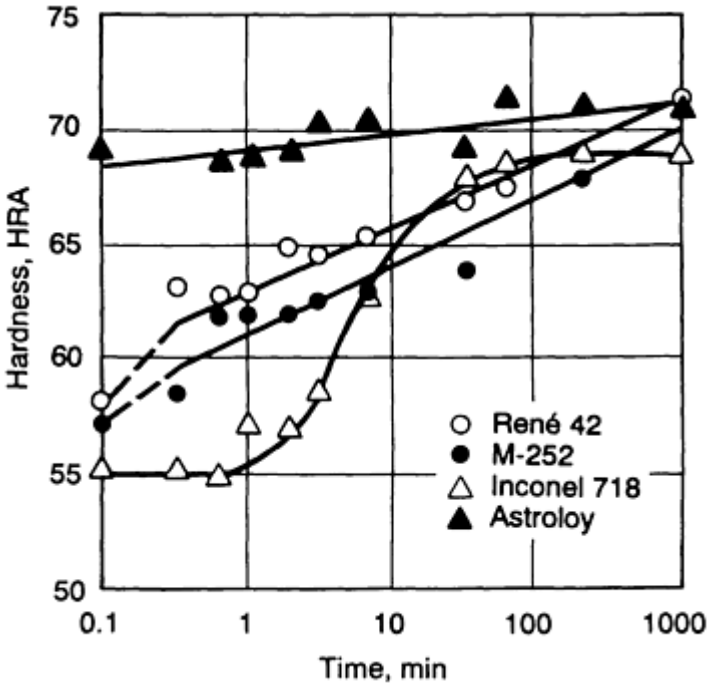

FIG. 2 PLOT OF HARDNESS VERSUS TIME TO SHOW AGE-HARDENING KINETICS OF SELECTED NICKEL-BASE ALLOYS. SOURCE: REF 3

Welded structures that require corrosion resistance but not high strength often will not need postweld heat, and can thus avoid strain-age cracking. However, if they are placed in service at elevated temperature, they may still crack during the initial heat-up cycle.

Strain-Age Cracking Susceptibility Curves. The circular-patch test is a high-restraint weld test that can be used to evaluate the sensitivity of an alloy to strain-age cracking. The test, when used with thermal treatments, can be used to produce crack-susceptibility C-curves. These are so named because of the characteristic "C" shape of the temperature-time space that separates the cracked from the uncracked behavior of this rate process. Figure 3 shows that, for a given C-curve behavior, different heating rates can produce cracked or uncracked plates. Figure 4 shows alloy chemistry variations that can affect the crack sensitivity of a given alloy.

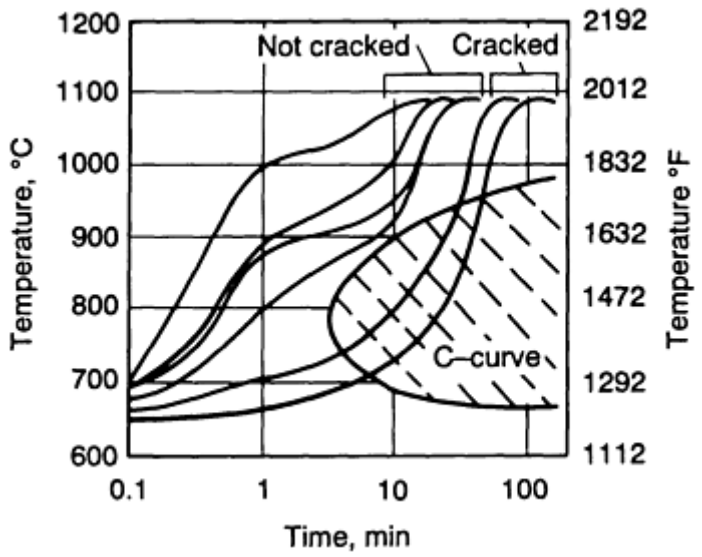

FIG. 3 EFFECT OF HEATING RATE ON THE CRACKING TENDENCY OF SOLUTION-ANNEALED (BEFORE WELDING) RENÉ 41 DURING POSTWELD HEAT TREATMENT. SOURCE: REF 4

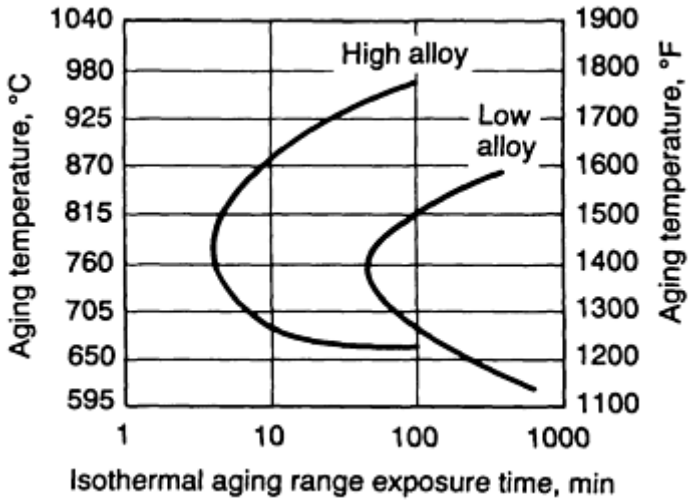

FIG. 4 EFFECT OF ALLOY COMPOSITION (HIGH ALLOY VERSUS LOW ALLOY CONCENTRATIONS OF IRON, SILICON, MANGANESE, AND SULFUR TAKEN COLLECTIVELY) ON THE CRACKING TENDENCY OF POSTWELD HEAT-TREATED RENÉ 41. SOURCE: REF 4

HAZ Liquation Cracking. Phases that form during solidification, such as MC carbides and Laves phases, have the potential to initiate melting in the HAZ during welding and spread along the grain boundaries (Fig. 5). The melting, often termed liquation, occurs because of a reaction between the dissolving precipitate and the matrix. When this melting is accompanied by sufficient thermal stress, cracks can form along the HAZ grain boundaries, and extend into the fusion zone. Such cracking may be termed liquation cracking, hot cracking, or microfissuring. A number of alloy systems are known to experience liquation cracking; some are listed in Table 2.

TABLE 2 CONSTITUTIONAL LIQUATION IN MULTICOMPONENT SYSTEMS

ALLOY SYSTEM	LIQUATING PHASE
HASTELLOY X	**M_6C**[(A)]
INCONEL 600	**CR_7C_3; TI(CN)**
18% MARAGING STEEL	**TITANIUM SULFIDE**[(B)]
AUSTENITIC ALLOY A-286	**TIC OR TI(CN)**
HIGH-STRENGTH MAGNESIUM-BASE	**ND; Y-CONTAINING PHASE ALLOY**

Source: Ref 5.

Source: Ref 7

(A)

(B)

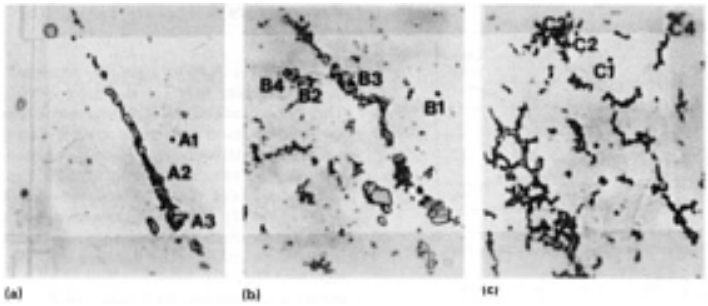

FIG. 5 LIQUATION OF A NIOBIUM CARBIDE STRINGER IN A NICKEL-BASE ALLOY 718 WIRE. (A) STRINGER BEFORE ONSET OF LIQUATION. (B) STRINGER IN INITIAL STAGE OF LIQUATION AS IT IS HEATED BY WELDING THERMAL CYCLE. (C) MOVEMENT OF STRINGER LIQUATION INTO GRAIN BOUNDARIES OF ALLOY. 500×

Liquid metal is invariably associated with the HAZ except in the unusual case of very pure, single-element metals. This is so because the HAZ stretches from the base metal to the edge of the fusion zone and will include all or part of the mushy zone (a pure metal has no mushy zone). This liquid is almost always found along the grain boundaries (Fig. 6). The few exceptions are alloys that have miscibility gaps, such as leaded brass. These alloys can have liquid from the low-melting-point phase, such as lead, which does not wet the grain boundaries. Such nonwetting behavior is associated with alloys where the solute is insoluble in the parent phase. It can be concluded that most engineering alloys contain a HAZ during welding that has a mushy zone full of intergranular liquid.

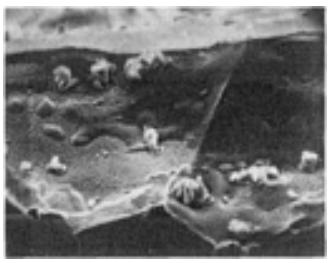

FIG. 6 INTERGRANULAR FRACTURE SURFACE SHOWING PARTIAL INTERGRANULAR WETTING WITH BOTH SOLID-SOLID AND LIQUID-LIQUID BONDING. 500×

The mushy-zone liquid generally does not contribute to poor weldability, because during the normal course of solidification it is always open to the fusion zone. The fusion zone acts as a source of liquid to backfill or heal shrinkage or cracks that might form.

Metallurgically, liquation cracking occurs when an alloy containing a susceptible second phase is heated at such a rate that the second phase cannot dissolve before the alloy reaches a system solidus that causes melting. This melting will invariably occur at the interface between the precipitate and the matrix, as can be shown with an analysis of the appropriate phase diagram. The molten liquid will spread along the grain boundaries if its solute is soluble in the matrix or if there is sufficient impurity to enhance wetting (Ref 10). This liquation can occur below the system solidus and thus be located remotely from the HAZ mushy zone. Such a location prevents backfilling and promotes liquation cracking. The fact that liquation from precipitates can extend well away from the fusion zone not only increases the chance of liquation cracking but also increases the potential length of the crack, accentuating the stress intensity of the crack.

Metallurgical evaluation of HAZ liquation reveals three stages of microstructural and compositional evolution (Fig. 7). An initial stage develops where the liquating precipitate is in contact with the liquid. In a later stage of evolution, the precipitate is completely liquated, but the intergranular liquid is stable and may even be growing. Finally, the intergranular liquid begins to solidify and may retract from the grain boundary.

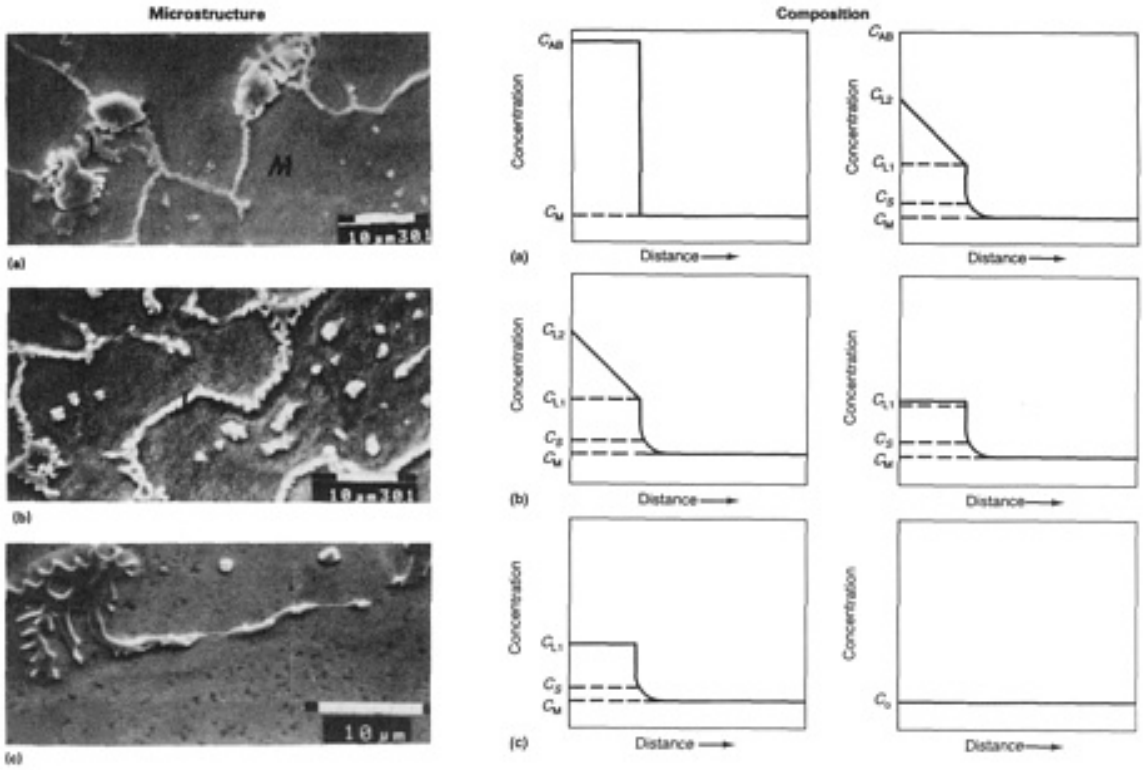

FIG. 7 THREE STAGES OF HAZ LIQUATION SHOWN RELATIVE TO THE TYPICAL TRANSFORMATION IN MICROSTRUCTURE AND COMPOSITION OF NICKEL-BASE ALLOY 718. (A) STAGE 1: PRECIPITATE LIQUATION. (B) STAGE 2: ELIMINATION OF COMPOSITION GRADIENT. (C) STAGE 3: SOLIDIFICATION

References cited in this section

1. M. PRAGER AND C.S. SHIRA, WELDING OF PRECIPITATION-HARDENING NICKEL-BASE ALLOYS, *WELD. RES. COUNC. BULL.*, NO. 128, 1968
2. H.L. EISELSTEIN, *ADVANCES IN THE TECHNOLOGY OF STAINLESS STEELS AND RELATED ALLOYS*, STP 369, ASTM, P 62-79
3. R.M. WILSON JR. AND L.W.G. BURCHFIELD, *WELD. J.*, VOL 35, 1956, P 32S
4. T.F. BERRY AND W.P. HUGHES, *WELD. J.*, VOL 46, 1969, P 505S
5. D.S. DUVALL AND W.A. OWCZARSKI, FURTHER HEAT-AFFECTED ZONE STUDIES IN HEAT RESISTANT NICKEL ALLOYS, *WELD. J.*, VOL 46, 1967, P 423S
7. J.J. PEPE AND W.F. SAVAGE, EFFECTS OF CONSTITUTIONAL LIQUATION IN 18-NI MARAGING STEEL WELDMENTS, *WELD. J.*, VOL 45, 1967, P 411S-422S
10. C.S. SMITH, GRAINS, PHASES AND INTERFACES: AN INTERPRETATION OF MICROSTRUCTURE, *TRANS. AIME*, VOL 175, 1948, P 15-51

R.G. Thompson, University of Alabama at Birmingham

Parameters Affecting Liquation Cracking

Grain Size. A large grain size promotes liquation cracking (Ref 11), as shown in Fig. 8. This can be understood in several ways. When the HAZ begins to accumulate strain from residual stress, grain boundary sliding is one mechanism

that operates to accommodate the strain. Large grain size does not accommodate the strain as readily as smaller grain size, and the potential for crack initiation at grain boundary triple points, and therefore liquation cracking, is increased (Ref 13). Another effect of grain size occurs when precipitates liquate and the liquid spreads along the boundaries. Material of large grain size will accumulate a thicker layer of liquid for a given amount (volume fraction) of precipitate, because larger grains have less grain boundary surface area (Ref 14). The thicker liquid layer takes longer to resolidify during cooling, as has been shown in alloy 718 (Ref 11) and through computer simulations (Ref 14, 15). Anything that increases the life of the intergranular liquid relative to the onset of residual stress accentuates liquation cracking.

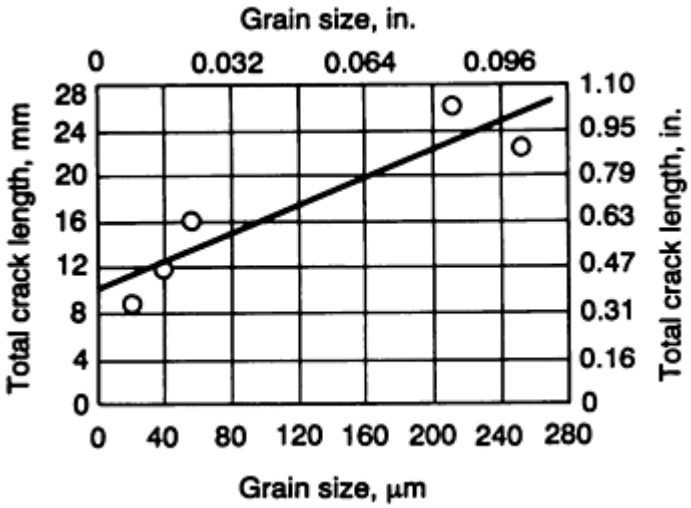

FIG. 8 PLOT OF TOTAL CRACK LENGTH VERSUS GRAIN SIZE TO SHOW EFFECT OF MICROFISSURING IN ALLOY 718 WHEN EVALUATING NICKEL-BASE ALLOY WITH SPOT VARESTRAINT TEST. SOURCE: REF 12

Liquation cracking is sensitive to the amount and location of second-phase precipitates. The size of precipitates in the HAZ, as well as the location relative to the position of grain boundaries, changes during the welding thermal cycle. Precipitates, especially those susceptible to constitutional liquation, dissolve during the thermal cycle (Ref 16).

Constitutional liquation can be illustrated with the simple binary eutectic shown in Fig. 9(a). Alloy C_O has a certain volume fraction of second-phase particles, AB, at room temperature. When the alloy is rapidly heated to a temperature, *T,* above the binary eutectic temperature, T_E, there may be insufficient time for complete dissolution of AB. Therefore, at temperatures above T_E, the AB phase is still present. Dissolution of AB above T_E takes place by the formation of a liquid phase that subsequently resolidifies in accordance with phase diagram requirements. The concentration gradients in the matrix adjacent to the AB particle are shown in Fig. 9(b). The terms C_{L1} and C_{L2} are the concentrations of liquid in equilibrium with γ and AB, respectively, at temperature *T.* The term C_S is the concentration of γ in equilibrium with liquid, and C_M is the concentration of the γ matrix in equilibrium with the AB particle at room temperature.

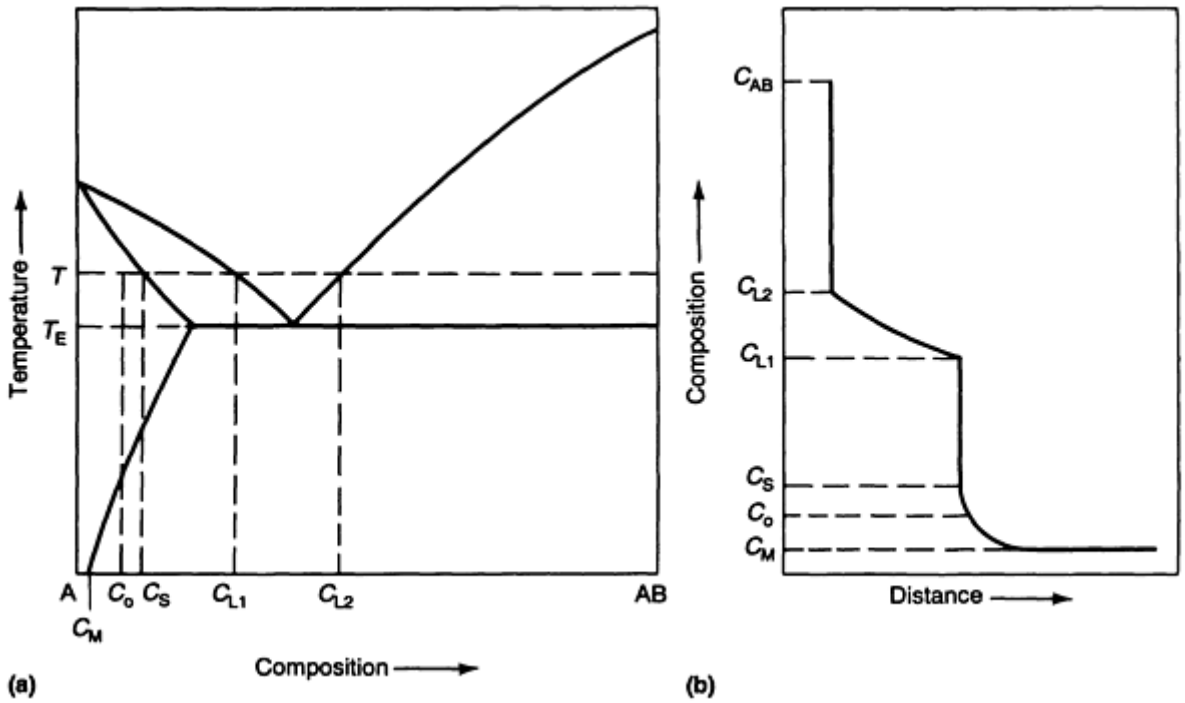

FIG. 9 EFFECT OF TEMPERATURE AND DISTANCE ON LIQUATION IN A BINARY SYSTEM. (A) CONSTITUTIONAL LIQUATION OF AB PARTICLES. (B) CONCENTRATION GRADIENTS IN FRONT OF THE LIQUATING AB PARTICLE

Behavior of NbC Dissolved in Nickel (Ref 16). A computer simulation of NbC dissolved in nickel is shown in Fig. 10. Some precipitates dissolve completely and disappear, while others become small and lose their attachment to the grain boundary. This is shown by computer simulation in Fig. 11, where *R* is the fraction of initial grain boundary precipitates remaining on the HAZ grain boundaries during heating.

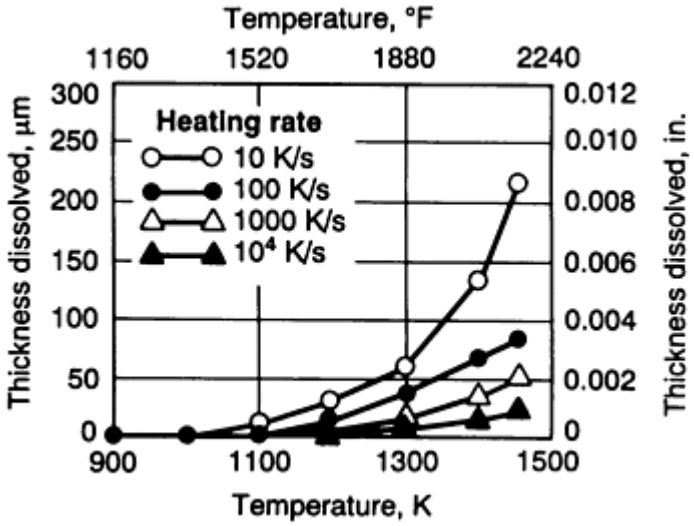

FIG. 10 DISSOLUTION KINETICS OF NBC PRECIPITATES IN NICKEL. SOURCE: REF 16

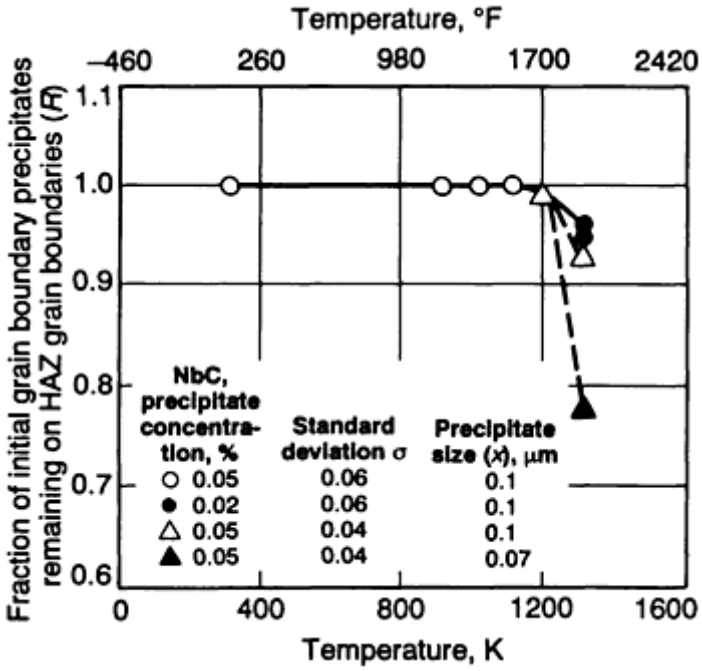

FIG. 11 PLOT OF *R* VERSUS TEMPERATURE AS A FUNCTION OF NBC PRECIPITATE CONCENTRATION, σ, AND *X* DURING CONTINUOUS 100 K/S (180 °F/S) HEATING. THE RATIO, *R*, HAS A STEEP DROP IN VALUE AS THE TEMPERATURE RISES ABOVE 1250 K (1790 °F). SOURCE: REF 16

Amount of Liquating Precipitate. A large amount of liquating precipitate can have both positive and negative effects relative to liquation cracking. On the negative side, a large amount of liquation produces a thicker layer of intergranular liquid. Just as for large-grain-size metal, a thicker layer takes longer to solidify and accentuate liquation cracking. However, on the positive side, a larger amount of liquation produces a wider path for backfilling from the mushy zone and thus can help heal cracking. This would be especially effective for liquation that occurs at a temperature near the bulk solidus. Because wrought alloys and many cast alloys are metallurgically designed to minimize liquation-type precipitates, the initial amount of precipitates is low (0.5 to 2.0 vol% for both wrought and cast alloy 718). Increasing an initially small amount of precipitate increases liquation cracking (Ref 11). Thus, using large amounts of precipitate to reduce liquation cracking would seem prudent only under closely guarded conditions where the precipitate is well connected to the HAZ mushy zone.

Finally, a more sophisticated analysis of the effect of precipitate volume fraction on liquation cracking must take into account the rate at which the precipitates dissolve before liquation (because all precipitates that liquate below the solidus try to dissolve first). While a large volume fraction of precipitates may be present in the HAZ before welding, those precipitates may disappear quickly during heating. Thus, the rate of precipitate dissolution and the welding thermal cycle must be known to predict the effect of precipitate volume fraction on cracking.

Type of Precipitate. Two types of precipitates liquate in the HAZ:

- CONSTITUTIONALLY LIQUATING PRECIPITATES (REF 7)
- EQUILIBRIUM MELTING PRECIPITATES (REF 12)

Constitutionally liquating precipitates can begin melting below the bulk solidus because their liquation is tied to the fact that the alloy has been forced to support their existence beyond some equilibrium limit. Such nonequilibrium processing can result from two factors: (1) a rapid heating rate that takes a normally low-temperature phase above its equilibrium stability temperature or (2) coring-type segregation during casting. Coring-type segregation causes the system to create a nonequilibrium phase (such as Laves phase in alloy 718) or an overabundance of an equilibrium phase (such as MC carbides). Both the nonequilibrium phase and the excessive fraction of the equilibrium phase can constitutionally liquate (Ref 4).

Equilibrium Melting Precipitates. The equilibrium phase melts when heated above its solidus temperature, producing HAZ liquid.

Precipitates Versus Liquation Cracking. The two types of precipitates described above are different relative to liquation cracking because their melting ranges are different relative to the mushy zone. Because equilibrium precipitates will always liquate at or above the bulk solidus, they will be connected with the mushy zone and have access to large volumes of liquid for backfilling and healing. The nonequilibrium precipitates will have the potential to liquate below the bulk solidus and thus be separated from backfilling liquid from the larger mushy zone. These nonequilibrium precipitates will have a greater potential for liquation cracking.

Solidification carbides such as MC carbides can be present in overabundance due to coring during solidification. Thus, they can be present in the nonequilibrium form but with a melting range that spans the subsolidus to the bulk liquidus. The liquation of the carbides should produce a continuous path to the mushy zone and thus provide a network for backfilling and healing cracks. However, the liquation of an MC carbide produces such great local solute enrichment at the groin boundary that the resolidification of these boundaries can be greatly delayed. This delay in resolidification separates them from the bulk solidification of the mushy zone and makes these boundaries potential sites for liquation cracking.

Impurities and Heat Treatment. Impurity metallic elements have long been the subject of intergranular-cracking investigations (Ref 17, 18, 19, 20, 21). Some elements (for example, sulfur, phosphorus, antimony, arsenic, bismuth, and tin) concentrate in the grain boundaries of various systems. Other elements (for example, boron), affect intergranular properties (for example, stress rupture strength).

Elements that have been identified as potential sources of liquation cracking are sulfur, phosphorus, boron, and lead. It has been suggested that if the impurity level restrictions shown below are observed, increased liquation cracking will not be observed (Ref 20):

ELEMENT	COMPOSITION, WT% (MAXIMUM)
SULFUR	**0.015**
PHOSPHORUS	**0.015**
SILICON	**0.02**
OXYGEN	**0.005**
NITROGEN	**0.005**

Some researchers separate the behavior of impurities into two groups: (1) those that are present as precipitates (for example, borides, sulfides, and so on) and (2) those that are not precipitated but are enriched at the grain boundary and the precipitate interfaces due to segregation. The latter category would also include elements such as boron and sulfur. However, the state in which the impurities reside is often debatable, and the issue here is their effect on HAZ hot cracking. Thus, no attempt will be made to differentiate between impurity precipitates or segregation.

Liquation is not necessarily caused by impurities. Impurities magnify the problem by:

- INCREASING THE WETTING OF THE INTERGRANULAR LIQUID (REF 11)
- DEPRESSING THE SOLIDUS TEMPERATURE
- FORMING LOW-MELTING-POINT PRECIPITATES/EUTECTICS
- INCREASING THE AMOUNT OF LIQUID PRESENT ON THE GRAIN BOUNDARIES

Sulfur and carbon provide a unique case. When the carbon content is increased in alloy 718, the amount of carbide and the potential for liquation cracking both increase (Fig. 12). If the sulfur content is increased, the potential for liquation cracking also increases about the same amount for both carbon levels (Fig. 12). One reason for the increased cracking susceptibility with sulfur is that the sulfur becomes trapped between the carbide and the matrix during casting (Table 3).

A high sulfur level reduces the solidification temperature of the carbide and appears to increase the wetting of the intergranular liquid in the HAZ during cooling (Ref 22).

TABLE 3 INTERFACIAL SULFUR LEVELS IN EXCESS OF SPUTTER-CLEANED SURFACES FOR HEAT-TREATED ALLOY 718 SPECIMENS RELATIVE TO AS-CAST ALLOY 718 FROM THE SAME HEAT

HEAT-TREATED CONDITION	SULFUR CONTENT, %	
	CARBIDE SURFACE	GRAIN BOUNDARY
AS-CAST	4.3	**0.11**
HOMOGENIZED	1.8	**0.03**
SOLUTION ANNEALED	1.1	**0.00**
STEP-COOLED	**0.1**	**2.20**

Source: Ref 21

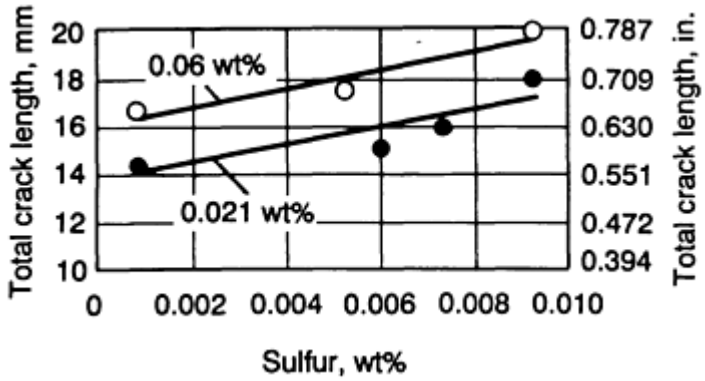

FIG. 12 PLOT OF TOTAL CRACK LENGTH VERSUS SULFUR CONTENT AS A FUNCTION OF TWO SELECTED BULK CARBON LEVELS TO SHOW MICROFISSURING SUSCEPTIBILITY OF CAST ALLOY 718. SOURCE: REF 11

Impurities may also affect the response of liquation cracking to heat treatment. Heat treatment has been shown to have either an adverse or a beneficial effect on liquation cracking (Ref 5, 23, 24). This has been shown for alloy 718 (Fig. 13) to be a function of carbon content. This effect might be partially explained by the change in impurity distribution (in this example, sulfur) during heat treatment (Ref 21, 25). As given in Table 3, sulfur moves from the carbide matrix interface onto the grain boundaries during age-hardening treatment. Simultaneously, liquation cracking increases during heat treatment. Conversely, the solution-anneal heat treatment cleans the grain boundary of any residual sulfur and reduces the potential for liquation cracking. Many other metallurgical events occur simultaneously during these heat treatments, and it has not been shown conclusively which of these events (if not all) affect cracking.

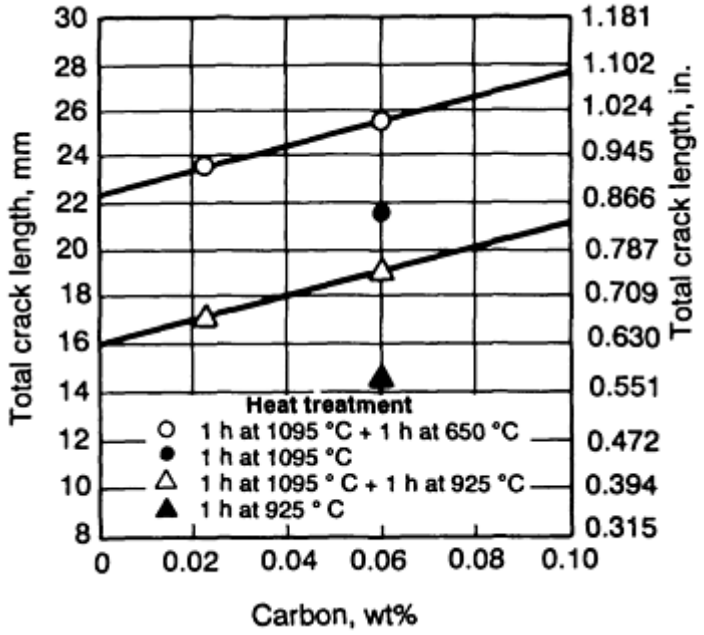

FIG. 13 PLOT OF TOTAL CRACK LENGTH VERSUS CARBON CONTENT AS A FUNCTION OF SELECTED HEAT TREATMENTS FOR CAST ALLOY 718 CONTAINING 0.009% S TO SHOW MICROFISSURING SUSCEPTIBILITY OF THE MATERIAL

Reducing Susceptibility to Liquation Cracking. Welding parameters and fabrication sequence can often be adjusted to reduce the possibility of liquation cracking. In addition, there are several metallurgical conditions that minimize HAZ liquation cracking:

- GRAIN SIZE SHOULD BE MINIMIZED
- IF PRECIPITATES ARE DESIRED FOR GRAIN SIZE CONTROL, SOLIDIFICATION PRECIPITATES SUCH AS MC CARBIDES SHOULD BE USED. THESE WILL MINIMIZE LIQUID PENETRATION INTO THE HAZ AND PROMOTE BACKFILLING AND HEALING OF CRACKS, BECAUSE THEIR LIQUATION TEMPERATURE IS SIMILAR TO THAT OF THE MUSHY ZONE
- THE AMOUNT OF PRECIPITATE THAT LIQUATES SHOULD BE MINIMIZED. IF A PARTICULARLY DIFFICULT CRACKING PROBLEM CANNOT BE RESOLVED ANY OTHER WAY, THEN INCREASING THE AMOUNT OF PRECIPITATE MAY PRODUCE ENOUGH LIQUATION TO INITIATE BACKFILLING FROM THE MUSHY ZONE AND PROMOTE HEALING OF CRACKS
- IMPURITY CONTENT SHOULD BE MINIMIZED
- WELDING SHOULD TAKE PLACE WHEN THE ALLOY HAS UNDERGONE SOME COMBINATION OF THE SOLUTIONED AND/OR HOMOGENIZED CONDITIONS, FOLLOWED BY RAPID COOLING (DIRECT QUENCHING SHOULD BE AVOIDED). THESE HEAT TREATMENTS MINIMIZE IMPURITY CONCENTRATION ON THE GRAIN BOUNDARIES

References cited in this section

4. T.F. BERRY AND W.P. HUGHES, *WELD. J.*, VOL 46, 1969, P 505S
5. D.S. DUVALL AND W.A. OWCZARSKI, FURTHER HEAT-AFFECTED ZONE STUDIES IN HEAT RESISTANT NICKEL ALLOYS, *WELD. J.*, VOL 46, 1967, P 423S
7. J.J. PEPE AND W.F. SAVAGE, EFFECTS OF CONSTITUTIONAL LIQUATION IN 18-NI MARAGING STEEL WELDMENTS, *WELD. J.*, VOL 45, 1967, P 411S-422S

11. R.G. THOMPSON, D.E. MAYO, AND B. RADHAKRISHNAN, ON THE RELATIONSHIP BETWEEN CARBON CONTENT, MICROSTRUCTURE, AND INTERGRANULAR HOT CRACKING IN CAST NICKEL ALLOY 718, *METALL. TRANS. A,* VOL 22, 1991, P 557-567
12. B. RADHAKRISHNAN AND R.G. THOMPSON, MODELING OF MICROSTRUCTURAL EVOLUTION IN THE WELD HAZ, *METAL SCIENCE OF JOINING,* M.J. CIESLAK *ET AL.,* ED., TMS, OCT 1991, P 31-40
13. R.G. THOMPSON, J.J. CASSIMUS, D.E. MAYO, AND J.R. DOBBS, THE RELATIONSHIP BETWEEN GRAIN SIZE AND MICROFISSURING IN ALLOY 718, *WELD. J.,* VOL 63, 1984, P 91S
14. B. RADHAKRISHNAN AND R.G. THOMPSON, THE KINETICS OF INTERGRANULAR LIQUATION IN THE HAZ OF ALLOY 718, *RECENT TRENDS IN WELDING SCIENCE AND TECHNOLOGY,* PROC. 2ND INT. CONF. TRENDS IN WELDING RESEARCH, ASM INTERNATIONAL, 1989, P 637-648
15. B. RADHAKRISHNAN AND R.G. THOMPSON, A MODEL FOR THE SOLIDIFICATION OF GRAIN BOUNDARY LIQUID IN THE HAZ OF WELDS, *METALL. TRANS.,* JUNE 1992
16. Y. SHEN, B. RADHAKRISHNAN, AND R.G. THOMPSON, MONTE CARLO SIMULATION OF GRAIN GROWTH IN THE HAZ, *PROC. 3RD LNT. CONF. TRENDS IN WELDING RESEARCH,* ASM INTERNATIONAL, JUNE 1992
17. T.J. MORRISON, C.S. SHIRA, AND L.A. WEISENBERG, EFFECTS OF MINOR ELEMENTS ON THE WELDABILITY OF HIGH NICKEL ALLOYS, *PROC. WELD. RES. SYMP.,* AWS, VOL 93, 1967
18. W.A. OWCZARSKI, *EFFECTS OF MINOR ELEMENTS ON THE WELDABILITY OF HIGH-NICKEL ALLOYS,* WELDING RESEARCH COUNCIL, 1969, P 6
19. W. YENISCAVICH AND C.W. FOX, *EFFECTS OF MINOR ELEMENTS ON THE WELDABILITY OF HIGH-NICKEL ALLOYS,* WELDING RESEARCH COUNCIL, 1969, P 24
20. D.A. CANONICO *ET AL., EFFECTS OF MINOR ELEMENTS ON THE WELDABILITY OF HIGH-NICKEL ALLOYS,* WELDING RESEARCH COUNCIL, 1969, P 68
21. R.G. THOMPSON, M.C. KOOPMAN, AND B.H. KING, GRAIN BOUNDARY CHEMISTRY OF ALLOY 718-TYPE ALLOYS, *SUPERALLOY 718, 625 AND DERIVATIVES,* E. LORIA, ED., TMS, 1991, P 53-70
22. C. CHEN, R.G. THOMPSON, AND D.W. DAVIS, A STUDY OF EFFECTS OF PHOSPHORUS, SULFUR, BORON AND CARBON ON LAVES AND CARBIDE FORMATION IN ALLOY 718, *SUPERALIOY 718, 625 AND DERIVATIVES,* E. LORIA, ED., TMS, 1991, P 81-96
23. R.G. THOMPSON AND S. GENCULU, MICROSTRUCTURAL EVALUATION IN THE HAZ OF INCONEL 718 AND CORRELATIONS WITH THE HOT DUCTILITY TEST, *WELD. J.,* VOL 62, 1983, P 337S-345S
24. R.G. THOMPSON, J.R. DOBBS, AND D.E. MAYO, THE EFFECT OF HEAT TREATMENT ON THE MICROFISSURING IN ALLOY 718, *WELD. J.,* VOL 65, 1986, P 299S-304S
25. R.G. THOMPSON, B. RADHAKRISHNAN, AND D.E. MAYO, GRAIN BOUNDARY CHEMISTRY CONTRIBUTIONS TO INTERGRANULAR HOT CRACKING, *J. PHYSIQUE-COLLOQUE C5,* SUPPL. NO. 10, 1988, P 471-482

Welding Metallurgy of Nonferrous High-Temperature Materials

R.G. Thompson, University of Alabama at Birmingham

References

1. M. PRAGER AND C.S. SHIRA, WELDING OF PRECIPITATION-HARDENING NICKEL-BASE ALLOYS, *WELD. RES. COUNC. BULL.,* NO. 128, 1968
2. H.L. EISELSTEIN, *ADVANCES IN THE TECHNOLOGY OF STAINLESS STEELS AND RELATED*

ALLOYS, STP 369, ASTM, P 62-79

3. R.M. WILSON JR. AND L.W.G. BURCHFIELD, *WELD. J.*, VOL 35, 1956, P 32S
4. T.F. BERRY AND W.P. HUGHES, *WELD. J.*, VOL 46, 1969, P 505S
5. D.S. DUVALL AND W.A. OWCZARSKI, FURTHER HEAT-AFFECTED ZONE STUDIES IN HEAT RESISTANT NICKEL ALLOYS, *WELD. J.*, VOL 46, 1967, P 423S
6. B. WEISS, G.E. GROTKE, AND R. STICKLER, *WELD. J.*, VOL 49, 1970, P 471S-487S
7. J.J. PEPE AND W.F. SAVAGE, EFFECTS OF CONSTITUTIONAL LIQUATION IN 18-NI MARAGING STEEL WELDMENTS, *WELD. J.*, VOL 45, 1967, P 411S-422S
8. J.R. BROOKS, *WELD J.*, VOL 53, 1974, P 517-523
9. W.A. BAESLACK III, S.J. SAVAGE, AND F.H. FROES, *J. MATER. SCI. LETT.*, 1986, P 935-939
10. C.S. SMITH, GRAINS, PHASES AND INTERFACES: AN INTERPRETATION OF MICROSTRUCTURE, *TRANS. AIME*, VOL 175, 1948, P 15-51
11. R.G. THOMPSON, D.E. MAYO, AND B. RADHAKRISHNAN, ON THE RELATIONSHIP BETWEEN CARBON CONTENT, MICROSTRUCTURE, AND INTERGRANULAR HOT CRACKING IN CAST NICKEL ALLOY 718, *METALL. TRANS. A*, VOL 22, 1991, P 557-567
12. B. RADHAKRISHNAN AND R.G. THOMPSON, MODELING OF MICROSTRUCTURAL EVOLUTION IN THE WELD HAZ, *METAL SCIENCE OF JOINING*, M.J. CIESLAK *ET AL.*, ED., TMS, OCT 1991, P 31-40
13. R.G. THOMPSON, J.J. CASSIMUS, D.E. MAYO, AND J.R. DOBBS, THE RELATIONSHIP BETWEEN GRAIN SIZE AND MICROFISSURING IN ALLOY 718, *WELD. J.*, VOL 63, 1984, P 91S
14. B. RADHAKRISHNAN AND R.G. THOMPSON, THE KINETICS OF INTERGRANULAR LIQUATION IN THE HAZ OF ALLOY 718, *RECENT TRENDS IN WELDING SCIENCE AND TECHNOLOGY*, PROC. 2ND INT. CONF. TRENDS IN WELDING RESEARCH, ASM INTERNATIONAL, 1989, P 637-648
15. B. RADHAKRISHNAN AND R.G. THOMPSON, A MODEL FOR THE SOLIDIFICATION OF GRAIN BOUNDARY LIQUID IN THE HAZ OF WELDS, *METALL. TRANS.*, JUNE 1992
16. Y. SHEN, B. RADHAKRISHNAN, AND R.G. THOMPSON, MONTE CARLO SIMULATION OF GRAIN GROWTH IN THE HAZ, *PROC. 3RD LNT. CONF. TRENDS IN WELDING RESEARCH*, ASM INTERNATIONAL, JUNE 1992
17. T.J. MORRISON, C.S. SHIRA, AND L.A. WEISENBERG, EFFECTS OF MINOR ELEMENTS ON THE WELDABILITY OF HIGH NICKEL ALLOYS, *PROC. WELD. RES. SYMP.*, AWS, VOL 93, 1967
18. W.A. OWCZARSKI, *EFFECTS OF MINOR ELEMENTS ON THE WELDABILITY OF HIGH-NICKEL ALLOYS*, WELDING RESEARCH COUNCIL, 1969, P 6
19. W. YENISCAVICH AND C.W. FOX, *EFFECTS OF MINOR ELEMENTS ON THE WELDABILITY OF HIGH-NICKEL ALLOYS*, WELDING RESEARCH COUNCIL, 1969, P 24
20. D.A. CANONICO *ET AL.*, *EFFECTS OF MINOR ELEMENTS ON THE WELDABILITY OF HIGH-NICKEL ALLOYS*, WELDING RESEARCH COUNCIL, 1969, P 68
21. R.G. THOMPSON, M.C. KOOPMAN, AND B.H. KING, GRAIN BOUNDARY CHEMISTRY OF ALLOY 718-TYPE ALLOYS, *SUPERALLOY 718, 625 AND DERIVATIVES*, E. LORIA, ED., TMS, 1991, P 53-70
22. C. CHEN, R.G. THOMPSON, AND D.W. DAVIS, A STUDY OF EFFECTS OF PHOSPHORUS, SULFUR, BORON AND CARBON ON LAVES AND CARBIDE FORMATION IN ALLOY 718, *SUPERALIOY 718, 625 AND DERIVATIVES*, E. LORIA, ED., TMS, 1991, P 81-96
23. R.G. THOMPSON AND S. GENCULU, MICROSTRUCTURAL EVALUATION IN THE HAZ OF INCONEL 718 AND CORRELATIONS WITH THE HOT DUCTILITY TEST, *WELD. J.*, VOL 62, 1983, P 337S-345S
24. R.G. THOMPSON, J.R. DOBBS, AND D.E. MAYO, THE EFFECT OF HEAT TREATMENT ON THE MICROFISSURING IN ALLOY 718, *WELD. J.*, VOL 65, 1986, P 299S-304S
25. R.G. THOMPSON, B. RADHAKRISHNAN, AND D.E. MAYO, GRAIN BOUNDARY CHEMISTRY

CONTRIBUTIONS TO INTERGRANULAR HOT CRACKING, *J. PHYSIQUE-COLLOQUE C5,* SUPPL. NO. 10, 1988, P 471-482

Postweld Heat Treatment of Nonferrous High-Temperature Materials

Steven C. Ernst, Haynes International, Inc.

Introduction

THE NONFERROUS HIGH-TEMPERATURE ALLOYS discussed in this article are based on nickel and on cobalt. These alloys can be generally categorized as either solid-solution strengthened or precipitation strengthened. The former category is not appreciably strengthened by heat treatment and is considered non-heat-treatable, whereas the latter category is typically used in the age-hardened or heat-treated, condition. It is important to distinguish between these two classes of alloys when considering postweld heat treatment. In general, alloys that contain significant amounts of age-hardening elements, such as aluminum, titanium, and niobium, are heat treatable. The compositions of selected nickel- and cobalt-base alloys in these two categories are shown in Table 1.

TABLE 1 NOMINAL COMPOSITION OF SELECTED NICKEL-BASE AND COBALT-BASE HIGH-TEMPERATURE ALLOYS

ALLOY	**UNS NO.**	COMPOSITION, WT%							
		C	**Cr**	**Ni**	**Co**	**Fe**	**Mo**	**W**	OTHERS
NICKEL-BASE SOLID-SOLUTION ALLOYS									
LNCONEL 600	N06600	0.08 (MAX)	15.5	BAL	. . .	8.0	. . .	. . .	**. . .**
LNCONEL 601	N06601	0.10 (MAX)	23.0	BAL	. . .	14.4	. . .	. . .	**1.4 AL**
INCONEL 617	N06617	0.07	22.0	BAL	12.5	1.5	9.0	. . .	**1.2 AL**
INCONEL 625	N06625	0.10 (MAX)	21.5	BAL	. . .	2.5	9.0	. . .	**3.6 NB**
HAYNES 230	N06230	0.1	22.0	BAL	. . .	3.0 (MAX)	2.0	14.0	**0.02 LA, 0.015 B (MAX)**
HAYNES HR-160	. . .	0.05	28.0	BAL	29.0	1.5	. . .	. . .	**2.75 SI**
HASTELLOY X	N06002	0.1	22.0	BAL	1.5	18.5	9.0	0.6	**. . .**
HASTELLOY W	N10004	0.12 (MAX)	5.0	BAL	2.5	6.0	24.0	. . .	**. . .**
HASTELLOY S	N06635	0.02 (MAX)	15.5	BAL	. . .	3.0 (MAX)	14.5	. . .	**0.05 LA, 0.015 B (MAX)**
RA 333	N06333	0.05	25.0	BAL	3.0	18.0	3.0	3.0	**. . .**
CHROMEL A (OR NICHROME 80)	. . .	. . .	20.0	BAL	. . .	. . .	. . .	. . .	**1.0 SI**
NIMONIC 75	. . .	0.10	19.5	BAL	. . .	. . .	. . .	. . .	**. . .**
NIMONIC 86	. . .	. . .	25.0	BAL	. . .	. . .	10.0	. . .	**0.03 CE**
COBALT-BASE SOLID-SOLUTION ALLOYS									
HAYNES 188	R30188	0.10	22.0	22.0	BAL	3.0 (MAX)	. . .	14.0	**0.04 LA**
HAYNES 25 (L-605)	R30605	0.10	20.0	10.0	BAL	3.0 (MAX)	. . .	15.0	**. . .**
HAYNES 150 (UMCO-50)	. . .	0.06	27.0	. . .	BAL	18.0	. . .	. . .	**. . .**

S-816	R30816	0.38	20.0	20.0	BAL	4.0	4.0	4.0	**4.0 NB**
MAR-M 918	. . .	0.05	20.0	20.0	BAL	. . .	. . .	. . .	**7.5 TA, 0.10 ZR**
MP35-N	R30035	. . .	20.0	35.0	BAL	. . .	10.0	. . .	**. . .**
MP159	. . .	. . .	19.0	25.5	BAL	9.0	7.0	. . .	**0.6 NB, 0.2 AL, 3.0 TI**
NICKEL-BASE PRECIPITATION-HARDENING ALLOYS									
LNCONEL 706	N09706	0.03	16.0	BAL	. . .	37.0	. . .	. . .	**1.8 TI, 0.2 AL, 2.9 NB**
INCONEL 718	N07718	0.04	18.0	BAL	. . .	18.5	3.0	. . .	**5.1 NB, 0.9 TI, 0.5 AL**
LNCONEL X-750	N07750	0.04	15.5	BAL	. . .	7.0	. . .	. . .	**2.5 TI, 0.7 AL, 1.0 NB**
LNCONEL 751	N07751	0.05	15.0	BAL	. . .	7.0	. . .	. . .	**2.5 TI, 1.1 AL, 1.0 NB**
NIMONIC 80A	N07080	0.06	19.5	BAL	. . .	. . .	. . .	. . .	**1.4 AL, 2.4 TI**
NIMONIC 90	N07090	0.07	19.5	BAL	16.5	. . .	. . .	. . .	**1.5 AL, 2.5 TI**
NIMONIC 91	. . .	. . .	28.5	BAL	20.0	. . .	. . .	. . .	**1.2 AL, 2.3 TI**
NIMONIC 105	. . .	0.08	15.0	BAL	20.0	. . .	5.0	. . .	**4.7 AL, 1.3 TI, 0.005 B**
NIMONIC 115	. . .	0.15	15.0	BAL	15.0	. . .	4.0	. . .	**5.0 AL, 4.0 TI**
RENÉ 41	N07041	0.09	19.0	BAL	11.0	5.0 (MAX)	10.0	. . .	**1.5 AL, 3.0 TI, 0.006 B**
RENÉ 95	. . .	0.15	14.0	BAL	8.0	. . .	3.5	3.5	**3.5 NB, 3.5 AL, 2.5 TI, 0.05 ZR**
RENÉ 100	. . .	0.16	9.5	BAL	15.0	. . .	3.0	. . .	**5.5 AL, 4.2 TI, 0.06 ZR, 0.015 B**
UDIMET 400	. . .	0.06	17.5	BAL	14.0	. . .	4.0	. . .	**0.5 NB, 1.5 AL, 2.5 TI, 0.06 ZR, 0.008 B**
UDIMET 500	. . .	0.08	18.0	BAL	18.5	. . .	4.0	. . .	**2.9 AL, 2.9 TI, 0.05 ZR, 0.006 B**
UDIMET 520	. . .	0.05	19.0	BAL	12.0	. . .	6.0	1.0	**2.0 AL, 3.0 TI, 0.005 B**
UDIMET 630	. . .	0.03	18.0	BAL	. . .	18.0	3.0	3.0	**6.5 NB, 0.5 AL, 1.0 TI**
UDIMET 700	. . .	0.03	15.0	BAL	18.5	. . .	5.2	. . .	**5.3 AL, 3.5 TI, 0.03 B**
UDIMET 710	. . .	0.07	18.0	BAL	15.0	. . .	3.0	1.5	**2.5 AL, 5.0 TI**
UDIMET 720	. . .	0.03	17.9	BAL	14.7	. . .	3.0	1.3	**2.5 AL, 5.0 TI, 0.03 ZR, 0.033 B**
WASPALOY ALLOY	N07001	0.08	19.0	BAL	14.0	. . .	4.3	. . .	**1.5 AL, 3.0 TI, 0.05 ZR, 0.006 B**
263	. . .	0.06	20.0	BAL	20.0	. . .	5.8	. . .	**0.5 AL, 2.2 TI**
UNITEMP AF2-1DA	. . .	0.35	12.0	BAL	10.0	. . .	3.0	6.0	**1.5 TA, 4.6 AL, 3.5 TI, 0.10 ZR**
UNITEMP AF2-1DA6	. . .	0.04	12.0	BAL	10.0	. . .	2.7	6.5	**1.5 TA, 4.0 AL, 2.8 TI, 0.1 ZR, 0.015 B**
ASTROLOY	. . .	0.06	15.0	BAL	17.0	. . .	5.3	. . .	**4.0 AL, 3.5 TI, 0.03 B**
D-979	N09979	0.05	15.0	BAL	. . .	27.0	4.0	4.0	**1.0 AL, 3.0 TI**
LNCONEL 100	N13100	0.15	10.0	BAL	15.0	. . .	3.0	. . .	**5.5 AL, 4.7 TI,**

									0.06 ZR, 1.0 V, 0.015 B
INCONEL 102	N06102	0.06	15.0	BAL	. . .	7.0	3.0	3.0	**3.0 NB, 0.4 AL, 0.6 TI, 0.02 MG, 0.03 ZR**
M252	N07252	0.15	20.0	BAL	10.0	. . .	10.0	. . .	**1.0 AL, 2.6 TI, 0.005 B**
PYROMET 31	N07031	0.04	22.5	BAL	. . .	15.0	2.0	. . .	**1.4 AL, 2.3 TI, 0.9 CU, 0.005 B**
PYROMET 860	. . .	0.05	13.0	BAL	4.0	28.9	6.0	. . .	**1.0 AL, 3.0 TI, 0.01 B**
REFRACTORY 26	. . .	0.03	18.0	BAL	20.0	16.0	3.2	. . .	**0.2 AL, 2.6 TI, 0.015 B**
ALLOY 625	N07716	0.02	20.0	BAL	. . .	5.0	9.0	. . .	**3.1 NB, 0.2 AL, 1.3 TI**
INCONEL 100 GATORIZED	**. . .**	**0.07**	**12.4**	**BAL**	**18.5**	**. . .**	**3.2**	**. . .**	**5.0 AL, 4.3 TI, 0.06 ZR, 0.02 B, 0.8 V**

Postweld Heat Treatment of Nonferrous High-Temperature Materials

Steven C. Ernst, Haynes International, Inc.

Types of Postweld Heat Treatment

Stress relieving is a process used to reduce residual welding stresses prior to further fabrication or service. An important result of a good stress-relief heat treatment is dimensional stability of a weldment during high-temperature service. Typical stress-relieving temperature ranges are less than those required for annealing or recrystallization. Accordingly, stress relieving can result in deleterious effects to the microstructure and corresponding mechanical properties. When considering a postweld stress-relief heat treatment, it is important to recognize these effects so that a suitable compromise can be made between dimensional stability and mechanical properties.

Annealing is a process performed above the recrystallization temperature to promote maximum softness in an alloy. This heat treatment is also effective at relieving residual welding stresses. Annealing should be conducted after welding age-hardenable alloys in highly restrained conditions. This annealing requires high heating rates to reduce the probability of strainage cracking.

Solution annealing is a high-temperature anneal carried out above the secondary carbide solvus. Because that temperature is significantly higher than the recrystallization temperature, significant grain coarsening can occur. The carbide dissolution and coarse grain structure can be beneficial to high-temperature rupture life.

Solution treating and quenching is a process used with precipitation-strengthened alloys to dissolve the principle aging phases and carbides formed during welding and to produce a supersaturated solid solution at room temperature. This heat treatment will put the weldment in optimum metallurgical condition for subsequent age hardening.

Aging treatments are performed in the intermediate temperature range, allowing precipitation of the strengthening phase(s) from the supersaturated solid solution. The aging response may not necessarily be uniform in all regions of a weldment because of segregation effects that occur during weld solidification.

Steven C. Ernst, Haynes International, Inc.

Postweld Heat Treatment of Solid-Solution-Strengthened Alloys

Solid-solution-strengthened alloys normally do not require postweld heat treatment to achieve or restore optimum mechanical properties. Postweld heat treatment is sometimes used to provide stress relief. Complete stress relief can be achieved with full solution anneal, which also gives the alloy an optimal metallurgical condition. Solution annealing will eliminate any prior cold work by recrystallization and will dissolve secondary $M_{23}C_6$-type carbides that may have formed upon cooling during welding. Typical solution annealing temperatures for solid-solution-strengthened alloys are given in Table 2. The time required can range from a few minutes to about an hour, followed by rapid quenching in water or air. A popular calculated time is 140 s/mm (1 h/in.) of cross-section thickness.

TABLE 2 TYPICAL SOLUTION ANNEALING AND MILL ANNEALING TEMPERATURES FOR SOLID-SOLUTION-STRENGTHENED ALLOYS

ALLOY	**SOLUTION ANNEALING TEMPERATURE RANGE**		MINIMUM TEMPERATURE FOR MILL ANNEALING	
	°C	**°F**	**°C**	°F
HASTELLOY X	1165-1190	2125-2175	1010	**1850**
HASTELLOY S	1050-1135	1925-2075	955	**1750**
ALLOY 625	1095-1205	2000-2200	925	**1700**
RA 333	1175-1205	2150-2200	1040	**1900**
INCONEL 617	1165-1190	2125-2175	1040	**1900**
HAYNES 230	1165-1245	2125-2275	1120	**2050**
HAYNES 188	1165-1190	2125-2175	1120	**2050**
HAYNES 25 (L-605)	**1175-1230**	**2150-2250**	**1040**	**1900**

In cases where stress relief is needed and a fine grain size is required, mill annealing is effective. The mill annealing heat treatment is similar to solution annealing. However, the lower temperatures involved are not sufficient to dissolve secondary carbides that may have precipitated intergranularly during welding. The mill annealing treatment may not develop the stress rupture properties in the weldment to their full potential. Examples of minimum mill annealing temperatures are given in Table 3.

TABLE 3 TYPICAL SOLUTION TREATMENT AND AGING CYCLES FOR PRECIPITATION-STRENGTHENED HIGH-TEMPERATURE ALLOYS

ALLOY	**SOLUTION TREATMENT**				AGING			
	TEMPERATURE		**TIME, H**	**COOLING PROCEDURE**	**TEMPERATURE**		**TIME, H**	COOLING PROCEDURE
	°C	**°F**			**°C**	**°F**		
INCONEL 718	980	1800	1	AIR COOL	720	1325	8	**FURNACE COOL**
					620	1150	8	**AIR COOL**
INCONEL X-750	1150	2100	2	AIR COOL	845	1550	24	**AIR COOL**
					705	1300	20	**AIR COOL**
NIMONIC 80A	1080	1975	8	AIR COOL	705	1300	16	**AIR COOL**
NIMONIC 90	1080	1975	8	AIR COOL	705	1300	16	**AIR COOL**

RENÉ 41	1065	1950	$\frac{1}{2}$	AIR COOL	760	1400	16	**AIR COOL**
UDIMET 500	1080	1975	4	AIR COOL	845	1550	24	**AIR COOL**
					760	1400	16	**AIR COOL**
WASPALOY	1080	1975	4	AIR COOL	845	1550	24	**AIR COOL**
					760	**1400**	**16**	**AIR COOL**

In terms of optimizing metallurgical structure, mechanical properties, and stress relief, annealing treatments are the best postweld heat treatments for solid-solution-strengthened alloys. When large or complex structures are involved, the high annealing temperatures can result in distortion problems during the heat treatment. In many cases, the best decision may be to completely avoid postweld heat treatment. If stress relief is mandatory, but the high annealing temperatures are not tolerable, a lower temperature may be used at the expense of the metallurgical condition. Some fabricators conduct stress relieving at a temperature about 100 °C (180 °F) above the intended service temperature to avoid distortion during service. A partial stress relief can be accomplished for many alloys in the range from 450 to 900 °C (840 to 1650 °F), concomitant with embrittlement caused by extensive precipitation of carbides and topologically close-packed (TCP) phases. Additionally, the weldment may display poor creep-rupture characteristics in service following a stress relief heat treatment in the 450 to 900 °C (840 to 1650 °F) temperature range. The magnitude of stress relief and property degradation vary for each alloy and stress-relief temperature. These factors should be carefully considered if stress relief is to be performed below the minimum mill annealing temperature.

Postweld Heat Treatment of Nonferrous High-Temperature Materials

Steven C. Ernst, Haynes International, Inc.

Postweld Heat Treatment of Precipitation-Strengthened Alloys

The precipitation-strengthened alloys are typically used in the solution-treated and aged condition. Solution treatment can be performed either above or below the γ' solvus temperature, depending on the desired microstructure. In wrought material, aging results in a homogeneous distribution of γ' and intergranular, secondary-type carbides. The γ' distribution in weld metal may or may not be homogeneous because of the segregational effects of weld solidification. In this situation, the weld metal may not strengthen to the same degree as the base metal. A two-step aging treatment that involves a stabilization followed by a lower-temperature aging treatment can be used in some cases. The stabilization heat treatment involves the formation of $M_{23}C_6$ carbides plus γ', which forms from a reaction between metal carbides (MC) and the matrix. Examples of typical solution treatment and aging cycles are shown in Table 3. For further information, see the article "Heat Treating of Superalloys" in *Heat Treating,* Volume 4 of the *ASM Handbook.*

The major problem that occurs when postweld heat treating the precipitation-hardenable alloys is strain-age cracking. The susceptibility of an alloy to strain-age cracking tends to increase with an increasing aluminum and titanium content. Alloys that contain niobium as a hardening element exhibit a sluggish aging response and are therefore less sensitive to strain-age cracking. Strain-age cracking is more prevalent in highly restrained weldments or in the presence of high residual stresses. Cracking is caused by the combination of stress, precipitation strengthening, and the volumetric contraction associated with γ' precipitation. Guidelines to follow to avoid strain-age cracking include:

- MINIMIZE RESIDUAL AND THERMALLY INDUCED STRESSES BY USING THE APPROPRIATE JOINT DESIGN, WELDING PROCESS, AND FILLER METAL.
- HEAT AS RAPIDLY AS POSSIBLE THROUGH THE REGION OF AGING TEMPERATURES WHEN STRESS-RELIEF ANNEALING.
- MINIMIZE HEAT INPUT DURING WELDING TO AVOID PARTIAL MELTING OF GRAIN BOUNDARIES ADJACENT TO THE FUSION LINE.
- HEAT TREAT IN AN INERT ATMOSPHERE IF POSSIBLE; THE PRESENCE OF OXYGEN TENDS TO INCREASE INTERGRANULAR EMBRITTLEMENT, WHICH CAN RESULT IN CRACKING.
- TO AVOID POSTWELD STRAIN-AGE CRACKING, ALWAYS STRESS-RELIEF ANNEAL BEFORE AGING. FOR HEAVY-SECTION WELDMENTS IN ALUMINUM-TITANIUM AGED

MATERIALS, MULTIPLE STRESS-RELIEF ANNEALS MAY BE NECESSARY DURING WELDING.

- AVOID WELDING ON MATERIAL WITH ROUGH OR POOR SURFACE CONDITIONS.

Special Metallurgical Welding Considerations for Nickel and Cobalt Alloys and Superalloys

S.D. Kiser, Inco Alloys International, Inc.

Introduction

THE DESIGN ENGINEER who wishes to use a welded structure for demanding service faces a challenging dilemma. On the one hand, the materials involved and the deposited weld metal must exhibit sufficient ductility to withstand the severe thermal cycle imposed by fusion welding. On the other hand, many applications demand that specimens taken from a qualification welded assembly be capable of passing 2*t* 180° side-bend testing (where *t* is the material thickness). This test requires 20% elongation of the outer fibers of the bend specimen. After welding, some applications for which the weldment is designed may demand different properties.

Most solid-solution (nonprecipitation-hardening) nonferrous alloys exhibit sufficient ductility to meet the above requirements. The weld fabrication of these materials is straightforward in that they usually do not require preheat or postheat, and interpass temperature control during welding normally is not critical.

The precipitation-hardenable materials are different from the above alloys in that they generate a second phase when exposed to temperatures for specified times in a particular range. They further distinguish themselves by exhibiting superior mechanical properties after being precipitation treated (aged). These materials are usually welded in the annealed (or solution-annealed) condition and are heat treated to precipitate the second phase as a final or near-final production step.

Both the solid-solution and the precipitation-hardening groups of alloys are typically austenitic (that is, the atoms of their basic structures fit together in a face-centered-cubic arrangement, often referred to as γphase). The precipitation-hardening alloys form a second phase, γ', as a result of controlled heat treatment. The development and dispersion of this second phase are made possible by additions of aluminum, titanium, and niobium. The γ' phase imparts great stiffness to these materials at room temperature and up to the upper limit of their aging-temperature ranges. When used at service temperatures above their aging ranges, these materials lose strength rapidly as a result of the agglomeration of their second phase. This condition, commonly referred to as overaging, results in relatively large γ' particles.

A subset of the precipitation-hardenable high-temperature materials is the secondary-carbide-strengthened materials. These alloys have an austenitic structure like the above groups, but do not contain sufficient alloy content to precipitate γ' phase. Instead, they contain generous additions of carbide-forming elements such as chromium, niobium (also forms γ"), and a supersaturating amount of carbon. These materials are primarily used as centrifugally cast tubes. They enjoy reasonably good weldability in the as-cast condition, but usually require special precautions for welding after they have been in service.

A final group of exceptionally strong high-temperature metals is the mechanically alloyed materials. These metals combine the high strength of the precipitation-hardened alloys by use of γ' strengthening up to about 705 °C (1300 °F) with dispersion strengthening with yttrium oxide (Y_2O_3) up to 1315 °C (2400 °F). These materials are produced by a combination of the mechanical forging of powder particles in a ball mill, followed by hot working and a 1315 °C (2400 °F) thermal treatment (Fig. 1). Joining these materials requires special precautions.

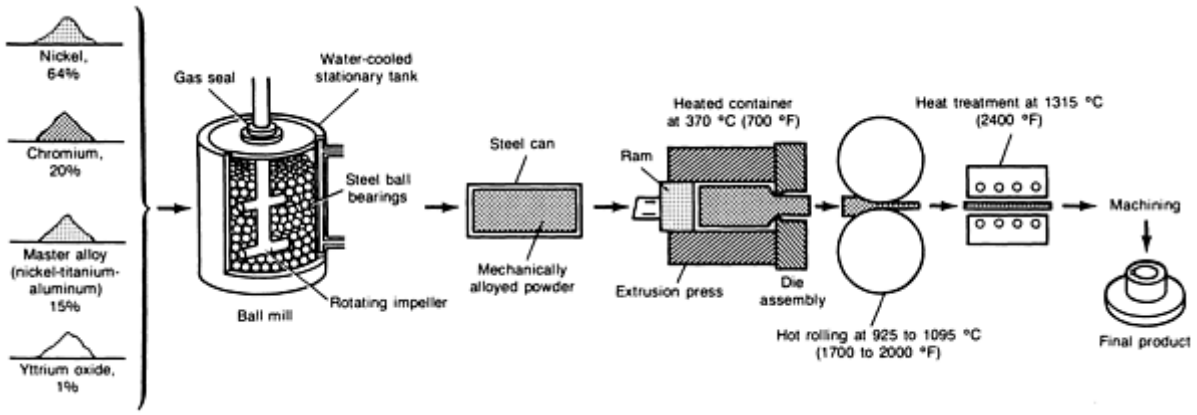

FIG. 1 SCHEMATIC SHOWING TYPICAL PROCESS OPERATIONS USED IN THE PRODUCTION OF MECHANICALLY ALLOYED OXIDE-DISPERSION-STRENGTHENED PRODUCTS

In many demanding applications, it is necessary to design components made of different materials. The process of making such assemblies often requires the welding of dissimilar metals, the welding of diffusion-bonded materials, and sometimes weld overlay cladding and even thermal spraying. These types of unusual welding and spraying applications require special knowledge and treatments that may have been developed specifically for each material.

Finally, in the service life of nearly every welded structure, there arises a need for alteration or repair. In many cases it becomes necessary to splice new materials into old. Most of the above materials require special conditioning before repair welding.

Special Metallurgical Welding Considerations for Nickel and Cobalt Alloys and Superalloys

S.D. Kiser, Inco Alloys International, Inc.

Solid-Solution Nickel Alloys

These materials have good weldability and are often used in the as-welded condition. The alloys are usually formed by additions to nickel of chromium, cobalt, molybdenum, iron, and sometimes small amounts of aluminum, silicon, and niobium (Table 1). While they do not develop abnormally high strength levels like the other groups, these alloys provide attractive creep resistance in conjunction with good thermal-fatigue resistance. Under moderate loading, alloys of this group can be used up to temperatures approaching 1150 °C (2100 °F). Typical applications are welded containers and fixtures for thermal processing, and headers and manifolds for chemical and petrochemical processing.

TABLE 1 COMPOSITION OF SELECTED SOLID-SOLUTION NICKEL ALLOYS FOR HIGH-TEMPERATURE APPLICATIONS UP TO 1150 °C (2100 °F)

ALLOY	UNS NO.	COMPOSITIONS, WT%									
		Ni	Cr	Fe	Cu	Co	Mo	Ti	Al	Nb	OTHERS
600	N06600	76.0	15.5	8.0	. . .	. . .	. . .	. . .	. . .	. . .	**. . .**
601	N06601	60.5	23.0	14.4	. . .	. . .	. . .	. . .	1.4	. . .	**. . .**
617	N06617	52.0	22.0	1.5	. . .	12.5	9.0	. . .	1.2	. . .	**. . .**
625	N06625	61.0	21.5	2.5	. . .	. . .	9.0	. . .	. . .	3.6	**. . .**
690	N06690	61.5	29.0	9.0	. . .	. . .	. . .	. . .	. . .	. . .	**. . .**
HX	. . .	47.5	21.8	18.5	. . .	1.5	9.0	. . .	. . .	. . .	**0.6 W**
800	N08800	32.5	21.0	46.0	. . .	. . .	. . .	. . .	. . .	. . .	**0.05 C**

800H	N08810	32.5	21.0	46.0	. . .	. . .	. . .	. . .	. . .	. . .	**0.08 C**
800HT	N08811	32.5	21.0	46.0	. . .	. . .	. . .	. . .	. . .	. . .	**0.08 C; 1.0 (AL + TI)**
802	N08802	32.5	21.0	46.0	. . .	. . .	. . .	. . .	. . .	. . .	**0.4 C**
DS	. . .	37.0	18.0	41.0	. . .	. . .	. . .	. . .	. . .	. . .	**1.0 MN; 2.3 SI**
330	N08330	35.5	18.5	44.0	. . .	. . .	. . .	. . .	. . .	. . .	**1.1 SI**
330HC	**. . .**	**31.5**	**18.5**	**48.0**	**. . .**	**. . .**	**. . .**	**. . .**	**. . .**	**. . .**	**1.2 SI; 0.4 C**

The potential problem in welding these materials is grain size. As grain size increases, weldability decreases. In some applications, a minimum grain size is specified for maximum creep resistance. The compromise normally implemented is to limit welding processes to those methods that use lower heat input (Ref 1).

Reference cited in this section

1. *WELDING--IAI-14,* INCO ALLOYS INTERNATIONAL, JULY 1991, TABLE 18, P 23

Special Metallurgical Welding Considerations for Nickel and Cobalt Alloys and Superalloys

S.D. Kiser, Inco Alloys International, Inc.

Precipitation-Hardenable Nickel Alloys

These materials are characterized by their distinctively high strength at room temperature through about 705 °C (1300 °F). They range in alloy content from the virtually pure nickel-aluminum Alloy 301 to nickel-copper Alloy K-500 through the nickel-chromium-iron Alloy 718 through the low-expansion nickel-iron Alloy 909. They enjoy the commonality of γ' strengthening by heat treatment because of additions of aluminum, titanium, and niobium. Table 2 lists selected precipitation-hardening alloys and their chemistries.

TABLE 2 COMPOSITION OF SELECTED PRECIPITATION-HARDENABLE NICKEL ALLOYS THAT RETAIN HIGH-STRENGTH PROPERTIES TO 705 °C (1300 °F)

ALLOY	**UNS NO.**	COMPOSITIONS, WT%									
		Ni	**Cr**	**Fe**	**Cu**	**Co**	**Mo**	**Ti**	**Al**	**Nb**	OTHERS
K-500	N05500	65.5	. . .	1.0	29.5	. . .	. . .	0.6	2.7	. . .	**. . .**
706	N07702	41.5	16.0	37.0	. . .	. . .	. . .	1.8	0.2	2.9	**. . .**
718	N07718	54.0	18.0	18.5	. . .	. . .	3.0	. . .	. . .	5.1	**. . .**
X-750	N07750	73.0	15.5	7.0	. . .	. . .	. . .	2.5	0.7	1.0	**. . .**
751	N07751	73.0	15.0	7.0	. . .	. . .	. . .	2.5	1.1	1.0	**. . .**
903	N19903	38.0	. . .	42.0	. . .	15.0	. . .	1.4	0.9	3.0	**. . .**
904	. . .	32.5	. . .	51.0	. . .	14.5	. . .	1.6	. . .	. . .	**. . .**
907	. . .	38.0	. . .	42.0	. . .	13.0	. . .	1.5	0.03	4.7	**0.15 SI**
909	. . .	38.0	. . .	42.0	. . .	13.0	. . .	1.5	0.03	4.7	**0.4 SI**
925	**. . .**	**44.0**	**21.0**	**28.0**	**1.8**	**. . .**	**3.0**	**2.1**	**0.3**	**. . .**	**0.01 C**

Most of these alloys have good weldability in the annealed condition. Because of this, most are formed, machined, and welded in the annealed condition. They are then reannealed after welding, and then aged, to obtain the desired properties.

Postweld Strain-Age Cracking (PWSAC). Because all these types of materials are at least somewhat prone to PWSAC, little welding is performed in the aged condition if the weldment is to be re-heat treated or put in elevated-temperature service. Postweld strain-age cracking occurs in precipitation-hardenable alloys when cold-work stresses,

weld-induced residual stresses, and the stress imparted by aging exceed the yield strength (and available ductility) of the material. The result is an instantaneous, catastrophic failure by cracking (Fig. 2).

FIG. 2 PWSAC FAILURE IN ALLOY X-750 INDUCED BY RESIDUAL WELDING STRESS AT A 50 MM (2 IN.) THICK JOINT. ALLOY WAS WELDED IN THE AGE-HARDENED CONDITION AND RE-AGED AT 705 °C (1300 °F) FOR 20 H AFTER WELDING.

Those alloys whose γ' phase is formed predominantly by nickel-aluminum-titanium age more rapidly than those using niobium. As a result, these alloy are more prone to PWSAC.

Alloy 718. In an effort to improve the weldability of precipitation-hardenable alloys, niobium was substituted for large amounts of aluminum and titanium. The result was nickel-chromium-iron Alloy 718, which showed greatly improved resistance to PWSAC. With Alloy 718, thicknesses up to 3.2 mm ($\frac{1}{8}$ in.) could be welded in the aged condition and directly re-aged without cracking. This combination of very high mechanical properties and fabricability has earned Alloy 718 a prominent spot in the aerospace industry.

Alloy 713C. Some precipitation-hardenable alloys often require welding in the aged condition. Alloy 713C, for example, is a nickel-chromium alloy with very high levels of aluminum and titanium that is used for gas-turbine vanes. It is normally produced as a casting that precipitation hardens during cool down. It is considered nonweldable by fusion processes. However, experience has shown that blade and vane tips can be restored by fusion welding with a nonhardenable filler metal (ERNiCrMo-3) without cracking (Ref 2). Thus, crack-free welds can sometimes be accomplished in very-difficult-to-weld materials where residual shrinkage stresses can be kept low and cooling rates are slow. Both conditions occur naturally when welding on an edge.

Alloy 301. Preliminary work has shown similar results when welding on nickel-aluminum Alloy 301 in the aged condition. This alloy exhibits high mechanical properties and very good thermal conductivity. It finds use in cooled glass molds and plastic extrusion equipment. It can be readily welded in the aged condition--fully restrained--when the recommended ductile ERNi-1 filler metal is added. Also, autogenous, low-stress welds (on an edge) can be made at high travel speeds without cracking. However, when fully restrained, autogenous welds are made in forging stock at 200 to 250 mm/min (8 to 10 in./min) travel speed, the cooling rate is so rapid that the aluminum-rich weld pool contains numerous large solidification cracks. Decreasing the travel speed to decrease the cooling rate allows crack-free autogenous welds to be made.

Low-Coefficient-of-Expansion Alloys. For the next group of precipitation-hardening alloys, the same guidelines apply (that is, to weld in the annealed condition). In this group of alloys, the chromium has been removed in order to maintain a low coefficient of thermal expansion. The fabrication sequence includes welding, annealing, heat treating, and in some cases coating. The coating applied is usually an oxidation-resisting ceramic coating.

Alloy 909. The most prominent member of this group is nickel-iron Alloy 909. It is primarily used for seals and rings in aircraft turbines. Its low coefficient of expansion allows close-tolerance designs, which increase the fuel efficiency of gas-turbine engines.

Mechanically Alloyed Products. The final group of precipitation-hardening alloys to be discussed merits the name superalloys. Mechanically alloyed products have a remarkable advantage over conventional materials in elevated-temperature stress-rupture strength. This advantage is gained by the combination of precipitation hardening and dispersion strengthening. Neither concept is revolutionary, but the combination of the two using the ball mill is. As shown in Fig. 1, various ingredients are added to the ball mill as metallic and intermetallic powders. Extended processing times of approximately 10 h in the mill cause the particles to become metallurgically homogeneous. This process is similar to the step of incorporation in Du Pont's early approach to making homogenous particles of gunpowder, each containing the correct ratio of charcoal, sulfur, and potassium nitrate.

Homogenization in the mill is followed by either hot rolling or extrusion. The form is then thermally treated at 1315 °C (2400 °F) to produce the exceptional strength characteristics. Tables 3 and 4 list the chemical compositions and selected properties for mechanically alloyed products.

TABLE 3 COMPOSITION OF SELECTED MECHANICALLY ALLOYED MATERIALS

ALLOY	COMPOSITIONS, WT%							
	Fe	**Cr**	**Al**	**Ti**	**Ni**	**C**	**Y_2O_3**	MO
MA 754	1.0	20.0	0.3	0.5	BAL	0.05	0.6	**. . .**
MA 956	BAL	20.0	4.5	0.5	. . .	. . .	0.5	**. . .**
MA 957	BAL	14.0	. . .	1.0	. . .	. . .	0.25	**0.3**
MA 6000	**. . .**	**15.0**	**4.5**	**2.5**	**BAL**	**0.5**	**0.6**	**. . .**

TABLE 4 PROPERTIES OF SELECTED MECHANICALLY ALLOYED MATERIALS

ALLOY	**DENSITY**		**YOUNG'S MODULUS**		**TENSILE STRENGTH(A)**		**YIELD STRENGTH(A)**		**ELONGATION AT FRACTURE, %(A)**	STRESS TO PRODUCE RUPTURE AT 1095 °C (2000 °F) FOR INDICATED ELAPSED TIME			
										100 H		1000 H	
	G/CM³	**LB/IN.³**	**GPA**	**10^6 PSI**	**MPA**	**KSI**	**MPA**	**KSI**		**MPA**	**KSI**	**MPA**	KSI
MA 754(B)	8.3	0.30	149	21.6	148	21.5	134	19.5	12.5	102	14.8	94	**13.6**
MA 956(B)	7.2	0.26	269	39.0	91	13.2	85	12.3	3.5	57	8.3	51	**7.4**
MA 957(C)	7.67	0.277	210(D)	30.0(D)	1150	167	1100	160	17	345	50	. . .	**. . .**
MA 6000(B)	**8.11**	**0.293**	**203**	**29.4**	**222**	**32.2**	**192**	**27.8**	**9**	**131**	**19**	**127**	**18.5**

(A) LONGITUDINAL.

(B) TEST TEMPERATURE, 1095 °C (2000 °F).

(C) TEST TEMPERATURE, 600 °C (1100 °F), WHICH IS THE INTENDED APPLICATION TEMPERATURE FOR ALLOY IN NUCLEAR REACTORS.

(D) AT 20 °C (70 °F)

Figure 3 shows the dramatic advantage in strength of mechanically alloyed products over the conventional dispersion-strengthened and cast nickel-base alloys. Unfortunately, making these materials weldable is difficult. While they can undergo diffusion bonding or brazing with little loss in properties, fusion welding produces a softened heat-affected zone (HAZ). This behavior is caused by the agglomeration of the dispersoid Y_2O_3. In addition, it is not possible to produce a weld that has properties similar to those of the alloys. Thus, for most applications, the mechanically alloyed products are joined mechanically, or diffusion bonded, or brazed.

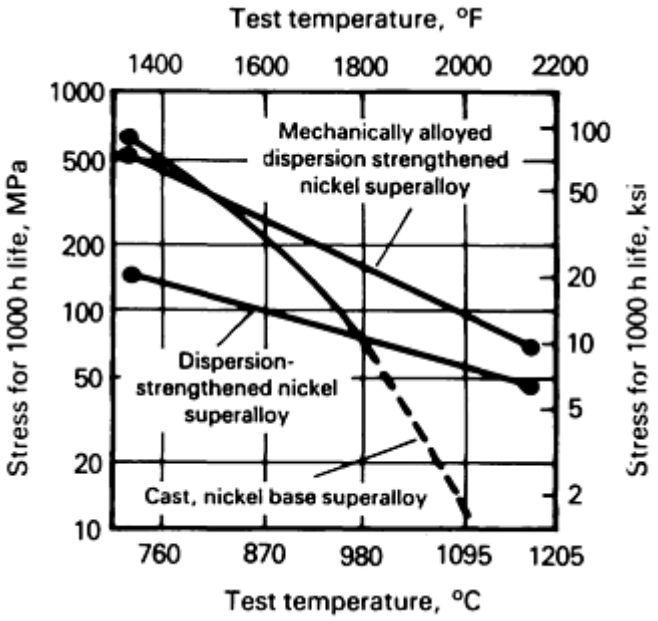

FIG. 3 STRESS-RUPTURE STRENGTH OF MECHANICALLY ALLOYED DISPERSION-STRENGTHENED NICKEL SUPERALLOY RELATIVE TO CONVENTIONAL DISPERSION-STRENGTHENED NICKEL SUPERALLOYS AND CAST NICKEL-BASE ALLOYS

Reference cited in this section

2. D.S. DUVALL AND J.R. DOYLE, *REPAIR OF TURBINE BLADES AND VANES,* PUBLICATION 73-GT-44, AMERICAN SOCIETY OF MECHANICAL ENGINEERS, 1973

Special Metallurgical Welding Considerations for Nickel and Cobalt Alloys and Superalloys

S.D. Kiser, Inco Alloys International, Inc.

Creep-Resistant Secondary Carbide-Strengthened Alloys Welded with Nickel Alloys

This group of alloys has become extremely popular in the chemical and petrochemical industries for the processing of hydrocarbon compounds. Such alloys are typically fabricated in the as-cast condition after being produced in a rotating, water-cooled mold. This production method, which incorporates rapid cooling, allows a supersaturated solution of carbon (0.40 to 0.45%) in nickel, chromium, and iron to retain the carbon in solution. This condition allows sufficient ductility in the as-cast condition to provide good weldability by most fusion processes.

Formation of Secondary Carbides. Once the assembly has been fabricated, it is normally put into service at temperatures of 760 to 1095 °C (1400 to 2000 °F). At these temperatures, the chromium (and sometimes niobium) combines with the carbon in a solid-state diffusion process that results in the precipitation of secondary carbides. These secondary carbides provide a tremendous strengthening effect for the intended high-temperature service. Figure 4 compares the stress-rupture strength of a typical centrifugal-cast carbide-strengthened alloy with that of a widely used nickel-alloy welding product that is needed to attain approximately equal strength. It is interesting to note that welds made in these alloys with near-matching composition welding products suffer failure at less than half the rupture life of welds made with ERNiCrCoMo-1 type welding products (Ref 3). (See Table 1 for the approximate chemical composition of ERNi-CrCoMo-1, identified as N06617.) In addition, transverse stress-rupture specimens welded with near-matching composition products routinely fail in the weld itself, while those welded with ERNiCrCoMo-1 products typically fail in the alloy casting.

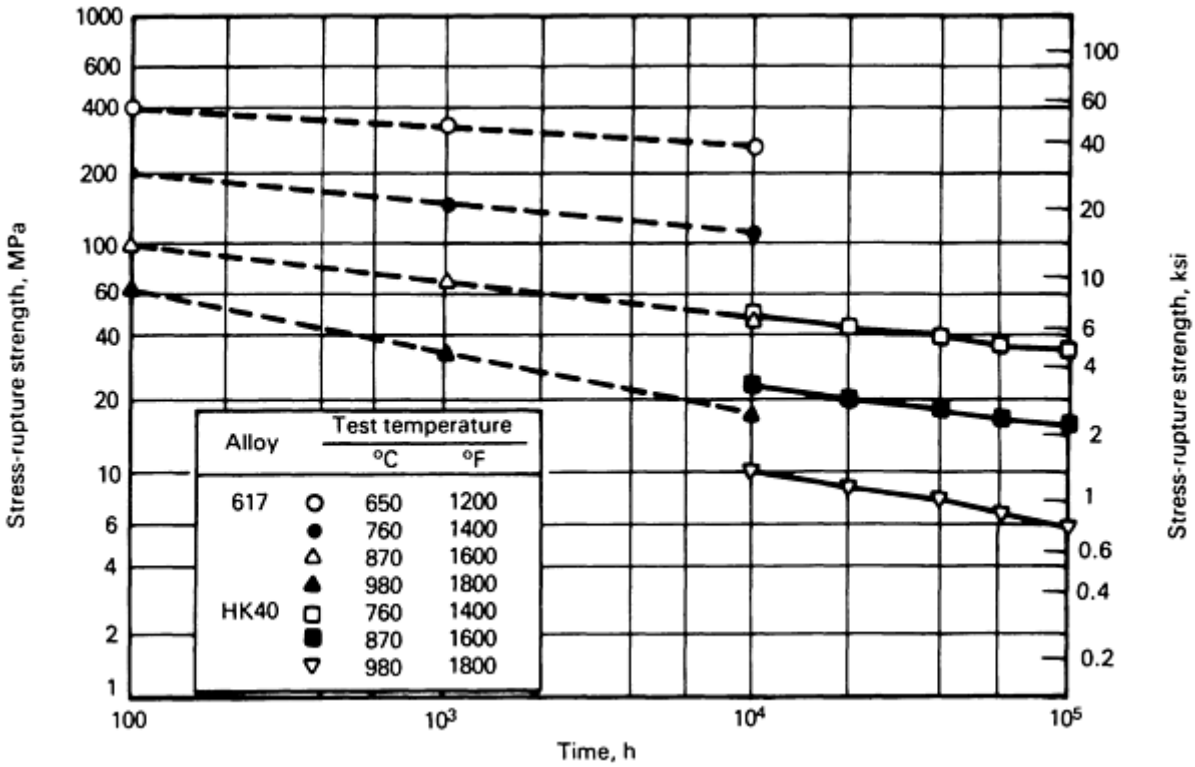

FIG. 4 STRESS-RUPTURE STRENGTH OF ALLOY 617 FILLER METAL RELATIVE TO CENTRIFUGAL-CAST CARBIDE-STRENGTHENED ALLOY HK40

Effect on Weldability. As might be expected, once these alloys have precipitated their secondary-phase carbides, their weldability decreases. Like the precipitation-hardenable, γ'-strengthened alloys, these materials undergo a drastic reduction in room-temperature ductility as a result of carbide precipitation. This result usually means that a secondary carbide-strengthened alloy cannot be welded by fusion processes immediately after service. It is customary to use a resolutioning heat treatment for used tubes in preparation for welding. Parts are exposed to 1095 to 1205 °C (2000 to 2200 °F) for several hours, usually followed by a forced-air cool (Ref 4). This practice restores ductility to near asproduced levels, and allows successful fusion welding without cracking of the base metal.

Castings. Most of the above-mentioned carbide-strengthened castings have good weldability in the proper thermally treated condition. Likewise, most of the solid-solution and precipitation-hardened nonferrous materials in previous sections can be produced as castings. Further, the weldability of these castings may be good if they are produced using clean foundry conditions and clean charge (raw) materials. However, castings are usually made to near-finished dimensions and do not require further hot working as wrought materials do. As a result, many castings do not have the good hot ductility and malleability of wrought materials, characteristics that contribute greatly to good weldability. Thus, a casting may be produced and delivered as a finished part if it simply solidifies from the liquid state without cracking.

In many cases, the customer may attempt to weld fabricate the casting into a larger design only to encounter HAZ cracking in the casting. Analysis usually discloses objectionable levels of low-melting-temperature elements as contaminants. Once the casting has been delivered, and welding difficulties discovered, options to produce good weldments are limited. Best results are obtained by using very low heat input, some-times coupled with buttering or overlaying joint surfaces before welding them together.

An alternate approach that generally yields successful results is for the buyer to specify in purchase documents that the casting must be weldable. To avoid sharply increased prices in quotations for castings, the buyer should not tightly specify chemical limits for damaging contaminating elements. Rather, a simple fusion weldability test can be written into the purchase specifications. Such a test is usually not seen as rigorously expensive to the foundry, and it ensures that the fabricator will get a weldable casting. The weldability test is usually a gas tungsten-arc weld made with no filler metal added on a ground surface of the casting (or testpiece). Amperage and travel speed are usually specified, along with

length of weld. A testing method, usually liquid-penetrant inspection, is employed to detect weld and HAZ discontinuities. Generally, the start and stop are excluded from inspection, and cause for rejection is any linear indication.

References cited in this section

3. C.W. COX AND S.D. KISER, FUSION WELDING OF DISSIMILAR METALS FOR HIGH TEMPERATURE STRENGTH, *WELD. J.*, VOL 5, MAY 1991, FIGURE 1, P 68
4. R.E. AVERY AND C.M. SCHILLMOLLER, REPAIR WELDING HIGH ALLOY FURNACE TUBES,*HYDROCARBON PROCESS.*, JAN 1988

Special Metallurgical Welding Considerations for Nickel and Cobalt Alloys and Superalloys

S.D. Kiser, Inco Alloys International, Inc.

Special Welded Product Conditions

Dissimilar Metals. The welding of dissimilar metals has been amply discussed (Ref 5, 6, 7). The materials discussed in this article have reasonably good dissimilar weldability provided the dissimilar alloy is not too different in liquidus and solidus temperatures and other characteristics important to sound weldments. For instance, nearly all the materials previously mentioned can be readily joined to steel, high-strength low-alloy (HSLA) steels, stainless steels, and other nickel alloys. A high-temperature nickel alloy filler metal is often used to make such dissimilar joints. Design and filler metal selection criteria usually include strength, corrosion resistance, and dilution tolerance of the filler metal for the elements present in the metals to be joined. In some cases, special design consideration is given to selecting filler metals with a specific coefficient of thermal expansion, thermal conductivity, electrical resistivity, and thermal fatigue resistance (Ref 8).

An example of a filler-metal-added dissimilar weld for high-temperature service can be found in hydrogen furnaces. In many applications, centrifugal-cast, secondary-carbide-strengthened furnace tubes are welded to collection headers of UNS 08800 using ERNiCrCoMo-1, to achieve a combination of strength, ductility, and corrosion resistance. An example of a successful autogenous dissimilar weld is the weld used in the manufacture of internal combustion engine turbochargers. In some of these, the difficult-to-weld Alloy 713C is friction-welded to an HSLA steel shaft such as 4340. Such a design economically uses the high-strength precipitation-hardenable alloy only where its high-temperature strength and corrosion resistance are needed.

Clad Metals and Overlays. A similar set of considerations also applies to filler metal selection for welding clad materials and for overlay cladding by welding. First, the materials selected must be capable of being mixed during welding without resulting cracks, and second, the resulting weldment must perform well in the intended service.

In overlay cladding and the welding of clad materials, the alloy contribution of the substrate to the final weld composition must be considered. For instance, if a one-layer overlay on steel is desired to have a minimum of 50 wt% Ni and 15 wt% Cr, and the chosen welding process yields 20 wt% dilution, then a filler metal with approximately 70 wt% Ni and 20 wt% Cr must be selected. In this case, ERNiCr-3 filler metal, which has 18 to 22 wt% Cr and 67 wt% (min) Ni, would yield a single-layer overlay chemistry of 16 wt% Cr and 54 wt% Ni.

Likewise, if two clad plates are to be welded together, it is usually desirable that the weld have a slightly richer alloy content than the cladding. In order to achieve this condition, a welding product of considerably higher alloy content than the cladding must be selected to allow for the dilution by the substrate. For example, refineries often use steel tubing with the inside surface clad with UNS08825 for elevated-temperature resistance to H_2S. This alloy cladding contains 42 wt% Ni, 20 wt% Cr, 3 wt% Mo, and 1 wt% Ti. In order to achieve a slightly enriched weld composition, it is welded using ERNiCrMo-3, which contains 60 wt% Ni, 22 wt% Cr, and 9 wt% Mo.

Outside-Diameter Clad Tubing. A more complex application is needed for butt welding boiler tubing made from UNS08800 that had been outside-diameter clad with a 45Cr-55Ni nickel alloy for resistance to molten salt and fuel-ash corrosion. The substrate was welded using ERNiCr-3 to develop sufficient stress-rupture strength, and the weld was

capped with two layers of a proprietary near-matching filler metal using a low-dilution-rate process. (A crack-free higher-chromium filler metal was unavailable.) In this application, the filler metal chosen for welding the substrate had to provide the necessary strength after having been diluted by the substrate and had to be compatible with the capping weld layers. Because both materials were nickel-chromium types, the procedure went smoothly, and the tubing has given nearly 20 years of service in a demanding corrosive environment.

Repair welding, or welding after service, has been briefly addressed in some previous sections of this article. It has also been thoroughly discussed in the literature (Ref 9). Primarily, the same fabrication requirements must be met; namely, a sound weld must be produced that is capable of giving usable service in a given environment. If service conditions such as corrosion have rendered the material unweldable, the corrosion layers must be removed or neutralized. The precipitation-hardenable alloys and the secondary-carbide-strengthened alloys usually must have weldability restored by thermal treatment before repair is attempted.

In some cases, the usefulness of a part can be restored without a 100% joint-efficient weld design. In the example of worn turbine blades, greatly extended service can be attained by repair welding without reannealing by using a lower-strength but more ductile filler metal.

In yet other applications only a small part of a welded assembly may have become inoperative due to corrosion or tertiary creep. In these situations, it is highly desirable to remove the damaged portions, remove corrosion deposits, restore weldability if necessary, and select a suitable filler metal. Then, the assembly can be successfully repaired with a proven welding procedure to provide the desired extension in service life.

Alternatively, corrosion attack such as oxidation or carburization may have completely penetrated the full thickness of all parts. In such cases, attempts to repair the weld will be unsuccessful. In addition, the formation of extensive creep voids or thermal-fatigue cracking may have permeated the materials to such an extent that repair welding is impossible. In these cases, good diagnostic analysis is important for preventing wasted effort when attempting to repair parts that cannot be salvaged.

References cited in this section

5. B. IRVING, DISSIMILAR METAL WELDING PAVES THE WAY TO NEW VENTURES, *WELD. J.*, VOL 5, MAY 1992, P 27-32
6. S.D. KISER, DISSIMILAR WELDING WITH NICKEL ALLOYS, *CAN. WELD. FABRICAT.*, JAN 1980
7. *PROCEEDINGS: SEMINAR ON DISSIMILAR WELDS IN FOSSIL-FIRED BOILERS,* EPRI-CS-3623, PROJECT 1874-1, JULY 1985
8. S.D. KISER, NICKEL ALLOYS CONSUMABLE SELECTION FOR SEVERE SERVICE CONDITIONS, *WELD. J.*, VOL 11, NOV 1990, P 30-35
9. S.D. KISER, REPAIR WELDING OF NICKEL ALLOYS, *CAN. WELD. FABRICAT.*, VOL 12, DEC 1980

Special Metallurgical Welding Considerations for Nickel and Cobalt Alloys and Superalloys

S.D. Kiser, Inco Alloys International, Inc.

References

1. *WELDING--IAI-14,* INCO ALLOYS INTERNATIONAL, JULY 1991, TABLE 18, P 23
2. D.S. DUVALL AND J.R. DOYLE, *REPAIR OF TURBINE BLADES AND VANES,* PUBLICATION 73-GT-44, AMERICAN SOCIETY OF MECHANICAL ENGINEERS, 1973
3. C.W. COX AND S.D. KISER, FUSION WELDING OF DISSIMILAR METALS FOR HIGH TEMPERATURE STRENGTH, *WELD. J.*, VOL 5, MAY 1991, FIGURE 1, P 68
4. R.E. AVERY AND C.M. SCHILLMOLLER, REPAIR WELDING HIGH ALLOY FURNACE

TUBES,*HYDROCARBON PROCESS.*, JAN 1988
5. B. IRVING, DISSIMILAR METAL WELDING PAVES THE WAY TO NEW VENTURES, *WELD. J.*, VOL 5, MAY 1992, P 27-32
6. S.D. KISER, DISSIMILAR WELDING WITH NICKEL ALLOYS, *CAN. WELD. FABRICAT.*, JAN 1980
7. *PROCEEDINGS: SEMINAR ON DISSIMILAR WELDS IN FOSSIL-FIRED BOILERS,* EPRI-CS-3623, PROJECT 1874-1, JULY 1985
8. S.D. KISER, NICKEL ALLOYS CONSUMABLE SELECTION FOR SEVERE SERVICE CONDITIONS, *WELD. J.*, VOL 11, NOV 1990, P 30-35
9. S.D. KISER, REPAIR WELDING OF NICKEL ALLOYS, *CAN. WELD. FABRICAT.*, VOL 12, DEC 1980

Special Metallurgical Welding Considerations for Refractory Metals

Bryan A. Chin, Probal Banerjee, Jiayan Liu, and Shaofeng Chen, Auburn University

Introduction

THE REFRACTORY METALS, which include niobium (also called columbium), tantalum, molybdenum, tungsten, and rhenium, have the highest melting temperatures and lowest vapor pressures of all metals, except osmium and iridium. The refractory metals are readily degraded by oxidizing environments at moderately low temperatures, a property that has restricted the applicability of the metals in low-temperature or nonoxidizing high-temperature environments.

This article is limited to a discussion of special metallurgical considerations during the fusion welding of refractory metal alloys. These alloys are discussed in order of decreasing weldability: tantalum, niobium, rhenium, molybdenum, and tungsten.

Special Metallurgical Welding Considerations for Refractory Metals

Bryan A. Chin, Probal Banerjee, Jiayan Liu, and Shaofeng Chen, Auburn University

Tantalum Alloys

Tantalum is a refractory metal that readily reacts with atmospheric gases, especially at high temperatures. This metal melts at 3000 °C (5430 °F), has a body-centered cubic (bcc) structure, and does not undergo an allotropic transformation. It also exhibits excellent corrosion resistance to a wide spectrum of reagents. However, it oxidizes readily at temperatures above 343 °C (650 °F).

Carbon, oxygen, nitrogen, and hydrogen actively react with tantalum, typically forming intermetallics that lead to weld embrittlement. Although tantalum and its alloys are generally considered to have the best weldability of the refractory metals, the formation of these brittle intermetallics makes it difficult to weld to most structural metals. Processes used for joining tantalum alloys include gas-tungsten arc welding (GTAW), solid-state diffusion bonding, friction welding, resistance welding, brazing, and explosion bonding (Ref 1). Trailing shields help reduce atmospheric contamination due to the active nature of tantalum.

Effect of Microstructure

The fusion zones generally contain large grains and, in the absence of hafnium, cellular substructures (Ref 2). The proportion of large grains is higher in alloys with low alloy contents, because of a narrow freezing range (Ref 3) and a single-phase structure. Metallographic sections along the cell growth direction typically consist of nearly parallel grain boundaries. However, transverse sections show hexagonal cells. Increasing alloy content produces a more delineated substructure (Ref 2). Extensive carbide precipitation at grain boundaries can lead to severe embrittlement after a silicide coating procedure in certain weld configurations in Ta-10W alloy (Ref 4).

Ductility. Differences in grain size or cell size do not appear to strongly affect ductility, but material quality, or impurity concentration, does have an influence. High interstitial contents in the alloys can lead to a large concentration of micropores. Only in special carbon-containing Ta-5W-2.5Mo alloys does weld hardness influence ductility (Ref 2). Ductility is reduced in surface-ground welded specimens. Welds in Ta-5W-2.5Mo and Ta-10W-2.5Mo have excellent bend ductility at room temperature.

The GTAW process results in an increase in sheet bend transition temperature in Ta-8W-2Hf, Ta-10W, and Ta-9.6W-2.4Hf-0.01C (T-222), with the highest increase being in the T-222 material (Ref 3). With an increasing tungsten content, alloys become brittle at room temperature (Ref 2). A postweld heat treatment of 1 h at 816 °C (1500 °F) can significantly reduce the 2*t* bend transition temperature for welds produced by the GTAW process. The bend transition temperature is the lowest temperature below which cracking develops in a weld bent at a radius of 2*t* (twice the thickness of the sheet) with an angle of at least 90 °. Welds produced by electron-beam welding (EBW), however, have slightly higher transition temperatures (Ref 2). Under elevated-temperature exposure, there is considerable grain growth, which reduces the cellular fusion zone substructure. This leads to an increased impurity concentration at grain boundaries. In alloys susceptible to impurities, elevated-temperature exposure leads to a decrease in ductility. Generally, total metallic alloy contents of less than 10 at.% produce ductile welds, whereas alloy contents of greater than 13 at.% produce brittle welds (Ref 2).

Tensile Properties. A postweld heat treatment of 1 h at 816 °C (1500 °F) reduces the susceptibility of tantalum-tungsten-molybdenum alloys to premature tensile failure (Ref 2). Joint efficiencies of welds in wrought material are lower than those of welds in recrystallized materials. However, room-temperature tensile strengths of welds in wrought material are higher than those of welds in recrystallized material. The tensile strengths of welds drop very sharply above 1649 °C (3000 °F). Tensile strengths decrease with an increase in tungsten content, whether testing is conducted at room temperature or at elevated temperatures. In general, tensile strengths decrease exponentially with an increase in testing temperature (Ref 3) (Fig. 1).

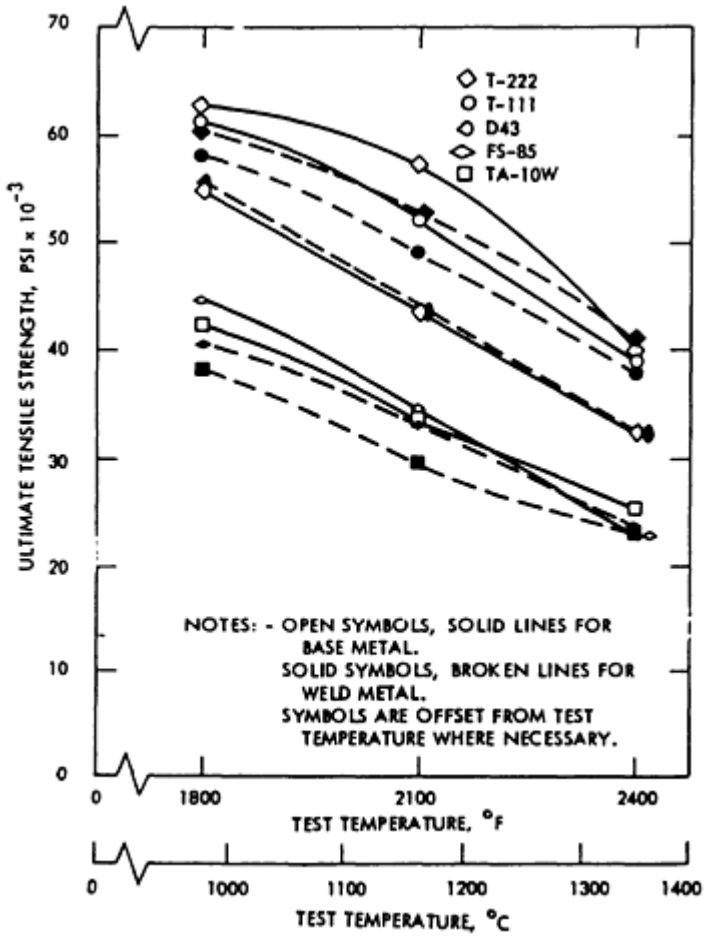

FIG. 1 ELEVATED-TEMPERATURE TENSILE STRENGTH OF ANNEALED BASE METAL AND TANTALUM ALLOY ARC WELDS. SOURCE: REF 3

Effect of Interstitial Impurities

Interstitial impurities can strongly influence the properties of welded tantalum materials. The average weld bend ductility is lower for gas-tungsten arc welds in low-interstitial-content materials. Generally, tantalum alloy sheet must have a low interstitial level (less than 100 ppm) to be weldable. Carbon contents of less than 100 ppm or hydrogen contents of less than 17 ppm do not significantly affect weld ductility (Ref 2).

Effect of Welding Conditions

Welding conditions can also be used to control properties in tantalum and its alloys. In low-interstitial-content sheets, arc travel speed and energy input do not appear to influence ductility. In high-interstitial-content sheets, ductility is better at high travel speeds (12.7 to 31.75 mm/s, or 30 to 75 in./min) and low energy inputs (98 to 118 J/mm, or 2500 to 3000 J/in.) (Ref 2).

Effect of Arc Oscillations

Arc oscillation has been found to reduce the columnar structure in the fusion zone (Ref 5), which promotes ductility. However, there is an optimum frequency that produces an equiaxed structure. If this frequency (10 Hz) is exceeded, then elongated grains result (Ref 5, 6).

Increased energy input results in larger heat-affected zone (HAZ) grains and fewer nucleation sites for fusion zone grains (Ref 2). There is an increase in hardness at the areas of metal deposition and at the HAZ in gas-tungsten arc welded tantalum (Ref 7).

References cited in this section

1. R.T. WEBSTER, JOINING OF TANTALUM AND NIOBIUM, *J. MET.*, VOL 36 (NO. 8), AUG 1984, P 43
2. P.A. KAMMER, R.E. MONROE, AND D.C. MARTIN, WELDABILITY OF TANTALUM ALLOYS, *WELD. J.*, JUNE 1972, P 304S-320S
3. G.G. LESSMAN, THE COMPARATIVE WELDABILITY OF REFRACTORY METAL ALLOYS, *WELD. J.*, DEC 1966, P 540S-560S
4. J. WADSWORTH AND C.M. PACKER, WELD EMBRITTLEMENT IN A SILICIDE-COATED TANTALUM ALLOY, *INT. J. REFRACT. HARD MET.*, VOL 2 (NO. 4), DEC 1983, P 164-169
5. A. GRILL, EFFECT OF ARC OSCILLATIONS ON THE TEMPERATURE DISTRIBUTION AND MICROSTRUCTURE IN GTA TANTALUM WELDS, *METALL. TRANS. B*, DEC 1981, P 667-674
6. Y. SHARIR, J. PELLEG, AND A. GRILL, EFFECT OF ARC VIBRATION AND CURRENT PULSES ON MICRO-STRUCTURE AND MECHANICAL PROPERTIES OF TIG TANTALUM WELDS, *MET. TECHNOL.*, JUNE 1978, P 190-196
7. H. HIROSE, K. SATO, AND T. HAYASHI, WELDING OF TANTALUM AND NIOBIUM, *WELD. LNT.*, AUG 1989, P 672-677

Special Metallurgical Welding Considerations for Refractory Metals

Bryan A. Chin, Probal Banerjee, Jiayan Liu, and Shaofeng Chen, Auburn University

Niobium Alloys

Niobium and its alloys are often selected for high-temperature use in fabricated systems. They can be easily welded by the GTAW, EBW, and laser-beam welding (LBW) processes, either autogenously or with matching filler metals in inert atmospheres. In special cases, resistance welding (RW), plasma arc welding (PAW), hot pressure welding (HPW), and explosion welding (EXW) can be considered.

Atmospheric contamination is a major cause of the embrittlement of niobium alloy welded joints. To avoid significant increases in the ductile-to-brittle transition temperature (DBTT) of welds (caused by interstitial contamination), welding atmospheres should have less than 600 ppm oxygen, 300 ppm nitrogen, and 150 ppm hydrogen.

Effect of Welding Atmosphere. Niobium and its alloys can be welded using an inert gas shield or a vacuum chamber. A vacuum-purged chamber backfilled with argon and helium is recommended for better-quality welds that are free from air contamination.

Effect of Microstructure. The DBTT of welds is also influenced by microstructural changes resulting from weld thermal cycles. The size of the HAZ and grain growth in this zone are major factors that affect the ductility of welds. Welding conditions that tend to increase the size of the HAZ, as well as the grains within it, will result in an upward shift in the transition temperature of welds. Furthermore, alloys with different strengthening mechanisms respond differently to weld heat input.

The solid-solution alloys, such as Nb-1Zr and Nb-10W-10Ta (SCb-291) show a continuous ductility loss with an increasing HAZ size and fusion zone grain size. A heat input limit, above which ductility impairment occurs, exists for solid-solution plus dispersion-strengthened alloys, such as Nb-10W-2.5Zr (Cb-752), Nb-27Ta-10W-1Zr (FS-85), Nb-10W-1Zr-0.2C (D-43), and Nb-5Mo-5V-1Zr (B-66). To reduce the tendency of grain growth in the HAZ and fusion zones, a high-energy-density welding process, such as EBW, is often more advantageous than GTAW.

Effect of Welding Conditions. The alloy Nb-1Zr can be easily welded using arc welding and EBW processes. The alloy B-66 has a hot tearing tendency during arc welding, which makes both manual and automatic welding more difficult. High-speed arc welding of Nb-10W-10Hf + Y (C-129Y) will cause gross shrinkage defects in the welds. Welds of D-43Y have the tendency to hot tear along the weld centerline and crack during welding. This factor, in conjunction with unmodified D-43, tends to produce high porosity in the weld.

Several alloys are temperature limited with respect to thermal stability. Welds of D-43 tend to lose strength with increasing aging time and temperature. Design stresses need to be reset for long-term applications of welded joints at temperatures above 1095 °C (2000 °F). During high-temperature aging, SCb-291 and B-66 welds gradually lose ductility, because of grain growth in both the weld and the HAZ.

Special Metallurgical Welding Considerations for Refractory Metals

Bryan A. Chin, Probal Banerjee, Jiayan Liu, and Shaofeng Chen, Auburn University

Rhenium Alloys

The weldability of rhenium is better than that of tungsten and molybdenum, but is slightly less than that of tantalum. Rhenium welds typically demonstrate a large degree of ductility. The only problem that can be encountered is porosity, which often occurs from welding a powder metallurgical product. It has been proposed that tungsten and molybdenum be alloyed with rhenium to improve both room-temperature ductility and weldability. The binary alloy of molybdenum with 50% rhenium can be easily welded using the GTAW and EBW processes. The welds retain nearly the same strength as the base metal and have good ductility.

Special Metallurgical Welding Considerations for Refractory Metals

Bryan A. Chin, Probal Banerjee, Jiayan Liu, and Shaofeng Chen, Auburn University

Molybdenum Alloys

Molybdenum and its alloys can be welded by the GTAW and EBW processes (Fig. 2), as well as most other welding methods. However, the weldability of molybdenum and its alloys is marginal, because of a high DBTT in the welded and recrystallized zones. Furthermore, the DBTT of molybdenum welds is significantly increased after the GTAW and EBW processes.

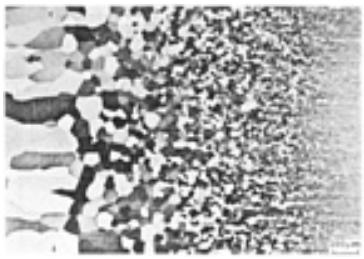

FIG. 2 WELD AND HAZ IN ELECTRON-BEAM WELDED TZM; ARROWS INDICATE FUSION LINE. SOURCE: REF 8

Effect of Welding Conditions. Heat input is a major factor influencing the ductility of welds. Electron-beam welding with relatively low heat input results in a lower DBTT than that obtained from the GTAW process. A high melting point, in conjunction with low ductility, also make molybdenum susceptible to failure by thermal impact during welding. Therefore, weldability can be improved by a weld preheat. If their DBTT values are below the ambient temperature, then molybdenum and most of its alloys with low DBTT values can be welded without a preheat. Alloys with high DBTT values must be preheated above their respective transition temperatures to avoid cracking during welding. Postweld annealing for stress relief helps improve weld ductility. The brittle behavior is principally the result of the large grain size in the HAZ and fusion zone. By reducing the grain size difference between the parent and weld metals through heat treatment, significant increases in ductility can be achieved. TZM (Mo-0.5Ti-0.1Zr) welds are not inherently as brittle as other molybdenum alloys (Ref 8).

Effect of Interstitial Impurities. Molybdenum and tungsten both have extremely low solubility limits for interstitials such as oxygen, nitrogen, and carbon (1 ppm or less). Of these three, oxygen is particularly harmful to ductility. Just several parts per million are enough to raise the DBTT from well below the ambient temperature to well above it. To prevent interstitial contamination, welding in vacuum or in an inert-gas-filled chamber is recommended. A high-purity shield gas is effective in promoting ductile joints.

Hot cracking and weld porosity represent other problems that can arise when welding powder metallurgy alloys. These problems often occur even when the welds are made in high vacuum. Large amounts of oxygen and other gases that are generally contained in the powder metallurgy base metal will react with the molybdenum during welding, leading to embrittlement.

Reference cited in this section

8. J. WADSWORTH, G.R. MORSE, AND P.M. CHEWEY, THE MICROSTRUCTURE AND MECHANICAL PROPERTIES OF A WELDED MOLYBDENUM ALLOY, *MATER. SCI. ENG.*, JUNE 1983, VOL 59, P 257-273

Special Metallurgical Welding Considerations for Refractory Metals

Bryan A. Chin, Probal Banerjee, Jiayan Liu, and Shaofeng Chen, Auburn University

Tungsten Alloys

Tungsten and tungsten alloys can be joined by welding (GTAW and EBW), brazing, diffusion bonding, and other joining techniques. Tungsten and its alloys are generally considered to have poor weldability, when compared with other refractory metals, such as niobium and tantalum. Welding problems encountered with tungsten and its alloys are generally traceable to physical metallurgy and properties. Chemical changes that are due primarily to atmospheric contamination during heating and cooling and microstructural changes that are due to thermal cycling can result in grain growth, hardening, and embrittlement. Embrittlement can often be traced to recrystallization and oxygen ingression along grain boundaries.

Of the refractory metals, tungsten has the highest modulus and melting point. This high melting point results in greater than normal cooling time intervals after joining and a large range of cooling temperatures over which sizeable thermal strains can be generated, because of differential thermal expansion and contraction. High elastic modulus, high yield strength, and resistance to plastic flow lead to a rapid rise in residual stress with an increase in thermal strain. High residual stresses are commonly encountered in tungsten welds. If the welds are made under restraint, then they may crack during cooling.

Effect of Alloy Production Technique. The weldability and properties of tungsten strongly depend on the process used to make the tungsten. Porosity and entrained gases in powder metallurgy tungsten products will result in weld porosity. This porosity usually concentrates along the fusion boundary. To a lesser extent, welds of chemical vapor deposition (CYD) tungsten products will show porosity along the fusion line and in the HAZ (Ref 9). Welds of arc cast tungsten materials can be made porosity free if proper welding procedures are followed. Tungsten weld embrittlement can be caused by contamination and/or recrystallization.

Effect of Interstitial Impurities. Tungsten, which is composed of a bcc crystal lattice, is sensitive to the presence of interstitial atoms such as carbon, oxygen, and nitrogen. Because the solubility of these elements in tungsten is very low, their embrittling effects are much greater. Tungsten has a particularly high affinity for carbon and oxygen, readily forming carbides (WC) and oxides (WO_2).

Carbon, oxygen, and nitrogen dramatically increase the bend ductility transition temperature and DBTT, as shown in Fig. 3. Typical sources of these contaminants are moisture/impurities in the shielding gas, surface films on the base metals and/or filler metals, and oils on the components being welded. Use of either a vacuum or an inert atmosphere chamber consisting of specially purified shielding gas (argon, helium, or combinations of the two) is necessary to control contamination.

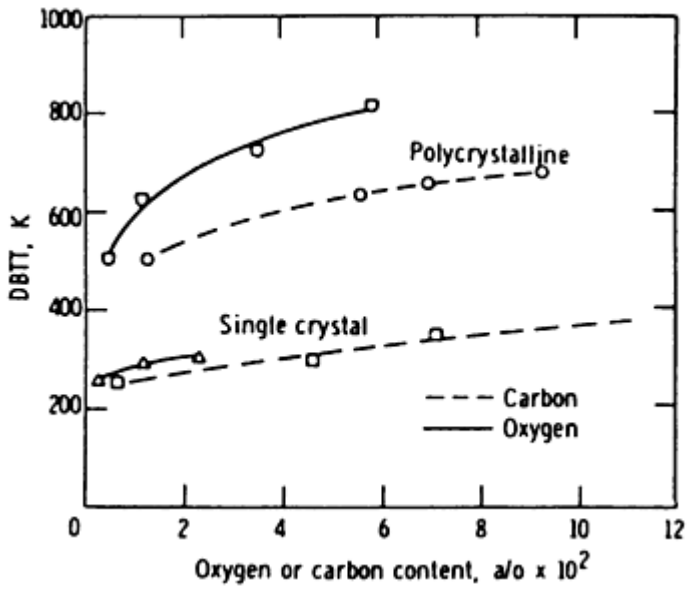

FIG. 3 EFFECTS OF OXYGEN AND CARBON ON DBTT OF TUNGSTEN. SOURCE: REF 10

Effect of Microstructure. Recrystallization and grain growth in the HAZ (Fig. 4) is another effect that can also contribute to embrittlement. Increasing grain size reduces the tensile strength, ductility, and toughness of tungsten alloys. Coarse grains in the HAZ have been found to increase the DBTT. The effect of grain size on DBTT is shown in Fig. 5. The effect of coarse grains on weldment ductility may be minimized by using a low heat input and by choosing proper welding procedures and parameters that limit recrystallization and grain growth effects. The EBW process can be used to obtain an extremely narrow HAZ. This technique has been shown to minimize embrittlement that is caused by recrystallization and grain growth.

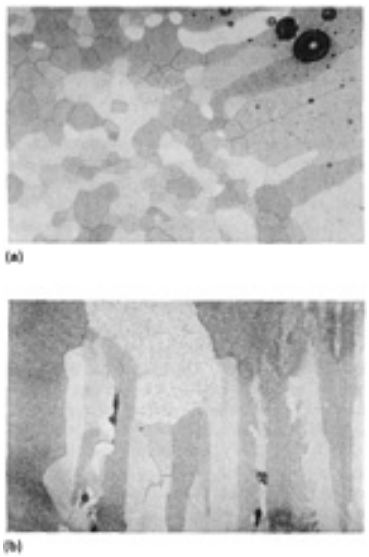

FIG. 4 COARSE GRAINS IN HAZ. 65×. (A) POWDER METALLURGY TUNGSTEN; POROSITY SHOWN ALONG FUSION LINE. (B) CVD TUNGSTEN

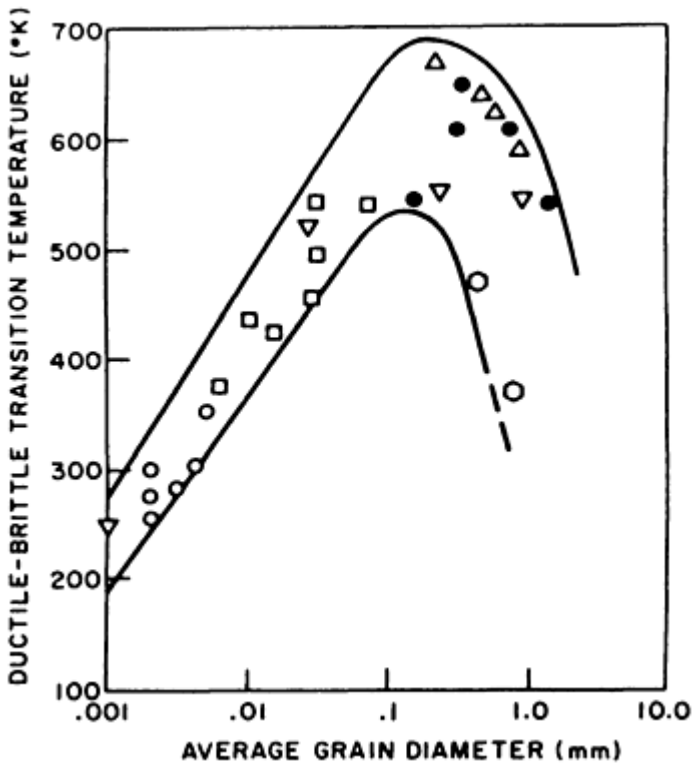

FIG. 5 EFFECT OF GRAIN SIZE ON DBTT OF TUNGSTEN. SOURCE: REF 10

Weld cracking usually can be avoided by preheating to above the DBTT. Welding tungsten-rhenium alloys or using the EBW process makes it possible to avoid preheat requirements. When CVD tungsten is welded, cracks are usually found in the columnar grain boundaries in the HAZ, having been caused by the growth and coalescence of small pores on the grain boundaries.

References cited in this section

9. K. FARRELL, J.T. HOUSTON, AND J.W. CHUMLEY, HOT CRACKING IN FUSION WELDS IN TUNGSTEN, *WELD. J.*, MARCH 1970, P 132S-137S
10. S.W.H. YIH AND C.T. WANG, *TUNGSTEN*, PLENUM PRESS, 1979

References

1. R.T. WEBSTER, JOINING OF TANTALUM AND NIOBIUM, *J. MET.*, VOL 36 (NO. 8), AUG 1984, P 43
2. P.A. KAMMER, R.E. MONROE, AND D.C. MARTIN, WELDABILITY OF TANTALUM ALLOYS, *WELD. J.*, JUNE 1972, P 304S-320S
3. G.G. LESSMAN, THE COMPARATIVE WELDABILITY OF REFRACTORY METAL ALLOYS, *WELD. J.*, DEC 1966, P 540S-560S
4. J. WADSWORTH AND C.M. PACKER, WELD EMBRITTLEMENT IN A SILICIDE-COATED TANTALUM ALLOY, *INT. J. REFRACT. HARD MET.*, VOL 2 (NO. 4), DEC 1983, P 164-169
5. A. GRILL, EFFECT OF ARC OSCILLATIONS ON THE TEMPERATURE DISTRIBUTION AND MICROSTRUCTURE IN GTA TANTALUM WELDS, *METALL. TRANS. B*, DEC 1981, P 667-674
6. Y. SHARIR, J. PELLEG, AND A. GRILL, EFFECT OF ARC VIBRATION AND CURRENT PULSES ON MICRO-STRUCTURE AND MECHANICAL PROPERTIES OF TIG TANTALUM WELDS, *MET. TECHNOL.*, JUNE 1978, P 190-196
7. H. HIROSE, K. SATO, AND T. HAYASHI, WELDING OF TANTALUM AND NIOBIUM, *WELD. LNT.*, AUG 1989, P 672-677
8. J. WADSWORTH, G.R. MORSE, AND P.M. CHEWEY, THE MICROSTRUCTURE AND MECHANICAL PROPERTIES OF A WELDED MOLYBDENUM ALLOY, *MATER. SCI. ENG.*, JUNE 1983, VOL 59, P 257-273
9. K. FARRELL, J.T. HOUSTON, AND J.W. CHUMLEY, HOT CRACKING IN FUSION WELDS IN TUNGSTEN, *WELD. J.*, MARCH 1970, P 132S-137S
10. S.W.H. YIH AND C.T. WANG, *TUNGSTEN*, PLENUM PRESS, 1979

Special Metallurgical Welding Considerations for Refractory Metals

Bryan A. Chin, Probal Banerjee, Jiayan Liu, and Shaofeng Chen, Auburn University

Selected References

- N.C. COLE, R.G. GILLILAND, AND G.M. SLAUGHTER, WELDABILITY OF TUNGSTEN AND ITS ALLOYS, *WELD. J.*, SEPT 1971, P 419S-426S
- E.S. ROBERT, *REFRACTORY METALS AND THEIR INDUSTRIAL APPLICATIONS*, STP 849, ASTM
- E.M. SAVITSKII, M.A. TYLKINA, AND K.B. POVAROVA, *RHENIUM ALLOYS*, ISRAEL PROGRAM FOR SCIENTIFIC TRANSLATIONS, 1970
- J. WADSWORTH, T.G. NIEH, AND J.J. STEPHENS, RECENT ADVANCES IN AEROSPACE REFRACTORY METAL ALLOYS, *INT. MATER. REV.*, VOL 33 (NO.3), 1988, P 131-150

Introduction to the Selection of Nonferrous Corrosion-Resistant Materials

S.J. Matthews, Haynes International, Inc.

Introduction

CORROSION has a tremendous cost impact on our industrial society, estimated to be on the order of $170 billion/year. There are many different forms of corrosion, and the interested reader is referred to *Corrosion,* Volume 13 of the *ASM Handbook*, for a detailed description of the subject. Improvement in corrosion performance of a component or structure can be achieved through proper design, surface protection, proper material selection, or combinations of all three parameters. This Section of the Handbook will address weldability and material selection issues associated with nonferrous corrosion-resistant alloys.

Stainless steel, as its generic name implies, has been a traditional material employed to resist corrosion. However, some corrosion service is so harsh that even stainless steels do not perform adequately. In the chemical process industry, for example, the manufacture of phosphoric, acetic, hydrochloric, and sulfuric acids requires highly corrosion-resistant materials. A boiling 1% HCI solution, for example, can totally dissolve type 316 stainless steel during laboratory corrosion testing. For many applications, nickel-base alloys are called upon to resist certain severe corrosion environments.

Pure nickel has good resistance to reducing environment corrosion and is an excellent base upon which to build corrosion-resistant alloys. The atomic size, outer-shell electron configuration, and face-centered cubic (fcc) crystal structure of nickel make this element amenable to solid-solution alloying with elements such as iron, copper, chromium, tungsten, and molybdenum. Each of these alloying elements can contribute unique corrosion resistance to specific forms of corrosion attack, such as chloride pitting, galvanic corrosion, and stress-corrosion cracking. A wealth of empirical evidence and experience is available regarding the effects of alloying elements, individually and cumulatively, on corrosion resistance in aqueous environments (Ref 1).

Because industrial corrosion environments are diverse and complex, very few alloys can be expected to resist all forms of corrosion. Hence, numerous different nickel-base alloys have evolved over the last 50 years, each with a different combination of alloying elements to serve a particular niche in the corrosion market. It is not the intent of this Section to cover all nonferrous corrosion-resistant alloys on the market today. Rather, this Section has been organized into three different groupings of corrosion-resistant alloys; the information contained in these articles should also apply to similar alloys not listed. The first article addresses a family of materials that includes pure nickel, nickel-copper alloys, nickel-chromium alloys, and nickel-chromium-iron alloys. Monel and Inconel alloys are well-known members of this group of alloys. The next article addresses families of nickel-base alloys containing appreciable amounts of molybdenum. Molybdenum additions to nickel substantially improve resistance to nonoxidizing acid environments. Hastelloy alloys are typical of alloys belonging to this category of materials. In the last article, weldability and material selection issues associated with corrosion-resistant materials not based on nickel are discussed. These materials include cobalt-base corrosion-resistant alloys and commercially pure titanium, zirconium, and tantalum.

Reference

1. N. SRIDHAR, J.B.C. WU, AND P.E. MANNING, CORROSION RESISTANT NI-CR-MO ALLOYS, *J. MET.*, NOV 1985

Introduction to the Selection of Nonferrous Corrosion-Resistant Materials

S.J. Matthews, Haynes International, Inc.

Corrosion Performance

Information presented in these articles about corrosion performance should be treated as generalized claims. Potential material users are advised to seek actual laboratory corrosion data or field test experience from the material producer

before selecting alloys for actual use. When communicating with a corrosion material specialist for the purposes of selecting alloys, it is important to identify five environmental parameters:

- CHEMICAL NATURE OF THE AQUEOUS (OR GASEOUS) ENVIRONMENT, INCLUDING IMPURITIES
- TEMPERATURE
- PH
- HALIDE CONCENTRATION (THAT IS, PRESENCE OF CHLORIDE OR FLUORIDE IONS)
- REDOX POTENTIAL (IF KNOWN)

Redox potential refers to the electrolytic nature of the aqueous environment. It determines whether the system is "oxidizing" or "reducing" to the exposed material and has an important influence on proper material selection.

Introduction to the Selection of Nonferrous Corrosion-Resistant Materials

S.J. Matthews, Haynes International, Inc.

Reference

1. N. SRIDHAR, J.B.C. WU, AND P.E. MANNING, CORROSION RESISTANT NI-CR-MO ALLOYS, *J. MET.*, NOV 1985

Selection of Nickel, Nickel-Copper, Nickel-Chromium, and Nickel-Chromium-Iron Alloys

Donald J. Tillack, D.J. Tillack and Associates

Introduction

THE NICKEL-BASE FAMILY OF ALLOYS was developed in the early 1900s, and significant amounts of nickel began to be used in engineering materials in the 1920s. Although nickel was discovered by a Swedish scientist in 1751, them were no useful applications of the element until the late 1800s.

In nature, nickel is found in two basic forms: in lateritic deposits (as oxides) and in a nickel-sulfide ore. Usually, nickel is found in combination with copper and numerous other elements. The ratio of nickel to copper in these ore bodies is normally 2:1. Therefore, it is not too surprising that the first major alloy based on a nickel-containing ore was composed of 67% nickel and 33% copper. This is also the same composition, roughly, of Monel alloy 400, which was patented in 1906 and first melted and cast commercially in the United States in 1921 by the International Nickel Company. Subsequently, numerous alloys that could be used in a wide variety of applications were developed.

The Monel composition was used extensively in corrosion-resisting applications early in its history, because stainless steel had not yet been invented. Kitchen and food preparation equipment, in particular, were made from "Monel metal," because of its corrosion resistance, ease of cleaning, and attractive appearance.

The consumption of high-nickel-content corrosion-resistant alloys grow at an impressive rate during the postwar years. The cost of nickel alloys was high after World War I and high cost per unit weight continues to be a primary concern in the present use of these alloys. Although these alloys are more expensive than some other materials, their high performance generally makes them cost effective in the long run. Although the current annual consumption of nickel alloys is a small fraction of the steel consumption total, the numbers are still impressive. In 1990, it was estimated that the Western nations consumed approximately 40×10^9 g (89×10^6 lb) of solid-solution corrosion-resistant nickel, nickel-copper, nickel-chromium, and nickel-chromium-iron alloys. Most (85%) were wrought products.

Because of their relatively high cost, these alloys are usually only specified when lower-cost alloys are unable to withstand the environment or are not strong enough. Often, the combination of these two criteria is the reason that nickel alloys are specified. No other alloy system combines the qualities of strength, environmental resistance, weldability, formability, and availability more completely than the nickel-base alloy family.

The compositions of some of the popular, commercially available, solid-solution wrought nickel, nickel-copper, nickel-chromium, and nickel-chromium-iron alloys are given in Table 1. This list does not include the molybdenum-rich alloys nor the precipitation-hardened alloys. The former are covered in the article "Selection of Nickel-Base Corrosion-Resistant Alloys Containing Molybdenum" in this Section of the Volume. The latter are described in the Section "Selection of Nonferrous High-Temperature Materials" in this Volume.

TABLE 1 COMPOSITIONS OF SELECTED NICKEL-BASE CORROSION-RESISTANT ALLOYS

ALLOY	COMPOSITION, WT%								
	Ni	Cr	Fe	Cu	C0	Si	Al	Ti	Mo
NICKEL ALLOYS									
200	99.5	. . .	. . .	. . .	0.08	0.2	. . .	. . .	. . .
201	99.5	. . .	. . .	. . .	0.01	0.2	. . .	. . .	. . .
NICKEL-COPPER ALLOY									
400	66.5	. . .	. . .	31.5	0.15	0.2	. . .	. . .	. . .
NICKEL-CHROMIUM ALLOYS									
600	76.0	15.5	8	. . .	0.08	0.2	. . .	. . .	. . .
601	60.5	23	14	. . .	0.08	0.2	1.3	. . .	. . .
690	60.0	30	9.3	. . .	0.03	0.2	0.3	0.2	. . .
NICKEL-CHROMIUM-IRON ALLOYS									
800	32.5	21	46	. . .	0.05	0.5	0.3	0.3	. . .
825	42	21	30	. . .	0.03	0.2	0.1	0.9	3

The commercially pure nickel grades are used extensively in applications that utilize their corrosion resistance, such as caustic service areas and food handling equipment, and in applications that utilize their electronic or magnetic characteristics, such as transducers. Alloy 201 has a low carbon content and is used in applications above 315 °C (600 °F), where long time exposure would cause the precipitation of embrittling graphite in alloy 200.

The nickel-copper alloys are used extensively in seawater applications, because of their excellent resistance to corrosion, cavitation, and erosion. Other significant applications include their use in the presence of chlorinated solvents, sulfuric acid, and alkalies. Typical industrial applications include valves and pumps, propeller shafts, marine fixtures and fasteners, chemical processing equipment, process vessels and piping, and heat exchangers.

The nickel-chromium alloys are used in severely corrosive environments at elevated temperatures, as well as at lower temperatures. Typical applications include furnace muffles and retorts, carburizing baskets, nuclear reactor components, thermocouple protection tubes, radiant furnace tubes, and chemical and food processing equipment.

The nickel-chromium-iron alloys are typically used in oxidizing and carburizing applications because of their resistance to these environments and their high strength. Typical applications include furnace components, heat exchangers and process piping, electric range heating-element sheathing, extruded tubing for ethylene and steam methane reforming furnaces, and chemical processing equipment.

All of the nickel-base alloys are resistant to sigma formation (that is, a hard, brittle, non-magnetic intermetallic intermediate phase with a tetragonal crystal structure) and to stress-corrosion cracking. They are austenitic throughout the range of temperatures in which they are normally used. This metallurgical stability enables designers to specify these alloys with the confidence that exposure to service temperatures will not cause premature structural damage to the materials.

The nickel and nickel-copper alloys are generally easier to fabricate than steels of the same thickness. The nickel-chromium and nickel-chromium-iron alloys are stronger than most steels, but can be formed with modest changes in

technique. For example, their spring-back is greater, but if these alloys are overbent slightly more than normal, they can usually be formed on the same equipment that is used for steels. The nickel-base alloys can be work hardened more quickly than steels and require anneals more frequently during forming operations.

Selection of Nickel, Nickel-Copper, Nickel-Chromium, and Nickel-Chromium-Iron Alloys

Donald J. Tillack, D.J. Tillack and Associates

General Welding Characteristics

Thermal Conductivity. Nickel is quite conductive and copper is extremely conductive. However, the addition of chromium or iron decreases the thermal conductivity of nickel or nickel-copper. Conductivity, whether thermal or electrical, always decreases when the solvent accepts solute atoms, as in alloying. The data in Table 2 illustrate this fact. Note that nickel has a thermal conductivity value of 75 W/m · K (45 Btu/ft · h · °F) and copper (not shown in Table 2) has a value of 391 W/m · K (225 Btu/fi · h · °F), but alloy 400, which contains roughly two-thirds nickel and one-third copper, has a lower thermal conductivity value (22 W/m · K, or 13 Btu/ft · h · °F) than either nickel or copper.

TABLE 2 PROPERTIES OF SELECTED NICKEL-BASE CORROSION-RESISTANT ALLOYS

ALLOY	DENSITY, G/CM^3	MELTING RANGE		COEFFICIENT OF THERMAL EXPANSION(A), 10^{-6}/K	THERMAL CONDUCTIVITY		ELECTRICAL RESISTIVITY, 10^{-8} Ω/M
		°C	°F		W/M^2·K	BTU/FT^2 · H · °F	
1020 CARBON STEEL(B)	7.9	1470-1530	2680-2790	12	46	27	19
304 STAINLESS STEEL(B)	8.0	1390-1450	2535-2640	17	16	9.3	72
200	8.9	1435-1502	2615-2735	14	75	44	9
201	8.9	1435-1502	2615-2735	14	79	46	8
400	8.8	1299-1349	2370-2460	16	22	13	51
600	8.4	1354-1413	2470-2575	14	15	8.7	103
601	8.1	1301-1368	2375-2495	15	11	6.4	119
690	8.2	1343-1377	2450-2510	14	12	7	115
800	7.9	1357-1385	2475-2525	16	12	7	99
825	8.1	1371-1399	2500-2550	15	11	6.4	113

(A) IN RANGE FROM 20 TO 260 °C (68 TO 500 °F).

(B) DATA PROVIDED FOR PURPOSE OF COMPARISON

Thermal conductivity plays an important function during welding because it influences heat flow and the amount of heat required to melt material into the weld puddle. A base material composition with a high level of thermal conductivity will conduct heat away from the fusion zone and therefore requires slightly more heat input during welding than would an alloy with low thermal conductivity, which retains the local heat of welding for a longer time.

The nickel-base alloys vary considerably in their thermal conductivity characteristics. The nickel-chromium and nickel-chromium-iron alloys have values lower than those of both the carbon steels and the austenitic stainless steels, whereas nickel and the nickel-copper alloys have values considerably higher than those of the steels.

The electrical resistivity of a material is especially important in the welding process itself, because the melting rate of an electrode or wire is influenced by the electrical characteristics of the material (Table 2). Usually, solid-solution alloys are not very good electrical conductors because the solute and solvent atoms are of different sizes, which distorts the crystal lattice structure of the material and impedes the passage of electrons. The alloys that are composed primarily of one element, such as 1020 steel and nickel-base alloys 200 and 201, have the lowest electrical resistivity values of the alloys listed in Table 2.

The thermal expansion characteristics of a material are important because the heat that is applied to weld joints causes localized expansion and/or contraction during heating and/or cooling. A material with a greater thermal expansion value will expand and contract more during the welding operation, thus creating a greater amount of stress on the weld joint. This is particularly important when the weld deposit is marginally crack sensitive. It is also a consideration when dissimilar metals are welded together, especially when them is a large difference in expansion characteristics. The section "Dissimilar Welding" in this article provides more details on this topic. The nickel-base alloys have thermal expansion values that are between those of carbon steel and the austenitic stainless steels, as shown in Table 2.

Liquidus-Solidus Temperature. The cracking resistance of a material is often associated with the difference in the liquidus and solidus temperatures, particularly when stress is involved. When a highly restrained structure is welded, considerable stress is generated during the welding operation. If a material has a relatively large spread between its liquidus and solidus temperatures, then there is more time that the material is in a vulnerable situation in terms of cracking. However, a material with a relatively narrow liquidus-solidus range will cool down fairly rapidly through the temperature range, and there will be less time for stress-related cracking to occur. This example assumes that other factors that influence cracking, such as grain size or structural mass, are equal. Table 2 lists the liquidus-solidus temperatures, or melting ranges, of several solid-solution nickel alloys.

Selection of Nickel, Nickel-Copper, Nickel-Chromium, and Nickel-Chromium-Iron Alloys

Donald J. Tillack, D.J. Tillack and Associates

Welding Metallurgy

The heat-affected zone (HAZ) is discussed below in terms of grain boundary precipitation, grain growth, and hot cracking.

Grain Boundary Precipitation. Grain boundaries are the weak link in a microstructure that is exposed to elevated temperature, whether that exposure occurs during service or, in the case of welding, during the thermal cycles that are part of the welding operation. Precipitates that form in the grain boundaries can vary in size and composition and can be either harmful or beneficial. Intermetallic compounds, such as carbides, act as barriers to grain growth and can be very beneficial. Intergranular carbides in alloys 600 and 690 can also deter stress-corrosion cracking during high-purity water exposure in nuclear reactor steam generator primary side environments (Ref 1).

Grain Growth. Generally, it is easier to make defect-free welds in material with a relatively fine grain size, because there is less of an undesirable element concentration that contributes to grain boundary cracking in a fine-grain network. With larger grains, there are fewer grain boundaries and the deleterious elements are more concentrated in them. However, it is not always possible to have a fine-grain structure to weld. Most high-temperature applications, for example, need a large grain size material to ensure elevated-temperature creep and rupture strength.

Even when a fine-grain material is welded, grain growth will occur in the HAZ. The width of this grain growth band depends on numerous variables, such as the welding process used, the heat input and travel speed, and the heat transfer characteristics of the base material. The electron-beam (EB) welding process, for example, will produce a narrower HAZ and a smaller band of grain growth than the gas-metal arc welding (GMAW) process.

Hot Cracking. In terms of constitutional liquation, HAZ fissures are seldom a problem in the nickel or nickel-copper alloys, but they have been the subject of considerable study in nickel-chromium and nickel-chromium-iron alloys.

Such fissures have been observed in alloy 600, for example, when relatively high heat inputs puts (2.4 MJ/m, or 45×10^3 J/in., and higher) were used. These fissures are typically narrow, linear intergranular separations that are perpendicular to the direction of weld travel. Fissures have been found in the HAZ of welds made by the GMAW, gas-tungsten arc welding (GTAW), and EB welding processes. An example of a typical fissure found in a nickel-chromium HAZ is shown in Fig. 1.

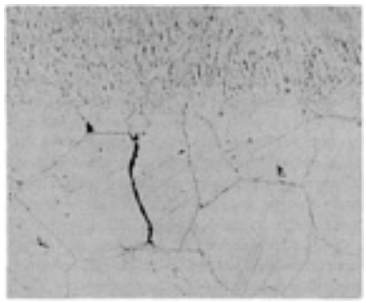

FIG. 1 PHOTOMICROGRAPH SHOWING A HEAT-AFFECTED ZONE MICROFISSURE IN A NICKEL-CHROMIUM ALLOY. SPECIMEN IS A GMAW 44.4 MM (1.75 IN.) PLATE. ELECTROLYTIC PHOSPHORIC ACID ETCHANT, 75×

Grain boundary liquation is one of the proposed mechanisms that causes fissuring (Ref 2). Grain boundary liquation occurs when a phase or particle causes the grain boundary to melt at a temperature below the bulk melting point. Because the liquated grain boundary has practically no strength, separation at the liquated grain boundary can occur, causing the fissure.

Constitutional liquation was proposed as a mechanism for hot cracking by Savage in 1959 and was described in detail in subsequent papers (Ref 3). In this theory, a relatively stable second-phase particle begins to dissolve during nonequilibrium, or rapid, heating and forms an intermediate phase with the matrix, which has a solidus temperature that is lower than that of either the second-phase particle or the matrix. In alloy 600, some experimenters have identified the precipitation of Cr_7C_3 at the grain boundary as the second-phase particle around which constitutional liquation occurs.

Chemical segregation at a grain boundary can also cause grain boundary liquation. Boron and sulfur are two elements that form lower melting point eutectics that can contribute to HAZ fissuring. Manganese segregation in alloy 600 has been identified as forming a binary compound (Mn-38Ni) with a 1000 °C (1832 °F) solidus temperature, which is considerably below the bulk melting range of the alloy.

Several approaches can be made to minimize the occurrence of HAZ fissuring, including the control of:

- HEAT INPUT DURING WELDING
- MICROSTRUCTURE, TO OBTAIN FAIRLY SMALL GRAIN SIZES
- CHEMISTRY, TO MINIMIZE THE AMOUNT OF DELETERIOUS MINOR ELEMENTS THAT ARE KNOWN TO CONTRIBUTE TO FISSURING

There are many minor elements that can contribute to HAZ fissuring in nickel-base alloys, including some that are intentionally added to enhance properties. Although these elements are considered minor because they are present in small amounts, they are far from being minor in their effect on fissuring. These elements include, but are not limited to, sulfur, phosphorus, lead, boron, zirconium, tin, zinc, selenium, tellurium, antimony, bismuth, silver, and gold. Boron and zirconium are two elements that are intentionally added to nickel-base alloys to enhance hot workability and elevated-temperature strength, but they can be detrimental during welding operations. More details on the effects of many of these elements are provided later in this article.

The fusion zone of autogenous welds is discussed below in terms of sensitivity to porosity formation, hot-cracking susceptibility, and microsegregation.

In terms of sensitivity to porosity, the nickel-base alloys can be divided into two groups: those that contain chromium and those that do not. Chromium has a natural affinity for the gases that form during the welding operation, notably oxygen, nitrogen, and hydrogen. Because the nickel and nickel-copper alloys lack chromium, they are sensitive to porosity formation during autogenous welding. Therefore, the protection of the weld puddle during melting and solidification is critical to the achievement of porosity-free autogenous welds in these two alloy classes. Dry torch gases and adequate gas protection are necessities. Although the use of filler metals helps in porosity control, because of the additions of gas-absorbing elements such as titanium and aluminum, proper precautions are still necessary.

Porosity control is much easier in the nickel-chromium and nickel-chromium-iron alloys because of their high chromium levels. This is not meant to imply that gas coverage is not important when autogenously welding the chromium-containing alloys, but it certainly is not as critical, compared with nickel and nickel-copper alloys.

Hot-Cracking Susceptibility. Hot cracking, or fissuring, is a grain boundary related mechanism that can occur, primarily, in the nickel-chromium and nickel-chromium-iron families of alloys. Although the nickel and nickel-copper alloys are not immune to this phenomenon, there have been more occurrences in the chromium-bearing nickel-base alloy materials.

A study of the weldability of alloy 800 (Ref 4) found that reducing the aluminum plus titanium content to extremely low levels (<0.06%) essentially eliminated hot cracking. It was noted that when normal levels of these elements were present, segregation of titanium and aluminum resulted in grain-boundary embrittlement and banding that was sufficiently severe to exhibit liquation during heating through a weld cycle. There also appeared to be a strong association between sulfur and titanium in the discrete inclusions observed in sulfur-bearing alloys.

Microsegregation. When a weld solidifies, an inhomogeneous dendritic structure forms. Solidification begins with the highest-melting-point liquid and continues until the whole structure is solid. A condition called microsegregation, or coring, occurs during this solidification process, and areas of the solidified microstructure can have great differences in composition. This becomes a problem in corrosion situations where an alloy was chosen for its particular resistance to corrosion. For example, because the dendritic weld material can have vastly different chromium and molybdenum levels, preferential corrosion may initiate and propagate at those areas of the microstructure that are lean in the element responsible for providing the corrosion resistance.

Microsegregation cannot be eliminated in a weld, but it can be minimized by judicious selection of welding parameters, such as the control of heat input. High-temperature heat treatments for several hours can partially equalize the composition gradients by diffusion. Cold working the weld structure, followed by annealing, can also break down this microsegregation, if the component lends itself to this type of treatment. Thin-sheet welds can be planished, for example. In addition to improving the corrosion resistance of the welds, cold working and annealing the weld area also increases weld ductility. Figure 2 illustrates how a dendritic weld structure can be reduced by cold working and annealing. After a 20% cold reduction followed by an anneal, the cast structure of the weld has been refined substantially and the wrought grain structure can be seen easily.

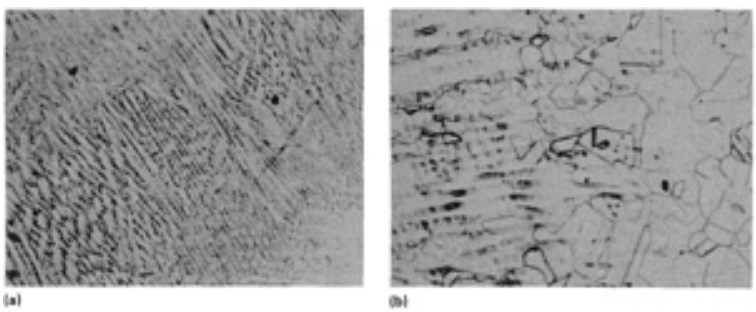

FIG. 2 MICROSTRUCTURES OF ALLOY 400 (UNS N04400) WELDED WITH FILLER METAL 60. (A) AS WELDED; CYANIDE PERSULFATE ETCHANT, 70×. (B) WELDED, PLUS 20% COLD REDUCTION, PLUS ANNEAL AT 871 °C (1600 °F)/2 H; CYANIDE PERSULFATE ETCHANT, 150×. SOURCE: REF 5

Unmixed Zone. For many years, it was assumed that there was complete mixing in the weld pool and that the composition of a fusion weld was homogeneous throughout. Now it is known that there are areas adjacent to the fusion line where mixing does not occur. This unmixed zone has been the subject of considerable research and is of concern to corrosion engineers because of the adverse effect that a cast base-metal structure can have on weld-associated corrosion. These zones are base material undiluted by filler metal and are, essentially, narrow bands of autogenous welds situated on the fusion line. Figure 3 shows an unmixed zone (Ref 6). There is a greater tendency for unmixed zones to be present in nickel-base welds, compared with steel and stainless steel welds. The sluggish nature of the molten nickel alloy weld metal tends to deter complete mixing during welding.

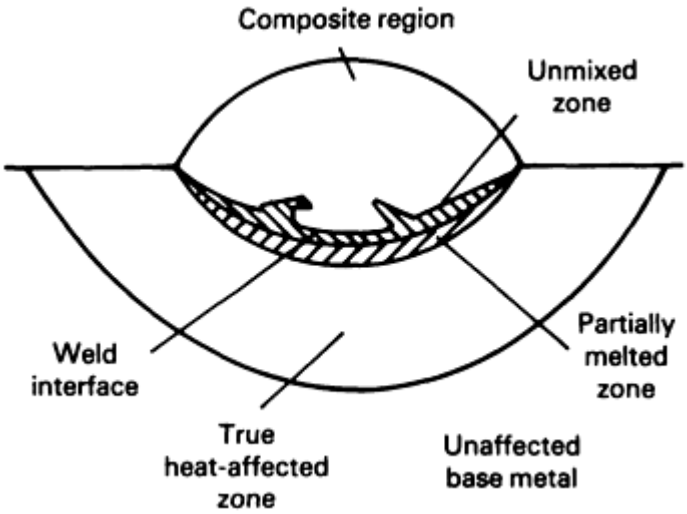

FIG. 3 SCHEMATIC SHOWING LOCATION OF UNMIXED ZONE IN A SOLIDIFIED WELDMENT. SOURCE: REF 6

These unmixed zones can be reduced or practically eliminated by controlling the welding procedures to ensure adequate mixing of the weld pool during welding. As an example, excessively fast travel speed promotes the formation of these zones. Slowing the travel speed and adjusting the other welding parameters to compensate for the slower travel speed will do a great deal to minimize the formation of unmixed zones.

The effects of alloying elements on the weldability of nickel-base alloys are described below.

Copper forms a complete series of solid-solution alloys with nickel and has little effect on the weldability of nickel. Metallurgically, the binary high-nickel-content alloys that contain from 15 to 40% Cu behave much like commercially pure nickel when welded. The nickel-copper alloys have about the same susceptibility to embrittlement by elements such as sulfur as does commercially pure nickel. The need for alloying to control gaseous porosity is not significantly reduced in the nickel-copper alloys, compared to that required for commercially pure nickel. As copper is increased up to the range of the copper-nickel alloys, such as 70Cu-30Ni and 80Cu-20Ni, the alloy behaves more like a copper alloy and reduced amounts of deoxidizers can be used. The presence of copper changes the high-temperature solubility of carbon to the point where graphitization is not encountered.

The chromium addition in alloys of commercial importance does not exceed the limit of solid-solution alloys and presents an attractively narrow freezing range. Chromium has the ability to form stable oxides and nitrides, which in turn greatly reduce the tendency for weld porosity, compared to that encountered in commercially pure nickel and nickel-copper welds. The chromium-bearing alloys are more susceptible than other high-nickel-content alloys to hot cracking when other elements, notably silicon, are present. For example, the hot-cracking susceptibility of a nickel-base weld metal containing 15% Cr is sharply increased as silicon increases from a few tenths of a percent to 1% and higher, whereas levels on the order of 1% Si are relatively innocuous in nickel and nickel-copper alloys.

Iron is commonly present in the nickel-chromium alloys, such as alloy 600, in amounts up to 8 wt%. It is not intended to enhance mechanical properties or weldability, but is added as a ferroalloy, along with other additives, and helps keep the cost of these alloys down. Up to this level, iron is not believed to appreciably effect welding behavior. As the amount of iron increases to the composition range of nickel-chromium-iron alloys (such as alloy 800, which contains about 46% Fe),

the alloy becomes increasingly hot-crack sensitive. When steel is melted into a high-nickel-content alloy weld, such as in an overlay or in dissimilar metal welding, there is some reason to believe that residual elements such as sulfur and phosphorus, which are normally present in more abundant quantities in steel than in nickel-base alloys, are more damaging to the properties of the weld than the iron itself.

Carbon is usually present in nickel and high-nickel-content weld metals in amounts ranging from 0.01 to 0.15 or 0.20%. The effect of carbon is a major concern with commercially pure nickel. The limit of carbon solubility in the temperature range from 371 to 649 °C (700 to 1200 °F) is about 0.02 to 0.03%. During welding, any graphitic carbon present in the HAZ is dissolved and held in a super-saturated solution as the metal rapidly cools. Subsequent exposure to the temperature range from 371 to 649 °C (700 to 1200 °F) causes carbon to precipitate in the form of intergranular graphite. Unwelded high-carbon commercially pure nickel would be similarly embrittled in this temperature range by carbon migration to the grain boundaries, but it would require a much longer time. Therefore, when the wrought commercially pure alloys are to be used at temperatures above 371 °C (700 °F), a maximum of 0.02% carbon is used, as in alloy 201. In weld metal, titanium is added to tie carbon up in the form of titanium carbide, thus preventing the formation of graphitic carbon.

In the nickel-base alloys, copper alters solubility to the point where graphitic embrittlement is not encountered up to carbon levels of 0.15 to 0.20%. The carbon content in nickel-copper alloys does have an effect on hot-cracking tendencies when iron is present. For example, nickel-copper alloys with over 0.20% C can tolerate only about 5% Fe; hot cracking may result at higher levels. Low-carbon nickel-copper alloys with less than 0.10% C can tolerate up to about 30 wt% Fe.

In nickel-chromium alloys, carbon combines with chromium to form chromium carbides, unless titanium or columbium are present to form their respective carbides. Although chromium depletion may occur in the HAZ of welds, as it does with the iron-base alloys in the absence of titanium or columbium, it is only in extremely corrosive media that corrosion resistance is impaired.

Manganese was considered to be relatively unimportant to welding metallurgy for many years. It is now well established that in both the nickel-chromium and nickel-copper alloys, manganese is beneficial in minimizing fissuring and in preventing hot cracking in welds of heavy sections, as well as in cases where excessive iron dilution may be encountered. Additions of up to 9 wt% Mn have been used in some commercially available welding electrodes.

Magnesium in wrought materials forms a stable high-melting-point magnesium sulfide preferentially to the extremely low-melting-point nickel-nickel sulfide eutectic. In welding, magnesium in the base metal serves to prevent hot cracking in the HAZ.

Silicon may be present in nickel-base alloys in amounts ranging from 0.01% to 4.0%. However, it is generally considered to have an adverse effect on welding because it increases the tendency for hot cracking. Therefore, wrought materials generally have less than 1% Si. The adverse behavior is associated with a eutectic melting that is more damaging to weld metal than to base metal. Pure nickel is most resistant, followed by nickel-copper alloys. Nickel-chromium alloys are the least resistant to the effects of silicon.

Both titanium and aluminum can be added to the weld metal and the base material to promote age hardening. In smaller amounts, the addition of titanium to nickel and nonchromium-bearing nickel-base alloys helps control gas porosity. Aluminum is added to wrought alloys as a deoxidizer. If substantial amounts of titanium and aluminum are added, the sensitivity of the weld metal to hot cracking increases.

Boron amounts that range from 0.003 to 0.10% improve the high-temperature mechanical properties of certain wrought and cast nickel-base alloys. These alloys are usually intended for elevated-temperature service, where grain boundary strengths are enhanced by boron additions. Unfortunately, boron contents of 0.03% or higher have a grossly damaging effect on weldability. At higher boron levels, the weld metal and HAZ are extremely hot-crack sensitive and considerable care must be exercised with respect to heat input and stress levels.

Zirconium acts similarly to boron in nickel-base alloys by promoting hot cracking in the weld metal and HAZ. However, the tolerance for zirconium is somewhat higher than it is for boron.

Sulfur is perhaps the most damaging of all elements that are involved in the welding metallurgy of nickel and high-nickel-content alloys. Sulfur is particularly damaging to nickel because of its extremely limited solid solubility and because of a nickel-nickel sulfide eutectic reaction that occurs at 649 °C (1200 °F).

Sulfur is different from most other elements that adversely affect weldability because it affects both the HAZ and the weld metal. Penetration occurs at the weld HAZ area that is heated above a threshold temperature while being in contact with sulfur-bearing material. The threshold temperature varies from 316 °C (600 °F) for pure nickel to about 649 °C (1200 °F) for chromium-bearing alloys. Magnesium and manganese are alloying additions that are used to control the effects of sulfur. Unusual diligence is required when handling the nickel-base alloys to avoid contamination from sulfur-containing compounds, which can include such commonly used materials as machining lubricants, marking crayons, temperature-indicating sticks, and shop dirt. Figure 4 shows the type of cracking that can occur when a sheet of alloy 200 is wiped with a dirty cloth containing sulfur compounds and then welded.

FIG. 4 SULFUR EMBRITTLEMENT OF A JOINT IN ALLOY 200 (UNS N02200). PRIOR TO WELDING, THE CRACKED SIDE OF JOINT WAS WIPED WITH DIRTY CLOTH ON WHICH SULFUR-CONTAINING RESIDUE HAD ACCUMULATED.

Lead causes hot shortness in high-nickel-content weld metal at about the same level as sulfur does. The metallurgical explanation of the subversive effect of lead is very similar to that of sulfur. In practice, lead contamination is less common than sulfur contamination, but probably only because there are fewer common sources of lead-containing contaminants in fabricating shops than there are sources of sulfur-containing contaminants.

Phosphorus can exhibit an effect similar to lead and sulfur in high-nickel-content weld metals. The solubility of phosphorus is quite limited and undergoes a eutectic reaction at about 871 °C (1600 °F). Severe weld metal cracking has been attributed to as little as a few hundredths of a percent of phosphorus.

References cited in this section

1. J.M. SARVER, J.R. CRUM, AND W.L. MANKINS, "CARBIDE PRECIPITATION AND THE EFFECT ON THERMAL TREATMENTS ON THE STRESS CORROSION CRACKING BEHAVIOUR OF INCONEL ALLOY 690," PAPER PRESENTED AT CORROSION '87, NACE, 1987
2. B.B. WEISS, G.E. ROTKE, AND R. STICKLER, PHYSICAL METALLURGY OF HOT DUCTILITY TESTING, *WELD. J.,* OCT 1970, P 471S-422S
3. W.F. SAVAGE AND J.J. PEPE, EFFECTS OF CONSTITUTIONAL LIQUATION IN 18-NI MARAGING STEEL WELDMENTS, *WELD. J.,* SEPT 1967, P 411S-422S
4. D.A. CANONICO, W.F. SAVAGE, W.J. WERNER, AND G.M. GOODWIN, EFFECTS OF MINOR ADDITIONS ON WELDABILITY OF INCOLOY 800, PROC. *WELDING RESEARCH COUNCIL SYMPOSIUM ON EFFECTS OF MINOR ELEMENTS ON THE WELDABILITY OF HIGH-NICKEL ALLOYS,* WELDING RESEARCH COUNCIL, OCT 1967
5. "WELDING TECHNICAL BULLETIN," INCO ALLOYS INTERNATIONAL, JULY 1991, P 29
6. W.F. SAVAGE, WELDMENTS, PHYSICAL METALLURGY AND FAILURE PHENOMENA, *PROC. FIFTH BOLTON LANDING CONF.,* AUG 1978, P 16

Donald J. Tillack, D.J. Tillack and Associates

Postweld Heat Treatment

Postweld heat treatments are usually not required for the non-precipitation-hardenable nickel and nickel-base alloy weldments. For example, the ASME boiler and pressure vessel code for unfired pressure vessels does not require postweld heat treatment, except as agreed upon between the user and the manufacturer. However, a dissimilar weldment between a nickel-base alloy and a steel is postweld heat treated because the steel side of the joint requires it. In this case, the heat treatment will normally have little consequence on the nickel-base alloy. Table 3 lists the typical annealing temperatures for many of the solid-solution nickel-base alloys.

TABLE 3 TYPICAL ANNEALING TEMPERATURES FOR CORROSION-RESISTANT NICKEL, NICKEL-COPPER, NICKEL-CHROMIUM, AND NICKEL-CHROMIUM-IRON ALLOYS

All alloys air cooled or water quenched

ALLOY	UNS NO.	TEMPERATURE[A]	
		°C	°F
200	N02200	830-871	1525-1600
201	N02201	830-871	1525-1600
400	N04400	871	1600
600	N06600	925-1040	1700-1900
601	N06601	1175	2150
690	. . .	1040	1900
800	N08800	1010-1175	1850-2150
825	N08825	940	1725

(A) ±14 °C (±25 °F)

In certain environments, it has been beneficial to perform a postweld heat treatment on some of the nickel-base alloy weldments. Alloys 200, 201, and 600 receive this treatment for caustic service applications, as does alloy 400 for hydrofluoric acid service applications. The recommended heat treatment procedures for these materials in these service environments are given in Table 4.

TABLE 4 RECOMMENDED HEAT TREATMENT PROCEDURES FOR SELECTED NICKEL-BASE CORROSION-RESISTANT ALLOYS

ALLOYS 200 AND 201 FOR CAUSTIC SERVICE
1. HOLD AT 704 °C (1300 °F) FOR A MINIMUM OF 0.5 H/25.4 MM (L IN.) OF THICKNESS
2. DETERMINE THE HEATING AND COOLING RATES, WHICH WILL VARY WITH THE SHAPE OF THE PART. COMPLEX SHAPES WITH NONUNIFORM THICKNESSES SHOULD HAVE HEATING AND COOLING RATES OF 111 °C (200 °F)/H. SHAPES WITH UNIFORM THICKNESSES CAN USE FAST HEATING AND AIR COOLING
ALLOY 600 FOR CAUSTIC SERVICE
1. HOLD AT 899 °C (1650 °F) FOR A MINIMUM OF I H/25.4 MM (1 IN.) OF THICKNESS OR AT 788 °C (1450 °F) FOR A MINIMUM OF 4 H/25.4 MM (1 IN.) OF THICKNESS
2. DETERMINE HEATING AND COOLING RATES PER GUIDELINES FOR ALLOYS 200 AND 201
ALLOY 400 FOR HYDROFLUORIC ACID SERVICE
1. HOLD AT 593 °C (1100 °F) FOR A MINIMUM OF 0.5 H/25.4 MM (1 IN.) OF THICKNESS
2. DETERMINE HEATING AND COOLING RATES PER GUIDELINES FOR ALLOYS 200 AND 201

Although determining the rates of heating and cooling after postweld heat treating is seldom a problem with the solid-solution nickel-base alloys, the cooling rate should generally be at least as fast as the rate of an air cool. When there are

large differences in cross-sectional areas in a welded structure, the heating and cooling rates may have to be controlled in order to minimize the distortion that might occur with a rapid rate of heating or cooling. Such structures could experience enough distortion to cause fit-up or assembly problems, particularly if a too-rapid cooling rate causes excessive stresses that are due to the mass differences in the structure.

The usual precautions regarding furnace atmosphere and temperature control should be followed when postweld heat treating these alloys. Because cracking caused by contaminants is always a concern, all surfaces should be thoroughly cleaned prior to being postweld heat treated.

Special Metallurgical Welding Considerations

Dissimilar welding of plate-to-plate, clad, and weld overlay cladding specimens are described below.

Plate-to-Plate. There can be drastic consequences related to complex metallurgical considerations when butt welding plates of different composition. The composition of the weld deposit is controlled not only by the filler metal, but by the amount of dilution from the two base metals. Many different dissimilar-metal combinations are possible, and the amount of dilution varies with the welding process, the operator technique, and the joint design.

In many cases, more than one welding product will satisfy the requirement of metallurgical compatibility. Selection should be based on the strength required, service environment, or the cost of the welding product. Table 5 lists the recommended filler metals to use when welding numerous dissimilar metal combinations.

TABLE 5 WELDING PRODUCTS FOR DISSIMILAR-METAL JOINTS BETWEEN NICKEL-BASE CORROSION-RESISTANT ALLOYS AND OTHER METALS

NICKEL-BASE ALLOY	WELDING PRODUCT FOR DISSIMILAR-METAL JOINT WITH									
	STAINLESS STEEL		CARBON AND LOW-ALLOY STEEL		5-9% NI STEEL		COPPER		NICKEL-COPPER	
	ELECTRODE	FILLER METAL	ELECTRODE	FILLER METAL	ELECTRODE	FILLER METAL	ELECTRODE	FILLER METAL	ELECTRODE	FILLER METAL
200, 201	ENICRFE-2 (LNCO WELD A)	ERNICR-3 (FM 82)	ENICRFE-2 (LNCO WELD A)	ERNICR-3 (FM 82)	ERNICRFE-2 (LNCO WELD A)	ERNICR-3 (FM 82)	ENICU-7 (WE 190)	ERNICU-7 (FM 60)	ENICU-7 (WE 190)	ERNICU-7 (FM 60)
400	ENICRFE-2 (INCO WELD A)	ERNICR-3 (FM 82)	ENICU-7 (WE 190)	ERNI-1 (FM 61)	ENICU-7 (WE 190)	ERNI-1 (FM 61)	ENICU-7 (WE 190)	ERNICU-7 (FM 60)	ENICU-7 (WE 190)	ERNICU-7 (FM 60)
600, 601	ENICRFE-2 (INCO WELD A)	ERNICR-3 (FM 82)	ENICRFE-2 (INCO WELD A)	ERNICR-3 (FM 82)	ENICRFE-2 (INCO WELD A)	ERNICR-3 (FM 82)	ENI-1 (WE 741)	ERNI-1 (FM 61)	ENI-1 (WE 141)	ERNI-1 (FM 61)
690	ENICRFE-2 (INCO WELD A)	ERNICR-3 (FM 82)	ENICRFE-2 (INCO WELD A)	ERNICR-3 (FM 82)	ENICRFE-2 (INCO WELD A)	ERNICR-3 (FM 82)	ENI-1[(A)] (WE 141)	ERNI-1[(A)] (FM 61)	ENI-1[(A)] (WE 141)	ERNI-1[(A)] (FM 61)
800	ENICRFE-2 (INCO WELD A)	ERNICR-3 (FM 82)	ENICRFE-2 (INCO WELD A)	ERNICR-3 (FM 82)	ENICRFE-2 (INCO WELD A)	ERNICR-3 (FM 82)	ENI-1 (WE 141)	ERNI-1 (FM 61)	ENI-1 (WE 141)	ERNI-1 (FM 61)
825	ENICRMO-3 (WE 112)	ERNICRMO-3 (FM 625)	ENICRMO-3 (WE 112)	ERNICRMO-3 (FM 625)	(WE 113)	ERNICRMO-3 (FM 625)	ENI-1 (WE 141)	ERNI-1 (FM 61)	ENI-1 (WE 141)	ERNI-1 (FM 61)

(A) PRECAUTION IS REQUIRED TO MINIMIZE COPPER DILUTION IN THE WELD, BECAUSE OF THE HIGH CHROMIUM LEVEL OF ALLOY 690. "BUTTERING" THE COPPER OR COPPER-NICKEL SIDE OF THE JOINT WITH NICKEL WELD METAL PRIOR TO WELDING MAY BE ADVISABLE.

The selection of the welding product involves extra considerations when dissimilar materials are being welded. In addition to dilution factors, the thermal expansion of the two metals being joined and of the filler metal should be reviewed in order to achieve a weld that will not fail prematurely.

In the power industry, for example, an austenitic stainless steel and a low-alloy steel represent a common joint. The expansion rate of the stainless steel side is higher than that of the low-alloy side (see Table 2). If this joint were welded with a stainless steel electrode, then both the weld and the stainless steel side of the joint would expand and contract during heating and cooling at the same rate, thus putting stress on the low-alloy side of the weld. Because the low-alloy steel has less strength than the stainless steel, the shifting of stress to this side of the joint is undesirable and could lead to premature fatigue or stress failure.

On the other hand, if a nickel-base alloy filler metal were used to weld this combination, both the weld and the low-alloy side of the joint would expand and contract together during temperature swings in the service environment and any stresses induced would be shifted to the stainless steel side of the joint, which is stronger than the low-alloy side. This would result in a longer service life for this weld.

Clad Material. Most clad specimens consist of a highly alloyed material, such as a nickel-base alloy, clad to a less-expensive material, usually steel. The nickel-base alloy provides corrosion resistance, whereas the steel, which usually constitutes at least 80% of the total thickness, provides backing strength and reduced costs. Because clad steels are frequently joined by welding, it is important to ensure that any weld joint surface that is exposed to corrosive media is at least as corrosion resistant as the cladding. This requirement influences both joint design and welding technique.

Butt joints should be used whenever possible. Figure 5 shows recommended designs for two thickness ranges. Both designs include a small edge of unbeveled steel above the cladding to protect the cladding when the steel is welded. The steel side should be welded first, using a low-hydrogen welding product. It is important to avoid cladding penetration during the first welding pass. Dilution of the steel weld with the nickel-alloy cladding can cause the deposit to crack. The clad side of the joint should be prepared by grinding or chipping, and it should be welded using the welding product that is recommended for solid sections of the cladding alloy. The weld metal will be diluted with steel. To maintain corrosion resistance, at least two layers should be applied, although three or more layers are preferable.

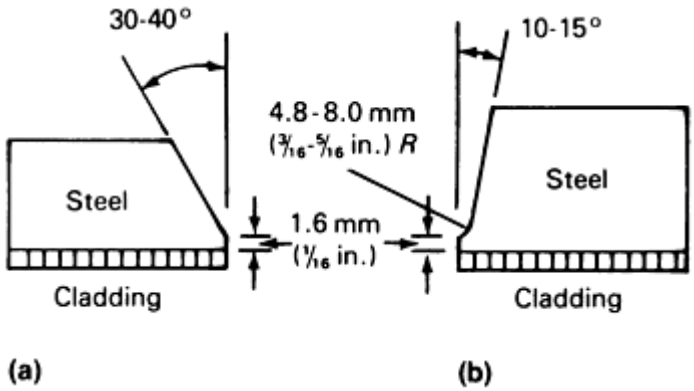

FIG. 5 JOINT DESIGNS FOR CLAD STEEL. (A) MATERIAL OF 4.8 TO 16 MM ($\frac{3}{16}$ TO $\frac{5}{8}$ IN.) THICKNESS. (B) MATERIAL OF 16 TO 25 MM ($\frac{5}{8}$ TO 1 IN.) THICKNESS. SOURCE: REF 7

The strip-back method is sometimes used instead of the procedure described above. The cladding is removed from the vicinity of the joint, as shown in Fig. 6. The remaining steel is then welded using a standard steel joint design and technique, and the nickel-alloy cladding is reapplied by weld overlaying. The advantage of the strip-back method is that it eliminates the possibility of cracking caused by steel weld metal penetration into the cladding (Ref 7).

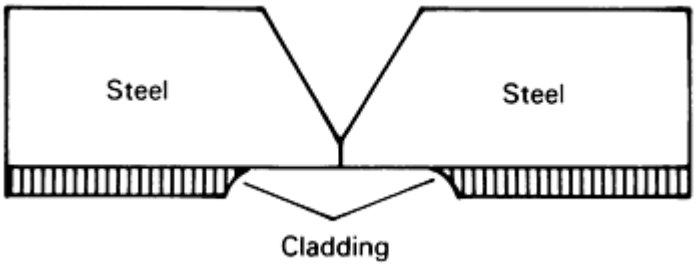

FIG. 6 STRIP-BACK METHOD OF JOINT PREPARATION. SOURCE: REF 7

Some joints, such as those in closed vessels or tubular products, are accessible only from the steel side. In such cases, a standard steel joint design is used, and the cladding at the bottom of the joint is welded first with nickel-base alloy weld metal. After the cladding is welded, the joint can either be completed with nickel-base alloy weld metal or a barrier layer of carbon-free iron can be applied and the joint completed with steel weld metal. If the steel thickness is 8.0 mm ($\frac{5}{16}$ in.) or less, it is generally more economical to complete the joint with nickel-base alloy weld metal.

Weld Overlay Cladding. Nickel-base alloy weld metals are readily applied as overlays on carbon steels, low-alloy steels, and other materials. The cleanliness of the surface to be overlaid is extremely important. All oxides and foreign materials must be removed prior to welding to ensure crack-free results and to minimize the possibility of oxide inclusions in the deposited weld metal. If the material being overlaid has a high sulfur or phosphorus content, then cracking is possible in the deposited nickel-base alloy weld layer. If this occurs, then the cracked layer should be ground or machined away and another layer deposited.

This sacrificial layer approach is just one solution to this situation. Other approaches would be to deposit the first layer with a more-tolerant weld metal composition or, if possible, to design the structure with a lower sulfur/phosphorus base material. Using a welding process and welding parameters that minimize dilution also is very helpful in avoiding problems in this type of situation.

Welding of Castings. Many of the wrought solid-solution nickel alloys discussed in this article have equivalent cast compositions that are modified slightly to enhance castability and properties. The largest modification usually is the increase in silicon content, which unfortunately has an adverse effect on weldability. It is not unusual to find silicon levels that exceed 1.5% in cast nickel-base alloys. Depending on other influences, such as restraint, amount of other minor elements, and the welding process used, this level of silicon may result in weld cracking. When welding surface defects that occurred during the casting process, which is a common welding procedure with castings, most welding methods can be used with most of the solid-solution nickel-base alloy castings.

Repair Welding. The solid-solution nickel-base alloy system does not undergo drastic metallurgical changes during either thermal cycling or exposure to commonly encountered service temperatures, as do many of the ferrous alloys. This is a definite benefit when it becomes necessary to repair weld a component. Except for exposure to surface-modifying environments, such as carburization, nickel-base alloys generally retain their excellent weldability, even after prolonged service exposure. In those cases where a general condition renders a component unusable, such as overall carburization or oxidation attack, very little can be done to repair weld the part. However, if a localized area fails, then there usually is a good chance that a repair weld can salvage the component.

There are occasions when a carburized area is the site of a failure, and if the carburization was not the primary reason for the failure, then sometimes the localized area can be ground free of the carburized layer and a successful repair weld made. If the carburization did-cause the failure, then localized repair welding would probably result in only a short extension of component life, because failure in another area of the carburized surface would undoubtedly occur quickly. This example illustrates how inspection and examination of the component is an important aspect when deciding whether or not to make a weld repair. Once the decision has been made that repair welding is feasible, an area of the component should be ground clean and a test weld made to determine whether the material can be successfully welded. If this test is positive, then the component should be thoroughly prepared by grinding the surface, if necessary, and cleaning it prior to

actual repair welding. If groove welding is necessary, then the previously described precautions concerning joint design should be followed in order to provide room for electrode manipulation.

Reference cited in this section

7. "WELDING TECHNICAL BULLETIN," INCO ALLOYS INTERNATIONAL, JULY 1991, P 23

Selection of Nickel, Nickel-Copper, Nickel-Chromium, and Nickel-Chromium-Iron Alloys

Donald J. Tillack, D.J. Tillack and Associates

References

1. J.M. SARVER, J.R. CRUM, AND W.L. MANKINS, "CARBIDE PRECIPITATION AND THE EFFECT ON THERMAL TREATMENTS ON THE STRESS CORROSION CRACKING BEHAVIOUR OF INCONEL ALLOY 690," PAPER PRESENTED AT CORROSION '87, NACE, 1987
2. B.B. WEISS, G.E. ROTKE, AND R. STICKLER, PHYSICAL METALLURGY OF HOT DUCTILITY TESTING, *WELD. J.*, OCT 1970, P 471S-422S
3. W.F. SAVAGE AND J.J. PEPE, EFFECTS OF CONSTITUTIONAL LIQUATION IN 18-NI MARAGING STEEL WELDMENTS, *WELD. J.*, SEPT 1967, P 411S-422S
4. D.A. CANONICO, W.F. SAVAGE, W.J. WERNER, AND G.M. GOODWIN, EFFECTS OF MINOR ADDITIONS ON WELDABILITY OF INCOLOY 800, PROC. *WELDING RESEARCH COUNCIL SYMPOSIUM ON EFFECTS OF MINOR ELEMENTS ON THE WELDABILITY OF HIGH-NICKEL ALLOYS*, WELDING RESEARCH COUNCIL, OCT 1967
5. "WELDING TECHNICAL BULLETIN," INCO ALLOYS INTERNATIONAL, JULY 1991, P 29
6. W.F. SAVAGE, WELDMENTS, PHYSICAL METALLURGY AND FAILURE PHENOMENA, *PROC. FIFTH BOLTON LANDING CONF.*, AUG 1978, P 16
7. "WELDING TECHNICAL BULLETIN," INCO ALLOYS INTERNATIONAL, JULY 1991, P 23

Selection of Nickel-Base Corrosion-Resistant Alloys Containing Molybdenum

S.J. Matthews, Haynes International, Inc.

Introduction

THE FAMILY OF nickel-base corrosion-resistant (CR) alloys containing molybdenum are described in this article both in terms of a historical perspective and an alloy utilization viewpoint. Table 1 gives the nominal chemical compositions of the most widely used materials in this family, but is not all inclusive. Although other molybdenum-bearing nickel-base alloys exist, the information presented below is relative to the joining of similar alloys.

TABLE 1 NOMINAL COMPOSITION OF SELECTED MOLYBDENUM-BEARING NICKEL-BASE CORROSION-RESISTANT ALLOYS

ALLOY TYPE	ALLOY	UNS NO.	COMPOSITION, WT %										
			Ni	Co	Fe	Cr	Mo	W	Mn	Si	C	Cu	OTHERS
NI-MO	B-2	N10665	69	1 MAX	2 MAX	1 MAX	28	. . .	1 MAX	0.1 MAX	0.01 MAX	. . .	. . .
LOW C,	C-4	N06455	65	2	3	16	16	. . .	1	0.08	0.01	. . .	0.7 TI

NI-MO-CR				MAX	MAX				MAX	MAX	MAX		MAX
	C-22	N06022	56	2.5 MAX	3	22	13	3	0.5 MAX	0.08 MAX	0.010	. . .	0.35 V MAX
	C-276	N10276	57	2.5 MAX	5	16	16	4	1	0.08 MAX	0.01 MAX	. . .	0.35 V MAX
	G-3	N06985	44	5 MAX	19.5	22	7	1.5 MAX	1 MAX	1 MAX	0.015 MAX	2.5	0.5 NB MAX
NI-CR-FE-MO-CU	G-30	N06030	43	5 MAX	15	30	5.5	2.5	1.5 MAX	1 MAX	0.03 MAX	2	1.5 NB MAX
NI-MO-CR-FE	N	N10003	71	0.2 MAX	5 MAX	7	16	0.5 MAX	0.8 MAX	1 MAX	0.08 MAX	0.35 MAX	0.5 (AL + TI) MAX

Alloy C Family. Hastelloy alloy C, developed in the early 1930s, is the grandfather of the nickel-chromium-molybdenum family of corrosion-resistant materials. Advances in process metallurgy and corrosion research has prompted the evolution of various C-type alloys. The minimum carbon content of the original alloy C composition was limited to about 0.05% C by the arc melting practices of the time.

The nickel-chromium-molybdenum alloys proved to be extremely important in the chemical processing industry, because they provided corrosion resistance over a wide range of reducing and oxidizing environments. However, grain boundary precipitation of carbides in the as-welded condition required a postweld solution heat treatment to restore optimum corrosion resistance. The deleterious effect of both carbon and silicon on corrosion resistance led to the development of alloy C-276.

An important factor in this new alloy was the development of a reliable quantitative method for determining susceptibility to intergranular attack in the original C-type alloy and the newer C-276 and C-4 alloys (Ref 1). The introduction of the argon-oxygen decarburization (AOD) process in the late 1960s made the production of alloy C-276 commercially viable. The maximum carbon content of alloy C-276 is 0.01% C with typical production compositions of about 0.005% C (Ref 2). Unfortunately, the optimum corrosion resistance of alloy C-276 was found to be hampered by the precipitation of an intermetallic compound rich in molybdenum and tungsten. The alloy is particularly susceptible to μ-phase formation when exposed to temperatures ranging from 650 to 1095 °C (1200 to 2000 °F).

Advances in alloy development theory, specifically the concept of electron vacancy number (N_v), led to the evolution of alloy C-4 in 1975. Alloy C-4 is essentially a tungsten-free, low-carbon, low-silicon ternary alloy of nickel, chromium, and molybdenum. Secondary carbide precipitation was further controlled by the addition of titanium to stabilize residual carbon that was not totally removed by AOD refining. Unfortunately, the removal of tungsten in order to reduce μ-phase precipitation also reduced the resistance of the alloy to localized corrosion attack, namely pitting and crevice corrosion (Ref 2).

A relatively recent (1985) development in the alloy C family is alloy C-22. Because it was recognized that molybdenum and tungsten had an opposing role to chromium in reducing versus oxidizing acid environments, alloy C-22 was developed with the proper balance of both elements to achieve versatility in a wide range of corrosive environments. The reduction of the molybdenum and tungsten content in alloy C-22, versus alloy C-276, also resulted in improved thermal stability (that is, resistance to intermetallic compound formation). An example of an alloy C-type application is in the lining of inlet and outlet ducts that are associated with the flue gas desulfurization (FGD) systems being installed by electric power utility companies.

Alloy B Family. Hastelloy alloy B-2 is unique in that it contains essentially no chromium, an element common to nearly all other CR alloys (Ref 3). It was originally developed to resist hydrochloric acid in all concentrations up to the boiling point and is used in many applications involving the production of this acid, as well as acetic acid and other chemicals. The alloy also resists sulfuric acid and pure phosphoric acid. Without chromium, however, this alloy is vulnerable to corrosion attack in reducing acids when oxidizing salts such as ferric or cupric chloride are present, even in the parts-per-million range.

Not unlike the old alloy C, which required postweld heat treatment to restore optimum corrosion properties, alloy B (the predecessor to alloy B-2) was improved by the evolution of a low-carbon (0.02% C maximum) and low-silicon version (0.08% Si maximum). Alloy B-2 is close to being a commercially "pure" binary alloy of nickel and molybdenum. It has a face-centered cubic (fcc) crystal structure and is quite ductile in the solution-annealed condition (that is, 60% room-temperature tensile elongation). However, the alloy forms intermetallic phases, Ni_3Mo and Ni_4Mo, with modest exposure

to the intermediate temperature range from 595 to 850 °C (1100 to 1560 °F). Precipitation of these intermetallic compounds can render alloy B-2 quite brittle. For example, its room-temperature ductility can drop to less than 5% elongation if it is exposed to 760 °C (1400 °F) for a period of 10 min.

A third-generation B-type alloy has recently been developed. Its composition was specially formulated to provide improved thermal stability while retaining the corrosion resistance of alloy B-2. This means that the reaction kinetics that drive the formation of Ni_3Mo and Ni_4Mo have been significantly retarded, greatly improving the fabricability of this family of alloys.

The alloy G family of alloys has excellent resistance to phosphoric acid and has been used in wet-process phosphoric acid evaporators, agitator shafts, pumps, and in the handling of superphosphoric acid (76% P_2O_5). Alloys G-3 and G-30 are newer versions of predecessor alloy G. Alloy G-3 is a lower-carbon version (0.015% C maximum versus 0.05% C maximum) and, hence, has improved resistance to heat-affected zone (HAZ) carbide precipitation. Improved resistance to hot cracking and improved weld metal bend ductility were also achieved by reducing the niobium plus tantalum content from nominally 2.0% (alloy G) to 0.5% maximum (alloy G-3). Alloy G-30 is a high-chromium (30% Cr) alloy designed to possess even greater resistance to HAZ corrosion attack. Recognizing that the phenomenon of sensitization involves not only the type and amount of HAZ precipitation, but also the depleted zones associated with the precipitates, the resistance of alloy G-30 to HAZ corrosion degradation is achieved by higher available chromium, even in the depleted zones. Alloy G-30 resists highly oxidizing acids such as the nitric plus hydrofluoric acid mixtures used in metal pickling baths and in nuclear waste reprocessing.

References

1. M.A. STREICHER, THE RELATIONSHIP OF HEAT TREATMENT AND MICROSTRUCTURE TO CORROSION RESISTANCE IN WROUGHT NI-CR-MO ALLOYS, *CORROSION*, VOL 19, 1963, P 272T-284T
2. M.A. STREICHER, THE EFFECT OF COMPOSITION AND STRUCTURE ON CREVICE, INTERGRANULAR, AND STRESS CORROSION OF SOME WROUGHT NI-CR-MO ALLOYS, *CORROSION,* VOL 32, 1976, P 79-93
3. A.I. ASPHAHANI AND F.G. HODGE, NICKEL-BASE MOLYBDENUM-CONTAINING ALLOYS FOR THE CHEMICAL PROCESS INDUSTRY, *ALLOYS FOR THE EIGHTIES,* R.Q. BARR, ED., CLIMAX MOLYBDENUM CO., 1980

Selection of Nickel-Base Corrosion-Resistant Alloys Containing Molybdenum

S.J. Matthews, Haynes International, Inc.

General Welding Characteristics

Because of similarities in heat capacity, density, and other physical properties, the welding characteristics of the alloys described in this article are quite similar to austenitic stainless steels. The major differences between these alloys and stainless steel are lower thermal expansion, lower thermal conductivity, and higher electrical resistivity. Generally, solidus temperatures are about 55 °C (100 °F) lower than type 304 stainless. Table 2 summarizes the comparative physical properties relevant to welding and joining operations.

TABLE 2 PHYSICAL PROPERTIES OF NICKEL-BASE MOLYBDENUM-BEARING CORROSION-RESISTANT ALLOYS RELATIVE TO CARBON STEEL AND STAINLESS STEELS

MATERIAL	MELTING TEMPERATURE RANGE	DENSITY	THERMAL CONDUCTIVITY	COEFFICIENT OF THERMAL EXPANSION	ELECTRICAL RESISTIVITY, $10^{-8}\Omega \cdot M$

	°C	°F	g/cm^3	$lb/in.^3$	w/m · k	$btu\ in./ft^2 \cdot h \cdot °f$	$10^{-6}/K$	$10^{-6}/°F$	
CARBON STEEL	1470-1530	2670-2785	7.9	0.285	0.46	3.2	11.7	6.51	19
AUSTENITIC STAINLESS STEEL	1390-1450	2535-2640	8.0	0.289	0.16	1.1	17.0	9.45	72
NICKEL-BASE CORROSION-RESISTANT ALLOYS									
ALLOY B-2	1350-1390	2460-2535	9.2	0.332	0.11	0.76	10.3	5.73	137
ALLOY C-22	1350-1390	2460-2535	8.7	0.314	0.10	0.69	12.4	6.89	114
ALLOY G-30	1300-1350	2370-2460	8.2	0.296	0.10	0.69	12.8	7.12	116

Welding Processes. Gas-tungsten arc welding (GTAW), gas-metal arc welding (GMAW), and shielded metal arc welding (SMAW) processes are commonly used to join this family of CR alloys.

A filler metal that matches the composition of the base material is usually recommended when welding the nickel-chromium-molybdenum CR alloys. Other processes, such as plasma arc welding (PAW), resistance spot welding (RSW), laser-beam welding (LBW), electron-beam welding (EBW), and friction welding, can be used. The plasma arc cutting process is commonly used to cut alloy plate into desired shapes and to prepare weld angles. Oxyacetylene cutting is not recommended, nor is the use of oxyacetylene welding (OAW) and submerged arc welding (SAW). Oxyacetylene welding is not recommended because of the possibility of carbon pickup from the flame, whereas submerged arc welding is not recommended because of its high heat input, chromium loss across the arc, and silicon pickup from the welding flux.

Generally, welding heat input is controlled in the low-to-moderate range. Wide weave beads are not recommended. Stringer bead welding techniques, with some electrode manipulation, are preferred. The nickel-chromium-molybdenum alloy weld metal is not as fluid as carbon steel and does not flow out as readily to "wet" the sidewalls. Therefore, the welding arc and filler metal must be manipulated so as to place the molten metal where it is needed. In addition to sluggishness, the penetration pattern of this alloy type is less than that of a typical carbon or stainless steel weld, and incomplete fusion is more likely to occur. Therefore, care must be taken to ensure that the groove opening is wide enough to allow proper torch or electrode manipulation and proper placement of the weld bead.

Cleaning, Edge Preparation, and Fit-Up. Proper penetration of the weld angles is a very important part of welding these nickel-base CR alloys. It is necessary to condition all thermal cut edges to bright, shiny metal prior to welding. This is particularly important if air arc gouging is being used, because of the possibility of carbon pickup from the carbon electrode.

In addition to the weld angle, a 25 mm (1 in.) wide band on both the top and bottom (face and root) surface of the weld zone should be conditioned to bright metal with about an 80-grit flapper wheel or disk. This procedure is particularly important for the SMAW of alloy B-2. If the mill scale is not removed, then the B-2 alloy welding flux can interact with it and cause cracking at the toe of the weld in the base material.

The welding surface and adjacent regions should be thoroughly cleaned with an appropriate solvent prior to any welding operation. All greases, oils, cutting oils, crayon marks, machining solutions, corrosion products, paints, scale, dye-penetrant solutions, and other foreign matter should be completely removed.

Stainless steel wire brushing is normally sufficient for interpass cleaning of GTAW and GMAW weldments. The grinding of starts and stops is recommended for all fusion welding processes. When the GMAW process is used, light grinding may be necessary between passes prior to wire brushing, depending on the composition of the shielding gas. Slag removal during SMAW will require chipping and grinding, followed by wire brushing.

Preheating the nickel-molybdenum and nickel-chromium-molybdenum alloys is not required. A preheat is generally specified as room temperature (typical shop conditions). Interpass temperature should be maintained below 95 °C (200 °F). Auxiliary cooling methods can be used to control the interpass temperature. Water quenching is acceptable. However, care must be taken to avoid contaminating the weld zone with traces of oil from shop air lines, grit/dirt from soiled water-soaked rags, or mineral deposits from hard water used to cool the weld joint. The safest way to maintain a low interpass temperature is to allow the assembly to cool naturally. When attaching hardware to the outside of a thin-walled vessel, it is good practice to provide auxiliary cooling to the inside (process side) to minimize the extent of the HAZ.

Selection of Nickel-Base Corrosion-Resistant Alloys Containing Molybdenum

S.J. Matthews, Haynes International, Inc.

Welding Metallurgy

Heat-Affected Zone. The phenomenon of HAZ grain boundary sensitization is addressed in the article "Selection of Austenitic Stainless Steels" in this Volume. However, it should be noted here that the solid solubility of carbon is considerably lower in nickel-base alloys than in stainless steels. The net effect is that during the welding of low-carbon nickel-molybdenum and nickel-chromium-molybdenum CR alloys, HAZ grain boundary precipitation is still a potential reality, despite the relatively low carbon content of these alloys. The amount and severity of precipitation will depend on the cooling rate through the intermediate temperature range from 1000 to 600 °C (1830 to 1110 °F). Some heat-to-heat variations in grain boundary precipitation have also been observed during simulated HAZ studies in alloy B-2 (Ref 4). The adverse effects of minor grain boundary precipitation depend on the severity of the corrosive environment. For example, the maximum corrosion penetration after testing in boiling 10% hydrochloric acid (HCl) varied little for simulated heat-affected zones in alloy B-2. However, when harsher autoclave testing environments were used (20% HCl at 150 °C, or 300 °F), penetration by corrosion increased as the simulated HAZ cooling rate decreased from 20 to 120 s through the critical intermediate temperature range (Ref 4). Despite these laboratory findings, most low-carbon nickel-molybdenum and nickel-chromium-molybdenum alloys have been put into corrosion service in the as-welded condition with good results. Occasionally, poor results are encountered. Metallographic examination of the corroded part will usually reveal evidence of grain boundary precipitation in the heat-affected zone (Fig. 1).

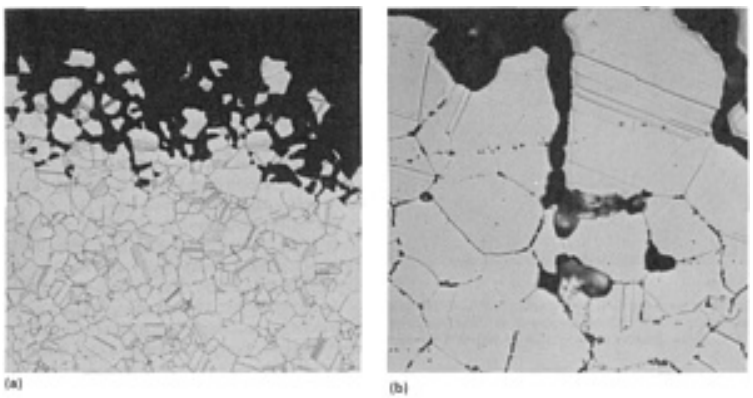

FIG. 1 PHOTOMICROGRAPHS SHOWING CORROSION ATTACK IN HASTELLOY C-276 (UNS N10276) CAUSED BY GRAIN BOUNDARY PRECIPITATION IN THE HEAT-AFFECTED ZONE OF THE WELD. THE SAMPLE WAS TAKEN FROM A PIPE REMOVED AFTER 18 MONTHS OF SERVICE IN A HYDROCHLORIC ACID VAPOR ENVIRONMENT IN A CHEMICAL PLANT. SAMPLE WAS ETCHED IN HCL AND OXALIC ACID. (A) 75×. (B) 375×

Aside from the possibility of grain growth, few other metallurgical HAZ problems have been reported for these alloys. HAZ hot cracking, especially of the type created by constitutional liquation of primary carbide particles, is not a problem with these alloys.

Fusion zone welding metallurgy of the nickel-molybdenum and nickel-chromium-molybdenum alloy family is important, because base materials are usually welded with filler metals of matching composition and because these alloys can be welded autogeneously (no filler added), as in the case of welded tubular products. Three issues should be considered in terms of the fusion zone:

- EFFECT OF WELD METAL SEGREGATION ON CORROSION RESISTANCE
- PROPENSITY TO FORM POROSITY
- SOLIDIFICATION HOT-CRACK SENSITIVITY

Segregation. Because of the segregation of solute elements upon solidification (principally molybdenum, which segregates to the cellular dendritic boundaries of the fusion zone), it is generally accepted that the corrosion resistance of the weld metal will be marginally less than that of the more homogeneous wrought base material. Differences in corrosion performance, however, depend heavily on the severity of the corrosion environment. In mild corrosion environments, little difference is observed. In severe environments, the fusion zone may be preferentially attacked, as illustrated in Fig. 2, a cross section of an as-welded alloy B-2 coupon exposed for about 1 year in a chemical plant process stream. Figure 3(a) is a high-magnification view of the surface attack on alloy B-2 weld metal when tested for 96 h in 20% HCl at 150 °C (300 °F) in an autoclave. Under these conditions, corrosion attack appears to be the most aggressive at the dendrite cores (molybdenum lean). Figure 3(b) shows the lack of corrosion attack on weld metal from a specially devised overalloyed B-type filler material (Ref 5). This alloy consists of 42% Mo, rather than the nominal 28% Mo. The higher-molybdenum nickel alloy solidifies as a nonequilibrium hypoeutectic structure consisting of a metastable α phase, with Ni_3Mo and NiMo in the interdendritic regions. In this case, despite solidification segregation, the dendrite core regions are sufficiently saturated with molybdenum to resist preferential fusion zone attack.

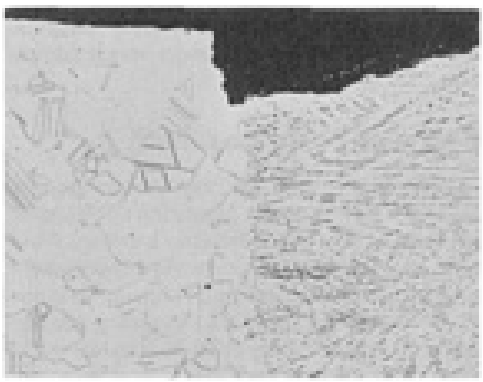

FIG. 2 METALLOGRAPHIC CROSS SECTION SHOWING PREFERENTIAL FUSION ZONE ATTACK IN HASTELLOY B-2 (UNS N10665). SAMPLE WAS A WELDED COUPON PLACED IN A CHEMICAL PLANT PROCESS STREAM FOR APPROXIMATELY 1 YEAR. HYDROCHLORIC AND CHROMIC ACID ETCH. 75×

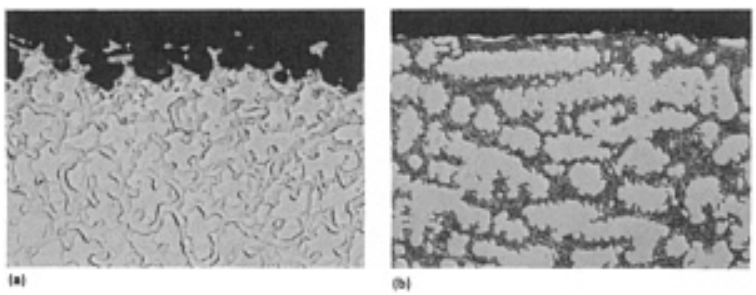

FIG. 3 METALLOGRAPHIC CROSS SECTIONS OF THE CORRODED SURFACE OF WELD DEPOSITS ON HASTELLOY B-2 (UNS N10665) AFTER TESTING IN AN AUTOCLAVE AT 150 °C (300 °F) FOR 96 H IN A 20% HCL ENVIRONMENT. (A) NI-28MO (UNS N10665) ALLOY FILLER METAL. 375×. (B) NI-42MO FILLER METAL. 375×. BOTH SAMPLES WERE ETCHED IN HYDROCHLORIC AND CHROMIC ACID. SEE TEXT FOR EXPLANATION.

It should be noted that although the microstructure of the Ni-42Mo material in Fig. 3(b) offers high corrosion resistance, the alloy is characterized by limited weld ductility (Ref 6). However, the use of overalloyed filler metals as a solution to preferential weld metal corrosion attack has been demonstrated elsewhere. For example, alloy C-22 (22% Cr) has been used successfully to refurbish corroded welds in an alloy C-276 (16% Cr) pulp and paper mill bleach-mixing device. Alloy G-30 (30% Cr) is also a logical choice as an overalloyed filler for certain alloy G-3 components.

Porosity. Recognizing that the solubility of gas is greater in the liquid state than in the solid state, the subject of weld porosity is relevant to fusion zone discussion. The three most logical origins of gas-generated porosity are carbon monoxide, hydrogen, and nitrogen. However, in welding the low-carbon nickel-molybdenum and nickel-chromium-molybdenum alloys, the cause of porosity is not believed to be from the formation of carbon monoxide. As long as there is a residual silicon or aluminum content in the weld deposit, the oxygen potential is too low for the formation of carbon monoxide. In order to produce a carbon monoxide "carbon boil" during welding, it would be necessary first to deplete all the aluminum, silicon, and any other deoxidizers that may be present.

Gas hole formation can be caused by hydrogen evolution. As is well known, even the smallest amount of water will be reduced by metal deoxidizers, releasing a sufficient volume of gas to create porosity. Hydrocarbons can also dissociate and go into solution. The lower the carbon content of the alloy, the more likely it is to pick up hydrogen from hydrocarbons. These reactions are favored as the carbon content of the alloy decreases. Gas hole formation that is due to hydrogen can be minimized by the well-known methods of keeping the joint area and the weld filler metal dry and oil-free. This approach is especially true when welding with coated electrodes. The ceramic coating ingredients can absorb sufficient moisture in humid weather to cause potential problems. It is because of this behavior that unused electrodes should be stored in a warm oven (110 °C, or 230 °F, minimum).

The third and only other possible cause of gas hole formation is nitrogen. As is well documented in the literature, a large quantity of nitrogen is capable of being picked up by the molten metal during arc welding processes whenever the gas in the arc contains any nitrogen. Nitrogen pickup from air, for example, might prove to be a problem whenever the weld pool is improperly shielded. Different alloys would be expected to have different susceptibilities to nitrogen-induced porosity. The ability of the solidified matrix plus secondary solid phases to hold or carry nitrogen is the primary difference between alloys. Alloys with a greater nitrogen-carrying capacity are apparently less susceptible to nitrogen-induced porosity. For example, a nickel-chromium alloy would be less susceptible to nitrogen porosity than pure nickel because of the increased solubility of nitrogen. Furthermore, because alloy B-2 contains no chromium, it possesses a lower nitrogen solubility than alloy C-22, and, thus, would be more prone to nitrogen porosity.

Hot-Crack Sensitivity. The final fusion zone issue is hot-crack sensitivity. Hot cracking of C-type alloys during solidification has been studied in depth by researchers equipped with sophisticated microanalysis equipment (Ref 7). Solidification hot cracking, as generated by the varestraint hot-cracking device, was found to increase as the tendency to form intermetallic secondary solidification constituents increased. In terms of general weldability ranking, alloy C-4 was found to be the least sensitive to solidification cracking, followed by alloy C-22, and then alloy C-276. It should be noted that all of the low-carbon nickel-chromium-molybdenum alloys of the C family are characterized by high weld metal ductility. Hot-cracking problems have rarely been reported under actual fabrication conditions.

References cited in this section

4. S.J. MATTHEWS, SIMULATED HEAT-AFFECTED ZONE STUDIES OF HASTELLOY ALLOY B-2, *WELD. J. RES. SUPPL.*, MARCH 1979
5. A.I. ASPHAHANI AND S.J. MATTHEWS, "HIGH MOLYBDENUM NICKEL-BASE ALLOY," U.S. PATENT 4,846,885, 11 JULY 1989
6. E.M. HORN, P. MATTERN, H. SCHLECKE, J. KORKHAUS, A.I. ASPHAHANI, AND S.J. MATTHEWS, HASTELLOY ALLOY B-42 WELD OVERLAY WELDING, *WERKST. KORROS.*, VOL 43, 1992, P 396-401
7. M.J. CIESLAK, T.J. HEADLEY, AND J. ROMIG, THE WELDING METALLURGY OF HASTELLOY ALLOYS C-4, C-22, AND C-276, *METALL. TRANS. A*, VOL 17A, NOV 1986, P 2035-2047

S.J. Matthews, Haynes International, Inc.

Postweld Heat Treatment

Because of their very low carbon contents (<0.02% C), the newer-generation CR alloys do not require heat treatment after welding. However, for certain critical corrosion environments, proper postweld annealing will maximize corrosion resistance of the HAZ. Annealing can also be performed to reduce residual stresses, which play a role in the susceptibility to stress-corrosion cracking in some environments. Annealing can be used to increase the corrosion resistance of the weld fusion zone by promoting diffusion of some elements.

Corrosion-resistant alloys are usually supplied in the mill-annealed condition, unless otherwise specified. The mill-annealing procedure has been designed to place the material in the optimum condition with respect to ductility and corrosion resistance. During fabrication of a vessel or component, several operations or conditions may require an anneal. For example, following any hot-forming operation, a reanneal of the material should be done to restore ductility and corrosion properties. Annealing is also performed after cold working to restore ductility. Generally, annealing is not required if the total cold work is below 7% outer fiber elongation. In general, the only heat treatment that is acceptable for these alloys is a full solution anneal. Table 3 lists the proper heat-treating temperatures and type of quench. Intermediate temperatures commonly used for stress-relieving steels, stainless steels, and other alloys are not effective and could promote precipitation that would be detrimental to corrosion resistance.

TABLE 3 SOLUTION ANNEALING TEMPERATURES FOR CORROSION-RESISTANT NICKEL-BASE ALLOYS CONTAINING MOLYBDENUM

Data are applicable for either water quench (WQ) or rapid air cool (RAC) quench.

ALLOY	UNS NO.	TEMPERATURE	
		°C ± 14°	°F ± 25°
B-2	N10665	1065	1950
C-4	N06455	1065	1950
C-22	N06022	1120	2050
C-276	N10276	1120	2150
G-3	N06905	1150	2100
G-30	N06030	1175	2150
N	N10003	1175	2150

Before heat treatment, grease, graphite, and other foreign materials must be removed from all surfaces. Tube products may require special care for complete removal of these contaminants from interior surfaces. Carburization of these materials at the heat-treating temperatures can reduce corrosion resistance, and sulfur embrittlement can cause severe cracking. Proper control of the temperature and time cycle are also critical. A flexible set of rules governing soaking-annealing time is generally followed, because of the many variations in furnace type, furnace operation, facilities for loading and unloading the furnace, and so on. The temperature should be monitored using thermocouples attached to the piece being annealed. The actual holding time should begin to be measured when the entire section is at the specified annealing temperature. It is important to remember that the center of a section does not reach the solutioning temperature as soon as the surface.

Normally, hold time should be in the range from 10 to 30 min, depending on section thickness. Thin-sheet components are held at the shorter time, whereas heavier sections are held at the longer time. Shorter annealing times can be used if the sole purpose is to remove the effect of cold work. Longer annealing times might be required if the objective is to promote homogenization of the fusion zone.

Rapid cooling is essential after solution heat treatment to prevent the precipitation of secondary phases and the resultant lowering of the corrosion resistance of these alloys. Water quenching is recommended on material thicker than 9.5 mm

($\frac{3}{8}$ in.). Although rapid air cooling can be used on sections thinner than 9.5 mm ($\frac{3}{8}$ in.), water quenching is preferred. The time from the furnace to the quench tank or to the start of rapid air cooling must be as short as possible (less than 3 min).

The requirements for proper annealing of alloy B-2 (UNS 10665) are quite demanding. In addition to the guidelines established above, the following factors should be considered very carefully. It is strongly recommended that the part being heat treated be charged into a furnace that is at the annealing temperature, and that the heating rate be as fast as possible. In addition, the thermal capacity of the furnace should be large to allow the temperature of the furnace to recover quickly after the part is charged into it. These steps are designed to shorten the time in the intermediate temperature range from 595 to 815 °C (1100 to 1500 °F). Extended exposure (greater than 15 min) at these intermediate temperatures can cause intergranular cracking because of phase transformations, especially if the part is in the cold-worked condition. Under certain conditions, shot peening prior to heat treatment may be beneficial to the elimination of residual tensile stresses. For example, it has been observed that shot peening the knuckle radius and straight flange regions of a cold-formed head prior to heat treatment can help reduce intermediate temperature intergranular cracking by lowering the residual stress patterns at the surface of the cold-formed component.

Other Welding Situations

Welding of dissimilar metals to nickel-base CR alloys does not present a problem in most cases. The nature of nickel as a "forgiving" solvent element renders most industrially encountered dissimilar metal combinations as metallurgically compatible. Filler materials designed to join the nickel-base side of the joint are usually recommended.

When joining a nickel-base alloy to a ferrous alloy (for example, mild steel or a stainless steel), electrodes of the nickel-base alloy should be used as filler metal, rather than steel or stainless electrodes, because excess superheat caused by melting temperature differences (Table 2) will tend to aggravate the HAZ on the nickel-base side of the joint.

The joining of clad plate (that is, steel plate that has been explosion clad or roll clad with a thinner nickel-base CR alloy) has been successfully performed. However, proper welding procedures need to be developed to ensure minimum iron dilution in the weld zone facing the corrosion environment.

The welding of cast CR alloys presents no unusual problems, as long as the integrity of the casting is sound (that is, free from shrinkage cavity and inclusions). Welding is often used to repair casting defects. Generally, the defective area is thoroughly removed by grinding, which eventually forms a cavity. The prepared cavity should be dye-penetrant inspected to ensure that all objectionable defects have been removed and then thoroughly cleaned prior to welding repair. Because these alloys have low-penetration characteristics, the ground cavity must be broad enough and have sufficient sidewall clearance in the weld groove to allow weld rod/weld bead manipulation. It is not recommended to heal cracks or wash out defects by autogeneously remelting weld beads or by depositing additional filler metal over the defect.

Repair welding of wrought alloy components and structures is accomplished using a similar technique. The good thermal stability of low-carbon CR alloys is such that solution annealing of material that has been in corrosion service for many years is generally not required prior to repair welding. In these situations, the repair is usually required because of accelerated corrosion of a localized area. The selection of higher-alloyed filler metals for such repairs should be considered.

Selection of Nickel-Base Corrosion-Resistant Alloys Containing Molybdenum

S.J. Matthews, Haynes International, Inc.

References

1. M.A. STREICHER, THE RELATIONSHIP OF HEAT TREATMENT AND MICROSTRUCTURE TO CORROSION RESISTANCE IN WROUGHT NI-CR-MO ALLOYS, *CORROSION,* VOL 19, 1963, P 272T-284T
2. M.A. STREICHER, THE EFFECT OF COMPOSITION AND STRUCTURE ON CREVICE, INTERGRANULAR, AND STRESS CORROSION OF SOME WROUGHT NI-CR-MO ALLOYS, *CORROSION,* VOL 32, 1976, P 79-93
3. A.I. ASPHAHANI AND F.G. HODGE, NICKEL-BASE MOLYBDENUM-CONTAINING ALLOYS FOR THE CHEMICAL PROCESS INDUSTRY, *ALLOYS FOR THE EIGHTIES,* R.Q. BARR, ED., CLIMAX MOLYBDENUM CO., 1980
4. S.J. MATTHEWS, SIMULATED HEAT-AFFECTED ZONE STUDIES OF HASTELLOY ALLOY B-2, *WELD. J. RES. SUPPL.,* MARCH 1979
5. A.I. ASPHAHANI AND S.J. MATTHEWS, "HIGH MOLYBDENUM NICKEL-BASE ALLOY," U.S. PATENT 4,846,885, 11 JULY 1989
6. E.M. HORN, P. MATTERN, H. SCHLECKE, J. KORKHAUS, A.I. ASPHAHANI, AND S.J. MATTHEWS, HASTELLOY ALLOY B-42 WELD OVERLAY WELDING, *WERKST. KORROS.,* VOL 43, 1992, P 396-401
7. M.J. CIESLAK, T.J. HEADLEY, AND J. ROMIG, THE WELDING METALLURGY OF HASTELLOY ALLOYS C-4, C-22, AND C-276, *METALL. TRANS. A,* VOL 17A, NOV 1986, P 2035-2047

Selection of Nickel-Base Corrosion-Resistant Alloys Containing Molybdenum

S.J. Matthews, Haynes International, Inc.

Selected References

• P.E. MANNING, J.D. SMITH, AND J.L. NICKERSON, NEW VERSATILE ALLOYS FOR THE CHEMICAL PROCESS INDUSTRY, *MATER. SELECT. DES.,* JUNE 1988, P 67-73

Selection of Cobalt-, Titanium-, Zirconium-, and Tantalum-Base Corrosion-Resistant Alloys

S.J. Matthews, Haynes International, Inc.

Introduction

A GREAT VARIETY of nonferrous corrosion-resistant (CR) alloys are available in the market. The common nickel-base corrosion-resistant alloys are covered in the preceding articles in this Section of the Handbook. This article will provide information about non-nickel-base alloys; however, no attempt will be made here to cover all such materials. The interested reader is referred to *Corrosion,* Volume 13 of the *ASM Handbook,* for information on the corrosion of specific alloy systems. The four corrosion-resistant materials of commercial significance that are briefly addressed here are based on:

- COBALT
- COMMERCIALLY PURE TITANIUM
- ZIRCONIUM
- TANTALUM

S.J. Matthews, Haynes International, Inc.

Cobalt-Base CR Alloys

Cobalt behaves much like nickel in terms of active-passive behavior in aqueous corrosion systems. Chromium additions reportedly are more effective in imparting passivity to cobalt than to nickel (Ref 1). Cobalt-chromium CR alloys typically contain sufficient additions of nickel or iron, which serve to stabilize the face-centered cubic (fcc) crystal structure and increase the stacking, fault energy of the fcc phase. Molybdenum and tungsten additions act as solid-solution strengtheners and enhance the corrosion resistance of cobalt-base alloys in nonoxidizing media. Cobalt-base CR alloys have been used in the pulp and paper, agrichemical, and chemical process industries in applications such as valves, pumps, nozzles, screw conveyors, and other components that are characterized by harsh environments aggravated by both corrosion and wear. Electrogalvanizing rolls are an example of a component exposed to both of these conditions. Cobalt-base CR alloys represent the premium materials for this application. The nominal composition of some cobalt-base corrosion-resistant alloys are given in Table 1.

TABLE 1 NOMINAL COMPOSITION OF SELECTED COBALT-BASE CORROSION-RESISTANT ALLOYS

ALLOY	UNS NO.	COMPOSITION, WT %							
		CO	Cr	Ni	Fe	Mo	W	C	N
ULTIMET	R31233	BAL	26	9	3	5	2	0.06	0.08
ALLOY 25	R30605	BAL	20	10	3 MAX	. . .	15	0.10	. . .
ALLOY 150	. . .	BAL	28	. . .	21	. . .	. . .	0.05 MAX	. . .
MP35-N MULTIPHASE	R30035	BAL	20	35	. . .	10	. . .	. . .	. . .

Weldability Characteristics. The fusion-welding characteristics of fcc-stabilized cobalt-base alloys are virtually identical to those of nickel-base alloys, because of similarities in melting range and physical properties. The only welding procedural idiosyncrasy of cobalt-base alloys relative to nickel is the potential for heat-affected zone (HAZ) cracking caused by copper surface contamination. Even minuscule amounts of copper inadvertently transferred to the surface of a sheet or plate will cause cracking if the contaminated surface corresponds to a HAZ of a subsequent weld (Ref 2). Cracking is caused by liquid-metal embrittlement (LME). Copper and cobalt are relatively insoluble in each other and form a classic LME couple (Ref 3). Nickel and copper exhibit 100% solid solubility; hence, nickel-base alloys are not prone to copper contamination cracking in the HAZ. Copper jigs and fixtures, especially those used in sheet welding, are a potential source of copper contamination. Chromium or nickel plating of copper fixtures will minimize the potential for inadvertent copper transfer when welding cobalt alloys.

Cobalt-base CR alloys are generally welded using a filler-metal composition that matches the composition of the base material. Like low-carbon nickel-base CR alloys, cobalt alloys have relatively good resistance to fusion-zone (FZ) solidification cracking. The lower the carbon content, the greater the resistance to hot cracking. Boron is particularly deleterious as a residual trace element and can cause welding problems.

Cobalt-chromium CR alloys with relatively low nickel or iron content (for example, UNS alloy R31233, Table 1) exhibit unique mechanical property characteristics in the as-welded condition. Weldments are characterized by high strength and low ductility, because of stress-induced localized transformation from a fcc crystal structure to a hexagonal close-packed (hcp) structure (Ref 4). The transformation products are not visible in optical photomicrographs (Fig. 1). Instead, thin-film electron microscopy is required to detect the hcp phase.

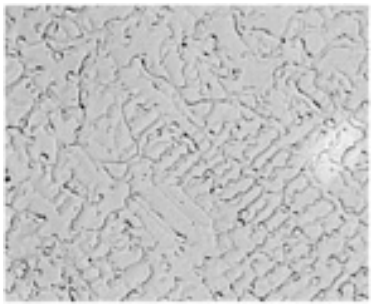

FIG. 1 TYPICAL WELD METAL MICROSTRUCTURE OF ULTIMET ALLOY (UNS R31233) OBTAINED WITH GMAW DEPOSIT WHEN SHORT-CIRCUITING MODE OF TRANSFER IS USED. SAMPLE WAS ETCHED WITH HCL AND OXALIC ACID. 500×

Tensile data comparing room-temperature elongation of weldments versus castings and annealed base material are given in Table 2. Castings generally have less residual stress in the as-cast condition than do weldments; hence, the observed difference in ductility. Table 2 also shows that a full postweld anneal at 1120 °C (2050 °F) will reduce the yield strength and improve the ductility of a welded structure. A postweld heat treatment is recommended, especially if the cold forming of a weldment after welding is a required part of the fabrication sequence.

TABLE 2 TENSILE PROPERTIES OF WELDED COBALT-BASE CORROSION-RESISTANT ALLOY UNS R31233 RELATIVE TO WROUGHT AND CAST PRODUCTS AT ROOM TEMPERATURE

PRODUCT FORM	CONDITION	YIELD STRENGTH AT 0.2% OFFSET		ULTIMATE TENSILE STRENGTH		ELONGATION, %
		MPa	ksi	MPa	ksi	
PLATE	ANNEALED	545	79	1020	148	36
CASTINGS[A]	AS CAST	395	57	770	112	35
WELD METAL[B]	AS WELDED	585	85	850	123	18
	ANNEALED (1120 °C, OR 2050 °F)	460	67	825	120	22

Source: Ref 4

(A) INVESTMENT CASTING.

(B) GMAW SPRAY TRANSFER.

References cited in this section

1. H.H. UHLIG AND A.I. ASPHAHANI, CORROSION BEHAVIOR OF COBALT BASE ALLOYS IN AQUEOUS MEDIA, *MATER. PERFORM.,* VOL 18 (NO. 11), NOV 1979
2. S.J. MATTHEWS, M.O. MADDOCK, AND W.F. SAVAGE, HOW COPPER SURFACE CONTAMINATION AFFECTS WELDABILITY OF COBALT SUPERALLOYS, *WELD. J.*, MAY 1972
3. W.F. SAVAGE AND M. MUSHALA, COPPER CONTAMINATION CRACKING IN THE WELD HEAT AFFECTED ZONE, *WELD. J.*, MAY 1978, P 145
4. S.J. MATTHEWS, P. CROOK, L.H. FLASCHE, AND J.W. TACKETT, WELDABILITY CHARACTERISTICS OF A NEW CORROSION- AND WEAR-RESISTANT COBALT ALLOY, *WELD. J.*, DEC 1991, P 331-337

Titanium-Base CR Alloys

Commercially pure (CP) titanium offers excellent corrosion resistance in most environments, except those media that contain fluoride ions. Titanium is more corrosion resistant than stainless steel in many industrial environments, and its use in the chemical process industry has been gradually increasing (Ref 5). Titanium has a density approximately one-half that of nickel- or cobalt-base alloys, and its cost effectiveness relative to these alloys is generally calculated using the cost per unit weight, the difference in density, the corrosion allowances, and other performance factors.

Titanium has moderate strength, good ductility, and excellent weldability relative to the more complex aerospace α-β titanium alloys. Various grades of CP titanium are classified on the basis of mechanical properties and interstitial impurities. In general, variations in strength are produced by differences in impurity content, primarily the interstitial elements (that is, oxygen, nitrogen, and carbon) and iron. As the content of these elements increases, strength also increases.

Titanium that is intentionally alloyed with trace amounts of palladium or molybdenum and nickel is also used to provide corrosion-resistant service. For example, the Ti-0.2Pd alloy and the Ti-0.3Mo-0.8Ni alloy are characterized by improved crevice corrosion resistance, as well as improved corrosion resistance in reducing environments.

Weldability Characteristics. Corrosion-resistant titanium materials are generally welded with matching filler-metal compositions. Welded joints will have essentially the same corrosion resistance as the base metal. However, any iron contamination of the weld metal that exceeds even 0.05% Fe will cause accelerated corrosion attack in nitric acid or in other strongly oxidizing solutions. Therefore, it is imperative that all potential sources of iron contamination be avoided. Steel wire brushes should not be used for interpass cleaning of titanium weldments.

Titanium is a single (α) phase material with a hcp crystal structure. However, an allotropic transformation occurs at temperatures above approximately 870 °C (1600 °F), where α transforms to a body-centered cubic (bcc) β phase. Accordingly, the heat-affected zone of CP titanium weldments will be characterized by large β grains, which form at high temperatures during welding but transform back to an acicular and serrated α phase upon cooling to room temperature.

Commercially pure titanium alloys are not heat treatable, that is, they do not develop significant differences in properties after heat treatment. However, a postweld anneal in the temperature range from 650 to 760 °C (1200 to 1400 °F) or a postweld stress relief from 480 to 595 °C (900 to 1100 °F) might be warranted for purposes of maintaining dimensional stability during subsequent machining operations. A postweld heat treatment may also improve resistance to stress-corrosion cracking (SCC), depending on the configuration of the weldment and the intended corrosion-resistant service.

The welding metallurgy of titanium and titanium alloys is discussed in greater depth in the Section "Selection of Nonferrous Low-Temperature Materials" in this Volume. Additional information can be found in the article "Welding of Titanium Alloys" in this Volume.

Reference cited in this section

5. F.E. KATEAK, I.D. SERVI, AND J.C. AGARWAL, NONAEROSPACE APPLICATIONS: TITANIUM'S SOLE OPPORTUNITY FOR GROWTH, *MET. BULL. MON.*, AUG 1991

Zirconium- and Tantalum-Base CR Alloys

The metals and alloys based on zirconium and tantalum have weldability characteristics similar to those of titanium. They readily react with oxygen and form very stable oxides. Like titanium, they have high solubilities for oxygen, nitrogen, and hydrogen at elevated temperatures. Small amounts of dissolved oxygen and nitrogen significantly increase the hardness of the metal, whereas dissolved hydrogen reduces toughness and increases notch sensitivity. Therefore, these metals must be welded or brazed in a shield of high-purity inert gas or in a vacuum (Ref 6).

Unalloyed zirconium is similar in characteristics to titanium, except that its density is about 50% higher. Like titanium, zirconium has a hcp crystal structure (α phase) up to approximately 865 °C (1590 °F), and it transforms to a bcc structure (β phase) above this temperature.

Zirconium is resistant to corrosive attack by most acids, strong alkalies, and some molten salts. Its corrosion-resistant behavior is due to the formation of a stable, dense, adherent, and self-healing zirconium oxide film on the metal surface. Zirconium is used for corrosion applications in the petrochemical, chemical process, and food processing industries. Zirconium alloys are also used in the nuclear industry for pressurized water reactor components, because of their low thermal neutron absorption characteristics.

Zirconium is readily welded using the same processes and procedures as titanium. Residual welding stresses are generally low because of its low modulus of elasticity. Zirconium also has a low coefficient of thermal expansion, which contributes to low distortion during welding. In addition, inclusions in welds are usually not a problem, because zirconium has a high solubility for its own oxide. Although some porosity is possible in zirconium welds, it can usually be minimized by properly adjusting welding parameters and by following sound welding practices with respect to precleaning and proper shielding during the welding process.

Additional information is available in the article "Welding of Zirconium Alloys" in this Volume.

Tantalum is a very dense (over 3.5 times the density of titanium) CR material. It is an inherently soft, fabricable metal that has a very high melting temperature, approximately 3000 °C (5400 °F). It has a bcc crystal structure, with no allotropic transformation at elevated temperature. Unlike many bcc metals, tantalum retains good ductility to very low temperatures, and exhibits a ductile-to-brittle transition temperature (DBTT) of approximately -250 °C (-420 °F).

Tantalum has excellent corrosion resistance to a wide variety of acids, alcohols, chlorides, sulfates, and other chemicals. For this reason, it is widely used for chemical equipment that operates at ambient temperatures.

Tantalum oxidizes in air above approximately 300 °C (570 °F) and is attacked by hydrofluoric, phosphoric, and sulfuric acids, and by chlorine and fluorine gases at temperatures above 150 °C (300 °F). Tantalum also reacts with carbon, hydrogen, and nitrogen at elevated temperatures. Because of the high per unit weight cost of tantalum and its high density, the cost effectiveness of this material has been increased by using clad, explosion clad, or resistance-welded clad products.

Like zirconium, tantalum is also readily welded by the processes and procedures used for titanium. The joining of tantalum-clad plate requires special procedures and precautions and is beyond the scope of this article.

Reference cited in this section

6. J.M. GERKIN *ET AL.*, TITANIUM, ZIRCONIUM, HAFNIUM, TANTALUM, AND COLUMBIUM, *WELDING HANDBOOK*, 7TH ED., VOL 4, *METALS AND THEIR WELDABILITY*, AWS, 1982

Selection of Cobalt-, Titanium-, Zirconium-, and Tantalum-Base Corrosion-Resistant Alloys

S.J. Matthews, Haynes International, Inc.

References

1. H.H. UHLIG AND A.I. ASPHAHANI, CORROSION BEHAVIOR OF COBALT BASE ALLOYS IN AQUEOUS MEDIA, *MATER. PERFORM.,* VOL 18 (NO. 11), NOV 1979
2. S.J. MATTHEWS, M.O. MADDOCK, AND W.F. SAVAGE, HOW COPPER SURFACE CONTAMINATION AFFECTS WELDABILITY OF COBALT SUPERALLOYS, *WELD. J.,* MAY 1972
3. W.F. SAVAGE AND M. MUSHALA, COPPER CONTAMINATION CRACKING IN THE WELD HEAT AFFECTED ZONE, *WELD. J.,* MAY 1978, P 145
4. S.J. MATTHEWS, P. CROOK, L.H. FLASCHE, AND J.W. TACKETT, WELDABILITY CHARACTERISTICS OF A NEW CORROSION- AND WEAR-RESISTANT COBALT ALLOY, *WELD. J.,* DEC 1991, P 331-337
5. F.E. KATEAK, I.D. SERVI, AND J.C. AGARWAL, NONAEROSPACE APPLICATIONS: TITANIUM'S SOLE OPPORTUNITY FOR GROWTH, *MET. BULL. MON.,* AUG 1991
6. J.M. GERKIN *ET AL.,* TITANIUM, ZIRCONIUM, HAFNIUM, TANTALUM, AND COLUMBIUM, *WELDING HANDBOOK,* 7TH ED., VOL 4, *METALS AND THEIR WELDABILITY,* AWS, 1982

Weldability Testing

Richard D. Campbell, Joining Services, Inc.; Daniel W. Walsh, California Polytechnic State University

Introduction

THIS ARTICLE describes many of the various weldability tests that have been developed through the years. Some of these tests are used extensively, while others find limited application. The purposes of this article are to briefly describe these tests, to show what material characteristics they provide, and to present some advantages and limitations of each. This discussion is limited to tests used to evaluate the weldability of base materials.

Additional Tests Used in Welding (Service Tests). This article does not cover the basic tests used for weld qualification, as specified in the numerous welding codes and standards. The tests for welding procedure qualification are used to establish the properties of the welded assembly (including any filler material) and determine that the weldment is capable of providing the required properties for the intended applications. Tests for welder performance qualification are intended to establish the ability of the welder to deposit sound weld metal. Examples of these tests are given in Table 1; information about these tests can be found in the Section "Joint Evaluation and Quality Control" in this Volume. These are often termed service tests because they measure the properties of the weldment under servicelike conditions.

TABLE 1 TYPICAL TESTS REQUIRED IN VARIOUS WELDING CODES AND STANDARDS FOR WELDING PROCEDURE QUALIFICATION AND WELDER PERFORMANCE QUALIFICATION

DESTRUCTIVE TESTS
MECHANICAL TESTS
TENSILE TESTS
GUIDED BEND TESTS
CHARPY V-NOTCH IMPACT TOUGHNESS TESTS
DROP WEIGHT NOTCH TOUGHNESS TESTS
FILLET WELD BREAK, SHEAR, OR FRACTURE TESTS
STUD WELD BEND OR TORQUE TESTS
METALLOGRAPHIC TESTS
MACROEXAMINATION TESTS
MACROETCH TESTS
MICROEXAMINATION TESTS
NONDESTRUCTIVE TESTS
VISUAL INSPECTION

LIQUID PENETRANT INSPECTION
MAGNETIC PARTICLE INSPECTION
RADIOGRAPHIC INSPECTION

Tests to evaluate the mechanical or corrosion properties of weldments are described in detail in several sources (Ref 1, 2). Other Volumes of the *ASM Handbook* present the basics of mechanical testing (Ref 3), metallographic techniques and etchants (Ref 4), and nondestructive testing methods (Ref 5).

This article does not cover tests for weld metal or weld wire. These tests, such as chemical analysis or mechanical testing of the deposited weld metal, are used to evaluate the properties of the weld filler material. Welding tests of filler material, such as spark tests, are performed to evaluate the welding characteristics of the wire.

References

1. "WELDING TECHNOLOGY," CHAPTER 12, *WELDING HANDBOOK*, VOL 1, 8TH ED., AMERICAN WELDING SOCIETY, 1987
2. "STANDARD METHODS FOR MECHANICAL TESTING OF WELDS," ANSI/AWS B4.0-85, AMERICAN WELDING SOCIETY, 1985
3. *MECHANICAL TESTING*, VOL 8, *ASM HANDBOOK*, AMERICAN SOCIETY FOR METALS, 1985
4. *METALLOGRAPHY AND MICROSTRUCTURES*, VOL 9, *ASM HANDBOOK*, AMERICAN SOCIETY FOR METALS, 1985
5. *NONDESTRUCTIVE EVALUATION AND QUALITY CONTROL*, VOL 17, *ASM HANDBOOK*, ASM INTERNATIONAL, 1989

Weldability Testing

Richard D. Campbell, Joining Services, Inc.; Daniel W. Walsh, California Polytechnic State University

General Characteristics of Weldability Tests

Weldability is defined as "*the capacity of a material to be welded under the imposed fabrication conditions into a specific, suitably designed structure and to perform satisfactorily in the intended service*" (Ref 6). The weldability tests described in this article are used to evaluate the effects of welding on such properties and characteristics as:

- BASE-METAL AND WELD-METAL CRACKING
- BASE-METAL AND WELD-METAL DUCTILITY
- WELD PENETRATION
- WELD POOL SHAPE AND FLUID FLOW

Because weldability testing is used to evaluate the welding characteristics of the base materials, many of these weldability tests are laboratory or research tests rather than "production" tests. Weldability tests are used extensively during alloy development. However, many are also used during weld procedure development to ensure the weldability of base materials before production commences. Each test is designed to evaluate a susceptibility to a specific weldability problem.

Obviously, the best tests evaluate the actual service conditions. However, because this is expensive and often impossible, standardized weldability tests and test methods have been developed. These tests evaluate various responses of the base material to different welding conditions or simulated welding conditions. Most of these tests utilize simple geometries and configurations, and loading conditions are typically simple and uniform. Thus, none of these tests duplicates the actual service conditions of a real weldment. Instead they provide a baseline for comparisons of base material responses.

The various weldability tests provide information on alloys, welding processes, and welding procedures. Data generated can be compared to data produced under the same testing conditions on other heats of material or to data produced with other welding processes or procedures (Ref 7). All of these tests provide qualitative information in that they are used to sort different materials or heats of the same materials, processes, procedures, and thermal cycles. None of these tests have any quantitative "acceptance" limits, such as the yield strength requirements of a specific alloy when tensile tested (Ref 7).

All weldability tests involve either actual welding or simulated welding. Those involving actual welding require that the test coupons be produced using an actual welding process. An example of this type of test is Varestraint hot crack testing using the gas-tungsten arc welding (GTAW) process. Simulated welding tests involve the application of heat through means other than welding, with or without loading. An example is Gleeble testing, in which a test specimen is resistance heated to simulate a weld heat-affected zone (Ref 7). Excellent reviews of various weldability tests are provided in Ref 8 and 9.

References cited in this section

6. "STANDARD WELDING TERMS AND DEFINITIONS," ANSI/AWS A3.0-89, AMERICAN WELDING SOCIETY, 1989
7. "WELDABILITY TESTING," CHAPTER 4, *WELDING HANDBOOK*, VOL 1, 8TH ED., AMERICAN WELDING SOCIETY, 1987
8. R.D. STOUT AND W.D. DOTY, *WELDABILITY OF STEELS*, WELDING RESEARCH COUNCIL, 1978
9. R.D. STOUT, *WELDABILITY OF STEELS*, WELDING RESEARCH COUNCIL, 1987

Richard D. Campbell, Joining Services, Inc.; Daniel W. Walsh, California Polytechnic State University

Weldability Tests for Evaluating Cracking Susceptibility

The majority of weldability tests have been developed to evaluate the susceptibility of the base materials (and any added filler material) to cracking. The purpose of these tests is to reduce or to eliminate the formation of these defects during fabrication or service. Cracking can be in the form of hot cracking, cold cracking, or lamellar tearing. Detailed information about these defects is available in the article "Cracking Phenomena Associated With Welding" in this Volume. Table 2 presents a comparison of several weldability tests for cracking susceptibility, their applications, and resultant types of data.

TABLE 2 WELDABILITY TESTS USED TO EVALUATE SUSCEPTIBILITY TO CRACKING

TEST	FIELDS OF USE	CONTROLLABLE VARIABLES	TYPE OF DATA	SPECIALIZED EQUIPMENT	RELATIVE COST
LEHIGH RESTRAINT TEST	WELD METAL HOT AND COLD CRACKING, ROOT CRACKING, HAZ HYDROGEN CRACKING, STRESS-RELATED CRACKING	JOINT GEOMETRY, PROCESS, FILLER METAL, RESTRAINT LEVEL, HEAT INPUT, PREHEAT	CRITICAL RESTRAINT, OR % HINDERED CONTRACTION	NONE	COSTLY MACHINING
SLOT TEST	HAZ HYDROGEN CRACKING	FILLER METAL, INTERPASS TIME, PREHEAT	TIME TO CRACK, CRITICAL PREHEAT	NONE	LOW COST
RIGID RESTRAINT (RRC) TEST	WELD METAL HOT AND COLD CRACKING, ROOT CRACKING, HAZ HYDROGEN CRACKING	JOINT GEOMETRY, PROCESS RESTRAINT LEVEL, FILLER METAL, HEAT INPUT, PREHEAT	CRITICAL RESTRAINT	RESTRAINING JIG	COSTLY MACHINING AND SET-UP
TEKKEN TEST	WELD METAL ROOT CRACKING, HAZ HYDROGEN CRACKING	JOINT GEOMETRY, PROCESS, FILLER METAL, HEAT INPUT, PREHEAT	CRITICAL PREHEAT	NONE	LOW-COST
CIRCULAR GROOVE TEST	WELD METAL HOT AND COLD CRACKING, HAZ HYDROGEN CRACKING	PROCESS, FILLER METAL, PREHEAT	GO-NO GO	NONE	COSTLY PREPARATION
IMPLANT TEST	HAZ HYDROGEN CRACKING, STRESS-RELIEF CRACKING	PROCESS, FILLER METAL, PREHEAT, PWHT	CRITICAL FRACTURE STRESS, CRITICAL PREHEAT	LOADING JIG	MEDIUM COST
TENSION RESTRAINT CRACKING (TRC) TEST	HAZ HYDROGEN CRACKING	PROCESS, FILLER METAL, HEAT INPUT, PREHEAT	CRITICAL FRACTURE STRESS, CRITICAL PREHEAT	LOADING JIG	COSTLY MACHINING AND SET-UP
VARESTRAINT TEST	WELD METAL AND HAZ HOT CRACKING	PROCESS, FILLER METAL, HEAT INPUT	CRACK LENGTH, % STRAIN	LOADING JIG	COSTLY PREPARATION AND ANALYSIS
LONGITUDINAL, BEAD-ON-PLATE TEST	HAZ HYDROGEN CRACKING	CURRENT, HEAT INPUT	% CRACKING	NONE	LOW COST

CONTROLLED THERMAL SEVERITY TEST	HAZ HYDROGEN CRACKING IN FILLET WELDS	CURRENT, COOLING RATE, PREHEAT	GO-NO GO (AT 2 COOLING RATES)	NONE	COSTLY PREPARATION
CRUCIFORM TEST	HAZ HYDROGEN CRACKING, WELD METAL ROOT CRACKS	PROCESS, HEAT INPUT, PREHEAT, FILLER METAL	GO-NO GO	NONE	COSTLY PREPARATION
LEHIGH CANTILEVER TEST	LAMELLAR TEARING	PROCESS, FILLER INPUT, HEAT INPUT, PREHEAT	CRITICAL RESTRAINT, STRESS AND STRAIN	LOADING JIG	COSTLY SPECIMEN PREPARATION
CRANFIELD TEST	LAMELLAR TEARING	FILLER METAL	NUMBER OF PASSES TO CRACK	NONE	LOW COST
NICK BEND TEST	WELD METAL SOUNDNESS	FILLER METAL	GO-NO GO	NONE	LOW COST

Source: Ref 9

Hot and Cold Cracking

Hot cracking occurs during weld solidification and can occur in the weld metal or in the heat-affected zone (HAZ). Hot cracking is caused by low melting temperature constituents, in addition to tensile stress on the weld. Other names for hot cracking include microfissuring, solidification cracking, reheat cracking, and liquation cracking. In actual weldments, the tensile stress may come from external loads on the structure, the weight of the structure producing stress on the weld, solidification shrinkage stresses, or combinations of these.

Cold cracking (also known as hydrogen-induced cracking) is a cracking phenomenon that occurs after the weld has solidified (Ref 6). It is also referred to as delayed cracking, because cracking is often "delayed" for minutes, hours, or even longer, after the weld has solidified. Cold cracking is most often associated with the presence of hydrogen in hardenable steels. The ductility and toughness of the welded structure are greatly reduced by cold cracking. Requisites for cold cracking include tensile stress (external loading or residual stress from welding), a crack-susceptible microstructure (martensite), and the presence of hydrogen. Cold cracking can occur in the weld fusion zone or in the HAZ.

Several weldability tests for evaluating cracking susceptibility are described in this article. Most tests are used to evaluate susceptibility to one type of cracking: cold cracking, hot cracking, underbead cracking, or lamellar tearing. Some tests are useful for both hot and cold cracks. The applicabilities of each test are discussed within the descriptions of the test. The weldability tests discussed in this section are classified as self-restraint tests or externally loaded tests.

Self-Restraint Tests

Self-restraint tests utilize the restraint, or stress, within the specimen to cause weld metal or base metal cracking. No external loading of the specimen occurs. The specimen is designed to produce variable restraint on the weld joint, thus causing cracking.

Lehigh Restraint Test (Hot and Cold Cracks). The Lehigh restraint test is illustrated in Fig. 1. This test, developed at Lehigh University, uses a plate with slots machined into the sides and ends. A groove weld joint is machined along the centerline of the plate, and a single-pass weld is produced along this groove. The restraint from the plate and slots produces a weld with various levels of cracking.

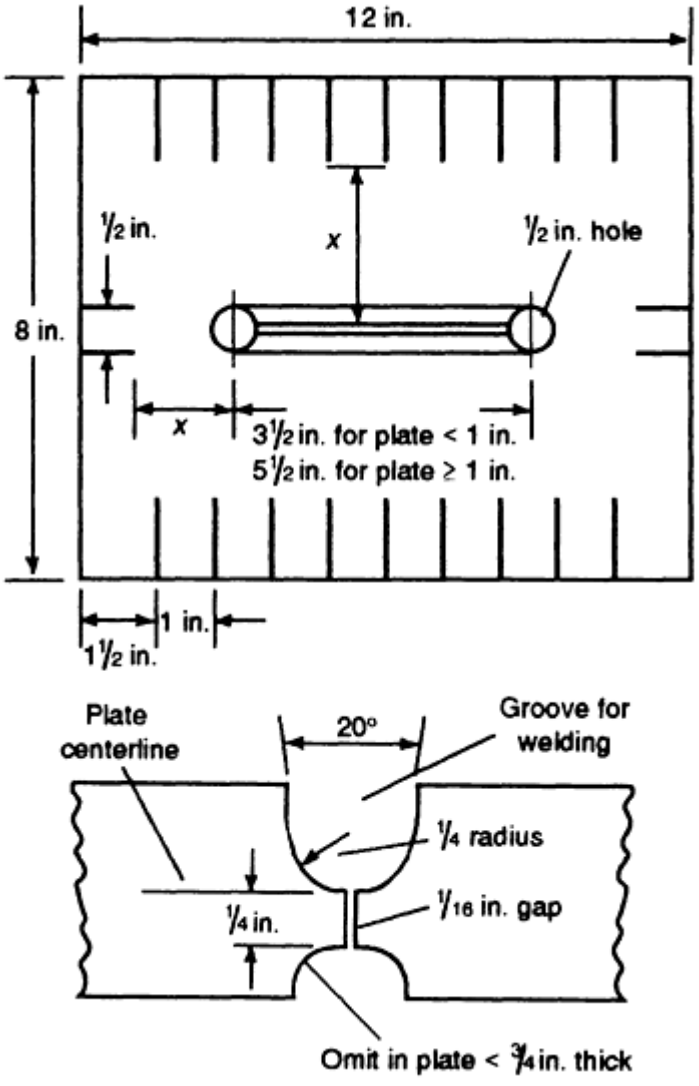

FIG. 1 SCHEMATIC SHOWING SLOTTED PLATE SPECIFICATIONS FOR LEHIGH RESTRAINT TEST. SOURCE: REF 8

This test compares quantitatively the degree of restraint at which cracking occurs in welds during cooling. The level of restraint is altered by changing the length of the slots (Ref 7). The restraint is quantified as 2*x*, where *x* is the distance from the centerline of the weld groove to the bottom of the slots. Numerous samples with different slot lengths are welded, and a threshold level of restraint is determined as the width that is just sufficient to cause cracking. Cracking can be evaluated by metallographic cross sections of the weld or by heat tinting and breaking open the weld to expose the cracked region. This test has also been used to evaluate reheat cracking in steels (Ref 7, 8, 9).

Keyhole Restraint Cracking Test (Hot and Cold Cracks). The Naval Research Laboratory (NRL) keyhole restraint crack test (Fig. 2) is a simplified version of the Lehigh test. The specimen is welded along the groove beginning at the open end and progressing toward the hole. This imposes a varying degree of restraint along the weld, with a maximum at the hole and a minimum at the edge where welding commenced. Cracks form at the hole and extend outward to a point where the restraint is low enough to arrest the crack growth. The crack length is the measure of crack susceptibility (Ref 8).

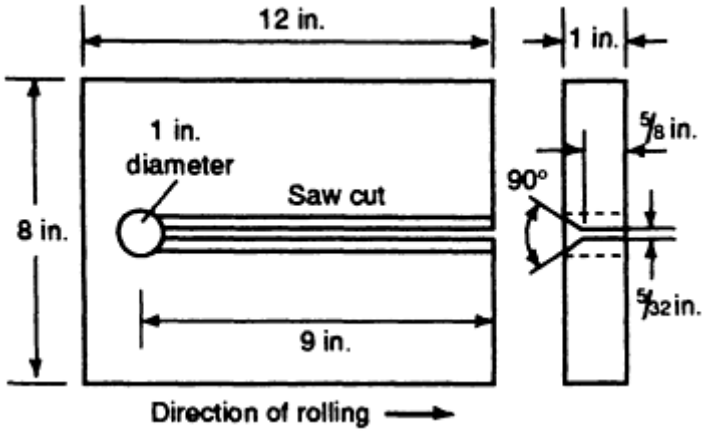

FIG. 2 PLATE SPECIFICATIONS FOR NRL KEYHOLE RESTRAINT TEST. SOURCE: REF 8

Houldcroft Crack Susceptibility Test (Hot Crack Test). The Houldcroft crack susceptibility test utilizes a design similar to the Lehigh test, but the slots vary in length from one end of the specimen to the other (Fig. 3). The Houldcroft test was developed for sheet steels. No weld joint is machined into the specimen, but rather a bead-on-plate, complete penetration weld (usually using the GTAW process) is made. Duplicate samples are produced, and the mean crack length of these specimens is used as an index of hot crack susceptibility (Ref 8).

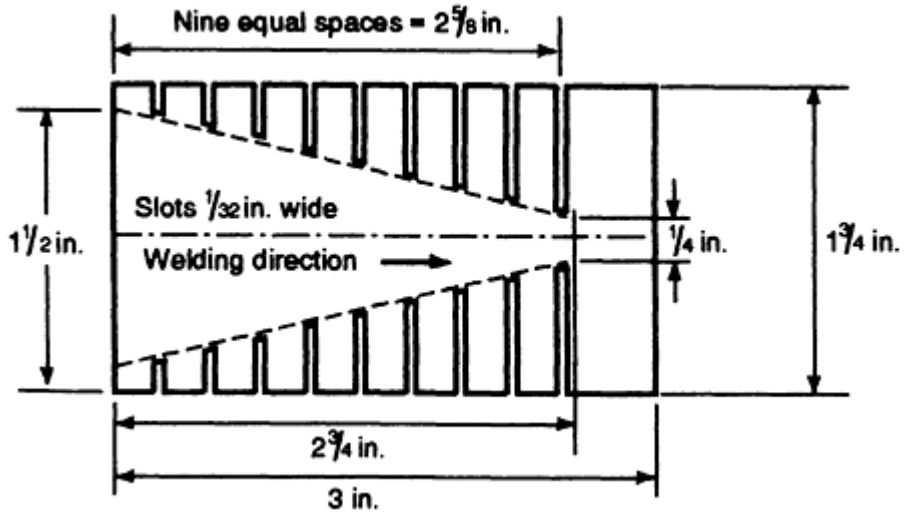

FIG. 3 SPECIMEN DIMENSIONS FOR HOULDCROFT CRACK SUSCEPTIBILITY TEST. SOURCE: REF 8

Keyhole Slotted-Plate Restraint Test (Hot Crack Test). A variation of the Houldcroft test for plate material is the keyhole slotted-plate restraint test (Fig. 4). This test was developed at Battelle and utilizes a groove weld, which begins at the low restraint end. Crack sensitivity is determined, in a manner similar to the Lehigh test, by the uncut width of the specimen at which the crack propagation ceases (Ref 8).

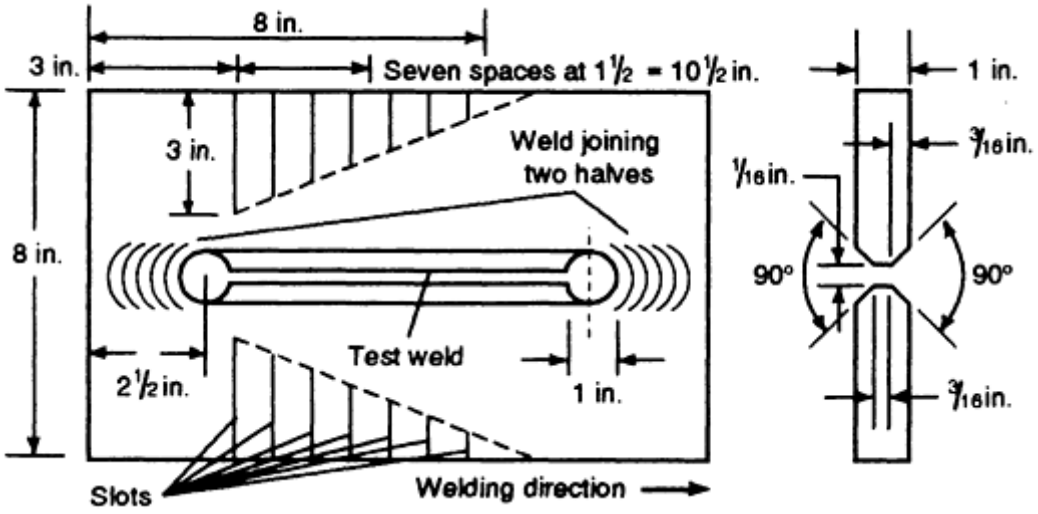

FIG. 4 SPECIMEN REQUIREMENTS FOR KEYHOLE SLOTTED-PLATE RESTRAINT TEST. SOURCE: REF 8

Tekken Test (Cold Crack Test). The Tekken Test, developed in Japan, uses several specimen dimensions and joint designs (Fig. 5). The Y joint provides more restraint than the U- or double-U joint designs. In these tests, preheat and welding parameters are varied to alter the stress state, rather than changing the specimen design. This test is used to evaluate HAZ cracks and underbead cracks.

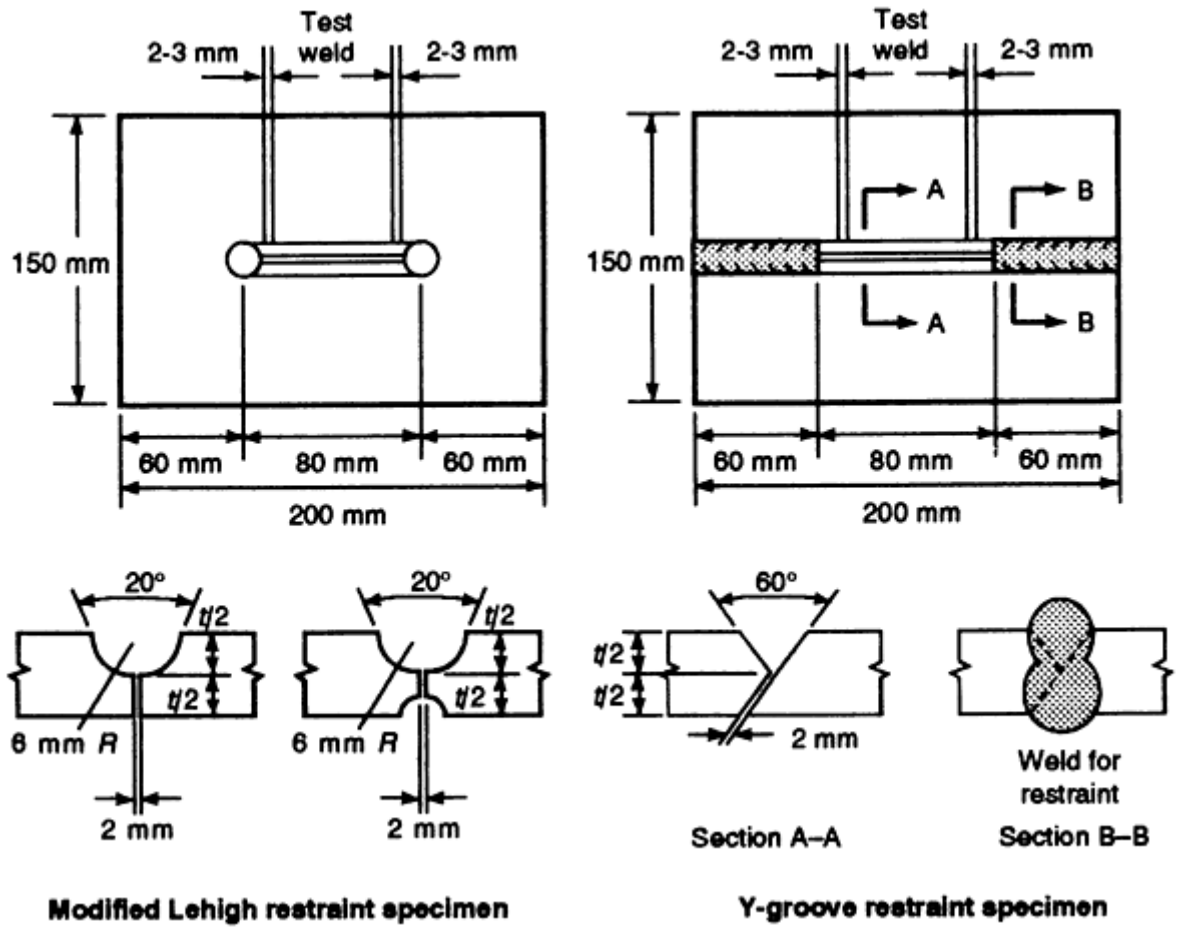

FIG. 5 SAMPLE SPECIFICATIONS FOR TEKKEN TEST. SOURCE: REF 9

Circular Patch Test (Cold and Hot Crack Test). The circular patch test (Fig. 6) utilizes a plate with a circular hole cut out and replaced by a patch. Both the plate and the patch have a weld joint machined into them. One or more weld passes are made in this circular groove, and cracking is detected by visual, radiographic, and/or liquid penetrant inspection. This test is used to generate and evaluate both hot cracks and cold cracks (Ref 8, 9).

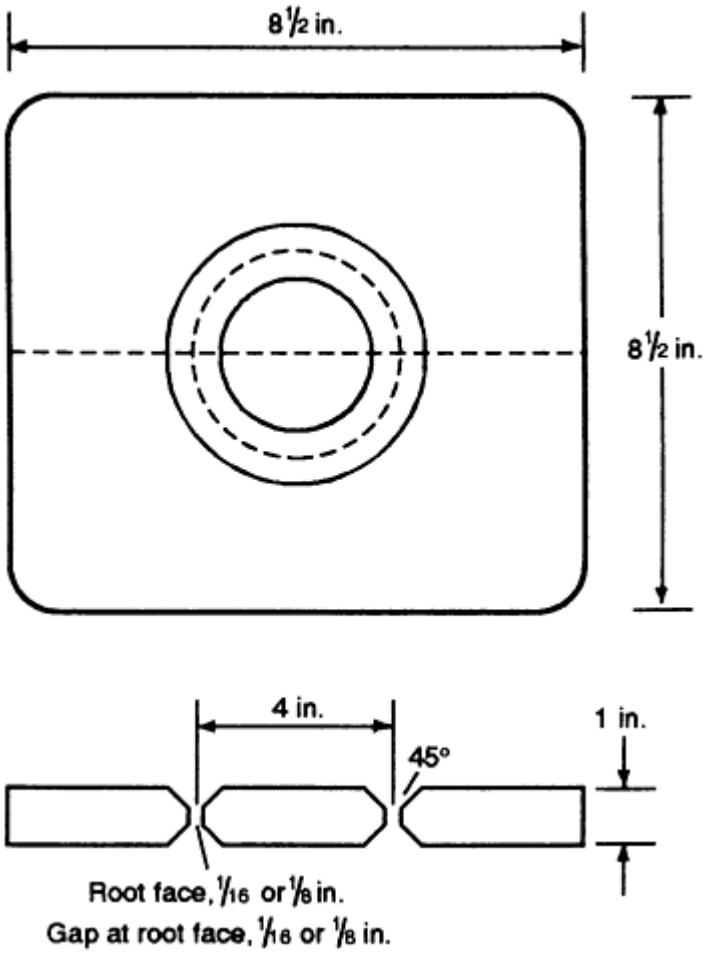

FIG. 6 PLATE SPECIFICATIONS FOR CIRCULAR PATCH TEST. SOURCE: REF 8

Navy Circular Patch Test (Cold and Hot Crack Test). The Navy circular patch test utilizes a much larger specimen (Fig. 7). This test is used for evaluating different electrodes on various base metals. A circular hole is cut in the plate, into which a patch is placed, with a backing ring to hold the plate and patch together. A multipass weld is made, one quadrant at a time, as shown in Fig. 7. Cracking evaluation is by visual, radiographic, and/or liquid penetrant inspection. Both hot cracks and cold cracks can be generated in this test (Ref 8).

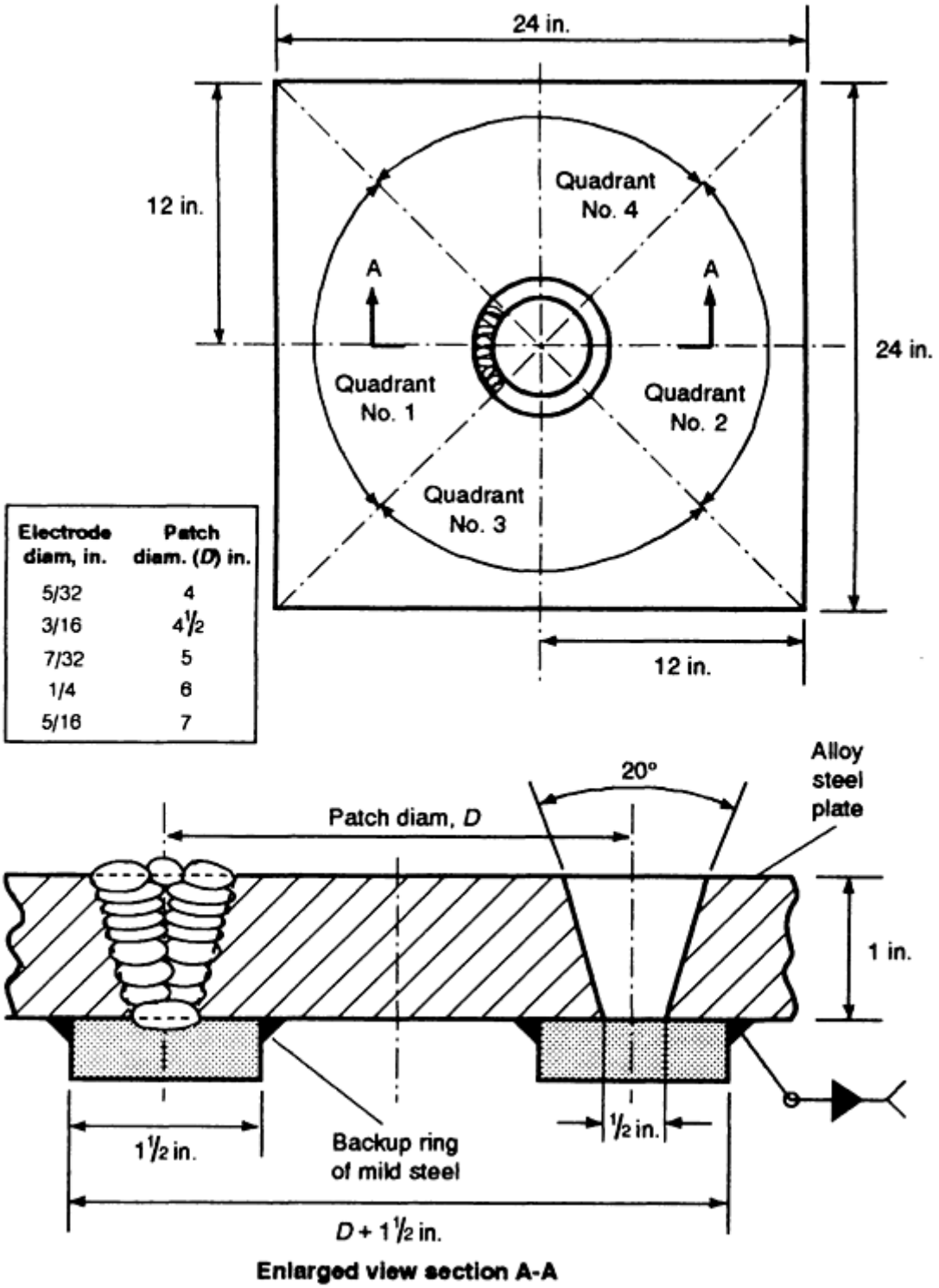

FIG. 7 PLATE REQUIREMENTS FOR NAVY CIRCULAR PATCH TEST. SOURCE: REF 8

Controlled-Thermal-Severity Test (Cold Crack Test). The controlled-thermal-severity test specimen consists of a square plate bolted and anchor welded to a larger rectangular plate (Fig. 8). After the anchor welds have cooled to room temperature, two test welds are made on the specimen. The fillet weld along the plate edges is made first. This weld, called the bithermal weld, has only two-dimensional heat flow. After this weld has cooled, the lap weld is made on the other edge of the top plate, near the center of the bottom plate. Because this weld has nearly three-dimensional heat flow, it is called a trithermal weld. The specimen is held for 72 h at room temperature, then the degree of cracking is determined by measuring crack length on three metallographic specimens cut from cross sections of the two welds.

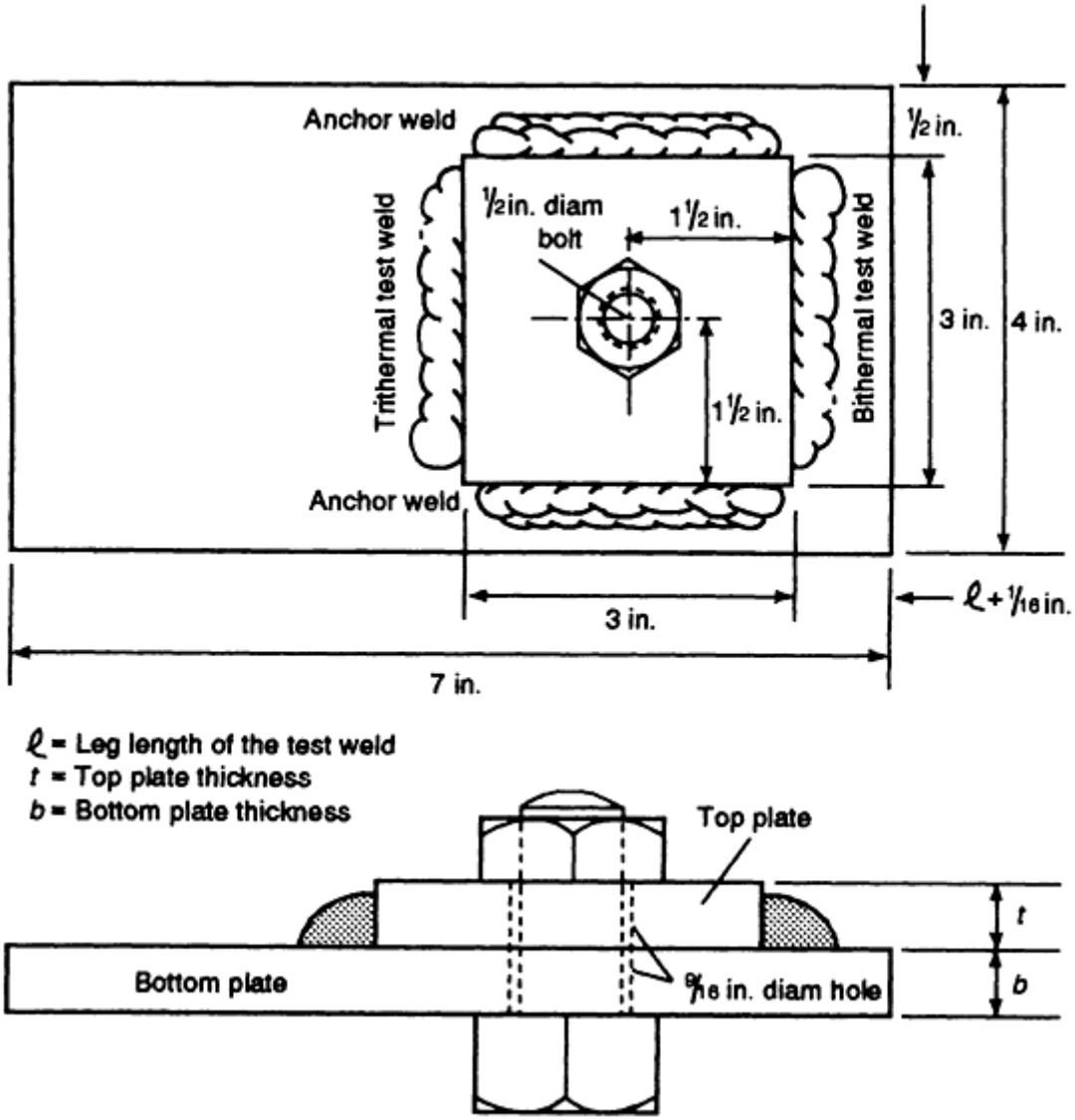

FIG. 8 PLATE DIMENSIONS FOR CONTROLLED THERMAL SEVERITY TEST. SOURCE: REF 8

Each specimen is assigned a thermal severity number (*TSN*) according to plate thickness using Eq 1 and 2. For bithermal welds:

$$TSN = 4(T + B) \qquad \textbf{(EQ 1)}$$

where *t* and *b* are the thicknesses of the top and bottom plates, respectively. For trithermal welds:

$$TSN = 4(T + 2B) \qquad \textbf{(EQ 2)}$$

A series of plate thicknesses, which provided varying cooling rates, are tested. The crack susceptibility of the base metal-filler material (welding wire or electrode) combination is determined by the minimum *TSN* that produces cracking. Controlled-thermal-severity testing is used to measure the cold crack sensitivity of steels under cooling rates controlled by the thickness of the plates and the differences in cooling rates between bithermal and trithermal welds. This test is primarily used to evaluate the crack sensitivity of hardenable steels (Ref 7, 9).

Cruciform Cracking Test (Cold Crack Test). The cruciform cracking test (Fig. 9) uses three plates that are surface ground along their interfaces to ensure consistent and reproducible fit-up. The ends are tack welded together to form a

double T-joint. Four test fillet welds are deposited in the sequence shown in Fig. 9, with complete cooling between passes. The specimen is held at room temperature for at least two days before stress relieving at about 620 °C (1150 °F) for 2 h (Ref 7). Cracking is determined by evaluation of metallographic cross sections of the four welds. The test data can be erratic and are very susceptible to sample preparation. Five to ten samples are typically required to provide reliable results for cracking sensitivity level (Ref 7, 8).

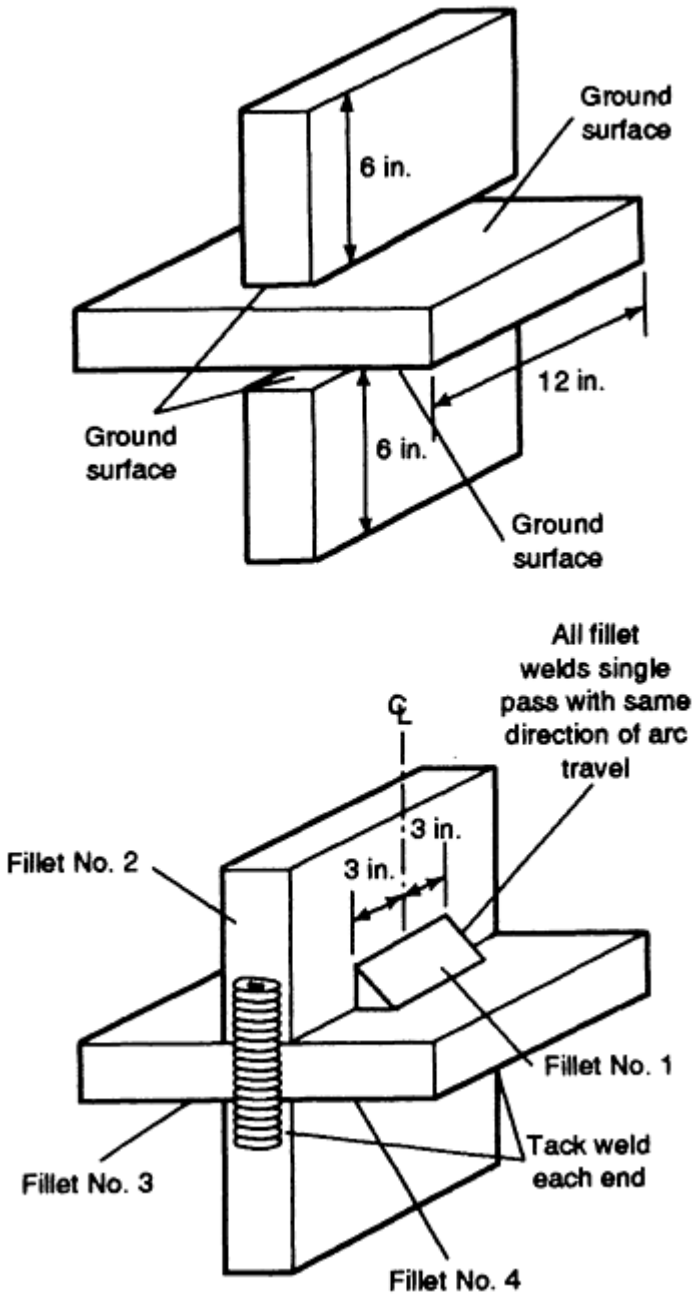

FIG. 9 SPECIFICATIONS FOR CRUCIFORM CRACKING TEST SPECIMENS. SOURCE: REF 8

Externally Loaded Tests

Externally loaded tests involve the application of an external load to the specimen during weld testing. This external load is typically varied to alter the stress state and thus the severity of cracking. This allows a more quantitative measure of stress than can be obtained from the self-restraint tests.

Implant Testing (Cold Crack Test). The implant test is used to evaluate hydrogen-induced cracking (HIC). A rod of the steel base metal to be tested is machined to the dimensions shown in Fig. 10, the end of the rod having either a circular groove or a helical groove machined into it (Ref 8). The rod is placed inside a hole in the center of a plate so the

top of the rod is flush with the top of the plate. A weld bead is made on the top surface of the plate and passes directly over the top of the rod. By making the weld over the rod, the groove in the rod is thus located in the coarse-grained HAZ, which is most susceptible to HIC.

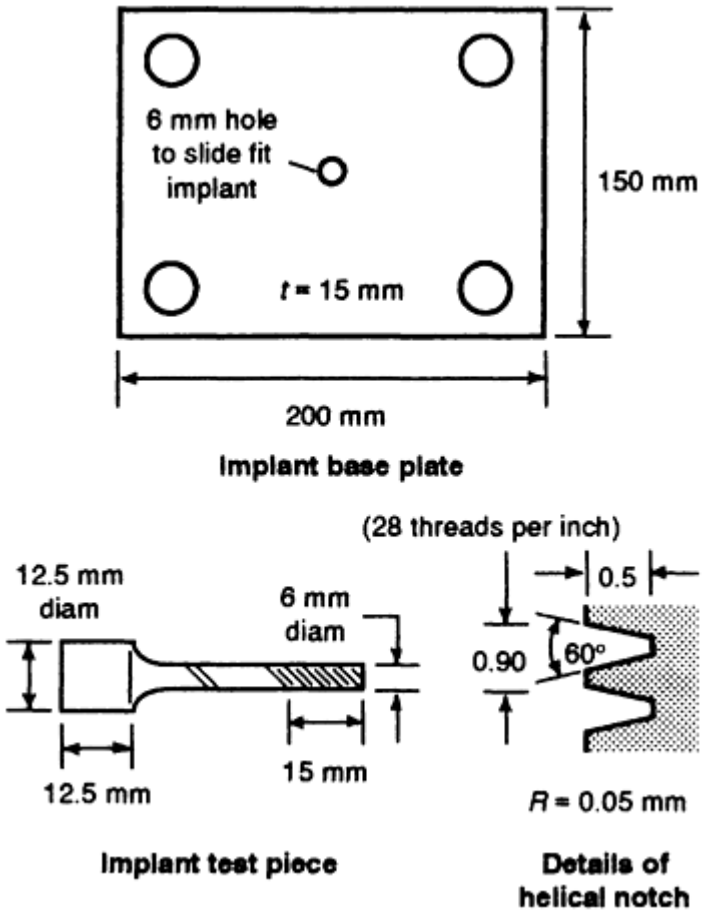

FIG. 10 SAMPLE SPECIFICATIONS FOR IMPLANT TEST SPECIMENS. SOURCE: REF 8

After welding (but within 60 s after weld completion), the test setup is placed in an apparatus that places a tensile stress on the rod, and this is maintained for 24 h, or until the weldment fails. Numerous samples are welded, then tested under different loads. The time to fail is plotted as a function of the loading stress. The crack susceptibility of the base metal is measured by the degree to which the failure stress is reduced with time.

Varestraint Test (Hot Crack Test). The Varestraint (variable restraint) test was developed at Rensselaer Polytechnic Institute (Ref 10). It is the most common test used to evaluate hot crack sensitivity. In this test, one end of a rectangular bar (typically 50 by 205 by 6.4 mm, or 2 by 8 by $\frac{1}{4}$ in.) is firmly mounted in a fixed position while the opposite end is attached to a hydraulic or pneumatic plunger (Fig. 11). A gas-tungsten arc weld is produced on the top side of the plate, along its longitudinal centerline, beginning at the unsupported end and moving toward the fixed end. When the welding arc reaches a predetermined location over a die block, the plate is bent to conform to the radius of the die block. This induces an augmented longitudinal strain on the welded surface of the specimen. The value of the strain is given approximately by:

$$e = \frac{t}{2R} \qquad \textbf{(EQ 3)}$$

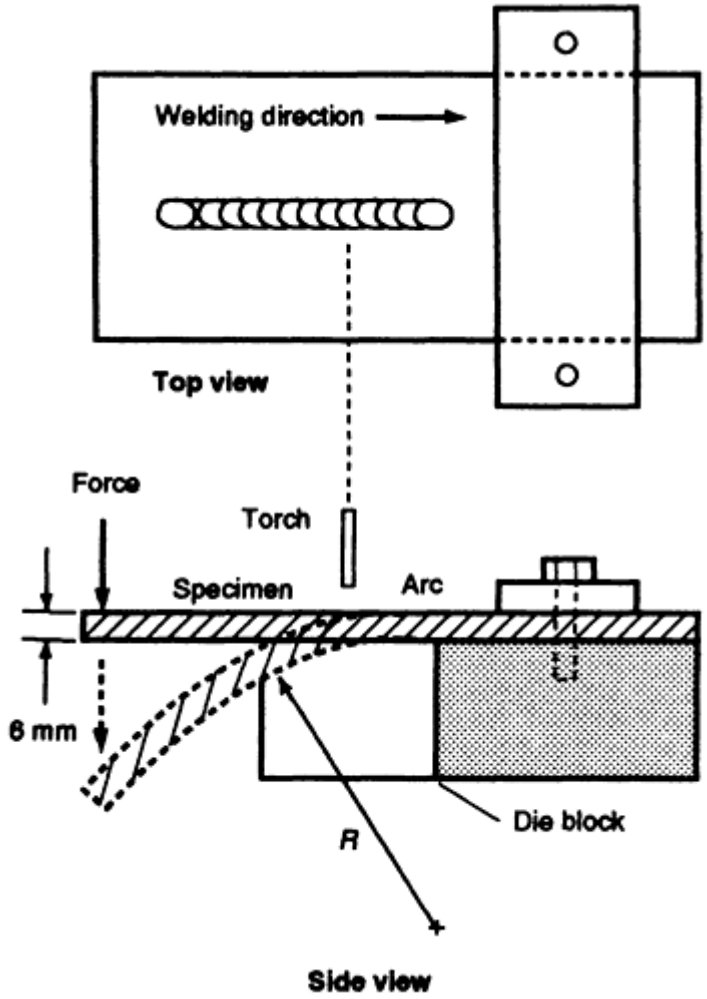

FIG. 11 SETUP AND SAMPLE SPECIFICATIONS FOR VARESTRAINT TEST. SOURCE: REF 7

Various die blocks with different radii can be used on samples of the same material to characterize the strain level at which cracking begins. Typically, for alloy evaluation, a single die block of known radius is used which will produce cracking in all samples. Hot cracks typically form radially along the trailing edge of the weld pool and in the HAZ. Duplicate samples of each alloy are tested, and mean values of total crack length, number of cracks, or maximum crack length are used as a quantitative means of base metal weldability (Ref 7).

The Varestraint test also has been used to test the hot crack susceptibility of filler material. By depositing filler wire on a plate (for example, with the gas-metal arc welding process) and then machining the specimen surface flush, a Varestraint test can be made using the GTAW process. This method has been used to evaluate the effect of base metal-filler material dilution on hot crack susceptibility.

The subscale Varestraint test uses a smaller sample (Fig. 12). This test uses the same testing equipment, but was developed for sheet material (Ref 11). Typical specimen size is 25 by 150 by 3.2 mm (1 by 6 by $\frac{1}{8}$ in.).

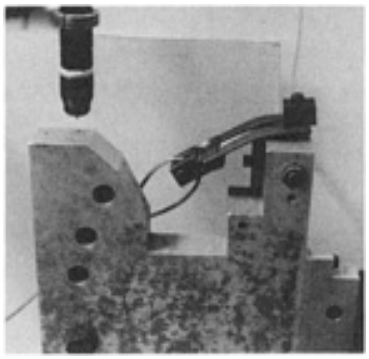

FIG. 12 PHOTO OF A TYPICAL SUBSCALE VARESTRAINT TEST APPARATUS. SOURCE: REF 11

Advantages of the Varestraint and subscale Varestraint tests are that they produce top surface cracks, both in the weld and the HAZ. Disadvantages are the cost of manufacturing or procuring the test equipment.

Another variation of this test is the trans Varestraint test, in which the sample is bent in a direction normal to the welding direction instead of the longitudinal direction. The loading in this test is tensile loading normal to the welding direction. This usually causes centerline cracks to form. The length of centerline cracks is used as a measure of hot crack susceptibility.

Spot Varestraint Test (Hot Crack Test). The spot Varestraint test is a modification of the Varestraint test; it is sometimes referred to as the TIG-A-MA-JIG test (Ref 10). In this test, a stationary welding torch is used to produce a gas-tungsten arc spot weld in the center of a rectangular sample (Fig. 13). The specimen size is typically 140 by 25 by 6.4 mm (5.5 by 1 by 0.25 in.). After the weld is established for a predetermined time, the test specimen is forced around a curved die block and the arc is extinguished. Hot cracks or hot tears form radially around the weld pool in the HAZ. The total crack length, maximum crack length, or strain level necessary to cause cracking is used as the measure of crack sensitivity. The spot Varestraint test is used mainly for evaluating susceptibility to HAZ hot cracking or liquation cracking (Ref 12).

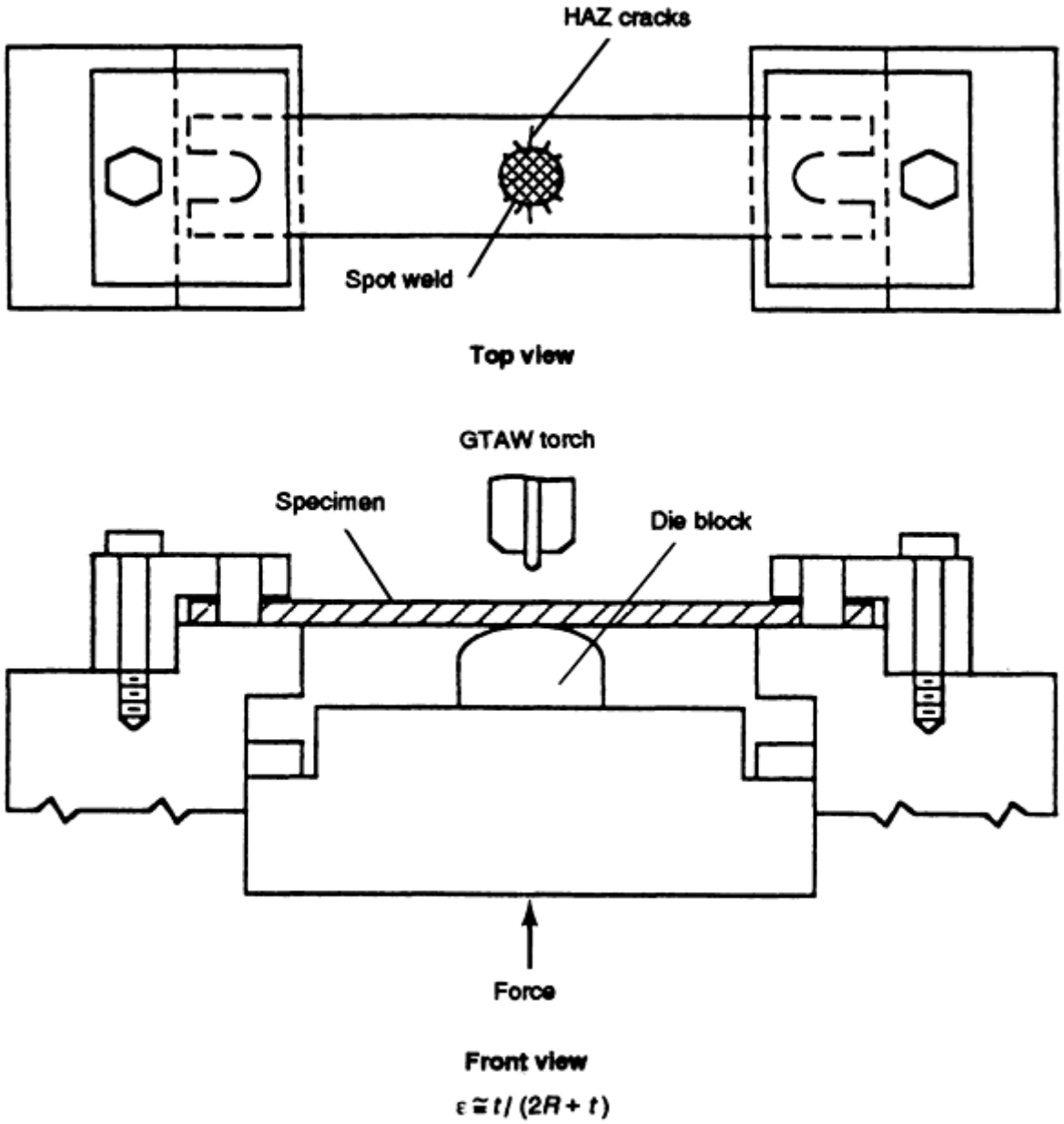

FIG. 13 SCHEMATIC SHOWING TOP AND FRONT VIEWS OF A SETUP USED IN SPOT VARESTRAINT TESTING. SOURCE: REF 12

One potential problem with the spot Varestraint test is that crater cracks often form, and they are difficult to distinguish from the other hot cracks. Also, extensive subsurface cracking often occurs, but cannot be detected without examination of metallographic cross sections. Reproducibility is difficult because slight variations often occur in welding conditions with the spot weld. A modified spot Varestraint test, developed at the University of Tennessee, moves the torch away from the pool prior to bending. This helps eliminate problems associated with crater cracks.

Sigmajig Test (Hot Crack Test). This test, developed at Oak Ridge National Laboratory, involves application of a transverse normal stress, σ, to a 50 by 50 mm (2 by 2 in.) sheet specimen (Fig. 14). An autogenous gas-tungsten arc weld is produced along the longitudinal centerline of the specimen. Numerous specimens are welded, with the stress being increased with each specimen, until centerline cracking occurs. A threshold stress level necessary to cause 100% cracking is used to quantify hot crack susceptibility (Ref 13). The advantages of this test are its usefulness for thin sheet, up to approximately 2.5 mm (0.1 in.).

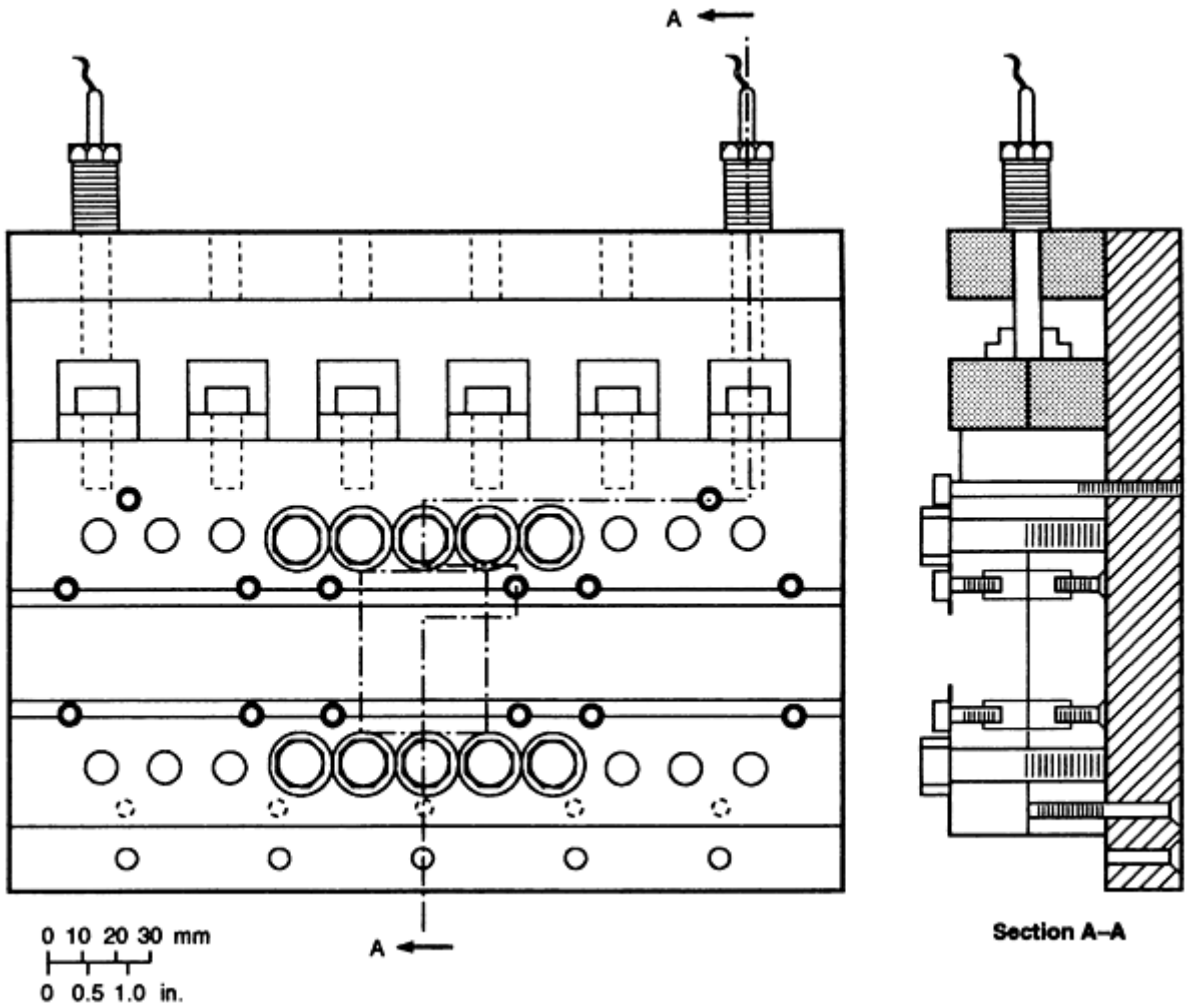

FIG. 14 RELATIONSHIP OF 50 BY 50 MM (2 BY 2 IN.) SHEET SPECIMEN TO APPARATUS USED IN SIGMAJIG TEST. SOURCE: REF 13

References cited in this section

6. "STANDARD WELDING TERMS AND DEFINITIONS," ANSI/AWS A3.0-89, AMERICAN WELDING SOCIETY, 1989
7. "WELDABILITY TESTING," CHAPTER 4, *WELDING HANDBOOK*, VOL 1, 8TH ED., AMERICAN WELDING SOCIETY, 1987
8. R.D. STOUT AND W.D. DOTY, *WELDABILITY OF STEELS*, WELDING RESEARCH COUNCIL, 1978
9. R.D. STOUT, *WELDABILITY OF STEELS*, WELDING RESEARCH COUNCIL, 1987
10. C.D. LUNDIN, A.C. LINGENFELTER, G.E. GROTKE, G.G. LESSMANN, AND S.J. MATTHEWS, THE VARESTRAINT TEST, *WELD. RES. COUNC. BULL.*, NO. 280, AUG 1982
11. R.D. CAMPBELL, "AN INVESTIGATION INTO THE PHYSICAL METALLURGY, WELDING METALLURGY, HOT CRACKING AND WELD POOL SHAPE OF FERRITIC STAINLESS STEELS," PH.D. THESIS, RENSSELAER POLYTECHNIC INSTITUTE, TROY, NEW YORK, 1987
12. W. LIN, J.C. LIPPOLD, AND W.A. BAESLACK, AN EVALUATION OF HEAT-AFFECTED ZONE LIQUATION CRACKING SUSCEPTIBILITY, PART I: DEVELOPMENT OF A METHOD FOR QUANTIFICATION, *WELD. J.*, VOL 72 (NO. 4), APRIL 1993, P 135-S TO 153-S
13. G.M. GOODWIN, DEVELOPMENT OF A NEW HOT-CRACKING TEST--THE SIGMAJIG, *WELD. J.*, VOL 66 (NO. 2), FEB 1987, P 33-S TO 38-S

Richard D. Campbell, Joining Services, Inc.; Daniel W. Walsh, California Polytechnic State University

Weldability Tests for Evaluating Weld Pool Shape, Fluid Flow, and Weld Penetration

Weld pool shape, fluid flow, and the subsequent weld penetration and weld profile are important characteristics in industrial welding applications. Improvements in material processing have resulted in alloys with much "cleaner" chemical analyses. Small changes in the amounts of certain trace elements have been shown to cause dramatic variations in weld pool shape and penetration (Ref 14). Predictable and reproducible weld shape and weld penetration are critical in many applications. As a result, several weldability tests have been developed to evaluate base material response characteristics. Although these tests are not as standardized as the others described above, they are becoming increasingly important, both for alloy development and for production welding applications.

Weld Penetration Tests. Individual companies have developed tests for evaluating the penetration behavior of base metals. A simple weld test utilizes a bar stock sample on which an autogenous gas-tungsten arc, bead-on-plate, partial-penetration weld is produced (Fig. 15). A single set of welding parameters and the same heat sinking are used to test different heats of the same base materials. After welding, the sample is metallographically cross sectioned and etched. Measurements are made of the weld bead width (*W*) and depth of penetration (*D*); from these dimensions, a depth-to-width ratio (*D*/*W*) is calculated.

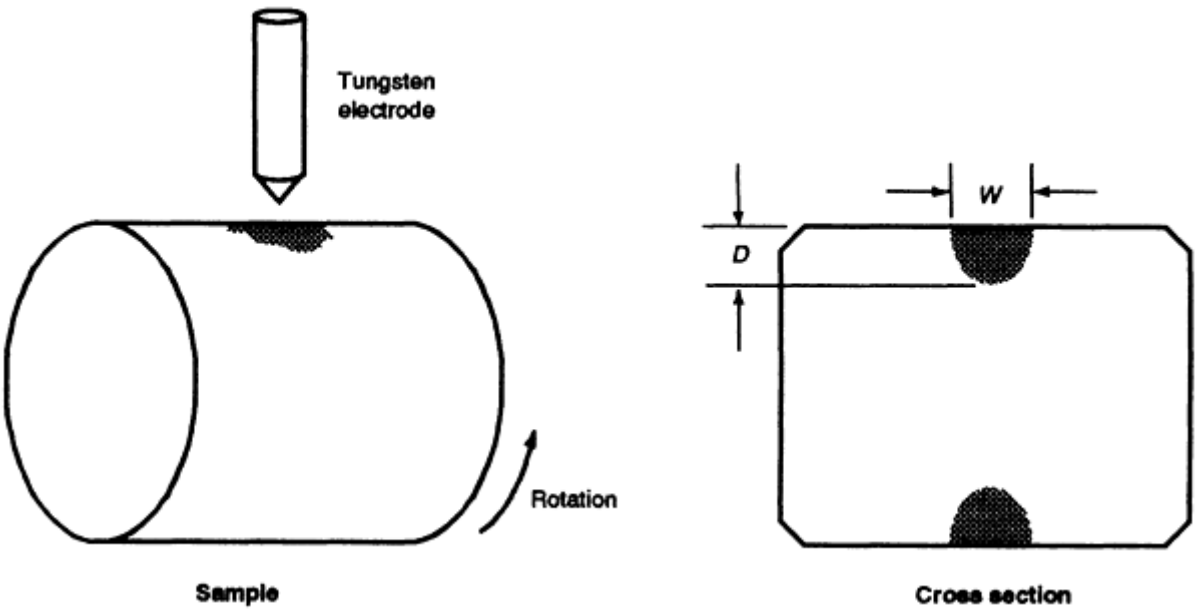

FIG. 15 POSITION OF WELD RELATIVE TO SOLID BAR STOCK IN PARTIAL PENETRATION WELD TEST. SOURCE: REF 14

The *D*/*W* ratio can be used to characterize the weld penetration characteristics of base materials and different heats of the same materials. For production applications, this provides information about the material response before components reach the production welding area. The advantage of this partial-penetration test is that measurements of the solidified weld bead are made. These data characterize the response of the material to all forces that affect weld bead shape, without the influence of a backside or underbead.

Full-penetration weld tests can also be used. These tests are applicable when the weldability test specimen is similar in geometry to the production weldment. However, full-penetration weld shape is complicated because, in some cases, three-dimensional heat flow applies, while in other cases, two-dimensional heat flow applies. Heat buildup on the backside,

weld joint shape, and-heat sinking dramatically affect the final weld shape. As a result, full-penetration weldability tests are useful only when the production geometry is used in the test (Ref 14).

Weld Pool Shape Tests. Weld pool shape is determined by a complex set of factors that include process and material variables (Ref 15, 16, 17). Pool shape determination is of interest for basic research and for production applications. Walsh, Campbell, and Savage (Ref 18) pointed out that determinations of pool shape based on metallographic cross sections are incomplete, and subject to error even in stationary welds. Any arc or weld pool motion that sweeps out a width or length greater than the instantaneous pool dimensions cannot be detected on metallographic cross sections. Many critical geometric features of the weld pool could be overlooked if a true three-dimensional measurement was not made.

Some work has been done to characterize the three-dimensional shape of weld pools (Ref 19, 20). However, techniques based on gravity and gunshots have drawbacks, principally lack of speed and contamination, respectively. A new weldability test, called an impulse decanting test, is shown in Fig. 16. This test utilizes a high-pressure jet of argon gas that is impulse-released through the bottom of a modified GTAW torch to decant, or expel, the liquid weld pool. A control box contains the necessary timing circuitry and system relays to extinguish the welding arc and fire the solenoid valve on an accumulator tank that holds the argon.

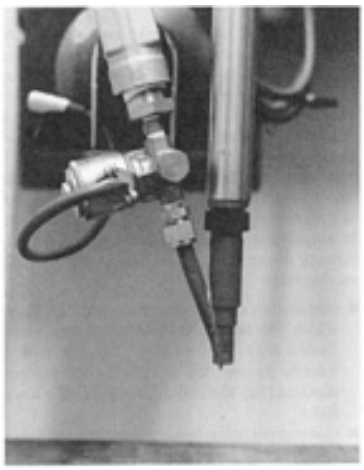

FIG. 16 TYPICAL SETUP USED TO MEASURE WELDABILITY USING THE IMPULSE DECANTING TEST. SOURCE: REF 11

The decanted weld pool shape can be evaluated by two methods:

- USING SILICONE RUBBER TO REPLICATE THE WELD POOL CAVITY
- VISUALLY MEASURING THE WELD POOL CAVITY DIMENSIONS ALONG THE SAMPLE TOP SURFACE, AND ALSO ON A METALLOGRAPHIC TRANSVERSE CROSS SECTION OF THE CAVITY

The silicone rubber replicas are the best method (Fig. 17), because they accurately provide the weld pool length, width, depth, volume, and surface area. This test method is extremely valuable to investigators of weld pool modeling.

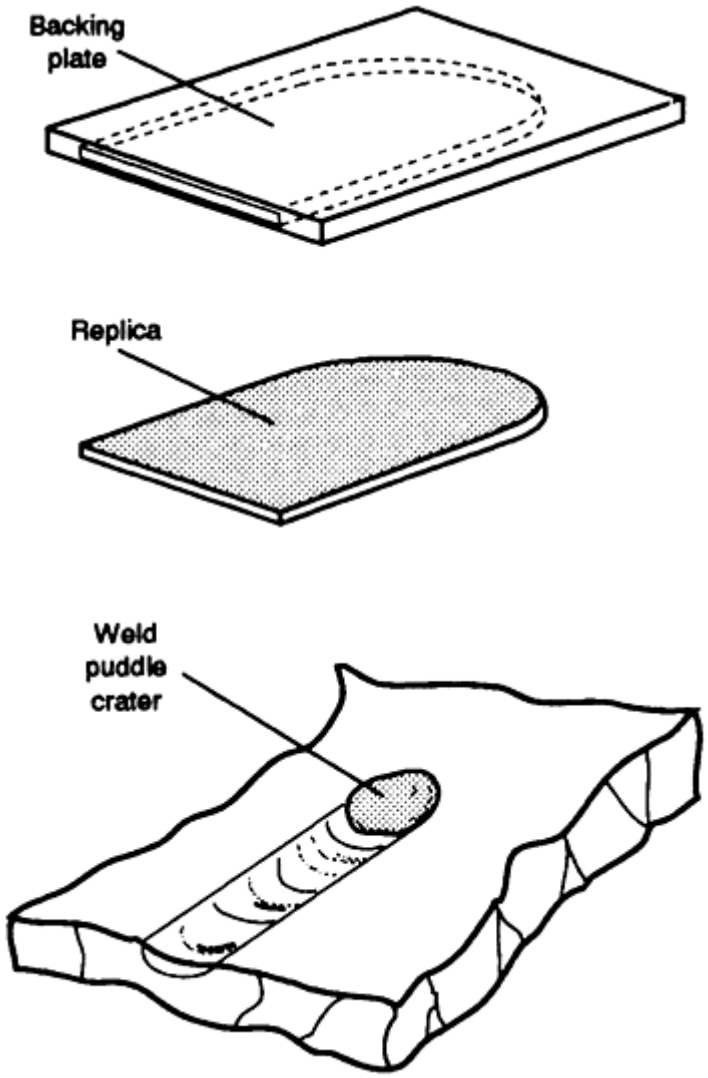

FIG. 17 SILICONE RUBBER REPLICATION TECHNIQUE USED TO EVALUATE DECANTED WELD POOL SHAPE. SOURCE: REF 21

References cited in this section

11. R.D. CAMPBELL, "AN INVESTIGATION INTO THE PHYSICAL METALLURGY, WELDING METALLURGY, HOT CRACKING AND WELD POOL SHAPE OF FERRITIC STAINLESS STEELS," PH.D. THESIS, RENSSELAER POLYTECHNIC INSTITUTE, TROY, NEW YORK, 1987
14. P. BURGARDT AND R.D. CAMPBELL, CHEMISTRY EFFECTS ON STAINLESS STEEL WELD PENETRATION, CHAPTER 13, *FERROUS ALLOY WELDMENTS*, TRANS TECH PUBLICATIONS, SWITZERLAND, 1992
15. D.W. WALSH AND W.F. SAVAGE, THE MECHANISM OF MINOR ELEMENT INTERACTION IN AUTOGENOUS WELD POOLS, *ADVANCES IN WELDING TECHNOLOGY INTERNATIONAL CONF. PROC.* (GATLINBURG, TN), 18 MAY 1986, AMERICAN SOCIETY FOR METALS, P 59-63
16. C.R. HEIPLE AND J.R. ROPER, EFFECTS OF MINOR ELEMENTS ON GTAW FUSION ZONE SHAPE, *TRENDS IN WELDING RESEARCH IN THE UNITED STATES*, CONF. PROC. (NEW ORLEANS, LA), NOV 1981
17. S.S. GLICKSTEIN AND W. YENISCAVICH, "A REVIEW OF MINOR ELEMENT EFFECTS ON THE WELDING ARC AND WELD PENETRATION," BULLETIN 226, WELDING RESEARCH COUNCIL, MAY 1977

18. D.W. WALSH, R.D. CAMPBELL AND W.F. SAVAGE, UNPUBLISHED RESEARCH, RENSSELAER POLYTECHNIC INSTITUTE, TROY, NY, 1986
19. F.J. ZANNER, PH.D. THESIS, RENSSELAER POLYTECHNIC INSTITUTE, TROY, NEW YORK, JUNE 1967
20. D.W. WALSH, "MINOR ELEMENT EFFECTS ON GAS TUNGSTEN ARC WELDS," PH.D. THESIS, RENSSELAER POLYTECHNIC INSTITUTE, TROY, NEW YORK, JUNE 1986
21. W.F. SAVAGE, E.F. NIPPES, AND F.J. ZANNER, *WELD. J.*, VOL 57 (NO. 7), JULY 1978, P 201

Richard D. Campbell, Joining Services, Inc.; Daniel W. Walsh, California Polytechnic State University

Gleeble Testing

The Gleeble, a thermomechanical testing device, has been used in a wide range of applications involving study of a variety of material problems. These include, but are not limited to, studies of hot ductility (Ref 22, 23, 24, 25), mechanical properties of the weld HAZ (Ref 26, 27, 28, 29, 30, 31, 32, 33, 34, 35), continuous cooling transformation diagrams (Ref 36, 37, 38), stress relief cracking (Ref 39), precipitation kinetics (Ref 40), basic weldability (Ref 41, 42, 43, 44, 45), strain age cracking (Ref 46, 47), constitutional liquation (Ref 48), liquid metal embrittlement (LME) (Ref 49, 50), and solidification of austenitic stainless steel weldments (Ref 51, 52). The Gleeble system permits simulation of virtually any thermomechanical process. The device is used in a variety of applications and is in no way limited by its historical application to welding.

The Gleeble test method is shown schematically in Fig. 18. Stainless steel samples being tested under load and no-load conditions are shown in Fig. 19(a) and 19(b), respectively. The Gleeble is a fully computer interfaced system, readily programmed to provide reference signals for closed loop control of both thermal and mechanical operations. Heating is accomplished by the flow of low-frequency alternating current in the specimen, and heating rates up to 20,000 °C/s (36,000 °F/s) per second can be obtained (Ref 54). The feedback signal necessary for closed-loop control is normally obtained from a fine wire thermocouple percussion welded to the specimen surface. However, for temperatures above the operating limits of thermocouples, a radiation pyrometer can be employed at some sacrifice in the overall response time of the system.

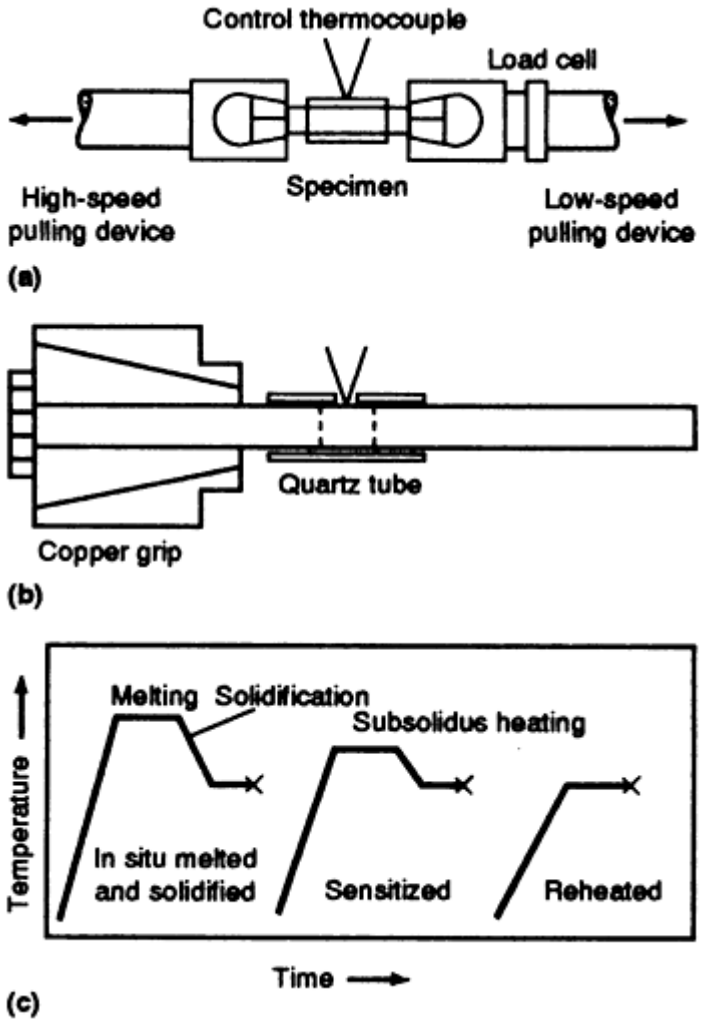

FIG. 18 GLEEBLE TEST METHOD. (A) PRIMARY COMPONENTS. (B) CLOSE-UP VIEW OF RESISTANCE HEATER. (C) PROGRAMMED THERMAL CYCLE. SOURCE: REF 53

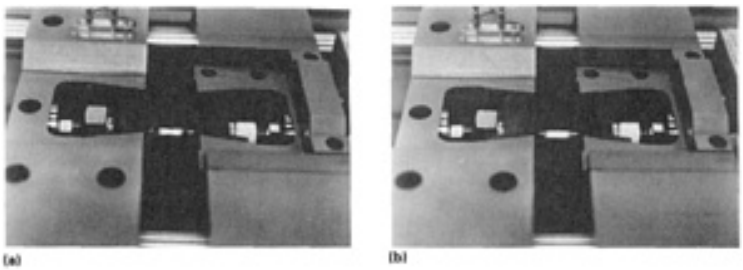

FIG. 19 GLEEBLE TESTING OF A 6 MM (0.236 IN.) DIAMETER STAINLESS STEEL BAR AT 1100 °C (2010 °F). (A) SAMPLE UNDER NO-LOAD CONDITION (NOTE UNIFORMITY OF REPRODUCIBLE THERMAL GRADIENT). (B) SAMPLE UNDER LOAD AT ELEVATED TEMPERATURES TO EVALUATE DUCTILITY

The Gleeble has a long and proven history as a tool for both the study of metallurgical phenomena at the research level and for materials testing to predict service behavior at the production level. A major advantage of the Gleeble is that it generates large volumes of microstructure that simulate small, hard-to-study regions in actual weldments.

Gleeble test samples take on an unlimited variety of sizes and shapes, based on material availability and project application. The following is a discussion of round bar samples, as they are the most typical samples studied. The concepts discussed can be extended to a variety of geometries.

A given test sample is a system in dynamic thermal equilibrium with its surroundings. Thus, to maintain any given temperature profile, heat is supplied by the electrical current passing through the specimen, and heat is lost by three mechanisms:

- CONDUCTION ALONG THE SPECIMEN ITSELF, IN WHICH THE HEAT IS TRANSFERRED TO THE WATER-COOLED JAWS. THE RATE OF THIS HEAT FLOW IS DIRECTLY PROPORTIONAL TO BOTH THE THERMAL GRADIENT AND THE THERMAL DIFFUSIVITY OF THE MATERIAL.
- CONVECTION IN THE GASEOUS ATMOSPHERE, WHICH REMOVES HEAT AND DISSIPATES IT TO THE SURROUNDINGS BY MIXING.
- RADIATION EMITTED BY THE SPECIMEN. THE AMOUNT OF HEAT LOST THROUGH THIS MODE IS PROPORTIONAL TO THE FOURTH POWER OF THE ABSOLUTE TEMPERATURE, AND THEREFORE BECOMES MORE IMPORTANT AT HIGH TEMPERATURES.

Thus, the thermal profile generated by a given peak temperature, jaw separation, specimen diameter, and material type is determined by a complex interplay of these mechanisms in establishing a thermal balance.

The Gleeble specimen may be treated as a uniform cylindrical bar with internal generation of heat. If convection and radiation losses are neglected, the principle of the conservation of energy leads to the following relationships for the instantaneous temperature distribution in the bar:

$$\frac{\partial T}{\partial t} = \frac{K}{r C_p} \nabla^2 T + \frac{t^2}{r C_p w^2 s} \qquad \textbf{(EQ 4)}$$

where C_p is the heat capacity at constant pressure; ∇ is the del operator; I is the current; ω is the area in cross section; σ is the electrical conductivity; K is the thermal conductivity; T is the temperature; ρ is the density; and t is the time.

If the system is simplified by limiting the heat flow to one dimension, Eq 4 becomes:

$$\frac{\partial T}{\partial t} = \frac{K}{r C_p} \frac{\partial^2 T}{\partial x^2} + \frac{t^2}{r C_p w^2 s} \qquad \textbf{(EQ 5)}$$

This relationship closely approximates the behavior of a resistance-heated specimen. If the temperature distribution within the bar is assumed to be steady state, Eq 5 reduces to the Poisson relation:

$$\frac{\partial^2 T}{\partial x^2} = \frac{-I^2}{K w^2 s} \qquad \textbf{(EQ 6)}$$

Therefore, if radiation and convection losses are ignored, the temperature distribution in the bar will be a parabolic one. This can be demonstrated by double integration of Eq 6 to obtain:

$$T(x) = \frac{-I^2}{K w^2 s} x^2 + c' + c'' \qquad \textbf{(EQ 7)}$$

The constants of c' and c'' can be determined for specific boundary conditions. Solutions to this equation exist in the literature (Ref 55) and have been applied to the determination of the lengths over which the temperature of the bar lies, between the maximum, T_{max}, and some arbitrary lower temperature, T_0. This length is given by the following:

$$L = L_o\left(\frac{\Delta T}{T_{\max} - T_o}\right)^{1/2} \qquad \textbf{(EQ 8)}$$

where L is the length at or above arbitrary temperature; L_0 is the jaw separation; T_0 is the temperature at the jaw; and ΔT is the difference between peak temperature and arbitrary temperature.

However, problems exist for this simplified treatment because experimental results do not fit the model well. Several factors contribute to this. The thermal conductivity, K, is not a constant, and being itself a function of temperature can be presented as:

$$K = K_0(1 - BT) \qquad \textbf{(EQ 9)}$$

where K_0 is the thermal conductivity at absolute zero if conductivity is treated linearly.

However, because the value of b is small, an average value of K can be used over a small range of temperatures without generating an excessively large error.

The mathematics of the system become more complex when treatments for either convection or radiation heat transfer are included. Heat loss by either mechanism will tend to flatten the parabolic profile predicted by Eq 7. Convection losses can be represented by adding a single term to the Poisson equation to obtain:

$$\frac{K}{rC_p}\frac{\partial^2 T}{\partial x^2} + \frac{-I^2}{rC_p w^2 s} - \frac{hg}{rC_p w}(T - T_o) = 0 \qquad \textbf{(EQ 10)}$$

where h is the convective heat transfer coefficient and γ is the dependent constant relative to geometry.

The inclusion of another temperature-dependent term makes the solution to the differential equation more complex, and leads to solutions involving hyperbolic functions. The addition of a term for radiation losses further complicates the solution because the radiative heat loss, Q_{12}, is proportional to the fourth power of absolute temperature:

$$Q_{12} = F_{12}\alpha(T_1^4 - T_2^4) \qquad \textbf{(EQ 11)}$$

where Q_{12} is the heat transfer from body 1 to body 2; F_{12} is the view factor, body 1 to body 2; T_1 is the temperature of body 1; and α is the Stefan-Boltzmann constant. The constants h, in the convective solution, and α, in the radiative solution, are small, and high temperatures are required before convection and radiation play a major role in determining the temperature profile in the bar.

Walsh, Savage and Cieslak (Ref 56) reported an empirical study of carbon and stainless steel that related test parameters to the extent of a uniform temperature region in Gleeble samples. They developed polynomial equations that describe longitudinal and radial thermal profiles that exist in test samples under a wide variety of operator-controlled conditions. At any particular peak temperature, a span in which the temperature lies within a specified percentage of the peak temperature can be generated by a judicious choice of operating conditions and specimen geometries.

Gleeble testing has been used to study a variety of phenomenon in electrically conductive materials. However, the discussion of its application to weldability testing will be limited to studies of hot cracking and hot ductility. Information about other applications of Gleeble testing is available in the References cited in this article.

Hot Ductility Testing. The development of high-performance materials and increasingly rigid standards for quality, coupled with the jux-taposition of very different materials in engineering assemblies, has led to significant increases in the difficulty associated with producing satisfactory weldments. The temperatures and steep thermal gradients associated with welding produce high stresses and complex transient stress patterns. These factors often combine to produce cracking in the weld and HAZ region. The rapid thermal cycle associated with the welding process produces a plethora of microstructures in the weld/HAZ region, and weld understood metallurgical transformations associated with heating and cooling become complex under the nonequilibrium conditions associated with the welding process.

Goodwin (Ref 57) has pointed out that hot cracking is an often-studied, yet poorly understood phenomena. Hot cracking results when a susceptible microstructure is subjected to tensile stresses, and it occurs while liquid and solid phases coexist. A successful hot cracking test must reproduce combinations of restraint and microstructure that can be used to differentiate the crack sensitivity of different materials (Ref 57). Several hot cracking tests are described in the section "Weldability Tests for Evaluating Cracking Susceptibility" in this article.

Borland (Ref 58) described features required of an ideal hot crack test--it should be inexpensive, simple, brief, directly correlatable to fabrication parameters and service conditions, reproducible, free from operator error, and applicable to all welding processes. In addition to these criteria, the test should also produce easily interpretable results, be amenable to modeling, be quantitative, and above all, be universally accepted (Ref 57). It is very difficult to conceive of a single test that could satisfy all these criteria; however, many investigators have found that the combination of Varestraint or Varestraint-like testing and Gleeble testing yields results that can be used to provide a state-of-the-art characterization of weldability. (The Varestraint test is described in the section "Varestraint Test (Hot Crack Test)" in this article.)

Gleeble testing provides a complete characterization of hot ductility related to hot crack susceptibility. In the Gleeble test, small cylindrical tensile samples are fractured during heating or during cooling from specified temperatures. Reduction-in-area and ultimate tensile strength data are used to generate strength and ductility curves upon cooling and upon heating. A number of factors are important to the test, including heating and cooling rates, peak temperatures, hold times, and stroke rates. A number of investigators have examined the effects of changes to these parameters and found that the peak temperature of the test is by far the most crucial. The magnitude of effects that changes to other parameters produce is a strong function of material and material condition.

Weiss, Grotke, and Stickler (Ref 25) discuss the physical metallurgy of hot ductility testing and the use of the Gleeble in studying alloy weldability. Hot cracking is caused by the presence of persistent liquid films on grain boundaries. These films are unable to accommodate strains that are produced by mechanical restraint and/or transient thermal distributions during cooling. Hot cracking will not occur unless a susceptible microstructure is exposed to critical level of restraint. Several characteristic temperatures that can be used to classify material weldability have been identified using the Gleeble. In hot ductility testing, the nil temperature (NDT) is the temperature upon heating at which the material ductility goes to zero; in essence, the temperature at which all surfaces are coated by a thin liquid layer. The nil strength temperature (NST) is the temperature upon heating at which the strength of a material drops essentially to zero; in essence, the temperature at which liquid layers thicken to the point that minimal capillarity exists. The ductility recovery temperature is the temperature upon cooling at which an arbitrary ductility is observed.

Investigators have used a wide variety of criteria to interpret hot ductility curves produced using the Gleeble. Nippes, Savage, and Grotke (Ref 23) published a classification of hot ductility curves encountered during testing of stainless steels and nickel-base alloys. The criteria most widely used include minimum arbitrary ductility, recovery rate of ductility, recovery rate of ultimate strength, zero-ductility range, and the presence of ductility dips (Ref 31). Kreischer (Ref 24) published a critical review of hot ductility testing and suggested that:

- WHEN THE NST IS USED AS THE PEAK TEMPERATURE IT PROVIDES MUCH MORE ACCURATE INDICATION OF HOT CRACK SUSCEPTIBILITY THAN THE NDT
- ALLOYS EXHIBITING HIGH DUCTILITIES UPON HEATING AND RAPID RECOVERY OF DUCTILITY UPON COOLING FROM THE NST ARE CRACK RESISTANT
- ALLOYS WITH HIGH TENSILE STRENGTH AT ELEVATED TEMPERATURES CAN BE CRACK RESISTANT DESPITE LOW DUCTILITIES
- ALLOYS WITH RELATIVELY LOW TENSILE STRENGTHS AT ELEVATED TEMPERATURE, IN CONCERT WITH ONLY MODERATE DUCTILITIES, ARE NORMALLY CRACK SENSITIVE

Lin, Lippold, and Baeslack (Ref 59, 60) have detailed a methodology for quantifying crack susceptibility using the Gleeble hot ductility test.

References cited in this section

22. E.F. NIPPES AND W.F. SAVAGE, AN INVESTIGATION OF THE HOT DUCTILITY OF HIGH-TEMPERATURE ALLOYS, *WELD. J.*, VOL 34 (NO. 4), 1955, P 183-S TO 196-S

23. E.F. NIPPES, W.F. SAVAGE, AND G. GROTKE, "FURTHER STUDIES OF THE HOT DUCTILITY OF HIGH-TEMPERATURE ALLOYS," BULLETIN SERIES VOL 33 (NO. 2), WELDING RESEARCH COUNCIL, 1957
24. C.H. KREISCHER, A CRITICAL ANALYSIS OF THE WELD HEAT-AFFECTED ZONE HOT DUCTILITY TEST, *WELD. J.,* VOL 42 (NO. 2), 1963, P 49-S TO 59-S
25. B. WEISS, B.E. GROTKE, AND R. STICKLER, PHYSICAL METALLURGY OF HOT DUCTILITY TESTING, *WELD. J.,* VOL 49 (NO. 10), 1970, P 471-S TO 487-S
26. E.F. NIPPES, W.F. SAVAGE, AND J.M. PAEZ, IMPACT CHARACTERISTICS OF HEAT-AFFECTED ZONES IN MN-MO ARMOR STEELS, *WELD. J.,* VOL 39 (NO. 1), 1960, P 31-S TO 39-S
27. K.C. WU, A STUDY OF THE WELD HEAT-AFFECTED ZONE OF CENTRIFUGALLY CAST 5% CHROMIUM STEEL, *WELD. J.,* VOL 42 (NO. 9), 1963, P 392-S TO 396-S
28. E.F. NIPPES AND E.W. EMMERICH, HEAT-AFFECTED ZONE STUDY OF AN EUTECTOID ULTRA-HIGH STRENGTH STEEL, *WELD. J.,* VOL 42 (NO. 12), 1963, P 547-S TO 556-S
29. W.A. PETERSON, WELD HEAT-AFFECTED ZONE OF 18% NICKEL MARAGING STEEL, *WELD. J.,* VOL 43 (NO. 9), 1964, P 428-S TO 432-S
30. W.F. SAVAGE AND B.M. KRANTZ, AN INVESTIGATION OF HOT CRACKING IN HASTELLOY X, *WELD. J.,* VOL 45 (NO. 1), 1966, P 13-S TO 25-S
31. W.A. OWCZARSKI, D.S. DUVAL, AND C.P. SULLIVAN, A MODEL FOR HEAT-AFFECTED ZONE CRACKING IN NICKEL-BASE SUPERALLOYS, *WELD. J.,* VOL 45 (NO. 4), 1966, P 145-S TO 155-S
32. L.P. CONNOR, A.M. RATHBONE, AND J.H. GROSS, EFFECTS OF COMPOSITION ON THE HEAT-AFFECTED ZONE TOUGHNESS OF CONSTRUCTIONAL ALLOY STEELS, *WELD. J.,* VOL 46 (NO. 5), 1967, P 217-S TO 234-S
33. R.A. MUELLER, D.G. HOWDEN, AND F.B. SIMMONS, HAZ THERMOCYCLE AND STRUCTURE SIMULATION, *WELD. J.,* VOL 52 (NO. 10), 1973, P 411-S TO 416-S
34. N.E. HANNERY, EFFECT OF CB ON HAZ DUCTILITY IN CONSTRUCTIONAL HT STEELS, *WELD. J.,* VOL 54 (NO. 5), 1975, P 162-S TO 168-S
35. S.J. MATTHEWS, SIMULATED HEAT-AFFECTED ZONE STUDIES OF HASTELLOY ALLOY B-2, *WELD. J.,* VOL 58 (NO. 3), 1979, P 91-S TO 95-S
36. R.F. FASTINI AND M. SEMCHYSHEN, THE EFFECT OF MOLYBDENUM ON THE CONTINUOUS COOLING TRANSFORMATION OF A 0.40% CARBON STEEL, *ASM TRANS. QUART.,* SEPT 1964
37. D.G. HOWDEN, ISOTHERMAL TRANSFORMATION CHARACTERISTICS OF A LOW-ALLOY STEEL USING A WELD THERMAL CYCLE SIMULATOR, *CAN. METALL. QUART.,* VOL 6 (NO. 3), 1967
38. K.C. WU, CONTINUOUS-COOLING TRANSFORMATION DIAGRAMS OF TI-8A1-MO-1V, *TRANS. ASM,* VOL 61, 1968, P 621-626
39. C.F. MEITZNER AND A.W. PENSE, STRESS-RELIEF CRACKING IN LOW-ALLOY STEEL WELDMENTS, *WELD. J.,* VOL 48 (NO. 10), 1969, P 431-S TO 440-S
40. A.W. DIX AND W.F. SAVAGE, SHORT TIME AGING CHARACTERISTICS OF INCONEL X-750, *WELD. J.,* VOL 52 (NO. 3), 1973, P 135-S TO 144-S
41. S.J. MATTHEWS, WELDABILITY OBSERVATIONS IN 70/30 COPPER-NICKEL TUBESHEET MATERIAL, *WELD. J.,* VOL 47 (NO. 4), 1968, P 155-S TO 161-S
42. K.C. WU AND T.A. KRINKE, WELDABILITY STUDIES FOR AFC-77--PART 1: MECHANICAL PROPERTIES, *WELD. J.,* VOL 47 (NO. 6), 1968, P 332-S TO 336-S
43. W.A. PETERSON, WELDABILITY OF A CHROMIUM STRENGTHENED COPPER-NICKEL ALLOY, *WELD. J.,* VOL 48 (NO. 10), 1969, P 425-S TO 430-S
44. J. GORDINE, THE WELDABILITY OF SOME ARTIC-GRADE LINE-PIPE STEELS, *WELD. J.,* VOL 56 (NO. 7), 1977, P 201-S TO 210-S
45. W.F. SAVAGE, E.F. NIPPES, AND J.E. CASTERAS, EFFECT OF ALLOYING ADDITIONS ON THE WELDABILITY OF 70 CU-30 NI, *WELD. J.,* VOL 57 (NO. 12), 1978, P 375-S TO 382-S

46. W.P. HUGHES AND T.F. BERRY, A STUDY OF THE STRAIN-AGE CRACKING CHARACTERISTICS IN WELDED RENE 41--PHASE 1, *WELD. J.*, VOL 46 (NO. 8), 1967, P 361-S TO 370-S
47. A.W. DIX AND W.F. SAVAGE, FACTORS INFLUENCING STRAIN-AGE CRACKING IN INCONEL X-750, *WELD. J.*, VOL 50 (NO. 6), 1971, P 247-S TO 252-S
48. J.J. PEPE AND W.F. SAVAGE, EFFECTS OF CONSTITUTIONAL LIQUATION IN 18-NI MARAGING STEEL WELDMENTS, *WELD. J.*, VOL 46 (NO. 9), 1967, P 411-S TO 422-S
49. W.F. SAVAGE, E.F. NIPPES, AND M.C. MUSHALA, COPPER-CONTAMINATION CRACKING IN THE WELD HEAT-AFFECTED ZONE, *WELD. J.*, VOL 57 (NO. 5), 1978, P 237-S TO 245-S
50. W.F. SAVAGE, E.F. NIPPES, AND M.C. MUSHALA, LIQUID-METAL EMBRITTLEMENT OF THE HEAT-AFFECTED ZONE BY COPPER CONTAMINATION, *WELD. J.*, VOL 57 (NO. 8), 1978, P 237-S TO 245-S
51. J.C. LIPPOLD AND W.F. SAVAGE, SOLIDIFICATION OF AUSTENITIC STAINLESS STEEL WELDMENTS: PART 1--A PROPOSED MECHANISM, *WELD. J.*, VOL 58 (NO. 12), 1979, P 362-S TO 374-S
52. J.C. LIPPOLD AND W.F. SAVAGE, SOLIDIFICATION OF AUSTENITIC STAINLESS STEEL WELDMENTS: PART 2--THE EFFECT OF ALLOY COMPOSITION ON FERRITE MORPHOLOGY, *WELD. J.*, VOL 59 (NO. 2), 1980, P 48-S TO 58-S
53. COMPUTERIZED THERMAL AND MECHANICAL TESTING MACHINE A SIGNIFICANT ASSET IN RESEARCH, DEVELOPMENT AND PRODUCTION, *INDUSTRIAL HEATING*, VOL 53 (NO. 12), DEC 1986
54. H. FERGUSON, METALWORKING PROCESS SIMULATIONS SAVE PRODUCTION HEADACHES, *MET. PROG.*, SEPT 1986, P 39-42
55. D.J. WIDGERY, THE DESIGN AND USE OF RESISTANCE HEATED WELD THERMAL SIMULATORS, *PROC. CONF. WELD THERMAL SIMULATORS FOR RESEARCH AND PROBLEM SOLVING*, THE WELDING INSTITUTE, CAMBRIDGE, ENGLAND, APRIL 1972
56. D.W. WALSH, M.J. CIESLAK, AND W.F. SAVAGE, TEMPERATURE MEASUREMENTS IN RESISTANCE HEATED SPECIMENS: LONGITUDINAL GRADIENTS, *WELD. J.*, VOL 65 (NO. 8), 1986, P 184-S TO 192-S
57. G.M. GOODWIN, *PROC. 1ST JAPAN-U.S. SYMPOSIUM ON ADVANCES IN WELDING METALLURGY* (SAN FRANCISCO, CA), JUNE 1990, P 27-39
58. J.C. BORLAND, *BR. WELD. J.*, VOL 7 (NO. 8), 1961, P 508-512
59. W. LIN, W.A. BAESLACK, AND J.C. LIPPOLD, HOT DUCTILITY TESTING OF HIGH-STRENGTH, LOW-EXPANSION SUPERALLOYS, *RECENT TRENDS IN WELDING AND TECHNOLOGY LNT. CONF. PROC.* (GATLINBURG, TN), 14 MAY 1989, ASM INTERNATIONAL, P 609-614
60. W. LIN, W.A. BAESLACK, AND J.C. LIPPOLD, A METHOD FOR QUANTIFYING HAZ LIQUATION CRACKING SUSCEPTIBILITY USING THE GLEEBLE HOT-DUCTILITY TEST, *PROC. INT. SYMP. PHYSICAL SIMULATION*, DELFT, 1992, P 93-99

Weldability Testing

Richard D. Campbell, Joining Services, Inc.; Daniel W. Walsh, California Polytechnic State University

---

References

1. "WELDING TECHNOLOGY," CHAPTER 12, *WELDING HANDBOOK*, VOL 1, 8TH ED., AMERICAN WELDING SOCIETY, 1987
2. "STANDARD METHODS FOR MECHANICAL TESTING OF WELDS," ANSI/AWS B4.0-85, AMERICAN WELDING SOCIETY, 1985

3. *MECHANICAL TESTING,* VOL 8, *ASM HANDBOOK,* AMERICAN SOCIETY FOR METALS, 1985
4. *METALLOGRAPHY AND MICROSTRUCTURES,* VOL 9, *ASM HANDBOOK,* AMERICAN SOCIETY FOR METALS, 1985
5. *NONDESTRUCTIVE EVALUATION AND QUALITY CONTROL,* VOL 17, *ASM HANDBOOK,* ASM INTERNATIONAL, 1989
6. "STANDARD WELDING TERMS AND DEFINITIONS," ANSI/AWS A3.0-89, AMERICAN WELDING SOCIETY, 1989
7. "WELDABILITY TESTING," CHAPTER 4, *WELDING HANDBOOK,* VOL 1, 8TH ED., AMERICAN WELDING SOCIETY, 1987
8. R.D. STOUT AND W.D. DOTY, *WELDABILITY OF STEELS,* WELDING RESEARCH COUNCIL, 1978
9. R.D. STOUT, *WELDABILITY OF STEELS,* WELDING RESEARCH COUNCIL, 1987
10. C.D. LUNDIN, A.C. LINGENFELTER, G.E. GROTKE, G.G. LESSMANN, AND S.J. MATTHEWS, THE VARESTRAINT TEST, *WELD. RES. COUNC. BULL.,* NO. 280, AUG 1982
11. R.D. CAMPBELL, "AN INVESTIGATION INTO THE PHYSICAL METALLURGY, WELDING METALLURGY, HOT CRACKING AND WELD POOL SHAPE OF FERRITIC STAINLESS STEELS," PH.D. THESIS, RENSSELAER POLYTECHNIC INSTITUTE, TROY, NEW YORK, 1987
12. W. LIN, J.C. LIPPOLD, AND W.A. BAESLACK, AN EVALUATION OF HEAT-AFFECTED ZONE LIQUATION CRACKING SUSCEPTIBILITY, PART I: DEVELOPMENT OF A METHOD FOR QUANTIFICATION, *WELD. J.,* VOL 72 (NO. 4), APRIL 1993, P 135-S TO 153-S
13. G.M. GOODWIN, DEVELOPMENT OF A NEW HOT-CRACKING TEST--THE SIGMAJIG, *WELD. J.,* VOL 66 (NO. 2), FEB 1987, P 33-S TO 38-S
14. P. BURGARDT AND R.D. CAMPBELL, CHEMISTRY EFFECTS ON STAINLESS STEEL WELD PENETRATION, CHAPTER 13, *FERROUS ALLOY WELDMENTS,* TRANS TECH PUBLICATIONS, SWITZERLAND, 1992
15. D.W. WALSH AND W.F. SAVAGE, THE MECHANISM OF MINOR ELEMENT INTERACTION IN AUTOGENOUS WELD POOLS, *ADVANCES IN WELDING TECHNOLOGY INTERNATIONAL CONF. PROC.* (GATLINBURG, TN), 18 MAY 1986, AMERICAN SOCIETY FOR METALS, P 59-63
16. C.R. HEIPLE AND J.R. ROPER, EFFECTS OF MINOR ELEMENTS ON GTAW FUSION ZONE SHAPE, *TRENDS IN WELDING RESEARCH IN THE UNITED STATES,* CONF. PROC. (NEW ORLEANS, LA), NOV 1981
17. S.S. GLICKSTEIN AND W. YENISCAVICH, "A REVIEW OF MINOR ELEMENT EFFECTS ON THE WELDING ARC AND WELD PENETRATION," BULLETIN 226, WELDING RESEARCH COUNCIL, MAY 1977
18. D.W. WALSH, R.D. CAMPBELL AND W.F. SAVAGE, UNPUBLISHED RESEARCH, RENSSELAER POLYTECHNIC INSTITUTE, TROY, NY, 1986
19. F.J. ZANNER, PH.D. THESIS, RENSSELAER POLYTECHNIC INSTITUTE, TROY, NEW YORK, JUNE 1967
20. D.W. WALSH, "MINOR ELEMENT EFFECTS ON GAS TUNGSTEN ARC WELDS," PH.D. THESIS, RENSSELAER POLYTECHNIC INSTITUTE, TROY, NEW YORK, JUNE 1986
21. W.F. SAVAGE, E.F. NIPPES, AND F.J. ZANNER, *WELD. J.,* VOL 57 (NO. 7), JULY 1978, P 201
22. E.F. NIPPES AND W.F. SAVAGE, AN INVESTIGATION OF THE HOT DUCTILITY OF HIGH-TEMPERATURE ALLOYS, *WELD. J.,* VOL 34 (NO. 4), 1955, P 183-S TO 196-S
23. E.F. NIPPES, W.F. SAVAGE, AND G. GROTKE, "FURTHER STUDIES OF THE HOT DUCTILITY OF HIGH-TEMPERATURE ALLOYS," BULLETIN SERIES VOL 33 (NO. 2), WELDING RESEARCH COUNCIL, 1957
24. C.H. KREISCHER, A CRITICAL ANALYSIS OF THE WELD HEAT-AFFECTED ZONE HOT DUCTILITY TEST, *WELD. J.,* VOL 42 (NO. 2), 1963, P 49-S TO 59-S
25. B. WEISS, B.E. GROTKE, AND R. STICKLER, PHYSICAL METALLURGY OF HOT DUCTILITY TESTING, *WELD. J.,* VOL 49 (NO. 10), 1970, P 471-S TO 487-S

26. E.F. NIPPES, W.F. SAVAGE, AND J.M. PAEZ, IMPACT CHARACTERISTICS OF HEAT-AFFECTED ZONES IN MN-MO ARMOR STEELS, *WELD. J.*, VOL 39 (NO. 1), 1960, P 31-S TO 39-S
27. K.C. WU, A STUDY OF THE WELD HEAT-AFFECTED ZONE OF CENTRIFUGALLY CAST 5% CHROMIUM STEEL, *WELD. J.*, VOL 42 (NO. 9), 1963, P 392-S TO 396-S
28. E.F. NIPPES AND E.W. EMMERICH, HEAT-AFFECTED ZONE STUDY OF AN EUTECTOID ULTRA-HIGH STRENGTH STEEL, *WELD. J.*, VOL 42 (NO. 12), 1963, P 547-S TO 556-S
29. W.A. PETERSON, WELD HEAT-AFFECTED ZONE OF 18% NICKEL MARAGING STEEL, *WELD. J.*, VOL 43 (NO. 9), 1964, P 428-S TO 432-S
30. W.F. SAVAGE AND B.M. KRANTZ, AN INVESTIGATION OF HOT CRACKING IN HASTELLOY X, *WELD. J.*, VOL 45 (NO. 1), 1966, P 13-S TO 25-S
31. W.A. OWCZARSKI, D.S. DUVAL, AND C.P. SULLIVAN, A MODEL FOR HEAT-AFFECTED ZONE CRACKING IN NICKEL-BASE SUPERALLOYS, *WELD. J.*, VOL 45 (NO. 4), 1966, P 145-S TO 155-S
32. L.P. CONNOR, A.M. RATHBONE, AND J.H. GROSS, EFFECTS OF COMPOSITION ON THE HEAT-AFFECTED ZONE TOUGHNESS OF CONSTRUCTIONAL ALLOY STEELS, *WELD. J.*, VOL 46 (NO. 5), 1967, P 217-S TO 234-S
33. R.A. MUELLER, D.G. HOWDEN, AND F.B. SIMMONS, HAZ THERMOCYCLE AND STRUCTURE SIMULATION, *WELD. J.*, VOL 52 (NO. 10), 1973, P 411-S TO 416-S
34. N.E. HANNERY, EFFECT OF CB ON HAZ DUCTILITY IN CONSTRUCTIONAL HT STEELS, *WELD. J.*, VOL 54 (NO. 5), 1975, P 162-S TO 168-S
35. S.J. MATTHEWS, SIMULATED HEAT-AFFECTED ZONE STUDIES OF HASTELLOY ALLOY B-2, *WELD. J.*, VOL 58 (NO. 3), 1979, P 91-S TO 95-S
36. R.F. FASTINI AND M. SEMCHYSHEN, THE EFFECT OF MOLYBDENUM ON THE CONTINUOUS COOLING TRANSFORMATION OF A 0.40% CARBON STEEL, *ASM TRANS. QUART.*, SEPT 1964
37. D.G. HOWDEN, ISOTHERMAL TRANSFORMATION CHARACTERISTICS OF A LOW-ALLOY STEEL USING A WELD THERMAL CYCLE SIMULATOR, *CAN. METALL. QUART.*, VOL 6 (NO. 3), 1967
38. K.C. WU, CONTINUOUS-COOLING TRANSFORMATION DIAGRAMS OF TI-8A1-MO-1V, *TRANS. ASM*, VOL 61, 1968, P 621-626
39. C.F. MEITZNER AND A.W. PENSE, STRESS-RELIEF CRACKING IN LOW-ALLOY STEEL WELDMENTS, *WELD. J.*, VOL 48 (NO. 10), 1969, P 431-S TO 440-S
40. A.W. DIX AND W.F. SAVAGE, SHORT TIME AGING CHARACTERISTICS OF INCONEL X-750, *WELD. J.*, VOL 52 (NO. 3), 1973, P 135-S TO 144-S
41. S.J. MATTHEWS, WELDABILITY OBSERVATIONS IN 70/30 COPPER-NICKEL TUBESHEET MATERIAL, *WELD. J.*, VOL 47 (NO. 4), 1968, P 155-S TO 161-S
42. K.C. WU AND T.A. KRINKE, WELDABILITY STUDIES FOR AFC-77--PART 1: MECHANICAL PROPERTIES, *WELD. J.*, VOL 47 (NO. 6), 1968, P 332-S TO 336-S
43. W.A. PETERSON, WELDABILITY OF A CHROMIUM STRENGTHENED COPPER-NICKEL ALLOY, *WELD. J.*, VOL 48 (NO. 10), 1969, P 425-S TO 430-S
44. J. GORDINE, THE WELDABILITY OF SOME ARTIC-GRADE LINE-PIPE STEELS, *WELD. J.*, VOL 56 (NO. 7), 1977, P 201-S TO 210-S
45. W.F. SAVAGE, E.F. NIPPES, AND J.E. CASTERAS, EFFECT OF ALLOYING ADDITIONS ON THE WELDABILITY OF 70 CU-30 NI, *WELD. J.*, VOL 57 (NO. 12), 1978, P 375-S TO 382-S
46. W.P. HUGHES AND T.F. BERRY, A STUDY OF THE STRAIN-AGE CRACKING CHARACTERISTICS IN WELDED RENE 41--PHASE 1, *WELD. J.*, VOL 46 (NO. 8), 1967, P 361-S TO 370-S
47. A.W. DIX AND W.F. SAVAGE, FACTORS INFLUENCING STRAIN-AGE CRACKING IN INCONEL X-750, *WELD. J.*, VOL 50 (NO. 6), 1971, P 247-S TO 252-S
48. J.J. PEPE AND W.F. SAVAGE, EFFECTS OF CONSTITUTIONAL LIQUATION IN 18-NI MARAGING STEEL WELDMENTS, *WELD. J.*, VOL 46 (NO. 9), 1967, P 411-S TO 422-S

49. W.F. SAVAGE, E.F. NIPPES, AND M.C. MUSHALA, COPPER-CONTAMINATION CRACKING IN THE WELD HEAT-AFFECTED ZONE, *WELD. J.*, VOL 57 (NO. 5), 1978, P 237-S TO 245-S
50. W.F. SAVAGE, E.F. NIPPES, AND M.C. MUSHALA, LIQUID-METAL EMBRITTLEMENT OF THE HEAT-AFFECTED ZONE BY COPPER CONTAMINATION, *WELD. J.*, VOL 57 (NO. 8), 1978, P 237-S TO 245-S
51. J.C. LIPPOLD AND W.F. SAVAGE, SOLIDIFICATION OF AUSTENITIC STAINLESS STEEL WELDMENTS: PART 1--A PROPOSED MECHANISM, *WELD. J.*, VOL 58 (NO. 12), 1979, P 362-S TO 374-S
52. J.C. LIPPOLD AND W.F. SAVAGE, SOLIDIFICATION OF AUSTENITIC STAINLESS STEEL WELDMENTS: PART 2--THE EFFECT OF ALLOY COMPOSITION ON FERRITE MORPHOLOGY, *WELD. J.*, VOL 59 (NO. 2), 1980, P 48-S TO 58-S
53. COMPUTERIZED THERMAL AND MECHANICAL TESTING MACHINE A SIGNIFICANT ASSET IN RESEARCH, DEVELOPMENT AND PRODUCTION, *INDUSTRIAL HEATING*, VOL 53 (NO. 12), DEC 1986
54. H. FERGUSON, METALWORKING PROCESS SIMULATIONS SAVE PRODUCTION HEADACHES, *MET. PROG.*, SEPT 1986, P 39-42
55. D.J. WIDGERY, THE DESIGN AND USE OF RESISTANCE HEATED WELD THERMAL SIMULATORS, *PROC. CONF. WELD THERMAL SIMULATORS FOR RESEARCH AND PROBLEM SOLVING*, THE WELDING INSTITUTE, CAMBRIDGE, ENGLAND, APRIL 1972
56. D.W. WALSH, M.J. CIESLAK, AND W.F. SAVAGE, TEMPERATURE MEASUREMENTS IN RESISTANCE HEATED SPECIMENS: LONGITUDINAL GRADIENTS, *WELD. J.*, VOL 65 (NO. 8), 1986, P 184-S TO 192-S
57. G.M. GOODWIN, *PROC. 1ST JAPAN-U.S. SYMPOSIUM ON ADVANCES IN WELDING METALLURGY* (SAN FRANCISCO, CA), JUNE 1990, P 27-39
58. J.C. BORLAND, *BR. WELD. J.*, VOL 7 (NO. 8), 1961, P 508-512
59. W. LIN, W.A. BAESLACK, AND J.C. LIPPOLD, HOT DUCTILITY TESTING OF HIGH-STRENGTH, LOW-EXPANSION SUPERALLOYS, *RECENT TRENDS IN WELDING AND TECHNOLOGY LNT. CONF. PROC.* (GATLINBURG, TN), 14 MAY 1989, ASM INTERNATIONAL, P 609-614
60. W. LIN, W.A. BAESLACK, AND J.C. LIPPOLD, A METHOD FOR QUANTIFYING HAZ LIQUATION CRACKING SUSCEPTIBILITY USING THE GLEEBLE HOT-DUCTILITY TEST, *PROC. INT. SYMP. PHYSICAL SIMULATION*, DELFT, 1992, P 93-99

Brazeability and Solderability of Engineering Materials

S.D. Brandi, Escola Politécnica da Universidade de São Paulo, Brazil; S. Liu, Colorado School of Mines; J.E. Indacochea and R. Xu, University of Illinois at Chicago

Introduction

ANALYSIS of the brazeability and solderability of engineering materials requires the following considerations:

- JOINING PROCESS CHARACTERISTICS (TYPE AND CHARACTERISTICS OF HEAT SOURCE)
- CHEMICAL COMPOSITION OF BASE METAL
- CLEANING PREPARATION AND AFTER-PROCESS CLEANING
- CHEMICAL COMPOSITION OF FILLER METAL
- JOINT PROTECTION AGAINST OXIDATION (FLUX, BATH COMPOSITION, PROTECTIVE ATMOSPHERES)
- JOINT TEMPERATURE AND TIME
- JOINT DESIGN (JOINT GEOMETRY, JOINT CLEARANCE, JOINING POSITION)

Each one of these topics influences wetting and spreading behavior, joint mechanical properties, corrosion resistance, and residual stress levels.

Brazeability and Solderability of Engineering Materials

S.D. Brandi, Escola Politécnica da Universidade de São Paulo, Brazil; S. Liu, Colorado School of Mines; J.E. Indacochea and R. Xu, University of Illinois at Chicago

Process Applications and Requirements

The use of high-performance materials in advanced engineering and manufacturing places demanding requirements on joining processes such as brazing and soldering. Appropriate design of the joints and proper selection of joining processes and filler metals can increase the application of brazed and soldered joints in sophisticated mechanical assemblies, such as aerospace equipment, chemical reactors, and high-value electronic assemblies.

Soldering in the electronics field has undergone many dramatic changes since the first radios were built. Between the 1920s and 1940s, all interconnections were made using the point-to-point wiring method, and the solder joints were made with soldering irons. With the end of World War II and a greater demand for consumer electronics, mass soldering techniques such as dip soldering were developed. By the late 1950s, wave soldering was developed in England and introduced to the United States soon after; this technique is still widely used on printed wiring boards.

Brazing has also evolved significantly. The introduction of torch brazing, furnace brazing, and vacuum brazing has expanded the application of brazing to different material systems such as aluminum, stainless steel, superalloys, titanium, and ceramics.

Recent developments in aluminum brazing in the automotive industry include the application of noncorrosive fluxes in conjunction with a dry nitrogen atmosphere in a continuous mesh belt furnace. Under these conditions, only a small amount of flux is required for joint protection, so flux removal after brazing is not necessary. Many other automotive parts are furnace brazed, such as pollution control tubing, water pump impellers, torque converters, and so on. While the torque converter is usually brazed with a copper filler metal, a nickel filler metal is used when additional strength is required (for example, for dynamometer testing or other high-stress applications). Stainless steel automotive assemblies are brazed in a low-dew-point atmosphere such as cryogenic nitrogen, with an addition of 20 to 50 vol% of dry hydrogen.

The potential applications of brazing and soldering have increased both in volume and significance with the introduction of advanced structural ceramics. Much emphasis has been placed on the application of these ceramics in aerospace, automotive, and electronics applications. A complete characterization and understanding of the existing brazing and soldering techniques for joining dissimilar materials will contribute to the further development of these techniques and to the joining of ceramic materials reliably. Improved brazing and soldering technology will also result in the establishment of optimized design criteria and high-yield, low-cost manufacturing processes.

Aerospace Applications

Jet engine components such as turbines blades and stators with very thin section are assembled by brazing. The vanes can be hollow, with passageways for dynamic cooling during operation. Yet the brazements must be designed to withstand loads that the part will experience throughout its service life. In the modem aircraft engine industry, most brazing is carried out in vacuum or hydrogen, using specialized brazing cycles. Typically, large components are brazed in vacuum furnaces at 0.13 to 0.013 Pa (10^{-3} to 10^{-4} torr). Other parts of engine systems are brazed in continuous hydrogen furnaces and batch hydrogen furnaces.

The interest of the aerospace industries in structural ceramics centers on the potential application in gas turbine engines. The severe service conditions encountered within a gas turbine, and the desire of design engineers to increase operating temperatures for higher efficiency, make several of the properties of structural ceramics particularly attractive. High-temperature strength, low thermal expansion coefficient, dimensional accuracy, and corrosion resistance are some of these properties.

The silicon-base ceramics, such as Si_3N_4, SiC, or Sialon ($Si_{5.5}Al_{0.5}O_{0.5}N_{7.5}$), have been considered for gas turbine parts (including bearings, shroud rings, and turbine blades). The bearings may be found either as ceramic balls or rollers in conventional bearings or shells. The use of ceramics for shroud rings allows for high-temperature operation while maintaining tight control of shroud clearances on the blades, because of their low thermal expansion coefficients. In the case of present turbine blades technology, the operating temperatures are already close to the maximum temperature limit. Therefore, the high-temperature strength of these ceramics is particularly desirable.

Ceramic materials are more difficult to braze because they are not easily wet by the standard commercial filler metals. When joined to metals, the different thermal expansion coefficients may result in residual stress generation and cracking of the ceramic component. Ceramic-to-metal joints must be specially designed to alleviate the residual stress problem. Techniques such as metallization and ductile reactive metal fillers can be utilized to promote wettability and minimize stress-induced cracking in the ceramic component.

Braze joints for heat engine applications require good mechanical properties at high temperatures. Thus, the combination of base metal and filler metal in the joint must be thermally stable. The presence of intermetallics at the interface of base metal and filler metal should be minimized, and the filler metal should not undergo any type of strengthening or softening mechanism, such as precipitation hardening, order/disorder reactions, or precipitate coarsening. Wetting and spreading are important to avoid lack of filling, which will create stress concentrations and, consequently, the premature failure of the component.

Nuclear Applications

Because of the need of structural integrity at high temperatures for components used in nuclear applications, refractory metals are targeted for those applications. Joints of significant dimensions with properties that are adequate to meet requirements of strength, ductility, and corrosion resistance are required. Brazing has been widely accepted as the joining method to satisfy these requirements.

For the past 30 years engineers have been attracted to the inherent properties of ceramic materials for potential use in nuclear reactors, which involve high temperatures and corrosive environments. Fuel element structures were one of the first applications for which experimental assemblies were designed and fabricated using ceramic materials. To demonstrate the use of ceramic brazing in advanced fuel elements, one element was made entirely of Al_2O_3 and compartmented ceramic plates were brazed after loading with fuel (Fig. 1).

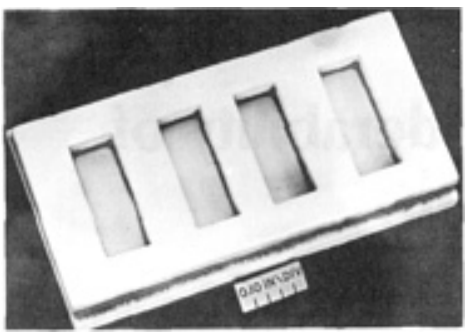

FIG. 1 ALUMINUM OXIDE COMPARTMENTED ASSEMBLY VACUUM BRAZED WITH 49TI-49CU-2BE (IN WT%) BRAZING FILLER METAL AT 980 °C (1795 °F) FOR 10 MIN

A BeO tubular assembly was also brazed, simulating a fuel bundle with ferrule spacers. The larger BeO tube diameters represent the fuel tubes, while the smaller tubes simulate the spacers. This assembly (Fig. 2) was brazed with the same brazing filler metal as the flat-plate assembly in Fig. 1 (vacuum, 1000 °C, or 1830 °F, for l0 min).

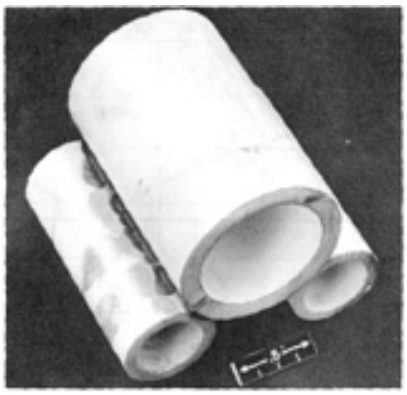

FIG. 2 BERYLLIUM OXIDE TUBULAR ASSEMBLY BRAZED WITH 49TI-49CU-2BE FILLER METAL

Another application is the advanced Tokamak fusion test reactor, being developed at Princeton University. The effort is aimed at achieving a commercially feasible magnetic-fusion reactor. In this reactor, large ceramic insulator rings are used to electrically insulate the vacuum-pumping and natural-beam injector system from the stainless steel vacuum vessel, in which the plasma is confined by surrounding magnetic fields.

The insulating rings for the fusion reactor are composed of ceramics, copper, and stainless steel, all of which must be brazed together successfully. To accomplish the task, titanium hydride was first applied to the ceramic mating surfaces, followed by silver-copper foil of 0.076 mm (0.003 in.) thick. The assembled parts, wrapped in titanium foil that acted as a getter to obtain a higher purity atmosphere, were then successfully brazed.

Heat Exchangers

Heat exchangers, particularly in the automotive industry. are fabricated from many different materials. such as copper. aluminum, copper-nickel alloys, steels, and titanium. Depending on the base metal selected, joint strength requirements, and assembly design, different brazing processes, such as torch, furnace, resistance brazing, and so on, can be used.

Temperature and humidity control within the atmospheres of space vehicles, space stations, and space suits can be realized with condensing heat exchangers. By use of the plate-fin design, units with high efficiency at minimum mass and volume may be tailored close to actual system requirements. Stainless steel cores, brazed together in vacuum with nickel-base filler metals, are used to meet these requirements.

A variety of ceramic materials have been considered for use in heat exchange systems, such as the main heat transfer surfaces (tubes, plates, and so on), seals, tube sheets, and insulation. They have been used primarily in these critical zones in an effort to minimize cost over metallic counterparts. Heat exchanger designs have ranged from all-ceramic to ceramic-metal hybrids with varying numbers of ceramic components. These parts are commonly brazed with ductile active metal fillers.

Brazeability/solderability in this application is related mainly to the corrosion resistance of the joint. The filler metal should be more noble than the base metal to minimize galvanic corrosion in the joint. Wetting and spreading are also important to prevent crevices that may generate crevice corrosion, especially when the environment has chloride ions in solution. The flux should be easily removed to avoid residues that can accelerate the corrosion rate in the joint.

Electronic Packaging

Filler metal compositions and forms for soldering have experienced significant changes to meet the needs of a growing number of process techniques and applications, from simple wires to foils, preforms, and pastes. The first electronic solder was 50Sn-50Pb wire, traditionally used by plumbers. Today, the selection of materials has expanded to eutectic tin-lead solders, neareutectic (60Sn-40Pb) solders, and ternary (62.5Sn-36.1Pb-l.4Ag) alloys in the form of foils, preforms, and pastes. Although the main emphasis has remained on the Sn-Pb eutectic and near-eutectic alloys, other alloys, such as the indium and gold-tin eutectics, have also been developed for more specialized applications.

Flux technology has also evolved. Environmental regulations have placed emphasis on the development of new flux types. Extensive work has been done with organic acids, that can be removed with aqueous media or low-residue fluxes which have eliminated cleaning altogether.

The use of mass soldering techniques has increased the need for adequate solderability of substrates. The large throughput of high-production-rate processes prohibits the repair of defective solder joints. In addition, modern components are more heat-sensitive. Lower soldering temperatures and less mechanical working have made it necessary to maintain the highest solderability to ensure a metallurgically sound and reliable joint on the first pass.

The service performance of a solder joint is a strong consideration in modem electronics. Many environments, such as aircraft avionics, telecommunications systems, dishwashers, and automobiles, impose a regular thermal cycle on the electronic equipment that results in thermal-mechanical strains. Failure by fatigue or creep becomes inevitable if the joint design is incorrect or if the joint has defects due to poor manufacturing control.

Solderability in this application describes the formation of a joint by adequate wetting of the entire surface by the molten solder to achieve good electrical contact. Base-metal dissolution by the molten solder should be minimized by processing variables (time, temperature, filler metal composition). The flux should promote the oxide removal and protect the molten solder against oxidation to prevent "cold weld," which may cause a misfunction of the electronic component.

Dissimilar Material Joints

Industrial machinery construction and electronic components fabrication require the joining of materials that exhibit highly different properties. An example is the joining of ceramics with metals that have quite different melting points and coefficients of thermal expansion. Various processes have been developed to join dissimilar materials. Usually the selection of the joining technique will depend on the materials used and on the specified joint properties. For instance, to obtain high mechanical strength or good heat resistance, the reaction layer must consist of high-melting-temperature products. For good dielectric properties, the reaction layer must contain oxide compounds. The use of vitreous phases in the interlayer may provide chemical resistance and high puncture-proofness. Presently, processes such as sintering of interfaces, spraying and sintering of coatings, and depositing of layers by chemical vapor deposition, soldering (metal-metal and metal-ceramic), and infiltration (joints of composite materials) are applied in joining dissimilar materials. In developing processes to join dissimilar materials, one must consider and solve such problems as wettability, chemical reactivity of the base materials and filler metals to be bonded under specific processing conditions, and the effect of the joining processes on the stress state in the joint during production and during operation.

Brazeability and Solderability of Engineering Materials

S.D. Brandi, Escola Politécnica da Universidade de São Paulo, Brazil; S. Liu, Colorado School of Mines; J.E. Indacochea and R. Xu, University of Illinois at Chicago

---

Materials Selection

Brazing and soldering are joining processes performed at temperatures below the base material solidus temperature. To fill the joint, the liquid filler metal must spread through the joint gap by capillarity or coat the substrate by spreading. Capillarity and spreading are related to the balance of surface tensions, which determines the wetting and spreading behavior of a liquid on a solid. Both wetting and spreading are results of interfacial reactions (physical and chemical reactions). The influence of material selection, joint design, and surface conditions on the mechanical properties and corrosion resistance of a brazed joint will be discussed below.

There is no precise definition of brazeability and solderability of a material. These properties are related to how easily a material can be joined, how closely a joint can fit its design function (mechanics, corrosion, electrical contact, and so on), and the most suitable joining process. As an example, in electronic applications solderability involves not only the soldering process characteristics but also the effect of heating on the electronic component characteristics.

Wetting and Spreading. Wetting is a surface phenomenon related to the balance of the solid-liquid surface tension, γ_{sl}, the solid-vapor surface tension, γ_{sv}, and the liquid-vapor surface tension, γ_{lv}. The contact angle, θ, between the solid and the liquid is defined in equilibrium conditions as the angle between the vectors that represents the liquid-vapor surface

tension and the solid-liquid surface tension. The relationship between the contact angle and the surface tensions is given by the Young-Dupré equation:

$$\gamma_{LV} \cdot \cos\theta = \gamma_{SV} - \gamma_{SL} \qquad \textbf{(EQ 1)}$$

A liquid is said to wet a solid when the contact angle is less than 90°. In this case, for constant γ_{lv} the solid-vapor surface tension is greater than the solid-liquid surface tension. On the other hand, if the solid-vapor surface tension is lower than the solid-liquid surface tension, the contact angle is greater than 90° and the liquid will not wet the solid. Figure 3 shows a wetting and a nonwetting system in a joint. In neither case did a reaction layer form between the solid and the liquid.

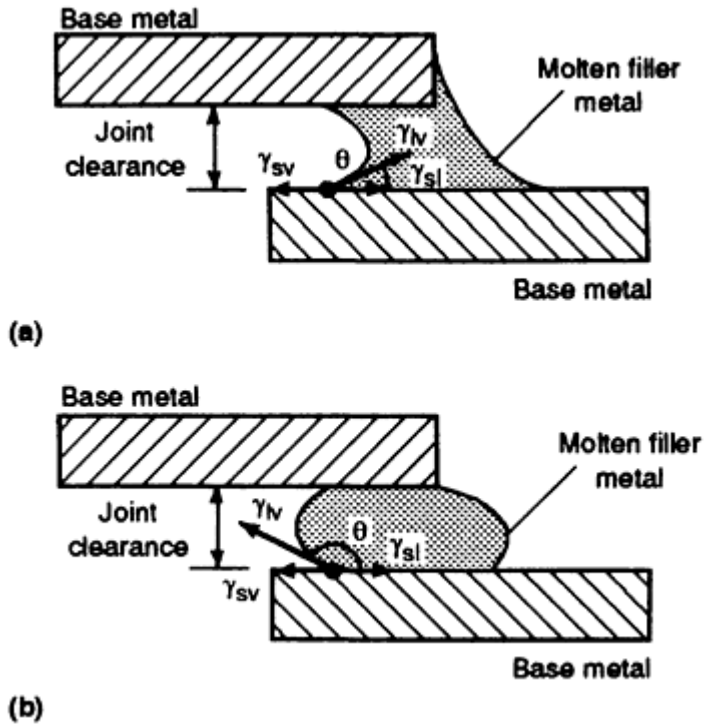

FIG. 3 SCHEMATIC SHOWING RELATIONSHIP OF CONTACT ANGLE TO SURFACE TENSION. (A) WETTING SYSTEM. (B) NONWETTING SYSTEM

Spreading is a dynamic process related to the contact angle θ and can be described as an increase in the liquid surface and the interfacial area, ΔA, with time. Based on Fig. 4, a liquid is said to completely spread over a solid surface when the contact angle tends to 0° (Fig. 4a). Alternatively, spreading is considered to proceed when the liquid surface area increases to a maximum, even if θis greater than 0° (Fig. 4b). Rate of spreading can be inhibited by the liquid inertia and/or the liquid viscosity.

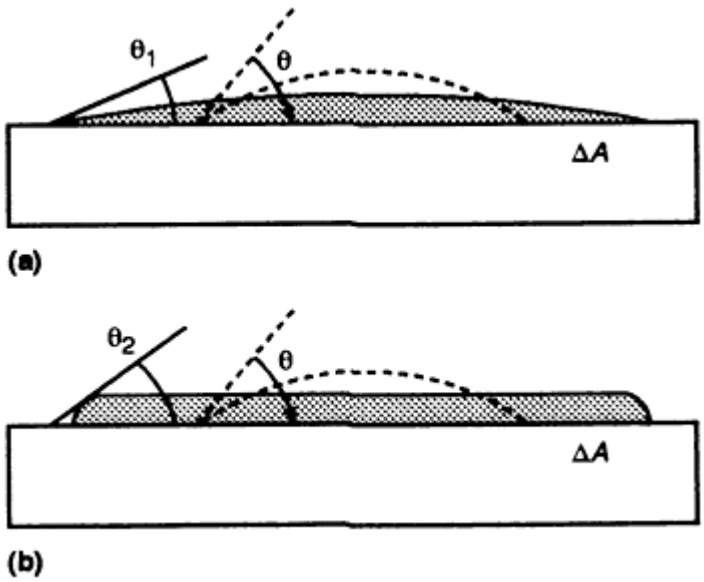

FIG. 4 SCHEMATIC SHOWING A LIQUID SPREADING THROUGH A SOLID SURFACE WITH θ< 90°. (A) θ_1 0°. (B) $\theta_2 = \theta_{EQUIL}$

From Eq 1, $\gamma_{lv} \cdot \cos \theta$can be considered as a resistance force that opposes a liquid to wet a solid, and ($\gamma_{sv} - \gamma_{sl}$) is a driving force for wetting. If $\gamma_{lv} \cdot \cos \theta$ is greater than ($\gamma_{sv} - \gamma_{sl}$), no wetting or spreading will occur. So it is important to decrease $\gamma_{lv} \cdot \cos \theta$and/or to increase ($\gamma_{sv} - \gamma_{sl}$) by means of a flux, a filler metal, or a suitable brazing atmosphere. γ_{lv} and γ_{sv} decrease when a deoxidation reaction takes place at the liquid and solid surfaces. γ_{sl} can be reduced by promoting a deoxidation reaction via alloying elements in the filler metal (such as phosphorus in BCuP filler in contact with a copper substrate), formation of a reaction layer, or adsorption of a chemical element at the solid-liquid interface. Figure 5 shows the effect of the atmosphere and filler metal composition on the surface tensions for a Cu-BCuP system.

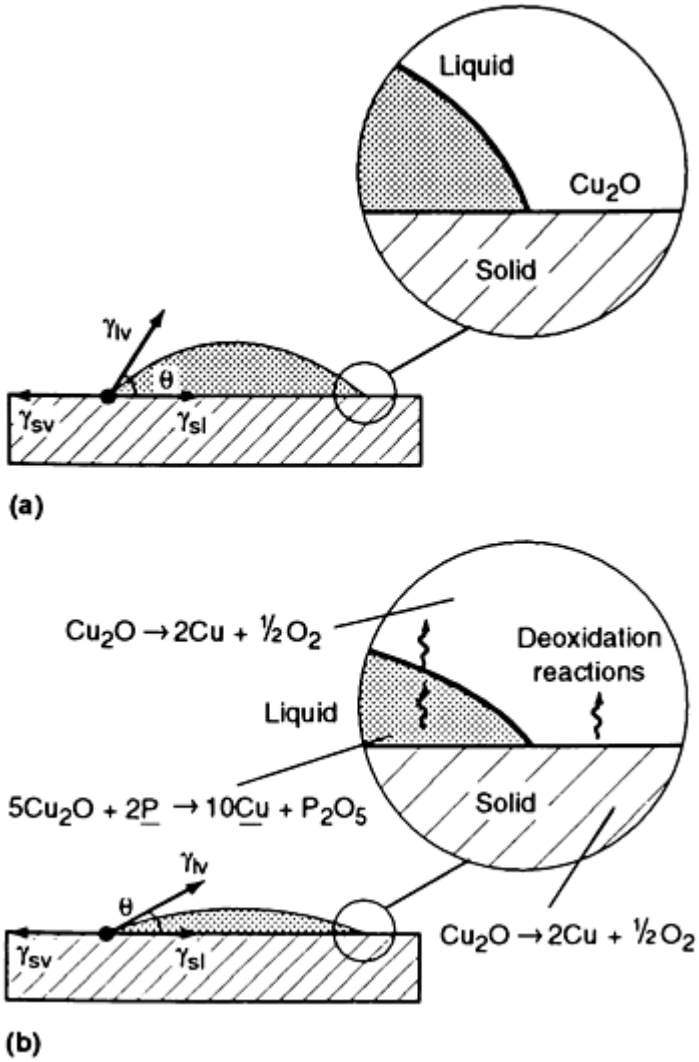

FIG. 5 SCHEMATIC SHOWING EFFECT OF THE SURROUNDING MEDIUM AND THE COMPOSITION OF THE FILLER METAL ON THE WETTING AND SPREADING BEHAVIOR OF COPPER-BCUP SYSTEM. (A) NEUTRAL OR OXIDIZING MEDIUM. (B) DEOXIDIZING MEDIUM

Interfacial Reactions. During brazing, the molten filler metal often reacts with the base metal. The product is a reaction layer that is sometimes too thin to be observed by optical microscopy. In fact, this layer modifies the wetting and spreading behavior of the liquid filler metal in contact with the base metal. Figure 6 shows the interfacial reaction during the brazing process.

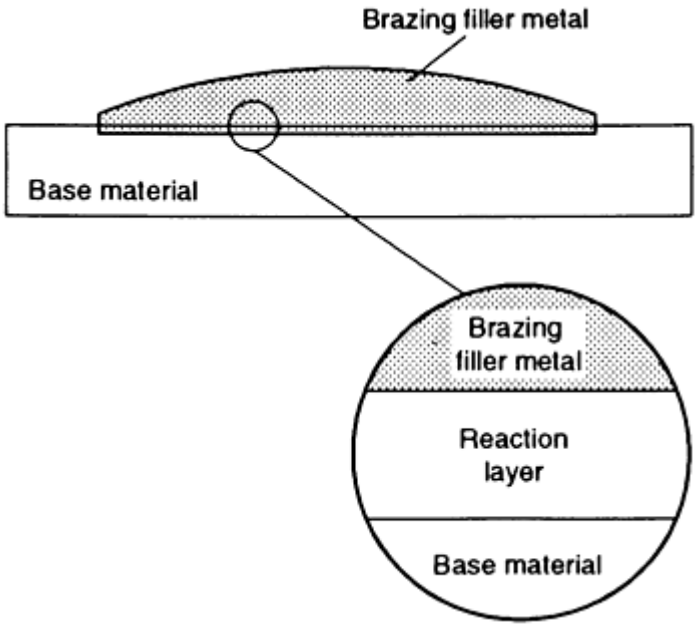

FIG. 6 REACTION LAYER FORMATION DURING THE BRAZING PROCESS

When an interfacial reaction occurs between the base metal and the liquid filler, the free energy of the reaction per unit area and unit time (ΔG_r) should be included in Eq 1, as follows:

$$\gamma_{SV} - (\gamma'_{SL} - \Delta G_R) = \gamma_{LV} \cdot \text{COS}\ \theta \qquad \textbf{(EQ 2)}$$

Due to a change in the solid-liquid interface by a chemical reaction, γ'_{sl} is lower than γ_{sl} of Eq 1. The variables γ'_{sl} and ΔG_r will increase the driving force for wetting. If the driving force is greater than $\gamma_{lv} \cdot \cos\ \theta$, spreading will occur until the liquid has reacted completely with the solid. This concept can be illustrated by the results of a sessile drop experiment in copper-silver systems, shown in Fig. 7.

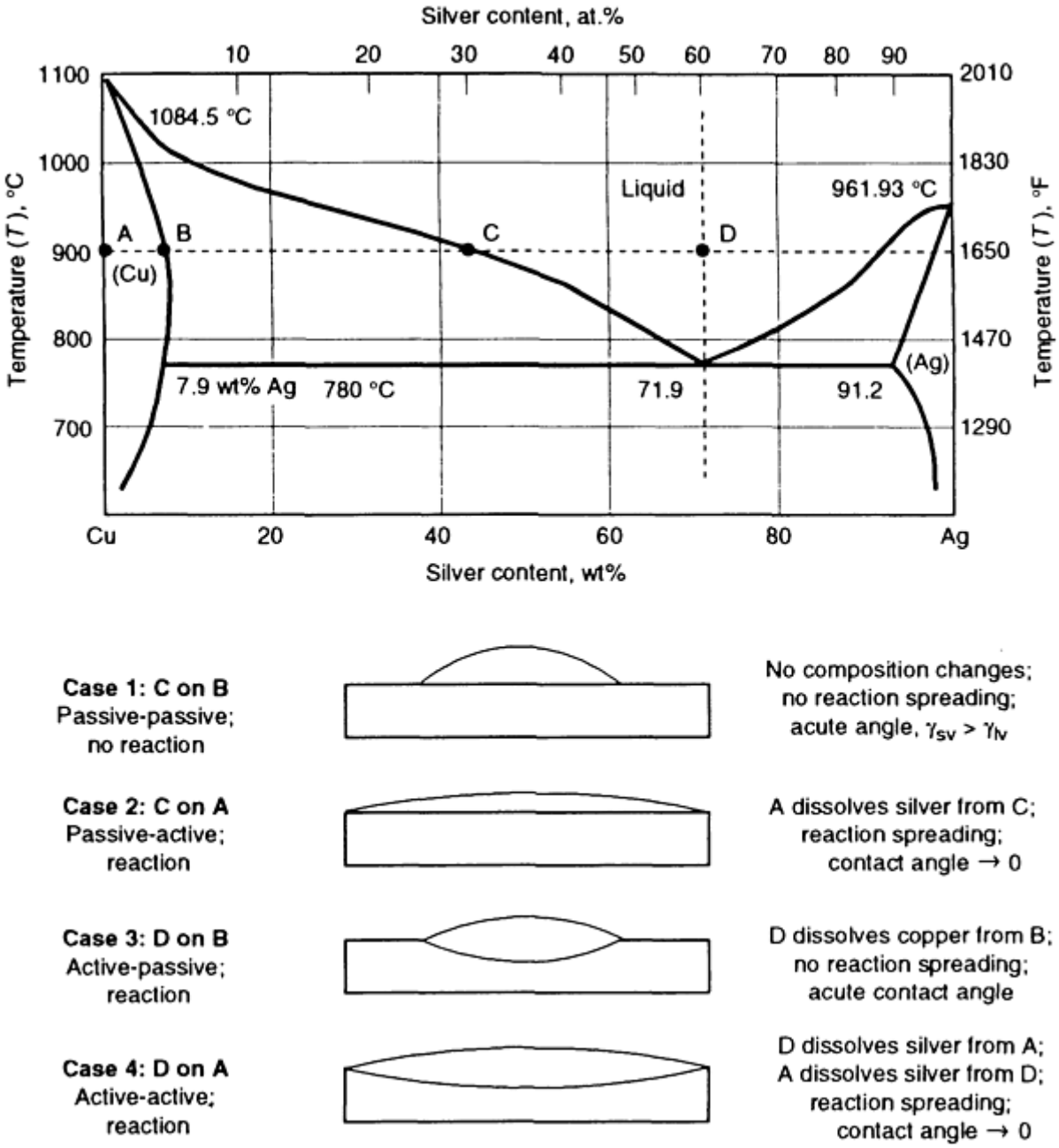

FIG. 7 RESULTS OF A SESSILE DROP TEST TO ANALYZE SPREADABILITY AS A FUNCTION OF THE SOLID AND LIQUID COMPOSITION. SOURCE: REF 1

Cases 1 and 2 in Fig. 7 show that no spreading occurred. In case 1 the solid and the liquid are in equilibrium (points B and C), and no composition change can occur as long as the brazing temperature is maintained. In case 3 the liquid dissolves copper from the solid to reach the equilibrium composition (point C). In both cases the chemical composition of the solid remains the same. This means that in cases 1 and 3 the solid has a passive behavior with respect to the liquid. On the other hand, cases 2 and 4 show the solid as the active element in the system. In other words, the chemical composition of solid A changes up to B, based on the phase diagram. In case 2, a spreading reaction occurs (that is, silver from the liquid diffuses into the solid and changes the composition at the solid-liquid interface). In case 4, both solid and liquid are active and a spreading reaction is expected to occur. It is important to point out that wetting will occur in all four cases, but only in cases 2 and 4 is spreading expected to take place.

Depending on the mechanical properties of the base metal and the filler metal, the mechanical behavior of the reaction layer may determine the strength of the braze joint. If a solid solution is formed, the reaction layer may be as tough as the base metal and the filler metal. On the other hand, if a brittle intermetallic compound is produced, the interfacial region

may degrade the joint properties. Phase diagrams are good tools to estimate the compatibility between the filler metal and the base metal.

Liquid Filler Flowability. Joint clearance is an important factor in the brazeability or solderability of a joint. Table 1 shows the recommended joint clearance at brazing temperatures for different filler metal groups. The BAlSi and BMg filler metals require larger clearances, while the BCu, BAu, BAg, and BCuP filler metals require smaller gaps. This difference can be related to the difficulty with which the first two filler metal groups wet and spread over a solid surface. The flowability of a liquid filler metal on a solid surface is related to the equilibrium conditions expressed through Eq 2, the dynamic properties such as liquid viscosity, and interfacial reaction kinetics, if applicable. So it is desirable that a filler metal has:

- HIGH WETTABILITY AS DESCRIBED BY EQ 2
- LOW VISCOSITY
- FASTER INTERFACE REACTION KINETICS

Figure 8 shows the effect of the chemical composition of a binary alloy on its viscosity. The eutectic composition will have the lowest viscosity. Filler metals with large solidification ranges tend to have higher viscosities. Notice that the chemical composition of the filler metal may change during brazing or soldering due to a dissolution reaction or an intermetallic formation. This will also affect the liquid flowability.

TABLE 1 RECOMMENDED JOINT CLEARANCE FOR SELECTED FILLER METALS AT BRAZING TEMPERATURE PER AWS B2.2 SPECIFICATION

AWS FILLER METAL CLASSIFICATION	FLUX OR BRAZING ATMOSPHERE	JOINT CLEARANCE[A]	
		mm	in.
BAG, BVAG	FLUX	0.05-0.12	0.002-0.005
	BRAZING ATMOSPHERE	0.00-0.05	0.000-0.002
BAU, BVAU	FLUX	0.05-0.12	0.002-0.005
	BRAZING ATMOSPHERE	0.00-0.05	0.000-0.002
BALSI	FLUX	0.05-0.21[B]	0.002-0.008[B]
	BRAZING ATMOSPHERE	0.21-0.25[C]	0.008-0.010[C]
BCUP	FLUX OR FLUXLESS	0.025-0.12	0.001-0.005
BCU, BVCU	BRAZING ATMOSPHERE	0.00-0.05	0.000--0.002
BCUZN, RBCUZN	FLUX	0.05-0.12	0.002-0.005
BNI1 THROUGH BNI5, BNI8, BCO1	FLUX OR BRAZING ATMOSPHERE	0.05-0.12	0.002-0.005
BNI6, BNI7	BRAZING ATMOSPHERE	0.00-.05	0.000-0.002
BMG	FLUX	0.10-0.25	0.004-0.010

(A) CLEARANCE ON THE RADIUS WHEN RINGS, PLUGS, OR TUBULAR MEMBERS ARE INVOLVED. ON SOME APPLICATIONS IT MAY BE NECESSARY TO USE THE RECOMMENDED CLEARANCE ON THE DIAMETER TO PREVENT EXCESSIVE CLEARANCE WHEN ALL THE CLEARANCE IS ON ONE SIDE. AN EXCESSIVE CLEARANCE WILL PRODUCE VOIDS. THIS IS PARTICULARLY TRUE WHEN BRAZING IS ACCOMPLISHED IN A HIGH-QUALITY ATMOSPHERE (GAS PHASE FLUXING).

(B) FOR A LAP LENGTH OF ≤ 6.35 MM ($\leq \frac{1}{4}$ IN.).

(C) FOR A LAP LENGTH OF >6.35 MM ($> \frac{1}{4}$ IN.)

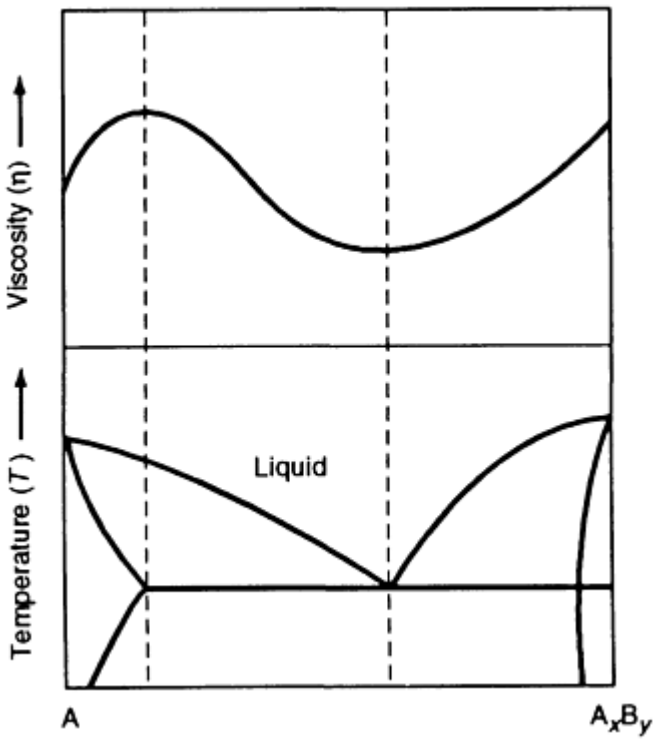

FIG. 8 EFFECT OF THE CHEMICAL COMPOSITION OF A BINARY ALLOY ON ALLOY VISCOSITY. SOURCE: REF 2

Joint design also affects filler metal flow. Figure 9 shows two different groove geometries for brazing with preplaced filler metals. In the case of a groove with sharp edges (Fig. 9a), the filler metal melts and starts to wet and spread through the groove surface. At the corner, however, the abrupt change in wall angle produces a barrier to the liquid's continued flow. Nearly all the liquid metal will accumulate at the corner, so that only a smaller amount of the molten filler is available to form the braze joint. On the other hand, the groove in Fig. 9(b) is designed to assist liquid filler flow to the outer joint surface by specifying a radius at the corner. Smooth changes in angles are preferred, to promote a more uniform flow of the liquid filler metal.

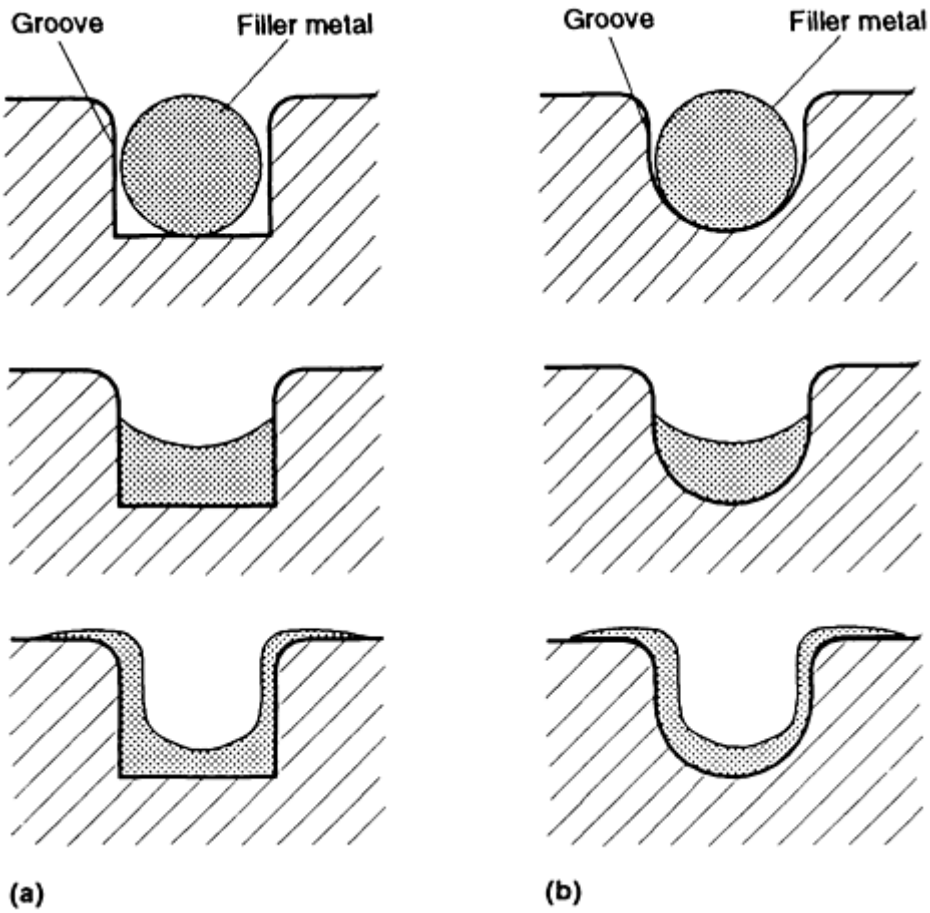

FIG. 9 EFFECT OF GROOVE GEOMETRY ON THE SPREADABILITY OF A PREPLACED FILLER METAL. (A) GROOVE WITH SHARP EDGES AND RECTANGULAR BOTTOM. (B) GROOVE WITH RADIUSED CORNERS AND SEMICIRCULAR BOTTOM WALL

Brazing position will also affect the flow rate of the liquid filler metal. A horizontal joint position is expected to offer a better flow characteristic than a vertical joint design. This is due to the gravitational field action in the vertical joint. The flow equation for the vertical and horizontal gaps are, respectively:

$$\frac{dh}{dt} = \frac{1}{4}\sqrt{\frac{g_{lv}.d.\cos q}{h.t}} \qquad \textbf{(EQ 3)}$$

$$\frac{dh}{dt} = \frac{1}{2}\sqrt{\frac{g_{lv}.d.\cos q}{h.t}} \qquad \textbf{(EQ 4)}$$

where h is the filler metal penetration in the joint, d is the joint clearance, η is the molten filler metal viscosity, t is brazing time, γ_{1v} is the surface tension between liquid and vapor, and θ is the wetting angle.

Joint Clearance. The effect of joint clearance on the behavior of a joint is about the same whether the joint is brazed or soldered. When shear strength is plotted as a function of joint clearance (Fig. 10), three different regions can be identified. At small clearances, region 1, the joint strength decreases as the clearance diminishes. The number of pores and the lack of joint filling caused by improper flow of the molten filler metal may be responsible for the lower shear strength observed. Surface discontinuity and/or entrapped flux are other factors that contribute to the joint performance. If intermetallic compounds form at the interface, a small joint clearance will invariably result in a higher volume fraction of brittle compounds, which degrade the joint properties.

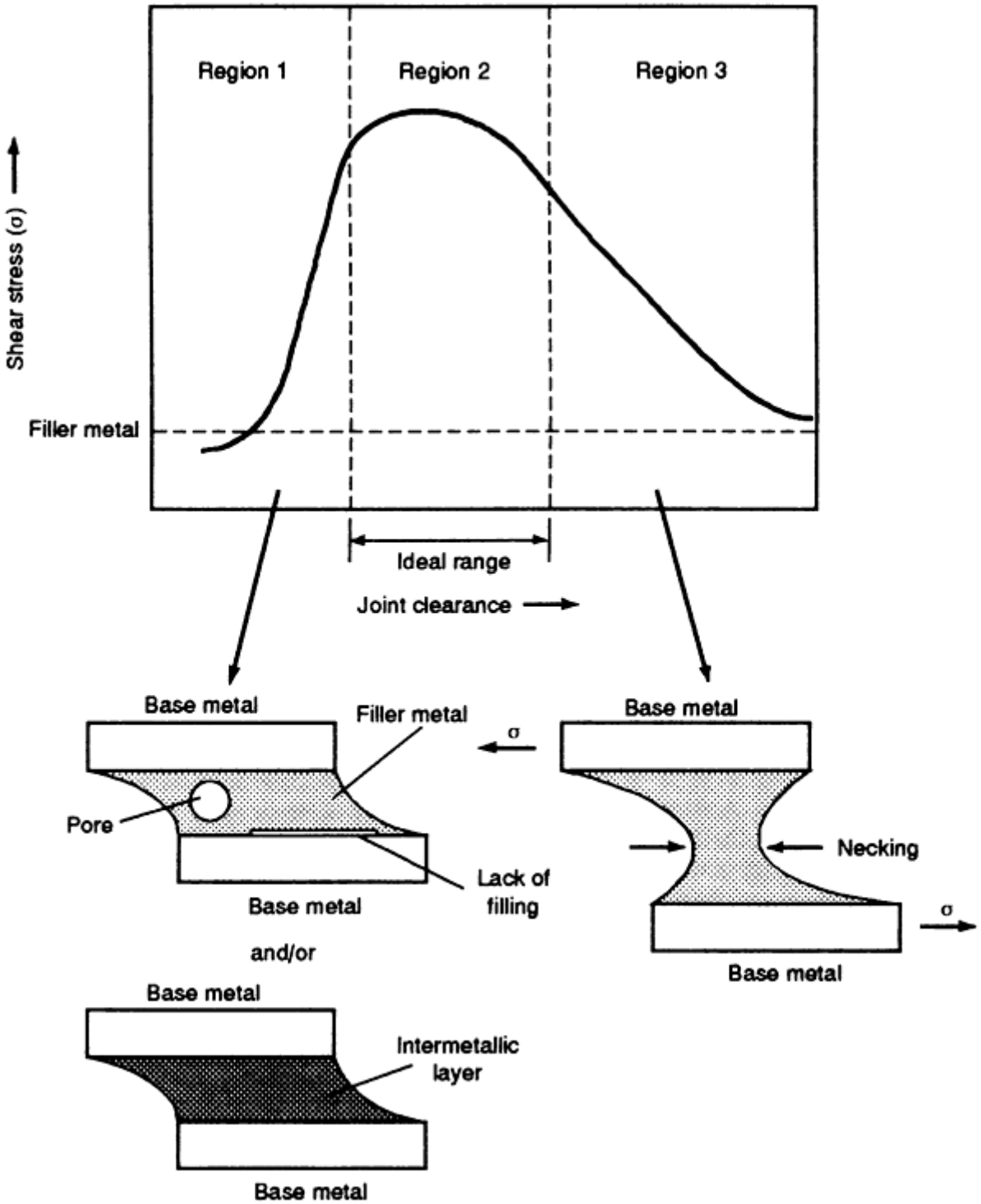

FIG. 10 EFFECT OF JOINT CLEARANCE ON THE STRENGTH OF A BRAZEMENT

With clearances indicated in region 2, the joint strength increases to a value close to that of the base metal, but only in the case of brazing. This increase in strength is due to a constraint generated by the base metal in the filler metal. As the clearance further increases, region 3, the constraint in the filler metal decreases and the mechanical properties of the filler metal will determine the strength of the joint. The lack of joint filling and the presence of voids can also affect the properties in this region.

Mutual Dissolution and Erosion. In the presence of the liquid filler metal, base metal dissolution can occur. Depending upon the mutual solubility of the base metal and the filler metal, excessive dissolution or erosion can result. Additionally, the alloying elements found in the filler metal may migrate into the base metal through solid-state diffusion or liquid

metal grain boundary penetration. Figure 11(a) shows a phase diagram that suggests complete solubility of the filler metal (fm) and the base metal (bm). The amount of base metal dissolution expected in the system represented by Fig. 11(a) will be higher than that expected in the eutectic phase diagram shown in Fig. 11(b). The effect of dissolution depends on the kinetics of the reaction. One example of mutual solubility is the brazing of nickel-base alloys with pure copper. The copper-nickel phase diagram is similar to Fig. 9(a).

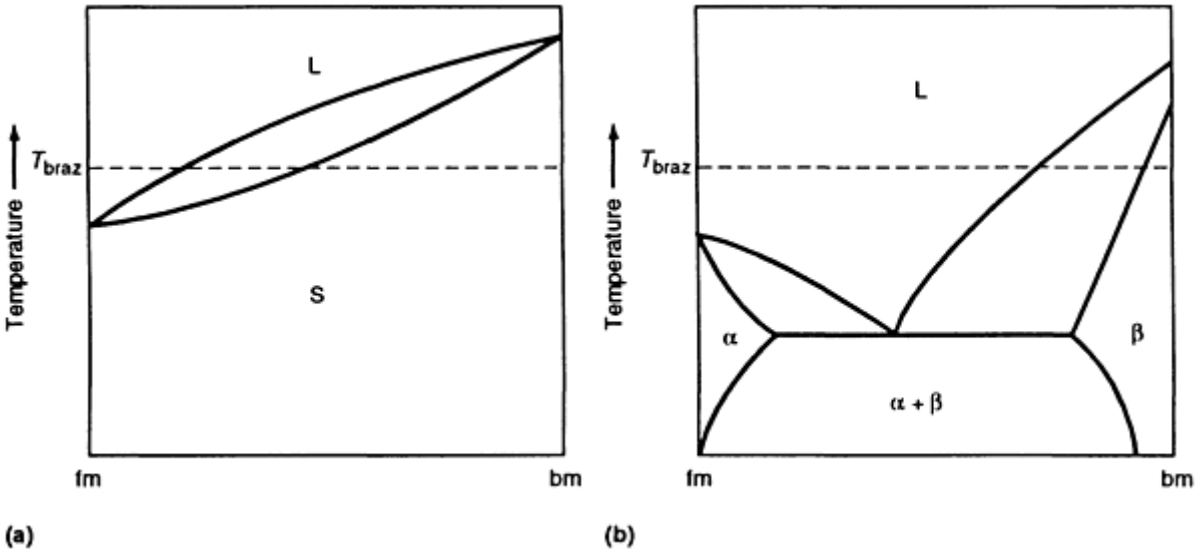

FIG. 11 HYPOTHETICAL PHASE DIAGRAMS BETWEEN FILLER METAL AND BASE METAL. (A) COMPLETE SOLUBILITY OF FILLER METAL AND BASE METAL. (B) EUTECTIC PHASE

Liquid penetration through grain boundaries may increase with decreasing mutual solubility. Copper is known to cause hot shortness in steel because of its limited solubility in steel (0.3 wt% at 590 °C, or 1095 °F) which favors the grain boundary liquid penetration.

Vapor Pressure. The vapor pressure of an element increases with increasing temperature. Furthermore, decreasing the surrounding pressure, such as in a vacuum, further increases the vaporization loss. This will cause variations in the chemical composition of the filler metal. As a consequence, the flowing behavior of the filler metal can be impaired. Metal vaporization may also promote porosity formation in the joint. Figure 12 summarizes the relationship between joining temperature, furnace pressure, and metal vapor pressure. Using silver as an illustration, the equilibrium vapor pressure at 1000 °C (1830 °F) is 13 Pa (10^{-1} mm Hg). If the furnace pressure is lower than 13 Pa (10^{-1} mm Hg), silver will vaporize. The loss due to vaporization is critical for soldering, especially when joined under vacuum.

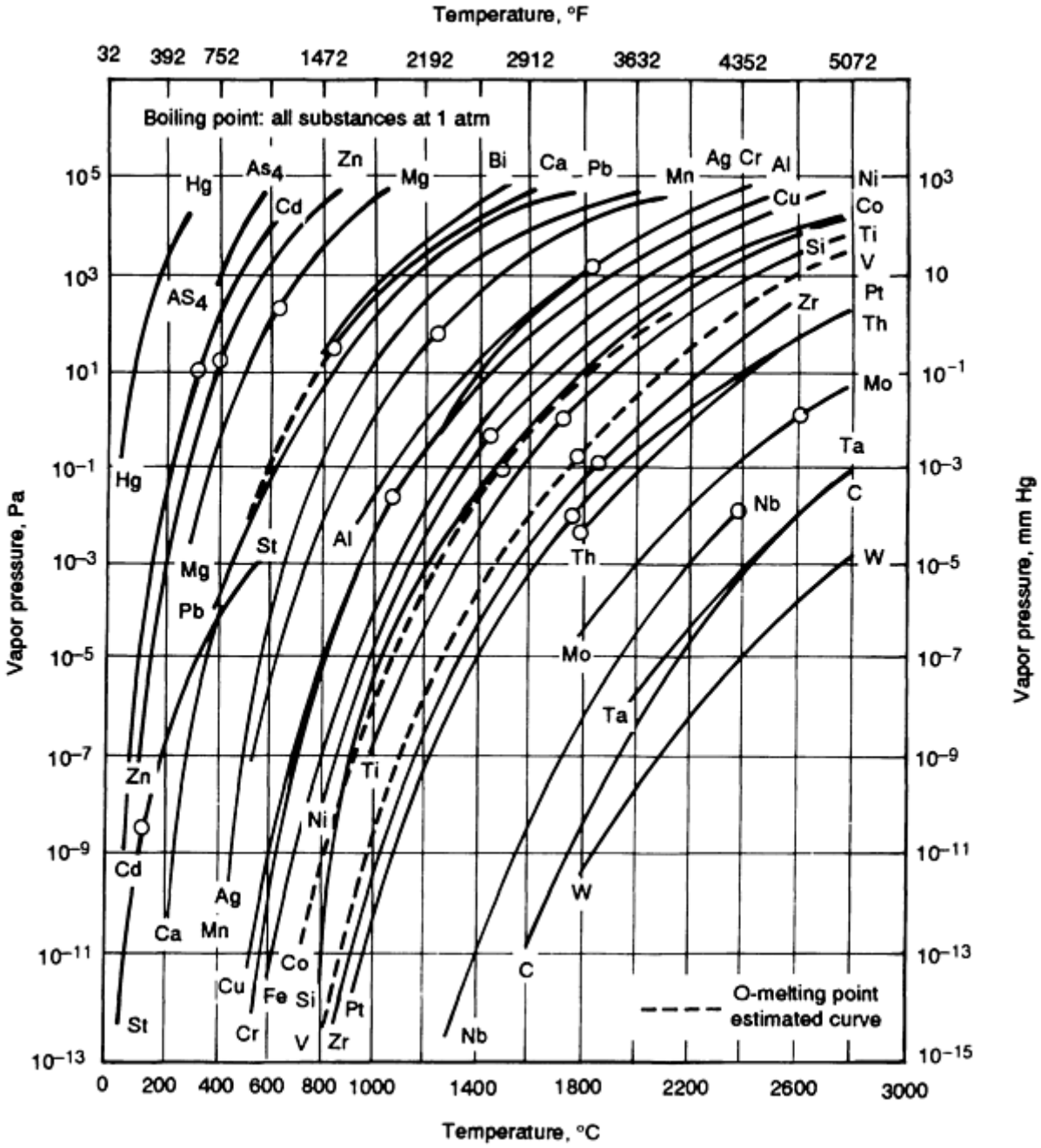

FIG. 12 VAPOR PRESSURE AS A FUNCTION OF TEMPERATURE. SOURCE: REF 3

Vapor pressure of metallic elements is particularly important in vacuum tube applications. The presence of high vapor pressure elements in the filler metal is restricted because of potential contamination inside the tube. The American Welding Society (AWS) filler metal specification for vacuum brazing limits the amount of high vapor pressure elements in the alloys. For elements that have vapor pressures higher than 13 μPa (10^{-7} torr) at 500 °C (930 °F), such as magnesium, antimony, potassium, sodium, lithium, thallium, sulfur, cesium, rubidium, selenium, tellurium, strontium, and calcium, the maximum allowed concentrations are 0.001 and 0.002 wt% for grades 1 and 2, respectively. In addition, the total sum of high vapor pressure elements, including zinc, cadmium, and lead, is limited to 0.010 wt%.

Fluxes and Atmospheres Selection. The major functions of fluxes in brazing and soldering are to remove oxides from the base metal surface by a reduction and/or dissolution reaction, to protect the clean surface from reoxidation, and to modify the surface tension of the molten metal. These functions can be achieved through chemical reactions that are, in general, thermally activated.

Chemical reactions typically occur between the surface oxide and the active components of the flux. The surface oxide can undergo a reduction reaction that results in the formation of a soluble compound, as exemplified below:

$$(MO)_{SURF} + (FLUX) \rightarrow M_{SURF} + O + \ldots \quad \textbf{(EQ 5)}$$

$$(MO)_{SURF} + (FLUX) \rightarrow M_{SURF} + (MO \cdot FLUX)_{VEHICLE\ SOLUB.} \quad \textbf{(EQ 6)}$$

$$\rightarrow M_{SURF} + (MO \cdot VEHICLE)_{FLUX\ SOLUB.} \quad \textbf{(EQ 6A)}$$

where MO is the metal oxide, M is the metal, and O is oxygen. The subscript *surf* indicates that the reaction is located at the surface. (MO · flux) and (MO · vehicle) represent metal oxides dissolved in the flux or vehicle. Equation 5 represents a reduction of a surface oxide by a flux, resulting in a metal at the surface plus the evolution of oxygen. Equations 6 and 6a(a) represent a reduction of a surface oxide by a flux succeeding in a metal at surface and the oxygen soluble in the vehicle flux (Eq 6) or in the flux (Eq 6aa).

The chemical activity of a flux is strongly dependent on temperature and on the properties of a flux, such as thermal stability, activation temperature, and deactivation temperature, that characterize the activation temperature range. Suitable joining processes require that the flux components be stable throughout the joining cycle. They should not evaporate or decompose. For example, in applications in which the boiling point of the flux vehicle is lower than the joining temperature, the flux is thermally stable and able to protect the clean surface from reoxidation. On the other hand, the flux vehicle may have a high boiling point and remain intact on the part surface. The liquid flux vehicle assists the flux solder to act as a physical barrier that ensures protection of the clean surface against reoxidation.

The activation temperature range is defined as the temperature range at which a flux reaches its maximum chemical activity. The deactivation temperature is the temperature at which the flux breaks down and is no long active. It is important that the joining temperature remains slightly higher than the minimum activation temperature for maximum activity. Figure 13 shows two temperature ranges. The first one corresponds to the maximum flux chemical activity and dissolution and reduction reactions. The second corresponds to the breakdown of the fluxes and a loss of flux chemical activity.

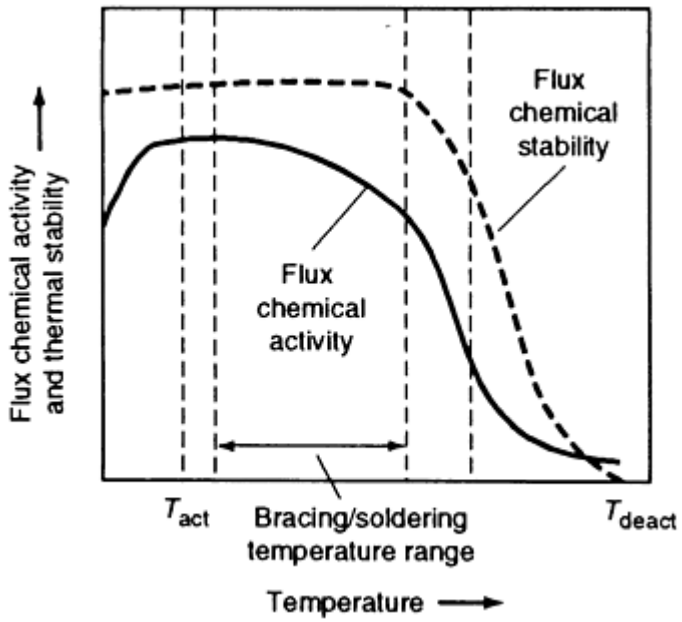

FIG. 13 EFFECT OF TEMPERATURE ON FLUX CHEMICAL ACTIVITY AND FLUX THERMAL STABILITY

Fluxes are not designed to remove grease, oil, dirt, or paint from the part surface. Thus, the joint surface must be free of these contaminants prior to joining.

Another common practice in brazing is the use of protective atmospheres. Combustion gases of different compositions, reducing gases such as NH_3 and hydrogen, and inert gases such as argon and nitrogen are typical examples of the gases used. In the case of combustion gases, the oxygen and carbon potentials of the gases determine the oxidation and reduction behavior of the alloying elements and surface oxides. Thermodynamic calculations can also be carried out to relate these potentials to the partial pressures of CO and CO_2. The water vapor content, similar to that of CO_2, is usually expressed as the dew point of the gas.

In the case of a hydrogen-rich atmosphere, it is the hydrogen-oxygen reaction alone that controls the oxidation-reduction behavior of the filler metal and base metal. For a particular brazing atmosphere and dew point, a threshold temperature must be reached to start to reduce the surface oxides that cover both the base metal and filler metal. This temperature is specific for each metal-metal oxide system and is related to the oxide stability.

Figure 14 shows the metal-metal oxide equilibria in pure hydrogen atmospheres. In this diagram the region under a metal-metal oxide curve represents the conditions under which the metal oxide can be reduced by hydrogen. For example, brazing a stainless steel at 925 °C (1700 °F) in a hydrogen-rich atmosphere can be successfully performed only if the dew point is lower than -43 °C (-45 °F). In this case the thermodynamic conditions are favorable to reduce the chromium oxide which will promote good wetting and spreading.

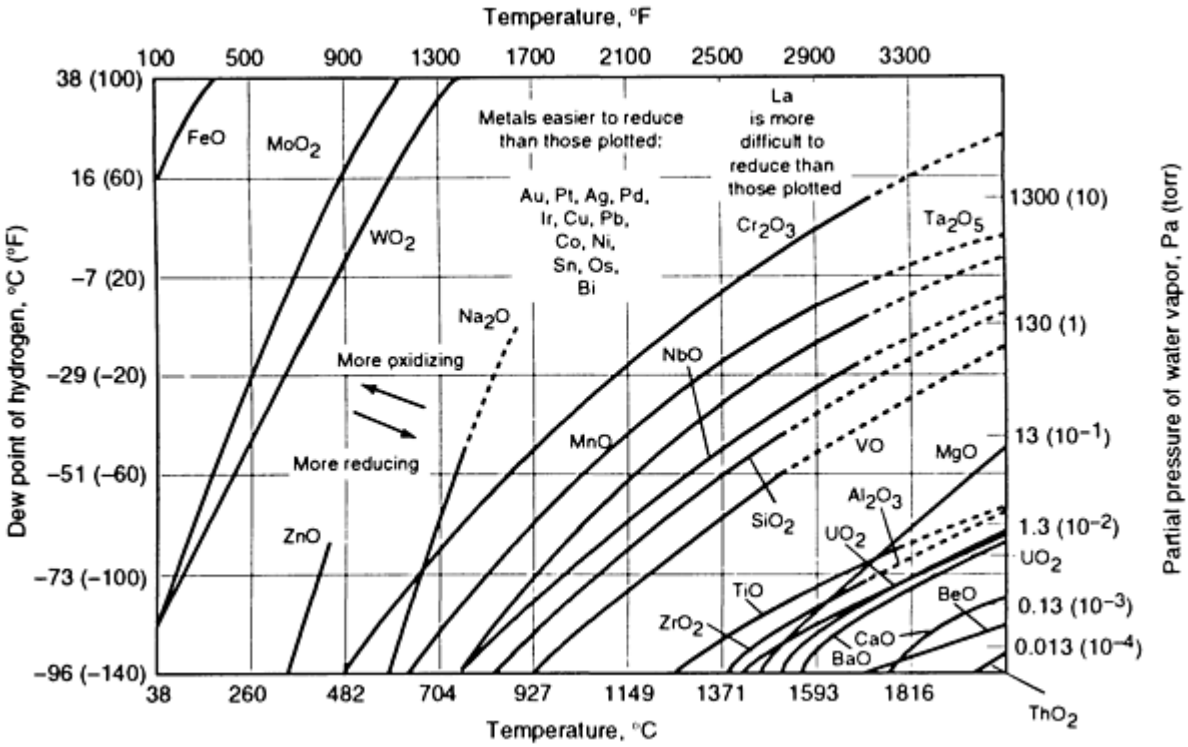

FIG. 14 METAL-METAL OXIDE EQUILIBRIA IN PURE HYDROGEN ATMOSPHERES. SOURCE: REF 4

Tables 2, 3, and 4 present the classifications of brazing fluxes, brazing atmospheres, and soldering fluxes. These tables are intended for general use only.

TABLE 2 BRAZING FLUX TYPES PER AWS SPECIFICATION B2.2

AWS BRAZING FLUX NO.	RECOMMENDED BASE METALS[(A)]	RECOMMENDED FILLER METALS	RECOMMENDED USEFUL TEMPERATURE RANGE		CONSTITUENTS
			°C	°F	
1	ALL BRAZEABLE	BALSI	370-	700-	CHLORIDES,

	ALUMINUM ALLOYS		645	1190	FLUORIDES
2	ALL BRAZEABLE MAGNESIUM ALLOYS	BMG	480-650	900-1200	CHLORIDES, FLUORIDES
3A	(B)	BCUP, BAG	565-870	1050-1600	BORIC ACID, BORATES, FLUORIDES, FLUOBORATES, WETTING AGENT
3B	(B)	BCU, BCUP, BAG, BAU, RBCUZN, BNI	730-1150	1350-2100	BORIC ACID, BORATES, FLUORIDES, FLUOBORATES, WETTING AGENT
4	ALUMINUM BRONZE, ALUMINUM BRASS, AND IRON-BASE OR NICKEL-BASE ALLOYS CONTAINING ALUMINUM OR TITANIUM	BAG, BCUP(C)	565-870	1050-1600	CHLORIDES, FLUORIDES, BORATES, WETTING AGENT
5	(B)	(D)	760-1205	1400-2200	BORAX BORIC ACID BORATES, WETTING AGENT

(A) NOT APPLICABLE, IN SOME CASES, TO TITANIUM-BASE AND ZIRCONIUM-BASE METALS.

(B) ALL EXCEPT THOSE LISTED UNDER 1, 2, AND 4.

(C) COPPER-BASE ALLOYS ONLY.

(D) SAME AS 3B (EXCLUDING BAG-1 THROUGH BAG-7)

TABLE 3 BRAZING ATMOSPHERE TYPES (PER AWS SPECIFICATION B2.2)

AWS BRAZING ATMOSPHERE NO.	SOURCE	DEW POINT MAXIMUM(A)		PRESSURE		COMPOSITION, WT%				
		°C	°F	PA	TORR	H_2	N_2	CO	CO_2	OTHER
1	COMBUSTED FUEL GAS	RT	RT	. . .	. . .	1-5	87	1-5	11-12	. . .
2	COMBUSTED FUEL GAS	RT	RT	. . .	. . .	14-15	70-71	9-10	5-6	. . .
3	COMBUSTED FUEL GAS	-40	-40	. . .	. . .	15-16	73-75	10-11	. . .	. . .
4	COMBUSTED FUEL GAS	-40	-40	. . .	. . .	38-40	41-45	17-19	. . .	. . .
5	DISSOCIATED AMMONIA	-54	-65	. . .	. . .	75	25	. . .	. . .	. . .
6	HYDROGEN	RT	RT	. . .	. . .	97-100	. . .	. . .	. . .	. . .
7	HYDROGEN	-59	-74	. . .	. . .	100	. . .	. . .	. . .	. . .
8	HEATED VOLATILE MATERIALS	. . .	. . .	. . .	. . .	. . .	. . .	. . .	. . .	INORGANIC VAPOR (E.G., ZN, CD, LI, MG, FLUORIDES)

9	PURIFIED INERT GAS	. . .	. . .	. . .	. . .	. . .	. . .	. . .	. . .	. . .
10	VACUUM	. . .	. . .	>265	>2	. . .	. . .	. . .	. . .	. . .
10A	VACUUM	. . .	. . .	>65-265	>0.5-2	. . .	. . .	. . .	. . .	. . .
10B	VACUUM	. . .	. . .	>0.13-65	>0.001-0.5	. . .	. . .	. . .	. . .	. . .
10C	VACUUM	. . .	. . .	≤0.13	≤0.001	. . .	. . .	. . .	. . .	. . .

(A) RT, ROOM TEMPERATURE

TABLE 4 CLASSIFICATION OF SOLDERING FLUXES

FLUX TYPE	USES	CONSTITUENTS	TEMPERATURE STABILITY	RECOMMENDED TEMPERATURE RANGE	
				°C	°F
CORROSIVE (INORGANIC)					
ACIDS	STRUCTURAL	HYDROCHLORIC, HYDROFLUORIC, ORTHOPHOSPHORIC	GOOD	150-450	300-840
SALTS	STRUCTURAL	ZINC CHLORIDE, AMMONIUM CHLORIDE, TIN CHLORIDE	EXCELLENT	150-450	300-840
INTERMEDIATE (ORGANIC)					
ACIDS	STRUCTURAL, ELECTRICAL	LACTIC, OLEIC, STEARIC, GLUTAMIC, PHTHALIC	FAIRLY GOOD	180-280	355-500
HALOGENS	STRUCTURAL, ELECTRICAL	ANILINE HYDROCHLORIDE, GLUTAMIC HYDROCHLORIDE, BROMIDE DERIVATIVES OF PALMITIC ACID, HYDRAZINE HYDROCHLORIDE (OR HYDROBROMIDE)	FAIRLY GOOD	180-280	355-500
AMINES AND AMIDES	STRUCTURAL, ELECTRICAL	UREA, ETHYLENE DIAMINE, MONOTRIETHANOL AMINE, TRIETHANOLAMINE	FAIR	180-280	355-500
NONCORROSIVE (ORGANIC)					
ROSIN NONACTIVATED (R)	ELECTRICAL	WATER-WHITE ROSIN	POOR	140-270	285-520
ROSIN MILDLY ACTIVATED (RMA)	ELECTRICAL	ROSIN WITH ACTIVATOR (HALIDE-BASE, ORGANIC ACID, AMINES, AMIDES . . .)	POOR	140-270	285-520
ROSIN ACTIVATED (RA)	ELECTRICAL, STRUCTURAL	ROSIN WITH MORE ACTIVATOR THAN RMA FLUX	FAIR	140-270	285-520

Source: Ref 5

Additional Metallurgical Considerations. Exposure to brazing temperatures can also result in base metal embrittlement. These embrittling conditions must be taken into consideration in the design of a brazed joint and brazing process parameters. Soldering occurs at lower temperatures than brazing, so embrittlement seldom happens in the base metal of a soldered joint because it is thermally activated. Embrittlement in the base metal can be caused by second-phase precipitation, hydrogen embrittlement, or the brazing of dissimilar metals.

Second-Phase Precipitation. The most common embrittlement phenomenon is second-phase precipitation of carbides at grain boundaries. Plain steels with low carbon contents can be embrittled by the precipitation of a cementite (Fe_3C) film at the grain boundary. For a steel with 0.02 wt% C, this phenomenon occurs at approximately 400 °C (750 °F).

Ferritic and austenitic stainless steels can have their corrosion behavior and toughness impaired by chromium carbide precipitation between 450 to 850 °C (750 to 1560 °F). This precipitation forms a chromium-depleted zone around the carbides and along the grain boundaries, which decreases the corrosion resistance of the alloy. This phenomenon is called sensitization. For the austenitic stainless steels, a low-carbon steel or a stabilized steel should be chosen to avoid the loss in corrosion resistance. Higher chromium diffusivity in the ferritic stainless steels results in a narrower chromium-depleted zone than that observed in the austenitic stainless steels. Thus, a heat treatment can remove the chromium-depleted zone and restore corrosion resistance. However, the toughness of the ferritic stainless steels will not be recovered by heat treatment.

Aluminum-magnesium alloys can experience an Al_3Mg_2 grain boundary precipitate that decreases the corrosion resistance of the alloy. In this case the difference between the corrosion potentials of the precipitate and the matrix increases the corrosion rate at the matrix-precipitate interface. Depending on the conditions, intergranular corrosion may take place, followed by stress-corrosion cracking.

Hydrogen Embrittlement. Hydrogen can cause severe embrittlement in many different materials. It can diffuse faster at room temperature and may cause a delayed embrittlement, mainly in steels. This type of embrittlement is not important for soldering.

In steels, hydrogen embrittlement occurs when four conditions are met: favorable microstructure (martensite, bainite, ferrite), hydrogen level, residual stress, and low temperature (<<100 °C, or 212 °F). These four conditions should be kept in mind when choosing a brazing procedure for steels. For example, steel brazing in a hydrogen-rich atmosphere may be inappropriate due to hydrogen pickup during joining.

Two mechanisms have been proposed for hydrogen embrittlement in nonferrous alloys: water vapor buildup and hydride precipitation. If an alloy has oxides precipitated along the grain boundaries, hydrogen will diffuse toward the oxides and may react with them to form water vapor. The pressure built up because of water vapor at the grain boundaries can separate the boundaries and promote embrittlement of the alloy. This is the case with electrolytic tough pitch copper that is brazed in a hydrogen-rich atmosphere.

Refractory metals such as titanium, zirconium, niobium, tantalum, tungsten, and molybdenum are very susceptible to the presence of interstitial elements (hydrogen, nitrogen, oxygen, and carbon). These interstitials distort the metal lattice, causing a strong interstitial solid solution hardening that diminishes the toughness of these metals. In a body-centered cubic (bcc) lattice, the solubility of the interstitial elements is reduced, which may result in the precipitation of the carbides and nitrides in these metals. In the case of hydrogen, a hydride will precipitate. The brazing conditions should be carefully selected to avoid interstitial pickup and the formation of a second interstitial-based phase during brazing.

Brazing of Dissimilar Materials. When different materials are brazed together, the possibility of intermetallics formation and the effect of the mismatch between the coefficients of thermal expansion must be considered. The formation of intermetallics was described above. The mismatch between the coefficients of thermal expansion generates residual stresses that influence the mechanical properties of the joint. Ultimately, fracture may occur, depending on the residual stress level. This effect is particularly important in the case of metal-to-ceramic brazing, in which the thermal expansion coefficients are very different. Table 5 presents some physical properties for selected materials.

TABLE 5 GENERAL PROPERTIES OF SELECTED MATERIALS

MATERIAL	MELTING POINT		DENSITY		EXPANSION COEFFICIENT		YOUNG'S MODULUS		TENSILE STRENGTH	
	°C	°F	g/cm^3	$lb/in.^3$	$10^{-6}/k$	$10^{-6}/°f$	GPa	10^6 psi	MPa	ksi
CERAMIC										
OXIDE										
AL_2O_3 (SAPPHIRE)	2050	3720	3.985	0.144	5.8	3.2	380	55.1	620	90
BEO	2530	4585	3.01	0.109	8.4-9.0	4.7-5.0	311	45.1	172-275	24.9-39.9
SIO_2 (VITREOUS)	1710	3110	2.19	0.079	0.54	0.30	69	10.0	110	16.0
ZRO_2 (Y_2O_3)	2960	5360	5.56	0.200	10	5.6	138	20.0	>300	>44
CARBIDE										
B_4C	2350	4260	2.51	0.091	5.6	3.1	440-470	64-68	310-350(B)	45-51(B)
SIC	2300-2580(A)	4170-4675(A)	3.17	0.115	4.3-4.6	2.4-2.6	414	60.0	450-520(C)	65-75(C)
TIC	3140	5685	4.93	0.178	7.7	4.3	462	67.0	275-450(C)	40-65(C)
WC	2770	5020	15.70	0.567	4.9	2.7	814	118	790-825	115-120
NITRIDE										
ALN	2400	4350	3.25	0.117	5.3	2.9	350	50.8	270	39(B)
SI_3N_4	1750-1900(A)	3180-3452(A)	3.19	0.115	3.3	1.8	304	44.1	400-580(B)	58-72.5
METAL										
AL	660	1220	2.70	0.098	23.5	13.1	69	10	50-195	7.3-28.3
CU	1083	1981	8.96	0.324	17.0	9.5	180	19	224-314	32.5-45.5
BRASS (70-30)	910-965	1670-1770	8.55	0.309	19-20	10.6-11.1	100-115	14.5-16.7	300-700	43.5-102
FE	1535	2795	7.87	0.284	12.1	6.7	197	28.5	180-210	26-30.5
AISI 304	1400-1455	2550-2650	7.93	0.286	18.0	10.0	190-210	27.6-30.4	460-1100	67-160
AISI 410	1480-1530	2695-2785	7.73	0.279	10-12	5.6-6.7	190-210	27.6-30.4	480-1500	70-220
NI	1453	2647	8.9	0.322	13.3	7.4	199	28.9	660	96
MO	2617	4743	10.22	0.369	5.1	2.8	324.8	47.1	458-690	66.4-100
NB	2468	4474	8.57	0.310	7.2	4.0	104.9	15.2	330-585	48-85
ZR	1852	3366	6.49	0.234	5.9	3.3	98	14.2	350-390	51-57
W	3410	6170	19.3	0.697	4.5	2.5	411	59.6	550-620	80-90
GRAPHITE										
GRAPHITE	3650	6600	2.26	0.082	0.6-4.3	0.3-2.4	6.9	10.0	28	41

(A) SUBLIMATION POINT.

(B) 5% POROSITY.

(C) 2% POROSITY

The strain developed during heating and cooling by mismatch of thermal expansion coefficients can be evaluated using Eq 7.

$$\Delta\varepsilon = \Delta\alpha \cdot \Delta T \qquad \textbf{(EQ 7)}$$

where $\Delta\varepsilon$ is the strain variation, $\Delta\alpha$ is the thermal expansion coefficient mismatch, and ΔT is the temperature variation below solidus temperature. However, more in-depth computations using finite-element analysis should be performed to identify stress concentrations as a function of the joint configuration.

In the case of a silicon nitride (Si_4N_3) part being joined to an austenitic stainless steel component at 1325 K (1925 °F) using a filler metal with a solidus temperature of 1298 K (1877 °F), the value of the strain is estimated at 16.7×10^{-3} (thermal expansion coefficient mismatch = 16.7×10^{-6} K). Correspondingly, a stress of 5.078 GPa (much higher than the strength of silicon nitride) is generated. Based on this estimation, it is very likely that cracks will nucleate and propagate in the brittle ceramic material. The actual value of the stress is, however, lower than the value calculated by Eq 7 once the metal deforms and the stress developed in the joint is alleviated.

One technique for decreasing the residual stress level in the joint is to perform brazing with a soft, ductile metal interlayer. In this case the interlayer will deform and will accommodate the residual stresses generated by the mismatch between the coefficients of thermal expansion. Figure 15 shows this technique.

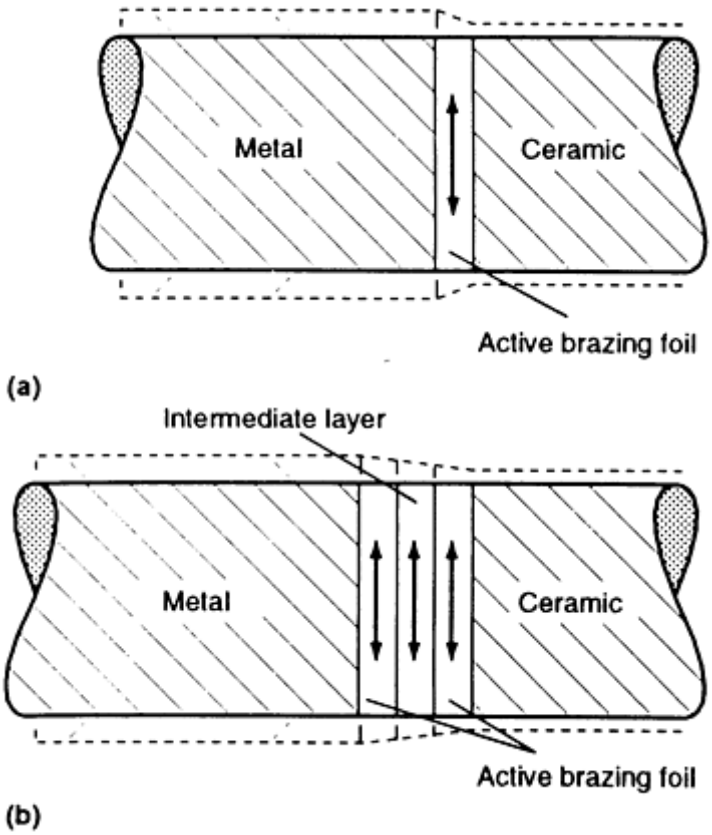

FIG. 15 ADDITION OF SOFT DUCTILE METAL INTERLAYER TO REDUCE RESIDUAL STRESSES IN A JOINT. (A) WITHOUT INTERLAYER. (B) WITH INTERLAYER

The mismatch in the strength may also generate a stress concentration in the joint under applied loads. In this case, assuming the same load and a metal-ceramic joint, the deformation in the ceramic is lower than that in the metal. Thus, as a result of the different deformation ($\varepsilon_{metal} - \varepsilon_{ceramic}$), a stress concentration is created at the interface, as shown in Fig. 16.

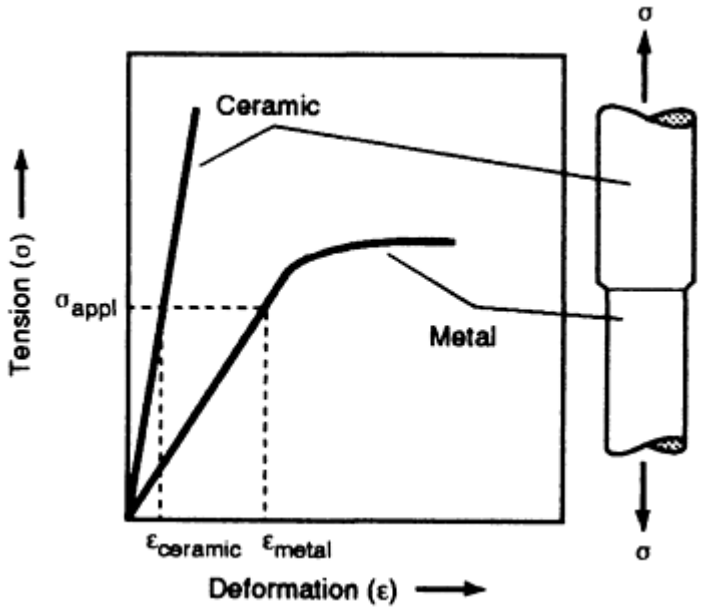

FIG. 16 STRESS CONCENTRATION AS A FUNCTION OF MISMATCHED STRENGTH

References cited in this section

1. P.R. SHARPS, A.P. TOMSIA, AND J.A. PASK, WETTING AND SPREADING IN THE CU-AG SYSTEM, *ACTA METALL.*, VOL 29 (NO. 5), 1981, P 855-865
2. V. KONDIC, *METALLURGICAL PRINCIPLES OF FOUNDING*, AMERICAN ELSEVIER, 1973
3. M.G. NICHOLAS AND D.A. MORTIMER, CERAMIC/METAL JOINING FOR STRUCTURAL APPLICATIONS, *MATER. SCI. TECHNOL.*, VOL 1 (NO. 9), 1985, P 657-665
4. D.R. MILNER AND R.L. APPS, *INTRODUCTION TO WELDING AND BRAZING*, PERGAMON PRESS, 1969
5. *SOLDERING MANUAL*, AMERICAN WELDING SOCIETY, 1977

Brazeability and Solderability of Engineering Materials

S.D. Brandi, Escola Politécnica da Universidade de São Paulo, Brazil; S. Liu, Colorado School of Mines; J.E. Indacochea and R. Xu, University of Illinois at Chicago

Brazing and Soldering Characteristics of Engineering Materials

To continue the discussion on brazeability and solderability of engineering materials, the joining process characteristics will be discussed. More detailed information about practices for brazing and soldering specific materials is available in the Section "Procedure Development and Practice Considerations for Brazing and Soldering" in this Volume.

All brazing and soldering processes consist of a cleaning operation, a filler metal addition, and a heating and cooling cycle. In some processes the material is heated faster than in others, which may require different temperature and time control. The faster the joining process, the lower the probability that intermetallics will be formed and the narrower the heat-affected zone (HAZ) in the base metal. On the other hand, fast heating may lead to high residual stress levels.

Depending on the joining process characteristics (heating and cooling cycles, joint design, protection of the joint, and so on), the mechanical and corrosion behavior could be different for brazed or soldered joints of the same base metal and filler metal. Figure 17 presents the thermal experience of a joint prepared using three different heating methods. Curve A

represents induction or resistance heating, characterized by faster heating and cooling. Torch heating is generally more diffused and performed at a slower rate. As a result, base metal heating is more extensive, as shown by curve B. The thermal performance of furnace heating is described by curve C, where uniform heat in both base metal and joint is achieved.

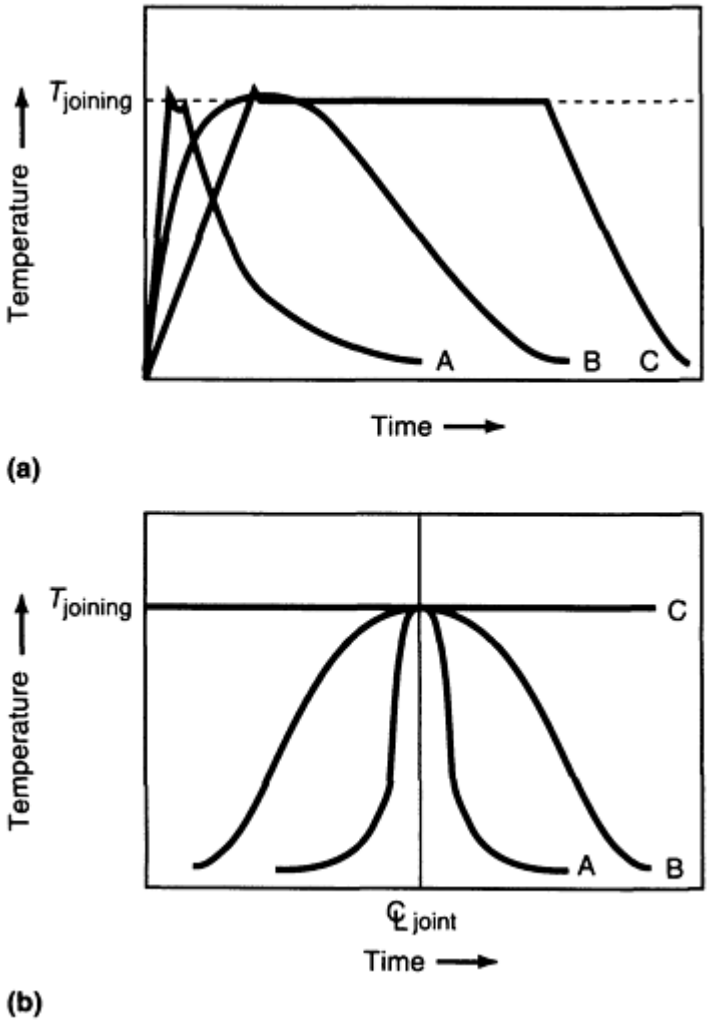

FIG. 17 THERMAL PERFORMANCE OF A JOINT AS A FUNCTION OF HEATING METHOD. (A) THERMAL CYCLE. (B) TEMPERATURE DISTRIBUTION. A, INDUCTION OR RESISTANCE HEATING; B, TORCH HEATING; C, FURNACE HEATING

The heating method is chosen according to base metal and filler metal characteristics, base metal-filler metal interaction, joint geometry, quality, cost, and productivity. Tables 6 and 7 summarize the common heating methods for brazing and soldering different materials.

TABLE 6 RELATIONSHIP OF TYPICAL HEATING METHOD, BASE METALS, AND FILLER METALS USED IN BRAZING

AWS FILLER-METAL CLASSIFICATION[A]	APPLICATION	HEATING METHOD[A]	AWS FLUX CLASSIFICATION[B]
BAG-1; BAG-1A; BAG-2; BAG-2A	GENERAL-PURPOSE (EXCEPT AL AND MG ALLOYS)	T, I, R, F(A), F(H)	FB3-A; FB3-C; FB3-D; FB3-E; FB3-F; FB3-G; FB3-H; FB3-I, FB3-J; FB3-K; FB4-A

BAG-3	GENERAL-PURPOSE (EXCEPT AL AND MG ALLOYS)	T, I, R	FB3-A; FB3-C; FB3-D; FB3-E; FB3-F; FB3-G; FB3-H; FB3-I, FB3-J; FB3-K; FB4-A
BAG-4; BAG-5; BAG-6; BAG-7; BAG-9; BAG-10; BAG-13; BAG-20; BAG-22; BAG-24; BAG-25; BAG-26; BAG-27; BAG-28	SPECIAL-PURPOSE	T, I, R, F(A), F(H)	FB3-A; FB3-C; FB3-D; FB3-E; FB3-F; FB3-G: FB3-H; FB3-I, FB3-J; FB3-K; FB4-A
BAG-8; BAG-8A; BAG-13A; BAG-19	SPECIAL-PURPOSE	F(V), F(H), F(A)	FB3-A; FB3-C; FB3-D; FB3-E; FB3-F; FB3-G; FB3-H; FB3-I, FB3-J; FB3-K; FB4-A
BAG-18; BAG-21; BAG-23	SPECIAL-PURPOSE	T, R, I, F(V), F(H), F(A)	FB3-A; FB3-C; FB3-D; FB3-E; FB3-F; FB3-G; FB3-H; FB3-I, FB3-J; FB3-K; FB4-A
BAU-1; BAU-2; BAU-3; BAU-4	SPECIAL-PURPOSE (STEEL, NI, CO = RESISTANCE TO CORROSION AND OXIDATION)	R, I, F(V), F(H), F(A)	FB3-D; FB3-I; FB3-J
BAU-5; BAU-6; BAU-7; BAU-8	SPECIAL-PURPOSE (STEEL, NI, CO = RESISTANCE TO CORROSION AND OXIDATION)	F(V), F(A)	FB3-D, FB3-I, FB3-J
BPD-I	SPECIAL-PURPOSE	F(V), F(A)	. . .
BALSI-2; BALSI-5	SPECIAL-PURPOSE	F(A), D	FB1-A; FB1-B; FB1-C
BALSI-3; BALSI-4	GENERAL-PURPOSE (AL ALLOYS)	T, D, I, R, F(V)	FB1-A; FB1-B; FB1-C
BALSI-6; BALSI-7; BALSI-8; BALSI-9; BALSI-10; BALSI-11	SPECIAL-PURPOSE	F(V)	FB1-A; FB1-B; FB1-C
BCUP-1	SPECIAL-PURPOSE (COPPER AND COPPER ALLOYS)	R, I	FB3-A; FB3-C; FB3-E; FB3-F; FB3-G; FB3-H; FB3-K; FB4-A
BCUP-2; BCUP-3; BCUP-4; BCUP-5; BCUP-6; BCUP-7	SPECIAL-PURPOSE (COPPER AND COPPER ALLOYS)	T, I, R, F(A), F(H)	FB3-A; FB3-C; FB3-E; FB3-F; FB3-G; FB3-H; FB3-K; FB4-A
BCU-1; BCU-1A; BCU-2	SPECIAL-PURPOSE (FERROUS AND NONFERROUS ALLOYS)	F(H), F(V)	FB3-D; FB3-I; FB3-J
RBCUZN-A, RBCUZN-C	SPECIAL-PURPOSE (FERROUS AND NONFERROUS ALLOYS)	T, F(H), F(A), I, R	FB3-D; FB3-I; FB3-J; FB3-K
RBCUZN-D	SPECIAL-PURPOSE (FERROUS AND NONFERROUS ALLOYS)	T, I, R	FB3-D; FB3-I; FB3-J; FB3-K
RBCUZN-E; RBCUZN-F; RBCUZN-G; RBCUZN-H	SPECIAL-PURPOSE (FERROUS AND	T, I, R	FB3-D; FB3-I; FB3-J; FB3-K

	NONFERROUS ALLOYS)		
BNI-1; BNI-1A; BNI-2; BNI-5; BNI-6; BNI-7	SPECIAL-PURPOSE (CORROSION AND HEAT RESISTANCE MATERIALS)	T, I, R, F(H)	FB3-D, FB3-I, FB3-J
BNI-3; BNI-4	SPECIAL-PURPOSE (CORROSION AND HEAT RESISTANCE MATERIALS)	T, I, R, F(H), F(V)	FB3-D; FB3-I; FB3-J
BNI-8	SPECIAL-PURPOSE (CORROSION AND HEAT RESISTANCE MATERIALS)	F(H), F(A), F(V)	FB3-D; FB3-I; FB3-J
BCO-1	SPECIAL-PURPOSE (HIGH-TEMPERATURE SERVICE)	F(V)	. . .
BMG-1	SPECIAL-PURPOSE (AZ1OA,K1A, AND M1A MG ALLOYS)	T, F(A), D	FB2-A

Source: Ref 3

(A) T, TORCH; I, INDUCTION; R, RESISTANCE; F(H), FURNACE WITH H_2 ATMOSPHERE; F(A), FURNACE WITH ARGON ATMOSPHERE; F(V), FURNACE WITH VACUUM; D, DIP BRAZING.

(B) IN SOME CASES, A FLUX IS NOT NECESSARY.

TABLE 7 RELATIONSHIP OF COMMON HEATING METHODS, BASE METALS, AND FILLER METALS USED IN SOLDERING

BASE METAL	**FILLER METAL**	**HEATING METHOD[(A)]**	**FLUX TYPE[(B)]**
COPPER AND COPPER ALLOYS	SN-PB	ALL	NC (CU, CU-SN, CU-ZN), IN (CU, CU-SN, CU-ZN), CO (ALL CU-BASE ALLOYS, ESPECIALLY CU-BE, SILICON BRONZE, AND ALUMINUM BRONZE)
STEEL	SN-PB (20-50%) (PREDOMINANTLY 40SN-60PB)	ALL	CO
AL COATED STEEL	40SN-60PB, 50SN-50PB, 60SN-40PB	I, R, US	CO
CD COATED STEEL	40SN-60PB, 50SN-50PB, 60SN-40PB	IR	NC
SN COATED STEEL	40SN-60PB, 50SN-50PB, 60SN-40PB	IR, I, D, T	NC
ZN COATED STEEL	40SN-60PB, 50SN-50PB, 60SN-40PB	DIFFICULT TO SOLDER	CO (SAME AS STAINLESS STEEL)
STAINLESS STEEL	SN-PB (SN > 50%)	ALL	CO
CAST IRON	SN-PB (20-50%)	ALL (AVOID OVERHEATING)	CO

NI AND NI ALLOYS	60SN-40PB, 50SN-50PB, 95SN-5SB	ALL	CO (CHLORIDE FLUX FOR NI, NI-CU), CO (HCI FLUX FOR NI-CR)
AL AND AL ALLOYS	SN-ZN, PB-BI, CD-ZN, ZN-AL	ALL (T, IR, AVOID OVERHEATING)	CO
MG AND MG ALLOYS	CD-ZN-SN, CD-ZN, SN-CD, SN-ZN	ALL	. . .
TIN AND TIN ALLOYS	63SN-37PB, 60SN-40PB	T, IR (AVOID OVERHEATING)	NC
PB AND PB ALLOYS	40SN-58PB-2SB	IR (WIPING)	NC
SILVER COATINGS AND FILMS	62SN-36PB-2AG	ALL	NC
GOLD COATINGS AND FILMS	53SN-29PB- 17IN-0.5ZN; 951N-5BI	ALL	NC
PLATINUM, PALLADIUM, RHODIUM COATINGS AND FILMS	60SN-40PB	ALL	NC
PRINTED CIRCUITS	63SN-37PB; 60SN-40PB	IR, D, W	NC

Source: Ref 5

(A) IR, SOLDERING IRONS; T, TORCH; D, DIP; I, INDUCTION; R, RESISTANCE; F, FURNACE; US, ULTRASONIC SOLDERING; FIR, FOCUSED INFRARED RADIATION; HG, HOT GAS; W, WAVE SOLDERING; VPC, VAPOR PHASE CONDENSATION; LB, LASER-BEAM SOLDERING.

(B) NC, NONCORROSIVE ORGANIC FLUX (BASE: ROSIN): IN. INTERMEDIATE ORGANIC FLUX (BASE: ORGANIC ACIDS, ORGANIC HYDROHALIDES, AMINES, AND AMIDES); CO, CORROSIVE INORGANIC FLUX (BASE: CHLORIDES AND ACIDS).

Low-Carbon Steels, Low-Alloy Steels, and Tool Steels

Brazing of low-carbon steels, low-alloy steels, and tool steels is a common practice. In this article, low-carbon steel is defined as a carbon steel with a maximum carbon content of 0.1 wt% and with silicon and manganese within the usual range. Low-alloy steels include not only the steels with a maximum total alloy content of 5.0 wt%, but also the high-strength low-alloy steels (microalloyed steels). Tool steels are high-alloy steels designed for high hardness and wear resistance. Tool steels can be further divided into two groups: carbon tool steels and high-speed tool steels. The mechanical properties of carbon tool steels depend mainly on the carbon content, which lies between 0.6 and 1.4 wt%. The high-speed tool steels are generally lower in carbon content, and their mechanical properties are mainly achieved by alloying elements such as tungsten, molybdenum, chromium, and vanadium. These elements are carbide formers. These carbides may affect the wetting and spreading behaviors of the braze alloy at the microstructural level. They also change the characteristics of iron oxide, making wetting and spreading more difficult.

Because each type of steel has a different set of mechanical properties, the brazing procedure for these steels should be determined as a function of the process characteristics and possible deterioration in material properties due to heating. In particular, the type of heating and heating cycle control (temperature and time), the kind of quenching medium (oil, water, air, and so on), and the optimal brazing conditions (filler metal type, flux or atmosphere type, cleaning conditions, joint geometry, fixtures, and so on) must be considered.

Low-carbon and low-alloy steels can be brazed by all brazing processes, but torch, furnace, induction, and dip brazing are most commonly used. Torch brazing of low-alloy steels should be performed with a neutral or slightly reducing flame, to minimize thermal effects on the base metal, filler metal, and flux. However, this process does not offer accurate temperature control, and excessive grain growth may occur. On the other hand, furnace brazing generally offers more

accurate temperature and brazing cycle control. The chemical composition of the atmosphere, if not adequately controlled, may lead to decarburization or hydrogen pickup, which eventually will degrade the steel properties.

The presence of surface oxides on steels affects the wetting of the molten filler metal. In general, surface oxides on low-carbon and low-alloy steel can be easily removed by means of a flux or atmosphere during brazing. AWS specification B2.2 recommends different brazing conditions for steels that have more than 1.0 wt% Cr and for those that contain aluminum and/or titanium. These three elements change the characteristics of the iron oxide on the surface. They increase the adherence of the oxides and decrease the diffusivity of oxygen in the oxide layer. Thus, the flux or brazing atmosphere must be able to reduce these oxides and promote wetting.

Carbon and low-alloy steels can be brazed with BCu, BAg, and RBCuZn filler metals. These filler metal groups present brazing temperature ranges of 1095 to 1150 °C (2000 to 2100 °F), 620 to 900 °C (1145 to 1650 °F), and 910 to 982 °C (1670 to 1800 °F), respectively. Based on the brazing temperature range, two different brazing techniques can be performed (Fig. 18). If the brazing temperature is higher than the austenitization temperature, A_1, of the steel (Fig. 18a and b), brazing can be done together with the first part of the heat treatment. In other cases, the brazing process may require lower temperatures so it can be performed simultaneously with the first or secondary tempering of the steel (Fig. 18c).

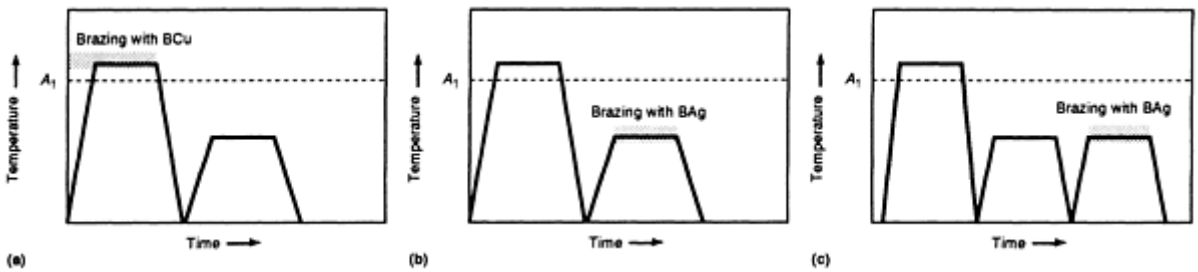

FIG. 18 INCORPORATION OF BRAZING OPERATION INTO HEAT TREATMENT CYCLE. (A) DURING AUSTENITIZATION PROCESS (BCU FILLER METAL). (B) DURING AUSTENITIZATION PROCESS (BAG FILLER METAL). (C) DURING TEMPERING PROCESS. A_1, AUSTENITIZATION TEMPERATURE

As a lower temperature process, soldering is related more to wetting phenomena than to microstructural changes in the steels. As with brazing, surface preparation and flux selection are fundamental to achieving a sound joint. Low-carbon and low-alloy steels present good solderability if the surfaces of the steels are properly cleaned and an aggressive flux is used.

Common filler metals used to solder steel belong to the tin-lead alloy group, with 20 to 50 wt% Sn. Because iron forms two intermetallics with tin, FeSn and Fe_2Sn, the amount and distribution of these intermetallics may impair the soundness of the joint. To minimize the presence of intermetallics, a solderable protective layer, such as copper and nickel, should be used. These layers present a limited intermetallic formation and can improve the solderability. The nickel layer must be protected from excessive oxidation by an overcoat of gold.

Tool steels having higher hardenability than the low-carbon, low-alloy steels, and the usual microstructure is tempered martensite with a fine dispersion of carbides. This microstructure is susceptible to thermal gradients, which may result in thermal cracking. During cooling, depending on the size of the component, the outer part transforms to martensite with volumetric expansion while the core remains untransformed and at a higher temperature. Together with different thermal expansion coefficients, this phase transformation may induce residual stresses and cracking in the transition region (between transformed and untransformed microstructure). Therefore, the heating and cooling of tool steels should be carefully controlled to minimize thermal gradients throughout the component.

Tool steels can be brazed by most brazing processes. However, torch brazing should be used carefully because of the lack of control in heating. As a result, thermal cracking is quite common. Induction brazing can be performed if a ductile metal insert is placed in the joint. The soft metal reduces the residual stresses generated and minimizes the cracking tendency. A composite filler metal (for example, copper-silver-copper sandwich) can be used to balance the shear stresses generated

during brazing. As indicated previously, furnace brazing presents the best temperature control, but the composition of the furnace atmosphere must be regulated to avoid decarburization of the base metal.

The filler metal groups are similar to those used to braze low-carbon and low-alloy steels. Some tool steels may have a higher chromium content, so the fluxes must be specially designed to promote wetting in spite of the oxidation potential of chromium.

Soldering of tool steel is not commonly done due to a lack of relevant applications.

Stainless steels are designed for better corrosion and oxidation resistance than ordinary steels. Chromium is responsible for this improvement. However, as the amount of chromium increases, the surface oxide changes from an $FeO/Fe_3O_4/Fe_2O_3$ to a more stable Cr_2O_3, which is difficult to wet. The presence of titanium, aluminum, manganese, and silicon in the stainless steels further modifies the nature of the surface oxide. The flux or the joining atmosphere must be able to promote reduction or dissolution of the oxide layer and enhance wetting and spreading behavior.

Stainless steels are often divided into five groups: austenitic, ferritic, martensitic, precipitation-hardened, and duplex. Filler metal selection will depend on the particular application:

- SERVICE CONDITIONS SUCH AS TEMPERATURE, STRESSES, AND ENVIRONMENT
- HEAT TREATMENT (ESPECIALLY FOR MARTENSITIC AND PRECIPITATION-HARDENING STAINLESS STEELS)
- BRAZING PROCESS CHARACTERISTICS (INCLUDING THERMAL CYCLE CONTROL)
- WETTING AND SPREADING BEHAVIOR
- METAL DISSOLUTION AND EROSION OF THE BASE METAL
- SECOND-PHASE PRECIPITATION (CARBIDES, σ PHASE)
- COST

Austenitic stainless steels exhibit good corrosion resistance, except in chloride-content environments. According to AWS specification B2.2, the austenitic and austenitic-alloyed-with-titanium stainless steels are classified into two groups. All other stainless steel groups are classified as one.

Corrosion resistance of an austenitic stainless steel is impaired by sensitization, which is a precipitation of chromium carbides along the grain boundaries when slowly heating or cooling the steel through the temperature range of 450 to 850 °C (750 to 1560 °F). The amount of precipitation depends on the temperature, time, carbon content, grain size, degree of plastic deformation, and the amount of stabilizers such as titanium and niobium. If not controlled, the heating cycle during brazing may sensitize the base metal. Based on Fig. 17, the best thermal experience to avoid sensitization is induction or resistance brazing (curve A). Furnace brazing (curve C) can give good results if joining is carried out at a temperature higher than the sensitization range, followed by a fast cooling.

Often the base metal that is susceptible to sensitization can be substituted with a low-carbon or a niobium-stabilized stainless steel, without the need to qualify a new brazing procedure (according to AWS B2.2).

Galvanic corrosion may also occur because of the potential difference between the base metal and the filler metal. In the case that the filler metal is less noble than the base metal, it will corrode faster and result in a crevice, which will further accelerate the corrosion process. A lack of joint filling (promoted by poor wetting) or void formation may also create a crevice that will corrode with or without galvanic action.

The chromium-nickel stainless steels are prone to stress-corrosion cracking (SCC). During brazing, the filler metal may penetrate along the grain boundaries of the base metal and form a grain boundary network of the filler metal. This grain boundary penetration, associated with tensile stresses and/or cyclic stresses and an aggressive medium, may promote stress-corrosion cracking. An example of stress-corrosion cracking at room temperature occurs when a sensitized austenitic stainless steel is exposed to fluorides (residual from brazing fluxes). Thus, cleaning after brazing is as important as the brazing operation to increase the life of brazed components.

Austenitic stainless steels have considerably higher coefficients of thermal expansion and lower thermal conductivities than other steels. The combination of these physical properties generally results in large distortions in a brazement. In the

case of localized heating, the broad heat source that heats up a large region may also induce plastic deformation in a large region, which generates residual stresses during cooling. For example, torch brazing of stainless steels should be used carefully when distortion is an important factor.

Stainless steels can be brazed using BCu, BAg, BNi, BCo, BPt, BPd, and BAu filler metal groups. Table 8 shows some filler metals and respective service temperatures of the brazement.

TABLE 8 BRAZING TEMPERATURES AND SERVICE TEMPERATURES FOR FILLER METALS USED IN THE BRAZING OF STAINLESS STEELS

FILLER METAL	BRAZING TEMPERATURE RANGE		SERVICE TEMPERATURE	
	°C	°F	°C	°F
BAG-1 THROUGH BAG-8A, BAG-24	620-900	1145-1650	205	400
BAG-13; BAG-19; BAG-21	800-980	1475-1800	370	700
BCU	1095-1150	2000-2100	425	800
CU-MN-NI	. . .	. . .	425-540	800-1000
BNI	925-1205	1700-2200	[GES]540	[GES]1000
BCO	1150-1230	2100-2250	[GES]540	[GES]1000
BAU	890-1230	1635-2250	[GES]540	[GES]1000
BPD	1220-1250	2225-2285	[GES]540	[GES]1000

Source: Ref 6

Stainless steels can be soldered using a nickel solderable coating and a gold protection finish to eliminate the need for harsh cleaning treatment.

Ferritic stainless steels usually have less chromium than austenitic grades. Sensitization is faster and at a slightly lower temperature range when compared with austenitic grades. So, the same brazing procedure should be followed to braze ferritic grades. A heating at the sensitization temperature range may eliminate the chromium-depleted zone, during or after brazing.

Ferritic stainless steel brazements are subjected to interfacial corrosion when brazed with some BAg alloys. A filler metal containing nickel can be used to minimize the corrosion rate. A special filler metal, BAg-21, was designed to braze AISI 403 ferritic stainless steel and reduce this corrosion attack.

Because the strength of ferritic grades is drastically reduced above 815 °C (1500 °F), special fixtures must be designed to maintain the shape of the component if brazing is to be performed at higher temperatures.

Martensitic and Precipitation-Hardening Stainless Steels. The brazing of a martensitic or a martensitic-type precipitation-hardening steel is similar to that of a martensitic low-alloy steel. The techniques shown in Fig. 18 can also be applied to these steels. The difference between the coefficients of thermal expansion of a transformed and an untransformed microstructure in a component must be considered to avoid residual stresses and subsequent cracking during cooling.

Some martensitic and precipitation-hardening stainless steels contain aluminum and titanium, which require special fluxes or a suitable atmosphere (dry H_2) to promote wetting. The hydrogen-rich atmosphere may cause hydrogen embrittlement of the martensitic stainless steels.

Duplex stainless steels generally contain a mixed microstructure of 50% ferrite and 50% austenite. They have better corrosion resistance than other stainless steels, and they have better mechanical properties than the austenitic and ferritic grades.

Few published data related to duplex stainless steel brazing are available. Compared with the austenitic grades, however, the duplex grades have higher chromium contents, so wetting and spreading problems may be expected.

Duplex stainless steels are susceptible to several embrittlement mechanisms, particularly chromium carbide formation, σ-phase precipitation, and 475 °C (885 °F) embrittlement. They all impair the corrosion resistance and the toughness of these steels. The effects of chromium carbide precipitation were discussed above. In many aspects, σ-phase precipitation is similar to sensitization in that it generates a chromium-depleted zone and occurs at almost the same temperature range (450 to 900 °C, or 840 to 1650 °F). Small amounts of σ phase (~1%) can reduce Charpy V-notch absorbed energy by 50%. Sigma phase also increases by at least eight times the corrosion rate of duplex stainless steels. To avoid σ-phase precipitation, brazing should be performed at high temperatures, greater than 950 °C (1740 °F).

The 475 °C (885 °F) embrittlement occurs in the ferrite phase at a temperature range from 300 and 500 °C (570 to 930 °F). It is characterized by the formation of a chromium-rich phase (α'), which causes a precipitation-hardening effect in the ferritic phase and, as a consequence, decreases the toughness of the steel. The presence of α' may also impair the corrosion resistance of the steel.

Duplex stainless steels also experience strength loss at temperatures near 1000 °C (1830 °F). Special fixtures must be designed to maintain the shape of the component during brazing.

Cast Irons

The brazing of gray, ductile, and malleable cast irons differs from the brazing of steel in two principal respects: special precleaning methods are necessary to remove graphite from the surface of the iron; and the brazing temperature is kept as low as feasible to avoid reduction in the hardness and strength of the iron. The processes used for brazing cast irons are the same as those used for steel--furnace, torch, induction, and dip brazing.

Because most cast irons are brazed at relatively low temperatures, the filler metals used are almost exclusively silver brazing alloys. Of these silver alloys, BAg-1 is most often used for brazing of cast iron, principally because it has the lowest brazing temperature range. A fluoride-type flux such as AWS type 3A is usually used with BAg-1 filler metal. Soldering of cast iron is not usual.

Relatively high silicon content and sand inclusions on as-cast surfaces have some adverse effects on the brazeability of cast iron. These effects, however, are less significant than the adverse effect of graphite, which is present in all gray, ductile, and malleable cast irons. Graphite has essentially the same effect on machined joint surfaces as on as-cast surfaces. Although gray, ductile, and malleable irons all have lower brazeabilities than carbon or low-alloy steels, the three types of iron are not equal in brazeability.

Malleable iron is generally considered the most brazeable of the three types of cast iron, largely because the total carbon content is somewhat lower (seldom over 2.70 wt%) and, therefore, graphitization is less. Brazeability is also enhanced because the graphite occurs in the form of approximately spherical nodules that are easier to remove or cover up (as by abrasive blasting). Also, malleable iron is lower in silicon than the other types of cast iron and thus is less graphitized, which makes it better suited for brazing.

Ductile iron and gray iron can have nearly the same composition. However, the graphite particles in ductile iron are spheroidal rather than flake-shaped. The spheroidal shape is more favorable for brazing. Gray iron, which is characterized by large flakes of graphite, is the most difficult type of cast iron to braze. Until the development of electrolytic salt-bath cleaning, brazing of gray iron was considered impractical.

A number of methods have been tried for preparing cast iron surfaces for brazing; most of them have been only partly successful. Abrasive blasting with steel shot or grit has proved reasonably successful for preparing the surfaces of ductile and malleable iron castings, but it is seldom suitable for preparing surfaces of gray iron casting. Electrolytic treatment in a molten salt bath, alternatively reducing and oxidizing, has been the most successful method for surface preparation and is applicable to all graphitic cast irons. Ordinary chemical cleaning methods, such as degreasing, detergent washing, or acid pickling, have the distinct disadvantage of not removing surface carbon, which interferes with bonding.

Before any procedure for cleaning is adopted, tests should be made by cleaning samples of the iron intended for use in the castings to be brazed, fluxing the samples, and applying filler metal (preferably on a smooth, flat surface). The samples are then heated to the pre-established brazing temperature, cooled, and examined visually. If the samples show that the filler metal has not uniformly wetted the test piece, the surface is not sufficiently clean.

Aluminum Alloys

Brazing of aluminum alloys was made possible by the development of fluxes that disrupt the oxide film on aluminum without harming the underlying metal and filler metals (aluminum alloys) that have suitable melting ranges and other desirable properties, such as corrosion and mechanical resistance. The aluminum-base filler metals used for brazing aluminum alloys have liquidus temperatures much closer to the solidus temperature of the base metal than those for brazing most other metals. For this reason, close temperature control is required in brazing aluminum. The brazing temperature should be approximately 40 °C (70 °F) below the solidus temperature of the base metal.

The non-heat-treatable wrought aluminum alloys, such as the 1*xxx*, 3*xxx*, and 5*xxx* (low-magnesium) series, have been brazed successfully. Alloys that contain higher magnesium contents are more difficult to braze by the usual flux methods because of poor wetting and excessive penetration by the filler metal. Filler metals that melt below the solidus temperatures of most commercial, non-heat-treatable wrought alloys are available.

The most commonly brazed heat-treatable wrought alloys are those of the 6*xxx* series. The 2*xxx* and 7*xxx* series of aluminum alloys have low melting points and therefore are not normally brazeable. Alloys 7072 (used as a cladding material only) and 7005 are the few exceptions. Alloys that have solidus temperatures above 595 °C (1100 °F) are easily brazed with commercial binary aluminum-silicon filler metals. Higher-strength, lower-melting-point alloys can be brazed with proper attention to filler metal selection and temperature control, but the brazing cycle must be short to minimize penetration by the molten filler metal. Sand and permanent mold casting alloys with high solidus temperatures are brazeable.

Commercial filler metals for brazing aluminum are aluminum-silicon alloys containing 7 to 12 wt% Si. Brazing fillers with lower melting points are attained, with some sacrifice in resistance to corrosion, by adding copper and zinc. Filler metals for vacuum brazing of aluminum usually contain magnesium.

The optimum brazing temperature range for an aluminum-base filler metal is determined by the melting range of the filler metal, the amount of molten filler metal needed to fill the joint, and the mutual solubility between the filler metal and the base metal.

Filler metals for separate application from the base metal to be brazed are available as wire and sheet.

Most filler metals are used for any of the common brazing processes and methods. Two alloys, 4004 and 4104, have been developed exclusively for use in fluxless vacuum brazing. They contain additions of magnesium and magnesium-bismuth, respectively, with a brazing temperature range of approximately 590 to 605 °C (1090 to 1120 °F). Similarly, a proprietary mixture of filler metal BAlSi-4 (alloy 4047) in powder form and a chemical compound is used exclusively with dip brazing. The manufacture of filler metal in sheet and wire forms becomes more difficult as the silicon content increases. Only BAlSi-2 (alloy 4343), BAlSi-4 (alloy 4047), and alloy 4004 are available as sheet.

Brazing of aluminum to other alloys should be performed only after considering the differences between:

- COEFFICIENTS OF THERMAL EXPANSION, WHICH CAN AFFECT THE RESIDUAL STRESS LEVEL AND CHANGE THE CLEARANCE OF THE JOINT
- THERMAL CONDUCTIVITIES, WHICH CAN GENERATE DIFFERENT HEATING RATES
- CORROSION RESISTANCES OF ALUMINUM AND THE OTHER MATERIAL, WHICH CAN GENERATE A GALVANIC CORROSION
- MECHANICAL PROPERTIES

Brazing of Aluminum to Ferrous Alloys. The steel component should be protected from oxidation during preheating and brazing to aluminum. In dip brazing, oxidation can be prevented by dipping unheated parts into molten flux, but this procedure has limited application because it is likely to cause warping and misalignment of the components.

Plated or coated steel can be brazed to aluminum more readily than bare steel. Copper, nickel, or zinc electroplates and aluminum, silver, tin, or hot dip zinc coatings are used to promote wetting of the steel and to minimize formation of brittle aluminum-iron compounds, thus producing a more ductile joint.

Brazing of aluminum to copper is difficult, because of the low melting temperature, 548 °C (1018 °F), of the aluminum-copper eutectic and its extreme brittleness. The eutectic is formed due to the dissolution of aluminum during

brazing. By heating and cooling rapidly, however, it is possible to make reasonably ductile joints for applications such as copper inserts in aluminum castings for electrical conductors. The usual filler metals and fluxes for aluminum-to-aluminum brazing can be used. Silver alloy filler metals, BAg-1 and BAg-1a, can also be used if heating and cooling are rapid (to minimize interdiffusion). Hot dipping the copper surfaces with solder or silver alloy filler metal improves wetting and permits shorter time at brazing temperatures. An example of brazing aluminum tubing to copper tubing is to use a transition tubing of steel with aluminum coating on one end of the tubing. The aluminum-coated end of the tubing is brazed to the aluminum, and the other end is silver brazed to the copper tubing.

Brazing of Aluminum to Other Nonferrous Metals. Aluminum-silicon filler metals are unsuitable for brazing aluminum to uncoated titanium because of the formation of brittle intermetallic compounds (titanium-aluminum and titanium-silicon). Titanium can be hot dip coated with aluminum, however, and then brazed to aluminum with the usual aluminum filler metals.

Under adequate conditions, nickel and nickel alloys are no more difficult to braze to aluminum than ferrous alloys. They can be brazed directly or precoated with aluminum. Although Monel alloys can be wetted directly, brazed joints are likely to be brittle; thus, Monel alloys are preferably precoated with aluminum.

Beryllium can be wetted directly by aluminum brazing alloys. Magnesium alloys can be brazed to aluminum, but the brazed joints have limited usefulness because of the extremely brittle aluminum-magnesium phases that form at the interface.

Soldering of aluminum and aluminum alloys is relatively simple. Compared with brazing, soldering presents advantages such as little loss of base metal temper, minimal distortion, and easy removal of flux. Aluminum is soldered at a minimum of 110 °C (200 °F) below the solidus temperature of the base metal.

Wetting and spreading are affected by the presence of an oxide at the faying surface of the joint. The nature of the aluminum oxide is different from alloy to alloy. The heat-treatable alloys present a more tenacious oxide that is more adherent and more difficult to remove. The oxides of the non-heat-treatable alloys are less tenacious and easier to remove. The action of a corrosive flux is enough to disrupt and displace the oxide layer in a non-heat-treatable aluminum alloy. However, the oxide layer of a heat-treatable alloy must be removed by chemical or mechanical means before soldering.

Solderability of aluminum alloys is influenced by alloying elements of the base metal. Generally, purer aluminum alloys are easily soldered. Table 9 presents the solderabilities of aluminum alloys. Analyzing this table, one can see that alloys of groups 1*xxx*, 3*xxx*, and 6*xxx* have good solderabilities.

TABLE 9 SOLDERABILITY OF ALUMINUM ALLOYS

ALLOY GROUP	TYPICAL ALLOY	SOLDERABILITY
1*XXX* (COMMERCIAL PURITY OR HIGHER)	1060	GOOD
	1100	GOOD
2*XXX* (AL-CU)	2014	FAIR[(A)]
3*XXX* (AL-MN)	3003	GOOD
4*XXX* (AL-SI)	4043	POOR[(B)]
5*XXX* (AL-MG OR AL-MG-MN)[(C)]	5005	GOOD
	5050, 5154	FAIR[(A)]
	5456, 5083	FAIR[(A)]
6*XXX* (AL-MG-SI)	6061	GOOD[(A)]
7*XXX* (AL-ZN)[(C)]	7072	GOOD
	7075	POOR
8*XXX* (AL-OTHER)[(C)]	8112	GOOD

Source: Ref 7

(A) SUSCEPTIBLE TO INTERGRANULAR PENETRATION BY SOLDER.

(B) SOLDERABLE ONLY WITH ABRASION OR ULTRASONIC TECHNIQUES.
(C) SOLDERABILITY GREATLY AFFECTED BY COMPOSITION.

Solderability is primarily affected by two alloying elements, magnesium and silicon. The presence of magnesium in an aluminum alloy not only reduces the wettability (more than 1 wt% Mg) but also increases the intergranular penetration (more than 0.5 wt% Mg). Magnesium content up to 1.0 wt% does not reduce the flux effectiveness, so it does not affect wetting and spreading of the molten filler metal. Alloys with less than 1.0 wt% Mg can be soldered with all flux types. Between 1.0 and 1.5 wt% Mg, the low-temperature organic-type flux is not effective to remove the surface oxide of the faying surface. When the amount of magnesium exceeds 1.5 wt%, the corrosive flux does not work either. Silicon plays the same role. Thus, if the amount of silicon is higher than 4.0 wt%, all flux types are ineffective. To solve this problem, a fluxless technique such as abrasion or ultrasonic soldering should be utilized.

Typical solders used for aluminum are shown in Table 10. The corrosion resistances of the filler metals are rated in this table. Solders that melt below 260 °C (500 °F) are called low-melting-point solders. Those that melt between 260 and 370 °C (500 and 700 °F) are called intermediate-melting-point solders. Those that melt between 370 and 440 °C (700 and 820 °F) are called high-melting-point solders.

TABLE 10 COMPOSITION AND TYPICAL PROPERTIES OF SOLDERS USED WITH ALUMINUM

SOLDER TYPE	COMPOSITION, WT%						MELTING RANGE, SOLIDUS - LIQUIDUS[A]		WETTING ABILITY[B]	FLUX TYPE[C]	CORROSION RESISTANCE[B]
	Sn	Zn	Al	Cd	Pb	Cu	°C	°F			
ZINC	. . .	100	. . .	. . .	. . .	. . .	419	787	G	C	VG
	. . .	94	4	. . .	. . .	2	380-395	720-740	G	C	VG
	. . .	95	5	. . .	. . .	. . .	375	710	G	C	VG
	. . .	90	5	. . .	. . .	5	380	720	G	C	VG
	2	79.6	10	0.4	3	5	275-400	527-750	. . .	. . .	. . .
ZINC-CADMIUM	. . .	90	. . .	10	. . .	. . .	265-405	509-760	G	C	F
	. . .	60	. . .	40	. . .	. . .	265-335	509-635	VG	C	F
	. . .	17.5	. . .	82.5	. . .	. . .	265	509	. . .	. . .	. . .
TIN-ZINC	20	15	0.8	64.2	. . .	. . .	110-275	230-530	. . .	. . .	. . .
	70	30	. . .	. . .	. . .	. . .	200-310	390-592	F	C	F
	30	70	. . .	. . .	. . .	. . .	200-190	390-710	G	C	G
TIN-LEAD	40	. . .	. . .	. . .	60	. . .	185-240	361-460	. . .	. . .	. . .
TIN-ZINC	60	39.4	. . .	. . .	0.1	0.5	200-340	390-645	G	C	G
TIN-LEAD	63	. . .	. . .	. . .	37	. . .	185-215	361-420	. . .	. . .	. . .
TIN-ZINC	69.3	28	0.7	. . .	2.0	. . .	195-335	385-635	. . .	. . .	. . .
	80	20	. . .	. . .	. . .	. . .	200-275	390-530	. . .	. . .	. . .
	91	9	. . .	. . .	. . .	. . .	205	400	F	OC	F

TIN-LEAD	36.9	. . .	. . .	3.8	59.3	. . .	145-230	290-450	. . .	. . .	. . .
	34	3	. . .	. . .	63	. . .	195-255	383-492	P	OC	P
	31.6	9	. . .	8	51	0.4	140-250	282-485	. . .	. . .	. . .
	40	15	0.8	. . .	44.2	. . .	170-355	335-675	. . .	. . .	. . .
TIN-CADMIUM	20	15	0.8	64.2	. . .	. . .	110-275	230-530	. . .	. . .	. . .
	50	. . .	. . .	. . .	50	. . .	180-215	360-420	P	OC	P
TIN-ZINC	91	9	. . .	. . .	. . .	. . .	200	391	F	O	P

Source: Ref 8

(A) SOLDERS WITH ONLY ONE TEMPERATURE GIVEN ARE EUTECTICS.

(B) VG, VERY GOOD; G, GOOD; F, FAIR; P, POOR.

(C) C, CORROSIVE; OC, ORGANIC CORROSIVE; O, ORGANIC.

Aluminum alloys can be soldered to all usual metals and nonmetallic materials. However, loss of corrosion resistance should be expected. The high-melting-point solders are suitable for soldering mild steel, stainless steel, nickel, copper, brass, zinc, and silver directly to aluminum. Magnesium, titanium, zirconium, niobium, tantalum, molybdenum, and tungsten may be soldered if they are plated with a solderable metal coating such as silver.

Copper and Copper Alloys

Most coppers and copper alloys can be brazed satisfactorily using one or more of the conventional brazing processes: furnace, torch, induction, resistance, and dip brazing. Their brazeabilities are rated from good to excellent.

Brazing of Tough Pitch Coppers. Tough pitch coppers are subject to embrittlement when heated at temperatures above 480 °C (900 °F) in reducing atmospheres containing hydrogen. Phosphorus-deoxidized and oxygen-free coppers can be brazed without flux in hydrogen-containing atmospheres without risk of embrittlement, provided self-fluxing filler metals (BCuP series) are used.

The coppers, including those that contain small additions of silver, lead, tellurium, selenium, or sulfur (generally no more than 1 wt%), are readily brazed with the self-fluxing BCuP filler metals, but wetting action is improved when a flux is used and when a sliding motion between components is provided while the filler metal is molten. Precipitation-hardenable copper alloys that contain beryllium, chromium, or zirconium form oxide films that impede the flow of filler metal. To ensure proper wetting action of the joint surface by the filler metal, beryllium copper parts, for example, should be freshly machined or mechanically abraded before being brazed. Removal of beryllium oxide from joint surfaces requires the use of a high-fluoride-content flux.

Brazing of Red and Yellow Brasses. Red and yellow brasses are readily brazed with a variety of filler metals. Flux is normally required for best results, especially when the zinc content is above 15 wt%. Low-melting filler metals should be used to avoid dezincification of the yellow brasses. If added to red brass or yellow brass, lead forms a dross on heating that can seriously impede wetting and the flow of filler metal. Consequently, in brazing leaded brasses, the use of a flux is mandatory to prevent dross formation in the joint area.

Brazing of Tin-Containing Brasses. Tin-containing brasses, which include admiralty brass, naval brass, and leaded naval brass, contain up to 1 wt% Sn and may contain other alloying elements, such as lead, manganese, arsenic, nickel, and aluminum. Except for the aluminum-containing alloys, these brasses are readily brazed; they have greater resistance to thermal shock and are less susceptible to hot cracking than the high-lead brasses. For proper wetting, brasses that contain aluminum require a special flux.

Brazing of Phosphor Bronzes. Phosphor bronzes contain small amounts of phosphorus, up to approximately 0.25 wt%, added as a deoxidizer. Although susceptible to hot cracking in the coldworked condition, alloys in this group have good brazeability and are adaptable to brazing with any of the common filler metals that have melting temperatures lower than that of the base metal. The use of a flux is generally preferred. To avoid cracking, parts made from phosphor bronzes should be stress-relieved at approximately 290 to 345 °C (550 to 650 °F) before brazing. Silicon bronzes, which contain up to about 3.25 wt% Si, when applied in a highly stressed condition, are susceptible to hot shortness and stress cracking by molten filler metal. To avoid cracking, the alloys should be stress-relieved at about 290 to 345 °C (550 to 650 °F) before brazing.

Because of the formation of aluminum oxide on the surface, aluminum bronzes are generally considered difficult to braze. The oxide, which inhibits the flow of filler metal, cannot be reduced in dry hydrogen. However, alloys containing 8 wt% Al or less are brazeable, provided AWS type 4 flux is used to dissolve the aluminum oxide. Use of the low-melting, high-silver filler metals is recommended for these bronzes.

Brazing of Copper Alloys to Other Alloys. Copper and copper alloys can be brazed to other alloys. Some characteristics to consider are: coefficients of thermal expansion, thermal conductivities, corrosion behavior, and mechanical properties.

Copper nickels, which may contain from about 5 to 40 wt% Ni, are susceptible both to hot cracking and to stress cracking by molten filler metal. The silver alloy filler metals (BAg series) are preferred for brazing these alloys. In general, the use of filler metals containing phosphorus should be avoided, because the copper nickels are susceptible to the formation of brittle nickel phosphides at the interface. Nickel silvers (brasses that contain up to about 20 wt% Ni but do not contain silver) are highly susceptible to hot cracking and should be stress-relieved at about 290 °C (550 °F) before being brazed. They should be heated and cooled uniformly because of their low thermal conductivity.

Most of the alloys belonging to any one of the above groups can be brazed to an alloy of another group. However, to achieve compatibility, some compromise may be required in the selection of brazing temperature, filler metal, and flux. For example, if a copper component is to be brazed to a component made of aluminum bronze, the brazing temperature should be predicated on the lower melting temperature of the bronze, and a suitable flux should be selected to accommodate the bronze.

Soldering of Copper and Copper Alloys. Copper and copper alloys are among the most frequently soldered engineering materials. The copper oxide is easily disrupted and displaced by most flux types. The presence of alloying elements such as beryllium, chromium, silicon, and aluminum modifies the nature of the oxide, making it more tenacious. For these alloys, a special flux is recommended to remove the oxide from the surface and enhance the solderability of these base metal groups.

The most common solders for copper are tin- or lead-base solders. Tin can react with copper and form two intermetallic phases, Cu_6Sn_5 and Cu_3Sn, at the solid-liquid interface. As the thickness of this reaction layer increases, the mechanical behavior of the joint became impaired. Therefore, a thin intermetallic layer is desirable. The kinetics of intermetallic phase growth are controlled by the amount of tin and other elements in the solder, the soldering temperature, and time. Thus, to minimize the thickness of the intermetallic phase, a low-tin solder or a short soldering time should be utilized. Another way to minimize the intermetallic formation is to use a barrier coating, such as nickel, silver, or gold. These copper-tin intermetallics may also cause a dewetting phenomenon. Dewetting is defined as the withdrawal of molten solder from a surface that was previously wetted. If the solderable surface is not well protected during soldering, the intermetallic can oxidize and the dewetting phenomenon takes place.

Nickel-Base Alloys

In the selection of a brazing process for a nickel-base alloy, the characteristics of the alloy must be carefully considered. The nickel-base alloy family includes alloys that differ significantly in physical metallurgy (such as precipitation-strengthened versus solid-solution strengthened) and in process history (such as cast versus wrought). These characteristics can have a profound effect on their brazeability.

Precipitation-hardenable alloys present several difficulties not normally encountered with solid-solution alloys. Precipitation-hardenable alloys often contain appreciable (greater than 1 wt%) quantities of aluminum and titanium. The oxides of these elements are almost impossible to reduce in a controlled atmosphere (vacuum, hydrogen). Therefore, nickel plating or the use of a flux is necessary to obtain a surface that allows wetting by the filler metal.

Because these alloys are hardened at temperatures of 540 to 815 °C (1000 to 1500 °F), brazing at or above these temperatures may alter the alloy properties. This frequently occurs when using silver-copper (BAg) filler metals, which occasionally are used on heat-resistant alloys.

Liquid metal embrittlement is another difficulty encountered in brazing precipitation-hardenable alloys. Many nickel-base, iron-base, and cobalt-base alloys crack when subjected to tensile stresses in the presence of molten metals. However, liquid-metal-induced cracking of these alloys is usually confined to the silver-copper (BAg) filler metals. If precipitation-hardenable alloys are brazed in the hardened condition, residual stresses are often high enough to initiate cracking.

Oxide dispersion-strengthened alloys (ODS) are powder metallurgy (P/M) alloys that contain stable oxide, evenly distributed throughout the matrix. The oxide does not go into solution in the alloy, even at the liquidus temperature of the matrix. However, once the oxide particles are rejected into the molten matrix (for example, during fusion welding), they cannot be redistributed evenly in the matrix on solidification. Therefore, these alloys are usually joined by brazing. There are two commercial alloy classes of ODS alloys: the dispersion-strengthened nickel, and the mechanically alloyed Inconel MA 754, Inconel MA 6000, and Incoloy MA 956.

Inconel MA 754, dispersion-strengthened nickel alloys, and dispersion-strengthened nickel-chromium alloys are the easiest to braze of the ODS alloys. Vacuum, hydrogen, or inert atmospheres can be used for brazing. Prebraze cleaning consists of grinding or machining with a solvent that evaporates without leaving a residue. Generally, brazing temperatures should not exceed 1315 °C (2400 °F) unless demanded by a specific application that has been well examined and tested. The brazing filler metals for use with these ODS alloys usually are not classified by AWS. In most cases, the brazing filler metals used with these alloys have brazing temperatures in excess of 1230 °C (2250 °F); these filler metals include proprietary alloys based on nickel, cobalt, gold, or palladium.

Inconel MA 6000 is a nickel-base ODS alloy that is also γ'-strengthened. The number of alloying elements plus the γ' precipitation presents a formidable challenge to the joining of this alloy. Inconel MA 6000 has a solidus temperature of 1300 °C (2372 °F); therefore, the brazing temperature should be no higher than 1250 °C (2280 °F). Additionally, because 1230 °C (2250 °F) is the γ' solution treatment temperature, it becomes important to carefully select the brazing filler metal and to heat treat the assembly after brazing. The BNi, BCo, and specially formulated filler metals have been used in this alloy. Inconel MA 6000 is used for its high-temperature strength and corrosion resistance; unfortunately, the passive oxide scale that provides good corrosion resistance also prevents wetting and flow of brazing filler metal. Therefore, correct cleaning procedures are very important.

The brazeability of these alloys is affected by the chromium content, oxide dispersion, and the manufacturing process of the component. Chromium forms a stable and adherent oxide that impairs the wetting and spreading of the molten filler metal. The oxide dispersion also may affect the wetting and spreading behavior since an oxide is not easily wettable. The P/M manufacturing process can introduce some porosity in the component, which will act as a barrier to molten metal flow.

References cited in this section

3. M.G. NICHOLAS AND D.A. MORTIMER, CERAMIC/METAL JOINING FOR STRUCTURAL APPLICATIONS, *MATER. SCI. TECHNOL.*, VOL 1 (NO. 9), 1985, P 657-665
5. *SOLDERING MANUAL*, AMERICAN WELDING SOCIETY, 1977
6. J.A. PASK, FROM TECHNOLOGY TO THE SCIENCE OF GLASS/METAL AND CERAMIC/METAL SEALING, *AM. SOC. CERAM. BULL.*, VOL 66 (NO. 11), 1987, P 1587-1592
7. H.H. MANKO, *SOLDERS AND SOLDERING*, 3RD ED., MCGRAW-HILL, 1992
8. *ALUMINUM SOLDERING HANDBOOK*, ALUMINUM ASSOCIATION, 1974

S.D. Brandi, Escola Politécnica da Universidade de São Paulo, Brazil; S. Liu, Colorado School of Mines; J.E. Indacochea and R. Xu, University of Illinois at Chicago

Heat-Resistant Alloys

Heat-resistant alloys are frequently referred to as superalloys because of their strength, oxidation resistance, and corrosion resistance at elevated temperatures. Superalloys can be subdivided into two categories: conventional cast and wrought alloys, and P/M products. Powder metallurgy products may be produced as conventional alloy compositions and as ODS alloys. Almost any metal or nonmetallic can be brazed to these heat-resistant alloys if it can withstand the heat of brazing.

The American Welding Society has classified several gold-base, nickel-base, and cobalt-base brazing filler metals that can be used for elevated-temperature service. In addition, there are many that are not classified by AWS. It should be noted that for lower service temperatures, copper (BCu) and silver (BAg) brazing filler metals have been used for many successful applications.

Generally, heat-resistant alloys are brazed with nickel-base or cobalt-base alloys containing boron and/or silicon, which serve as melting-point depressants and as oxide-reducing agents. In many commercial brazing filler metals, the levels are 2 to 3.5 wt% B and 3 to 10 wt% Si. Phosphorus is another effective melting-point depressant for nickel and is used in filler metals from 0.02 to 15 wt%. It is also used where good flow is important in applications of low stress, where temperatures do not exceed 760 °C (1400 °F). Chromium is often present to provide oxidation and corrosion resistance. The amount may be as high as 20 wt%, depending on the service conditions. Higher amounts, however, tend to lower brazement strength.

Cobalt-base filler metals are used mainly for brazing cobalt-base components, such as first-stage turbine vanes for jet engines. Most cobalt-base filler metals are proprietary. In addition to boron and silicon, these alloys usually contain chromium, nickel, and tungsten to provide corrosion and oxidation resistance and to improve strength. As discussed in the section "Stainless Steels" of this article, the presence of chromium in higher amounts affects the wetting and spreading behavior of the flux during brazing.

Titanium and Titanium Alloys

Titanium is one of the chemical elements that reacts readily with oxygen to form an adherent and stable oxide. This oxide gives titanium and titanium alloys excellent corrosion resistance. Properties such as corrosion resistance, light weight, and high strength make titanium especially attractive in aerospace and chemical applications.

On cooling, pure titanium undergoes an allotropic transformation from β(bcc) to α(hcp) at 882.5 °C (1621 °F). Some alloying elements stabilize the α phase, others, the β phase. Figure 19 shows the αand β stabilizers and their effects on a binary phase diagram. In this case, α and β represent a solid solution and γ represents an intermetallic compound. Table 11 shows the classification for some commercial titanium alloys according to the prevailing microstructure.

TABLE 11 CLASSIFICATION OF SELECTED COMMERCIAL TITANIUM ALLOYS

ALLOY	CLASSIFICATION
TI-5AL-2.5SN	α
TI-8AL-1MO-1V[(A)]	α + β
TI-6AL-2SN-4ZR-2MO[(A)]	α + β
TI-6AL-4V	α + β
TI-6AL-2SN-6V	α + β
TI-3AL-2.5V	α + β
TI-6AL-2SN-4ZR-6MO[(B)]	α + β
TI-5AL-2SN-2ZR-4CR-4MO[(B)]	α + β

TI-3AL-10V-2FE[B]	α + β
TI-13V-11CR-3AL	β
TI-15V-3CR-3AL-3SN	β
TI-4MO-8V-6CR-4ZR-3AL	β
TI-8MO-8V-2FE-3AL[C]	β
TI-11.5MO-6ZR-4.5SN	β

Source: Ref 9

(A) NEAR- α; THE TERMS "LEAN- β " AND "SUPER- α " MAY ALSO BE USED.

(B) NEAR- β.

(C) OBSOLETE ALLOY.

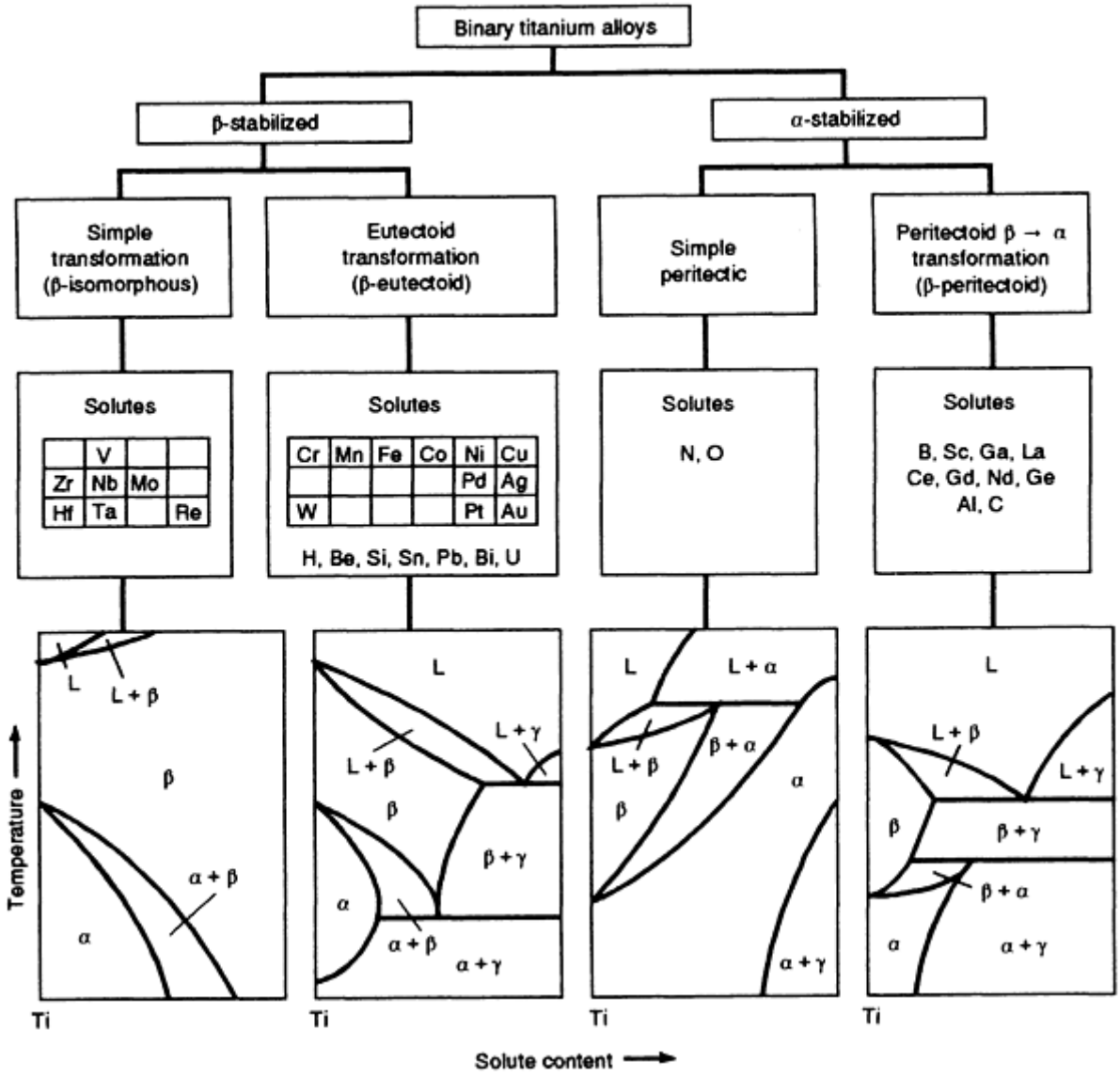

FIG. 19 FLOWCHART SHOWING EFFECT OF α' AND β STABILIZERS ON A BINARY PHASE DIAGRAM. SOURCE: REF 9

The β alloys present a ductile-to-brittle transition temperature (DBTT). Thus, depending on the temperature, β alloys can be brittle. On the other hand, α alloys have no DBTT. These characteristics determine some applications of the two alloys. The α alloys have, in general, good strength, toughness, and creep resistance, and they are suitable for cryogenic applications. The β alloys are not designed for low-temperature applications, but they present good formability and a high

strength-to-weight ratio. The α+ βalloys are also formable with high room-temperature strength and moderate elevated-temperature strength. The volumetric fraction of β in these alloys is between 10 to 50%, but alloys with over 20 vol% β phase are not joinable.

Titanium and titanium alloys are not directly solderable due to the formation of an adherent stable oxide.

Commercially Pure Titanium, α and Near-α Titanium Alloys. Because these alloys are not strengthened by heat treatment, the brazing thermal cycle has little effect on their mechanical properties. The filler metals used to braze titanium and titanium alloys are shown in Table 12. During brazing there is a dissolution of the base metal and a diffusion of the alloying elements toward the base metal and/or the filler metal. These phenomena will form a reaction layer, which may consist of brittle titanium intermetallics. Titanium can combine with copper, nickel, aluminum, and silver to form intermetallics. The first three intermetallics (titanium-copper, titanium-nickel, and titanium-aluminum) are harder and have a lower ductility than a titanium-silver intermetallic. Therefore, the filler metal should have a lower amount of these elements, or the brazing process should be as fast as possible, to minimize the intermetallic formation.

TABLE 12 TEMPERATURE SPECIFICATIONS FOR FILLER METALS USED TO BRAZE TITANIUM ALLOYS

FILLER METAL	SERVICE TEMPERATURE		BRAZING TEMPERATURE	
	°C	°F	°C	°F
AG	425	800	925	1700
AG-5AL, AG-7.5CU	425	800	870-925	1600-1700
AG-5AL-0.5MN	425	800	870-900	1600-1650
AL, AL-SI (4040), AL-MN (3003)	260	500	650-690	1200-1275
TI-48ZR-4BE, TI-43ZR-12NI-2BE	540	1000	870-1095	1600-2000
AG-9PD-9GA	. . .	. . .	880-920	1615-1690

Source: Ref 4

Titanium and titanium alloys are very resistant to corrosion. The filler metal should be selected carefully to avoid galvanic corrosion.

Titanium and its alloys are usually brazed by induction or furnace processes with a protective atmosphere. The brazing atmosphere is usually a vacuum with less than 13 mPa (10^{-4} torr) or an inert atmosphere with dew point lower than -55 °C (-70 °F). Vacuum brazing with filler metals that contain silver or gallium must be performed with an argon back pressure to avoid the vaporization loss of these elements.

In induction brazing, the chemical elements of the filler metal must alloy readily with titanium, due to the fast heating cycle. However, furnace brazing requires a filler metal with a chemical composition that does not alloy excessively with titanium, due to longer periods at elevated temperatures. Torch brazing is not usually done because special fluxes and a skilled operator are required.

β and α+ β titanium alloys can be strengthened by heat treatment. The basic heat treatment consists of heating in a single-phase field (β alloys) or in a two-phase field (α + βalloys), followed by a quenching. The aging is performed between 480 and 650 °C (900 and 1200 °F). During aging, α or other compounds will precipitate in a β matrix, increasing the strength and toughness of the alloy. Thus, the thermal cycle during brazing may affect the mechanical properties of the base metal. The β alloys should be brazed at a temperature close to the solubility temperature. Brazing at higher temperatures will reduce the ductility of these alloys. The α + β alloys should be brazed at a temperature below the α-to-β transition temperature. Table 13 shows the α-to-β transition temperature for some titanium alloys.

TABLE 13 α-TO-β TRANSITION TEMPERATURE FOR TITANIUM AND TITANIUM ALLOYS

ALLOY	α -TO- β TRANSITION

	TEMPERATURE	
	°C ± 15°	°F ± 25°
COMMERCIALLY PURE TI, 0.25 MAX O_2	915	1675
COMMERCIALLY PURE TI, 0.40 MAX O_2	945	1735
α AND NEAR- α ALLOYS		
TI-5AL-2.5SN	1050	1925
TI-8AL-1MO-1V	1040	1900
TI-6AL.4ZR-2MO-2SN	995	1820
TI-6AL-2CB- 1TA-0.8MO	1015	1860
TI-0.8NI-0.3MO	880	1615
α - β ALLOYS		
TI-6AL-4V	1000(A)	1830(B)
TI-6AL-6V-2SN	945	1735
TI-3AL-2.5V	935	1715
TI-6AL-6MO-4ZR-2SM	940	1720
TI-7AL-4MO	1005	1840
TI-8MN	800(C)	1475(D)
β OR NEAR- β ALLOYS		
TI-13V-11CR-3AL	720	1330
TI- 11.5MO-6ZR-4.5SN	760	1400
TI-3AL-8V-6CR-4ZR-4MO	795	1460

Source: Ref 4

(A) ±20°.

(B) ±30°.

(C) ±35°.

(D) ±50°.

The fixture material for brazing a titanium alloy should be chosen carefully to avoid contamination or solid-state bonding between them. For example, nickel forms an eutectic with titanium at 940 °C (1725 °F) and can be bonded to titanium at approximately 816 °C (1500 °F). Thus, a physical contact between titanium alloys and nickel-containing alloys, such as austenitic stainless steels, should be avoided.

Cobalt-Base Alloys

The brazing of cobalt-base alloys is readily accomplished with the same techniques used for nickel-base alloys. Because most of the popular cobalt-base alloys do not contain appreciable amounts of aluminum or titanium, brazing atmosphere requirements are less stringent. Several cobalt-base alloys can be brazed in either a hydrogen atmosphere or a vacuum. Filler metals are usually nickel-base alloys, cobalt-base alloys, or gold-palladium compositions. Silver or copper brazing filler metals may not have sufficient strength and oxidation resistance in many high-temperature applications. Although cobalt-base alloys do not contain appreciable amounts of aluminum or titanium, an electroplate or flash of nickel is often used to better promote wetting of the brazing filler metal.

Cobalt alloys, much like nickel alloys, may become susceptible to liquid metal embrittlement or stress-corrosion cracking when brazed under residual or dynamic stresses. This frequently is observed when using silver or silver-copper (BAg) filler metals. Liquid metal embrittlement of cobalt-base alloys by copper (BCu) filler metals occurs with or without the application of stress; therefore, BCu filler metals should be avoided when brazing cobalt.

Refractory Metals

The mechanical properties of the refractory metals are affected markedly by their DBTT behavior, recrystallization temperature, and reactions with carbon and selected gases. These characteristics must be considered when procedures for

brazing refractory metals are established. The strength and ductility of the refractory metals are adversely affected by microstructural changes that occur when the recrystallization temperatures of these metals are exceeded.

The recrystallization temperature range also varies with alloying additions, interstitial content, fabrication method (including degree of cold working), and time at temperature. Some applications permit brazing with brazing filler metals that melt below the recrystallization temperature range. Other applications require the use of brazing filler metals that melt above this temperature range. As a result, a joint must be designed to accommodate the loss in mechanical properties associated with recrystallization.

The environment in which the refractory metals are brazed is determined by the reactivity of these metals with oxygen, hydrogen, carbon, and nitrogen, and the effect of these elements on the mechanical properties of the refractory metals. All of the refractory metals react with oxygen at moderately elevated temperatures, but they form different types of oxides. Niobium and tantalum form hard adherent oxides at temperatures above 205 and 400 °C (400 and 750 °F), respectively. On the other hand, molybdenum and tungsten form volatile oxides at temperatures above 400 and 510 °C (750 and 950 °F), respectively. In either case, the surfaces of the refractory metals must be protected from oxidation during brazing to ensure wetting by the braze filler metal. Also, these metals must be coated with an oxidation-resistant material, such as nickel or silver plating, if they are exposed to air at elevated temperatures. For such service conditions, the brazing filler metal must be compatible with both the base metal and the coating.

Niobium is used mainly for nuclear and aerospace applications. As a result, research has been directed toward the development of brazing filler metals with characteristics that are compatible with the base metal and its intended use. For example, brazing filler metals have been developed to produce joints that are resistant to liquid alkali metals, such as sodium, and that possess useful properties at 705 to 815 °C (1300 to 1500 °F). The base metal Nb-lZr has been vacuum brazed at 1250 °C (2280 °F) with the Ti-28V-4Be brazing filler metal.

Other niobium alloys--for example, D-43 (Nb-10W-IZr-0.1C), Cb-752 (Nb-10W-2.5Zr), and C-129Y (Nb-10W-11Hf-0.07Y)--have been successfully brazed with two brazing filler metals (B120VCA and Ti-8.5si) at 1455 °C (2650 °F).

Molybdenum. Copper-base and silver-base brazing filler metals can be used to braze molybdenun for low-temperature service. For high-temperature applications, molybdenum can be brazed with gold, palladium, and platinum filler metals, nickel-base filler metals, reactive metals, and refractory metals that melt at lower temperatures than molybdenum. It should be noted, however, that nickel-base alloys have limited applicability for high-temperature service, because nickel and molybdenum form an intermetallic compound that melts at 1315 °C (2400 °F). Two binary brazing filler metals (V-35Nb and Ti-30V) have been evaluated for use with the Mo-0.5Ti molybdenum base metal.

Molybdenum alloy TZM (0.5Ti-0.08Zr-Mo) has also been successfully vacuum brazed at 1400 °C (2550 °F) with molybdenum powder added to the Ti-8.5Si brazing filler metal. Molybdenum has an extremely low coefficient of thermal expansion, which should be considered in the design of brazed joints, particularly when molybdenum is joined to other metals.

Tantalum. Nickel-base brazing filler metals (such as the nickel-chromium-silicon filler metals) have been used to braze tantalum. Tantalum forms a homogeneous solid solution with nickel at concentrations up to 36 wt% with the liquidus temperature reducing from 1450 to 1350 °C (2640 to 2460 °F). These brazing filler metals are satisfactory for service temperatures below 982 °C (1800 °F). Copper-gold alloys with less than 40 wt% Au can be used as brazing filler metals. When gold is added in amounts between 40 to 90 wt%, the alloys tend to form brittle age-hardening compounds. Because tantalum and its alloys are usually used for elevated-temperature applications (1650 °C, or 3000 °F, and above), only a few brazing filler metals have been developed. Most of the brazing filler metals currently available for tantalum are in powder form, which is difficult to work with at elevated temperatures. New powder brazing filler metals (for example, Hf-7Mo, Hf-40Ta, and Hf-19Ta-2.5Mo) are being developed for tantalum as foil-type brazing filler metals.

Tungsten can be brazed in much the same manner as molybdenum and its alloys, using many of the same brazing filler metals. Brazing can be accomplished in a vacuum or in a dry argon, helium, or hydrogen atmosphere. To some extent, the selection of the brazing atmosphere depends on the brazing filler metal used. For example, brazing filler metals that contain elements with high vapor pressures at the brazing temperature cannot be used effectively in a high vacuum.

Ceramic Materials

Ceramic materials can be joined by two different methods: by metallization of the ceramic surface or by using a ductile active filler metal. In the first method, a coating of a metal such as molybdenum and manganese is used as a transition between the ceramic and metal. It may be followed by a nickel coating to improve the wetting and spreading of the filler metal. The disadvantage of this method is that the heating, cycles used to sinter these coatings can crack the ceramic substrate. In the second method, an active metal in the filler reduces the ceramic to promote the bond between a metal and a ceramic. This filler metal should be ductile to relieve the residual stresses built up during cooling. A uniform heating of all components, such as in furnace joining, should be used to minimize the presence of cracking due to thermal stresses.

Graphite. Brazeability of graphite is strongly influenced by the presence of impurities, such as oxygen and moisture, and by pore size and pore distribution. Data from Table 5 indicate that graphite has a low coefficient of thermal expansion and low strength; these properties make joining graphite to other engineering materials a difficult task. A metal with a coefficient of thermal expansion close to that of graphite (for example, tungsten, molybdenum, tantalum, and zirconium), should be chosen as a transition piece. Graphite is also difficult to wet, so a coating or a filler metal with a strong tendency to form carbide must be used to form the joint. Sometimes, a ductile metal such as copper is used to decrease the residual stress developed in the joint.

At least two commercially available filler metals are used to join graphite. One has a nominal chemical composition of 68Ag-27Cu-4.5Ti (in wt%) with a solidus temperature of 830 °C (1525 °F) and a liquidus temperature of 849 °C (1560 °F). The other filler metal has a chemical composition of 70Ti- 15Cu- 15Ni (in wt%) with a solidus temperature of 910 °C (1670 °F) and a liquidus temperature of 960 °C (1760 °F).

Figure 20 shows a sandwich technique for brazing graphite to an austenitic stainless steel. The filler metal is 68Ag-27Cu-4.5Ti with alternate layers of copper and molybdenum to match as closely as possible the coefficients of thermal expansion of graphite and stainless steel. A special fixturing system was designed to create compression in the joint to compensate for the mismatch in the coefficients of thermal expansion.

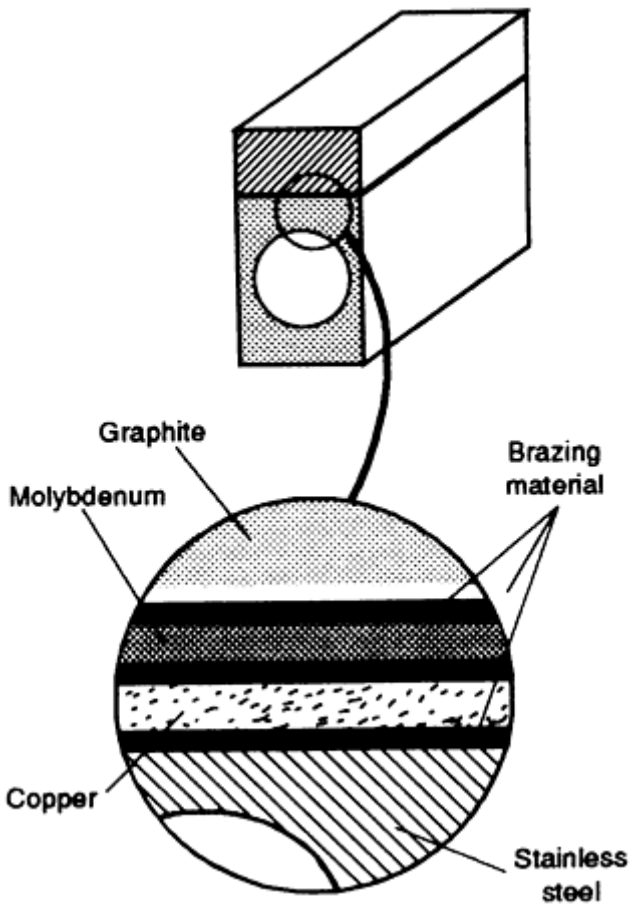

FIG. 20 APPLICATION OF SANDWICH TECHNIQUE TO BRAZE GRAPHITE TO AN AUSTENITIC STAINLESS STEEL WITH 68AG-27CU-4.5TI FILLER METAL. SOURCE: REF 10

Another example of graphite brazing also used transition inserts of gradient composition. In this case, graphite was joined to a nickel-base alloy, and the transition piece consisted of seven rings of tungsten-nickel-iron alloys. The first ring contained 97.5 wt% W to match the coefficient of thermal expansion of graphite, and the last ring contained 40 wt% W to match the coefficient of thermal expansion of the nickel-base alloy.

Carbides. The discussion of carbide brazing will be divided into two parts: brazing of carbide tools and brazing of silicon carbide (ceramic).

Carbide Tools. This group includes tungsten carbide with cobalt binder (3 to 25 wt%); tungsten carbide plus titanium and tantalum carbides, or niobium carbide with cobalt binder; titanium or tantalum carbides plus tungsten carbide with nickel or cobalt binder; chromium carbides with nickel or cobalt binders, and other carbide combinations.

Filler metals from the BAg group have been used to perform the carbide-to-steel joining. The filler metals that contain nickel (BAg-3, BAg-4, and BAg-22) promote a better wettability, because nickel improves the wettability in carbide-metal systems. RBCuZn-D and BCu have also been used, particularly where a post-braze heat treatment is required. Filler metals BAg-23 or 52.5Cu-38Mn-9.5Ni have been used when the brazements will be subjected to elevated temperature or additional wetting, as in the case of brazing titanium-base or chromium-base carbides.

In the case of tungsten-base carbide, the use of composite filler metal (consisting of a sandwich of two layers of a silver-base filler metal and a copper shim) has been reported. The ductile copper layer deforms during brazing to decrease the residual stress generated in the joint. A wider joint requires a thicker copper shim. Figure 21 shows this technique.

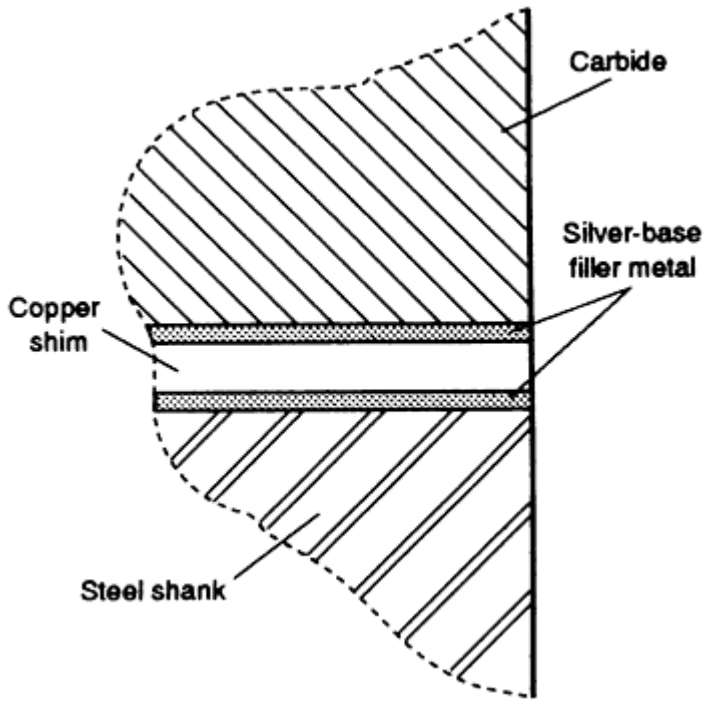

FIG. 21 USE OF COMPOSITE BRAZING FILLER METAL (TWO LAYERS OF SILVER-BASE FILLER METAL AND A COPPER SHIM) TO JOIN TUNGSTEN CARBIDE TO STEEL

Joint design is important in carbide tool brazing. The mismatch in the coefficients of thermal expansion must be taken into account and to avoid cracking during brazing, which decreases tool life. Figure 22 shows some optimum tool joint designs. In each set, the right-most drawing represents an improved design with longer expected tool life.

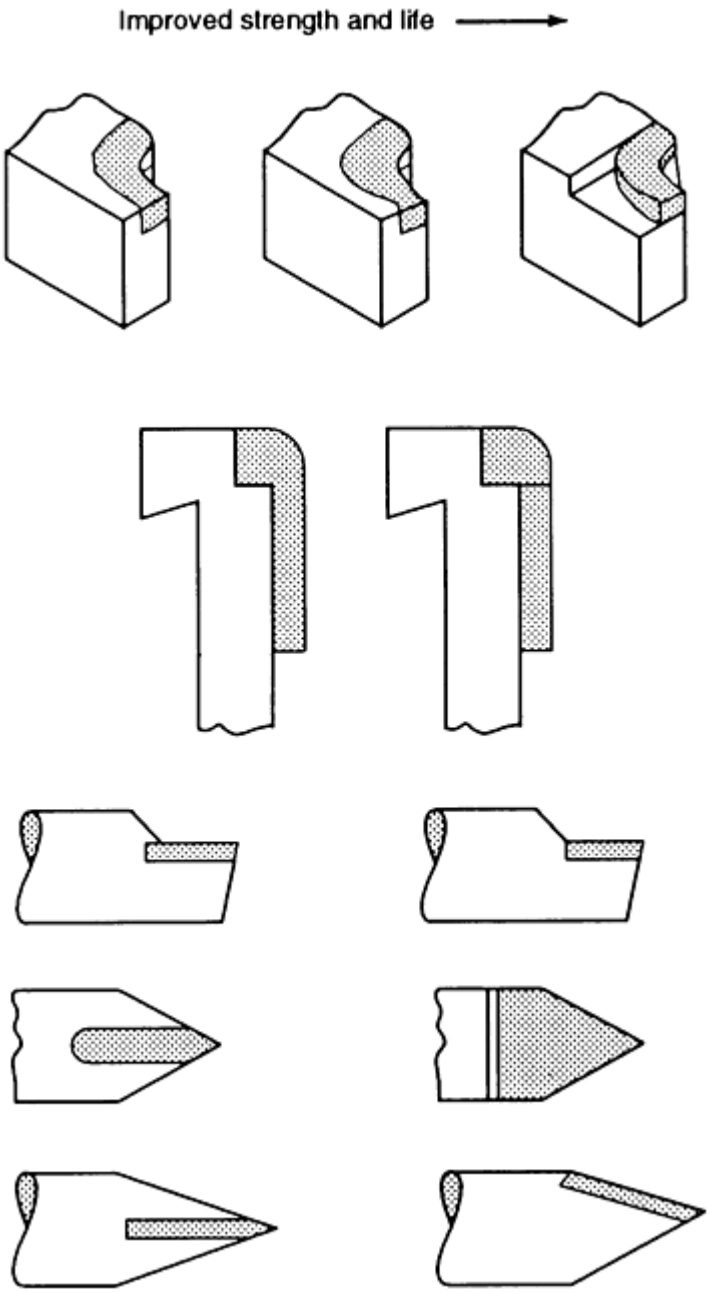

FIG. 22 JOINT DESIGNS TO OPTIMIZE STRENGTH AND TOOL LIFE OF BRAZED CARBIDE TOOL ASSEMBLIES. IN EACH SET, THE RIGHT-MOST DRAWING REPRESENTS AN IMPROVED DESIGN.

Silicon carbide can usually be brazed using a titanium-base filler metal according to the following reaction:

$$SiC + Ti_{fm} \rightarrow TiC_i + \underline{Si}_{fm} \qquad \textbf{(EQ 8)}$$

The subscripts *fm* and *i* denote the filler metal and interface, respectively. Commercial silver-titanium, silver-copper-titanium, and silver-copper-indium-titanium alloys can be used as filler metals to join silicon carbide to silicon carbide or to other alloys. The amount of copper in the filler metal must be controlled, because copper dissolves silicon from silicon carbide to form a copper-silicon alloy and graphite and changes the characteristics of the ceramic material close to the joint.

Some experimental results show that a Ni-13.4Cr-40Si (in at.%) filler metal can also be used to braze silicon carbide to silicon carbide components with good results. On the other hand, an experimental filler metal Fe-34Si (in at.%) used to join silicon carbide to Inconel 600 showed extensive chemical reaction with formation of low-melting-point silicides.

To increase the work temperature range of brazed silicon carbide components, a filler metal with higher solidus temperature is needed. Ni-50Ti (in at.%) has been reported to perform well. Table 14 presents some filler metals commonly used to braze silicon carbide.

TABLE 14 FILLER METALS COMMONLY USED IN SILICON CARBIDE BRAZING APPLICATIONS

BRAZING FILLER METAL SYSTEM	COMPOSITION, WT%					SOLIDUS TEMPERATURE		LIQUIDUS TEMPERATURE		BRAZING TEMPERATURE	
	Cu	In	Ti	Ag	Ni	°C	°F	°C	°F	°C	°F
SILVER-COPPER-TITANIUM	27.5	. . .	2	70.7	. . .	780	1435	795	1465	840	1545
	26.5	. . .	3	70.5	. . .	803	1475	857	1575	950	1740
	6	. . .	3	91	. . .	875	1605	917	1685	970	1780
SILVER-COPPER-INDIUM-TITANIUM	23.5	14.5	1.25	60.75	. . .	605	1120	715	1320	760	1400
	19.5	5	3	72.5	. . .	732	1350	811	1490	950	1740
NICKEL-TITANIUM	. . .	. . .	55.1	. . .	44.9	985	1805	130	2390	1550	2820

Oxide ceramics such as Al_2O_3, ZrO_2, and MgO are not easily wetted. Consequently, an active element must be present in the filler metal to reduce the oxide. Titanium is the active element most frequently added in the filler metals, although zirconium, niobium, aluminum, chromium, and vanadium have also been used. The oxide reduction by titanium is represented by:

$$M_xO_y + y\underline{Ti}_{fm} \rightarrow yTiO_i + x\underline{M}_{fm} \qquad \textbf{(EQ 9)}$$

Depending on the brazing system, a dissolution reaction may occur instead of the reduction of the oxide ceramics. In the case of the Al_2O_3-Cu-Cu_2O system, a spinel $CuAlO_2$ is reported to form at the interface. This spinel makes the metal/ceramic transition to promote a good bond between both types of material.

The nature of the oxide formed at the ceramic oxide-filler metal interface is very important to the wetting and spreading of the molten filler metal and to the integrity of the joint. The metallic-type conductivity and metallic-ionic bonding of titanium gives it a metallic characteristic. On the other hand, Ti_2O_3 has only ionic bonding, giving it a typical ceramic characteristic.

To protect the titanium in the filler metal against "premature" oxidation or other reactions during the joining, a high vacuum or an inert atmosphere (that is, non-nitrogen) is recommended. Table 15 shows active brazing conditions for some oxide ceramics.

TABLE 15 TYPICAL ACTIVE BRAZING PARAMETERS FOR OXIDE CERAMICS

JOINT	FILLER METAL	BRAZING TEMPERATURE		STRENGTH	
		°C	°F	MPA	KSI
AL_2O_3/AL_2O_3	CU-44AG-4SN-4TI	800-900	1470-1650	80-120	12-17
AL_2O_3/AL	AL INTERLAYERS (40 μM, OR 0.0016 IN., THICK)	1000	1830	73-89	11-13
AL_2O_3/FE-29NI-18CO	AG-27CU-3TI	900	1650	185	27
	AG-25CU-15IN-1TI	900	1650	162	23

AL_2O_3/TI-6AL-4V	CU-40AG-5TI	850-890	1560-1635	. . .	. . .
PSZ ZRO_2/PSZ ZRO_2	CU-44AG-4SN-4TI	800-850	1470-1560	>400	>58
	CU-44AG-4SN-4TIK	900	1650	248	36
TZP ZRO_2/STEEL[B]	AG-4TI	1050	1920	151	22

(A) (A) PSZ, PARTIALLY STABILIZED ZIRCONIA.

(B) TZP, TETRAGONAL ZIRCONIA POLYCRYSTALS

Nitride Ceramics. Nonoxide ceramics are more easily reduced by chemical reactions than oxide ceramics. Thus, the brazing techniques developed for oxide ceramics should be used judiciously in joining nonoxide ceramics.

Joining of nitrides using a glass bonding agent or by active metal brazing has been reported. A glass bonding agent such as $70SiO_2$-$27MgO$-$3Al_2O_3$ (in wt%) is used to join Si_3N_4. Si_2N_2O is formed at the ceramic-glass interface to promote the joining.

Active brazing of nitrides follows the same principles as outlined in the section "Oxide Ceramics" in this article. An active element reduces the ceramic at the interface between the ceramics and the molten filler metal. The general equation for a nitride reduced by a titanium-rich filler metal is:

$$M_xN_y + y\underline{Ti}_{fm} \rightarrow yTiN_i + x\underline{M}_{fm} \qquad \textbf{(EQ 10)}$$

TiN is formed at the filler metal-nitride interface, and it has a character similar to TiO in promoting wetting. Depending on which active metal is contained in the filler metal, a silicide or an aluminide may form first at the interface. In the case of copper-niobium filler metal for silicon nitride joining, niobium silicide may form before the niobium nitride. Table 16 shows some typical brazing conditions for the nitride ceramics.

TABLE 16 TYPICAL PARAMETERS FOR BRAZING OF NITRIDE CERAMICS

JOINT	FILLER METAL	BRAZING TEMPERATURE		STRENGTH	
		°C	°F	MPA	KSI
BN/BN	AL	1000	1830	6[A]	0.9[A]
AIN/MO	CU-42TI	1100	2010	167[A]	24.2[A]
	CU-71TI	1100	2010	49[A]	7.1[A]
	AG-35CU-4TI	980	1795	192[A]	27.8[A]
SI_3N_4/SI_3N_4	AL	1000	1830	450-500[B]	65-72.5[B]
	AL-SI (0.06-10.6)	800	1470	>400[B]	>58[B]
	AG-27CU-2TI	850	1560	270[A]	39[A]
	AG-CU-IN-1.25TI	700	1290	219-427[B]	31.8-61.9[B]
	$70SIO_2$-$27MGO$-$3AL_2O_3$	1500	2730	450[B]	65[B]
SI_3N_4/MO	AG-35CU-4TI	980	1795	195[A]	28.3[A]
SI_3N_4/FE-29NI-18CO	AG-28CU-2TI	800	1470	95[B]	14[B]
	AG-25CU-15IN-1TI	900	1650	51[B]	7.4[B]
SIALON/SIALON	AL	1000	1830	61[A]	8.8[A]

(A) SHEAR TEST.

(B) FOUR-POINT BEND TEST

The presence of these compounds, as a reaction layer, is necessary to promote wetting and spreading and to make a good bond between ceramic and metal. The growth of the reaction layer is affected by brazing temperature, time, reactivity,

and the amount of active element in the filler metal. Thus, the joining conditions should be carefully controlled to produce a thin layer and promote the optimum mechanical behavior of the joint.

References cited in this section

4. D.R. MILNER AND R.L. APPS, *INTRODUCTION TO WELDING AND BRAZING,* PERGAMON PRESS, 1969
9. E.W. COLLINGS, *THE PHYSICAL METALLURGY OF TITANIUM ALLOYS,* AMERICAN SOCIETY FOR METALS, 1984
10. M.M. SCHWARTZ, *CERAMIC JOINING,* ASM INTERNATIONAL, 1990

S.D. Brandi, Escola Politécnica da Universidade de São Paulo, Brazil; S. Liu, Colorado School of Mines; J.E. Indacochea and R. Xu, University of Illinois at Chicago

References

1. P.R. SHARPS, A.P. TOMSIA, AND J.A. PASK, WETTING AND SPREADING IN THE CU-AG SYSTEM, *ACTA METALL.,* VOL 29 (NO. 5), 1981, P 855-865
2. V. KONDIC, *METALLURGICAL PRINCIPLES OF FOUNDING,* AMERICAN ELSEVIER, 1973
3. M.G. NICHOLAS AND D.A. MORTIMER, CERAMIC/METAL JOINING FOR STRUCTURAL APPLICATIONS, *MATER. SCI. TECHNOL.,* VOL 1 (NO. 9), 1985, P 657-665
4. D.R. MILNER AND R.L. APPS, *INTRODUCTION TO WELDING AND BRAZING,* PERGAMON PRESS, 1969
5. *SOLDERING MANUAL,* AMERICAN WELDING SOCIETY, 1977
6. J.A. PASK, FROM TECHNOLOGY TO THE SCIENCE OF GLASS/METAL AND CERAMIC/METAL SEALING, *AM. SOC. CERAM. BULL.,* VOL 66 (NO. 11), 1987, P 1587-1592
7. H.H. MANKO, *SOLDERS AND SOLDERING,* 3RD ED., MCGRAW-HILL, 1992
8. *ALUMINUM SOLDERING HANDBOOK,* ALUMINUM ASSOCIATION, 1974
9. E.W. COLLINGS, *THE PHYSICAL METALLURGY OF TITANIUM ALLOYS,* AMERICAN SOCIETY FOR METALS, 1984
10. M.M. SCHWARTZ, *CERAMIC JOINING,* ASM INTERNATIONAL, 1990

Brazeability and Solderability of Engineering Materials

S.D. Brandi, Escola Politécnica da Universidade de São Paulo, Brazil; S. Liu, Colorado School of Mines; J.E. Indacochea and R. Xu, University of Illinois at Chicago

Selected References

- *BRAZING MANUAL,* AMERICAN WELDING SOCIETY, 1992
- J.A. DEVORE, SOLDERING AND MOUNTING TECHNOLOGY, *ELECTRONIC MATERIALS HANDBOOK,* VOL 1, *PACKAGING,* ASM INTERNATIONAL, 1987
- G. ELSSNER AND G. PETZOW, METAL/CERAMIC JOINING, *ISIJ LNT.,* VOL 30 (NO. 12), 1990, P 1011-1032

- H.H. MANKO, *SOLDERING HANDBOOK FOR MOUNTED CIRCUITS AND SURFACE MOUNTING,* VAN NOSTRAND REINHOLD, 1986
- Y. NAKAO, RESEARCH ON JOINING OF CERAMICS IN JAPAN, *1ST U.S.-JAPAN SYMP. ADVANCES IN WELDING METALLURGY,* AWS/JWS, JWES, 1990, P 79-101
- M.G. NICHOLAS, REACTIVE METAL BRAZING, *JOINING CERAMICS, GLASS AND METAL,* W. KRAFT, ED., DGM INFORMATIONSGESELLSCHAFT-VERLAG, 1989
- R.L. PEASLEE, BRAZING: YESTERDAY'S ART HAS BECOME TODAY'S SCIENCE, *WELD. J.,* VOL 71 (NO. 10), NOV 1992, P 25-31
- S.L. RICHLEN AND W.P. PARKS, JR., HEAT EXCHANGERS, *ENGINEERED MATERIALS HANDBOOK,* VOL 4, *CERAMICS AND GLASSES,* ASM INTERNATIONAL, 1991
- M.M. SCHWARTZ, *BRAZING,* ASM INTERNATIONAL, 1987
- R.J. KLEIN WASSINK, *SOLDERING IN ELECTRONICS,* ELECTROCHEMICAL PUBLICATIONS, 1989
- WELDING, *BRAZING, AND SOLDERING, METALS HANDBOOK,* 9TH ED., VOL 6, AMERICAN SOCIETY FOR METALS, 1982
- *WELDING PROCESSES, WELDING HANDBOOK,* 8TH ED., VOL 2, AMERICAN WELDING SOCIETY, 1991
- W. WLOSINSKI, INTERFACES IN DISSIMILAR MATERIAL JOINTS, *2ND INTERNATIONAL KOLLOQUIM BAD NAUHEIM,* MARCH 1985, P 27-29

Arc Welding of Carbon Steels

Ronald B. Smith, The ESAB Group, Inc.

Introduction

CARBON STEELS are defined as those steels containing up to 2% C, 1.65% Mn, 0.60% Si, and 0.60% Cu, with no deliberate addition of other elements to obtain a desired alloying effect. Tables 1(a) and 1(b) list some of the common grades of carbon steel that are covered in this article. The weldability of these steels greatly depends on their carbon and manganese contents and impurity levels.

TABLE 1(A) COMPOSITION OF SELECTED CARBON STEELS USED IN ARC WELDING APPLICATIONS

SAE-AISI NO.	COMPOSITION, WT %[A]				
	C	Mn	P	S	OTHER
1006	0.08	0.45	0.040	0.050	. . .
1010	0.08-0.13	0.30-0.60	0.040	0.050	. . .
1020	0.17-0.23	0.30-0.60	0.040	0.050	. . .
1030	0.27-0.34	0.60-0.90	0.040	0.050	. . .
1040	0.36-0.44	0.60-0.90	0.040	0.050	. . .
1050	0.47-0.55	0.60-0.90	0.040	0.050	. . .
1060	0.55-0.66	0.60-0.90	0.040	0.050	. . .
1070	0.65-0.73	0.60-0.90	0.040	0.050	. . .
1080	0.74-0.88	0.60-0.90	0.040	0.050	. . .
1095	0.90-1.04	0.30-0.50	0.040	0.050	. . .
MANGANESE-CARBON					
1513	0.10-0.16	1.10-1.40	0.040	0.050	. . .
1527	0.22-0.29	1.20-1.50	0.040	0.050	. . .
1541	0.36-0.44	1.35-1.65	0.040	0.050	. . .
1566	0.60-0.71	0.85-1.15	0.040	0.050	. . .
FREE-MACHINING					
1108	0.08-0.13	0.50-0.80	0.040	0.08-0.13	. . .
1139	0.35-0.43	1.35-1.65	0.040	0.13-0.20	. . .
1151	0.48-0.55	0.70-1.00	0.040	0.08-0.13	. . .
1212	0.13	0.70-1.00	0.07-0.12	0.16-0.23	. . .
12L14	0.15	0.85-1.15	0.04-0.09	0.26-0.35	0.15-0.35 PB

(A) SINGLE VALUES ARE MAXIMUMS.

TABLE 1(B) COMPOSITION AND MECHANICAL PROPERTIES OF SELECTED CARBON STEELS USED IN ARC WELDING APPLICATIONS

ASTM DESIGNATION		COMPOSITION, WT%[A]			ULTIMATE TENSILE STRENGTH[B]		YIELD STRENGTH[B]		COMMENTS[C]
SPECIFICATION	GRADE OR TYPE	c	mn	si[d]	mpa	ksi	mpa	ksi	
STRUCTURAL STEELS									
A 36	. . .	0.29	0.80-1.20	0.15-0.40	400-550	58-80	220-250	32-36	. . .

A 131	B	0.21	0.80-1.10	0.35	400-500	58-71	220	32	. . .
	E	0.18	0.70-1.35	0.10-0.35	400-500	58-71	220	32	NORMALIZED
	CS	0.16	1.00-1.35	0.10-0.35	400-500	58-71	220	32	NORMALIZED
A 283	A	0.14	0.90	0.04	310-415	45-60	165	24	. . .
	B	0.17	0.90	0.04	345-450	50-65	185	27	. . .
	C	0.24	0.90	0.04	380-485	55-70	205	30	. . .
	D	0.27	0.90	0.04	415-515	60-75	230	33	. . .
A 284	C	0.36	0.90	0.15-0.40	415	60	205	30	. . .
	D	0.35	0.90	0.15-0.40	415	60	230	33	. . .
A 573	58	0.23	0.60-0.90	0.10-0.35	400-500	58-71	220	32	. . .
	65	0.26	0.85-1.20	0.15-0.40	450-530	65-77	240	35	. . .
	70	0.28	0.85-1.20	0.15-0.40	485-620	70-90	290	42	. . .
A 285	A	0.17	0.90	0.35	310-450	45-65	165	24	. . .
	B	0.22	0.90	0.35	345-485	50-70	185	27	. . .
	C	0.28	0.90	0.35	380-515	55-75	205	30	. . .
A 442	55	0.24	0.80-1.10	0.15-0.40	380-515	55-75	205	30	. . .
	60	0.27	0.80-1.10	0.15-0.40	415-550	60-80	220	32	. . .
A 515	55	0.28	0.90	0.15-0.40	380-515	55-75	205	30	NORMALIZED IF *T* > 38 MM (1.5 IN.)
	60	0.31	0.90	0.15-0.40	415-550	60-80	220	32	NORMALIZED IF *T* > 38 MM (1.5 IN.)
	65	0.33	0.90	0.15-0.40	450-585	65-85	240	35	NORMALIZED IF *T* > 38 MM (1.5 IN.)
	70	0.35	1.20	0.15-0.40	485-620	70-90	260	38	NORMALIZED IF *T* > 38 MM (1.5 IN.)
A 516	55	0.26	0.60-1.20	0.15-0.40	380-515	55-75	205	30	NORMALIZED IF *T* > 38 MM (1.5 IN.)
	60	0.27	0.60-1.20	0.15-0.40	415-550	60-80	220	32	NORMALIZED IF *T* > 38 MM (1.5 IN.)
	65	0.29	0.85-1.20	0.15-0.40	450-585	65-85	240	35	NORMALIZED IF *T* > 38 MM (1.5 IN.)
	70	0.31	0.85-1.20	0.15-0.40	485-620	70-90	260	38	NORMALIZED IF *T* > 38 MM (1.5 IN.)
A 537	C1.1	0.24	0.70-1.60	0.15-0.50	450-585	65-85	310	45	NORMALIZED
	C1.2	0.24	0.70-	0.15-	515-	75-	380	55	QUENCHED AND

			1.60	0.50	655	95			TEMPERED
A 662	A	0.14	0.90-1.50	0.15-0.40	400-540	58-78	275	40	NORMALIZED
	B	0.19	0.85-1.60	0.15-0.40	450-585	65-85	275	40	NORMALIZED IF *T* > 38MM (1.5 IN.)
	C	0.20	1.00-1.60	0.15-0.50	485-620	70-90	295	43	NORMALIZED IF *T* > 38MM (1.5 IN.)
PIPE STEELS									
A 53	A	0.25	0.95	. . .	330	48	205	30	. . .
	B	0.30	1.20	. . .	415	60	240	35	. . .
A 106	A	0.25	0.27-0.93	0.10	330	48	205	30	. . .
	B	0.30	0.29-1.06	0.10	415	60	240	35	. . .
	C	0.35	0.29-1.06	0.10	485	70	275	40	. . .
A 381	Y42	0.26	1.40	. . .	415	60	290	42	. . .
	Y52	0.26	1.40	. . .	495	72	360	52	. . .
	Y60	0.26	1.40	. . .	540	78	415	60	. . .
CAST STEELS									
A 27	60-30	0.30	0.60	0.80	415	60	205	30	HEAT-TREATED
	70-40	0.25	1.20	0.80	485	70	275	40	HEAT-TREATED
A 216	WCA	0.25	0.70	0.60	415-585	60-85	205	30	HEAT-TREATED
	WCB	0.30	1.00	0.60	485-655	70-95	250	36	HEAT-TREATED
	WCC	0.25	1.20	0.50	485-655	70-95	275	40	HEAT-TREATED
SAE J435C	0025	0.25	0.75	0.80	415	60	205	30	HEAT-TREATED
	0050A	0.40-0.50	0.50-0.90	0.80	585	85	310	45	HEAT-TREATED

(A) SINGLE VALUES ARE MAXIMUMS.

(B) SINGLE VALUES ARE MINIMUMS.

(C) *T*, PLATE THICKNESS.

(D) SILICON CONTENT VARIES WITH DEOXIDATION PRACTICE USED.

At low carbon levels (less than 0.15% C), the steels are nonhardening and weldability is excellent. The bulk of the steels in this carbon range are used for flat-rolled products (sheet and strip), which may contain up to 0.5% Mn. Most of these steels are now aluminum-killed, continuous-cast product supplied in the cold-rolled and annealed condition. The lower available oxygen in the killed sheet makes it easier to arc weld without porosity formation. Typical uses for these steels are automobile body panels, appliances, and light-walled tanks.

In the range of 0.15 to 0.30% C, the steels are generally easily welded, but because hardening is a possibility, precautions such as preheating may be required at higher manganese levels, in thicker sections, or at high levels of joint restraint. Much of the steel in this carbon range is used for rolled structural plate and tubular products. These steels are generally killed or semi-killed and are usually supplied in the hot-rolled condition. The presence of surface scale (iron oxide) from the high-temperature rolling process increases the likelihood of porosity formation during welding and may require the use of welding electrodes with higher levels of deoxidizers, or removal of the scale prior to welding. Some carbon steel plate may be heat-treated (normalized or quenched and tempered) to enhance properties. In such cases, careful selection of the welding consumable must be made in order to match the base metal properties. Welding heat input may have to be controlled so as not to diminish the properties in the heat-affected zone (HAZ) of the base metal, or postweld heat treatment may be necessary to restore the strength and/or toughness of the HAZ.

Medium-carbon steel--steel that contains 0.30 to 0.60% C--can be successfully welded by all of the arc welding processes, provided suitable precautions are taken. The higher carbon content of these steels, along with manganese from 0.6 to 1.65%, makes these steels more hardenable. For this reason, they are commonly used in the quenched and tempered condition for such applications as shafts, couplings, gears, axles, crankshafts, and rails. Because of the greater likelihood of martensite formation during welding, and the higher hardness of the martensite formed, preheating and postheating treatments are necessary. Low-hydrogen consumables and procedures should also be used to reduce the likelihood of hydrogen-induced cracking. The higher strength level of these steels may require the use of an alloyed electrode to match the base metal properties. It may also be necessary to postweld heat treat the part in order to restore the strength and/or toughness of the HAZ.

Higher-carbon steel--steel that contains 0.60 to 2.00% C--has poor weldability because of the likelihood of formation of a hard, brittle martensite upon weld cooling. Steels of this type are used for springs, cutting tools, and abrasion-resistant applications. Low-hydrogen consumables and procedures, preheating, interpass control, and stress relieving are essential if cracking is to be avoided. Austenitic stainless steel electrodes are sometimes used to weld high-carbon steels. These electrodes will reduce the risk of hydrogen-induced cracking but may not match the strength of the high-carbon steel base metal.

The 11*xx* and 12*xx* series steels contain large amounts of sulfur, phosphorus, or lead for improved machinability. Both series are difficult to weld because of solidification cracking and porosity formation.

Carbon steel castings can be made in the same wide range of compositions as the wrought types. The major differences are that castings are always fully killed (0.3 to 1.0% Si) and are generally heat-treated. For a given composition, the weldabilities of the cast and wrought carbon steels are similar. Casting defects are often repaired by welding. Care in the selection of a welding electrode is required if the casting is to be heat-treated. Low-alloy steel electrodes are frequently used because they match the casting properties better after heat treatment. Low-hydrogen electrodes and procedures are commonly used, depending on casting size and carbon content.

Arc Welding of Carbon Steels

Ronald B. Smith, The ESAB Group, Inc.

Weldability Considerations for Carbon Steels

As a group, the carbon steels are among the most weldable of materials, yet they are susceptible, to one degree or another, to:

- HYDROGEN-INDUCED CRACKING
- SOLIDIFICATION CRACKING
- LAMELLAR TEARING
- WELD METAL POROSITY
- WELD METAL AND HAZ MECHANICAL PROPERTY VARIATIONS

Additional information about the weldability of carbon steel is available in the Section "Selection of Carbon and Low-Alloy Steels" in this Volume.

Hydrogen-Induced Cracking (Ref 1, 2)

Hydrogen-induced cracking (also referred to as cold cracking, delayed cracking, or underbead cracking) is the most serious problem affecting weldability. Any hardenable carbon steel is susceptible. This type of cracking results from the combined effects of four factors:

- A SUSCEPTIBLE ("BRITTLE") MICROSTRUCTURE
- THE PRESENCE OF HYDROGEN IN THE WELD METAL

- TENSILE STRESSES IN THE WELD AREA
- A SPECIFIC TEMPERATURE RANGE, -100 TO 200 °C (-150 TO 390 °F)

Hydrogen-induced cracking occurs after weld cooling (hence the term cold cracking) and is often delayed for many hours while atomic hydrogen diffuses to areas of high tensile stress. At microstructural flaws in a tensile stress field, the hydrogen changes to its molecular form, causing cracking. Cracking may occur in the HAZ or weld metal, and it may be longitudinal or transverse (Fig. 1). For carbon steels, cracking is more likely to occur in the HAZ because carbon steel electrodes are usually low in carbon and the weld metal is generally not hardenable. Exceptions would be if a highly alloyed electrode were being used, if the weld metal were made more hardenable by dilution of carbon from the base material, or in certain submerged arc welds where the use of excessive arc voltage and active fluxes results in high manganese and/or silicon pickup from the flux (see the section "Submerged Arc Welding" in this article).

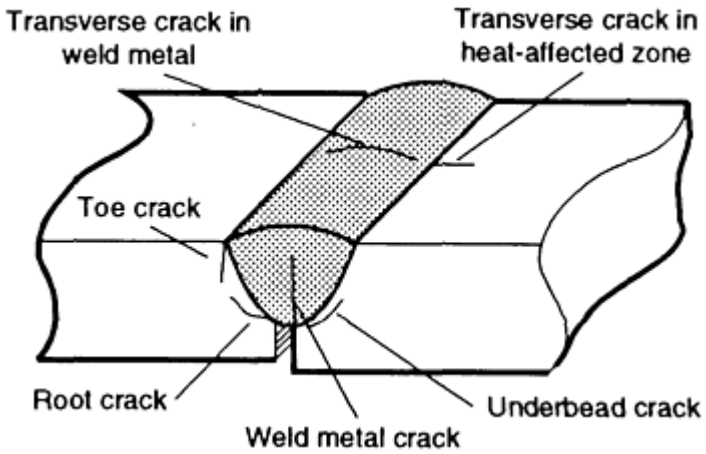

FIG. 1 SCHEMATIC SHOWING LOCATION OF HYDROGEN-INDUCED CRACKS IN CARBON STEEL WELDMENTS. SOURCE: REF 1

Cracks in the HAZ are most often longitudinal. Underbead cracks lie more or less parallel to the fusion line. They do not normally extend to the surface and may therefore be difficult to detect. Underbead cracks will form at relatively low stress levels in martensite when high levels of hydrogen are present.

Toe cracks and root cracks start in areas of high stress concentration. Cracking may therefore occur in less susceptible microstructures or at relatively low hydrogen levels. This type of cracking is often delayed while the necessary hydrogen diffuses to the area.

Transverse cracking in the HAZ is less common. It will occur in high-carbon martensite under conditions of high longitudinal stresses (for example, outside fillet welds on heavy plate).

Weld metal cracks may be longitudinal or transverse. Longitudinal cracks start due to stress concentrations at the root of the weld. Transverse cracking starts at hydrogen-containing defects subject to longitudinal stresses. Weld metal cracks do not always extend to the surface. In submerged arc weld metal made with damp fluxes, a unique crack morphology known as chevron cracking can occur. Here the cracks lie at 45° to the weld axis.

One of the serious problems with hydrogen-induced cracking is the difficulty in detecting the presence of a crack. The delayed nature of some of the cracks demands that inspection not be carried out too soon, especially in welds that will have external stresses applied when put in service. Because some of the cracks do not extend to the surface, they are not detectable by visual inspection methods (for example, liquid penetrant, or magnetic particle inspection, which requires the defect to be near the surface). Radiography is most sensitive to volumetric flaws, and it may not detect cracks that are too fine or of the wrong orientation. Ultrasonic inspection is capable of detecting the crack if the operator knows where to look. Given the difficulty in detecting hydrogen-induced cracks and the possibility of this cracking leading to in-service failure, it is prudent to observe the precautions necessary to avoid cracking in the first place.

Susceptible Microstructures. A susceptible microstructure is any hard, brittle transformation product formed in the HAZ or weld metal. Martensite is by far the most susceptible microstructure found in carbon steels. In all but high-carbon steel weld zones, the martensite, when formed, is usually mixed with other, less susceptible transformation products (for example, pearlite). Nevertheless, these mixed microstructures are susceptible to cracking, depending on the level of hardening. Martensite itself may be more or less susceptible, depending on its carbon content. Higher-carbon martensite is harder, more brittle, and more susceptible to cracking. Figure 2 shows the effect of carbon content on the hardness of carbon steel for various percentages of martensite formed upon rapid cooling.

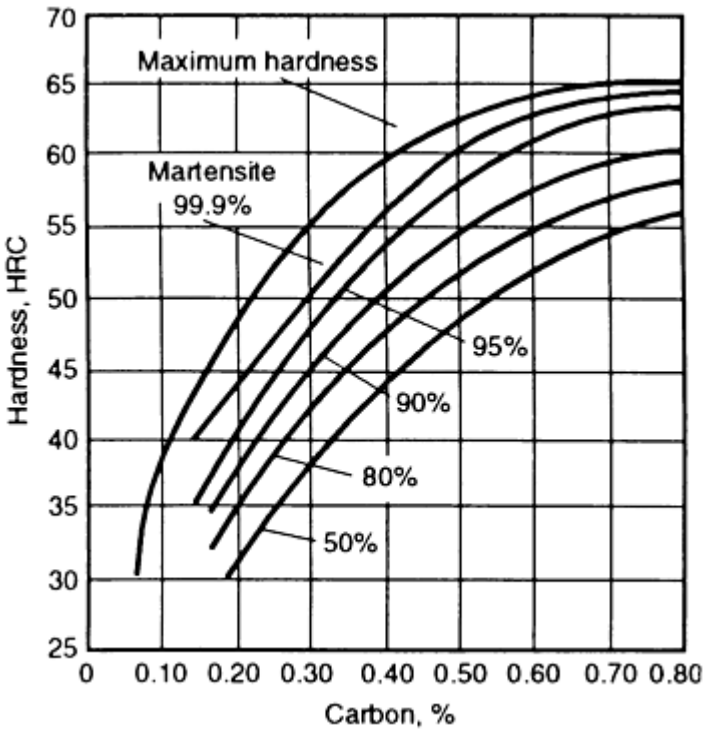

FIG. 2 PLOT OF HARDNESS VERSUS CARBON CONTENT AS A FUNCTION OF MARTENSITE FORMATION IN CARBON STEEL THAT HAS COOLED RAPIDLY

The hardenability of the steel also increases as the carbon content increases. Figure 3 presents hardenability curves for five carbon steels (as determined by end-quench tests). As the cooling rate (top scale) decreases, the lower-carbon steels show a more rapid decline in hardness (that is, less martensite is being formed at the slower cooling rates). Higher carbon steels are more likely to form martensite upon cooling, and the martensite formed will be harder and thus more susceptible to hydrogen-induced cracking.

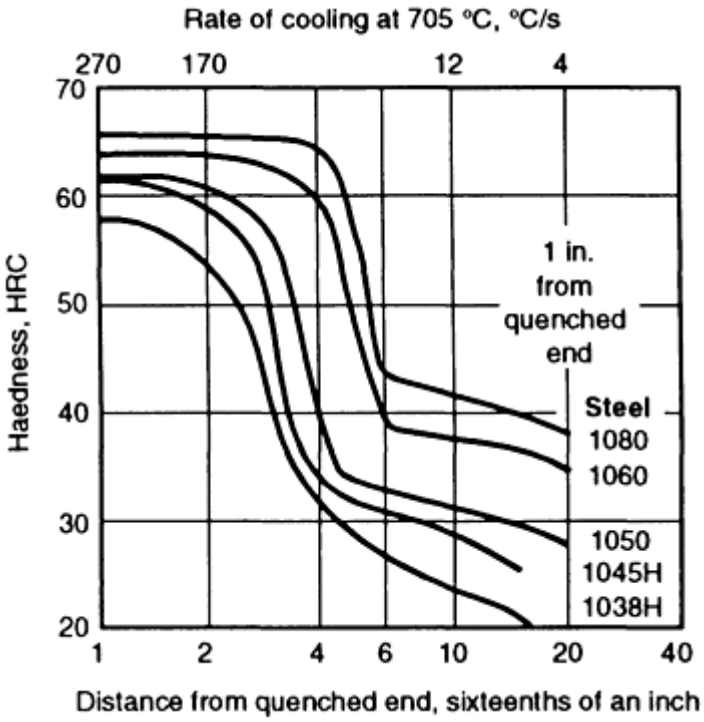

FIG. 3 HARDENABILITY CURVES FOR FIVE CARBON STEELS AS DETERMINED BY END-QUENCH TESTING

Martensite formation is also a function of grain size. The HAZ adjacent to the fusion line will have large austenite grains, which more readily form martensite than smaller grains.

Presence of Hydrogen in Weld Metal. The exact role that hydrogen plays in cold cracking is unknown, but its presence is necessary for this type of cracking to occur. Hydrogen is generally introduced into the weld area during welding. The sources are:

- MOISTURE IN THE FLUX COATING OF SHIELDED METAL ARC WELDING ELECTRODES, IN SUBMERGED ARC FLUXES, OR IN THE CORE OF FLUX-CORED ELECTRODES
- HYDROGEN-CONTAINING LUBRICANTS LEFT ON THE SURFACE OF WIRE ELECTRODES OR IN THE SEAMS OF CORED ELECTRODES
- HYDROGEN-CONTAINING COMPOUNDS OR RESIDUES LEFT ON THE PLATE SURFACE (THESE CAN INCLUDE GREASE, OIL, PAINT, RUST, AND SO ON)
- LEAKING WATER-COOLED TORCHES, BROKEN GAS LINES, OR HIGH MOISTURE IN THE SHIELDING GAS
- ASPIRATION OF MOISTURE-LADEN AIR INTO THE WELD AREA

The principal source of hydrogen is the welding consumable.

Hydrogen, ionized to its atomic form by the intense heat of the arc, is very soluble in liquid iron. This solubility decreases with decreasing temperature. Rapid cooling (in a weld, for example) can result in significant supersaturation of atomic hydrogen in the solidified metal. Because atomic hydrogen diffuses relatively easily through ferrite, a certain amount of the initial hydrogen present when the weld has cooled to ambient temperatures will subsequently diffuse out of the weld metal. This diffusible hydrogen, whose exit from the weld metal is accelerated by higher temperatures, may be measured using standardized test methods (such as those outlined in AWS A4.3). The results, measured in mL of hydrogen per 100 g of weld metal, give an indication of the amount of hydrogen potentially available to induce cracking. These tests are now widely used to measure diffusible hydrogen and to classify arc welding electrodes.

The distribution of hydrogen in the weld metal and HAZ and the subsequent susceptibility to cold cracking is a function of the phase transformations that take place upon cooling. Three examples are described below.

HAZ Hardens but Weld Metals Do Not. If the HAZ hardens (transforms to martensite) but the weld metal does not (for example, welding a medium-carbon steel with a low-carbon, mild-steel electrode), the weld metal undergoes transformation to a ferritic structure at relatively high temperatures. Because hydrogen diffuses easily in ferrite, it will diffuse to and migrate across the fusion boundary into the still-austenitic HAZ, which has a higher solubility for hydrogen but a lower diffusivity. At a much lower temperature, the HAZ transforms to martensite. The area near the fusion boundary is highly concentrated in hydrogen. Cracking may then occur.

Weld Metal More Hardenable than Base Material. If the weld metal is more hardenable than the base material (for example, highly alloyed electrode picks up substantial carbon from a carbon steel base plate), the HAZ transforms first. The weld metal, which is austenitic, will retain the hydrogen. When the weld metal transforms, it will be in the presence of high hydrogen, which may lead to cracking in the weld metal. The HAZ, which is low in hydrogen, will not crack.

No Lower Temperature Transformation in Austenitic Weld Metal. If an austenitic filler metal is used to weld a hardenable base metal (for example, high-carbon steel), there is no lower temperature transformation in the weld metal, which remains austenitic with a high tolerance for hydrogen. Little hydrogen migrates across the fusion boundary, and so the HAZ transforms to martensite with a low hydrogen content and cracking is avoided.

Once hydrogen is present in a hardenable microstructure, the exact mechanism by which it engenders cracking is unknown. The hydrogen is thought to diffuse to defects and areas of triaxial stress, where it interacts with tensile stress to enlarge and extend discontinuities.

Tensile Stresses in Weld Area. The stresses that a weldment is subjected to may be either externally or internally generated. External stresses are those applied when the weld is put in service. Internal, or residual, stresses are those that arise from the welding process, due mainly to thermal gradients, unequal thermal expansion and contraction of the base metal and weld metal, and volume changes resulting from phase transformations during cooling. The residual stresses can be reduced by unrestrained movement of the parts being welded, thermal treatments, and proper weld design.

Movement of the parts can be actual physical displacement or an elastic or plastic deformation. An example of the former would be offsetting the parts prior to welding and allowing them to rotate into the desired final position. An example of the latter is the use of a lower strength ferritic filler metal or of an austenitic filler metal to weld a medium- or high-carbon steel. The weaker, more ductile weld metal of these deposits is able to absorb some of the stress (by elastic or plastic deformation) and reduce the level in the more vulnerable HAZ.

Any condition that limits the movement of welded parts will increase the residual stresses and the likelihood of hydrogen-induced cracking. Thicker, more massive plates, high clamping pressure, or rigid surrounding structures reduce the freedom of motion of the welded parts and result in high residual stresses. Thicker, more massive weld structures also cool faster because of the large heat sink, thus increasing the likelihood of martensite formation. The use of preheat to reduce the risk of martensite formation will also reduce and delay the onset of maximum residual stresses (and allow more time for hydrogen to escape). Postweld stress relief reduces residual stresses by heating the weldment to a temperature at which the yield point drops low enough for plastic flow to occur, thus relaxing the stresses.

Joint designs that reduce the volume of weld metal needed will result in lower residual stresses. The smallest groove angles and root openings that allow good access should be used. The smallest fillet weld size that meets shear strength requirements should be used. The presence of notches or gaps in the weld joint will also increase the incidence of cracking because they produce a localized concentration of stress. Accumulation of relatively low levels of hydrogen in these areas may be sufficient to cause cracking.

Temperature Range for Hydrogen-Induced Cracking. Hydrogen-induced cracking will not normally occur outside of the temperature range of -100 to 200 °C (-150 to 390 °F). Below -100 °C (-150 °F), the hydrogen probably diffuses too slowly to reach a critical concentration in a susceptible area, while above 200 °C (390 °F) the hydrogen diffuses so rapidly out of the weld area that it does not have time to reach a critical accumulation.

Prevention of Hydrogen-Induced Cracking. The major preventative measures to avoid cold cracking are:

- PREHEAT, INCLUDING MAINTENANCE OF PROPER INTERPASS TEMPERATURE

- HEAT INPUT CONTROL
- POSTWELD HEAT TREATMENT
- BEAD TEMPERING
- USE OF LOW-HYDROGEN PROCESSES AND CONSUMABLES
- USE OF ALTERNATE FILLER MATERIALS (FOR EXAMPLE, AUSTENITIC ELECTRODES)

Preheating of the weld area is the most effective and widely used method for avoiding hydrogen-induced cracking. Its primary function is to reduce the weld metal cooling rate so that transformation to martensite is avoided or reduced below a certain critical level. The slower cooling also gives hydrogen more time to diffuse out of the weld area and delays the onset of maximum residual stresses. Many specifications and codes require the use of specific preheat and interpass temperatures for welding hardenable steels. AWS D1.1 (Ref 3) and CSA W59 (Ref 4) specify minimum preheat and interpass temperatures for various thicknesses of structural carbon steels (Table 2). Table 3 gives suggested preheat and postheat treatments for steels. Various methods are also available that allow one to determine the required preheat by taking into account the steel composition, restraint level, and hydrogen level. These methods are discussed in the section "Methods for Determining Preheat/Heat Input" in this article. Some are available as software packages. For example, PREHEAT is a software package from The Welding Institute that is based on BS 5135 (Ref 6) and is available from the Edison Welding Institute.

TABLE 2 RECOMMENDED PREHEAT AND INTERPASS TEMPERATURES FOR SELECTED THICKNESSES OF STRUCTURAL CARBON STEELS

CATEGORY	ASTM DESIGNATIONS	WELDING PROCESS	THICKNESS OF THICKEST PART AT POINT OF WELDING (*T*)		MINIMUM TEMPERATURE[A][B][D]	
			MM	IN.	°C	°F
A	A 36(C); A 53, GRADE B; A 106, GRADE B; A 131, GRADES A, B, CS, D, DS, AND E; A 139, GRADE B; A 381, GRADE Y35; A 500, GRADES A AND B; A 501; A 516; A 524, GRADES I AND II; A 529; A 570[H]; A 573, GRADE 65; A 709, GRADE 36[C]; API 5L[F], GRADES B AND X42; ABS[G], GRADES A, B, D, CS, DS, AND E	SHIELDED METAL ARC WELDING WITH OTHER THAN LOW HYDROGEN ELECTRODES	≤ 19	$\leq \frac{3}{4}$	[E]	[E]
			$19 < T \leq 38.1$	$\frac{3}{4} < T \leq 1\frac{1}{2}$	66	150
			$38.1 < T \leq 63.5$	$1\frac{1}{2} < T \leq 2\frac{1}{2}$	107	225
			>63.5	$>2\frac{1}{2}$	150	300
B	A 36[C]; A 53, GRADE B; A 106, GRADE B; A 131, GRADES A, B, CS, D, DS, E, AH 32, AH 36, DH 32, DH 36, EH 32, AND EH 36; A 139, GRADE B; A 242; A 381, GRADE Y35; A 441; A 500, GRADES A AND B; A 501; A 516, GRADES 55, 60, 65, AND 70; A 524, GRADES I AND II; A 529; A 537, CLASSES 1 AND 2; A 570[H]; A 572, GRADES 42 AND 50; A 573, GRADE 65; A 588; A 595, GRADES A, B, AND C; A 606, A 607, GRADES 45, 50, AND 55; A 618; A 633, GRADES A, B, C, AND D; A 709, GRADES 36, 50, AND 50W[C]; A 808; API 5L[F], GRADES B AND X42; API 2H[F], GRADES 42 AND 50; ABS[G], GRADES AH 32, AH 36, DH 32, DH 36, EH 32, EH 36, A, B, D, CS, DS, AND E	SHIELDED METAL ARC WELDING WITH LOW-HYDROGEN ELECTRODES, SUBMERGED ARC WELDING, GAS-METAL ARC WELDING, FLUX-CORED ARC WELDING	≤ 19	$\leq \frac{3}{4}$	[E]	[E]
			$19 < T < 38.1$	$\frac{3}{4} < T \leq 1\frac{1}{2}$	10	50
			$38.1 < T < 63.5$	$1\frac{1}{2} < T \leq 2\frac{1}{2}$	66	150
			>63.5	$>2\frac{1}{2}$	107	225
C	A 572, GRADES 60 AND 65; A 633, GRADE E; API 5L[F], GRADE X52	SHIELDED METAL ARC WELDING WITH LOW-HYDROGEN ELECTRODES, SUBMERGED ARC WELDING, GAS-METAL ARC WELDING, FLUX-CORED	≤ 19	$\leq \frac{3}{4}$	10	50
			$19 < T < 38.1$	$\frac{3}{4} < T$	66	150

				$\leq 1\frac{1}{2}$		
			38.1 < T < 63.5	$1\frac{1}{2}$ < T $\leq 2\frac{1}{2}$	107	225
			>63.5	$>2\frac{1}{2}$	150	300
D	A 514; A 517; A 709, GRADES 100 AND 100W	SHIELDED METAL ARC WELDING WITH LOW-HYDROGEN ELECTRODES, SUBMERGED ARC WELDING WITH CARBON OR ALLOY STEEL WIRE, NEUTRAL FLUX, GAS-METAL ARC WELDING, OR FLUX-CORED ARC WELDING	≤ 19	$\leq \frac{3}{4}$	10	50
			19 < T < 38.1	$\frac{3}{4}$< T $\leq 1\frac{1}{2}$	50	125
			38.1 < T < 63.5	$1\frac{1}{2}$ < T $\leq 2\frac{1}{2}$	80	175
			>63.5	$>2\frac{1}{2}$	107	225
E	A 710, GRADE A[I]	. . .	. . .	. . .	[J]	[J]

Source: Ref 3

(A) WELDING SHALL NOT BE DONE WHEN THE AMBIENT TEMPERATURE IS LOWER THAN -18 °C (O °F). TEMPERATURE OF -18 °C (0 °F) DOES NOT MEAN THE AMBIENT ENVIRONMENTAL TEMPERATURE BUT THE TEMPERATURE IN THE IMMEDIATE VICINITY OF THE WELD. THE AMBIENT ENVIRONMENTAL TEMPERATURE MAY BE BELOW -18 °C (0 °F) BUT A HEATED STRUCTURE OR SHELTER AROUND THE AREA BEING WELDED COULD MAINTAIN THE TEMPERATURE ADJACENT TO THE WELDMENT AT -18 °C (0 °F) OR HIGHER. WHEN THE BASE METAL IS BELOW THE TEMPERATURE LISTED FOR THE WELDING PROCESS BEING USED AND THE THICKNESS OF MATERIAL BEING WELDED, IT SHALL BE PREHEATED (EXCEPT AS OTHERWISE PROVIDED) IN SUCH MANNER THAT THE SURFACES OF THE PARTS ON WHICH WELD METAL IS BEING DEPOSITED ARE AT OR ABOVE THE SPECIFIED MINIMUM TEMPERATURE FOR A DISTANCE EQUAL TO THE THICKNESS OF THE PART BEING WELDED, BUT NOT LESS THAN 75 MM (3 IN.) IN ALL DIRECTIONS FROM THE POINT OF WELDING. PREHEAT AND INTERPASS TEMPERATURES MUST BE SUFFICIENT TO PREVENT CRACK FORMATION. TEMPERATURE ABOVE THE MINIMUM SHOWN MAY BE REQUIRED FOR HIGHLY RESTRAINED WELDS. FOR A 514, A 517, AND A 709, GRADES 100 AND 100W STEEL, THE MAXIMUM PREHEAT AND INTERPASS TEMPERATURE SHALL NOT EXCEED 205 °C (400 °F) FOR THICKNESS UP TO 38.1 MM ($1\frac{1}{2}$ IN.) INCLUSIVE, AND 230 °C (450 °F) FOR GREATER

THICKNESS. HEAT INPUT WHEN WELDING A 514, A 517, AND A 709 GRADES 100 AND 100W STEEL SHALL NOT EXCEED THE STEEL PRODUCER'S RECOMMENDATION.

(B) IN JOINTS INVOLVING COMBINATIONS OF BASE METALS, PREHEAT SHALL BE AS SPECIFIED FOR THE HIGHER STRENGTH STEEL BEING WELDED.

(C) ONLY LOW-HYDROGEN ELECTRODES SHALL BE USED WHEN WELDING A 86 OR A 709 GRADE 36 STEEL MORE THAN 25.4 MM (1 IN.) THICK FOR DYNAMICALLY LOADED STRUCTURES.

(D) WHEN THE BASE METAL TEMPERATURE IS BELOW 0 °C (32 °F), THE BASE METAL SHALL BE PREHEATED TO AT LEAST 21 °C (70 °F) AND THIS MINIMUM TEMPERATURE MAINTAINED DURING WELDING.

(E) NONE.

(F) AMERICAN PETROLEUM INSTITUTE (API) SPECIFICATION.

(G) AMERICAN BUREAU OF SHIPPING (ABS) SPECIFICATION.

(H) ALL GRADES.

(I) ALL CLASSES.

(J) PREHEAT IS NOT REQUIRED FOR THE BASE METAL. PREHEAT FOR E80XX-X FILLER METAL SHALL BE AS FOR GROUP C; FOR HIGHER STRENGTH FILLER METAL TREAT AS GROUP D.

TABLE 3 RECOMMENDED PREHEAT AND INTERPASS TEMPERATURES FOR SELECTED CARBON STEELS

AISI-SAE STEEL SPECIFICATIONS	RECOMMENDED WELDING CONDITIONS										
	CARBON RANGE, %[A]	THICKNESS RANGE		MINIMUM PREHEAT AND INTERPASS TEMPERATURE				POSTWELD HEAT TREATMENT			PEENING MAY BE NECESSARY
				LOW HYDROGEN		OTHER THAN LOW HYDROGEN		DESIRABLE OR OPTIONAL	TEMPERATURE RANGE		
		MM	IN.	°C	°F	°C	°F		°C	°F	
1008, 1010, 1011, 1012, 1013	WITHIN SPECIFICATION	≤50	≤2	AMBIENT[B]		AMBIENT[B]		OPTIONAL	590-675	1100-1250	. . .
		>50 TO 100	>2 TO 4	38	100	65	150	OPTIONAL	590-675	1100-1250	YES
1015, 1016	WITHIN SPECIFICATION	≤50	≤2	AMBIENT[B]		AMBIENT[B]		OPTIONAL	590-675	1100-1250	. . .
		>50 TO 100	>2 TO 4	38	100	93	200	OPTIONAL	590-675	1100-1250	YES
1017, 1018, 1019	WITHIN SPECIFICATION	≤50	≤2	AMBIENT[B]		AMBIENT[B]		OPTIONAL	590-675	1100-1250	. . .
		>50 TO 100	>2 TO 4	38	100	121	250	OPTIONAL	590-675	1100-1250	YES
1020, 1021, 1022, 1023	WITHIN SPECIFICATION	≤50	≤2	AMBIENT[B]		38	100	OPTIONAL	590-675	1100-1250	. . .
		>50 TO 100	>2 TO 4	93	200	149	300	OPTIONAL	590-675	1100-1250	YES
1024, 1027	0.18-0.25	≤25	≤1	AMBIENT[B]		38	100	OPTIONAL	590-675	1100-1250	. . .
		>25 TO 50	>1 TO 2	38	100	93	200	OPTIONAL	590-675	1100-1250	. . .
		>50 TO 100	>2 TO 4	93	200	149	300	OPTIONAL	590-675	1100-1250	YES
	0.25-0.29	≤13	≤ 1/2	10	50	65	150	OPTIONAL	590-675	1100-1250	. . .

		>13 TO 25	> 1/2 TO 1	65	150	149	300	OPTIONAL	590-675	1100-1250	. . .
		>25 TO 50	>1 TO 2	121	250	149	300	OPTIONAL	590-675	1100-1250	. . .
		>50 TO 100	>2 TO 4	149	300	177	350	OPTIONAL	590-675	1100-1250	YES
1025	WITHIN SPECIFICATION	≤25	≤1	AMBIENT(B)		AMBIENT(B)		OPTIONAL	590-675	1100-1250	. . .
		>25 TO 50	>1 TO 2	AMBIENT(B)		38	100	OPTIONAL	590-675	1100-1250	. . .
		>50 TO 100	>2 TO 4	38	100	93	200	OPTIONAL	590-675	1100-1250	YES
1026, 1029, 1030	0.25-0.30	≤25	≤1	AMBIENT(B)		38	100	DESIRABLE	590-675	1100-1250	. . .
		>25 TO 50	>1 TO 2	38	100	93	200	DESIRABLE	590-675	1100-1250	YES
		>50 TO 100	>2 TO 4	93	200	149	300	DESIRABLE	590-675	1100-1250	YES
	0.31-0.34	≤13	≤ 1/2	AMBIENT(B)		38	100	DESIRABLE	590-675	1100-1250	. . .
		>13 TO 25	> 1/2 TO 1	38	100	93	200	DESIRABLE	590-675	1100-1250	. . .
		>25 TO 50	>1 TO 2	93	200	149	300	DESIRABLE	590-675	1100-1250	YES
		>50 TO 100	>2 TO 4	121	250	177	350	DESIRABLE	590-675	1100-1250	YES
1035, 1037	WITHIN SPECIFICATION	≤13	≤ 1/2	AMBIENT(B)		38	100	DESIRABLE	590-675	1100-1250	. . .
		>13 TO 25	> 1/2 TO 1	38	100	93	200	DESIRABLE	590-675	1100-1250	. . .

		>25 TO 50	>1 TO 2	93	200	149	300	DESIRABLE	590-675	1100-1250	YES
		>50 TO 100	>2 TO 4	149	300	205	400	DESIRABLE	590-675	1100-1250	YES
1036, 1041	0.30-0.35	≤13	$\leq \frac{1}{2}$	38	100	93	200	DESIRABLE	590-675	1100-1250	. . .
		>13 TO 25	$> \frac{1}{2}$ TO 1	65	150	149	300	DESIRABLE	590-675	1100-1250	. . .
		>25 TO 50	>1 TO 2	121	250	149	300	DESIRABLE	590-75	100-1250	YES
		>50 TO 100	>2 TO 4	149	300	177	350	DESIRABLE	590-675	1100-1250	YES
	0.36-0.40	≤13	$\leq \frac{1}{2}$	65	150	93	200	DESIRABLE	590-675	1100-1250	. . .
		>13 TO 25	$> \frac{1}{2}$ TO 1	93	200	149	300	DESIRABLE	590-675	1100-1250	. . .
		>25 TO 50	>1 TO 2	149	300	177	350	DESIRABLE	590-675	100-1250	YES
		>50 TO 100	>2 TO 4	177	350	205	400	DESIRABLE	590-675	1100-1250	YES
	0.41-0.44	≤13	$\leq \frac{1}{2}$	93	200	149	300	DESIRABLE	590-675	1100-1250	. . .
		>13 TO 25	$> \frac{1}{2}$ TO 1	149	300	177	350	DESIRABLE	590-675	1100-1250	. . .
		>25 TO 50	>1 TO 2	177	350	205	400	DESIRABLE	590-675	1100-1250	YES
		>50 TO 100	>2 TO 4	205	400	230	450	DESIRABLE	590-675	1100-1250	YES
1038, 1039, 1040	0.34-0.40	≤13	$\leq \frac{1}{2}$	38	100	93	200	DESIRABLE	590-675	1100-1250	. . .

		>13 TO 25	> 1/2 TO 1	93	200	149	300	DESIRABLE	590-675	1100-1250	. . .
		>25 TO 50	>1 TO 2	121	250	177	350	DESIRABLE	590-675	1100-1250	YES
		>50 TO 100	>2 TO 4	149	300	205	400	DESIRABLE	590-675	1100-1250	YES
	0.41-0.44	≤13	≤ 1/2	65	150	121	250	DESIRABLE	590-675	1100-1250	. . .
		>13 TO 25	> 1/2 TO 1	93	200	149	300	DESIRABLE	590-675	1100-1250	. . .
		>25 TO 50	>1 TO 2	149	300	177	350	DESIRABLE	590-675	1100-1250	YES
		>50 TO 100	>2 TO 4	205	400	230	450	DESIRABLE	590-675	1100-1250	YES
1042, 1043	WITHIN SPECIFICATION	≤13	≤ 1/2	93	200	149	300	DESIRABLE	590-675	1100-1250	YES
		>13 TO 25	> 1/2 TO 1	121	250	149	300	DESIRABLE	590-675	1100-1250	YES
		>25 TO 50	>1 TO 2	149	300	177	350	DESIRABLE	590-675	1100-1250	YES
		>50 TO 100	>2 TO 4	205	400	230	450	DESIRABLE	590-675	1100-1250	YES
1044, 1045, 1046	WITHIN SPECIFICATION	≤13	≤ 1/2	149	300	177	350	DESIRABLE	590-675	1100-1250	YES
		>13 TO 100	> 1/2 TO 4	205	400	230	450	DESIRABLE	590-675	1100-1250	YES
1048, 1049, 1050, 1052, 1053	0.43-0.50	≤25	≤1	93	200	149	300	DESIRABLE	590-675	1100-1250	YES
		>25 TO 50	>1 TO 2	149	300	177	350	DESIRABLE	590-675	1100-1250	YES

		>50 TO 100	>2 TO 4	205	400	230	450	DESIRABLE	590-675	1100-1250	YES
1108, 1109, 1110	WITHIN SPECIFICATION	≤50	≤2	AMBIENT[B]		NOT RECOMMENDED		OPTIONAL	590-675	1100-1250	. . .
		>50 TO 100	>2 TO 4	38	100	NOT RECOMMENDED		OPTIONAL	590-675	1100-1250	YES
1116, 1117, 1118, 1119	WITHIN SPECIFICATION	≤25	≤1	AMBIENT[B]		NOT RECOMMENDED		OPTIONAL	590-675	1100-1250	. . .
		>25 TO 100	>1 TO 4	93	200	NOT RECOMMENDED		OPTIONAL	590-675	1100-1250	YES
1132, 1137, 1139, 1140, 1141, 1144, 1145, 1146, 1151	0.27-0.30	≤13	$\leq \frac{1}{2}$	10	50	NOT RECOMMENDED		OPTIONAL	590-675	1100-1250	. . .
		>13 TO 25	$>\frac{1}{2}$ TO 1	38	100	NOT RECOMMENDED		DESIRABLE	590-675	1100-1250	. . .
		>25 TO 50	>1 TO 2	93	200	NOT RECOMMENDED		DESIRABLE	590-675	1100-1250	YES
		>50 TO 100	>2 TO 4	121	250	NOT RECOMMENDED		DESIRABLE	590-675	1100-1250	YES
	0.31-0.35	≤13	$\leq \frac{1}{2}$	38	100	NOT RECOMMENDED		DESIRABLE	590-675	1100-1250	. . .
		>13 TO 25	$>\frac{1}{2}$ TO 1	65	150	NOT RECOMMENDED		OPTIONAL	590-675	1100-1250	. . .
		>25 TO 50	>1 TO 2	121	250	NOT RECOMMENDED		DESIRABLE	590-675	1100-1250	YES
		>50 TO 100	>2 TO 4	149	300	NOT RECOMMENDED		DESIRABLE	590-675	1100-1250	YES
	0.36-0.40	≤13	$\leq \frac{1}{2}$	65	150	NOT RECOMMENDED		DESIRABLE	590-675	1100-1250	. . .
		>13 TO 25	$>\frac{1}{2}$	93	200	NOT RECOMMENDED		DESIRABLE	590-675	1100-1250	. . .

			TO 1							
		>25 TO 100	>1 TO 4	149	300	NOT RECOMMENDED	DESIRABLE	590-675	1100-1250	YES
	0.41-0.45	≤13	≤ $\frac{1}{2}$	93	200	NOT RECOMMENDED	DESIRABLE	590-675	1100-1250	. . .
		>13 TO 25	> $\frac{1}{2}$ TO 1	149	300	NOT RECOMMENDED	DESIRABLE	590-675	1100-1250	. . .
		>25 TO 100	>1 TO 4	177	350	NOT RECOMMENDED	DESIRABLE	590-675	1100-1250	YES
	0.45-0.50	≤13	≤ $\frac{1}{2}$	149	300	NOT RECOMMENDED	DESIRABLE	590-675	1100-1250	. . .
		>13 TO 25	> $\frac{1}{2}$ TO 1	205	400	NOT RECOMMENDED	DESIRABLE	590-675	1100-1250	. . .
		>25 TO 100	>1 TO 4	230	450	NOT RECOMMENDED	OPTIONAL	590-675	1100-1250	YES
1211, 1212, 1213, 1215, B1111, B1112, B1113	WITHIN SPECIFICATION	≤50	≤2	AMBIENT[B]		NOT RECOMMENDED	OPTIONAL	590-675	1100-1250	. . .
		>50 TO 100	>2 TO 4	38	100	NOT RECOMMENDED	OPTIONAL	590-675	1100-1250	YES
12L 13[C], 12L 14[C]	WITHIN SPECIFICATION	≤50	≤2	AMBIENT[B]		NOT RECOMMENDED	OPTIONAL	590-675	1100-1250	. . .
		>50 TO 100	>2 TO 4	38	100	NOT RECOMMENDED	OPTIONAL	590-675	1100-1250	YES
1330, 1335, 1340, 1345	0.27-0.33	≤13	≤ $\frac{1}{2}$	121	250	NOT RECOMMENDED	DESIRABLE	550-565	1025-1050	. . .
		>13 TO 25	> $\frac{1}{2}$ TO 1	149	300	NOT RECOMMENDED	DESIRABLE	550-565	1025-1050	. . .
		>25 TO 50	>1 TO 2	177	350	NOT RECOMMENDED	DESIRABLE	550-565	1025-1050	YES

	0.33-0.38	≤13	≤ $\frac{1}{2}$	149	300	NOT RECOMMENDED	DESIRABLE	550-565	1025-1050	. . .
		>13 TO 25	> $\frac{1}{2}$ TO 1	205	400	NOT RECOMMENDED	DESIRABLE	550-565	1025-1050	. . .
		>25 TO 50	>1 TO 2	205	400	NOT RECOMMENDED	DESIRABLE	550-565	1025-1050	YES
	0.38-0.43	≤13	≤ $\frac{1}{2}$	177	350	NOT RECOMMENDED	DESIRABLE	550-565	1025-1050	. . .
		>13 TO 25	> $\frac{1}{2}$ TO 1	230	450	NOT RECOMMENDED	DESIRABLE	550-565	1025-1050	. . .
		>25 TO 50	>1 TO 2	290(D)	550(D)	NOT RECOMMENDED	DESIRABLE	550-565	1025-1050	YES
	0.43-0.49	≤13	≤ $\frac{1}{2}$	205	400	NOT RECOMMENDED	DESIRABLE	550-565	1025 1050	. . .
		>13 TO 25	> $\frac{1}{2}$ TO I	260(D)	500	NOT RECOMMENDED	DESIRABLE	550-565	1025-1050	. . .
		>25 TO 50	>1 TO 2	315	600(D)	NOT RECOMMENDED	DESIRABLE	550-565	1025-1050	YES
1513, 1518, 1522, 1525	≤0.20	≤25	≤1	AMBIENT(B)		AMBIENT(B)	OPTIONAL	590-675	1100-1250	. . .
		>25 TO 50	> 1 TO 2	AMBIENT(B)		38	100	OPTIONAL	590-675	1100-1250	. . .
		>50 TO 100	>2 TO 4	38	100	93	200	OPTIONAL	590-675	1100-1250	YES
	0.21-0.25	≤25	≤1	AMBIENT(B)		38	100	OPTIONAL	590-675	1100-1250	. . .
		>25 TO 50	>1 TO 2	38	100	93	200	OPTIONAL	590-675	1100-1250	. . .
		>50 TO 100	>2 TO 4	93	200	149	300	OPTIONAL	590-675	1100-1250	YES
	0.26-0.29	≤13	≤ $\frac{1}{2}$	10	50	65	150	OPTIONAL	590-675	1100-1250	. . .

		>13 TO 25	> 1/2 TO 1	65	150	149	300	OPTIONAL	590-675	1100-1250	. . .
		>25 TO 50	>1 TO 2	121	250	149	300	OPTIONAL	590-675	1100-1250	. . .
		>50 TO 100	>2 TO 4	149	300	177	350	OPTIONAL	590-675	1100-1250	YES
1524, 1526, 1527	≤ 0.25	≤ 25	≤ 1	10	50	38	100	OPTIONAL	590-675	1100-1250	. . .
		>25 TO 50	>1 TO 2	38	100	93	200	OPTIONAL	590-675	1100-1250	. . .
		>50 TO 100	>2 TO 4	93	200	149	300	OPTIONAL	590-675	1100-1250	YES
	0.26-0.29	≤ 25	≤ 1	65	150	121	250	DESIRABLE	590-675	1100-1250	. . .
		>25 TO 50	>1 TO 2	121	250	149	300	DESIRABLE	590-675	1100-1250	. . .
		>50 TO 100	>2 TO 4	149	300	177	350	DESIRABLE	590-675	1100-1250	YES
1536, 1541	≤ 0.35	≤ 13	≤ 1/2	38	100	93	200	DESIRABLE	590-675	1100-1250	. . .
		>13 TO 25	> 1/2 TO 1	65	150	149	300	DESIRABLE	590-675	1100-1250	. . .
		>25 TO 50	>1 TO 2	121	250	149	300	DESIRABLE	590-675	1100-1250	YES
		>50 TO 100	>2 TO 4	149	300	177	350	DESIRABLE	590-675	1100-1250	YES
	0.364-0.40	≤ 13	≤ 1/2	65	150	93	200	DESIRABLE	590-675	1100-1250	. . .
		>13 TO 25	> 1/2 TO 1	93	200	149	300	DESIRABLE	590-675	1100-1250	. . .

		>25 TO 50	>1 TO 2	149	300	177	350	DESIRABLE	590-675	1100-1250	YES
		>50 TO 100	>2 TO 4	177	350	205	400	DESIRABLE	590-675	1100-1250	YES
	0.414-0.44	≤ 13	≤ $\frac{1}{2}$	93	200	149	300	DESIRABLE	590-675	1100-1250	. . .
		>13 TO 25	> $\frac{1}{2}$ TO 1	149	300	177	350	DESIRABLE	590-675	1100-1250	. . .
		>25 TO 50	>1 TO 2	177	350	205	400	DESIRABLE	590-675	1100-1250	YES
		>50 TO 100	>2 TO 4	205	400	230	450	DESIRABLE	590-675	1100-1250	YES
1547, 1548	0.43-0.52	≤ 13	≤ $\frac{1}{2}$	149	300	177	350	DESIRABLE	590-675	1100-1250	. . .
		>13 TO 100	> $\frac{1}{2}$ TO 4	205	400	230	450	DESIRABLE	590-675	1100-1250	YES

Source: Ref 5

(A) RANGES ARE INCLUSIVE.

(B) AMBIENT ABOVE -12 °C (10 °F).

(C) DUE TO LEAD CONTENT, MANUFACTURING OPERATIONS INVOLVING ELEVATED TEMPERATURES IN THE RANGE OF THOSE ENCOUNTERED IN GAS CUTTING OR WELDING SHOULD BE CARRIED OUT WITH ADEQUATE VENTILATION.

(D) HOLD AT TEMPERATURE FOR 1 H AFTER WELDING IS COMPLETED.

Particular care must be exercised when dealing with weldments made at low heat inputs (high cooling rates). Tack welds are usually short, low-heat-input welds that cool rapidly. The first pass of a multipass weld in a large structure may be made at low heat input (to avoid bum-through) or on a relatively cold workpiece. Again, cooling rates may be high. It is essential that proper preheat be used under these circumstances, because the likelihood of martensite formation is much greater, given the rapid cooling rates.

Heat input control can also be used to reduce the cooling rate. The use of a higher heat input to slow cooling may not always be commensurate with good welding practice. For example, the resultant bead size may be too large, or the welding parameters (current, voltage, travel speed) needed to achieve the required heat input level may be outside the operating window of the electrode.

Postweld heat treatment may involve holding the completed weld at or near the interpass temperature for a period of time sufficient to allow hydrogen to escape the weld area. This temperature should be above the temperature range where cracking occurs (approximately 200 °C, or 390 °F).

If the interpass and postweld soak temperature are held above the martensite start temperature, M_s, for a sufficient length of time, isothermal transformation to a less susceptible microstructure will occur (for example, bainitic structure with some ferrite). A tempered martensite, however, will generally have better toughness than the isothermal transformation product, so this procedure should be used only when a stress relief is not possible.

The use of a proper postweld treatment may allow a reduction in the preheat temperature because both treatments serve the same purpose (that is, reducing the weld metal cooling rate). A lower preheat will increase operator comfort.

In the event that martensite formation cannot be avoided (as may be the case in a medium- to high-carbon steel), or when joint restraint is high, it is advisable to postweld heat treat the weldment to produce a less brittle, tempered martensite. The weldment should be held at or near the interpass temperature until postweld heat treatment can be done. This will reduce the possibility of cracking before the postweld heat treatment. Postweld heat treating of carbon steels is normally performed in the 600 to 650 °C (1110 to 1200 °F) range. The soak time is usually 1 h/in. of the thickest member. Many codes (for example, the ASME Boiler and Pressure Vessel Code) define when postweld heat treatment is to be done. Figure 4 can also be used as a guide for determining when postweld heat treatment should be done.

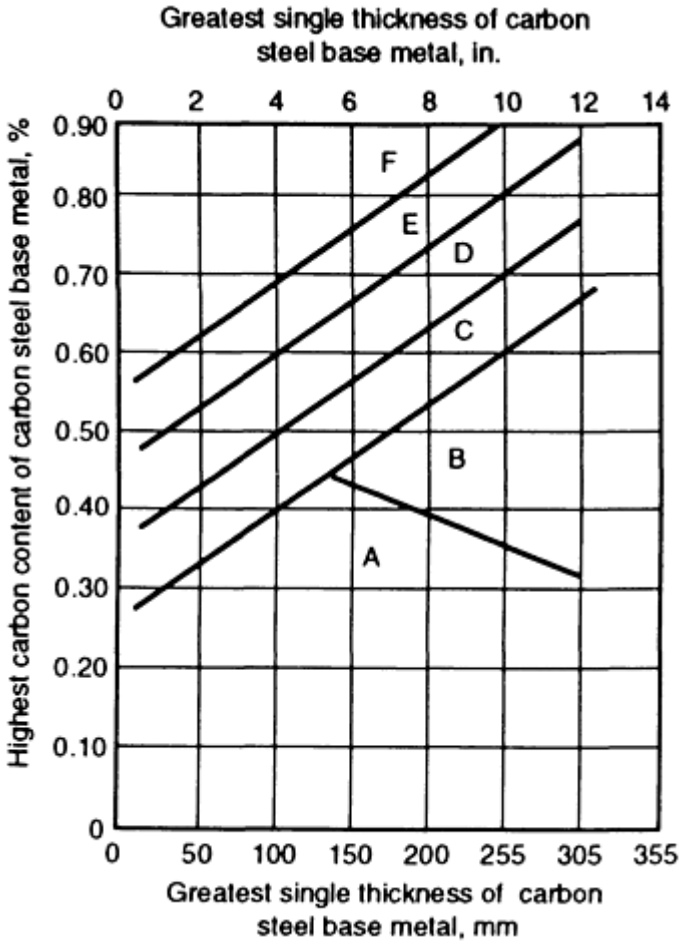

FIG. 4 PLOT OF BASE-METAL CARBON CONTENT VERSUS BASE-METAL THICKNESS OF CARBON STEELS TO SHOW DEGREE OF STRESS RELIEF REQUIRED. A, POSTWELD HEATING IS SELDOM REQUIRED. B, POSTWELD HEATING IS REQUIRED ONLY FOR DIMENSIONAL STABILITY, AS WHEN PARTS ARE TO BE FINISH MACHINED AFTER WELDING. C, POSTWELD STRESS RELIEF IS HIGHLY DESIRABLE FOR REPETITIVELY LOADED OR SHOCK-LOADED STRUCTURES AND FOR RESTRAINED JOINTS HAVING A THICKNESS GREATER THAN 25 MM (1 IN.). D, POSTWELD STRESS RELIEF IS REQUIRED FOR ALL REPETITIVELY LOADED OR SHOCK-LOADED STRUCTURES, FOR ALL RESTRAINED JOINTS, AND FOR ALL THICKNESSES OVER 50 MM (2 IN.); IT IS ALSO DESIRABLE FOR STATICALLY LOADED STRUCTURES. E, POSTWELD STRESS RELIEF IS RECOMMENDED FOR ALL APPLICATIONS; NO INTERMEDIATE COOLDOWN SHOULD BE PERMITTED FOR RESTRAINED STRUCTURES OR FOR BASE METAL HAVING A THICKNESS GREATER THAN 50 MM (2 IN.). F, SAME AS E, EXCEPT HAZARDS ARE GREATER

Bead Tempering. In a multipass weld, the underlying weld metal is subjected to repeated thermal cycles. This extends the time for hydrogen to diffuse out of the weld area, and it tempers any martensite that may have previously formed. Each bead also provides the preheat for the subsequent weld pass. The final bead and the HAZ it creates will not receive this same benefit. If the base metal is crack-sensitive, the final bead should be placed so that the HAZ does not form in the base metal (Fig. 5).

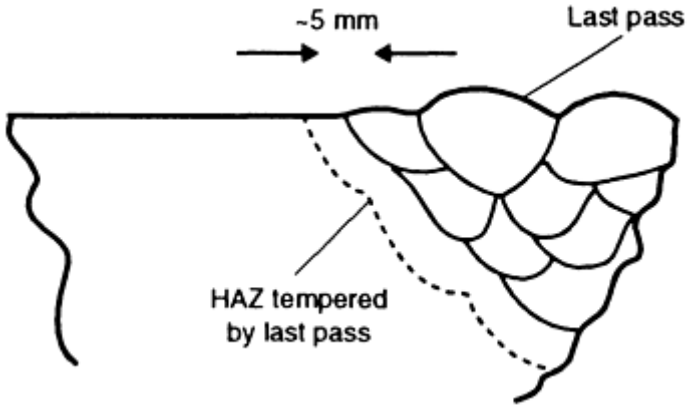

FIG. 5 BEAD TEMPERING. THE LAST BEAD IS PLACED SO ITS HAZ IS FORMED IN THE WELD METAL RATHER THAN IN THE MORE HARDENABLE BASE METAL. SOURCE: REF 1

Use of Low-Hydrogen Processes and Consumables. The principal source of weld metal hydrogen is the welding consumable(s). Careful selection of low-hydrogen consumables or low-hydrogen processes (such as gas-metal arc welding) can greatly reduce hydrogen pickup. This is especially important with medium- to high-carbon steels, in which the formation of a hard, brittle martensite is more likely. Many new specifications (for example, AWS A5.*x* filler metal specifications) now provide methods for consumable classification based on the diffusible hydrogen levels of their deposited weld metals. A standardized procedure is prescribed for measuring the diffusible hydrogen (for AWS specifications, this is AWS A4.3, while in many other parts of the world ISO 3690 is used). Designators are then used to indicate the maximum hydrogen level that an electrode will produce. The AWS uses a logarithmic scale; the International Institute of Welding method uses a linear system (Table 4).

TABLE 4 CLASSIFICATION OF CONSUMABLES RELATIVE TO THE DIFFUSIBLE HYDROGEN LEVELS OF THEIR DEPOSITED WELD METALS

SPECIFICATION	HYDROGEN LEVELS AT INDICATED DESIGNATIONS, ML/100 G		
	VERY LOW	LOW	HYDROGEN-CONTROLLED
AWS	<4[A]	<8[B]	<16[C]
IIW	<5	<10	<15

(A) H4.
(B) H8.
(C) H16

The extension of the AWS series down to diffusible hydrogen levels of less than 2 mL/100 g is feasible (for example, for gas-metal arc welding, flux-cored arc welding, or submerged arc welding). In both systems, an electrode that produces hydrogen in excess of the maximum, 16 mL/100 g (or 15 mL/100 g), is not considered hydrogen-controlled.

Use of Alternate Filler Materials. Often, the use of a softer, more ductile weld metal can help to absorb some of the high residual stresses in the weld area. The use of a lower-strength carbon steel electrode with greater ductility will reduce the high residual stresses in the HAZ and reduce the likelihood of cracking in the HAZ. Care must be exercised to be sure the decreased weld metal strength does not compromise the usefulness of the welded structure.

In higher carbon steels, austenitic weld metals are often used. They not only help reduce the stress level in the HAZ, but they also absorb and hold weld metal hydrogen. Austenite has a higher solubility for hydrogen, and the relatively low diffusivity of hydrogen in austenite ensures that little hydrogen will diffuse into the more susceptible HAZ. Caution must also be exercised here. The strength of the austenitic deposit will be lower than that of a carbon or alloy steel deposit. The austenitic filler material should be selected carefully to avoid other problems (for example, solidification cracking).

Methods for Determining Preheat/Heat Input. It is common practice to find preheat information by using published tables (for example, WRC Bulletin No. 326) or tables in applicable codes (for example, AWS D1.1). There are also various methods available that allow the fabricator to determine the necessary preheat (and/or heat input) by taking into account the effect of important variables such as steel composition, amount of restraint, and hydrogen level. Many codes, such as AWS D1.1 (Ref 3), Canadian Standard W59 (Ref 4), and British Standard 5135 (Ref 6), provide methods that the fabricator can use to determine preheat and/or heat input. The method used depends on the hardenability of the steel.

For lower hardenability steels, a hardness control method is used. The basis of this method is that welding conditions can be chosen that will give cooling rates slow enough to avoid the formation of a hard, brittle microstructure in the HAZ. Critical hardness levels, below which cracking is unlikely to occur, have been established. For high-hydrogen consumables, this critical hardness value is 350 HV, while for low-hydrogen consumables (<10 mL/100 g of diffusible hydrogen) it increases to 400 HV.

The cooling rate required to keep the HAZ hardness below the critical value is a function of the composition of the steel (this can be seen in Fig. 2). A carbon equivalent (CE) is used as an indicator of the hardenability of the steel. If the CE is known, Fig. 6 can be used to determine the cooling rate necessary to avoid cracking. Then the heat input and, if necessary, preheat to produce that cooling rate can be determined by using published data for various plate thicknesses. This is done graphically in AWS D1.1 (Ref 3) and CSA W59 (Ref 4) for determining the heat inputs necessary to make crackfree fillet welds without the need to preheat. Figure 7 is an example for submerged arc fillets with 13 mm ($\frac{1}{2}$ in.) flanges. Reference 7 (upon which specification BS 5135 is based) provides a more thorough treatment that allows one to determine the required heat inputs and, if necessary, preheat. An example of the graphical presentation is given in Fig. 8. Knowing the carbon equivalent, one can determine an energy input/preheat combination for a variety of plate thicknesses. The hardness control method is used for carbon steels up to CE = 0.6.

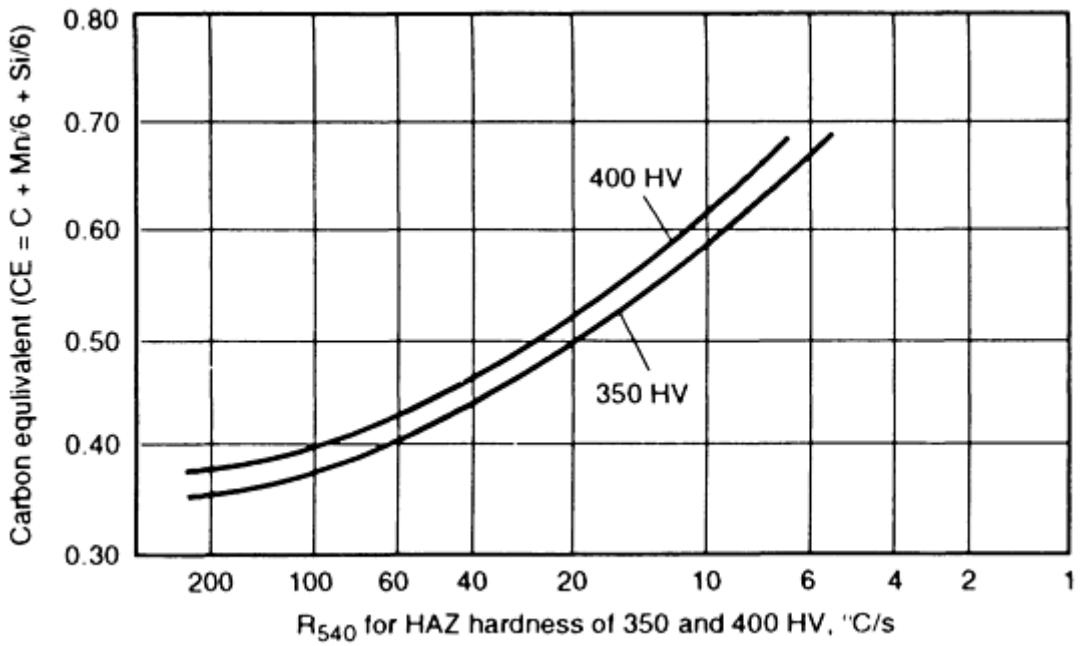

FIG. 6 CRITICAL COOLING RATES TO OBTAIN HARDNESS OF 350 HV (HIGH-HYDROGEN CONSUMABLES) AND 400 HV (LOW-HYDROGEN CONSUMABLES). R_{540} IS COOLING RATE AT 540 °C (1005 °F). SOURCE: REF 3

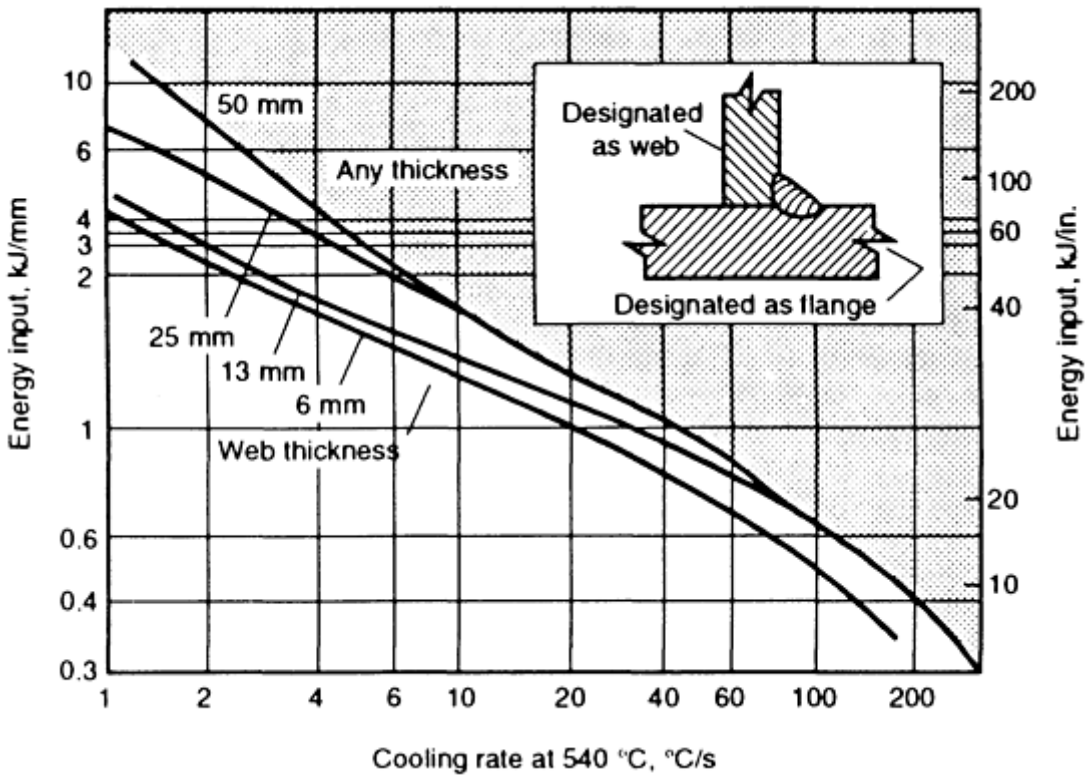

FIG. 7 PLOT OF MINIMUM ENERGY INPUT VERSUS CRITICAL COOLING RATE TO WELD SINGLE-PASS SAW FILLET WELD (WITH 13 MM, OR $\frac{1}{2}$ IN., FLANGES) WITHOUT PREHEAT. SOURCE: REF 3

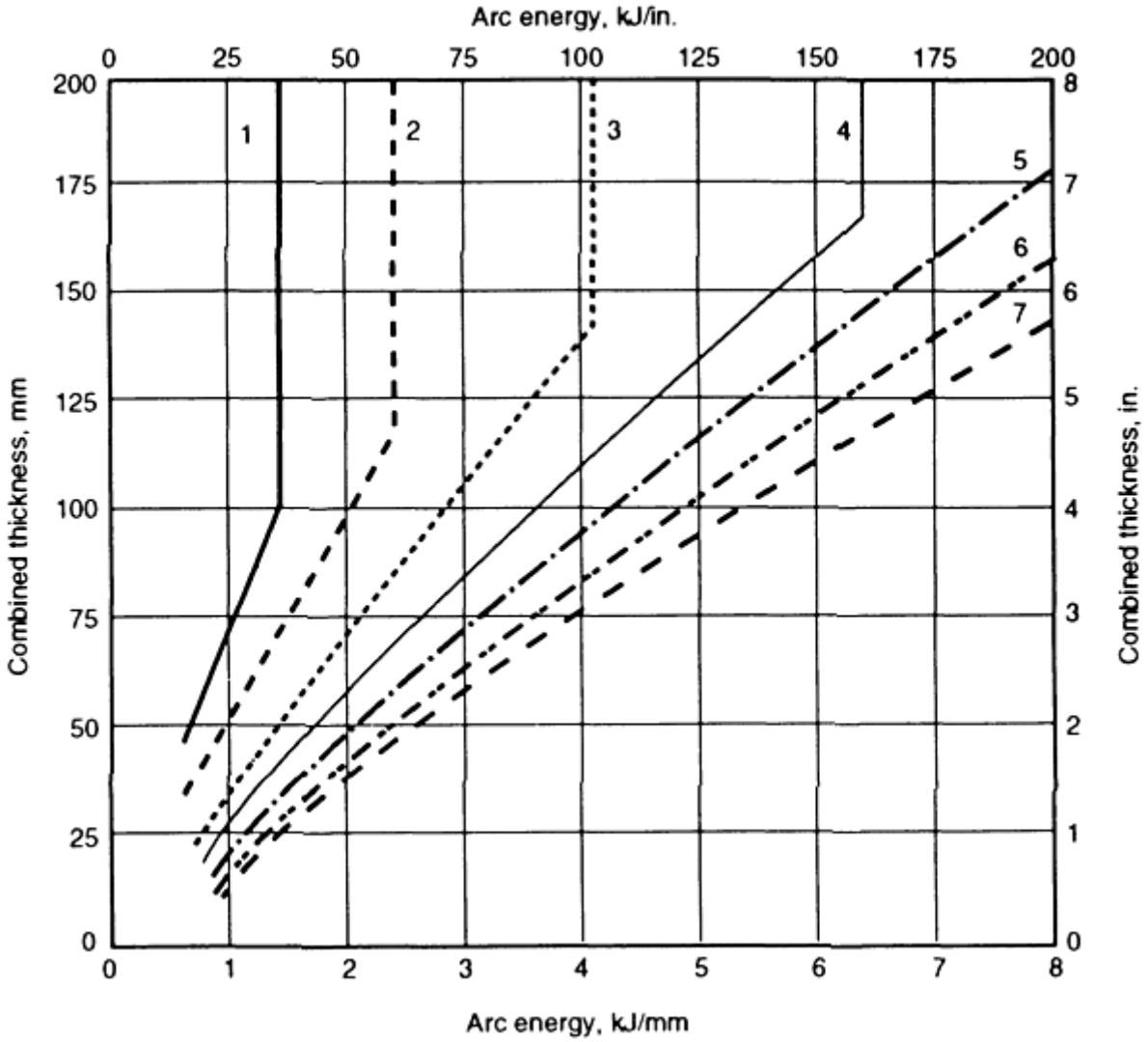

LINE	MINIMUM PREHEAT TEMPERATURE	
	°C	°F
1	175	**345**
2	150	**300**
3	125	**255**
4	100	**212**
5	75	**165**
6	20	**70**
7	**0**	**32**

CARBON EQUIVALENT OF STEEL	**AT HYDROGEN SCALE**	EQUIVALENT DIFFUSIBLE H_2, ML/100 G
≤0.47	A	**> 15**
≤0.49	B	**10-15**
≤0.51	C	**5-10**
≤0.57	**D**	**< 5**

FIG. 8 PLOT USED TO OBTAIN HEAT INPUT/PREHEAT COMBINATIONS FOR SPECIFIC CARBON EQUIVALENTS.

THE SCALES A, B, C, AND D REFER TO THE LEVEL OF DIFFUSIBLE HYDROGEN AS CERTIFIED BY THE ELECTRODE MANUFACTURER. SOURCE: REF 7

For higher hardenability steels, a hydrogen control method is used. Even slow cooling rates cannot prevent the formation of hard, brittle microstructures. In order to avoid cracking, a hydrogen control method is used. The hydrogen control method consists of holding the weld at an elevated temperature, above the range where cracking occurs, so that hydrogen can diffuse out of the weld area more rapidly. This method requires a preheat, an interpass temperature to maintain the heat, and a postweld soak to hold the heat after welding. Both AWS D1.1 (Appendix XI) (Ref 3) and CSA W59 (Appendix P) (Ref 4) provide a hydrogen control method that was designed for low-alloy steels and that may yield conservative results for carbon steels. Reference 7 provides a variety of data for different grades of steel. Figure 9 can be used for medium-carbon steels with up to 0.45% C.

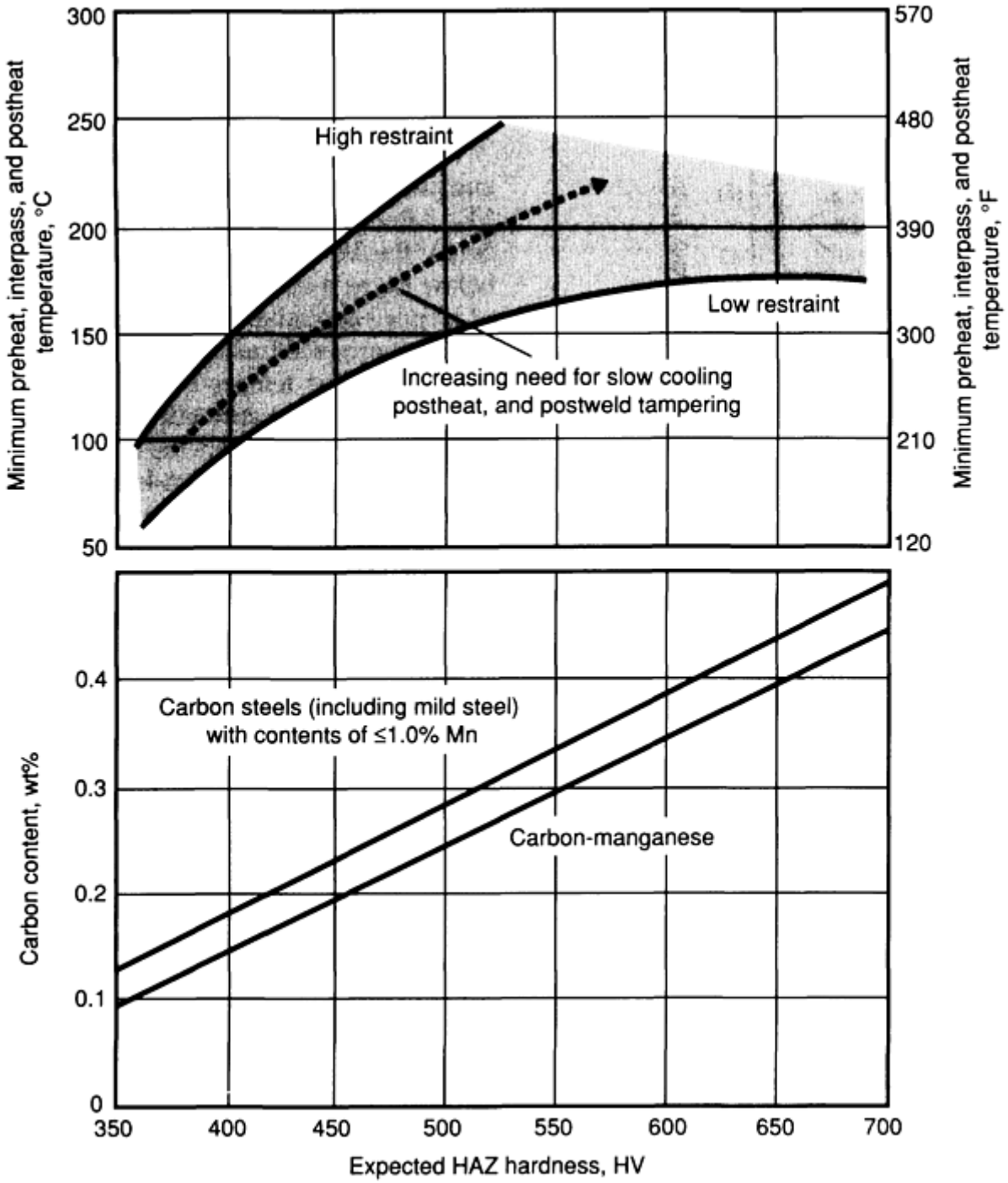

FIG. 9 PLOT FOR SELECTING PREHEAT, INTERPASS, AND POSTWELD SOAK TEMPERATURES FOR FULLY HARDENED CARBON STEELS USING HYDROGEN CONTROL METHOD. SOURCE: REF 7

Medium-carbon steels are often stress-relieved, especially at higher carbon levels, at higher restraint, and for welds exposed to shock or fatigue loading. When stress relief is not possible, an isothermal transformation method may be used. The use of this method requires knowledge about the isothermal transformation characteristics of the steel. By maintaining preheat, interpass, and postweld soak temperatures above the M_s for a sufficient length of time, a nonmartensitic microstructure is formed. This microstructure (usually bainite) will be less susceptible to hydrogen-induced cracking than martensite, but more susceptible than tempered martensite. For this reason, stress relieving is preferred when it can be done.

When even minimal preheat cannot be used with medium- or high-carbon steels, the use of an austenitic filler material should be considered. However, it should be noted that an austenitic filler cannot meet the yield strength requirements of a medium- or high-carbon steel. The high solubility of hydrogen in the austenitic weld metal and the slow diffusion rates limit the amount of hydrogen in the HAZ. At higher base-plate carbon levels (>0.4% C), a 150 °C (300 °F) preheat is recommended to reduce cracking tendency.

For high-carbon steels, the preheat, interpass, and postweld temperature should be equal to the M_s. After welding, the weld should be cooled below the M_s (60 to 70 °C, or 110 to 125 °F, below M_s as a minimum) to reduce the amount of retained austenite. A double temper treatment is then introduced as an additional heat treatment. The first temper treatment converts the remaining retained austenite to martensite. The second treatment tempers the martensite.

Overview of Hydrogen-Induced Cracking in Carbon Steels. The following guidelines apply to hydrogen-induced cracking in carbon steels.

Carbon steels with less than 0.2% C are generally not susceptible to cracking, and precautions are usually unnecessary.

Mild steels can be welded with hardness control methods. Up to CE of 0.40, cooling rates can be controlled by energy input, and preheat is usually not necessary except for thick plates. Above CE of 0.40, preheat is required except in thin sections. The use of low-hydrogen consumables is recommended at higher carbon and manganese levels and will reduce preheat requirements at all carbon equivalents. A heat-treated mild steel may require a low-alloy steel weld metal to match its properties. The resultant weld metal itself may be susceptible to hydrogen-induced cracking, and suitable precautions should be taken (such as using the hydrogen control method based on weld metal composition). Low-hydrogen consumables should be used.

Medium-carbon steels up to CE = 0.6 can be welded with hardness control methods. Above CE = 0.6, hydrogen control methods (preheat, interpass, and postweld soak) should be used with low-hydrogen consumables. Stress relief is recommended at high carbon levels (>0.45% C), for highly restrained welds, or for welds subjected to fatigue or shock loading. When stress relief is not possible, the isothermal transformation method should be considered.

High-carbon steels require preheat equal to the martensite start temperature, followed by a double temper. When tempering or isothermal transformation is not possible, the use of an austenitic filler material should be considered. Procedure testing for each specific application of high-carbon steel welding is essential.

Solidification Cracking

Solidification cracking occurs at high temperature, at the terminal stages of solidification. The cracks are easily recognized because they usually follow the weld centerline, although they do not always come to the surface. The cracks often appear towards the end of the weld, due to stresses arising from the thermal field. The crack surfaces are heavily oxidized, and dendritic structures can often be found upon examination with scanning electron microscopy.

Solidification cracks arise due to the formation of low melting compounds at grain boundaries. When a coherent solid network forms upon solidification, stresses start to build across the weld due to shrinkage. The low melting compounds remain molten, and the grain boundaries rupture under the shrinkage stresses. The conditions that control the extent of solidification cracking are the amount of impurities, the shape of the weld, and the stress level.

Impurities. Sulfur and phosphorus are the main causes of solidification cracking in carbon steel weld metal. Both will segregate to grain boundaries and form low melting compounds. In the case of sulfur, this is FeS, which tends to form a continuous film at the grain boundaries. The addition of a sufficient amount of manganese to the weld metal will cause MnS to form in preference to FeS. Manganese sulfide solidifies at a higher temperature and forms as globules, a morphology much less prone to cracking. Figure 10 shows the ratio of manganese to sulfur necessary to avoid cracking. Carbon also has a very strong effect, with the cracking tendency increasing with carbon content. At higher carbon levels, increasing the manganese-to-sulfur ratio is less effective, and it is more beneficial to lower the carbon content to avoid cracking. The effect of carbon is believed to be related to the phase, δ-ferrite or austenite, that forms upon solidification. At lower carbon contents, δ-ferrite, which has a relatively high solubility for sulfur and phosphorus, is the primary phase formed. As the carbon content increases, more austenite is formed upon solidification. Because austenite has a low solubility for sulfur and phosphorus, more of these impurities are rejected upon solidification and tend to build up at interdendritic boundaries.

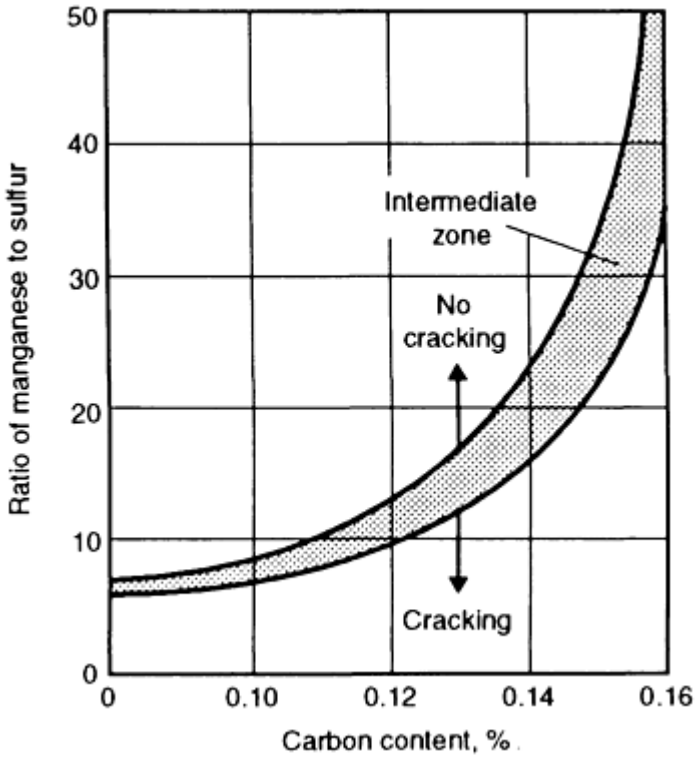

FIG. 10 EFFECT OF MANGANESE-TO-SULFUR RATIO AND CARBON CONTENT ON SOLIDIFICATION CRACKING TENDENCIES IN CARBON STEEL WELD METAL. SOURCE: REF 8

Welding consumables are kept deliberately low in sulfur and phosphorus to avoid problems. Base plates are the primary contributors of these impurities. Any high-dilution welding procedure or process (for example, submerged arc welding) will promote the pickup of impurities.

The shape of the weld bead and the solidification grain structure also affect solidification cracking (Fig. 11). Concave weld beads have a greater tendency to crack because their outer surface is stressed in tension. A slightly convex bead is always preferred. Deep narrow beads also have a greater tendency to crack. The depth-to-width ratio (d/w) should always be between 0.5 and 0.8.

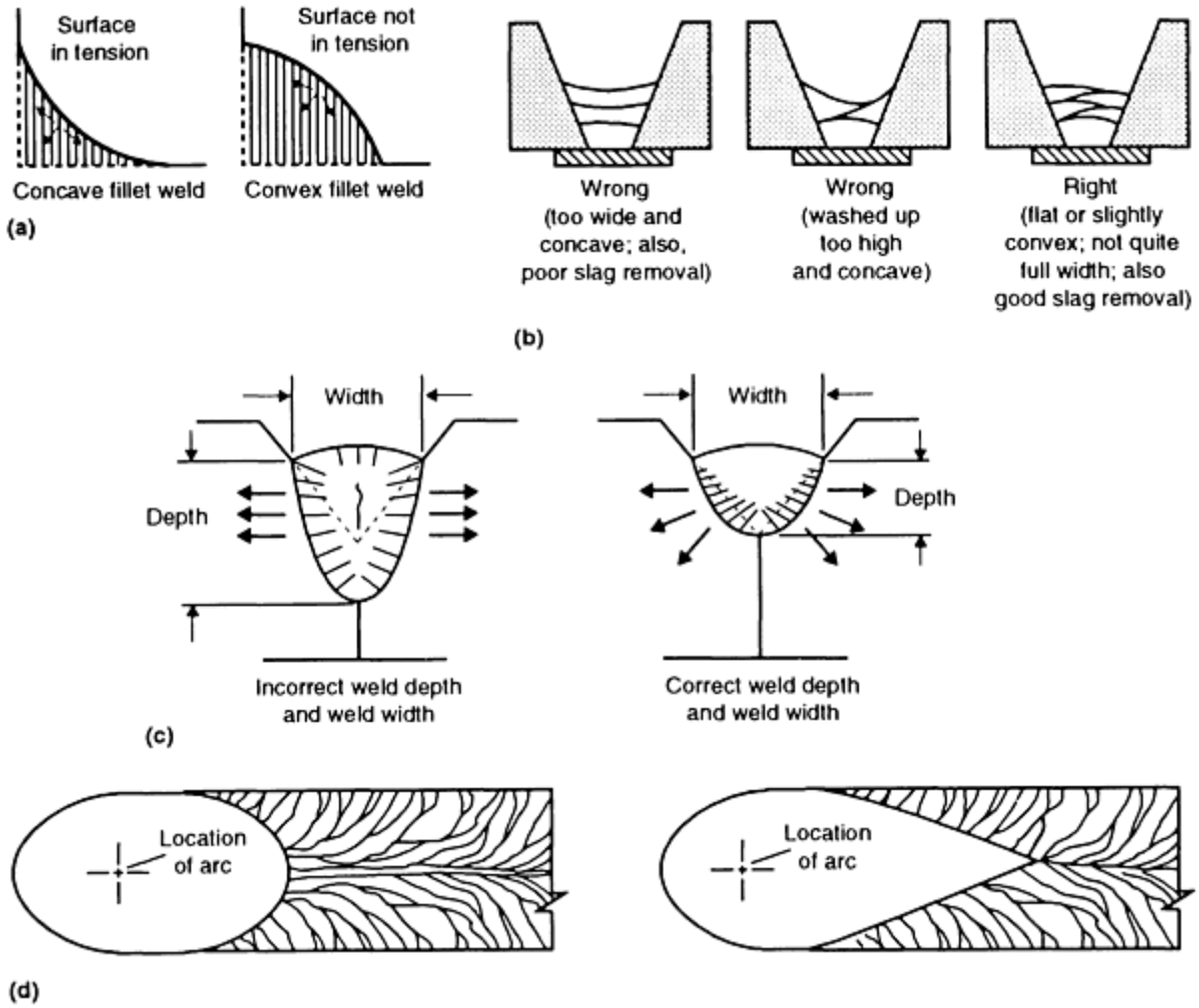

FIG. 11 EFFECT OF WELD BEAD SHAPE AND SOLIDIFICATION PATTERN ON SOLIDIFICATION CRACKING. (A) AND (B) CONCAVE VERSUS CONVEX BEAD SHAPES. SLIGHTLY CONVEX BEAD SHAPES ARE PREFERRED. (C) PREFERRED DEPTH AND WIDTH OF WELD BEAD. DEEP, NARROW BEADS SHOULD BE AVOIDED. (D) EFFECT OF TRAVEL SPEED ON CRACKING POTENTIAL. HIGH TRAVEL SPEEDS (TEARDROP-SHAPED PUDDLE, ON RIGHT) RESULT IN MORE CENTERLINE SEGREGATION AND A GREATER CHANCE OF CRACKING. SOURCE: REF 9, 10

High travel speeds tend to cause the dendrites growing from either side of the weld to meet head on. This results in heavy segregation of impurities at the weld centerline and a greater likelihood of centerline cracking. Teardrop-shaped puddles, which produce this type of solidification pattern, should be avoided if the weld metal is susceptible to hot cracking.

Weld Configuration. The greater the restraint in a joint, the greater the likelihood of solidification cracking. Particular care must be taken with root beads. They are generally small, highly diluted beads (a problem if the steel is high in carbon, sulfur, or phosphorus) that can be subjected to very high stresses. Concave weld beads should be avoided here also. A convex bead gives a better stress distribution and increases the throat dimension, thus providing more cross-sectional area to carry the stresses. A slight offset of the plates (Fig. 12) and freedom for them to move will reduce the residual stresses. If no offset is used, a gap at the root should be provided to allow for shrinkage movement. When welding higher-carbon steels, a low-carbon electrode will reduce the weld metal carbon level and decrease the likelihood of cracking.

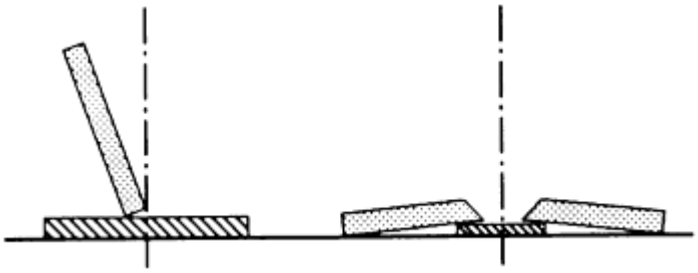

FIG. 12 DESIGN FOR OFFSETTING PLATES THAT ALLOWS THEM TO MOVE INTO FINAL POSITION, THEREBY REDUCING RESIDUAL STRESSES. SOURCE: REF 11

Welding of Free-Machining Steels. SAE-AISI series 11*xx* and 12*xx* steels are a particular problem because they contain high amounts of sulfur, phosphorus, or lead for improved machinability (see Tables 1(a) and 1(b)). The 11*xx* series steels are all resulfurized. The 12*xx* series steels are resulfurized and rephosphorized. The letter "L" after the first two numbers in any steel designation indicates the presence of lead.

All of these steels are susceptible to solidification cracking because of the high sulfur and phosphorus contents. High sulfur contents can also cause weld metal porosity. Lead can cause weld metal porosity or embrittlement, but the main concern is toxic fumes. Special precautions are required to ensure good ventilation during the welding of leaded steels.

When free-machining steels must be welded, a low-hydrogen consumable with a basic slag system is recommended. Low hydrogen will reduce the formation of hydrogen sulfide porosity, while the basic slag system reduces the sulfur and phosphorus content of the weld metal. Shielded metal arc welding electrodes such as E7015, E7016, and E7018 are preferred because they are the basic electrodes that produce the least base plate dilution. For gas-shielded flux-cored electrodes, E70T-5 and E71T-5 types are preferred over T-1 electrodes. Self-shielded flux-cored electrodes of the T-4, T-7 and T-8 types are recommended. Low currents should be used with all electrodes in order to minimize base plate dilution.

There is no guarantee that these precautions will eliminate the problem. Sometimes the best that can be achieved is a reduced level of cracking and/or porosity. The best advice is not to weld free-machining steel at all. Welding specifications can state that no component in a welded assembly should be produced from these materials. Overall, this will lead to the lowest total cost for the welded assembly.

Lamellar Tearing

Lamellar tearing is a form of cracking that occurs in the base metal beneath the weld (Fig. 13). It is caused by a combination of high, localized stresses from weld contraction and poor through-thickness ductility in the steel. The tearing is initiated by the separation of the interface between inclusions and metal (delamination) or by fracture of an inclusion itself. The cracks enlarge by linkage of delaminations in the same plane and by shear steps that join cracks on different planes. The controlling factors in lamellar tearing are:

- QUANTITY AND MORPHOLOGY OF NONMETALLIC INCLUSIONS (USUALLY SULFIDES OR SILICATES)
- MAGNITUDE OF THE INDUCED STRESSES NORMAL TO THE PLATE SURFACE

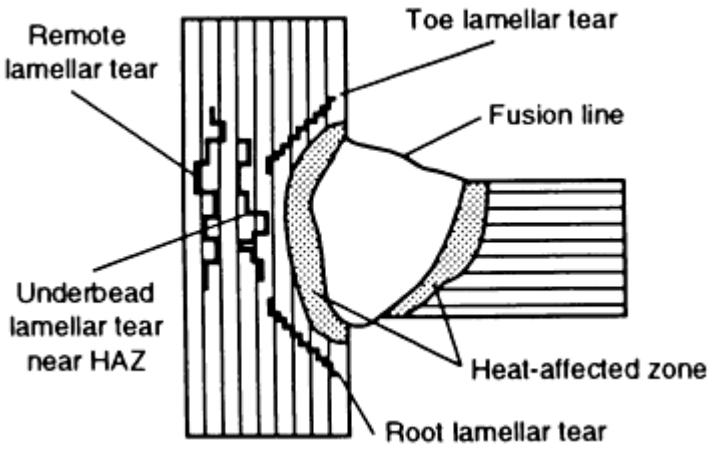

FIG. 13 ORIENTATION OF LAMELLAR TEARS IN A BASE METAL BELOW THE WELD. SOURCE: REF 4

During the hot rolling of plate, the inclusions become elongated in the rolling direction and tend to flatten out parallel to the surface of the plate. The ductility in the through-thickness direction is reduced because the bond between the inclusions and steel is much weaker than the steel itself. If the quantity of inclusions is high and if they have been sufficiently flattened during hot rolling, the steel may fail under high stresses in the thickness direction.

The magnitude of the induced stresses depends on the joint design, the degree of restraint imposed on the joint, the plate thickness, the orientation of the weld, and the size of the weld. Restrained corner or T-joints are the most susceptible to lamellar tearing because the fusion boundary is roughly parallel to the plate surface (Fig. 14) and through-thickness contraction stresses are high. Lamellar tearing in butt welds is rare. Thick-plate, high-imposed restraint (for example, rigid clamping) and large weld beads all increase residual stresses and the likelihood of tearing.

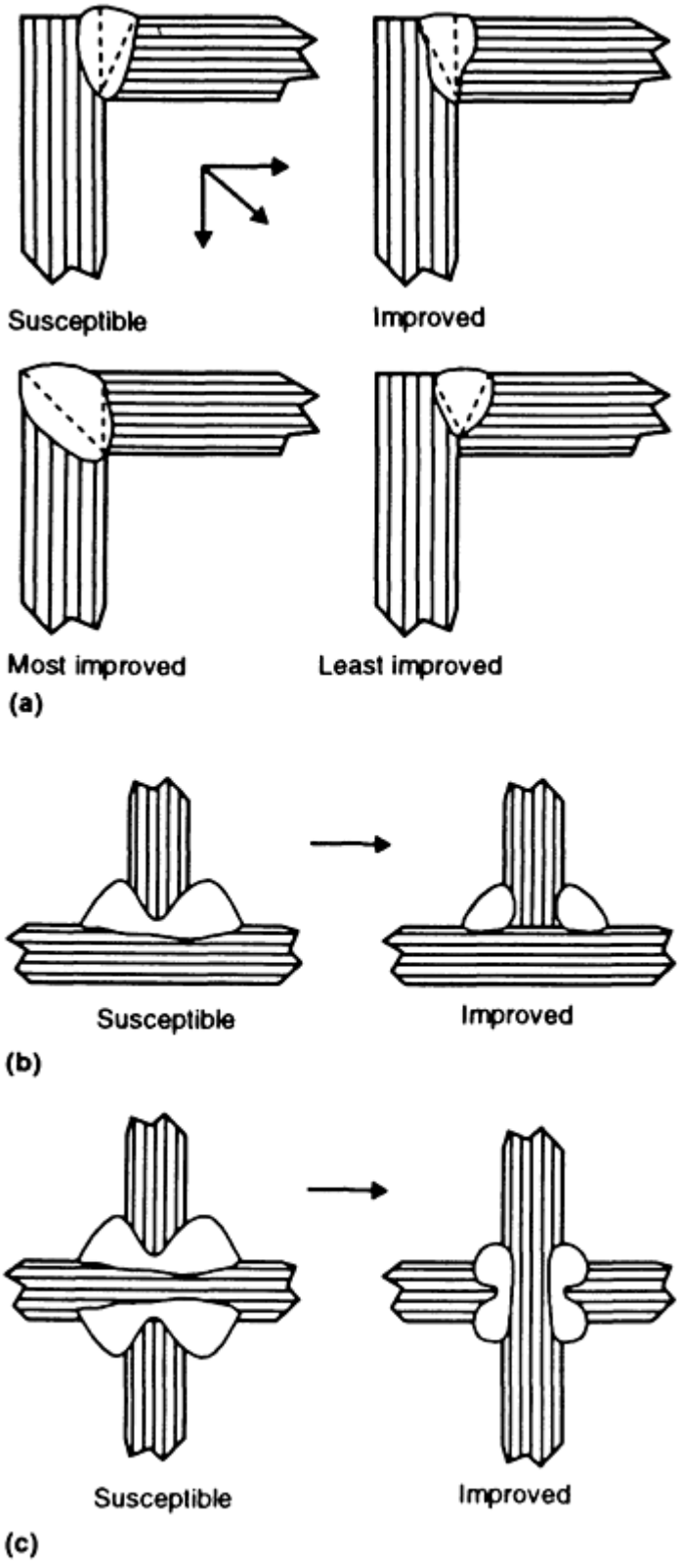

FIG. 14 METHODS USED TO REDUCE LAMELLAR TEARING. (A) ANGLING THE WELD FUSION LINE TO AVOID SHRINKAGE STRESSES IN THE THROUGH-THICKNESS DIRECTION. (B) USE OF SMALLER PARTIAL-PENETRATION WELDS TO REDUCE JOINT RESTRAINT. (C) PLACEMENT OF WELDING BEADS ON THE THINNER PLATE (WHEN WELDING PLATES OF DIFFERENT THICKNESSES) SO THAT SMALLER BEADS CAN BE USED. SOURCE: REF 4

Hydrogen has also been found to increase susceptibility to lamellar tearing. For this reason, a moderate preheat is sometimes beneficial in reducing the tendency to lamellar tearing. The use of low-hydrogen consumables is also beneficial.

Steps to avoid lamellar tearing include:

- USE OF PLATE MATERIAL WITH IMPROVED THROUGH-THICKNESS PROPERTIES. A REDUCTION IN OXYGEN CONTENT (BY ALUMINUM KILLING, FOR EXAMPLE) OR A REDUCTION IN SULFUR CONTENT WILL REDUCE THE AMOUNT OF INCLUSIONS IN THE STEEL. SULFUR UNDER 0.01% WILL GREATLY REDUCE THE RISK OF LAMELLAR TEARING. SULFIDE SHAPE CONTROL, THROUGH THE ADDITION OF RARE EARTHS OR CALCIUM TREATMENT DURING STEELMAKING, WILL ALTER THE INCLUSION MORPHOLOGY FROM STRINGERS TO DISCONTINUOUS GLOBULES.
- CHANGE THE JOINT DESIGN TO MINIMIZE THROUGH-THICKNESS CONTRACTION STRESSES (SEE FIG. 14 FOR EXAMPLES).
- USE LOWER-STRENGTH WELDING CONSUMABLES. THIS WILL ABSORB AND REDUCE SOME OF THE THROUGH-THICKNESS STRESS.
- IN EXTREME CASES, THE SURFACE OF THE PLATE MAY BE GROUND OR MACHINED TO A LEVEL BELOW WHERE LAMELLAR TEARING IS ANTICIPATED. THE AREA CAN THEN BE BUTTERED WITH WELD METAL AND THE ATTACHMENT WELD CAN BE MADE.

Porosity

Porosity in carbon steel weld metal may result from excessive amounts of carbon monoxide, nitrogen, hydrogen, or hydrogen sulfide remaining in the weld pool upon solidification.

Carbon monoxide is formed when oxygen combines with carbon in the weld puddle. The oxygen may come from the arc atmosphere, the welding consumables (especially fluxes), or the steel base material. Rimmed and capped steels contain low silicon (<0.05%) and high oxygen. When these types of steels are welded, the carbon and oxygen from the steel will react to form carbon monoxide, unless there is sufficient deoxidizer in the weld metal to prevent it. This deoxidizer (usually silicon) must come from the welding consumable. Higher levels of deoxidizer in the welding electrode are required when welding rimmed and capped steels. A killed steel is fully deoxidized during manufacture by the addition of silicon and/or aluminum or by vacuum treatment. Because it is the least costly, silicon (0.15 to 0.30%) is often used, although aluminum killing is becoming much more common. Killed steels are much less prone to carbon monoxide porosity, and consumables with a lower silicon level may often be used to weld them. A semikilled steel (0.05 to 0.10% Si) has a behavior that is intermediate to the rimmed and killed steels. It is important that the fabricator realize what deoxidation practice was used on the base material, especially for processes like autogenous gas-tungsten arc welding where no filler material is used.

The surface condition of the base material can also affect porosity levels. Millscale (iron oxide) or rust (hydrated iron oxide) adds additional oxygen to the weld puddle. Higher levels of deoxidizers in the consumables will be needed to prevent carbon monoxide porosity.

Nitrogen in the weld metal is most often the result of poor shielding. The amount of pickup will be increased by the use of excessive voltage (longer arc length), excessive travel speeds (effectively outrunning the shielding), broken electrode coatings, or unstable arc conditions (such as arc blow). A nitrogen-containing residue may be left on the surface of plasma cut plate when nitrogen is used as a cutting gas. Grinding of the surface may be necessary to avoid weld metal porosity.

Hydrogen has numerous sources, including atmospheric moisture, welding consumables (especially fluxes), and plate contaminants. The major source of hydrogen is the welding consumable. Hydrogen sources and pickup were discussed more fully in the section "Hydrogen-Induced Cracking" in this article.

Hydrogen sulfide is formed when high-hydrogen weld metal combines with high-sulfur (>0.04%) base plate. This type of porosity was discussed in the section "Welding of Free-Machining Steels" in this article.

There are many potential causes of porosity, too numerous to be covered in this article. Detailed information is available in the Section "Fusion Welding Processes" and the article "Overview of Weld Discontinuities" in this Volume.

References cited in this section

1. B.A. GRAVILLE, *THE PRINCIPLES OF COLD CRACKING CONTROL IN WELDS,* DOMINION BRIDGE COMPANY, 1975
2. H. GRANJON, *FUNDAMENTALS OF WELDING METALLURGY,* ABINGTON PUBLISHING, 1991, P 156-177
3. STRUCTURAL WELDING CODE, STEEL, AWS D1.1, AMERICAN WELDING SOCIETY, 1992
4. *WELDED STEEL CONSTRUCTION (METAL ARC WELDING),* CSA W59, CANADIAN STANDARDS ASSOCIATION, 1989
5. R.D. STOUT, *WELDABILITY OF STEELS,* 4TH ED., WELDING RESEARCH COUNCIL, 1987, P 420-426
6. *PROCESS OF ARC WELDING CARBON & CARBON MANGANESE STEELS,* BS5135, BRITISH STANDARDS INSTITUTE, 1984
7. F.R. COE, *WELDING STEELS WITHOUT HYDROGEN CRACKING,* THE WELDING INSTITUTE, 1973
8. J.F. LANCASTER, *THE METALLURGY OF WELDING,* 4TH ED., ALLEN AND UNWIN, 1987, P 157
9. *THE PROCEDURE HANDBOOK OF ARC WELDING,* LINCOLN ELECTRIC COMPANY, 1973, CHAPTERS 5 AND 12
10. W.F. SAVAGE AND A.H. ARONSON, *PREFERRED ORIENTATION IN THE WELD FUSION ZONE,* VOL 46, 1966
11. *WELDING HANDBOOK,* 8TH ED., VOL 1, AMERICAN WELDING SOCIETY, 1987, P 261

Arc Welding of Carbon Steels

Ronald B. Smith, The ESAB Group, Inc.

Process Selection

All of the arc welding processes are suitable for welding carbon steels. Choosing the best process to use for a particular application must take into account not only the material characteristics (sensitivity to porosity or cracking and the required mechanical properties), but also the details of the joint (plate thickness, joint design, welding position, and location) and weld economics (deposition rates and efficiencies, cost of labor, cost of consumables, capital cost of equipment, number of spare parts required, operator skills or training needed, set-up, and cleanup cost, and so on). There are many excellent reviews (Ref 9, 11, 12, 13) that discuss process selection and cost calculation details. Table 5 provides a brief guide that can be used to select a process for welding carbon steels.

TABLE 5 PROCESS SELECTION GUIDELINES FOR ARC WELDING CARBON STEELS

PARAMETERS	**SMAW**	**GMAW**	**FCAW**	**GTAW/PAW**	**SAW**	**EGW/ESW**	SW
USABILITY	VERY ADAPTABLE, ALL-POSITION PROCESS. CAN BE USED OUTDOORS. GIVES EXCELLENT JOINT ACCESSIBILITY. VERY PORTABLE. CAN BE USED ON CARBON STEELS DOWN TO 18 GAGE. JOINT PREPARATION IS REQUIRED ON THICKNESSES OVER 3.2 MM ($\frac{1}{8}$ IN.). UNLIMITED UPPER THICKNESS BUT OTHER PROCESSES (GMAW, FCAW, OR SAW) ARE USUALLY MORE ECONOMICAL.	AN ALL-POSITION PROCESS IN THE SHORT-ARC OR PULSED MODE. MODERATELY ADAPTABLE, BUT USE LIMITED OUTSIDE WHERE LOSS OF SHIELDING IS POSSIBLE. USABLE ON STEEL DOWN TO <0.25 MM (0.010 IN.) THICK. ABOVE 4.8 MM ($\frac{3}{16}$ IN.), REQUIRES JOINT PREPARATION. NO UPPER LIMIT OF PLATE THICKNESS.	ALL-POSITION PROCESS. EQUIPMENT SIMILAR TO GMAW, BUT SELF-SHIELDED VERSION HAS BETTER PORTABILITY AND IS USABLE OUTDOORS. MINIMUM PLATE THICKNESS IS 18 GAGE. FOR SELF-SHIELDED MATERIAL ABOVE 6.4 MM ($\frac{1}{4}$ IN.), REQUIRES JOINT PREPARATION. WITH CO_2 SHIELDING, MATERIALS ABOVE 13 MM ($\frac{1}{2}$ IN.) REQUIRE JOINT PREPARATION. THERE IS NO UPPER LIMIT ON PLATE THICKNESS.	AN ALL-POSITION PROCESS WITH FAIR JOINT ACCESSIBILITY. LIMITED OUTDOOR USE. CAN WELD VERY THIN MATERIAL IN ALL POSITIONS; GTAW--<0.13 MM (0.005 IN.) MIN. THICKNESS, JOINT PREP. OVER 3.2 MM ($\frac{1}{8}$ IN.) PAW--<0.13 MM (0.005 IN.) MIN. THICKNESS, JOINT PREP OVER 6.4 MM ($\frac{1}{4}$ IN.). NO UPPER LIMIT ON THICKNESS BUT OTHER PROCESSES ARE MORE EFFICIENT.	LIMITED TO FLAT AND HORIZONTAL POSITION. SEMI-AUTOMATIC VERSION HAS SOME ADAPTABILITY BUT PROCESS IS MOST OFTEN MECHANIZED AND HAS LIMITED PORTABILITY. MINIMUM MATERIAL THICKNESS IS 1.6 MM ($\frac{1}{16}$ IN.) (MECHANIZED). JOINT PREPARATION IS REQUIRED ON MATERIAL ABOVE 13 MM ($\frac{1}{2}$ IN.) THICK. THE PROCESS LENDS ITSELF TO WELDING THICK MATERIALS.	LIMITED TO VERTICAL OR NEAR-VERTICAL. O.K. OUTSIDE. FAIR PORTABILITY. EGW USED ON PLATE 9.5 TO 102 MM ($\frac{3}{8}$ TO 4 IN.) THICK. ESW USED ON PLATE 19 TO 900 MM ($\frac{3}{4}$ TO 36 IN.) HICK.	**ALL-POSITION. O.K. OUTSIDE. FAIR PORTABILITY. USED ON PLATE 1.0 MM (0.04 IN.) AND ABOVE. NO JOINT PREPARATION REQUIRED.**
COST FACTORS	A LOW-DEPOSITION-RATE PROCESS (UP TO 9 KG/H, OR 20 LB/H) WITH LOW DEPOSIT EFFICIENCY (TYPICALLY 65%).	DEPOSITION RATES (TO 16 KG/H, OR 35 LB/H) ARE HIGHER THAN SMAW. DEPOSITION EFFICIENCY (90-	DEPOSITION RATES (UP TO 18 KG/H, OR 40 LB/H) ARE HIGHER THAN GMAW. DEPOSITION EFFICIENCIES (80-90%) ARE LOWER	LOW DEPOSITION RATES (UP TO 5.4 KG/H, OR 12 LB/H) BUT HIGH DEPOSITION EFFICIENCY (99%). IF AUTOMATED,	DEPOSITION RATES ARE VERY HIGH (OVER 45 KG/H, OR 100 LB/H WITH MULTIWIRE SYSTEMS). DEPOSITION EFFICIENCY IS 99%	HIGH JOINT COMPLETION RATE. HIGH DEPOSITION EFFICIENCY (SOLID WIRES--99%, CORED WIRES LOWER).	**EQUIPMENT COST IS MODERATE.**

	LOW OPERATOR FACTOR. EQUIPMENT COST IS LOW AND SPARE PARTS ARE MINIMAL. WELDING SPEEDS ARE GENERALLY LOW. HOUSEKEEPING IS REQUIRED TO DESLAG AND DISPOSE OF FLUX AND ELECTRODE STUBS.	95%) AND OPERATOR FACTOR (TYPICAL 50%) ARE ALSO HIGHER. EQUIPMENT AND SPARE PARTS COST ARE MODERATE TO HIGH (PULSED-ARC POWER SUPPLIES ARE HIGHER COST). WELDING SPEEDS ARE MODERATE TO HIGH (BURIED ARC CO_2 CAN WELD AT OVER 2540 MM/MIN (100 IN./MIN). CLEANUP IS MINIMAL.	BUT OPERATOR FACTORS (50%) ARE SIMILAR TO GMAW. EQUIPMENT COST IS MODERATE. GOOD OUT-OF-POSITION DEPOSITION RATES CAN BE ACHIEVED WITH CONVENTIONAL POWER SOURCES. WELDING SPEEDS ARE MODERATE TO HIGH. SLAG AND SPATTER REMOVAL AND DISPOSAL IS REQUIRED.	THE OPERATOR FACTOR IS HIGH. EQUIPMENT AND SPARE PARTS COST IS MODERATE TO HIGH, DEPENDING ON COMPLEXITY (PAW IS SLIGHTLY MORE EXPENSIVE). CLEANUP IS GENERALLY UNNECESSARY DUE TO NO FLUX OR SPATTER.	BUT THAT DOES NOT INCLUDE THE FLUX (A 1:1 FLUX-TO-WIRE RATIO IS COMMON). BECAUSE THE PROCESS IS USUALLY MECHANIZED, OPERATOR FACTORS ARE HIGH. COST IS MODERATE FOR SINGLE-WIRE SYSTEMS. HIGH WELDING SPEEDS ARE ACHIEVABLE. HIGHER HOUSEKEEPING COSTS RESULT FROM THE NEED TO HANDLE THE SLAG AND UNFUSED FLUX.	HIGH OPERATOR FACTOR. HIGH EQUIPMENT AND SET-UP COST.	
WELD METAL QUALITY	STRONGLY DEPENDENT ON THE SKILL OF THE WELDER. LACK OF FUSION OR SLAG INCLUSIONS ARE POTENTIAL PROBLEMS. THE RELATIVELY SMALL BEADS USUALLY RESULT IN A HIGH PERCENTAGE OF REFINING IN MULTIPASS WELDS, AND VERY GOOD TOUGHNESS IS ACHIEVABLE WITH SOME	VERY GOOD QUALITY. POROSITY OR LACK OF FUSION CAN BE A PROBLEM. LESS TOLERANT OF RUST AND MILLSCALE THAN FLUX-USING PROCESSES. VERY GOOD TOUGHNESS IS ACHIEVABLE.	GOOD QUALITY. WELD METAL TOUGHNESS IS FAIR TO GOOD (BEST WITH BASIC ELECTRODES). SLAG INCLUSIONS ARE A POTENTIAL PROBLEM.	HIGH QUALITY, BUT REQUIRES CLEAN PLATE. EXCELLENT TOUGHNESS POSSIBLE DUE TO SMALL BEAD SIZE (HIGH REFINED WELD METAL, FINER GRAIN SIZE).	VERY GOOD. GOOD WELD METAL TOUGHNESS IS POSSIBLE. HANDLES RUST AND MILLSCALE WELL WITH PROPER FLUX SELECTION. HIGH-DILUTION PROCESS.	LARGE COLUMNAR GRAIN STRUCTURE RESULTS IN ONLY FAIR TOUGHNESS. HIGH DILUTION OF BASEPLATE (UP TO 35% FOR EGW, UP TO 50% FOR ESW).	**MINIMAL WELD SIZE. USUALLY FINE-GRAINED DUE TO FAST COOLING. WELD STRUCTURE IS AS CAST.**

	ELECTRODES.						
EFFECT ON BASE METAL	LOW HEAT INPUTS CAN CAUSE RAPID HAZ COOLING. FLUX COATINGS ARE A POTENTIAL SOURCE OF HYDROGEN.	GENERALLY A LOW-HYDROGEN PROCESS.	FLUX CORE CAN CONTRIBUTE HYDROGEN.	A LOW-HYDROGEN PROCESS. LOW HEAT INPUTS CAN CAUSE RAPID HAZ COOLING.	HIGHER HEAT INPUTS CAN RESULT IN LARGE HAZ AND POSSIBLE DETERIORATION OF BASEPLATE PROPERTIES (ESPECIALLY QUENCHED AND TEMPERED PLATE). FLUX IS A SOURCE OF HYDROGEN.	HIGH HEAT INPUT RESULTS IN LARGE HAZ AND GRAIN GROWTH. NOT RECOMMENDED FOR QUENCHED AND TEMPERED STEELS UNLESS REHEAT TREATMENT IS TO BE DONE. SLOW WELD COOLING ALLOWS HYDROGEN TO ESCAPE WELD AREA.	**CAUSES RAPID COOLING OF HAZ.**
GENERAL COMMENTS	**VERY VERSATILE, LOW-COST PROCESS. ESPECIALLY STRONG ON NON-ROUTINE OR REPAIR JOBS. USUALLY NOT ECONOMICAL ON STANDARD THICK WELDS OR ON REPETITIVE JOBS THAT CAN BE MECHANIZED.**	**RELATIVELY VERSATILE. EQUIPMENT MORE COSTLY, COMPLEX, AND LESS PORTABLE THAN SMAW. EASILY MECHANIZED. A CLEAN PROCESS WITH HIGHER DEPOSITION RATES AND EFFICIENCIES THAN SMAW.**	**RELATIVELY VERSATILE (SELF-SHIELDED VERSION CAN BE USED OUTSIDE). HIGHER DEPOSITION RATES THAN GMAW (HIGHER FUMES ALSO). WELDS EASILY OUT-OF-POSITION. READILY MECHANIZED.**	**EXTREMELY GOOD WELDS IN ALL POSITIONS. REQUIRES MORE PREPARATION. LOW DEPOSITION RATES LIMIT PROCESS TO THINNER PLATES.**	**A HIGH-DEPOSITION, HIGH-PENETRATION PROCESS, BUT THIN MATERIAL CAN BE WELDED AT HIGH SPEEDS. EASILY MECHANIZED. NATURAL FOR WELDING THICKER PLATES. HOUSEKEEPING AND POSITION LIMITATION CAN BE A PROBLEM.**	**HIGH JOINT COMPLETION RATE, BUT LIMITED TO VERTICAL. USED MAINLY ON LONG VERTICAL WELDS. HIGH HEAT INPUT CAN LIMIT BASEPLATES.**	**SPECIALIZED PROCESS FOR ATTACHING STUDS TO STEEL PLATE. USUALLY MORE ECONOMICAL THAN DRILLING AND TAPPING.**

SMAW, shielded metal arc welding; GMAW, gas-metal arc welding; FCAW, flux-cored arc welding; GTAW, gas-tungsten arc welding; PAW, plasma arc welding; SAW, submerged arc welding; EGW, electrogas welding; ESW, electroslag welding; SAW, stud arc welding

The effect of the welding process on carbon steel base metal is a function of the heat input (and cooling rate) imposed by the process and the amount of hydrogen contributed. Low-heat-input processes, such as gas-tungsten arc welding (GTAW), plasma arc welding (PAW), shielded metal arc welding (SMAW), short-arc gas-metal arc welding (GMAW), and stud welding (SW), result in a narrow, rapidly cooled HAZ. Greater care needs to be exercised when using these processes to weld hardenable carbon steels. On the other hand, a higher-heat-input process, like electrogas welding (EGW), will produce a much wider HAZ, produce more grain coarsening, and may cause a deterioration in the properties of heat-treated carbon steels. Heat input limits or a process change may be necessary when welding quenched and tempered carbon steels.

The arc welding processes that employ flux or flux-containing consumables contribute hydrogen to the weld area if the consumables are not adequately dried or protected from moisture. Examples are SMAW, flux-cored arc welding (FCAW), and submerged arc welding (SAW). Each of these processes offers low-hydrogen consumable types that should be used when welding hardenable carbon steels. Procedures are available, or will soon be available, in AWS electrode specifications to allow classification of arc welding electrodes based upon the weld metal diffusible hydrogen produced. This is a safe approach to use when welding hardenable carbon steels, because there can be wide variations between electrodes, even in the so-called "low-hydrogen" processes.

Weld metal properties as a function of process are a bit more complex. Not only are the heat input and hydrogen contributions important, but also the amount of base metal dilution, rust and scale tolerance, and pickup of atmospheric gases. The high-heat-input processes, particularly EGW, and electroslag welding (ESW) will result in large columnar grains and resulting lower toughness. The lower-heat-input processes (particularly GTAW, PAW, and SMAW) produce finer grain size. For a given weld chemistry, the higher-heat-input processes will produce a weaker weld deposit because of the formation of coarser, high-temperature transformation products. Hydrogen-induced cracking is generally not as serious a problem in weld metal as it is in the HAZ, because weld metal is usually low in carbon. Excessive carbon pickup (by dilution) or the use of an alloyed electrode would make the weld metal more vulnerable.

High dilution processes (for example, SAW and EGW) will incorporate a large amount of base metal into the weld. In square-butt submerged arc welds, over 60% of the weld metal can be diluted base metal. Obviously, this has a major effect on the properties of the weld metal. It also illustrates the importance of conducting procedure qualification testing to determine the actual mechanical and chemical properties of the production joint. The pickup of impurities (for example, sulfur, phosphorus, or nitrogen) from the base plate could lead to problems such as solidification cracking, porosity, or toughness deterioration.

The tolerance of the process to plate contaminants, such as rust, scale, or organic compounds (oil, grease, and so on) can be important. The nonflux processes are generally less tolerant of rust and scale. Processes such as GTAW, GMAW, and PAW are particularly sensitive and require clean plate. The submerged arc process is sensitive to porosity caused by organic compounds. In the open arc processes, the compounds can be vaporized by the heat of the arc before steel melting occurs. In submerged arc welding, the flux blanket acts to block the radiant heat from the arc, and the compound becomes incorporated in the weld metal.

Pickup of nitrogen and oxygen can also cause problems. Porosity is one outcome; toughness deterioration is another. Figure 15 shows the levels of weld metal oxygen and nitrogen produced by several arc welding processes. The GTAW and PAW processes produce the lowest gaseous impurity level. The arc in both of these processes is short and extremely stable, and the shielding gases (for example, argon or argon-helium mixtures) are inert and make no contribution. GMAW deposits are higher in both oxygen and nitrogen. A longer, less stable arc allows a greater chance of pickup. The use of Ar-O_2, Ar-CO_2, or CO_2 shielding gases also raises the oxygen level of the weld metal.

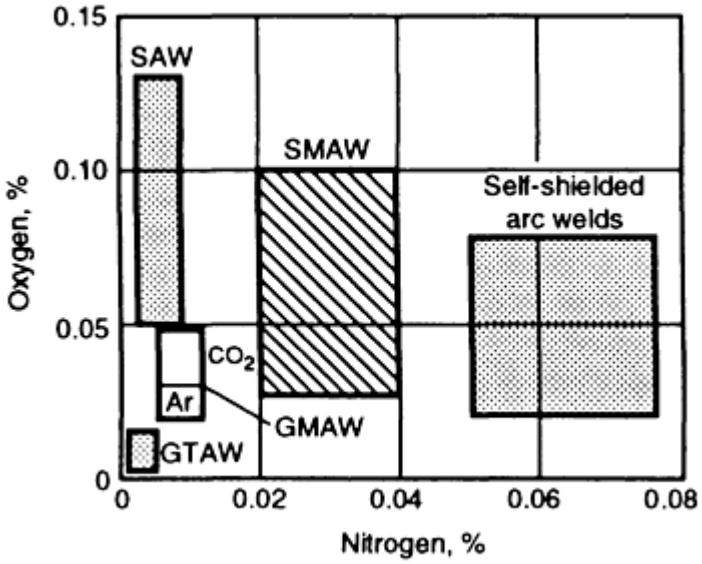

FIG. 15 TYPICAL OXYGEN AND NITROGEN LEVELS OBTAINED IN WELD METAL FROM SELECTED ARC WELDING PROCESSES. SOURCE: REF 14

The flux-using processes (that is, SMAW, FCAW, and SAW) can all pick up oxygen from decomposition of metal oxides contained within the flux. More basic flux systems produce lower oxygen levels. The two open arc, self-shielded processes (that is, SMAW and self-shielded FCAW) do not produce an even, well-directed gas shield. As a result, aspiration of air is higher than with the externally gas-shielded processes. Strong denitriders (for example, aluminum) are added to self-shielded flux-cored wires to counteract this pickup. Some submerged arc welds are more prone to nitrogen pickup when alternating current (ac) power is used.

All of the arc welding processes are susceptible to aspiration of air when long arc lengths (excessive arc voltages) are used. A longer arc length increases the time of exposure of the molten drops on transfer and increases the likelihood of gaseous impurity pickup.

References cited in this section

9. *THE PROCEDURE HANDBOOK OF ARC WELDING,* LINCOLN ELECTRIC COMPANY, 1973, CHAPTERS 5 AND 12
11. *WELDING HANDBOOK,* 8TH ED., VOL 1, AMERICAN WELDING SOCIETY, 1987, P 261
12. H.B. CARY, *MODERN WELDING TECHNOLOGY,* 2ND ED., PRENTICE-HALL, 1989, P 204-206
13. P.T. HOULDCROFT, *WHICH PROCESS?,* ABINGTON PUBLISHING, 1990
14. S. KOU, *WELDING METALLURGY,* JOHN WILEY & SONS, 1987, P 63

Arc Welding of Carbon Steels

Ronald B. Smith, The ESAB Group, Inc.

Welding Consumable Selection and Procedure Development

When choosing a welding consumable, the following should be considered:

- MECHANICAL PROPERTIES REQUIRED

- WELDABILITY CONSIDERATIONS
- PERFORMANCE FEATURES NEEDED OR DESIRED

Codes or customer specifications may define the mechanical properties required. Some codes will specify the types of electrodes to be used, while others limit the selection to certain products from certain manufacturers who have performed tests to qualify their products. If this information is not available, then it is customary to try to match or slightly exceed the base plate strength. There may be conditions where an undermatching weld metal strength is actually preferred--this is a function of the weld design and type of loading. The toughness level and other properties (for example, hardness) are dictated by service conditions and are more difficult to define. Code requirements can be used as guidelines.

Weldability considerations (that is, potential cracking or porosity problems in carbon steel) should then be assessed. A medium-carbon steel, for instance, will require a low-hydrogen consumable, preheat, and perhaps a postweld heat treatment to avoid hydrogen-induced cracking. The effect of this treatment on candidate consumables should be considered.

Certain performance features may be necessary, or at least desired. They allow the welding to be performed more economically. These types of choices are more frequently made with the flux-using processes where the formulations are designed to do certain things (for example, weld out-of-position, at high travel speeds, or at high deposition rates). Even nonflux processes require choices. For example, for GTAW of very thin steel tubing an ER70S-2 electrode (which contains some aluminum) produces a more viscous puddle that is easier to control out-of-position.

Once a consumable is chosen, a suitable process and procedure must be specified. American Society for Quality Control (ASQC) Standard Q91 (or ISO 9001) treats welding as a special process because the results cannot be fully verified by subsequent inspection and testing of the product. Therefore, documented work instructions, monitoring and control of process, approval of process and equipment, and criteria for workmanship shall be stipulated. In addition, ASQC Standard Q94 requires verifying the results of this special processing and determining to what extent equipment, environments, and operators are able to affect these final desired results.

In welding, the documented work instruction is usually referred to as a welding procedure specification (WPS) or just welding procedure (Fig. 16). In some fabrication specifications (for example, AWS D1.1), the WPS can be prequalified if it is specified within certain guidelines, such as equipment settings and methods. In other fabrication specifications, the WPS must be qualified, usually with the rules of the qualification standard such as the ASME Boiler and Presser Vessel Code Section IX or MIL STD 248. In all cases, a welding procedure specification that addresses all the important process variables must be documented. If these variables change, then a new WPS may have to be prepared to reflect these changes. Whether the WPS must be requalified when revised always depends on which variables are being revised. The qualification standard will identify which changes require requalification.

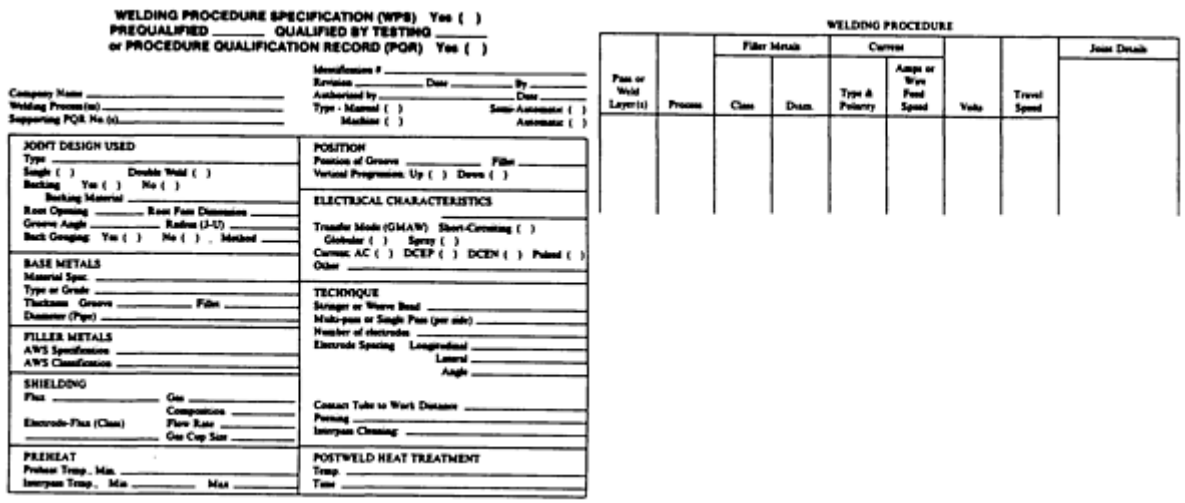

FIG. 16 WELDING PROCEDURE SPECIFICATION FORM. SOURCE: REF 3

All welding procedure specifications must be qualified by actual mechanical testing of welds made in accordance with the WPS. If this testing fails to meet the requirements of a customer or code, then a new WPS must be prepared and tested. Detailed information about procedure qualification is available in the article "Weld Procedure Qualification" in this Volume and in Ref 15.

Once a welding procedure specification is prepared, then the welding operators who will be applying this process should establish through testing that they are proficient in its application. This testing of worker proficiency is usually termed a welder or welding operator performance qualification test. Again, the qualification specification will outline the guidelines in which the welder or welding operator can be qualified with each test. As long as the worker continues to perform within those guidelines on a periodic basis without significant faults, the worker's qualification remains in effect. If the worker does not use the process for an extended period of time, uses it outside the guideline limits for performance qualification, or fails to achieve acceptable quality, then disqualification may occur with further training and testing as a corrective action, if deemed necessary. Repeated disqualification may necessitate reassignment to a less-skilled job. Adequate records are required to show continuity of process application for each qualified worker within the certifying organization.

Shielded Metal Arc Welding

Shielded metal arc welding is widely used for joining all classes of carbon steels. Detailed information is available in the article "Shielded Metal Arc Welding" in this Volume.

A wide variety of electrode types exist, each designed to work in a specific way and each possessing unique characteristics. Proper electrode selection is essential to achieve good welding performance and weld quality. AWS A5.1 (covering carbon steel electrodes) (Ref 16) and A5.5 (covering low-alloy steel electrodes) (Ref 17) are widely used to classify SMAW electrodes suitable for welding carbon steels. The low-alloy steel versions are used to weld higher carbon steels when higher strength is required.

E60XX electrodes (415 MPa, or 60 ksi, minimum tensile strength) are suitable for welding carbon steels containing up to about 0.3% C. They are not made with low-hydrogen coatings and should not be used to weld hardenable steels, especially under conditions of high joint restraint.

E70XX electrodes (485 MPa, or 70 ksi, minimum tensile strength) are suitable for steels with a wide range of strength values. The E7015, E7016, E7018, E7018M, E7028, and E7048 types are low-hydrogen electrodes and may be used in situations where hydrogen-induced cracking is a possibility. Table 6 summarizes some of the features and characteristics of the different carbon steel electrode types (see the Section "Fusion Welding Procedures" in this Volume or the appendices of Ref 16 and 17 for a more thorough discussion).

TABLE 6 CARBON STEEL ELECTRODES FOR SMAW WELDING APPLICATIONS

ELECTRODE	COATING TYPE	POSITION[A]	CURRENT TYPE	MINIMUM IMPACT ENERGY (CHARPY V-NOTCH)		GENERAL COMMENTS	APPLICATIONS
				J	J · LBF		
E6010	HIGH-CELLULOSE SODIUM	ALL	DCEP	27[B]	20[B]	GOOD PENETRATION. DIRECT FORCEFUL ARC. HIGH WELD METAL HYDROGEN.	**USED ON ALL TYPES OF JOINTS**
E6011	HIGH-CELLULOSE POTASSIUM	ALL	DCEP, AC	27[B]	20[B]	SIMILAR TO 6010 EXCEPT THAT IT HAS A MORE STABLE ARC AND IS SLIGHTLY LESS PENETRATING	**USED ON ALL TYPES OF JOINTS**
E6012	HIGH-RUTILE SODIUM	ALL	DCEN, AC	[C]	[C]	LOWER PENETRATION, HIGHER TRAVEL SPEEDS	**THIN SHEET METAL**
E6013	HIGH-RUTILE POTASSIUM	ALL	DCEN, DCEP, AC	[C]	[C]	HIGHER TRAVEL SPEEDS, LOWER PENETRATION. BETTER ON AC THAN E6012.	**THIN SHEET METAL**
E7014	RUTILE, IRON POWDER	ALL	DCEN, DCEP, AC	[C]	[C]	HIGHER-DEPOSITION-RATE VERSION OF E6013	**INCLINED AND SHORT FILLETS**
E6019	IRON OXIDE, RUTILE POTASSIUM	ALL	DCEN, DCEP, AC	27[D]	20[D]	MEDIUM-PENETRATION FLUID SLAG, ONLY SMALLER DIAMETER USED OUT-OF-POSITION (NO VERTICAL DOWN)	**MULTIPASS WELDS (TO 25 MM, OR 1 IN.), SOME OUT-OF-POSITION USE**
E6020	HIGH-IRON OXIDE	HF FLAT	DCEN, AC DCEN, DCEP, AC	[C]	[C]	SPRAY-LIKE ARC, HEAVY FLUID SLAG	**DOWNHAND WELDING OF THICKER PLATE**
E7024	RUTILE, IRON POWDER	HF, FLAT	DCEN, DCEP, AC	[C][E]	[C][E]	VERY HIGH-DEPOSITION-RATE VERSION OF E7014. THICK COATING OF FLUX. GOOD ARC CHARACTERISTICS.	**FILLETS AT HIGH TRAVEL SPEEDS. GRAVITY WELDING.**
E6027	HIGH-IRON OXIDE, IRON POWDER	HF FLAT	DCEN, AC DCEN, DCEP, AC	27[B]	20[B]	MEDIUM PENETRATION. HIGH-DEPOSITION-RATE VERSION OF E6020.	**FLAT FILLETS OR GROOVE WELDS**
E7027	HIGH-IRON OXIDE, IRON POWDER	HF FLAT	DCEN, AC DCEN, DCEP, AC	27[B]	20[B]	HIGHER TENSILE VERSION OF 6027	**SAME AS 6027**
LOW-HYDROGEN ELECTRODES							
E7015	LOW-HYDROGEN SODIUM	ALL	DCEP	27[B]	20[B]	THE ORIGINAL LOW-HYDROGEN ELECTRODE, NOT WIDELY USED TODAY	**USED ON ALL TYPES OF JOINTS WHERE LOW HYDROGEN IS NEEDED**

E7016	LOW-HYDROGEN POTASSIUM	ALL	DCEP, AC	27[B][F]	20[B][F]	SIMILAR TO E7015, BUT A MORE STABLE ARC	**USED ON ALL TYPES OF JOINTS WHERE LOW HYDROGEN IS NEEDED**
E7018	LOW-HYDROGEN POTASSIUM, IRON POWDER	ALL	DCEP, AC	27[B][G]	20[B][G]	MODERN LOW-HYDROGEN ELECTRODE. BETTER ARC AND OPERATING CHARACTERISTICS.	**USED ON ALL TYPES OF JOINTS, ESPECIALLY WHEN LOW HYDROGEN IS NEEDED**
E7018M	LOW-HYDROGEN IRON POWDER	ALL	DCEP	68[B]	50[B]	A LOW-MOISTURE VERSION OF 7018	**JOINING CARBON STEELS TO HIGH-STRENGTH LOW-ALLOY STEELS**
E7028	LOW-HYDROGEN POTASSIUM, HIGH-IRON POWDER	FLAT, HF	DCEP, AC	27[D]	20[D]	E7018 WITH HIGH IRON POWDER, HIGH DEPOSITION RATES	**HIGH TRAVEL SPEEDS ON FILLETS AND GROOVE WELDS**
E7048	**LOW-HYDROGEN POTASSIUM, IRON POWDER**	**FLAT, OH, HORIZONTAL, V-DOWN**	**DCEP, AC**	**27[B]**	**20[B]**	**SIMILAR TO E7018 WITH EXCELLENT VERTICAL-DOWN WELDING CHARACTERISTICS**	**VERTICAL DOWN WELDING**

(A) HF, HORIZONTAL FLAT; OH, OVERHEAD; V, VERTICAL.

(B) AT -30 °C (-20 °F).

(C) NOT REQUIRED.

(D) AT - 20 °C (0 °F).

(E) 7024-1 SPECIFICATIONS: 27 J (20 FT · LBF) AT -20 °C (0 °F).

(F) 7016-1 SPECIFICATIONS: 27 J (20 FT · LBF) AT -45 °C (-50 °F).

(G) 7018-1 SPECIFICATIONS: 27 J (20 FT · LBF) AT -45 °C (-50 °F)

Low-Alloy Steel Electrodes. Most low-alloy steel electrodes have low-hydrogen coatings (EXX15, EXX16, and EXX18), but some may not. Because low-alloy steel electrodes are used to weld higher-carbon, more hardenable steels, it is recommended that only the low-hydrogen versions be used. Consideration should also be given to the hydrogen-induced cracking tendencies of the low-alloy steel weld metal, especially if it is heavily diluted with carbon from the baseplate. The low-hydrogen electrodes have been specially formulated and processed to give low coating moistures. It is important that they be stored and handled properly in order to avoid moisture absorption. Once removed from their storage cans, they should be held in a vented oven at 110 to 150 °C (230 to 300 °F). If the electrodes have absorbed excessive moisture, they can be restored by baking at 250 to 425 °C (480 to 800 °F) for 1 to 2 h (consult the manufacturer of the electrode for the exact temperature).

Because SMAW is a lower-heat-input process and cooling rates can be high, it is especially important to control hydrogen when welding higher-carbon steels. The newer revisions of the AWS specifications will have optional procedures for choosing electrodes on the basis of the weld metal diffusible hydrogen produced.

Gas-Metal Arc Welding

Detailed information about this process is in the article "Gas-Metal Arc Welding" in this Volume. The process is unique in that it operates in a number of different modes, each with its own distinct method of metal transfer, using different shielding gases, operating at different heat input levels, and having different penetration (dilution) characteristics. The resultant weldment properties may vary significantly, depending on the mode used. For this reason, it is important to be cautious about generalizations regarding the process and to perform procedure qualifications.

Electrodes for GMAW are available as solid-or metal-cored wires. AWS A5.18 (Ref 19) classifies carbon steel filler metals. AWS A5.28 (Ref 18) classifies low-alloy steel electrodes, used to weld medium- and high-carbon steels where a higher-strength deposit is needed. Compositions of GMAW electrodes are given in Table 7. Mechanical property requirements are given in Table 8.

TABLE 7 COMPOSITION REQUIREMENTS FOR GMAW ELECTRODES USED TO WELD CARBON STEELS

AWS CLASSIFICATION[A]	COMPOSITION, WT%													
	C	Mn	Si	P	S	Ni	Cr	Mo	V	Cu[B]	Ti	Zr	Al	TOTAL OTHER ELEMENTS[C]
ER70S-2	0.07	0.90-1.40	0.40-0.70	0.025	0.035	[D]	[D]	[D]	[D]	0.50	0.05-0.15	0.02-0.12	0.05-0.15	...
ER70S-3	0.06-0.15	0.90-1.40	0.45-0.70	0.025	0.035	[D]	[D]	[D]	[D]	0.50	...	...	...	...
ER70S-4	0.07-0.15	1.00-1.50	0.65-0.85	0.025	0.035	[D]	[D]	[D]	[D]	0.50	...	...	...	...
ER70S-5	0.07-0.19	0.90-1.40	0.30-0.60	0.025	0.035	[D]	[D]	[D]	[D]	0.50	...	...	0.50-0.90	...
ER70S-6	0.07-0.15	1.40-1.85	0.80-1.15	0.025	0.035	[D]	[D]	[D]	[D]	0.50	...	...	...	...
ER70S-7	0.07-0.15	1.50-2.00[E]	0.50-0.80	0.025	0.035	[D]	[D]	[D]	[D]	0.50	...	...	...	...
ER70S-G	**NO CHEMICAL REQUIREMENTS[F]**													
ER80S-NI1	...	...	...	...	...	0.80-1.10	0.15	0.35	0.05	...	...	...	...	...
ER80S-NI2	0.12	1.24	0.40-	0.025	0.025	2.0-2.75	...	...	...	0.35	...	...	...	**0.50**

			0.80											
ER80S-NI3	. . .	. . .	. . .	. . .	. . .	3.0-3.75	. . .	. . .	. . .	. . .	. . .	. . .	. . .	**. . .**
ER80S-D2	0.07 - 0.12	1.60-2.10	0.50 - 0.80	0.025	0.025	0.15	. . .	0.40 - 0.60	. . .	0.50	. . .	. . .	. . .	**0.50**
ER100S-1	0.08	1.25-1.30	0.20 - 0.50	0.010	0.010	1.40 - 2.10	0.30	0.25 - 0.55	0.05	0.25	. . .	. . .	. . .	**. . .**
ER100S-2	0.12	1.25-1.80	0.20 - 0.60	0.010	0.010	0.80 - 1.25	0.30	0.20 - 0.55	0.05	0.35 - 0.65	0.10	0.10	0.10	**0.50**
ER110S-1	0.09	1.40-1.80	0.20 - 0.55	0.010	0.020	1.90 - 2.60	0.50	0.25 - 0.55	0.04	0.25	. . .	. . .	. . .	**. . .**
ER120S-1	0.10	1.40-1.80	0.25 - 0.60	0.010	0.010	2.0-2.80	0.60	0.30 - 0.65	0.03	0.25	. . .	. . .	. . .	**. . .**
ERXXS-G	**SUBJECT TO AGREEMENT BETWEEN SUPPLIER AND PURCHASER**													

Note: Single values shown are maximums. Analysis shall be made for the elements for which specific values are shown in this table. If, however, the presence of other elements is indicated in the course of routine analysis, further analysis shall be made to determine that the total of these other elements, except iron, is not present in excess of the limits specified for "Total other elements" in the last column of this table.

Source: Ref 18

(A) ELECTRODES CLASSIFIED E70S-1B PREVIOUSLY ARE NOW CLASSIFIED ER80S-D2. THE SUFFIXES B2, NIL, AND SO ON, DESIGNATE THE CHEMICAL COMPOSITION OF THE ELECTRODE AND ROD CLASSIFICATION.

(B) THE MAXIMUM WEIGHT PERCENT OF COPPER IN THE ROD OR ELECTRODE DUE TO ANY COATING PLUS THE RESIDUAL COPPER CONTENT IN THE STEEL SHALL COMPLY WITH THE STATED VALUE.

(C) OTHER ELEMENTS, IF INTENTIONALLY ADDED, SHALL BE REPORTED.

(D) THESE ELEMENTS MAY BE PRESENT BUT ARE NOT INTENTIONALLY ADDED.

(E) IN THIS CLASSIFICATION, THE MAXIMUM MANGANESE MAY EXCEED 2.0%. IF IT DOES, THE MAXIMUM CARBON MUST BE REDUCED 0.01% FOR EACH 0.05% INCREASE IN MANGANESE OR PART THEREOF.

(F) FOR THIS CLASSIFICATION, THERE ARE NO CHEMICAL REQUIREMENTS FOR THE ELEMENTS LISTED, WITH THE EXCEPTION THAT THERE SHALL BE NO INTENTIONAL ADDITION OF NICKEL, CHROMIUM, MOLYBDENUM, OR VANADIUM.

(G) TO MEET THE REQUIREMENTS OF THE G CLASSIFICATION, THE ELECTRODE MUST HAVE AS A MINIMUM ONE OF EITHER 0.50% NI, 0.30% CR, OR 0.20% MO.

TABLE 8 MECHANICAL-PROPERTY REQUIREMENTS FOR WELD-METAL DEPOSITS OF GMAW ELECTRODES

AWS CLASSIFICATION	**SHIELDING GAS**	**CURRENT AND POLARITY**	**MINIMUM TENSILE STRENGTH**		**MINIMUM YIELD STRENGTH 0.2% OFFSET**		**ELONGATION IN 50 MM (2 IN.) MIN, %**	**CONDITION**	MINIMUM REQUIRED IMPACT PROPERTIES	
			MPA	**KSI**	**MPA**	**KSI**			**J**	FT · LBF
ER70S-2	CO_2[A]	DCEP	495[B]	72[B]	415[B]	60[B]	22	AS WELDED	27[F]	**20[F]**
ER70X-3	CO_2[A]	DCEP	495[B]	72[B]	415[B]	60[B]	22	AS WELDED	27[G]	**20[G]**
ER70S-4	CO_2[A]	DCEP	495[B]	72[B]	415[B]	60[B]	22	AS WELDED	[H]	**[H]**

ER70S-5	CO_2[A]	DCEP	495[B]	72[B]	415[B]	60[B]	22	AS WELDED	[H]	**[H]**
ER70S-6	CO_2[A]	DCEP	495[B]	72[B]	415[B]	60[B]	22	AS WELDED	27[F]	**20[F]**
ER70S-7	CO_2[A]	DCEP	495[B]	72[B]	415[B]	60[B]	22	AS WELDED	27[F]	**20[F]**
ER70S-G	[C]	DCEP	495[B]	72[B]	415[B]	60[B]	22	AS WELDED	[C]	**[C]**
ER80S-NI1	ARGON + 1 TO 5% OXYGEN	DCEP	550	80	470	68	24	AS WELDED	27[I][J][K]	**20[I][J][K]**
ER80S-NI2	ARGON + 1 TO 5% OXYGEN	DCEP	550	80	470	68	24	PWHT[D]	27[J][L][M]	**20[J][L][M]**
ER80S-NI3	ARGON + 1 TO 5% OXYGEN	DCEP	550	80	470	68	24	PWHT[D]	27[J][M][N]	**20[J][M][N]**
ER80S-D2	CO_2	DCEP	550	80	470	68	17	PWHT[D]	27[F]	**20[F]**
ER100S-1	ARGON + 2% OXYGEN	DCEP	670	100	605-705	88-102	16	AS WELDED	27[F][J][K]	**20[F][J][K]**
ER100S-2	ARGON + 2% OXYGEN	DCEP	670	100	605-705	88-102	16	AS WELDED	68[O]	**50[O]**
ER110S-1	ARGON + 2% OXYGEN	DCEP	760	110	655-740	95-107	15	AS WELDED	68[O]	**50[O]**
ER120S-1	ARGON + 2% OXYGEN	DCEP	830	120	725-840	105 - 122	14	AS WELDED	68[O]	**50[O]**
ERXXS-G	[C]	DCEP	[E]	[E]	[C]	[C]	[C]	AS WELDED	[C]	**[C]**
EXXC-G	**[C]**	**DCEP**	**[E]**	**[E]**	**[C]**	**[C]**	**[C]**	**AS WELDED**	**[C]**	**[C]**

Source: Ref 18

(A) CARBON DIOXIDE SHIELDING GAS. THE USE OF CO_2 FOR CLASSIFICATION PURPOSES SHALL NOT BE CONSTRUED TO RESTRICT THE USE OF ARGON-CO_2 OR ARGON-O_2 SHIELDING GAS MIXTURES. A FILLER METAL CLASSIFIED WITH CO_2 WILL ALSO MEET THE REQUIREMENTS OF THIS SPECIFICATION WHEN USED WITH ARGON-CO_2 OR ARGON-O_2 MIXTURES.

(B) FOR EACH INCREASE OF ONE PERCENTAGE POINT IN ELONGATION OVER THE MINIMUM, THE YIELD STRENGTH, OR TENSILE STRENGTH, OR BOTH MAY DECREASE 7 MPA (1 KSI) TO A MINIMUM OF 485 MPA (70 KSI) FOR THE TENSILE STRENGTH AND 400 MPA (58 KSI) FOR THE YIELD STRENGTH.

(C) SUBJECT TO AGREEMENT BETWEEN SUPPLIER AND PURCHASER.

(D) PWHT, POSTWELD HEAT TREATED IN ACCORDANCE WITH AWS A5.28-79.

(E) TENSILE STRENGTH SHALL BE CONSISTENT WITH THE LEVEL PLACED AFTER THE "ER" OR "E" PREFIX; E.G., ER90S-G SHALL HAVE 620 MPA (90 KSI) MINIMUM ULTIMATE TENSILE STRENGTH.

(F) AT -30 °C (-20 °F).

(G) AT -20 °C (0 °F).

(H) NOT REQUIRED.

(I) AT -45 °C (-50 °F).

(J) THE LOWEST AND THE HIGHEST VALUES OBTAINED SHALL BE DISREGARDED FOR THIS TEST. TWO OF THE THREE REMAINING VALUES SHALL BE GREATER THAN THE SPECIFIED 27 J (20 FT · LBF) ENERGY LEVEL; ONE OF THE THREE MAY BE LOWER BUT

SHALL NOT BE LESS THAN 20 J (15 FT · LBF). THE COMPUTED AVERAGE VALUE OF THE THREE VALUES SHALL BE EQUAL TO OR GREATER THAN THE 68 J (20-FT · LBF) ENERGY LEVEL.

(K) AS-WELDED IMPACT PROPERTIES.

(L) AT -60 °C (-80 °F).

(M) REQUIRED IMPACT PROPERTIES AFTER POSTWELD HEAT TREATMENT (SEE AWS A5.28-79).

(N) AT -75 °C (-100 °F).

(O) IMPACT PROPERTIES FOR THE ER100S-1, ER100S-2, ER110S-1, AND ER120S-1 SHALL BE OBTAINED AT TEST TEMPERATURE SPECIFIED IN THE TABLE ±1.7 °C (± 3 °F). THE LOWEST AND THE HIGHEST IMPACT VALUES THUS OBTAINED SHALL BE DISREGARDED FOR THIS TEST. TWO OF THE THREE REMAINING VALUES SHALL BE GREATER THAN THE SPECIFIED 68 J (50-FT · LBF) ENERGY LEVEL; ONE OF THE THREE MAY BE LOWER BUT SHALL NOT BE LESS THAN 54 J (40 FT · LBF); THE COMPUTED AVERAGE VALUES OF THESE THREE SHALL BE GREATER THAN THE SPECIFIED 68 J (50-FT · LBF) LEVEL.

Carbon steel electrodes are welded using CO_2, argon-oxygen, or argon-CO_2 shielding gases. Concern about welding fume levels has led to the increased use of the argon-base shielding gases. The low-alloy steel electrodes are commonly welded with argon-oxygen (2 to 5% O) or argon-CO_2 (5 to 12% CO_2) to avoid the loss of alloy during arc transfer. For carbon steel metal-cored electrodes, argon-CO_2 or argon-oxygen mixtures are used. The performance of welds is generally enhanced at higher argon levels.

The major difference between the carbon steel electrodes is the deoxidizer content. As the oxygen level of the molten weld pool increases, so must the deoxidizer level in the welding electrode if excessive porosity is to be avoided. The sources of oxygen are CO_2 or O_2 in the shielding gas, rust or millscale on the plate surface, and the baseplate oxygen (left from the deoxidation practice employed during steel manufacture. The ER70S-3 (1.1Mn-0.55Si) electrodes are the most widely used type, because of low cost, but they also have the lowest deoxidizer level. When welding rimmed steels with CO_2 shielding gas, porosity may be a problem. In that case an ER70S-4 (1.3Mn-0.75Si) electrode would do a better job. When heavier rest or scale is present or when high current welds are made (more baseplate dilution), it may be necessary to use an ER70S-6 (1.7Mn-0.9Si) electrode, which will tolerate most conditions, including high-speed welding. The ER70S-7 (1.8Mn-0.6Si) electrodes also have a higher deoxidizer level, better bead shape, and higher strength compared to ER70S-3 electrodes. The ER70S-5 (1.2Mn-0.5Si-0.7Al) electrodes, which contain high aluminum for deoxidation, are not readily available and are rarely used.

The ER70S-2 (low carbon, 1.2% Mn, 0.6% Si) electrodes contain small amounts of aluminum, titanium, and zirconium. Because these are strong deoxidizers, the ER70S-2 electrodes also produce good-quality welds at high weld puddle oxygen levels. The aluminum content makes the weld puddle more viscous, and this electrode is suitable for out-of-position welding because of ease of control. The low carbon content, and the fact that aluminum, titanium, and zirconium are strong denitriders, also make this electrode ideal for root passes. The highest weld quality is obtained when shielding gases higher in oxygen or CO_2 content are used. The viscous nature of the weld puddle can lead to an entrapment of gas that creates weld porosity. Higher oxygen and carbon dioxide components in the shielding gas improve puddle fluidity and minimize porosity levels.

Low-alloy electrodes contain sufficient deoxidizers to avoid porosity on relatively clean plate, but the silicon levels are kept low so as not to decrease toughness. An exception is ER80S-D2 electrodes, which contain higher silicon and can therefore be used with CO_2 or Ar-25CO_2 shielding.

Metal-cored electrodes may also be used. They produce higher deposition rates for a given heat input than do solid electrodes. Some users also claim that they provide a better bead profile and less chance of burn-through in root passes.

The GMAW process is considered a low-hydrogen process, but hydrogen can vary, depending on wire lubricant levels. Revisions of AWS A5.18 (Ref 18) and A5.28 (Ref 19) will include optional provisions for specification based on weld metal diffusible hydrogen.

Flux-Cored Arc Welding

Flux-cored arc welding may be used with or without an external shielding gas (see the article "Flux-Cored Arc Welding" in this Volume). Electrodes for flux-cored arc welding are classified under AWS A5.20 (covering carbon-steel electrodes) (Ref 20) and AWS A5.29 (covering low-alloy steel electrodes) (Ref 21).

Gas-shielded electrodes are designed to be used only with an external shielding gas (usually CO_2 or Ar-CO_2). The characteristics of these electrodes are given in Table 9. The majority of these electrodes are rutile-base and have excellent operating characteristics. The larger diameter versions (2.0 mm, or $\frac{5}{64}$ in., and larger) are used for flat and horizontal fillet welding, usually with CO_2 shielding gas. High penetration (high dilution), high heat inputs, and high deposition rates are characteristic of these electrodes. The T-1 group of large-diameter wires are used for single- and multiple-pass welding. The T-2 group contains higher levels of deoxidizer (manganese and silicon) to handle rust, scale, or rimmed steels, and is designed primarily for single-pass welding.

TABLE 9 ELECTRODES FOR FCAW APPLICATIONS

AWS ELECTRODE TYPE	**POLARITY**	**WELDING POSITION**	CHARACTERISTICS
GAS-SHIELDED ELECTRODES			
EXOT-1	DCEP	FLAT, HORIZONTAL	**RUTILE-BASE SPRAY-LIKE ARC, LOW SPATTER, FLAT BEAD SHAPE, EASY-PEELING SLAG, DEEP PENETRATION, HIGH DEPOSITION RATE. SINGLE- AND MULTIPASS WELDING. CO_2 NORMALLY USED.**
EXIT-1	DCEP	ALL	**SMALL-DIAMETER VERSIONS OF EXOT-1. CO_2 OR AR-CO_2 SHIELDING USED. SOME MICROALLOY VERSIONS CAPABLE OF GOOD LOW-TEMPERATURE TOUGHNESS.**
EXOT-2	DCEP	FLAT, HORIZONTAL	**OPERATE SIMILARLY TO EXOT-1 ELECTRODES BUT CONTAIN HIGHER LEVELS OF SILICON AND MANGANESE FOR IMPROVED PERFORMANCE OVER RUST AND MILLSCALE**
EXOT-5	DCEP	FLAT, HORIZONTAL	**BASIC ELECTRODE, MORE GLOBULAR ARC, ROUNDED BEAD, THIN SLAG COVER. PRODUCES VERY GOOD LOW-TEMPERATURE TOUGHNESS AND VERY LOW WELD-METAL HYDROGEN. USED FOR SINGLE-PASS AND MULTIPASS WELDS WHERE LOW HYDROGEN AND GOOD TOUGHNESS ARE REQUIRED. CO_2 SHIELDING NORMALLY USED.**
EXIT-5	DCEN	ALL	**SMALL-DIAMETER VERSIONS OF EXOT-5. USE CO_2 OR AR-CO_2 SHIELDING. OPERATING CHARACTERISTICS NOT AS GOOD AS T-1 ELECTRODES.**
SELF-SHIELDED ELECTRODES			
EXOT-3	DCEP	FLAT, HORIZONTAL	**DESIGNED FOR HIGH WELDING SPEEDS. SPRAY-LIKE ARC. USED ON THIN GAGE MATERIAL ONLY (<5 MM, OR 0.2 IN.).**
EXOT-4	DCEP	FLAT, HORIZONTAL	**HIGH-DEPOSITION-RATE ELECTRODE. GLOBULAR ARC. GOOD RESISTANCE TO SOLIDIFICATION CRACKING. USED FOR SINGLE-PASS AND MULTIPASS WELDING.**

EXOT-6	DCEP	FLAT, HORIZONTAL	**SPRAY-LIKE ARC WITH GOOD ROOT PENETRATION AND SLAG PEELING. PRODUCES GOOD LOW-TEMPERATURE TOUGHNESS. SINGLE-PASS AND MULTIPASS USE.**
EXOT-7	DCEN	FLAT, HORIZONTAL	**DESIGNED FOR SINGLE-PASS OR MULTIPASS WELDING IN ALL POSITIONS**
EXIT-7	DCEN	ALL	**GOOD CRACK-RESISTANCE WELD METAL**
EXOT-8	DCEN	FLAT, HORIZONTAL	**DESIGNED FOR SINGLE-PASS OR MULTIPASS WELDS IN ALL POSITIONS. GOOD LOW-TEMPERATURE TOUGHNESS.**
EXIT-8	DCEN	ALL	
EXOT-10	DCEN	FLAT, HORIZONTAL	**HIGH-SPEED SINGLE-PASS WELDS ON ANY THICKNESS PLATE**
EXOT-11	DCEN	FLAT, HORIZONTAL	**VERY WELL-OPERATING, GENERAL PURPOSE, ALL-POSITION ELECTRODE. TENSILE DUCTILITY MAY BE POOR ON WELDS IN PLATE >19 MM ($\frac{3}{4}$ IN.).**
EXIT-11	**DCEN**	**ALL**	

Source: Ref 20, 21

The smaller diameter (1.6 mm, or $\frac{1}{16}$ in., and under) rutile-base electrodes are used in all positions. They are widely used because of the ease of use and the high deposition rates possible when out-of-position. Carbon dioxide shielding or Ar-CO_2 shielding is used. The Ar-CO_2 mixture (typically with 20 to 25% CO_2) gives better operating characteristics and less loss of elements during arc transfer. Many electrodes are specifically designed to work in one gas or the other, so manufacturer recommendations should be followed. The weld metal toughness of these electrodes can vary from fair to very good. Newer, microalloyed versions, both carbon and low-alloy steel, are capable of achieving good low-temperature toughness and low-hydrogen characteristics. Small quantities of titanium and boron are added to modify transformation characteristics and promote the formation of acicular ferrite. The quantities of titanium and boron transferred to the weld metal are critical. The use of the recommended shielding gas and tight control of welding variables (especially arc voltage) are necessary to achieve optimum results. There is the possibility of solidification cracking with excessive amounts of boron in the weld metal.

The basic electrodes (T-5 types) do not have operating characteristics as good as those of the rutile types, but they are capable of producing excellent low-temperature toughness and low diffusible hydrogen. They are mainly used for multipass welding or where resistance to cracking (both hydrogen-induced and solidification) is required. Some smaller-diameter versions can be used for out-of-position welding, but the performance features are inferior to those of rutile-base electrodes.

Self-shielded electrodes are designed to be used only without a shielding gas. The weld metal is protected from atmospheric contamination by denitriders, deoxidizers, and gas formers in the core. Compared to the gas-shielded types, the self-shielded electrodes require closer control of welding parameters to achieve consistent results. This is because the balance of denitriders/deoxidizers to atmospheric gases, N_2 and O_2, is critical to performance and weld metal mechanical properties. An increase in arc length, for instance, will reduce the transfer of aluminum and titanium to the weld metal, but it will increase the amount of nitrogen and oxygen absorbed. This interaction with the atmosphere also makes weld metal hydrogen levels more dependent on atmospheric moisture. Self-shielded electrodes can be classified as being either controlled-hydrogen or low-hydrogen, provided that welding parameters, including proper electrode stickout parameters are maintained. These electrodes also have the special ability to make quality welds, even in windy conditions.

T-3 and T-10 Types. Self-shielded electrodes are differentiated according to the intended application and the mechanical properties achieved. The T-3 types are single-pass electrodes for use on sheet metal and plate under 5 mm (0.2 in.) thick. The fast travel speeds and high cooling rate of a thicker material result in poor weld metal ductility. The T-

10 types are also designed for high-speed, single-pass welding. They operate at lower travel speeds, but the deposit is less hardenable and they are not limited by plate thickness.

The T-4, T-7, and T-11 types are intended for single-pass or multipass applications, but none of them is required to meet minimum weld metal toughness levels. The T-4 and large diameter T-7 types are for horizontal and flat use. Both produce high deposition rates, but the T-7 is capable of higher travel speeds. The T-11 electrodes have very good operating characteristics and are frequently used for out-of-position welding of thin plate and gage materials. The higher hardenability of the T-11 deposit may require preheat when welding plate over 19 mm ($\frac{3}{4}$ in.) thick.

T-6 and T-8 Types. T-6 electrodes are intended for single-pass and multipass welding where good toughness is needed in the flat and horizontal position. T-8 electrodes provide good toughness single-pass or multipass welds in all positions. The T-8 slag system forms the basis for many of the higher-toughness, low-alloy steel electrodes.

Gas-Tungsten Arc and Plasma Arc Welding

These two processes are so similar that they can be treated together. Their main use on carbon steels is for welding thinner material components (especially thin-walled tubing) and for making root passes in pipe joints. (Detailed information is available in the articles "Gas-Tungsten Arc Welding" and "Plasma Arc Welding" in this Volume.) Both processes produce very clean, high-quality weld metal because of the use of inert shielding gases and a tightly-controlled arc. Each is considered a low-hydrogen process, with the major contribution coming from the filler material, if one is used. Heat inputs are relatively low, so care must be exercised when welding hardenable carbon steels.

A choice must be made whether to use a filler material or to weld autogenously (without a filler material). Generally, thin carbon steels are welded autogenously up to 3 mm ($\frac{1}{8}$ in.) thick (for GTAW) or 6 mm ($\frac{1}{4}$ in.) thick (for PAW) unless a metallurgical problem precludes the use of either process. If the baseplate sulfur or phosphorus levels are high, then a low-carbon, high-manganese filler material may have to be used to prevent solidification cracking. High oxygen levels in the steel (rimmed) will require a high-deoxidizer-containing filler material to counteract porosity. Consumable inserts are sometimes used in root-pass welds. These inserts are of a specific steel composition (some have compositions equal to the filler wires) and are preplaced in the root of weld. They are melted and become part of the root-pass weld metal. Their use generally results in more consistent weld-bead fusion and underbead formation. Consumable inserts are covered in AWS A5.30-79 (Ref 22).

Filler metals for GTAW or PAW joining of carbon steels are the same as those used for GMAW (see Tables 7 and 8). The same guidelines prevail (that is, higher oxygen weld puddles require higher deoxidizer levels in the filler material). Because much of the welding is done-out-of-position or in root passes, the ER70S-2 filler rod is very popular. This is due to its viscous, easier-to-control weld puddle and to the low carbon level that reduces the likelihood of solidification cracking in root beads. Manual GTAW or PAW processing is normally done with straight length rods. Spooled or coiled product is used for mechanized setups.

Submerged Arc Welding

Submerged arc welding is a high-current process capable of high heat input, high penetration, high rate of travel, and high deposition rates (see the article "Submerged Arc Welding" in this Volume).

The high heat inputs associated with this process lead to slow weld metal cooling rates. The presence of a flux blanket tends to slow down the rate of cooling even more. This promotes formation of microstructures less susceptible to hydrogen-induced cracking and allows longer times for hydrogen to escape. Excessive heat inputs, however, can result in low strength and perhaps low toughness in the weld metal and HAZ.

High penetration results in high baseplate dilution. It is not uncommon to have over 60% dilution in one- or two-pass, square butt welds. This addition of base material must be taken into consideration when selecting procedures and consumables to meet specific mechanical property requirements. Procedure tests should always be run. Impurities in the baseplate (for example, sulfur, phosphorus, oxygen, and nitrogen) can lead to problems in heavily diluted weld metal.

High travel speeds increase the probability of solidification cracking, especially in small, more diluted root passes. Under such circumstances, special attention should be paid to baseplate chemistry (carbon, sulfur, and phosphorus) and bead shape control.

Consumable selection involves choosing both a flux and an electrode. They are an interactive pair that together determine the properties of the weld. Fluxes and electrodes for welding carbon steels are classified under AWS A5.17 (carbon steels) (Ref 23) and AWS A5.23 (low-alloy steels) (Ref 24). Solid electrodes are classified on the basis of chemistry. The flux/electrode combination is classified on the basis of weld metal mechanical properties (tensile and Charpy V-notch) and, for low-alloy electrodes only, deposit chemistry. Preliminary selection based on mechanical properties is thus fairly easy. Procedure tests should always be run, because production welding conditions rarely match the AWS test procedures (which are low-dilution, moderate-heat-input welds).

Flux Selection. Selection for performance features is more difficult. Performance characteristics are largely determined by the flux. Past experience or manufacturer recommendations can be used. Caution must be exercised in the selection of a flux.

Active fluxes (those that contain, and contribute to the weld metal, significant amounts of silicon and manganese) are designed to tolerate high weld puddle oxygen. Their use is mainly for single- or limited-pass welding on scaled or rusty plate. In the absence of oxides, the deoxidizers enter the weld metal and may cause excessive hardness. Therefore, their use may be limited on multipass welds. Transfer of metals from the flux to the weld metal is enhanced at higher arc voltages, where more flux is consumed per unit of electrode. Close control of arc voltage is required with active fluxes, or weld metal cracking might occur. Low-alloy steel electrodes should not be used with active fluxes.

Neutral fluxes (those that contain and contribute no or low amounts of silicon and manganese) are not as tolerant to rust and millscale and are intended for welding on clean plate or in multipass welding.

Intermediate Activity Fluxes. Some fluxes have intermediate activity. This provides them with some tolerance to rust and millscale, and it allows their use for multipass welding with less probability of excessive manganese and silicon pickup.

Wall Neutrality Number Method. The appendices of AWS A5.17 (Ref 23) and A5.23 (Ref 24) describe a method, the wall neutrality number, that may be used to quantify the activity of a flux.

Basic fluxes are generally used for multipass welding where good low-temperature toughness is required.

Acid fluxes generally have better performance features than basic fluxes. Acid fluxes deslag more easily and may give better visual bead appearance. However, overall performance may be lacking due to silicon pickup or carbon depletion in heavier thicknesses.

Flux Storage. Submerged arc welding can be a low-hydrogen process if the fluxes are properly stored and handled. Flux exposed to the atmosphere can pick up moisture, especially under humid conditions. This moisture can be removed by drying the flux. The manufacturer should be consulted for proper procedures. Heated flux hoppers, which hold the flux above 120 °C (250 °F), are frequently used to maintain low moisture during usage, especially when welding crack-sensitive steels.

Electrogas Welding

From a metallurgical viewpoint, the primary feature of the electrogas welding process is the protracted thermal cycle that results from the relatively slow progression rate of the welding arc (see the article "Electroslag and Electrogas Welding" in this Volume). The slow heat-up and cool-down results in a wide, grain-coarsened HAZ and large columnar grains in the weld metal. Low toughness can be a problem in some applications. Control of welding conditions to limit heat input will improve HAZ properties. Low-alloy electrodes are often used when low-temperature weld-metal toughness is required. Table 10 gives typical applications of steels based on grade. Electrogas welding of quenched and tempered carbon steels can result in serious degradation of strength and toughness properties in the HAZ. A postweld heat treatment may be necessary to restore the properties. Some codes (for example, AWS D1.1, Ref 3) prohibit the use of EGW on quenched and tempered steels.

TABLE 10 SELECTED STEEL GRADES COMMONLY JOINED BY ELECTROGAS WELDING PROCESS

GRADE	
AISI	ASTM
PLAIN CARBON STEELS	
1010	**. . .**
1018	**. . .**
1020	**. . .**
STRUCTURAL STEELS	
. . .	**A 36**
. . .	**A 131**
. . .	**A 242**
. . .	**A 283**
. . .	**A 441**
. . .	**A 572**
. . .	**A 573**
. . .	**A 588**
PRESSURE VESSEL STEELS	
. . .	**A 36**
. . .	**A 285**
. . .	**A 515**
. . .	**A 516**
. . .	**A 537**

Source: Ref 25

On the positive side, the formation of hard, crack-sensitive microstructures is less likely to occur because of the slow cooling rates, and the elevated time at temperature allows more time for hydrogen to escape (electrogas welding is a low-hydrogen process). Preheating is not normally required.

Baseplate dilution can vary with welding parameters. High voltage and low current will increase sidewall penetration. Up to about 35% dilution is possible. Because this will have a major effect on weld metal properties, it is very important to run procedure qualification tests.

Electrodes for electrogas welding are classified in accordance with AWS A5.26 (Ref 26). The process utilizes either solid electrodes (Table 11) or composite electrodes (Table 12). The composite electrodes can be flux-cored or metal-cored and require either shielding gas or self shielding. Typical properties of carbon steel grades in the as-welded condition are given in Table 13. Carbon dioxide or Ar-CO_2 mixtures are used for the shielded flux-cored and solid-wire electrodes. The solid electrodes used are similar to those used for GMAW. The flux-cored electrodes used for electrogas welding are not the same as those used for FCAW. They have a lower level of slag formers. Flux-cored electrodes offer an advantage over solid electrodes in that they have a higher deposition rate (approximately 20%). This will result not only in faster joint completion rates, but also in lower heat inputs.

TABLE 11 CHEMICAL COMPOSITION FOR SOLID CARBON STEEL ELECTRODES USED IN ELECTROGAS WELDING

AWS CLASSIFICATION[B]	COMPOSITION, %[A]											
	C	**Mn**	**P**	**S**	**Si**	**Ni**	**Cr**	**Mo**	**Cu[C]**	**Ti**	**Zr**	Al
EGXXS-1	0.07-0.19	0.90-1.40	0.025	0.035	0.30-0.50	. . .	. . .	. . .	0.35	. . .	. . .	**. . .**
EGXXS-D2[D]	0.07-0.12	1.60-2.10	0.025	0.035	0.50-0.80	0.15	. . .	0.40-0.60	0.35	. . .	. . .	**. . .**

EGXXS-G	**NO CHEMICAL REQUIREMENTS[E]**											
EGXXS-2	0.06	0.90-1.40	0.025	0.035	0.40-0.70	. . .	. . .	. . .	0.35	0.05-0.15	0.02-0.12	**0.05-0.15**
EGXXS-3	0.06-0.15	0.90-1.40	0.025	0.035	0.45-0.70	. . .	. . .	. . .	0.35	. . .	. . .	**. . .**
EGXXS-5	0.07-0.19	0.90-1.40	0.025	0.035	0.30-0.60	. . .	. . .	. . .	0.35	. . .	. . .	**0.50-0.90**
EGXXS-6	**0.07-0.15**	**1.40-1.85**	**0.025**	**0.035**	**0.80-1.15**	**. . .**	**. . .**	**. . .**	**0.35**	**. . .**	**. . .**	**. . .**

(A) SINGLE VALUES ARE MAXIMUMS.

(B) THE LETTERS "XX" (AS IN 6Z, 60, 62, 7Z, 70, 72, AND 8Z, 80, AND 82) ARE MECHANICAL PROPERTY DESIGNATIONS.

(C) THE COPPER LIMIT INCLUDES COPPER THAT MAY BE APPLIED AS A COATING ON THE ELECTRODE.

(D) FORMERLY EGXXS-1B.

(E) COMPOSITION SHALL BE REPORTED; THE REQUIREMENTS ARE THOSE AGREED TO BY THE PURCHASER AND THE SUPPLIER.

TABLE 12 COMPOSITION OF WELD METAL OBTAINED WHEN USING COMPOSITE FLUX-CORED AND METAL-CORED ELECTRODES

AWS CLASSIFICATION[A]	**SHIELDING GAS**	**COMPOSITION, WT%[B]**										OTHER ELEMENTS (TOTAL)
		C	**Mn**	**P**	**S**	**Si**	**Ni**	**Cr**	**Mo**	**Cu**	**V**	
EGXXT-1	NONE	[C]	1.7	0.03	0.03	0.50	0.30	0.20	0.35	0.35	0.08	**0.50**
EGXXT-2	CO_2	[C]	2.0	0.03	0.03	0.90	0.30	0.20	0.35	0.35	0.08	**0.50**
EGXXT-NIL (FORMERLY EGXXT-3)	CO_2	0.10	1.O-1.8	0.03	0.03	0.50	0.7-1.1	. . .	0.30	0.35	. . .	**0.50**
EGXXT-NM1 (FORMERLY EGXXT-4)	AR/CO_2 OR CO_2	0.12	1.0-2.0	0.02	0.03	0.15-0.50	1.5-2.0	0.20	0.40-0.65	0.35	0.05	**0.50**
EGXXT-NM2 (FORMERLY EGXXT-6)	CO_2	0.12	1.10-2.10	0.03	0.03	0.20-0.60	1.1-2.0	0.20	0.10-0.35	0.35	0.05	**0.50**
EGXXT-W (FORMERLY EGXXT-5)	CO_2	0.12	0.50-1.3	0.03	0.03	0.30-0.80	0.40-0.80	0.45-0.70	. . .	0.30-0.75	. . .	**0.50**
EGXXT-G	**NOT SPECIFIED[D]**											

Source: Ref 25

(A) THE LETTERS "XX" (FOR EXAMPLE, 6Z, 60, 62, 7Z, 70, 72, 8Z, 80 OR 82) REFER TO MECHANICAL PROPERTY DESIGNATIONS.

(B) SINGLE VALUES ARE MAXIMUMS.

(C) COMPOSITION RANGE FOR CARBON NOT SPECIFIED FOR THESE CLASSIFICATIONS, BUT THE AMOUNT SHALL BE DETERMINED AND REPORTED.

(D) COMPOSITION SHALL BE REPORTED; THE REQUIREMENTS ARE THOSE AGREED TO BETWEEN THE PURCHASER AND SUPPLIER.

TABLE 13 TYPICAL AS-WELDED MECHANICAL PROPERTIES OF ELECTROGAS WELDS OBTAINED WHEN USING FLUX-CORED ELECTRODES

ASTM GRADE	APPLICATION	THICKNESS		ELECTRODE CLASS (A5.26)	SHIELDING GAS	TENSILE PROPERTIES					TEST TEMPERATURE		IMPACT ENERGY (CHARPY V-NOTCH)			
						YIELD STRENGTH		TENSILE STRENGTH		ELONGATION IN 50 MM (2 IN.), %			WELD METAL		HAZ	
		MM	IN.			MPA	KSI	MPA	KSI		°C	°F	J	FT · LBF	J	FT · LBF
1020[A]	STRUCTURAL	12	15/32	EG72T1	. . .	496	72	552	80	28	-29	-20	58	43	. . .	. . .
		25	1	EG72T1	. . .	441	64	545	79	27	-29	-20	45	33	. . .	. . .
A 36	STRUCTURAL	25	1	EG72T1	. . .	448	65	545	79	27	-29	-20	56	41	. . .	. . .
		25	1	EG72T4	CO_2	483	70	634	92	26	-30	-22	47	35	. . .	. . .
		75	3	EG72T4	CO_2	462	67	614	89	26	-30	-22	42	31	. . .	. . .
		75	3	EG72T4	80AR-20CO_2	. . .	. . .	600	87	23	-18	-0.4	72	53	. . .	. . .
A 131-C	SHIPBUILDING	38	1 1/2	EG72T3	CO_2	. . .	. . .	490	71	30	-34	-29	61	45	41	**30**
A 441	STRUCTURAL	19	3/4	EG72T1	. . .	510	74	565	82	23	-29	-20	56	41	. . .	. . .
		25	1	EG72T1	. . .	455	66	558	81	23	-29	-20	49	36	. . .	. . .
		50	2	EG72T1	. . .	448	65	558	81	24	-29	-20	41	30	. . .	. . .
		50	2	EG72T4	CO_2	468	68	634	92	24	-18	-0.4	41	30	. . .	. . .
A 572	STRUCTURAL	25	1	EG72T4	80AR-20CO_2	. . .	. . .	. . .	. . .	. . .	-10	14	83	61	46	**34**
A 572-50	STRUCTURAL	38	1 1/2	EG72T1	. . .	393	57	531	77	23	-18	-0.4	19	14	. . .	. . .
A 588	STRUCTURAL	76	3	EG72T4	CO_2	. . .	. . .	655	95	23	-18	-0.4	76	56	. . .	. . .
A 203	PRESSURE VESSEL	41	1 5/8	EG72T4	80AR-20CO_2	365	53	496	72	32	-40	-40	31	23	. . .	. . .

A 516	PRESSURE VESSEL	25	1	EG72T1	. . .	400	58	510	74	26	-29	-20	38	28	. . .	**. . .**
		38	$1\frac{1}{2}$	EG72T4	80AR-20CO_2	538	78	621	90	29	-29	-20	56	41	87	**64**
A 537-1	PRESSURE VESSEL	19	$\frac{3}{4}$	EG72T1	. . .	483	70	593	86	24	-20	-4	58	43	. . .	**. . .**
		25	1	EG72T4	CO_2	427	62	572	83	29	-29	-20	46	34	53	**39**
		28	$1\frac{1}{8}$	EG72T4	80AR-20CO_2	510	74	689	100	26	-30	-22	62	46	. . .	**. . .**
A 633	**PRESSURE VESSEL**	**25**	**1**	**EG72T1**	**. . .**	**510**	**74**	**614**	**89**	**25**	**-18**	**-0.4**	**84**	**62**	**. . .**	**. . .**

Source: Ref 25

(A) AMERICAN IRON AND STEEL INSTITUTE (AISI) DESIGNATION.

Electroslag Welding (Ref 27, 28)

Electroslag welding (ESW) is similar in many respects, to electrogas welding (see the article "Electroslag and Electrogas Welding" in this Volume). Both are used to complete large, vertical welds in a single pass. High heat inputs and protracted thermal cycles are characteristic of these processes. Weld-metal hydrogen levels are low, and preheat is usually not required. The residual stresses and angular distortion are generally low. Weld-metal soundness is excellent provided the welding can be completed without stopping. The slow heating and cooling cycles, however, result in a wide, coarse-grained heat-affected zone and coarse, columnar weld metal. Low toughness and strength can be a problem in certain applications. Some codes, such as AWS D1.1, have restrictions on the use of these processes.

Electroslag welding is not an arc welding process. An arc is used only to initiate melting of a flux in order to form a molten slag. The molten slag, which is conductive, then extinguishes the arc and the heat necessary to complete the weld is generated by electrical resistance to the current passing through the slag. The molten slag also acts to shield the weld metal from the atmosphere. The fluxes used for electroslag welding are unique to the process. Most SAW fluxes will not work in ESW applications. Unlike electrogas welding, electroslag welding may use multiple electrodes. This allows thicker materials (up to 900 mm, or 36 in.) to be welded. Dilution from the baseplates can be quite high (up to 50%), so procedure qualifications are essential.

Process Variations. There are two variations of the process in general use. The conventional method uses a wire electrode (either solid or cored) and a nonconsumable guide to direct the electrode into the molten bath. The welding head moves up the plate as the weld progresses, and sliding copper shoes hold the molten puddle in position.

The consumable guide method employs a consumable guide tube that extends down the length of the joint. The welding head remains stationary at the top of the joint, and a wire electrode (either solid or cored) is fed down the center of the guide tube into the molten puddle. The steadily rising weld puddle consumes both the electrode and the guide tube. Some guide tubes are coated with flux. This provides electrical insulation and supplements the slag, some of which plates out onto the weld surface. Copper dams are used to hold the molten pool in place.

Metallurgically, there is little difference between the variations except that the consumable guide tubes (which comprise 5 to 10% of the weld metal in a 50 mm, or 2 in., plate weld) may not be available in the same range of chemistries as the wire electrodes.

Electrode chemistries and required properties for ESW are given in Ref 29. Typical mechanical properties of electroslag welds in carbon and alloy steels and in structural steels are given in Tables 14 and 15, respectively.

TABLE 14 TYPICAL MECHANICAL PROPERTIES OF WELD METAL FROM ELECTROSLAG WELDS IN CARBON AND ALLOY STEELS

BASE METAL (ASTM SPECIFICATION)	THICKNESS		ELECTRODE		HEAT TREATMENT[A]	YIELD STRENGTH		TENSILE STRENGTH		ELONGATION IN 50 MIN (2 IN.), %	IMPACT ENERGY (CHARPY V-NOTCH) AT 12.2 °C (10 °F) FOR INDICATED NOTCH LOCATION					
											WMFG[B]		WMCG[C]		BM HAZ[D]	
	IN.	MM	TYPE	QUANTITY		MPA	KSI	MPA	KSI		J	FT · LBF	J	FT · LBF	J	FT · LBF
A 204-A	$3\frac{1}{2}$	89	MN-MO	1	NT	382	55.5	562	81.5	27	46	34	39	29	18	**13**
A 515 GR70	$1\frac{1}{2}$	38	MN-MO	1	SR	358	52.0	579	84.1	26	61	45	35	26	10	**7**
	2	51	MN-MO	1	SR	469	68.1	587	85.2	23	63	46	29	21	7	**5**
	$3\frac{3}{8}$	86	MN-MO	2	NT	396	57.5	537	78.0	29	46	34	45	33	30	**22**
	$6\frac{3}{4}$	171	MN-MO	2	NT	313	45.5	512	74.3	31	33	24	29	21	16	**12**
A 302-B	3	76	MN-MO-NI	1	NT	393	57.0	565	82.0	28	72	53	71	52	86	**63**
A 387-C	3	76	$1\frac{1}{4}$CR-$\frac{1}{2}$MO	2	NT	320	46.5	503	73.0	29	95	70	103	76	78	**57**
A 387-D	$3\frac{1}{4}$	83	$2\frac{1}{4}$CR-1MO	1	SR	396	57.5	565	82.0	25	63	46	68	50	65	**48**
	$7\frac{1}{2}$	**191**	**$2\frac{1}{4}$CR-1MO**	**2**	**SR**	**551**	**80.0**	**658**	**95.5**	**20**	**84[E]**	**62[E]**	**102[E]**	**75[E]**	**113[E]**	**83[E]**

Source: Ref 28

(A) NT, NORMALIZED AND TEMPERED; SR, STRESS-RELIEVED.

(B) WMFG, WELD METAL, FINE GRAIN.

(C) WMCG, WELD METAL, COARSE GRAIN.

(D) BM HAZ, BASE METAL, HEAT-AFFECTED ZONE.

(E) IMPACTS AT 10 °C (50 °F).

TABLE 15 TYPICAL MECHANICAL PROPERTIES OF WELD METAL (IN AS-WELDED CONDITION) OBTAINED WITH ELECTROSLAG WELDS IN STRUCTURAL STEELS

Using solid-wire electrodes and applying consumable guide method

BASE METAL, ASTM	THICKNESS		ELECTRODE		YIELD STRENGTH		TENSILE STRENGTH		ELONGATION IN 50 MM (2 IN.), %	REDUCTION IN AREA, %	IMPACT ENERGY[A]	
	MM	IN	TYPE (AWS)	QUANTITY	MPA	KSI	MPA	KSI			J	FT · LBF
A 441	25	1	EM13K-EW	1	344	49.9	523	75.8	28.0	59.0	23	**17**
	64	$2\frac{1}{2}$	EM13K-EW	1	316	45.8	505	73.3	26.5	66.0	37	**27**
A 36	152	6	EM13K-EW	2	317	46.0	548	79.5	28.5	52.8	. . .	**. . .**
	305	12	EM13K-EW	2	255	37.0	464	67.3	33.5	71.0	. . .	**. . .**
A 572 GRADE 42	203	8	EM13K-EW	2	400	58.2	585	84.8	25.0	67.6	38	**28**
GRADE 60	**57**	**2** $\frac{1}{4}$	**EH10MO-EW**	**1**	**423**	**61.5**	**680**	**98.5**	**18.0**	**35.6**	**. . .**	**. . .**

Source: Ref 28

(A) AT -17.8 °C (0 °F).

Stud Arc Welding

Stud arc welding is commonly used to attach carbon steel studs to carbon steel plate (see the article "Stud Arc Welding" in this Volume). A primary characteristic of this process is the rapid heating and cooling cycle. Both the HAZ and the weld-metal area are relatively small. The rapid cooling rate can be a problem with medium-carbon and high-carbon steels because the likelihood of martensite formation is high. Preheat is essential for welding medium-carbon and high-carbon steels but is not required for low-carbon steels. Procedure tests should be run on high-carbon steels. Stud arc welding is a low-hydrogen process if the plate surface and studs are free of hydrogen-containing materials.

Studs for attachment to carbon steels are chosen based on their strength. Low-carbon steel studs are made from cold-drawn bar stock in grades 1006 to 1020 (killed or semi-killed). A minimum tensile strength of 380 to 415 MPa (55 to 60 ksi) is required. A stronger heat-treated steel stud (830 MPa, or 120 ksi, tensile strength) is also available. Most carbon steel studs require a flux (affixed to the end of the stud) for deoxidation. Aluminum is commonly used for this purpose.

References cited in this section

3. STRUCTURAL WELDING CODE, STEEL, AWS D1.1, AMERICAN WELDING SOCIETY, 1992
15. *WELDING HANDBOOK,* 8TH ED., VOL 1, AMERICAN WELDING SOCIETY, 1987, P 437-464
16. SPECIFICATION FOR CARBON STEEL FOR SHIELDED METAL ARC WELDING, A5.1-91, AMERICAN WELDING SOCIETY, 1991
17. SPECIFICATION FOR LOW-ALLOY STEEL COVERED ARC WELDING ELECTRODES, A5.5-81, AMERICAN WELDING SOCIETY, 1981
18. SPECIFICATION FOR LOW-ALLOY STEEL FILLER METALS FOR GAS-SHIELDED ARC WELDING, A5.28-79, AMERICAN WELDING SOCIETY, 1979
19. SPECIFICATION FOR CARBON STEEL FILLER METALS FOR GAS-SHIELDED ARC WELDING, A5.18-79, AMERICAN WELDING SOCIETY, 1979
20. SPECIFICATION FOR CARBON STEEL ELECTRODES FOR FLUX-CORED ARC WELDING, A5.20-79, AMERICAN WELDING SOCIETY, 1979

21. SPECIFICATION FOR LOW-ALLOY STEEL ELECTRODES FOR FLUX-CORED ARC WELDING, A5.29-80, AMERICAN WELDING SOCIETY, 1980
22. SPECIFICATION FOR CONSUMABLE INSERTS, A5.30-79, AMERICAN WELDING SOCIETY, 1979
23. SPECIFICATION FOR CARBON STEEL ELECTRODES AND FLUXES FOR SUBMERGED ARC WELDING, A5.17-89, AMERICAN WELDING SOCIETY, 1989
24. SPECIFICATION FOR LOW-ALLOY STEEL ELECTRODES AND FLUXES FOR SUBMERGED ARC WELDING, A5.23-90, AMERICAN WELDING SOCIETY, 1990
25. *WELDING HANDBOOK,* 8TH ED., VOL 2, AMERICAN WELDING SOCIETY, 1991, P 234-269
26. SPECIFICATION FOR CARBON AND LOW-ALLOY STEEL ELECTRODES FOR ELECTROGAS WELDING, A5.26-91, AMERICAN WELDING SOCIETY, 1991
27. *WELDING HANDBOOK,* 8TH ED., VOL 1, AMERICAN WELDING SOCIETY, 1987, P 13-16
28. *WELDING HANDBOOK,* 8TH ED., VOL 2, AMERICAN WELDING SOCIETY, 1991, P 272-294
29. SPECIFICATION FOR CARBON AND LOW-ALLOY STEEL ELECTRODES AND FLUXES FOR ELECTROSLAG WELDING, A5.25-91, AMERICAN WELDING SOCIETY, 1991

Arc Welding of Carbon Steels

Ronald B. Smith, The ESAB Group, Inc.

References

1. B.A. GRAVILLE, *THE PRINCIPLES OF COLD CRACKING CONTROL IN WELDS,* DOMINION BRIDGE COMPANY, 1975
2. H. GRANJON, *FUNDAMENTALS OF WELDING METALLURGY,* ABINGTON PUBLISHING, 1991, P 156-177
3. STRUCTURAL WELDING CODE, STEEL, AWS D1.1, AMERICAN WELDING SOCIETY, 1992
4. *WELDED STEEL CONSTRUCTION (METAL ARC WELDING),* CSA W59, CANADIAN STANDARDS ASSOCIATION, 1989
5. R.D. STOUT, *WELDABILITY OF STEELS,* 4TH ED., WELDING RESEARCH COUNCIL, 1987, P 420-426
6. *PROCESS OF ARC WELDING CARBON & CARBON MANGANESE STEELS,* BS5135, BRITISH STANDARDS INSTITUTE, 1984
7. F.R. COE, *WELDING STEELS WITHOUT HYDROGEN CRACKING,* THE WELDING INSTITUTE, 1973
8. J.F. LANCASTER, *THE METALLURGY OF WELDING,* 4TH ED., ALLEN AND UNWIN, 1987, P 157
9. *THE PROCEDURE HANDBOOK OF ARC WELDING,* LINCOLN ELECTRIC COMPANY, 1973, CHAPTERS 5 AND 12
10. W.F. SAVAGE AND A.H. ARONSON, *PREFERRED ORIENTATION IN THE WELD FUSION ZONE,* VOL 46, 1966
11. *WELDING HANDBOOK,* 8TH ED., VOL 1, AMERICAN WELDING SOCIETY, 1987, P 261
12. H.B. CARY, *MODERN WELDING TECHNOLOGY,* 2ND ED., PRENTICE-HALL, 1989, P 204-206
13. P.T. HOULDCROFT, *WHICH PROCESS?,* ABINGTON PUBLISHING, 1990
14. S. KOU, *WELDING METALLURGY,* JOHN WILEY & SONS, 1987, P 63
15. *WELDING HANDBOOK,* 8TH ED., VOL 1, AMERICAN WELDING SOCIETY, 1987, P 437-464
16. SPECIFICATION FOR CARBON STEEL FOR SHIELDED METAL ARC WELDING, A5.1-91, AMERICAN WELDING SOCIETY, 1991
17. SPECIFICATION FOR LOW-ALLOY STEEL COVERED ARC WELDING ELECTRODES, A5.5-81, AMERICAN WELDING SOCIETY, 1981

18. SPECIFICATION FOR LOW-ALLOY STEEL FILLER METALS FOR GAS-SHIELDED ARC WELDING, A5.28-79, AMERICAN WELDING SOCIETY, 1979
19. SPECIFICATION FOR CARBON STEEL FILLER METALS FOR GAS-SHIELDED ARC WELDING, A5.18-79, AMERICAN WELDING SOCIETY, 1979
20. SPECIFICATION FOR CARBON STEEL ELECTRODES FOR FLUX-CORED ARC WELDING, A5.20-79, AMERICAN WELDING SOCIETY, 1979
21. SPECIFICATION FOR LOW-ALLOY STEEL ELECTRODES FOR FLUX-CORED ARC WELDING, A5.29-80, AMERICAN WELDING SOCIETY, 1980
22. SPECIFICATION FOR CONSUMABLE INSERTS, A5.30-79, AMERICAN WELDING SOCIETY, 1979
23. SPECIFICATION FOR CARBON STEEL ELECTRODES AND FLUXES FOR SUBMERGED ARC WELDING, A5.17-89, AMERICAN WELDING SOCIETY, 1989
24. SPECIFICATION FOR LOW-ALLOY STEEL ELECTRODES AND FLUXES FOR SUBMERGED ARC WELDING, A5.23-90, AMERICAN WELDING SOCIETY, 1990
25. *WELDING HANDBOOK*, 8TH ED., VOL 2, AMERICAN WELDING SOCIETY, 1991, P 234-269
26. SPECIFICATION FOR CARBON AND LOW-ALLOY STEEL ELECTRODES FOR ELECTROGAS WELDING, A5.26-91, AMERICAN WELDING SOCIETY, 1991
27. *WELDING HANDBOOK*, 8TH ED., VOL 1, AMERICAN WELDING SOCIETY, 1987, P 13-16
28. *WELDING HANDBOOK*, 8TH ED., VOL 2, AMERICAN WELDING SOCIETY, 1991, P 272-294
29. SPECIFICATION FOR CARBON AND LOW-ALLOY STEEL ELECTRODES AND FLUXES FOR ELECTROSLAG WELDING, A5.25-91, AMERICAN WELDING SOCIETY, 1991

Arc Welding of Carbon Steels

Ronald B. Smith, The ESAB Group, Inc.

Selected References

- S. GANESH AND R.D. STOUT, MATERIAL VARIABLES AFFECTING LAMELLAR TEARING SUSCEPTIBILITY IN STEELS, *WELD. J.*, NOV 1976
- P.F. HOULDCROFT, *SUBMERGED ARC WELDING*, 2ND ED., ABINGTON PUBLISHING, 1989
- D.J. KOTECKI, HYDROGEN RECONSIDERED, *WELD. J.*, AUG 1992
- G.E. LINNERT, *WELDING METALLURGY*, VOL 2, AMERICAN WELDING SOCIETY, 1967
- W. LUCAS, *TIG AND PLASMA WELDING*, ABINGTON PUBLISHING, 1990
- *ASM HANDBOOK*, VOL 1, ASM INTERNATIONAL, 1990
- *MIG WELDING HANDBOOK*, L-TEC WELDING AND CUTTING SYSTEMS, 1987
- *SUBMERGED ARC WELDING HANDBOOK*, L-TEC WELDING AND CUTTING SYSTEMS, 1987
- *TIG WELDING HANDBOOK*, L-TEC WELDING AND CUTTING SYSTEMS, 1987
- *WELDING HANDBOOK*, 7TH ED., VOL 4, AMERICAN WELDING SOCIETY, 1982

Welding of Low-Alloy Steels

F.J. Winsor, Welding Consultant

Introduction

THE DETERMINATION of appropriate procedures and practices for low-alloy steels (those containing up to 10% Cr) involves a systematic evaluation of factors such as:

- DESIGN REQUIREMENTS
- AVAILABILITY AND PRACTICABILITY OF USING A PARTICULAR ARC WELDING PROCESS
- PRODUCTIVITY REQUIREMENTS
- CHARACTERISTICS OF FILLER METALS AND OTHER CONSUMABLES
- PROPERTIES OF WELD DEPOSITS
- PREHEATING AND POSTWELD HEAT-TREATMENT REQUIREMENTS DETERMINED BY THE METALLURGICAL CHARACTERISTICS OF THE LOW-ALLOY STEEL

When compared with other steels, the arc welding of low-alloy steels can require greater emphasis on some of these factors, because of unique mechanical property or service requirements, as well as metallurgical characteristics, such as hardenability and hydrogen embrittlement.

This article discusses factors involved in selecting welding processes and consumables and establishing procedures and practices for the arc welding of low-alloy steels. Because of their different design or service requirements and their often different welding characteristics, the low-alloy steels discussed in this article are categorized as:

- HIGH-STRENGTH LOW-ALLOY (HSLA) STRUCTURAL STEELS
- HIGH-STRENGTH LOW-ALLOY QUENCHED AND TEMPERED (HSLA Q&T) STRUCTURAL STEELS
- LOW-ALLOY STEELS FOR PRESSURE VESSELS AND PIPING
- MEDIUM-CARBON HEAT-TREATABLE (QUENCHED AND TEMPERED) LOW-ALLOY (HTLA) STEELS
- ULTRAHIGH-STRENGTH LOW-ALLOY STEELS
- LOW-ALLOY TOOL AND DIE STEELS

Welding Processes. All of the common arc welding processes can be used with low-alloy steels. Shielded metal arc, gas-tungsten arc, gas-metal arc, flux-cored arc, and submerged arc welding processes are used for most applications.

Electroslag and electrogas processes can be used to weld some of the low-alloy structural and pressure vessel steels, although restrictions may be imposed by some codes.

Welding of Low-Alloy Steels

F.J. Winsor, Welding Consultant

Welding Consumables

General information is provided below in terms of filler metals and fluxes and shielding gases.

Filler Metals and Fluxes

The selection of consumables for the arc welding of low-alloy steels is greatly facilitated by reference to American National Standards Institute/American Welding Society (ANSI/AWS) Filler Metal Specifications (Ref 1). These specifications define the requirements for classifying welding consumables in accordance with established parameters for chemical composition, mechanical properties, and usability. The ANSI/AWS specifications are often incorporated into the materials requirements of fabrication codes.

Shielding Gases

Gas-Tungsten Arc Welding (GTAW) and Plasma Arc Welding (PAW). The shielding gas most commonly used in the GTAW and PAW of low-alloy steels is 100% welding grade (99.995%) argon. Although argon is commonly used when gas backing is specified, nitrogen can also be used satisfactorily as a backing gas for many applications.

Gas-Metal Arc Welding (GMAW), Flux-Cored Arc Welding (FCAW), and Electrogas Welding (EGW). The selection of shielding gases used in these processes often depends on filler metal characteristics. Information should be obtained from the filler metal manufacturer or supplier regarding the proper shielding gas or mixture to be used. Use of a shielding gas other than that which is recommended can result in inferior welding performance or unsatisfactory weld metal chemical composition and/or properties.

Argon-oxygen and argon-carbon dioxide mixtures are commonly used for the GMAW and FCAW of low-alloy steels. Either argon-helium-carbon dioxide mixtures or 100% carbon dioxide are used for low-heat-input welding that utilizes small-diameter electrodes and a short-circuiting mode of metal transfer. Carbon dioxide shielding can also be used with larger-diameter electrodes, when its characteristic high spatter level can be tolerated and its resulting weld metal mechanical properties are acceptable.

The type of shielding gas has a significant effect on the mechanical properties of welds in low-alloy steels. A change in shielding from 100% CO_2 to a mixture of 75% Ar and 25% CO_2 generally results in a 10% increase in tensile strength of the weld metal in the as-deposited condition. This is due to greater retention of strengthening elements, such as manganese, silicon, and chromium, in the weld metal when the oxidizing effect of the arc atmosphere is lowered by the decrease in percentage of carbon dioxide. Depending on the original carbon content of the electrode, a carbon dioxide shielding atmosphere can result in either an increase or decrease in the carbon content of undiluted weld metal. If the carbon content of the electrode is less than 0.05%, then the weld metal tends to pick up carbon from the CO_2 shielding gas. If the carbon content of the electrode is greater than 0.10%, then the weld metal tends to lose carbon.

Reference cited in this section

1. "ANSI/AWS FILLER METAL SPECIFICATIONS," AWS, 1979-1992

Welding of Low-Alloy Steels

F.J. Winsor, Welding Consultant

High-Strength Low-Alloy (HSLA) Structural Steels

The HSLA structural steels typically contain less than 0.2% C and less than 2% alloy. They are different from other alloy steels in the sense that they are designed to meet specific mechanical property requirements, rather than a specified chemical composition. The steels have minimum yield strengths that range from 275 to 550 MPa (40 to 80 ksi) and tensile strengths that range from 415 to 655 MPa (60 to 95 ksi). ASTM specifications for typical HSLA as-rolled pearlitic structural steels include A 242, A 440, A 441, A 572, A 588, A 606, A 607, A 618, A 633, A 656, A 690, A 710, and A 715. Other HSLA steels are covered by Society of Automotive Engineers (SAE) Recommended Practice J410c. Some HSLA structural steels contain copper, phosphorus, nickel, chromium, and silicon in various combinations and amounts that provide a level of corrosion resistance that is up to four times better than that of carbon steel. The chemical compositions of typical ASTM HSLA structural steels are given in Table 1.

TABLE 1 TYPICAL COMPOSITION AND STRENGTH PROPERTIES OF HSLA STRUCTURAL STEELS

ASTM SPECIFICATION	TYPE OR GRADE	COMPOSITION, %[A]										MINIMUM TENSILE STRENGTH		MINIMUM YIELD STRENGTH	
		C	Mn	P	S	Si	Cr	Ni	Mo	V	OTHER	MPA	KSI	MPA	KSI
A 242	1	0.15	1.00	0.15	0.05	. . .	. . .	. . .	. . .	. . .	0.20 MIN CU	435-485	63-70	290-345	**42-50**
A 441	1	0.22	0.85-1.25	0.04	0.05	0.30	. . .	. . .	. . .	. . .	0.20 MIN CU; 0.02 MIN V	415-485	60-70	275-345	**40-50**
A 572	42[B]	0.21	1.35	0.04	0.05	0.30	. . .	. . .	. . .	. . .	0.20 MIN CU	415	60	290	**42**
	50[B]	0.23	1.35	0.04	0.05	0.30	. . .	. . .	. . .	. . .	0.20 MIN CU	450	65	345	**50**
	60[B]	0.26	1.35	0.04	0.05	0.30	. . .	. . .	. . .	. . .	0.20 MIN CU	515	75	415	**60**
	65[B]	0.26	1.65	0.04	0.05	0.30	. . .	. . .	. . .	. . .	0.20 MIN CU	550	80	450	**65**
A 588	A	0.10-0.19	0.90-1.25	0.04	0.05	0.15-0.30	0.40-0.65	. . .	. . .	0.02-0.10	0.25-0.40 CU	435-485	63-70	290-345	**42-50**
	B	0.20	0.75-1.25	0.04	0.05	0.15-0.30	0.40-0.70	0.25-0.50	. . .	0.01-0.10	0.20-0.40 CU	435-485	63-70	290-345	**42-50**
	C	0.15	0.80-1.35	0.04	0.05	0.15-0.30	0.30-0.50	0.25-0.50	. . .	0.01-0.10	0.20-0.50 CU	435-485	63-70	290-345	**42-50**
	D	0.10-0.20	0.75-1.25	0.04	0.05	0.50-0.90	0.50-0.90	. . .	. . .	. . .	0.30 CU; 0.05-0.15 ZR; 0.04 NB	435-485	63-70	290-345	**42-50**
	E	0.15	1.20	0.04	0.05	0.15-0.30	. . .	0.75-1.25	0.10-0.25	0.05	0.50-0.80 CU	435-485	63-70	290-345	**42-50**
	F	0.10-0.20	0.50-1.00	0.04	0.05	0.30	0.30	0.40-1.10	0.10-0.20	0.01-0.10	0.30-1.00 CU	435-485	63-70	290-345	**42-50**
	G	0.20	1.20	0.04	0.05	0.25-0.70	0.50-1.00	0.80	0.10	. . .	0.30-0.50 CU; 0.07 TI	435-485	63-70	290-345	**42-50**
	H	0.20	1.25	0.035	0.040	0.25-0.75	0.10-0.25	0.30-0.60	0.15	0.02-0.10	0.20-0.35 CU; 0.005-0.030 TI	435-485	63-70	290-345	**42-50**
	J	0.20	0.60-1.00	0.04	0.05	0.30-0.50	. . .	0.50-0.70	. . .	. . .	0.30 MIN CU; 0.03-0.05 TI	435-485	63-70	290-345	**42-50**
A 633	A	0.18	1.00-1.35	0.04	0.05	0.15-0.50	. . .	. . .	. . .	. . .	0.05 NB	435-570	63-83	290	**42**
	C	0.20	1.15-1.50	0.04	0.05	0.15-0.50	. . .	. . .	. . .	. . .	0.01-0.05 NB	450-620	65-90	315-345	**46-50**

	D	0.20	0.70-1.60	0.04	0.05	0.15-0.50	0.25	0.25	0.08	. . .	0.35 CU	450-620	65-90	315-345	**56-50**
	E	0.22	1.15-1.50	0.04	0.05	0.15-0.50	. . .	. . .	. . .	0.04-0.11	0.01-0.03 N	515-700	75-100	380-415	**55-50**
A 710	A	0.07	0.40-0.70	0.025	0.025	0.35	0.60-0.90	0.70-1.00	0.15-0.25	. . .	1.00-1.30 CU; 0.02 MIN NB	450-620	65-90	380-585	**55-85**
	B	**0.06**	**0.40-0.65**	**0.025**	**0.025**	**0.20-0.35**	**. . .**	**1.20-1.50**	**. . .**	**. . .**	**1.00-1.30 CU; 0.02 MIN NB**	**605-620**	**88-90**	**515-585**	**75-85**

Source: Ref 2

(A) SINGLE VALUES ARE MAXIMUM UNLESS OTHERWISE NOTED.

(B) THESE GRADES MAY CONTAIN NIOBIUM, VANADIUM, OR NITROGEN.

Filler Metal Selection

The predominant factor in most applications of HSLA steels is tensile strength; the alloy content is incidental. Consequently, filler metal is selected, most frequently, on the basis of providing a weld metal with minimum yield and tensile strength values that are at least equal to those of the base metal. However, HSLA steels are also often used because of their resistance to atmospheric corrosion. Such applications require that the alloy content and corrosion resistance of the weld deposit be considered.

Shielded Metal Arc Welding (SMAW). Some types of carbon steel electrodes (classified in ANSI/AWS specification A5.1) used in this process will deposit weld metal that has mechanical properties that are adequate to match those of some of the HSLA structural steels. Low-alloy steel covered electrodes are classified in ANSI/AWS specification A5.5. Table 2 shows the welding consumables for HSLA structural steels, based on ANSI/AWS D1.1 (Ref 3). This specification requires the use of low-hydrogen filler metals for welding HSLA structural steels in order to satisfy the conditions established for the prequalification of welding procedures.

TABLE 2 GUIDELINES FOR SELECTING CONSUMABLES TO WELD HSLA STRUCTURAL STEELS

PROCESS	**FILLER METAL**		BASE MATERIAL			
			ASTM SPECIFICATION	**THICKNESS**		GRADE
	ANSI/AWS SPECIFICATION	**CONSUMABLE[A]**		**MM**	**IN.**	
SMAW	A5.1	E7015; E7016; E7018; E7028; E7048	A 242	≤100	≤4	**. . .**
			A 441	ALL	ALL	**. . .**
			A 572	. . .	. . .	**42; 50**
			A 588	≤100	≤4	**. . .**
			A 633	≤65	$\leq 2\frac{1}{2}$	**A, B, C, D**
	A5.5	E8015-XX; E8016-XX; E8018-XX[B]	A 572	. . .	. . .	**60, 65**
			A 633	. . .	. . .	**E**
SAW	A5.17	F7XXX-EXXX	A 242	≤100	≤4	**. . .**
			A 441	ALL	ALL	**. . .**
			A 572	. . .	. . .	**42; 50**
			A 588	≤100	≤4	**. . .**
			A 633	≤65	$\leq 2\frac{1}{2}$	**A, B, C, D**
	A5.23	F8XX-EXXX-XX[B]	A 572	. . .	. . .	**60; 65**
			A 633	. . .	. . .	**E**
GMAW	A5.18	ER70S-X	A 242	≤100	≤4	**. . .**
			A 441	ALL	ALL	**. . .**
			A 572	. . .	. . .	**42; 50**
			A 588	≤100	≤4	**. . .**
			A 633	≤65	$\leq 2\frac{1}{2}$	**A, B, C, D**
	A5.28	ER80S-XX[B]	A 572	. . .	. . .	**60; 65**
			A 633	. . .	. . .	**E**
FCAW	A5.20	E7XT-1; E7XT-4; E7XT-5; E7XT-6; E7XT-7; E7XT-8; E7XT-11; E7XT-G	A 242	≤100	≤4	**. . .**
			A 441	ALL	ALL	**. . .**
			A 572	. . .	. . .	**42; 50**
			A 588	≤100	≤4	**. . .**
			A 633	≤65	$\leq 2\frac{1}{2}$	**A, B, C, D**
	A5.29	E8XTX-XX[B]	A 572	. . .	. . .	**60; 65**

			A 633	**. . .**	**. . .**	**E**

Source: Ref 3

(A) CONSULT THE APPROPRIATE ANSI/AWS FILLER METAL SPECIFICATION FOR INFORMATION ON THE SIGNIFICANCE OF "X" USED IN THE FILLER METAL DESIGNATIONS. OTHER CLASSIFICATIONS OF FILLER METAL (FOR EXAMPLE, A5.5; E80XX-XX, E7018-W, OR E8018-W COVERED ELECTRODES), AND CORRESPONDING ELECTRODES FOR SAW, GMAW, AND FCAW PROCESSES MAY BE REQUIRED TO ACHIEVE NOTCH TOUGHNESS REQUIREMENTS OR TO MATCH ATMOSPHERIC CORROSION AND WEATHERING CHARACTERISTICS.

(B) FOR BRIDGES, THE WELD METAL SHALL HAVE A MINIMUM CHARPY V-NOTCH IMPACT STRENGTH OF 27 J (20 FT · LBF) AT -20 °C (0 °F).

The low-temperature impact properties, as well as the tensile strength of the weld deposit, can be an important factor when selecting filler metals for the welding of HSLA steels. Various electrodes in ANSI/AWS specifications A5.1 and A5.5 have minimum Charpy impact test requirements at temperatures ranging from -20 to -100 °C (0 to -150 °F). In addition to relying on either the requirements of electrode specifications or typical test results furnished by electrode producers, it is often necessary to run procedure qualification tests to determine the impact properties of the weld metal and heat-affected zones (HAZs), because of code requirements or other considerations.

As indicated in footnote [(a)] of Table 2, low-alloy steel weld metal compositions are available to match the resistance to atmospheric weathering afforded by some HSLA structural steels. Because of the risk of hydrogen cracking when welding HSLA structural steels, most steel producers recommend the use of low-hydrogen electrodes. However, the use of electrodes that are not low in hydrogen may be acceptable in some applications, if the parts are relatively thin and the joints are not restrained or if a higher preheating temperature can be used.

Gas-Metal Arc Welding (GMAW) and Gas-Tungsten Arc Welding (GTAW). Suggested filler metals for the GMAW of low-alloy structural steels are given in Table 2. Similar filler metals can also be employed for GTAW, although this process is not often used for structural welding. The chemical compositions of the low-alloy steel filler metals included in ANSI/AWS specification A5.28 are generally comparable to the weld metal compositions provided by low-alloy steel SMAW electrodes. Some of the filler metals identified in this specification have minimum impact property requirements. This information is useful when selecting filler metals for application where low-temperature notch ductility is important.

Flux-Cored Arc Welding (FCAW). Flux-cored electrodes used for welding HSLA structural steels are classified in ANSI/AWS specifications A5.20 and A5.29. Weld metal compositions are generally comparable to those available from SMAW electrodes. Several classifications of flux-cored electrodes also have specified impact test requirements. Some types of flux-cored electrodes (self-shielding) require no external gas shielding. E80T1-W electrodes provide weld metal that has weathering characteristics similar to those of some low-alloy structural steels. Suggested electrodes for the FCAW of low-alloy structural steels are given in Table 2.

Submerged Arc Welding (SAW). Electrodes and fluxes used for the SAW of HSLA structural steels are classified in ANSI/AWS specifications A5.17 and A5.23. Inasmuch as numerous different electrode/flux combinations can be suitable for a specific application, it is not possible to suggest in this article anything other than broad categories, as shown in Table 2. When selecting electrodes and fluxes, it is often necessary to refer to producer literature for information on available electrode/flux combinations, performance characteristics of fluxes, and typical properties of weld deposits, as well as the electrode/flux specifications. In addition, procedure development tests may be necessary in order to determine the results obtained under representative fabricating conditions.

For the welding of HSLA steels exposed to outdoor environments in the unpainted condition, SAW compositions that match the weathering characteristics, as well as the mechanical properties of several HSLA steels, are available. Producers can offer recommendations on consumables for such applications.

Electroslag Welding (ESW) and Electrogas Welding (EGW). Solid and metal-cored electrodes used in the ESW of HSLA structural steels are classified in ANSI/AWS specification A5.25. Weld metal compositions are similar to those of many of the electrodes available for GMAW and SAW. Chromium-molybdenum, nickel, or nickel-chromium-copper

low-alloy steel weld metals are recommended for exposed, bare, and unpainted applications of ASTM A 588 steel. Classifications EWT2, EWT4, and EWS-EW are useful for other weather-resistant applications.

Flux-cored and solid electrodes classified in ANSI/AWS specification A5.26 for the EGW of HSLA structural steels are similar in composition to many of the flux-cored electrodes classified in ANSI/AWS specification A5.29 and the solid electrodes classified in ANSI/AWS specification A5.28 for GMAW.

The higher-energy input associated with ESW and EGW can result in weld metal and HAZ properties that are significantly different from those obtained with other arc welding processes. To select appropriate consumables, a consultation with producers and welding procedure development tests are recommended.

Welding Procedures and Practices

Preheating. The successful welding of HSLA structural steels requires consideration of a preheat. Generally, the need for preheating increases with increasing carbon and alloy content and with increasing steel thickness. The recommended minimum preheat and interpass temperatures for several HSLA structural steels are given in Table 3.

TABLE 3 MINIMUM PREHEAT AND INTERPASS TEMPERATURES TO WELD HSLA STRUCTURAL STEELS USING LOW-HYDROGEN WELDING PROCESSES

TEMPERATURE AT INDICATED THICKNESS								BASE METAL	
AT ≤20 MM (≤ 3/4 IN.)		**AT 20-40 MM (3/4-1 1/2 IN.)**		**AT 40-65 MM (1 1/2-2 1/2 IN.)**		**AT >65 MM (2 1/2 IN.)**			
°C	**°F**	**°C**	**°F**	**°C**	**°F**	**°C**	**°F**	**ASTM SPECIFICATION**	GRADE
0	32	10	50	65	150	105	225	A 242	**. . .**
								A 441	**. . .**
								A 572	**42**
									50
								A 588	**. . .**
								A 633	**A**
									B
									C
10	50	65	150	105	225	150	300	A 572	**60**
									65
								A 633	**E**

Source: Ref 3

Information on recommended preheat temperatures for other HSLA structural steels can be obtained from steel producers. If the preheat temperature is not sufficiently high, weld cracking can occur, particularly with highly restrained joints. When different preheat temperatures are specified for the joining of different thicknesses or types of HSLA steels, the higher preheat temperature should be used.

Postweld heat treatment is seldom required for welds in HSLA structural steels. However, it may be necessary to consider postweld heat treatment if:

- THE WELDMENT IS EXPOSED TO AN ENVIRONMENT THAT CAN CAUSE STRESS-CORROSION CRACKING
- CONTROL OF DIMENSIONS DURING MACHINING IS IMPORTANT
- IMPROVED DUCTILITY IS REQUIRED

When postweld heat treatment is required, the vanadium content of the weld metal should be no greater than 0.05%. The recommended postweld heat-treatment range for many HSLA structural steels is from 595 to 675 °C (1100 to 1250 °F). For proprietary steels, the postweld heat-treatment recommendations of the producer should be followed.

References cited in this section

2. CHAPTERS 1, 3, 4, *WELDING HANDBOOK*, 7TH ED., VOL 4, *METALS AND THEIR WELDABILITY*, AWS, 1982
3. "STRUCTURAL WELDING CODE--STEEL," ANSI/AWS D1.1-92, AWS, 1992

F.J. Winsor, Welding Consultant

High-Strength Low-Alloy Quenched and Tempered (HSLA Q&T) Structural Steels

HSLA Q&T structural steels typically contain less than 0.25% C and less than 5% alloy. These steels combine high yield and tensile strengths with good ductility, notch toughness, atmospheric corrosion resistance, and weldability. They are strengthened primarily by quenching and tempering to produce microstructures that contain martensite, bainite, and, in some compositions, ferrite. Some types are produced with a precipitation-hardening treatment that follows hot rolling or quenching. Yield strength values range from approximately 345 to 895 MPa (50 to 130 ksi), and tensile strength values range from 485 to 1035 MPa (70 to 150 ksi), depending on chemical composition, thickness, and heat treatment.

Many of the steels are included in ASTM specifications such as A 514, A 517, and A 543. However, a few steels, such as HY-80, HY-100, and HY-130, are covered by military specifications. The HSLA Q&T steels are furnished primarily as plate, although some are produced as either forgings or castings. The chemical compositions of typical steels are given in Table 4. Heat treatments used by the producers of these steels and the resulting microstructures are shown in Table 5.

TABLE 4 NOMINAL COMPOSITION AND TENSILE PROPERTIES OF SELECTED QUENCHED AND TEMPERED LOW-ALLOY STRUCTURAL STEELS

ASTM SPECIFICATION OR COMMON DESIGNATION	GRADE	COMPOSITION, %[A]										MINIMUM TENSILE STRENGTH[C]		MINIMUM YIELD STRENGTH[C]	
		C	Mn	P	S	Si	Cr	Ni	Mo	Cu	OTHER	MPA	KSI	MPA	KSI
A 514; A 517	A	0.15-0.21	0.80-1.10	0.035	0.04	0.40-0.80	0.50-0.80	. . .	0.18-0.28	. . .	ZR, 0.05-0.15; B, 0.0025	700-895; 725-930	100-130; 105-135	620-700	**90-100**
	B	0.12-0.21	0.70-1.00	0.035	0.04	0.20-0.35	0.40-0.65	. . .	0.15-0.25	. . .	V, 0.03-0.08; TI, 0.01-0.03; B, 0.0005-0.005	700-895; 725-930	100-130; 105-135	620-700	**90-100**
	C	0.10-0.20	1.10-1.50	0.035	0.04	0.15-0.30	. . .	. . .	0.20-0.30	. . .	B, 0.001-0.005	700-895; 725-930	100-130; 105-135	620-700	**90-100**
	D	0.13-0.20	0.40-0.70	0.035	0.04	0.20-0.35	0.85-1.20	. . .	0.15-0.25	0.20-0.40	TI, 0.004-0.10[B]; B, 0.0015-0.005	700-895; 725-930	100-130; 105-135	620-700	**90-100**
	E	0.12-0.20	0.40-0.70	0.035	0.04	0.20-0.35	1.40-2.00	. . .	0.40-0.60	0.20-0.40	TI, 0.04-0.10[A]; B, 0.0015-0.005	700-895; 725-930	100-130; 105-135	620-700	**90-100**
	F	0.10-0.20	0.60-1.00	0.035	0.04	0.15-0.35	0.40-0.65	0.70-1.00	0.40-0.60	0.15-0.50	V, 0.03-0.08; B, 0.0005-0.006	700-895; 725-930	100-130; 105-135	620-700	**90-100**
	G	0.15-0.21	0.80-1.10	0.035	0.04	0.50-0.90	0.50-0.90	. . .	0.40-0.60	. . .	ZR, 0.05-0.15; B, 0.0025	700-895; 725-930	100-130; 105-135	620-700	**90-100**
	H	0.12-0.21	0.95-1.30	0.035	0.04	0.20-0.35	0.40-0.65	0.30-0.70	0.20-0.30	. . .	V, 0.03-0.08; B, 0.0005-0.005	700-895; 725-	100-130; 105-	620-700	**90-100**

												930	135		
	J	0.12-0.21	0.45-0.70	0.035	0.04	0.20-0.35	. . .	. . .	0.50-0.65	. . .	B, 0.001-0.005	700-895; 725-930	100-130; 105-135	620-700	**90-100**
	K	0.10-0.20	1.10-1.50	0.035	0.04	0.15-0.30	. . .	. . .	0.45-0.55	. . .	B, 0.001-0.005	700-895; 725-930	100-130; 105-135	620-700	**90-100**
	L	0.13-0.20	0.40-0.70	0.035	0.04	0.20-0.35	1.15-1.65	. . .	0.25-0.40	0.20-0.40	TI, 0.04-0.10[(B)]; B, 0.0015-0.005	700-895; 725-930	100-130; 105-135	620-700	**90-100**
	M	0.12-0.21	0.45-0.70	0.035	0.04	0.20-0.35	. . .	1.20-1.50	0.45-0.60	. . .	B, 0.001-0.005	700-895; 725-930	100-130; 105-135	620-700	**90-100**
	N	0.15-0.21	0.80-1.10	0.035	0.04	0.40-0.90	0.50-0.80	. . .	0.25	. . .	ZR, 0.05-0.15; B, 0.0005-0.0025	700-895; 725-930	100-130; 105-135	620-700	**90-100**
	P	0.12-0.21	0.45-0.70	0.035	0.04	0.20-0.35	0.85-1.20	1.20-1.50	0.45-0.60	. . .	B, 0.001-0.005	700-895; 725-930	100-130; 105-135	620-700	**90-100**
	Q	0.14-0.21	0.95-1.30	0.035	0.04	0.15-0.35	1.00-1.50	1.20-1.50	0.40-0.60	. . .	V, 0.03-0.08	700-895; 725-930	100-130; 105-135	620-700	**90-100**
A 543	B	0.23	0.40	0.020	0.020	0.20-0.40	1.50-2.00	2.60-4.00	0.45-0.60	. . .	V, 0.03	620-930	90-135	480-700	**70-100**
	C	0.23	0.40	0.020	0.020	0.20-0.40	1.20-1.50	2.25-3.50	0.45-0.60	. . .	V, 0.03	620-930	90-135	480-700	**70-100**
HY-80	. . .	0.12-0.18	0.10-0.40	0.025	0.025	0.15-0.35	1.00-1.80	2.00-3.25	0.20-0.60	0.25	V, 0.03; TI, 0.02	. . .	. . .	550	**80**
HY-100	. . .	0.12-0.20	0.10-0.40	0.025	0.025	0.15-0.35	1.00-1.80	2.25-3.50	0.20-0.60	0.25	V, 0.03; TI, 0.02	. . .	. . .	700	**100**

HY-130	**. . .**	**0.12**	**0.60-0.90**	**0.010**	**0.015**	**0.15-0.35**	**0.40-0.70**	**4.75-5.25**	**0.30-0.65**	**. . .**	**V, 0.05-0.10**	**. . .**	**. . .**	**895**	**130**

Source: Ref 2

(A) WHEN A SINGLE VALUE IS SHOWN, IT IS A MAXIMUM LIMIT.

(B) VANADIUM MAY BE SUBSTITUTED FOR PART OR ALL OF TITANIUM CONTENT ON A ONE-FOR-ONE BASIS.

(C) LIMITING VALUES VARY WITH THE PLATE THICKNESS.

TABLE 5 TYPICAL HEAT TREATMENTS FOR QUENCHED AND TEMPERED LOW-ALLOY STRUCTURAL STEELS THAT YIELD BAINITE AND MARTENSITE MICROSTRUCTURES

BASE METAL ASTM SPECIFICATION OR COMMON DESIGNATION	**AUSTENITIZING TEMPERATURE**		**QUENCHING MEDIUM**	TEMPERING TEMPERATURE	
	°C	**°F**		**°C**	°F
A 514; A 517	900	1650	WATER OR OIL	620	**1150**
A 543, TYPE B	900	1650	WATER	540	**1000**
HY-80; HY-100	900	1650	WATER	650	**1200**
HY-130	**815**	**1500**	**WATER**	**540**	**1000**

Welding Processes

Any of the common arc welding processes can be used to join the quenched and tempered low-alloy structural steels that have minimum yield strengths of ≤1035 MPa (≤150 ksi). However, the GMAW and GTAW processes are preferred for welding steels with minimum yield strengths of [ges]700 MPa ([ges]100 ksi), such as HY-130, because they afford a higher level of notch toughness in the weld metal.

Filler Metals

Welding filler metals and electrode/flux combinations are available for welding most of the HSLA Q&T structural steels. Many of these consumables are classified in ANSI/AWS filler metal specifications for low-alloy steels. The selection of consumables is usually based on factors such as tensile strength, composition, and notch toughness of the weld metal. For some steels, more than one type or classification of welding consumable may satisfy the fabrication requirements.

The selection of welding consumables for a specific application should be based on a thorough evaluation of the design requirements and knowledge of the available weld metal properties, such as tensile strength, ductility, and impact strength. In general, the deposited weld metal should have properties that either match or exceed those of the base metal. However, for welds that are subject to relatively low stresses, the use of a weld metal that has a lower strength than that of the base metal may be acceptable. Typical examples are fillet welds stressed in longitudinal shear, welds carrying low secondary stresses, and welds that join a lower-strength steel to a HSLA Q&T steel. In cases where the design permits, lower-strength weld metal can be advantageous, allowing highly restrained welds to resist the tendency for toe cracking (that is, cracking at the toe of a fillet weld) or lamellar tearing in the steel, especially with corner and T-joints.

Weld Metal Hydrogen

The weld metal hydrogen content must be maintained at very low levels when welding HSLA Q&T steels, in order to avoid hydrogen-induced cracking. The maximum acceptable moisture, or hydrogen content, of covered electrodes, bare filler metal, and fluxes decreases as the strength of the weld metal increases. Welding consumables must be produced, packaged, stored, and used in a manner that limits the weld metal hydrogen content to a low level.

Weld Design

In order to employ HSLA Q&T structural steels advantageously, it is necessary to use appropriate joint designs, careful workmanship, and adequate inspection. Weld joints should be designed and located to avoid abrupt changes in cross section or other stress raisers in regions of high stress. Joints should permit good accessibility for welding and inspection. Groove welds are preferred over fillet welds for many applications, because of inherent stress concentrations associated with fillet welds and because groove welds are more amenable to volumetric methods of examination, such as radiographic or ultrasonic testing. The weld metal should blend smoothly into the base metal, with no abrupt ridges or valleys, and excessive reinforcement should be avoided.

Preheat and Interpass Temperature Control

The successful welding of HSLA Q&T structural steels often requires preheating in order to prevent cracking. However, caution must be exercised, because the preheat temperature affects the cooling rate during welding, thereby possibly affecting the microstructures and properties of the weld metal and HAZs. A preheat or interpass temperature that is too

high can decrease the rate of cooling of the weld metal and HAZs sufficiently to result in the transformation of austenite to either ferrite (containing regions of high-carbon martensite) or coarse bainite. Both structures lack high strength and good toughness. Next to the reaustenitized portion of the HAZ, a region of previously tempered base metal may be overtempered, causing a loss in strength.

Suggested preheat and interpass temperature ranges for some HSLA Q&T steels are given in Table 6. Information on preheating can be obtained from producers of HSLA Q&T steels. Exceeding the recommended maximum temperature should be avoided. If a preheat temperature of 40 °C (100 °F) or less is used, precautions must be taken to ensure that the surfaces to be welded are dry.

TABLE 6 TYPICAL PREHEAT AND INTERPASS TEMPERATURE RANGES TO WELD QUENCHED AND TEMPERED HSLA STRUCTURAL STEELS

BASE METAL ASTM SPECIFICATION OR COMMON DESIGNATION	**THICKNESS**		PREHEAT AND INTERPASS TEMPERATURE RANGE	
	MM	**IN.**	**°C**	°F
A 514; A517	≤20	$\leq \frac{3}{4}$	10-95	**50-200**
	>20-40	$>\frac{3}{4}\text{-}1\frac{1}{2}$	50-135	**125-275**
	>40-65	$>1\frac{1}{2}\text{-}2\frac{1}{2}$	80-165	**175-325**
	>65	$>2\frac{1}{2}$	105-190	**225-375**
A 543	≤12.5	$\leq \frac{1}{2}$	40-120	**100-250**
	>12.5-20	$>\frac{1}{2}\text{-}\frac{3}{4}$	50-135	**125-275**
	>20-25	$>\frac{3}{4}\text{-}1$	65-150	**150-300**
	>25-50	>1-2	95-175	**200-350**
	>50	>2	150-230	**300-450**
HY-80, HY-100	≤12.5	$\leq \frac{1}{2}$	15-150	**60-300**
	>12.5-28.7	$>\frac{1}{2}\text{-}1.13$	50-150	**125-300**
	>28.9	>1.14	95-150	**200-300**
HY-130	≤16	≤0.63	25-65	**75-150**
	16.3-22.4	0.64-0.88	50-95	**125-200**
	22.6-35.1	0.89-1.38	95-135	**200-275**
	>35.1	**>1.38**	**105-150**	**225-300**

Heat Input

In addition to preheat and interpass temperature, the heat (energy) input during welding and the base metal thickness are factors that affect the cooling rate, and thereby affect the microstructures and mechanical properties of the weld metal and HAZs. As is the case with too high a preheat and interpass temperature, excessive heat input can decrease the rate of cooling sufficiently to produce unfavorable microstructures and properties. Welding heat input is of greater concern in steels with a minimum yield strength of 700 MPa (100 ksi) than it is in lower-strength HSLA Q&T steels.

The welding heat input can be calculated as follows:

$$H = \frac{E.I.60}{S.1000} \qquad \textbf{(EQ 1)}$$

where H is heat input (arc energy), in units of kJ/in.; E is arc voltage, in V; I is welding current, in A; and S is arc travel speed, in units of in./min.

Table 7 shows the maximum permissible welding heat input for butt joints in ASTM A 514/A 517, grade F steel, depending on the preheat temperature and section thickness. Exceeding the maximum specified heat input can result in undesirable microstructures and unacceptable mechanical properties. Because of the different metallurgical characteristics that are possible, other types of steel may require different heat input limitations.

TABLE 7 MAXIMUM WELDING HEAT INPUT FOR BUTT JOINTS IN ASTM SPECIFICATION A 514 AND A 517 GRADE F QUENCHED AND TEMPERED HSLA STEEL

PREHEAT TEMPERATURE		MAXIMUM HEAT INPUT FOR INDICATED SECTION THICKNESS[A]															
		AT 4.8 MM (0.19 IN.)		**AT 6.35 MM (0.25 IN.)**		**AT 12.7 MM (0.5 IN.)**		**AT 19.1 MM (0.75 MIN.)**		**AT 25.4 MM (1.0 IN.)**		**AT 31.8 MM (1.25 IN.)**		**AT 38.1 MM (1.5 IN.)**		AT 50.8 MM (2.0 IN.)	
°C	**°F**	**KJ/MM**	**KJ/IN.**	**KJ/MM**	**KJ/IN.**	**KJ/MM**	**KJ/IN.**	**KJ/MM**	**KJ/IN.**	**KJ/MM**	**KJ/IN.**	**KJ/MM**	**KJ/IN.**	**KJ/MM**	**KJ/IN.**	**KJ/MM**	KJ/IN.
20	70	1.1	27	1.4	36	2.8	70	4.8	121	(B)	(B)	(B)	(B)	(B)	(B)	(B)	**(B)**
95	200	0.83	21	1.1	29	2.2	56	3.9	99	6.8	173	(B)	(B)	(B)	(B)	(B)	**(B)**
150	300	0.67	17	0.94	24	1.9	47	3.2	82	5.0	126	6.9	175	(B)	(B)	(B)	**(B)**
205	**400**	**0.51**	**13**	**0.75**	**19**	**1.6**	**40**	**2.6**	**65**	**3.7**	**93**	**5.0**	**127**	**6.5**	**165**	**(B)**	**(B)**

Source: Ref 2

(A) FOR INTERMEDIATE PREHEAT TEMPERATURES AND THICKNESSES, INTERPOLATE TO OBTAIN HEAT INPUT LIMIT. THIS LIMIT CAN BE INCREASED 25% FOR FILLET WELDS.

(B) NO HEAT INPUT LIMIT FOR MOST ARC WELDING PROCESSES. HIGH HEAT INPUT PROCESSES SHOULD NOT BE USED.

Heat input limitations apply to each weld pass and are not considered cumulatively. They also limit the size of weld beads. Large weld beads typically have poor notch toughness. Therefore, a good welding practice for Q&T steels is to deposit many small stringer beads. This technique produces a weld metal that has good notch toughness as a result of the grain refining and tempering effect of successive weld passes.

These heat input limitations are applicable only for single-arc welding processes. Multiple-arc processes, with the arcs in tandem, generally do not allow sufficient time for the metal deposited by the first arc to cool before the second arc passes over it, supplying additional heat. This can significantly influence the transformation of austenite in the weld metal and HAZs and adversely affect the weld properties. Multiple-arc processes should not be used to weld HSLA Q&T steels prior to conducting welding procedure development tests to prove their suitability.

The cooling rates of welds made using the SMAW, GMAW, FCAW, and GTAW processes are usually sufficiently rapid, under normal conditions, so that the mechanical properties of the HAZ approach those of the unaffected quenched and tempered base metal. The use of high heat input welding processes, such as ESW, EGW, or multiple-wire SAW, generally should be avoided when welding HSLA Q&T steels. Such processes may require complete heat treatment (quenching and tempering) of the weldment in order to obtain acceptable mechanical properties.

Postweld Heat Treatment

Postweld heat treatment is seldom required for welds in HSLA Q&T structural steels, except where heavy sections are involved. The mechanical properties of either the base metal or the weld metal can be adversely affected by postweld heat treatment. When weldments of some HSLA Q&T structural steels are heated to above 510 °C (950 °F), intergranular cracking can occur in the coarse-grained region of the weld HAZ. Cracking occurs by stress rupture, usually early in the heat-treatment cycle.

In situations where postweld heat treatment is necessary, some practices may be used singly or in combination to minimize cracking during postweld heat treatment. These practices involve:

- SELECTING A WELD LOCATION, WELD JOINT DESIGN, AND ASSEMBLY SEQUENCE THAT WILL MINIMIZE RESIDUAL STRESSES AND STRESS CONCENTRATIONS
- USING A TYPE OF WELD METAL THAT HAS SIGNIFICANTLY LOWER STRENGTH THAN THAT OF THE HAZ AT THE POSTWELD HEAT-TREATMENT TEMPERATURE
- PEENING EACH WELD LAYER, EXCEPT THE ROOT AND FINAL LAYERS
- HEATING TO THE POSTWELD HEAT-TREATMENT TEMPERATURE RANGE AS RAPIDLY AS POSSIBLE

In the postweld heat treatment of quenched and tempered steels, the mill tempering temperature used by the steel producer should not be exceeded. To avoid unnecessary risks, the steel producer should be consulted prior to reaching a decision regarding postweld heat treatment of a HSLA Q&T structural steel.

Of the available HSLA Q&T structural steels, only ASTM A 514 and A 517 are customarily given postweld heat treatments when the section thickness exceeds a specified amount.

Reference cited in this section

2. CHAPTERS 1, 3, 4, *WELDING HANDBOOK,* 7TH ED., VOL 4, *METALS AND THEIR WELDABILITY,* AWS, 1982

Welding of Low-Alloy Steels

F.J. Winsor, Welding Consultant

Low-Alloy Steels for Pressure Vessels and Piping

A variety of low-alloy steels containing from 0.10 to 0.30% C and up to 10% total alloy are used for welded pressure vessels and piping. Alloy additions include manganese, silicon, molybdenum, chromium, nickel, vanadium, copper, and niobium. Table 8 gives the nominal chemical composition and minimum specified tensile strength values of representative low-alloy steels used in pressure vessels and piping. These steels are usually furnished in the as-rolled, as-forged, or annealed condition. Some steels, such as those shown in Table 9, also may be obtained in the normalized, normalized and tempered, or quenched and tempered condition to provide enhanced mechanical properties.

TABLE 8 TYPICAL AS-ROLLED, AS-FORGED, OR ANNEALED LOW-ALLOY STEELS USED FOR PRESSURE VESSELS AND PIPING

PRODUCT TYPE	**BASE METAL ASTM SPECIFICATION**	**GRADE**	**NOMINAL COMPOSITION, WT%**			MAXIMUM SPECIFIED TENSILE STRENGTH	
			Cr	**Mo**	**Ni**	**MPA**	KSI
PLATE	A 203	A	. . .	. . .	2.25	450	**65**
		B	. . .	. . .	2.25	480	**70**
		D	. . .	. . .	3.50	450	**65**
		E	. . .	. . .	3.50	480	**70**
		F (≤50 MM, OR 2 IN.)	. . .	. . .	3.50	550	**80**
		(>50 MM, OR 2 IN.)	. . .	. . .	3.50	515	**75**
	A 204	A	. . .	0.5	. . .	450	**65**
		B	. . .	0.5	. . .	480	**70**
		C	. . .	0.5	. . .	515	**75**
	A 387	2	0.5	0.5	. . .	380	**55**
		12	1	0.5	. . .	380	**55**
		11	1.25	0.5	. . .	415	**60**
		22	2.25	1	. . .	415	**60**
		21	3	1	. . .	415	**60**
		5	5	0.5	. . .	415	**60**
		7	7	0.5	. . .	415	**60**
		9	9	1	. . .	415	**60**
PIPE	A 369	FP1	. . .	0.5	. . .	380	**55**
		FP2	0.5	0.5	. . .	380	**55**
		FP5	5	0.5	. . .	415	**60**
		FP7	7	0.5	. . .	415	**60**
		FP9	9	1	. . .	415	**60**
		FP11	1.25	0.5	. . .	415	**60**
		FP12	1	0.5	. . .	415	**60**
		FP21	3	1	. . .	415	**60**
		FP22	**2.25**	**1**	**. . .**	**415**	**60**

TABLE 9 SELECTED NORMALIZED, NORMALIZED AND TEMPERED, OR QUENCHED AND TEMPERED LOW-ALLOY STEELS USED FOR PRESSURE VESSEL AND PIPING APPLICATIONS

PRODUCT TYPE	**ASTM SPECIFICATION**	**GRADE**	**COMPOSITION, WT%**	MAXIMUM SPECIFIED TENSILE

								STRENGTH	
			Ni	**Cr**	**Cu**	**Mn**	**Mo**	**MPA**	KSI
PIPE FITTINGS	A 420	WPL 9	1.9	. . .	1	. . .	. . .	435	**63**
		WPL 3	3.5	. . .	. . .	. . .	. . .	450	**65**
		WPL 8	9	. . .	. . .	. . .	. . .	690	**100**
FORGINGS	A 508	CLASS 2	0.75	0.35	. . .	. . .	0.65	550	**80**
		CLASS 3	0.70	. . .	. . .	. . .	0.50	550	**80**
		CLASS 4	3.50	1.75	. . .	. . .	0.50	725	**105**
		CLASS 5	3.50	1.75	. . .	. . .	0.50	725	**105**
	A 541	CLASS 2	0.75	0.35	. . .	. . .	0.65	550	**80**
		CLASS 3	0.70	. . .	. . .	. . .	0.50	550	**80**
		CLASS 5	. . .	1.25	. . .	. . .	0.50	550	**80**
		CLASS 6	. . .	2.25	. . .	. . .	1	725	**105**
		CLASS 7	3.35	1.6	. . .	. . .	0.50	725	**105**
		CLASS 8	3.35	1.6	. . .	. . .	0.50	725	**105**
FLAGES, FITTINGS, AND VALVES	A 522	TYPE I	9	. . .	. . .	. . .	. . .	725	**100**
		TYPE II	8	. . .	. . .	. . .	. . .	725	**100**
PLATES	A 533	TYPE A	. . .	. . .	. . .	1.3	0.5	550[A] 620[B] 690[C]	**80[A]** **90[B]** **100[C]**
		TYPE B	0.55	. . .	. . .	1.3	0.5	550[A] 620[B] 690[C]	**80[A]** **90[B]** **100[C]**
		TYPE C	0.85	. . .	. . .	1.3	0.5	550[A] 620[B] 690[C]	**80[A]** **90[B]** **100[C]**
		TYPE D	**0.30**	**. . .**	**. . .**	**1.3**	**0.5**	**550[A]** **620[B]** **690[C]**	**80[A]** **90[B]** **100[C]**

(A) CLASS 1.

(B) CLASS 2.

(C) CLASS 3

The choice of low-alloy steel to be used for a pressure vessel or piping system is usually made on the basis of one or more desired properties in service, such as tensile strength, resistance to hydrogen attack, resistance to creep and oxidation at elevated temperatures, or low-temperature notch ductility. Weldability is an important consideration, as well.

Heat-resisting low-alloy steels used for pressure vessels and pipe generally contain up to 0.25% C, plus alloy additions such as chromium, molybdenum, vanadium, and silicon. When compared with plain carbon steels, the heat-resisting steels offer greater tensile and creep-rupture strengths at elevated temperatures and greater resistance to oxidation and hydrogen attack. Steels with from 1 to 9% Ni provide greater resistance to notch embrittlement than do carbon steels or many other low-alloy steels and are widely used in low-temperature service.

Welding Processes and Practices

All of the common arc welding processes can be used to join low-alloy steels used for pressure vessels and piping. SMAW, GTAW, GMAW, FCAW, and SAW are used for most applications. Successful welding requires consideration of preheating and control of weld metal hydrogen content. The use of low-hydrogen consumables and practices is essential in welding most low-alloy steels that contain more than minor amounts of alloying elements. When notch toughness requirements are important, control of heat input must be considered.

ESW and EGW can be used for many low-alloy steels. However, careful evaluation is required when good notch toughness in the weld metal and HAZ is important. A postweld grain refinement heat treatment may be required by some codes and specifications. Preheating is not normally necessary with these high heat input processes.

Filler Metal Selection

In order to provide weld metals that match or exceed the service performance characteristics of low-alloy steel base metals used in pressure vessels and piping, it is frequently necessary to base the filler metal selection on considerations of chemical composition and mechanical properties. In most cases, the content of critical elements in the weld metal must either match or exceed that of the base metal.

Shielded Metal Arc Welding. Electrodes for the SMAW of low-alloy steels used for pressure vessels and piping are classified in ANSI/AWS specification A5.5. In addition, 5%Cr-0.5%Mo and 9%Cr-1%Mo electrodes are classified in ANSI/AWS specification A5.4. Nearly all welding of low-alloy steels is done using low-hydrogen electrodes. However, electrodes that are not low in hydrogen can be used satisfactorily in a few applications where base metals are relatively thin and/or where higher preheat temperatures are feasible. Examples include the welding of C-Mo steel pipe and tubing and the welding of the root pass of groove welds in low Cr-Mo pipe and tubing. All-position electrodes that are not low in hydrogen may have better usability than low-hydrogen types for out-of-position welding, especially where frequent changes in welding position are necessary, as in the welding of pipe in the fixed horizontal position.

At present, SMAW electrodes that will deposit weld metal that has a nominal content of 9% Ni, to match that of ASTM A 353 or A 333, grade 8, base metal, for example, are not commercially available. To weld this material, it is common industry practice to use either an austenitic stainless steel electrode classified in ANSI/AWS specification A5.4 or a nickel-chromium-iron or nickel-chromium-molybdenum alloy electrode classified in ANSI/AWS specification A5.11. The selection of dissimilar alloy covered electrodes or other consumables for the welding of 9% Ni steels must be done carefully, based on the design tensile strength and low-temperature impact requirements.

For cyclic temperature service, consideration should be given to the possible adverse effect of the greater coefficient of linear thermal expansion of austenitic stainless steel, compared to that of nickel-base alloy weld metals.

Gas-Tungsten Arc Welding and Gas-Metal Arc Welding. Bare filler metals for the gas-shielded arc welding of low-alloy steels used for pressure vessels and piping are classified in ANSI/AWS specifications A5.28 and A5.9 (classifications ER502 and ER505). The chemical compositions of low-alloy steel bare filler metals are generally comparable to the deposits produced by covered electrodes for SMAW. As with covered electrodes, there is no standard matching composition of bare welding filler metal for joining 9% Ni steel. To weld this material, it is common practice to use a stainless steel filler metal classified in ANSI/AWS specification A5.9 or a nickel-chromium or nickel-chromium-iron alloy filler metal classified in ANSI/AWS specification A5.14, selected to provide the required tensile strength and impact properties in the weld metal.

ANSI/AWS specification A5.9 classifies matching ER502 and ER505 filler metals for the welding of 5Cr-0.5Mo and 9Cr-lMo base metals, respectively. Filler metal of 9Cr-1Mo is also used to weld 7Cr-0.5Mo base metal.

Flux-Cored Arc Welding. Low-alloy steel electrodes for the FCAW of low-alloy steels used in pressure vessels and piping are classified in ANSI/AWS specification A5.29. Also, ANSI/AWS specification A5.22 classifies E502T-X and E505T-X flux-cored electrodes for welding 5Cr-0.5Mo, 7Cr-0.5Mo, and 9Cr-1Mo base metals.

Submerged Arc Welding. Electrodes and fluxes used for the SAW of low-alloy steels for pressure vessels and piping are classified in ANSI/AWS specification A5.23. Low-alloy steels are most often welded using a neutral flux and an alloy steel electrode. Occasionally, a carbon steel electrode can be used with a particular alloy flux designed to yield weld metal of the desired alloy composition.

When selecting electrodes and fluxes for submerged arc welding, it is often necessary or desirable to consult producers of electrodes and fluxes for information on the characteristics of their fluxes, recommendations on electrode/flux combinations, and data on typical properties of weld deposits, in addition to referring to ANSI/AWS specification A5.23. Such information can often be of great assistance in narrowing the search for suitable SAW consumables. Most pressure vessel and piping applications require procedure qualification testing to demonstrate that a particular electrode/flux combination will deposit weld metal that has the required chemical composition and mechanical properties.

To avoid hydrogen-induced cracking, care should be taken to maintain the flux and electrode in a dry condition. Producers should be consulted for recommendations concerning the storage and reconditioning of submerged arc welding flux.

Electroslag and Electrogas Welding. Low-alloy steel electrodes for ESW are classified in ANSI/AWS specification A5.25, whereas low-alloy steel electrodes for EGW are classified in ANSI/AWS A5.26. Only a few of the low-alloy steel compositions in these specifications satisfy requirements for matching chemical compositions of low-alloy steels used for pressure vessels. However, in some situations, nonmatching compositions may be acceptable. Fortunately, electrodes classified in various other filler metal specifications are useful for electroslag and electrogas welding. Thus, solid and metal-cored electrodes classified in ANSI/AWS A5.23 (for SAW) and in ANSI/AWS A5.28 (for GMAW) may also be useful for ESW and EGW. Appropriate testing is required to ensure that the required weld metal chemical composition and mechanical properties are obtained.

Welding Procedures and Practices

Preheating. The successful welding of low-alloy steels used for pressure vessels and piping requires the consideration of preheating. The suggested minimum preheat and interpass temperatures for several low-alloy steels are given in Table 10. The appropriate sections of the ASME Boiler and Pressure Vessel Code (Ref 4) or the American Society of Mechanical Engineers (ASME) B31.1 Power Piping Code and B31.3 Chemical Plant and Petroleum Piping Code should be consulted for preheat recommendations or requirements regarding boilers, pressure vessels, and code piping.

TABLE 10 RECOMMENDED MINIMUM PREHEAT AND INTERPASS TEMPERATURES TO WELD LOW-ALLOY STEEL PRESSURE VESSELS AND PIPES

PRODUCT TYPE AND ALLOY CLASSIFICATION	ASTM SPECIFICATION	GRADE	THICKNESS		MINIMUM PREHEAT AND INTERPASS TEMPERATURE		MAXIMUM TENSILE STRENGTH	
			mm	in.	°C	°F	MPA	KSI
PRESSURE VESSEL PLATE								
NICKEL	A 203	A	(A)	(A)	120	250	(B)	**(B)**
		B	(A)	(A)	120	250	(B)	**(B)**
		D	(A)	(A)	150	300	(B)	**(B)**
		E	(A)	(A)	150	300	(B)	**(B)**
		F	(A)	(A)	150	300	(B)	**(B)**
MOLYBDENUM	A 204	. . .	<12.5	<0.5	10	50	485	**70**
					80	175	>485	**>70**
			[GES]12.5	[GES]0.5	80	175	(B)	**(B)**
MANGANESE-	A 302	A; B	<12.5	<0.5	10	50	485	**70**

MANGANESE-MOLYBDENUM NICKEL			[GES]12.5	[GES]0.5	80	175	(B)	**(B)**
9% NICKEL	A 353	. . .	(A)	(A)	10	50	(B)	**(B)**
CHROMIUM-NICKEL	A 387	11; 12	≤12.5	≤0.5	10	50	415	**60**
			>12.5	>0.5	120	250	415	**60**
			(A)	(A)	120	250	>415	**>60**
		5; 22	(A)	(A)	150	300	415	**60**
					205	400	>415	**>60**
PIPE								
SEAMLESS AND WELDED FOR LOW-TEMPERATURE SERVICE	A 333	3	(A)	(A)	150	300	(B)	**(B)**
		7	(A)	(A)	120	250	(B)	**(B)**
		8	(A)	(A)	10	50	(B)	**(B)**
SEAMLESS FERRITIC FOR HIGH-TEMPERATURE SERVICE	A 335	P1	<12.5	<0.5	10	50	485	**70**
					80	175	>485	**>70**
			[GES]12.5	[GES]0.5	80	175	(B)	**(B)**
		P5	(A)	(A)	150	300	415	**60**
					205	400	>415	**>60**
		P11;P12	≤12.5	≤0.5	10	50	415	**60**
			>12.5	>0.5	120	250	415	**60**
			(A)	(A)	120	250	>415	**>60**
		P22	(A)	(A)	150	300	415	**60**
					205	400	>415	**>60**
ELECTRIC-FUSION WELDED FOR HIGH-PRESSURE SERVICE AT MODERATE TEMPERATURES	A 672	H75; H80	<12.5	<0.5	10	50	485	**70**
					80	175	>485	**>70**
			[GES]12.5	**[GES]0.5**	**80**	**175**	**(B)**	**(B)**

(A) ALL AVAILABLE SIZES PER ASTM SPECIFICATIONS.

(B) VALUES VARY WITH SIZE.

Postweld heat treatment is often essential for welds in low-alloy steels used for pressure vessels and piping. Various sections of the ASME Boiler and Pressure Vessel Code (Ref 4), the ASME Piping Codes, and military specifications specify requirements for postheat treatment of welds in low-alloy steels. Frequently, purchasers of equipment refer to proprietary specifications that contain postweld heat-treatment requirements. For some materials with certain categories and thicknesses of joints, the codes or other fabrication specifications may allow exemptions from postweld heat-treatment requirements. Because of the differences in various codes and specifications, it is not feasible to provide a universally adequate and reliable summary here of all postweld heat-treatment requirements and practices for low-alloy steel pressure vessel and pipe welding.

Table 11 presents a general view of some of the different postweld heat-treatment temperatures involved in welding low-alloy steels for pressure vessels and piping. The applicable section of the ASME Boiler and Pressure Vessel Code (Ref 4), the ASME Piping Codes, military specifications, or purchaser specifications should be consulted for specific detailed postweld heat-treatment requirements. When dealing with applications that may not fall within the scope of a code or specification, it is a good policy to consult various codes for information to use in determining postweld heat-treatment practices.

TABLE 11 POSTWELD HEAT TREATMENT TEMPERATURES FOR LOW-ALLOY STEELS USED IN

PRESSURE VESSEL AND PIPE APPLICATIONS

PRODUCTS TYPE AND ALLOY CLASSIFICATION	**ASTM CLASSIFICATION**	**GRADE**	POSTWELD HEAT TREATMENT TEMPERATURE RANGE	
			°C	°F
PRESSURE VESSEL PLATE				
NICKEL	A 203	A; B; D; E; F	595-635	**1100-1175**
MOLYBDENUM	A 204	. . .	595-720	**1100-1325**
MANGANESE-MOLYBDENUM; MANGANESE-MOLYBDENUM NICKEL	A 302	A; B	595-720	**1100-1325**
9% NICKEL	A 353	. . .	550-585	**10265-1085**
CHROMIUM-NICKEL	A 387	11; 12	595-745	**1100-1375**
		5; 22	675-760	**1250-1400**
PIPE				
SEAMLESS AND WELDED FOR LOW-TEMPERATURE SERVICE	A 333	3; 7	595-635	**1100-1175**
		8	550-585	**1025-1085**
SEAMLESS FERRITIC FOR HIGH-TEMPERATURE SERVICE	A 335	P1	595-720	**1100-1325**
		P5; P22	675-760	**1250-1400**
		P11; P12	595-745	**1100-1375**
ELECTRIC-FUSION WELDED FOR HIGH-PRESSURE SERVICE AT MODERATE TEMPERATURES	**A 672**	**H75; H80**	**595-720**	**1100-1325**

Reference cited in this section

4. "ASME BOILER AND PRESSURE VESSEL CODE," ASME, 1992

Welding of Low-Alloy Steels

F.J. Winsor, Welding Consultant

Heat-Treatable Low-Alloy (HTLA) Steels

The term heat-treatable low-alloy steels applies to medium-carbon HSLA Q&T steels, which typically contain up to 5% of total alloy content and from 0.25 to 0.50% C. The carbon content of these steels is significantly higher than the 0.10 to 0.25% C range that is found in quenched and tempered structural low-alloy steels or low-alloy steels used for pressure vessels and piping.

Medium-carbon low-alloy steels are strengthened by quenching to produce a martensitic structure, followed by tempering to obtain the desired levels of hardness, strength, and ductility. The combination of high carbon content, which promotes high maximum hardness levels, and high hardenability, which is produced by the carbon and alloy content, results in a greater susceptibility to weld cracking.

The high hardness of many of these steels in their final hardened and tempered condition often precludes their being welded in that condition, because of the strong tendency for cold cracking (that is, cracking that develops after solidification is complete). Except for weld repairs, these steels are normally welded in the annealed or over-tempered condition, and then the complete weldment is heat treated to obtain the desired level of hardness or strength. The compositions of several typical HTLA steels are given in Table 12.

TABLE 12 COMPOSITION OF SELECTED HEAT-TREATABLE LOW-ALLOY (HTLA) STEELS

AISI-SAE OR OTHER DESIGNATION	COMPOSITION, WT%						
	C	**Mn**	**Si**	**Cr**	**Ni**	**Mo**	V
1330	0.28-0.33	1.60-1.90	0.15-0.30	. . .	. . .	. . .	**. . .**
1340	0.38-0.43	1.60-1.90	0.15-0.30	. . .	. . .	. . .	**. . .**
4023	0.20-0.25	0.70-0.90	0.15-0.30	. . .	. . .	0.20-0.30	**. . .**
4028	0.25-0.30	0.70-0.90	0.15-0.30	. . .	. . .	0.20-0.30	**. . .**
4047	0.45-0.50	0.70-0.90	0.15-0.30	. . .	. . .	0.20-0.30	**. . .**
4118	0.18-0.23	0.70-0.90	0.15-0.30	0.40-0.60	. . .	0.08-0.15	**. . .**
4130	0.28-0.33	0.40-0.60	0.15-0.30	0.80-1.10	. . .	0.15-0.25	**. . .**
4140	0.38-0.43	0.75-1.00	0.15-0.30	0.80-1.10	. . .	0.15-0.25	**. . .**
4150	0.48-0.53	0.75-1.00	0.15-0.30	0.80-1.10	. . .	0.15-0.25	**. . .**
4320	0.17-0.22	0.45-0.65	0.15-0.30	0.40-0.60	1.65-2.00	0.20-0.30	**. . .**
4340	0.38-0.43	0.60-0.80	0.15-0.30	0.70-0.90	1.65-2.00	0.20-0.30	**. . .**
4620	0.17-0.22	0.45-0.65	0.15-0.30	. . .	1.65-2.00	0.20-0.30	**. . .**
5120	0.17-0.22	0.70-0.90	0.15-0.30	0.70-0.90	. . .	. . .	**. . .**
5145	0.40-0.48	0.70-0.90	0.15-0.30	0.70-0.90	. . .	. . .	**. . .**
6150	0.48-0.53	0.70-0.90	0.20-0.35	0.80-1.10	. . .	. . .	**0.15-0.25**
8620	0.18-0.33	0.70-0.90	0.15-0.30	0.40-0.60	0.40-0.70	0.15-0.25	**. . .**
8630	0.28-0.33	0.70-0.90	0.15-0.30	0.40-0.60	0.40-0.70	0.15-0.25	**. . .**
8640	**0.38-0.43**	**0.70-0.90**	**0.15-0.30**	**0.40-0.60**	**0.40-0.70**	**0.15-0.25**	**. . .**

Welding Processes and Practices

Any of the common arc welding processes, such as SMAW, SAW, GMAW, GTAW, and FCAW, can be used to join the HTLA steels. It is important to use low-hydrogen welding consumables and processes in order to minimize cold cracking.

Because of its versatility, simple equipment requirements, and availability of electrode choices, the SMAW process is very often used in the fabrication or repair welding of HTLA steels. GTAW is capable of producing welds with the lowest hydrogen content, and this process is often preferred for critical applications. Both GTAW and GMAW processes provide good control of weld metal composition and cleanliness. For some applications, automatic and semiautomatic GTAW, GMAW, FCAW, and SAW processes offer the advantages of greater productivity and higher weld quality, compared with manual welding.

To avoid porosity and to minimize cracking problems, all materials involved in the welding operation must be clean and free of moisture, oil, grease, dirt, paint, or other contaminants. This includes the base metal, weld filler metal, submerged arc fluxes, gloves, fixtures, and handling devices.

The successful welding of HTLA steels requires not only the selection of the proper welding process and filler metal, but the consideration of several other factors:

- PREHEAT AND INTERPASS TEMPERATURE REQUIREMENTS
- ACHIEVEMENT OF A LOW HYDROGEN CONTENT IN THE WELD METAL, ESPECIALLY WHEN THE PREHEAT TEMPERATURE IS LESS THAN 205 °C (400 °F)
- NEED TO MAINTAIN PREHEAT AFTER WELDING IS COMPLETED UNTIL THE COMMENCEMENT OF POSTWELD HEAT TREATMENT

Filler Metals

Shielded Metal Arc Welding. Low-hydrogen electrodes are nearly always recommended for the welding of HTLA steels to minimize weld metal and HAZ cracking. Electrodes that deposit weld metal that has a response to heat treatment matching that of the base metal are available from some electrode manufacturers for use in welding a few HTLA steels

that are quenched and tempered after welding. The chemical composition of the weld metal deposited by these electrodes sometimes, but not always, matches that of the base metal for which they are intended. The main objective is to achieve a weld deposit that responds to a quench and temper heat treatment in a manner similar to that of the base metal. Sometimes this objective can be achieved with weld metal that has a lower carbon and higher alloy content than the base metal. This is advantageous in reducing weld-cracking tendencies. Medium-carbon HTLA steel welding electrodes are not classified in ANSI/AWS specification A5.5 or other standard filler metal specifications. Rather, they are proprietary types designed for welding steels such as American Iron and Steel Institute-Society of Automotive Engineers (AISI-SAE) types 4130, 4140, and 8630. Electrode manufacturers should be consulted for information on the availability of HTLA steel electrodes and applications.

Some applications of HTLA steels do not require that the hardness and strength of the weld match those of the base metal. The location of weld joints and the orientation of applied stresses can be such that weld properties need not match base metal properties after a quench and temper heat treatment. In some repair situations, it may be possible to use the steel in the annealed or over-tempered condition. In this case, after welding the material in that condition, the weldment is placed in service after a stress-relieving or tempering treatment. For such applications, a variety of low-hydrogen carbon steel, low-alloy steel, stainless steel, and nickel alloy covered electrodes may be useful.

Some types of electrodes that deposit non-heat-treatable weld metal can be used to a limited extent for the welding of HTLA steels in the hardened condition, as in repair welding, where it may not be feasible to anneal or over-temper the steel prior to welding nor to stress relieve the weld upon completion. Weld metal from austenitic stainless steel electrodes, such as ANSI/AWS A5.4 E309 (25Cr-12Ni), E310 (25Cr-20Ni), and E312 (29Cr-9Ni), and from nickel alloy electrodes, such as ANSI/AWS A5.11 ENiCrFe-2 and ENiCrFe-3, can tolerate a rather large amount of dilution from the medium-carbon low-alloy steel base metal without cracking. Additionally, these weld deposits have lower strength and greater ductility than the quenched and tempered base metal. Consequently, high shrinkage stresses during welding can result in plastic deformation of the weld deposit, rather than in cracking of the base metal.

Table 13 shows classifications of carbon steel and low-alloy steel covered electrodes commonly used for the welding of HTLA steels in applications that do not require a properties match between the weld metal and the base metal in the quenched and tempered condition. In some instances, the weld metal compositions include one or more of the principal alloying elements in the associated base metal. Also, a weld metal that has a higher strength in the as-welded condition is associated with steels that have higher alloy and carbon contents, which are often heat treated to higher hardness and strength levels. However, it should be noted that all of the weld deposits listed have a low carbon content. Therefore, even though the alloy content of the weld deposit may match that of the base metal, it is unlikely that the carbon content of the weld, even with considerable dilution from the base metal, will be high enough to result in weld metal hardness and strength values that match those of the base metal after a post-weld quench and temper heat treatment. It may be necessary to use one of the higher-strength weld metals in order to satisfy a higher design strength requirement for the weld in the as-welded or stress-relieved condition. If this is not necessary, then the use of a lower-strength weld metal is recommended to decrease the susceptibility to cracking.

TABLE 13 COVERED ELECTRODES COMMONLY USED FOR SHIELDED METAL ARC WELDING OF HTLA STEELS

ELECTRODE CLASSIFICATION	TYPE OF STEEL[(A)]
E7018	**1330**
E7018-A1	**4023; 4028; 4118; 4320; 8620**
E8016-C1	**4620**
E8016-B2	**5120**
E9016-B3	**5145**
E10016-D2	**1340; 4047; 4130**
E11018-M	**8630**
E12018-M	**4140; 4150; 4340; 4640; 8640**

(A) WELD METAL PROPERTIES DO NOT MATCH BASE METAL PROPERTIES IN THE QUENCHED AND TEMPERED CONDITION.

Gas-Tungsten Arc Welding and Gas-Metal Arc Welding. There are no standard filler metal specifications that classify medium-carbon, heat-treatable bare electrodes and rods for gas-shielded arc welding processes. Bare filler metal of a composition similar to the base metal can be used for the GTAW and GMAW processes. It is desirable to have the lowest possible phosphorus and sulfur contents, and, in some instances, it may be permissible to use weld metal that has a lower carbon content than the base metal, with the objectives of reducing weld metal hot cracking tendencies and improving weld metal ductility. Many of the standard AISI-SAE steel compositions are available in wire form that is suitable for gas-shielded arc welding. The results of transverse tensile tests of GMAW and GTAW joints in some representative low-alloy steels after quenching and tempering are shown in Table 14.

TABLE 14 TYPICAL TRANSVERSE TENSILE PROPERTIES OF ARC WELDED JOINTS IN SELECTED LOW-ALLOY STEELS AFTER QUENCHING AND TEMPERING

WELDING PROCESS AND STEEL DESIGNATION	THICKNESS		FILLER METAL	TEMPERING TEMPERATURE		WELDED JOINT					APPROXIMATE BASE METAL TENSILE STRENGTH	
						TENSILE STRENGTH		YIELD STRENGTH		ELONGATION IN 2 IN., %		
	MM	IN.		°C	°F	MPA	KSI	MPA	KSI		MPA	KSI
GAS-METAL ARC WELDING (GMAW)												
4130	6.35	0.25	(A)	510	950	1170	170	1145	166	7	1170	**170**
4140	12.7	0.50	4140	480	900	1305	189	1225	178	8(E)	1310	**190**
4340	25.4	1.0	4340	510	950	1307	189.5	1251	181.5	11	1310	**190**
			(B)	510	950	1320	191.5	1224	177.5	8	1310	**190**
GAS-TUNGSTEN ARC WELDING (GTAW)												
4335V	6.35	0.25	4340	205	400	1760	255	1530	222	9	1785	**259**
D6	2.36	0.093	(C)	315	600	1860	270	1635	237	6(E)	1895	**275**
			D6	315	600	1780	258	1505	218	6	1825	**265**
D6	**12.7**	**0.50**	**(D)**	**540**	**1000**	**1545**	**224**	**1425**	**207**	**7**	**1585**	**230**

Source: Ref 2

(A) COMPOSITION: 0.18 C-1.50 MN-0.44 SI-1.2 NI-0.34 MO-0.65 CR.

(B) COMPOSITION: 0.25 C-1.17 MN-0.65 SI-1.8 NI-0.80 MO-1.17 CR-0.21 V.

(C) COMPOSITION: 0.25 C-0.28 MN-0.03 SI-1.29 MO-0.98 CR-0.56 V.

(D) COMPOSITION: 0.25 C-0.55 MN-0.65 SI-0.50 SI-1.25 CR-0.30 V.

(E) ELONGATION IN 25 MM (1 IN.) GAGE LENGTH.

The surface condition of the filler metal can have a critical effect on arc welding operations. Welding filler metal producers or specialty wire suppliers who are familiar with welding requirements usually are the best sources of bare welding filler metals.

In cases where service requirements do not dictate the need for weld deposits that are heat treatable by quenching and tempering after welding, the carbon steel filler metals classified in ANSI/AWS specification A5.18 or the low-alloy steel filler metals classified in ANSI/AWS A5.28 can be used. Also, nonheat-treatable austenitic stainless steel or nickel alloy filler metals may be acceptable choices for some applications.

Flux-Cored Arc Welding. There are no standard specifications for FCAW electrodes that provide weld deposits that respond similarly to heat treatment as do medium-carbon low-alloy steel-base metals. However, FCAW electrodes of special composition can often be obtained more readily than solid filler metals of similar composition. For example, to achieve weld strength requirements equivalent to a quenched and tempered AISI 4130 steel (0.30C-0.95Cr-0.20Mo) weldment, a FCAW electrode was specially formulated to produce a weld deposit with a composition of 0.15% C, 1.50 to 1.70% Mn, 0.50 to 0.60% Si, 0.60 to 0.80% Cr, and 0.60 to 0.90% Mo. Producers of flux-cored electrodes should be consulted regarding the availability of special electrodes.

Where service requirements do not dictate the need for weld deposits that are heat treatable by quenching and tempering after welding, ANSI/AWS A5.20 carbon steel flux-cored electrodes or ANSI/AWS A5.29 low-alloy steel flux-cored electrodes can be used. A T5 slag system is preferred to T1, because weld deposits often have a higher toughness and lower hardness. Carbon steel deposits can fail, because of low strength, if the fillet size is small or high restraint exists. When selecting FCAW electrodes, it may be helpful to refer to commonly used SMAW electrodes (shown in Table 13). Also, either the non-heat-treatable austenitic stainless steel flux-cored electrodes listed in ANSI/AWS specification A5.22 or proprietary nickel alloy flux-cored electrodes may be suitable choices for some applications.

Submerged Arc Welding. Some low-alloy steel weldments that require a quench and temper heat treatment after welding can be welded by the SAW process. Submerged arc weld metal usually has lower toughness than welds made by GTAW, particularly after heat treatment to a high strength level. Neutral or basic fluxes generally produce welds with better notch toughness. Manufacturers of electrodes and fluxes, as well as steel producers, should be consulted to determine the availability of consumables, recommended welding parameters and heat treatment, and information on mechanical properties for specific applications of SAW. If such information is not available, then welding procedure development tests will be needed.

Preheating

In low-alloy steels, the carbon and alloy contents determine the transformation characteristics (microstructure) of the steel upon cooling from a high temperature. The higher the carbon content, the higher the maximum hardness of as-quenched martensite. If the weld metal and HAZs are allowed to cool rapidly to room temperature during welding of low-alloy steels that have high carbon and high alloy content, then hard, crack-sensitive martensite is likely to form. The risk of cracking is greatly increased by the presence of hydrogen. By slowing the cooling rate, preheating may lower the risk of cracking through the reduction of stresses imposed on the weld metal and HAZs during the transformation to martensite or to martensite and bainite. In some steels, preheating may promote the formation of softer bainite instead of hard martensite. Preheating also promotes the evolution of dissolved hydrogen. Steels with an identical alloy content, but different carbon contents, usually require an increase in preheat temperature with increasing carbon content.

The minimum preheat and interpass temperature required to prevent cracking during the welding of HTLA steels depends on the:

- CARBON AND ALLOY CONTENT OF THE BASE METAL AND WELD METAL
- CONDITION OF HEAT TREATMENT PRIOR TO WELDING
- BASE METAL THICKNESS
- AMOUNT OF RESTRAINT
- AMOUNT OF AVAILABLE HYDROGEN

Figure 1, an isothermal transformation diagram for AISI 4340 steel, shows a M_s temperature (the temperature at which martensite starts to form from austenite upon cooling) of approximately 290 °C (550 °F). At 315 °C (600 °F), the diagram

shows about 30 min of elapsed time, and, at 370 °C (700 °F) about 3 h time, required for isothermal transformation of austenite (A) to bainite (ferrite and carbides, F + C). When welding this steel by using a preheat and interpass temperature ranging from 315 to 345 °C (600 to 650 °F), and maintaining this temperature for a minimum of 3 h after completion of welding, followed by slow cooling, a bainitic microstructure can be obtained in the HAZ and in weld metal of matching composition. It is essential to maintain the preheat after welding for a sufficient time to allow for variations that could result in a longer transformation time. Maintaining preheat after welding also promotes the evolution of hydrogen and reduces the risk of hydrogen-induced cracking.

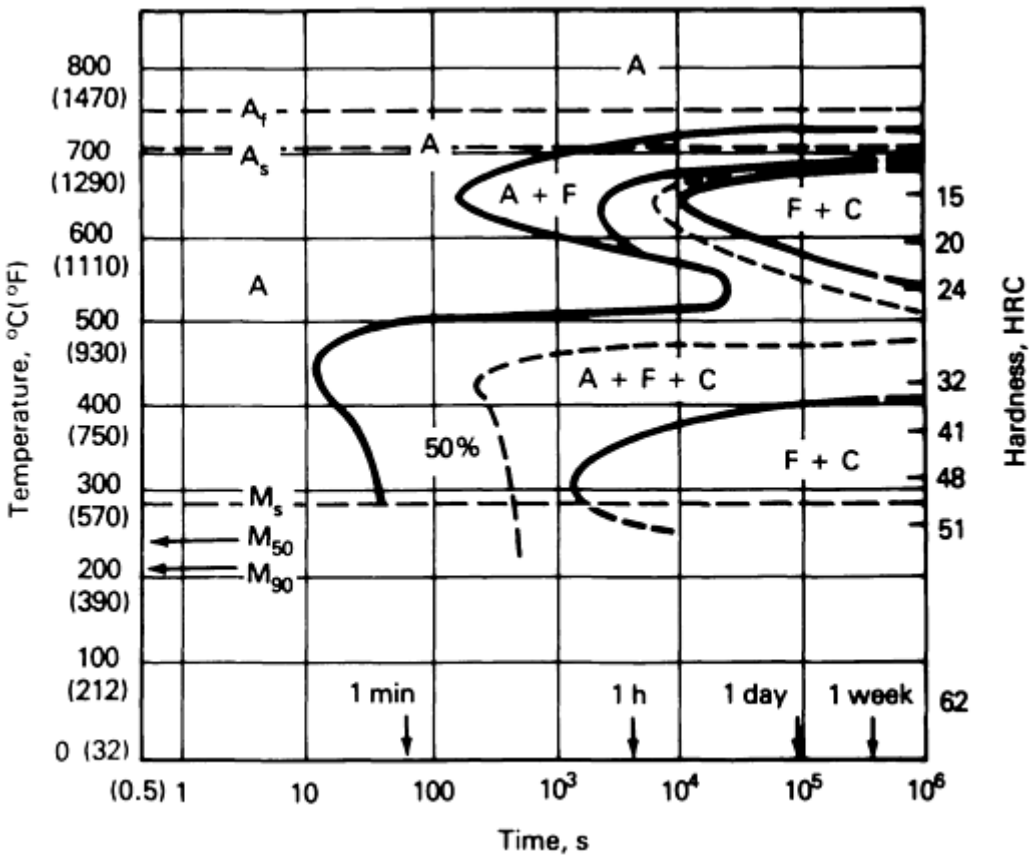

FIG. 1 ISOTHERMAL TRANSFORMATION DIAGRAM FOR AISI 4340 STEEL. SOURCE: REF 5

Unfortunately, preheat and interpass temperatures above about 290 °C (550 °F) promote the formation of a thin oxide layer on the joint surfaces and can also contribute to welder discomfort. These factors can have an adverse effect on weld quality and should be considered when planning the welding operation.

The isothermal transformation diagram in Fig. 2 for AISI 8620 steel, which has a lower carbon and lower total alloy content than AISI 4340, indicates a considerably higher M_s temperature of 405 °C (760 °F). M_s temperatures for HTLA steels with relatively low carbon and alloy contents are usually so high that it is often not feasible to employ a preheat and interpass temperature that is above the M_s temperature for the particular steel. However, with a lower carbon and lower alloy content, these steels have lower hardenability. This means that, with moderate rates of cooling from the welding temperature, there is a possibility for obtaining at least partial transformation to ferrite and carbides, rather than complete transformation to martensite. When martensite does form, its hardness will be lower, because of the lower carbon content. In addition, for steels that have a high martensite formation temperature range, the use of a preheat and interpass temperature below this range can permit partial tempering of the martensite. Because of these factors, lower preheat and interpass temperatures can be used satisfactorily when welding lower carbon and lower alloy content steels.

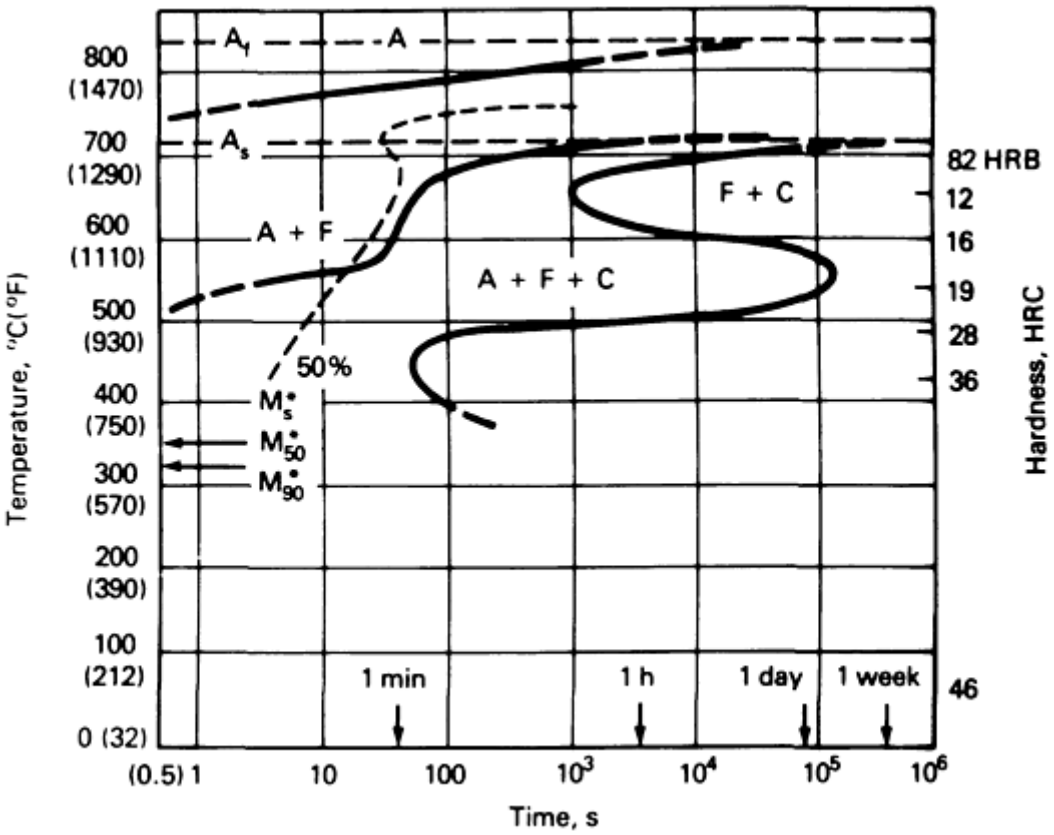

FIG. 2 ISOTHERMAL TRANSFORMATION DIAGRAM FOR AISI 8620 STEEL. * INDICATES ESTIMATED TEMPERATURE. SOURCE: REF 5

For a given initial base metal temperature (preheat) and level of energy input during welding, increasing the section thickness will increase the cooling rate. Therefore, when welding steels of intermediate hardenability, the likelihood of martensite formation also increases with increasing thickness, and it may be necessary to increase the preheat temperature as the section thickness is increased.

Suggested preheat and interpass temperatures for several HTLA steels are given in Table 15. Other than the inherent metallurgical characteristics of the steel, some factors that may permit the use of lower preheat and interpass temperatures than might otherwise be the case are:

- WELDING THE STEEL IN THE FULLY ANNEALED OR OVER-TEMPERED CONDITION
- LOCATING THE WELD IN AREAS OF LEAST SECTION THICKNESS OR WHERE RESTRAINT CONDITIONS MAY BE LEAST SEVERE
- SELECTING PROCESSES AND FILLER METALS THAT OFFER THE LOWEST AMOUNT OF AVAILABLE HYDROGEN
- USING FILLER METALS THAT HAVE THE LOWEST CARBON AND ALLOY CONTENT CONSISTENT WITH OBTAINING THE REQUIRED WELD METAL MECHANICAL PROPERTIES

TABLE 15 RECOMMENDED PREHEAT AND INTERPASS TEMPERATURES FOR SELECTED HTLA STEELS

STEEL DESIGNATION	PREHEAT AND INTERPASS TEMPERATURE RANGE FOR INDICATED SECTION THICKNESS

	AT ≤13 MM (≤ 1/2 IN.)		AT 13-25 MM (1/2-1 IN.)		AT 25-50 MM (1-2 IN.)	
	°C	°F	°C	°F	°C	°F
1330	175-230	350-450	205-260	400-500	230-290	**450-550**
1340	205-260	400-500	260-315	500-600	315-370	**600-700**
4023	[GES]40	[GES]100	95-150	200-300	120-170	**250-350**
4028	95-150	200-300	120-175	250-350	205-260	**400-500**
4047	205-260	400-500	230-290	450-550	260-315	**500-600**
4118	95-150	200-300	175-230	350-450	205-260	**400-500**
4130	150-205	300-400	205-260	400-500	230-290	**450-550**
4140	175-230	350-450	230-290	450-550	290-345	**550-650**
4150	205-260	400-500	260-315	500-600	315-370	**600-700**
4320	95-150	200-300	175-230	350-450	205-260	**400-500**
4340	290-345	550-650	315-370	600-700	315-370	**600-700**
4620	[GES]40	[GES]100	95-150	200-300	120-175	**250-350**
4640	175-230	350-450	205-260	400-500	230-290	**450-550**
5120	[GES]40	[GES]100	95-150	200-300	120-175	**250-350**
5145	205-260	400-500	230-290	450-550	260-315	**500-600**
8620	[GES]40	[GES]100	95-150	200-300	120-175	**250-350**
8630	95-150	200-300	120-175	250-350	175-230	**350-450**
8640	**120-175**	**250-350**	**175-230**	**350-450**	**205-260**	**400-500**

Note: Data are for low-hydrogen welding processes and low-hydrogen filler metals.

Heat Input

Low-to-moderate levels of heat input are usually preferred for the welding of HTLA steels. High heat input levels tend to promote wide HAZs with enlarged grain size and reduced notch ductility. High heat input also increases the risk of hot cracking (solidification cracking) in the weld metal and the HAZs.

Postweld Heat Treatment

The type of heat treatment required after welding the HTLA steels (that is, postweld stress relieving or tempering or a quench and temper heat treatment of the completed weldment) depends on the metallurgical characteristics of the steel and the mechanical property requirements. Postweld heat treatment details often depend on the preheat and interpass temperature used in welding.

For the higher carbon and higher alloy content steels, welding with low-to-moderate heat input and using preheat and interpass temperatures that are below the M_s temperature of the particular steel will result in the partial or complete transformation to martensite of some or all of the austenite in the weld metal and HAZs. The amount of martensite that forms depends on the preheat temperature and its relation to the martensite transformation temperature range (essentially between M_s and M_{90}, as shown in Fig. 2). If the martensite transformation is incomplete at the preheat temperature, subsequent cooling from that temperature will result in additional martensite formation. Rapid cooling to room temperature can result in weld or HAZ cracking in higher-carbon HTLA steels. If partial or complete transformation to martensite has occurred, then heating the part to a higher temperature for a sufficient time will temper the martensite.

Steels of lower alloy and carbon content have higher temperature ranges of martensite formation (compare AISI 8620 in Fig. 2 to AISI 4340 in Fig. 1), and they are less susceptible to weld cracking than higher carbon and higher alloy content steels. Preheat and interpass temperatures for steels with lower carbon and lower alloy content usually are within or below the martensite-forming temperature ranges, and weldments are given a tempering heat treatment after welding, unless a quench and temper heat treatment is required.

In order to avoid weld metal or HAZ cracking in the higher carbon and higher alloy content steels, it is necessary, upon completion of welding, to proceed immediately with postweld heat treatment without interrupting the preheating. Even with less crack-sensitive steels, it is preferable to start the postweld heat treatment as soon as possible after welding. If a stress relief or tempering heat treatment is specified immediately after welding (usually 595 to 675 °C, or 1100 to 1250

°F), and if the preheat temperature used in welding is within the martensite-formation temperature range for the steel, then the weldment should first be allowed to cool slowly and uniformly to just below the M_{90} temperature, where transformation to martensite will be essentially complete.

Next, the weldment should be immediately heated to the stress-relieving temperature where the martensite will be softened by tempering. After holding at temperature for a sufficient time (usually ~1 h/in. of joint thickness), the weldment can be cooled to room temperature without danger of cracking. It may not always be practical to start the postweld heat treatment immediately after completion of welding. When cooling to room temperature is necessary after welding, it should be done slowly and uniformly to avoid cracking.

References cited in this section

2. CHAPTERS 1, 3, 4, *WELDING HANDBOOK*, 7TH ED., VOL 4, *METALS AND THEIR WELDABILITY*, AWS, 1982
5. "ISOTHERMAL TRANSFORMATION DIAGRAMS," UNITED STATES STEEL CORP., 1963

Welding of Low-Alloy Steels

F.J. Winsor, Welding Consultant

Ultrahigh-Strength Low-Alloy Steels

The ultrahigh-strength alloy steels used for structural applications have a minimum yield strength of 1240 MPa (180 ksi) and minimum tensile strength of 1380 MPa (200 ksi), combined with good fracture toughness. General types of ultrahigh-strength steels include the nickel-chromium-molybdenum-vanadium steels, nickel-cobalt steels, and the 5% chromium-molybdenum-vanadium steels. The latter are also known as hot-work die steels and are included among the steels discussed in the section "Tool and Die Steels" in this article.

Welded joints in the nickel-cobalt steels generally do not require postweld heat treatment, except for stress relieving in certain applications. Steels in the Ni-Cr-Mo-V series are represented by Aerospace Material Specifications (AMS) 6434, 300M, and D-6a. Some medium-carbon low-alloy steels, such as AISI 4140 and 4340, discussed in the section "Heat-Treatable Low-Alloy (HTLA) Steels," also may be included among the ultrahigh-strength steels. Compositions of several typical ultrahigh-strength steels are given in Table 16.

TABLE 16 TYPICAL COMPOSITION OF SELECTED ULTRAHIGH-STRENGTH LOW-ALLOY STEELS

STEEL DESIGNATION	COMPOSITION, WT%								
	C	**Mn**	**Si**	**Cr**	**Ni**	**Mo**	**V**	**Co**	OTHER
AF1410	0.16	0.05 MAX	0.1 MAX	2 MAX	10	1	0.1	14	**0.15 AL; 0.01 TI (MAX)**
AMS 6434	0.31-0.38	0.60-0.80	0.20-0.35	0.65-0.90	1.65-2.00	0.30-0.40	0.17-0.20	. . .	**. . .**
300M	0.40-0.46	0.65-0.90	1.45-1.80	0.70-0.95	1.65-2.00	0.30-0.45	0.05 MIN	. . .	**. . .**
D-6A	0.42-0.48	0.60-0.90	0.15-0.30	0.90-1.20	0.40-0.70	0.90-1.10	0.05-0.10	. . .	**. . .**
H11 MOD	0.37-0.43	0.20-0.40	0.80-1.00	4.75-5.25	. . .	1.20-1.40	0.40-0.60	. . .	**. . .**
H13	0.32-0.45	0.20-0.50	0.80-1.20	4.75-5.50	. . .	1.10-1.75	0.80-1.20	. . .	**. . .**

HP 9-4-20	0.16-0.23	0.20-0.40	0.20 MAX	0.65-0.85	8.50-9.50	0.90-1.10	0.06-0.12	4.25-4.75	. . .
HP 9-4-30	0.29-0.34	0.10-0.35	0.20 MAX	0.90-1.10	7.0-8.0	0.90-1.10	0.06-0.12	4.25-4.75	. . .
HY-180	**0.09-0.13**	**0.05-0.25**	**0.15 MAX**	**1.8-2.2**	**9.5-10.5**	**0.90-1.10**	**. . .**	**7.5-8.5**	**0.025 AL (MAX); 0.02 TI (MAX)**

Welding Processes and Filler Metals

For many important applications of ultrahigh-strength alloy steels, the mechanical properties of the weld metal and the HAZs must be equal to those of the base metal. The required weld metal strength and toughness can only be achieved with very low levels of impurities such as oxygen, hydrogen, nitrogen, carbon, sulfur, and phosphorus.

The preferred process for achieving maximum strength and toughness in both weld metal and HAZs is gas-tungsten arc welding. Plasma arc welding (PAW) can also be used. Dry and pure argon, helium, or mixtures of both can be used for shielding. Shielding gases should be essentially free from oxygen, nitrogen, and hydrogen.

Premium-quality filler metals are produced from selected raw materials by vacuum induction melting (VIM) and vacuum arc remelting (VAR). Filler metals of matching chemical composition are generally recommended for the welding of nickel-cobalt steels. For the 5Cr-Mo-V steels and the medium-carbon low-alloy steels, the filler metal can either have the same composition as the base metal or, for some applications, lower alloy and lower carbon content filler metal can be used, with some sacrifice in strength.

Welding Procedures and Practices

Joint Design, Workmanship, and Inspection. To utilize the properties of ultrahigh-strength steels and to achieve good serviceability of weldments, it is necessary to provide appropriate joint designs, good workmanship, and adequate inspection. In order to minimize cracking tendencies, welded joints in these steels should not be located in areas of abrupt changes in cross section or high stress concentration. Joints should be located to provide good accessibility for welding and inspection. Groove welds are preferable to fillet welds for many applications, because of the inherent stress concentrations usually associated with fillet welds and because groove welds are more amenable to volumetric methods of examination, such as radiographic or ultrasonic methods. Weld metal should blend smoothly with the adjacent base metal, and excessive weld reinforcement should be avoided.

Nickel-cobalt alloy steels are often welded in the quenched and tempered condition. Preferably, the 5% chromium-molybdenum-vanadium steels and the medium-carbon low-alloy steels are welded in the annealed condition. Successful welding of ultrahigh-strength alloy steels requires careful control of welding conditions. Low nitrogen, oxygen, and hydrogen contents in the weld metal are essential. The filler metal, base metal, weld joint area, and deposited weld metal all must be exceptionally clean. An important monitor of weld metal cleanliness is total oxygen content. The oxygen level must be very low to achieve maximum weld metal properties.

In HY-180 weldments, for example, an oxygen content of less than 50 ppm is necessary. Only GTAW and PAW processes are capable of achieving the required low oxygen levels in the weld metal. The oxygen content of weld metals deposited by GMAW is seldom less than 150 ppm, and it is far higher for slag shielded welding processes.

Welding heat input must be controlled to a low and consistent level to produce grain refinement in previously deposited weld beads and to minimize degradation of the properties of the HAZ. GTAW or PAW with cold wire feed is generally recommended for these steels in preference to GMAW or to GTAW or PAW with hot wire feed. For some applications, high-energy welding processes can be used successfully, if the weld metal oxygen content is kept low and some degradation of mechanical properties can be tolerated.

Preheating

Suggested preheat and interpass temperatures for welding ultrahigh-strength steels are given in Table 17. Preheating generally is not required for welding the nickel-cobalt alloy steels, but it is essential in welding the medium-carbon low-alloy steels and the 5Cr-Mo-V alloy steels in order to prevent cracking in the weld metal and HAZs.

TABLE 17 RECOMMENDED PREHEAT AND INTERPASS TEMPERATURES TO WELD SELECTED ULTRAHIGH-STRENGTH STEELS

STEEL DESIGNATION	PREHEAT AND INTERPASS TEMPERATURE RANGE FOR INDICATED SECTION THICKNESS					
	AT ≤13 MM (≤ $\frac{1}{2}$ IN.)		**AT 13-25 MM ($\frac{1}{2}$-1 IN.)**		AT 25-50 MM (1-2 IN.)	
	°C	**°F**	**°C**	**°F**	**°C**	°F
AMS 6434	175-230	350-450	230-290	450-550	260-315	**500-600**
300M	290-345	550-650	290-345	550-650	315-370	**600-700**
D-6A	230-290	450-550	260-315	500-600	290-345	**550-650**
H11 MOD	315-540	600-1000	315-540	600-1000	315-540	**600-1000**
H13	315-540	600-1000	315-540	600-1000	315-540	**600-1000**
HP 9-4-20	(A)	(A)	(A)	(A)	(A)	**(A)**
HP 9-4-30	(A)	(A)	(A)	(A)	(A)	**(A)**
AF1410	(A)	(A)	(A)	(A)	(A)	**(A)**
HY-180	**(A)**	**(A)**	**(A)**	**(A)**	**(A)**	**(A)**

(A) PREHEATING NOT REQUIRED

Preferred preheat and interpass temperatures for the 5Cr-Mo-V steels (H11 mod and H13) are at least 30 to 55 °C (50 to 100 °F) above the M_s temperature for the steel. The M_s temperature is about 290 °C (550 °F) for H11 mod and about 345 °C (650 °F) for H13 steel. Maintaining the preheat and interpass temperature above the M_s temperature will prevent martensite formation in the weld metal and HAZs during welding. However, high preheat and interpass temperatures can cause welding problems, because of oxidation of the joint faces. The oxide can lead to occasional weld metal porosity or lack of fusion. Although the use of a lower preheat and interpass temperature will overcome this problem, it will allow some of the austenite in the weld zone to transform to martensite. A preheat temperature of about 230 °C (450 °F) can be used without excessive oxidation. For thin sections welded by the GTAW process, a preheat and interpass temperature of 150 °C (300 °F) can be suitable.

If the completed weldment is cooled from the preheat temperature to room temperature, then the remaining austenite will transform to martensite. The volumetric expansion accompanying the martensite transformation will produce high local stresses and can result in cracking of the weld metal or HAZs, especially if the cooling is rapid or nonuniform. In order to avoid this, heat treatment immediately after welding is recommended.

Postweld Heat Treatment

The nickel-cobalt high-strength steels generally do not require postweld heat treatment. Weldments of HP9-4-20 and HP9-4-30 steels can be stress relieved at 540 °C (1000 °F) for 24 h. This postweld heat treatment has no adverse effect on the strength or toughness of either weld metal or base metal. Aging of weldments in HY-180 and AF 1410 steels for a short time at 480 to 510 °C (900 to 950 °F) appears to improve tensile properties and toughness. However, these properties decrease with longer aging times.

The problem of weld metal or HAZ cracking that is due to martensite formation when welding the 5Cr-Mo-V steels and the medium-carbon low-alloy steels can be avoided by postweld heat treatment immediately after welding, rather than allowing the weldment to cool to room temperature. One approach is to raise the temperature after welding to about 55 °C (100 °F) above the M_s temperature and hold it for a sufficient time (indicated by the isothermal transformation diagram) to allow the austenite to transform to a reasonably ductile bainitic structure. The weldment can then be cooled to room temperature without much risk of cracking. A subsequent tempering treatment is required to produce a desirable microstructure in the weld metal and HAZs.

An alternative approach to postweld heat treatment is to allow the weldment to cool slowly and uniformly from the preheat temperature to approximately 95 °C (200 °F), which allows the retained austenite to transform to martensite. The weldment should then be heated to the recommended tempering temperature for the steel to relieve residual welding stresses and to temper the martensite.

Tool and Die Steels

Welding applications for tool and die steels are generally divided into five work operations:

- ASSEMBLY OF COMPONENTS INTO A SINGLE TOOL OR DIE
- FABRICATION OF A COMPOSITE TOOL BY DEPOSITING AN OVERLAY OF TOOL STEEL WELD METAL ON SPECIFIC AREAS OF A CARBON STEEL OR LOW-ALLOY STEEL BASE METAL
- REBUILDING OF WORN SURFACES AND EDGES
- ALTERATION OF A TOOL OR DIE TO MEET A DIFFERENT APPLICATION REQUIREMENT
- REPAIR OF CRACKED, BROKEN, OR OTHERWISE DAMAGED TOOLS, DIES, OR OTHER COMPONENTS

The assembly of components by welding permits the use of less-expensive steels for parts of the assembly that do not require the special properties of tool steel, such as hardness or wear resistance. This practice also permits the use of a tougher steel to provide support for tool steel components or weld overlays. Applications covered by the second and third bullets listed above include most of the welding that is done on tools or dies by hard surfacing, often using special hard-facing alloys, rather than tool steel weld metals. The use of arc welding has significant application for the repair of crocked or broken tools and dies, restoration of worn areas to original dimensions, and alteration of tools and dies to produce modified parts.

Because the manufacturing of complicated tools and dies involves a high material cost, and because premature failures incur the cost of downtime, welding procedures and operations should be carefully planned and controlled to ensure that the required properties are achieved in the completed weldment.

Welding of Low-Alloy Steels

F.J. Winsor, Welding Consultant

Description of Steels

Tool steels are categorized by AISI and the SAE into seven major groups (listed in Table 18) according to the normal hardening medium or the general applications of the alloys. Tool and die steels are produced in small tonnage quantities by processes that yield clean, homogeneous material with close control of chemical composition.

TABLE 18 COMPOSITION OF TOOL AND DIE STEEL GROUPS

GROUP	**STEEL TYPE**	**LETTER SYMBOL**	PRINCIPAL ALLOYING ELEMENTS
WATER-HARDENING	PLAIN CARBON,	W	**. . .**
	HIGH-CARBON, LOW-ALLOY	W	**. . .**
SHOCK-RESISTING	MEDIUM-CARBON, LOW-ALLOY	S	**CR, MN, MO, SI, W**
COLD-WORK	HIGH-CARBON, LOW-ALLOY	S	**CR, MN, MO, SI, W**
	HIGH-CARBON, MEDIUM-	A	**CR, MN, MO, NI, V, W**

	ALLOY		
	HIGH-CARBON, HIGH-CHROMIUM	D	**CO, CR, MO, V**
HOT-WORK	CHROMIUM	H	**CO, CR, MO, V, W**
	TUNGSTEN	H	**CR, V, W**
	MOLYBDENUM	H	**CR, MO, V, W**
HIGH-SPEED	TUNGSTEN	T	**CO, CR, MO, V, W**
	MOLYBDENUM	M	**CO, CR, MO, V, W**
MOLD STEELS	LOW-TO-MEDIUM CARBON, LOW-ALLOY	P	**CR, MO, NI**
SPECIAL PURPOSE	**MEDIUM-TO-HIGH CARBON, LOW-ALLOY**	**L**	**CR, MO, NI, V**

Welding Processes

All of the common arc welding processes can be used to fabricate or repair tools and dies. Process selection primarily depends on the size and complexity of the work, the requirements for preheat and interpass temperature control and postweld heat treatment, and the availability of filler metal.

The SMAW process is most widely used for these reasons: it often affords more flexibility with regard to accessibility to the joint area and position of welding, it requires relatively simple and portable equipment, and it offers a variety of weld metal compositions based on readily available covered electrodes.

The SMAW, GTAW, GMAW, FCAW, and PAW processes are widely used to repair damaged or worn areas or to fabricate composite tools. Both GTAW and PAW are particularly well suited for use on small areas, thin sections, or sharp edges where greater control of the process is advantageous. To deposit large volumes of weld metal, as in building up large die blocks, filling large cavities, or repairing deep cracks, SMAW that utilizes special large electrodes of up to 19 mm ($\frac{3}{4}$ in.) in diameter can be used, as well as SAW, GMAW, FCAW, and hot-wire PAW. Filler metals for semiautomatic and automatic processes can either be solid wires or composite metal-cored or flux-cored tubular products. SAW process modifications can include the use of alloy-enriched fluxes and the direct addition of metal powders into the weld pool.

Welding of Low-Alloy Steels

F.J. Winsor, Welding Consultant

Filler Metals

Factors that must be considered when selecting a filler metal for a specific application include:

- COMPOSITION OF THE BASE METAL
- HEAT-TREATED CONDITION OF THE BASE METAL (ANNEALED OR HARDENED AND TEMPERED)
- SERVICE REQUIREMENTS OF THE WELD DEPOSIT
- POSTWELD HEAT TREATMENT

For many tool steel welds, it is essential that the weld metal and the base metal respond similarly to heat treatment, so that the weld metal hardness will be equal to that of the base metal after a quench and temper heat treatment. Although this often means that the weld metal chemical composition must match that of the base metal, that is not always the case. It is sometimes possible to develop the same final hardness or strength in the weld using a weld deposit that has a lower carbon and higher alloy content than the base metal. Where possible, lowering the carbon content of the weld metal generally minimizes the risk of weld cracking and improves the toughness of the weld deposit.

For some applications, either when fabricating a tool or die from components or when repairing a damaged tool or die, the region of welding may not involve the working surface of the tool or die. In those cases, matching the composition or heat-treatment response of the weld metal to that of the base metal may not be essential. A weld deposit composition that offers greater resistance to weld cracking and improved ductility and toughness often is a better choice.

When selecting filler metals for the welding of tools or dies in the hardened condition, the location of the required weld with respect to the working area of the part should be considered. If the location of the weld deposit is in a functional area of the tool, such as a cutting edge or a wear surface, then it is necessary to select a weld metal that will have the desired hardness or strength in the as-welded condition or, possibly, in the stress-relieved or tempered condition, without a hardening heat treatment. If the weld deposit is located away from the working area of the tool or die, then selection of the filler metal can often be based on achieving maximum crack resistance, ductility, and toughness in the weld deposit.

Filler metals for welding tool steels can be divided into three main categories. The first includes those that produce weld deposits that correspond in hardenability or composition to those of some of the basic tool steel types: water-, oil-, and air-hardening; hot-work; and high-speed. Table 19 shows proprietary compositions of typical tool steel weld metals available from covered electrodes and bare solid and cored filler metals. Such weld deposits will be hard in the as-welded condition. These types of filler metal are not included in standard filler metal specifications.

TABLE 19 COMPOSITION OF SELECTED PROPRIETARY HEAT-TREATABLE WELD DEPOSITS USED TO WELD NUMEROUS TYPES OF TOOL STEEL

AISI STEEL TYPE	**FILLER-METAL TYPE**	NOMINAL WELD DEPOSIT COMPOSITION, WT%[(A)]							
		C	**Mn**	**Si**	**Cr**	**Ni**	**V**	**W**	Mo
W1; W2	WATER-HARDENING	0.95	0.30	0.20	. . .	. . .	0.20	. . .	**. . .**
S1; S5; S7	HOT-WORK	0.33	0.40	1.00	5.00	. . .	. . .	1.25	**1.35**
O1; O6	OIL-HARDENING	0.92	1.28	0.30	0.50	. . .	. . .	0.50	**. . .**
A2; A4; D2	AIR-HARDENING	0.95	0.40	0.30	5.25	. . .	0.25	. . .	**1.10**
H11; H12; H13	HOT-WORK	0.33	0.40	1.00	5.00	. . .	. . .	1.25	**1.35**
M1; M2; M10; T1; T2; T4	**HIGH-SPEED**	**0.90**	**0.30**	**0.35**	**4.00**	**. . .**	**1.00**	**1.50**	**8.00**

(A) COMPOSITIONS OF SIMILAR TYPES OF WELD METAL FROM DIFFERENT PRODUCERS CAN VARY.

The second category of filler metals includes carbon and low-alloy steels that have moderate hardness and toughness properties at room temperature in the as-welded or stress-relieved condition. Although some deposit compositions can respond to a quench and temper heat treatment, most of the filler metals in this category are intended for applications where the properties of the weld deposit are not required to match those of the tool steel in the hardened condition. These filler metals are included in ANSI/AWS specifications for carbon steel and low-alloy steel filler metals.

The third category of filler metals includes austenitic stainless steels and the nickel-chromium-iron, nickel-copper, and copper-nickel alloys. These nonhardenable filler metals are often used for the repair welding of tools in the hardened condition, where high weld metal ductility is advantageous in resisting weld metal and base metal cracking. They can also be useful in providing ductile deposits for building up worn tools. Some types of nonhardenable deposit can be overlaid with a hardfacing deposit to provide a hard, wear-resistant surface. Nonhardenable filler metals are included in ANSI/AWS filler metal specifications for stainless steels, nickel alloys, and copper alloys.

F.J. Winsor, Welding Consultant

Welding Procedures and Practices

It is preferable to conduct the welding of tool and die steels with the part in the annealed condition whenever feasible. Tool steels welded in the hardened and tempered condition are more susceptible to cracking. However, many items are successfully repaired in the hardened and tempered condition. When this can be done safely, it avoids the need for annealing before the repair, hardening and tempering afterwards, and the possible costly correction of dimensional changes caused by such heat treatment. If a tool or die has previously been hardened but not yet tempered, then it cannot be safely welded. Annealing is necessary prior to welding.

Preheating. In order to avoid cracking, tools and dies should never be welded without preheating, regardless of composition or heat-treatment condition (annealed or hardened). The preheat and interpass temperature depends on the composition and thickness of the steel and, sometimes, on the heat-treatment condition. Typical preheat and interpass temperatures for welding different types of tool steel are given in Table 20.

TABLE 20 TYPICAL PREHEAT AND INTERPASS TEMPERATURES TO WELD SELECTED TOOL STEELS

AISI STEEL TYPE	PREHEAT AND INTERPASS TEMPERATURE RANGE			
	ANNEALED BASE METAL		HARDENED BASE METAL	
	°C	**°F**	**°C**	°F
W1; W2	120-230	250-450	120-230	**250-450**
S1; S5; S7	150-260	300-500	150-260	**300-500**
O1; O6	150-205	300-400	150-205	**300-400**
A2; A4	150-260	300-500	150-205	**300-400**
D2	370-480	700-900	370-480	**700-900**
H11; H12; H13	480-650	900-1200	370-540	**700-1000**
M1; M2; M10; T1; T2; T4	**510-595**	**950-1100**	**510-565**	**950-1050**

Source: Ref 2

Preheat and interpass temperatures for welding should not be confused with temperatures used for preheating a tool prior to austenitizing during a hardening treatment. The preheat and interpass temperature for welding a hardened tool steel should not exceed the recommended tempering temperature for the steel. Use of a higher preheat temperature will over-temper and soften the tool. If the tempering temperature is unknown, the preheat and interpass temperature should be at the low end of the range recommended for the particular steel.

To weld annealed tool steels in massive sections, the preheat and interpass temperatures should be near the upper end of the recommended range. For thin sections, the lower portion of the range is satisfactory.

Postweld Heat Treatment. *Heat Treating,* Volume 4 of the *ASM Handbook,* contains information on the heat treatment of tool steel materials. The producers of tool and die steels also can be consulted regarding heat-treatment procedures for their products.

Depending on the type of tool steel and weld metal, the weld metal and HAZ can be very hard and brittle in the as-welded condition and susceptible to cracking if the tools are allowed to cool completely to room temperature after welding and before postweld heat treatment.

With tool steels in the annealed condition prior to welding, it is usually necessary to harden and temper the part after welding in order to provide desired performance characteristics. It is often preferable to heat the part to the hardening

temperature as soon as welding is completed, without allowing the part to cool. With some steels, it can be necessary to heat to the hardening temperature in stages in order to avoid cracking. With less-crack-sensitive tool steels, it may not be necessary to proceed with the hardening and tempering heat treatments immediately after completion of welding. In those cases, after welding is completed, the part can be allowed to cool slowly and uniformly to room temperature.

For steels welded in the hardened and tempered condition, reference to isothermal transformation diagrams (Ref 5) can assist in developing postweld heat-treatment practices. For example, with some steels it may be possible to use a preheat and interpass temperature that, if maintained for a reasonable length of time after welding, allows isothermal transformation of austenite to a bainitic microstructure rather than to martensite. Postweld heat treatment involving isothermal transformation of AISI 4340 steel is discussed in the section on welding structural HTLA steels, with reference to Fig. 1, the isothermal transformation diagram for AISI 4340 steel. If the preferred welding preheat and interpass temperature (see Table 20) does not coincide with the desired isothermal transformation temperature, then the temperature of the part should be raised or lowered, as necessary, after welding is completed.

An alternative postweld heat-treatment practice for some tool steels welded in the hardened and tempered condition is to allow the part to cool slowly and uniformly after welding to a temperature from 30 to 55 °C (50 to 100 °F) lower than the M_{90} temperature shown in Fig. 1, permitting transformation to martensite. Then the part should be immediately heated to the recommended tempering temperature.

References cited in this section

2. CHAPTERS 1, 3, 4, *WELDING HANDBOOK*, 7TH ED., VOL 4, *METALS AND THEIR WELDABILITY*, AWS, 1982
5. "ISOTHERMAL TRANSFORMATION DIAGRAMS," UNITED STATES STEEL CORP., 1963

F.J. Winsor, Welding Consultant

Repair Practices for Tools and Dies

Base Metal. The type of tool steel to be repaired and its heat-treatment condition are best determined from the original specifications for the tool or die. If this information is not available, then a chemical analysis must be made to determine the carbon and alloy content of the steel. The heat-treatment condition (either hardened and tempered or annealed) can be determined by a hardness test.

Surface Preparation for Welding. Surfaces of tool and die materials must be clean and dry before welding. Prior to repair welding, all cracks and the tool marks produced in removing damaged areas should be removed. Metal removal can be accomplished by machining, grinding, or thermal cutting, depending on the hardness. Preheating is essential before thermal cutting and gouging, and is often desirable before grinding on hardened tools, as well.

Preparation of Repair Area. For the partial repair of cutting edges or working surfaces, the damaged areas should be machined or ground to a uniform depth that will permit a deposit thickness with the required hardness and wear characteristics. Dilution of the weld metal by fusion with the base metal must be considered, particularly when repairing a composite tool that has a carbon steel or a lower alloy steel base supporting the working surface. A groove depth of about 3.2 mm ($\frac{1}{8}$ in.) is commonly used. When it is necessary to repair the entire cutting or working edge, the edge should be chamfered at 45° for a sufficient depth.

Cracks are generally ground in order to remove the damaged base metal and produce a suitable groove for repair welding. Thermal gouging is also used where extensive excavation is required.

Whether the repair requires a full- or partial-penetration weld depends on many factors, such as the location of the repair area, the stresses that will be imposed on the area in service, the type of weld metal required, and the condition of heat

treatment. If the repair requires a hardenable alloy steel weld deposit, or if it is necessary to harden and temper the part after welding, then a partial-penetration weld is generally unsatisfactory, because cracks are likely to propagate from the unwelded root of the repair area.

Welding Processes. The SMAW process is very versatile for the repair welding of small areas. Some types of SMAW electrodes that are available in very large sizes are also used to repair deep cracks or to rebuild large surface areas in massive parts. Some large repairs can be accomplished more economically with semiautomatic or automatic welding processes, such as GMAW, FCAW, SAW, and hot-wire PAW.

Manual GTAW is generally used to repair small areas or edges of parts. Automatic GTAW, using hot or cold wire feed, and hot-wire PAW processes can be used for larger areas.

Repair Practices. If a repair is in a working area of a tool in the annealed condition and is shallow in depth, then a heat-treatable type of deposit that will respond to heat treatment in a manner similar to that of the base metal will be required. If the area has sufficient depth, it can be partially built up with a nonhardenable filler metal and then completed with a tool steel filler metal. The built-up layer should have sufficient strength to support the tool steel deposit under working conditions of the tool. The tool steel deposit should be thick enough to compensate for dilution with the built-up deposit, and it should have adequate wear properties after the quench and temper heat treatment.

A weld deposit used to repair the working surface of a tool in the hardened and tempered condition should have adequate properties after tempering. Alternatively, a hardfacing deposit that does not require heat treatment can be used.

In some cases, the required repairs of either hardened or annealed tools can be in noncritical areas, and a nonhardenable type of filler metal can be used.

When repair welding a cutting edge, the weld metal should be allowed to flow or roll over the edge so that the repaired area can be machined or ground to produce a finished edge without notches or depressions.

Peening is often required to reduce distortion and prevent the cracking of weld deposits. In order to be effective, peening must be done properly; generally, when the deposit is red. Insufficient peening will not relieve stresses, whereas excessive peening can cause cracking.

Welding of Low-Alloy Steels

F.J. Winsor, Welding Consultant

References

1. "ANSI/AWS FILLER METAL SPECIFICATIONS," AWS, 1979-1992
2. CHAPTERS 1, 3, 4, *WELDING HANDBOOK*, 7TH ED., VOL 4, *METALS AND THEIR WELDABILITY*, AWS, 1982
3. "STRUCTURAL WELDING CODE--STEEL," ANSI/AWS D1.1-92, AWS, 1992
4. "ASME BOILER AND PRESSURE VESSEL CODE," ASME, 1992
5. "ISOTHERMAL TRANSFORMATION DIAGRAMS," UNITED STATES STEEL CORP., 1963

Welding of Stainless Steels

D.J. Kotecki, The Lincoln Electric Company

Introduction

STAINLESS STEELS can be defined as alloys that contain at least 10.5% Cr, no more than 1.5% C, and more iron than any other single element. There are five major families of stainless steels, based on microstructure and properties:

- MARTENSITIC STAINLESS STEELS
- FERRITIC STAINLESS STEELS
- AUSTENITIC STAINLESS STEELS
- PRECIPITATION-HARDENING (PH) STAINLESS STEELS
- DUPLEX FERRITIC-AUSTENITIC STAINLESS STEELS

Each family requires different weldability considerations, because of the varied phase transformation behavior upon cooling from solidification to room temperature or below.

Often, the optimal filler metal is not the one that most closely matches the base-metal composition. The most successful procedures for one family are often markedly different from those that are appropriate for another family.

This article addresses consumable selection and procedure development for the welding of stainless steels. Additional information about the selection and weldability of these alloys is available in the Section "Selection of Stainless Steels" in this Volume.

Stainless steel base metals and, therefore, the welding filler metals used with them, are almost invariably chosen on the basis of adequate corrosion resistance for the intended application. This usually means that the welding filler metal must at least match (and sometimes overmatch) the contents of the base metal in terms of specific alloying elements, such as chromium, nickel, and molybdenum.

After considering corrosion resistance, the avoidance of cracking becomes the unifying theme in filler-metal selection and procedure development for the welding of stainless steels. Cracking can occur at temperatures that are just below the bulk solidus temperature of the alloy(s) being welded. This hot cracking, as it is called, can appear as large weld-metal cracks, usually along the weld centerline. However, it can also appear as small, short cracks (microfissures) in the weld metal or in the heat-affected zone (HAZ) at the fusion line and, usually, perpendicular to it. Hot cracking in stainless steel welds is of most concern in austenitic weld metals, although it can occur in all types of stainless steel weldments.

Cracking can also occur at rather low temperatures of, typically, 150 °C (300 °F) or below, because of the interaction of high weld stresses, high-strength metal, and diffusible hydrogen. This cold cracking commonly occurs in martensitic weld metals, as well as HAZs, including those of PH stainless steels. Cold cracking can also occur in ferritic stainless steel weldments that have become embrittled by grain coarsening and/or second-phase particles.

In many instances of cold cracking, where the resulting weld has acceptable properties, the substitution of a mostly austenitic filler metal (with appropriate corrosion resistance) for a martensitic or ferritic filler metal serves as a remedy. When hot cracking occurs in an austenitic weld metal, a common remedy is to use a mostly austenitic filler metal that includes a small amount of ferrite. However, another approach toward avoiding hot cracking may be necessary in situations that require low magnetic permeability, high toughness at cryogenic temperatures, resistance to media that selectively attack ferrite (such as urea), or postweld heat treatments (PWHT) that embrittle ferrite, because their requirements may severely limit the amount of ferrite that is acceptable.

Welding engineers who are responsible for filler-metal selection and procedure development for stainless steel welds will often estimate the microstructure of the weld metal, taking the dilution effects into consideration. This task is best accomplished with a constitution diagram for the stainless steel weld metals. Several diagrams that have been developed over the years are described below.

Welding of Stainless Steels

D.J. Kotecki, The Lincoln Electric Company

Constitution Diagrams

In 1949, Anton Schaeffler (Ref 1) published what has become known as the Schaeffler diagram (Fig. 1). This diagram proposed a relationship among alloy elements that promote the formation of ferrite (chromium-equivalent elements) and elements that promote the formation of austenite and the suppression of ferrite (nickel-equivalent elements). To use this diagram, both the chromium and nickel equivalents are first calculated from the composition of a given weld bead. Next, these equivalents are plotted as coordinates on the Schaeffler diagram. This allows an estimated weld-metal microstructure to be determined from the boundaries given in the diagram. Experience has shown that the Schaeffler diagram is reasonably accurate for conventional "300 series" stainless steel weld deposits from covered electrodes. However, it is of limited use when less-conventional compositions are used and when a high level of nitrogen is present.

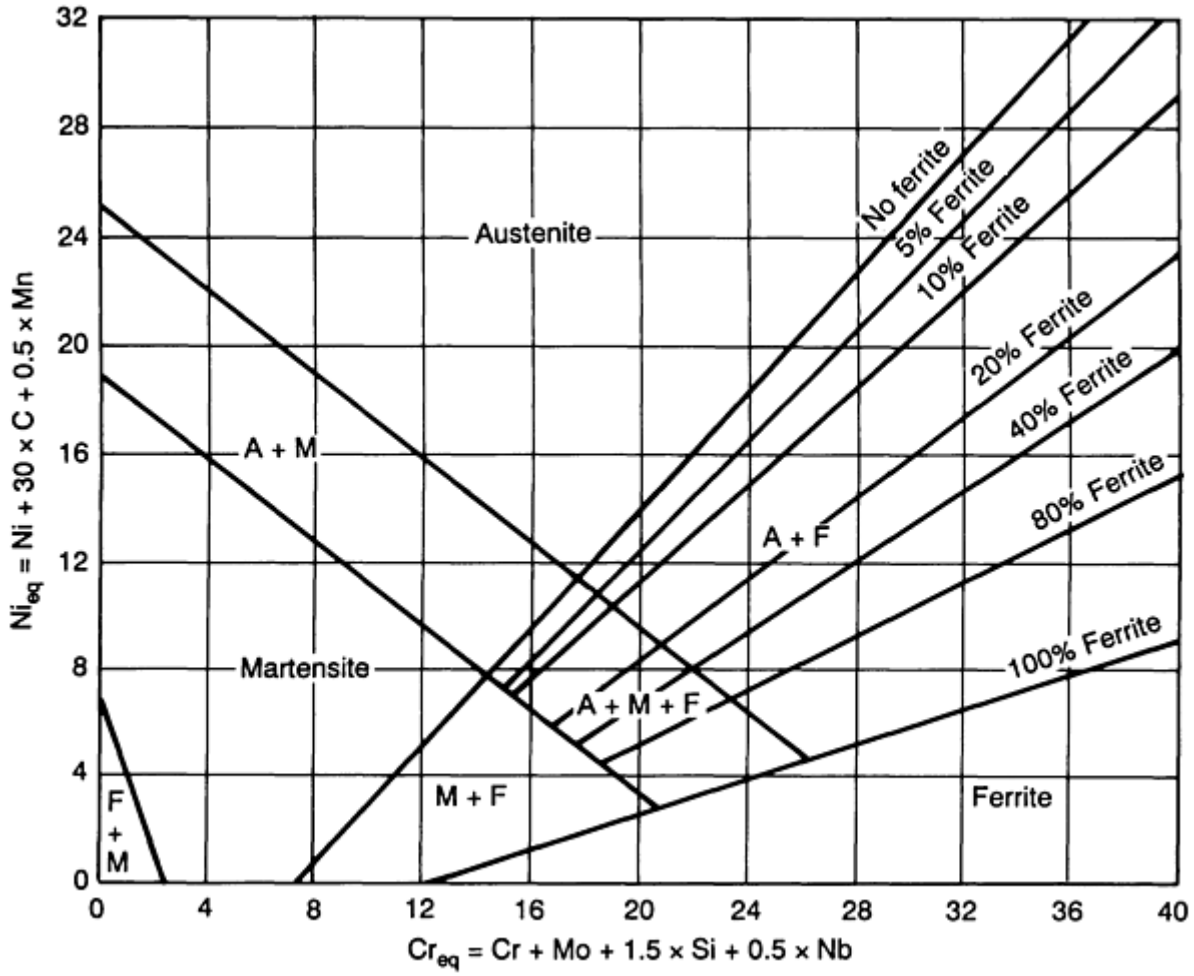

FIG. 1 SCHAEFFLER CONSTITUTION DIAGRAM FOR STAINLESS STEEL WELD METAL

W.T. DeLong recognized the effect of nitrogen in promoting austenite at the expense of ferrite, and he developed a new diagram (Ref 2) that covered a more-restricted composition range and included the effect of nitrogen (Fig. 2). Specifically, a nickel equivalent of 30 × %N was added. To use this diagram, the nickel and chromium equivalents are calculated from the weld-metal analysis. If a nitrogen analysis of the weld metal is not available, then a value of 0.06% should be assumed for the gas-tungsten arc welding (GTAW) process and covered electrodes and a value of 0.08% assumed for gas-metal arc welded metals. If the chemistry is accurate, then the diagram predicts the Welding Research Council (WRC) Ferrite Number within ±3 in approximately 90% of the tests for the alloy 308, 309, 316, and 317 families.

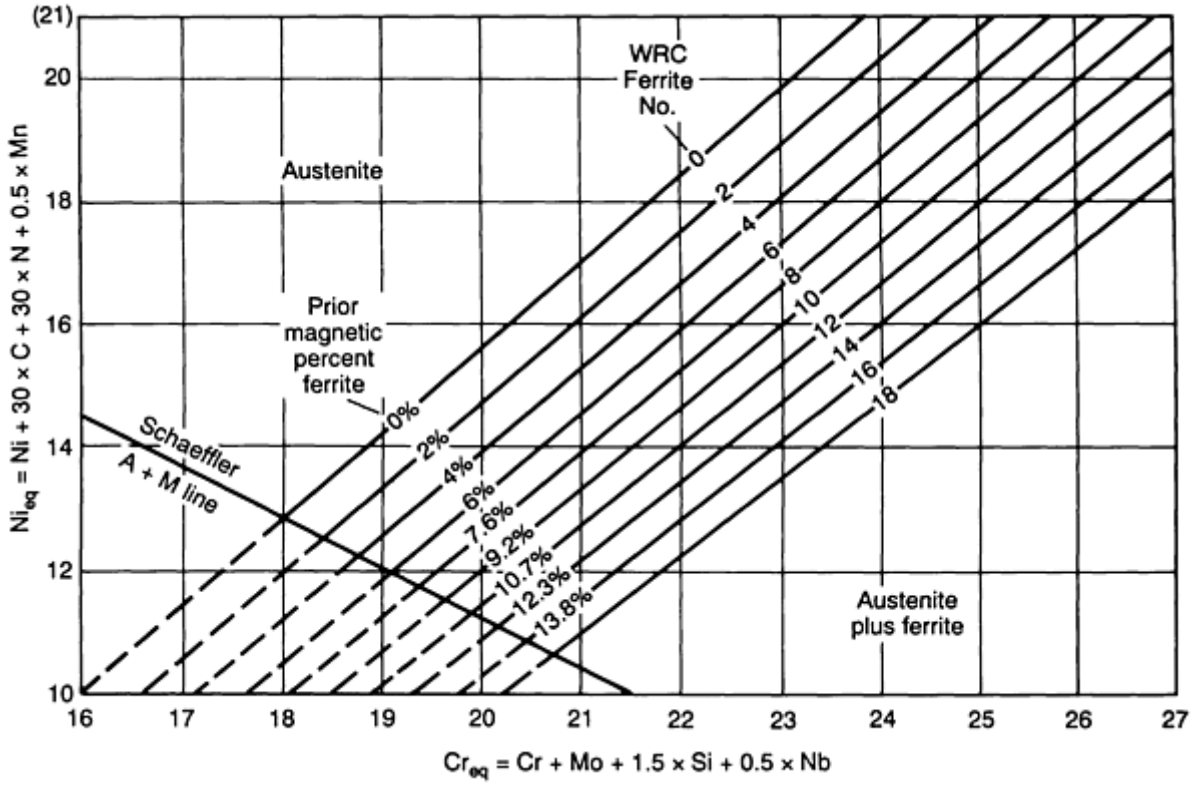

FIG. 2 DELONG CONSTITUTION DIAGRAM FOR STAINLESS STEEL WELD METAL. THE SCHAEFFLER AUSTENITE-MARTENSITE BOUNDARY IS INCLUDED FOR REFERENCE.

In the DeLong diagram, the Ferrite Numbers for alloy 308, 308L, and 347 covered electrodes are similar to those in the Schaeffler diagram, but the alloy 309, 316, and 317 families have Ferrite Numbers that are about two to four times higher. Generally, the DeLong diagram correlates better with GTAW and gas-metal arc welding (GMAW) weld metals than does the Schaeffler diagram, because it allows for nitrogen pickup.

In 1974, at about the time the DeLong diagram was being published, the measurement of ferrite in nominally austenitic stainless steel weld metals was standardized by the ANSI/AWS A4.2 specification in terms of magnetically determined Ferrite Numbers (FN), rather than the metallographically determined "percent ferrite" used by the Schaeffler diagram. The DeLong diagram became part of the "Boiler and Pressure Vessel Code" of the American Society of Mechanical Engineers (ASME).

The DeLong diagram was subsequently discovered to seriously underestimate the ferrite content of weld metals with high manganese contents and overestimate the FN of highly alloyed weld metals, such as alloy 309. Consequently, the Welding Research Council both funded and collected data for the development of a new, more-accurate diagram using computer mapping techniques (Ref 3, 4). A joint effort was conducted by the Colorado School of Mines and the U.S. National Institute of Standards and Technology (NIST). The product of this effort, known as the WRC-1988 diagram (Fig. 3), covers a broader range of compositions than does the DeLong diagram and removes the two errors noted above.

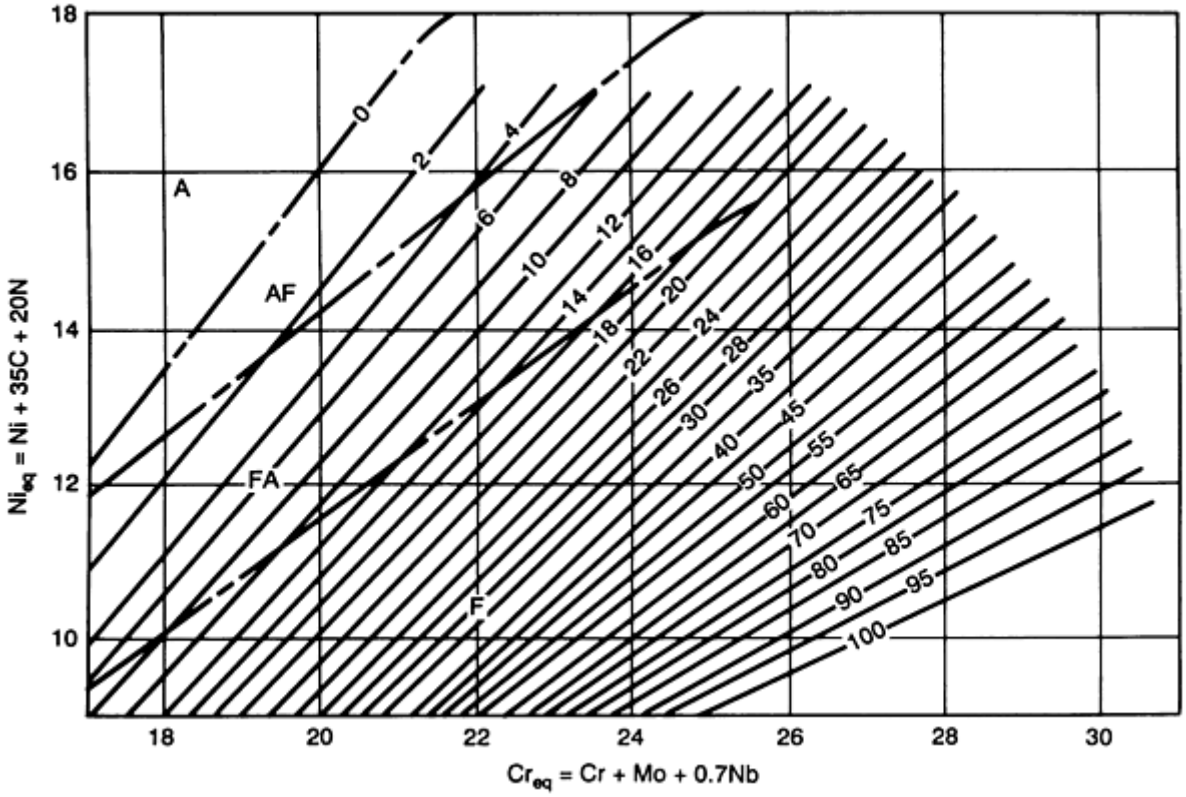

FIG. 3 WRC-1988 DIAGRAM, INCLUDING SOLIDIFICATION-MODE BOUNDARIES

A modification of the WRC-1988 diagram, which allowed the nickel equivalent to include a coefficient for copper, was first proposed by F.B. Lake in 1990 (Ref 5). This modification and an extension of the chromium-equivalent and nickel-equivalent axes were incorporated into the most recent constitution diagram, the WRC-1992 diagram (Ref 6) shown in Fig. 4. Its extended axes permit graphical estimation of the ferrite content of weld metal that comprises very different base metal(s) and filler metal, as could be done less precisely with the Schaeffler diagram.

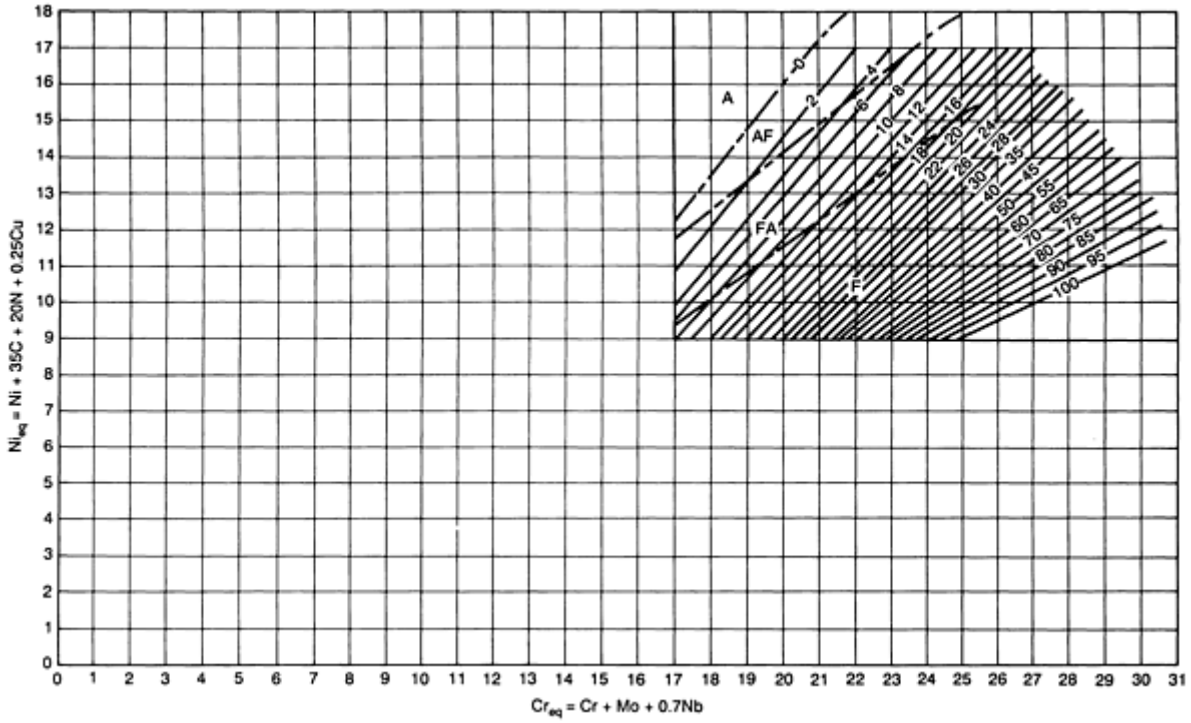

FIG. 4 WRC-1992 DIAGRAM WITH EXPANDED SCALE FOR DILUTION CALCULATIONS. ALTHOUGH EXTENDED AXES ALLOW A WIDE RANGE OF COMPOSITIONS TO BE LOCATED, THE FN PREDICTION IS ONLY ACCURATE FOR WELD COMPOSITIONS THAT FALL WITHIN THE BOUNDS OF THE ISO-FN LINES (0 TO 100 FN). LIMITS OF WRC DIAGRAM WERE DETERMINED BY EXTENT OF DATA BASE, AND EXTENSION OF THE LINES COULD RESULT IN ERRONEOUS PREDICTIONS. SOURCE: REF 6

Although the WRC-1992 diagram is more accurate in predicting ferrite content for many weld metals, the Schaeffler diagram still retains some utility because it can offer reasonably accurate predictions in terms of martensite in lean stainless steel compositions. This is because the WRC-1992 diagram does not include manganese. Manganese has been found (Ref 7) to have no effect on the high-temperature transformation of ferrite to austenite during cooling. Therefore, it does not figure in the nickel equivalent of the WRC-1992 diagram. However, it does have a significant effect on the low-temperature transformation of austenite to martensite during further cooling. It tends to stabilize austenite at low temperatures (Ref 8). Without a manganese effect, it is not possible to put a boundary for the martensite phase in the WRC-1992 diagram.

If the weld deposit is austenitic, then a Ferrite Number around 4 or 5, minimum, typically suffices to prevent hot cracking (Ref 9). In addition, a deposit that is primarily austenitic will not cold crack. These two considerations often influence filler-metal selection and procedure development. In the following sections of this article, the WRC-1992 diagram and, occasionally, the Schaeffler diagram, are used to illustrate the rationale behind many filler-metal choices.

It is appropriate to keep in mind that the ferrite that survives at room temperature after solidification is only a fraction of what existed during solidification. In terms of the utility of constitution diagrams like the WRC-1992 diagram, it is currently thought (Ref 10) that finding ferrite at room temperature is only an indirect indication of the solidification mode. According to this theory, if the weld metal solidifies as ferrite first, with austenite appearing only in the latter stages of solidification, if at all, then the weld metal will be crack resistant. However, if the weld metal solidifies as austenite first, with ferrite only appearing in the latter stages of solidification, if at all, then the weld metal is at risk for cracking.

The dividing line between compositions that solidify as austenite first and compositions that solidify as ferrite first is approximated by the dashed line between the fields labeled "AF" (primary austenite solidification) and "FA" (primary ferrite solidification) in Fig. 3 and 4. This line is not parallel to the isoferrite lines. Rather, it is at a small angle to them, which means that more ferrite is needed at room temperature to represent evidence of primary ferrite solidification in higher-alloyed stainless steel weld metals than in lower-alloyed stainless steel weld metals.

References cited in this section

1. A.L. SCHAEFFLER, CONSTITUTION DIAGRAM FOR STAINLESS STEEL WELD METAL, *MET. PROG.*, VOL 56 (NO. 11), 1949, P 680-680B
2. W.T. DELONG, FERRITE IN AUSTENITIC STAINLESS STEEL WELD METAL, *WELD. J.*, VOL 53 (NO. 7), 1974, P 273S-286S
3. T.A. SIEWERT, C.N. MCCOWAN, AND D.L. OLSON, FERRITE NUMBER PREDICTION TO 100 FN IN STAINLESS STEEL WELD METAL, *WELD J.*, VOL 67 (NO. 12), 1988, P 289S-298S
4. C.N. MCCOWAN, T.A. SIEWERT, AND D.L. OLSON, "STAINLESS STEEL WELD METAL: PREDICTION OF FERRITE CONTENT," WELDING RESEARCH COUNCIL BULLETIN 342, WRC, 1989
5. F.B. LAKE, "EFFECT OF CU ON STAINLESS STEEL WELD METAL FERRITE CONTENT," PAPER PRESENTED AT 1990 AMERICAN WELDING SOCIETY ANNUAL MEETING, AS YET UNPUBLISHED
6. D.J. KOTECKI AND T.A. SIEWERT, WRC-1992 CONSTITUTION DIAGRAM FOR STAINLESS STEEL WELD METALS: A MODIFICATION OF THE WRC-1988 DIAGRAM, *WELD. J.*, VOL 71 (NO. 5), 1992, P 171S-178S
7. E.R. SZUMACHOWSKI AND D.J. KOTECKI, MANGANESE EFFECT ON STAINLESS STEEL WELD METAL FERRITE, *WELD. J.*, VOL 71 (NO. 5), 1984, P 156S-161S
8. J.A. SELF, D.K. MATLOCK, AND D.L. OLSON, AN EVALUATION OF AUSTENITIC FE-MN-NI WELD METAL FOR DISSIMILAR METAL JOINING, *WELD. J.*, VOL 63 (NO. 9), 1984, P 282S-288S
9. C.D. LUNDIN, W.T. DELONG, AND D.F. SPOND, FERRITE-FISSURING RELATIONSHIP IN AUSTENITIC STAINLESS STEEL WELD METALS, *WELD. J.*, VOL 54 (NO. 8), 1975, P 241S-246S
10. J.C. LIPPOLD AND W.F. SAVAGE, SOLIDIFICATION OF AUSTENITIC STAINLESS STEEL WELDMENTS: PART III--THE EFFECT OF SOLIDIFICATION BEHAVIOR ON HOT CRACKING SUSCEPTIBILITY, *WELD. J.*, VOL 61 (NO. 12), 1982, P 388S-396S

Welding of Stainless Steels

D.J. Kotecki, The Lincoln Electric Company

Martensitic Stainless Steels

Basic Metallurgy. At high temperatures, the equilibrium microstructure of martensitic stainless steels is either entirely or almost entirely austenite. At room temperature, the equilibrium microstructure of these steels is a mixture of ferrite and carbides. The reformation of austenite upon heating occurs very rapidly, but the transformation back to ferrite upon cooling is extremely slow. As a result, these steels have a very high tendency to transform to martensite upon cooling from temperatures at which austenite is the stable phase. In fact, it is very difficult to avoid martensite in these steels. They are air hardening, which means that even upon slow cooling in heavy sections, they form martensite.

The binary iron-chromium phase diagram shown in Fig. 5 indicates that above a level of approximately 12% Cr, binary alloys will not form austenite at any temperature, so they cannot be hardened by heating and cooling. However, the addition of carbon to iron-chromium alloys increases the range of chromium contents over which austenite can be formed at elevated temperatures (Fig. 6). It should be noted that nitrogen, nickel, copper, and, possibly, manganese, also expand this range. Even with 17% Cr, a fully austenitic microstructure can be achieved with about 0.4% C at 1250 °C (2280 °F). It can then be fully hardened. When the corrosion-resisting properties of iron-chromium alloys were first discovered early in the 20th century, it was extremely difficult to remove carbon from melts of iron-chromium alloys. Thus, the first stainless steels, which were discovered more or less simultaneously in Germany and England, were martensitic.

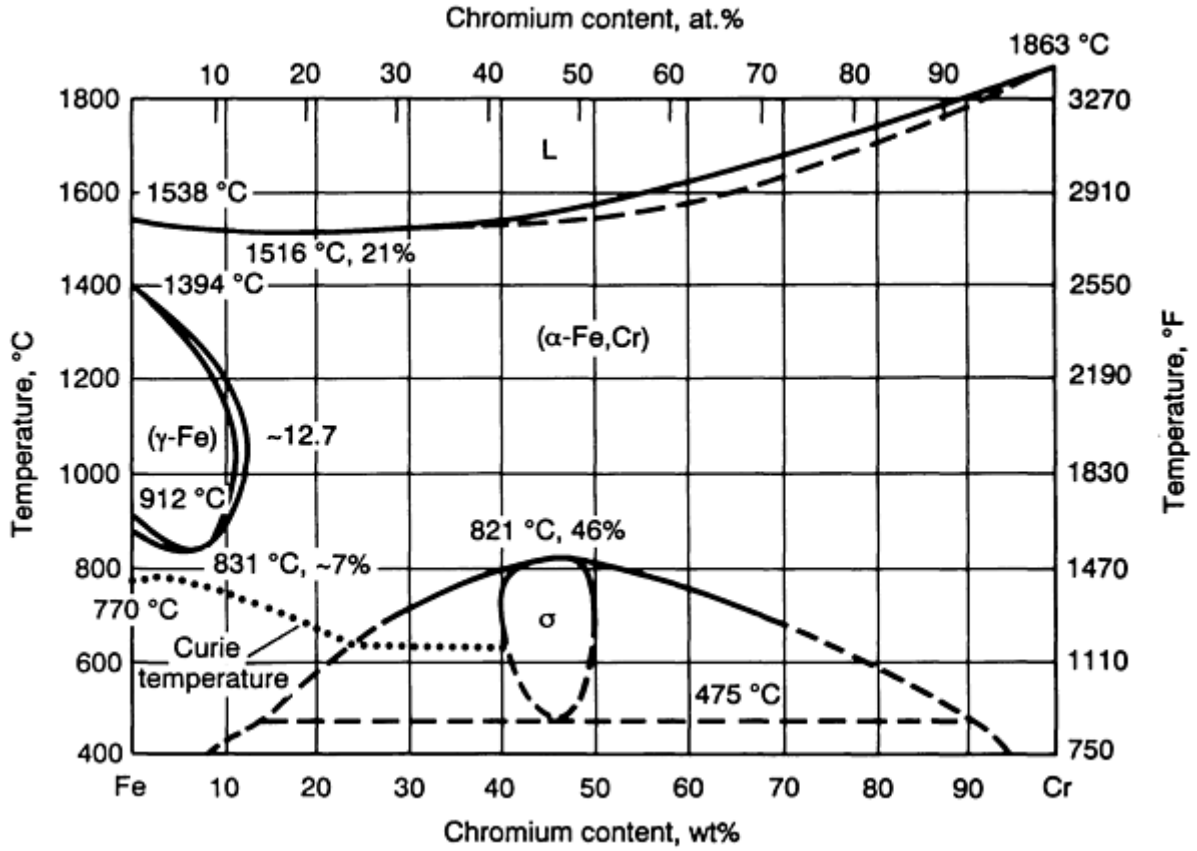

FIG. 5 BINARY IRON-CHROMIUM EQUILIBRIUM PHASE DIAGRAM. SOURCE: REF 11

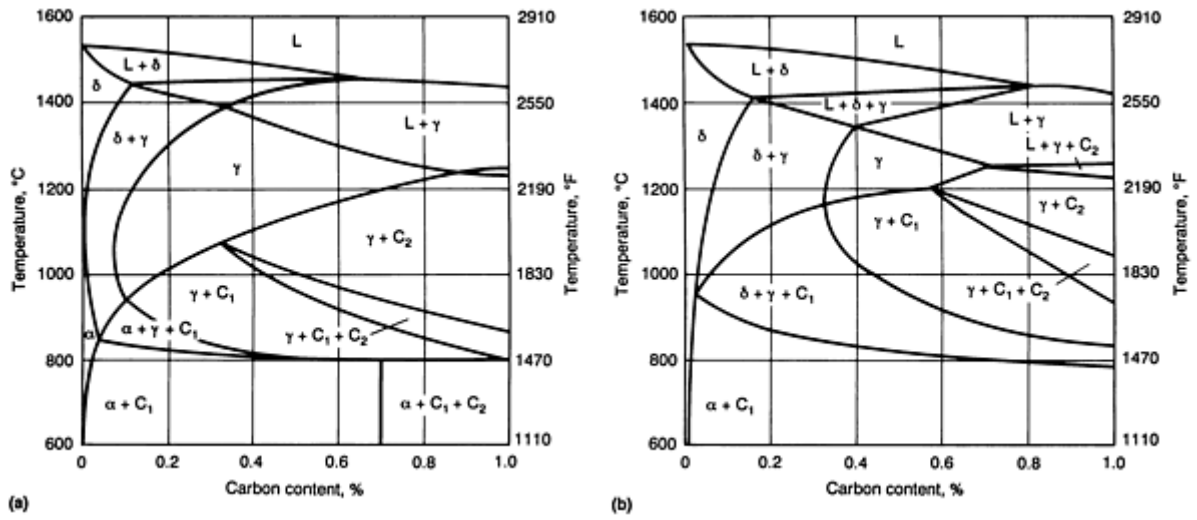

FIG. 6 CONCENTRATION PROFILE IN TERNARY IRON-CHROMIUM-CARBON CONSTITUTION DIAGRAM. (A) 13% CR. (B) 17% CR. SOURCE: REF 12

Carbon content almost entirely determines the hardness of martensite. If virtually 100% martensite can be achieved in a steel, then Fig. 7 shows several relationships that have been found experimentally between carbon and hardness. In particular, it shows that as little as 0.10% C in martensite will result in a hardness value of approximately 35 HRC. The hardness of martensite increases to over 60 HRC at approximately 0.5% C, and it does not change significantly at higher levels of carbon, at least on a macroscale.

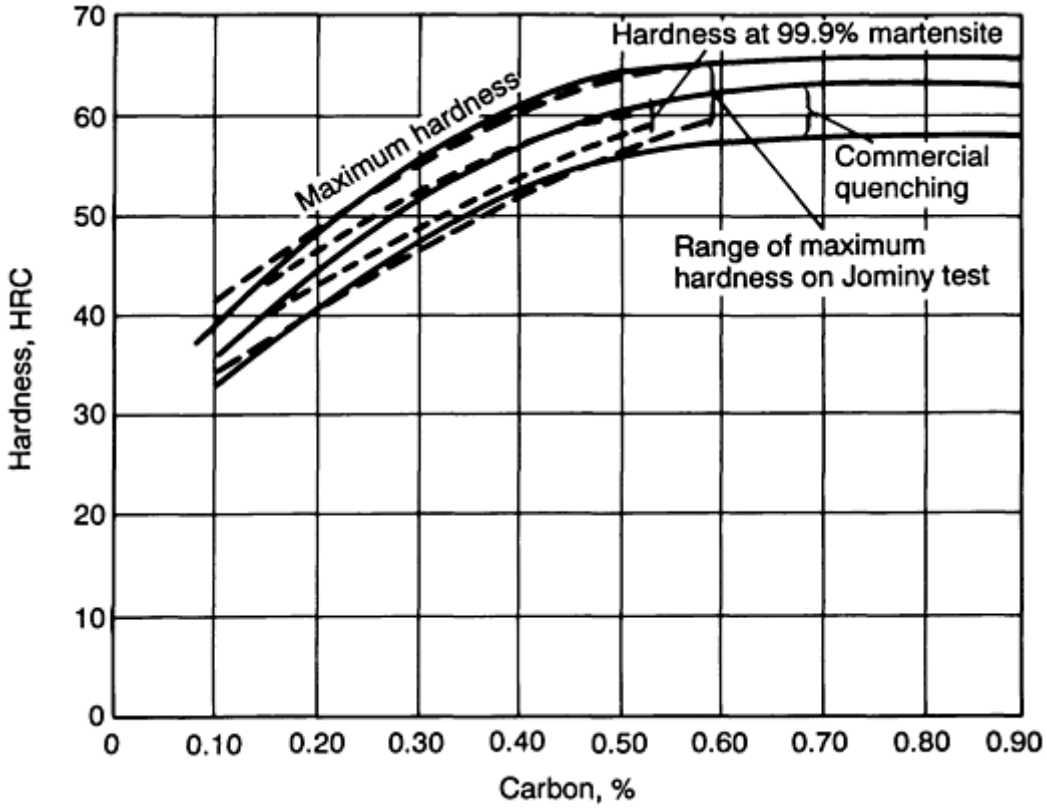

FIG. 7 HARDNESS VALUES OF FULLY HARDENED STEELS WITH A RANGE OF CARBON CONTENTS. SOURCE: REF 13

Figure 7 presents the situation if essentially all martensite is obtained. In carbon and low-alloy steels, rapid cooling is usually necessary to avoid the formation of ferrite. However, as more alloy is added, the avoidance of ferrite becomes easier. At a 12% Cr level, nearly any cooling rate will result in virtually 100% martensite. The prototype of all martensitic stainless steels is type 410 (approximately 12% Cr and 0.10% C). The isothermal transformation diagram for type 410 stainless steel (Fig. 8) indicates that, after cooling from high temperatures and being held at approximately 700 °C (1290 °F), it will take approximately 2 min before any ferrite forms, and several hours will be required before the transformation to ferrite with carbides is complete. Cooling to a holding temperature of 400 °C (750 °F) will require more than 1 week before any ferrite forms.

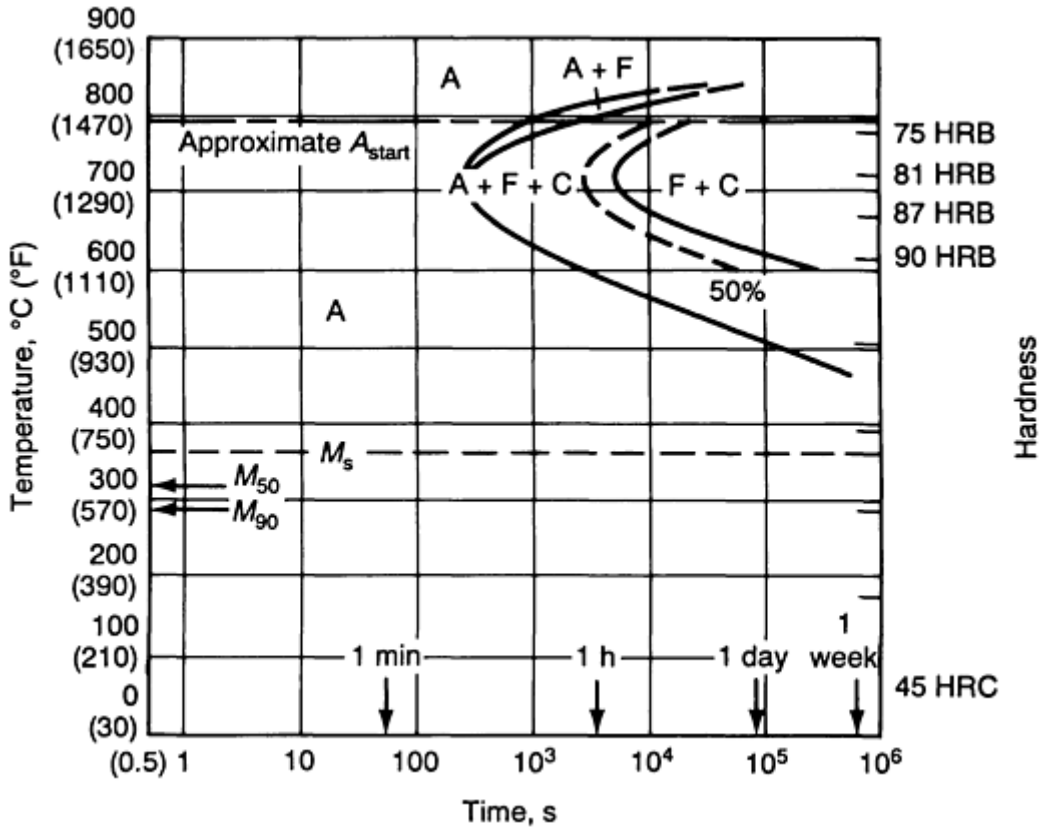

FIG. 8 ISOTHERMAL TRANSFORMATION DIAGRAM FOR TYPE 410 STAINLESS STEEL (12CR-0.1C) AUSTENITIZED AT 980 °C (1800 °F), WITH GRAIN SIZE OF 6 TO 7. A, AUSTENITE; F, FERRITE; C, CARBIDE; M, MARTENSITE; B, BAINITE; P, PEARLITE. SOURCE: REF 14

Figure 8 further shows that martensite begins to form at about 350 °C (660 °F) on cooling type 410 stainless steel and is finished when cooling reaches about 250 °C (480 °F). Alloying at levels that are either above or in addition to 12% Cr serves to further delay ferrite formation and further reduces the martensite-start (M_s) temperature. In the extreme case, some austenite will exist indefinitely, even at room temperature, and refrigeration or complex heat treatments (such as double tempering) may be necessary to induce complete martensite transformation in highly alloyed martensitic stainless steels. Therefore, in any fusion welding process, it must be assumed that regardless of the condition of heat treatment of the base metal, the HAZ and any nearly matching filler metal for martensitic stainless steels in the as-welded condition will be freshly formed martensite. The martensite will be hard and, unless it is very low carbon martensite, it will also be quite brittle and crack-sensitive. Therefore, a standard rule to follow when welding martensitic stainless steels is to weld hot, that is, a high preheat, high interpass temperature, and high heat input are, in most cases, beneficial to accomplishing the weld without incurring cracking.

Martensitic Stainless Steel Base Metals. A number of martensitic stainless steel base metals are identified in Table 1(a). Welding filler metals that have approximately matching compositions, as classified by the American Welding Society (AWS), are also listed in Table 1(b), but only for selected base metals.

TABLE 1(A) COMPOSITIONS OF NOMINALLY MARTENSITIC STAINLESS STEELS

DESIGNATION	UNS NO.	ASTM SPECIFICATION	COMPOSITION, WT%									
			C	Mn	P (max)	S	Si (max)	Cr	Ni	Mo	N	OTHER
XM-32	K64152	A 565	0.08-0.15	0.50-0.90	0.025	0.025 MAX	0.35	11.00-12.50	2.00-3.00	1.50-2.00	0.01-0.05	**V, 0.25-0.40**
403	S40300	A 479	0.15 MAX	1.00 MAX	0.040	0.030 MAX	0.50	11.50-13.00	. . .	. . .	. . .	**. . .**
410	S41000	A 240	0.15 MAX	1.00 MAX	0.040	0.030 MAX	1.00	11.50-13.50	0.75 MAX	. . .	. . .	**. . .**
410S	S41008	A 240	0.08 MAX	1.00 MAX	0.040	0.030 MAX	1.00	11.50-13.50	0.60 MAX	. . .	. . .	**. . .**
XM-30	S41040	A 479	0.18 MAX	1.00 MAX	0.040	0.030 MAX	1.00	11.50-13.50	. . .	. . .	. . .	**NB + TA, 0.05-0.30**
. . .	S41041	A 565	0.13-0.18	0.40-0.60	0.030	0.030 MAX	1.50	11.50-13.00	0.50 MAX	0.20 MAX	. . .	**NB + TA, 0.15-0.45; AL, 0.05 MAX**
. . .	S41050	A 240	0.040 MAX	1.00 MAX	0.040	0.030 MAX	1.00	10.50-12.50	0.60-1.10	. . .	0.10 MAX	**. . .**
414	S41400	A 479	0.15 MAX	1.00 MAX	0.040	0.030 MAX	1.00	11.50-13.50	1.25-2.50	. . .	. . .	**. . .**
410NIMO	S41500	A 240	0.05 MAX	0.5-1.0	0.030	0.030 MAX	0.60	11.5-14.0	3.5-5.5	0.5-1.0	. . .	**. . .**
416	S41600	A 473	0.15 MAX	1.25 MAX	0.06	0.15 MIN	1.00	12.00-14.00	. . .	0.60 MAX	. . .	**. . .**
XM-6	S41610	A 582	0.15 MAX	1.50-2.50	0.06	0.15 MIN	1.00	12.00-14.00	. . .	. . .	. . .	**. . .**
416SE	S41623	A 473	0.15 MAX	1.25 MAX	0.06	0.06 MAX	1.00	12.00-14.00	. . .	. . .	. . .	**SE, 0.15 MIN**
615	S41800	A 565	0.15-0.20	0.50 MAX	0.040	0.030 MAX	0.50	12.00-14.00	1.80-2.20	0.50 MAX	. . .	**W, 2.50-3.50**
420	S42000	A 276	0.15 MIN	1.00 MAX	0.040	0.030 MAX	1.00	12.00-14.00	. . .	. . .	. . .	**. . .**
. . .	S42010	A 276	0.5-0.30	1.00 MAX	0.040	0.030 MAX	1.00	13.50-15.00	0.35-0.85	0.40-0.85	. . .	**. . .**

420F	S42020	A 565	0.30-0.40	1.25 MAX	0.06	0.15 MIN	1.00	12.00-14.00	0.50 MAX	. . .	. . .	**CU, 0.60 MAX**
420FSE	S42023	A 565	0.20-0.40	1.25 MAX	0.06	0.06 MAX	1.00	12.00-14.00	0.50 MAX	. . .	. . .	**CU, 0.60 MAX; SE, 0.15 MIN**
616	S42200	A 565	0.20-0.25	0.50-1.00	0.025	0.025 MAX	0.50	11.00-12.50	0.50-1.00	0.90-1.25	. . .	**V, 0.20-0.30; W, 0.90-1.25**
619	S42300	A 565	0.27-0.32	0.95-1.35	0.025	0.025 MAX	0.50	11.00-12.00	0.50 MAX	2.50-3.00	. . .	**V, 0.20-0.30**
431	S43100	A 479	0.20 MAX	1.00 MAX	0.040	0.030 MAX	1.00	15.00-17.00	1.25-2.50	. . .	. . .	**. . .**
440A	S44002	A 276	0.60-0.75	1.00 MAX	0.040	0.030 MAX	1.00	16.00-18.00	. . .	0.75	. . .	**. . .**
440B	S44003	A 276	0.75-0.95	1.00 MAX	0.040	0.030 MAX	1.00	16.00-18.00	. . .	0.75	. . .	**. . .**
440C	S44004	A 276	0.95-1.20	1.00 MAX	0.040	0.030 MAX	1.00	16.00-18.00	. . .	0.75	. . .	**. . .**
440F	S44020	A 582	0.95-1.20	1.25 MAX	0.06	0.15 MIN	1.00	16.00-18.00	0.50 MAX	. . .	. . .	**CU, 0.60 MAX**
440FSE	S44023	A 582	0.95-1.20	1.25 MAX	0.06	0.06 MAX	1.00	16.00-18.00	0.50 MAX	. . .	. . .	**CU, 0.60 MAX; SE, 0.15 MIN**
CA-15	. . .	A 743	0.15 MAX	1.00 MAX	0.04	0.04 MAX	1.50	11.5-14.0	1.00 MAX	0.50 MAX	. . .	**. . .**
CA-15M	. . .	A 743	0.15 MAX	1.00 MAX	0.040	0.040 MAX	0.65	11.5-14.0	1.0 MAX	0.15-1.0	. . .	**. . .**
CA-40	. . .	A 743	0.20-0.40	1.00 MAX	0.04	0.04 MAX	1.50	11.5-14.0	1.0 MAX	0.5 MAX	. . .	**. . .**
CA-40F	. . .	A 743	0.20-0.40	1.00 MAX	0.04	0.20-0.40	1.50	11.5-14.0	1.0 MAX	0.5 MAX	. . .	**. . .**
CA6N	. . .	A 743	0.06 MAX	0.50 MAX	0.02	0.02 MAX	1.00	10.5-12.5	6.0-8.0	. . .	. . .	**. . .**
CA-6NM	. . .	A 743	0.06 MAX	1.00 MAX	0.04	0.03 MAX	1.00	11.5-14.0	3.5-4.5	0.40-1.0	. . .	**. . .**
CA-28MWV	**. . .**	**A 743**	**0.20-0.28**	**0.50-1.00**	**0.030**	**0.030 MAX**	**1.0**	**11.0-12.5**	**0.50-1.00**	**0.90-1.25**	**. . .**	**V, 0.20-0.30; W, 0.90-1.25**

TABLE 1(B) PROPERTIES AND FILLER METALS FOR NOMINALLY MARTENSITIC STAINLESS STEELS

DESIGNATION	UNS NO.	ASTM SPECIFICATION	TENSILE STRENGTH		YIELD STRENGTH		ELONGATION, %	MATCHING FILLER METALS		
			MPA	KSI	MPA	KSI		A5.4	A5.9[A]	A5.22
XM-32	K64152	A 565	1000	145	790	115	15	. . .	. . .	. . .
403	S40300	A 479	480	70	275	40	20	E410-XX	ER410	E410T-X
410	S41000	A 240	450	65	205	30	20	E410-XX	ER410	E4101-X
410S	S41008	A 240	415	60	205	30	22	E410-XX	ER410	E410T-X
XM-30	S41040	A 479	480	70	275	40	13	. . .	. . .	. . .
. . .	S41041	A 565	790	115	520	75	15	. . .	. . .	. . .
. . .	S41050	A 240	415	60	205	30	22	. . .	. . .	. . .
414	S41400	A 479	790	115	620	90	15	. . .	. . .	. . .
410NIMO	S41500	A 240	790	115	620	90	15	E410NIMO-XX	ER410NIMO	E410NIMOT-X
416	S41600	A 473	480	70	275	40	20	NCW	NCW	NCW
XM-6	S41610	A 582	NS	NS	NS	NS	NS	NCW	NCW	NCW
416SE	S41623	A 473	480	70	275	40	20	NCW	NCW	NCW
615	S41800	A 565	970	140	760	110	115	. . .	. . .	. . .
420	S42000	A 276	NS	NS	NS	NS	NS	. . .	ER420	. . .
. . .	S42010	A 276	NS	NS	NS	NS	NS	. . .	. . .	. . .
420F	S42020	A 565	NS	NS	NS	NS	NS	NCW	NCW	NCW
420FSE	S42023	A 565	NS	NS	NS	NS	NS	NCW	NCW	NCW
616	S42200	A 565	970	140	760	110	13	. . .	. . .	. . .
619	S42300	A 565	970	140	760	110	8	. . .	. . .	. . .
431	S43100	A 479	790	115	620	90	15	. . .	. . .	. . .
440A	S44002	A 276	NS	NS	NS	NS	NS	. . .	. . .	. . .
440B	S44003	A 276	NS	NS	NS	NS	NS	. . .	. . .	. . .
440C	S44004	A 276	NS	NS	NS	NS	NS	. . .	. . .	. . .
440F	S44020	A 582	NS	NS	NS	NS	NS	NCW	NCW	NCW
440FSE	S44023	A 582	NS	NS	NS	NS	NS	NCW	NCW	NCW
CA-15	. . .	A 743	620	90	450	65	18	E410-XX	ER4109	E410T-X
CA-15M	. . .	A 743	620	90	450	65	18	. . .	. . .	. . .
CA-40	. . .	A 473	690	100	480	70	15	. . .	ER420	. . .
CA-40F	. . .	A 743	690	100	480	70	12	NCW	NCW	NCW

CA6N	. . .	A 743	970	140	930	135	15	. . .	. . .	**. . .**
CA-6NM	. . .	A 743	760	110	550	80	15	E410NIMO-XX	ER410NIMO	**E410NIMOT-X**
CA-28MWV	**. . .**	**A 743**	**970**	**140**	**760**	**110**	**10**	**. . .**	**. . .**	**. . .**

NS, not specified; NCW, not considered weldable.

(A) METAL-CORED ELECTRODES, INDICATED BY A "C" IN PLACE OF THE "R" IN THE CLASSIFICATION, ARE ALSO INCLUDED.

Of these base metals, the lower carbon content alloys, especially type 410 and CA-6NM (410NiMo), are often used for turbines in hydroelectric and similar types of facilities. They provide resistance to mild corrosion, cavitation, and moderate abrasion, and they possess relatively high strength. CA-6NM is also used in fittings, valves, and pumps for sour (H_2S-containing) oil and gas service. In this application, the alloy usually must be heat treated to a hardness value that does not exceed 22 HRC. This usually requires a double temper treatment consisting of 2 h at 675 °C (1250 °F) (intercritical temperature range), an air cool to room temperature, and then 4 h at 615 °C (1140 °F) (below lower critical temperature).

Type 420 and similar alloys are used in cutlery, valve parts, gears, shafts, and rollers. One extensive application is a weld overlay on rolls for steel mill continuous casters. This type of alloy is quite brittle in the freshly hardened condition and usually must be tempered to obtain useful toughness properties.

The higher carbon content martensitic stainless steels, such as types 440A, 440B, and 440C, can be hardened to values near 60 HRC. Then, they can be tempered at temperatures up to 480 °C (900 °F) to toughen without experiencing much loss of hardness. In this condition, they serve well as cutting edges and as bearings.

Martensitic stainless steels generally develop full hardness upon air cooling from about 1000 °C (1830 °F). They can be softened by tempering at temperatures ranging from approximately 500 to 750 °C (930 to 1380 °F), unless they contain significant amounts of nickel, in which case the maximum temperature for tempering is reduced. After tempering at 650 to 750 °C (1200 to 1380 °F), their hardness values generally drop to about 30 HRC or lower. This can be useful if it is necessary to soften a martensitic stainless steel before welding to allow enough ductility in the bulk of the material to accommodate shrinkage stresses associated with welding. However, such high-temperature tempering produces rather coarse chromium carbides, which damage the corrosion resistance of the metal. Then, it may be necessary after welding to austenitize, air cool to room temperature, and temper at a low temperature (less than 450 °C, or 840 °F) to restore corrosion resistance.

Engineering for Use in the As-Welded Condition. Except for very small weldments or very low carbon base metals, martensitic stainless steels are not usually used in the as-welded condition. This is due to the very brittle weld area that normally results. This area includes the weld metal itself, if it has a matching or near-matching composition to that of the base metal, and the heat-affected zone. However, repair situations can necessitate that the engineer work with these circumstances.

If a weldment of martensitic stainless steel must be used in the as-welded condition, then it is usually best to avoid both autogenous welds (no filler metal) and welds with matching filler metals. Small parts that are welded by laser-beam welding (LBW), electron-beam welding (EBW), or GTAW processes are an exception, because residual stresses can be very low and the welding processes generate almost no diffusible hydrogen.

If at all possible, an austenitic filler metal, such as type 309 or 309L stainless, or a duplex ferritic-austenitic stainless filler metal, such as type 312 stainless, should be chosen, depending on the base metal. The filler-metal choice should provide for a small amount of ferrite in the weld metal, in order to avoid hot cracking. This can be anticipated by using the extended WRC-1992 diagram (Fig. 4). If the weld metal is austenite with a little ferrite, then the weld metal itself will have appreciable ductility, and only the HAZ will be at risk for cold cracking. This possibility can be minimized by using high preheat temperatures (200 °C, or 390 °F, minimum for type 410 base metal and 350 °C, or 660 °F, minimum for types 440A, 440B, and 440C base metals) and slow cooling after welding.

Example 1: Type 410 base metal (0.10C-12.5Cr-0.04N), Cr_{eq} = 12.5 and Ni_{eq} = 4.3; to be welded with E309-16 manual electrode (0.05C-23.5Cr-13.0Ni-0.06N all-weld metal composition), Cr_{eq} = 23.5 and Ni_{eq} = 15.95.

If the type 410 base metal is plotted in Fig. 9 (point A), along with the all-weld metal composition of the E309-16 electrode (point B), then all possible mixtures of these two metals must lie along the line connecting these two points. If the root pass is diluted with 30% base metal (a typical result to expect), then the actual root pass composition will lie along the tie line, 30% of the distance from point B to point A. This composition is shown as point C in Fig. 9. It would correspond to slightly over 8 FN, which is quite safe in terms of the likelihood of hot cracking. Furthermore, because the tie line is nearly parallel to the isoferrite lines in the diagram, major changes in dilution would have practically no effect on weld-metal ferrite content. Additional weld passes on top of the root pass would have compositions that are also along the tie line, but closer to the E309-16 all-weld metal composition. Therefore, E309-16 would be a very good filler metal

choice if a nonhardenable weld deposit is acceptable. By similar reasoning, type 309 (or 309L) would be an excellent choice for gas-metal arc weld wire, flux-cored wire, or submerged arc wire.

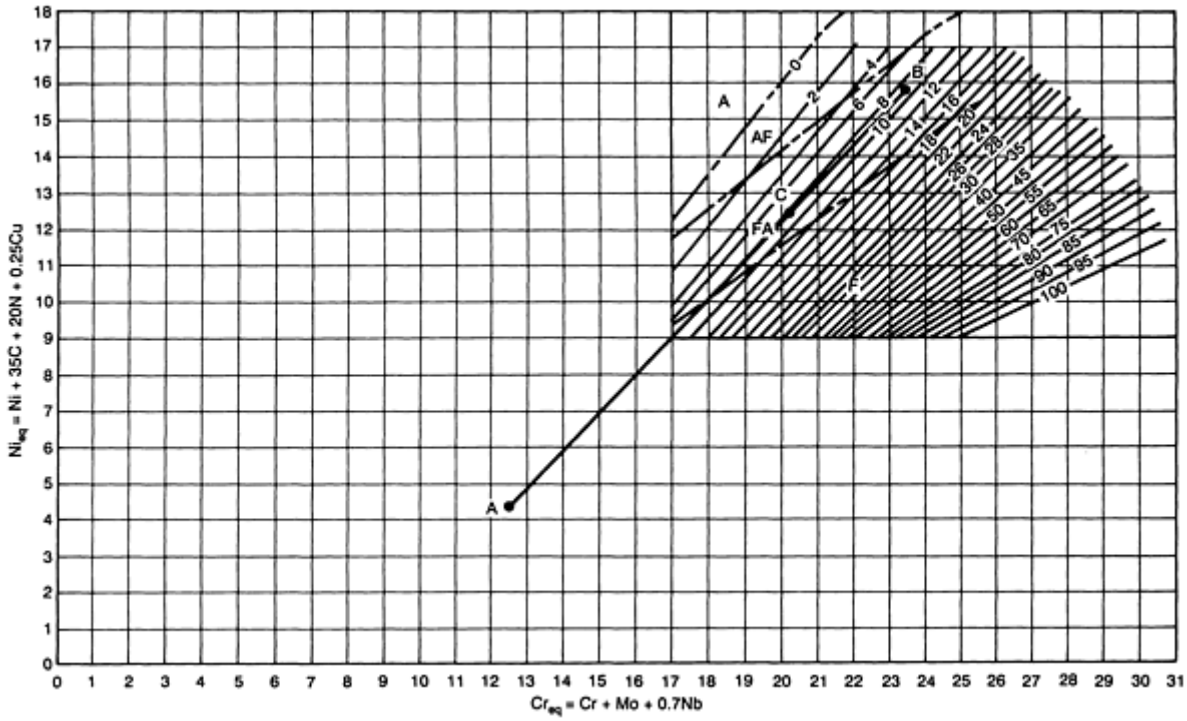

FIG. 9 WRC-1992 DIAGRAM WITH EXPANDED SCALE FOR DILUTION CALCULATIONS, IN WHICH FERRITE IS CALCULATED FOR TYPE 410 STAINLESS STEEL WELDED WITH E309-16 (REFER TO EXAMPLE 1)

Example 2: Type 440A base metal (0.7C-17.0Cr-0.04N), Cr_{eq} = 17.0 and Ni_{eq} = 25.3; to be welded with E309-16 manual electrode (0.05C-23.5Cr-13.0Ni-0.06 N all-weld metal composition), Cr_{eq} = 23.5 and Ni_{eq} = 15.95.

Because the type 440A base metal cannot be plotted on the WRC-1992 diagram, it is necessary to calculate the weld Cr_{eq} and Ni_{eq}. Assuming a 30% dilution, the weld Cr_{eq} = 0.7 (E309-16 Cr_{eq}) + 0.3(440A Cr_{eq}) = 0.7(23.5) + 0.3(17.0) = 21.55; and the weld Ni_{eq} = 0.7(E309-16 Ni_{eq}) + 0.3(440A Ni_{eq}) = 0.7(15.95) + 0.3(25.3) = 18.8. Because the weld-metal composition would clearly lie above and to the left of the 0 FN line in Fig. 4, there would be no ferrite in such a weld deposit. Therefore, E309-16 would not be a good choice for welding type 440A base metal.

Example 3: Type 440A base metal (0.7C-17.0Cr-0.04N), Cr_{eq} = 17.0 and Ni_{eq} = 25.3; to be welded with E312-16 manual electrode (0.10C-29.0Cr-8.8Ni-0.06N), Cr_{eq} = 29.0 and Ni_{eq} = 13.3.

Because the type 440A base metal cannot be plotted on the WRC-1992 diagram, it is necessary to calculate the weld Cr_{eq} and Ni_{eq}. Assuming a 30% dilution, the weld Cr_{eq} = 0.7(E312-16 Cr_{eq}) + 0.3(440A Cr_{eq}) = 0.7(29.0) + 0.3(17) = 25.4; and the weld Ni_{eq} = 0.7(E312-16 Ni_{eq}) + 0.3(440A Ni_{eq}) = 0.7(13.3) + 0.3(25.3) = 16.9. Plotting the weld Cr_{eq} and Ni_{eq} on the WRC-1992 diagram shows this composition corresponds to about 12 FN. Therefore, E312-16 would be a good choice for welding type 440A base metal, if a nonhardenable weld is acceptable.

However, unlike the situation in Example 1, the tie line from the E312-16 electrode all-weld metal composition on the WRC-1992 diagram to the type 440A base-metal composition is nearly perpendicular to the isoferrite lines. This means that large changes in dilution would have a strong effect on weld-metal ferrite content. In particular, it can be calculated that an increase in dilution to just over 35% would put the weld composition into the primary austenite solidification mode and, therefore, at risk of hot cracking. Because higher dilution is normal in submerged arc welding (SAW) and spray-transfer GMAW processes, the avoidance of these processes would be suggested by this example. However, the GMAW process using short-circuiting transfer with type 312 filler wire should be acceptable.

Although the welding filler metals of Examples 1 and 3 seem appropriate choices for avoiding hot cracking in joints in the martensitic stainless steels used in these examples, the weld metals would considerably undermatch the strengths of the base metals, unless the base metals were annealed. The base metals could easily have tensile strength values that exceed 1000 MPa (145 ksi), depending on their condition of heat treatment before welding, whereas the weld metals are likely to have tensile strengths on the order of 550 to 600 MPa (80 to 90 ksi). Furthermore, the austenitic weld metals cannot be hardened by heat treatment. If higher-strength weld metal is essential, then a martensitic filler metal is necessary, which almost always requires a PWHT to obtain reasonable ductility in the weld metal.

Engineering for Use after Postweld Heat Treatment. Because of the major weld-metal strength (hardness) undermatch that often occurs when martensitic stainless steel base metals are welded with austenitic filler metals, these base metals are usually welded with martensitic stainless steel filler metals, and the weldment is subsequently heat treated to improve the properties of the weld area. Heat treatment after welding usually takes one of two forms. The weldment could be either tempered by heat treatment below the austenitic-start temperature or heated above the austenitic-finish temperature to austenitize the entire mass, and then cooled back to nearly room temperature to fully harden it, and then heated again, but to a temperature below the austenitic-start temperature in order to temper the metal to desired properties. Tempering heat treatments at temperatures between the austenitic-start and austenitic-finish temperatures are generally avoided, because they result in a mixture of heavily tempered martensite and fresh untempered martensite, although it is possible to follow such a temper (after cooling to near-room temperature) with a second temper just below the austenitic-start temperature. Such a "double temper" has been successfully used to obtain low hardness and high toughness properties in weldments of CA-6NM (410NiMo).

Tempering at temperatures up to approximately 450 °C (840 °F) has little effect on the hardness of martensitic stainless steels, compared with the hardness of the same steel in the untempered condition. Tempering above 450 °C (840 °F) causes the hardness to fall rapidly with increasing tempering temperatures (Fig. 10), but at the same time, ductility increases. The tempering temperature upper limit is the austenite-start temperature, which is about 800 °C (1470 °F) for the nickel-free alloys, such as types 410, 420, and 440 (Fig. 6 and 8). The addition of nickel to a martensitic alloy reduces the austenite-start temperature appreciably. For CA-6NM, it is about 640 °C (1180 °F).

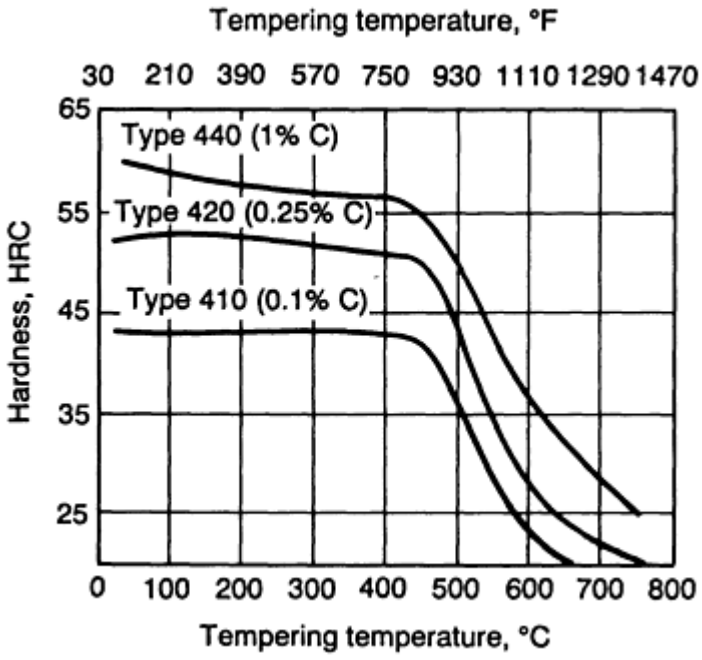

FIG. 10 TEMPERING RESPONSE OF MARTENSITIC STAINLESS STEELS. SOURCE: REF 15

Tempering at temperatures above 450 °C (840 °F), but below the austenitic-start temperature, also can be useful *before* welding, because the base metal is softened and made more ductile, which better accommodates the shrinkage strains that accompany cooling of the weld metal. This helps to avoid weldment cracking during cooling.

With all but the lowest carbon content martensitic stainless steel base metals, high preheat and high interpass temperatures are usually necessary to avoid cracking when the weld metal is also martensitic stainless steel. The alloy CA-6NM only requires approximately 140 °C (280 °F), minimum, whereas types 410 and 420 require approximately 200 °C (390 °F), and type 440 requires approximately 260 °C (500 °F), minimum. However, for a sizable weldment, a safer procedure is to perform all welding at temperatures above the martensite-start temperature of the weld metal, so that no martensite forms in the weld until welding is completed. Preheat and interpass temperatures ranging from 300 to 500 °C (570 to 930 °F) are successfully used. In either case, the weldment must be very slowly cooled to below 100 °C (212 °F) to complete martensite transformation of the weld metal and HAZ without cracking, once welding is finished.

Only after martensite transformation is completed (when the weldment is below 100 °C, or 212 °F) should tempering of the weldment be undertaken. If untransformed austenite is still present, tempering followed by cooling will result in fresh martensite formation when the weldment reaches room temperature, and unexpected hardness (possibly accompanied by cracking) is likely to be encountered.

The availability of matching filler metals is a problem for some martensitic stainless steels. For covered electrodes, only E410-XX and E410NiMo-XX types are commercially significant, as indicated by the ANSI/AWS A5.4 classification. The same compositions are also the only entries in the flux-cored electrode standard, ANSI/AWS A5.22. These compositions, as well as the ER420 classification, are given as solid wires in the ANSI/AWS A5.9 standard. Therefore, Table 1(b), which designates matching filler metals along with selected base metals, has many voids in the filler-metal listings. A few filler-metal producers can produce special orders, such as tubular metal-cored electrodes, in compositions to match the other base metals. Otherwise, the fabricator may be forced to choose a filler metal that does not match the base metal.

One special case deserves mention. Literally thousands of tons of filler metal in the form of tubular wires have been deposited by submerged arc overlay of type 420 and modified-composition weld metals on low-alloy steel rolls for continuous casters. In service, these rolls typically crack from thermal shock. After a period ranging from 6 months to 1 year, their surfaces are sufficiently damaged so that they must be removed from service. If cracking is not too deep, then the cracks can be machined off and the roll rewelded as before.

A very successful welding procedure has been to maintain preheat and interpass temperatures of at least 350 °C (660 °F) from the start to the finish of welding. Because this temperature is above the martensite-start temperature of the weld metal, the weld metal remains as austenite during welding, which may last 1 day or longer. As many as three welding heads, each using 400 to 900 A, can be used on a roll that is about 2 m (6.5 ft) long, which helps to keep the roll hot. The welded roll is covered with insulating material and left to slow cool to nearly room temperature. Then, it is tempered, typically at temperatures of 450 °C (840 °F) or higher, to soften the overlay enough to make it machinable. Molybdenum, vanadium, and, sometimes, niobium, can be added to the basic type 420 composition to modify the tempering response (as well as service performance). Figure 11 illustrates the change in tempering response that results from the alloy modifications.

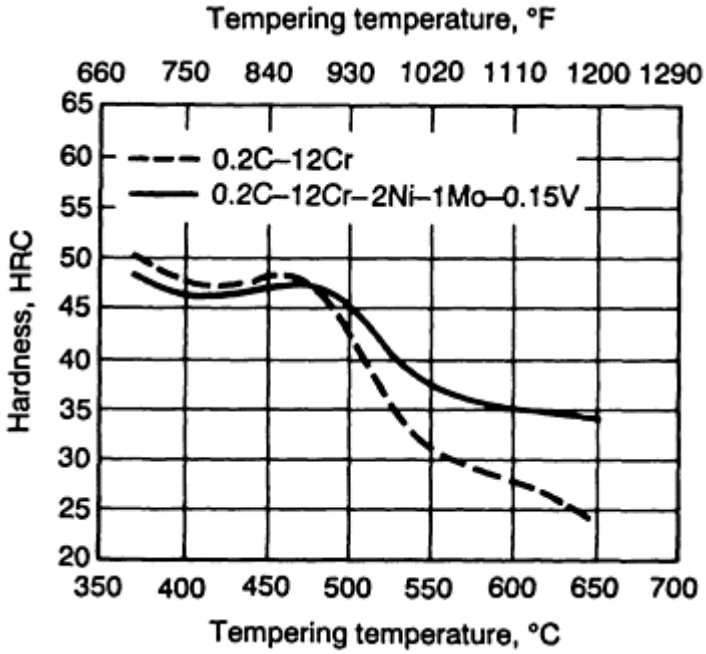

FIG. 11 TEMPERING RESPONSE (2 H AT TEMPERATURE) OF TYPES 420 AND MODIFIED 420 CONTINUOUS CASTER ROLL OVERLAY. SOURCE: REF 16

References cited in this section

11. *METALS HANDBOOK,* 8TH ED., VOL 8, AMERICAN SOCIETY FOR METALS, 1973, P 291
12. E. FOLKHARD, *WELDING METALLURGY OF STAINLESS STEELS,* SPRINGER-VERLAG, 1984, P 17
13. M.A. GROSSMANN AND E.C. BAIN, *PRINCIPLES OF HEAT TREATMENT,* 5TH ED., AMERICAN SOCIETY FOR METALS, 1964, P 49
14. *ATLAS OF ISOTHERMAL TRANSFORMATION AND COOLING TRANSFORMATION DIAGRAMS,* AMERICAN SOCIETY FOR METALS, 1977, P 324
15. "CARPENTER STAINLESS STEELS--WORKING DATA," CARPENTER TECHNOLOGY CORPORATION, 1983
16. "ENGINEERING REPORT ES-489," THE LINCOLN ELECTRIC COMPANY, 1991

D.J. Kotecki, The Lincoln Electric Company

Ferritic Stainless Steels

Basic Metallurgy. There are essentially three generations of ferritic stainless steels. The first--in which carbon is not very low, so that chromium needs to be high--dates from the early decades of the 20th century, when the decarburization of iron-chromium alloys was quite inefficient. The prototype alloy is type 430 stainless, typically 0.08C-17Cr. Figure 6(b) indicates that this alloy would be fully ferritic at temperatures above approximately 1250 °C (2280 °F). At lower temperatures, ferrite and austenite would co-exist to about 1030 °C (1890 °F). Further cooling would cause carbides to appear as well. Then, at about 920 °C (1690 °F), the austenite would disappear and only ferrite and some carbides would remain at room temperature, under equilibrium conditions. Type 446 stainless (typically, 0.1C-25Cr) is also of this first generation, and it behaves similarly.

It is something of a misnomer to call these first-generation ferritic stainless steels "ferritic" because some austenite appears at certain high temperatures. This austenite has a beneficial effect in that it retards grain growth, which has an important embrittling effect when it occurs. However, because it also tends to transform to martensite under welding conditions, first-generation ferritic stainless steels generally have hard spots after welding (see Fig. 12). In addition, normal weld cooling will cause some supersaturation of the ferrite with carbon, because of declining carbon solubility in the ferrite with falling temperatures below 950 °C (1740 °F). A PWHT at about 760 °C (1400 °F) simultaneously tempers the martensite where austenite existed at higher temperatures, and causes the excess carbon in the ferrite to precipitate as carbides. Both of these effects act to significantly improve the ductility and toughness of type 430 after welding. Type 446 is not ductile at room temperature, even before welding.

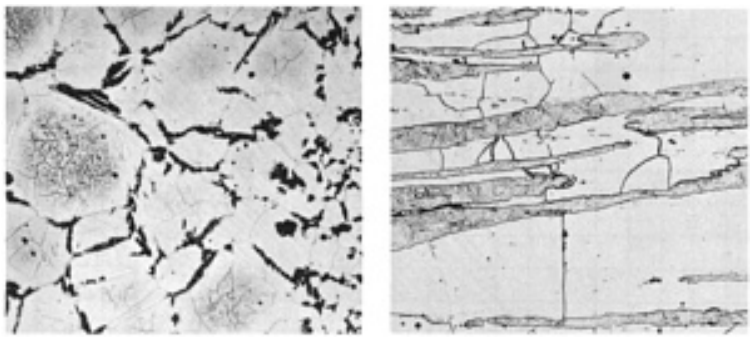

FIG. 12 MICROSTRUCTURE OF TYPE 430 FERRITE STAINLESS STEEL. (A) BASE METAL, 25 MM (1 IN.) THICK PLATE, AS HOT ROLLED; SPECIMEN FROM LONGITUDINAL DIRECTION. FERRITE MATRIX CONTAINS ELONGATED LAYERS OF MARTENSITE AND TRANSFORMATION PRODUCTS. PICRAL AND HYDROCHLORIC ACID ETCH, 100×. (B) WELD HEAT-AFFECTED ZONE. PROGRESSIVE COARSENING OF FERRITE GRAINS AND DISTRIBUTION OF MARTENSITE (DARK) AT GRAIN BOUNDARIES AS DISTANCE FROM WELD ZONE (RIGHT) INCREASES. TEMPERED 10 MIN AT 593 °C (1100 °F) TO CAUSE MARTENSITE TO BE DARK-ETCHING. PICRIC ACID (5%) AND HYDROCHLORIC ACID (3%) IN ALCOHOL, 150×. SOURCE: REF 17

The second generation of ferritic stainless steels have lower-carbon and low-nitrogen contents, to which a stabilizer is added to tie up whatever carbon and/or nitrogen is present. The prototype of this second generation is type 409, typically 0.04C-11Cr-0.5Ti. The titanium ties up both carbon and nitrogen, leaving all of the chromium free. Surplus titanium is also a ferritizer. Therefore, the alloy is ferritic at all temperatures. Type 405 is a similar alloy, but it is stabilized with aluminum, which ties up nitrogen, but not carbon. Aluminum is also a powerful ferritizer. The various carbides and/or nitrides produced by the addition of stabilizers help to resist embrittling grain growth in second-generation ferritic stainless steels during welding.

The third generation of ferritic stainless steels arose circa 1970, with the advent of more-efficient decarburization techniques in steelmaking. Carbon and nitrogen levels are typically 0.02% or less, and stabilizers, such as titanium and/or niobium, are often added to tie up any free interstitials. The prototype alloy is type 444 (18Cr-2Mo). There are also a number of proprietary alloys that are not yet covered by an ASTM designation.

The third-generation ferritic stainless steel alloys are austenite-free at all temperatures. However, they can be embrittled by the formation of intermetallic phases at elevated temperatures. They are sensitive to "475 °C (885 °F) embrittlement," because of precipitation of the chromium-rich α' phase, and to embrittlement by σ, χ, and other phases at higher temperatures. Figure 5 indicates that the αphase is approximately FeCr, whereas α' is a chromium-rich ferrite that precipitates from the iron-rich ferrite. The χ phase is a complex iron-chromium-molybdenum intermetallic, which can only appear in molybdenum-bearing steels. Except in the case of α' embrittlement, which disappears rapidly upon exposure to temperatures above approximately 575 °C (1070 °F), temperatures that are high enough to dissolve all of these phases are also high enough to cause severe grain growth in the ferrite. Because this grain growth also has an embrittling effect, heat treatment alone is not usually desirable. In general, hot working to reduce grain size is necessary to restore full ductility and toughness once the alloy is embrittled by σ, χ, or other high-temperature intermetallic compounds.

Ferritic stainless steels of the third generation can be severely embrittled by interstitial contamination during welding, because of improper or contaminated gas shielding. Although nitrogen contamination is most common, carbon, hydrogen,

and oxygen also have detrimental effects on ductility and toughness. Cleanliness, inert backing gas, and high-purity gas shielding conducted with precautions to avoid disturbances are essential if the best weldment properties are to be obtained.

Ferritic Stainless Steel Base Metals. Tables 2(a) and 2(b) list selected ferritic stainless steel base metals, their minimum mechanical property requirements, and some corresponding welding filler metals. Ferritic stainless steels cannot offer the range of mechanical properties (depending on heat treatment) that martensitic stainless steels offer. Whereas the martensitic stainless steels offer only moderate corrosion resistance, that of the ferritic stainless steels can range from moderate, for types 430 or 409, to outstanding, for the third-generation "super ferritics" such as type 444 and UNS Nos. S44627, S44635, S44660, S44700, and S44800. Types 405 and 409 have resistance to atmospheric corrosion. Type 430 also resists mild oxidizing acids and organic acids, and is therefore used in food-handling equipment, sinks, and such. The super ferritics offer exceptional resistance to localized corrosion induced by exposure to aqueous chlorides. Localized corrosion, such as pitting, crevice corrosion, and stress-corrosion cracking, are problems that plague many austenitic stainless steels. Therefore, the super ferritics are often used in heat exchangers and piping systems for chloride-bearing aqueous solutions and seawater.

TABLE 2(A) COMPOSITIONS OF NOMINALLY FERRITIC STAINLESS STEELS

DESIGNATION	UNS NO.	ASTM SPECIFICATION	COMPOSITION, WT%									
			C	Mn	P (max)	S	Si (max)	Cr	Ni	Mo	N	OTHER
XM-34	S18200	A 582	0.08 MAX	2.50 MAX	0.04	0.15 MIN	1.00	17.50-19.50	. . .	1.50-2.50	. . .	
. . .	S18235	A 582	0.025 MAX	0.50 MAX	0.030	0.15-0.30	1.00	17.50-18.50	1.00 MAX	2.00-2.50	0.025 MAX	**C + N, 0.035 MAX; TI, 0.30-1.00**
405	S40500	A 240	0.08 MAX	1.00 MAX	0.040	0.030 MAX	1.00	11.50-14.50	0.60 MAX	. . .	. . .	**AL, 0.10 TO 0.30**
409	S40900	A 240	0.08 MAX	1.00 MAX	0.045	0.030 MAX	1.00	10.50-11.75	0.50 MAX	. . .	. . .	**TI, 6 × C MIN TO 0.75 MAX**
429	S42900	A 240	0.12 MAX	1.00 MAX	0.040	0.030 MAX	1.00	14.00-16.00	0.75 MAX	. . .	. . .	**. . .**
430	S43000	A 240	0.12 MAX	1.00 MAX	0.040	0.030 MAX	1.00	16.00-18.00	0.75 MAX	. . .	. . .	**. . .**
430F	S43020	A 473	0.12 MAX	1.25 MAX	0.06	0.15 MAX	1.00	16.00-18.00	0.75 MAX	0.60 MAX	. . .	
430F SE	S43023	A 473	0.12 MAX	1.25 MAX	0.06	0.06 MAX	1.00	16.00-18.00	0.75 MAX	. . .	. . .	**SE, 0.15 MIN**
439	S43035	A 240	0.07 MAX	1.00 MAX	0.040	0.030 MAX	1.00	17.00-19.00	0.50 MAX	. . .	0.04 MAX	**TI, 0.20 + 4 (C + N) MIN TO 1.10 MAX; AL, 0.15 MAX**
444	S44400	A 240	0.025 MAX	1.00 MAX	0.040	0.030 MAX	1.00	17.5-19.5	1.00 MAX	1.75-2.50	0.035 MAX	**TI + NB, 0.20 + 4 (C + N) MIN TO 0.80 MAX**
446	S44600	A 276	0.20 MAX	1.50 MAX	0.040	0.030 MAX	1.00	23.00-27.00	. . .	. . .	0.25 MAX	**. . .**
XM-27	S44627	A 240	0.010	0.40	0.020	0.020 MAX	0.40	25.00-27.50	0.50 MAX	0.75-1.50	0.015 MAX	**NB + TA, 0.05-0.20; AL, 0.20 MAX; NI + CU, 0.50 MAX**
XM-33	S44626	A 240	0.06	0.75	0.040	0.020	0.75	25.00-	0.50	0.75-	0.04	**TI, 7 × (C + N)**

			MAX	MAX		MAX		27.00	MAX	1.50	MAX	**MIN AND 0.02-1.00; CU, 0.20 MAX**
. . .	S44635	A 240	0.025 MAX	1.00 MAX	0.040	0.030 MAX	0.75	24.5-26.0	3.5-4.5	3.5-4.5	0.035 MAX	**TI + NB, 0.20 + 4 × (C + N) MIN TO 0.80 MAX**
. . .	S44660	A 240	0.030 MAX	1.00 MAX	0.040	0.030 MAX	1.00	25.0-28.0	1.0-3.50	3.00-4.00	0.040 MAX	**TI + NB, 6 × (C + N) MIN AND 0.20 TO 1.00**
29-4	S44700	A 240	0.010 MAX[(A)]	0.30 MAX	0.025	0.020 MAX	0.20	28.0-30.0	0.15 MAX	3.5-4.2	0.020 MAX[(A)]	
29-4-2	S44800	A 240	0.010 MAX[(A)]	0.30 MAX	0.025	0.020 MAX	0.20	28.0-30.0	2.0-2.5	3.5-4.2	0.020 MAX[(A)]	
. . .	S44735	A 240	0.030 MAX	1.00 MAX	0.040	0.030 MAX	1.00	28.00-30.00	1.00 MAX	3.60-4.20	0.045 MAX	**TI + NB, 6 × (C + N) MIN AND 0.20 TO 1.00**
CB-30	. . .	A 743	0.30 MAX	1.00 MAX	0.04	0.04 MAX	1.50	18.0-21.0	2.00 MAX	. . .	. . .	**. . .**
CC-50	**. . .**	**A 743**	**0.50 MAX**	**1.00 MAX**	**0.04**	**0.04 MAX**	**1.50**	**26.0-30.0**	**4.00 MAX**	**. . .**	**. . .**	**. . .**

(A) (C + N) = 0.025 MAX, CU = 0.015 MAX

TABLE 2(B) PROPERTIES AND FILLER METALS FOR NOMINALLY FERRITIC STAINLESS STEELS

DESIGNATION	UNS NO.	ASTM SPECIFICATION	TENSILE STRENGTH		YIELD STRENGTH		ELONGATION, %	MATCHING FILLER METALS		
			MPA	KSI	MPA	KSI		A5.4	A5.9[A]	A5.22
XM-34	S18200	A 582	NS	NS	NS	NS	NS	NCW	NCW	**NCW**
. . .	S18235	A 582	NS	NS	NS	NS	NS	NCW	NCW	**NCW**
405	S40500	A 240	415	60	170	25	20	. . .	. . .	**E409T-X**
409	S40900	A 240	380	55	170	25	20	. . .	ER409	**E409T-X**
429	S42900	A 240	450	65	205	30	22	. . .	. . .	**. . .**
430	S43000	A 240	450	65	205	30	22	E430-XX	ER430	**E430T-X**
430F	S43020	A 473	480	70	275	40	20	NCW	NCW	**NCW**
430F SE	S43023	A 473	480	70	275	40	20	NCW	NCW	**NCW**
439	S43035	A 240	415	60	205	30	22	. . .	. . .	**. . .**
444	S44400	A 240	415	60	275	40	20	. . .	. . .	**. . .**
446	S44600	A 276	450	65	275	40	20	. . .	. . .	**. . .**
XM-27	S44627	A 240	450	65	275	40	22	. . .	ER446LMO	**. . .**
XM-33	S44626	A 240	470	68	310	45	20	. . .	. . .	**. . .**
. . .	S44635	A 240	620	90	520	75	20	. . .	. . .	**. . .**
. . .	S44660	A 240	585	85	450	65	18	. . .	. . .	**. . .**
29-4	S44700	A 240	550	80	415	60	20	. . .	. . .	**. . .**
29-4-2	S44800	A 240	550	80	415	60	20	. . .	. . .	**. . .**
. . .	S44735	A 240	550	80	415	60	18	. . .	. . .	**. . .**
CB-30	. . .	A 743	450	65	205	30	. . .	. . .	. . .	**. . .**
CC-50	**. . .**	**A 743**	**380**	**55**	**. . .**	**. . .**	**. . .**	**. . .**	**. . .**	**. . .**

NS, not specified; NCW, not considered weldable.

(A) METAL-CORED ELECTRODES, INDICATED BY A "C" IN PLACE OF THE "R" IN THE CLASSIFICATION, ARE ALSO INCLUDED.

Because of 475 °C (885 °F) embrittlement and σ-phase formation, long-term service temperatures for most ferritic stainless steels are usually limited to 250 °C (480 °F), maximum. However, 475 °C (885 °F) embrittlement does not seem to be a serious problem in the low-chromium types 409 and 405, which have been extensively used in automobile exhaust systems (where temperatures can exceed 575 °C, or 1070 °F, at times, which can dissolve α'). Another exception to the maximum service temperature limit is type 446, which offers outstanding resistance to scaling in air at high temperatures, because of its high chromium content. It is used in compressive loading, as the supports in heat-treat furnaces and the like, where brittleness at room temperature is not an important issue. Because ferritic stainless steels lose toughness and ductility at low temperatures, their use below ambient temperatures is very limited.

The ferritic stainless steels generally require rapid cooling from hot-working temperatures to avoid grain growth and embrittlement from the α phase. As a result, most ferritic stainless steel is used in relatively thin gages, especially in alloys that are high in chromium. The super ferritics are limited to thin plate, sheet, and tube forms. To avoid embrittlement in welding, the general rule is to "weld cold," which means to weld with either no or low preheating; a low interpass temperature; and a low level of welding heat input, commensurate with adequate fusion, to avoid cold laps and other defects.

Engineering for Use in the As-Welded Condition. In contrast to martensitic stainless steels, weldments in ferritic stainless steels (at least in the stabilized grades or super ferritics, that is, second- and third-generation alloys), are usually used in the as-welded condition. If the "weld cold" rule is followed, then embrittlement that is due to grain coarsening in the HAZ can be avoided. However, it is not as easy to avoid coarse grains in the fusion zone if the weld metal is fully ferritic. As a result, a considerable amount (but not all) of the filler metal used to join ferritic stainless steels is austenitic, usually with considerable ferrite.

If an austenitic filler metal is contemplated, then consideration should be given to differences in corrosion resistance (especially localized corrosion resistance) across the joint, as well as to differences in properties, such as the coefficient of thermal expansion (CTE) between austenitic filler metal and ferritic base metal. Nickel-base alloy filler metals are another possible alternative, especially for the third-generation ferritic stainless steels, which have the highest corrosion resistance requirements. High molybdenum content nickel-base alloy filler metals of the ANSI/AWS A5.11 specification, covered-electrode classifications ENiCrMo-3, ENiCrMo-4, and ENiCrMo-10, as well as the ANSI/AWS A5.14 specification, solid-wire classifications ERNiCrMo-3, ERNiCrMo-4, and ERNiCrMo-10, have been successfully used for the most corrosion resistant ferritic stainless steels.

Undoubtedly, the greatest quantity of ferritic stainless steel welded at the present time is type 409, which is used for automobile exhaust system components. The welds are virtually all single-pass fillet or lap welds. The most common filler metal is a matching composition supplied as a 1.1 mm (0.045 in.) diameter metal-cored wire (ANSI/AWS A5.9-92 classification EC409 or EC409Cb), which is used for gas-metal arc welding with argon-oxygen gas mixtures, such as the popular 98Ar-2O_2 mixture. This filler metal is often used in robotic welding, at high travel speeds, in the vertical-down position on rotating pieces that are 18 gage or less in thickness. Welding is done in a short-circuiting transfer mode, or nearly so.

Example 4:

An alternative procedure for welding type 409 base metal in automotive exhaust applications is to use 0.9 mm (0.035 in.) diameter solid austenitic stainless wire, in the short-circuiting transfer mode, with an argon-oxygen gas mixture. Because of the thin gage of the base metal, dilution that is on the order of 40% can be anticipated. Because the filler metal ER308LSi would exceed the corrosion resistance of the type 409 base metal, it could be considered. If the type 409 composition were 0.04C-0.5Mn-0.4Si-11.0Cr-0.5Ti (WRC-1988 Cr_{eq} = 11.0 and Ni_{eq} = 1.4; FN, off the diagram), and if the ER308LSi composition were 0.02C-1.5Mn-0.8Si-19.7Cr-10.2Ni-0.2Mo-0.04N (WRC-1988 Cr_{eq} = 19.9 and Ni_{eq} = 11.7; FN = 9.7), then the 40% dilution weld metal would have Cr_{eq} = 16.34, Ni_{eq} = 7.58, and FN would be off the diagram. Recalculating the chromium and nickel equivalents according to Schaeffler (Fig. 1), the weld metal would be deeply into the A + M + F field, that is, on the order of 50% martensite could be expected in the weld metal. This could be a problem for cracking or forming after welding. Therefore, ER308LSi may not be a good choice for welding type 409 base metal.

Example 5:

Assume that ER309LSi is substituted for the ER308LSi of Example 4. If the ER309LSi composition were 0.02C-1.5Mn-0.8Si-23.5Cr-13.5Ni-0.2Mo-0.04N (WRC-1988 Cr_{eq} = 23.7 and Ni_{eq} = 15.0; FN = 12.8), then the 40% dilution weld metal would have Cr_{eq} = 18.6, Ni_{eq} = 9.56, and FN = 12.6. Recalculating the chromium and nickel equivalents according to Schaeffler (Fig. 1) puts the weld metal just at the upper edge of the A + M + F field, that is, a trace of martensite, at most, would be present in the weld metal. Furthermore, because the calculated weld-metal FN is almost exactly the same as the calculated wire FN, the tie line from the wire composition to the base-metal composition must be nearly parallel to the isoferrite lines in the WRC-1988 diagram. This means that the weld-metal FN will be immune to changes in dilution, although excess dilution should be avoided because it would lead to more martensite. Thus, the ER309LSi filler metal would be a good choice for welding type 409 base metal.

The third generation of ferritic stainless steels, the super ferritics, are often supplied in the form of thin-walled tubing and are used in heat exchangers that handle chloride solutions. Tube-to-tube or tube-to-tubesheet weld joints are often made by orbital GTAW machines at relatively high speeds, without filler metal. The tube-to-tube weld is, of course, fully ferritic, and the high-speed "weld cold" procedure avoids excessive grain growth in materials such as type 444 ferritic stainless steel (18Cr-2Mo). However, the tubesheet in such a heat exchanger is often not type 444, but type 316L.

Example 6:

Type 444 tube welded to type 316L tube sheet by the GTAW process, without filler metal, makes an interesting material combination. If the Type 444 is 0.01C-0.5Mn-0.2Si-18.0Cr-2.0Mo-0.01N-0.4Nb (WRC-1988 Cr_{eq} = 20.28 and Ni_{eq} = 0.55; FN, out of range), and if the type 316L is 0.02C-1.5Mn-0.4Si-17.0Cr-2.2Mo-0.03N (WRC-1988 Cr_{eq} = 19.2, Ni_{eq} = 12.8, and FN = 3.4), and if each base metal is assumed to contribute equally to the weld metal, then the weld metal will have Cr_{eq} = 19.7, Ni_{eq} = 6.7, and FN will be out of range. Recalculating chromium and nickel equivalents for the Schaeffler diagram indicates approximately 40% ferrite, with the remainder being primarily austenite, with some martensite. This would not be the best situation, in terms of weld-metal ductility, but many such combinations have been welded this way and have provided satisfactory service.

Engineering for Use in the Postweld Heat-Treated Condition. In general, only the first-generation ferritic stainless steels are postweld heat treated, especially type 430. If it were welded with matching filler metal (or no filler metal), then both the weld metal and the HAZ would contain fresh martensite in the as-welded condition. In addition, some carbon would have gone into solution in the ferrite at elevated temperatures, and the rapid cooling after welding would result in ferrite in both the weld metal and the HAZ being supersaturated with carbon. Thus, the joint would be quite brittle, compared with the unwelded condition. Ductility could be significantly improved by a PWHT at 760 °C (1400 °F) for 1 h, followed by rapid cooling to avoid the 475 °C (885 °F) embrittlement phenomenon.

Example 7:

Type 430 could also be welded with type 308 or 308L filler metals, which are readily available and would exceed the corrosion resistance of the type 430 base metal in most environments. Then, only the HAZ would suffer embrittlement that is due to welding. For a type 430 composition of 0.06C-0.5Mn-0.2Si-17Cr-0.02N (WRC-88 Cr_{eq} = 17.0 and Ni_{eq} = 2.5; FN, off the diagram), and an E308L-16 electrode with all-weld metal composition of 0.03C-1.0Mn-0.4Si-19Cr-10Ni-0.08Mo-0.06N (WRC-1988 Cr_{eq} = 19.08 and Ni_{eq} = 12.25; calculated FN = 4.4), with 30% dilution, the first weld pass would have Cr_{eq} = 18.46, Ni_{eq} = 9.33, and the calculated FN = 12.9. Further, the weldment could be postweld heat treated for 1 h at 760 °C (1400 °F) to improve the HAZ ductility without harming the weld metal, and a very satisfactory joint would result.

Reference cited in this section

17. *METALS HANDBOOK*, 8TH ED., VOL 7, AMERICAN SOCIETY FOR METALS, 1972, P 144-145

Welding of Stainless Steels

D.J. Kotecki, The Lincoln Electric Company

Austenitic Stainless Steels

Basic Metallurgy. Nominally austenitic stainless steels cover a very broad spectrum of compositions. Many, but by no means all, solidify at least partly as ferrite, which transforms under equilibrium cooling, or hot working, to austenite at high temperatures (above 1000 °C, or 1830 °F) by a diffusion-controlled reaction. The austenite is stable, or at least metastable, to room temperature and below. Some of the leaner austenitic alloys can be induced to transform to martensite, at least in part, by cold work and/or by refrigeration to cryogenic temperatures.

In order to understand the weldability of nominally austenitic stainless steels, it is necessary to first understand their solidification and high-temperature transformation behavior. Austenitic stainless steel compositions are based on a balance between alloy elements that promote ferrite formation and those that promote austenite formation. The prototype ferritizing element is chromium, but molybdenum, niobium, titanium, aluminum, tungsten, and vanadium also promote ferrite. The prototype austenitizing element is nickel, but carbon, nitrogen, and copper all promote transformation of ferrite to austenite at high temperatures. In addition, while manganese does not seem to promote transformation of ferrite to austenite at high temperatures, it clearly does tend to stabilize austenite with respect to transformation to martensite at low temperatures. Further, manganese promotes the solubility of nitrogen in steel (as does chromium), making possible a low-nickel family of austenitic stainless steels that are high in manganese and nitrogen.

The solidification and high-temperature transformation behavior of austenitic stainless steels can be understood by examining sections of the ternary iron-chromium-nickel phase diagram. Figure 13 presents three levels of iron: 70 wt%, 60 wt%, and 55 wt%. Each diagram has a eutectic triangle (labeled "γ+δ+L"), which indicates compositions in which austenite, ferrite, and liquid metal can all coexist.

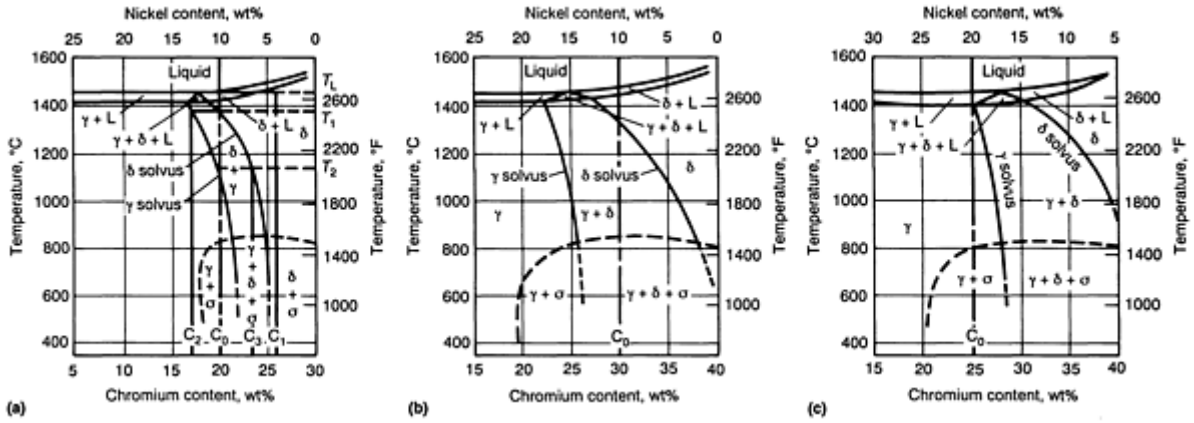

FIG. 13 IRON-CHROMIUM-NICKEL PSEUDO-BINARY DIAGRAM. (A) 70 WT% FE. (B) 60 WT% FE. (C) 55 WT% FE. SOURCE: REF 10

On the left (nickel-rich) side of each diagram are compositions that solidify entirely as austenite and remain austenite to room temperature, for example, an alloy of 10Cr-20Ni in the 70% iron diagram. Close to, and within the left side of, the eutectic triangle are compositions (for example, 17Cr-13Ni) that solidify as austenite in the early stages of solidification, but in which some ferrite will appear in the last stages of solidification. This is called "primary austenite solidification." Further cooling can cause that ferrite to transform to austenite under equilibrium conditions, but under the relatively rapid cooling conditions of welding, some of this ferrite may survive to room temperature.

Close to, and within the right side of, the eutectic triangle are compositions (for example, 19Cr-11Ni) that solidify as ferrite in the early stages of solidification, but in which some austenite will appear in the last stages of solidification. This is called "primary ferrite solidification." Further cooling can cause that ferrite to transform to austenite under equilibrium conditions, but under the relatively rapid cooling conditions of welding, some of this ferrite may, and usually does, survive to room temperature.

Further to the right in Fig. 13 are compositions that solidify entirely as ferrite, but, upon further cooling under equilibrium conditions, transform either partly or entirely to austenite. An alloy of 20Cr-10Ni would be entirely ferrite when solidification was completed, but would begin to transform to austenite at a temperature (T_1 in Fig. 13) slightly below the end of solidification, and would be completely transformed to austenite at a still lower temperature (T_2 in Fig. 13). However, an alloy of 23Cr-7Ni would only partially transform to austenite, that is, some ferrite would be stable at room temperature. Under the relatively rapid cooling conditions of welding, not as much ferrite transforms to austenite, as Fig. 13 indicates, because the diffusion of atoms must occur. As a result, the 20Cr-10Ni alloy weld metal would still contain some ferrite at room temperature, and the 23Cr-7Ni alloy would contain more ferrite than Fig. 13 indicates.

Finally, there are compositions (still further to the right of the eutectic triangle in Fig. 13) that will not form any austenite at any temperature. These are ferritic stainless steels.

Considerable research has shown that alloys that solidify as primary ferrite are the most resistant to hot cracking. Alloys that solidify entirely as austenite are the most susceptible to hot cracking. Alloys that solidify as primary austenite are more susceptible than all alloys in this system, except those that solidify entirely as austenite. Alloys that solidify entirely as ferrite are more resistant to hot cracking than any other alloys, except those that solidify as primary ferrite. Therefore, from a welding viewpoint, the preferred order of solidification is primary ferrite, fully ferritic, primary austenite, and, last, fully austenitic. In the WRC-1988 diagram (Fig. 3), the dashed lines divide the range of chromium equivalents and nickel equivalents into those that solidify fully austenitic (Region A), those that solidify as primary austenite (Region AF), those that solidify as primary ferrite (Region FA), and those that solidify fully ferritic (Region F).

Figures 3 and 13, when considered together, indicate that the ferrite that remains in a nominally austenitic weld metal when it reaches room temperature is only a fraction of that which existed during solidification. Most of the initial ferrite is transformed to austenite. Thus, the more-fundamental piece of information about a given weld metal is its solidification mode. However, this is difficult and time-consuming to assess, whereas the Ferrite Number, measured at room temperature after the fact, is easy to measure using any number of instruments calibrated to the ANSI/AWS A4.2 specification, and the interlaboratory reproducibility of measurement is very high. The conventional wisdom accumulated over numerous years indicates that a 4 FN minimum ill ensure freedom from hot cracking problems in most nominally austenitic stainless steel weld metals. An examination of Fig. 3 indicates that 4 FN is comfortably within the FA region for lower-alloyed weld metals and barely within the FA region for highly alloyed weld metals.

Several caveats need to be remembered when applying the "4 FN minimum" convention. First, it is based on measurement *along the top centerline of an as-welded weld bead.* This means that applying such a rule, either after PWHT or at all points across a multipass overlay, is inappropriate because heat treatment or reheating by a subsequent weld pass reduces ferrite toward its equilibrium value (which may be zero).

Second, this convention derives from experience with normal impurity levels (primarily sulfur and phosphorus). Extraordinarily high impurities, as in free-machining stainless steels, often renders the metal susceptible to hot cracking at any ferrite level. On the other hand, extraordinarily low impurity levels can make low or zero ferrite weld metals fairly crack resistant.

Third, one cannot determine, from a ferrite measurement on unwelded base metal, what its hot cracking susceptibility in autogenous (no filler metal) welding is likely to be. Because hot working erases ferrite, hot-rolled plate is likely to indicate zero ferrite. On the other hand, cold working causes lean alloys, such as types 201, 301, 302, and 304, to transform to martensite, which is ferromagnetic and gives a false ferrite reading with instruments based on magnetic principles. Ferrite can be either estimated from the composition of a base metal (including nitrogen), using the WRC-1988 diagram, or measured by first making a gas-tungsten arc melt of the base metal without using filler metal, and then using a calibrated instrument along the weld centerline.

Fourth, a certificate of test from a filler metal manufacturer that indicates a FN greater than 4 only indicates that the filler metal was properly designed. It cannot take into account the ability of a careless welder to change the Ferrite Number by permitting nitrogen from the air to enter the welding arc. Practices such as long arc length in shielded metal arc welding (SMAW) or self-shielded flux-cored arc welding (FCAW); the disturbance of shielding gas by drafts in gas-shielded welding; or the loss of flux cover, as evidenced by arc "flashing" in the SAW process, can produce enough nitrogen pickup to reduce the ferrite of an otherwise satisfactory weld deposit to an unacceptably low level, which makes hot cracking possible.

Fifth, very lean alloy weld metals, such as ER16-8-2, can solidify as crack-resistant primary ferrite, even when the weld metal measures nearly zero FN.

Sixth, the minimum 4 FN convention is really only applicable to weld metals that solidify under cooling rates normal for conventional SMAW, GMAW, GTAW, and single-electrode SAW. The slow cooling rates of strip cladding can produce lower than normal FN measurements when the weld metal solidifies as primary ferrite. Furthermore, the very rapid cooling rates associated with EBW or LBW can produce marked departures from the expected solidification mode and ferrite content (see Ref 18). Nevertheless, the minimum 4 FN convention has been a very successful guideline in normal welded fabrication of nominally austenitic stainless steels.

Arc welding heats the base metal adjacent to the weld deposit, which can produce undesirable metallurgical reactions. In austenitic stainless steels, a principal concern is grain-boundary carbide precipitation. Whatever carbides were initially present before welding can be dissolved at temperatures above approximately 1000 °C (1830 °F). Then, subsequent slow

cooling through the temperature range from approximately 950 °C (1740 °F) down to approximately 500 °C (900 °F) can cause chromium carbides to precipitate again, usually on austenite grain boundaries. This precipitation can leave the metal adjacent to the grain boundaries depleted in chromium and, therefore, susceptible to intergranular corrosion. The steel is said to be "sensitized." Improper heat treatment can do this to an entire base metal.

Figure 14 gives the times and temperatures that produce sensitization. In particular, it indicates that carbides, although they form quickly, must be quite extensive in order to make the metal susceptible to intergranular corrosion. Generally, a selection of low-carbon (less than 0.03%) base metal is nearly immune to sensitization that is due to welding. Another alternative is to choose a base metal to which a strong carbide-forming element (titanium or niobium) is added, which ties up the available carbon and leaves the chromium free to provide corrosion resistance.

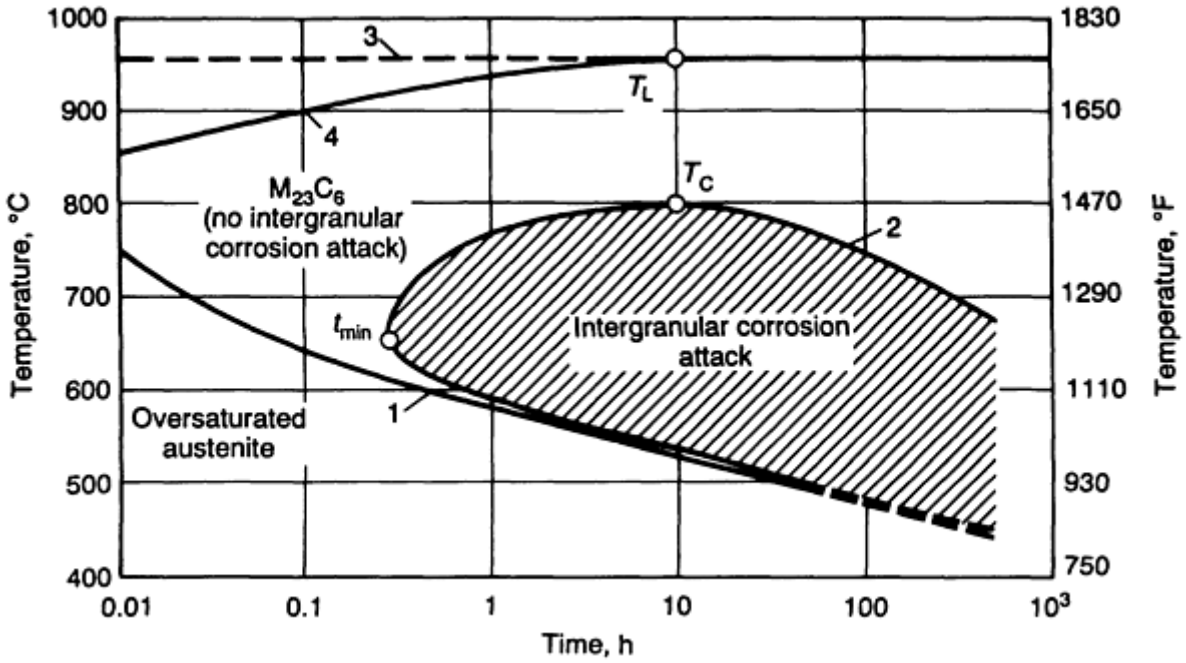

FIG. 14 PRECIPITATION OF CARBIDE $M_{23}C_6$ AND AREA OF INTERGRANULAR CORROSION ATTACK OF STAINLESS STEEL GRADE AISI 304 (0.042C-0.59SI-1.23MN-17.46CR-10.58NI-0.046N). SOURCE: REF 19

The σ phase precipitates slowly in austenite, but more rapidly in ferrite. In nominally austenitic weld metal with some ferrite, cooling rates are still high enough that σ is seldom encountered in the as-welded condition. However, a PWHT at 700 to 900 °C (1290 to 1650 °F) for even 1 h will convert some ferrite to the σ phase, as indicated by Fig. 15. High levels of chromium, molybdenum, silicon, titanium, and/or niobium can greatly accelerate σ formation. The segregation of these elements during solidification can promote σ formation. Because of sensitization and the σ phase, it is best to avoid the heat treatment of nominally austenitic weld metals at temperatures between 500 and 900 °C (930 and 1650 °F).

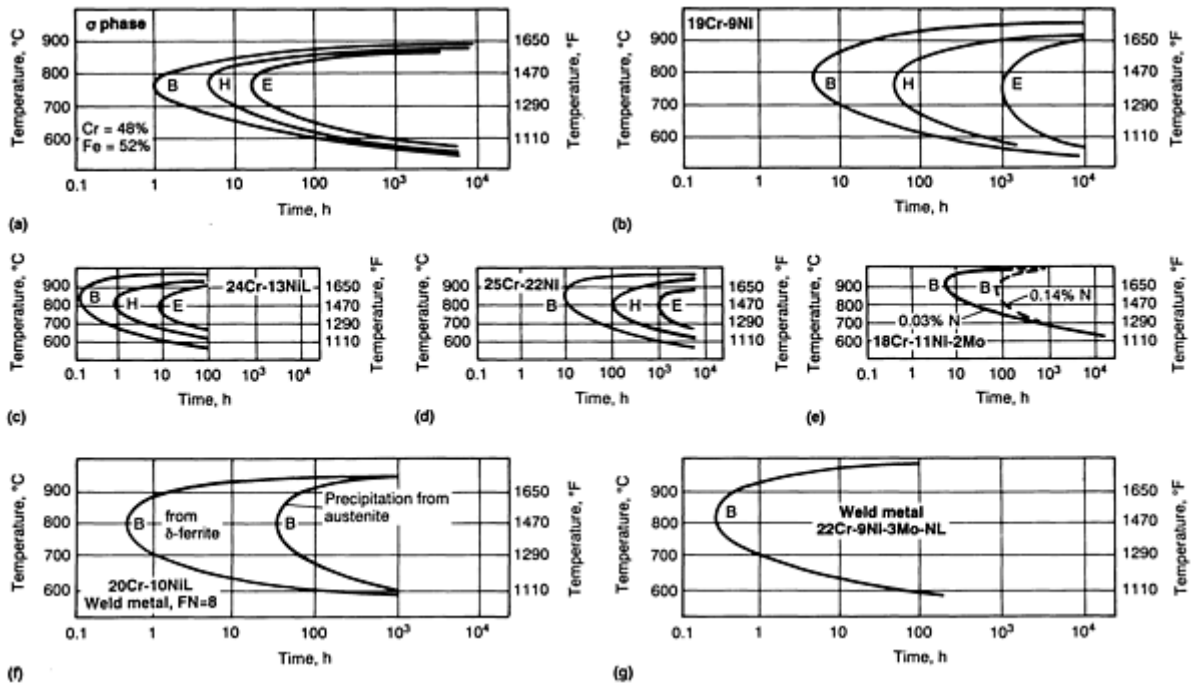

FIG. 15 DIAGRAM OF σ-PHASE PRECIPITATION IN SOLUTION ANNEALED AND QUENCHED STAINLESS STEELS AND IN WELD METAL (AS-WELDED STATE). B, BEGINNING OF PRECIPITATION; H, HALF-WAY THROUGH PRECIPITATION; E, END OF PRECIPITATION. (A) PURE σPHASE. (B) AUSTENITIC 19CR-8NI STEEL (AISI 304). (C) AUSTENITIC 24CR-13NI STEEL (AISI 309S) WITH APPROXIMATELY 15% DELTA FERRITE. (D) AUSTENITIC 25CR-22NI STEEL (AISI 310). (E) AUSTENITIC 18CR-11NI-2MO STEELS (AISI 316) WITH VARYING NITROGEN CONTENTS. (F) AUSTENITIC WELD METAL WITH LOW CONTENT OF DELTA FERRITE (FN = 8) OF THE TYPE 20CR-10NI-L (AWS E308L). (G) AUSTENITIC-FERRITIC DUPLEX WELD METAL WITH 24 TO 27% DELTA FERRITE OF THE TYPE 22CR-9NI-3MO-LN. SOURCE: REF 20

Austenitic Stainless Steel Base Metals. Tables 3(a) and 3(b) list numerous nominally austenitic stainless steel base metals and their minimum mechanical property requirements, as well as corresponding welding filler metals. The yield strengths of these materials are rather modest, and are comparable to those of mild steels. Austenitic stainless steels cannot be hardened by heat treatment, but they do work harden rapidly. Therefore, high strength is possible in cold-worked forms, especially in drawn wire, in which a tensile strength of 1200 MPa (175 ksi) or higher is achievable. The heat of welding will soften the HAZ of heavily cold-worked austenitic stainless steel.

TABLE 3(A) COMPOSITIONS OF NOMINALLY AUSTENITIC STAINLESS STEELS

DESIGNATION	UNS NO.	ASTM SPECIFICATION	COMPOSITION, WT%									
			C	Mn	P	S	Si	Cr	Ni	Mo	N	OTHER
. . .	S01815	A 167	0.018 MAX	2.0 MAX	0.02 MAX	0.02 MAX	3.7-4.3	17.0-18.5	14.0-15.5	0.20 MAX	. . .	. . .
201	S20100	A 240	0.15 MAX	5.50-7.50	0.060 MAX	0.030 MAX	1.00 MAX	16.00-18.00	3.50-5.50	. . .	0.25 MAX	. . .
201	S20100	A 666	0.15 MAX	5.50-7.50	0.060 MAX	0.030 MAX	0.75 MAX	16.00-18.00	3.50-5.50	. . .	0.25 MAX	. . .
. . .	S20161	A 479	0.15 MAX	4.00-6.00	0.040 MAX	0.040 MAX	3.00-4.00	15.00-18.00	4.00-6.00	. . .	0.08-0.20	. . .
202	S20200	A 240	0.15 MAX	7.50-10.0	0.060 MAX	0.030 MAX	1.00 MAX	17.00-19.00	4.00-6.00	. . .	0.25 MAX	. . .
202	S20200	A 666	0.15 MAX	7.50-10.0	0.060 MAX	0.030 MAX	0.75 MAX	17.00-19.00	4.00-6.00	. . .	0.25 MAX	. . .
XM-1	S20300	A 582	0.08 MAX	5.00-6.50	0.04 MAX	0.18-0.35	1.00 MAX	16.00-18.00	5.00-6.50	. . .	. . .	**CU, 1.75-2.25**
205	S20500	A 666	0.12-0.25	14.00-15.00	0.060 MAX	0.030 MAX	0.75 MAX	16.50-18.00	1.00-1.75	. . .	0.32-0.40	. . .
XM-19	S20910	A 240	0.06 MAX	4.00-6.00	0.040 MAX	0.030 MAX	0.75 MAX	20.50-23.50	11.50-13.50	1.50-3.00	0.20-0.40	**NB + TA, 0.10-0.30;V, 0.10-0.30**
XM-31	S21400	A 240	0.12 MAX	14.00-16.00	0.045 MAX	0.030 MAX	0.30-1.00	17.00-18.50	1.00 MAX	. . .	0.35 MIN	. . .
XM-14	S21460	A 666	0.12 MAX	14.00-16.00	0.060 MAX	0.030 MAX	0.75 MAX	17.00-19.00	5.00-6.00	. . .	0.35-0.50	. . .
XM-17	S21600	A 240	0.08 MAX	7.50-9.00	0.045 MAX	0.030 MAX	0.75 MAX	17.50-22.00	5.00-7.00	2.00-3.00	0.25-0.50	. . .

DESIGNATION	UNS NO.	ASTM SPECIFICATION	COMPOSITION, WT%									
			C	Mn	P	S	Si	Cr	Ni	Mo	N	OTHER
XM-18	S21603	A 240	0.03 MAX	7.50-9.00	0.045 MAX	0.030 MAX	0.75 MAX	17.50-22.00	5.00-7.00	2.00-3.00	0.25-0.50	. . .
. . .	S21800	A 240	0.10 MAX	7.00-9.00	0.060 MAX	0.030 MAX	3.50-4.50	16.00-18.00	8.00-9.00	. . .	0.08-0.18	. . .
XM-10	S21900	A 276	0.08 MAX	8.00-10.00	0.060 MAX	0.030 MAX	1.00 MAX	19.00-21.00	5.50-7.50	. . .	0.15-0.40	. . .
XM-11	S21904	A 666	0.04 MAX	8.00-10.00	0.060 MAX	0.030 MAX	0.75 MAX	19.00-21.50	5.50-7.50	. . .	0.15-0.40	. . .
XM-29	S24000	A 240	0.08 MAX	11.50-14.50	0.045 MAX	0.030 MAX	0.75 MAX	17.00-19.00	2.25-3.75	. . .	0.20-0.40	. . .
XM-28	S24100	A 276	0.15 MAX	11.00-14.00	0.060 MAX	0.030 MAX	1.00 MAX	16.50-19.00	0.50-2.50	. . .	0.20-0.45	. . .
. . .	S28200	A 276	0.15 MAX	17.00-19.00	0.045 MAX	0.030 MAX	1.00 MAX	17.00-19.00	. . .	0.75 1.25	0.40-0.60	**CU, 0.75-1.25**
301	S30100	A 666	0.15 MAX	2.00 MAX	0.045 MAX	0.030 MAX	0.75 MAX	16.00-18.00	6.00-8.00	. . .	. . .	. . .
302	S30200	A 240	0.15 MAX	2.00 MAX	0.045 MAX	0.030 MAX	0.75 MAX	17.00-19.00	8.00-10.00	. . .	0.10 MAX	. . .
302	S30200	666	0.15 MAX	2.00 MAX	0.045 MAX	0.030 MAX	0.75 MAX	17.00-19.00	8.00-10.00	. . .	. . .	. . .
302B	S30215	A 167	0.15 MAX	2.00 MAX	0.045 MAX	0.030 MAX	2.00-3.00	17.00-19.00	8.00-10.00	. . .	0.10 MAX	. . .
303	S30300	A 473	0.15 MAX	2.00 MAX	0.20 MAX	0.15 MIN	1.00 MAX	17.00-19.00	8.00-10.00	0.60 MAX	. . .	. . .
XM-5	S30310	A 582	0.15 MAX	2.50-4.50	0.20 MAX	0.25 MIN	1.00 MAX	17.00-19.0	7.00-10.0	. . .	. . .	. . .

DESIGNATION	UNS NO.	ASTM SPECIFICATION	COMPOSITION, WT%									
			C	Mn	P	S	Si	Cr	Ni	Mo	N	OTHER
								0	0			
303SE	S30323	A 473	0.15 MAX	2.00 MAX	0.20 MAX	0.06 MAX	1.00 MAX	17.00-19.00	8.00-10.00	. . .	. . .	**SE, 0.15 MIN**
XM-2	S30345	A 582	0.15 MAX	2.00 MAX	0.05 MAX	0.11-0.16	1.00 MAX	17.00-19.00	8.00-10.00	0.40-0.60	. . .	**. . .**
XM-3	S30360	A 582	0.15 MAX	2.00 MAX	0.04 MAX	0.12-0.15	1.00 MAX	17.00-19.00	8.00-10.00	. . .	. . .	**PB, 0.12-0.30**
304	S30400	A 240, A 666	0.08 MAX	2.00 MAX	0.045 MAX	0.030 MAX	0.75 MAX	18.00-20.00	8.00-10.50	. . .	0.10 MAX	**. . .**
TP304	. . .	A 376	0.08 MAX	2.00 MAX	0.040 MAX	0.030 MAX	0.75 MAX	18.0-20.0	8.00-11.0	. . .	. . .	**. . .**
304L	S30403	A 240, A 666	0.030 MAX	2.00 MAX	0.045 MAX	0.030 MAX	0.75 MAX	18.00-20.00	8.00-12.00	. . .	0.10 MAX	**. . .**
304H	S30409	A 240	0.04-0.10	2.00 MAX	0.045 MAX	0.030 MAX	0.75 MAX	18.00-20.00	8.00-10.50	. . .	. . .	**. . .**
TP304H	. . .	A 376	0.04-0.10	2.00 MAX	0.040 MAX	0.030 MAX	0.75 MAX	18.0-20.0	8.00-11.0	. . .	. . .	**. . .**
. . .	S30415	A 240	0.04-0.06	0.30 MAX	0.045 MAX	0.030 MAX	1.00-2.00	18.00-19.00	9.00-10.00	. . .	0.12-0.18	**CE, 0.03 TO 0.08**
XM-7	S30430	A 276	0.10 MAX	2.00 MAX	0.045 MAX	0.030 MAX	1.00 MAX	17.00-19.00	8.00-10.00	. . .	. . .	**CU, 3.00-4.00**
304N	S30451	A 240	0.08 MAX	2.00 MAX	0.045 MAX	0.030 MAX	0.75 MAX	18.00-20.00	8.00-10.50	. . .	0.10-0.16	**. . .**
304N	. . .	A 376	0.08 MAX	2.00 MAX	0.040 MAX	0.030 MAX	0.57 MAX	18.0-20.0	8.00-11.0	. . .	. . .	**. . .**
XM-21	S30452	A 240	0.08 MA	2.00 MA	0.045	0.030	0.75 MA	18.00-	8.00-	. . .	0.16-	**. . .**

DESIGNATION	UNS NO.	ASTM SPECIFICATION	COMPOSITION, WT%									
			C	Mn	P	S	Si	Cr	Ni	Mo	N	OTHER
			X	X	MAX	MAX	X	20.00	10.50		0.30	
304LN	S30453	A 240	0.030 MAX	2.00 MAX	0.045 MAX	0.030 MAX	0.75 MAX	18.00-20.00	8.00-12.00	. . .	0.10-0.16	. . .
304LN	S30453	A 666	0.030 MAX	2.00 MAX	0.045 MAX	0.030 MAX	0.75 MAX	18.00-20.00	8.00-10.50	. . .	0.10-0.15	. . .
TP304LN	. . .	A 376	0.035 MAX	2.00 MAX	0.040 MAX	0.030 MAX	0.75 MAX	18.0-20.0	8.00-11.0	. . .	0.10-0.16	. . .
. . .	S30454	A 276	0.03 MAX	2.00 MAX	0.045 MAX	0.030 MAX	0.75 MAX	18.00-20.00	8.00-10.50	. . .	0.16-0.30	. . .
305	S30500	A 240	0.12 MAX	2.00 MAX	0.045 MAX	0.030 MAX	0.75 MAX	17.00-19.00	10.50-13.00	. . .	. . .	. . .
306	S30600	A 240	0.018 MAX	2.00 MAX	0.020 MAX	0.020 MAX	3.7-4.3	17.0-18.5	14.0-15.5	0.20 MAX	. . .	. . .
RA85H	S30615	A 240	0.16-0.24	2.00 MAX	0.030 MAX	0.030 MAX	3.20-4.00	17.00-19.00	13.50-16.00	. . .	. . .	**AL, 0.80-1.50**
308	S30800	A 167	0.08 MAX	2.00 MAX	0.045 MAX	0.030 MAX	0.75 MAX	19.00-21.00	10.00-12.00	. . .	. . .	. . .
. . .	S30815	A 167, A 240	0.05-0.10	0.80 MAX	0.040 MAX	0.030 MAX	1.40-2.00	20.00-22.00	10.00-12.00	. . .	0.14-0.20	**CE, 0.03 TO 0.08**
309	S30900	A 167	0.20 MAX	2.00 MAX	0.045 MAX	0.030 MAX	0.75 MAX	22.00-24.00	12.00-15.00	. . .	. . .	. . .
309S	S30908	A 240	0.08 MAX	2.00 MAX	0.045 MAX	0.030 MAX	0.75 MAX	22.00-24.00	2.00-15.00	. . .	. . .	. . .
309H	S30909	A 240	0.04-0.10	2.00 MAX	0.045 MAX	0.030 MAX	0.75 MAX	22.00-24.00	12.00-15.00	. . .	. . .	. . .
309CB	S309	A 240	0.08	2.00	0.04	0.03	0.75	22.0	12.0	. . .	. . .	**NB + TA, 10 ×**

DESIGNATION	UNS NO.	ASTM SPECIFICATION	COMPOSITION, WT%									
			C	Mn	P	S	Si	Cr	Ni	Mo	N	OTHER
	40		MAX	MAX	5 MAX	0 MAX	MAX	0-24.00	0-16.00			**C TO 1.10**
309HCB	S30949	A 240	0.04-0.10	2.00 MAX	0.045 MAX	0.030 MAX	0.75 MAX	22.00-24.00	12.00-16.00	. . .	. . .	**NB + TA, 10 × C TO 1.10**
310	S31000	167	0.25 MAX	2.00 MAX	0.045 MAX	0.030 MAX	1.50 MAX	24.00-26.00	19.00-22.00	. . .	. . .	**. . .**
310S	S31008	A 240	0.08 MAX	2.00 MAX	0.045 MAX	0.030 MAX	1.50 MAX	24.00-26.00	19.00-22.00	. . .	. . .	**. . .**
310H	S31009	A 240	0.04-0.10	2.00 MAX	0.045 MAX	0.030 MAX	0.75 MAX	24.00-26.00	19.00-22.00	. . .	. . .	**. . .**
310CB	S31040	A 240	0.08 MAX	2.00 MAX	0.045 MAX	0.030 MAX	1.50 MAX	24.00-26.00	19.00-22.00	. . .	. . .	**NB + TA, 10 × C TO 1.10**
310HCB	S31049	A 240	0.04-0.10	2.00 MAX	0.045 MAX	0.030 MAX	0.75 MAX	24.00-26.00	19.00-22.00	. . .	. . .	**NB + TA, 10 × C TO 1.10**
310MOLN	S31050	A 240	0.030 MAX	2.00 MAX	0.030 MAX	0.010 MAX	0.50 MAX	24.00-26.00	21.00-23.00	2.00-3.33	0.10-0.16	**. . .**
254SMO	S31254	A 240	0.020 MAX	1.00 MAX	0.030 MAX	0.010 MAX	0.80 MAX	19.50-20.50	17.50-18.50	6.00-6.50	0.18-0.22	**CU, 0.50-1.00**
314	S31400	A 276	0.25 MAX	2.00 MAX	0.045 MAX	0.030 MAX	1.50-3.00	23.00-26.00	19.00-22.00	. . .	. . .	**. . .**
316	S31600	A 240	0.08 MAX	2.00 MAX	0.045 MAX	0.030 MAX	0.75 MAX	16.00-18.00	10.00-14.00	2.00-3.00	0.10 MAX	**. . .**
316	S31600	A 666	0.08 MAX	2.00 MAX	0.045 MAX	0.030 MAX	0.75 MAX	16.00-18.00	10.00-14.00	2.00-3.00	. . .	**. . .**
TP316	. . .	A 376	0.08 MAX	2.00 MAX	0.040 MAX	0.030 MAX	0.75 MAX	16.0-18.0	11.0-14.0	2.00-3.00	. . .	**. . .**

DESIGNATION	UNS NO.	ASTM SPECIFICATION	COMPOSITION, WT%									
			C	Mn	P	S	Si	Cr	Ni	Mo	N	OTHER
316L	S31603	A 240	0.030 MAX	2.00 MAX	0.045 MAX	0.030 MAX	0.75 MAX	16.00-18.00	10.00-14.00	2.00-3.00	0.10 MAX	. . .
316L	S31603	A 666	0.030 MAX	2.00 MAX	0.045 MAX	0.030 MAX	0.75 MAX	16.00-18.00	10.00-14.00	2.00-3.00	. . .	. . .
316H	S31609	A 240	0.04-0.10	2.00 MAX	0.045 MAX	0.030 MAX	0.75 MAX	16.00-18.00	10.00-14.00	2.00-3.00	. . .	. . .
TP316H	. . .	A 376	0.04-0.10	2.00 MAX	0.040 MAX	0.030 MAX	0.75 MAX	16.0-18.0	11.0-14.0	2.00-3.00	. . .	. . .
316TI	S31635	A 240	0.08 MAX	2.00 MAX	0.045 MAX	0.030 MAX	0.75 MAX	16.00-18.00	10.00-14.00	2.00-3.00	. . .	**TI, 5 × (C + N) TO 0.70**
316CB	S31640	A 240	0.08 MAX	2.00 MAX	0.045 MAX	0.030 MAX	0.75 MAX	16.00-18.00	10.00-14.00	2.00-3.00	0.10 MAX	**NB + TA, 10 × C TO 1.10**
316N	S31651	A 240	0.08 MAX	2.00 MAX	0.045 MAX	0.030 MAX	0.75 MAX	16.00-18.00	10.00-14.00	2.00-3.00	0.10-0.16	. . .
316N	S31651	A 666	0.08 MAX	2.00 MAX	0.045 MAX	0.030 MAX	0.75 MAX	16.00-18.00	10.00-14.00	2.00-3.00	0.10-0.16	. . .
316N	. . .	A 376	0.08 MAX	2.00 MAX	0.040 MAX	0.030 MAX	0.75 MAX	16.0-18.0	11.0-14.0	2.00-3.00	0.10-0.16	. . .
316LN	S31635	A 240	0.030 MAX	2.00 MAX	0.045 MAX	0.030 MAX	0.75 MAX	16.00-18.00	10.00-14.00	2.00-3.00	0.10-0.16	. . .
T316LN		A 376	0.035 MAX	2.00 MAX	0.040 MAX	0.030 MAX	0.75 MAX	16.0-18.0	11.0-14.0	2.00-3.00	0.10-0.16	. . .
	S31654	A 276	0.03 MAX	2.00 MAX	0.045 MAX	0.030 MAX	0.75 MAX	16.00-18.00	10.00-14.00	2.00-3.00	0.16-0.30	. . .
317	S31700	A 240	0.08 MAX	2.00 MAX	0.045 MA	0.030 MA	0.75 MAX	18.00-20.0	11.00-15.0	3.00-4.00	0.10 MAX	. . .

DESIGNATION	UNS NO.	ASTM SPECIFICATION	COMPOSITION, WT%									
			C	Mn	P	S	Si	Cr	Ni	Mo	N	OTHER
					X	X		0	0			
317L	S31703	A 240	0.030 MAX	2.00 MAX	0.045 MAX	0.030 MAX	0.75 MAX	18.00-20.00	11.00-15.00	3.00-4.00	0.10 MAX	**. . .**
317LM	S31725	A 240	0.030 MAX	2.00 MAX	0.045 MAX	0.030 MAX	0.75 MAX	18.00-20.00	13.50-17.50	4.0-5.0	0.10 MAX	**. . .**
317LM	S31725	A 376	0.03 MAX	2.00 MAX	0.040 MAX	0.030 MAX	0.75 MAX	18.0-20.0	13.5-17.5	4.0-5.0	0.10 MAX	**CU, 0.75 MAX**
317LMN	S31726	A 240	0.030 MAX	2.00 MAX	0.045 MAX	0.030 MAX	0.75 MAX	18.00-20.00	13.50-17.50	4.0-5.0	0.10-0.20	**. . .**
317LMN	S31726	A 376	0.03 MAX	2.00 MAX	0.040 MAX	0.030 MAX	0.75 MAX	17.0-20.0	13.5-17.5	4.0-5.0	0.10-0.20	**CU, 0.75 MAX**
317LN	S31753	A 240	0.030 MAX	2.00 MAX	0.045 MAX	0.030 MAX	0.75 MAX	18.00-20.00	11.00-15.00	3.00-4.00	0.10-0.22	**. . .**
321	S32100	A 240	0.08 MAX	2.00 MAX	0.045 MAX	0.030 MAX	0.75 MAX	17.00-19.00	9.00-12.00	. . .	0.10 MAX	**TI, 5 × (C + N) TO 0.70**
TP321		A 376	0.08 MAX	2.00 MAX	0.040 MAX	0.030 MAX	0.75 MAX	17.0-20.0	9.00-13.0	. . .	. . .	**TI, 5 × C TO 0.60**
321H	S32109	A 240	0.04-0.10	2.00 MAX	0.045 MAX	0.030 MAX	0.75 MAX	17.00-19.00	9.00-12.00	. . .	0.10 MAX	**TI, 4 × (C + N) TO 0.70**
TP321H	. . .	A 376	0.04-0.10	2.00 MAX	0.040 MAX	0.030 MAX	0.75 MAX	17.0-20.0	9.00-13.0	. . .	. . .	**TI, 4 × C TO 0.60**
. . .	S32615	A 240	0.07 MAX	2.00 MAX	0.045 MAX	0.030 MAX	4.8-6.0	16.5-19.5	19.0-22.0	0.30-1.5	. . .	**CU, 1.5-2.5**
347	S34700	A 240	0.08 MAX	2.00 MAX	0.045 MAX	0.030 MAX	0.75 MAX	17.00-19.00	9.00-13.00	. . .	. . .	**NB + TA, 10 × C TO 1.00**
TP347	. . .	A 376	0.08 MA	2.00 MA	0.040	0.030	0.75 MA	17.0-	9.00-	. . .	. . .	**NB + TA, 10 × C TO 1.00**

DESIGNATION	UNS NO.	ASTM SPECIFICATION	COMPOSITION, WT%									
			C	Mn	P	S	Si	Cr	Ni	Mo	N	OTHER
			X	X	MAX	MAX	X	20.0	13.0			
347H	S34709	A 240	0.04-0.10	2.00 MAX	0.045 MAX	0.030 MAX	0.75 MAX	17.00-19.00	9.00-13.00	. . .	. . .	**NB + TA, 8 × C TO 1.00**
TP347H	. . .	A 376	0.04-0.10	2.00 MAX	0.040 MAX	0.030 MAX	0.75 MAX	17.0-20.0	9.00-13.0	. . .	. . .	**NB + TA, 8 × C TO 1.00**
348	S34800	A240	0.08 MAX	2.00 MAX	0.045 MAX	0.030 MAX	0.75 MAX	17.00-19.00	9.00-13.00	. . .	. . .	**NB + TA, 10 × C TO 1.00; CO, 0.20 MAX; TA, 0.10 MAX**
TP348	. . .	A 376	0.08 MAX	2.00 MAX	0.040 MAX	0.030 MAX	0.75 MAX	17.0-20.0	9.00-13.0	. . .	. . .	**NB + TA, 10 × C TO 1.00**
348H	S34809	A 240	0.04-0.10	2.00 MAX	0.045 MAX	0.030 MAX	0.75 MAX	17.00-19.00	9.00-13.00	. . .	. . .	**NB + TA, 8 × C TO 1.00; CO, 0.20 MAX; TA, 0.10 MAX**
16-8-2H	. . .	A 376	0.05-0.10	2.00 MAX	0.040 MAX	0.030 MAX	0.75 MAX	14.5-16.5	7.50-9.50	1.5 2.0	. . .	**. . .**
XM-15	S38100	A 240	0.08 MAX	2.00 MAX	0.030 MAX	0.030 MAX	1.50-2.50	17.00-19.00	17.50-18.50	. . .	. . .	**. . .**
320	N08020	B 463	0.07 MAX	2.00 MAX	0.045 MAX	0.035 MAX	1.00 MAX	19.00-21.00	32.00-38.00	2.00-3.00	. . .	**NB + TA, 8 × C TO 1.00; CU, 3.00-4.00**
SANICRO 28	N08028	B 709	0.030 MAX	2.50 MAX	0.030 MAX	0.030 MAX	1.00 MAX	26.0-38.0	30.0-34.0	3.0-4.0	. . .	**CU, 0.6-1.4**
330	N08330	B 536	0.10 MAX	2.00 MAX	0.03 MAX	0.03 MAX	0.75-1.50	17.0-20.0	34.0-37.0	. . .	. . .	**CU, 1.00 MAX**
AL-6XN	N08367	B 688	0.030 MAX	2.00 MAX	0.040 MAX	0.030 MAX	1.00 MAX	20.00-22.00	23.50-25.50	6.00-7.00	. . .	**CU, 0.75 MAX**
904L	N08904	B 625	0.020 MAX	2.00 MAX	0.045 MAX	0.035 MAX	1.00 MAX	19.00-2300	23.00-28.00	4.0-5.0	. . .	**CU, 1.0-2.0**

DESIGNATION	UNS NO.	ASTM SPECIFICATION	COMPOSITION, WT%									
			C	Mn	P	S	Si	Cr	Ni	Mo	N	OTHER
25-6MO	N08925	B 625	0.020 MAX	1.00 MAX	0.045 MAX	0.030 MAX	0.50 MAX	19.00-21.00	24.00-26.00	6.0-7.0	0.10-0.20	**CU, 0.8-1.5**
CF-8	. . .	A 743	0.08 MAX	1.50 MAX	0.04 MAX	0.04 MAX	2.0 MAX	18.0-21.0	8.0-11.0	. . .	. . .	**. . .**
CG-12	. . .	A 743	0.12 MAX	1.50 MAX	0.04 MAX	0.04 MAX	2.00 MAX	20.0-23.0	10.0-13.0	. . .	. . .	**. . .**
CF-20	. . .	A 743	0.20 MAX	1.50 MAX	0.04 MAX	0.04 MAX	2.00 MAX	18.0-21.0	0.8-11.0	. . .	. . .	**. . .**
CF-8M	. . .	A 743, A 744	0.08 MAX	1.50 MAX	0.04 MAX	0.04 MAX	2.00 MAX	18.0-21.0	9.0-12.0	2.0-3.0	. . .	**. . .**
CF-8C	. . .	A 743, A 744	0.08 MAX	1.50 MAX	0.04 MAX	0.04 MAX	2.00 MAX	18.0-21.0	9.0-12.0	. . .	. . .	**NB + TA = 8 × C TO 1.0 (9 × C TO 1.1 AT HI TA)**
CF-16F	. . .	A 743	0.16 MAX	1.50 MAX	0.04 MAX	0.04 MAX	2.00 MAX	18.0-21.0	9.0-12.0		. . .	**S, MO, P, SE ADDED ABOVE LIMITS GIVEN FOR MACHINABILITY**
CH-20	. . .	A 743	0.20 MAX	1.50 MAX	0.04 MAX	0.04 MAX	2.00 MAX	22.0-26.0	12.0-15.0	. . .	. . .	**. . .**
CK-20	. . .	A 743	020 MAX	2.00 MAX	0.04 MAX	0.04 MAX	2.00 MAX	23.0-27.0	19.0-22.0	. . .	. . .	**. . .**
CE-30	. . .	A 743	0.30 MAX	1.50 MAX	0.04 MAX	0.04 MAX	2.00 MAX	26.0-30.0	8.0-11.0	. . .	. . .	**. . .**
CF-3	. . .	A 743, A 744	0.03 MAX	1.50 MAX	0.04 MAX	0.04 MAX	2.0 MAX	17.0-21.0	8.0-11.0	. . .	. . .	**. . .**
CF10SMNN	. . .	A 743	0.10 MAX	7.00-9.00	0.060 MAX	0.030 MAX	3.50-4.50	16.0-18.0	8.0-9.0	. . .	0.08-0.18	**. . .**
CF-3M	. . .	A 743, A 744	0.03 MAX	1.50 MAX	0.04 MAX	0.04 MAX	1.50 MAX	17.0-21.0	9.0-13.0	2.0-3.0	. . .	**. . .**
CF-3MN	. . .	A 743	0.03 MAX	1.50 MAX	0.040 MAX	0.040 MAX	1.50 MAX	17.0-22.0	9.0-13.0	2.0-3.0	0.10-0.20	**. . .**
CG6MM	. . .	A 743	0.06	4.00	0.04	0.03	1.00	20.5	11.5	1.50	0.20	**NB + TA, 0.10-**

DESIGNATION	UNS NO.	ASTM SPECIFICATION	COMPOSITION, WT%									
			C	Mn	P	S	Si	Cr	Ni	Mo	N	OTHER
N			MAX	- 6.00	MAX	MAX	MAX	- 23.5	- 13.5	- 3.00	- 0.40	**0.30; V, 0.10-0.30**
CG-8M	. . .	A 743, A 744	0.08 MAX	1.50 MAX	0.04 MAX	0.04 MAX	1.50 MAX	18.0 - 21.0	9.0-13.0	3.0-4.0	. . .	**. . .**
CN-3M	. . .	A 743	0.03 MAX	2.0 MAX	0.03 MAX	0.03 MAX	1.0 MAX	20.0 - 22.0	23.0 - 27.0	4.5-5.5	. . .	**. . .**
CN-7M	. . .	A 743, A 744	0.07 MAX	1.50 MAX	0.04 MAX	0.04 MAX	1.50 MAX	19.0 - 22.0	27.5 - 30.5	2.0-3.0	. . .	**CU, 3.0-4.0**
CN-7MS	. . .	A 743, A 744	0.07 MAX	1.00 MAX	0.04 MAX	0.03 MAX	2.50 - 3.50	18.0 - 20.0	22.0 - 25.0	2.5-3.0	. . .	**CU, 1.5-2.0**
CK-3MCUN	**. . .**	**A 743, A 744**	**0.025 MAX**	**1.20 MAX**	**0.045 MAX**	**0.010 MAX**	**1.00 MAX**	**19.5 - 20.5**	**17.5 - 19.5**	**6.0-7.0**	**0.180-0.240**	**CU, 0.50-1.00**

TABLE 3(B) PROPERTIES AND FILLER METALS FOR NOMINALLY AUSTENITIC STAINLESS STEELS

DESIGNATION	UNS NO.	ASTM SPECIFICATION	COMMENTS	TENSILE STRENGTH		YIELD STRENGTH		ELONGATION, %	MATCHING FILLER METALS		
				MPA	KSI	MPA	KSI		A5.4	A5.9[A]	A5.22
. . .	S01815	A 167	. . .	540	78	240	35	40	. . .	. . .	. . .
201	S20100	A 240	201-1, BOTH SPECIFICATIONS	655	95	260	38	40	E240-XX	ER240	. . .
201	S20100	A 666	201-2, BOTH SPECIFICATIONS	655	95	310	45	40	E240-XX	ER240	. . .
. . .	S20161	A 479	. . .	860	125	345	50	40	E240-XX	ER240	. . .
202	S20200	A 240	. . .	620	90	260	38	40	E240-XX	ER240	. . .
202	S20200	A 666	. . .	620	90	260	38	40	E240-XX	ER240	. . .
XM-1	S20300	A 582	. . .	NS	NS	NS	NS	NCW	NCW	NCW	. . .
205	S20500	A 666	. . .	790	115	450	65	40	E240-XX	ER240	. . .
XM-19	S20910	A 240	NITRONIC 50	690	100	380	55	35	E209-XX	ER209	. . .
XM-31	S21400	A 240	SHEET HIGHER STRENGTH	720	105	380	55	40	E240-XX	ER240	. . .
XM-14	S21460	A 666	. . .	720	105	380	55	40	E240-XX	ER240	. . .
XM-17	S21600	A 240	SHEET HIGHER STRENGTH	620	90	345	50	40	E209-XX	ER209	. . .
XM-18	S21603	A 240	SHEET HIGHER STRENGTH	620	90	345	50	40	E209-XX	ER209	. . .
. . .	S21800	A 240	NITRONIC 60	655	95	345	50	35	E240-XX	ER218	. . .
XM-10	S21900	A 276	NITRONIC 40	620	90	345	50	45	E219-XX	ER219	. . .
XM-11	S21904	A 666	SHEET HIGHER STRENGTH	620	90	345	50	45	E219-XX	ER219	. . .
XM-29	S24000	A 240	NITRONIC 33	690	100	380	55	40	E240-XX	ER240	. . .
XM-28	S24100	A 276	NITRONIC 32	690	100	380	55	30	. . .	. . .	. . .
. . .	S28200	A 276	. . .	760	110	415	60	35	. . .	. . .	. . .
301	S30100	A 666	LOWER STRENGTH IN A 167	620	90	205	30	40	. . .	. . .	. . .
302	S30200	A 240	. . .	515	75	205	30	40	E308-XX	ER308	**E308T-X**
302	S30200	666	. . .	515	75	205	30	40	E308-XX	ER308	**E308T-X**
302B	S30215	A 167	. . .	515	75	205	30	40	. . .	. . .	. . .
303	S30300	A 473	. . .	515	75	205	30	40	NCW	NCW	**NCW**
XM-5	S30310	A 582	. . .	NS	NS	NS	NS	NS	NCW	NCW	**NCW**

DESIGNATION	UNS NO.	ASTM SPECIFICATION	COMMENTS	TENSILE STRENGTH		YIELD STRENGTH		ELONGATION, %	MATCHING FILLER METALS		
				MPA	KSI	MPA	KSI		A5.4	A5.9[A]	A5.22
303SE	S30323	A 473	. . .	515	75	205	30	40	NCW	NCW	**NCW**
XM-2	S30345	A 582	. . .	NS	NS	NS	NS	NS	NCW	NCW	**NCW**
XM-3	S30360	A 582	. . .	NS	NS	NS	NS	NS	NCW	NCW	**NCW**
304	S30400	A 240, A 666	. . .	515	75	205	30	40	E308-XX	ER308	**E308T-X**
TP304	. . .	A 376	. . .	515	75	205	30	35	E308-XX	ER308	**E308T-X**
304L	S30403	A 240, A 666	. . .	480	70	170	25	40	E308L-XX	ER308L	**E308LT-X**
304H	S30409	A 240	. . .	515	75	205	30	40	E308H-XX	ER308H	**E308T-X**
TP304H	. . .	A 376	. . .	515	75	205	30	35	E308H-XX	ER308H	**E308-X**
. . .	S30415	A 240	. . .	600	87	290	42	40	. . .	. . .	**. . .**
XM-7	S30430	A 276	. . .	480	70	170	25	40	. . .	. . .	**. . .**
304N	S30451	A 240	. . .	550	80	240	35	30	. . .	. . .	**. . .**
304N	. . .	A 376	. . .	550	80	240	35	35	. . .	. . .	**. . .**
XM-21	S30452	A 240	SHEET HIGHER STRENGTH	585	85	275	40	30	. . .	. . .	**. . .**
304LN	S30453	A 240	. . .	515	75	205	30	40	. . .	. . .	**. . .**
304LN	S30453	A 666	. . .	550	80	240	35	40	. . .	. . .	**. . .**
TP304LN	. . .	A 376	. . .	515	75	205	30	35	. . .	. . .	**. . .**
. . .	S30454	A 276	. . .	620	90	245	50	30	. . .	. . .	**. . .**
305	S30500	A 240	LOWER STRENGTH IN A 167	515	75	205	30	40	E308-XX	ER308	**E308T-X**
306	S30600	A 240	. . .	540	78	240	35	40	. . .	. . .	**. . .**
RA85H	S30615	A 240	. . .	620	90	275	40	35	. . .	. . .	**. . .**
308	S30800	A 167	. . .	515	75	205	30	40	E308-XX	ER308	**E308T-X**
. . .	S30815	A 167, A 240	. . .	600	87	310	45	40	. . .	. . .	**. . .**
309	S30900	A 167	. . .	515	75	205	30	40	E309-XX	ER309	**E309T-X**
309S	S30908	A 240	. . .	515	75	205	30	40	E309-XX	ER309	**E309T-X**
309H	S30909	A 240	. . .	515	75	205	30	40	E309-XX	ER309	**E309T-X**
309CB	S30940	A 240	. . .	515	75	205	30	40	E309CB-XX	. . .	**. . .**
309HCB	S30949	A 240	. . .	515	75	205	30	40	E309CB-XX	. . .	**. . .**
310	S31000	.167	. . .	515	75	205	30	40	E310-XX	ER310	**E310T-X**
310S	S31008	A 240	. . .	515	75	205	30	40	E310-XX	ER310	**E310T-X**

DESIGNATION	UNS NO.	ASTM SPECIFICATION	COMMENTS	TENSILE STRENGTH		YIELD STRENGTH		ELONGATION, %	MATCHING FILLER METALS		
				MPA	KSI	MPA	KSI		A5.4	A5.9[A]	A5.22
310H	S31009	A 240	. . .	515	75	205	30	40	E310-XX	ER310	**E310T-X**
310CB	S31040	A 240	. . .	515	75	205	30	40	E310CB-XX	. . .	**. . .**
310HCB	S31049	A 240	. . .	515	75	205	30	40	E310CB-XX	. . .	**. . .**
310MOLN	S31050	A 240	. . .	550	80	240	35	30	. . .	. . .	**. . .**
254SMO	S31254	A 240	. . .	650	94	305	44	35	. . .	. . .	**. . .**
314	S31400	A 276	. . .	515	75	205	30	40	. . .	. . .	**. . .**
316	S31600	A 240	. . .	515	75	205	30	40	E316-XX	ER316	**E316T-X**
316	S31600	A 666	. . .	515	75	205	30	40	E316-XX	ER316	**E316T-X**
TP316	. . .	A 376	. . .	515	75	205	30	35	E316-XX	ER316	**E316T-X**
316L	S31603	A 240	. . .	480	70	170	25	40	E316L-XX	ER316L	**E316LT-X**
316L	S31603	A 666	. . .	480	70	170	25	40	E316L-XX	ER316L	**E316LT-X**
316H	S31609	A 240	. . .	515	75	205	30	40	E316H-XX	ER316H	**E316T-X**
TP316H	. . .	A 376	. . .	515	75	205	30	35	E316H-XX	ER316H	**E316T-X**
316TI	S31635	A 240	. . .	515	75	205	30	40	E318-XX	ER318	**. . .**
316CB	S31640	A 240	. . .	515	75	205	30	40	E318-XX	ER318	**. . .**
316N	S31651	A 240	. . .	550	80	240	35	35	. . .	. . .	**. . .**
316N	S31651	A 666	. . .	550	80	240	35	40	. . .	. . .	**. . .**
316N	. . .	A 376	. . .	550	80	240	35	35	. . .	. . .	**. . .**
316LN	S31653	A 240	. . .	515	75	205	30	40	. . .	. . .	**. . .**
TP316LN	. . .	A 376	. . .	515	75	205	30	35	. . .	. . .	**. . .**
. . .	S31654	A 276	. . .	620	90	345	50	30	. . .	. . .	**. . .**
317	S31700	A 240	. . .	515	75	205	30	35	E317-XX	ER317	**E317LT-X**
317L	S31703	A 240	. . .	515	75	205	30	40	E317L-XX	ER317L	**E317LT-X**
317LM	S31725	A 240	. . .	515	75	205	30	40	. . .	. . .	**. . .**
317LM	S31725	A 376	. . .	515	75	205	30	35	. . .	. . .	**. . .**
E17LMN	S31726	A 240	. . .	550	80	240	35	40	. . .	. . .	**. . .**
317LMN	S31726	A 376	. . .	550	80	240	35	35	. . .	. . .	**. . .**
317LN	S31753	A 240	. . .	550	80	240	35	40	. . .	. . .	**. . .**

DESIGNATION	UNS NO.	ASTM SPECIFICATION	COMMENTS	TENSILE STRENGTH		YIELD STRENGTH		ELONGATION, %	MATCHING FILLER METALS		
				MPA	KSI	MPA	KSI		A5.4	A5.9[A]	A5.22
321	S32100	A 240	. . .	515	75	205	30	40	E347-XX	ER321	**E347T-X**
TP321	. . .	A 376	. . .	515	75	205	30	35	E347-XX	ER321	**E347T-X**
321H	S32109	A 240	. . .	515	75	205	30	40	E347-XX	ER321	**E347T-X**
TP321H	. . .	A 376	. . .	515	75	205	30	35	E347-XX	ER321	**E347T-X**
. . .	S32615	A 240	. . .	550	80	220	32	25	. . .	. . .	**. . .**
347	S34700	A 240	. . .	515	75	205	30	40	E347-XX	ER347	**E347T-X**
TP347	. . .	A 376	. . .	515	75	205	30	35	E347-XX	ER347	**E347T-X**
347H	S34709	A 240	. . .	515	75	205	30	40	E347-XX	ER347	**E347T-X**
TP347H	. . .	A 376	. . .	515	75	205	30	35	E347-XX	ER347	**E347T-X**
348	S34800	A 240	. . .	515	75	205	30	40	E347-XX	ER347	**E347T-X**
TP348	. . .	A 376	. . .	515	75	205	30	35	E347-XX	ER347	**E347T-X**
348H	S34809	A 240	. . .	515	75	205	30	40	E347-XX	ER347	**E347T-X**
16-8-2H	. . .	A 376	. . .	515	75	205	30	35	E16-8-2-XX	ER16-8-2	**. . .**
XM-15	S38100	A 240	. . .	515	75	205	30	40	. . .	. . .	**. . .**
320	N08020	B 463	. . .	550	80	240	35	30	E320-XX	ER320	**. . .**
SANICRO 28	N08028	B 709	. . .	505	73	215	31	40	E383-XX	ER383	**. . .**
330	N08330	B 536	. . .	480	70	205	30	30	E330-XX	ER330	**. . .**
AL-6XN	N08367	B 688	. . .	690	100	310	45	30	. . .	. . .	**. . .**
904L	N08904	B 625	. . .	490	71	215	31	35	E385-XX	ER385	**. . .**
25-6MO	N08925	B 625	. . .	600	87	295	43	40	. . .	. . .	**. . .**
CF-8	. . .	A 743	. . .	480	70	205	30	35	E308-XX	ER308	**E308T-X**
CG-12	. . .	A 743	. . .	480	70	195	28	35	E309-XX	ER309	**E309T-X**
CF-20	. . .	A 743	. . .	480	70	205	30	30	E308-XX	ER308	**E308T-X**
CF-8M	. . .	A 743, A 744	. . .	480	70	205	30	30	E316-XX	ER316	**E316T-X**
CF-8C	. . .	A 743, A 744	. . .	480	70	205	30	30	E347-XX	ER321	**E347T-X**
CF-16F	. . .	A 743	. . .	480	70	205	30	25	. . .	. . .	**. . .**
CH-20	. . .	A 743	. . .	480	70	205	30	30	E309-XX	ER309	**E309T-X**
CK-20	. . .	A 743	. . .	450	65	195	28	30	E310-XX	ER310	**E310T-X**
CE-30	. . .	A 743	. . .	550	80	275	40	10	. . .	. . .	**. . .**
CF-3	. . .	A 743, A 744	. . .	480	70	205	30	35	E308L-XX	ER308L	**E308LT-X**
CF10SMNN	. . .	A 743	. . .	585	85	290	42	30	. . .	. . .	**. . .**

DESIGNATION	UNS NO.	ASTM SPECIFICATION	COMMENTS	TENSILE STRENGTH		YIELD STRENGTH		ELONGATION, %	MATCHING FILLER METALS		
				MPA	KSI	MPA	KSI		A5.4	A5.9(A)	A5.22
CF-3M	. . .	A 743 , A 744	. . .	480	70	205	30	30	E316L-XX	ER316L	**E316LT-X**
CF-3MN	. . .	A 743	. . .	515	75	255	37	35	. . .	. . .	**. . .**
CGMMN	. . .	A 743	. . .	585	85	290	42	30	. . .	. . .	**. . .**
CG-8M	. . .	A 743 , A 744	. . .	515	75	240	35	25	E317-XX	ER317	**E317LT-X**
CN-3M	. . .	A 743	. . .	435	63	170	25	30	E385-XX	. . .	**. . .**
CM-7M	. . .	A 743, A 744	. . .	425	62	170	25	35	E320-XX	ER320	**. . .**
CM-7MS	. . .	A 743, A 744	. . .	480	70	205	30	35	. . .	. . .	**. . .**
CK-3MCUN	**. . .**	**A 743, A 744**	**. . .**	**550**	**80**	**260**	**38**	**35**	**. . .**	**. . .**	**. . .**

NS, not specified; NCW, not considered weldable.

(A) ELECTRODES WITH HIGHER SILICON (0.65-1.00%), INDICATED BY "SI" ADDED AT THE END OF THE CLASSIFICATION WERE INCLUDED. METAL-CORED ELECTRODES, INDICATED BY A "C" IN PLACE OF THE "R" IN THE CLASSIFICATION, ARE ALSO INCLUDED.

Even the leanest austenitic stainless steels (such as types 302 and 304, which can be considered the base alloys of the austenitic stainless steels) offer general corrosion resistance in the atmosphere, in many aqueous media, in the presence of foods, and in oxidizing acids such as nitric acid. Types 321 and 347 are essentially type 304 with additions of either titanium or niobium, respectively, which stabilize carbides against sensitization.

The addition of molybdenum in type 316L provides pitting resistance in phosphoric and acetic acids and dilute chloride solutions, as well as corrosion resistance in sulfurous acid (H_2SO_3). An even higher molybdenum content, as in type 317L (3%), and even richer alloys further enhance pitting resistance.

Nitrogen is added to enhance strength at room temperature and, especially, at cryogenic temperatures (as in type 304LN, for example). Nitrogen is also added to reduce the rate of chromium carbide precipitation and, therefore, the susceptibility to sensitization. Nitrogen is also added to molybdenum-containing alloys to increase resistance to chloride-induced pitting and crevice corrosion.

Higher amounts of chromium and/or nickel are used to enhance high-temperature oxidation resistance (as in types 309, 310, and 330, for example). Copper and nickel can be added to enhance resistance to reducing acids, such as sulfuric acid (type 320). Nickel and molybdenum, when present in sufficient amounts, promote resistance to chloride-induced stress-corrosion cracking. As indicated by this discussion and Tables 3(a) and 3(b), there is an enormous number of austenitic stainless steel types.

Engineering for Use in the As-Welded Condition. Most weldments in nominally austenitic stainless steel base metals are put into service in the as-welded condition. In contrast to the situations with martensitic and ferritic stainless steel base metals, many of the nominally austenitic stainless steel base metals have matching, or near-matching, welding filler metals (see Tables 3(a) and 3(b)). In many cases, a nearly matching filler metal is a good choice.

Filler-metal selection and welding procedure development for austenitic stainless steel base metals primarily depend on whether or not ferrite is possible and acceptable in the weld metal. In general, if ferrite is both possible and acceptable, then the suitable choices of filler metals and procedures are broad. If the weld metal solidifies as primary ferrite, then the range of acceptable welding procedures can be as broad as it would be for ordinary mild steel. However, if ferrite in the weld metal is neither possible nor acceptable, then the filler metal and procedure choices are much more restricted, because of hot-cracking considerations.

Most filler-metal compositions are available in a variety of forms. When the presence of ferrite is possible, some filler-metal manufacturers will tailor it to meet specific needs, at least in filler metals that are composites (for SMAW, FCAW, and metal-cored wires for GMAW or SAW processes). For example, in type 308 or 308L filler metals, which are typically selected for joining base-metal types 302, 304, 304L, 305, CF-8, or CF-3, the filler metal can be designed for zero ferrite, more than 20 FN, or any FN value between these extremes, and still be within the composition limits for the classification in the relevant AWS filler-metal specification.

In solid wires of type 308 or 308L, which are used for GMAW, GTAW, or SAW processes, the potential ferrite content of all-weld metal is often designed by the steel producer to provide maximum yield from the heat of steel. Stainless steel producers have generally found that the yield from a heat of steel, which will be reduced to "green rod" for supply to a filler-metal producer, is maximized when the ferrite content ranges from 3 to 8 FN, based on the WRC-1988 diagram. Weld rod demand is usually for a minimum of 8 FN. Poor yields make the production of metal with more than 10 FN uneconomical and, thus, limit its availability. A lack of demand limits production and, thus, the availability of green rod with less than 8 FN. Therefore, most solid-wire compositions are designed to achieve approximately 8 to 10 FN. Solid wires with compositions that are much beyond this range (as in austenitic grades that generally contain some ferrite) usually require special order, heat quantities (of 18 Mg, or 40,000 lb), long lead times, and they command premium prices.

With composite filler metals, the manufacturer can adjust both composition and ferrite content via alloying in either the electrode coating of SMAW electrodes or the core of flux-cored and metal-cored wires. Tailoring composition and ferrite for special applications is much more easily accomplished than it is for solid wires. For most off-the-shelf composite filler metals, the filler-metal manufacturer has a target all-weld metal FN in mind when designing the filler metal. For a given alloy type, such as 308L, the target FN is likely to depend on the economics of filler-metal design, the appropriate Ferrite Number for the specific type of filler metal to avoid hot cracking, and market requirements.

For example, the ANSI/AWS A5.4 classification system recognizes three all-position coating types. In general, E308L-15 electrodes provide better hot-cracking resistance at low or no levels of ferrite than do E308L-16 electrodes, which, in turn, provide better hot-cracking resistance than do E308L-17 electrodes when little or no ferrite is present in the deposit. This difference in cracking resistance without ferrite primarily stems from bead shape. The E308L-15 electrodes tend to produce a convex bead shape. Convexity provides something of a riser, as in a casting, which tends to resist hot cracking. The E308L-16 electrodes tend to produce a nearly flat profile, which provides little or no riser. The E308L-17 electrodes tend to produce a concave profile (as well as a high silicon deposit), which makes this the least crack resistant coating type when there is little or no ferrite in the deposit. Further, the sensitivity to nitrogen pickup with a long arc (and the consequent loss of ferrite) is least with E308L-15 and greatest with E308L-17 electrodes.

As a result, filler-metal manufacturers generally aim their off-the-shelf E308L-15 electrodes toward a lower FN than they do their E308L-16 electrodes, which, in turn, are aimed toward lower FN values than are their E308L-17 electrodes. Of course, the same tendencies apply to other alloy compositions with the same coating types, which can be generalized as EXXX-15, EXXX-16, or EXXX-17, where "XXX" stands for 308, 308L, 309, 309L, 316, 316L, and so on.

Until 1992, the EXXX-17 coating type was not recognized by the ANSI/AWS A5.4 specification as being a distinct type, although the electrodes have been available for many years. Because electrodes that are properly classified as EXXX-17 generally weld satisfactorily on both direct current (dc) and alternating current (ac), they had to be classified as EXXX-16 electrodes until the publication of ANSI/AWS A5.4-92 introduced the EXXX-17 classifications. Using these electrodes and meeting the vertical-up fillet weld size and convexity requirements of the EXXX-16 classifications were difficult to achieve, at best.

Although the EXXX-17 classifications have relaxed vertical-up fillet size and convexity requirements, some electrode manufacturers have been reluctant to change the classification of certain brand names (originally classified as EXXX-16) in order to more correctly reflect the true vertical-up capabilities of the electrodes. The knowledgeable fabricator can detect an electrode that is classified by its manufacturer as EXXX-16, when it properly ought to be classified as EXXX-17, either by attempting to meet the vertical-up fillet requirements of the EXXX-16 classification or by examining the all-weld metal composition that the electrode produces. The EXXX-17 electrodes all produce deposits of low manganese and high silicon. In general, a nominally austenitic electrode with an all-weld metal silicon content that is nearly as high as, or higher than, its manganese content (that is, silicon content approaches the 0.9% maximum of the specification) is in all probability properly classified as an EXXX-17 electrode.

Flux-cored and metal-cored electrodes do not have the clear distinctions that exist among the three main coating types. In general, both off-the-shelf flux-cored and metal-cored electrodes tend to have higher ferrite numbers, more like those of EXXX-17 electrodes, because the higher heat input that normally accompanies the use of these products tends to make the weld metal less crack resistant when little or no ferrite is present.

If a fully austenitic stainless steel as-welded deposit, or one with almost no ferrite, is necessary, and solidification as primary austenite, or fully austenitic solidification, is expected, then the choices of both filler metals and procedures are more restricted. When designing filler metals with low or no ferrite, the producer tries to obtain raw materials with minimal sulfur and phosphorus contents. Generally, high-silicon compositions are avoided, because of their hot-cracking tendencies. Concave beads and high heat input are best avoided in procedure development. As a result, little or no filler metals are even offered commercially as EXXX-17 SMAW electrodes without ferrite. Submerged arc joining with fully austenitic filler metals is usually avoided, because of cracking problems, although submerged arc cladding is more successful. The GMAW process is often restricted to a short-circuiting transfer mode.

A general rule to follow in procedure development for fully austenitic weld metals, in order to avoid or minimize cracking problems, is to "weld ugly." In particular, this means that if cracking is encountered, then welding procedures that produce markedly convex beads can overcome it. For compositions that are very crack sensitive, it may be necessary to make individual weld beads that are so convex that part of the weld bead must be ground away before the next bead is deposited. For the most crack sensitive steels, such as type 320, crack-free welding with matching filler metal may be possible only with either small-diameter (1.6 through 2.4 mm, or 0.06 through 0.10 in.) E320-15 electrodes that are welded on the low side of the recommended current range or small-diameter ($\leq$0.9 mm, or 0.04 in.) GMAW wire in the short-circuiting transfer mode.

Niobium, phosphorus, and sulfur in such alloys generally tend to make hot-cracking problems more severe. As a result, for type 320 stainless steel, both SMAW electrodes (E320LR-15) and GMAW wires (ER320LR) are available with reduced residual elements, as well as low carbon, so that niobium can be minimized without loss of the stabilization of carbides.

Additional welding procedure approaches to eliminating hot cracking with weld metals that solidify either fully austenitic or as primary austenite include those that reduce heat buildup in the steel. Low welding heat input and low preheat and interpass temperatures are all beneficial.

Weld puddle shape has a strong influence on hot-cracking tendencies. Narrow, deep puddles crack more readily than wide, shallow puddles. In particular, it is helpful to adjust welding conditions to obtain a weld pool that is elliptical in surface shape and to avoid tear-drop-shaped weld pools, the sharp tail of which tends to promote hot cracking. Low current and slow travel speed favor an elliptical pool shape. Copper chill blocks also can help to extract heat and speed cooling.

With fully austenitic or primary austenite solidification, it is essential to backfill weld craters to avoid crater cracks, which are a form of localized hot cracking. This means stopping the travel of the arc while continuing to add filler metal, with a down-sloping current, if possible, before breaking the arc, so that the crater becomes convex, rather than concave.

It was noted earlier that the usual choice for a filler metal for austenitic stainless steel is a matching or near-matching composition to that of the base metal. However, one situation generally requires an exception. This situation occurs when a high-molybdenum base metal is chosen for pitting or crevice corrosion resistance in a chloride-containing aqueous solution. Although the high molybdenum content of the weld metal provides resistance to localized corrosion, it invariably has segregation of molybdenum on a microscopic scale. The center of each dendrite is leaner in molybdenum than are the interdendritic spaces. The center of a dendrite then becomes a preferential site for localized corrosion.

It has been found that this preferential localized corrosion in the weld metal can be overcome by using a filler metal that is higher in molybdenum than is the base metal. Thus, a 3% Mo base metal (such as type 317L) requires a filler metal of at least 4% Mo. A 4% Mo base metal (such as type 904L) requires a filler metal of at least 6% Mo. A 6% Mo base metal requires a filler metal of at least 8% Mo. However, stainless steel weld metal that contains more than 5% Mo often has poor mechanical properties. Therefore, a nickel-base alloy of at least 8% Mo is usually chosen for filler metal when joining stainless steels with contents of 4% Mo and higher. The most common filler metals selected are the ENiCrMo-3 or ENiCrMo-10 covered-electrode classifications in ANSI/AWS A5.11 and the ERNiCrMo-3 or ERNiCrMo-10 bare-wire classifications in the ANSI/AWS A5.14 specification.

Engineering for Use in the Postweld Heat-Treated Condition. Austenitic stainless steel weldments are usually put into service in the as-welded condition, except in the situations described below. When non-low-carbon grades are welded and sensitization that is due to chromium carbide precipitation cannot be tolerated, then annealing at 1050 to 1150 °C (1920 to 2100 °F), followed by a water quench, can be used to dissolve all carbides (and any intermetallic compounds, such as σ phase) and to maintain a solid solution. This annealing heat treatment also causes much of the ferrite that is present to transform to austenite.

Autogenous welds in high-molybdenum stainless steel, such as longitudinal seams in pipe, represent another exception. Annealing is used to cause the diffusion of molybdenum to erase the microsegregation of the as-welded condition, thus allowing the weld to match the pitting and crevice corrosion resistance of the base metal. Because these welds generally contain no ferrite in the as-welded condition, no ferrite is lost.

A third exception is the joints between austenitic stainless steel and carbon or low-alloy steel or the weld overlay of carbon or low-alloy steel with austenitic stainless steel filler metal. Type 309 filler metal often has been used for such a joint or overlay, so that the weld metal (especially in a multipass weld where type 309 is used throughout) contains an appreciable amount of ferrite. The HAZ of the carbon or low-alloy steel may require a PWHT at various temperatures from 600 to 700 °C (1110 to 1290 °F), depending on the specific alloy. These temperatures produce both carbide precipitation in the austenitic base metal and weld metal and transformation of ferrite to σ phase in the weld metal.

In the weld metal, carbide precipitation works against σ-phase formation because the carbides tend to precipitate where chromium is highest: at the ferrite-austenite interface. Because carbide precipitation reduces the chromium in the adjacent ferrite, some of it becomes unstable and transforms to austenite. This reduces the amount of ferrite available for σ formation. In a joint, but not in an overlay, corrosion resistance of the weld metal is seldom of concern because of the proximity of carbon or low-alloy steel. At the same ferrite content in the as-welded condition, less ferrite will be available for σ formation in type 309 than in type 309L weld metal. Therefore, the higher-carbon filler metal is often preferred for such applications.

At the same time, carbon from the mild steel or low-alloy steel immediately adjacent to the fusion line migrates to the higher-chromium weld metal, producing a layer of carbides along the fusion line in the weld metal and a carbon-depleted layer in the HAZ of the base metal. This carbon-depleted layer is weak at elevated temperatures. If the weldment is in service at suitable temperatures, then creep failure can occur there. There is also a serious mismatch in the CTE between austenitic stainless steel filler metal and carbon steel or low-alloy steel base metal. Therefore, thermal cycling produces strain accumulations along the interface and can lead to premature failure in creep, as has occurred in joints of chromium-molybdenum low-alloy steels to stainless steels. As a result, such dissimilar joints intended for elevated-temperature service are often welded with nickel-base alloy filler metals.

Although PWHT can be used for stress relief in austenitic stainless steel weldments, the yield strength of austenitic stainless steels falls much more slowly with rising temperature than does the yield strength of carbon or low-alloy steel. In addition, carbide precipitation and σ-phase embrittlement occur in the temperature range (600 to 700 °C, or 1110 to 1290 °F) where carbon steels and low-alloy steels are normally stress relieved. Significant improvement in relieving residual stresses without damaging corrosion resistance is only accomplished with a full anneal at temperatures ranging from 1050 to 1150 °C (1920 to 2100 °F), followed by rapid cooling to avoid carbide precipitation in unstabilized grades.

In stabilized grades, heat treatment at these temperatures causes niobium or titanium carbides to precipitate in part, which accomplishes much of the stabilization. However, rapid cooling is still necessary to obtain full corrosion resistance. In either case, the rapid cooling often reintroduces residual stresses, which means that this approach has to be used carefully. At the annealing temperatures, significant surface oxidation occurs in air. This oxide is tenacious on stainless steels and must be removed by pickling, followed by a water rinse, and then passivation, in order to restore full corrosion resistance.

References cited in this section

10. J.C. LIPPOLD AND W.F. SAVAGE, SOLIDIFICATION OF AUSTENITIC STAINLESS STEEL WELDMENTS: PART III--THE EFFECT OF SOLIDIFICATION BEHAVIOR ON HOT CRACKING SUSCEPTIBILITY, *WELD. J.*, VOL 61 (NO. 12), 1982, P 388S-396S
18. S.A. DAVID, J.M. VITEK, AND T.L. HEBBLE, EFFECT OF RAPID SOLIDIFICATION ON STAINLESS STEEL WELD METAL MICROSTRUCTURES AND ITS IMPLICATIONS ON THE SCHAEFFLER DIAGRAM, *WELD. J.*, VOL 66 (NO. 10), 1987, P 289S-300S
19. E. FOLKHARD, *WELDING METALLURGY OF STAINLESS STEELS*, SPRINGER-VERLAG, 1984, P 105
20. E. FOLKHARD, *WELDING METALLURGY OF STAINLESS STEELS*, SPRINGER-VERLAG, 1984, P 126

Welding of Stainless Steels

D.J. Kotecki, The Lincoln Electric Company

Precipitation-Hardening Stainless Steels

Basic Metallurgy. PH stainless steels can be divided into three groups, based on microstructure and precipitation behavior. Martensitic PH stainless steels are solutionized at a high temperature and transform to low-carbon martensite during cooling to room temperature. Then, they are further hardened by aging at an intermediate temperature to precipitate a second phase, which can be an intermetallic compound or a single component, such as copper. Both martensite and the precipitates harden the steel.

Semiaustenitic PH stainless steels can be cooled from their solutionizing temperature to room temperature without martensite formation, remaining rather soft austenite as they cool. Then, they are aged at an intermediate temperature, which causes carbides or an intermetallic compound to precipitate. This precipitation removes alloying elements and, possibly, carbon, from the solid solution, which destabilizes the austenite, allowing it to transform to martensite upon cooling from the aging temperature. Again, both martensite and the precipitates harden the steel.

Austenitic PH stainless steels contain enough alloys to be stable austenite upon cooling from their solutionizing temperature to room temperature. They are still stable austenite upon cooling from their aging temperature after

intermetallic compounds are precipitated. In the case of austenitic PH stainless steels, only the precipitate hardens the alloy. As a result, the austenitic PH stainless steels cannot achieve tensile strengths as high as can be achieved with the martensitic or semiaustenitic grades.

Some of the PH stainless steels (some martensitic and semiaustenitic grades) can solidify as primary ferrite and have very good resistance to hot cracking. Because martensite is also ferromagnetic, a magnetic Ferrite Number loses meaning in terms of ensuring freedom from hot cracking. In the highly alloyed austenitic PH stainless steels, no ferrite is possible, and it is difficult to weld these without hot cracking.

Precipitation-Hardening Base Metals. Table 4(a) lists several PH stainless steels. Most of their applications are in the aerospace and other high-technology industries. Only one composition, the martensitic type 630 (17-4PH), is made as a welding filler metal in sufficient volume to warrant AWS classification of a matching filler metal, as can be seen in Table 4(b).

TABLE 4(A) COMPOSITIONS OF PRECIPITATION-HARDENING STAINLESS STEELS

DESIGNATION	UNS NO.	ASTM SPECIFICATION	COMPOSITION, WT%									
			C	MN	P (MAX)	S (MAX)	SI (MAX)	CR	NI	MO	N	OTHER
630	S17400	A 564	0.07 MAX	1.00 MAX	0.040	0.030	1.00	15.00-17.50	3.00-5.00	. . .	. . .	**NB + TA, 0.15-0.45; CU, 3.00-5.00**
631	S17700	A 564	0.09 MAX	1.00 MAX	0.040	0.030	1.00	16.00-18.00	6.50-7.75	. . .	. . .	**AL, 0.75-1.50**
632	S15700	A 564	0.09 MAX	1.00 MAX	0.040	0.030	1.00	14.00-16.00	6.50-7.75	2.00-3.00	. . .	**AL, 0.75-1.50**
633	S35000	A 693	0.07-0.11	0.50-1.25	0.040	0.030	0.50	16.00-17.00	4.00-5.00	2.50-3.25	0.07-0.13	**. . .**
634	S35500	564	0.10-0.15	0.50-1.25	0.040	0.030	0.50	15.00-16.00	4.00-5.00	2.50-3.25	0.07-0.13	**. . .**
635	S17600	A 564	0.08 MAX	1.00 MAX	0.040	0.030	1.00	16.00-17.50	6.00-7.50	. . .	. . .	**TI, 0.40-1.20; AL, 0.40 MAX**
XM-9	S36200	A 564	0.05 MAX	0.50 MAX	0.030	0.030	0.30	14.00-14.50	6.25-7.00	0.3 MAX	. . .	**TI, 0.60-0.90 AL, 0.10 MAX**
XM-12	S15500	A 564	0.07 MAX	1.00 MAX	0.040	0.030	1.00	14.00-15.50	3.50-5.50	. . .	. . .	**NB + TA, 0.15-0.45; CU, 2.50-4.50**
XM-13	S13800	A 564	0.05 MAX	0.20 MAX	0.010	0.008	0.10	12.25-13.25	7.50-8.50	2.00-2.50	0.01 MAX	**AL, 0.90-1.35**
XM-16	S45500	A 564	0.03 MAX	0.50 MAX	0.015	0.015	0.50	11.00-12.50	7.50-9.50	0.50 MAX	. . .	**NB + TA, 0.10-0.50; TI, 0.90-1.40; CU, 1.50-2.50**
. . .	S45503	A 564	0.010 MAX	0.50 MAX	0.010	0.010	0.20	11.00-12.50	7.50-9.50	0.50 MAX	. . .	**NB + TA, 0.10-0.50; TI, 1.00-1.35; CU, 1.50-2.50**
XM-25	S45000	A 564	0.05 MAX	1.00 MAX	0.030	0.030	1.00	14.00-16.00	5.00-7.00	0.50-1.00	. . .	**NB + TA, 8 × C MIN; CU, 1.25-1.75**

660 (A286)	S66286	A 638, A 453	0.08 MAX	2.00 MAX	0.040	0.030	1.00	13.50-16.00	24.00-27.00	1.00-1.50	. . .	**B, 0.0010-0.010; TI, 1.90-2.35; AL, 0.35 MAX; V, 0.10-0.50**
662	**K66220**	**A 638**	**0.08 MAX**	**1.50 MAX**	**0.040**	**0.030**	**1.00**	**12.00-15.00**	**24.00-28.00**	**2.50-3.50**	**. . .**	**B, 0.0010-0.010; TI, 1.55-2.00; CU, 0.50 MAX; AL, 0.35 MAX**

TABLE 4(B) PROPERTIES AND FILLER METALS FOR PRECIPITATION-HARDENING STAINLESS STEELS

DESIGNATION	UNS NO.	ASTM SPECIFICATION	COMMENTS	TENSILE STRENGTH		YIELD STRENGTH		ELONGATION, %	MATCHING FILLER METALS		
				MPA	KSI	MPA	KSI		A5.4	A5.9[A]	A5.22
630	S17400	A 564	480 °C (900 °F) AGE	1310	190	1170	170	10	E630-XX	ER630	...
631	S17700	A 564	510 °C (950 °F) AGE	1280	185	1030	150	6	...	...	...
632	S15700	A 564	510 °C (950 °F) AGE	1380	200	1210	175	7	...	...	...
633	S35000	A 693	450 °C (850 °F) AGE	1280	185	1030	150	8	...	...	...
634	S35500	564	540 °C (1000 °F) AGE	1170	170	1070	155	12	...	...	...
635	S17600	A 564	510 °C (950 °F) AGE	1310	190	1170	170	8	...	...	...
XM-9	S36200	A 564	AGE NOT SPECIFIED	1240	180	1210	175	10	...	...	...
XM-12	S15500	A 564	480 °C (900 °F) AGE	1310	190	1170	170	10	...	...	...
XM-13	S13800	A 564	510 °C (950 °F) AGE	1520	220	1410	205	10	...	...	...
XM-16	S45500	A 564	480 °C (900 °F) AGE	1620	235	1520	220	8	...	...	...
...	S45503	A 564	480 °C (900 °F) AGE	1620	235	1520	220	8	...	...	...
XM-25	S45000	A 564	480 °C (900 °F) AGE	1240	180	1170	170	10	...	...	...
660 (A286)	S66286	A 638, A 453	730 °C (1350 °F) AGE	900	130	590	85	15	...	...	...
662	**K66220**	**A 638**	**650 °C (1200 °F) AGE**	**860**	**125**	**550**	**80**	**15**	**...**	**...**	**...**

(A) METAL-CORED ELECTRODES, INDICATED BY A "C" IN PLACE OF THE "R" IN THE CLASSIFICATION, ARE ALSO INCLUDED.

Type 630 base metal (17Cr-4Ni-3Cu) is also the prototype martensitic PH stainless steel. In the solution-annealed (martensitic) condition, its yield strength is already above 750 MPa (110 ksi). The PH phase is copper, which, after aging at 480 °C (900 °F), is so fine that it can only be detected with a high-powered electron microscope. A yield strength of more than 1200 MPa (170 ksi) is obtained after this aging treatment. Higher aging temperatures coarsen the precipitate and reduce the strength.

Type 632 base metal (15Cr-7Ni-2Mo-1Al) is an example of a semiaustenitic PH stainless steel. In the solution-annealed (austenitic) condition, its yield strength is only on the order of 380 MPa (55 ksi), which is not very different from that of an ordinary austenitic stainless steel. Heat treatment at 955 °C (1750 °F) precipitates carbides and destabilizes the austenite, which transforms to martensite upon subsequent cooling. Then, aging at 510 °C (950 °F) precipitates nickel-aluminum intermetallic compounds. The aged martensite can exhibit a strength of approximately 1500 MPa (220 ksi). Again, aging at a higher temperature coarsens the precipitates and softens the steel.

Type 660 (A286) is the prototype austenitic PH stainless steel. Its high alloy content (15Cr-25Ni-1Mo-2Ti) provides higher corrosion resistance than that of the martensitic or semiaustenitic types. Furthermore, it contains no magnetic phases, which makes it suitable for use in high magnetic fields, such as those associated with superconducting magnets used for fusion energy research. Aging at about 730 °C (1350 °F) causes nickel-titanium intermetallic compound particles to precipitate, hardening the alloy. Its fully hardened yield strength (approximately 590 MPa, or 86 ksi), however, is considerably lower than that available from the martensitic or semiaustenitic grades.

Engineering for Use in the As-Welded Condition. Because PH stainless steels achieve their high strength by heat treatment, it is not reasonable to expect the weld metal to match the properties of the base metal in the as-welded condition. Therefore, the design of a weldment to be used in the as-welded condition generally must assume that the weld metal will under-match the strength of the base metal. If that is acceptable, then austenitic filler metals, such as types 308 and 309, can be suitable filler metals for the martensitic and semiaustenitic PH stainless steels. As with many of the other filler-metal selections in this article, consideration should be given to obtaining some ferrite in the weld metal to avoid hot cracking.

Example 8: Type 630 base metal (0.04C-16.5Cr-4Ni-4Cu-0.3Nb-0.02N, WRC-1992 Cr_{eq} = 16.71 and Ni_{eq} = 6.80; FN, off the diagram) to be welded with E308-16 electrode (0.05C-19.8Cr-9.6Ni-0.06N, WRC-1992 Cr_{eq} = 19.8 and Ni_{eq} = 12.55; FN = 6.2).

Assuming 30% dilution, the first weld bead would have Cr_{eq} = 18.87, Ni_{eq} = 10.83, and the calculated FN = 8.6. This is comfortably safe to ensure freedom from cracking during welding, and the weld composition is sufficiently rich in alloy that the weld metal will be stable as regards transformation of austenite to martensite. Thus, E308-16 is a good filler-metal selection, if its low strength, when compared with that of type 630 base metal, is acceptable. Clearly, type 309 filler metal would do as well.

Type A286 PH stainless steel, which is fully austenitic, presents a different situation if it is to be used in the as-welded condition. If nonmagnetic weld metal is essential, then type 310 filler metal is often the choice. Type 310 probably has the best cracking resistance of all of the fully austenitic filler metals. However, the first bead on A286 would be most at risk for hot cracking, because of the elements picked up from the A286 in the weld metal. Because a joint always presents a greater risk of hot cracking than does an overlay, a possible strategy to adopt is to first butter the A286 with type 310 weld metal. Then, welding type 310 to itself is less risky. In any event, the "weld ugly" practice of low heat input, convex beads, and so on, is always appropriate for crack-sensitive fully austenitic welds.

On the other hand, if a partially magnetic weld joint is acceptable and the weldment will not experience elevated temperatures where embrittlement could occur, then type 312 filler metal (at least for the weld deposits directly on A286) will provide the weld metal with ferrite and minimal hot-cracking risk. Once the A286 is covered with type 312 filler metal, the joint could be finished with a filler metal having a much lower ferrite content, such as type 308 or 309. However, type 309 will not provide ferrite when deposited directly on A286 with normal weld dilution.

Engineering for Use in the Postweld Heat Treated Condition. Normally, PWHT is done on a weldment of PH stainless steel because a weld-metal strength that is comparable to that of the base metal is desired. This, in turn, generally means that the weld metal must also be a PH stainless steel. Many PH stainless steel weldments are light-gage materials that readily lend themselves to autogeneous GTAW or LBW processes. Then, the weld metal matches the base metal and responds similarly to heat treatment.

Except for type 630, matching filler metals for the PH stainless steels are not very easy to locate and do not have AWS classifications. Some are covered by Aerospace Material Specifications (AMS) as bare wires only, which match base-metal compositions. These wires, used for GTAW or GMAW processes, are most likely to be available from suppliers to the aerospace industry. Alternatively, the shearing of base metal into narrow strips can provide filler metal for the GTAW process.

It is a common practice to use type 630 as a filler metal with several of the martensitic and semiaustenitic PH stainless steel base metals. The best weldment properties can then be obtained by a full-solution heat treatment, rapid cooling to room temperature, reheating to age harden at about 480 °C (900 °F), and cooling to room temperature. Because type 630 filler metal will transform to martensite upon cooling from solidification, it is also possible to obtain nearly full-strength weld metal, when using this filler metal, by simply cooling to room temperature and then aging at 480 °C (900 °F) to harden the weld metal. This presupposes that the weld metal does not pick up enough alloying elements by dilution to stabilize austenite and therefore does transform to martensite. When the weldment is simply aged after welding, without first using a solution heat treatment, some portion of the HAZ will have been overaged by the heat of welding and will become the weak link in the weldment. Then, 100% joint efficiency cannot be expected. A procedure qualification test becomes necessary to determine if the weldment strength will be adequate.

Welding of Stainless Steels

D.J. Kotecki, The Lincoln Electric Company

Duplex Ferritic-Austenitic Stainless Steels

Basic Metallurgy. Duplex ferritic-austenitic stainless steels solidify as essentially 100% ferrite. At high temperatures (on the order of 1300 °C, or 2370 °F), austenite nucleates and grows, first, at ferrite grain boundaries and, later, along preferred crystallographic directions within the ferrite grains. Diffusion of alloying elements must occur as the transformation of ferrite to austenite proceeds, with austenite-stabilizing elements (carbon, nickel, nitrogen, and copper) concentrating in the austenite, and ferrite-stabilizing elements (chromium, molybdenum, and tungsten) concentrating in the ferrite. The extent of the transformation depends not only on the balance between austenite-stabilizing elements and ferrite-stabilizing elements in the alloy, but on the time available for diffusion and on the actual diffusion of specific elements. It is possible to quench a duplex stainless steel from near the solidification temperature and to obtain nearly 100% ferrite at room temperature. Slow cooling, annealing, and hot working promote transformation of ferrite to austenite by promoting diffusion.

In a duplex ferritic-austenitic stainless steel, the optimum phase balance is usually approximately equal amounts of ferrite and austenite. Base-metal compositions are usually adjusted to obtain this phase balance as the equilibrium structure at approximately 1040 °C (1900 °F) after hot working and/or annealing. Of the alloying elements that affect the phase balance, carbon is generally undesirable for reasons of corrosion resistance. All of the other elements are slow to diffuse substitutional alloy elements, except for nitrogen. The other alloy elements contribute to determining the equilibrium phase balance, but nitrogen is most important in determining the relative ease of achieving a near-equilibrium phase balance. In developing the earliest duplex stainless steels (such as types 329 and CD-4MCu), nitrogen was not a deliberate alloying element. Therefore, under normal weld cooling conditions, the weld HAZs and matching weld metals reached room temperature with very little austenite, and had poor mechanical properties and corrosion resistance. To obtain useful properties, the welds required an annealing heat treatment, followed by quenching to avoid embrittlement of the ferrite by σ and other phases.

Overalloying of the weld filler metal with nickel causes the transformation to begin at a higher temperature, where diffusion is more rapid. Using this approach, a better phase balance can be obtained in the as-welded condition in the weld metal. However, this approach does nothing for the HAZ. Alloying with nitrogen, in the newer duplex stainless steels, usually solves the HAZ problem. With normal welding heat input and about 0.15% Ni, a reasonable phase balance is achieved in the HAZ. In addition, the nitrogen, when it diffuses to the austenite, imparts improved pitting resistance. On the other hand, if the cooling rate is too rapid and nitrogen is trapped in ferrite, then chromium nitride precipitates, damaging corrosion resistance. Therefore, low welding heat inputs should be avoided with duplex stainless steels.

The ferrite in the duplex stainless steels behaves much like a fully ferritic stainless steel in terms of formation of intermetallic compounds during heat treatment. The α, χ, and other phases can form in the temperature range from 500 to

1000 °C (930 to 1830 °F) in the base metals. High-nickel weld metals can extend the σ range to 1050 °C (1920 °F) or even higher (Ref 21). An α' embrittlement (475 °C, or 885 °F, embrittlement) can occur at temperatures as low as 250 °C (480 °F) to as high as 550 °C (1020 °F), depending on composition and time at temperature. An α' embrittlement occurs extremely slowly below approximately 350 °C (660 °F). Therefore, the American Society of Mechanical Engineers (ASME) code allows the use of UNS No. S31803 alloy at service temperatures up to 315 °C (600 °F). But, generally, the PWHT of duplex stainless steels needs to be done at temperatures above 1040 °C (1900 °F), or not at all.

It has been shown that duplex stainless steel weldments can suffer from hydrogen-induced cracking at very high hydrogen levels (Ref 22), and that lower levels damage ductility (Ref 23). This presents a special problem in duplex stainless steel weld metals, because austenite that occurs along original ferrite grain boundaries acts as a barrier to hydrogen escape. Therefore, the damage to ductility, caused by hydrogen, can remain indefinitely, in contrast to the easy escape of hydrogen from ferritic weld metals. Fortunately, α' embrittlement at 250 °C (480 °F) requires over 1000 h at temperature, whereas hydrogen escape from a 12 mm (0.5 in.) thick weldment can be achieved in about 100 h at this temperature (Ref 22). A postweld soak at this temperature can restore ductility to a hydrogen-damaged weldment.

Duplex Ferritic-Austenitic Base Metals. Tables 5(a) and 5(b) list selected duplex ferritic-austenitic stainless steel base metals and their compositions and mechanical property requirements, along with a limited number of "matching" filler metals. It is noteworthy that the yield strength of these steels is on the order of twice that of ordinary austenitic stainless steels, such as type 304 or 316L. The duplex stainless steels provide resistance to stress-corrosion cracking (SCC) in aqueous chloride-containing media. The level of resistance is generally superior to that of ordinary austenitic stainless steels, but may not be as good as that of the third-generation ferritic stainless steels described above. The newer duplex stainless steels, alloyed with nitrogen and molybdenum, also provide pitting resistance in aqueous chloride-containing media.

TABLE 5(A) COMPOSITIONS OF DUPLEX FERRITIC-AUSTENITIC STAINLESS STEELS

DESIGNATION	**UNS NO.**	**ASTM SPECIFICATION**	COMPOSITION, WT%									
			C (max)	**Mn**	**P (max)**	**S (max)**	**Si**	**Cr**	**Ni**	**Mo**	**N**	OTHER
XM-26	S31100	A 276	0.06	1.00 MAX	0.040	0.030	1.00 MAX	25.00-27.00	6.00-7.00	. . .	. . .	**TI, 0.25 MAX**
. . .	S31200	A 240	0.030	2.00 MAX	0.045	0.030	1.00 MAX	24.0-26.0	5.5-6.5	1.2-2.0	0.14-0.20	**. . .**
. . .	S31260	A 240	0.03	1.00 MAX	0.030	0.030	0.75 MAX	24.0-26.0	5.50-7.50	2.50-3.50	0.10-0.30	**CU, 0.20-0.08; W, 0.10-0.50**
. . .	S31500	A 790	0.030	1.20-2.00	0.030	0.030	1.40-2.00	18.0-19.0	4.25-5.25	2.50-3.00	0.05-0.1	**. . .**
2205	S31803	A 240, A 790	0.030	2.00 MAX	0.030	0.020	1.00 MAX	21.0-23.0	4.50-6.50	2.50-3.50	0.08-0.20	**. . .**
2304	S32304	A 790	0.030	2.50 MAX	0.040	0.040	1.0 MAX	21.5-24.5	3.0-5.5	0.05-0.60	0.05-0.20	**CU, 0.05-0.60**
255	S32550	A 240, A 790	0.04	1.5 MAX	0.040	0.030	1.0 MAX	24.0-27.0	4.5-6.5	2.9-3.9	0.10-0.25	**CU, 1.5-2.5**
2507	S32750	A 790	0.030	1.2 MAX	0.035	0.020	0.8 MAX	24.0-26.0	6.0-8.0	3.0-5.0	0.24-0.32	**CU, 0.5 MAX**
329	S32900	A 240, A 790	0.08	1.00 MAX	0.040	0.030	0.75 MAX	23.0-28.0	2.50-5.00	1.0-2.0	. . .	**. . .**
. . .	S32950	A 240, A 790	0.03	2.00 MAX	0.035	0.010	0.60 MAX	26.00-29.00	3.50-5.20	1.00-2.50	0.15-0.35	**. . .**
CD-4MCU	**. . .**	**A 743**	**0.40**	**1.00 MAX**	**0.04**	**0.04**	**1.00 MAX**	**24.5-26.5**	**4.75-6.00**	**1.75-2.25**	**. . .**	**CU, 2.75-3.35**

TABLE 5(B) PROPERTIES AND FILLER METALS FOR DUPLEX FERRITIC-AUSTENITIC STAINLESS STEELS

DESIGNATION	UNS NO.	ASTM SPECIFICATION	TENSILE STRENGTH		YIELD STRENGTH		ELONGATION, %	MATCHING FILLER METALS		
			MPA	KSI	MPA	KSI		A5.4	A5.9(A)	A5.22
XM-26	S31100	A 276	620	90	450	65	20	. . .	. . .	. . .
. . .	S31200	A 240	690	100	450	65	25	. . .	. . .	. . .
. . .	S31260	A 240	690	100	480	70	20	. . .	. . .	. . .
. . .	S31500	A 790	635	92	440	64	30	. . .	. . .	. . .
2205	S31803	A 240, A 790	620	90	450	65	25	E2209-XX	ER2209	. . .
2304	S32304	A 790	600	87	400	58	25	. . .	. . .	. . .
255	S32550	A 240, A 790	760	110	550	80	15	E2553-XX	ER2553	. . .
2507	S32750	A 790	800	116	550	80	15	. . .	. . .	. . .
329	S32900	A 240, A 790	620	90	480	70	15	. . .	. . .	. . .
. . .	S32950	A 240, A 790	690	100	480	70	15	. . .	. . .	. . .
CD-4MCU	**. . .**	**A 743**	**690**	**100**	**480**	**70**	**16**	**E2553-XX**	**ER2553**	**. . .**

(A) METAL-CORED ELECTRODES, INDICATED BY A "C" IN PLACE OF THE "R" IN THE CLASSIFICATION, ARE ALSO INCLUDED.

It is common to estimate pitting resistance of these alloys according to a pitting resistance equivalent (PRE_N). Various expressions have been used to calculate pitting resistance. The most common is (Ref 24):

$$PRE_N = \%CR + 3.3(\%MO) + 16(\%N)$$

When the PRE_N exceeds 40, the duplex stainless steel is said to be a "super duplex." A critical pitting temperature (CPT) of approximately 80 °C (180 °F) in a 6% ferric chloride solution is typically observed with super duplex stainless grades. New alloy developments in this area have led to several proprietary grades that are not yet addressed in ASTM standards.

Of the duplex stainless steels, the most common is probably type 2205. It is used in pressure vessels, piping, valves, fittings, and pumps for offshore oil collection and processing; chemicals handling; desalinization; and paper mills. Its CPT is on the order of 30 °C (85 °F). More-severe environments may require the use of a duplex stainless steel with 25% Cr, of which alloy 255 is the most common. It generally offers a CPT of 35 °C (95 °F) or higher. For the most severe environments that promote SCC, pitting, and crevice corrosion, the super duplex stainless steels are finding increasing application.

Because of their high yield strengths, duplex stainless steels are more difficult to cold form than are the austenitic stainless steels. Further, because of the various high-temperature embrittlements that can occur in these alloys, forging and other hot-working processes require more care than do the same processes with austenitic stainless steels.

Engineering for Use in the As-Welded Condition. As noted above, a weld metal with a matching composition to that of duplex stainless steels often has inferior ductility and toughness, because of a high ferrite content. This problem is less critical with inert gas-shielded weld metals (GTAW or GMAW process), when compared with flux-shielded weld metals (SMAW, SAW, or FCAW processes), but it is still significant. The safest procedure for the as-welded condition is to use a filler metal that matches the base metal in all respects, except that is has a higher nickel content. It is usually better to avoid autogenous welds, especially with the very rapid cooling rates that are typical of EBW or LBW processes. With the GTAW process, especially for the root pass, it is important to design the welding procedure to limit dilution of the weld metal by the base metal. This often means using a wider than normal root opening and more filler metal in the root than one would use for an austenitic stainless steel joint.

The AWS specifications only classify two filler-metal compositions for the duplex stainless steels. The 2209 filler metal composition, used as a covered electrode for the SMAW process or as a bare wire for SAW, GTAW, GMAW, plasma arc welding (PAW), and other welding processes, is a match for type 2205 base metal, except that it has a higher nickel content, which is necessary for proper ferrite control, ductility, and toughness. It can also be used for any lower-alloyed duplex stainless. The 2553 filler metal composition, used as a covered electrode or as a bare wire, is a match for alloy 255 base metal. In general, it can also be used for all lower-alloyed base metals. This leaves only the super duplex alloys, such as 2507, without an acceptable matching or overmatching filler metal in the AWS specifications. The supplier of such base metals should be contacted for welding filler-metal recommendations.

For submerged arc welding of the duplex stainless steels, high-basicity fluxes generally provide the best results, especially if weld-metal toughness is a concern. The toughness of duplex stainless steel weld metal is strongly sensitive to oxygen content, and basic fluxes provide the lowest weld-metal oxygen content with a given wire. Because fluxes for submerged arc welding of stainless steels are not classified by the AWS, the manufacturer is the best source of information regarding flux selection.

Welding procedure development for use in the as-welded condition, in addition to filler-metal selection, involves hydrogen considerations, preheat, interpass temperature, and welding heat input. In the past, argon-hydrogen gas mixtures have been utilized to some extent in the GTAW process to achieve better wetting and bead shape. However, instances of significant hydrogen embrittlement of GTAW weldments made with argon-hydrogen gas mixtures have occurred, and this practice is best avoided for weldments used in the as-welded condition.

Covered electrodes for use in the SMAW process should be treated as low-hydrogen electrodes for low-alloy steels, that is, they should be kept in sealed containers provided by their manufacturer until they are ready for use. Alternatively, they should be held in heated ovens, typically at 125 to 175 °C (260 to 350 °F), and exposure to a humid atmosphere should be limited to a few hours, at most.

In contrast to the situation with low-alloy steels, preheat and interpass temperature control are not practiced with duplex stainless steel weldments for the purpose of hydrogen cracking protection, but for HAZ microstructure control. A minimum preheat of 100 °C (212 °F) and a maximum interpass temperature of 200 °C (390 °F) can be recommended for most duplex stainless steel weldments. This modest preheat/interpass temperature helps to slow the cooling rate to promote more-extensive austenite formation in the HAZ, without posing potential problems with α' embrittlement.

A limitation on welding heat input also serves to promote austenite formation in the HAZ, as well as in the weld metal. Heat input below approximately 1.2 kJ/mm (30 kJ/in.) tends to result in undesirably high ferrite content in the HAZ and, sometimes, in the weld metal. Further, heat input levels above approximately 4 kJ/mm (100 kJ/in.) tend to produce excessive grain growth in the HAZ and, sometimes, in the weld metal, which reduces toughness and may also promote chromium nitride precipitation (Ref 25).

Engineering for Use in the Postweld Heat Treated Condition. Longitudinal seams in pipe lengths, welds in forgings, and repair welds in castings are often annealed after welding. This involves heating to 1040 °C (1900 °F) or higher, followed by rapid cooling, usually a water quench, to avoid σ phase. Annealing permits the use of either an exactly matched filler metal or no filler metal at all, because proper annealing adjusts the phase balance to near equilibrium. Slow heating to annealing temperature permits σand other phases to precipitate during heating, because the precipitation of σ phase occurs in only a few minutes at 800 °C (1470 °F). The production of pipe lengths often includes very rapid induction heating of the pipe, so that the σ phase is completely avoided during heating, and only a brief hold near 1040 °C (1900 °F) is necessary to accomplish phase balance control.

Furnace annealing can produce slow heating. Therefore, σ phase can be expected to form during heating. It is necessary to hold at the annealing temperature for longer times (perhaps an hour or more) to ensure that all σ is dissolved. However, properly mn continuous furnaces can provide high heating rates, especially for light-wall tubes and other thin sections. If the precipitation of σ phase during heating can be avoided, long anneals are not necessary. The extremely low creep strength of duplex stainless steels at their annealing temperatures can result in severe distortion during annealing. Rapid cooling to avoid σ phase also can contribute to distortion that is due to annealing.

High-nickel filler metals can present a special problem when the weldment is to be annealed. A higher nickel content raises the minimum temperature needed to dissolve the σ phase; temperatures as high as 1100 °C (2010 °F) may be needed at levels of 9 to 10% nickel (Ref 21), especially when the molybdenum content exceeds about 3%.

A very significant loss in weld metal yield strength occurs during the annealing of duplex stainless steel weld metals (Ref 21). In the as-welded condition, the yield strength of duplex stainless weld metal, whether matching nickel (approximately 5 to 6% Ni in the weld, as in the base metal) or high nickel (approximately 8 to 10% Ni in the weld), far exceeds base-metal minimum requirements. But after annealing, especially a furnace anneal, the yield strength of the weld metal usually falls to near (or even below) base-metal minimum requirements. It is thought that the strength loss is due to loss of coherence at the austenite-ferrite interfaces. Wrought base metal does not seem to be as badly affected, partly because hot working markedly textures it, that is, it aligns ferrite and austenite in stringers parallel to the rolling direction. Higher nitrogen contents (over 0.2%) in the weld metal may be necessary to maintain weld metal-yield strength after annealing (Ref 21).

Annealing in air causes a tenacious oxide to form on the surface of the duplex stainless steels. This must be removed to obtain optimal corrosion resistance of the weldment. Pickling with nitric plus hydrofluoric acid solutions, rinsing with clear water, and passivation with a nitric acid solution usually produces the optimum corrosion resistance with duplex stainless steels. The steel supplier can provide optimal solution concentrations for each alloy.

References cited in this section

21. D.J. KOTECKI, HEAT TREATMENT OF DUPLEX STAINLESS STEEL WELD METALS, *WELD. J.*, VOL 68 (NO. 11), 1989, P 431S-441S
22. C.D. LUNDIN, K. KIKUCHI, AND K.K. KHAN, "PHASE 1 REPORT: MEASUREMENT OF DIFFUSIBLE HYDROGEN CONTENT AND HYDROGEN EFFECTS ON THE CRACKING POTENTIAL OF DUPLEX STAINLESS STEEL WELDMENTS," WELDING RESEARCH COUNCIL, MARCH 1991
23. U. FEKKEN, L. VAN NASSAU, AND M. VERWEY, "HYDROGEN INDUCED CRACKING IN

AUSTENITIC/FERRITIC DUPLEX STAINLESS STEEL," PAPER 26, INTERNATIONAL CONFERENCE ON DUPLEX STAINLESS STEEL (THE HAGUE), NEDERLANDS INSTITUUT VOOR LASTECHNIEK, 26-28 OCT 1986

24. L. VAN NASSAU, H. MEELKER, AND J. HILKES, "WELDING DUPLEX AND SUPER-DUPLEX STAINLESS STEELS," DOCUMENT II-C-893-92, INTERNATIONAL INSTITUTE OF WELDING, 1992
25. I. VAROL, W.A. BAESLACK III, AND J.C. LIPPOLD, "FINAL REPORT: WELD CRACKING AND SOLID-STATE PHASE TRANSFORMATION CHARACTERISTICS IN DUPLEX STAINLESS STEELS," WELDING RESEARCH COUNCIL, 30 JUNE 1989

Welding of Stainless Steels

D.J. Kotecki, The Lincoln Electric Company

Welding Process and Parameter Selection for Stainless Steels

Stainless steels of all types are weldable by virtually all welding processes. In part, process selection is often dictated by available equipment. Perhaps the simplest and most universal welding process is manual SMAW with coated electrodes. It has been applied to material as thin as 1.2 mm (0.05 in.), and there is no upper limit on thickness. Other very commonly used processes for stainless steels are GTAW, GMAW, SAW, FCAW, and several forms of resistance welding. The PAW, LBW, and EBW processes are also used.

Detailed discussion of all of the possible processes and parameters is beyond the scope of this article. However, the common arc welding processes are briefly discussed below, especially with regard to procedure and technique errors that can lead to loss of ferrite control with the common austenitic stainless steel weld metals that are designed to contain a small amount of ferrite (that is, solidify as primary ferrite) for protection from hot cracking.

Shielded-Metal Arc Welding. The ANSI/AWS A5.4-92 specification provides for five different electrode coating types. If the alloy to be deposited were type 308, then the five coating types would be typified by the following five electrode classifications: E308-15, E308-16, E308-17, E308-25, and E308-26. Of these, the E308-25 and E308-26 are typically very heavily coated electrodes, often made with mild-steel or lower-alloyed core wire, with all or most of the alloying elements in the coating. For these two coating types (-25 and -26), the various commercial products are not sufficiently alike to permit a statement to be made about typical current ranges for the various sizes. The -25 coating type is recommended only for direct current, electrode positive (DCEP). The -26 coating type is recommended for alternating current, as well as DCEP. Both the -25 and -26 coating types are generally limited to welding in the flat and horizontal positions. The remaining three coating types are very well standardized in existing commercial products, although the -17 type has been classified separately from the -16 type only since the 1992 edition of the ANSI/AWS A5.4 specification.

The -15 coating type is recommended for welding on DCEP only. Its slag system, which generally consists of lime and fluorspar, permits the easiest out-of-position welding of all of the stainless steel electrode coating types, especially for fixed-position pipe welding. It tends to produce a convex weld surface profile, which provides the best cracking resistance when primary ferrite solidification is not achieved. It usually requires more welder skill to make attractive-appearing welds, but it also has the greatest resistance to porosity when the electrode is exposed to moisture or when the careless welder draws a long arc. Its arc is relatively harsh, and surface ripple is coarse. In general, it produces more spatter than the other coating types.

The -16 coating type is recommended for welding both DCEP and alternating current. Its slag system, which is very high in titanium dioxide, permits fairly easy out-of-position welding, but it is generally necessary to weave slightly for vertical-up welding, which is not necessary for the -15 coating type. It tends to produce a nearly flat surface profile. The characteristics of the -16 coating that are not quite as good as those of the -15 coating type, but are more than adequate for most purposes, are its weld metal cracking resistance when no ferrite is formed; the resistance of the coating to porosity, which is due to either moisture pickup or the drawing of a long arc; and its out-of-position weldability. Its weld surface appearance, spatter level, and slag removal are generally more attractive than those of the -15 coating type.

The -17 coating type is a modification of the -16 coating type, produced by substituting silica and silicates for some of the titanium dioxide, which welds both DCEP and alternating current. The use of this coating type and a comparison to the -16 coating type were described earlier in the section on engineering for use of austenitic stainless steels in the as-welded condition.

Table 6 lists typical welding current ranges for the three more-standardized electrode coating types. Welding voltage is determined by the arc length that the welder holds. Some -16 coated electrodes, and most -17 electrodes, can be used by dragging the coating on the base-metal surface, which maintains a short arc length. This length is generally desirable, because a longer arc length permits more air to enter the arc and the weld metal. Nitrogen from the air can be picked up by the weld metal and become an alloying element. This means that the careless welder who draws a long arc with an electrode designed to produce primary ferrite solidification can add enough nitrogen to change the solidification mode to primary austenite (refer to Fig. 3, which shows that nitrogen promotes austenite and suppresses ferrite). This can result in hot cracks in a weld metal, caused by electrodes designed to produce sufficient ferrite to avoid hot cracking. The -15 coating type is the least sensitive to this error, whereas the -17 coating type is generally the most sensitive.

TABLE 6 TYPICAL CURRENT RANGES FOR STAINLESS STEEL SMAW ELECTRODES

ELECTRODE DIAM		CURRENT (DCEP), A		
MM	**IN.**	**FOR E3XX-15**	**FOR E3XX-16(A)**	FOR E3XX-17(A)
1.6	1/16	20-40	20-40	**. . .**
2.0	5/64	30-50	30-50	**35-55**
2.4	3/32	30-70	40-70	**40-80**
3.2	1/8	45-95	60-100	**75-110**
4.0	5/32	75-130	90-140	**95-150**
4.8	3/16	95-165	120-185	**130-200**
6.4	1/4	**150-225**	**200-300**	**. . .**

(A) CURRENT RANGES ARE TYPICALLY 10% HIGHER WHEN ALTERNATING CURRENT IS USED FOR E3XX-16 OR E3XX-17 ELECTRODES.

Figure 16 provides the suggested procedures for the SMAW of butt joints in stainless steel sheet and plate in the flat position. Figure 17 provides the suggested procedures for butt welds in the vertical and overhead positions. Figure 18 addresses fillet welds in the flat or horizontal positions. Figure 19 considers lap joints, and Fig. 20 considers comer joints. The information in these figures is meant only as a starting point in procedure development. Although originally developed for austenitic stainless steels, the procedures are also reasonable starting points for other stainless steels within the guidelines given elsewhere in this article.

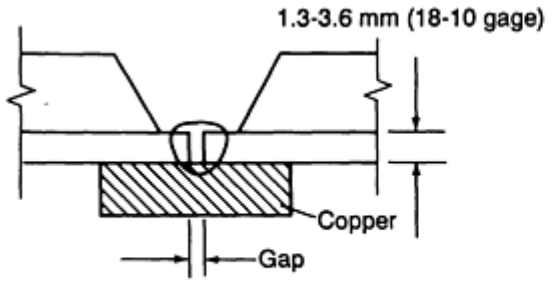

Joint A

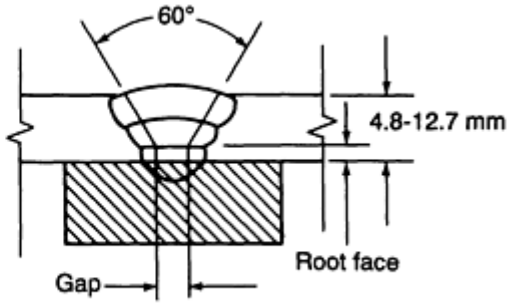

Joint B

PLATE THICKNESS			ELECTRODE DIAMETER				CURRENT (DCEP)[A], A		ARC SPEED				AMOUNT OF ELECTRODE REQUIRED		TOTAL TIME OF WELD		GAP		ROOT FACE	
			FIRST PASS		ADDITIONAL PASSES				FIRST PASS		ADDITIONAL PASSES									
mm	**in.**	**gage**	**mm**	**in.**	**mm**	**in**	**First pass**	**Additional passes**	**mm/s**	**in./min**	**mm/s**	**in./min**	**kg/m**	**lb/ft**	**h/m**	**h/ft**	**mm**	**in.**	**mm**	in.
JOINT A																				
1.3	0.050	18	2.0	5/64	. . .	. . .	40[B]	. . .	5.9-6.8	14-16	. . .	. . .	0.030	0.020	0.0436	0.0133	0	0	0	**0**
2.0	0.078	14	2.4	3/32	. . .	. . .	60	. . .	4.9-5.3	11.5-12.5	. . .	. . .	0.057	0.038	0.0548	0.0167	0.8	1/32	0	**0**
3.6	0.140	10	3.2	1/8	. . .	. . .	85	. . .	3.6-4.0	8.5-9.5	. . .	. . .	0.119	0.080	0.0728	0.0222	0.8	1/32	0	**0**
JOINT B																				
4.8	0.19	. . .	4.0	5/32	. . .	. . .	125	. . .	2.8-3.1	6.7-7.3	. . .	. . .	0.223	0.150	0.0938	0.0286	1.6	1/16	1.6	1/16
6.4	0.25	. . .	4.0	5/32	4.8[C]	3/16 [C]	125	160[C]	2.4-2.7	5.7-6.3	3.2-3.6(C)	7.6-8.5[C]	0.506	0.340	0.1913	0.0583	2.4	3/32	1.6	1/16
9.5	0.38	. . .	4.0	5/32	4.8[D]	3/16 [D]	125	160[D]	2.4-2.7	5.7-6.3	2.4-2.7[D]	5.7-6.3[D]	0.968	0.650	0.3281	0.100	2.4	3/32	1.6	1/16
12.7	**0.50**	**. . .**	**4.0**	5/32	**4.8[E]**	3/16 **[E]**	**125**	**160[E]**	**2.4-2.7**	**5.7-6.3**	**2.4-2.7[E]**	**5.7-6.3[E]**	**1.579**	**1.06**	**0.5479**	**0.167**	**2.4**	3/32	**1.6**	1/16

(A) ALTERNATING CURRENT CAN BE USED WITH 10% INCREASE IN CURRENT; E3XX-15 ELECTRODE CAN BE USED WITH 10% DECREASE IN CURRENT.

(B) USE DCEN.

(C) PASS 2.

(D) PASSES 2 AND 3.

(E) PASSES 2 THROUGH 5

FIG. 16 SUGGESTED PROCEDURES FOR SMAW OF BUTT JOINTS IN AUSTENITIC STAINLESS STEEL FROM 1.3 MM (0.05 IN., OR 18 GAGE) TO 12.7 MM (0.5 IN.) IN THICKNESS IN THE FLAT POSITION. E3XX-16 ELECTRODE. SOURCE: REF 26

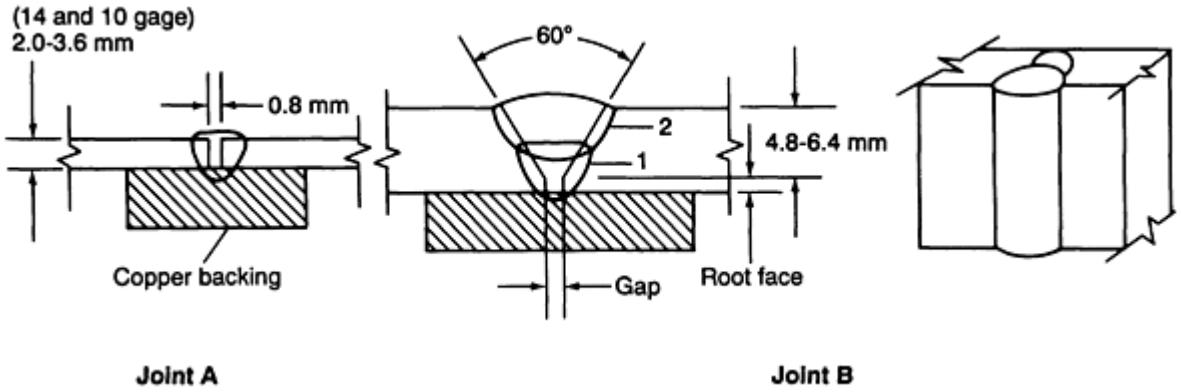

PLATE THICKNESS			ELECTRODE DIAMETER		CURRENT (DCEP), A	ARC SPEED				AMOUNT OF ELECTRODE REQUIRED		TOTAL TIME OF WELD		GAP		ROOT FACE	
						FIRST PASS		SECOND PASS									
MM	IN.	GAGE	MM	IN.		mm/s	in./min	mm/s	in/min	kg/m	lb/ft	h/m	h/ft	mm	in.	mm	in.
JOINT A																	
2.0[A]	0.078[A]	14	2.4	3/32	50	5.9-6.8	14-16	. . .	. . .	0.045	0.030	0.0436	0.0133	0	0	0	**0**
3.6	0.140	10	3.2	1/8	75	2.8-3.1	6.7-7.3	. . .	. . .	0.136	0.091	0.0938	0.0286	0	0	0	**0**
JOINT B																	
4.8	3/16	. . .	4.0	5/32	110	2.2-2.5	5.2-5.8	. . .	. . .	0.238	0.160	0.1194	0.0364	1.6	1/16	1.6	1/16
6.4	1/4	**. . .**	**4.0**	5/32	**L10**	**2.2-2.5**	**5.2-5.8**	**1.8-2.0**	**4.3-4.7**	**0.551**	**0.370**	**0.2651**	**0.0808**	**2.4**	1/16	**1.6**	1/16

FIG. 17 SUGGESTED PROCEDURES FOR SMAW OF BUTT JOINTS IN AUSTENITIC STAINLESS STEEL FROM 2.0 MM (0.08 IN., OR 14 GAGE) TO 6.4 MM (0.25 IN.) IN THICKNESS IN THE VERTICAL AND OVERHEAD POSITIONS. E3XX-15 ELECTRODE. SOURCE: REF 26

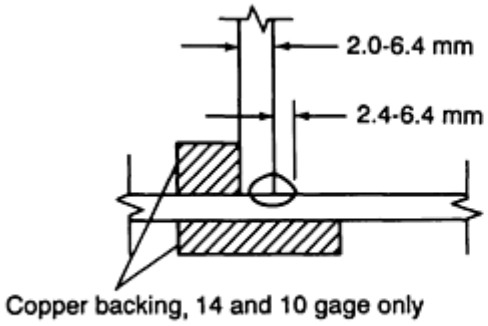

Joint A

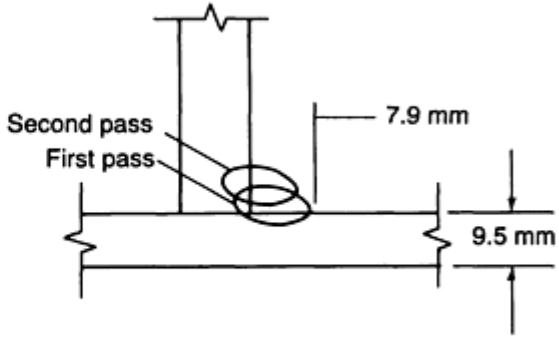

Joint B

PLATE THICKNESS			WELD SIZE		ELECTRODE DIAMETER		CURRENT (DCEP)(A), A	ARC SPEED				AMOUNT OF ELECTRODE REQUIRED		TOTAL TIME OF WELD	
								FIRST PASS		SECOND PASS					
mm	in.	gage	mm	in.	mm	in.		mm/s	in./min	mm/s	in./min	kg/m	lb/ft	h/m	h/ft
JOINT A															
2.0	0.078	14	2.4	3/32	2.4	3/32	60	5.3-5.7	12.5-13.5	. . .	. . .	0.054	0.036	0.051	**0.0154**
3.6	0.140	10	3.2	1/8	3.2	1/8	85	5.3-5.7	12.5-13.5	. . .	. . .	0.083	0.056	0.051	**0.0154**
4.8	3/16	. . .	4.8	3/16	4.0	5/32	120	3.6-4.0	8.6-9.4	. . .	. . .	0.178	0.120	0.073	**0.0222**
6.4	1/4	. . .	6.4	1/4	4.8	3/16	160	2.6-2.9	6.2-6.8	. . .	. . .	0.328	0.220	0.101	**0.0308**
JOINT B															
9.5	3/8	**. . .**	**7.9**	5/16	**4.8**	3/16	**170**	**2.6-2.9**	**6.2-6.8**	**2.8-3.1**	**6.7-7.3**	**0.640**	**0.430**	**0.195**	**0.0594**

Note: For vertical and overhead welding position, use same procedures as for vertical and overhead butt welds.

(A) ALTERNATING CURRENT CAN BE USED WITH A 10% INCREASE IN CURRENT; E3XX-15 ELECTRODE CAN BE USED WITH A 10% DECREASE IN CURRENT.

FIG. 18 SUGGESTED PROCEDURES FOR SMAW OF FILLET JOINTS IN AUSTENITIC STAINLESS STEEL FROM 2.0 MM (0.08 IN., OR 14 GAGE) TO 9.5 MM (0.38 IN.) IN THICKNESS IN THE FLAT OR HORIZONTAL POSITIONS. E3XX-16 ELECTRODE. SOURCE: REF 26

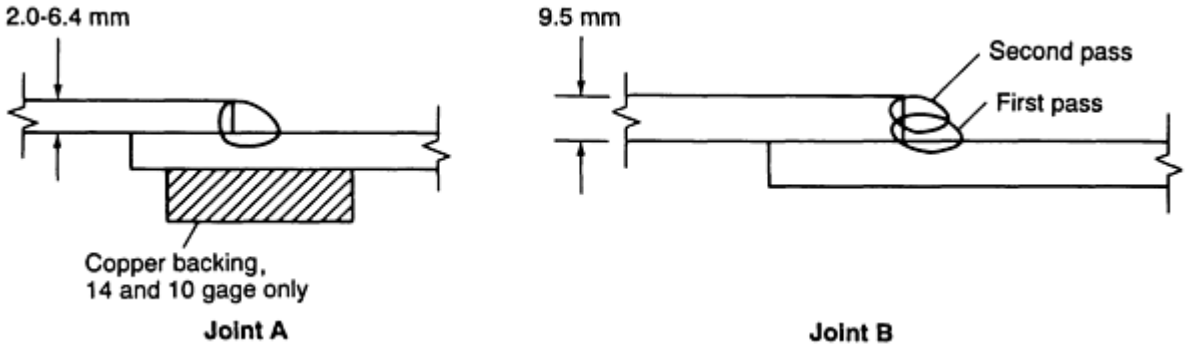

PLATE THICKNESS			ELECTRODE DIAMETER		CURRENT (DCEP)[A], A	ARC SPEED				AMOUNT OF ELECTRODE REQUIRED		TOTAL TIME OF WELD	
						FIRST PASS		SECOND PASS					
mm	**in.**	**gage**	**mm**	**in.**		**mm/s**	**in./min**	**mm/s**	**in./min**	**kg/m**	**lb/ft**	**h/m**	h/ft
JOINT A													
2.0	0.078	14	2.4	3/32	60	5.3-5.7	12.5-13.5	. . .	. . .	0.054	0.036	0.051	**0.0154**
3.6	0.140	10	3.2	1/8	90	5.3-5.7	12.5-13.5	. . .	. . .	0.083	0.056	0.051	**0.0154**
4.8	3/16	. . .	4.0	5/32	125	3.6-4.0	8.6-9.4	. . .	. . .	0.194	0.130	0.073	**0.0222**
6.4	1/4	. . .	4.8	3/16	170	2.6-2.9	6.2-6.8	. . .	. . .	0.357	0.240	0.101	**0.0308**
JOINT B													
9.5	3/8	**. . .**	**4.8**	3/16	**175**	**2.6-2.9**	**6.2-6.8**	**2.8-3.1**	**6.7-7.3**	**0.685**	**0.460**	**0.195**	**0.0594**

(A) ALTERNATING CURRENT CAN BE USED WITH A 10% INCREASE IN CURRENT; E3XX-15 ELECTRODE CAN BE USED WITH A 10% DECREASE IN CURRENT.

FIG. 19 SUGGESTED PROCEDURE FOR SMAW OF LAP JOINTS IN AUSTENITIC STAINLESS STEEL FROM 2.0 MM (0.08 IN., OR 14 GAGE) TO 9.5 MM (0.38

IN.) IN THICKNESS IN THE HORIZONTAL POSITION. E3XX-16 ELECTRODE. SOURCE: REF 26

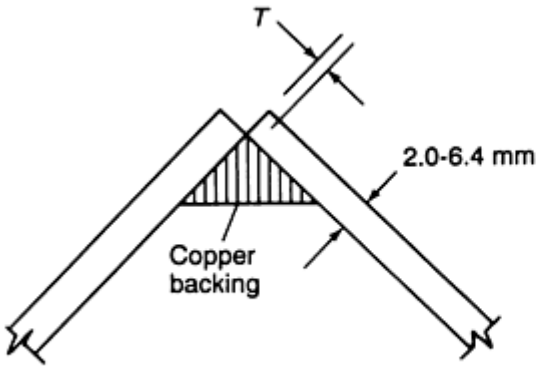

Joint A

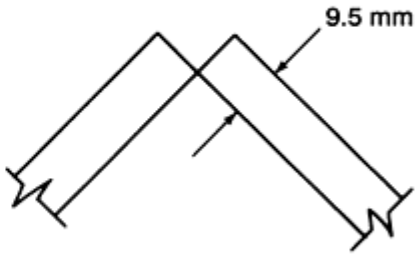

Joint B

PLATE THICKNESS			ELECTRODE DIAMETER		CURRENT (DCEP)[A], A		ARC SPEED				AMOUNT OF ELECTRODE REQUIRED		TOTAL TIME OF WELD		THICKNESS, *T*	
							FIRST PASS		SECOND PASS							
mm	**in.**	**gage**	**mm**	**in.**	**FIRST PASS**	**SECOND PASS**	**mm/s**	**in./min**	**mm/s**	**in./min**	**kg/m**	**lb/ft**	**h/m**	**h/ft**	**mm**	in.
JOINT A																
2.0	0.078	14	2.4	3/32	60	. . .	5.9-6.8	14-16	. . .	. . .	0.042	0.028	0.0436	0.0133	1.0	**0.04**
3.6	0.140	10	3.2	1/8	85	. . .	5.3-5.7	12.5-13.5	. . .	. . .	0.083	0.056	0.0505	0.0154	0.8	1/32
4.8	3/16	. . .	4.0	5/32	125	. . .	4.4-4.9	10.5-11.5	. . .	. . .	0.140	0.094	0.0597	0.0182	1.2	3/64
6.4	1/4	. . .	4.8	3/16	160	. . .	2.6-2.9	6.2-6.8	. . .	. . .	0.33	0.22	0.101	0.0308	1.6	1/16
JOINT B																
9.5	3/8	**. . .**	**4.8**	3/16	**160**	**175**	**2.6-2.9**	**6.2-6.8**	**2.4-2.7**	**5.7-6.3**	**0.67**	**0.45**	**0.210**	**0.0641**	**0**	**0**

FIG. 20 SUGGESTED PROCEDURE FOR SMAW OF CORNER JOINTS IN AUSTENITIC STAINLESS STEEL FROM 2.0 MM (0.08 IN., OR 14 GAGE) TO 9.5 MM (0.38 IN.) IN THICKNESS IN THE FLAT POSITION. E3XX-16 ELECTRODE. SOURCE: REF 26

Submerged Arc Welding. The ANSI/AWS A5.9-92 specification classifies both solid and composite (metal-cored tubular or stranded) wires that can be used for several welding processes, including submerged arc welding. Wires are classified only on the basis of their composition and whether they are solid or composite. For the ferrite-containing austenitic grades, the chromium content of a wire of a given alloy type is generally shifted to a higher level for the wires, compared with SMAW electrodes. For example, the chromium content for E308-XX electrodes ranges from 18.0 to 21.0%, but for ER308 wire, it is 19.5 to 22.0%. There is a good reason for this. The composition requirements for SMAW electrodes are for the all-weld metal deposit, that is, the finished weld, whereas the requirements for the wires are for the wire composition, the tool that is used to produce the finished weld. Some loss of chromium is to be expected in transferring the metal across the arc in SAW, as well as in gas-shielded processes. In the SAW process, chromium recovery depends strongly on the specific flux chosen and on the choice of welding parameters.

The AWS filler-metal specifications do not classify fluxes for the submerged arc welding of stainless steels. However, practical experience indicates that there are essentially three groupings of SAW fluxes with respect to chromium recovery. In submerged arc welding of carbon steels and low-alloy steels, it is common to describe fluxes as "neutral" or "active," depending on whether manganese and silicon content of the deposited weld metal vary appreciably with changes in arc voltage or flux-to-wire ratio. However, a flux that is neutral with respect to manganese and silicon recovery may be very aggressive in removing chromium from the weld metal. Therefore, "neutral" and "active" descriptions from the ANSI/AWS A5.17 (mild-steel submerged arc) or ANSI/AWS A5.23 (low-alloy submerged arc) specifications have no meaning with regard to stainless steel.

A somewhat quantitative grouping of fluxes for stainless steels relates all-weld metal chromium content to wire chromium content. A number of fluxes that are high in manganese silicate and the other oxides that are less stable than chromium oxide tend to deplete the chromium of the deposit on the order of 2%, or even more, in absolute terms. With such a flux, a wire of 21% Cr is likely to produce a deposit of only 19% Cr, which fits well with the higher chromium content of the wires of ANSI/AWS A5.9, when compared with the electrodes of ANSI/AWS A5.4. With such fluxes, a higher arc voltage, or any other change that tends to increase the ratio of flux melted to wire melted, will tend to reduce the chromium recovery further. These fluxes are sometimes referred to as "acid" fluxes.

A second group of fluxes for stainless steels are those composed primarily of oxides of calcium, magnesium, titanium, and aluminum, along with calcium fluoride. These compounds are more stable than chromium oxide. Fluxes of this group tend to produce only a small loss of chromium, typically on the order of 0.5 to 1.0%, in absolute terms, when compared with the wire compositions. With such fluxes, a higher voltage, or any other change that tends to increase the ratio of flux melted to wire melted, produces only a small increase in chromium loss. These fluxes are sometimes referred to as "basic" fluxes.

A third group of fluxes for stainless steels are those that include, in the individual flux particles, particles of chromium metal or alloy. The amount of this chromium is usually only slightly more than that needed to make up for the chromium that is lost to oxidation during welding. Therefore, a small chromium increase, typically on the order of 0.5 to 1%, is observed in the weld metal, when compared with the wire. This chromium gain may increase with increase in arc voltage, or with any other welding parameter change that increases the ratio of flux melted to wire melted. These fluxes are sometimes referred to as "chromium-compensating" fluxes.

Loss of chromium not only means loss of some corrosion resistance, but also loss of ferrite in nominally austenitic stainless steel weld metals that are intended to contain some ferrite. The use of an acid flux is likely to produce about 5 FN less than the Ferrite Number calculated from the wire composition using Fig. 3. The use of a basic flux is likely to produce almost the same Ferrite Number as that calculated from the wire composition using Fig. 3. The use of a chromium-compensating flux is likely to produce as much as 5 FN, or more, greater than the FN value calculated from the wire composition using Fig. 3.

A further consideration in flux selection is carbon recovery with martensitic stainless steels. The acid fluxes tend to remove considerable carbon from high-carbon stainless steels, so that the ability to achieve a given hardness level is affected. The basic fluxes tend to recover nearly all of the wire carbon. The chromium-compensating fluxes can do either, depending on the specific oxide balance in a given flux. The use of either an acid flux or a chromium-compensating flux with a martensitic stainless steel wire like ER410 may produce ferrite stringers in what ought to be a fully martensitic deposit. As a result, the mechanical properties may be inferior.

Submerged arc welding permits much broader ranges of current for a given electrode size than does the SMAW process. Current is largely determined by wire feed speed, although increased electrode extension ("stickout") will decrease current at a given wire feed speed. Figure 21 presents typical wire feed speed ranges for a variety of solid electrode sizes

and the corresponding welding currents with austenitic filler metals. Other current ranges result when either composite or martensitic wires are used, because the electrical resistance of these wires differs from that of the austenitic wires. Nevertheless, Fig. 21 can provide a starting point. In general, as the wire feed speed is increased, a corresponding voltage increase is appropriate for the best bead shape. Typically, 26 to 28 V produce the best results at the bottom end of the wire feed speed range, and 32 to 36 V produce the best results at the top end of the wire feed speed range.

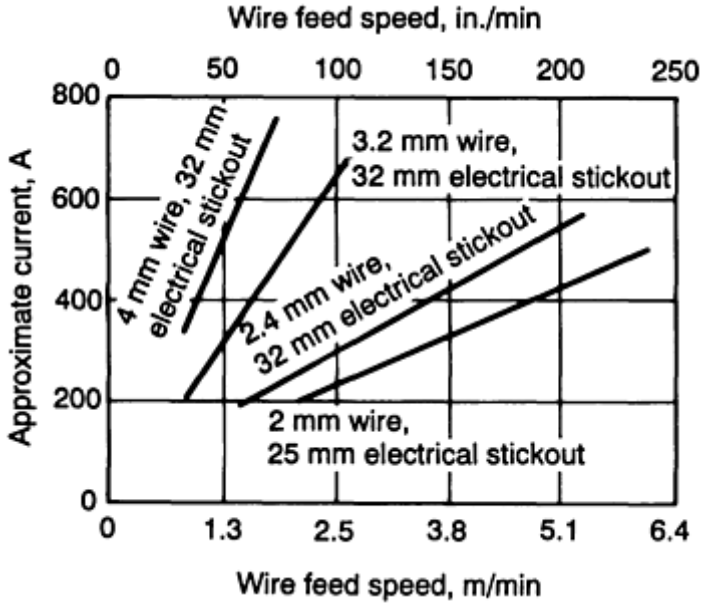

FIG. 21 CURRENT (DCEP) VERSUS WIRE FEED SPEED FOR SUBMERGED ARC WELDING WITH E3XX STAINLESS STEEL ELECTRODES. SOURCE: REF 27

Because there is no classification system for submerged arc fluxes for stainless steels, and because the broad range of chromium recovery that is possible depends on the specific flux chosen, either the advice or literature of the flux manufacturer should be obtained before using an unfamiliar flux.

Figures 22 and 23 provide joint preparations that have proven useful in submerged arc butt welding of stainless steel plate. Figure 24 provides copper backing information for one-side butt welding using the SAW process. Circumferential welding on tubular components is usually done by off-setting the welding head from top-dead-center, so that solidification occurs in the flat position, slightly uphill or slightly downhill. This affects the weld profile, as shown in Fig. 25.

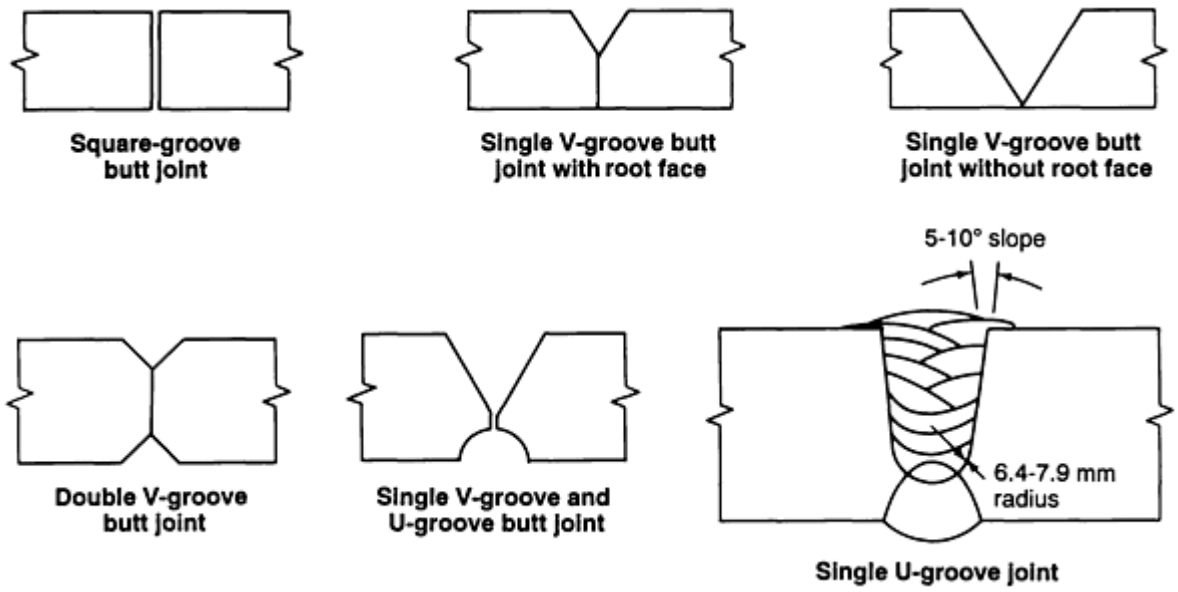

FIG. 22 BUTT JOINT DESIGNS FOR SUBMERGED ARC WELDING. SOURCE: REF 26

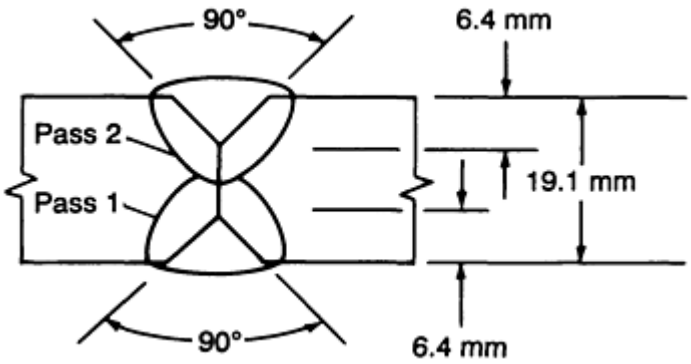

FIG. 23 TYPICAL DOUBLE-V WELD IN TYPE 304 PLATE. PASS 1 WAS MADE AT 700 A AND 33 V, AT 6.8 MM/S (16 IN./MIN). PASS 2 WAS MADE AT 950 A AND 35 V, AT 5.1 MM/S (12 IN./MIN). POWER, DCEP; TYPE 308 ELECTRODE, 4.8 MM ($\frac{3}{16}$ IN.) DIAM; NEUTRAL FLUX. SOURCE: REF 26

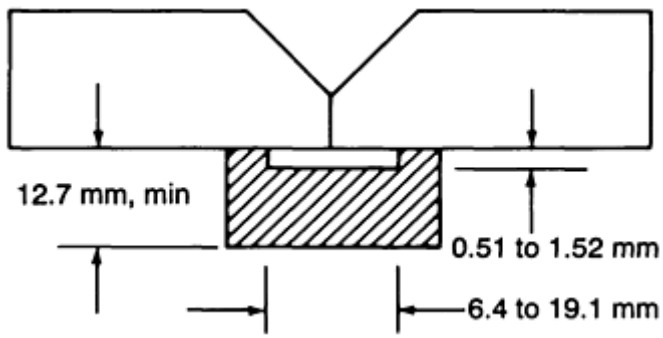

FIG. 24 RECOMMENDED GROOVE DIMENSIONS FOR COPPER BACKING BARS IN THE SUBMERGED ARC WELDING OF STAINLESS STEELS. SOURCE: REF 26

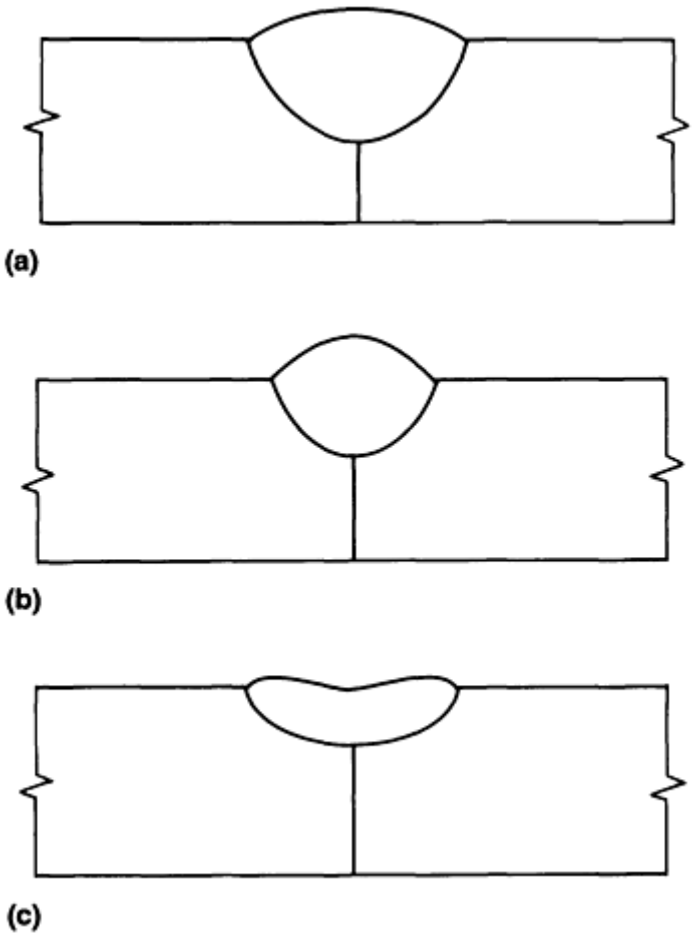

FIG. 25 WELD PROFILES. (A) CONTOUR OF A WELD BEAD IN THE FLAT POSITION WITH THE WORK HORIZONTAL. (B) WELDING SLIGHTLY UPHILL. (C) WELDING SLIGHTLY DOWNHILL. SOURCE: REF 26

Gas-Tungsten Arc Welding. The GTAW process is widely used for welding stainless steels, especially for full-penetration welds in thin-gage materials and root passes in thicker materials. For almost all gas-tungsten arc welding of stainless steels, thoriated tungsten electrodes (ANSI/AWS A5.12 classification EWTh-2) are preferred, and welding utilizes argon gas shielding with direct current, electrode negative (DCEN) polarity. For heavy sections, sometimes helium or argon-helium mixes can be used to achieve greater heat input or higher welding speeds.

Additions of hydrogen (on the order of 5%) to argon gas shielding have also been used, primarily for austenitic stainless steels, to provide higher heat input and a cleaner weld surface. Hydrogen additions are a possible source of embrittlement for all other types of stainless steels. Both manual and automatic procedures are suitable. In automatic welding, a voltage-controlled head can be used to maintain a constant arc length, and either cold-wire or hot-wire filler-metal additions are used.

Many welds in tubing and light-gage material are made without filler-metal additions, using square butt joints, lap joints, edge joints, corner joints, and the like. Then, the weld metal has nearly the same composition as the base metal. When welding austenitic stainless steels such as type 304 or 316, ferrite is usually desirable in the weld metal, but attempts to measure ferrite in the base metal before welding will generally detect no ferrite. This is not a cause for alarm, because the hot-working operations that were conducted to reduce the original stainless steel ingot to the final form generally cause all ferrite in the base metal to be transformed to austenite. Steelmakers generally prefer to adjust the composition of a stainless steel ingot to contain a small amount (typically 3 to 8 FN) of ferrite as cast, because this improves resistance to the ingot breaking up during the first reductions. Thus, their interest is similar to that of the welding engineer. Although no ferrite may be present after hot working, remelting during welding will return the original as-cast ferrite, which means that ferrite is usually found in the weld metal of autogenous joints in types 304, 316, and similar stainless steel alloys.

The potential for ferrite in an autogenous joint can be assessed from the base-metal certified material test report (CMTR) using the WRC-1988 diagram. To be truly useful for this purpose, the CMTR should include nitrogen. If the CMTR indicates that no ferrite is likely in the autogenous weld, then the addition of a filler metal that will provide ferrite ought to be considered, at least for base metals that normally can be expected to provide some ferrite in near-matching weld-metal compositions.

Filler metals for the GTAW process are classified according to the ANSI/AWS A5.9 specification, and many are listed in Tables 1(a), 1(b), 2(a), 2(b), 3(a), 3(b), 4(a), 4(b), 5(a), and 5(b). Similar compositions in the form of consumable inserts, classified to the ANSI/AWS A5.30 specification, are also available for full-penetration root-pass welding. The consumable inserts provide a little surplus filler metal in order to attain an underside profile that is slightly convex. Consumable inserts can also be purchased with a variety of special shapes that assist in joint alignment, especially for welding pipe.

Pipe and tube welds are often made with a backing gas inside in order to prevent oxidation of the root surface. Although argon backing gas is the safest choice, it is more expensive than nitrogen, which has also been used. Small amounts of nitrogen from backing gas can be picked up in the weld metal, and cases are known where such nitrogen pickup was responsible for loss of ferrite and consequent hot cracking. Nevertheless, many successful welds have been made with nitrogen backing gas.

In the gas-tungsten arc welding of fully austenitic stainless steels, it is often advisable to add filler metal even when it does not appear to be needed. The proper addition of filler metal can be used to obtain a convex bead shape, which has better resistance to hot cracking than does the flat or slightly concave weld shape that often results when no filler metal is added. This can be of critical importance when welding fully austenitic stainless steels without cracking.

The successful gas-tungsten arc welding of nominally austenitic stainless steels (the weld metals of which are designed to contain a little ferrite) can depend on the integrity of the gas shield. Drafts, low gas-flow rates, or excessively high gas-flow rates can cause air (which is about 80% nitrogen) to enter the arc. Nitrogen is then picked up by the weld metal, and a weld, which ought to contain ferrite, can be rendered ferrite-free and sensitive to hot cracking. Proper gas-flow rates, typically 0.3 to 0.8 m^3/h (10 to 30 ft^3/h), and barriers that prevent moving air from reaching the arc area can be used to prevent nitrogen pickup. Special attention to the integrity of both shielding gas and backing gas can be especially important in the successful welding of third-generation ferritic stainless steels, which can be embrittled by traces of nitrogen that are picked up during welding.

Gas-tungsten arc welding can be done with a broad range of welding currents for most applications, with travel speed adjusted to make the proper size of weld for the current chosen. Each individual tungsten electrode size has a corresponding proper current range. These current ranges are not particular to stainless steels. Figure 26 provides some welding procedure information for beginning procedure development in the gas-tungsten arc welding of stainless steels.

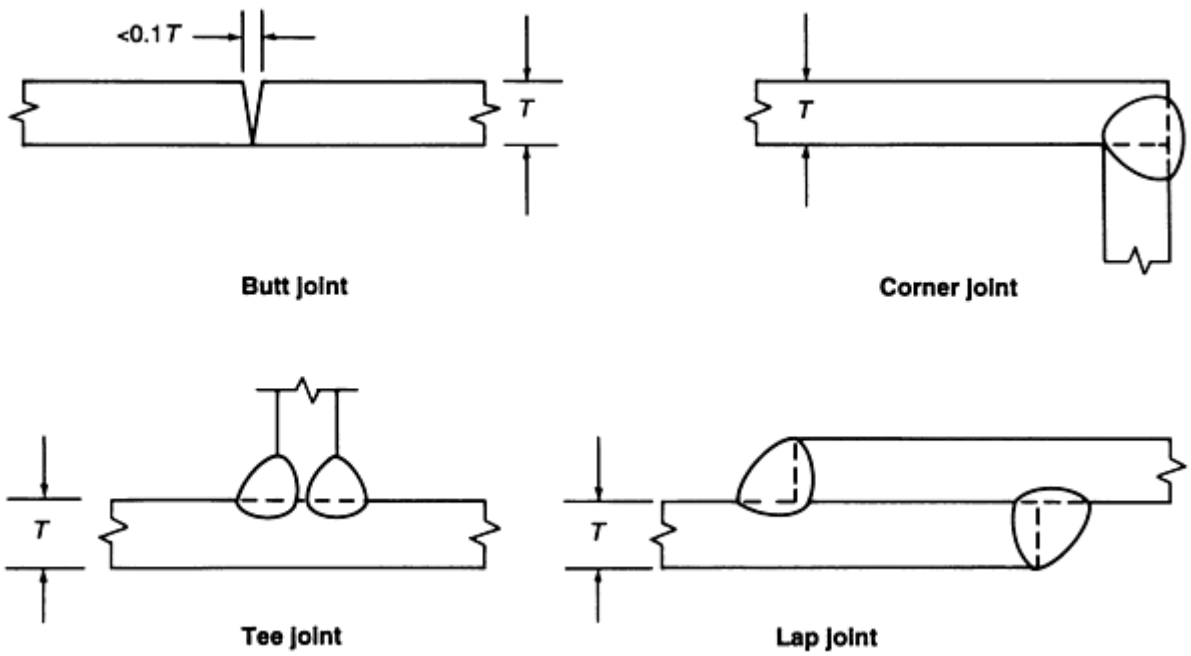

PLATE THICKNESS, *T*		CURRENT DCEN[(A)], A	ELECTRODE DIAMETER		ARGON GAS FLOW		FILLER ROD DIAMETER		ARC SPEED		TOTAL TIME OF WELD	
mm	**in.**		**mm**	**in.**	**m^3/h**	**ft^3/h**	**mm**	**in.**	**mm/s**	**in./min**	**h/m**	h/ft
BUTT AND CORNER JOINTS												
1.6	1/16	80-100	1.6	1/16	0.3	10	1.6	1/16	5.1	12	0.0548	**0.0167**
2.4	3/32	100-120	1.6	1/16	0.3	10	1.6	1/16	5.1	12	0.0548	**0.0167**
3.2	1/8	120-140	1.6	1/16	0.3	10	2.4	3/32	5.1	12	0.0548	**0.0167**
4.8	3/16	200-250	2.4	3/32	0.4	15	3.2	1/8	4.2	10	0.0656	**0.0200**
6.4	1/4	200-350	3.2	1/8	0.56	20	3.2	1/8	3.4	8	0.0820	**0.0250**
12.7	1/2	225-375	3.2	1/8	0.7	25	3.2	1/8	3.4	8	0.0820	**0.0250**
TEE AND LAP JOINTS												
1.6	1/16	90-110	1.6	1/16	0.3	10	1.6	1/16	4.2	10	0.0656	**0.0200**
2.4	3/32	110-130	1.6	1/16	0.3	10	1.6	1/16	4.2	10	0.0565	**0.0200**
3.2	1/8	130-150	1.6	1/16	0.3	10	2.4	3/32	4.2	10	0.0656	**0.0200**
4.8	3/16	225-275	2.4	3/32	0.4	15	3.2	1/8	3.4	8	0.0820	**0.0250**
6.4	1/4	225-350	3.2	1/8	0.56	20	3.2	1/8	3.4	8	0.0820	**0.0250**
12.7	1/2	**225-375**	**3.2**	1/8	**0.7**	**25**	**3.2**	1/8	**3.4**	**8**	**0.0820**	**0.0250**

(A) FOR VERTICAL-UP AND OVERHEAD POSITIONS, DECREASE CURRENT 10 TO 20%.

FIG. 26 SUGGESTED PROCEDURES FOR GTAW OF BUTT, CORNER, TEE, AND LAP JOINTS IN STAINLESS STEELS. SOURCE: REF 26

Special attention should be given to the role of sulfur and other surface-active elements in controlling penetration in full-penetration GTAW welds. It has been amply demonstrated that sulfur levels on the order of 0.005% and lower tend to produce penetration profiles with very low depth-to-width ratios, because of surface tension gradient effects. On the other hand, sulfur levels of 0.010% and higher seem to ensure a high depth-to-width ratio, which is desirable for full-penetration butt welds (Ref 28).

When searching for a small amount of filler metal for a GTAW application, especially in repair situations, it is not uncommon for the welder and/or engineer to be tempted to remove the coating from a covered electrode of nominally matching composition to a given base metal, and to use the core wire for GTAW filler metal. This can be a very risky approach, because the coating of many covered stainless steel electrodes provides alloy elements. The core wire may not be close to the weld-metal composition. For example, it is not uncommon to produce type 347 weld metal from a covered electrode whose core wire is type 308, and has all of the niobium in the coating. It is also not uncommon to produce type 317L covered electrodes using type 316L core wire. Some stainless steel electrodes are made from mild-steel core wire, and have all of the alloy in the coating. Therefore, before attempting a gas-tungsten arc weld with the core wire from a covered electrode, those concerned should contact the electrode manufacturer to determine what core wire was used to make the electrode.

Gas-Metal Arc Welding. The GMAW process is extensively used for joining both thin and thick stainless steel base metals. Filler metals are classified to the ANSI/AWS A5.9 specification, as are filler metals for submerged arc or gas-tungsten arc welding. For many applications with nominally austenitic filler metals that are intended to contain a little ferrite, high-silicon versions of the basic classifications are preferred for better wetting and bead shape. These high-silicon versions contain from 0.65 to 1.00% Si, versus 0.30 to 0.65% for the normal grades.

With thin materials, the short-circuiting transfer mode is primarily used, with 0.9 mm (0.035 in.) and 1.1 mm (0.045 in.) diameters being the most common. The preferred shielding gas is often a mixture of 90% He, 7.5% Ar, and 2.5% CO_2. Helium-rich gases provide higher voltage in short-circuiting transfer welding, resulting in better wetting and fewer problems with lack-of-fusion defects than occur with argon-rich gases. However, argon-rich gas may be preferred for welding on very thin materials. Typical welding conditions for short-circuiting transfer welding are given in Table 7 and Fig. 27. Short-circuiting transfer is usable both in the flat position and out of position.

TABLE 7 PROCEDURE RANGE FOR GAS-METAL ARC WELDING WITH ER3XXLSI ELECTRODES BY SHORT-CIRCUIT TRANSFER MODE

CHARACTERISTICS	**WIRE FEED SPEED**		**APPROXIMATE CURRENT, A**	**ARC VOLTAGE, V(A)**	DEPOSITION RATE	
	M/MIN	**IN./MIN**			**KG/H**	LB/H
FOR A 0.9 MM (0.035 IN.) DIAM ELECTRODE WEIGHING 5.11 G/M (0.003 LB/FT), USING DCEP AND A 13 MM ($\frac{1}{2}$ IN.) ELECTRICAL STICKOUT, WITH A SHIELDING GAS OF 90HE-7$\frac{1}{2}$AR-2$\frac{1}{2}CO_2$	3.0	120	55	19-20	0.9	**2.0**
	3.8	150	75	19-20	1.2	**2.5**
	4.6	180	85	19-20	1.4	**3.0**
	5.2	205	95	19-20	1.6	**3.4**
	5.8	230	105	20-21	1.8	**3.9**
	6.9	275	110	20-21	2.1	**4.6**
	7.6	300	125	20-21	2.3	**5.0**
	8.3	325	130	20-21	2.5	**5.4**
	8.9	350	140	21-22	2.7	**5.9**
	9.5	375	150	21-22	2.9	**6.3**
	10.2	400	160	22-23	3.1	**6.7**
	10.8	425	170	22-23	3.3	**7.1**
FOR A 1.1 MM (0.045 IN.) DIAM ELECTRODE WEIGHING 7.63 G/M (0.0045 LB/FT), USING DCEP AND A 13 MM ($\frac{1}{2}$ IN.) ELECTRICAL STICKOUT, WITH A SHIELDING GAS OF 90HE-7 $\frac{1}{2}$AR-2$\frac{1}{2}CO_2$	2.5	100	100	19-20	1.1	**2.8**
	3.2	125	120	19-20	1.5	**3.5**
	3.8	150	135	21	1.7	**4.2**
	4.4	175	140	21	2.0	**4.8**
	5.6	220	170	22	2.6	**6.1**
	6.4	250	175	22-23	2.9	**6.9**
	7.0	**275**	**185**	**22-23**	**3.2**	**7.6**

(A) ARC VOLTAGES ARE MEASURED FROM THE WIRE FEEDER GUN CABLE BLOCK TO WORK.

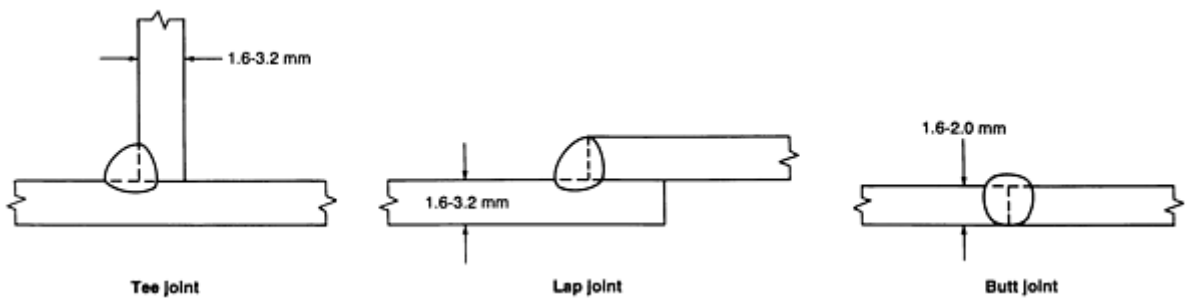

PLATE THICKNESS		**CURRENT (DCEP), A**	**VOLTAGE, V(A)**	**WIRE FEED SPEED**		**WELDING SPEED**		**AMOUNT OF ELECTRODE REQUIRED**		TOTAL TIME OF WELD	
mm	**in.**			**mm/s**	**in./min**	**mm/s**	**in./min**	**kg/m**	**lb/ft**	**h/m**	h/ft

TREE AND LAP JOINTS											
1.6	0.063	85	15	78	184	7.2-8.0	17-19	0.037	0.025	0.0364	**0.0111**
2.0	0.078	90	15	81	192	5.5-6.3	13-15	0.051	0.034	0.0469	**0.0143**
2.4	0.093	105	17	98	232	5.9-6.8	14-16	0.058	0.039	0.0436	**0.0133**
3.2	0.125	125	17	119	280	5.9-6.8	14-16	0.069	0.046	0.0436	**0.0133**
BUTT JOINT											
1.6	0.063	85	15	78	184	8.0-8.9	19-21	0.034	0.023	0.0328	**0.0100**
2.0	**0.078**	**90**	**15**	**81**	**192**	**4.9-5.3**	**11.5-12.5**	**0.058**	**0.039**	**0.0548**	**0.0167**

(A) FOR AR-25 CO_2 OR AR-2O; VOLTAGE IS 6 TO 7V HIGHER FOR HE-7$\frac{1}{2}$AR-2$\frac{1}{2}CO_2$.

FIG. 27 SUGGESTED PROCEDURES FOR GMAW OF BUTT FILLET AND LAP JOINTS IN 200 AND 300 SERIES STAINLESS STEELS USING THE SHORT-CIRCUITING TRANSFER MODE. SHIELDING GAS, ARGON PLUS 25% CO_2 OR ARGON PLUS 2% O_2; GAS FLOW, 0.4 TO 0.6 M^3/H (15 TO 20 FT^3/H); ELECTRODE, 0.8 MM (0.030 IN.) DIAM. SOURCE: REF 26

With thicker materials, the spray-transfer mode is most often used. In addition to the same two common diameters used in short-circuiting transfer, a 1.6 mm ($\frac{1}{16}$ in.) diameter is often used. The most common shielding gases are argon-rich mixtures, such as argon with from 1% to 5% O, argon with a few percent of carbon dioxide, or argon with both oxygen and carbon dioxide added. Typical welding conditions for spray transfer are given in Table 8 and Fig. 28. Spray-transfer welding is limited to the flat and horizontal positions.

TABLE 8 PROCEDURE RANGE FOR GAS-METAL ARC WELDING WITH ER3XXLSI ELECTRODES BY AXIAL SPRAY TRANSFER

CHARACTERISTICS	**WIRE FEED SPEED**		**APPROXIMATE CURRENT, A**	**ARC VOLTAGE, V(A)**	DEPOSITION RATE	
	m/min	**in./min**			**kg/h**	lb/h
FOR A 0.9 MM (0.035 IN.) DIAM ELECTRODE WEIGHING 5.11 G/M (0.003 LB/FT), USING DCEP AND A 13 MM ($\frac{1}{2}$ IN.) ELECTRICAL STICKOUT, WITH A SHIELDING GAS OF 98AR-2O_2	10.2	400	180	23	3.1	**6.7**
	10.8	425	190	24	3.3	**7.1**
	11.4	450	200	24	3.5	**7.5**
	12.1	475	210	25	3.7	**8.0**
FOR A 1.1 MM (0.045 IN.) DIAM ELECTRODE WEIGHING 7.63 G/M (0.0045 LB/FT), USING DCEP AND A 19 MM ($\frac{3}{4}$ IN.) ELECTRICAL STICKOUT, WITH A SHIELDING GAS OF 98AR-2O_2	6.1	240	195	24	2.8	**6.6**
	6.6	260	230	25	3.0	**7.2**
	7.6	300	240	25	3.5	**8.3**
	8.3	325	250	26	3.8	**9.0**
	9.1	360	260	26	4.2	**10.0**
FOR A 1.6 MM ($\frac{1}{16}$ IN.) DIAM ELECTRODE WEIGHING 16.14 G/M (0.01 LB/FT), USING DCEP AND A 19 MM ($\frac{3}{4}$ IN.) ELECTRICAL STICKOUT, WITH A SHIELDING GAS OF 98AR-2O_2	4.4	175	260	26	4.3	**9.2**
	5.1	200	310	29	4.9	**10.5**
	6.4	250	330	29	6.2	**13.1**
	7.0	275	360	31	6.8	**14.4**
	7.6	**300**	**390**	**32**	**7.4**	**15.8**

(A) ARC VOLTAGES ARE MEASURED FROM THE WIRE FEEDER GUN CABLE BLOCK TO WORK.

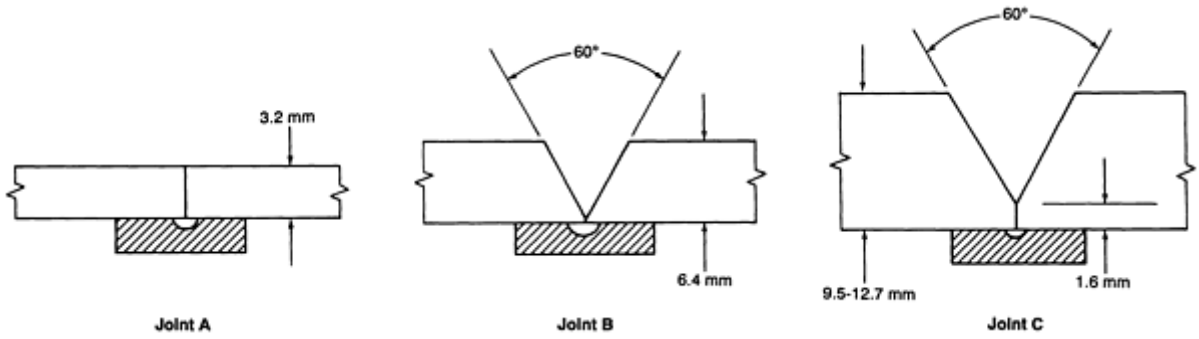

PLATE THICKNESS		ELECTRODE DIAMETER		NUMBER OF PASSES	CURRENT (DCEP), A	WIRE FEED SPEED		ARC SPEED		AMOUNT OF ELECTRODE REQUIRED		TOTAL TIME OF WELD	
mm	**in.**	**mm**	**in**			**mm/s**	**in./min**	**mm/s**	**in./min**	**kg/m**	**lb/ft**	**h/m**	h/ft
JOINT A													
3.2	1/8	1.6	1/16	1	225	60	140	8.0-8.9	19-21	0.112	0.075	0.033	**0.010**
JOINT B													
6.4	1/4	1.6	1/16	2	275	74	175	8.0-8.9	19-21	0.282	0.189	0.066	**0.020**
JOINT C													
9.5	3/8	1.6	1/16	2	300	85	200	6.3-7.2	15-17	0.405	0.272	0.082	**0.025**
12.7	1/2	**2.4**	3/32	**4**	**325**	**95**	**225**	**6.3-7.2**	**15-17**	**0.737**	**0.495**	**0.164**	**0.050**

FIG. 28 SUGGESTED PROCEDURES FOR GMAW OF BUTT JOINTS IN 200 AND 300 SERIES STAINLESS STEELS USING THE SPRAY-ARC TRANSFER MODE. SHIELDING GAS, ARGON PLUS 1% O_2; GAS FLOW, 1 M^3/H (35 FT^3/H). SOURCE: REF 26

With special pulsing power sources, a spray-like transfer can be produced at a much lower average welding current, more like that of the short-circuiting transfer mode. Pulsed gas-metal arc welding can permit out-of-position welding. So-called "synergic" power sources are claimed to automatically adjust pulse frequency to produce the transfer of a single drop with each pulse, despite variations in electrical stickout or wire feed speed. The pulsed GMAW process is an area of rapid technological development at the present time.

All gas-metal arc welding conducted with nominally austenitic filler metals that are intended to produce a little ferrite is sensitive to the integrity of the gas shielding, as is the GTAW process. Drafts and gas turbulence can permit air to enter the gas stream, resulting in nitrogen pickup and loss of ferrite. As with gas-tungsten arc welding, proper gas-flow rates (0.8 to 1.1 m^3/h, or 30 to 40 ft^3/h) and the use of barriers to exclude drafts from the arc area are essential to shielding gas integrity.

Flux-Cored Arc Welding. The ANSI/AWS A5.22 specification provides for three different classifications of a given alloy type, based on recommended shielding. Using type 308L as an example, an electrode can be classified as E308LT-1 (carbon dioxide shielding), E308LT-2 (Ar-2O shielding), or E308LT-3 (no gas shielding).

In practice, E308LT-1 (and other alloy wires designed for carbon dioxide gas shielding) are usually used in small diameters, that is, 1.6 mm ($\frac{1}{16}$ in.) and 1.1 mm (0.045 in.). Even 0.9 mm (0.035 in.) diameters are becoming available. Despite the use of carbon dioxide shielding gas, low-carbon-deposit compositions can be produced. Many of these wires, especially in 1.1 mm (0.045 in.) and smaller diameters, are welded in the vertical-up and overhead positions, as well as in the downhand position. Although the wires are classified with carbon dioxide gas shielding, in many cases they weld better in the vertical-up and overhead positions with Ar-25CO_2 shielding. The small-diameter wires are generally made from austenitic stainless steel strip (often type 304L), which work hardens very much during reduction to its final diameter. Thus, these wires are mechanically rather hard and tolerate high feed-roll pressures. Equipment for feeding such wires can be the same as for GMAW solid wires.

It is doubtful that there are any flux-cored stainless steel wires that are correctly classified with Ar-2O. The reason for this statement is that the scope of the ANSI/AWS A5.22 specification requires that a wire classified as flux cored must contain a minimum of 5% nonmetallics, by weight of the electrode. This much slag is not compatible with very high argon gas shielding. Certain metal-cored electrodes seem to be improperly classified as EXXXT-2, but they have almost no nonmetallic ingredients and are more properly classified as composite electrodes, according to the ANSI/AWS A5.9 specification.

In practice, E308LT-3 electrodes (and other stainless steel alloy compositions designed for welding without gas shielding) are commonly available in somewhat larger sizes than are the carbon dioxide classifications. The most popular size is still 2.4 mm ($\frac{3}{32}$ in.), although 2.0 mm ($\frac{5}{64}$ in.) and 1.6 mm ($\frac{1}{16}$ in.) sizes are also popular. These wires are generally usable only in the downhand and horizontal positions. In contrast to the carbon dioxide shielded wires, these wires generally produce rather shallow penetration. This feature can require somewhat higher welder skill levels to make sound x-ray quality welds, because of the dangers of slag entrapment. Higher travel speed is usually necessary when this defect is encountered. On the other hand, this shallow penetration is a major advantage for cladding operations, and these electrodes have been extensively used to achieve fully alloyed low-carbon overlays in a minimum number of layers.

The 2.4 mm (0.10 in.) electrodes, typified by E308LT-3, are generally made from thin, mild-steel strip, with all alloying elements in the core. This makes for a mechanically soft wire that often requires special U-grooved gear drive rolls for the wire feeder. Such drive rolls can grip the wire positively all around its circumference and do not tend to flatten the wire, which results in the best feeding characteristics. Special drive-roll conversion kits are offered for feeding these and other very soft wires. Some 2.0 mm (0.08 in.) diameter wires are also very soft, and similar drive rolls may be necessary.

The flux-cored wires designed for use without gas shielding are virtually immune to any effects of drafts on weld-metal ferrite content. They generally produce a fairly heavy fume plume, which means that fume extracting welding guns or other local exhaust systems can be desirable. Because of their immunity to drafts, these wires lend themselves very well to local exhaust.

On the other hand, the wires designed for use without shielding gas are sensitive to nitrogen pickup that is due to excessive arc length, as are SMAW coated electrodes. A proper balance between wire feed speed (current) and voltage will ensure proper ferrite control with such electrodes (Ref 29).

The wires designed for use with carbon dioxide (or Ar-25CO_2) are sensitive to loss of shielding gas, caused by drafts or inappropriate gas-flow rates, although less so than solid wires in the GMAW process. Protection from drafts is necessary for ferrite control, and local exhaust must be used with care so as not to disturb the gas shield. Otherwise, nitrogen can be picked up by the weld and ferrite can be lost. These wires also appear to have a greater tendency to pick up moisture from humid air if they are carelessly stored for long periods of time. Moisture pickup is often evidenced by "worm track" porosity (surface porosity elongated parallel to the solidification direction). This can often be eliminated by increasing the electrical stickout to preheat the wire, but care must be used to avoid loss of gas shielding.

A simple technique is to recess the contact tip approximately 5 to 10 mm (0.2 to 0.4 in.) behind the end of the shielding gas cup, and to then weld with normal distance between the gas cup and the workpiece. In extreme cases of moisture pickup, the wire may require a bake at 260 to 315 °C (500 to 600 °F) to remove the moisture. In humid weather, it is best to return gas-shielded flux-cored stainless steel wires to their packaging, or to store them in a tight plastic bag or in a low-temperature oven (100 °C, or 212 °F), if the wire is not to be used overnight.

References cited in this section

26. J.M. GERKEN AND D.J. KOTECKI, "STAINLESS STEELS," PUBLICATION NO. M250, THE LINCOLN ELECTRIC COMPANY, 1990
27. "ENGINEERING REPORT PROD/ES533," THE LINCOLN ELECTRIC COMPANY, 1992
28. C.R. HEIPLE AND J.R. ROPER, MECHANISM OF MINOR ELEMENT EFFECT ON GTA FUSION ZONE GEOMETRY, *WELD. J.*, VOL 61 (NO. 4), 1982, P 97S-102S
29. D.J. KOTECKI, WELDING PARAMETER EFFECTS ON OPEN-ARC STAINLESS STEEL WELD METAL FERRITE, *WELD. J.*, VOL 57 (NO. 4), 1978, P 109S-117S

References

1. A.L. SCHAEFFLER, CONSTITUTION DIAGRAM FOR STAINLESS STEEL WELD METAL, *MET. PROG.*, VOL 56 (NO. 11), 1949, P 680-680B
2. W.T. DELONG, FERRITE IN AUSTENITIC STAINLESS STEEL WELD METAL, *WELD. J.*, VOL 53 (NO. 7), 1974, P 273S-286S
3. T.A. SIEWERT, C.N. MCCOWAN, AND D.L. OLSON, FERRITE NUMBER PREDICTION TO 100 FN IN STAINLESS STEEL WELD METAL, *WELD J.*, VOL 67 (NO. 12), 1988, P 289S-298S
4. C.N. MCCOWAN, T.A. SIEWERT, AND D.L. OLSON, "STAINLESS STEEL WELD METAL: PREDICTION OF FERRITE CONTENT," WELDING RESEARCH COUNCIL BULLETIN 342, WRC, 1989
5. F.B. LAKE, "EFFECT OF CU ON STAINLESS STEEL WELD METAL FERRITE CONTENT," PAPER PRESENTED AT 1990 AMERICAN WELDING SOCIETY ANNUAL MEETING, AS YET UNPUBLISHED
6. D.J. KOTECKI AND T.A. SIEWERT, WRC-1992 CONSTITUTION DIAGRAM FOR STAINLESS STEEL WELD METALS: A MODIFICATION OF THE WRC-1988 DIAGRAM, *WELD. J.*, VOL 71 (NO. 5), 1992, P 171S-178S
7. E.R. SZUMACHOWSKI AND D.J. KOTECKI, MANGANESE EFFECT ON STAINLESS STEEL WELD METAL FERRITE, *WELD. J.*, VOL 71 (NO. 5), 1984, P 156S-161S
8. J.A. SELF, D.K. MATLOCK, AND D.L. OLSON, AN EVALUATION OF AUSTENITIC FE-MN-NI WELD METAL FOR DISSIMILAR METAL JOINING, *WELD. J.*, VOL 63 (NO. 9), 1984, P 282S-288S
9. C.D. LUNDIN, W.T. DELONG, AND D.F. SPOND, FERRITE-FISSURING RELATIONSHIP IN AUSTENITIC STAINLESS STEEL WELD METALS, *WELD. J.*, VOL 54 (NO. 8), 1975, P 241S-246S
10. J.C. LIPPOLD AND W.F. SAVAGE, SOLIDIFICATION OF AUSTENITIC STAINLESS STEEL WELDMENTS: PART III--THE EFFECT OF SOLIDIFICATION BEHAVIOR ON HOT CRACKING SUSCEPTIBILITY, *WELD. J.*, VOL 61 (NO. 12), 1982, P 388S-396S
11. *METALS HANDBOOK*, 8TH ED., VOL 8, AMERICAN SOCIETY FOR METALS, 1973, P 291
12. E. FOLKHARD, *WELDING METALLURGY OF STAINLESS STEELS*, SPRINGER-VERLAG, 1984, P 17
13. M.A. GROSSMANN AND E.C. BAIN, *PRINCIPLES OF HEAT TREATMENT*, 5TH ED., AMERICAN SOCIETY FOR METALS, 1964, P 49
14. *ATLAS OF ISOTHERMAL TRANSFORMATION AND COOLING TRANSFORMATION DIAGRAMS*, AMERICAN SOCIETY FOR METALS, 1977, P 324
15. "CARPENTER STAINLESS STEELS--WORKING DATA," CARPENTER TECHNOLOGY CORPORATION, 1983

16. "ENGINEERING REPORT ES-489," THE LINCOLN ELECTRIC COMPANY, 1991
17. *METALS HANDBOOK,* 8TH ED., VOL 7, AMERICAN SOCIETY FOR METALS, 1972, P 144-145
18. S.A. DAVID, J.M. VITEK, AND T.L. HEBBLE, EFFECT OF RAPID SOLIDIFICATION ON STAINLESS STEEL WELD METAL MICROSTRUCTURES AND ITS IMPLICATIONS ON THE SCHAEFFLER DIAGRAM, *WELD. J.,* VOL 66 (NO. 10), 1987, P 289S-300S
19. E. FOLKHARD, *WELDING METALLURGY OF STAINLESS STEELS,* SPRINGER-VERLAG, 1984, P 105
20. E. FOLKHARD, *WELDING METALLURGY OF STAINLESS STEELS,* SPRINGER-VERLAG, 1984, P 126
21. D.J. KOTECKI, HEAT TREATMENT OF DUPLEX STAINLESS STEEL WELD METALS, *WELD. J.,* VOL 68 (NO. 11), 1989, P 431S-441S
22. C.D. LUNDIN, K. KIKUCHI, AND K.K. KHAN, "PHASE 1 REPORT: MEASUREMENT OF DIFFUSIBLE HYDROGEN CONTENT AND HYDROGEN EFFECTS ON THE CRACKING POTENTIAL OF DUPLEX STAINLESS STEEL WELDMENTS," WELDING RESEARCH COUNCIL, MARCH 1991
23. U. FEKKEN, L. VAN NASSAU, AND M. VERWEY, "HYDROGEN INDUCED CRACKING IN AUSTENITIC/FERRITIC DUPLEX STAINLESS STEEL," PAPER 26, INTERNATIONAL CONFERENCE ON DUPLEX STAINLESS STEEL (THE HAGUE), NEDERLANDS INSTITUUT VOOR LASTECHNIEK, 26-28 OCT 1986
24. L. VAN NASSAU, H. MEELKER, AND J. HILKES, "WELDING DUPLEX AND SUPER-DUPLEX STAINLESS STEELS," DOCUMENT II-C-893-92, INTERNATIONAL INSTITUTE OF WELDING, 1992
25. I. VAROL, W.A. BAESLACK III, AND J.C. LIPPOLD, "FINAL REPORT: WELD CRACKING AND SOLID-STATE PHASE TRANSFORMATION CHARACTERISTICS IN DUPLEX STAINLESS STEELS," WELDING RESEARCH COUNCIL, 30 JUNE 1989
26. J.M. GERKEN AND D.J. KOTECKI, "STAINLESS STEELS," PUBLICATION NO. M250, THE LINCOLN ELECTRIC COMPANY, 1990
27. "ENGINEERING REPORT PROD/ES533," THE LINCOLN ELECTRIC COMPANY, 1992
28. C.R. HEIPLE AND J.R. ROPER, MECHANISM OF MINOR ELEMENT EFFECT ON GTA FUSION ZONE GEOMETRY, *WELD. J.,* VOL 61 (NO. 4), 1982, P 97S-102S
29. D.J. KOTECKI, WELDING PARAMETER EFFECTS ON OPEN-ARC STAINLESS STEEL WELD METAL FERRITE, *WELD. J.,* VOL 57 (NO. 4), 1978, P 109S-117S

Welding of Cast Irons*

Roger A. Bushey, The ESAB Group, Inc.

Introduction

THE FIRST STEP in selecting the type of welding process and consumable to use for welding cast iron is to determine what type or grade of casting needs to be welded. This discussion is not intended to cover all types of cast irons available on the market today (Table 1), but will discuss the major types of cast irons (that is, gray, ductile, malleable, white, and compacted graphite).

TABLE 1 CLASSIFICATION OF CAST IRON BY COMMERCIAL DESIGNATION, MICROSTRUCTURE, AND FRACTURE

COMMERCIAL DESIGNATION	CARBON-RICH PHASE	MATRIX[A]	FRACTURE	FINAL STRUCTURE AFTER
GRAY IRON	LAMELLAR GRAPHITE	P	GRAY	SOLIDIFICATION
DUCTILE IRON	SPHEROIDAL GRAPHITE	F, P, A	SILVER-GRAY	SOLIDIFICATION OR HEAT TREATMENT
COMPACTED GRAPHITE IRON	COMPACTED VERMICULAR GRAPHITE	F, P	GRAY	SOLIDIFICATION
WHITE IRON	FE_3C	P, M	WHITE	SOLIDIFICATION AND HEAT TREATMENT[B]
MOTTLED IRON	LAMELLAR GR + FE_3C	P	MOTTLED	SOLIDIFICATION
MALLEABLE IRON	TEMPER GRAPHITE	F, P	SILVER-GRAY	HEAT TREATMENT
AUSTEMPERED DUCTILE IRON	SPHEROIDAL GRAPHITE	AT	SILVER-GRAY	HEAT TREATMENT

(A) F, FERRITE; P, PEARLITE; A, AUSTENITE; M, MARTENSITE; AT, AUSTEMPERED (BAINITE).

(B) WHITE IRONS ARE NOT USUALLY HEAT TREATED, EXCEPT FOR STRESS RELIEF AND TO CONTINUE AUSTENITE TRANSFORMATION.

Cast iron can be described as an alloy of predominantly iron, carbon, and silicon. Commercially produced irons contain manganese and may be alloyed with nickel, chromium, copper, molybdenum, tin, antimony, vanadium, and various other elements either by themselves or in combinations.

Cast iron is produced by adding excess amounts of carbon to an austenite structure. During solidification, a portion of this carbon separates from the melt as either iron carbide or graphite. The form that the excess carbon takes is determined by the rate of cooling. If the cooling is rapid, the carbon will solidify as iron carbide. If the cooling is slow, the carbon will solidify as graphite. The type of carbon present and its shape will determine the type and, in particular, the properties of the cast iron. These properties are of prime importance when considering the welding procedure to be used. A flowchart illustrating the structure of the common types of commercial cast irons, as well as the processing required to obtain them, is shown in Fig. 1.

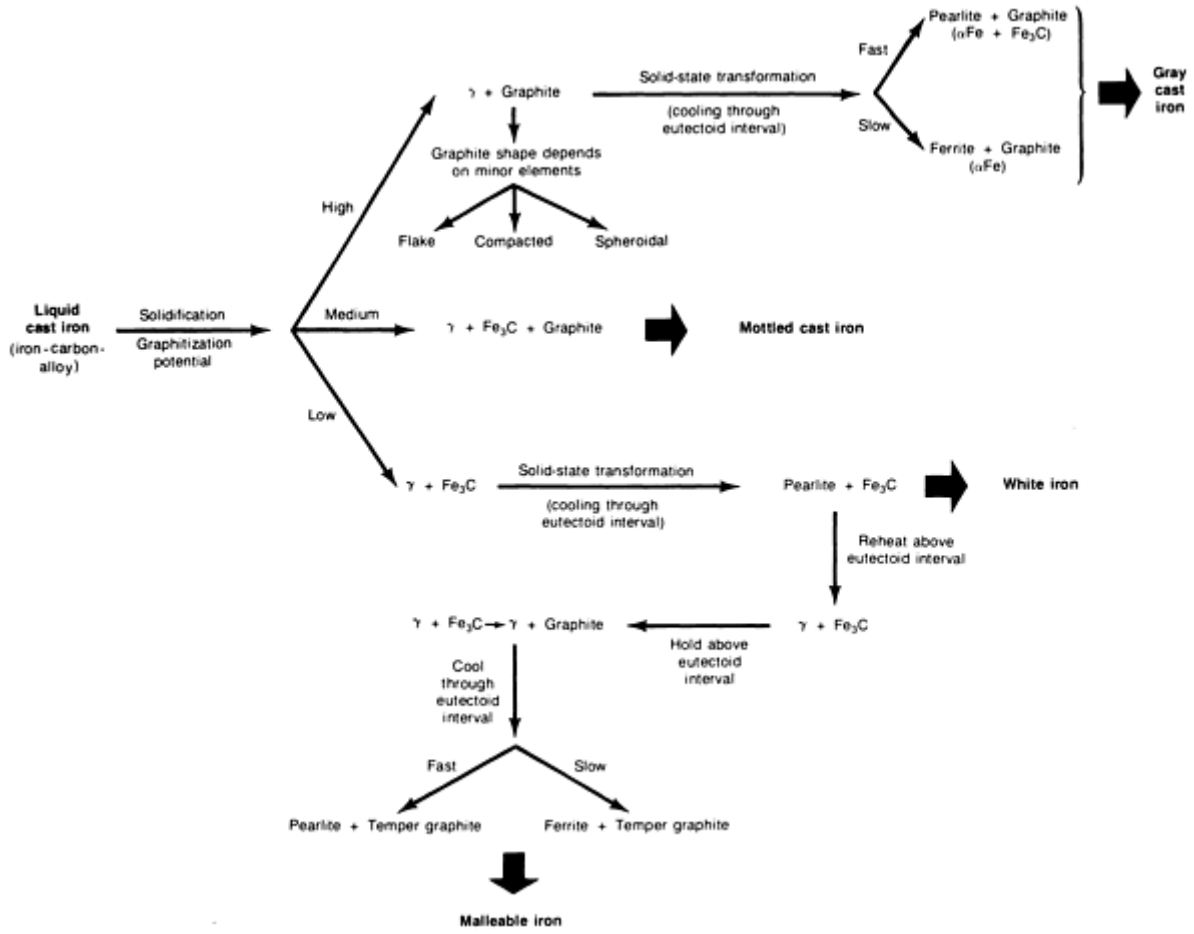

FIG. 1 FLOWCHART SHOWING BASIC MICROSTRUCTURES AND PROCESSING STEPS REQUIRED TO OBTAIN COMMON COMMERCIAL CAST IRONS

Note

* PORTIONS OF THIS ARTICLE WERE ADAPTED FROM "GUIDE FOR WELDING IRON CASTINGS," ANSI/AWS D11.2-89, AMERICAN WELDING SOCIETY, 1989.

Welding of Cast Irons*

Roger A. Bushey, The ESAB Group, Inc.

Classification

Historically, the first classification of cast iron was based on its fracture. Two types of iron were initially recognized:

- *WHITE IRON:* EXHIBITS A WHITE, CRYSTALLINE FRACTURE SURFACE BECAUSE FRACTURE OCCURS ALONG THE IRON CARBIDE PLATES; IT IS THE RESULT OF METASTABLE SOLIDIFICATION (FE_3C EUTECTIC)
- *GRAY IRON:* EXHIBITS A GRAY FRACTURE SURFACE BECAUSE FRACTURE OCCURS ALONG THE GRAPHITE PLATES (FLAKES); IT IS THE RESULT OF STABLE SOLIDIFICATION (GR EUTECTIC)

With the advent of metallography, and as the body of knowledge pertinent to cast iron increased, other classifications based on microstructural features became possible:

- *GRAPHITE SHAPE:* LAMELLAR (FLAKE) GRAPHITE, SPHEROIDAL (NODULAR) GRAPHITE, COMPACTED (VERMICULAR) GRAPHITE, AND TEMPER GRAPHITE; TEMPER GRAPHITE RESULTS FROM A SOLID-STATE REACTION (MALLEABILIZATION)
- *MATRIX:* FERRITIC, PEARLITIC, AUSTENITIC, MARTENSITIC, BAINITIC (AUSTEMPERED)

This classification is seldom used by the floor foundryman. The most widely used terminology can be made in two categories:

- *COMMON CAST IRONS:* FOR GENERAL-PURPOSE APPLICATIONS, THEY ARE UNALLOYED OR LOW-ALLOY
- *SPECIAL CAST IRONS:* FOR SPECIAL APPLICATIONS, GENERALLY HIGH-ALLOY

The correspondence between commercial and microstructural classification, as well as the final processing stage in obtaining common cast irons, is given in Table 1. Special cast irons differ from the common cast irons mainly in the higher content of alloying elements (>3%). Higher alloy content promotes microstructures with special properties for elevated-temperature applications, corrosion resistance, and wear resistance.

Gray Cast Iron

Gray cast iron is the most common form of cast iron. The excess carbon solidifies as flakes of graphite. This type of cast iron has moderate strength, excellent damping and machinability, but poor ductility. It contains 2 to 4% C, 1 to 3% Si, and up to 1% Mn, and has a tensile strength of up to 275 MPa (40 ksi).

The properties and the microstructure of gray iron can be altered with additions of alloying elements. The tensile strength of these alloyed gray cast irons can be as high as 550 MPa (80 ksi). Because of these many variables and different alloying systems, special welding procedures may be required. Because of the alloys added, some gray iron can be considered unweldable.

White Cast Iron

If cooling is rapid, then the excess carbon remains in the metastable form of iron carbide. This material is referred to as white cast iron. Because it contains a large amount of this intermetallic compound, white cast iron is very brittle, greatly reducing its ductility and weldability. The formation of iron carbide does improve hardness and abrasion resistance in these cast irons.

If large amounts of this iron carbide (also referred to as cementite) are present, the material is prone to cracking and is considered unweldable. White cast iron contains 2.5 to 3.8% C, 0.2 to 2.8% Si, and as much as 5.5% Ni, 30% Cr, 6.5% Mo, and 30% Mn, if designed for wear resistance. Tensile strengths can range from 160 to 620 MPa (23 to 90 ksi).

Malleable Cast Iron

White iron, if given the proper heat treatment, can transform into a ductile form of cast iron known as malleable iron. The iron carbides present are dissociated during a high-temperature anneal above 870 °C (1600 °F) for more than 60 h. During this process, irregularly shaped graphite nodules are precipitated and grow in the solid iron matrix. If the atmosphere in the furnace is of an oxidizing nature, some of the carbon will be oxidized, producing a white-heart malleable iron that is considered weldable. If the atmosphere is of a reducing nature, the entire amount of carbon is retained, and the material is a blackheart malleable iron, considered unweldable.

Malleable cast iron contains 2 to 2.8% C and 1 to 1.7% Si. Tensile strengths can range from 310 to 620 MPa (45 to 90 ksi) and elongations from 2 to 20%.

Ductile Cast Iron

Adding nodularizers, such as manganese or rare earths, makes the carbon solidify as small spheroids instead of flakes. Graphite in spheroidal form causes minimal interruption in the continuity of the metallic matrix. This is the most favorable form in which the graphite can be dispersed in order to achieve the desired mechanical properties. Ductile cast irons possess the highest strength and ductility of the cast irons. They combine the principal advantages of gray iron (machinability) with the advantages of steel (high strength, toughness, ductility, hot workability, and hardenability).

Ductile iron (also known as spheroidal graphite or nodular iron) typically contains 3 to 4% C, 1.8 to 2.8% Si, and a maximum of 0.7% Mn. Manganese levels are sometimes restricted if impact properties are important. Higher manganese content in the heat-affected zone during welding can reduce the impact resistance of the weld. Ductile iron has tensile strengths of 415 to 830 MPa (60 to 120 ksi). Alloying additions are sometimes made to ductile irons to improve heat and corrosion resistance. These alloyed grades can contain 2 to 3% C, 1 to 6% Si, 0.7 to 2.4% Mn, 18 to 36% Ni, and up to 5.5% Cr.

The matrix of ductile irons can be varied by heat treatment, alloying, or casting practices. The common as-cast product is 65-45-12. This designation means it has a tensile strength of 65 ksi (450 MPa), a yield strength of 45 ksi (310 MPa), and a tensile elongation of 12%. If this matrix, which has a 10 to 20% pearlite structure, is annealed, the structure becomes ferritic, producing a 60-40-18 iron material. Many different types of higher-strength grades can be produced. In general, as the strength of the iron increases, so do the problems that can be experienced during welding.

Compacted Graphite

Compacted graphite, or vermicular graphite, irons have structures and properties that are in between those of gray irons and ductile irons. The graphite forms interconnected flakes as in a graphite iron, but the flakes are thicker. Compacted graphite iron has better machinability and damping characteristics than ductile iron, but has improved ductility.

Welding of Cast Irons*

Roger A. Bushey, The ESAB Group, Inc.

Weldability

Many microstructural and mechanical properties can be obtained in a cast iron. Therefore, there is a wide range to their weldability. White cast iron is generally considered unweldable, while a ductile iron is generally easier to weld than gray iron.

During welding, a full spectrum of thermal gradients is experienced across the weldment and into the heat-affected zone of the cast iron. This results in many different microstructures and properties. The various microstructures can be classified into different zones and regions, as shown in Fig. 2. The nature and relative size of these zones will be determined by the heat generated during welding, the composition of the iron casting being welded, and the welding consumable used. Each zone will be discussed separately to provide a better understanding of the zones themselves and how welding procedures can affect their characteristics.

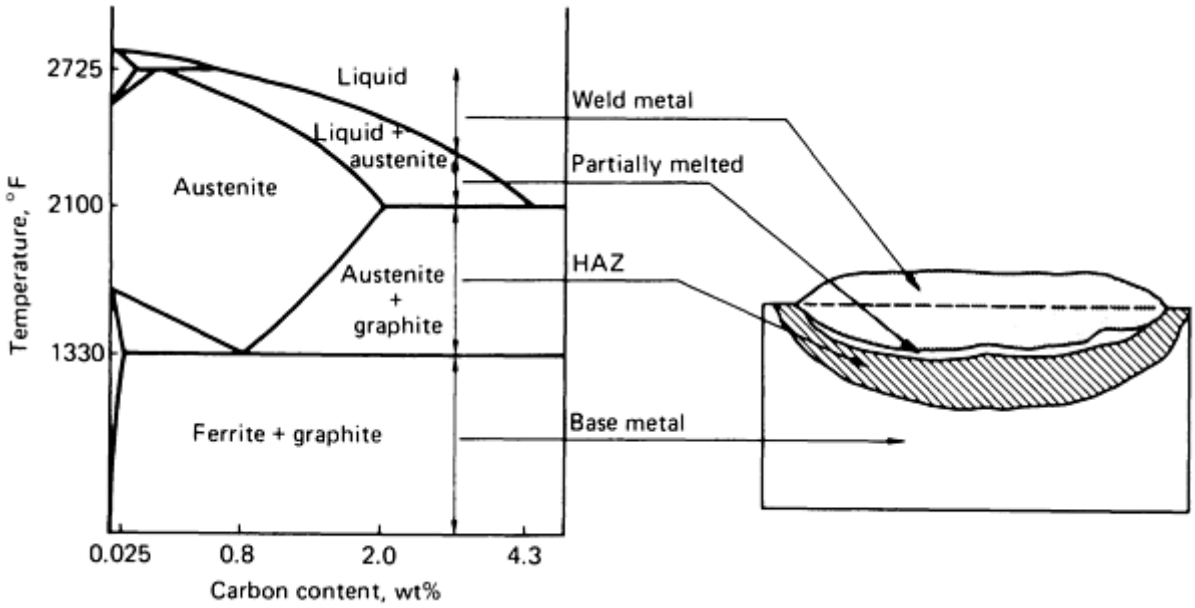

FIG. 2 SCHEMATIC REPRESENTATION OF THE TEMPERATURE ZONES IN A TYPICAL CAST IRON WELDING

Heat-Affected Zone (HAZ). The welding process by its nature is characterized by rapid cooling when compared to a casting procedure. Therefore, the properties of the weld--as well as the sections of the casting exposed to these high temperatures, known as the heat-affected zone--can be different from the rest of the casting.

During welding, the carbon can diffuse into the austenite. When cooling occurs, this austenite transforms to martensite. This martensitic structure is very brittle and susceptible to cracking. The amount of martensite formed depends on the chemistry or type of cast iron and on the thermal history. The brittle martensitic structure can be modified by tempering using preheat and interpass temperature control, by multiple-pass welding (stringer beads), or by a postweld heat treatment.

The partially melted region is an area next to the HAZ where the heat of the weld has been high enough to cause partial melting of the base metal, near the fusion line. This is the most critical zone in the weld, because upon cooling, this area freezes as white iron (that is, when held at high temperature long enough for carbon to dissolve) due to the high cooling rates. The region is very complex and may contain many different types of microstructures. If the amount of graphite dissolved during welding is high enough and forms a continuous molten matrix, it is likely that the carbide network will also be continuous, leading to problems. Because the partially melted region contains a great proportion of hard products, it is the hardest zone of the weld.

The high hardness and resulting low toughness make this region responsible for many of the mechanical problems experienced in the welding of cast iron. The most effective way to reduce the severity of cracking problems is to reduce the peak temperatures and the duration at the high temperatures. This can be controlled by heat input, preheat, interpass temperature, and proper filler metal selection.

The use of a low melting point filler metal will help reduce the peak temperature experienced in the partially remelted region. However, if a weldment is sufficiently small and a high heat input was used, the temperature of the base metal may be raised enough to cause severe fusion line problems even if no preheat was used. If, on the other hand, a high preheat temperature was used to prevent the formation of martensite in the HAZ and reduce the stresses, fusion line cracking may occur even with a low heat input. Some amount of trial-and-error procedure testing may be necessary. A welding procedure that can handle the partially melted region and the HAZ will likely produce a successful weld.

Fusion Zone. The properties and microstructure of the fusion zone are dictated by the welding consumable used. This area is made up of the melted filler metal consumable and some dilution from the iron casting. Because of the turbulence of the weld pool, the weld deposit has a relatively uniform composition. All efforts should be made to minimize the dilution.

Identification of Iron Casting. It is important to determine the type of casting to be welded in order to ensure the best weldment possible. If the type of casting is not known, it will be necessary to try and obtain this information. Records kept on the material purchased may indicate the type or manufacturer of the iron casting. Examination of a small piece under the microscope will indicate its structure. Some of the newer types of cast irons available today are difficult to distinguish from one another; much experience is usually needed. A detailed chemical analysis and hardness level of the cast iron will also help in classifying the material. If all else fails, the casting should be assumed to be a gray cast iron, and caution should be exercised when proceeding.

Weldability of a Casting. One attempt to classify the weldability of a casting is given in Ref 1. The document describes techniques to determine a no-crack temperature based on a carbon equivalent (CE) number. In order to obtain an accurate CE number, the following new CE formula was devised:

$$CE = C + 0.31\ SI + 0.33\ P + 0.45\ S - 0.028$$
$$Mn + Mo + Cr - 0.02\ Ni - 0.01\ Cu$$

The no-crack temperature can then be found for the specific casting under test by using Fig. 3. The procedure was used to show a correlation between the CE of a casting and a no-crack temperature. These data should be used only as a guide to establish a preheat temperature for a casting. Many factors other than preheat affect the ability to produce a sound weld. These include filler metal selection, peening, heat input, local contaminants, trapped sand, and absorbed lubricants in the casting.

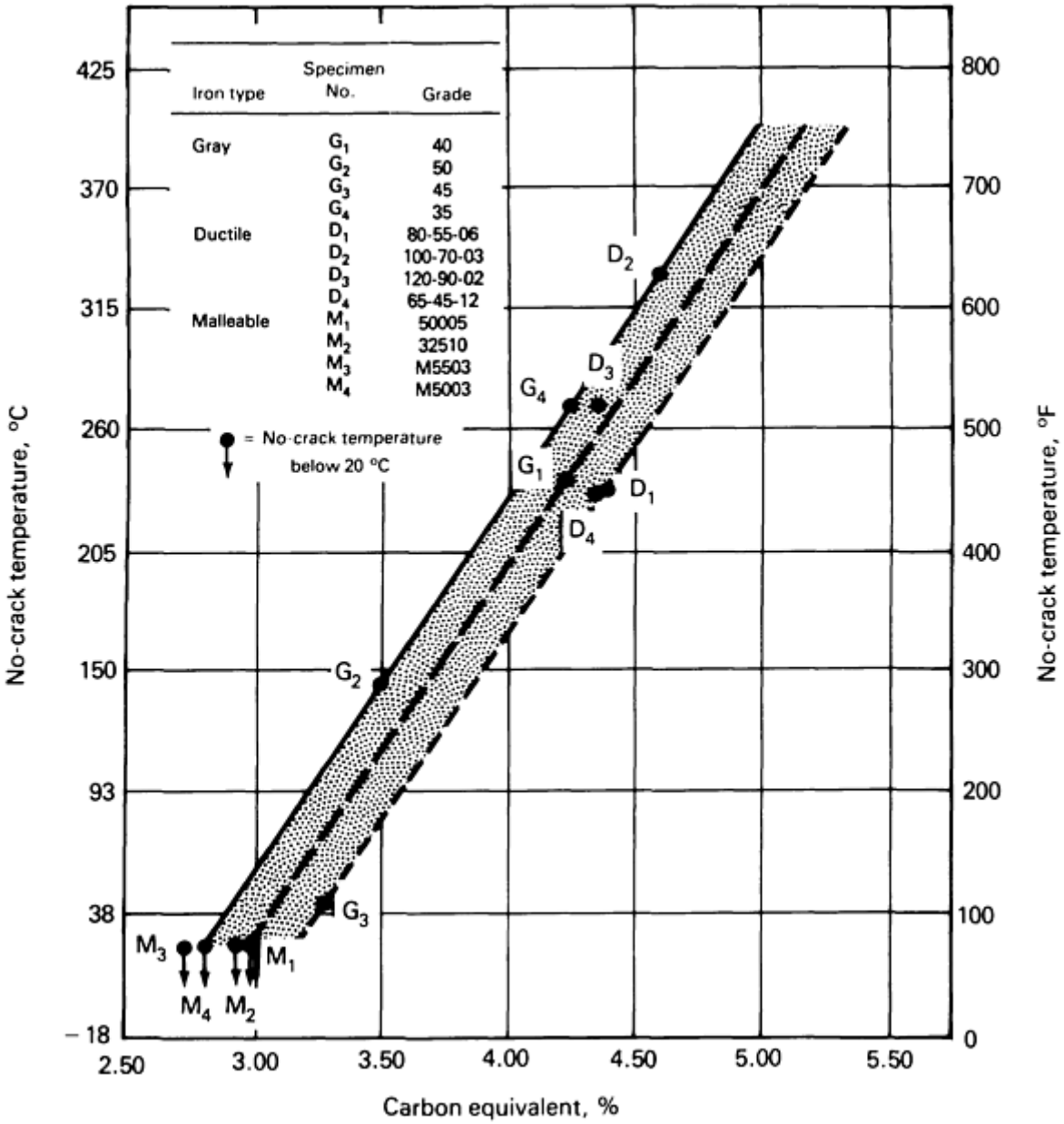

FIG. 3 EFFECT OF CARBON EQUIVALENT ON NO-CRACK TEMPERATURE FOR SELECTED GRADES OF IRON CASTINGS. SOURCE: REF 1

Preheat. One of the most important considerations in welding cast irons is the use of preheat. It:

- PREVENTS CRACKING CAUSED BY TEMPERATURE GRADIENTS AND THERMAL STRESSES
- REDUCES RESIDUAL STRESSES IN THE CASTING
- REDUCES DISTORTION
- REDUCES HARDNESS OF THE HAZ
- REDUCES TEMPERATURE GRADIENTS WHEN WELDING DISSIMILAR BASE METALS
- REDUCES HYDROCARBON CONTAMINANTS IN CASTINGS THAT HAVE BEEN IN SERVICE (CONTAMINANTS ARE BURNED OFF)

How much preheat to give a cast iron is debatable, but the following are some general guidelines:

- THE HIGHER THE CE, THE HIGHER THE PREHEAT TEMPERATURE
- IF THE TYPE OF CASTING IS KNOWN BUT THE SPECIFIC CHEMISTRY IS NOT, THEN THE PREHEAT SHOULD BE BASED ON THE MICROSTRUCTURE AND THE STRENGTH OF THE CASTING
- LOW-STRENGTH CAST IRONS USUALLY REQUIRE LOWER PREHEAT TEMPERATURE THAN HIGH-STRENGTH CAST IRONS
- A CASTING WITH A COMPLEX SHAPE WILL USUALLY REQUIRE A HIGHER PREHEAT TEMPERATURE TO CONTROL DISTORTION OR RESIDUAL STRESSES
- WHEN WELDING THIN METAL TO A THICK BASE METAL, IT IS RECOMMENDED TO PREHEAT THE THICK MEMBER TO DECREASE ITS HEAT SINK CAPACITY AND TO REDUCE THERMAL STRESSES
- MALLEABLE OR DUCTILE CAST IRONS USUALLY REQUIRE LOWER PREHEAT TEMPERATURES THAN GRAY OR WHITE CAST IRON

Preheat is applied to control the microstructure of the weld area. The influence of preheat on the microstructure in a typical cast iron is indicated below:

PREHEAT TEMPERATURE		RESULTING MICROSTRUCTURE
°C	**°F**	
22	72	**MARTENSITE**
100	212	**PEARLITE TRANSFORMATIONS OCCUR.**
200	392	**A GREATER PORTION OF MARTENSITE AND CARBIDES ARE REPLACED BY PEARLITE.**
300	572	**ALMOST ALL MARTENSITE IS REPLACED BY PEARLITE.**
400	**752**	**ALL MARTENSITE IS TRANSFORMED.**

Source: Ref 1

Preheating to temperatures above 315 °C (600 °F) slows the cooling rate to the point that formation of martensite is minimized, reducing the tendency of the cast iron to crack. Slow cooling also helps minimize residual stresses.

Preheating needs to be done properly. Preheat should be applied so that the weld joint is in compression, not tension (Fig. 4). If the proper method is used while the weld metal is contracting during cooling, the base metal will also contract.

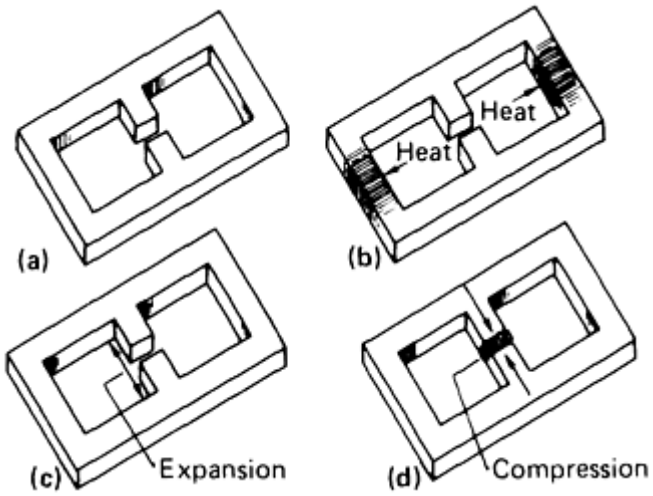

FIG. 4 PROPER METHOD OF PREHEATING CAST IRON CASTINGS TO PREPARE SAMPLES FOR WELDING. (A) CASTING AT ROOM TEMPERATURE. (B) HEAT APPLIED TO PERIMETER OF CASTING. (C) VERTICAL MEMBERS OF CASTING IN TENSION. (D) VERTICAL MEMBERS IN COMPRESSION READY TO BE WELDED

The need to weld complex shapes may necessitate preheating the entire structure. This helps eliminate stresses due to thermal gradients. The area to be welded should be brought to an even higher temperature if necessary. After welding, the entire structure should then be slow cooled to reduce stresses.

Preweld Testing. Cast irons, because they are porous, can collect many contaminants during service. Preheating the casting before welding can help bum out some of these contaminants (for example, grease, oils, or certain chemicals). Another technique uses the electrode selected for the repair. In the area to be repaired, a small stringer bead of 50 to 75 mm (2 to 3 in.) is deposited. The bead is then removed by grinding until the weld bead is back to the original surface of the casting. If a dense porosity-free weld exists, then the possibility is good that the casting contains limited amounts of contaminants. If, however, porosity does exist, then the contaminants must be removed prior to welding. Castings that have excessive amounts of contaminants will exhibit porosity throughout the entire weld. However, if the level of contaminants is lower, then the weld bead will appear to be sound. The only way to determine lack of fusion or porosity due to contaminants is to grind to the base of the weld metal. This procedure can be done without preheat, provided the area tested will not require subsequent machining.

Base-Metal Preparation. The only way to deposit a sound weld on a cast iron is to begin with a sound, clean base metal. When a known crack or defect is to be repaired, it should be completely removed before welding can begin. This also applies when repairing other defects, such as casting tears, porosity, shrinkage defects, and inclusions. The entire defect should be removed before attempting the repair.

Contaminants such as casting skin, coatings, sand, rust, paint, oil, grease, moisture, dirt, and other foreign materials should be removed prior to welding. Castings exposed to high temperatures may have surfaces that are heavily oxidized or carburized, and these surfaces should be removed before attempting a repair.

Baking the casting at temperatures from 370 to 480 °C (700 to 900 °F) will remove most of the organic materials, such as oil and grease. Castings that are impregnated with silt or sand cause additional problems. One method is to apply a weld, then grind, and examine the weld. If the weld metal is not free of porosity, the procedure should be repeated until a sound weld is obtained.

Many of the methods used for removing defects in the castings may make the crack or defect worse unless special procedures are used. One technique is to pin the defect before starting any procedure. This is done by locating the ends of the defect, either visually or with magnetic particle or liquid penetrant testing, followed by drilling holes at this location. The crack or defect will terminate in the hole and not propagate through the casting.

An alternative method involves welding a ductile weld bead perpendicular to the direction of the crack or defect. A nickel or nickel-iron electrode can be used. The defect can then be excavated or removed.

There are several methods of cutting and gouging the iron castings before repair. The air carbon arc process is the most commonly used. Either direct or alternating current can be used with cast irons. The arc length should be kept to a minimum, but the carbon electrode should not be allowed to touch the casting. This will prevent the formation of a high melting point slag on the surface of the casting, which will interfere with cutting. To prevent the formation of large HAZs in the castings, the heat input used for this procedure should be kept to a minimum. The HAZ should be removed by grinding or other mechanical means before welding.

An alternative method is the use of shielded metal arc cutting electrodes. These can be used provided they do not require supplemental compressed air or a special torch. The electrodes have special exothermic flux coatings that concentrate the heat into a very small crater at the tip of the electrode. When the electrode tip is placed in contact with the iron casting, the high concentration of heat from the arc causes the metal to melt.

Once the contaminants and defects are removed, the casting must be prepared for welding. This will require the casting to be machined or ground to achieve a proper joint configuration. The design of the weld groove is important in the casting in order to achieve a sound weld and to provide useful performance. Factors such as base metal thickness, type of base metal, filler metal, service application, and accessibility will determine the design of the groove.

Welds in thin cast irons can be made with single V or U grooves. Standard steel weld groove designs can be used for superficial repairs. However, if a nickel-base filler metal is required, the groove angles need to be increased to allow for the manipulation of the sluggish weld pool. Figure 5 illustrates some of the suggested joint preparations.

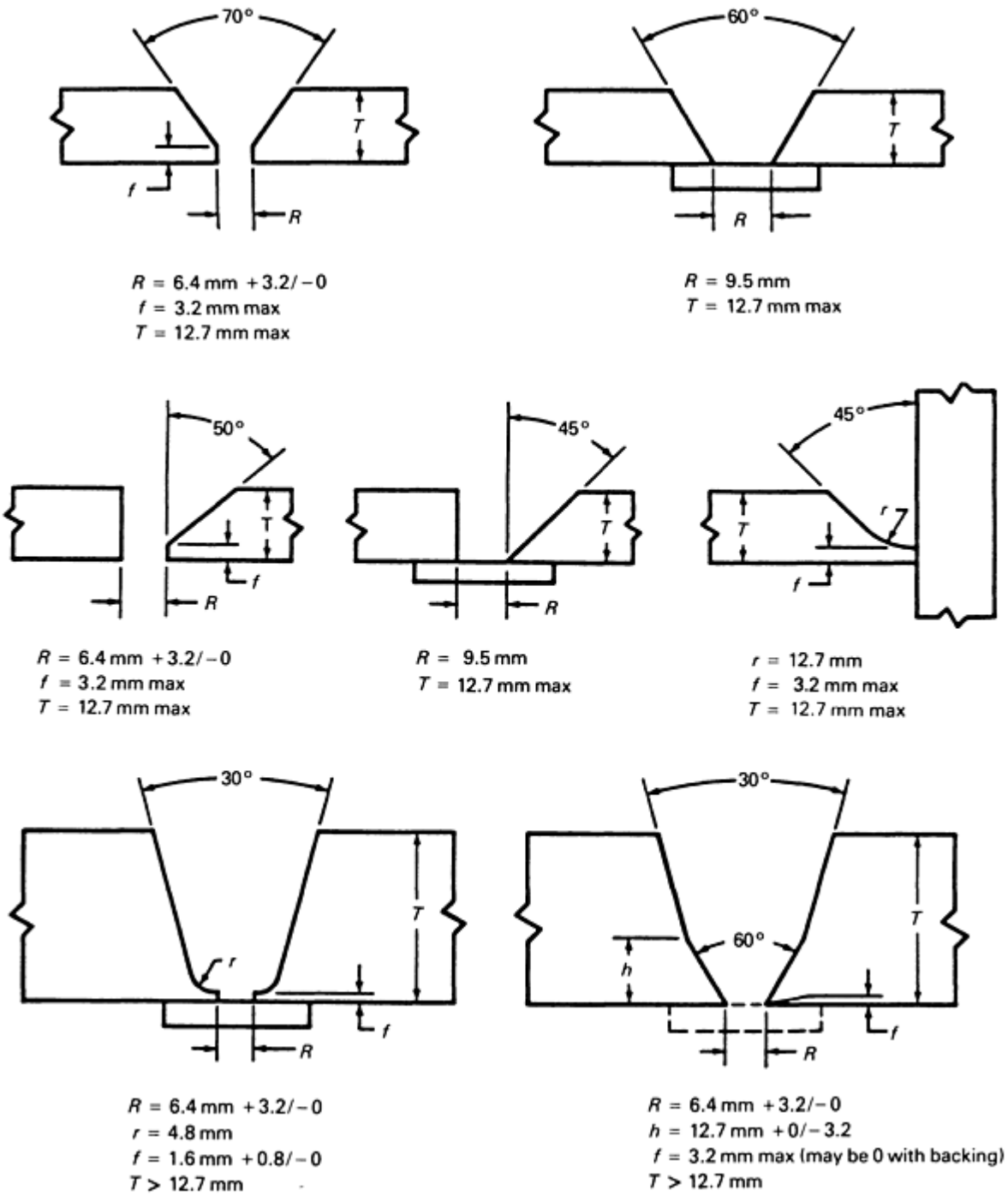

FIG. 5 RECOMMENDED JOINT PREPARATION FOR WELDS USING SINGLE U OR V GROOVES. SOURCE: REF 1

For castings thicker than 13 mm ($\frac{1}{2}$ in.), the groove must be designed so that the stresses caused by welding can be distributed uniformly in the casting. Double-welded joints are used in such applications when possible. For thicknesses up to 19 mm ($\frac{3}{4}$ in.), a double-V groove or a double-bevel groove is recommended. For thicknesses over 19 mm ($\frac{3}{4}$ in.), a double-U groove or double-J groove is recommended. When only one side of the section is accessible, a modified U groove can be used. This type of joint allows access to the joint root and decreases the width of the weld face, helping to decrease the mass of the weld metal and shrinkage stresses. These joints are illustrated in Fig. 6. When welding thick material, the groove faces are sometimes buttered to help minimize stresses.

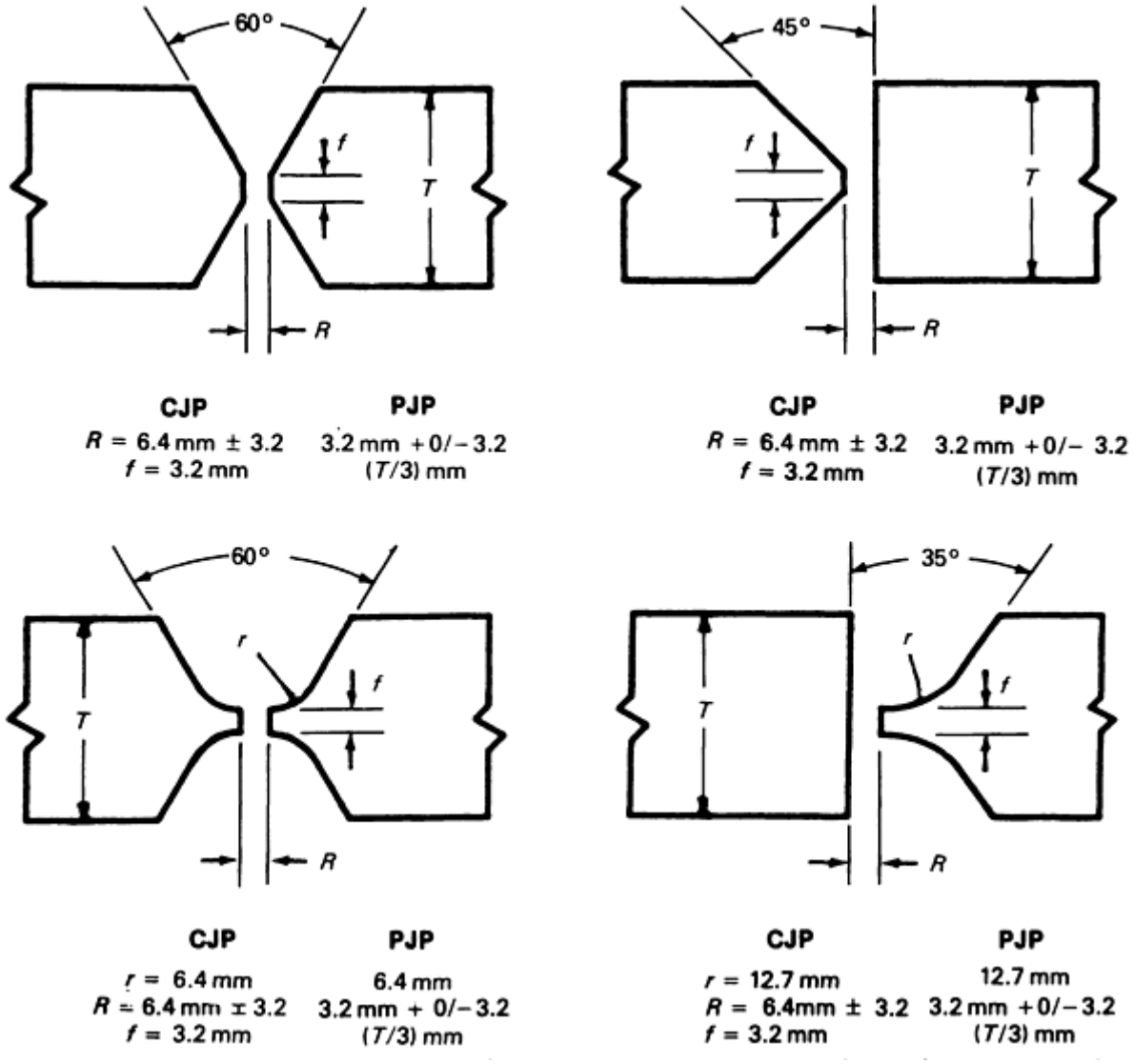

FIG. 6 RECOMMENDED DIMENSIONS FOR COMPLETE JOINT PENETRATION (CJP) AND PARTIAL JOINT PENETRATION (PJP) GROOVES. SOURCE: REF 1

The joint penetrations for braze welding a cast iron are essentially the same as those for arc welding, except the edges are rounded (Fig. 7). This facilitates access, flow, and finishing.

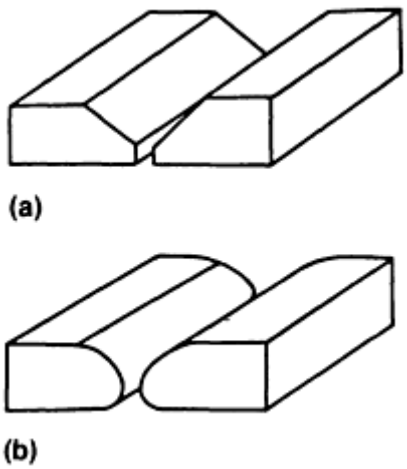

FIG. 7 RECOMMENDED GROOVE CONFIGURATIONS FOR JOINING CAST IRONS. (A) ARC WELDING. (B) BRAZE WELDING. SOURCE: REF 1

The degree of joint preparation required depends on several factors, such as the relative strength of the weld metal, the strength of the base plate, the stresses the casting will see in service, and the thickness of the casting being welded. If there is a question, then a complete joint penetration is preferred. The savings in time and filler metal should be weighed carefully against the conditions in the service environment.

Thick castings of gray iron are sometimes joined with welds having less than complete joint penetration. When nickel-base welding consumables are used, the welds are stronger than the gray cast iron, making partial-penetration welds acceptable. For castings over 13 mm ($\frac{1}{2}$ in.) thick, welding only two-thirds of the thickness should be adequate, and a double-U groove is recommended.

When welding other castings having higher strength levels, such as ductile iron, a complete joint penetration is recommended. Welds to be exposed to fatigue loading, or welds used for pipe applications, should always be complete joint penetration welds.

Special Techniques. The strength of a weld or its fitness for service can be improved by using various special techniques:

- GROOVE FACE GROOVING
- STUDDING
- JOINT DESIGN MODIFICATIONS
- PEENING

Groove Face Grooving. The face of the weld is grooved as shown in Fig. 8. The grooves are then filled with a weld, after which the joint is filled. As a result, the weld interface is irregular so that the path of a crack, if initiated, would not be straight.

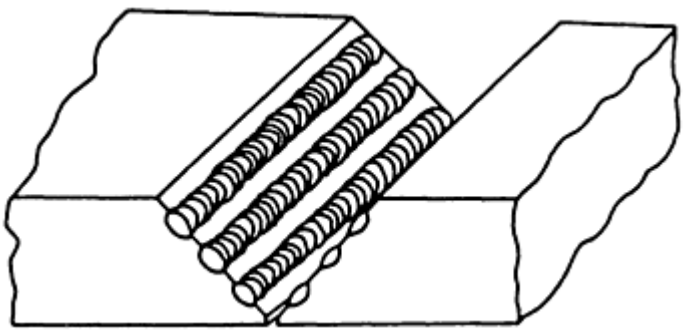

FIG. 8 GROOVE FACE GROOVING FOR WELDING OF CAST IRONS. SOURCE: REF 1

Studding is a mechanical means used to increase the strength and quality of a joint. The studs are either threaded or driven into the joint and must be made of a material compatible with the filler metal used (Fig. 9).

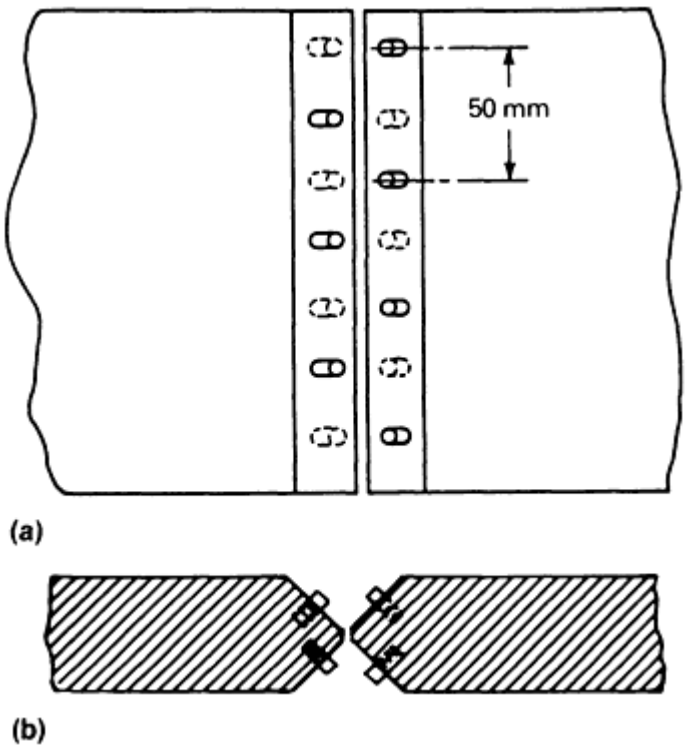

FIG. 9 APPLICATION OF STAGGERED STUD PATTERN TO PROVIDE INCREASED STRENGTH AT WELD INTERFACE. (A) TOP VIEW. (B) FRONT VIEW. SOURCE: REF 1

Joint design modifications in iron castings can improve the service of the welds. Figure 10 shows some samples of these improvements. Figure 10(a) shows a partial joint penetration weld (left) compared with a complete penetration weld (right). Figure 10(b) shows how to improve the casting design to help eliminate problems with changes in metal thickness, so that the weld is not in a highly stressed region. Figure 10(c) shows the addition of a fillet weld to help eliminate the flexing between the two members, again helping to reduce stress concentrations at the weld joint.

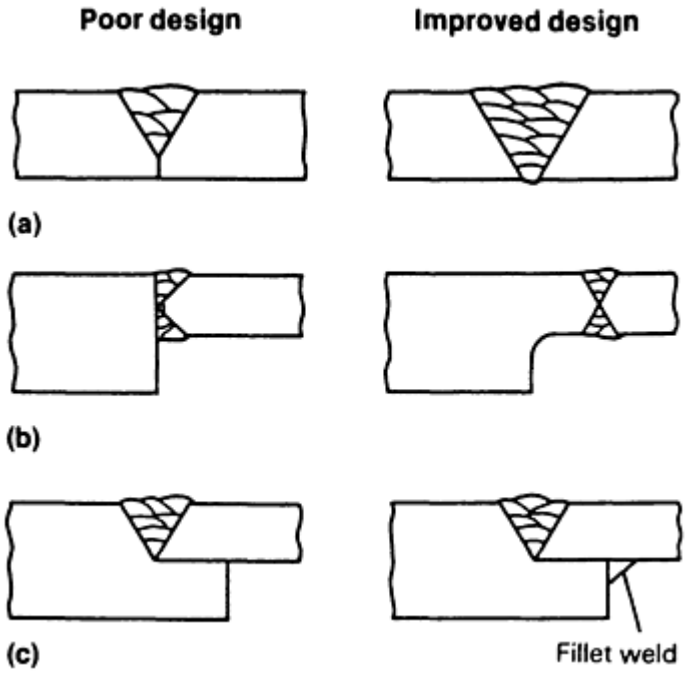

FIG. 10 MODIFICATION OF JOINTS TO PRODUCE OPTIMUM WELD. (A) PARTIAL JOINT PENETRATION WELD (LEFT) CHANGED TO COMPLETE JOINT PENETRATION WELD (RIGHT). (B) PART MODIFIED TO ALLEVIATE PROBLEMS CAUSED BY CHANGES IN METAL THICKNESS. (C) ADDITION OF SECONDARY FILLET WELD TO REDUCE STRESS CONCENTRATIONS OF PRIMARY WELD. SOURCE: REF 1

Peening can help distribute the stresses associated with a weld. A 13 to 19 mm ($\frac{1}{2}$ to $\frac{3}{4}$ in.) rounded ballpeen hammer is used to make repeated, moderate strikes perpendicular to the weld surface. The weld metal should be maintained at or near red hot and not allowed to cool below 540 °C (1000 °F). If a reciprocating air hammer is used, it should be operated at 620 kPa (90 psi) on welds up to 75 mm (3 in.) in length. The tool used should be no wider than the weld bead and should have a tip radius equivalent to one-half the tip width. Travel speed would be 750 to 1000 mm/min (30 to 40 in./min).

Reference cited in this section

1. "GUIDE FOR WELDING IRON CASTINGS," ANSI/AWS D11.2-89, AMERICAN WELDING SOCIETY, 1989

Welding of Cast Irons*

Roger A. Bushey, The ESAB Group, Inc.

Postwelding Treatment

The final stress level of a welded casting is affected by the rate at which the casting is cooled after welding. The casting should be allowed to cool slowly to minimize the residual stresses caused by welding. This can be accomplished by:

- BURYING THE ENTIRE CASTING IN SAND OR VERMICULITE
- POSTHEATING THE CASTING WITH A TORCH
- TRANSFERRING THE CASTING TO A FURNACE
- COVERING THE CASTING WITH AN INSULATING BLANKET

A postweld heat treatment may be necessary to:

- IMPROVE THE DUCTILITY OF THE HAZ
- IMPROVE THE MACHINABILITY OF THE WELD AND HAZ
- TRANSFORM THE MARTENSITIC MICROSTRUCTURE FORMED DURING WELDING TO A LESS BRITTLE PHASE
- RELIEVE RESIDUAL STRESSES IN THE CASTING

The need for postweld heat treatment will depend on the condition of the casting, possible distortion during subsequent machining, the desired finish of the machined surfaces, and prior heat treatment. Thermal stress cracking due to temperature variations in the casting can be avoided by keeping postweld heating and cooling rates below 55 °C/h (100 °F/h) for complex parts; slower rates may be necessary under some circumstances. Table 2 gives the recommended holding temperatures and cooling rates for the postweld heat treatment of gray and ductile cast irons.

TABLE 2 RECOMMENDED POSTWELD HEAT TREATMENT PRACTICE FOR SELECTED GRAPHITIC

CAST IRONS

HEAT TREATMENT	TEMPERATURE		HOLDING TIME (PER WORKPIECE THICKNESS)	COOLING RATE
	°C	°F		
DUCTILE IRON				
STRESS RELIEF	510-565[A]	950-1050[A]	1H/IN.	(F)
	565-595[B]	1050-1100[A]	1H/IN.	(F)
	540-650[C]	1000-1200[C]	1H/IN.	(F)
	620-675[D]	1150-1250[D]	1H/IN.	(F)
FERRITIZE ANNEAL	900-955	1650-1750	1H + 1 H/IN.	(G)
FULL ANNEAL	870-900	1600-1650	1H/IN.	(H)
GRAPHITIZING ANNEAL	. . .	. . .	. . .	. . .
NORMALIZING ANNEAL	. . .	. . .	. . .	. . .
NORMALIZING AND TEMPERING ANNEAL	900-940	1650-1725	2H/IN.[E]	(I)
GRAY IRON				
STRESS RELIEF	595-650	1100-1200	1H/IN.	(F)
FERRITIZE ANNEAL	705-760	1300-1400	1H/IN.	(F)
FULL ANNEAL	790-900	1450-1650	1H/IN.	(F)
GRAPHITIZING ANNEAL	900-955	1650-1750	1-3 H + 1 H/IN.	(F)
NORMALIZING ANNEAL	**870-955**	**1600-1750**	**1-3 H + 1 H/IN.**	(J)

(A) UNALLOYED.

(B) LOW ALLOY.

(C) HIGH ALLOY.

(D) AUSTENITIC.

(E) 2 H MINIMUM.

(F) FURNACE COOL TO 315 °C (600 °F) AT 55 °C/H (100 °F/H), AIR COOL TO ROOM TEMPERATURE (RT).

(G) FURNACE COOL TO 690 °C (1275 °F); HOLD AT 690 °C (1275 °F) FOR 5 H + 1 H/IN. OF THICKNESS, FURNACE COOL TO 345 °C (650 °F) AT 55 °C/H (100 °F/H); AIR COOL TO RT.

(H) FURNACE COOL TO 345 °C (650 °F) AT 55 °C/H (100 °F/H); AIR COOL TO RT.

(I) FAST COOL WITH AIR TO 540 TO 640 °C (1000 TO 1200 °F), FURNACE COOL TO 345 °C (650 °F) AT 55 °C (100 °F/H), AIR COOL TO RT.

(J) AIR COOL FROM ANNEALING TEMPERATURE TO BELOW 480 °C (900 ° F) TO RT.

Welding of Cast Irons*

Roger A. Bushey, The ESAB Group, Inc.

Welding Processes and Consumables

Oxyfuel welding (OFW) is any welding process that uses oxygen and a fuel gas as a heating medium. It involves melting the base plate and filler metal with a welding torch flame. The fuel gas and oxygen are mixed in the proper

proportions in a mixing chamber. Molten metal from the groove faces and filler metal intermix and, upon cooling, form a continuous deposit.

The major advantage of the OFW process is the control the welder has over the rate of heat input, the temperature of the weld zone, and the oxidizing and reducing potential of the welding torch flame. The weld bead size and shape, as well as the viscosity of the weld pool, can be controlled because the filler metal is added independently of the welding flame. The OFW process is ideal for welding thin sections, tubes, and small-diameter pipe.

Acetylene is the preferred fuel gas. Other fuel gases (for example, methylacetylene propadiene, propylene, propane, natural gas, and several proprietary gases) are excessively oxidizing and do not develop sufficient heat to properly weld cast irons.

Oxyfuel welding is widely used to repair minor defects in gray cast iron and is used less frequently for ductile iron castings. The slow heating rate of OFW causes a large HAZ to develop but prevents the formation of the brittle martensitic structure.

The consumables for the oxyfuel welding of gray iron are normally cast with higher levels of carbon and silicon than the castings; this compensates for losses experienced during welding. The weld metal has a graphitic structure, making it machinable, and is a good color match. The chemical compositions for three gray iron welding rods are given in Table 3. The RCI filler material is used to join Class 20 through 35 gray irons, and RCI-A is used for gray castings with higher levels of nickel and molybdenum of Class 35 through 45.

TABLE 3 COMPOSITION OF WELDING RODS USED FOR OXYFUEL WELDING OF GRAY IRONS

GRAY IRON WELDING APPLICATION	**AWS FILLER METAL CLASSIFICATION(B)**	**UNS NO.**	COMPOSITION, WT%(A)									
			C	**Mn**	**Si**	**P**	**S**	**Fe**	**Ni(c)**	**Mo**	**Mg**	CE
CONVENTIONAL	RCI	F10090	3.2 - 3.5	0.60 - 0.75	2.7 - 3.0	0.50 - 0.75	0.10	BAL	TRACE	TRACE	. . .	**. . .**
HIGH-STRENGTH ALLOY	RCI-A	F10091	3.2 - 3.5	0.50 - 0.70	2.0 - 2.5	0.20 - 0.40	0.10	BAL	1.2-1.6	0.25-0.45	. . .	**. . .**
MALLEABLE AND NODULAR	**RCI-B**	**F10092**	**3.2 - 4.0**	**0.10 - 0.40**	**3.2 - 3.8**	**0.05**	**0.015**	**BAL**	**0.50**	**. . .**	**0.04 - 0.10**	**0.20**

Source: Ref 2

(A) SINGLE VALUES SHOWN ARE MAXIMUM.

(B) COPPER-BASE FILLER METALS FREQUENTLY USED IN THE BRAZE WELDING OF CAST IRONS ARE NO LONGER INCLUDED IN THIS SPECIFICATION. FOR INFORMATION PERTAINING TO THESE MATERIALS SEE ANSI/AWS A7.6.

(C) NICKEL PLUS INCIDENTAL COBALT.

These consumables, along with some proprietary filler metals, have been designed to furnish weld metal having adequate strength and a minimum level of iron carbide. This is achieved by alloying with elements that promote solid solution strengthening in combination with a graphitizing agent. Nickel, manganese, molybdenum, and silicon are the most common. The addition of phosphorus promotes fluidity of the molten iron. If the phosphorus level is high, then a hard, brittle, iron/iron phosphide eutectic can be formed.

The RCI-B filler material given in Table 3, along with additional proprietary filler metals, is designed for welding ductile iron castings. A ductile iron welding rod contains additions of nodularizing elements such as magnesium or cerium. These types of filler metals are capable of producing weld metal with a nodular graphite structure, provided the magnesium or cerium is high enough to compensate for losses incurred during welding. Cerium-containing rods may be the preferred

nodularizing element to minimize porosity. Rods containing magnesium can develop a scum during welding unless enough flux is used. This scum is hard to remove and can cause contaminated and low-strength welds.

The filler metals listed in Table 3 have been used for welding malleable cast iron. However, the OFW process can create a wide HAZ of brittle white iron, lowering the ductility of the base metal and making it more prone to cracking. Some foundries repair the rough castings while still having a white iron microstructure before the malleabilizing heat treatment.

Fluxes are used to protect the molten metal from oxidation, to increase the fluidity of the slag formed, and to help dissolve oxides and other impurities. Fluxes used for OFW when utilizing acetylene fuel gas contain sodium borate, or boric acid, soda ash, and some iron oxide powder. Some fluxes are designed specifically for welding ductile iron by lowering the melting point; otherwise, the fluxes are used for both gray and ductile iron.

The weld preparation for OFW must be wider than that for the arc-welding processes to allow for manipulation of the welding rod and torch. Groove angles of 90 to 120° are common.

A preheating temperature of 540 to 650 °C (1000 to 1200 °F) is recommended for the oxyfuel welding of cast irons. This allows for a quick repair and provides slow cooling. If possible, the entire casting should be preheated to minimize local thermal stresses. Gray iron is especially susceptible to cracking due to thermal stresses introduced by localized preheating. If done carefully with a torch, localized preheating can be used successfully on small castings.

After the proper preheating temperature is reached, the repair should be done immediately before the base metal adjacent to the weld area is allowed to cool. The casting should not be allowed to cool below 315 to 425 °C (600 to 800 °F). If the casting cools below this temperature during welding, or if welding is interrupted, the casting should be reheated before welding is resumed. The casting should not be exposed to extreme temperatures during welding to help reduce thermal stresses. During OFW, the area being repaired should not exceed 675 °C (1250 °F). Excessive preheating and welding time may introduce additional stresses, may distort the casting, and may reduce tensile strength.

The temperature of the casting must be monitored during welding. The recommended practice is to preheat the entire casting in a furnace, maintain an interpass temperature during welding, and cool slowly in a furnace. If a permanent furnace is not available, a temporary furnace can be made from sheet metal and fire brick on top of several gas burners.

Several techniques are unique to OFW when welding cast irons:

- THE SIZE OF THE WELDING TORCH SHOULD BE SIMILAR TO THOSE USED FOR MILD STEEL.
- A NEUTRAL FLAME OR SLIGHTLY REDUCING FLAME IS RECOMMENDED. AN OXIDIZING FLAME IS NOT RECOMMENDED, BECAUSE IT CAN CAUSE LOSS OF SILICON, LEADING TO THE FORMATION OF WHITE CAST IRON AND POROSITY.
- AFTER THE CASTING IS AT THE PROPER PREHEAT TEMPERATURE, THE FLUX IS SPRINKLED ONTO THE GROOVE FACES TO BE WELDED. THE CONE OF THE FLAME SHOULD BE KEPT APPROXIMATELY 3.2 TO 6.4 MM ($\frac{1}{8}$ TO $\frac{1}{4}$ IN.) FROM THE BASE METAL. CONTACTING THE CONE TO THE BASE METAL SHOULD BE AVOIDED, BECAUSE IT COULD CAUSE OXIDATION OF SILICON AND CARBON, RESULTING IN HARD SPOTS.
- WHEN THE BOTTOM OF THE GROOVE HAS MELTED, THE TORCH FLAME IS MOVED FROM SIDE TO SIDE TO MELT BOTH GROOVE FACES. AT THIS POINT, THE WELDING ROD IS ADDED SLOWLY TO FORM THE WELD POOL. FURTHER ADDITION OF THE ROD SHOULD BE DONE BY MELTING THE ROD IN THE WELD POOL, NOT IN THE FLAME.
- FURTHER ADDITION OF FLUX SHOULD BE DONE BY HEATING THE TIP OF THE WELDING ROD IN THE OUTER PORTION OF THE WELDING FLAME AND DIPPING THE ROD INTO THE FLUX. WHITE SPOTS AND GAS BUBBLES IN THE WELD POOL INDICATE THAT IMPURITIES ARE PRESENT AND THAT ADDITIONAL FLUX IS NEEDED.
- USING A STIRRING ACTION WITH THE WELDING ROD HELPS THE IMPURITIES FLOAT TO THE SURFACE IN THE SLAG AND HELPS MAINTAIN A GOOD FUSION WITH THE GROOVE FACES. EXCESSIVE STIRRING SHOULD BE AVOIDED IN ORDER TO MINIMIZE

OXIDATION.

One recommended practice for depositing the filler metal is called block sequence (Fig. 11). This procedure requires depositing welds approximately 25 mm (1 in.) long in different sections of the joint. The ends of each length should be staggered. Care must be taken to obtain complete fusion between each section and both groove faces. Excess molten metal that might have run ahead of the block must be remelted before welding over it. Another method, called the cascade method, involves depositing thin layers in succession, where each layer is longer than the previous one (Fig. 11). The repaired casting can then be given a postweld heat treatment. Large castings with complex shapes or castings that require excessive machining should be given a postweld stress relief immediately after welding. This requires holding the casting at 540 to 650 °C (1000 to 1200 °F) for 1 h per inch of thickness, followed by slow cooling.

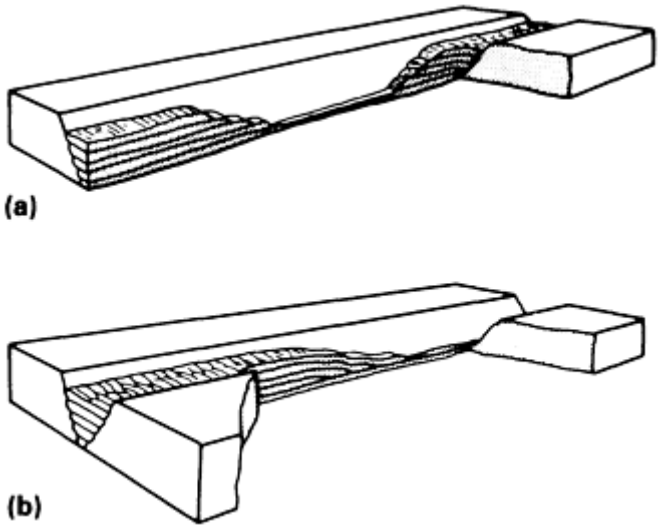

FIG. 11 METHODS APPLIED TO THE OFW PROCESS TO DEPOSIT FILLER METAL WITH MINIMUM WELD STRESS. (A) BLOCK SEQUENCE. (B) CASCADE SEQUENCE

Flame spraying (FLSP) of gray iron is mainly used to repair worn areas, defects, and broken corners on gray iron glass molds. The FLSP process is preferred because deposits as thin as 0.10 to 0.13 mm (0.004 to 0.005 in.) can be applied uniformly to a complex contour of a casting. Finishing time is minimal, and the deposits can be hand filed or machined back to the original contours of the casting. Flame spraying allows a high-strength bond with varying hardness values.

The FLSP process uses a special acetylene torch designed to store and inject powder particles into the gas stream ahead of the flame. These particles then become semimolten as they pass through the flame before striking the casting.

The powders used for FLSP are manufactured by an atomization process and then blended to become an aggregate of various-sized particles. The correct mesh size distribution is necessary in order to obtain an efficient flow of powder through the torch and to maintain reasonable efficiency in thermal spraying deposition.

Various powders have been developed to conform to the Aerospace Material Specification 4779 standard. The standard has the following specifications:

ELEMENT	CONTENT, WT%
CARBON	**0.6 MAX**
SILICON	**4.0-5.0**
IRON	**1.5 MAX**

BORON	**1.0-2.2**
NICKEL	**BAL**

Altering the percentage of each element causes variations in performance and hardness. The hardness range can vary from 165 to 392 HV (85 HRB to 40 HRC).

The area of the casting to be sprayed must be cleaned beforehand. All oxides must be removed. Sand blasting is not recommended, because small particles of silica can become embedded in the casting and cause bonding problems.

The preheat temperature for FLSP is 260 to 315 °C (500 to 600 °F). The preheated area is then sprayed completely with a layer 0.10 to 0.18 mm (0.004 to 0.007 in.) thick. With the torch flame only, the area is then heated to 1010 to 1150 °C (1850 to 2100 °F), starting at one edge until complete fusion is obtained. After the initial deposit has been fused, additional layers can be deposited using the same technique.

Braze welding is a welding process in which the filler metal has a melting point above 450 °C (840 °F) but below the melting point of the casting. Unlike brazing, the filler metal in braze welding is not distributed in the joint by capillary action.

Braze welding was originally developed to repair cracks or broken cast iron parts. Because the process does not require the casting to be melted, the temperature is lower, reducing the formation of brittle cementite, and thus reducing the tendency toward cracking.

The molten filler metal must wet the hot base casting in order for a proper metallic bond to be created between the filler metal and the unmelted casting. This heat is generated with an oxyfuel gas torch.

Flux must be used to properly clean and protect both the base metal and weld metal. The filler metal is fed into the heated groove face in one or more passes until the groove is completely filled. The joint design is similar to joints used for oxyfuel gas welding. Typical groove and joint designs are shown in Fig. 5, 6, 7, 8, 9, and 10.

Advantages. There are some distinct advantages of braze welding over fusion welding:

- BECAUSE LESS HEAT IS REQUIRED, THERE IS LESS DISTORTION AND SUSCEPTIBILITY TO CRACKING.
- THE DEPOSITED WELD METAL IS RELATIVELY SOFT AND DUCTILE, RESULTING IN DEPOSITS THAT HAVE EXCELLENT MACHINABILITY AND LOW RESIDUAL STRESSES.
- JOINTS CAN BE PRODUCED WITH ADEQUATE STRENGTH FOR MANY APPLICATIONS.
- EQUIPMENT REQUIRED IS VERY SIMPLE AND RELATIVELY EASY TO USE.
- CAST IRONS, WHICH ARE VERY SENSITIVE TO TEMPERATURE GRADIENTS OR THERMAL SHOCK, CAN BE BRAZE WELDED WITHOUT EXCESSIVE PREHEATING.

Limitations of braze welding include:

- THE JOINT STRENGTH IS CONTROLLED BY THE WELD METAL OR WELD INTERFACE.
- THE SERVICE TEMPERATURES WILL BE LOWER THAN THOSE IN FUSION WELDS DUE TO THE LOWER MELTING TEMPERATURES OF THE FILLER METAL. IF A COPPER ALLOY IS USED, IT IS LIMITED TO 260 °C (500 °F) OR LOWER.
- BRAZE-WELDED JOINTS WILL NOT MATCH THE COLOR OF THE CASTING.
- DEFECTS ARE HARDER TO LOCATE IN THE BRAZE-WELDED JOINTS, MAKING THEM MORE DIFFICULT TO INSPECT THAN FUSION-WELDED JOINTS.

Equipment and Techniques. The equipment used for braze welding consists of a welding torch and associated components. Braze welding can be used to join castings to other castings or castings to other metals (for example, steel or stainless steel), provided the proper filler metal is used.

A preferred technique of braze welding is to butter one or both faces of the groove prior to welding. The buttered layer can be the same alloy as the filler metal or a different filler metal that will act as a buffer between the two metals to be joined.

The filler metal used for this process is predominantly a 60Cu-40Zn brass alloy. Tin, iron, manganese, silicon, and nickel are added to improve flow characteristics, lower the melting temperature, decrease the volatilization of zinc, react with oxygen, and increase strength and hardness. Table 4 gives the chemical composition and properties of several filler metal rods. Even though the minimum tensile strengths of these alloys range from 275 to 485 MPa (40 to 70 ksi), they may decrease if the service temperature is above 260 °C (500 °F).

TABLE 4 COMPOSITION AND PROPERTIES OF RODS AND ELECTRODES USED FOR BRAZE WELDING OF CAST IRONS (WITH JOINT CONFIGURATIONS SIMILAR TO THOSE APPLIED TO OFW PROCESSING) PER AWS SPECIFICATION A5.27

FILLER METAL TYPE	COMPOSITION, WT%											TENSILE STRENGTH[(A)]		LIQUIDUS TEMPERATURE		APPLICATIONS
	CU	ZN	SN	FE	NI	MN	AL	SI	PB	P	TOTAL OTHER	MPA	KSI	°C	°F	
RBCUZN-A	57.0-61.0	BAL	0.25-1.00	. . .	. . .	. . .	0.01	0.04-41.15	0.05	. . .	0.50	275	40	900	1650	**A LOW-FUMING BRONZE USED ON COPPER SHEET, MILD TUBE STEEL, DEEP-DRAWING STEEL, AND CAST IRON**
RBCUZN-B	56.0-60.0	BAL	0.80-1.10	0.25-1.2	0.20-0.80	0.01-0.50	0.01	0.04-0.15	0.05	. . .	0.50	344	50	890	1630	**HIGHER STRENGTH, USED TO SURFACE OR BRAZE WELD COPPER, STEEL, CAST IRON, OR WROUGHT IRON**
RBCUZN-C	56.0-60.0	BAL	0.80-1.10	0.25-1.2	. . .	0.01-0.50	0.01	0.04-0.15	0.05	. . .	0.50	344	50	890	1630	**BETTER COLOR MATCH WITH MILD STEEL, CAST IRON, AND WROUGHT IRON**
RBCUZN-D	**46.0-50.0**	**BAL**	**. . .**	**. . .**	**9.0-11.0**	**. . .**	**0.01**	**0.40-0.25**	**0.05**	**0.25**	**0.50**	**413**	**60**	**935**	**1715**	**NICKEL-SILVER-BRONZE FILLER METAL PROVIDING BEST STRENGTH AND COLOR MATCH WITH CAST IRON AND WROUGHT IRON**

Source: Ref 1

(A) MINIMUM AT ROOM TEMPERATURE.

Fluxes for braze welding are basic fluxes of alkali fluoride and borax mixtures. They are designed to clean the base metal casting and weld metal, and are active over the full melting range of the filler metal. Braze-welding fluxes contain some iron oxide or manganese dioxide, which combines with the free carbon on the cast iron surface to promote wetting. Fluxes are applied by dipping the heated filler metal into the flux or by brushing onto the joint. They are also precoated on filler metal or applied through the oxyfuel gas flame.

The cleanliness of the castings to be braze welded is very important, because contaminants will inhibit the wetting of the filler metal. This wetting is necessary to accomplish the metallic bond between the filler metal and the casting. Both the groove faces and the surfaces adjacent to the joint must be cleaned of all contaminants and foreign materials. This includes graphite smears caused by machining. Graphite smears will adversely affect the wetting of the filler metal. Smears can be removed by quickly heating the cast iron to a dull red color with a slightly oxidizing flame and then wire brushing after cooling. Malleable iron, because of its lower carbon content and rough graphite nodules, can be cleaned by abrasive blasting.

The joints used for braze welding are similar to those used for oxyfuel welding. For thicknesses over 2.4 mm ($\frac{3}{32}$ in.), single and double-V grooves are prepared, with groove angles between 90 and 120°. This allows a large weld-interface area between the base metal and the weld metal. Square grooves can be used for thicknesses of 2.4 mm ($\frac{3}{32}$ in.) or less. In large casting repairs, studs may be inserted into the groove surfaces to increase the strength of the repair (Fig. 9).

The malleable cast iron grades are the easiest to braze weld. Ductile iron is more difficult to braze weld because of its higher total carbon content. The graphite flakes in gray cast iron make it the most difficult to braze weld; special groove preparation will be necessary. The groove surfaces need to be cleaned with caustic or decarburized with an oxidizing oxyfuel flame.

Preheating can be done locally, or the entire part can be heated, depending on the complexity of the part. The part should be preheated to 425 to 480 °C (800 to 900 °F) and slow cooled after welding.

Braze welding uses an oxyfuel gas torch with a slightly oxidizing flame. This is obtained by increasing the oxygen/fuel ratio until the feather disappears and the cone becomes slightly necked. Once the smeared graphite is removed from the groove surfaces, this type of flame is no longer required.

The technique for braze welding is as follows:

- THE BRAZE-WELDING FLUX IS APPLIED TO THE GROOVE FACES AND FILLER METAL TO BE USED.
- THE BASE METAL CASTING IS HEATED UNTIL THE FILLER METAL MELTS, WETS THE CASTING, AND FLOWS ONTO THE GROOVE FACES.
- THE GROOVE IS THEN FILLED WITH ONE OR MORE PASSES. THE CONE OF THE GAS FLAME SHOULD NOT BE DIRECTED ON THE COPPER-ZINC FILLER METAL OR ON IRON-BASE METALS.

References cited in this section

1. "GUIDE FOR WELDING IRON CASTINGS," ANSI/AWS D11.2-89, AMERICAN WELDING SOCIETY, 1989
2. "SPECIFICATION FOR WELDING RODS AND COVERED ELECTRODES FOR CAST IRON," ANSI/AWS A5.15-90, AMERICAN WELDING SOCIETY, 1990

Welding of Cast Irons*

Roger A. Bushey, The ESAB Group, Inc.

Arc-Welding Processes

The arc-welding processes used for welding cast irons are shielded metal arc welding, gas-metal arc welding, flux-cored arc welding, gas-tungsten arc welding, and submerged arc welding.

More than 90% of all industrial welding is done by arc welding. Arc welding has a lower heat input than oxyfuel gas welding because it has a faster welding speed and higher deposition rate. Arc welding may achieve temperatures in excess of 5000 °C (9000 °F) in the arc. Such intense heat allows necessary fusion while heating only a small portion of the weldment. This causes high cooling rates and results in large thermal expansion and contraction stresses. The high cooling rate may also cause more HAZ problems than normally encountered with oxyfuel gas welding. Arc-welding processes are capable of producing welds of high quality when the proper procedure and consumables are used.

Shielded Metal Arc Welding

Shielded metal arc welding (SMAW) is the most widely used process. It uses the heat of the arc to melt the base metal and the tip of the consumable-covered electrode. Protection of the weld pool is achieved by decomposition of the electrode covering.

The electrode and the part to be welded constitute a circuit that also includes the power source, welding leads, and electrode holder. Once an arc is established between the electrode and the base metal, globules of molten metal rapidly form on the tip of the electrode. The molten metal is then transferred through the arc stream into the weld pool. Filler metal is then deposited as this covered electrode is consumed.

The current used can be either an alternating current (ac) or direct current (dc). Any power source capable of supplying the proper range, type and polarity of current, and open circuit voltage may be used.

The advantages of this welding process include a wide range of consumables, good availability, low-cost power sources, and all-position capabilities.

The consumables used for welding cast irons are quite varied. Economic considerations and weld requirements will determine the appropriate electrode for each application.

Cast iron electrodes are covered with a flux to improve arc stability, to reduce porosity, and to add alloying elements. These electrodes produce a composition, mechanical properties, microstructure, and matching color similar to cast iron.

Steel electrodes are made with carbon-steel-core wire and are classified as ESt (Table 5). This classification comes from ANSI/AWS A5.15-90 specification. These steel electrodes are specifically designed for the welding of cast iron, and are different from ordinary mild steel electrodes. The welds deposited by these electrodes are not readily machinable, and it is almost impossible to prevent the formation of hard weld metal with low ductility.

TABLE 5 COMPOSITION OF ELECTRODES FOR THE SHIELDED METAL ARC AND FLUX-CORED ARC WELDING OF CAST IRONS

ELECTRODE PRODUCT FORM	**AWS CLASSIFICATIONS**	**UNS NO.**	COMPOSITION, WT%									
			C	**Mn**	**Si**	**P**	**S**	**Fe**	**Ni**	**Cu**	**Al**	OTHER ELEMENTS (TOTAL)
SHIELDED METAL ARC WELDING ELECTRODES												
UNDILUTED WELD	ENI-CI	W82001	2.0	2.5	4.0	. . .	0.03	8.0	85[A]	2.5	1.0	**1.0**

METAL	ENI-CI-A	W82003	2.0	2.5	4.0	. . .	0.03	8.0	85[A]	2.5	1.0 - 3.0	**1.0**
	ENIFE-CI	W82002	2.0	2.5	4.0	. . .	0.03	BAL	45-60	2.5	1.0	**1.0**
	ENIFE-CI-A	W82004	2.0	2.5	4.0	. . .	0.03	BAL	45-60	2.5	1.0 - 3.0	**1.0**
	ENIFEMN-CI	W82006	2.0	10-14	1.0	. . .	0.03	BAL	35-45	2.5	1.0	**1.0**
	ENICU-A	W84001	0.35 - 0.55	2.3	0.75	. . .	0.025	3.0-6.0	50-60	35 - 45	. . .	**1.0**
	ENICU-B	W84002	0.35 - 0.55	2.3	0.75	. . .	0.025	3.0-6.0	60-70	25 - 35	. . .	**1.0**
CORE WIRE	EST	K01520	0.15	0.60	0.15	0.04	0.04	BAL	. . .	. . .	. . .	**. . .**
FLUX-CORED ARC WELDING ELECTRODES												
UNDILUTED WELD METAL	**ENIFET3-CI**	**W82032**	**2.0**	**3.0-5.0**	**1.0**	**. . .**	**0.03**	**BAL**	**45-60**	**2.5**	**1.0**	**1.0**

(A) MINIMUM

This electrode is normally used to repair small pits, cracks, and other defects when the casting does not require machining. Because the shrinkage of steel is greater than that of cast iron, high tensile stresses develop upon cooling, possibly causing cracking. Groove preparation, as shown in Fig. 5, 6, 7, 8, and studs, as shown in Fig. 9, are recommended for any sizable casting.

Preheating the casting is recommended only when absolutely necessary in order to prevent excessive stresses. Steel electrodes are used at low current to limit the amount of dilution from the casting. The recommended polarity and current for this electrode is dc reverse (electrode positive). The weld beads deposited by these electrodes should be short and widely separated, followed by a light peening after each deposit. After welding, the slag should be completely removed, especially prior to painting.

The hardness level of the weld deposit of a steel electrode depends on dilution of the casting. Small single beads with high dilution have hardnesses as high as 500 HB. Heavier beads with less dilution and multiple passes will have lower hardness levels.

Low-hydrogen electrodes, such as E7016 and E7018, are sometimes used to weld cast irons. They are generally used for cosmetic repair in nonstructural applications where machining is not necessary and cracking is not a major concern. These electrodes are classified in ANSI/AWS A5.1, are readily available at low cost, and are easy to use. The color match of their weld deposit to the casting is good. Because of the dilution of the casting, the weld metal deposit of these electrodes will contain carbon levels of 0.8 to 1.5%. As a result, the deposit will have a high level of hardness and, with rapid cooling, can produce crack-sensitive martensitic microstructures. This can be minimized by using preheat, slow cooling, and postweld annealing.

Stainless steel electrodes are generally not used for welding cast irons. This is due to the formation of chromium carbides during the welding operation, resulting in a crack-prone brittle microstructure. Cracking in the HAZ is likely to occur as a result of differences in tensile strength and coefficient of expansion between the stainless steel weld deposit and the casting.

Nickel-base electrodes are widely used to weld cast irons. Nickel, unlike iron, does not form carbides and has a low solubility for carbon. As the weld metal solidifies and cools, carbon is rejected from solution as graphite. This increases the volume of the weld metal, reducing shrinkage stresses and reducing the likelihood of cracking.

Nickel-base electrodes can be classified into four categories:

- PREDOMINANTLY NICKEL
- 50NI-50FE
- NICKEL-IRON-MANGANESE
- NICKEL COPPER

Predominantly Nickel Electrodes. The electrodes classified as ENi-CI and ENi-CI-A (see Table 5 for composition) produce a weld deposit having a high nickel content; therefore, it is soft and machinable. The "A" designation is used for electrodes to which aluminum has been added to levels from 1 to 3%. These electrodes are used for surfacing applications and where the diluted weld deposit must be machined.

50Ni-50Fe Electrodes. The electrodes classified as ENiFe-CI and ENiFe-CI-A (see Table 5 for composition) have approximately the same level of nickel and iron. These electrodes are different from the high-nickel electrodes in that the:

- WELDS ARE STRONGER AND MORE DUCTILE.
- STRENGTH OF THE ELECTRODES MAKES THEM SUITABLE FOR WELDING DUCTILE AND HIGH-STRENGTH GRAY IRONS.
- ELECTRODES CAN BE USED FOR DISSIMILAR JOINTS, SUCH AS CAST IRON TO CARBON STEEL AND NICKEL-BASE ALLOYS. IF THE DISSIMILAR JOINT USES CAST IRON WELDED TO A CHROMIUM-CONTAINING STEEL SUCH AS STAINLESS STEEL, THEN A BUTTERING LAYER SUCH AS ENI-1 ELECTRODE (ANSI/AWS 5.11) SHOULD BE USED ON THE CAST IRON. THIS WILL HELP PREVENT THE FORMATION OF CHROMIUM CARBIDES IN THE WELD DEPOSIT.
- ELECTRODES CAN BE USED TO WELD GRAY IRONS HAVING HIGH LEVELS OF PHOSPHORUS BECAUSE THE IRON IN THE WELD METAL CAN TOLERATE PHOSPHORUS BETTER THAN NICKEL.

At a chemical composition of 30% Ni and 70% Fe, the nickel-iron alloy has its lowest coefficient of expansion. The weld deposit from ENiFe-CI and ENiFe-CI-A electrodes has approximately this 30Ni-70Fe composition because of base metal dilution. Therefore, these electrodes can be used for thicker sections of casting than the high-nickel electrodes.

Because of the formation of nickel-iron compositions, the weld hardness levels are higher than those made with high-nickel electrodes. Therefore, the use of ENi-CI-A is preferred when machinability is important. In multipass welds, each pass is tempered by each subsequent pass, reducing the hardness and resulting in improved machinability. Typical hardness levels are given in Table 6.

TABLE 6 MECHANICAL PROPERTIES OF WELDS OBTAINED WITH NICKEL-BASE ELECTRODES USED IN SMAW OF CAST IRONS

ELECTRODE	HARDNESS FOR TYPE OF WELD METAL INDICATED								TENSILE STRENGTH		YIELD STRENGTH (0.2% OFFSET)		ELONGATION IN 50 MM (2 IN.), %
	HIGHLY DILUTED BEAD		MODERATELY DILUTED BEAD		MULTIPLE LAYER WELD[A]								
					WELD FACE		ROOT SURFACE						
	HV	HB	HV	HB	HV	HB	HV	HB	MPA	KSI	MPA	KSI	
ENI-CI	220	209	182	173	. . .	. . .	. . .	. . .	276[B]	40[B]	263[B]	38[B]	**3-6[B]**
ENIFE-CI	364	345	209	199	183	174	187	174	400-579[B]	58-84[B]	296-434[B]	43-63[B]	**6-13[B]**
									449-500[C]	65-72[C]	310-358[C]	45-62[C]	**8-19[C]**
									544[D]	**79[D]**	**420-462[D]**	**61-67[D]**	**6-10[D]**

Source: Ref 1

(A) BUTT JOINT OF 12.7 MM ($\frac{1}{2}$ IN.) PLATE USING 60° V AND 4.8 MM ($\frac{3}{16}$ IN.) ROOT OPENING.

(B) AS-WELDED CONDITION.

(C) ANNEALED AT 900 °C (1650 °F) FOR 4 H, FURNACE COOLED.

(D) ANNEALED AT 845 TO 900 °C (1550 TO 1650 °F) FOR 3 H, FURNACE COOLED TO 690 °C (1275 °F) FOR 5 H, FURNACE COOLED SLOWLY TO 595 °C (1100 °F), AIR COOL.

Nickel-Iron-Manganese Electrodes. When manganese is added to the nickel-iron alloy, it improves strength, ductility, and resistance to cracking. The composition of this electrode is given in Table 5 as ENiFeMn-CI. The strength of this alloy is sufficient for joining nodular irons up to the 80-55-06 grades. It is also used where increased wear resistance is needed on surfacing or buildup applications.

Nickel-copper electrodes are also used for welding cast irons, but because of their sensitivity to iron dilution, they will have limited usage. They are to be used with low-penetration procedures because the dilution with iron may cause weld cracking.

Copper-base electrodes are mainly used for surfacing iron castings on bearing surfaces to improve corrosion and wear resistance, or for joining cast irons to dissimilar metals. As described in the section "Base-Metal Preparation" in this article, base metal cleanliness when welding cast iron is very important, especially prior to using copper-base electrodes.

Copper-base electrodes are classified in ANSI/AWS A5.6-84, and the composition and mechanical property requirements are given in Table 7. The coverings developed for these copper-base electrodes perform satisfactorily on cast iron.

TABLE 7 COMPOSITION AND MECHANICAL PROPERTIES FOR COVERED COPPER ALLOY WELDING ELECTRODES USED IN SMAW APPLICATIONS TO JOIN CAST IRONS

AWS CLASSIFICATION	**COMPOSITION, WT %[A][B]**										MECHANICAL PROPERTIES			
											HARDNESS, HB	**TENSILE STRENGTH[F]**		ELONGATION IN 50 MM (2 IN.), %[F]
	Cu + Ag	**Sn**	**Mn**	**Fe**	**Si**	**Ni[C]**	**P**	**Al**	**Pb[D]**	**OTHER ELEMENTS TOTAL[E]**		**MPA**	**KSI**	
ECUSN-A	BAL	4.0-6.0	. . .	0.25	. . .	. . .	0.05-0.35	0.01	0.02	0.50	70-85[G]	240	35	**20**
ECUSN-C	BAL	7.0-9.0	. . .	0.25	. . .	. . .	0.05-0.35	0.01	0.02	0.50	85-100[G]	280	40	**20**
ECUA1-A2	BAL	. . .	. . .	0.5-5.0	1.0	. . .	. . .	7.0-9.0	0.02	0.60	130-150[H]	410	60	**20**
ECUMNNIAL	**BAL**	**. . .**	**11.0-13.0**	**2.0-6.0**	**1.5**	**1.0-2.5**	**. . .**	**5.5-7.5**	**0.02**	**0.60**	**160-200[H]**	**520**	**75**	**15**

Source: ANSI/AWS A5.6-84

(A) PER SPECIFICATION A5.6.

(B) SINGLE VALUES ARE MAXIMUM PERCENTAGES.

(C) INCLUDES COBALT.

(D) MUST BE INCLUDED IN DETERMINING THE VALUE FOR TOTAL OTHER ELEMENTS.

(E) MAXIMUM.

(F) MINIMUM.

(G) 4-9 KN (500 KGF) LOAD.

(H) 30 KN (3000 KGF) LOAD.

Phosphor-Bronze Electrodes. The electrodes classified as ECuSn-A and ECuSn-C are referred to as phosphor-bronze because of the residual phosphorus used for deoxidizing the molten metal during their manufacture. These electrodes, because of their chemical makeup, flow sluggishly and require preheat and interpass temperatures of at least 205 °C (400 °F) on thick base metal. Eliminating moisture from the surface of the metals requires that the electrodes be baked at 120 to 150 °C (250 to 300 °F) prior to use.

The ECuSn-C electrodes have a higher tin content than the ECuSn-A electrodes, resulting in a weld deposit with a higher hardness, tensile strength, and yield strength. Hardness levels for the ECuSn-C electrode deposit range from 85 to 100 HB; for the ECuSn-A electrode deposit, from 70 to 85 HB.

Aluminum-bronze electrodes are also used for welding cast irons. The ECuAl-2 electrode is classified in ANSI/AWS A5.6, and the composition and mechanical property requirements are given in Table 7. This electrode has a weld deposit that has a higher tensile strength than the tin-bronze electrodes (minimum of 415 MPa, or 60 ksi) and a hardness of 130 to 150 HB. Aluminum-bronze electrodes also require close attention to the cleanliness of the base plate prior to welding.

The ECuMnNiAl electrode is also listed in Table 7. This electrode is used for the repair of cast irons where a higher tensile strength is needed than that provided by the ECuAl-A2, ECuSn-A, or ECuSn-C electrode deposit. The ECuMnNiAl electrodes vary the level of aluminum and have higher levels of iron, manganese, and nickel than the ECuAl-A2 electrode. This results in higher minimum tensile strengths of 515 MPa (75 ksi) and hardness levels of 160 to 200 HB.

Gas-Metal Arc Welding

Gas-metal arc welding (GMAW) produces coalescence of metals by heating them with an arc between a continuously fed filler metal electrode and the cast iron to be welded. Shielding is obtained from an externally supplied gas.

This process can produce high deposition rates, high heat input, and deep-penetration welds by varying the arc voltage, gas shielding, and wire-feed speeds of the electrode. These electrodes will function in all positions if used at the proper settings.

The transfer of the molten metal from the electrode to the cast iron being welded can occur in three different modes:

- SPRAY
- GLOBULAR
- SHORT CIRCUITING

The mode of transfer is determined by the heat input and the type of shielding gas used.

Spray transfer takes place at the highest heat input of the three modes and is used in the flat position. An inert gas is required, such as argon or helium or a mixture of the two gases. Spray transfer gives the highest deposition rates and the greatest penetration of the three modes of transfer. It is also the most likely to cause cracking due to the high heat input, resulting in the largest HAZ. Additional information is available in the article "Transfer of Heat and Mass to the Base Metal in Gas-Metal Arc Welding" in this Volume.

The globular transfer mode gives a slightly lower heat input, with the metal transferring as large droplets. This lower heat input makes globular transfer less likely to cause cracking and results in welds having lower penetration than with the spray transfer mode. Globular transfer can be used in all positions, but may require a very experienced welder for the vertical and overhead positions.

The short-circuiting transfer mode is the lowest-heat-input and lowest-penetration mode. This is achieved by having the welding electrode actually contact the weld pool many times per second. As a result, short circuiting produces the smallest HAZ and the lowest crack sensitivity of the three transfer modes. Shielding gases for this process include argon, helium, carbon dioxide, or mixtures of these gases. Short circuiting should be used only on thin sections or with high preheat in order to avoid incomplete-fusion and incomplete-penetration defects.

Choosing the Right Transfer Mode. Selection of transfer mode is dictated by the size and complexity of the casting to be welded, the deposition required, and the weld position to be used. Generally, the low-heat-input processes are preferred because they minimize the melting of the cast iron and stresses introduced by arc welding.

Consumable Electrodes. The consumables of this welding process closely parallel those of SMAW. Steel, nickel-base, nickel-iron, nickel-iron-manganese, and copper-base electrodes are used.

Steel Electrodes. A typical application that uses steel electrodes is the repair of casting defects in noncritical areas of the casting that will not be machined. The color match that steel electrodes provide is excellent. Because the weld will be hard due to the increase in carbon level from dilution of the casting in the weld deposit, steel electrodes should not be used where machining is required. Areas to be welded should be preheated, and parameters should be chosen to minimize penetration--for example, short-circuiting transfer and the use of small-diameter electrodes with a carbon dioxide or C-25 ($75Ar/25CO_2$) shielding gas. The typical welding electrodes used that fall into this category are ER70S-3 and ER70S-6. These electrodes are designed with significant quantities of deoxidizers such as manganese and silicon.

Nickel-base electrodes containing 95% or higher levels of nickel are used to weld cast iron. These electrodes are used when there is highly diluted weld metal and the deposit must be machined. The most common is electrode containing 99% or greater nickel, with no additional deoxidizers. Another electrode that falls into this category is the ERNi-1 electrode classified in ANSI/AWS A5.14. This electrode contains approximately 4% Ti as a deoxidizer, which leads to the formation of titanium carbides, increasing the hardness of the deposit. Table 8 gives recommended shielding gas and welding parameters.

TABLE 8 GMAW PARAMETERS FOR NICKEL-BASE ELECTRODES USED TO WELD CAST IRONS

ELECTRODE DIAMETER		**SHIELDING GAS**	**WIRE-FEED SPEED**		**ARC VOLTAGE, V**	**CURRENT[A], A**	**ELECTRODE EXTENSION**		TRAVEL SPEED	
mm	**in.**		**in./min**	**mm/s**			**in.**	**mm**	**in./min**	mm/s
0.9	0.035	$75AR/25CO_2$	300	130	24	130	1/2	13	15	**6.5**
			400	170	25	160	1/2	13	15	**6.5**
			500	210	27	200	1/2	13	15	**6.5**
		CO_2	300	130	24	125	1/2	13	15	**6.5**
			400	170	25	155	1/2	13	15	**6.5**
			500	210	26	180	1/2	13	15	**6.5**
			575	245	27	200	1/2	13	15	**6.5**
		ARGON	300	130	26	150	1/2	13	15	**6.5**
			400	170	27	190	1/2	13	15	**6.5**
			500	210	28	220[B]	1/2	13	15	**6.5**
			575	245	29	250[B]	1/2	13	15	**6.5**
1.2	0.045	$75AR/25CO_2$	250	105	27	180	5/8	16	15	**6.5**
			300	130	28	190	5/8	16	15	**6.5**

			350	150	29	220	5/8	16	17	**7.0**
			400	170	30	240	5/8	16	20	**8.5**
			500	210	32	280	5/8	16	25	**10.5**
		CO_2	250	105	26	165	5/8	16	15	**6.5**
			300	130	27	180	5/8	16	15	**6.5**
			350	150	28	220	5/8	16	17	**7.0**
			400	170	29	230	5/8	16	20	**8.5**
			500	210	31	270	5/8	16	25	**10.5**
		ARGON	250	105	27	190	5/8	16	15	**6.5**
			300	130	28	220	5/8	16	15	**6.5**
			350	150	29	240(B)	5/8	16	17	**7.0**
			400	170	30	275(B)	5/8	16	20	**8.5**
			500	210	32	310(B)	5/8	16	25	**10.5**
1.6	0.062	75AR/25CO_2	150	65	27	235	5/8	16	17	**7.0**
			175	75	28	235	5/8	16	17	**7.0**
			200	85	29	285	5/8	16	20	**8.5**
			225	95	30	320	5/8	16	25	**10.5**
		CO_2	150	65	27	220	5/8	16	17	**7.0**
			175	75	28	245	5/8	16	17	**7.0**
			200	85	29	265	5/8	16	20	**8.5**
			225	95	30	285	5/8	16	25	**10.5**
		ARGON	150	65	27	240	5/8	16	17	**7.0**
			175	75	28	265	5/8	16	17	**7.0**
			200	85	29	300(B)	5/8	16	20	**8.5**
			225	**95**	**30**	**350(B)**	5/8	**16**	**25**	**10.5**

Source: Ref 1

(A) POLARITY, DCEP.
(B) SPRAY TRANSFER.

Nickel-iron electrodes are also used for the GMAW process. They will deposit a harder weld metal and, therefore, are more sensitive to cracking than the high-nickel electrodes.

Nickel-Iron-Manganese Electrodes. As stated in the section "Shielded Metal Arc Welding" of this article, the addition of manganese increases the crack resistance and strength of the weld deposit. As a result, this consumable is suitable for welding the higher-strength grades of ductile iron, such as 65-45-12 and 80-55-06. The typical hardness level of the weld deposit is 80 to 95 HRB. The composition of this electrode is 12% Mn, 44% Ni, and the remainder iron.

Copper-Base Electrodes. Electrodes containing predominantly copper can be used to join or surface cast iron. The electrodes are classified as ERCuSn-A, ERCuAl-A2, and ERMnNiAl in ANSI/AWS A5.7. Table 9 gives the chemical composition and minimum mechanical properties of these electrodes.

TABLE 9 COMPOSITION AND MECHANICAL PROPERTIES OF COPPER-BASE ELECTRODES USED TO JOIN OR SURFACE CAST IRON IN GMAW APPLICATIONS

AWS CLASSIFICATION	COMPOSITION, WT%[A]											MECHANICAL PROPERTIES		
	CU + AG	ZN	SN	MN	FE	SI	NI + CO	P	AL	PB	OTHER ELEMENTS (TOTAL)[B]	HARDNESS, HB	TENSILE STRENGTH[C]	
													MPA	KSI
ECUSN-A	93.5[C]	[D]	4.0-6.0	[D]	[D]	[D]	[D]	0.10-0.35	0.01[D]	0.02[D]	0.50	70-85[E]	240	**35**
ERCUA1-A2	BAL	0.02	. . .	. . .	1.5	0.10	. . .	. . .	9.0-11.0	0.02[D]	0.50	130-150[F]	415	**60**
ERCUMNNIA 1	**BAL**	**0.15**	**. . .**	**11.0-14.0**	**2.0-4.0**	**0.10**	**1.5-3.0**	**[D]**	**7.0-8.5**	**0.02[D]**	**0.50**	**160-200[F]**	**515**	**75**

Source: Ref 1

(A) SINGLE VALUES ARE MAXIMUMS.

(B) VALUES, INCLUDING ELEMENTS MARKED WITH (D), SHALL NOT EXCEED VALUE SPECIFIED.

(C) MINIMUM.

(D) TOTAL OF THESE ELEMENTS CANNOT EXCEED THOSE IN (B).

(E) 4.9 KN (500 KGF) LOAD.

(F) 30 KN (3000 KGF) LOAD.

Flux-Cored Arc Welding

Flux-cored arc welding (FCAW) produces coalescence of metals by heating them with an arc between a continuous filler metal electrode and the workpiece. The equipment used for GMAW can also be used for FCAW. Shielding may be provided by the decomposition of the flux fill (self-shielding) or as an external shielding gas (gas-shielded).

Core Composition. The electrode core contains slag formers, arc stabilizers, deoxidizers, and metal alloys. Depending on the makeup and the shielding gas, the electrode may achieve a deep- or shallow-penetration weld.

Electrode Types. The different types of FCAW electrodes include steel, iron-nickel, and nickel-iron-manganese.

Steel electrodes are classified in ANSI/AWS A5.20. They are classified based on type of slag system and gas-shielding requirements. The gas-shielded types EXXT-1 and EXXT-2 are futile-or acid-base, and EXXT-5 is basic. The EXXT-5 electrodes are preferred for welding cast iron, because they have lower penetration, resulting in less dilution and therefore greater crack resistance.

The EXXT-4, EXXT-7, and EXXT-8 electrodes are steel electrodes that are classified as self-shielding or require no external shielding gas. These electrodes can be used to weld cast iron.

The weld deposit of these steel flux-cored electrodes will become hardenable steel with the pickup of carbon from the cast iron. This will make these deposits hard to machine and susceptible to cracking.

Iron-Nickel Electrodes. Flux-cored electrodes having a 70/30 iron-nickel ratio are used to repair heavy cast iron vessels. These heavy castings include the pouring ladles and molds in foundries and steel plants. The high hardness of the weld metal is not detrimental, because all it is required to do in service is to fill in voids and maintain the proper contours.

Nickel-iron-manganese electrodes are flux-cored electrodes with the nickel-iron-manganese matrix described previously. The typical composition is 1% C, 5% Mn, 40% Fe, and the balance nickel. The addition of manganese improves the strength, ductility, and machinability of the weld deposit. These electrodes are used for upgrading or repairing castings, fabrication, surfacing, and welding dissimilar metals. Typical welding conditions for the nickel-iron-manganese electrodes are given in Table 10.

TABLE 10 TYPICAL WELDING PARAMETERS FOR FCAW OF CAST IRONS WITH NICKEL-IRON-MANGANESE ELECTRODES

ELECTRODE DIAMETER		WELD TYPE	AWS POSITION SPECIFICATION	WIRE FEED SPEED		CURRENT		VOLTAGE, V
MM	IN.			MM/S	IN./MIN	A	POLARITY	
2.0	5/64	FLAT BUTT OR FILLET	1G,F	101	240	300	DCEP	**30**
2.0	5/64	VERTICAL BUTT OR FILLET	3G,F	55	130	180	DCEP	**18-25**
2.4	3/32	FLAT BUTT OR FILLET	1G,F	90	215	320	DCEP	**32**
2.4	3/32	FLAT OVERLAY(A)	. . .					
		FIRST LAYER	. . .	88	210	250	DCEN	**29-33**
		REMAINING LAYERS	**. . .**	**113**	**270**	**350**	**DCEP**	**28-30**

(A) OSCILLATION RECOMMENDED: 19 TO 25 MM ($\frac{3}{4}$ TO 1 IN.) WIDTH, 26 TO 40 CYCLES PER MINUTE. OVERLAP PREVIOUS BEAD 6.4 TO 9.6 MM ($\frac{1}{4}$ TO $\frac{3}{8}$ IN.).

Gas-Tungsten Arc Welding

Gas-tungsten arc welding (GTAW) produces the coalescence of metals by heating them with an arc between a tungsten electrode (nonconsumable) and the workpiece. Shielding is obtained from an inert gas such as argon or gas mixtures. This process can make autogenous welds or welds using a filler metal. The filler metals would be the same as those used for GMAW; however, the ENi-1 electrode containing titanium is not recommended.

The GTAW process is used for the welding of cast iron utilizing nickel or nickel-base filler metal with an argon shielding gas. The procedure for GTAW welding should minimize dilution of the weld by the base metal.

Again, it is of utmost importance to make sure that the groove surface to be welded is free of contaminants. The joint design must be wide enough to facilitate manipulation of the torch and retention of the external shielding gas.

Submerged Arc Welding

Submerged arc welding (SAW) produces the coalescence of metals by heating them with an arc or multiple arcs between a bare metal electrode(s) and the workpiece. The arc, as well as the molten metal, is protected by a granular flux. This welding process is capable of producing welds only in the flat position.

The electrode used for SAW can be either solid or flux-cored. The SAW process is designed and used for high-deposition welding. The equipment used is similar to that for GMAW. The flux can be added manually or by some automatic feeding system.

The only filler metals used for SAW are nickel-base materials. Further alloy additions can be made by variations in the flux, by using powdered metals, or by adding welding wire. The nickel-iron-manganese electrode can be used for groove, fillet, or surfacing applications. This alloy is more resistant to cracking and therefore is more widely used than other nickel-base electrodes.

The selection of the flux is also very important for ensuring a quality weld. The flux must be matched to the filler metal to be used, alloy requirements, strength requirements, and multiple-pass requirements. Welding conditions for SAW are given in Table 11.

TABLE 11 RECOMMENDED PARAMETERS FOR SAW OF CAST IRONS WITH NICKEL-BASE ELECTRODES

WELD TYPE	CURRENT	VOLTAGE,V	ELECTRODE EXTENSION		TRAVEL SPEED		OSCILLATION		
							WIDTH		FREQUENCY, CYCLES/MIN
			mm	in.	mm/s	in./min	mm	in.	
OVERLAY	250	32-34	25	1	2	$4\frac{1}{2}$	29	$1\frac{1}{8}$	**60**
GROOVE/FILLET	**250**	**32**	**25**	**1**	**4.3**	**10**	**. . .**	**. . .**	**. . .**

Source: Ref 1

Surfacing and Overlaying

Surfacing processes are used to restore surfaces or to improve the surface properties of iron castings damaged by corrosion, spalling, or wear. Any process used for the fabrication, maintenance, or repair of iron castings can be used successfully for surfacing.

Materials for surfacing can be any material normally used for the brazing or welding of iron castings. Ceramic powders and hardfacing alloys not normally associated with cast iron are gaining wide acceptance.

Oxyfuel gas welding was first used for buildup. The total heat input to the base metal is high, producing a large HAZ; however, the cooling rate is quite slow, reducing the residual stresses and the formation of hard martensitic microstructures. This process allows good control of the metal size, shape, and thickness, thus requiring less expensive equipment. However, it is a low-deposition process.

The arc-welding processes are the most commonly used for surfacing cast irons. Process selection depends on the application, grade or type of cast iron, degree of dilution allowable, thickness of the deposit desired, and the intended service.

Thermal spraying processes are employed for surfacing to improve wear or corrosion properties, to salvage mismachined parts, and to improve the service life of a cast iron.

Flame spraying uses the heat from a fuel gas and oxygen to melt surfacing material in the form of cord, powder, rod, or wire. Compressed air is used to propel the melted particles onto the cast iron to be surfaced. The fuel gas usually used for this process is acetylene. Flame spraying can produce bond strengths of 17 to 41 MPa (2.5 to 6.0 ksi), depending on the surfacing material used. Bond strengths of 70 MPa (10 ksi) can be obtained by using special techniques, such as high-energy compressed gas with detonation gun systems. Powders containing boron and silicon can be fused after spraying, producing a homogeneous metallurgical structure with the substrate.

Arc spraying uses the heat produced between two electrically conductive wires. Compressed air is then used to atomize and propel the molten surfacing metal particles to the surface of cast iron. Arc spraying has the highest deposition rate of all the surfacing processes. Bond strengths of 35 to 70 MPa (5 to 10 ksi) are possible, but strength depends on the surfacing metal used.

Plasma spraying involves the use of a water-cooled gun containing a tungsten cathode surrounded by a copper anode nozzle. The arc generated in the gun produces a plasma, which is forced through a small orifice in the copper nozzle by an ionized shielding gas. An additional envelope of inert or mixed carrier gas is added to the stream as it passes out of the gun. The metal or ceramic powders used for surfacing cast iron are pressure fed into the gas stream, melted, then propelled to the cast iron. A clean surface is of utmost importance for achieving a good bond between the thermal spray deposit and the cast iron substrate being surfaced.

Additional processes, such as laser and electron beam, can be used to melt surfacing material to produce layers of deposited metal on cast iron. The surfacing material can take many forms, such as powder, rod, wire, or strip, as long as they can be fed into the beam. Laser remelting is used on thermal spray deposits when a denser deposit with a metallic bond is required.

Surfacing Materials. Filler metals used for surfacing and overlaying are the same as those used in the other welding processes described. Copper alloys are used for corrosion resistance or to build up surfaces for wear. Alloys designed for corrosion resistance are covered under ANSI/AWS A5.6 and A5.7. Classifications, such as CuSn-A, CuSn-C, CuAl-A2, and Cu-NiAl, are used for this purpose.

Hardfacing alloys, as covered in ANSI/AWS A5.13, are used for surfacing cast irons. Copper alloys, such as the CuZn grades B, C, and D, are used for bearing surfaces. A buttering layer of CuAl-2 is recommended before trying to apply a surface of the CuZn grades. If several layers are required, then a stress relieving of 315 °C (600 °F) is recommended after each layer is added.

Stainless steels, not typically used for joining or repairing iron castings, are used for surfacing to increase corrosion and oxidation resistance. Carbon absorption into the stainless steel is a problem. It can cause the formation of chromium carbide and can lower the crack resistance by reducing the level of ferrite. This can be eliminated by first surfacing with a low-carbon nickel electrode before adding the stainless steel surface. The stainless steel deposit may increase in nickel level as a result of the buttering, thus lowering the volume of ferrite, but the formation of chromium carbides is eliminated. The amount of dilution can be minimized by overlapping the beads.

A deposit with a convex shape is recommended. This will help eliminate the tendency of the weld to separate from the casting due to differences in the coefficient of expansion between stainless steel and cast iron.

High-nickel alloys are used for surfacing to correct machining errors, to provide surface machinability in castings containing high phosphorus, and to improve resistance to caustic attack. Classifications such as ENi-CI and ENi-CI-A, which are discussed in the "Shielded Metal Arc Welding" of this article, are used. In addition, alloys covered in ANSI/AWS A5.11 and A5.14 are also used.

The corrosion resistance of a nickel overlay can be greatly reduced if it becomes diluted with iron and carbon from the cast iron. This dilution can be minimized by overlapping beads up to one-half the bead width. Stringer beads are the

preferred method except for the SAW process. Widely oscillated beads with straight polarity (electrode negative) are used for SAW surfacing applications. Again, a buffer layer of nickel should be added to reduce the effects caused by differences in the coefficient of expansion between the surfacing material and the iron casting.

Cast iron alloys are used for buildup when comparable microstructure is required in the application. These electrodes are available in gray, ductile, and malleable iron compositions. The use of preheat, the proper interpass temperature, and a postweld heat treatment may be necessary to ensure a crack-free deposit.

Hardfacing alloys are specified in ANSI/AWS A5.13 and A5.21. They are used for over-laying when wear is the main concern. These alloys may increase the low-stress abrasion resistance, hot hardness, and corrosion resistance of the casting. For more demanding service conditions, nickel- or cobalt-base alloys may be used.

Special precautions must be taken when using hardfacing alloys containing high levels of chromium carbides, which are designed to stress crack in service. Several layers of an iron-nickel alloy, such as ENiFe-CI or ENiFe-CI-A are used to obtain a buffer zone between the hardfacing alloy and the iron casting. Preheating and techniques for minimizing dilution are required when welding these high-chromium alloys.

Ceramic materials or other refractory materials can be overlayed on cast iron when thermal distortion of the casting is important. Other materials, such as alumina and chromium oxide, are used in high-temperature wear and corrosion-resistance applications. Tungsten carbide is applied when surface temperatures up to 540 °C (1000 °F) will be encountered in service or when abrasion resistance is the main concern.

Minimizing dilution of the base iron casting into the weld deposit can be kept to a minimum by:

- MAXIMIZING THE AMOUNT OF METAL DEPOSITED PER UNIT LENGTH. THE BEADS BEING DEPOSITED SHOULD BE OVERLAPPED AS MUCH AS POSSIBLE
- MINIMIZING THE AMOUNT OF HEAT INPUT IN ORDER TO REDUCE THE AMOUNT OF BASE METAL MELTING. THE USE OF STRAIGHT-POLARITY DC CURRENT WILL HELP DECREASE THE PENETRATION
- USING MULTIPLE LAYERS INSTEAD OF ONLY ONE LAYER

Caution must be exercised when considering the reduction in penetration or melting of the cast iron substrate. The deposited weld metal must melt part of the casting to adhere properly. A rule of thumb is that a minimum of 5 to 10% dilution is needed for complete fusion.

Reference cited in this section

1. "GUIDE FOR WELDING IRON CASTINGS," ANSI/AWS D11.2-89, AMERICAN WELDING SOCIETY, 1989

Welding of Cast Irons*

Roger A. Bushey, The ESAB Group, Inc.

References

1. "GUIDE FOR WELDING IRON CASTINGS," ANSI/AWS D11.2-89, AMERICAN WELDING SOCIETY, 1989
2. "SPECIFICATION FOR WELDING RODS AND COVERED ELECTRODES FOR CAST IRON," ANSI/AWS A5.15-90, AMERICAN WELDING SOCIETY, 1990

Welding of Aluminum Alloys

Paul B. Dickerson, Aluminum Company of America (retired)

Introduction

ALUMINUM AND ITS ALLOYS can be joined by as many or more methods than any other metal. The primary methods used are the gas-shielded arc welding processes, which are described in detail in this article. Other methods are briefly reviewed.

Aluminum has several chemical and physical properties that need to be understood when using the various joining processes. The specific properties that affect welding are its oxide characteristics; the solubility of hydrogen in molten aluminum; its thermal, electrical, and nonmagnetic characteristics; its lack of color change when heated; and its wide range of mechanical properties and melting temperatures that result from alloying with other metals. Various property values are provided in Tables 1, 2, 3, and 4.

TABLE 1 COMPOSITION, PHYSICAL PROPERTIES, AND WELDABILITY OF SELECTED NON-HEAT-TREATABLE WROUGHT ALUMINUM ALLOYS

BASE ALLOY	NOMINAL COMPOSITION, WT%					APPROXIMATE MELTING RANGE		THERMAL CONDUCTIVITY AT 25 °C (77 °F)		ELECTRICAL CONDUCTIVITY[A], %IACS	WELDABILITY[B]				
	Al	Cu	Mn	Mg	Cr	°C	°F	W/M · K	BTU/FT · H · °F		GAS	ARC WITH FLUX	ARC WITH INERT GAS	RESISTANCE	PRESSURE
1060	[GES]99.6	. . .	. . .	. . .	. . .	646-657	1195-1215	234	135	62	A	A	A	B	**A**
1100	[GES]99.0	. . .	. . .	. . .	. . .	643-657	1190-1215	222	128	59	A	A	A	A	**A**
1350	[GES]99.5	. . .	. . .	. . .	. . .	646-657	1195-1215	234	135	62	A	A	A	B	**A**
3003	REM	0.12	1.2	. . .	. . .	643-654	1190-1210	193	112	50	A	A	A	A	**A**
3004	REM	. . .	1.2	1.0	. . .	629-654	1165-1210	163	94	42	B	A	A	A	**B**
5005	REM	. . .	. . .	0.8	. . .	632-654	1170-1210	200	116	52	A	A	A	A	**A**
5050	REM	. . .	. . .	1.4	. . .	624-652	1155-1205	193	112	50	A	A	A	A	**A**
5052, 5652	REM	. . .	. . .	2.5	. . .	607-649	1125-1200	138	80	35	A	A	A	A	**B**
5083	REM	. . .	0.7	4.4	0.15	574-638	1065-1180	117	67.5	29	C	C	A	A	**C**
5086	REM	. . .	0.45	4.0	0.15	585-641	1085-1185	125	72.5	31	C	C	A	A	**B**
5154, 5254	REM	. . .		3.5	0.25	593-643	1100-1190	125	72.5	32	C	C	A	A	**B**
5454	REM	. . .	0.8	2.7	0.12	602-646	1115-1195	134	77.5	34	B	B	A	A	**B**
5456	**REM**	**. . .**	**0.8**	**5.1**	**0.12**	**568-638**	**1055-1180**	**117**	**67.5**	**29**	**C**	**C**	**A**	**A**	**C**

(A) EQUAL VOLUME AT 20 °C (68 °F).

(B) WELDABILITY RATINGS: A, READILY WELDABLE; B, WELDABLE IN MOST APPLICATIONS, BUT MAY REQUIRE SPECIAL TECHNIQUE OR FILLER ALLOY; C, LIMITED WELDABILITY

TABLE 2 COMPOSITION, PHYSICAL PROPERTIES, AND WELDABILITY OF SELECTED HEAT-TREATABLE WROUGHT ALUMINUM ALLOYS

BASE ALLOY	NOMINAL COMPOSITION OF ALLOYING ELEMENTS, WT%								APPROXIMATE MELTING RANGE		THERMAL CONDUCTIVITY AT 25 °C (77 °F)		ELECTRICAL CONDUCTIVITY[A], %IACS	WELDABILITY[B]				
	CU	SI	MN	MG	ZN	CR	AL	OTHERS	°C	°F	W/M · K	BTU/FT · H · °F		GAS	ARC WITH FLUX	ARC WITH INERT GAS	RESISTANCE	PRESSURE
2014	4.4	0.8	0.8	0.50	. . .	. . .	REM	. . .	507-593	945-1100	154	89	40	X	C	B	B	**C**
2024	4.4	. . .	0.6	1.5	. . .	. . .	REM	. . .	502-638	935-1180	121	70	30	X	C	C	B	**C**
2090	2.7	. . .	. . .	. . .	. . .	. . .	REM	2.2 LI; 0.12 ZR	560-643	1040-1190	88	51	17	X	X	B	B	**C**
2219	6.3	. . .	0.30	. . .	. . .	. . .	REM	0.6 TI; 0.10 V; 0.18 ZR	543-643	1010-1190	121	70	30	X	C	A	B	**C**
2618	2.3	0.18	. . .	1.6	. . .	. . .	REM	1.1 FE; 1.0 NI; 0.07 TI	549-638	1020-1180	161	93	37	X	C	B	B	**C**
6009	0.40	0.8	0.50	0.6	0.25	0.10	REM	. . .	560-649	1040-1200	167	97	44	C	C	B	B	**B**
6013	0.9	0.25	0.35	0.95	. . .	. . .	REM	. . .	579-649	1075-1200	150	87	38	C	C	B	A	**B**
6061	0.28	0.6	. . .	1.0	. . .	0.20	REM	. . .	582-652	1080-1205	167	97	43	A	A	A	A	**B**
6063	. . .	0.40	. . .	0.7	. . .	. . .	REM	. . .	616-654	1140-1210	200	116	53	A	A	A	A	**B**
6101	. . .	0.50	. . .	0.6	. . .	. . .	REM	. . .	621-654	1150-1210	218	126	57	A	A	A	A	**B**
6262	0.28	0.6	. . .	1.0	. . .	0.09	REM	0.6 PB; 0.6 BI	582-652	1080-1205	172	99	44	C	C	B	A	**B**
6351	. . .	1.0	0.6	1.0	. . .	. . .	REM	. . .	596-652	1105-1205	176	102	46	A	A	A	A	**B**
6951	0.28	0.35	. . .	0.6	. . .	. . .	REM	. . .	616-654	1140-1210	198	114	52	A	A	A	A	**A**
7005	. . .	. . .	0.45	1.4	4.5	0.13	REM	0.15 ZR; 0.04 TI	607-646	1125-1195	. . .	. . .	. . .	X	X	A	A	**B**

7039	. . .	. . .	0.30	2.8	4.0	0.20	REM	. . .	577-638	1070-1180	154	89	34	X	X	A	A	**B**
7075	1.6	. . .	. . .	2.5	5.6	0.23	REM	. . .	477-635	890-1175	130	75	33	X	X	C	B	**C**
7079	0.6	. . .	0.20	3.3	4.3	0.20	REM	. . .	482-638	900-1180	125	72	32	X	X	C	B	**C**
7178	**2.0**	**. . .**	**. . .**	**2.8**	**6.8**	**0.23**	**REM**	**. . .**	**477-629**	**890-1165**	**125**	**72**	**31**	**X**	**X**	**C**	**B**	**C**

(A) EQUAL VOLUME AT 20 °C (68 °F).

(B) WELDABILITY RATINGS: A, READILY WELDABLE; B, WELDABLE IN MOST APPLICATIONS, BUT MAY REQUIRE SPECIAL TECHNIQUE OR FILLER ALLOY; C, LIMITED WELDABILITY; X, METHOD NOT RECOMMENDED

TABLE 3 COMPOSITION, PHYSICAL PROPERTIES, AND WELDABILITY OF SELECTED NON-HEAT-TREATABLE CAST ALUMINUM ALLOYS

BASE ALLOY	NOMINAL COMPOSITION OF ALLOYING ELEMENTS, WT%					APPROXIMATE MELTING RANGE		THERMAL CONDUCTIVITY AT 25 °C (77 °F)		ELECTRICAL CONDUCTIVITY[A], %IACS	WELDABILITY[B]				
	CU	SI	MG	ZN	OTHERS	°C	°F	W/M · K	BTU/FT · H · °F		GAS	ARC WITH FLUX	ARC WITH INERT GAS	RESISTANCE	PRESSURE
SAND CASTINGS															
208.0	4.0	3.0	. . .	. . .	. . .	521-632	970-1170	121	70	31	C	C	B	B	**X**
443.0	. . .	5.25	. . .	. . .	. . .	577-632	1070-1170	146	84	37	A	A	A	A	**X**
511.0	. . .	0.50	4.0	. . .	. . .	588-638	1090-1180	141	82	36	X	X	A	A	**X**
512.0	. . .	1.8	4.0	. . .	. . .	588-632	1090-1170	146	84	38	X	X	B	B	**X**
514.0	. . .	. . .	4.0	. . .	. . .	599-638	1110-1180	137	79	35	X	X	A	A	**X**
535.0	. . .	. . .	6.9	. . .	0.18 MN; 0.18 TI; 0.005 BE	549-632	1020-1170	99	58	23	X	X	A	A	**X**
710.0	0.50	. . .	0.7	6.5	. . .	599-649	1110-1200	137	79	35	C	C	B	B	**X**
712.0	. . .	. . .	0.6	5.8	0.50 CR; 0.20 TI	599-638	1110-1180	159	92	40	C	C	A	B	**X**
PERMANENT MOLD CASTINGS															
208.0	4.0	3.0	. . .	. . .	. . .	521-632	970-1170	121	70	31	C	C	B	B	**X**
238.0	10.0	4.0	0.25	. . .	. . .	510-599	950-1110	104	60	25	C	C	B	A	**X**
443.0	. . .	5.25	. . .	. . .	. . .	577-632	1070-1170	146	84	37	A	A	A	A	**X**
A444.0	. . .	7.0	. . .	. . .	. . .	577-632	1070-1170	159	92	41	A	A	A	A	**X**
513.0	. . .	. . .	4.0	1.8	. . .	582-638	1080-1180	133	77	34	X	X	A	A	**X**
711.0	0.50	. . .	0.35	6.5	1.0 FE	599-643	1110-1190	159	92	40	B	B	A	A	**X**
DIE CASTINGS															
360.0	. . .	9.5	0.50	. . .	. . .	571-588	1060-1090	146	84	37	C	X	C	B	**X**

380.0	3.5	8.5	. . .	. . .	. . .	521-588	970-1090	108	62	27	C	X	C	B	**X**
413.0	. . .	12.0	. . .	. . .	. . .	577-588	1070-1090	154	89	39	C	X	C	B	**X**
518.0	**. . .**	**. . .**	**8.0**	**. . .**	**. . .**	**538-621**	**1000-1150**	**99**	**58**	**24**	**X**	**X**	**C**	**B**	**X**

(A) EQUAL VOLUME AT 20 °C (68 °F).

(B) WELDABILITY RATINGS: A, READILY WELDABLE; B, WELDABLE IN MOST APPLICATIONS, BUT MAY REQUIRE SPECIFIC TECHNIQUE OR FILLER ALLOY; C, LIMITED WELDABILITY; X, JOINING METHOD NOT RECOMMENDED

TABLE 4 COMPOSITION, PHYSICAL PROPERTIES, AND WELDABILITY OF SELECTED HEAT-TREATABLE CAST ALUMINUM ALLOYS

BASE ALLOY	NOMINAL COMPOSITION OF ALLOYING ELEMENTS, WT%					APPROXIMATE MELTING RANGE		THERMAL CONDUCTIVITY AT 25 °C (77 °F)		ELECTRICAL CONDUCTIVITY[A], %IACS	WELDABILITY[B]				
	CU	SI	MG	NI	OTHERS	°C	°F	W/M · K	BTU/FT · H · °F		GAS	ARC WITH FLUX	ARC WITH INERT GAS	RESISTANCE	PRESSURE
ONLY SAND CASTINGS															
A201.0	4.5	. . .	0.25	. . .	0.7 AG; 0.30 MN; 0.25 TI	571-649	1060-1200	121	70	30	C	C	B	B	**X**
240.0	8.0	. . .	6.0	. . .	0.50 MN	516-604	960-1120	95	55	23	X	X	C	B	**X**
A242.0	4.1	. . .	1.5	2.0	0.20 CR; 0.13 TI	527-638	980-1180	146	84	38	X	X	B	B	**X**
295.0	4.5	1.1	. . .	. . .	. . .	521-643	970-1190	141	82	35	C	C	B	B	**X**
520.0	. . .	. . .	10.0	. . .	. . .	449-599	840-1110	87	50	21	C	C	B	C	**X**
ONLY PERMANENT MOLD CASTINGS															
332.0	3.0	9.5	1.0	. . .	1.0 ZN	521-582	970-1080	104	60	26	X	X	B	B	**X**
333.0	3.5	9.0	0.30	. . .	. . .	521-588	970-1090	117	68	29	X	X	B	B	**X**
336.0	1.0	12.0	1.0	2.5	. . .	538-571	1000-1060	117	68	29	C	C	B	B	**X**
354.0	1.8	9.0	0.50		. . .	538-599	1000-1110	125	72	32	C	C	B	B	**X**
SAND AND PERMANENT MOLD CASTINGS															
222.0	10.0	. . .	0.25	. . .	. . .	521-627	970-1160	130	75	33	X	X	B	B	**X**
242.0	4.0	. . .	1.5	2.0	. . .	527-638	980-1180	133	77	34	X	X	C	B	**X**
319.0	3.5	6.0	. . .	. . .	. . .	521-604	970-1120	112	65	27	C	C	B	B	**X**
355.0	1.3	5.0	0.50	. . .	. . .	549-621	1020-1150	150	87	39	B	B	B	B	**X**
C355.0	1.3	5.0	0.50	. . .	. . .	549-621	1020-1150	146	84	39	B	B	B	B	**X**
356.0	. . .	7.0	0.35	. . .	. . .	560-616	1040-1140	150	87	41	A	A	A	A	**X**

A356.0	. . .	7.0	0.35	. . .	. . .	560-610	1040-1130	150	87	40	A	A	A	A	**X**
A357.0	. . .	7.0	0.55	. . .	0.5 BE	554-610	1030-1130	159	92	40	B	B	A	A	**X**
359.0	**. . .**	**9.0**	**0.6**	**. . .**	**. . .**	**566-599**	**1050-1110**	**137**	**79**	**35**	**B**	**B**	**A**	**A**	**X**

(A) EQUAL VOLUME AT 20 °C (68 °F).

(B) WELDABILITY RATINGS: A, READILY WELDABLE; B, WELDABLE IN MOST APPLICATIONS, BUT MAY REQUIRE SPECIAL TECHNIQUE OR FILLER ALLOY; C, LIMITED WELDABILITY; X, JOINING METHOD NOT RECOMMENDED

Welding of Aluminum Alloys

Paul B. Dickerson, Aluminum Company of America (retired)

Properties of Aluminum

Oxide. Aluminum has a strong chemical affinity for oxygen and it will oxidize immediately upon exposure to air. Thermal treatments and moist storage conditions will increase oxide thickness, as will electrochemical "anodizing" treatments applied for ornamental, architectural, and wear-resistance applications. The natural oxide is thin enough to be removed by either inert-gas welding arcs or fluxes. However, the thicker oxide should be reduced by chemical or mechanical means prior to welding.

Aluminum oxide melts at about 2050 °C (3720 °F), which is much higher than the melting point of the base alloy. If the oxide is not removed or displaced, the result is incomplete fusion. The fluxes used with some joining processes in order to remove the oxide contain chlorides and fluorides that must be removed after the joining operation to avoid a possible corrosion problem in service. This has led to a wide acceptance of the inert-gas arc welding processes, which remove the oxide without use of a flux.

Aluminum oxide is an electrical insulator. If it is thick enough, as in anodic coatings, then it can prevent arc initiation. In this case, oxide reduction is required not only in the weld joint, but also at the location of the ground lead connection. A thick oxide on a gas-metal arc welding (GMAW) electrode (from a thermal treatment or storage in a humid atmosphere) can produce erratic electrical commutation in the contact tube of the gun, with poor welding results.

Hydrogen Solubility. Hydrogen dissolves very rapidly in molten aluminum. However, hydrogen has almost no solubility in solid aluminum and it has been determined to be the primary cause of porosity in aluminum welds. High temperatures of the weld pool allow a large amount of hydrogen to be absorbed, and as the pool solidifies, the solubility of hydrogen is greatly reduced. Hydrogen that exceeds the effective solubility limit forms gas porosity, if it does not escape from the solidifying weld.

Any source of hydrogen--such as lubricant on the base metal or filler, moisture on the surface or in the form of a hydrated oxide on the base or filler metals, moisture leaks or condensation inside the nozzle of a water-cooled torch, or moisture in the shielding gas--must be eliminated in order to produce sound welds. The aluminum-magnesium (5*xxx* series) alloys are most sensitive to forming a hydrated oxide, and spooled bare electrode must be stored in a dry, heated area. The moisture cannot be removed from the hydrated oxide by heating, as is done with flux-coated electrodes.

Electrical Conductivity. When arc welding, the ground connection can be attached anywhere on the part. This is preferred to the attachment of the ground cable to a steel work table, because the insulating oxide on the aluminum and rust on the steel can both cause a poor transfer of the electric current. Arcing at contact points can occur and can mar the aluminum surface. Aluminum alloys possess high electrical conductivity and pure aluminum has 62% that of pure copper, as shown in Tables 1, 2, 3, and 4.

High electrical conductivity permits the use of long contact tubes in GMAW guns, because resistance heating of the electrode does not occur, as is experienced with ferrous electrodes. Long contact tubes are desirable to provide multiple contact points for good current commutation. Arcing in short contact tubes is common with aluminum, because of its natural insulating oxide, when only a couple of contacts are available. This is especially true when the arc is being initiated using a constant-voltage power supply and a fast electrode "run-in" speed, which cause a high-current surge.

The nonmagnetic property of aluminum minimizes problems of "arc blow" and makes it a suitable material for clamps and fixtures when arc welding other materials. Vacuum attachments, rather than magnetic devices, are required for lifting or attaching portable welding tracks and the like.

Thermal Characteristics. The thermal conductivity of aluminum is about 6 times that of steel. Although the melting temperature of aluminum alloys is substantially below that of ferrous alloys, higher heat inputs are required to weld aluminum because of its high specific heat. Even so, if a slow welding pace is employed, then the heat can be conducted

ahead of the arc, requiring continuous adjustments of welding parameters. Most uniform welding conditions dictate high heat inputs with moderate welding speeds.

High thermal conductivity makes aluminum very sensitive to fluctuations in heat input by the welding process. Specifically, a steady heat input is required with the faster welding processes, such as GMAW, to avoid variations in penetration and fusion. For instance, both of these discontinuities can result from the fluctuations in current that occur in the root pass of a groove or fillet weld when manipulating a GMAW gun powered by a constant-voltage machine. For assemblies subjected to radiographic examination, the use of a constant-current (drooping volt-ampere characteristic) power supply with the GMAW process is preferred in order to produce the soundest welds in aluminum.

The thermal expansion of aluminum is about twice that of steel, and aluminum welds shrink about 6% by volume during solidification. Thin material must be fixtured or "tack welded" closely to keep the edges of the joint in alignment. Shrinkage must be balanced by the welding sequence to control distortion. Weld termination craters must be given more attention and avoided in order to prevent shrinkage voids and crater cracking.

Aluminum does not change color as it is heated. Therefore, the welder must be in a position to see the melting under the arc in order to control the degree of melting as the weld progresses.

Forms of Aluminum. Most forms of aluminum can be welded. All the wrought forms (sheet, plate, extrusions, forgings, rod, bar, and impact extrusions), as well as sand and permanent mold castings, can be welded. Welding on conventional die castings produces excessive porosity in both the weld and the base metal adjacent to the weld because of internal gas. Vacuum die castings, however, have been welded with excellent results. Powder metallurgy (P/M) parts also may suffer from porosity during welding because of internal gas.

The alloy composition is a much more significant factor than the form in determining the weldability of an aluminum alloy. Compositions of the major wrought base alloys and their relative weldability ratings are given in Tables 1 and 2. Similar data are listed in Tables 3 and 4 for the common casting alloys.

Welding of Aluminum Alloys

Paul B. Dickerson, Aluminum Company of America (retired)

Filler Alloy Selection Criteria

When choosing the optimum filler alloy, the end use of the weldment and its desired performance must be prime considerations. Many alloys and alloy combinations can be joined using any one of several filler alloys, but only one filler may be optimal for a specific application. Table 5 lists the chemical composition and melting range of standard aluminum filler alloys.

TABLE 5 NOMINAL COMPOSITION AND MELTING RANGE OF STANDARD ALUMINUM FILLER ALLOYS

ALUMINUM ALLOY	NOMINAL COMPOSITION, WT%								APPROXIMATE MELTING RANGE	
	SI	CU	MN	MG	CR	TI	AL	OTHERS	°C	°F
1100	. . .	0.12	. . .	. . .	. . .	. . .	[GES]99.00	. . .	643-657	**1190-1215**
1188	. . .	. . .	. . .	. . .	. . .	. . .	[GES]99.88	. . .	657-660	**1215-1220**
2319	. . .	6.3	0.30	. . .	. . .	0.15	REM	0.18 ZR; 0.10 V	543-643	**1010-1190**
4009[A]	5.0	1.25	. . .	0.50	. . .	. . .	REM	. . .	546-621	**1015-1150**
4010[B]	7.0	. . .	. . .	0.35	. . .	. . .	REM	. . .	557-613	**1035-1135**
4011[C]	7.0	. . .	. . .	0.58	. . .	0.12	REM	0.55 BE	557-613	**1035-1135**
4043	5.25	. . .	. . .	. . .	. . .	. . .	REM	. . .	574-632	**1065-1170**
4047	12.0	. . .	. . .	. . .	. . .	. . .	REM	. . .	577-582	**1070-1080**
4145	10.0	4.0	. . .	. . .	. . .	. . .	REM	. . .	521-585	**970-1085**
4643	4.1	. . .	. . .	0.20	. . .	. . .	REM	. . .	574-635	**1065-1175**

5183	. . .	. . .	0.75	4.75	0.15	. . .	REM	. . .	579-638	**1075-1180**
5356	. . .	. . .	0.12	5.0	0.12	0.13	REM	. . .	571-635	**1060-1175**
5554	. . .	. . .	0.75	2.7	0.12	0.12	REM	. . .	602-646	**1115-1195**
5556	. . .	. . .	0.75	5.1	0.12	0.12	REM	. . .	568-635	**1055-1175**
5654	. . .	. . .	. . .	3.5	0.25	0.10	REM	. . .	593-643	**1100-1190**
C355.0	5.0	1.25	. . .	0.50	. . .	. . .	REM	. . .	546-621	**1015-1150**
A356.0	7.0	. . .	. . .	0.35	. . .	. . .	REM	. . .	557-613	**1035-1135**
A357.0	**7.0**	**. . .**	**. . .**	**0.58**	**. . .**	**0.12**	**REM**	**0.55 BE**	**557-613**	**1035-1135**

(A) WROUGHT ALLOY WITH COMPOSITION IDENTICAL TO CAST ALLOY C355.0.

(B) WROUGHT ALLOY WITH COMPOSITION IDENTICAL TO CAST ALLOY A356.0.

(C) WROUGHT ALLOY WITH COMPOSITION IDENTICAL TO CAST ALLOY A357.0

The primary factors commonly considered when selecting a welding filler alloy are:

- EASE OF WELDING OR FREEDOM FROM CRACKING
- TENSILE OR SHEAR STRENGTH OF THE WELD
- WELD DUCTILITY
- SERVICE TEMPERATURE
- CORROSION RESISTANCE
- COLOR MATCH BETWEEN THE WELD AND BASE ALLOY AFTER ANODIZING

Each of these factors is addressed below.

Sensitivity to Weld Cracking. Ease of welding is the first consideration for most welding applications. In general, the non-heat-treatable aluminum alloys can be welded with a filler alloy of the same basic composition as the base alloy. In some cases, as shown in Table 5, a small amount of grain refiner, such as titanium, is added to the filler alloy to minimize cracking during welding. For example, filler alloys 5554 and 5556 are identical to base alloys 5454 and 5456, respectively, except that titanium is added to the filler alloy.

The heat-treatable aluminum alloys are some-what more complex, metallurgically, and are more sensitive to "hot short" cracking, which results from heat-affected zone (HAZ) liquidation during the welding operation. Generally, a dissimilar alloy filler having higher levels of solute (for example, copper or silicon) is used in this case. At high solute levels, there is sufficient eutectic liquid available for the back-filling (healing) of tears that formed during solidification. Typically, alloys used as filler for welding heat-treatable aluminum alloys have a lower melting temperature than the base alloy. By allowing the low-melting-point constituents of the base alloy adjacent to the weld to solidify before the weld metal, stresses are minimized on the base metal during its hot short condition, and tendencies for intergranular cracking are greatly reduced. One heat-treatable base alloy that exhibits low sensitivity to hot short cracking is 2219, which can be welded with a similar filler alloy, 2319.

A simple inverted "T" fillet weld test (Ref 1, 2) can be used to determine the compatibility of a filler alloy with a base alloy. It is a measure of weldability in terms of resistance to weld metal hot cracking. This test requires that a continuous fillet weld be made joining 13 to 25 mm ($\frac{1}{2}$ to 1 in.) plate by the gas-tungsten arc welding (GTAW) process. The total length of cracking that results from a given combination of base and filler alloys provides a quantitative comparison with other alloy combinations. When no cracking is observed in the continuous fillet weld, a more sensitive discontinuous weld test can be used. In this case, a weld nugget is deposited and allowed to solidify before depositing an overlapping weld nugget. Typical weld cracking results obtained from the fillet weld test and similar tests (Ref 3, 4, 5, 6) are shown in Fig. 1 and 2. These tests, as well as field experience, have indicated that:

- THE HIGH-PURITY L*XXX* SERIES ALLOYS AND 3003 ARE EASY TO WELD WITH BASE ALLOY FILLER, 1100 ALLOY, OR AN ALUMINUM-SILICON ALLOY FILLER, SUCH AS 4043.
- ALLOY 2219 EXHIBITS THE BEST WELDABILITY OF THE 2*XXX* SERIES BASE ALLOYS AND IS EASILY WELDED WITH 2319, 4043, AND 4145 FILLERS.
- ALUMINUM-SILICON-COPPER FILLER ALLOY 4145 PROVIDES THE LEAST

SUSCEPTIBILITY TO WELD CRACKING WITH 2*XXX* SERIES WROUGHT COPPER BEARING ALLOYS, AS WELL AS ALUMINUM-COPPER AND ALUMINUM-SILICON-COPPER ALUMINUM ALLOY CASTINGS.

- THE CRACKING SENSITIVITY OF ALUMINUM-MAGNESIUM ALLOY WELDS DECREASES AS THE MAGNESIUM CONTENT OF THE WELD INCREASES ABOVE 2%. THE HIGH-MAGNESIUM CONTENT ALUMINUM FILLER ALLOYS 5356, 5183, AND 5556 CAN BE USED TO WELD THE ALUMINUM-MAGNESIUM WROUGHT AND CAST ALUMINUM ALLOYS WITH RELATIVE EASE, USING THE GAS-SHIELDED ARC WELDING PROCESSES.
- THE 6*XXX* SERIES BASE ALLOYS ARE MOST EASILY WELDED WITH THE ALUMINUM-SILICON TYPE FILLER ALLOYS, SUCH AS 4043 AND 4047. HOWEVER, THE ALUMINUM-MAGNESIUM TYPE FILLER ALLOYS CAN ALSO BE EMPLOYED SATISFACTORILY WITH THE LOW-COPPER BEARING 6*XXX* ALLOYS WHEN HIGHER ASWELDED SHEAR STRENGTH AND WELD METAL DUCTILITY ARE REQUIRED. THE 6*XXX* ALLOYS SHOULD NOT BE WELDED WITH BASE ALLOY FILLER OR WITHOUT A FILLER ADDITION, BECAUSE IT CAN RESULT IN CRACKING. WHEN 4043 FILLER ALLOY IS USED, THE WELD METAL SHOULD POSSESS A MINIMUM OF 50% 4043; WITH 5356 FILLER ALLOY, THE WELD METAL SHOULD CONSIST OF 70% 5356, MINIMUM (REF 7). JOINTS IN 6*XXX* SERIES ALLOYS ARE OFTEN BEVELED OR SPACED TO PERMIT THE EXCESS FILLER ALLOY DILUTION.
- THE 7*XXX* SERIES (ALUMINUM-ZINC-MAGNESIUM) ALLOYS EXHIBIT A WIDE RANGE OF CRACK SENSITIVITY DURING WELDING. ALLOYS 7005 AND 7039, WITH A LOW (<0.1%) COPPER CONTENT, HAVE A NARROW MELTING RANGE AND CAN BE READILY JOINED WITH THE HIGH-MAGNESIUM CONTENT FILLER ALLOYS 5356, 5183, AND 5556. THE 7*XXX* SERIES ALLOYS THAT POSSESS A SUBSTANTIAL AMOUNT OF COPPER, SUCH AS 7075 AND 7178, HAVE A VERY WIDE MELTING RANGE WITH A LOW SOLIDUS TEMPERATURE AND ARE EXTREMELY SENSITIVE TO WELD CRACKING WHEN ARC WELDED.
- THE RECENTLY INTRODUCED ALUMINUM-LITHIUM ALLOYS ARE WELDABLE WHEN CORRECT FILLER ALLOYS ARE SELECTED. ALLOYS 2090 AND 2095 CAN BE EASILY WELDED WITH 2319 ALLOY.

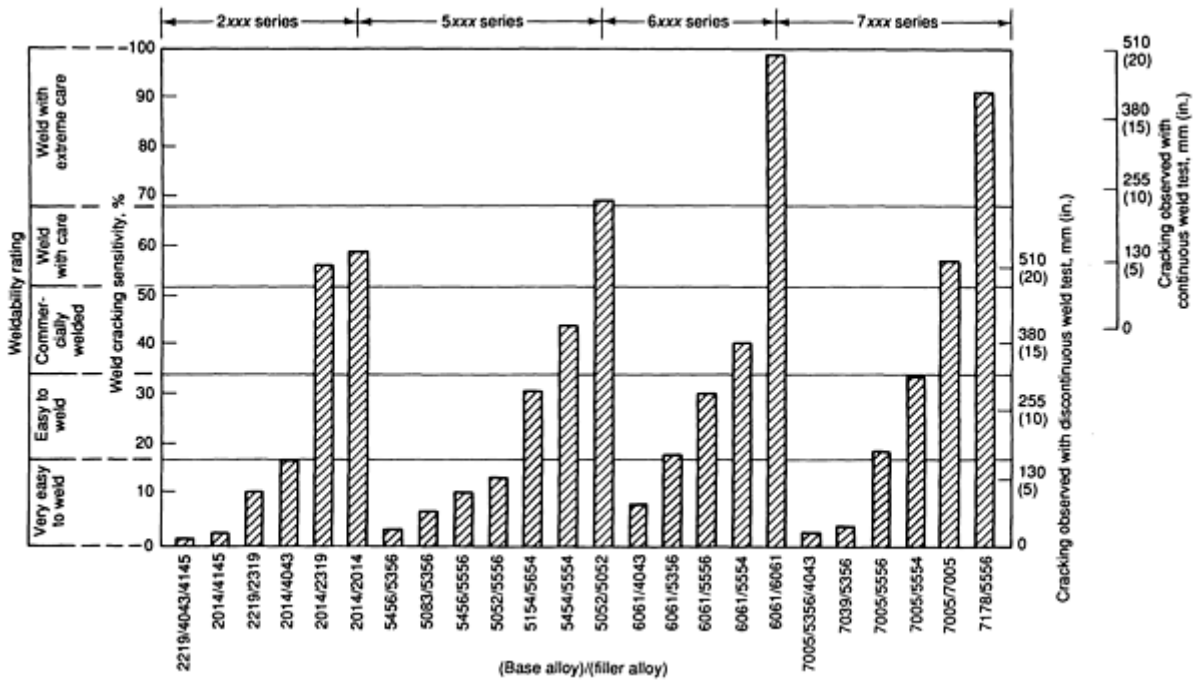

FIG. 1 RELATIVE CRACK SENSITIVITY RATINGS OF SELECTED ALUMINUM (BASE ALLOY/FILLER ALLOY) COMBINATIONS

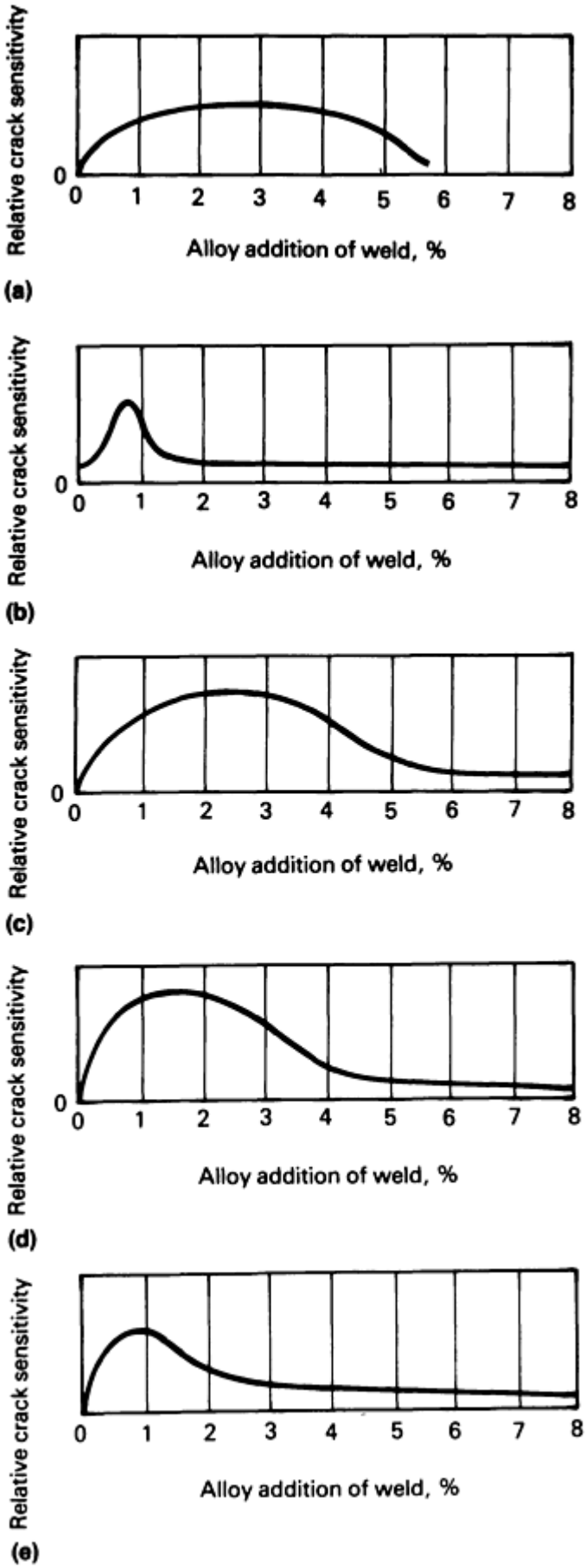

FIG. 2 EFFECT OF ALLOYING ADDITIONS ON SOLIDIFICATION CRACK SENSITIVITY OF SELECTED ALUMINUM

ALLOY SYSTEMS. (A) ALUMINUM-LITHIUM. (B) ALUMINUM-SILICON. (C) ALUMINUM-COPPER. (D) ALUMINUM-MAGNESIUM. (E) ALUMINUM-MAGNESIUM SILICIDE. SOURCE: REF 1, 3, 4, 5, AND 6

Groove weld strength is another major consideration when selecting a proper filler alloy. The heat of welding softens the aluminum alloys adjacent to the weld if they are in any temper other than annealed. In most groove welds, the HAZ of the base alloy will control the as-welded strength of the joint.

For non-heat-treatable aluminum alloys, the zone adjacent to the weld will be completely annealed, as illustrated in Fig. 3. A few seconds at a temperature above 343 °C (650 °F) will completely remove any effect of work hardening for 25 to 38 mm (1 to 1 $\frac{1}{2}$ in.) in any direction from the weld in these alloys. The welding procedure and choice of fusion welding process have little effect on the transverse ultimate tensile strength of groove welds; they simply affect the width of the HAZ. The mechanical properties of groove welds in common non-heat-treatable alloys are listed in Table 6.

TABLE 6 MECHANICAL PROPERTIES OF GAS-SHIELDED ARC WELDED BUTT JOINTS IN SELECTED NON-HEAT-TREATABLE ALUMINUM ALLOYS

BASE ALLOY	**FILLER ALLOY**	**ULTIMATE TENSILE STRENGTH**				**MINIMUM ULTIMATE YIELD STRENGTH[A]**		**TENSILE ELONGATION, % IN 50.8 MM (2 IN.)**	FREE BEND ELONGATION, %
		TYPICAL		**MINIMUM**					
		MPA	**KSI**	**MPA**	**KSI**	**MPA**	**KSI**		
1060	1188	69	10	55	8	17.2	2.5	29	**63**
1100	1100	90	13	75.8	11	31	4.5	29	**55**
1350	1188	69	10	55	8	17.2	2.5	29	**63**
3003	1100	110	16	96.5	14	48.3	7	24	**54**
5005	1100	110	16	96.5	14	48.3	7	15	**32**
5050	5356	159	23	124	18	55.2	8	18	**36**
5052	5356	193	28	172	25	90	13	19	**39**
5083	5183	296	43	276[B]	40[B]	165	24	16	**34**
5086	5356	262	38	241[C]	35[C]	117	17	17	**38**
5154	5654	228	33	207	30	103	15	17	**39**
5454	5554	234	34	214	31	110	16	17	**40**
5456	**5556**	**317**	**46**	**290[B]**	**42[B]**	**179**	**26**	**14**	**28**

(A) 0.2% OFFSET IN 254 MM (10 IN.) GAGE LENGTH.

(B) FOR THICKNESSES UP TO 38 MM (1.5 IN) PLATE

(C) FOR THICKNESSES UP TO 51 MM (2 IN.) PLATE

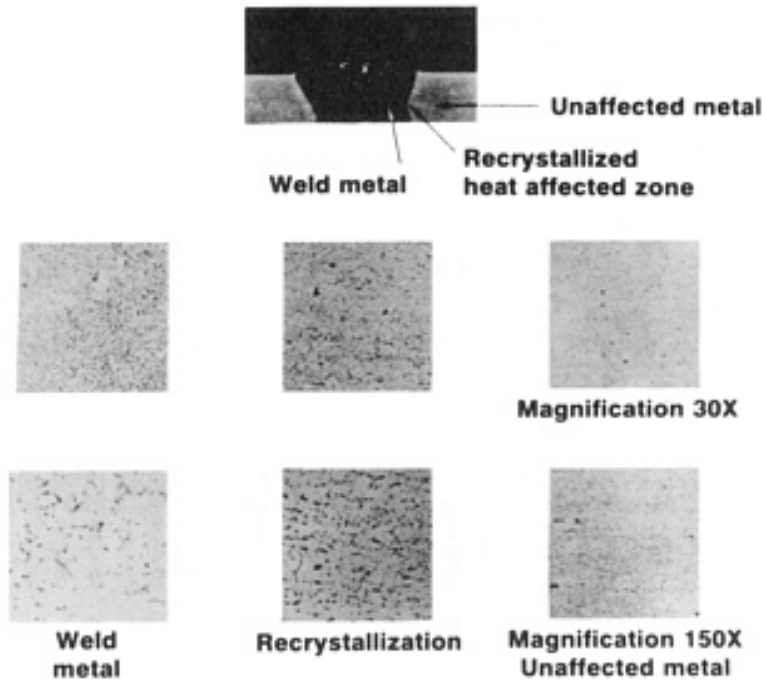

FIG. 3 PHOTOMICROGRAPHS SHOWING HAZ MICROSTRUCTURES OF A SINGLE-PASS GAS-METAL ARC WELD ON 6.35 MM (0.25 IN.) THICK 5083-H116 ALLOY. KELLER'S REAGENT USED AS ETCHANT

The heat-treatable alloys require 2 to 3 h at their annealing temperature, combined with slow cooling, for a complete anneal. This does not occur during welding, and the HAZ will consist of several stages of dissolution and varying degrees of precipitation, based on the thermal conditions, as shown in Fig. 4. The degree of softening in the HAZ is quite sensitive to the peak temperature reached at a specific location, as well as the time at temperature.

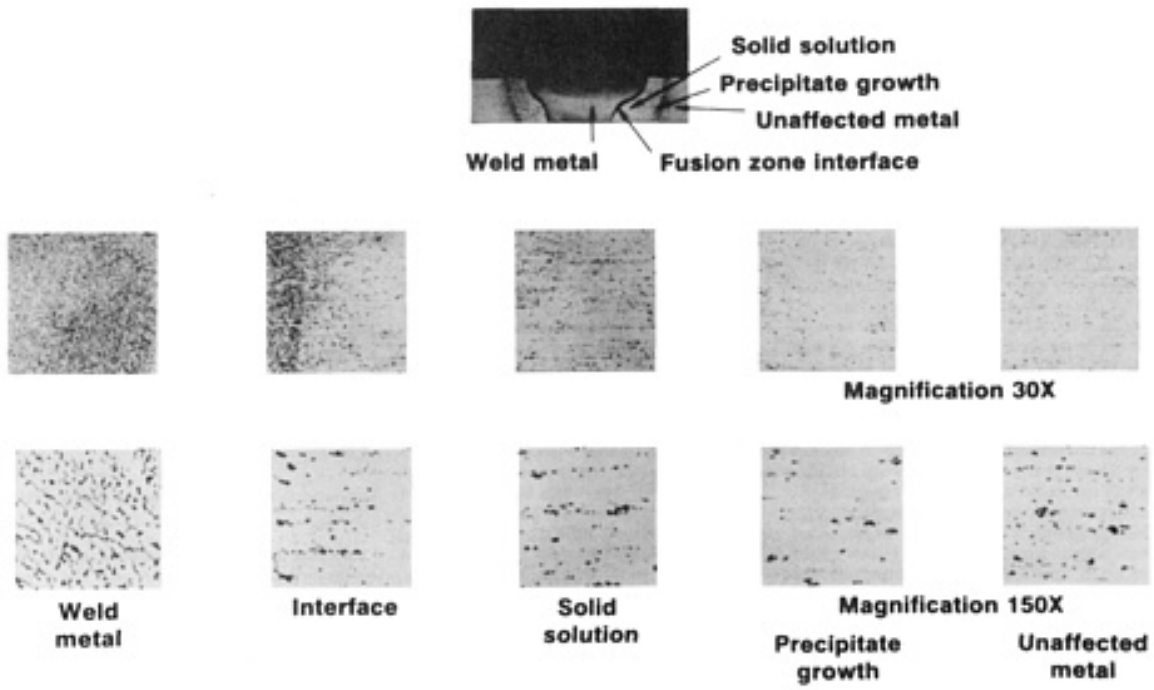

FIG. 4 PHOTOMICROGRAPHS SHOWING HAZ MICROSTRUCTURES OF A SINGLE-PASS GAS-METAL ARC WELD ON 6.35 MM (0.25 IN.) THICK 6061-T6 ALLOY. KELLER'S REAGENT USED AS ETCHANT

Factors such as preheat temperature, interpass cooling, heat input of the joining process and welding technique, use of "chill" bars, and rate of cooling all have an effect on the degree of softening that results from welding the heat-treatable aluminum alloys. Preheat, lack of interpass cooling, and slow, weaving weld passes all increase peak temperatures and extend high temperatures farther from the weld, as well as increase the time at these high temperatures so as to reduce the mechanical properties in the HAZ. These factors alone, as well as the use of too small a specimen to provide an adequate "heat sink," can create sufficient overheating that the minimum values required for procedure qualification may not be met. The weldable 7*xxx* series alloys 7005 and 7039 are least sensitive to these variables and will naturally age (dissolved precipitate will reprecipitate) at room temperature for 2 to 4 weeks following the welding operation to provide high strength without a postweld thermal operation. Typical mechanical properties for groove welds in the heat-treatable aluminum alloys are listed in Table 7.

TABLE 7 TYPICAL MECHANICAL PROPERTIES OF GAS SHIELDED ARC WELDED BUTT JOINTS IN SELECTED WROUGHT HEAT-TREATABLE ALUMINUM ALLOYS

BASE ALLOY AND TEMPER	FILLER ALLOY	AS WELDED						POSTWELD HEAT TREATED AND AGED					
		TENSILE STRENGTH		YIELD STRENGTH[A]		ELONGATION		TENSILE STRENGTH		YIELD STRENGTH[A]		ELONGATION	
		MPA	KSI	MPA	KSI	TENSILE, % IN 50.8 MM (2 IN.)	FREE BEND, %	MPA	KSI	MPA	KSI	TENSILE, % IN 50.8 MM (2 IN.)	FREE BEND, %
2014-T6	4043	234	34	193	28	4	9	345	50	. . .	. . .	2	**5**
2014-T6	2319	241	35	193	28	5	. . .	414	60	317	46	5	**. . .**
2219-T81, T87	2319	241	35	179	26	3	15	379	55	262	38	7	**5**
2219-T31, T37	2319	241	35	179	26	3	15	276[B]	40[B]	228[B]	33[B]	2[B]	**12[B]**
6009-T4	4043	221	32	138	20	9	. . .	303[B]	44[B]	. . .	. . .	. . .	**. . .**
6061-T6	4043	186	27	124	18	8	16	303[C]	44[C]	276[C]	40[C]	5[C]	**11[C]**
6061-T6	5356	207	30	131	19	11	25	. . .	. . .	. . .	. . .	. . .	
6061-T4	4043	186	27	124	18	8	16	241[B]	35[B]	165[B]	24[B]	3[B]	**. . .**
6063-T6	4043	138	20	83	12	8	16	207	30	. . .	. . .	13	**11**
6063-T6	5356	138	20	83	12	12	25	. . .	. . .	. . .	. . .	. . .	**. . .**
7005-T53	5356	317[D]	46[D]	207[D]	30[D]	10[D]	33[D]	. . .	. . .	. . .	. . .	. . .	**. . .**
7039-T61	**5556**	**324[D]**	**47[D]**	**221[D]**	**32[D]**	**10[D]**	**21[D]**	**. . .**	**. . .**	**. . .**	**. . .**	**. . .**	**. . .**

(A) 0.2% OFFSET IN 50.8 MM (2 IN.) GAGE LENGTH.

(B) POSTWELD ARTIFICIALLY AGED ONLY.

(C) FOR THICKNESSES GREATER THAN 19 MM ($\frac{3}{4}$ IN.), 4643 FILLER IS REQUIRED.

(D) POSTWELD AGED AT ROOM TEMPERATURE FOR 30 DAYS

When heat-treatable alloy weldments are given a postweld solution heat treatment and artificial aging, the filler selection is limited. The heat-treatable filler alloy 2319 will provide the highest strength for 2014 and 2219 base alloys. Heat-treatable alloy castings are often repaired or welded with a filler of the same composition as the base alloy and can be postweld heat treated to the desired strength. In most cases, the filler is either not a heat-treatable alloy or is one that is only mildly responsive to strengthening thermal treatments. In these cases, dilution of the base alloy into the weld metal is necessary to obtain a weld metal alloy that can be postweld heat treated.

Filler alloy 4043 (5% Si, balance Al) is a non-heat-treatable alloy. When it is used to weld 6061 alloy, some magnesium from the 6061 must be alloyed with it to provide an aluminum-silicon-magnesium mixture in the weld metal. This new weld metal mixture will respond to a postweld solution heat treatment and produce a groove weld with a tensile strength equal to that of the original 6061-T6. When thick sections, that is, 19 mm ($\frac{3}{4}$ in.) and thicker, are welded, the bevel is normally so wide that the dilution effect may not reach the center of the weld. Filler alloy 4643, which contains some magnesium itself, has been used to provide the highest strength in these cases, as shown for a 76 mm (3 in.) groove weld in Table 8. This filler is also useful for fillet welds in thinner metal.

TABLE 8 EFFECT OF WELDING CONDITIONS ON 6061 ALLOY WELD STRENGTH

BASE METAL ALLOY AND TEMPER	THICKNESS		WELDING PROCESS AND CONDITIONS	AS-WELDED					ONLY AGED AFTER WELDING					POSTWELD SOLUTION HEAT TREATED AND AGED				
				TENSILE STRENGTH		YIELD STRENGTH(A)		ELONGATION IN 51 MM (2 IN.), %	TENSILE STRENGTH		YIELD STRENGTH(A)		ELONGATION IN 51 MM (2 IN.), %	TENSILE STRENGTH		YIELD STRENGTH(A)		ELONGATION IN 51 MM (2 IN.), %
	MM	IN.		MPA	KSI	MPA	KSI		MPA	KSI	MPA	KSI		MPA	KSI	MPA	KSI	
6061-T6[B]	3.2	1/8	DCEN-GTAW, 15 MM/S (35 IN./MIN)	248	36	165	24	6	. . .	. . .	. . .	. . .	. . .	303	44	276	40	**5**
6061-T4[B]	3.2	1/8	DCEN-GTAW, 8.5 MM/S (20 IN./MIN)	234	34	145	21	8	283	41	179	26	3	303	44	276	40	**5**
6061-T6[B]	6.4	1/4	AUTOMATIC GMAW, ONE PASS EACH SIDE 17 MM/S (40 IN./MIN)	255	37	138	20	6	. . .	. . .	. . .	. . .	. . .	296	43	276	40	**5**
6061-T4[B]	76	3	AUTOMATIC GMAW, MULTIPASS DOUBLE-V	172	25	90	13	L0	. . .	. . .	. . .	. . .	. . .	234	34	. . .	. . .	**4**
6061-T6[C]	**76**	**3**	**AUTOMATIC GMAW, MULTIPASS DOUBLE-V**	**186**	**27**	**97**	**14**	**13**	**. . .**	**. . .**	**. . .**	**. . .**	**. . .**	**310**	**45**	**276**	**40**	**4**

(A) 0.2% OFFSET IN 50.8 MM (2 IN.) GAGE LENGTH.

(B) 4043 FILLER WAS USED.

(C) 4643 FILLER WAS USED.

Complete re-solution heat treatment is not always practical, because the rapid quench from a high temperature can cause distortion of a welded assembly. An alternate method for increasing the welded strength of heat-treatable alloys is to weld them in the solution heat-treated temper (T4) and age them after welding is complete. To accomplish this effectively, a welding procedure that keeps the heat input relatively low and short in duration should be employed (Ref 8, 9, 10). Tables 7 and 8 compare mechanical properties for postweld solution heat treating and aging versus artificial aging only for 2219 and 6061 alloys. An example of this is highway light poles tapered in a very workable 6*xxx*-T4 alloy, welded to the base, and artificially aged to the T6 temper.

Filler alloys 5183, 5356, 5556, and 5654, which contain over 3% Mg, are not normally recommended for use when parts are to be postweld aged. These high-magnesium content aluminum alloys can be sensitized to stress-corrosion cracking (SCC) when subjected to a relatively long-time precipitation heat treatment (artificial aging) under conditions of high residual stress (Ref 11, 12).

Fillet weld strength represents a significant consideration when selecting a welding filler alloy. Minimum shear strength values for several common filler alloys are listed in Table 9 (Ref 13). Filler alloy 5556 produces the highest fillet weld strength in the as-welded condition. This is nearly twice the shear strength of 4043 fillet welds.

TABLE 9 MINIMUM SHEAR STRENGTHS OF SELECTED FILLET WELDS

FILLER ALLOY	SHEAR STRENGTH			
	LONGITUDINAL		TRANSVERSE	
	MPA	**KSI**	**MPA**	KSI
1100	51.7	7.5	51.7	**7.5**
2319[(A)(B)]	110	16.0	110	**16.0**
2319[(C)]	152	22.0	200	**29.0**
4043	79.3	11.5	103	**15.0**
4643	93.1	13.5	138	**20.0**
5183	128	18.5	193	**28.0**
5356	117	17.0	179	**26.0**
5554	117	17.0	159	**23.0**
5556	138	20.0	207	**30.0**
5654	**82.7**	**12.0**	**124**	**18.0**

(A) AS-WELDED.

(B) ARTIFICIALLY AGED AFTER WELDING.

(C) SOLUTION HEAT-TREATED AND AGED AFTER WELDING

Because several filler alloys can be used to weld many base alloys, the higher-strength weld metal can provide an economic advantage in some applications. For instance, 6061 is commonly welded with 4043 filler, although 5556 filler can also be used. For a symmetrical design requiring a force per unit length of 875 N/mm (5000 lbf/in.) of fillet weld length, an 11 mm ($\frac{7}{16}$ in.) fillet would be required for the 4043 filler versus a 6.4 mm ($\frac{1}{4}$ in.) fillet for 5556 filler. The 6.4 mm ($\frac{1}{4}$ in.) fillet can be made in a single weld pass, but three passes normally would be required for the 11 mm ($\frac{7}{16}$ in.) fillet size. Not only can the 5556 weld be made in one-third of the time, but distortion from the volume of weld metal shrinkage is also minimized by the smaller weld.

The ductility of aluminum welds is excellent for the non-heat-treatable alloys when like filler alloys are used. Using free-bend elongation values as the measure of weld metal ductility, the highest ductility is observed with the pure aluminum alloys. Excellent ductility is also experienced in 5*xxx* series alloys welded with 5*xxx* series fillers. Tables 6 and 7 list the free-bend elongation of butt joints in commonly welded base alloys.

Welds in the heat-treatable alloys do not exhibit as high ductility as the non-heat-treatable alloys. In addition, postweld heat treatments generally reduce ductility, compared to the as-welded condition. About a 50% higher ductility level is

obtained when a 5*xxx* series filler is used with 6061 and 6063 base alloys, rather than an aluminum-silicon filler alloy, such as 4043.

Low weld ductility results when welding the aluminum-copper alloys with 4043 or 4145 filler alloys. However, moderate ductility can be obtained when the aluminum-copper alloys are welded with 2319 filler. In addition, 2319 produces the highest weld metal ductility with the aluminum-copper alloys after postweld heat treatments.

Welds in Al-Zn-Mg-Cu alloys, such as 7075 and 7178, possess very low ductility (1% or less). This, in addition to their high sensitivity to cracking when arc welded, generally discourages their use for arc welded applications. The low copper content 7*xxx* series alloys, 7005 and 7039, exhibit good weld ductility with 5183, 5356, and 5556 fillers.

Low ductility is experienced at the weld fusion zone when joining a high silicon content alloy (such as 356.0 casting) to a high magnesium content base alloy (such as 5083). No favorable filler selection is available. If an aluminum-magnesium filler compatible with 5083 is used, then a low-ductility interface of Mg_2Si occurs on the 356.0 side of the weld. Use of an aluminum-silicon filler compatible with the 356.0 casting moves the low-ductility interface to the 5083 side of the weld. A desirable solution is to weld either the 5083 to an aluminum-magnesium casting or the 356.0 (7 Si) casting to a wrought alloy, such as 6061, which is also welded with an aluminum-silicon filler alloy.

Temperature Versus Performance. Aluminum alloys lose a substantial portion of their strength as temperatures exceed 200 °C (390 °F). The aluminum-copper 2*xxx* series alloys exhibit the best elevated-temperature properties, as indicated in Table 10. The 5*xxx* series base and filler alloys with nominal magnesium contents that exceed 3% are not recommended for use at sustained temperatures above 66 °C (150 °F) because they can be sensitized to SCC (Ref 11). Base alloy 5454 and its companion filler alloy 5554 were developed specifically to provide the highest strength among the 5*xxx* alloys for sustained elevated-temperature service. Filler alloy selections suitable for welding common wrought and cast alloys for sustained elevated-temperature service are listed in Table 11.

TABLE 10 ULTIMATE TENSILE STRENGTH AT SELECTED TEMPERATURES FOR GAS-SHIELDED ARC WELDED GROOVE JOINTS IN ALUMINUM ALLOYS

ALLOY AND TEMPER	**FILLER ALLOY**	ULTIMATE TENSILE STRENGTH AT INDICATED TEMPERATURE											
		-184 °C (-300 °F)		**-129 °C (-200 °F)**		**-73 °C (-100 °F)**		**38 °C (100 °F)**		**149 °C (300 °F)**		260 °C (500 °F)	
		MPA	**KSI**	**MPA**	**KSI**	**MPA**	**KSI**	**MPA**	**KSI**	**MPA**	**KSI**	**MPA**	KSI
2219-T37(A)	2319	334	48.5	276	40.0	248	36.0	241	35.0	214	31.0	131	**19.0**
2219(B)	2319	445	64.5	410	59.5	379	55.0	345	50.0	262	38.0	152	**22.0**
3003	1100	190	27.5	148	21.5	121	17.5	97	14.0	66	9.5	34	**5.0**
5052	5356(C)	262	38.0	214	31.0	183	26.5	172	25.0	145	21.0	72	**10.5**
5083	5183	376	54.5	317	46.0	279	40.5	276	40.0	(D)	(D)	(D)	**(D)**
5086	5356	331	48.0	279	40.5	245	35.5	241	35.0	(D)	(D)	(D)	**(D)**
5454	5554	303	44.0	255	37.0	221	32.0	214	31.0	179	26.0	103	**15.0**
5456	5556	386	56.0	328	47.5	293	42.5	290	42.0	(D)	(D)	(D)	**(D)**
6061-T6(A)	4043	238	34.5	207	30.0	183	26.5	165	24.0	138	20.0	41	**6.0**
6061-T6(B)	**4043(E)**	**379**	**55.0**	**341**	**49.5**	**317**	**46.0**	**290**	**42.0**	**217**	**31.5**	**48**	**7.0**

(A) AS WELDED.

(B) POSTWELD SOLUTION HEAT TREATED AND ARTIFICIALLY AGED.

(C) 5554 FILLER ALLOY USED AT >38 °C (> 100 °F).

(D) ALLOY NOT RECOMMENDED FOR USE AT SUSTAINED OPERATING TEMPERATURES ABOVE 66 °C (150 °F).

(E) 4643 FILLER ALLOY FOR [GES] 19 MM ([GES] $\frac{3}{4}$ IN.) BASE METAL

TABLE 11 FILLER ALLOYS FOR WELDING SELECTED ALUMINUM ALLOYS USED FOR SUSTAINED ELEVATED-TEMPERATURE SERVICE

ALUMINUM ALLOYS	ACCEPTABLE

WROUGHT	CAST	FILLER ALLOYS
1*XXX* SERIES	. . .	**BASE ALLOY, 1100, 1188, 4043, 4047**
2014, 2219	222.0, 295.0, 319.0, 333.0	**2319, 4043, 4145**
3003, 5005, 5050	. . .	**1100, 4043, 4047**
5052, 5454, 6061, 6063, 7005	. . .	**4043, 4047, 5554**
. . .	354.0, 355.0, C355.0	**4009, 4145, C355.0**
. . .	356.0, A356.0, A357.0, 359.0	**4010, 4011, 4043, 4047, 4643, A356.0, A357.0**
. . .	**413.0, 443.0, A444.0**	**4043, 4047**

With decreasing temperature, aluminum alloys and their weldments gain strength (Table 10). Rather than becoming brittle, the aluminum alloys either maintain or increase in ductility as the temperature decreases below 0 °C. Typical properties for 5083 plate welded with 5183 alloy filler are shown in Fig. 5. The high magnesium content 5*xxx* series alloys have very good cryogenic properties and, because of their excellent weldability, have been used widely for the storage and transport of liquid oxygen and liquid natural gas. Additional information is available in the Section "Selection of Nonferrous Low-Temperature Materials" and the article "Welding for Cryogenic Service" in this Volume.

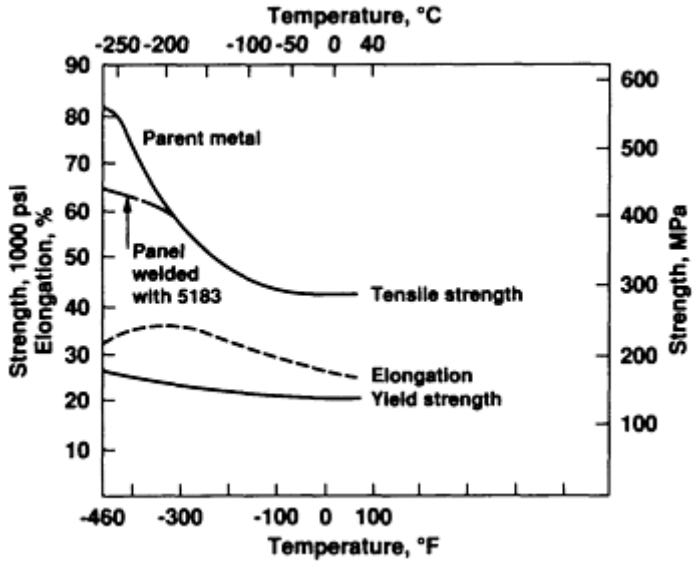

FIG. 5 TYPICAL ROOM-TEMPERATURE AND LOW-TEMPERATURE TENSILE PROPERTIES OF 5083-O BASE ALLOY PLATE WELDED WITH 5183 ALLOY FILLER

Corrosion resistance of the non-heat-treatable alloys is not altered significantly by the heat of welding. The aluminum-magnesium-silicon heat-treatable alloys, such as 6061 and 6063, also have high corrosion resistance in the welded condition. The 2*xxx* and 7*xxx* series heat-treatable alloys, which contain substantial amounts of copper and zinc, respectively, can have their resistance to corrosion altered by the heat of welding. For example, in the aluminum-copper alloys, the HAZ becomes cathodic, whereas in the aluminum-zinc alloys, it becomes anodic to the remainder of the weldment in the presence of water or other electrolytes (Ref 12). The solution potentials across the weld zone for a 5*xxx*, 2*xxx*, and 7*xxx* series weldment are shown in Fig. 6.

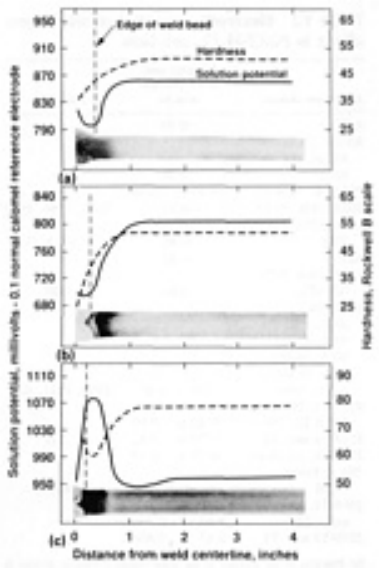

FIG. 6 PLOT OF SOLUTION POTENTIAL AND HARDNESS VERSUS DISTANCE FROM WELD CENTERLINE TO SHOW EFFECT OF THE HEAT OF WELDING ON METALLURGICAL CHANGES IN SELECTED ALUMINUM ALLOYS. (A) 5456-H321 BASE ALLOY WELDED WITH 5556 ALLOY FILLER. GMAW-DCEP, THREE PASSES. (B) 2219-T87 BASE ALLOY WELDED WITH 2319 ALLOY FILLER. GTAW-DCEN, TWO PASSES. (C) 7039-T651 BASE ALLOY WELDED WITH 5183 ALLOY FILLER. GTAW-DCEN, TWO PASSES

Different aluminum alloy compositions produce slightly different electrode potentials in the presence of various solutions. Selective corrosion can result in immersed service, where the base alloy and weld metal possess significant differences in potential. Table 12 lists the solution potentials for common aluminum alloys in a salt solution.

TABLE 12 ELECTRODE POTENTIAL OF ALUMINUM ALLOYS IN NACL-H_2O_2 SOLUTION

ALUMINUM ALLOY[A]	**POTENTIAL VOLTS 0.1 *N* CALOMEL SCALE**[B]	FILLER ALLOY
A712.0	-0.99	**. . .**
ALCLAD. 3003, ALCLAD. 6061, 7072	-0.96	**. . .**
7005-T6, 7039-T6	-0.93 TO -0.96	**. . .**
5083, 5456, 514.0	-0.87	**5183, 5356, 5556**
5154, 5254, 5454, 5086	-0.86	**5554, 5654**
5052	-0.85	**. . .**
1350, 3004, 5050, 7075-T73	-0.84	**1188**
1100, 3003, 5005, 6061-T6, 6063, ALCLAD 2014, ALCLAD 2024, 413.0, 443.0, A444.0	-0.82 TO -0.83	**1100, 4043, 4047**
6061-T4, 7075-T6, 356.0-T6, 360.0	-0.80 TO -0.81	**. . .**
2219-T6 AND -T8	-0.79 TO -0.82	**2319**
2014-T6, 355.0-T6	-0.78 TO -0.79	
380.0, 319.0, 333.0	-0.75	**4145**
2014-T4, 2024-T3 AND -T4	-0.68 TO -0.70[C]	**. . .**
2219-T3 AND -T4	**-0.63 TO -0.65**[C]	**. . .**

(A) POTENTIAL OF ALL TEMPERS IS THE SAME UNLESS A SPECIFIC TEMPER IS DESIGNATED.

(B) MEASURED IN AN AQUEOUS SOLUTION OF 53 G NACL + 3 G H_2O_2 PER LITER AT 25 °C (77 °F).

(C) POTENTIAL VARIES WITH QUENCHING RATE DURING FABRICATION.

The alloy with the more negative potential in the weldment will attempt to protect the other part. Thus, if the weld metal is anodic to the base metal (as is a 5356 weld in 6061-T6), the small weld can be attacked preferentially to protect the larger surface area of the base metal. The greater the area to be protected and the greater the difference in electrode potential, the more rapidly will corrosive action occur.

Optimum corrosion resistance is obtained when the solution potential of the filler is the same as that of the base alloy, as shown in Table 12 for 4043 filler alloy and 6061-T6. If this is not practical, then a preferred arrangement is to have the larger base alloy surface area be anodic to the weld metal, such as 7005-T6 welded with 5356 filler.

For the welds shown in Fig. 6, the HAZ in the 5*xxx* alloy is mildly cathodic, whereas the 2*xxx* alloy exhibits a greater cathodic differential. The 7*xxx* series HAZ is anodic to the unaffected material and would be of greatest concern. Fabrications in the 7*xxx* alloys are usually painted to avoid galvanic corrosion. However, as an additional safety precaution in some cases, the weld area is metallized with another aluminum alloy to prevent galvanic corrosion if a void occurs in the paint coating. Most unprotected aluminum-base and filler alloy combinations are very satisfactory for general atmospheric conditions.

In some cases, an alloy constituent can be formed by alloying components of the base and filler alloys to produce an anodic zone at the transition of the weld and base metal. If a 5*xxx* alloy is welded with an aluminum-silicon filler, or vice versa, then a magnesium silicide constituent can be formed. For certain immersed conditions, such as a mild acid condition, the magnesium silicide can be highly anodic to all other parts of the weldment (Ref 14, 15). A very selective knifelike corrosive attack can result from this immersed service.

Some chemical exposures or special circumstances can require special controls within the elements of an alloy. In the case of hydrogen peroxide exposure, the manganese and copper impurities have been controlled to low limits in 5652 and 5254 base alloys, as well as 5654 filler alloy. In some cases, a high-purity aluminum alloy is chosen for special exposure. A filler alloy of equal or higher purity to that of the base alloy is generally acceptable in these cases, and filler alloy 1188 would meet most of these requirements.

Weld and Base Metal Color Match. A good color match between the weld metal and the base metal is often desired for ornamental or architectural applications that are given either chemical or electrochemical finishes. The final color of the alloy depends on the chemical composition of the alloy. Ideally, a filler alloy should possess the same composition as the base alloy for an optimum color match. This can be accomplished for most of the non-heat-treatable alloys, but it is not practical with the majority of the heat-treatable aluminum alloys because of weld cracking sensitivity. Thus, dissimilar alloys with the same color response to the final surface treatment are used with these alloys. The two alloying elements of primary interest are silicon and chromium. Silicon in an alloy will create a gray-to-black color, depending on the percentage of silicon (Fig. 7). Thus, welds made with aluminum-silicon filler alloys would exhibit a sharp color contrast with all but the aluminum-silicon base alloys or those clad with an aluminum-silicon alloy. Chromium causes an alloy to take on a yellow or gold shading when anodically treated. Of lesser concern is manganese, which causes a faint gray color.

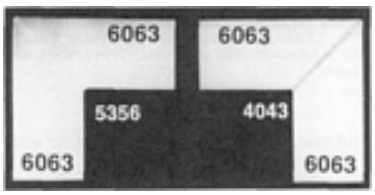

FIG. 7 CLEAR ANODIC COATING ON 6063 WELDS MADE WITH ALUMINUM-MAGNESIUM (5356) AND ALUMINUM-SILICON (4043) FILLERS

The filler alloys that are recommended to obtain a good color match with various base alloys are listed in Table 13. Base alloys 6061 and 6063, which are most commonly welded with 4043 alloy filler, are of the most concern. Because a black weld results when a 4043 weld is anodized, filler alloy 5356 is preferred for the best color match (Fig. 7).

TABLE 13 RECOMMENDED FILLER ALLOYS USED TO OBTAIN BEST COLOR MATCH WITH

ALUMINUM ALLOYS

ALUMINUM ALLOY	FILLER ALLOY
1100, 3003, 5005, 5050	**1188**
5052, 5154	**5654**
6061, 6063, 511.0, 514.0, 535.0	**5356**
5083, 5086, 5454, 5456	**5183 OR 5556**
356.0, A356.0, A357.0, 443.0, A444.0	**4010, 4043, OR 4047**

Filler Alloy Choices. The final determination of the optimal filler alloy for joining an aluminum alloy or combination of alloys should be made after a thorough analysis of the final performance desired from the weldment. Usually, a filler alloy can be selected to meet the service conditions with little or no compromise in the ease-of-welding characteristic. The criteria discussed for an alloy type can be applied to the cast aluminum alloys, as well as to the wrought aluminum alloys.

Table 14 provides a comprehensive matrix for selecting a filler alloy for the GTAW and GMAW processes, based on the various requirements or service conditions presented previously. Commonly welded wrought and cast aluminum alloys are included to assist in selecting a filler for welding an alloy to itself or to another aluminum alloy. The corrosion data are based on performance in fresh or salt water and do not necessarily apply to other exposure conditions. In addition, all ratings are based on as-welded performance and may not apply when the weldment is subjected to postweld thermal treatments.

TABLE 14 RELATIVE RATING OF SELECTED ALUMINUM FILLER ALLOYS USED TO FILLET WELD OR BUTT WELD TWO COMPONENT BASE ALLOYS

Data are for welded assemblies not heat treated after welding.

BASE ALLOYS TO BE JOINED		**FILLER ALLOYS**	FILLER ALLOY CHARACTERISTIC[(A)]					
ALLOY 1	**ALLOY 2**		**W**	**S**	**D**	**C**	**T**	M
319.0, 333.0, 354.0, 355.0, C355.0, 380.0	1060, 1350	4043	B	A	A	A	A	**A**
		4145	A	A	B	A	A	**A**
	1100	4043	B	A	A	A	A	**A**
		4145	A	A	B	A	A	**A**
	2014, 2036	2319	B	A	A	A	A	**A**
		4043	C	C	B	C	A	**A**
		4145	A	B	C	B	A	**A**
	2219	2319	B	A	A	A	A	**A**
		4043	C	C	B	C	A	**A**
		4145	A	B	C	B	A	**A**
	3003, ALCLAD 3003	4043	B	B	A	A	A	**A**
		4145	A	A	B	A	A	**A**
	3004	4043	B	B	A	A	A	**A**
		4145	A	A	B	A	A	**A**
	ALCLAD 3004	4043	B	B	A	A	A	**A**
		4145	A	A	B	A	A	**A**
	5005, 5050	4043	B	B	A	A	A	**A**
		4145	A	A	B	A	A	**A**
	5052, 5652	4043	A	A	A	A	A	**A**
	5083, 5456	4043	A	A	A	A	. . .	**A**
	5086, 5356	4043	A	A	A	A	. . .	**A**
	514.0, A514.0, B514.0, F514.0, 5154, 5254	4043	A	A	A	A	. . .	**A**
	5454	4043	A	A	A	A	A	**A**
	6005, 6063, 6101, 6151, 6201, 6351, 6951	4043	B	B	A	A	A	**A**
		4145	A	A	B	A	A	**A**
	6061, 6070	4043	B	B	A	A	A	**A**
		4145	A	A	B	A	A	**A**
	7005, 7021, 7039, 7046, 7146,	4043	B	B	A	A	A	**A**

	A712.0, C712.0	4145	A	A	B	A	A	**A**
	413.0, 443.0, 444.0, 356.0, A356.0, A357.0, 359.0	4043	B	B	A	A	A	**A**
		4145	A	A	B	A	A	**A**
	319.0, 333.0, 354.0, 355.0, C355.0, 380.0	2319	B	A	A	A	A	**A**
		4145	A	B	B	B	A	**A**
413.0, 443.0, 444.0, 356.0, A356.0, A357.0, 359.0	1060, 1350	4043	A	A	A	A	A	**A**
		4145	A	A	B	B	A	**. . .**
	1100	4043	A	A	A	A	A	**A**
		4145	A	A	B	B	A	**. . .**
	2014, 2036	4043	B	B	A	A	A	**A**
		4145	A	A	B	A	A	**. . .**
	2219	4043	B	B	A	A	A	**A**
		4145	A	A	B	A	A	**. . .**
	3003, ALCLAD 3003	4043	A	A	A	A	A	**A**
		4145	A	A	B	B	A	**. . .**
	3004	4043	A	A	A	A	A	**A**
	ALCLAD 3004	4043	A	A	A	A	A	**A**
	5005, 5050	4043	A	A	A	A	A	**A**
	5052, 5652	4043	A	B	A	A	A	**A**
		5356	B	A	B	B	. . .	**A**
	5083, 5456	4043	A	B	B	A	. . .	**A**
		5356	A	A	A	A	. . .	**A**
	5086, 5356	4043	A	B	B	A	. . .	**A**
		5356	A	A	A	A	. . .	**A**
	514.0, A514.0, B514.0, F514.0, 5154, 5254	4043	A	B	B	A	. . .	**A**
		5356	A	A	A	B	. . .	**A**
	5454	4043	A	B	B	A	A	**A**
		5356	A	A	A	B	. . .	**A**
	6005, 6063, 6101, 6151, 6201, 6351, 6951	4043	A	B	A	A	A	**A**
		4145	A	A	B	B	A	**. . .**
	6061, 6070	4043	A	B	A	A	A	**A**
		4145	A	A	B	B	A	**. . .**
	7005, 7021, 7039, 7046, 7146, A712.0, C712.0	4043	A	B	B	A	A	**A**
		4145	A	A	B	B	A	**. . .**
		5356	A	A	A	A	. . .	**B**
	413.0, 443.0, 444.0, 356.0, A356.0, A357.0, 359.0	4043	A	B	A	A	A	**A**
		4145	A	A	B	B	A	**. . .**
7005, 7021, 7039, 7046, 7146, A712.0, C712.0	1060, 1350	4043	A	A	C	A	A	**. . .**
		5183	B	A	B	A	. . .	**A**
		5356	B	A	A	A	. . .	**A**
		5556	B	A	B	A	. . .	**A**
	1100	4043	A	A	C	A	A	**. . .**
		5183	B	A	B	A	. . .	**A**
		5356	B	A	A	A	. . .	**A**
		5556	. . .	A	B	A	. . .	**A**
	2014, 2036	4043	B	B	A	A	A	**. . .**
		4145	A	A	B	A	A	**. . .**
	2219	4043	B	B	A	A	A	**. . .**
		4145	A	A	B	A	A	**. . .**
	3003, ALCLAD 3003	4043	A	B	C	A	A	**. . .**
		5183	B	A	B	A	. . .	**A**
		5356	B	A	A	A	. . .	**A**
		5556	B	A	B	A	. . .	**A**
	3004	4043	A	D	C	B	A	**. . .**
		5183	B	A	B	A	. . .	**A**
		5356	B	B	A	A	. . .	**A**
		5554	C	C	A	A	A	**A**
		5556	B	A	B	A	. . .	**A**
		5654	C	C	A	A	. . .	**B**
	ALCLAD 3004	4043	A	D	C	B	A	**. . .**
		5183	B	A	B	A	. . .	**A**

		5356	B	B	A	A	. . .	**A**
		5554	C	C	A	A	A	**A**
		5556	B	A	B	A	. . .	**A**
		5654	C	C	A	A	. . .	**B**
	5005, 5050	4043	A	B	C	B	A	**. . .**
		5183	B	A	B	A	. . .	**A**
		5356	B	A	A	A	. . .	**A**
		5554	C	A	A	A	A	**A**
		5556	B	A	B	A	. . .	**A**
		5654	C	A	A	A	. . .	**A**
	5052, 5652	4043	B	D	C	B	A	**. . .**
		5183	A	A	B	A	. . .	**A**
		5356	A	B	A	A	. . .	**A**
		5554	B	C	A	A	A	**A**
		5556	A	A	B	A	. . .	**A**
		5654	B	C	A	A	. . .	**A**
	5083, 5456	5183	A	A	B	A	. . .	**A**
		5356	A	B	A	A	. . .	**A**
		5556	A	A	B	A	. . .	**A**
	5086, 5356	5183	A	A	B	A	. . .	**A**
		5356	A	B	A	A	. . .	**A**
		5556	A	A	B	A	. . .	**A**
	514.0, A514.0, B514.0, F514.0, 5154, 5254	5183	A	A	B	A	. . .	**A**
		5356	A	B	A	A	. . .	**A**
		5554	B	C	A	A	. . .	**A**
		5556	A	A	B	A	. . .	**A**
		5654	B	C	A	A	. . .	**A**
	5454	5183	A	A	B	A	. . .	**A**
		5356	A	B	A	A	. . .	**A**
		5554	B	C	A	A	A	**A**
		5556	A	A	B	A	. . .	**A**
		5654	B	C	A	A	. . .	**A**
	6005, 6063, 6101, 6151, 6201, 6351, 6951	4043	A	D	C	B	A	**. . .**
		5183	A	A	B	A	. . .	**A**
		5356	A	B	A	A	. . .	**A**
		5554	B	C	A	A	A	**A**
		5556	A	A	B	A	. . .	**A**
		5654	B	C	A	A	. . .	**A**
	6061, 6070	4043	A	D	C	B	A	**. . .**
		5183	A	A	B	A	. . .	**A**
		5356	A	B	A	A	. . .	**A**
		5554	B	C	A	A	A	**A**
		5556	A	A	B	A	. . .	**A**
		5654	B	C	A	A	. . .	**A**
	7005, 7021, 7039, 7046, 7146, A712.0, C712.0	4043	B	D	C	B	A	**. . .**
		5183	A	A	B	A	. . .	**A**
		5356	A	B	A	A	A	**A**
		5554	B	C	A	A	. . .	**A**
		5556	A	A	B	A	. . .	**A**
		5654	B	C	A	A	. . .	**A**
6061, 6070	1060, 1350	4043	A	A	C	A	A	**. . .**
		4145	A	A	D	B	A	**. . .**
		5183	B	A	B	. . .	. . .	**A**
		5356	B	A	A	. . .	. . .	**A**
		5556	B	A	B	. . .	. . .	**A**
	1100	4043	A	A	C	A	A	**. . .**
		4145	A	A	D	B	A	**. . .**
		5183	B	A	B	. . .	. . .	**A**
		5356	B	A	A	. . .	. . .	**A**
		5556	B	A	B	. . .	. . .	**A**
	2014, 2036	4043	B	B	A	A	A	**. . .**

		4145	A	A	B	A	A	**...**
	2219	4043	B	B	A	A	A	**...**
		4145	A	A	B	A	A	**...**
	3003, ALCLAD 3003	4043	A	B	C	A	A	**...**
		4145	A	A	D	B	A	**...**
		5183	B	A	B	...	...	**A**
		5356	B	A	A	...	...	**A**
		5556	B	A	B	...	...	**A**
	3004	4043	A	D	C	A	A	**...**
		4145	B	C	D	B	A	**...**
		5183	B	A	B	...	...	**A**
		5356	B	B	A	...	...	**A**
		5556	B	A	B	...	...	**A**
	ALCLAD 3004	4043	A	D	C	A	A	**...**
		4145	B	C	D	B	A	**...**
		5183	B	A	B	...	...	**A**
		5356	B	B	A	...	...	**A**
		5556	B	A	B	...	...	**A**
	5005, 5050	4043	A	B	C	A	A	**...**
		4145	A	B	D	B	A	**...**
		5183	B	A	B	...	...	**A**
		5356	B	A	A	...	...	**A**
		5556	B	A	B	...	...	**A**
	5052, 5652	4043	A	D	C	A	A	**...**
		5183	B	A	B	C	...	**B**
		5356	B	B	A	C	...	**A**
		5554	C	C	A	B	A	**B**
		5556	B	A	B	C	...	**B**
		5654	C	C	A	B	...	**A**
	5083, 5456	4043	A	D	C	A	...	**...**
		5183	A	A	B	A	...	**A**
		5356	A	B	A	A	...	**A**
		5554	B	C	A	A	...	**A**
		5556	A	A	B	A	...	**A**
		5654	B	C	A	A	...	**B**
	5086, 5356	4043	A	D	C	A	...	**...**
		5183	A	A	B	A	...	**A**
		5356	A	B	A	A	...	**A**
		5554	B	C	A	A	...	**A**
		5556	A	A	B	A	...	**A**
		5654	B	C	A	A	...	**B**
	514.0, A514.0, B514.0, F514.0, 5154, 5254	4043	A	D	C	A	...	**...**
		5183	B	A	B	C	...	**B**
		5356	B	B	A	C	...	**A**
		5554	C	C	A	B	...	**B**
		5556	B	A	B	C	...	**B**
		5654	C	C	A	B	...	**A**
	5454	4043	A	D	C	B	A	**...**
		5183	B	A	B	C	...	**A**
		5356	B	B	A	C	...	**A**
		5554	C	C	A	A	A	**A**
		5556	B	A	B	C	...	**A**
		5654	C	C	A	B	...	**B**
	6005, 6063, 6101, 6151, 6201, 6351, 6951	4043	A	C	B	A	A	**...**
		5183	B	A	A	C	...	**A**
		5356	B	A	A	C	...	**A**
		5554	C	B	A	B	B	**A**
		5556	B	A	A	C	...	**A**
		5654	C	B	A	B	...	**B**
	6061, 6070	4043	A	C	B	A	A	**...**
		5183	B	A	A	C	...	**B**

		5356	B	B	A	C	. . .	**A**
		5554	C	B	A	B	B	**B**
		5556	B	A	A	C	. . .	**B**
		5654	C	B	A	B	. . .	**B**
6005, 6063, 6101, 6151, 6201, 6351, 6951	1060, 1350	4043	A	A	C	A	A	**. . .**
		4145	A	A	D	B	A	**. . .**
		5183	B	A	B	. . .	. . .	**A**
		5356	B	A	A	. . .	. . .	**A**
		5556	B	A	B	. . .	. . .	**A**
	1100	4043	A	A	C	A	A	**. . .**
		4145	A	A	D	B	A	**. . .**
		5183	B	A	B	. . .	. . .	**A**
		5356	B	A	A	. . .	. . .	**A**
		5556	B	A	B	. . .	. . .	**A**
	2014, 2036	4043	B	B	A	A	A	**. . .**
		4145	A	A	B	A	A	**. . .**
	2219	4043	B	B	A	A	A	**. . .**
		4145	A	A	B	A	A	**. . .**
	3003, ALCLAD 3003	4043	A	B	C	A	A	**. . .**
		4145	A	A	D	B	A	**. . .**
		5183	B	A	B	. . .	. . .	**A**
		5356	B	A	A	. . .	. . .	**A**
		5556	B	A	B	. . .	. . .	**A**
	3004	4043	A	D	C	A	A	**. . .**
		4145	B	C	D	B	A	**. . .**
		5183	B	A	B	. . .	. . .	**A**
		5356	B	B	A	. . .	. . .	**A**
		5556	B	A	B	. . .	. . .	**A**
	ALCLAD 3004	4043	A	D	C	A	A	**. . .**
		4145	B	C	D	B	A	**. . .**
		5183	B	A	B	. . .	. . .	**A**
		5356	B	B	A	. . .	. . .	**A**
		5556	B	A	B	. . .	. . .	**A**
	5005, 5050	4043	A	B	C	A	A	**. . .**
		4145	A	B	D	B	A	**. . .**
		5183	B	A	B	. . .	. . .	**A**
		5356	B	A	A	. . .	. . .	**A**
		5556	B	A	B	. . .	. . .	**A**
	5052, 5652	4043	A	D	C	A	A	**. . .**
		5183	B	A	B	C	. . .	**B**
		5356	B	B	A	C	. . .	**A**
		5554	C	C	A	B	A	**B**
		5556	B	A	B	C	. . .	**B**
		5654	C	C	A	B	. . .	**A**
	5083, 5456	4043	A	B	C	A	. . .	**. . .**
		5183	A	A	B	A	. . .	**A**
		5354	A	A	A	A	. . .	**A**
		5556	B	A	A	A	. . .	**A**
		5556	A	A	B	A	. . .	**A**
		5654	B	A	A	A	. . .	**B**
	5086, 5356	4043	A	B	C	A	. . .	**. . .**
		5183	A	A	B	A	. . .	**A**
		5356	A	A	A	A	. . .	**A**
		5554	B	A	A	A	. . .	**A**
		5556	A	A	B	A	. . .	**A**
		5654	B	A	A	A	. . .	**B**
	514.0, A514.0, B514.0, F514.0, 5154, 5254	4043	A	B	C	A	. . .	**. . .**
		5183	B	A	B	C	. . .	**A**
		5356	B	A	A	C	. . .	**A**
		5554	C	A	A	B	. . .	**A**
		5556	B	A	B	C	. . .	**A**

		5654	C	A	A	B	. . .	**B**
	5454	4043	A	B	C	B	A	**. . .**
		5183	B	A	B	C	. . .	**A**
		5356	B	A	A	C	. . .	**A**
		5554	C	A	A	A	A	**A**
		5556	B	A	B	C	. . .	**A**
		5654	C	A	A	B	. . .	**B**
	6005, 6063, 6101, 6151, 6201, 6351, 6951	4043	A	C	B	A	A	**. . .**
		5183	B	A	A	C		**A**
		5356	B	A	A	C	. . .	**A**
		5554	C	B	A	B	B	**A**
		5556	B	A	A	C	. . .	**A**
		5654	C	B	A	B	. . .	**B**
5454	1060, 1350	4043	A	B	C	C	A	**. . .**
		5183	B	A	B	B	. . .	**A**
		5356	B	A	A	B	. . .	**A**
		5554	C	A	A	A	A	**A**
		5556	B	A	B	B	. . .	**A**
	1100	4043	A	B	C	C	A	**. . .**
		5183	B	A	B	B	. . .	**A**
		5356	B	A	A	B	. . .	**A**
		5554	C	A	A	A	A	**A**
		5556	B	A	B	B	. . .	**A**
	2014, 2036	(B)	. . .	. . .	. . .	. . .	. . .	**. . .**
	2219	4043	A	A	A	A	A	**. . .**
	3003, ALCLAD 3003	4043	A	B	C	C	A	**. . .**
		5183	B	A	B	B	. . .	**A**
		5356	B	A	A	B	. . .	**A**
		5554	C	A	A	A	A	**A**
		5556	B	A	B	B	. . .	**A**
	3004	4043	A	D	C	C	A	**. . .**
		5183	B	A	B	B	. . .	**A**
		5356	B	B	A	B	. . .	**A**
		5554	C	C	A	A	A	**A**
		5556	B	A	B	B	. . .	**A**
	ALCLAD 3004	4043	A	D	C	C	A	**. . .**
		5183	B	A	B	B	. . .	**A**
		5356	B	B	A	B	. . .	**A**
		5554	C	C	A	A	A	**A**
		5556	B	A	B	B	. . .	**A**
	5005, 5050	4043	A	B	C	C	A	**. . .**
		5183	B	A	B	B	. . .	**A**
		5356	B	A	A	B	. . .	**A**
		5554	C	A	A	A	A	**A**
		5556	B	A	B	B	. . .	**A**
	5052, 5652	4043	A	D	C	C	A	**. . .**
		5183	A	A	A	B	. . .	**A**
		5356	A	B	A	B	. . .	**A**
		5554	C	C	A	A	A	**A**
		5556	A	A	B	B	. . .	**A**
		5654	B	C	A	B	. . .	**B**
	5083, 5456	5183	A	A	B	B	. . .	**A**
		5356	A	B	A	B	. . .	**A**
		5554	B	C	A	A	. . .	**A**
		5556	A	A	B	B	. . .	**A**
	5086, 5356	5183	A	A	B	B	. . .	**A**
		5356	A	B	A	B	. . .	**A**
		5554	B	C	A	A	. . .	**A**
		5556	A	A	B	B	. . .	**A**
	514.0, A514.0, B514.0, F514.0, 5154, 5254	5183	A	A	B	B	. . .	**A**
		5356	A	B	A	B	. . .	**A**

		5554	B	C	A	A	. . .	**A**
		5556	A	A	B	B	. . .	**A**
		5654	B	C	A	A	. . .	**B**
	5454	5183	A	A	B	B	. . .	**A**
		5356	A	B	A	B	. . .	**A**
		5554	B	C	A	A	A	**A**
		5556	A	A	B	B	. . .	**A**
		5654	B	C	A	B	. . .	**B**
514.0, A514.0, B514.0, F514.0, 5154, 5254	1060, 1350	4043	A	B	C	C	. . .	**. . .**
		5183	B	A	B	B	. . .	**A**
		5356	B	A	A	B	. . .	**A**
		5554	C	A	A	A	. . .	**A**
		5556	B	A	B	B	. . .	**A**
		5654	C	A	A	A	. . .	**B**
	1100	4043	A	B	C	C	. . .	**. . .**
		5183	B	A	B	B	. . .	**A**
		5356	B	A	A	B	. . .	**A**
		5554	C	A	A	A	. . .	**A**
		5556	B	A	B	B	. . .	**A**
		5654	C	A	A	A	. . .	**B**
	2014, 2036	[B]	. . .	. . .	. . .	. . .	. . .	**. . .**
	2219	4043	A	A	A	A	. . .	**. . .**
	3003, ALCLAD 3003	4043	A	B	C	C	. . .	**. . .**
		5183	B	A	B	B	. . .	**A**
		5356	B	A	A	B	. . .	**A**
		5554	C	A	A	A	. . .	**A**
		5556	B	A	B	B	. . .	**A**
		5654	C	A	A	A	. . .	**B**
	3004	4043	A	D	C	C	. . .	**. . .**
		5183	B	A	B	B	. . .	**A**
		5356	B	B	A	B	. . .	**A**
		5554	C	C	A	A	. . .	**A**
		5556	B	A	B	B	. . .	**A**
		5654	C	C	A	A	. . .	**B**
	ALCLAD 3004	4043	A	D	C	C	. . .	**. . .**
		5183	B	A	B	B	. . .	**A**
		5356	B	B	A	B	. . .	**A**
		5554	C	C	A	A	. . .	**A**
		5556	B	A	B	B	. . .	**A**
		5654	C	C	A	A	. . .	**B**
	5005, 5050	4043	A	B	C	C	. . .	**. . .**
		5183	B	A	B	B	. . .	**A**
		5356	B	A	A	B	. . .	**A**
		5554	C	A	A	A	. . .	**A**
		5556	B	A	B	B	. . .	**A**
		5654	C	A	A	A	. . .	**B**
	5052, 5652	4043	A	D	C	C	. . .	**. . .**
		5183	A	A	B	B	. . .	**B**
		5356	A	B	A	B	. . .	**A**
		5554	C	C	A	A	. . .	**B**
		5556	A	A	B	B	. . .	**B**
		5654	B	C	A	A	. . .	**A**
	5083, 5456	5183	A	A	B	A	. . .	**A**
		5356	A	B	A	A	. . .	**A**
		5554	B	C	A	A	. . .	**A**
		5556	A	A	B	A	. . .	**A**
		5654	B	C	A	A	. . .	**B**
	5086, 5356	5183	A	A	B	A	. . .	**A**
		5356	A	B	A	A	. . .	**A**
		5554	B	C	A	A	. . .	**A**
		5556	A	A	B	A	. . .	**A**

		5654	B	C	A	A	. . .	**B**
	514.0, A514.0, B514.0, F514.0, 5154, 5254	5183	A	A	B	B	. . .	**B**
		5356	A	B	A	B	. . .	**A**
		5554	B	C	A	A	. . .	**B**
		5556	A	A	B	B	. . .	**B**
		5654	B	C	A	A	. . .	**A**
5086, 5356	1060, 1350	4043	A	B	C	B	. . .	**. . .**
		5183	A	A	B	A	. . .	**A**
		5356	A	A	A	A	. . .	**A**
		5556	A	A	B	A	. . .	**A**
	1100	4043	A	B	C	B	. . .	**. . .**
		5183	A	A	B	A	. . .	**A**
		5356	A	A	A	A	. . .	**A**
		5556	A	A	B	A	. . .	**A**
	2014, 2036	(B)	. . .	. . .	. . .	. . .	. . .	**. . .**
	2219	4043	A	A	A	A	. . .	**. . .**
	3003, ALCLAD 3003	4043	A	B	C	B	. . .	**. . .**
		5183	A	A	B	A	. . .	**A**
		5356	A	A	A	A	. . .	**A**
		5556	A	A	B	A	. . .	**A**
	3004	4043	A	C	C	B	. . .	**. . .**
		5183	A	A	B	A	. . .	**A**
		5356	A	B	A	A	. . .	**A**
		5556	A	A	B	A	. . .	**A**
	ALCLAD 3004	4043	A	C	C	B	. . .	**. . .**
		5183	A	A	B	A	. . .	**A**
		5356	A	B	A	A	. . .	**A**
		5556	A	A	B	A	. . .	**A**
	5005, 5050	4043	A	B	C	B	. . .	**. . .**
		5183	A	A	B	A	. . .	**A**
		5356	A	A	A	A	. . .	**A**
		5556	A	A	B	A	. . .	**A**
	5052, 5652	5183	A	A	B	A	. . .	**A**
		5356	A	B	A	A	. . .	**A**
		5554	C	C	A	A	. . .	**A**
		5556	A	A	B	A	. . .	**A**
		5654	B	C	A	A	. . .	**B**
	5083, 5456	5183	A	A	B	A	. . .	**A**
		5356	A	B	A	A	. . .	**A**
		5556	A	A	B	A	. . .	**A**
	5086, 5356	5183	A	A	B	A	. . .	**A**
		5356	A	B	A	A	. . .	**A**
		5556	A	A	B	A	. . .	**A**
5083, 5456	1060, 1350	4043	A	B	C	B	. . .	**. . .**
		5183	A	A	B	A	. . .	**A**
		5356	A	A	A	A	. . .	**A**
		5556	A	A	B	A	. . .	**A**
	1100	4043	A	B	C	B	. . .	**. . .**
		5183	A	A	B	A	. . .	**A**
		5356	A	A	A	A	. . .	**A**
		5556	A	A	B	A	. . .	**A**
	2014, 2036	(B)	. . .	. . .	. . .	. . .	. . .	**. . .**
	2219	4043	A	A	A	A	. . .	**. . .**
	3003, ALCLAD 3003	4043	A	B	C	B	. . .	**. . .**
		5183	A	A	B	A	. . .	**A**
		5356	A	A	A	A	. . .	**A**
		5556	A	A	B	A	. . .	**A**
	3004	4043	A	C	C	B	. . .	**. . .**
		5183	A	A	B	A	. . .	**A**
		5356	A	B	A	A	. . .	**A**
		5556	A	A	B	A	. . .	**A**

	ALCLAD 3004	4043	A	C	C	B	. . .	**. . .**
		5183	A	A	B	A	. . .	**A**
		5356	A	B	A	A	. . .	**A**
		5556	A	A	B	A	. . .	**A**
	5005, 5050	4043	A	B	C	B	. . .	**. . .**
		5183	A	A	B	A	. . .	**A**
		5356	A	A	A	A	. . .	**A**
		5556	A	A	B	A	. . .	**A**
	5052, 5652	5183	A	A	B	A	. . .	**A**
		5356	A	B	A	A	. . .	**A**
		5554	C	C	A	A	. . .	**A**
		5556	A	A	B	A	. . .	**A**
		5654	B	C	A	A	. . .	**B**
	5083, 5456	5183	A	A	B	A	. . .	**A**
		5356	A	. . .	A	A	. . .	**A**
		5556	A	A	B	A	. . .	**A**
5052, 5652	1060, 1350	4043	A	B	C	A	A	**. . .**
		5183	B	A	B	. . .	. . .	**A**
		5356	B	A	A	. . .	. . .	**A**
		5556	B	A	B	. . .	. . .	**A**
	1100	4043	A	B	C	A	A	**. . .**
		5183	B	A	B	. . .	. . .	**A**
		5356	B	A	A	. . .	. . .	**A**
		5556	B	A	B	. . .	. . .	**A**
	2014, 2036	4043	A	A	A	A	A	**. . .**
	1219	4043	A	A	A	A	A	**. . .**
	3003, ALCLAD 3003	4043	A	B	C	A	A	**. . .**
		5183	B	A	B	. . .	. . .	**A**
		5356	B	A	A	. . .	. . .	**A**
		5556	B	A	B	. . .	. . .	**A**
	3004	4043	A	C	C	A	A	**. . .**
		5183	B	A	B	. . .	. . .	**A**
		5356	B	B	A	. . .	. . .	**A**
		5556	B	A	B	. . .	. . .	**A**
	ALCLAD 3004	4043	A	C	C	A	A	**. . .**
		5183	B	A	B	. . .	. . .	**A**
		5356	B	B	A	. . .	. . .	**A**
		5556	B	A	B	. . .	. . .	**A**
	5005, 5050	4043	A	B	C	A	A	**. . .**
		5183	B	A	B	. . .	. . .	**A**
		5356	B	A	A	. . .	. . .	**A**
		5556	B	A	B	. . .	. . .	**A**
	5052, 5652	4043	A	D	C	B	A	**. . .**
		5183	A	A	B	C	. . .	**B**
		5356	A	B	A	C	. . .	**A**
		5554	C	C	A	A	A	**B**
		5556	A	A	B	C	. . .	**B**
		5654	B	C	A	B	. . .	**A**
5005, 5050	1060, 1350	1100	C	B	A	A	A	**A**
		4043	A	A	C	A	A	**. . .**
		4145	B	A	D	B	A	**. . .**
		5183	C	A	B	. . .	. . .	**B**
		5356	C	A	B	. . .	. . .	**B**
		5556	C	A	B	. . .	. . .	**B**
	1100	1100	C	B	A	A	A	**A**
		4043	A	A	C	A	A	**. . .**
		4145	B	A	D	B	A	**. . .**
		5183	C	A	B	. . .	. . .	**B**
		5356	C	A	B	. . .	. . .	**B**
		5556	C	A	B	. . .	. . .	**B**
	2014, 2036	4043	B	B	A	A	A	**. . .**

		4145	A	A	B	A	A	**. . .**
	2219	4043	B	B	A	A	A	**. . .**
		4145	A	A	B	A	A	**. . .**
	3003, ALCLAD 3003	1100	C	C	A	A	A	**A**
		4043	A	B	C	A	A	**. . .**
		4145	B	B	D	B	A	**. . .**
		5183	C	A	B	C	. . .	**B**
		5356	C	A	B	C	. . .	**B**
		5556	C	A	B	C	. . .	**B**
	3004	4043	A	B	C	A	A	**. . .**
		5183	B	A	B	. . .	. . .	**A**
		5356	B	A	A	. . .	. . .	**A**
		5556	B	A	B	. . .	. . .	**A**
	ALCLAD 3004	4043	A	B	C	A	A	**. . .**
		5183	B	A	B	B	. . .	**A**
		5356	B	A	A	B	. . .	**A**
		5556	B	A	B	B	. . .	**A**
	5005, 5050	1100	B	. . .	A	A	A	**A**
		4043	A	B	D	A	A	**. . .**
		5183	B	A	C	. . .	. . .	**B**
		5356	B	A	B	. . .	. . .	**B**
		5556	B	A	C	. . .	. . .	**B**
ALCLAD 3004	1060, 1350	1100	D	B	A	A	A	**A**
		4043	A	A	C	A	A	**. . .**
		4145	B	A	D	B	A	**. . .**
		5183	C	A	B	C	. . .	**B**
		5356	C	A	B	C	. . .	**B**
		5556	C	A	B	C	. . .	**B**
	1100	1100	D	B	A	A	A	**A**
		4043	A	A	C	A	A	**. . .**
		4145	B	A	D	B	A	**. . .**
		5183	C	A	B	C	. . .	**B**
		5356	C	A	B	C	. . .	**B**
		5556	C	A	B	C	. . .	**B**
	2014, 2036	4043	B	B	A	A	A	**. . .**
		4145	A	A	B	A	A	**. . .**
	2219	4043	B	B	A	A	A	**. . .**
		4145	A	A	B	A	A	**. . .**
	3003, ALCLAD 3003	1100	C	C	A	A	A	**A**
		4043	A	B	C	A	A	**. . .**
		4145	B	B	D	B	A	**. . .**
		5183	C	A	B	C	. . .	**A**
		5356	C	A	B	C	. . .	**A**
		5556	C	A	B	C	. . .	**A**
	3004	4043	A	D	D	A	A	**. . .**
		5183	B	A	C	C	. . .	**A**
		5356	B	B	B	C	. . .	**A**
		5554	C	C	A	B	A	**A**
		5556	B	A	C	C	. . .	**A**
	ALCLAD 3004	4043	A	D	D	A	A	**. . .**
		5183	B	A	C	C	. . .	**A**
		5356	B	B	B	C	. . .	**A**
		5554	C	C	A	B	A	**A**
		5556	B	A	C	C	. . .	**A**
3004	1060, 1350	1100	D	B	A	A	A	**A**
		4043	A	A	C	A	A	**. . .**
		4145	B	A	D	B	A	**. . .**
		5183	C	A	B	. . .	. . .	**B**
		5356	C	A	B	. . .	. . .	**B**
		5556	C	A	B	. . .	. . .	**B**
	1100	1100	D	B	A	A	A	**A**

		4043	A	A	C	A	A	. . .
		4145	B	A	D	B	A	. . .
		5183	C	A	B	. . .	. . .	**B**
		5356	C	A	B	. . .	. . .	**B**
		5556	C	A	B	. . .	. . .	**B**
	2014, 2036	4043	B	B	A	A	A	. . .
		4145	A	A	B	A	A	. . .
	2219	4043	B	B	A	A	A	. . .
		4145	A	A	B	A	A	. . .
	3003, ALCLAD 3003	1100	C	C	A	A	A	**A**
		4043	A	B	C	A	A	. . .
		4145	B	B	D	B	A	. . .
		5183	C	A	B	C	. . .	**A**
		5356	C	A	B	C	. . .	**A**
		5556	C	A	B	C	. . .	**A**
	3004	4043	A	B	D	A	A	. . .
		5183	B	A	C	C	. . .	**A**
		5356	B	B	B	C	. . .	**A**
		5554	C	C	A	B	A	**A**
		5556	B	A	C	C	. . .	**A**
3003, ALCLAD 3003	1060, 1350	1100	B	B	A	A	A	**A**
		4043	A	A	B	A	A	. . .
		4145	A	A	C	B	A	. . .
	1100	1100	B	B	A	A	A	**A**
		4043	A	A	B	A	A	. . .
		4145	A	A	C	B	A	. . .
	2014, 2036	4043	B	A	A	A	A	. . .
		4145	A	A	B	A	A	. . .
	2219	4043	B	A	A	A	A	. . .
		4145	A	A	B	A	A	. . .
	3003, ALCLAD 3003	1100	B	B	A	A	A	**A**
		4043	A	A	B	A	A	. . .
		4145	A	A	C	B	A	. . .
2219	1060, 1350	4043	B	A	A	A	A	. . .
		4145	A	A	B	A	A	. . .
	1100	4043	B	A	A	A	A	. . .
		4145	A	A	B	A	A	. . .
	2014, 2036	2319	B	A	A	A	A	**A**
		4043	B	C	B	C	A	. . .
		4145	A	B	C	B	A	. . .
	2219	2319	A	A	A	A	A	**A**
		4043	B	C	B	C	A	. . .
		4145	A	B	C	B	A	. . .
2014, 2036	1060, 1350	4043	B	A	A	A	A	. . .
		4145	A	A	B	A	A	. . .
	1100	4043	B	A	A	A	A	. . .
		4145	A	A	B	A	A	. . .
	2014, 2036	2319	C	A	A	A	A	**A**
		4043	B	C	B	C	A	. . .
		4145	A	B	C	B	A	. . .
1100	1060, 1350	1100	B	B	A	A	A	**A**
		4043	A	A	B	A	A	. . .
	1100	1100	B	B	A	A	A	. . .
		4043	A	A	B	A	A	. . .
1060, 1350	1060, 1350	1100	B	B	A	A	A	**B**
		1188	C	C	A	A	A	**A**
		4043	A	A	B	A	A	. . .
		5554	C	C	A	B	A	**A**
		5556	**B**	**A**	**C**	**C**	**. . .**	**A**

Note: Combinations having no ratings are not recommended.

Source: Aluminum Company of America

(A) A, B, C, AND D REPRESENT RELATIVE RATINGS (WHERE A IS BEST AND D IS WORST) OF THE PERFORMANCE OF THE TWO COMPONENT BASE ALLOYS COMBINED WITH EACH GROUP OF SELECTED FILLER ALLOYS. W, EASE OF WELDING (RELATIVE FREEDOM FROM WELD CRACKING); S, STRENGTH OF WELDED JOINT IN AS-WELDED CONDITION (RATING APPLIES SPECIFICALLY TO FILLET WELDS, BUT ALL RODS AND ELECTRODES RATED WILL DEVELOP PRESENTLY SPECIFIED MINIMUM STRENGTHS FOR BUTT WELDS); D, DUCTILITY (RATING BASED ON FREE BEND ELONGATION OF THE WELD); C, CORROSION RESISTANCE IN CONTINUOUS OR ALTERNATE IMMERSION OF FRESH OR SALT WATER; T, PERFORMANCE IN SERVICE AT SUSTAINED TEMPERATURES >65 °C (>150 °F); M, COLOR MATCH AFTER ANODIZING.

(B) NO FILLER SUITABLE.

Quality control requirements for bare aluminum filler rod and electrode are stated in Ref 16. To maintain the quality level to which they are produced, the filler wire must be protected during shipment, storage, handling, and use. The spooled filler wire, which is most critical, is normally packaged in a sealed plastic bag and carton. The best storage place is a dry, heated area. If stored in an unheated area, then the packaged product should be brought to the production area and allowed to reach that ambient temperature before the carton is opened. If the temperature of the wire is more than 9 °C (16 °F) below the room temperature when the package is opened, moisture in the atmosphere can condense on the wire, creating a hydrated oxide. The 5*xxx* (aluminum-magnesium) series filler alloys are most sensitive to this situation and can be ruined after just a few seconds of exposure, because the hydrated oxide can cause excessive porosity in the weld. For the same reason, the spooled product should be removed from the welding apparatus at the completion of work and stored in a cabinet where the relative humidity is kept below 35%. A small resistance heating unit in an electrical socket on the inside of a sealed cabinet will accomplish this. If the product is not removed from the equipment, a small resistance heater inside the spool enclosure can also be effective.

References cited in this section

1. J.D. DOWD, WELD CRACKING OF ALUMINUM ALLOYS, *WELD. J.*, RESEARCH SUPPLEMENT, VOL 31, 1952, P 448S-456S
2. J.H. DUDAS AND F.R. COLLINS, PREVENTING WELD CRACKS IN HIGH-STRENGTH ALUMINUM ALLOYS, *WELD. J.*, RESEARCH SUPPLEMENT, VOL 45 (NO. 6), JUNE 1966, P 241S-249S
3. C.E. CROSS, PH.D. THESIS, COLORADO SCHOOL OF MINES, 1986, P 144
4. A.R.E. SINGER AND P.H. JENNINGS, HOT SHORTNESS OF THE ALUMINUM-SILICON ALLOYS OF COMMERCIAL QUALITY, *J. INST. MET.*, VOL 73, 1947, P 197-212
5. W.I. PUMPHREY AND J.V. LYONS, CRACKING DURING THE CASTING AND WELDING OF THE MORE COMMON BINARY ALUMINUM ALLOYS OF COMMERCIAL QUALITY, *J. INST. MET.*, VOL 74, 1948, P 439-455
6. P.H. JENNINGS, A.R.E. SINGER, AND W.I. PUMPHREY, HOT-SHORTNESS OF SOME HIGH PURITY ALLOYS IN THE SYSTEMS ALUMINUM-COPPER AND ALUMINUM-MAGNESIUM-SILICON, *J. INST. MET.*, VOL 74, 1948, P 227-248
7. N.F. GITTOS AND M.H. SCOTT, HEAT AFFECTED ZONE CRACKING OF AL-MG-SI ALLOYS, *WELD. J.*, RESEARCH SUPPLEMENT, JUNE 1981, P 95S-103S
8. W.L. BURCH, THE EFFECT OF WELDING SPEED ON THE STRENGTH OF 6061-T4 ALUMINUM JOINTS, *WELD. J.*, RESEARCH SUPPLEMENT, VOL 37 (NO. 8), AUG 1958, P 361S-367S
9. G.E. METZGER, SOME MECHANICAL PROPERTIES OF WELDS IN 6061 ALUMINUM ALLOY SHEET, *WELD. J.*, RESEARCH SUPPLEMENT, VOL 46 (NO. 10), OCT 1967, P 457S-469S
10. F.R. COLLINS, F.G. NELSON, AND I.B. ROBINSON, ALUMINUM 2219--NEW ALLOY FOR HIGH-STRENGTH WELDED STRUCTURES, *MET. PROG.*, NOV 1961
11. E.H. DIX, W.H. ANDERSON, AND M.B. SHUMAKER, INFLUENCE OF SERVICE TEMPERATURE

ON THE RESISTANCE OF WROUGHT ALUMINUM-MAGNESIUM ALLOYS TO CORROSION, *CORROSION*, VOL 15 (NO. 2), FEB 1959, P 55T-62T

12. M.B. SHUMAKER, R.A. KELSEY, D.O. SPROWLS, AND J.G. WILLIAMSON, "EVALUATION OF VARIOUS TECHNIQUES FOR STRESS-CORROSION TESTING WELDED ALUMINUM ALLOYS," PRESENTED AT ASTM STRESS-CORROSION TESTING SYMPOSIUM, JUNE 1966
13. F.G. NELSON AND R.L. ROLF, SHEAR STRENGTHS OF ALUMINUM ALLOY FILLET WELDS, *WELD. J.*, RESEARCH SUPPLEMENT, VOL 45 (NO. 2), FEB 1966, P 82S-84S
14. S.L. WÖHLER AND O. SCHLIEPHAKE, ÜBEREINEM GERS., DURCH POTENTIALMESSUNGER DAS AUFGREGEN DER VERB. MG_2SI ZU BESTÄTIGEN, *Z. ANORG. CHEM.*, 1962, P 151
15. G.W. AKIMOW AND A.S. OLESCHKO, GMELINS HANDBUCH DER ANORGANISCHEN CHEMIE, (NO. 8), AUFLAGE, 1942, P 393
16. "SPECIFICATION FOR BARE ALUMINUM AND ALUMINUM ALLOY WELDING ELECTRODE AND ROD," ANSI/AWS A5.10-92, AMERICAN WELDING SOCIETY, 1992

Welding of Aluminum Alloys

Paul B. Dickerson, Aluminum Company of America (retired)

Preparation for Welding

Joint Designs. Typical joint geometries for ac-GTAW and GMAW processes used with aluminum are shown in Fig. 8. Because good penetration control can be obtained with GTAW, welds can be made from a single side without backing. When mechanizing the GTAW process and when using the GMAW process by manual or mechanical means, the use of a temporary grooved backing is very helpful in controlling the uniformity of penetration for single-sided welds. When welding from both sides, a temporary support of the initial weld pass can be given by an angle or rod when a thin land is employed, or the land can be thickened to provide support. In either case, back gouging to sound weld metal is required before application of the initial root pass.

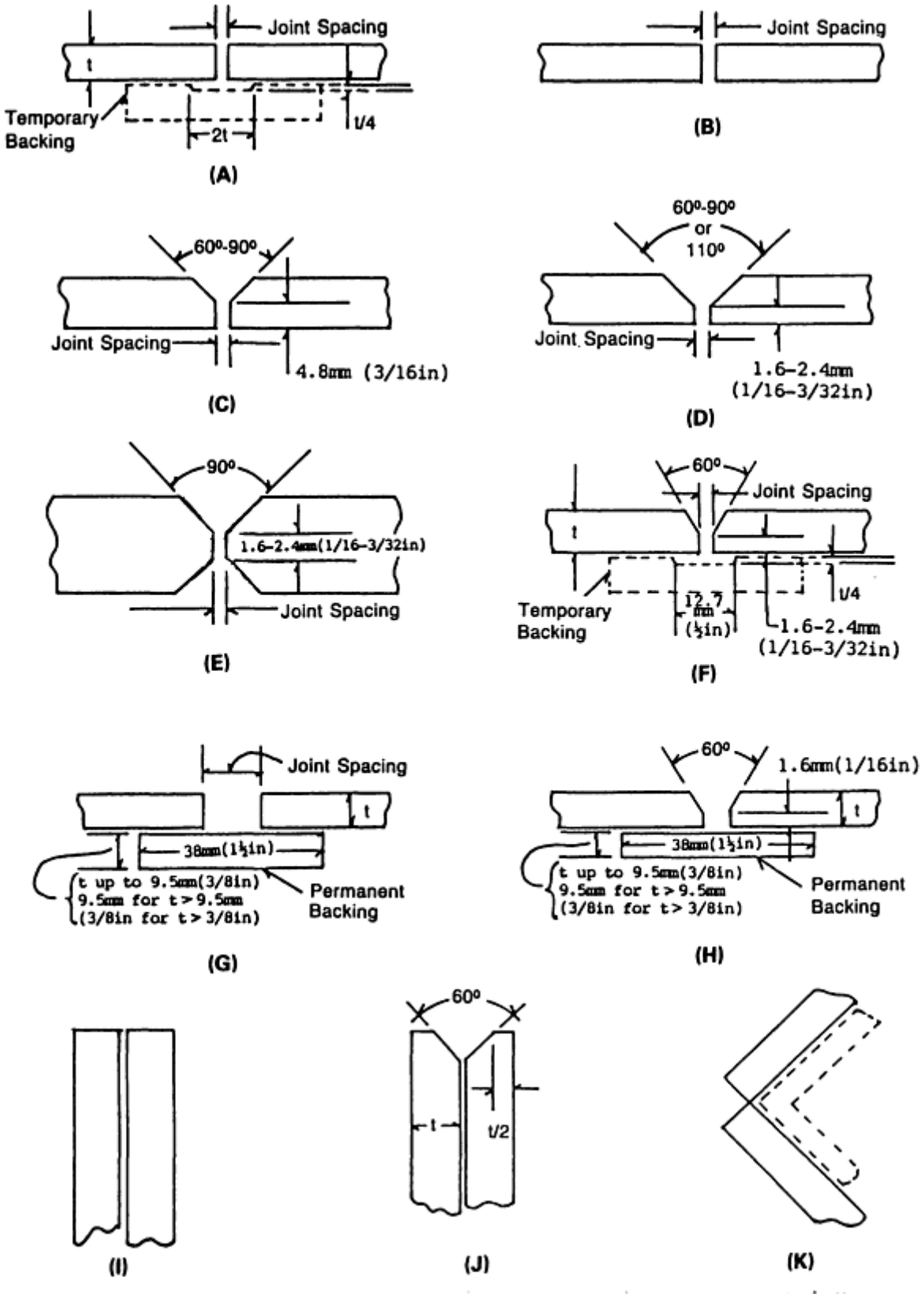

FIG. 8 TYPICAL JOINT GEOMETRIES USED FOR AC-GTAW AND GMAW OF ALUMINUM COMPONENTS. LETTERS CORRESPOND TO EDGE PREPARATIONS IN TABLES 15, 17, AND 18. SOURCE: AMERICAN WELDING SOCIETY

A 60° included "V" bevel is standard for GMAW. For GTAW, the bevel varies from 60° to 90°, and for overhead groove welds, a 110° minimum "V" bevel is required for root pass control. The large angles are needed to allow the gas nozzle access to the joint to provide adequate inert-gas shielding of the root passes. For proper nozzle access with 25 mm (1 in.)

and thicker material, single "U" and double "U" bevels are required. A special joint design used for aluminum pipe and other single-sided access joints, which permits uniform and complete penetration welds without backing, is shown in Fig. 9 (Ref 17).

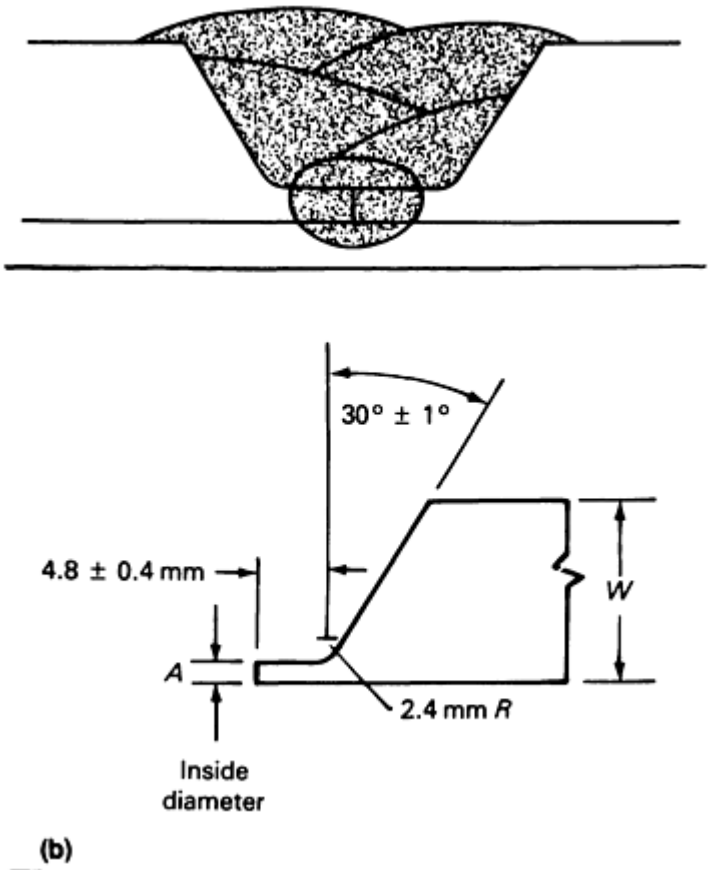

PIPE SIZE		*A*		W_{MAX}	
MM	**IN.**	**MM**	**IN.**	**MM**	IN.
3.2-64	$\frac{1}{8}$ -2 $\frac{1}{2}$	1.6 ± 0.4	$\frac{1}{16} \pm \frac{1}{64}$	7.01	**0.276**
76-305	**3-12**	**2.4 ± 0.4**	$\frac{3}{32} \pm \frac{1}{64}$	**12.7**	**0.500**

FIG. 9 EXTENDED-LAND BEVEL USED TO WELD ALUMINUM PIPE. (A) TYPICAL MULTIPLE-PASS WELD USED TO JOIN PIPE WITH EXTENDED-LAND BEVEL. (B) RECOMMENDED EXTENDED-LAND BEVEL SPECIFICATIONS FOR 3.2 TO 305 MM ($\frac{1}{8}$ TO 12 IN.) DIAM PIPE WITH 7.01 TO 12.7 MM (0.276 TO 0.500 IN.) WALL THICKNESS. SOURCE: AMERICAN WELDING SOCIETY

When welding from a single side, the oxide on the opposite side is not removed by the action of the arc and inert-gas shield. Therefore, it must be physically stretched (Fig. 10) out of the way to permit complete root fusion for full-penetration welds. To accomplish this, the depth of the penetration reinforcement needs to be greater than the levels normally allowed by specifications governing other metals. Practical values for the root reinforcement (*R*) are (Ref 18):

THICKNESS, *T*		ROOT REINFORCEMENT, *R*	
mm	**in.**	**mm**	in.
$T \le 1.6$	$T \le \frac{1}{16}$	$1.5T$	**$1.5T$**
$1.6 < T \le 6.4$	$\frac{1}{16} < T \le \frac{1}{4}$	2.4	$\frac{3}{32}$
$6.4 < T \le 12.7$	$\frac{1}{4} < T \le \frac{1}{2}$	3.2	$\frac{1}{8}$
$12.7 < T \le 25.4$	$\frac{1}{2} < T \le 1$	4.0	$\frac{5}{32}$
$T > 25.4$	**$T > 1$**	**4.8**	$\frac{3}{16}$

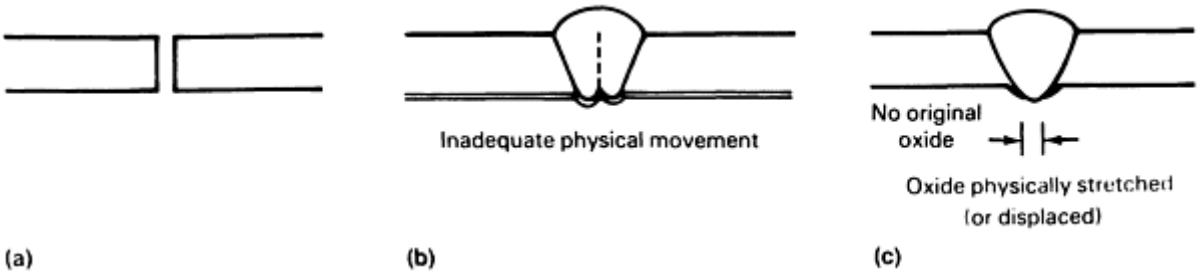

FIG. 10 EFFECT OF PHYSICAL STRETCHING ON ROOT FUSION. (A) ORIGINAL OXIDE SURFACES. (B) INCOMPLETE (POOR) ROOT FUSION. (C) COMPLETE (PROPER) ROOT FUSION

When an integral aluminum backing is used, the base metal edge spacing must be adequate to permit the arc cleaning action to remove the oxide from the backing surface and thus allow proper fusion. An opening of about 1*t* (one times the thickness) is required for thicknesses up to 9.5 mm ($\frac{3}{8}$ in.). For thicker material, the edge spacing should be sufficient to allow two root passes--one along each edge. Integral backings should either be flush with the base metal or possess a shallow groove and should be tack welded to the base metal. Any projections up into the joint to control edge spacing can result in poor fusion along each side of the projection because the oxide cannot be displaced.

Back gouging is normally done mechanically with pneumatic chisels, portable milling cutters, and routers. The gouge should possess a 3.2 mm ($\frac{1}{8}$ in.) minimum radius at its base. Sharp diamond-shaped chisels and sharp saw cuts do not permit proper fusion at their root when welded. Plasma arc cutting can be used to make square and beveled cuts that are free from surface contaminants. The plasma arc welding (PAW) process can also be used for back gouging. Argon-hydrogen gas mixtures are preferred for the best surface smoothness. Surface cracks can occur when arc cutting or gouging the heat-treatable aluminum alloys. These cracks can extend about 2.3 mm (0.090 in.) into the metal and must be mechanically removed before welding over that surface.

Surface Preparation. All surface lubricants on the base metal must be removed following metal working, sawing, and machining operations in order to avoid porosity. Vapor degreasers and any chlorinated solvent must be isolated from the welding area, because the arc radiation can alter these cleaning solutions chemically, resulting in toxic gases. Petroleum-base solvents can be used satisfactorily in the welding area.

Water stains, heat-treating oxides, chemical conversion coatings, and anodic finishes must be removed by chemical etching or mechanical means. Stainless steel brushes are preferred to avoid rust contamination of the joint. If a power brush is used, then a light pressure should be applied to remove the thick oxide. A high force can embed the oxide or contaminant into the surface and increase, rather than eliminate, weld discontinuities.

Surface moisture can be removed by a slight preheat of the joint prior to welding. A brief exposure at a maximum temperature of 120 °C (250 °F) should be controlled with the 5*xxx* series and heat-treatable aluminum alloys to avoid lowering corrosion resistance and reducing mechanical properties, respectively.

Optimal welding occurs when the metal is clean and dry, and possesses a minimum oxide thickness. In multiple-pass welds, it is common to wire brush the previously deposited surface in order to minimize the oxide or surface "smut" and thereby facilitate the subsequent weld pass.

References cited in this section

17. "RECOMMENDED PRACTICES FOR GAS SHIELDED ARC WELDING OF ALUMINUM AND ALUMINUM ALLOY PIPE," ANSI/AWS D10.7-86, AMERICAN WELDING SOCIETY, 1986
18. "STRUCTURAL WELDING CODE--ALUMINUM," ANSI/AWS D1.2-90, AMERICAN WELDING SOCIETY, 1990

Welding of Aluminum Alloys

Paul B. Dickerson, Aluminum Company of America (retired)

Welding Processes

The GTAW process has been used to weld thicknesses from 0.25 to 150 mm (0.010 to 6 in.) and can be used in all weld positions. Because it is relatively slow, it is highly maneuverable for welding tubing, piping, and variable shapes. It permits excellent penetration control and can produce welds of excellent soundness. Weld termination craters can be filled easily as the current is tapered down by a foot pedal or electronic control.

The ac-GTAW process provides an arc cleaning action to remove the surface oxide during the positive electrode half of the cycle and a penetrating arc when the electrode is operated at negative polarity. It is used primarily to weld thicknesses up to 6.3 mm ($\frac{1}{4}$ in.) and can be used for manual, mechanized, or automated applications. Typical manual welding procedures are listed in Tables 15, 16, and 17.

TABLE 15 TYPICAL AC-GTAW PROCEDURES FOR GROOVE WELDING OF ALUMINUM

See also AWS D10.7, "Recommended Practices for Gas Shielded Arc Welding of Aluminum and Aluminum Alloy Pipe"

BASE METAL THICKNESS		**WELD POSITION[A]**	**EDGE PREPARATION[B]**	**ROOT OPENING**		**WELD PASSES**	**FILLER DIAMETER**		**PURE TUNGSTEN ELECTRODE DIAMETER**		**GAS CUP INSIDE DIAMETER**		**ARGON GAS FLOW**		**BALANCED WAVE AC, A**	ARC TRAVEL SPEED	
MM	**IN.**			**MM**	**IN.**		**MM**	**IN.**	**MM**	**IN.**	**MM**	**IN.**	**L/MIN**	**FT^3/H**		**MM/S**	IN./MIN
1.6	1/16	F, V, H	A OR B	0-1.6	0-1/16	1	2.4	3/32	1.6-2.4	1/16 - 3/32	9.5	3/8	9	20	70-100	3-4	**8-10**
		O	A OR B	0-1.6	0-1/16	1	2.4	3/32	1.6	1/16	9.5	3/8	12	25	60-75	3-4	**8-10**
2.4	3/32	F	A OR B	0-2.4	0-3/32	1	3.2	1/8	2.4-3.2	3/32 - 1/8	9.5	3/8	9	20	95-115	3-4	**8-10**
		V, H	A OR B	0-2.4	0-3/32	1	2.4-3.2	3/32 - 1/8	2.4	3/32	9.5	3/8	9	20	85-110	3-4	**8-10**
		O	A OR B	0-2.4	0-3/32	1	2.4-3.2	3/32 - 1/8	2.4-3.2	3/32 - 1/8 1/8	9.5	3/8	12	25	90-110	3-4	**8-10**
3.2	1/8	F	A OR B	0-2.4	0-3/32	1-2	3.2-4.0	1/8 - 5/32	3.2	1/8	11.1	7/16	9	20	125-150	4-5	**10-12**
		V, H	A OR B	0-2.4	0-3/32	1-2	3.2	1/8	3.2	1/8	11.1	7/16 7/16	9	20	110-140	4	**10**
		O	A OR B	0-2.4	0-3/32	1-2	3.2-4.0	1/8 - 5/32	3.2	1/8	11.1	7/16	12	25	115-140	4-5	**10-12**

4.8	3/16	F	D-60°	0-3.2	0-1/8	2	4.0-4.8	5/32-3/16	4.0-4.8	5/32-3/16	11.1-12.7	7/16-1/2	12	25	170-190	4-5	**10-12**
		V	D-60°	0-2.4	0-3/32	2	4.0	5/32	4.0	5/32	11.1	7/16	12	25	160-175	4-5	**10-12**
		H	D-90°	0-2.4	0-3/32	2	4.0	5/32	4.0	5/32	11.1	7/16	12	25	155-170	4-5	**10-12**
		O	D-110°	0-2.4	0-3/32	2	4.0	5/32	4.0	5/32	11.1	7/16	14	30	165-180	4-5	**10-12**
6.3	1/4	F	D-60°	0-3.2	0-1/8	2	4.8	3/16	4.8-6.3	3/16-1/4	12.7	1/2	14	30	220-275	3-4	**8-10**
		V	D-60°	0-2.4	0-3/32	2	4.8	3/16	4.8	3/16	12.7	1/2	14	30	200-240	3-4	**8-10**
		H	D-90°	0-2.4	0-3/32	2-3	4.0-4.8	5/32-3/16	4.0-4.8	5/32-3/16	12.7	1/2	14	30	190-225	3-4	**8-10**
		O	D-110°	0-2.4	0-3/32	2	4.8	3/16	4.8	3/16	12.7	1/2	16	35	210-250	3-4	**8-10**
9.5(C)	3/8(C)	F	D-60°	0-3.2	0-1/8	2	4.8-6.3	3/16-1/4	6.3	1/4	15.8	5/8	16	35	315-375	3-4	**8-10**
		F	E	0-2.4	0-3/32	2	4.8-6.3	3/16-1/4	6.3	1/4	15.8	5/8	16	35	340-380	3-4	**8-10**
		V	E-60°	0-2.4	0-3/32	3	4.8	3/16	4.8-6.3	3/16-1/4	15.8	5/8	16	35	260-300	3-4	**8-10**

		V, H, O	E	0-2.4	0-3/32	2	4.8	3/16	4.8-6.3	3/16 - 1/4	15.8	5/8	16	35	240-300	3-4	**8-10**
		H	D-90°	0-2.4	0-3/32	3	4.8	3/16	4.8-6.3	3/16 - 1/4	15.8	5/8	16	35	240-300	3-4	**8-10**
		O	**D-110°**	**0-2.4**	**0-3/32**	**3**	**4.8**	3/16	**4.8-6.3**	3/16 - 1/4	**15.8**	5/8	**19**	**40**	**260-300**	**3-4**	**8-10**

(A) F, FLAT; V, VERTICAL; H, HORIZONTAL; O, OVERHEAD.

(B) THESE ARE JOINTS SHOWN IN FIG. 8.

(C) PREHEATING IS OPTIONAL UP TO 177 °C (350 °F), HOWEVER, THIS MAY REDUCE THE WELD STRENGTH OF HEAT-TREATABLE ALLOYS.

TABLE 16 TYPICAL AC-GTAW PROCEDURES FOR FILLET AND LAP WELDING OF ALUMINUM COMPONENTS

BASE METAL THICKNESS		WELD POSITION[A]	WELD PASSES	FILLER DIAMETER		PURE TUNGSTEN ELECTRODE DIAMETER		GAS CUP INSIDE DIAMETER		ARGON GAS FLOW		BALANCED WAVE AC, A	ARC TRAVEL SPEED	
MM	IN.			MM	IN.	MM	IN.	MM	IN.	L/MIN	FT^3/H		MM/S	IN./MIN
1.6	1/16	F, H, V	1	2.4	3/32	1.6-2.4	1/16 - 3/32	9.5	3/8	8	16	70-100	3-4	**8-10**
		O	1	2.4	3/32	1.6-2.4	1/16 - 3/32	9.5	3/8	9	20	65-90	3-4	**8-10**
2.4	3/32	F	1	2.4-3.2	3/32 - 1/8	3.2-4.0	1/8 - 5/32	9.5	3/8	8	18	110-145	3-4	**8-10**
		H, V	1	2.4	3/32	2.4-3.2	3/32 - 1/8	9.5	3/8	8	18	90-125	3-4	**8-10**
		O	1	2.4	3/32	2.4-3.2	3/32 - 1/8	9.5	3/8	9	20	110-135	3-4	**8-10**
3.2	1/8	F	1	3.2	1/8	3.2-4.0	1/8 - 5/32	11.1	7/16	9	20	135-175	4-5	**10-12**
		H, V	1	3.2	1/8	2.4-3.2	3/32 - 1/8	9.5	3/8	9	20	115-145	3-4	**8-10**
		O	1	3.2	1/8	2.4-3.2	3/32 - 1/8	11.1	7/16	12	25	125-155	3-4	**8-10**
4.8	3/16	F	1	4.0	5/32	4.0-4.8	5/32 - 3/16	12.7	1/2	12	25	190-245	3-4	**8-10**
		H, V	1	4.0	5/32	4.0-4.8	5/32 - 3/16	12.7	1/2	12	25	175-210	3-4	**8-10**
		O	1	4.0	5/32	4.0-4.8	5/32 - 3/16	12.7	1/2	14	30	180-225	3-4	**8-10**
6.3	1/4	F	1	4.8	3/16	4.8-6.3	3/16 - 1/4	12.7	1/2	14	30	240-295	3-4	**8-10**
		H,V	1	4.8	3/16	4.8	3/16	12.7	1/2	14	30	220-265	3-4	**8-10**
		O	1	4.8	3/16	4.8	3/16	12.7	1/2	16	35	230-275	3-4	**8-10**
9.5[B]	3/8 [B]	F	2	4.8	3/16	6.3	1/4	16	5/8	16	35	325-375	3-4	**8-10**

		V	2	4.8	3/16	4.8-6.3	3/16 - 1/4	16	5/8	16	35	280-315	3-4	**8-10**
		H	3	4.8	3/16	4.8-6.3	3/16 - 1/4	16	5/8	16	35	270-300	3-4	**8-10**
		O	**3**	**4.8**	3/16	**4.8-6.3**	3/16 - 1/4	**16**	5/8	**19**	**40**	**290-335**	**3-4**	**8-10**

(A) F, FLAT; V, VERTICAL; H, HORIZONTAL; O, OVERHEAD.

(B) PREHEATING IS OPTIONAL UP TO 177 °C (350 °F); HOWEVER, THIS MAY REDUCE THE WELD STRENGTH OF HEAT-TREATABLE ALLOYS.

TABLE 17 TYPICAL AC-GTAW PROCEDURES FOR CORNER AND EDGE WELDING OF ALUMINUM COMPONENTS

BASE METAL THICKNESS		**WELD POSITION[A]**	**NUMBER OF WELD PASSES**	**FILLER DIAMETER**		**PURE TUNGSTEN ELECTRODE DIAMETER**		**GAS CUP INSIDE DIAMETER**		**ARGON GAS FLOW**		**BALANCED WAVE AC, A**	ARC TRAVEL SPEED	
MM	**IN.**			**MM**	**IN.**	**MM**	**IN.**	**MM**	**IN.**	**L/MIN**	**FT^3/H**		**MM/S**	IN./MIN
1.6	1/16	I, K	1	2.4	3/32	1.6	1/16	9.5	3/8	9	20	60-85	4-7	**10-16**
2.4	3/32	I, K	1	3.2	1/8	2.4	3/32	9.5	3/8	9	20	90-120	4-7	**10-16**
3.2	1/8	I, K	1	3.2-4.0	1/8 - 5/32	3.2	1/8	9.5	3/8	9	20	115-150	4-7	**10-16**
4.8	3/16	J, K	1	4.0	5/32	4.0	5/32	11.1	7/16	12	25	160-210	4-7	**10-16**
6.3	1/4	**J, K**	**2**	**4.8**	3/16	**4.8**	3/16	**12.7**	1/2	**14**	**30**	**200-250**	**3-5**	**8-12**

(A) JOINT DESIGNS AS SHOWN IN FIG. 8.

(B) HIGHER CURRENTS AND WELDING SPEEDS CAN BE EMPLOYED IF A TEMPORARY BACKING IS USED FOR COMER JOINTS.

(C) USE LOW SIDE OF CURRENT RANGE FOR HORIZONTAL AND VERTICAL JOINTS.

Optimal control of penetration in groove welds is obtained with a balanced ac wave, which permits a wide tolerance in the welding current or heat input between insufficient and excessive penetration. The fairly wide melting pattern does not penetrate readily into narrow grooves or corners and tends to bridge the root of fillet welds. When a wave balance control is available on the power supply, an increase in the percentage of the negative polarity can be beneficial, as long as adequate arc cleaning action is maintained.

The ac-GTAW process is particularly useful for welding aluminum pipe. An integral backing is suitable for structural and electrical bus applications; however, for fluid flow of water, gas, oil, and chemicals, crevice corrosion can result at the backing interface within the pipe. The joint configuration shown in Fig. 9 has been used for all-position GTAW of aluminum pipe and is considered standard for this purpose (Ref 17).

Argon shielding gas is normally used. However, for increased penetration capabilities and use on thick base metal, a mixture of argon with 25 to 50% helium can be used. Welding operations must be protected from wind gusts, which can disturb the inert-gas shielding, when welding near open doors and windows or when welding outdoors.

The alternating current arc (whether sinusoidal or square wave) requires a superimposed high-frequency power to maintain the ionized gas circuit when the current changes polarity. This avoids rectification, which reduces the arc cleaning action and arc stability.

Pure or zirconia-tungsten electrodes, which form a ball on the end during welding, should be used with ac-GTAW. Fine spitting of thoria-tungsten electrodes will occur when used with alternating current and should be limited to direct current (dc) operations.

The dc-GTAW Process. Negative electrode polarity direct current can be used to weld aluminum by manual and mechanized means. Helium gas shielding or a mixture of helium with 5 to 10% argon is used with a thoria-tungsten electrode. Because no arc cleaning occurs, the oxide must be minimized on the surface prior to welding. This is normally accomplished by chemical etching, followed by a mechanical "scraping" of the joint surfaces immediately prior to welding. Internal oxide stringers and associated poor fusion can occur if this cleaning is not done thoroughly. The deep, narrow penetration allows welding of square groove joints in thicknesses up to 12.7 mm ($\frac{1}{2}$ in.) and permits welding of heat-treatable alloys with a lower heat input than does ac-GTAW. This can result in higher as-welded mechanical properties with the heat-treatable alloys. The process is most widely used by the aerospace industry for this purpose.

Manual dc-GTAW using negative electrode polarity has been applied primarily to the repair of thick castings or weldments in thick plate. Agitation of the weld pool with the filler rod is sometimes required to break up the surface oxide for proper weld fusion. An excellent fabrication technique utilizing this process has been tack welding of fillet joints in 4.8 mm ($\frac{3}{16}$ in.) and thicker non-heat-treatable alloys, such as 5083 and 5456. A very small fillet reinforcement possessing deep penetration can be made, and there is little or no interference when the continuous weld is produced.

Variable Polarity PAW. This inert-gas process provides good arc cleaning action and sufficient penetration capabilities, such that a "keyhole" is created. It is best used in the vertical weld position so that when the keyhole is generated, the weld metal backfills the joint. The process is only used in mechanized or automated environments, and the equipment is very expensive. The weld is less sensitive to oxide conditions than those produced by either ac- or dc-GTAW, and high-quality welds can be made. Inert-gas backing is desirable for some of the aluminum alloys, such as the aluminum-copper-lithium type. Square groove joints up to 16 mm ($\frac{5}{8}$ in.) can be welded in a single pass.

GMAW is the major high-speed production process for arc welding aluminum. The equipment is portable, and the process can be easily used in all weld positions. It uses positive electrode dc power, which gives it a continuous cleaning action and concentrates the arc to produce rapid melting. Widely varying thicknesses can be welded without the need to preheat. Spooled aluminum wire is automatically fed through the welding gun, melted at the arc, and then sprayed across the arc. Because the electrode and filler are the same, the process is a one-handed operation that is easily mechanized or adapted for robotic operations. Manual travel speeds normally range from 7.6 to 15.2 mm/s (18 to 36 in./min). However, mechanized welds have been made at speeds that exceed 42 mm/s (100 in./min). Initially, GMAW was limited to 3.2 mm

($\frac{1}{8}$ in.) and thicker material. However, the availability of pull-type wire feed apparatus and pulsed-dc power supplies has extended its use with smaller electrodes and lower average currents to weld thicknesses of less than 1 mm (0.040 in.).

GMAW is best used in lap, fillet, or groove welds with integral or temporary backing. Typical welding procedures are listed in Tables 18 and 19. It is not recommended for corner or edge joints, unless the metal is thick enough to provide a substantial ledge or trough upon which to deposit the filler. Heat input needs to be constant for uniform penetration. A constant voltage power supply can be used for straight stringer passes. However, when the arc is oscillated transversely or in line with the joint, wide current excursions produce variable penetration and fusion. Weld starts with short contact tubes and fast electrode feed rates, as used in equipment designed for welding ferrous metals, and a constant voltage power supply often results in poorly fused starts, arcing in the contact tube, and excessive "burn backs" when used with aluminum.

TABLE 18 TYPICAL SEMIAUTOMATIC GMAW PROCEDURES FOR GROOVE WELDING OF ALUMINUM COMPONENTS

BASE METAL THICKNESS		WELD POSITION[A]	EDGE PREPARATION[B]	JOINT SPACING		TYPE AND NUMBER OF WELD PASSES[C]	ELECTRODE DIAMETER		CURRENT (DC, POSITIVE ELECTRODE)[D], A	ARC VOLTAGE[D], V	ARGON GAS FLOW		ARC TRAVEL SPEED	
MM	IN.			MM	IN.		MM	IN.			L/MIN	FT^3/H	MM/S	IN./MIN
1.6	1/16	F	A	. . .	. . .	1	0.8	0.030	70-110	15-20	12	25	10-19	**25-45**
		F	G	2.4	3/32	1	0.8	0.030	70-110	15-20	12	25	10-19	**25-45**
2.4	3/32	F	A	. . .	. . .	1	0.8-1.2	0.030-3/64	90-150	18-22	14	30	10-19	**25-45**
		F, V, H, O	G	3.2	1/8	1	0.8	0.030	110-130	18-23	14	30	10-13	**23-30**
3.2	1/8	F, V, H	A	0-2.4	0-3/32	1	0.8-1.2	0.030-3/64	120-150	20-24	14	30	10-13	**24-30**
		F, V, H, O	G	4.8	3/16	1	0.8-1.2	0.030-3/64	110-135	19-23	14	30	8-12	**18-28**
4.8	3/16	F, V, H	B	0-1.6	0-1/16	1F, 1R	0.9-1.2	0.035-3/64	130-175	22-26	16	35	10-13	**24-30**
		F, V, H	F	0-1.6	0-1/16	1	1.2	3/64	140-180	23-27	16	35	10-13	**24-30**
		O	F	0-1.6	0-1/16	2F	1.2	3/64	140-175	23-27	28	60	10-13	**24-30**
		F, V	H	3.2-4.8	1/8-3/16	2	1.2-1.6	3/64-1/16	140-185	23-27	16	35	10-13	**24-30**
		H, O	H	4.8	3/16	3	0.9-1.2	0.035-3/64	130-175	23-27	28	60	10-15	**25-35**

6.3	1/4	F	B	0-2.4	0-3/32	1F, 1R	1.2-1.6	3/64-1/16	175-200	24-28	19	40	10-13	**24-30**
		F	F	0-2.4	0-3/32	2	1.2-1.6	3/64-1/16	185-225	24-29	19	40	10-13	**24-30**
		V, H	F	0-2.4	0-3/32	3F, 1R	1.2	3/64	165-190	25-29	21	45	10-15	**25-35**
		O	F	0-2.4	0-3/32	3F, 1R	1.2-1.6	3/64-1/16	180-200	25-29	28	60	10-15	**25-35**
		F, V	H	3.2-6.3	1/8-1/4	2-3	1.2-1.6	3/64-1/16	175-225	25-29	19	40	10-13	**24-30**
		O, H	H	6.3	1/4	4-6	1.2-1.6	3/64-1/16	170-200	25-29	28	60	11-17	**25-40**
9.5	3/8	F	C-90°	0-2.4	0-3/32	1F, 1R	1.6	1/16	225-290	26-29	23	50	8-13	**20-30**
		F	F	0-2.4	0-3/32	2F, 1R	1.6	1/16	210-275	26-29	23	50	10-15	**24-35**
		V, H	F	0-2.4	0-3/32	3F, 1R	1.6	1/16	190-220	26-29	26	55	10-13	**24-30**
		O	F	0-2.4	0-3/32	5F, 1R	1.6	1/16	200-250	26-29	38	80	11-17	**25-40**
		F, V	H	6.3-9.5	1/4-3/8	4	1.6	1/16	210-290	26-29	23	50	10-13	**24-30**
		O, H	H	9.5	3/8	8-10	1.6	1/16	190-260	26-29	38	80	11-17	**25-40**
19.0	3/4	F	C-60°	0-2.4	0-3/32	3F, 1R	2.4	3/32	340-400	26-31	28	60	6-8	**14-20**

		F	F	0-3.2	0-1/8	4F, 1R	2.4	3/32	325-375	26-31	28	60	7-8	**16-20**
		V, H, O	F	0-1.6	0-1/16	8F, 1R	1.6	1/16	240-300	26-30	38	80	10-13	**24-30**
		F	E	0-1.6	0-1/16	3F, 3R	1.6	1/16	270-330	26-30	28	60	7-10	**16-24**
		V, H, O	**E**	**0-1.6**	**0-1/16**	**6F, 6R**	**1.6**	1/16	**230-280**	**26-30**	**38**	**80**	**7-10**	**16-24**

(A) F, FLAT; V, VERTICAL; H, HORIZONTAL; O, OVERHEAD.

(B) JOINTS AS SHOWN IN FIG. 8.

(C) F, FACE PASSES; R, ROOT PASSES. BACK GOUGING SHOULD BE DONE PRIOR TO THE APPLICATION OF FIRST ROOT PASS.

(D) FOR 5*XXX* SERIES ELECTRODES, USE A WELDING CURRENT IN THE HIGH SIDE OF THE RANGE AND AN ARC VOLTAGE IN THE LOWER PORTION OF THE RANGE. FOR 1*XXX*, 2*XXX*, AND 4*XXX* SERIES ELECTRODES, USE THE LOWER CURRENTS AND THE HIGHER ARC VOLTAGES.

TABLE 19 TYPICAL SEMIAUTOMATIC GMAW PROCEDURES FOR FILLET AND LAP WELDING OF ALUMINUM COMPONENTS

BASE METAL THICKNESS		**WELD POSITION[A]**	**WELD PASSES[B]**	**ELECTRODE DIAMETER**		**CURRENT (DC, POSITIVE ELECTRODE)[C], A**	**ARC VOLTAGE[C], V**	**ARGON GAS FLOW**		ARE TRAVEL SPEED	
MM	**IN.**			**MM**	**IN.**			**L/MIN**	**FT^3/H**	**MM/S**	IN./MIN
2.4	3/32	F, V, H, O	1	0.8	0.030	100-130	18-22	14	30	10-13	**24-30**
3.2	1/8	F	1	0.8-1.2	0.030-3/64	125-150	20-24	14	30	10-13	**24-30**
		V, H	1	0.8	0.030	110-130	19-23	14	30	10-13	**24-30**
		O	1	0.8-1.2	0.030-3/64	115-140	20-24	19	40	10-13	**24-30**
4.8	3/16	F	1	1.2	3/64	180-210	22-26	14	30	10-13	**24-30**
		V, H	1	0.8-1.2	0.030-3/64	130-175	21-25	16	35	10-13	**24-30**
		O	1	0.8-1.2	0.030-3/64	130-190	22-26	21	45	10-13	**24-30**
6.3	1/4	F	1	1.2-1.6	3/64-1/16	170-240	24-28	19	40	10-13	**24-30**
		V, H	1	1.2	3/64	170-210	23-27	21	45	10-13	**24-30**
		O	1	1.2-1.6	3/64-1/16	190-220	24-28	28	60	10-13	**24-30**
9.5	3/8	F	1	1.6	1/16	240-300	26-29	23	50	8-10	**18-25**
		V, H	3	1.6	1/16	190-240	24-27	28	60	10-13	**24-30**
		O	3	1.6	1/16	200-240	25-28	40	85	10-13	**24-30**
19.0[D]	3/4 [D]	F	4	2.4	3/32	360-380	26-30	28	60	8-10	**18-25**
		V, H	4-6	1.6	1/16	260-310	25-29	33	70	10-13	**24-30**
		O	**10**	**1.6**	1/16	**275-310**	**25-29**	**40**	**85**	**10-13**	**24-30**

(A) F, FLAT; V, VERTICAL; H, HORIZONTAL; O, OVERHEAD.

(B) NUMBER OF WELD PASSES GIVEN IS FOR ONE SIDE ONLY.

(C) FOR 5*XXX* SERIES ELECTRODES, USE A WELDING CURRENT IN THE HIGH SIDE OF THE RANGE GIVEN AND AN ARC VOLTAGE IN THE LOWER PORTION OF THE RANGE; FOR 1*XXX*, 2*XXX*, AND 4*XXX* SERIES ELECTRODES, USE THE LOWER CURRENTS AND THE HIGHER VOLTAGES IN THEIR RANGES.

(D) METAL THICKNESSES OF [GES]19.0 MM ([GES] $\frac{3}{4}$ IN.) FOR FILLET WELDS CAN EMPLOY A DOUBLE-VEE BEVEL OF [GES]50° INCLUDED VEE WITH 2.4-3.2 MM ($\frac{3}{32}$ - $\frac{1}{8}$ IN.) LAND THICKNESS IN THE ABUTTING MEMBER.

The optimal equipment for the GMAW of aluminum to meet radiographic standards and to overcome excessive downtime in maintaining the equipment consists of:

- A CONSTANT-ENERGY (CONSTANT-CURRENT, OR "DROOPER") TYPE POWER SUPPLY
- A WIRE FEEDER POSSESSING A "TOUCH-START" OR SLOW RUN-IN FEATURE AND RADIUSED TOP AND BOTTOM DIVE ROLLS
- A WELDING GUN POSSESSING A CONTACT TUBE OF 100 MM (4 IN.) OR MORE IN LENGTH
- NONMETALLIC GUIDES AND LINERS FOR THE ELECTRODE CIRCUITRY

For 1.2 mm ($\frac{3}{64}$ in.) and smaller diameter electrodes, as well as for robotic installations, the wire feeding apparatus should be a pull or push-pull type.

Argon gas shielding is most often used. However, when welding with 5*xxx* series electrode alloys and in facilities that possess highly loaded power circuits, a mixture of argon with 50 to 75% helium will provide improved weld quality.

Other arc welding processes include shielded metal arc welding (SMAW), as well as electroslag and electrogas welding (ESW, EGW). SMAW with flux-coated rods has been replaced to a very substantial degree by the GMAW process. SMAW can be effective on 9.5 mm ($\frac{3}{8}$ in.) and thicker aluminum where high heat inputs are used. However, it produces porous and erratic welds on thinner metal. Excessive spatter limits its use overhead, and the flux requires removal after welding. Because a flux is used, the alloys that can be welded are limited (refer to Tables 1, 2, 3, 4).

The ESW and EGW processes have been used experimentally, but the processes are not in commercial use with aluminum. GMAW can be used for the few applications appropriate for the ESW and EGW processes.

The oxyfuel gas welding (OFW) process uses a flux and either an oxyacetylene or oxyhydrogen gas flame. When the oxyacetylene flame is used, a slightly reduced flame is required, which causes a carbonaceous deposit that obscures the weld and slows the travel speed. The best visibility, control, and weld speed are obtained when an oxyhydrogen flame is used with aluminum alloys. The flux (composed of chlorides and fluorides) must be removed after welding to avoid corrosion in service. For this reason, GTAW has generally replaced OFW of aluminum alloys. The use of a flux limits the alloys for which it is suitable (Tables 1, 2, 3, 4) and produces the greatest heat input. This results in the lowest mechanical properties and highest sensitivity to weld cracking with heat-treatable aluminum alloys. The advantage of the OFW process is the low equipment investment.

Electron-beam welding (EBW) in a vacuum chamber produces a very deep, narrow penetration at high welding speeds. The low overall heat input produces the highest as-welded strengths in the heat-treatable alloys. The high thermal gradient from the weld into the base metal creates very limited metallurgical modifications and is least likely to cause intergranular cracking in butt joints when no filler is added. Fixturing to provide transverse compressive loading on the joint can be very helpful in avoiding intergranular cracking in the fusion zones or HAZs. Alloys are more prone to have porosity when welded in a vacuum.

For lap joints and butt joints with an integral backing, a shim of filler alloy is commonly placed at the interface of the heat-treatable aluminum alloys to prevent transverse cracking at the interface. For the 6*xxx* series and for 2014, 2024, and 7075 alloys, a filler alloy shim is often desirable between the abutting edges of square groove welds. This adds two additional oxide layers to the joint and can result in weld inclusions.

Laser-beam welding (LBW) is now considered to be a viable fusion joining process for aluminum with the advent of commercially available, stable, high-power laser systems. Because of aluminum's high reflectivity, effective coupling of the laser beam and aluminum requires a relatively high power density. High power densities are obtained by minimizing the focused spot size of the beam through optical considerations and higher power levels.

When sufficient power densities are obtained (that is, on the order of 10^6 W/cm^2, or 6×10^6 W/in.^{2}), successful laser-beam welds on aluminum can be produced, with minimal distortion, and at high processing speeds. Inert gas shielding is commonly used. Filler metal is required when welding heat-treatable aluminum alloys.

Reference cited in this section

17. "RECOMMENDED PRACTICES FOR GAS SHIELDED ARC WELDING OF ALUMINUM AND ALUMINUM ALLOY PIPE," ANSI/AWS D10.7-86, AMERICAN WELDING SOCIETY, 1986

Joining Aluminum to Other Metals

Very brittle intermetallic compounds are formed when metals such as steel, copper, magnesium, or titanium are fusion welded to aluminum. Bimetallic transition materials in sheet, plate, and tubular forms are commercially available in combinations of aluminum to such other metals as steel, stainless steel, and copper. These are made by rolling, explosion welding, fiction welding, flash welding, or hot pressure welding and provide the easiest method for fusion welding aluminum to other metals. Conventional GTAW and GMAW methods, as well as resistance spot welding, are used to join the aluminum side of the transition piece to the intended component. The dissimilar metal is joined to the opposite side of the bimetallic transition.

A wide range of dissimilar metals can be joined directly to aluminum by such means as ultrasonic welding, pressure welding, friction welding, explosion welding, and soldering. Hot dip or electroplated coatings on the dissimilar metal facilitate diffusion bonding and the brazing of aluminum to these metals.

Welding of Aluminum Alloys

Paul B. Dickerson, Aluminum Company of America (retired)

References

1. J.D. DOWD, WELD CRACKING OF ALUMINUM ALLOYS, *WELD. J.*, RESEARCH SUPPLEMENT, VOL 31, 1952, P 448S-456S
2. J.H. DUDAS AND F.R. COLLINS, PREVENTING WELD CRACKS IN HIGH-STRENGTH ALUMINUM ALLOYS, *WELD. J.*, RESEARCH SUPPLEMENT, VOL 45 (NO. 6), JUNE 1966, P 241S-249S
3. C.E. CROSS, PH.D. THESIS, COLORADO SCHOOL OF MINES, 1986, P 144
4. A.R.E. SINGER AND P.H. JENNINGS, HOT SHORTNESS OF THE ALUMINUM-SILICON ALLOYS OF COMMERCIAL QUALITY, *J. INST. MET.*, VOL 73, 1947, P 197-212
5. W.I. PUMPHREY AND J.V. LYONS, CRACKING DURING THE CASTING AND WELDING OF THE MORE COMMON BINARY ALUMINUM ALLOYS OF COMMERCIAL QUALITY, *J. INST. MET.*, VOL 74, 1948, P 439-455
6. P.H. JENNINGS, A.R.E. SINGER, AND W.I. PUMPHREY, HOT-SHORTNESS OF SOME HIGH PURITY ALLOYS IN THE SYSTEMS ALUMINUM-COPPER AND ALUMINUM-MAGNESIUM-SILICON, *J. INST. MET.*, VOL 74, 1948, P 227-248
7. N.F. GITTOS AND M.H. SCOTT, HEAT AFFECTED ZONE CRACKING OF AL-MG-SI ALLOYS, *WELD. J.*, RESEARCH SUPPLEMENT, JUNE 1981, P 95S-103S
8. W.L. BURCH, THE EFFECT OF WELDING SPEED ON THE STRENGTH OF 6061-T4 ALUMINUM JOINTS, *WELD. J.*, RESEARCH SUPPLEMENT, VOL 37 (NO. 8), AUG 1958, P 361S-367S
9. G.E. METZGER, SOME MECHANICAL PROPERTIES OF WELDS IN 6061 ALUMINUM ALLOY

SHEET, *WELD. J.*, RESEARCH SUPPLEMENT, VOL 46 (NO. 10), OCT 1967, P 457S-469S

10. F.R. COLLINS, F.G. NELSON, AND I.B. ROBINSON, ALUMINUM 2219--NEW ALLOY FOR HIGH-STRENGTH WELDED STRUCTURES, *MET. PROG.*, NOV 1961
11. E.H. DIX, W.H. ANDERSON, AND M.B. SHUMAKER, INFLUENCE OF SERVICE TEMPERATURE ON THE RESISTANCE OF WROUGHT ALUMINUM-MAGNESIUM ALLOYS TO CORROSION, *CORROSION*, VOL 15 (NO. 2), FEB 1959, P 55T-62T
12. M.B. SHUMAKER, R.A. KELSEY, D.O. SPROWLS, AND J.G. WILLIAMSON, "EVALUATION OF VARIOUS TECHNIQUES FOR STRESS-CORROSION TESTING WELDED ALUMINUM ALLOYS," PRESENTED AT ASTM STRESS-CORROSION TESTING SYMPOSIUM, JUNE 1966
13. F.G. NELSON AND R.L. ROLF, SHEAR STRENGTHS OF ALUMINUM ALLOY FILLET WELDS, *WELD. J.*, RESEARCH SUPPLEMENT, VOL 45 (NO. 2), FEB 1966, P 82S-84S
14. S.L. WÖHLER AND O. SCHLIEPHAKE, ÜBEREINEM GERS., DURCH POTENTIALMESSUNGER DAS AUFGREGEN DER VERB. MG_2SI ZU BESTÄTIGEN, *Z. ANORG. CHEM.*, 1962, P 151
15. G.W. AKIMOW AND A.S. OLESCHKO, GMELINS HANDBUCH DER ANORGANISCHEN CHEMIE, (NO. 8), AUFLAGE, 1942, P 393
16. "SPECIFICATION FOR BARE ALUMINUM AND ALUMINUM ALLOY WELDING ELECTRODE AND ROD," ANSI/AWS A5.10-92, AMERICAN WELDING SOCIETY, 1992
17. "RECOMMENDED PRACTICES FOR GAS SHIELDED ARC WELDING OF ALUMINUM AND ALUMINUM ALLOY PIPE," ANSI/AWS D10.7-86, AMERICAN WELDING SOCIETY, 1986
18. "STRUCTURAL WELDING CODE--ALUMINUM," ANSI/AWS D1.2-90, AMERICAN WELDING SOCIETY, 1990

Welding of Nickel Alloys

Revised by E.B. Hinshaw, Inco Alloys International, Inc.

Introduction

NICKEL ALLOYS can be joined reliably by all types of welding processes or methods, with the exception of forge welding and oxyacetylene welding. Because the majority of consumables are used with arc welding processes, it is those processes that are discussed in this article. The wrought nickel alloys listed in Table 1 can be welded under conditions similar to those used to weld austenitic stainless steels. Cast nickel alloys, particularly those with a high silicon content, present difficulties in welding. The arc welding of heat-resistant and corrosion-resistant nickel alloys is described in the Sections "Selection of Nonferrous Corrosion-Resistant Materials" and "Selection of Nonferrous High-Temperature Materials" in this Volume.

TABLE 1 NOMINAL COMPOSITIONS OF SELECTED WELDABLE WROUGHT NICKEL AND NICKEL ALLOYS

UNS NO.	ALLOY	COMPOSITION, WT%											
		Ni	**C**	**Mn**	**Fe**	**S**	**Si**	**Cu**	**Cr**	**Al**	**Ti**	**Nb**	OTHER
N02200	200	99.5	0.08	0.18	0.2	0.005	0.18	0.13	. . .	. . .	. . .	. . .	**. . .**
N02201	201	99.5	0.01	0.18	0.2	0.005	0.18	0.13	. . .	. . .	. . .	. . .	**. . .**
N02205	205	99.5	0.08	0.18	0.10	0.004	0.08	0.08	. . .	. . .	0.03	. . .	**0.05 MG**
N0233	233	99.64	0.06	0.19	0.05	0.004	0.03	0.01	. . .	. . .	0.002	. . .	**0.01 MG**
N02270	270	99.98	0.01	<0.001	0.003	<0.001	<0.001	<0.001	<0.001	. . .	0.001	. . .	**<0.001 MG <0.001 CO**
N03300	300	98.67	0.30	0.11	0.05	0.002	0.06	0.01	. . .	. . .	0.46	. . .	**. . .**
N03301	301	94.18	0.17	0.25	0.06	0.001	0.42	0.01	. . .	4.48	0.43	. . .	**. . .**
N04400	400	66.5	0.15	1.0	1.25	0.012	0.25	31.5	. . .	. . .	. . .	. . .	**. . .**
N04401	401	42.5	0.05	1.6	0.38	0.008	0.13	BAL	. . .	. . .	. . .	. . .	**. . .**
N04404	404	54.5	0.08	0.05	0.25	0.012	0.05	44.0	. . .	0.03	. . .	. . .	**. . .**

N04405	R-405	66.5	0.15	1.0	1.25	0.043	0.25	31.5	. . .	. . .	. . .	. . .	**. . .**
N05500	K-500	66.5	0.13	0.75	1.00	0.005	0.25	29.5	. . .	2.73	0.60	. . .	**. . .**
N06600	600	76.0	0.08	0.5	8.0	0.008	0.25	0.25	15.5	. . .	. . .	. . .	**. . .**
N06601	601	60.5	0.05	0.5	14.1	0.007	0.25	0.50	23.0	1.35	. . .	. . .	
N06617	617	54.5	0.07	. . .	. . .	. . .	. . .	. . .	22.0	1.0	. . .	. . .	**12.5 CO, 9.0 MO**
N06022	622	59.4	0.01	. . .	2.3	<0.001	. . .	. . .	20.5	. . .	. . .	. . .	**3.2 W, 14.2 MO**
N06625	625	61.0	0.05	0.25	2.5	0.008	0.25	. . .	21.5	0.2	0.2	3.65	**9.0 MO**
N06686	686	57	<0.01	0.25	1.0	<0.001	. . .	. . .	20.5	0.2	0.03	. . .	**16.5 MO, 4.0 W**
N10276	C-276	57	0.01	. . .	6.0	<0.001	. . .	. . .	15.5	. . .	. . .	. . .	**16.0 MO, 3.9 W**
N06690	690	60.0	0.03	. . .	9.0	<0.001	0.20	. . .	29.0	0.25	0.25	. . .	**. . .**
N07702	702	79.5	0.05	0.50	1.0	0.005	0.35	0.25	15.5	3.25	0.63	. . .	**. . .**
N09706	706	41.5	0.03	0.18	40.0	0.008	0.18	0.15	16.0	0.20	1.75	2.9	**. . .**
N07718	718	52.5	0.04	0.18	18.5	0.008	0.18	0.15	19.0	0.50	0.90	5.13	**3.05 MO**
N07725	725	57.0	<0.01	. . .	8.0	. . .	. . .	. . .	21.5	0.2	1.4	3.5	**8.0 MO**
N07750	X-750	73.0	0.04	0.50	7.0	0.005	0.25	0.25	15.5	0.70	2.50	0.95	**. . .**
N07751	751	72.5	0.05	0.5	7.0	0.005	0.25	0.25	15.5	1.20	2.30	0.95	**. . .**
N08800	800	32.5	0.05	0.5	39.5	0.008	0.50	0.50	21.0	0.40	0.40	. . .	**. . .**
N08810	800H	32.5	0.075	0.5	39.5	0.008	0.50	0.50	21	0.40	0.37	. . .	**. . .**
N08811	800HT	32.5	0.08	0.5	39.5	0.008	0.50	0.50	21	0.40	0.37	. . .	**1.0 MAX (AL + TI)**
N08801	801	32.0	0.05	0.75	44.5	0.008	0.50	0.50	20.5	. . .	1.13	. . .	**. . .**
N08802	802	32.5	0.35	0.75	46.0	0.008	0.38	0.38	21.0	0.58	0.75	. . .	**. . .**
N08825	825	42.0	0.03	0.50	30.0	0.015	0.25	0.25	21.5	0.10	0.90	. . .	**3.0 MO**
N09902	902	42.25	0.03	0.40	48.5	0.02	0.50	0.50	5.33	0.55	2.58	. . .	**. . .**
N19903	903	38.2	0.03	0.13	41.13	0.002	0.19	. . .	. . .	0.86	1.38	3.00	**. . .**
N19907	907	37.42	0.02	0.05	41.78	0.004	0.09	. . .	0.13	0.05	1.55	4.72	**14.33 CO, 0.005 B**
. . .	908	50.0	0.15	0.05	40.5	<0.002	0.20	0.01	4.0	1.0	1.5	3.0	**0.15 CO**
N19909	909	38.0	<0.01	0.025	42.0	<0.001	0.30	0.10	0.10	0.07	1.60	4.8	**13.0 CO, 0.04 MO**
K09925	925	44.0	0.01	. . .	28.0	. . .	. . .	1.8	21.0	0.3	2.1	. . .	**3.0 MO**
K93600	36	35.8	0.05	0.40	63.2	0.010	. . .	. . .	. . .	. . .	. . .	. . .	**. . .**
K94100	42	40.63	0.03	0.36	58.9	0.004	0.21	. . .	0.02	. . .	. . .	. . .	**. . .**
K94800	48	48	0.03	0.40	52.0	0.010	. . .	. . .	. . .	. . .	. . .	. . .	**. . .**
N06333	RA333	45	0.05	. . .	18.0	. . .	. . .	. . .	25.0	. . .	. . .	. . .	**. . .**
N08020	20CB3	35.0	0.07	2.0	BAL	. . .	1.0	3.5	20.0	. . .	. . .	1.0	**. . .**
N08028	28	31.0	0.03	2.5	BAL	0.030	1.00	1.0	27.0	. . .	. . .	. . .	**3.5 MO**
N06030	G-30	BAL	0.03	1.5	15.0	0.02	0.8	1.6	29.7	. . .	. . .	0.9	**5.0 CO, 0.4 P, 2.7 W**
N10665	B-2	BAL	0.02	1.0	2.0	0.03	0.10	. . .	1.0	. . .	. . .	. . .	**1.0 CO, 28.0 MO, 0.04 P**
N08925	25-6MO	25.0	0.01	0.7	BAL	<0.001	0.30	1.0	20.0	. . .	. . .	. . .	**6.5 MO, 0.18 N**
N06985	**G-3**	**BAL**	**0.01**	**0.8**	**19.0**	**0.03**	**0.40**	**1.8**	**22.5**	**. . .**	**. . .**	**. . .**	**3.4 CO, 7.0 MO. 1.0 W**

The most widely employed processes for welding the non-age-hardenable (solid solution-strengthened) wrought nickel alloys are gas-tungsten arc welding (GTAW), gas-metal arc welding (GMAW), and shielded metal arc welding (SMAW). Submerged arc welding (SAW) and electroslag welding (ESW) have limited applicability, as does plasma arc welding (PAW). Although the GTAW process is preferred for welding the precipitation-hardenable alloys, both the GMAW and SMAW processes are also used.

Heat Treatment of Nickel Alloys

Preweld Heating and Heat Treating. Preweld heating of wrought alloys is not required, unless the base metal is below 16 °C (60 °F), in which case a path that is 255 to 305 mm (10 to 12 in.) wide on both sides of the joint should be warmed to 16 to 21 °C (60 to 70 °F) to avoid the condensation of moisture that can cause porosity in the weld metal.

Nickel alloys are usually welded in the solution-treated condition. Precipitation-hardenable (PH) alloys should be annealed before welding if they have undergone any operations that introduce high residual stresses (see the section "Welding of Precipitation-Hardenable Alloys" in this article).

Postweld Treatment. No postweld treatment, either thermal or chemical, is required to maintain or restore corrosion resistance, although in some cases a full solution anneal will improve corrosion resistance. Heat treatment may be necessary to meet specification requirements, such as stress relief of a fabricated structure to avoid age hardening or stress-corrosion cracking (SCC) of the weldment in hydrofluoric acid vapor or caustic soda. If welding induces moderate-to-high residual stresses, then the PH alloys would require a stress-relief anneal after welding and before aging (see the section "Welding of Precipitation-Hardenable Alloys" in this article).

Welding of Nickel Alloys

Revised by E.B. Hinshaw, Inco Alloys International, Inc.

Cleaning of Workpieces

Nickel and nickel alloys are susceptible to embrittlement by lead, sulfur, phosphorus, and other low-melting-point elements. These materials can exist in grease, oil, paint, marking crayons or inks, forming lubricants, cutting fluids, shop dirt, and processing chemicals. Work-pieces must be completely free of foreign material before they are heated or welded. Both sides of the workpiece should be cleaned in the area that will be heated by the welding operations. When no subsequent heating is involved, the cleaned area may be restricted to 50 mm (2 in.) on each side of the joint.

Shop dirt, oil, and grease can be removed by either vapor degreasing or swabbing with acetone or another nontoxic solvent. Paint and other materials that are not soluble in degreasing solvents may require the use of methylene chloride, alkaline cleaners, or special proprietary compounds. If alkaline cleaners that contain sodium carbonate are used, then the cleaners themselves must be removed prior to welding. Spraying or scrubbing with hot water is recommended. Marking ink can usually be removed with alcohol. Processing material that has become embedded in the work metal can be removed by grinding, abrasive blasting, and swabbing with a 10 vol% HCl solution, followed by a thorough water wash. Further information on the cleaning of nickel and nickel alloys is given in the article "Nickel Alloy Plating" in *Surface Engineering*, in Volume 5, *ASM Handbook*.

Oxides must also be removed from the area involved in the welding operation, primarily because of the difference between the oxide and base metal melting points. Oxides are normally removed by grinding, machining, abrasive blasting, or pickling.

Welding of Nickel Alloys

Revised by E.B. Hinshaw, Inco Alloys International, Inc.

Joint Design

Various joint designs are used in the arc welding of nickel alloys (Fig. 1). Although the same design can be used for GTAW and SMAW processes, the GMAW and SAW processes require special considerations. A joint design developed for other metals is not necessarily suitable for nickel alloys and should not be used unless it proves to be satisfactory, based on either experience or tests.

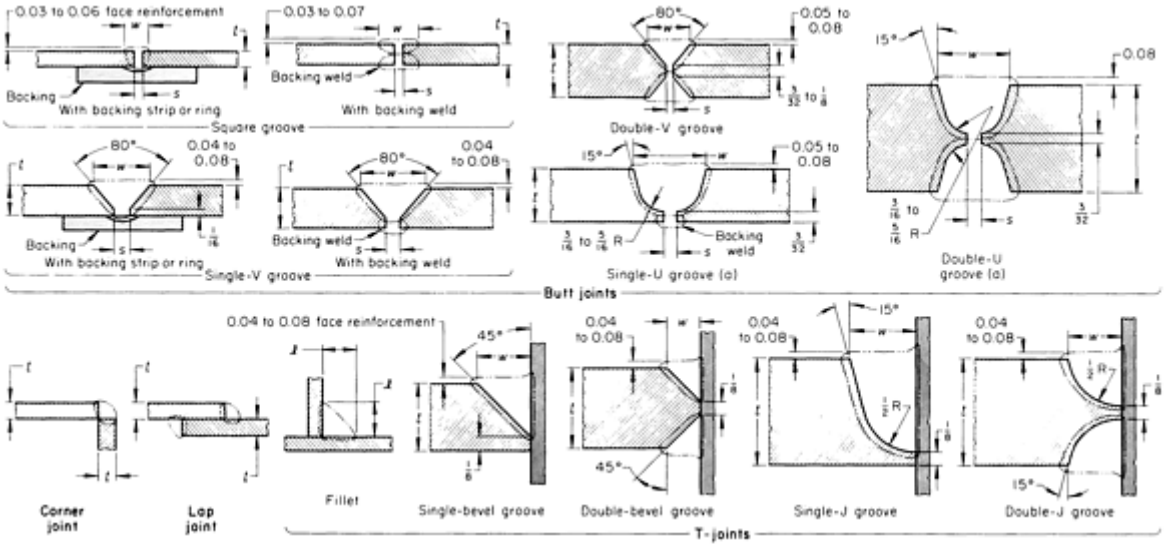

BASE-METAL THICKNESS(*T*)		WIDTH OF GROOVE OR BEAD (*W*)		MAXIMUM ROOT OPENING (*S*)		APPROXIMATE AMOUNT OF METAL DEPOSITED		APPROXIMATE WEIGHT OF ELECTRODE	
mm	**in.**	**mm**	**in.**	**mm**	**in.**	**kg/m**	**lb/ft**	**kg/m**	lb/ft[(a)]
SQUARE-GROOVE BUTT JOINT WITH BACKING STRIP OR RING									
0.94	0.037	3.2	1/8	0	0	0.03	0.02	0.038	**0.025**
1.27	0.050	4.0	5/32	0	0	0.06	0.04	0.07	**0.05**
1.57	0.062	4.8	3/16	0	0	0.06	0.04	0.09	**0.06**
2.36	0.093	4.8-6.4	3/16 - 1/4	0.8	1/32	0.09	0.06	0.12	**0.08**
3.18	0.125	6.4	1/4	1.6	1/16	0.10	0.07	0.13	**0.09**
SQUARE-GROOVE BUTT JOINT WITH BACKING WELD									
3.2	1/8	6.4	1/4	0.8	1/32	0.16	0.11	0.22	**0.15**
4.8	3/16	9.5	3/8	1.6	1/16	0.36	0.24	0.48	**0.32**
6.4	1/4	22	7/8	2.4	3/32	0.46	0.31	0.62	**0.42**
SINGLE-V-GROOVE BUTT JOINT WITH BACKING STRIP OR RING									
4.8	3/16	8.89	0.35	3.2	1/8	0.338	0.227	0.46	**0.31**
6.4	1/4	12.9	0.51	4.8	3/16	0.659	0.443	0.91	**0.61**

7.9	$\frac{5}{16}$	15.5	0.61	4.8	$\frac{3}{16}$	0.866	0.582	1.19	**0.80**
9.5	$\frac{3}{8}$	18.0	0.71	4.8	$\frac{3}{16}$	1.11	0.745	1.52	**1.02**
13	$\frac{1}{2}$	23.1	0.91	4.8	$\frac{3}{16}$	1.73	1.16	2.37	**1.59**
16	$\frac{5}{8}$	29.5	1.16	4.8	$\frac{3}{16}$	2.40	1.61	3.29	**2.21**
SINGLE-V-GROOVE BUTT JOINT WITH BACKING WELD									
6.4	$\frac{1}{4}$	10.4	0.41	2.4	$\frac{3}{32}$	0.62	0.42	0.86	**0.58**
7.9	$\frac{5}{16}$	12.9	0.51	2.4	$\frac{3}{32}$	0.80	0.54	1.10	**0.74**
9.5	$\frac{3}{8}$	16.5	0.65	3.2	$\frac{1}{8}$	1.09	0.73	1.49	**1.00**
13	$\frac{1}{2}$	21.6	0.85	3.2	$\frac{1}{8}$	1.80	1.21	2.48	**1.67**
16	$\frac{5}{8}$	26.9	1.06	3.2	$\frac{1}{8}$	2.17	1.46	2.98	**2.00**
DOUBLE-V-GROOVE BUTT JOINT									
13	$\frac{1}{2}$	10.2	0.40	3.2	$\frac{1}{8}$	1.32	0.89	1.73	**1.16**
16	$\frac{5}{8}$	12.4	0.49	3.2	$\frac{1}{8}$	1.61	1.08	2.20	**1.48**
19	$\frac{3}{4}$	15.7	0.62	3.2	$\frac{1}{8}$	2.17	1.46	2.98	**2.00**
25	1	20.6	0.81	3.2	$\frac{1}{8}$	3.60	2.42	4.97	**3.34**
32	$1\ \frac{1}{4}$	26.2	1.03	3.2	$\frac{1}{8}$	4.34	2.92	5.95	**4.00**
SINGLE-BEVEL-GROOVE T-JOINT									
6.4	$\frac{1}{4}$	3.18	0.125	. . .	. . .	0.10	0.07	0.13	**0.09**
7.9	$\frac{5}{16}$	4.78	0.188	. . .	. . .	0.19	0.13	0.25	**0.17**
9.5	$\frac{3}{8}$	6.35	0.250	. . .	. . .	0.28	0.19	0.39	**0.26**
13	$\frac{1}{2}$	9.52	0.375	. . .	. . .	0.57	0.38	0.77	**0.52**
16	$\frac{5}{8}$	12.7	0.500	. . .	. . .	0.94	0.63	1.28	**0.86**
19	$\frac{3}{4}$	15.9	0.625	. . .	. . .	1.38	0.93	1.90	**1.28**
25	1	22.2	0.875	. . .	. . .	2.64	1.77	3.60	**2.42**
DOUBLE-BEVEL-GROOVE T-JOINT									
13	$\frac{1}{2}$	4.78	0.188	. . .	. . .	0.37	0.25	0.51	**0.34**
16	$\frac{5}{8}$	6.35	0.250	. . .	. . .	0.58	0.39	0.80	**0.54**
19	$\frac{3}{4}$	7.95	0.313	. . .	. . .	0.83	0.56	1.15	**0.77**
25	1	11.1	0.438	. . .	. . .	1.47	0.99	2.02	**1.36**
32	$1\ \frac{1}{4}$	14.3	0.563	. . .	. . .	2.29	1.54	3.20	**2.15**
38	$1\ \frac{1}{2}$	17.5	0.688	. . .	. . .	3.29	2.21	4.51	**3.03**
44	$1\ \frac{3}{4}$	20.7	0.813	. . .	. . .	4.46	3.00	6.09	**4.09**

50	2	23.8	0.938	. . .	. . .	5.80	3.90	7.96	**5.35**
SINGLE-U-GROOVE BUTT JOINT[B]									
13	$\frac{1}{2}$	17.2	0.679	3.2	$\frac{1}{8}$	1.53	1.03	2.10	**1.41**
16	$\frac{5}{8}$	18.9	0.745	3.2	$\frac{1}{8}$	2.05	1.38	2.83	**1.90**
19	$\frac{3}{4}$	20.7	0.813	3.2	$\frac{1}{8}$	2.50	1.68	3.42	**2.30**
25	1	24.3	0.957	3.2	$\frac{1}{8}$	3.91	2.63	5.36	**3.60**
32	$1\ \frac{1}{4}$	27.3	1.073	3.2	$\frac{1}{8}$	5.39	3.62	7.38	**4.96**
38	$1\ \frac{1}{2}$	30.9	1.215	3.2	$\frac{1}{8}$	7.13	4.79	9.75	**6.55**
44	$1\ \frac{3}{4}$	34.3	1.349	3.2	$\frac{1}{8}$	8.90	5.98	12.2	**8.19**
50	2	37.7	1.485	3.2	$\frac{1}{8}$	11.0	7.40	15.1	**10.12**
DOUBLE-U-GROOVE BUTT JOINT[B]									
25	1	17.2	0.679	3.2	$\frac{1}{8}$	3.07	2.06	4.20	**2.82**
32	$1\ \frac{1}{4}$	18.9	0.745	3.2	$\frac{1}{8}$	4.11	2.76	5.65	**3.80**
38	$1\ \frac{1}{2}$	20.7	0.813	3.2	$\frac{1}{8}$	5.00	3.36	6.84	**4.60**
50	2	24.3	0.957	3.2	$\frac{1}{8}$	7.83	5.26	10.7	**7.20**
64	$2\ \frac{1}{2}$	27.3	1.073	3.2	$\frac{1}{8}$	10.8	7.24	14.8	**9.92**
CORNER AND LAP JOINT									
1.6	$\frac{1}{16}$	. . .	. . .	. . .	. . .	0.03	0.02	0.06	**0.04**
3.2	$\frac{1}{8}$	. . .	. . .	. . .	. . .	0.07	0.05	0.10	**0.07**
4.8	$\frac{3}{16}$	. . .	. . .	. . .	. . .	0.15	0.10	0.21	**0.14**
6.4	$\frac{1}{4}$	. . .	. . .	. . .	. . .	0.28	0.19	0.39	**0.26**
9.5	$\frac{3}{8}$	. . .	. . .	. . .	. . .	0.62	0.42	0.85	**0.57**
13	$\frac{1}{2}$	. . .	. . .	. . .	. . .	1.04	0.74	1.52	**1.02**
T-JOINT WITH FILLET									
. . .	. . .	. . .	. . .	3.2	$\frac{1}{8}$	0.04	0.03	0.06	**0.04**
. . .	. . .	. . .	. . .	4.8	$\frac{3}{16}$	0.10	0.07	0.15	**0.10**
. . .	. . .	. . .	. . .	6.4	$\frac{1}{4}$	0.18	0.12	0.24	**0.16**
. . .	. . .	. . .	. . .	7.9	$\frac{5}{16}$	0.28	0.19	0.39	**0.26**
. . .	. . .	. . .	. . .	9.5	$\frac{3}{8}$	0.40	0.27	0.55	**0.37**
. . .	. . .	. . .	. . .	13	$\frac{1}{2}$	0.70	0.47	0.95	**0.64**
. . .	. . .	. . .	. . .	16	$\frac{5}{8}$	1.10	0.74	1.50	**1.01**

. . .	. . .	. . .	. . .	19	$\frac{3}{4}$	1.59	1.07	2.17	**1.46**
. . .	. . .	. . .	. . .	25	1	2.83	1.90	3.87	**2.60**
SINGLE-J-GROOVE T-JOINT									
25	1	15.9	0.625	. . .	. . .	2.65	1.78	3.6	**2.4**
32	$1\frac{1}{4}$	18.3	0.719	. . .	. . .	3.72	2.50	5.1	**3.4**
38	$1\frac{1}{2}$	19.8	0.781	. . .	. . .	4.81	3.23	6.5	**4.4**
44	$1\frac{3}{4}$	22.2	0.875	. . .	. . .	6.09	4.09	8.3	**5.6**
50	2	24.6	0.969	. . .	. . .	7.34	4.93	10.1	**6.8**
57	$2\frac{1}{4}$	26.2	1.031	. . .	. . .	8.63	5.80	11.9	**8.0**
64	$2\frac{1}{2}$	27.8	1.094	. . .	. . .	10.3	6.94	14.1	**9.5**
DOUBLE-J-GROOVE T-JOINT									
25	1	12.7	0.500	. . .	. . .	2.20	1.48	3.0	**2.0**
32	$1\frac{1}{4}$	14.3	0.563	. . .	. . .	2.83	1.90	3.9	**2.6**
38	$1\frac{1}{2}$	15.1	0.594	. . .	. . .	3.81	2.56	5.2	**3.5**
44	$1\frac{3}{4}$	15.9	0.625	. . .	. . .	4.63	3.11	6.4	**4.3**
50	2	16.7	0.656	. . .	. . .	5.67	3.81	7.7	**5.2**
57	$2\frac{1}{4}$	17.5	0.688	. . .	. . .	6.71	4.51	9.2	**6.2**
64	$\mathbf{2\frac{1}{2}}$	**19.1**	**0.750**	**. . .**	**. . .**	**7.84**	**5.27**	**10.7**	**7.2**

(A) TO OBTAIN LINEAR FEET OF WELD PER POUND OF CONSUMABLE ELECTRODE, TAKE THE RECIPROCAL OF POUNDS PER LINEAR FOOT. IF THE UNDERSIDE OF THE FIRST BEAD IS CHIPPED OUT AND WELDED, ADD 0.31 KG/M (0.21 LB/FT) OF METAL DEPOSITED (EQUIVALENT TO 0.43 KG/M, OR 0.29 LB/FT, OF CONSUMABLE ELECTRODE).

(B) FOR GMAW (EXCEPT WITH THE SHORT-CIRCUITING ARC), ROOT RADIUS SHOULD BE ONE-HALF THE VALUE SHOWN AND BEVEL ANGLE SHOULD BE TWICE AS GREAT.

FIG. 1 TYPICAL JOINT CONFIGURATIONS AND DIMENSIONS FOR GTAW, GMAW, AND SMAW APPLICATIONS. DIMENSIONS IN SCHEMATIC GIVEN IN INCHES

Beveled Joints. Beveling is usually not required for metal that is 2.4 mm (0.093 in.) or less in thickness, although thinner sections of certain alloys are sometimes beveled. Metal thicker than 2.4 mm (0.093 in.) should be beveled to form a V-, U-, or J-shaped groove and should be welded using either a backing material or a gas, unless welding from both sides. Otherwise, erratic penetration can result, leading to crevices and voids that are potential areas for joint weakness and accelerated corrosion in the underside of the joint. To attain the best underbead contour on joints that cannot be welded from both sides, the GTAW process should be used for the root pass.

For metal that is more than 9.5 mm ($\frac{3}{8}$ in.) thick, a double U- or V-shaped groove design is preferred. The added cost of preparation is justified, because less welding time and material are required and less residual stress is developed than with a single-groove design.

Beveling is best accomplished by machine, usually a plate planer or other machine tool. Plasma arc and electric arc cutting can be used for joint penetration, but all oxidized metal must be removed from the joint area by grinding or chipping for a depth of 0.8 to 1.6 mm ($\frac{1}{32}$ to $\frac{1}{16}$ in.).

Corner and lap joints can be welded when service stresses will not be excessive. However, they should be avoided if service temperatures are high or if service conditions involve thermal or mechanical cycling. When comer joints are used, a full-penetration weld must be made, usually with a fillet weld on the root side. Lap joints should be welded on both sides.

Design Considerations. Molten nickel alloy weld metal does not flow as easily as steel weld metal. This characteristic cannot be compensated for by using extra heat input or pooling, because serious loss of residual deoxidizers may result. For joints in metal up to 16 mm ($\frac{5}{8}$ in.) thick, ample accessibility is provided by V-groove butt joints beveled to a 60° groove angle. For thicker metal, U-groove butt joints are machined to a 15° bevel angle and a 4.8 to 7.9 mm ($\frac{3}{16}$ to $\frac{5}{16}$ in.) radius. Single bevels used to form T joints should have an angle of 45°. The bottom radius of a J-shaped groove for T joints should be at least 9.5 mm ($\frac{3}{8}$ in.), and the bevel angle described above should be used for J- and U-shaped grooves. For full-penetration welds, the bevel and groove angles should be about 30% more than those used for carbon steels.

Welding of Nickel Alloys

Revised by E.B. Hinshaw, Inco Alloys International, Inc.

Welding Fixtures

Proper fixturing and clamping hold the workpieces firmly in place, minimize buckling, maintain alignment, and, when needed, provide compressive stress in the weld metal. A backing bar, or any portion of a fixture that might contact the workpiece, should be made of copper. This metal has such a high thermal conductivity that inadvertent welding against the copper will reduce the chance that the bar will fuse to the weldment. In addition, the grooves in copper bars are often used to contour, without sticking, the side underneath the weld.

Backing bars, when used, should incorporate a groove of suitable contour to permit penetration of weld metal and avoid the possibility of trapping gas or flux at the bottom of the weld. Grooves in backing bars used in the GMAW process usually have a shallow semielliptical shape that is 0.38 to 0.89 mm (0.015 to 0.035 in.) deep and 4.8 to 6.4 mm ($\frac{3}{16}$ to $\frac{1}{4}$ in.) wide. Square corner grooves are used with the GMAW and GTAW processes to accommodate the backing gas. A machined passageway is connected to the gas supply, and holes that are 1.6 mm ($\frac{1}{16}$ in.) in diameter are drilled 75 mm (3 in.) apart from the bottom of the groove to the passageway, permitting the backing gas to flow along the weld. The gas flows out of the groove at the ends of the bar. Figure 2 shows groove designs for backing bars.

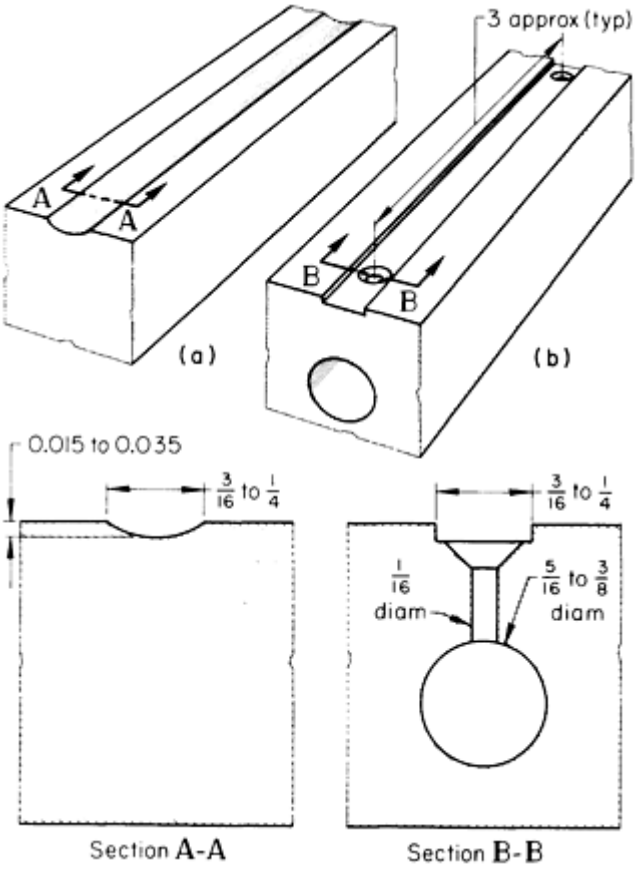

FIG. 2 GROOVE CONFIGURATIONS FOR BACKING BARS. (A) STANDARD GROOVE FOR USE WITHOUT A BACKING GAS. (B) SQUARE-CORNER GROOVE EMPLOYED WITH BACKING GAS (GROOVE DEPTH DEPENDS ON GAS FLOW REQUIRED AND LENGTH OF BAR). DIMENSIONS GIVEN IN INCHES

The clamping and restraint requirements for nickel alloys are about the same as for low-carbon steel. The hold-down bars should be located close enough to the line of the weld to maintain alignment and provide the proper degree of heat transfer. Generally, hold-down pressure should be just enough to maintain alignment, but high restraint can be advantageous when welding square groove joints in thin metals using the GMAW process without a filler metal. When the pieces to be welded are positioned with a zero root opening and hold-down bars are brought very close to the line of welding, and when a high hold-down pressure is used, the heat of welding creates an expansive force that results in compression in the line of the weld. This compression will have an upsetting effect on the hot weld metal and can cause the weld to develop a slight top and bottom crown, or weld reinforcement, without the use of filler metal.

Welding of Nickel Alloys

Revised by E.B. Hinshaw, Inco Alloys International, Inc.

Welding of Precipitation-Hardenable Alloys

The PH alloys require special welding procedures because of their susceptibility to cracking. Cracks can occur in the base-metal heat-affected zone (HAZ) upon aging or in service at temperatures above the aging temperature, as a result of residual welding stress and stress induced by precipitation. Before welding these alloys, a full-solution anneal is usually performed. After welding, the appropriate aging heat treatment is performed. To further improve alloy properties, a full anneal after welding, followed by a postweld heat treatment, can be incorporated in the welding procedure.

Preweld and Postweld Treatments. Any part that has been subjected to severe bending, drawing, or other forming operations should be annealed before welding. If possible, heating should be done in a controlled-atmosphere furnace to limit oxidation and minimize subsequent surface cleaning.

The aluminum and titanium hardened alloys must be stress relieved (solution treated) after welding and before precipitation hardening. To avoid prolonged exposure of the welded structure to temperatures within the precipitation-hardening range, rapid heating in a furnace preheated to the appropriate temperature is recommended. When the workpiece is large, compared with the furnace area, it may be necessary to preheat the furnace to a temperature that is 110 to 280 °C (200 to 500 °F) above the solution-treatment temperature and then to reset the furnace controls when the workpiece has reached the solution-treatment temperature. The stresses created by repair or alteration welding must be relieved in a similar fashion by rapid heating to the solution-treating temperature prior to re-aging. If satisfactory stress relief of the weldment is not feasible, particularly if the structure is complicated, then preweld overaging treatments may be helpful. Preheating, however, is not a satisfactory substitute for postweld heat treatment. Although PH alloys can be welded in the aged condition, if temperatures encountered in service are in the PH range, then the weldment must be solution treated and reaged.

General Welding Procedures. Precipitation-hardenable alloys are usually welded by the GTAW process, but SMAW and GMAW processes are also applicable. Heat input during the welding operations should be held to a moderately low level in order to obtain the highest possible joint efficiency and minimize the extent of the HAZ. For multiple-bead or multiple-layer welds, many narrow stringer beads should be used, rather than a few large, heavy beads.

Any oxides that form during welding should be removed by abrasive blasting or grinding. If such films are not removed as they accumulate on multiple-pass welds, then they can become thick enough to inhibit weld fusion and produce unacceptable laminar-type oxide stringers along the weld axis.

Welding of Nickel Alloys

Revised by E.B. Hinshaw, Inco Alloys International, Inc.

Welding of Cast Nickel Alloys

Cast nickel alloys can be joined by the GTAW, GMAW, and SMAW processes. For optimum results, castings should be solution annealed before welding to relieve some of the casting stresses and provide some homogenization of the cast structure.

Light peening of solidified metal after the first pass will relieve stresses and, thus, reduce cracking at the junction of the weld metal and the cast metal. The peening of subsequent passes is of little, if any, benefit. Stress relieving after welding is also desirable.

Welding of Nickel Alloys

Revised by E.B. Hinshaw, Inco Alloys International, Inc.

Gas-Tungsten Arc Welding

Nickel alloys, both cast and wrought and either solid-solution-strengthened or precipitation-hardenable, can be welded by the GTAW process. The addition of filler metal is usually recommended. Direct current electrode negative (DCEN) is recommended for both manual and machine welding. Parameters for manual GTAW of alloy 400 are given in Table 2.

TABLE 2 PARAMETERS FOR MANUAL GTAW OF 1.6 MM (0.062 IN.) THICK ALLOY 400

JOINT TYPE	**BEVELED BUTT, 1.6 MM ($\frac{1}{16}$ IN.) ROOT OPENING**
ELECTRODE	**2.4 MM ($\frac{3}{32}$ IN.) DIAM EWTH-2, TAPERED TO 0.4 MM ($\frac{1}{64}$ IN.) DIAM**
FILLER METAL	**1.6 MM ($\frac{1}{16}$ IN.) DIAM ERNICU-7**
NUMBER OF PASSES	**3**
WELDING CURRENT, A	**70-90 (DCEN)**
VOLTAGE, V	**10-12**
SHIELDING GAS:	
AT TORCH, M^3/H (FT^3/H)	**0.6 (20)**
BACKING GAS, M^3/H (FT^3/H)	**0.08-0.14 (3-5)**
PREHEAT AND POSTHEAT TREATMENT	**NONE**
INTERPASS TEMPERATURE, °C (°F)	**175 (350) MAXIMUM**

The welding torch should be set or held at an angle of 90° to the work. A slight deviation is permissible to provide a better view of the work, but an acute angle can lead to aspiration of the surrounding air and contamination of the shielding gas. The largest gas nozzle size applicable to the job should be used, and a minimum practical distance between the nozzle and the work should be maintained. A gas lens should be used to improve shielding gas flow and coverage (see the article "Gas-Tungsten Arc Welding" in this Volume).

Shielding Gas. Either argon or helium, or a mixture of the two, is used as a shielding gas for welding nickel and nickel alloys. Additions of oxygen, carbon dioxide, or nitrogen to argon gas will usually cause porosity or erosion of the electrode. Argon with small quantities of hydrogen (typically 5%) can be used and may help avoid porosity in pure nickel, as well as aid in reducing oxide formation during welding. The advantages and disadvantages of using helium, rather than argon, when welding thin metal without the addition of filler metal, are:

- *IMPROVED SOUNDNESS:* POROSITY-FREE WELDS ARE MORE EASILY OBTAINED IN ALLOY 400, AND THE POROSITY OF WELDS IN NICKEL 200 IS LESS.
- *INCREASED WELDING SPEED:* WITH DCEN, WELDING SPEED CAN BE INCREASED AS MUCH AS 40% OVER THAT ACHIEVED WITH ARGON AT THE SAME CURRENT SETTING, BECAUSE WELDING SPEED IS A FUNCTION OF HEAT INPUT, AND HEAT INPUT IS CONSIDERABLY GREATER WITH HELIUM.
- *DECREASED ARC STABILITY:* AT LOWER CURRENT LEVELS (<120 A), ARC STABILITY IS LOWERED AS HELIUM CONTENT IS INCREASED. MIXTURES OF ARGON AND HELIUM HELP STABILIZE THE ARC WHILE MAINTAINING THE BENEFITS OF THE HELIUM SHIELDING GAS.

Because the purity and dryness of the welding gas are important, welding-grade shielding gas should be used. Furthermore, the welding area should be screened to avoid drafts, because disruption of the shielding atmosphere and drawing in of air can cause porosity in the weld metal.

Electrodes. Pure-tungsten electrodes or tungsten alloyed with thoria or zirconia can be used. The alloyed electrodes are more economical, because of their lower vaporization loss. Overheating that is due to the use of excessive amperage must be avoided at all times.

The best arc stability and penetration control are achieved by tapering the electrode tip. The taper angle should be approximately 30°, with a flat land of about 0.38 mm (0.015 in.) diameter on the tip end. Larger taper angles are used to produce a narrower bead and deeper penetration. After its selection, the taper angle should be maintained, because changes in the angle can affect penetration and bead width.

Electrode extension (stick out) should be short, and the amount should be based on joint design. For example, a maximum extension of 4.8 mm ($\frac{3}{16}$ in.) can be used for butt welds in thin metal, but a 9.5 to 13 mm ($\frac{3}{8}$ to $\frac{1}{2}$ in.) extension is required for some fillet welds or for reaching the bottom of the groove welds.

The electrode should be inclined slightly in the forehand position. Filler metal, when used, should be added carefully at the leading edge of the weld pool to avoid contact with and contamination of the electrode. If contamination occurs, then the electrode should be cleaned and reshaped.

Filler Metals. Compositions of the filler metals used with the GTAW process are, in general, similar to those of the base metals with which they are used. Because of high welding temperatures, filler metals are alloyed to resist porosity and hot cracking of the weld metal. Filler-metal additions and dilution ratios should be adjusted to ensure that the weld metal contains about 75% filler metal.

Table 3 lists the compositions of filler metals used for the gas-tungsten arc welding of nickel and nickel alloys. Filler metals of the ERNi-1 classification are used for welding the high-nickel-content alloys (for example, Nickel 200 and 201), whereas those of the ERNiCu-7 classification are used for welding nickel-copper alloys (for example, alloys 400 and 404).

TABLE 3 COMPOSITION OF FILLER METALS FOR GTAW, GMAW, AND SAW APPLICATIONS OF NICKEL ALLOYS

UNS NO.	ELECTRODE	COMPOSITION, WT%[A]													
		C MAX	MN	FE	S	SI	CU	NI + CO	AL MAX	TI	P	NB + TA	MO	CR	OTHER
N02061	ERNI-1	0.15	1.0	1.0	0.015	0.75	0.25	93.0 MIN	1.5	2.0-3.5	0.03	. . .	. . .	. . .	. . .
N04060	ERNICU-7	0.15	4.0	2.5	0.015	1.25	BAL	62.0-69.0	1.25	1.5-3.0	0.02	. . .	. . .	. . .	. . .
N08065	ERNIFECR-1	0.05	1.0	22.0 MIN	0.03	0.50	1.5-3.0	38.0-46.0	0.20	0.60-1.2	0.03	. . .	2.50-3.50	19.5-23.5	. . .
N07092	ERNICRFE-6	0.03	2.0-2.7	8.0	0.015	0.35	0.50	67.0 MIN	. . .	2.5-3.5	0.03	. . .	. . .	14.0-17.0	. . .
N06082	ERNICR-3	0.10	2.5-3.5	3.0	0.015	0.50	0.50	67.0 MIN	. . .	0.75	0.03	2.0-3.0	. . .	18.0-22.0	. . .
N06062	ERNICRFE-5	0.08	1.0	6.0-10.0	0.015	0.35	0.50	70.0 MIN	. . .	. . .	. . .	1.5-3.0	. . .	14.0-17.0	. . .
N06052	ERNICRFE-7	0.04	1.0	7.0-11.0	0.015	0.50	0.30	BAL	1.10	1.10	0.020	0.10	0.50	28.0-31.5	. . .
N06007	ERNICRMO-1	0.05	1.0-2.0	18.0-21.0	0.04	1.0	1.5-2.5	BAL	. . .	. . .	0.04	1.75-2.50	5.5-7.5	21.0-23.5	. . .
N06625	ERNICRMO-3	0.10	0.50	5.0	0.015	0.50	0.50	58 MM	0.40	0.40	0.02	3.15-4.15	8.0-10.0	20.0-23.0	. . .
N10276	ERNICRMO-4	0.02	1.0	4.0-7.0	0.03	0.08	0.50	BAL	. . .	. . .	0.04	2.5	15.0-17.0	14.5-16.5	**2.5 CO, 0.35 V, 3.0-4.5 W**
N06985	ERNICRMO-9	0.015	1.0	18.0-21.0	0.03	1.0	1.5-2.5	BAL	. . .	. . .	0.04	. . .	6.0-8.0	21.0-23.5	**1.5 W, 5.0 CO**
N06022	ERNICRMO-10	0.02	1.0	2.0-6.0	0.015	0.20	. . .	BAL	. . .	. . .	0.03	. . .	12.5-14.5	20-22.5	**2.5-3.5 W**
N07718	ERNIFECR-2	0.08	0.35	BAL	0.015	0.35	0.30	50-55	0.2-0.8	0.65-1.15	0.015	4.75-5.50	2.8-3.3	17.0-21.0	**0.006 B**
N06617	ERNICRCOMO-1	0.05-0.15	1.0	3.0 MAX	0.015	1.0	0.50	BAL	0.8-1.5	0.60	0.03	. . .	8.0-10.0	20.0-24.0	. . .
N10665	ERNIMO-7	0.02	8.0	2.0	0.03	0.10	0.50	BAL	. . .	. . .	0.04	. . .	26.0-30.0	1.0	**1.0 CO**
N06030	ERNICRMO-11	0.03	1.5	13.0-	0.02	0.80	1.0-	BAL	. . .	. . .	0.04	0.30-	4.0-	28.0-	**5.0 CO, 1.5-**

				17.0			2.4					1.50	6.0	31.5	**4.0 W**
N10004	ERNIMO-3	0.12	1.00	4.0-7.0	0.03	1.00	0.50	BAL	. . .	. . .	0.04	. . .	23.0-26.0	4.0-6.0	**2.5 CO, 0.60 V**
N10001	**ERNIMO-1**	**0.08**	**1.00**	**4.0-7.0**	**0.025**	**1.00**	**0.50**	**BAL**	**. . .**	**. . .**	**0.03**	**. . .**	**26.0-30.0**	**1.00**	**2.5 CO, 0.20-0.40 V**

(A) SINGLE VALUES ARE MAXIMUM (EXCEPT WHERE OTHERWISE SPECIFIED).

Joint Design. All joint designs shown in Fig. 1 can be used when welding nickel alloys by the GTAW process. If no filler metal is used, then the sections to be joined must be held tightly together to promote satisfactory fusion.

Welding Techniques. When a filler metal is used, the wire diameter should be related to the work-metal thickness. For example, a 1.6 mm ($\frac{1}{16}$ in.) diameter wire is generally used to weld 1.6 mm ($\frac{1}{16}$ in.) thick sheet. During welding, the hot end of the wire must remain under the shielding gas to avoid oxidation. A short arc length should be maintained to ensure that deoxidizing elements transfer to the weld pool.

To ensure a sound weld, the arc should be maintained at the shortest possible length. When no filler metal is added, the arc length should be 1.3 mm (0.05 in.), maximum, and preferably 0.5 to 0.8 mm (0.02 to 0.03 in.). When filler metal is used, the arc should be kept as short as possible, consistent with filler-metal diameter, to avoid loss of gas coverage. This loss can result in oxidation and reduced penetration. A short arc also reduces weld spatter with filler wire.

The speed of welding affects penetration, weld width, and weld soundness, especially when no filler metal is added. For a given thickness of metal, there is a range of welding speeds that results in minimum porosity. Speeds outside this range, either faster or slower, can result in increased porosity. When welding thinner-gage material, the required heat input is considerably lower. This contributes to increased porosity, which is due to the increased solidification rate of the molten weld pool.

Complete-penetration welds require the use of grooved backing bars that permit local gas shielding (Fig. 2b), or the purging of the inside of the workpiece. The surface condition affects the porosity level in thin sheet material to a much larger degree, because the surface layer makes up a larger percentage of the overall thickness of material.

Welding of Nickel Alloys

Revised by E.B. Hinshaw, Inco Alloys International, Inc.

Gas-Metal Arc Welding

The solid-solution nickel-base alloys can be joined by the GMAW process. In addition, the use of special procedures allows PH alloys (for example, alloy K-500) to be gas-metal arc welded.

Spray, globular, and short-circuiting metal transfer methods are suitable. Varying the power input produces the different types of metal transfer. The pulsed arc process is also used. In these methods, the filler metal is a current-carrying consumable and is typically 0.89, 1.14, or 1.57 mm (0.035, 0.045, or 0.062 in.) in diameter. Table 4 lists typical conditions for the welding of nickel-base alloys using spray-type metal transfer (Table 4(a)), short-circuiting metal transfer (Table 4(b)), and pulsed-arc transfer (Table 4(c)) with various nickel-base filler metals.

TABLE 4 TYPICAL PARAMETERS FOR GMAW APPLICATIONS OF NICKEL 200 AND ALLOY 400

PARAMETER	**SPRAY METAL TRANSFER(A)**		**SHORT-CIRCUITING METAL TRANSFER(B)**		PULSED-ARC METAL TRANSFER(C)	
	NICKEL 200	**ALLOY 400**	**NICKEL 200**	**ALLOY 400**	**NICKEL 200**	ALLOY 400
ELECTRODE WIRE DESIGNATION	ERNI-1	ERNICU-7	ERNI-1	ERNICU-7	ERNI-1	**ERNICU-7**
AVERAGE VOLTAGE, V	29-31	28-30	20-21	16-18	21-22	**21-22**
PEAK VOLTAGE, V	. . .	. . .	. . .	. . .	46	**40**
AVERAGE CURRENT, A	375	290	160	130-135	150	**110**
WIRE FEED RATE, MM/S (IN./MIN)	**87 (205)**	**85 (200)**	**152 (360)**	**116-123 (275-290)**	**68 (160)**	**59 (140)**

(A) ARGON SHIELDING GAS FLOW RATE AT 1.7 M^3/H (60 FT^3/H); FLAT WELDING POSITION; 1.57

MM (0.062 IN.) DIAM ELECTRODE WIRE.

(B) ARGON-HELIUM SHIELDING GAS FLOW RATE AT 1.4 M^3/H (50 FT^3/H); VERTICAL WELDING POSITION; 0.89 MM (0.035 IN.) DIAM WIRE.

(C) ARGON OR ARGON-HELIUM SHIELDING GAS FLOW RATE AT 0.71 TO 0.99 M^3/H (25 TO 35 FT^3/H); VERTICAL WELDING POSITION 1.14 MM (0.045 IN.) DIAM ELECTRODE

TABLE 4(A) TYPICAL PARAMETERS FOR SPRAY TRANSFER GMAW OF NICKEL-BASE ALLOYS

Workpiece was flat welded with argon shielding gas (flow rate of 1.7 m^3/h, or 60 ft^3/h).

FILLER METAL	**WIRE DIAMETER**		**WIRE FEED RATE**		**VOLTAGE, V**	CURRENT, A
	MM	**IN.**	**M/MIN**	**IN./MIN**		
ERNI-1	0.9	0.035	10.8-13.2	425-520	26-32	**200-300**
	1.1	0.045	7.0-8.1	275-320	26-32	**250-325**
	1.6	0.062	4.4-5.6	175-220	27-33	**275-350**
ERNICU-7	0.9	0.035	12.1-13.2	475-520	26-32	**175-230**
	1.1	0.045	6.4-7.6	250-300	26-32	**225-300**
	1.6	0.062	3.8-5.1	150-200	27-33	**250-300**
ERCUNI	0.9	0.035	12.1-14.6	475-575	26-32	**200-300**
	1.1	0.045	6.4-8.1	250-320	26-32	**250-325**
	1.6	0.062	4.4-5.8	175-230	27-33	**275-350**
ERNICRFE-5	0.9	0.035	10.8-13.2	425-520	26-32	**175-240**
	1.1	0.045	6.4-7.9	250-310	26-32	**225-300**
	1.6	0.062	4.4-5.6	175-220	27-33	**250-330**
ERNICR-3, ERNIFECR-1, ERNICRMO-1	0.9	0.035	11.4-13.2	450-520	26-32	**175-240**
	1.1	0.045	6.4-7.9	250-310	26-32	**225-300**
	1.6	0.062	3.2-5.1	125-200	27-33	**250-330**
ERNICRFE-6	0.9	0.035	11.4-13.2	450-520	26-32	**175-240**
	1.1	0.045	6.4-8.1	250-320	26-32	**225-300**
	1.6	0.062	3.2-5.1	125-200	27-33	**250-330**
ERNICRCOMO-1, ERNICRMO-3, ERNICRMO-4 THROUGH -11	0.9	0.035	11.4-15.2	450-600	26-32	**180-245**
	1.1	0.045	6.4-8.9	250-350	26-32	**225-300**
	1.6	**0.062**	**3.2-5.7**	**125-225**	**27-33**	**250-330**

TABLE 4(B) TYPICAL PARAMETERS FOR SHORT-CIRCUITING TRANSFER GMAW OF NICKEL-BASE ALLOYS

Data applicable to vertical welding of 3.18 mm (0.125 in.) thick base metal using 65Ar-35H_2 shielding gas at a flow rate of 0.99 m^3/h (35 ft^3/h)

FILLER METAL[A]	OPEN-CIRCUIT VOLTAGE, V		WELDING VOLTAGE, V		WELDING CURRENT, A		WIRE FEED RATE				SECONDARY INDUCTANCE[B]		SLOPE[B]	
							M/MIN		IN./MIN					
	RANGE	TYPICAL	RANGE	TYPICAL	RANGE	TYPICAL	RANGE	TYPICAL	RANGE	TYPICAL	RANGE	TYPICAL	RANGE	TYPICAL
ERNI-1	28-34	30	20-24	22	90-150	110	5.1-11.4	6.0	200-450	235	5-12	10	$6\frac{1}{2}$-$8\frac{1}{2}$	$7\frac{1}{2}$
ERNICU-7	27-33	30	19-24	22	90-150	110	5.1-11.4	7.0	200-450	275	7-12	10	$6\frac{1}{2}$-$8\frac{1}{2}$	**8**
ERCUNI	27-36	28	19-25	20	100-175	130	5.7-11.4	7.0	225-450	275	5-14	$7\frac{1}{2}$	6-$7\frac{1}{2}$	$6\frac{1}{2}$
ERNICR-3	29-36	33	21-26	23	90-150	115	4.4-9.5	7.0	175-375	275	10-17	15	7-$9\frac{1}{2}$	$9\frac{1}{2}$
ERNICRMO-3	**29-36**	**33**	**21-26**	**23**	**90-150**	**110**	**4.4-9.5**	**7.0**	**175-375**	**275**	**10-17**	**15**	**7-$9\frac{1}{2}$**	**$9\frac{1}{2}$**

(A) ROD DIAMETER OF 0.9 MM (0.035 IN.).

(B) RELATIVE VALUES ONLY. HIGHER NUMBERS DENOTE GREATER SECONDARY INDUCTANCE OR SLOPE.

TABLE 4(C) TYPICAL PARAMETERS FOR PULSED-ARC TRANSFER GMAW OF NICKEL-BASE ALLOYS

Data applicable for vertical welding with 1.1 mm (0.045 in.) wire and argon shielding gas flowing at 0.8 m^3/h (30 ft^3/h)

FILLER METAL	TYPICAL WIRE FEED RATE		PEAK VOLTAGE, V		AVERAGE VOLTAGE, V		CURRENT, A	
	M/MIN	IN./MIN	RANGE	TYPICAL	RANGE	TYPICAL	RANGE	TYPICAL
ERNI- 1	4.1	160	45-46	46	21-22	21	90-150	**130**
ERNICU-7	3.6	140	39-40	40	21-22	21	90-150	**125**
ERNICR-3	**3.6**	**140**	**43-44**	**44**	**20-22**	**21**	**90-150**	**110**

Welding current is most often provided by constant-voltage power supplies, although all standard direct current (dc) power supplies are satisfactory. Direct current electrode positive (DCEP) is used because it is virtually impossible to transfer metal in a controlled manner when using DCEN. The amperage should be well within the maximum rating of the equipment, but it should be sufficient to obtain the desired melting rate.

The shielding gas used in the gas-metal arc welding of nickel alloys by spray or globular transfer can be argon, which yields good results. The addition of 15 to 20% He is beneficial when welding nickel alloys with short-circuiting arc or pulsed-arc transfer methods. As the helium content increases from 0 to 20%, the weld beads become progressively wider and flatter, and penetration decreases. The addition of oxygen or carbon dioxide to argon stabilizes the arc, but results in heavily oxidized and irregular bead surfaces. With standard constant-voltage GMAW power sources, helium alone has been used as a shielding gas, but it creates an unsteady arc with excessive weld spatter and is a difficult atmosphere in which to initiate an arc. With pulsed GMAW power sources in which the waveform can be controlled, helium can be very effective for overlaying, resulting in low base metal dilution.

Gas flow rates vary from 0.71 to 2.8 m^3/h (25 to 100 ft^3/h), depending on joint design and position. A flow rate of 1.4 m^3/h (50 ft^3/h) is used most frequently. The choice of gas used with short-circuiting metal transfer is influenced by the type of equipment available. Argon, without additions, is suitable for use with equipment that has both inductance and slope control. Argon gas produces convex beads, which may cause cold lapping (lack of fusion), but it also provides a pronounced pinch effect that can be controlled by inductance. The addition of helium is helpful when induction and slope cannot be varied. Helium imparts a wetting action, and the arc is hotter. These factors greatly decrease the possibility of cold lapping. As the percentage of helium increases, the gas flow rate must be increased to ensure adequate protection.

The size of the gas nozzle is important when using a short-circuiting arc. When a 1:1 mixture of argon and helium is used at a flow rate of 1.1 m^3/h (40 ft^3/h) through a 9.5 mm ($\frac{3}{8}$ in.) diameter nozzle, at a wire feed rate of 6.4 m/min (250 in./min), and a wire diameter of 1.1 mm (0.045 in.) the current can be increased to 160 to 180 A without adversely affecting weld quality. An argon-helium mixture is recommended as the shielding gas with the pulsed-arc GMAW process. The gas flow rate should range from 0.42 to 1.3 m^3/h (15 to 45 ft^3/h). An excessive flow rate can interfere with the arc.

Filler metals used in the GMAW process are listed in Table 3. The appropriate wire diameter depends on the method used and the thickness of the base metal. With globular or spray transfer, 0.89, 1.14, and 1.57 mm (0.035, 0.045, and 0.062 in.) diameter wire is used. The short-circuiting and pulsed-arc processes generally require wire that is 1.14 mm (0.045 in.) or less in diameter.

Joint designs recommended for the GMAW process are shown in Fig. 1. For U-shaped groove designs that use globular or spray transfer methods, the root radius should be decreased by about 50%, and the bevel angle should be doubled. With these transfer methods, the use of high amperage on small-diameter wire produces a high level of arc force. As a result, the arc cannot be deflected from a straight line, as is possible when the welding process utilizes covered electrodes. Because the arc must contact all areas to be fused, the joint design must provide an intersection with the arc force line. When a short-circuiting arc is used, the U-shaped groove designs are the same as those employed with the other arc welding processes.

Welding Techniques. Positioning the electrode holder vertically along the centerline of the joint yields the best results. Some inclination is permissible to allow a better view of the work, but excessive displacement can cause the surrounding atmosphere to be drawn into the shielding gas, causing porous or heavily oxidized welds. Arc length is also important. Too short an arc causes spatter, and too long an arc results in loss of control and reduced penetration.

Because arc length is directly proportional to voltage, particular care must be paid to the voltage setting to ensure properly controlled arc length. In addition, once a procedure has been qualified, consistent torch-to-work positioning should be maintained to prevent possible changes in transfer mode caused by loss (or gain) of energy available at the arc. The alteration in energy at the arc is caused by I^2R energy changes corresponding to wire extension changes.

Cold lapping (lack of fusion) can occur with the short-circuiting, globular, and pulsed-arc processes if manipulation is faulty. The torch should be advanced at a rate that will keep the arc in contact with the base metal, just ahead of the weld pool. The manipulation and angle used with the pulsed-arc torch are similar to those used in the SMAW process. To avoid undercutting, a slight pause should be made at the limit of the weave. Excessive welding speeds and improper torch positioning can cause oxides on the surface of underlying passes to become entrapped between weld passes. Slower

welding speeds and good torch positioning allow the arc to reduce certain oxides and/or allow time to float the oxides to the surface of the molten weld puddle.

Plasma Arc Welding

Using the keyholing mode, the PAW process can produce acceptable welds in nickel alloys that are up to about 7.6 mm (0.3 in.) thick. Argon-hydrogen mixtures are used as orifice and shielding gases. Levels from 5 to 8% H_2 are optimum. The amount of current needed for keyholing decreases as hydrogen content increases (up to about 7% H_2). Above this level, torch starting becomes more difficult. If helium or hydrogen is used, then the arc starting ability is subsequently reduced.

Typical travel speed and current parameters for keyhole welding are:

TRAVEL SPEED		CURRENT, A	
MM/MIN	**IN./MIN**	**NICKEL 200**	ALLOY 400
205	8	185	**155**
255	L0	200	**175**
305	12	220	**195**
355	**14**	**235**	**215**

Typical conditions for welding 5.97 mm (0.235 in.) thick Nickel 200 using 95% Ar-5% H_2 gas are: current, 245 A; voltage, 31.5 V; feed rate, 355 mm/min (14 in./min); and gas flow, 0.28 m^3/h (10 ft^3/h) (orifice) and 1.3 m^3/h (45 ft^3/h) (shielding) (Ref 1, 2).

References cited in this section

1. A.C. LINGENFELTER, *WELD. ENG.*, JAN 1970, P 42-45
2. A.C. LINGENFELTER *ET AL.*, *WELD. J.*, MAY 1966, P 417-422

Welding of Nickel Alloys

Revised by E.B. Hinshaw, Inco Alloys International, Inc.

Shielded Metal Arc Welding

The SMAW process can be used for welding nickel and nickel alloys. Although the minimum metal thickness is usually about 1.3 mm (0.050 in.), thinner metal can be welded when appropriate fixtures are provided. The types of joints used, as well as bead and groove dimensions, are given in Fig. 2.

Electrodes. The composition of electrodes used in the SMAW process are given in Table 5. Electrode composition is selected to be similar to that of the base metal with which the electrode is to be used. Electrodes of the ENi-1 classification are used to weld wrought and cast forms of nickel and nickel alloys to themselves and to steel. ENiCu electrodes can be used to weld nickel-copper alloys to themselves, to surface steel with a nickel-copper alloy, to weld the

clad side of a nickel-copper-clad steel, and to weld nickel-copper alloys to steel. ECuNi electrodes can be used to weld nickel-copper, copper-nickel, and nickel wrought alloys when overlaying steel. A buttering layer of ENi-1 is usually placed onto the steel surface before a copper-nickel surface layer is made.

TABLE 5 COMPOSITION OF ELECTRODES USED FOR SMAW OF NICKEL-ALLOYS, HIGH-NICKEL CONTENT ALLOYS, AND NICKEL-COPPER ALLOYS

UNS NO.	ELECTRODE	COMPOSITION, WT %														
		C	MN	FE	S	SI	CU	NI + CO	AL	TI	NB + TA	CR	MO	P	W	OTHER
W82141	ENI-1	0.10	0.75	0.75	0.02	1.25	0.25	92.0 MIN	1.0	1.0-4.0	. . .	. . .	. . .	. . .	. . .	**. . .**
W84190	ENICU-7	0.15	4.00	2.5	0.015	1.5	BAL	62.0-69.0	0.75	1.0	. . .	. . .	. . .	0.02	. . .	**. . .**
W60715	ECUNI	0.15	1-2.5	0.4-.75	0.015	0.5	BAL	29 MIN	. . .	0.5	. . .	. . .	. . .	0.02	. . .	**. . .**
W86112	ENICRMO-3	0.10	1.0	7.0	0.02	0.75	0.50	55.0 MIN	. . .	. . .	3.15-4.15	20.0-23.0	8.0-10.0	0.03	. . .	**2.5 CO, 0.35 V**
W80276	ENICRMO-4	0.02	1.0	4.0-7.0	0.03	0.2	0.50	BAL	. . .	. . .	. . .	14.5-16.5	15.0-17.0	0.04	3.0-4.5	**. . .**
W86985	ENICRMO-9	0.02	1.0	18.0-21.0	0.03	1.0	1.5-2.5	BAL	. . .	. . .	0.5	21.0-23.5	6.0-8.0	0.04	1.5	**5.0 CO**
W86022	ENICRMO-10	0.02	1.0	2.0-6.0	0.015	0.2	0.5	BAL	. . .	. . .	. . .	20.0-22.5	12.5-14.5	0.03	2.5-3.5	**0.35 V, 2.5 CO**
W86030	ENICRMO-11	0.03	1.5	13.0-17.0	0.02	1.0	1.0-2.4	BAL	. . .	1.5-4.0	0.3-1.5	28.0-31.5	4.0-6.0	0.04	1.5-4.0	**5.0 CO**
W86040	ENICRMO-12	0.03	2.2	5.0	0.02	0.7	0.50	BAL	. . .	. . .	1.0-2.8	20.5-22.5	8.8-10.0	0.03	. . .	**. . .**
W86132	ENICRFE-1	0.08	3.5	11.0	0.015	0.75	0.50	62.0 MIN	. . .	. . .	1.5-4.0	13.0-17.0	. . .	0.03	. . .	**. . .**
W86133	ENICRFE-2	0.10	1.0-3.5	12.0	0.02	0.75	0.50	62.0 MIN	. . .	. . .	0.5-3.0	13.0-17.0	0.50-2.50	0.03	. . .	**0.50-2.50 V**
W86134	ENICRFE-3	0.10	5.0-9.5	10.0	0.015	1.0	0.50	59.0 MIN	. . .	1.0	1.0-2.5	13.0-17.0	. . .	0.03	. . .	**. . .**
W80001	ENIMO-1	0.07	1.0	4.0-7.0	0.03	1.0	0.50	BAL	. . .	. . .	. . .	1.0	26.0-30.0	0.04	1.0	**0.60 V, 2.5 CO**
W80665	ENIMO-7	0.02	1.75	2.0	0.03	0.2	0.50	BAL	. . .	. . .	. . .	1.0	26.0-30.0	0.04	1.0	**1.0 CO**
W86152	ENICRFE-7	0.05	5.0	7.0-12.0	0.015	0.75	0.5	BAL	0.50	0.50	1.0-2.5	28-31.5	0.50	0.030	. . .	**. . .**

W86117	**ENICRCOMO-1**	**0.05-0.15**	**0.3-2.5**	**5.0**	**0.015**	**0.75**	**0.50**	**BAL**	**. . .**	**. . .**	**1.0**	**21.0-26.0**	**8.0-10.0**	**0.03**	**. . .**	**9.0-15.0 CO**

(A) SINGLE VALUES ARE MAXIMUM (EXCEPT WHERE OTHERWISE SPECIFIED).

ENiCrMo-3 electrodes typically are used to join a wide range of pitting and crevice corrosion-resistant alloys. The lowest alloyed materials employed with these electrodes are the molybdenum-modified type 317 stainless steels. ENiCrMo-3 electrodes are used for richer alloy compositions of the nickel-chromium-iron-molybdenum families, up to and including alloy 625. Intermediate alloys welded with ENiCrMo-3 include alloy 825, alloy 20, alloy G, and alloy G-3. This type of electrode is widely used because its high nickel content allows good dissimilar weldability, whereas the high molybdenum content matches or exceeds the pitting resistance of the base alloys being welded. Because of the strength of the ENiCrMo-3 electrode, welding to many high-strength low-alloy (HSLA) grade steels can be performed without sacrificing strength.

Other electrodes in this alloy group, such as ENiCrMo-4 and ENiCrMo-10, are used to join alloys to themselves or to steel. They are also used to join alloys in the ENi-Cr-Mo group to each other. Usually, the base metal is welded with a higher alloyed welding electrode to counteract the microsegregation that occurs in the weld deposit. For example, in a pitting environment, such as the SO_2 environments found in flue gas desulfurization (FGD) applications, the choice would be a nickel-chromium-molybdenum alloy group with a higher molybdenum-containing welding electrode family.

Nickel-chromium-iron electrodes, such as ENiCrFe-2 and ENiCrFe-3, are designed to weld the same family of alloys, as well as dissimilar metal joints involving carbon steel, stainless steel, nickel, and nickel-base alloys. Other welding electrodes with the ENi-Cr-Fe electrode grouping are special-application chemistry electrodes, such as ENi-Cr-Fe-7, which are used to weld alloy 690 to itself, to alloy 600, and to butt weld alloy 690 to steel or to overlay certain grades of steel in nuclear boiler and pressure water reactor applications.

Nickel-chromium-cobalt-molybdenum electrodes, such as ENi-Cr-Co-Mo-1, are readily used to join nickel-chromium-iron alloys, especially when service temperatures will exceed 790 °C (1450 °F) and could reach up to 1150 °C (2100 °F) in oxidizing atmospheres.

Nickel-molybdenum electrodes, such as ENMo-1, are designed to weld nickel-molybdenum alloys to themselves and to other nickel-, cobalt-, and iron-base metals. They are normally used in the flat position only.

Covered electrodes should be kept in sealed, moisture-proof containers in a dry storage area prior to their use. All opened containers of unused electrodes should be stored in a cabinet equipped with a dessicant or heated to 6 to 8 °C (10 to 15 °F) above ambient temperature prior to use. If the electrodes are exposed to excessive moisture, then they can be reclaimed by rebaking at 260 °C (500 °F) for 2 h or at 315 °C (600 °F) for 1 h. The electrode diameter should be chosen on the basis of quality requirements and position of welding, rather than on speed of production.

Welding Current. The SMAW process utilizes DCEP. Each electrode size has an optimum amperage range in which good arcing characteristics prevail and outside of which the arc becomes unstable or the electrode overheats. Suggested electrode diameters and current settings for various metal thicknesses are shown in Table 6. Variables such as type of backing, tightness of clamping, and joint design influence the required amount of current density. Actual welding currents should be developed by making sample welds in metal of the same composition and thickness as the metal to be welded.

TABLE 6 RECOMMENDED ELECTRODE DIAMETER AND WELDING CURRENT FOR SMAW OF SELECTED THICKNESSES OF HIGH-NICKEL-CONTENT ALLOYS AND NICKEL-COPPER ALLOYS IN THE FLAT POSITION

BASE-METAL THICKNESS		**ELECTRODE DIAMETER**[A]		CURRENT[B], A
MM	**IN.**	**MM**	**IN.**	
HIGH-NICKEL-CONTENT ALLOYS				
0.94	0.037	2.4	$\frac{3}{32}$	[C]
1.09	0.043	2.4	$\frac{3}{32}$	[C]
1.27	0.050	2.4	$\frac{3}{32}$	[C]
1.57	0.062	2.4	$\frac{3}{32}$	**75**

1.98	0.078	2.4	3/32	**80**
2.36	0.093	2.4	3/32	**85**
2.77	0.109	3.2	1/8	**105**
3.18	0.125	3.2	1/8	**150**
3.18	0.125	2.4-4.0	3/32 - 5/32	**80-150**
3.56	0.140	4.0	5/32	**130**
3.96	0.156	4.0	5/32	**135**
[GES]4.75	[GES]0.187	4.0	5/32	**150**
NICKEL-COPPER ALLOYS				
0.94	0.037	2.4	3/32	**(C)**
1.09	0.043	2.4	3/32	**(C)**
1.27	0.050	2.4	3/32	**(C)**
1.57	0.062	2.4	3/32	**50**
1.98	0.078	2.4	3/32	**55**
2.36	0.093	2.4	3/32	**60**
2.77	0.109	2.4	3/32	**60**
2.77	0.109	3.2	1/8	**65**
3.18	0.125	2.4-4.0	3/32 - 5/32	**60-140**
3.56	0.140	2.4-4.0	3/32 - 5/32	**60-140**
3.96	0.156	2.4-4.0	3/32 - 5/32	**60-140**
6.35	0.250	2.4-4.0	3/32 - 5/32	**60-140**
9.53	0.375	2.4-4.8	3/32 - 3/16	**60-180**
[GES]12.7	**[GES]0.500**	**2.4-4.8**	3/32 - 3/16	**60-180**

(A) WHERE A RANGE IS SHOWN, THE SMALLER DIAMETER ELECTRODES ARE USED FOR THE FIRST PASSES AT THE BOTTOM OF THE GROOVE, AND THE JOINTS ARE COMPLETED WITH THE LARGER DIAMETER ELECTRODES.

(B) CURRENT SHOULD BE IN THE RANGE RECOMMENDED BY THE ELECTRODE MANUFACTURER.

(C) USE MINIMUM AMPERAGE AT WHICH ARC CONTROL CAN BE MAINTAINED.

Welding Position. Flat-position welding should be used whenever possible, because it is faster, more economical, and produces a weld of good quality. The recommended electrode position for flat-position welding is an inclination of about 20° from the vertical, ahead of the weld pool. This position facilitates control of the molten flux and prevents slag entrapment. A short arc must be maintained to prevent atmospheric contamination of the arc and weld and to prevent porosity.

For vertical welding, the arc should be slightly shorter than for flat-position welding, and the amperage should be 10 to 20% lower than the values in Table 6. The electrode should be approximately a 90° angle to the joint. For overhead welding, the arc should be slightly shorter than for flat-position welding, and the welding current should be reduced by 5 to 15 A from the values shown in Table 6.

Welding Techniques. Because molten nickel alloy weld metal is not as free flowing as iron-base alloys, it must be deposited where it is needed. Therefore, a slight weave is required. The amount of weave will depend on joint design, welding position, and type of electrode. Although a straight stringer bead made without weaving can be used for single-pass work, and is satisfactory at the bottom of a deep groove on thicker sections, a weave is generally desirable.

When a weave is used, it should be no wider than approximately three times the electrode diameter. Some deviation from this role may be necessary during vertical welding. A slight weave, if it is not excessive, can help prevent possible centerline solidification cracking problems.

Weld spatter should be avoided. Spatter indicates that the arc is too long, that excessive amperage is being used, or that the current is straight polarity (DCEN). Other causes of spatter are wet electrodes or base metal and slag that run under the arc during welding.

Arc blow may occur when one or both of the metals being welded is magnetic. The arc is deflected from its normal path by a magnetic force in the base metal. One method of overcoming arc blow is to change the location of the ground connection on the workpiece or to change the direction of the electrical path to the arc. A dissimilar joint (for example, steel welded to a nickel-base alloy) can cause considerable arc blow toward the steel side of the joint.

When the arc is to be broken, it should be shortened slightly, and the rate of travel should be increased to reduce the size of the weld pool. This practice reduces the probability of crater cracking, ensures that the crater does not develop a rolled leading edge, and prepares the way for restriking the arc. Another technique to prevent crater cracking is called crater filling, in which the weld pool is held stationary for a short period of time before the arc is broken. This technique is usually incorporated at the end of a weld.

The manner in which the arc is restruck has a significant effect on the soundness of the weld. A reverse (or T) restrike is recommended. The arc should be struck at the leading edge of the crater and carried back to the extreme rear of the crater at a normal welding speed. The direction is then reversed, weaving is commenced, and the weld is continued. Advantages of this procedure are:

- THE WELDER HAS AN OPPORTUNITY TO ESTABLISH THE CORRECT ARC LENGTH BEFORE ACTUAL WELDING COMMENCES.
- SOME PREHEAT IS APPLIED TO THE COLD CRATER.
- THE FIRST DROPS OF RAPIDLY COOLED WELD METAL ARE DEPOSITED WHERE THEY WILL BE REMELTED, THUS RESTRICTING THE POROSITY TO A MINIMUM.

Another technique is to make the restrike where the weld metal can be readily removed (for example, 13 to 25 mm, or $\frac{1}{2}$ to 1 in., behind the crater on top of the previous pass). Later, the restrike area can be ground to be level with the rest of the bead. This technique is used when the weld must meet rigid radiographic standards and calls for less welder skill than the reverse-restrike method.

Welding procedures should be qualified before production begins. In one plant where this was not done, qualifying tests of the welding procedure were conducted before further welds were made when cracks appeared in the weld metal of a joint in a 13 mm ($\frac{1}{2}$ in.) thick Nickel 200 cylinder.

The original procedure for this weld specified a V-shaped groove butt joint with a 60° included angle, a 3.2 mm ($\frac{1}{8}$ in.) root face, and zero root opening (Fig. 3a). An ENi-1 electrode that was 355 mm (14 in.) long by 48 mm ($\frac{3}{16}$ in.) wide was used with a welding current of 235 A. On the first pass, a weld bead that was 165 mm ($6\frac{1}{2}$ in.) long was deposited with each electrode. On the second pass, a weld bead that was 75 mm (3 in.) long was deposited with each electrode. A cross section of the completed weld is shown in Fig. 3(b). An investigation showed that cracks in the weld metal were caused by the high welding current and low travel speed, which had resulted in the weld pool being held in a superheated condition for an excessively long time.

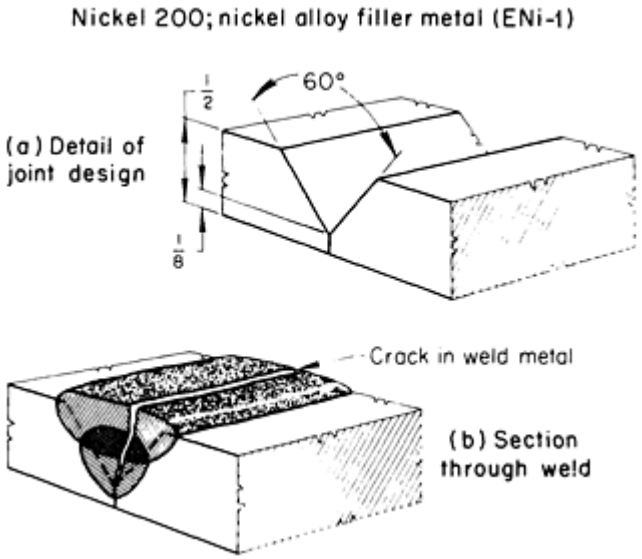

FIG. 3 JOINT CONFIGURATIONS FOR WELDING 13 MM ($\frac{1}{2}$ IN.) NICKEL 200 AND SUBSEQUENT CRACK IN WELD METAL CAUSED BY EXCESSIVE HEAT INPUT. DIMENSIONS GIVEN IN INCHES

Therefore, a qualified procedure was established, specifying a welding current of 210 A and an increased travel speed, which resulted in a 305 mm (12 in.) long weld for each electrode on the first pass and 230 mm (9 in.) long welds per electrode on the second pass. Electrode type and length, and all other welding conditions, were unchanged. An included angle of 80° and a 1.6 to 2.4 mm ($\frac{1}{16}$ to $\frac{3}{32}$ in.) root face would have produced a better welded joint, but the workpieces had been machined and roll formed before the problem arose.

Cleaning the Weld Bead. In multiple-pass welding, all flux and slag must be removed before each succeeding bead is deposited. All slag should be completely removed from completed welds, especially if service involves high temperatures. The slag is easily removed with either hand tools or a hand or power wire brush.

Welding of Nickel Alloys

Revised by E.B. Hinshaw, Inco Alloys International, Inc.

Submerged Arc Welding

Submerged arc welding can be used to join solid-solution nickel alloys. Alloy 400, Nickel 200, and several Ni-Cr-Fe alloys are most frequently welded by this process. Joints in metal up to 75 mm (3 in.) thick have met American Society of

Mechanical Engineers (ASME) codes and other specification requirements. The SAW process cannot be used to weld the PH nickel alloys.

Joint Design. Some joint designs used in the submerged arc welding of nickel-alloy plate are shown in Fig. 4. Single compound-angle grooves, single U-grooves, and double U-grooves are used for metal that is 19 mm ($\frac{3}{4}$ in.) or more thick. The double U-groove is usually preferred, because it results in a lower level of residual stress and can be completed in less time, with less filler metal. A single V-groove is used for stock up to 13 mm (1 in.) thick.

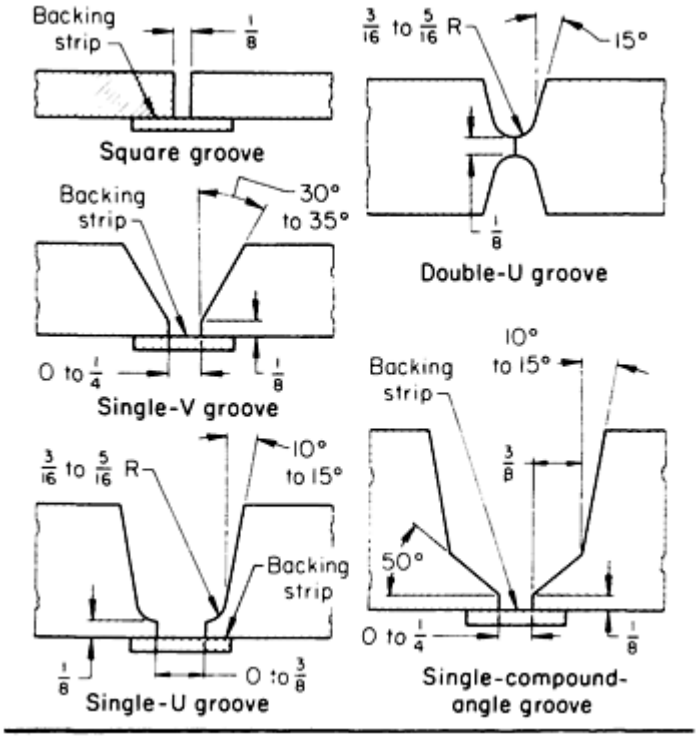

FIG. 4 TYPICAL DIMENSIONS FOR SAW OF NICKEL ALLOYS. BACKING STRIPS ARE OPTIONAL WITH ZERO ROOT OPENINGS. DIMENSIONS GIVEN IN INCHES

Electrodes. The compositions of the electrode wires used in the SAW process are the same as those of the filler metals or electrode wires used in GTAW and GMAW processes (Table 3). Submerged arc welding is possible with the following electrodes: ERNi-1, ER-CuNi, ERNiCu-7, ERNiCr-3, ERNiCrFe-5, and ERNiCrMo-3.

Wire that ranges from 1.14 to 2.36 mm (0.045 to 0.093 in.) in diameter can be used for all nickel alloys. The 1.6 mm ($\frac{1}{16}$ in.) diameter wire is generally preferred. Small-diameter wires are used to weld metal that is up to 13 mm ($\frac{1}{2}$ in.) thick, and 2.4 mm ($\frac{3}{32}$ in.) diameter wires are used for heavier sections. The approximate amounts of filler metal needed for a single compound angle, a single U-groove, and a single V-groove are given in Table 7.

TABLE 7 QUANTITY OF FILLER METAL REQUIRED TO PRODUCE SUBMERGED ARC WELDS IN THREE TYPES OF GROOVES

JOINT DESIGN								APPROXIMATE AMOUNT OF METAL REQUIRED (IN POUNDS PER LINEAR FOOT) FOR INDICATED PLATE THICKNESS (IN INCHES) OF:								
ANGLE	**ANGLE β**	**RADIUS (*R*)**		**ROOT OPENING (*S*)**		**DIMENSIONS (S_1)**										
		MM	**IN.**	**MM**	**IN.**	**MM**	**IN.**	**1**	**$1\frac{1}{4}$**	**$1\frac{1}{2}$**	**$1\frac{3}{4}$**	**2**	**$2\frac{1}{2}$**	**3**	**$3\frac{1}{2}$**	4
SINGLE-COMPOUND-ANGLE GROOVE																
10°	40°	. . .	. . .	0	0	9.5	$\frac{3}{8}$	2.19	3.10	4.10	5.17	6.33	8.90	11.77	14.95	**18.50**
10°	40°	. . .	. . .	0	0	13	$\frac{1}{2}$	2.74	3.56	4.84	6.16	7.61	10.45	13.73	17.32	**21.00**
10°	50°	. . .	. . .	0	0	9.5	$\frac{3}{8}$	1.95	2.83	3.79	4.82	5.93	8.40	11.18	14.00	**17.70**
15°	50°	. . .	. . .	0	0	9.5	$\frac{3}{8}$	2.03	2.95	4.08	5.29	6.62	9.68	13.20	17.30	**21.78**
10°	50°	. . .	. . .	6.4	$\frac{1}{4}$	9.5	$\frac{3}{8}$	2.87	3.98	5.17	6.43	7.77	10.70	13.94	17.22	**21.38**
10°	40°	. . .	. . .	6.4	$\frac{1}{4}$	9.5	$\frac{3}{8}$	3.11	4.25	5.48	6.78	8.17	11.20	14.53	18.17	**22.18**
SINGLE U-GROOVE																
10°	. . .	4.8	$\frac{3}{16}$	0	0	. . .	. . .	1.46	2.07	2.76	3.53	4.37	6.33	8.60	11.20	**14.10**
10°	. . .	6.4	$\frac{1}{4}$	0	0	. . .	. . .	1.77	2.47	3.25	4.12	5.06	7.20	9.67	12.45	**15.60**
10°	. . .	7.9	$\frac{5}{16}$	0	0	. . .	. . .	2.03	2.86	3.68	4.71	5.76	8.10	10.70	13.70	**17.00**
15°	. . .	4.8	$\frac{3}{16}$	0	0	. . .	. . .	1.60	2.36	3.23	4.22	5.34	7.94	11.00	14.60	**18.68**
15°	. . .	6.4	$\frac{1}{4}$	0	0	. . .	. . .	1.90	2.73	3.68	4.76	5.96	8.74	12.00	15.78	**20.00**
15°	. . .	7.9	$\frac{5}{16}$	0	0	. . .	. . .	2.17	3.08	4.14	5.30	6.60	9.55	12.90	16.90	**21.40**
10°	. . .	4.8	$\frac{3}{16}$	6.4	$\frac{1}{4}$	. . .	. . .	2.38	3.22	4.14	5.14	6.21	8.63	11.36	14.42	**17.78**

10°	. . .	6.4	$\frac{1}{4}$	6.4	$\frac{1}{4}$	. . .	. . .	2.69	3.62	4.63	5.73	6.90	9.50	12.43	15.67	**19.28**
SINGLE V-GROOVE																
30°	. . .	. . .	. . .	0	0	. . .	. . .	1.63	. . .	. . .	. . .	. . .	. . .	. . .	. . .	**. . .**
35°	. . .	. . .	. . .	0	0	. . .	. . .	1.96	. . .	. . .	. . .	. . .	. . .	. . .	. . .	**. . .**
30°	**. . .**	**. . .**	**. . .**	**6.4**	$\frac{1}{4}$	**. . .**	**. . .**	**2.55**	**. . .**	**. . .**	**. . .**	**. . .**	**. . .**	**. . .**	**. . .**	**. . .**

Fluxes. The fluxes used in the submerged arc welding of carbon and stainless steels are not satisfactory when welding nickel alloys. Special proprietary fluxes are available and must be used. Loss of alloy elements (especially chromium), poor weld contour, flux entrapment, weld cracking, and inclusions can result when the wrong flux is used.

Only enough flux cover to prevent arc flashing should be used because excessive flux can cause a deformed bead surface. Slag entrapment can be prevented by appropriate joint design and by correct placement of beads. Slag is easily removed from welds in the bottom of grooves. Fused flux is self-lifting from exposed welds and should be discarded. Unfused flux can be recovered by means of a vacuum system, and it can be reused, if clean. Screening to adjust particle size is not required.

Fluxes should be stored in dry storage areas. Opened containers should be resealed to prevent moisture pickup. However, flux that has absorbed moisture can be reclaimed by drying at 315 °C (600 °F) for 1 h. Hoppers used for fluxes appropriate for the welding of steel and other metals should be thoroughly cleaned before being filled with flux appropriate for the welding of nickel alloys.

Welding Current. Direct current electrode negative (typically used for groove plus cladding applications) or direct current electrode positive (typically used for cladding applications) can be used. Reverse polarity (DCEP) is preferred for butt welding, because it produces a flatter bead with deeper penetration at a rather low arc voltage (30 to 33 V). Straight polarity (DCEN) results in a slightly higher rate (typically 30% higher) of deposition at increased voltage (over 35 V) and requires oscillation. The flux covering, however, must be appreciably deeper. Consequently, flux consumption and the risk of slag entrapment increase. Alternating current and the two wire series technique for multiple arc welding are not suitable for use with the available fluxes.

Bead Deposition. The bead location in a multiple-pass layer should provide an open, or reasonably wide, root area for the next bead. Slightly convex beads are preferred to concave beads. Bead contour is controlled by voltage, travel speed, and the position of the electrode.

Welding of Nickel Alloys

Revised by E.B. Hinshaw, Inco Alloys International, Inc.

Minimizing Weld Defects

The defects and metallurgical difficulties encountered in the arc welding of nickel alloys include:

- POROSITY
- SUSCEPTIBILITY TO HIGH-TEMPERATURE EMBRITTLEMENT BY SULFUR AND OTHER CONTAMINANTS
- CRACKING IN THE WELD BEAD, CAUSED BY HIGH HEAT INPUT AND EXCESSIVE WELDING SPEEDS
- STRESS-CORROSION CRACKING IN SERVICE

Porosity. Oxygen, carbon dioxide, nitrogen, or hydrogen can cause porosity in welds. In the SMAW and SAW processes, porosity can be minimized by using electrodes that contain deoxidizing or nitride-forming elements, such as aluminum and titanium. These elements have a strong affinity for oxygen and nitrogen and form stable compounds with them. Presence of deoxidizers in either type of electrode serves to reduce porosity. In addition, porosity is much less likely to occur in chromium-bearing nickel alloys than in non-chromium-bearing alloys.

In the GMAW and GTAW processes, porosity can be avoided by preventing the access of air to the molten weld metal. Gas backing on the underside of the weld is sometimes used.

In the GTAW process, the use of argon with up to 10% H_2 as a shielding gas helps to prevent porosity. Bubbles of hydrogen that form in the weld pool gather the diffusing nitrogen. Too much hydrogen (>15%) in the shielding gas can result in hydrogen porosity.

Cracking. Hot shortness of welds can result from contamination by sulfur, lead, phosphorus, cadmium, zinc, tin, silver, boron, bismuth, or any other low-melting-point elements, which form intergranular films and cause severe liquid-metal embrittlement at elevated temperatures. Many of these elements are found in soldering and brazing filler metals. Hot cracking of the weld metal usually results from such contamination. Cracking in the heat-affected zone is often caused by intergranular penetration of contaminants from the base-metal surface. Sulfur, which is present in most cutting oils used for machining, is a common cause of cracking in nickel alloys. The removal of foreign material from the surfaces of the work metal is imperative (see the section "Cleaning of Workpieces" in this article). Weld metal cracking also can be caused by heat input that is too high, as a result of high welding current and low welding speed (Fig. 3). Welding speeds have a large effect on the solidification pattern of the weld. High welding speeds create a tear-drop molten weld pool, which leads to uncompetitive grain solidification at the center of the weld. At the weld centerline, residual elements will collect and cause centerline hot cracking or lower transverse tensile properties.

In addition, cracking may result from undue restraint. When conditions of high restraint are present, as in circumferential welds that are self restraining, all bead surfaces should be slightly convex. Although convex beads are virtually immune to centerline splitting, concave beads are particularly susceptible to centerline cracking. In addition, excessive width-to-depth or depth-to-width ratios can result in cracking that may be internal (that is, subsurface cracking).

Stress-Corrosion Cracking. Nickel and nickel alloys do not experience any metallurgical changes, either in the weld metal or in the HAZ, that affect normal corrosion resistance. When the alloys are intended to contact substances such as concentrated caustic soda, fluorosilicates, and some mercury salts, however, the welds may need to be stress relieved to avoid stress-corrosion cracking. Nickel alloys have good resistance to dilute alkali and chloride solutions. Because resistance to stress-corrosion cracking increases with nickel content, the stress relieving of welds in the high-nickel-content alloys is not usually needed.

Effect of Slag on Weld Metal. Because fabricated nickel alloys are ordinarily used in high-temperature service and in aqueous corrosive environments, all slag should be removed from finished weldments. If slag is not removed in the latter type of application, then crevices and accelerated corrosion can result. Slag inclusions between weld beads reduce the strength of the weld. If the service temperature approximates the melting point of the slag, then severe corrosion can occur when slag is present on the weld surfaces, particularly in oxygen-containing atmospheres. Fluorides in the slag can react with moisture or elements in the environment to create highly corrosive compounds.

Slag also acts as an accumulator of sulfur, particularly in reducing atmospheres, which can lead to service failure in atmospheres that would be considered adequately low in sulfur. In one instance, although only 0.01% S was present in the atmosphere, the sulfur content of the slag on the weld surface rose from 0.02% to 2 or 3% after a one-month exposure. Sulfur pickup also depresses the melting temperature of the weld slag and, consequently, the maximum safe operating temperature of the weldment.

Welding of Nickel Alloys

Revised by E.B. Hinshaw, Inco Alloys International, Inc.

Joining of Dissimilar Metals

Nickel and nickel alloys have been successfully joined to other nickel alloys and carbon and low-alloy steels, stainless steel, and a number of copper alloys. Filler metal, or consumable electrode, must be selected to ensure a compatible metallurgical relationship between the two base metals. Several factors are involved:

- DIFFERENCES IN THERMAL EXPANSION OF THE BASE METALS
- POSSIBILITY OF PERMANENT CHANGES IN VOLUME AFTER EXTENDED SERVICE AT ELEVATED TEMPERATURE
- EFFECT OF WELD-METAL DILUTION AT THE INTERFACES WITH THE BASE METAL

All of these factors influence the choice of filler metal and welding process.

An example of a good metallurgical combination is the welding of nickel to alloy 400. Because these metals are completely compatible, they can be welded to each other by any welding process, using any compatible filler metal.

Dilution of Weld Metal. The composition of the weld metal can be expected to differ from that of the filler metal, or consumable electrode, and the base metals being joined, because some elements are lost through the arc when they are transferred from the filler-metal electrode to the weld metal during welding. Filler metal and base metal mixing results in the formation of a unique alloy. The composition of the weld metal is fairly uniform for a given bead, except in a narrow band at the edge of the weld, just adjacent to the fusion line in the near heat-affected zone of the weld. This area is sometimes referred to as the "unmixed zone." Although this region can never entirely be eliminated, its size can be minimized by lowering the overall heat input during welding. The amount of dilution varies from bead to bead. The welding process, current density, deposition rate, welding speed, weld-metal thickness, and welding technique have a significant influence on the amount of base-metal dilution that occurs in the weld deposit. Another region that forms in the near heat-affected zone of the weld is the "partially melted zone." This region can lower the overall corrosion resistance of the weldment, but can be controlled by lowering or limiting the heat input during welding.

The dilution of a nickel-base alloy by a dissimilar metal can be tolerated only to a limited degree. When a stainless steel filler metal is used to weld alloy 400 to an austenitic stainless steel, any significant amount of copper pickup from the alloy 400 causes the weld metal to become hot short and to crack. Thus, stainless steel filler metal should not be used when the welding process can cause a considerable amount of dilution. Neither nickel-copper nor copper-nickel types of filler metal can be used in this instance, because chromium from the stainless steel dilutes the weld metal and causes cracking. Although nickel or a nickel-chromium-iron or nickel-chromium-molybdenum filler metal is best, they should only be used after the welding procedure has been qualified by tests.

Filler Metals/Welding Electrodes. Selection of the correct filler metal helps produce a weld that meets the service requirements for strength, corrosion resistance, and soundness and tolerates dilution without causing cracking susceptibility in the weld metal. Crack sensitivity of the weld metal is proportional to the amount of dilution, especially when there is a considerable difference in the composition of a base metal and a filler metal.

Some combinations of base metal and filler metal produce undesirable weld-metal compositions:

- A FERRITIC WELD-METAL DEPOSIT DILUTED BY NICKEL, CHROMIUM, OR COPPER
- AN 18-8 STAINLESS STEEL WELD-METAL DEPOSIT DILUTED BY MORE THAN 3% CU
- AN 18-8 TYPE OF WELD-METAL DEPOSIT SUFFICIENTLY DILUTED BY NICKEL OR CHROMIUM TO RESULT IN THE FULLY AUSTENITIC CRACK-SENSITIVE WELD-METAL COMPOSITION (FOR EXAMPLE, 35% NI AND 15% CR)
- ANY NICKEL-COPPER OR COPPER-NICKEL ALLOY WELD-METAL DEPOSIT DILUTED BY MORE THAN 6 TO 8% CR

Manipulation of the welding arc so that it impinges primarily on the base metal nearest in composition to the filler metal helps reduce dilution. For most combinations of dissimilar metals, filler-metal suppliers should be consulted before a filler metal is selected. The addition of ample filler metal to the root pass helps lower the amount of base-metal dilution and also prevents the probability of producing a concave weld deposit profile, instead of the preferred convex shape.

The coefficients of thermal expansion (CTEs) of the base metals must be considered when selecting filler metals for joining dissimilar metal combinations. CTE differences are a major factor in situations where there is temperature cycling (for example, welding of 300 series stainless steel to carbon or low-alloy steel at temperatures above 425 °C, or 800 °F). A large difference in CTE values can induce stresses of sufficient magnitude to produce cracking in the weld metal. Some of the nickel-base electrodes (ENiCr, ENiCrFe, ERNiCr, and ERNiCrFe) and matching filler metals can be used to weld a wide range of base-metal combinations. These electrodes and filler metals can tolerate considerable dilution without loss of strength or ductility. Filler-metal ERNiMo-6 can be used to join nickel-base alloys, cobalt-base alloys, and stainless steels to themselves and to other metals and alloys. The low chromium content of this filler metal, however, should be carefully considered when welding oxidation-resistant materials.

Although GTAW and GMAW processes can be employed, the SMAW process is the most widely used to join nickel and nickel alloys to dissimilar metals. The welding current should be maintained near the middle of the recommended range for the electrode in order to control dilution. Dilution usually can be kept below 25% by manipulating the electrode to

dissipate the arc force on already-deposited weld metal. When depositing the first bead, the arc should be directed toward the member from which dilution of the weld metal will be least detrimental. Welding procedures that reduce the amount of penetration, which can cause dilution of the weld metal by the base metal, will increase the probability of securing a good weld. Table 8 gives recommended welding consumables for joining selected nickel-base alloys.

TABLE 8 SELECTION OF WELDING CONSUMABLES FOR NICKEL-BASE ALLOY JOINING APPLICATIONS

WELDING ELETRODE OR FILLER METAL	PRIMARY APPLICATIONS
COATED ELECTRODES	
ENI-1	**NICKEL 200 AND NICKEL 201; THE CLAD SIDE OF NICKEL-CLAD STEEL; JOINING OF STEELS TO NICKEL ALLOYS**
ENICU-7	**ALLOY 400 TO ITSELF, TO LOW-ALLOY AND CARBON STEELS, TO COPPER AND COPPER-NICKEL ALLOYS; SURFACING OF STEELS**
ECUNI	**ALLOY 450; WELDABLE GRADES OF CAST AND WROUGHT 70/30, 80/20, AND 90/10 COPPER-NICKEL ALLOYS**
ENICRFE-1	**ALLOY 600; ALLOY 330**
ENICRFE-3	**ALLOYS 600 AND 601, SURFACING OF STEEL; DISSIMILAR COMBINATIONS OF STEELS AND NICKEL ALLOYS**
ENICRMO-3	**ALLOYS 625 AND 601; PIT-RESISTANT ALLOYS; DISSIMILAR COMBINATIONS OF STEELS AND NICKEL ALLOYS; SURFACING OF STEELS**
ENICRCOMO-1	**ALLOY 617; ALLOY 800HT; DISSIMILAR COMBINATIONS OF HIGH-TEMPERATURE ALLOYS**
ENICRMO-3	**ALLOY 825; ALLOY 686, ALLOY 622, ALLOY C-276; OTHER PIT-RESISTANT ALLOYS; SURFACING OF STEELS**
ENICRMO-3, ENICRMO-9	**ALLOYS G AND G-3; OTHER PIT-RESISTANT ALLOYS; DISSIMILAR COMBINATIONS OF STEELS AND NICKEL ALLOYS; SURFACING OF STEELS**
ENICRFE-3, ENICRFE-7	**ALLOY 600 AND ALLOY 690 TO THEMSELVES AND TO DISSIMILAR COMBINATIONS WITH STEEL; SURFACING OF STEELS**
FILLER METALS	
ERNI-1	**NICKEL 200 AND NICKEL 201; DISSIMILAR COMBINATIONS OF NICKEL ALLOYS AND STEELS; SURFACING OF STEELS**
ERNICU-7	**ALLOYS 400, R-405, AND K-500; SURFACING OF STEEL**
ERCUNI	**ALLOY 450; WELDABLE GRADES OF 70/30, 80/20, AND 90/10 COPPER-NICKEL ALLOYS**
ERNICR3, ERNICRFE-7	**ALLOY 600, ALLOY 690; DISSIMILAR COMBINATION TO STEELS; SURFACING OF STEELS**
ERNICR-3	**ALLOYS 600 AND 601; ALLOYS 800 AND 800HT; ALLOY 330; DISSIMILAR COMBINATIONS OF STEELS AND NICKEL ALLOYS; SURFACING OF STEELS**
ERNICR-3, ERNICRMO-3	**DISSIMILAR COMBINATIONS OF STEELS AND NICKEL ALLOYS**
ERNICRCOMO-1	**ALLOY 617; ALLOY 800HT; DISSIMILAR COMBINATIONS OF HIGH-TEMPERATURE ALLOYS**
ERNICRMO-3	**ALLOYS 625 AND 601; PIT-RESISTANT ALLOYS; DISSIMILAR COMBINATIONS OF STEELS AND NICKEL ALLOYS; SURFACING OF STEELS**
ERNIFECR-2	**ALLOYS 718 AND X-750**
ERNICRMO-3	**ALLOY 825**
ERNICRMO-4 THROUGH -10	**ALLOY 686, ALLOY 622, ALLOY C-276; OTHER PIT-RESISTANT ALLOYS; SURFACING OF STEELS**

Example 1: Elimination of Weld Cracking and Distortion.

The welding of an alloy 400 skirt box to a low-carbon steel (ASTM A 285) cover for a fluorine generator resulted in cracking of the weld metal and warping of the cover (Fig. 5). Cracks resulting from excessive dilution were eliminated by modifying the way in which the beads were deposited. Weld crater cracks were prevented by taking care when ending the weld bead and breaking the arc. The alloy 400 skirt boxes replaced low-carbon steel skirt boxes that had corroded.

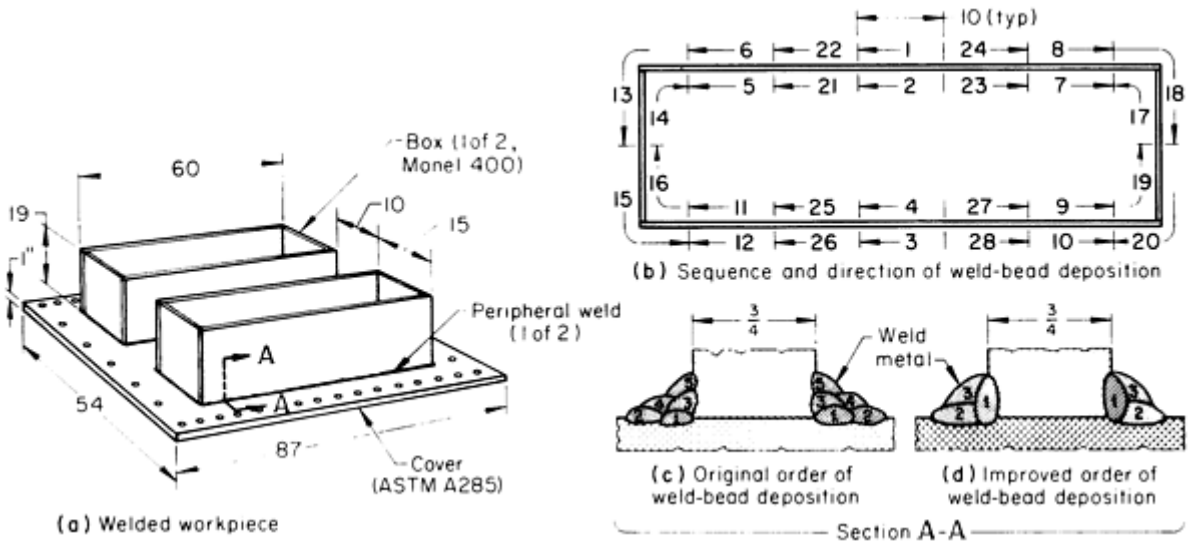

PARAMETER	**ALLOY 400 WELDED TO ALLOY 400**		ALLOY 400 WELDED TO LOW-CARBON STEEL	
	ORIGINAL METHOD	**IMPROVED METHOD**	**ORIGINAL METHOD**	IMPROVED METHOD
WELDING PASSES	1	1	5	**3**
FIXTURES	NONE	CLAMPS	NONE	**CLAMPS**
ELECTRODE TYPE[A]	4 MM ($\frac{5}{32}$ IN.) DIAM ENICU-4	4 MM ($\frac{5}{32}$ IN.) DIAM ENICU-4	4 MM ($\frac{5}{32}$ IN.) DIAM ENICU-1	**4.8 MM ($\frac{3}{16}$ IN.) DIAM ENICU-1**
WELDING CURRENT	130 A (DCEP)	130 A (DCEP)	154 A (DCEP)	**145 TO 150 A (DCEP)**
LEAK TEST[B]	WELDS REJECTED	WELDS ACCEPTED	WELDS REJECTED	**WELDS ACCEPTED**
WELDING TIME PER COVER	40 H	25 H	40 H	**25 H**
WELD PENETRATION:				
BEAD 1	1.6 MM ($\frac{1}{16}$ IN.) INTO STEEL	3.2 MM ($\frac{1}{8}$ IN.) INTO ALLOY 400, 0.4 MM ($\frac{1}{64}$ IN.) INTO STEEL	1.6 MM ($\frac{1}{16}$ IN.) INTO STEEL	**3.2 MM ($\frac{1}{8}$ IN.) INTO ALLOY 400, 0.4 MM ($\frac{1}{64}$ IN.) INTO STEEL**
BEAD 2	1.6 MM ($\frac{1}{16}$ IN.) INTO STEEL	0.8 MM ($\frac{1}{32}$ IN.) INTO STEEL	1.6 MM ($\frac{1}{16}$ IN.) INTO STEEL	**0.8 MM ($\frac{1}{32}$ IN.) INTO STEEL**
BEAD 3	1.6 MM ($\frac{1}{16}$ IN.) INTO ALLOY 400	0.8 MM ($\frac{1}{32}$ IN.) INTO ALLOY 400	1.6 MM ($\frac{1}{16}$ IN.) INTO ALLOY 400	**0.8 MM ($\frac{1}{32}$ IN.) INTO ALLOY 400**
BEAD 4	NONE IN BASE METAL	. . .	NONE IN BASE METAL	**. . .**
BEAD 5	0.8 MM ($\frac{1}{32}$ IN.) INTO ALLOY 400	. . .	0.8 MM ($\frac{1}{32}$ IN.) INTO ALLOY 400	**. . .**
IRON IN WELD METAL:				
BEAD 1	30%	7%	30%	**7%**
BEAD 2	30%	10%	30%	**10%**

BEAD 3	20%	4%	20%	**4%**
BEAD 4 AND 5	**7%**	**. . .**	**7%**	**. . .**

(A) NEITHER ENICU-1 NOR ENICU-4 ELECTRODES ARE CURRENTLY PRODUCED; BOTH HAVE BEEN REPLACED BY ENICU-7 ELECTRODE WHICH HAS 2.5% FE CONTENT.

(B) HELIUM MASS SPECTROMETER WITH INTERNAL VACUUM OF 3.3 PA (0.025 MM HG)

FIG. 5 FLUORINE-GENERATOR COVER MADE BY SMAW OF SIMILAR (ALLOY 400 TO ALLOY 400) AND DISSIMILAR (ALLOY 400 TO LOW-CARBON STEEL) MATERIALS. (ASTM A 285). BOTH WELDS USED NICKEL ALLOY FILLER METAL. A CORNER JOINT AND DOUBLE FILLET WELD WAS UTILIZED TO JOIN THE SIMILAR ALLOYS. A T-JOINT AND DOUBLE FILLET WELD WAS UTILIZED TO JOIN THE DISSIMILAR MATERIALS. PARAMETERS COMMON TO BOTH SETUPS: POWER SUPPLY, 400 A (DC); STRESS RELIEF, 1 H AT 620 ± 14 °C (1150 ± 25 °F)

The original procedure for removing corroded skirt boxes, making new boxes, and welding the new boxes to the cover plate was:

1. REMOVE CORRODED LOW-CARBON STEEL SKIRT BOXES BY AIR-CARBON ARC CUTTING.
2. CLEAN SURFACES OF LOW-CARBON STEEL COVER BY SURFACE GRINDING.
3. CLEAN ALL JOINT AREAS ON THE ALLOY 400 PLATES WITH TRICHLOROETHYLENE AND REMOVE MILL SCALE WITH A SURFACE GRINDER.
4. ASSEMBLE THE ALLOY 400 SKIRT BOX AND WELD THE FOUR COMERS IN ONE PASS EACH WITH A 4.0 MM ($\frac{5}{32}$ IN.) DIAMETER ENICU-4 ELECTRODE, USING A WELDING CURRENT OF 130 A.
5. WELD THE ALLOY 400 SKIRT BOX TO THE LOW-CARBON STEEL COVER WITH INTERMITTENT WELDS, USING THE SEQUENCE OF WELD BEAD DEPOSITION SHOWN IN FIG. 5(B). (THE BOX AND COVER WERE FIRST TACK WELDED AT THE STARTING PLACE FOR EACH OF THE 255 MM, OR 10 IN., LONG WELDS.) DEPOSIT FIVE BEADS AS SHOWN IN FIG. 5(C), WITH A 4.0 MM ($\frac{5}{32}$ IN.) DIAMETER ENICU-1 ELECTRODE, USING A WELDING CURRENT OF 154 A.
6. STRESS RELIEVE AT 620 ± 14 °C (1150 ± 25 °F) FOR 1 H IN A REDUCING ATMOSPHERE. (THE ASSEMBLY WAS PLACED IN THE FURNACE WHEN THE FURNACE TEMPERATURE WAS LESS THAN 315 °C (600 °F), AND, AFTER HEATING, WAS ALLOWED TO COOL TO 315 °C, OR 600 °F, BEFORE IT WAS REMOVED.)
7. TEST THE WELDS WITH A HELIUM MASS SPECTROMETER UNDER AN INTERNAL VACUUM OF 3.3 PA (0.025 MM HG). (WELDS THAT FAILED THE TEST WERE REWELDED.)

During deposition of the first bead, considerable arc blow toward the alloy 400 skirt box was encountered. The ground connection was repositioned several times, but no improvement was obtained. When the welds were tested with a helium mass spectrometer, leakage caused by cracks in the weld beads was detected. An investigation revealed that some cracks had resulted from excessive dilution of the weld metal by iron (analysis showed 30% Fe in bead 1 in Fig. 5b), a result of the high welding heat, and that cracks in the weld craters had been caused by ending beads too abruptly. In addition to the cracking, there was excessive distortion of the cover, where the cover edges were warped upward toward the skirt boxes for 3.2 mm ($\frac{1}{8}$ in.) maximum, along the sides and about 6.4 mm ($\frac{1}{4}$ in.) across the ends. The distortion was not reduced during stress relieving (step 6).

Experimentation resulted in the adoption of a new welding procedure (step 5) that minimized distortion and eliminated weld-metal cracking. The remaining steps in the original procedure were retained, unchanged. In the new procedure, when welding the box to the cover plate, both parts were securely clamped to a welding surface plate. The sequence of weld-bead deposition was the same as for the original method (Fig. 5b), but only firm weld beads were deposited (Fig.

5d). Bead 1 was placed mostly on the alloy 400, which resulted in considerably less dilution by iron (7%, compared with 30%). The bead was ended very slowly to avoid the danger of subsequent crater cracking. The welds were made with an electrode that was slightly larger than the original (4.8 mm, or $\frac{3}{16}$ in., diameter instead of 4.0 mm, or $\frac{5}{32}$ in., diameter), using from 145 to 150 A welding current, instead of 154 A. These modifications reduced the current density and, thus, the heat input.

When the clamps were released, no significant distortion of the cover plate was observed. All joints passed the helium leak-detection test.

Welding of Nickel Alloys

Revised by E.B. Hinshaw, Inco Alloys International, Inc.

References

1. A.C. LINGENFELTER, *WELD. ENG.*, JAN 1970, P 42-45
2. A.C. LINGENFELTER *ET AL.*, *WELD. J.*, MAY 1966, P 417-422

Welding of Nickel Alloys

Revised by E.B. Hinshaw, Inco Alloys International, Inc.

Selected References

• "WELDING," BROCHURE IAI-14-1, INCO ALLOYS INTERNATIONAL, MAY 1989, P 15-36

Welding of Copper Alloys

Revised by M. Ned Rogers, Batesville Casket Company

Introduction

COPPER AND COPPER ALLOYS offer a unique combination of material properties that makes them advantageous for many manufacturing environments. They are widely used because of their excellent electrical and thermal conductivities, outstanding resistance to corrosion, ease of fabrication, and good strength and fatigue resistance. Other useful characteristics include spark resistance, metal-to-metal wear resistance, low-permeability properties, and distinctive color.

Copper and copper alloys find their greatest use for electrical conductors and in the manufacture of electrical components. In its pure form, copper has a face-centered cubic crystal structure and a density of 8.968 g/cm^3 (0.32 lb/in.^{3}), which is about three times the density of aluminum. The electrical conductivity of copper is only slightly lower than that of silver, but it exceeds the electrical and thermal conductivity of aluminum by one-and-a-half times. The electrical conductivity reference standard of engineering materials is copper with a rating of 100% IACS (International Annealed Copper Standard). All other materials are compared on a conductivity basis to the IACS standard. Special processing of copper can produce some forms which reach 102% IACS.

Their excellent resistance to fresh water, salt water, and alkaline solutions makes copper alloys ideally suited for fabrication of tubing, valve fittings, heat exchangers, and chemical equipment. Copper reacts with sulfur and ammonia compounds. Ammonium hydroxide solutions will rapidly attack copper and its alloys, causing severe corrosion.

Many copper alloys are used for bearings and wear surfaces. Their excellent metal-to-metal wear resistance and lack of galling makes them excellent bearing surfaces. The good malleability and formability of copper and its alloys, as well as its aesthetically pleasing color, make it a prime candidate for architectural applications such as ornamentation and roofing.

In manufacturing, copper is often joined by welding. The arc welding processes are of prime concern. Arc welding can be performed using shielded metal arc welding (SMAW), gas-tungsten arc welding (GTAW), gas-metal arc welding (GMAW), plasma arc welding (PAW), and submerged arc welding (SAW). These joining processes will be discussed with reference to specific copper alloy groups. The effects of various alloying agents are also discussed relative to welding metallurgy and process considerations. Examples of standard joint geometry, process parameters, and specific applications are described.

Welding of Copper Alloys

Revised by M. Ned Rogers, Batesville Casket Company

Alloy Metallurgy and Weldability

Many common metals are alloyed with copper to produce the various copper alloys. The most common alloying elements are aluminum, nickel, silicon, tin, and zinc. Other elements and metals are alloyed in small quantities to improve certain material characteristics, such as corrosion resistance or machinability. Copper and its alloys are divided into nine major groups. These major groups are:

- *COPPERS,* WHICH CONTAIN A MINIMUM OF 99.3% CU
- *HIGH-COPPER ALLOYS,* WHICH CONTAIN UP TO 5% ALLOYING ELEMENTS
- *COPPER-ZINC ALLOYS (BRASSES),* WHICH CONTAIN UP TO 40% ZN
- *COPPER-TIN ALLOYS (PHOSPHOR BRONZES),* WHICH CONTAIN UP TO 10% SN AND 0.2% P
- *COPPER-ALUMINUM ALLOYS (ALUMINUM BRONZES),* WHICH CONTAIN UP TO 10% AL
- *COPPER-SILICON ALLOYS (SILICON BRONZES),* WHICH CONTAIN UP TO 3% SI
- *COPPER-NICKEL ALLOYS,* WHICH CONTAIN UP TO 30% NI
- *COPPER-ZINC-NICKEL ALLOYS (NICKEL SILVERS),* WHICH CONTAIN UP TO 27% ZN AND 18% NI
- *SPECIAL ALLOYS,* WHICH CONTAIN ALLOYING ELEMENTS TO ENHANCE A SPECIFIC PROPERTY OR CHARACTERISTIC, FOR EXAMPLE, MACHINABILITY

Many copper alloys have common names, such as oxygen-free copper (99.95% Cu min), beryllium copper (0.2 to 2.0% Be), Muntz metal (Cu-40Zn), Naval brass (Cu-39.25Zn-0.75Sn), and commercial bronze (Cu-10Zn).

A more standardized system of identification is the Unified Numbering System (UNS). In this system, wrought alloys of copper are designated by numbers 1*xxxx* to 7*xxxx*, and cast alloys are designated 8*xxxx* to 9*xxxx*; thus, the same alloy can be produced as a wrought and cast product.

Table 1 lists various copper alloys that are frequently arc welded, their UNS numbers, and their physical properties. Many of the physical properties of copper alloys are important to the welding processes, including melting temperature, coefficient of thermal expansion, and electrical and thermal conductivity. As shown in Table 1, certain alloying elements greatly decrease the electrical and thermal conductivities of copper and copper alloys. This will in turn significantly affect the weldability of the alloys. The copper and copper alloys listed in Table 1 are rated for their relative weldability using SMAW, GTAW, and GMAW.

TABLE 1 NOMINAL COMPOSITIONS, MELTING POINTS, RELATIVE THERMAL CONDUCTIVITIES, AND WELDABILITIES OF WROUGHT COPPERS AND COPPER ALLOYS THAT ARE COMMONLY ARC

WELDED

UNS NO.	ALLOY NAME	NOMINAL COMPOSITION, %	MELTING POINT (LIQUIDUS)		RELATIVE THERMAL CONDUCTIVITY[A]	WELDABILITY[B] BY		
			°C	°F		GTAW	GMAW	SMAW
OFC AND ETP COPPERS								
C10200	OXYGEN-FREE COPPER (OFC)	99.95 CU	1083	1981	100	G	G	**NR**
C11000	ELECTROLYTIC TOUGH PITCH (ETP) COPPER	99.90 CU, 0.04 O_2	1083	1981	100	F	F	**NR**
DEOXIDIZED COPPERS								
C12000	PHOSPHORUS-DEOXIDIZED COPPER, LOW-P	99.9 CU, 0.008 P	1083	1981	99	E	E	**NR**
C12200	PHOSPHORUS-DEOXIDIZED COPPER, HIGH-P	99.9 CU, 0.02 P	1083	1981	87	E	E	**NR**
BERYLLIUM COPPERS								
C17000	HIGH-STRENGTH BERYLLIUM COPPER	98.3 CU, 1.7 BE	982	1800	27-33[C]	G	G	**G**
C17200	HIGH-STRENGTH BERYLLIUM COPPER	98.1 CU, 1.9 BE	982	1800	27-33[C]	G	G	**G**
C17500	HIGH-CONDUCTIVITY BERYLLIUM COPPER	96.9 CU, 0.6 BE, 2.5 CO	1068	1955	53-66[C]	F	F	**F**
LOW-ZINC BRASSES								
C21000	GILDING	95 CU, 5 ZN	1065	1950	60	G	G	**NR**
C22000	COMMERCIAL BRONZE	90 CU, 10 ZN	1043	1910	48	G	G	**NR**
C23000	RED BRASS	85 CU, 15 ZN	1026	1880	41	G	G	**NR**
C24000	LOW BRASS	80 CU, 20 ZN	999	1830	36	G	G	**NR**
HIGH-ZINC BRASSES								
C26000	CARTRIDGE BRASS	70 CU, 30 ZN	954	1750	31	F	F	**NR**
C26800	YELLOW BRASS	65 CU, 35 ZN	932	1710	30	F	F	**NR**
C28000	MUNTZ METAL	60 CU, 40 ZN	904	1660	31	F	F	**NR**
TIN BRASSES								
C44300	ADMIRALTY BRASS	71 CU, 28 ZN, 1 SN[D]	937	1720	28	F	F	**NR**
C46400	NAVAL BRASS	60 CU, 39.25 ZN, 0.75 SN[D]	899	1650	30	F	F	**NR**
SPECIAL BRASSES								
C67500	MANGANESE BRONZE A	58.5 CU, 39 ZN, 1.4 FE, 1 SN, 0.1 MN	888	1630	27	F	F	**NR**
C68700	ALUMINUM BRASS, ARSENICAL	77.5 CU, 20.5 ZN, 2 AL (0.06 AS)	971	1780	26	F	F	**NR**
NICKEL SILVERS								
C74500	NICKEL SILVER	65 CU, 25 ZN, 10 NI	1021	1870	12	F	F	**NR**
C75200	NICKEL SILVER	65 CU, 17 ZN, 18 NI	1110	2030	8	F	F	**NR**
C75400	NICKEL SILVER	65 CU, 20 ZN, 15 NI	1076	1970	9	F	F	**NR**
C75700	NICKEL SILVER	65 CU, 23 ZN, 12 NI	1037	1900	10	F	F	**NR**
C77000	NICKEL SILVER	55 CU, 27 ZN, 18	1054	1930	8	F	F	**NR**

		NI						
PHOSPHOR BRONZES								
C50500	PHOSPHOR BRONZE, 1.25% E	98.7 CU, 1.3 SN (0.2 P)	1076	1970	53	G	G	**F**
C51000	PHOSPHOR BRONZE, 5% A	95 CU, 5 SN (0.2 P)	1049	1920	18	G	G	**F**
C52100	PHOSPHOR BRONZE, 8% C	92 CU, 8 SN (0.2 P)	1026	1880	16	G	G	**F**
C52400	PHOSPHOR BRONZE, 10% D	90 CU, 10 SN (0.2 P)	999	1830	13	G	G	**F**
ALUMINUM BRONZES								
C61300	ALUMINUM BRONZE D, SN-STABILIZED	89 CU, 7AL, 3.5 FE (0.35 SN)	1046	1915	14	G	E	**G**
C61400	ALUMINUM BRONZE D	91 CU, 6-8 AL, 1.5-3.5 FE, 1 MAX MN	1046	1915	17	G	E	**G**
C63000	ALUMINUM BRONZE E	82 CU, 10 AL, 5 NI, 3 FE	1054	1930	10	G	G	**G**
SILICON BRONZES								
C65100	LOW-SILICON BRONZE B	98.5 CU, 1.5 SI	1060	1940	15	E	E	**F**
C65500	HIGH-SILICON BRONZE A	97 CU, 3 SI	1026	1880	9	E	E	**F**
COPPER-NICKEL								
C70600	COPPER NICKEL	88.6 CU, 9-11 NI, 1.4 FE, 1.0 MN	1149	2100	12	E	E	**G**
C71500	**COPPER NICKEL**	**70 CU, 30 NI**	**1238**	**2260**	**8**	**E**	**E**	**E**

(A) BASED ON THE THERMAL CONDUCTIVITY OF ALLOY C10200 (2553.8 KJ/M^2 IN METERS PER HOUR AT 20 °C) AS 100. FOR COMPARISON, CARBON STEEL HAS A THERMAL CONDUCTIVITY OF 339 KJ/M^2 IN METERS PER HOUR AT 20 °C WHICH IS 13 ON THIS SCALE.

(B) E, EXCELLENT; G, GOOD; F, FAIR; NR, NOT RECOMMENDED.

(C) IN THE PRECIPITATION-HARDENED CONDITION.

(D) ALLOYS C44300 AND C46400 CONTAIN NOMINAL 0.06% AS; ALLOYS C44400 AND C46600, A NOMINAL 0.06% SB; ALLOYS C44500 AND 46700, A NOMINAL 0.06% P.

Several alloying elements have pronounced effects on the weldability of copper and copper alloys. Small amounts of volatile, toxic alloying elements are often present in copper and its alloys. As a result, the requirement of an effective ventilation system to protect the welder and/or the welding machine operator is more critical than when welding ferrous metals.

Zinc reduces the weldability of all brasses in relative proportion to the percent of zinc in the alloy. Zinc has a low boiling temperature, which results in the production of toxic vapors when welding copper-zinc alloys. Effective forced ventilation is mandatory, and source-capture systems are necessary to contend with the fumes.

Tin increases the hot-crack susceptibility during welding when present in amounts from 1 to 10%. These alloys are typically the phosphor bronzes and tin brasses. Tin, when compared with zinc, is far less volatile and toxic. During welding, tin may preferentially oxidize relative to copper. The results will be an oxide entrapment, which may reduce the strength of the weldment.

Beryllium, aluminum, and nickel form tenacious oxides that must be removed prior to welding. The formation of these oxides during the welding process must be prevented by shielding gas or by fluxing, in conjunction with the use of the appropriate welding current. The oxides of nickel interfere with arc welding less than those of beryllium or aluminum. Consequently, the nickel silvers and copper-nickel alloys are less sensitive to the type of welding current used during manufacture. Beryllium-containing alloys also produce toxic fumes during welding.

Silicon has a beneficial effect on the weldability of copper-silicon alloys because of its deoxidizing and fluxing actions. The combination of this effect and the low thermal conductivity makes silicon bronzes the most weldable of the copper alloys for any arc process.

Phosphorus is beneficial to certain copper and copper alloys as a strengthener and deoxidizer. When added to brass, phosphorus inhibits dezincification corrosion. In the amounts normally present in most copper alloys, phosphorus does not adversely affect or hinder welding.

Chromium, like beryllium and aluminum, can form a refractory oxide on the surface of the molten weld pool. Arc welding should be done in an inert protective atmosphere to prevent formation of chromium oxides.

Cadmium has no serious effect on the weldability of copper. However, the low boiling temperature of cadmium does result in evaporation of this alloy at welding temperatures, thereby creating a potential health hazard. Cadmium will also form an oxide in the molten weld metal, but the oxide can be easily reduced by fluxing agents.

Oxygen can cause porosity and reduce the strength of welds made in certain copper alloys that do not contain sufficient quantities of phosphorus or other deoxidizers. Oxygen may be found as a free gas or as cuprous oxide. Most commonly welded copper alloys contain deoxidizing elements--usually phosphorus, silicon, aluminum, iron, or manganese. These elements will readily combine with oxygen and eliminate the potential for porosity. The same deoxidizers are also included in the filler metals. The soundness and strength of arc welds made in commercial coppers depend upon the cuprous oxide content. As the oxide content decreases, weld soundness increases. Deoxidized coppers provide the best results because they are free from cuprous oxides and contain residual amounts of phosphorus.

Iron and manganese do not significantly affect the weldability of the alloys that contain them. Iron is typically present in some special brasses, aluminum bronzes, and copper-nickel alloys in amounts of 1.4 to 3.5%. Manganese is commonly used in these same alloys, but at lower concentrations than iron.

Free-Machining Additives. Lead, selenium, tellurium, and sulfur are added to copper alloys to improve machinability. Bismuth is beginning to be used for this purpose as well when lead-free alloys are desired. These minor alloying agents, while improving machinability, adversely affect the weldability of copper alloys by rendering the alloys hot-crack susceptible. The adverse effect on weldability begins to be evident at about 0.05% of the additive and is more severe with larger concentrations. Lead is the most harmful of the alloying agents with respect to hot-crack susceptibility. However, alloys that contain 0.5 to 4% Pb are not ordinarily welded and are not included in Table 1.

Welding of Copper Alloys

Revised by M. Ned Rogers, Batesville Casket Company

Factors Affecting Weldability

Besides the alloying elements that comprise a specific copper alloy, several other factors affect weldability. These factors are the thermal conductivity of the alloy being welded, the shielding gas, the type of current used during welding, the joint design, the welding position, and the surface condition and cleanliness. The effects of the shielding gas, type of current, and joint design used during welding are discussed under the sections for each individual process and alloy, described later in this article.

Effect of Thermal Conductivity. The behavior of copper and copper alloys during welding is strongly influenced by the thermal conductivity of the alloy. Table 1 shows the relative thermal conductivities based on the conductivity of alloy C10200 (oxygen-free copper). As shown in Table 1, the thermal conductivity varies greatly from this baseline value, which is 339 kJ/m^2 in meters per hour at 20 °C (226 Btu/ft^2 in feet per hour at 68 °F). The range is from 100, for alloys C10200 and C11000, to lows of 8 to 12 for nickel silvers and copper-nickel alloys and 9 for alloy C65500. In comparison, carbon steel has a thermal conductivity of 13 on this scale.

When welding commercial coppers and lightly alloyed copper materials with high thermal conductivities, the type of current and shielding gas must be selected to provide maximum heat input to the joint. This high heat input counteracts the rapid head dissipation away from the localized weld zone. Depending on section thickness, preheating may be required for copper alloys with lower thermal conductivities. The interpass temperature should be the same as for preheating. Copper alloys are not postweld head treated as frequently as steels, but some alloys may require controlled cooling rates to minimize residual stresses and hot shortness.

Welding Position. Due to the highly fluid nature of copper and its alloys, the flat position is used whenever possible for welding. The horizontal position is used in some fillet welding of corner joints and T-joints.

Vertical and overhead positions and the horizontal position are less frequently used in welding butt joints. These positions are ordinarily restricted to GTAW, GMAW, and PAW of the less conductive aluminum bronzes, silicon bronzes, and copper-nickel alloys. Small-diameter electrodes and filler-metal wires are used in conjunction with low welding currents for out-of-position welding. Current pulsation is used with GTAW, GMAW, and PAW, to control weld pool fluidity.

When using SMAW, out-of-position welding is usually limited to the joining of aluminum bronzes and copper-nickel alloys, but it can also be done on some phosphor bronzes and silicon bronzes.

Precipitation-Hardenable Alloys. The most important precipitation-hardening reactions are obtained with beryllium, chromium, boron, nickel, silicon, and zirconium. Care must be taken when welding precipitation-hardenable copper alloys to avoid oxidation and incomplete fusion. Whenever possible, the components should be welded in the annealed condition, and then the weldment should be given a precipitation-hardening heat treatment.

Hot Cracking. Copper alloys, such as copper-tin and copper-nickel, are susceptible to hot cracking at solidification temperatures. This characteristic is exhibited in all copper alloys with a wide liquidus-to-solidus temperature range. Severe shrinkage stresses produce interdendritic separation during metal solidification. Hot cracking can be minimized by reducing restraint during welding, preheating to slow the cooling rate and reduce the magnitude of welding stresses, and reducing the size of the root opening and increasing the size of the root pass.

Porosity. Certain elements (for example, zinc, cadmium, and phosphorus) have low boiling points. Vaporization of these elements during welding may result in porosity. When welding copper alloys containing these elements, porosity can be minimized by fast weld speeds and a filler metal low in these elements.

Surface Condition. Grease and oxide on work surfaces should be removed before welding. Wire brushing or bright dipping can be used. Millscale on the surfaces of aluminum bronzes and silicon bronzes is removed for a distance from the weld region of at least 13 mm (0.5 in.), usually by mechanical means. Grease, paint, crayon marks, shop dirt, and similar contaminants on copper-nickel alloys may cause embrittlement and should be removed before welding. Millscale on copper-nickel alloys must be removed by grinding or pickling; wire brushing is not effective.

Welding of Copper Alloys

Revised by M. Ned Rogers, Batesville Casket Company

Arc Welding Processes

Copper and most copper alloys can be joined by arc welding. The commercial alloys that are readily arc welded are listed in Table 1. Welding processes that use gas shielding are generally preferred, although SMAW can be used for many noncritical applications.

Argon, helium, or mixtures of the two are used as shielding gases for GTAW, PAW, and GMAW. Generally, argon is used when manually welding material that is less than 3 mm (0.13 in.) thick, has low thermal conductivity, or both. Helium or a mixture of 75% helium and 25% argon is recommended for machine welding of thin sections and for manual welding of thicker sections of alloys that have high thermal conductivity. Small amounts of nitrogen can be added to the argon shielding gas to increase the effective heat input.

Shielded metal arc welding can be used to weld a wide range of thicknesses of copper alloys. Covered electrodes for SMAW of copper alloys are available in standard sizes ranging from 2.4 to 4.8 mm ($\frac{3}{32}$ to $\frac{3}{16}$ in.). Other sizes are available in certain electrode classifications, and the reader is referred to ANSI/AWS A5.6 "Specification for Covered Copper and Copper Alloy Arc Welding Electrodes."

Higher thermal conductivity and thermal expansion of copper and copper alloys result in greater weld distortion than in comparable steel welds. The use of preheat, fixtures, proper welding sequence, and tack welds can minimize distortion or warping.

Gas-Tungsten Arc Welding

Gas-tungsten arc welding is well suited for copper and copper alloys because of its intense arc, which produces an extremely high temperature at the joint and a narrow heat-affected zone (HAZ). In welding copper and the more thermally conductive copper alloys, the intensity of the arc is important in completing fusion with minimum heating of the surrounding, highly conductive base metal. A narrow HAZ is particularly desirable in the welding of copper alloys that have been precipitation-hardened.

The most frequent use of GTAW for copper and copper alloys is on sections up to 3 mm (0.13 in.) thick that have been prepared with a square edge. Often no filler metal is used in joining these thicknesses. Filler metal is usually required in GTAW of sections thicker than 3 mm (0.13 in.). Gas-tungsten arc welding of sections thicker than 13 mm (0.5 in.) is performed only if GMAW equipment is not available or if special conditions exist. These conditions would include hot shortness of the base metal or adjacent heat-sensitive features that make it necessary to limit the heat input to the base material. Under certain conditions, pulsed GMAW would be the preferred process.

Type of Current. Direct current electrode negative (DCEN) is used for GTAW of most copper and copper alloys. This permits the use of an electrode that has a minimum diameter for a given welding current and that provides maximum penetration of the base material. Alternating current stabilized by high frequency is used on beryllium coppers and aluminum bronzes to prevent the buildup of tenacious oxide film on the base metals.

Electrodes. Many of the standard tungsten or alloyed tungsten electrodes can be used in GTAW of copper and copper alloys. The selection factors normally considered for tungsten electrodes apply in general to the copper and copper alloys. Except as noted for the specific classes of copper alloys, thoriated tungsten (usually EWTh-2) is preferred for its better performance, longer life, and greater resistance to contamination.

Gas-Metal Arc Welding

Gas-metal arc welding is used to join all of the coppers and copper alloys listed previously in Table 1. Gas-tungsten arc welding is preferred for thicknesses less than 3 mm (0.13 in.), while GMAW is preferred for section thicknesses above 3 mm (0.13 in.) and for the joining of aluminum bronzes, silicon bronzes, and copper-nickel alloys.

The major application of GMAW of copper alloys is in the joining of material thicknesses between 3 and 13 mm (0.13 and 0.5 in.) thick, and the process is almost invariably selected for arc welding sections of copper alloys thicker than 13 mm (0.5 in.). The high deposition rate for GMAW is a major advantage in this application when compared to GTAW or SMAW. The greater heat input to the weld, compared with that for GTAW, is a disadvantage in some applications due to the formation of a wider HAZ.

Direct current electrode positive (DCEP) is used exclusively for GMAW of copper alloys. Typically, argon is used as a shielding gas. Helium or mixtures of argon and helium are often used when hotter arc voltages are needed with standard operating current levels. A square-groove joint is not ordinarily used for welding thicknesses greater than 3 mm (0.13 in.), except for coppers. Single-V-grooves are used for thicknesses of 3 to 13 mm (0.13 to 0.5 in.). When section thicknesses exceed 13 mm (0.5 in.), double-V-grooves or double-U-grooves are used as joint preparations.

Welding Position. Most GMAW of copper alloys is done in the flat position with spray transfer; fillet welds acceptable for many applications can be produced in a horizontal position. Gas-metal arc welding is preferred to GTAW or SMAW when weld positions other than flat are required. Out-of-position welding is usually restricted to the less-fluid copper alloys, such as aluminum bronzes, silicon bronzes, and copper-nickel alloys. Small-diameter filler metals and low welding currents are preferred for such applications, and a globular or short-circuiting transfer is ordinarily used. The development of pulsed spray transfer has been quite advantageous for welding of coppers and copper alloys. Small- to medium-diameter wires can be readily used out-of-position for vertical and overhead welding of most alloys.

Shielded Metal Arc Welding

When compared with SMAW of low-carbon steels, SMAW of copper and copper alloys uses larger root openings, wider groove angles, more tack welds, higher preheat and interpass temperatures, and higher welding currents. Welding of coppers and copper alloys using SMAW is almost always restricted to flat-position welding. Out-of-position welding using this process is usually limited to the joining of phosphor bronzes and copper-nickel alloys.

Plasma Arc Welding

The welding of coppers and copper alloys using PAW is comparable to GTAW of these alloys. Argon, helium, or mixtures of the two are used for the welding of all alloys. Hydrogen gas should never be used when welding coppers. Plasma arc welding has two distinct advantages over GTAW: (1) the tungsten is concealed and entirely shielded, which greatly reduces contamination of the electrode, particularly for alloys with low-boiling-temperature constituents such as brasses, bronzes, phosphor bronzes, and aluminum bronzes; and (2) the constricted arc plume gives rise to higher arc energies while minimizing the growth of the HAZ. As with GTAW, current pulsation and current ramping may also be used. Plasma arc welding equipment has been miniaturized for intricate work, known as microplasma welding.

Plasma arc welding of coppers and copper alloys may be performed either autogenously or with filler metal. Filler metal selection is identical to that outlined for GTAW. Automation and mechanization of this process is readily performed and is preferable to GTAW where contamination can restrict production efficiencies. Welding positions for PAW are identical to those for GTAW. However, the plasma keyhole mode has been evaluated for thicker sections in a vertical-up position. Generally, all information presented for GTAW is applicable to PAW.

Submerged Arc Welding

The welding of thick gage material, such as seamed pipe formed from heavy plate, can be achieved by continuous metal-arc operation under a granular flux. Effective deoxidation and slag-metal reactions to form the required weld-metal composition are critical, and the SAW process is still under development for copper-base materials. A variation on this process can be used for weld cladding or hardfacing. Promising results have been seen with the copper-nickel alloys for section thicknesses greater than 13 mm (0.5 in.). V-groove and U-groove joint designs similar to those used in GMAW are satisfactory.

Commercially available fluxes should be used for the copper-nickel alloys. Welding conditions, which are greatly dependent upon the flux used, are provided by the flux manufacturer. Special attention should be given to the weld bead sequence when multi-pass welds are deposited, to ensure complete fusion while maintaining proper bead contour. X-ray quality results can be obtained when the technique is correctly performed.

Welding of Copper Alloys

Revised by M. Ned Rogers, Batesville Casket Company

Filler Metals

Both covered electrodes and bare electrode wire and rods are available for welding copper and copper alloys. Tables 2, 3, and 4 list the various American Welding Society (AWS) classifications for the filler metals for GTAW, GMAW, and SMAW, respectively.

TABLE 2 FILLER METALS FOR GTAW OF COPPER AND COPPER ALLOYS

FILLER METAL	**AWS CLASSIFICATION**	PRINCIPLE CONSTITUENTS[B]
COPPER	ERCU	**98.0 MIN CU + AG, 1.0 SN, 0.5 MU, 0.50 SI, 0.15 P**
PHOSPHOR BRONZE	ERCUSN-A	**93.5 MIN CU + AG, 4.0-6.0 SN, 0.10-0.35 P**
ALUMINUM BRONZE	ERCUAL-A2	**1.5 FE, 9.0-11.0 AL, REM CU + AG**
ALUMINUM BRONZE	ERCUAL-A3	**3.0-4.25 FE, 11.0-12.0 AL, REM CU + AG**
SILICON BRONZE	ERCUSI-A	**94.0 MIN CU + AG, 2.8-4.0 SI, 1.5 ZN, 1.5 SN, 1.5 MN, 0.5 FE**
COPPER-NICKEL	**ERCUNI**	**1.00 MN, 0.40-0.70 FE, 29.0-32.0 NI + CO, 0.20-0.50 TI, REM CU + AG**

(A) NOTE: THESE DATA ARE BASED ON AWS A5.27, A5.6, AND A5.7; SEE CURRENT EDITIONS OF THOSE SPECIFICATIONS FOR COMPLETE COMPOSITIONS AND QUALIFICATIONS.

(B) SINGLE PERCENTAGES ARE MAXIMUMS UNLESS OTHERWISE STATED. OPTIONAL ELEMENTS AND IMPURITIES HAVE BEEN OMITTED.

TABLE 3 FILLER METALS FOR GMAW OF COPPER AND COPPER ALLOYS

ELECTRODE DESIGNATION[(A)]	**COMMON NAME**	BASE-METAL APPLICATIONS
ERCU	COPPER	**COPPERS**
ERCUSI-A	SILICON BRONZE	**SILICON BRONZES, BRASSES**
ERCUSN-A	PHOSPHOR BRONZE	**PHOSPHOR BRONZES, BRASSES**
ERCUNI	COPPER-NICKEL	**COPPER-NICKEL ALLOYS**
ERCUAL-A2	ALUMINUM BRONZE	**ALUMINUM BRONZES, BRASSES, SILICON BRONZES, MANGANESE BRONZES**
ERCUAL-A3	ALUMINUM BRONZE	**ALUMINUM BRONZES**
ERCUNIAL	. . .	**NICKEL-ALUMINUM BRONZES**
ERCUMNNIAL	. . .	**MANGANESE-NICKEL-ALUMINUM BRONZES**
RBCUZN-A	NAVAL BRASS	**BRASSES, COPPER**
RCUZN-B	LOW-FUMING BRASS	**BRASSES, MANGANESE BRONZES**
RCUZN-C	**LOW-FUMING BRASS**	**BRASSES, MANGANESE BRONZES**

(A) SEE THE MOST RECENT EDITION OF AWS A5.7, "SPECIFICATION FOR COPPER AND COPPER ALLOY BARE WELDING RODS AND ELECTRODES," OR AWS A5.27, "SPECIFICATION FOR COPPER AND COPPER ALLOY GAS WELDING RODS."

TABLE 4 FILLER METAL FOR SMAW OF COPPER AND COPPER ALLOYS

COVERED ELECTRODE[(A)]	**COMMON NAME**	BASE-METAL APPLICATIONS
ECU	COPPER	**COPPERS**
ECUSI	SILICON BRONZE	**SILICON BRONZES, BRASSES**
ECUSN-A, ECUSN-C	PHOSPHOR BRONZE	**PHOSPHOR BRONZES, BRASSES**
ECUNI	COPPER-NICKEL	**COPPER-NICKEL ALLOYS**
ECUAL-A2	ALUMINUM BRONZE	**ALUMINUM BRONZES, BRASSES, SILICON BRONZES, MANGANESE BRONZES**
ECUAL-B	ALUMINUM BRONZE	**ALUMINUM BRONZES**
ECUNIAL	. . .	**NICKEL-ALUMINUM BRONZES**
ECUMNNIAL	**. . .**	**MANGANESE-NICKEL-ALUMINUM BRONZES**

(A) SEE THE MOST RECENT EDITION OF AWS A5.6, "SPECIFICATION FOR COVERED COPPER AND COPPER ALLOY ARC WELDING COVERED ELECTRODES."

Copper Filler Metals. The electrodes and rods used to weld the coppers, primarily deoxidized and electrolytic tough pitch (ETP) coppers, are designated as ERCu and have a minimum copper content of 98%. These filler metals, which can be used with GMAW, GTAW, and PAW processes, have electrical conductivity ratings of 25 to 40% IACS.

The covered electrodes used for SMAW are designated as ECu. These are normally used with DCEP. Compared to carbon steel electrodes of the same diameter, the required welding current for ECu electrodes is typically 30 to 40% greater.

Copper-Zinc Filler Metals. Copper-zinc (brass) weld rods are available in three classifications: RBCuZn-A (Naval Brass), RCuZn-B (Low-Fuming Brass), and RCuZn-C (Low-Fuming Brass). These particular welding rods are used for braze welding of copper, bronze, and nickel alloys. Their electrical conductivity is about 25% IACS; thermal-conductivity values are about 30% of those of copper.

Copper-zinc filler metals cannot be used as electrodes for the arc welding processes. The high zinc content tends to become volatile during arc welding and boils from the molten weld pool. This boiling of the low-melting-temperature constituents results in a porous weld.

Copper-Tin Filler Metals. The copper-tin (phosphor bronze) welding electrodes and rods are designated as ECuSn-A, ERCuSn-A, and ECuSn-C. The ECuSn-A and ECuSn-C electrodes contain approximately 5 and 8% Sn, respectively. Phosphorus is used as a deoxidizer for both electrodes. These electrodes are suitable for welding bronze, brass, and copper if the presence of tin in the weld metal is not objectionable. These filler metals are also commonly used for repair welding of castings. Greater weld-metal strength and hardness are obtained with the ECuSn-C electrodes than with the ECuSn-A electrodes.

The ERCuSn-A rods can be used with GTAW and PAW for joining phosphor bronzes. Preheat temperatures of about 200 °C (400 °F) are required when welding with these electrodes, particularly for heavy sections.

Copper-Silicon Filler Metals. Copper-silicon (silicon bronze) electrodes are used in barewire form for GMAW, GTAW, PAW, and sometimes for oxyfuel welding. The designation for these electrodes is ERCuSi-A. Chemical compositions contain between 2.8 and 4.0% Si with approximately 1.5% Mn, 1.0% Sn, and 1.0% Zn. These filler metals are frequently used to weld silicon bronzes and brasses. They are also used for braze welding of galvanized steel. The electrical conductivity is about 6.5% IACS, and the thermal conductivity is approximately 8.4% of that of copper. The covered electrodes in this filler metal classification are designated as ECuSi and are used primarily for welding copper-zinc alloys with the DCEP setting. The covered electrode can also be used for welding of silicon bronze, copper, and galvanized steel. Weld-metal mechanical properties are slightly higher than those of silicon bronze base metal.

Copper-Aluminum Filler Metals. There are a number of copper-aluminum (aluminum) bronze filler metals for both hardfacing and joining applications. The first of these is designated as ERCuAI-A and is an iron-free aluminum bronze. It is used as a surfacing alloy for wear-resistant surfaces with relatively light loads and for resistance to corrosive media, such as salt water and some commonly used acids. This alloy is not recommended for joining applications. Another hardfacing filler metal is ECuAl-B, which is a covered electrode containing 7.5 to 10% AI. These electrodes are used for surfacing applications and repair welding of aluminum bronze castings with similar compositions.

The covered electrodes for SMAW are designated as ECuAl-A2 and contain from 6.5 to 9% A1. The bare-wire electrodes for GTAW, GMAW, and PAW contain from 8.5 to 11% Al and are designated as ERCuAl-A2. This electrode has a higher strength than the covered electrode. Both filler metals can be used for joining aluminum bronzes, silicon bronzes, copper-nickel alloys, copper-zinc alloys, manganese bronzes, and many combinations of dissimilar metals.

ERCuAl-A3 electrodes and rods are used for repair welding of aluminum bronze castings using GMAW and GTAW. The high aluminum content produces welds with less tendency to crack in highly stressed cross sections.

Repair of both wrought and cast aluminum bronze materials containing nickel can be performed with copper-nickel-aluminum electrodes and bare wire. The designations for these metals are ECuNiA1 and ERCuNiA1. These electrodes offer good corrosion resistance as well as good cavitation resistance in both salt water and brackish water.

Joining of manganese-nickel-aluminum bronzes is performed with covered electrodes, designated as ECuMnNiAl, and bare filler metals, designated as ERCuMnNiAl. Like the copper-nickel-aluminum electrodes, these electrodes have good resistance to cavitation, erosion, and corrosion.

Copper-Nickel Filler Metals. Covered electrodes for this classification are designated as ECuNi, and bare electrode wire and rods are designated as ERCuNi. The nominal compositions are 70% Cu and 30% Ni. Titanium is used as a deoxidizer in these filler metals, which are used for the joining of copper-nickel alloys.

Welding of Copper Alloys

Revised by M. Ned Rogers, Batesville Casket Company

Welding of Coppers

As indicated in Table 1, coppers include oxygen-free, ETP, and deoxidized grades that contain [ges]99% Cu (UNS Numbers C10100 to C 15760). The coppers are welded using GTAW, GMAW, and SMAW. Additional information on the properties and applications of coppers can be found in Volume 2 of the *ASM Handbook.*

Gas-Tungsten Arc Welding

When using GTAW to join commercial coppers, weld quality will differ depending on the cuprous oxide content of the copper. The nominal welding conditions, however, for a given thickness and joint design are approximately the same. Table 5 lists several representative welding conditions for GTAW of commercial coppers.

TABLE 5 NOMINAL CONDITIONS FOR GTAW OF COMMERCIAL COPPERS USING EWTH-2 ELECTRODES, ERCU WELDING ROD, AND DCEN

WORKPIECE THICKNESS		ROOT OPENING[A]		ELECTRODE DIAMETER		WELDING ROD DIAMETER		SHIELDING GAS[B]	GAS FLOW RATE		CURRENT, A	TRAVEL SPEED		PREHEAT		NUMBER OF PASSES
MM	IN.	MM	IN.	MM	IN.	MM	IN.		L/MIN	FT^3/H		M/MIN	IN./MIN	°C	°F	
BUTT JOINTS--SQUARE GROOVE																
1.6	1/6	0	0	1.6	1/6	NONE USED		ARGON	7.1	15	110-114	0.30	12	NONE USED		**1**
3.2	1/8	0	0	2.4	3/32	NONE USED		ARGON	7.1	15	175-225	0.28	11	NONE USED		**1**
3.2	1/8	3.2	1/8	2.4	3/32	2.4	3/32	ARGON	7.1	15	175-225	0.28	11	NONE USED		**1**
4.8	3/16	4.8	3/16	3.2	1/8	3.2	1/8	HELIUM	15.0	30	190-225	0.25	10	95	200	**1**
BUTT JOINTS--60° SINGLE-V-GROOVE, 1.6 MM (1/16 IN.) ROOT FACE																
6.4	1/4	1.6	1/16	3.2	1/8	3.2	1/8	HELIUM	15.0	30	225-260	0.23	9	150	300	**1**
9.5	3/8	1.6	1/16	4.8	3/16	4.8	3/16	HELIUM	18.9	40	280-320	. . .	. . .	260	500	**2**
BUTT JOINTS--60° DOUBLE-V-GROOVE, 3.2 MM (1/8 IN.) ROOT FACE[C]																
12.7	1/2	1.6	1/16	6.4	1/4	6.4	1/4	HELIUM	18.9	40	375-525	. . .	. . .	260	500	**3**
LAP JOINTS--FILLET WELDED[D]																
1.6	1/16	0	0	1.6	1/16	1.6	1/16	ARGON	7.1	15	130-150	0.25	10	NONE USED		**1**
3.2	1/8	0	0	2.4	3/32	3.2	1/8	ARGON	7.1	15	200-250	0.23	9	NONE USED		**1**
4.8	3/16	0	0	3.2	1/8	3.2	1/8	HELIUM	15.0	30	205-250	0.20	8	95	200	**1**
6.4	1/4	0	0	3.2	1/8	3.2	1/8 1/8	HELIUM	15.0	30	250-280	0.18	7	150	300	**1**
9.5	3/8	0	0	4.8	3/16	4.8	3/16	HELIUM	18.9	40	300-340	. . .	. . .	260	500	**3**
OUTSIDE CORNER JOINTS--SQUARE GROOVE																

3.2	1/8	3.2	1/8	2.4	3/32	3.2	1/8	ARGON	7.1	15	170-225	0.28	11	NONE USED		**1**
4.8	3/16	4.8	3/16	3.2	1/8	3.2	1/8	HELIUM	15.0	30	190-225	0.25	10	95	200	**1**
6.4	1/4	4.8	3/16	3.2	1/8	3.2	1/8	HELIUM	15.0	30	225-260	0.23	9	150	300	**1**
9.5	3/8	6.4	1/4	4.8	3/16	4.8	3/16	HELIUM	18.9	40	280-320	. . .	. . .	260	500	**2**
OUTSIDE CORNER JOINTS--50° SINGLE-BEVEL-GROOVE, 1.6 MM (1/16 IN.) ROOT FACE																
4.8	3/16	1.6	1/16	3.2	1/8	3.2	1/8	HELIUM	15.0	30	205-250	0.20	8	95	200	**1**
6.4	1/4	1.6	1/16	3.2	1/8	3.2	1/8	HELIUM	15.0	30	250-280	0.18	7	150	300	**1**
9.5	3/8	1.6	1/16	4.8	3/16	4.8	3/16	HELIUM	18.9	40	300-340	. . .	. . .	260	500	**3**
INSIDE CORNER JOINTS--SQUARE GROOVE, FILLET WELDED																
3.2	1/8	3.2	1/8	2.4	3/32	3.2	1/8	ARGON	7.1	15	200-250	0.23	9	NONE USED		**1**
T-JOINTS--FILLET WELDED																
3.2	1/8	1.6	1/16	2.4	3/32	3.2	1/8	ARGON	7.1	15	200-250	0.23	9	NONE USED		**1**
4.8	3/16	1.6	1/16	3.2	1/8	3.2	1/8	HELIUM	15.0	30	205-250	0.20	8	95	200	**1**
6.4	1/4	1.6	1/16	3.2	1/8	3.2	1/8	HELIUM	15.0	30	250-280	0.18	7	150	300	**1**
9.5	3/8	**1.6**	1/16	**4.8**	3/16	**4.8**	3/16	**HELIUM**	**18.9**	**40**	**300-340**	**. . .**	**. . .**	**260**	**500**	**3**

Note: The data in this table are intended to serve as starting points for the establishment of optimum joint design and conditions for welding of parts on which previous experience is lacking. They are subject to adjustments necessary to meet the special requirements of individual applications.

(A) COPPER, CARBON, GRAPHITE, OR CERAMIC TAPE BACKING STIPS OR RINGS MAY BE USED (SEE TEXT).

(B) MIXTURES OF ARGON AND HELIUM ARE ALSO USED (SEE TEXT).

(C) DEPTH OF BACK V IS 9.5 MM (3/8 IN.) OF STOCK THICKNESS.

(D) USE OF FILLER METAL IS OPTIONAL FOR THICKNESSES OF 6.4 MM ($\frac{1}{4}$ IN.) OR LESS.

Effect of Cuprous Oxide. Cuprous oxide may be present within the base metal or introduced through oxidation of the molten weld pool during the arc welding process. Migration of cuprous oxides to the grain boundaries lowers the strength and ductility of the weld and adversely affects fatigue properties.

The best results in the arc welding of copper are obtained on the deoxidized coppers because these alloys are free of cuprous oxides and they contain residual phosphorus. This phosphorus combines with oxygen, which is absorbed during the heating or welding, and prevents the formation of cuprous oxide. The strength, ductility, and porosity of welds made in alloy C10200 (oxygen-free copper) are intermediate between the same properties for welds made in deoxidized coppers (alloys C12000 and C12200) and those made in alloy C11000 (ETP copper), which contains 0.02 to 0.5% oxygen.

While cuprous oxide does have an adverse effect on the mechanical properties of coppers, weld properties of arc welded coppers containing cuprous oxide are superior to those obtained from oxyacetylene welding of oxygen-bearing coppers. Welds made by oxyfuel welding are subject to gassing and embrittlement.

Shielding Gases. Argon is the preferred shielding gas when welding copper sections up to 1.6 mm (0.06 in.) thick. As sections grow thicker, slower travel speeds and higher preheat temperatures are required when using argon shielding gas. For sections in excess of 1.6 mm (0.06 in.), helium is the preferred gas. The risk of oxide entrapment in the weld pool is greatly reduced when using helium. Also, compared to argon, helium provides deeper penetration or higher travel speed for the same welding current.

Mixtures of argon and helium shielding gases result in intermediate welding characteristics. For welding positions other than the flat position, a mixture of 65 to 75% He with argon provides a good balance between the penetrating effect of helium and the ease of control for argon. Gas flow rate usually ranges from 7.1 to 19 L/min (15 to 40 ft^3/h), with higher values being used for high currents in the welding of thick sections.

Type of Current. As indicated in Table 5, DCEN is preferred for GTAW of commercial coppers.

Electrodes. In GTAW of coppers, best results for electrode life and maintenance are obtained using a thoriated tungsten electrode containing 2% thoria (EWTh-2). Proper electrode preparation for the welding of copper is usually a pointed electrode with an included angle of 60°. The tip of the point is truncated with a diameter approximately one-third the diameter of the electrode.

Welding Without Filler Metal. Square-groove butt joints on copper up to 3 mm (0.13 in.) thick can be gas-tungsten arc welded without the use of filler metal. However, filler metal is sometimes required as thicknesses approach this value. Copper sections greater than 3 mm (0.13 in.) may be gas-tungsten arc welded without the use of filler metal by making two passes, one from each side.

Filler Metals. As shown in Table 5, copper sections greater than 3 mm (0.13 in.) that are joined by GTAW typically require the use of filler metals. As discussed above, the adverse effect of the formation of cuprous oxide requires that the filler metal contain a residual deoxidizer. The deleterious effect of oxygen is even more severe within the filler metal than within the base metal, because the filler metal has greater exposure to welding heat.

In most cases, copper filler metal is selected that contains a maximum of 0.15% P and 0.50% Si as deoxidizers. This filler metal is known as ERCu, as shown in Table 2. Alloys such as C12000 and C12200 (deoxidized coppers) do not contain enough residual phosphorus to ensure sound welds and are not used as filler metal. The ERCu filler metal has other advantages, such as relatively high electrical conductivity (30 to 40% IACS) and good color match to the copper base metal. Any of the other filler metals listed in Table 2 can be used in GTAW of commercial coppers. Most of the alloys contain adequate amounts of deoxidizing elements such as phosphorus, silicon, iron, aluminum, or titanium. These filler metals offer the advantage of greater joint strengths, but they have lower electrical conductivity and poor color match.

Welding Technique. Either the forehand or backhand welding technique can be used when GTAW is used for coppers. Forehand welding is preferred for all welding positions. It produces a smaller and more uniform bead size than is possible with backhand welding; however, a greater number of passes may be required to fill the joint.

The weld joint should be filled using one or more stringer beads or narrow weave beads. Wide oscillation of the arc while welding should be avoided, lest the edges of the bead be intermittently exposed to the atmosphere and consequently to oxidation. The first bead should penetrate the root of the joint and be relatively thick, to provide time for deoxidation of the weld metal and to avoid cracking of the bead.

Joint Designs. Welding of butt joints with thicker cross sections requires the use of filler metal and a root opening, due to the high thermal conductivity of copper. Clearance is needed to prevent the base metal from conducting the heat away too rapidly and solidifying the filler metal, thus choking the joint before it is filled.

Because of the high fluidity of copper, backing rings or strips are ordinarily used in GTAW of butt joints. The backing rings are typically made of copper, carbon, graphite, or ceramic tape. Backing is needed both for tightly fitted butt joints used in thin metal and for loosely fitted butt joints in thick metal, to prevent the loss of the fluid weld pool. Backing may also be used when needed for this purpose with other joint geometries.

Preheating. For GTAW of sections greater than 3 mm (0.13 in.), preheating of the base material is typically required to maintain the base metal at welding temperature. Without preheating, the high thermal conductivity of coppers results in excessive loss of heat away from the weld zone. The small arc that is typically used in GTAW cannot maintain sufficient welding heat in thick sections of copper, even under the most favorable conditions. Preheat temperatures are also shown in Table 5.

Deoxidized Copper. When copper weldments require the strength of the base metal, deoxidized coppers are usually used. Even with the localized heat input of GTAW, special fixturing and other welding conditions may be needed to minimize distortion, as shown in the following example.

Example 1: Redesign of Joint and Fixture to Minimize Distortion in GTAW of Alloy C12000.

A wafer of nuclear fuel was encapsulated in a can and cover assembly constructed of alloy C12000 using automatic GTAW. The completed weldment is shown in Fig. 1(a). As shown in detail A in Fig. 1, the can has a machined recess for the wafer and a 0.13 mm (0.005 in.) thick bottom. The can-to-cover joint had raised lips, which eliminated the need for filler metal.

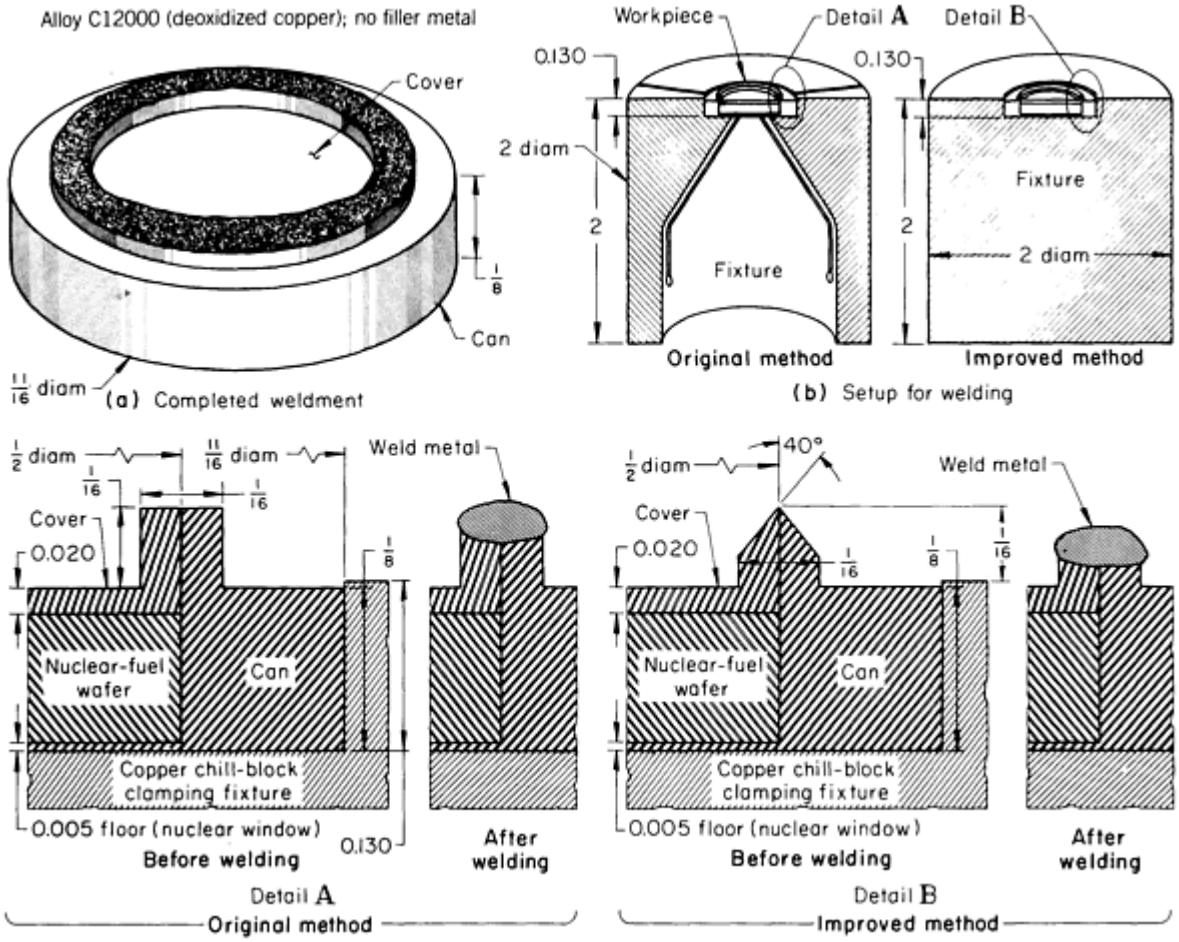

Erro! •

AUTOMATIC GTAW	
JOINT TYPE	**CIRCUMFERENTIAL EDGE**
WELD	**EDGE FLANGE**
POWER SUPPLY	**250 A RECTIFIER**
ELECTRODE	**1.0 MM (0.040 IN.) DIAM EWTH-2**
TORCH	**110 A, AIR-COOLED**[A]
FILLER METAL	**NONE**
FIXTURE	[B]
CURRENT	**16 A (DCEN)**[C]
ARC STARTING	[D]
ARC LENGTH	**0.38 MM (0.015 IN.)**
SHIELDING GAS	**ARGON**[E]
WELDING POSITION	**FLAT**
TRAVEL SPEED	**0.14 M/MIN (5.5 IN./S)**

(A) MODIFIED BY ELIMINATION OF CERAMIC CUP AND BY USE OF BARE CONNECTION CABLE TO AVOID THE PRESENCE OF ORGANIC MATERIAL IN THE CHAMBER.

(B) COPPER CHILL-BLOCK CLAMPING FIXTURE HELD BY A SMALL CHUCK THAT WAS ROTATED BY A VARIABLE-SPEED DRIVE.

(C) WITH CONTINUOUS SUPERIMPOSED HIGH-FREQUENCY CURRENT, FOR ARC STABILITY.

(D) SUPERIMPOSED HIGH-FREQUENCY CURRENT, WHICH WAS CONTINUOUS AS DESCRIBED IN NOTE[C].

FIG. 1 CONDITIONS FOR GTAW OF A NUCLEAR FUEL CONTAINER. DISTORTION IN WELDING WAS MINIMIZED BY INCREASING THE MASS OF THE FIXTURE TO INCREASE HEAT WITHDRAWAL AND BY CHAMFERING JOINT EDGES TO PERMIT REDUCTION OF WELDING CURRENT.

The weld had to provide a hermetic seal without distortion of the assembly, including the thin can bottom that was only 4.8 mm (0.19 in.) from the welded area. A mass spectrometer was used to conduct leak testing of the weldment.

The welds were made in a controlled atmosphere chamber with the can mounted in a rotating copper chill-block clamping fixture underneath a stationary electrode. Welding conditions are given in the table accompanying Fig. 1.

Originally the fixture and joint shown in Fig. 1 and detail A were used. However, at currents high enough for fusion, the welds were porous, the joint leaked, and the can warped unacceptably.

The porosity that caused leaking resulted from the machining operation of the can. The lubricant was wiped under the surface of the metal by the cutting tool, and subsequent cleaning operations failed to remove it. Machining without a lubricant eliminated the difficulty. To minimize distortion, the joint and fixture were improved as follows. The square lips of the joint were chamfered (40°) to a sharp edge, as shown in detail B in Fig. 1. This was done to reduce the heat input required to make the weld. With the chamfered lips, the welding current could be lowered because a smaller mass of metal was being melted at any instant. The mass of the fixture was increased, as shown in Fig. 1(b), to increase heat withdrawal. The redesigned fixture also provided complete support for the thin can bottom against pressure during leak testing.

Before welding, the assembly was retained in the fixture, which was held by a small chuck with all of the 0.13 mm (0.005 in.) thick can bottom resting on the thick copper backing, as shown in detail B of Fig. 1. The fixture assembly was welded in a chamber that was first vacuum-purged and then filled with 100% Ar under slightly positive pressure.

The torch was rigidly mounted on a sliding base with locating stops with which the electrode tip was positioned over the seam and clamped into position. In the argon atmosphere it was not necessary to provide a shielding gas to the electrode tip or to use an electrode cup. The electrode was ground to a sharp point to reduce current flow and arc wander.

During welding, the chuck holding the fixture was rotated by a variable-speed drive. Arc stability was maintained by a superimposed high-frequency current that was continuous. Current upslope was not controlled. Two revolutions at 3.5 rev/min were used, because slight variations in pressure between the cover and the can caused variations in the thickness of the weld bead after the first revolution. The second revolution smoothed out these irregularities and ensured adequate penetration of the base metal along the circumference of the joint. After the second revolution, the current was tapered to 0 A in 5 s.

Distortion was minimized because of the low welding current, the high heat-sink efficiency, and rigid support by the fixture. Control of heat input was also helpful in preventing excessive internal gas expansion after the joint was closed.

After welding, the chamber was evacuated to 1.3×10^{-4} Pa (10^{-6} torr). The interior of the can remained at approximately 0.1 MPa (15 psi). Under the pressure differential, the can, still in the fixture, was inspected for leaks by use of a mass spectrometer. The fixture supported the can bottom against internal pressure.

Oxygen-Free and ETP Coppers. Compared to GMAW or other processes with nonlocalized heat input, GTAW is preferred for the joining of either oxygen-free copper (alloy C10200) or ETP copper (alloy C11000) for thicknesses up to approximately 13 mm (0.5 in.).

Because of the absence of a deoxidizer, gas-tungsten arc welds in alloy C 10200 have slightly lower strength and ductility and are slightly more porous. Gas-tungsten arc welds in alloy C11000 have somewhat lower tensile strength than those in deoxidized coppers, and they are also more porous (see the section "Effect of Cuprous Oxide" in this article). However, the properties of gas-tungsten arc welds in ETP copper are acceptable in many applications involving welded electrical conductors, particularly when tensile strength is relatively unimportant, as in the induction-coil weldment described in the following example.

Example 2: Automatic GTAW of Joints between Alloy C11000 Bar and Tubing.

A solid bar approximately 9 m (30 ft) long of alloy C11000 was gas-tungsten arc welded automatically to a comparable length of tubing of the same alloy. The weldment was used in making water-cooled induction coils for low frequency (60 to 180 Hz) induction heating that required more cross-sectional area for electrical conduction than was provided by the tubular section alone. Figure 2 shows a weldment with a cross section of typical size. The 9 m (30 ft) length was standard for inductor stock. The weldment was bent into coils with an inside diameter of 100 mm (4 in.). The bar stock was located to the inside of the coil. The requirement of the joint was to maintain good electrical conductivity.

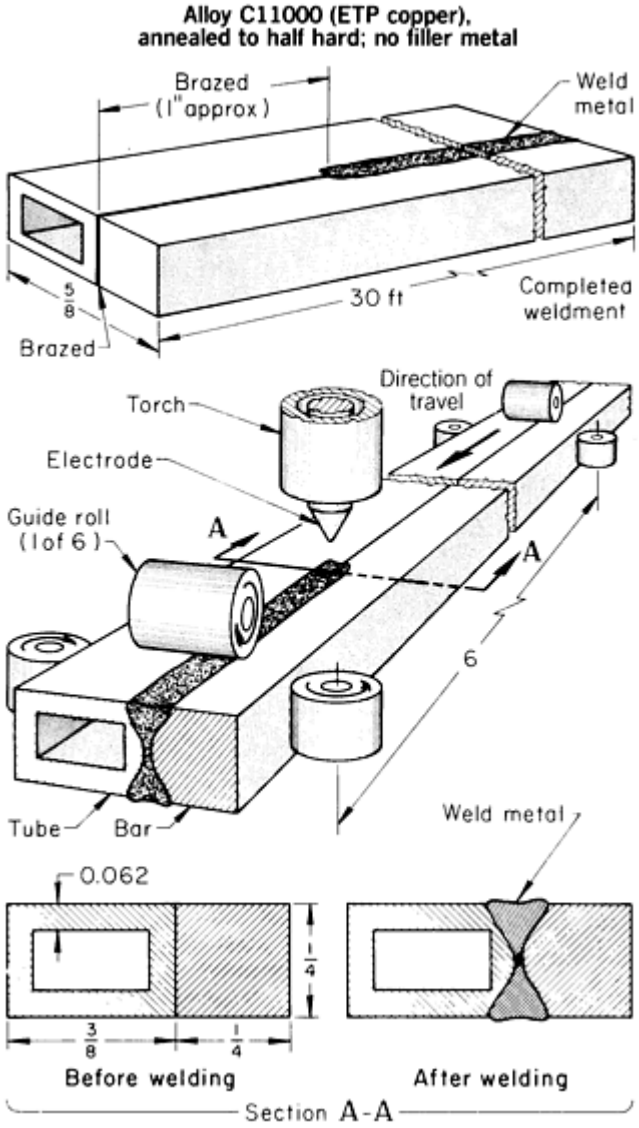

AUTOMATIC GTAW	
JOINT TYPE	**BUTT**
WELD TYPE	**SQUARE GROOVE, ZERO ROOT OPENING**
POWER SUPPLY	**500 A RECTIFIER[A]**
ELECTRODE	**3.2 MM ($\frac{1}{8}$ IN) DIAM EWTH-2[B]**
TORCH	**350 A, WATER-COOLED[C]**
FILLER METAL	**NONE**
FIXTURE	**6 GUIDE ROLLS[D]**
NUMBER OF PASSES	**2 (ONE PER SIDE)**
CURRENT	**220 A (DCEN)**
ARC STARTING	**TORCH START**
ARC LENGTH	**3.2 MM ($\frac{1}{8}$ IN.)**
SHIELDING GAS (HELIUM) FLOW RATE	**9.5 L/MIN (20 FT^3/H)**
WELDING POSITION	**FLAT**
TRAVEL SPEED	**0.33 M/MIN (13 IN./MIN)**

CUP-TO-WORK DISTANCE	**7.9 MM ($\frac{5}{16}$ IN.)**
PREHEAT/POSTHEAT	**NONE**

(A) CONSTANT VOLTAGE.
(B) TAPER GROUND.
(C) FIXED, ON AN ADJUSTABLE MOUNT.
(D) VARIABLE-SPEED DRIVE AND CHAIN USED TO PULL ASSEMBLY THROUGH ROLLS

FIG. 2 CONDITIONS FOR AUTOMATIC GTAW OF ALLOY C11000 TUBING AND BAR INDUCTOR COILS. THE POSITIONS OF THE ASSEMBLY, GUIDE ROLLS, AND TORCH DURING WELDING ARE SHOWN.

Originally, the bar and tubing were torch brazed along the entire length using a silver alloy filler metal. Not only was the filler metal expensive, but brazing was slow, requiring two operators to handle the lengths of tubing and bar. A faster and less costly method was developed by mechanizing a GTAW procedure in which no filler metal was used, thus increasing the production rate.

Welding conditions for the application are given in the table accompanying Fig. 2. The fixture, designed to accommodate the sizes of inductor bar and tubing regularly used, consisted of six guide rolls, as shown in Fig. 2. These guide rolls properly aligned the assembly during welding. A chain and variable-speed drive was used to pull the assembly through the rolls during welding. Positioning of the torch over the joint was achieved by using an adjustable mount.

The first 25 mm (1 in.) of the leading edge of the joint was brazed prior to welding, to prepare the assembly for feeding through the guide rolls. The position of the assembly, guide rolls, and electrode holder during welding is shown in Fig. 2. The relative travel speed of the assembly as pulled through the rolls was 5.5 mm/s (13 in./min). A single pass was used without coolant for each side of the weldment and the ends were trimmed after welding.

The high thermal conductivity of alloy C11000 caused rapid dissipation of the heat energy. However, this difficulty was overcome without preheating by the use of helium as the shielding gas. Helium provided a hotter arc than could be obtained with argon. Thus, it was possible to produce the relatively deep, narrow beads at the stated travel speed. Oxygen from the oxide in alloy C11000 caused some porosity, but this was minimized by the fast freezing promoted by the high travel speed. The required joint properties were obtained in spite of the potential for porosity.

Gas-Metal Arc Welding

As has been previously discussed, oxygen has a detrimental effect when copper is welded. The resulting porosity and reduced weld strength described for GTAW of copper are more pronounced in GMAW. This is due to the greater heat input associated with the process. Gas-metal arc welds of deoxidized coppers compare favorably in density and strength with the welds made using GTAW. However, the greater heat input and lesser localization of heat obtained with GMAW result in greater porosity and lower strength in the HAZ of the welds. This is especially true in coppers that contain insufficient amounts of deoxidizer, particularly ETP copper. Consequently, GMAW has less applicability than GTAW to the welding of ETP copper, oxygen-free copper, or low-phosphorus-deoxidized copper up to approximately 13 mm (0.5 in.) thick.

Nominal Conditions. Table 6 gives the nominal conditions for gas-metal arc butt welding of copper and copper alloys. In welding joints for which the root opening is between 2.5 and 3 mm (0.10 and 0.13 in.), mixtures of helium and argon are used as shielding gas instead of pure argon. This results in lower requirements for preheat, deeper penetration into the weld joint, and higher rates of filler metal deposition.

TABLE 6 NOMINAL CONDITIONS FOR GAS-METAL ARC BUTT WELDING OF COMMERCIAL COPPERS AND COPPER ALLOYS

WELD TYPES FOR BUTT JOINTS, AS DESCRIBED	WORKPLACE THICKNESS		ROOT FACE		ROOT OPENING[B]		ELECTRODE TYPE	ELECTRODE DIAMETER		SHIELDING GAS[C]	GAS FLOW RATE		CURRENT (DCEP), A	VOLTAGE, V	TRAVEL SPEED		PREHEAT TEMPERATURE		NUMBER OF PASSES
	MM	IN.	MM	IN.	MM	IN.		MM	IN.		L/MIN	FT^3/H			M/MIN	IN./MIN	°C	°F	
COMMERCIAL COPPERS																			
SQUARE GROOVE[B]	3.2	1/8	3.2	1/8	0	0	ERCU	1.6	1/16	ARGON	15	30	310	27	0.76	30	NONE USED		**1**
SQUARE GROOVE[C]	3.2	1/8	3.2	1/8	0-1.6	0-1/16	ERCU	1.6	1/16	ARGON[D]	15-16.5	30-35	325-350	28-33	. . .	. . .	NONE USED		**1**
SQUARE GROOVE	6.4	1/4	6.4	1/4	0	0	ERCU	2.4	3/32	ARGON	15	30	460	26	0.50	20	95	200	**2**
	6.4	1/4	6.4	1/4	0	0	ERCU	2.4	3/32	ARGON	15	30	500	27	0.50	20	95	200	**1**
75-90° SINGLE-V-GROOVE[C]	6.4	1/4	3.2	1/8	0-3.2	0-1/8	ERCU	1.6	1/16	ARGON[D]	15-16.5	30-35	400-425	32-36	. . .	. . .	200-260	400-500	**2**
	12.7	1/2	0-3.2	0-1/8	0-3.2	0-1/8	ERCU	1.6	1/16	ARGON[D]	15-16.5	30-35	425-450	35-40	. . .	. . .	425-480	800-900	**4**
90° SINGLE-V-GROOVE[C]	9.5	3/8	4.8	3/16	0	0	ERCU	2.4	3/32	ARGON	15	30	500	27	0.35	14	200	400	**(E)**
	9.5	3/8	4.8	3/16	0	0	ERCU	2.4	3/32	ARGON	15	30	550	27	0.35	14	200	400	**(E)**
	12.7	1/2	6.4	1/4	0	0	ERCU	2.4	3/32	ARGON	15	30	540	27	0.30	12	200	400	**(E)**
	12.7	1/2	6.4	1/4	0	0	ERCU	2.4	3/32	ARGON	15	30	600	27	0.25	10	200	400	**(E)**
ALLOYS C17000 AND C17200 (HIGH-STRENGTH BERYLLIUM COPPERS)[F]																			
90° SINGLE-V-GROOVE	6.4-9.5	1/4-	0.8-1.6	1/32-	. . .	. . .	ALLOY C17000, C17500	1.2	0.045	5AR/HE	21	45	175-200	. . .	. . .	. . .	150-200	300-400	**3-4[G]**

		1/2		1/16														
30° DOUBLE-U-GROOVE[I]	19-38.1	3/4-1 1/2	1.6	1/16	. . .	. . .	ALLOY C17000, C17500	1.6	1/16	AR/HE	28	60	325-350	. . .	. . .	. . .	150-200	300-400	**10-20[H]**
ALLOY C17500 (HIGH-CONDUCTIVITY BERYLLIUM COPPERS)[F]																		
90° SINGLE-V-GROOVE	6.4-9.5	1/4-1/2	0.8	1/32	. . .	. . .	ALLOY C17500	1.2	0.045	AR/HE	15	30	200-240	. . .	. . .	. . .	315	600	**3-4[J]**
	19.0	3/4	0.8	1/32	. . .	. . .	ALLOY C17500	1.2	0.045	AR/HE	15	30	200-240	. . .	. . .	. . .	480	900	**6[J]**
LOW-ZINC BRASSES																		
SQUARE GROOVE[C]	3.2	1/8	3.2	1/8	0	0	ERCUSI-A	1.6	1/16	ARGON	15	30	275-285	25-28	. . .	. . .	NONE USED		**1**
	3.2	1/8	3.2	1/8	0	0	ERCUSI-A	1.6	1/16	HELIUM	16.5	35	275-285	25-28	. . .	. . .	NONE USED		**1**
60° SINGLE-V-GROOVE[C]	9.5	3/8	0	0	3.2	1/8	ERCUSI-A	1.6	1/16	ARGON	15	30	275-285	25-28	. . .	. . .	NONE USED		**2**
	12.7	1/2	0	0	3.2	1/8	ERCUSI-A	1.6	1/16	ARGON	15	30	275-285	25-28	. . .	. . .	NONE USED		**4**
70° SINGLE-V-GROOVE[C]	9.5	3/8	0	0	3.2	1/8	ERCUSN-A	1.6	1/16	HELIUM	16.5	35	275-285	25-28	. . .	. . .	260[K]	500[K]	**2**
	12.7	1/2	0	0	3.2	1/8	ERCUSN-A	1.6	1/16	ARGON	15	30	275-285	25-28	. . .	. . .	260[K]	500[K]	**4**
HIGH-ZINC BRASSES, TIN BRASSES, SPECIAL BRASSES, NICKEL SILVERS																		
SQUARE GROOVE[C]	3.2	1/8	3.2	1/8	0	0	ERCUSN-A	1.6	1/16	ARGON	15	30	275-285	25-28	. . .	. . .	NONE USED		**1**
70° SINGLE-V-GROOVE[C]	9.5	3/8	0	0	3.2	1/8	ERCUSN-A	1.6	1/16	ARGON	15	30	275-285	25-28	. . .	. . .	NONE USED		**2**
	12.7	1/2	0	0	3.2	1/8	ERCNSN-A	1.6	1/16	ARGON	15	30	275-285	25-28	. . .	. . .	NONE USED		**4**
PHOSPHOR BRONZES[L]																		
90° SINGLE-V-	9.5	3/8	0	0	3.2	1/8	ERCUSN-A	1.6	1/16	HELIUM	16.5	35	275-285	25-28	. . .	. . .	95-150	200-300	**3-4[M]**

V-GROOVE(C)	12.7	1/2	0	0	3.2	1/8	ERCUSN-A	1.6	1/16	HELIUM	16.5	35	275-285	25-28	. . .	. . .	175-200	350-400	**5-6(M)**
ALUMINUM BRONZES(N)																			
SQUARE GROOVE(O)	3.2	1/8	3.2	1/8	0	0	ERCUAL-A2	1.6	1/16	ARGON	15	30	280-290	27-30	. . .	. . .	NONE USED		**1**
60-70° SINGLE V-GROOVE(C)	9.5	3/8	0	0	3.2	1/8	ERCUAL-A2	1.6	1/16	ARGON	15	30	280-290	27-30	. . .	. . .	NONE USED		**2**
	12.7	1/2	0	0	3.2	1/8	ERCUAL-A2	1.6	1/16	ARGON	15	30	280-290	27-30	. . .	. . .	NONE USED		**3**
SILICON BRONZES(P)																			
SQUARE GROOVE(Q)	3.2	1/8	3.2	1/8	0	0	ERCUSI-A	1.6	1/16	ARGON	15	30	260-270	27-30	. . .	. . .	NONE USED		**1**
70° SINGLE-V-GROOVE(C)	9.5	3/8	0	0	3.2	1/8	ERCUSI-A	1.6	1/16	ARGON	15	30	260-270	27-30	. . .	. . .	NONE USED		**2**
	12.7	1/2	0	0	3.2	1/8	ERCUSI-A	1.6	1/16	ARGON	15	30	260-270	27-30	. . .	. . .	NONE USED		**3**
COPPER NICKELS																			
SQUARE GROOVE(C)	3.2	1/8	3.2	1/8	0	0	ERCUNI	16	1/16	ARGON	15	30	280	27-30	. . .	. . .	NONE USED		**1**
60° SINGLE-V-GROOVE(C)	9.5	3/8	0	0	3.2	1/8	ERCUNI	1.6	1/16	ARGON	15	30	280	27-30	. . .	. . .	NONE USED		**2**
	12.7	1/2	**0**	**0**	**3.2**	1/8	**ERCUNI**	**16**	1/16	**ARGON**	**15**	**30**	**280**	**27-30**	**. . .**	**. . .**	**NONE USED**		**4**

Note: The data in this table are intended to serve as starting points for the establishment of optimum joint design and conditions for welding of parts on which previous experience is lacking. They are subject to adjustments necessary to meet the special requirements of individual applications.

(A) THICKNESSES UP TO 38.1 MM (1 1/2 IN.) ARE SOMETIMES WELDED BY USE OF SLIGHTLY HIGHER CURRENT AND LOWER TRAVEL SPEED THAN SHOWN FOR A THICKNESS OF 12.7 MM (1/2 IN.).

(B) COPPER BACKING.

(C) GROOVED COPPER BACKING.

(D) OR 75AR-25HE.

(E) SPECIAL WELDING SEQUENCE IS USED (SEE TEXT).

(F) SEE TABLE 1 FOR COMPOSITIONS.

(G) THE FINAL PASS IS MADE ON THE ROOT SIDE AFTER BACK CHIPPING. WIRE BRUSH AFTER EACH PASS.

(H) SEVERAL PASSES ARE MADE ON THE FACE SIDE, THEN SEVERAL ON THE BACK SIDE, UNTIL THE WELD IS COMPLETED. BACK CHIP THE ROOT PASS BEFORE MAKING THE FIRST PASS ON THE BACK SIDE. WIRE BRUSH AFTER EACH PASS.

(I) SIMILAR TO THE DOUBLE V-GROOVE WELD, BUT WITH A GROOVE RADIUS OF 9.5 MM ($\frac{3}{8}$ IN.).

(J) THE FINAL PASS IS MADE ON THE ROOT SIDE AFTER BACK CHIPPING.

(K) SHOULD NOT BE OVERHEATED; AS LITTLE PREHEAT AS POSSIBLE SHOULD BE USED.

(L) WELDING CONDITIONS BASED ON ALLOYS C51000, C52100, AND C52400; CURRENT IS INCREASED OR SPEED IS DECREASED FOR ALLOY C50500.

(M) HOT PEENING BETWEEN PASSES IS RECOMMENDED FOR MAXIMUM STRENGTH.

(N) SLIGHT PREHEAT MAY BE NEEDED ON HEAVY SECTIONS; INTERPASS TEMPERATURE SHOULD NOT EXCEED 315 °C (600 °F).

(O) WITH ALUMINUM BRONZE BACKING.

(P) NO PREHEAT IS USED ON ANY THICKNESS; INTERPASS TEMPERATURE SHOULD NOT EXCEED 95 °C (200 °F).

(Q) WITH SILICON BRONZE BACKING

Filler Metals (Electrode Wires). The recommended ERCu electrode contains phosphorus, tin, silicon, and manganese as deoxidizers to minimize porosity. The electrode produces sound, trouble-free welds that also provide good color match to the copper base metal and have good electrical conductivity. The ERCu electrode was used as a basis for the conditions listed in Table 6.

Copper electrodes of higher purity than ERCu are seldom used in GMAW of copper, because these usually result in welds that are porous, due to the absence of deoxidizers. Most of the electrodes listed in Table 3 can be used. Any of the electrodes other than ERCu will produce dense, strong welds, but they will result in poor color match and unacceptable electrical conductivities. Filler metals should be deposited as stringer beads or narrow weave beads using the spray-transfer mode; weaving of the electrodes may result in oxidation at the edges of the weld.

Welding Technique. The forehand welding technique should be used in the flat position. For vertical-position welding, an upward progression should be utilized. Gas-metal arc welding of copper is not recommended for the overhead position due to poor bead contour. The preferred process for overhead-position welding is GTAW.

Joint Design. A square-groove joint is used for the single-pass welding of coppers up to 3 mm (0.13 in.) thick. A backing bar is used for zero root openings, and a grooved copper backing bar is used for root openings of 1.6 mm (0.06 in.) maximum. The square-groove joint can also be used for one-pass-per-side welding of coppers up to 6 mm (0.25 in.) thick.

Single-V-groove joints are used when welding coppers of sections above 6 mm (0.25 in.). The filler metal is deposited on one side using three or more passes, and the root pass is back gouged to sound metal before the last pass is applied to the back of the joint. In some applications, the root pass is applied using GTAW and subsequent passes are completed via GMAW for rapid buildup.

If heavy sections (thicker than 13 mm, or 0.5 in.) are to be welded, these should be prepared with a double-V- or a double-U-groove joint. Welding is performed by applying alternating passes to opposite sides of the joint, if readily accessible, to minimize distortion. In a small, closed vessel, limited access may prevent the use of this technique, and in addition, heat buildup often prevents welding on both sides.

Preheating. Because of the high thermal conductivity of copper, sections thicker than 6 mm (0.25 in.) are usually preheated. As shown in Table 6, single-V-groove joints in 6 mm (0.25 in.) thick copper, welded using 1.6 mm ($\frac{1}{16}$ in.) diameter filler metal, are also preheated.

Deoxidized Coppers. Heavy-wall copper pressure vessels (up to about 40 mm, or 1.5 in., wall thickness), which are usually made from phosphorus-deoxidized copper, are frequently gas-metal arc welded. Residual phosphorus helps obtain maximum weld strength while minimizing porosity. In order to meet the high heat demand in welding these heavy-walled vessels, welding currents and preheat temperatures may be higher than those shown in Table 6.

Similar operating conditions are employed in welding crucibles for arc melting of refractory metals in controlled atmospheres. These crucibles are typically heavy-wall deoxidized copper cylinders with wall thicknesses up to 32 mm (1.25 in.), diameters of 0.3 to 1.2 m (1 to 4 ft), and lengths of 1 to 7.5 m (3 to 25 ft). Formed and welded copper plate is used, because seamless tubes of this size are not available. Longitudinal seams are welded, and flanges are welded to each end of the cylinders by GMAW. Such cylinders are preheated to 650 °C (1200 °F) before welding. Welding is done automatically, to avoid exposing operators to such heavy sections at elevated temperatures.

Oxygen-Free and ETP Coppers. The GMAW process is also used for welding oxygen-free copper in the production of the crucibles previously described. These crucibles are also used for arc melting of refractory metals. However, the weld properties are inferior to those produced with deoxidized copper. Because oxygen-free copper contains no residual deoxidizer, heating and welding cycles must be kept as short as possible, and gas shielding must be completely effective to avoid excessive porosity. Although the strength and soundness of welds in oxygen-bearing coppers, such as ETP copper, are substantially less than in oxygen-free copper, the reduced properties are seldom important for welds in electrical conductors. Busbars made of ETP copper are frequently joined using the GMAW process. The use of filler metals such as ERCu or another of the standard filler metals listed in Table 3 significantly lowers the electrical conductivity of the joint. In order to minimize this adverse effect, large root faces are used to increase the contact area at the joint line. For improved electrical conductivity, a filler metal with chemical composition approximately 0.75% Sn, 0.25% Si, and 0.20% Mn is sometimes used for welding ETP copper busbars.

Shielded Metal Arc Welding

Problems with porosity and low weld strength, due to oxygen content of the base metal and oxygen absorption during welding, are more severe in joining coppers by SMAW than by the gas-shielded processes. The resulting lower mechanical properties greatly limit the usefulness of weldments produced using SMAW. Additionally, electrical conductivity suffers greatly.

Welding of Copper Alloys

Revised by M. Ned Rogers, Batesville Casket Company

Welding of High-Strength Beryllium Coppers

The wrought high-strength beryllium coppers include alloys C17000 and C17200, which contain nominally 1.7 and 1.9% Be, respectively, and up to 0.25% Co. A free-machining grade version of C17200 is available that is modified with a small lead addition, but this grade is not recommended for welding. The high-strength beryllium coppers are joined by GTAW and GMAW. Additional information on the properties and application of these materials can be found in Volume 2 of the *ASM Handbook.*

Gas-Tungsten Arc Welding

Copper alloys C17000 and C17200, high-strength beryllium coppers, are readily welded using GTAW. These alloys are more easily welded than the high-conductivity beryllium coppers, which exhibit higher melting temperature and less fluidity. Gas-tungsten arc welding can be used for section thicknesses in excess of 13 mm (0.5 in.) when the use of the preferred GMAW process is not practical.

Nominal Conditions. Table 7 lists the suggested starting points for nominal conditions for GTAW of high-strength beryllium coppers. The shielding gas is usually a mixture of argon and helium to obtain a hot arc, smooth and spatter-free welds, and maximum electrode life.

TABLE 7 NOMINAL CONDITIONS FOR GTAW OF BERYLLIUM COPPERS

For butt joints having zero root opening; welding with a zirconiated tungsten electrode, filler metal of the same composition as the base metal, argon-helium gas at 12 L/min (25 ft^3/h)

WORKPIECE THICKNESS		**BUTT-JOINT GROOVE**	**ELECTRODE DIAMETER**		**CURRENT[A], A**	**TRAVEL SPEED**		**PREHEAT TEMPERATURE**		NUMBER OF PASSES
MM	**IN.**		**MM**	**IN.**		**M/MIN**	**IN./MIN**	**°C**	**°F**	
ALLOY C17500 (HIGH-CONDUCTIVITY BERYLLIUM COPPER)[B]										
0-2.4	0-3/32	SQUARE	2.4	3/32	150	0.13-0.25	5-10	NONE USED		**1**
2.4-3.2	3/32-1/8	90° SINGLE-V[C]	4.8	3/16	250	0.13-0.25	5-10	NONE USED		**1-2**
6.4	1/4	90° SINGLE-V[C]	4.8	3/16	250	0.13-0.25	5-10	425	800	**4-5**
ALLOYS C17000 AND C172000 (HIGH-STRENGTH BERYLLIUM COPPERS[C]										
0-2.4	0-3/32	SQUARE	2.4	3/32	150	0.13-0.25	5-10	NONE USED		**1**
2.4-3.2	3/32-1/8	90° SINGLE-V[C]	2.4	3/32	180	0.13-0.25	5-10	NONE USED		**1**
6.4-12.7[D]	1/4-1/2 [D]	90° SINGLE-V[C]	4.8	3/16	250	0.13-0.25	5-10	150	300	**3-4**
12.7[D]	1/2 **[D]**	**90° SINGLE-V[C]**	**4.8**	3/16	**250**	**0.13-0.25**	**5-10**	**200**	**400**	**5-8**

Note: The data in this table are intended to serve as starting points for the establishment of optimum joint design and conditions for welding of parts on which previous experience is lacking. They are subject to adjustments necessary to meet the special requirements of individual applications.

(A) HIGH-FREQUENCY-STABILIZED ALTERNATING CURRENT IS PREFERRED; DCEN, WITH A THORIATED TUNGSTEN ELECTRODE, IS SUITABLE UNDER SOME CONDITIONS (SEE TEXT).

(B) FOR COMPOSITION, SEE TABLE 1.

(C) MAXIMUM ROOT FACE IS 1.6 MM (1/16 IN.).

(D) GAS-TUNGSTEN ARC WELDING IS USED ON THESE THICKNESSES ONLY WHEN GMAW CANNOT BE USED.

Electrodes. The preferred electrode when using alternating current is zirconiated tungsten (EWZr); noncritical applications can use the more economical pure tungsten (EWP). For DCEN, the thoriated electrodes (such as EWTh-2) are preferred.

Filler Metals. The addition of filler metals is almost always required to provide proper fill for the joint or to provide joint reinforcement in a V-groove weld. This is due to the high concern for strength when welding these alloys. Rods or strips of the same composition as the base metal are generally used as filler metals; the standard filler metals of other copper alloys are weaker and offer no advantages.

Joint Design. As Table 7 indicates, the typical joint designs for GTAW of high-strength beryllium copper are square-groove or 90° single-V-groove butt joints with a 1.5 mm (0.06 in.) maximum root face and zero root opening. The 90° single-V-groove butt welds can be used for thicknesses in excess of 13 mm (0.5 in.).

Preheating and Postweld Heat Treatment. As shown in Table 7, preheat temperatures of 150 to 200 °C (300 to 400 °F) are recommended for GTAW of section thicknesses greater than 3 mm (0.13 in.). Maximum weld strength is obtained by solution annealing and aging after welding. Aging treatments are 3 h at 315 °C (600 °F) for alloy C17000 and 3 h at 345 °C (650 °F) for alloy C17200. This postweld treatment does not consistently provide the full strength of solution-annealed and aged base metal, even for welds made under optimum conditions. Higher strength can be obtained by cold working the annealed metal to a higher temper and modifying the aging treatment.

For some applications, the intermediate weld metal strength obtained by aging after welding, without a solution anneal, is adequate. Omission of solution annealing avoids the expense and distortion associated with this high-temperature operation. Following are three applications of GTAW of high-strength beryllium coppers. Welding conditions for GTAW for three applications are shown in Table 8.

TABLE 8 THREE APPLICATIONS OF GTAW OF HIGH-STRENGTH BERYLLIUM COPPERS

	PRESSURE VESSEL (EXAMPLE 3)	**GENERATOR LINER (EXAMPLE 4)**	COVER TO HOUSING (EXAMPLE 5)
ALLOY	C17000	C17000 TO C17200	**CAST BE-CU (1.7% BE) TO C17000**
SIZE OF WORKPIECE	483 MM DIAM BY 1016 MM (19 IN. DIAM BY 40 IN.)	495 MM DIAM BY 1219 MM (19.5 IN. DIAM BY 48 IN.)	**295 MM (11.6 IN.)**
THICKNESS OF WORK METAL	19 MM ($\frac{3}{4}$ IN.)	(A)	**1.6 MM ($\frac{1}{16}$ IN.)**
FILLER METAL	1.6 MM ($\frac{1}{16}$ IN.) DIAM ALLOY C17200	NONE	**NONE**
CURRENT, A	100-150 DCEN	122, AC(B)	**275, AC(B)**
SHIELDING GAS	ARGON AND HELIUM	ARGON AND HELIUM	**ARGON AND HELIUM**
GAS FLOW RATE	12 L/MIN (25 FT^3/H)	12 L/MIN (25 FT^3/H)	**9.5 L/MIN (20 FT^3/H)**
TRAVEL SPEED	0.50 M/MIN (20 IN./MIN)	0.25 M/MIN (10 IN./MIN)	**0.30 M/MIN (12 IN./MIN)**
NUMBER OF PASSES	10	1	**1**
POSTWELD HEAT	345 °C (650 °F), 3 H	NONE	**NONE**
TESTING METHOD	**X-RAY(C)**	. . .	(D)

(A) REINFORCING RINGS, 40 BY 32 MM ($1\frac{1}{2}$ BY $1\frac{1}{4}$ IN.) WELDED TO 6 BY 6 MM ($\frac{1}{4} \times \frac{1}{4}$ IN.) LONGITUDINAL RIBS.

(B) HIGH-FREQUENCY-STABILIZED.

(C) WELD WAS TESTED BY DYE-PENETRATION TECHNIQUES; LEAK TESTING WAS BY HELIUM MASS SPECTROMETRY AND X-RAY RADIOGRAPHY.

(D) WELD DEPTH OF 1.6 MM ($\frac{1}{16}$ IN.) MINIMUM WAS DETERMINED ULTRASONICALLY; WELD

WAS LEAK-TESTED BY HELIUM MASS SPECTROMETRY AT 76 MPA (11 KSI).

Example 3: Gas-Tungsten Arc Welding of High-Strength Beryllium Coppers in an Alloy C17000 Pressure Vessel.

The pressure vessel was used to scavenge propane from a freon bubble chamber. Use of GTAW was dictated because the vessel could not be solution-annealed after welding because of danger of warpage. The service conditions for this vessel included pressure of 41 MPa (6 ksi) and rapid thermal cycling. This application is shown in Table 8.

Example 4: Gas-Tungsten Arc Welding of High-Strength Beryllium Copper in a Cylindrical Generator Liner.

A cylindrical generator liner was constructed using alloy C17000 and alloy C17200. It was back-extruded from a cast billet. Longitudinal rings about 6 by 6 mm (0.25 by 0.25 in.) were machined on the outer surface. Nine reinforcing rings were rolled from extruded alloy C17000, equally spaced along the longitudinal rings, and welded to them. The reinforcing rings measured 40 mm (1.5 in.) wide and 32 mm (1.25 in.) high. The liner, used in a magneto-hydrodynamic electrical power generator, contained plasma at 1650 to 1925 °C (3000 to 3500 °F). This application is shown in Table 8.

Example 5: Gas-Tungsten Arc Welding of High-Strength Beryllium Copper in a Cover-to-Housing Weldment.

For ocean-cable use, a cast beryllium copper cover made from alloy C17000 was welded to a housing of the same alloy. The cast cover was welded to an extruded housing to produce a joint that was watertight at 83 MPa (12 ksi). This application is shown in Table 8.

Gas-Metal Arc Welding

Alloys C17000 and C17200 are more easily welded using the GMAW process than is high-conductivity alloy C17500. These alloys have lower melting temperatures, greater fluidity, and 50% lower thermal conductivities. The GMAW process is generally preferred for the welding of precipitation-hardened, high-strength beryllium coppers in thicknesses of 6 mm (0.25 in.) and greater. This process is also preferred for thicknesses from 6 mm (0.25 in.) down to 2.5 mm (0.1 in.) if heat treatment is to be done after welding.

Nominal Conditions. Table 6 gives the nominal welding conditions for GMAW of high-strength beryllium coppers. The shielding gas used for GMAW is typically a mixture of argon and helium. Direct current electrode positive is used to prevent the buildup of oxides during welding. The filler metal is ordinarily of the same composition as the base metal, for joints requiring maximum strength. However, electrode wires ERCuSi-A and ERCuA1-A2 can be used when joint strength is less critical. Preheating, postweld heat treating, and joint designs are generally the same as discussed in the section on GTAW of high-strength beryllium coppers.

Welding of Copper Alloys

Revised by M. Ned Rogers, Batesville Casket Company

Welding of High-Conductivity Beryllium Copper

The traditional wrought high-conductivity alloys (C17500 and C17510) contain 0.2 to 0.7% Be and nominal 2.5% Co (or 2% Ni). The leanest and most recently developed high-conductivity alloy is C17410, which contains somewhat less than 0.4% Be and 0.6% Co. This section will describe the GTAW and GMAW of alloy C17500, the most frequently welded high-conductivity beryllium copper alloy. Additional information on the properties and applications of these materials can be found in Volume 2 of the *ASM Handbook.*

Gas-Tungsten Arc Welding

Gas-tungsten arc welding of precipitation-hardened copper alloy C17500 (high-conductivity beryllium copper) is performed for thicknesses up to 6 mm (0.25 in.). This process produces a narrow HAZ, which is desirable. Ordinarily, the maximum thickness that can be gas-tungsten arc welded without substantial decrease in strength is about 13 mm (0.5 in.). However, thicker sections have been gas-tungsten arc welded. For weldments that require postweld heat treatments, GTAW is generally used only for thicknesses up to 2.5 mm (0.1 in.), with GMAW being used for thicker sections.

High-conductivity beryllium copper is more difficult to weld than the high-strength beryllium coppers because of its higher thermal conductivity, which is about twice that of the high-strength beryllium coppers. A difficulty common to the beryllium coppers is the formation of surface oxides, both beryllium oxide and cuprous oxide. The beryllium oxide is a tenacious oxide that inhibits wetting and fusion during welding. Cleanliness of the joint faces and surrounding surfaces before and during welding is necessary to ensure weld soundness.

Nominal Conditions. Table 7 gives the nominal starting conditions for GTAW of high-conductivity beryllium copper alloy C17500. Shielding gas, type of current, and electrode type are the same as for C17000 and C17200 high-strength alloys.

Type of Current. Variation in arc length or welding speed during GTAW can result in the formation of tenacious films on beryllium coppers. For this reason, high-frequency stabilized alternating current is preferred in automatic welding and must be used in manual welding. The alternating current continually breaks up the oxide coating, and high-frequency adds to the cleaning action during welding. Direct current electrode negative can be employed in the automatic welding of beryllium coppers. The advantage is found with the high heat input to the work and the deep penetration of this polarity. Close control of the arc length and welding speed must be maintained to minimize oxide formation.

High-conductivity beryllium coppers are more susceptible to porosity and cracking than welds made in high-strength beryllium copper. This is particularly true in multi-pass welding. However, successfully welded joints exhibit improved mechanical properties in HAZ compared with similar joints in high-strength beryllium coppers.

Filler Metals. Material with the same composition as the base alloy (C17500) is generally used, since high electrical conductivity is desired in the welds. If maximum electrical conductivity through the weld joint is not a requirement, silicon bronze filler metal is satisfactory. Aluminum bronze filler metals can be used but are less satisfactory than silicon bronze.

Joint Design. As Table 7 indicates, the usual joint designs for GTAW of high-conductivity beryllium copper are square-groove or 90° single-V-groove butt joints with a 1.6 mm (0.06 in.) root face and zero root opening. All joints should be backed with grooved copper or graphite backing strips or rings.

Preheating. Preheating is not ordinarily needed for welding alloy C17500 up to about 3 mm (0.13 in.) thick. However, thicker stock that may require multipass welds is usually preheated to approximately 425 °C (800 °F).

Gas-Metal Arc Welding

Gas-metal arc welding is preferred to GTAW for joining alloy C17500 with section thicknesses greater than 2.5 mm (0.1 in.) when the weldment is to be heat treated to obtain maximum weld strength. It is also the process of choice for joining thicknesses in excess of 6 mm (0.25 in.) if the welding is done on precipitation-hardened material. Gas-metal arc welding can be used for thicknesses up to 19 mm (0.75 in.).

As pointed out in the discussion of GTAW of alloy C17500, the three important factors in arc welding this alloy are: (1) high thermal and electrical conductivities; (2) oxide-forming characteristics; and (3) responsiveness to heat treatment. Although compromise is necessary between weld strength and conductivity, high thermal conductivities are typically the prime objectives in welding assemblies using this alloy.

Nominal Conditions. Table 6 lists the typical conditions for GMAW of high-conductivity beryllium coppers. Typically, DCEP is used. Argon is a suitable shielding gas; however, greater heat input, which is usually required when welding this alloy, can be obtained through the use of an argon-helium gas mix.

Filler Metals. As with GTAW for high-conductivity beryllium coppers, GMAW utilizes a filler metal of similar composition to the base metal. If reduced conductivity is an acceptable result of the weld metal, wires made of high-strength beryllium copper alloys C17000 and C17200 can be used for greater welding ease. Because of the precipitation-

hardening characteristics of beryllium coppers, the joint strength is always somewhat lower than that of the base material and depends on the initial condition of the base metal, the welding conditions, and the filler-metal selection.

Other electrodes, such as ERCuSi-A or ERCuAl-A2, can be used for GMAW of alloy C17500. Because of their lack of beryllium content, however, these alloys do not develop the high strength attained when beryllium copper filler metal is used.

Preheating and Postweld Aging. Section thicknesses of alloy C17500 greater than 3 mm (0.13 in.) are usually preheated at 315 to 480 °C (600 to 900 °F), depending on section thickness. When a beryllium copper filler metal is used, strength can be increased by aging after welding. The aging heat treatment for alloy C17500 is 480 °C (900 °F) for 3 h.

Properties of Weldments. Based on its high thermal conductivity and moderate to high strength, alloy C17500 is used for welded water-cooled assemblies such as tuyeres for blast furnaces, attrition mills for grinding beryllium chips to powder, and molds for the continuous casting of steel. While some strength is lost in the weld metal and the adjoining HAZ when alloy C17500 is welded, the magnitude of this decrease is affected by the condition and thicknesses of the base metal, and by joint design, welding process, and parameters.

Welding of Cadmium and Chromium Coppers

Typically, the welding procedures for GTAW of coppers are a satisfactory basis for determining initial welding parameters for cadmium and chromium coppers. These alloys have lower thermal and electrical conductivities than copper, and they can be welded with lower preheats and heat inputs than those required for copper. Section thickness limitations are the same as for GTAW of coppers. In addition to GTAW, GMAW can be used for the joining of cadmium and chromium coppers. The nominal conditions previously stated for GMAW welding of coppers are satisfactory for the welding of cadmium and chromium coppers.

The filler metal types, welding currents, polarities, and shielding gas mixtures for either GTAW or GMAW of coppers are suitable for the joining of cadmium and chromium coppers. These alloys should be welded using the standard joint geometries listed for GTAW and GMAW of coppers.

Welding of Copper Alloys

Revised by M. Ned Rogers, Batesville Casket Company

Welding of Copper-Zinc Alloys

Brasses are basically copper-zinc alloys and are the most widely used group of copper alloys. As shown in Table 1, brasses can be categorized as low-zinc brasses (5 to 20% Zn), high-zinc brasses (30 to 40% Zn), tin brasses, and special brasses. Copper-zinc alloys are joined by GTAW, GMAW, and SMAW. Additional information on the properties and applications of copper-zinc (brass) alloys can be found in Volume 2 of the *ASM Handbook.*

Gas-Tungsten Arc Welding

Table 1 lists the copper-zinc (brass) alloys and shows their relative weldability. The low-zinc brasses are shown to have good weldability using GTAW. High-zinc brasses, tin brasses, special brasses, and nickel silvers have only fair weldability. This is because of the high zinc content or the moderate zinc content in combination with other elements, such as oxide-forming aluminum or nickel.

Gas-tungsten arc welding is sometimes used for the welding of copper-zinc alloys with 20% Zn or less. Alloys containing up to 1% Pb can also be welded with this process. Gas-tungsten arc welding is used because of its ability to weld rapidly with a highly localized heat input. It should be noted that most leaded copper alloys are generally not recommended for arc welding.

Section thicknesses of copper-zinc alloys ordinarily welded using GTAW are limited to about 9.5 mm (0.4 in.). However, thick sections of cast alloys such as manganese bronze are sometimes repair welded in localized areas. Preheating is not normally required for the welding of these alloys.

Shielding Gas. Selection of the proper shielding gas for GTAW of copper-zinc alloys is influenced by the heat required to fuse the metals together. This requirement is directly related to the thermal conductivity of the base metal. Normally argon is used for GTAW of the less conductive materials. Helium or helium mixes are the preferred shielding gases for alloys having higher thermal conductivities. However, the use of helium and helium-rich gas mixes can reduce the fumes produced when welding the less conductive alloys, such as high-zinc brasses, tin brasses, special brasses, and nickel silvers.

Filler Metals. Filler metals used in GTAW of copper-zinc alloys should not contain zinc. The addition of filler metal is recommended when welding sections greater than 1.6 mm (0.06 in.) thick. The arc is concentrated on the filler metal, thus reducing the zinc loss and fuming of the base material. For the welding of low-zinc brass, ERCuSn-A is recommended; ERCuSi-A and ERCuAl-2 are recommended for high-zinc alloys.

The silicon found in ERCuSi-A helps to decrease the zinc fumes. For this reason and to provide reinforcement, ERCuSi-A is sometimes used, with alternating current, on copper-zinc alloys 1.3 mm (0.05 in.) or less. Thinner sections of high-zinc alloys are sometimes gas-tungsten arc welded using ERCuAl-A2. The addition of this filler metal produces sound welds but does not decrease zinc vaporization.

Thin brass sheets less than 1.6 mm (0.06 in.) thick can be welded without the addition of filler metal. Zinc fuming can be limited through the use of high electrode travel speed, which generates short weld pool arc times. Tube sheet joints can be made with brass members, using the same kind of joint preparation, if high electrode speed is maintained.

Gas-Metal Arc Welding

Unleaded brasses can be welded using GMAW. These brasses include both the low-zinc alloys (red brasses) and the high-zinc alloys (including yellow brasses, tin brasses, and special brasses). Copper-zinc alloys are not used as filler metals for GMAW due to the violent fuming and loss of zinc that accompanies arc welding of these zinc-bearing alloys.

Low-Zinc Brasses. Table 6 lists nominal conditions for butt welding of low-zinc brasses, using GMAW. These alloys include up to 20% Zn. Direct current electrode positive is always used.

Silicon bronze (ERCuSi-A) wire provides easy welding, since it has good fluidity at low welding currents. A 60° single-V-groove is used with this filler metal. When ERCuSn-A electrode wire is used, its sluggish flow characteristics make a 70° V-groove advisable for heavier sections, as shown in Table 6. ERCuSn-A is primarily used for a better color match on low-zinc copper alloys. The wider groove provided with the 70° V-groove joint allows more room for manipulation of the molten weld pool. Except for color, weld metal properties are comparable when using either of these two types of electrodes. A preheat in the range of 95 to 315 °C (200 to 600 °F) is sometimes required for low-zinc brasses due to their relatively high thermal conductivities.

High-Zinc Copper Alloys. Nonleaded copper alloys that have zinc contents from 20 to 40% or more can be gas-metal arc welded. However, the weldability is less than with nonleaded low-zinc brasses. The evolution of zinc fumes is more severe, and the welds experience greater porosity and lower strength than with low-zinc brasses. Both wrought and cast alloys can be joined by GMAW. Massive sections, such as for manganese bronze ship propellers, are regularly repair welded using this process.

The nominal conditions for gas-metal arc butt welding of high-zinc copper alloys (yellow brasses, tin brasses, special brasses, and nickel silvers) are given in Table 6. Welding parameters and variables are generally the same when using either ERCuAl-A2 or ERCuSn-A filler metals. The difference between the two filler metals is a higher weld-metal strength with ERCuAl-A2 and better color match with ERCuSn-A. Preheating is seldom necessary since these alloys have

relatively low thermal conductivities. However, preheating does help to limit zinc fuming in some applications, because it permits the use of lower welding amperages.

Shielded Metal Arc Welding

Brasses can be welded using SMAW. A variety of covered electrodes can be used, including phosphor bronze, silicon bronze, or aluminum bronze (ECuSi, ECuSn-A, ECuSn-C, ECuAl-A2, ECuAl-B). Relatively large welding grooves are required for good joint penetration and to avoid the entrapment of slag. Welding is typically done using a backing strip of copper or brass.

Phosphor bronze electrodes, such as ECu-Sn-A and ECuSn-C, have been used for SMAW of low-zinc brasses. Preheating of the base metal from 200 to 260 °C (400 to 500 °F) is required. Application of filler metal should be in narrow, shallow stringer beads.

The high-zinc copper alloys can be welded with aluminum bronze (ECuAl-A2) electrodes. Preheat and interpass temperatures are 260 to 370 °C (500 to 700 °F). The arc is held directly on the molten weld pool rather than toward the base metal, and it is advanced slowly to minimize zinc volatilization and fuming.

Welding of Copper Alloys

Revised by M. Ned Rogers, Batesville Casket Company

Welding of Phosphor Bronzes

The phosphor bronzes (C50100-C52400) contain additions of tin (up to 10%) and phosphorus (0.2%), which produce good resistance to flowing seawater and to most nonoxidizing acids (except hydrochloric acid). Phosphor bronzes are joined by GTAW, GMAW, and SMAW. Additional information on the properties and applications of phosphor bronzes can be found in Volume 2 of the *ASM Handbook.*

Gas-Tungsten Arc Welding

Sheet and other wrought forms of phosphor bronze can be gas-tungsten arc welded up to approximately 13 mm (0.5 in.). The process can also be used to join or repair phosphor bronze castings. Copper-tin alloys solidify with large, weak, dendritic grain structures that are susceptible to cracking. Hot peening each layer of multi-pass welds reduces cracking and stresses and therefore the likelihood of weld metal cracking.

Nominal Conditions. The use of GTAW for joining nonleaded phosphor bronzes is described in Table 9. Square-groove butt joints are employed, and the current used is DCEN or a stabilized alternating current arc.

TABLE 9 NOMINAL CONDITIONS FOR GTAW OF SQUARE-GROOVE BUTT JOINTS IN PHOSPHOR BRONZES

WORKPIECE THICKNESS		ROOT OPENING		ELECTRODE (EWTH-2) DIAMETER		WELDING ROD DIAMETER[(A)]		SHIELDING GAS	GAS FLOW RATE		CURRENT (DCEN), A	TRAVEL SPEED		PREHEAT TEMPERATURE		NUMBER OF PASSES
MM	IN.	MM	IN.	MM	IN.	MM	IN.		L/MIN	FT^3/H		M/MIN	IN./MIN	°C	°F	
1.6	1/16	0	0	3.2	1/8	NONE USED		ARGON	15	30	90-150	1.78	70	NONE USED		1
3.2	1/8	1.6	1/16	3.2	1/8	3.2	1/8	ARGON	15	30	100-220	1.27	50	NONE USED		1

Notes: (1) The data in this table are intended to serve as starting points for the establishment of optimum joint design and conditions for welding of parts on which previous experience is lacking. They are subject to adjustments necessary to meet the special requirements of individual applications. (2) Higher welding current or lower welding travel speed is used in welding alloy C50500.

(A) ERCUSN-A, OR ROD OF COMPOSITION CLOSE TO THAT OF THE BASE METAL

The nominal conditions shown in Table 9 are based primarily on the three phosphor bronzes given in Table 1, which have low thermal conductivities. These include alloys C51000, C52100, and C52400. When welding alloy C50500, higher welding currents or slower welding travel speeds are required. This alloy, commonly known as phosphor bronze-1.25% E, contains approximately 98.7% Cu and has 3 to 4 times the thermal conductivity of the other alloys in this grouping.

Shielding Gas. The use of argon as a shielding gas is most common, since argon restricts the size of the HAZ. This minimizes the area where mechanical properties are decreased. When necessary for thicker sections, helium shielding gas can be used, along with an argon backup gas shield.

Filler metal may be added to the weld joint using either ERCuSn-A or wire of approximately the same composition as the base metal. When matching the composition of the base metal is not essential, ERCuSi-A filler metal can be used instead, producing stronger welds. When welding section thicknesses less than 3 mm (0.13 in.), phosphor bronze strip can be butt welded using autogenous GTAW.

Preheating is not normally required for GTAW of thin sections of phosphor bronzes. Thick sections usually require preheating to 175 or 200 °C (350 or 400 °F) and are slowly cooled after welding. Due to the hot-short nature of phosphor bronze, weld layers should be thin, and interpass temperature should not exceed 200 °C (400 °F). Hot peening is often used to refine grain size and minimize distortion.

Gas-Metal Arc Welding

Table 6 gives the nominal conditions for GMAW of butt joints using phosphor bronze. Lead-bearing or other free-machining types are not welded. Table 10 gives GMAW conditions that can be used as starting points for establishing welding conditions for joining phosphor bronzes. As with GTAW, the welding conditions are based on three poorly conductive phosphor bronze alloys (C51000, C52100, and C52400). When welding the more conductive alloy C50500, higher welding currents or slower welding speeds are needed. For joining thicknesses of 9.5 to 13 mm (0.4 to 0.5 in.), 90° single-V grooves are used rather than the narrow grooves used for most other poorly conductive alloys.

TABLE 10 SUGGESTED CONDITIONS FOR GMAW OF PHOSPHOR BRONZES

WORKPIECE THICKNESS		JOINT DESIGN			ELECTRODE DIAMETER[A]		ARC VOLTAGE, V	WELDING CURRENT (DCEP), A[A]
		GROOVE TYPE	ROOT OPENING					
MM	IN.		MM	IN.	MM	IN.		
1.6	1/16	SQUARE	1.3	0.05	0.8	0.030	25-26	130-140
3.2	1/8	SQUARE	2.4	0.09	0.9	0.035	26-27	140-160
6.4	1/4	V	1.6	0.06	1.2	0.045	27-28	165-185
12.7	1/2	V	2.4	0.09	1.6	0.062	29-30	315-335
19.0	3/4	DOUBLE-V OR DOUBLE-U	2.4	0.09	2.0	0.078	31-32	365-385
25.4	1.0	DOUBLE-V OR DOUBLE-U	2.4	0.09	2.4	0.094	33-34	440-460

(A) ERCUSN-A PHOSPHOR BRONZE ELECTRODES AND ARGON SHIELDING GAS

Filler Metals. For joining phosphor bronzes, ERCuSn-A electrode wire is generally used. The filler metal wire that contains about 0.5% Si is sometimes used to minimize porosity in the weld.

Preheating. As with other copper alloys, preheating of the phosphor bronzes helps in obtaining complete fusion. Also, porosity is minimized because the freezing rate of the weld pool is decreased, and more gas is permitted to evolve before solidification. However, preheating increases the susceptibility of the weld to the formation of large columnar grains and the risk of hot cracking. This susceptibility requires that welding be performed with a stringer bead technique and that

each weld layer be peened. A small weld pool and rapid electrode travel speed are required. Interpass temperatures while welding should not exceed the preheat temperatures because of the hot shortness of the phosphor bronze alloys.

Shielded Metal Arc Welding

Shielded metal arc welding is done on a limited basis for phosphor bronzes. The covered electrodes typically used are ECuSn-A and ECu-Sn-C. These electrodes may be used interchangeably and are designed for use with DCEP.

Preheating is required in the range of 150 to 200 °C (300 to 400 °F), since the phosphor bronzes are very sluggish. However, because of the hot shortness of these alloys, the interpass temperature must not exceed the preheat temperature. This is extremely important in thicker sections. Stringer beads with rapid travel speed are normally used. In groove welding, the first two passes are made with a weaving technique. The width of the weave should not exceed two electrode diameters. The remaining passes are made without appreciable traverse weaving and with the use of narrow stringer beads. The development of the coarse, dendritic structure with low strength and ductility is minimized by the control of preheat and interpass temperatures. Hot peening is often used after welding to reduce grain size. For the maximum ductility, the welded assembly should be postweld heat treated to 480 °C (900 °F) and cooled rapidly. Groove joints should be wide, with an included angle of 80 to 90° to achieve proper washing and tie-in at the walls of the groove.

Welding of Copper Alloys

Revised by M. Ned Rogers, Batesville Casket Company

Welding of Aluminum Bronzes

As shown in Table 1, aluminum bronzes (C60600-C64400) are complex alloys based on the Cu-Al-Ni-Fe-Si-Sn system. They are welded using GTAW, GMAW, or SMAW. Some aluminum bronzes are also used as hardfacing alloys (see the article "Hardfacing, Weld Cladding, and Dissimilar Metal Joining" in this Volume). Additional information on the properties and applications of aluminum bronzes can be found in Volume 2 of the *ASM Handbook.*

Gas-Tungsten Arc Welding

Gas-tungsten arc welding is readily used for joining aluminum bronzes up to 9.5 mm (0.4 in.). Aluminum bronze castings are also repair welded by GTAW. Conditions differ somewhat from those of most other copper alloys. Porosity is minimized in the weld metal by the presence of iron, manganese, or nickel in the filler metal or base metal.

Nominal Conditions. Table 11 lists the nominal conditions for welding of aluminum bronze alloys. Conditions must be selected to avoid difficulties that result from the tenacious refractory aluminum oxide films that form almost instantaneously during any heating process such as welding unless oxygen is completely excluded from the metal. Heat input requirements are not high, since aluminum bronzes have a thermal conductivity near that of carbon steel.

TABLE 11 NOMINAL CONDITIONS FOR GTAW OF ALUMINUM BRONZES

WORKPIECE THICKNESS		ROOT OPENING		ELECTRODE DIAMETER[B]		WELDING ROD DIAMETER[C]		FLOW RATE OF ARGON		CURRENT (AC, HF-STABILIZED), A[D]	NUMBER OF PASSES
mm	in.	mm	in.	mm	in.	mm	in.	l/min	ft³/h		
SQUARE-GROOVE BUTT JOINTS											
0-1.6	0-1/16	0	0	1.6	1/16	1.6	1/16 [E]	9.5-15	20-30	25-80	1
1.6-3.2	1/16-1/8	1.6 MAX	1/16 MAX	2.4	3/32	3.2	1/8	9.5-15	20-30	60-175	1

3.2	$\frac{1}{8}$	3.2 MAX	$\frac{1}{8}$ MAX	4.8	$\frac{3}{16}$	4.0	$\frac{5}{32}$	15	30	210	1
70° SINGLE-V-GROOVE BUTT JOINTS											
9.5	$\frac{3}{8}$	0	0	4.8	$\frac{3}{16}$	4.0	$\frac{5}{32}$	15	30	210-330	4
FILLET-WELDED T-JOINTS OR SQUARE-GROOVE INSIDE CORNER JOINTS											
9.5	$\frac{3}{8}$	(F)		4.8	$\frac{3}{16}$	4.0	$\frac{5}{32}$	15	30	225	3

Note: The data in this table are intended to serve as starting points for the establishment of optimum joint design and conditions for welding of parts on which previous experience is lacking. They are subject to adjustments necessary to meet the special requirements of individual applications.

(A) PREHEATING IS NOT ORDINARILY USED IN WELDING THE THICKNESSES SHOWN.

(B) ZIRCONIATED OR UNALLOYED ELECTRODES ARE RECOMMENDED WITH HIGH-FREQUENCY-STABILIZED ALTERNATING CURRENT.

(C) PREFERRED WELDING ROD IS ERCUAL-A2; OTHERWISE ERCUAL-A3 OR ROD OF THE SAME COMPOSITION AS THE BASE METAL.

(D) DIRECT CURRENT ELECTRODE NEGATIVE CAN ALSO BE USED IN MAKING SINGLE-PASS WELDS (SEE TEXT).

(E) USE OF WELDING ROD IS OPTIONAL FOR THICKNESSES UP TO 1.6 MM ($\frac{1}{16}$ IN.).

(F) ZERO ROOT OPENING FOR T-JOINTS; 9.5 MM ($\frac{3}{8}$ IN.) MAX FOR CORNER JOINTS

Shielding Gas. Argon is typically used with alternating current as a shielding gas for the welding of aluminum bronzes. For better penetration or faster travel speed, direct current can be used with argon, helium, or a mixture of these two gases. While the shielding gas protects the weld pool and adjacent base metal, the use of a special flux augments the shielding effect of the gas. The flux is applied to the edge of the weld joints to increase fluidity and help protect the base metal from oxide formation. Aluminum oxide forms even at room temperature, and the flux prevents air from reaching the prepared edges until the protective argon shielding gas can become effective in the localized area.

Type of Current. As stated above, alternating current is used for GTAW of aluminum bronzes. The alternating current is stabilized by continuous high frequency and is preferred to DCEN, since it prevents oxide formation on the surface of the weld pool. High-frequency-stabilized alternating current is particularly desirable when multi-pass welding of these alloys is performed. Direct current electrode negative can be used in a single-pass welding, particularly for automatic welding. Surfaces must be well cleaned and protected, and the arc must be closely controlled.

Electrodes. Gas-tungsten arc welding of aluminum bronzes typically uses zirconiated tungsten (EWZr) or unalloyed tungsten (EWP) electrodes. Thoriated tungsten electrodes are used with direct current; however, these electrodes cause the arc to wander when they are used with alternating current. The thoriated tungsten gives a longer tip life and is easier to start. Electrode preparation for use with direct current is a tapered cone-shaped tip. For alternating current, the end of the electrode is typically balled via an arc melting process.

Filler Metals. ERCuAl-A2 is ordinarily used for joining aluminum bronzes. ERCuAl-A3 or other aluminum bronze wire of matching chemical composition can be used when the composition and color of the weld metal must closely match that of the base metal.

Preheating of aluminum bronzes for GTAW of sections thinner than approximately 6 mm (0.25 in.) is not necessary. Aluminum bronzes have a low thermal conductivity but may require preheating for section thicknesses greater then 6 mm (0.25 in.). When preheating is required, the preheat and interpass temperature should not exceed 150 °C (300 °F) for alloys with less than 10% Al. In the following example, preheating was used for joining of a 9.5 mm (0.4 in.) thick aluminum bronze.

Example 6: Use of GTAW versus GMAW to Avoid Melt-Through of Neighboring Sections.

The propeller housing for the Kort nozzle shown in Fig. 3 was originally made as a one-piece sand casting from aluminum bronze alloy 9B (ASTM B148), which contains 10% Al and 1% Fe. Difficulties were experienced in the coring necessary to produce the thin outer shell. This led to the production of this outer shell as a separate piece that was welded to the casting to make a two-piece structure.

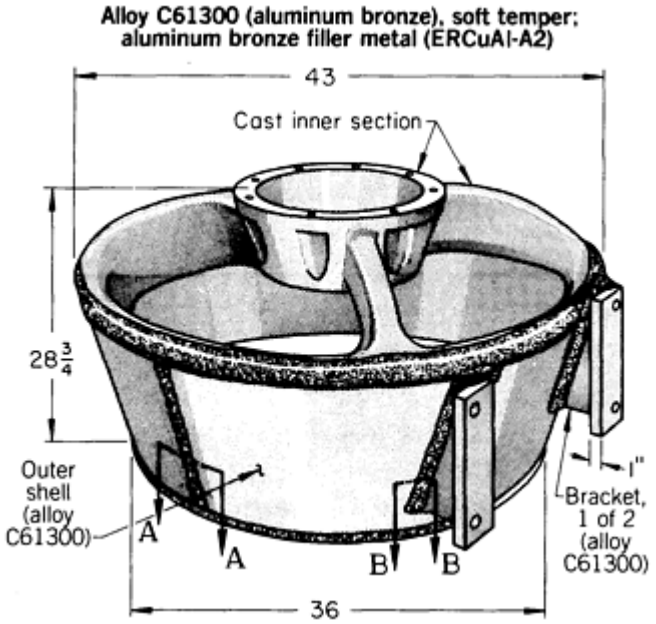

Circumferential welds joining outer shell to cast inner section were made by gas metal arc welding

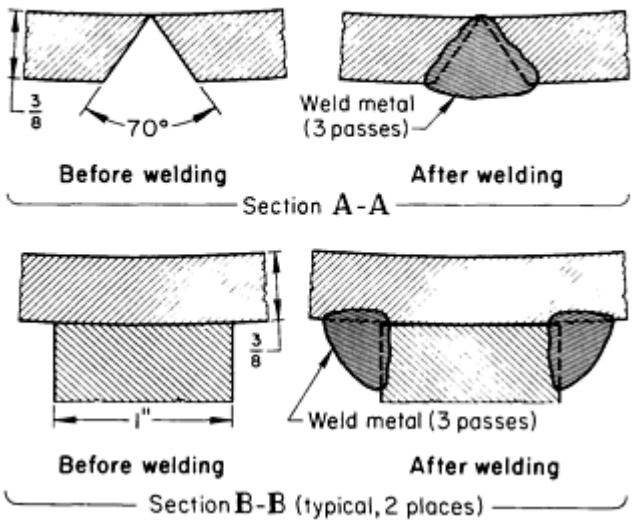

Erro! •

CONDITIONS FOR GTAW	
JOINT TYPES	BUTT AND T
WELD TYPES	SINGLE-V-GROOVE AND FILLET
WELDING POSITION	FLAT
NUMBER OF PASSES	3
POWER SUPPLY	300 A RECTIFIER, CONSTANT-CURRENT TYPE
TORCH	WATER-COOLED
ELECTRODE	2.4 MM ($\frac{3}{32}$ IN.) DIAM EWTH-2

FILLER METAL	2.4 MM ($\frac{3}{32}$ IN.) DIAM ERCUAL-A2
SHIELDING GAS	ARGON; FLOW RATE, 9.5 L/MIN (20 FT^3/H)
PREHEAT AND INTERPASS TEMPERATURE	150 °C (300 °F)
VOLTAGE	35 V
CURRENT	225 A (DCEN)
ARC STARTING	CONTACT AND HIGH FREQUENCY

FIG. 3 CONDITIONS FOR GTAW OF A PROPELLER HOUSING. THE WELDMENT REPLACED A SINGLE-PIECE CASTING, THEREBY REDUCING COST AND IMPROVING SERVICEABILITY.

The inner section was cast in propeller bronze as one intricate piece that included a central hub and shaft-mounting flange connected to the main body of the nozzle by four arms. The outer shell was cut from 9.5 mm (0.4 in.) thick alloy C61300 (aluminum bronze) with soft temper and was wrapped around the cast intersection after being cold formed into a truncated cone. Before cold forming, all edges of the shell were machined to a 35° bevel to provide a groove for subsequent welding.

The assembly was tack welded together, and then circumferential seams at the top and bottom were gas-metal arc welded. Next, to avoid melt-through of the cast intersection (and resultant poor effect on the propeller stream), GTAW was used for the longitudinal seam in the shell and for joining two brackets to the shell. The brackets were used for mounting the shell to the hull of the vessel. Figure 3 illustrates the weldment as constructed.

Not only was the cost of production reduced by eliminating the complex and expensive coring in the casting, but the weight of the welded housing was less than that of the completed cast housing. Furthermore, the cast housing had been made of an alloy that, although easy to cast, did not resist erosion, corrosion, or cavitation as well as did the alloys used in the welded assembly.

Gas-Metal Arc Welding

Gas-metal arc welding with aluminum bronze electrode wire is the preferred technique for welding aluminum bronzes. Because of the comparatively high surface tension of the molten weld pool and the relatively low thermal conductivity of the base metal, welding can be performed in all positions. Welding in the vertical and overhead positions is usually performed with either the globular or short-circuiting mode of metal transfer, using filler metal up to 1.6 mm ($\frac{1}{16}$ in.) in diameter.

Nominal Conditions. The nominal conditions for gas-metal arc butt welding of aluminum bronze are given in Table 6. Backing strips or rings of aluminum bronze are used when welding material up to 3 mm (0.13 in.) thick. These conditions make it necessary to use helium or argon-helium mixes for shielding gas instead of the argon shown in Table 6. These hotter shielding gases provide adequate heat input.

Filler Metals. ERCuAl-A2 ordinarily is used in the GMAW of aluminum bronze. The 1.5% Fe present in this wire reduces the hot-short cracking susceptibility of the weld metal. The use of ERCuAl-A3 also produces welds that are free from hot shortness. Joints made with ERCuAl-A3 are also stronger and harder, but lower in ductility.

Joint Design. The joining of aluminum bronzes thicker than 13 mm (0.5 in.) requires wider root openings and groove angles than those indicated in Table 6. This is necessary to avoid incomplete fusion and to improve the penetration resulting from the use of a thicker section, which increases the weld heat-sink characteristics.

Preheating. For most thin sections of aluminum bronzes, preheating is not required prior to welding. If preheat is used, the preheat and interpass temperatures should not exceed 150 °C (300 °F) for alloys that contain less than 10% Al. When aluminum content exceeds 10%, preheat temperatures should be elevated to 260 °C (500 °F). Again, interpass temperatures should not exceed preheat temperatures, due to the hot shortness of these alloys.

Shielded Metal Arc Welding

Aluminum bronzes are readily welded using SMAW for both the wrought and cast forms. The fluxing action of the electrode coating removes the aluminum oxides that form on the surface of the alloys.

Except for thin sections, a 70 to 90° V-groove joint is used. Typically, a backing strip of the same composition as the base metal is also utilized. Deposition technique and bead thickness are not critical, because the weld metal has excellent hot strength and ductility.

Electrodes. Aluminum bronze electrodes ECuAl-A2 and ECuAl-B are used for SMAW of aluminum bronze alloys C61300 and C61400. Preheating of thick sections of these alloys may be needed and is usually in the range of 200 °C (400 °F) with a controlled interpass temperature not exceeding 200 °C (400 °F). Depending upon section thickness and overall mass, preheat and interpass temperatures may vary from 65 to 425 °C (150 to 800 °F). Weldments made of aluminum bronze alloys containing 7% Al need not be heat treated after welding. Aluminum bronzes having an aluminum content greater than 7% are usually welded with electrodes that contain more aluminum than do ECuAl-A2 and ECuAl-B. These higher-aluminum bronze electrodes, ECuAl-C, ECuAl-D, and ECuAl-E, are best known as surfacing electrodes and have nominal aluminum contents of 12.5, 13.5, and 14.5%, respectively. These electrodes are described in AWS A5.13 and have strength corresponding to the aluminum content. In welding high-aluminum bronzes, thick sections may require preheating up to 620 °C (1150 °F), and fan cooling may be necessary to avoid cracking. These alloys may also require annealing at 620 °C (1150 °F), followed by fan cooling for stress relief.

Welding of Copper Alloys

Revised by M. Ned Rogers, Batesville Casket Company

Welding of Silicon Bronzes

Silicon bronzes (C64700-C66100), which are based on the Cu-Si-Sn system, are the most weldable of the copper alloys. Silicon bronzes can be welded by most arc welding processes, the most commonly utilized being GTAW, GMAW, and SMAW. Additional information on the properties and applications of silicon bronzes can be found in Volume 2 of the *ASM Handbook.*

Gas-Tungsten Arc Welding

Silicon bronze alloys that do not contain lead can be gas-tungsten arc welded in thin and moderately thick sections. These alloys are typically the most weldable of all copper alloys. Inherent characteristics of these bronzes that contribute to their weldability include low thermal conductivity, good deoxidation of the weld metal by silicon, and protection offered by the resulting slag. Silicon bronzes have a relatively narrow hot-short range just below the solidus, and they must be rapidly cooled through this range to avoid weld cracking.

Nominal Conditions. Table 12 lists the nominal welding conditions for GTAW of silicon bronzes. The data for manual welding include welding conditions for various positions. Because of their low fluidity, silicon bronzes are the only group of copper alloys where GTAW is applied extensively in the vertical and overhead positions. Direct current electrode negative with argon or helium shielding can be used for section thicknesses less than 1.6 mm (0.06 in.). Zirconiated (EWZr) or pure tungsten (EWP) electrodes are recommended.

TABLE 12 NOMINAL CONDITIONS FOR GTAW OF SILICON BRONZES USING ZERO ROOT OPENING, NO PREHEAT, EWTH-2 ELECTRODES, ERCUSI-A WELDING ROD, AND ARGON SHIELDING GAS

WORKPIECE THICKNESS[A]		ELECTRODE DIAMETER		WELDING ROD DIAMETER[B]		GAS FLOW RATE		CURRENT (DCEN), A	TRAVEL SPEED		NUMBER OF PASSES
mm	in.	mm	in.	mm	in.	l/min	ft^3/h		M/MIN	IN./MIN	
AUTOMATIC WELDING											
SQUARE-GROOVE BUTT JOINTS, FLAT POSITION											
0.3-1.3	0.012-0.050	3.2	$\frac{1}{8}$	NONE USED		7.1-16.5	15-35	80-140	1.52-2.03	60-80	1

1.6-3.2	1/16-1/8	3.2	1/8	NONE USED		7.1-16.5	15-35	90-210	1.14-1.52	45-60	1
3.2	1/8	3.2	1/8	1.6	1/16	7.1-16.5	15-35	250	0.46-0.50	18-20	1
MANUAL WELDING											
SQUARE-GROOVE BUTT JOINTS, FLAT POSITION											
1.6	1/16	1.6	1/16	1.6	1/16	7.1	15	100-120	0.30	12	1
3.2	1/8	1.6	1/16	2.4	3/32	7.1	15	130-150	0.30	12	1
4.8	3/16	2.4	3/32	3.2	1/8	9.5	20	150-200	. . .	. . .	1
6.4	1/4	3.2	1/8	3.2	1/8	9.5	20	250-300	. . .	. . .	1
6.4	1/4	3.2	1/8	3.2	1/8	9.5	20	150-200	. . .	. . .	3
SQUARE-GROOVE BUTT JOINTS, VERTICAL AND OVERHEAD POSITIONS											
1.6	1/16	1.6	1/16	1.6	1/16	7.1	15	90-110	. . .	. . .	1
3.2	1/8	1.6	1/16	2.4	3/32	7.1	15	120-140	. . .	. . .	1
60° SINGLE-V-GROOVE BUTT JOINTS, FLAT POSITION											
9.5	3/8	3.2	1/8	3.2	1/8	9.5	20	230-280	. . .	. . .	3-4
12.7	1/2	3.2	1/8	4.8	3/16	9.5	20	250-300	. . .	. . .	4-5
19.0	3/4	3.2	1/8	4.8	3/16	9.5	20	300-350	. . .	. . .	9-10
25.4	1	3.2	1/8	6.4	1/4	9.5	20	300-350	. . .	. . .	13
FILLET-WELDED LAP JOINTS, FLAT POSITION											
1.6	1/16	1.6	1/16	1.6	1/16	7.1	15	110-130	0.25	10	1
3.2	1/8	2.4	3/32	2.4	3/32	7.1	15	140-160	0.25	10	1
4.8	3/16	2.4	3/32	3.2	1/8	9.5	20	175-225	. . .	. . .	1
6.4	1/4	2.4	3/32	3.2	1/8	9.5	20	175-225	. . .	. . .	3
9.5	3/8	3.2	1/8	4.8	3/16	9.5	20	250-300	. . .	. . .	3
12.7	1/2	3.2	1/8	4.8	3/16	9.5	20	275-325	. . .	. . .	6
19.0	3/4	3.2	1/8	4.8	3/16	9.5	20	300-350	. . .	. . .	12
25.4	1	3.2	1/8	6.4	1/4	9.5	20	325-350	. . .	. . .	16
FILLET-WELDED LAP JOINTS, VERTICAL AND OVERHEAD POSITIONS											
1.6	1/16	1.6	1/16	1.6	1/16	7.1	15	100-120	. . .	. . .	1
3.2	1/8	2.4	3/32	2.4	3/32	7.1	15	130-150	. . .	. . .	1
SQUARE-GROOVE OUTSIDE CORNER JOINTS, FLAT POSITION											

1.6	1/16	1.6	1/16	1.6	1/16	7.1	15	100-130	0.30	12	1
3.2	1/8	1.6	1/16	2.4	3/32	7.1	15	130-150	0.30	12	1
4.8	3/16	2.4	3/32	3.2	1/8	9.5	20	150-200	. . .	. . .	1
SQUARE-GROOVE OUTSIDE CORNER JOINTS, VERTICAL AND OVERHEAD POSITIONS											
1.6	1/16	1.6	1/16	1.6	1/16	7.1	15	90-110	. . .	. . .	1
3.2	1/8	1.6	1/16	2.4	3/32	7.1	15	120-140	. . .	. . .	1
50° SINGLE-BEVEL-GROOVE OUTSIDE CORNER JOINTS, FLAT POSITION[C]											
6.4	1/4	2.4	3/32	3.2	1/8	9.5	20	175-225	. . .	. . .	3
9.5	3/8	3.2	1/8	4.8	3/16	9.5	20	230-280	. . .	. . .	3
12.7	1/2	3.2	1/8	4.8	3/16	9.5	20	275-325	. . .	. . .	7
19.0	3/4	3.2	1/8	4.8	3/16	9.5	20	300-350	. . .	. . .	14
25.4	1	3.2	1/8	6.4	1/4	9.5	20	325-350	. . .	. . .	20
FILLET-WELDED SQUARE-GROOVE INSIDE CORNER JOINTS, FLAT POSITION[D]											
1.6	1/16	1.6	1/16	1.6	1/16	7.1	15	110-130	0.25	10	1
3.2	1/8	2.4	3/32	2.4	3/32 3/32	7.1	15	140-150	0.25	10	1
4.8	3/16	2.4	3/32	3.2	1/8	9.5	20	175-225	. . .	. . .	1
FILLET-WELDED T-JOINTS, FLAT POSITION											
1.6	1/16	1.6	1/16	1.6	1/16	7.1	15	110-130	0.25	10	1
3.2	1/8	2.4	3/32	2.4	3/32	7.1	15	140-160	0.25	10	1
4.8	3/16	2.4	3/32	3.2	1/8	9.5	20	175-225	. . .	. . .	1
6.4	1/4	2.4	3/32	3.2	1/8	9.5	20	175-225	. . .	. . .	3
9.5	3/8	3.2	1/8	4.8	3/16	9.5	20	230-280	. . .	. . .	3
12.7	1/2	3.2	1/8	4.8	3/16	9.5	20	275-325	. . .	. . .	7
19.0	3/4	3.2	1/8	4.8	3/16	9.5	20	300-350	. . .	. . .	14
25.4	1	3.2	1/8	6.4	1/4	9.5	20	325-350	. . .	. . .	20

Note: The data in this table are intended to serve as starting points for the establishment of optimum joint design and conditions for welding of parts on which previous experience is lacking. They are subject to adjustments necessary to meet the special requirements of individual applications.

(A) THICKNESSES GREATER THAN ABOUT 12.7 MM (1/2 IN.) ARE GAS-TUNGSTEN ARC WELDED ONLY WHEN IT IS NOT PRACTICAL TO USE GMAW.

(B) WIRE FEED RATE OF 2.9-3.2 M/MIN (115-125 IN./MIN).

(C) ROOT FACE IS 1.6 MM ($\frac{1}{16}$ IN.) FOR THICKNESSES OF 12.6 MM ($\frac{1}{2}$ IN.) OR LESS, AND 3.2 MM ($\frac{1}{8}$ IN.) FOR THICKNESSES GREATER THAN 12.7 MM ($\frac{1}{2}$ IN.)

(D) MAXIMUM ROOT OPENING IS EQUAL TO BASE METAL THICKNESS, *T*.

Filler Metals. The conventional silicon bronze filler metal, ERCuSi-A, which is similar in composition to alloy C65500 (high-silicon bronze A), can be used to weld any of the silicon bronzes. Alloy C65500 is the most commonly used of all the silicon bronzes. Thin sections of this alloy are readily welded using GTAW without the addition of filler metal.

Joint Design. On metal thicknesses greater than 6 mm (0.25 in.) a V-groove with a 60° included angle is used. Butt joints in thin sections can be welded without special preparation.

Preheating. Silicon bronzes have the lowest thermal conductivity of all copper alloys. The thermal conductivity of these alloys is less than that of carbon steels. Further, these alloys exhibit hot shortness. Based on this, preheating can be harmful to the welding of these alloys, and interpass temperature on multi-pass welds should not exceed 95 °C (200 °F).

Gas-Metal Arc Welding

The nonleaded silicon bronzes are readily welded using GMAW. Nominal conditions for GMAW of silicon bronzes in various thicknesses and joint designs are given in Table 6. This process is used for section thicknesses greater than 6 mm (0.25 in.). Rapid travel speeds (minimum of 3.5 mm/s, or 8 in./min) should be used to avoid excessive heat buildup. As shown in Table 6, the welding current used for these alloys is slightly lower than that used for other copper alloys. Because of the low thermal conductivity of silicon bronzes (Table 1), the resulting low heat input to the weld is adequate for complete fusion and good penetration. Argon shielding gas is preferred. A thin layer of oxide forms on the weld metal after each pass and must be removed by wire brushing prior to the next weld pass.

All silicon bronze alloys can be gas-metal arc welded using ERCuSi-A filler metal. The chemical composition of this wire is similar to that of alloy C65500 (high-silicon bronze A), which is the most frequently used silicon bronze. These wires may include up to 1.5% Sn instead of, or in addition to, the 1.5% Mn specified as a maximum for alloy C65500.

Joint Preparation. Metal thicknesses of 6 to 19 mm (0.25 to 0.75 in.) should utilize a single 60° V-groove. For silicon bronze alloys of section thicknesses greater than 19 mm (0.75 in.), U-grooves or 60° double-V-groove joints can be used.

Preheating. As with GTAW of silicon bronze alloys, preheating is not required and should not be used with GMAW of silicon bronze. Interpass temperatures must be held below 95 °C (200 °F) to prevent weld cracking. Stress relieving of silicon bronze weldment is recommended to prevent stress-corrosion cracking failures.

Shielded Metal Arc Welding

Shielded metal arc welding of silicon bronze alloys is usually done using ECuAl-A2 aluminum bronze electrodes. Welding temperatures are easily attained, due to the low thermal conductivity of silicon bronzes. As with other arc welding processes, preheat and interpass temperatures should not exceed 95 °C (200 °F) to prevent hot-short cracking.

Groove dimensions are similar to those used for steel joints. Metal thicknesses up to 4 mm (0.16 in.) can be welded with square grooves. Thicker sections can be welded with a single-V-or double-V-groove of 60° included angle.

Weld properties in silicon bronzes joined using SMAW are usually substantially lower than those of welds made by the gas-shielded processes. Based on this, these welds may not meet code or design requirements for strength. Peening of welds reduces residual stress and minimizes weld distortion.

Revised by M. Ned Rogers, Batesville Casket Company

Welding of Copper-Nickel Alloys

Copper-nickel alloys (C70000-C79900) are the most corrosion-resistant copper-base alloys. Alloy C71500 (Cu-30Ni) has the best general resistance to aqueous corrosion, but alloy C70600 (Cu-10Ni) is often selected because it offers good resistance at lower cost. Copper-nickel alloys are readily welded by GTAW, GMAW, and SMAW. Additional information on the properties and applications of copper-nickel alloys can be found in Volume 2 of the *ASM Handbook.*

Gas-Tungsten Arc Welding

Gas-tungsten arc welding is the preferred process for joining copper-nickel alloys with section thicknesses up to 1.6 mm (0.06 in.). This process may also be used for thicker sections. Automatic welding produces satisfactory results in thin sections of tube sheets. Manual welding is normally used for sheet and plate thicknesses up to 6 mm (0.25 in.).

Nominal Conditions. Conditions by which copper-nickel alloys can be manually and automatically welded using GTAW are given in Table 13. These include butt joints with square- and single-V-groove preparation.

TABLE 13 NOMINAL CONDITIONS FOR GAS-TUNGSTEN ARC BUTT WELDING OF COPPER-NICKEL ALLOYS

WORKPIECE THICKNESS		BUTT-JOINT GROOVE	ELECTRODE DIAMETER(A)		ERCUNI WELDING ROD DIAMETER(B)		FLOW RATE OF ARGON		CURRENT (DCEN), A	TRAVEL SPEED		NUMBER OF PASSES
mm	in.		mm	in.	mm	in.	l/min	ft^3/h		M/MIN	IN./MIN	
AUTOMATIC WELDING OF ALLOY C70600 (COPPER-NICKEL, 10%)												
3.2	1/8	SQUARE	4.8	3/16	1.6	1/16	15	30	310-320	0.38-0.46	15-18	1
MANUAL WELDING OF ALLOY C70600 (COPPER-NICKEL, 10%)												
3.2	1/8	SQUARE	4.8	3/16	3.2	1/8	15	30	300-310	0.13	5	1
9.5	3/8	70-80° SINGLE-V	4.8	3/16	4.8	3/16	15	30	300-310(C)	0.15	6	2-4
MANUAL WELDING OF ALLOY C71500 (COPPER-NICKEL, 30%)												
3.2	1/8	SQUARE	4.8	3/16	3.2	1/8	15	30	270-290	0.13	5	1
9.5	3/8	70-80° SINGLE-V	4.8	3/16	4.0	5/32	15	30	270-290(C)	0.15	6	4

Notes: (1) The data in this table are intended to serve as starting points for the establishment of optimum joint design and conditions for welding of parts on which previous experience is lacking. They are subject to adjustments necessary to meet the special requirements of individual applications. (2) Root opening is zero. Preheating is not needed.

(A) PREFERRED ELECTRODE MATERIAL IS EWTH-2.

(B) FILLER METAL (ERCUNI) MUST BE USED ON ALL WELDED JOINTS (SEE TEXT).

(C) CURRENT SHOULD BE INCREASED IN EQUAL INCREMENTS WITH EACH PASS, UP TO A MAXIMUM OF ABOUT 375 A, WITH LARGER WELDING RODS.

Preferred conditions include the use of argon shielding gas, DCEN, and thoriated tungsten electrodes. However, these variables are not critical for copper-nickel, since these alloys have low heat conductivities. Helium may be substituted for argon as a shielding gas, but argon provides better arc control and stability. Alternating current can be employed for automatic welding if there is adequate control of arc length.

During GTAW of alloy C70600, slightly higher welding currents or slower travel speeds should be used, due to the higher thermal conductivity of this alloy. Preheating is not necessary, and backing strips or rings can be used. Backing strips or rings should be made of copper or copper-nickel alloy, not carbon, graphite, or steel.

Filler Metals. ERCuNi is used as a filler metal in GTAW of copper-nickel alloys. This filler metal contains 0.20 to 0.50% Ti to minimize porosity and the possibility of oxygen embrittlement in either the weld metal or the HAZ. Because the standard copper-nickel alloys do not contain titanium or a comparable deoxidizer, filler metal should be used even in welding thin sheets of copper-nickel. This will avoid the formation of porosity. However, special compositions of alloys C70600 and C71500 are available that do contain titanium. Thin sheets of these special alloys can be welded without the use of a filler metal. In multi-pass welding of copper-nickel alloys, the filler metal diameter and welding current may be increased with successive passes to provide efficient deposition. Autogenous welds can sometimes be made on sheet thicknesses up to 1.6 mm (0.06 in.), but porosity may be a problem due to the absence of deoxidizers in the base metal.

Gas-Metal Arc Welding

Gas-metal arc welding is the preferred welding process for non-leaded copper-nickel alloys thicker than approximately 1.6 mm (0.06 in.). Table 14 lists welding conditions for GMAW of copper-nickel alloy plate. The preferred welding position is the flat position. Argon is the preferred shielding gas; however, argon-helium mixes give better penetration on thick sections. Direct current electrode positive is recommended.

TABLE 14 SUGGESTED CONDITIONS FOR GMAW OF COPPER-NICKEL ALLOY PLATE

WORKPIECE THICKNESS		ELECTRODE FEED[A]		ARC VOLTAGE, V	WELDING CURRENT (DCEP), A[A]
mm	in.	m/min	in./min		
6.4	$\frac{1}{4}$	4.5-5.6	180-220	25-26	130-140
9.5	$\frac{3}{8}$	5.1-6.1	200-240	26-27	140-160
12.7	$\frac{1}{2}$	5.6-6.1	220-240	27-28	165-185
19.0	$\frac{3}{4}$	5.6-6.1	220-240	29-30	315-335
25.4	1.0	5.6-6.1	220-240	31-32	365-385
>25.4	1.0	6.1-6.6	240-260	33-34	440-460

(A) ERCUNI ELECTRODE, 1.6 MM ($\frac{1}{16}$ IN.), ARGON SHIELDING GAS

Nominal conditions for gas-metal arc butt welding of non-leaded copper-nickel alloys for various joint designs and thicknesses are given in Table 6. These alloys can be satisfactorily welded using either spray or short-circuiting transfer. Spray transfer is normally used for sections greater than 6 mm (0.25 in.). Pulsed spray transfer or short-circuiting transfer can be used to weld thin sections. These transfer methods provide better control of the molten weld pool when welding in the vertical and overhead positions. Selection of processing conditions is not critical in GMAW of these poorly heat-conductive alloys. Alloy C70600 is usually welded at a slightly higher current or slower travel speed than alloy C71500.

Filler Metals. ERCuNi electrode wire is the common choice for GMAW of copper-nickel alloys. This wire resembles alloy C71500 in composition, since it has a 70 to 30 copper-to-nickel ratio. ERCuNi contains 0.15 to 1.00% Ti, which serves as a deoxidizer to minimize porosity and prevent oxygen embrittlement. Titanium also improves the fluidity of the weld pool.

Joint Design. For GMAW of butt joints in non-leaded copper nickels 3 mm (0.13 in.) thick, the joint design usually includes a square-groove weld and grooved copper backing. This is indicated in Table 6. For thicknesses between 3 and 13 mm (0.13 and 0.5 in.), single-V-grooves of 60 to 80° and grooved copper backing are typically used. For section

thicknesses greater than 13 mm (0.5 in.), double-V-groove or double-U-groove joints are used. As with GTAW of copper-nickel alloys, backing material should be made of copper or copper-nickel rather than carbon, graphite, or steel.

Preheating and Postheating. The copper-nickel alloys have thermal conductivity equal to or lower than that of low-carbon steel. Therefore, no preheating or postheating is needed. However, interpass temperatures should be maintained below 65 °C (150 °F).

Shielded Metal Arc Welding

Both wrought and cast forms of copper-nickel alloys can be welded using SMAW. The weldability of these alloys is similar to that of low-carbon steels, because the thermal conductivity of these alloys is quite similar to that of steel. Copper-nickel electrode ECuNi is used in welding the copper-nickel alloys C70600 and C71500 with DCEP.

The weld deposits ordinarily have a high center crown, and the slag is viscous when molten and quite adherent when cold. Therefore, special care is needed to ensure complete slag removal before complete solidification of the weld metal, to prevent slag entrapment when cleaning between passes. Welding in both the vertical and overhead positions using SMAW provides good results in these alloys, although best results are obtained in the flat position. This process is preferred in some applications where access to the joint is limited, as in the butt welding of copper-nickel pipe.

Welding of Copper Alloys

Revised by M. Ned Rogers, Batesville Casket Company

Welding of Dissimilar Metals

Copper and many copper alloys can be welded to other (dissimilar) copper alloys, to carbon and alloy steels, to stainless steels, and to nickel and nickel alloys using GTAW and GMAW. Tables 15 and 16 provide guidelines for joining copper and copper alloys to dissimilar metals.

TABLE 15 ELECTRODES AND PREHEAT AND INTERPASS TEMPERATURES USED IN GTAW OF COPPER AND COPPER ALLOYS TO DISSIMILAR METALS

METAL TO BE WELDED	ELECTRODES (WITH PREHEAT AND INTERPASS TEMPERATURES) FOR WELDING METAL IN COLUMN 1 TO:				
	COPPERS	PHOSPHOR BRONZES	ALUMINUM BRONZES	SILICON BRONZES	COPPER-NICKEL ALLOYS
COPPER ALLOYS					
LOW-ZINC BRASSES	ERCUSN-A OR ERCU (540 °C, OR 1000 °F)	. . .	. . .	. . .	. . .
PHOSPHOR BRONZES	ERCUSN-A OR ERCU (540 °C, OR 1000 °F)	. . .	. . .	. . .	. . .
ALUMINUM BRONZES	ERCUAL-A2 (540 °C, OR 1000 °F)	ERCUAL-A2 OR ERCUSN-A (200 °C, OR 400 °F)	. . .	. . .	. . .
SILICON BRONZES	ERCUSN-A OR ERCU (540 °C, OR 1000	ERCUSI-A (65 °C MAX, OR 150 °F	ERCUAL-A2 (65 °C MAX, OR 150 °F MAX)	. . .	. . .

	°F)	MAX)			
COPPER-NICKEL ALLOYS	ERCUAL-A2 OR ERCUNI OR ERCU (540 °C, OR 1000 °F)	ERCUSN-A (65 °C MAX, OR 150 °F MAX)	ERCUAL-A2 (65 °C MAX, OR 150 °F MAX)	ERCUAL-A2 (65 °C MAX, OR 150 °F MAX)	. . .
NICKEL ALLOYS					
NICKEL AND NI-CU ALLOYS	ERCUNI OR ERCUNI-7 (540 °C, OR 1000 °F)	(A)	(A)	(A)	ERCUNI OR ERCUNI-7 (65 °C MAX, OR 150 °F MAX)
NI-CR, NI-FE, AND NI-CR-FE ALLOYS	ERCUNI-3 (540 °C, OR 1000 °F)	(A)	(A)	(A)	ERCUNI-3 (65 °C MAX, OR 150 °F MAX)
STEELS					
LOW-CARBON STEELS	ERCUAL-A2 OR ERCU OR ERCUNI-3 (540 °C, OR 1000 °F)	ERCUSN-A (200 °C, OR 400 °F)	ERCUAL-A2 (150 °C, OR 300 °F)	ERCUAL-A2 (65 °C MAX, OR 150 °F MAX)	ERCUAL-A2 OR ERCUNI-3 (65 °C MAX, OR 150 °F MAX)
MEDIUM-CARBON STEELS	ERCUAL-A2 OR ERCU OR ERCUNI-3 (540 °C, OR 1000 °F)	ERCUSN-A (200 °C, OR 400 °F)	ERCUAL-A2 (200 °C, OR 400 °F)	ERCUAL-A2 (65 °C MAX, OR 150 °F MAX)	ERCUAL-A2 OR ERCUNI-3 (65 °C MAX, OR 150 °F MAX)
HIGH-CARBON STEELS	ERCUAL-A2 OR ERCU OR ERCUNI-3 (540 °C, OR 1000 °F)	ERCUSN-A (260 °C, OR 500 °F)	ERCUAL-A2 (260 °C, OR 500 °F)	ERCUAL-A2 (200 °C, OR 400 °F)	ERCUAL-A2 OR ERCUNI-3 (65 °C MAX, OR 150 °F MAX)
LOW-ALLOY STEELS	ERCUAL-A2 OR ERCU OR ERCUNI-3 (540 °C, OR 1000 °F)	ERCUSN-A (260 °C, OR 500 °F)	ERCUAL-A2 (260 °C, OR 500 °F)	ERCUAL-A2 (200 °C, OR 400 °F)	ERCUAL-A2 OR ERCUNI-3 (65 °C MAX, OR 150 °F MAX)
STAINLESS STEELS	ERCUAL-A2 OR ERCU OR ERCUNI-3 (540 °C, OR 1000 °F)	ERCUSN-A (200 °C, OR 400 °F)	ERCUAL-A2 (65 °C MAX, OR 150 °F MAX)	ERCUAL-A2 (65 °C MAX, OR 150 °F MAX)	ERCUAL-A2 OR ERCUNI-3 (65 °C MAX, OR 150 °F MAX)

Notes: (1) Filler metal selections shown are based on weldability except where mechanical properties are usually more important. (2) Preheating usually is used only when at least one member is thicker than 3.2 mm ($\frac{1}{8}$ in.) or is highly conductive (see text). Preheat and interpass temperatures are subject to adjustment based on size and shape of weldment.

(A) THESE COMBINATIONS ARE SELDOM WELDED; AS A STARTING POINT IN DEVELOPING WELDING PROCEDURES, USE OF ERCUAL-A2 FILLER METALS IS RECOMMENDED, EXCEPT FOR COMBINATIONS INCLUDING PHOSPHOR BRONZE.

TABLE 16 ELECTRODES AND PREHEAT AND INTERPASS TEMPERATURES USED IN GMAW OF COPPER AND COPPER ALLOYS TO DISSIMILAR METALS

METAL TO BE WELDED	**ELECTRODES (WITH PREHEAT AND INTERPASS TEMPERATURES) FOR WELDING METAL IN COLUMN 1 TO:**						
	COPPERS	**LOW-ZINC**	**HIGH-ZINC**	**PHOSPHOR BRONZES**	**ALUMINUM BRONZES**	**SILICON BRONZES**	**COPPER-NICKEL**

		BRASSES	BRASSES, TIN BRASSES, AND SPECIAL BRASSES				ALLOYS
COPPER ALLOYS							
LOW-ZINC BRASSES	ERCUSN-A OR ERCU (540 °C, OR 1000 °F)	. . .	. . .	. . .	. . .	. . .	. . .
HIGH-ZINC, TIN, SPECIAL BRASSES	ERCUSI-A OR ERCUSN-A OR ERCU (540 °C, OR 1000 °F)	ERCUSN-A (315 °C, OR 600 °F)	. . .	. . .	. . .	. . .	. . .
PHOSPHOR BRONZES	ERCUSN-A OR ERCU (540 °C, OR 1000 °F)	ERCUSN-A (260 °C, OR 500 °F)	ERCUSN-A (315 °C. OR 600 °F)	. . .	. . .	. . .	. . .
ALUMINUM BRONZES	ERCUAL-A2 (540 °C, OR 1000 °F)	ERCUAL-A2 (315 °C, OR 600 °F)	ERCUAL-A2 (315 °C, OR 600 °F)	ERCUAL-A2 OR ERCUSN-A (200 °C, OR 400 °F)	. . .	. . .	. . .
SILICON BRONZES	ERCUSN-A OR ERCU (540 °C, OR 1000 °F)	ERCUAL-A2 OR ERCUSI-A (65 °C, OR 150 °F)	ERCUAL-A2 OR ERCUSI-A 65 °C, OR 150 °F)	ERCUSI-A (65 °C, OR 150 °F)	ERCUAL-A2 (65 °C, OR 150 °F)	. . .	. . .
COPPER-NICKEL ALLOYS	ERCUAL-A2 OR ERCUNI OR ERCU (540 °C, OR 1000 °F)	ERCUAL-A2 (65 °C, OR 150 °F)	ERCUAL-A2 (65 °C, OR 150 °F)	ERCUSN-A (65 °C, OR 150 °F)	ERCUAL-A2 (65 °C, OR 150 °F)	ERCUAL-A2 (65 °C, OR 150 °F)	. . .
NICKEL ALLOYS							
NICKEL AND NI-CU ALLOYS	ERCUNI OR ERCUNI-7 (540 °C, OR 1000 °F)	(A)	(A)	(A)	(A)	(A)	ERCUNI OR ERCUNI-7 (65 °C, OR 150 °F)
NI-CR, NI-FE, AND NI-CR-FE ALLOYS	ERCUNI-3 (540 °C, OR 1000 °F)	(A)	(A)	(A)	(A)	(A)	ERCUNI-3 (65 °C, OR 150 °F)
STEELS							
LOW-CARBON STEELS	ERCUAL-A2 OR ERCU OR ERCUNI-3 (540 °C, OR 1000 °F)	ERCUSN-A (315 °C, OR 600 °F)	ERCUAL-A2 (260 °C, OR 500 °F)	ERCUSN-A (200 °C, OR 400 °F)	ERCUAL-A2 (150 °C, OR 300 °F)	ERCUAL-A2 (65 °C, OR 150 °F)	ERCUAL-A2 OR ERCUNI-3 (65 °C, OR 150 °F)
MEDIUM-CARBON STEELS	ERCUAL-A2 OR ERCU OR ERCUNI-3 (540 °C, OR 1000 °F)	ERCUAL-A2 (315 °C, OR 600 °F)	ERCUAL-A2 (260 °C, OR 500 °F)	ERCUSN-A (200 °C, OR 400 °F)	ERCUAL-A2 (150 °C, OR 300 °F)	ERCUAL-A2 (65 °C, OR 150 °F)	ERCUAL-A2 OR ERCUNI-3 (65 °C, OR 150 °F)
HIGH-CARBON STEELS	ERCUAL-A2 OR ERCU	ERCUAL-A2 (315 °C,	ERCUAL-A2 (260 °C, OR	ERCUSN-A (260 °C, OR 500 °F)	ERCUAL-A2 (260 °C, OR 500 °F)	ERCUAL-A2 (200 °C, OR	ERCUAL-A2 OR ERCUNI-3

	OR ERCUNI-3 (540 °C, OR 1000 °F)	OR 600 °F)	500 °F)			400 °F)	(65 °C, OR 150 °F)
LOW-ALLOY STEELS	ERCUAL-A2 OR ERCU OR ERCUNI-3 (540 °C, OR 1000 °F)	ERCUAL-A2 (315 °C, OR 600 °F)	ERCUAL-A2 (315 °C, OR 600 °F)	ERCUSN-A (260 °C, OR 500 °F)	ERCUAL-A2 (260 °C, OR 500 °F)	ERCUAL-A2 (200 °C, OR 400 °F)	ERCUAL-A2 OR ERCUNI-3 (65 °C, OR 150 °F)
STAINLESS STEELS	ERCUAL-A2 OR ERCU OR ERCUNI-3 (540 °C, OR 1000 °F)	ERCUAL-A2 OR ERCUSN-A (315 °C, OR 600 °F)	ERCUAL-A2 (315 °C, OR 600 °F)	ERCUSN-A (200 °C, OR 400 °F)	ERCUAL-A2 (95 °C MAX, OR 200 °F MAX)	ERCUAL-A2 (95 °C MAX, OR 200 °F MAX)	ERCUAL-A2 OR ERCUNI-3 (65 °C MAX, OR 150 °F MAX)
CAST IRONS							
GRAY AND MALLEABLE IRONS	ERCUAL-A2 OR ERCU (540 °C, OR 1000 °F)	ERCUAL-A2 OR ERCUSN-A (315 °C, OR 600 °F)	ERCUAL-A2 (315 °C, OR 600 °F)	ERCUSN-A (200 °C, OR 400 °F)	ERCUAL-A2 (200 °C, OR 400 °F)	ERCUAL-A2 OR ERCUSI-A (150 °C, OR 300 °F)	ERCUAL-A2 OR ERCUNI (65 °C MAX, OR 150 °F MAX)
DUCTILE IRONS	ERCUAL-A2 OR ERCU (540 °C, OR 1000 °F)	ERCUAL-A2 (315 °C, OR 600 °F)	ERCUAL-A2 (315 °C, OR 600 °F)	ERCUSN-A (200 °C, OR 400 °F)	ERCUAL-A2 (95 °C MAX, OR 200 °F MAX)	ERCUAL-A2 OR ERCUSI-A (150 °C MAX, OR 300 °F)	ERCUAL-A2 OR ERCUNI (65 °C MAX, OR 150 °F MAX)

Notes: (1) Electrode selections in table are based on weldability, except where mechanical properties are usually more important. (2) Preheating usually is used only when at least one member is thicker than 3.2 mm ($\frac{1}{8}$ in.) or is highly conductive (see text). Preheat and interpass temperature are subject to adjustment based on size and shape of weldment.

(A) THESE COMBINATIONS ARE SELDOM WELDED; AS A STARTING POINT IN DEVELOPING WELDING PROCEDURES, USE OF ERCUAL-A2 ELECTRODES IS RECOMMENDED, EXCEPT FOR COMBINATIONS INCLUDING PHOSPHOR BRONZE.

Gas-Tungsten Arc Welding

Copper and many copper alloys can be gas-tungsten arc welded to other materials with good results. The use of a filler metal is typically required. Copper and its alloys have been readily gas-tungsten arc welded to steels, stainless steels, nickel, and nickel alloys. Gas-tungsten arc welding for the joining of these dissimilar metals is usually restricted to thin sections less than 3 mm (0.13 in.) thick. Preliminary surface welding, also known as buttering, is ordinarily not required for thin sections. For section thicknesses exceeding 3 mm (0.13 in.), the preferred joining process is GMAW or SMAW. Usually, when GTAW is used to join copper alloys to dissimilar metals, the arc is directed at the more conductive metal being welded. Table 15 shows combinations of dissimilar metals that are joined by GTAW with the aid of copper alloy or nickel alloy filler metals. The recommended filler metals, preheat temperature, and interpass temperature for each combination are given.

Except when one or both members of the joint being welded have high thermal conductivity, preheating is not required for GTAW of copper and dissimilar metals. This is restricted to section thicknesses of 3 mm (0.13 in.) or less.

Gas-Metal Arc Welding

The GMAW process can be used for joining nearly all combinations of the weldable copper alloys. Two major considerations when developing the GMAW procedures are: (1) the composition of the welding wire to be used as an

electrode; and (2) the preheat temperatures required. As with the other arc welding processes, the arc is typically directed at the more conductive material to concentrate the heat energy on this base metal.

The electrodes as well as preheat and interpass temperatures for GMAW of copper and copper alloys to dissimilar metals are given in Table 16. This table includes all alloys listed in Table 15 for GTAW, plus the high-zinc brasses, tin brasses, and special brasses. As is shown in Table 16, ERCu-A1-A2 comes close to being the universal electrode for GMAW of dissimilar copper alloys. However, this filler metal is incompatible with phosphor bronzes. Silicon bronze (ERCuSi-A) and phosphor bronze (ERCuSn-A) electrodes are useful for many combinations of copper alloys that do not contain nickel. Copper electrodes (ERCu) are suitable for final welding passes (cap or cover passes) of coppers to any of the commonly welded copper alloys. Underlying or preliminary weld deposits are typically made with alloy electrodes. For joining copper to copper-nickel alloys, ERCuNi (copper-nickel) electrodes are generally used.

Generally, for welding dissimilar copper alloys, the electrode selected should be suitable for welding one of the materials within the combination to itself. The primary exception to this general rule is in the welding of silicon bronzes to copper-nickel alloys. The only electrode that can be used successfully for the joining of this combination is ERCuAl-A2.

As has been stated in the sections of this article dealing with specific alloy groups, alloys which have susceptibility to hot cracking, oxide formation, or other deterrents to weld strength characteristics should be noted when welding a dissimilar-metal combination. Typically, the restrictions for preheat, interpass temperature, and surface cleansing that apply to the individual alloy also apply to that alloy when joining it to other copper alloys or other metal groups. Of particular importance is preheat and interpass temperature for alloys that exhibit hot shortness.

For GMAW of copper or copper alloys to ferrous or nickel alloys, the primary consideration is dilution. Strength is not a factor because it is quite easy to generate weld metal whose strength is equal to that of the two base materials. The difficulty is in retaining the ductility demanded by the in-service requirements of the weldment. The most serious effect of excessive dilution is the formation of shrinkage cracks. These can start in the weld metal itself and propagate into the base metal.

Two methods are frequently used to control dilution in GMAW of combinations involving copper alloys. The first is to braze one side of the joint, thus promoting a minimum amount of dilution on that side, and weld the other side of the joint. The second technique is to overlay one or both joint surfaces with a buffer material. This technique, known as buttering, is typically used on thicker sections. Filler-metal selection again should be based upon the composition of the base alloy and the requirements for weld-metal strength and ductility. Additional information on buttering can be found in the article "Hardfacing, Weld Cladding, and Dissimilar Metal Joining" in this Volume.

Welding of Copper Alloys

Revised by M. Ned Rogers, Batesville Casket Company

Safe Welding Practices

Many of the elements used in producing copper alloys, as well as copper itself, have low or very low permissible exposure limits, as set by the American Conference of Governmental Industrial Hygienists. These would include such elements as arsenic, beryllium, cadmium, chromium, lead, manganese, and nickel. When welding, brazing, or soldering copper or copper alloys, adequate ventilation is required to ensure that contaminant levels do not exceed the human exposure limits. Precautions may include local exhaust ventilation, general area exhaust ventilation, operator respiratory protection, or a combination of these. The reader is referred to ANSI/AWS Z49.1, "Safety in Welding and Cutting," for detailed information.

Copper alloys that contain appreciable amounts of beryllium, cadmium, or chromium may present health hazards to the welder and others. Exposure to welding fumes containing these elements can produce adverse health defects. The user should consult the Occupational Safety and Health Administration guidelines for the specific element.

Fumes and dust of copper and zinc can cause irritation of the upper respiratory tract, nausea, metal-fume fever, skin irritation, dermatitis, and eye problems. It should be noted that cadmium and beryllium fumes are toxic when inhaled.

Fluxes used during welding, brazing, and soldering of certain copper alloys may contain fluorides and chlorides. Again, these fumes can be irritating to the eyes, nose, throat, and skin. Additionally, some fluorine compounds are toxic.

Proper personal hygiene must be emphasized, particularly before eating. Food and beverages should not be stored or consumed in and/or around the work area. Contaminated clothing should be changed. For more detailed information on safety considerations, see the article "Safe Practices" in this Volume.

Welding of Copper Alloys

Revised by M. Ned Rogers, Batesville Casket Company

Selected References

- H.B. CARY, *MODERN WELDING TECHNOLOGY,* 2ND ED., PRENTICE-HALL, 1991
- "GUIDE TO THE WELDING OF COPPER-NICKEL ALLOYS," INTERNATIONAL NICKEL COMPANY, 1979
- E.F. NIPPES, ED., 9TH ED., VOL 6, *METALS HANDBOOK,* AMERICAN SOCIETY FOR METALS, 1984
- "SAFETY IN CUTTING AND WELDING," ANSI/ IAWS Z49.1, AMERICAN WELDING SOCIETY, 1988
- "SPECIFICATION FOR COPPER AND COPPER ALLOY BARE WELDING RODS AND ELECTRODES," AWS A5.7, AMERICAN WELDING SOCIETY, 1984
- "SPECIFICATION FOR COPPER AND COPPER ALLOY ELECTRODES," AWS A5.6, AMERICAN WELDING SOCIETY, 1984
- "SPECIFICATION FOR COPPER AND COPPER ALLOY GAS WELDING RODS," AWS A5.27, AMERICAN WELDING SOCIETY, 1979
- *WELDING HANDBOOK,* 8TH ED., VOL 2, AMERICAN WELDING SOCIETY, 1991

Introduction

MOST MAGNESIUM ALLOYS can be joined by gas-tungsten arc welding (GTAW) and gas-metal arc welding (GMAW). Relative weldability ratings, joint design and surface preparation, and the use of filler metals and shielding gases suitable to arc welding are discussed in this article. For more information on arc welding, see the Section "Fusion Welding Processes" in this Volume.

Weldability

Table 1 lists some magnesium alloys that are weldable, along with their respective weldability ratings based on a scale of A (excellent) to D (limited). This rating is based largely on freedom from susceptibility to cracking, and to some extent on joint efficiency. Under optimum welding conditions, including favorable joint design, joint efficiencies of 60 to 100% can be obtained for virtually all of the magnesium alloys. Alloys rated A in Table 1 are likely to have high joint efficiency ratings.

TABLE 1 RELATIVE ARC WELDABILITY OF MAGNESIUM ALLOYS

A, excellent; B, good; C, fair; D, limited weldability

ALLOY	RATING
CASTING ALLOYS	
AM100A	B+
AZ63A	C
AZ81A	B+
AZ91C	B+
AZ92A	B
EK30A	B
EK41A	B
EQ21	B
EZ33A	A
HK31A	B+
HZ32A	B
K1A	A
QE22A	B
ZE41A	B
QH21A	B
WE43	B-
WE54	B-
ZC63	B-
ZH62A	C-
ZK51A	D
ZK61A	D
WROUGHT ALLOYS	
AZCOML	A
AZ10A	A
AZ31B,C	A

AZ80A	B
HK31A	A
HM21A	A
HM31A	A
ZE10A	A
ZK21A	B

In the magnesium-aluminum-zinc alloys (AZ31B, AZ61A, AZ63A, AZ80A, AZ81A, AZ91C, and AZ92A), aluminum content up to about 10% (Table 2) aids weldability by helping to refine the grain structure, while zinc content of more than 1% increases hot shortness, which may cause weld cracking. Alloys with high zinc content (ZH62A, ZK51A, ZK60A, and ZK61A) are highly susceptible to cracking and have poorer weldability. Thorium-containing alloys (HK31A, HM21A, and HM31A) have excellent arc weldability and are rated B + or A in Table 1.

TABLE 2 COMPOSITION OF SELECTED MAGNESIUM ALLOYS

DESIGNATION		**COMPOSITION, WT%**									
ASTM	**UNS NO.**	**Al**	**Li**	**Mn**	**Rare earths**	**Th**	**Zn**	**Zr**	**Ca**	**Cu**	**Fe**
9980A	M19980	. . .	. . .	0.10	. . .	. . .	. . .	. . .	. . .	0.02	. . .
9980B	M19981	. . .	. . .	0.10	. . .	. . .	. . .	. . .	. . .	0.021	. . .
9990A	M19990	0.003	. . .	0.004	. . .	. . .	. . .	. . .	. . .	. . .	0.04
9990B	M19991	0.005	. . .	0.004	. . .	. . .	. . .	. . .	. . .	. . .	0.011
9995A	M19995	0.010	. . .	0.004	. . .	. . .	. . .	. . .	. . .	. . .	0.003
9998A	M19998	0.004	. . .	0.002	. . .	. . .	. . .	. . .	. . .	0.0005	0.002
A3A	M10030	2.5-3.5	. . .	0.005	0.001	. . .	0.10	. . .	. . .	0.005	0.005
AM60A	M10600	5.5-6.5	. . .	0.13 MIN	. . .	. . .	0.22	. . .	. . .	0.35	. . .
AM80A	M10800	8.0-9.0	. . .	0.18 MIN	. . .	. . .	0.20	. . .	. . .	0.08	. . .
AM90A	M10900	8.5-9.5	. . .	0.15 MIN	. . .	. . .	0.20	. . .	. . .	0.10	0.008
AM100A	M10100	9.3-10.7	. . .	0.10 MIN	. . .	. . .	0.30	. . .	. . .	0.10	. . .
AM100B	M10102	9.4-10.6	. . .	0.13 MIN	. . .	. . .	. . .	. . .	. . .	0.08	. . .
AS41A	M10410	3.5-5.0	. . .	0.20-0.50	. . .	. . .	0.12	. . .	. . .	0.06	. . .
AZ10A	M11100	1.0-1.5	. . .	0.20 MIN	. . .	. . .	0.20-0.6	. . .	0.04	0.10	0.005
AZ21A	M11210	1.6-2.5	. . .	0.15	. . .	. . .	0.8-1.6	. . .	0.10-0.25	0.05	0.005
AZ31A	M11310	2.5-3.5	. . .	0.20 MIN	. . .	. . .	0.6-1.4	. . .	0.30	0.05	0.005
AZ31B	M11311	2.5-3.5	. . .	0.20 MIN	. . .	. . .	0.6-1.4	. . .	0.04	0.05	0.005
AZ31C	M11312	2.4-3.6	. . .	0.15 MIN	. . .	. . .	0.50-1.5	. . .	. . .	0.10	. . .
AZ61A	M11610	5.8-7.2	. . .	0.15 MIN	. . .	. . .	0.40-1.5	. . .	. . .	0.05	0.005

AZ63A	M11630	5.3-6.7	. . .	0.15 MIN	. . .	. . .	2.5-3.5	. . .	. . .	0.25	. . .
AZ80A	M11800	7.8-9.2	. . .	0.12 MIN	. . .	. . .	0.20-0.8	. . .	. . .	0.05	0.005
AZ81A	M11810	7.0-8.1	. . .	0.13 MIN	. . .	. . .	0.40-1.0	. . .	. . .	0.10	. . .
AZ90A	M11900	8.5-9.5	. . .	0.15 MIN	. . .	. . .	0.20	. . .	. . .	0.02	0.015
AZ91A	M11910	8.5-9.5	. . .	0.15 MIN	. . .	. . .	0.45-0.9	. . .	. . .	0.08	. . .
AZ91B	M11912	8.5-9.5	. . .	0.15 MIN	. . .	. . .	0.45-0.9	. . .	. . .	0.25	. . .
AZ91C	M11914	8.1-9.3	. . .	0.13 MIN	. . .	. . .	0.40-1.0	. . .	. . .	0.10	. . .
AZ92A	M11920	8.3-9.7	. . .	0.10 MIN	. . .	. . .	1.6-2.4	. . .	. . .	0.25	. . .
AZ101A	M11101	9.5-10.5	. . .	0.13 MIN	. . .	. . .	0.75-1.25	. . .	. . .	0.05	0.005
AZ125A	M11125	11.0-13.0	. . .	. . .	. . .	. . .	4.5-5.5	. . .	. . .	. . .	. . .
EK30A	M12300	. . .	. . .	. . .	2.5-4.0	. . .	0.30	0.20 MIN	. . .	0.10	. . .
EK41A	M12410	. . .	. . .	. . .	3.0-5.0	. . .	0.30	0.40-1.0	. . .	0.10	. . .
EZ33A	M12330	. . .	. . .	. . .	2.5-4.0	. . .	2.0-3.1	0.50-1.0	. . .	0.10	. . .
HK31A	M13310	. . .	. . .	. . .	. . .	2.5-4.0	0.30	0.40-1.0	. . .	0.10	. . .
HM21A	M13210	. . .	. . .	0.45-1.1	. . .	1.5-2.5	. . .	. . .	. . .	. . .	. . .
HM31A	M13312	. . .	. . .	1.2 MIN	. . .	2.5-3.5	. . .	. . .	. . .	. . .	. . .
HZ32A	M13320	. . .	. . .	. . .	0.10	2.5-4.0	1.7-2.5	0.50-1.0	. . .	0.10	. . .
K1A	M18010	. . .	. . .	. . .	. . .	. . .	. . .	0.40-1.0	. . .	. . .	. . .
LA141A	M14141	1.0-1.5	13.0-15.0	0.15 MIN	. . .	. . .	. . .	. . .	. . .	0.005	. . .
LS141A	M14142	0.05	12.0-15.0	0.15	. . .	. . .	. . .	. . .	. . .	0.05	0.005
LZ145A	M14145	0.05	12.0-15.0	0.15	. . .	. . .	4.5-5.0	. . .	. . .	0.05	0.005
M1A	M15100	. . .	. . .	1.2 MIN	. . .	. . .	. . .	. . .	0.30	0.05	. . .
M1B	M15101	. . .	. . .	1.3 MIN	. . .	. . .	. . .	. . .	. . .	0.08	. . .
M1C	M15102	0.01	. . .	0.9-1.2	. . .	. . .	. . .	. . .	. . .	0.02	0.03
TA54A	M18540	3.0-4.0	. . .	0.20 MIN	. . .	. . .	0.30	. . .	. . .	0.05	. . .
QE22A	M18220	. . .	. . .	. . .	1.8-2.5[(A)]	. . .	. . .	0.40-1.0	. . .	0.10	. . .
QH21A	M18210	. . .	. . .	. . .	0.6-	0.6-	0.20	0.40-	. . .	0.10	. . .

					1.5[B][C]	1.6[C]		1.0[D]			
ZE10A	M16100	. . .	. . .	. . .	0.12-0.22	. . .	1.0-1.5	. . .	. . .	. . .	. . .
ZE41A	M16410	. . .	. . .	0.15	0.75-1.75	. . .	3.5-5.0	0.40-1.0	. . .	0.10	. . .
ZE63A	M16630	. . .	. . .	. . .	2.1-3.0	. . .	5.5-6.0	0.40-1.0	. . .	0.10	. . .
ZH62A	M16620	. . .	. . .	. . .	. . .	1.4-2.2	5.2-6.2	0.50-1.0	. . .	0.10	. . .
ZK21A	M16210	. . .	. . .	. . .	. . .	. . .	2.0-2.6	0.45-0.8	. . .	0.10	. . .
ZK40A	M16400	. . .	. . .	. . .	. . .	. . .	3.5-4.5	0.45 MIN	. . .	0.10	. . .
ZK51A	M16510	. . .	. . .	. . .	. . .	. . .	3.6-5.5	0.50-1.0	. . .	. . .	. . .
ZK60A	M16600	. . .	. . .	. . .	. . .	. . .	4.8-6.2	0.45 MIN	. . .	. . .	. . .
ZK60B	M16601	. . .	. . .	. . .	. . .	. . .	4.8-6.8	0.45 MIN	. . .	. . .	. . .
ZK61A	M16610	. . .	. . .	. . .	. . .	. . .	5.5-6.5	0.6-1.0	. . .	. . .	. . .

DESIGNATION		**COMPOSITION, WT%**					**OTHER ELEMENTS**			**Mg**
ASTM	**UNS NO.**	**Si**	**Ag**	**Cd**	**Ni**	**Pb**	**OTHER**	**EACH**	**TOTAL**	
9980A	M19980	. . .	. . .	. . .	0.001	0.01	0.01 SN	0.05	. . .	99.80 MIN
9980 B	M19981	. . .	. . .	. . .	0.005	0.01	0.01 SN	0.05	. . .	99.80 MIN
9990A	M19990	0.005	. . .	0.0001	0.001	. . .	0.00007 B	0.01	. . .	99.90 MIN
9990B	M19991	0.005	. . .	. . .	0.001	. . .	. . .	0.01	. . .	99.90 MIN
9995A	M19995	0.005	. . .	0.00005	0.001	. . .	0.00003 B 0.01 TI	0.005	. . .	99.95 MIN
9998A	M19998	0.003	. . .	0.00005	0.00005	0.001	0.00003 B 0.001 TI	0.005	. . .	99.98 MIN
A3A	M10030	. . .	0.001	0.001	0.001	. . .	. . .	. . .	0.30	BAL
AM60A	M10600	0.50	. . .	. . .	0.03	. . .	. . .	. . .	0.30	BAL
AM80A	M10800	0.20	. . .	. . .	0.01	. . .	. . .	. . .	0.30	BAL
AM90A	M10900	0.15	0.008	. . .	0.005	. . .	. . .	0.02	0.10	BAL
AM100A	M10100	0.30	. . .	. . .	0.01	. . .	. . .	. . .	0.30	BAL
AM100B	M10102	1.0	. . .	. . .	0.01	. . .	. . .	. . .	0.30	BAL
AS41A	M10410	0.50-1.5	. . .	. . .	0.03	. . .	. . .	. . .	0.30	BAL
AZ10A	M11100	0.10	. . .	. . .	0.005	. . .	. . .	. . .	0.30	BAL
AZ21A	M11210	0.05	. . .	. . .	0.002	. . .	. . .	. . .	0.30	BAL
AZ31A	M11310	0.30	. . .	. . .	0.005	. . .	. . .	. . .	0.30	BAL
AZ31B	M11311	0.10	. . .	. . .	0.005	. . .	. . .	. . .	0.30	BAL
AZ31C	M11312	0.10	. . .	. . .	0.03	. . .	. . .	. . .	0.30	BAL
AZ61A	M11610	0.10	. . .	. . .	0.005	. . .	. . .	. . .	0.30	BAL

AZ63A	M11630	0.30	. . .	. . .	0.01	. . .	. . .	. . .	0.30	BAL
AZ80A	M11800	0.10	. . .	. . .	0.005	. . .	. . .	. . .	0.30	BAL
AZ81A	M11810	0.30	. . .	. . .	0.01	. . .	. . .	. . .	0.30	BAL
AZ90A	M11900	0.20	. . .	. . .	0.005	. . .	. . .	0.07	0.30	BAL
AZ91A	M11910	0.20	. . .	. . .	0.01	. . .	. . .	. . .	0.30	BAL
AZ91B	M11912	0.20	. . .	. . .	0.01	. . .	. . .	. . .	0.30	BAL
AZ91C	M11914	0.30	. . .	. . .	0.01	. . .	. . .	. . .	0.30	BAL
AZ92A	M11920	0.30	. . .	. . .	0.01	. . .	. . .	. . .	0.30	BAL
AZ101A	M11101	0.05	. . .	. . .	0.005	. . .	. . .	0.0002-0.0008 BE	0.30	BAL
AZ125A	M11125	. . .	. . .	. . .	. . .	. . .	. . .	0.0002-0.0008 BE	0.30	BAL
EK30A	M12300	. . .	. . .	. . .	0.01	. . .	. . .	. . .	0.30	BAL
EK41A	M12410	. . .	. . .	. . .	0.01	. . .	. . .	. . .	0.30	BAL
EZ33A	M12330	. . .	. . .	. . .	0.01	. . .	. . .	. . .	0.30	BAL
HK31A	M13310	. . .	. . .	. . .	0.01	. . .	. . .	. . .	0.30	BAL
HM21A	M13210	. . .	. . .	. . .	. . .	. . .	. . .	. . .	0.30	BAL
HM31A	M13312	. . .	. . .	. . .	. . .	. . .	. . .	. . .	0.30	BAL
HZ32A	M13320	. . .	. . .	. . .	0.01	. . .	. . .	. . .	0.30	BAL
K1A	M18010	. . .	. . .	. . .	0.01	. . .	. . .	. . .	0.30	BAL
LA141A	M14141	0.004	. . .	. . .	0.005	. . .	0.005 NA	. . .	0.20	BAL
LS141A	M14142	0.50-0.6	. . .	. . .	0.005	. . .	0.005 NA	. . .	. . .	BAL
LZ145A	M14145	1.5-2.0	2.0-3.0	. . .	0.005	. . .	0.005 NA	. . .	0.20	BAL
M1A	M15100	0.10	. . .	. . .	0.01	. . .	. . .	. . .	0.30	BAL
M1B	M15101	0.10	. . .	. . .	0.01	. . .	. . .	. . .	0.20	BAL
M1C	M15102	. . .	. . .	. . .	0.001	. . .	. . .	0.05	0.30	BAL
TA54A	M18540	0.30	. . .	. . .	0.01	. . .	4.0-6.0 SN	. . .	0.30	BAL
QE22A	M18220	. . .	2.0-3.0	. . .	0.01	. . .	. . .	. . .	0.30	BAL
QH21A	M18210	. . .	2.0-3.0	. . .	0.01	. . .	. . .	. . .	0.30	BAL
ZE10A	M16100	. . .	. . .	. . .	. . .	. . .	. . .	. . .	0.30	BAL
ZE41A	M16410	. . .	. . .	. . .	0.01	. . .	. . .	. . .	0.30	BAL
ZE63A	M16630	. . .	. . .	. . .	0.01	. . .	. . .	. . .	0.30	BAL
ZH62A	M16620	. . .	. . .	. . .	0.01	. . .	. . .	. . .	0.30	BAL
ZK21A	M16210	. . .	. . .	. . .	0.01	. . .	. . .	. . .	0.30	BAL
ZK40A	M16400	. . .	. . .	. . .	0.01	. . .	. . .	. . .	0.30	BAL
ZK51A	M16510	. . .	. . .	. . .	. . .	. . .	. . .	. . .	0.30	BAL
ZK60A	M16600	. . .	. . .	. . .	. . .	. . .	. . .	. . .	0.30	BAL
ZK60B	M16601	. . .	. . .	. . .	. . .	. . .	. . .	. . .	0.30	BAL
ZK61A	M16610	. . .	. . .	. . .	. . .	. . .	. . .	. . .	0.30	BAL

Source: Ref 1

(A) RARE EARTH ELEMENTS ARE IN THE FORM OF DIDYMIUM.

(B) DIDYMIUM, NOT LESS THAN 70% NEODYMIUM ANY REMAINDER SUBSTANTIALLY PRAESODYMIUM.

(C) THORIUM AND DIDYMIUM TOTAL 1.5 TO 2.4.

(D) ZIRCONIUM SOLUBLE 0.40 MIN, BUT DETERMINATION NOT REQUIRED FOR ROUTINE ACCEPTANCE.

Welds in magnesium alloys are characterized by a fine grain size averaging less than 0.25 mm (0.01 in.). Magnesium alloys containing more than 1.5% Al are susceptible to stress corrosion, and residual welding stresses must be relieved.

Reference cited in this section

1. "STANDARD PRACTICE FOR CODIFICATION OF CERTAIN NONFERROUS METALS AND ALLOYS, CAST AND WROUGHT," B 275, *1989 ANNUAL BOOK OF STANDARDS,* VOL 2.02, *DIE-CAST METALS; ALUMINUM AND MAGNESIUM ALLOYS,* ASTM, 1989, P 325-326

Welding of Magnesium Alloys

Filler Metals

Compositions of the four most commonly used electrode wires for GMAW and filler metals (when used) for GTAW are given in Table 3. The choice of electrode wire or filler metal is governed by the composition of the base metal (Table 4).

TABLE 3 COMPOSITIONS OF ELECTRODES AND FILLER METALS USED IN GAS SHIELDED ARC WELDING OF MAGNESIUM ALLOYS PER AWS A5.19

FILLER METAL	COMPOSITION, WT%											
	Al	Be	Mn	Zn	Zr	Rare earth	Cu	Fe	Ni	Si	OTHERS (TOTAL)	MG
ER AZ61A	5.8-7.2	0.0002-0.0008	0.15 MIN	0.40-1.5	. . .	. . .	0.05 MAX	0.005 MAX	0.005 MAX	0.05 MAX	0.30 MAX	BAL
ER AZ101A	9.5-10.5	0.0002-0.0008	0.13 MIN	0.75-1.25	. . .	. . .	0.05 MAX	0.005 MAX	0.005 MAX	0.05 MAX	0.30 MAX	BAL
ER AZ92A	8.3-9.7	0.0002-0.0008	0.15 MIN	1.7-2.3	. . .	. . .	0.05 MAX	0.005 MAX	0.005 MAX	0.05 MAX	0.30 MAX	BAL
ER EZ33A	. . .	. . .	. . .	2.0-3.1	0.45-1.0	2.5-4.0	. . .	. . .	. . .	. . .	0.30 MAX	BAL

TABLE 4 SELECTION GUIDE FOR USING FILLER METAL TO JOIN TWO MAGNESIUM-BASE ALLOYS

BASE ALLOY	FILLER METAL FOR USE WITH INDICATED BASE ALLOYS																				
	AM100A	**AZ10A**	**AZ31, AZ31C**	**AZ61A**	**AZ63A**	**AZ80A**	**AZ81A**	**AZ91C**	**AZ92A**	**EK41A**	**EZ33A**	**HK31A**	**HM21A**	**HM31A**	**HZ32A**	**K1A**	**LA141A**	**M1A, MG1**	**QE22A**	**ZE10A**	**ZE41A**	**ZX21A**	**ZH62A, ZK51A, ZK60A, ZK61A**
AM100A	AZ92A, AZ101	... ...	... ...	... ...	... ...	... ...	... ...	... ...	... ...	... ...	... ...	... ...	... ...	... ...	... ...	... ...	... ...	... ...	... ...	... ...	... ...	... ...	... ...
AZ10A	AZ92A	AZ61A, AZ32A	... ...	... ...	... ...	... ...	... ...	... ...	... ...	... ...	... ...	... ...	... ...	... ...	... ...	... ...	... ...	... ...	... ...	... ...	... ...	... ...	... ...
AZ31B, AZ31C	AZ92A	AZ61A, AZ92A	AZ61A, AZ92A	... ...	... ...	... ...	... ...	... ...	... ...	... ...	... ...	... ...	... ...	... ...	... ...	... ...	... ...	... ...	... ...	... ...	... ...	... ...	... ...
AZ61A,	AZ92A	AZ61A, AZ92A	AZ61A, AZ92A	AZ61A, AZ92A	... ...	... ...	... ...	... ...	... ...	... ...	... ...	... ...	... ...	... ...	... ...	... ...	... ...	... ...	... ...	... ...	... ...	... ...	... ...
AZ63A	[A]	[A]	[A]	[A]	AZ92A	... ...	... ...	... ...	... ...	... ...	... ...	... ...	... ...	... ...	... ...	... ...	... ...	... ...	... ...	... ...	... ...	... ...	... ...
AZ80A	AZ92A	AZ61A, AZ92A	AZ61A, AZ92A	AZ61A, AZ92A	[A]	AZ61A, AZ92A	... ...	... ...	... ...	... ...	... ...	... ...	... ...	... ...	... ...	... ...	... ...	... ...	... ...	... ...	... ...	... ...	... ...
AZ81A	AZ92A	AZ92A	AZ92A	AZ92A	[A]	AZ92A	AZ92A, AZ101	... ...	... ...	... ...	... ...	... ...	... ...	... ...	... ...	... ...	... ...	... ...	... ...	... ...	... ...	... ...	... ...
AZ91C	AZ92A	AZ92A	AZ92A	AZ92A	[A]	AZ92A	AZ92A	AZ92A, AZ101	... ...	... ...	... ...	... ...	... ...	... ...	... ...	... ...	... ...	... ...	... ...	... ...	... ...	... ...	... ...
AZ92	AZ92	AZ9	AZ9	AZ9	[A]	AZ9	AZ9	AZ9	AZ1	...	...	...	...	...	...	...	...	...	...	...	...	...	...

A	A	2A	2A	2A		2A	2A	2A	01													
EK41 A	AZ92 A	AZ92A	AZ92A	AZ92A	(A)	AZ92A	AZ92A	AZ92A	AZ92A	EZ33A	. . .	. . .	. . .	. . .	. . .	. . .	. . .	. . .	. . .	. . .	. . .	. . .
EZ33 A	AZ92 A	AZ92A	AZ92A	AZ92A	(A)	AZ92A	AZ92A	AZ92A	AZ92A	EZ33A	EZ33A	. . .	. . .	. . .	. . .	. . .	. . .	. . .	. . .	. . .	. . .	. . .
HK31 A	AZ92 A	AZ92A	AZ92A	AZ92A	(A)	AZ92A	AZ92A	AZ92A	AZ92A	EZ33A	EZ33A	EZ33A	. . .	. . .	. . .	. . .	. . .	. . .	. . .	. . .	. . .	. . .
HM21 A	AZ92 A	AZ92A	AZ92A	AZ92A	(A)	AZ92A	AZ92A	AZ92A	AZ92A	EZ33A	EZ33A	EZ33A	EZ33A	. . .	. . .	. . .	. . .	. . .	. . .	. . .	. . .	. . .
HM31 A	AZ92 A	AZ92A	AZ92A	AZ92A	(A)	AZ92A	AZ92A	AZ92A	AZ92A	EZ33A	EZ33A	EZ33A	EZ33A	EZ33A	. . .	. . .	. . .	. . .	. . .	. . .	. . .	. . .
HZ32 A	AZ92 A	AZ92A	AZ92A	AZ92A	(A)	AZ92A	AZ92A	AZ92A	AZ92A	EZ33A	EZ33A	EZ33A	EZ33A	EZ33A	EZ33A	. . .	. . .	. . .	. . .	. . .	. . .	. . .
K1A	AZ92 A	AZ92A	AZ92A	AZ92A	(A)	AZ92A	AZ92A	AZ92A	AZ92A	EZ33A	EZ33A	EZ33A	EZ33A	EZ33A	EZ33A	EZ33A	. . .	. . .	. . .	. . .	. . .	. . .
M1A, MG1	AZ92 A	AZ61A, AZ92A	AZ61A, AZ92A	AZ61A, AZ92A	(A)	AZ61A, AZ92A	AZ92A	AZ92A	AZ92A	AZ92A	AZ92A	AZ92A	AZ92A	AZ92A	AZ92A	AZ92A	(B)	AZ61A, AZ92A	. . . . .	. . . . .	. . . . .	. . . . .
ZE41 A	(B)	(B)	(B)	(B)	(A)	(B)	(B)	(B)	(B)	EZ33A	EZ33A	EZ33A	EZ33A	EZ33A	EZ33A	EZ33A	(B)	(B)	EZ33A	(B)	EZ33A	. . .	. . .
ZX21 A	AZ92 A	AZ61A, AZ92A	AZ61A, AZ92A	AZ61A, AZ92A	(A)	AZ61A, AZ92A	AZ92A	AZ92A	AZ92A	AZ92A	AZ92A	AZ92A	AZ92A	AZ92A	AZ92A	AZ92A	(B)	AZ61A, AZ92A	AZ92A	AZ61A, AZ92A	AZ92A	AZ61A, AZ92A	. . . . .
ZH62A, ZK51A, ZK60A, ZK61A	(A)	(A)	(A)	(A)	(A)	(A)	(A)	(A)	(A)	(A)	(A)	(A)	(A)	(A)	(A)	(A)	(A)	(A)	(A)	(A)	(A)	(A)	EZ33A

(A) WELDING NOT RECOMMENDED.

(B) WELDING DATA NOT AVAILABLE

Electrode wires or filler metals having compositions conforming to ER AZ61A or ER AZ92A (Mg-Al-Zn) are considered satisfactory for welding alloys AZ10A, AZ31B, AZ31C, AZCOML, AZ61A, AZ80A, ZE10A, and ZK21A to themselves or to each other. ER AZ61A is usually preferred for welding aluminum-containing wrought products because of its tendency to resist crack sensitivity. The ER AZ92A filler metal shows less crack sensitivity for welding the cast magnesium-aluminum-zinc and magnesium-aluminum alloys. The same electrode wires or filler metals are used for joining any one of the above alloys to high-temperature alloys HK31A, HM21A, and HM31A. However, when the high-temperature alloys are joined to each other, ER EZ33A is recommended. Joints of wrought or cast alloys welded with ER EZ33A filler metal exhibit good mechanical properties at high temperatures.

The choice of electrode wire or filler metal for welding wrought alloys to cast alloys should be based on the recommendations outlined above, except that ER AZ101A may be used instead of ER AZ61A or ER AZ92A.

When aluminum-containing cast alloys are joined to aluminum-containing cast alloys, ER AZ101A or ER AZ92A electrode wire or filler metal is usually recommended. However, for joining HK31A and HZ32A to themselves or to each other, ER EZ33A is preferred; for joining HK31A and HZ32A to any of the other cast alloys, ER AZ101A is used. Filler rod of the same composition as the base metal should be used for most welds.

Shielding Gases

Only the inert gases are used for shielding in arc welding of magnesium alloys. Argon is the most widely used. Helium and various mixtures of argon and helium have also proved satisfactory, but because of the higher cost per unit volume of helium, and because two to three times more helium than argon is required for the same degree of shielding, the use of pure helium has gradually decreased. Pure helium is also undesirable because it raises the current required for spray arc transfer and increases weld spatter. The factors determining shielding-gas selection for magnesium alloys are similar to those for aluminum.

Joint Design

Typical joint designs for gas shielded arc welding of various thicknesses of magnesium alloy sheet and plate are presented in Table 5. The metal thickness ranges vary for GTAW in accordance with the type of current used (alternating current; direct current electrode negative, DCEN; and direct current electrode positive, DCEP) and vary for GMAW in accordance with the mode of metal transfer.

TABLE 5 TYPICAL JOINT DESIGNS USED FOR GAS SHIELDED ARC WELDING OF SELECTED THICKNESSES OF MAGNESIUM ALLOY SHEET AND PLATE

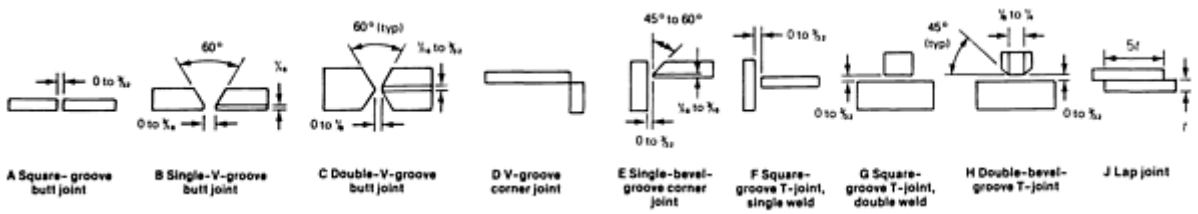

TYPE OF JOINT	APPLICABLE RANGE OF WORK-METAL THICKNESS[A]											
	GTAW[B]						GMAW[C]					
	AC		DCEN		DCEP		SHORT CIRCUITING		PULSED ARC		SPRAY ARC	
	mm	in.	mm	in.	mm	in.	mm	in.	mm	in.	mm	in.
A[D]	0.64-6.4	0.025-1/4	0.64-13	0.025-1/2	0.64	0.025-3/16	0.64-4.8	0.025-3/16	2.3-6.4	0.090-1/4	4.8-9.5	3/16-

												3/8
B[E]	6.4-9.5	1/4 3/8 3/8	6.4-9.5	1/4 - 3/8	4.8-9.5	3/16 - 3/8	[F]	[F]	4.8-6.4	3/16 - 1/4	6.4-13	1/4 - 1/2
C[G]	9.5[H]	3/8 [H]	9.5[H]	3/8 [H]	9.5[H]	3/8 [H]	[F]	[F]	[F]	[F]	13[H]	1/2 [H]
D[I]	1.0-6.4	0.04-1/4	1.0-6.4	0.040-1/4	1.0-6.4	0.040-1/4	1.6-4.8	1/16 - 3/16	1.6-6.4	1/16 - 1/4	4.8-13	3/16 - 1/2
E[J]	4.8[H]	3/16 [H]	4.8[H]	3/16 [H]	4.8[H]	3/16 [H]	[F]	[F]	3.2-6.4	1/8 - 1/4	6.4[H]	1/4 [H]
F[K]	0.64-6.4	0.025-1/4	0.64-13	0.025-1/2	0.64-4.0[H]	0.025-5/32 [H]	1.6-4.0	1/16 - 5/32	2.3-4.8	0.090-3/16	4.0-9.5	5/32 - 3/8
G[L]	1.6-4.8	1/16 - 3/16	1.6-9.5	1/16 - 3/8	1.6-3.2	1/16 - 1/8	1.6-4.0	1/16 - 5/32	2.3-6.4	0.090-1/4	4.0-19	5/32 - 3/4
H[M]	4.8[H]	3/16 [H]	9.5[H]	3/8 [H]	3.2[H]	1/8 [H]	[F]	[F]	6.4-9.5	1/4 - 3/8	9.5[H]	3/8 [H]
J[N]	1.0[H]	0.040[H]	1.0[H]	0.040[H]	0.64[H]	0.025[H]	1.0-4.0	0.040-5/32	2.3-6.4	0.090-1/4	4.0[H]	5/32 [H]

(A) SUGGESTED MINIMUM AND MAXIMUM THICKNESS LIMITS.

(B) USING 300 A AC OR DCEN, OR 125 A DCEP.

(C) USING 400 A DCEP.

(D) SINGLE-PASS FULL-PENETRATION WELD. SUITABLE FOR THIN MATERIAL.

(E) FULL-PENETRATION WELD. SUITABLE FOR THICK MATERIAL. ON MATERIAL THICKER THAN SUGGESTED MAXIMUM, USE DOUBLE-V-GROOVE BUTT JOINT TO MINIMIZE DISTORTION.

(F) NOT RECOMMENDED BECAUSE SPRAY ARC WELDING IS MORE PRACTICAL OR ECONOMICAL, OR BOTH.

(G) FULL-PENETRATION WELD. USED ON THICK MATERIAL. MINIMIZES DISTORTION BY EQUALIZING SHRINKAGE STRESS ON BOTH SIDES OF JOINT.

(H) NO MAXIMUM. THICKEST MATERIAL IN COMMERCIAL USE COULD BE WELDED IN THIS TYPE OF JOINT.

(I) SINGLE-PASS FULL-PENETRATION ESPECIALLY IF A SQUARE CORNER IS REQUIRED.

(J) SINGLE-PASS OR MULTIPLE-PASS FULL-PENETRATION WELD. USED ON THICK MATERIAL TO MINIMIZE WELDING. PRODUCES SQUARE JOINT CORNERS.

(K) SINGLE WELD T-JOINT. THICKNESS LIMITS ARE BASED ON 40% JOINT PENETRATION.

(L) DOUBLE WELD T-JOINT. SUGGESTED THICKNESS LIMITS BASED ON 100% JOINT PENETRATION.

(M) DOUBLE WELD T-JOINT. USED ON THICK MATERIAL REQUIRING 100% JOINT PENETRATION.

(N) SINGLE OR DOUBLE WELD JOINT. STRENGTH DEPENDS ON SIZE OF FILLET. MAXIMUM STRENGTH IN TENSION ON DOUBLE WELD JOINTS IS OBTAINED WHEN LAP EQUALS FIVE TIMES THE THICKNESS OF THE THINNER MEMBER.

Edges are prepared by milling, sawing, shearing, arc cutting, chipping, planing, routing, sanding, or filing. Sheet up to about 2.03 mm (0.080 in.) thick is generally single sheared; double shearing is preferred for sheet thicker than 2.03 mm (0.080 in.). Double-bevel edges are preferred over single-bevel edges because less distortion occurs during welding.

Fit-Up. Components of weldments should fit closely at abutting edges, preferably with no root opening, although a root opening up to 1.6 mm ($\frac{1}{16}$ in.) is usually permissible. If tack welds are used, the first tack should be a short distance from the end of a seam. The best practice in tack welding is to use 3.2 mm ($\frac{1}{8}$ in.) tacks spaced 25 to 50 mm (1 to 2 in.) on centers for sheet up to 1.65 mm (0.065 in.) thick, and 6.4 mm ($\frac{1}{4}$ in.) tacks spaced 100 to 125 mm (4 to 5 in.) on centers for sheet or plate from 1.65 to 6.4 mm (0.065 to $\frac{1}{4}$ in.) thick.

Welding fixtures must be rigid enough to resist movement of the workpieces during welding. Hold-down bars must exert enough pressure to keep the edges from overlapping or rising away from the backing bar or plate. A backing bar or strip normally is used when welding sheet metal components to help control joint penetration, root surface contour, and heat removal. The gas is usually supplied through holes in the backing strip. When a backing strip cannot be used because of space limitations, a chemical flux is sometimes painted on the root side of the joint to smooth the root surface and control joint penetration. Backing plates are made of mild steel, stainless steel, magnesium, aluminum, or copper and are cut with a small groove that is positioned directly under the seam. They prevent excessive metal drop-through and minimize distortion. Depth of the grooves in backing plates depends on base-metal thickness, the welding process used, and the absence or presence of a root opening in the joint. Typical groove depths are given in Table 6. When a temporary backing bar or strip is used, the root side of the joint should be shielded with inert gas to prevent oxidation of the root surface.

TABLE 6 TYPICAL DEPTH OF GROOVES IN BACKING BARS OR PLATES USED IN ARC WELDING OF MAGNESIUM ALLOYS

BASE-METAL THICKNESS		DEPTH OF GROOVE					
		GTAW		GMAW			
				NO ROOT OPENING(A)		ROOT OPENING	
mm	in.	mm	in.	mm	in.	mm	in.
0.64	0.025	0.38	0.015	0.51	0.020	0.51	0.020
1.02	0.040	0.51	0.020	0.76	0.030	0.51	0.020
1.60	0.063	0.64	0.025	1.02	0.040	0.76	0.030
2.29	0.090	0.76	0.030	1.52	0.060	1.02	0.040
3.18	0.125	0.76	0.030	1.78	0.070	1.02	0.040
4.06	0.160	1.02	0.040	1.78	0.070	1.27	0.050
4.83	0.190	1.02	0.040	1.78	0.070	1.27	0.050
6.35	0.250	1.27	0.050	1.78	0.070	1.52	0.060
9.53	0.375	1.52	0.060	2.03	0.080	1.52	0.060

(A) WITH NO ROOT OPENING, GROOVES IN BACKING BARS OR PLATES ARE DEEPER TO PERMIT BETTER BALANCE BETWEEN TOP AND BOTTOM WELD REINFORCEMENT. USE OF A ROOT OPENING PERMITS BALANCING REINFORCEMENT WITH A SHALLOWER GROOVE DEPTH.

Surface Preparation

Magnesium alloys are usually supplied with either an oil coating, an acid pickled surface, or a chromate coated surface. Surfaces and edges must be cleaned just before welding to remove oxides and dirt picked up during forming, assembly,

and fixturing. Electrode wire or filler metal must be mechanically or chemically cleaned. A partly used spool of electrode wire or filler metal should be properly stored to protect it from dirt.

Mechanical cleaning with aluminum or stainless steel wool, aluminum oxide abrasive cloth, or power wire brushes with stainless steel bristles is preferred for most production jobs. In shops where chemical finishing equipment is available, a cleaning bath of 190 mL/L (24 oz/gal) chromic acid, 40 mL/L ($5\frac{1}{3}$ oz/gal) ferric nitrate, 0.5 mL/L ($\frac{1}{16}$ oz/gal) potassium fluoride, and water to make 3.8 L (1 gal) can be used. Parts are dipped in this bath, which is maintained at 20 to 30 °C (70 to 90 °F), for about 3 min, then are rinsed thoroughly in hot water and dried in air. Ceramic or stainless steel tanks are preferred; tanks lined with lead, synthetic rubber, or a vinyl-based material are also acceptable.

Welding of Magnesium Alloys

Preheating

The need for preheating castings is determined largely by section thickness and amount of restraint. Thick sections, particularly if the magnitude of joint restraint is small, seldom need preheating. Thin sections and highly restrained joints often require preheating to prevent weld cracking, particularly in the high-zinc alloys. Maximum preheat temperatures for all of the common cast magnesium alloys are given in Table 7. In practice, if preheating is used, the temperature is usually less than the maximum shown in Table 7.

TABLE 7 PREHEAT TEMPERATURES AND POSTWELD HEAT TREATMENTS FOR MAGNESIUM ALLOY CASTINGS

ALLOY	TEMPER OF ALLOY[A]		MAXIMUM PREHEAT TEMPERATURE[B]		POSTWELD HEAT TREATMENT[C]
	BEFORE WELDING	AFTER TREATMENT	°C	°F	
AZ63A	T4	T4	380	720	$\frac{1}{2}$ H AT 390 °C (730 °F)
	T4 OR T6	T6	380	720	$\frac{1}{2}$ H AT 390 °C (730 °F) + 5 H AT 220 °C (425 °F)
	T5	T5	260[D]	500[D]	5 H AT 220 °C (425 °F)
AZ81A	T4	T4	400	750	$\frac{1}{2}$ H AT 415 °C (780 °F)
AZ91C	T4	T4	400	750	$\frac{1}{2}$ H AT 415 °C (780 °F)
	T4 OR T6	T6	400	750	$\frac{1}{2}$ H AT 415 °C (780 °F) + 4 H AT 215 °C (420 °F)[E]
AZ92A	T4	T4	400	750	$\frac{1}{2}$ H AT 410 °C (770 °F)
	T4 OR T6	T6	400	750	$\frac{1}{2}$ H AT 410 °C (770 °F) + 4 H AT 260 °C (500 °F)
AM100A	T6	T6	400	750	$\frac{1}{2}$ H AT 415 °C (780 °F) + 5 H AT 220 °C (425 °F)
EK30A	T6	T6	260[D]	500[D]	16 H AT 205 °C (400 °F)
EK41A	T4 OR T6	T6	260[D]	500[D]	16 H AT 205 °C (400 °F)
	T5	T5	260[D]	500[D]	16 H AT 205 °C (400 °F)
EQ21	T4 OR T6	T6	300	570	1 H AT 505 °C (940 °F)[F] + 16 H AT

					200 °C (390 °F)
EZ33A	F OR T5	T5	260[D]	500[D]	2 H AT 345 °C (650 °F)[G] + 5 H AT 215 °C (420 °F)
HK31A	T4 OR T6	T6	260	500	1 H AT 315 °C (600 °F)[G] + 16 H AT 205 °C (400 °F)
HZ32A	F OR T5	T5	260	500	16 H AT 315 °C (600 °F)
K1A	F	F	NONE	NONE	NONE
QE22A	T4 OR T6	T6	260	500	8 H AT 530 °C (985 °F)[F] + 8 H AT 205 °C (400 °F)
WE43	T4 OR T6	T6	300	570	1 H AT 510 °C (950 °F)[F] + 16 H AT 250 °C (480 °F)
WE54	T4 OR T6	T6	300	570	1 H AT 510 °C (950 °F)[F][H] + 16 H AT 250 °C (480 °F)[I]
ZC63	F OR T4	T6	250	480	1 H AT 425 °C (795 °F)[F] + 16 H AT 180 °C (355 °F)[I]
ZE41A	F OR T5	T5	315	600	2 H AT 330 °C (625 °F) + 16 H AT 175 °C (350 °F)[G]
ZH62A	F OR T5	T5	315	600	2 H AT 330 °C (625 °F) + 16 H AT 175 °C (350 °F)
ZK51A	F OR T5	T5	315	600	2 H AT 330 °C (625 °F) + 16 H AT 175 °C (350 °F)[G]
ZK61A	F OR T5	T5	315	600	48 H AT 150 °C (300 °F)
	T4 OR T6	T6	315	600	2-5 H AT 500 °C (930 °F) + 48 H AT 130 °C (265 °F)

(A) T4, SOLUTION HEAT TREATED; T6, SOLUTION HEAT TREATED AND ARTIFICIALLY AGED; T5, ARTIFICIALLY AGED; F, AS CAST. "AFTER TREATMENT" MEANS AFTER POSTWELD HEAT TREATMENT.

(B) HEAVY AND UNRESTRAINED SECTIONS USUALLY NEED NO PREHEAT; THIN AND RESTRAINED SECTIONS MAY NEED PREHEATING, UP TO MAXIMUM TEMPERATURES SHOWN, TO AVOID WELD CRACKING. A SULFUR DIOXIDE OR CARBON DIOXIDE ATMOSPHERE IS RECOMMENDED WHEN TEMPERATURE EXCEEDS 370 °C (700 °F).

(C) TEMPERATURES SHOWN ARE MAXIMUM ALLOWABLE. FURNACE CONTROLS SHOULD BE SET SO TEMPERATURE DOES NOT EXCEED INDICATED MAXIMUM. A SULFUR DIOXIDE OR CARBON DIOXIDE ATMOSPHERE IS RECOMMENDED WHEN TEMPERATURE EXCEEDS 370 °C (700 °F).

(D) FOR $1\frac{1}{2}$ H MAX.

(E) 16 H AT 170 °C (335 °F) MAY BE USED INSTEAD OF 4 H AT 215 °C (420 °F).

(F) QUENCH IN WATER AT 60 TO 105 °C (140 TO 220 °F) BEFORE SECOND HEAT TREATMENT.

(G) THIS PHASE OF HEAT TREATMENT IS OPTIONAL AND SERVES TO INDUCE GREATER STRESS RELIEF. SOME LOSS IN HIGH-TEMPERATURE CREEP STRENGTH MAY OCCUR IN EZ33A DUE TO THE 345 °C (650 °F) STRESS RELIEF.

(H) AIR COOL AFTER QUENCHING.

(I) AIR COOL AFTER SECOND HEAT TREATMENT

Welding of Magnesium Alloys

Gas-Metal Arc Welding

Power supplies used for welding magnesium alloys furnish DCEP. Constant-voltage machines must be used for short circuiting welding and are generally preferred for spray arc welding. Constant-current (drooping volt-ampere output)

machines can be used for spray arc welding and are sometimes advantageous for welding that is performed at a current level near the minimum for spray transfer because weld spatter is less. Special constant-voltage machines that are designed to pulse the current output must be used in pulsed arc welding. For detailed information on power supplies and modes of metal transfer, see the article "Power Sources" and "Transfer of Heat and Mass to the Base Metal in Gas-Metal Arc Welding" in this Volume.

Electrode holders, wire feeders, and related equipment used for GMAW of magnesium alloys are generally the same as those used for welding other metals.

Metal Transfer. Three modes of metal transfer are suitable for welding magnesium alloys: short circuiting, pulsed arc, and spray transfer. Pulsed arc transfer can be achieved only with a power supply designed to produce a pulsing secondary current. Without the pulsing feature, the type of transfer that would be obtained in the specific operating range of current, wire feed, and wire size for this process would be globular, which is not suitable for welding magnesium alloys.

Each of the three modes of transfer is best suited to a specific (sometimes overlapping) range of base-metal thickness and welding current, as shown in Table 8. Curves that show the relationship among current, electrode wire size, and wire-feed rate for each mode are presented in Fig. 1.

TABLE 8 TYPICAL OPERATING CONDITIONS FOR GAS-METAL ARC BUTT WELDING OF MAGNESIUM ALLOYS AT WELDING SPEED OF 610 TO 915 MM/MIN (24 TO 36 IN./MIN)

BASE-METAL THICKNESS		TYPE OF GROOVE	NO. OF PASSES	ELECTRODE DIAMETER		ELECTRODE FEED RATE		ELECTRODE CONSUMPTION OF WELD		CURRENT, A	VOLTAGE, V	ARGON FLOW RATE	
mm	in.			mm	in.	m/min	in./min	kg/m	lb/ft			m^3/h	ft^3/h
SHORT CIRCUITING MODE OF METAL TRANSFER													
0.64	0.025	SQUARE[A]	1	1.02	0.040	3.6	140	0.009	0.006	25	13	1.1-1.7	40-60
1.02	0.040	SQUARE[A]	1	1.02	0.040	5.8	230	0.013	0.009	40	14	1.1-1.7	40-60
1.60	0.063	SQUARE[A]	1	1.60	0.063	4.7	185	0.027	0.018	70	14	1.1-1.7	40-60
2.29	0.090	SQUARE[A]	1	1.60	0.063	6.2	245	0.036	0.024	95	16	1.1-1.7	40-60
3.18	0.125	SQUARE[B]	1	2.39	0.094	3.4	135	0.045	0.030	115	14	1.1-1.7	40-60
4.06	0.160	SQUARE[B]	1	2.39	0.094	4.2	165	0.055	0.037	135	15	1.1-1.7	40-60
4.83	0.190	SQUARE[B]	1	2.39	0.094	5.2	205	0.068	0.046	175	15	1.1-1.7	40-60
PULSED ARE MODE OF METAL TRANSFER[C]													
1.60	0.063	SQUARE[A]	1	1.02	0.040	9.1	360	0.021	0.014	50	21	1.1-1.7	40-60
3.18	0.125	SQUARE[A]	1	1.60	0.063	7.1	280	0.042	0.028	110	24	1.1-1.7	40-60

4.83	0.190	SQUARE[A]	1	1.60	0.063	12.1	475	0.070	0.047	175	25	1.1 - 1.7	40 - 60
6.35	0.250	SINGLE-V, 60°[D]	1	2.39	0.094	7.4	290	0.097	0.065	210	29	1.1 - 1.7	40 - 60
SPRAY ARC MODE OF METAL TRANSFER[E]													
6.35	0.250	SINGLE-V, 60°[D]	1	1.60	0.063	13.5	530	0.062	0.042	240	27	1.4 - 2.3	50 - 80
9.53	0.375	SINGLE-V, 60°[D]	1	2.39	0.094	7.2-7.9	285-310	0.085	0.057	320-350	24-30	1.4 - 2.3	50 - 80
12.7	0.500	SINGLE-V, 60°[D]	2	2.39	0.094	8.1-9.1	320-360	0.158	0.106	360-400	24-30	1.4 - 2.3	50 - 80
15.9	0.625	DOUBLE-V, 60°[F]	2	2.39	0.094	8.4-9.4	330-370	0.186	0.125	370-420	24-30	1.4 - 2.3	50 - 80
25.4	1.000	DOUBLE-V, 60°[F]	4	2.39	0.094	8.4-9.4	330-370	0.310	0.208	370-420	24-30	1.4 - 2.3	50 - 80

(A) ZERO ROOT OPENING.

(B) ROOT OPENING, 2.3 MM (0.090 IN.).

(C) PULSE VOLTAGE OF 55 V, EXCEPT FOR METAL 4.83 MM (0.190 IN.) THICK, WHICH USES A PULSE VOLTAGE OF 52 V.

(D) 1.6 MM ($\frac{1}{16}$ IN.) ROOT FACE AND ZERO ROOT OPENING.

(E) SETTINGS ALSO APPLY TO FILLET WELDS IN THE SAME THICKNESS OF METAL.

(F) 3.2 MM ($\frac{1}{8}$ IN.) ROOT FACE AND ZERO ROOT OPENING

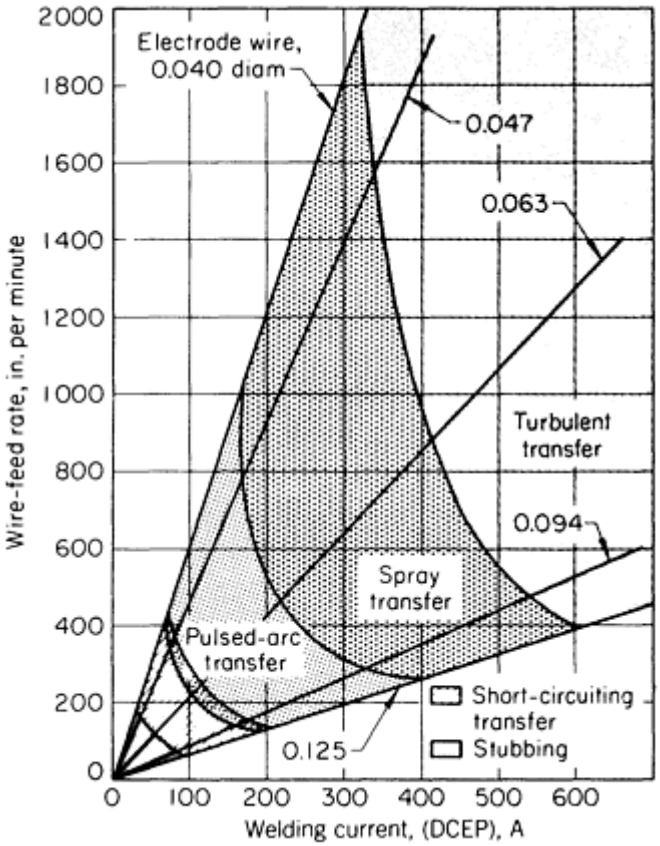

FIG. 1 PLOT OF WIRE-FEED RATE VERSUS WELDING CURRENT AS A FUNCTION OF ELECTRODE WIRE DIAMETER AND MODE OF METAL TRANSFER

Welding positions are restricted to flat, horizontal, and vertical-up by the high deposition rate and fluidity of the weld metal.

Typical operating conditions for gas metal arc butt welding of magnesium alloys in the thickness range from 0.64 to 25 mm (0.025 to 1 in.) are presented in Table 8. These operating conditions are intended as a guide and should be altered to the extent required by experience with specific applications.

Gas-Tungsten Arc Welding

Gas-tungsten arc welding is used more extensively than GMAW for joining magnesium alloys. It is well suited for welding thin sections. Control of heat input and the molten weld pool is better with GTAW than GMAW. Alternating current machines with a high-frequency current superimposed on the normal welding current for arc stabilization and direct current machines with continuous amperage control are used. For thin sheets, both alternating current and DCEP are used. On material over 4.8 mm ($\frac{3}{16}$ in.) thick, alternating current is preferred because it provides deeper penetration. Direct current electrode negative is seldom used on magnesium alloys because the arc lacks cathodic cleaning action. Alternating current machines should be equipped with a primary contactor, actuated by a switch on the torch or by a foot switch, for starting and stopping the arc. Otherwise, the arcing that occurs while the electrode approaches or draws away from the workpiece may result in burned spots on the work. Pure tungsten, zirconiated, and thoriated electrodes, from 0.25 to 6.35 mm (0.010 to 0.250 in.) in diameter, are used for GTAW of magnesium alloys. Additional information on power supplies, electrodes, and related items for GTAW is given in the article "Gas-Tungsten Arc Welding" in this Volume.

Manual Welding. Data on current settings, electrode diameter, shielding-gas flow, filler-metal diameter, and filler-metal consumption for manual GTAW of butt joints in magnesium alloys 1.0 to 12.7 mm (0.040 to 0.500 in.) thick are given in Table 9. For best results, the electrode should be held close to the work to produce an arc about 0.8 mm ($\frac{1}{32}$ in.) long. The preferred angles of torch, joint, and filler metal are given in Fig. 2. Welding should be done at a uniform speed in a straight line. A weaving or rotary motion should be used only for fillet welds or large corner joints. Forehand welding is preferred; a minimal number of stops produces the best results. If stops are required, the weld should be restarted on weld metal about 13 mm ($\frac{1}{2}$ in.) from the end of the previous weld.

TABLE 9 TYPICAL PARAMETERS FOR MANUAL GTAW OF BUTT JOINTS WITH MAGNESIUM ALLOYS

BASE-METAL THICKNESS		JOINT DESIGN(A)	NO. OF PASSES	ELECTRODE DIAMETER		AC CURRENT(B), A	ARGON FLOW RATE		FILLER METAL			
									DIAMETER		CONSUMPTION	
mm	in.			mm	in.		m^3/h	ft^3/h	mm	in.	kg/m	lb/ft
1.02	0.040	A	1	1.6	$\frac{1}{16}$	35	0.34	12	2.4	$\frac{3}{32}$	0.006	0.004
1.60	0.063	A	1	2.4	$\frac{3}{32}$	50	0.34	12	2.4	$\frac{3}{32}$	0.007	0.005
2.03	0.080	A	1	2.4	$\frac{3}{32}$	75	0.34	12	2.4	$\frac{3}{32}$	0.009	0.006
2.54	0.100	A	1	2.4	$\frac{3}{32}$	100	0.34	12	2.4	$\frac{3}{32}$	0.012	0.008
3.18	0.125	A	1	2.4	$\frac{3}{32}$	125	0.34	12	3.2	$\frac{1}{8}$	0.013	0.009
4.83	0.190	A	1	3.2	$\frac{1}{8}$	160	0.42	15	3.2	$\frac{1}{8}$	0.016	0.011
6.35	0.250	B	2	4.0	$\frac{5}{32}$	175	0.57	20	3.2	$\frac{1}{8}$	0.039	0.026
9.53	0.375	B	3	4.0	$\frac{5}{32}$	175	0.57	20	4.0	$\frac{5}{32}$	0.085	0.057
9.53	0.375	C	2	4.8	$\frac{3}{16}$	200	0.57	20	3.2	$\frac{1}{8}$	0.036	0.024
12.7	0.500	C	2	4.8	$\frac{3}{16}$	250	0.57	20	3.2	$\frac{1}{8}$	0.070	0.047

(A) A, SQUARE GROOVE BUTT JOINT, ZERO ROOT OPENING; B, 60° BEVEL, SINGLE-V-GROOVE BUTT JOINT 1.6 MM ($\frac{1}{16}$ IN.) ROOT FACE, ZERO ROOT OPENING; C, 60° BEVEL, DOUBLE-V-GROOVE BUTT JOINT 4 MM ($\frac{3}{32}$ IN.) ROOT FACE, ZERO ROOT OPENING.

(B) THORIUM-CONTAINING ALLOYS WILL REQUIRE ABOUT 20% HIGHER CURRENT. WITH HELIUM SHIELDING, REQUIRED WELDING CURRENT WILL BE REDUCED BY ABOUT 20 TO 30 A.

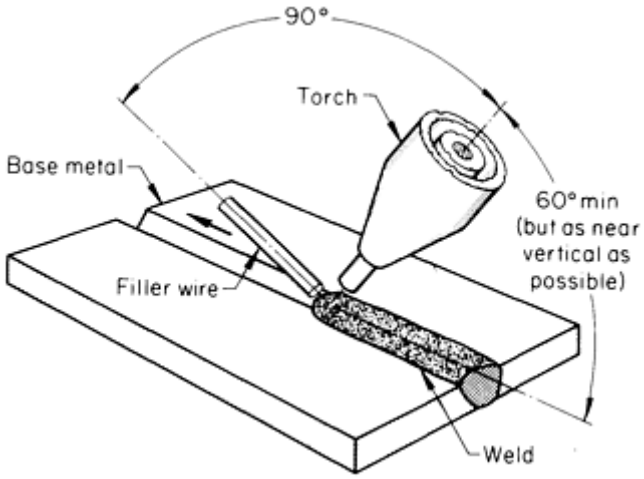

FIG. 2 RECOMMENDED GTAW SETUP FOR JOINING TWO MAGNESIUM ALLOY PLATES

To minimize the risk of weld cracking, either of the methods shown in Fig. 3 should be used: method A, in which starting and runoff plates (or tabs) are used to start and end the weld; or method B, in which the weld is made in two increments by passes that begin in the middle and progress toward opposite ends. Also, the base metal (and fixture, if used) should be preheated to at least 95 to 150 °C (200 to 300 °F). If the thickness of the two compositions to be welded differs by 6.4 mm ($\frac{1}{4}$ in.) or more, the thicker section should be preheated to approximately 150 °C (300 °F).

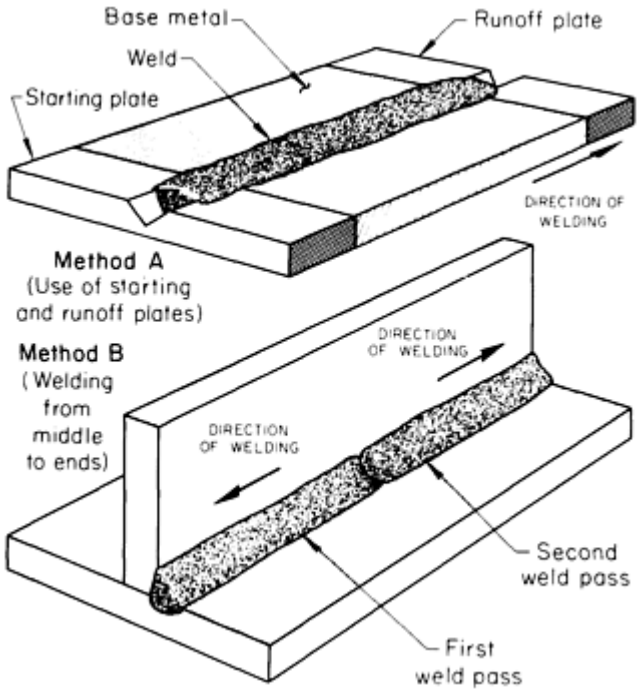

FIG. 3 TECHNIQUES TO PREVENT CRACKING OF WELD WHEN JOINING MAGNESIUM ALLOY PLATES

Short-Run Production. In short production runs for which the cost of elaborate fixtures cannot be justified, tooling costs can be minimized by fabricating the components so that they can be tack welded into position.

Example 1: Tack Welding for Short-Run Production.

To minimize tooling costs on short production runs of electronic deck assemblies, which were essentially two rectangular boxes 50 by 50 by 100 mm (2 by 2 by 4 in.), as shown in Fig. 4, tack welds were used instead of fixturing to position some of the component pieces. Formed sheet sections of 1.3 mm (0.050 in.) thick AZ31B-H24 were tack welded into position by GTAW, using 1.6 mm ($\frac{1}{16}$ in.) diam ER AZ61A filler wire. The tack welds were 3.2 mm ($\frac{1}{8}$ in.) long and were spaced on 50 mm (2 in.) centers (starting at each comer). A tool plate and toggle clamps held the pieces for tack welding. Tack welds were not used to hold angle pieces.

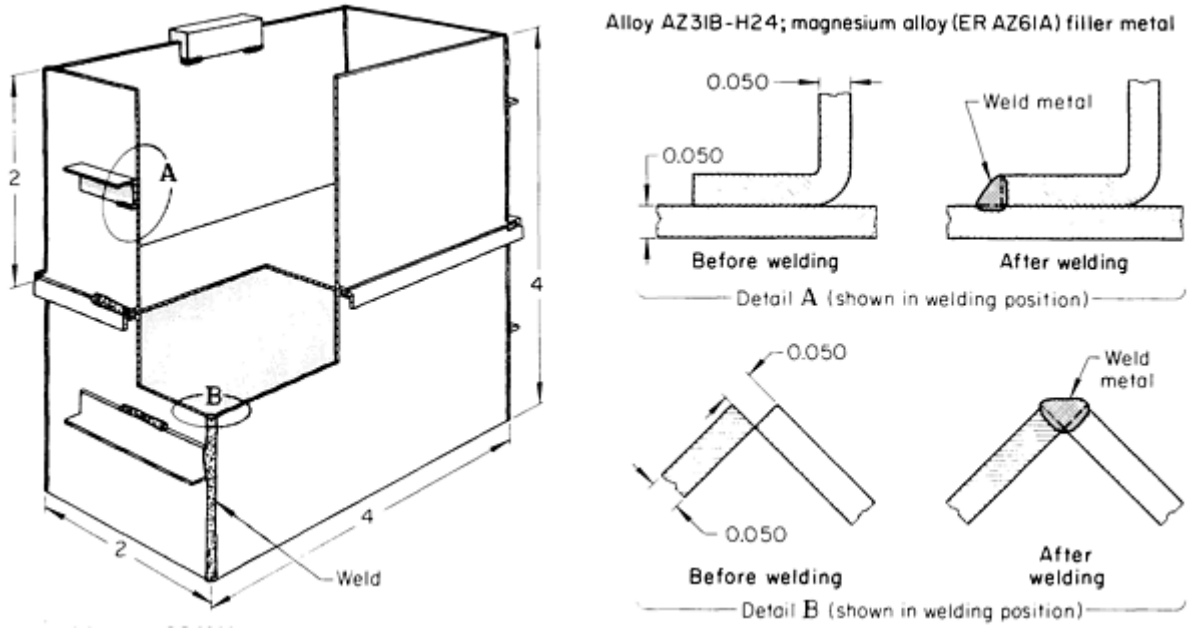

CONDITIONS FOR MANUAL GTAW	
JOINT TYPES	LAP AND CORNER
WELD TYPES	FILLET AND SINGLE-V-GROOVE
WELDING POSITIONS	HORIZONTAL AND FLAT
PREWELD CLEANING	WIRE BRUSHING
PREHEAT	NONE
FIXTURES	TOOL PLATE AND TOGGLE CLAMPS
SHIELDING GAS	HELIUM, AT 0.71 M^3/H (25 FT^3/H)
ELECTRODE	1.02 MM (0.040 IN.) DIAM EWP
FILLER METAL	1.6 MM ($\frac{1}{16}$ IN.) DIAM ER AZ61A(A)
TORCH	350 A, WATER COOLED(B)
POWER SUPPLY	300 A TRANSFORMER(C)
CURRENT, FILLET WELDS	25 A, AC
CURRENT, V-GROOVE WELDS	40 A, AC
POSTWELD HEAT TREATMENT	175 °C (350 °F) FOR $3\frac{1}{2}$ H

(A) 915 MM (36 IN.) LONG ROD.
(B) CERAMIC NOZZLE.

FIG. 4 MANUAL GTAW OF ELECTRONIC DECK ASSEMBLY

Welding of the assembled and tack welded components was completed by manual GTAW with 1.6 mm ($\frac{1}{16}$ in.) diam ER AZ61A filler wire. The comer joints were welded with continuous beads about 50 mm (2 in.) long, and the flanged bottom of the top part of the assembly was joined to the sides with 25 mm (1 in.) long fillet welds. Extruded angle sections were fillet welded to the ends of the boxes with welds about 25 mm (1 in.) long (Fig. 4, detail A).

The assembly was repositioned manually so that all welds could be made in either the flat or the horizontal position. A standard alternating current power supply with a high-frequency arc stabilizer was used. Helium was selected as the shielding gas because a hotter and more stable arc was produced than would have been possible with argon shielding gas. Preheating was not used, but after welding, the assemblies were stress relieved at 175 °C (350 °F) for $3\frac{1}{2}$ h to prevent stress-corrosion cracking. Welds were inspected visually.

Example 2: Manually Welded T-Joint.

The welding of a single 3.2 mm ($\frac{1}{8}$ in.) fillet in a 205 mm (8 in.) long T-joint between sheets of alloy AZ31B, 1.6 and 3.2 mm ($\frac{1}{16}$ and $\frac{1}{8}$ in.) thick (see Table 10), was used as a quick shop test for welder qualification. The welder adjusted the machine settings, gas flow, and welding speed to produce a sound weld with proper contour and adequate penetration, using manual GTAW. After welding, the joint was broken by striking a blow against the unwelded side of the vertical stem to open and expose the root of the weld. The fracture was then examined for depth of penetration, porosity, lack of fusion, and other defects. Welding conditions and a view of the joint are given in Table 10.

TABLE 10 MANUAL GTAW OF ALLOY AZ31B

Argon shielding gas; flow rate, 0.51 m^3/h (18 ft^3/h)

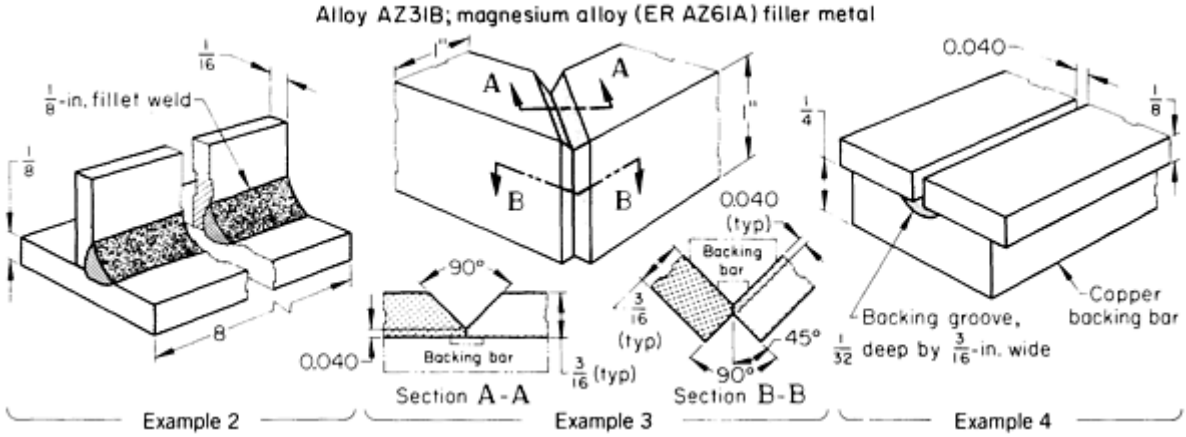

ITEM	EXAMPLE 2	EXAMPLE 3	EXAMPLE 4
JOINT TYPE	T	CORNER; BUTT	BUTT
WELD TYPE	SINGLE FILLET	SINGLE-V-GROOVE	SQUARE GROOVE
WELDING POSITION	HORIZONTAL	VERTICAL-UP; FLAT	FLAT
ELECTRODE (EWP) DIAMETER, MM (IN.)	2.4 ($\frac{3}{32}$)	3.2 ($\frac{1}{8}$)	3.2 ($\frac{1}{8}$)
FILLER METAL (ER AZ61A) DIAMETER, MM (IN.)	1.6 ($\frac{1}{16}$)	2.4 ($\frac{3}{32}$)	1.6 ($\frac{1}{16}$)
CURRENT (AC, HF-STABILIZED)[A]	110 A	125 A	135 A
WELDING SPEED	255 MM/MIN (10 IN./MIN)	5 UNITS/H[B]	255 MM/MIN (10 IN./MIN)

POSTWELD HEAT TREATMENT	260 °C (500 °F) FOR 15 MIN	175 °C (350 °F) FOR 1 $\frac{1}{2}$ H	175 °C (350 °F) FOR 1 $\frac{1}{2}$ H

(A) A 300 A AC/DC POWER SUPPLY WITH CONTINUOUS HIGH FREQUENCY WAS USED FOR ALL THREE APPLICATIONS, WITH A LIGHT-DUTY WATER-COOLED WELDING TORCH. ALL WORKPIECES WERE PREWELD CLEANED BY CHROMIC-SULFURIC PICKLING. NO PREHEAT WAS USED.

(B) INCLUDES FIXTURING, WELDING, AND UNLOADING

Example 3: Manually Welded Single-V-Groove Butt and Corner Joints.

Structural frames were fabricated by welding the mitered ends of 25 by 25 by 4.8 mm (1 by 1 by $\frac{3}{16}$ in.) angles extruded from alloy AZ31B. One of the four right angle corners of one of these structural frames is shown in Table 10. Manual GTAW was used because production quantity was less than 50 pieces per month.

The procedure consisted of mitering, edge beveling, cleaning, assembling on a fixture, and welding. Horizontal joint edges were beveled 45° with a 1.0 mm (0.040 in.) deep root face; vertical joint edges were beveled to form a similar root face for a 90° corner joint. After acid pickling and rinsing, the angles were assembled on a clamping fixture with flat backing bars for the horizontal joints and corner backing bars for the vertical joints. The backing bars for both the horizontal and vertical joints were provided with backing grooves that were 3.2 mm ($\frac{1}{8}$ in.) wide by 0.51 mm (0.020 in.) deep. The outside corner joint was single-pass welded, vertical-up; the grooved butt joint was single-pass welded in the flat position. No preheat was used, but the frames were postweld stress relieved at 175 °C (350 °F) for 1 $\frac{1}{2}$ h. Welding conditions are given in Table 10.

Example 4: Square-Groove-Welded Butt Joints.

Gas-metal arc welding was to be used on the square-groove-welded butt joints (with 1.0 mm, or 0.040 in., root opening) in 3.2 mm ($\frac{1}{8}$ in.) thick AZ31B-H24 sheet, but contact tube arcing occurred and contamination of the filler metal resulted. Rather than delay production while the arcing problem was being eliminated, manual GTAW was used instead. Good mechanical properties were obtained in single-pass welds, using argon shielding on the torch side and a grooved copper backing bar, but no gas backing, on the underside. Joint alignment was maintained with bolted hold-down bars. Welding conditions are given in Table 10.

Automatic welding of magnesium alloys by GTAW is similar to manual welding, except that higher currents and welding speeds are used. Table 11 can be used as a guide to determine settings for automatic welding. Alternating current is best, although DCEP can be used. A balanced-wave alternating current machine, or a conventional alternating current machine equipped with a battery bias for wave balancing, should be used.

TABLE 11 OPERATING PARAMETERS FOR AUTOMATIC GTAW OF AZ31B MAGNESIUM ALLOY BUTT JOINTS

Helium shielding gas; flow rate, 0.6 m^3/h (20 ft^3/h)

TYPE OF CURRENT	CURRENT A	DIAMETER OF TUNGSTEN ELECTRODE		ARC LENGTH		ER AZ61A OR ER AZ92A FILLER METAL, 1.60 MM (0.063 IN.) DIAM				TRAVEL SPEED	
						FEED RATE		CONSUMPTION OF WELD			
		mm	in.	mm	in.	m/min	in./min	kg/m	lb/ft	mm/min	in./min
AZ31B, 1.60 MM (0.063 IN.) THICK											
AC,	55	2.39	0.094	0.64	0.025	0.89	35	0.010	0.007	255	12

WAVE	70	3.18	0.125	0.64	0.025	1.37	54	0.006	0.004	915	36
	95	3.18	0.125	0.64	0.025	2.44	96	0.007	0.005	1145	45
	170	4.76	0.188	0.64	0.025	4.06	160	0.007	0.005	1780	70
	195	4.76	0.188	0.64	0.025	4.83	190	0.009	0.006	2030	80
	200	4.76	0.188	0.64	0.025	5.16	203	0.007	0.005	2415(A)	95(A)
DCEN	75	3.18	0.125	0.64	0.025	2.03	80	0.006	0.004	1220	48
DCEP	120	6.35	0.250	0.51	0.020	4.67	184	0.007	0.005	2030(A)	80(A)
AZ31B, 4.83 MM (0.190 IN.) THICK											
AC, BALANCED WAVE	300		0.250	0.51	0.020	4.04	159	0.016	0.011	865	34
DCEN	170		0.125	0.76	0.030	1.78	70	0.012	0.008	510	20
DCEP	120		0.250	0.51	0.020	0.25	10(B)	0.012	0.008(B)	180(A)	7(A)

(A) MAXIMUM SPEED LIMITATION BECAUSE OF UNDERCUTTING OR ARC INSTABILITY.

(B) DIAMETER OF FILLER METAL, 2.39 MM (0.094 IN.)

Constant alignment of electrode and filler metal is important in automatic welding. Filler metal is fed into the arc at a low angle to the work so that the filler rod touches the weld surface just ahead of the electrode. The arc length shown in Table 11 should be preset and maintained. Travel speeds up to 2410 mm/min (95 in./min) can be used on thin sheet, but 610 to 915 mm/min (24 to 36 in./min) is more common. Automatic welding is not necessarily restricted to high-production applications; sometimes the high degree of control that can be attained with automatic welding is required regardless of quantity.

Example 5: Automatic Welding of Extrusions.

Airtight doors for an aerospace application were made by welding panels of alloy AZ31B-H24 sheet to frames extruded from AZ31B. The frames, which acted as stiffeners, also contained a groove for an air seal. Cross sections of similar offset butt joints in two designs of door assemblies are shown as joints A and B in Fig. 5. The offset lip of the extruded frames provided a single-bevel groove butt joint and supplied backing for the weld; the lap joint on the underside was not welded. Although production quantities were low, automatic GTAW was used because weld quality was good and the equipment was available. Automatic travel was obtained by mounting the welding equipment on the motorized carriage of a cutting machine. Differences in welding conditions for the two joints resulted from operator choice or judgment. Both procedures produced satisfactory welds, but the difference in welding speeds would have been significant had production quantities been large.

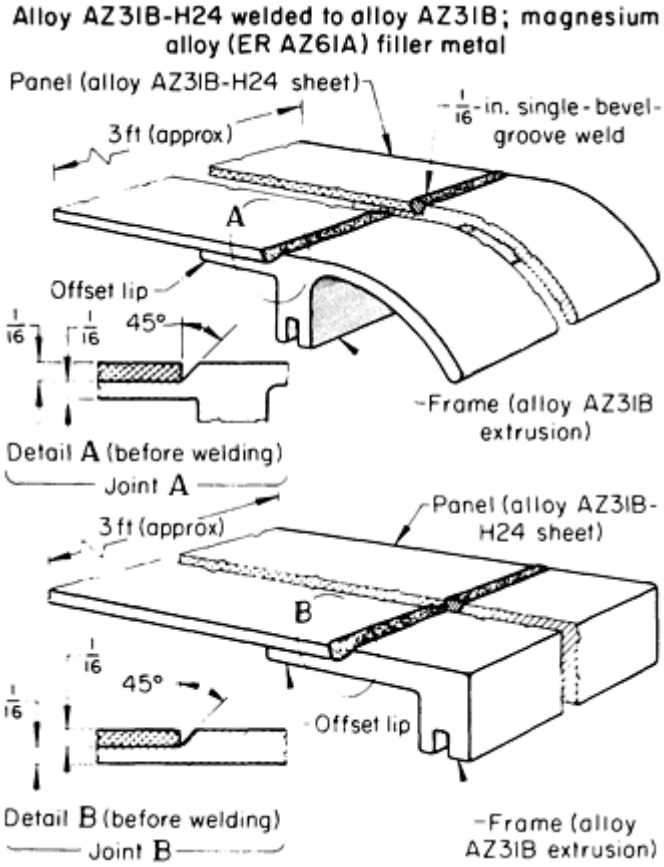

AUTOMATIC GTAW	
JOINT TYPE	OFFSET BUTT
WELD TYPE	SINGLE-BEVEL GROOVE
PREWELD CLEANING	CHROMIC-SULFURIC PICKLE
WELDING POSITION	FLAT
PREHEAT	NONE
SHIELDING GAS	ARGON, 0.51 M^3/H (18 FT^3/H) FOR JOINT A; ARGON, 0.45 M^3/H (16 FT^3/H) FOR JOINT B
ELECTRODE	3.2 MM ($\frac{1}{8}$ IN.) DIAM EWP
FILLER METAL	1.6 MM ($\frac{1}{16}$ IN.) DIAM ER AZ61A
TORCH	WATER COOLED
POWER SUPPLY	300 A AC (HF-STABILIZED)
CURRENT (AC)	175 A FOR JOINT A; 135 A FOR JOINT B
WIRE-FEED RATE	1650 MM/MIN (65 IN./MIN)
TRAVEL SPEED	510 MM/MIN (20 IN./MIN) FOR JOINT A; 380 MM/MIN (15 IN./MIN FOR JOINT B)
POSTWELD HEAT TREATMENT	175 °C (350 °F) FOR $1\frac{1}{2}$ H

FIG. 5 AUTOMATIC GTAW OF AZ31B ALLOY SHEET AND EXTRUDED MATERIAL

Repair Welding of Castings

A significant portion of the total amount of welding that is done on magnesium alloy castings is for repair. Repair welding is usually limited to the repair of defects in clean metal, including broken sections, sand or blowholes, cracks, and cold shuts. Repair welding is not recommended in areas containing flux or oxide inclusions or excessive porosity. Castings that have been organically impregnated for pressure tightness or that may contain oil in pores should not be welded. Many magnesium castings are aircraft parts that are heat treated to meet strength requirements. These castings must be heat treated again after welding. The type, size, and location of defects in castings vary so much that each job presents its own welding problems; procedures cannot be standardized. However, to complete most repairs:

- CASTINGS MUST BE STRIPPED OF PAINT AND DEGREASED BEFORE WELDING; CONVERSION COATINGS SHOULD BE REMOVED FROM DEFECTIVE AREAS WITH STEEL WOOL OR WITH A POWER WIRE BRUSH HAVING STAINLESS STEEL BRISTLES; A ROTARY DEBURRING TOOL IS RECOMMENDED FOR REMOVING DEFECTS AND PREPARING THE WORKPIECE FOR WELDING.
- CASTINGS SHOULD BE CLAMPED IN PLACE, AND THE SURFACE ADJOINING THE FRACTURE SHOULD BE BEVELED FOR THE WELD (TABLE 5).
- PREHEATING, IF NECESSARY, SHOULD BE DONE AT THE TEMPERATURES RECOMMENDED IN TABLE 7. EITHER LOCAL HEATING WITH A TORCH OR FURNACE HEATING CAN BE USED. THE USE OF A PROTECTIVE ATMOSPHERE DURING FURNACE HEATING WILL REDUCE THE POSSIBILITY OF OXIDATION AT TEMPERATURES ABOVE 370 °C (700 °F).
- WELDING SHOULD BE DONE IMMEDIATELY AFTER PREHEATING. REHEATING MAY BE NECESSARY IF THE TEMPERATURE OF THE CASTING DROPS SIGNIFICANTLY BELOW THE PREHEAT TEMPERATURE.
- MEDIUM-SIZE WELD BEADS SHOULD BE USED.
- WELDING SHOULD PROGRESS FROM THE CENTER OF THE BREAK TO THE OUTSIDE EDGES. THE ARC SHOULD NOT BE ALLOWED TO DWELL TOO LONG IN ANY ONE AREA BECAUSE WELD CRACKING MAY RESULT.
- HIGH WELDING CURRENT, WHICH MAY CAUSE WELD CRACKING OR INCIPIENT MELTING IN THE HEAT-AFFECTED ZONE (HAZ), SHOULD BE AVOIDED; LOW WELDING CURRENTS, WHICH MAY CAUSE COLD LAPS, OXIDE CONTAMINATION, OR POROSITY, SHOULD ALSO BE AVOIDED.
- A FOOT CONTROL SHOULD BE USED TO FADE IN AND OUT THE ARC GRADUALLY TO MINIMIZE THERMAL SHOCK FROM ARC STOPS. THERMAL SHOCK MAY CAUSE CRACKING.

The examples that follow describe procedures that were used in successful repair welding of specific castings.

Example 6: Repair of an Aircraft Wheel Rim Casting.

After machining, aircraft wheel film castings of AZ91C-T4 were occasionally found to have small sand holes (Fig. 6). Defects, of a size that could be removed by cutting a groove about 3.2 mm ($\frac{1}{8}$ in.) deep and 13 mm ($\frac{1}{2}$ in.) wide, were repaired by welding. The defective area was cleaned by cutting a smoothly blended groove (see Fig. 6, Before welding), using a burring tool. After complete removal of defective material was verified by liquid-penetrant inspection, the groove and surrounding area were wire brushed to prepare for GTAW. The relatively thick section of the casting in the repair area and the wide groove for the deposit ensured that the weld would be under low restraint; therefore, preheating was not necessary. Ordinarily, a standard filler metal, such as ER AZ92A or ER AZ101A, would prove satisfactory for welding the AZ91C base metal; in this application, a filler metal of the same composition as the base metal was specified. The weld was made by striking the arc at the bottom of the groove and proceeding in a circular direction along the groove wall to fill the groove, as shown in the "After welding" view in Fig. 6.

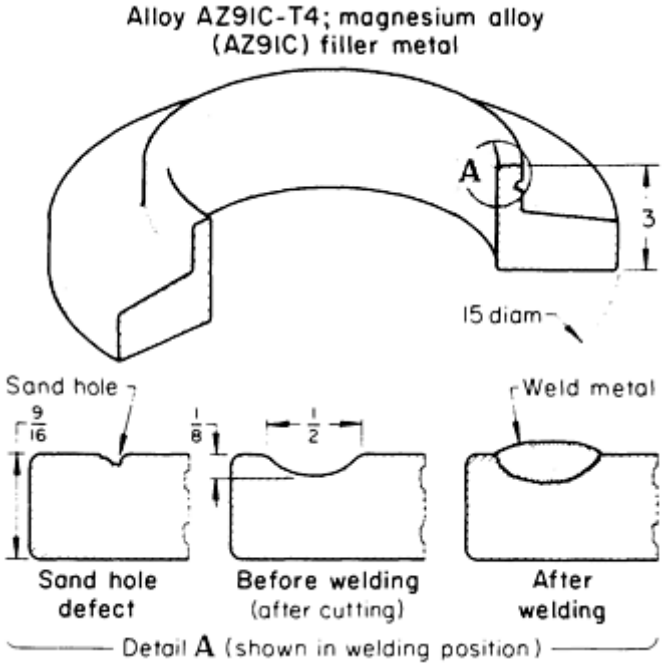

MANUAL GTAW	
WELD TYPE	SURFACING, FOR REPAIR
WELDING POSITION	FLAT
PREHEAT	NONE
SHIELDING GAS	HELIUM, 0.6 M^3/H (20 FT^3/H)
ELECTRODE	2.4 MM ($\frac{3}{32}$ IN.) DIAM EWP
FILLER METAL	3.2 MM ($\frac{1}{8}$ IN.) DIAM AZ91C
TORCH	300 A, WATER COOLED
POWER SUPPLY	300 A TRANSFORMER, WITH HIGH-FREQUENCY GENERATOR
CURRENT	60 A, AC
POSTWELD HEAT TREATMENT	415 °C (780 °F) FOR $\frac{1}{2}$H PLUS 215 °C (420 °F) FOR 4 H

FIG. 6 REPAIR WELDING OF AZ91C ALLOY AIRCRAFT WHEEL RIM CASTING

After welding, the weld reinforcement was ground to 0.8 mm ($\frac{1}{32}$ in.) above the base-metal surface, and surface weld quality was verified by liquid-penetrant inspection. After passing inspection, the casting was heat treated to the T6 condition. The casting was accepted after radio-graphic inspection indicated satisfactory internal weld quality.

Example 7: Repair Welding of a Jet Engine Casting.

During an aircraft jet engine overhaul, fluorescent-penetrant inspection revealed a 64 mm ($2\frac{1}{2}$ in.) long crack near a rib in the cast AZ92A-T6 compressor housing shown in Fig. 7. The thickness of the section containing the crack ranged from

4.8 to 7.9 mm ($\frac{3}{16}$ to $\frac{5}{16}$ in.). Repair welding was permissible. The part was vapor degreased to remove surface grease and dirt and soaked in a commercial alkaline paint remover. The crack was then marked with a felt-tip marker, and the part was stress relieved at 205 °C (400 °F) for 2 h. The crack was removed by slotting the flange through to the periphery. Each side of the slot was beveled to approximately 30° from vertical to form a 60° double-V-groove. The area to be welded was cleaned with a power wire brush with stainless steel bristles. Welding was done by manual GTAW, without preheating.

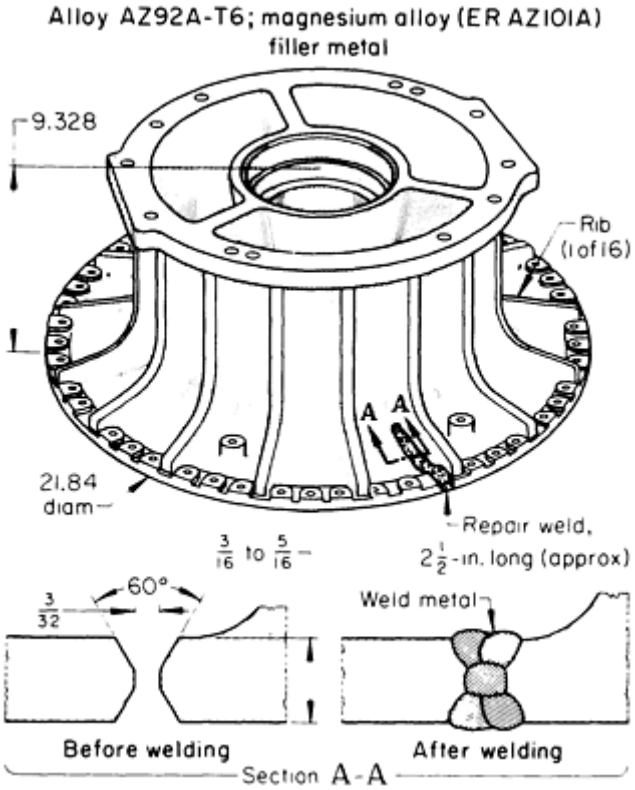

MANUAL GTAW	
JOINT TYPE	BUTT
WELD TYPE	60° DOUBLE-V-GROOVE REPAIR
SHIELDING GAS	ARGON, 0.6 M^3/H (20 FT^3/H)(A)
ELECTRODE	1.6 MM ($\frac{1}{16}$ IN.) DIAM EWTH-2
FILLER METAL	1.6 MM ($\frac{1}{16}$ IN.) DIAM ER AZ101A
TORCH	WATER COOLED
POWER SUPPLY	300 A TRANSFORMER, WITH HIGH-FREQUENCY STARTING
CURRENT	UNDER 70 A, AC(B)
POSTWELD STRESS RELIEF	205 °C (400 °F) FOR 2 H(C)
INSPECTION	FLUORESCENT PENETRANT

(A) ALSO USED FOR BACKING.

(B) CURRENT WAS REGULATED BY A FOOT SWITCH.

FIG. 7 REPAIR WELDING OF A CAST AZ92A ALLOY COMPRESSOR HOUSING

The welding technique maintained a low-amperage arc (less than 70 A) directed onto the base metal while filler metal was deposited on the sides of the groove, working from the innermost point outward. After a molten weld pool formed, the arc was weaved slightly while depositing a bead on the sides of the groove. During welding, heat input was adjusted by a foot-operated current-control rheostat to maintain a uniform weld pool. After welding was completed on one side of the slot, the casting was turned over. Excess drop-through and areas of incomplete penetration were removed by grinding. The underside was then welded by the same technique used for the first side. After welding, the casting was stress relieved at 205 °C (400 °F) for 2 h and inspected by the fluorescent-penetrant method.

Sand casting repairs can be made with manual GTAW. Figure 8 shows three repairs for the correction of surface flaws that occur in machining, defects resulting from the casting process, and deficiencies in design. Welding was done with high-frequency stabilized alternating current. The castings were preheated and maintained at temperature during welding to avoid cracking. To avoid distortion, the postweld heat treatments were used as a compromise between stress relieving and an aging treatment. However, when repair-welded areas were large enough so that the heat of welding caused a significant reduction in mechanical properties, welding was followed by a full heat treatment. Radiographic inspection was used in establishing the welding procedure, and all repair welds were subjected to fluorescent-penetrant inspection. Fillet welds were left as welded; other types of welds were finished to conform to the contour of the casting or to the desired shape.

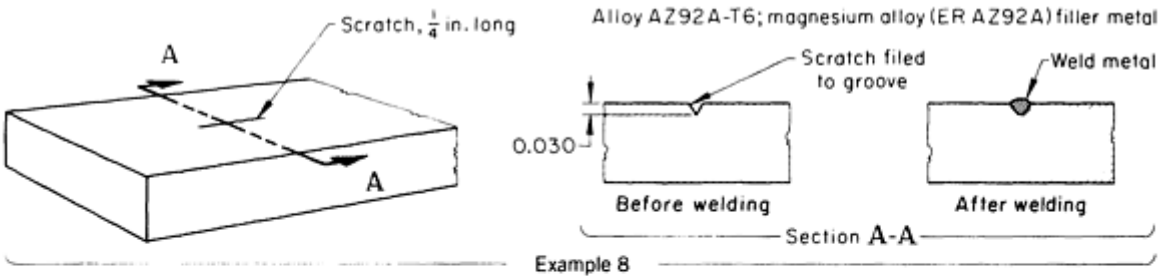

Example 8

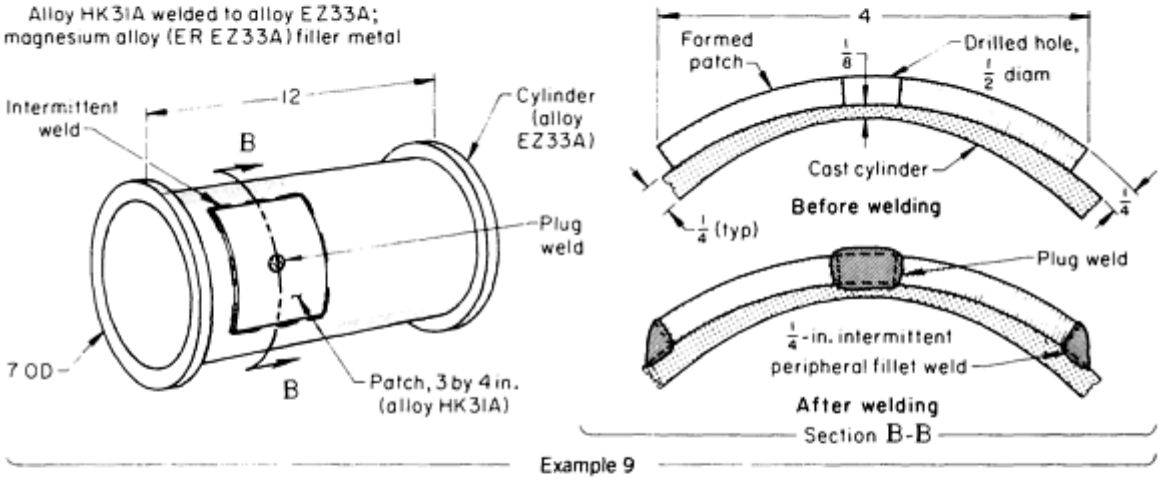

Example 9

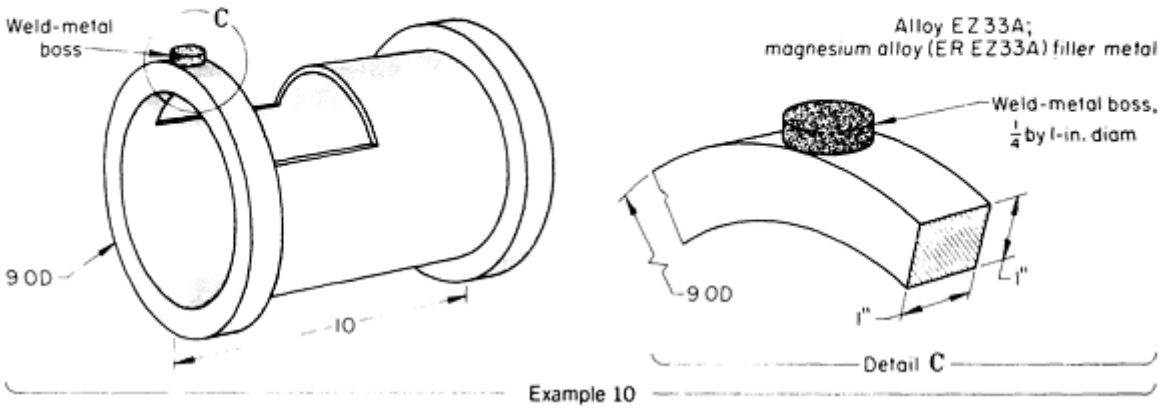

Example 10

WELDING CONDITION	EXAMPLE 8	EXAMPLE 9	EXAMPLE 10
CONDITIONS FOR MANUAL GTAW[A]			
FIXTURES	NONE	PLATES	NONE
WELDING POSITION	FLAT	FLAT	FLAT
SHIELDING GAS	ARGON; 0.57-0.68 M^3/H (20-24 FT^3/H)	ARGON; 0.68-0.79 M^3/H (24-28 FT^3/H)[B]	ARGON; 0.68-0.79 M^3/H (24-28 FT^3/H)
ELECTRODE, 3.2 MM ($\frac{1}{8}$ IN.) DIAM	EWP	EWP	EWP
FILLER METAL, 1.6 MM ($\frac{1}{16}$ IN.) DIAM	ER AZ92A	ER EZ33A	ER EZ33A
CURRENT (AC, HF-STABILIZED)	80-140 A	160-180 A	160-180 A
PREHEAT AND INTERPASS	120 °C (250 °F)	150 °C (300 °F)	120-175 °C (250-

TEMPERATURE			350 °F)
POSTWELD HEAT TREATMENT	150 °C (300 °F) FOR 3 H	205 °C (400 °F) FOR 2 H	150 °C (300 °F) FOR 4 H
TOTAL TIME PER PIECE(C)	$\frac{1}{2}$H	2 H	$\frac{1}{2}$H

(A) FOR ALL THREE APPLICATIONS, PREWELD CLEANING WAS DONE WITH A WIRE BRUSH OR A ROTARY FILE, POWER SUPPLY WAS A 300 A TRANSFORMER WITH HIGH-FREQUENCY (BALANCED WAVE) STABILIZER, AND ELECTRODE HOLDER WAS A 300 A WATER-COOLED TYPE.

(B) HELIUM AT 0.23 M^3/H (8 FT^3/H) WAS USED FOR BACKING.

(C) NOT INCLUDING TIME FOR POSTWELD HEAT TREATMENT

FIG. 8 MANUAL GTAW REPAIR OF SAND CASTINGS

Example 8: Repair Welding of a Machining Scratch.

The views at the top in Fig. 8 show a portion of an alloy AZ92A-T6 sand casting with a machining scratch 6.4 mm ($\frac{1}{4}$ in.) long and 0.76 mm (0.030 in.) deep. This scratch was repaired by gas tungsten arc surface welding. Machining flaws up to 9.5 mm ($\frac{3}{8}$ in.) square in castings of various shapes and sizes have been corrected by this method.

Example 9: Repair Welding of Wall Thinning.

The middle views in Fig. 8 show a flanged cylindrical alloy EZ33A sand casting that was one of about 200 such castings in which core shift caused the 6.4 mm ($\frac{1}{4}$ in.) wall to thin to 3.2 mm ($\frac{1}{8}$ in.), beginning about 25 mm (1 in.) away from one of the flanges. To repair these thin areas without distortion of the cylinder, a 75 by 100 mm (3 by 4 in.) piece of 6.4 mm ($\frac{1}{4}$ in.) alloy HK31A plate was formed to fit the outside wall of the cylinder, drilled in the center with a 13 mm ($\frac{1}{2}$ in.) diam hole, and clamped in place over the thin area. The patch was tack welded at the four corners and then gas tungsten arc welded along the periphery with intermittent 6.4 mm ($\frac{1}{4}$ in.) fillet welds 25 mm (1 in.) long. During welding, the inside of the cylinder was flushed with helium to prevent oxidation of heated portions. After the patch had been fillet welded to the cylinder, the center hole was plug welded, using successive small beads to ensure fusion to the wall of the casting and to minimize the possibility of cracking, which can occur when large beads are deposited. The part was then finish machined using plates to hold the flanges.

Example 10: Application of an All-Weld-Metal Boss.

Because a design change was made after the first run of flanged cylindrical alloy EZ33A castings had been produced, a boss had to be added to one of the flanges on each casting, as shown in the views at the bottom in Fig. 8. Using a buildup welding procedure of successive small beads, a cylindrical boss 25 mm (1 in.) in diameter by 6.4 mm ($\frac{1}{4}$ in.) high was produced on the flange by manual GTAW. In later production, the pattern was changed, and the boss was cast integrally with the flange.

Defects in Repair Welds. Oxide inclusions are caused by (1) welding on unsound base metal, (2) inadequate cleaning of base metal or filler metal, (3) maintaining too long an arc, (4) insufficient flow of shielding gas, (5) leaky gas connections, and (6) defective shielding-gas hoses that allow the drawing in of air.

Tungsten inclusions are caused by maintaining too long an arc, using too high a current, and touching the weld pool, base metal, or filler metal with the electrode.

Porosity is usually caused by welding on unsound base metal, poor preweld cleaning of base metal or filler metal, and contamination of the shielding gas.

Microshrinkage, a defect consisting of interdendritic voids detectable on magnification, is caused by too rapid current decay at the end of a weld, which results in too rapid freezing of the weld pool. As a result, the weld pool is unable to serve as a riser to feed the solidifying weld metal below.

Base-metal cracks are usually caused by excessive heat input or by carrying the arc too far over onto the base-metal surface during repair welding.

In repair welds of magnesium alloys that contain rare earth elements or thorium, a light-colored area at the HAZ of the weld is often visible on a radiograph taken with the x-ray beam parallel and the x-ray film perpendicular to the weld edge. This is caused by eutectic-enriched material with high atomic numbers absorbing substantially more radiation. Eutectic enrichment is caused by the melting of eutectic material at a lower temperature and heat expansion of the parent grains, squeezing this material into a layer at the edge of the weld. Below this layer is a darker area on the radiograph where eutectic material has vacated. Above the eutectic-rich layer appears another eutectic-depleted zone due to the first solidification of higher melting constituents. The effect can be minimized by avoiding preheat and by rapid welding.

Heat Treatment After Welding

Heat treated castings are often heat treated again after welding. The heat treatments shown in Table 7 depend on the temper before welding and the temper required after welding. Only the minimum heat-treating time ($\frac{1}{2}$ h) for complete solution is used for welded AZ81A, AZ91C, AZ92A, and QE22A castings to avoid abnormal grain growth in the deposited weld metal. As noted in Table 7, some solution treatments require an SO_2 or CO_2 atmosphere.

If complete solution treatment is not required, magnesium alloys containing more than 1.5% Al should always be stress relieved to prevent stress-corrosion cracking in service. Postweld stress-relieving temperatures and times are given in Table 12.

TABLE 12 POSTWELD TREATMENTS TO OBTAIN 80 TO 95% STRESS RELIEF IN MAGNESIUM ALLOYS

ALLOY	TEMPERATURE		TIME
	°C	°F	
SHEET			
AZ31B-O[(B)]	260	500	15 MIN
AZ31B-H24[(B)]	150	300	1 H
HK31A-H24	315	600	30 MIN
HM21A-T8	370	700	30 MIN
HM21A-T81	400	750	30 MIN
ZE10A-O	230	450	30 MIN
ZE10A-H24	135	275	1 H
EXTRUSIONS			
AZ10A-F	260	500	15 MIN
AZ31B-F[(B)]	260	500	15 MIN
AZ61A-F[(B)]	260	500	15 MIN
AZ80A-F[(B)]	260	500	15 MIN
AZ80A-T5[(B)]	205	400	1 H
HM31A-T5[(A)]	425	800	1 H
AZCOML	260	500	15 MIN
CASTINGS[(C)]			

AM100A	260	500	1 H
AZ63A	260	500	1 H
AZ81A	260	500	1 H
AZ91C	260	500	1 H
AZ92A	260	500	1 H
EZ33	330	625	2-4 H
EQ21	505	940	1 H
QE22	505	940	1 H
ZE41	330	625	2-4 H
ZC63	425	795	1 H
WE43	510	950	1 H
WE54	510	950	1 H

(A) 70% STRESS RELIEF IS PROVIDED.

(B) REQUIRES POSTWELD HEAT TREATMENT TO AVOID STRESS-CORROSION CRACKING.

(C) REQUIRES POSTWELD HEAT TREATMENT FOR MAXIMUM STRENGTH (SEE TABLE 7 FOR POSTWELD HEAT TREATMENTS)

References

1. "STANDARD PRACTICE FOR CODIFICATION OF CERTAIN NONFERROUS METALS AND ALLOYS, CAST AND WROUGHT," B 275, *1989 ANNUAL BOOK OF STANDARDS*, VOL 2.02, *DIE-CAST METALS; ALUMINUM AND MAGNESIUM ALLOYS*, ASTM, 1989, P 325-326
2. H.B. CARY, *MODERN WELDING TECHNOLOGY*, 2ND ED., PRENTICE-HALL, 1989, P 526-527

Introduction

COMMERCIALLY PURE TITANIUM and most titanium alloys can be welded by procedures and equipment used in welding austenitic stainless steel and aluminum. Because of the high reactivity of titanium and titanium alloys at temperatures above 550 °C (1020 °F), additional precautions must be applied to shield the weldment from contact with air. Also, titanium base metal and filler metal must be clean to avoid contamination during welding.

Welding of Titanium Alloys

Revised by R. Terrence Webster, Consultant

Weldability

Unalloyed titanium and all alpha titanium alloys are weldable. Although the alpha-beta alloy Ti-6Al-4V and other weakly beta-stabilized alloys are also weldable, strongly beta-stabilized alpha-beta alloys are embrittled by welding. Most beta alloys can be welded, but because aged welds in beta alloys can be quite brittle, heat treatment to strengthen the weld by age hardening should be used with caution.

Unalloyed titanium is generally available in several grades, ranging in purity from 98.5 to 99.5% Ti. These grades are strengthened by variations in oxygen, nitrogen, carbon, and iron. Strengthening by cold working is possible but is seldom used. All grades are usually welded in the annealed condition. Welding of cold-worked alloys anneals the heat-affected zone (HAZ) and negates the strength produced by cold working.

Alpha alloys Ti-5Al-2.5Sn, Ti-6Al-2Sn-4Zr-2Mo, Ti-5Al-5Sn-2Zr-2Mo, Ti-6Al-2Nb-1Ta-1Mo, and Ti-8Al-1Mo-1V are always welded in the annealed condition.

Alpha-beta alloys of Ti-6Al-4V can be welded in the annealed condition or in the solution-treated and partially aged condition, with aging completed during postweld stress relieving. In contrast to unalloyed titanium and the alpha alloys, which can be strengthened only by cold work, the alpha-beta and beta alloys can be strengthened by heat treatment.

The low weld ductility of most alpha-beta alloys is caused by phase transformation in the weld zone or in the HAZ. Alpha-beta alloys can be welded autogeneously or with various filler metals. It is common to weld some of the lower-alloyed materials with matching filler metals. Filler metal of an equivalent grade or one grade lower is used to ensure good weld strength and ductility. Filler metal of matching composition is used to weld the Ti-6Al-4V alloy. This extra-low-interstitial (ELI) grade improves ductility and toughness. The use of filler metals that improve ductility may not prevent embrittlement of the HAZ in susceptible alloys. In addition, low-alloy welds can be embrittled by hydride precipitation. However, with proper joint preparation, filler-metal storage, and shielding, hydride precipitation can be avoided.

Sheet thicknesses 2.54 mm (0.100 in.) and thinner can be welded without filler metal additions by the fused-root welding technique. Filler metal may be added to repair unfused and sunken weld-metal areas. The lack of a joint line on the root face of the weld indicates 100% penetration.

Metastable beta alloys Ti-3Al-13V-11Cr, Ti-11.5Mo-6Zr-4.5Sn, Ti-8Mo-8V-2Fe-3Al, Ti-15V-3Cr-3Al-3Sn, and Ti-3Al-8V-6Cr-4Zr-4Mo are weldable in the annealed or solution heat treated condition. In the as-welded condition, welds are low in strength but ductile. Beta alloy weldments are sometimes used in the as-welded condition. Welds in the Ti-3Al-13V-11Cr alloy embrittle more severely when age hardened. To obtain full strength, the metastable beta alloys are welded in the annealed condition; the weld is cold worked by peening or planishing, and the weldment is then solution treated and aged. This procedure also obtains adequate ductility in the weld.

For additional information on the weldability of titanium alloys, see the Section "Selection and Weldability of Nonferrous Low-Temperature Materials" in this Volume.

Welding of Titanium Alloys

Revised by R. Terrence Webster, Consultant

Process Selection

The following fusion-welding processes are used for joining titanium and titanium alloys:

- GAS-TUNGSTEN ARC WELDING (GTAW)
- GAS-METAL ARC WELDING (GMAW)
- PLASMA ARC WELDING (PAW)
- ELECTRON-BEAM WELDING (EBW)
- LASER-BEAM WELDING (LBW)
- FRICTION WELDING (FRW)
- RESISTANCE WELDING (RW)

Fluxes cannot be used with these processes because they combine with titanium to cause brittleness and may reduce corrosion resistance. The welding processes that use fluxes are electroslag welding, submerged arc welding, and flux-

cored arc welding. These processes have been used on a limited basis. However, they are not considered to be economical because they require high-cost, fluoride-base fluxes.

Gas-tungsten arc welding is the most widely used process for joining titanium and titanium alloys except for parts with thick sections. Square-groove butt joints can be welded without filler metal in base metals up to 2.5 mm (0.10 in.) thick. For thicker base metals, the joint should be grooved, and filler metal is required. The heated weld metal in the weld zone must be shielded from the atmosphere to prevent contamination with oxygen, nitrogen, and carbon, which will degrade the weldment ductility.

Welding may be done manually or automatically. Local shielding can be accomplished by the use of backup shields (Fig. 1) and torch-trailing shields (Fig. 2). For complex weld geometries, rigid or collapsible plastic bags purged and filled with inert gas (usually argon) may be used. For welds with high chemical purity requirements, the use of vacuum weld chambers is recommended.

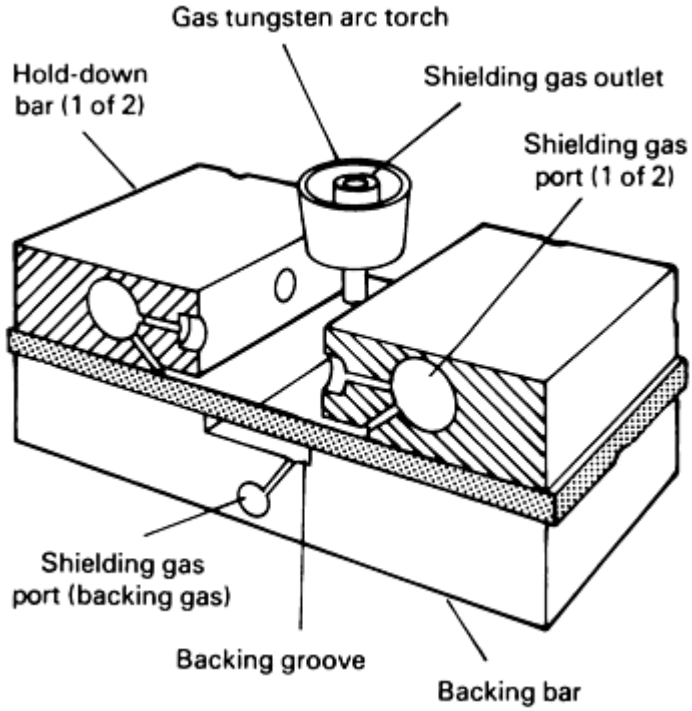

FIG. 1 SETUP FOR INERT GAS SHIELDING FOR GTAW OF TITANIUM ALLOYS OUTSIDE A WELDING CHAMBER. GAS SHIELDING IS FROM THE TORCH AND THROUGH PARTS IN HOLD-DOWN BARS, BACKING BARS, AND FROM TRAILING AND BACKUP SHIELDS.

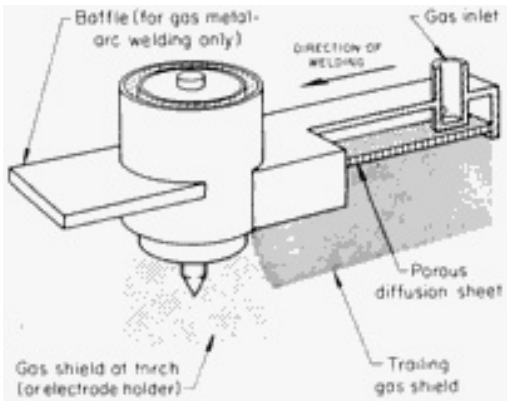

FIG. 2 ARRANGEMENT FOR SHIELDED AUTOMATIC WELDING OF TITANIUM ALLOYS IN AIR. THE BAFFLE SHOWN ON THE LEADING SIDE OF THE TORCH (OR ELECTRODE HOLDER) IS SELDOM USED FOR GTAW, BUT

IS USED FOR GMAW.

Gas-metal arc welding is used to join titanium and titanium alloys more than 3.18 mm (0.125 in.) thick. It is applied using pulsed current or the spray mode and is less costly than GTAW, especially when the base metal thickness is greater than 13 mm (0.50 in.).

Plasma arc welding is also applicable to joining titanium and titanium alloys. It is faster than GTAW and can be used on thicker sections, such as one-pass welding of plate up to 13 mm (0.50 in.) thick, using square-butt and keyhole techniques.

Electron-beam welding is used in the aircraft and aerospace industries for producing high-quality welds in titanium and titanium alloy plates ranging from 6.4 mm (0.25 in.) to more than 76 mm (3 in.) thick. Because the welding is performed in a high-vacuum atmosphere, low contamination of the weldment is achieved.

Laser-beam welding is increasingly being used to join titanium and titanium alloys. Square-butt weld joint configurations can be used, and the welding process does not require the use of vacuum chambers; gas shielding is still required. This process is more limited than electron-beam welding regarding base metal thickness, which cannot usually exceed 13 mm (0.50 in.).

Friction welding is useful in joining tube, pipe, or rods, where joint cleanliness can be achieved without shielding.

Resistance welding is used to join titanium and titanium alloy sheet by either spot welds or continuous seam welds. The process is also used for welding titanium sheet to dissimilar metals, that is, cladding titanium to carbon or stainless steel plate.

Welding of Titanium Alloys

Revised by R. Terrence Webster, Consultant

Filler Metals

For welding titanium thicker than about 2.5 mm (0.10 in.) by the GTAW process, a filler metal must be used. For PAW, a filler metal may be used for welding metal less than 13 mm (0.5 in.) thick.

Composition. Thirteen titanium and titanium alloy filler-metal (or electrode) classifications are given in AWS A5.16. Five of these are essentially unalloyed titanium, and the remainder are titanium alloy filler metals. Maximums are set on carbon, oxygen, hydrogen, and nitrogen contents. Compositions for titanium and titanium alloy filler metals are given in Table 1.

TABLE 1 CHEMICAL COMPOSITION REQUIREMENTS FOR TITANIUM AND TITANIUM ALLOY ELECTRODES AND RODS

AWS CLASSIFICATION		UNS NUMBER	COMPOSITION, WT%								
1990	1970		C	O	H	N	Al	V	Sn	Fe	OTHER
ERTI-1	ERTI-1	R50100	0.03	0.10	0.005	0.015	. . .	. . .	. . .	0.10	. . .
ERTI-2	ERTI-2	R50120	0.03	0.10	0.008	0.020	. . .	. . .	. . .	0.20	. . .
ERTI-3	ERTI-3	R50125	0.03	0.10-0.15	0.008	0.020	. . .	. . .	. . .	0.20	. . .
ERTI-4	ERTI-4	R50130	0.03	0.15-0.25	0.008	0.020	. . .	. . .	. . .	0.30	. . .
ERTI-5	ERTI-6A1-	R56400	0.05	0.18	0.015	0.030	5.5-	3.5-	. . .	0.30	0.005 Y

	4V						6.7	4.5			
ERTI-5ELI	ERTI-6AL-4V-1	R56402	0.03	0.10	0.005	0.012	5.5-6.5	3.5-4.5	. . .	0.15	0.005 Y
ERTI-6	ERTI-5A 1-2.5SN	R54522	0.08	0.18	0.015	0.050	4.5-5.8	. . .	2.0-3.0	0.50	0.005 Y
ERTI-6ELI	ERTI-5AL-2.5SN-1	R54523	0.03	0.10	0.005	0.012	4.5-5.8	. . .	2.0-3.0	0.20	0.005 Y
ERTI-7	ERTI-0.2PD	R52401	0.03	0.10	0.008	0.020	. . .	. . .	. . .	0.20	0.12/0.25 PD
ERTI-9	ERTI-3AL-2.5V	R56320	0.03	0.12	0.008	0.020	2.5-3.5	2.0-3.0	. . .	0.25	0.005 Y
ERTI-9ELI	ERTI-3AL-2.5V-1	R56321	0.03	0.10	0.005	0.012	2.5-3.5	2.0-3.0	. . .	0.20	0.005 Y
ERTI-12	. . .	R53400	0.03	0.25	0.008	0.020	. . .	. . .	. . .	0.30	0.2/0.4 MO 0.6/0.9 NI
ERTI-15	ERTI-6AL-2CB-1TA-1MO	R56210	0.03	0.10	0.005	0.015	5.5-65	. . .	. . .	0.15	0.5/1.5 MO 1.5/2.5 NB 0.5/1.5 TA

Notes: Titanium constitutes the remainder of the composition. Single values are maximum. Analysis of the interstitial elements carbon, oxygen, hydrogen, and nitrogen shall be conducted on samples of filler metal taken after the filler metal has been reduced to its final diameter and all processing operations have been completed. Analysis of the other elements may be conducted on these same samples or it may have been conducted on samples taken from the ingot or the rod stock from which the filler metal is made. In case of dispute, samples from the finished filler metal shall be the referee method. Residual elements, total, shall not exceed 0.02%, with no single such element exceeding 0.05%. Residual elements need not be reported unless a report is specifically required by the purchaser. Residual elements are those elements (other than titanium) that are not listed in Table 1 for the particular classification, but which are inherent in the raw material or the manufacturing practice. Residual elements can be present only in trace amounts and they cannot be elements that have been intentionally added to the product.

Source: ANSI/AWS A5.16-90, American Welding Society, 1990

Filler-metal composition is usually matched to the grade of titanium being welded. For improved joint ductility in welding the higher strength grades of unalloyed titanium, filler metal of yield strength lower than that of the base metal is occasionally used. Because of the dilution that occurs during welding, the weld deposit acquires the required strength. Unalloyed filler metal is sometimes used to weld Ti-5Al-2.5Sn and Ti-6Al-4V for improved joint ductility. The use of unalloyed filler metals lowers the beta content of the weldment, thereby reducing the extent of the transformation that occurs and improving ductility. Engineering approval, however, is recommended when using pure filler metal to ensure that the weld meets strength requirements. Another option is filler metal containing lower interstitial content (oxygen, hydrogen, nitrogen, and carbon) or alloying contents that are lower than the base metal being used. The use of filler metals that improve ductility does not preclude embrittlement of the HAZ in susceptible alloys. In addition, low-alloy welds may enhance the possibility of hydrogen embrittlement.

Preparation. The filler metal, as well as the base metal, should be clean at the time of welding. As shown in Fig. 3, wires used for filler metals have a large surface-to-volume ratio. Therefore, if the wire surface is slightly contaminated, the weld may be severely contaminated. Some procedures require that the filler wire be cleaned immediately before use. The use of an acetone-soaked, lint-free cloth serves to assess surface contamination caused by the die lubricant used in the wire drawing operation, in addition to cleaning the filler wire. Pickling in nitric-hydrofluoric acid solution is also used for cleaning.

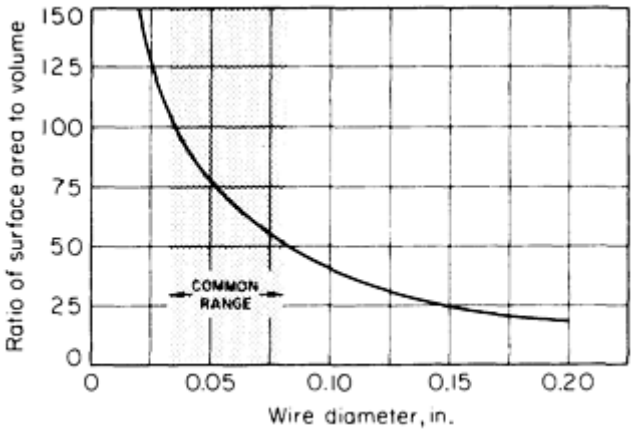

FIG. 3 RATIO OF FILLER-METAL (ELECTRODE) WIRE SURFACE AREA TO VOLUME FOR VARIOUS WIRE DIAMETERS. "COMMON RANGE" INDICATES RANGE OF WIRE DIAMETERS MOST OFTEN USED FOR WELDING TITANIUM.

Shielding Gases

In welding titanium and titanium alloys, only argon and helium, and occasionally a mixture of these two gases, are used for shielding. Because it is more readily available and less costly, argon is more widely used. Argon shielding gas was used in the examples given in this article.

Because of its high purity (99.985% min.) and low moisture content, a liquid argon supply is often preferred. The argon gas should have a dew point of -60 °C (-75 °F) or lower. The hose used for the shielding gas should be clean, nonporous, and flexible, and may be made of Tygon or vinyl plastic. Because rubber hose absorbs air, it should not be used. Excessive gas flow rates that cause turbulence should be avoided, and flowmeters are usually employed for all gas shields. Pressure gages may be used for trailing and backup shields.

Characteristics. The type of shielding gas used affects the characteristics of the arc. At a given welding current, the arc voltage is much greater with helium than with argon. Because the heat energy liberated in helium is about twice that in argon, higher welding speeds can be obtained, weld penetration is deeper, and thicker sections can be welded more rapidly using helium shielding. However, when using pure helium for welding, arc stability and weld-metal control are sacrificed.

Argon is used when welding thin and thick sections where the arc length can be altered without appreciably changing the heat input. Argon-helium mixtures are also used, particularly 75% argon, which improves arc stability, and 25% helium, which increases penetration. The 75Ar-25He mixture is also frequently utilized as the shielding gas at the torch in automatic operations. Furthermore, helium is used in shielding out-of-position welds.

Welding of Titanium Alloys

Revised by R. Terrence Webster, Consultant

Joint Preparation

If welding is done outside a controlled-atmosphere welding chamber, joints must be carefully designed so that both the top and the underside of the weld can be shielded (Fig. 1). Dimensions of typical joints are given in Table 2. For welding titanium alloys, joint fit-up should be better than for welding other metals, because of the possibility of entrapping air in the joint. The joint should be clamped to prevent separation during welding.

TABLE 2 DIMENSIONS OF TYPICAL JOINTS FOR WELDING TITANIUM AND TITANIUM ALLOYS

BASE-METAL THICKNESS		ROOT OPENING[A]	GROOVE ANGLE, DEGREES	WELD-BEAD WIDTH[A]
mm	in.			
SQUARE-GROOVE BUTT JOINT				
0.254-2.29	0.010-0.090	0	. . .	. . .
0.787-3.18	0.0314-0.125	0-0.10*T*	. . .	. . .
SINGLE-V-GROOVE BUTT JOINT				
1.57-3.18	0.062-0.125	0-0.10*T*	30-60	0.10-0.25*T*
2.29-3.18	0.090-0.125	[B]	90	. . .
3.18-6.35	0.125-0.250	0-0.10*T*	30-60	0.10-0.25*T*
DOUBLE-V-GROOVE BUTT JOINT				
6.35-12.7	0.250-0.500	0-0.20*T*	30-120	0.10-0.25*T*
SINGLE-U-GROOVE BUTT JOINT				
6.35-19.1	0.250-0.750	0-0.10*T*	15-30	0.10-0.25*T*
DOUBLE-U-GROOVE BUTT JOINT				
19.1-38.1	0.750-1.500	0-0.10*T*	15-30	0.10-0.25*T*
FILLET WELD				
0.787-3.18	0.031-125	0-0.10*T*	0-45	0-0.25*T*
3.18-12.7	0.125-0.500	0-0.10*T*	30-45	0.10-0.25*T*

Source: J.J. Vagi *et al.,* "Welding Procedures for Titanium and Titanium Alloys," NASA TMX 53432, 1965

(A) *T,* BASE-METAL THICKNESS.

(B) ROOT FACE, 0.76 MM (0.030 IN.).

Welding of Titanium Alloys

Revised by R. Terrence Webster, Consultant

Cleaning

To obtain a good weld, the joint and the surfaces of the workpiece at least 51 mm (2 in.) beyond the width of the gas trailing shield on each side of the weld groove must be meticulously cleaned. The cleaning procedure depends on whether the oxide layer in the joint area is light or heavy.

Degreasing. Grease and oil accumulated during forming and machining must be removed before welding to avoid weld contamination. Scale-free metal requires only degreasing. Degreasing precedes descaling for metal with an oxide scale. Methods of degreasing include steam cleaning, alkaline cleaning, vapor degreasing, and solvent cleaning.

For vapor degreasing, toluene rather than a chlorinated solvent should be used, because residues from chlorinated solvents (and also from silicated solvents) may contribute to cracking of titanium weldments. Solvent cleaning is frequently used, especially for large components that cannot conveniently be placed in a vapor degreaser or washer for alkaline cleaning. Solvents applied include methyl ethyl ketone, toluene, acetone, and other chlorine-free solvents. Because methyl alcohol has reportedly caused stress corrosion, it is prohibited for use on aerospace hardware.

In solvent cleaning, the joint areas are hand-wiped with the solvent just before welding. All wiping should be done with clean, lint-free cloths or a cellulose sponge. Plastic or lint-free gloves should be worn; rubber gloves are likely to leave traces of plasticizer that can cause porosity in the weld metal. Handprints are also a source of contamination.

After a lightly oxidized joint area has been degreased, it should be pickled for a short time. A typical mixture is 4 wt% hydrofluoric acid and 40 wt% nitric acid. Because hydrogen is detrimental to the properties of titanium, causing embrittlement and sometimes contributing to weld porosity, pickling should be performed cautiously. Industrial practice usually is to maintain the acid bath at a high oxidation potential of 30 wt% or more nitric acid, which simultaneously holds the ratio of nitric acid to hydrofluoric acid at 10 to 1 strictly as a factor of safety. If the nitric acid content falls below 30 wt% and the ratio of nitric acid to hydrofluoric acid falls below 10 to 1, excessive hydrogen pickup is possible.

Oxide Removal. Lightly oxidized joint areas may also be cleaned by brushing with a stainless steel wire brush or by draw filing. When weld corrosion resistance is important, however, these cleaning methods should be followed immediately by acid pickling. Steel wool or abrasives should never be used, because of the danger of contamination.

If grinding is required, the use of silicon carbide burrs is preferred, because wheels produce residues of rubber or resin on the surface that contaminate the weld. To prevent burning, excessive heat should be avoided while grinding, and low rotating speeds should be used.

If titanium has been exposed to temperatures above 540 °C (1000 °F), a more complex removal treatment, such as chemical, salt bath, mechanical, or combinations of these treatments is required. The salt baths are basically sodium hydroxide to which oxidizing agents or hydrogen has been added to form sodium hydride.

One procedure for removing heavy scale involves subjecting the parts to liquid abrasive blasting or salt-bath descaling after degreasing. These treatments are usually followed by pickling in nitric-hydrofluoric acid for the removal of light scale. When salt-bath descaling is used, oxide removal can be hastened by removing the workpieces from the bath, scrubbing them with brushes, and then re-immersing them. To prevent hydrogen pickup during salt-bath descaling, cycle time must be short (preferably no more than 2 min) and bath temperature must be carefully controlled.

Selection of cleaning method depends largely on the size and shape of the parts and on the cleaning methods available in a particular plant.

Welding of Titanium Alloys

Revised by R. Terrence Webster, Consultant

Equipment for Gas-Tungsten Arc Welding

Power Supplies. Inverters are the preferred power supply for welding titanium, because the current can be controlled more closely than with motor-generator sets; slight variations in welding current may cause variations in penetration. Transformer-rectifiers may also be used. Direct current electrode negative (DCEN) is always used for GTAW of titanium because deeper weld penetration and a narrower bead can be obtained than with direct current electrode positive (DCEP). Also, in manual welding, DCEN is easier to control.

The power supply should include accessories for arc initiation because of the danger of tungsten contamination of the weld if the arc is struck by torch starting. If welding is to be done in air, controls for extinguishing the arc without pulling the torch away from the workpiece are needed, so that shielding-gas flow continues and the hot weld metal is not contaminated by air.

Electrodes. The conventional thoriated tungsten types of electrodes (EWTh-1 or EWTh-2) are used for GTAW of titanium. Electrode size is governed by the smallest diameter able to carry the welding current. To improve arc initiation and control the spread of the arc, the electrode should be ground to a point. The electrode may extend one and a half times the size of the diameter beyond the end of the nozzle.

Shielding. To ensure a diffuse, nonturbulent flow of shielding gas, nozzles of torches for welding titanium are larger than those used for welding other metals. With a 0.8 mm ($\frac{1}{32}$ in.) diam electrode, a 14 mm ($\frac{9}{16}$ in.) ID nozzle is ordinarily used, and with a 1.6 mm ($\frac{1}{16}$ in.) diam electrode, a 19 mm ($\frac{3}{4}$ in.) ID nozzle is used.

Because titanium has low thermal conductivity, the area ahead of the arc does not exceed 540 °C (1000 °F); therefore, leading shields are seldom required when welding is done by the GTAW process. For welding operations where a trailing shield (Fig. 2) is not adaptable, the nozzle of the torch is fitted with a concentric outer shroud through which a supplementary supply of shielding gas is fed. In Fig. 4, which shows this type of torch, a shielding gas is diffused through copper shavings contained in the outer shroud that cool the gas substantially, helping to protect the metal near the weld.

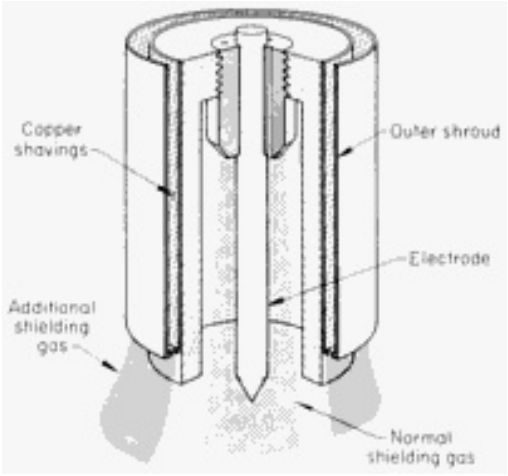

FIG. 4 SECTIONAL VIEW OF A TORCH NOZZLE EQUIPPED WITH AN OUTER SHROUD. COPPER SHAVINGS IN THE OUTER SHROUD PROVIDE ADDITIONAL GAS SHIELDING FOR MANUAL INERT GAS WELDING.

Shielding of the underside of a weld is provided by slotted backing bars, usually copper, through which a diffuse flow of argon or helium is maintained (Fig. 1). Gas channels in the clamping fixtures also provide diffuse flow of inert gas to the weld area. These fixtures are placed close to the weld to avoid the danger of air contamination.

Fixtures. Copper fixtures are usually employed for GTAW. Although other metals are sometimes used, they should be nonmagnetic; arc blow tends to occur with magnetic metal fixtures. Metal fixtures are sometimes water cooled, but this method introduces the possibility of moisture from the air condensing on the fixtures.

Welding of Titanium Alloys

Revised by R. Terrence Webster, Consultant

Stress Relieving

Most titanium weldments are stress relieved after welding to prevent weld cracking and susceptibility to stress-corrosion cracking in service. Stress relief also improves fatigue strength. An assembly subjected to a substantial amount of welding and severe fixturing restraint may require intermediate stress relieving of the partially welded structure, which should be done in an inert atmosphere. Otherwise, the unwelded joints may have to be recleaned before being welded.

With unalloyed titanium and alpha titanium alloys, time and temperature should be controlled to prevent grain growth. Stress relieving times and temperatures for several weldable titanium alloys are given in Table 3. For alloys not mentioned in this table, tests should be conducted to ensure that stress relieving does not reduce fracture toughness, creep strength, or other important properties.

TABLE 3 STRESS-RELIEVING TIMES AND TEMPERATURES FOR SELECTED TITANIUM ALLOYS

GRADE	TEMPERATURE		TIME, H
	°C	°F	
UNALLOYED TI-0.15PD	425	800	8
	480	900	0.75
	540	1000	0.5
TI-5AL-2.5SN(A)	480	900	20
	540	1000	6
	595	1100	2
	650	1200	1
TI-6AL-4V:			
ANNEALED(A)	480	900	20
	540	1000	2
	595	1100	1
SOLUTION-TREATED	480	900	15
	540	1000	4
AGED	480	900	15
	540	1000	5
TI-8AL-1MO-IV:			
SINGLE- AND DOUBLE-ANNEALED	595	1100	2
	650	1200	1.5
	705	1300	0.5
TRIPLE-ANNEALED	595	1100	5
	650	1200	2
	750	1300	0.5
TI-3AL-2.5V	540	1000	0.5
	595	1100	2
TI-13V-11CR-3AL	480	900	0.5
	540	1000	6

(A) DATA ALSO APPLY TO EXTRA-LOW-INTERSTITIAL (ELI) MODIFICATIONS.

Stress relieving of Ti-13V-11Cr-3Al weldments causes aging and subsequent embrittlement of the weld and HAZ and, therefore, is not recommended. Re-solution heat treatment (re-annealing) may be used to relieve stresses if the welded assembly is amenable to such treatment. All titanium surfaces should be free of dirt, fingerprints, grease, and residues before stress relieving. Contaminated surface metal must be removed from the entire weldment by machining or descaling and pickling to remove 0.025 to 0.050 mm (0.001 to 0.002 in.) per surface.

Welding of Titanium Alloys

Revised by R. Terrence Webster, Consultant

Repair Welding

Repair welds should follow the established specification requirements for the original welds and be made prior to final heat treatment. Manual or automatic GTAW is generally used for repairing butt and fillet welds. Repairs can also feature a combination of welding processes such as GTAW and the initial welding process (GMAW, PAW, or hot wire welding).

Repair welds must always be carefully executed, and all traces of liquid-penetrant inspection material must be removed. Generally, inspection is performed on both faces of the repair weld and several inches beyond the repaired area.

Welding of Zirconium Alloys

R. Terrence Webster, Consultant

Introduction

ZIRCONIUM is a corrosion-resistant structural metal that has many physical and mechanical properties similar to titanium and austenitic stainless steels. Zirconium alloys are weldable; procedures and equipment are similar to those used for welding titanium and austenitic stainless steels. Zirconium has a low coefficient of thermal expansion, which contributes to low distortion during welding.

Because of the reactivity of zirconium with oxygen, nitrogen, and hydrogen, the metal must be shielded during welding with high-purity inert gas or a good vacuum. Furthermore, zirconium should be free of oil, grease, and dirt to avoid the dissolving of carbon- and oxygen-containing materials, which can embrittle the metal or create porosity and may reduce the corrosion-resistant properties of the metal.

Zirconium and its alloys are available in two general categories: commercial grade and reactor grade. Commercial-grade zirconium designates zirconium that contains hafnium as an impurity. Reactor-grade zirconium designates zirconium from which most of the hafnium has been removed to make it suitable for nuclear reactor applications. Because pure zirconium has relatively low mechanical properties, various alloying elements are added to enhance its mechanical properties.

Zirconium and its alloys are available in plate, sheet, bar, rod, and tubing form in a variety of material specifications. The four most common grades of commercial zirconium alloys, as specified in ASTM B 550, are given in Table 1. For reactor grades, the hafnium content is reduced to a minimum and other impurities are closely controlled. Chemical compositions of the most common grades of nuclear-grade Zircaloys, as specified in ASTM B 351, are given in Table 2.

TABLE 1 CHEMICAL COMPOSITIONS OF COMMERCIAL ZIRCONIUM AND ZIRCONIUM ALLOYS PER ASTM SPECIFICATION B 550-92

ELEMENT	COMPOSITION, WT%		
	R60702	R60704	R60705
ZIRCONIUM + HAFNIUM, MIN	99.2	97.5	95.5
HAFNIUM, MAX	4.5	4.5	4.5
IRON + CHROMIUM	0.2 MAX	0.2-0.4	0.2 MAX
TIN	. . .	1.0-2.0	. . .
HYDROGEN, MAX	0.005	0.005	0.005
NITROGEN, MAX	0.025	0.025	0.025
CARBON, MAX	0.05	0.05	0.05
NIOBIUM	. . .	. . .	2.0-3.0
OXYGEN, MAX	0.16	0.18	0.18

TABLE 2 CHEMICAL COMPOSITIONS OF THE MOST COMMON GRADES OF NUCLEAR-GRADE ZIRCALOYS PER ASTM SPECIFICATION B 351-92

ELEMENT	COMPOSITION WT%		
	R60802 (ZIRCALOY-2)	R60804 (ZIRCALOY-4)	R60901 (ZR-2.5NB)
TIN	1.20-1.70	1.20-1.70	. . .
IRON	0.07-0.20	0.18-0.24	. . .
CHROMIUM	0.05-0.15	0.07-0.13	. . .

NICKEL	0.03-0.08	. . .	. . .
NIOBIUM	. . .	. . .	2.40-2.80
OXYGEN	. . .	. . .	0.09-0.13
IRON + CHROMIUM + NICKEL	0.28-038	. . .	. . .
IRON + CHROMIUM	. . .	0.28-0.37	. . .
HAFNIUM	0.010	0.010	0.010
ZIRCONIUM	BAL	BAL	BAL

Zirconium can only be welded to itself or to other reactive metal alloys, such as titanium, niobium, or tantalum. When welded to nonreactive metals, intermetallics that embrittle the weld metal are formed.

Welding of Zirconium Alloys

R. Terrence Webster, Consultant

Process Selection

Zirconium alloys are highly reactive to oxygen and nitrogen in air at high temperatures. Consequently, the selected welding processes and procedures must be capable of shielding the weldment and heat-affected zones (HAZ) from contamination. The use of fluxes is generally avoided, because reactivity with the chemicals in the fluxes causes brittleness and may reduce the corrosion resistance of zirconium weldments.

The following welding processes can be used for welding any of the zirconium alloys:

- GAS-TUNGSTEN ARC WELDING (GTAW)
- GAS-METAL ARC WELDING (GMAW)
- PLASMA ARC WELDING (PAW)
- ELECTRON-BEAM WELDING (EBW)
- LASER-BEAM WELDING (LBW)
- FRICTION WELDING (FRW)
- RESISTANCE WELDING (RW)
- RESISTANCE SPOT WELDING (RSW)
- RESISTANCE SEAM WELDING (RSEW)

The selection of a welding process depends on several factors: weld joint, tensile and corrosion-resistant property requirements, cost, and design configuration.

Gas-tungsten arc welding is the most widely used process for joining zirconium alloys. It employs techniques similar to those used for welding stainless steel, that is, the direct current power supply is connected for straight polarity (electrode negative, DCEN). Two desirable features are a contactor for making and breaking the arc and high-frequency arc starting. Recommended electrodes are thoriated tungsten, Type EWTh2.

Plasma arc welding is also commonly used, especially for autogenous welding of butt joint thicknesses from 3.18 to 1.52 mm (0.125 to 0.600 in.).

Gas-metal arc welding is occasionally used for joint thicknesses from 3.18 mm (0.125 in.) or more, because of its more-rapid weld time and the consequent savings in shielding gas and production time. Weld quality is more difficult to maintain, because of weld spatter and arc instability, which result in weld contamination and weld defects.

Electron-beam welding is rarely used, because of high equipment operating cost as well as weld chamber size limitations.

Laser-beam welding has had very limited use in joining zirconium and has been applied primarily in nuclear reactors.

Friction welding is used to join zirconium tubes to zirconium rods, as well as to dissimilar metal alloys (for example, zirconium to stainless steel) for heat-exchanger applications.

Resistance welding is especially useful for the seam or spot welding of thin sheets, because no shielding is required.

Shielding Gases

High-purity argon (99.996% Ar; -65 °C, or -85 °F, dew point), helium, or a mixture of the two gases are used to weld zirconium alloys. Argon has the advantage over helium in terms of lower cost, and it provides good stability and weld metal control. Helium is used to obtain deeper penetration into the joint, and mixtures of argon and helium are frequently used in automatic operations. Helium is the gas most often used to fabricate nuclear reactor equipment.

Filler-Metal Selection

Three zirconium and zirconium-alloy electrodes are identified in American .Welding Society (AWS) specification A5.24-90 (Table 3). The filler-metal composition is selected to match the base-metal composition. Type ERZr2 is used to weld commercially pure zirconium (grade R60702); type ERZr3 to weld Zr-1.5Sn alloy (grade R60704); and type ERZr4 to weld Zr-2.5Nb alloy (grades R60705 and R60706). For critical nuclear applications, the impurities are more closely controlled and the hafnium level is minimized. The nuclear-grade zirconium alloys (Table 1) are welded with filler wire of the same grade chemical composition.

TABLE 3 CHEMICAL COMPOSITIONS OF ZIRCONIUM AND ZIRCONIUM-ALLOY ELECTRODES

ELEMENT	COMPOSITION, WT%		ERZR4 (R60705)
	ERZR2 (R60702)	ERZR3 (R60704)	
CARBON	0.05	0.05	0.05
CHROMIUM + IRON	0.20	0.20-0.40	0.20
NIOBIUM	. . .	. . .	2.0-3.0
HAFNIUM	4.5	4.5	4.5
HYDROGEN	0.005	0.005	0.005
NITROGEN	0.025	0.025	0.025
TIN	. . .	1.00-2.00	. . .
ZIRCONIUM + HAFNIUM	99.01 MIN	97.5 MIN	95.5 MIN

Source: AWS A5.24-90

Process Procedures

Joints and welding wire should be cleaned before welding. Most welding wire is adequately acid cleaned prior to spooling or packaging. When cut lengths of wire are found to be dirty, it is good practice to wipe each piece with a clean cloth and solvent prior to use. If it is necessary to clean spooled wire, then a wipe with solvents will usually be satisfactory. If wire is acid cleaned, then the acid bath should be fresh and should not contain iron or any other contaminant that will remain on the wire surface.

Heavy grease and machining oil on the work-piece can be removed using degreasing solvents or reagent methanol, acetone, methyl ethyl ketone (MEK), or the equivalent. If acetone is used, then an alcohol rinse should follow.

Heavy mill scale (usually gray in color) should be removed by grinding. The blue surface oxide that develops when the metal is heated above 315 to 425 °C (600 to 800 °F) can be removed either by wire brushing (with a clean austenitic stainless steel wire brush not used for other metals) or by grinding or acid pickling, which are more effective than wire brushing. A common treatment is to soak from 2 to 5 min in room-temperature solution of 35% HNO_3 and 5% HF in water, followed by a thorough clean-water rinse and air drying.

A joint cleaned by degreasing can still be covered by a very light oil film that is approximately the equivalent thickness of the residue left by fingerprints. This can be effectively removed by abrasive or detergent cleaning, using common household cleansers or detergents, followed by air drying. Air drying can be accelerated by rinsing with methanol, acetone, or other solvents.

Joints cleaned by abrasive, detergent, or acid pickling should be kept entirely clean of dirt, including fingerprints. Generally, it is good practice to clean and to weld a joint within the same work shift. When this is not possible, the joint should be covered with paper or bagged with plastic sheet or another material to minimize the accumulation of dust and dirt.

ASTM specification B 614 ("Descaling and Cleaning Zirconium and Zirconium Alloy Surfaces") should be consulted for cleaning details.

Preheating is not normally required for zirconium welding. The commercial alloys have enough ductility to prevent weld cracking (of uncontaminated welds). Preheating is an aid to moisture removal and is good practice where the shop temperature is low or the humidity is high (it is better to control temperature and humidity in the welding area). Heat can be applied by any conventional means. However, if torch heating is used, then the torch should be moved continuously to avoid local heating of the metal.

Interpass cleaning is not required if the weld deposit is bright and shiny. Light temper colors (straw to light blue) should be removed by brushing with a clean austenitic stainless steel brush.

To prevent weld contamination from the oxygen and nitrogen in air, the weld must be shielded during welding and cooling to below 480 °C (896 °F).

The commercial grades of zirconium will most often be welded in air, and the weldments will require gas shielding on the torch side and the back side of the weld. For sheet, plate, and pipe welds, this requires a gas trailing shield on the torch side and a back-up gas shield for the back side. The shielding gases must envelope the weldment during welding and cooling.

Complex assemblies that are difficult to shield in air can be welded in a chamber. The chamber can be capable of either being evacuated and back filled with argon or helium or it can be supply purged with shielding gas before and during the welding operation. Taping a plastic bag over the part to be welded and sealing the bag at the point where the welding cables enter the bag will simulate an enclosed chamber when helium is introduced into the bag system as a shielding gas.

Heat Treatment. Preweld heat treatment is not required. Postweld stress relief for commercial grades R60702 and R60704 can be used when high residual stresses occur. Grade R60705 must be stress relieved within 14 days after welding to prevent delayed hydride cracking (DHC). Commercial-grade zirconium alloys can be heat treated in air or in an inert atmosphere. Nuclear-grade zirconium alloys are usually heat treated in an inert atmosphere.

Introduction

SURFACING, as applied to welding technology, refers to the deposition of a filler metal on a base metal (substrate) to impart some desired property to the surface that is not intrinsic to the underlying base metal. There are several types of surfacing: hardfacing, buildup, weld cladding, and buttering.

Hardfacing is a form of surfacing that is applied for the purpose of reducing wear, abrasion, impact, erosion, galling, or cavitation. As will be described in the first section of this article, hardfacing alloys may be deposited by oxyfuel welding, various arc welding methods, laser welding, and thermal spray processes.

The term buildup refers to the addition of weld metal to a base metal surface for the restoration of the component to the required dimensions. Buildup alloys are generally not designed to resist wear, but to return the worn part back to, or near, its original dimensions or to provide adequate support for subsequent layers of true hardfacing materials.

A weld clad is a relatively thick layer of filler metal applied to a carbon or low-alloy steel base metal for the purpose of providing a corrosion-resistant surface. Weld cladding is normally carried out by arc welding, the subject of the second section of this article. It should be pointed out, however, that cladding can also be accomplished by solid-state welding processes (roll cladding or explosion cladding) and vacuum brazing. These non-fusion techniques are described elsewhere in this Volume.

Buttering also involves the addition of one or more layers of weld metal to the face of the joint or surface to be welded. It differs from buildup in that the primary purpose of buttering is to satisfy some metallurgical consideration. It is used primarily for the joining of dissimilar metal base metals, as is described in the final section of this article.

Many of the principles associated with successful welding of dissimilar metals are also addressed in the sections on "Hardfacing" and "Weld Cladding" in this article, because these processes also involve a combination of materials with significantly different chemical, mechanical, and physical properties. Such combinations pose a number of challenges for the welding engineer, as evidenced by the discussions of dilution control found throughout this article.

Hardfacing, Weld Cladding, and Dissimilar Metal Joining

J.R. Davis, Davis & Associates

Hardfacing

Hardfacing is the application of a hard, wear-resistant material to the surface of a component by welding, thermal spraying, or allied welding processes to reduce wear or loss of material by abrasion, impact, erosion, galling, and cavitation (Ref 1). The stipulation that the surface be modified by welding, thermal spraying, or allied welding processes excludes the use of heat treatment or surface modification processes such as flame hardening, nitriding, or ion implantation as a hardfacing process. The stipulation that the surface be applied for the main purpose of reducing wear excludes the application of materials primarily used for prevention or control of corrosion or high-temperature scaling. Weld overlays to control corrosion are described in the section on "Weld Cladding" in this article. Corrosion and/or high-temperature scaling may, however, have a major effect on the wear rate and, hence, may become a significant factor in the selection of proper materials for hardfacing.

Hardfacing applications for wear control vary widely, ranging from very severe abrasive wear service, such as rock crushing and pulverizing, to applications to minimize metal-to-metal wear, such as control valves where a few thousandths of an inch of wear is intolerable. Hardfacing is used for controlling abrasive wear, such as that encountered by mill hammers, digging tools, extrusion screws, cutting shears, parts of earthmoving equipment, ball mills, and crusher

parts. It is also used to control the wear of unlubricated or poorly lubricated metal-to-metal sliding contacts such as control valves, undercarriage parts of tractors and shovels, and high-performance bearings.

Hardfacing is also used to control combinations of wear and corrosion, as encountered by mud seals, plows, knives in the food processing industry, valves and pumps handling corrosive liquids, or slurries. In most instances, parts are made of either plain carbon steel or stainless steel, materials that do not provide desirable wear on their own. Hardfacing alloys are applied to critical wear areas of original equipment or during reclamation of worn parts.

Hardfacing Materials

Hardfacing materials include a wide variety of alloys, carbides, and combinations of these materials. Conventional hardfacing materials, also referred to as weld overlays, are normally classified as steels or low-alloy ferrous materials, high-chromium white irons or high-alloy ferrous materials, carbides, nickel-base alloys, or cobalt-base alloys. A few copper-base alloys are sometimes used for hardfacing applications, but for the most part, hardfacing alloys are either iron-, nickel-, or cobalt-base. Out of a total hardfacing market of about 18×10^6 kg (40×10^6 lb) per year, it has been estimated that iron-base hardfacing alloys account for about 90% by weight, but only about 75% by dollar volume (Ref 2).

Microstructurally, hardfacing alloys generally consist of hard phase precipitates such as borides, carbides, or intermetallics bound in a softer iron-, nickel, or cobalt-base alloy matrix. Carbides am the predominant hard phases in iron- and cobalt-base hardfacing alloys. Carbon contents of iron- and cobalt-base hardfacing alloys generally range up to 4 wt%. Borides, as well as carbides, are the predominant hard phases in nickel-base hardfacing alloys. Combined carbon plus boron contents generally range up to 5 wt%. The specific carbide and/or boride phases that form are determined by matrix alloying additions.

The matrix alloys in most cobalt-, nickel-and high-alloy iron-base hardfacing alloys generally contain up to 35% Cr, up to 30% Mo, and up to 13% W, with smaller amounts of silicon and manganese.

Thermal spray materials, which encompass an extremely wide range of metals and alloys, carbides, ceramics, and polymers, are described in the section on "Thermal Spraying" in this article.

Hardfacing Alloy Categories (Ref 2)

Hardfacing (weld overlay) materials can be grouped into five general categories:

- BUILDUP ALLOYS
- METAL-TO-METAL WEAR ALLOYS
- METAL-TO-EARTH ABRASION ALLOYS
- TUNGSTEN CARBIDES (FOR EXTREME EARTH SLIDING AND CUTTING WEAR)
- NONFERROUS ALLOYS

The buildup alloys include low-alloy pearlitic steels and highly alloyed austenitic manganese steels. For the most part, these alloys are not designed to resist wear but to return a worn part back to, or near, its original dimensions and to provide adequate support for subsequent layers of true hardfacing materials. However, austenitic manganese steels are used as wear-resistant materials under mild wear conditions. Typical examples of applications where buildup alloys are used for wearing surfaces include tractor rails, railroad rail ends, steel mill table rolls, and large slow-speed gear teeth.

The metal-to-metal wear alloys are martensitic air-hardening steels that, with care, can be applied (without cracking) to wearing areas of machinery parts (hence, these materials are commonly referred to as machinery hardfacing alloys). Typical applications of this alloy family include undercarriage components of tractors and power shovels, steel mill work rolls, and crane wheels.

The metal-to-earth abrasion alloys are high-chromium white irons in which chromium carbides are formed during alloy solidification. The metal-to-earth alloys possess resistance to sliding and crushing (that is, low- and high-stress abrasion) on a moderate scale. Typical applications for these material types include shovel teeth, rock crusher parts, plowshares, and auger flights.

Tungsten carbides are actually composite materials, and their use involves the transfer of discrete tungsten carbide particles (which in the welding consumable forms are encased in a steel tube) across the welding arc and into the molten weld pool, where they are subsequently "frozen" into the overlay structure by the matrix formed from the melting of the steel tube. The tungsten carbides are intended for use under extreme sliding and cutting conditions. Typical applications for these tungsten carbides include cutting teeth and edge-holding surfaces of rock drill bits, and quarrying, digging, and earthmoving equipment.

The nonferrous hardfacing alloys are used in environments that are too aggressive for the ferrous hardfacing alloys or where high resistance to a specific type of wear (other than abrasion) is required. For the purpose of this article, they are classified as follows:

- COBALT-BASE, INCLUDING CARBIDE-CONTAINING ALLOYS AND LAVES PHASE ALLOYS
- NICKEL-BASE, INCLUDING BORIDE-CONTAINING ALLOYS, CARBIDE-CONTAINING ALLOYS, AND LAVES PHASE ALLOYS
- COPPER-BASE ALLOYS

Also included in this section is a discussion of several cobalt-substitute materials, some iron-base or nickel-base, which share with the cobalt-base alloys resistance to a variety of wear conditions and corrosive media.

Whereas the ferrous hardfacing alloys and tungsten carbide composites find extensive use in agriculture, mining, construction, and the steel industry, the nonferrous alloys are typically used in the chemical processing, power, automotive, and oil industries, all of which require resistance to a hostile environment in addition to resistance to wear. The cobalt-base alloys are especially resistant to deformation and chemical attack at high temperatures (500 °C < $T \leq 900$ °C, or 930 °F < $T \leq 1650$ °F) and are used to protect dies and guide rolls in the steel industry. Other common applications of the nonferrous hardfacing alloys include valve seating surfaces (both control valves and diesel exhaust valves), pump parts, extrusion screw flights, rock bit bearings, marine bearings, and glass molding hardware.

Iron-Base Alloys (Ref 1)

As described above, iron-base hardfacing alloys are more widely used than cobalt- and/or nickel-base hardfacing alloys and constitute the largest volume use of hardfacing alloys. Iron-base hardfacing alloys offer low cost and a broad range of desirable properties. Most equipment that undergoes severe wear, such as crushing and grinding equipment and earthmoving equipment, is usually very large and rugged. Parts subjected to wear usually require downtime for repair. For this reason, there is a general temptation to hardface them with the lowest cost and most readily available materials. As a result, literally hundreds of iron-base hardfacing alloys are in use today.

Due to the great number of alloys involved, iron-base hardfacing alloys are best classified by their suitability for different types of wear and their general microstructures rather than by chemical composition. Most iron-base hardfacing alloys can be divided into the following classes:

- PEARLITIC STEELS
- AUSTENITIC STEELS
- MARTENSITIC STEELS
- HIGH-ALLOY IRONS

Pearlitic steels are essentially low-alloy steels with minor adjustments in composition to achieve weldability. These alloys contain low carbon (<0.2% C) and low amounts of other alloying elements (for example, up to 2% Cr), resulting in a pearlitic structure. Pearlitic steels are useful as buildup overlays, primarily to rebuild carbon steel or low-alloy steel machinery parts back to size. Examples include shafts, rollers, and other parts in heavy machinery subjected to rolling, sliding, or impact loading. Typically, this group of alloys has high impact resistance and low hardness (in the range 25 to 37 HRC), as well as excellent weldability. Table 1 lists the composition and properties of a typical low-alloy pearlitic steel (EFe1) used for buildup applications.

TABLE 1 COMPOSITIONS, HARDNESS, AND ABRASION DATA FOR A PEARLITIC LOW-ALLOY STEEL (EFE1) AND AUSTENITIC MANGANESE STEELS (EFEMN-C AND EFEMN-CR) USED FOR BUILDUP OVERLAYS AND AIR-HARDENING OF MARTENSITIC STEELS USED FOR METAL-TO-METAL WEAR APPLICATIONS

ALLOY	COMPOSITION, WT%							HARDNESS, HRC	ABRASION, VOLUME LOSS			
									LOW-STRESS[C]		HIGH-STRESS[D]	
	Fe	Cr	C	Si	Mn	Mo	Ni		MM^3	$IN.^3 \times 10^{-3}$	MM^3	$IN.^3 \times 10^{-3}$
BUILDUP WELD OVERLAY												
EFE1[A]	BAL	2	0.1	1.0	1	1.5	. . .	37	88	5.4	49	3.0
EFEMN-C[A]	BAL	4	0.8	1.3	14	. . .	4	18	65	4.0	57	3.5
EFEMN-CR[A]	BAL	15	0.5	1.3	15	2.0	1	24	93	5.7	46	2.8
METAL-TO-METAL WELD OVERLAY												
EFE2[A]	BAL	3	0.2	1.0	1	1.0	1	48	54	3.3	66	4.0
EFE3[A]	BAL	6	0.7	1.0	1	1.0	. . .	59	60	3.7	68	4.1
ER420[B]	BAL	12	0.3	1.0	2	. . .	. . .	45	84	5.1	62	3.8

(A) TWO-LAYER SMA DEPOSIT PROCESS.

(B) TWO-LAYER SAW DEPOSIT PROCESS.

(C) DRY SAND/RUBBER WHEEL TEST (ASTM G 65, PROCEDURE B): LOAD 13.6 KG (30 LB); 2000 REV.

(D) SLURRY/STEEL WHEEL TEST (ASTM B 611, MODIFIED): LOAD 22.7 KG (50 LB); 250 REV

Austenitic steels are usually stabilized by manganese additions. Austenitic iron-base hardfacing alloys essentially are modeled after Hadfield steels. Most commercially available alloys in this category can be broadly subdivided into low-chromium and high-chromium alloys.

Low-chromium alloys usually contain up to 4% Cr and 12 to 15% Mn and some nickel or molybdenum (Table 1). Low-chromium austenitic steels generally are used to build up manganese steel machinery parts subjected to high impact (impact crusher or shovel lips).

High-chromium austenitic steels, which may normally contain 12 to 17% Cr in addition to about 15% Mn, are used for the buildup and joining of austenitic manganese steels as well as carbon and low-alloy steels. In addition, the as-deposited hardness of high-chromium steels is higher (~24 HRC) than that of low-chromium steels (~18 HRC).

The high strength of the austenitic manganese steels is the result of a synergism between manganese and carbon (Ref 3). In suppressing the formation of phases other than austenite, manganese not only increases carbon solubility at lower temperatures but also encourages carbon supersaturation of the structure. Both high inherent strength and a high work-hardening rate result from this.

Because the austenitic manganese steels are metastable, problems of carbide embrittlement tend to arise when the alloys are cooled slowly or reheated. Manganese steel components are therefore kept as cool as possible during the buildup (repair) process. Often, the bulk of the part is submerged in water during the welding process. Compositions and properties of austenitic manganese steel hardfacing alloys used for buildup applications are given in Table 1.

Martensitic steels are designed to form martensite on normal air cooling of the weld deposit. As a result, these steels are often termed "self-hardening" or "air-hardening," and they resemble tool steels with hardnesses in the range of 45 to 60 HRC. The carbon content of the martensitic steels ranges up to 0.7%. Other elements such as molybdenum, tungsten, nickel, and chromium (up to 12%), are added to increase hardenability and strength and to promote martensite formation. Manganese and silicon usually are added to aid weldability.

The major hardfacing applications for martensitic steels include unlubricated metal-to-metal rolling or sliding parts such as undercarriage parts of tractors. The impact resistance of martensitic steels is inferior to that of pearlitic or austenitic alloys, but there is a compensating increase in hardness and resistance to abrasive wear.

In hostile environments, a higher chromium content is beneficial. AWS ER420 and modified versions containing nickel, molybdenum, and niobium (or vanadium) are therefore the natural choice when high temperatures and mildly corrosive environments are encountered. For applications using steel mill hot-work rolls (which demand considerable hot hardness, resistance to oxidation, and resistance to thermal fatigue) both ER420 and EFe3 have been found suitable. Other applications for the metal-to-metal martensitic wear alloys in Table 1 include crane wheels (EFe2), pincer guide shoes (EFe3), and blast furnace bells (ER420).

The high-chromium irons encompass a wide range of compositions in which chromium may vary between approximately 6 and 35 wt%, and carbon may vary from about 2 to 6 wt%. Other possible alloying additions include molybdenum, manganese, and silicon.

The most important microstructural feature in the high-chromium irons, at least from a wear standpoint, is an M_7C_3 carbide, which forms in abundance during solidification and contains chromium, iron, and (if present) molybdenum. The matrix around these carbide particles can be austenitic, pearlitic, or martensitic (Ref 4). In general, the austenitic alloys rely on manganese for austenite stability.

Carbon content is a good indicator of abrasion resistance for this class of materials. To illustrate this fact, low- and high-stress data are plotted for selected alloys in Fig. 1. This information was generated by the use of six different alloys (open arc/flux-cored wires) and nine different sets of welding parameters (Ref 5). The carbon contents referred to in the figures are those of the second layer of the two-layer overlays tested. The use of a shaded zone, rather than a line, indicates that there was considerable scatter in the data (particularly at the lower carbon contents, in the case of high-stress abrasion). The test methods and parameters were identical to those described in the footnotes to Table 1 in this article.

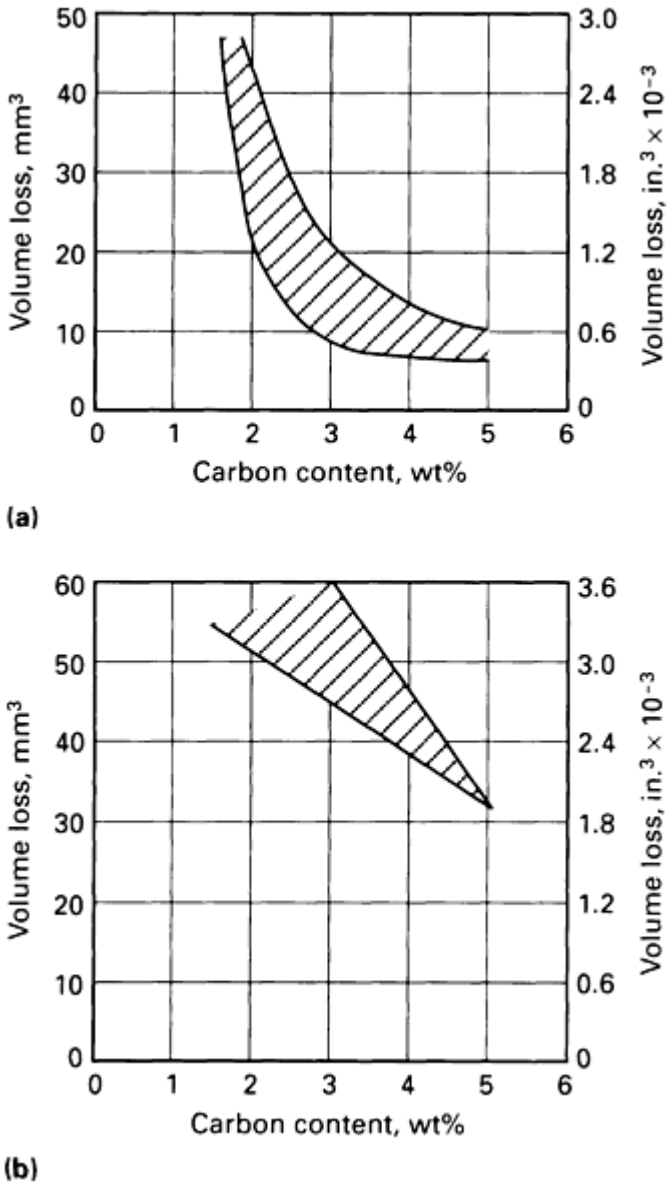

FIG. 1 PLOT OF VOLUME LOSS VERSUS CARBON CONTENT FOR HIGH-CHROMIUM WHITE IRON METAL-TO-EARTH ABRASION HARDFACING ALLOYS. (A) LOW-STRESS CONDITION. (B) HIGH-STRESS CONDITION. SOURCE: REF 5

At high carbon and chromium levels, the formation of a hypereutectic microstructure, containing large, spinelike carbide particles (with a hexagonal cross section), is favored. At lower carbon and chromium contents, the microstructure is hypoeutectic. The microstructures of three high-chromium irons (as deposited by the open arc welding process) are shown in Fig. 2. The nominal compositions of the same three alloys are presented in Table 2. As can be seen, ERFeCr-A3 (at a chromium content of 11 wt% and a carbon content of 2.6 wt%) exhibits a hypoeutectic (primary austenite) microstructure. The other two alloys, ERFeCr-A4(Mod) (29Cr-3.5C) and ERFeCr-A2 (28Cr-4.3C), possess a hypereutectic (primary carbide) structure. In Fig. 2, the large, spinelike carbides are shown in cross section.

TABLE 2 COMPOSITIONS OF HIGH-CHROMIUM WHITE IRONS USED FOR METAL-TO-EARTH ABRASION APPLICATIONS

ALLOY	COMPOSITION, WT%							
	Cr	C	Si	Mn	Mo	Ni	B	Fe

ERFECR-A3	11	2.6	1.3	1.8	1.5	. . .	. . .	BAL
ERFECR-A4(MOD)	29	3.5	1.1	0.9	. . .	2.6	0.7	BAL
ERFECR-A2	28	4.3	0.8	1.7	1.4	. . .	. . .	BAL

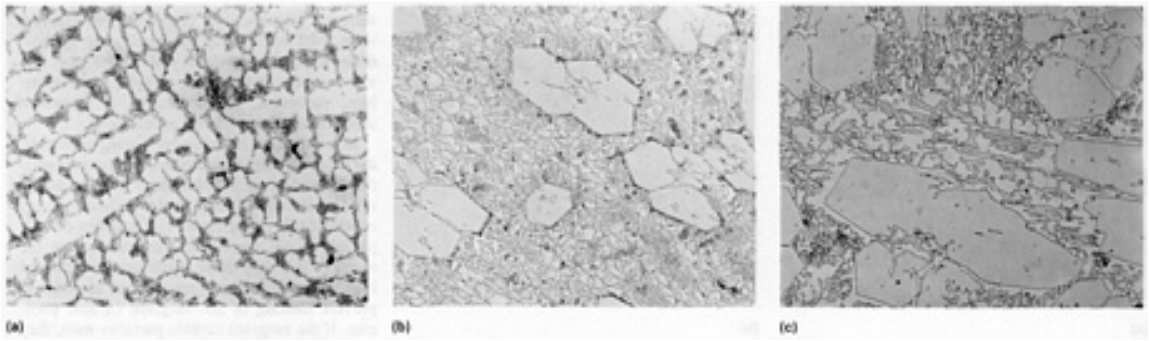

FIG. 2 MICROSTRUCTURES OF HIGH-CHROMIUM WHITE IRON METAL-TO-EARTH ABRASION ALLOYS HARDFACED WITH TWO-LAYER FLUX-COLORED OPEN ARC DEPOSIT. (A) ERFECR-A3. (B) ERFECR-A4(MOD). (C) ERFECR-A2. 300×. SOURCE: REF 2

In addition to M_7C_3, deposits of ERFeCr-A2 contain small quantities of M_6C, and deposits of ERFeCr-A4(Mod) contain small quantities of both M_6C and M_3C. With regard to the matrix, both ERFeCr-A3 and ERFeCr-A4(Mod) exhibit a face-centered cubic (fcc) austenitic structure as deposited. ERFeCr-A2 is largely austenitic but may also contain small quantities of ferrite or martensite. The presence of martensite in the matrix structure of a high-chromium iron is believed to be beneficial to its high-stress abrasion resistance, because of the additional support martensite provides to surface carbides.

For a given hardfacing consumable, deposit (overlay) microstructure is strongly influenced by the welding process and parameters used. Factors of concern, in this regard, include:

- OVERLAY/SUBSTRATE INTERMIXING
- CHANGES IN COMPOSITION DUE TO LOSSES IN THE ARC
- DEPOSIT COOLING RATE

With regard to industrial applications of the high-chromium metal-to-earth abrasion alloys, the low-carbon (2 to 3% C) hypoeutectic materials are usually selected for situations involving moderate abrasion and impact, whereas the higher-carbon (4 to 6% C) hypereutectic alloys are used in applications involving severe abrasion and little or no impact. Specific uses include crusher cones and pump casings (ERFeCr-A3), bulldozer blades and crusher hammers [ERFeCr-A4(Mod)], and coal pulverizer liners and gravel pumps (ERFeCr-A2).

Carbides (Ref 1, 2)

The amount of carbides used for hardfacing applications is small compared to iron-base hardfacing alloys, but carbides are extremely important for severe abrasion and cutting applications. Historically, tungsten-base carbides were used exclusively for hardfacing applications. Recently, however, carbides of other elements, such as titanium, molybdenum, tantalum, vanadium, and chromium, have proved useful in many hardfacing applications.

In contrast to the other hardfacing materials, the tungsten carbide composites do not rely upon the formation of suitable hard phases during weld pool solidification. Instead, these overlay materials rely on the transfer of tungsten carbide particles from the welding consumable to the overlay. It is important, therefore, to limit the heat input of the welding process in order to prevent melting of the tungsten carbide particles. If the tungsten carbide particles melt, they mix with iron to form much softer iron-tungsten carbides, thus reducing abrasion resistance. For this reason, oxyacetylene deposits usually exhibit higher abrasion resistance than arc-welded tungsten carbide overlays. An advantage of the tungsten carbide composites is that the size of the hard particles in the overlay can be controlled. This is important because abrasion resistance is dependent upon the size relationship between microstructural features (such as carbides) and the

abrading particles. It is believed that if the abrading particles are large in comparison to the microstructural particles, then, after a running-in period (during which the softer matrix material at the surface is worn down), the abrading particles ride over the hard microstructural outcrops. On the other hand, if the abrading particles are small in comparison to the microstructural particles, it is believed that the opportunity exists for wear of the matrix around the microstructural particles. Eventually, these may drop out, having played only a small role in resisting abrasion.

Several tungsten carbide composites are available in a variety of tubular product forms. Popular compositions are 40, 50, 55, and 60 wt% tungsten carbide, with a carbon steel tube making up the balance. For each composition, several carbide size ranges are available. As an example, for the 60% tungsten carbide oxyacetylene welding consumable, four mesh size ranges are available:

AWS DESIGNATION	MESH SIZE RANGE
RWC-12/20	12-20
RWC-20/30	20-30
RWC-30/40	30-40
RWC-40/120	40-120

The same composition is also available in flux-coated form for shielded metal arc welding and as a continuous wire (with an internal flux) for open arc welding.

Tungsten carbide composites generally possess very high resistance to abrasion and very low impact strength. Performance in a given situation is dependent upon:

- CARBIDE VOLUME FRACTION
- SIZE RELATIONSHIP BETWEEN THE CARBIDES AND THE ABRASIVE MEDIUM
- WELDING TECHNIQUE APPLIED

Important factors are the distribution of carbides in the overlay (because the particles tend to sink, turbulence in the molten weld pool is an advantage), and the amount of carbide dissolution and reprecipitation in the steel matrix during welding. Impact strength generally decreases with increasing carbide volume fraction.

Table 3 relates tungsten carbide composites and the previously mentioned alloys on the basis of low-stress and high-stress abrasion data (generated under identical test conditions). These values should be compared with the values in Table 1 and Fig. 1. Micrographs of the test deposits are shown in Fig. 3. Noteworthy features include:

- THE DIFFERENCE IN SIZE OF THE TUNGSTEN CARBIDE PARTICLES IN THE TWO MATERIALS
- THE EXTENT TO WHICH SECONDARY CARBIDES HAVE PRECIPITATED WITHIN THE MATRIX

TABLE 3 ABRASION DATA FOR TUNGSTEN CARBIDE HARDFACING MATERIALS

MATERIAL		ABRASION, VOLUME LOSS			
		LOW-STRESS(A)		HIGH-STRESS(B)	
CARBIDE, WT%	MESH SIZE	mm^3	$in.^3 \times 10^{-3}$	mm^3	$in.^3 \times 10^{-3}$
60	20-30	7.3	0.45	28.7	1.75
61	100-250	10.6	0.65	24.4	1.49

(A) DRY SAND/RUBBER WHEEL TEST (ASTM G 65. PROCEDURE B): LOAD 13.6 KG (30 LB); 2000

REV.

(B) SLURRY/STEEL WHEEL TEST (ASTM B 611, MODIFIED): LOAD 22.7 KG (50 LB): 250 REV

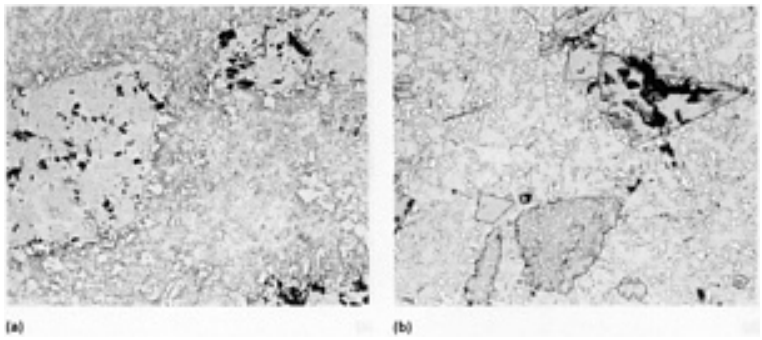

FIG. 3 MICROSTRUCTURES OF TUNGSTEN CARBIDE COMPOSITES WITH CARBIDES OF DIFFERENT SIZES IN THE HARDFACING MATERIAL. (A) 60% TUNGSTEN CARBIDE, 20 TO 30 MESH PARTICLES. (B) 61% TUNGSTEN CARBIDE, 100 TO 250 MESH PARTICLES. HARDFACING PROCESS APPLIED IS ONE-LAYER SHIELDED METAL ARC DEPOSIT. 120 ×. SOURCE: REF 2

The tungsten carbide composites have been used to solve a wide variety of industrial sliding and drilling abrasion problems. Some of the common applications are plowshares, ditchdigger teeth, ripper teeth, and oil well drilling tools. For extremely hostile environments, some nonferrous tungsten carbide products (cobalt- and nickel-base products in the form of bare cast rods) are available. Also, several alternative composite materials, utilizing other carbides (for example, vanadium, titanium, or niobium), are available that have the advantage of creating a more homogeneous deposit because of their lower densities.

Cobalt-Base Alloys (Ref 1, 2)

The two types of commercially available cobalt-base hardfacing alloys are carbide-containing alloys and alloys containing Laves phase. Compositions and properties of cobalt-base hardfacing alloys are given in Tables 4 and 5, respectively.

TABLE 4 COMPOSITIONS OF SELECTED COBALT-BASE HARDFACING ALLOYS

ALLOY	COMPOSITION, WT%					
	CR	MO	W	SI	C	CO
CARBIDE-CONTAINING ALLOYS						
ERCOCR-A	28	. . .	5	. . .	1.2	BAL
ERCOCR-B	29	. . .	8	. . .	1.5	BAL
ERCOCR-C	31	. . .	13	. . .	2.5	BAL
ERCOCR-E	27	6	. . .	. . .	0.2	BAL
LAVES PHASE ALLOYS						
T-400	9	29	. . .	2.5	. . .	BAL
T-800	18	29	. . .	3.5	. . .	BAL

TABLE 5 PROPERTIES OF SELECTED COBALT-BASE HARDFACING ALLOYS

PROPERTY	ALLOY 21[(A)]	RCOCRA	RCOCRB	RCOCRC	TRIBALOY T-800
DENSITY, G/CM^3 (LB/IN.^{3})	8.3 (0.30)	8.3 (0.30)	8.6 (0.31)	8.6 (0.31)	8.6 (0.31)
ULTIMATE COMPRESSIVE STRENGTH,	1295	1515	1765	1930	1780

MPA (KSI)	(188)	(220)	(256)	(280)	(258)
ULTIMATE TENSILE STRENGTH, MPA (KSI)	710 (103)	834 (121)	827 (120)	620 (90)	. . .
ELONGATION, %	8	1.2	1	1	
COEFFICIENT OF THERMAL EXPANSION, $°C^{-1}$ ($°F^{-1}$)	14.8×10^{-6}	15.7×10^{-6}	14×10^{-6}	13.1×10^{-6}	12.3×10^{-6}
	(8.2×10^{-6})	(8.7×10^{-6})	(7.8×10^{-6})	(7.3×10^{-6})	(6.8×10^{-6})
HOT HARDNESS, DPH AT:					
445 °C (800 °F)	150	300	345	510	659
540 °C (1000 °F)	145	275	325	465	622
650 °C (1200 °F)	135	260	285	390	490
760 °C (1400 °F)	115	185	245	230	308
WEAR					
UNLUBRICATED SLIDING WEAR[B], MM^3 ($IN.^3 \times 10^3$) AT:					
670 N (150 LBF)	5.2 (0.32)	2.6 (0.16)	2.4 (0.15)	0.6 (0.04)	1.7 (0.11)
1330 N (300 LBF)	14.5 (0.90)	18.8 (1.17)	18.4 (1.14)	0.8 (0.05)	2.1 (0.13)
ABRASIVE WEAR[C], MM^3 ($IN.^3 \times 10^{-3}$)					
OAW	. . .	29 (1.80)	12 (0.75)	8 (0.50)	. . .
GTAW	86 (5.33)	64 (3.97)	57 (3.53)	52 (3.22)	24 (1.49)
UNNOTCHED CHARPY IMPACT STRENGTH, J (FT · LBF)	37 (27)	23 (17)	5 (4)	5 (4)	1.4 (1)
CORROSION RESISTANCE[D]:					
65% NITRIC ACID AT 65 °C (150 °F)	U	U	U	U	S
5% SULFURIC ACID AT 65 °C (150 °F)	E	E	E	E	. . .
50% PHOSPHORIC ACID AT 400 °C (750 °F)	E	E	E	E	E

(A) CO-27CR-5MO-2.8NI-0.2C.

(B) WEAR MEASURED FROM TESTS CONDUCTED ON DOW-CORNING LFW-1 AGAINST 4620 STEEL RING AT 80 REV/MIN FOR 2000 REV VARYING THE APPLIED LOAD.

(C) WEAR MEASURED FROM DRY SAND RUBBER WHEEL ABRASION TESTS. TESTED FOR 2000 REV AT A LOAD OF 135 N (30 LBF) USING A 230 MM (9 IN.) DIAM RUBBER WHEEL AND AMERICAN FOUNDRYMEN'S SOCIETY TEST SAND.

(D) E, LESS THAN 2 MILS/YEAR; S, OVER 20 TO LESS THAN 50 MILS/YEAR; G, LESS THAN 20 MILS/YEAR; U, MORE THAN 50 MILS/YEAR

Carbide-containing cobalt-base alloys have been widely used since the early 1900s, when a cobalt-base alloy with the nominal composition of Co-28Cr-4W-1.1C was first developed. The chief difference between the various carbide-containing cobalt-base alloys is in carbon content (hence, carbide volume fraction, room-temperature hardness, and level of abrasion resistance). Chromium-rich M_7C_3 is the predominant carbide in these alloys, although tungsten-rich M_6C is evident in those alloys having a high tungsten content, and chromium-rich $M_{23}C_6$ is common in the low-carbon alloys. Figure 4 relates the carbon content and the resistance to low-stress abrasion for the carbide-containing cobalt-base alloys (ERCoCr-A, -B, -C, and -E). The low-stress abrasion data in this figure were generated using the ASTM G 65 dry sand/rubber wheel test.

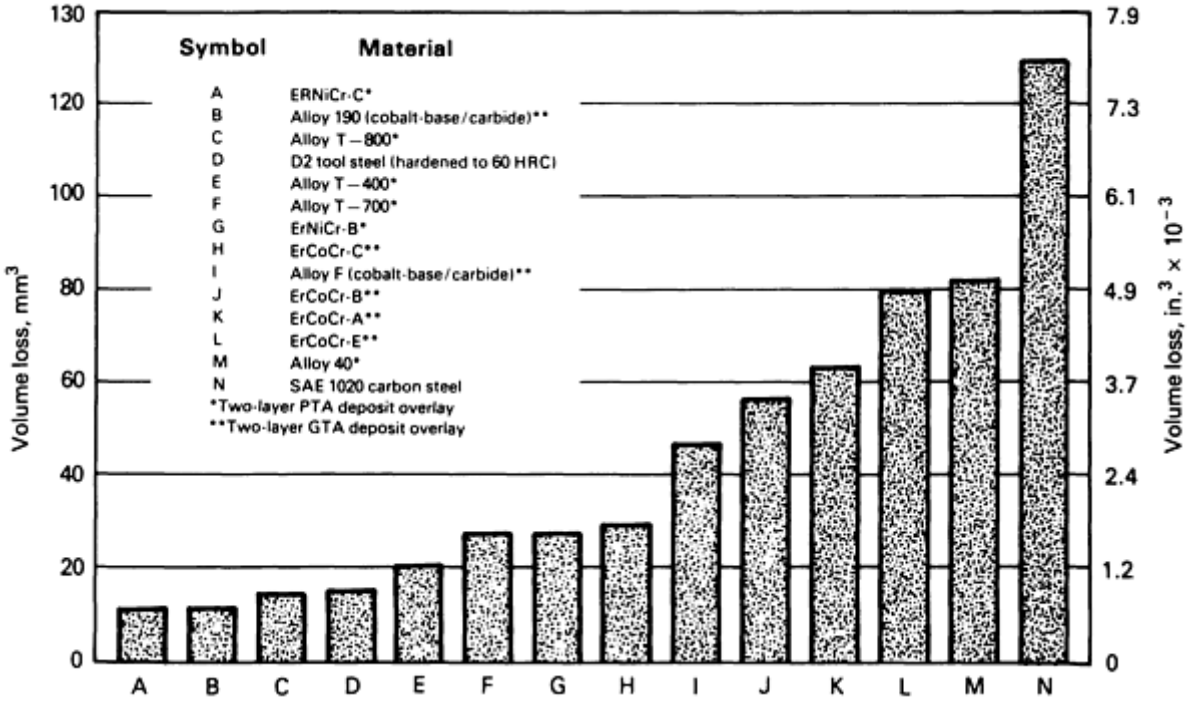

FIG. 4 COMPARISON OF NONFERROUS HARDFACING ALLOYS TO TOOL STEEL AND CARBON STEEL REFERENCE MATERIALS USING ASTM G 65 LOW-STRESS ABRASION TEST. G 65 TEST PARAMETERS: PROCEDURE B; ROOM TEMPERATURE; 13.6 KG (30 LBF) LOAD; QUARTZ GRAIN SAND DIAMETER OF 212 TO 300 μM; 2000 REV AT 200 REV/MIN; 390 G/MIN (0.86 LB/MIN) FEED RATE. SOURCE: REF 2

Micrographs of plasma-transferred arc (two-layer) deposits of three carbide-containing cobalt-base alloys are shown in Fig. 5. The differences in carbide volume fraction and geometry are evident from these micrographs.

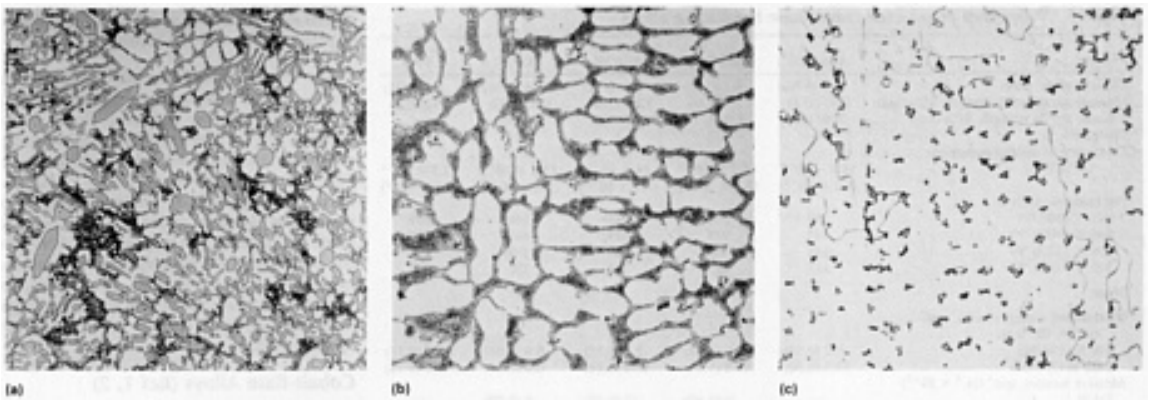

FIG. 5 MICROSTRUCTURES OF TWO-LAYER PLASMA TRANSFERRED ARC DEPOSIT CARBIDE-CONTAINING COBALT-BASE HARDFACING ALLOYS. (A) ERCOCR-C. (B) ERCOCR-A. (C) ERCOCR-E. 425×. SOURCE: REF 2

Laves Phase Alloys. Laves phase is a type of topologically closed-packed intermetallic compound. Historically, metallurgists have avoided the presence of Laves phase in most alloys because of its detrimental effect on mechanical properties. However, in the early 1960s, the usefulness of Laves phase in resisting metal-to-metal wear was discovered; subsequently, alloys containing Laves phase have become commercially available. As listed in Table 4, there are two different Laves phase-containing cobalt-base alloys commercially available for hardfacing applications: Co-29Mo-9Cr-2.5Si (T-400) and Co-29Mo-18Cr-3.5Si (T-800). Both of these alloys contain at least 50 vol% of Laves phase, bound in a cobalt-base matrix alloyed with chromium and molybdenum.

Because the Laves intermetallic phase is so abundant in these alloys, its presence governs all the material properties. Accordingly, the effects of the matrix composition in these alloys are less pronounced than is the case for the carbide-containing cobalt-base alloys. for example. The Laves phase is specifically responsible for outstanding abrasion resistance, but it severely limits the material ductility and the impact strength. In fact, it is difficult to attain crack-free overlays on all but the smallest components given adequate preheat. For this reason, these alloys have been more successful as thermal spray materials. Figure 4 compares the abrasion resistance of various nonferrous hardfacing alloys, including T-400 and T-800 Laves phase cobalt-base alloys. The microstructure of a two-layer plasma transferred arc (PTA) deposit of alloy T-800 is shown in Fig. 6.

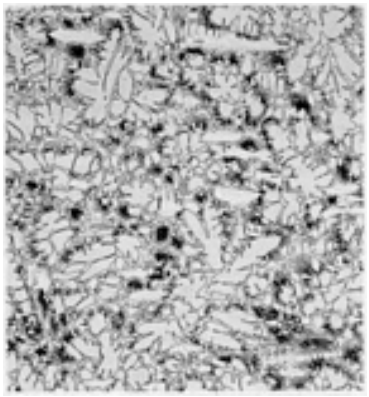

FIG. 6 MICROSTRUCTURE OF T-800 (TWO-LAYER PLASMA TRANSFERRED ARC DEPOSIT) COBALT-BASE LAVES PHASE HARDFACING ALLOY. 200×. SOURCE: REF 2

Nickel-Base Alloys (Ref 1, 2)

Most commercially available nickel-base hardfacing alloys can be divided into three groups: boride-containing alloys, carbide-containing alloys, and Laves phase-containing alloys. The compositions of some typical nickel-base hardfacing alloys are listed in Table 6. Selected properties of these alloys are listed in Table 7.

TABLE 6 COMPOSITION OF NICKEL-BASE AND HIGH-NICKEL-CONTENT HARDFACING ALLOYS

ALLOY	COMPOSITION, WT%								
	Fe	Cr	Mo	W	Si	C	B	Co	Ni
BORIDE-CONTAINING ALLOYS									
ALLOY 40	1.5	7.5	. . .	. . .	3.5	0.3	1.5	. . .	BAL
ERNICR-B	3	11	. . .	. . .	4	0.5	2.5	. . .	BAL
ERNICR-C	4	16	. . .	. . .	4	0.7	3.5	. . .	BAL
CARBIDE-CONTAINING ALLOYS									
ALLOY N-6	3	29	5.5	2	1.5	1.1	0.6	3	BAL
ALLOY 716	BAL	26	3	3.5	1.5	1.1	0.5	11	23
LAVES PHASE ALLOYS									
T-700	. . .	16	33	. . .	3.5	. . .	. . .	. . .	BAL

TABLE 7 PROPERTIES OF SELECTED NICKEL-BASE HARDFACING ALLOYS

PROPERTY	RNICRC	RNICRB	HASTELLOY C (NI-17CR-17MO-0.12C)	TRIBALOY T-700
DENSITY, G/CM^3 (LB/IN.^{3})	7.8 (0.28)	8.0 (0.29)	8.6 (0.32)	8.6 (0.32)
COEFFICIENT OF THERMAL EXPANSION, °C^{-1} (°F^{-1})	14.3 (8.0)	14.3 (8.0)	13.7 (7.6)	11.9 (6.6)
HOT HARDNESS, DPH AT: 425 °C (800 °F)				

425 °C (800 °F)	555	. . .	190	500
540 °C (1000 °F)	440	. . .	185	485
650 °C (1200 °F)	250	. . .	170	400
760 °C (1400 °F)	115	. . .	145	280
WEAR				
UNLUBRICATED SLIDING WEAR[A], MM^3 ($IN.^3 \times 10^{-3}$) AT:				
670 N (150 LBF)	0.15 (0.009)	0.3 (0.018)	0.4 (0.024)	0.1 (0.006)
1330 N (300 LBF)	0.3 (0.018)	0.4 (0.024)	. . .	0.3 (0.018)
ABRASIVE WEAR[B], MM^3 ($IN.^3 \times 10^{-3}$)				
OAW	12 (0.73)	18 (1.10)	. . .	. . .
GTAW	11 (0.67)	12 (0.73)	105 (6.40)	43 (2.62)
UNNOTCHED CHARPY IMPACT STRENGTH, J (FT · LBF)	3 (2)	3 (2)	39 (29)	1.4 (1)
CORROSION RESISTANCE AT 65 °C (150 °F)[C]: 65% NITRIC ACID				
65% NITRIC ACID	U	U	E	E
5% SULFURIC ACID	U	U	E	E
50% PHOSPHORIC ACID	U	U	E	E

(A) WEAR MEASURED FROM TESTS CONDUCTED ON DOW-CORNING LFW-1 AGAINST 4620 STEEL RING AT 80 REV/MIN FOR 2000 REV VARYING THE APPLIED LOADS.

(B) WEAR MEASURED FROM DRY SAND RUBBER WHEEL ABRASION TESTS. TESTED FOR 2000 REV AT A LOAD OF 135 N (30 LBF) USING A 230 MM (9-IN.) DIAM RUBBER WHEEL AND AMERICAN FOUNDRYMEN'S SOCIETY TEST SAND.

(C) E, LESS THAN 2 MILS/YEAR; S, OVER 20 TO LESS THAN 50 MILS/YEAR; G, LESS THAN 20 MILS/YEAR; U, MORE THAN 50 MILS/YEAR

The boride-containing nickel-base alloys were first commercially produced as spray-and-fuse powders. The alloys are currently available from most manufacturers of hardfacing products under various tradenames and in a variety of forms, such as bare cast rod, tube wires, and powders for plasma weld and manual torch. This group of alloys is primarily composed of nickel, chromium, boron, silicon, and carbon. Usually, the boron content ranges from 1.5 to 3.5%, depending on chromium content, which can be as high as 16%. The higher chromium alloys generally contain a large amount of boron, which forms very hard chromium borides with hardnesses of approximately 1800 DPH (kg/mm^2).

Of all the hardfacing alloys, the boride-containing nickel-base alloys are microstructurally the most complex. The complexity of this type of alloy structure is evident in Fig. 7, which shows a two-layer PTA deposit of ERNiCr-C (see Table 6 for composition). The alloy compositions represent a progression in terms of iron, chromium, boron, and carbon contents. Iron content is largely incidental, allowing the use of ferrocompounds during manufacture. Together with nickel, the other three elements determine the level and type of hard phase within the structure upon solidification, boron being the primary hard-phase forming element (for which nickel and chromium. compete) and carbon being the secondary hard-phase former. The actual phases that form in boride-containing nickel-base alloys are listed in Table 8 on the basis of chromium content.

TABLE 8 PHASES FORMED IN BORIDE-CONTAINING NICKEL-BASE HARDFACING ALLOYS

CHROMIUM CONTENT	SECONDARY PHASES		DOMINANT HARD PHASE
	COMPOUND FORMED	REQUIRED CONDITIONS	
LOW (~5 WT%)	NI_3SI	>3 WT% SI	NI_3B
MEDIUM (~15 WT%)	NI_3SI	>2.5 WT% SI	NI_3B AND CHROMIUM BORIDE (USUALLY CRB, ALTHOUGH CR_2B AND CR_3B_2 MAY ALSO BE PRESENT)
HIGH (~25	NI_3SI	>3 WT% SI	CRB AND CR_5B_3

WT%)			
ALL LEVELS	. . .	. . .	COMPLEX CARBIDES OF $M_{23}C_6$ AND M_7C_3 TYPES

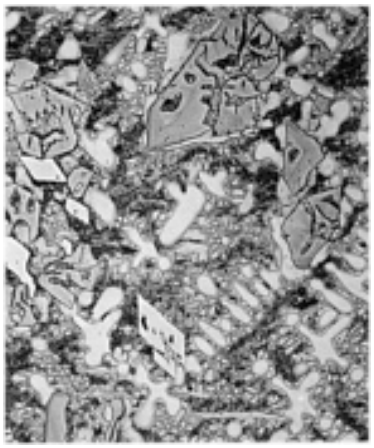

FIG. 7 MICROSTRUCTURE OF ERNICR-C (TWO-LAYER PLASMA TRANSFERRED ARC DEPOSIT) BORIDE-CONTAINING NICKEL-BASE HARDFACING ALLOY. 425×. SOURCE: REF 2

The chief purpose of silicon in the material is to provide, in conjunction with boron, self-fluxing characteristics. However, as an important matrix element and as a potential promoter of intermetallic precipitates, it also has a powerful influence on the wear properties of the alloys.

Boron content influences the level of silicon required for silicide (Ni_3Si) formation. The higher the boron content, the lower is the silicon content required to form silicides.

Because of the boride and carbide dispersions within their microstructures, the boride-containing nickel-base alloys exhibit excellent resistance to abrasion (ERNiCr-C, ERNiCr-B, and Alloy 40 in Fig. 4). Low-stress abrasion resistance generally increases with boron and carbon contents, hence the hard-phase volume fraction for these materials. Although their performance is not as good under self-mated sliding conditions as that of cobalt-base materials, the boride-containing nickel-base alloys possess moderate resistance to galling. Of the nonferrous materials, the boride-containing nickel-base alloys are the least resistant to corrosion. This is attributed to the lack of chromium in the matrix that follows boride and carbide formation.

Originally, the boride-containing nickel-base alloys were developed from brazing alloy compositions specifically for use with the spray-and-fuse process (for which their self-fluxing properties are ideal). During the fusing cycle of this process, it is believed that oxides within the sprayed coating combine with some of the silicon and boron to form a borosilicate slag (which floats to the surface of the deposit). The only other commercially significant spray-and-fuse alloys are some silicon-containing and boron-containing derivatives of the carbide-containing cobalt-base materials. Microstructurally, and in a property sense, these alloys bear little resemblance to their traditional counterparts because the presence of boron markedly changes the matrix chromium content and the types of hard phase that form during solidification. Additional information on the spray-and-fuse process can be found later in this article in the section on "Thermal Spraying."

Carbide-Containing Alloys. The use of carbide-containing nickel-base alloys has been somewhat limited to date. However, these alloys are gaining popularity as alternatives to cobalt-base hardfacing alloys. This is particularly applicable in the nuclear power industry, where it has been found that high-cobalt hardfacing alloys are sources of the highly radioactive ^{60}Co isotope that deposits in pipes, fittings, and valve bodies (Ref 6). Wear and corrosion of hardfacing alloys lead to the release of ^{59}Co into the primary coolant. The ^{59}Co deposits on the reactor core, where it is transmuted to the radioactive ^{60}Co isotope, which is then released back to the coolant. The most popular and widely used cobalt-free alloys are in the Ni-Cr-Mo-C and Ni-Cr-Fe-C systems. Table 6 lists several compositions of these alloys.

Generally, carbide-containing nickel-base alloys have poor oxyacetylene weldability, which has made then unsuitable for hardfacing applications in the past. Carbide-containing nickel-base alloys of the Ni-Cr-Mo-Co-Fe-W-C system are more

readily weldable by oxyacetylene methods and are gaining popularity as low-cost alternatives to cobalt-base alloys. These alloys, depending on precise composition, contain M_7C_3- or M_6C-type carbides similar to cobalt-base alloys.

Laves Phase Alloys. Only one Laves phase-containing nickel-base alloy is commercially available: Ni-33Mo-16Cr-3.5Si (T-700 in Table 6). This alloy, like most nickel-base alloys, is difficult to weld using the oxyacetylene process, but it can be readily welded using gas-tungsten arc welding or the PTA process. It can also be applied using the plasma or high-velocity oxyfuel thermal spray techniques. Although it has excellent metal-to-metal wear resistance and moderate abrasive wear resistance, it possesses poor impact resistance.

High-Silicon Stainless Steels (Ref 2)

Recently, several new high-silicon stainless steels have been introduced that may also be considered as alternate materials to cobalt-base alloys. These exhibit identical anti-galling characteristics and possess equal resistance to cavitation erosion. Some of these have been developed for general use and others for specific applications (for example, hydroelectric turbines and nuclear valves). Some are based on type 200 (manganese- and nitrogen-containing) austenitic stainless steel; others are based on type 300 stainless steel. One of these latter compositions is as follows (Ref 7):

ELEMENT	COMPOSITION, WT%
CARBON	0.12
CHROMIUM	21.0
NICKEL	8.0
SILICON	5.0
MANGANESE	6.5
IRON	BAL

These high-silicon hardfacing alloys differ from the traditional carbide-containing cobalt-base alloys in terms of their corrosion resistance (they are better in some aqueous media and worse in others), their mechanical properties (particularly at high temperatures), and their thermal stability.

Copper-Base Alloys (Ref 2)

Copper-base hardfacing alloys fall in the aluminum bronze category. Examples include ECu-AlB (Cu-9Al-4Fe-1Si) and ECuAl-D (Cu-13.5Al-4Fe). Silicon and other types of bronze are also available in welding consumable form for hardfacing. Aluminum, silicon, and iron are added to the bronzes to strengthen the solid solution, and, in excess of their solubility limits (about 8%, in the case of aluminum), to provide precipitation hardening.

Wear tests have shown that the aluminum bronzes possess anti-galling characteristics (self-coupled) comparable to those of ER-CoCr-E; low-stress abrasion resistance of the aluminum bronzes, however, was very low. Components typically protected using the aluminum bronzes include gears, cams, bearings, and cold drawing/forming dies. These alloys are not recommended for elevated-temperature use because their mechanical properties considerably decrease at temperatures >200 °C (>390 °F).

Hardfacing Alloy Selection (Ref 1)

Hardfacing alloy selection is guided primarily by wear and cost considerations. However, other manufacturing and environmental factors must also be considered, such as base metal; deposition process; and impact, corrosion, oxidation, and thermal requirements. The factors affecting hardfacing process selection are discussed in the next section of this article. Usually, the hardfacing process dictates the hardfacing or filler-metal product form.

Hardfacing alloys usually are available as bare rod, flux-coated rod, long-length solid wires, long-length tube wires (with and without flux), or powders. The most popular processes, and the forms most commonly associated with each process, are (Ref 2):

HARDFACING PROCESS	CONSUMABLE FORM
OXYFUEL/OXYACETYLENE (OFW/OAW)	BARE CAST OR TUBULAR ROD
SHIELDED METAL ARC (SMAW)	COATED SOLID OR TUBULAR ROD (STICK ELECTRODE)
GAS-TUNGSTEN ARC (GTAW)	BARE CAST OR TUBULAR ROD
GAS-METAL ARC (GMAW)	TUBULAR OR SOLID WIRE
FLUX-CORED OPEN ARC	TUBULAR WIRE (FLUX CORED)
SUBMERGED ARC (SAW)	TUBULAR OR SOLID WIRE
PLASMA TRANSFERRED ARC (PTA)	POWDER
LASER BEAM	POWDER

In general, the impact resistance of hardfacing alloys decreases as the carbide content increases. As a result, in a situation where a combination of impact and abrasion resistance is desired, a compromise between the two must be made. In applications where impact resistance is extremely important, austenitic manganese steels are used to build up worn parts.

Frequently, wear is accompanied by aqueous corrosion from acids or alkalis, such as those encountered in the chemical processing or petroleum industries or in flue gas scrubbers. Few of the iron-base hardfacing alloys possess the necessary corrosion resistance in such aqueous media. As a result, nickel- or cobalt-base hardfacing alloys generally are recommended when corrosion resistance combined with wear resistance is required. For example, a knife used to cut tomatoes in a food processing plant can last many times longer than a tool steel knife if the edge is made of a cobalt-base alloy.

Oxidation and hot corrosion resistance of iron-base alloys is also generally poor. Typically, boride-containing nickel-base alloys do not contain sufficient chromium in the matrix to resist oxidation. Hence, Laves phase-containing or carbide-containing nickel- or cobalt-base alloys typically are recommended for applications in which wear resistance combined with oxidation or hot corrosion resistance is required.

The ability of an alloy to retain strength at elevated temperatures is important for wear applications such as hot forging dies or valves for service at 870 °C (1600 °F), as well as service in coal gasification/liquefaction applications. Iron-base alloys with martensitic structures lose hardness at elevated temperatures. Generally, the high-temperature strength retention of a hardfacing alloy increases with its tungsten or molybdenum content. In applications requiring elevated-temperature strength and wear resistance, cobalt-base alloys or Laves phase alloys are recommended.

Wear-resistant materials typically are classified by type and alloy content, which largely determines their properties. These materials have structures consisting of hard phases (carbides, borides, or Laves phases) in a matrix hardened to a level that depends on the desired alloy properties.

Table 9 provides an extensive list of hardfacing materials along with their specific advantages and applications. Such recommendations are also available from producers of hardfacing alloys. The following steps should be taken in selecting a hardfacing alloy:

- ANALYSIS OF THE SERVICE CONDITIONS TO DETERMINE THE TYPE OF WEAR AND ENVIRONMENTAL RESISTANCE REQUIRED
- SELECTION OF SEVERAL HARDFACING ALLOY CANDIDATES
- ANALYSIS OF THE COMPATIBILITY OF THE HARDFACING ALLOYS WITH THE BASE METAL, TAKING INTO CONSIDERATION THERMAL STRESSES AND POSSIBLE CRACKING
- FIELD TESTING OF HARDFACED PARTS
- SELECTION OF AN OPTIMUM HARDFACING ALLOY, CONSIDERING COST AND WEAR LIFE
- SELECTION OF THE HARDFACING PROCESS FOR PRODUCTION OF WEAR COMPONENTS, CONSIDERING DEPOSITION RATES, THE AMOUNT OF DILUTION, DEPOSITION,

EFFICIENCY, AND OVERALL COST, INCLUDING THE COST OF CONSUMABLES AND PROCESSING

TABLE 9 SELECTION GUIDE FOR HARDFACING ALLOYS

TYPES OF MATERIALS	ADVANTAGES	APPLICATIONS
LOW HARDNESS		
PEARLITIC STEELS	LOW COST, CRACK-RESISTANT	A BUILDUP MATERIAL TO RESTORE DIMENSION OR AS A LOW-COST BASE FOR SURFACING APPLICATIONS
MILD STEELS	AN EXCELLENT BASE FOR HARDFACING	
LOW-ALLOY STEELS	SOME TOUGHNESS FOR BUILDUP OF WORN AREAS	
AUSTENITIC STEELS	EXCELLENT FOR HEAVY IMPACT, TOUGH	FOR METAL-TO-METAL WEAR UNDER HEAVY IMPACT CONDITIONS
LOW-CARBON NI-CR STAINLESS	GOOD CORROSION RESISTANCE	CORROSION-RESISTANT SURFACING OF LARGE TANKS, NUCLEAR VESSELS
HIGH-CARBON NI-CR STAINLESS	OXIDATION AND HOT WEAR RESISTANT	FURNACE PARTS, RED HEAT FRICTIONAL WEAR
14% MN, CR-NI	HIGH YIELD STRENGTH AUSTENITIC	BUILDUP, CRACK REPAIR, JOINING MANGANESE ALLOYS OR MANGANESE TO MILD STEEL
14% MN, 1% MO	FAIR ABRASION AND CORROSION RESISTANCE, WORK HARDENS	RAILWAY TRACK BUILDUP
14% MN, 3% NI	WORK HARDENS	BUILDUP AND JOINING OF MANGANESE PARTS
SEMIAUSTENITIC STEELS	LOW-COST CRACK-RESISTANT MATERIALS	HARDFACING APPLICATIONS
COPPER ALLOYS	RESISTANCE TO SEIZING UNDER FRICTIONAL WEAR CONDITIONS	FOR BUILDUP OF BEARING SURFACES
MEDIUM HARDNESS		
NICKEL-BASE ALLOYS	GOOD CORROSION RESISTANCE AND EXCELLENT HOT HARDNESS	FOR APPLICATIONS WHERE HOT HARDNESS IS IMPORTANT
NICKEL-CHROMIUM	RESISTANCE TO OXIDATION	FOR CORROSIVE WEAR CONDITIONS
NICKEL-CHROMIUM-MOLYBDENUM	RESISTANCE TO EXHAUST GAS CORROSION	FOR HARDFACING TRUCK, BUS, AND AIRCRAFT ENGINE VALVES
NICKEL-CHROMIUM-MOLYBDENUM-TUNGSTEN	CORROSION-RESISTANT PROPERTIES	FOR SURFACING APPLICATIONS
NICKEL-CHROMIUM-BORON	CORROSION-RESISTANT AS WELL AS ABRASIVE-	PUMPING SERVICE APPLICATIONS, ESPECIALLY IN THE OIL FIELDS

	RESISTANT PROPERTIES	
MARTENSITIC ALLOY IRONS	EXCELLENT ABRASION RESISTANCE	FOR OVERCOMING ABRASIVE WEAR WHERE LIGHT OR NO IMPACT IS INVOLVED
CHROMIUM-MOLYBDENUM	ABRASION RESISTANCE WHILE WITHSTANDING LIGHT IMPACT	FOR THE BUILDUP OF MACHINE PARTS SUBJECT TO REPETITIVE METAL-TO-METAL WEAR WITH OR WITHOUT LIGHT IMPACT
CHROMIUM-TUNGSTEN	HIGH COMPRESSIVE STRENGTHS	
AUSTENITIC ALLOY IRONS	BETTER CRACK-RESISTANT PROPERTIES THAN THE MARTENSITIC ALLOY IRONS	WHERE EROSIVE WEAR WITH OR WITHOUT LIGHT IMPACT IS PRESENT
CHROMIUM-MOLYBDENUM	GOOD CRACK-RESISTANT QUALITIES	PUMP AND TURBINE BUILDUP
NICKEL-CHROMIUM	CRACK-RESISTANT, LIGHT IMPACT	FOR EROSIVE WEAR WITH LIGHT IMPACT
MARTENSITIC STEELS	ABRASION RESISTANCE WITH MEDIUM IMPACT	FOR A VARIETY OF ABRASIVE WEAR CONDITIONS WHERE THERE MAY ALSO BE INVOLVEMENT WITH MEDIUM IMPACT
LOW CARBON (UP TO 0.30% C)	LEAST EXPENSIVE, TOUGH	
MEDIUM CARBON (0.30-0.65% C)	GOOD RESISTANCE TO MEDIUM IMPACT	
HIGH CARBON (0.65-1.7% C)	FAIR ABRASION RESISTANCE	
HIGH HARDNESS		
HIGH-CHROMIUM IRONS	EXCELLENT EROSION-RESISTANT PROPERTIES	FOR GENERAL USE WHERE HOT GASES OR MATERIALS ARE INVOLVED
AUSTENITIC	GOOD ABRASION-RESISTANT QUALITIES	FOR FARM AND EARTH-MOVING EQUIPMENT WORKING IN SANDY SOILS
MARTENSITIC	ABILITY TO BE REHARDENED AFTER ANNEALING	AS A HARDFACING IN STEEL MILLS AND REFINERIES WHERE HOT EROSION (595 °C, OR 1100 °F) IS A WEAR PROBLEM
TUNGSTEN-MOLYBDENUM ALLOYS	HIGH RED HARDNESS	FOR HARDFACING OF COKE OVEN PARTS AS WELL AS OTHER HOT (425 TO 650 °C, OR 800 TO 1200 °F) STEEL MILL APPLICATIONS
CHROMIUM-TUNGSTEN-COBALT ALLOYS	HIGH RED HARDNESS, HIGH HOT STRENGTH AND CREEP-RESISTANT QUALITIES	FOR MOST HARDFACING APPLICATIONS, BUT BEST SUITED TO THOSE APPLICATIONS WHERE HOT WEAR AND ABRASION (ABOVE 650 °C, OR 1200 °F) ARE INVOLVED (JET ENGINE TURBINE BLADES, GAS ENGINE EXHAUST VALVE)
LOW CARBON (UP TO 1.0% C)	GOOD OXIDATION RESISTANCE, TOUGH	
MEDIUM	RESISTANT TO ABRASION AND	

CARBON (1.4% C)	OXIDATION	
HIGH CARBON (2.5% C)	GOOD ABRASION RESISTANCE, BRITTLE	
TUNGSTEN CARBIDES	THE ULTIMATE IN ABRASION-RESISTANT QUALITIES	A VARIETY OF MATERIALS USED FOR HARDFACING TO MEET AN EXTREMELY WIDE RANGE OF SEVERE ABRASIVE CONDITIONS, ESPECIALLY OIL WELL DRILL BITS, TOOL JOINTS, ROCK DRILL BITS
FINE-GRAIN TUBULAR RODS	A RELATIVELY SMOOTH, EXTREMELY WEAR-RESISTANT SURFACE, GAS WELD	
COARSE GRANULAR TUBE ROD	DEVELOPS A ROUGH CUTTING SURFACE AS THE DEPOSITED BINDER WEARS AWAY	
GRANULES OR INSERTS	DEVELOPS AN EXTREMELY ROUGH ABRASIVE CUTTING SURFACE AS GRANULES OR INSERTS BECOME MORE EXPOSED. HIGHLY ABRASIVE, BUT BRITTLE UNDER IMPACT CONDITIONS	

Source: Ref 8

Hardfacing Process Selection (Ref 1)

Hardfacing process selection may be as important as hardfacing alloy selection, depending on the engineering application. Service performance requirements not only dictate hardfacing alloy selection, but also have a strong influence on hardfacing process selection. Other technical factors involved in hardfacing process selection include (but are not limited to) hardfacing property and quality requirements, physical characteristics of the workpiece, metallurgical properties of the base metal, form and composition of the hardfacing alloy, and welder skill. Ultimately, economic considerations predominate, and cost is the determining factor in the final process selection.

The term "hardfacing" is sometimes used to describe true welding processes, in which both the filler material and a small amount of the base metal are molten and are bonded metallurgically. Such processes, which include oxyfuel, arc, and laser welding methods, are preferred for applications that require dense and relatively thick coatings with excellent bonding between the hardfacing material and the base metal. Thermal spray processes are used for applications that require a thin, hard coating applied with minimum work distortion and where a purely mechanical bond between the hardfacing material and the base metal is acceptable.

Property and Quality Requirements. Welded hardfacing deposits are, in effect, mini-castings characterized by variable composition (segregation) and solidification kinetics that influence deposit microstructure. It is not surprising, therefore, that the properties and quality of welded hardfacing deposits should depend on welding process and technique, as well as on alloy selection.

Composition variations also derive from base-metal dilution during welding, although carbon pickup in oxyfuel gas welding (OFW) processes and solute volatilization during arc welding processes are additional factors. Dilution is the inter-alloying of the hardfacing alloy and the base metal and is usually expressed as the percentage of base metal in the hardfacing deposit. A dilution of 10% means that the deposit contains 10% base metal and 90% hardfacing alloy (see the section on "Weld Cladding" in this article for more detailed information). The wear resistance and other desirable properties of the hardfacing alloy are generally thought to degrade as dilution increases. The maximum amount of allowable dilution depends on specific service requirements. Welding process and technique should, however, be selected so as to control dilution to less than 20% for the hardest layer. More dilution is acceptable for buildup layers.

Dilution is nil in thermal spraying processes and tends to be acceptably low in conventional OFW processes. Dilution is generally more of a problem in arc weld hardfacing processes, ranging from approximately 5% in plasma arc welding

(PAW) hardfacing processes to as much as 50% in submerged arc welding (SAW). Laser hardfacing dilution is also low, ranging generally from 1 to 10%. High-dilution welding processes can be tolerated in applications requiring relatively thick hardfacings that can be applied in multiple layers. The effects of dilution on the microstructure of a high-chromium, white iron hardfacing alloy deposited in multiple layers on low-carbon steel substrate using shielded metal arc welding (SMAW) are illustrated in Fig. 8. The first layer (Fig. 8a) microstructure in this particular case was hypoeutectic with interdendritic eutectic and exhibited a hardness of 55 HRC. The second layer (Fig. 8b) consisted of a fine hypereutectic microstructure with a large percentage of eutectic and exhibited a hardness of 57 HRC. The third (Fig. 8c) and fifth (Fig. 8d) layers were microstructurally equivalent, consisting of primary M_7C_3 carbides in eutectic matrices. The hardness in the third and subsequent layers ranged from 60 to 61 HRC.

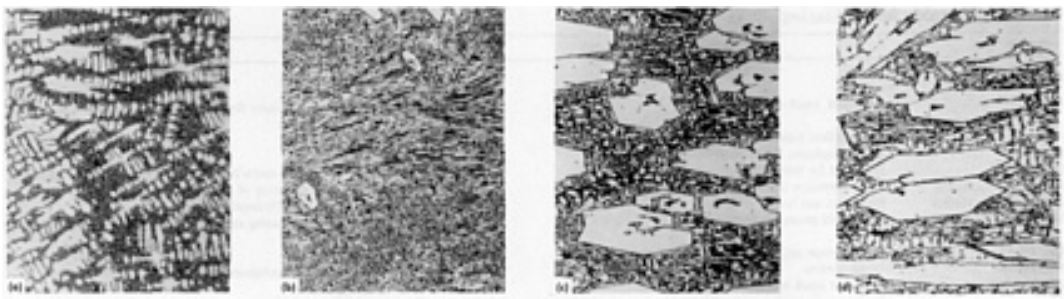

FIG. 8 EFFECT OF DILUTION ON THE MICROSTRUCTURE OF A FE-28CR-4MO-0.4MN-4.6C HARDFACING ALLOY. (A) FIRST LAYER OVER MILD STEEL SHOWING A HYPOEUTECTIC STRUCTURE OF METAL DENDRITES AND INTERDENDRITIC EUTECTIC, 55 HRC. (B) SECOND LAYER SHOWING A FINE HYPOEUTECTIC STRUCTURE WITH A LARGE PERCENTAGE OF EUTECTIC MATRIX, 57 HRC. (C) THIRD LAYER SHOWING A COARSE HYPEREUTECTIC STRUCTURE OF PRIMARY M_7C_3 CARBIDES IN A EUTECTIC MATRIX, 61 HRC. (D) FIFTH LAYER SHOWING A STRUCTURE SIMILAR TO BOTH THE THIRD AND FOURTH PASSES, 60 HRC. SOURCE: REF 1

The microstructures and mechanical properties of hardfacing deposits, like castings, vary depending on solidification kinetics as well as on dilution. Solidification generally is rapid in thermal spray processes, with nearly amorphous structures being achieved with some thermal spray processes. Solidification kinetics tend to be somewhat slower in conventional weld hardfacing processes. As a rule, hardfacing deposits produced by OFW processes tend to solidify more slowly than hardfacing deposits produced by arc welding processes. These differences in solidification rate produce widely different microstructures and widely different properties regardless of dilution. The effects of welding process on the microstructure of a cobalt-base (ERCoCr-A) hardfacing alloy deposited on a low-carbon steel substrate are illustrated in Fig. 9.

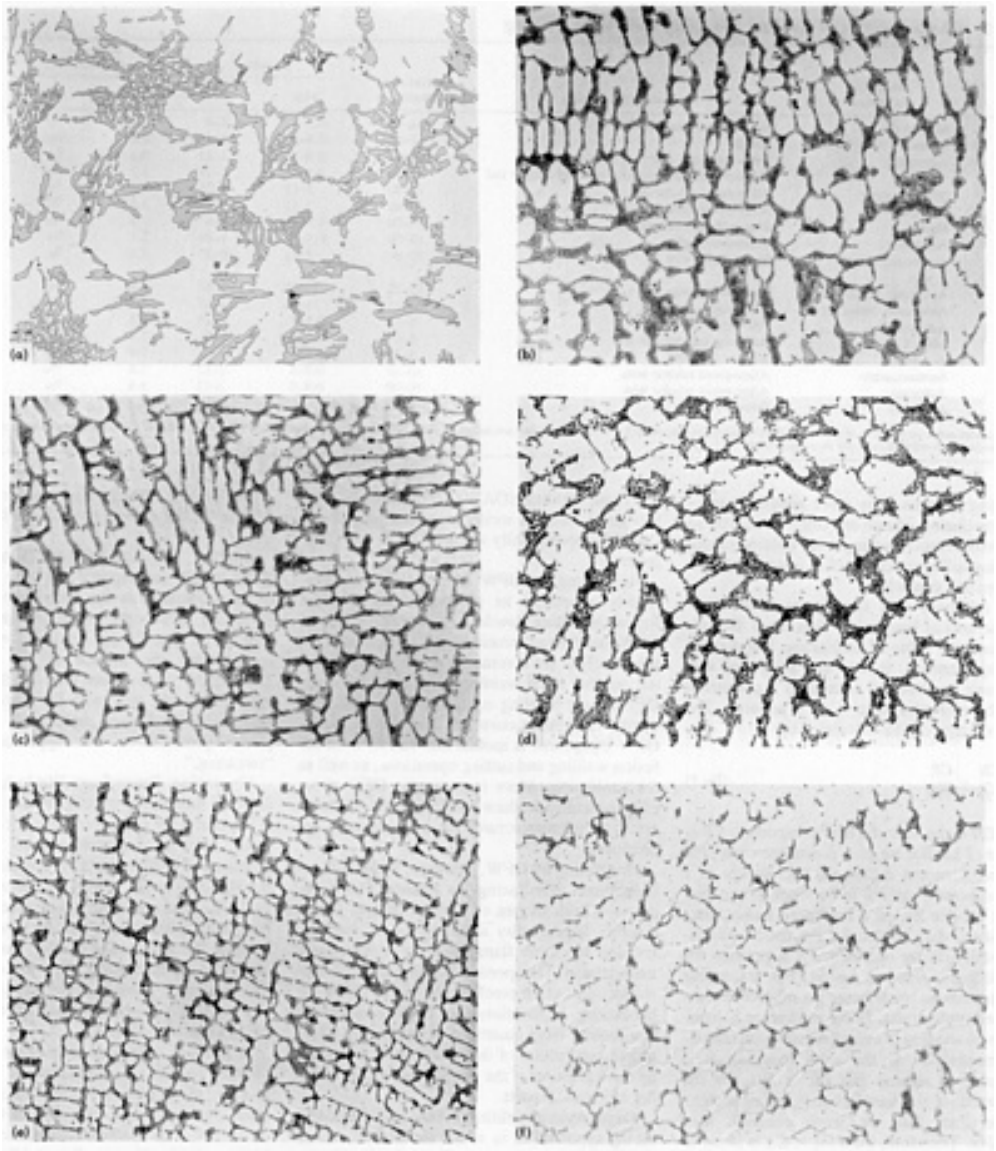

FIG. 9 EFFECT OF WELDING PROCESS ON THE MICROSTRUCTURE OF AN ERCOCR-A HARDFACING ALLOY. (A) OXYFUEL GAS WELDING. (B) PLASMA TRANSFERRED ARC WELDING. (C) GAS-TUNGSTEN ARC WELDING. (D) FLUX-CORED OPEN ARC WELDING. (E) SUBMERGED ARC WELDING. (F) SHIELDED METAL ARC WELDING. SOURCE: REF 1

Physical Characteristics of the Workpiece. The size, shape, and weight of the workpiece have a strong influence on hardfacing process selection. Large, heavy workpieces that are difficult to transport are most conveniently hardfaced using manual or semiautomatic hardfacing processes in which the hardfacing equipment can be moved to the workpiece. Gas shielded metal arc and open arc welding processes, for which portable equipment is readily available, are well suited to field applications involving inaccessible surfaces on large, difficult-to-transport workpieces. Thermal spraying processes and equipment also are available for *in situ* field hardfacing applications.

Hardfacing process selection is more involved in applications where the workpiece is sufficiently small so that it can be readily transported to the welding equipment. Thermal spraying processes and OFW, SAW, gas-tungsten arc welding (GTAW), PAW, and gas-tungsten arc welding (GMAW) are all well suited to in-plant hardfacing of small workpieces. Preference is usually given to thermal spraying and/or OFW or GTAW for small workpieces requiring thin, accurately placed hardfacing deposits. Large quantities of small workpieces can usually be hardfaced most economically using dedicated, specially designed, fully automatic hardfacing equipment and processes.

Metallurgical Characteristics of the Base Metal. As described below, base-metal surface preparation is important in thermal spray hardfacing processes. However, base-metal composition, melting temperature range, and thermal expansion and contraction characteristics have a significant effect on welding process selection.

Steels are generally suitable base metals for hardfacing. Low-alloy and medium-carbon steels with carbon contents up to 0.4% can be easily hardfaced by all welding processes with generally excellent results. Higher-carbon steels are similarly readily amenable to hardfacing, but preheating is necessary to minimize deleterious martensitic reactions in the heat-affected zone (HAZ). Austenitic stainless steels, with the exception of the free-machining grades, and most nickel-base alloys can also be easily hardfaced by all welding processes with excellent results. Martensitic stainless steels, tool steels, die steels, and cast irons are also amenable to hardfacing, but greater attention to preheat, interpass temperature, and postweld heat treatment is required. Age-hardenable base metals present special hardfacing problems and generally require solution and/or overaging heat treatments prior to hardfacing, as well as careful attention to preheat, interpass temperature, and postheat.

Hardfacing welding processes require that the base metal melting temperature range be higher than or at least equal to that of the hardfacing alloy. Thermal spraying processes, on the other hand, do not require a base metal melting temperature advantage.

Base metal thermal expansion and contraction characteristics affect solidification strain. Workpieces frequently have to be uniformly heated to relatively high temperatures during welding to enable the deposition of crack-free hardfacing alloys. Welding process selection is important in that it directly affects heat input and preheat requirements.

Thermal expansion and contraction differences between the hardfacing alloy and base metal are important in applications involving thermal cyclic service conditions. Large differences can result in shear failures in thermal spray deposits or thermal fatigue failures in welded deposits. Buffer layers are often deposited between the base metal and hardfacing alloy to counteract large differences in thermal expansion and contraction characteristics. Frequently, dilution, which is generally regarded to be detrimental, can be used to good advantage to form *in situ* buffer layers and to minimize the risk of thermal fatigue failure. Hardfacing process selection is an important consideration in this regard.

Hardfacing Product Forms. Hardfacing process selection is often limited by product form. Hardfacing alloys normally are available as bare cast rod, covered electrodes, wire, and powders. However, not all alloys are available in all product forms.

Virtually all hardfacing alloys can be produced in powder form, and most hardfacing alloys can be produced in rod form. Rods generally are available in bare cast form or in tubular form. Bare cast rod diameters are limited to a large extent by alloy characteristics and casting processes to a range of 3.2 to 8.0 mm ($\frac{1}{8}$ to $\frac{5}{16}$ in.). Bare cast rod lengths usually range from 250 to 700 mm (10 to 28 in.), but some hardfacing alloys can be cast in extra long, continuous lengths with diameters as small as 3.2 mm ($\frac{1}{8}$ in.). Tubular rods consist of highly alloyed powder cores encased in low-alloy sheaths. Tubular rods can be produced in discrete lengths or in spooled continuous coils. Discrete-length tube rods generally are available in the same diameter range as bare cast rod. Long-length tube rods, or tube wire as they are properly named, normally are available in diameters ranging from 4.0 to 1.6 mm ($\frac{5}{32}$ to $\frac{1}{16}$ in.). Some of the tougher, more ductile hardfacing alloys can be produced as solid drawn wire. Some of the more brittle hardfacing alloys can be produced, at a premium cost, as solid wire using extrusion techniques.

Welder Skill. It is essential to consider hardfacing quality requirements in relation to welder/operator skill, as well as in relation to the hardfacing process. As a rule, hardfacing by manual welding processes such as OFW or GTAW requires high welder proficiency, whereas hardfacing by automatic welding processes, such as SAW, requires a minimum of operator skill, assuming machine control settings have previously been established. Thermal spraying and related powder welding processes generally require intermediate welder/operator skills.

Manual GTAW can be used to obtain high-quality deposits on relatively small areas, such as the interlock regions of turbine blades. In this type of application, thin layers can be deposited with dilution as low as 10%, but relatively high welder skill and close control of the welding operation are necessary. In contrast, earthmoving and mining equipment can be hardfaced adequately in the field by relatively unskilled welders. Selection of process is usually based on maximum deposition rate: high dilution rates seldom significantly affect the suitability of the coating for service.

Cost is ultimately the determining factor in hardfacing process selection. Hardfacing costs basically consist of labor, materials, and in some instances, new equipment cost. Transportation cost also must be considered.

Labor costs depend primarily on the level of welder skill required and process deposition rates, but surface preparation and finishing costs also must be considered. Deposition rates are normally lowest with manual hardfacing processes. Considerably higher deposition rates are possible with automatic arc welding hardfacing processes. Deposition rates as high as 27 kg/h (60 lb/h) are possible with multiwire or powder and wire submerged arc hardfacing processes, but dilution is also high. An ideal welding process for hardfacing would be one with the ability to limit dilution while achieving a high deposition rate. Typical dilution percentages; deposition rates; and minimum deposit thicknesses for different welding processes and various forms, compositions, and modes of application of hardfacing alloys are given in Table 10.

TABLE 10 CHARACTERISTICS OF WELDING PROCESSES USED IN HARDFACING

WELDING PROCESS	MODE OF APPLICATION	FORM OF HARDFACING ALLOY	WELD-METAL DILUTION, %	DEPOSITION		MINIMUM THICKNESS[A]		DEPOSIT EFFICIENCY, %
				kg/h	lb/h	mm	in.	
OAW	MANUAL	BARE CAST ROD, TUBULAR ROD	1-10	0.5-2	1-4	0.8	MATH OMITTED	100
	MANUAL	POWDER	1-10	0.5-2	1-4	0.8	1/32	85-95
	AUTOMATIC	EXTRA-LONG BARE CAST ROD, TUBULAR WIRE	1-10	0.5-7	1-15	0.8	1/32	100
SMAW	MANUAL	FLUX-COVERED CAST ROD, FLUX-COVERED TUBULAR ROD	10-20	0.5-5	1-12	3.2	1/8	65
OPEN ARC	SEMIAUTOMATIC	ALLOY-CORED TUBULAR WIRE	15-40	2-11	5-25	3.2	1/8	80-85
	AUTOMATIC	ALLOY-CORED TUBULAR WIRE	15-40	2-11	5-25	3.2	1/8	80-85
GTAW	MANUAL	BARE CAST ROD, TUBULAR ROD	10-20	0.5-3	1-6	2.4	3/32	98-100
	AUTOMATIC	VARIOUS FORMS[B]	10-20	0.5-5	1-10	2.4	3/32	98-100
SAW	AUTOMATIC, SINGLE WIRE	BARE TUBULAR WIRE	30-60	5-11	10-25	3.2	1/8	95
	AUTOMATIC, MULTIWIRE	BARE TUBULAR	15-25	11-27	25-60	4.8	3/16	95

		WIRE						
	AUTOMATIC, SERIES ARC	BARE TUBULAR WIRE	10-25	11-16	25-35	4.8	$\frac{3}{16}$	95
PAW	AUTOMATIC	POWDER[C]	5-15	0.5-7	1-15	0.8	$\frac{1}{32}$	85-95
	MANUAL	BARE CAST ROD, TUBULAR ROD	5-15	0.5-4	1-8	2.4	$\frac{3}{32}$	98-100
	AUTOMATIC	VARIOUS FORMS[B]	5-15	0.5-4	1-8	2.4	$\frac{3}{32}$	98-100
GMAW	SEMIAUTOMATIC	ALLOY-CORED TUBULAR WIRE	10-40	0.9-5	2-12	1.6	$\frac{1}{16}$	90-95
	AUTOMATIC	ALLOY-CORED TUBULAR WIRE	10-40	0.9-5	2-12	1.6	$\frac{1}{16}$	90-95
LASER	AUTOMATIC	POWDER	1-10	[D]	[D]	0.13	0.005	85-95

(A) RECOMMENDED MINIMUM THICKNESS OF DEPOSIT.

(B) BARE TUBULAR WIRE; EXTRA-LONG (2.4 M, OR 8 FT) BARE CAST ROD; TUNGSTEN CARBIDE POWDER WITH CAST ROD OR BARE TUBULAR WIRE.

(C) WITH OR WITHOUT TUNGSTEN CARBIDE GRANULES.

(D) VARIES WIDELY DEPENDING ON POWDER FEED RATE AND LASER INPUT POWER

Hardfacing material costs depend on the prevailing price of raw materials and product form. Raw material cost is predominant in tungsten-, cobalt-, and nickel-base hardfacing alloys, whereas product form is the predominant cost in iron-base hardfacing alloys. As a rule, tubular rod and wire are the least expensive hardfacing product forms. In contrast, solid wire is the most expensive hardfacing product form. Cast rod and powder are generally intermediate in cost. Powder, depending on specific powder size requirements, tends to be less expensive than cast rod. However, deposit efficiency, measured as the percentage of hardfacing consumable retained on the workpiece surface, is generally slightly lower for hardfacing processes that utilize powder consumables than for hardfacing processes that utilize rod consumables. Thermal spraying processes are particularly poor in this regard, with typical deposit efficiencies as low as 70%.

Equipment costs vary from simple arc welding equipment to fully automated laser beam hardfacing systems. The more advanced automatic hardfacing equipment often costs 100 to 1000 times as much as simple arc welding equipment, depending on the level of instrumentation and computer control.

It is relatively easy to estimate or predetermine the cost of hardfacing. It is more difficult to estimate the value of hardfacing. For maintenance applications, it has been suggested that hardfacing is preferred over total replacement when the cost advantage (*CA*) is positive. The cost advantage can be calculated by:

$$CA = \frac{CN}{PN} - \frac{CR}{PR} \qquad \textbf{(EQ 1)}$$

where *CN* is the cost of a new component; *CR* is the cost of hardfacing plus downtime costs; *PN* is the work output during the service life of a new component; and *PR* is the work output during the service life of a hardfaced component. Most of the data needed for the above calculation usually can be obtained; *PR* is perhaps the most difficult value to assess, but reasonable estimates can be made based on relative laboratory wear test results. If the workpiece is hardfaced with an alloy of essentially the same chemical composition as the wom material, it is reasonable to assume that *PR* = *PN.* On the

other hand, if the hardfacing material is more wear-resistant than the worn material, then *PR* > *PN*. Therefore, from Eq 1, *CA* is likely to be positive, which is the primary objective of hardfacing.

Hardfacing by Oxyfuel Gas Welding

Oxyfuel gas welding (OFW) is a process in which the heat from a gas flame is used to melt hardfacing materials onto workpiece surfaces. During hardfacing, the workpiece is only superficially melted. The gas flame is created by the combustion of a hydrocarbon gas and oxygen. Acetylene is the most widely used fuel for OFW. In fact, OFW is commonly referred to as oxyacetylene welding (OAW), even though other fuel gases, such as methylacetylene propadiene (MAPP), occasionally are used in certain OFW processes.

Hardfacing by OFW is a versatile process, readily adaptable to all hardfacing product forms, including powder. As described below, OFW hardfacing processes that use fillers in powder form are commonly referred to as manual powder torch welding or powder welding. Oxyfuel gas welding equipment is simple, and capital equipment costs are low. Furthermore, OFW equipment is mobile and can be used for fusion welding and cutting operations, as well as for hardfacing. More importantly, OFW processes generally produce hardfacing deposits with optimum microstructures for wear-resistant applications.

Hardfacing by OFW, however, is not without limitations. Hardfacing by manual OAW requires a high degree of welder skill to obtain smooth, high-quality deposits, as the welding rod and the torch flame have to be separately manipulated. The speed of welding and low deposition rates often preclude the use of OAW for hardfacing applications on large components that require large quantities of hardfacing alloy, unless automation of the operation is warranted by configuration of the surface and a large number of identical parts.

Oxyacetylene welding is best suited to hardfacing applications in which the surface area to be hardfaced is minimal. Thus, for hardfacing steam valves, automotive and diesel engine valves, cutter blades for wood and plastic, chain saw bars, and plowshares and other agricultural implements, it is often the most satisfactory process as it can be easily employed in field applications.

Most steel workpieces can be hardfaced by OFW processes. High-manganese and high-sulfur steels are exceptions. High-speed steel workpieces are difficult to hardface and should be fully annealed before hardfacing. Cast iron workpieces also can be hardfaced by OFW processes, but cast iron substrates generally require the use of fluxes and special welding precautions.

Dilution is generally low (1 to 10%) in OFW hardfacing deposits, as only the surface of the workpiece in the immediate area being hardfaced is brought to the melting temperature. The hardfacing rod is melted and spread over the surface of the workpiece. The melted rod does not mix or alloy with the base metal, but only with the melted surface. Superficial workpiece melting of steel workpieces produces a wet appearance, called "sweating."

Operating Procedures. Workpiece surfaces must be thoroughly cleaned before hardfacing. If impurities are present on surfaces of the workpiece, or if an excessive amount of oxide is produced in heating (usually, a neutral or reducing flame is used), it may be necessary to dislodge the solid contaminants by prodding or rubbing with a hardfacing rod tip. Oxide trapped beneath the hardfacing overlay can react with carbon in the hardfacing alloy to produce a gas and thus cause porosity. Hardfacing alloys usually contain a deoxidizer that controls a moderate amount of oxidation.

It is often necessary to preheat workpieces prior to hardfacing, regardless of the welding process, to prevent cracks in the hardfacing deposit. Preheating not only reduces tensile strain associated with thermal contraction differences between the hardfacing alloy and the workpiece, but in the case of OFW, also permits the use of a softer flame and results in less dilution. Small low-carbon steel workpieces can be preheated locally with a torch, but large workpieces are best preheated with gas burners in a brick muffle furnace, allowing sufficient soak time to ensure even heating.

With practice, one-layer hardfacing deposits up to 1.6 mm ($\frac{1}{16}$ in.) thick can be deposited, particularly if the workpiece is inclined so that the deposition is slightly uphill. Alternatively, thick deposits can be applied in several layers. Hardfacing deposits by OFW can be remelted as necessary to improve deposit quality or surface appearance.

Common Flaws. Hardfacing deposits applied by OFW generally are characterized by low dilution and high deposit quality. Discontinuities are possible, however, depending on the skill of the welder and the quality of the filler material.

Porosity is probably the most common flaw observed in hardfacing deposits applied by OFW. Porosity in hardfacing deposits, like porosity in castings, can result from inadequate feeding or gas evolution during solidification. Porosity resulting from inadequate feeding is sometimes referred to as microshrinkage. Microshrinkage is most common at the termination of the hardfacing deposit and usually results from the inability of the hardfacing deposit to accommodate solidification shrinkage after the flame is withdrawn. This type of flaw can be minimized or prevented by withdrawing the flame very slowly and allowing solidification to progressively occur from the bond line to the surface.

Porosity can also occur by gas evolution during solidification if the total gas content in the molten deposit is greater than the solid solubility limit. Gas-induced porosity generally derives from slag or non-metallic inclusions trapped in or on the surface of the base metal. However, the initial gas content of the filler materials and possible gas pickup during OFW are also contributing factors.

Manual Powder Torch Welding (Ref 9)

Also termed "powder welding," manual powder torch welding is a modified OFW process in which powder application and fusion occur in a single operation using a special oxyacetylene torch. Powder is fed from a small hopper mounted on a gas welding torch into the fuel gas supply and conveyed through the flame to the workpiece surface. By following general oxyacetylene surfacing practice, smooth, thin, dense deposits are obtained. Deposit thickness is controlled by powder flow rate and movement of the torch. A dilution of 1 to 5% in the deposit occurs from this process.

Deposits ranging from 0.75 to 3 mm (0.030 to 0.125 in.) in thickness can be applied at a rate of 1.3 mm (0.050 in.) per pass. Sweating of the base metal during surfacing generates a fusion-type bond with the hardfacing alloy. Ease of application and material recovery are enhanced because of close control of the powder flow into the welding flame.

Oxyacetylene torch flame adjustment is essential to produce good powder deposition. The amount of excess acetylene required for hardfacing varies depending on alloy composition. The amount of excess acetylene is conveniently measured in terms of the flame geometry as the ratio between the length of the oxyacetylene feather and the length of the inner cone. The length of the inner cone, indicated by the value *X*, is the distance from the torch tip to the extreme end of the inner cone.

The length of the oxyacetylene feather is measured from the torch tip to the extreme end of the intermediate zone, generally expressed in multiples of the length of the inner cone. A neutral flame is thus classified as 1×. Cobalt-base powders are usually applied using 2× to 3× flame. The oxyacetylene feather is two to three times the length of the inner cone.

Tungsten carbide-containing composite powders should be applied using a 1.5× flame. Nickel-base powders are welded with a neutral or slightly oxidizing flame. Because flame characteristics change somewhat when powder is being sprayed, the powder feed handle should be depressed and final flame adjustment made while the powder is being sprayed. Alloys commonly welded with this process contain boron and silicon, which combine with any oxide skin to form an easily removed slag and to provide a clean weld pool.

The manual torch process is well suited for small repairs or for hardfacing of small areas requiring a wide range of hardnesses (about 20 to 60 HRC). Typical applications of manual torch welding include glass dies and molds, brick molding equipment, components for the cement industry, cast iron parts for foundries, feed screws, hammer mill hammers, and pump parts.

Hardfacing by Arc Welding (Ref 1)

In hardfacing by arc welding, the heat from an electric arc is used to melt the hardfacing material onto the workpiece surface. The electric arc is developed by impressing a voltage between an electrode and the workpiece. The voltage required to sustain the arc varies with the distance between the electrode and workpiece and with the arc welding process. The filler material is provided by the electrode used to form the arc or can be externally introduced into the arc. Arc welding processes in which the filler derives directly from the electrode are sometimes referred to as consumable electrode processes. Arc welding processes in which the filler is externally introduced into the arc are sometimes referred to as nonconsumable electrode processes. As a rule, nonconsumable electrode processes are accomplished at lower power requirements than are consumable electrode processes, resulting in less dilution and lower deposition rates. Consumable and nonconsumable electrode hardfacing processes both require that the filler materials be protected from oxidation as they are melted and joined to the workpiece surfaces.

Filler materials in consumable electrode hardfacing processes are sometimes protected by fluxes as in SMAW, SAW, and flux-cored open arc welding, or by inert gases, as in GMAW. The selection of a particular consumable or nonconsumable electrode hardfacing process depends on consideration of the factors discussed in the section on "Hardfacing Process Selection" in this article.

Shielded Metal Arc Welding. The electrodes used in the SMAW consumable electrode hardfacing process generally consist of discrete lengths of filler material rod covered with specially formulated coatings. The filler material rod generally ranges in diameter from 3.2 to 8.0 mm ($\frac{1}{8}$ to $\frac{5}{16}$ in.) and may be cast or of tubular construction. The electrode coating protects the filler material during welding by chemical reaction as the electrode melts. The coating can be fortified to increase alloy content during melting, as well as to simply provide molten metal protection. Coating ingredients also determine or affect the shape of the weld, amount of penetration, cooling rate of the weld, stabilization of the arc, and refinement of the hardfacing deposit.

The selection of the proper power supply for SMAW consumable electrode hardfacing is not a serious problem. Motor-generators, direct current rectifiers, and alternating current transformers can be used. Direct current electrode positive (DCEP) normally is recommended for hardfacing. Direct current electrode negative (DCEN) can be used to increase deposition rates slightly, but there is a tendency for the weld beads to be high and narrow. Although direct current is recommended, alternating current has been used in many applications with reasonably good success. Arc stability and burnoff characteristics are not quite as good by this method.

Speed of travel, position of the electrode in relation to the weld pool, arc voltage, and amperage are modified to minimize penetration and the consequent dilution of the deposit. Typical welding currents for small 3.2 mm ($\frac{1}{8}$ in.) diam hardfacing electrodes range from 60 to 130 A, depending on the alloy. Welding currents for larger 6.4 mm ($\frac{1}{4}$ in.) diam hardfacing electrodes range from 150 to 330 A.

Depending on the surface area to be hardfaced, the bead-deposit pattern may be of the stringer or weave type, with or without staggering of beads, as dictated by service requirements. Selection of the bead pattern and sequence also depends on the accessibility of the surface to be hardfaced and the distortion limits of the workpiece.

Deposition rates vary considerably with welding conditions. Normally from 1.4 to 1.8 kg (3 to 4 lb) of metal per hour of arc time can be applied. The recovery of alloy in the deposit generally ranges from 65 to 75% of the electrode weight, excluding stub loss. The average stub loss is approximately 75 mm (3 in.), which corresponds to about 20% of a 350 mm (14 in.) long electrode.

There are many advantages to the SMAW consumable electrode process. The intense heat of the arc permits the hardfacing of large parts without preheat. Small areas of parts machined or fabricated to close tolerances can be hardfaced without distorting the entire part. Difficult-to-reach areas are best accessed with coated electrodes. The overall process is relatively fast, as preheat and high interpass temperatures do not have to be maintained. Another attractive feature of this process is the portability of the equipment. Gasoline engine-driven generators can be readily taken into the field.

There are also some disadvantages to the SMAW consumable electrode process that must be considered. Penetration tends to be high, and dilution rates of 20% or more are not uncommon. This results in lower hardness and less resistance to abrasion. Two or three layers of weld metal normally are required to obtain maximum wear properties. Coated electrodes also leave a slag covering on the surface of the weld deposit which must be removed prior to each succeeding pass. Because coated electrodes usually are deposited with no more than a small amount of preheat, cracking or cross checking may occur, especially with the higher alloy electrodes that produce hard overlays.

The hardfacing material is at its maximum temperature, and hence its maximum thermal expansion, as it is being deposited. The workpiece, by contrast, may be near ambient temperature during the welding process and may be considerably less expanded than the hardfacing material. Severe strains develop in the hardfacing deposit as it cools after welding. These strains are accommodated by plastic deformation, in the case of a ductile hardfacing material or by cracking and cross checking, in the case of more brittle hardfacing materials. Cracking or cross checking does not affect the wear resistance of the overlay in many applications.

Submerged arc welding is a consumable electrode hardfacing process in which the area between the electrode and workpiece is shielded by a blanket of granular, fusible flux material. Electrodes in the SAW hardfacing process consist of continuous lengths, or coils, of filler materials--generally in tubular wire form.

The fluxes used for hardfacing by SAW are mineral compositions specially formulated to protect the molten filler metal without appreciable gas evolution. Submerged arc fluxes are generally finely divided, free-flowing granules in the solid state, which are placed by gravity along the surface to be hardfaced in advance of the electrode. The flux becomes molten and highly conductive under the arc, creating localized conditions conducive to high deposition rates.

Hardfacing filler materials can be deposited over a wide range of welding currents, voltages, and travel speeds, each of which can be controlled independently. Generally, however, the current, voltage, and workpiece travel speed are adjusted for hardfacing applications to produce a bead approximately 15 mm ($\frac{5}{8}$ in.) wide with a slightly convex surface and sides tapering into the base metal. Welding current usually ranges from 300 to 500 A for most SAW hardfacing applications. However, it is not uncommon to increase current to as much as 900 A to increase deposition rate.

A number of features make SAW particularly attractive for hardfacing. Because it is an automatic process, SAW requires little skill on the part of the operator for efficient operation. High deposition rates are possible, usually ranging as high as 4.5 to 9.0 kg/h (10 to 20 lb/h), depending on the job. The process is capable of making porosity-free deposits that are smooth and even on the surface and that either can be used aswelded or require only a minimum of grinding to clean up. The filler metal is protected from the atmosphere by flux, which also completely surrounds the arc, requiring no shielding for the operator.

The major disadvantages of hardfacing by SAW are that: (1) it is generally limited to hardfacing simple cylindrical or flat workpieces; and (2) it is not particularly adaptable to the surfacing of small parts. Hardfacing in other than the flat position requires special flux retainers. Preheating the workpiece in excess of 315 °C (600 °F) usually makes slag removal extremely difficult unless the slag is designed for easy hot slag removal. Occasionally, small portable units are used, but normally SAW units are fairly large and are mounted on stationary tracks, thus limiting their use for field operations. It is imperative that the flux be kept dry prior to use; therefore, storage can be a problem. Dilution is relatively high. It is not uncommon to find interalloying with the base metal, reaching or exceeding levels of 30%. Consequently, two or three layers of weld metal may be required for maximum wear resistance. Dilution can be reduced by long stickout techniques and by heavy overlap of individual weld beads.

Flux-cored open arc welding is a semiautomatic or automatic process in which the arc between the electrode and workpiece is shielded by a self-generated or self-contained gas or flux. Flux-cored open arc electrodes are continuous lengths, or coils, of filler material in tubular wire form. Open arc tubular filler materials are generally of low-carbon steel sheath construction with alloying elements, deoxidants, arc stabilizers, and a shielding gas source and/or flux contained in the core as powder or granules. High-alloy filler materials are generally shielded by a self-generated CO_2 gas deriving from the reaction between carbonaceous materials contained in the core and the atmosphere, or by vaporization of fluorides in the corn. Arc shielding is often supplemented in low-alloy filler materials with flux and/or aluminum or magnesium additions, which serve as deoxidizers.

Low equipment cost is one of the primary advantages of the flux-cored open arc hardfacing process. Neither flux-handling nor gas-regulating equipment is required. Thus the flux-cored open arc hardfacing process is a simple semiautomatic welding process requiring only a torch and a device to feed the continuous electrode wire. Conventional power, supplied with drooping voltage-amperage characteristics, is well adapted to flux-cored open arc hardfacing equipment. Motor-generator units are frequently used for field applications because of their portability. In-plant operations normally make use of direct current rectifiers. Although flux-cored open arc hardfacing is a semiautomatic process, it is not necessary to have a constant-potential power supply for its operation.

Flux-cored open arc equipment generally is designed for small-diameter welding wires, usually 1.2 mm ($\frac{3}{64}$ in.), 1.6 mm ($\frac{1}{16}$ in.), or 2.8 mm ($\frac{7}{64}$ in.). Most ferrous metals can be hardfaced with ease. Cast iron and chilled iron should be handled cautiously. Open arc is a high-energy process capable of much higher deposition rates than SMAW. The 2.8 mm ($\frac{7}{64}$ in.) diam rod can be deposited with welding currents as high as 500 A. The flux-cored open arc hardfacing process is closely related to the submerged arc process, except that it does not require a flux burden over the bead; consequently,

them is little or no slag to be removed from the overlay. Most hardfacing alloys can be deposited by the flux-cored open arc process without preheat, and there is good recovery of elements across the arc. Hardfacing by fluxcored open arc welding is an easy process to use, and only a short time is required to train an operator for the average application.

Arc stability and melting rates are excellent. The best hardfacing characteristics are obtained from DCEP. However, good results can be obtained with an alternating current supply at 26 to 30 V. Hardfacing deposits are comparable in soundness to deposits made with covered electrodes, at deposition rates three to five times faster than with covered electrodes.

Hardfacing by flux-cored open arc welding is not without disadvantages. Because the arc is not shielded with inert gas or a blanket of granular flux, considerable spatter and some porosity can be expected with this process. In addition, because of high welding currents, it is not particularly well adapted to the hardfacing of small parts. The recovery of weld metal from the tube wire to the deposit normally averages near 80 to 85% or higher. The amount of cross cracking and distortion is comparable to that of other arc welding processes.

Gas-metal arc welding is a consumable electrode hardfacing process in which the filler material and workpiece surfaces are protected by a flowing shielding gas--carbon dioxide, argon, or helium, either singly or in combination with a small amount of oxygen. The GMAW process is suitable for semiautomatic hardfacing, and the versatility of the process lends itself to the hardfacing of complex shapes. Hardfacing using GMAW can be fully mechanized. The hardfacing deposit is visible at all times in GMAW, thereby enabling high-quality deposits. Hardfacing by GMAW utilizes small-diameter (generally 1.6 mm, or $\frac{1}{16}$ in., or less) hardfacing filler wires or electrodes. Gas-metal arc hardfacing wires can be deposited in either spray arc or short arc modes. The spray arc mode produces a continuous stream of droplets about the same diameter as the hardfacing wire, which are projected by electromagnetic force from the tip of the wire. Deposition rates are high, as is dilution. In the short arc mode, lower voltages are used, and transfer of the molten hardfacing wire is more globular, usually resulting in more spatter.

Hardfacing by GMAW, unlike SMAW, requires a constant-potential power source with voltage, slope, and wire-feed rate controls. Best results for 1.6 mm ($\frac{1}{16}$ in.) diam cobalt-base hardfacing wires in the spray arc mode are generally obtained at 18 to 26 V, with wire-feed rates ranging from 45 to 65 mm/s (110 to 150 in./min.). Best results in the short arc mode are generally obtained at 16 to 18 V, with wire-feed rates ranging between 35 to 40 mm/s (80 to 100 in./min.). The use of auxiliary shielding gases adds to the cost of hardfacing by GMAW. However, the higher cost is generally offset by the higher deposit quality associated with GMAW.

Gas tungsten arc welding is a nonconsumable electrode arc process in which the heated area of the workpiece, molten hardfacing alloy, and the nonconsumable electrode are shielded from the atmosphere by a flow of shielding gas fed through the torch. Thoriated tungsten is the preferred nonconsumable electrode material. Conventional power supplies with drooping voltage-amperage characteristics are normally used for hardfacing. Motor-driven generators can be used, as can alternating current transformers with continuous high-frequency current. Direct current electrode negative is always used to minimize tungsten contamination in the hardfacing deposit. Argon generally is used as the shielding gas, but helium is also suitable.

Hardfacing by manual GTAW is a useful alternative to hardfacing by OAW techniques, particularly when large components or reactive base metals are involved. Gas-tungsten arc welding is preferred for hardfacing on reactive base metals such as titanium-stabilized stainless steels or aluminum-bearing nickel-base alloys. Gas-tungsten arc welding also is preferred over OAW for hardfacing applications in which carbon pickup is unacceptable or in applications involving filler materials that tend to boil under the influence of an oxyacetylene flame. The localized, intense heat of GTAW generally results in more base metal dilution than OAW. Base metal dilution can be minimized by torch oscillation, by using no more amperage than is necessary, and/or by concentrating the arc on the hardfacing deposit rather than on the workpiece. Hardfacing deposition rates generally are comparable in manual GTAW and OAW, despite the difference in base metal dilution.

Hardfacing by GTAW can be accomplished automatically by simply attaching the torch to an oscillating mechanism and using a mechanized device to feed the hardfacing filler material into the arc region. This, of course, requires long-length filler rod or continuous wire. High-quality, reproducible hardfacing deposits can be produced by automatic GTAW by controlling filler-metal feed rates, torch oscillation, and travel speed. Current-delay controls can be used to control the final stages of solidification in the hardfacing deposit to minimize shrinkage and crater cracking.

The arc action in GTAW is generally smoother, quieter, and freer of weld spatter than in other consumable electrode arc welding processes. The use of a separate filler rod or wire enables greater operator control of deposit shape. Gas-tungsten arc welding is more adaptable to hardfacing small intricate parts and generally produces higher-quality deposits than other hardfacing processes.

Plasma Arc Welding. Hardfacing by PAW is similar to hardfacing by GTAW in that both processes employ a gas-shielded arc between a nonconsumable tungsten electrode and the workpiece as the primary heat source for hardfacing. The processes differ in that the PAW process maximizes the use of plasma as a secondary heat source. The plasma is formed by ionizing the gas flowing in a nozzle surrounding the electrode. The electrode generally is recessed into the nozzle. The plasma gas generally emerges from a constricting orifice arrangement. The PAW process can use bare rod or wire as a hardfacing consumable, but more often powder is used as the consumable. When powder is used, the process is often referred to as the plasma transferred arc (PTA) process.

Plasma transferred arc surfacing, as shown schematically in Fig. 10, is a welding process in which the powder is introduced into a combined arc/plasma stream to form a molten pool on the workpiece. The resulting deposit is homogeneous and dense, with excellent metallurgical bonding with the base metal (workpiece). This process uses a constricted arc. The alloy is carried from a powder feeder to the plasma torch in a stream of argon gas, which forms the plasma and is directed away from the torch into the arc effluent, where it is melted and fusion-bonded to the base metal. A direct current power source connecting the tungsten electrode and the workpiece provides energy for the transferred arc.

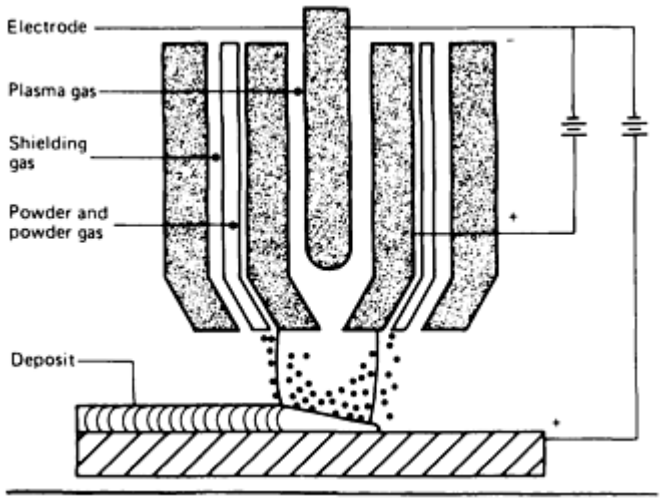

FIG. 10 SCHEMATIC OF THE PLASMA TRANSFERRED ARC HARDFACING PROCESS. SOURCE: REF 1

A second direct current power source connecting the tungsten electrode and the arc-constricting orifice supports a nontransferred arc. This nontransferred arc supplements the heat of the transferred arc and serves as a pilot arc to initiate the transferred arc. Argon is passed through a gas diffuser to provide a blanket of shielding gas in and around the arc zone.

Hardfacing with the PTA process has many advantages. Deposits ranging from 0.64 to 3.2 mm (0.025 to 0.125 in.) thick can be produced rapidly in a single pass. A dilution of 5 to 20% in the deposit is typical. Powder recoveries as high as 95%, with deposition rates up to 4.5 kg/h (10 lb/h), are possible, depending on the size and shape of the part being hardfaced. Still higher deposition rates ranging up to 18 kg/h (40 lb/h) are possible using the plasma arc hot wire process, which, as its name implies, uses wire hardfacing consumables and two independently controlled systems operating in one weld pool to melt and fuse a hardfacing alloy to a substrate. This process, however, is considered a weld cladding operation and is described later in this article.

Hardfacing by the PTA process has some disadvantages. The equipment is relatively expensive and is limited to straight-line or cylindrical parts, except when special tooling is provided. Usually, several parts are needed for setup, which makes the process somewhat unattractive to the low-volume job shop. The torch is mounted on a carriage and track that require permanent installation. There are two circuits employed in this process; therefore, either a special power supply or two separate conventional power units are required. Argon consumption is somewhat higher than with GTAW. Argon has to

be supplied to the center of the torch to protect the electrode. Shielding gas is necessary to protect the weld metal, and argon is also used as a carrier for the powder. Large parts being faced with hard alloys normally require preheat. This is a serious potential problem with the PAW process, if excessive preheats and prolonged hardfacing times cause overheating of the torch.

Laser Hardfacing (Ref 10)

Laser hardfacing, also commonly referred to as laser cladding, differs little in principle from traditional forms of hardfacing; the primary difference is the use of a high-energy laser beam heat source rather than an arc or gas flame. Laser beams offer potential in applying thin overlays or when access to the surface to be hardfaced can be achieved more readily by a laser beam than with an electrode or torch.

Cobalt-, nickel-, and tungsten carbide-base hardfacing alloys are the usual cladding materials used for laser hardfacing. As with conventional hardfacing methods, the materials are used in applications involving metal-to-metal contact, impact, erosion, and abrasion wear resistance. Other laser hardfacing materials include titanium carbide, Fe-Cr-Ni-B alloys, aluminum bronzes, and ceramics. Substrates have included carbon and low-alloy steels, stainless steels, nickel-base alloys (including superalloys), aluminum, cast irons, and tool steels (Ref 11).

Hardfacing material selection depends on its metallurgical compatibility with the substrate material. Alloys that form brittle intermetallic phases with the substrate are undesirable. For example, cobalt forms harmful intermetallics with titanium, and cobalt-base hardfacing alloys would be unsuitable on titanium alloy substrates.

Processing. The hardfacing alloy is melted by a laser beam and allowed to spread freely and freeze over the substrate. The beam also melts a very thin layer of the substrate, which combines with the liquid weld metal to the least extent necessary and solidifies to form a strong metallurgical bond. A good fusion bond can be achieved with a dilution zone that is only 10 to 20 μm thick.

The hardfacing alloy can be in several forms, examples of which are a prealloyed powder that is applied to the sample surface with or without a binder, a self-fluxing powder that is flame-sprayed, a hardfacing alloy that is plasma-sprayed, or a chip that is preplaced. Laser consolidation of these coatings results in densification and smoothening, eliminates channels to the substrate, improves the bonding between coating and substrate, and reduces porosity, all of which contribute to the strength and integrity of the hardfacing layer. Processing parameters for laser cladding are a power density that ranges from 10 to 1000 MW/m^2 and an interaction time from 0.1 to 1 s. The shielding gas could be any of the inert gases or a combination of gases, such as He/Ar and H_2/Ar.

To date the most successful application of laser hardfacing involves a proprietary process that utilizes a specially designed powder-feed apparatus. Using such equipment, the powder and an assist gas are fed to the weld area through a ceramic nozzle; a shielding gas of helium and argon surrounds the powder-gas mixture as it leaves the nozzle (Fig. 11). The powder delivery nozzle is positioned in such a manner as to flood the entire melt pool with powder. The feeding angle is generally from 35 to 45° to the horizontal, and the feed tube, which typically has a 3 mm (0.12 in.) diam, is positioned 10 to 12 mm (0.4 to 0.5 in.) from the substrate. Typically, the powder flow rate is from 0.005 to 0.1 cm^3/s (0.0003 to 0.006 $in.^3/s$), particle velocity is from 1 to 2 m/s (3.3 to 6.6 ft/s), and carrier gas velocity is from 3 to 7 m/s (10 to 23 ft/s). Desirable dilutions are from 3 to 8%. Overlay thickness can be varied from 0.15 to 4 mm (0.005 to 0.15 in.). Uniform feeding of the powder ensures uniform surfacing layers. Unlike plasma-sprayed coatings, porosity and unmelted powder particles are almost never observed within a laser hardfacing layer.

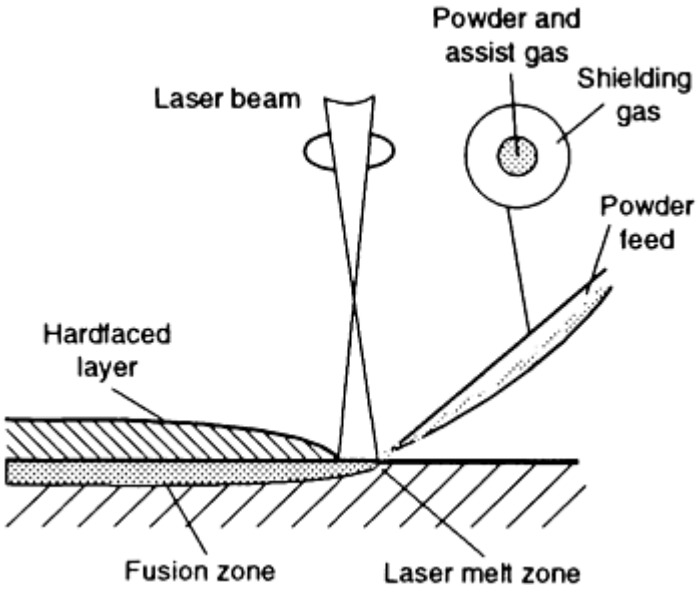

FIG. 11 SCHEMATIC OF THE LASER HARDFACING PROCESS USING DYNAMIC POWDER FEED. COURTESY OF QUANTUM LASER CORPORATION

Laser hardfacing deposits are commonly achieved by relatively large doughnut-shape beams, or by somewhat focused beams that are oscillated. These ensure a desirable deposit profile. Hardfacing material can also be added in rod, wire, or sheet form, but special procedures are needed because of reflectivity problems.

Thermal stresses in the weld metal can cause harmful cracking, but this can be eliminated by an appropriate preheating practice. Low power densities, large beam diameters, and slow sample translation rates tend to produce crack-free deposits.

Laser Hardfacing Applications. Because one of the primary goals of laser hardfacing is to improve the tribological properties of components, several applications have been found for the technique. Some of them are in the exploratory stage, others are in the pilot-plant stage, and a few have reached the production stage.

Ayers and Gnanamuthu (Ref 12) give several examples of laser hardfacing for improved wear resistance, such as Tribaloy T-800 on powder-coated ASTM A 387 steel, Haynes Stellite alloy No. 1 cast rods placed on AISI 4815 steel, and a mixture of WC and iron powder applied without binder on AISI 1018 steel.

In addition to stainless steel on mild steel, Steen (Ref 13) has reported successful laser hardfacing of nickel, bronze, Fe-B, and Stellite SF6 on mild steel; chromium on titanium; stainless on aluminum; mild steel on stainless; and Stellite on brass. Other examples of laser hardfacing are AISI 1016 steel clad with a mixture of chromium, manganese, and carbon powders (Ref 14) and gray cast iron hardfaced with a powder-fed mixture of molybdenum, chromium-carbide (Cr_3C_2), chromium, nickel, and silicon (Ref 15).

Bruck (Ref 16) demonstrated laser hardfacing within a confined space by coating the inside surface of small-bore pipes (inside diameter of 50 to 100 mm, or 2 to 4 in., and length of 0.3 to 1.2 m, or 1 to 4 ft). An oscillating mirror placed in the pipe formed a 12.5 mm (0.5 in.) wide melt pass, into which the hardfacing alloy powder was fed. The pipe was rotated and translated to cover the entire inner surface. Previously, chromium plating was used, but the laser technique appreciably improved galling resistance. Using suitable cooling techniques, the pipe temperature was maintained below 500 °C (930 °F) to avoid deterioration of the core properties, as well as distortion.

La Rocca (Ref 17) describes laser hardfacing of exhaust valves with a cobalt-base alloy at an Italian automotive manufacturer. The cobalt-base powder was fed into the laser melt pool. The laser hardfacing material was superior to GTAW material in terms of thickness uniformity, uniform microstructure and elemental distributions, and adhesion. When compared to GTAW, excess-metal removal was reduced by 10 to 15%. One British automotive manufacturer used production-stage laser hardfacing of a nickel-alloy turbine blade shroud interlock by powder feeding either a Tribaloy

alloy or a Nimonic alloy (Ref 18). Previously, a manual arc melting technique was used. Laser hardfacing reduced hardfacing time from 14 min to 75 s, improved productivity and quality, reduced cost by 85%, and reduced powder consumption by 50%. Table 11 lists components that are laser hardfaced for commercial applications.

TABLE 11 TYPICAL APPLICATIONS FOR LASER HARDFACING

COMPONENT	HARDFACING ALLOY	HARDFACING TECHNIQUE	COMPANY
GATE AND SEAT OF STEEL VALVES FOR OIL-FIELD, GEOTHERMAL, AND NUCLEAR ENERGY PRODUCTION, AND CHEMICAL PROCESSING	STELLITE 6	POWDER FEED	W-K-M DIV. OF JOY MFG., HOUSTON, TX
DIESEL ENGINE VALVE	STELLITE SF6	PREPLACED POWDER PASTE	CABOT CORP., KOKOMO, IN
GATE VALVE SEAT	DELORO 60	PREPLACED POWDER PASTE	CABOT CORP., KOKOMO, IN
GAS TURBINE BLADE "Z" NOTCH	CO-BASE ALLOY	POWDER FEED	QUANTUM LASER, EDISON, NJ
LEADING EDGE OF TURBINE BLADES	CO-BASE ALLOY	POWDER FEED	QUANTUM LASER, EDISON, NJ
PUMP BUSHINGS AND IMPELLERS	CO-BASE ALLOY	POWDER FEED	QUANTUM LASER, EDISON, NJ
ENGINE VALVE BASES	NI-CR ALLOY	POWDER FEED	QUANTUM LASER, EDISON, NJ
OIL-FIELD VALVE GATES	WC AND CO ALLOY	POWDER FEED	QUANTUM LASER, EDISON, NJ
TRACTOR BUSHINGS	STELLITE 6	POWDER FEED	QUANTUM LASER, EDISON, NJ
TURBINE BLADES, PUMP VALVE SEATS	STELLITE, COLMOLOY, BLENDED POWDER	PREPLACED BEDS, GRAVITY FEED	WESTINGHOUSE, PITTSBURGH, PA
VALVE STEM, VALVE SEAT, ALUMINUM BLOCK	CRC_2, CR, NI, MO/CAST FE	PREPLACED POWDER	FIAT, TURIN, ITALY
OFF-SHORE DRILLING AND PRODUCTION PARTS, VALVE COMPONENTS, BOILER FIREWALL	STELLITE, COLMONOY, ALLOYS/CARBIDES	POWDER FEED	COMBUSTION ENG., OH
AEROSPACE COMPONENTS	STELLITE, TRIBALOY	POWDER FEED	ROCKWELL INT., CA
TURBINE BLADE SHROUD INTERLOCKS	PWA 694, NIMONICS	PREPLACED CHIP	PRATT & WHITNEY, WEST PALM BEACH, FL

Source: Ref 10

References cited in this section

1. K.C. ANTONY *ET AL.*, HARDFACING, *WELDING, BRAZING, AND SOLDERING,* 9TH ED., VOL 6, *METALS HANDBOOK,* AMERICAN SOCIETY FOR METALS, 1983, P 771-793
2. P. CROOK AND H.N. FARMER, FRICTION AND WEAR OF HARDFACING ALLOYS, *FRICTION,*

LUBRICATION, AND WEAR TECHNOLOGY, VOL 18, *ASM HANDBOOK,* ASM INTERNATIONAL, 1992, P 758-765

3. D.K. SUBRAMANYAM, A.E. SWANSIGER, AND H.S. AVERY, AUSTENITIC MANGANESE STEELS, *PROPERTIES AND SELECTION: IRONS, STEELS, AND HIGH-PERFORMANCE ALLOYS,* VOL 1, *ASM HANDBOOK,* ASM INTERNATIONAL, 1990, P 822-840
4. H.S. AVERY AND H.J. CHAPIN, *WELD J.,* VOL 31, 1952, P 917
5. R.D. ZORDAN, REPORT 10890, CABOT CORPORATION, KOKOMO, IN, 1982
6. H. OCKEN AND A.K. VELAN, ED., "LABORATORY EVALUATIONS OF COBALT-FREE, NICKEL-BASED HARDFACING ALLOYS FOR NUCLEAR APPLICATIONS," REPORT NP-4993, PROJECT 1935, ELECTRIC POWER RESEARCH INSTITUTE, PALO ALTO, CA, MARCH 1987
7. P.J. HOFMANN, B.C. FRIEDRICH, AND H. OCKEN, ED., "LABORATORY EVALUATIONS OF IRON-BASED HARDFACING ALLOYS," REPORT NP-5874, PROJECT 1935-11, ELECTRIC POWER RESEARCH INSTITUTE, PALO ALTO, CA, JUNE 1988
8. WELD DESIGN AND FABRICATION, DATA SHEET 420, *WELD. DES. FABR.,* VOL 48 (NO. 8), 1975, P 50
9. K.M. KULKARNI AND V. ANAND, METAL POWDERS USED FOR HARDFACING, *POWDER METALLURGY,* 9TH ED., VOL 7, *ASM HANDBOOK,* AMERICAN SOCIETY FOR METALS, 1984, P 823-836
10. K.P. COOPER, LASER SURFACE PROCESSING, *FRICTION, LUBRICATION, AND WEAR TECHNOLOGY,* VOL 18, *ASM HANDBOOK,* ASM INTERNATIONAL, 1992, P 861-872
11. A.G. BLAKE, *ET AL.,* "LASER COATING TECHNOLOGY: A COMMERCIAL REALITY," BULLETIN OF QUANTUM LASER CORPORATION, EDISON, NJ
12. J.D. AYERS AND D.S. GNANAMUTHU, HARDENING OF METAL SURFACES BY LASER PROCESSING, *WELDING, BRAZING, AND SOLDERING,* 9TH ED., VOL 6, *ASM HANDBOOK,* AMERICAN SOCIETY FOR METALS, 1983, P 793-803
13. W.M. STEEN, *PROC. NATO ADVANCED STUDY INSTITUTE ON LASER SURFACE TREATMENT OF METALS,* C.W. DRAPER AND P. MAZZOLDI, ED., MARTINUS NIJHOFF, 1986, P 369
14. J. MAZUMDER AND J. SINGH, *PROC. NATO ADVANCED STUDY INSTITUTE ON LASER SURFACE TREATMENT OF METALS,* C.W. DRAPER AND P. MAZZOLDI, ED., MARTINUS NIJHOFF, 1986, P 297
15. A. BELMONDO AND M. CASTAGNA, *SOURCEBOOK ON APPLICATIONS OF THE LASER IN METALWORKING,* E. METZBOWER, ED., AMERICAN SOCIETY FOR METALS, 1981, P 310
16. G.J. BRUCK, *J. MET.,* VOL 39 (NO. 2), 1987, P 10
17. A.V. LA ROCCA, *PROC. NATO ADVANCED STUDY INSTITUTE ON LASER SURFACE TREATMENT OF METALS,* C.W. DRAPER AND P. MAZZOLDI, ED., MARTINUS NIJHOFF, 1986, P 521
18. R.M. MACINTYRE, *PROC. NATO ADVANCED STUDY INSTITUTE ON LASER SURFACE TREATMENT OF METALS,* C.W. DRAPER AND P. MAZZOLDI, ED., MARTINUS NIJHOFF, 1986, P 545

Hardfacing, Weld Cladding, and Dissimilar Metal Joining

J.R. Davis, Davis & Associates

Thermal Spraying

Thermal spraying comprises a group of processes in which divided molten metallic or nonmetallic material is sprayed onto a prepared substrate to form a coating. The sprayed material is originally in the form of wire, rod, or powder. As the coating materials are fed through the spray unit, they are heated to a molten or plastic state and propelled by a stream of compressed gas onto the substrate. As the particles strike the surface, they flatten and form thin platelets that conform and

adhere to the irregularities of the prepared surface and to each other. They cool and accumulate, particle by particle, into a lamellar, castlike structure. In general, the substrate temperature can be kept below approximately 200 °C (400 °F), eliminating metallurgical change of the substrate material. The spray gun generates the necessary heat for melting through combustion of gases, an electric arc, or a plasma. Figure 12 illustrates a general thermal spraying process.

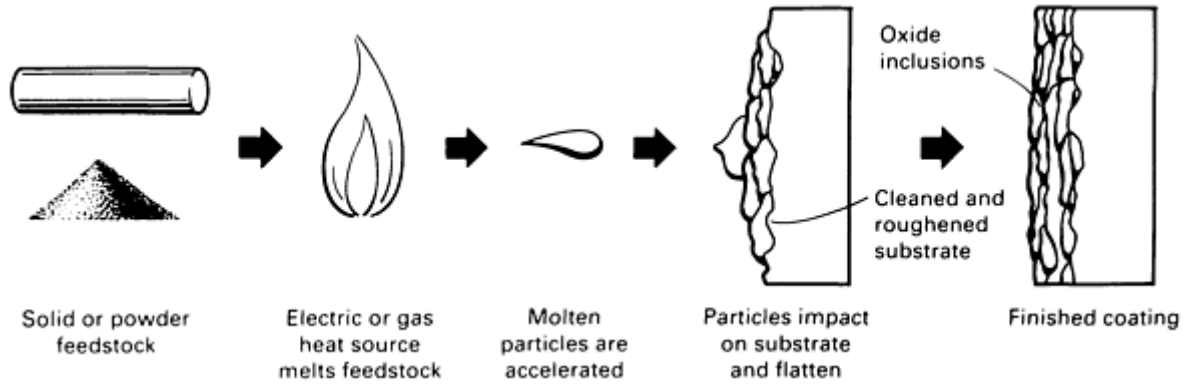

FIG. 12 SCHEMATIC OF THE GENERAL THERMAL SPRAY PROCESS. SOURCE: REF 20

The deposited structures of thermal spray coatings differ from those of the same material in the wrought form because of the incremental nature of the coating buildup and because the coating composition is often affected by reaction with the process gases and the surrounding atmosphere while the materials are in the molten state. For example, where air or oxygen is used as the process gas, oxides of the material applied may be formed and become part of the coating. The as-applied structures of all thermal spray coatings are similar in their lamellar nature; the variations in structure depend on the particular thermal spray process used, the processing parameters and techniques employed, and the material applied. Figure 13 illustrates the microstructure that results from the thermal spray process. As shown in this figure, the molten particles spread out and deform (splatter) as they impact the substrate, at first locking onto irregularities on the roughened surface, then interlocking with each other.

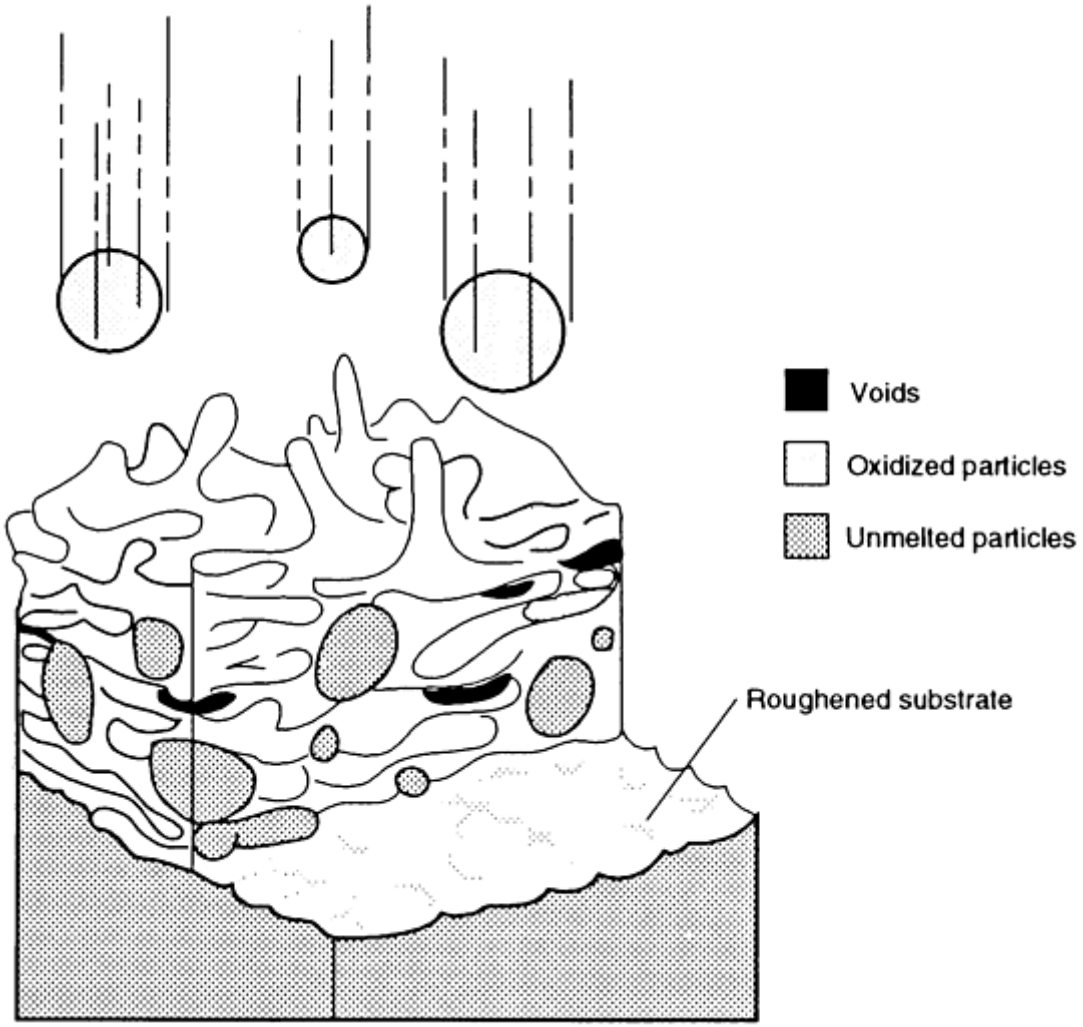

FIG. 13 SCHEMATIC SHOWING THE BUILDUP OF A THERMAL SPRAY COATING. MOLTEN PARTICLES SPREAD OUT AND DEFORM (SPLATTER) AS THEY STRIKE THE TARGET, AT FIRST LOCKING ONTO IRREGULARITIES ON THE SUBSTRATE, THEN INTERLOCKING WITH EACH OTHER. VOIDS CAN OCCUR IF THE GROWING DEPOSIT TRAPS AIR. PARTICLES OVERHEATED IN THE FLAME BECOME OXIDIZED. UNMELTED PARTICLES MAY SIMPLY BE EMBEDDED IN THE ACCUMULATING DEPOSIT. COURTESY OF THE MATERIALS ENGINEERING INSTITUTE, ASM INTERNATIONAL

The bond between the sprayed coating and the substrate is generally mechanical. Proper surface preparation of the substrate before spraying is often the most critical influence on the bond strength of the coating. Surface preparation techniques will be discussed later in this section.

Thermal spraying is a very versatile technique in that it can be used both in-shop or on-site. The thermal spray process permits rapid application of high-performance material in thicknesses from a few mils to more than 25 mm (1 in.) thick on parts of a variety of sizes and geometries. A list of applications would include coatings for:

- WEAR RESISTANCE
- OXIDATION RESISTANCE
- CORROSION RESISTANCE
- DIMENSIONAL RESTORATION
- THERMAL BARRIERS
- ELECTRICAL CONDUCTIVITY OR RESISTIVITY
- BIOMEDICAL DEVICES

Thermal Spray Processes (Ref 19, 20)

Currently, five different commercially available thermal spray methods are in use:

- OXYFUEL WIRE (OFW) SPRAY
- ELECTRIC ARC WIRE (EAW) SPRAY
- OXYFUEL POWDER (OFP) SPRAY
- PLASMA ARC (PA) POWDER SPRAY
- HIGH-VELOCITY OXYFUEL (HVOF) POWDER SPRAY

Of these, the plasma arc process is most commonly used. Market studies indicate that by the year 2000, plasma spraying will capture about 48% of the market, the HVOF process 25%, the electric-arc method 15%, and the combustion methods (OFW and OFP) a combined 12% (Ref 21). Table 12 compares important process characteristics associated with these techniques. Selection of the appropriate thermal spray method is typically determined by:

- DESIRED COATING MATERIAL
- COATING PERFORMANCE REQUIREMENTS
- ECONOMICS
- PART SIZE AND PORTABILITY

TABLE 12 COMPARISON OF THERMAL SPRAY PROCESSES

PROCESS	GAS FLOW		FLAME OR EXIT PLASMA TEMPERATURE		PARTICLE IMPACT VELOCITY		RELATIVE ADHESIVE STRENGTH[(A)]	COHESIVE STRENGTH	OXIDE CONTENT, %	RELATIVE PROCESS COST[(A)]	MAXIMUM SPRAY RATE		POWER		ENERGY REQUIRED TO MELT	
	M^3/H	FT^3/H	°C	°F	M/S	FT/S					KG/H	LB/H	KW	HP	KW/KG	KW/LB
FLAME POWDER: POWDER FEEDSTOCK, ASPIRATED INTO THE OXYGEN/FUEL-GAS FLAME, IS MELTED AND CARRIED BY THE FLAME ONTO THE WORKPIECE. PARTICLE VELOCITY IS RELATIVELY LOW, AND BOND STRENGTH OF DEPOSITS IS LOW. POROSITY IS HIGH AND COHESIVE STRENGTH IS LOW. SPRAY RATES ARE USUALLY IN THE 0.5 TO 9 KG/H (1 TO 20 LB/H) RANGE. SURFACE TEMPERATURES CAN RUN QUITE HIGH.	11	400	2200	4000	30	100	3	LOW	6	3	7	15	25-75	34-100	11-22	5-10
FLAME WIRE: IN FLAME WIRE SPRAYING, THE ONLY FUNCTION OF THE FLAME IS TO MELT THE MATERIAL. A STREAM OF AIR THEN DISINTEGRATES THE MOLTEN MATERIAL AND PROPELS IT ONTO THE WORKPIECE. SPRAY RATES FOR MATERIALS SUCH	71	2500	2800	5000	180	600	4	MEDIUM	4	3	9	20	50-100	70-135	11-22	5-10

AS STAINLESS STEEL ARE IN THE RANGE OF 0.5 TO 9 KG/H (1 TO 20 LB/H). SUBSTRATE TEMPERATURES ARE FROM 95 TO 205 °C (200 TO 400 °F) BECAUSE OF THE EXCESS ENERGY INPUT REQUIRED FOR FLAME MELTING.																
WIRE ARC: TWO CONSUMABLE WIRE ELECTRODES ARE FED INTO THE GUN, WHERE THEY MEET AND FORM AN ARC IN AN ATOMIZING AIR STREAM. THE AIR FLOWING ACROSS THE ARC/WIRE ZONE STRIPS OFF THE MOLTEN METAL, FORMING A HIGH-VELOCITY SPRAY STREAM. THE PROCESS IS ENERGY EFFICIENT; ALL INPUT ENERGY IS USED TO MELT THE METAL. SPRAY RATE IS ABOUT 2.3 KG/H/KW (5 LB/H/KW). SUBSTRATE TEMPERATURE CAN BE LOW BECAUSE ENERGY INPUT PER POUND OF METAL IS ONLY ABOUT ONE-EIGHTH THAT OF OTHER SPRAY METHODS.	71	2500	5500	10,000	240	800	6	HIGH	0.5-3	1	16	35	4-6	5-8	0.2-0.4	0.1-0.2
CONVENTIONAL PLASMA: CONVENTIONAL	4.2	150	5500	10,000	240	800	6	HIGH	0.5-1	5	5	10	30-80	40-110	13-22	6-10

PLASMA SPRAYING PROVIDES FREE-PLASMA TEMPERATURES IN THE POWDER HEATING REGION OF 5500 °C (10,000 °F) WITH ARGON PLASMA, AND 4400 °C (8000 °F) WITH NITROGEN PLASMA--ABOVE THE MELTING POINT OF ANY KNOWN MATERIAL. TO GENERATE THE PLASMA, AN INERT GAS IS SUPERHEATED BY PASSING IT THROUGH A *DC* ARC. POWDER FEEDSTOCK IS INTRODUCED AND IS CARRIED TO THE WORKPIECE BY THE PLASMA STREAM. PROVISIONS FOR COOLING OR REGULATION OF THE SPRAY RATE MAY BE REQUIRED TO MAINTAIN SUBSTRATE TEMPERATURES IN THE 95 TO 205 °C (200 TO 400 °F) RANGE. TYPICAL SPRAY RATE IS 0.1 KG/H/KW (0.2 LB/H/KW).																
DETONATION GUN: SUSPENDED POWDER IS FED INTO A 1 M (3 FT) LONG TUBE ALONG WITH OXYGEN AND FUEL GAS. A	11	400	3900	7000	910	3000	8	VERY HIGH	0.1	10	1	2	100-270	135-360	220	100

SPARK IGNITES THE MIXTURE AND PRODUCES A CONTROLLED EXPLOSION. THE HIGH TEMPERATURES AND PRESSURES (1 MPA, OR 150 PSI) THAT ARE GENERATED BLAST THE PARTICLES OUT OF THE END OF THE TUBE TOWARD THE SUBSTRATE.																
HIGH-VELOCITY OXYFUEL: IN HVOF SPRAYING, A FUEL GAS AND OXYGEN ARE USED TO CREATE A COMBUSTION FLAME AT 2500 TO 3100 °C (4500 TO 5600 °F). THE COMBUSTION TAKES PLACE AT VERY HIGH CHAMBER PRESSURE, EXITING THROUGH A SMALL-DIAMETER BARREL TO PRODUCE A SUPERSONIC GAS STREAM AND VERY HIGH PARTICLE VELOCITIES. THE PROCESS RESULTS IN EXTREMELY DENSE, WELL-BONDED COATINGS, MAKING IT ATTRACTIVE FOR MANY CORROSION-RESISTANT APPLICATIONS.	28-57	1000-2000	3100	5600	610-1060	2000-3500	8	VERY HIGH	0.2	5	14	30	100-270	135-360	22-200	10-90

EITHER POWDER OR WIRE FEEDSTOCK CAN BE SPRAYED, AT TYPICAL RATES OF 2.3 TO 14 KG/H (5 TO 30 LB/H).																
HIGH-ENERGY PLASMA: THE HIGH-ENERGY PLASMA PROCESS PROVIDES SIGNIFICANTLY HIGHER GAS ENTHALPIES AND TEMPERATURES, ESPECIALLY IN THE POWDER HEATING REGION, DUE TO A MORE STABLE, LONGER ARC AND HIGHER POWER DENSITY IN THE ANODE NOZZLE. THE ADDED POWER (TWO TO THREE TIMES THAT OF CONVENTIONAL PLASMA) AND GAS FLOW (TWICE AS HIGH) PROVIDE A LARGER, HIGHER TEMPERATURE POWDER INJECTION REGION AND REDUCED AIR ENTRAINMENT. ALL THIS LEADS TO IMPROVED POWDER MELTING, FEWER UNMELTS, AND HIGH PARTICLE IMPACT VELOCITY.	17-28	600-1000	8300	15,000	240-1220	800-4000	8	VERY HIGH	0.1	4	23	50	100-250	135-335	9-13	4-6
VACUUM PLASMA: VACUUM PLASMA USES A CONVENTIONAL PLASMA TORCH IN A CHAMBER AT	8.4	300	8300	15,000	240-610	800-2000	9	VERY HIGH	(B)	10	10	24	50-100	70-135	11-22	5-10

PRESSURES IN THE RANGE OF 10 TO 50 KPA (0.1 TO 0.5 ATM). AT LOW PRESSURES THE PLASMA IS LARGER IN DIAMETER, IS LONGER, AND HAS A HIGHER VELOCITY. THE ABSENCE OF OXYGEN AND THE ABILITY TO OPERATE WITH HIGHER SUBSTRATE TEMPERATURES PRODUCE DENSER, MORE ADHERENT COATINGS HAVING MUCH LOWER OXIDE CONTENTS.																

Source: Ref 21

(A) 1 (LOW) TO 10 (HIGH).

(B) PPM LEVELS.

The oxyfuel wire spray process (also called wire flame spraying or the combustion wire process) is the oldest of the thermal spray coating methods and among the lowest in capital investment. The process utilizes an oxygen-fuel gas flame as a heating source and coating material in wire form. Any material in the form of wire and capable of being melted below 2480 °C (4500 °F) can be flame-sprayed. Solid-rod feed stock has also been used. During operation, the wire is drawn into the flame by drive rolls that are powered by an adjustable air turbine or electric motor. The tip of the wire is melted as it enters the flame, atomized into particles by a surrounding jet of compressed air, and propelled to the workpiece. Figure 14 shows a schematic of the OFW spray process.

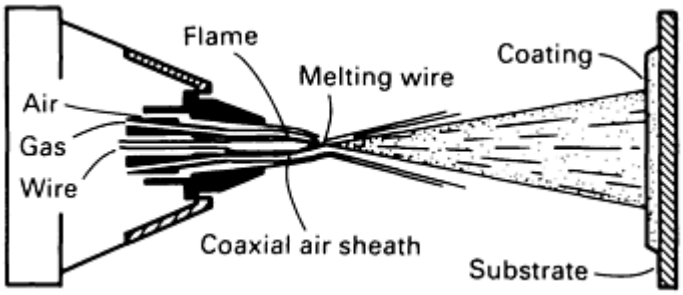

FIG. 14 SCHEMATIC OF THE OXYFUEL WIRE SPRAY PROCESS. SOURCE: REF 20

Spray rates for this process range from 0.5 to 10 kg/h (1 to 20 lb/h) and are dictated by the melting point of the material and the choice of fuel gas. Common fuel gases are acetylene, MAPP gas, propane, propylene, and natural gas, each combined with oxygen. The wire spray gun is most commonly used as a hand-held device for on-site application, although an electric-motor-driven gun is recommended for fixed-mounted use in high-volume, repetitive production work.

The OFW process is widely used for corrosion protection of large outdoor structures, such as bridges and storage tanks, and for restoration of dimension to worn machinery components. It is a good choice for all-purpose spraying. Coatings can be applied rapidly and at low cost, and a wide variety of metal coating materials are available. Typical spray materials include austenitic and martensitic stainless steels, nickel aluminide, nickel-chromium alloys, bronze, Monel, babbitt, aluminum, zinc, and molybdenum. In general, oxyfuel wire flame-sprayed coatings exhibit lower bond strengths, higher porosity, a narrower working temperature range, and higher heat transmittal to the substrate than plasma or electric arc-sprayed coatings.

Electric arc wire spraying also applies coatings of selected metals in wire form. Push-pull motors feed two electrically charged wires through the arc gun to contact tips at the gun head. An arc is created that melts the wires at temperatures above 5500 °C (10,000 °F). Compressed air atomizes the molten metal and projects it onto a prepared surface. Figure 15 shows a schematic of the EAW spray process.

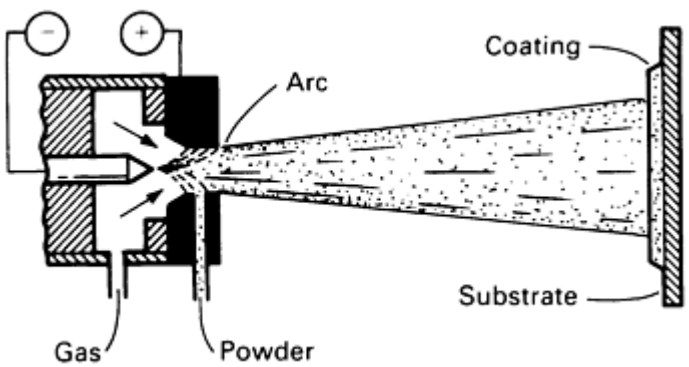

FIG. 15 SCHEMATIC OF THE ELECTRIC ARC WIRE SPRAY PROCESS. SOURCE: REF 20

The EAW process is excellent for applications that require heavy coating buildup or have large surfaces to be sprayed. The arc system can produce a spray pattern ranging from 50 to 300 mm (2 to 12 in.) and can spray at high speeds. It has built-in flexibility, allowing coating characteristics, such as hardness or surface texture, to be tailored to specific applications.

The EAW method is characterized by strong coating adhesion because of the high particle temperatures produced. Because the process uses only electricity and compressed air, it allows equipment to be moved relatively easily from one installation to another, and it eliminates the need to stock oxygen and fuel gas supplies. Materials applied by the EAW method are similar to those used in the OFW process.

The oxyfuel powder spray method, which also uses combustion gases as the heat source, extends the range of available coatings and subsequent applications to include ceramics, cermets, carbides, and fusible hardfacing coatings. Using either gravity flow or pressurized feed, powder is fed into the gun and carried to the gun nozzle, where it is melted and projected by the gas stream onto a prepared surface (Fig. 16). For general-purpose spraying, the gravity-flow system is used. When exacting coating consistency and/or high spray rates are desired, the pressurized feed system is used. Oxyfuel powder guns are the lowest-cost thermal spray equipment, are easiest to set up, and make it easy to change coating materials. The OFP method finds widest use in short-run machinery maintenance work and in the production spraying of abradable clearance-control seals for gas turbine engines. The OFP spray equipment is lighter and more compact than other forms of thermal spray equipment, but because of the lower particle velocities obtained, the coatings generally have lower bond strength, higher porosity, and a lower overall cohesive (interparticle) strength than the coatings produced by other thermal spray processes.

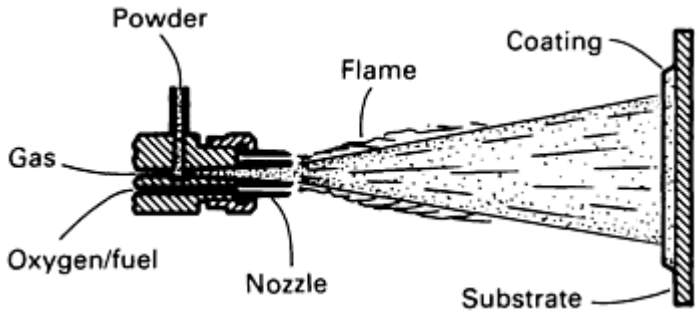

FIG. 16 SCHEMATIC OF THE OXYFUEL POWDER SPRAY PROCESS. SOURCE: REF 20

Flame spray and fuse is a modification of the OFP spray method. The materials used for coating are self-fluxing, fusible materials which require postspray heat treatment. In general, these are the boride-containing nickel-base alloys described earlier in this article. In practice, parts are prepared and coated as in other thermal spray processes and then fused. Fusing is accomplished using one of several techniques, such as flame or torch; induction; or in vacuum, inert, or hydrogen furnaces. These alloys generally fuse between 1010 to 1175 °C (1850 to 2150 °F), depending upon composition.

Spray-and-fuse coatings are used in applications where excessive wear is a problem. Coating hardnesses can be as high as 65 HRC. The use of spray-and-fuse coatings is limited to substrate materials that can tolerate the 1010 to 1175 °C (1850 to 2150 °F) fusing temperatures. Fusing temperatures may alter the heat-treated properties of some alloys. However, the coating will usually withstand additional heat treatment of the substrate.

Plasma arc spraying is one of the most sophisticated and versatile thermal spray methods. The PA spray process uses coating materials in the form of powders, which are heated with a plasma heat source (Fig. 17). Temperatures that can be obtained with commercial plasma equipment have been calculated to be greater than 11,000 °C (20,000 °F) and are far above the melting or even the vaporization point of any known material. Decomposition of materials during spraying is minimized because of the high gas velocities produced by the plasma, resulting in extremely short residence time in the thermal environment. The plasma process also provides a controlled atmosphere for melting and transport of the coating material, thus minimizing oxidation, and the high gas velocities produce coatings of high density.

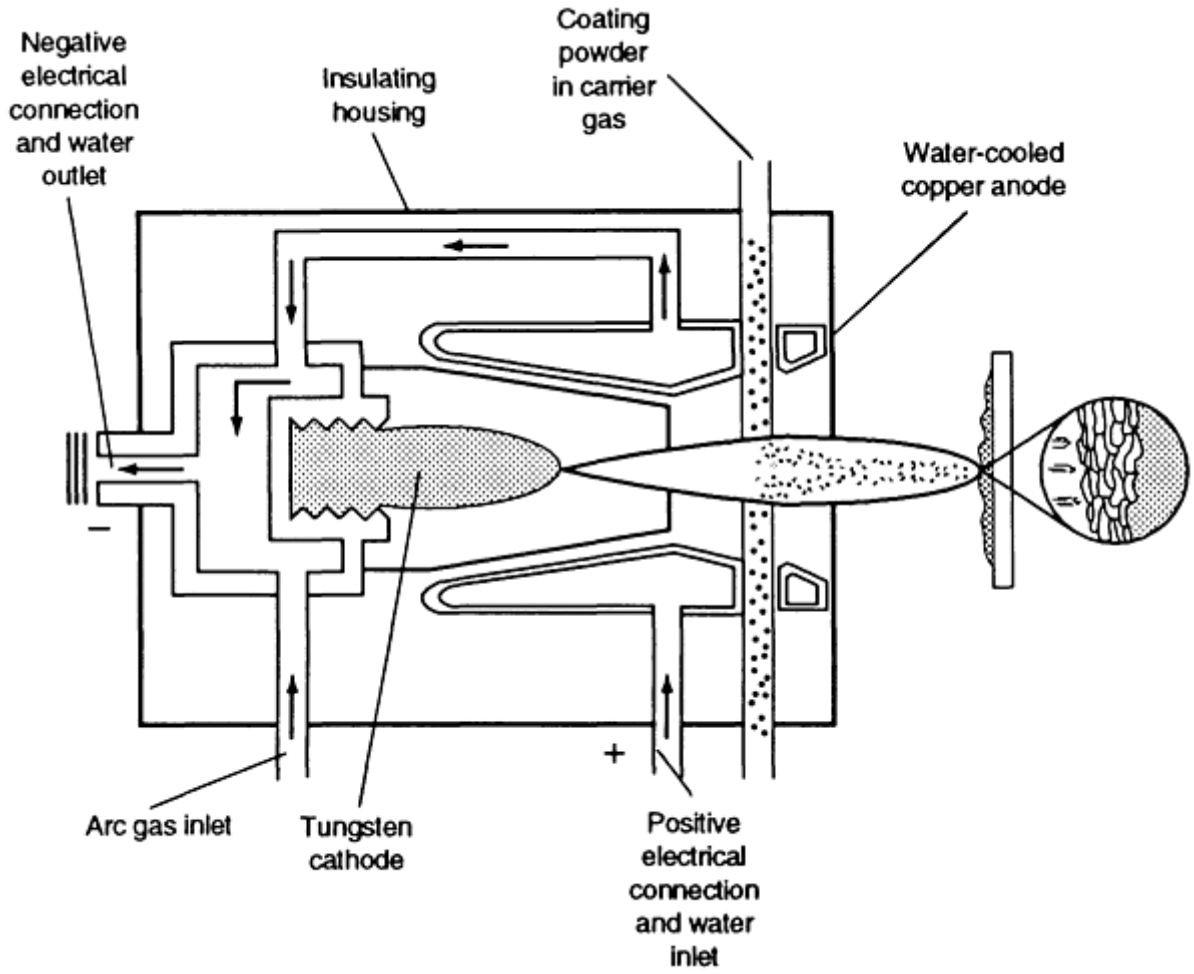

FIG. 17 SCHEMATIC OF THE PLASMA ARC SPRAY PROCESS. COURTESY OF D. BAXTER, *ADVANCED MATERIALS & PROCESSES*

The plasma gun operates on the principle of raising the energy state of a gas by passing it through an electric arc. The release of energy in returning the gas to its ground state results in exceedingly high temperatures. A gas such as nitrogen or argon enters a direct-current arc between a tungsten cathode and a copper anode that make up the nozzle (Fig. 17). Both components are cooled by a constant flow of water through internal passages. Here the plasma gas first dissociates (in the case of nitrogen, into two atoms), followed by ionization that releases free electrons. The electrons recombine outside the electric arc, and energy is released as heat and light. In addition, frequent collisions transfer energy from the electrons to the positive ions, accelerating them until the plasma reaches a state of equilibrium. The result is a thermal plasma in which the energy of the electrons has been turned into enthalpy, or heat content. At this point, powdered coating material suspended in a gas is injected into the plasma and is subsequently melted and propelled at high velocity to the workpiece. In practice, a small amount of a secondary gas, such as hydrogen or helium, is mixed with the primary plasma gas to increase operating voltage and thermal energy.

The high temperatures and high gas velocities produced by the plasma process result in coatings that are superior in mechanical and metallurgical properties to low-velocity OFW or OFP coatings. The plasma process is particularly efficient for spraying high-quality coatings of ceramic materials, such as zirconium oxide for turbine engine combustors and chromium oxide for printing rolls. The plasma process is also readily field-portable and is thus used for large on-site applications such as power utility plant boiler tubes.

Current plasma spray technology permits fully automatic start/stop operation and closed-loop computer control for power level, plasma gas flow, and powder feed rate. System problems can be diagnosed via computer modem to the equipment manufacturer, and system performance can be documented and stored on a digital recorder or data logger.

With any thermal spray powder method, the degree to which a given flame effectively melts and accelerates the powder depends on the type of coating material and the size and shape of the particles. Each particular coating material and gun combination has an optimum particle size. Particles much smaller than ideal will overheat and vaporize; much larger particles will not melt and may fall from the flame or rebound from the target. For the highest coating density, powders are sized between about 44 μm (325 mesh) and 10 μm (Ref 1, 9). The lower limit ensures free flow. Coarser powder may be sized up to 100 μm, with typical distribution falling between 88 μm (170 mesh) and 44 μm (325 mesh). Powder shape ranges from spherical to acicular; spherical is best because of reduced surface area and consistent flow.

Any material that melts without subliming and is available as a properly sized powder has potential as a plasma spray process coating. Plasma spray coatings may be elemental (aluminum, molybdenum, nickel, or chromium), alloyed (nickel-, iron-, or cobalt-base), ceramics and cermets (Al_2O_3, Cr_2O_3, or Cr_3C_2), composites (nickel-aluminum, cobalt-bonded tungsten carbide, or clad Al_2O_3), or mechanical blends.

In one process variation, the plasma gun and workpiece are enclosed in a vacuum chamber, and the entire operation is carried out in an inert atmosphere at low pressure (7 kPa, or 50 torr). Advantages of this low-pressure plasma technique include improved bonding and density of the deposit, improved control over coating thickness (even with an irregular work surface), and higher deposit efficiency. However, facility cost is higher, and workpiece size is limited by the vacuum chamber size. This modification is suitable for coating turbine airfoils, blade tips, and shroud segments with complex coatings such as NiCrAlY and other MCrAlY-type alloys. Very fine powder (-325 mesh) generally is used for low-pressure plasma spraying to achieve maximum density. If high-purity coatings are also desired, then the powder must be manufactured under inert cover and atomized in an inert gas to preserve purity.

The high-velocity oxyfuel powder spray process represents the state of the art for thermal spray coatings. The HVOF process uses extremely high kinetic energy and controlled thermal energy output to produce very-low-porosity coatings that exhibit high bond strength, fine as-sprayed surface finish, and low residual stresses. Both pulsed-combustion and continuous-combustion HVOF methods are used.

Pulsed-Combustion HVOF. The detonation gun (or D-gun) process was the first HVOF method introduced and was initially developed for the deposition of hard, wear-resistant materials such as oxides and carbides (Ref 1, 9). The extremely high particle velocities achieved in the detonation gun result in coatings with higher density, greater internal strength, and superior bond strength than can be achieved with conventional plasma spraying or oxyfuel powder spraying. Detonation gun coatings have been successfully applied to critical areas of precision components made from virtually all commercial alloys. The typical coating thickness is less than 0.75 mm (0.030 in.), but many applications require only 0.075 mm (0.003 in.) or less of finished coating.

This process, which is depicted schematically in Fig. 18, uses a controlled series of explosions of a mixture of oxygen and acetylene to blast the powder onto the surface of the workpiece. The detonation gun consists of a water-cooled barrel several feet long, with an inside diameter of about 25 mm (1 in.), and associated gas- and powder-metering equipment. In operation, a mixture of oxygen and acetylene is fed into the barrel along with a charge of powder. The gas is then ignited, and the detonation wave accelerates the powder to about 760 m/s (2500 ft/s), while heating it close to, or above, its melting point. Temperatures up to 3900 °C (7000 °F) are reached inside the gun. The distance that the powder is entrained in the high-velocity gas is much longer than in a plasma or flame spray device, which accounts for the high particle velocity. After the powder has exited the barrel, a pulse of nitrogen purges the barrel. The gun discharges four to eight times per second.

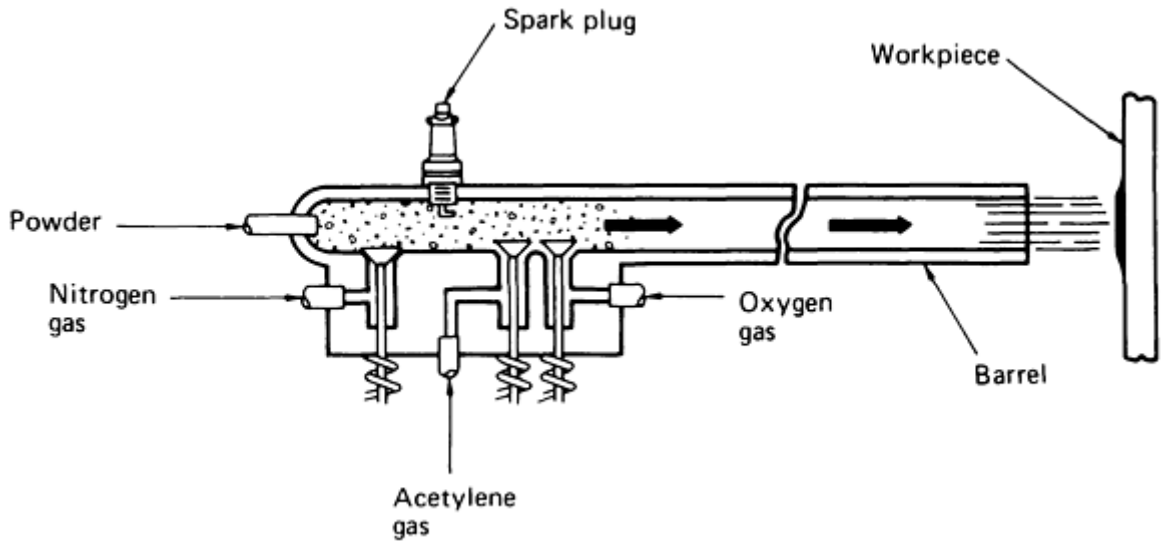

FIG. 18 SCHEMATIC OF THE DETONATION GUN (D-GUN) HVOF PROCESS. SOURCE: REF 1

Suitable materials for detonation gun coatings include pure metals, alloys, oxides, carbides, composites, and mechanical blends of two or more components. Historically, the detonation gun has proven particularly advantageous in applying hard wear-resistant carbide and oxide coatings. Detonation gun coatings have been successfully applied to critical areas of precision parts made from virtually all commercial alloys. The substrate surface is seldom heated above 150 °C (300 °F) during the coating process. As a result, a part can be fabricated and fully heat treated prior to coating. In addition, very high melting point materials (such as WC-Co) can be deposited on relatively low melting point substrates (such as aluminum). Usually, there is little or no distortion, and the substrate microstructure and strength are not changed by the coating process.

Continuous-combustion HVOF processes, which also feature internal, confined combustion, operate with an oxyfuel mixture consisting of oxygen and either propylene, propane, hydrogen, and even liquid fuels such as kerosene. High-velocity oxyfuel guns have combustor sections (air- or water-cooled), which combust the fuel/oxygen mixtures under pressure and accelerates the combusted gas streams down a confined cooled tube. Powders, with carrier gases, are fed into the nozzle where the particles are entrained with the confined, high-pressure combusting gases.

The high-velocity gases produce uniquely characteristic multiple shock diamond patterns, which are visible in the flame (Fig. 19). Combustion temperatures approach 2750 °C (5000 °F) and form a circular flame configuration. Powder is injected into the flame axially to provide uniform heating, and powder particles are accelerated by the high velocity gases, which typically approach speeds ranging from 1370 m/s (4500 ft/s) to as high as 2160 m/s (7100 ft/s). Particle velocities range from 760 m/s (2500 ft/s) to more than 900 m/s (3000 ft/s).

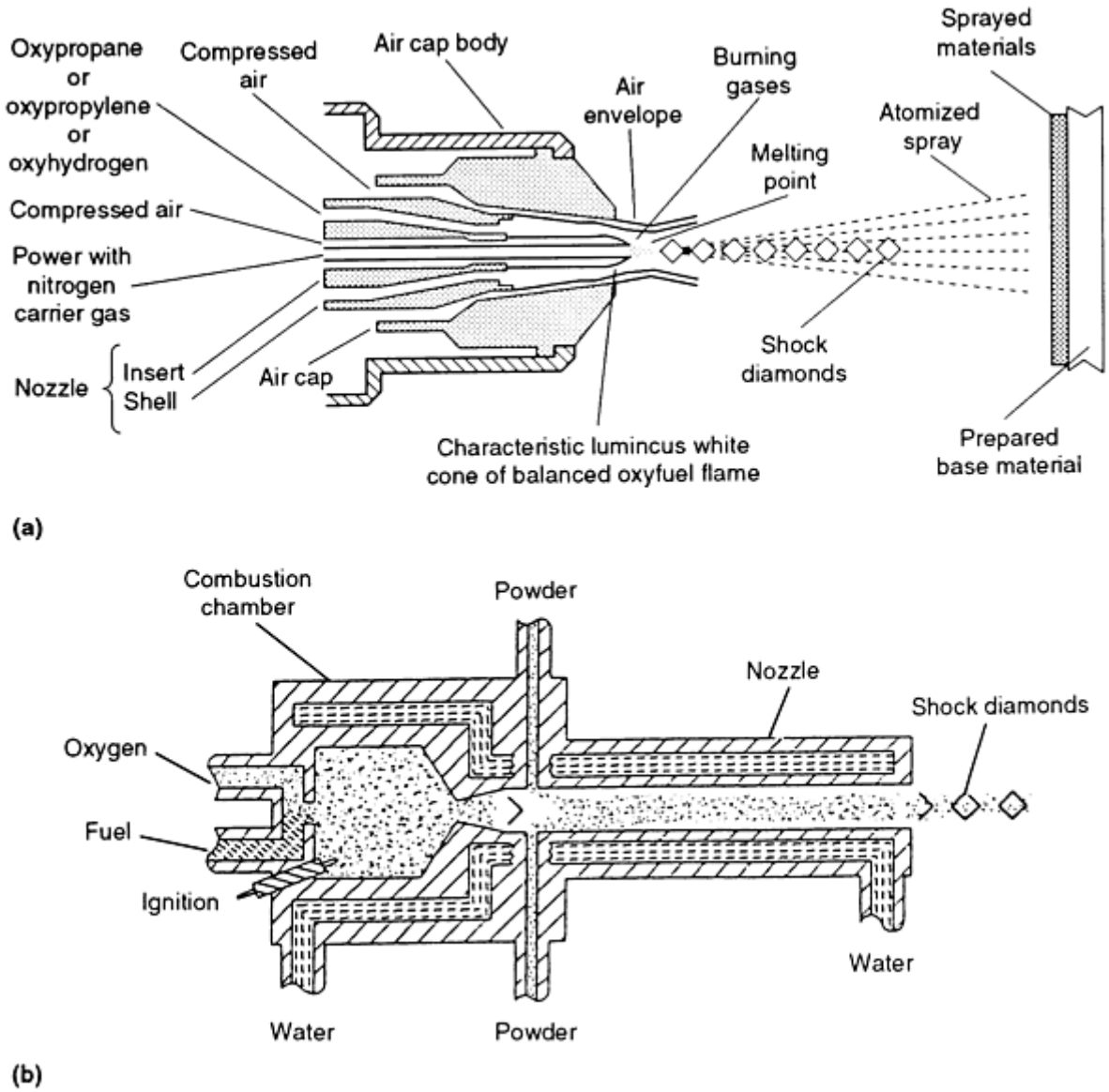

FIG. 19 SCHEMATICS OF (A) AIR-COOLED AND (B) WATER-COOLED CONTINUOUS COMBUSTION HVOF THERMAL SPRAY PROCESSES. (A) COURTESY OF METCO PERKIN ELMER. (B) SOURCE: REF 22

Continuous-combustion HVOF spray coating processes are separated into four major designs: (1) internal combustion, with the hot gases directed into a chamber where they mix with and heat a mixture of carrier gas and powder particles; (2) simultaneous injection of powder into a combustion chamber, where the mixture continuously bums and heats the particles; (3) confined combustion into which a stream of powder with carrier gas is injected; and (4) high-pressure liquid fuel systems with radial injection of powders downstream of the combustor exit. Figure 19 illustrates two of these variations. Common to all HVOF methods is that the gases are being burned under higher-than-atmospheric pressures, with the combustion gases, carrier gas, and an entrained distribution of powders being accelerated in the tube. The length of the nozzle, the design of heating chambers, the geometry/location of powder feed, and the cooling, either by water or air, are the major features which differ.

The low residual coating stress produced in the continuous-combustion HVOF process allows significantly greater thickness capability than the plasma method, while providing lower porosity, lower oxide content, and higher coating adhesion. Coatings produced by the continuous-combustion HVOF process also have much better machinability compared with other methods, and coating porosity has closely approached wrought materials, as verified by gas permeability testing. Continuous-combustion HVOF systems are available with closed-loop computer control and robotics capability. Figures 20 and 21 compare the bond strengths and hardness of coatings deposited with various thermal spray processes. The correlation between hardness and particle velocity is shown in Fig. 22.

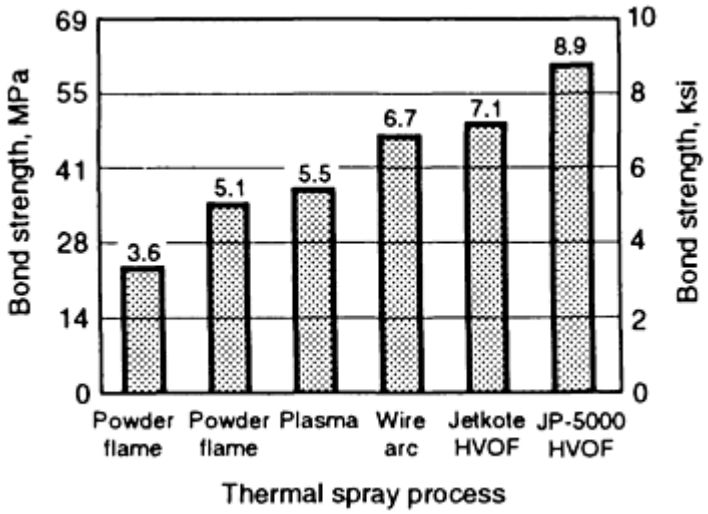

FIG. 20 BOND STRENGTHS OF TYPE 316 STAINLESS STEEL COATINGS DEPOSITED BY VARIOUS THERMAL SPRAY PROCESSES. JETKOTE IS A REGISTERED TRADENAME OF THERMODYNE, INC.; JP-5000 IS A REGISTERED TRADENAME OF HOBART TAFA TECHNOLOGIES, INC. SOURCE: REF 22

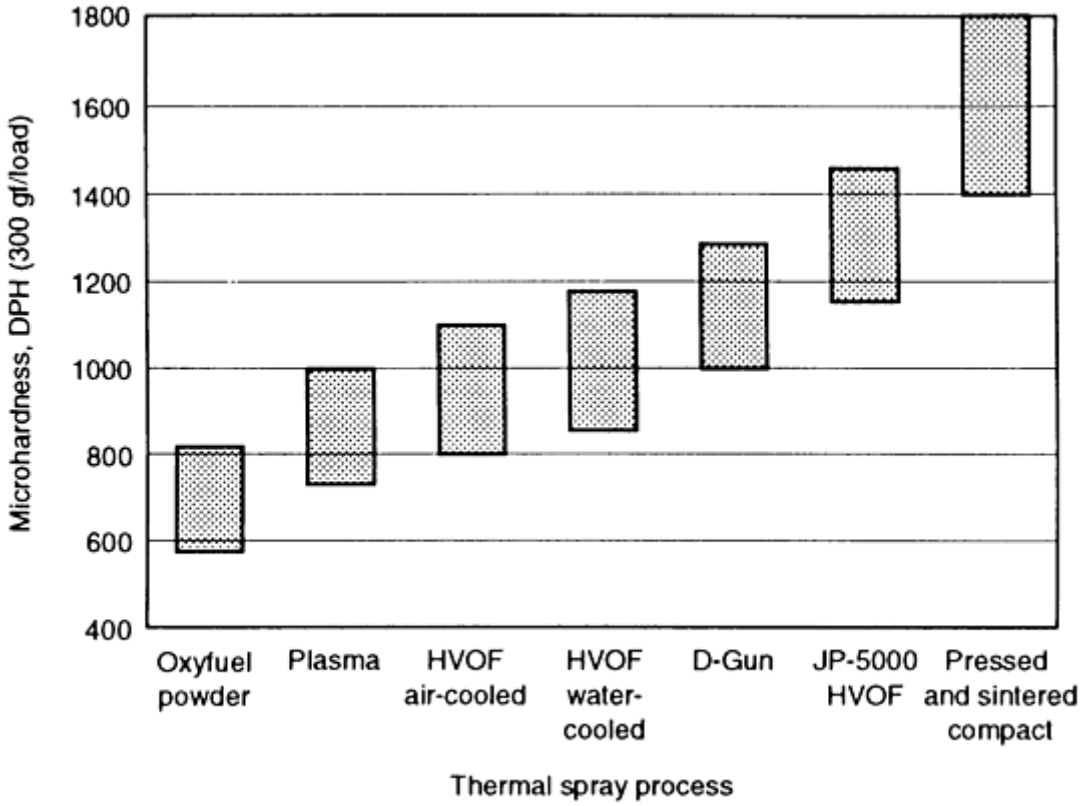

FIG. 21 HARDNESS OF WC-CO COATING VERSUS THERMAL SPRAY PROCESS. JP-5000 IS A REGISTERED TRADENAME OF HOBART TAFA TECHNOLOGIES, INC. SOURCE: REF 22

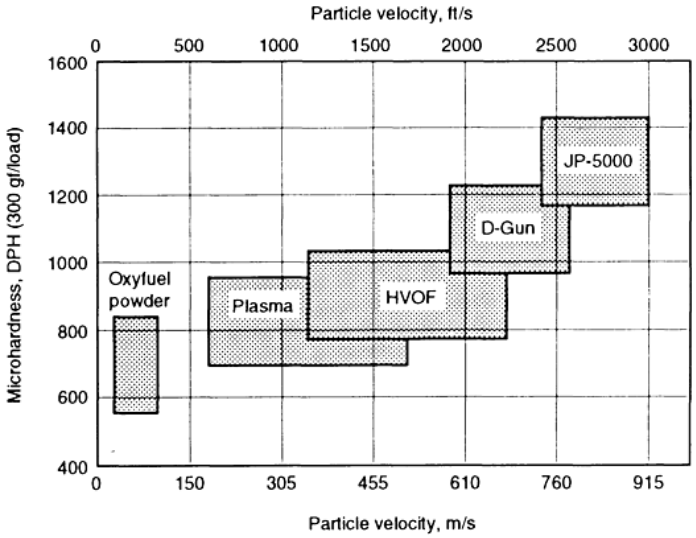

FIG. 22 HARDNESS OF WC-CO COATING VERSUS THERMAL SPRAY PROCESS PARTICLE VELOCITY. JP-5000 IS A REGISTERED TRADENAME OF HOBART TAFA TECHNOLOGIES, INC. SOURCE: REF 22

Surface Preparation (Ref 20)

Thermal spray coatings rely primarily on mechanical bonding to the substrate surface. Because bonding relies on this mechanical interlocking of spray particles with the substrate surface, preparation of the surface is critical to a successful coating. Preparation of the substrate before spraying is virtually the same for all thermal spray processes. More detailed information on surface preparation can be found in Ref 23.

Chemical Cleaning. Chemical cleaning is used on parts that are contaminated or impregnated with material that cannot be removed by other methods. Surfaces can be chemically cleaned by vapor degreasing, steam, hot detergent washing, or application of an industrial cleaning solvent. Degreasing is usually the most economical and a fast way to remove lubricants and oils.

Grit blasting is the most frequently used surface preparation procedure. The roughening cleans the surface of contamination that may inhibit bonding and creates an irregular profile of minute surface irregularities. This enhances the adhesion of the coating. Before application of the thermal spray coating, the cleaned substrate should be blasted to a white-metal condition (according to Steel Structures Painting Council specification SSPC-SP5-82) with a minimum surface profile of 6 μm (250 μm) R_a (arithmetic average surface roughness). Sharp angular grit (18 to 24 mesh average) should be used. Typical-grit blasting materials include chilled iron grit, alumina (Al_2O_3), silica sand, crushed flint, crashed garnet, silicon carbide, and crushed slag.

Rough threading is often used in conjunction with grit blasting for cylindrical surfaces. It consists essentially of machining a thread form on the area to be sprayed. This type of preparation provides excellent adhesion of the coating to the substrate.

Bond coats are often used when an extremely high bond strength is desired or when mechanical deformation of the substrate is not possible or practical. This involves spraying materials that are exothermic and self-bonding. Nickel-aluminum alloys (Ni-5 to 20Al) and molybdenum are the most commonly used bond materials. A thin coating (normally about 50 to 125 μm, or 2 to 5 mils) of bond material is generally applied before the thermally sprayed overcoat. Care should be taken to ensure that the bond material is compatible with the overcoat and that a galvanic cell will not be created, which may be detrimental to the performance of the coating system.

Preheating of the substrate is often beneficial. Preheating to 65 to 95 °C (150 to 200 °F) will eliminate surface condensation and will reduce shrink differentials between the coating and the substrate. It is generally employed only with the flame spray processes, which use their flame as the heat source for warming the substrate.

Finishing Treatment

Thermal spray coatings usually exhibit two common features in the as-deposited condition, a sandpaper-like surface finish and a structure with inherent porosity. A typical surface roughness of an as-sprayed coating ranges from 5.0 to 13 μm (200 to 500 μin.) R_a. The porosity usually ranges from 2 to 17 vol%, depending on the process by which the coating is deposited and the material sprayed. In many cases, thermal spray coatings are applied to machine elements where the coated component must conform to close dimensional tolerances or have a high surface finish. In many applications, coatings are exposed to corrosive solutions or hydraulic fluids, which can infiltrate the pores, resulting in fluid leakage or corrosion of the base material. These conditions can contribute to the premature failure of the coating. Many applications require the coating to be sealed before finishing by machining or grinding, to protect the thermal spray coating.

Sealing is the process by which the pores of a coating are filled to eliminate the possibility of infiltration by fluids or corrosive media that can contribute to premature failure. Sealing materials, which may be applied by brushing, spraying, or dipping, include petroleum-based waxes and organic materials such as phenolics, epoxy resins, polyesters, polyurethanes, and polyimides.

Coating Finishing Method. Thermal spray coatings are finished to dimension either by single-point machining or by grinding. Hard surfacing materials such as ceramics and carbides are restricted to grind finishing, typically with diamond wheels. Thermal spray coatings are sufficiently different from the same material in wrought form that different grinding wheel and finishing tool recommendations are almost always required. Therefore, tools and wheels should not be chosen based on experience with the parent material in wrought or cast form.

Most thermal spray coatings exhibit some degree of porosity. However, the HVOF method produces coatings closest in machining and grinding behavior to wrought materials. In general, thermal spray coatings can be machined to 1 to 2 μm (40 to 80 μin.) R_a and ground to 0.25 to 0.5 μm (10 to 20 μin.) R_a. Many plasma spray ceramic coatings can be lapped down to 0.025 to 0.05 μm (1 to 2 μin.) R_a.

References cited in this section

1. K.C. ANTONY *ET AL.*, HARDFACING, *WELDING, BRAZING, AND SOLDERING,* 9TH ED., VOL 6, *METALS HANDBOOK,* AMERICAN SOCIETY FOR METALS, 1983, P 771-793
9. K.M. KULKARNI AND V. ANAND, METAL POWDERS USED FOR HARDFACING, *POWDER METALLURGY,* 9TH ED., VOL 7, *ASM HANDBOOK,* AMERICAN SOCIETY FOR METALS, 1984, P 823-836
19. B.A. KUSHNER AND E.R. NOVINSKI, THERMAL SPRAY COATINGS, *FRICTION, LUBRICATION, AND WEAR TECHNOLOGY,* VOL 18, *ASM HANDBOOK,* ASM INTERNATIONAL, 1992, P 829-833
20. R.H. UNGER, THERMAL SPRAY COATINGS, *CORROSION,* 9TH ED., VOL 13, *ASM HANDBOOK,* ASM INTERNATIONAL, 1987, P 459-462
21. M.L. THORPE, THERMAL SPRAY: INDUSTRY IN TRANSITION, *ADV. MATER. PROCESS.*, VOL 143 (NO. 5), 1993, P 50-56
22. G. IRONS, "HIGHER VELOCITY THERMAL SPRAY PROCESSES PRODUCE BETTER AIRCRAFT ENGINE COATINGS," SAE TECHNICAL PAPER 920947, PRESENTED AT THE 28TH ANNUAL AEROSPACE/AIRLINE PLATING AND METAL FINISHING FORUM AND EXPOSITION (SAN DIEGO, CA), APRIL 1992
23. F.N. LONGO, PROCESSING AND DESIGN, LESSON 3, COURSE 51, *THERMAL SPRAY TECHNOLOGY,* MATERIALS ENGINEERING INSTITUTE, ASM INTERNATIONAL, 1992

J.R. Davis, Davis & Associates

Thermal Spray Materials and Applications

The most outstanding feature of thermal spray coatings is probably their diverse applicability. There are two primary reasons for this. First, materials selection is almost unlimited. In fact, more than 200 coating materials with different characteristics of toughness, coefficient of friction, hardness, and other properties are available. These materials can be grouped as follows:

- PURE METALS
- METAL ALLOYS
- CERMETS
- CERAMICS
- CARBIDES
- POLYMERS
- SPECIAL COMPOSITE MATERIALS SUCH AS NICKEL-ALUMINUM AND NICKEL-GRAPHITE COMPOSITE POWDERS

Second, the thermal spray process, properly controlled, imparts very little heat to the substrate (100 to 260 °C, or 200 to 500 °F), avoiding metallurgical change, distortion, and oxidation. This allows thermal spray coatings to be applied to practically any substrate (metals, plastics, composites, etc.). Also, such coatings can often be applied to the finish machined part, a practice unthinkable with welding, heat treating, or other high-temperature processes.

Thermal spray coatings provide the design engineer with many options. They offer material properties not available in wrought metals. Coatings can be applied to selected areas rather than treating the entire part. Manufacturing costs can be reduced by eliminating unnecessary processing steps. Extraordinary performance characteristics can be designed into a part to extend its useful life, creating a new, marketable product in the process.

Thermal spray coatings provide the solution to many mechanical, electrical, and corrosion resistance problems involving metal parts and assemblies. However, there are certain applications where such coatings should not be used. Before a thermal spray coating is specified, its suitability can usually be determined according to these criteria (Ref 24):

- NO STRENGTH IS IMPARTED TO THE BASE MATERIAL BY A SPRAYED DEPOSIT. THE COMPONENT TO BE SPRAYED MUST, IN ITS PREPARED FORM, BE ABLE TO WITHSTAND ANY MECHANICAL LOADING THAT WILL BE EXPERIENCED IN SERVICE. (IN A FEW APPLICATIONS, SOME STRENGTH CAN BE ADDED BY A THERMAL SPRAY COATING; HOWEVER, SUCH USES ARE UNUSUAL AND SHOULD BE CAREFULLY TESTED.)
- IF THE AREA ON A PART TO BE SPRAYED OR ANY SECTION OF THE TOTAL AREA WILL BE SUBJECTED TO SHEAR LOADING IN SERVICE, THE PART IS NOT A SUITABLE CANDIDATE FOR THERMAL SPRAYING. GEAR TEETH, SPLINES, AND THREADS ARE EXAMPLES.
- POINT LOADING WITH LINE CONTACT ON A SPRAYED METAL DEPOSIT WILL EVENTUALLY SPREAD THE DEPOSIT, CAUSING DETACHMENT. IF THE DEPOSIT IS ON A MOVING COMPONENT WITH SUCH LOADING, IT WILL FAIL RAPIDLY. FOR EXAMPLE, NEEDLE AND ROLLER BEARING SEATS, WHERE THE BEARING ELEMENTS ARE IN DIRECT CONTACT WITH THE SPRAYED DEPOSIT, MAY NOT BE GOOD THERMAL SPRAY CANDIDATES.
- IF THE BASE METAL OF A COMPONENT TO BE TREATED HAS BEEN NITRIDED, NON-HVOF THERMAL SPRAYING IS NOT RECOMMENDED UNLESS THE NITRIDING IS FIRST REMOVED. OTHER FORMS OF SUBSTRATE HARDENING REQUIRE SPECIAL TREATMENT, SUCH AS INTENSIVE GRIT BLASTING. THERMAL SPRAYING OF NITRIDED TURBINE ENGINE COMPONENTS USING HVOF METHODS IS DESCRIBED IN REF 25.

To date, the most common application area for thermal spraying has been advanced aircraft gas turbine components such as compressor blades, compressor stator vanes, beating housings, and labyrinth seals. Common coating materials include cobalt-base (Laves phase) alloys T-400 and T-800, tungsten carbide-cobalt materials, and chromium carbide-nickel chromium cermets (Cr_3C_2-20 to 30% NiCr). Other key application areas are listed below.

Wear coatings are used to resist abrasion, erosion, cavitation, and fretting, and to reduce friction. These coatings consist of a wide range of metals and their alloys, ceramics, cermets, carbides, and even low-friction plastics. Typical coating hardness ranges from 20 to 70 HRC. Metal matrices are hardened by rapid solidification, by dispersions introduced from the spray process, by the addition of separate hard phases (for example, carbides of chromium, tungsten, titanium and/or tantalum), or by oxide inclusions. Table 13 lists friction and wear applications for various thermal spray materials.

TABLE 13 THERMAL SPRAY COATINGS USED FOR HARDFACING APPLICATIONS

TYPE OF WEAR	COATING MATERIAL	COATING PROCESS[(A)]	APPLICATIONS
ADHESIVE WEAR	SOFT BEARING COATINGS:		
	ALUMINUM BRONZE	OFW, EAW, OFP, PA, HVOF	BABBITT BEARINGS, HYDRAULIC PRESS SLEEVES, THRUST BEARING SHOES, PISTON GUIDES, COMPRESSOR CROSSHEAD SLIPPERS
	TOBIN BRONZE	OFW, EAW	
	BABBITT	OFW, EAW, OFP	
	TIN	OFW, EAW, OFP	
	HARD BEARING COATINGS:		
	MO/NI-CR-B-SI BLEND	PA	BUMPER CRANKSHAFTS FOR PUNCH PRESS, SUGAR CANE GRINDING ROLL JOURNALS, ANTIGALLING SLEEVES, RUDDER BEARINGS, IMPELLER SHAFTS, PINION GEAR JOURNALS, PISTON RINGS (INTERNAL COMBUSTION); FUEL PUMP ROTORS
	MOLYBDENUM	OFW, EAW, PA	
	HIGH-CARBON STEEL	OFW, EAW	
	ALUMINA/TITANIA	OFP, PA	
	TUNGSTEN CARBIDE	OFP, PA, HVOF	
CO-MO-CR-SI	PA, HVOF		
FE-MO-C	PA		
ABRASIVE WEAR	ALUMINUM OXIDE	PA	SLUSH-PUMP PISTON RODS, POLISH ROD LINERS, AND SUCKER ROD COUPLINGS (OIL INDUSTRY); CONCRETE MIXER SCREW CONVEYORS; GRINDING HAMMERS (TOBACCO INDUSTRY); CORE MANDRELS (DRY-CELL BATTERIES); BUFFING AND POLISHING FIXTURES; FUEL-ROD MANDRELS
	CHROMIUM OXIDE	PA	
	TUNGSTEN CARBIDE	PA, HVOF	
	CHROMIUM CARBIDE	PA, HVOF	
	NI-CR-B-SIC/WC (FUSED)	OFP, HVOF	
	NI-CR-B-SIC (FUSED)	OFP, HVOF	
	NI-CR-B-SIC (UNFUSED)	HVOF	
SURFACE FATIGUE WEAR			
FRETTING:	MOLYBDENUM	OFW, PA	SERVOMOTOR SHAFTS, LATHE

			COMBUSTION), CYLINDER LINERS
FRETTING: SMALL-AMPLITUDE OSCILLATORY DISPLACEMENT APPLICATIONS:			
LOW TEMPERATURE (<540 °C, OR 1000 °F)	ALUMINUM BRONZE	OFW, EAW, PA, HVOF	AIRCRAFT FLAP TRACKS (AIR-FRAME COMPONENT); EXPANSION JOINTS AND MID-SPAN SUPPORTS (JET ENGINE COMPONENTS)
	CU-NI-IN	PA, HVOF	
	CU-NI	PA, HVOF	
HIGH TEMPERATURE (>540 °C, OR 1000 °F)	CO-CR-NI-W	PA, HVOF	COMPRESSOR AIR SEALS, COMPRESSOR STATORS, FAN DUCT SEGMENTS AND STIFFENERS (ALL JET ENGINE COMPONENTS)
	CHROMIUM CARBIDE	PA, HVOF	
EROSION	CHROMIUM CARBIDE	PA, HVOF	EXHAUST FANS, HYDROELECTRIC VALVES, CYCLONE DUST COLLECTOR, DUMP VALVE PLUGS AND SEATS, EXHAUST VALVE SEATS
	TUNGSTEN CARBIDE	PA, HVOF	
	WC/NI-CR-B-SIC (FUSED)	OFP, HVOF	
	WC/NI-CR-B-SIC (UNFUSED)	OFP, HVOF	
	CHROMIUM OXIDE	PA	
CAVITATION	NI-CR-B-SIC-AL-MO	PA	WEAR RINGS (HYDRAULIC TURBINES), WATER TURBINE BUCKETS, WATER TURBINE NOZZLES, DIESEL ENGINE CYLINDER LINES PUMPS
	NI-AL/NI-CR-B-SIC	PA	
	TYPE 316 STAINLESS STEEL	PA	
	NI-CR-B-SIC (FUSED)	OFP, HVOF	
	NI-CR-B-SIC (UNFUSED)	HVOF	
	ALUMINUM BRONZE	PA, HVOF	
	CU-NI	PA, HVOF	

(A) OFW, OXYFUEL WIRE SPRAY; EAW, ELECTRIC ARC WIRE SPRAY; OFP, OXYFUEL POWDER SPRAY; PA, PLASMA ARC SPRAY; HVOF, HIGH-VELOCITY OXYFUEL POWDER SPRAY

Corrosion Resistance. Zinc and aluminum and their alloys are the metals most widely used for thermal spray anticorrosion coatings. They are extensively used for the corrosion protection of iron and steel in a wide range of environments and have been shown to provide very long-term protection (over 20 years) in both marine and industrial locations. Properties and applications of zinc and aluminum thermal spray coatings are described in the article "Thermal Spraying Coatings" in this Volume.

Other coating materials for corrosion-resistant applications include austenitic stainless steels, aluminum bronze, nickel-base alloys, and MCrAlY materials. Selection of a specific alloy depends on the particular environment. When using these alloys, it must be understood that these coatings will not galvanically protect the underlying steel. This can be a particular problem due to the porosity of thermal spray coatings. Great care must be taken to ensure that these coatings are properly sealed in order to prevent penetration of the corrosive medium to the underlying steel and subsequent corrosion at the coating/substrate interface.

Oxidation Protection. Thermal spray coatings are extensively used by industry to protect steel components and structures from heat oxidation at surface temperatures to 1095 °C (2000 °F). By ensuring long-term protection, thermal spray coatings show real economic advantages during the service lives of such items. Coatings are particularly effective in protecting low-alloy and carbon steels. Table 14 lists thermal spray coatings for use in high-temperature applications.

TABLE 14 THERMAL SPRAY COATINGS USED FOR ELEVATED-TEMPERATURE SERVICE

SERVICE TEMPERATURE	COATING METAL OR ALLOY	COATING THICKNESS	
		µm	mils
UP TO 550 °C (1020 °F)	ALUMINUM	175	7
UP TO 550 °C (1020 °F) IN THE PRESENCE OF SULFUROUS GASES	NI-43CR-2TI	375	15
550-900 °C (1020-1650 °F)	ALUMINUM OR ALUMINUM-IRON	175	7
900-1000 °C (1650-1830 °F)	NICKEL-CHROMIUM OR MCRALY	375	15
900-1000 °C (1650-1830 °F) IN THE PRESENCE OF SULFUROUS GASES	NICKEL-CHROMIUM, FOLLOWED BY ALUMINUM	375	15
		100	4

Source: Ref 20

Aluminum has been widely used to protect such steels in a number of applications involving high surface temperatures up to 550 °C (1020 °F). Nickel-chromium alloys and some of the MCrAlY alloys have also provided protection in severe environments (up to 1000 °C, or 1830 °F).

Thermal insulation provides low-thermal-conductivity zirconium and/or aluminum oxides that are deposited as coatings to reduce heat conduction to base metals. These insulating oxide coatings can also reduce heat loss, reduce thermal transient effects, and reduce the high-temperature oxidation/corrosion effects by lowering temperatures of the coated base metals. Thermal spray processes usually introduce a controlled level of porosity, which further enhances the coating insulation and increases its thermal shock resistance.

Thermal barrier coatings consist of a low-conductivity (thermal) ceramic deposited over an MCrAlY bond coat. The ceramic of choice is partially-stabilized zirconia (7 to 8 wt% Y_2O_3-ZrO_2) deposited at a thickness of 0.25 mm (0.010 to 0.040 in.) with 10 to 15% porosity. A bond coat of NiCrAlY or CoCrAlY is used at a thickness of 0.125 mm (0.005 in.). Both coatings are used on components used in gas turbine engines and adiabatic engines to improve efficiency and reduce metal temperatures or cooling requirements.

Electrically conductive coatings include silver, copper, aluminum, zinc, and bronze alloys. Typical conductivities of these sprayed metals are reported to be 40 to 90% of wrought materials, depending on the spray coating method. In addition, superconducting plasma-sprayed Y-Ba-Cu-O, Cu/Nb_3Sn, and Nb_3Sn materials that have zero resistance at low to intermediate temperatures of 100 K (-280 °F) have been deposited by thermal spraying. Conductive coatings designed to shield electronic components against radio frequency or electromagnetic interference such as aluminum, zinc, and tin coatings, are also sprayed.

Dimensional Restorative Coatings. Thermal spray is used as a coating to repair or resurface (up to 3 mm, or 0.12 in. thick) worn and/or corroded parts, as well as to repair new part errors (for example, undersize parts), to repair nicks or other blemishes, or to renew surfaces that are corroded or worn in use.

Medically Compatible Coatings. Interactive bonding coatings on implants use thermal spray coatings to provide biocompatible titanium (commercially pure Ti or Ti-6Al-4V alloy) and/or ceramic (calcium phosphates) surfaces on both dental and orthopedic devices, to improve wear surface and/or tissue adhesion. Coating porosity and high surface roughness can be produced in thermal spray coatings to improve further tissue adherence.

References cited in this section

20. R.H. UNGER, THERMAL SPRAY COATINGS, *CORROSION*, 9TH ED., VOL 13, *ASM HANDBOOK,* ASM INTERNATIONAL, 1987, P 459-462

24. M.L. THORPE, THERMAL SPRAYING BECOMES A DESIGN TOOL, *MACH. DES.*, 24 NOV 1983

25. P.O. BUZBY AND J. NIKITICH, HVOF THERMAL SPRAYING OF NITRIDED PARTS, *ADV. MATER. PROCESS.*, DEC 1991, P 35-36

Hardfacing, Weld Cladding, and Dissimilar Metal Joining

J.R. Davis, Davis & Associates

Weld Cladding

The term weld cladding usually denotes the application of a relatively thick layer ([ges]3 mm, or $\frac{1}{8}$ in.) of weld metal for the purpose of providing a corrosion-resistant surface. Hardfacing, as described earlier in this article, produces a thinner surface coating than a weld cladding and is normally applied for dimensional restoration or wear resistance. Typical base metal components that are weld-cladded include the internal surfaces of carbon and low-alloy steel pressure vessels, paper digesters, urea reactors, tubesheets, nuclear reactor containment vessels, and hydrocrackers. The cladding material is usually an austenitic stainless steel or a nickel-base alloy, although certain copper-base alloys are also sometimes used. Some specialized cladding is also carried out using silver filler metal. Weld cladding is usually performed using the submerged arc welding process (SAW). However, flux-cored (either self-shielded or gas-shielded), plasma arc, and electroslag welding methods can also produce weld claddings. Filler metals are available as covered electrodes, coiled electrode wire, and strip electrodes. Table 15 lists some of the filler metals for stainless steel weld claddings.

TABLE 15 STAINLESS STEEL FILLER METALS FOR WELD CLADDING APPLICATIONS

WELD OVERLAY TYPE	FIRST LAYER		SUBSEQUENT LAYERS	
	COVERED ELECTRODE(A)	BARE ROD OR ELECTRODE(B)	COVERED ELECTRODE(A)	BARE ROD OR ELECTRODE(B)
304	E309	ER309	E308	ER308
304L	E309L	ER309L	E308L	ER308L
	E309CB			
321	E309CB	ER309CB	E347	ER347
347	E309CB	ER309CB	E347	ER347
309	E309	ER309	E309	ER309
310	E310	ER310	E310	ER310
316	E309MO	ER309MO	E316	ER316
316L	E309MOL	ER309MOL	E316L	ER316L
	E317L	ER317L		
317	E309MO	ER309MO	E317	ER317
	E317	ER317		
317L	E309MOL	ER309MOL	E317L	ER317L
	E317L	ER317L		
20 CB	E320	ER320	E320	ER320

Note: Columbium (Cb) is also referred to as niobium (Nb).

(A) REFER TO AWS SPECIFICATION A5.4.

(B) REFER TO AWS SPECIFICATION A5.9.

Application Considerations (Ref 26)

The technique of weld cladding is an excellent method to impart properties to the surface of a substrate that are not available from that base metal, or to conserve expensive or difficult-to-obtain materials by using only a relatively thin surface layer on a less expensive or abundant base material. This technique has several inherent limitations or possible problems that must be considered when planning for weld cladding. The thickness of the required surface must be less than the maximum thickness of the overlay that can be obtained with the particular process and filler metal selected.

Welding position also must be considered when selecting an overlay material and process. Certain processes are limited in their available welding positions; for example, SAW can be used only in the flat position. In addition, when using a high-deposition-rate process that exhibits a large liquid pool, welding vertically or overhead may be difficult or impossible. Some alloys exhibit eutectic solidification, which leads to large molten pools that solidify instantly rather than with a "mushy" (liquid plus solid) transition. Such materials are also difficult to weld except in the flat position.

Composition Control of Stainless Steel Weld Overlays (Ref 26)

The economics of stainless steel weld cladding are dependent on achieving the specific chemistry at the highest practical deposition rate in a minimum number of layers. The fabricator selects the filler wire and welding process, whereas the purchaser specifies the surface chemistry and thickness, along with the base metal. The most outstanding difference between welding a joint and depositing an overlay is in the area of dilution. The percentage of dilution equals the amount of base metal melted (x) divided by the sum of base metal melted and filler metal added ($x + y$), the quotient of which is multiplied by 100.

$$\%dilution = \frac{x}{x+y} x100 \qquad \textbf{(EQ 2)}$$

For stainless steel cladding, a fabricator must understand how the dilution of the filler metal with the base metal affects the composition and metallurgical balance, such as the proper ferrite level to minimize hot cracking, absence of martensite at the interface for bond integrity, and carbon at a low level to ensure corrosion resistance. The prediction of the microstructures and properties (such as hot cracking and corrosion resistance) for the austenitic stainless steels has been the topic of many studies (Ref 27). During the last two decades, four microstructure prediction diagrams have found the widest application. These include the Schaeffler diagram, the DeLong diagram, and the Welding Research Council (WRC) diagrams (WRC-1988 and WRC-1992). Each of these is described below.

The Schaeffler diagram (Fig. 23), published in 1949, has been extensively used for estimating the ferrite content of stainless steel weld metals (Ref 28). The diagram contains phase fields and iso-ferrite lines that permit prediction of the weld structure from the composition. It is still widely used for predicting the ferrite content of dissimilar weld deposits. This involves calculating a "chromium equivalent" (Cr_{eq}) and a "nickel equivalent" (Ni_{eq}) for each base metal and for the proposed filler metal, plotting each equivalent on the Schaeffler diagram, and drawing tie lines between the plotted points, proportioned according to expected dilution, to obtain an estimate of the weld metal ferrite content.

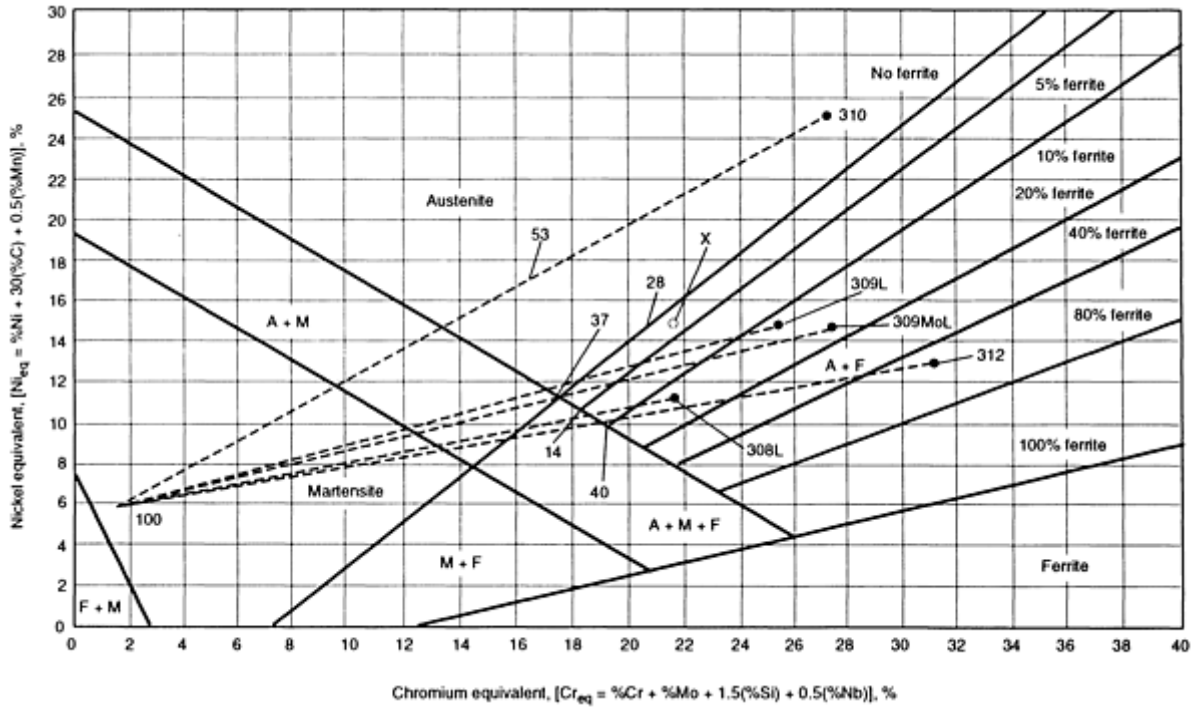

FIG. 23 SCHAEFFLER DIAGRAM FOR STAINLESS STEEL WELD METAL. A, AUSTENITE; F, FERRITE; M, MARTENSITE. POINT 100 IS ASTM A 387A STEEL. EXAMPLE: POINT X ON THE DIAGRAM INDICATES THE EQUIVALENT COMPOSITION OF TYPE 318 (316 CB) WELD DEPOSIT CONTAINING 0.07% C, 1.55% MN, 0.57% SI, 19.02% CR, 11.87% NI, 2.16% MO, AND 0.80% NB. EACH OF THESE PERCENTAGES WAS MULTIPLIED BY THE "POTENCY FACTOR" INDICATED FOR THE ELEMENT IN QUESTION ALONG THE AXES OF THE DIAGRAM TO DETERMINE THE CHROMIUM AND THE NICKEL EQUIVALENT. WHEN THESE WERE PLOTTED AS POINT X, THE CONSTITUTION OF THE WELD WAS INDICATED AS AUSTENITE PLUS FROM 0 TO 5% FERRITE; MAGNETIC ANALYSIS OF THE ACTUAL SAMPLE REVEALED AN AVERAGE FERRITE CONTENT OF 2%. FOR AUSTENITE-PLUS-FERRITE (A+F) STRUCTURES, THE DIAGRAM PREDICTS THE PERCENTAGE OF FERRITE WITHIN 4% FOR THE FOLLOWING STAINLESS STEELS: 308, 309, 309 CB, 310, 312, 316, 317, 318 (316 CB), AND 347. SOURCE: REF 26

As an example of the use of the Schaeffler diagram, suppose a type 304L clad surface is specified (shown as a triangle in Fig. 23). A desirable composition is approximately 20% Cr equivalent and 11% Ni equivalent. If an ASTM A 387A plate (point 100 on the diagram) is specified, all combinations of weld deposit lie on a line connecting point 100 with a proposed filler metal. As an example, note the line connecting point 100 with type 310 stainless steel. The diagram shows that weld-deposit compositions with up to 53% dilution (53% of the length of the line connecting the base metal and the filler metal) will be fully austenitic. Although sufficient alloy might be present, at least for a first layer, the absence of ferrite may make the deposit sensitive to fissuring. The same procedure can be used to estimate the usefulness of other filler metals.

Good metallurgical practice dictates that the first layer contain no martensite, shown as M in the diagram. This limits the dilution. If a process can be found that has less than 14% dilution, then a type 308L could be deposited with absence of martensite. On the other hand, if a first layer is made using type 312 stainless, any dilution factor less than 40% prevents the formation of martensite. Choosing a filler metal for the first layer that falls in the A + F region with 3 to 15% ferrite and no martensite meets the metallurgical requirements of a sound deposit. Proper composition and thickness may be achieved in a single layer, but more often a second layer is required.

Special consideration must be given to carbon levels for the austenitic stainless steels. Figure 24 predicts the carbon in the deposit once the base metal carbon and cladding process dilution factors have been established. To illustrate its use, suppose a base metal plate with 0.20% C and a welding process that results in 30% dilution are established. The diagram indicates that the deposit chemistry will contain approximately 0.07% C. If the specification requires 0.04% C maximum, a second layer would be required to achieve the necessary carbon level. Using the same diagram with the first layer

composition of 0.07% C, and assuming the same dilution factor, the diagram predicts that a second layer will contain approximately 0.03% C. This would meet the specification of 0.04% C maximum.

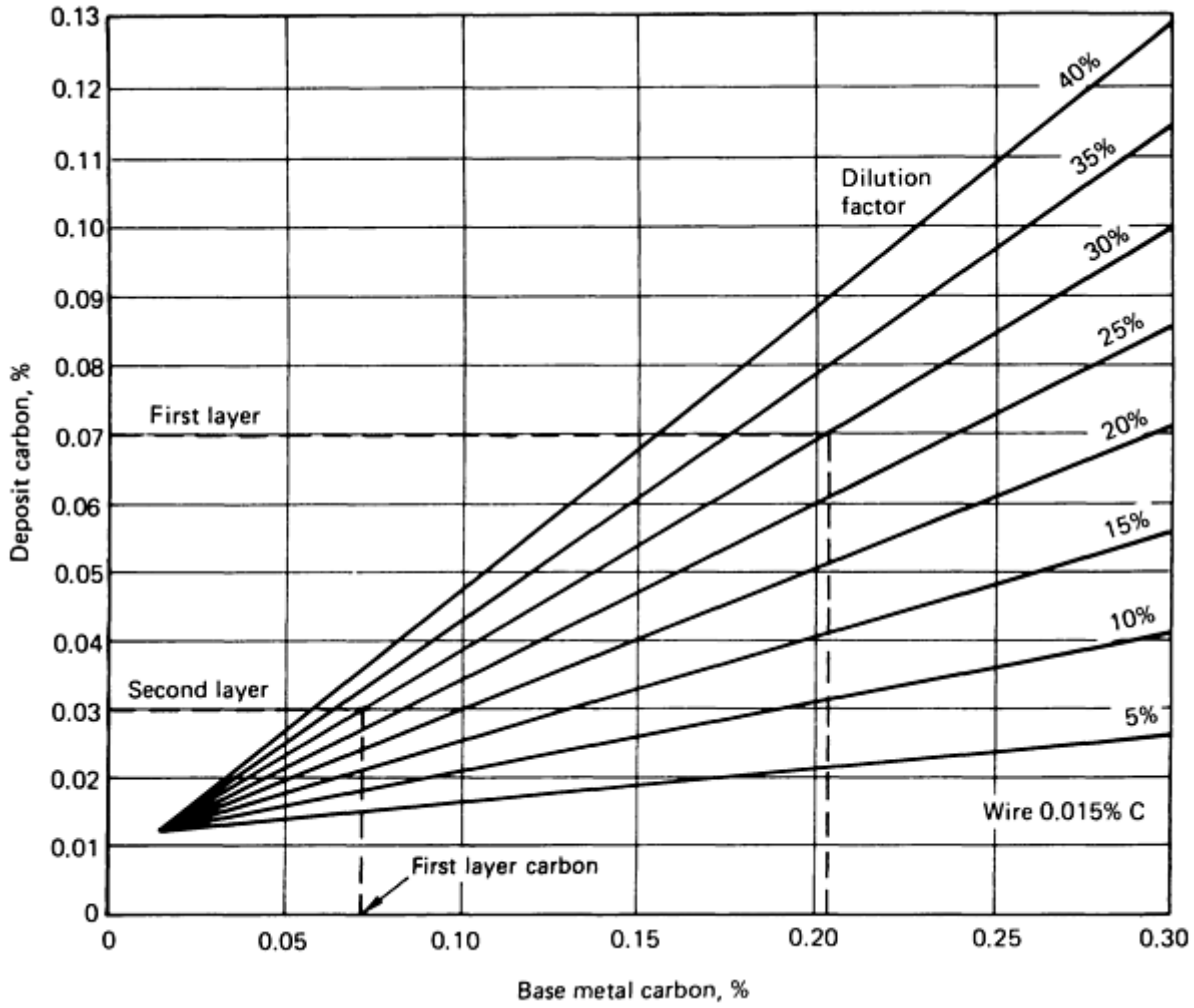

FIG. 24 PERCENTAGE OF CARBON IN THE DEPOSIT AFTER BASE METAL CARBON AND CLADDING DILUTION FACTORS HAVE BEEN ESTABLISHED. SOURCE: REF 26

Several problems have been identified when using the Schaeffler diagram for predicting the physical and mechanical properties of a weld. The Schaeffler diagram does not consider the effect of nitrogen in promoting austenite at the expense of ferrite, and it is incorrect in its treatment of manganese. Manganese does not promote the high-temperature formation of austenite at the expense of ferrite, as predicted by the diagram, although manganese does stabilize austenite in its low-temperature transformation to martensite. Also, the Schaeffler diagram makes its predictions in terms of percent ferrite. This has been found to be imprecise, and the magnetically based Ferrite Number (FN) unit was developed for the specification and determination of ferrite content. The basis for the FN scale is described in the American Welding Society standard AWS 4.2, "Standard Procedures for Calibrating Magnetic Instruments to Measure the Delta Ferrite Content of Austenitic and Duplex Austenitic Ferritic Steel."

The DeLong Diagram. A second widely used prediction diagram, the DeLong diagram (Fig. 25) was published in 1974 and incorporated some improvements (Ref 29). It has an FN scale and includes a coefficient for nitrogen in the Ni_{eq}, though the range of compositions is more limited than for the Schaeffler diagram.

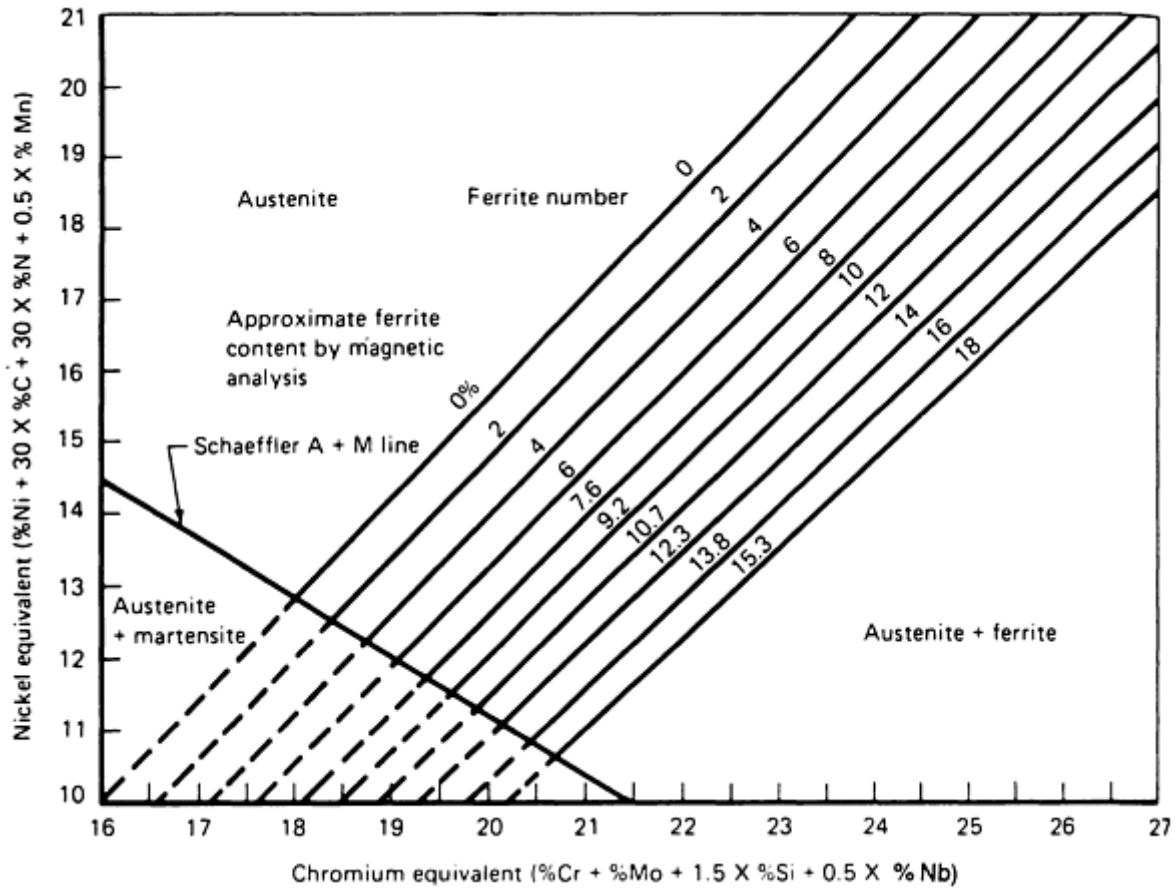

FIG. 25 THE DELONG CONSTITUTION DIAGRAM, REVISED JANUARY 1973 TO CONVERT IT TO THE WELDING RESEARCH COUNCIL'S FERRITE NUMBER (FN) SYSTEM FOR WELD METALS

The difference in the applicability of the Schaeffler and DeLong diagrams is substantial (Ref 30). The DeLong diagram is a finely tuned subset of the Schaeffler range, designed specifically for the 300-series stainless steel welds containing small amounts of ferrite. Its widely accepted use with these alloys is documented by its inclusion in the AWS filler metal specifications A5.4 and A5.9 and in the American Society of Mechanical Engineers (ASME) Boiler and Pressure Vessel Code. Prediction of FN for compositions that fall outside the range of the DeLong diagram (for example, duplex stainless steels) is the most quantitative use of the Schaeffler diagram; however, its extension to fully ferritic compositions and the inclusion of martensitic regions provides much qualitative information about the general effect of alloying elements and characteristic mechanical properties of alloy families.

In effect, the DeLong diagram traded improved prediction accuracy for a more limited composition range, but a range that included all the common austenitic stainless steel weld metals. However, it has been found to incorrectly handle manganese (as does the Schaeffler diagram) and to overestimate the FN of more highly alloyed compositions, such as type 309 (Ref 30). It also has had limited application to dissimilar metal joints.

The WRC-1988 diagram (Fig. 26) overcomes many of the problems associated with the Schaeffler and DeLong diagrams (Ref 30). It was developed with data measured by the most recent definition of the FN scale. It removed the erroneous manganese coefficient from the Ni_{eq}, and it eliminated the systematic overestimation of FN for highly alloyed weld metals. While it covers a much broader range of compositions than does the DeLong diagram, it has a narrower composition range than the Schaeffler diagram, because it extends only over the composition range of the commercial alloys with which it was developed.

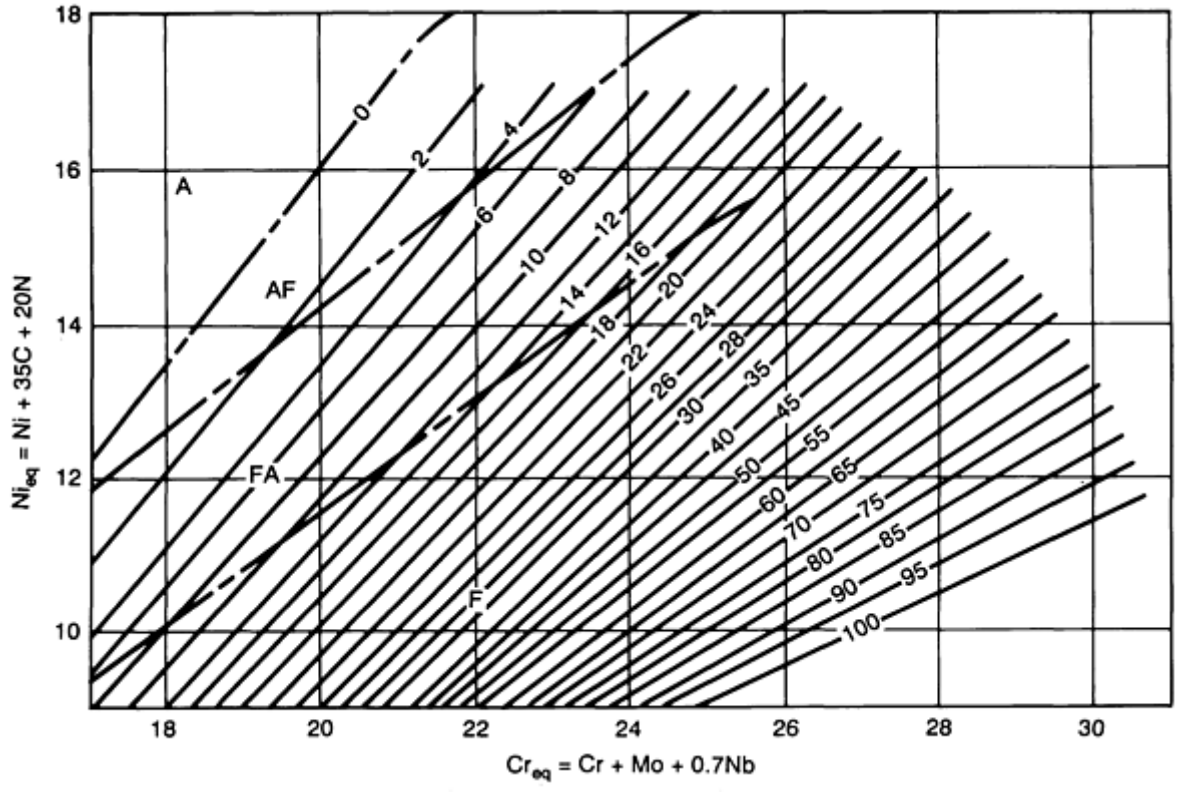

FIG. 26 THE WRC-1988 DIAGRAM, INCLUDING SOLIDIFICATION-MODE BOUNDARIES. SOURCE: REF 30

In the interval since the WRC-1988 diagram first appeared, it has been subjected to considerable evaluation and review. Independent data from more than 200 weld metals have confirmed the improved prediction accuracy of the WRC-1988 over that of its predecessors (Ref 31). The WRC-1988 diagram predicts the ferrite content of the conventional 300-series stainless steels with a higher degree of accuracy than the DeLong diagram, is more accurate than the Schaeffler diagram for predicting the ferrite content of duplex stainless steels, and is suitable for new alloys containing extended compositional ranges. It also includes primary solidification-mode data to reveal relationships to the FN response. Recent studies have emphasized that the solidification mode is more accurate than the FN for predicting the resistance to hot cracking (Ref 30). These studies indicate that the initial solidification structure (primary austenite or ferrite) directly determines the sensitivity to cracking by controlling the solubility of elements that promote cracking at these temperatures.

The WRC-1992 Diagram. In recent years, duplex ferritic-austenitic stainless steels have been used more frequently. Some of these steels and their welds contain significant amounts of copper (often about 2 wt%). While these compositions might be plotted on the WRC-1988 diagram, greater accuracy can be obtained with the modified WRC-1992 diagram (Ref 32). Whereas the Schaeffler diagram offers predictions for Cr_{eq} from 0 to 40 and Ni_{eq} from 0 to 32, the WRC-1992 diagram is more limited, considering Cr_{eq} from 17 to 31 and Ni_{eq} from 9 to 18 (Fig. 27). As indicated in the following example, the WRC-1992 diagram is useful for predicting the FN for dissimilar metal joints.

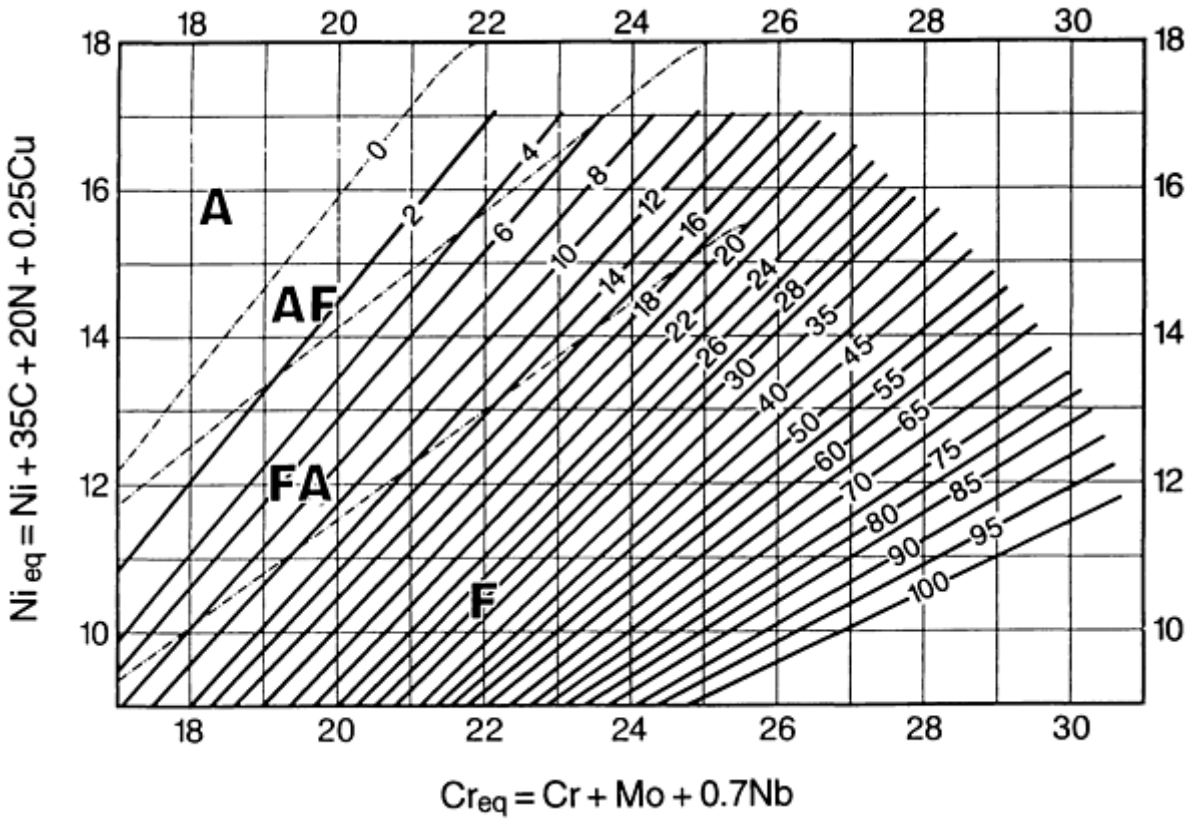

FIG. 27 THE WRC-1992 DIAGRAM. SOURCE: REF 32

Example 1: Weld Cladding of AISl 1050 Steel with AWS A5.4 Class E312-16 Electrode

(Ref 32). Table 16 lists typical plate composition and all-weld-metal composition produced with this electrode. The Cr_{eq} and Ni_{eq} for the AISI 1050 steel (0.0 and 17.50, respectively) do not permit an FN calculation for this material. The Cr_{eq} and Ni_{eq} for the E312-16 electrode all-weld-metal composition (29.0 and 11.9, respectively) result in a predicted 88.2 FN for this material. If the Cr_{eq} and Ni_{eq} for each composition is plotted in Fig. 28 and a line drawn between the point corresponding to the AISI 1050 composition (Point A in Fig. 28) and the point corresponding to the E312-16 composition (Point B in Fig. 28), then all possible mixtures of these two materials must lie along this line.

TABLE 16 BASE METAL AND WELD METAL COMPOSITIONS PRODUCED WHEN AISI 1050 CARBON STEEL WAS WELD CLAD USING E312-16 STAINLESS STEEL FILLER METAL

See Example 1 in text.

MATERIAL	AISI 1050	E312-16 ALL-WELD-METAL	30% DILUTION CLADDING
C, %	0.50	0.060	0.192
MN, %	0.30	1.20	0.93
SI, %	0.02	0.60	0.43
CR, %	. . .	29.00	20.30
NI, %	. . .	8.60	6.02
N, %	0.004	0.06	0.043
CR_{EQ}	0.00	29.00	20.30
NI_{EQ}	17.58	11.90	13.60
WRC-1988 FN	. . .	88.2	4.6

Source: Ref 32

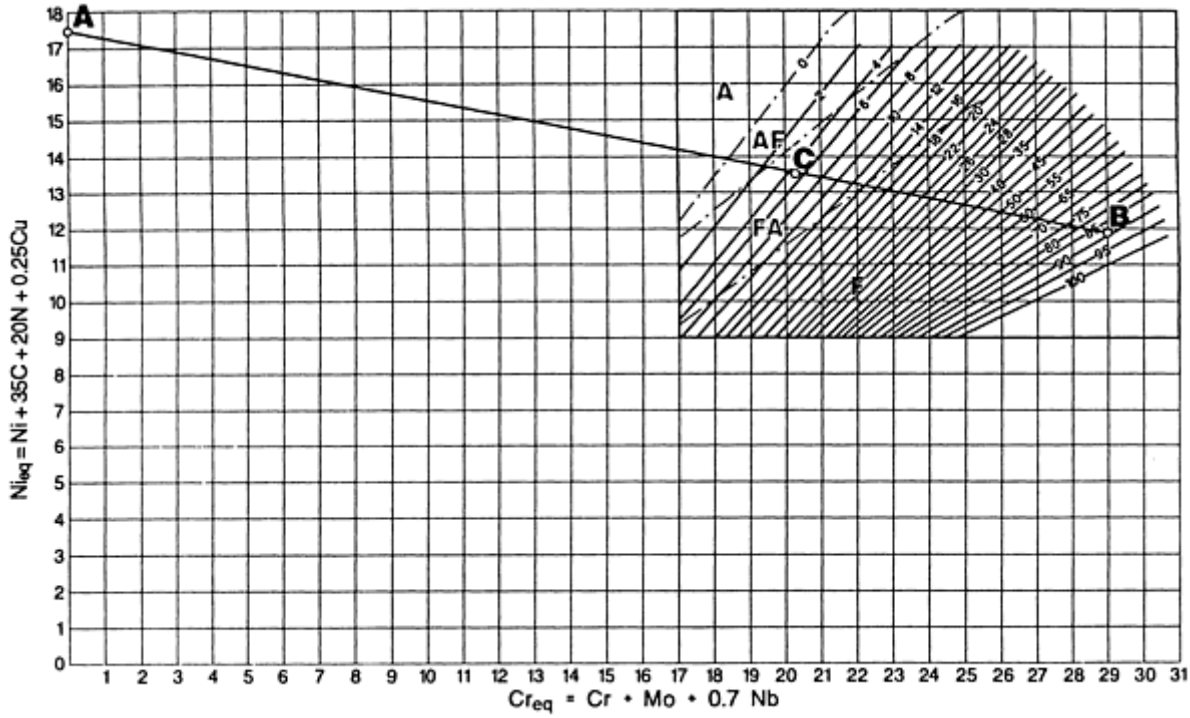

FIG. 28 DILUTION CALCULATION IN EXAMPLE 1 USING THE WRC-1992 DIAGRAM. SOURCE: REF 32

The lever rule is then used to estimate the position of the weld metal. In SMAW, typical dilution is 30%. A weld pass of E312-16 with 30% dilution from AISI 1050 steel would lie at a Point C, located 30% of the distance from Point B to Point A in Fig. 28. Mathematically, this can be calculated as:

$$CR_{EQ}(C) = 0.7\ CR_{EQ}(B) + 0.3\ CR_{EQ}(A)$$
$$= 0.7(29.00) + 0.3(0.00) = 20.30 \quad \textbf{(EQ 3)}$$

$$NI_{EQ}(C) = 0.7\ NI_{EQ}(B) + 0.3\ NI_{EQ}(A)$$
$$= 0.7(11.90) + 0.3(17.58) = 13.60 \quad \textbf{(EQ 4)}$$

The Cr_{eq} and Ni_{eq} of Point C correspond to 4.6 FN, which indicates that the weld pass will have sufficient FN to avoid fissuring (Ref 30). Any additional passes overlapping part of this first pass will also lie along the line between Point B and Point A, but they will be closer to Point B than is Point C, so all subsequent passes will contain even more ferrite than the first pass and the weld cladding should be crack-free.

Control of dilution plays an important part in the economics of the weld cladding process. Although each process has an expected dilution factor, experimenting with the welding parameters can minimize dilution. A value between 10 and 15% is generally considered optimum. Less than 10% raises the question of bond integrity, and greater than 15% increases the cost of the filler metal. Unfortunately, most welding processes have considerably greater dilution.

Because of the importance of dilution in weld cladding as well as hardfacing applications, each welding parameter must be carefully evaluated and recorded. Many of the parameters that affect dilution in weld cladding applications are not so closely controlled when arc welding a joint. These parameters include:

- *AMPERAGE:* INCREASED AMPERAGE (CURRENT DENSITY) INCREASES DILUTION. THE ARC BECOMES HOTTER, IT PENETRATES MORE DEEPLY, AND MORE BASE METAL MELTING OCCURS.
- *POLARITY:* DIRECT CURRENT ELECTRODE NEGATIVE (DCEN) GIVES LESS PENETRATION AND RESULTING LOWER DILUTION THAN DIRECT CURRENT ELECTRODE POSITIVE

(DCEP). ALTERNATING CURRENT RESULTS IN A DILUTION THAT LIES BETWEEN DCEN AND DCEP.

- *ELECTRODE SIZE:* THE SMALLER THE ELECTRODE, THE LOWER THE AMPERAGE, WHICH RESULTS IN LESS DILUTION.
- *ELECTRODE EXTENSION:* A LONG ELECTRODE EXTENSION FOR CONSUMABLE ELECTRODE PROCESSES DECREASES DILUTION. A SHORT ELECTRODE EXTENSION INCREASES DILUTION.
- *TRAVEL SPEED:* A DECREASE IN TRAVEL SPEED DECREASES THE AMOUNT OF BASE METAL MELTED AND INCREASES PROPORTIONALLY THE AMOUNT OF FILLER METAL MELTED, THUS DECREASING DILUTION.
- *OSCILLATION:* GREATER WIDTH OF ELECTRODE OSCILLATION REDUCES DILUTION. THE FREQUENCY OF OSCILLATION ALSO AFFECTS DILUTION--THE HIGHER THE FREQUENCY OF OSCILLATION, THE LOWER THE DILUTION.
- *WELDING POSITION:* DEPENDING ON THE WELDING POSITION OR WORK INCLINATION, GRAVITY CAUSES THE WELD POOL TO RUN AHEAD OF, REMAIN UNDER, OR RUN BEHIND THE ARC. IF THE WELD POOL STAYS AHEAD OF OR UNDER THE ARC, LESS BASE METAL PENETRATION AND RESULTING DILUTION WILL OCCUR. IF THE POOL IS TOO FAR AHEAD OF THE ARC, THERE WILL BE INSUFFICIENT MELTING OF THE SURFACE OF THE BASE METAL, AND COALESCENCE WILL NOT OCCUR.
- *ARC SHIELDING:* THE SHIELDING MEDIUM, GAS OR FLUX, ALSO AFFECTS DILUTION. THE FOLLOWING LIST RANKS VARIOUS SHIELDING MEDIUMS IN ORDER OF DECREASING DILUTION: GRANULAR FLUX WITHOUT ALLOY ADDITION (HIGHEST), HELIUM, CARBON DIOXIDE, ARGON, SELF-SHIELDED FCAW, AND GRANULAR FLUX WITH ALLOY ADDITION (LOWEST).
- *ADDITIONAL FILLER METAL:* EXTRA METAL (NOT INCLUDING THE ELECTRODE), ADDED TO THE WELD POOL AS POWDER, WIRE, STRIP, OR WITH FLUX, REDUCES DILUTION BY INCREASING THE TOTAL AMOUNT OF FILLER METAL AND REDUCING THE AMOUNT OF BASE METAL THAT IS MELTED.

Procedures for Stainless Steel Weld Cladding (Ref 26)

Submerged arc welding is by far the most commonly used process for weld cladding. The process is adaptable for use with single wires as the electrode filler metal, multiple wires, or strip. Alternating current is often used, but direct current, with either reverse or straight polarity, has been found preferable in numerous instances. Oscillation of the filler metal is frequently found desirable. Typical welding parameters for stainless steel weld cladding by SAW are given in Table 17.

TABLE 17 TYPICAL WELDING PARAMETERS FOR STAINLESS STEEL WELD CLADDING BY SAW

FORM OF ELECTRODE	SIZE OF ELECTRODE		POWER SOURCE	CURRENT, A	VOLTAGE, V	TRAVEL SPEED		OSCILLATION		PRODUCTIVITY		DILUTION[A], %
	mm	in.				mm/min	in./min	mm	in.	kg/h	lb/h	
SINGLE WIRE	1.6	1/16	DCEN[B]	240	34	130	5	19	3/4	4	9	15-20
	2.4	3/32	DCEN[B]	350	42	150	6	32	1 1/4	9	20	15-20
	2.4	3/32	AC	350	30	280	11	NONE		5.0	11	20-25
	3.2	1/8	AC	450	32	280	11	NONE		5.4	12	20-25
	4.0	5/32	AC	500	34	280	11	NONE		5.9	13	20-25
SERIES ARC												
TWO WIRES	4.0	5/32	AC[B]	400	26	255	10	NONE		19	41	20-25
THREE WIRES	4.0	5/32	AC[B]	480	28	355	14	NONE		20	43	15-20
SIX WIRE												
FIRST WIRE	1.6	1/16	DCEP	255	27	130	5	16	5/8	28	83	15-20
OTHERS	1.6	1/16	DCEN	1125	30	130	5	16	5/8	28	83	15-20
STRIP	0.5 × 30	0.020 × 1.2	DCEP[B]	400	25	180	7	NONE		35	16	15-20
	0.5 × 61	0.020 × 2.4	DCEP[B]	700	27	180	7	NONE		15	32	15-20
	0.5 × 88	0.020 × 3.5	DCEP[B]	1250	27	130	5	NONE		27	60	15-20
	0.5 × 119	0.020 × 4.7	DCEP[B]	1550	27	130	5	NONE		35	78	15-20
	0.64 × 25	0.025 × 1	DCEP[B]	525	27	305	12	NONE		14	30	10-15
	0.64 ×	0.025 × 2	DCEP[B]	1050	27	305	12	NONE		27	60	10-15

	50										
	0.64 × 100	0.025 × 4	DCEP[B]	2100	27	305	12	NONE	54	120	10-15

(A) VARIATIONS IN CURRENT, VOLTAGE, AND TRAVEL SPEED AFFECT PERCENTAGE OF DILUTION.

(B) CONSTANT POTENTIAL

The single-wire process is largely used for overlaying limited areas or where it is necessary to limit the heat input. Wires from 1.6 to 4.8 mm (or $\frac{1}{16}$ to $\frac{3}{16}$ in.) diam are practical. The small-size wires are generally employed with oscillation to keep dilution low, to provide a wide (up to about 25 mm, or 1 in.) weld bead, and to give uniformly good tie-ins with the adjacent beads. Either alternating or direct current may be employed for single-wire overlays.

Productivity (deposition rate) is greatly increased by the use of multiple wires (Table 17). Two-wire series arc (each wire connected to the poles of an alternating current power source) is a frequently used method for producing type 347 stainless steel weld cladding of petrochemical pressure vessels. The wire size is usually either 3.2 or 4.0 mm ($\frac{1}{8}$ or $\frac{5}{32}$ in.) in diameter. Alternating current is essential to achieve uniform fusion of both wires. The height of the welding head over the base metal greatly influences the penetration and hence the dilution. If the base metal has a non-uniform surface, or if the head cannot be accurately controlled above the base metal, the process may not be acceptable because of variations in dilution, or even lack of penetration in spots.

"Shingling" is a technique used to minimize dilution in single- or two-wire weld claddings. By providing an overlap of as much as 70% of a bead width, it is possible to reduce the dilution from 30 or 35% to 15 or 20%. In some applications, this allows the cladding to be deposited in a single layer at considerable cost savings as compared with two-layer overlays.

To further improve productivity, fabricators have increased the number of wires deposited by a single welding head. Up to six wires have been used with oscillation to deposit beads 150 mm (6 in.) or more in width. Usually, the wire sizes are 1.6 to 4.0 mm ($\frac{1}{16}$ to $\frac{5}{32}$ in.) in diameter. Direct current electrode negative has been found best for relatively low dilution (around 15%). Sometimes the wire that overlaps the previously deposited bead is connected to the positive tap of the power source (DCEP), which gives somewhat greater penetration and ensures good tie-in with the previous bead.

For weld cladding the inside surfaces of large pressure vessels, as shown in Fig. 29(a)and 29(b), wide beads produced by oscillated multiple-wire systems or strip electrodes have become the means to improve productivity and minimize dilution while offering a uniformly smooth surface. Welding parameters for stainless steel strip weld overlays are illustrated in Fig. 30, 31, 32. In Fig. 30, the effect of increased current on dilution, penetration, and bead thickness of a 60 mm (2.4 in.) strip is shown. Figure 31 illustrates the effect of travel speed on dilution, penetration, and bead dimensions using a 60 mm (2.4 in.) strip. Productivity of different strip sizes (deposition rate versus arc current) is shown in Fig. 32.

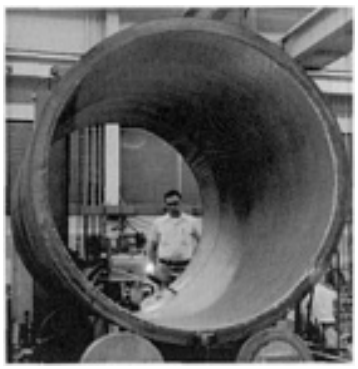

FIG. 29(A) WELD CLADDING OF A 1.8 M (6 FT) INNER DIAMETER PRESSURE VESSEL SHELL WITH 50 MM (2 IN.) WIDE, 0.64 MM (0.025 IN.) THICK STAINLESS STEEL STRIP. COURTESY OF J.J. BARGER, ABB COMBUSTION ENGINEERING

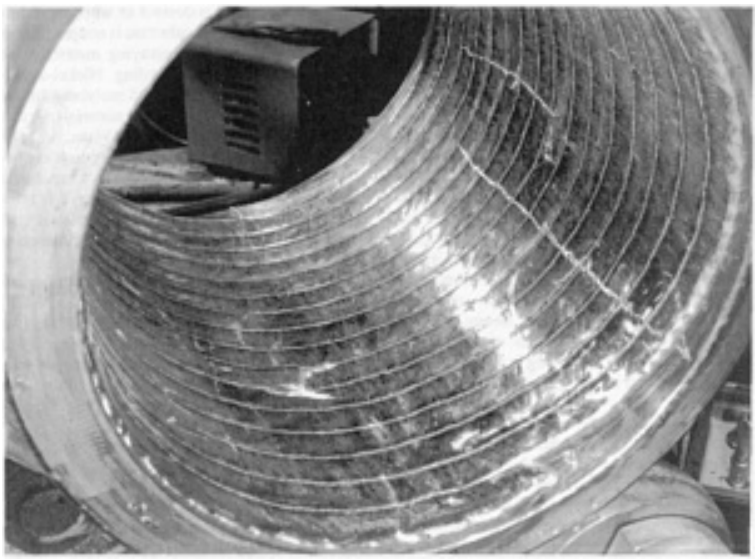

FIG. 29(B) CLOSEUP VIEW OF THE 25 MM (1 IN.) WIDE BY 0.64 MM (0.025 IN.) THICK STAINLESS STEEL STRIP USED TO CLAD A 300 MM (12 IN.) INNER DIAMETER PRESSURE VESSEL NOZZLE. COURTESY OF J.J. BARGER, ABB COMBUSTION ENGINEERING

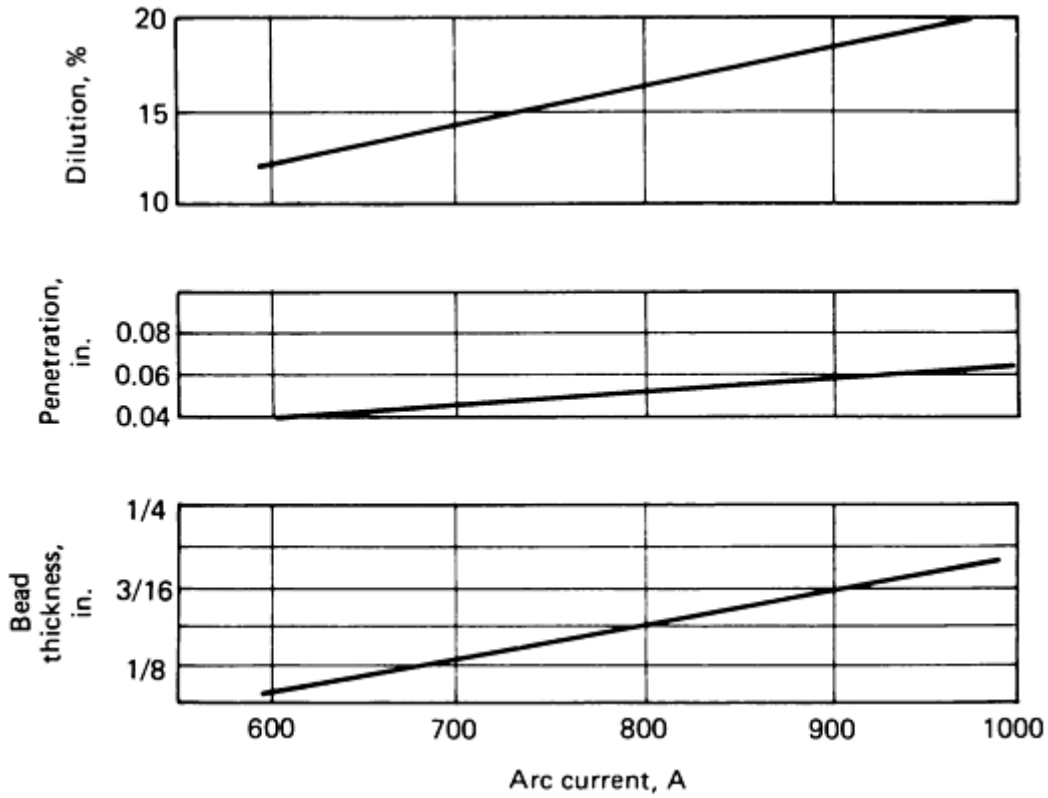

FIG. 30 DILUTION, PENETRATION, AND BEAD THICKNESS USING 60 MM (2.4 IN.) STRIP AT VARIOUS CURRENTS. SOURCE: REF 26

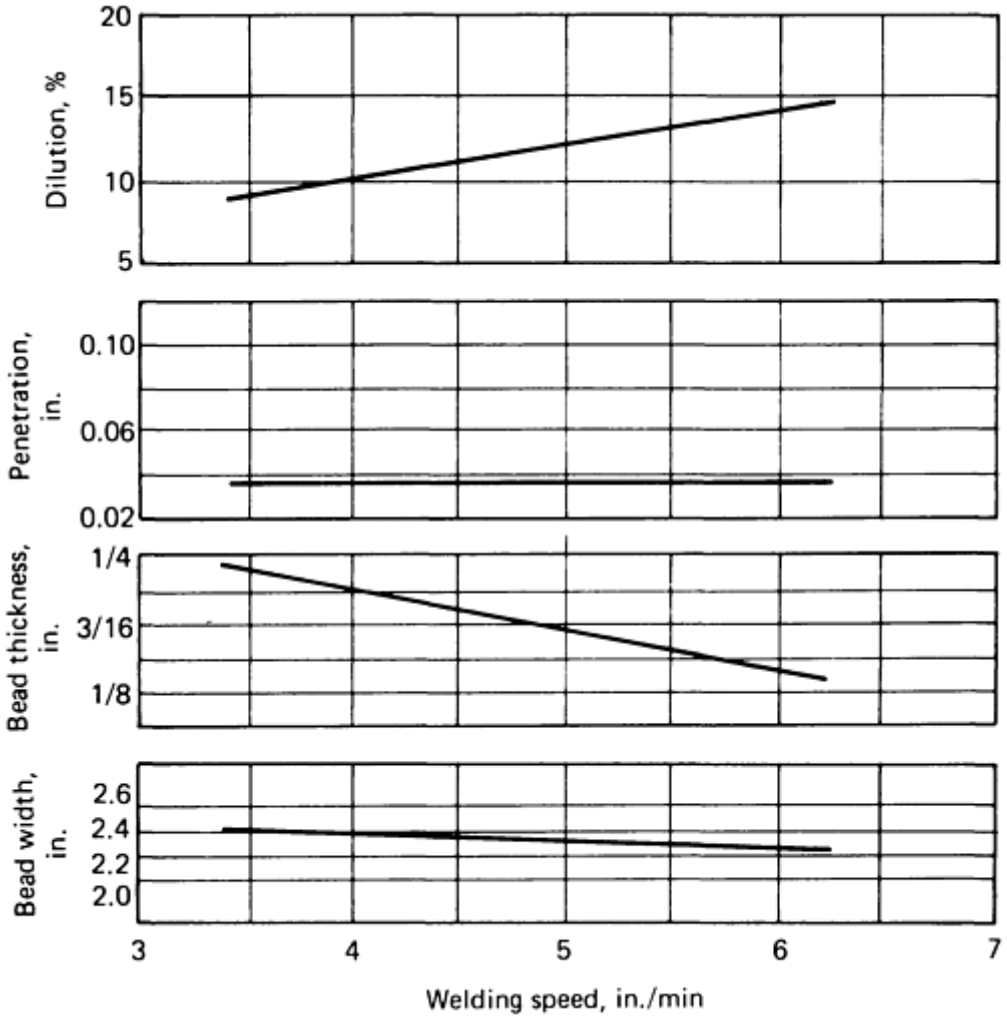

FIG. 31 INFLUENCE OF TRAVEL SPEED ON DILUTION, PENETRATION, AND BEAD THICKNESS USING 60 MM (2.4 IN.) STRIP. SOURCE: REF 26

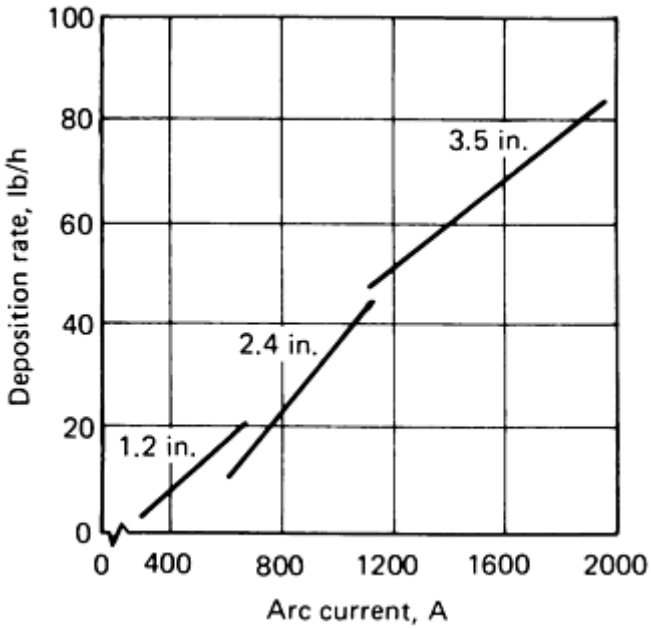

FIG. 32 DEPOSITION RATE (100% DUTY CYCLE) AS A FUNCTION OF CURRENT AND DIFFERENT STRIP SIZES. SOURCE: REF 26

The fluxes for submerged arc overlays should have low bulk density, especially for wide weld beads produced with multiple wire or strip electrodes. Standard fused fluxes, therefore, are usually unsuitable. Agglomerated fluxes, which have much lower bulk density, are commonly used for this purpose. Low-bulk-density fused fluxes have been successfully produced by a manufacturing process known as foaming. Such foamed fluxes have even lower bulk density than agglomerated fluxes.

Agglomerated fluxes (or bonded fluxes) have a distinct advantage over fused fluxes in that it is possible to introduce alloying elements by means of the flux. When this is done, they are known as reinforced, or alloyed, fluxes. For stainless steel weld claddings, chromium is commonly added to the fluxes to overcome the oxidation of chromium, which is characteristic of SAW of stainless alloys, and to compensate for the dilution with the non-chromium or low-chromium base metal. Other alloying elements often added to reinforced fluxes are manganese, nickel, molybdenum, and niobium. With reinforced fluxes, it is possible to produce various modified stainless weld overlays using a single filler metal as an electrode, for example, a type 347 overlay with a 308 or 309 filler metal using a niobium-alloyed flux. Table 18 lists variations in chemical compositions of series-arc weld deposits using an agglomerated flux and type 308 or 309 wire.

TABLE 18 CHEMICAL COMPOSITION VARIATIONS IN SERIES-ARC WELD CLADDING DEPOSITS USING AN AGGLOMERATED FLUX AND TYPE 308 OR 309 WIRE

WELDING CONDITIONS	WIRE SIZE		ANGLE BETWEEN WIRES, DEGREES	CURRENT (AC), A	VOLTAGE, V	TRAVEL SPEED	
	mm	in.				mm/min	in./min
TYPE 308 OVERLAY	4.0	5/32	45	500	20-25	255	10
TYPE 309 OVERLAY	4.0	5/32	45	540	26-30	330	13

CHEMICAL ANALYSIS	COMPOSITION, %						
	C	Mn	Si	S	P	Cr	Ni
308 FILLER WIRE	0.04	1.74	0.30	0.011	0.022	21.30	**9.83**
TOP OR THIRD LAYER	0.05	1.39	0.61	0.007	0.028	20.95	**9.57**
SECOND LAYER	0.06	1.36	0.63	0.010	0.029	20.29	**9.02**
FIRST LAYER	0.07	1.20	0.58	0.006	0.026	18.08	**8.16**
CARBON STEEL BASE	0.07	0.51	. . .	0.013	0.016	. . .	**. . .**
309 FILLER WIRE	0.05	1.81	0.32	0.016	0.022	24.68	**13.36**
TOP OR THIRD LAYER	0.06	1.49	0.93	0.005	0.043	24.43	**13.14**
SECOND LAYER	0.06	1.55	0.84	0.006	0.040	24.37	**11.08**
FIRST LAYER	0.07	1.36	0.84	0.008	0.039	21.79	**11.43**
CARBON STEEL BASE	**0.07**	**0.51**	**. . .**	**0.013**	**0.016**	**. . .**	**. . .**

Another method for providing the desired stainless steel cladding composition is to introduce a layer of powdered metal under the submerged arc flux. This procedure is sometimes known as bulk welding. It is suitable for use either with single-wire or strip electrodes. The powdered metal not only provides the alloying elements needed in the overlay, but it also greatly reduces the dilution. A schematic of the process is shown in Fig. 33.

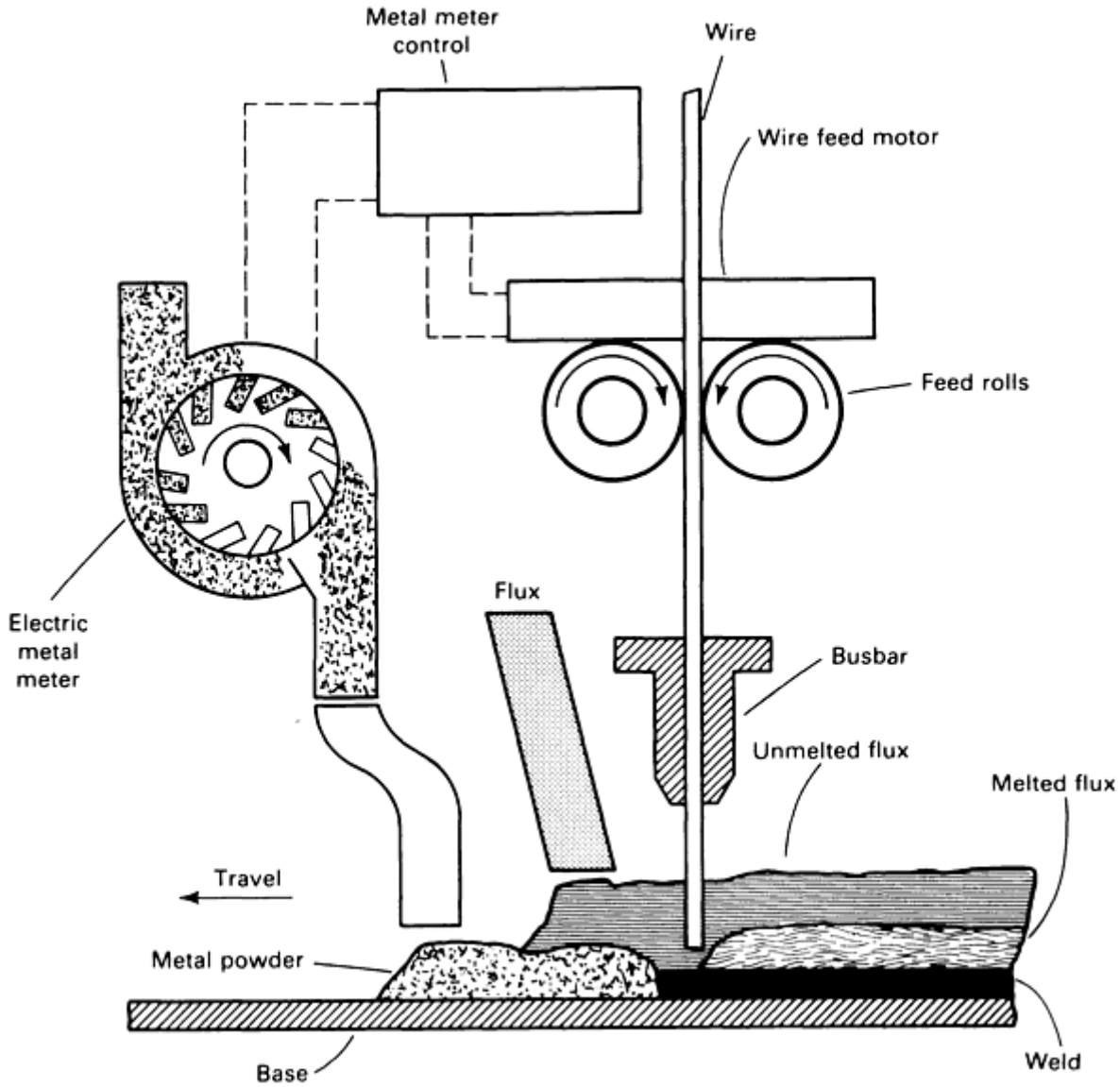

FIG. 33 SCHEMATIC OF THE BULKWELDING PROCESS USING METAL POWDER JOINT FILL. SOURCE: REF 9

Either method of adding alloying elements by using powdered alloys, either as an ingredient of the flux or separately underneath the flux, is subject to variability of the deposit composition. When reinforced fluxes are employed, the recovery of the alloying ingredient is dependent on the arc voltage, with a measurable difference in recovery by a change of as little as 1 or 2 V. This is not the case when the powdered alloys are separately fed below the flux, but in this case variability results if the height of the powder layer varies. Thus, it is unwise to rely on these methods of alloy adjustment of the weld overlay composition for more than three percentage points.

Still another method of providing the desired composition for the cladding is to use tubular wire for the filler metal. Whereas the solid wire producer is limited in the compositions that can be produced and still provide hot workability and cold drawing capability, the producer of tubular wire is virtually unlimited as to the compositions that can be produced. For example, the strip can be chromium or chromium-nickel steel, to which the core ingredients are added to give a weld deposit of austenitic stainless steel, rich enough in the essential alloys to compensate for both oxidation and dilution losses. Another distinct advantage of tubular wires is for relatively small production applications of compositions that are not available as "shelf items" in solid-wire form. Small quantities of tubular wires can also be prepared for experiments to determine the optimum composition for a particular application. The effective cross section of tubular wire for current-carrying ability is substantially less than solid wire of the same diameter. Welding parameters that have been established for solid wires will have to be adjusted to take this and other differences into account.

Self-Shielded Flux-Cored Wire. Tubular wires are produced that contain not only the alloying ingredients, but also the fluxing and gas-shielding ingredients. This permits the deposition of weld claddings without the need of an external flux, as is needed with SAW, or an external gas, as is needed with gas-shielded solid wire welding. Weld claddings are produced by manually directed welding guns for limited areas using a single tubular filler wire.

High productivity procedures have been developed using multiple wires in a manner similar to six-wire SAW. These wires have inherently low penetration characteristics, making them highly suitable for cladding. Deposition rates of 35 to 45 kg/h (80 to 100 lb/h) are often achieved. In addition, improved wire feed roll mechanisms have lessened the problems of kinking and crushing of these thin-wall electrodes during the wire-feeding process, thereby increasing the productivity of multiple-wire applications. Some fabricators who use self-shielded flux-cored wires prefer to limit the automatic cladding process to two or three wires, particularly because the gain in productivity with increasing numbers of wires diminishes. A three-wire welding head for overlay applications is shown in Fig. 34.

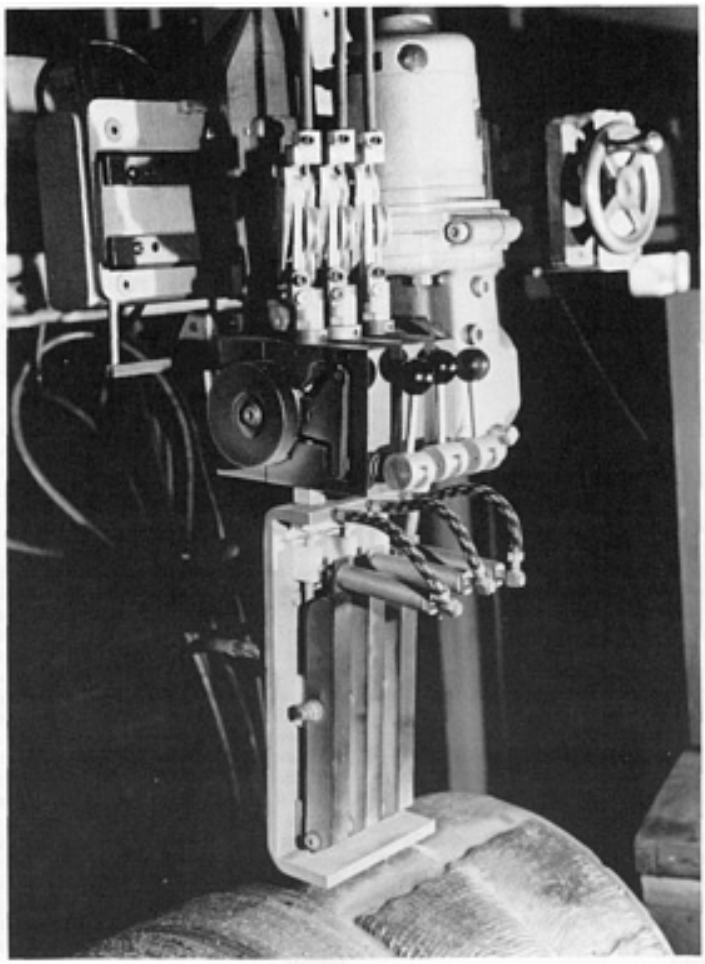

FIG. 34 THREE-WIRE WELDING HEAD FOR WELD CLADDING APPLICATIONS. COURTESY OF STOODY COMPANY

Metallurgically, flux-cored wires offer potentially higher alloyed claddings, permitting a considerable cost saving to produce the desired composition in a single layer. Also, dilution is minimized with this process. Furthermore, carbon content can be kept to much lower levels than is possible with solid wires, partly due to the ability to have very low-carbon ingredients in the flux-cored wire and partly due to the low dilution. Typical welding parameters for stainless steel weld cladding using self-shielded flux-cored wires are given in Table 19.

TABLE 19 TYPICAL WELDING PARAMETERS FOR STAINLESS STEEL WELD CLADDING USING SELF-SHIELDED FLUX-CORED WIRES

NO. OF 2.4 MM ($\frac{8}{32}$ IN.) DIAM WIRES	**CONSTANT POTENTIAL POWER SOURCE CAPACITY[(A)]**	**CURRENT, A**	**VOLTAGE, V**	**TRAVEL SPEED**		**OSCILLATION, CYCLES/MIN**	**PRODUCTIVITY**		DILUTION, %
				MM/MIN	**IN./MIN**		**KG/H**	**LB/H**	
1	400	300	27	510	20	NONE	5.4	12	**20**
2	800	600	27	115	4.5	20	14	30	**12**
3	1200	900	27	100	4.0	20	20	45	**12**
6	**1200 EACH (50 MM, OR 2 IN., PARALLEL)**	**1800**	**27**	**90**	**3.5**	**20**	**39**	**85**	**12**

(A) 100% DUTY CYCLE

The plasma arc hot wire process is used for depositing stainless steel claddings on pressure vessels subjected to corrosive, high-temperature, and high-pressure hydrogen environments. The setup for this process is illustrated in Fig. 35. Using this method, two filler-metal wires are fed at a constant speed through individual hot wire nozzles to intersect in the weld pool beneath the plasma arc. The filler metals are electrically connected in series and energized by an alternating current constant-potential power supply. Resistance heating occurs in each electrode between the wire contact tip and the weld pool. Input power is selected for a given filler-metal feed rate so that maximum resistance heating is induced into both electrodes without resulting in an open arc between them. While a single hot wire increases the deposition rate considerably over the cold wire or powder methods, a dual hot wire process permits deposition rates as high as 18 to 32 kg/h (40 to 70 lb/h), thus making the hot wire process commercially competitive with other weld cladding processes. A continuously made stainless steel weld overlay made by the hot wire process is shown in Fig. 36.

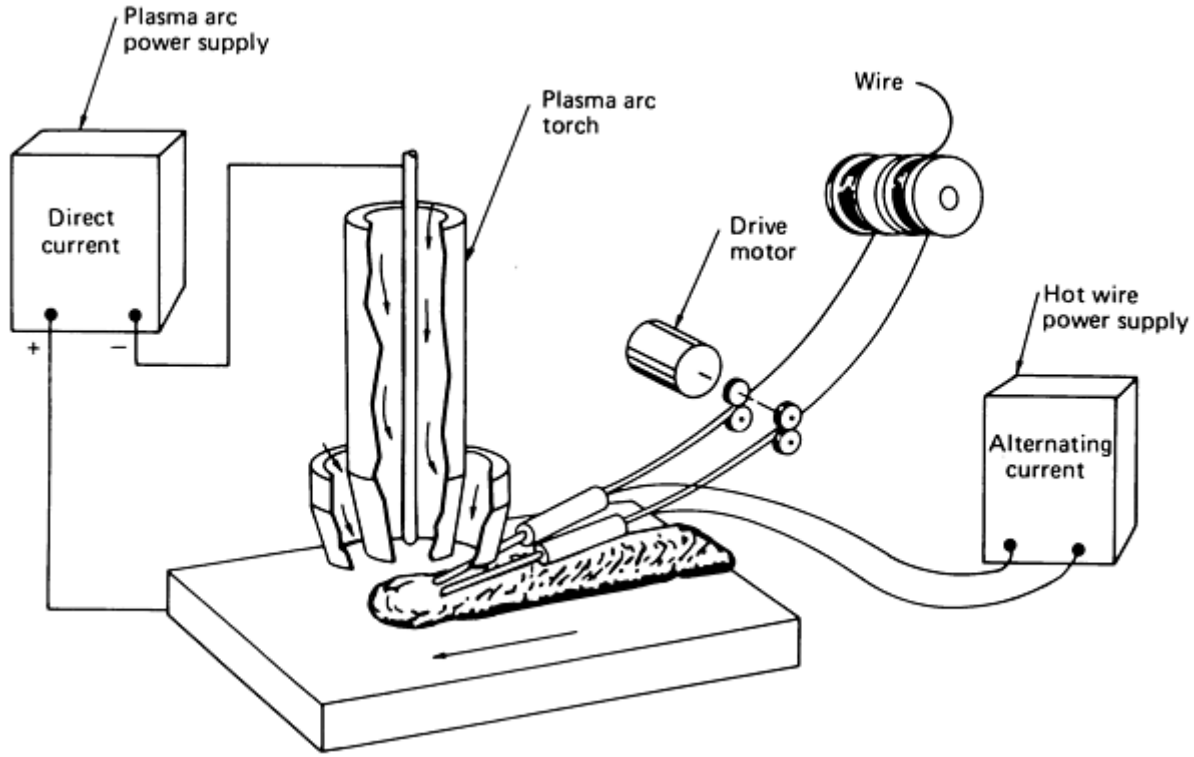

FIG. 35 SCHEMATIC OF THE PLASMA ARC HOT WIRE WELD CLADDING PROCESS. SOURCE: REF 1

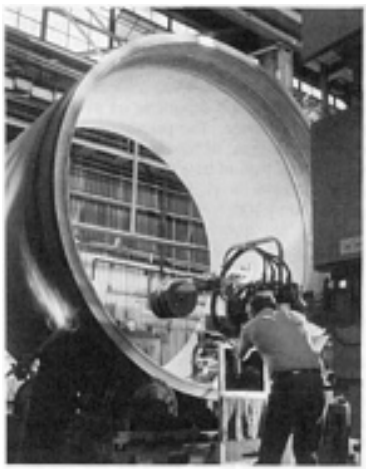

FIG. 36 PLASMA ARC HOT WIRE PROCESS FOR WELD CLADDING THE INTERNAL SURFACE OF A PRESSURE VESSEL SHELL. COURTESY OF NOOTER CORPORATION

Advantages of the hot wire process include:

- ACCURATE CONTROL OF DILUTION AND THUS COMPOSITION OF THE OVERLAY
- LITTLE OR NO CHANGES DUE TO OXIDATION OF THE ELEMENTS IN THE PROCESS
- PARAMETERS THAT CAN BE INDEPENDENTLY AND ACCURATELY CONTROLLED
- SINGLE-LAYER OVERLAYS THAT CAN BE PRODUCED IN THICKNESSES RANGING FROM 4.0 TO 8.0 MM ($\frac{5}{32}$ TO $\frac{5}{32}$ IN.)
- APPLICABILITY TO MANY CORROSION-RESISTANT ALLOYS, SUCH AS MONEL, INCONEL, AND HASTELLOY ALLOYS

Typical welding parameters for stainless steel weld cladding by the plasma arc process are given in Table 20.

TABLE 20 TYPICAL WELDING PARAMETERS FOR STAINLESS STEEL WELD CLADDING BY THE PLASMA ARC PROCESS

TORCH CONDITIONS				FILLER-WIRE CONDITIONS				TRAVEL SPEED		PRODUCTIVITY		DILUTION, %
CURRENT, A	VOLTAGE, V	GAS FLOW RATES		NO. OF WIRES	SIZE		CURRENT, A					
		$mm^3/h \times 10^6$	$in.^3/h$		mm	in.		mm/min	in./min	kg/h	lb/h	
440	38	1.4	85	2	1.6	$\frac{1}{16}$	160	205	8	18-23	40-50	**8-12**
480	38	1.4	85	2	1.6	$\frac{1}{16}$	180	230	9	23-27	50-60	**8-12**
500	39	1.4	85	2	1.6	$\frac{1}{16}$	200	230	9	27-32	60-70	**8-15**
500	**39**	**1.4**	**85**	**2**	**2.4**	$\frac{3}{32}$	**240**	**255**	**10**	**27-32**	**60-70**	**8-15**

Electroslag Overlays. The electroslag welding process has been adapted to produce stainless steel weld claddings. This process offers the ability to use wider strip (up to 300 mm, or 12 in.) than the submerged arc process and more uniform penetration into, and lower dilution with, the base metal. Its principal disadvantages are operator exposure to the radiant heat from the molten slag and a sharper compositional change at the fusion line, which may give unsatisfactory service in certain high-temperature pressure vessels (for example, disbonding in hydrocracker or hydrosulfurizer service).

For large heavy-wall pressure vessels, the electroslag overlay process typically uses strip 4.0 mm (0.16 in.) thick by 150 mm (6 in.) wide. The effect of electroslag welding parameters on dilution using a 150 mm (6 in.) strip is shown in Fig. 37. As in SAW, energy is created by ohmic resistance as the electric current flows from the strip to the work through the molten slag; no arc exists. Unlike SAW, however, the slag bath is relatively thin. To provide the required electrical resistance, viscosity, and other properties, the fluxes must be significantly higher in fluorides than for SAW (Ref 26). A typical fused flux composition comprises 49% CaF_2, 21% CaO, 21% SiO_2, and 9% Al_2O_3.

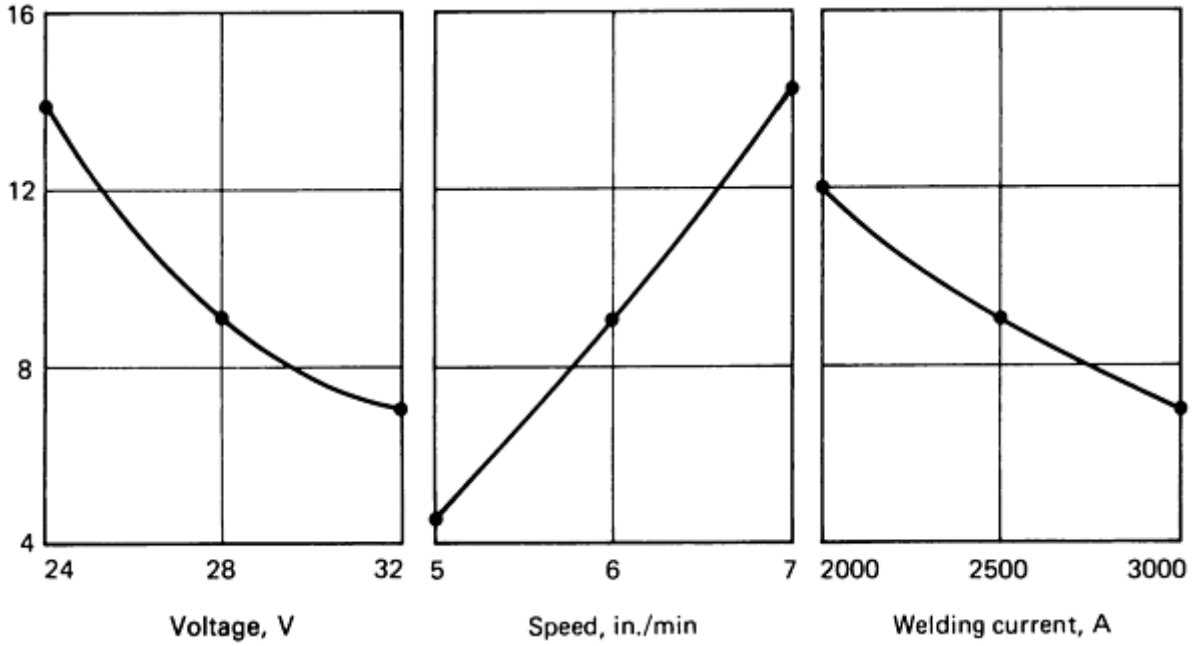

FIG. 37 EFFECT OF WELDING PARAMETERS ON DILUTION USING 150 MM (6 IN.) STRIP IN ELECTROSLAG WELD CLADDING PROCESS. SOURCE: REF 26

Because of disbonding of weld claddings deposited on pressure vessels in a hydrogen environment, electroslag weld claddings are not used for single-layer overlays; but where two-layer overlayers are specified, the electroslag process is used for the second layer. Higher productivity and a smoother surface are thus obtained, the first layer having been deposited by the SAW.

Extremely low carbon levels are possible because of low dilution with the base metal and a removal of carbon through oxidation in the process. Using a 0.18% C base metal and a 0.01% C strip, one investigator produced weld-metal carbon levels of 0.02% in the first layer and 0.01% in the second (Ref 26). The electroslag weld cladding process also can be applied for weld overlays of nickel-chromium (Inconel) alloys in the same manner as for stainless steel.

Weld Overlays Other Than Stainless Steel (Ref 26)

Many of the procedures described for stainless steel weld cladding are applicable to other alloys. Generally, nickel-base alloys can be produced successfully using essentially the same procedures as for stainless steels. Some of the common alloy filler metals used are given in Table 21. Figure 38 shows the use of both Inconel and stainless steel strip overlays used to clad a large pressure vessel shell.

TABLE 21 NONFERROUS FILLER METALS USED FOR WELD CLADDING OF STEELS

WELD OVERLAY TYPE	**COVERED ELECTRODE**		BARE ROD OR ELECTRODE	
	AWS SPECIFICATION NO.	**CLASSIFICATION NO.**	**AWS SPECIFICATION NO.**	CLASSIFICATION NO.
ALUMINUM-BRONZE	A5.6	ECUAL-A2	A5.7	**ERCUAL-AL**
SILICON-BRONZE	A5.6	ECUSI	A5.7	**ERCUSI**
COPPER-NICKEL	A5.6	ECUNI[(A)]	A5.7	**ERCUNI[(A)]**
NICKEL	A5.11	ENI-1	A5.14	**ERNI-1**
MONEL	A5.11	ENICU-7	A5.14	**ENICU-7**
LNCONEL	A5.11	ENICRFE-3	A5.14	**ERNICR-3**
LNCONEL 625	A5.11	ENICRMO-3	A5.14	**ERNICRMO-3**
HASTELLOY B	A5.11	ENIMO-7	A5.14	**ERNIMO-7**

HASTELLOY C	**A5.11**	**ENICRMO-4**	**A5.14**	**ERNICRMO-4**

(A) FIRST LAYER MUST BE EITHER NICKEL OR MONEL.

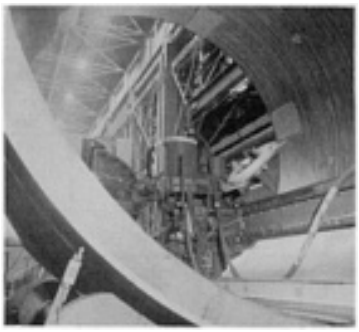

FIG. 38 WELD CLADDING OF A 1.8 M (6 FT) INNER DIAMETER PRESSURE VESSEL SHELL USING 100 MM (4 IN.) WIDE BY 0.64 MM (0.025 IN.) THICK STAINLESS STEEL STRIP. NOTE SMALL "WINDOWS" THAT HAVE BEEN CLAD WITH 50 MM (2 IN.) WIDE BY 0.64 MM (0.025 IN.) THICK INCONEL STRIP. COURTESY OF J.J. BARGER, COMBUSTION ENGINEERING

Metals and alloys that do not tolerate significant amounts of iron cannot be used in weld overlays on steels. Titanium, zirconium, magnesium, and aluminum are examples of incompatible metals for cladding steel. Pure copper is also unsatisfactory, but some copper alloys, such as aluminum-bronze and silicon-bronze, can be applied to steels. The incompatible metals are usually bonded by explosion cladding or roll bonding techniques, which are described elsewhere in this Volume.

References cited in this section

1. K.C. ANTONY *ET AL.*, HARDFACING, *WELDING, BRAZING, AND SOLDERING,* 9TH ED., VOL 6, *METALS HANDBOOK,* AMERICAN SOCIETY FOR METALS, 1983, P 771-793
9. K.M. KULKARNI AND V. ANAND, METAL POWDERS USED FOR HARDFACING, *POWDER METALLURGY,* 9TH ED., VOL 7, *ASM HANDBOOK,* AMERICAN SOCIETY FOR METALS, 1984, P 823-836
26. R.D. THOMAS *ET AL.*, WELD OVERLAYS, *WELDING, BRAZING, AND SOLDERING*, 9TH ED., VOL 6, *METALS HANDBOOK*, AMERICAN SOCIETY FOR METALS, 1983, P 804-819
27. D.L. OLSON, PREDICTION OF AUSTENITIC WELD METAL MICROSTRUCTURE AND PROPERTIES, *WELD. J.*, VOL 64 (NO. 10), 1985, P 2815-2955
28. A.L. SCHAEFFLER, CONSTITUTION DIAGRAM FOR STAINLESS STEEL WELD METAL, *MET. PROG.*, VOL 56 (NO. 11), 1949, P 680-680B
29. W.T. DELONG, FERRITE IN AUSTENITIC STAINLESS STEEL WELD METAL, *WELD. J.*, VOL 53 (NO. 7), 1974, P 2735-2865
30. T.A. SIEWERT, C.N. MCCOWAN, AND D.L. OLSON, FERRITE NUMBER PREDICTION TO 100 FN IN STAINLESS STEEL WELD METAL, *WELD. J.*, VOL 67 (NO. 12), 1988, P 2895-2985
31. D.J. KOTECKI, "VERIFICATION OF THE NBS-CSM FERRITE DIAGRAM," INTERNATIONAL INSTITUTE OF WELDING DOCUMENT II-C-834-88, 1988
32. D.J. KOTECKI AND T.A. SIEWERT, WRC-1992 CONSTITUTION DIAGRAM FOR STAINLESS STEEL WELD METALS: A MODIFICATION OF THE WRC-1988 DIAGRAM, *WELD. J.*, MAY 1992, P 171S-178S

Dissimilar Metal Joining

Because various portions of a process system operate at different service conditions, different structural alloys are used in the design, and hence, dissimilar-metal welded joints may be required. Many factors must be considered when welding dissimilar metals, and the development and qualification of adequate procedures for the various metals and sizes of interest for a specific application must be undertaken.

Most combinations of dissimilar metals can be joined by solid-state welding (diffusion welding, explosion welding, friction welding, or ultrasonic welding), brazing, or soldering where alloying between the metals is normally insignificant. In these cases, only the differences in the physical and mechanical properties of the base metals and their influence on the serviceability of the joint should be considered. When dissimilar metals are joined by fusion welding processes, alloying between the base metals and a filler metal, when used, becomes a major consideration. The resulting weld metal can behave much differently from one or both base metals during subsequent processing or in service.

In this section, the principal factors that are responsible for failure (cracking) of dissimilar metal arc welds are described. These include:

- GENERAL ALLOYING PROBLEMS (BRITTLE PHASE FORMATION AND LIMITED MUTUAL SOLUBILITY) OF THE TWO METALS
- WIDELY DIFFERING MELTING POINTS
- DIFFERENCES IN COEFFICIENTS OF THERMAL EXPANSION
- DIFFERENCES IN THERMAL CONDUCTIVITY

In addition, service considerations that can result in dissimilar-metal weld failure by carbon migration or by corrosion/oxidation are addressed. Lastly, a brief review of specific dissimilar metal combinations and filler metal selection guidelines are presented. Additional information on welding dissimilar metals can be found throughout this Volume and in Ref 33 and 34.

Factors Influencing Joint Integrity (Ref 33)

Weld Metal. In the fusion welding of dissimilar-metal joints, the most important consideration is the weld metal composition and its properties. Its composition depends upon the compositions of the base metals; the filler metal, if used; and the relative dilutions of these. The weld metal composition is usually not uniform, particularly with multipass welds, and a composition gradient is likely to exist in the weld metal adjacent to each base metal.

These solidification characteristics of the weld metal are also influenced by the relative dilutions and the composition gradients near each base metal. These characteristics are important with respect to hot cracking of the weld metal during solidification.

The basic concepts of alloying, the metallurgical characteristics of the resultant alloy, and its mechanical and physical properties must be considered when designing a dissimilar-metal joint. For the fusion welding processes it is important to investigate the phase diagram of the two metals involved. If there is mutual solubility of the two metals, the joint can usually be made successfully. If there is little or no solubility between the two metals to be joined, the weld joint will not be successful. The intermetallic compounds that are formed between the dissimilar metals must be investigated to determine their crack sensitivity, ductility, susceptibility to corrosion, and so on. The microstructure of this intermetallic compound is extremely important. In some cases, it is necessary to use a third metal that is soluble with each metal in order to produce a successful joint.

Dilution. In dissimilar-metal welding, the filler metal must alloy readily with the base metals to produce a weld metal that has a continuous, ductile matrix phase. Specifically, the filler metal must be able to accept dilution (alloying) by the base metals without producing a crack-sensitive microstructure (dilution was defined and described earlier in this article in the sections on "Hardfacing" and "Weld Cladding"). The weld metal microstructure must also be stable under the expected service conditions. A successful weld between dissimilar metals is one that is as strong as the weaker of the two metals being joined, that is, possessing sufficient tensile strength and ductility so that the joint will not fail.

In multipass welding, the composition of each weld bead should be relatively uniform. However, definite compositional differences are likely in succeeding weld beads, especially between a root bead, the beads adjacent to the base metals, and the remaining fill beads. The average composition of the whole weld metal can be calculated when: (1) the ratio of the volumes of base metals melted to the entire weld metal volume can be determined; and (2) the compositions of the base and filler metals are known. The dilution can be based on area measurements on a transverse cross section through a test weld. Figure 39 illustrates how to determine the dilution by two base metals, A and B, when welding with filler metal F.

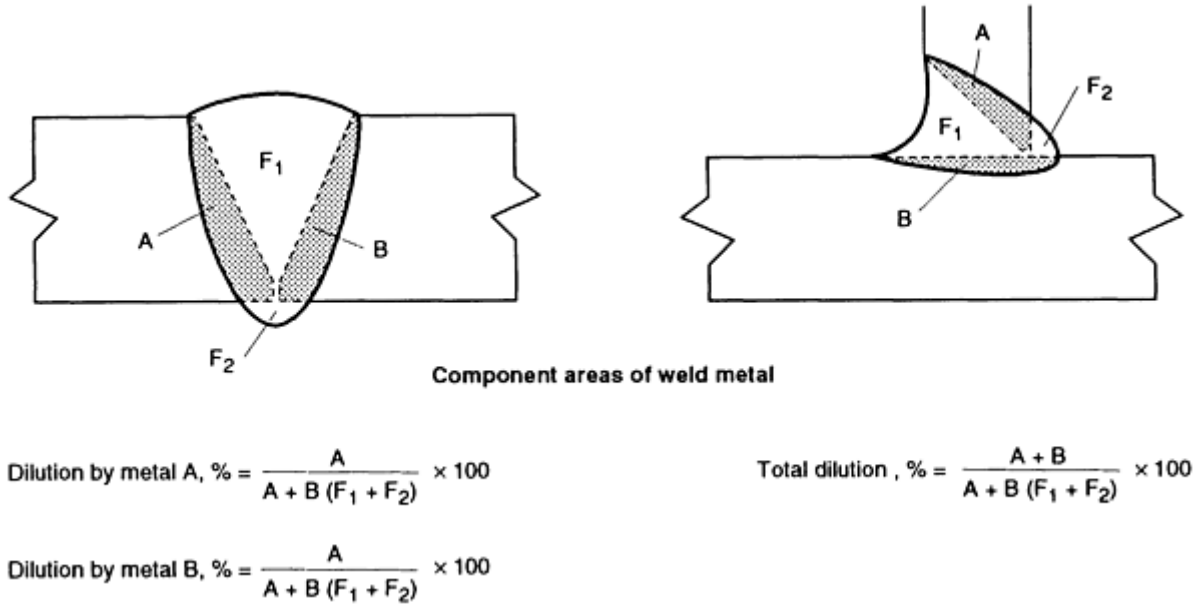

FIG. 39 DILUTION IN A DISSIMILAR-METAL WELDED JOINT. SOURCE: REF 33

The average percentage of a specific alloying element in the diluted weld metal can be calculated using the following equation developed by the American Welding Society (Ref 33):

$$X_W = (D_A)(X_A) + (D_B)(X_B) + (1 - D_T)(X_F) \quad \textbf{(EQ 5)}$$

where X_w is the average percentage of element X in the weld metal; X_A is the percentage of element X in base metal A; X_B is the percentage of element X in base metal B; X_F is the percentage of element X in the filler metal F; D_A is the percent dilution by base metal A, expressed as a decimal; D_B is the percent dilution by base metal B, expressed as a decimal; and D_T is the percent total dilution by base metals A and B, expressed as a decimal.

To illustrate the calculation of weld metal composition, assume that type 316 stainless steel is welded to a 2.25Cr-1Mo (UNS K21590) low-alloy ferritic pressure vessel steel with a nickel-chromium alloy filler metal ERNiCr3. The nominal chemical compositions of the three alloys are:

ALLOY	COMPOSITION, WT%			
	CR	**NI**	**MO**	FE
2.25CR-1MO	2.5	. . .	1.0	**95.5**
TYPE 316	17.0	12.0	2.5	**63.0**
ERNICR-3	**20.0**	**72.0**	**. . .**	**3.0**

Assuming that the total dilution is 35%, 15% by the Cr-Mo alloy steel and 20% from the type 316 stainless steel, the average percentages of Cr, Ni, and Mo in the weld metal are calculated as follows:

$$CR, \% = 0.15(2.5) + 0.20(17) + 0.65(20) = 16.8 \quad \textbf{(EQ 6)}$$

$$NI, \% = 0.20(12) + 0.65(72) = 49.2 \quad \textbf{(EQ 7)}$$

$$MO, \% = 0.15(1) + 0.20(2.5) = 0.65 \quad \textbf{(EQ 8)}$$

Melting Temperatures. The difference in melting temperatures of the two metals that are to be joined must also be considered. This is of primary interest when a fusion welding process utilizing considerable heat is involved, since one metal may be molten long before the other when subjected to the same heat source. Significant difference between the melting temperatures of the two base metals or between those of the weld metal and a base metal can result in rupture of the metal having the lower melting temperature. Solidification and contraction of the metal with the higher melting temperature will induce stresses in the other metal while it is in a weak, partially solidified condition. This problem may be solved by depositing one or more layers of a filler metal of intermediate melting temperature on the face of the base metal with the higher melting temperature. This procedure is known as buttering. The weld is then made between the buttered face and the other base metal. The buttering layer should serve to reduce the melting temperature differential. Buttering may also be used to provide a transition between materials with substantially different coefficients of thermal expansion but which must endure cycling temperatures in service. Similarly, buttering may be used to provide a barrier layer that will slow the migration of undesirable elements from the base metal to the weld metal during postweld heat treatment or in service at elevated temperatures.

Thermal Conductivity. Most metals and alloys are relatively good conductors of heat, but some are much better than others. Rapid conduction of heat from the molten weld pool by an adjacent base metal may affect the energy input required to locally melt the base metal. When two dissimilar metals of significantly different thermal conductivities are welded together (for example, plain carbon steels and copper-base alloys), the welding procedure must provide for this difference. Often the welding heat source must be directed at the metal having the higher thermal conductivity to obtain the proper heat balance.

When welding dissimilar metals, heat loss to the base metals can be balanced somewhat by selectively preheating the metal having the higher thermal conductivity. Dilution is more uniform with balanced heating.

Preheating the base metal of higher thermal conductivity also reduces the cooling rate of the weld metal and the HAZ. The net effect of preheating is to reduce the heat needed to melt that base metal.

The coefficient of thermal expansion of the two dissimilar base metals is another important factor. Large differences in thermal expansion coefficients of adjacent metals during cooling will induce tensile stress in one metal and compressive stress in the other. The metal subject to tensile stress may hot crack during welding, or it may cold crack in service unless the stresses are relieved thermally or mechanically. This factor is particularly important in joints that will operate at elevated temperatures in a cyclic temperature mode. A common example of this is austenitic stainless steel/ferritic steel pipe butt joints used in energy conversion plants.

Ideally, the thermal expansion coefficient of the weld metal should be intermediate between those of the base metals, especially if the difference between those of the two base metals is large. If the difference is small, the weld metal may have an expansion coefficient equivalent to that of one of the base metals.

Welding Considerations (Ref 33)

Welding Process. The three most popular arc welding processes utilized for joining dissimilar metals are SMAW, GMAW, and GTAW. Selecting the welding process to make a given dissimilar-metal joint is almost as important as selecting the proper filler metal. As described in the articles in this Volume that cover the various fusion welding processes, the depth of fusion into the base metals and the resulting dilution may vary with different welding processes and techniques.

It is not uncommon with SMAW for the filler metal to be diluted up to 30% with base metal. The amount of dilution can be modified somewhat by adjusting the welding technique. For example, the electrode can be manipulated so that the arc impinges primarily on the previously deposited weld metal. The dilution rate can be kept below 25% with this technique. If dilution from one base metal is less detrimental than from the other, the arc should be directed toward that metal. This

technique is also applicable to GTAW. Other means to control dilution are described in the section on "Weld Cladding" in this article.

Dilution rates with GMAW can range from 10 to 50%, depending upon the type of metal transfer and the welding gun manipulation. Spray transfer gives the greatest dilution; short-circuiting transfer, the least dilution. Penetration with SAW can be greater, depending on polarity, and can result in more dilution.

Regardless of the process, dilution is also affected by other factors, including joint design and fit-up. It is always best to have a minimum uniform dilution along the joint. Variations in dilution may produce inconsistent joint properties.

Selection of a suitable filler metal is an important factor in producing a dissimilar-metal joint that will perform well in service. One objective of dissimilar-metal welding is to minimize undesirable metallurgical interactions between the metals. The filler metal should be compatible with both base metals and be capable of being deposited with a minimum of dilution.

Two important criteria that should govern the selection of a proper filler metal for welding two dissimilar metals are as follows:

- THE CANDIDATE FILLER METAL MUST PROVIDE THE JOINT DESIGN REQUIREMENTS, SUCH AS MECHANICAL PROPERTIES OR CORROSION RESISTANCE.
- THE CANDIDATE FILLER METAL MUST FULFILL THE WELDABILITY CRITERIA WITH RESPECT TO DILUTION, MELTING TEMPERATURE, AND OTHER PHYSICAL PROPERTY REQUIREMENTS OF THE WELDMENT.

The Schaeffler diagram is commonly used to predict weld metal microstructure and subsequent filler metal selection when joining a stainless steel to a carbon or low-alloy steel. Figure 40 illustrates the procedure with an example of a single-pass weld joining mild steel to type 304 stainless steel with ER309 stainless steel filler metal. First a connecting line is drawn between the two points representing the base metal compositions, based on their chromium and nickel equivalents. Point X, representing the relative dilutions contributed by each base metal is then located on this line. If the relative dilutions are equal, point X is at the midpoint of the line. A second line is drawn between point X and the point representing the ER309 filler metal composition. The composition of the weld pass lies somewhere on this line, the exact location depending upon the total dilution. With 30% dilution, the composition would be at point Y and would be considered acceptable. If a succeeding pass joins the first pass to mild steel, the dilution with the mild steel should be kept to a minimum, to avoid martensite formation in the weld metal.

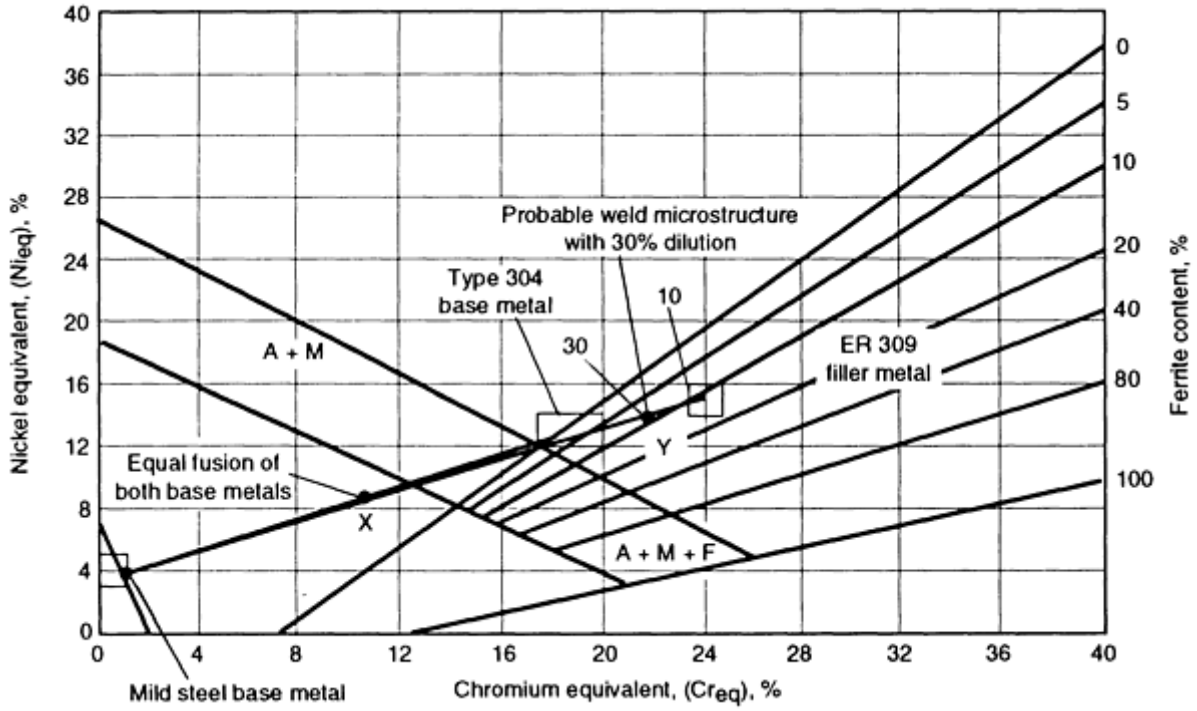

FIG. 40 PREDICTION OF WELD METAL COMPOSITION FROM THE SCHAEFFLER DIAGRAM. A, AUSTENITE; F, FERRITE, M, MARTENSITE. SEE TEXT FOR DETAILS. SOURCE: REF 33

For improved accuracy in predicting the microstructure of dissimilar-metal welds, the WRC-1988 or WRC-1992 diagrams should be used. The following example demonstrates the use of the WRC-1992 diagram for predicting the microstructure of a structural steel/stainless steel weld.

Example 2: Joining Type 304 Stainless Steel to ASTM A 36 Structural Steel with E309L-16 Electrode

(Ref 32). Table 22 lists typical plate compositions and all-weld-metal composition from the electrode. The Cr_{eq} and Ni_{eq} for the A 36 steel (0.00 and 7.08, respectively) do not permit an FN calculation for this material. The Cr_{eq} and Ni_{eq} for the type 304 stainless steel (18.83 and 12.45, respectively) result in a calculated 3.2 FN for this material. The Cr_{eq} and Ni_{eq} for these two base metals are shown in Fig. 41 and Point D (A 36) and Point E (type 304). Any mixture of these two base metals will lie along the line connecting Point D to E. If each base metal contributes equally to the weld metal, then the overall base metal contribution is given by the midpoint of the line between Point D and Point E, indicated in Fig. 41 as Point F. If one base metal contributed more than the other to the joint (for example, due to unequal plate thickness of a complex joint design), the Point F would slide along this line proportionately toward the greater contributor. In any case, the average base metal contribution to the weld pool would be along this line.

TABLE 22 BASE METAL AND WELD METAL COMPOSITIONS PRODUCED WHEN ASTM A 36 STRUCTURAL STEEL AND TYPE 304 STAINLESS STEEL WERE JOINED BY SMAW USING E309L-16 FILLER METAL

See Example 2 in text.

MATERIAL	**AISI 304**	**ASTM A 36**	**E309L-16 ALL-WELD-METAL**	70% E309L-16, 15% AISI 304, 15% A 36
C, %	0.05	0.20	0.03	**0.059**
MN, %	1.60	0.80	1.40	**1.34**
SI, %	0.40	0.20	0.60	**0.51**
CR, %	18.75	. . .	24.40	**19.89**

NI, %	9.90	. . .	12.70	**10.38**
MO, %	0.08	. . .	0.20	**0.15**
N, %	0.04	0.004	0.06	**0.049**
CR_{EQ}	18.83	0.00	24.60	**20.04**
NI_{EQ}	12.45	7.08	14.95	**13.39**
WRC-1988 FN	**3.2**	**. . .**	**17.4**	**4.3**

Source: Ref 32

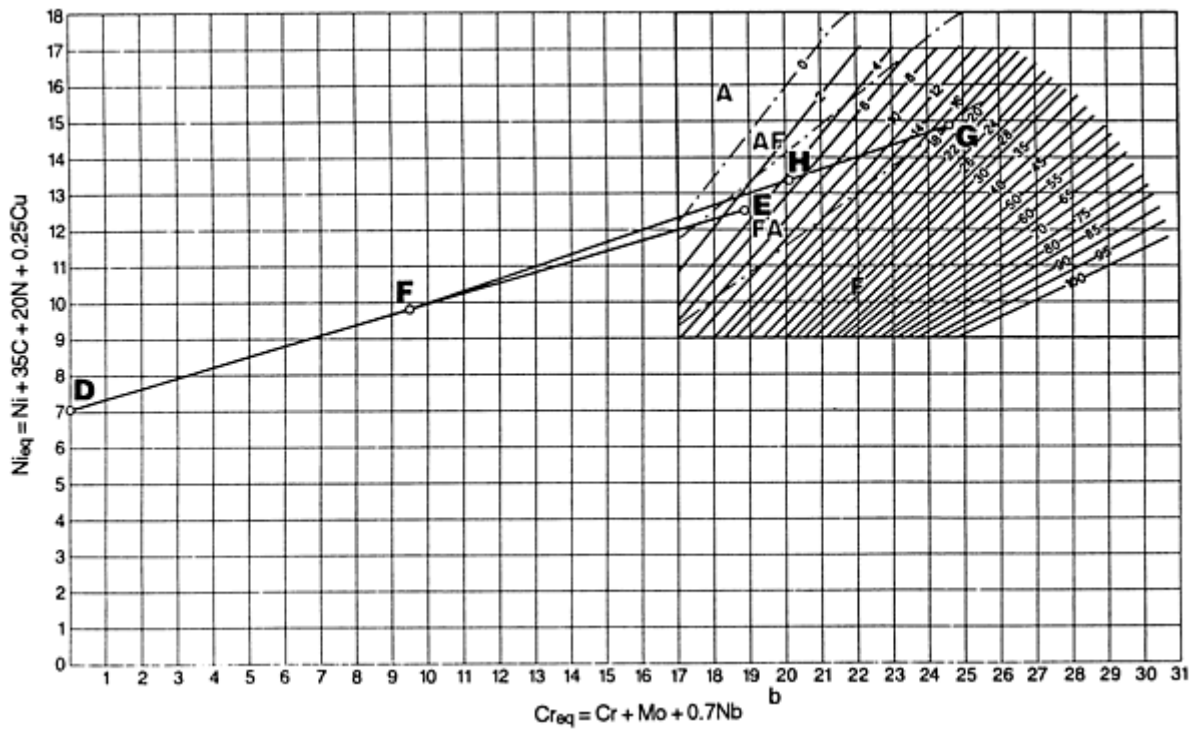

FIG. 41 DILUTION CALCULATION IN EXAMPLE 2 USING THE WRC-1992 DIAGRAM. SOURCE: REF 32

The all-weld-metal Cr_{eq} and Ni_{eq} (24.60 and 14.95, respectively) for the E309L-16 electrode is shown as Point G in Fig. 41, and a 17.4 FN would be predicted for that electrode. The root pass weld metal, consisting of the E309L-16 electrode and equal parts of the two base metals, must lie along the line from Point G to Point F in Fig. 41. Assuming the normal 30% base metal dilution with the shielded metal arc process, the root pass weld would lie 30% of the distance along the line from Point G to Point F. This is shown as Point H in Fig. 41. The calculations to reach Point H are as follows:

$$CR_{EQ}(F) = 0.5\ CR_{EQ}(D) + 0.5\ CR_{EQ}(E)$$
$$= 0.5(0.00) + 0.5(18.83) = 9.47 \quad \textbf{(EQ 9)}$$

$$NI_{EQ}(F) = 0.5\ NI_{EQ}(D) + 0.5\ NI_{EQ}(E)$$
$$= 0.5(7.08) + 0.5(12.45) = 9.77 \quad \textbf{(EQ 10)}$$

$$CR_{EQ}(H) = 0.7\ CR_{EQ}(G) + 0.3\ CR_{EQ}(F)$$
$$= 0.7(24.60) + 0.3(9.47) = 20.04 \quad \textbf{(EQ 11)}$$

$$NI_{EQ}(H) = 0.7\ NI_{EQ}(G) + 0.3\ NI_{EQ}(F)$$
$$= 0.7(14.95) + 0.3(9.77) = 13.39 \quad \textbf{(EQ 12)}$$

Point H corresponds to 4.3 FN, which would be expected to result in a crack-free root pass in this joint. Higher dilution, or excess dilution from the A 36 side of the joint, could reduce the ferrite content and increase the likelihood of cracking.

Buttering. If dilution of austenitic stainless steel filler metal is a problem, it may be controlled by first buttering the joint face of the carbon or low-alloy steel with one or two layers of type 309 or 310 stainless steel filler metal, as shown in Fig. 42(a) and 42(b). After machining and inspecting the buttered layer (Fig. 42c), the joint between the stainless steel component and the buttered steel part can be made using conventional welding procedures and the appropriate filler metal for welding the stainless steel base metal (Fig. 42d and 42e). A low-alloy steel component can be heat-treated after the buttering operation, then joined to the stainless steel part. This avoids a postweld heat treatment that might sensitize the austenitic stainless steel to intergranular corrosion. Additional information on buttering can be found in the article "Dissimilar Welds with Stainless Steels" in this Volume.

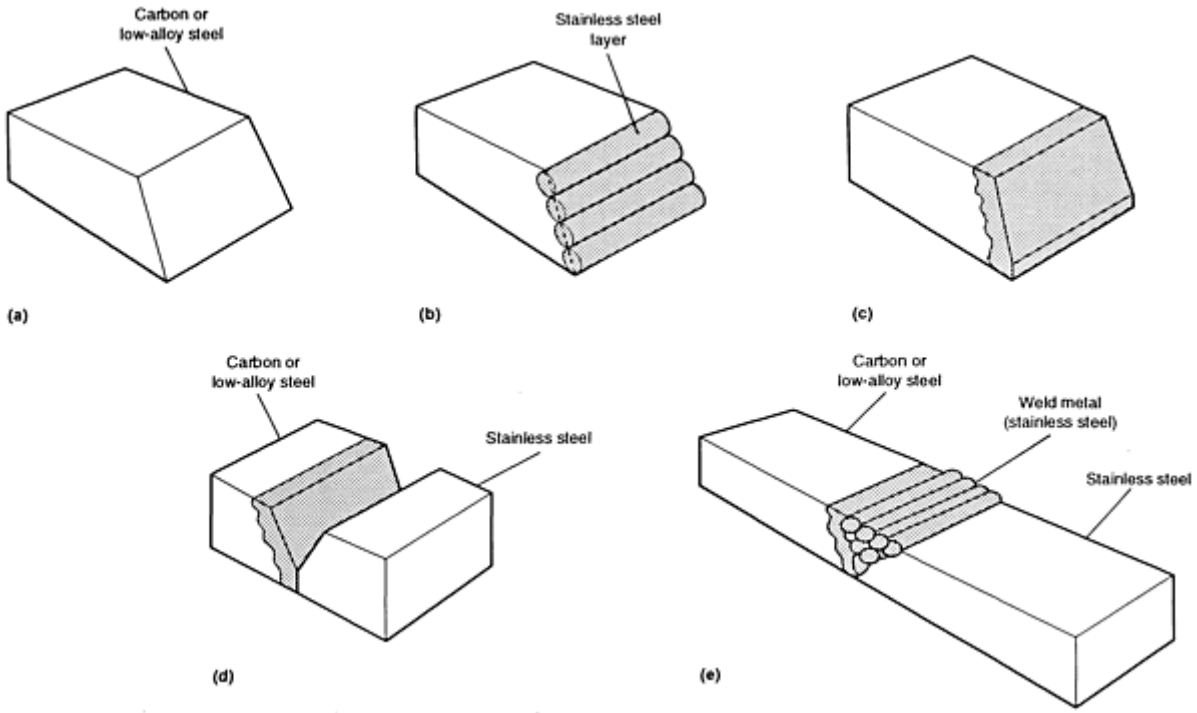

FIG. 42 BUTTERING TECHNIQUE USED TO ASSIST WELDING STAINLESS STEEL TO CARBON OR LOW-ALLOY STEEL. (A) EDGE PREPARED FOR BUTTERING. (B) FACE BUTTERED WITH FILLER METAL. (C) BUTTERED FACE PREPARED FOR WELDING. (D) JOINT ALIGNED FOR WELDING. (E) JOINT WELDED WITH STAINLESS STEEL FILLER METAL. SOURCE: REF 33

Joint Design. When designing butt joints between dissimilar metals, consideration must be given to the melting characteristics of each base metal and the filler metal, as well as to dilution effect. Large grooves decrease dilution, permit better control of viscous weld metal, and provide room for better manipulation of the arc for good fusion.

The joint design should provide for appropriate dilution in the first few passes placed in the joint when welding from one side. Improper dilution could result in a layer of weld metal possessing mechanical properties that are inappropriate for the intended service, particularly when the joint will be exposed to cyclic stresses. When welding from both sides, back gouging of the first weld can provide better control of dilution in the first few passes of the second weld.

Dissimilar-metal joints are often made with groove geometries similar to those used in conventional similar-metal welds and are left in the as-welded condition. However, removing the excess penetration of the weld root eliminates possible defects that may be present in the root of the joint, and it eliminates notches and crevices associated with backing rings. Removing the weld root also improves the capabilities of nondestructive tests (radiography, liquid penetrant, and ultrasonic). Provision can also be made for removing the exterior reinforcement to eliminate stress concentrations associated with undercutting and with the change in section thickness across the as-welded joint. Again, inspection capabilities are improved.

Preheat and Postweld Heat Treatments. Selection of an appropriate preheat or postweld heat treatment (PWHT) for a welded joint can present a problem with some dissimilar metal combinations. The appropriate heat treatment for one component of the weldment may be deleterious to the other component for the intended service conditions. For example,

if an age-hardenable nickel-chromium alloy is welded to a nonstabilized austenitic stainless steel, exposure of the weldment to the aging treatment for the nickel-chromium alloy would sensitize the stainless steel and decrease its resistance to intergranular corrosion (weld decay).

One solution is to use a stabilized austenitic stainless steel if that is acceptable. Another solution might be to butter the face of the age-hardenable, nickel-chromium alloy component with a similar alloy that is not age-hardenable. This component is then heat-treated to obtain the desired properties. Finally, the buttered surface is welded to the stainless steel component.

Service Considerations (Ref 33)

Property Considerations. A dissimilar metal joint normally contains weld metal having a composition different from that of one or both base metals. The properties of the weld metal depend on the filler metal composition, the welding procedures, and the relative dilution with each base metal. There also two different HAZs, one in each base metal adjacent to the weld metal. The mechanical and physical properties of the weld metal as well as those of the two HAZs, must be considered for the intended service.

Special considerations are generally given to dissimilar-metal joints intended for elevated-temperature service. A favorable situation exists when the joint will operate at constant temperatures. During elevated-temperature service, internal stresses can decrease by relaxation and reach an equilibrium. However, it is best to reduce the effect of large differences in coefficients of thermal expansion when large temperature fluctuations cannot be avoided in service. The problem can be avoided by selecting base metals with similar thermal expansion characteristics.

Figure 43 gives the mean linear thermal expansion coefficients as a function of temperature for several alloys commonly associated with transition butt joints for steam plant applications. The thermal expansion coefficient of 2.25Cr-1Mo steel is about 25% less than that of types 304 and 316 austenitic stainless steel. In certain applications, transition joints between austenitic stainless steel and low-alloy steel may experience numerous temperature changes during operation. For a given change in temperature, the stress imposed at the weld joint is proportional to the difference in their coefficients of thermal expansion. Stress analyses of welded joints between these two types of steel indicate that the stresses introduced by thermal change are nearly an order of magnitude greater than those produced by the operating pressures and any thermal gradients across the joint.

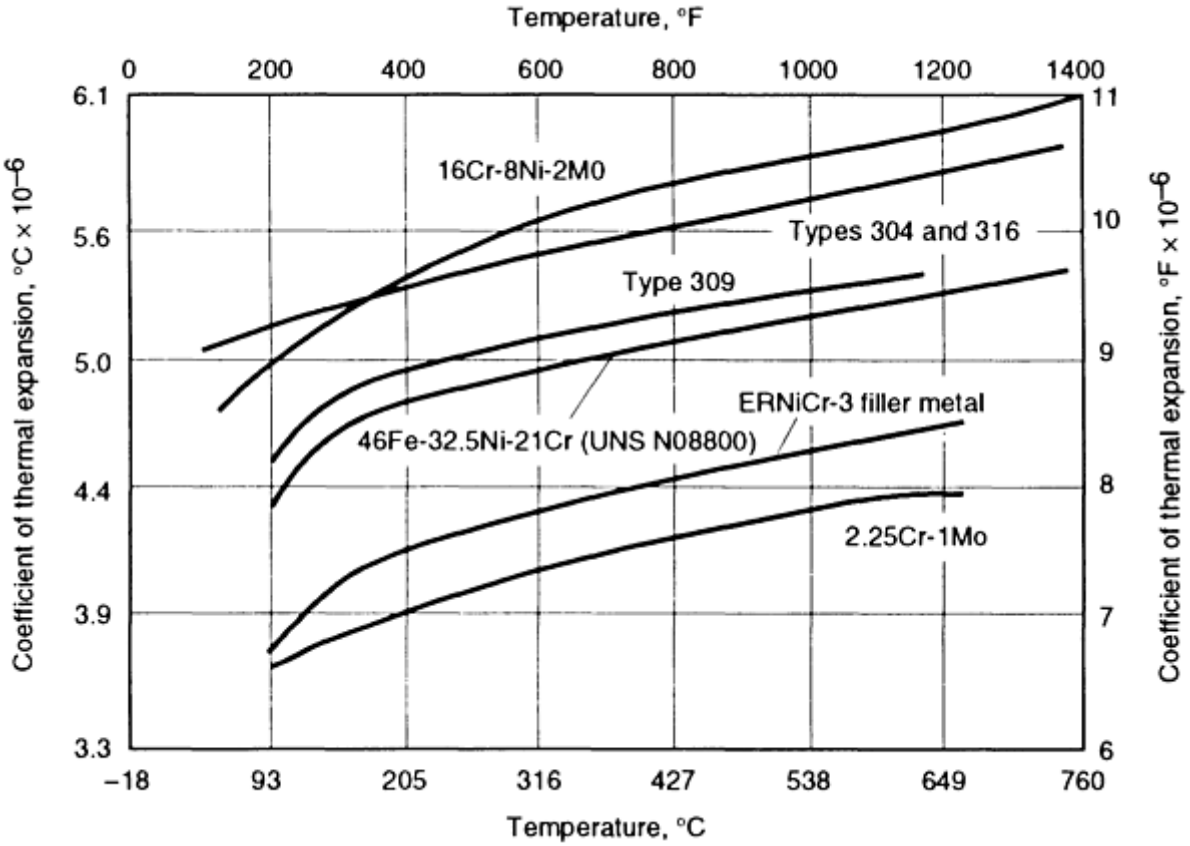

FIG. 43 MEAN COEFFICIENTS OF THERMAL EXPANSION AS A FUNCTION OF TEMPERATURE FOR TRANSITION BUTT-JOINT MATERIALS. SOURCE: REF 33

Experience with dissimilar-metal transition joints has shown a significant number of failures in less than the expected service life. The majority of the transition joint failures in austenitic steel/ferritic steel joints occur in the ferritic steel HAZ, adjacent to the weld interface. These failures are generally attributed to one or more of the following causes:

- HIGH STRESSES AND THE RESULTING CREEP AT THE INTERFACE AS A RESULT OF THE DIFFERENCES BETWEEN THE COEFFICIENTS OF THERMAL EXPANSION OF THE WELD AND BASE METALS
- CARBON MIGRATION FROM THE FERRITIC STEEL INTO THE STAINLESS STEEL, WHICH WEAKENS THE HAZ IN THE FERRITIC STEEL
- PREFERENTIAL OXIDATION AT THE INTERFACE, ACCELERATED BY THE PRESENCE OF STRESS

Carbon Migration. There is the likelihood of significant chemical composition gradients in the weld metal, particularly in the regions adjacent to the base metals. In addition, operation at elevated temperatures can cause interdiffusion between the weld metal and the base metal that, in turn, results in microstructure changes. A dissimilar-metal weld made between a low-alloy steel and an austenitic stainless steel, with an austenitic stainless steel filler metal, illustrates this problem. Chromium in steel has a greater affinity for carbon than does iron. When a carbon or low-alloy steel is welded with a steel filler metal containing a significant amount of chromium, carbon will diffuse from the base metal into the weld metal at temperatures above about 425 °C (800 °F). The diffusion rate is a function of temperature and exposure time, and it increases rather rapidly at 595 °C (1100 °F) and above. Carbon migration can take place during PWHT heat treatment or service at elevated temperatures.

Austenitic steel has a greater solubility for carbon than does ferritic steel. Therefore, carbon depletion in a carbon or low-alloy steel is greater when an austenitic stainless steel filler metal is used in preference to a ferritic steel filler metal. On the other hand, carbon migration is not as serious a problem when a nickel-chromium-iron filler metal is used.

If carbon migration is extensive, it will be indicated by a lightly etching, low-carbon band in the carbon steel HAZ and a dark, high-carbon zone in the stainless steel weld metal, as seen in a transverse metallographic section. The extent of carbon migration during PWHT or elevated-temperature service should be determined during welding procedure qualification. It is known to influence long-time stress-rupture strength during elevated-temperature service.

During cyclic temperature service, the HAZ will be subjected to varying shear stresses because of the differences in coefficients of thermal expansion of the base and weld metals. These stresses may produce fatigue failure in the decarburizing band next to the weld interface.

Corrosion and Oxidation Resistance. The weld metal and both base metals have specific corrosion behaviors that must be considered by the designer in the initial selection of materials. For example, with dissimilar metal weldments, the formation of galvanic cells can cause corrosion of the most anodic metal or phase in the joint. Also, the weld metal is usually composed of several microstructural phases, and very localized cells between phases can result in galvanic corrosion at the microstructural level. To minimize galvanic corrosion, the composition of the weld metal can be adjusted to provide cathodic protection to the base metal that is most susceptible to galvanic attack. However, other design requirements should not be seriously compromised to do this. Instead, some other form of protection should be used.

A galvanic cell associated with a high-strength steel may promote hydrogen embrittlement in the HAZ of that steel if it is the cathode of the cell. Hydrogen embrittlement must be considered if the service temperature of the weldment will be in the range of -40 to 95 °C (-40 to 200 °F), and the weld will be in a highly stressed area of the assembly. Residual stresses developed in the weld zone are often sufficient to promote hydrogen embrittlement and stress-corrosion cracking.

Chemical compositional differences in a dissimilar-metal weld can also cause high-temperature corrosion problems. Compositional variations at the interfaces between the different metals can result in selective oxidation when operating at high temperatures in air and formation of notches at these locations. Such notches are potential stress-raisers in the joint and can cause oxidation failure along the weld interface under cyclic thermal conditions.

Specific Dissimilar Metal Combinations (Ref 33)

The emphasis in the following section will be on joining carbon and low-alloy steels to various dissimilar materials (both ferrous and nonferrous) by arc welding. See other articles in this Section of the Handbook for additional information (for example, "Welding of Nickel Alloys" and "Welding of Copper Alloys").

Stainless Steels to Carbon or Low-Alloy Steels. Austenitic, ferritic, or martensitic stainless steels can be readily fusion welded to carbon or low-alloy steels using a filler metal that can tolerate dilution by both base metals without formation of flaws in the joint. An austenitic stainless steel or nickel alloy filler metal is commonly used. The choice depends on the application and the service conditions.

Generally, carbon or low-alloy steels are joined to 300-type stainless steels using austenitic filler metals, such as types E/ER 308, 309, 316, and 347. Such filler metals are used for service applications below 425 °C (800 °F). For higher temperatures or when high-temperature cyclic service is a concern, high-nickel filler metals such as ERNiCr-3 and ENiCrFe-3 are used. The coefficients of thermal expansion of high-nickel alloys approximate those of ferritic steels, and during cyclic-temperature service, the major differential expansion stresses are located primarily at the tough stainless steel/weld metal interface. Another advantage of a nickel-base weld metal is that it markedly reduces carbon migration from the ferritic steels to the weld metal. Extensive carbon migration into stainless steel weld metal weakens the HAZ of the carbon or low-alloy steel.

The problem of cracking between ferritic steels, such as the 2.25Cr-1Mo steel described earlier, and austenitic stainless steels is a recurring problem in such operations as the petrochemical industry and electric utility generating plants. Cracking has been repeatedly observed in HAZs of the ferritic portions of dissimilar-metal welds, particularly those that have been subjected to a large number of thermal cycles and extended time at elevated temperatures around 565 °C (1050 °F). Such cracking must be minimized, since repair maintenance and non-productive downtime are costly. High-nickel filler metals have proven useful in such applications.

Buttering is also used to improve the weldability between ferritic and austenitic stainless steel joints. A thick overlay (13 mm, or $\frac{1}{2}$ in., or greater) of a highly austenitic weld metal, such as type 309 stainless steel, can be deposited on carbon or low-alloy steel components so that stainless steel/stainless steel welds can be made subsequently in the field. This technique has limited reliability for high-temperature cyclic service and has not been used extensively for material combinations other than ferritic steels, stainless steels, and some high-nickel alloys.

A filler metal for joining a 4*xx*-series stainless steel to a carbon or low-alloy steel can be selected using the following general rules:

- FOR WELDING ONE HARDENABLE CHROMIUM STEEL TO ANOTHER WITH A HIGHER CHROMIUM CONTENT, FILLER METAL CONTAINING CHROMIUM EQUAL TO THAT OF EITHER STEEL MAY BE USED. FURTHERMORE, ANY FILLER METAL WHOSE CHROMIUM CONTENT LIES BETWEEN THESE LIMITS IS EQUALLY SATISFACTORY, PROVIDED THE WELDMENT IS PROPERLY HEAT-TREATED.
- A GENERAL RULE FOR WELDING ANY CHROMIUM STEEL TO ANY LOW-ALLOY STEEL IS TO USE A FILLER METAL THAT HAS THE SAME COMPOSITION AS THE LOW-ALLOY STEEL, PROVIDED THAT IT MEETS THE SERVICE REQUIREMENTS OF THE APPLICATION. WITH ANY LOW-ALLOY STEEL FILLER METAL, THE CHROMIUM THAT IS PICKED UP BY DILUTION WITH THE CHROMIUM STEEL BASE METAL MUST BE CONSIDERED.
- FOR WELDING ANY CHROMIUM STEEL TO A CARBON STEEL, CARBON STEEL FILLER METAL CAN BE USED. A CHROMIUM STEEL FILLER METAL CAN ALTERNATIVELY BE USED, BUT IT IS PREFERABLE TO USE A LESS HARDENABLE FILLER METAL.

When the properties of the HAZ in the chromium stainless steel are important, both the stainless steel and other steel can be buttered with type 309 or 310 austenitic stainless steel weld metal. An appropriate preheat or PWHT can be used to obtain desired properties in the buttered components. The stainless steel surfaces can then be welded together without preheat using a suitable austenitic stainless steel filler metal, such as type 308.

Nickel-Base Alloys to Steels. Nickel alloys can easily be welded to steels using a suitable filler metal and proper control of dilution. Nickel-base filler metals are generally used because of their good ductility and tolerance of dilution by iron. Suggested nickel-base filler metals for welding nickel alloys to steel or stainless steel are listed in Table 23.

TABLE 23 SUGGESTED FILLER METALS FOR WELDING NICKEL-BASE ALLOYS TO CARBON AND LOW-ALLOY STEELS

NICKEL ALLOY		**FILLER METAL FORM**	FILLER METAL FOR WELDING TO	
UNS NO.	**COMMON DESIGNATION**		**CARBON OR LOW-ALLOY STEEL**	STAINLESS STEEL
N02200	COMMERCIALLY PURE NICKEL	COVERED ELECTRODE	ENI-1, ENICRFE-2	**ENI-1, ENICRFE-2, ENICRFE-3**
		BARE WIRE	ERNI-1, ERNICR-3	**ERNI-1, ERNICR-3, ERNICRFE-6**
N04400	MONEL 400	COVERED ELECTRODE	ENICU-7, ENI-1	**ENICRFE-2, ENICRFE-3**
N05500	MONEL K-500	BARE WIRE	ERNI-1	**ERNICR-3, ERNICRFE-6**
N05502	MONEL 502			
N06600	INCONEL 600	COVERED ELECTRODE	ENICRFE-2, ENICRFE-3	**ENICRFE-2, ENICRFE-3**
N08800	INCOLOY 800	BARE WIRE	ERNICR-3, ERNICRFE-6	**ERNICR-3, ERNICRFE-6**
N08825	INCOLOY 825	COVERED ELECTRODE	ENICRMO-3	**ENICRMO-3**
		BARE WIRE	ERNICRMO-3	**ERNICRMO-3**

N10665	HASTELLOY B-2	COVERED ELECTRODE	ENIMO-7	**ENIMO-7**
		BARE WIRE	ERNIMO-7	**ERNIMO-7**
N10276	HASTELLOY C-276	COVERED ELECTRODE	ENICRMO-4	**ENICRMO-4**
		BARE WIRE	ERNICRMO-4	**ERNICRMO-4**
N06455	HASTELLOY C-4	COVERED ELECTRODE	ENICRMO-4	**ENICRMO-4**
		BARE WIRE	ERNICRMO-7	**ERNICRMO-7**
N06007	HASTELLOY G	COVERED ELECTRODE	ENICRMO-9	**ENICRMO-9**
		BARE WIRE	**ERNICRMO-1**	**ERNICRMO-1**

Source: Ref 33

Sulfur and phosphorus in nickel and nickel alloys cause hot cracking. The melting techniques used to produce nickel and its alloys are designed to keep the content of these elements to low levels. By contrast, the sulfur and phosphorus contents in some steels are typically higher. Consequently, dilution should be carefully controlled when joining a steel to a nickel alloy with a nickel alloy filler metal, to avoid hot cracking in the weld metal.

Most nickel-base weld metals can accept a substantial amount of iron dilution, but the dilution limit generally varies with the welding process. Weld metal deposited with nickel- or nickel-chromium-covered electrodes can tolerate up to approximately 40% iron dilution. With bare nickel or nickel-chromium filler metals, however, dilution should be kept to about 25%.

Acceptable limits of iron dilution for nickel-copper weld metal vary, depending on the weld process. With SMAW, iron dilution of up to about 30% can be tolerated. Submerged arc weld metal should not be diluted by more than 25%.

With the gas-shielding processes, nickel-copper weld metal is less tolerant of iron dilution, especially if the weld is to be thermally stress-relieved. The maximum limits for iron dilution in a welded joint are 10% when it will be used as-welded and 5% when it will be stress-relieved. A buttering layer of nickel or nickel-copper weld metal should be applied to the steel face in order to avoid exceeding these limits.

Nickel-copper weld metal has a maximum dilution tolerance for chromium of about 8%. Consequently, nickel-copper filler metal should not be used to join nickel-copper alloys to stainless steels (see Table 23).

Cobalt-Base Alloys to Steels. Metallurgically, cobalt-base alloys behave similarly to the high-temperature nickel-chromium alloys with respect to welding. When joining a cobalt alloy to a stainless steel, a filler metal with a composition similar to that of the cobalt alloy is recommended. A nickel alloy filler metal may also be suitable for some applications. In any case, the filler metal selection, welding process, and welding procedure for the application should be established by suitable tests.

Copper-Base Alloys to Steels. As described in the article "Welding of Copper Alloys" in this Volume, copper and many copper-base alloys can be joined to carbon, low-alloy, and stainless steels by GTAW, GMAW, and SMAW. Iron dilution can be minimized by the use of appropriate welding procedures or by placement of a buttering layer of nickel on the steel. Tables 24 and 25 show combinations of dissimilar metals by GTAW and GMAW with the aid of copper-base or nickel-base filler metals.

TABLE 24 FILLER METALS AND PREHEAT AND INTERPASS TEMPERATURES USED IN GAS-TUNGSTEN ARC WELDING OF COPPERS AND COPPER-BASE ALLOYS TO STEELS

METAL TO BE WELDED	FILLER METALS (AND PREHEAT AND INTERPASS TEMPERATURES) FOR WELDING METAL IN COLUMN 1 TO[(A)]:				
	COPPERS	**PHOSPHOR BRONZES**	**ALUMINUM BRONZES**	**SILICON BRONZES**	COPPER NICKELS
LOW-CARBON STEEL	ERCUAL-A2 OR ERCU OR ERNI-3	ERCUSN-A (205 °C, OR 400 °F)	ERCUAL-A2 (150 °C, OR 300 °F)	ERCUAL-A2 (65 °C, OR 150 °F	**ERCUAL-A2 OR ERNI-3 (65 °C, OR**

	(540 °C, OR 1000 °F)			MAX)	**150 °F MAX)**
MEDIUM-CARBON STEEL	ERCUAL-A2 OR ERCU OR ERNI-3 (540 °C, OR 1000 °F)	ERCUSN-A (205 °C, OR 400 °F)	ERCUAL-A2 (205 °C, OR 400 °F)	ERCUAL-A2 (65 °C, OR 150 °F MAX)	**ERCUAL-A2 OR ERNI-3 (65 °C, OR 150 °F MAX)**
HIGH-CARBON STEEL	ERCUAL-A2 OR ERCU OR ERNI-3 (540 °C, OR 1000 °F)	ERCUSN-A (260 °C, OR 500 °F)	ERCUAL-A2 (260 °C, OR 500 °F)	ERCUAL-A2 (205 °C, OR 400 °F)	**ERCUAL-A2 OR ERNI-3 (65 °C, OR 150 °F MAX)**
LOW-ALLOY STEEL	ERCUAL-A2 OR ERCU OR ERNI-3 (540 °C, OR 1000 °F)	ERCUSN-A (260 °C, OR 500 °F)	ERCUAL-A2 (260 °C, OR 500 °F)	ERCUAL-A2 (205 °C, OR 400 °F)	**ERCUAL-A2 OR ERNI-3 (65 °C, OR 150 °F MAX)**
STAINLESS STEEL	**ERCUAL-A2 OR ERCU OR ERNI-3 (540 °C, OR 1000 °F)**	**ERCUSN-A (205 °C, OR 400 °F)**	**ERCUAL-A2 (65 °C, OR 150 °F MAX)**	**ERCUAL-A2 (65 °C, OR 150 °F MAX)**	**ERCUAL-A2 OR ERNI-3 (65 °C, OR 150 °F MAX)**

(A) FILLER-METAL SELECTIONS SHOWN IN TABLE ARE BASED ON WELDABILITY, EXCEPT WHERE MECHANICAL PROPERTIES ARE USUALLY MORE IMPORTANT. PREHEATING IS ORDINARILY USED ONLY WHEN AT LEAST ONE MEMBER IS THICKER THAN ABOUT 3.2 MM ($\frac{1}{8}$ IN.) OR IS HIGHLY CONDUCTIVE (SEE TEXT). PREHEAT AND INTERPASS TEMPERATURES ARE SUBJECT TO ADJUSTMENT ON THE BASIS OF THE SIZE AND SHAPE OF THE WELDMENT.

TABLE 25 FILLER METALS AND PREHEAT AND INTERPASS TEMPERATURES USED IN GAS-METAL ARC WELDING OF COPPERS AND COPPER-BASE ALLOYS TO STEELS

METAL TO BE WELDED	ELECTRODES (AND PREHEAT AND INTERPASS TEMPERATURES) FOR WELDING METAL IN COLUMN 1 TO[(A)]:						
	COPPERS	**LOW-ZINC BRASSES**	**HIGH-ZINC BRASSES, TIN BRASSES, SPECIAL BRASSES**	**PHOSPHOR BRONZES**	**ALUMINUM BRONZES**	**SILICON BRONZES**	COPPER NICKELS
LOW-CARBON STEEL	ERCUAL-A2 OR ERCU OR ERNI-3 (540 °C, OR 1000 °F)	ERCUSN-A (315 °C, OR 600 °F)	ERCUAL-A2 (260 °C, OR 500 °F)	ERCUSN-A (205 °C, OR 400 °F)	ERCUAL-A2 (150 °C, OR 300 °F)	ERCUAL-A2 (65 °C, OR 150 °F MAX)	**ERCUAL-A2OR ERNI-3 (65 °C, OR 150 °F MAX)**
MEDIUM-CARBON STEEL	ERCUAL-A2 OR ERCU OR ERNI-3 (540 °C, OR 1000 °F)	ERCUAL-A2 (315 °C, OR 600 °F)	ERCUAL-A2 (260 °C, OR 500 °F)	ERCUSN-A (205 °C, OR 400 °F)	ERCUAL-A2 (205 °C, OR 400 °F)	ERCUAL-A2 (65 °C, OR 150 °F MAX)	**ERCUAL-A2 OR ERNI-3 (65 °C, OR 150 °F MAX)**
HIGH-CARBON STEEL	ERCUAL-A2 OR ERCU OR ERNI-3 (540 °C, OR 1000 °F)	ERCUAL-A2 (315 °C, OR 600 °F)	ERCUAL-A2 (260 °C, OR 500 °F)	ERCUSN-A (260 °C, OR 500 °F)	ERCUAL-A2 (260 °C, OR 500 °F)	ERCUAL-A2 (205 °C, OR 400 °F)	**ERCUAL-A2 OR ERNI-3 (65 °C, OR 150 °F MAX)**
LOW-ALLOY STEEL	ERCUAL-A2 OR ERCU OR ERNI-3 (540 °C, OR 1000 °F)	ERCUAL-A2 (315 °C, OR 600 °F)	ERCUAL-A2 (315 °C, OR 600 °F)	ERCUSN-A (260 °C, OR 500 °F)	ERCUAL-A2 (260 °C, OR 500 °F)	ERCUAL-A2 (205 °C, OR 400 °F)	**ERCUAL-A2, OR ERNI-3 (65 °C, OR 150 °F MAX)**
STAINLESS STEEL	**ERCUAL-A2 OR ERCU OR ERNI-3 (540 °C, OR 1000 °F)**	**ERCUAL-A2 OR ERCUSN-A (315 °C, OR 600 °F)**	**ERCUAL-A2 (315 °C, OR 600 °F)**	**ERCUSN-A (205 °C, OR 400 °F)**	**ERCUAL-A2 (65 °C, OR 150 °F MAX)**	**ERCUAL-A2 (65 °C, OR 150 °F MAX)**	**ERCUAL-A2 OR ERNI-3 (65 °C, OR 150 °F MAX)**

(A) ELECTRODE SELECTIONS IN TABLE ARE BASED ON WELDABILITY, EXCEPT WHERE MECHANICAL PROPERTIES ARE USUALLY MORE IMPORTANT. PREHEATING USUALLY IS USED ONLY WHEN AT LEAST ONE MEMBER IS THICKER THAN 3.2 MM ($\frac{1}{8}$ IN.) OR IS HIGHLY CONDUCTIVE (SEE TEXT). PREHEAT AND INTERPASS TEMPERATURES ARE SUBJECT TO ADJUSTMENT BASED ON SIZE AND SHAPE OF WELDMENT.

Aluminum-Base Alloys to Steels. With respect to fusion welding, iron and aluminum are not compatible metals. Their melting temperatures differ greatly: 660 °C (1220 °F) for aluminum versus 1538 °C (2800 °F) for iron. Both metals have almost no solubility for the other in the solid state, especially iron in aluminum, and several brittle intermetallic phases can form ($FeAl_2$, Fe_2Al_5, or $FeAl_3$). Consequently, fusion welds joining iron and aluminum are brittle. In addition, high welding stresses would be expected because of the significant differences in the thermal expansion coefficients, thermal conductivities, and specific heats of iron and aluminum. Aluminum can be joined to carbon or stainless steel by brazing, solid-state welding or by high-energy processes such as electron-beam welding.

References cited in this section

32. D.J. KOTECKI AND T.A. SIEWERT, WRC-1992 CONSTITUTION DIAGRAM FOR STAINLESS STEEL WELD METALS: A MODIFICATION OF THE WRC-1988 DIAGRAM, *WELD. J.*, MAY 1992, P 171S-178S
33. DISSIMILAR METALS, *WELDING HANDBOOK*, 7TH ED., VOL 4, AMERICAN WELDING SOCIETY, 1982, P 514-547
34. DISSIMILAR-WELD FAILURE ANALYSIS AND DEVELOPMENT PROGRAM, VOL 1-4, REPORT CS-4252, ELECTRIC POWER RESEARCH INSTITUTE, PALO ALTO, CA

Hardfacing, Weld Cladding, and Dissimilar Metal Joining

J.R. Davis, Davis & Associates

References

1. K.C. ANTONY *ET AL.*, HARDFACING, *WELDING, BRAZING, AND SOLDERING*, 9TH ED., VOL 6, *METALS HANDBOOK*, AMERICAN SOCIETY FOR METALS, 1983, P 771-793
2. P. CROOK AND H.N. FARMER, FRICTION AND WEAR OF HARDFACING ALLOYS, *FRICTION, LUBRICATION, AND WEAR TECHNOLOGY*, VOL 18, *ASM HANDBOOK*, ASM INTERNATIONAL, 1992, P 758-765
3. D.K. SUBRAMANYAM, A.E. SWANSIGER, AND H.S. AVERY, AUSTENITIC MANGANESE STEELS, *PROPERTIES AND SELECTION: IRONS, STEELS, AND HIGH-PERFORMANCE ALLOYS*, VOL 1, *ASM HANDBOOK*, ASM INTERNATIONAL, 1990, P 822-840
4. H.S. AVERY AND H.J. CHAPIN, *WELD J.*, VOL 31, 1952, P 917
5. R.D. ZORDAN, REPORT 10890, CABOT CORPORATION, KOKOMO, IN, 1982
6. H. OCKEN AND A.K. VELAN, ED., "LABORATORY EVALUATIONS OF COBALT-FREE, NICKEL-BASED HARDFACING ALLOYS FOR NUCLEAR APPLICATIONS," REPORT NP-4993, PROJECT 1935, ELECTRIC POWER RESEARCH INSTITUTE, PALO ALTO, CA, MARCH 1987
7. P.J. HOFMANN, B.C. FRIEDRICH, AND H. OCKEN, ED., "LABORATORY EVALUATIONS OF IRON-BASED HARDFACING ALLOYS," REPORT NP-5874, PROJECT 1935-11, ELECTRIC POWER RESEARCH INSTITUTE, PALO ALTO, CA, JUNE 1988
8. WELD DESIGN AND FABRICATION, DATA SHEET 420, *WELD. DES. FABR.*, VOL 48 (NO. 8), 1975, P 50
9. K.M. KULKARNI AND V. ANAND, METAL POWDERS USED FOR HARDFACING, *POWDER METALLURGY*, 9TH ED., VOL 7, *ASM HANDBOOK*, AMERICAN SOCIETY FOR METALS, 1984, P 823-836
10. K.P. COOPER, LASER SURFACE PROCESSING, *FRICTION, LUBRICATION, AND WEAR TECHNOLOGY*, VOL 18, *ASM HANDBOOK*, ASM INTERNATIONAL, 1992, P 861-872
11. A.G. BLAKE, *ET AL.*, "LASER COATING TECHNOLOGY: A COMMERCIAL REALITY," BULLETIN OF QUANTUM LASER CORPORATION, EDISON, NJ

12. J.D. AYERS AND D.S. GNANAMUTHU, HARDENING OF METAL SURFACES BY LASER PROCESSING, *WELDING, BRAZING, AND SOLDERING*, 9TH ED., VOL 6, *ASM HANDBOOK*, AMERICAN SOCIETY FOR METALS, 1983, P 793-803
13. W.M. STEEN, *PROC. NATO ADVANCED STUDY INSTITUTE ON LASER SURFACE TREATMENT OF METALS*, C.W. DRAPER AND P. MAZZOLDI, ED., MARTINUS NIJHOFF, 1986, P 369
14. J. MAZUMDER AND J. SINGH, *PROC. NATO ADVANCED STUDY INSTITUTE ON LASER SURFACE TREATMENT OF METALS*, C.W. DRAPER AND P. MAZZOLDI, ED., MARTINUS NIJHOFF, 1986, P 297
15. A. BELMONDO AND M. CASTAGNA, *SOURCEBOOK ON APPLICATIONS OF THE LASER IN METALWORKING*, E. METZBOWER, ED., AMERICAN SOCIETY FOR METALS, 1981, P 310
16. G.J. BRUCK, *J. MET.*, VOL 39 (NO. 2), 1987, P 10
17. A.V. LA ROCCA, *PROC. NATO ADVANCED STUDY INSTITUTE ON LASER SURFACE TREATMENT OF METALS*, C.W. DRAPER AND P. MAZZOLDI, ED., MARTINUS NIJHOFF, 1986, P 521
18. R.M. MACINTYRE, *PROC. NATO ADVANCED STUDY INSTITUTE ON LASER SURFACE TREATMENT OF METALS*, C.W. DRAPER AND P. MAZZOLDI, ED., MARTINUS NIJHOFF, 1986, P 545
19. B.A. KUSHNER AND E.R. NOVINSKI, THERMAL SPRAY COATINGS, *FRICTION, LUBRICATION, AND WEAR TECHNOLOGY*, VOL 18, *ASM HANDBOOK*, ASM INTERNATIONAL, 1992, P 829-833
20. R.H. UNGER, THERMAL SPRAY COATINGS, *CORROSION*, 9TH ED., VOL 13, *ASM HANDBOOK*, ASM INTERNATIONAL, 1987, P 459-462
21. M.L. THORPE, THERMAL SPRAY: INDUSTRY IN TRANSITION, *ADV. MATER. PROCESS.*, VOL 143 (NO. 5), 1993, P 50-56
22. G. IRONS, "HIGHER VELOCITY THERMAL SPRAY PROCESSES PRODUCE BETTER AIRCRAFT ENGINE COATINGS," SAE TECHNICAL PAPER 920947, PRESENTED AT THE 28TH ANNUAL AEROSPACE/AIRLINE PLATING AND METAL FINISHING FORUM AND EXPOSITION (SAN DIEGO, CA), APRIL 1992
23. F.N. LONGO, PROCESSING AND DESIGN, LESSON 3, COURSE 51, *THERMAL SPRAY TECHNOLOGY*, MATERIALS ENGINEERING INSTITUTE, ASM INTERNATIONAL, 1992
24. M.L. THORPE, THERMAL SPRAYING BECOMES A DESIGN TOOL, *MACH. DES.*, 24 NOV 1983
25. P.O. BUZBY AND J. NIKITICH, HVOF THERMAL SPRAYING OF NITRIDED PARTS, *ADV. MATER. PROCESS.*, DEC 1991, P 35-36
26. R.D. THOMAS *ET AL.*, WELD OVERLAYS, *WELDING, BRAZING, AND SOLDERING*, 9TH ED., VOL 6, *METALS HANDBOOK*, AMERICAN SOCIETY FOR METALS, 1983, P 804-819
27. D.L. OLSON, PREDICTION OF AUSTENITIC WELD METAL MICROSTRUCTURE AND PROPERTIES, *WELD. J.*, VOL 64 (NO. 10), 1985, P 2815-2955
28. A.L. SCHAEFFLER, CONSTITUTION DIAGRAM FOR STAINLESS STEEL WELD METAL, *MET. PROG.*, VOL 56 (NO. 11), 1949, P 680-680B
29. W.T. DELONG, FERRITE IN AUSTENITIC STAINLESS STEEL WELD METAL, *WELD. J.*, VOL 53 (NO. 7), 1974, P 2735-2865
30. T.A. SIEWERT, C.N. MCCOWAN, AND D.L. OLSON, FERRITE NUMBER PREDICTION TO 100 FN IN STAINLESS STEEL WELD METAL, *WELD. J.*, VOL 67 (NO. 12), 1988, P 2895-2985
31. D.J. KOTECKI, "VERIFICATION OF THE NBS-CSM FERRITE DIAGRAM," INTERNATIONAL INSTITUTE OF WELDING DOCUMENT II-C-834-88, 1988
32. D.J. KOTECKI AND T.A. SIEWERT, WRC-1992 CONSTITUTION DIAGRAM FOR STAINLESS STEEL WELD METALS: A MODIFICATION OF THE WRC-1988 DIAGRAM, *WELD. J.*, MAY 1992, P 171S-178S
33. DISSIMILAR METALS, *WELDING HANDBOOK*, 7TH ED., VOL 4, AMERICAN WELDING SOCIETY, 1982, P 514-547
34. DISSIMILAR-WELD FAILURE ANALYSIS AND DEVELOPMENT PROGRAM, VOL 1-4, REPORT

Introduction

RESISTANCE WELDING (RW) encompasses a group of processes in which the heat for welding is generated by the resistance to the flow of electrical current through the parts being joined. These processes are most commonly used to weld two overlapping sheets or plates that may have different thicknesses. A pair of electrodes clamp the workpieces under pressure to provide good electrical contact and to contain the molten metal in the joint. The electrodes conduct electrical current to the joint; resistance to the flow of current heats the faying surfaces, forming a weld (Ref 1).

The required heat generated through the electrical resistance of the two bodies to be joined is given by

$$H = I^2RT \qquad \textbf{(EQ 1)}$$

where H is the heat generated in joules; I is the current in amperes; R is the resistance in ohms; and t is the time of current flow, in seconds. The actual temperature rise at the joint depends on the interrelationship of the three component variables. These variables are affected by:

- COOLING EFFECT OF THE ELECTRODE
- EFFECT OF FOLLOW UP ON RESISTANCE
- EFFECT OF SHUNTING

Pressure is applied even before the current is activated to ensure a good bond. Accurate control and timing of the electric current and application of pressure is an essential feature of resistance welding.

The strength of the bond also depends on the cleanliness of the mating surfaces, although the process is more tolerant of the presence of oxide layers and contaminants than other welding processes. Resistance welding processes require specialized machinery, but they have the major advantages of not requiring filler metals, shielding gases, or flux.

The three major resistance welding processes are resistance spot welding (RSW), resistance seam welding (RSEW), and projection welding (PW). Flash welding (FW) is also classified as a resistance welding process, but it is unique in that the heat for welding is created at the faying surfaces of the joint not only by resistance to the flow of electric current, but also by arcs across the interface. Upset welding (UW) differs from flash welding in that no arc is generated by the process. Capacitor discharge stud welding incorporates a stud which serves as a weld member and is a process similar to flash welding. High-frequency resistance welding (HFRW) concentrates current of the surface of the part to heat the base metal and cause the coalescence of metal.

This article addresses procedure development and considerations for using these processes to join specific types of materials. Additional information about these processes can be found in the Section "Fusion Welding Processes" in this Volume.

Acknowledgements

Special thanks are due to David M. Beneteau of CenterLine (Windsor) Limited, who offered suggestions about revisions for portions of this article. His participation was arranged through the Resistance Welder Manufacturers Association.

Reference

1. L.P. CONNER, ED., *WELDING HANDBOOK*, 8TH ED., VOL 1, AWS, 1987, P 16

Resistance Spot Welding

Resistance spot welding is the most common form of resistance welding. It is a process in which laying surfaces are joined in one or more overlapping spots by the heat generated by resistance to the flow of electric current through workpieces that are held together under force by electrodes. The contacting surfaces in the region of current concentration are heated by a short-time pulse of low-voltage, high-amperage current to form a fused nugget of weld metal. When the flow of current ceases, the electrode force is maintained while the weld metal rapidly cools and solidifies. The electrodes are retracted after each weld, which usually is completed in a fraction of a second.

The size and shape of the individually formed welds are limited primarily by the size and contour of the electrode faces. The weld nugget forms at the faying surfaces (Fig. 1), but does not extend completely to the outer surfaces. In a cross section, the nugget in a properly formed spot weld is obround or oval in shape; in plan view, it has the same shape as the electrode face (which usually is round) and approximately the same size. The spots should be at a sufficient distance from the edge of the workpiece (edge distance) so that there is enough base metal to withstand the electrode force and to ensure that the local distortion during welding does not allow expulsion of metal from the weld. Additional information is available in the article "Resistance Spot Welding" in this Volume.

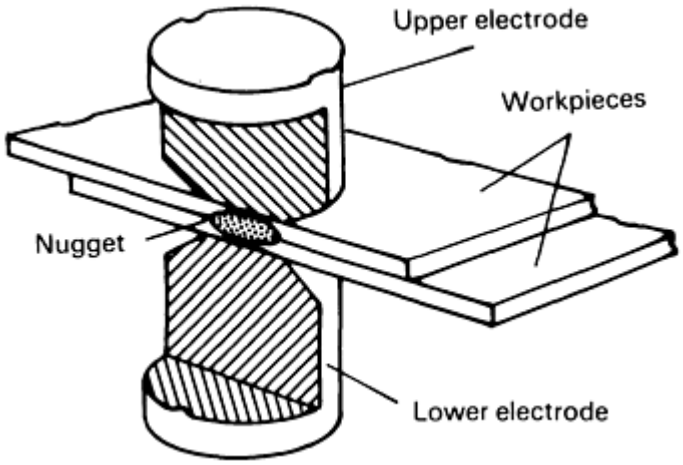

FIG. 1 CUTAWAY VIEW SHOWING LOCATION AND SHAPE OF WELD NUGGET RELATIVE TO THE INNER AND OUTER SURFACES OF WORKPIECES IN A RESISTANCE SPOT WELDING SETUP

RSW Applications

Weldability and the thickness of the metals joined are key factors in determining whether two materials can be resistance spot welded.

Material Selection (Ref 2). Practically all combinations of ductile metals and alloys can be spot welded (Table 1). Some, like copper to aluminum, and aluminum to magnesium, form alloys having little strength. Others, such as zinc and some of the high-chromium alloys, experience grain growth even during a very short welding period. Although welding times are relatively short, the material is adversely affected by the heat conducted through the sheet to the point that the physical properties such as the strength and corrosion resistance of the material surface are typically reduced in value. The short welding period is also necessary in stainless steel to prevent carbide precipitation when the carbon content is high enough to permit it. High-carbon steels weld readily, but the weld will be in the full-hardened state and will require subsequent heat treatment. This can be accomplished automatically by a control that applies preheating, postheating, or both as part of the welding cycle. To ensure that the control can apply the compensating quench or temper cycle, the electrodes must open immediately after the cycle is complete. Excessive hold time will quench the joint, negating the benefits associated with this control function.

TABLE 1 RELATIVE WELDABILITY RATINGS OF SELECTED METAL AND ALLOY COMBINATIONS USED FOR RESISTANCE SPOT WELDING OPERATIONS

A, excellent; B, good; C, fair; D, poor; E, very poor; F, impractical

METALS	ALUMINUM	STAINLESS STEEL	BRASS	COPPER	GALVANIZED IRON	STEEL	LEAD	MONEL	NICKEL	NICHROME	TINPLATE	ZINC	PHOSPHOR BRONZE	NICKEL SILVER	TERNEPLATE
ALUMINUM	B	E	D	E	C	D	E	D	D	D	C	C	C	F	C
STAINLESS STEEL	F	A	E	E	B	A	F	C	C	C	B	F	D	D	B
BRASS	D	E	C	D	D	D	F	C	C	C	D	E	C	C	D
COPPER	E	E	D	F	E	E	E	D	D	D	E	E	C	C	E
GALVANIZED IRON	C	B	D	E	B	B	D	C	C	C	B	C	D	E	B
STEEL	D	A	D	E	B	A	E	C	C	C	B	F	C	D	A
LEAD	E	F	F	E	D	E	C	E	E	E	. . .	C	E	E	D
MONEL	D	C	C	D	C	C	E	A	B	B	C	F	C	B	C
NICKEL	D	C	C	D	C	C	E	B	A	B	C	F	C	B	C
NICHROME	D	C	C	D	C	C	E	B	B	A	C	F	D	B	C
TINPLATE	C	B	D	E	B	B	. . .	C	C	C	C	C	D	D	C
ZINC	C	E	E	E	C	F	C	F	F	F	C	C	D	F	C
PHOSPHOR BRONZE	C	D	C	C	D	C	E	C	C	D	D	D	B	B	D
NICKEL SILVER	F	D	C	C	E	D	E	B	B	B	D	F	B	A	D
TERNEPLATE	C	B	D	E	B	A	D	C	C	C	C	C	D	D	B

Source: Ref 3

Zinc-alloy die castings can be welded with little loss of strength, but the ductility is reduced. Free-turning Bessemer screw-machine steel frequently refuses to weld, or results in brittle welds, and hence its use for welded parts should be avoided. Usually, however, when clean, properly prepared metal parts are spot welded, the strength of the welds is perfectly satisfactory. Table 1 lists combinations that have been successfully welded. Many other combinations may also be satisfactorily welded. Copper and silver are difficult to weld, but they may be welded by the use of low-conductivity electrodes (for example, refractory alloys such as Elkonite and Trodaloy). Copper alloys are more commonly resistance brazed. In many applications, the weldability of copper is increased if it has a tinned surface.

Thickness Parameters (Ref 4). Parts of widely different thicknesses may be spot welded. For example, 0.4 mm ($\frac{1}{64}$ in.) material can be welded to a 150 mm (6 in.) thick piece and would require only slightly more power input and pressure than to weld two pieces of 0.4 mm ($\frac{1}{64}$ in.) material, as it is not necessary to heat the 150 mm (6 in.) piece through, and the push-up is obtained on the thinner piece. The thickness of the thinner component is referred to as the governing metal thickness because it dictates the heat input. However, the thermal mass of the larger component may make RSW applications impractical because the thick section may not reach fusion temperature before the thin piece is melted. The limit to welding pieces of equal thickness with an uninterrupted flow of current seems to be approximately 3.2 mm ($\frac{1}{8}$ in.). Greater thicknesses may be welded by a technique known as pulsation welding. In the pulsation welding method, the current is turned off during the weld at intervals that allow the electrodes to cool the electrode/workpiece surface. This ensures that the heat will be generated as desired, primarily at the faying surface.

Sheet Steel Limitations. Spot welded lap joints are widely used in joining sheet steel up to about 3.2 mm ($\frac{1}{8}$ in.) thick (Table 2) and are used occasionally in joining steel 6.4 mm ($\frac{1}{4}$ in.) or more in thickness, *t*. Thicknesses of 25 mm (1 in.) or more have been joined by spot welding, but this requires special equipment and would not ordinarily be economical. Many assemblies of two or more sheet metal stampings that do not require gastight or liquid-tight joints can be more economically joined by high-speed RSW than by mechanical methods.

TABLE 2 MINIMUM DIMENSIONS FOR SINGLE-IMPULSE SPOT WELDS IN LOW-CARBON STEEL

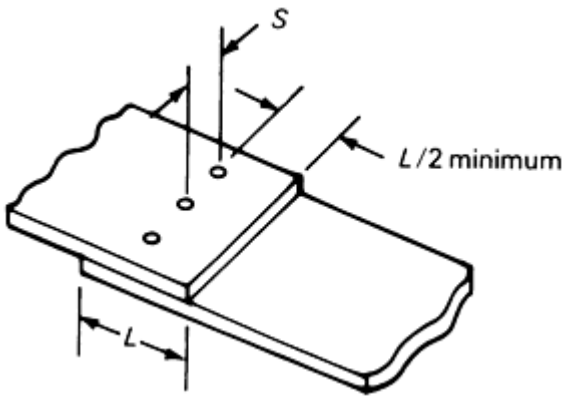

STOCK THICKNESS		**MINIMUM WELD SPACING, *S***		MINIMUM OVERLAP OF MATERIAL, *L*	
mm	**in.**	**mm**	**in.**	**mm**	in.
0.25	0.010	6.3	0.250	9.5	**0.375**
0.53	0.021	9.5	0.375	11	**0.433**
0.80	0.031	13	0.500	11	**0.433**
1.0	0.040	19	0.750	13	**0.500**
1.3	0.050	22	0.875	14	**0.551**
1.6	0.063	27	1.062	16	**0.625**

2.0	0.078	35	1.375	17	**0.669**
2.4	0.094	41	1.625	19	**0.750**
2.8	0.109	46	1.813	21	**0.827**
3.2	**0.125**	**51**	**2.000**	**22**	**0.875**

Source: Ref 5

For aluminum and magnesium welds, minimum spot spacing, *S*, should equal 8*t*. A spot spacing value of 16*t* would be even better if the strength requirements of the joint permit such spacing (Ref 5).

Joint Design Recommendations. Like other welds, resistance spot welds are subject to shrinkage on cooling. To minimize distortion, welds should be positioned to balance shrinkage forces (Fig. 2).

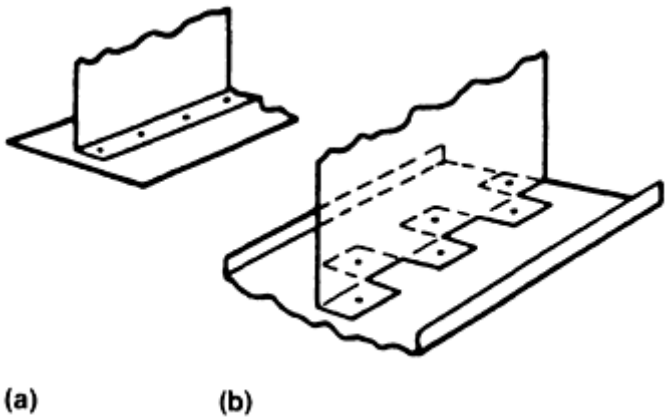

FIG. 2 PLACEMENT OF WELDS TO JOIN TWO SHEETS OF METAL IN A T-JOINT. (A) CONFIGURATION NOT RECOMMENDED DUE TO UNBALANCED SHRINKAGE FORCES. (B) PREFERRED SETUP THAT RESULTS IN BALANCED FORCES AND MINIMUM DISTORTION

Distortion can also result from electrode skidding. This is related to stress introduced at the time of electrode impact and machine deflection under high electrode force. The components must be designed to provide methods of accommodating variations (for example, by incorporating slip joints and minimizing material stackups).

Even when welding of multiple spot thicknesses is feasible, it can be more troublesome than simple welds of two sheet thicknesses. Scalloped edges permit alternate welding of spots in two thicknesses only (Fig. 3). However, scalloped edges are rarely used and the current trend is toward triple-metal-thickness welding as a method of reducing capital cost.

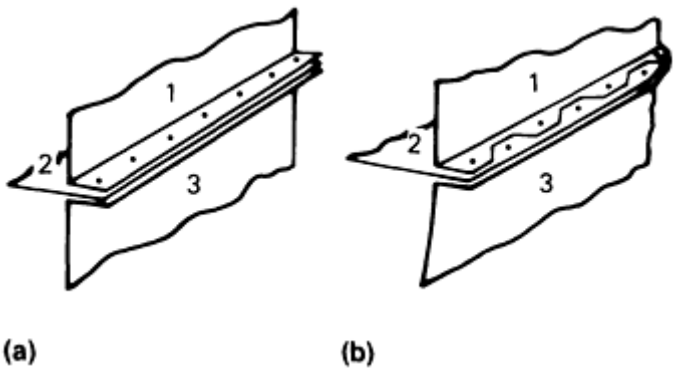

FIG. 3 PLACEMENT OF WELDS TO JOIN THREE SHEETS OF METAL IN A T-JOINT. (A) CONFIGURATION THAT CAN BE USED TO JOIN THREE STOCK THICKNESSES. (B) RECOMMENDED CONFIGURATION INCORPORATING

SCALLOPED EDGES TO PERMIT ALTERNATE WELDING OF SPOTS IN TWO THICKNESSES ONLY

Spot-welded assemblies should be designed so that joint areas are readily accessible to the electrode and simple, inexpensive electrodes can be used. When special electrode shapes are required, every effort should be made to avoid extremes of shape and to provide as accessible a joint as possible. Deep, narrow joint areas should be avoided. Figure 4 provides guidelines for accessibility of joints.

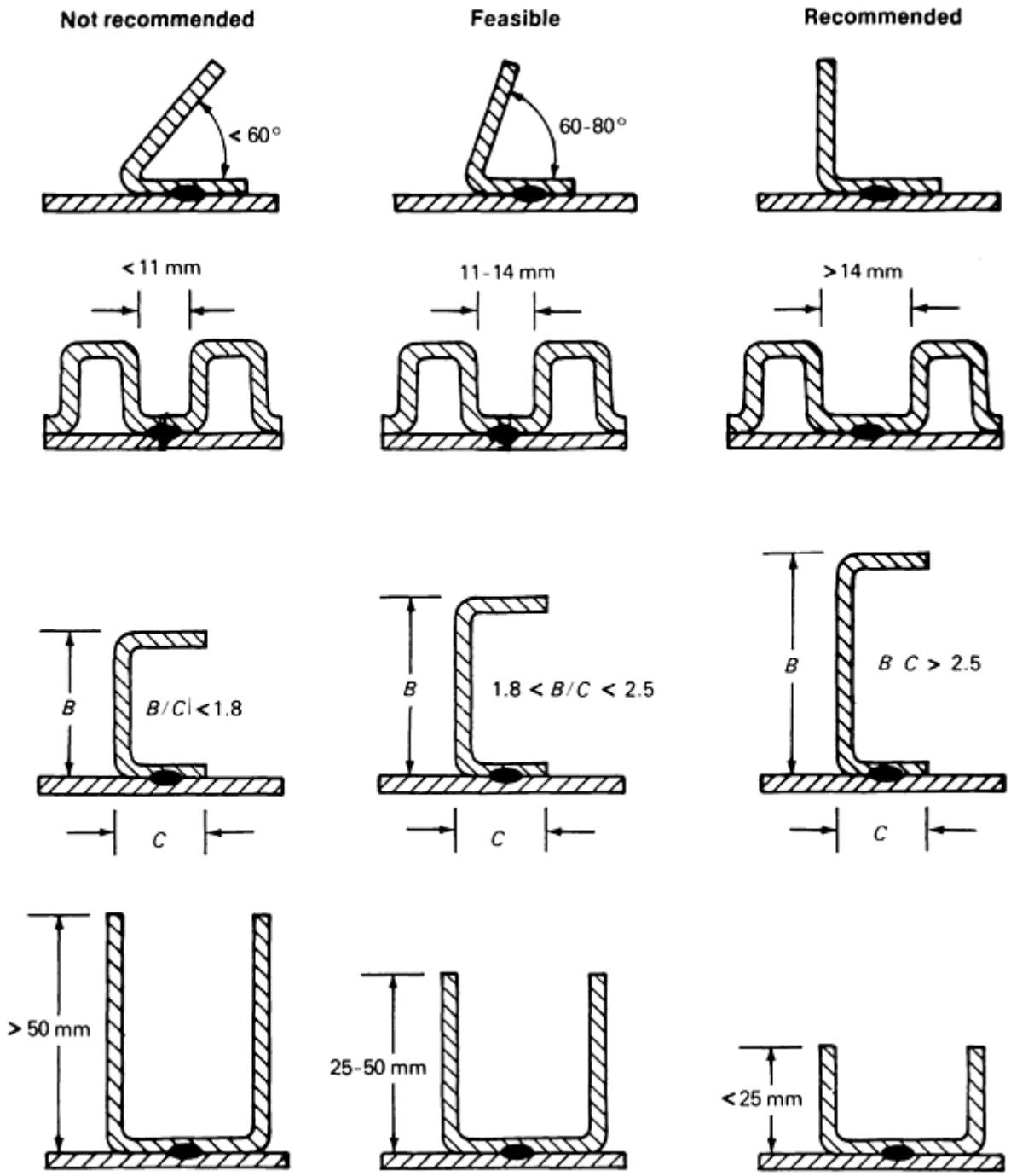

FIG. 4 GRADUAL IMPROVEMENTS IN JOINT DESIGN THAT PROVIDE OPTIMUM ACCESS TO SELECTED JOINT CONFIGURATIONS USING STANDARD ELECTRODES

Weld Strength in RSW Joints. The strength of a single spot weld in shear depends on the cross-sectional area of the nugget in the plane of the faying surfaces.

Lap joints may fail either by shear through the nugget, or by tearing of the base metal adjacent to the weld nugget. Low weld strengths are typically associated with weld nugget shear failure, and high strengths are typically associated with base metal tearing. A minimum nugget diameter that is unique to the type of base material, surface condition, and metal gage used, is required in order to obtain failure by base metal tearing.

Increasing the nugget diameter above this minimum value can produce an increase in the weld strength. Figure 5 shows the slight increase in strength values obtained for low-carbon steel as a result of increases in nugget size.

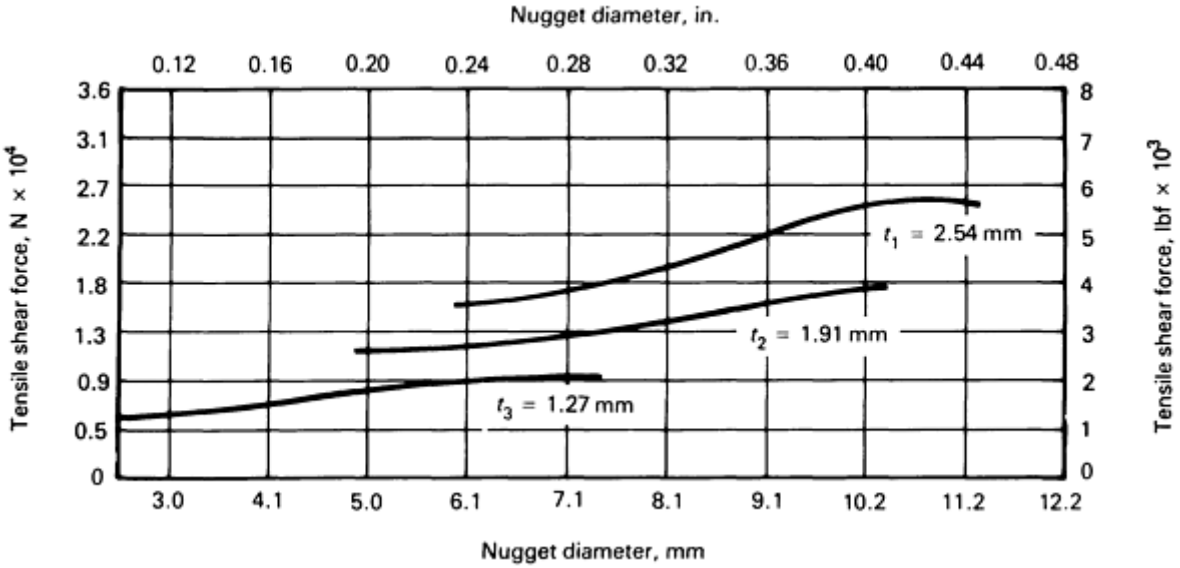

FIG. 5 PLOT OF TENSILE SHEAR STRENGTH VERSUS WELD NUGGET DIAMETER AS A FUNCTION OF SHEET THICKNESS, *T*, FOR 1008 LOW-CARBON STEEL

The strength of multiple spot-welded joints depends on material thickness, spot weld spacing, and weld pattern. The spacing between adjacent spot welds may alter the joint weld strength due to current shunting through previous welds. As the spacing between adjacent spot welds decreases, the joint shear strength may decrease.

Table 3 summarizes the relationship between resistance spot welding variables and joint strength for uncoated low-carbon steel.

TABLE 3 RECOMMENDED PARAMETERS FOR RESISTANCE SPOT WELDING OF UNCOATED LOW-CARBON STEEL SHEET PRODUCED FOR AUTOMOTIVE APPLICATIONS

Data are average values.

SHEET THICKNESS		**ELECTRODE**				**FORCE[C]**		**WELD TIME, CYCLES (60 HZ)**	**WELDING CURRENT, A**	**MINIMUM CONTACT OVERLAP**		**MINIMUM WELD SPACING[D]**				**MINIMUM SHEAR STRENGTH**		BUTTON DIAMETER	
		FACE DIAMETER		**SHAPE[A]**	**BEVEL ANGLE[B]**							**TWO STACK**		**THREE STACK**					
MM	**IN.**	**MM**	**IN.**			**KN**	**LBF**			**MM**	**IN.**	**MM**	**IN.**	**MM**	**IN.**	**KN**	**LBF**	**MM**	IN.
0.51	0.020	4.78	0.188	E,A,B	45 °	1.8	400	7	8,500	11.2	0.44	9.7	0.38	15.8	0.62	1.43	320	2.5	**0.10**
0.64	0.025	4.78	0.188	E,A,B	45 °	2.0	450	8	9,500	11.9	0.47	15.8	0.62	22.4	0.88	2.02	450	3.1	**0.12**
0.76	0.030	6.35	0.250	E,A,B	45 °	2.2	500	9	10,500	11.9	0.47	15.8	0.62	22.4	0.88	2.58	575	3.6	**0.14**
0.89	0.035	6.35	0.250	E,A,B	45 °	2.7	600	9	11,500	13.5	0.53	19.1	0.75	26.9	1.06	3.36	750	4.1	**0.16**
1.02	0.040	6.35	0.250	E,A,B	45 °	3.1	700	10	12,500	13.5	0.53	19.1	0.75	26.9	1.06	4.14	925	4.6	**0.18**
1.14	0.045	6.35	0.250	E,A,B	45 °	3.4	750	11	13,000	15.0	0.59	24.9	0.94	30.0	1.18	5.15	1150	4.8	**0.19**
1.27	0.050	7.92	0.312	E,A,B	30°	3.6	800	12	13,500	15.0	0.59	24.9	0.94	30.0	1.18	6.05	1350	5.1	**0.20**
1.40	0.055	7.92	0.312	E,A,B	30°	4.0	900	13	14,000	16.0	0.63	26.9	1.06	33.3	1.31	7.53	1680	5.3	**0.21**
1.52	0.060	7.92	0.312	E,A,B	30°	4.5	1000	14	15,000	16.0	0.63	26.9	1.06	33.3	1.31	8.29	1850	5.8	**0.23**
1.78	0.070	7.92	0.312	E,A,B	30°	5.4	1200	16	16,000	16.8	0.66	30.0	1.18	38.1	1.50	10.3	2300	6.4	**0.25**
2.03	0.080	7.92	0.312	E,A,B	30°	6.3	1400	18	17,000	18.3	0.72	35.1	1.38	40.6	1.60	12.1	2700	6.6	**0.26**
2.29	0.090	9.53	0.375	E,A,B	30°	7.2	1600	20	18,000	19.8	0.78	39.6	1.56	47.8	1.88	15.5	3450	6.9	**0.27**
2.67	0.105	9.53	0.375	E,A,B	30°	8.1	1800	23	19,500	21.3	0.84	42.7	1.68	50.8	2.00	18.6	4150	7.1	**0.28**
3.05	**0.120**	**9.53**	**0.375**	**E,A,B**	**30°**	**9.4**	**2100**	**26**	**21,000**	**22.4**	**0.88**	**46.0**	**1.81**	**63.5**	**2.50**	**22.4**	**5000**	**7.6**	**0.30**

Source: Ref 6

(A) SHAPE DEFINITIONS: E, TRUNCATED CONE; A, POINTED; B, 75 MM (3 IN.) RADIUS.

(B) APPLIES TO TRUNCATED CONE ELECTRODES ONLY AND IS MEASURED FROM THE PLANE OF THE ELECTRODE FACE.

(C) FOR INTERMEDIATE THICKNESSES, FORCE AND WELD TIME MAY BE INTERPOLATED.

(D) MINIMUM WELD SPACING IS MEASURED FROM CENTERLINE TO CENTERLINE.

Power Requirements. Nearly all RSW of low-carbon steel is direct-energy welding, in which single- or three-phase 60-cycle alternating current, drawn ordinarily from 220 or 440 V implant power lines and stepped down to about 2 to 20 V, is fed directly to the electrodes as each weld is made.

Direct and Series Welding

Spot welds are classified as either direct or series welds.

Direct Single-Spot Welding. Single-spot welds are usually made by direct welding. Figure 6 shows schematically three arrangements used for making this type of weld; these arrangements may be modified to meet special requirements. In all of the arrangements shown, one transformer secondary circuit makes one spot weld.

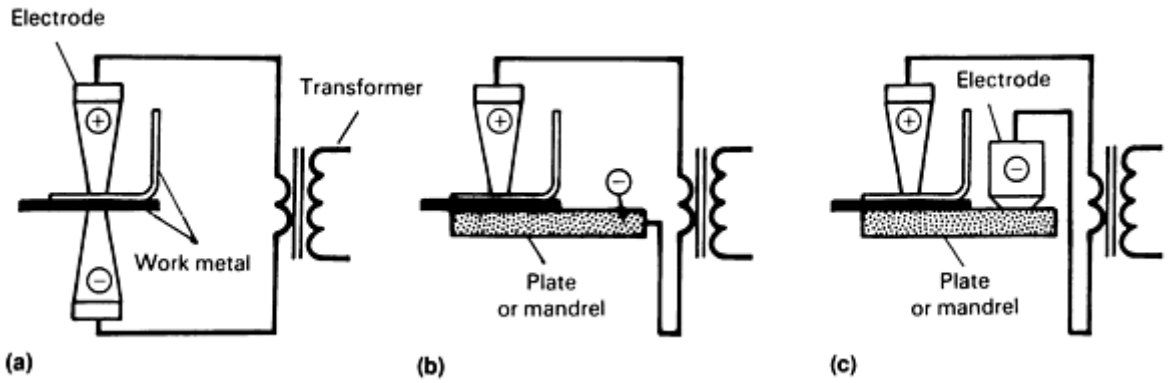

FIG. 6 RELATION OF WORK METAL TO ELECTRODES WHEN MAKING SINGLE-SPOT WELDS BY DIRECT WELDING

The simplest and most common arrangement in which two workpieces are sandwiched between opposing upper and lower electrodes, is shown in Fig. 6(a). In Fig. 6(b), a conductive plate or mandrel having a large contacting surface is used as the lower electrode; this reduces marking on the lower workpiece and conducts heat away from the weld more rapidly and may be necessary because of the shape of the workpiece. In the arrangement in Fig. 6(c), a conductive plate or mandrel beneath the lower workpiece is used for the same purposes but in conjunction with a second upper electrode.

Direct Multiple-Spot Welding. Two arrangements of the secondary circuit for making two or more spot welds simultaneously by direct welding are shown in Fig. 7(a) and 7(b). In direct multiple-spot welding (as well as in series multiple-spot welding, described below), tip contour and surface condition must be the same for each electrode. Also, the force exerted by all the electrodes on the workpieces must be equal, regardless of inequalities in work-metal thickness. The force can be equalized by using a spring-loaded electrode holder or a hydraulic equalizing system. The use of a conductive plate or mandrel, as in Fig. 7(b), minimizes weld marks on the lower workpiece.

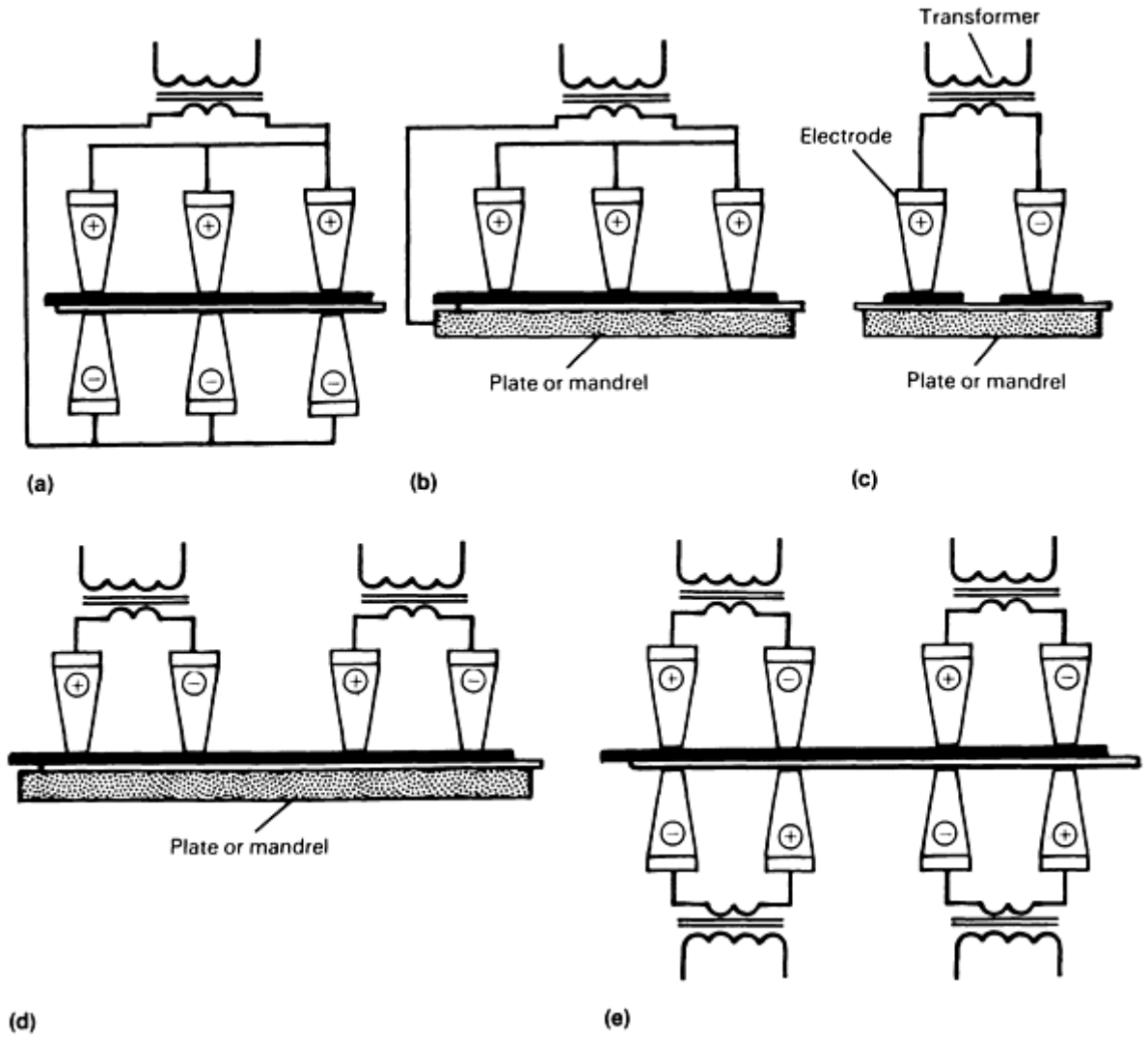

FIG. 7 RELATION OF WORK METAL TO ELECTRODES WHEN MAKING MULTIPLE-SPOT WELDS. (A) AND (B) DIRECT WELDING. (C), (D), AND (E) SERIES WELDING

Series Multiple-Spot Welding. Three arrangements for making a number of spot welds simultaneously by series welding are shown in Fig. 7(c), 7(d), and 7(e). In Fig. 7(d), each of the two transformer secondary circuits makes two spot welds. A portion of the current bypasses the weld nuggets through the upper workpiece.

Push-Pull Welding. Figure 7(e) is commonly referred to as push-pull welding. The advantage to this process is that the secondary loop area is quite small. This is common for components such as floor pans where a normal welding unit would have a throat several feet deep.

References cited in this section

2. J.F. YOUNG AND R.S. SHANE, ED., *MATERIALS AND PROCESSES, PART B: PROCESSES,* 3RD ED., MARCEL DEKKER, 1985, P 11257-1126
3. J.G. BRALLA, ED., *HANDBOOK OF PRODUCT DESIGN FOR MANUFACTURING,* MCGRAW-HILL, 1986, P 7-35
4. J.F. YOUNG AND R.S. SHANE, ED., *MATERIALS AND PROCESSES, PART B: PROCESSES,* 3RD ED., MARCEL DEKKER, 1985, P 1127

5. J.G. BRALLA, ED., *HANDBOOK OF PRODUCT DESIGN FOR MANUFACTURING,* MCGRAW-HILL, 1986, P 7-38
6. R.L. O'BRIEN, ED., *WELDING HANDBOOK,* 8TH ED., VOL 2, AWS, 1991, P 552

Procedure Development and Practice Considerations for Resistance Welding

Resistance Seam Welding

Resistance seam welding is a process in which heat caused by resistance to the flow of electric current in the work metal is combined with pressure to produce a welded seam. This seam, consisting of a series of overlapping spot welds, is normally gastight or liquid-tight. Two rotating, circular electrodes (electrode wheels), or one circular and one bar-type electrode, are used for transmitting the current to the work metal. When two electrode wheels are used, one or both wheels are driven either by means of a gear-driven shaft or by a knurl or friction drive that contacts the peripheral surface of the electrode wheel.

The series of spot welds is made without retracting the electrode wheels or releasing the electrode force between spots, although the electrode wheels may advance either continuously or intermittently.

Additional information is available in the article "Resistance Seam Welding" in this Volume.

Seam Welding Machines

A seam welding machine is similar in construction to a spot welding machine, except that one or two electrode wheels are substituted for the spot welding electrodes. Generally, seam. Welding is done in a press-type resistance welding machine.

There are four basic types of RSEW machines:

- *CIRCULAR:* AXIS OF ROTATION OF THE ELECTRODE WHEELS IS AT RIGHT ANGLES TO THE FRONT OF THE MACHINE (FIG. 8A).
- *LONGITUDINAL:* AXIS OF ROTATION OF THE ELECTRODE WHEELS IS PARALLEL TO THE FRONT OF THE MACHINE (FIG. 8B), AND THROAT DEPTH IS TYPICALLY 305 TO 915 MM (12 TO 36 IN.).
- *UNIVERSAL:* A SWIVEL-TYPE HEAD AND INTER-CHANGEABLE LOWER ARMS ALLOW THE AXIS OF ROTATION OF THE ELECTRODE WHEELS TO BE SET EITHER AT RIGHT ANGLES OR PARALLEL TO THE FRONT OF THE MACHINE.
- *PORTABLE:* WORK IS CLAMPED IN A FIXTURE, AND A PORTABLE WELDING HEAD IS MOVED OVER THE SEAM. THIS TYPE OF MACHINE IS USED FOR WORKPIECES THAT ARE TOO BULKY TO BE HANDLED BY REGULAR MACHINES

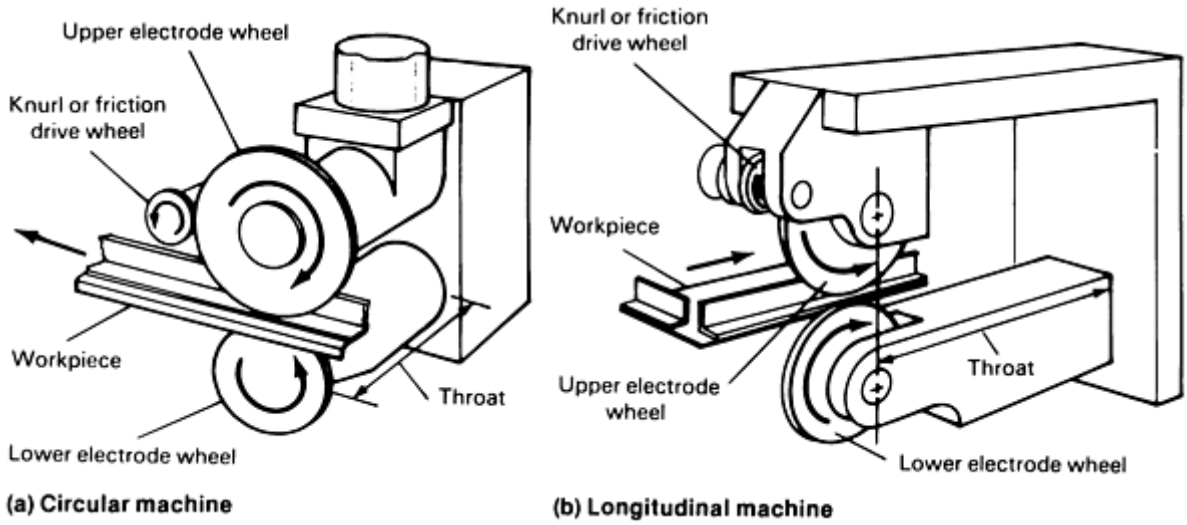

FIG. 8 RELATION OF ELECTRODE WHEELS TO OTHER COMPONENTS IN CIRCULAR AND LONGITUDINAL RSEW MACHINES

Electrodes

Electrode wheels made of Resistance Welder Manufacturers Association (RWMA) class 1 material were once used for seam welding of aluminum and magnesium alloys, galvanized steel, and tin-plated steel. However, class 1 material is now uncommon because of the restrictions on cadmium exposure. Typically, class 2, 3, or 20 materials are used (similar to spot welding electrodes).

Electrode wheels range in diameter from 50 to 610 mm (2 to 24 in.). Table 4 shows the diameters and body widths of commonly used electrodes, in relation to the size of the welding machine. Narrower wheels are used in machines with knurl or friction drive; wider wheels, in gear drive and idler machines.

TABLE 4 COMMON SIZES OF ELECTRODE WHEELS USED FOR RESISTANCE SEAM WELDING APPLICATIONS

MACHINE SIZE	**WHEEL DIAMETER**		WHEEL WIDTH[A]	
	mm	**in.**	**mm**	in.
SMALL	18	7	9.5	$\frac{3}{8}$
MEDIUM	20	8	9.5-13	$\frac{3}{8}$ - $\frac{1}{2}$
LARGE	**25-30**	**10-12**	**9.5-19**	$\frac{3}{8}$ - $\frac{3}{4}$

(A) DATA ARE FOR BODY WIDTH.

A small-diameter electrode wheel (Fig. 9a), or a large-diameter wheel mounted on a canted axis (Fig. 9b), can be used to avoid interference with a sidewall when a narrow flange is being welded on an inside radius or on a re-entrant curve. Beads, fibs, and other extensions on the surfaces to be seam welded can be passed over by cutting notches in the electrode wheels (Fig. 10).

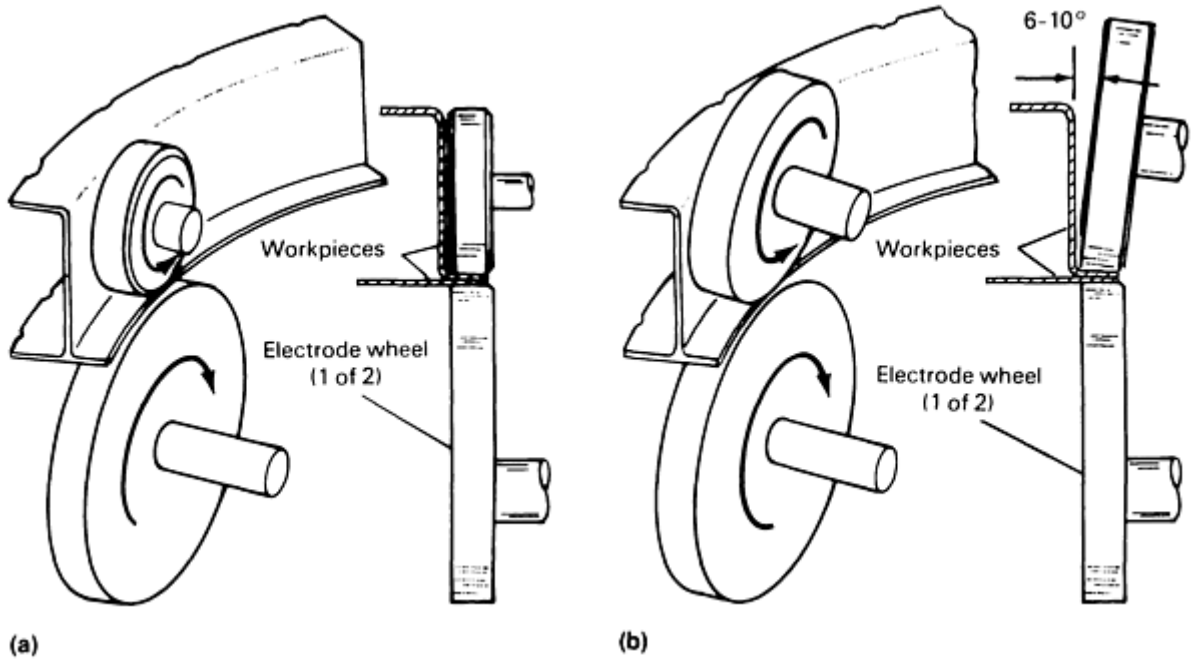

FIG. 9 UPPER ELECTRODE WHEELS DESIGNED TO AVOID INTERFERENCE WITH A SIDEWALL. (A) SMALL-DIAMETER WHEEL. (B) CANTED LARGE-DIAMETER WHEEL

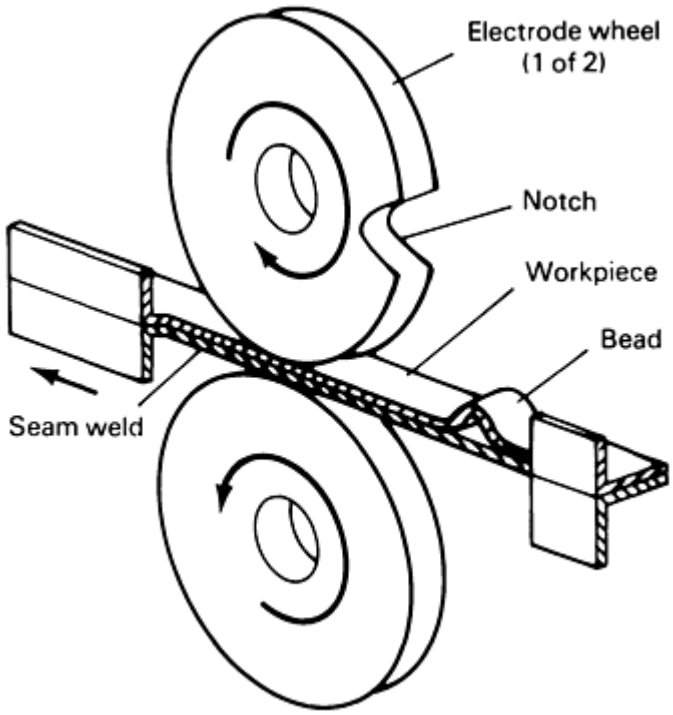

FIG. 10 NOTCH ELECTRODE WHEEL USED TO SEAM WELD A WORKPIECE HAVING AN OBSTRUCTION IN THE PATH OF THE WHEEL

Process Variations

Seam welding operations vary primarily in terms of travel speed and duration of the welding current. In continuous-motion welding, the electrodes (or workpieces) are driven at a constant speed, and welding current is either interrupted or

flows continuously. In either case, a continuous, leaktight seam is generated. This method is generally used for metals less than about 4.8 mm ($\frac{3}{16}$ in.) thick.

In intermittent-motion welding, rotation of the electrode wheels is automatically stopped to produce a spot weld; the electrodes are then rotated to move the workpiece the required distance for the next weld. This method is often used for aluminum and steel alloys less than 4.8 mm ($\frac{3}{16}$ in.) thick and selected metals greater than 4.8 mm ($\frac{3}{16}$ in.) thick.

Lap Seam Welding. In this process (also known as stitch or roll welding), the on and off cycling of the current while the electrodes continuously rotate actually determines the weld spacing (Fig. 11a). The minimum joint overlap is the same as for spot welding. There is generally no forging (that is, mash-down) with lap seam welding.

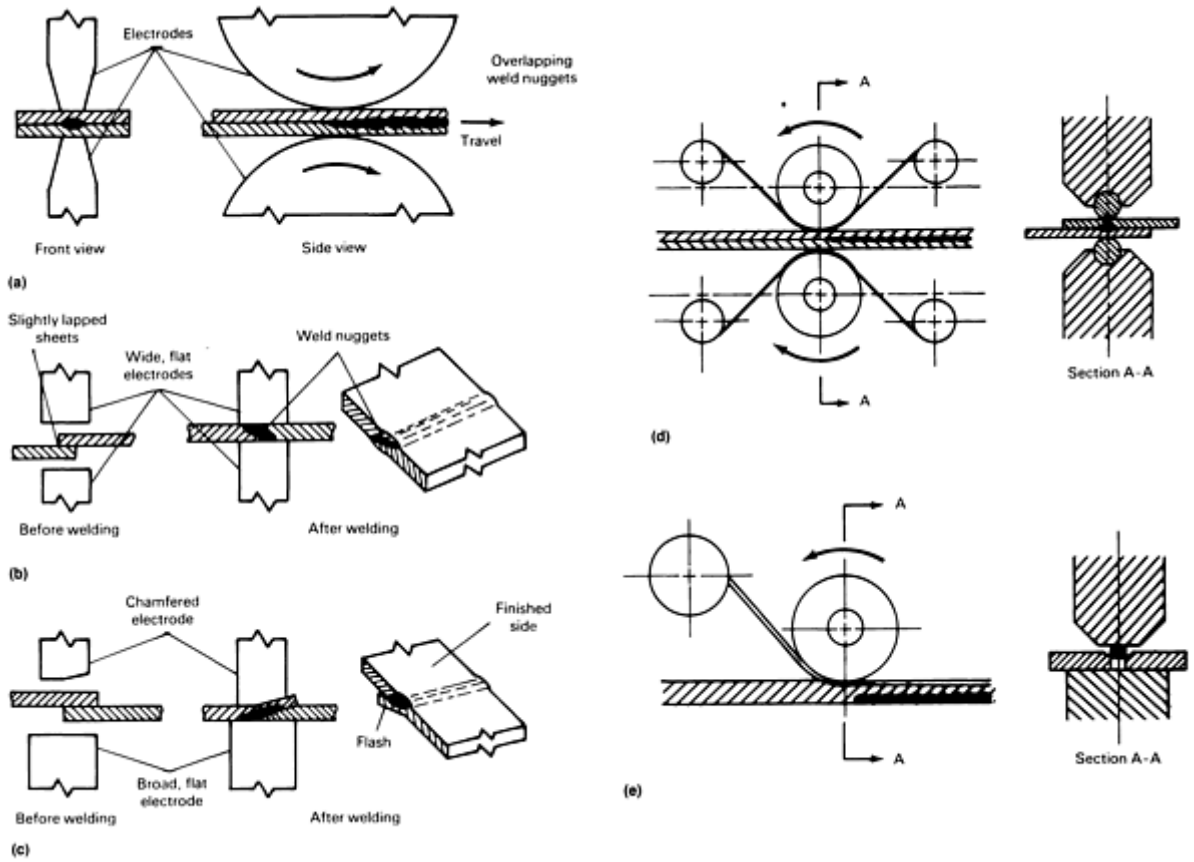

FIG. 11 PROCESS VARIATIONS OF SEAM WELDING. (A) LAP SEAM WELDING. (B) MASH SEAM WELDING. (C) METAL FINISH SEAM WELDING. (D) ELECTRODE WIRE SEAM WELDING. (E) FOIL BUTT SEAM WELDING

Mash seam welding generally has less overlap than lap seam welding and produces more mash-down (electrode force) with its continuous current (Fig. 11b). Joint thicknesses after welding usually vary from 120 to 150% of the sheet thickness. Continuous seams produced by this method have smooth appearance, but rigid workholding fixtures are required to minimize distortion.

Metal Finish Seam Welding. This process uses a chamfered electrode wheel, and one side of the joint is mashed down while the other side of the joint has a smooth, flat finish (Fig. 11c). Overlap is greater than for mash seam welding, and higher current amperages and electrode forces are also required.

Electrode wire seam welding is an internationally patented process that requires an intermediate wire electrode between each wheel electrode and the workpiece (Fig. 11d). The electrode wire seam welding process is used almost

exclusively for seam welding of tin mill products to fabricate cans. The copper wire travels around the wheel electrodes at the welding speed. The circular or flat cross-section of copper wire electrode provides a continuously renewed surface, but it is not consumed in the welding operation. The tin build-up which would occur on a copper wheel electrode is thus avoided. The process requires specially designed welding systems. The seam welds may be made with two wheel electrodes, or one wheel electrode and a mandrel electrode.

Foil Butt Seam Welding. This process requires metal foil to be placed on one or both sides of a butt joint prior to seam welding (Fig. 11e). The foil distributes current to the edges of the sheet, provides additional electrical resistance, helps to contain the molten metal, and also serves as a filler.

Applications

Resistance seam welding can be applied to a variety of workpiece shapes. Girth welds can be made in round, square, or rectangular parts by using electrode wheels of suitable diameter. Longitudinal welds can also be made.

Advantages of RSEW, as compared with resistance spot and projection welding, are:

- GASTIGHT OR LIQUID-TIGHT JOINTS CAN BE PRODUCED
- OVERLAP CAN BE LESS THAN FOR RESISTANCE SPOT WELDS OR PROJECTION WELDS, AND SEAM WIDTH CAN BE LESS THAN THE DIAMETER OF SPOT OR PROJECTION WELDS (TABLE 5)
- ROLLED SECTIONS ARE FREQUENTLY WELDED IN-LINE, THEREBY ELIMINATING SUBSEQUENT OPERATIONS

TABLE 5 RECOMMENDED PRACTICE FOR SEAM WELDING OF 1010 LOW-CARBON STEEL

Data are for material free of scale, oxide, paint, grease, and oil. Welding conditions determined by thickness of thinnest outside piece.

THICKNESS, *T*, OF THINNEST OUTSIDE PIECE[A]		**ELECTRODE DIMENSIONS**				**NET ELECTRODE FORCE**		**HEAT TIME, CYCLES (60 HZ)**	**COOL TIME (PRESSURE TIGHT), CYCLES (60 HZ)**	**WELDING SPEED**		**WELDS PER MM**	**WELDS PER IN.**	**APPROXIMATE WELDING CURRENT, A**	MINIMUM CONTACTING OVERLAP[C]	
		WHEEL WIDTH (*W*)[B]		**FACE WIDTH (*W*)[B]**												
mm	**in.**	**mm**	**in.**	**mm**	**in.**	**kn**	**lbf**			**mm/min**	**in./min**				**MM**	IN.
0.25	0.010	9.5	3/8	4.8	3/16	1.8	400	2	1	200	80	0.60	15	8,000	9.5	3/8
0.53	0.021	9.5	3/8	4.8	3/16	2.5	550	2	2	190	75	0.48	12	11,000	11	7/16
0.80	0.031	13	1/2	6.4	1/4	3.1	700	3	2	185	72	0.40	10	13,000	13	1/2
1.02	0.040	13	1/2	6.4	1/4	4.0	900	3	3	170	67	0.36	9	15,000	13	1/2
1.27	0.050	13	1/2	7.9	5/16	4.7	1050	4	3	165	65	0.32	8	16,500	14	9/16
1.57	0.062	13	1/2	7.9	5/16	5.3	1200	4	4	160	63	0.28	7	17,500	16	5/8
1.98	0.078	16	5/8	9.5	3/8	6.7	1500	6	5	140	55	0.24	6	19,000	17.5	11/16
2.39	0.094	16	5/8	11	7/16	7.6	1700	7	6	125	50	0.24	6	20,000	19	3/4
2.77	0.109	19	3/4	13	1/2	8.7	1950	9	6	120	48	0.20	5	21,000	20.5	13/16
3.18	**0.125**	**19**	3/4	**13**	1/2	**9.8**	**2200**	**10**	**7**	**115**	**45**	**0.20**	**5**	**22,000**	**22**	7/8

(A) DATA FOR TOTAL THICKNESS OF PILE-UP NOT EXCEEDING 4*T*. MAXIMUM RATIO BETWEEN THICKNESSES, 3 TO 1.

(B) FOR RWMA CLASS 2 ELECTRODE MATERIAL (MINIMUM CONDUCTIVITY, 75% IACS; MAXIMUM HARDNESS, 75 HRB). WHEEL WIDTH IS OVERALL WIDTH OF A FIAT-FACE WHEEL OR OF A WHEEL WITH A 75 MM (3 IN.) RADIUS FACE; FACE WIDTH IS THAT OF THE CONTACTING SURFACE OF FLAT-FACE WHEELS.

(C) FOR LARGER ASSEMBLIES, MINIMUM CONTACTING OVERLAP INDICATED SHOULD BE INCREASED 30%.

Limitations of RSEW, apart from those it shares with spot and projection welding, are:

- THE WELD ORDINARILY MUST PROCEED IN A STRAIGHT OR UNIFORMLY CURVED LINE
- OBSTRUCTIONS ALONG WITH THE PATH OF THE ELECTRODE WHEEL MUST BE AVOIDED OR BE COMPENSATED FOR IN THE DESIGN OF THE WHEEL
- SHARP CORNER RADII OR ABRUPT CHANGES IN CONTOUR ALONG THE PATH OF THE ELECTRODE WHEEL MUST BE AVOIDED (TABLE 6)
- FATIGUE LIFE OF RESISTANCE SEAM WELDS IS USUALLY SHORTER THAN THAT OF WELDS MADE BY OTHER SEAM WELDING METHODS

The shorter fatigue life is due to two factors. First, the most common method of cooling the electrode is flood cooling, which quenches the weld. Second, RSEW electrodes move continuously, preventing the application of postweld heat treatment to temper the weld.

TABLE 6 RECOMMENDED MINIMUM RADII OF CURVATURE FOR SEAM WELDED ALUMINUM AND STEEL COMPONENTS

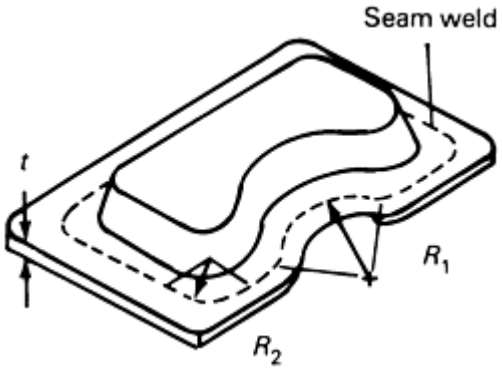

BASE MATERIAL	MINIMUM RADIUS			
	INSIDE RADIUS, R_1		OUTSIDE RADIUS, R_2	
	MM	**IN.**	**MM**	IN.
ALUMINUM	250	10	75	**3**
STEEL	**150**	**6**	**50**[A] **57**[B] **64**[C] **75**[D]	**2**[A] **$2\frac{1}{4}$**[B] **$2\frac{1}{2}$**[C] **3**[D]

Source: Ref 7

(A) 0.8 MM $\leq T \leq$ 1.3 MM (0.031 IN. $\leq T \leq$ 0.051 IN.).

(B) $T \leq$ 1.6 MM ($T \leq$ 0.063 IN.).

(C) $T \leq$ 2.0 MM ($T \leq$ 0.079 IN.).

(D) $T \leq$ 3.0 MM ($T \leq$ 0.12 IN.).

Metals Welded. Low-carbon, high-carbon, low-alloy, high-strength low-alloy (HSLA), stainless, and many coated steels can be resistance seam welded satisfactorily. Alloys with carbon levels above about 0.15% may tend to form areas of hard martensite upon cooling.

Reference cited in this section

7. J.G. BRALLA, ED., *HANDBOOK OF PRODUCT DESIGN FOR MANUFACTURING,* MCGRAW-HILL, 1986, P 7-39

Procedure Development and Practice Considerations for Resistance Welding

Projection Welding

Resistance projection welding (RPW) is a welding process in which current flow and heating are localized at a point or points predetermined by the design or shape of one or both of two parts to be welded (Fig. 12). The process is closely related to resistance spot welding (RSW), in which current flow and heating are localized by one or both electrode contact faces, which determine the location, size, and shape of the weld produced.

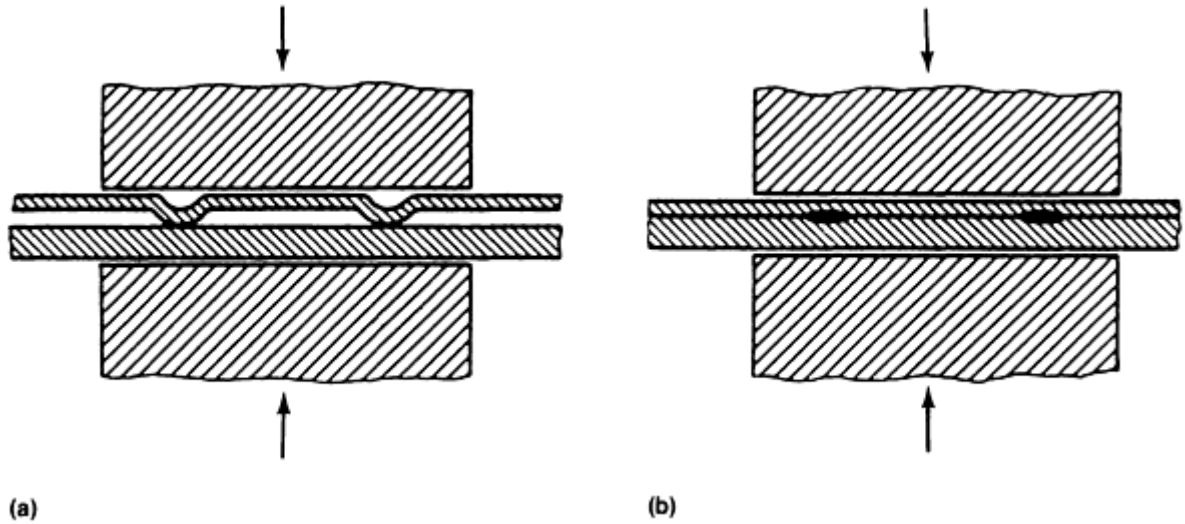

FIG. 12 RELATION OF WELD NUGGETS TO EMBOSSED REGIONS OF METAL SHEETS USED IN PROJECTION WELDING. (A) ELECTRICAL CIRCUIT LOOP IS COMPLETED WHEN CURRENT TRAVELS THROUGH EMBOSSED PROJECTION CONTACT POINTS. (B) ADDITION OF PRESSURE AFTER WELDING CURRENT IS TURNED OFF CAUSES PLASTIC DEFORMATION WHICH FLATTENS THE PROJECTIONS.

Projections may be of any practical shape that can properly concentrate the welding current (Fig. 13). In cross-wire projection welding, the curved surfaces of two intersecting wires perform the function of a projection. The shapes of parts may also take the place of conventional projections in projection welding of special types of joints.

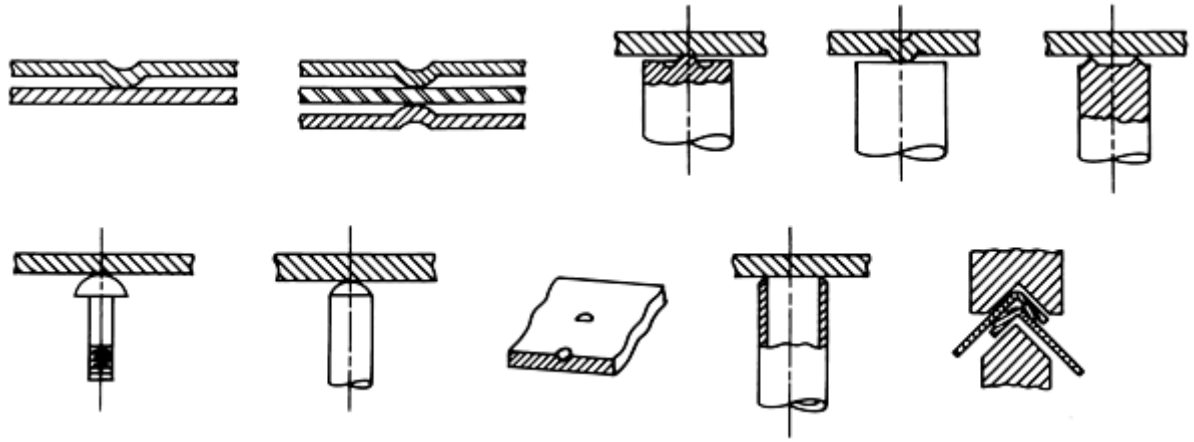

FIG. 13 SCHEMATICS SHOWING SELECTED SETUPS WHICH CAN BE USED IN PROJECTION WELDING OPERATIONS

Additional information is available in the article "Projection Welding" in this Volume.

Formation of the Weld. The formation of a projection weld nugget, which depends on the design of the projection, the selection of welding conditions, and the adequacy of the resistance welding equipment, is shown in Fig. 14. In this application, 2.33 mm (0.092 in.) thick low-carbon steel is projection welded using embossed spherical projections and a weld time of 20 cycles ($\frac{1}{3}$ s).

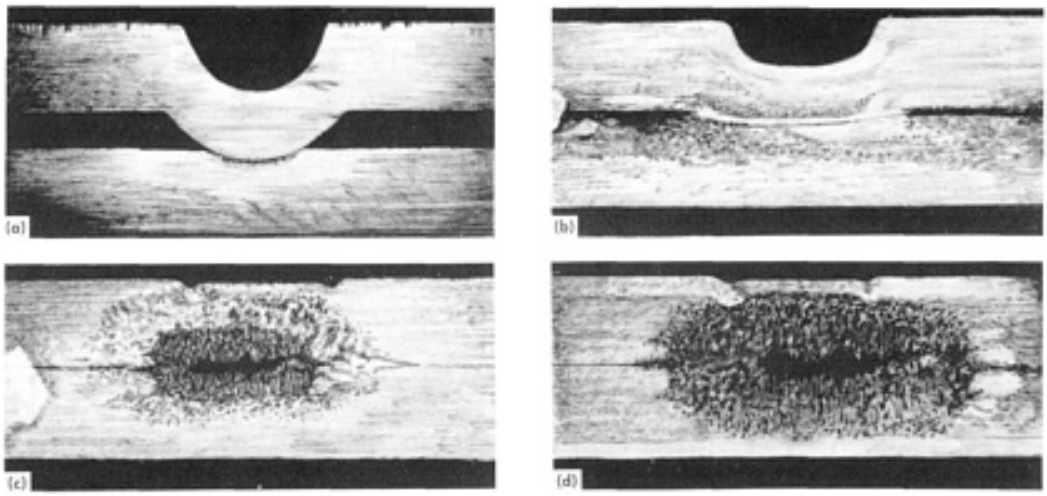

FIG. 14 FORMATION OF A WELD NUGGET DURING PROJECTION WELDING OF AN EMBOSSED SPHERICAL PROJECTION. SEE TEXT FOR EXPLANATION.

In the first stage of fabrication (Fig. 14a), the workpieces are brought together under pressure without application of welding current, and the projection may be slightly compressed and indented into the surface of the mating workpiece. Figures 14(b), 14(c), and 14(d) show the stages of formation of a typical weld at 20, 60 to 70, and 100% of the weld time (or heat time).

At about 20% of weld time (Fig. 14b), collapse of the projection is nearly complete, and a pressure weld is formed. A nugget of fused weld metal does not begin to form until about 50% of the weld time has elapsed. At about 60 to 70% of weld time (Fig. 14c), fusion has progressed a sufficient distance from the interface to produce a well-defined weld nugget that has about half its final thickness (penetration) and diameter. Sheet separation adjacent to the weld nugget has been

reduced to zero, and the softened metal above the nugget has been flattened against the face of the upper electrode (compare with Fig. 14b). Nugget diameter, penetration, and shear strength continue to increase as weld time progresses. Figure 14(d) shows the fully developed weld nugget.

Applicability

Projection welding is used where there is a high thickness ratio (for example, nuts welded to sheet), and where the appearance of the sheets must be controlled (for example, appliance surfaces). The principal application of projection welding is the joining of stamped low-carbon, low-alloy, and high-strength low-alloy (HSLA) steel parts. During stamping (punching, drawing, or forming), one of the parts must have a projection which has been formed during the stamping operation to enable projection welding. Projection welding is also used for joining screw-machine parts to stamped parts; the projection is machined or cold formed on the end of the screw-machine part.

Projection welding is most successful in workpieces 0.56 to 3.18 mm (0.022 to 0.125 in.) thick. Stock 0.25 mm (0.010 in.) thick has been projection welded; projection design is critical, however, and machines with low-inertia heads and fast follow-up are needed. Sections less than 0.25 mm (0.010 in.) thick are more adaptable to spot welding.

Advantages. The principal advantages of projection welding are:

- THE NUMBER OF WELDS THAT CAN BE MADE SIMULTANEOUSLY WITH ONE OPERATION OF THE WELDING MACHINE IS LIMITED ONLY BY THE ABILITY OF THE CONTROLS TO REGULATE CURRENT AND FORCE.
- BECAUSE OF GREATER CURRENT CONCENTRATION AT THE WELD, AND THUS LESS CHANCE OF SHUNTING, NARROWER FLANGES CAN BE WELDED, AND WELDS CAN BE SPACED CLOSER TOGETHER BY PROJECTION WELDING THAN BY SPOT WELDING.
- ELECTRODES USED IN PROJECTION WELDING HAVE FACES LARGER THAN THE PROJECTIONS AND LARGER THAN THE FACES OF ELECTRODES USED FOR MAKING SPOT WELDS OF COMPARABLE NUGGET DIAMETER. CONSEQUENTLY, BECAUSE OF LOWER CURRENT DENSITY, ELECTRODES REQUIRE LESS MAINTENANCE THAN DO SPOT WELDING ELECTRODES.
- PROJECTION WELDS CAN BE MADE IN METAL THAT IS TOO THICK TO BE JOINED BY RSW.
- FLEXIBILITY IN SELECTION OF PROJECTION SIZE AND LOCATION ALLOWS WELDING OF WORKPIECES IN THICKNESS RATIOS OF 6 (OR MORE) TO 1. WORK-PIECES IN THICKNESS RATIOS GREATER THAN ABOUT 3 TO 1 SOMETIMES ARE DIFFICULT TO SPOT WELD.
- THE PROCESS CAN BE USED TO MAKE LEAKPROOF JOINTS (FOR EXAMPLE, RING PROJECTIONS).

Limitations of projection welding include:

- FORMING OF ONE OR MORE PROJECTIONS ON ONE OF THE WORKPIECES MAY REQUIRE EXTRA OPERATIONS UNLESS THE PARTS ARE PRESS FORMED TO DESIGN SHAPE.
- WHEN SEVERAL WELDS ARE MADE AT ONCE WITH THE SAME ELECTRODE, ALIGNMENT OF THE WORK AND DIMENSIONS (PARTICULARLY HEIGHT) OF THE PROJECTIONS MUST BE HELD TO CLOSE TOLERANCES TO OBTAIN CONSISTENT WELD QUALITY.
- WHEN MAKING SIMULTANEOUS PROJECTION WELDS, THE PROJECTION LAYOUT WILL BE DICTATED BY THE SHUNT CURRENT PATHS, WHICH MAY NOT COINCIDE WITH THE DESIRED LOCATION.
- BECAUSE TWO PARTS ARE MOVING RELATIVE TO EACH OTHER DURING THE WELDING PROCESS, PROPER GAGING IS DIFFICULT.

Cross-Wire Welding

Resistance welding of crossed wires is a type of projection welding process. In practice, it usually consists of welding a number of parallel wires at right angles to one or more other wires or rods. There are many specific ways to perform the welding operation, depending upon production requirements, but the final finished product is essentially the same regardless of the method used.

Typical crossed-wire products include items such as stove and refrigerator racks, grills of all kinds, lamp shade frames, poultry equipment, wire baskets, fencing, grating and concrete rein-forcing mesh.

Welding Machines

Press-type machines, with either single-phase or three-phase transformers, usually are used for projection welding. The welding head in these machines is guided by bearings or ways and moves in a straight line. Platens with T-slots or tapped holes are used for mounting the welding dies or electrodes. Rocker-arm machines generally are not used for projection welding because the electrode moves in an arc that can cause slippage between the components as the projection collapses.

At the start of the welding stroke (Fig. 15a), equal air pressure is applied to the top of the piston and to the diaphragm. By the time the piston has completed its travel, the diaphragm has been compressed by the retraction of the internal shaft. Retraction of the internal shaft simultaneously compresses the diaphragm and closes the welding-current switch; the control lever for the switch rides in the shaft collar.

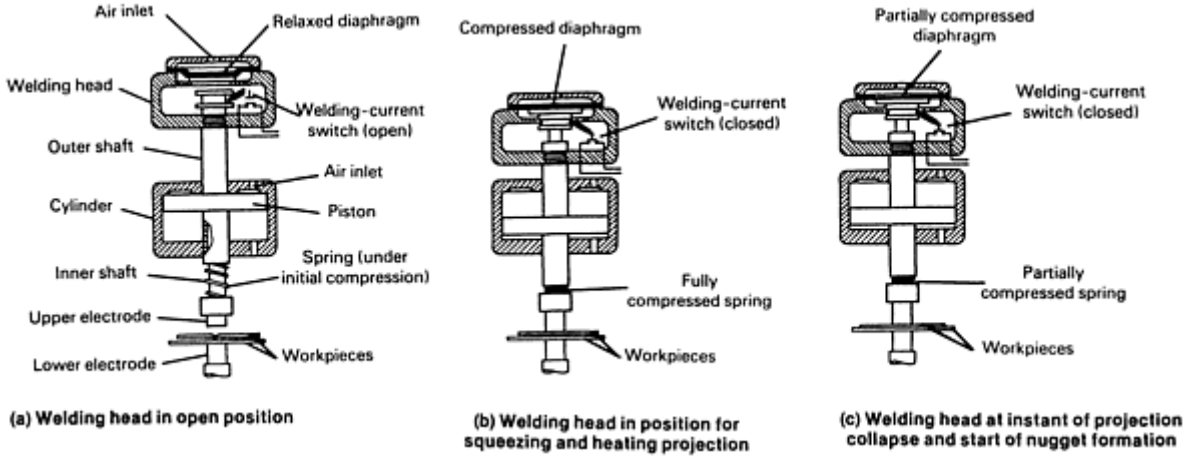

FIG. 15 SCHEMATIC SHOWING MOTION OF INTERNAL COMPONENTS IN A LOW-INERTIA WELDING HEAD USED FOR PROJECTION WELDING OPERATIONS

When the welding current is initiated (Fig. 15b), the only remaining mass to be moved is the internal shaft and its attached electrode. Air pressure acting on the diaphragm and the force of the compressed spring between the inner and outer shafts easily overcome the low inertia of the system and move the upper electrode downward as the projection collapses. Thus, the workpieces are kept in close contact under partial electrode force until the welding head follows and forges the weld region with the full electrode force (Fig. 15c). This setup, however, is no longer used because diaphragm cylinders are now classified as obsolete technology.

Process Variables

The major variables that affect projection welding are welding current, electrode force, and weld time.

Specifications for projection welding of stainless steels relative to low-carbon steel from 0.36 to 3.18 mm (0.014 to 0.125 in.) thick are given in Table 7. These data are intended to serve as starting points and should be adjusted to suit the specific application and the equipment used.

TABLE 7 RECOMMENDED ELECTRODE FORCE AND WELDING CURRENT SPECIFICATIONS FOR PROJECTION WELDING OF SELECTED STAINLESS STEELS RELATIVE TO 1010 LOW-CARBON STEEL

Thickness of thinnest outside piece, *T* (a)		Minimum electrode face diameter, *d* (b)				1010 low-carbon steel			Stainless steel(e)		
						Net electrode force			Net electrode force		
mm	in.	mm	in.	Weld time(c), cycles	Hold time(d), cycles	kN	lbf	Welding current at electrodes (f), A	kN	lbf	Welding current at electrodes(f), A
0.36	0.014	3.2	1/8		7	15	0.78	175	5,000	1.33	300	4,500
0.53	0.021	4.0	5/32		10	15	1.33	300	6,000	2.22	500	4,750
0.79	0.031	4.8	3/16		15	15	1.78	400	7,000	3.11	700	5,750
1.12	0.044	6.4	1/4		20	15	1.78	400	7,000	3.11	700	6,000
1.57	0.062	7.9	5/16		25	15	3.11	700	9,500	5.34	1,200	7,500
1.98	0.078	9.5	3/8		30	30	5.34	1,200	13,000	8.45	1,900	10,000
2.39	0.094	11.1	7/16		30	30	5.34	1,200	14,500	8.45	1,900	10,000
2.77	0.109	12.7	1/2		30	45	7.56	1,700	16,000	12.45	2,800	13,000
3.18	0.125	14.3	9/16		30	45	7.56	1,700	17,000	12.45	2,800	14,000

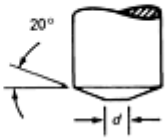

(a) Data based on thickness of thinner sheet and for two thicknesses only. Maximum ratio between two thicknesses, 3:1. (b) Flat-faced electrodes and dies are normally used. Dimension *d* is absolute minimum (*d* = 2× projection diameter). (c) Based on 60 Hz current. (d) Based on 60 cycles/s. (e) AISI types 309, 310, 316, 317, 321, 347, and 349 (nonhardenable, 0.15% C max). (f) 60 Hz ac. Source: Ref 8

Parameters for projection welding of low-carbon steel wire are given in Table 8.

TABLE 8 GUIDELINES FOR PROJECTION WELDING OF LOW-CARBON STEEL WIRE

WIRE DIAMETER		WELD TIME[B], CYCLES	CONDITIONS FOR 15% SETDOWN[A]					CONDITIONS FOR 30% SETDOWN[A]					CONDITIONS FOR 50% SETDOWN[A]				
			ELECTRODE FORCE		WELDING CURRENT, A	WELD STRENGTH		ELECTRODE FORCE		WELDING CURRENT, A	WELD STRENGTH		ELECTRODE FORCE		WELDING CURRENT, A	WELD STRENGTH	
MM	IN.		KN	LBF		KN	LBF	KN	LBF		KN	LBF	KN	LBF		KN	LBF
COLD-DRAWN WIRE																	
1.6	1/16	5	0.45	100	600	2.0	450	0.67	150	800	2.2	500	0.89	200	1,000	2.4	**550**
3.2	1/8	10	0.56	125	1,800	4.3	975	1.2	260	2,650	5.0	1,125	1.6	350	3,400	5.6	**1,250**
4.8	3/16	17	1.6	360	3,300	8.9	2,000	2.7	600	5,000	10.7	2,400	3.3	750	6,000	11.1	**2,500**
6.4	1/4	23	2.6	580	4,500	16.4	3,700	3.8	850	6,700	18.7	4,200	5.5	1240	8,600	19.6	**4,400**
7.9	5/16	30	3.7	825	6,200	22.7	5,100	6.4	1450	9,300	27.1	6,100	8.9	2000	11,400	28.9	**6,500**
9.5	3/8	40	4.9	1100	7,400	29.8	6,700	9.2	2060	11,300	37.1	8,350	13.3	3000	14,400	39.1	**8,800**
11	7/16	50	6.2	1400	9,300	42.7	9,600	12.9	2900	13,800	50.3	11,300	19.8	4450	17,400	52.9	**11,900**
13	1/2	60	7.6	1700	10,300	54.3	12,200	15.1	3400	15,800	60.5	13,600	23.6	5300	21,000	64.9	**14,600**
HOT-DRAWN WIRE																	
1.6	1/16	5	0.45	100	600	1.6	350	0.67	150	800	1.8	400	0.89	200	1,000	2.0	**450**
3.2	1/8	10	0.56	125	1,850	3.3	750	1.2	260	2,770	3.8	850	1.6	350	3,500	4.0	**900**
4.8	3/16	17	1.6	360	3,500	6.7	1,500	2.7	600	5,100	7.6	1,700	3.3	750	6,300	8.0	**1,800**
6.4	1/4	23	2.6	580	4,900	12.5	2,800	3.8	850	7,10	13.3	3,000	5.5	1240	9,000	13.8	**3,100**
7.9	5/16	30	3.7	825	6,600	20.5	4,600	6.4	1450	9,600	22.2	5,000	8.9	2000	12,000	23.6	**5,300**
9.5	3/8	40	4.9	1100	7,700	27.6	6,200	9.2	2060	11,800	30.2	6,800	13.3	3000	14,900	32.0	**7,200**

11	$\frac{7}{16}$	50	6.2	1400	10,000	39.1	8,800	12.9	2900	14,000	42.7	9,600	19.8	4450	18,000	45.4	**10,200**
13	$\frac{1}{2}$	**60**	**7.6**	**1700**	**11,000**	**51.1**	**11,500**	**15.1**	**3400**	**16,500**	**55.2**	**12,400**	**23.6**	**5300**	**22,000**	**57.8**	**13,000**

Source: Ref 9

(A) SETDOWN, % = (DECREASE IN JOINT HEIGHT ÷ DIAMETER OF SMALLER WIRE) × 100.

(B) FOR 15.30, AND 50% SETDOWN.

Welding current required for projection welding, although slightly less per weld than that needed for spot welding, must be high enough to cause fusion before the projection is completely flattened. The recommended current is the highest current that, when used with the current electrode pressure, does not cause excessive expulsion of metal.

Electrode force used in projection welding depends on the work metal, the size and design of the projection, the number of projections in the joint, and the welding machine. Excessive force causes the projections to collapse before the weld area has reached the proper temperature, resulting in the formation of ring welds, in which fusion occurs around the periphery of the projection but is incomplete at the center. For best weld appearance, the electrode force should be such that the projection is flattened completely after the metal has reached welding temperature.

Weld time for a given type and thickness of work metal depends on welding current and rigidity of the projection. Weld time is less important than electrode force in projection welding of low-carbon, low-alloy, and HSLA steel, provided that the time is sufficient to produce a nugget of adequate size at the chosen welding current. A short weld time creates higher production efficiency and less discoloration and distortion of the workpiece. After the proper electrode force and welding current are determined, the weld time is adjusted to make the desired weld.

Electrodes

An electrode designed for RSW can be used for projection welding if the electrode face is large enough to cover the projection being welded, or the pattern of projections being welded simultaneously. To minimize marking and indentation of workpieces, the recommended electrode-face diameter for making a single projection weld usually is two or more times the diameter of the projection. In multiple-projection welding, the electrode face should be large enough to extend beyond the boundaries of the pattern of projections by approximately the diameter of one projection. RWMA class 2 electrode materials generally are preferred as general-purpose materials because they provide the best compromise among electrical and conductivity, strength, hardness, and temperature resistance. Typically, class 10, 11, or 12 materials are used on the bottom side of the weld to resist damage from the high localized force.

Reference cited in this section

9. *RESISTANCE WELDING MANUAL,* 3RD ED., VOL 1, RESISTANCE WELDER MANUFACTURERS ASSOCIATION, 1956, P 88

Flash Welding

Flash welding (FW) commonly is used to join sections of metals and alloys in production quantities. It is a resistance/forge welding process in which the items to be welded are securely clamped to electric current-carrying dies, heated by the electric current, and upset (Fig. 16). Clamping ensures good electrical contact between the current-carrying dies and the workpiece and prevents the parts from slipping during the upsetting action. Flash welding equipment must be durable to withstand high clamping force and upset pressures without deflecting. If deflection occurs, misalignment of workpieces may occur during welding. Flash welding is rapid and economical, and when properly executed, welds of uniform high quality are produced. A typical flash welding machine comprises a horizontal press-transformer combination with conducting work-clamping dies mounted on the press platens.

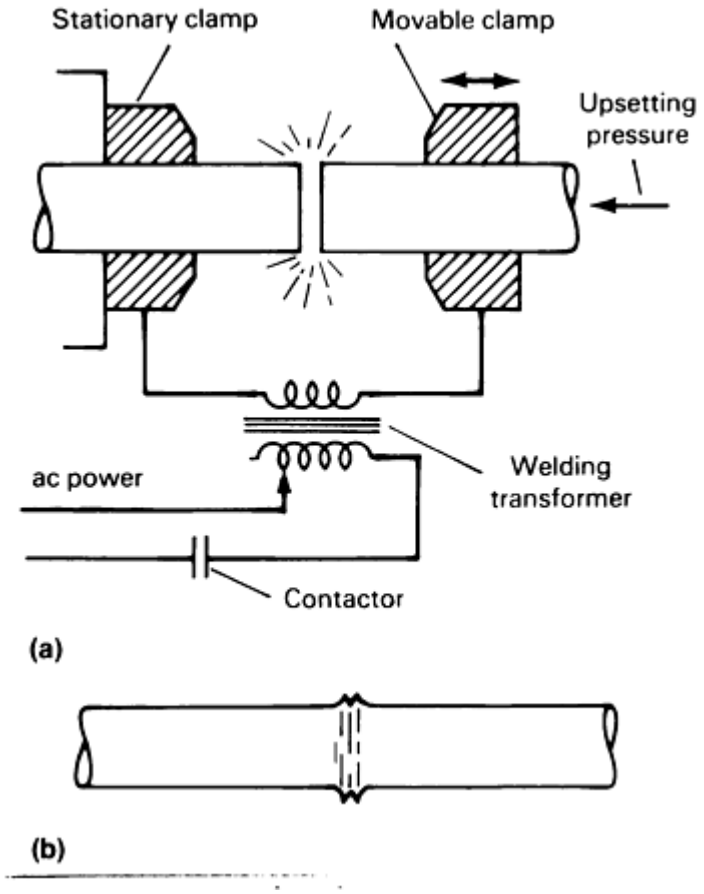

FIG. 16 WELD PRODUCED WHEN USING THE FLASH WELDING PROCESS. (A) WORKPIECES SECURELY CLAMPED IN CURRENT-CARRYING DIES BEFORE UPSETTING OPERATION IS INITIATED. (B) FINISHED WELD PRODUCED AFTER UPSETTING OPERATION

Additional information is available in the article "Flash Welding" in this Volume.

Applications

Flash welding can be used for joining many ferrous and nonferrous alloys and combinations of dissimilar metals. In addition to low-carbon steels, metals that are flash welded on a production basis include low-alloy steels, tool steels, stainless steels, aluminum alloys, magnesium alloys, nickel alloys, and copper alloys. Table 9 gives typical upsetting pressures for numerous classes of alloys.

TABLE 9 RECOMMENDED UPSETTING PRESSURES FOR FLASH WELDING OF SELECTED ALLOYS

STRENGTH CLASSIFICATION	**UPSET PRESSURE**		ALLOYS	
	MPA	**KSI**	**SAE DESIGNATION**	OTHERS
LOW FORGING	69	10	1020, 1112, 1315	**HIGH-STRENGTH LOW-ALLOY (HSLA) STEELS**
MEDIUM FORGING	103	15	1045, 1065, 1335, 3135, 4130, 4140, 8620, 8630	
HIGH FORGING	172	25	4340, 4640, 300M	**TOOL STEELS, TITANIUM, ALUMINUM**

EXTRA-HIGH FORGING	**241**	**35**	**A-286, 19-9 DL**	**NICKEL-BASE ALLOYS, (A)**

Source: Ref 10

(A) MATERIALS EXHIBITING EXTRA-HIGH COMPRESSIVE STRENGTH AT ELEVATED TEMPERATURES.

Welding Parameters

Fundamentally, flash welding involves heating the ends of the pieces to be welded and subsequently forging them together. During the heating phase, a thermal distribution pattern is established along the axial length of the pieces being joined, which is characterized by a steep temperature gradient.

The major difference between the temperature pattern developed in flash welding and that developed in resistance welding is that flash welding produces a much steeper thermal gradient. This steep thermal gradient, combined with the resulting characteristic upset pattern, enables flash welding to accommodate a much greater variety of materials and shapes than can be welded by resistance welding.

Once the proper temperature-distribution pattern has been established, the abutting surfaces are rapidly forced together. The parts must be securely held together during the forging process to prevent slipping. Three distinct peaks are characteristic of flash welds (Fig. 17). The two peaks on either side of the weld line represent the material displaced by the upsetting action; the center peak is the molten metal extruded out of the weld, including oxides or contaminants formed during heating.

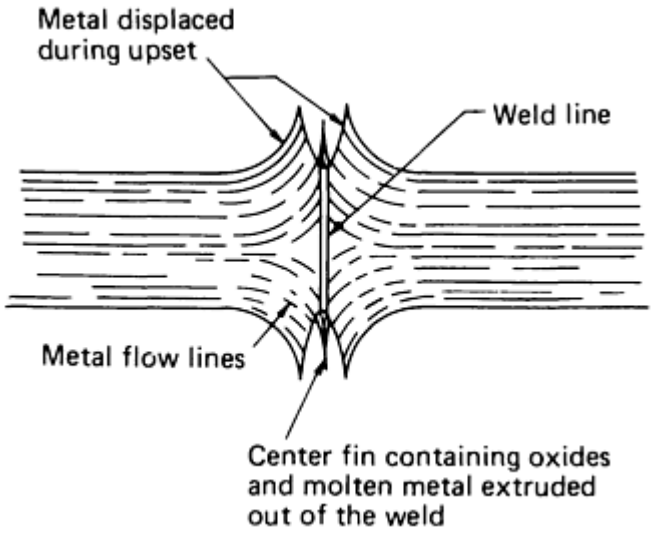

FIG. 17 SCHEMATIC SHOWING CROSS-SECTIONAL VIEW OF TYPICAL PEAKS AND FLOW LINES GENERATED IN A FLASH WELD

Heat (Energy) Sources

One of the major considerations for flash welding is the electrical power service. Flashing is a term used to describe the major heating process during flash welding. When the ends of the workpiece are brought together under light pressure, an electrical short circuit is established through the material. Because the abutting surfaces are not perfectly matched, the short-circuit current flows across the joint only at a few small contact areas. The large amount of current flowing through a relatively small area causes very rapid heating to the melting point. Heating is so rapid and intense that molten metal is expelled explosively from the joint area. Following this expulsion, a brief period of arcing occurs. Arcing is not sustained due to the low voltages employed. Studies have shown that stable flashing can be maintained with as low as $2\frac{1}{2}$ to 3 V, but typically the flashing voltage for alternating-current machines is from 5 to 10 V.

Following the expulsion of molten metal and subsequent arcing, small craters are formed on the ends of the abutting surfaces. The pieces are steadily advanced toward one another, and other short circuits are formed and additional molten metal is expelled. This process continues as random melting, arcing, and expulsion occur over the entire cross-sectional surface. During flashing, many active areas are in various stages of this sequence (Fig. 18). Flashing surfaces act as heat sources, and the steep thermal profile is established primarily from these heat sources. Temperatures of the flashes are at or above the melting point of the material and are progressively lower as distance progresses from the flashing surface toward the clamp.

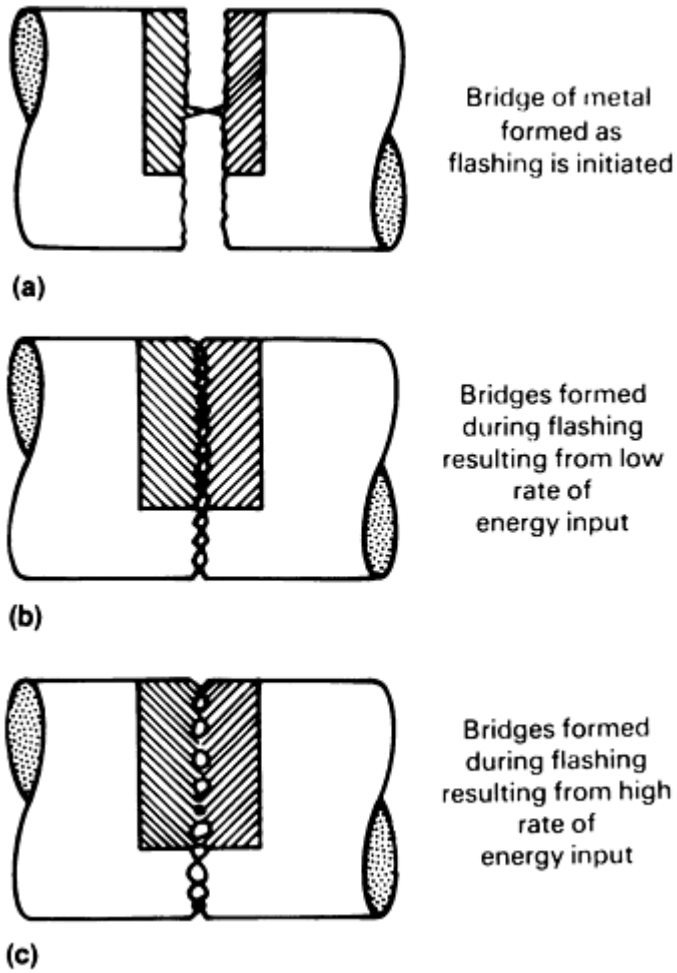

FIG. 18 GROWTH OF CONTACT POINTS PRODUCED BY ENERGY INPUT DURING FLASH WELDING

Force

Parts to be welded must be clamped or fixtured securely to provide good electrical contact with current-carrying dies and to transmit the upset forces. Also, a reliable source of force for the upsetting action is required. Systems for generating these forces vary greatly and are determined by the cross sections to be welded. The simplest welding machines derive their power for clamping and upsetting from the operator (that is, the parts are clamped to the dies via screw, lever, cam, or toggle force-multiplying linkages). Upset forces are generated in a similar manner. In larger machines, these forces are generated by pneumatic systems, oil hydraulic systems, combination air/oil hydraulic systems, or motor-driven cam systems.

Machines

Machines used for flash welding generally consist of a mainframe; a low-impedance welding transformer; a stationary platen; a movable platen on which clamping dies, electrodes, and other tools needed to position and hold the work-pieces are mounted; flashing and upsetting mechanisms; and the necessary electrical, air, or hydraulic controls (Fig. 19).

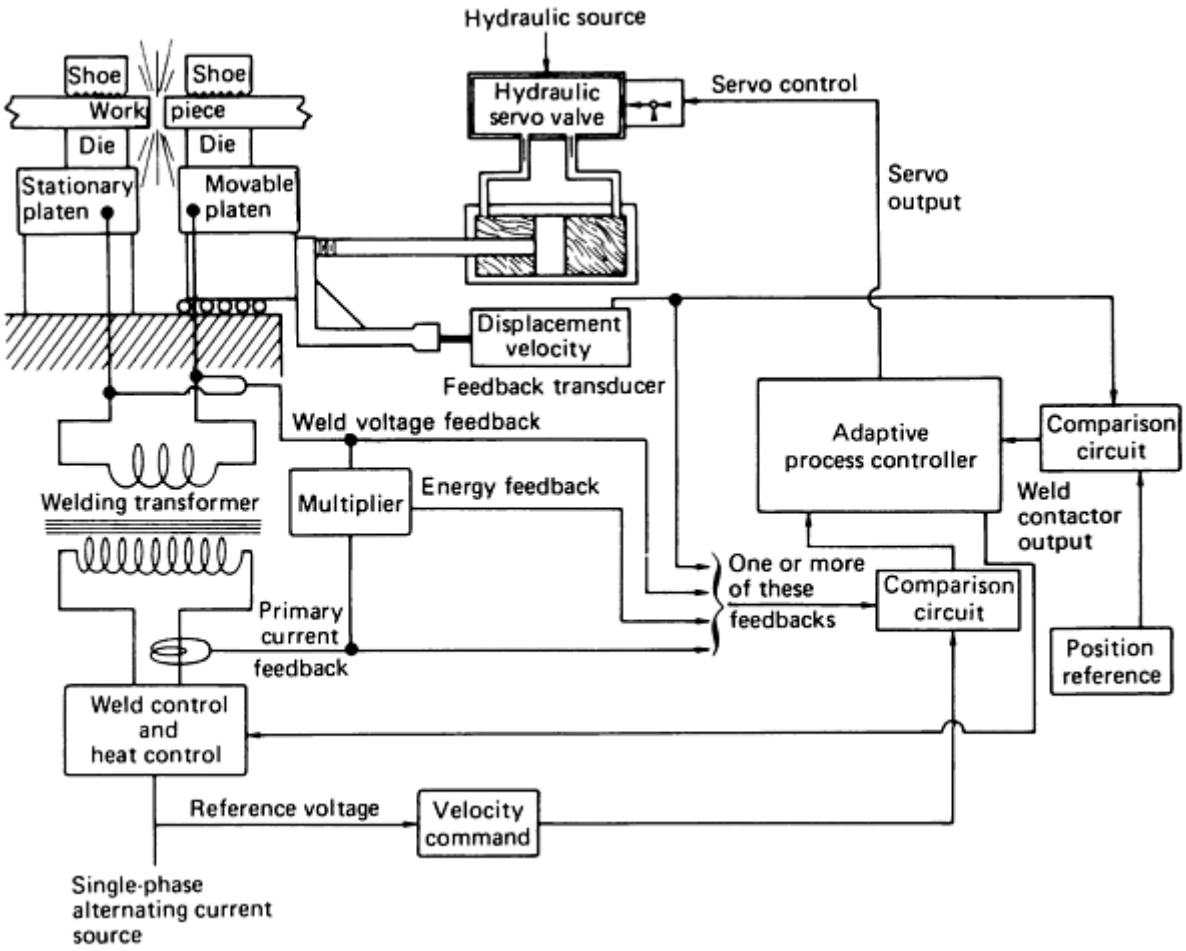

FIG. 19 FLOW DIAGRAM SHOWING ADAPTIVE CONTROLS USED TO CONTROL AND MONITOR FLASH WELDING PROCESS

Flash welding machines may be manual, semiautomatic, or fully automatic. With manual operation, the operator controls the speed of the platen from the time flashing is initiated until the upset is completed. In semiautomatic operation, the operator manually initiates flashing and then actuates an automatic cycle that completes the weld. In fully automatic operation, after the operator initiates the welding sequence, a fully automatic cycle can be used through the use of position-indicating devices and timers. Values for the various welding parameters are preselected by the operator. Automatic feedback control is used in some applications. These fully adaptive circuits vary from current to voltage feedback circuits, and data are obtained to control the welding sequences. Figure 19 shows various adaptive controls used by different flash welding unit manufacturers.

Transformers are used to supply electrical energy for the welding operation. The transformer tap switch frequently is a rotary, eight-step, knife-type, fully enclosed locking switch, which provides convenient adjustment of the welding voltage to suit work requirements. Voltages from 4 to 16 V are common.

Clamping Dies and Fixtures

Workpieces must be accurately clamped to maintain alignment, to allow the secondary current to pass into the workpieces, and to apply the upsetting force properly. Generally, the parts of the clamping mechanism that actually grip the workpiece are the electrodes, often called clamping dies. The surface of the material in contact with the dies must be cleaned of scale, rust, paint, or contaminants to ensure proper current flow.

The materials commonly used for clamping dies are RWMA class 3 and hardened tool steels such as H11, L6, and O1. Bronze and other copper-base electrode materials can be used in some applications. The die half (upper or lower) that

conducts the current usually is made of a copper-base material. The other half is made of the same copper-base material or of hardened steel.

Cooling of Electrodes. The need for water cooling of flash welding electrodes depends on the size of the electrode, die, or fixture, the magnitude of the flashing current, and the production rate. When the mass of the electrodes is large compared with that of the workpiece, the heat sink generally is large enough to dissipate the heat generated by the resistance to current flow and the heat absorbed from the workpiece. With high flashing currents and high production rates, electrodes generally must be cooled.

Shape and Size of Clamping Dies. Generally, the shape of the clamping-die surface is such that the die encompasses almost the entire workpiece surface. The required area of clamping-die contact depends on the current needed for heating the workpiece and the pressure needed for holding it. Semicircular dies are used where the line contact provided by V-shape dies gives insufficient surface for the current to flow without burning the workpiece, or for holding the workpiece without marking it.

Table 10 gives the minimum lengths of clamping dies for welding rounds, tubing, and other sections of various diameters or minimum dimensions; these data are for welding steels of low or medium forging strength.

TABLE 10 MINIMUM LENGTHS OF CLAMPING DIES, WITH AND WITHOUT BACKUP, FOR FLASH WELDING SELECTED DIAMETERS OF WORKPIECES MADE FROM STEELS OF LOW OR MEDIUM FORGING STRENGTH

WORKPIECE DIAMETER(A)		**MINIMUM LENGTH OF CLAMPING DIE**				**WORKPIECE DIAMETER(A)**		**MINIMUM LENGTH OF CLAMPING DIE WITH BACKUP**		**WORKPIECE DIAMETER(A)**		MINIMUM LENGTH OF CLAMPING DIE WITH BACKUP	
		WITH BACKUP		**WITHOUT BACKUP(B)**									
mm	**in.**	**mm**	**in.**	**mm**	**in.**	**mm**	**in.**	**mm**	**in.**	**mm**	**in.**	**mm**	in.
6.35, 7.92	0.250, 0.312	9.53	0.375	25.4	1.00	50.8	2.00	31.8	1.25	152	6.00	82.3	**3.25**
9.53	0.375	9.53	0.375	38.1	1.50	63.5	2.50	44.5	1.75	165	6.50	88.9	**3.50**
12.70	0.500	9.53	0.375	44.5	1.75	76.2	3.00	50.8	2.00	178	7.00	95.3	**3.75**
19.05	0.750	12.70	0.500	50.8	2.00	88.9	3.50	57.2	2.25	191	7.50	102	**4.00**
25.40	1.000	19.05	0.750	63.5	2.50	102	4.00	63.5	2.50	203	8.00	108	**4.25**
38.10	1.50	25.40	1.000	76.2	3.00	114	4.50	69.9	2.75	216	8.50	114	**4.50**
						127	5.00	69.9	2.75	229	9.00	121	**4.75**
						140	**5.50**	**76.2**	**3.00**	**241**	**9.50**	**127**	**5.00**

(A) DIAMETER OF ROUNDS OR TUBING, OR MINIMUM DIMENSION OF OTHER SECTIONS.

(B) BACKUP IS RECOMMENDED FOR ALL WORKPIECE DIAMETERS OR MINIMUM DIMENSIONS OVER 38.1 MM (1.50 IN.).

Preweld Processing

Parts that are flash welded come in a variety of forms, including forgings; rolled or extruded bar; sheet, strip, or plate, ring preforms; and castings. Each of the above parts or assemblies requires preweld preparation.

Cleaning. As a minimum precaution, the ends of the workpiece that are clamped on the current-conducting die must be free from dirt, scale, surface oxidation, and grease. In addition, the ends of the workpiece that extend into the weld zone must be free from any contamination that could react with the base metal at the high temperatures developed during welding. Cleaning is needed because of the high current densities developed in the workpiece at the current-conducting dies. If insufficient electrical contact is made, weld quality is poor and localized hot spots can develop between the current-conducting dies and the workpiece. These localized hot spots are called "die burns." Many of the alloys welded have tightly adherent, highly resistive oxides that must be removed prior to welding.

In addition, poor fit-up, loose scale, and grease may cause the parts to slip during upsetting. Common cleaning techniques include (1) abrading the surfaces by grinding, grit blasting, or wire brushing; (2) pickling or chemical descaling; and (3) vapor degreasing.

End Preparation. Die burns, upset slippage, and inferior welds may be caused by poor fit-up between the current-conducting dies and the workpiece. In some cases, the ends of the workpiece must be machined or ground to fit the dies, particularly in welding of rough forgings or castings. Also, a chamfer may be required on the ends of the workpiece to initiate flashing action.

Alignment of Workpiece. After the workpieces are clamped in the welding unit, the alignment of the workpieces with respect to each other along the axis of upset must be maintained. After the flashing process and during upsetting, any misalignment may cause the parts to overlap one another or cause a skewed weld. If this occurs, insufficient metal will be extruded out of the weld zone during upsetting and a poor-quality weld will be formed (Fig. 20).

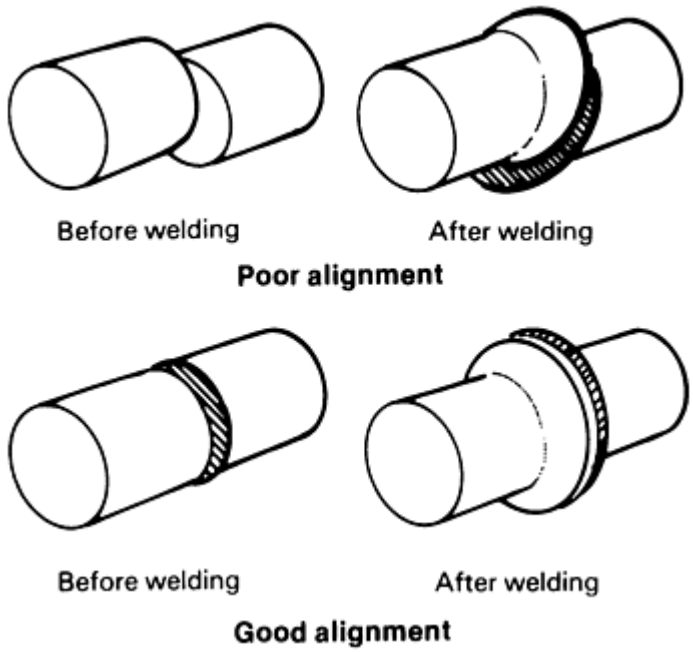

FIG. 20 EFFECT OF WORKPIECE ALIGNMENT ON JOINT QUALITY AND WELD UPSET

Dimensional Tolerances. Some combinations of joint length and stock thickness are difficult or even impossible to weld. Table 11 gives relationships between joint length (sheet width) and sheet thickness that have proven successful in a large number of production jobs. Relationships of tube diameter to wall thickness that have been successfully welded are listed in Table 12.

TABLE 11 LENGTHS OF JOINTS COMMONLY FLASH WELDED IN SELECTED THICKNESSES OF FLAT SHEET

SHEET THICKNESS		JOINT LENGTH	
mm	**in.**	**mm**	in.
0.25	0.010	25	**1**
0.51	0.020	125	**5**
0.76	0.030	255	**10**
1.02	0.040	380	**15**
1.27(A)	0.050(A)	510	**20**
1.52(A)	0.060(A)	635	**25**
2.03(A)	0.080(A)	890	**35**
2.54(A)	0.100(A)	1145	**45**
3.18(A)	0.125(A)	1458	**57**
4.75(A)	**0.187(A)**	**2235**	**88**

(A) LENGTH OF JOINTS IN STOCK THICKNESSES OF 1.27 MM (0.050 IN.) AND GREATER CAN BE UP TO 2540 MM (100 IN.) DEPENDING ON MATERIAL EXTENSION, PLATEN TRAVEL, DIE ALIGNMENT, AND CLAMPING.

TABLE 12 MAXIMUM FLASH-WELDABLE DIAMETERS OF TUBING OF SELECTED WALL THICKNESSES

WALL THICKNESS		MAXIMUM DIAMETER	
mm	**in.**	**mm**	in.
0.51	0.020	13	$\frac{1}{2}$
0.76	0.030	19	$\frac{1}{4}$
1.27	0.050	32	$\mathbf{1}\frac{1}{4}$
1.57	0.062	38	$\mathbf{1}\frac{1}{2}$
2.03	0.080	50	**2**
2.54	0.100	75	**3**
3.18	0.125	100	**4**
4.75	0.187	150	**6**
6.35	0.250	230	**9**
9.52	0.375	380	**15**
12.7	**0.500**	**510**	**20**

Burnoff. After the parts are clamped in the welding machine and the welding power is activated, the abutting surfaces are brought together for a brief period of violent flashing. This phase of the welding sequence is called "burnoff." It serves the function of squaring off the abutting surfaces and compensates for inconsistencies in end preparation.

Preheating is a resistive heating phase of the welding process in which the heat is generated by the electrical resistance of the workpieces. It is accomplished by bringing the workpieces together under light pressure, creating a short circuit. The pressure must be great enough to prevent flashing, but not so great that workpieces are prematurely welded.

In practice, preheating is performed in a cyclic manner, workpieces are brought together briefly, then separated for a brief period to allow the heat generated to diffuse into them. This sequence is repeated several times. Fully automatic machines perform this function, thus eliminating operator variables.

Flashing. The primary purpose of flashing is to generate enough heat to produce a plastic zone that permits adequate upsetting. The rate of energy input must be in proper proportion to the travel of the platen or movable die, so that constant flashing is maintained until the appropriate amount of metal is flashed off and the required plastic zone is obtained.

Upsetting (Forging). Bonding takes place during the upsetting action, and some metal must be extruded from the weld zone to remove slag and other inclusions not expelled during flashing. The extruded metal must extend beyond the cross-sectional boundaries of the workpiece to ensure that maximum amounts of slag and inclusions are removed when the weld upset is removed during subsequent trimming. When the weld upset is removed, no evidence of the weld should remain. Porosity near the outer surface on an etched section of the weld, or a crevice around the workpiece after the weld upset has been removed, indicates incomplete bonding because of either insufficient upsetting force or insufficient plasticity during upsetting.

A large upset produced by an excessive upsetting force can be detrimental to weld quality, can waste metal, and indicates that most of the plastic metal has been extruded, requiring bonding to take place in metal where plasticity may not have been sufficient to ensure a good weld.

Reference cited in this section

10. R.L. O'BRIEN, ED., *WELDING HANDBOOK,* 8TH ED., VOL 2, AWS, 1991, P 593

Procedure Development and Practice Considerations for Resistance Welding

Upset Welding (Ref 11)

Upset welding (UW) is a resistance welding process that produces coalescence over the entire area of faying surfaces or progressively along a butt joint by the heat obtained from the resistance to the flow of welding current through the area where those surfaces are in contact. Pressure is applied before heating is started and is maintained throughout the heating period (Fig. 21). The equipment used for upset welding is very similar to that used for flash welding. It can be used only if the parts to be welded are equal in cross-sectional area. Upset welding differs from flash welding in that the parts are clamped in the welding machine and force is applied to bring the parts tightly together. High-amperage current is then passed through the joint, which heats the abutting surfaces. When they have been heated to a suitable forging temperature, an upsetting force is applied and the current is stopped. The high temperature of the work at the abutting surfaces, plus the high pressure, causes coalescence to take place. After cooling, the force is released and the weld is completed. There is no arc or flash in upset welding. The area at the joint is usually enlarged over its original dimension.

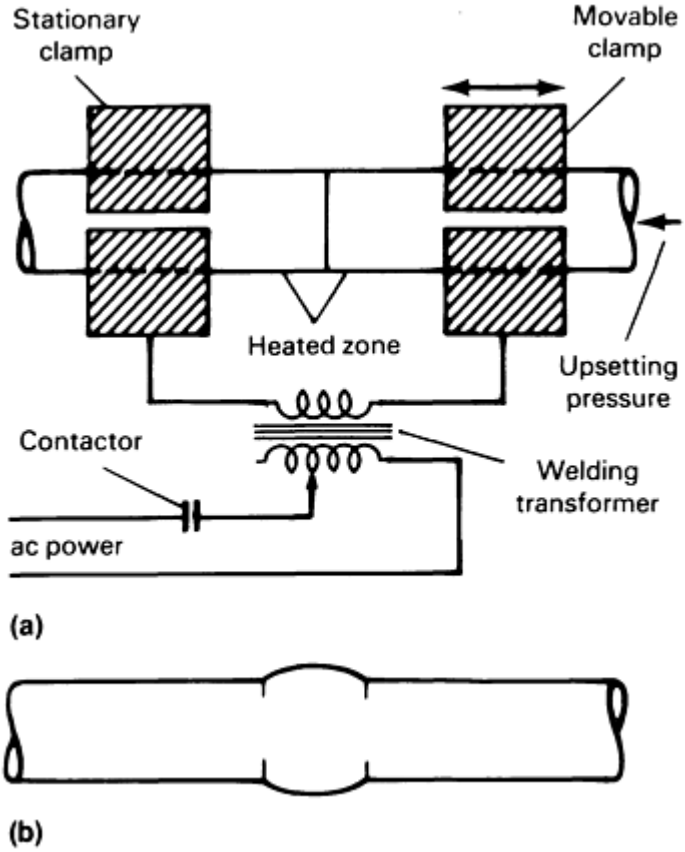

FIG. 21 WELD OBTAINED WHEN USING THE UPSET WELDING PROCESS. (A) WORKPIECES SECURELY CLAMPED IN CURRENT-CARRYING DIES WHILE PRESSURE AND CURRENT ARE APPLIED. (B) FINISHED WELD PRODUCED AFTER WELDING OPERATION IS COMPLETED

This process is used for welding small wires, tubing, piping, rings, and strips where the cross-sectional areas of both pieces are identical. If intimate contact is not obtained because of improper joint preparation, the weld will be defective.

Additional information is available in the article "Upset Welding" in this Volume.

Reference cited in this section

11. H.B. CARY, *MODERN WELDING TECHNOLOGY*, 2ND ED., PRENTICE-HALL, 1989, P 251-252

Procedure Development and Practice Considerations for Resistance Welding

High-Frequency Resistance Welding

High-frequency resistance welding (HFRW) is a resistance welding process that produces coalescence of metals by the heat generated from the resistance of the workpieces to a high-frequency current (10 to 500 kHz) and the rapid application of an upsetting force once heating is completed. The current is applied to the base metal by using electrodes that are held against the surface of the workpiece. The principal applications of HFRW are for making such structural shapes as pipe and tubing from continuous strips of metal. Two process variations of HFRW are continuous seam welding (Fig. 22a, b, c, d, e, and f) and finite-length butt welding (Fig. 22g), which is a variation of induction upset welding (UW-I).

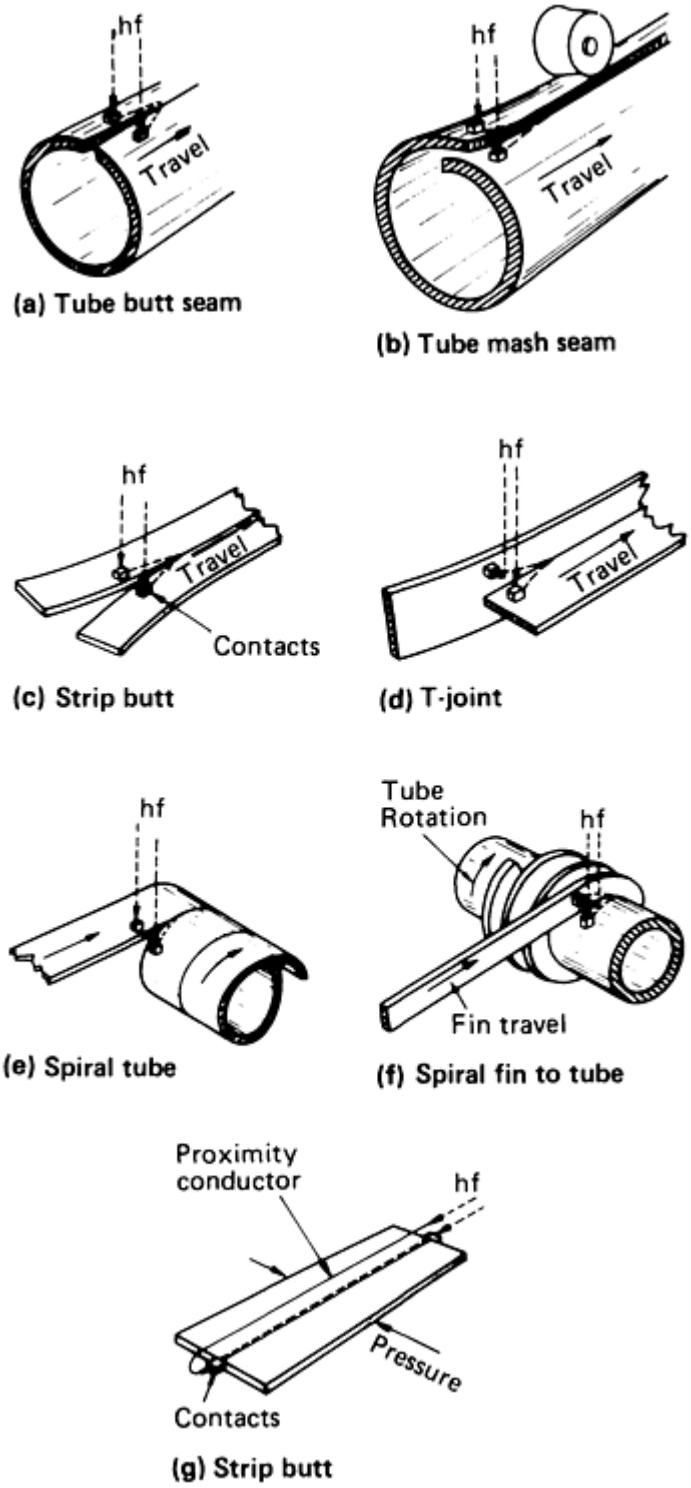

FIG. 22 TYPICAL HIGH-FREQUENCY WELDING APPLICATIONS USED TO JOIN PLATES AND TO FORM TUBES

Detailed information is available in the article "High-Frequency Welding" in this Volume.

Continuous seam welding can be described by its most common application, high-frequency upset welding (UW-HF) of a tube (Fig. 23). A pair of electrodes is placed on either side of an open V formed by the converging edges of the strip being made into tubing. The angle of this V typically varies from 4 to 7°. The edges of the strip converge between the weld pinch rolls, where a certain degree of forging upset is accomplished.

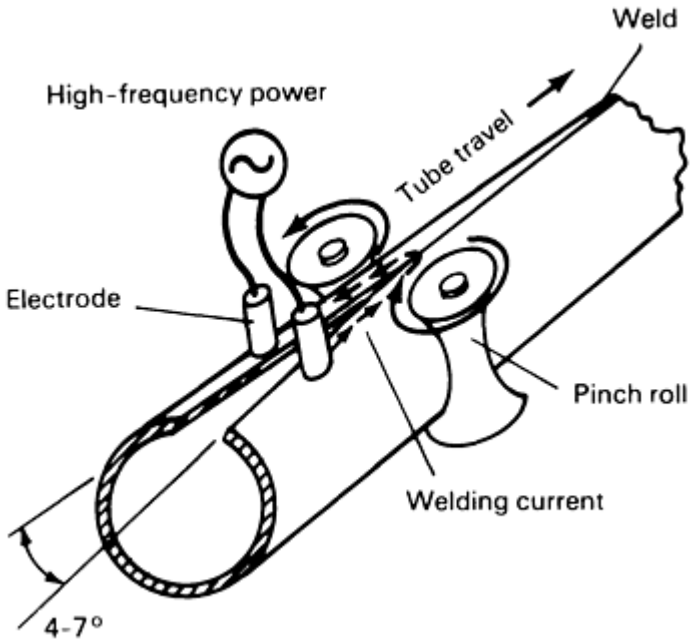

FIG. 23 HIGH-FREQUENCY LONGITUDINAL BUTT SEAM WELDING OF A TUBE

As the material moves through the rolls from the contacts to the point of welding, high-frequency current introduced at the electrodes flows on the opposing faying surfaces of the strip, down one side of the V to the point of welding, and back to the other electrode. Because this process is performed at frequencies of about 400 kHz, the depth of heating is quite shallow and heating occurs rapidly. Power is adjusted to bring the edges to a welding temperature at the time they join, and contaminants on the surfaces, as well as most of the molten material, are squeezed out of the seam toward the inside and outside of the tube when the weld is completed. This upset material can be trimmed off flush to the surfaces of the tube if desired.

The other applications of continuous high-frequency resistance seam welding (Fig. 23) vary from tube welding only in the shape of the workpiece. Contacts introduce current at the open part of a V that is being closed by rolls at the point at which the material has been heated to a high enough temperature to weld.

Finite-Length Welding. The process shown in Fig. 22(g), in which a butt joint of finite length is welded between two parts, is used for applications in coil end joining as well as in the manufacture of strip and sheet blanks for subsequent press forming. In this process, heating is accomplished along a seam that has already been closed under light pressure. The path of the heating current is controlled by the use of a proximity conductor positioned over the seam. The high-frequency heating causes the edges to be brought to welding temperature, after which pressure is increased to weld the joint. The appropriate frequency is selected to achieve heating through the material thickness. For example, 10 kHz can be used up to 6.4 mm (0.25 in.) thickness. Joints made this way can be produced very quickly, typically in 1 s. Compared to flash welding, the amount of upset is small, no shower of sparks and debris is emitted from the weld, and very little metal is consumed in making the joint.

Welding Parameters. Table 13 gives typical HFRW weld speeds as a function of wall thickness for tube and pipe products.

TABLE 13 TYPICAL WELD RATES FOR HIGH-FREQUENCY RESISTANCE WELDING OF TUBE AND PIPE

WALL THICKNESS	SPEED	
	200 KW, 76 MM (3.0 IN.)	600 KW, 305 MM (12 IN.)

		DIAMETER		DIAMETER	
MM	**IN.**	**M/S**	**FT/MIN**	**M/S**	FT/MIN
1.52	0.06	2.91	571	. . .	**. . .**
2.03	0.08	2.17	428	. . .	**. . .**
3.05	0.12	1.45	285	. . .	**. . .**
4.06	0.16	1.08	213	. . .	**. . .**
6.10	0.24	0.67	132	2.00	**393**
8.13	0.32	0.41	81	1.38	**272**
9.91	0.39	. . .	. . .	0.97	**191**
11.94	0.47	. . .	. . .	0.70	**137**
13.97	0.55	. . .	. . .	0.50	**99**
16.00	**0.63**	**. . .**	**. . .**	**0.35**	**69**

Capacitor Discharge Stud Welding

The capacitor discharge process uses direct current produced by the rapid discharge of a capacitor bank to create an electric arc and the heat needed for melting both stud and workpiece. The weld time is very short, ranging from 1 to 6 ms. Because the weld time is so short, no ferrule or fluxing is required. The equipment consists of a stud gun, capacitor discharge power/control unit, and suitable weld cable. Figure 24 illustrates a portable capacitor discharge stud welding system.

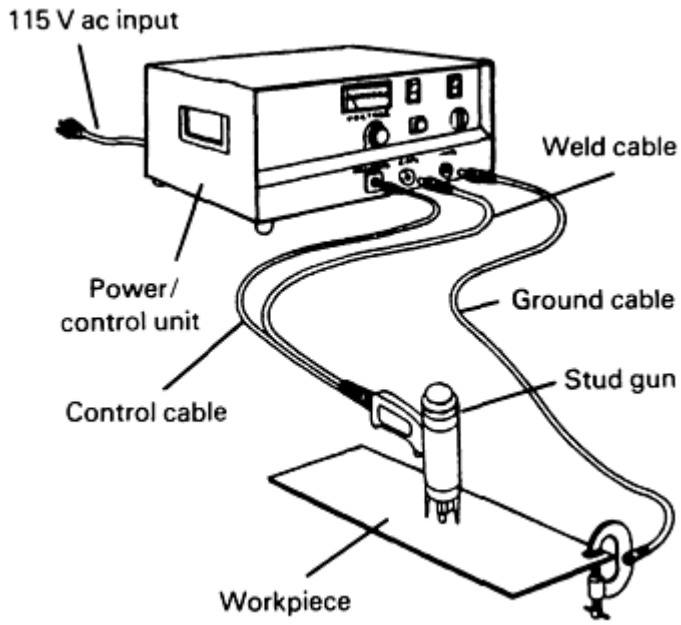

FIG. 24 KEY COMPONENTS OF A PORTABLE CAPACITOR DISCHARGE STUD WELDING SYSTEM

The three different methods of capacitor discharge stud welding include: initial contact, initial gap (Fig. 25), and drawn arc. The difference among these three methods is in the manner of arc initiation. The initial contact and initial gap methods utilize a small, specially engineered projection or tip to obtain arc initiation, whereas the drawn arc method initiates the arc by drawing the stud away from the workpiece.

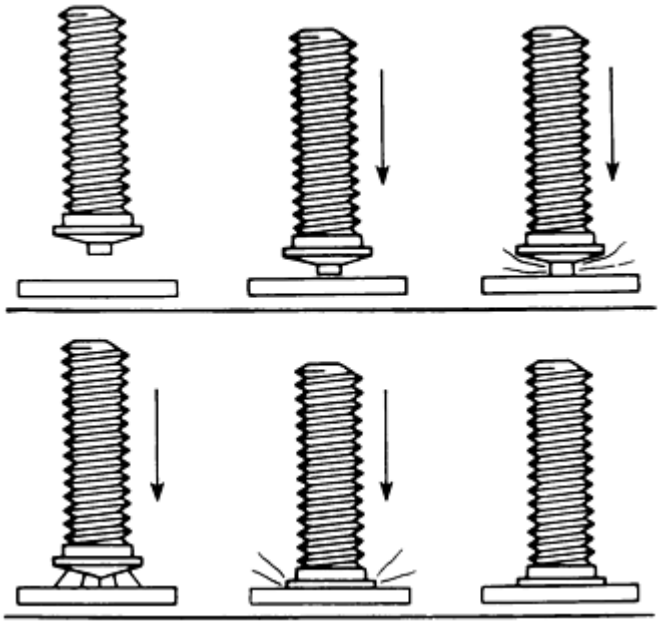

FIG. 25 SEQUENCE OF OPERATIONS REQUIRED TO WELD A STUD TO A WORKPIECE USING THE INITIAL GAP METHOD OF CAPACITOR DISCHARGE STUD WELDING

Studs. Low-carbon steel, stainless steel, aluminum, and brass are the materials used most often for studs welded commercially with the capacitor discharge method. The preferred weld base of a capacitor discharge welding stud is round, and the shank may be of almost any shape--threaded, unthreaded, round, square, rectangular, tapered, or grooved. The maximum weld-base diameter being welded commercially with the capacitor discharge welding process is 13 mm ($\frac{1}{2}$ in.).

Weld Current/Weld Time Relationships. The weld current process ranges from approximately 600 to 25,000 A, depending on stud size and weld method. The weld current range with the drawn arc method is approximately 600 to 3000 A, whereas with the initial contact or gap method the range is approximately 2500 to 25,000 A. Weld time with the drawn arc method is generally in the range of 4 to 6 ms, whereas with the initial contact and gap method it is generally in the range of 1 to 3 ms.

Metals Welded. The capacitor discharge stud welding process is an arc welding process, but differs from other arc welding processes in that the weld is made in a few milliseconds. For this reason, acceptable metallurgical results can be obtained without shielding the arc or using a flux. The welding of aluminum using the drawn arc method of capacitor discharge stud welding does require a shielding gas, however. Because of the speed at which the weld takes place, very little metal is melted. Weld penetration is slight, and very little stud metal intermixes with the plate metal. Therefore, studs may be welded to very thin metals without melt-through, and many dissimilar metals can be welded with acceptable results. Various stud and plate material combinations can be welded (Table 14).

TABLE 14 BASE METAL/STUD METAL COMBINATIONS THAT CAN BE SUCCESSFULLY JOINED USING CAPACITOR DISCHARGE STUD WELDING

BASE METAL	STUD METAL				
	LOW-CARBON STEEL[A]	**STAINLESS STEEL (300 SERIES)[B]**	**LEAD-FREE COPPER ALLOY**	**ALUMINUM ALLOY (1100 SERIES, 5000 SERIES, 6000 SERIES)**	TITANIUM OR TITANIUM ALLOY

LOW-CARBON STEEL (1006-1025)	X	X	X	. . .	. . .
STAINLESS STEEL (300 SERIES, 400 SERIES)	X	X	X	. . .	. . .
ALUMINUM ALLOY (1100 SERIES, 3000 SERIES, 5000 SERIES, 6000 SERIES)	. . .	. . .	. . .	X	. . .
COPPER ALLOY (LEAD-FREE BRASS)	X	X	X	. . .	. . .
ZINC ALLOY (DIE CAST)	. . .	. . .	. . .	X	. . .
TITANIUM OR TITANIUM ALLOY	. . .	. . .	. . .	. . .	**X**

(A) COMPOSITION: 0.23% C (MAX), 0.60% MN (MAX), 0.04% P (MAX), 0.05% S (MAX).

(B) WITH EXCEPTION OF FREE-MACHINING TYPE 303 STAINLESS STEEL

Procedure Development and Practice Considerations for Resistance Welding

Resistance Welding of Stainless Steels

Stainless steels are readily resistance welded by spot, seam, projection, flash, upset, high-frequency, and capacitor discharge. Generally, the weld time and welding current are less than those used for welding carbon steel, but the electrode force is usually greater. Austenitic stainless steels of the 300 series are resistance welded more often than any other metal except lowcarbon steel. Ideally, stainless steel to be resistance welded should contain a maximum of 0.08% C (as in types 304, 316, and 347), although steels of higher carbon content (such as types 301, 302, 309, and 310) can be successfully resistance welded.

The martensitic and ferritic types of stainless steel can be welded satisfactorily. The martensitic types are less frequently resistance welded, because joints made in them are hard and brittle in the as-welded condition.

Equipment

Resistance welding of stainless steel requires less transformer capacity than for equivalent thicknesses of other metal, under the same conditions. The welding machines use a singlephase alternating-current power supply, a three-phase rectifier, or a frequency-converter power supply. A weld made with a three-phase power supply usually requires slightly higher current and a longer weld time than a weld made with a single-phase supply.

Factors Affecting Resistance Welding of Stainless Steels

The characteristics of stainless steel that affect resistance welding include electrical resistivity, thermal conductivity, melting temperature, strength at elevated temperatures, coefficient of thermal expansion, and contact resistance.

Electrical Resistivity. Stainless steels have much higher electrical resistance than carbon steels. As a result, more heat is generated in a stainless steel with the same current. Therefore, resistance welding of a stainless steel requires lower currents or shorter weld times than welding of a carbon steel.

Thermal Conductivity. Stainless steel has a lower thermal conductivity than carbon steel and, therefore, heat is conducted away from the weld zone more slowly. This, in conjunction with the electrical resistivity, means that less heat has to be applied to reach the melting temperature.

Melting temperatures of stainless steels have an effect on the amount of heat required to produce fusion for welding. The austenitic stainless steels melt in various ranges between 1370 and 1455 °C (2500 and 2650 °F), and the martensitic and ferritic alloys melt in ranges between 1400 and 1530 °C (2550 and 2790 °F). Plain low-carbon steels melt at temperatures between 1480 and 1540 °C (2700 and 2800 °F).

Coefficient of Thermal Expansion. Austenitic and nitrogen-strengthened austenitic stainless steel expands and contracts with changing temperature almost 50% more than does plain carbon steel. These dimensional changes and the slower heat diffusion in austenitic grades result in greater thermal stress, which leads to warping. The ferritic, martensitic, and precipitation-hardening grades of stainless steel have coefficients of thermal expansion from 6 to 11% lower than that of plain carbon steel.

High strength at room and elevated temperatures of nitrogen-strengthened stainless steels and, to a lesser extent, of straight-chromium grades makes it necessary to use greater electrode force than is required for carbon steel to bring the work-metal surfaces together for the required intimate contact at points of welding.

Contact resistance of stainless steel is higher than that of carbon steel and, therefore, greater electrode pressure is needed to make good resistance welds. In addition, the welding process is more stable because the base material is not as susceptible to surface contamination.

Welding Characteristics of Stainless Steels

Austenitic Stainless Steels. All of the austenitic stainless steels in the solution-annealed condition contain carbon in solution. When the steel is heated to the temperature range of 425 to 815 °C (800 to 1500 °F), as in the weld heat-affected zone (HAZ), carbon combines with chromium, resulting in chromium carbide precipitation at the grain boundaries. Precipitation of chromium carbide (sensitization) makes the material susceptible to intergranular corrosion. Sensitization to intergranular corrosion is influenced in austenitic stainless steel by (1) the carbon content, (2) the solubility of the carbon, (3) the presence of one or more stabilizing elements, (4) the proximity of the actual metal temperature to 1200 °F, and (5) the time period during which the metal is held in that temperature range. The first three factors are controllable only through selection of composition; the latter two are controllable by adjustment of welding conditions such as heat input, size of spot, production rate, and provisions for cooling.

Martensitic stainless steels most often welded are types 403,410,414, and 431. These steels can be resistance welded in the annealed, hardened or hardened-and-tempered condition. Regardless of prior condition, welding produces a hardened martensitic zone adjacent to the weld. The hardness of this zone depends mainly on carbon content, although it can be controlled to a degree by welding procedure. As the hardness of the metal in the HAZ increases, its susceptibility to cracking increases and its toughness decreases. Steels having a maximum carbon content of 0.15%, such as types 403 and 410, often produce satisfactory welds without postweld heat treatment. Steels with higher carbon content, such as types 420 and 440A, generally require postweld heat treatment.

Ferritic grades of stainless steel most often welded are types 405,430,442, and 446. Resistance welds in these steels exhibit reduced ductility at room temperature because of grain growth in the HAZ. Ferritic stainless steels can also become embrittled if heated to approximately 475 °C (885 °F). This phenomenon, known as "885 °F embrittlement," may be encountered in the HAZ of a ferritic stainless steel weld. If properties in the as-welded condition are unsuitable, annealing must follow welding. Postweld annealing, in addition to improving ductility, helps restore normal corrosion resistance.

Precipitation-hardening grades of stainless steel can be resistance welded in the annealed or aged (hardened) condition. If they are welded in the aged condition, the strength of the weld area is significantly reduced because the heat of welding anneals the material subjected to it. Generally, most of the strength may be restored by simply re-aging the weldment. When maximum strength is required in the weld area, it is best to resistance weld these grades in the annealed condition and then age the weldment.

Procedure Development and Practice Considerations for Resistance Welding

Resistance Welding of Aluminum Alloys

Aluminum alloys, both of the non-heat-treatable and heat-treatable types, either wrought or cast, can be resistance welded. Some of these alloys are welded more readily than others. Gas shielding may be required to maximize joint quality. Characteristics of aluminum alloys include comparatively high thermal and electrical conductivity, a relatively narrow plastic range (about 95 to 205 °C, or 200 to 400 °F, temperature differential between softening and melting), considerable shrinkage during cooling, a troublesome surface oxide, and an affinity for copper electrode materials.

Base-Metal Characteristics

Although aluminum alloys can be resistance spot and seam welded, some alloys or combinations of alloys have higher as-welded properties than others. Table 15 gives melting ranges, electrical and thermal conductivities, and resistance weldability of some wrought alloys and casting alloys.

TABLE 15 MELTING RANGES, ELECTRICAL AND THERMAL CONDUCTIVITIES, AND RESISTANCE WELDABILITY OF COMMON ALUMINUM ALLOYS

Wrought and casting alloys are identified by Aluminum Association designations.

ALLOY AND TEMPER	**MELTING RANGE**		**ELECTRICAL CONDUCTIVITY, %IACS[A]**	**RELATIVE THERMAL CONDUCTIVITY[B],%**	RESISTANCE WELDABILITY[C]
	°C	**°F**			
NON-HEAT-TREATABLE WROUGHT ALUMINUM ALLOYS					
1350-H19	646-657	1195-1215	62	60	**ST**
1060-H18	646-657	1195-1215	61	57	**ST**
1100-H18	643-657	1190-1215	57	55	**RW**
3003-H18	643-654	1190-1210	40	39	**RW**
3004-H38	629-652	1165-1205	42	42	**RW**
5005-H38	632-652	1170-1205	52	51	**RW**
5050-H38	627-652	1160-1205	50	49	**RW**
5052-H38	593-649	1100-1200	35	35	**RW**
5083-H321	574-638	1065-1180	29	30	**RW**
5086-H34	584-640	1084-1184	31	32	**RW**
5154-H38	593-643	1100-1190	32	32	**RW**
5182-O	574-640	1065-1185	31	31	**RW**
5454-H34	602-646	1115-1195	34	34	**RW**
5456-H321	571-638	1060-1180	29	30	**RW**
HEAT-TREATABLE WROUGHT ALUMINUM ALLOYS					
2014-T6	510-638	950-1180	40	39	**ST**
2024-T361	501-638	935-1180	30	31	**ST**
2036-T4	554-649	1030-1200	41	40	**RW**
2219-T37	543-643	1010-1190	28	29	**ST**
6009-T4	560-649	1040-1200	44	43	**RW**
6010-T4	585-	1085-	39	38	**RW**

	649	1200			
6061-T6	593-649	1100-1200	43	43	**RW**
6063-T6	615-654	1140-1210	53	51	**RW**
6101-T6	615-652	1140-1205	57	55	**RW**
7075-T6	477-638	890-1180	33	33	**ST**
ALUMINUM CASTING ALLOYS					
413.0-F	574-582	1065-1080	31	32	**LW**
443.0-F	574-632	1065-1170	37	37	**RW**
308.0-F	521-613	970-1135	37	37	**ST**
238.0-F	507-599	945-1110	25	26	**LW**
513.0-F	579-638	1075-1180	34	34	**ST**
520.0-T4	449-604	840-1120	21	22	**NR**
333.0-T6	516-585	960-1085	29	30	**ST**
C355.0-T61	546-621	1015-1150	39	38	**ST**
356.0-T6	557-613	1035-1135	39	38	**ST**
712-F	**604-643**	**1120-1190**	**40**	**39**	**RW**

(A) INTERNATIONAL ANNEALED COPPER STANDARD. VOLUME BASIS AT 20 °C (68 °F). FOR COMPARISON, COPPER ALLOY 102 (OXYGEN-FREE COPPER) IS 101% AND LOW-CARBON (1010) STEEL ABOUT 14%.

(B) BASED ON COPPER ALLOY 102 AS 100%. WHICH HAS A THERMAL CONDUCTIVITY OF 391 W/M · K (226 BTU/FT · H · °F) AT 20 °C (68 °F). LOW CARBON STEEL HAS A THERMAL CONDUCTIVITY OF ABOUT 13% ON THIS RELATIVE SCALE.

(C) RW, READILY WELDABLE; ST, WELDABLE IN MOST APPLICATIONS BUT MAY REQUIRE SPECIAL TECHNIQUES FOR SPECIFIC APPLICATIONS; LW. LIMITED WELDABILITY AND USUALLY REQUIRES SPECIAL TECHNIQUES; NR. WELDING NOT RECOMMENDED

Alclad Alloys. Resistance welding is also done on Alclad products made by roll cladding some of the alloys listed in Table 15 with a thin layer of aluminum or aluminum alloy. Because this layer is anodic to the core alloy, it provides electrochemical protection for exposed areas of the core. Alclad alloys 2219, 3003, 3004, 6061, and 7075 have a cladding of alloy 7072, which contains 1% Zn; Alclad alloy 2014 has a cladding of alloy 6003 or sometimes alloy 6053, both of which contain about 1.2% Mg; and Alclad alloy 2024 has a cladding of alloy 1230, which contains a minimum of 99.3% Al.

Effects on Weldability. The hardness of an alloy is one variable influencing weldability. Any alloy in the annealed condition (O temper) is more difficult to weld than the same alloy in a harder temper. In general, alloys in the softer tempers are much more susceptible to excessive indentation and sheet separation and to low or inconsistent weld strength. Greater deformation under the welding force causes an increase in the contact area and variations in the distribution of current and pressure. Therefore, welding of aluminum alloys in the annealed condition or in the softer tempers is not recommended without special electromechanical or electronic controls.

High-strength alloys such as 2024 and 7075 are easy to resistance weld, but may require applications of a forge pressure, because they are more susceptible to cracking and porosity than the lower-strength alloys.

Resistance Welding Machines

Aluminum alloys can be resistance welded with single-phase direct-energy, three-phase direct-energy, and stored-energy machines. Best results are obtained by using a machine that has these features:

- ABILITY TO HANDLE HIGH WELDING CURRENTS FOR SHORT WELD TIMES
- SYNCHRONOUS ELECTRONIC CONTROLS FOR WELD TIME AND WELDING CURRENT
- LOW-INERTIA WELDING HEAD FOR RAPID FOLLOW-UP OF ELECTRODE FORCE
- SLOPE CONTROL (FOR SINGLE-PHASE WELDING MACHINES)
- MULTIPLE-ELECTRODE-FORCE SYSTEM TO PERMIT PROPER FORGING OF THE WELD NUGGET AND REDRESSING OF ELECTRODES

Electrodes and Electrode Holders

Selection of electrode material and face shape, maintenance of the face, and cooling of the electrode are important in producing consistent spot and seam welds in aluminum alloys.

Copper Alloy Electrodes. Resistance Welder Manufacturers Association (RWMA) classes 1, 2, and 3 are used for welding aluminum alloys. These electrode materials have high electrical and thermal conductivities, which combined with adequate cooling help keep the temperature of the electrode below the temperature at which aluminum will alloy with copper and cause electrode pickup.

Design of spot welding electrodes suitable for spot welding of aluminum includes both straight and offset electrodes. Construction details of each are shown in Fig. 26. Straight electrodes should be used whenever possible, because deflection and skidding may occur with offset electrodes under similar welding conditions. If offset electrodes are used, the amount of offset should be the minimum permitted by the shape of the assembly being welded.

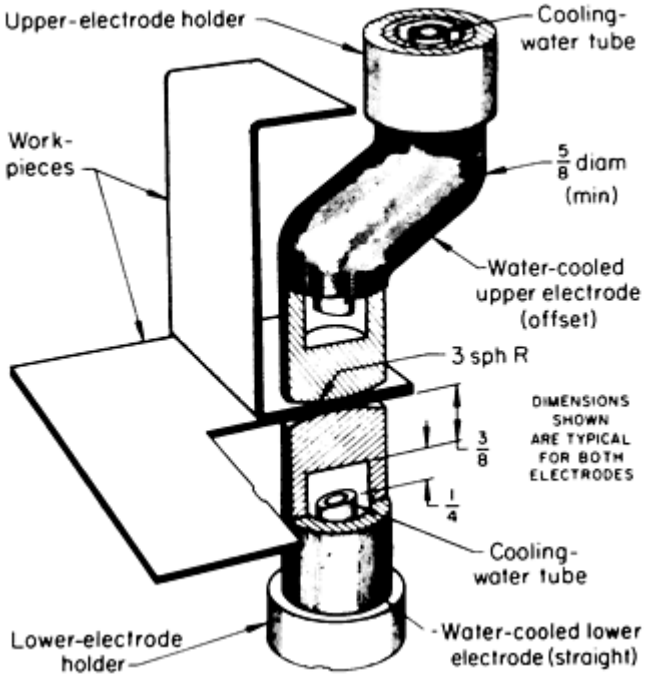

FIG. 26 CUTAWAY VIEW SHOWING INTERNAL COMPONENTS OF STRAIGHT AND OFFSET RADIUS-FACE ELECTRODES USED IN RESISTANCE SPOT WELDING OF ALUMINUM ALLOYS

Only electrodes that have the cooling-water hole within 9.5 mm ($\frac{3}{8}$ in.) of the face surface should be used.

Preweld Surface Preparation

Although welds for some purposes can be made satisfactorily without any preweld surface preparation, welds that are free of cracks, porosity and sheet separation, and that have the most uniform strength and symmetry, are obtained only with correct procedures for cleaning and reduction or removal of oxide film. In addition, adequate surface preparation reduces electrode contamination.

Procedure Development and Practice Considerations for Resistance Welding

Resistance Welding of Copper and Copper Alloys

Resistance spot welding is widely used for joining copper and copper alloys. Principal applications include welding sections up to about 1.52 mm (0.060 in.) thick, particularly those alloys with low electrical conductivities. Many copper alloys with low conductivities can be seam welded easily. Coppers with a low weldability factor are difficult to seam weld. Projection welding is not recommended for copper or for most brasses. Bronzes can be projection welded with satisfactory results in many applications.

Welding Characteristics

The resistance weldability of any copper alloy is inversely proportional to its electrical and thermal conductivities. Generally, alloys with lower conductivities are easier to weld. Compared with steel, most copper alloys require shorter weld time, lower electrode force, higher current, and different electrode materials that are compatible with the alloy being welded.

Welding Equipment

Single-phase and three-phase direct-energy and electrostatic stored-energy (capacitor-discharge) welding machines are used for resistance welding of copper and copper alloys. The addition of slope control to single-phase direct-energy welding machines is not necessary for spot welding most copper alloys. In welding high-zinc brasses, the use of upslope can result in an increase of as much as 20% in weld strength. Downslope is not recommended for welding of any of the copper alloys.

Welding Machine Controls. Copper alloys are particularly sensitive to variations in welding conditions, and therefore all direct-energy machines used for welding these alloys should be equipped with synchronous electronic controls, especially in applications requiring short weld times. These devices are capable of controlling weld time and welding current for repeated operations with extreme accuracy.

Electrodes

The current used for resistance welding of copper alloys is much higher than that used for welding low-carbon steel, and therefore, the electrode must have high electrical conductivity to minimize heat buildup.

Electrode Materials. The Resistance Welder Manufacturers Association (RWMA) class 1 electrode materials (typically tungsten or molybdenum alloys), containing copper and cadmium, are sometimes used for welding copper and high-conductivity brass and bronze. Class 2 materials, containing copper and chromium, are used on low-conductivity brass and bronze and the copper-nickel alloys. Class 3 materials are used in electrodes for seam welding.

Electrodes must be sufficiently water cooled to minimize sticking to the work metal and to prolong their life. Face contours must be carefully prepared and the electrodes must be properly aligned for welding.

Selection of Process

Weldability of the work metal often determines which process should be used for a given application. Some of the coppers and copper alloys can be spot welded, but not seam welded because of high conductivity, and not projection welded because of low compressive strength of the projections at elevated temperature.

Coppers

Coppers and copper alloys having electrical conductivity higher than about 30% IACS are the least well suited for resistance spot, projection, or seam welding, mainly because of severe electrode pickup.

Thin copper stock can be welded using electrodes faced with RWMA class 13 (tungsten) or class 14 (molybdenum), but surface appearance is poor and frequent electrode maintenance is required. A tinned coating on wire or sheet is helpful in welding copper.

Beryllium Copper

Beryllium copper alloys can be resistance welded most successfully in thin gages. Spot welding produces satisfactory welds; seam welding is less successful. Projection welding is satisfactory, provided that the projections can be formed with the work metal in the annealed condition and without cracking the work metal around the projection. Close control of welding conditions is required for consistent weld size and joint strength.

Oxide films produced by heat treating must be removed to ensure low and consistent contact resistance. Work metals that have not been heated after rolling frequently need only degreasing before welding.

Low electrical conductivity (22% IACS for alloys C17000 and C17200) contributes to the weldability of beryllium copper alloys. However, they are more difficult to resistance weld than low-carbon steel. Alloy C17500 has an electrical conductivity of 45% IACS and is more difficult to resistance weld than higher-strength, lower-conductivity beryllium copper.

Low- and High-Zinc Brasses

The low-zinc brasses are difficult to weld, although easier than copper, and are subject to electrode pickup. Welds made in these brasses may lack strength, principally because of comparatively high electrical conductivity (32 to 56% IACS).

The high-zinc brasses have an electrical conductivity of 27 to 28% IACS and can be both spot and projection welded over a wide range of conditions. Electrode pickup can be a problem unless weld time, welding current, and electrode force are properly selected.

Excessive electrode pickup and blowthrough of the weld may occur when long weld times, high energy input, and low electrode forces are used. Yellow brasses (alloys C26800 and C27000) are less susceptible to electrode pickup than cartridge brass except when long weld times and high energy input are used. Electrode force should be sufficient to prevent arcing or expulsion of molten metal, to which these alloys are subject because of their 30 to 40% Zn content, which boils at about 905 °C (1665 °F). As shown in Table 16, the recommended electrode force, when using electrodes having a face diameter of 4.8 mm ($\frac{3}{16}$ in.), is approximately 1.8 kN (400 lbf).

TABLE 16 GUIDELINES FOR RESISTANCE SPOT WELDING OF SELECTED COPPER ALLOYS

UNS NO.	**ALLOY NAME**	WELDING PARAMETER[A]			
		WELD TIME, CYCLES	**ELECTRODE FORCE**		WELDING CURRENT,A
			KN	**LBF**	
C23000	RED BRASS	6	1.8	400	**25,000**
C24000	LOW BRASS	6	1.8	400	**24,000**
C26000	CARTRIDGE BRASS	4	1.8	400	**25,000**
C26800-C27000	YELLOW BRASS	4	1.8	400	**24,000**
C28000	MUNTZ METAL	4	1.8	400	**21,000**

C51000-C52400	PHOSPHOR BRONZE	6	2.3	510	**19,500**
C62800	ALUMINUM BRONZE	4	2.3	510	**21,000**
C65100-C65500	SILICON BRONZE	6	1.8	400	**16,500**
C66700	MANGANESE BRASS	6	1.8	400	**22,000**
C68700	ALUMINUM BRASS	4	1.8	400	**24,000**
C69200	**SILICON BRASS**	**6**	**2.3**	**510**	**22,000**

(A) FOR SPOT WELDING 0.91 MM (0.036 IN.) THICK SHEET USING RWMA TYPE E ELECTRODES WITH 4.8 MM ($\frac{3}{16}$ IN.) DIAM FACE AND 30 ° CHAMFER AND MADE OF RWMA CLASS 1 MATERIAL

Copper Nickels

The copper-nickel alloys have electrical conductivities of 4.5 to 11% IACS, are readily spot and seam welded with relatively low welding current, and generally do not alloy with the electrode material and cause electrode pickup.

Bronzes

The phosphor bronzes, except alloy C50500, which is not recommended for resistance spot and seam welding because of its high electrical conductivity (48% IACS), have relatively low electrical conductivity (11 to 20% IACS) and am readily spot and seam welded using low welding currents. Electrode pickup can be reduced by use of a type F (radius) electrode face and frequent redressing to keep the face clean and smooth. Hot shortness can be minimized by supporting the workpieces to prevent strain during welding and by using a greater minimum overlap than recommended by the data in Table 17.

TABLE 17 GUIDELINES FOR RESISTANCE SPOT WELDING OF HIGH-ZINC BRASSES

THICKNESS OF THINNEST SHEET		**MINIMUM SPOT SPACING**		**MINIMUM CONTACTING OVERLAP[(A)]**		SHEAR LOAD OF JOINT	
mm	**in.**	**mm**	**in.**	**mm**	**in.**	**kn**	lbf
0.81	0.032	16	$\frac{5}{8}$	13	$\frac{1}{2}$	1.47	**330**
1.27	0.050	16	$\frac{5}{8}$	16	$\frac{5}{8}$	2.28	**512**
1.63	0.064	19	$\frac{3}{4}$	19	$\frac{3}{4}$	3.02	**680**
2.39	0,094	25	1	25	1	5.20	**1168**
3.18	**0.125**	**38**	**1** $\frac{1}{2}$	**32**	**1** $\frac{1}{4}$	**8.33**	**1872**

(A) MINIMUM EDGE DISTANCE IS EQUAL TO ONE HALF THE CONTACTING OVERLAP.

Nickel Silvers

Nickel silvers, which have about the same conductivities (6 to 10.9% IACS) as copper nickels, are spot welded as readily as copper nickels but are more difficult to seam weld. Surface contaminants such as lead and bismuth (which form low-melting eutectics with copper and nickel) or sulfur (which may be introduced in forming) must be removed before resistance welding.

References

1. L.P. CONNER, ED., *WELDING HANDBOOK*, 8TH ED., VOL 1, AWS, 1987, P 16
2. J.F. YOUNG AND R.S. SHANE, ED., *MATERIALS AND PROCESSES, PART B: PROCESSES*, 3RD ED., MARCEL DEKKER, 1985, P 11257-1126
3. J.G. BRALLA, ED., *HANDBOOK OF PRODUCT DESIGN FOR MANUFACTURING*, MCGRAW-HILL, 1986, P 7-35
4. J.F. YOUNG AND R.S. SHANE, ED., *MATERIALS AND PROCESSES, PART B: PROCESSES*, 3RD ED., MARCEL DEKKER, 1985, P 1127
5. J.G. BRALLA, ED., *HANDBOOK OF PRODUCT DESIGN FOR MANUFACTURING*, MCGRAW-HILL, 1986, P 7-38
6. R.L. O'BRIEN, ED., *WELDING HANDBOOK*, 8TH ED., VOL 2, AWS, 1991, P 552
7. J.G. BRALLA, ED., *HANDBOOK OF PRODUCT DESIGN FOR MANUFACTURING*, MCGRAW-HILL, 1986, P 7-39
8. "RECOMMENDED PRACTICES FOR RESISTANCE WELDING," AWS C1.1-66, AWS, 1966
9. *RESISTANCE WELDING MANUAL*, 3RD ED., VOL 1, RESISTANCE WELDER MANUFACTURERS ASSOCIATION, 1956, P 88
10. R.L. O'BRIEN, ED., *WELDING HANDBOOK*, 8TH ED., VOL 2, AWS, 1991, P 593
11. H.B. CARY, *MODERN WELDING TECHNOLOGY*, 2ND ED., PRENTICE-HALL, 1989, P 251-252

Procedure Development and Practice Considerations for Electron-Beam Welding

Introduction

ELECTRON-BEAM WELDING (EBW) can produce deep, narrow, and almost parallel-sided welds with low total heat input and relatively narrow heat-affected zones in a wide variety of common and exotic metals. In many applications, a single pass is sufficient to weld the components. When initially applied to industrial applications in the 1950s, EBW had to be performed totally in a vacuum environment. In this form, EBW was primarily used because of its ability to reliably produce very high quality welds in materials normally considered extremely difficult to join (for example, refractory metals, oxidizable metals, stainless steels, and superalloys). This made it ideally suited for use in aerospace, nuclear, and other similar (high-technology) manufacturing industries.

During the 1960s, the capability of employing the EBW process for medium-vacuum and nonvacuum welding tasks was developed. This increased production capacity helped make EBW more attractive to other industries desiring to take advantage of the numerous joining benefits it provided. However, the use of EBW required that all applications have a demonstrated capacity for fairly high-volume production.

Today, EBW is used to join not only difficult-to-weld materials but also common materials such as steel ($\leq$150 mm, or 6 in., thick), aluminum ($\leq$305 mm, or 12 in., thick), and copper ($\leq$100 mm, or 4 in., thick) (Ref 1). These and other metals (in thicknesses ranging from foil to plate dimensions) can be electron-beam welded. In addition, EBW can be used to join numerous combinations of dissimilar metals. See the Section "Fusion Welding Processes" in this Handbook for a description of EBW systems and equipment.

Reference

1. A. SANDERSON AND K.R. NIGHTINGALE, *WELD. J.*, APRIL 1990, P 45

Procedure Development and Practice Considerations for Electron-Beam Welding

Weld Geometry

Part Configuration. Whether a component is welded in a vacuum or at atmospheric pressure (nonvacuum), part configuration and the corresponding joint designs used are critical parameters in the successful application of EBW. A circular weld in the axial direction, for example, that joins a disk-shaped member (gear or cup) to a shaft (Fig. 1) may

experience severe constraint. Such joints are practical in easily welded metals--those that are soft, have low yield points, and exhibit low shrinkage--but not in difficult-to-weld steels that have high strength, hardenability, or machinability due to high sulfur content.

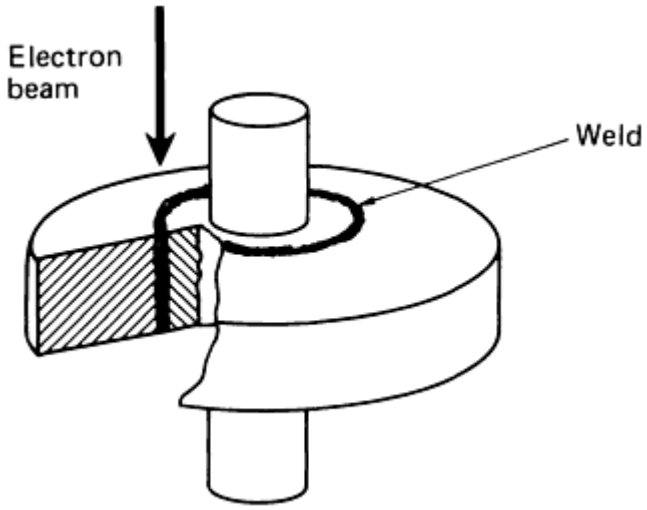

FIG. 1 CUTAWAY VIEW SHOWING LOCATION AND PENETRATION OF A CIRCULAR ELECTRON-BEAM WELD JOINING A DISK-SHAPED COMPONENT TO A SHAFT

The difficulties encountered in welding shapes such as those shown in Fig. 1 are aggravated if the weld zone is broadened by defocusing the electron beam. This is a frequent problem if exact beam position cannot be controlled, either because of beam instability, magnetism of the parts, or excessive tolerances in fixturing on high throughput machines. The need for beam broadening can be eliminated by the use of closed-loop beam position control systems.

Shrinkage stress is minimal in radial welds, as shown in Fig. 2. The volume of molten metal is less constrained by the axial direction if the gear hub is allowed to move by using push fit and no restraints. The weld must also have root clearances--the weld zone must not extend into the shaft. Stresses are lower if the melt zone has parallel side boundaries. Triangular weld zones that are caused by broadened beams, uneven beam power distribution, or incomplete penetration have more complex stresses which may result in cracking.

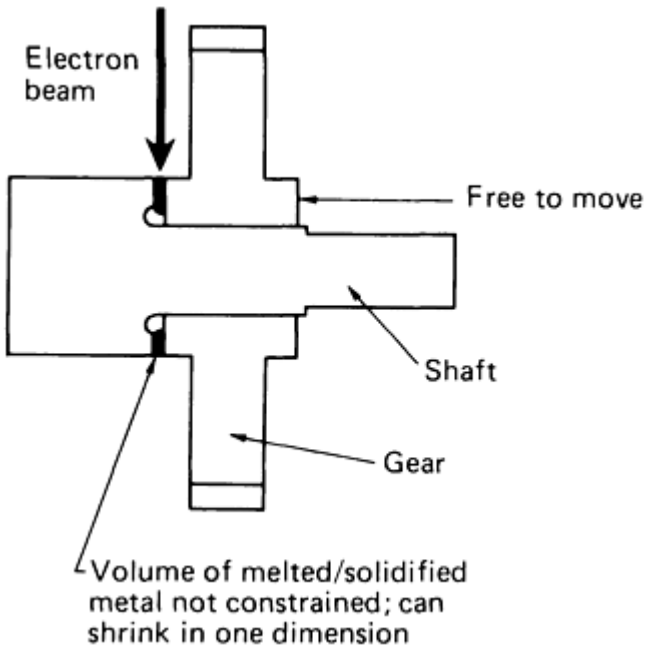

FIG. 2 SHRINKAGE STRESS IN A RADIAL WELD

The same principles of joint design discussed above for joints between shafts and disklike members apply equally to T-joints and comer joints between plates. Figure 3 shows recommended and nonrecommended weld configurations. Although true for all welding methods, it is essential in EBW (which is usually performed in a single pass) that constraints on the volume of the melt must be avoided by self-aligning interlocking steps in the joint. In multilayer arc welds, the individual weld bead is less constrained in volume and shrinks from its surface downward. Functionally, it is not useful to make the cross section of the joint any less thick than the plates that are being joined. If two welds are made in succession, the second weld may be constrained by the first (Fig. 3), which may lead to solidification cracking. It is thus advisable to direct the beam at the joint parallel to the faying surfaces and to cause melting over the whole contact area.

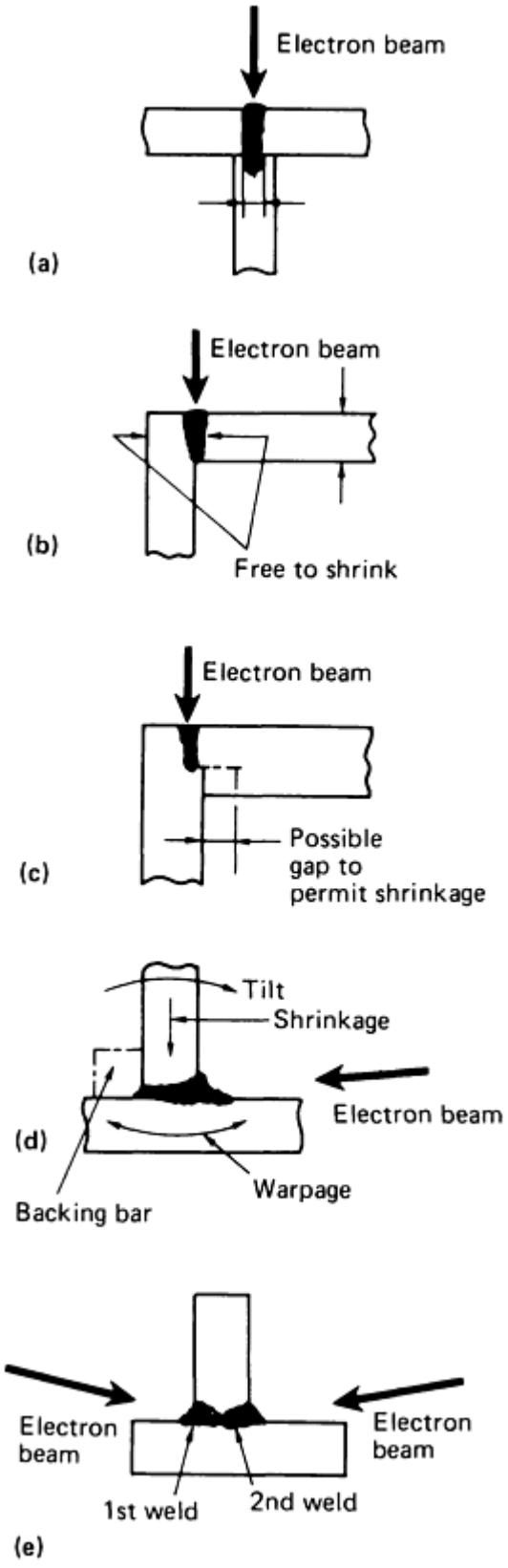

FIG. 3 OPTIMUM VERSUS LEAST DESIRABLE WELD CONFIGURATIONS. (A) NOT RECOMMENDED--MAXIMUM CONFINEMENT OF MOLTEN METAL, MINIMUM JOINING CROSS SECTION (ARROWS); WASTES BEAM ENERGY FOR MELTING, NONFUNCTIONAL METAL. (B) MOST FAVORABLE--VOLUME OF MELT NOT CONFINED; MAXIMUM JOINING CROSS SECTION (ARROWS). (C) NOT RECOMMENDED--MAXIMUM CONFINEMENT OF MELT (UNLESS GAP IS PROVIDED); JOINING CROSS SECTION LESS THAN PLATE CROSS SECTION. (D) MOST FAVORABLE--MINIMUM CONSTRAINT AND CONFINEMENT OF MELT; MINIMUM INTERNAL STRESSES; WARPAGE CAN BE OFFSET BY BENDING PRIOR TO WELDING; TILT CAN BE OFFSET BY LOCATION OF T-ARM AT LESS THAN 90°

TO BASE PRIOR TO WELDING. FILLET OBTAINED BY PLACING WIRE IN RIGHT CORNER AND MELTING IT WITH THE BEAM. (E) NOT RECOMMENDED--TWO SUCCESSIVE WELDS; SECOND WELD IS FULLY CONSTRAINED BY THE FIRST WELD AND SHOWS STRONG TENDENCY TO CRACK.

Surface Geometry. Usually, EBW does not use or need filler wire. Therefore, neither V-grooves nor corners can be filled; in fact, they are detrimental. Surface tension pulls some of the molten metal up the V-shaped surfaces so that it is no longer available to fill the space created by the keyhole that is generated by the moving beam. Voids remain in the actual joint plane (Fig. 4).

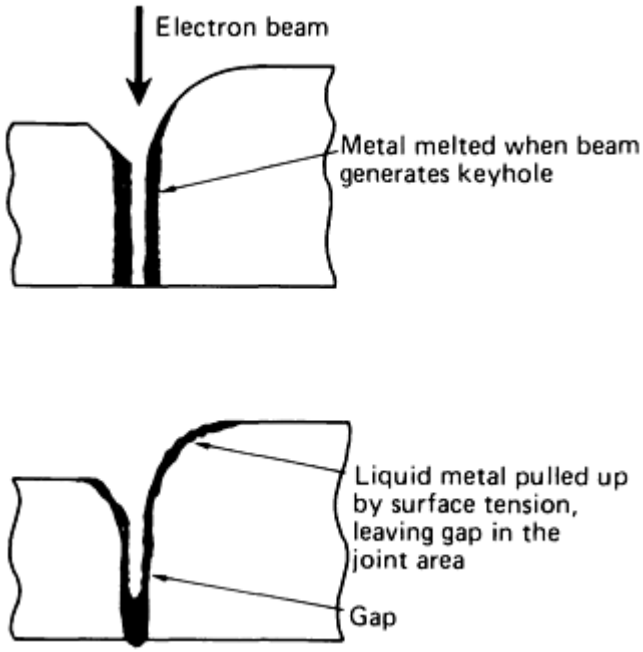

FIG. 4 GAP IN JOINT PLANE CREATED BY SURFACE TENSION

A step in the surfaces at the joint line is also undesirable. Any small lateral shift of the beam from the low to the high side, and vice versa, changes the penetration to some extent. In the extreme case, this shift may be equal to the height of the step, as shown in Fig. 5. On circular welds, with joint configurations similar to Fig. 5(a), a noncircular weld profile may develop with irregularities that can lead to uneven applied stresses. By contrast, a mere shift in the melt zone, as shown in Fig. 5(b), does not affect weld quality, as long as the entire joint line is covered.

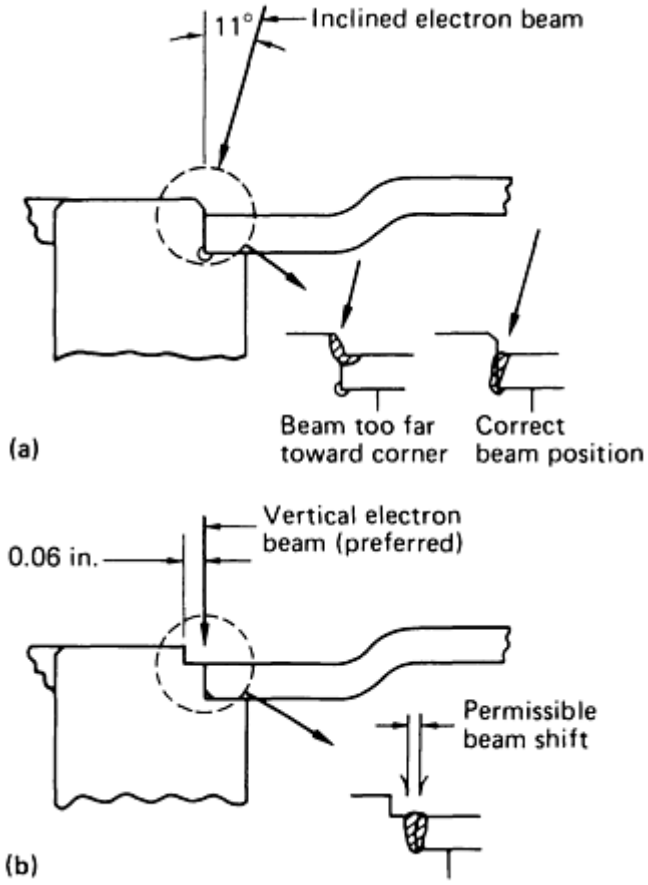

FIG. 5 EFFECT OF BEAM AND MELT ZONE POSITION ON WELD PENETRATION. (A) INCLINED ELECTRON BEAM. (B) VERTICAL ELECTRON BEAM

Configurations for Wide Welds Bridging a Gap. The high speed and autogenous nature of an electron-beam weld can be advantageous when a wide weld (6.5 to 13 mm, or $\frac{1}{4}$ to $\frac{1}{2}$ in.) is needed without great depth-to-width ratio. The atmospheric electron beam has been used extensively to make such welds in mass-production automotive parts such as catalytic converter cases and die-cast aluminum intake manifolds.

The easiest weld to make with an electron beam is an edge-weld in the vertical position of the beam (weld horizontal and flat), as illustrated by the edge-flange weld in Fig. 6. In vacuum, the beam must be defocused; in air, the standoff must be short enough to prevent substantial beam scattering. The standoff is not critical because energy flow is not influenced by standoff as it is in electric arc welding.

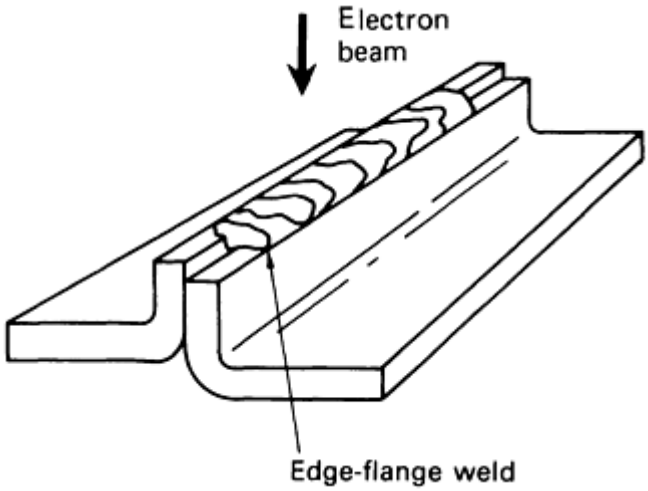

FIG. 6 EDGE-FLANGE WELD TYPICALLY USED TO JOIN THIN PANELS

For edge welds, changes in energy input per unit length and changes in power density affect only the amount of molten metal. Offset and gaps up to the thickness of the sheet to be joined often can be tolerated (Ref 2). In making an edge-flange weld (Fig. 6), the same advantages exist, provided the flange is high enough. For joining thinner sheet that is tightly clamped, edge welds also can be made with the electron beam in the horizontal position.

The nonvacuum EBW (EBW-NV) process can tolerate and fill large gaps if sufficient sacrificial metal is available to be melted by the beam (Fig. 7). If not, surface tension may pull whatever metal is melted to either side of the weld joint.

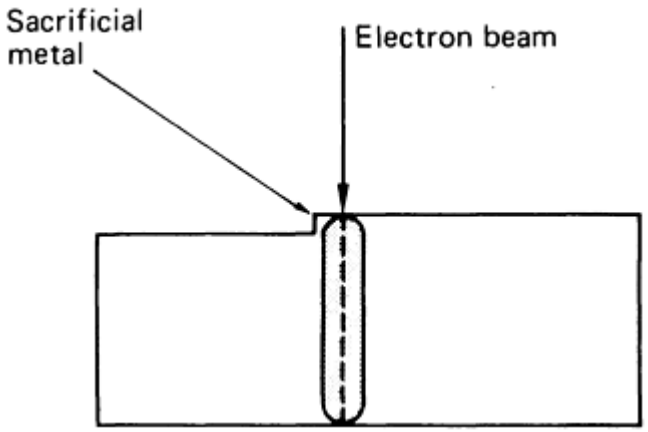

FIG. 7 USE OF SACRIFICIAL METAL TO FILL A LARGE GAP IN A SQUARE-GROOVE WELD

Melt-Zone Configuration. Welds with parallel sides of the melt zone (Fig. 8a) show minimum warpage and only transverse shrinkage when they are unconstrained. Triangular melt zones (Fig. 8b) cause warpage. If there are constraints, the hindered warpage and shrinkage cause internal stresses. A parallel-sided melt zone is preferred in either case; to obtain this configuration, joint design must allow for a full-penetration weld.

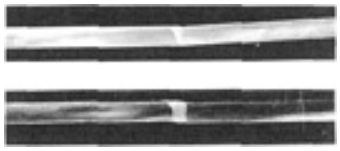

FIG. 8 VARIATION IN BEAM VELOCITY AND SUBSEQUENT WARPAGE OF 0.25 MM (0.10 IN.) THICK TYPE 304 STAINLESS STEEL JOINED BY A BUTT WELD. (A) BEAM TRAVERSE, 7110 MM/MIN (280 IN./MIN); TRIANGULAR MELT ZONE. (B) BEAM TRAVERSE, 4190 MM/MIN (165 IN./MIN); PARALLEL-SIDED MELT ZONE. WELD PARAMETERS: 12 KW BEAM POWER; 11.4 MM (0.45 IN.) STANDOFF; HELIUM SHIELDING GAS

Reference cited in this section

2. J.F. LOWRY, J.H. FINK, AND B.W. SCHUMACHER, A MAJOR ADVANCE IN HIGH-POWER ELECTRON BEAM WELDING IN AIR, *J. APPL. PHYS.*, VOL 47, 1976, P 95-106

Procedure Development and Practice Considerations for Electron-Beam Welding

Joint Design

Figures 9, 10, 11, 12, and 13 show the commonly used joint and weld types for EBW. Different joint preparations, joint designs, and welding positions are used to meet special requirements. For preferred joint configurations and shrinkage stresses encountered in various joint designs, see the section on weld geometry for electron-beam welding in this article.

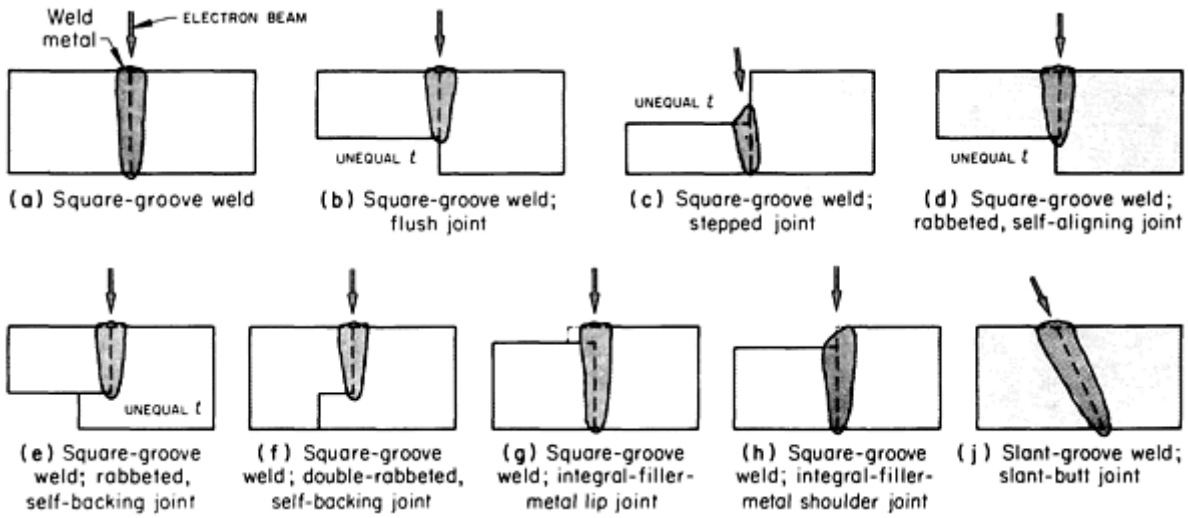

FIG. 9 TYPES OF BUTT JOINTS AND WELDS TYPICALLY GENERATED BY EBW

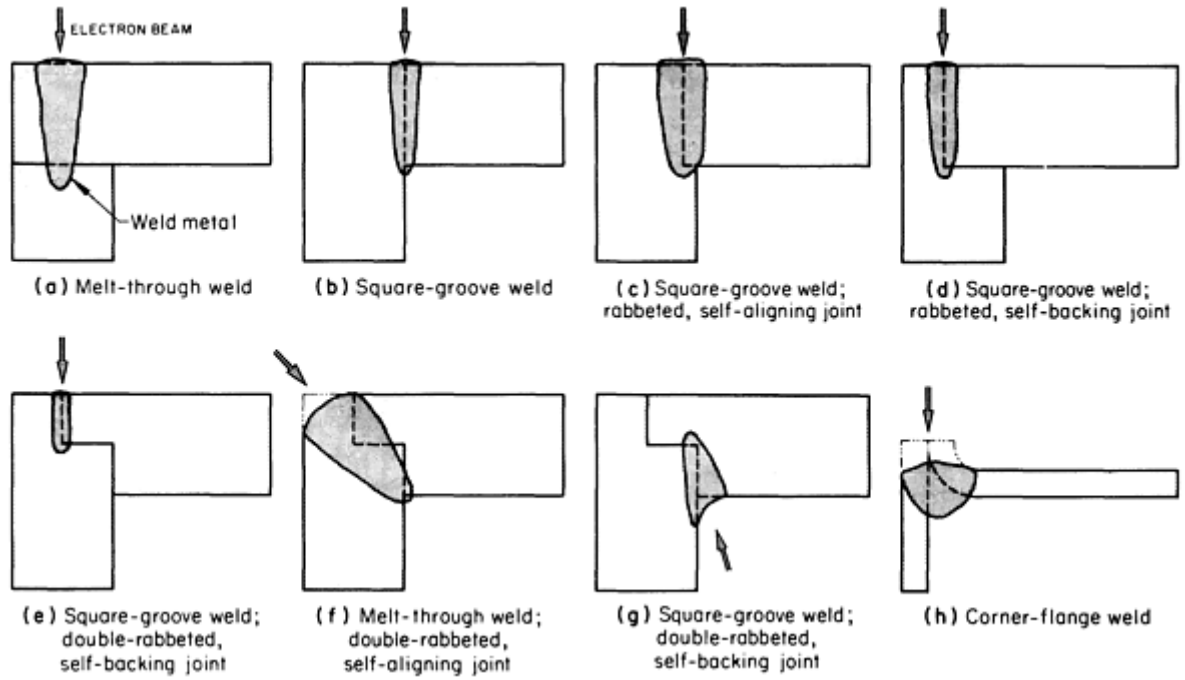

FIG. 10 TYPES OF CORNER JOINTS AND WELDS TYPICALLY OBTAINED WITH EBW

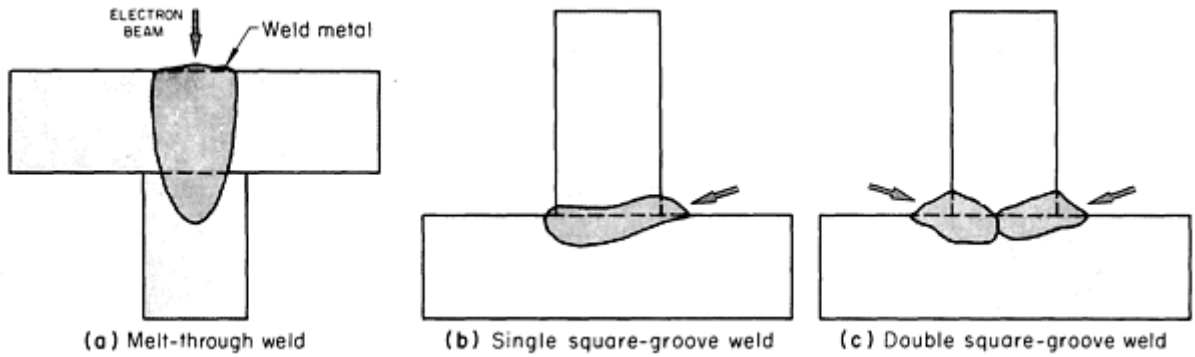

FIG. 11 TYPICAL WELDS PRODUCED BY EBW OF T-JOINTS

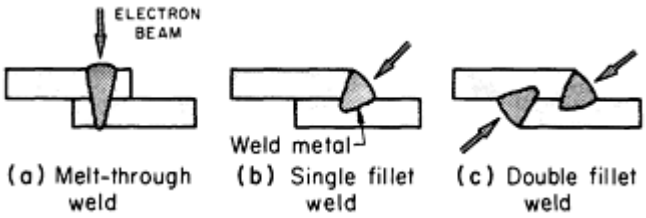

FIG. 12 TYPICAL WELDS OBTAINED BY EBW OF LAP JOINTS

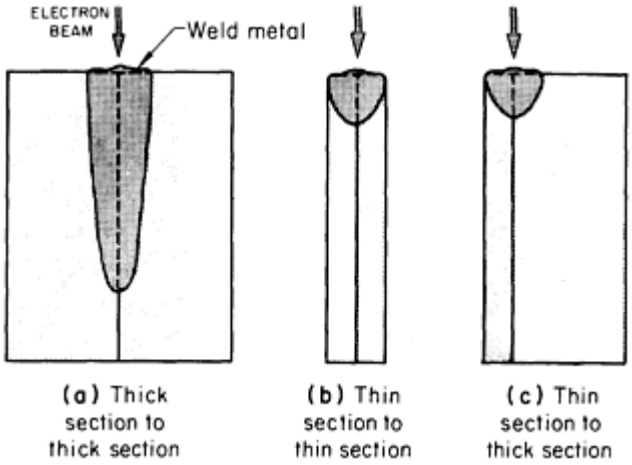

FIG. 13 TYPICAL WELDS GENERATED BY EBW OF EDGE JOINTS HAVING COMPONENTS OF EQUAL AND UNEQUAL SECTION THICKNESSES

Welds in Butt Joints

Butt joints are the most common of the five basic joint types used in EBW. The basic square-groove weld, which is shown in Fig. 9(a), 9(b), and 9(c), needs only the simplest and least expensive joint preparation. It is suitable for either partial- or full-penetration welds. Good fit-up and external fixtures are needed. The flush joint (Fig. 9b) is preferred to the stepped joint (Fig. 9c) for joining unequal thicknesses, chiefly because control of conditions for making sound full-penetration welds is less critical than for the stepped joint. A wider beam is used in welding the stepped joint, and the beam angle must he carefully controlled to avoid scarfing the upper edge of the thicker member (angle too small) or missing the bottom of the joint (angle too large), especially if the thinner member is more than about 9.5 mm ($\frac{3}{8}$ in.) thick.

In Fig. 9(d), the joint is rabbeted to make it self-aligning, but the offset is small to avoid leaving an unwelded seam near the root of the weld (compare Fig. 9e). In Fig. 9(d) to (g), the joints are self-aligning and may be self-fixturing in circular, circumferential, and certain other joint arrangements. In Fig. 9(e) and 9(f), the joints are both self-aligning and self-backing; each, however, leaves an unwelded seam near the root of the weld.

In Fig. 9(g) and 9(h), two ways are shown of providing integral and filler metal. The lip of the joint in Fig. 9(g) provides more filler metal than the shoulder of the joint in Fig. 9(h), but because it conceals the joint, a scribed line or other means for beam placement and for scanning must be provided before the welding operation can proceed.

The slant-groove weld (also called angular or scarf) shown in Fig. 9(j) is used in butt joints to facilitate fixturing. It is also used where limitations on the beam location prevent fusion for the entire groove depth if the basic square-groove weld (Fig. 9a) were used. Greater weld depth, as measured parallel to the beam axis, is needed for full penetration of a given metal thickness than with the square-groove weld. This type of weld and variations of it are used both in butt joints and in corner joints.

A slant-butt joint can also be welded with beam alignment set at 90° to the surface of the work. This beam angle permits the production of defect-free welds where fit-up is poor or where the joint opening is larger than can be tolerated when the beam is aligned with the groove. In a related type of weld, the joint has a square-groove preparation, and the beam is at an angle to the groove. The main reason for using this type of weld is difficulty of access with other types of welds.

Welds in Corner Joints

Eight types of electron-beam welds frequently made in corner joints are shown in Fig. 10. Corner joints are second only to butt joints in frequency of use for EBW.

Important differences between butt and corner joints are notch sensitivity and suitability for nondestructive testing. To compare alignment, self-fixturing, and the occurrence of portions of unwelded seam, see Fig. 9 and 10.

The two simplest and most economical welds in corner joints are the melt-through (Fig. 10a) and basic square-groove (Fig. 10b) welds. Neither is self-aligning or self-fixturing; manipulation of the work for weld (b) in Fig. 10 can be simplified by using a horizontal electron beam and corresponding work orientation (rotated 90° from the orientation shown). The melt-through weld (Fig. 10a), unless made with a fusion zone wide enough to eliminate the unwelded seam completely, is weaker than the square-groove weld and is notch sensitive.

The corner-flange weld (Fig. 10h), usually made only on thin stock, requires precision forming of the 90° bend. Welds in corner joints are subject to high stress concentrations.

Welds in T-Joints

Three types of electron-beam welds made in T-joints are shown in Fig. 11. The melt-through or blind weld (Fig. 11a), like melt-through welds in butt or corner joints, leaves an unwelded seam with resulting low strength, notch sensitivity, and corrosion susceptibility. Figure 11(b) is the preferred joint design. The double-square-groove weld (Fig. 11c) is used primarily on sections 25 mm (1 in.) or more thick. For welds similar to Fig. 11(b) and 11(c), filler metal can be added.

Welds in Lap Joints

Three types of electron-beam welds made in edge joints are shown in Fig. 13. Thick sections can be joined by deep, narrow square-groove welds (Fig. 13a). Shallow welds made with a low-power, partially defocused beam are used to join thin sections to each other or to thick sections, as shown in Fig. 13(b) and 13(c). Shallow edge welds can be made at high speed. Welds of this type are particularly useful on hermetically sealed assemblies, which may be designed for planned salvage by removal of the weld region and subsequent rewelding.

Butt Joints Versus Corner and T-Joints

The concentration of bending stresses at the weld in corner and T-joints is sometimes avoided by designing the work for a butt joint on a straight section near the corner or T (flange neck or welding neck construction). This principle of design is applicable also to butt joints between members having different thicknesses, and it can be applied to straight line, circular, and circumferential joints.

In welding such a joint in magnetic metals, if the beam path is too close to the corner, T, or shoulder, the beam may be deflected away from the metal that it passes near on its way to the joint, causing it to enter the work at an angle and possibly to miss the lower portion of the joint. To avoid this, the beam clearance should be 0.8 mm (0.030 in.) or more, depending on the height of the magnetic projection (Fig. 14).

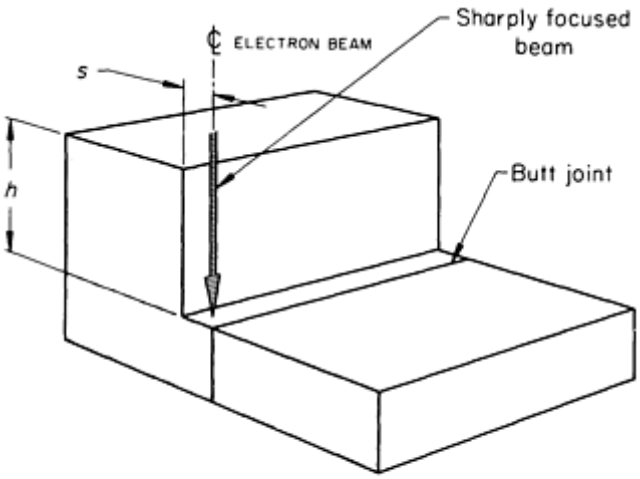

FIG. 14 JOINT LOCATION AND BEAM CLEARANCE FOR AN EBW BUTT JOINT NEAR A PROJECTING CORNER, T, OR SHOULDER CONSISTING OF MAGNETIC WORK METAL

Procedure Development and Practice Considerations for Electron-Beam Welding

Special Joints and Welds

Many variations of the basic joint and weld types described in the preceding section and illustrated in Fig. 9, 10, 11, 12, and 13 are used to meet the needs of individual applications. Some of these special joints and welds are discussed below.

Plug and puddle welds are usually made by manually (or automatically) manipulating the work under a fixed beam at low power. Filler metal used for plug welds is often preplaced at the weld site. Puddle welding is used mainly to fuse shallow defects together locally.

Multiple-Pass Welds. Most electron-beam welds produce the desired penetration in a single pass. Tack welds and cosmetic or smoothing passes are not considered penetration passes. Welds several inches deep can be made in most metals in a single pass. Weld depth obtainable in a single pass can be nearly doubled by welding from both the face and the back of the work.

In a variation on straight-through two-pass welding from opposite sides, separate welds that meet or almost meet can be made at an angle of 90° to each other in a rabbeted square-groove joint.

Tangent-tube welds are longitudinal welds joining two parallel tangent tubes (or cylinders). The tubes may differ in size; the beam is perpendicular, or nearly perpendicular, to the common axial plane of the two tubes. Added filler metal may be used for reinforcement. Thinner wall tubes can be joined more easily by EBW than by arc welding methods.

Three-Piece Welds. Welds can be made that join three or more pieces in which there is penetration in a single pass into all of the pieces. Many of the difficulties encountered in welding very thin metal or foil are eliminated by sandwiching it between two thicker sections.

Multiple-tier welds are welds made simultaneously in in-line, separated joints (usually butt joints) in a single pass of the electron beam. A more detailed discussion is given in the section of this article on multiple-tier welding .

Welds using integral filler metal may be of the types shown in Fig. 9(g) and 9(h), in which an overhanging lip or a shoulder provides filler metal to a butt joint, or both members may be made thicker at the joint than elsewhere.

EBW in High Vacuum

Most EBW is done in a vacuum environment where the maximum ambient pressure is less than 0.13 Pa (1×10^{-3} torr). Maintenance of this degree of vacuum is important because of the effect that ambient pressure has on both the beam and the weld produced, as discussed below.

Applications. High-precision applications that require welding to be done in a high-purity environment to avoid contamination by oxygen or nitrogen are ideally suited for high-vacuum EBW (EBW-HV). These applications include the nuclear, aircraft, missile, and electronics industries. Typical products include nuclear fuel elements, pressure vessels for rocket propulsion systems, special alloy jet engine components, and hermetically sealed vacuum devices. Welding of reactive metals such as zirconium and titanium in high vacuum is preferred over medium- or nonvacuum EBW because of the affinity of reactive metals to oxygen and nitrogen.

Effect of Pressure on Beam. Under ambient high-vacuum conditions, the frequency of collisions between beam electrons and residual gas molecules is extremely low, and any dispersion (i.e., beam-broadening effect) that would result from such scattering collisions is minimal. However, because the frequency of scattering collisions increases with the density of gas molecules present, this effect becomes greater as the surrounding environment pressure is increased. Only at ambient pressure values below 0.13 Pa (1×10^{-3} torr) is the effect of scattering insignificant enough that the beam can be held in sharp focus over distances of several feet (depending on the particular characteristics of the electron gun and electron optics being employed) to achieve maximum effectiveness in producing relatively deep, narrow welds.

Beam scattering from collisions with residual gas molecules begins to occur at ambient pressures above 0.13 Pa (1×10^{-3} torr) and initially results in decreased penetration and increased weld width. This scattering effect reduces the maximum working distance that can be employed for producing a similar electron-beam weld as obtained under high-vacuum conditions at ambient pressures greater than 0.13 Pa (1×10^{-3} torr).

In EBW-NV, where the ambient pressure is 10 MPa (760 torr) and above, the scattering dispersion of the beam increases so that penetration and working distance capacity are appreciably reduced below values obtainable in either high- or medium-vacuum processes. However, the penetration and working distance capabilities of EBW-NV are appreciably greater than those of conventional arc welding processes. Electron-beam dispersion characteristics and their effect on weld penetration at various ambient pressures are shown in Fig. 15.

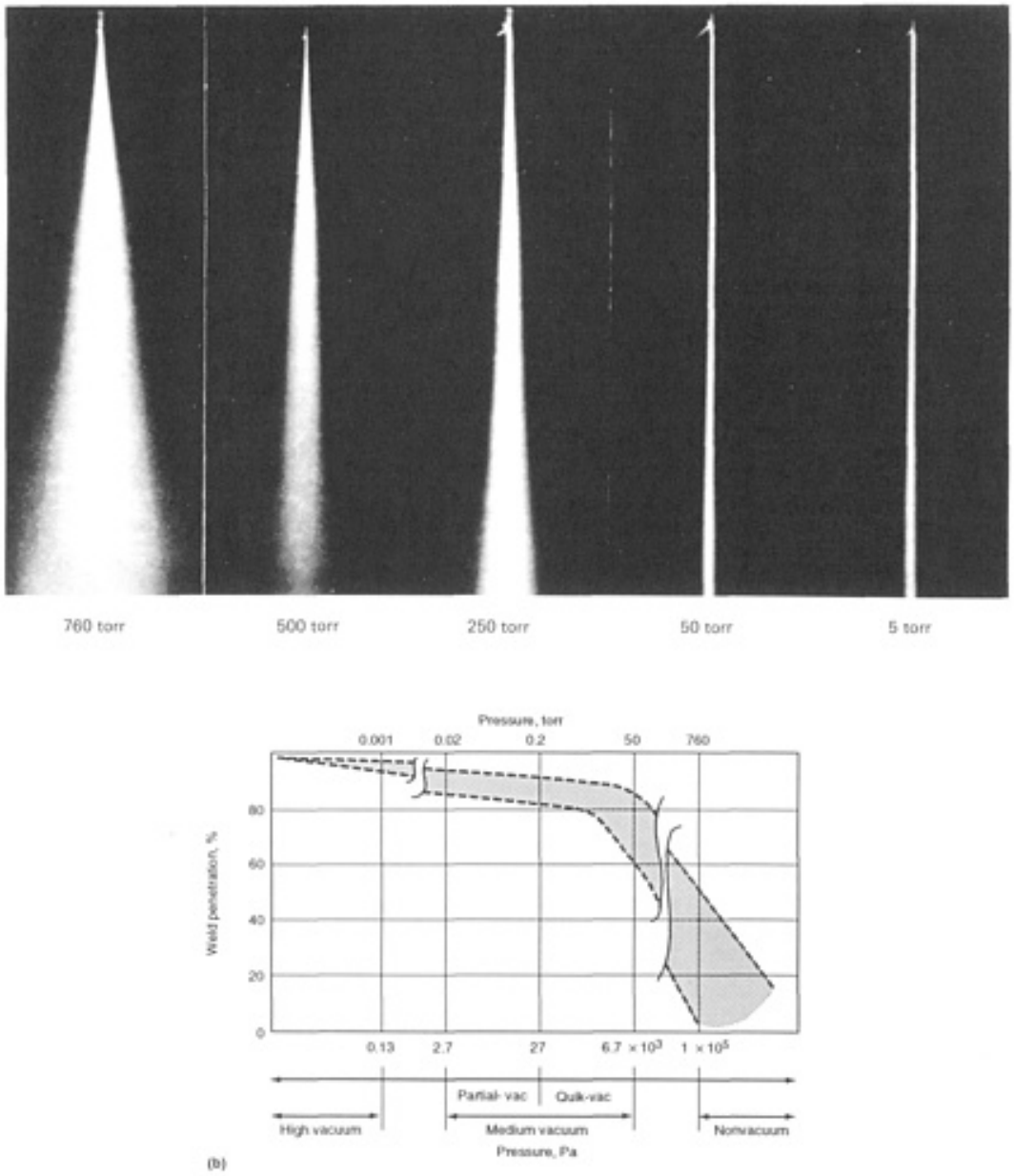

FIG. 15 EFFECT OF PRESSURE ON BEAM INTENSITY AND RESULTING WELD QUALITY. (A) DISPERSION PATTERNS OF ELECTRON BEAM AT SELECTED PRESSURES. (B) WELD PENETRATION AS A FUNCTION OF AMBIENT PRESSURE LEVEL. ADDITIONAL PARAMETERS SUCH AS BEAM VOLTAGE, BEAM TRAVEL DISTANCE, AND TYPE OF AMBIENT GAS USED CAN PRODUCE A WIDE RANGE OF VALUES, THUS ACCOUNTING FOR THE SPREAD IN THE PENETRATION DATA.

Effect of Pressure on Weld and Heat-Affected Zone. The maintenance of a high vacuum in the work chamber protects the weld metal and the HAZ from oxidation and contamination by harmful gases, serving the same function as inert shielding gases do in arc welding, while also degassing the weld. The contamination level as a function of pressure is discussed in the section EBW in Medium Vacuum in this article.

The nearly complete absence of gaseous impurities eliminates the serious contamination difficulties that usually are encountered when attempting to arc weld relative metals such as titanium and zirconium.

Width of Weld and Heat-Affected Zone. Electron-beam welds made in a high vacuum are narrower and have a narrower HAZ than comparable welds made in medium vacuum or at atmospheric pressure, and they are much narrower than the narrowest welds made in production welding by GTAW. The narrow width of the heat-affected zone in

hardenable steels and other hardenable alloys permits welding of these metals after heat treatment, in many instances without loss of strength.

Limitations. A major limitation in the use of high vacuum in the work chamber is the effect on unit production time, because of the need to pump the chamber down before each load is welded. Pumpdown time is typically about 3 min for a 0.85 m^3 (30 ft^3) chamber and 10 min for an 8.5 m^3 (300 ft^3) chamber. The above pumpdown times are realistic only for a very clean and well-maintained system. In production, pumpdown may be nearly double the above times.

The effect of this limitation on unit production time is reduced by welding a number of assemblies in each load and by keeping chamber size as small as possible. Small chambers specially designed for use with small workpieces have typical pumpdown times of I min (3.69×10^6 mm^3, or 225 $in.^3$, chamber) and 15 s or less (1.0×10^6 mm^3, or 60 $in.^3$, chamber).

A second major limitation in the use of high vacuum is that work size is limited by chamber dimensions. This limitation is sometimes circumvented by the use of a chamber having special openings and seals that permit oversize work to extend outside the chamber, or by the use of a portable clamp-on chamber.

Welding Conditions. Welding in high vacuum is done with low-voltage, as well as high-voltage, equipment. Beam voltage ranges from 15 to 185 kV; beam current, 2 to 1000 mA; and welding speed, 100 to 5000 mm/min (4 to 200 in./min) for most applications. However, higher welding speeds are used for special thin section applications. The energy input to the work needed to produce a weld of the required depth of penetration and width is the basis for selecting the welding conditions.

Depth of penetration is increased by increasing the voltage or current for greater beam power, or by decreasing the welding speed. Table 1 lists approximate energy inputs per inch of weld length for making narrow single-pass electron-beam welds 6.4 to 75 mm (0.25 to 3 in.) deep in the weldable alloys of copper, iron, nickel, aluminum, and magnesium. These values are intended to serve as guidelines for establishing conditions for welding work for which no previous experience is available. Energy-input requirements for specific applications depend on the alloy composition and special operating conditions such as the use of beam oscillation or a defocused beam.

TABLE 1 ENERGY INPUT AT THE WELD FOR SINGLE-PASS EBW IN HIGH VACUUM FOR VARIOUS DEPTHS OF PENETRATION

DEPTH OF PENETRATION		ENERGY INPUT PER WELD LENGTH FOR INDICATED METAL[(A)]									
		Cu		**Fe**		**Ni**		**Al**		Mg	
mm	**in.**	**kj/mm**	**kj/in.**	**kj/mm**	**kj/in.**	**kj/mm**	**kj/in.**	**kj/m**	**kj/in.**	**kj/mm**	kj/in.
6.35	0.25	0.3	0.7	0.2	5	0.2	4	0.1	2	0.04	**1**
12.7	0.50	0.6	0.15	0.4	10	0.3	8	0.2	5	0.1	**3**
19.1	0.75	1.0	0.25	0.7	18	0.6	15	0.3	8	0.2	**5**
25.4	1.00	1.5	0.37	1.1	27	0.9	22	0.5	13	0.3	**8**
38.1	1.50	2.4	0.62	1.8	46	1.5	39	0.9	23	0.6	**15**
50.8	2.00	3.4	0.87	2.7	68	2.4	60	1.4	35	0.9	**22**
63.5	2.50	4.4	112	3.5	90	3.1	80	1.9	47	1.1	**29**
76.2	**3.00**	**5.4**	**137**	**4.4**	**112**	**3.9**	**100**	**2.3**	**59**	**1.4**	**36**

(A) VALUES ARE APPROXIMATE AND APPLY TO THE COMMONLY WELDED ALLOYS OF THE METALS. THEY ARE INTENDED TO SERVE AS STARTING POINTS FOR ESTABLISHING CONDITIONS FOR MAKING NARROW WELDS. ENERGY INPUT MAY VARY SUBSTANTIALLY FROM THESE VALUES IN SPECIFIC APPLICATIONS, DEPENDING ON THE COMPOSITION OF THE ALLOY AND SPECIAL OPERATING CONDITIONS. ENERGY INPUT AT WELD = [(BEAM VOLTAGE) (BEAM CURRENT) 0.6]/WELDING SPEED, WHERE ENERGY INPUT IS IN KJ/IN.; BEAM VOLTAGE IS IN KV; BEAM CURRENT IS IN MA; AND WELDING SPEED IS IN IN./MIN.

EBW in Medium Vacuum

Electron-beam welding in a medium vacuum (EBW-MV) usually is performed at a welding (work) chamber pressure of about 10 Pa (7.5×10^{-2} torr), or at a work chamber pressure ranging from 0.4 to 40 Pa (3×10^{-3} to 3×10^{-1} torr)--the total partial-vacuum region. The gun chamber, where the beam is generated, is held at 1.3 to 13 mPa (10^{-5} to 10^{-4} torr), as in high-vacuum welding. A diffusion pump is required to provide this gun chamber vacuum, but only a mechanical-type pump is required to evacuate the work chamber to the final partial vacuum welding pressure desired.

Comparison with High-Vacuum EBW. The chief advantage of welding in medium vacuum, compared with welding in high vacuum, is the short pumpdown time for the welding chamber, which ordinarily does not exceed 40 s for a general-purpose chamber (of about 0.11 m^3, or 4 ft^3) and which is less than 5 s for the specially designed chambers used in welding small parts. Accordingly, EBW-MV permits mass production of parts, using a chamber of minimum volume.

Production rates for welding in medium vacuum depend on part design and other factors; maximum production rate is typically about 60 pieces per hour for general-purpose, manually operated equipment; upwards of 600 pieces per hour for specially tooled semiautomatic machines; and 1500 pieces per hour for fully automatic single-purpose machines. General-purpose chambers and tooling are used for short runs.

Welds on reactive metals and other welds for which the effects of contamination by gases are especially critical are preferably made in high vacuum. The contamination level of air (total concentration of gases present) is proportional to pressure, as follows:

PRESSURE		GASES, PPM
PA	**TORR**	
0.0013	10^{-5}	**0.01**
0.13	10^{-3}	**1.3**
13	10^{-1}	**132**
50	**4×10^{-1}**	**500**

Lower contamination levels are obtainable than those actually observed for arc welding with inert-gas shielding.

Penetration and Weld Shape. Penetration at a given power level is ordinarily 5 to 10% less than for EBW-HV, and welds are wider and slightly more tapered. These changes are caused by the scattering of the electrons in the beam by collision with gas molecules, which makes the beam broader.

The effect of welding chamber pressure on penetration and weld shape is shown in Fig. 16 for welds made on type 304 stainless steel, using a beam length of 405 mm (16 in.) without changing focus. Maximum penetration shown in Fig. 16 is approximately 13 mm ($\frac{1}{2}$ in.). Welding conditions were 150 kV, 30 mA, and 1525 mm/min (60 in./min). Penetration drops off rapidly at pressures of 13 Pa (10^{-1} torr) or more at this beam length and at somewhat lower pressures when the beam path is longer.

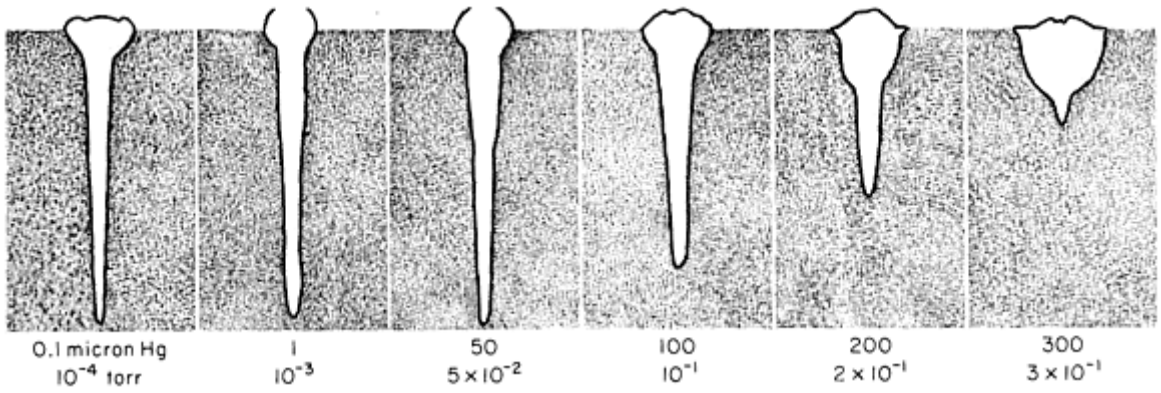

FIG. 16 EFFECT OF WELDING-CHAMBER PRESSURE ON PENETRATION AND WELD SHAPE FOR TYPE 304 AUSTENITIC STAINLESS STEEL

Comparison With Nonvacuum EBW Welding. Disadvantages of medium-vacuum welding, compared with welding at atmospheric pressure, include limitations on work size imposed by the need to enclose the work in a vacuum chamber and the time needed for chamber pumpdown.

Beam deflection and oscillation, which cannot be used in welding at atmospheric pressure, can be used in EBW-MV.

Applications. Most parts that can be welded in high vacuum can also be welded in medium vacuum. Depth of penetration is less than in high-vacuum welding, and depth-to-width ratio is less than about 10 to 1. Reactive metals are less readily welded in medium vacuum than in high vacuum. Medium-vacuum welding can be acceptable, however, for refractory metal welding when absorption of small amounts of oxygen can be tolerated. Medium-vacuum welding has been used for welding mass-produced automobile parts, such as gears and shafts, that are welded to close tolerances and that are not subsequently finished.

Procedure Development and Practice Considerations for Electron-Beam Welding

Nonvacuum (Workpiece Out-of-Vacuum) Welding

In EBW-NV (workpiece out-of-vacuum), which is also referred to as atmospheric EBW, the work to be welded is not enclosed in a vacuum chamber. Instead, it is welded at atmospheric pressure. A radiation-tight enclosure or chamber, similar to that used in high- or medium-vacuum EBW, surrounds the weld area. A vacuum, however, is not provided in this welding enclosure.

A nonvacuum electron beam is generated at high vacuum in the same manner as in high- and medium-vacuum welding. It is focused down through a series of individually pumped stages, each connected to the other by concentrically aligned orifices, decreasing in diameter in the direction of increasing pressure; this differential pumping scheme provides the high vacuum (gun region) to atmospheric (workpiece region) pressure gradient necessary to allow the beam to pass down through the column and exit out into the ambient atmosphere.

Figure 17 depicts a typical EBW-NV gun/column assembly. This unit can be mounted in either a vertical or a horizontal position and is capable of motion during welding. The gun/column assembly depicted in Fig. 17 is capable of beam power levels greater than 35 kW and beam transmission efficiencies in excess of 90%.

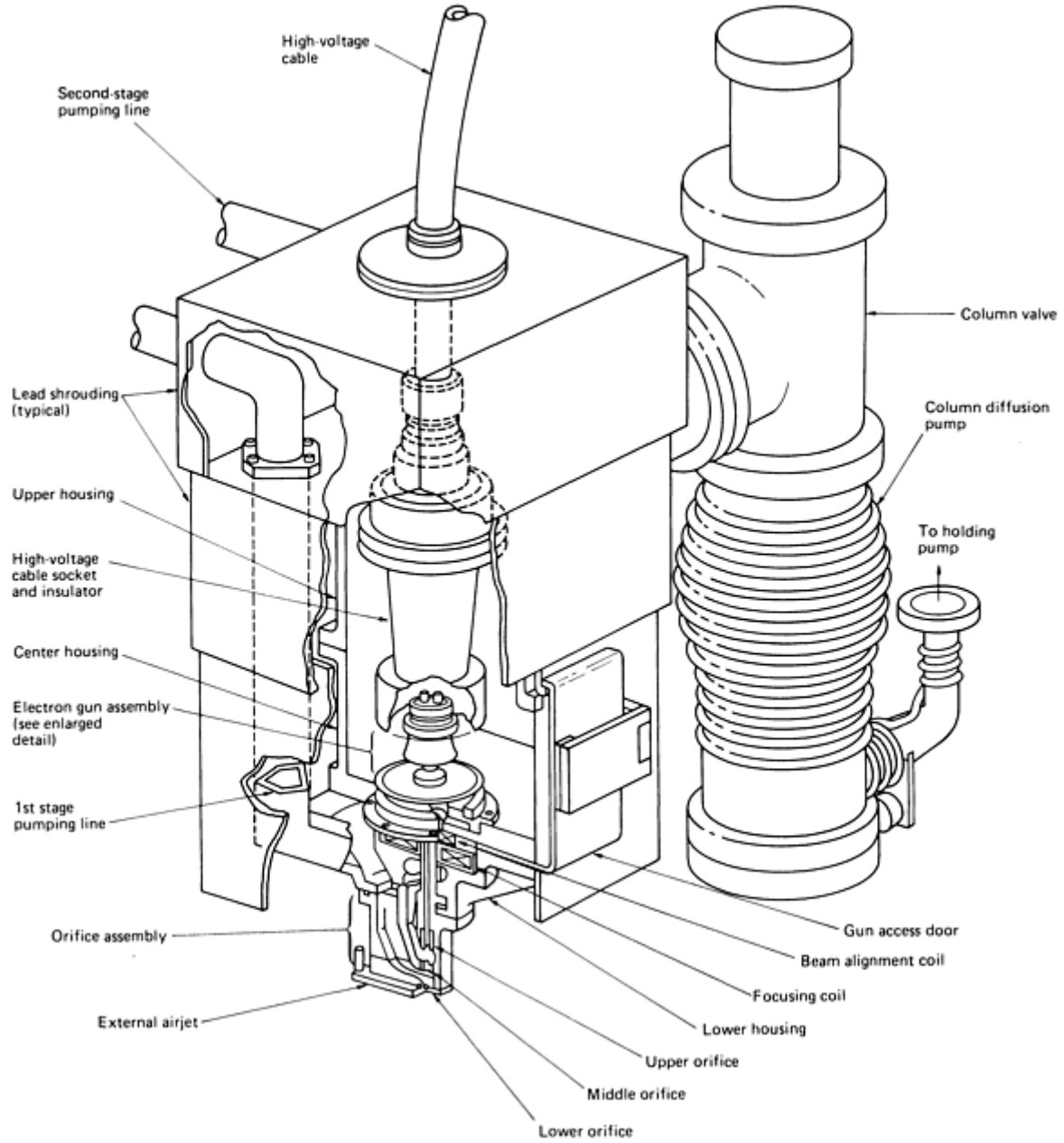

FIG. 17 SCHEMATIC WITH CUTAWAY VIEW SHOWING PRIMARY COMPONENTS OF A TYPICAL EBW-NV GUN/COLUMN APPARATUS. COURTESY OF LEYBOLD-HERAEUS VACUUM SYSTEMS INC.

Production rates are generally much higher for EBW-NV than for EBW-HV and EBW-MV, because no work chamber vacuum pumpdown time is required for each chamber load. This results in a lower per part production cost. Because pumpdown time for high- and medium-vacuum welding varies with chamber cleanliness and ambient humidity, elimination of work chamber pumpdown time in EBW-NV produces appreciable time savings. This saving, however, is gained at the expense of a reduction in penetration and working distance capability, thus imposing limits on the thickness and shape of the workpiece. Additionally, most (but not all) out-of-vacuum welds cannot be made as narrow and parallel sided as welds made in a vacuum.

When welding in ambient atmospheric air alone, the practical working distance of the nonvacuum process is normally limited to the range of from 9.5 to 22 mm ($\frac{3}{8}$ to $\frac{7}{8}$ in.); however, when welding in the presence of a lighter ambient gas, such as helium, this practical working distance range is extended to 25 to 50 mm (1 to 2 in.). For this reason, most commercial nonvacuum EBW units are equipped to provide a "helium blowdown," which is an effluent of helium that

extends out from the nonvacuum column and along the beam travel path. The effect of this helium effluent is that it reduces the degree of beam scattering incurred using only air, thus allowing the working distance capability of the nonvacuum unit to be approximately doubled.

Most metals that can be arc welded or electron-beam welded in a vacuum also can be welded in nonvacuum. As stated previously, inert-gas shielding of the weld zone can be provided when the molten weld metal (or HAZ) cannot be exposed to air. On readily welded metals, weld properties approach those of welds made in a vacuum; on difficult-to-weld metals, weld properties are usually lower than those of welds made in a vacuum.

Ordinarily, filler metal is not used in EBW-NV. The addition of a suitable filler metal may be helpful, however, in joining metallurgically incompatible metals or in avoiding weld cracking caused by hot shortness. Selection of the filler-metal composition in such applications is critical.

Operating conditions for nonvacuum welding differ substantially from those for welding in high or medium vacuum. Because beam dispersion increases in proportion to pressure and distance traveled, at pressures above the high-vacuum level, the nonvacuum beam becomes dispersed at travel distances greater than several inches in air at atmospheric pressure.

To provide an electron beam of sufficient energy to minimize the scattering effect of collisions with residual gas molecules within the electron-beam transfer column (i.e., the differentially pumped gun/column assembly), the applied gun voltage is held at a constant high value (from 150 to 200 kV). This also helps extend the work distance of the beam after it has exited the column and entered the ambient atmosphere. The practical working distance (standoff distance) for nonvacuum welding, as measured from the bottom of the final exit orifice to the top of the workpiece, ranges from 13 to 50 mm ($\frac{1}{2}$ to 2 in.), although some nonvacuum welding is performed at both shorter and longer standoff distances.

With voltage held constant, beam current, working distance, and welding speed are selected to provide the required penetration and weld shape for a sound weld. Because it is usually desirable to keep working distance as short as possible and welding speed high, beam current is the primary control variable in nonvacuum welding.

The small size of the exit orifice on the electron gun makes it necessary to focus the beam at or very close to the exit orifice. Accordingly, it is not possible to vary weld characteristics to a significant degree by changing focus. Similarly, beam deflection and oscillation are not possible. The absence of these adjustment capabilities in nonvacuum welding is not a handicap, because beam width is ordinarily great enough so that it does not promote undercutting or porosity at the root of the electron-beam weld.

A cosmetic pass is seldom needed on electron-beam welds made at atmospheric pressure, because a smooth surface is produced on welds in most metals. The smoothness of the crown also improves the ease of nondestructive inspection of the as-welded surface; wire brushing is often adequate preparation for radiographic or liquid-penetrant inspection.

The limitation on workpiece shape imposed by the need for a short working distance can be overcome to some degree by the use of electron gun nozzles specially designed to extend into restricted spaces. Filler metal is not ordinarily used except where necessary for weld reinforcement to produce the desired weld properties or to avoid cracking.

A stream of dry filtered air, or an inert shielding gas such as argon or helium, is passed across the weld region in the space between the work and the electron gun, or may be supplied through a special insert nozzle assembly that is part of the exit orifice and is designed to minimize entrance of welding vapors and other contaminants into the gun. Auxiliary inert-gas shielding is supplied where needed for complete protection of the molten weld metal and the HAZ from gaseous contaminants. Welds are sometimes made on carbon and alloy steel and other readily weldable metals without using shielding gas. However, shielding gas is often used; helium is the preferred gas. Weld shape can be changed by varying the flow of helium.

Penetration. Nonvacuum electron-beam welds are seldom deeper than 9.5 mm ($\frac{3}{8}$ in.). Welds having penetration much greater than 25 mm (1 in.) are easily produced, but ordinarily this requires a reduction in welding speed, with a corresponding increase in production cost. Figure 18 provides a comparison of penetration, as a function of weld speed, in steel and aluminum, employing a fixed power level and work distance and using a helium shield to improve power density.

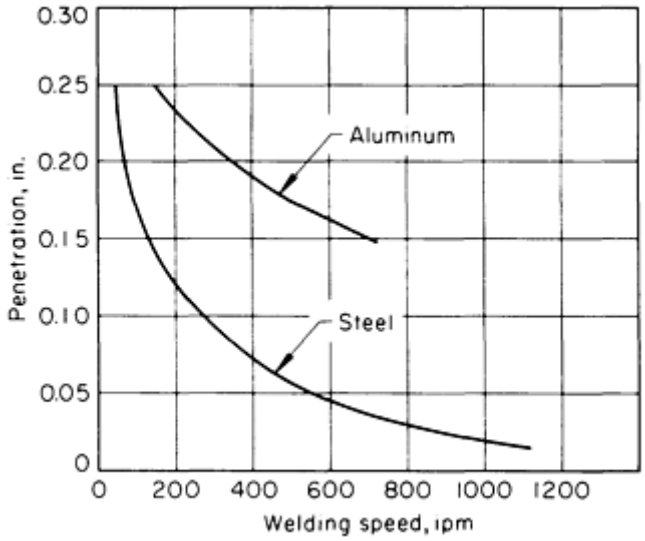

FIG. 18 PLOT OF PENETRATION VERSUS WELDING SPEED AS A FUNCTION OF MATERIAL AT A BEAM POWER OF 9 KW

Studies made of nonvacuum welding of steel pipe showed that, at speeds of 2.5 to 25 m/min (100 to 1000 in./min), full-penetration welds could be made in metal twice as thick if helium shielding gas was used instead of air. Table 2 gives the results of this comparison in terms of welding speed for joining steel pipe 1.3 to 3.8 mm (0.050 to 0.150 in.) thick in air or in helium. Welding speeds were 2.16 to 2.24 times greater in helium as in air. Beam power used was 12 kW.

TABLE 2 SPEEDS FOR NONVACUUM FULL-PENETRATION WELDING OF CARBON AND LOW-ALLOY STEEL PIPE AT A BEAM POWER OF 12 KW

WALL THICKNESS		WELDING SPEEDS				RELATIVE WELDING SPEED IN HELIUM(A)
		IN AIR		IN HELIUM		
mm	in.	m/min	in./min	m/min	in./min	
1.27	0.050	10.6	417	22.9	900	**2.16**
2.03	0.80	6.12	241	13.4	528	**2.20**
2.54	0.100	4.75	187	10.5	412	**2.21**
3.81	**0.150**	**3.00**	**118**	**6.68**	**264**	**2.24**

(A) BASED ON WELDING SPEED IN AIR BEING EQUIVALENT TO 1.00

Weld Shape and Heat Input. Nonvacuum electron-beam welds are generally wider and more tapered than high-vacuum welds (medium-vacuum welds differ only slightly in shape from high-vacuum welds).

Weld shrinkage across nonvacuum electron-beam welds is generally less than half that of gas-tungsten arc welds on the same work metal and thickness and is typically about twice that for high-vacuum electron-beam welds.

Tooling generally is designed specifically for welding a particular assembly in mass production. Providing fixtures and equipment that permit welding at high speeds and efficient work handling is the key to obtaining high production rates and low cost.

The work-handling equipment is at atmospheric pressure instead of in a vacuum; hence, general-purpose welding positioners and related fixtures usually are satisfactory. Hold-down clamping devices can be simpler than those often needed for arc welding similar parts, because angular distortion or dihedral warpage is generally low. Locating and alignment mechanisms are simpler than for welding in a vacuum, because of their accessibility and because beams are

wider and lower accuracy is required in tracking the joint. Maintenance of work-handling equipment is greatly simplified by its out-of-chamber location.

Applications. Nonvacuum electron-beam welding is used in the production of transmission-train components, steering column jackets, die-cast aluminum intake manifolds, and catalytic converters. In addition, several appliance (and other consumer-related) items also are produced using the EBW-NV process. Figure 19 shows a catalytic converter that was nonvacuum electron-beam welded with the beam in a horizontal position.

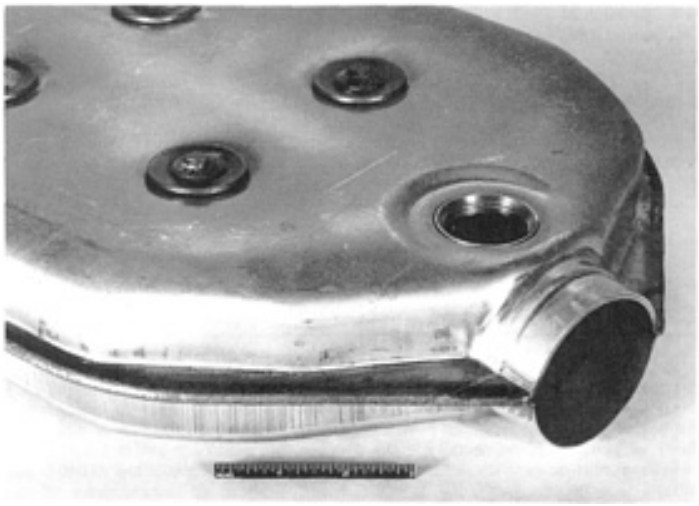

FIG. 19 CATALYTIC CONVERTER ASSEMBLY CONSISTING OF SEAMS JOINED BY EBW-NV PROCESS

Controlling Heat Effects

The extent of heat-affected base metal in EBW is controlled mainly by regulating the welding speed, width, and shape of the weld. In general, the width of the HAZ is proportional to the average width of the weld, which also strongly influences shrinkage and distortion.

Damage to heat-sensitive attachments, inserts, or encapsulated materials close to the weld joint is controlled mainly by regulating the width and shape of the weld bead. Damage to nearby finished functional surfaces on the workpieces or to nearby drilled or tapped holes or other crucial features of the workpieces can often be avoided in EBW because of the narrowness of the welds.

Joint designs that provide constricted sections near the weld to retard heat transfer from the weld, or that provide an integral heat sink, and the use of external heat sinks or chill bars are also helpful in controlling heat effects in EBW.

Narrow, closely controlled electron-beam welds, with low heat input, can be made in close proximity to heat-sensitive attachments, inserts, or encapsulated materials without damaging them, often when no other welding process can meet this requirement.

Procedure Development and Practice Considerations for Electron-Beam Welding

Welding of Thin Metal

Electron-beam welding can be advantageous for joints in which at least one member is made of thin metal (<2.4 mm, or $\frac{3}{32}$ in., and as thin as 0.025 mm, or 0.001 in.). Applications include instrument parts, instrument enclosures, pressure or hermetic seals, diaphragms, encapsulations, electrical connectors, and electronic devices, of various metals.

The joint area must be heated to melting temperatures in joining thin sections, just as in joining thick sections, but the rate of heat transfer away from the joint is much lower because of the reduced cross section. Hence, local heat buildup is greater, which increases weld width and decreases depth-to-width ratio. In addition, minimum beam spot size has a much greater effect on depth-to-width ratio in joining thin metal than in joining thick metal. The minimum usable beam spot size obtainable generally ranges from about 0.13 to 0.51 mm (0.005 to 0.020 in.) in diameter. Because of these conditions, depth-to-width ratio for full-penetration welds joining two sections thinner than about 2.4 mm ($\frac{3}{32}$ in.) usually does not exceed about 5 to 1 and may be less than 1 to 1.

When voltage, current, welding speed, and other variables have been optimized for a specific joint, use of a heat sink may still be necessary to avoid overheating thin material, depending on the base-metal properties (melting point, specific heat, and thermal conductivity) and metal thickness. Best results usually are obtained by the use of copper chill blocks machined to fit the workpiece closely at the joint area. Fixtures made of other metals may be effective as chill blocks if the contact area is sufficiently large and close to the heat source.

Joining Thin Sections to Thick Sections. In joining thin sections to thick sections by EBW, the joint is usually designed so that the thick member serves as a heat sink for the thin member, and the point of beam impingement is slightly removed from the thin metal. When these precautions are taken, welding behavior and heat dissipation are generally the same as in welding thick sections under similar conditions. Depth of penetration in the thicker section is usually made only slightly greater than the thickness of the thin section.

Even with the aid of the heat-sink capacity of a thicker member, heat input by arc welding often cannot be localized sufficiently and controlled closely enough to avoid damage to metal foil thickness. In some applications, using EBW instead of gas-metal arc welding can eliminate excessive foil melting.

Partial-Penetration Welds. The precise control of heat input obtainable in EBW permits partial-penetration welds having uniform depth to be made in metals as thin or thinner than 0.25 mm (0.010 in.).

Work-metal thickness must be uniform, and workpiece fixture arrangement and dimensions must be selected to provide a constant rate of heat loss adjacent to the path of the weld along its entire length, with special provisions made for weld starting and stopping. Beam power, focus, and workpiece travel speed must be closely regulated to minimize variation in penetration.

For the closest control of penetration, both beam power and focus can be regulated by sensitive, fast-response closed-loop servomechanisms or feedback controllers, and workpiece travel speed can be held within extremely narrow limits by precision, mechanical worktable traverse, or rotary-motion systems. To compensate automatically for the effect of any variation in voltage on focus, the servomechanism regulating the beam focus can be coupled to the voltage supply by solid-state devices that have a response time of less than 17 μs.

Partial-penetration welds in thin metal are not subject to root voids, root porosity, or cold shuts, which are flaws frequently encountered in partial-penetration welds in thick metal, because such welds in thin metal have relatively low depth-to-width ratios and a wide-angle V-shape with a gently radiused bottom.

Data on the relation of depth to width for high-vacuum partial-penetration welds in thin sections are given in Table 3. The ratio of depth to width is lower for the welds in the thinner sections. Penetration was from 50 to 85% of the work-metal thickness, and all welds were made with chill bars in intimate contact with the underside of the work at the weld location.

TABLE 3 RELATION OF DEPTH TO WIDTH (*D*/*W*) FOR PARTIAL-PENETRATION ELECTRON-BEAM WELDS OF THIN SECTIONS IN A HIGH VACUUM

WORK METAL[A]	THICKNESS,		WELD DIMENSIONS[A]				*D*/*W* FOR WELD
			DEPTH, *D*		WIDTH, *W*[B]		
	mm	in.	mm	in.	mm	in.	
ALUMINUM ALLOYS							
6061-T6	0.13	0.005	0.008	0.003	0.38	0.015	**0.2**
5052	0.25	0.010	0.013	0.005	0.30	0.012	**0.4**

	0.51	0.020	0.43	0.017	0.38	0.015	**1.1**
STAINLESS STEELS							
17-4 PH	0.13	0.005	0.10	0.004	0.36	0.014	**0.3**
TYPE 301	**0.25**	**0.010**	**0.15**	**0.006**	**0.28**	**0.011**	**0.5**

(A) CHILL TOOLING WAS IN INTIMATE CONTACT WITH THE UNDERSIDE OF THE WORK AT THE WELD LOCATION.

(B) WIDTH OF THE WELD AT THE CROWN, WHICH WAS THE GREATEST WIDTH FOR THE GENTLY RADIUSED WIDE-ANGLE V-SHAPED WELDS

Depth of penetration generally varies 10 to 15% from a mean value for a work thickness of about 0.51 mm (0.020 in.), and the percentage variation is greater for welds in thinner metal. Accordingly, partial-penetration welds are not ordinarily made in metal about 0.25 mm (0.010 in.). Beam oscillation is sometimes used to smooth out variations in penetration, but such oscillation must be controlled closely in order to be effective.

Procedure Development and Practice Considerations for Electron-Beam Welding

EBW of Thick Metal

For joining thick sections, electron-beam welding in a vacuum has three principal advantages over other welding processes:

- MUCH DEEPER PENETRATION CAN BE OBTAINED IN A SINGLE PASS. EXTREMELY NARROW, ONLY SLIGHTLY TAPERED WELDS AND A SMALL HAZ CAN BE PRODUCED.
- FOR JOINTS ON MOST WELDABLE METALS, NO FILLER METAL IS NEEDED. WHERE A FILLER METAL IS REQUIRED, THE QUANTITY IS USUALLY VERY SMALL.
- JOINTS HAVE CLOSELY FITTED PARALLEL GROOVE FACES REQUIRING NO EDGE PREPARATION, INSTEAD OF V-GROOVES OR U-GROOVES.

The disadvantages of EBW for joining thick metal include: high equipment cost, size limitations imposed by the dimensions of the vacuum chamber in which the work must be placed, and the time needed for evacuating the chamber.

Deep welds made in a vacuum are usually narrow; weld width for penetration deeper than 6.4 mm ($\frac{1}{4}$ in.) is typically about $\frac{1}{5}$ to $\frac{1}{20}$ of the section thickness, except for a somewhat greater width at the crown of the weld. Welds may be either full or partial penetration.

Effects of Pressure. Penetration capability is greatest for EBW in high vacuum. The effect that welding pressure has on penetration of steel is shown in Table 4. A constant weld speed of 890 mm/min (35 in./min) and beam power of 7.5 kW from 150 kV/50 mA for high and medium vacuum, and 175 kV/43 mA for nonvacuum were used to obtain the data in Table 4.

TABLE 4 TYPICAL PRESSURE AND BEAM TRAVEL DISTANCE SPECIFICATIONS REQUIRED TO OBTAIN MAXIMUM WELD PENETRATION OF STEEL

TYPE OF SYSTEM	**AMBIENT WORKPIECE PRESSURE**		**BEAM TRAVEL DISTANCE**		MAXIMUM PENETRATION	
	pa	**torr**	**mm**	**in.**	**mm**	in.
HIGH VACUUM	0.013	1×10^{-4}	455	18	25	**1**
MEDIUM VACUUM	130	1	205	8	16	$\frac{5}{8}$

NONVACUUM	**1.0×10^5**	**760**	**13**	$\frac{1}{2}$	**4.0**	$\frac{5}{32}$

Full-Penetration Welds. In welding carbon steel, single-pass, full-penetration, vacuum (high/medium) electron-beam welds are made commercially in thicknesses up to approximately 100 mm (4 in.); production EBW-HV has been done on aluminum alloy plates 150 mm (6 in.) thick, and 230 mm (9 in.) thick aluminum alloy sections have been welded experimentally under near-optimum conditions.

Two-Pass Full-Penetration Welding. Penetration can be nearly doubled by making two passes, one on each side of the work, but cold shuts, voids, and porosity are encountered at the root of the second weld unless conditions are adjusted for the pass made on the second, or back, side. A broader second-side weld with a larger radius at the root helps to reduce the incidence and severity of these flaws, but they often remain a problem.

Partial-Penetration Welding. Welds that do not penetrate completely through the work metal are satisfactory in many applications in welding thick metal; joint design and product requirements often rule out full penetration.

Problems and Flaws. In making vacuum electron-beam welds 3.2 to 13 mm ($\frac{1}{8}$ to $\frac{1}{2}$ in.) deep in weldable metals, weld quality is ordinarily equal to or better than that of arc welds in the same metal. Special precautions are needed to avoid certain types of discontinuities in welds about 13 mm ($\frac{1}{2}$ in.) deep or deeper. Fusion-zone porosity, gas pockets, and cold shuts are more serious problems than in arc welding, particularly in deep welds.

Reducing the welding speed usually helps to reduce porosity and gas entrapment. Extreme care in cleaning the work metal may be necessary where the problem is severe. When flaws are found near the root of the weld, they can be avoided or minimized by any adjustment of welding conditions that broadens the weld and increases the radius of the weld at the root. Sometimes the joint can be designed so that any root flaws are in a noncritical region, or in integral or separate backup metal that will be machined away after welding.

As in arc welding, cold shuts (incomplete fusion) are sometimes encountered at the root of a deep partial-penetration weld or of a full-penetration weld that has a poorly fitted backing strip. These discontinuities are troublesome because they are difficult to detect. Normally they cannot be detected by radiographic methods. Ultrasonic testing can detect the larger cold shuts. Many cannot be observed on roughly polished macrosections of electron-beams welds, but require a metallographic polish and examination at a magnification of at least 100 diameters for detection. Cold shuts can usually be avoided or minimized by reducing the welding speed or by otherwise changing conditions so as to broaden the weld and increase the radius of the weld at the root.

Poor fit-up or excessive joint gap can cause excessive shrinkage, underfill, undercut, voids, and cold shuts. Joint gap should not exceed 0.25 mm (0.010 in.) for narrow welds deeper than about 13 mm ($\frac{1}{2}$ in.) in most metals, although sound welds have been obtained using joint gaps of 0.76 mm (0.030 in.), by use of a procedure that increased weld width.

Welding with the beam at a slight angle to the joint is helpful in avoiding flaws related to poor fit-up, but may increase weld width excessively and require an unduly low welding speed for deep welds.

Excessive mismatch can cause discontinuities of the same general types as poor fit-up; mismatch limits depend on joint design and dimensions, and on operating conditions. Weld quality in joining thick sections is ordinarily unaffected by changes in surface roughness of the joint faces between about 1.60 to 2.50 μm (63 and 1000 μin.).

A problem that is unpredictable and inconsistent in making electron-beam welds deeper than about 13 mm ($\frac{1}{2}$ in.) is arc-outs, or sudden failures of electron emission during welding. However, problems of arc-out have decreased with the newer machines and experience accumulated in operation.

Work-metal composition and quality also influence arc-outs, which are more frequent when welding materials with low vaporization points, or when welding materials susceptible to outgassing in a vacuum or those that contain nonmetallic inclusions.

Use of Filler Metal

Fusion of closely fitted groove faces generally provides sufficient weld metal, or extra metal is provided where necessary by including extra stock thickness or integral shoulders or lips in the joint preparation. Where product requirements or other circumstances prevent the use of a joint preparation and welding conditions that will provide sufficient weld metal, filler metal is added.

Prevention of Cracking. Filler-metal (shim stock) additions can prevent cracking in electron-beam welds in a crack-susceptible metal or combination of dissimilar metals. It may be needed even when joint design, fit-up, and operating conditions are selected to achieve minimum joint restraint and residual stress. In other applications, the use of preplaced filler metal can provide weld metal that is less brittle than would be obtained by welding a base metal (or metals) alone.

Among the base metals for which added filler metal is often required are heat-treatable aluminum alloys 6061, 6063, and 6066, free-machining steels, and other free-machining alloys.

Many combinations of dissimilar metals that are susceptible to cracking when welded directly, usually because of the formation of brittle intermetallic phases, can be electron-beam welded with the aid of filler metal that has a composition compatible with both metals of the combination.

Preventing Porosity. The EBW of rimmed steel without filler metal ordinarily results in severe porosity in the weld, even when welding speed is slow and other conditions are selected to increase the time during which gas can escape from the molten weld metal. Inserting a filler metal that contains a deoxidizer such as aluminum, manganese, or silicon helps to minimize porosity.

Copper alloys C11000 (tough pitch copper) and other types of copper that do not contain residual deoxidizers also produce porous welds when joined without filler metal, but sound welds can be made with the aid of nickel filler metal or a deoxidizing filler metal.

Preplacement of Filler Metal. The technique most frequently used for the addition of filler metal in EBW, especially for deep welds, is preplacement. A shim of filler metal, usually of foil thickness, can be inserted between the groove faces when the joint is assembled for welding, or a wire or other suitable shape can be preplaced over the joint, being held in position by tack welding, if necessary.

Filler-Wire Feeding. Electrically operated filler-wire feeding systems that are modifications of wire-feed equipment used in GTAW, or specially designed electron-beam wire feeders, are sometimes used in the vacuum chamber. Usually, filler-wire feeding does not help in joining incompatible metals unless they are very thin.

The design of the wire-feeding nozzle and the technique with which it is used are important in guiding the wire so that it intercepts the weld pool. Any filler metal inserted into the beam path absorbs energy and affects penetration.

The wire-feeding nozzle is normally held as close to the weld pool as is possible without damage to the nozzle, and the wire is directed into the forward edge of the pool. The tip of the nozzle should be made of a heat-resistant material and should be coated so as to prevent molten weld metal from adhering to it if inadvertent contact is made. The nozzle is usually pointed in the direction of workpiece travel.

Wire-Feeding Equipment. Several design features are desirable in a wire feeder for EBW. These include means of making positioning adjustments from outside the vacuum chamber during welding, such as changing the proximity of the nozzle to the weld pool, changing the angle of incidence between the workpiece and nozzle, and controlling the movement of the wire relative to the beam to ensure accurate interception.

A simple, variable-resistance, controlled motor drive is ordinarily satisfactory, as a 10% variation in wire speed causes no adverse effect other than a slight variation in weld width. It is desirable to be able to control the timing so that wire feed can be started and stopped independently of the beam and table. Being able to adjust the timing of the wire feeder eliminates sticking of the wire to the workpiece at the end of the weld. Vibrating the nozzle at subsonic rates promotes flow of molten metal into the weld joint and results in less wire sticking at the end of the weld.

Welding Technique When Feeding Filler Wire. The wire-feed rate is usually set at approximately the same rate as the welding speed. Beam power must be sufficient to melt the wire as fast as it is fed. The wire diameter is selected so as to provide 1.25 times the volume of filler metal needed to fill the joint cavity. Where needed, backing strips or rings are used to prevent loss of molten weld metal.

The filler metal can be deposited during the weld pass, using a low welding speed to allow time for the molten metal to fill the joint gap, but for deep welds it is preferably deposited in a separate pass. If cracking is a problem, another method used on thin metal is to deposit filler metal on the joint, and then make the welding pass to distribute the filler metal more effectively. Additional information on the wire-feed process and related equipment can be found in the section Electron Beam Welding as a Repair Method of this article.

Tack Welding

In fixturing work for EBW, clamping often is supplemented or replaced by tack welding, which is usually done with the electron beam. Fixturing time and cost are often substantially reduced by the effective use of tack welds.

In some applications, selection of the tack welding procedure is critical to avoid unacceptable variation in the shape and dimensions of the final weld bead and to avoid root porosity or cold shuts. Reduced power and other special operating conditions are often used.

Techniques. Perhaps the most common technique is to make one or more suitably spaced tack welds at full or reduced beam power before making the welding pass. For circular or circumferential welds, one or more tack welds are usually made. Melt-through (spike) tack welds can be used on straight-line lap joints.

A shallow seal pass at reduced beam power can also be made along the full length of the joint to keep the workpieces aligned, to be followed by the full-power penetration pass. For some applications, it is convenient to leave occasional unwelded gaps as an aid for tracking the joint during the penetration pass.

EBW of Poorly Accessible Joints

One of the advantages of EBW is the capability of reaching into areas lying deep within narrow openings. This is accomplished by virtue of the electron beam having a small diameter, long working distance, and frequently, the capability of being projected at an angle. Many joints that are inaccessible for welding by other processes can be electron-beam welded. This capability is used both in fabrication and in repair work. It is especially useful in salvaging intricate castings.

Workpiece Requirements. For limited-access welding, the workpiece must satisfy three general requirements: (1) the weld area must be on a line-of-sight path from the beam source; (2) there must be sufficient sidewall clearance to avoid beam-fringe interference; and (3) the beam path must be free of magnetic fields.

Beam characteristics that determine applicability of EBW to poorly accessible joints are beam diameter and the working distance or effective beam length available between the exit end of the beam transfer column and the work. These characteristics in turn depend on the beam power used, which is selected to produce the desired penetration, and on beam focal length, which is influenced by the design of the gun, the chamber, and the focusing coil.

Sidewall Clearance. Parts intended for fabrication by EBW can often be designed with sufficient sidewall clearance for the beam power required. Where insufficient sidewall clearance exists in repair welding, lowering the beam power or slightly changing the angle of incidence of the beam often avoids interference. In repair welding, tests should be made on simulated joints, using the same type of work metal and the required beam power, rather than risking damage to difficult-to-replace parts.

Where close sidewall clearances are involved, it is especially important to avoid magnetic fields, which can cause damage to the part by deflecting the beam. A test run on low power is commonly used to detect beam deflection; however,

allowance must be made for the increase in deflection at full welding power. Magnetically soft materials with induced magnetism can usually be demagnetized with magnetic-particle inspection equipment or with coils.

Minimum beam clearance for making welds close to magnetic metal that projects above the work surface at the joint is given in Fig. 14.

Multiple-Tier Welding

The deep-penetration properties of the electron beam make it possible to weld two or more tiers of joints simultaneously. The joints can be separated by an air space as great as several inches, provided that the space can be evacuated and the joints aligned in the path of the beam. This type of weld cannot be made by any other welding process.

In multiple-tier welding, the electron beam must pierce at least the upper tiers in such a way that the molten metal flows in behind the advancing beam, as in keyholing. The molten weld metal is held in place by the combined forces of capillarity, surface tension, and viscosity. Welding conditions must be carefully selected and controlled.

Difficulties. ln-line welds are progressively different in shape and size, because of the scattering and reduction in beam density and other effects on the beam that take place when it penetrates each layer of metal in turn.

Internal weld spatter may cause difficulty if it interferes with service performance and there is no access for cleaning. Other difficulties such as undercut, underfill, and excessive root bead may be correctable. Hidden welds, which are difficult or impossible to inspect, require some acceptable indirect method of controlling joint reliability.

Applications. Multiple-tier welding has been applied to a variety of joints. Two-tier joints separated by as much as 75 mm (3 in.) have been welded in a single pass in joining honeycomb panels to end frames or structural shapes where only one side was accessible.

Welding With Extreme Accuracy

The development of feedback servomechanisms for controlling variations in beam power and beam spot size, as well as in work travel and speed, permits EBW within tolerances of a few thousandths of an inch in high-vacuum machines.

With the use of closed-loop feedback control systems, variations in beam voltage and current can be held to approximately 1% for a 10% variation in the supply line, which is well within the tolerances that can be maintained by the remainder of the system.

Although the diameter of the beam spot cannot be measured directly with special techniques, it can be estimated by measuring the width of the weld or by calibrating the controls for the focusing and beam-power settings. Depending on machine characteristics, beam spots effective for most welding purposes can be set up in the range of 0.25 to 0.76 mm (0.010 to 0.030 in.) in diameter without difficulty. Assuming a very small beam variation, an application requiring a beam spot of only 0.25 mm (0.010 in.) diam would require a means of holding the joint-to-beam coincidence with a runout of less than ±0.13 mm (±0.005 in.).

For welding with a 0.25 mm (0.010 in.) diam beam, a pileup of manufacturing tolerances could easily cause the beam to miss the joint. Therefore, for most production purposes, small beam spots are not economically feasible.

Various types of travel mechanisms of rigid construction are available with runout tolerances of approximately 80 μm/m (0.001 in./ft) or with total deviations of 0.08 to 0.12 mm (0.003 to 0.005 in.) for a complex traverse pattern. However, joint runout depends also on the manufacturing tolerances of the part and on accuracy of fit-up and fixturing. In some applications, 20 to 25 possible sources of error, such as magnetic deflection of the beam, and human and systematic errors in beam alignment, can be found.

Use of Scanning

Scanning is a method of checking the runout between the beam spot and the joint to be welded. Its purpose is to indicate the final adjustments needed to align the beam with respect to the joint and to expose possible unsuspected discrepancies in beam behavior or workpiece travel that would interfere with welding. Details of the procedure vary with joint design and the type of equipment available; in one widely used method, a low-power beam is used for visual scanning of the joint during a simultaneous welding pass.

Accuracy of Beam Alignment. Beam alignment is generally a matter of workpiece alignment, as even guns of the adjustable type are usually fixed during welding. Where the gun does traverse the joint, the principles of alignment are the same. Most joints are designed for simple path shapes--straight lines and circles--that can be adequately traced with precision-made carriages, cross-feeds, turntables, eccentric tables, and spindles.

Scanning Procedure. The workpiece is fixtured, and the joint is aligned for travel direction and is moved to its approximate location under the gun. The chamber is closed and pumped down to a vacuum sufficient for safe operation of the gun. A low-power beam is turned on and focused sharply on the workpiece surface. The specific power settings will vary with the working distance selected and the power ratings of the machine; however, they should be sufficient only to create a detectable spot without overheating the workpiece.

The joint line is then adjusted to its precise location with respect to the beam spot, the workpiece is traversed through a complete cycle, and the runout is equalized. Maximum allowable tolerance on runout is determined from a consideration of joint design and weld width, which is mainly a function of the spot size and travel speed.

Considerable latitude in required accuracy of alignment can be gained where beam oscillation can be used. Usually, if the runout approaches one-half the effective welding beam spot width (spot size plus oscillation amplitude), the cause must be determined and corrected. If the runout is within tolerances, production parts ordinarily need only periodic scanning as a quality-control measure.

Problems in Scanning. Some of the causes of excessive runout and other difficulties encountered during scanning are as follows:

- POOR JOINT DESIGN, INACCURATE JOINT PREPARATION
- IMPROPER FIT-UP, INADEQUATE FIXTURING
- LACK OF PRECISION IN WORKPIECE TRAVERSING MECHANISM
- OBSTRUCTIONS IN THE BEAM PATH
- INDISTINCT OR UNDETECTABLE JOINT LINE
- BEAM DEFLECTION BY ELECTRIC OR MAGNETIC FIELDS

The corrections required for mechanical discrepancies are self-evident; the effects of electric and magnetic fields may be less obvious.

The negatively charged electrons that comprise the electron beam constitute a negative space charge. When the electrons strike an insulated metal part, negative charges are built up, causing mutual repulsion between the part and the beam. By grounding the part, excess electrons are conducted away. To avoid unintentional deflection of the beam by nearby magnetic fields, workpieces, fixtures, and tooling components made of magnetic materials should be demagnetized before welding.

Scanning techniques vary in detail, depending on the type of equipment used and also on joint design. It is not always necessary to position the beam spot precisely on the joint line. When welding dissimilar metals, dissimilar thicknesses of the same metal, or certain self-locating joints, it is often necessary to position the beam a short distance from the visible joint line. A corner edge or a scribed line can often serve as a reference, or measurement can be made with an optical grid.

Some special-purpose EBW machines are not intended for scanning. Nearly all general-purpose machines, however, make some provision for this operation. On machines with a fixed gun located in an upper section of the vacuum chamber, a built-in internal optical viewing system is generally provided for scanning. Machines having movable guns can be equipped with external telescopes and internal mirror systems.

Optical Scanning. Optical systems usually consist of horizontally mounted monocular or binocular telescopes with internal illumination and reflecting mirrors that provide a line of sight coaxial with the beam path. Magnifying power may be 10 to 40 times, depending partly on working distance. High-precision alignment can be obtained.

There are two common methods of using this equipment. One method makes use of a low-power beam that is sighted telescopically on the workpiece surface. Using a calibrated grid, measurements to 0.025 mm (0.001 in.) can be made. In the other method, the beam is centered on a crosshair reticle embodied in the optical system. The beam is then turned off and the workpiece joint is moved into coincidence with the crosshair, under internal illumination. The advantage of the latter method is that, after the beam is turned off, the chamber need no longer remain under vacuum, and further alignment work can be done in the open, if necessary.

Before scanning, the mirror surfaces of the internal optical system should be cleaned, because vapor deposition takes place during welding. The frequency of cleaning may vary from a few to many hours of operation, depending on the amount of vapor created and the proximity of the weld. Mirror surfaces are usually protected with glass shields that can be removed for cleaning or replacement.

Scanning Without Optics. Scanning can also be done without visual aids where great precision is not required. On machines that are not equipped with viewing optics, scanning is done by direct observation through sight-glass ports. From one to four such ports may be located in the chamber wall, usually spaced 90° apart, to permit checking beam alignment from several angles. The beam spot is generated the same as for optical scanning.

Electronic Scanning. Checking the location of an electron beam with respect to the joint can be done with an electronic device that displays the relationship on an oscilloscope. The equipment makes use of a low-power electron beam that is made to oscillate at 60 Hz transversely across the joint. The amplitude of the oscillation is sufficient to display the workpiece surface for a short distance on either side of the joint, as well as the joint line itself. In addition, each oscillation pulse is interrupted momentarily to permit the beam to assume its normal welding position, causing a relatively large spot to appear on the display. When the spot coincides with the joint line of the display, the beam is accurately aligned for welding.

Figure 20(a) shows the display condition for a beam centered exactly on the joint. The V represents the joint line, with the beam spot centered accurately; the two horizontal arms (of equal length with a centered beam) at the top of the V represent the adjacent workpiece surface. The broken lines above the work (at left in Fig. 20a) show the plane of oscillation; the wavy line along the joint in the same view shows the approximate amplitude of oscillation.

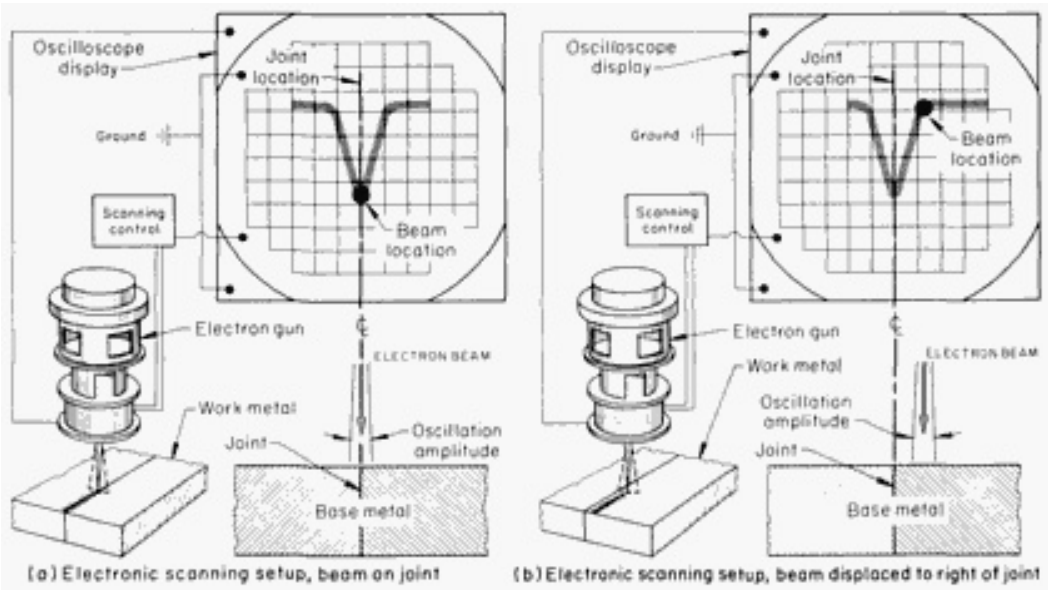

FIG. 20 ELECTRONIC SCANNING APPARATUS WITH CRT DISPLAY TO SHOW ALIGNMENT OF ELECTRON BEAM RELATIVE TO WELD BEFORE WELDING OPERATION IS CARRIED OUT. (A) ELECTRON BEAM CENTERED ALONG LENGTH OF JOINT. (B) ELECTRON BEAM DISPLACED FROM CENTERLINE OF JOINT

If the beam location were displaced to the right of the joint, the display would look like Fig. 20(b); an opposite-handed display would indicate displacement to the left. By the relative depth of the V, the display also indicates the amount of joint separation from apparent zero to approximately 0.15 mm (0.006 in.). A joint mismatch of a few thousandths of an inch is indicated by the relative height of the horizontal arms. In setting up for electronic scanning (under vacuum), the work is provisionally aligned as for optical scanning, making sure that the joint line is parallel to the direction of travel.

Joint Tracking

Joints that have a path that deviates from a straight line or circle usually require an automatic tracking device for EBW of production quantities. For small production lots, manual tracking, using a coordinate drive having separate controls, sometimes can be used. Whether the method is controlled manually or automatically, the motion required to generate the curve is usually imparted to the workpiece, although limited motion can be imparted to some guns.

Manual Joint Tracking. In manual tracking, the welding operator must closely observe the joint at the point where the weld is being made to anticipate any change in direction. The conditions best suited to this type of operation are: (1) a joint path consisting of a smooth curve, (2) slow travel speed, and (3) a low-power beam with oscillation, to form a weld as wide as possible. The welding operator is capable of regulating two motions of the workpiece (or gun) by manually adjusting the remote controls of the travel mechanism.

For a low heat input, to permit the use of the low welding speeds needed when manual tracking is used, beam pulsation can be combined with beam oscillation.

Automatic Joint Tracking. Mechanical, electromechanical, numerical control, and computerized systems are sometimes used for welding joints that deviate from straight lines or circles. The use of computerized numerical control (CNC) has become highly prevalent in EBW equipment. The capability of a CNC for allowing the weld seam path of a part to be quickly "digitized" and "edited" makes it an ideal tool for programming and tracking the actual weld seam path.

Electromechanical joint tracking systems make use of a stylus, or probe, that rides in the joint. Lateral movements of the stylus (which precedes the beam), resulting from a change in joint position, are converted to electrical signals by a transducer. The electrical signals drive a positioning servomotor that maintains preset alignment of the joint-to-gun focus. These electrical signals define a right error, a left error, and the correct gun position. Precision is usually better, response-delay time is shorter, and other problems associated with mechanical tracking with templates are avoided.

Tape-Controlled Joint Tracking. Workpiece (or gun) motion can be programmed for the complete welding cycle by conventional numerical-control equipment. The actual position of the workpiece with respect to the programmed tape input can be controlled to approximately ±0.025 mm (±0.001 in.). As with other tracking systems in which the generated motion is independent of the joint path, the two paths must coincide. There must be a high degree of assurance that the prior processing of the workpiece, its fixturing, and beam alignment have been done with repeatable accuracy. The tape input information must be sufficiently fine to generate the curve within the desired accuracy.

Beam Oscillations

Through the use of a two-axis deflection coil, either a static (fixed) or an oscillatory (periodic) motion can be imparted to the beam spot through a separate deflection control module. Generally, this control consists of a set of amplifiers for driving the *x-y* axes and a function generator for programming the beam spot motion desired. Beam spot motions employed comprise a variety of shapes and may consist of straight, fixed, or periodic deflection, or a combination of both. Square wave, circular, hyperbolic, or parabolic beam spot motions can easily be programmed, employing angular beam deflections of up to 15° and frequencies greater than 5000 Hz. This beam oscillation capability allows wider welds, slower cooling rates, and more uniform weld shapes to be produced, without necessarily using beam defocusing. Also, beam oscillation capability reduces the need for accurate beam-to-seam alignment and makes precise joint tracking less critical. In addition, programmed beam oscillation can be used to control microshuts and porosity in partial-penetration welds, thus reducing undercut and underfill for better bead control and for maximizing penetration capability.

Use of a Pulsed Beam

Beam operation can be changed from continuous to intermittent on machines equipped with pulsing controls. Although available repetition rates (frequencies) and pulse lengths depend on the control unit, frequencies in the range of 0.1 to 3000 Hz with pulses up to about 60 to 70 ms in duration are representative. Beam pulsation reduces the rate of heat input, but is independent of other beam conditions. Therefore, pulsation can be combined with oscillation and deflection, as well as travel speed, to influence weld behavior.

At very low frequencies, such as 1 Hz, with a 5 to 10 ms pulse length, each pulse produces a separate weld, even at low travel speed. By increasing travel speed and adjusting pulse frequency and pulse length, tack welds, spot welds, or intermittent welds can be made at normal production rates. Increasing pulse frequency to approximately 35 to 100 Hz while maintaining short pulse lengths makes it possible to overlap the successive welds to form a continuous weld at speeds suitable for manual tracking.

Pulsed beams generally result in lower peak temperatures, especially in the area adjacent to the weld, as compared to continuous welding, although total heat input may be greater because of the slower welding speed used. At higher pulse frequencies, pulsation has been used to control the solidification pattern of the weld and the microstructure of the HAZ. Pulsation also has been used in rewelding to fuse cold shuts, fill gas pockets, and smooth irregular root areas.

Procedure Development and Practice Considerations for Electron-Beam Welding

Electron Beam Welding as a Repair Method

Restoration of worn or damaged components traditionally has been an important application for welding technology. Some repairs are approached by welding a new detail in the area requiring restoration. However, it is frequently more suitable and cost effective to use a weld buildup process to restore the dimensions and structural integrity of the affected area. Welding processes such as manual or automatic GTAW or GMAW traditionally have been utilized for this type of repair; these processes facilitate the addition of filler wire to accomplish a weld buildup. While these processes enable efficient and relatively fast buildup of filler metal, they have a potential drawback of relatively high heat input, which may cause distortion when section thicknesses are small.

The EBW process has been employed extensively for original equipment manufacture mainly because of its ability to minimize or eliminate distortion through high weld speed, small HAZ, and small bead size. In the past, application of EBW for repair has been relatively limited, confined primarily to butt welding of repair insert details, penetration of parent metal (e.g., to eliminate a crack), or melting of preplaced filler wire. The matching of automatic wire-feed equipment to EBW equipment, however, has led to the development of a system that incorporates the inherent advantages of EBW systems and offers the additional capability of achieving a precise, multiple-pass weld buildup with minimum heat input. The addition of this capability has greatly increased the utilization of EBW as a repair mechanism.

Electron-Beam Wire-Feed Process and Equipment for Repairs

Electron-beam welding units used for weld buildup repairs are high-voltage, high-vacuum machines (150 kV, 13 mPa, or 10^{-4} torr). The availability of a highly controlled welding atmosphere is a distinct advantage for the electron-beam process, particularly when welding reactive materials such as titanium. High-voltage, high-vacuum EBW machines are equipped with signal generators that oscillate and deflect the beam in the *x-y* directions. They are also capable of making circles and other geometric figures. Beam deflection frequency can be varied, and the beam can be focused above or below the point of impingement. Beam pulsing and modulation of the pulse are also possible. All these tools can be used in weld buildup repairs. Current electron-beam vacuum chambers can accommodate parts up to 1525 mm (60 in.) in diameter. On the floor of the chamber is an *x-y* table; fixed to this table is a variable-speed rotary table. The component to be repaired, typically a cylindrical ring or case, is fixtured to this rotary table. An automatic filler-wire feeder delivers wire to the beam impingement point, enabling a continuous multiple-pass weld buildup when the component is rotated under the beam. Typically, a fused spot is less than 0.51 mm (0.020 in.) in diameter, allowing for an extremely small HAZ.

The wire-feed equipment is an adaptation of standard GTAW wire-feed equipment, and the technique is similar to that employed in cold wire circumferential automatic GTAW. The precision wire feeder delivers wire through a nozzle, which can be positioned in the *x*, *y*, and *z* directions and which is easily visible in the coaxial optical system of the electron-beam welding machine. Wire entry angle, nozzle position, wire speed, weld speed, accelerating voltage, focal position,

deflection, and amperage are critical factors in EBW buildup. Both inside and outside surfaces can be restored, depending on the position of the wire feeder within the chamber.

A relatively small filler-wire diameter (≤0.89 mm, or 0.035 in.) typically is employed to attain a precise low-heat input and a weld buildup typically 1.0 to 1.3 mm (0.040 to 0.050 in.) wide and 2.54 to 7.62 mm (0.100 to 0.300 in.) high, although much larger buildups could possibly be attained by multiple applications of the process. Electron-beam weld buildup lends itself readily to automation, thereby opening the process to use by less skilled operators. On some machines, all parameters are preset. The operator merely lines the machine up on the surface to be welded and pushes the start button. The wire feeder automatically activates and adjusts itself to produce a smooth, precise buildup.

Application of Electron-Beam Wire-Feed Process for Repairs

The electron-beam wire-feed process has been applied primarily for restoration of worn or damaged gas turbine aircraft engine components, which are typically cylindrical in shape with diameters ranging from 100 to 1525 mm (4 to 60 in.), lengths from 25 to 915 mm (1 to 36 in.), and section sizes from 1.3 to 12.7 mm (0.050 to 0.500 in.). Repair of gas turbine engine components has become increasingly attractive to commercial and military operators because of the cost and lead time involved in the procurement of spare parts. Repairs are typically conducted at 50 to 70% of the cost of a new component, with three to six times improvement in replacement time.

One of the key gas turbine engine component repairs is the restoration of the rotating labyrinth-type air seals used to maximize engine pressure gradients. As seals wear or are damaged, engine efficiency drops and fuel consumption rises. Hence, restoring minimal seal clearances has become increasingly attractive. Seal design is typically of the straight knife edge or tapered knife edge type (Fig. 21). Materials vary from iron-base alloys (AMS 6508 and A-286) to high-nickel alloys (Incoloy 901 and Waspaloy) to titanium alloys (Ti-6Al-4V, Ti-8Al-1Mo-1V, and Ti-6Al-2Sn-4Zr-2Mo).

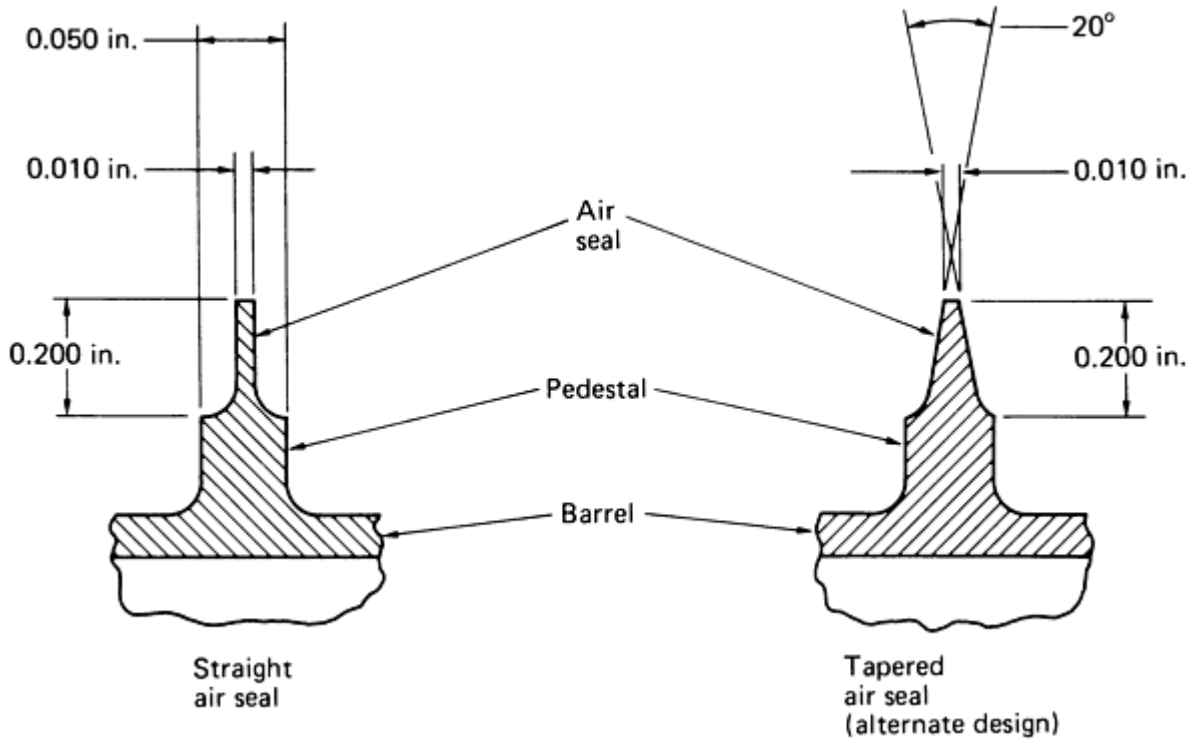

FIG. 21 SCHEMATIC COMPARING CROSS SECTIONS OF STRAIGHT AND TAPERED AIR SEALS

Currently, virtually all air seal restoration is done by welding. Gas-tungsten arc welding, gas-metal arc welding, and electron-beam welding have all been successfully applied depending on requirements of engine manufacturers, component design, material, and experience and equipment of repair stations. Prior to the establishment of the electron-beam wire-feed process, utilization of the standard electron-beam weld process for this type of repair was limited to

competitive weld buildup processes (GTAW and GMAW) and was primarily applied where distortion and HAZ size were a primary concern.

Initial application of the standard electron-beam process involved welding a machining ring onto a premachined pedestal on which the worn air seal was removed, as shown in Fig. 22. The knife edge configuration was then machined into the welded ring. Later, a split ring concept was introduced. In this procedure, an edge-rolled ring was assembled into a shallow groove premachined into the pedestal top (Fig. 22). Circumferential spike welds from each side welded the ring in place and the ends of the split ring were radiused to blend the discontinuity in the ring. The wall thickness of the as-rolled ring was the finished thickness of the knife edge, typically about 0.25 mm (0.010 in.), and the outside diameter was finish machined after welding. Disadvantages of this weld buildup system include ring detail cost and the amount of post-repair machining required.

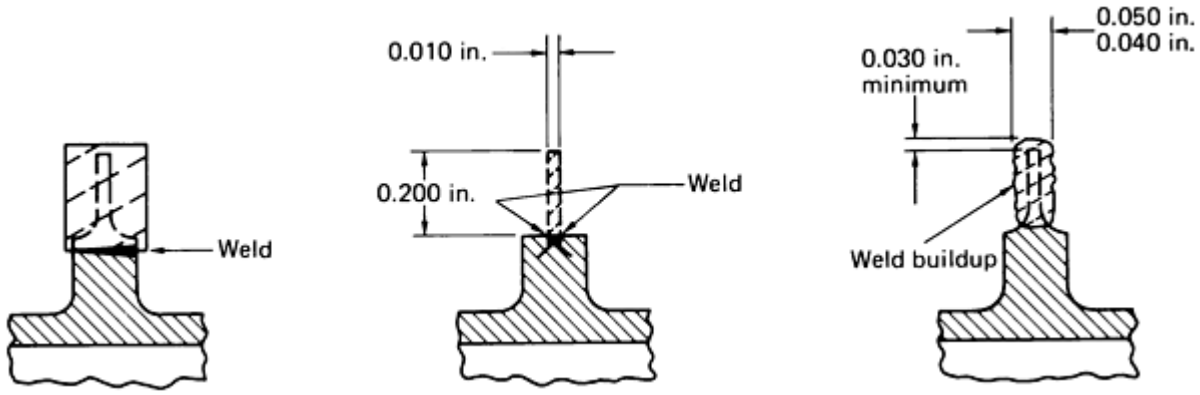

FIG. 22 SEQUENCE OF OPERATIONS REQUIRED FOR EBW REPAIR OF AN AIR SEAL. SEE TEXT FOR DETAILS.

The application of the precision wire-feed electron-beam process (Fig. 22) to gas turbine seal repairs provides both the material application efficiency and cost advantages of weld buildup systems and the inherent low heat input and controlled atmosphere advantages of the EBW process. A typical automatic wire-feed electron-beam air seal repair, applied to a compressor rotor spacer for a gas turbine engine, is shown in Fig. 23. This part is made from a titanium (Ti-6Al-4V) forging. The outside diameter of the knife edges wear in service, and the knife edges must be restored to maintain the proper tip clearance. The knife edge material is machined close to the diameter of the pedestal; a weld buildup is made using Ti-6Al-4V titanium filler wire, and a new knife edge is machined. The multiple-pass technique typically deposits 0.25 to 0.38 mm (0.010 to 0.015 in.) of radial buildup per pass. Penetration of the HAZ below the pedestal top typically does not exceed 0.38 mm (0.015 in.). Because the entire weld buildup operation is performed in a vacuum, there is no weld metal or HAZ oxidation. Cost is minimized by the high speed of the EBW process, which substantially exceeds that of the standard GTAW buildup process.

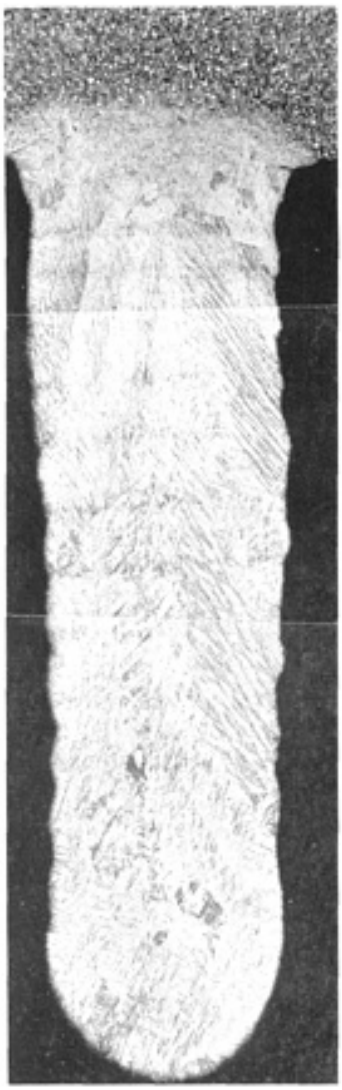

FIG. 23 PHOTOMICROGRAPH OF A TYPICAL AUTOMATIC WIRE-FEED ELECTRON-BEAM REPAIR OF AN AIR SEAL. 15×

Air seal repairs also are routinely performed on steel and nickel alloy parts. Experience with nickel-base superalloys containing relatively high percentages of gamma prime that form hardening elements has shown these alloys to be crack sensitive during welding or postweld heat treatment. Crack-free precision wire-feed EBW buildup repairs, however, are achieved when appropriate process parameters are utilized.

In applying the process to steel alloys, parameters should be optimized to avoid a pronounced swirl pattern at the buildup interface which may be encountered due to uneven mixing of the weld buildup and substrate. Potential swirling is associated with certain steel alloys and may be a potential source of porosity or cracking.

Quality assurance testing is an integral part of all gas turbine engine repairs. The high degree of control inherent in the precision wire-feed electron-beam repair process facilitates in-process control and quality assurance. Because of the high degree of control the electron-beam process offers, process variables can be kept to a minimum. This built-up consistency tends to ensure a long-term high level of quality assurance.

Weld parameters are developed by the analysis of microsections of sample welds and by nondestructive testing. Once an acceptable process has been established for a component, a weld schedule is initiated and weld parameters are maintained. Any changes in equipment or process must be qualified by the analysis of new microsections. Quality of finished air seals is ensured by one or more of the following tests, depending on customer requirements:

- VISUAL
- LIQUID PENETRANT
- FLUORESCENT MAGNETIC PARTICLE
- X-RAY
- ETCH INSPECTION

Future Applications for Repair

Although the most common application of the precision wire-feed electron-beam buildup process has been in the repair of gas turbine engine air seals, the process is not limited to this type of application. Various other wear restoration applications have been developed, including spline and groove buildups. Although the process is most efficiently utilized as a continuous multiple-pass process on cylindrical components, planar buildup can be achieved by utilizing sequential weld pass patterns or oscillation. The process is also potentially applicable for new part manufacture to enable a component to be machined from a smaller, less costly forging with selective electron-beam buildup to provide material for specific structural features (for example, outside diameter bosses on cylindrical cases).

Procedure Development and Practice Considerations for Electron-Beam Welding

Joining of Dissimilar Metals

The joining of dissimilar metals is an important application of EBW. The weldability of two dissimilar metals or alloys depends primarily on their physical properties, such as melting points, thermal conductivities, and coefficients of thermal expansion. Weldability generally can be determined by examination of the phase diagram of the alloys to be welded. If intermetallic compounds are formed by the metals to be welded, the weld metal will be brittle. However, many combinations that are difficult to weld or unweldable by other processes can be welded by the electron-beam process.

Procedure Development and Practice Considerations for Electron-Beam Welding

EBW of Low-Carbon Steel

Low-carbon steels are readily electron-beam welded. Grain size in both the weld and the heat-affected zone (HAZ) is significantly smaller than in arc welds, because of the lower heat input and extremely rapid heating and cooling. Rimmed steel causes excessive gassing. A technique used to weld rimmed steel is to sandwich an aluminum alloy shim about 0.25 mm (0.010 in.) thick in the joint to provide deoxidizing action during welding. Welding at a low travel speed or otherwise adjusting welding conditions to produce a more tapered weld and thus to allow more time for the escape of gases from the molten weld metal also helps to reduce porosity. Semikilled steel is easier to weld than rimmed steel, but some oxygen may remain to cause porosity. Fully killed steel is readily weldable.

Procedure Development and Practice Considerations for Electron-Beam Welding

EBW of Hardenable Steel

The variation in weldability by EBW among hardenable steel follows the same pattern as for arc welding of these steels. Properties of electron-beam welds in a given hardenable steel differ from those of arc welds mainly because of the narrowness of the fusion and HAZ and the extremely rapid heat-melt-cool cycles.

Hardness traverses across the midpoint of electron-beam (high-vacuum) and gas tungsten arc welds in 1.57 mm (0.062 in.) thick heat treated 4340 steel are plotted in Fig. 24. For both welds, maximum hardness was produced uniformly in the weld metal, and hardness dropped off abruptly at the edge of the weld metal.

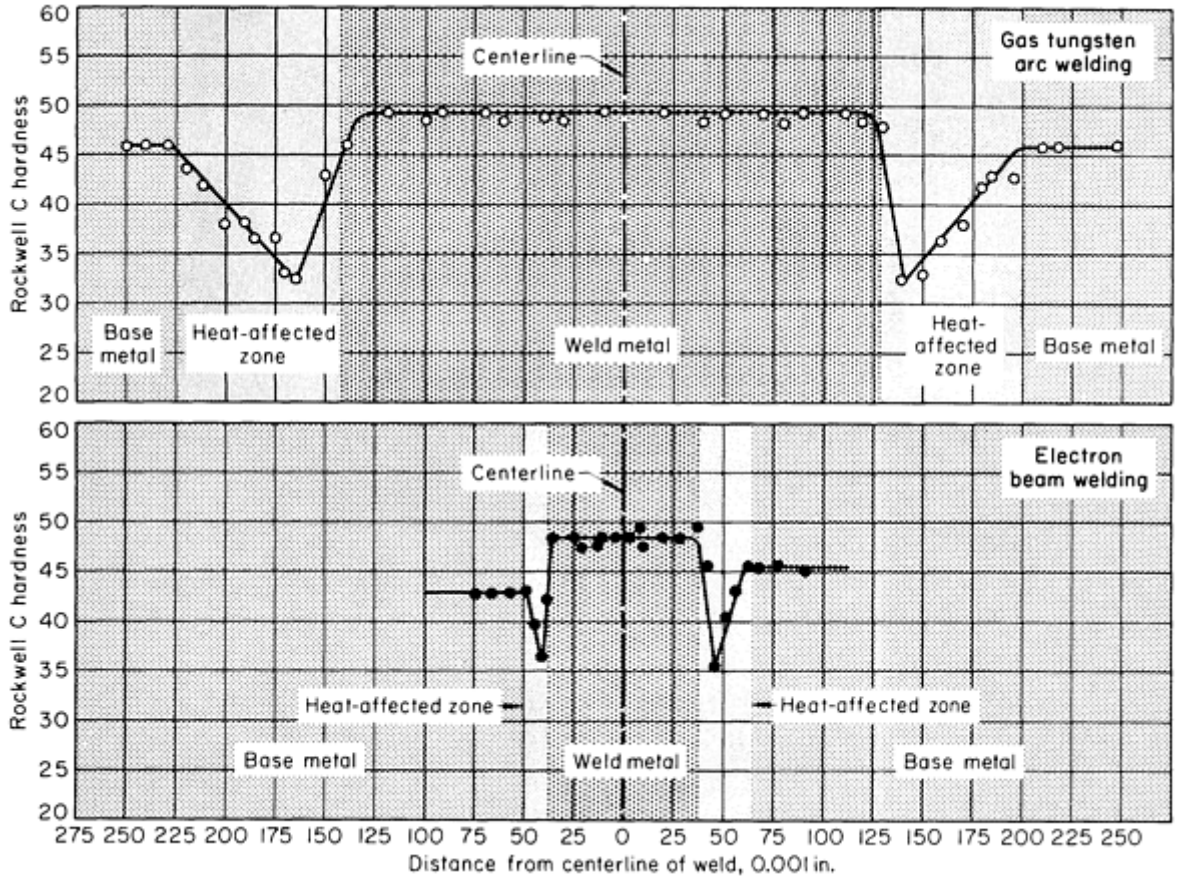

FIG. 24 HARDNESS PROFILE OF HIGH-VACUUM EBW AND GTAW BUTT JOINTS USED TO JOIN 1.57 MM (0.062 IN.) THICK MEDIUM-CARBON ULTRAHIGH-STRENGTH STEEL

Similar hardness traverses for electron-beam welds in 9.65 mm (0.380 in.) thick heat-treated 1024 (modified) are shown in Fig. 25. The hardness profile across this weld was similar to that for the electron-beam welds in 1.57 mm (0.062 in.) thick 4340 steel. Tempering after welding eliminated or minimized the hardness differential in the HAZ (Fig. 25).

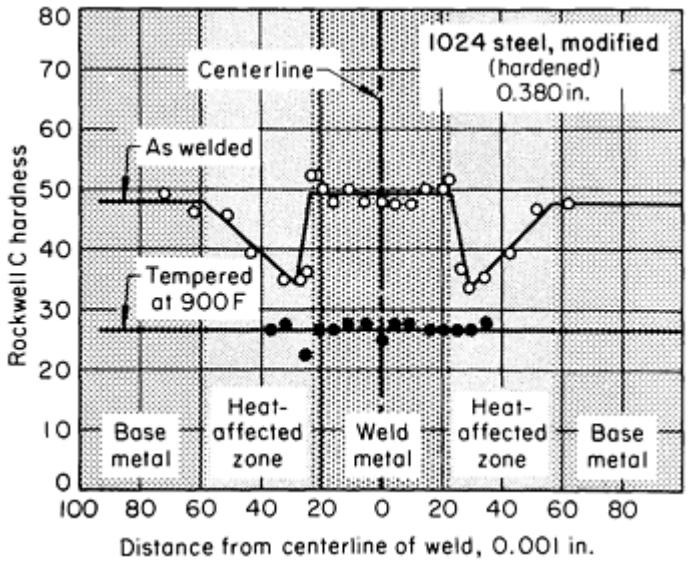

FIG. 25 HARDNESS-PROFILE OF HIGH-VACUUM EBW BUTT JOINT USED TO JOIN 9.65 MM (0.380 IN.) THICK

Prevention of Cracking. Cracking can be a problem in EBW of hardenable steel, just as in arc welding, if the weld is made in a highly restrained joint, especially in welding parts that have been hardened. Deep circular welds in heavy sections are particularly troublesome. Partial-penetration welds are more likely to crack under restraint than full-penetration welds. It is desirable to place the joint in a location that will allow the part to shrink freely as it cools after welding. Welding through carburized or nitrided cases is not recommended.

Cracking of electron-beam welds in hardenable steels can also be minimized by reducing the welding speed to allow more buildup of heat in the base metal, and by preheating, postheating, and allowing the work to cool in the chamber after welding.

Medium-carbon steels except for the free-machining types, are readily electron-beam welded (for hardness traverses, see Fig. 25). Weldability decreases with increasing carbon content.

Low-alloy steels containing less than 0.30% C are usually electron-beam welded without preheating or postheating. When preheating is used--to prevent cracking in highly restrained joints, for example--a temperature of 260 to 315 °C (500 to 600 °F) is usually adequate. If the part has been hardened and tempered prior to welding, the postweld tempering must be done at a temperature slightly below that at which the base metal was originally tempered.

Two of the most frequently electron-beam-welded alloy steels of this type are 8620 and 9310. Components made of these steels often are case hardened, then assembled by EBW, without distortion or heat damage to the case. Before welding, the case should be removed from the immediate vicinity of the joint to prevent microcracks from forming in it.

High-strength alloy steels containing more than 0.30% C are electron-beam welded either in the annealed or the normalized condition or in the quenched and tempered condition, although weldability is better for the annealed or normalized condition. The hardness profile for electron-beam welds in hardened high-strength alloy steel sections no thicker than about 65 mm ($\frac{1}{4}$ in.) is ordinarily like that shown for 1.57 mm (0.062 in.) thick heat-treated 4340 steel in Fig. 24, and joint strength can approach that of the base metal, without preheating or postweld treatment other than stress relief.

When a shielding gas is substituted for air in nonvacuum welding, assuming the same operating conditions, penetration is greater when a gas is used that has a lower molecular weight (or nominal density) than that of air. Penetration is less when a gas that has a higher molecular weight than that of air is used. In tests on welding 4340 steel, using a fixed beam power of 6.4 kW, working distances of 6.4, 13, and 25 mm ($\frac{1}{4}$, $\frac{1}{2}$, and 1 in.), and welding speeds of about 380 to 2030 mm/min (15 to 80 in./min), penetration was increased when helium was substituted for air and was decreased when argon was substituted for air, as shown in Fig. 26. The relative capacities of helium, air, and argon to scatter the electrons of the beam by collisions of electrons with gas molecules are controlled by their molecular weights and relative densities. On the average, when helium was used as a shielding gas, penetration depth was about twice that obtained when welding was done in air, and when argon was used, penetration depth was about half that when welding was done in air. Thus, with helium shielding, penetration averaged about four times that with argon, especially at higher welding speeds. The speed at which a given thickness of 4340 steel could be welded with full penetration, using helium, was two to four times that with air. Using argon, speed was 25 to 50% that with air.

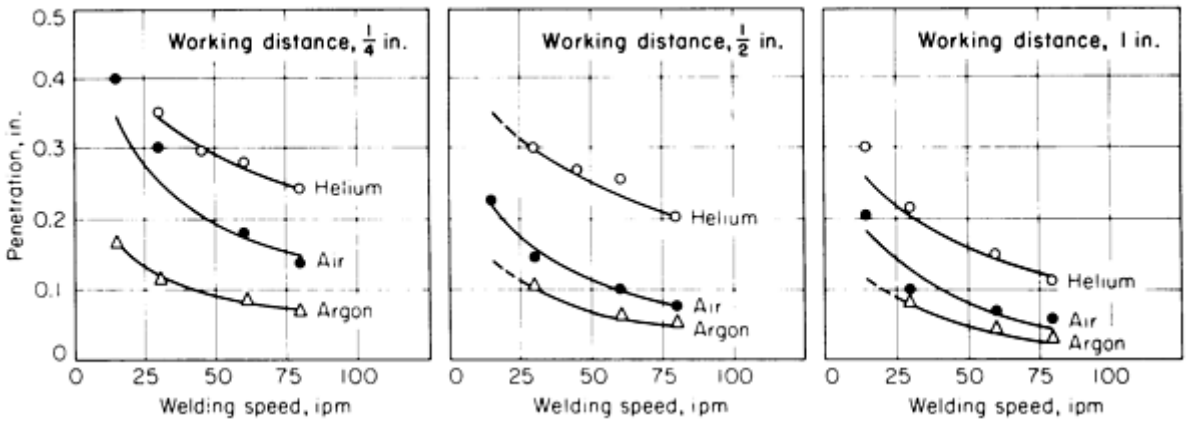

FIG. 26 PLOT OF PENETRATION VERSUS WELDING SPEED AS A FUNCTION OF SHIELDING GASES AND WORKING DISTANCES FOR NONVACUUM EBW OF 4340 MEDIUM-CARBON ULTRAHIGH-STRENGTH STEEL. BEAM POWER WAS 6.4 KW.

In EBW of thicker sections of high-strength alloy steels, preheating or postheating, or both, is usually needed to prevent cracking. In studies on full-penetration, single-pass welding of 15 mm (0.6 in.) thick annealed D-6ac steel, which is used frequently for missile castings, cracking was observed when preheating was not used and was eliminated by preheating at 540 to 565 °C (1000 to 1050 °F). Welding was started with the joint at a temperature of 370 °C (700 °F), and the joint temperature remained above 345 °C (650 °F) for 8 to 10 min after completion of the weld. Hardness profiles for the joints welded with and without preheat are shown in Fig. 27. Sound welds were also obtained in 55.9 mm (2.2 in.) thick annealed D-6ac steel, after preheating to 425 to 455 °C (800 to 850 °F); welding was started when joint temperature was no lower than 260 °C (500 °F).

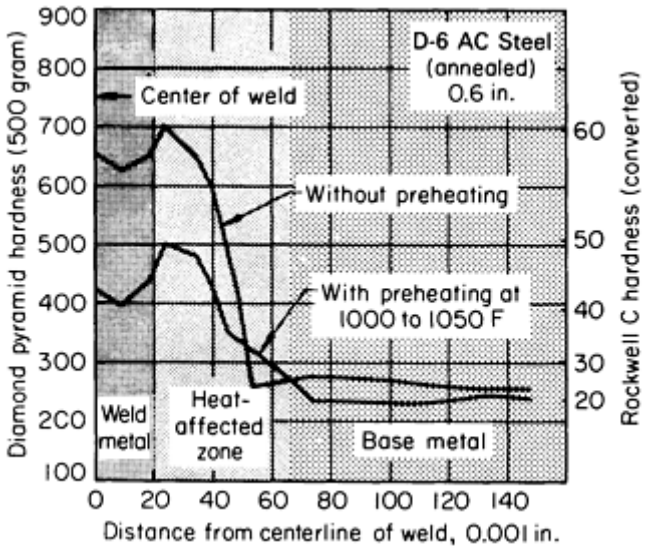

FIG. 27 EFFECT OF PREHEATING ON THE HARDNESS OF 15 MM (0.6 IN.) THICK D-6AC LOW-ALLOY ULTRAHIGH-STRENGTH STEEL

High-Carbon Steels. Because of the low total heat input and the rapid thermal cycling that are characteristic of EBW, weld cracking of steels containing more than 0.50% C is less likely than in arc welding. Even bearing steels such as 52100, which are seldom arc welded, have been electron-beam welded on a high-production basis. The 52100 steel is welded in the spheroidize-annealed condition in applications where joint performance is not critical to the function of the part and where service stresses in the joint are low. Preheating and postheating are not necessary.

EBW of Tool Steels

The chief advantage of EBW over other welding processes in joining tool steels is its ability to produce joints at high speed without annealing or other heat-treating operations. Hardness profiles similar to those shown for low-alloy steels in Fig. 24 and 25 were also obtained for H11 tool steel. For full-penetration butt welds on hardened (50 HRC) sections 5.72 ram (0.225 in.) thick, the hardness of the weld metal and the immediately adjacent base metal was 56 to 57 HRC, and hardness dropped to a minimum of 43 to 46 HRC in the HAZ, as measured after double tempering at 550 °C (1025 °F). The overtempered portion of the HAZ was only 0.13 mm (0.005 in.) wide.

Small dies of D2 tool steel have been electron-beam welded in production. A larger operation is the production of bimetal band saws. Specially designed high-vacuum machines, which are referred to as "air-to-air" machines, are used to produce band-saw blades by welding 1.6 mm ($\frac{1}{16}$ in.) wide M2 high-speed-steel cutting-edge strips to 6150 steel bands. The composite blade is about 0.8 mm ($\frac{1}{32}$ in.) thick and is welded at speeds above 7.6 m/min (300 in./min) in a special vacuum chamber. In "air-to-air" bimetallic strip welding, the backing band and edging strip are continuously fed through slots in a series of differentially pumped chambers and welded in a high vacuum without any interruption of this continuous product flow.

EBW of Hardened and Work-Strengthened Metals

The full properties of hardened and work-strengthened base metals can be retained on functional surfaces very close to the narrow electron-beam weld zone. In addition to confining the decrease in base-metal properties to a very narrow zone, EBW of hardened or work-strengthened metals also produces joint quality superior to that produced by arc welding. Some high-strength steels, however, cannot be electron-beam welded in the hardened condition without cracking or without an unacceptable decrease in strength and hardness. These steels, such as 52100 beating steel, are normally annealed before welding and given a postweld heat treatment for controlled strength and hardness. In Example 1, EBW was chosen over gas-tungsten arc welding (GTAW) because of the narrow fusion zone and HAZ obtained by the electron-beam process.

Example 1: Selection of Electron-Beam Welding to Minimize Tempering in the Heat-Affected Zone.

Fabrication of armor for military aircraft involved the welding of corner joints in 7.9 mm ($\frac{5}{16}$ in.) thick armor plate. The armor plate was made by roll-bonding H 11 tool steel to an alloy steel (AMS 6545) containing 9% Ni, 4% Co, and 0.30% C. Welding was done with the plate in the hardened condition; the H11 steel was hardened to 60 HRC and the alloy steel to 50 HRC. The plate was not difficult to weld. Either GTAW or EBW could be used to obtain sound welds using the joint designs shown in Fig. 28.

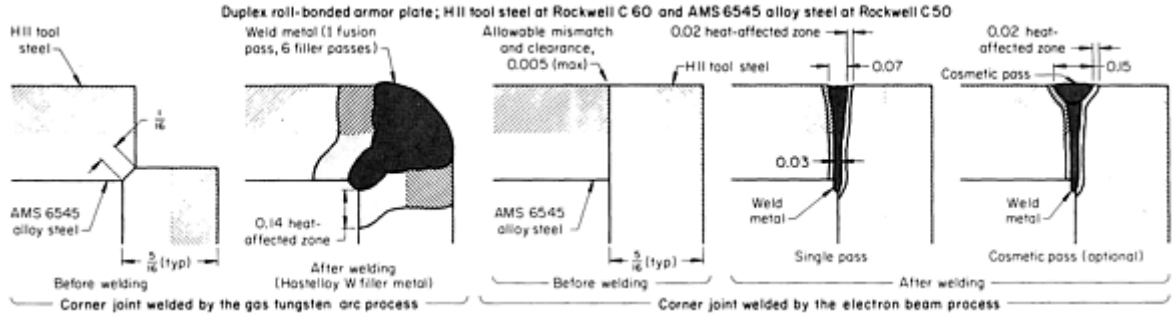

FIG. 28 SCHEMATIC OF CROSS SECTIONS THROUGH CORNER JOINTS AND WELDS TO SHOW VARIATION IN THE SIZE OF WELDS AND HAZ THAT ARE OBTAINED WITH EBW AND GTAW

The weld and HAZ of the electron-beam process are compared with those of GTAW in Fig. 28. Joint designs differed; if the joint for GTAW had been made the same as the joint for EBW, a V-groove would have been required, and about the same amount of weld metal would have been needed. Gas-tungsten arc welding was done in one fusion pass and six filler-metal passes, using 1.57 mm (0.062 in.) diam Hastelloy W wire.

Electron-beam welding was done in a single pass. Because of the occasional undercutting, a second (cosmetic) pass was sometimes used. Even when the second pass was used, the weld and the HAZ were much narrower than were those created by arc welding, and they were unaffected below the crown of the weld. Because the general effect of the welding heat was to decrease the hardness and strength of the base metal, EBW, which produced less heat, was selected.

There were no unusual problems associated with the EBW procedure. Plates were machined square and then were degreased. Just before welding, surface films were removed from all surfaces to be welded by brushing with a stainless steel wire brush followed by wiping with alcohol. The plates were then fixtured into an assembly roughly resembling a bathtub having sides about 250 mm (10 in.) high and a floor area of about 510 by 1015 mm (20 by 40 in.). A maximum tolerance of 0.13 mm (0.005 in.) was allowed on fit-up for joint mismatch and clearance. Starting and runoff tabs, made of the same duplex plate, were attached to joint ends to contain variations in beam initiation and termination. The fixture was a simple arrangement of toggle clamps and stainless steel blocks that could be set up for flat-position welding on a track-guided carriage in the vacuum chamber.

After beam alignment and vacuum pump-down, each joint was welded in a single pass without tack welding and without beam oscillation. Because undercutting occurred where fit-up approached the maximum tolerance, a second (cosmetic) pass occasionally was used. The effect of the cosmetic pass on the weld cross section is shown in Fig. 28; the machine settings for the defocused beam used to make the cosmetic pass are in the table with Fig. 28.

Procedure Development and Practice Considerations for Electron-Beam Welding

EBW of Stainless Steels

The properties and the welding metallurgy of stainless steels are discussed in the Section "Selection of Stainless Steel" in this Volume.

Austenitic Stainless Steels

The high cooling rates typical of EBW help to inhibit carbide precipitation, because of the short time during which the steel is in the sensitizing-temperature range. Filler metal is used in welding joints that cannot be fitted together closely.

Effect of Air and Helium Atmospheres on Selected Parameters. Figure 29 shows the effect of welding speed on penetration of nonvacuum welds made in austenitic stainless steel and the effect of ambient gas and power on the penetration versus speed curve. Curves identified as helium penetration-versus-speed curves were performed using a helium effluent-style lower orifice design, that is, using a lower (exit) orifice that is capable of blowing helium into the atmosphere with enough directed flow to provide a helium gas column in which the beam can travel.

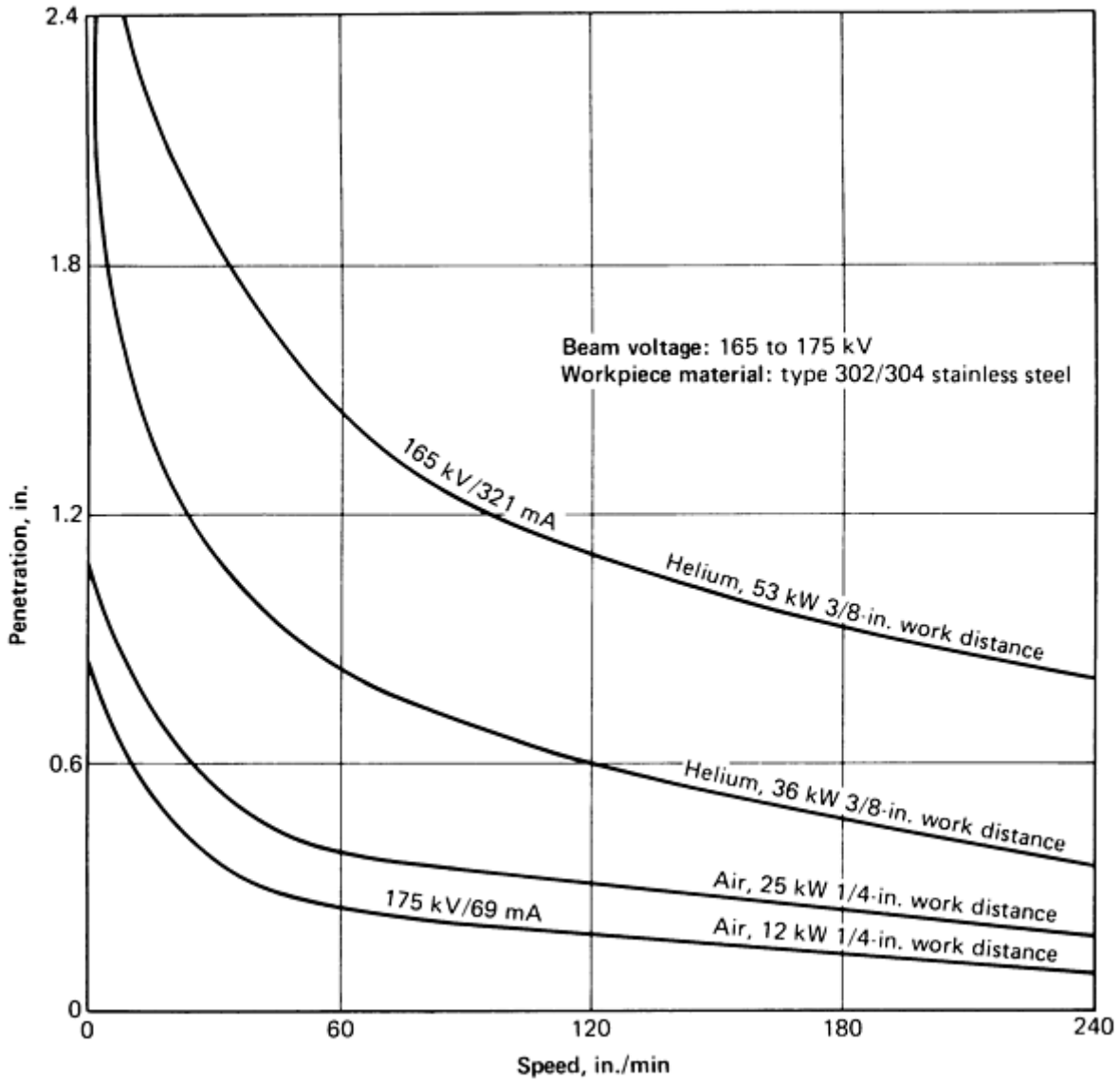

FIG. 29 PLOT OF PENETRATION VERSUS WELDING SPEED AS A FUNCTION OF SELECTED BEAM VOLTAGES, ATMOSPHERES, POWER LEVELS, AND WORK DISTANCES TO WELD TYPE 302 TO TYPE 304 AUSTENITIC STAINLESS STEELS

Example 2: Melt-Through Welding of 0.05 mm (0.002 in.) Thick Foil.

A rupture-disk assembly (Fig. 30) designed for gas-pressure relief consisted of three components: (1) a 50 mm (2 in.) diam nozzle of 2.5 mm (0.100 in.) thick type 304 stainless steel attached to an outer pressure vessel (not shown); (2) a 0.05 mm (0.002 in.) thick cupped rupture disk of type 304 stainless steel; and (3) a 1.02 mm (0.040 in.) thick cap, also of stainless steel, containing an off-center flued-in hole with downward-pointing knife edges.

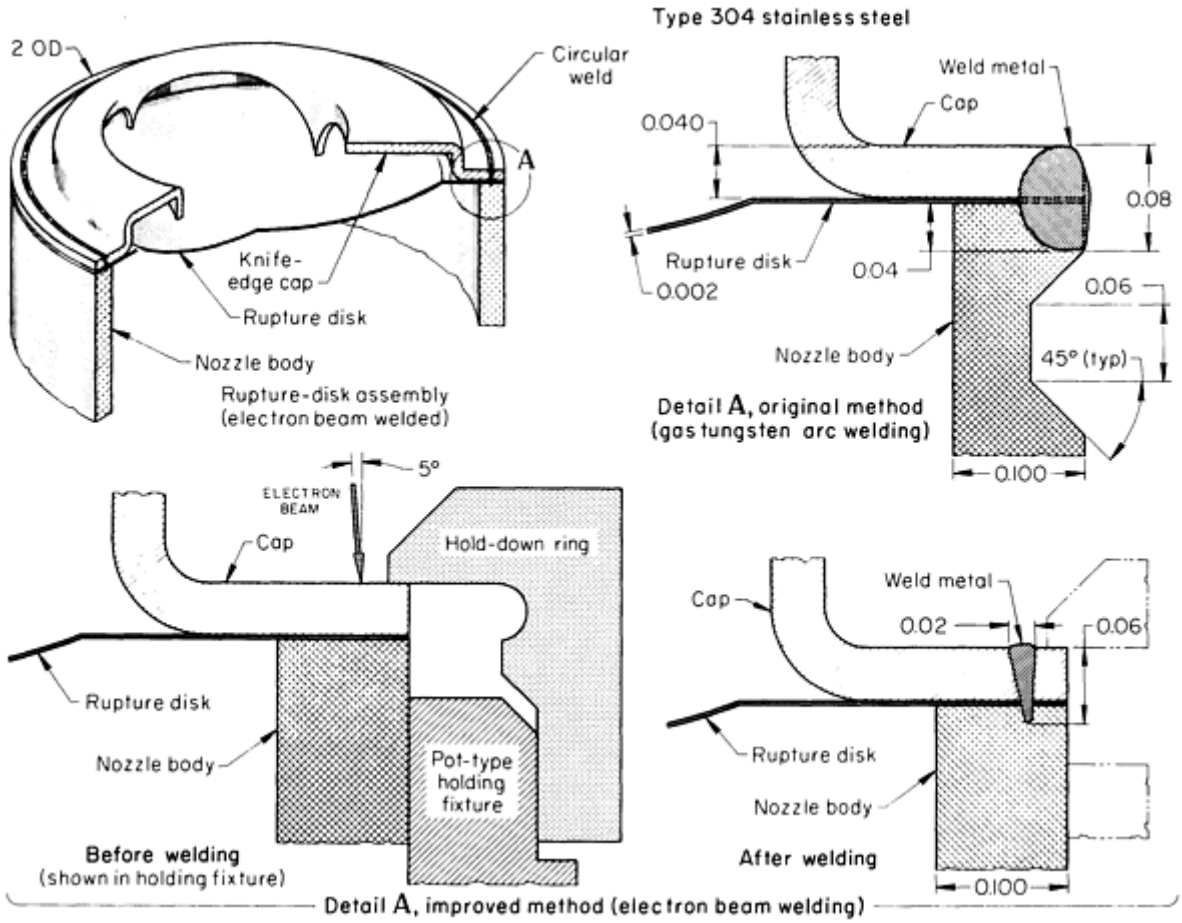

JOINT TYPE	**CIRCULAR, THREE-PIECE COMER**
WELD TYPE	**MELT-THROUGH (SPIKE)**
MACHINE CAPACITY	**50 KV AT 250 MA**
GUN TYPE	**DIODE; FIXED DURING WELDING**
VACUUM CHAMBER	**STEEL: 1370 × 1220 × 1220 MM (54 × 48 × 48 IN.) WITH FULL-WIDTH END DOORS**
FIXTURES	**56-PIECE HOLDING TOOL WITH INDIVIDUAL ROTATION; TABLE WITH *X-Y* MOTION**
WELDING POWER	**26 KV AT 16 MA**
WELDING VACUUM	**0.65 MPA (5×10^{-6} TORR)**
PUMPDOWN TIME	**10 MIN**
WORKING DISTANCE	**38 MM (1.5 IN.)**
BEAM FOCAL POINT	**SHARP AT WORK SURFACE**
BEAM SPOT SIZE	**∼0.51 MM**

	(~0.020 IN.) DIAM
WELDING SPEED	**2540 MM/MIN (100 IN./MIN)**
NUMBER OF PASSES	**ONE, PLUS 30° DOWNSLOPE**
SETUP TIME	**48 MIN**
PRODUCTION RATE	**44 $\frac{1}{2}$ PIECES/H**

FIG. 30 COMPARISON OF EBW AND GTAW WELDS APPLIED TO A TYPE 304 STAINLESS STEEL RUPTURE DISK ASSEMBLY

The three components were joined by a single weld that was required to have a leak rate of less than 10^{-8} cm^3/s (6×10^{-10} $in.^3/s$) when tested with a helium mass spectrometer. When pressure in the nozzle exceeded the design limit, the cupped rupture disk reversed its shape from concave to convex, puncturing itself against the knife-edge of the cap. Leaktightness, rather than high tensile strength, was the welding objective. The material was selected for long, maintenance-free service, rather than for resistance to a corrosive environment.

Originally, the components were joined in one pass by GTAW, using the design shown in detail A, original method, Fig. 30. A circular groove was cut in the nozzle wall to help localize the weld bead, which was made without filler metal. Light pressure was applied at both ends of the assembly to hold the parts in alignment for welding.

This procedure resulted in numerous rejects because of leaks. Often, difficulty was encountered in getting the disks to lie absolutely flat on the joint surface. The 0.05 mm (0.002 in.) thick rupture disks, having been blanked and formed in the work-hardened condition, were tough, springy, and sometimes burred. As a result, they occasionally were burned back, instead of being fused into the weld bead, causing leaks. It was usually impossible to salvage this type of defect by rewelding.

To eliminate these difficulties, the operation was converted to EBW, even though initial equipment and tooling costs were high. The EBW machine used for this application had a relatively large vacuum chamber with full-width doors to facilitate loading and unloading of large, multiple-part fixtures. The holding fixture used had 56 receptacles to position and individually rotate 56 assemblies under a stationary gun. The fixture was mounted on a horizontal table equipped with *x-y* motion control to permit optical alignment of the beam for welding each part in turn.

Each assembly was fitted into a cylindrical receptacle or pot that was equipped with a hold-down ring that forced the periphery of the disks and caps into close alignment, as shown in detail A, improved method, Fig. 30. A melt-through or spike weld was made, rather than an edge-flange weld at the periphery.

With this setup, the blanking and forming operations on the disks could be allowed the more realistic tolerance of ±0.05 mm (±0.002 in.) on flatness. The electron beam was angled slightly and was positioned close to the hold-down ring so that, in the event of a leak, the joint could be rewelded by running a second weld just inside the first weld.

The weld-localizing groove needed for the original GTAW was eliminated, and the electron-beam melt-through weld was made at a heat input of 0.0098 kJ/mm (0.25 kJ/in.) of weld length, which was much lower than for arc welding. The hold-down ring provided a slight chill effect, but enabled the nozzle body to function effectively as a heat sink.

Welding results from the electron-beam procedure were good. Joint defects of all types dropped to 3%, and most of the rejects could be salvaged by rewelding. A production rate of $44\frac{1}{2}$ assemblies per hour was a significant improvement over the original arc method.

Martensitic Stainless Steels

Although these steels can be electron-beam welded in almost any heat-treated condition, welding will produce a hardened, martensitic HAZ. Hardness and susceptibility to cracking increase with increasing carbon content and cooling rate.

Precipitation-Hardenable Stainless Steels

Precipitation-hardenable stainless steels can, in general, be electron-beam welded to produce good mechanical properties in the joint. The semiaustenitic types, such as 17-7 PH and PH 14-8 Mo, can be welded as readily as the 18-8 types of austenitic stainless steel. The weld metal becomes austenitic during welding and remains austenitic during cooling. In the more martensitic types, such as 17-4 PH and 15-5 PH, the low-carbon content precludes formation of hard martensite.

Some of the precipitation-hardenable stainless steels have poor weldability because of their high phosphorus content. Steels 17-10 P and HNM are not usually electron-beam welded.

EBW of Heat-Resistant Alloys

Because of the marked differences in composition and weldability among heat-resistant alloys (nickel-base, iron-base, and cobalt-base), generalizations concerning EBW of these alloys are not useful.

Solid-Solution Nickel-Base Alloys. Hastelloy N, Hastelloy X, and Inconel 625 are readily electron-beam welded. Hastelloy B and Inconel 600 can be welded to type 304 stainless steel and to themselves.

Precipitation-hardenable nickel-base alloys that are rated good in weldability by the electron-beam process include Inconel 700, alloy 718, Inconel X-750, and René 41. Alloy 718 can be welded in either the annealed or the aged condition. Inconel X-750 should be welded in the annealed condition, and René 41 should be welded in the solution-treated condition. Alloys of this group that have fair weldability include casting alloys 713C and GMR-235 and wrought Udimet 700 and Waspaloy.

Iron-Nickel-Chromium Base Alloys. This group of alloys is also known as the iron-base heat-resistant alloys. The most readily welded alloy of this group, using EBW, is 19-9 DL, which has excellent weldability and which produces the best results when preheating is used. Alloy N-155 has good weldability, and alloys 16-25-6 and A-286 are rated fair. Alloy A-286 is usually welded in the solution-treated condition; hot cracking may result if welded in the aged condition.

Cobalt-Base Alloys. HS-21 has good weldability in unrestrained joints (and is generally poor in restrained joints). Cast alloy H-31 (X-40) has fair-to-good weldability, and alloy S-816 has fair weldability.

EBW of Refractory Metals

Electron-beam welding is the preferred technique for welding of refractory metals and their alloys. These materials, with melting temperatures in excess of 2200 °C (4000 °F), can be processed more efficiently with the intense heat source of the electron beam, which allows for localized fusion without excessive heating of the adjacent base metal. Weld-zone properties in refractory metals and alloys are particularly sensitive to contamination by interstitial elements such as carbon, hydrogen, nitrogen, and oxygen, which increase the already high ductile-to-brittle transition temperature of the weld zone and increase the notch sensitivity beyond the limits required for practical processing of these materials.

The possibility of atmospheric contamination during welding is essentially eliminated by EBW in a high-vacuum environment. Interstitial impurities already present in the base metal, however, have a significant effect on the weldability of the metal and alloy system. The Group V metals (e.g., niobium and tantalum) are softer, less subject to strain hardening, and less prone to the brittle behavior usually associated with the Group VI metals (molybdenum and tungsten). The very low room-temperature ductility of the Group VI metals gives rise to cracking problems due to cyclic thermal stresses during welding. Preheating above 300 °C (575 °F) reduces the susceptibility to this problem.

Excessive grain growth in the weld HAZ and fusion zones can produce cracking during the welding process or during subsequent application of the weldment. Grain coarsening can be controlled to some extent by specifying a fine-grained starting material and minimizing the total heat input during welding. The morphology of the fusion zone is also important. High welding speeds (>610 mm/min, or 24 in./min) selected to minimize heat input can promote pronounced directionality of grain growth in the weld pool, leading to a plane of weakness at the weld centerline. High-frequency (>1

kHz) beam oscillation can be applied to restore an elliptical weld-pool geometry at high travel speeds and eliminate the pronounced delineation of the weld centerline.

As with any low-ductility weldment, the degree of restraint imposed on the joint during the welding operation should be minimized. Most refractory metals and alloys can be welded in thin (<1.0 mm, or 0.04 in.) sheet. The weldability decreases with increasing section thickness in accordance with the increase in restraint. Weld joints should be designed to reduce the restraint by effective use of flange butt and standing edge designs, and by the incorporation of relief grooves to accommodate elastic/plastic strain in the material adjacent to the weld zone.

In contrast to many other alloy systems, the weldability of refractory metals tends to improve with the addition of alloying elements. Specific alloying elements can improve the low-temperature ductility of refractory metals and thus directly affect the weldability and weld mechanical properties. The overall weldability of tungsten is improved by the addition of substitutional alloying elements such as rhenium and molybdenum. As indicated previously, interstitials also raise the transition temperature; this effect can be reduced by alloying with elements that form stable carbides, oxides, and nitrides. For example, titanium and zirconium in molybdenum "scavenge" the interstitial impurities to improve low-temperature ductility and provide a dispersion-strengthening effect. Examples of successful electron-beam welds made in refractory metals and alloys are given in Table 5.

TABLE 5 TYPICAL APPLICATIONS AND CONDITIONS FOR EBW OF REFRACTORY METALS AND ALLOYS

APPLICATION	**BEAM SETUP**					COMMENTS
	KV	**MA**	**mm/min**	**in./min**	**FOCUS**	
TUNGSTEN HEAT PIPE, FLANGE-BUTT JOINT, 2.54 MM (0.100 IN.) PENETRATION	100	6	760	30	SURFACE	**PREHEAT TO 800 °C (1475 °F)**
TUNGSTEN CRUCIBLES, STANDING EDGE JOINT, 2.03 MM (0.080 IN.)	100	10	1525	60	ABOVE SURFACE	**PREHEAT WITH BEAM TO 800 °C (1475 °F)**
MOLYBDENUM HEAT PIPE, STEP JOINT/PARTIAL-PENETRATION WELD TO ROOT OF STEP, 1.57 MM (0.062 IN.) PENETRATION	125	25	760	30	SURFACE	**HIGH-FREQUENCY (~3 KHZ) DEFLECTION TO PRODUCE ELLIPTICAL POOL**
MO-TZM ALLOY STRAIGHT BUTT WELD IN HEAT SHIELD, 1.52 MM (0.060 IN.) PENETRATION	125	15	760	30	ABOVE SURFACE	**DUCTILITY OF WELD ZONE IMPROVED BY POSTWELD HEAT TREATMENT**
NB-1ZR REACTOR TUBING, BUTT WELD 1.52 MM (0.060 IN.) PENETRATION	100	10	760	30	. . .	**FULL-PENETRATION WELD, EXCELLENT AS-WELDED PROPERTIES**
MO-13 WT% RE TEST REACTOR TUBE 0.81 MM (0.032 IN.) PENETRATION	**100**	**7**	**760**	**30**	**SHARP**	**EXCELLENT WELD APPEARANCE, NO TEST DATA AVAILABLE**

Tungsten is the most difficult refractory metal to weld because of its high melting point (3410 °C, or 6170 °F), sensitivity to thermal shock, and room-temperature brittleness of welds and the HAZ. High-purity tungsten sheet can be electron-beam welded if the weld area is preheated and if external restraint is minimal. Successful welds have been made in sections as thick as 4.1 mm (0.16 in.); however, the resulting as-welded material is brittle and highly notch sensitive. Tungsten metal, manufactured by a chemical vapor deposition process, has also been proven to be weldable in sections <0.5 mm (<0.02 in.).

Molybdenum can be readily welded by EBW if chemical purity, grain size, and texture of the base metal are carefully monitored. Partly because of its lower melting point (2610 °C, or 4730 °F), molybdenum has better thermal shock resistance than tungsten; thus, narrower welds and higher welding speeds can be used. Preheating may or may not be necessary, depending on the starting material and the degree of restraint on the weld joint. When preheating is used, the workpiece should be heated to 205 °C (400 °F) or higher, followed by a postweld stress relief at 870 to 980 °C (1600 to 1800 °F).

Figure 31 shows an electron-beam weld zone in high-purity molybdenum. Penetration is approximately 3.05 mm (0.12 in.) to the root of a step-butt weld joint. This weld was made without preheat but with a high-frequency oscillation to

maintain an elliptical weld pool and influence the direction of grain growth in the solidifying metal. The growth direction at the center of the fusion zone is parallel to the welding direction, and the section is therefore an end view of the columnar grains. This type of solidification structure should not be confused with the grain refinement phenomena sometimes claimed to result from stirring of the weld pool. Because solidification in high-purity metals is essentially a columnar-planar growth, refinement most probably cannot be achieved by stirring the weld pool.

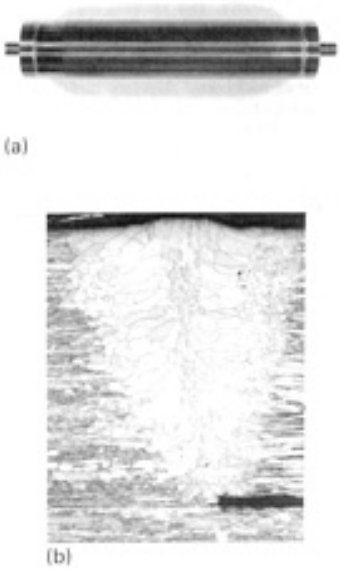

FIG. 31 ELECTRON-BEAM WELD ZONE IN HIGH-PURITY MOLYBDENUM. (A) MOLYBDENUM HEAT PIPE TEST ASSEMBLY SHOWING END CAPS JOINED BY EBW. (B) PHOTOMICROGRAPH SHOWING MORPHOLOGY OF WELD FUSION ZONE. 25×

Titanium and zirconium are the common alloying elements added to molybdenum to scavenge interstitial impurities and improve low-temperature ductility. The transition temperatures of welds in these alloys, however, are still above room temperature. Significant increases in the low-temperature ductility of these alloys can be obtained by solution and aging heat treatments. The greatest improvements in ductility are obtained by solution and aging heat treatments. The greatest improvements in ductility are obtained by the addition of rhenium; a 50 wt% addition of rhenium lowers the transition temperature of recrystallized molybdenum from approximately 52 to 205 °C (125 to 400 °F).

Niobium, which melts at 2468 °C (4474 °F), is easier to weld than molybdenum or tungsten. Gas-tungsten arc welding is often used, but EBW provides better protection, narrower welds, and lower heat input. Preheating is not necessary, but postweld vacuum stress relief is used to restore ductility and toughness, especially in the niobium alloys.

Unalloyed niobium is easily electron-beam welded, but has relatively low strength. More alloys have been developed, mainly for higher strength, than for the other refractory metals. Alloying usually reduces weldability, but most weld joints in alloys retain about 75% efficiency, and good structural properties can be obtained for service temperatures in the range of about 1095 to 1650 °C (2000 to 3000 °F), depending on the alloy. Chill tooling is often used, but copper, nickel, and stainless steel should be avoided to prevent contamination of the weld metal.

Tantalum is the most easily weldable of the four refractory metals. Because of its high melting point (2996 °C, or 5425 °F) and good thermal conductivity, thicknesses of 1.52 mm (0.060 in.) or more must be rapidly heated to high temperatures for welding. Copper chills are used to avoid distortion and weld sagging and to shorten the time the assembly has to remain in the vacuum chamber, thus limiting grain growth.

Weldability of tantalum alloys containing other refractory elements is somewhat lower than that of unalloyed titanium; however, successful welds have been made in alloys Ta-10W, T-111 (Ta-8.0W-2.5Hf-0.003C), and T-222 (Ta-9.64W-2.4Hf-0.01C). Because of high vapor pressure, alloys containing vanadium are better welded by the gas-tungsten arc process.

EBW of Aluminum Alloys

Single-pass, full-penetration welds with depth-to-width ratios of more than 20 to 1 have been made in 150 mm (6 in.) thick aluminum alloy plates. The low heat input, narrow HAZ, and short heat cycle result in minimum decrease in mechanical properties, especially in assemblies of some of the heat-treatable alloys.

Non-Heat-Treatable Alloys. The mechanical properties of electron-beam welds in the non-heat-treatable alloys (1*xxx*, 3*xxx*, and 5*xxx* series) are virtually the same as those obtained by GTAW. If the alloy is in a strain-hardened condition, the weld properties closely approach the annealed properties of the base metal.

Heat-treatable alloys of the 2*xxx*, 6*xxx*, and 7*xxx* series are crack sensitive to varying degrees when welded. Some may also be prone to porosity. The condition of the zone immediately adjacent to the weld is critical in determining weldability.

The effect on penetration of varying working distance (within practical operating limits and with other variables held constant) is shown in Fig. 32 for 6.4 mm ($\frac{1}{4}$ in.) thick aluminum alloy 2219. When maximum working distance was used, penetration was only about 80%, and maximum weld width was about one-third greater than with minimum working distance.

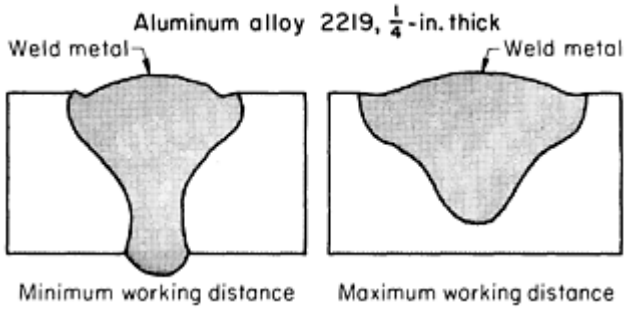

FIG. 32 VARIATION IN PENETRATION OF 6.5 MM ($\frac{1}{4}$ IN.) THICK 2219 ALUMINUM ALLOY AS A FUNCTION OF WORKING DISTANCE WHEN USING NONVACUUM EBW

Typical shapes of full-penetration welds made in 5.69 mm (0.224 in.) thick aluminum alloy 2219 by nonvacuum EBW (EBW-NV) and high-vacuum EBW (EWB-HV) and by GTAW are shown in Fig. 33.

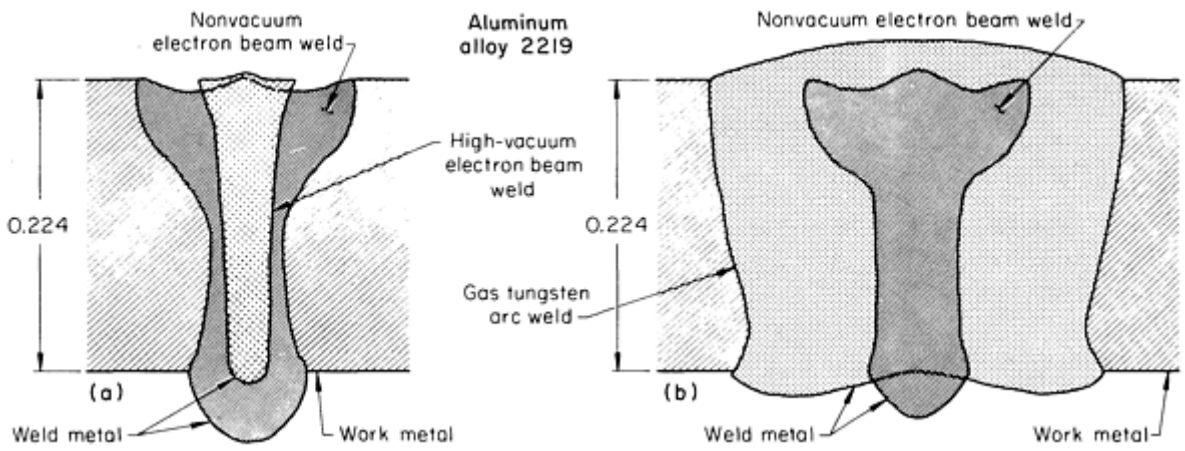

WELDING CONDITIONS	EBW-NV VERSUS EBW-HV		EBW-NV VERSUS GTAW	
	HIGH-VACUUM EBW	**NONVACUUM EBW**	**GTAW**	NONVACUUM EBW
VOLTAGE, KV	150	140	13V	**140**
CURRENT, MA	20	30	270A	**20**
WELDING SPEED, MM/MIN (IN./MIN)	2540 (100)	2540 (100)	510 (20)	**510 (50)**
WELDING ENERGY, KJ/MM (KJ/IN.)	**0.071 (1.8)**	**0.098 (2.5)**	**0.41 (10.5)**	**0.13 (3.36)**

FIG. 33 COMPARISON OF FULL-PENETRATION WELDS OBTAINED BY SELECTED WELDING PROCESSES TO JOIN 2219 ALUMINUM ALLOY. (A) EBW-NV VERSUS EBW-HV. (B) EBW-NV VERSUS GTAW

Comparing the nonvacuum and high-vacuum electron-beam welds in Fig. 33(a), heat input for the nonvacuum weld was about 40% greater, producing a midpoint weld width about 33% greater and a maximum crown width 160% greater than those of the high-vacuum weld. Comparing the nonvacuum electron-beam weld to the gas-tungsten arc weld in Fig. 33(b), heat input for the typical nonvacuum weld was 32% of that for the arc weld, producing a midpoint weld width about 25% and a maximum weld width about 56% of the corresponding widths for the arc weld. Compared to the arc weld, the widest weld produced by EBW-NV under workable operating conditions was about 42% as wide at midpoint and about 70% as wide at the crown.

Studies on welding 6.4 mm ($\frac{1}{4}$ in.) thick aluminum alloy 2219 showed average shrinkage of 0.08 to 0.13 mm (0.003 to 0.005 in.) for high-vacuum welds and shrinkage of 0.36 mm (0.014 in.) for high-heat-input nonvacuum welds, compared with a normal shrinkage of 0.76 mm (0.030 in.) for gas-tungsten arc welds.

The 6*xxx* series alloys are only slightly affected by the heat cycles of EBW. Alloys 2219, 7039, and 7005 appear to be the least affected alloys of their respective series. The techniques used to prevent cracking in EBW of the heat-treatable aluminum alloys are:

- SPECIAL CARE IN PREWELD CLEANING TO AVOID POROSITY AND OXIDE INCLUSIONS IN THE WELD METAL
- PRESTRESSING JOINTS IN COMPRESSION BY USING INTERFERENCE FITS WHEN POSSIBLE
- USE OF A DUCTILE FILLER METAL, USUALLY IN THE FORM OF A THIN STRIP PREPLACED IN THE JOINT, WHICH WILL YIELD UNDER SHRINKAGE STRESS AND FILL JOINT OPENINGS
- SELECTION OF BEAM POWER, BEAM SPOT SIZE, AND WELDING SPEED TO CREATE AS NARROW WELDS AS PRACTICAL DURING SHORT WELDING HEAT CYCLES, THUS AVOIDING EXCESSIVE GRAIN-BOUNDARY MELTING
- USE OF POSTWELD HEAT TREATMENT TO RESTORE THE STRENGTH AND DUCTILITY OF THE WELD AND HAZ
- DESIGNING OR LOCATING JOINTS TO BE FREE OF EXTERNALLY IMPOSED RESTRAINTS, REINFORCING JOINT AREAS, AND, WHEN POSSIBLE, WELDING IN THE SOLUTION-TREATED CONDITION, WITH POSTWELD AGING

Some aluminum alloy welded joints (for example, 38.1 ram, or 1.5 in., thick, welded 7075-T651 plate) exhibit lower mechanical properties than unwelded plate due to overaging in the HAZ. Postweld solution and aging heat treatments improve joint properties. At high travel speeds, porosity can develop in the weld from vaporization of certain elements,

such as zinc, in the alloy. Aluminum alloy 7075, which contains 5.6% Zn, is an example of this. Travel speed should be reduced in EBW of high-zinc aluminum alloys so that the vapor has time to escape to the surface before the weld metal solidifies. Zinc-free alloys (the 6*xxx* series alloys, for example) can be welded at higher speeds without the threat of porosity.

EBW of Copper and Copper Alloys

The EBW of copper and its alloys is influenced by the same factors that affect the arc welding of these metals (see the article "Welding of Copper Alloys" in this Volume). The high thermal conductivity of copper causes less difficulty in electron-beam welding than in arc welding.

Molten metal may be expelled from the weld joint during EBW of nondeoxidized coppers (especially alloy C11000, tough pitch copper), causing spatter and uneven weld surfaces. This can usually be remedied by the use of a cosmetic pass. The vacuum environment eliminates possible hydrogen embrittlement; nevertheless, root voids and porosity still can occur.

The presence of low-melting elements ordinarily makes the welding of free-machining copper alloys impractical, and the volatility of zinc prevents the welding of the brasses and other zinc-containing copper alloys. The remaining zinc-free copper alloys can generally be electron-beam welded without any unusual problems.

EBW of Magnesium Alloys

Electron-beam welding is used to a limited extent, chiefly for repair, on commercial wrought and cast magnesium alloys that contain less than 1% Zn. The relative suitability of alloys for EBW is generally the same as for arc welding, as discussed in the article "Welding of Magnesium Alloys" in this Volume.

Techniques. Special techniques and close control of operating variables are needed to prevent voids and porosity at the root of the weld, because of the high vapor pressure of magnesium, which has the lowest boiling point (1107 °C, or 2025 °F) of any commonly welded metal. This difficulty is aggravated by the presence of zinc, which has an even lower boiling point (906 °C, or 1663 °F). It is usually impractical to electron-beam weld magnesium alloys that contain more than 1% Zn.

Circular oscillation of the beam or the use of a slightly defocused beam is helpful in obtaining sound welds. The most satisfactory technique is to use integral or tightly fitted backing of the same alloy and to ensure that welding conditions are held to values that trial welds have shown will either minimize porosity and voids or localize them in an area where they can be tolerated or removed by machining.

EBW of Titanium Alloys

All of the commercial alloys of titanium that can be joined by arc welding can also be joined by EBW. Their relative weldability and response to heat cycling in EBW are generally the same as in arc welding, which is discussed in the article "Welding of Titanium Alloys" in this Volume.

Applicability. The vacuum environment of EBW prevents exposure to the atmospheric contaminants that cause embrittlement of titanium alloys, whereas arc welding processes must use elaborate and costly shielding methods to accomplish this. Cost studies show that direct labor costs for EBW of titanium sections more than 25 mm (1 in.) thick are less than for arc welding, provided a suitably large vacuum chamber is available.

Techniques. Filler metal is not ordinarily used, and the work is not preheated. Tack welding, contrary to experience in GTAW, presents no difficulties in EBW. For optimum results, welding is done in a high vacuum, but medium-vacuum welding is satisfactory for many applications.

Alloy Ti-6Al-4V, the alloy most frequently used in assemblies to be welded, can be electron-beam welded in either the annealed or the solution-treated-and-aged condition. For weldments that will be used at elevated temperatures, a preferred process sequence is anneal, weld, solution treat, and age. For other service conditions, a process sequence of solution treat, age, and weld gives almost the same strength properties and only slightly lower fracture toughness.

Procedure Development and Practice Considerations for Electron-Beam Welding

EBW of Beryllium

Beryllium is well suited for EBW. Narrow fusion zone and low heat input help control cracking. Also, the vacuum atmosphere controls toxic beryllium fumes and prevents oxidation. Weldability primarily is affected by the chemical composition of the metal. Beryllium oxide is the major contaminant in powder source material. Lower beryllium oxide content has been found to improve ductility, as well as weldability (Ref 3). Generally, the beryllium oxide content is limited to 1.5 wt% maximum. Lower aluminum content also is reported to improve weldability by decreasing crack susceptibility. The aluminum tends to produce a hot short condition. This hot short condition is reduced if the aluminum is tied up in a compound, such as $AlFeBe_4$, rather than existing as free aluminum in the grain boundaries (Ref 4).

Autogenous Welds. Cracking can be minimized in autogenous welds (no filler metal added) by reducing joint restraint during cooling. This is accomplished by appropriate fixturing, proper joint design, thin members, and good part fit-up. Most welding must be accomplished at sharp focus to minimize the size of the fusion zone. For deep welds, preheat has been found to improve weldability. For example, welds 1.3 mm (0.050 in.) thick have been made without preheat in low-oxide powder source beryllium (Ref 5). The same metal can be welded up to 2.5 mm (0.1 in.) thick with a preheat of approximately 345 °C (650 °F). In addition to cracking, high oxide levels can cause porosity and excessive cratering in the weld. Typical parameters for autogenous welds are given in Table 6.

TABLE 6 EFFECT OF PREHEAT ON THE WELDABILITY OF BERYLLIUM AND CONDITIONS FOR FULL-PENETRATION WELDS

THICKNESS		VOLTAGE, KV	CURRENT, MA	TRAVEL SPEED		PREHEAT TEMPERATURE TO PREVENT CRACKING	
MM	IN.			MM/MIN	IN./MIN	°C	°F
2.54	0.100	110	7.5	510	20	500	**500**
1.90	0.075	100	7.0	510	20	500	**500**
1.40	**0.055**	**90**	**5.0**	**510**	**20**	**120**	**250**

Braze Welds. The greatest success in EBW of beryllium is obtained by using a ductile filler metal in the weld; generally, aluminum is used. Optimum properties are obtained when the fusion-zone microstructure consists of beryllium dendrites surrounded by a ductile aluminum matrix. A fusion zone with less than 30% Al contains large beryllium dendrites which are susceptible to microcracking (Ref 4). Welds can be made with less than 30% Al in the fusion zone, but caution must be used.

Filler metal may be added by several methods. One method is to preplace aluminum shim stock in the joint. Care must be taken to ensure the shim stays in the joint during the weld. This may be accomplished by tack welding the joint prior to the penetration pass. By using a 0.51 mm (0.020 in.) thick by 2.54 mm (0.100 in.) deep 1100 aluminum shim, welds to 3.05 mm (0.120 in.) penetration have been made without preheat. A typical weld is shown in Fig. 34.

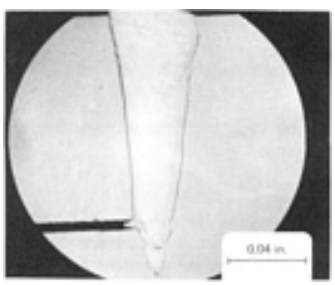

FIG. 34 ELECTRON-BEAM BRAZE WELD IN BERYLLIUM. COURTESY OF ROCKWELL INTERNATIONAL ENERGY SYSTEMS GROUP

An alternative method to brazing welds is to use an electron-beam cold wire-feed process similar to that used for stainless steel (Ref 6). In this process, a narrow, deep groove in the beryllium is filled with aluminum wire fed into the weld pool. A typical joint uses 718 aluminum wire, 0.76 mm (0.030 in.) in diameter, fed into a modified J-groove. The weld joint has a 0.64 mm (0.025 in.) root radius with a 10° 20' included angle. Welds to 2.54 mm (0.100 in.) have been successfully made this way (Fig. 35).

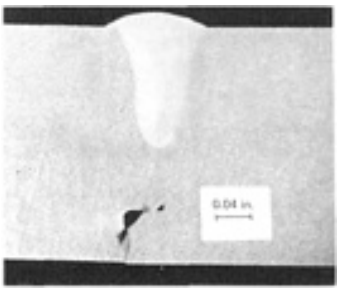

FIG. 35 ELECTRON-BEAM COLD WIRE-FEED WELD IN BERYLLIUM. COURTESY OF ROCKWELL INTERNATIONAL ENERGY SYSTEMS GROUP

References cited in this section

3. D. HAUSER, H.W. MISHLER, R.E. MONROE, AND D.C. MARTIN, *WELD. J.*, DEC 1967, P 525S-540S
4. C.R. HEIPLE AND R.D. DIXON, *WELD. MET. FABR.*, JUNE 1979, P 309-316
5. R.P. CAMPBELL, R.D. DIXON, AND A.L. LIBY, "ELECTRON BEAM FUSION WELDING OF BERYLLIUM," RFP-2621, ROCKWELL INTERNATIONAL, ROCKY FLATS PLANT, GOLDEN, CO, 1978
6. F.K. BENCH AND G.W. ELLISTON, *WELD. J.*, DEC 1974, P 763-766

Procedure Development and Practice Considerations for Electron-Beam Welding

References

1. A. SANDERSON AND K.R. NIGHTINGALE, *WELD. J.*, APRIL 1990, P 45
2. J.F. LOWRY, J.H. FINK, AND B.W. SCHUMACHER, A MAJOR ADVANCE IN HIGH-POWER ELECTRON BEAM WELDING IN AIR, *J. APPL. PHYS.*, VOL 47, 1976, P 95-106
3. D. HAUSER, H.W. MISHLER, R.E. MONROE, AND D.C. MARTIN, *WELD. J.*, DEC 1967, P 525S-540S
4. C.R. HEIPLE AND R.D. DIXON, *WELD. MET. FABR.*, JUNE 1979, P 309-316
5. R.P. CAMPBELL, R.D. DIXON, AND A.L. LIBY, "ELECTRON BEAM FUSION WELDING OF BERYLLIUM," RFP-2621, ROCKWELL INTERNATIONAL, ROCKY FLATS PLANT, GOLDEN, CO, 1978
6. F.K. BENCH AND G.W. ELLISTON, *WELD. J.*, DEC 1974, P 763-766

Procedure Development and Practice Considerations for Laser-Beam Welding

J. Mazumder, University of Illinois at Urbana-Champaign

Introduction

LASER-BEAM WELDING (LBW) is a joining process that produces coalescence of material with the heat obtained from the application of a concentrated coherent light beam impinging upon the surface to be welded. The principles of laser beams and the LBW process are discussed in the article "Laser-Beam Welding" in this Volume. In the present article, the steps that must be considered when selecting the LBW process will be described. Included will be a review of the individual process variables that influence procedure development of the process. In addition, joint design and special practices related to LBW will be discussed.

Procedure Development and Practice Considerations for Laser-Beam Welding

J. Mazumder, University of Illinois at Urbana-Champaign

Process Selection

Laser-beam welding is characterized by its low distortion and low specific energy input. It is an accurate inertialess method capable of high welding speeds for most materials, including many difficult-to-join materials. The process is often selected for high-volume, high-speed applications for joining materials/components that pose problems during arc welding, such as titanium alloys used for pacemakers. Often the selection criteria depends on economics, which is related to joining rate, welding speed, distortion, and postwelding treatment needs, among many other considerations. Another important consideration is whether the higher speeds can offset the higher initial capital costs within a reasonable time period. Low specific energy input is responsible for applications such as pace-makers because it reduces the possibility of thermal damage of the sophisticated electronics contained in such devices. Some manufacturers of cigarette lighters are now using LBW as an alternative to resistance welding because of the lower porosity in laser welds.

Economics combined with the smaller HAZ and higher overall weld toughness associated with LBW makes it a popular joining method for high-volume automotive applications. For example, multiple pieces of different compositions are joined by LBW to form blanks for automobile body components such as side-frame panels. These blanks need considerable weld toughness to withstand the stresses induced during subsequent press forming operations. Weld geometry is another consideration for the selection of the process. Since a smaller volume of material is melted due to the low specific energy input, weld defects such as undercuts are also minimized. This is especially important for applications involving dissimilar workpiece thicknesses, which have a higher probability of undercuts.

Another example where the narrow HAZ combined with high welding speed makes LBW a preferred method is the welding of planetary gears used in automobile powertrains. Planetary gear teeth are so closely spaced that it is difficult to access the weld joint without melting the neighboring gear teeth using conventional (arc) welding. This is one of the oldest LBW applications and it is routinely carried out worldwide.

Metallurgical considerations are sometimes responsible for the selection of the LBW process. The characteristic low specific energy input for this process results in a higher cooling rate. Higher cooling rates are often needed to suppress precipitation of harmful intermetallic compounds (which may promote brittle fracture) during the solidification of the weld pool. This is an important criteria for welding of many superalloys. For titanium alloys, high cooling rate limits the grain growth and oxidation during solidification, making it possible to weld titanium alloys outside a vacuum chamber with modest inert gas shielding. High cooling rates also help to avoid sensitization during welding of stainless steels. On the other hand, high cooling rates may cause problems in many ferrous alloys by promoting martensitic transformation and higher residual stresses; however, this is often balanced by the smaller size of the HAZ.

In many applications where resistance spot welding has been traditionally used, laser welding can offer many advantages, including single-side access and reductions in weight and costs by removing the tab* needed in resistance welding. Up to 60 kg (130 lb) of steel can be saved from an automobile by replacing resistance spot welding with laser welding and taking advantage of the design flexibility (Ref 1).

Another key factor in the successful implementation of laser welding is the selection of the right laser for a given application. Characteristics and parameters of commercial lasers available for welding are listed in Table 2 of the article

"Laser-Beam Welding" in this Volume. Carbon dioxide (CO_2) lasers with up to 25 kW power capacities and pulsed Nd:YAG lasers with up to 500 W peak power have been the workhorse for the industry until recently. The majority of the CO_2 laser applications involve lasers up to 5 kW. Recently, continuous Nd:YAG lasers with power capacities up to 2.5 kW have been made available.

In addition to welding speed and depth of penetration, which are the most important LBW attributes, the flexibility and precision of beam delivery are also important criteria for selecting LBW. Multiaxis workstations and robotics are already available in the market for CO_2 laser applications. However, one of the major advantages of the Nd:YAG laser is its capability to deliver the energy through a fiber. Unfortunately, no fibers are yet available for CO_2 lasers with a 10.6 μm wavelength. Most of the high-speed and deep-penetration welding are carried out with CO_2 lasers with power in excess of 1 kW. Continuous Nd:YAG lasers can outperform CO_2 lasers with the same power capacity, but they are limited by the maximum power of 2.5 kW. For reflective materials such as aluminum, Nd:YAG has better coupling, especially for conduction-mode welding, due to their shorter wavelength (1.06 μm). For deep-penetration welding, the coupling advantage is not significant.

Reference cited in this section

1. F.A. DIPIETRO, ROBOTIC LASER WELDING SYSTEMS IN THE AUTOMOTIVE INDUSTRY, *PROCEEDINGS OF LASER SYSTEMS APPLICATIONS IN INDUSTRY,* ATA, TORINO, ITALY, 1990, P 103-119

Note cited in this section

* *TABS CONSIST OF EXTRA MATERIAL PROVIDED DURING THE FABRICATION OF THE SQUARE FRAME IN RESISTANCE WELDING THAT ENABLE THE ELECTRODES TO PUSH THE EXCESS MATERIAL TOGETHER TO COMPLETE THE WELDING PROCESS. ADAPTING JOINT DESIGNS SUCH AS BUTT WELDS TO THE LASER WELDING PROCESS ELIMINATES THE NEED FOR TABS.

Procedure Development and Practice Considerations for Laser-Beam Welding

J. Mazumder, University of Illinois at Urbana-Champaign

Procedure Development

The key factor for procedure development is the selection of optimum independent and dependent process variables. The independent process variables for laser welding include incident laser-beam power, incident laser-beam diameter, traverse speed, absorptivity, shielding gas, depth of focus and focal position, and weld design and gap size. The important dependent variables are depth of penetration, microstructure and mechanical properties of laser-welded joints, and weld pool geometry. Detailed discussions of most of these variables are provided in Ref 2. They are discussed below in view of their role in procedure development.

Power density is defined as the incident power per unit area. In any welding process it is the power density that determines the depth of penetration and joining rate for the process, not the total power of the source. Therefore, beam diameter and spatial distribution of the laser-beam energy play an extremely important role because they determine the area of incidence. Two other variables affecting the ultimate power density driving the welding process are absorptivity and plasma-beam interaction, such as refraction. Position of focus with respect to the substrate and depth of focus of the beam also affects the power density and penetration depth.

Spatial distribution of the energy is generally constant for a given laser whereas absorptivity is a function of the substrate, its surface condition, and the laser-beam wavelength. Therefore, the most common practice for process development with a given laser and material is the selection of focusing optics for optimum power density and working distance by controlling the beam diameter. Thus, a working knowledge of the focusing optics is important for an engineer developing the laser welding process. Important formulae related to the laser as a welding tool will be summarized in following subsections dealing with process variables.

Interaction time is defined as the time a particular point on the substrate spends under the laser beam. In simple terms, it is the ratio of the beam diameter to the traverse speed. Strictly on the basis of heat transfer, one should account for the total time of heating and cooling at the point above the ambient temperature. This is, however, a much more difficult quantity to keep track of compared to the ratio of the traverse speed and beam diameter. Again, it is the interaction time which controls the weld pool profile, not the traverse speed alone. Laser welding procedure development involves the selection of optimum power density and interaction time after the selection of the laser.

Laser-Beam Power. As mentioned in the article "Laser-Beam Welding" in this Volume, laser-beam power is one of the primary variables in determining the penetration depth in laser welding. For process development, the first caution one should take is to calibrate the laser output power with the power delivered at the substrate. There is often a measurable loss due to the reflective and transmissive optics used to deliver the beam from the laser to the workpiece. For systems with fiber delivery, input coupling is often responsible for part of this loss. Fibers also scramble the spatial distribution resulting in poor focusing properties. Almost all commercial lasers are equipped with some kind of power-measuring device based either on a flowing-water calorimeter where the full beam is dumped, or a solid-state detector where a fraction of the laser energy is continuously deposited. Additional calorimetric devices should be maintained to measure power at the workpiece for periodic calibration of output power with the power delivered at the weld pool. For lasers with power in excess of a few hundred watts, water-cooled calorimeters are the most popular. For on-line monitoring many multi-kilowatt systems also use precalibrated solid-state detectors, usually behind one of the cavity mirrors which has a small leak around 1% or less. Several vendors offer both types of power meters. An excellent source of laser-beam device vendors is *Laser Focus World* buyer's guide, which is published annually (Ref 3).

In addition to the absolute power measurement, the beam mode (that is, the spatial distribution of energy) and beam diameter should be monitored since they also strongly affect the power density.

Laser-beam diameter is one of the most important variables since it determines the power density for a given total power (see the article "Laser-Beam Welding" for a more detailed discussion). The spatial distribution of energy in the beam affects the focusing characteristics of the beam. For a Gaussian beam, the diameter is defined as the $1/e^2$ of the central value (Fig. 1) and it contains almost 86% of the total power. The diffraction limited focal spot size, d_{min}, for such a Gaussian beam is given by the following relationship:

$$d_{mim} = \frac{1.27\, f\, l}{D} \qquad \textbf{(EQ 1)}$$

where D is unfocused beam diameter, f is the focal length of the focusing optics, and λ is the wavelength of the laser beam. This is an ideal situation and often the focused beam diameter will be larger due to aberrations and other imperfections in the focusing optics.

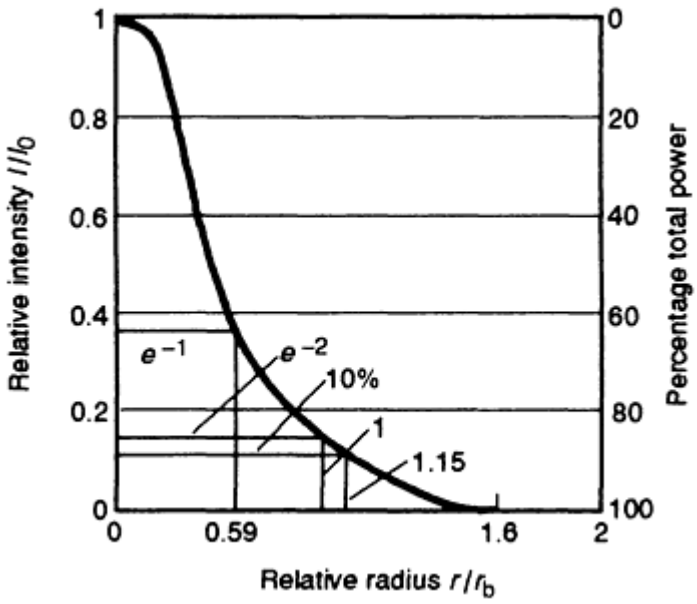

FIG. 1 VARIATION OF RELATIVE INTENSITY AND PERCENTAGE OF TOTAL POWER WITH RADIUS FOR A GAUSSIAN BEAM. SOURCE: REF 4

Diffraction limited spot size for various types of laser beam can be estimated using the relationships given in Eq 2, 3, 4. For a rectangular beam with a plane wave front:

$$d_{mim} = \frac{2 f l}{D} \qquad \textbf{(EQ 2)}$$

For a circular beam with a plane wave front:

$$d_{mim} = \frac{2.44 f l}{D} \qquad \textbf{(EQ 3)}$$

For a multimode beam (or a transverse electromagnetic mode (TEM_{mnq}) as described in the following subsection on laser-beam spatial distribution) with a plane wave front:

$$d_{mim} = \frac{2.44 f l}{D}(2m + n + 1) \qquad \textbf{(EQ 4)}$$

For example, if a 25 mm (1 in.) $TEM_{01}CO_2$ laser beam is focused by a 100 mm (4 in.) focal-length lens, the diffraction limited spot diameter is:

$$d_{mim} = \frac{2.44x100x10.6x10^{-3}}{25}(2.0 + 1 + 1) = 0.21mm$$

However, as indicated earlier, these are estimates for the theoretically possible minimum spot size. One of the more popular means for evaluation of beam quality is the recently developed "M^2 concept" (Ref 5), which is defined as:

$$M = \frac{\text{divergence of actual beam}}{\text{divergence of ideal gaussian Beam}} = \frac{q\,Actual}{q\,gaussian}$$

The correlated beam diameter based on the M^2 concept is:

$$d_{mim} = \frac{4M^2 f l}{p D} \qquad \textbf{(EQ 5)}$$

In this case, M has to be measured at two known locations in the beam propagation path. This reinforces to the point that a proper measurement technique for beam diameter is imperative for estimating the actual beam diameter and the power density.

There are several commercial systems now available for beam diameter measurement. Sasnet, *et al.* (Ref 5) describe one system which is specifically designed for beam evaluation based on the M^2 concept. This instrument is capable of measuring the beam width within 0.5 μm accuracy in two mutually perpendicular transverse directions. Knife edges are used to scan the beam and a set of lenses are traversed in the direction of the beam propagation to change the positions of the beam width. The measurement procedure and data acquisition and display are computer controlled.

Another commercial system is based on a hollow rotating needle which samples the beam. This is based on the research carried out by Loosen, *et al.* (Ref 6) and Lim and Steen (Ref 7) which resulted in the development of a laser-beam analysis system based on a rotating needle which reflects part of the beam to a set of detectors.

Although beam quality related to the ideal Gaussian beam is a good starting point, there is evidence that for high-power laser processing, this characterization may not be sufficient (Ref 8). Spatial coherence and temporal and local fluctuations are generally ignored, but they do affect the processing behavior. Many European research groups are working on characterizing the beam in terms of the mode coherence coefficient (MCC) which is based on a set of suitable modes and averaged intensity distribution and which takes into account the partial coherence properties of the beam.

Another complication of high-power laser welding is interaction with the plasma column. Rockstroh, *et al.* (Ref 9) found that free electrons in the plasma column cause absorption and refractions. For welding of aluminum with a CO_2 laser, as much as 30% of the energy is lost in the plasma and the refracted beam diameter is 8% larger. This measurement is based on the electron density measurement using emission spectroscopic technique. This observation is subsequently supported by similar measurements made by Lober, *et al.* (Ref 10, 11). Complete characterization of beam diameter will require both measurement at the focal spot before processing and monitoring of the beam refraction during the process using spectroscopic techniques.

Laser-Beam Spatial Distribution. Every laser resonator cavity, defined by the mirrors of the laser, has certain stable configurations of the electromagnetic field called "modes." A well-defined mode has a definite spatial distribution for the laser beam. As evident from Eq 4, the mode affects the focused beam diameter and leads to higher spot size for a given $f\lambda$ focusing optics. The general convention for indexing a mode is TEM_{mn} (transverse electromagnetic mode with *m* number of radial zero fields and *n* number of angular zero fields). TEM_{00} is the ideal Gaussian beam and will provide the smallest focused spot and highest power density. Most of the fast axial-flow lasers offer a TEM_{00} or TEM_{01} beam. Most of the transverse-flow lasers offer TEM_{01} (donut-shaped spatial distribution).

Intensity distribution for different modes can be calculated using the Hermite polynomial for rectangular coordinates and the LaGuerre polynomial for polar coordinates using the expressions for a TEM_{mn} mode beam given in Eq 6, 7, 8. For a rectangular coordinate:

$$\sqrt{\mathrm{I}_{mn}(x,y)} = \{H_m(\sqrt{2.x/R_b})H_n(\sqrt{2.y/R_b}).\exp[-(x^2+y^2)/R_b^2]^2\} \qquad \textbf{(EQ 6)}$$

For a polar coordinate:

$$\mathrm{I}_{mn}(r,q) = [L_m^n(2r^2/R_p^2)]^2(\sqrt{2.r/R_o})^{2n}.\exp[-2r^2/R_b^2]\cos^2 nq \qquad \textbf{(EQ 7)}$$

For a Gaussian beam with TEM_{00} mode:

$$1(\lambda) = \mathrm{EXP}(-2R^2/R_b^2) \qquad \textbf{(EQ 8)}$$

In Eq 6, 7, and 8, *x* is a variable, *r* is the radial position, 0 is the angular position of the beam, R_b is the beam radius at the $1/e^2$ point, H_m is the Hermite polynomial of order *m*, and L_m^n is the generalized LaGuerre polynomial.

A schematic of intensity distributions for different beam modes is shown in Fig. 2. For process development, the lowest-order mode available is the best choice for achieving the highest power density from a given power.

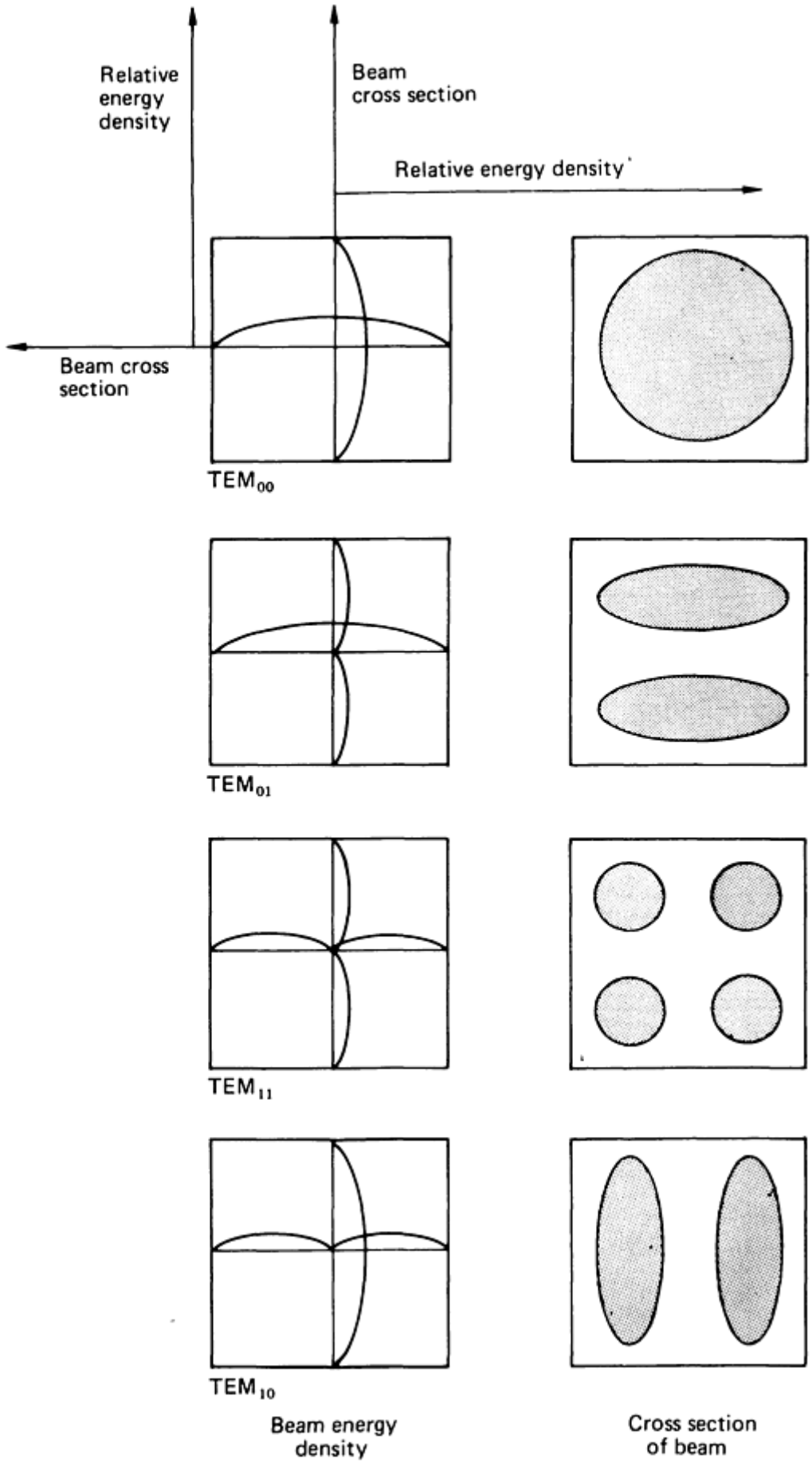
Relative energy density
Beam cross section
Relative energy density
Beam cross section
TEM00
TEM01
TEM11
TEM10
Beam energy density
Cross section of beam

FIG. 2 BEAM CROSS SECTIONS FOR FOUR DIFFERENT TEM MODES. SOURCE: REF 12

The position of focus with respect to the substrate surface influences the weld pool profile and penetration during laser welding. The optimum position for the focal point of the laser beam with respect to the substrate was investigated by Wilgoss, *et al.* (Ref 13). Figure 3 shows the transverse profiles generated by moving the focus point in 2.5 mm (0.1 in.) steps perpendicular to the plane of the workpiece. The reported plate thickness for this study was 6 mm (0.25 in.). When the focal point was positioned deep inside the workpiece, a V-shaped weld resulted necessitating more precise alignment than that for a parallel-sided weld of the same cross section. When the beam was focused well above the level of the workpiece surface, a large "nail head" with a consequent loss of penetration was observed.

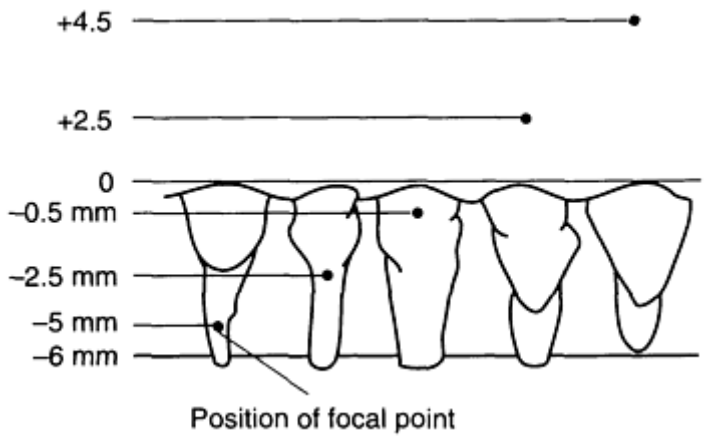

FIG. 3 TRANSVERSE PROFILES AS A FUNCTION OF FOCUS POSITION FOR A LASER-BEAM WELDED TYPE 310 STAINLESS STEEL. NEGATIVE AND POSITIVE NUMBERS INDICATE POSITION OF FOCAL POINT BELOW AND ABOVE, RESPECTIVELY, SURFACE OF PLATE. BEAM POWER, 5 KW. TRAVERSE WELDING SPEED, 16 MM/S (38 IN./MIN). SOURCE: REF 13

Wilgoss, *et al.* (Ref 13), concluded that the optimum focus is approximately 1 mm (0.04 in.) below the level of the workpiece surface. This produced welds with little or no "nail head" and nearly parallel sides.

Engel (Ref 14) reported that for several metals the optimum position of the focus is 1.25 mm to 2.5 mm (0.05 to 0.1 in.) below the surface. Research work by Alexander (Ref 15) using a 10 kW laser and 1.9 mm ($\frac{3}{4}$ in.) thick AISI 1020 steel revealed that the optimum position of focus was 2 mm (0.08 in.) below the surface. When the beam was focused 4 mm (0.16 in.) below the surface, the depth of penetration was almost the same as that for the 2 mm (0.08 in.) focus depth. The general consensus is that the optimum position for the focal point is below the surface, but the exact distance is dependent on the thickness of the workpiece and the laser power used.

Depth of focus is extremely important for welding thin-section materials because for a shallow depth of focus, the substrate comes in and out of the focal position due to thermal distortion. Depth of focus is defined as the distance over which the focus beam has the same approximate intensity. According to the Laser Institute of America, depth of focus is defined as the range over which the focused spot radius is increased by 5%. Based on this definition the depth of focus (Z) is given by:

$$Z = \pm \frac{0.32p\,R_b^{\,2}}{l} \approx \pm \frac{R_b^{\,2}}{l} = \frac{2.33(F\,l)^2}{l} = 1.488F^2\,l \qquad \textbf{(EQ 9)}$$

where F equals $f\lambda$ of the optics.

One can see from the above expression that as the *F* number of the focusing optics increases, depth of focus also increases. However, this is also accompanied by an increased beam diameter and decreased power density. As a result, these variables must be optimized for each particular application.

A common practice in determining the focal position and depth of focus is to carry out a trial bead-on-plate weld on an inclined plate and use the position where the plasma seems to be the visually strongest. This is a quick, but not necessarily the most accurate approach, for establishing the focal position.

Absorptivity. The importance of absorptivity and its role in laser welding is discussed in the aforementioned article "Laser-Beam Welding." For deep-penetration welding with power densities exceeding 10^6 W/cm^2, keyhole formation leads to high absorption by trapping the beam inside the hole by total internal reflection. However, the absorption during the initial transient period is dependent on wavelength and surface conditions. There are several techniques to enhance the initial absorption (Ref 16). They include nonmetallic absorbing coatings, preheating, surface roughening, periodic surface structure or induced grating structure**, and the application of an electric field of the correct sign.

Traverse Speed. The role of traverse speed during laser welding is also discussed in the article "Laser-Beam Welding." Generally, welding speed increases with increasing laser power as shown in Fig. 4. For a given thickness and power, a range of speed can be used to make successful welds. However, the fusion zone size will increase with the decreased speed within that range. For process development, the nugget size or fusion zone size is often prescribed by the design engineer for strength considerations. The laser welding engineer needs to select an optimum combination of speed and power to deliver the required nugget size.

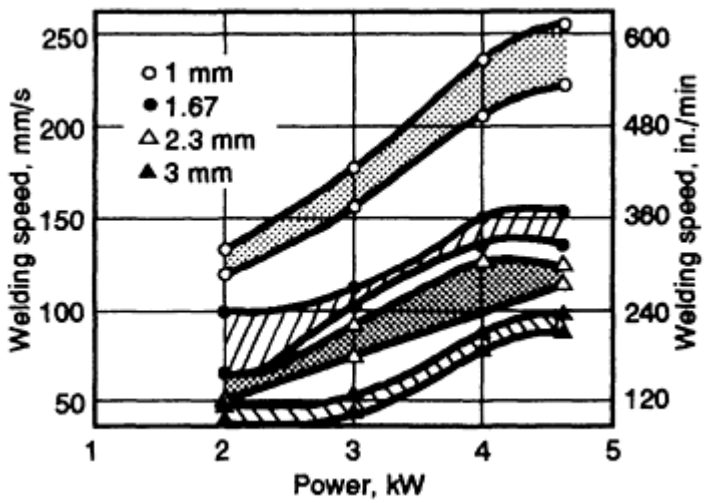

FIG. 4 WELDING SPEED VERSUS LASER POWER FOR A 5 KW CO_2 LASER. THE BASE METAL IS TI-6AL-4V. SOURCE: REF 17

Shielding Gas. The plasma produced during laser welding absorbs and scatters the laser beam. It is necessary, therefore, to remove or suppress plasma. The higher the power, the more clearly the phenomenon can be observed. An example of the way in which the depth of penetration decreases with the amount of beam absorption caused by plasma is shown in Fig. 5. Plasmas of this type can be removed by supplying a shielding gas such as helium. Shielding gas is also required to protect the weld surfaces from oxidation. Both the composition and flow rate of the shielding gas influence the depth of penetration (Ref 19, 20).

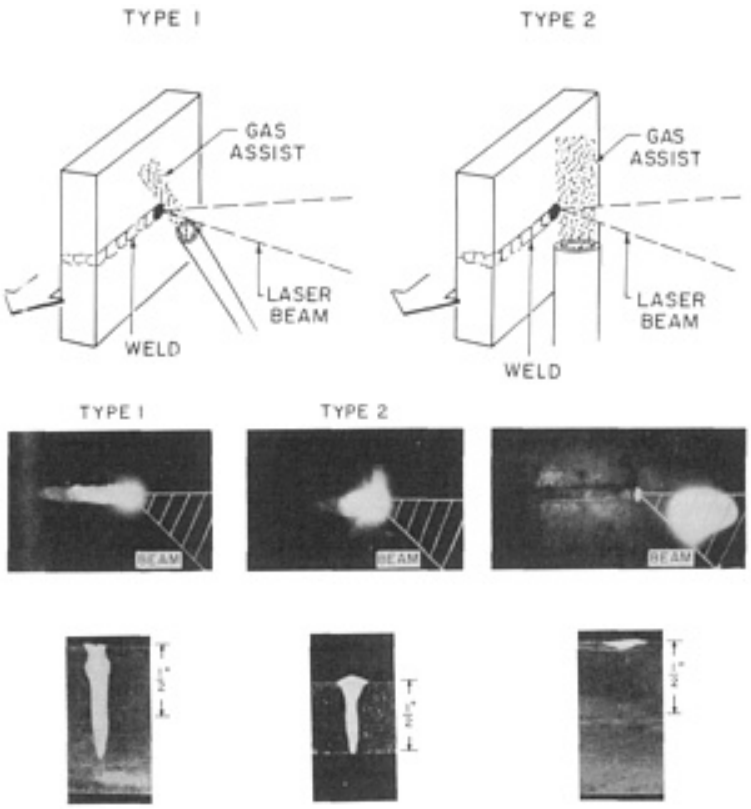

FIG. 5 EFFECT OF GAS ASSIST ON THE CROSS SECTION OF THE WELD. SOURCE: REF 18

Seaman (Ref 19) studied the role of shielding gas in high-power continuous-wave CO_2 laser welding. Weld cross sections made with various shielding gases and gas mixtures show a 60% difference in penetration. However, gases that permit the greatest penetration do not necessarily blanket (displace air from above the weld rapidly) the weld effectively at characteristically high laser welding speeds. This means that compromises are necessary to permit sound, deep-penetration laser welds (Ref 19).

The effect of the composition of the shielding gas on depth of penetration was studied by Seaman (Ref 19) and Rein, *et al.* (Ref 20). Generally, helium is used as the shielding gas for high-power laser welding. As shown in Fig. 6, helium seems to improve beam transmission whereas argon can cause severe beam blockage (Ref 19). This is probably due to the lower ionization potential of argon (15 eV) compared to that of helium (25 eV). The effects of air and CO_2 on beam transmission lie between the extremes represented by argon and helium (Fig. 7). Rein, *et al.* (Ref 20) have shown that the addition of small quantities of hydrogen, sulfur hexafluoride, and CO_2 to the helium enhances penetration at welding speeds below 40 mm/s (95 in./min).

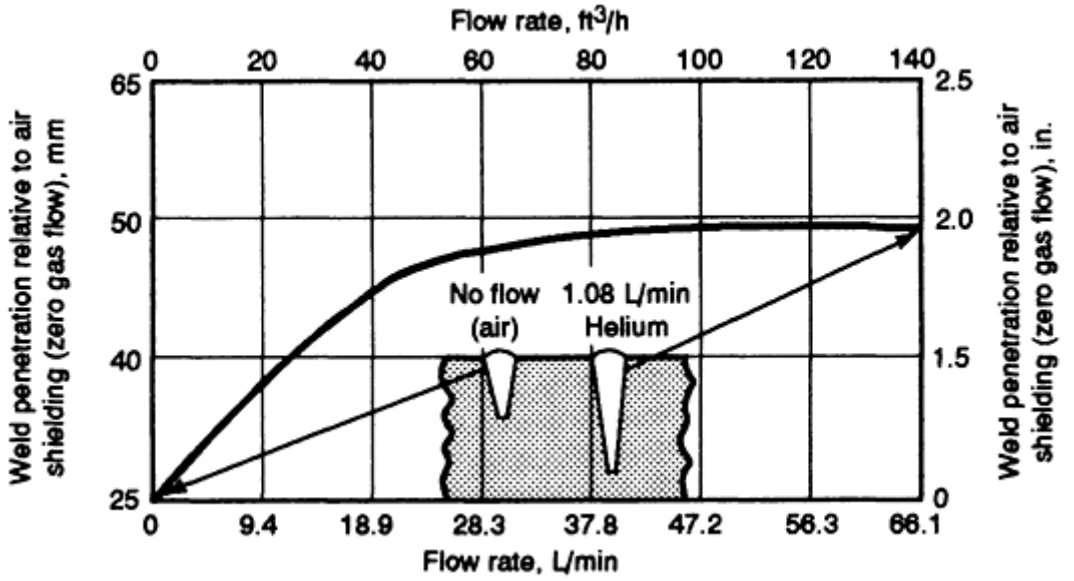

FIG. 6 EFFECT OF SHIELDING GAS ON DEPTH OF PENETRATION DURING LBW OF AN AUSTENITIC STAINLESS STEEL. LASER POWER, 15 KW. TRAVEL SPEED, 25 MM/S (60 IN./MIN). SOURCE: REF 19

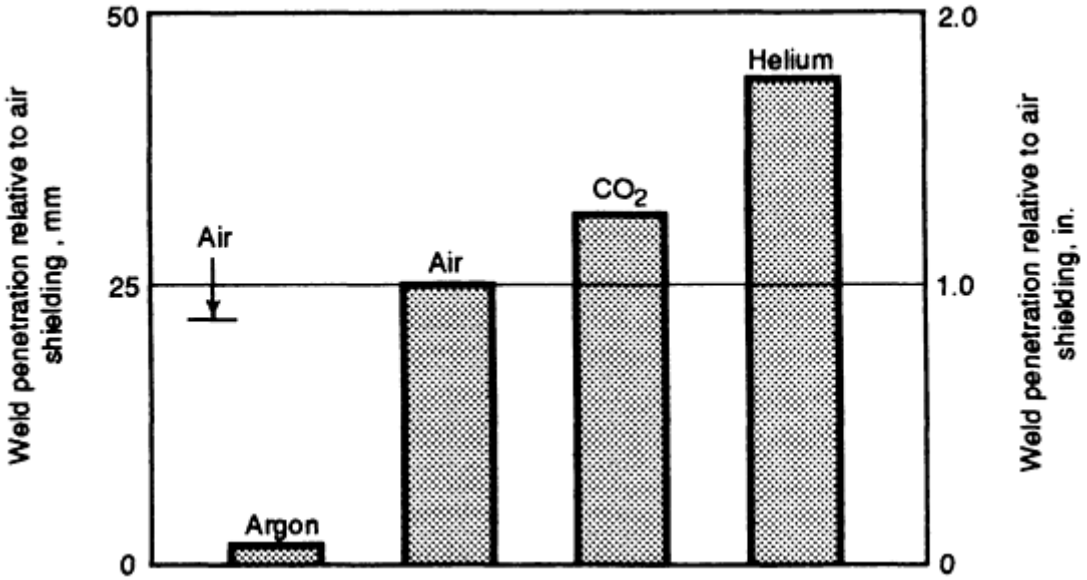

FIG. 7 COMPARISON OF LASER WELD PENETRATION ACHIEVED WITH DIFFERENT SHIELDING GASES. SOURCE: REF 9

The ionization potential of the shielding gas is not the only consideration for laser welding, especially at higher speeds. This is because gases with higher ionization potentials have lower atomic numbers and lower masses. These lighter gases are less effective in displacing air from the laser/material interaction area in the short time available in high-speed welding. Heavier gases are better able to displace air in a short time. Therefore, a mixture of heavier and lighter gases will result in optimum penetration. Figure 8 shows that as speed increases, the improvement resulting from the addition of a small amount of argon to helium (10% Ar and 90% He) becomes more noticeable.

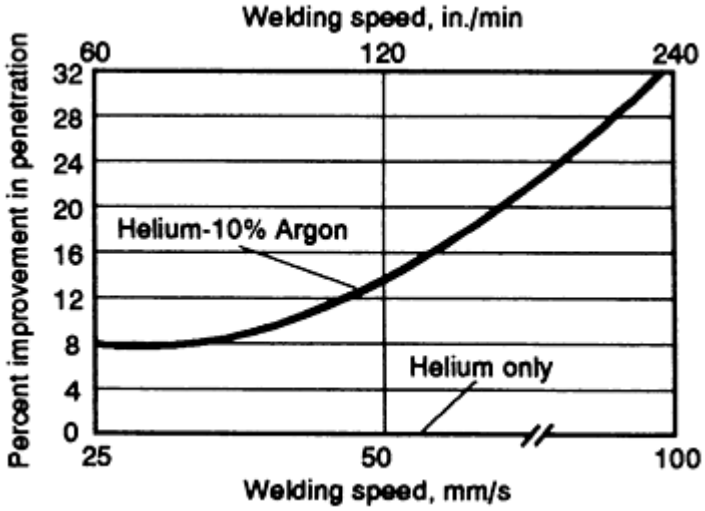

FIG. 8 IMPROVEMENTS IN WELD PENETRATION RESULTING FROM THE BLANKETING EFFECT OF A 10% ARGON ADDITION TO A HELIUM SHIELDING GAS. SOURCE: REF 19

For mass-scale production, the cost of shielding gas is also an important consideration. Recently, Chrysler Corporation replaced helium with CO_2 for plasma suppression during laser welding (Ref 21). The shielding gas is delivered from the side at an angle to suppress the plasma and remove metal vapor from the interaction point. For 14 kW laser power, a welding speed of 20 m/min (65 ft/min), and a shielding gas flow rate of 40 L/min (85 ft^3/h), CO_2 shielding resulted in a wider weld nugget size but mechanical properties were acceptable. The cost for helium gas is estimated to be $403,000 (3 shifts/day, 7 days a week) for a year compared to $80,600 for CO_2 gas; therefore, for process development, there is room for optimization of gas selection. However, one should remember that the use of CO_2 gas for a CO_2 laser may cause problems for the concentric gas shield due to preferential absorption.

Proper implementation of a shielding gas for plasma suppression can also be applied for joining difficult-to-weld materials with volatile alloying elements such as aluminum alloy 5083. Blake and Mazumder (Ref 22) demonstrated that with a properly designed helium suppression jet, magnesium losses and porosity formation could be minimized during laser welding of 5083 aluminum alloy. The resulting weld had a tensile strength equal to its parent material. This demonstrates that for process development, shielding gas can also be used to control the chemistry and weld defects.

References cited in this section

2. J. MAZUMDER, LASER WELDING, *LASER MATERIALS PROCESSING*, M. BASS, ED., NORTH HOLLAND, AMSTERDAM, 1983, P 113-200
3. *LASER FOCUS WORLD*, PENNWELL PUBLISHING COMPANY, TULSA, OK, 1993
4. J.E. HARRY, *INDUSTRIAL APPLICATION OF LASERS*, MCGRAW-HILL, UNITED KINGDOM, 1974
5. M.W. SASNETT AND T.F. JOHNSON, JR., LASER BEAM DIAGNOSTICS, *SPIE*, VOL 1414, 1991, P 21-32
6. P. LOOSEN, A. DRENKER, G. HERZIGER, R. KRAMER, AND U. STURM, DIAGNOSTICS OF HIGH POWER LASER BEAMS, *SPIE PROC.*, VOL 1024, 1988
7. G.C. LIM AND W.M. STEEN, *J. PHYS. E SCI. INSTRUM.*, VOL 17, 1984, P 999-1007
8. G. HERZIGER, LASER PROCESSING RESEARCH IN EUROPE, *LAMP '92*, A. MATSUNAWA AND S. KATAYAMA, ED., JAPAN HIGH TEMPERATURE SOCIETY, 1992, P 23-28
9. T. ROCKSTROH AND J. MAZUMDER, *J. APPL. PHYS.*, VOL 61 (NO. 3), 1987, P 917-923
10. R. LOBER, "SPECTROSCOPIC DIAGNOSTIC OF ARGON-ALUMINUM PLASMA DURING LASER-METAL INTERACTION," M.S. THESIS, UNIVERSITY OF ILLINOIS, 1989

11. R. LOBER AND J. MAZUMDER, SUBMITTED TO *J. APPL. PHYS.*, 1993
12. E.A. METZBOWER *ET AL.*, LASER BEAM WELDING, VOL 6, 9TH ED., *METALS HANDBOOK*, AMERICAN SOCIETY FOR METALS, 1984, P 647-671
13. R.A. WILGOSS, J.H.P.C. MEGAW, AND J.N. CLARK, *WELD. MET. FAB.*, MARCH 1979, P117
14. S.L. ENGEL, *LASER FOCUS*, FEB 1976, P 44
15. J. ALEXANDER, "PENETRATION STUDIES IN LASER AND ARC AUGMENTED LASER WELDING," PH.D. THESIS, LONDON UNIVERSITY, 1982
16. W.W. DULEY, "LASER SURFACE TREATMENT OF METALS," C.W. DRAPER AND P. MAZZOLDI, ED., NATO ASI SERIES E, NO. 115, MARTINUS NIJHOFT PUBLISHERS, THE NETHERLANDS, 1986
17. J. MAZUMDER AND W.M. STEEN, *MET. CONSTR.*, VOL 12 (NO. 9), 1980, P 423
18. E.V. LOCK, E. HOAG, AND R. HELLA, *WELD J.*, VOL 51, 1972, P 2455
19. F. SEAMAN, "ROLE OF SHIELDING GAS IN LASER WELDING," TECHNICAL PAPER NO. MR77-982, SOCIETY OF MANUFACTURING ENGINEERS, DEARBORN, MICHIGAN, 1977
20. R.M. REIN, *ET AL.*, PATENT 1448740, UNITED KINGDOM, 1972
21. M. OGLE, AUTOMOTIVE LASER APPLICATION WORKSHOP '93, INDUSTRIAL DEVELOPMENT DIVISION OF UNIVERSITY OF MICHIGAN, ANN ARBOR, MICHIGAN, 1993
22. A. BLAKE AND J. MAZUMDER, *ASME J. ENG. IND.*, VOL 107 (NO. 3), 1985, P 275-280

Note cited in this section

** *OPTICAL GRATINGS HAVE PERIODIC PEAKS AND VALLEYS, AND THEIR SPACING DETERMINES THE PREFERENTIAL ABSORPTION OF A CERTAIN WAVELENGTH OF LASER LIGHT. SIMILAR SURFACE PERIODIC STRUCTURE CAN BE USED TO ENHANCE ABSORPTION OF THE WAVELENGTH OF INTEREST.

Procedure Development and Practice Considerations for Laser-Beam Welding

J. Mazumder, University of Illinois at Urbana-Champaign

Joint Preparation, Fit-up, and Weld Design

Most weld joint geometries used in conventional fusion welding processes (for example, autogenous automatic gas-tungsten arc welding or electron-beam welding) are suitable for LBW. However, it must be remembered that the laser beam is focused to a spot of a few hundred micrometers in diameter and thus fit-up tolerances and alignment requirements are also of that order of magnitude.

Different types of joint design reported for laser-beam welding were reviewed by Shewell (Ref 23). Some of the important joint geometries are illustrated in Fig. 9 and 10.

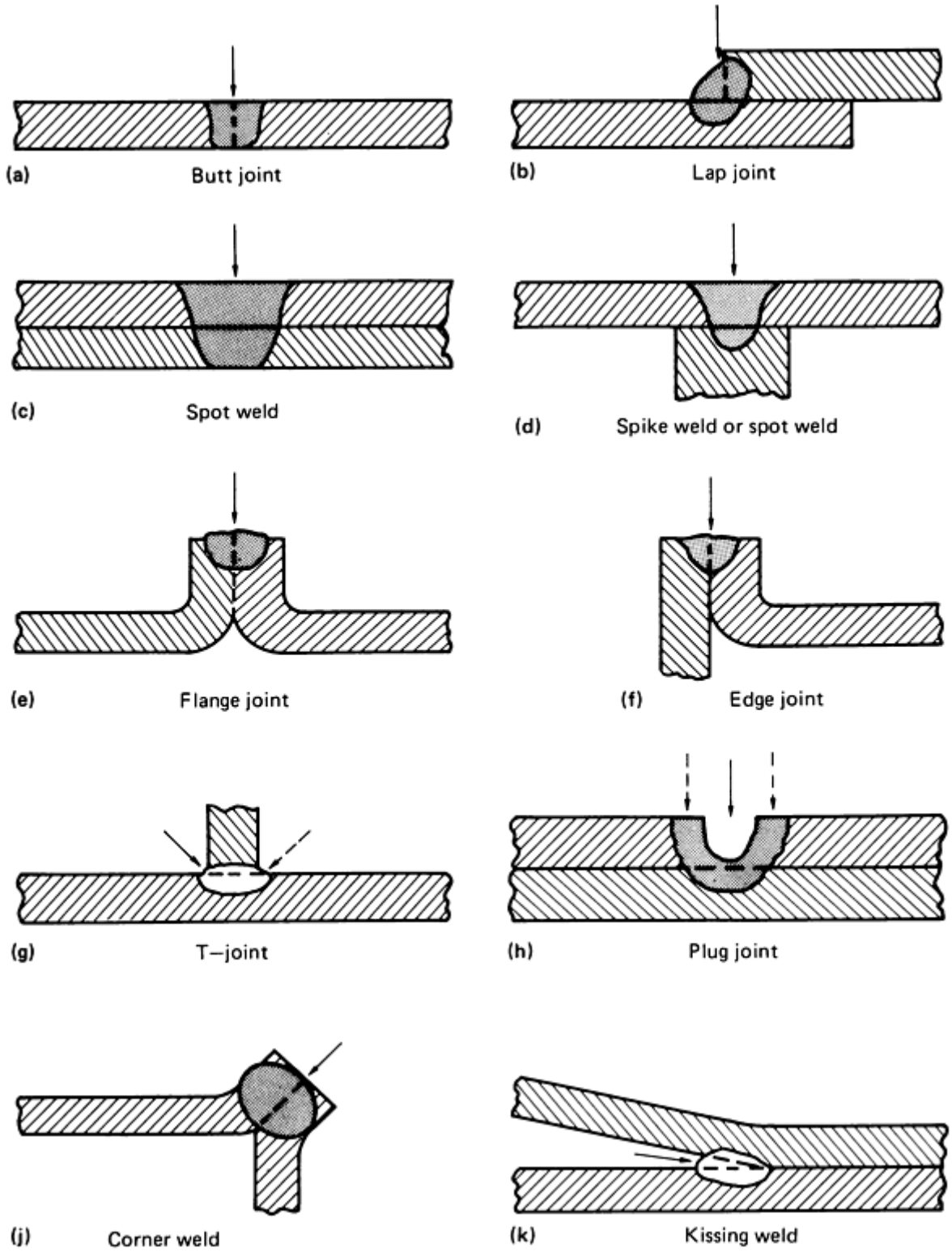

FIG. 9 JOINT DESIGNS FOR LASER-BEAM WELDS ON SHEET METAL. ARROWS SHOW DIRECTION OF LASER BEAM. SOURCE: REF 23

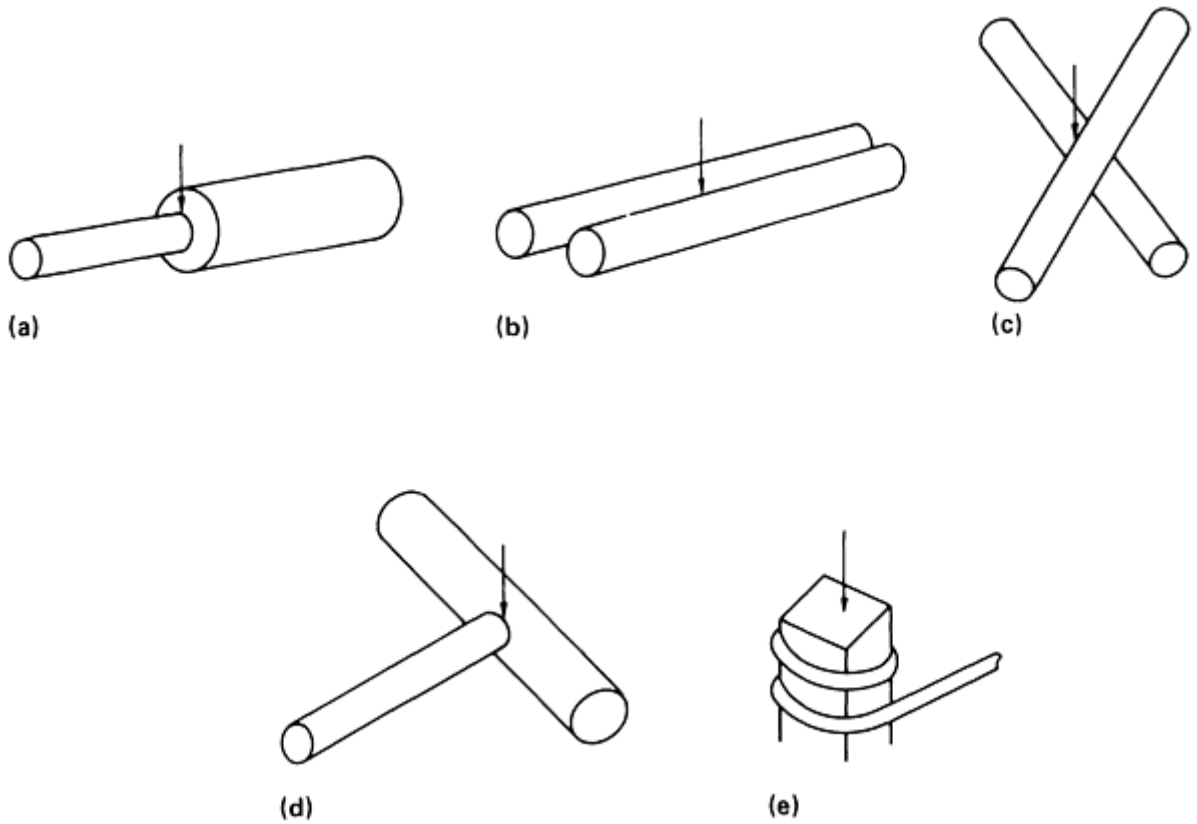

FIG. 10 JOINT DESIGNS FOR LASER-BEAM WELDS ON WIRE. ARROWS SHOW DIRECTION OF LASER BEAM. (A) BUTT WELD. (B) ROUND-TO-ROUND LAP WELD. (C) CROSS-JOINT WELD. (D) SPOT WELD FOR T-JOINT. (E) TERMINAL OR LUG WELD

Butt Joint--Full-Penetration Type. Material to be laser welded does not need beveled edges. Sheared edges are acceptable if square and straight (Ref 24, 25). The fit-up tolerance should be within 15% of the workpiece thickness. Misalignment and out-of-flatness should be less than 25% of material thickness, as shown in Fig. 11(a), to keep the laser beam from wandering. The transverse alignment should be kept within half of the focused beam diameter (Ref 17, 26). Clamping is recommended and buckling is not troublesome except when welding material thinner than 0.25 mm (0.01 in.) (Ref 24).

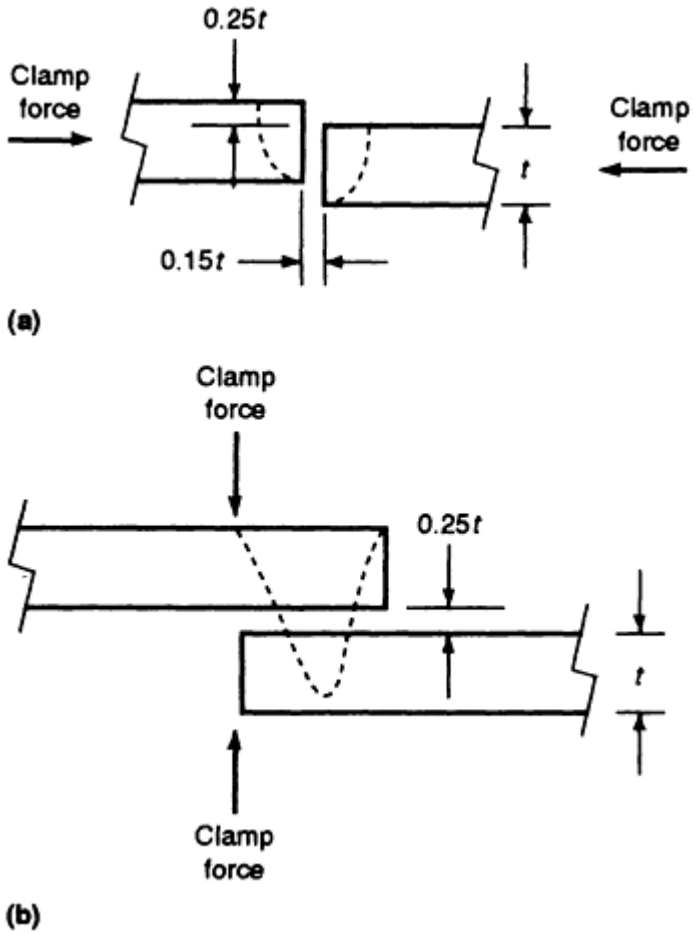

FIG. 11 CLAMPING AND TOLERANCES FOR A BUTT JOINT (A) AND A LAP JOINT (B). DIMENSIONS ARE IN UNITS OF PERCENT OF MATERIAL THICKNESS *T.* SOURCE: REF 25

Lap Joints. Air gaps severely limit penetration and welding speeds (Ref 24). Compressive clamping, as shown in Fig. 11(b), should be used to maintain a separation of less than 25% of the material thickness (Ref 25). For welding of dissimilar thicknesses, the thinner material should be placed on top to be welded to the thicker one (Ref 25).

Pulsed laser spot lap joints demand tighter tolerances than joints produced with continuous power laser welding. The maximum gap for ferrous and nickel alloys is 15% of the material thickness, and the gap must be less for higher conductivity materials (Ref 23). Baranov, *et al.* (Ref 27) studied the influence of gap size on the formation and strength of spot lap joints in laser welding. They reported for laser spot lap joints of 0.4 mm (0.016 in.) thick steel and 0.33 mm (0.013 in.) thick nickel, a gap of up to 0.1 mm (0.004 in.) has little influence on joint strength as there is almost no change in the diameter of the fusion zone. On the other hand, the shape of the weld pool changes with the gap size. It has also been observed that the presence of air in the gap may lead to the formation of porosity and nonfusion (Ref 27). Micropores sometimes form in the fusion zone and the number of pores and their size increase with increasing gap size.

Flange joints, as with butt joints, require straight, square edges, good fit-up, clamping, and precise transverse alignment. Flange joints are suitable for welding high-shrinkage metals such as aluminum (Ref 24).

Kissing Welds. This type of joint is called a kissing weld because the weld pool forms where two pieces just "kiss." This offers a small angle between the two parts that traps most of the energy of the laser beam. Very little (if any) pressure is required during welding, but the facing surfaces must fit well (Ref 23). A gap between the sheets will allow radiation to escape. This joint successfully joins thin foils in situations where spot welding would produce melt through.

Polarization Effect on Kissing Weld. One of the unique advantages of a kissing weld is the ability to take advantage of the polarization behavior of the laser light. If the laser light is polarized perpendicular to the wall of the metal, the beam is

preferentially reflected and it delivers all the energy at the joint. This increases the joint efficiency considerably. This idea was originally proposed by Sepold in 1987 (Ref 28). Subsequently, this concept is used for laser welding of pipes.

Wire Joints. The joint configurations for wires shown in Fig. 10 were developed by the electronics industry. For wire-to-wire joints, the two wires must share the incident laser energy. In a cross joint, for example, the laser beam should be directed at the intersection of the wires so that both wires are exposed directly to the beam.

References cited in this section

17. J. MAZUMDER AND W.M. STEEN, *MET. CONSTR.,* VOL 12 (NO. 9), 1980, P 423
23. J.R. SHEWELL, *WELD DES. FABR.,* JUNE 1977, P 106
24. S.L. ENGEL, *WELD DES. FABR.,* JAN 1978, P 62
25. M.M. SCHWARTZ, *METALLURGICAL JOINING MANUAL,* MCGRAW-HILL, 1979
26. J. MAZUMDER, "LASER WELDING OF TITANIUM AND TINPLATE," PH.D. THESIS, LONDON UNIVERSITY, 1978
27. M.S. BARANOV, B.A. VERSHOK, I.N. GEINRIKHS, AND V.I. PRIVEZENSTEV, *WELD. PROD.,* VOL 23 (NO. 5), 1976, P 19
28. G. SEPOLD, R. ROTHE, AND K. TESKE, *LAMP '87*, Y. ARATA, ED., JAPAN HIGH TEMPERATURE SOCIETY, 1987, P 151-156

Use of Consumables and Special Welding Practices

Laser welding is ideal for autogenous welding. The main consumable for laser welding is the shielding gas which was discussed earlier. For thick-section welding, a filler wire can be used to make multipass welds. Sometimes filler metals (or injected powders) are used during laser welding to control the weld bead geometry. The most common use of filler metals, however, is to prevent undercutting. The use of filler materials to control the weld chemistry is also common. For example, insertion of aluminum foil during butt welding of semikilled steel results in a porosity-free sound weld. Vaporization losses during laser welding of some alloys can be compensated for by the addition of filler materials or powder of desired composition. Energy consumption during LBW is lower with powder injection than with wire-fed filler metals. The wire surface reflects considerable amounts of energy and reduces the energy efficiency of the process.

As with arc welding processes, metallurgical considerations such as preweld and postweld heat treatments are also applicable to laser welding. The primary differences between LBW and other welding processes are the narrower HAZ associated with laser welds as well as the high cooling rates that result in higher localized residual stresses. These high cooling rates can be used beneficially for materials with brittle intermetallic phases. High cooling rate leads to extension of solid solubility and avoids brittle precipitates for many alloys.

Procedure Development and Practice Considerations for Laser-Beam Welding

J. Mazumder, University of Illinois at Urbana-Champaign

References

1. F.A. DIPIETRO, ROBOTIC LASER WELDING SYSTEMS IN THE AUTOMOTIVE INDUSTRY, *PROCEEDINGS OF LASER SYSTEMS APPLICATIONS IN INDUSTRY,* ATA, TORINO, ITALY, 1990, P

103-119

2. J. MAZUMDER, LASER WELDING, *LASER MATERIALS PROCESSING*, M. BASS, ED., NORTH HOLLAND, AMSTERDAM, 1983, P 113-200
3. *LASER FOCUS WORLD*, PENNWELL PUBLISHING COMPANY, TULSA, OK, 1993
4. J.E. HARRY, *INDUSTRIAL APPLICATION OF LASERS*, MCGRAW-HILL, UNITED KINGDOM, 1974
5. M.W. SASNETT AND T.F. JOHNSON, JR., LASER BEAM DIAGNOSTICS, *SPIE*, VOL 1414, 1991, P 21-32
6. P. LOOSEN, A. DRENKER, G. HERZIGER, R. KRAMER, AND U. STURM, DIAGNOSTICS OF HIGH POWER LASER BEAMS, *SPIE PROC.*, VOL 1024, 1988
7. G.C. LIM AND W.M. STEEN, *J. PHYS. E SCI. INSTRUM.*, VOL 17, 1984, P 999-1007
8. G. HERZIGER, LASER PROCESSING RESEARCH IN EUROPE, *LAMP '92*, A. MATSUNAWA AND S. KATAYAMA, ED., JAPAN HIGH TEMPERATURE SOCIETY, 1992, P 23-28
9. T. ROCKSTROH AND J. MAZUMDER, *J. APPL. PHYS.*, VOL 61 (NO. 3), 1987, P 917-923
10. R. LOBER, "SPECTROSCOPIC DIAGNOSTIC OF ARGON-ALUMINUM PLASMA DURING LASER-METAL INTERACTION," M.S. THESIS, UNIVERSITY OF ILLINOIS, 1989
11. R. LOBER AND J. MAZUMDER, SUBMITTED TO *J. APPL. PHYS.*, 1993
12. E.A. METZBOWER *ET AL.*, LASER BEAM WELDING, VOL 6, 9TH ED., *METALS HANDBOOK*, AMERICAN SOCIETY FOR METALS, 1984, P 647-671
13. R.A. WILGOSS, J.H.P.C. MEGAW, AND J.N. CLARK, *WELD. MET. FAB.*, MARCH 1979, P117
14. S.L. ENGEL, *LASER FOCUS*, FEB 1976, P 44
15. J. ALEXANDER, "PENETRATION STUDIES IN LASER AND ARC AUGMENTED LASER WELDING," PH.D. THESIS, LONDON UNIVERSITY, 1982
16. W.W. DULEY, "LASER SURFACE TREATMENT OF METALS," C.W. DRAPER AND P. MAZZOLDI, ED., NATO ASI SERIES E, NO. 115, MARTINUS NIJHOFT PUBLISHERS, THE NETHERLANDS, 1986
17. J. MAZUMDER AND W.M. STEEN, *MET. CONSTR.*, VOL 12 (NO. 9), 1980, P 423
18. E.V. LOCK, E. HOAG, AND R. HELLA, *WELD J.*, VOL 51, 1972, P 2455
19. F. SEAMAN, "ROLE OF SHIELDING GAS IN LASER WELDING," TECHNICAL PAPER NO. MR77-982, SOCIETY OF MANUFACTURING ENGINEERS, DEARBORN, MICHIGAN, 1977
20. R.M. REIN, *ET AL.*, PATENT 1448740, UNITED KINGDOM, 1972
21. M. OGLE, AUTOMOTIVE LASER APPLICATION WORKSHOP '93, INDUSTRIAL DEVELOPMENT DIVISION OF UNIVERSITY OF MICHIGAN, ANN ARBOR, MICHIGAN, 1993
22. A. BLAKE AND J. MAZUMDER, *ASME J. ENG. IND.*, VOL 107 (NO. 3), 1985, P 275-280
23. J.R. SHEWELL, *WELD DES. FABR.*, JUNE 1977, P 106
24. S.L. ENGEL, *WELD DES. FABR.*, JAN 1978, P 62
25. M.M. SCHWARTZ, *METALLURGICAL JOINING MANUAL*, MCGRAW-HILL, 1979
26. J. MAZUMDER, "LASER WELDING OF TITANIUM AND TINPLATE," PH.D. THESIS, LONDON UNIVERSITY, 1978
27. M.S. BARANOV, B.A. VERSHOK, I.N. GEINRIKHS, AND V.I. PRIVEZENSTEV, *WELD. PROD.*, VOL 23 (NO. 5), 1976, P 19
28. G. SEPOLD, R. ROTHE, AND K. TESKE, *LAMP '87*, Y. ARATA, ED., JAPAN HIGH TEMPERATURE SOCIETY, 1987, P 151-156

Procedure Development and Practice Considerations for Diffusion Welding

S.B. Dunkerton, The Welding Institute

Introduction

THE JOINING OF MATERIALS IN THE SOLID STATE can be an attractive alternative to fusion-welding processes. In fact, metals that are conventionally difficult to weld and combinations of dissimilar materials can only be welded using a solid-state process. The wide range of techniques that are available for solid-phase joining have various modes of heat and pressure application.

Diffusion welding represents one extreme within this range, in that it involves minimal pressurization, but relatively high temperatures and long periods of time. In its simplest form, the process involves holding premachined and cleaned parts in intimate contact, and then heating them in a protective atmosphere. As its name implies, diffusion has a major role in the joining of mating parts, although other mechanisms, such as microyielding and oxide dissolution, are also critical steps in successful welding.

The process of diffusion welding has been utilized for many years, although it did not attain industrial acceptance until the 1970s or 1980s, and then, only for specialized applications. A comprehensive, although somewhat dated, review of systems that have been successfully joined using diffusion welding is provided in Ref 1.

The specific advantages of the process include its ability to join most metals and some nonmetals in like or dissimilar combinations, the minimal amount of deformation that results, and the fact that the weld area is mostly independent of welding time. These advantages are offset by the need to machine paris to fairly tight tolerances on component fit-up, as well as on surface finish. However, the requirements that are generally specified can readily be achieved using standard machine shop practices.

Reference

1. W.A. OWCZARSKI AND D.F. PAULONIS, APPLICATION OF DIFFUSION WELDING IN THE USA, *WELD. J.*, FEB 1981, P 22-33

Procedure Development and Practice Considerations for Diffusion Welding

S.B. Dunkerton, The Welding Institute

Process Variants

Solid-Phase Process. The more-conventional form of diffusion welding utilizes uniaxial loading, which can be applied by dead weight, mechanical, pneumatic, or hydraulic means. The applied load is such that macrodeformation of the parent material(s) does not have to be reached. Because deformation also depends on welding temperature, temperatures that range from 50 to 75% of the melting point are usually employed. Heat can be applied by radiant, induction, and either direct or indirect resistance heating. Most welding operations are performed in vacuum or inert gas atmospheres, although welding in air has been reported (Ref 2). When welding noble metals, the requirements for a clean atmosphere are less stringent, but protection can prevent parent-metal oxidation while maintaining a clean weld interface.

An examination of the proposed sequence of stages in diffusion welding (Ref 3, 4) emphasizes the importance of the original surface finish. In forming a bond, it is necessary for the two metal surfaces to come into atomic contact (Fig. 1). Hence, microasperities and surface contaminants must be removed from the bonding faces. The applied load first causes the plastic deformation of surface asperities, thereby reducing interfacial voids. Bond development then continues by diffusion-controlled mechanisms, including grain-boundary diffusion and power-law creep.

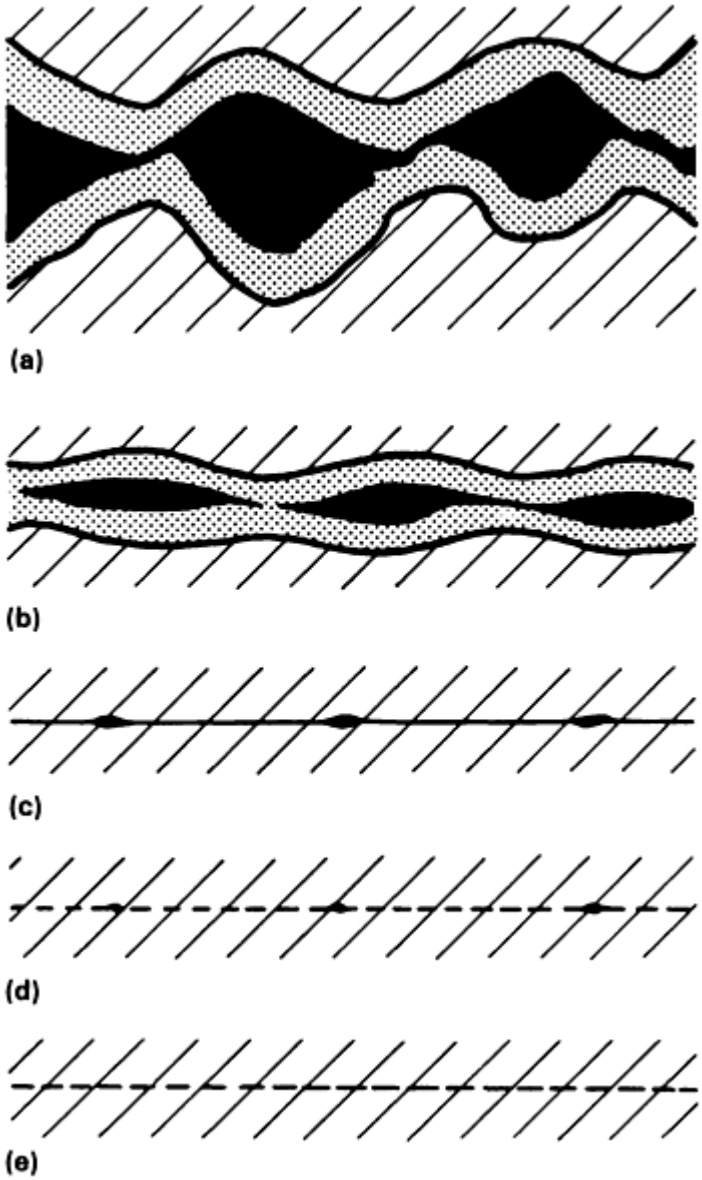

FIG. 1 MECHANISM OF DIFFUSION WELDING. (A) INITIAL "POINT" CONTACT AND OXIDE CONTAMINANT LAYER. (B) AFTER SOME "POINT" YIELDING AND CREEP, A THINNER OXIDE LAYER WITH LARGE VOIDS RESULTS. (C) AFTER FINAL YIELDING AND CREEP, SOME VOIDS REMAIN WITH VERY THIN OXIDE LAYER. (D) CONTINUED VACANCY DIFFUSION ELIMINATES OXIDE LAYER AND LEAVES FEW SMALL VOIDS. (E) COMPLETION OF BONDING

Premachined parts for uniaxial diffusion welding should have a surface finish of greater than 0.4 μm (16 μin.), roughness average (RA). Swabbing with acetone or petroleum ether, which should occur immediately prior to set-up in the welding machine, can suffice as a degreasing measure. Ultrasonic cleaning also has been used. Many researchers have examined the removal of oxide, prior to welding, by ion bombardment or other means. This can be applicable to certain metals if welding is to be carried out in the same vacuum chamber, or if the parts are in-vacuo coated with an oxide-resistant material. However, the additional cost and time involved in this procedure make it impractical for most industrial applications.

The liquid-phase process is applicable only to dissimilar material combinations or to like materials in situations where a dissimilar metal insert is used. Solid-state diffusional processes lead to the formation of a different phase at the weld interface. The liquid-phase welding temperature is based on the temperature at which this phase (usually, eutectic) melts. This thin layer of liquid spreads along the interface to form a joint at a lower temperature than the melting point of either of the parent metals. A reduction in welding temperature leads to the solidification of the melt. At the point where this phase is diffused into the parent metals, by holding at temperature, the process is known as transient liquid-phase

diffusion welding. The optimal welding time and temperature can be estimated using the applicable phase diagram and solidification kinetics (Ref 5).

The superplastic forming/diffusion welding (SPF/DW) technique has been developed specifically within the aerospace industry. Its industrial importance is such that it is worthy of separate consideration. The process is used commercially for titanium and its alloys, specifically those that exhibit superplastic properties at elevated temperatures within defined strain-rate conditions (Ref 6, 7, 8). This process also has been successfully utilized for advanced aluminum alloys (Ref 9). Because the temperature and pressure conditions coincide with the conditions required for welding, the two processes have been combined into one manufacturing operation.

Hot Isostatic Pressing (HIP). HIP welding is a solid-phase process that involves the application of a high-temperature, high-pressure gas to components. Isostatic pressurization allows the welding of more-complex geometries than the uniaxial welding process can handle.

A hot isostatic press consists of a furnace within a gas pressure vessel. Its size can range from a diameter of 100 mm (4 in.) to a diameter of 1.1 m (44 in.) and a height of 2.2 m (88 in.). Argon gas is typically used, and there is a need to encapsulate the bond interfaces to prevent the gas from entering the site of the bond. This is most often achieved by locating the specimen in an evacuated and sealed steel can, although various other means can be used, as well.

The pressures associated with HIP welding are significantly higher than those used in uniaxial welding. However, because the pressure is isostatic, the level of deformation is extremely low. In addition, less premachining is required. Typical HIP cycles can last from 6 to 16 h, but because many components can be fitted into one furnace, the unit costs on large production runs can be low. Bryant (Ref 10) has developed a graphical procedure to determine the minimum pressure and temperature required for the HIP welding of several metals and alloys.

References cited in this section

2. O.S. SPANSWICK, DIFFUSION BONDING--A CASE STUDY, REPRINT R269/10/B4, *WELD. INST. RES. BULL.*, THE WELDING INSTITUTE, 1984
3. B. DERBY AND E.R. WALLACH, THEORETICAL MODEL FOR DIFFUSION BONDING, *MET. SCI.*, VOL 16, JAN 1982, P 49-56
4. B. DERBY AND E.R. WALLACH, DIFFUSION BONDING: DEVELOPMENT OF THEORETICAL MODEL, *MET. SCI.*, VOL 18, SEPT 1984, P 427-431
5. I. TUAH-POKU, M. DOLLAR, AND T.B. MASSALSKI, A STUDY OF THE TRANSIENT LIQUID PHASE BONDING PROCESS APPLIED TO AG/CU/AG SANDWICH JOINT, *METALL. TRANS. A*, VOL 19, MARCH 1988, P 675-686
6. J. PILLING, THE KINETICS OF ISOSTATIC DIFFUSION BONDING IN SUPERPLASTIC MATERIALS, *MATER. SCI. ENG.*, VOL 100, 1988, P 137-144
7. J. PILLING, D.W. LIVESEY, J.B. HAWKYARD, AND N. RIDLEY, SOLID STATE BONDING IN SUPERPLASTIC TI-6AL-4V, *MET. SCI.*, VOL 18, MARCH 1984, P 117-122
8. Y. MAEHARA, Y. KOMIZO, AND T.G. LANGDON, PRINCIPLES OF SUPERPLASTIC DIFFUSION BONDING, *MATER. SCI. TECHNOL.*, VOL 4, AUG 1988, P 669-674
9. J. PILLING AND N. RIDLEY, SOLID STATE BONDING OF SUPERPLASTIC AA7475, *MATER. SCI. TECHNOL.*, VOL 3, MAY 1987, P 353-359
10. W.A. BRYANT, A METHOD FOR SPECIFYING HOT ISOSTATIC PRESSURE WELDING PARAMETERS, *WELD. J.*, DEC 1975, P 433-S TO 435-S

Procedure Development and Practice Considerations for Diffusion Welding

S.B. Dunkerton, The Welding Institute

Carbon and Low-Alloy Steels

Although diffusion welding is applicable to this class of steels, industrial applications are limited. The process is used in situations where it is essential to avoid or minimize distortion and postweld machining, and for complicated geometries that involve internal features.

These steels are generally welded without the use of filler material (interlayer). The parts themselves are machined to a good surface finish (<0.4 μm, or 16 μin., RA surface roughness, and flat) and assembled in a heating unit such that force can be applied uniaxially or isostatically.

In terms of uniaxial diffusion welding, a wide range of bonding conditions have been shown to give sound joints, that is, temperatures of 900 to 1200 °C (1650 to 2190 °F), pressures of 5 to 14 MPa (0.7 to 2 ksi) and times of 5 to 120 min. Because the parameters are interdependent, as temperature increases, the load and/or time can be reduced and vice versa. Figure 2 depicts a typical cross section of a joint in 0.4% C steel, in which a layer of ferrite indicates the bond line of the sound bond that has formed.

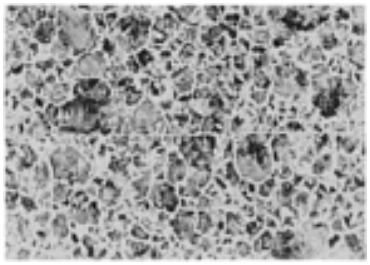

FIG. 2 CROSS SECTION OF DIFFUSION WELD IN 0.4% C STEEL. 50×

Tensile strength develops as temperature/pressure/time increase. Parent-metal tensile strength is readily achieved; failure occurs away from the joint interface, even when welding is not complete. Work has shown that only 80% bonding is necessary to achieve the equivalent parent-metal strength (Ref 11). However, ductility and joint-line toughness require a greater level of bond integrity.

Joints made in 0.4% C steel and a 1Cr-0.25Mo alloy steel have shown low Charpy impact values, when compared with the parent steels (Ref 12, 13). With the 0.4% C steel, it is possible to improve the toughness properties by using a postweld normalizing heat treatment (equivalent to the thermally cycled and normalized parent material). However, although the chromium-molybdenum steel had an improved microstructure after a postweld quench and temper heat treatment, it still had low joint-line toughness. This indicates the greater difficulty in forming a sound joint as alloy content increases.

Therefore, when diffusion welding carbon and low-alloy steels, the final application and service requirements should be considered carefully. The process is useful in low-stress applications, but when impact toughness is required, the fitness of a particular steel for the specific purpose needs to be examined. For higher-carbon-content steels and low-alloy steels, a suitable postweld heat treatment is recommended to return the steel to its original condition. However, it should be noted that some of the high temperatures referred to earlier ([ges]1100 °C, or 2010 °F) can cause significant grain coarsening.

The HIP welding of these steels also can be used when typical conditions involve a temperature of 1100 °C (2010 °F), a pressure of 100 MPa (14.5 ksi), and a bonding time of 4 h. Again, grain coarsening and the property considerations described above need to be reviewed.

References cited in this section

11. C.E. THORNTON AND E.R. WALLACH, IMPACT STRENGTH OF STEEL DIFFUSION BONDS, *MET. CONSTR.*, JULY 1985, P 450R-455R

12. S. ELLIOT, "PROPERTIES OF DIFFUSION BONDS IN A 0.4 C STEEL," REPORT 131/1980, THE WELDING INSTITUTE, 1980
13. S.B. DUNKERTON, "DIFFUSION BONDING OF A 0.4 CARBON CHROMIUM/MOLYBDENUM STEEL," REPORT 178/1982, THE WELDING INSTITUTE, 1982

High-Strength Steels

Although diffusion welding has not been widely applied to high-strength steels, it is a feasible process, and guidelines similar to those identified for carbon and low-alloy steels will apply. Because diffusion welding relies on microplastic yielding in the early stages of bonding, it is necessary to use parameters at the higher end of the ranges specified previously, that is, temperatures above 1000 °C (1830 °F) and pressures of 7 MPa (1 ksi) and above.

Although good tensile properties can be achieved, the as-bonded toughness will be low. In addition, a postweld heat treatment to restore the parent microstructure is recommended.

Procedure Development and Practice Considerations for Diffusion Welding

S.B. Dunkerton, The Welding Institute

Stainless Steels

Stainless steels can be diffusion welded using conditions similar to those that are used for high-strength steels. These steels are normally covered by a thin adherent oxide (chromium oxide) that must be broken up and/or dissolved during the welding process. This is possible when higher temperatures and/or higher pressures are used. Alternatively, stainless steels can be welded in dry hydrogen, which will reduce the oxide film, or the oxide can be removed prior to welding. The latter measure has been accomplished by anodic cleaning of the steel surfaces, followed immediately by copper plating to protect the surfaces from reoxidation. Again, if a dry hydrogen atmosphere is used, then the copper oxide will be reduced during welding and a sound bond will be attained.

Although few property data are available on the diffusion welding of stainless steels, it is known that tensile strength is readily achieved, whereas toughness is more difficult. If high welding temperatures are employed, then it will generally be necessary to use a postweld heat treatment to restore properties.

Procedure Development and Practice Considerations for Diffusion Welding

S.B. Dunkerton, The Welding Institute

Aluminum-Base Alloys

Diffusion welding of aluminum alloys is difficult, because of the presence of a tenacious surface oxide film. The surface oxide can be disrupted by the use of large deformations and/or high temperatures in, for example, roll bonding. However, for low-deformation diffusion welding, interlayers of similar or dissimilar materials have been used. The specific procedures to be followed for aluminum alloys vary, depending on the alloy system.

For aluminum-magnesium-silicon alloys (specifically, Al-0.6Mg-0.9Si-0.5Mn), diffusion welding without an interlayer has yielded tensile strengths of 145 MPa (21 ksi) for a welding temperature of 550 °C (1020 °F) (Ref 14). However, this

does induce deformation of the components. It has been more attractive to use copper or silver interlayers, which can be applied as a coating or a foil. These interlayers can be used to provide a solid-state weld or a transient liquid-phase (eutectic) weld. Care needs to be taken to achieve the latter, to ensure that the heating rate is not so slow as to allow the interlayer to be diffused away before the eutectic temperature is reached. Solid-state diffusion welds made with either copper or silver have yielded joint strengths of 85 MPa (12 ksi) for bonding temperatures as low as 450 °C (840 °F).

More attention has been directed to the diffusion welding of alloys that are of interest to the aerospace industries, that is, 7010 (Ref 15), 7475 (Ref 16, 17) and 8090 (Ref 18, 19, 20, 21). No clear guidelines exist as to the best practice for welding these alloys, because researchers have investigated many techniques and the results point in sometimes conflicting directions. Welding the alloys without an interlayer is possible, if disruption of the oxide can take place during welding. Some success has been achieved by welding the 7475 alloy with a "rough" surface (that is, brushed in air), by surface grinding the alloy in an argon atmosphere prior to welding, and by grit blasting with fine alumina particles followed by chemical cleaning in hot 30 wt% NaOH solution. Long welding times have been used for this material and high strengths have been reported by welding at 515 °C (960 °F) under a load of 5 MPa (0.7 ksi) for 5 h, followed by a postweld heat treatment to T6 condition. In instances where interlayers have been used for this alloy system, the material that has shown the greatest promise is zinc.

Aluminum-lithium alloys are currently attracting great attention for applications in the aerospace industries. This is because lithium significantly increases the elastic modulus of aluminum, by approximately 6% for each wt% addition of lithium, and simultaneously decreases its density by 3%. For aerospace applications, improvements in specific modulus and strength can lead directly to weight savings. In addition, it has been shown that aluminum-lithium alloys can develop superplastic behavior after appropriate thermomechanical processing, which means that advantage can be taken of the SPF/DW procedures already established in this industry.

Superplastic forming after welding restricts the welding temperature that can be used. Ideally, the temperature should be lower than or equal to the superplastic temperature for the alloy. In addition, the welding time must be restricted to avoid grain growth in the parent sheet, which could affect the superplastic-forming properties.

Aluminum-lithium alloys have been bonded with no interlayer and with interlayers of zinc, copper, zinc-copper, pure aluminum, and aluminum alloys. Surfaces have been prepared by a number of techniques, such as grinding with emery paper, shot peening, chemical etching, and degreasing. All techniques have shown some degree of success, but it is difficult to compare results, because the testing methods to achieve shear strength are varied. Generally, all of these welds require some form of postweld heat treatment to restore properties (for example, solution treatment at 535 °C, or 995 °F, followed by quenching). A section through a diffusion weld containing a pure aluminum interlayer is shown in Fig. 3. The position of the original aluminum foil is discernible by the presence of spheroidal precipitates, similar in size and shape to those precipitated in the grain boundaries of the aluminum alloy.

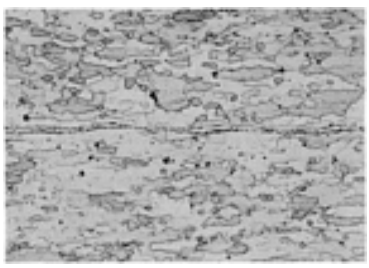

FIG. 3 CROSS SECTION OF DIFFUSION WELD IN ALUMINUM-LITHIUM ALLOY CONTAINING PURE ALUMINUM INTERLAYER. 75×

In order to avoid surface contamination during heating to the welding temperature, greater care needs to be taken with the aluminum-lithium alloys, because of the reactivity of lithium. However, this reactivity is also claimed to make this alloy system somewhat easier to weld than other less-reactive aluminum alloys.

References cited in this section

14. A.E. DRAY AND E.R. WALLACH, "DIFFUSION BONDING OF ALUMINIUM ALLOYS," PAPER PRESENTED AT INTERNATIONAL CONFERENCE ON DIFFUSION BONDING (CRANFIELD, UK), 1987
15. D.V. DUNFORD, C.G. GILMORE, AND P.G. PARTRIDGE, "EFFECT OF SILVER COATING THICKNESS ON THE SHEAR STRENGTH OF DIFFUSION BONDED CLAD AL-ZN-MG (7010) ALLOY," PAPER PRESENTED AT INTERNATIONAL CONFERENCE ON DIFFUSION BONDING (CRANFIELD, UK), 1987
16. N. RIDLEY *ET AL.*, "DIFFUSION BONDING OF SUPERPLASTIC ALUMINIUM ALLOYS," PAPER PRESENTED AT INTERNATIONAL CONFERENCE ON DIFFUSION BONDING (CRANFIELD, UK), 1987
17. D.W. LIVESEY AND N. RIDLEY, DIFFUSION BONDING OF SUPERPLASTIC ALUMINIUM ALLOYS USING A TRANSIENT LIQUID PHASE INTERLAYER (ZINC), *DIFFUSION BONDING 2*, ELSEVIER APPLIED SCIENCE, 1991
18. R.A. RICKS *ET AL.*, DEVELOPMENT OF DIFFUSION BONDING TECHNIQUES FOR AL-LI BASE ALLOY AA8090, *DIFFUSION BONDING 2*, ELSEVIER APPLIED SCIENCE, 1991
19. H.M. TENSI AND M. WITTMAN, INFLUENCE OF SURFACE PREPARATION ON THE DIFFUSION WELDING OF HIGH STRENGTH ALUMINIUM ALLOYS, *DIFFUSION BONDING 2*, ELSEVIER APPLIED SCIENCE, 1991
20. D.V. DUNFORD, P.G. PARTRIDGE, AND C.G. GILMORE, DIFFUSION BONDING OF AL-LI 8090 ALLOY, *DIFFUSION BONDING 2*, ELSEVIER APPLIED SCIENCE, 1991
21. A. URENA AND S.B. DUNKERTON, "DIFFUSION BONDING OF AN ALUMINIUM-LITHIUM ALLOY (AA 8090)," REPORT 403/1989, THE WELDING INSTITUTE, 1989

Procedure Development and Practice Considerations for Diffusion Welding

S.B. Dunkerton, The Welding Institute

Reactive and Refractory Metals

The diffusion welding of titanium alloys is well documented, because of its commercial application and importance to the aerospace industry. Many titanium airframe structures are now manufactured using the SPF/DW process, which provides significant benefits through weight and cost savings. Typical examples include hot-air nozzles, landing-gear doors, intricately shaped housings, keel sections, and heat-exchanger ducts. Most of the detailed procedures for welding are commercially sensitive. The factors that are important are (Ref 22):

- METALLURGICAL CONDITION OF THE STARTING MATERIAL
- CHARACTERIZATION OF THE SUPERPLASTICITY OF THE MATERIAL
- SURFACE CLEANLINESS
- TOOLING MATERIAL AND SURFACE CONDITION
- WELDING ATMOSPHERE
- FORMING AND WELDING PARAMETERS
- PART GEOMETRY

The primary alloy that is used is Ti-6Al-4V. It has been established that commercially available sheet material containing an equiaxed, uniform, small grain size (preferably, <10 μm, or 400 μin.) is suitable for superplastic forming. Conventional cutting processes are used for the preparation of sheet material, which is then subjected to an etching treatment prior to placement in the press. Although tooling is typically made of a 22Cr-4Ni-9Mn stainless steel with appropriate surface-parting compounds, ceramic-faced tooling has also been used. During the application of heat at temperatures ranging from 900 to 930 °C (1650 to 1710 °F), argon gas provides a protective atmosphere that is also utilized, under pressure, to

effect forming and diffusion welding. Tool-to-titanium sealing, in order to contain the forming/bonding pressure of 2 to 4 MPa (0.3 to 0.6 ksi), is of paramount importance to leakage prevention.

Multiple-sheet fabrication requires the application of a stop-off material (typically, yttria and a binder) after conventional titanium cleaning. The application of a stop-off material utilizes a silk-screen technique that allows complex patterns to be transferred to the sheet. The multiple-sheet pack is plumbed with stainless steel capillary tubes for internal gas pressurization (between the sheets), as opposed to single-sheet processing, where gas pressure access is achieved directly through tooling parts. The process allows formed titanium shapes that are far more complex than those produced by conventional forming methods. Parts can feature integral end flanges, deep beads, corner beads, and small-bend radii. In addition, compound contour; multiple, variable, hollow sections; and complex sandwich (including circular) structures with varying core configurations can be fabricated.

Zirconium and its alloys also have been joined by diffusion welding, as have the refractory metals of tungsten, tantalum, niobium, and molybdenum (Ref 23).

References cited in this section

22. R.J. REHDER AND D.T. LOVELL, PROCESS DEVELOPMENT FOR DIFFUSION WELDING TI-6AL-4V, *WELD. J.*, MAY 1970, P 213-S TO 218-S
23. A.T. D'ANNESSA, THE SOLID-STATE BONDING OF REFRACTORY METALS, *WELD. J.*, MAY 1964, P 232-S TO 240-S

Other Alloys

Other alloy systems have been diffusion welded, but with few industrial applications. Copper bonds to itself readily, if the surface oxide can be disrupted, and temperatures ranging from 850 to 950 °C (1560 to 1740 °F) have been employed. Alternatively, a liquid-phase procedure that uses silver as an interlayer has been adopted to reduce welding times. The nickel- and cobalt-base alloys are bondable, but some alloy systems exhibit good high-temperature strength that inhibits the microyielding required for diffusion welding. Beryllium alloys also can be bonded at low temperatures (Ref 24).

The noble metals, such as gold, bond readily because of their very thin surface oxide. Gold, in particular, is often used as an interlayer material when welding temperatures are restricted, because bonds can be achieved at temperatures as low as 250 to 350 °C (480 to 660 °F), if the surfaces and atmosphere are clean.

Reference cited in this section

24. J.L. KNOWLES AND T.H. HAZLETT, HIGH-STRENGTH LOW-TEMPERATURE BONDING OF BERYLLIUM AND OTHER METALS, *WELD. J.*, VOL 49, JULY 1970, P 301-S TO 310-S

Dissimilar Metal Combinations

Ferrous-to-Ferrous Combinations. Dissimilar steel joints have not bee extensively investigated in diffusion-welding research, primarily because it was initially believed that the process would mostly be used to join material combinations that were difficult to join by other, more-conventional methods. However, this is not strictly true, and in situations where multiple joints can be formed in one welding operation, the process can be economically viable for dissimilar steel joints.

The literature on steel includes the bonding of high-speed steels to carbon steels for prismatic cutting tools (Ref 25) and the joining of pure iron to a range of carbon steels (Ref 26). In this latter work, the bond tensile strength was greater than 430 MPa (62 ksi), which exceeds that of the weaker parent metal. A slight increase in tensile strength occurred with a decrease in welding temperature from 1000 to 900 °C (1830 to 1650 °F).

Nonferrous-to-Nonferrous Combinations. Many combinations have been studied within this category, but the most common one uses aluminum as one of the parent materials (Ref 27, 28, 29).

The diffusion welding of aluminum to copper and titanium results in the formation of intermetallic compounds at the bond interface. With copper, it has been found that the aluminum/copper intermetallic can reach 15 μm (600 μin.) in thickness before a reduction in the joint strength occurs (Ref 30). Also described in this work is the fact that the parent aluminum strength was not achieved, even before the excessive growth of the intermetallic, which suggests that full bonding can be achieved only after the time necessary for extensive intermetallic formation. However, aluminum-to-titanium diffusion bonds can reach a tensile strength that is equal to that of the parent aluminum, and it is claimed that intermetallic thicknesses of up to 10 μm (400 μin.) can be tolerated (Ref 31). Again, an interlayer of silver can be used to promote bonding between the aluminum and titanium, such that the parent aluminum strength can be achieved in shorter welding times.

The aerospace and nuclear industries have driven the development of a wide variety of special alloy and dissimilar-metal combinations. Examples of materials that have been successfully joined include nickel-stainless steel (Ref 32), uranium-stainless steel (Ref 33), beryllium-nickel (Ref 34), beryllium-stainless steel (Ref 34), thorium dioxide dispersion-strengthened-nickel alloys (Ref 35), zirconium-steel (Ref 36), and copper-Monel (Ref 37).

Ferrous-to-Nonferrous Combinations. The joining of aluminum to steel has received a great deal of interest. This subject has been reviewed by Elliot and Wallach (Ref 38), who recognized that the two major problems associated with this metal combination are:

- THE TENACIOUS OXIDE LAYER ON THE ALUMINUM, WHICH, BEING STOICHIOMETRIC AND HIGHLY STABLE, INHIBITS WELD FORMATION
- THE FORMATION OF BRITTLE INTERMETALLICS, SUCH AS THE $FEAL_3$ AND FE_2AL_5 TYPES, AT THE JOINT INTERFACE

These problems are generally overcome by using interlayers, both to promote welding and to prevent the formation of brittle intermetallic compounds. Silver has been successfully used as an interlayer, either as a foil interlayer or applied by electroplating (Ref 39, 40), vapor deposition (Ref 41, 42), or sputter deposition (Ref 43) on one or both surfaces. Both solid- and liquid-phase joints have been produced, the latter of which involves melting of the aluminum-silver eutectic.

Other interlayer materials that have been examined include nickel and a multilayer system of zinc and silver. However, both of these have disadvantages. The nickel also forms brittle intermetallics with iron that inhibit joint strength. In the multilayer system, the zinc was found to erode the silver, thereby removing the diffusion barrier. In addition, aluminum and steel alloys can be diffusion welded without any interlayer by a careful evaluation of the process parameters and with a higher amount of aluminum deformation.

The diffusion welding of refractory metals to steels has been another major research area. Molybdenum has been welded directly to steel, but the formation of brittle intermetallics limits the strength of the joints. Lison and Stelzer (Ref 25) have investigated the interlayers required to give good joint properties for this metal combination, based on metallurgical compatibility and the coefficients of thermal expansion. A complex multilayer system was devised, in which tantalum, vanadium, nickel, and copper were positioned in the following order: Mo-Ta-Ni-Cu-steel. Initially, the Mo-Ta-V combination was bonded at 1500 °C (2730 °F) for 40 min, whereas the remaining bonds were formed at 850 °C (1560 °F) in 20 min. The mechanical properties of such a joint are not given, but metallographic examination revealed full bond formation.

Metal-Ceramic Joining. Recent developments in gas-turbine and ceramic-engine technology have created an interest in the diffusion welding of ceramics to steels, because the low temperatures used for joining minimize the residual stresses created by thermal mismatch. Silicon nitride and zirconium oxide are two examples of oxides that have been successfully welded to steel using the diffusion welding process (Ref 44, 45).

References cited in this section

25. R. LISON AND J.F. STELZER, DIFFUSION WELDING OF REACTIVE AND REFRACTORY METALS TO STAINLESS STEELS, *WELD. J.*, VOL 58 (NO. 10), 1979, P 306-314
26. V.F. SHATINSKI *ET AL.*, THE DIFFUSION BONDING OF REFRACTORY ALLOYS TO A STEEL WITH A DECARBURIZED SURFACE, *WELD. PROD.*, VOL 24 (NO. 12), 1977
27. E.R. NAIMON, J.H. DOYLE, C.R. RICE, D. VIGIL, AND D.R. WALMSLEY, DIFFUSION WELDING OF ALUMINUM TO STAINLESS STEEL, *WELD. J.*, NOV 1981, P 17-20
28. P.D. CALDERON, D.R. WALMSLEY, AND Z.A. MUNIR, AN INVESTIGATION OF DIFFUSION WELDING OF PURE AND ALLOYED ALUMINUM TO TYPE 316 STAINLESS STEEL, *WELD. J.*, APRIL 1985, P 104-S TO 112-S
29. C.H. CRANE, D.T. LOVELL, W.A. BAGINSKI, AND M.G. OLSEN, DIFFUSION WELDING OF DISSIMILAR METALS, *WELD. J.*, VOL 46, P 23-S TO 31-S
30. T. ENJYO *ET AL.*, DIFFUSION WELDING OF COPPER TO ALUMINIUM, *TRANS. JWRI*, VOL 8, 1979, P 77-83
31. T. ENJYO *ET AL.*, DIFFUSION BONDING OF ALUMINIUM TO TITANIUM, *TRANS. JWRI*, VOL 6 (NO. 1), 1977, P 123-130
32. G.R. KAMAT, SOLID-STATE DIFFUSION WELDING OF NICKEL TO STAINLESS STEEL, *WELD. J.*, JUNE 1988, P 44-46
33. R.S. ROSEN, D.R. WALMSLEY, AND Z.A. MUNIR, THE PROPERTIES OF SILVER-AIDED DIFFUSION WELDS BETWEEN URANIUM AND STAINLESS STEEL, *WELD. J.*, VOL 65, APRIL 1986, P 83-S TO 92-S
34. W. FEDUSKA AND W.L. HORIGAN, DIFFUSION BONDING OF HIGH-TEMPERATURE ALLOYS WITH BERYLLIUM, *WELD. J.*, JAN 1962, P 28-S TO 35-S
35. T.J. MOORE AND K.H. HOLKO, SOLID STATE WELDING OF TD-NICKEL BAR, *WELD. J.*, SEPT 1970, P 395-S TO 409-S
36. M.L. WAYMAN, R.R. SMITH, AND M.G. WRIGHT, THE DIFFUSION BONDING OF ZR-2.5% NB TO STEEL, *METALL. TRANS. A*, VOL 17, MARCH 1986, P 429-433
37. J.T. NIEMANN, R.P. SOPHER, AND P.J. RIEPPEL, DIFFUSION BONDING BELOW 1000 °F, *WELD. J.*, AUG 1958, P 337-S TO 342-S
38. S. ELLIOT AND E.R. WALLACH, JOINING ALUMINIUM TO STEEL, PART 1--DIFFUSION BONDING, *MET. CONSTR.*, VOL 13 (NO. 3), 1981, P 167-171
39. J.W. DINI, USE OF ELECTRODEPOSITION TO PROVIDE COATINGS FOR SOLID-STATE BONDING, *WELD. J.*, NOV 1982, P 33-39
40. J.W. DINI, W.K. KELLEY, W.C. COWDEN, AND E.M. LOPEZ, USE OF ELECTRODEPOSITED SILVER AS AN AID IN DIFFUSION WELDING, *WELD. J.*, JAN 1984, P 26-S TO 34-S
41. C. SCHALANSKY, Z.A. MUNIR, AND D.L. WALMSLEY, AN INVESTIGATION ON THE BONDING OF HOT-HOLLOW CATHODE DEPOSITED SILVER LAYERS TO TYPE 304 STAINLESS STEEL, *J. MATER. SCI.*, VOL 22, 1987, P 745-751
42. P.S. MACLEOD AND G. MAH, THE EFFECT OF SUBSTRATE BIAS VOLTAGE ON THE BONDING OF EVAPORATED SILVER COATINGS, *J. VAC. SCI. TECHNOL. II*, VOL 1, JAN/FEB 1974, P 119-121
43. R.S. ROSEN AND M.E. KASSNER, DIFFUSION WELDING OF SILVER INTERLAYERS COATED ONTO BASE METALS BY PLANAR-MAGNETRON SPUTTERING, *J. VAC. SCI. TECHNOL.*, VOL

A8 (NO. 1), JAN/FEB 1990, P 19-29

44. K. SUGANUMA, T. OKAMOTO, M. KOIZUMI, AND M. SHIMADA, SOLID-STATE BONDING OF PARTIALLY STABILIZED ZIRCONIA TO STEEL WITH TITANIUM INTERLAYER, *J. MATER. SCI. LETT.*, VOL 5, 1986, P 1099-1100
45. K. SUGANUMA, T. OKAMOTO, Y. MIYAMOTO, M. SHIMADA, AND M. KOIZUMI, JOINING SI_3N_4 TO TYPE 405 STEEL WITH SOFT METAL INTERLAYERS, *MATER. SCI. TECHNOL.*, VOL 2, NOV 1986, P 1156-1161

Procedure Development and Practice Considerations for Diffusion Welding

S.B. Dunkerton, The Welding Institute

References

1. W.A. OWCZARSKI AND D.F. PAULONIS, APPLICATION OF DIFFUSION WELDING IN THE USA, *WELD. J.*, FEB 1981, P 22-33
2. O.S. SPANSWICK, DIFFUSION BONDING--A CASE STUDY, REPRINT R269/10/B4, *WELD. INST. RES. BULL.*, THE WELDING INSTITUTE, 1984
3. B. DERBY AND E.R. WALLACH, THEORETICAL MODEL FOR DIFFUSION BONDING, *MET. SCI.*, VOL 16, JAN 1982, P 49-56
4. B. DERBY AND E.R. WALLACH, DIFFUSION BONDING: DEVELOPMENT OF THEORETICAL MODEL, *MET. SCI.*, VOL 18, SEPT 1984, P 427-431
5. I. TUAH-POKU, M. DOLLAR, AND T.B. MASSALSKI, A STUDY OF THE TRANSIENT LIQUID PHASE BONDING PROCESS APPLIED TO AG/CU/AG SANDWICH JOINT, *METALL. TRANS. A*, VOL 19, MARCH 1988, P 675-686
6. J. PILLING, THE KINETICS OF ISOSTATIC DIFFUSION BONDING IN SUPERPLASTIC MATERIALS, *MATER. SCI. ENG.*, VOL 100, 1988, P 137-144
7. J. PILLING, D.W. LIVESEY, J.B. HAWKYARD, AND N. RIDLEY, SOLID STATE BONDING IN SUPERPLASTIC TI-6AL-4V, *MET. SCI.*, VOL 18, MARCH 1984, P 117-122
8. Y. MAEHARA, Y. KOMIZO, AND T.G. LANGDON, PRINCIPLES OF SUPERPLASTIC DIFFUSION BONDING, *MATER. SCI. TECHNOL.*, VOL 4, AUG 1988, P 669-674
9. J. PILLING AND N. RIDLEY, SOLID STATE BONDING OF SUPERPLASTIC AA7475, *MATER. SCI. TECHNOL.*, VOL 3, MAY 1987, P 353-359
10. W.A. BRYANT, A METHOD FOR SPECIFYING HOT ISOSTATIC PRESSURE WELDING PARAMETERS, *WELD. J.*, DEC 1975, P 433-S TO 435-S
11. C.E. THORNTON AND E.R. WALLACH, IMPACT STRENGTH OF STEEL DIFFUSION BONDS, *MET. CONSTR.*, JULY 1985, P 450R-455R
12. S. ELLIOT, "PROPERTIES OF DIFFUSION BONDS IN A 0.4 C STEEL," REPORT 131/1980, THE WELDING INSTITUTE, 1980
13. S.B. DUNKERTON, "DIFFUSION BONDING OF A 0.4 CARBON CHROMIUM/MOLYBDENUM STEEL," REPORT 178/1982, THE WELDING INSTITUTE, 1982
14. A.E. DRAY AND E.R. WALLACH, "DIFFUSION BONDING OF ALUMINIUM ALLOYS," PAPER PRESENTED AT INTERNATIONAL CONFERENCE ON DIFFUSION BONDING (CRANFIELD, UK), 1987
15. D.V. DUNFORD, C.G. GILMORE, AND P.G. PARTRIDGE, "EFFECT OF SILVER COATING THICKNESS ON THE SHEAR STRENGTH OF DIFFUSION BONDED CLAD AL-ZN-MG (7010) ALLOY," PAPER PRESENTED AT INTERNATIONAL CONFERENCE ON DIFFUSION BONDING (CRANFIELD, UK), 1987

16. N. RIDLEY *ET AL.*, "DIFFUSION BONDING OF SUPERPLASTIC ALUMINIUM ALLOYS," PAPER PRESENTED AT INTERNATIONAL CONFERENCE ON DIFFUSION BONDING (CRANFIELD, UK), 1987
17. D.W. LIVESEY AND N. RIDLEY, DIFFUSION BONDING OF SUPERPLASTIC ALUMINIUM ALLOYS USING A TRANSIENT LIQUID PHASE INTERLAYER (ZINC), *DIFFUSION BONDING 2*, ELSEVIER APPLIED SCIENCE, 1991
18. R.A. RICKS *ET AL.*, DEVELOPMENT OF DIFFUSION BONDING TECHNIQUES FOR AL-LI BASE ALLOY AA8090, *DIFFUSION BONDING 2*, ELSEVIER APPLIED SCIENCE, 1991
19. H.M. TENSI AND M. WITTMAN, INFLUENCE OF SURFACE PREPARATION ON THE DIFFUSION WELDING OF HIGH STRENGTH ALUMINIUM ALLOYS, *DIFFUSION BONDING 2*, ELSEVIER APPLIED SCIENCE, 1991
20. D.V. DUNFORD, P.G. PARTRIDGE, AND C.G. GILMORE, DIFFUSION BONDING OF AL-LI 8090 ALLOY, *DIFFUSION BONDING 2*, ELSEVIER APPLIED SCIENCE, 1991
21. A. URENA AND S.B. DUNKERTON, "DIFFUSION BONDING OF AN ALUMINIUM-LITHIUM ALLOY (AA 8090)," REPORT 403/1989, THE WELDING INSTITUTE, 1989
22. R.J. REHDER AND D.T. LOVELL, PROCESS DEVELOPMENT FOR DIFFUSION WELDING TI-6AL-4V, *WELD. J.*, MAY 1970, P 213-S TO 218-S
23. A.T. D'ANNESSA, THE SOLID-STATE BONDING OF REFRACTORY METALS, *WELD. J.*, MAY 1964, P 232-S TO 240-S
24. J.L. KNOWLES AND T.H. HAZLETT, HIGH-STRENGTH LOW-TEMPERATURE BONDING OF BERYLLIUM AND OTHER METALS, *WELD. J.*, VOL 49, JULY 1970, P 301-S TO 310-S
25. R. LISON AND J.F. STELZER, DIFFUSION WELDING OF REACTIVE AND REFRACTORY METALS TO STAINLESS STEELS, *WELD. J.*, VOL 58 (NO. 10), 1979, P 306-314
26. V.F. SHATINSKI *ET AL.*, THE DIFFUSION BONDING OF REFRACTORY ALLOYS TO A STEEL WITH A DECARBURIZED SURFACE, *WELD. PROD.*, VOL 24 (NO. 12), 1977
27. E.R. NAIMON, J.H. DOYLE, C.R. RICE, D. VIGIL, AND D.R. WALMSLEY, DIFFUSION WELDING OF ALUMINUM TO STAINLESS STEEL, *WELD. J.*, NOV 1981, P 17-20
28. P.D. CALDERON, D.R. WALMSLEY, AND Z.A. MUNIR, AN INVESTIGATION OF DIFFUSION WELDING OF PURE AND ALLOYED ALUMINUM TO TYPE 316 STAINLESS STEEL, *WELD. J.*, APRIL 1985, P 104-S TO 112-S
29. C.H. CRANE, D.T. LOVELL, W.A. BAGINSKI, AND M.G. OLSEN, DIFFUSION WELDING OF DISSIMILAR METALS, *WELD. J.*, VOL 46, P 23-S TO 31-S
30. T. ENJYO *ET AL.*, DIFFUSION WELDING OF COPPER TO ALUMINIUM, *TRANS. JWRI*, VOL 8, 1979, P 77-83
31. T. ENJYO *ET AL.*, DIFFUSION BONDING OF ALUMINIUM TO TITANIUM, *TRANS. JWRI*, VOL 6 (NO. 1), 1977, P 123-130
32. G.R. KAMAT, SOLID-STATE DIFFUSION WELDING OF NICKEL TO STAINLESS STEEL, *WELD. J.*, JUNE 1988, P 44-46
33. R.S. ROSEN, D.R. WALMSLEY, AND Z.A. MUNIR, THE PROPERTIES OF SILVER-AIDED DIFFUSION WELDS BETWEEN URANIUM AND STAINLESS STEEL, *WELD. J.*, VOL 65, APRIL 1986, P 83-S TO 92-S
34. W. FEDUSKA AND W.L. HORIGAN, DIFFUSION BONDING OF HIGH-TEMPERATURE ALLOYS WITH BERYLLIUM, *WELD. J.*, JAN 1962, P 28-S TO 35-S
35. T.J. MOORE AND K.H. HOLKO, SOLID STATE WELDING OF TD-NICKEL BAR, *WELD. J.*, SEPT 1970, P 395-S TO 409-S
36. M.L. WAYMAN, R.R. SMITH, AND M.G. WRIGHT, THE DIFFUSION BONDING OF ZR-2.5% NB TO STEEL, *METALL. TRANS. A*, VOL 17, MARCH 1986, P 429-433
37. J.T. NIEMANN, R.P. SOPHER, AND P.J. RIEPPEL, DIFFUSION BONDING BELOW 1000 °F, *WELD. J.*, AUG 1958, P 337-S TO 342-S

38. S. ELLIOT AND E.R. WALLACH, JOINING ALUMINIUM TO STEEL, PART 1--DIFFUSION BONDING, *MET. CONSTR.*, VOL 13 (NO. 3), 1981, P 167-171
39. J.W. DINI, USE OF ELECTRODEPOSITION TO PROVIDE COATINGS FOR SOLID-STATE BONDING, *WELD. J.*, NOV 1982, P 33-39
40. J.W. DINI, W.K. KELLEY, W.C. COWDEN, AND E.M. LOPEZ, USE OF ELECTRODEPOSITED SILVER AS AN AID IN DIFFUSION WELDING, *WELD. J.*, JAN 1984, P 26-S TO 34-S
41. C. SCHALANSKY, Z.A. MUNIR, AND D.L. WALMSLEY, AN INVESTIGATION ON THE BONDING OF HOT-HOLLOW CATHODE DEPOSITED SILVER LAYERS TO TYPE 304 STAINLESS STEEL, *J. MATER. SCI.*, VOL 22, 1987, P 745-751
42. P.S. MACLEOD AND G. MAH, THE EFFECT OF SUBSTRATE BIAS VOLTAGE ON THE BONDING OF EVAPORATED SILVER COATINGS, *J. VAC. SCI. TECHNOL. II*, VOL 1, JAN/FEB 1974, P 119-121
43. R.S. ROSEN AND M.E. KASSNER, DIFFUSION WELDING OF SILVER INTERLAYERS COATED ONTO BASE METALS BY PLANAR-MAGNETRON SPUTTERING, *J. VAC. SCI. TECHNOL.*, VOL A8 (NO. 1), JAN/FEB 1990, P 19-29
44. K. SUGANUMA, T. OKAMOTO, M. KOIZUMI, AND M. SHIMADA, SOLID-STATE BONDING OF PARTIALLY STABILIZED ZIRCONIA TO STEEL WITH TITANIUM INTERLAYER, *J. MATER. SCI. LETT.*, VOL 5, 1986, P 1099-1100
45. K. SUGANUMA, T. OKAMOTO, Y. MIYAMOTO, M. SHIMADA, AND M. KOIZUMI, JOINING SI_3N_4 TO TYPE 405 STEEL WITH SOFT METAL INTERLAYERS, *MATER. SCI. TECHNOL.*, VOL 2, NOV 1986, P 1156-1161

Procedure Development and Practice Considerations for Inertia and Direct-Drive Friction Welding

Tim Stotler, Edison Welding Institute

Introduction

FRICTION WELDING (FRW) is a solid-state welding process that uses the compressive force of the workpieces that are rotating or moving relative to one another, producing heat and plastically displacing material from the faying surfaces, thereby creating a weld. Process variations include inertia, direct-drive, linear, and orbital radial friction welding, as well as friction surfacing. (Additional information is available in the articles "Fundamentals of Friction Welding,", "Friction Welding,", "Radial Friction Welding,", and "Friction Surfacing" in this Volume.) This article provides information about practice considerations for the two most common variations: inertia and direct-drive friction welding.

Inertia welding obtains heat for welding that is supplied by stored rotational kinetic energy. Figure 1 depicts the parameter characteristics of the process. The inertia of the system is changed by either adding or removing flywheels from the rotating spindle that provides rotary motion and/or by changing the spindle speed.

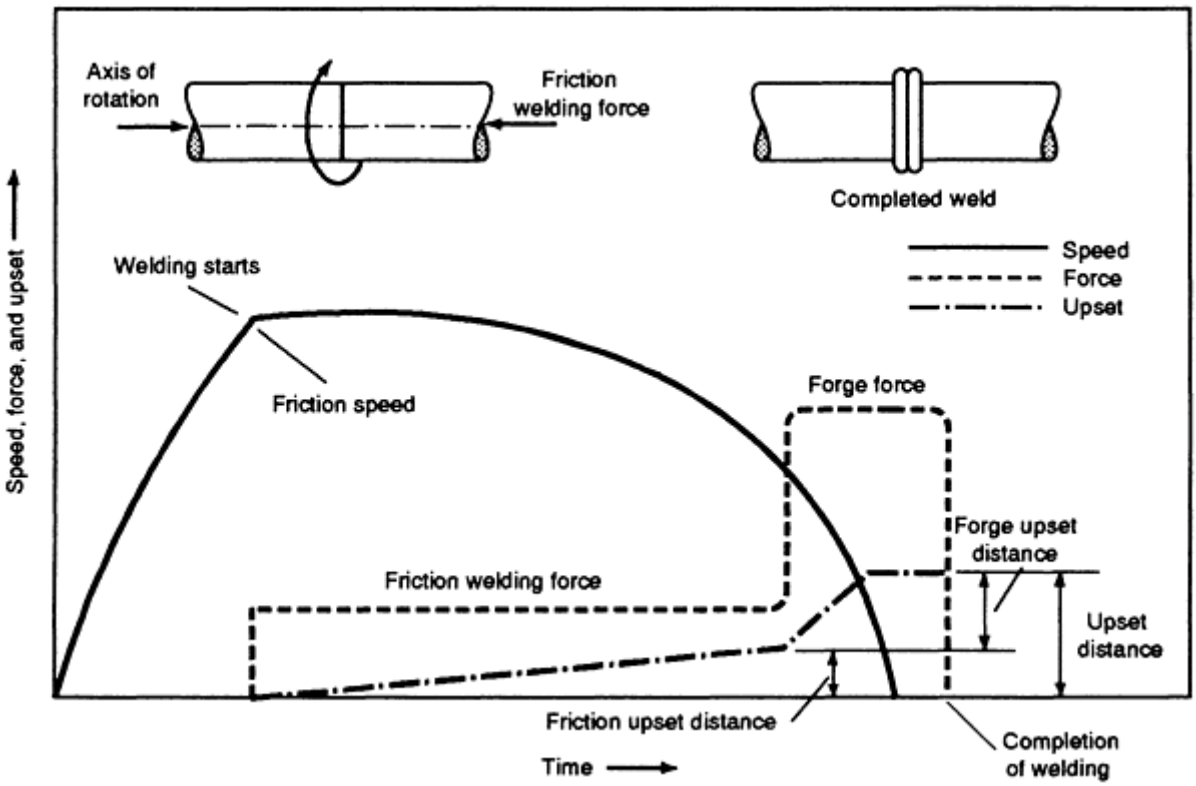

FIG. 1 INERTIA WELDING PARAMETER CHARACTERISTICS. SOURCE: ANSI/AWS C6.1-89

After the inertial mass is set, the parts are loaded in the machine (one in the spindle and one in the fixture/tailstock). The spindle speed and welding forces are set to predetermined levels. The spindle is then accelerated to velocity. After this velocity is attained, the drive system is disengaged, allowing the flywheel (and the part in the spindle) to effectively coast. The stationary part is then brought into contact with the rotating one, under a given applied force, and frictional heating begins. The flywheel is stopped by the transitioning of its kinetic energy into thermal energy (frictional heating) at the welding interface. This energy heats the part and allows forging to occur by displacing material at the interface.

Direct-drive friction welding differs from inertia welding, primarily in how the energy is delivered to the joint. Figure 2 depicts the characteristics of this process. In direct-drive friction welding, like inertia welding, one of the parts is loaded into a rotating spindle while the other is held stationary. However, the spindle is of a given mass and is not changed, as it is in inertia welding. To start the process, the spindle is set into motion at a constant rotational velocity (rev/min). The parts are then brought into contact under a low force (termed first friction force, or preheat force) and allowed to heat for a preset time or distance. In most applications, a higher welding force (termed second friction force, or welding force) is then applied, which increases the rate and amount of material extruded from the joint. The second friction force is controlled through a preset time or distance. After the preset time or distance has been reached for the first two friction stages, the rotating spindle is brought to a stop using some type of braking mechanism. This is typically a caliper brake(s) system and/or an electric-type brake in the spindle drive motor. In most cases, a third increase in the welding force (usually referred to as the upset force) is applied at the start of or after braking, which consolidates the joint. In contrast to inertia welding, where the microstructure at the interface reflects a rotational-type forging, direct-drive friction welding produces an axially forged microstructure in the weld. However, if braking times are increased, allowing the upset force to be applied while the spindle may still be rotating, some rotational-type forging can be obtained.

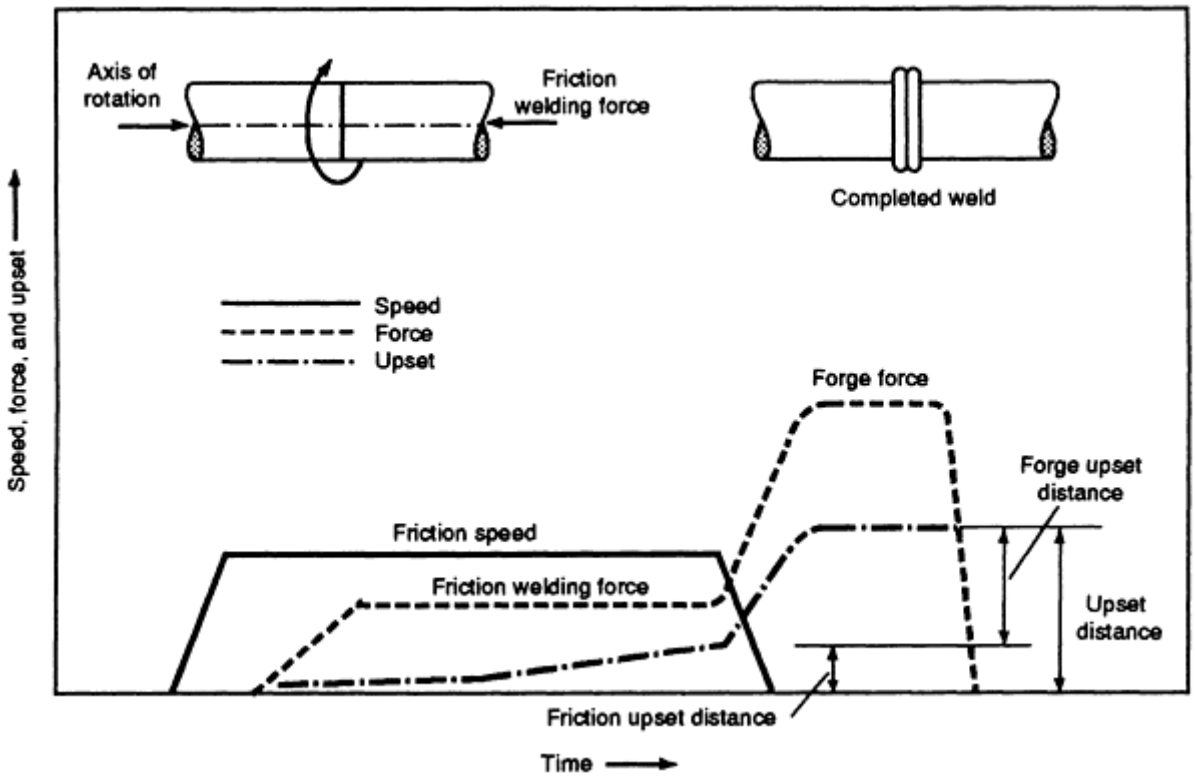

FIG. 2 DIRECT-DRIVE FRICTION WELDING PARAMETER CHARACTERISTICS. SOURCE:ANSI/AWS C6.1-89

One advantage that direct-drive friction welding possesses is reduced torque peaks, compared with those experienced in inertia welding. The initial torque peak is reduced by applying a low initial welding force (first friction), which reduces the rate at which heating occurs. This practice typically is used to reduce the power requirements at the beginning of the welding cycle. In addition, the spindle rotation in this process is either nearly or completely stopped before the final upset of the parts, thus minimizing the final torque peak. This is advantageous when welding thin-walled tubes, the walls of which could tend to tear under high torque peaks. Although torque peaks in inertia welding can be reduced by using lower welding forces, they will still be larger than those of direct-drive friction welding.

Procedure Development and Practice Considerations for Inertia and Direct-Drive Friction Welding

Tim Stotler, Edison Welding Institute

Inertia Welding Parameter Calculations

Differences in part geometry (bar-to-bar, tube-to-tube, bar-to-plate, and so on) affect welding parameter calculations. The calculation procedures described here are based on carbon steel. For a given alloy system, inertia welding spindle speeds are set within a specified range of surface velocities. The actual surface velocity depends on the size of the part to be joined. Surface velocities for welding carbon steels in all geometries typically range from 90 to 610 m/min (300 to 2000 ft/min). The actual spindle speed (rev/min) is calculated by:

$$rev/mim = \frac{c\,S}{p\,OD} \qquad \textbf{(EQ 1)}$$

where χ, the conversion factor, is 12 for the U.S. customary unit and 1000 for the metric SI unit, S is the surface velocity (m/min or ft/min), and OD is the outside diameter of the part (mm or in.).

For solid bars and a fixed welding force, lower surface velocities tend to reduce center heating. Center heating is not a problem with tube-type geometries, which means there is greater flexibility in the surface velocities used. The effect of surface velocity on the heat pattern in a solid bar is shown in Fig. 3.

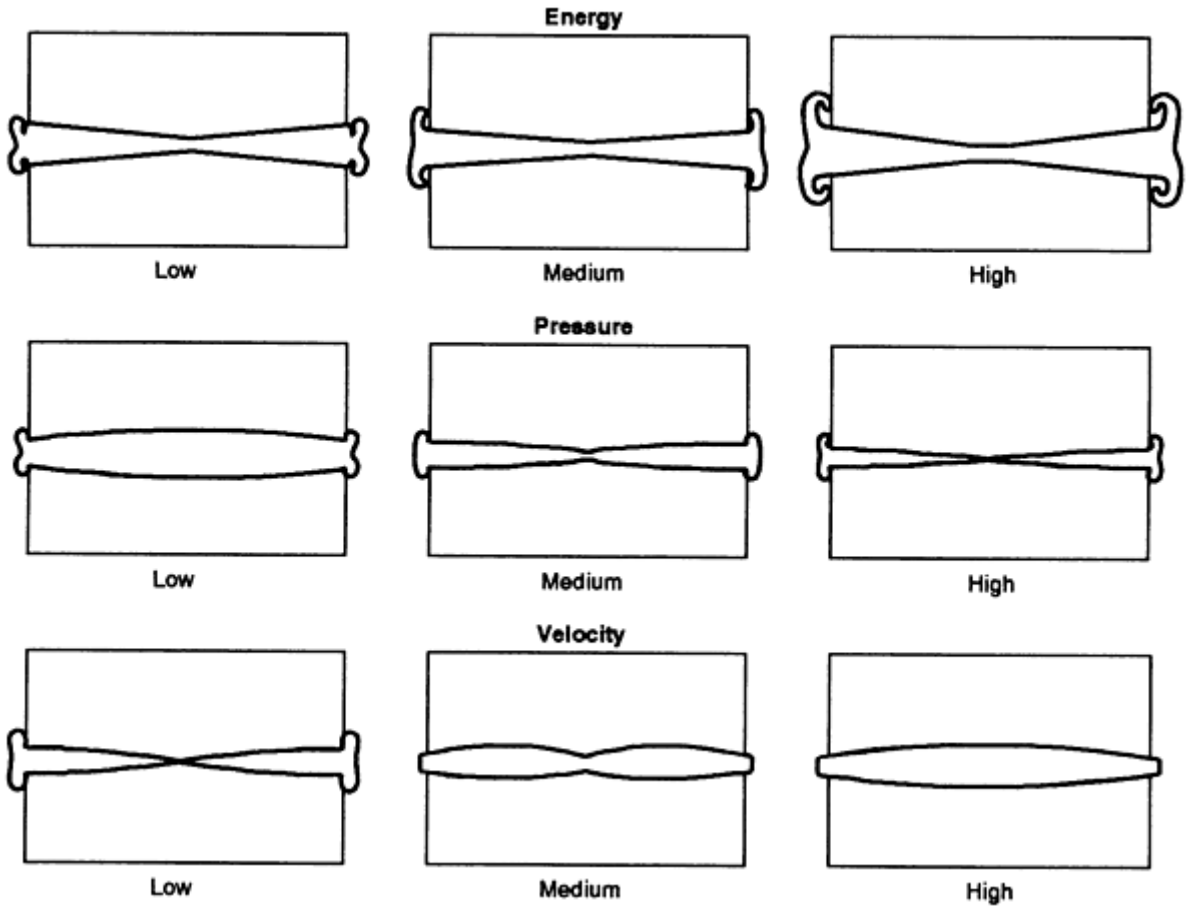

FIG. 3 EFFECT OF WELDING VARIABLES ON THE HEAT PATTERN AT THE INTERFACE AND FLASH FORMATION OF INERTIA WELDS

As mentioned in the introduction of this article, rotating flywheels are the source of energy for joining in the inertia welding process. During the welding-force stage where spindle deceleration occurs (see Fig. 1), the process is characterized by a loss of material from the interface to the flash. Larger inertias prolong the welding cycle. In addition, while maintaining a constant applied energy (combination of spindle speed and mass), rotational forging may be extended using larger flywheels and lower surface velocities.

The calculation of the flywheel energy that is needed to produce a weld depends on the surface velocity, material type, and joint geometry. As shown in Table 1 for a solid bar of low-carbon steel, the moment of inertia (expressed as wK^2 in mass units) is 0.18 kg · m^2 (4.2 lb · ft^2). This is found by using Eq 2 and the approximate flywheel energy (E_T) of 63 N · m/mm^2 (30,000 ft · lbf/$in.^2$) for the inertia welding of low-carbon steels per square inch:

$$wK^2 = \frac{E_T C}{(rev/mim)^2} \qquad \textbf{(EQ 2)}$$

where the value of C is 5873 for the U.S. customary unit and 182.4 for the SI unit, E_T is the total flywheel energy, and the $(rev/min)^2$ value is that for the spindle, which was calculated in Eq 1.

TABLE 1 TYPICAL INERTIA WELDING CONDITIONS FOR LOW-CARBON STEEL

PARAMETER	VALUE
BAR-TO-BAR	
DIAMETER, MM (IN.)	**25.4 (1)**
WELD AREA, MM^2 ($IN.^2$)	**506 (0.78)**
TOTAL MOMENT OF INERTIA, WK^2, $KG \cdot M^2$ ($LB \cdot FT^2$)	**0.18 (4.2)**
SPEED	
ANGULAR VELOCITY, REV/MIN	**5725**
SURFACE VELOCITY, M/MIN (FT/MIN)	**460 (1500)**
TOTAL FORCE, KN (LBF)	**68.9 (15,500)**
UPSET DISTANCE, MM (IN.)	**3.8 (0.150)**
TUBE-TO-TUBE	
OUTSIDE DIAMETER, MM (IN.)	**50.8 (2)**
INSIDE DIAMETER, MM (IN.)	**38.1 (1.5)**
WELD AREA, MM^2 ($IN.^2$)	**886 (1.37)**
TOTAL MOMENT OF INERTIA, WK^2, $KG \cdot M^2$ ($LB \cdot FT^2$)	**1.23 (29.3)**
SPEED	
ANGULAR VELOCITY, REV/MIN	**2875**
SURFACE VELOCITY, M/MIN (FT/MIN)	**460 (1500)**
TOTAL FORCE, KN (LBF)	**91.7 (20,600)**
UPSET DISTANCE, MM (IN.)	**5.1 (0.200)**

In the inertia welding process, there is flexibility in how the welding force can be applied, although a single force followed by an upset force is often used. The typical forces for welding carbon steels range from 96.5 to 207 MPa (14 to 30 ksi). The second-stage force (forging force), which can vary from 1.5 to nearly 4 times the welding force, is usually determined through experimentation. The effect of the welding force on the size of the heat-affected zone (HAZ) is inverse to that of surface velocity, that is, welds made at low welding forces have heat-affected areas resembling those produced with high surface velocities (see Fig. 3).

When designing an initial set of inertia welding parameters, the normal order of selection can be summarized as:

- CHOOSE THE DESIRED SPINDLE SPEED (REV/MIN)
- CALCULATE THE TOTAL MOMENT OF INERTIA (WK^2) THAT IS NEEDED FOR THE REQUIRED ENERGY LEVEL, E_T
- CHOOSE THE NEAREST AVAILABLE TOTAL MOMENT OF INERTIA (WK^2) LEVEL ON THE WELDING MACHINE
- RECALCULATE THE NECESSARY REV/MIN WITH THE TOTAL MOMENT OF INERTIA (WK^2) THAT IS AVAILABLE ON THE MACHINE
- CALCULATE THE NECESSARY WELDING FORCE (AND UPSET FORCE, IF USED)

Procedure Development and Practice Considerations for Inertia and Direct-Drive Friction Welding

Tim Stotler, Edison Welding Institute

Direct-Drive Friction Welding Parameter Calculations

Like those of inertia welding, the parameters for direct-drive friction welding were originally developed on carbon steel. Parameter calculations also involve only welding forces and spindle speeds. The same equation (Eq 1) is used for calculating the spindle rev/min value. Surface velocities for the direct-drive friction welding of carbon steels range from

76 to 182 m/min (250 to 600 ft/min). Tubes require slightly higher surface velocities than do bars. Typical welding pressure values for carbon steels range from 83 to 166 MPa (12 to 24 ksi) for the second friction force and from 166 to 332 MPa (24 to 48 ksi) for the upset force. Although first friction forces vary, they are typically 10 to 20% of the second friction force. Examples of welding parameters for bar-to-bar and tube-to-tube direct-drive welds are shown in Table 2.

TABLE 2 TYPICAL DIRECT-DRIVE FRICTION WELDING CONDITIONS FOR LOW-CARBON STEEL

PARAMETER	VALUE
BAR-TO-BAR	
DIAMETER, MM (IN.)	**25.4 (1)**
WELD AREA, MM^2 ($IN.^2$)	**506 (0.785)**
SPEED	
ANGULAR VELOCITY, REV/MIN	**1100**
SURFACE VELOCITY, M/MIN (FT/MIN)	**88 (290)**
SECOND FRICTION FORCE, KN (LBF)	**35.6 (8000)**
UPSET FORCE, KN (LBF)	**71.2 (16,000)**
UPSET DISTANCE, MM (IN.)	**4.6 (0.180)**
TUBE-TO-TUBE	
OUTSIDE DIAMETER, MM (IN.)	**50.8 (2)**
INSIDE DIAMETER, MM (IN.)	**38.1 (1.5)**
WELD AREA, MM^2 ($IN.^2$)	**886 (1.37)**
SPEED	
ANGULAR VELOCITY, REV/MIN	**900**
SURFACE VELOCITY, M/MIN (FT/MIN)	**143 (470)**
SECOND FRICTION FORCE, KN (LBF)	**48.9 (11,000)**
UPSET FORCE, KN (LBF)	**97.9 (22,000)**
UPSET DISTANCE, MM (IN.)	**3.2 (0.125)**

Carbon Steels

Generally, most metals that can be hot forged can readily be friction welded with either process variant. Carbon steels, which fall into this category, have been the fundamental basis of welding-parameter calculations for both inertia and direct-drive friction welding. Low- and medium-carbon steels are the easiest to weld and generally require no postweld heat treatments. Higher carbon and alloy steels also are easily joined, but the welding-parameter window is narrower than it is for low-carbon steels. This is primarily due to the reduced forgeability characteristics of the higher-carbon steels. Steels that contain significant amounts of free-machining elements, such as lead, also can be friction welded. However, these free-machining elements can cause undesirable directional properties near the bond line and may also act as dry lubricants that reduce frictional heating. Heat-treatable steels also can be friction welded. The rapid quenching of the weld area can present hardenability problems and a subsequent tempering or annealing procedure may be required. Hardenable steels such as these should be welded with longer heating times in order to reduce the cooling rate.

Procedure Development and Practice Considerations for Inertia and Direct-Drive Friction Welding

Tim Stotler, Edison Welding Institute

Stainless Steels

Stainless steels are commonly joined using either friction welding process. Austenitic and ferritic stainless steels are easily joined to each other and to themselves using either process. Because the heat-treatable stainless steels are sensitive

to temperature and pressure, a post-weld thermal treatment may be necessary to achieve the desired weld properties. Precipitation-hardenable stainless steels are often solution heat treated and aged after welding. In some cases, however, heat-treated base material must be stress relieved.

Welding parameters for stainless steels are similar to those used with carbon steels. Surface velocities for both bars and tubes fall within the same range as for carbon steels for both process variants. The flywheel energies, E_T, and welding forces for the inertia welding of stainless steels are typically 30 to 50% higher than those for carbon steels. For direct-drive friction welding, the welding forces are nearly the same as those used for carbon steel. Another factor relevant to the friction welding of stainless steel is the location of the weld when subjected to a corrosive environment. If possible, it should be located outside of the corrosive environment. In some instances, an increased corrosion rate occurs near the weld. This can be a concern, depending on the application.

Procedure Development and Practice Considerations for Inertia and Direct-Drive Friction Welding

Tim Stotler, Edison Welding Institute

Aluminum-Base Alloys

Aluminum alloys are commonly joined by either of the friction welding processes. In inertia welding, rotational forging will form flow lines with radial patterns, as opposed to the straight flow patterns produced with direct-drive friction welding or flash welding. An advantage of direct-drive friction welding is that thin-walled aluminum tubes are somewhat easier to join. This is because the rotation of the spindle can be stopped prior to forging. Because severe hot working of the materials will occur, the heat-affected regions of friction welds are very narrow and have a fine-grained structure. In addition, the severe hot working leads to dynamic recrystallization at the interface.

Parameters for the inertia welding of aluminum alloys differ somewhat from those used for carbon steel. The differences are due to the higher thermal conductivity of these materials. The surface velocities used for welding aluminum alloys are approximately 30 to 50% higher than those used for carbon steel. Inertia welding pressures are significantly lower than they are for carbon steels, ranging from 20 to 50% of those used for a similar-sized carbon steel part. The flywheel energy is from 20 to 50% of that for carbon steel. For direct-drive friction welding, the surface velocities are 10 to 50% higher than they are for carbon steel, depending on the type of aluminum alloy. Welding and upset pressures are typically 30 to 50% of those used for carbon steel.

Procedure Development and Practice Considerations for Inertia and Direct-Drive Friction Welding

Tim Stotler, Edison Welding Institute

Reactive and Refractory Metals

The reactive metals comprise titanium and zirconium, whereas the refractory metals comprise tungsten, tantalum, niobium, and molybdenum. Of all these metals, the titanium alloys have been studied most extensively, primarily because of their application in the aerospace industry. In the inertia welding process, titanium alloys have flywheel energies that are similar to those of steel. Surface velocities are typically at the higher end of the scale, ranging from values that are equivalent to those used for carbon steel to values that are 40% greater. However, welding forces are very low, typically ranging from 10 to 30% of those used for welding carbon steel. This difference is attributed primarily to the lower thermal conductivity of titanium.

Work has been done using direct-drive friction welding for titanium, although to a lesser degree than inertia welding. The welding parameters for the direct-drive friction welding of titanium are similar to those of steel, with a slight reduction in the welding forces. Most friction-welded joints in titanium can be used in the as-welded condition. However, somewhat better tensile and fatigue properties are obtained if stress relieving or solution annealing and aging procedures are used.

Zirconium has properties that are very similar to those of titanium. Therefore, initial welding parameters should be based on the parameters for titanium.

Both friction welding processes can be used to join molybdenum and tungsten. Current applications include the friction welding of molybdenum and tungsten wires in drawing operations for the lighting industry. Although there is not much friction welding currently being performed on niobium and tantalum, it is expected that these alloys could also be successfully welded. Tantalum has a very high melting temperature and very good low-temperature ductility. This suggests that a forge-welding process could be applicable.

Copper-, Nickel-, and Cobalt-Base Materials

Copper and nickel are commonly friction welded. Copper alloys are typically used in a dissimilar-metal welding application with aluminum. In the inertia welding process, surface velocities are nearly twice those of carbon steel, because of the high thermal conductivity of copper. Flywheel energies and welding forces are approximately 50% of those used for carbon steel.

For direct-drive friction welding, higher surface velocities would be required, given the high thermal conductivity of copper. However, welding forces would be lower, because the strength of copper is lower than that of carbon steel.

Nickel-base alloys also are commonly joined using the inertia welding process. Surface velocities are much lower than those of steel, typically ranging to a level that is no higher than 50% of that for carbon steel. However, because of increased elevated-temperature properties, flywheel energies and welding forces are nearly double those required for carbon steels. After inertia welding, the joint in heat-treatable nickel-base alloys is often subjected to a solution and aging treatment. This is needed to precipitate second-phase particles (that is, γ' and γ'') that have been taken back into solution by the thermal cycle of the weld.

In direct-drive friction welding, the surface velocities are approximately half those used for carbon steel, whereas welding forces are nearly double those used for carbon steel. The welding procedures for cobalt-base alloys are similar to those for nickel-base alloys.

Procedure Development and Practice Considerations for Inertia and Direct-Drive Friction Welding

Tim Stotler, Edison Welding Institute

Dissimilar Metals

In terms of process requirements for the inertia or direct-drive friction welding of dissimilar material combinations, it is typically found that the welding parameters tend to be closer to those used for the higher-strength material in the combination. This results in a significant loss of the lower-strength material during welding and upsetting. As in any other joining process, it must also be remembered that the strength of the bond can be no higher than that of the lower-strength material. The combinations of metals that have been joined using the friction welding processes are shown in Fig. 4. Other combinations may be possible, with additional procedure development.

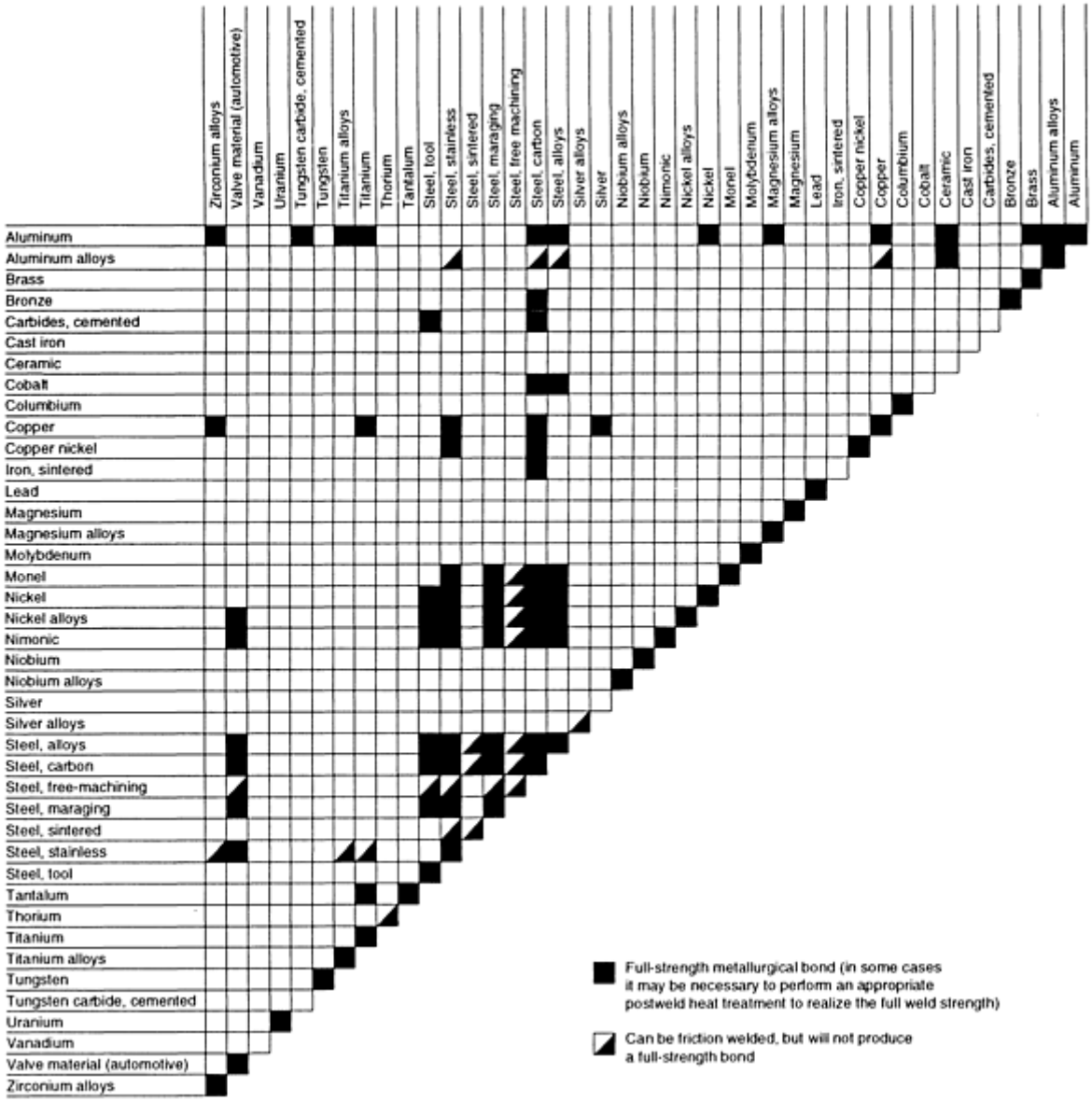

FIG. 4 MATERIAL COMBINATIONS THAT ARE WELDABLE BY FRICTION WELDING PROCESSES. LIST OF ALLOYS WAS COMPILED FROM AVAILABLE FRICTION WELDING LITERATURE. SOURCE: ANSI/AWS C6.1-89

Two of the most common dissimilar joints produced using the friction welding processes are:

- COPPER TO ALUMINUM
- ALUMINUM TO STEEL OR STAINLESS STEEL

In such applications, some surface preparation may be required prior to joining, because of oxidation of the aluminum surface. In most cases where aluminum is used in a joint, a dry machining or chemical etching of the aluminum is preferred. As mentioned previously, a majority of the forging (material loss) will occur in the aluminum, especially for the aluminum-to-steel joint.

The joining of aluminum to ceramics has also been performed, primarily for the electrical industry. Steel has also been attached to ceramics using an aluminum interlayer. This is performed by first welding the steel to the aluminum, followed by welding the bimetal joint to the ceramic. Using an interlayer for applications such as this is common when two

incompatible materials require joining. The interlayer materials must be selected on the basis of their forgeability and compatibility with the two parent materials.

Procedure Development and Practice Considerations for Inertia and Direct-Drive Friction Welding

Tim Stotler, Edison Welding Institute

Selected References

- *METALS HANDBOOK,* 9TH ED., VOL 6, AMERICAN SOCIETY FOR METALS
- "RECOMMENDED PRACTICES FOR FRICTION WELDING," ANSI/AWS C6.1-89, AMERICAN WELDING SOCIETY
- T. STOTLER AND J.E. GOULD, "INERTIA WELDING OF STEEL TO A STRUCTURAL CERAMIC," 73RD AWS MEETING (CHICAGO, IL), AWS, 1992
- A. SUZUMURA, T. ONZAWA, A. OHMORI, AND Y. ARATA, "FRICTION WELDING OF CERAMICS TO ALUMINUM-CLAD STEEL," DOCUMENT NO. III-890-87, 40TH ANNUAL ASSEMBLY OF INTERNATIONAL INSTITUTE OF WELDING (SOFIA, BULGARIA), IIW, 1987
- V.I. VILL, *FRICTION WELDING OF METALS*, AMERICAN WELDING SOCIETY, 1962
- *WELDING HANDBOOK,* 7TH ED., VOL 3, AMERICAN WELDING SOCIETY
- *WELDING HANDBOOK,* 7TH ED., VOL 4, AMERICAN WELDING SOCIETY
- *WELDING HANDBOOK,* 8TH ED., VOL 2, AMERICAN WELDING SOCIETY

Procedure Development and Practice Considerations for Ultrasonic Welding

Janet Devine, Sonobond Ultrasonics, Inc.

Introduction

ULTRASONIC WELDING (USW) is effectively used to join both similar and dissimilar metals with lap-joint welds. Various metals differ in weldability based on their compositions and properties. The metals that are considered more difficult to weld are those that require either high power or long weld times, or both, and those that incur operational problems, such as tip sticking or short tip life. Most ductile metals can be welded together. Figure 1 identifies some of the monometallic and bimetallic combinations that currently can be ultrasonically welded on a commercial basis.

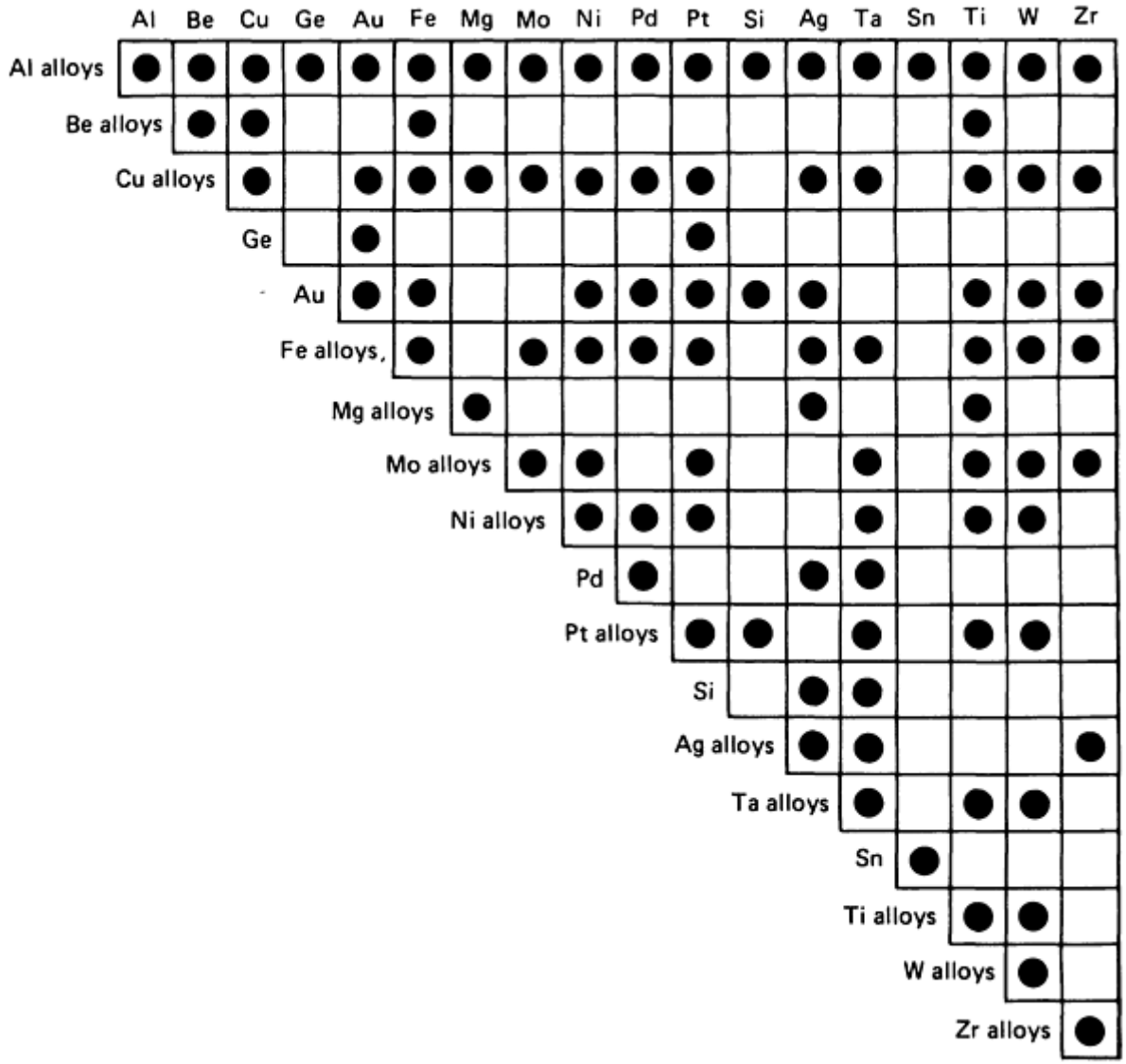

FIG. 1 CHART SHOWING ULTRASONICALLY WELDABLE METAL COMBINATIONS. BLANK AREAS IN THE CHART REPRESENT COMBINATIONS THAT HAVE NOT BEEN SUCCESSFULLY JOINED OR IN WHICH WELDING HAS NOT BEEN ATTEMPTED. SOURCE: AMERICAN WELDING SOCIETY

In ultrasonic welding, the temperature at the weld is not raised to the melting point. Therefore, there is no nugget similar to that formed in resistance welding. Weld strength is equal to the strength of the base metal. However, ultrasonic welding is typically restricted to relatively thin materials (foil or extremely thin gage thicknesses). The process, which can also be used for joining plastics, is finding wider applications in that field than in metals joining.

Ultrasonic welding is used extensively in the electronics, aerospace, and instrument industries. It is also used for producing packages and containers and for sealing applications.

This article describes procedure considerations for the ultrasonic welding of specific material types. For descriptions of USW processes and equipment, see the article "Ultrasonic Welding" in this Volume.

Procedure Development and Practice Considerations for Ultrasonic Welding

Janet Devine, Sonobond Ultrasonics, Inc.

Difficult-to-Weld Alloys

Satisfactory welds can be made in certain ferrous alloys. Frequently, however, low tip life and poor peel strength are encountered.

Carbon and Low-Alloy Steels. A weld between a 0.9% C steel and iron is shown in Fig. 2. Because many other processes are available for joining ferrous metals, ultrasonic welding usually is not chosen. Copper flash or copper plating on steel will sometimes improve the quality of the weld.

FIG. 2 PHOTOMICROGRAPH SHOWING WELD INTERFACE CROSS SECTION OF 0.81 MM (0.032 IN.) THICK HIGH-CARBON (0.9 WT% C) STEEL ULTRASONICALLY WELDED TO 0.81 MM (0.032 IN.) THICK IRON. 1000×

High-Strength Steels. Ultrasonic welding of high-strength steels is not considered to be viable.

Stainless Steels. A weld in 0.35 mm (0.014 in.) thick half-hard AISI 300-series stainless steel is shown in Fig. 3. Although it is possible to produce welds in stainless steels using ultrasonic welding, it is not the process of choice.

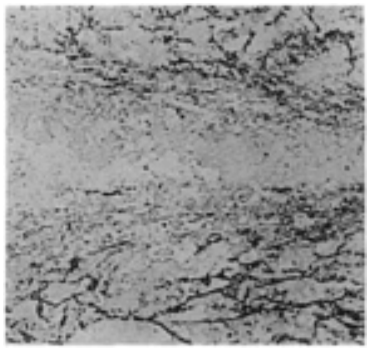

FIG. 3 PHOTOMICROGRAPH SHOWING WELD INTERFACE CROSS SECTION OF TWO 0.36 MM (0.014 IN.) THICK PIECES OF HALF-HARD AISI 300-SERIES STAINLESS STEEL THAT ARE ULTRASONICALLY WELDED TO EACH OTHER. 500×

Procedure Development and Practice Considerations for Ultrasonic Welding

Janet Devine, Sonobond Ultrasonics, Inc.

Weldable Materials

Aluminum Alloys. All combinations of aluminum alloys are ultrasonically weldable. The significant diffusion that is typical of ultrasonic welds in aluminum is shown in Fig. 4. In general, the hardness of work-hardenable aluminum should range from quarter-hard to half-hard. Annealed materials exhibit high deformation when ultrasonically welded.

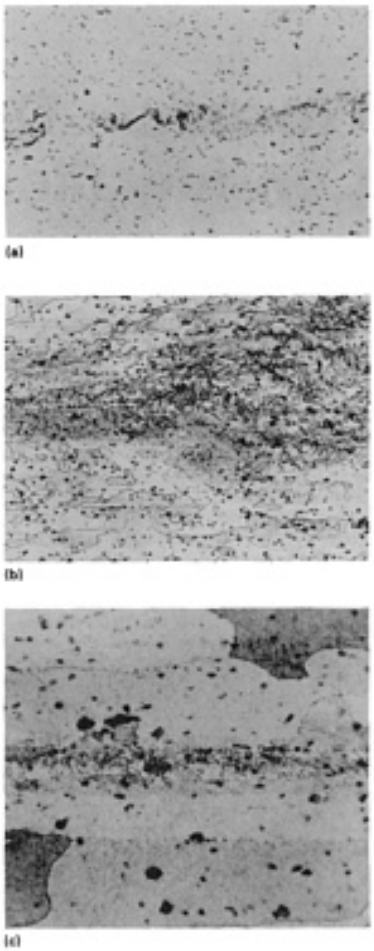

FIG. 4 PHOTOMICROGRAPHS OF WELD INTERFACE CROSS SECTIONS OF SELECTED ULTRASONICALLY WELDED ALUMINUM ALLOYS. (A) TWO PIECES OF 0.30 MM (0.012 IN.) THICK 1100 H14 ALLOY. 500×. (B) TWO PIECES OF 0.81 MM (0.032 IN.) THICK 2024-T3 BARE ALUMINUM ALLOY. 150×. (C) TWO PIECES OF 1.02 MM (0.040 IN.) THICK 2020 ALLOY. 750×

Some aluminum alloys (particularly the 1100 series and 2036 alloy) tend to stick to the welding tip. Tip sticking can sometimes be overcome by using high power and a short welding time. Hardened tool steel tips exhibit the most satisfactory results. Other solutions include using a mechanical stripper where light sticking occurs or placing a thin-gage steel shim between the vibrating tip and the weldment.

Various tip geometries and surface finishes can be used for welding aluminum, including circular radiused, flat cross-hatched, bulls-eye, and serrated types. Tips can be circular, rectangular, line-shaped, and so on, as suits the end use of the workpiece.

The aluminum adjacent to the tip should be less than 2.5 mm (0.1 in.) thick for the highest strength results. The material to which it is welded does not require a thickness limitation. Solid wires with diameters up to 3.18 mm (0.125 in.) or stranded wires with diameters up to 6.4 mm (0.25 in.) also can be welded.

Commercial applications of ultrasonically welded aluminum alloys include:

- SEAM WELDING OF LIGHT-GAGE FOILS
- WELDING OF STRANDED WIRE TO TERMINALS
- JOINING MULTIPLE LAYERS OF ALUMINUM FOIL TO A CAPACITOR TERMINAL
- JOINING ALUMINUM FRAMES TO ALUMINUM GRILLES FOR HEATING DUCTS
- AIRCRAFT PANEL WELDING FOR THE A-10 AIRCRAFT

- ALUMINUM INTERCONNECT WELDING ON PHOTOVOLTAIC PANELS

Reactive and Refractory Base Metals. The photomicrographs in Fig. 5 show ultrasonic welds in molybdenum. This material, as well as other reactive and refractory metal alloys, are difficult, but not impossible, to join using the ultrasonic welding process. In general, weldability appears to depend on the hardness and the ductility of the materials. Softer, more-ductile materials are more likely to weld, whereas hard, brittle materials tend to exhibit stress crocks under ultrasonic activation.

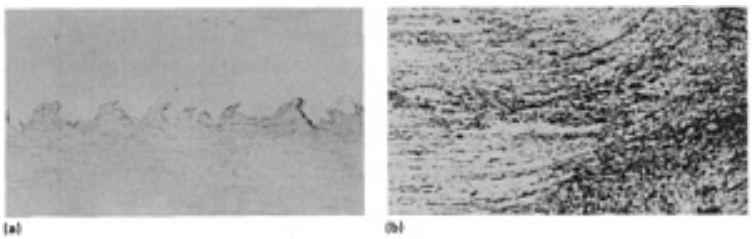

FIG. 5 PHOTOMICROGRAPHS OF WELD INTERFACE CROSS SECTIONS OF SELECTED ULTRASONICALLY WELDED MOLYBDENUM ALLOYS. (A) 0.13 MM (0.005 IN.) THICK NICKEL JOINED TO 0.51 MM (0.02 IN.) THICK MOLYBDENUM. 200×. (B) TWO PIECES OF 0.20 MM (0.008 IN.) THICK ARC CAST MOLYBDENUM WELDED TOGETHER. 140×

The welding of materials in this class is limited to thin sections with thicknesses under 0.4 mm (0.016 in.).

Titanium alloys, which have a very hard oxide layer, should be chemically etched before welding is attempted. Oxide removal should occur not more than 24 h prior to welding, unless the material is sealed and stored in an inert atmosphere.

Copper Alloys. The greatest industrial use of ultrasonic welding is in the joining of copper and brass materials. Copper alloys can be joined together or to other materials, such as aluminum, with great success. Various tip geometries and surface finishes can be used.

Welds in copper sheet that is up to 2 mm (0.08 in.) thick provide excellent joint strength. Stranded wires for wire harness applications represent one common use. Bundles that have a cross-sectional area up to 30 mm^2 (0.05 $in.^2$) are readily weldable.

The high thermal conductivity of copper is not the deterrent to ultrasonic welding that it is with fusion welding. Applications include:

- STRANDED WIRE TO STRANDED WIRE JOINTS FOR AUTOMOTIVE, TRUCK, AND APPLIANCE HARNESSES
- STRANDED WIRES JOINED TO TERMINALS FOR AUTOMOTIVE AND OTHER ELECTRICAL HARNESSES
- JOINING OF STRANDED WIRES TO SOLID WIRES
- SOLID WIRE TO SOLID WIRE JOINTS IN COMMUTATORS FOR AUTOMOTIVE ENGINE STARTER MOTORS
- JOINING OF COPPER STRIP TO COPPER STRIP FOR ELECTRICAL GROUNDING GRIDWORK
- JOINING OF FLAT WIRE TO FLAT WIRE FOR AUTOMOTIVE ENGINE STARTERS AND COILS
- JOINING OF FLAT COPPER SLUG TO ALUMINUM PLATE FOR AUTOMOTIVE ENGINE IGNITION MODULES
- JOINING OF ENAMELED WIRE TO STEEL HOUSING FOR SOLENOID COIL GROUND
- JOINING OF COPPER TUBE CLOSURES FOR HEATING, VENTILATING, AND AIR CONDITIONING (HVAC) INDUSTRY

- JOINING OF BRASS U-SHAPED SECTION TO A BRASS PLATE FOR A BRUSH HOLDER
- JOINING OF COPPER STEEL LAMINATE TO ITSELF FOR A COMMUNICATIONS CABLE SHEATHING

Precious Metals. Most of the precious metals (that is, gold, silver, platinum, and their alloys) are weldable ultrasonically. Materials plated with such metals are also ultrasonically weldable.

Nickel-Base Alloys. Many nickel-base alloys and nickel-plated materials are ultrasonically weldable. Figure 6 is a photomicrograph of nickel ultrasonically welded to gold-plated Kovar.

FIG. 6 PHOTOMICROGRAPH SHOWING WELD INTERFACE CROSS SECTION OF 0.08 MM (0.003 IN.) THICK NICKEL ULTRASONICALLY WELDED TO 0.08 MM (0.003 IN.) THICK GOLD-PLATED KOVAR. 300×

Figure 7 shows a weld in the nickel-base alloy Inconel X. A heat-affected zone (HAZ) is produced in nickel. Significant penetration across the interface is exhibited. Nickel sulfamate plating gives better results than electroless nickel plating when joining nickel-plated materials.

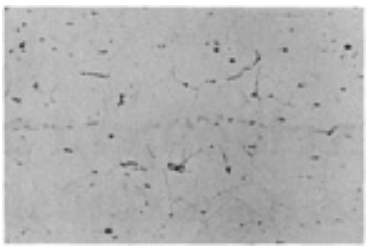

FIG. 7 PHOTOMICROGRAPH SHOWING WELD INTERFACE CROSS SECTION OF TWO 0.30 MM (0.012 IN.) THICK PIECES OF SOLUTION HEAT TREATED AND AGED INCONEL X THAT WERE ULTRASONICALLY WELDED TO EACH OTHER. 150×

Procedure Development and Practice Considerations for Ultrasonic Welding

Janet Devine, Sonobond Ultrasonics, Inc.

Dissimilar Metal (Nonferrous-to-Nonferrous) Combinations

Perhaps one of the most useful characteristics of ultrasonic welding is its ability to weld dissimilar material combinations. Primarily used to join copper and aluminum alloys, this technique promotes the advantages of using aluminum as a backing plate and the solderability of copper for attaching circuitry. [For example, copper slugs are ultrasonically welded to an aluminum backing plate for automotive-engine ignition modules and for antilock braking system (ABS) sensors]. The copper is more suitable for soldering the circuitry and provides a better match to the expansion coefficient of the chip carrier. This is important if the stress of thermal cycling is to be overcome.

When using aluminum for electrical wiring applications, one of the major causes of failure has occurred at the mechanical crimp between the aluminum wire and the connector. Problems have involved corrosion and loosening of the wire at the joint, as a result of thermal stress. In some applications, a copper "pigtail" inserted between the aluminum wire and the connector can eliminate this problem.

Other typical applications include:

- CONSTRUCTION OF A LITHIUM BATTERY, WHICH REQUIRED THE JOINING OF EITHER THIN ALUMINUM, COPPER, OR NICKEL SHEETS TO EXPANDED NICKEL MESH. ALL THREE VARIATIONS PROVIDED ELECTRICALLY AND THERMALLY SOUND JOINTS OF ADEQUATE STRENGTH
- COPPER WIRES WELDED TO COPPER-FLASHED STEEL PLATE TO MAKE A CARBON BRUSH HOLDER FOR A LOCOMOTIVE ELECTRIC TRACTION MOTOR. THE ULTRASONIC WELDED ASSEMBLY REPLACED A COMPLICATED PROCESS THAT REQUIRED RIVETING AND FORMING OF THE "BRIDGE" FOR THE BRUSH
- COPPER WIRES WELDED TO COPPER-PLATED STEEL FOR AN AUTOMOBILE SEAT SWITCH
- COPPER WIRES WELDED TO STAINLESS STEEL AS PART OF A PHOTOVOLTAIC ASSEMBLY
- COPPER WIRES AND STRIPS WELDED TO SILVER-PLATED TERMINALS

Procedure Development and Practice Considerations for Explosion Welding

Vonne D. Linse, Edison Welding Institute

Introduction

EXPLOSION WELDING (EXW), like all other welding or joining processes, has a well-defined set of input parameters or conditions that must fall within certain limits for the desired weld quality to be achieved. Contrary to other joining processes, however, the EXW occurs so rapidly (within a time period of a few microseconds) that there is no time for in-process adaptive control or modification of the welding parameters or conditions. Therefore, a total quality joining approach must be taken to ensure that proper process parameters are applied and controlled to consistently achieve high-quality welds. The quality must be built into the prewelding stages of the preparation of the process materials and setups before welding takes place. It is necessary to be thoroughly familiar with every aspect of the process and the quality level that must be applied in order to ensure the consistent quality of the end-product weld.

This article provides a general overview of the important mechanistic aspects of EXW, the process-material interactions, and the critical aspects or parameters that must be controlled. The procedure for ensuring control is also discussed. This type of approach to setting and controlling process parameters is particularly important when explosion welding dissimilar or metallurgically incompatible metals. Metallurgically incompatible combinations, such as titanium and steel, aluminum and steel, and zirconium and steel, will form brittle intermetallic compounds at the explosion weld interface if excessive energies are used during welding. The intermetallic compounds result in poor-quality welds. Setting and controlling process parameters are also important when welding the newer advanced materials, which have little tolerance for parametric variation (Table 1). Information about the principles underlying this process is available in the article "Fundamentals of Explosion Welding" in this Volume. Information about EXW equipment and applications can be found in the article "Explosion Welding" in this Volume.

TABLE 1 COMMERCIALLY USED METALS AND ALLOYS THAT CAN BE JOINED WITH EXW

METAL NO. 1	METAL NO. 2[(A)]														
	ZIRCONIUM	**MAGNESIUM**	**COBALT ALLOYS**	**PLATINUM**	**GOLD**	**SILVER**	**NIBIUM**	**TANTALUM**	**TITANIUM**	**NICKEL ALLOYS**	**COPPER ALLOYS**	**ALUMINUM ALLOYS**	**STAINLESS STEELS**	**ALLOY STEELS**	CARBON STEELS
CARBON STEELS	X	X	X	. . .	X	X	X	X	X	X	X	X	X	X	**X**
ALLOY STEELS	X	X	X	. . .	. . .	. . .	X	X	X	X	X	X	X	X	
STAINLESS STEELS	X	. . .	X	. . .	X	X	X	X	X	X	X	X	X		
ALUMINUM ALLOYS	X	X	. . .	. . .	X	X	X	X	X	X	X	X			
COPPER ALLOYS	X	. . .	. . .	. . .	X	X	X	X	X	X	X				
NICKEL ALLOYS	X	X	X	X	X	. . .	X	X	X	X					
TITANIUM	X	X	. . .	. . .	. . .	X	X	X	X						
TANTALUM	X	. . .	. . .	. . .	X	. . .	X	X							
NIOBIUM	. . .	. . .	. . .	X	. . .	. . .	X								
SILVER	. . .	. . .	. . .	. . .	. . .	X									
GOLD	. . .	. . .	. . .	. . .	. . .										
PLATINUM	. . .	. . .	. . .	X											
COBALT ALLOYS	. . .	. . .	X												
MAGNESIUM	X	X													
ZIRCONIUM	**X**														

Source: Adapted from Ref 1

(A) EXES INDICATE EXW IS AN APPLICABLE PROCESS.

Reference

1. *WELDING HANDBOOK*, VOL 2, 8TH ED., R.L. O'BRIEN, ED., AWS, 1991, P 772

Critical Process Parameters

In order to fully understand EXW and its control, it is helpful to know the general characteristics of the process, particularly the rates, pressures, and energies involved. The following are the general process parameters:

TRAVERSE RATE, M/S (FT/S)	**2000-3000 (6600-9800)**
PRESSURE, GPA (10^6 PSI)	**1.5-6.0 (0.22-0.88)**
PRESSURE TIME DURATION, μS	**5-20**
ENERGY DEPOSITION/UNIT AREA, J/CM^2 (BTU/FT^2)	**100-300 (90-260)**
ENERGY DEPOSITION RATE, MJ/S (BTU/H)	**20-90 (70×10^6 - 310×10^6)**

By comparison, standard fusion welding processes will typically have traverse rates of a fraction of a meter/second and energy depositions/unit area in the range of 10,000 to 30,000 J/cm^2 (9000 to 26,000 Btu/ft^2). The low-energy input of EXW and the high rate of deposition at the weld interface allow the weld to be made with an absolute minimum of thermal excursion and no resultant beat-affected zone (HAZ).

Procedure Development and Practice Considerations for Explosion Welding

Vonne D. Linse, Edison Welding Institute

Fundamentals of EXW

The overall mechanisms of EXW are well known and are shown in Fig. 1. In general, the energy from an explosive accelerates one of the two components being welded (prime or clad) across a gap or standoff to collide with the second component (base) and form a solid-state metallurgical weld or bond between the two. The various aspects or mechanisms of the process have been investigated and reported over the years; however, the process is still largely controlled by most commercial users on a more or less empirical basis. Important process-input parameters are selected primarily on the basis of past experience and usually are not calculated from basic principles of theory. The following sections ("Explosives and Explosive Detonation" , "Component Acceleration" , and "Component Collision") cover the latter approach to understanding and controlling EXW on a more fundamental basis. This requires breaking down and treating each mechanistic aspect of the process in a step-by-step sequence.

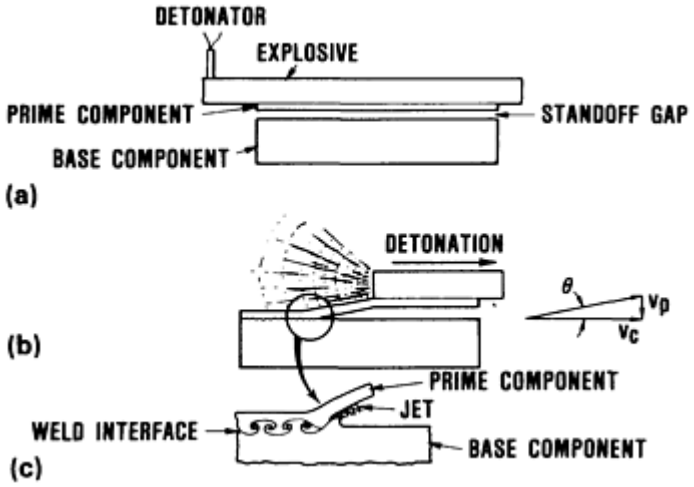

FIG. 1 SCHEMATIC SHOWING MECHANICS OF EXW. (A) ALIGNMENT OF COMPONENTS TO BE JOINED BEFORE DETONATION. (B) MOTION OF COMPONENTS AT DETONATION TO FORM WELD PLUS VECTOR DIAGRAM OF VELOCITY COMPONENTS. (C) CLOSE-UP VIEW OF WAVELIKE WELD INTERFACE CHARACTERISTIC OF EXW PROCESS

Explosives and Explosive Detonation

The explosive is the energy source for the process. It releases its energy in a very specific manner during detonation. It is, therefore, necessary to first understand the manner in which the welding explosive detonates and how its energy is delivered to the prime or cladding component.

In almost all instances, the explosives used for welding can be classified as nonideal. They do not detonate in a manner that can be easily defined by the physics equations-of-state typically used for extremely-high-velocity military or weapons explosives. This results from the fact that these explosives are almost always granular in nature, with the primary ingredient typically being ammonium nitrate (NH_4NO_3). Other ingredients (for example, sensitizers, density control agents, and diluents) are then blended to produce an explosive that yields the desired detonation velocity, pressure, and duration of pressure.

The detonation characteristics of the explosive are controlled by its composition, particle size distribution, pour or packing density, layer thickness, confinement, moisture content, and, in some instances, age. The detonation performance of the explosive should be tailored to match the metals or alloy combination being welded with respect to the density, thickness, and sonic or shock wave velocity of the prime component, as well as the sonic velocity of the base component (if it is different from that of the prime component).

Detonation is a progressive event that starts at the detonator and progresses into the undetonated explosive at a rate known as the detonation velocity. Within the detonation region itself (Fig. 2), the detonation front consists of an initial high-pressure shock wave intense enough to trigger the high-pressure chemical reaction that follows in the reaction zone. In an ideal explosive, the reaction goes almost instantaneously to completion; therefore, the reaction zone is extremely short (usually <1 mm, or 0.04 in.). In a nonideal explosive, however, the reaction zone is much longer (5 to 25 mm, or 0.2 to 1 in.) because the reaction takes longer to complete. While the pressure in the reaction zone of a nonideal explosive is much lower than that in the initial shock wave, it has a much longer duration in which the high-pressure gases in the zone can deliver their impulse to accelerate the prime component. Behind the reaction zone is the third and final region of relatively low-pressure expanding gases, which contribute little, if any, to the impulse delivered to the acceleration of the prime component. Each type of explosive has characteristic detonation velocity, pressure, and duration factors that can be applied to predict the specific velocity, pressure, and duration for a given thickness and density of that explosive. For welding, it is usually desirable for nonideal explosives to detonate in the range of 2000 to 3000 m/s (6600 to 9800 ft/s). If the explosive is manufactured to exacting specifications, it is possible to control the detonation velocity within ±2% of the target terminal velocity. With nonideal explosives, however, such factors as run-up regions near the initiation point and predetonation compression due to the precursor shock wave in the prime component ahead of the EXW collision front can cause nonsteady-state detonation conditions, which in turn can result in nonuniform weld quality.

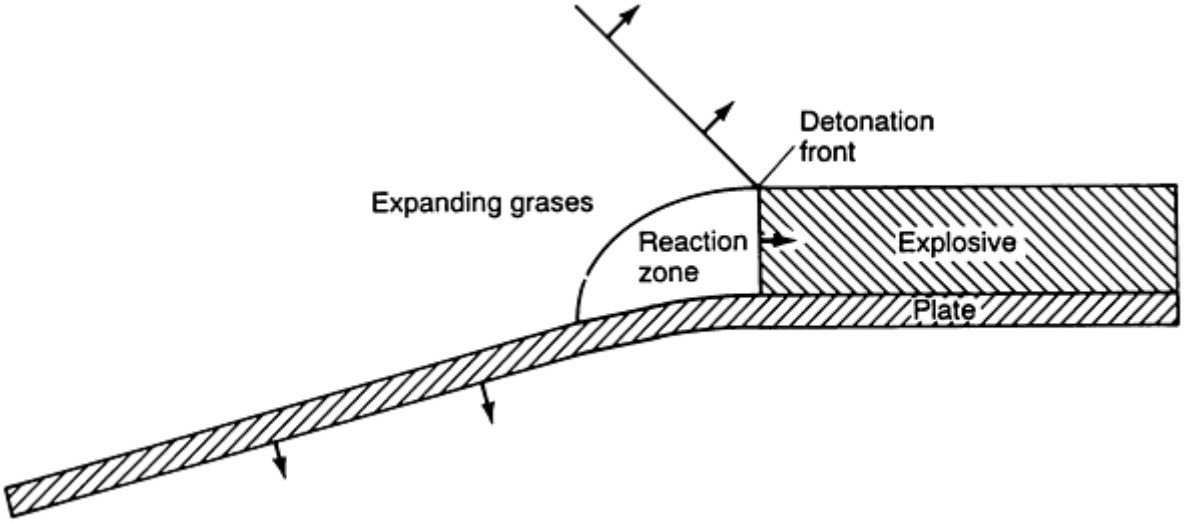

FIG. 2 SCHEMATIC SHOWING DETONATION REGIONS IN A NONIDEAL EXPLOSIVE AND THE ASSOCIATED ACCELERATION OF THE PRIME COMPONENT

Component Acceleration

For welding, the explosive is distributed over the top or exposed surface of the prime component and is detonated such that the detonation front progresses in a grazing or tangential manner over the length of the prime component. In doing so, the explosive delivers a specific level of impulse to the prime component that causes it to be accelerated to a terminal bend angle, θ, and velocity, v_p, as shown in Fig. 1. For explosion welding, the acceleration region before terminal conditions are reached is the important region.

The acceleration of the prime component actually results from the two separate zones of the detonation region in the explosive. First is the contribution of the high-pressure shock front in the explosive. This imparts a high-pressure shock wave into the prime component. The shock wave traverses back and forth, or rattles, between the opposite surfaces of the component, causing it to accelerate quickly in its early stages. The effects of this contribution diminish quickly and cause the component to reach only approximately 80% of the full-potential bend angle (Fig. 3) and velocity. As the effects of the shock component begin to diminish, the expanding high-pressure gas from the trailing reaction zone takes over and continues the acceleration more gradually until the terminal angle and velocity are obtained when the reaction is completed. This contribution (Fig. 3) plus the shock contribution yields the total impulse delivered to the prime component. In an ideal explosive, nearly all of the acceleration comes from the extremely high pressure of the shock wave and very little from the trailing reaction zone; therefore, the primary component reaches terminal conditions much more quickly with an ideal or near-ideal explosive.

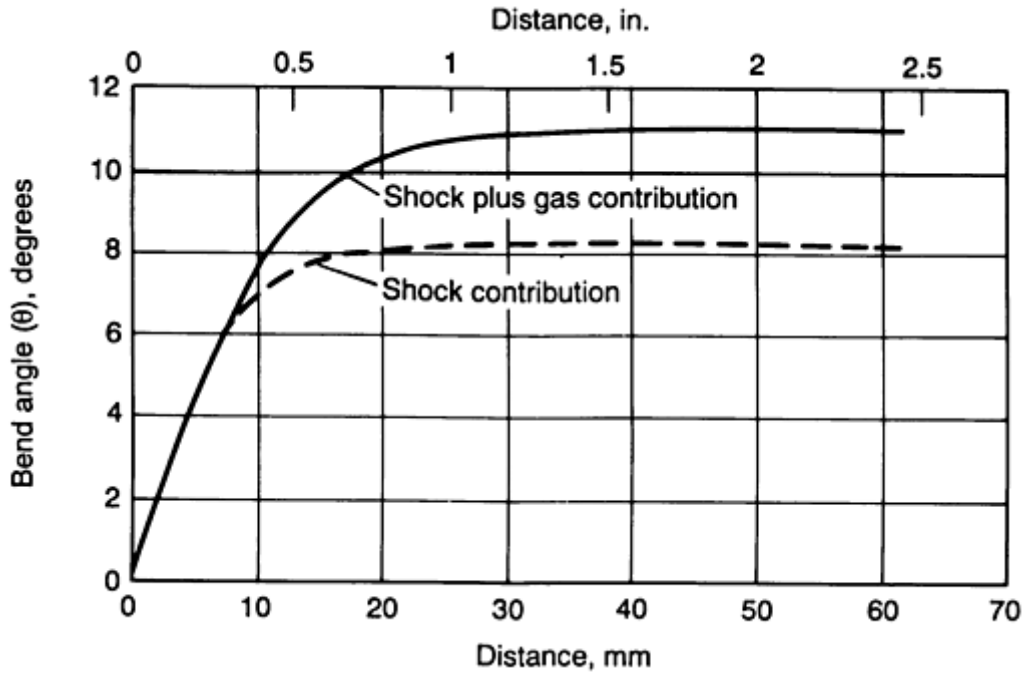

FIG. 3 PLOT OF PRIME PLATE COMPONENT BEND ANGLE VERSUS DISTANCE TO SHOW CONTRIBUTION OF SHOCK WAVE AND GAS PRESSURE TO ACCELERATION

The prime component acceleration depends on the following parameters:

- EXPLOSIVE PRESSURE (SHOCK AND GAS)
- DURATION OF THE EXPLOSIVE PRESSURE PULSE
- SONIC OR SHOCK WAVE VELOCITY OF THE PRIME COMPONENT
- THICKNESS OF THE PRIME COMPONENT
- DENSITY OF THE COMPONENT MATERIAL

With the above variables, the acceleration characteristics of the prime component can be calculated. In addition, techniques exist to directly measure the acceleration of a prime component (Ref 2). Precise knowledge of the acceleration achieved for a specific prime component/explosive combination is extremely important. It allows the exact standoff or separation distance to be set between the prime and base components to obtain the required collision angle and prime component velocity in the next step of EXW (that is, the collision and welding step).

Component Collision

Once the accelerated prime component crosses the standoff gap, it collides with the stationary base component. The exact collision angle and prime component velocity achieved at the time of the collision will, of course, depend on the combination of the acceleration characteristics of the prime component and the standoff distance selected for the system. The standoff distance is usually selected to ensure that the collision occurs while the prime component is still undergoing acceleration, usually in its final stages.

The collision is characterized by:

$$V_p = 2v_c \sin\left(\frac{q}{2}\right) \qquad \textbf{(EQ 1)}$$

where v_p is the velocity of the prime component or the relative velocity of the prime and base components; v_c is the collision point velocity of the welding front, which also equals the detonation velocity, v_d, of the explosive; and θ is the collision angle. If any two of the above variables are known, it is then easy to calculate the third variable. The relative component velocity, v_p, at the time of the collision is very important in that it determines the equation-of-state pressure generated at the collision point. This pressure, which must be sufficient to generate hydrodynamic flow of both materials at the collision point, can be determined from the characteristic pressure versus plate (or particle) velocity for the material or materials being welded. Figure 4 shows a high pressure versus particle velocity plot for a similar material collision (Fig. 5). Initially, the pressure required for dynamic yielding of the two materials being welded is calculated. This pressure is then located on the curve, and a mirror image of the curve is drawn through the selected pressure. The point at which the mirror-image curve intersects the zero pressure line or abscissa is the minimum prime plate velocity necessary to obtain the desired pressure and accompanying dynamic flow and jetting necessary for welding to occur.

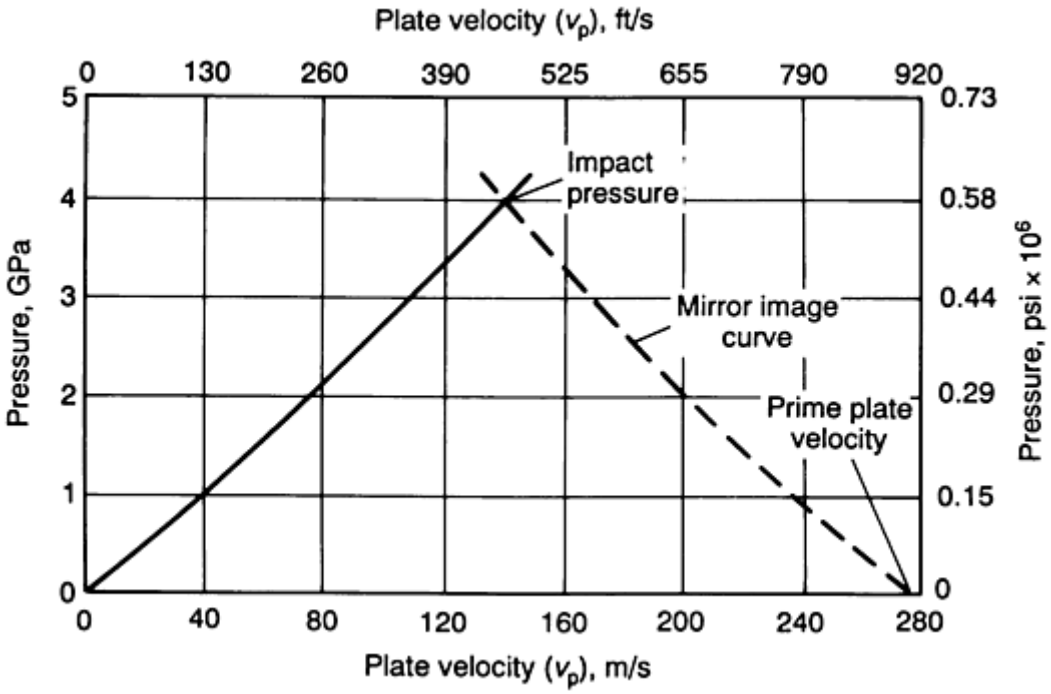

FIG. 4 PLOT OF HIGH PRESSURE VERSUS PARTICLE VELOCITY TYPICALLY USED TO DETERMINE THE PRIME COMPONENT VELOCITY NECESSARY TO ACHIEVE DYNAMIC YIELDING AND WELDING

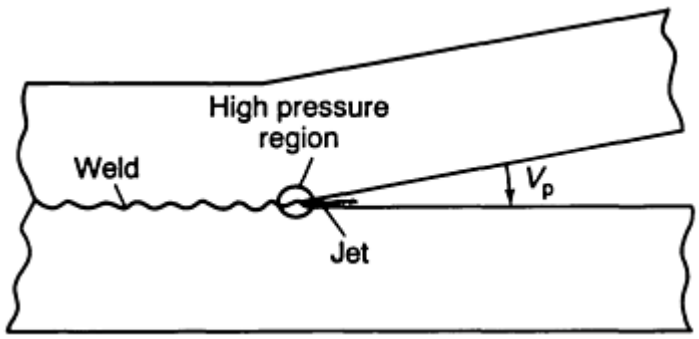

FIG. 5 JET FORMATION AT THE COLLISION POINT TO GENERATE WELD DURING EXW

Reference cited in this section

2. E.G. SMITH, JR. AND V.D. LINSE, THE ACCELERATION CHARACTERISTICS OF EXPLOSIVELY

DRIVEN FLYER PLATES, *PROC. SIXTH INT. CONF. HIGH ENERGY RATE FABRICATION* (ESSEN, WEST GERMANY), 13-16 SEPT 1977

Jetting and Weld Formation

When the required minimum collision pressure, a minimum duration of the pressure pulse, and a minimum collision angle are obtained, the surfaces of the two materials being joined locally flow in the immediate region of the collision point. Because of the angular geometry of the collision, these surfaces at the collision point are forced to reverse their flow direction with severe shearing flow and to be ejected out ahead of the advancing collision point in the form of a fine fingerlike mist (that is, a jet) (Fig. 5). Under the extremely high hydrodynamic pressures involved, this jet, which consists of a combination of both parent materials, has an extremely high temperature. When the collision conditions of the weld are within an appropriate range (as discussed in the section "Parametric Limits for Welding" in this article), most of the jet, with its attendant heat, is ejected out of the weld interface with little or no effect on the remaining weld zone. Of greatest importance, however, is that the surface-scarfing action of the jet removes the surface layers containing the oxides and other contaminants that typically inhibit solid-state interaction. This allows the two metals to directly weld or bond under the substantial residual pressure of the collision, which continues to act from some period of time on the two metals at the weld interface. This residual pressure on the interface after the collision also counteracts any reflected stress waves from separating the weld while it is forming.

Procedure Development and Practice Considerations for Explosion Welding

Vonne D. Linse, Edison Welding Institute

Weld Characteristics

Of particular importance is the nature or characteristics of the explosion weld itself. When properly made, it is, in essence, a solid-state bond or weld without any HAZ to degrade its strength, as is typical of all other heat-dependent welding or joining processes.

Weld Interface. Morphologically, two types of explosion weld interfaces can be created. First is the flat or straight-line interface, which occurs only when the collision conditions are at or near the lower limits for jetting and welding. This type of condition is typically avoided in most instances because a slight drop in collision conditions or parameters during welding would stop the welding and leave a nonwelded region.

In most cases, the explosion weld interface will have a wave morphology that is exclusively characteristic of the process. A typical, wavy explosion weld interface between copper and niobium is shown in Fig. 6. This wave formation, which has been the subject of considerable investigation (Ref 3, 4), results from the localized dynamic compression of the two metals in the region immediately adjacent to the collision point and weld interface. The compression causes localized bulk flow of the metals, which become unstable and make the weld interface oscillate above and below the theoretical plane of the interface. The size of the wave pattern is the one postwelding characteristic that can be used to determine the collision conditions used to make the weld and to allow for adjustments in subsequent welds of the same material type and thickness. The wavelengths or frequency of the interfacial wave in an explosion weld is directly related to the thickness of the prime or cladding plate and its angle of collision with the base plate (Ref 5, 6), as shown in Fig. 7. For practical purposes, this relationship is relatively independent of the types or combinations of metals or alloys being welded. It also shows that the wave formation ceases at collision angles of 4° or less.

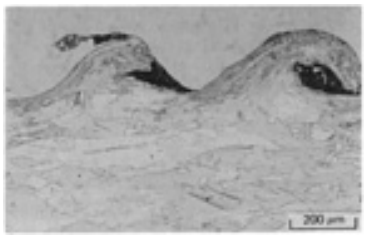

FIG. 6 PHOTOMICROGRAPH SHOWING TYPICAL WAVY WELD INTERFACE OBTAINED WHEN NIOBIUM AND COPPER ARE JOINED BY EXW

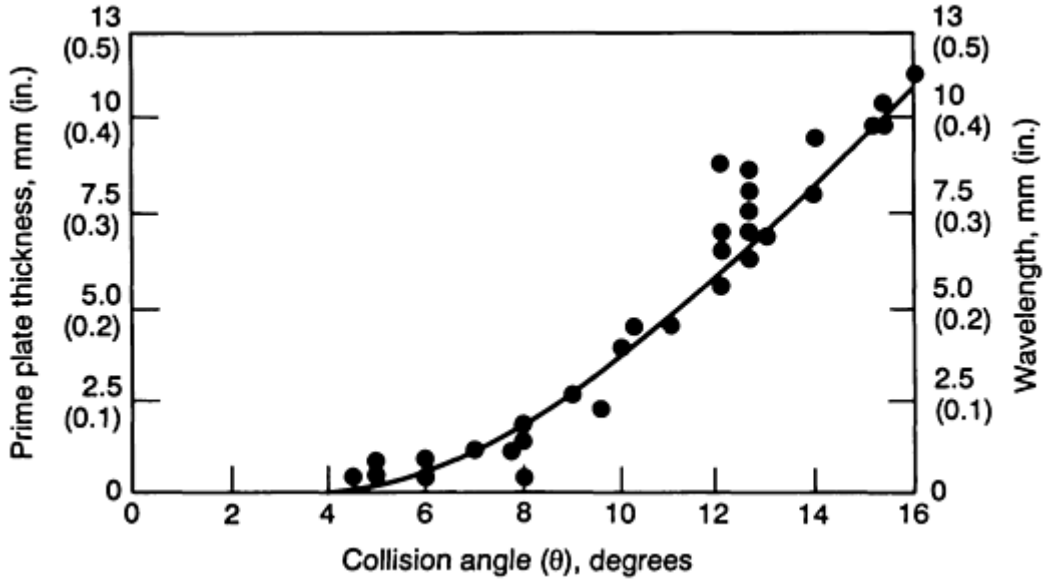

FIG. 7 RELATIONSHIP OF WAVELENGTH TO PLATE THICKNESS AS A FUNCTION OF COLLISION ANGLE

Wave Amplitude. The amplitude of the waves, on the other hand, is more difficult to predict. It depends on several factors, including the relative flow characteristics of the two metals being joined and the collision point velocity of the EXW process.

Control of the wave size, particularly the wavelength, is an important part of controlling several aspects of the explosion weld because:

- WAVE SIZE DETERMINES THE AMOUNT OF LOCALIZED FLOW AND WORK HARDENING IN AND ADJACENT TO THE EXPLOSION WELD INTERFACE.
- EXCESSIVE COLLISION ENERGIES AND WAVE SIZES CAN RESULT IN THE FORMATION OF LARGER MELT POCKETS ON THE FRONT AND BACK SLOPES OF THE WAVES, ALONG WITH RESIDUAL HEAT EFFECTS ON THE REGION IN AND ADJACENT TO THE WELD INTERFACE, WHICH WILL AFFECT THE MECHANICAL PROPERTIES OF THE WELD.
- WAVE SIZE IS AN EXTREMELY CRITICAL FACTOR IN PREVENTING ADIABATIC SHEAR DEFECTS OR CRACKS FROM FORMING ADJACENT TO THE WELD INTERFACE IN SPECIFIC ALLOYS (FOR EXAMPLE, CERTAIN HIGH-STRENGTH NICKEL-BASE AND TITANIUM ALLOYS).

Parametric Limits for Welding. All the above considerations and an understanding of the EXW and its controlling parameters can be assembled to produce a parametric envelope or window of parameters within which a high-quality

explosion weld can be consistently produced. The basic concept of the boundaries defining the envelope has been advanced by several researchers (Ref 7, 8, 9).

A typical parametric envelope is defined by four distinct boundary segments (Fig. 8). The lower boundary (1) is controlled by the collision pressure and dwell time of the pressure pulse. The left boundary (2), although somewhat complicated, is primarily controlled by the sonic velocities of the two materials being welded. The right boundary (3) is controlled by the upper sonic-velocity limit at which a jet will form. It is almost never of concern because EXW is typically conducted at collision velocities significantly below this limit. The upper limit (4 or 4A) is primarily controlled by the kinetic-energy release generated at the collision point. In similar or metallurgically compatible combinations of metals or alloys, increasingly higher amounts of energy in this area of the envelope result in increasingly greater amounts of residual heat effects (for example, large melt pockets, interface voids, and a general degradation of the weld quality and properties). Therefore, this boundary (4) cannot be sharply defined in this instance. In metallurgically incompatible systems, however, this upper boundary (4A) becomes very sharply defined because it corresponds to the energy level at which a brittle intermetallic compound begins to form. Welding at or above this limit produces a weld that is typically brittle and can fail catastrophically in service. Typically, this boundary is relatively close to the lower boundary (1), thus leaving a relatively small amount of latitude in collision parameters permissible to obtain a high-quality weld.

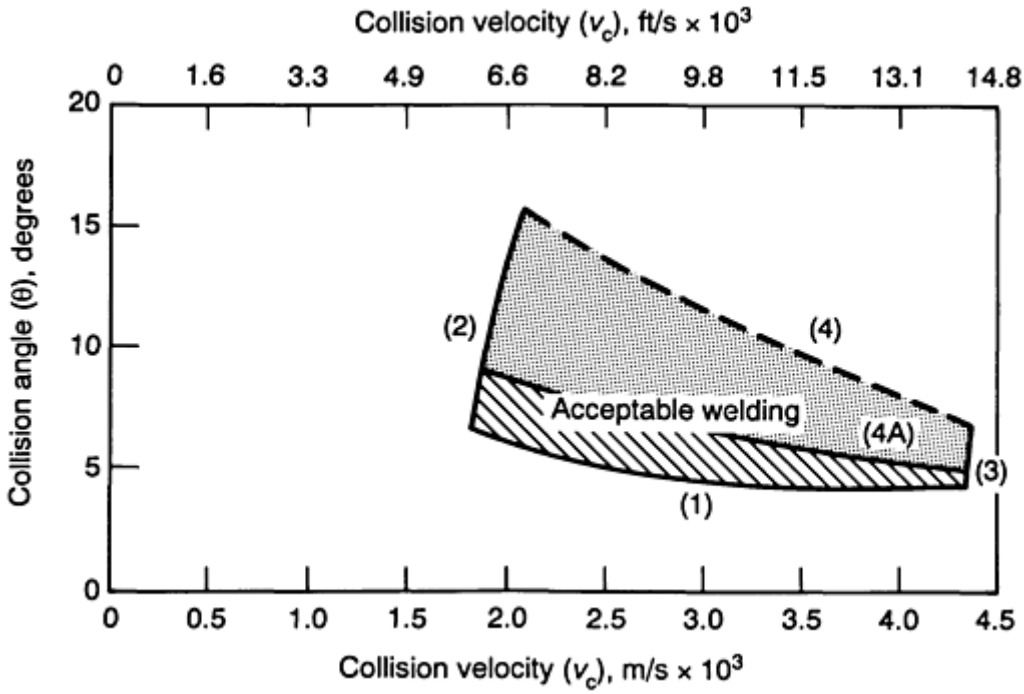

FIG. 8 PLOT OF COLLISION ANGLE VERSUS COLLISION VELOCITY TO OBTAIN TYPICAL EXW PROCESS PARAMETRIC ENVELOPE FOR BOTH SIMILAR AND DISSIMILAR METAL COMBINATIONS. SEE TEXT FOR DETAILS.

Each of the above boundaries can be calculated with relative accuracy for almost all material combinations and thicknesses to be explosion welded. With these limits defined, the collision conditions must then be maintained to fall within the boundaries sufficiently away from the edges to allow for minor variations in the collision conditions during EXW. If this is accomplished, then a reproducible, high-quality explosion weld can always be expected and produced.

References cited in this section

3. A.S. BAHRANNI, T.G. BLACK, AND B. CROSSLAND, THE MECHANICS OF WAVE FORMATION IN EXPLOSIVE WELDING, *PROC. R. SOC.*, VOL 296 (NO. 1445), 1967, P 123-126
4. J.N. HUNT, WAVE FORMATION IN EXPLOSIVE WELDING, *PHILOS. MAG.*, VOL 17 (NO. 148), APRIL 1968, P 669-680

5. A.A. DERIBAS, SIMULATION OF THE PROCESS IN WAVE FORMATION IN EXPLOSIVE WELDING, *COMBUSTION, EXPLOSION AND SHOCK WAVES,* VOL 4 (NO. 1), USSR, 1968
6. UNPUBLISHED DATA, BATTELLE COLUMBUS LABORATORIES
7. K.T. CHRISTENSEN, N.S. EGLEY, AND L. ATLING, EXPLOSIVE WELDING OF TUBES TO TUBE-PLATES, *PROC. FOURTH INT. CONF. CENTER FOR HIGH ENERGY FORMING* (VAIL, CO), 9-13 JULY 1973
8. R.H. WITTMAN, THE INFLUENCE OF COLLISION PARAMETERS ON THE STRENGTH AND MICROSTRUCTURE OF AN EXPLOSION WELDED ALUMINUM ALLOY, *PROC. SECOND INT. SYMP., USE OF EXPLOSIVE ENERGY IN MANUFACTURING METALLIC MATERIALS OF NEW PROPERTIES* (MARIANSKE LAZNE, CZECHOSLOVAKIA), 9-12 OCT 1973
9. A.A. DERIBAS, CLASSIFICATION OF FLOWS APPEARING ON OBLIQUE COLLISIONS OF METALLIC PLATES, *PROC. SECOND INT. SYMP., USE OF EXPLOSIVE ENERGY IN MANUFACTURING METALLIC MATERIALS OF NEW PROPERTIES* (MARIANSKE LAZNE, CZECHOSLOVAKIA), 9-12 OCT 1973

Procedure Development and Practice Considerations for Explosion Welding

Vonne D. Linse, Edison Welding Institute

References

1. *WELDING HANDBOOK,* VOL 2, 8TH ED., R.L. O'BRIEN, ED., AWS, 1991, P 772
2. E.G. SMITH, JR. AND V.D. LINSE, THE ACCELERATION CHARACTERISTICS OF EXPLOSIVELY DRIVEN FLYER PLATES, *PROC. SIXTH INT. CONF. HIGH ENERGY RATE FABRICATION* (ESSEN, WEST GERMANY), 13-16 SEPT 1977
3. A.S. BAHRANNI, T.G. BLACK, AND B. CROSSLAND, THE MECHANICS OF WAVE FORMATION IN EXPLOSIVE WELDING, *PROC. R. SOC.,* VOL 296 (NO. 1445), 1967, P 123-126
4. J.N. HUNT, WAVE FORMATION IN EXPLOSIVE WELDING, *PHILOS. MAG.,* VOL 17 (NO. 148), APRIL 1968, P 669-680
5. A.A. DERIBAS, SIMULATION OF THE PROCESS IN WAVE FORMATION IN EXPLOSIVE WELDING, *COMBUSTION, EXPLOSION AND SHOCK WAVES,* VOL 4 (NO. 1), USSR, 1968
6. UNPUBLISHED DATA, BATTELLE COLUMBUS LABORATORIES
7. K.T. CHRISTENSEN, N.S. EGLEY, AND L. ATLING, EXPLOSIVE WELDING OF TUBES TO TUBE-PLATES, *PROC. FOURTH INT. CONF. CENTER FOR HIGH ENERGY FORMING* (VAIL, CO), 9-13 JULY 1973
8. R.H. WITTMAN, THE INFLUENCE OF COLLISION PARAMETERS ON THE STRENGTH AND MICROSTRUCTURE OF AN EXPLOSION WELDED ALUMINUM ALLOY, *PROC. SECOND INT. SYMP., USE OF EXPLOSIVE ENERGY IN MANUFACTURING METALLIC MATERIALS OF NEW PROPERTIES* (MARIANSKE LAZNE, CZECHOSLOVAKIA), 9-12 OCT 1973
9. A.A. DERIBAS, CLASSIFICATION OF FLOWS APPEARING ON OBLIQUE COLLISIONS OF METALLIC PLATES, *PROC. SECOND INT. SYMP., USE OF EXPLOSIVE ENERGY IN MANUFACTURING METALLIC MATERIALS OF NEW PROPERTIES* (MARIANSKE LAZNE, CZECHOSLOVAKIA), 9-12 OCT 1973

Selection Criteria for Brazing and Soldering Consumables

A. Rabinkin, AlliedSignal Amorphous Metals

Introduction

THE ULTIMATE GOAL of brazing and soldering technologies is to join parts into an assembly through metallurgical bonding (Ref 1, 2, 3, 4, 5). This can be achieved by placing a relatively low-melting-temperature alloy, or filler metal, in the clearance, or gap, between the base materials to be joined, and then heating the assembly until the filler metal has melted and spread throughout the gap. The molten metal that fills the gap reacts with the parts being joined and, after solidification, forms an integral whole. The basic brazing/soldering process is depicted in Fig. 1. Assembly heating can be carried out using a variety of means, including electromagnetic induction, Joule heating, ovens, flames, and other forms.

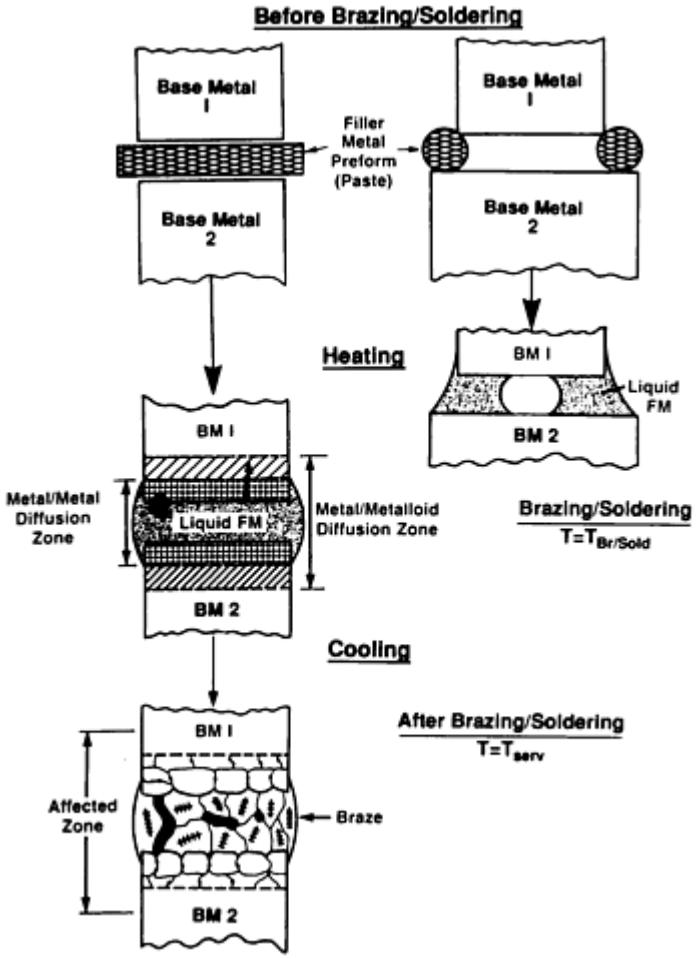

FIG. 1 FUNDAMENTALS OF BRAZING/SOLDERING PROCESSES

References

1. *BRAZING HANDBOOK,* 4TH ED., AWS, 1991
2. M.M. SCHWARTZ, *BRAZING,* ASM INTERNATIONAL, 1987
3. R.J. KLEIN-WASSINK, *SOLDERING IN ELECTRONICS,* ELECTROCHEMICAL PUBLICATIONS, 1984
4. M.M. SCHWARTZ, *CERAMIC JOINING,* ASM INTERNATIONAL, 1990
5. A. RABINKIN AND H.H. LIEBERMANN, CHAPTER 21, BRAZING AND SOLDERING WITH

RAPIDLY SOLIDIFIED ALLOYS,*RAPIDLY SOLIDIFIED ALLOYS: PROCESSES, STRUCTURES, AND PROPERTIES, AND APPLICATIONS*, MARCEL DEKKER, 1993, P 691-735

Selection Criteria for Brazing and Soldering Consumables

A. Rabinkin, AlliedSignal Amorphous Metals

Process Stages

There are three major stages in any brazing or soldering process. The first stage occurs during the heating of an assembled workpiece, when the filler metal melts, flows, and completely fills the gap between the parts. Because this gap is usually rather small, ranging from approximately 10 to several hundred μm (0.4 to ~10 mils), the degree to which a molten alloy penetrates into the gap is primarily determined by surface tension effects and, of course, by the chemical-reaction-driven phenomenon that plays an important role in wetting. Because physical properties of the filler metal and base material, such as part dimensions and surface tension forces, have a major role, this first stage can be conditionally called the physical stage.

The second stage, which normally occurs at a given joining temperature, is characterized by an intensive solid-liquid interaction, accompanied by a substantial mass-transfer through the interface with strongly uneven rates. The base material volume that immediately adjoins the liquid filler metal either dissolves or is reacted with the filler metal in this stage. At the same time, a small amount of elements from the liquid phase penetrates into the solid base material. Such mass-transfer unbalance is due to dramatically different diffusion rates in the solid and liquid phases. This redistribution of components in the joint area results in changes to the filler-metal composition, and sometimes, the onset of solidification of the filler metal.

Because all of the processes in this second joining stage have a distinctly metallurgical character, it is called the metallurgical stage. In soldering, these processes proceed to a lesser degree than they do in the brazing process, because of the substantially lower melting temperature of the solder alloys. Here, the dissolution of the base material and mutual diffusion occur to a lesser degree than they do in brazing, but because they can still be significant, protection of the base-material surface is required.

The last stage, which overlaps with the second, is characterized by the formation of the final joint microstructure and progresses during the solidification and cooling of the joint. Here, the crystallization process takes place. Post-solidification cooling causes annealing of the filler metal and partial relief of the thermal stresses induced upon cooling. This stage has very similar features in both brazing and soldering processes.

Cleaning the base-material components being joined and protecting them from oxidation during heating are essential in both brazing and soldering processes. Chemically active substances, called fluxes, are commonly used to provide such cleaning and shielding. The use of nonmetallic agents in fluxes is generally undesirable, because of the increased propensity for their entrapment and the resultant formation of voids in the finished joint. However, the use of certain active elements that can be added to filler-metal alloys to act as a flux can be advantageous. However, this concept usually only works with brazing filler metals. For solders, working temperatures are generally too low for the reduction reactions to take place with adequate speed, although in some cases these reactions do indeed occur.

Selection Criteria for Brazing and Soldering Consumables

A. Rabinkin, AlliedSignal Amorphous Metals

Product Forms and Joint Considerations

Basic forms of both brazing and solder filler metals include solid preforms and powders, which are used mostly in the compound form of paste; plastic-bonded tape (brazing filler metals); and rosin-core wire. Conventional paste forms of joining alloys, which consist of a filler-metal powder, fluxing agent, and a binder/solvent, are applied at externally

accessible locations of the clearance between the base-material components. This practice requires substantial filler-metal flow during joining to achieve constituent filler-metal-phase fusion and binder/solvent extraction. In addition, organic binders in a brazing filler metal decompose when used in the high-vacuum brazing of parts intended for critical, high-temperature service. Such binder decomposition can result in the formation of soot in the joint, which can degrade the performance of expensive vacuum equipment.

A basic requirement for any joint is that its strength and ductility be adequate for the service requirements. Generally, the strength of any materialincreases with decreasing grain size, whereas ductility is affected by the presence of brittle phases, which will be discussed later. Therefore, it is important to limit grain size and the amount of brittle phases, in addition to limiting the porosity in joints. Ideally, the maximum size that the grains in a joint should achieve is equal to half the width or even the complete width of the clearance between the base-material components. Thus, the use of a smaller clearance necessarily limits the maximum grain size, promotes higher cooling rates of the filler-metal alloy, and thereby results in a refined joint microstructure (grain size). A smaller clearance also promotes improved retention of base-material properties, because of curtailed base-material erosion achieved by using a smaller volume of filler metal. The size of the grains and the extent of the brittle intermetallic phases in the parent filler metal directly affect the strength of the brazed joint. This consideration is particularly important under transient heating/cooling conditions, such as torch or belt oven brazing, and during automatic solder die bonding, because of the increase in filler-metal grain size and the growth of brittle phases under both liquid and solid-state diffusion processes. The rapid dissolution of constituent filler-metal alloy phases allows the use of higher joining throughput speeds and/or lower joining temperatures. The choice of a specific filler-metal alloy composition depends on the composition of the base material, conditions being compatible with the base material during the joining operation, and the ability of the entire joint to meet the service requirements of the device. Other considerations include a low filler-metal surface tension and, in the case of brazing alloys, the need to reduce surface oxides on the base material. Specific parameters that determine the soundness of a metallic bond include:

- FILLER-METAL MELTING TEMPERATURE SHOULD BE LOWER THAN THAT OF THE CORRESPONDING BASE MATERIAL.
- TO PROVIDE THE DRIVING FORCE NECESSARY FOR JOINING, FILLER-METAL SURFACE TENSION (IN BOTH SOLID AND LIQUID STATES) SHOULD BE LOWER THAN THAT OF THE BASE MATERIAL.
- TO FORM A GOOD METALLIC BOND, BOTH FILLER METAL AND BASE MATERIAL MUST BE SIMILAR RELATIVE TO STRUCTURE, COMPOSITION, AND PHYSICAL PROPERTIES.
- TO REMOVE THE OXIDE FILM PRESENT ON THE BASE MATERIAL, THE FILLER METAL MUST CONTAIN ELEMENTS THAT PROMOTE THE CHEMICAL REDUCTION/DECOMPOSITION OR THE PHYSICAL REMOVAL OF THE OXIDE LAYER.

Brazing Filler Metals

Brazing filler metal alloy compositions can be grouped into four categories. The first and largest group is eutectic-type alloys that have aluminum, nickel, cobalt, or copper as a base, to which silicon/boron (in the case of aluminum- and nickel-base alloys) and phosphorus (in the case of copper- and nickel-base alloys) are added. The presence of one or more of these elements in the alloys tends to impart lower melting temperatures and surface tensions to the filler metal, as well as compatibility with the base material in terms of structure, composition, and properties. Silicon combined with a small amount of magnesium is what lowers the surface tension and melting temperature of aluminum-base alloys, whereas the magnesium addition serves as a fluxing agent. Boron and silicon are used in high-temperature brazing alloys in which the presence of phosphorus (another potential melting-temperature depressant element) could cause unacceptable joint brittleness. Of the alloy additions that promote the self-fluxing of the filler metal during brazing, boron has the greatest "penetrating power." On the other hand, phosphorus is a beneficial fluxing element for use in copper (low-temperature brazing), whereas silicon, for example, would cause unacceptable copper-joint brittleness. The boron- and phosphorus-containing alloys are brittle because various intermetallic phases precipitate when ingot manufacturing technology is used.

This brittle character has limited the available forms of conventionally produced brazing alloys to just powder forms. Fortunately, it was discovered that the presence of silicon, phosphorus, and boron in many conventional filler-metal alloys that have near-eutectic compositions facilitates the conversion of such alloys into ductile, thin, amorphous alloy foil forms when rapid solidification (RS) technology is used. In many cases, a foil filler metal produced by the RS process is very

well suited for use in brazing applications. The advantageous utilization of microcrystalline/amorphous RS soldering or brazing foil has been growing since the early 1980s (Ref 5).

The second group of brazing filler metals, which are characterized by a phase diagram that includes a peritectic reaction (for copper-tin alloys) or a minimum in the liquidus curve (for gold-nickel alloys), are used primarily in vacuum-brazing applications and, therefore, require no alloying elements to serve as fluxing agents.

The third group of alloys, which is probably the most widely used, is based on the copper-silver binary eutectic system that is modified by substantial additions of zinc and cadmium (both providing fluxing activity) and minor additions of tin and nickel. However, applicability of cadmium-containing alloys is limited, because of more-stringent Environmental Protection Agency restrictions on cadmium usage.

The fourth group of brazing filler-metal alloys consists of eutectic titanium/zirconium-base alloys to which copper and/or nickel are added. These materials may be used extensively in the brazing of titanium-base alloys in the near future.

The first three groups of conventional brazing filler metals have been classified by the American Welding Society into seven well-defined categories (Table 1).

TABLE 1 MAJOR CLASSES OF BRAZING FILLER METALS

NO.	ALLOY FAMILY AND TYPE	AWS DESIGNATION	FORMS	BASE MATERIALS JOINED	MAJOR APPLICATIONS
1	AI-SI, EUTECTIC	BALSI	PREFORMS, WIRE, RODS, FOIL, POWDER, RS FOIL[A]	ALUMINUM AND ALUMINUM ALLOYS, STEEL TO ALUMINUM AND ALUMINUM TO BERYLLIUM	CAR RADIATORS, HEAT EXCHANGERS, HONEYCOMB AIRCRAFT STRUCTURES, STRUCTURAL PARTS
2	CU-X, SOLID SOLUTION CU-ZN PERITECTIC CU-SN, PERITECTIC	BCU RBCUZN NONE	PREFORMS, WIRE, RODS, FOIL, POWDER, RS FOIL	COPPER AND COPPER ALLOYS, COPPER TO MILD STEEL, COPPER TO STAINLESS STEEL	HEAT EXCHANGERS, STRUCTURAL PARTS, AUTOMOTIVE PARTS
3	CU-P, EUTECTIC	BCUP	PREFORMS, WIRE, RODS, FOIL, POWDER, RS FOIL	COPPER TO COPPER, COPPER TO SILVER/OXIDE POWERED METAL COMPOSITES	ELECTRICAL CONTACTS, BUS BARS, HEAT EXCHANGERS
4	CU-AG, EUTECTIC	BAG	PREFORMS, FOIL, POWDER	MOST FERROUS AND NONFERROUS METALS, EXCEPT ALUMINUM AND MAGNESIUM	MOST WIDELY USED UTILITY FILLER METALS
5	TM-SI-B[B], EUTECTIC (NI/FE + CR)-SI-B	BNI	POWDER, TAPE[C], RS FOIL	AISI 300 AND 400 SERIES STEELS AND NICKEL- AND COBALT-BASE SUPERALLOYS; CARBON STEELS; LOW-ALLOY STEELS; AND COPPER	AIRCRAFT TURBINE COMPONENTS, AUTOMOTIVE PARTS, HEAT EXCHANGERS, HONEYCOMB STRUCTURES
	(NI, PD)-SI-B	NONE	POWDER, TAPE, RS FOIL	AISI 300 SERIES STAINLESS STEELS, CEMENTED CARBIDE, SUPERALLOYS	HONEYCOMB STRUCTURES, CEMENTED CARBIDE/POLYCRYSTALLINE DIAMOND TOOLS, ORTHODONTICS, CATALYTIC CONVERTERS
	(CO,CR)-SI-B	BCO	POWDER, TAPE, RS FOIL	COBALT-BASE HEAT-RESISTANT CORROSION-RESISTANT SUPERALLOYS	AIRCRAFT ENGINES, HONEYCOMB MARINE STRUCTURES

6	AU-NI, SOLID SOLUTION	BAU	PREFORMS, WIRE, RODS, FOIL, TAPE	NICKEL-BASE HEAT-RESISTANT ALLOYS, STEELS	HONEYCOMB STRUCTURES, STRUCTURAL TURBINE PARTS
7	CU-(TI,ZR)-NI EUTECTIC AND PERITECTIC	NONE	CLADDED STRIP, RS FOIL	TITANIUM/ZIRCONIUM-BASE ALLOYS	TITANIUM TUBING, AIRCRAFT ENGINES, HONEYCOMB AIRCRAFT STRUCTURES, AIRCRAFT STRUCTURAL PARTS, CHEMICAL REACTORS

Source: Ref 1

(A) MAY BE PRODUCED AS RAPIDLY SOLIDIFIED, DUCTILE, AMORPHOUS/MICROCRYSTALLINE FOIL.

(B) THIS GROUP INCLUDES ALLOYS BASED ON TRANSITION METALS, SUCH AS NICKEL, IRON, AND COBALT.

(C) BRAZING FILLER METAL IS CARRIED ON A PLASTIC-BONDED TAPE.

References cited in this section

1. *BRAZING HANDBOOK,* 4TH ED., AWS, 1991
5. A. RABINKIN AND H.H. LIEBERMANN, CHAPTER 21, BRAZING AND SOLDERING WITH RAPIDLY SOLIDIFIED ALLOYS,*RAPIDLY SOLIDIFIED ALLOYS: PROCESSES, STRUCTURES, AND PROPERTIES, AND APPLICATIONS,* MARCEL DEKKER, 1993, P 691-735

Selection Criteria for Brazing and Soldering Consumables

A. Rabinkin, AlliedSignal Amorphous Metals

Solders

Despite a long history of development and usage, those solders used today are still lead- or tin-base alloy systems to which a small amount of silver, zinc, antimony, bismuth, indium, or a combination thereof, have been added. The filler-metal and base-material reactions of many solders are characterized by the formation of intermetallic phases in the bulk of the joint as well as at the joint interfaces. Intermetallic phases with low plasticity play a dual role: on one hand, they improve soldered joint strength; on the other hand, they lessen the long-term fatigue life expectancy. The latter is of paramount importance for the reliable service of electronic devices, particularly surface-mount circuit boards and silicon dice that are connected by soldering and continuously experience power and thermal cycling. It is well known that materials with large intermetallic crystals have low resistance to fatigue because of high stress concentration in the vicinity of the crystals. The size of the intermetallic crystals formed in joints upon crystallization with transient soldering processes is determined by the initial size of the crystals in the starting solder filler metal and by the dissolution and precipitation processes initiated during the soldering operation. Here again, RS solders that possess a very uniform microcrystalline structure can have an advantage over conventional solders, because their application results in a strong and uniform joint that has a high resistance to fatigue (Ref 5).

Reference cited in this section

5. A. RABINKIN AND H.H. LIEBERMANN, CHAPTER 21, BRAZING AND SOLDERING WITH RAPIDLY SOLIDIFIED ALLOYS,*RAPIDLY SOLIDIFIED ALLOYS: PROCESSES, STRUCTURES, AND PROPERTIES, AND APPLICATIONS,* MARCEL DEKKER, 1993, P 691-735

Selection Criteria for Brazing and Soldering Consumables

A. Rabinkin, AlliedSignal Amorphous Metals

References

1. *BRAZING HANDBOOK,* 4TH ED., AWS, 1991
2. M.M. SCHWARTZ, *BRAZING,* ASM INTERNATIONAL, 1987
3. R.J. KLEIN-WASSINK, *SOLDERING IN ELECTRONICS,* ELECTROCHEMICAL PUBLICATIONS, 1984
4. M.M. SCHWARTZ, *CERAMIC JOINING,* ASM INTERNATIONAL, 1990
5. A. RABINKIN AND H.H. LIEBERMANN, CHAPTER 21, BRAZING AND SOLDERING WITH RAPIDLY SOLIDIFIED ALLOYS,*RAPIDLY SOLIDIFIED ALLOYS: PROCESSES, STRUCTURES, AND PROPERTIES, AND APPLICATIONS,* MARCEL DEKKER, 1993, P 691-735

Brazing of Cast Irons and Carbon Steels

Ann Severin, Lucas-Milhaupt, Inc.

Introduction

CAST IRONS AND CARBON STEELS are brazeable materials, although the brazeability of cast iron is lower than that of carbon steel. Similar heating methods and brazing procedures are used for both types of materials. However, there are differences between the two that must be considered when making cleaning and filler-metal decisions.

Brazing of Cast Irons and Carbon Steels

Ann Severin, Lucas-Milhaupt, Inc.

Base-Metal Brazeability

Cast irons are lower in brazeability than carbon steels, because of their higher carbon and silicon contents (Table 1), and because of sand inclusions on as-cast surfaces. Carbon, in the form of graphite, inhibits the wettability of a filler metal on a base metal. Silicon promotes graphite formation. Because the different types of cast irons listed in Table 1 have varying carbon and silicon contents, the form of the graphite will vary, giving each type distinct wetting characteristics.

TABLE 1 CHEMICAL COMPOSITION RANGES FOR TYPICAL UNALLOYED CAST IRONS AND PLAIN CARBON STEELS

MATERIAL	COMPOSITION, %				
	C	**SI**	**MN**	**S**	P
GRAY IRON	2.5-4.0	1.00-3.00	0.25-1.00	0.02-0.25	**0.05-1.00**
MALLEABLE IRON	2.00-2.60	1.10-1.60	0.20-1.00	0.04-0.18	**0.18**$^{(A)}$
DUCTILE IRON	3.00-4.00	1.80-2.80	0.10-1.00	0.03$^{(A)}$	**0.10**$^{(A)}$
PLAIN CARBON STEELS	**0.08-1.03**	**0.3**$^{(A)}$	**0.25-1.00**	**0.050**$^{(A)}$	**0.040**$^{(A)}$

Source: Ref 1

(A) MAXIMUM.

Malleable iron is considered to be the most brazeable of the three types of cast iron, because it has low carbon and silicon contents, and because it experiences a heat treatment that causes the graphite to form in irregularly shaped nodules. The nodules can be easily removed by mechanical means, such as shot or grit blasting.

Ductile Iron. The free carbon of ductile iron also is in the form of nodules. These nodules, which are spherical in shape, are formed when a minute amount of magnesium is added to the molten iron. The chemical composition of ductile iron is similar to that of gray iron, but with lower limits on the amounts of sulfur and phosphorus. Ductile iron also can be cleaned for brazing by mechanical means.

Gray iron is the least brazeable of the cast irons, because it forms large graphite flakes that inhibit the wetting of the metal surface. This material is brazeable only in conjunction with special cleaning methods, which are described in the cleaning section of this article.

Carbon steels are easily brazed using a wide variety of heating methods and filler metals, but the heat-treatment requirements and the service conditions need to be considered when choosing the heating method and the filler metal.

Dissimilar metals can be joined to carbon steels and cast irons by means of brazing. This method of joining two or more different materials is successful because the low interaction between the base metals generally results in a ductile joint. Coefficients of thermal expansion (CTE) (Table 2) are the major consideration when designing joints that comprise two different materials. The joints should be designed so that the filler metal is in compression, rather than tension, after brazing. The joint also should be designed so that an adequate gap exists at the brazing temperature to allow the flow of filler metal. The ideal gap, when brazing with the BAg series of materials, is approximately 0.050 to 0.127 mm (0.002 to 0.005 in.).

TABLE 2 COEFFICIENTS OF THERMAL EXPANSION FOR SELECTED MATERIALS

Values represent high and low sides of a range of typical values.

	COEFFICIENT OF THERMAL EXPANSION			
	HIGH		LOW	
	10^{-5}/K	**10^{-6}/°F**	**10^{-5}/K**	10^{-6}/°F
ZINC AND ITS ALLOYS[A]	3.5	19.3	1.9	**10.8**
LEAD AND ITS ALLOYS[A]	2.9	16.3	2.6	**14.4**
MAGNESIUM ALLOYS[B]	2.8	16	2.5	**14**
ALUMINUM AND ITS ALLOYS[A]	2.5	13.7	2.1	**11.7**
TIN AND ITS ALLOYS[A]	2.3	13	. . .	**. . .**
TIN AND ALUMINUM BRASSES[A]	2.1	11.8	1.8	**10.3**
PLAIN AND LEADED BRASSES[A]	2.1	11.6	1.8	**10**
SILVER[A]	2.0	10.9	. . .	**. . .**
CR-NI-FE SUPERALLOYS[C]	1.9	10.5	1.7	**9.2**
HEAT-RESISTANT ALLOYS (CAST)[C]	1.9	10.5	1.1	**6.4**
NODULAR OR DUCTILE IRONS (CAST)[A]	1.9	10.4	1.2	**6.6**
STAINLESS STEELS (CAST)[C]	1.9	10.4	1.1	**6.4**
TIN BRONZES (CAST)[A]	1.8	10.3	1.8	**10**
AUSTENITIC STAINLESS STEELS[A]	1.8	10.2	1.6	**9**
PHOSPHOR SILICON BRONZES[A]	1.8	10.2	1.7	**9.6**
COPPERS[A]	1.8	9.8	. . .	**. . .**
NICKEL-BASE SUPERALLOYS[C]	1.8	9.8	1.4	**7.7**
ALUMINUM BRONZES (CAST)[A]	1.7	9.5	1.6	**9**
COBALT-BASE SUPERALLOYS[D]	1.7	9.4	1.2	**6.8**
BERYLLIUM COPPER[A]	1.7	9.3	. . .	**. . .**
CUPRO-NICKELS AND NICKEL SILVERS[A]	1.7	9.5	1.6	**9**

NICKEL AND ITS ALLOYS[C]	1.7	9.2	1.2	**6.8**
CR-NI-CO-FE SUPERALLOYS[C]	1.6	9.L	1.4	**8**
ALLOY STEELS[C]	1.5	8.6	1.1	**6.3**
CARBON FREE-CUTTING STEELS[C]	1.5	8.4	1.5	**8.1**
ALLOY STEELS (CAST)[C]	1.5	8.3	1.4	**8**
AGE-HARDENABLE STAINLESS STEELS[A]	1.5	8.2	1.0	**5.5**
GOLD[A]	1.4	7.9	. . .	**. . .**
HIGH-TEMPERATURE STEELS[C]	1.4	7.9	1.1	**6.3**
ULTRAHIGH-STRENGTH STEELS[C]	1.4	7.6	1.0	**5.7**
MALLEABLE IRONS[C]	1.3	7.5	1.0	**5.9**
TITANIUM CARBIDE CERMET[C]	1.3	7.5	0.8	**4.3**
WROUGHT IRONS[A]	1.3	7.4	. . .	**. . .**
TITANIUM AND ITS ALLOYS[C]	1.3	7.1	0.9	**4.9**
COBALT[C]	1.2	6.8	. . .	**. . .**
MARTENSITIC STAINLESS STEELS[A]	1.2	6.5	1.0	**5.5**
NITRIDING STEELS[A]	1.2	6.5	. . .	**. . .**
PALLADIUM[A]	1.2	6.5	. . .	**. . .**
BERYLLIUM[B]	1.1	6.4	. . .	**. . .**
CHROMIUM CARBIDE CERMET[A]	1.1	6.3	1.0	**5.8**
THORIUM[B]	1.1	6.2	. . .	**. . .**
FERRITIC STAINLESS STEELS[A]	1.1	6	1.0	**5.8**
GRAY IRONS (CAST)[A]	1.1	6	. . .	**. . .**
BERYLLIUM CARBIDE[C]	1.0	5.8	. . .	**. . .**
LOW-EXPANSION NICKEL ALLOYS[A]	1.0	5.5	0.3	**1.5**
BERYLLIA AND THORIA[D]	0.9	5.3	. . .	**. . .**
ALUMINA CERMETS[C]	0.9	5.2	0.8	**4.7**
MOLYBDENUM DISILICIDE[A]	0.9	5.1	. . .	**. . .**
RUTHENIUM[B]	0.9	5.1	. . .	**. . .**
PLATINUM[A]	0.9	4.9	. . .	**. . .**
VANADIUM[B]	0.9	4.8	. . .	**. . .**
RHODIUM[B]	0.8	4.6	. . .	**. . .**
TANTALUM CARBIDE[C]	0.8	4.6	. . .	**. . .**
BORON NITRIDE[C]	0.8	4.3	. . .	**. . .**
NIOBIUM AND ITS ALLOYS	0.7	4.1	0.68	**3.8**
TITANIUM CARBIDE[C]	0.7	4.1	. . .	**. . .**
STEATITE[A]	0.7	4	0.6	**3.3**
TUNGSTEN CARBIDE CERMET[A]	0.7	3.9	0.4	**2.5**
IRIDIUM[B]	0.7	3.8	. . .	**. . .**
ALUMINA CERAMICS[A]	0.7	3.7	0.6	**3.1**
ZIRCONINM CARBIDE[C]	0.7	3.7	. . .	**. . .**
OSMIUM AND TANTALUM[B]	0.6	3.6	. . .	**. . .**
ZIRCONIUM AND ITS ALLOYS[B]	0.6	3.6	0.55	**3.1**
HAFNIUM[B]	0.6	3.4	. . .	**. . .**
ZIRCONIA[D]	0.6	3.1	. . .	**. . .**
MOLYBDENUM AND ITS ALLOYS	0.6	3.1	0.5	**2.7**
SILICON CARBIDE[D]	0.4	2.4	0.39	**2.2**
TUNGSTEN[B]	0.4	2.2	. . .	**. . .**
ELECTRICAL CERAMICS[A]	0.4	2	. . .	**. . .**
ZIRCON[A]	0.3	1.8	0.2	**1.3**
BORON CARBIDE[D]	0.3	1.7	. . .	**. . .**
CARBON AND GRAPHITE[A]	**0.3**	**1.5**	**0.2**	**1.3**

Source: Ref 2

(A) VALUE FOR A TEMPERATURE RANGE BETWEEN ROOM TEMPERATURE AND 100-390 °C (212-750 °F).

(B) VALUE AT ROOM TEMPERATURE ONLY.

(C) VALUE FOR A TEMPERATURE RANGE BETWEEN ROOM TEMPERATURE AND 540-980 °C (1000-1800 °F).

(D) VALUE FOR A TEMPERATURE RANGE BETWEEN ROOM TEMPERATURE AND 1205-1580 °C (2200-2875 °F).

Figure 1 shows a cross section of the interface of a joint made by the silver brazing of cast iron to carbon steel. The cast iron had been cleaned by the fused-salt method described in the section "Cleaning and Fixturing Procedures." In Fig. 1, note the clean line at the interface of the steel, versus the irregular shape of the cast iron interface. This is caused by the cleaning process, which removes surface impurities and leaves an irregular, but iron-rich, surface. These surface irregularities greatly increase the joint area, so that after the proper fused-salt cleaning, it is possible to produce a brazed bond that exceeds the strength of the cast iron base metal. It should also be noted that the low interaction between the base metal and the filler metal results in a very ductile joint between two materials that would otherwise be difficult to join by other methods.

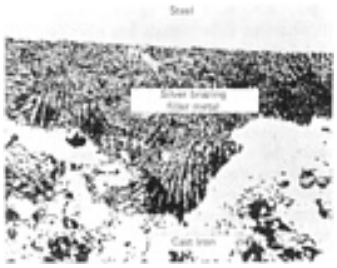

FIG. 1 INTERFACE OF BRAZED CAST IRON AND STEEL AFTER FUSED-SALT CLEANING

References cited in this section

1. C.F. WALTON, ED., *GRAY AND DUCTILE IRON CASTINGS HANDBOOK*, GRAY AND DUCTILE IRON FOUNDERS' SOCIETY, INC, 1971
2. *THE BRAZING BOOK*, HANDY AND HARMAN, 1991

Brazing of Cast Irons and Carbon Steels

Ann Severin, Lucas-Milhaupt, Inc.

Filler-Metal Selection

The most common filler metals used for the brazing of carbon steels and cast irons are those in the American Welding Society (AWS) BAg and BCu series. Filler metals from the RBCuZn series also have been used successfully. However, the BAg series is used because they melt and flow at low temperatures, whereas the BCu series are used because they are inexpensive, when compared with the silver-base filler metals. The trade-off is that the use of BCu materials requires more heat to melt the filler metal. The BCu materials are generally brazed in an atmosphere furnace, which necessitates capital investment in a furnace. The BAg materials, on the other hand, may be brazed by using a torch, an induction heater, a furnace, a resistance heater, or a variety of other means (Ref 2).

The BNi series also can be used in special applications that require chemical or oxidation resistance. The RBCuZn filler metals can be used with a torch, induction heater, or furnace. These alloys can be used either in the typical manner, which relies on capillary flow to make the joint, or in the process known as braze welding, which distributes filler metal by deposition, rather than by capillary flow.

Service Conditions. Temperature and environment are the two factors that need to be evaluated when choosing a filler metal for cast irons and carbon steels. The BAg series of filler metals generally has good long-term strength at temperatures up to 205 °C (400 °F) (Ref 3). Some of the higher-temperature filler metals, such as BAg-13 and BAg-13a, can be used for joints that require high strength up to 425 °C (800 °F) (Ref 4).

The BCu filler metals are generally used for service up to 480 °C (900 °F). The addition of nickel and manganese to copper has created filler-metal alloys with improved high-temperature properties. These materials are not covered by AWS specifications.

Service environment factors that need to be considered when choosing a filler metal include the expected exposure to corrosive environments, water, vibration, and loads. An example of a potential problem is the use of a high-zinc-content filler metal in an application involving contact with flowing water. There have been documented cases of the dezincification of filler-metal joints that eventually failed in service because of the loss of strength in the brazed joint (Ref 5).

A detailed and thorough testing program should be completed for the design and brazement of any critical component, in order to ensure that the finished part will withstand the intended service conditions.

The brazed joint design is another factor in filler-metal selection. Most filler metals are available in either wrought forms (wire, strip, or preformed part) or as a paste (powdered metal in a binder suspension with or without flux, depending on use). Some filler metals are available in limited forms, because of manufacturing difficulties. Ideally, the specific form will allow the brazer to utilize easy assembly and inspection methods and to produce a quality brazed joint. The joint must be designed to accommodate the specific filler-metal form.

In a silver-brazed joint, the greatest strength is achieved when the gap between the two mating parts ranges from 0.0381 to 0.0762 mm (0.0015 to 0.003 in.). Then, the strength of the joint can be equal to or greater than that of the base metal. It is difficult to make a joint that has a narrower gap, because the filler metal would not flow properly between the mating surfaces. When gaps are beyond 0.127 mm (0.005 in.), joint strength drops off, and approaches the tensile strength of the filler metal. If the gap gets too large, then capillary action can be inhibited and the filler metal may not fill the joint, which lowers joint strength even further.

Different silver brazing filler metals have varying degrees of fluidity. Generally, the narrower the melting range (solidus-liquidus), the more fluid the alloy. If the gaps are designed to be tight, then a more fluid filler metal, such as BAg-1 or BAg-7, would be appropriate. If the gaps are larger than 0.102 mm (0.004 in.), then BAg-3 would be a better choice.

Carbon steel and cast iron joints brazed with pure copper should be designed to have a 0.0508 mm (0.002 in.) press fit to a 0.0127 mm (0.0005 in.) gap. Any gap beyond this size will not be filled by pure copper, which is very fluid and has no gap-filling ability. A different filler metal would be required.

If possible, the design should allow visual examination of a joint to ensure that a brazed joint has been made. If a ring can be buried in a fitting/tube joint, then a fillet is evidence that the filler metal has melted and flowed up through the joint to make the fillet.

The heat source is also a factor in determining the type and form of filler metal best suited for a particular brazing cycle. Furnace brazing requires preplaced paste, rings, washers, or other shapes of preforms. Manual brazing can use either the forms described above or bulk wire that is hand fed into the joint when the part reaches a temperature that is higher than the liquidus of the filler metal. Vacuum brazing requires filler metals that will not volatilize in a vacuum at the brazing temperature. Therefore, filler metals with high vapor pressure elements, such as zinc and cadmium, should be avoided. However, these elements are desirable when torch brazing, because they aid wetting and depress melting points.

Heat-treatment requirements will also guide filler-metal selection. The chosen filler metal should allow one of three options when it is used to braze a carbon steel or cast iron that requires a heat treatment.

The first option is that brazing and heat treatment occur at the same temperature. This assumes that the brazing time is short enough to prevent base-metal and filler-metal interactions that can cause erosion or liquid-metal embrittlement. If quenching is required, then it should be conducted after solidification at a temperature that is below that of the filler metal.

The second option is for heat treatment followed by a subsequent brazing operation. In this case, brazing is usually done at the lowest temperature and shortest time possible to minimize the effects on the prior heat treatment. The effect of time at temperatures on heat-treated parts is shown in Table 3.

TABLE 3 EFFECT OF BRAZING TEMPERATURE ON HARDNESS OF SELECTED STEELS

BASE METAL	**CONDITION**	**HARDNESS BEFORE BRAZING**	**HARDNESS AFTER BRAZING SHORT TIME AT 635 °C (1175 °F)**	**HARDNESS AFTER BRAZING SHORT TIME AT 705 °C (1300 °F)**	HARDNESS AFTER BRAZING SHORT TIME AT 760 °C (1400 °F)
LOW-CARBON STEEL	ANNEALED	55-70 HRB	55-70 HRB	55-70 HRB	**55-70 HRB**
	COLD ROLLED	60-90 HRB	55-80 HRB	55-75 HRB	**55-70 HRB**
LOW-ALLOY OR LOW-CARBON STEEL (0.40-0.50 C)	ANNEALED	90-100 HRB	90-100 HRB	90-100 HRB	(A)
	HEAT TREATED TO 1030 MPA (150 KSI)	32 HRC	22-32 HRC	18-25 HRC	(A)
CARBON AND LOW-ALLOY TOOL STEEL	HARDENED AND TEMPERED	50-65 HRC	28-32 HRC	20-25 HRC	(B)
HIGH-SPEED STEEL	**HARDENED**	**65 HRC**	**59-63 HRC**	**46-50 HRC**	**. . .**

Source: Ref 6

(A) MAY HARDEN SLIGHTLY.

(B) MAY HARDEN.

The third option is to braze first and then heat treat. In this case, brazing is done at a temperature above the required heat-treatment temperature. This option usually is used with the BCu filler metals. The subsequent heat treatment is conducted at a low enough temperature to avoid affecting the braze. This is especially useful for parts that need to be case hardened or carburized in situations where brazing after heat treatment would soften or distort the parts.

If high hardness is a requirement and the part must be brazed after hardening, then a different material such as a high-speed tool steel should be considered. Hardened high-speed tool steels and other hot-worked steels exhibiting secondary hardening are only slightly softened by the lower-temperature filler metals in the AWS BAg series.

Before a part is brazed, its physical requirements in finished form must be known in order to select the heat treatment and filler metal that will provide the correct properties. The *ASM Handbook,* Volume 1, *Properties and Selection: Irons, Steels, and High-Performance Alloys,* and Volume 4, *Heat Treating,* offer valuable data for the selection of the appropriate heat treatment.

References cited in this section

2. *THE BRAZING BOOK,* HANDY AND HARMAN, 1991
3. "SILVER BRAZING FOR USE UP TO 400 °F (205 °C)," AMS 2665D, SAE, 1983
4. "SILVER BRAZING FOR USE UP TO 800 °F (425 °C)," AMS 2664D, SAE, 1982
5. *METALS HANDBOOK,* 8TH ED., VOL 10, 1975, P 372
6. "SILVER FILLER METAL BRAZING AND ITS RELATIONSHIP TO HEAT TREATMENT OF THE PARTS JOINED," BRAZING TECHNICAL BULLETIN NO. T-6 (REVISED), HANDY AND HARMAN, 1991

Brazing of Cast Irons and Carbon Steels

Ann Severin, Lucas-Milhaupt, Inc.

Cleaning and Fixturing Procedures

Many processes are used for the brazing of cast irons and carbon steels. All of them involve the same basic considerations, as described below.

Because of the difficulty in wetting cast irons, trials for cleaning the cast irons prior to production should be conducted. Samples should be made that will reflect the cleaning, flux, filler metals, and selected process in order to check the wettability of the base metal. If the samples are not uniformly wetted or if the contact angle is great, then the variables should be changed until uniform wetting and a small contact angle are achieved. Testing is also useful on steel parts, but is not as critical, because they are much easier to braze. It is advisable to run sample parts prior to brazing expensive machined parts, in order to check furnace atmospheres and other processing variables.

Cleaning

The first step required, when making a brazed joint, is to clean all parts, whether they are cast iron or carbon steel. They must be free from grease, dirt, oxides, and other contaminants in order for the filler metal to wet and flow on the surface of the base metal. Therefore, all processing fluids and mill scale must be removed. Generally, solvents or alkaline detergent-type cleaners are used for this purpose. It is important to match the cleaning method to the type of contaminant to be removed (that is, water based for water-based coolants, and solvents or alkaline degreasers for oily residues). Special procedures for specific materials are described below.

Cleaning of Cast Irons. Prior to brazing, cast irons require special cleaning procedures. Ductile and malleable cast iron are usually cleaned by abrasive blasting with steel or nickel shot to remove the graphite, silicon, and sand inclusions on the surface. Other methods for preparing ductile and malleable cast irons include various pickling and other chemical treatments, searing with an oxidizing flame, and heating to temperatures between 870 and 900 °C (1600 and 1650 °F) in a strongly decarburizing atmosphere.

Gray cast irons generally require cleaning in fused salts prior to brazing, because that method has proved to be the most effective. The fused-salt bath generally is maintained at temperatures between 400 and 480 °C (750 and 900 °F). At these temperatures, salt baths exhibit the required high chemical activity that is necessary to remove surface oxides, graphite, and sand from the iron surface. This action is further enhanced by the induction of direct current into the bath. By changing the polarity, the action of the bath can be changed from oxidizing to reducing, and vice versa.

Castings are immersed in the bath, suspended from bus bars or fixtures that are insulated from the tank of molten salt. Generally, the castings are attached to the negative polarity and the tank is made positive, which creates a reducing action in the bath that is capable of removing oxides and sand from the casting surfaces. The polarity is then reversed and the oxidation reaction begins. During this portion of the cycle, the graphite is removed. The current is then reversed again (to a reducing action) to remove the iron oxide that formed in the oxidation reaction. After the castings are rinsed in water and dried, they are ready for brazing. Although it is generally not necessary, ductile and malleable cast irons also can be cleaned by the fused-salt method.

In some applications, the brazing of all types of cast irons has been accomplished without special cleaning by using a black-type flux (AWS FB3-C or AMS 3411) and by silver brazing with a filler metal that contains nickel, such as BAg-3, BAg-4, or BAg-24. Brazing with RBCuZn-type filler metals has also been done without prior precleaning. If joint integrity, repeatability, and consistency are important, then prior precleaning is recommended.

Cleaning of low-carbon steels is generally accomplished by either chemical or mechanical means, the former of which is more popular. Chemical methods include alkaline detergents, solvents, vapor degreasing, and acid pickling. Mechanical methods include dry or wet abrasive blast cleaning, wire brushing, machining, or grinding. The selected cleaning method must provide a chemical match to the contaminant being removed. Some of the newer synthetic lubricants and coolants are easily removed with water-based cleaners, but not by vapor degreasing. Although the part may appear clean, residues of these materials can remain and will inhibit the wetting of the steel.

Chemical Cleaning. Alkaline cleaning, including soak, spray, and barrel cleaning, is widely used for removing oily, semisolid, or solid soils from steel. It is generally satisfactory for removing most cutting and grinding fluids, grinding and polishing abrasives, and some pigmented drawing compounds.

Solvent cleaning is capable of removing oil, grease, loose metal chips, and other contaminants from steel components. Parts are immersed and soaked in a common organic solvent. Spray methods can be employed, as well.

Vapor degreasing utilizes the hot vapors from a boiling chlorinated hydrocarbon solvent to remove surface contaminants such as oils, greases, and waxes. To supplement the vapor, some degreasing units are equipped with facilities for immersing the work in the hot solvent or for spraying with clean solvent. Others are equipped with ultrasonic equipment to remove oils and greases from crevices.

Mechanical Cleaning. Although mechanical methods are less widely used than chemical methods, they are usually preferred for removing heavy scale, and they can be indispensable in removing the more tenacious lubricants, such as a pigmented drawing compound. Mechanical methods are also useful in surface preparation that involves abrading or roughening, which may be required on a very smooth surface to promote wetting and filler-metal flow.

In dry grit blasting, the grits that are used on carbon and low-alloy steels consist of metallic particles of chilled cast iron nickels or of hardened cast steel. Wet blasting employs abrasives of many different types and sizes, suspended in a liquid carrier. Certain ingredients in the liquid carrier, such as rust inhibitors and the minerals in the water, can adversely affect the wetting action in brazing and could necessitate an additional cleaning process to remove all traces of liquid carrier from the work.

Fixturing

Fixturing is necessary to hold parts in alignment during the brazing process. The considerations are the same, whether brazing cast irons or carbon steels. Ideally, the parts would be self-fixturing by virtue of gravity, press fitting (copper filler metal only), tack welding, knurling, staking, expanding, interlocking, or other mechanical means. If tack welding is used, then the area surrounding the tack should be mechanically cleaned to remove any oxides that form during the welding operation. A mechanical method must avoid introducing contaminants, grease, or oils, or else a final cleaning process must be added.

If the part cannot be designed to be self-fixturing, then external fixturing must be designed. A fixture for torch brazing should be lightweight and have as little actual contact as possible with the parts to be brazed, to prevent it from acting as a heat sink.

The fixture material that is used will depend on the temperature and atmosphere of the brazing operation, how many times the fixture is to be used, the base metal, and the brazing process to be used. Fixtures are generally constructed of steel, stainless steel, nickel-base alloy, molybdenum, graphite, or ceramic. Regardless of the process or base metal, the differences in CTE between the base metal and the fixture material must be considered, in order to prevent warpage or damage to the brazed part. CTE differences can also be used advantageously to pull parts into place during the heating process.

Brazing of Cast Irons and Carbon Steels

Ann Severin, Lucas-Milhaupt, Inc.

Filler Metal and Flux/Atmosphere Procedures

Filler metal can be supplied to the joint by hand or by using automatic feeding methods when the base metal reaches the brazing temperature. It also can be preplaced in the joint prior to heating. Hand feeding is the simplest method, however, because it requires no equipment. The choice of wire gage is important, because a wire of large diameter will act as a heat sink, cooling the joint when it touches a part. This requires that the part be heated to a higher temperature, which could cause base-metal degradation. The amount of filler metal that is applied is determined by the operator.

Automatic wire feed machines are used on rotary torch brazing tables. Although this type of machine supplies a measured amount of filler metal to the joint, the wire can act as a heat sink if the wire gage is too large.

Preforms, in the form of wire or foil products, can supply filler metal to the joint in a consistently measured amount. Preforms can be used in any type of brazing operation in which the filler metal can or must be preplaced in the joint prior to heating.

Another common form of filler metal is a paste product, in which a powdered filler metal is mixed with either a binder or a flux/binder system. The choice of paste is determined by the brazing temperature and the atmosphere in which brazing occurs.

The best joint is made by preplacing the filler metal at the base of a joint (Fig. 2) and drawing it up, in order to form a joint. This gives the smallest, most even fillet, and ensures that a joint is formed over the entire shear length of the mating surfaces. However, it is not always practical to create a joint in this manner.

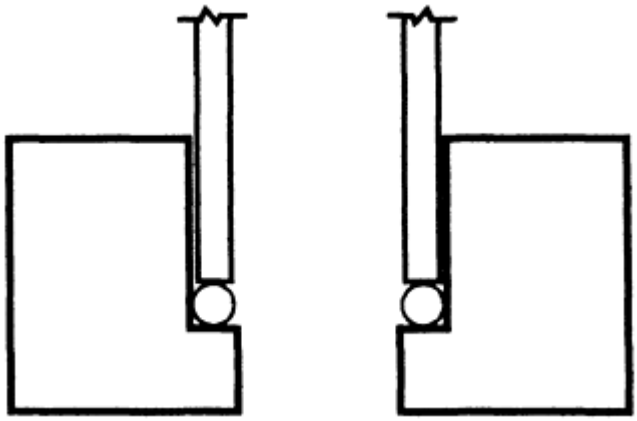

FIG. 2 SCHEMATIC OF A CROSS SECTION OF A PART WITH A BURIED RING OF BRAZING FILLER METAL PRIOR TO BRAZING

Fluxes and/or atmospheres are necessary when making a joint on carbon steels or cast irons. The fluxes used with these materials usually consist of borates and fluorides. Some may have additions of boron to promote wetting, especially on cast irons. Brazing fluxes act to prevent oxidation of both base metal and filler metal and to clean off any residual oxides on the base metal.

Fluxes that conform to AWS FB3A or FB3C can be used when torch brazing with the BAg filler metals. High-temperature torch brazing with RBCuZn filler metals can utilize either a vapor flux that is supplied in the flame or a high-temperature flux that conforms to FB3D. Furnace brazing should utilize a flux that is designed to be active for long periods of time; this type of flux is not covered by AWS designations. The selected flux must be compatible with the combination of base metal and filler metal and with the temperature range in which brazing occurs. Fluxes that are spent by overheating will not allow the filler metal to flow properly.

Brazing atmospheres act in a manner similar to fluxes, by providing a gas atmosphere to protect the part from oxidation and to remove residual oxides. High-temperature brazing using a BCu or a high-temperature copper alloy filler metal can be conducted in hydrogen or dissociated ammonia atmospheres. Low-temperature brazing using BAg filler metals also is possible when hydrogen or dissociated ammonia atmospheres are used. Endothermically generated atmospheres containing from 14 to 16% hydrogen can be used for carbon steels and properly cleaned cast irons. Flux should be used to prevent the vaporization of zinc whenever zinc-containing filler metals are used. Vacuum could be used, if it is available, but it generally is not used, because of the cost.

Brazing of Cast Irons and Carbon Steels

Ann Severin, Lucas-Milhaupt, Inc.

Heating Methods

The heating methods used for the brazing of carbon steel and cast iron are varied. Often, the choice of heating method depends on the process that provides the best results for the lowest cost. When determining the best-suited process and heating method, factors such as part size, planned production and lot sizes, filler-metal and base-metal combinations, and heat-treatment requirements need to be considered.

Torch brazing is commonly used to braze cast irons and carbon steels. This method is particularly suited for cast irons, because the short cycle times preclude the formation of graphite from free carbide or pearlite, which would lower the high-temperature properties of the cast iron. Torch brazing is used for the brazing of single pieces or numerous pieces. Generally, the lower-temperature BAg filler metals are used, although the RBCuZn filler metals can be used, as well. Torch size must be adjusted for the size of part being brazed. Usually, smaller parts or parts that must be brazed in place are the most suitable for torch brazing.

The induction brazing of cast irons and carbon steels is useful on parts that need very fast and localized heating to maintain heat-treatment properties at the maximum level, while ensuring a sound brazed joint. Both cast iron and carbon steel induct heat well, and the only limitations are the size of the part and accessibility to the joint area. Nearly any part shape can be brazed using induction heating, as long as a suitable inductor can be designed to give the desired heating pattern. Induction heating equipment tends to be expensive, but relatively inexpensive fixturing and inductors make it suitable for a wide variety of parts. When making steel parts, induction is useful for simultaneous brazing and hardening operations. When brazing dissimilar metals using an induction method, attention should be given to the differential heating rate of the two metals. The cycle and the coil placement must be such that the two metals are brought to temperature evenly, or else a cold joint can result.

A cold joint occurs when the filler metal melts, but cannot bond to one or both of the base metals because they have not reached the melting temperature of the filler metal. When the molten filler metal hits the colder base metal, it freezes, without making a bond.

Salt-bath brazing is another suitable method for the brazing of cast irons and carbon steels, but it is becoming less common, because of the environmental requirements associated with maintaining a salt bath. Salt-bath brazing is suited to applications where many joints must be made at once, such as the joining of tubing to headers for heat exchangers. This process generally uses the BAg, RBCuZn, or BCu filler metals. The selection of a suitable salt depends on the temperature that is needed for the filler metal to melt and flow. The carburizing of steels can be accomplished by using a carburizing salt. Generally, the higher-temperature copper-zinc filler metals are used in this process. Salt-bath brazing also is suited to applications that would involve daily use of the bath, because of the cost of maintaining and heating the bath.

Furnace brazing of cast irons and carbon steels is generally used when:

- THE PARTS ARE LARGE.
- THERE IS A WIDE VARIETY IN THE GAGES OF THE MATERIALS TO BE BRAZED.
- THERE ARE MANY JOINTS PER PART.
- LARGE PRODUCTION VOLUMES ARE REQUIRED.
- A PROTECTIVE ATMOSPHERE IS REQUIRED.

Furnace brazing is only practical when the filler metal can be preplaced in or at the joint during assembly and held in position during the brazing cycle.

The process can take place in different types of furnaces, such as batch or continuous belt ovens, which can operate in air, hydrogen, nitrogen, argon, or combusted gas atmospheres. Cast irons and carbon steels that are brazed in air need flux,

and postcleaning is required, as well. When brazing without flux, the atmosphere must be able to reduce the oxides that are present and prevent the formation of new ones. The reduction of oxides must take place below the solidus temperature of the filler metal, in order to enable the filler metal to wet the base metal and flow into the braze joint.

When furnace brazing, the parts are cleaned and assembled with the filler metal preplaced at or in the joint. Calculations should be made to determine the amount of filler metal needed, and a preformed ring, slug, or shim should be designed to provide the correct amount of filler metal. A paste form of filler metal also can be used.

Fixtures may be necessary to hold parts in the proper alignment during brazing. They should be lightweight and should not hinder the natural expansion or shrinkage of the base metal during heating and cooling. Restriction may cause base-metal distortion and/or brazed-joint cracking. The furnace brazing of cast irons and carbon steels generally employs BAg, BCu, and RBCuZn filler metals.

Regardless of the selected heating method, fluxes must be removed because they are corrosive and may contaminate systems and/or mask leaks. Fluxes are best removed by hot-water rinses or by using proprietary solutions that remove them, along with surface scale and oxidation products.

Brazing of Cast Irons and Carbon Steels

Ann Severin, Lucas-Milhaupt, Inc.

References

1. C.F. WALTON, ED., *GRAY AND DUCTILE IRON CASTINGS HANDBOOK*, GRAY AND DUCTILE IRON FOUNDERS' SOCIETY, INC, 1971
2. *THE BRAZING BOOK*, HANDY AND HARMAN, 1991
3. "SILVER BRAZING FOR USE UP TO 400 °F (205 °C)," AMS 2665D, SAE, 1983
4. "SILVER BRAZING FOR USE UP TO 800 °F (425 °C)," AMS 2664D, SAE, 1982
5. *METALS HANDBOOK*, 8TH ED., VOL 10, 1975, P 372
6. "SILVER FILLER METAL BRAZING AND ITS RELATIONSHIP TO HEAT TREATMENT OF THE PARTS JOINED," BRAZING TECHNICAL BULLETIN NO. T-6 (REVISED), HANDY AND HARMAN, 1991

Brazing of Stainless Steels

Revised by Matthew J. Lucas, Jr., General Electric Aircraft Engines

Introduction

STAINLESS STEEL ALLOYS as a group are not difficult to braze, but those alloys that also contain titanium or aluminum require additional precautions to prevent alloy oxidation during the brazing cycle. Excellent results can be obtained when standard wrought stainless steels are brazed.

The brazeability and weldability of these steels do vary with composition. The quality of brazed joints depends on the selection of the brazing process, process temperature, filler metal, and the type of protective atmosphere or flux that is used. These choices must be compatible with the intended performance of the brazed item.

Acknowledgements

Special thanks are due to Robert L. Peaslee and W. Daniel Kay of Wall Colmonoy Corporation for providing three of the examples cited in this article.

Brazing of Stainless Steels

Revised by Matthew J. Lucas, Jr., General Electric Aircraft Engines

Applicability

Brazing is often used to join stainless steels to a variety of dissimilar metals, such as carbon steels, low-alloy steels, and copper alloys, in combinations that would not otherwise weld satisfactorily. This capability is a principal advantage of the brazing process.

A wide variety of brazing filler-metal compositions are available to achieve compatibility, strength, corrosion resistance, and other desirable properties when joining dissimilar metals. When the appropriate heating techniques are employed, brazing provides a means to obtain strong, corrosion-resistant, leak-tight joints in small or thin-walled components with minimal buckling or warpage. Brazing also can produce joints in delicate assemblies and in very thin-gage metals that would be difficult or impossible to obtain if conventional welding techniques were used. Brazing is also suitable for the mass production of small- and medium-sized assemblies on various types of continuous furnace equipment. Finally, brazing enables the production of joints in inaccessible locations by the preplacement of filler metal and the subsequent heating of the workpiece. Often, such joints cannot be made by other joining processes.

Brazing of Stainless Steels

Revised by Matthew J. Lucas, Jr., General Electric Aircraft Engines

Brazeability

As a class, stainless steels are no more difficult to braze than carbon and low-alloy steels. The high quantities of chromium that are present in stainless steels cause the chromium oxide films that are on the surfaces of all stainless steels, as well as the films of titanium oxide that form on the surfaces of titanium-stabilized stainless steels, such as type 321. If these oxides, which are both refractory and strongly adherent, are inadequately removed, they will prevent the molten filler metal from wetting the base metal, and thus will prevent a capillary joint from being formed between the metals being joined.

The formation of chromium oxide is accelerated when stainless steels are heated in air. Although the oxide may have been removed from the surface by chemical cleaning at room temperature, a new oxide layer that seriously interferes with wetting will rapidly form when the steel is heated in air to the brazing temperature. The adverse effect of oxides on wetting can be alleviated by:

- CHEMICALLY CLEANING THE SURFACE OXIDE FROM THE STEEL AT ROOM TEMPERATURE, QUICKLY FOLLOWED BY HEATING TO THE BRAZING TEMPERATURE IN A CHEMICALLY INERT GASEOUS ATMOSPHERE, SUCH AS ARGON
- HEATING THE STEEL DIRECTLY TO THE BRAZING TEMPERATURE IN A STRONGLY REDUCING ATMOSPHERE, SUCH AS HYDROGEN, AFTER A LESS-INTENSE CLEANING, WHICH CHEMICALLY REDUCES THE OXIDE AND THEREBY PROMOTES WETTING ACTION
- COATING THE AREA AT THE JOINT WITH A CHEMICALLY ACTIVE FLUX THAT DISSOLVES THE OXIDE DURING HEATING TO THE BRAZING TEMPERATURE
- HEATING IN A VACUUM (AFTER CLEANING), WHICH REDUCES MANY OXIDES, SUCH AS CHROMIUM OXIDE, AND PREVENTS THE GROSS FORMATION OF OTHER OXIDES
- DEGREASING ALONE, IF THE PROPER FLUX OR CONTROLLED ATMOSPHERE IS USED, PRIOR TO BRAZING STAINLESS STEELS WITH CLEAN SURFACES, THAT IS, WITHOUT BLACK OR GREEN OXIDE COATINGS
- SELECTING LOWER-MELTING-POINT BRAZING FILLER METALS TO REDUCE OXIDATION

POTENTIAL

Inclusions and Surface Contaminants. When brazing stainless steel, base-metal inclusions and surface contaminants are even more deleterious than they are when brazing carbon steel. Base-metal inclusions, such as oxides, sulfides, and nitrides, interfere with the flow of filler metal. Flow is also impeded by surface contaminants, which may include lubricants, such as oil, graphite, molybdenum, disulfide, and lead, which are applied during machining, forming, and grinding. Other contaminants are the aluminum oxide particles that are produced either by grit blasting or by grinding with aluminum oxide wheels or belts.

Some filler-metal powders that are used in paste form with stainless steel contain organic binders. Acrylics and other plastics are often used for this purpose. Although some powders form a soot residue, it usually does not interfere with filler-metal flow.

The brazing characteristics of stainless steel can also be seriously impaired by unsuitable fixturing materials, such as graphite, or by a protective atmosphere that contains nitrogen. Carbon in graphite fixtures unites with hydrogen to form methane (CH_4), which carburizes stainless steel and impairs its corrosion resistance. Dissociated ammonia will result in nitriding of the stainless steel, unless the ammonia is sufficiently dry and completely (100%) dissociated. Both carburizing and nitriding interfere with brazing quality.

Brazing Processes. Stainless steels can be brazed by all conventional brazing processes, including furnace, torch, induction, resistance, and salt-bath dip brazing. Furnace brazing is most widely used, because applications generally require brazing in protective atmospheres, including a vacuum. Most of the applications described in this article utilize furnace brazing.

Brazing of Stainless Steels

Revised by Matthew J. Lucas, Jr., General Electric Aircraft Engines

---

Brazing Filler Metal

Most stainless steels can be brazed with any one of several different filler-metal families, including silver, nickel, copper, and gold. In most applications, filler metals are selected on the basis of their mechanical properties, corrosion resistance, service temperature, and compatibility with the base metal. This selection leads to the required brazing temperature, based on service use or manufacturing sequence, and to the required heating method. Table 1 lists the composition requirements of the filler metals that are most commonly used to braze stainless steels. A complete list of brazing filler metals can be found in ANSI/AWS A5.8, which specifies filler metals for the brazing and braze welding processes.

TABLE 1 TYPICAL COMPOSITIONS AND PROPERTIES OF STANDARD BRAZING FILLER METALS FOR BRAZING STAINLESS STEEL

BRAZING FILLER METAL	**COMPOSITION[(A)], %**									**SOLIDUS TEMPERATURE**		**LIQUIDUS TEMPERATURE**		BRAZING TEMPERATURE RANGE	
	Ag	**Cu**	**Zn**	**Cd**	**Ni**	**Sn**	**Li**	**Mn**	**OTHER ELEMENTS TOTAL**	**°C**	**°F**	**°C**	**°F**	**°C**	°F
SILVER															
BAG-1	44.0-46.0	14.0-16.0	14.0-18.0	23.0-25.0	. . .	. . .	. . .	. . .	0.15	610	1125	620	1145	620-760	**1145-1400**
BAG-	49.	14.	14.	17.	. .	. . .	. . .	. . .	0.15	630	1160	635	1175	635-	**1175-**

1A	0-51.0	5-16.5	5-18.5	0-19.0	.								760	**1400**
BAG-2	34.0-36.0	25.0-27.0	19.0-23.0	17.0-19.0	. . .	. . .	. . .	. . .	0.15	610	1125	700	1295	700-845	**1295-1550**
BAG-2A	29.0-31.0	26.0-28.0	21.0-25.0	19.0-21.0	. . .	. . .	. . .	. . .	0.15	610	1125	710	1310	710-845	**1310-1550**
BAG-3	49.0-51.0	14.5-16.5	13.5-17.5	15.0-17.0	2.5-3.5	. . .	. . .	. . .	0.15	630	1170	690	1270	690-815	**1270-1500**
BAG-4	39.0-41.0	29.0-31.0	26.0-30.0	. . .	1.5-2.5	. . .	. . .	. . .	0.15	670	1240	780	1435	780-900	**1435-1650**
BAG-5	44.0-46.0	29.0-31.0	23.0-27.0	. . .	. . .	. . .	. . .	. . .	0.15	680	1250	745	1370	745-845	**1370-1550**
BAG-6	49.0-51.0	33.0-35.0	14.0-18.0	. . .	. . .	. . .	. . .	. . .	0.15	690	1270	775	1425	775-870	**1425-1600**
BAG-7	55.0-57.0	21.0-23.0	15.0-19.0	. . .	. . .	4.5-5.5	. . .	. . .	0.15	620	1145	650	1205	650-760	**1205-1400**
BAG-8	71.0-73.0	BAL	. . .	. . .	. . .	. . .	. . .	. . .	0.15	780	1435	780	1435	780-900	**1435-1650**
BAG-8A	71.0-73.0	BAL	. . .	. . .	. . .	. . .	0.25-0.50	. . .	0.15	770	1410	765	1410	765-870	**1410-1600**
BAG-9	64.0-66.0	19.0-21.0	13.0-17.0	. . .	. . .	. . .	. . .	. . .	0.15	670	1240	720	1325	720-845	**1325-1550**
BAG-10	69.0-71.0	19.0-21.0	8.0-12.0	. . .	. . .	. . .	. . .	. . .	0.15	690	1275	740	1360	740-845	**1360-1550**
BAG-13	53.0-55.0	BAL	4.0-6.0	. . .	0.5-1.5	. . .	. . .	. . .	0.15	720	1325	860	1575	860-970	**1575-1775**
BAG-13A	55.0-57.0	BAL	. . .	. . .	1.5-2.5	. . .	. . .	. . .	0.15	770	1420	895	1640	870-980	**1600-1800**
BAG-18	59.0-61.0	BAL	. . .	. . .	. . .	9.5-10.5	. . .	. . .	0.15	600	1115	720	1325	720-845	**1325-1550**
BAG-19	92.0-93.0	BAL	. . .	. . .	. . .	. . .	0.15-0.30	. . .	0.15	760	1400	890	1635	875-980	**1610-1800**
BAG-	29.	37.	30.	. . .	. .	. . .	. . .	. . .	0.15	680	1250	765	1410	765-	**1410-**

20	0-31.0	0-39.0	0-34.0		.									870	**1600**
BAG-21	62.0-64.0	27.5-29.5	. . .	. . .	2.0-3.0	5.0-7.0	. . .	. . .	0.15	690	1275	800	1475	800-900	**1475-1600**
BAG-22	48.0-50.0	15.0-17.0	21.0-25.0	. . .	4.0-5.0	. . .	. . .	7.0-8.0	0.15	680	1260	700	1290	700-830	**1290-1525**
BAG-23	84.0-86.0	. . .	. . .	. . .	. . .	. . .	. . .	REMAINDER	0.15	960	1760	970	1780	970-1040	**1780-1900**
BAG-24	49.0-51.0	19.0-21.0	26.0-30.0	. . .	1.5-2.5	. . .	. . .	. . .	0.15	660	1220	705	1305	710-843	**1305-1550**
BAG-25	19.0-21.0	39.0-41.0	33.0-37.0	. . .	. . .	. . .	. . .	4.5-5.5	0.15	740	1360	790	1455	790-846	**1455-1555**
BAG-26	24.0-26.0	37.0-39.0	31.0-35.0	. . .	1.5-2.5	. . .	. . .	1.5-2.5	0.15	710	1305	800	1475	800-870	**1475-1600**
BAG-27	24.0-26.0	34.0-36.0	24.5-28.5	12.5-14.5	. . .	. . .	. . .	. . .	0.15	610	1125	745	1375	745-860	**1375-1575**
BAG-28	39.0-41.0	29.0-31.0	26.0-30.0	. . .	. . .	1.5-2.5	. . .	. . .	0.15	650	1200	710	1310	710-845	**1310-1550**
BAG-33	24.0-26.0	29.0-31.0	26.5-28.5	16.5-18.5	. . .	. . .	. . .	. . .	0.15	610	1125	680	1260	680-760	**1260-1400**
BAG-34	**37.0-39.0**	**31.0-33.0**	**26.0-30.0**	**. . .**	**. . .**	**1.5-2.5**	**. . .**	**. . .**	**0.15**	**650**	**1200**	**720**	**1330**	**720-845**	**1330-1550**

BRAZING FILLER METAL	**COMPOSITION[A], %**					**SOLIDUS TEMPERATURE**		**LIQUIDUS TEMPERATURE**		BRAZING TEMPERATURE RANGE	
	Cu	**P**	**Pb**	**Al**	**OTHER ELEMENTS TOTAL**	**°C**	**°F**	**°C**	**°F**	**°C**	°F
COPPER											
BCU-1	99.90[B]	0.075	0.02	0.01	0.10	1080	1981	1080	1981	1095-1150	**2000-2100**
BCU-1A	99.0[B]	. . .	. . .	. . .	0.30	1080	1981	1080	1981	1095-1150	**2000-2100**
BCU-2	**86.5[B]**	**. . .**	**. . .**	**. . .**	**0.50**	**1080**	**1981**	**1080**	**1981**	**1095-1150**	**2000-2100**

BRAZING FILLER METAL	**COMPOSITION[A], %**													**SOLIDUS TEMPERATURE**		**LIQUIDUS TEMPERATURE**		BRAZING TEMPERATURE RANGE	
	Cr	**B**	**Si**	**Fe**	**C**	**P**	**S**	**Al**	**Ti**	**Mn**	**Cu**	**Zr**	**Ni**	**OTHER ELEM**	**°C**	**°F**	**°C**	**°F**	**°C**	°F

														ENTS TOTAL						
NICKEL[C]																				
BNI-1	13.0-15.0	2.75-3.50	4.0-5.0	4.0-5.0	0.6-0.9	0.02	0.02	0.05	0.05	. . .	. . .	0.05	BAL	0.50	975	1790	1035	1900	1065-1205	**1950-2200**
BNI-1A	13.0-15.0	2.75-3.50	4.0-5.0	4.0-5.0	0.06	0.02	0.02	0.05	0.05	. . .	. . .	0.05	BAL	0.50	975	1790	1075	1970	1075-1205	**1970-2200**
BNI-2	6.0-8.0	2.75-3.50	4.0-5.0	2.5-3.5	0.06	0.02	0.02	0.05	0.05	. . .	. . .	0.05	BAL	0.50	990	1780	1000	1830	1010-1175	**1850-2150**
BNI-3	. . .	2.75-3.50	4.0-5.0	0.5	0.06	0.02	0.02	0.05	0.05	. . .	. . .	0.50	BAL	0.50	980	1800	1035	1900	1010-1175	**1850-2150**
BNI-4	. . .	1.5-2.2	3.0-4.0	1.5	0.06	0.02	0.02	0.05	0.05	. . .	. . .	0.05	BAL	0.50	980	1800	1065	1950	1010-1175	**1850-2150**
BNI-5	18.5-19.5	0.03	9.75-10.50	. . .	0.10	0.02	0.02	0.05	0.05	. . .	. . .	0.05	BAL	0.50	1080	1975	1135	2075	1150-1205	**2100-2200**
BNI-6	. . .	. . .	. . .	. . .	0.10	10.0-12.0	0.02	0.05	0.05	. . .	. . .	0.05	BAL	0.50	880	1610	875	1610	925-1095	**1700-2000**
BNI-7	13.0-15.0	0.01	0.10	0.2	0.08	9.7-10.5	0.02	0.05	0.05	0.04	. . .	0.05	BAL	0.50	890	1630	890	1630	925-1095	**1700-2000**
BNI-8	. . .	. . .	6.0-8.0	. . .	0.10	0.02	0.02	0.05	0.05	21.5-24.5	4.0-5.0	0.05	BAL	0.50	980	1800	1010	1850	1010-1095	**1850-2000**
BNI-9	**13.5-16.5**	**3.25-4.0**	**. . .**	**1.5**	**0.06**	**0.02**	**0.02**	**0.05**	**0.05**	**. . .**	**. . .**	**0.05**	**BAL**	**0.50**	**1055**	**1930**	**1055**	**1930**	**1065-1205**	**1950-2200**

BRAZING FILLER METAL	**COMPOSITION[A], %**					**SOLIDUS TEMPERATURE**		**LIQUIDUS TEMPERATURE**		BRAZING TEMPERATURE RANGE	
	Au	**Cu**	**Pd**	**Ni**	**OTHER ELEMENTS TOTAL**	**°C**	**°F**	**°C**	**°F**	**°C**	°F
PRECIOUS METALS											
BAU-1	37.0-38.0	REMAINDER	. . .	. . .	0.15	990	1815	1015	1860	1015-1095	**1860-2000**
BAU-2	79.5-80.5	REMAINDER	. . .	. . .	0.15	890	1635	890	1635	890-1010	**1635-1850**

BAU-3	34.5 - 35.5	REMAINDER	. . .	2.5-3.5	0.15	975	1785	1030	1885	1030-1090	**1885-1995**
BAU-4	81.5 - 82.5	. . .	. . .	REMAINDER	0.15	950	1740	950	1740	950-1005	**1740-1840**
BAU-5	29.5 - 30.5	. . .	33.5 - 34.5	35.5-36.5	0.15	1135	2075	1165	2130	1165-1230	**2130-2250**
BAU-6	**69.5 - 70.5**	**. . .**	**7.5-8.5**	**21.5-22.5**	**0.15**	**1010**	**1845**	**1045**	**1915**	**1045-1120**	**1915-2050**

BRAZING FILLER METAL	**COMPOSITION[(A)], %**													**SOLIDUS TEMPERATURE**		**LIQUIDUS TEMPERATURE**		BRAZING TEMPERATURE RANGE	
	Cr	**Ni**	**Si**	**W**	**Fe**	**B**	**C**	**P**	**S**	**Al**	**Ti**	**Zr**	**Co**	**OTHER ELEMENTS TOTAL**	**°C**	**°F**	**°C**	**°F**	**°C**	°F
COBALT																				
BCO-1	**18.0-20.0**	**16.0-18.0**	**7.5-8.5**	**3.5-4.5**	**1.0**	**0.7-0.9**	**0.35-0.45**	**0.02**	**0.02**	**0.05**	**0.05**	**0.05**	**REMAINDER**	**0.50**	**1120**	**2050**	**1150**	**2100**	**1150-1230**	**2100-2250**

Source: AWS A5.8-81, "Specification for Brazing Filler Metals"

(A) SINGLE VALUES ARE MAXIMUM PERCENTAGES, UNLESS OTHERWISE INDICATED.

(B) MINIMUM.

(C) ALL BNI ALLOYS HAVE A LIMIT OF 0.10 CO AND 0.005 SE.

Silver brazing filler metals, specifically the BAg group, are the most widely used type of filler metal in the brazing of stainless steels. The BAg-3 filler metal, which contains 3% Ni, is probably selected most frequently, although several other filler metals also can be used successfully. Silver brazing filler metals, especially those that contain zinc and chlorine, are primarily used in torch brazing where flux is applied and should not be considered for furnace brazing.

Joints brazed with silver-base filler metals cannot be used for high-temperature service applications. The recommended maximum service temperature is 370 °C (700 °F) (BAg-3). The recommended joint fitting allowances for silver brazing are relatively loose, that is, the diametral clearance is generally from 0.05 to 0.10 mm (0.002 to 0.004 in.).

Of the silver brazing filler metals shown in Table 1, all except BAg-19 and, possibly, BAg-13, are used at brazing temperatures that fall within the effective range of sensitizing temperatures (540 to 870 °C, or 1000 to 1600 °F) for austenitic stainless steels. Chromium carbide precipitation occurs in the sensitizing temperature range, which impairs the corrosion resistance of the base metal. Carbide precipitation, however, depends on time as well as temperature, and exposure to the sensitizing temperature range for only a few minutes is unlikely to result in a significant amount of precipitate. Nevertheless, the lower melting temperatures of the silver brazing filler metals prohibit the resolution treatment of the base metal after brazing. If corrosion resistance in service is sufficiently critical, an extra-low-carbon, titanium-stabilized or niobium-tantalum-stabilized type should be selected instead of a nonstabilized type of austenitic stainless steel.

Ferritic and martensitic stainless steels that contain little or no nickel are susceptible to interface corrosion in plain water or moist atmospheres, when they are brazed with nickel-free silver brazing filler metals, using a liquid or paste flux. Filler metal that contains nickel helps to prevent interface corrosion. However, for complete protection, special silver brazing filler metals that contain nickel and tin (for example, BAg-21) could be used, and brazing should be done in a protective atmosphere without flux.

Most silver brazing filler metals contain appreciable amounts of copper and zinc, either singly or in combination. Overheating or heating for an excessive period of time may result in extensive penetration of grain boundaries by copper and zinc, thereby embrittling the brazed joint.

Cadmium, which is added to some silver brazing filler metals to lower the melting temperature and improve wetting, also penetrates grain boundaries. The effect is accelerated when parts are brazed under tensile stress. Cadmium-containing fumes are extremely toxic, and operators must take every precaution to avoid inhaling them. Many new alloys that have similar brazing and functional characteristics of the cadmium-bearing alloys, but without their environmental and safety concerns, are being introduced to the market. Filler metals that contain cadmium and/or zinc should not be used in a protective atmosphere, including vacuum, because cadmium gases off readily. Because the loss of zinc or cadmium raises the melting point of the filler metal, brazeability is adversely affected.

Virtually all of the silver brazing filler metals are suitable for brazements that are used in fabricating vacuum chambers and pumps, where pressures as low as 1.3×10^{-3} Pa (10^{-5} torr) are encountered. However, for high-vacuum work (pressures of less than 1.3×10^{-4} Pa, or 10^{-6} torr), the filler metal must not contain cadmium or zinc. Vaporization of these metals interferes with the production of the vacuum and can contaminate the vacuum chamber and pumps. Selection of a suitable silver brazing filler metal for service in vacuum at a pressure below 1.3×10^{-3} Pa (10^{-5} torr) is considered in Example 1.

Nickel brazing filler metals are the next most frequently used filler metals for stainless steels. The BNi group of nickel brazing filler metals provides joints that have excellent corrosion resistance and high-temperature strength. These filler metals are typically supplied in the form of powders mixed with a binder. A limited number of filler metals are also available as sintered rods, preforms, and foils. However, these filler metals may alloy with stainless steel, forming intermetallic phases with two undesirable characteristics. First, the phases are considerably less ductile than either the base metal or the filler metal, even at elevated temperatures, and are therefore a potential source of rupture. Second, the alloys formed with stainless steel are higher-melting-point alloys that are likely to freeze at brazing temperatures, thus blocking further flow into the joint during brazing. To achieve flow in deep joints, diametral clearances as large as 0.10 to 0.20 mm (0.004 to 0.008 in.) are necessary. Knurling of male members sometimes helps in the centering of loosely fitting components. With such large clearances, joints that are brazed with nickel brazing filler metals do not develop their greatest strength. The brazed joint is much stronger with a clearance of 0.025 to 0.076 mm (0.001 to 0.003 in.).

Because of the relatively high brazing temperatures required for the nickel brazing filler metals, their use is generally limited to furnace brazing in a controlled atmosphere (including vacuum), although there are occasional exceptions, as will be seen when Fig. 15 is discussed. Torch brazing with BNi brazing filler metals is used to braze small parts and small quantities.

Copper Brazing Filler Metals. The high brazing temperature and the need for a protective atmosphere generally limits the use of copper filler metals to furnace applications. The BCu brazing filler metals (which are practically pure copper) melt at approximately 1080 °C (1980 °F), and flow freely at 1120 °C (2050 °F).

Copper is not recommended for exposure to certain corrosive substances, such as the sulfur in jet fuel and in sulfur-beating atmospheres. Furthermore, copper brazing filler metals exhibit poor oxidation resistance at elevated temperatures and should not be exposed to service temperatures higher than 430 °C (800 °F). When copper brazing filler metal is used, the recommended diametral allowance on joint fit ranges from a 0.10 mm (0.004 in.) clearance to a 0.05 mm (0.002 in.) interference.

Gold brazing filler metals (the BAu group) are sometimes used for the brazing of stainless steel, although their high cost restricts their use to specialized applications, such as the fabrication of aerospace equipment (Example 4). When gold brazing filler metal is used, them is minimal alloying with the stainless steel base metal. As a result, joints exhibit good ductility, strength, and corrosion resistance. When maximum corrosion resistance is needed, BAu-4 should be used.

Cobalt brazing filler metals (the BCo-1 group) are very rarely used for the brazing of stainless steels. However, this type of filler metal is included in Table 1, and it is available for that purpose.

Fluxes

Flux usually is not required for furnace brazing in strongly reducing or inert atmospheres. However, in some furnace brazing applications, flux is necessary. It is always required for torch brazing and is usually required for induction and resistance brazing, unless atmospheric protection is provided.

Any of the American Welding Society (AWS) types of FB3-A through FB3-J fluxes are suitable for all stainless steel brazing applications where flux is needed. The ANSI/AWS 5.31 specification for fluxes used in brazing and braze welding processes provides more details. There are basically three groups of these fluxes, based on their activity range, and they are further classified by their form (powder, paste, slurry, or liquid). The FB3-A, -F, and -G types of flux contain borates and fluorides and have an effective temperature range from 570 to 870 °C (1050 to 1600 °F). These fluxes are suitable for use with silver brazing filler metals.

Type FB3-C flux contains the same ingredients as type FB3-A, except for the addition of boron, and it has a higher effective temperature range from 570 to 930 °C (1050 to 1700 °F). This flux has an extended heating time capability.

The FB3-D, -I, and -J types of flux also contain borates and fluorides, such that its activity ranges from 760 to 1200 °C (1400 to 2200 °F). These fluxes are often selected for use with silver brazing filler metals if the brazing temperature is above 730 °C (1350 °F). They are well suited for use with copper, nickel, and gold brazing filler metals.

Brazing of Stainless Steels

Revised by Matthew J. Lucas, Jr., General Electric Aircraft Engines

Torch Brazing

For stainless steel, the fundamentals of torch brazing, as well as the advantages and limitations, are basically the same as for carbon steels. However, because of the metallurgical characteristics of stainless steel and its requirements for corrosion resistance, the best results are obtained when special consideration is given to the type of flame at the torch and to the filler-metal composition.

Flame Adjustment. To aid in reducing the oxide that is already present, and to prevent further oxidation of the workpiece surfaces, a flame that ranges from neutral to slightly reducing should be used when torch brazing stainless steel to itself. A reducing flame is also satisfactory for brazing stainless steel to nickel alloys or carbon steels. Although a slightly oxidizing flame is typically best for brazing oxide-containing (tough pitch) copper, a slightly reducing flame is usually best when brazing stainless steel to copper. Use of a reducing flame to braze copper is not recommended because this type of flame will remove oxygen from the copper and can also cause hydrogen embrittlement.

Filler Metals. The silver brazing filler metals that flow at relatively low temperatures are used almost exclusively for the torch brazing of stainless steels. BAg-3 is most often used, because it flows well in the temperature range from 700 to 760 °C (1300 to 1400 °F) and provides joints that have greater resistance to corrosion than those brazed with filler metals such as BAg-1 or BAg-1a (although these filler metals are also used). The use of brazing filler metals that require temperatures higher than approximately 760 °C (1400 °F) results in excessive oxidation, thus making it difficult to obtain adequate wetting of the brazed joint. In special applications, higher-melting-point filler metals must be used (Example 1).

Flux. Type FB3-A flux is most widely used for the torch brazing of stainless steel because it has a working range from 560 to 870 °C (1050 to 1600 °F) and is well suited for use with the lower-melting-point silver brazing filler metals. However, in some applications, other types of FB3 fluxes are preferred.

Example 1: Torch Brazing of Parts for High-Vacuum Service.

The sleeve and tube assembly shown in Fig. 1 is typical of brazements used in vacuum systems. The tubes and the sleeve are type 304L austenitic stainless steel. The BAg-18 (60Ag-10Sn-30Cu) brazing filler metal, which has proved satisfactory for the brazing of assemblies used in high-vacuum service, was used with type FB3-B flux. This silver brazing filler metal does not contain zinc or cadmium. It should be noted that vacuum grades of the silver brazing filler metals, such as BVAg-18, are available, and that they limit the amount of impurities that can be detrimental to components of the vacuum tube industry. Again, ANSI/AWS A5.8 should be consulted for further details.

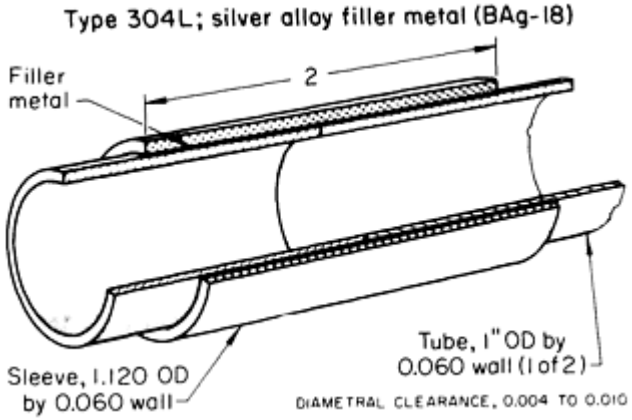

FIG. 1 ASSEMBLY THAT WAS TORCH BRAZED WITH A SILVER BRAZING FILLER METAL FOR USE IN A HIGH VACUUM ATMOSPHERE SYSTEM

Brazing was conducted with a manually manipulated oxyacetylene torch and a strong reducing flame. The assembly shown in Fig. 1 could have been brazed in a furnace or by induction, but production was small and did not justify the investment for such equipment.

Example 2: Torch Brazing of Stainless Steel to Nickel.

The brazed assembly shown in Fig. 2, which consists of a type 304 stainless steel tube and a pure nickel tube, was resistance heated in service. Requirements for this assembly were:

- TRANSMISSION OF ELECTRICITY WITHOUT DEVELOPING HOT SPOTS
- STRAIGHTNESS AND SMOOTHNESS, BECAUSE THE ASSEMBLY HAD TO SLIDE INTO A LARGER ASSEMBLY
- JOINING AT MINIMUM TEMPERATURE, BECAUSE NUMEROUS SMALL INSULATED WIRES WERE IN THE ASSEMBLY AT THE TIME OF JOINING AND WERE SUBJECT TO DAMAGE IF THE JOINING TEMPERATURE WAS TOO HIGH

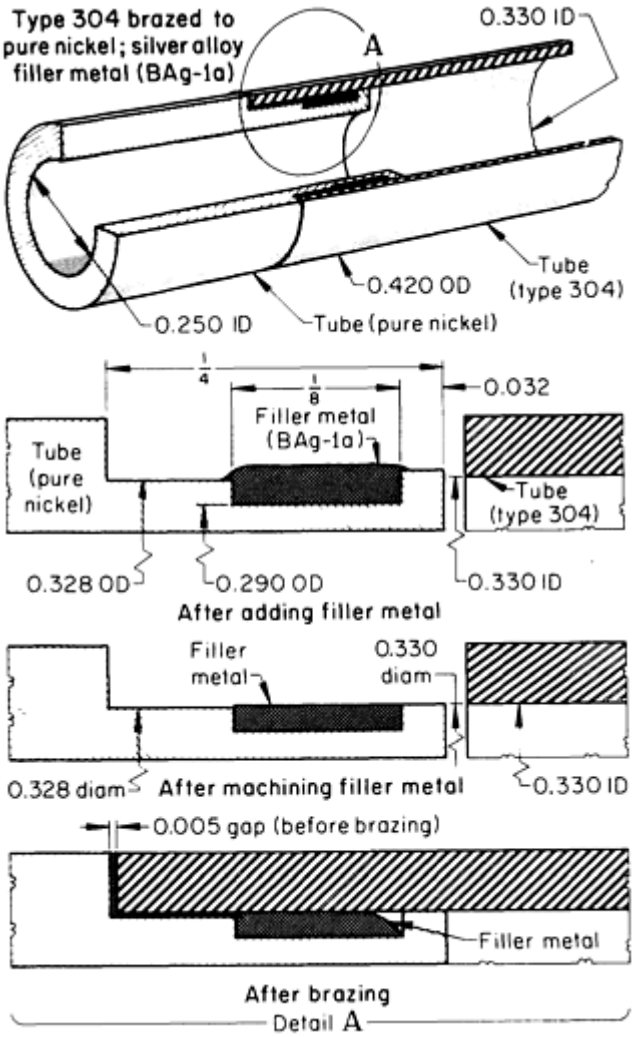

FIG. 2 TORCH-BRAZED ASSEMBLY OF A STAINLESS STEEL TUBE AND A PURE NICKEL TUBE

Torch brazing with silver brazing filler metal proved to be a desirable way to make the joint, because of the relatively low brazing temperature, high electrical conductivity of the joint, minimal distortion, ease of removing excess filler metal, and ease of radiographic inspection.

The joint design (Fig. 2) allowed the preplacement of the brazing filler metal (BAg-1a) in a 3.2 mm ($\frac{1}{8}$ in.) wide groove that was machined into the shoulder of the nickel tube. The filler metal was then melted with a torch, and both filler metal and shoulder were machined to match the inside diameter of the stainless tube (zero-clearance fit).

Several heating methods were tried in an attempt to braze the nickel tube to the stainless steel tube, including induction heating in an inert gas and multiple-torch heating. However, the use of a single oxyacetylene torch operated by a skilled technician proved to be the most successful method. The sequence of operations for single-torch brazing was:

- COMPONENTS WERE CLEANED WITH ACETONE
- FLUX PASTE WAS PLACED ON THE NICKEL TUBE IN THE AREA TO BE BRAZED
- THE TWO TUBES WERE ASSEMBLED IN A FIXTURE WITH A 0.13 MM (0.005 IN.) GAP THAT SHOWED SURFACE (DETAIL A IN FIG. 2)
- THE ASSEMBLY WAS HEATED WITH A TORCH UNTIL THE FILLER METAL FLOWED TO THE OUTSIDE SURFACE (FLOW TEMPERATURE OF 640 °C, OR 1175 °F, FOR BAG-1A)

- EXCESS FLUX THAT FLOWED TO THE SURFACE WAS REMOVED MANUALLY

It was possible to inspect the entire joint by making two radiographs. Only scattered porosity was detected in a routine radiographic inspection of the brazed joints.

Brazing of Stainless Steels

Revised by Matthew J. Lucas, Jr., General Electric Aircraft Engines

Furnace Brazing

Almost all furnace brazing of stainless steel is done in a protective atmosphere (including vacuum). One exception is the application described in Example 11, in which air was the furnace atmosphere. In this case, a liquid flux was used and the time at brazing temperature was short, which helped to prevent excessive oxidation.

The protective atmospheres most often used in furnace brazing of stainless steel are dry hydrogen and dissociated ammonia. These atmospheres are effective in reducing oxides, protecting the base metal, and promoting the flow of brazing filler metal. The low-cost exothermic atmospheres that are widely used in furnace brazing of low-carbon steel are not suitable for stainless steel. An inert gas, such as argon, or a vacuum environment, can be used to satisfy special requirements and to provide protection in applications for which hydrogen or hydrogen-bearing gases are unsatisfactory.

Selection of the furnace atmosphere depends on the degree of protection that must be given to the base metal or metals, the flow characteristics of the brazing filler metal, the brazing temperature, and cost. Special requirements that arise from the brazing of dissimilar metals are often a major factor in atmosphere selection. The availability of equipment can also be an important consideration.

Furnace Brazing in Dry Hydrogen. A dry hydrogen atmosphere is preferred for many stainless steel brazing applications. Hydrogen, which is the most strongly reducing protective atmosphere, reduces chromium oxide and promotes excellent wetting by many filler metals without the need for flux. The principal disadvantages of hydrogen are its cost, its difficulty in drying sufficiently, the need for special furnace equipment, and the potential danger involved in improper storage and handling. The following examples describe applications in which a specific type of stainless steel was joined to either the same or another type of stainless steel.

Example 3: Selection of BAg-13 Silver Brazing Filler Metal for Brazing at 930 °C (1700 °F).

The type 347 stainless steel retainer assembly shown in Fig. 3 was furnace brazed in dry hydrogen, using BAg-13 silver brazing filler metal, which was selected in preference to lower-melting-point silver brazing filler metals because the upper limit of its brazing temperature range (860 to 970 °C, or 1575 to 1775 °F) permitted brazing at 930 °C (1700 °F). At furnace temperatures above 980 °C (1800 °F), dry hydrogen is strongly reducing, and the use of a brazing flux is not required for satisfactory wetting action. Thus, by judicious selection of the brazing filler metal and the furnace atmosphere, the extra cost of applying the flux and of removing flux residue after brazing was avoided.

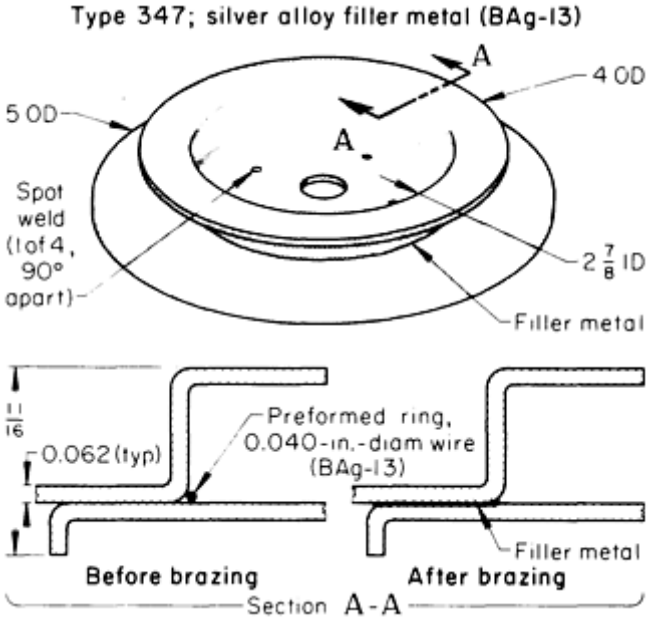

FURNACE BRAZING IN DRY HYDROGEN	
FURNACE	**CONTINUOUS CONVEYOR[A]**
FIXTURES	**NONE**
FURNACE TEMPERATURE, °C (°F)	**980 ± 5 (1800 ± 10)**
BRAZING TEMPERATURE, °C (°F)	**925 ± 5 (1700 ± 10)**
HYDROGEN DEW POINTS, °C (°F)	**-75 (-100)[B]; -60 (-70)[C]**
HYDROGEN FLOW RATE, M^3/H (FT^3/H)	**11 (400)**
FILLER METAL[D]	**BAG- 13**
JOINT POSITION DURING BRAZING	**HORIZONTAL**
CONVEYOR TRAVEL SPEED, M/H (FT/H)	**9 (30)**
TIME AT BRAZING TEMPERATURE, MIN[E]	**5**
PRODUCTION RATE, ASSEMBLIES/H	**120**

(A) ELECTRICITY HEATED (60 KW), CONSTRUCTED WITH HEATING CHAMBER HIGHER THAN ENTRANCE AND DISCHARGE ENDS.

(B) INCOMING.

(C) EXHAUST.

(D) IN FORM OF 1 MM (0.040 IN.) DIAMETER WIRE-RING PREFORMS.

FIG. 3 RETAINER ASSEMBLY FURNACE BRAZED WITH BAG-13 FILLER METAL

The components were vapor degreased, assembled (keeping their outside diameters concentric), and spot welded (to make them self-jigging) at four locations 90° apart (Fig. 3). A ring of brazing filler metal wire in a 1 mm (0.040 in.) diameter was preplaced at the joint, and assemblies were loaded two-across on the mesh belt of a conveyor-type furnace. The heating chamber of the furnace was elevated from the entrance and discharge level to conserve the lighter-than-air hydrogen and to prevent oxygen in the atmosphere from mixing with the hydrogen, which could either raise the dew point or cause an explosion.

Quality standards for brazed assemblies, which were checked by 100% visual inspection, required that the joint exhibit full braze penetration (360° fillets on both sides of the joint) and be pressure-tight.

Example 4: Use of a Gold Brazing Filler Metal for Brazing in an Aerospace Heat Exchanger.

In the fabrication of a high-reliability heat exchanger for manned space flights, 2552 fins of 0.10 mm (0.004 in.) thick type 347 stainless steel were brazed to 0.64 mm (0.025 in.) thick type 347 stainless steel side panels, as shown in Fig. 4. The 5104 fin-to-panel joints had to be strong and corrosion resistant.

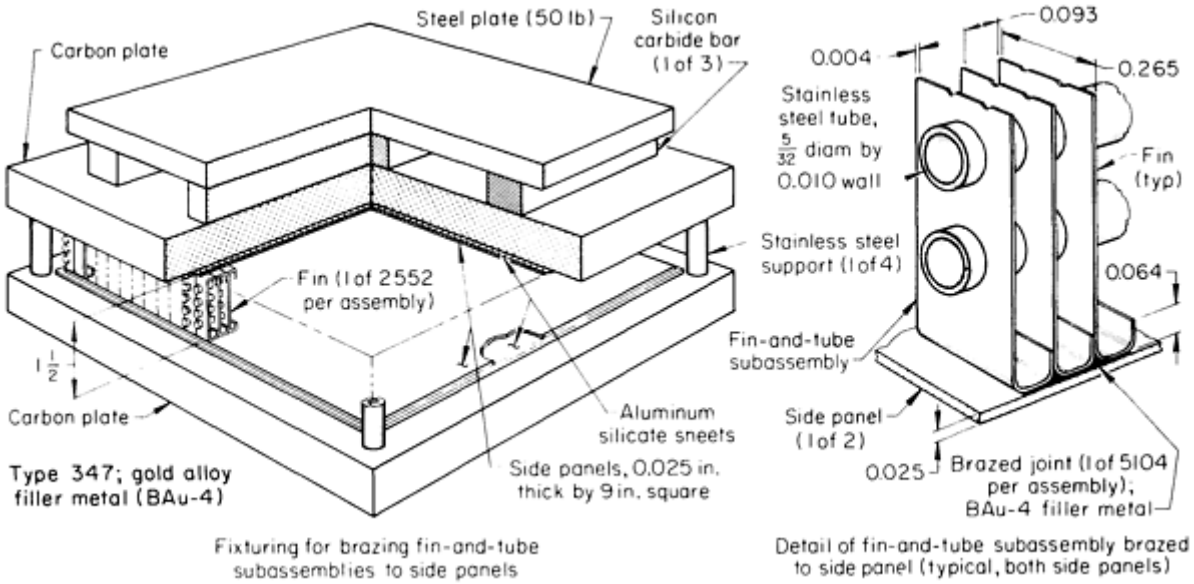

Fixturing for brazing fin-and-tube subassemblies to side panels

Detail of fin-and-tube subassembly brazed to side panel (typical, both side panels)

FURNACE BRAZING IN DRY HYDROGEN	
FURNACE	**BELL**[A]
FIXTURES	**(SEE ILLUSTRATION)**
BRAZING TEMPERATURE, °C (°F)	**1015 (1860)**
HYDROGEN DEW POINT (MAX), °C (°F)	**-60 (-80)**[B]
PURGING[C]	**5**
FILLER METAL[D]	**BAU-4**
NUMBER OF ASSEMBLIES PER LOAD	**1**
PROCESSING TIME PER ASSEMBLY	
CLEAN COMPONENTS, MIN	**45**
PREPLACE FILLER METAL, H	**1.25**
ASSEMBLE COMPONENTS IN FIXTURE, H	**4**
TIME AT BRAZING TEMPERATURE, MIN	**7-10**
TOTAL TIME IN FURNACE[E], H	**4**
INSPECT, H	**1**
PRESSURE TEST, H	**40**

(A) ELECTRICALLY HEATED, WITH 36 IN. DIAM RETORT WITH WATER-COOLED RUBBER SEALS.

(B) HYDROGEN WAS PURCHASED AS CYLINDER HYDROGEN, THEN PASSED THROUGH AN ELECTROLYTIC DRIER.

(C) NUMBER OF VOLUME CHANGES IN RETORT.

(D) 200-MESH POWDER SUSPENDED IN AN ORGANIC BINDER.

(E) INCLUDING COOLING TO 150 °C (300 °F) IN RETORT, WHICH WAS PURGED WITH ARGON BEFORE BEING OPENED

FIG. 4 HEAT-EXCHANGER ASSEMBLY IN BRAZING FIXTURE AND DETAIL OF JOINTS BRAZED WITH GOLD BRAZING FILLER METAL

Silver and copper brazing filler metals could not be used, because of their incompatibility with sulfur-bearing rocket fuel. The BNi series of nickel brazing filler metals had the necessary compatibility, but made nonductile joints that were unreliable under tension peel stress. Therefore, gold brazing filler metals were used. The necessary brazing characteristics for the fin-to-panel joints were present in BAu-4 (nominal composition, 82Au-18Ni). The strength and ductility of the resulting brazed joints justified the high cost of this particular brazing filler metal.

The fins and side panels were cleaned by vapor degreasing. The side panels were then pickled, rinsed in clean water, and dried. The brazing filler metal was deposited on the panels in the form of a powder suspended in an organic binder. Multiple lap joints were made between the flat-crown-hairpin ends of the fins and the flat side panels. The assembly was placed in a fixture (Fig. 4), and then the entire assembly and fixture were placed in the retort of a bell-type furnace and sealed. The sealed retort was purged with a volume of hydrogen that was equivalent to five times that of the retort. The retort was then heated to a brazing temperature of 1020 °C (1860 °F) and held for 7 to 10 min. The joint gaps at brazing temperature ranged from 0.000 to 0.254 mm (0.010 in.). After brazing, the retort was purged with argon while being cooled to 150 °C (300 °F) and was not opened until after purging and cooling.

The joints brazed by this procedure were the final brazed joints in the assembly. In a prior brazing operation, tubes had been joined to the fins (Fig. 4) by brazing at 1080 °C (1970 °F) using a higher-melting-point gold brazing filler metal of 70Au-22Ni-8Pd.

The completed assemblies were visually inspected and pressure tested at pressures that far exceeded those of the intended service environment: 1.86 MPa (270 psi) on the outside of the tubes and 11.8 MPa (1710 psi) on the inside. Acceptance pressure test values were 3.7 MPa (540 psi) on the outside and 15.7 MPa (2275 psi) on the inside of the tubes. Selected brazed assemblies were tested to bursting. These assemblies were required to withstand at least three times the service pressures before bursting. The assemblies that were brazed with gold brazing filler metals passed all tests and had three times the bursting strength of the assemblies brazed with undiffused nickel brazing filler metal.

Example 5: Combination Brazing and Solution Heat Treatment of an Assembly of Three Types of Stainless Steel.

Three different stainless steels were selected to make the cover for a hermetically sealed switch. The switching action had to be transmitted through the cover without breaking the seal. This was accomplished by providing a diaphragm through which a shoulder pin was inserted, as shown in Fig. 5. The switch was actuated by depressing the pin, which in turn deflected the diaphragm. The pin (type 303), the diaphragm (PH 15-7 Mo), and the cover (type 305) were assembled as shown in Fig. 3, and then brazed using a silver-base filler metal in a furnace with dry hydrogen.

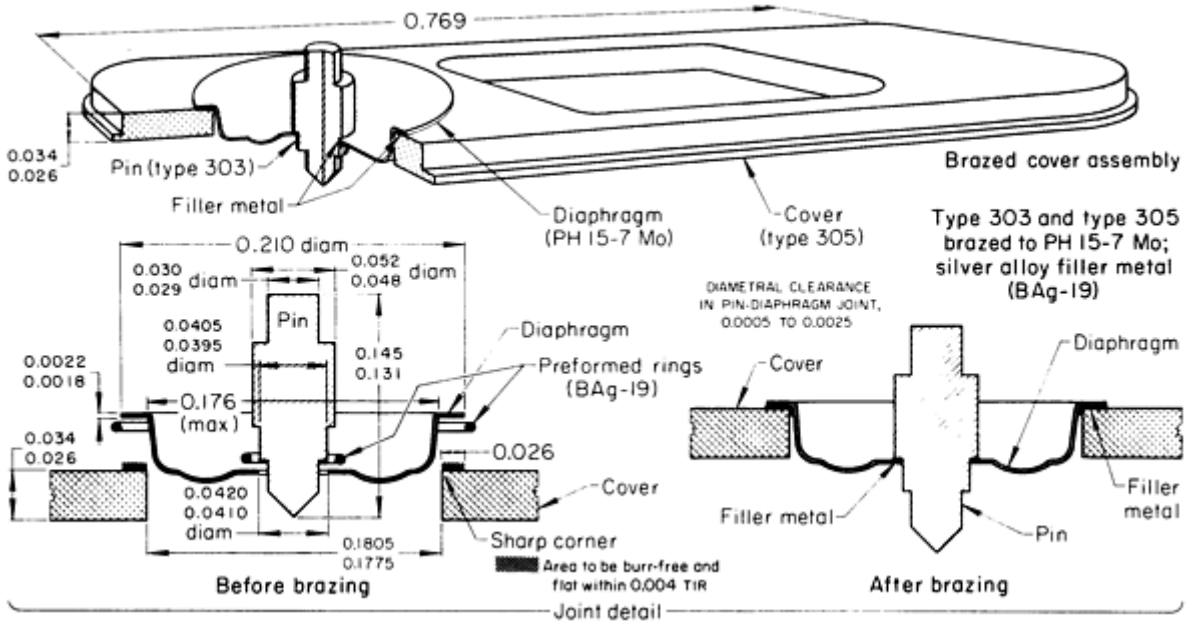

FURNACE BRAZING IN DRY HYDROGEN	
FURNACE[A]	**BATCH-TYPE TUBE**
FIXTURE MATERIAL[B]	**STAINLESS STEEL**
BRAZING TEMPERATURE, °C (°F)	**955 ± 8 (1750 - 15)**
FILLER METAL[C]	**BAG-19**
TIME AT BRAZING TEMPERATURE, MIN	**10**
TIME IN FIRST COOLING ZONE[D], MIN	**5**
TIME IN FINAL COOLING ZONE[D], MIN	**5**

(A) THREE-ZONE FURNACE WITH A HIGH-HEAT ZONE 125 MM (5 IN.) IN DIAMETER BY 460 MM (18 IN.) LONG.

(B) FIXTURE LOCATED AND HELD COMPONENTS OF ASSEMBLY TOGETHER AND WAS PLACED ON A STAINLESS STEEL SLED FOR TRANSPORT THROUGH THE FURNACE.

(C) PREFORMED WIRE RINGS.

(D) AT 540 °C (1000 °F).

(E) WATER-COOLED ZONE, IN WHICH ASSEMBLY WAS COOLED TO ROOM TEMPERATURE. TO COMPLETE HEAT TREATMENT OF THE PH 15-7 MO DIAPHRAGM, ASSEMBLY WAS

FIG. 5 THREE-STEEL SWITCH-COVER ASSEMBLY THAT UTILIZED BRAZING TEMPERATURE AS PART OF SOLUTION HEAT TREATMENT

Silver brazing filler metal BAg-19 was chosen because it flowed at a temperature that coincided with the solution heat-treating temperature for the PH 15-7 Mo diaphragm (950 °C, or 1750 °F). A holding fixture was needed to keep the PH 15-7 Mo diaphragm in position during the brazing cycle. To avoid carburizing the diaphragm, the material selected for the fixture was stainless steel, rather than graphite. The furnace was a batch-type tube furnace with a 120 mm (5 in.) diameter high-heat zone that was 460 mm (18 in.) long. The moisture content of the hydrogen atmosphere was carefully controlled, because the lithium-containing filler metal flowed too freely when the atmosphere was too dry, and it did not seal the joints.

After being cleaned, the components were assembled with two preform rings of BAg-19 wire. Tweezers were used to avoid contaminating the cleaned surfaces. Each assembly was held in a stainless steel fixture, which in turn was placed on a stainless steel furnace sled. The sled was pushed into the high-heat zone of the furnace and held at 950 °C (1750 °F) for 10 min, before being pulled into an intermediate cooling zone at 1830 °C (1000 °F) and held for 5 min. Finally, it was pulled to the water-cooled zone, where it cooled to room temperature. The brazing of the two joints and the solution treating of the PH 15-7 Mo diaphragm were accomplished simultaneously at the brazing temperature of 950 °C (1750 °F). To complete the heat-treating process, the assembly was cooled to -70 °C (-100 °F), held for 8 h, and then aged at 510 °C (950 °F) for 1 h.

A 25 mm (1 in.) square piece of PH 15-7 Mo was processed with each batch of cover assemblies and used as a hardness test specimen to verify that the diaphragms had been correctly heat treated. Brazed assemblies were inspected by the brazing operator. The joints were required to be fully sealed and to not have any voids. The pins were required to be perpendicular within 4°. Perpendicularity was measured on a comparator. Randomly selected samples were given a push-out test, in which joints had to withstand a push of 60 N (14 lbf). All assemblies were given 100% visual inspection at high magnification.

Example 6: Simultaneous Brazing of a Heat-Exchanger Assembly.

An air-to-air heat-exchanger assembly, shown in Fig. 6, consisted of 185 thin-walled (0.20 mm or 0.008 in.) tubes and two 1.6 mm ($\frac{1}{16}$ in.) thick headers. All components were made of type 347 stainless steel. The tubes were assembled with the headers by flaring the tube ends to lock them in place and provide metal-to-metal contact for the brazing filler metal. All 370 joints were brazed during a single pass through a continuous conveyor-type electric furnace.

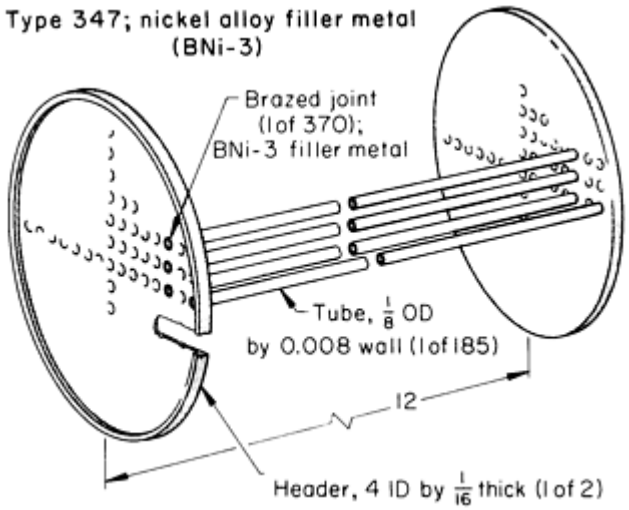

FURNACE BRAZING IN DRY HYDROGEN	
FURNACE[A]	**CONTINUOUS CONVEYOR**
FIXTURE MATERIAL[B]	**TYPE 347 STAINLESS STEEL**
FURNACE TEMPERATURE, °C (°F)	**1120 ± 5 (2050 ± 10)**
BRAZING TEMPERATURE, °C (°F)	**1065 ± 5 (1950 ± 10)**
HYDROGEN DEW POINTS, °C (°F)	**-75 (-100)[C]; -60 (-70)[D]**
HYDROGEN FLOW RATE, M^3/H (FT^3/H)	**17 (600)**
FILLER METAL[E]	**BNI-3 POWDER**
CONVEYOR TRAVEL SPEED, M^3/H (FT^3/H)	**9 (30)**
TIME AT BRAZING TEMPERATURE, MIN	**5**
COOLING	**IN HYDROGEN ATMOSPHERE**
ASSEMBLY PRODUCTION RATE/H	**15**

(A) ELECTRICALLY HEATED (60 KW), CONSTRUCTED WITH HEATING CHAMBER HIGHER THAN ENTRANCE AND DISCHARGE ENDS.

(B) HOLDING FIXTURE FABRICATED FROM 3.2 MM ($\frac{1}{8}$ IN.) THICK SHEET.

(C) INCOMING.

(D) EXHAUST.

(E) MIXED TO A SLURRY WITH ACRYLIC RESIN AND XYLENE THINNER; POWDER-TO-VEHICLE RATIO, 70/30

FIG. 6 HEAT-EXCHANGER ASSEMBLY WITH TUBE-TO-HEADER JOINTS BRAZED IN ONE PASS THROUGH A FURNACE

Although a nickel brazing filler metal was preferred for this high-temperature application, because of the resistance to heat and corrosion that it provides, the selection of a specific nickel brazing filler metal presented a problem. Higher-melting-point, boron-containing nickel brazing filler metals, such as BNi-1 and BNi-3, will react with the base metal, partially dissolve, and therefore are likely to erode thin materials. Fortunately, the extent of erosion can be modified by controlling the brazing temperature and time, as well as the amount of filler metal.

Although there are nickel brazing filler metals that contain silicon in place of boron, they generally require much higher brazing temperatures, which can result in grain coarsening in the base metal. Therefore, after numerous tests, BNi-3 filler metal was selected on the basis of its brazing temperature and excellent fluidity. The problem of applying the correct amount of filler metal to avoid erosion was solved by preparing a slurry from an accurately controlled mixture of filler-metal powder, acrylic-resin binder, and xylene thinner.

Before the filler metal was applied, the heat-exchanger assembly was cleaned ultrasonically in acetone and carefully weighed to determine the proportionate weight of filler metal that would be required. Half of the total amount of filler metal was then applied to one end of the assembly by spraying. The assembly was reweighed, and the remaining filler metal was applied to the opposite end. At all stages of processing, the assembly was handled by operators wearing clean, lint-free cotton gloves.

The assembly was placed on a holding fixture made of stainless steel sheet, on which a stop-off compound had been applied to prevent the assembly from brazing to the fixture if the brazing filler metal flowed excessively. Assemblies were placed 300 mm (12 in.) apart on the conveyor, as they traveled through the furnace at 9 m/h (30 ft/h) under the protection of dry hydrogen.

After brazing, each side was subjected to 100% visual inspection to detect the presence of fillets, and the assemblies were pressure tested in accordance with customer requirements. Because of the thin-walled (0.20 mm, or 0.008 in.) tubing, this assembly was brazed more consistently and at a lower cost than could have been achieved by other joining processes.

Example 7: Combined Brazing and Hardening of a Shaft Assembly.

The shaft assembly shown in Fig. 7 consists of three bars or screw machine products (a shaft, a drive pin, and a guide pin) and two stampings (upper and lower mounting plates), all made from type 410 stainless steel and furnace brazed together using four joints. By brazing with copper filler metal at 1120 °C (2050 °F), it was possible to austenitize and harden the assembly to the required minimum hardness value of 40 HRC during the brazing and cooling operations, thereby avoiding separate hardening operations after brazing.

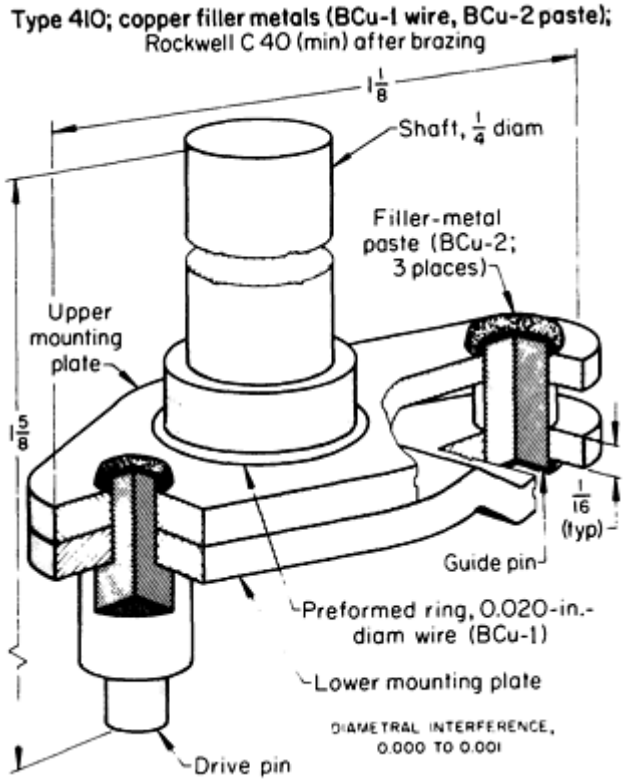

FURNACE BRAZING IN DRY HYDROGEN	
FURNACE[A]	**CONTINUOUS CONVEYOR**
FIXTURES[B]	**NONE**
FURNACE TEMPERATURE, °C (°F)	**1175 ± 5 (2150 ± 10)**
BRAZING TEMPERATURE, °C (°F)	**1120 ± 5 (2050 ± 10)**
HYDROGEN DEW POINTS, °C (°F)	**-75 (-100)[C]; -60 (-75)[D]**
HYDROGEN FLOW RATE, M^3/H (FT^3/H)	**11 (400)**
FILLER METAL[E]	**BCU-1 WIRE, BCU-2 PASTE**
CONVEYOR TRAVEL SPEED, M/H (FT/H)	**6 (20)**
TIME AT BRAZING TEMPERATURE [F], MIN	**8**
COOLING	**IN HYDROGEN ATMOSPHERE**
ASSEMBLY PRODUCTION RATE/H	**800**

(A) ELECTRICALLY HEATED (60 KW), CONSTRUCTED WITH HEATING CHAMBER HIGHER THAN ENTRANCE AND DISCHARGE ENDS.

(B) COMPONENTS WERE STAKED, FOR SELF-FIXTURING. ASSEMBLIES, SUPPORTED BY CERAMIC SPACERS TO KEEP SHAFT END UP, WERE BRAZED ON TRAYS.

(C) INCOMING.

(D) EXHAUST.

ONE END OF DRIVE PIN, BOTH ENDS OF GUIDE PIN.
(F) ASSEMBLIES WERE IN HIGH HEAT ZONE FOR ABOUT 10 MIN.

FIG. 7 FOUR-JOINT SHAFT ASSEMBLY THAT WAS SIMULTANEOUSLY FURNACE BRAZED AND HEATED FOR HARDENING

Because the joints were all relatively short, an interference fit of 0.000 to 0.025 mm (0.001 in.) was satisfactory. Typically, a clearance fit between mating parts is required with longer joints in stainless steel. The automatic staking of components was used to make the assembly self-fixturing.

As shown in Fig. 7, a full ring of 0.50 mm (0.020 in.) diameter BCu-1 copper wire was preplaced around the 13 mm ($\frac{1}{2}$ in.) diameter shaft to braze the shaft to the upper and lower mounting plates. A small amount of BCu-2 copper paste was applied at one end of the drive pin to braze it to the two mounting plates. Because of the separation between the two plates on the guide-pin side, a small amount of BCu-2 copper paste was manually applied on each end of the guide pin. The assemblies were placed in brazing trays, with the shaft in a vertical position, and were supported in this position by ceramic spacers.

The brazing trays were then placed on the mesh belt of a continuous-type conveyor furnace containing a dry hydrogen atmosphere. They were transported up an incline to the horizontal preheat and high-heat chambers at a speed of 6 m/h (20 ft/h). Because the assemblies were small, they became heated to the brazing temperature in about 2 min. After 8 min at the brazing temperature, the assemblies were conveyed into water-jacketed cooling chambers, where they cooled rapidly in the hydrogen atmosphere to room temperature. Brazed assemblies that were bright and oxidation-free emerged from the exit end of the furnace.

The brazed assemblies were 100% visually inspected for complete joint coverage. Hardness tests on a sampling basis were used to determine whether the assemblies had responded properly to hardening. Tempering to the desired final hardness followed the simultaneous brazing and hardening operation.

Example 8: Medical Device Brazed, Rather than Welded, in Hydrogen.

Because of the need for strong, corrosion-resistant, and leak-proof joints in a stainless steel blood-cell washer (Fig. 8), the process that was selected was hydrogen furnace brazing with BNi-7 brazing filler metal. The devices are used to expedite and standardize cell-washing procedures in blood banks and hematology laboratories. Therefore, neither voids nor cracks could be tolerated, because the possibility of breeding bacteria in the devices had to be avoided.

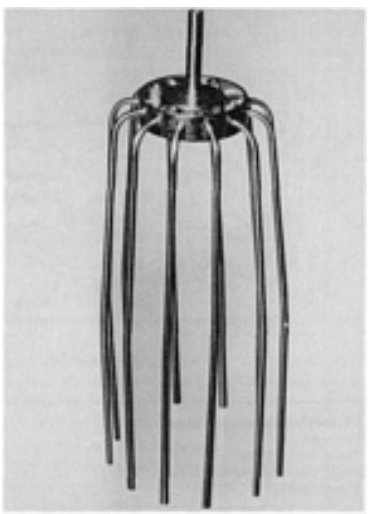

FIG. 8 MANIFOLD AND CANNULAS TUBE ASSEMBLY OF A BLOOD-CELL WASHER THAT WAS HYDROGEN FURNACE BRAZED WITH BNI-7 BRAZING FILLER METAL AT 1040 °C (1900 °F). COURTESY OF WALL

COLMONOY CORPORATION

Brazing, rather than welding, was chosen to join the manifold and the delicate tube parts of the washer, a rake-like component with twelve prong-like cannulas tubes that extend approximately 150 mm (6 in.) from a cylindrical manifold.

The manifold assembly was brazed using BNi-7 nickel brazing filler metal in a hydrogen atmosphere at 1040 °C (1900 °F). After assembling the tubes to the manifold, the brazing filler metal was applied to the joints and the assembly was placed in the furnace. Components were wired to stainless steel fixtures to maintain uniform tube spacing.

The brazing permitted the filler metal to flow completely around the thin-walled tubes, which was not possible with welding, leaving smooth fillets without voids that could trap harmful bacterial particles. Additional advantages of brazing were that it: minimized the amount of assembly distortion, eliminated flux hazards, simplified inspection procedures, and prevented the oxidation.

Brazing of Stainless Steels

Revised by Matthew J. Lucas, Jr., General Electric Aircraft Engines

---

Furnace Brazing in Dissociated Ammonia

When ammonia is free of moisture and is 100% dissociated, it becomes a suitable atmosphere for the brazing of stainless steel using selected brazing filler metals without requiring a flux. Although dissociated ammonia is strongly reducing, it is less so than pure, dry hydrogen. Consequently, it will promote wetting action by reducing chromium oxide on the surface of stainless steel, but it may not be sufficiently reducing to promote the flow of some brazing filler metals, such as copper oxide powders. Because of its high (75%) hydrogen content, dissociated ammonia forms explosive mixtures with air and must be handled with the same precautions as those required for the handling of hydrogen.

A dissociated-ammonia atmosphere is prepared by heating anhydrous liquid ammonia in the presence of an iron or nickel catalyst. The decomposition of ammonia to form hydrogen and nitrogen begins at 315 °C (600 °F), and the rate of decomposition increases with temperature. Unless the atmosphere used in brazing stainless steel is completely decomposed, that is, 100% dissociated, even minute amounts of raw ammonia (NH_3) in the atmosphere will cause the nitriding of stainless steel, especially steels containing little or no nickel. In addition, because of the solubility of ammonia in water, the atmosphere that comes from the dissociator must be extremely dry (preferably having a dew point of -60 °C, or -80 °F, or lower). To ensure a very low dew point, the atmosphere that comes from the dissociator is commonly processed by being passed through a molecular-sieve dryer. To avoid the oxidation of base metal and brazing filler metal, the atmosphere must be kept pure and dry while it is inside the furnace. In the following examples of production practices, dissociated ammonia was used successfully in the furnace brazing of austenitic and precipitation-hardening (PH) stainless steels.

Example 9: Brazing in Dissociated Ammonia Without Flux.

The pressure gage subassembly shown in Fig. 9 comprises five diaphragms of 17-7 PH stainless steel, a deep-drawn cup and a top fitting of type 304 stainless steel, and a connector of copper alloy 145 (tellurium-bearing copper). Originally, these subassemblies were furnace brazed with a silver brazing filler metal that required a flux. Because applying flux and assembling the fluxed components with gloved hands was time consuming, the decision was made to change to fluxless brazing in an atmosphere of dissociated ammonia. Although this necessitated using a more-expensive brazing filler metal (BAg-19), the higher cost was offset by the greater productivity of each operator. In addition, subassemblies brazed with BAg-19 in dissociated ammonia exhibited fewer leaks and had improved corrosion resistance and a better appearance than those brazed with the original filler metal and a flux.

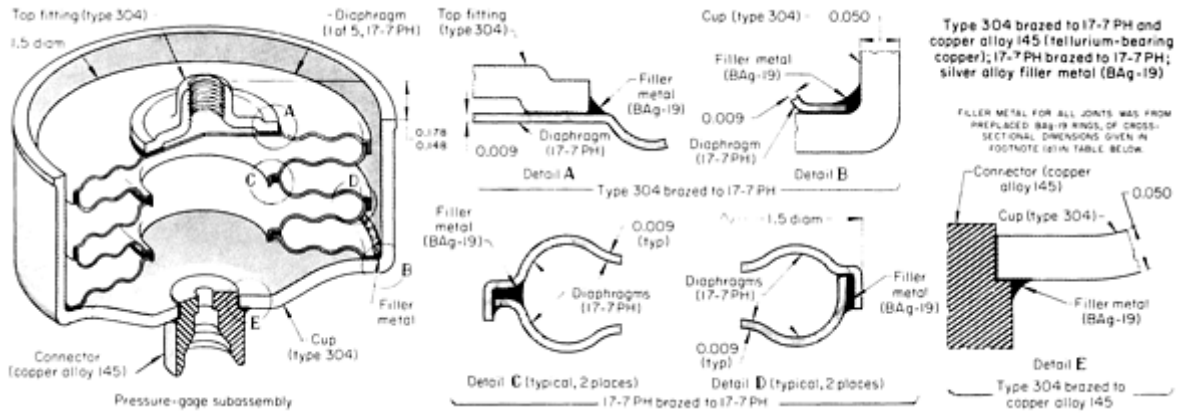

FURNACE BRAZING IN DISSOCIATED AMMONIA	
FURNACE[A]	**CHAIN-BELT CONVEYOR**
FURNACE TEMPERATURE[B], °C (°F)	**980 (1800)**
DISSOCIATED-AMMONIA DEW POINT[C], °C (°F)	**-60 (-80)**
FILLER METAL[D]	**BAG-19**
FLUX[E]	**NONE**
FURNACE BELT SPEED, MM/MIN (IN./MIN)	**255 (10)**
HEATING TIME, MIN	**5**
COOLING-CHAMBER TEMPERATURE[F], °C (°F)	**15 (60)**
PRECIPITATION-HARDENING TEMPERATURE[G], °C (°F)	**510 (950)**

(A) ELECTRICALLY HEATED, WITH ELEVATED HIGH-BEAT ZONE.

(B) FOR BRAZING THE SUBASSEMBLY AND SIMULTANEOUSLY SOLUTION HEAT TREATING THE 17-7 PH DIAPHRAGMS.

(C) ACHIEVED BY RUNNING THE DISSOCIATED AMMONIA THROUGH A MOLECULAR-SIEVE DRYER AFTER CRACKING.

(D) CROSS-SECTIONAL DIMENSIONS (AND PRODUCT FORMS) OF PREPLACED RINGS WERE: FOR JOINT BETWEEN DIAPHRAGM AND TOP FITTING (DETAIL A), 1.3 MM (0.050 IN.) WIDE BY O.10 TO 0.13 MM (0.004 TO 0.005 IN.) THICK STAMPING; FOR OUTSIDE JOINTS BETWEEN DIAPHRAGM SEGMENTS (DETAIL D) AND JOINT BETWEEN DIAPHRAGM AND CUP (DETAIL B), THICK (RIBBON); FOR INSIDE JOINTS BETWEEN DIAPHRAGM SEGMENTS (DETAIL C), 0.76 MM (0.030 IN.) WIDE BY 0.13 MM (0.005 IN.) THICK (RIBBON); AND FOR JOINT BETWEEN CUP AND CONNECTOR (DETAIL E), 1.52 BY 0.254 MM (0.060 BY 0.010 IN.) (WIRE).

(E) USE OF BAG-19 ELIMINATED THE NEED FOR FLUX, WHICH HAD BEEN REQUIRED WITH THE SILVER FILLER METAL ORIGINALLY USED.

(F) TO COOL RAPIDLY FROM 980 °C (1800 °F) AND ENSURE SOLUTION TREATMENT OF THE 17-7 PH DIAPHRAGMS.

(G) IN DRY DISSOCIATED AMMONIA, AFTER SUBASSEMBLY HAD BEEN COOLED TO -40 °C (-

FIG. 9 PRESSURE-GAGE SUBASSEMBLY THAT COMBINED FURNACE BRAZING WITH SOLUTION HEAT TREATMENT

Prior to brazing, the deep-drawn type 304 cups were fully annealed at 1090 °C (2000 °F). Annealing served to avoid the erosive penetration of brazing filler metal in zones of high residual stress. All components were chemically cleaned and then assembled by hand, along with seven preplaced rings of brazing filler metal. The assemblies were placed on holding fixtures, which were loaded on the belt of a conveyor furnace heated to 980 °C (1800 °F). The cooling chamber of the furnace was cooled to below 15 °C (60 °F) to ensure rapid cooling of the 17-7 PH diaphragms from the solution-treating temperature, thereby combining solution treating with the brazing operation.

After brazing, the assemblies were cooled to -40 °C (-40 °F), dried, and then heated to 510 °C (950 °F) in dry, dissociated ammonia to harden the diaphragms to 44 to 48 HRC. Brazed assemblies were pressure tested in a bellows halogen leak detector by applying Freon at 520 kPa (75 psi) and then adding compressed air to bring the total pressure up to 2.1 MPa (300 psi). Leakage of Freon in the gas-air mixture would have been detected by the halogen leak detector. The requirement was for no leakage at the most sensitive setting of the leak detector.

The rejection rate for leakage, based on the 750,000 bellows that were produced, dropped from 2.8%, with the original silver brazing filler metal, to 1.0%, with the BAg-19 brazing filler metal. Field corrosion returns dropped 96%. By eliminating the stains caused by flux, it was no longer necessary to paint the assemblies.

Brazing of Stainless Steels

Revised by Matthew J. Lucas, Jr., General Electric Aircraft Engines

---

Furnace Brazing in Argon

Argon is occasionally used as a furnace atmosphere when brazing stainless steels to other stainless steels or to reactive metals such as titanium (Example 10). Argon has the advantage of being chemically inert in relation to all metals. Therefore, it is a useful protective atmosphere for metals that can combine with or absorb reactive atmospheres such as hydrogen. Because an argon atmosphere has the disadvantage of being unable to reduce oxides, the surface of stainless steel components must be exceptionally clean and oxide-free when brazed in argon.

Example 10: Brazing in an Argon Atmosphere.

A manufacturer of jet engines designed a gear-reduction box of commercially pure titanium. This complicated fabrication was made from assemblies of stampings and machined forgings, most of which were joined by gas-tungsten arc welding (GTAW) in argon-filled welding chambers. However, brazing was more appropriate for the joining of some assemblies.

A typical assembly that was furnace brazed in argon is shown in Fig. 10. This assembly consisted of a machined forging of commercially pure titanium (per Aerospace Material Specification 4921) and a length of seamless type 347 stainless steel tubing that was flared or expanded for a distance of approximately 8 mm ($\frac{5}{16}$ in.) to accept the titanium forging.

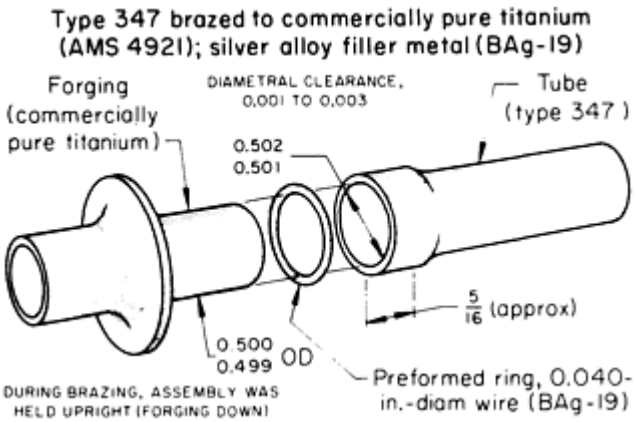

FURNACE BRAZING IN ARGON	
FURNACE[A]	**PIT**
RETORT[B]	**INCONEL**
FIXTURE MATERIAL[C]	**TITANIUM SHEET**
FURNACE TEMPERATURE, °C (°F)	**925 ± 5 (1700 ± 10)**
BRAZING TEMPERATURE, °C (°F)	**900 ± 5 (1650 ± 10)**
ARGON DEW POINTS, °C (°F)	**-65 (-85)[D]; -60 (-70)[E]**
ARGON FLOW RATE (PURGING TO COOLING), M^3/H (FT^3/H)	**4 (150)**
FILLER METAL[F]	**BAG-19**
TIME AT BRAZING TEMPERATURE, MIN	**<1**
COOLING	**IN ARGON, TO ROOM TEMPERATURE**
ASSEMBLY PRODUCTION LOT PER CYCLE	**1-20**

(A) GAS FIRED, 1.8 M (72 IN.) DIAMETER, 1.8 M (72 IN.) DEEP.

(B) 610 MM (24 IN.) DIAMETER AND LENGTH.

(C) HOLDING FIXTURE, TO KEEP ASSEMBLY UPRIGHT (FORGING DOWN) DURING BRAZING.

(D) INCOMING.

(E) EXHAUST.

(F) 1 MM (0.040 IN.) DIAMETER WIRE

FIG. 10 STAINLESS STEEL AND TITANIUM ASSEMBLY THAT WAS FURNACE BRAZED IN AN ARGON ATMOSPHERE

The outside diameter of the titanium forging was held to 12.70 mm (0.500 in.), +0.000 and -0.025 mm (-0.001 in.). The inside diameter of the stainless steel tube was held to 12.73 mm (0.501 in.), +0.025 mm (+0.001 in.) and -0.000 mm or in. This allowed for a diametral clearance of 0.025 to 0.076 (0.001 to 0.003 in.) between components at room temperature. From 0 to 900 °C (32 to 1650 °F), the mean coefficient of thermal expansion (CTE) of commercially pure titanium is $10.3^{-6}/K$. From 0 to 870 °C (32 to 1600 °F), the mean CTE of type 347 stainless steel is $20 \times 10^{-6}/K$. Calculation of the expansion that would occur when both components were heated to 900 °C (1650 °F) indicated a 0.102 mm (0.004 in.) diametral clearance between the titanium and the stainless steel. Adding the diametral clearance at room temperature (0.025 to 0.076 mm, or 0.001 to 0.003 in.) to the 0.102 mm (0.004 in.) clearance gave a total diametral clearance at brazing temperature of 0.127 to 0.178 mm (0.005 to 0.007 in.), which is within a range that will result in a successful joint.

The selected brazing filler metal was the BAg-19 silver, because it has high fluidity in an argon atmosphere and a brazing temperature that is lower than that of pure silver. Most alloy elements in silver brazing filler metals form brittle intermetallic compounds with titanium, which result in unreliable joints. With the exception of a minute amount of lithium, the only alloying element contained in BAg-19 is 7.5% Cu. By limiting the time at brazing temperature, sound ductile joints were made, and the formation of the titanium copper intermetallic phase was minimized.

Prior to assembly, the titanium forging was degreased and cleaned in a solution that contained 40% nitric acid plus 2% hydrofluoric acid. The stainless steel tubing and the brazing filler metal (preformed rings of 0.102 mm, or 0.004 in., diameter BAg-19 wire) were cleaned by washing in acetone. Operators wore clean, lint-free, white cotton gloves for all subsequent handling of the components during assembly, and kept them on until after brazing was completed.

The titanium forging was inserted into the expanded end of the stainless steel tube until it was completely seated. A brazing filler metal ring was placed around the outside diameter of the titanium tube at the joint intersection. The

assembly was placed upright (forging down) in a titanium sheet-metal-holding fixture and was loaded into an Inconel retort. The retort was designed for displacement purging with an inlet and exit manifold for the argon atmosphere. After loading, the retort cover was seal welded to its base, using the GTAW process.

The retort was purged for 30 min with pure, dry argon at 4.2 m^3/h (150 ft^3/h) and then placed in a gas-fired pit-type furnace. The retort was heated to 315 °C (600 °F), and it was held at that temperature for an additional 30 min, or until the dew point of the exiting argon was -60 °C (-70 °F), as recorded on an electrolytic water analyzer. The furnace temperature was then raised until the assembly temperature reached 900 °C (1650 °F), as indicated by a Chromel-Alumel thermocouple attached to the titanium holding fixture within the retort. As soon as this temperature was reached, the retort was removed from the furnace and fan-cooled to room temperature.

The retort cover was opened by grinding away the seal weld, and the assemblies were removed. The titanium and stainless steel components emerged bright and clean, with evidence of excellent brazing filler metal flow. Radiographic inspection showed over 95% joint coverage. All joints were visually inspected on both sides.

Brazing of Stainless Steels

Revised by Matthew J. Lucas, Jr., General Electric Aircraft Engines

---

Furnace Brazing in an Air Atmosphere

The principal advantages of furnace brazing are high production rates and a means for using controlled protective atmospheres at controlled dew points, which often precludes the use of a flux to obtain satisfactory wetting action. In most furnace-brazing applications, both of these advantages are exploited. Occasionally, however, furnace brazing is selected solely on the basis of production rate, and brazing is performed without a protective atmosphere, but with a suitable flux. Under these conditions, the lower-melting-point brazing filler metals are generally selected, as in the following application.

Example 11: Substitution of Furnace Brazing in Air Atmosphere for Torch Brazing.

The gas-valve bobbin assembly shown in Fig. 11 was satisfactorily brazed by both the torch and furnace brazing processes. The choice of process primarily depended on the required production rate. Cost data proved that furnace brazing increased the production rate per hour, reduced the direct labor rate per hour, and reduced the direct labor cost per assembly.

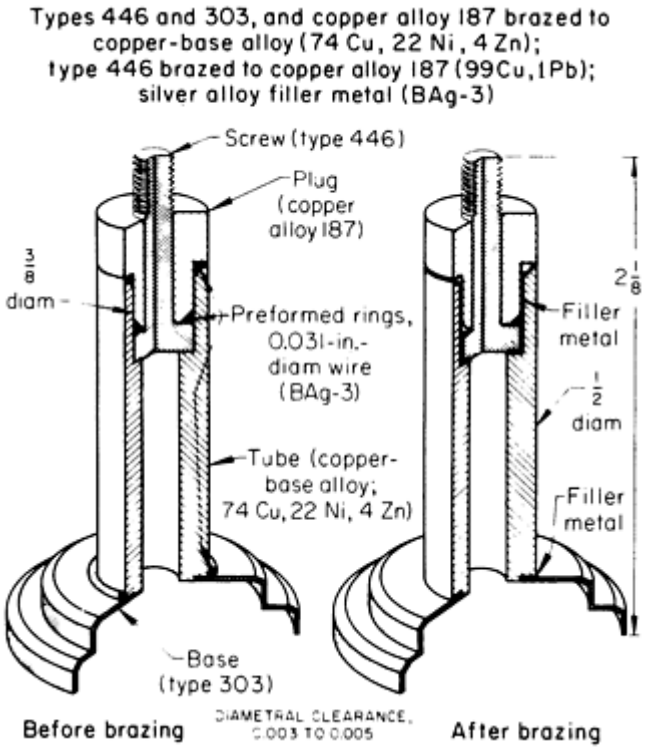

FURNACE BRAZING IN AIR ATMOSPHERE	
FURNACE[A]	**CONTINUOUS BELT**
FURNACE TEMPERATURE, °C (°F)	**745-790 (1370-1450)**
FILLER METAL[B]	**BAG-3**
FLUX	**AMS 3410D (AWS TYPE 3A)**
TIME AT BRAZING TEMPERATURE, MIN	**1 (MAX)**
ASSEMBLY PRODUCTION RATE/H	**140**

(A) AIR ATMOSPHERE.

(B) PREFORMED RINGS, PREPLACED AS SHOWN IN ILLUSTRATION, 0.8 MM (0.031 IN.)

FIG. 11 STAINLESS STEEL AND COPPER GAS-VALVE BOBBIN THAT WAS FURNACE BRAZED IN AN AIR ATMOSPHERE

As Fig. 11 shows, the bobbin assembly consisted of four parts: a screw made of type 446 stainless steel, a base made of type 303 stainless steel, a tube made of a copper alloy closely related to nickel-silver (74Cu-22Ni-4Zn), and a plug made of copper alloy 187 (99Cu-1Pb), which held the screw in place and blocked gas passage through the tube.

All components were thoroughly vapor degreased before brazing. They were assembled with two preformed rings of 0.787 mm (0.031 in.) diameter BAg-3 brazing filler metal wire. The diametral clearance on the joints was 0.076 to 0.127 mm (0.003 to 0.005 in.). One preform, with a 9.5 mm ($\frac{3}{8}$ in.) internal diameter, was placed over the neck of the plug. The other, with a 12.7 mm (0.5 in.) internal diameter, was placed over the tube adjacent to the base joint. The joint areas were coated with type FB3-A brazing flux, and the assemblies were brazed in a continuous-belt conveyor furnace. Brazing filler metal BAg-3 was chosen, in preference to BAg-1 or BAg-1a, in order to avoid the risk of interface corrosion.

Revised by Matthew J. Lucas, Jr., General Electric Aircraft Engines

Furnace Brazing in a Vacuum Atmosphere

The majority of vacuum brazing is performed in two types of equipment utilizing either hot- or cold-walled furnaces. The hot-walled structure utilizes a retort that is evacuated and placed into a furnace, which provides the heat source. The retort can be single-pumped, providing a vacuum to temperatures up to 980 °C (1800 °F), or double-pumped for temperatures above 980 °C (1800 °F) to prevent the retort from collapsing. Limitations of the hot-walled furnace (retort) include longer cycle times, because the retort is heated externally; a 1200 °C (2200 °F) temperature limit; and slower cooling rates. Some advantages of hot-walled furnaces are lower initial capital expenditures, reduced contamination from the retort, and easy upkeep and maintenance.

The cold-walled vacuum furnace is typically designed with a water-cooled outer jacket that is protected by radiation shielding adjacent to the inner wall. The heating elements are exposed directly to the workload. A braze cycle may have temperatures that exceed 2200 °C (4000 °F), depending on the heating element material and the load-support structure. Heating and cooling rates for cold-walled vacuum furnaces are substantially less than they are for the hot-walled vacuum retort. Higher braze temperatures, in excess of 1260 °C (2300 °F), are obtainable in vacuum furnaces and are frequently employed.

Effect of Filler-Metal Composition. Vacuum brazing of many structural configurations made of austenitic stainless steels offers excellent heat and corrosion resistance for high-temperature service applications. Brazing filler metals, such as gold, gold-palladium, and nickel, offer greater high-temperature strength and oxidation resistance. Problems can occur when brazing the 300 series of stainless steels, because of the carbide precipitation and loss of corrosion resistance that results when brazing in the temperature range from 480 to 815 °C (900 to 1500 °F). Brazing at temperatures in excess of 815 °C (1500 °F), using brazing filler metals with melting points that are higher than this temperature, followed by rapid cooling, will reduce carbide precipitation and improve corrosion properties.

Occasionally, wetting does not occur with a particular lot of stainless steel. Generally, alloying elements such as titanium and aluminum contribute to poor wettability.

Martensitic stainless steels, such as the 400 series, can be brazed successfully in vacuum. The use of a suitable brazing filler metal can result in austenitizing and brazing at the same time, followed by rapid cooling to harden the stainless steel.

Care must be exercised when selecting brazing filler metals for use in vacuum. Silver brazing filler metals, such as BAg-1, BAg-1a, and BAg-3, contain alloying elements of zinc and cadmium, which have very high vapor pressures. These elements vaporize if the furnace pressure is too low or the brazing temperature is excessive, or if a combination of these conditions exists. Copper and silver also vaporize under low-pressure conditions at higher brazing temperatures. Therefore, if brazing alloys containing copper or silver are to be used in vacuum, the furnace chamber must be backfilled with an appropriate atmosphere to 300 to 500 μm (12 to 20 mils) until melting occurs to prevent the loss of these elements. Caution must be exercised with the furnace exit gases because these gases are extremely toxic. Two materials that should never be put in a vacuum furnace under any condition are zinc and cadmium. It is recommended that specific alloys (for example, BAg-8 or BAg-13a) or other alloys free of zinc or cadmium be used when brazing in a vacuum furnace. A partial pressure may still be required for many of the alloys to prevent the vaporization of the silver.

Example 12: Vacuum Brazing to Improve Beverage Can Filling Nozzles.

Because of a continuous problem in obtaining uniform and void-free fillets when using silver brazing filler metals and induction brazing methods, a switch was made to vacuum furnace brazing using a nickel brazing filler metal. The beverage filling nozzle shown in Fig. 12 is an assembly consisting of 16 short tubes brazed to a cast body section that connects to the supply piping. The tubes are pressed into the holes that are drilled at angles through the body, and then brazed to form a tight joint. Both the body and tubes are made from type 304 stainless steel.

FIG. 12 STAINLESS STEEL TYPE 304 BEVERAGE CAN FILLING NOZZLE. TUBES ARE VACUUM BRAZED WITH A NICKEL BRAZING FILLER METAL AT 1120 °C (2050 °F). LEFT, LOCATION WHERE PASTE ALLOY IS PLACED AROUND TUBE. RIGHT, COMPLETED NOZZLE, SHOWING SMOOTH, VOID-FREE FILLETS. COURTESY OF WALL COLMONOY CORPORATION

The nozzles require a smooth surface that will not harbor bacteria. This means that the brazed joints must have uniform, smooth fillets and full-length void-free filler metal penetration. In addition, the entire assembly must be resistant to chemical attack by the beverages being handled, by steam, or by cleaning compounds.

The prior method of brazing using silver-base filler metals was not very successful in obtaining void-free joints or consistent results. In addition, many of the beverages being handled did attack the silver brazing filler metal, causing corrosion and discoloration in the joint area.

The nickel brazing filler metal selected for this application was BNi-9 (81.5Ni-15Cr-3.5B), because of its excellent capillary flow characteristics, low base-metal erosion, and self-fluxing properties. In addition, the alloy would be unaffected by subsequent processing operations, which include passivation and electropolishing.

The stainless parts were degreased and a small bead of the nickel brazing filler metal was placed around each tube. The brazing was done in a vacuum furnace at 1135 °C (2075 °F), where the part was heated and cooled at a controlled rate to ensure thermal stability. Careful control of the brazing cycle is the key element in obtaining the uniform fillets and void-free joints required for the nozzles.

Example 13: Cryogenic Valve Nickel Brazed in Vacuum.

Cryogenic valves that are used to handle liquid nitrogen and liquid hydrogen require construction that provides high strength and impact resistance at extremely low temperatures, as well as light weight and good corrosion resistance (Fig. 13). Valves that are part of the propellant loading systems for ballistic missiles were used at temperatures of -250 °C (-425 °F), and at pressures of nearly 41.4 MPa (6 ksi). The body, flanges, seat, and bonnet were brazed with BNi-2 brazing filler metal in a vacuum furnace.

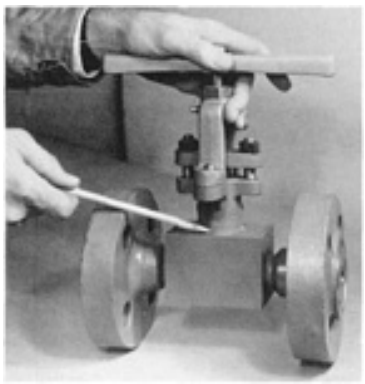

FIG. 13 CRYOGENIC VALVE THAT WAS VACUUM BRAZED WITH BNI-2 BRAZING FILLER METAL. ALL JOINTS ON THE BODY, FLANGES, SEAT, AND BONNETS WERE BRAZED SIMULTANEOUSLY. COURTESY OF WALL

COLMONOY CORPORATION

The valve seat and disc were cast from 17-7 or 17-4 PH steel or from stellite. They were brazed in place at the same time the assembly was brazed. Brazing replaced the welding of the seat, which in this case had trouble in terms of weld deposit cracking. All parts, except the valve seat, were finish-machined before brazing. By eliminating the need for machining after brazing, costs were reduced enough to pay for the brazing operation.

Brazing of Stainless Steels

Revised by Matthew J. Lucas, Jr., General Electric Aircraft Engines

---

Induction Brazing

The behavior of stainless steels, in terms of heating via electrical induction, depends on the metallurgical and physical properties of the particular material. This behavior can be considerably different from that of carbon and low-alloy steels, as well as from that of the more widely used nonferrous metals. In addition, the response of the steel to induction heating varies considerably, depending on whether a stainless steel is magnetic or nonmagnetic at room temperature. Differences in specific heat and electrical conductivity markedly affect the response to heating by induction.

Ferritic and martensitic (SAE 400 series) stainless steels are ferromagnetic at all temperatures, up to the Curie temperature. Thus, given the same power input, these steels generally heat faster than austenitic stainless steels, which are nonmagnetic in the annealed condition. Although cold working may induce slight magnetism in the austenitic chromium steels, the 400 series of chromium-nickel steels are strongly magnetic. The rate of heating to the temperature at which the filler metal flows usually affects induction-coil design and coupling. It may also influence the selection of power output frequency and other processing variables.

Stainless steels can be induction brazed in an air atmosphere, using a suitable flux. However, for critical applications, induction brazing is sometimes done in a protective or a vacuum atmosphere (refer to Example 14). In other applications, an inert gas, such as argon, can be used as a protective atmosphere to either minimize or prevent oxidation.

Example 14: Brazing a Tube to an End Blank.

The assembly shown in Fig. 14, which is part of a solenoid, consisted of a type 321 stainless steel brazed to a type 416 end blank. The former material is a nonmagnetic austenitic steel, whereas the latter is martensitic and ferromagnetic. Consequently, although both metals were easily brazed, the achievement of a proper joint clearance between the two components was complicated by the marked differences in the CTEs of the two steels. Thus, calculations were needed to determine the room-temperature clearance required to provide a suitable clearance at the brazing temperature.

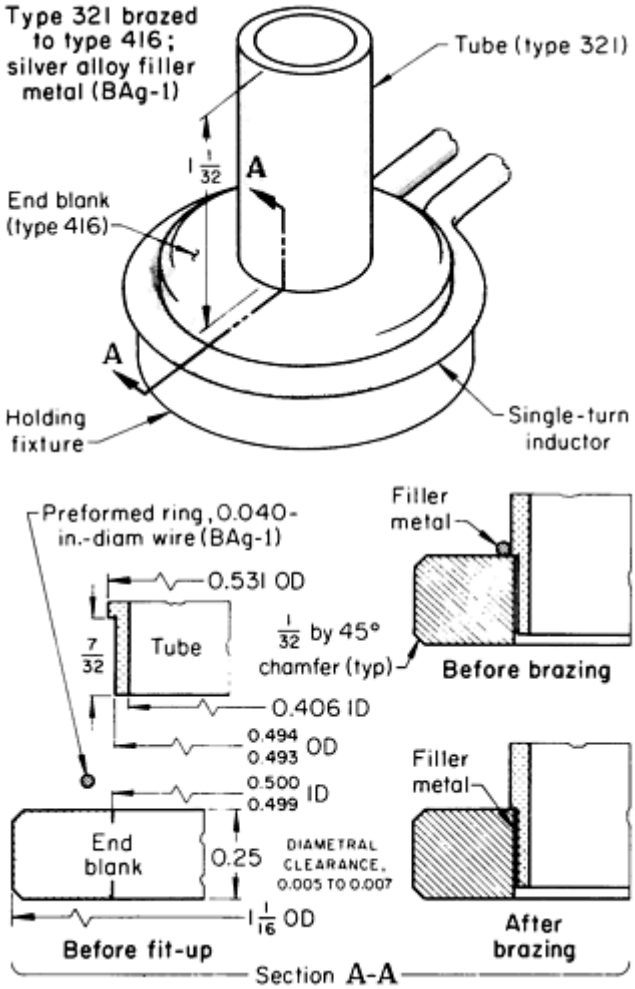

INDUCTION BRAZING	
POWER SUPPLY[(A)], KW; KHZ	**20; 450**
INDUCTOR	**SINGLE-TURN, COPPER TUBE**
BRAZING TEMPERATURE, °C (°F)	**650 (1200)**
FILLER METAL[(B)]	**BAG-1**
FLUX	**AWS TYPE FB3A**
TIME AT BRAZING TEMPERATURE, S	**10**
COOLING TIME IN FIXTURE, S	**10**
ASSEMBLY PRODUCTION RATE/H	**140**

(A) VACUUM TUBE.

FIG. 14 INDUCTION-BRAZED ASSEMBLY

Because the assembly was not intended for high-temperature service, the selection of the low-melting-point silver brazing filler metal (BAg-1) and a relatively low brazing temperature of 650 °C (1200 °F) were utilized to minimize heating and oxidation of the stainless steel components.

For brazing that is conducted at this temperature, calculations based on CTE values showed that the following dimensions and tolerances in the joining area would be satisfactory: for the tube diameter, 12.4 mm (0.494 in.) +0.000, -0.025 mm (-

0.001 in); and for the inside diameter of the end blank, 12.7 mm (0.500 in.) +0.000, -0.025 mm (-0.001 in.). Thus, the diametral clearance at room temperature ranged from 0.127 to 0.178 mm (0.005 to 0.007 in.).

The shape of the assembly and the low melting point and brazing temperatures favored brazing by induction. The end blank was in the hardened and tempered condition prior to brazing, and the short induction heating cycle (10 s) did not reduce the hardness to less than the required minimum.

Prior to brazing, the components were vapor degreased. The end of the tube was dipped in flux and inserted in the end blank. A preformed ring of filler-metal wire was slipped over the tube and positioned at the top of the joint. Then, the end blank was placed on a holding fixture, positioned in a single-turn inductor (Fig. 14), and heated for 10 s. After brazing, the assembly was cooled in air for 10 s before being removed from the holding fixture. The assembly was then washed in hot water to remove the flux residue.

Example 15: Induction Brazing in a Vacuum Atmosphere.

A distinctive advantage of induction brazing, as applied to stainless steel, is its suitability for simple setups that permit brazing in vacuum. Closed, nonmetallic containers with reasonably good strength and dielectric properties can provide an enclosure for the assembly to be brazed and can be evacuated prior to brazing. Because the inductor can be placed outside the container, it can heat the assembly efficiently without being part of the vacuum system.

Stainless steel collar-and-tube assemblies (Fig. 15) were brazed in a simple setup that combined induction heating and the protection afforded by heating in vacuum. The vacuum container consisted of a high-silica, low-expansion glass tube with copper end fittings connected to a vacuum system. The collar-and-tube components, with preformed BNi-7 filler-metal rings pressed into place on the shoulder of each collar, were positioned and held inside the glass tube by means of a simple holding fixture. The tube was sealed and evacuated with a multiple-turn inductor, outside the tube, in position to heat one of the collars. When the vacuum reached 0.133 Pa (10^{-3} torr), heating was started. The collar was heated slowly to 970 °C (1775 °F). After 4 min, the power was shut off. The tube was then repositioned to bring the second collar into the field of the inductor, and the heating sequence was repeated.

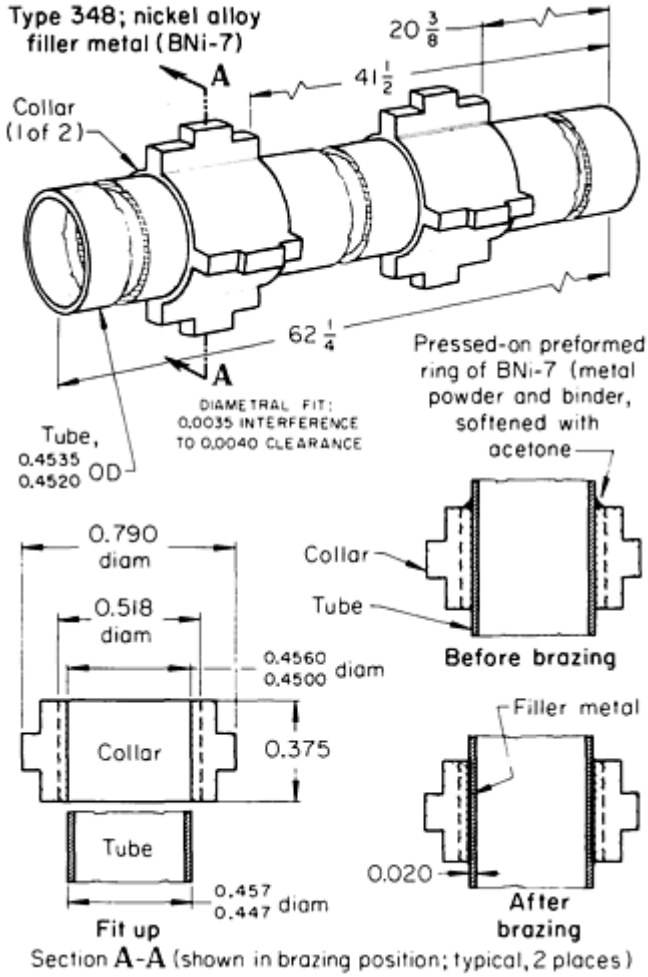

FIG. 15 COLLAR AND TUBE ASSEMBLY THAT WAS INDUCTION BRAZED IN VACUUM

When the second collar had cooled to the point at which no glow was visible in normal light, the tube was backfilled for 5 min with argon. Brazed joints were inspected visually and metallographically. They were found to be sound and acceptable in all respects. The induction heating source was an 8 kVA spark-gap converter with an operating frequency of 175 to 200 kHz. The water-cooled external inductor coil was made of 6.4 mm ($\frac{1}{4}$ in.) diameter copper tubing. The production rate was 22 assemblies per day.

Brazing of Stainless Steels

Revised by Matthew J. Lucas, Jr., General Electric Aircraft Engines

Dip Brazing in a Salt Bath

The brazing of stainless steel by immersing either all or a portion of the assembly in molten salt offers essentially the same advantages and limitations that would apply to the brazing of similar assemblies made of carbon steel.

Example 16: Change From Torch or Induction Brazing to Dip Brazing.

The television wave-guide assembly shown in Fig. 16 consisted of a type 304 stainless steel flange brazed to a tube of copper alloy 230 (red brass, 85Cu-15Zn). Satisfactory end use depended on minimal distortion. When the assembly was

brazed by torch or induction brazing, the rejection rate sometimes reached 70%, because of distortion caused by uneven heating. When dip brazing was adopted, the rejection rate dropped to nearly zero.

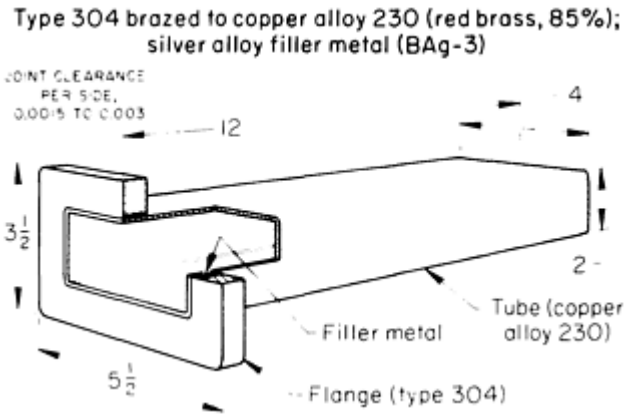

FIG. 16 TELEVISION WAVE-GUIDE ASSEMBLY JOINED BY SALT-BATH DIP BRAZING

Prior to brazing, the stainless steel flange was degreased and pickled, and the brass tube was degreased and bright dipped. Then, the flange was placed on the tube, the tube end was flared outward slightly, a preform of the BAg-3 filler metal was placed over the tube adjacent to the flange, and FB3-A flux (AMS 3410D) flux was applied to the joint. The assembly was suspended flange-down over an electrically heated salt bath to preheat the flange and dry the flux. Next, the assembly was lowered slowly into the molten bath, which was maintained at 730 °C (1350 °F) for a distance of approximately 25 mm (1 in.) above the flange. After being held in the bath for 0.5 min, the assembly was removed and air cooled. The flux residue was removed by rinsing the assembly in 60 °C (140 °F) water. The production rate was 30 assemblies per hour.

Brazing of Stainless Steels

Revised by Matthew J. Lucas, Jr., General Electric Aircraft Engines

High-Energy-Beam Brazing

High-energy-beam brazing techniques, such as those based on electron or laser beams, have been used to a limited extent. Both electron- and laser-beam brazing are performed in a manner similar to electron- and laser-beam welding, except that the beam is defocused to provide a larger beam and to reduce the power density to prevent the base metal from melting. Generally, the speed at which the beam is swept is increased so that a larger area of the part is heated and more uniform heating of the part occurs.

In electron-beam brazing, the high vacuum used in the work chamber (0.0133 to 0.00133 Pa, or 10^{-4} to 10^{-5} torr) permits the adequate flow of brazing filler metal on properly cleaned joints without the use of a reducing atmosphere or flux. Thus, flux entrapment does not occur, and the work does not require cleaning after brazing. The high-vacuum atmosphere and the absence of flux provide a brazing environment that avoids the problems associated with prepared atmospheres, which are encountered when brazing some stainless steels, as well as the more-reactive metals (such as titanium).

In laser-beam brazing, the paris are normally protected with a shielding gas to prevent the occurrence of oxidation. If necessary, the beam spot diameter can be enlarged substantially, depending on the type of equipment, while providing an adequate amount of heat input for brazing. A work movement technique can be used if an area substantially larger than the beam spot size is to be heated, and the work can be rotated or indexed under the beam for uniform heating. In high-energy brazing, the brazing temperatures are quickly attained, and heat can be localized to minimize grain growth, the softening of cold-worked metal, and, in austenitic stainless steels, the sensitizing of the material by carbide precipitation.

Applications. Electron-beam brazing is a convenient method for brazing small assemblies, such as instrument packages. It combines the versatility and close controllability of electron-beam heating with the advantages of vacuum brazing. Packaged devices can be encapsulated with an internal vacuum without damaging the basic package.

Tube-to-header joints in small heat-transfer equipment made of heat-resistant alloys and refractory metals are sometimes brazed using an electron beam. In one technique, the tube-to-header joint is electron-beam welded on the top side of the header. The heat of the beam causes the brazing filler metal that is preplaced on the reverse side of the header at the joint to melt and flow. Small-diameter, thin-walled stainless steel tubes are readily joined by electron-beam brazing, as in the following example.

Example 17: Use of Defocused Beam for the Electron-Beam Brazing of Small Tubes.

Capillary and other small-diameter tubes used in instrument packages required that leak-tight joints be made without overheating the other portions of the assembly. The avoidance of flux was also necessary, because entrapped flux would be either difficult or impossible to remove. These conditions were satisfied by electron-beam brazing.

Figure 17 shows a typical joint in type 304 tubing with a 2.55 mm (0.100 in.) outside diameter and a 0.254 mm (0.010 in.) thick wall that was brazed by the electron-beam process. The joint design was based on the use of a 19 mm ($\frac{3}{4}$ in.) long socket coupling that was counterbored with a diametral clearance of 0.076 to 0.127 mm (0.003 to 0.005 in.) over the tube diameter and to a depth of 6.4 mm ($\frac{1}{4}$ in.). The average joint clearance (per side) was therefore 0.050 mm (0.002 in.). Tubes and socket couplings were deburred and solvent cleaned. They were then assembled with two wire-ring preforms of BCu-1a brazing filler metal, as shown in Fig. 17. The tubes were held in position with a small clamping fixture, and the assembly was mounted in a fixed position on a table in the vacuum chamber.

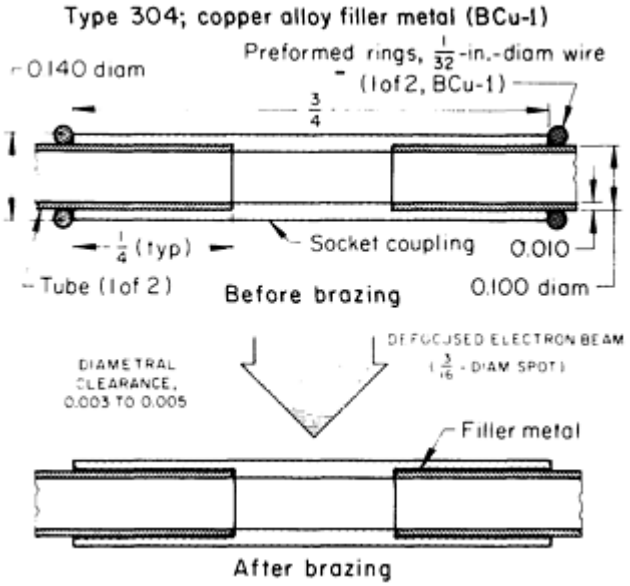

ELECTRON-BEAM BRAZING	
JOINT TYPE	**CYLINDRICAL SLEEVE**
FILLER METAL[(A)]	**BCU-1**
MACHINE CAPACITY, KW	**3**
GUN TYPE	**FIXED DIODE**
VACUUM CHAMBER DIAMETER, MM (IN.)	**610 (24)**
MAXIMUM VACUUM, PA (TORR)	**0.00133 (1×10^{-5})**
FIXTURE	**HOLDING JIG**

PUMPDOWN TIME, MIN	**30**
BRAZING POWER, KV; MA	**18; 20-30**
BEAM SPOT SIZE DIAMETER, MM (IN.)	**4.76 ($\frac{3}{16}$)**
BRAZING VACUUM, PA (TORR)	**0.00133 (1×10^{-5})**
BRAZING TIME, S	**30**

(A) WIRE FORM IN 0.03 MM ($\frac{1}{32}$ IN.) DIAMETER

FIG. 17 JOINT BETWEEN TWO CAPILLARY TUBES OF AN INSTRUMENT PACKAGE, MADE BY ELECTRON-BEAM BRAZING USING A LOW-POWER DEFOCUSED BEAM IN A HIGH-VACUUM ATMOSPHERE

After pumpdown, the joint was brought to the brazing temperature by moving the table back and forth under the defocused electron beam, which caused the heat of the 4.76 mm ($\frac{3}{16}$ in.) diameter beam spot to be applied primarily to the central portion of the coupling. After being heated by conduction at a relatively low beam power, the brazing filler metal melted and flowed through the joint in approximately 30 s.

About ten assemblies were brazed, at a rate of one per pumpdown, using the machine settings and other brazing conditions specified in Fig. 17. Sensitizing the austenitic stainless steel was not a problem in this application, because the service environment was not significantly corrosive. The relatively short-time brazing cycle minimized grain growth and the dilution of the thin-walled tubing with copper brazing filler metal.

Brazing of Heat-Resistant Alloys, Low-Alloy Steels, and Tool Steels

Revised by Darrell Manente, Vac-Aero International Inc.

Introduction

PROCEDURES for brazing heat-resistant alloys, low-alloy steels, and tool steels share much in common. This article focuses primarily on brazing of heat-resistant alloys; some information about particulars involved in the brazing of low-alloy steels and tool steels is also provided.

Brazing of Heat-Resistant Alloys, Low-Alloy Steels, and Tool Steels

Revised by Darrell Manente, Vac-Aero International Inc.

Brazing of Heat-Resistant Alloys

Heat-resistant alloys are frequently referred to as superalloys, because of their strength, oxidation resistance, and corrosion resistance at elevated service temperatures (650 to 1205 °C, or 1200 to 2200 °F). This article discusses primarily nickel- and cobalt-base alloys. Superalloys can also be subdivided (according to manufacturing technology) into two categories: conventional cast and wrought alloys and powder metallurgy (P/M) products. Powder metallurgy products may be produced in conventional alloy compositions and as oxide-dispersion-strengthened (ODS) alloys. Almost any metal, as well as nonmetallics, can be brazed to these heat-resistant alloys, if it can withstand the heat of brazing. For additional information on these alloys, see Volume 1 of the *ASM Handbook.*

Brazing Filler Metals

The American Welding Society (AWS) has classified several gold-, nickel-, and cobalt-base brazing filler metals which can be used for elevated-temperature service (Table 1). These brazing filler metals are suitable for high-temperature service; however, if the application is for temperatures above 980 °C (1800 °F) or in severe environments, the required brazing filler metal may not be in Table 1. It should be noted that for lower service temperatures, copper (BCu) (below 480 °C, or 900 °F) and silver (BAg) (below 425 and 200 °C, or 800 and 400 °F) brazing filler metals have been used for many successful applications.

TABLE 1 AWS BRAZING ALLOYS FOR ELEVATED-TEMPERATURE SERVICE

AWS CLASSIFICATION	COMPOSITION, WT%														SOLIDUS		LIQUIDUS		BRAZING RANGE	
	Cr	B	Si	Fe	C	P	S	Al	Ti	Mn	Cu	Zr	Ni	OTHER ELEMENTS TOTAL	°C	°F	°C	°F	°C	°F
NICKEL-BASE ALLOY FILLER METALS[A]																				
BNI-1	13.0-15.0	2.75-3.50	4.0-5.0	4.0-5.0	0.6-0.9	0.02	0.02	0.05	0.05	. . .	. . .	0.05	BAL	0.50	975	1790	975	1900	1065-1205	**1950-2200**
BNI-1A	13.0-15.0	2.75-3.50	4.0-5.0	4.0-5.0	0.06	0.02	0.02	0.05	0.05	. . .	. . .	0.05	BAL	0.50	975	1790	1075	1970	1075-1205	**1970-2200**
BNI-2	6.0-8.0	2.75-3.50	4.0-5.0	2.5-3.5	0.06	0.02	0.02	0.05	0.05	. . .	. . .	0.05	BAL	0.50	970	1780	1000	1830	1010-1175	**1850-2150**
BNI-3	. . .	2.75-3.50	4.0-5.0	0.5	0.06	0.02	0.02	0.05	0.05	. . .	. . .	0.05	BAL	0.50	980	1800	1040	1900	1010-1175	**1850-2150**
BNI-4	. . .	1.5-2.2	3.0-4.0	1.5	0.06	0.02	0.02	0.05	0.05	. . .	. . .	0.05	BAL	0.50	980	1800	1065	1950	1010-1175	**1850-2150**
BNI-5	18.5-19.5	0.03	9.75-10.50	. . .	0.10	0.02	0.02	0.05	0.05	. . .	. . .	0.05	BAL	0.50	1080	1975	1135	2075	1150-1205	**2100-2200**
BNI-6	. . .	. . .	. . .	. . .	0.10	10.0-12.0	0.02	0.05	0.05	. . .	. . .	0.05	BAL	0.50	875	1610	875	1610	925-1095	**1700-2000**
BNI-7	13.0-15.0	0.01	0.10	0.2	0.08	9.7-10.5	0.02	0.05	0.05	0.04	. . .	0.05	BAL	0.50	890	1630	890	1630	925-1095	**1700-2000**
BNI-8	**. . .**	**. . .**	**6.0-8.0**	**. . .**	**0.10**	**0.02**	**0.02**	**0.05**	**0.05**	**21.5-24.5**	**4.0-5.0**	**0.05**	**BAL**	**0.50**	**980**	**1800**	**1010**	**1850**	**1010-1095**	**1850-2000**

AWS CLASSIFICATION	COMPOSITION, WT%					SOLIDUS		LIQUIDUS		BRAZING RANGE	
	AU	CU	PD	NI	OTHER ELEMENTS TOTAL	°C	°F	°C	°F	°C	°F
PRECIOUS METALS											
BAU-1	37.0-38.0	BAL	. . .	. . .	0.15	990	1815	1015	1860	1015-1095	**1860-2000**
BAU-2	79.5-80.5	BAL	. . .	. . .	0.15	890	1635	890	1635	890-1010	**1635-1850**
BAU-3	34.5-35.5	BAL	. . .	2.5-3.5	0.15	975	1785	1030	1885	1030-1090	**1885-1995**
BAU-4	81.5-82.5	. . .	. . .	BAL	0.15	950	1740	950	1740	950-1005	**1740-1840**
BAU-5	**29.5-30.5**	**. . .**	**33.5-34.5**	**35.5-36.5**	**0.15**	**1135**	**2075**	**1165**	**2130**	**1165-1230**	**2130-2250**

AWS CLASSIFICATION	COMPOSITION, WT%														SOLIDUS		LIQUIDUS		BRAZING RANGE	
	Cr	Ni	Si	W	Fe	B	C	P	S	Al	Ti	Zr	Co	OTHER ELEMENTS TOTAL	°C	°F	°C	°F	°C	°F
COBALT-BASE ALLOY FILLER METALS																				

BCO-1	**18.0-20.0**	**16.0-18.0**	**7.5-8.5**	**3.5-4.5**	**1.0**	**0.7-0.9**	**0.35-0.45**	**0.02**	**0.02**	**0.05**	**0.05**	**0.05**	**BAL**	**0.50**	**1120**	**2050**	**1150**	**2100**	**1150-1230**	**2100-2250**

Source: AWS 5.8

(A) IF DETERMINED, COBALT IS 0.1% MAXIMUM UNLESS OTHERWISE SPECIFIED.

Many nickel-palladium-base brazing filler metals exhibiting good wetting and flow are not classified by AWS but are also available. These filler metals have been developed to replace gold-containing (BAu) brazing filler metals, which are more expensive.

Another group of brazing filler metals not classified by AWS are used for repair and overhaul of nickel- and cobalt-base superalloy aerospace and industrial turbine engine components. Many of these brazing filler metals are proprietary compositions of the engine manufacturer for which they were developed. However, a good variety of these filler metals are commercially available. These "diffusion braze" filler metals do not contain silicon. However, they do contain boron, which acts as a melting point suppressant. Both boron and silicon react with metals (such as chromium and molybdenum) to form intermetallic phases. These intermetallic phases are very hard and brittle and can seriously weaken a brazed joint. It is possible to perform annealing heat treatments on diffusion brazed joints that result in the diffusion of the boron out of the brazed joint and into the base metal. The result is a brazed joint in which intermetallic phases are partially dissolved or eliminated completely (Fig. 1). Diffusion heat treatment increases the strength and ductility of the brazed joint.

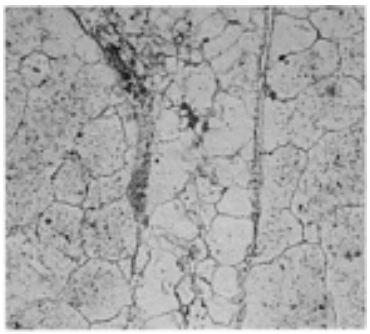

FIG. 1 PHOTOMICROGRAPH OF THE CRACK REPAIR OF A DIFFUSION BRAZED JOINT BY HEAT TREATING OF THE IN-792 BASE METAL. SAMPLE WAS ETCHED WITH KALLING'S REAGENT. 76×

Silicon atoms do not diffuse as easily as boron atoms (because silicon atoms are larger and sit on a regular lattice site, whereas boron atoms sit on interstitial sites, providing much faster diffusion paths). Therefore, similar heat treatments do not tend to dissolve or eliminate silicon intermetallic phases.

These boron-containing filler metals (used on their own or mixed with base metal powder to act as a gap filler) are used to fill cracks and eroded areas on turbine engine components. Some type of cleaning operation (such as hydrogen fluoride cleaning or mechanical cleaning) is employed before the brazing operation in order to remove oxides on the components and thus facilitate brazing filler metal wetting.

A second group of filler metals not classified by AWS are used for wide gaps (1.52 mm, or 0.060 in., and greater) and eroded areas. These filler metals are generally nickel- or cobalt-base superalloys that have additions of a melting point suppressant. These filler metals do not tend to flow away from the area in which they are placed. The microstructure of the joint formed using these filler metals is homogeneous and more closely approximates the base metal microstructure (Fig. 2).

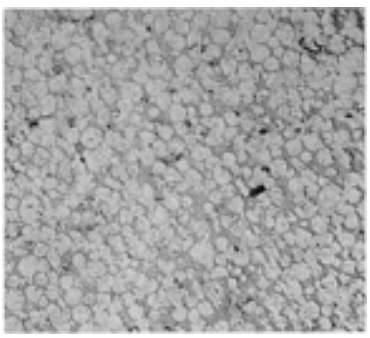

FIG. 2 MICROSTRUCTURE OF A WIDE GAP FILLER METAL BRAZE REPAIR. SAMPLE WAS ETCHED WITH KALLING'S REAGENT. 40×

Generally, heat-resistant alloys are brazed with nickel- or cobalt-base alloys containing boron and/or silicon, which serve as melting-point depressants. In many commercial brazing filler metals, the levels are 2 to 3.5% B and 3 to 10% Si. Phosphorus is another effective melting-point depressant for nickel and is used in filler metals from 0.02 to 10%. It is also used where good flow is important in applications of low stress, where service temperatures do not exceed 760 °C (1400 °F).

In addition to boron, silicon, and phosphorus, chromium is often present to provide oxidation and corrosion resistance. The amount may be as high as 20%, depending on the service conditions. Higher amounts, however, tend to lower brazement strength.

Cobalt-base filler metals are used mainly for brazing cobalt-base components, such as first-stage turbine vanes for jet engines. Most cobalt-base filler metals are proprietary. In addition to containing boron and silicon, these alloys usually contain chromium, nickel, and tungsten to provide corrosion and oxidation resistance and to improve strength.

Product Forms. Available forms of AWS classified and proprietary brazing filler metals include wire, foil, tape, paste, and powder. The form used can be dictated by the application or by the composition of the filler metal. If the filler metal required for a specific application is only available as a dry powder, then brazing aids such as cements and pastes are available to help position the brazing filler metal.

Brazing filler metal powders usually are gas atomized and sold in a range of specified particle sizes, which ensures uniform heating and melting of the brazing filler metal during the brazing cycle. These powders can be mixed with plasticizers or organic cements to facilitate positioning. If the mixture must support its own weight until the brazing cycle begins, an organic binder or cement is required. These binders burn off in atmosphere brazing and little or no residue results. When the brazing filler metal is supplied as a paste, it is simply a premixed powder and binder.

Brazing Tapes and Foils. Brazing filler metals in the form of tapes and amorphous foils appear similar, but the foils are usually made by rapid solidification during melt spinning operations and tend to exhibit homogeneous amorphous structures. Brazing tapes are made of powder that is held together by a binder and formed into a rather fragile sheet. Most amorphous foils have a high metalloid (phosphorus, silicon, boron) content, while tapes can be made from brazing filler metals that have no metalloid content. The metalloids usually are melting-point depressants and frequently form brittle phases. In some cases, where the composition is workable, such as BAu, foils can be made by cold rolling. Foil products can also be produced by rolling an alloy of suitable composition into a foil before adding the metalloids. Tapes and foils are best suited for applications requiring a large area joint, good fit-up, or where brazing flow and wetting may be a problem.

Brazing wires of nonfabricable alloys usually are made by P/M processes from gas atomized powder, which is held together by a binder or by extruding powder into wire and sintering. This form of brazing filler metal is better able to support itself than are pastes and powders of filler metal, but is not used to replace tapes or amorphous foils where precision is needed in preplacing the filler metal, such as joint gaps less than 0.13 mm (0.005 in.).

Surface Cleaning and Preparation

Cleaning of all surfaces that are involved in the formation of the desired brazed joint is necessary to achieve successful and repeatable brazed joints. All obstruction to wetting, flow, and diffusion of the molten brazing filler metal must be removed from both surfaces to be brazed prior to assembly. The presence of contaminants on one or both surfaces to be brazed may result in void formation, restricted or misdirected filler-metal flow, and contaminants included within the solidified brazed area, which reduces the mechanical properties of the resulting brazed joint. Common contaminants are oils, greases, residual liquid penetrant fluids, pigmented markings, residual casting or coring materials, and oxides formed either through previous thermal exposures or by exposures to contaminating environments or engine service.

Chemical cleaning methods are most widely used. As part of any chemical cleaning procedure for preprocessing assemblies for brazing, a degreasing solvent should be used to remove all oils and greases and to ensure wettability of the chemicals used for cleaning. Oils and greases form a very thin film on metals, which prevents wettability by both the

subsequent chemical cleaning and/or the molten filler metals. Oils and grease removers that are widely used include degreasing solutions such as stabilized perchloroethylene or stabilized trichloroethylenes. These may be used as simple manual soaks, sprays, or by suspending the parts in a hot vapor of the aforementioned chemicals, commonly referred to as a vapor degreasing process. In conjunction with these processes, anodic and cathodic electrolytic cleaning can be used.

Other cleaning methods include alkaline-based cleaners and emulsion-type cleaners. Alkaline-based cleaners use mixtures of phosphates, carbonates, silicates, soaps, detergents, and hydroxides. Emulsion-type cleaners contain wetting agents, surface actuators, fatty acids, and hydrocarbons.

A chemical cleaning procedure can be a simple single-step process or may involve multistep operations. If the surfaces of the brazed joint are in the machined condition, vapor degreasing may be sufficient to remove machining oils, handling oils, and liquid penetrant fluids to yield a sound, clean surface for brazing. If, on the other hand, one or both of the surfaces to be brazed is not a machined surface, then additional chemical cleanings should be employed. Once vapor degreasing is accomplished, care must be taken to maintain the surface cleanliness of the brazed components by handling in an environmentally clean atmosphere. Additional methods of chemical cleaning to remove oxides and other adherent metallic contaminants include immersion in phosphate acid cleaners or acid pickling solutions, which are comprised of nitric, hydrochloric, or sulfuric acids or combinations of these.

Care must be taken in time of exposure for both acid cleaning and acid pickling of heat-resistant base metals. Overexposure during chemical cleaning can lead to excessive metal loss, grain-boundary attack, and selective attack on microstructural phases. As the last step in chemical cleaning, an ultrasonic cleaning in alcohol or clean hot water is recommended to ensure removal of all traces of previous cleaning solutions.

If no subsequent mechanical cleaning is used, the components to be brazed should be stored and transported to the braze preparation areas in dry, clean containers, such as plastic bags. The time between cleaning and braze application to the assembled joints should be kept as short as manufacturing processes allow.

Mechanical cleaning usually is confined to those metals with heavy tenacious oxide films or to repair brazing on components exposed to service. (Nickel- or cobalt-base superalloy components that require repair brazing can be processed in hydrogen fluoride atmospheres in order to remove oxide films.) Mechanical methods are standard machining processes--abrasive grinding, grit blasting, filing, or wire brushing (stainless steel bristles must be used). These are used not only to remove surface contaminants, but to slightly roughen or fray the surfaces to be brazed.

Care must be taken that the surfaces are not burnished and that mechanical cleaning materials are not embedded in the metals to be brazed. In grit blasting, choice of the blasting medium is critical. Wet and dry grit blasting commonly are used, but wet mediums are subject to additional cleaning requirements to remove the embedded grit. The mediums used are iron grits, silicon carbide grits, and grits composed of brazing filler metals. Grit sizes as coarse as No. 30 (0.589 mm, or 0.0232 in.) are recommended for cleaning forgings and castings. Finer grits (No. 90 and No. 100, 0.165 and 0.150 mm [0.0065 and 0.0059 in.], respectively) are used for general blasting. All grit mediums should be changed frequently, as extensive reuse of the same medium results in loss of sharp angles or facets. Once these configurations are lost or markedly reduced in the grit medium, burnishing rather than cleaning occurs. Overused medium results in the entrapment of oxides in the metal. If possible, the angle of grit blasting should be less than 90° to the surfaces to be cleaned. This also reduces the chances of embedding the oxides or medium in the surfaces to be brazed.

Care must be taken to remove all blasting medium from the surface after mechanical cleaning, as these mediums will contaminate the braze. Iron grit may impart an iron film which oxidizes as a rust. Aluminum oxides, if not removed, prevent wetting and flow of the brazing filler metal; thus, use of aluminum oxides are not recommended. Silicon carbide is extremely hard and has sharp facets. Consequently, it becomes embedded if an improper blasting angle is used. Blasting with a nickel-base brazing filler metal or similar alloy gives the best results; stainless steel blasting medium is also acceptable.

After mechanical cleaning, air blasting or ultrasonic cleaning should be used to remove all traces of loosened oxides or cleaning medium. Care must be taken to ensure maintenance of the clean surfaces and components; once cleaned, they should be assembled and brazed as soon as possible.

Hydrogen Fluoride Cleaning. The successful repair of superalloy components requires that oxides formed during service, on external surfaces and within cracks, be removed prior to brazing to ensure proper wetting and flow of the braze material. For cobalt-base superalloy parts, heating in a hydrogen-rich atmosphere (hydrogen reduction) is generally

successful in this regard. However, hydrogen reduction is not effective in reducing oxides of aluminum and titanium that are formed on nickel-base superalloy parts in service because these oxides exhibit a high degree of thermodynamic stability. Hydrogen fluoride reduction, on the other hand, has been shown capable of reducing these oxides from the surfaces of nickel-base parts.

Oxides of aluminum and titanium are changed to their respective metallic fluorides by the fluoride ions created in the hydrogen fluoride process. Oxides of chromium are also changed to chromium fluoride by the fluoride ions. In addition, workpiece surfaces are depleted of aluminum and titanium so that oxides of these metals do not tend to reform during subsequent operations, such as braze repair (Fig. 3).

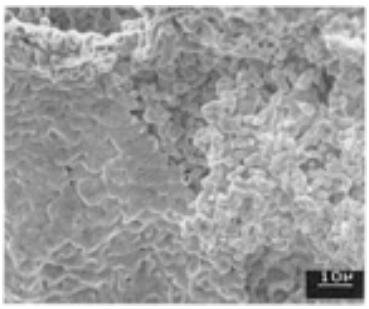

FIG. 3 SEM PHOTOMICROGRAPH OF A RENÉ 125 AEROSPACE ENGINE COMPONENT THAT WAS CLEANED WITH HYDROGEN FLUORIDE TO DEPLETE THE ELEMENTS AT THE SURFACE

Nickel Flashing. Certain heat-resistant alloys that are used as base metals in brazed assemblies--particularly nickel-base alloys containing high percentages of aluminum and titanium (such as Inconel 718)--may require a surface pretreatment to ensure maintenance of the cleaned surfaces. This surface pretreatment after cleaning is generally an electroplate of nickel, commonly referred to as nickel flashing. Thickness of the plate flashing is kept under 0.015 mm (0.0006 in.) for alloys with less than 4% (Ti + Al) and 0.020 to 0.030 mm (0.0008 to 0.0012 in.) for alloys with greater than 4% (Ti + Al). This promotes wettability in the braze joint without seriously affecting the braze strength and other mechanical properties of the braze. The thickness of nickel plating may have to be increased as the brazing temperature is increased and as the time above 980 °C (1800 °F) is increased. Titanium and aluminum will diffuse to the surface of the nickel plating upon heating.

Fixturing

One prerequisite to successful brazing that is often neglected is proper fixturing. Two types of fixtures are used: "cold" fixtures and "hot" fixtures.

Cold fixtures are used primarily for assembly purposes. In most cases, cold fixtures are made of hot or cold rolled iron, stainless alloys, nonferrous alloys, or nonmetals, such as phenolics and laminates. These fixtures are used for assembly and subsequent tack welding of parts to be brazed. They need not be massive or heavy, but should be sturdy enough to assemble components as required by design.

Hot fixtures (fixtures used in the furnace for brazing) must have good stability at elevated temperatures and the ability to cool rapidly. Metals can be used but generally are not stable enough to maintain tolerances during the brazing cycle. Therefore, ceramic, carbon, or graphite assemblies often are used for hot fixturing. Ceramics, due to their high processing cost, are used for small fixtures and for spacer blocks to maintain gaps during brazing of small components. Graphite has

been found to be the most suitable material for maintaining flatness in a high vacuum or argon atmosphere, and it provides faster cooling because of its high thermal conductivity, which is partially due to its porosity. Graphite should be coated with an Al_2O_3 slurry to prevent carburization of parts during the brazing cycle. It should not be used in a pure dry hydrogen atmosphere as it will cause carburization of the base metals by gaseous transfer. Molybdenum and tungsten may be used, but they are generally avoided because of their cost.

Controlled Atmospheres

Controlled atmospheres (including vacuum) are used to prevent the formation of oxides during brazing and to reduce the oxides present so that the brazing filler metal can wet and flow on clean base metal. Controlled-atmosphere brazing is widely used for the production of high-quality joints. Large tonnages of assemblies of a wide variety of base metals are mass produced by this process.

Controlled atmospheres are not intended to perform the primary cleaning operation for the removal of oxides, coatings, grease, oil, dirt, or other foreign materials from the parts to be brazed. All parts for brazing must be subjected to appropriate prebraze cleaning operations as dictated by the particular metals. Controlled atmospheres commonly are employed in furnace brazing; however, they may also be used with brazing processes that utilize induction, resistance, infrared, laser, and electron-beam heat sources. In applications where a controlled atmosphere is used, postbraze cleaning is generally not necessary. In special cases, flux may be used with a controlled atmosphere (1) to prevent the formation of oxides of titanium and aluminum when brazing in a gaseous atmosphere, (2) to extend the useful life of the flux, and (3) to minimize postbraze cleaning. Fluxes should not be used in a vacuum environment. Some types of equipment, such as metallic muffle furnaces and vacuum systems, may be damaged or contaminated by the use of flux.

The use of controlled atmospheres inhibits the formation of oxides and scale over the whole part and permits finish machining to be done before brazing in many applications. In some applications, such as the manufacture of electronic tubes, eliminating flux is tremendously important.

Pure dry hydrogen is used as a protective atmosphere because it dissociates the oxides of many elements. Hydrogen with a dew point of -51 °C (-60 °F) dissociates the oxides of most elements found in heat-resistant alloys, with the notable exception of aluminum and titanium, which are found in most of the high-strength heat-resistant base metals.

Inert gases, such as helium and argon, do not form compounds with metals. In equipment designed for brazing at ambient pressure, inert gases reduce the evaporation rate of volatile elements, in contrast to brazing in a vacuum. Inert gases permit the use of weaker retorts than required for vacuum brazing. Elements such as zinc and cadmium, however, vaporize in pure dry inert atmospheres.

Vacuum. An increasing amount of brazing of heat-resistant alloys, particularly precipitation-hardenable alloys that contain titanium and aluminum, is done in a vacuum. Vacuum brazing in the range of 13 mPa (10^{-4} torr) has proved adequate for brazing most of the nickel-base superalloys. By removal of gases to a suitably low pressure, including gases that are evolved during heating to brazing temperature, very clean surfaces are obtainable. A vacuum is particularly useful in the manufacture of parts for the aerospace, electronic tube, and nuclear fields, and where metals that react chemically with a hydrogen atmosphere are used or where entrapped fluxes or gases are intolerable. The maximum tolerable pressure for successful brazing depends on a number of factors that are primarily determined by the composition of the base metals, the brazing filler metal, and the gas that remains in the evacuated chamber.

Vacuum brazing is economical for fluxless brazing of many similar and dissimilar basemetal combinations. Vacuums are especially suited for brazing very large, continuous areas where (1) solid or liquid fluxes cannot be removed adequately from the interfaces after brazing, and (2) gaseous atmospheres are not completely efficient because of their inability to purge occluded gases evolved from close-fitting brazing interfaces. It is interesting to note that a vacuum system evacuated to 1.3 mPa (10^{-5} torr) contains only 0.00000132% residual gases based on a starting pressure of 100 kPa (760 torr).

Vacuum brazing has the following advantages and disadvantages compared with brazing that is carried out under other high-purity brazing atmospheres:

- VACUUM REMOVES ESSENTIALLY ALL GASES FROM THE BRAZING AREA, THEREBY ELIMINATING THE NECESSITY FOR PURIFYING THE SUPPLIED ATMOSPHERE. COMMERCIAL VACUUM BRAZING GENERALLY IS DONE AT PRESSURE VARYING FROM

0.0013 TO 13 PA (10^{-5} TO 10^{-1} TORR), DEPENDING ON THE MATERIALS BRAZED, THE FILLER METALS BEING USED, THE AREA OF THE BRAZING INTERFACES, AND THE DEGREE TO WHICH GASES ARE EXPELLED BY THE BASE METALS DURING THE BRAZING CYCLE.

- CERTAIN OXIDES THAT FORM ON BASE METALS (PARTICULARY ON COPPER-BASE METALS) DISSOCIATE IN VACUUM AT BRAZING TEMPERATURES.
- DIFFICULTIES SOMETIMES EXPERIENCED WITH CONTAMINATION OF BRAZING INTERFACES, DUE TO EXPULSION OF GASES FROM THE PARTS TO BE BRAZED, ARE NEGLIGIBLE IN VACUUM BRAZING.
- LOW PRESSURE EXISTING AROUND THE BASE AND FILLER METALS AT ELEVATED TEMPERATURES REMOVES VOLATILE IMPURITIES AND GASES FROM THE METALS. FREQUENTLY, THE PROPERTIES OF BASE METALS ARE IMPROVED. THIS CHARACTERISTIC IS ALSO A DISADVANTAGE WHEN ELEMENTS IN THE FILLER METAL OR BASE METALS VOLATILIZE AT BRAZING TEMPERATURES, THUS CHANGING THE MELTING POINT OF THE FILLER METAL OR PROPERTIES OF THE BASE METAL. THIS TENDENCY MAY, HOWEVER, BE CORRECTED BY EMPLOYING PARTIAL-PRESSURE VACUUM BRAZING TECHNIQUES.

Nickel-Base Alloys

In the selection of a brazing process for a nickel-base alloy, the characteristics of the alloy must be carefully considered. The nickel-base alloy family includes alloys that differ significantly in physical metallurgy (such as the mechanism of strengthening) and in process history (cast versus wrought). These characteristics can have a profound effect on their brazeability.

Precipitation-hardening alloys present several difficulties not normally encountered with solid-solution alloys. Precipitation-hardening alloys often contain appreciable (greater than 1%) quantities of aluminum and titanium for improved strength and corrosion resistance. The oxides of these elements are almost impossible to reduce in a controlled (vacuum or hydrogen) atmosphere. Therefore, nickel plating or the use of a flux is necessary to obtain a surface that allows wetting by the filler metal.

Because these alloys are hardened at temperatures of 540 to 815 °C (1000 to 1500 °F), brazing at or above these temperatures may alter the alloy properties. This frequently occurs when using silver-copper filler metals, which occasionally are used on heat-resistant alloys.

Liquid metal embrittlement is another difficulty encountered in brazing of precipitation-hardening alloys. Many nickel-, iron-, and cobalt-base alloys crack when stressed parts are exposed to molten metals. This is usually confined to the silver-copper filler metals. If precipitation-hardening alloys are brazed in the hardened condition, residual stresses am often high enough to initiate cracking.

Cleanliness, as in all metallurgical joining operations, is important when brazing nickel and nickel-base alloys. Cleanliness of base metal, filler metal, flux (when used for torch or induction brazing), and purity of atmosphere should be as high as practical to achieve the required joint integrity. Elements that cause surface contamination or interfere with braze wetting or flow should be avoided in prebraze processing. All forms of surface contamination such as oils, chemical residues, scale, or other oxide products should be removed by using suitable cleaning procedures. The use of nickel-base filler metals can offer some cost effectiveness in this regard because certain nickel-base brazing filler metals containing boron and/or silicon are known to be self-fluxing and thus more forgiving to slight imperfections in cleanliness.

Attempting to braze over the refractory oxides of titanium and aluminum that may be present on precipitation-hardenable nickel-base alloys must be avoided. Procedures to prevent or inhibit the formation of these oxides before and/or during brazing include special treatments of the surfaces to be joined or brazing in a highly controlled atmosphere. Surface treatments include electrolytic nickel plating and reducing the oxides to metallic form. As stated earlier in this section, a typical practice is to nickel plate the joint surface of any alloy that contains aluminum and/or titanium. For vacuum brazing of alloys containing aluminum and titanium in trace amounts, use of 0.0025 to 0.0075 mm (0.0001 to 0.0003 in.) thick plate is considered optimal. Alloys with up to 4% AI and/or titanium require 0.010 to 0.015 mm (0.0004 to 0.0006 in.) thick plate, and alloys with aluminum and/or titanium contents greater than 4% require 0.020 to 0.030 mm (0.0008 to

0.0012 in.) thick plate. When brazing in a pure dry hydrogen atmosphere, thicker plating (0.025 to 0.038 mm, or 0.001 to 0.0015 in.) is desirable for alloys with high (>4%) aluminum and/or titanium contents.

Atmospheres. Dry, oxygen-free atmospheres that are frequently used include inert gases, reducing gases, and vacuum. The brazing atmosphere, whether gaseous or vacuum, should be free from harmful constituents such as sulfur, oxygen, and water vapor. When brazing in a gaseous atmosphere, monitoring of the water vapor content of the atmosphere (that is, the dew point) is the common practice. A dew point of -50 °C (-60 °F) results in average brazeability; average; -60 °C (-80 °F) or below produces a better quality braze.

Stresses. During brazing, residual or applied tensile stress should be eliminated or minimized as much as possible. Also, inherent stresses present in the precipitation-hardening alloys may lead to stress-corrosion cracking. Therefore, stress relieving or annealing prior to brazing is also recommended for all furnace, induction, or torch brazing operations. Brazing filler metals that melt below the annealing temperature are likely to cause stress-corrosion cracking of the base metal.

Thermal Cycles. Consideration must be given to the effect of the brazing thermal cycle on the base metal. Filler metals that are suitable for brazing nickel-base alloys may require relatively high temperatures. This is particularly true for the filler-metal alloy systems most frequently used in brazing of nickel-base alloys--the nickel-chromium-silicon or nickel-chromium-boron systems.

Solid-solution-strengthened nickel-base alloys such as Inconel 600 may not be adversely affected by brazing temperatures of 1010 to 1230 °C (1850 to 2250 °F). Precipitation-strengthened alloys such as Inconel 718 may, however, display adverse property effects when exposed to brazing cycles with maximum temperatures that are higher than their normal solution heat treatment temperatures. Inconel 718, for example, is solution heat treated at 955 °C (1750 °F) for optimum stress-rupture life and ductility. Braze temperatures of 1010 °C (1850 °F) or above result in grain growth and a corresponding decrease in stress-rupture properties, which cannot be recovered by subsequent heat treatment.

Consideration of base-metal property requirements for service enables selection of an appropriate braze alloy. Lower melting temperature (below 1040 °C, or 1900 °F) braze filler metals are available within the nickel-base alloy family and within other brazing filler-metal systems (see Table 1).

Inconel 718 is often used in the fabrication of air diffusers for aerospace turbine engines. One manufacturer found that vacuum brazing of diffuser components at 10^{-4} torr in a cold-walled vacuum furnace provided the best results. Prior to brazing, all joint surfaces were nickel plated to 0.005 to 0.015 mm (0.0002 to 0.0006 in.) thicknesses. Plating was done in accordance with specification AMS 2424 or equivalent. Prior to assembly, application of BNi-2 braze filler metal tape (approximately 0.11 mm, or 0.0045 in., thick) was preplaced between all joint surfaces. After assembly, an additional braze slurry of BNi-2 filler metal was applied to all joints to ensure joint soundness.

Brazing of ODS Alloys

Oxide dispersion-strengthened alloys are P/-M alloys that contain stable oxides evenly distributed throughout the matrix. The oxide does not go into solution in the alloy even at the liquidus temperature of the matrix. However, the oxide is usually rejected from the matrix upon melting of the matrix, which occurs during fusion welding, and cannot be redistributed in the matrix on solidification; therefore, these alloys are usually joined by brazing. There are two commercial classes of ODS alloys: the dispersion-strengthened nickel, and mechanically alloyed Inconel MA 754, Inconel MA 6000, and Incoloy MA 956.

Inconel MA 754, dispersion-strengthened nickel alloys, and dispersion-strengthened nickel-chromium alloys are the easiest to braze of the family of ODS alloys. Vacuum, hydrogen, or inert atmospheres can be used for brazing. Prebraze cleaning consists of grinding or machining the faying surfaces and washing with a solvent that evaporates without leaving a residue. Generally, brazing temperatures should not exceed 1315 °C (2400 °F) unless demanded by a specific application that has been well examined and tested. The brazing filler metals for use with these ODS alloys usually are not classified by AWS. In most cases, the brazing filler metals used with these alloys have brazing temperatures in excess of 1230 °C (2250 °F). These include proprietary alloys that are based on nickel, cobalt, gold, or palladium.

Brazements made of ODS alloys to be used at elevated temperature must be tested at elevated temperature to prove fitness-for-purpose. In the case of stress-rupture testing, AWS specification C3.2 may be used as a guide because it gives

the actual joint configuration. The configuration shown in Fig. 4 is preferred by some as a test model, although any test configuration without stress raisers is adequate. The elevated-temperature brazement properties for Inconel alloy MA 754 should meet the following requirements:

SHEAR STRESS		**TEMPERATURE**		SERVICE LIFE, H
MPA	**KSI**	**°C**	**°F**	
26	3.8	980	1800	>**1000**
9.0	**1.3**	**1095**	**2000**	>**1000**

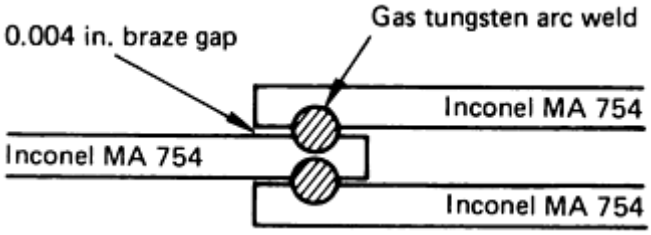

FIG. 4 BRAZING SPECIMEN ASSEMBLY USED TO EVALUATE STRESS-RUPTURE PROPERTIES OF BRAZED INCONEL MA 754

Inconel MA 6000 is a nickel-base ODS alloy that is also γ' strengthened. The amount of alloying elements in the base metal matrix plus the γ' precipitations cause an interesting problem in the brazing of this alloy. Inconel MA 6000 has a solidus temperature of 1300 °C (2372 °F); therefore, the brazing temperature should be no higher than 1250 °C (2282 °F). Additionally, because 1230 °C (2250 °F) is the γ' solution treatment temperature, it becomes important to carefully select the brazing filler metal and to heat treat the assembly after brazing. The AWS-specified BNi and BCo filler metals, as well as specially formulated filler metals, have been used for this alloy.

Inconel MA 6000 is used for its high-temperature strength and corrosion resistance; unfortunately, the passive oxide scale that provides good corrosion resistance also prevents wetting and flow of brazing filler metal. Therefore, correct cleaning procedures are very important. Surfaces to be brazed should be mechanically cleaned with a water-cooled, low-speed belt or wheel of approximately 320-grit and stored in a solvent, such as methanol, until immediately before the beginning of the brazing cycle.

Cobalt-Base Alloys

The brazing of cobalt-base alloys is readily accomplished with the same techniques used for nickel-base alloys. Because most of the popular cobalt-base alloys do not contain substantial amounts of aluminum or titanium, brazing atmosphere requirements are less stringent. Table 2 gives typical compositions of several cobalt-base alloys. These materials can be brazed in either a hydrogen atmosphere or a vacuum. Filler metals are usually nickel- or cobalt-base alloys or gold-palladium compositions. Silver- or copper-base brazing filler metals may not have sufficient strength and oxidation resistance in many high-temperature applications. Although cobalt-base alloys do not contain appreciable amounts of aluminum or titanium, an electroplate or flash of nickel is often used to promote better wetting of the brazing filler metal.

TABLE 2 TYPICAL COMPOSITIONS OF SELECTED COBALT-BASE ALLOYS

ALLOY[A]	NOMINAL COMPOSITION, WT%															CHARACTERISTICS AND TYPICAL APPLICATIONS
	C	Mn	Si	Cr	Ni	Co	Mo	W	Nb	Ti	Al	B	Zr	Fe	OTHER	
AIRESIST 13[B]	0.45	0.5[C]	. . .	21	1.0[C]	BAL	. . .	11	2.0	. . .	3.5	. . .	. . .	2.5[C]	0.1 Y	**HIGH-TEMPERATURE PARTS**
AIRESIST 213	0.18	. . .	. . .	19	. . .	BAL	. . .	4.7	. . .	. . .	3.5	. . .	0.15	. . .	6.5 TA, 0.1 Y	**SHEETS, TUBING; RESISTANT TO HOT CORROSION**
AIRESIST 215[B]	0.35	. . .	. . .	19	. . .	BAL	. . .	4.5	. . .	. . .	4.3	. . .	0.13	. . .	7.5 TA, 0.17 Y	**NOZZLE VANES; RESISTANT TO HOT CORROSION**
ELGILOY	0.15	2.0	. . .	20.0	15.0	40.0	7.0	. . .	. . .	. . .	. . .	. . .	. . .	BAL	0.04 BE	**SPRINGS; CORROSION RESISTANT, HIGH STRENGTH**
FSX-414[B]	0.25	1.0[C]	1.0[C]	29.5	10.5	BAL	. . .	7.0	. . .	. . .	. . .	0.012	. . .	2.0[C]	. . .	**GAS TURBINE VANES**
FSX-418[B]	0.25	1.0[C]	1.0[C]	29.5	10.5	BAL	. . .	7.0	. . .	. . .	. . .	0.012	. . .	2.0[C]	0.15 Y	**GAS TURBINE VANES; IMPROVED OXIDATION RESISTANCE**
FSX-430[B]	0.40	. . .	. . .	29.5	10.0	BAL	. . .	7.5	. . .	. . .	. . .	0.027	0.9	. . .	0.5 Y	**GAS TURBINE VANES; IMPROVED STRENGTH AND DUCTILITY**
X-40[B]	0.50	0.50	0.50	25	10	BAL	. . .	7.5	. . .	. . .	. . .	. . .	. . .	1.5	. . .	**GAS TURBINE PARTS, NOZZLE VANES**
HAYNES 150	0.08	0.65	0.35	28	3.0[B]	BAL	1.5[B]	. . .	. . .	. . .	. . .	. . .	. . .	20.0	. . .	**RESISTS THERMAL SHOCK, HIGH-TEMPERATURE CORROSION (AIR AND AIR-SO_2)**
HAYNES 188 (SHEET)	0.10	1.25[B]	0.3	22	22	BAL	. . .	14	. . .	. . .	. . .	. . .	. . .	3.0[B]	0.04 LA	**BETTER OXIDATION RESISTANCE THAN HASTELLOY X**

MAR-M302[B]	0.85	0.10	0.20	21.5	. . .	BAL	. . .	10.0	. . .	. . .	. . .	0.005	0.15	. . .	9.0 TA	**JET ENGINE BLADES, VANES**
MAR-M322[B]	1.00	0.10	0.10	21.5	. . .	BAL	. . .	9.0	. . .	0.75	. . .	. . .	2.25	. . .	4.5 TA	**JET ENGINE BLADES, VANES**
MAR-M509[B]	0.60	0.10[C]	0.10[C]	21.5	10	BAL	. . .	7.0	. . .	0.2	. . .	0.010[C]	0.50	1.0	3.5 TA	**JET ENGINE BLADES, VANES**
MAR-M918	0.05	0.2[C]	0.2[C]	20	20	BAL	. . .	. . .	. . .	. . .	. . .	. . .	0.16	0.5[C]	7.5 TA	**HIGH-TEMPERATURE SHEET**
MP35N	. . .	. . .	. . .	20.0	35.0	35.0	10.0	. . .	. . .	. . .	. . .	. . .	. . .	. . .	. . .	**STRESS-CORROSION RESISTANT, HIGH-STRENGTH FASTENERS**
NASA CO-W-RE[B]	0.40	. . .	. . .	3	. . .	BAL	. . .	25	. . .	1.0	. . .	. . .	1.0	. . .	2.0 RE	**HIGH-TEMPERATURE SPACE APPLICATIONS**
S-816	0.38	1.20	0.40	20	20	BAL	4.0	4.0	4.0	. . .	. . .	. . .	. . .	4	. . .	**GAS TURBINE BLADES, BOLTS, SPRINGS**
V-36	0.27	1.00	0.40	25	20	BAL	4.0	2.0	2.0	. . .	. . .	. . .	. . .	3	. . .	**HIGH-TEMPERATURE SHEET**
WF-11, L605, HAYNES 25	0.10	1.50	0.50	20	10	BAL	. . .	15	. . .	. . .	. . .	. . .	. . .	3.0[B]	. . .	**JET ENGINE PARTS, SHEET**
WF-31	0.15	1.42	0.42	20	L0	BAL	2.6	10.7	. . .	1.0	. . .	. . .	. . .	. . .	. . .	**HIGH-TEMPERATURE SHEETS**
WI-52[B]	0.45	0.50[C]	0.50[C]	21	1.0[C]	BAL	. . .	11	2.0	. . .	. . .	. . .	. . .	2.0	. . .	**GAS TURBINE PARTS, NOZZLE VANES**
X-45[B]	**0.25**	**1.0[C]**	**. . .**	**25.5**	**10.5**	**BAL**	**. . .**	**7.0**	**. . .**	**. . .**	**. . .**	**0.010**	**. . .**	**2.0[C]**	**. . .**	**NOZZLE VANES**

(A) SOME SUPERALLOYS ARE MADE BY MORE THAN ONE MANUFACTURER. THE PROPRIETARY DESIGNATIONS FOR SUCH ALLOYS HAS BEEN USED IN THIS COMPILATION.

(B) CAST ALLOY.

(C) MAXIMUM COMPOSITION

Nickel-base brazing alloys such as AWS BNi-3 have been used successfully on Haynes 25 for honeycomb structures. After brazing, a diffusion cycle was reportedly used to raise the braze joint remelt temperature to 1260 to 1315 °C (2300 to 2400 °F). Table 3 presents the effects of a high-temperature braze (1225 °C, or 2240 °F, for 15 rain) on the mechanical properties of Haynes 25. One cobalt-base brazing filler metal (AWS BCo-1, see Table 1) appears to offer a good combination of strength, oxidation resistance, and remelt temperature for use on Haynes 25 foil.

TABLE 3 EFFECT OF BRAZING ON MECHANICAL PROPERTIES OF HAYNES 25

CONDITION	**TEST TEMPERATURE(A)**		**ULTIMATE STRENGTH**		**0.2% OFFSET YIELD STRENGTH**		ELONGATION, %
	°C	**°F**	**MPA**	**KSI**	**MPA**	**KSI**	
TENSILE TESTING							
MILL ANNEAL	RT	RT	1020	147.9	477	69.2	**56**
AFTER BRAZE CYCLE	RT	RT	747	108.3	477	69.2	**12**
MILL ANNEAL	815	1500	396	57.4	210	30.5	**17**
AFTER BRAZE CYCLE	815	1500	393	57.0	229	33.2	**24**
MILL ANNEAL	980	1800	145	21.0	125	18.1	**35**
AFTER BRAZE CYCLE	**980**	**1800**	**148**	**21.5**	**130**	**18.8**	**35**

CONDITION	**TEST TEMPERATURE**		**STRESS**		TIME TO RUPTURE, H
	°C	**°F**	**MPA**	**KSI**	
STRESS-RUPTURE TESTING					
MILL ANNEAL	815	1500	169	24.5	**82**
AFTER BRAZE CYCLE	815	1500	169	24.5	**72.3**
MILL ANNEAL	900	1650	103	15.0	**56**
AFTER BRAZE CYCLE	900	1650	103	15.0	**36**
MILL ANNEAL	980	1800	45	6.5	**110**
AFTER BRAZE CYCLE	**980**	**1800**	**45**	**6.5**	**120**

(A) RT, ROOM TEMPERATURE

Cobalt-base alloys, much like nickel-base alloys, can be subject to liquid metal embrittlement or stress-corrosion cracking when brazed under residual or dynamic stresses. This frequently is observed when using silver- or silver-copper-base (BAg) filler metals. Liquid metal embrittlement of cobalt-base alloys by copper-base (BCu) filler metals occurs with or without the application of stress; therefore, BCu filler metals should be avoided when brazing cobaltbase alloys.

Brazing of Heat-Resistant Alloys, Low-Alloy Steels, and Tool Steels

Revised by Darrell Manente, Vac-Aero International Inc.

Brazing of Low-Alloy Steels and Tool Steels

Low-alloy steels constitute a category of ferrous materials that exhibit mechanical properties superior to plain carbon steels as the result of additions of such alloying elements as manganese, nickel, chromium, and molybdenum. Total alloy content can range from 2.07% up to levels just below that of stainless steels, which contain a minimum of 10% Cr. For many low-alloy steels, the primary function of the alloying elements is to increase hardenability in order to optimize mechanical properties and toughness after heat treatment. In some cases, however, alloy additions are used to reduce environmental degradation under certain specific service conditions. For compositions of specific low-alloy steels, see the article "Classification and Designation of Carbon and Low-Alloy Steels" in Volume 1 of the *ASM Handbook.*

Tool steels are any steels used to make tools for cutting, forming, or otherwise shaping a material into a part or component adapted to a definite use. Tool steels could be classified as low-alloy steels, but they are generally considered to be a separate group. Table 4 lists selected tool steels and their typical uses.

TABLE 4 PRINCIPAL TYPES OF TOOL STEELS

AISI/SAE DESIGNATION	**DESCRIPTION**	TYPICAL USES
W1, W2	WATER-HARDENING GRADES	**COLD-HEADING DIES, WOODWORKING TOOLS**
S1, S5	SHOCK-RESISTING TOOL STEELS	**CHISELS, HAMMERS, RIVET SETS**
O1, O2	OIL-HARDENING COLD-WORK TOOL STEELS	**SHORT-RUN COLD-FORMING DIES, CUTTING TOOLS**
A2, A5	AIR-HARDENING MEDIUM-ALLOY COLD-WORK TOOL STEELS	**THREAD ROLLING AND SLITTING DIES, INTRICATE DIE SHAPES**
D2, D3, D4	HIGH-CARBON HIGH-CHROMIUM COLD-WORK STEELS	**USES UNDER 480 °C (900 °F), GAGES, LONG-RUN FORMING AND BLAKING DIES**
H12, H13, H16	CHROMIUM HOT-WORK STEELS	**ALUMINUM OR MAGNESIUM EXTRUSION DIES, DIE-CASTING DIES, MANDRELS, HOT SHEARS, FORGING DIES**
H21, H23	TUNGSTEN HOT-WORK STEELS	**HOT EXTRUSION DIES FOR BRASS, NICKEL. AND STEEL; HOT-FORGING DIES**
T1, T15[(A)]	TUNGSTEN HIGH-SPEED STEELS	**ORIGINAL HIGH-SPEED CUTTING STEEL**
M1. M2. M3, M10, M15[(A)]	**MOLYBDENUM HIGH-SPEED STEELS**	**85% OF ALL CUTTING TOOLS IN UNITED STATES MADE FROM THIS GROUP**

(A) MOST WEAR-RESISTANT GRADE

Brazing Filler Metals

The AWS BAg, BCu, and BNi brazing filler metals can be used effectively to braze low-alloy steels or tool steels. The specific type of brazing filler metal used depends on the application, the available brazing equipment, and the strength requirements of the braze joint. Many BAg brazing filler metals are used for torch or induction brazing. BCu and BNi brazing filler metals are used for furnace brazing. High-solidus-point brazing filler metals can be chosen so that a component can be brazed and then heat treated. For example, a plate assembly made from 4340 material can be brazed with copper filler metal at 1120 °C (2050 °F) for 10 min. The plates are then kept at a temperature of 845 °C (1550 °F) for 1 h in order to austenitize the base metal and subsequently quenched in oil. The plates are tempered at 510 °C (950 °F) for 2 h in order to produce a hardness of about 40 HRC. The copper braze filler is not affected by the heat treatment due to its relatively high melting point.

Precleaning

The surface condition of the material will determine the cleaning method that is chosen. For example, a newly machined component would normally require only a vapor degreasing operation or a solvent wipe in order to remove machining lubricants. A component with a light oxide layer on the surface might be grit blasted with Al_2O_3 and then vapor degreased. This component could also be cleaned with emery paper or a stainless steel wire brush and wiped with a solvent.

A component with a heavy oxide layer on the surface would require a combination of mechanical and chemical cleaning in order to ensure that the oxide layer was removed. Another option available for removing oxides is to furnace clean

components in an atmosphere of vacuum or hydrogen. While this method will reduce oxides of iron and nickel, other oxides may not be reduced (Fig. 4).

Fixturing

Fixturing methods for heat-resistant alloys are also suitable for low-alloy steels and tool steels. However, greater use can be made of metal fixturing because many of these brazements are made at lower temperatures.

Atmospheres and Fluxes

Low-alloy steels and tool steels can be brazed in air, vacuum, hydrogen, nitrogen or endothermic or exothermic atmospheres. Components can also be torch or induction brazed in air using fluxes containing fluorides, borates, or chlorides.

Components brazed with AWS BNi brazing filler metals are usually brazed in a vacuum. Vacuum nitrogen, or hydrogen atmospheres are generally used for brazing components with BCu or BAg brazing filler metals. Care must be taken to ensure that the chosen atmosphere does not cause carburization or decarburization of the component.

Brazing of Copper, Copper Alloys, and Precious Metals

Roy E. Beal, Amalgamated Technologies, Inc. Rodger E. Cook, The Wilkinson Company

---

Introduction

COPPER, COPPER ALLOYS, AND PRECIOUS METALS are probably the most easily brazed metals available. A wide range of brazing filler metals is used to join the many different coppers, copper alloys, and precious metals that are manufactured. The selection of the brazing process and the filler metal depends on the alloy or material composition, the shape and dimension of the parts to be joined, and the intended application. Gold, silver, and the platinum group metals are well known for their resistance to oxidation at high temperatures. Not only does this characteristic make the precious metals desirable in industrial and medical applications, it helps enhance the brazeability of components made from them.

Brazing of Copper, Copper Alloys, and Precious Metals

Roy E. Beal, Amalgamated Technologies, Inc. Rodger E. Cook, The Wilkinson Company

---

Copper and Copper Alloys

Because the brazeability of most copper alloys is very good, the material considerations are generally not as difficult as those of some other metals. However, the specific metallurgy of the individual copper or copper alloy is an important factor and should be considered when selecting a manufacturing method. Most brazing operations will result in recrystallization of the copper alloy being joined. Fine grain sizes can be eliminated and the cold-working step removed, which may or may not be desirable. Often, electrical conductivity is an important factor in a copper alloy brazed joint when overall resistance across the joint must be controlled. Therefore, the finished metallurgical structures, grain sizes, and mechanical properties of the specific copper alloy must be considered when brazing is utilized.

The metallurgical structures of brazed joints are largely those of the brazing filler metal, enriched with copper from the parent material. Because some surface melting of the copper alloys being joined occurs, the interfaces usually show primary dendrites of a copper-rich phase growing from the copper alloy and braze metal interface. The brazing filler metal becomes more copper-rich, producing additional dendritic growth with increased brazing temperature and time.

The widely used oxygen-containing coppers must be carefully handled when heated. Brazing temperatures are normally above 480 °C (900 °F), which allows the dispersed copper oxides in the material to react with a hydrogen atmosphere, creating a high-pressure steam within the solid metal. Tough-pitch coppers cannot be satisfactorily brazed by furnace

techniques that utilize hydrogen as the atmosphere, either in the form of exothermic or endothermic gases or in the form of dissociated ammonia. Because the torch brazing of tough-pitch coppers also can cause problems with embrittlement, it generally should be avoided.

Copper metals that have been deoxidized by phosphorus or other elements and oxygen-free coppers can be readily brazed in hydrogen-containing atmospheres with no embrittlement. Brazing can also be accomplished without flux, if a copper-phosphorus brazing filler metal is used. When other copper materials, such as those containing lead, tellurium, silver, and other elements, are brazed, a copper-phosphorus filler metal can be used without flux, although flux is sometimes recommended.

The brazing characteristics of most copper filler metals and alloys are improved when a flux is used. In this case, phosphorus-deoxidized and oxygen-free coppers can be joined with a brazing filler metal from the silver series, which may contain zinc, cadmium, or nickel.

High-copper-content or copper alloys that contain metals that are more refractory, such as chromium or zirconium, will form oxide films that slow or prevent the flow of the brazing filler metal. Under these conditions, cleaning operations are often needed to remove the surface oxides prior to brazing. The brazing operation is then carried out in either a protective atmosphere or one that has essentially reducing conditions. Fluxes can be used to assist in the surface oxide removal or to prevent their reformation during the brazing process.

Some of the high-copper-content materials, such as chromium copper, are effectively hardened by the presence of the chromium element. In these cases, it is important to heat treat the material. This can sometimes be carried out in conjunction with the brazing operation when an appropriate brazing filler metal is selected.

Brass represents the largest group of copper alloys. Brass compositions usually contain from 5 to 40% zinc. The higher zinc contents require the use of fluxes in most brazing applications, especially when the zinc level is above 15%. Other elements are added to generate special properties, such as when lead is added to improve machining. This addition makes brazing very difficult. At a lead level of 8%, brazing is essentially impossible. Tin is added to produce a range of materials, including admiralty and naval brass. Modifications may contain other elements, such as manganese and nickel. Brasses with some aluminum content are more difficult to join than the other brasses mentioned and require specially made fluxes.

The next-largest group is bronze alloys, the most important of which are phosphor-bronze, silicon-bronze, and aluminum-bronze. Although phosphor-bronze alloys can be joined by most methods, this material has a weakness for hot cracking in cold-worked conditions. Therefore, parts should be stress relieved at temperatures from 290 to 345 °C (550 to 650 °F) before brazing. Similar problems, such as hot shortness, can be encountered with silicon-bronze alloys. Aluminum-bronze or silicon-bronze alloys that contain aluminum require special attention, because of the tenacity of the surface oxides. Generally, a special American Welding Society (AWS) type 4 flux is used in conjunction with low-melting-point, high-silver-percentage filler metals.

Copper-nickel alloys are widely used for corrosion protection and for durability in marine environments. Filler metals that contain phosphorus are not acceptable because of brittle nickel-phosphide formation. Most copper alloys can be joined to other coppers and copper alloys. Compatibility is important and can require compromise to suit the individual characteristics of the two metals involved. For example, when copper alloys that contain aluminum need to be joined to any other copper material, the AWS type FB4-A flux is required for good results.

Thus, the first step in the successful brazing of copper and copper alloys is to understand the metallurgy of the alloy involved and the effect of alloy additions on the properties of the surface to be brazed. The finished joints between the same or dissimilar metals must have a sufficiently matched composition in order to avoid joint brittleness, adverse diffusion, and large nonuniform phases. Ductility values also must be satisfactory.

Filler Metals

More filler metals are available for copper and copper alloys than for any other metal system. They vary widely in composition and cost. Standard alloys are listed by AWS reference code in Table 1. Many of the alloys contain high percentages of silver and copper, because these elements form a eutectic at a 77% silver level. Because of the high cost of silver, alloys containing phosphorus, zinc, cadmium, and other elemental additions were developed.

TABLE 1 COMPOSITIONS AND SELECTED PROPERTIES OF FILLER METALS USED IN BRAZING OF COPPER AND COPPER ALLOYS

AWS FILLER METAL DESIGNATION	NOMINAL COMPOSITION, %							SOLIDUS TEMPERATURE		LIQUIDUS TEMPERATURE		CONDUCTIVITY[A], %IACS	TYPICAL DIAMETRAL JOINT CLEARANCE	
	Ag	Cu	P	Zn	Cd	Ni	OTHER	°C	°F	°C	°F		MM	IN.
RBCUZN-A	. . .	59.25	. . .	40	. . .	. . .	0.75 SN	890	1630	900	1650	26	0.05-0.13	**0.002-0.005**
BCUZN-D	. . .	48	. . .	42	. . .	10	. . .	920	1690	935	1715	. . .	. . .	**. . .**
BCUP-1	. . .	95	5	. . .	. . .	. . .	. . .	710	1310	900	1650	. . .	0.05-0.13	**0.002-0.005**
BCUP-2	. . .	92.75	7.25	. . .	. . .	. . .	. . .	710	1310	795	1460	. . .	0.025-0.075	**0.011-0.003**
BCUP-4	6	86.75	7.25	. . .	. . .	. . .	. . .	645	1190	725	1335	. . .	0.025-0.075	**0.001-0.003**
BCUP-5	15	80	5	. . .	. . .	. . .	. . .	645	1190	800	1475	10	0.025-0.13	**0.001-0.005**
BAG-1	45	15	. . .	16	24	. . .	. . .	605	1125	620	1145	28	0.05-0.13	**0.002-0.005**
BAG-1A	50	15.5	. . .	16.5	18	. . .	. . .	625	1160	635	1175	24	0.05-0.13	**0.002-0.005**
BAG-2	35	26	. . .	21	18	. . .	. . .	605	1125	700	1295	29	0.05-0.13	**0.002-0.005**
BAG-3	50	15.5	. . .	15.5	16	3	. . .	630	1170	690	1270	18	0.05-0.13	**0.002-0.005**
BAG-5	45	30	. . .	25	. . .	. . .	. . .	675	1250	745	1370	19	0.05-0.13	**0.002-0,005**
[B]	75	22	. . .	3	. . .	. . .	. . .	. . .	. . .	740	1365	. . .	0.05-0.13	**0.002-0.005**
BAG-8	77	23	. . .	. . .	. . .	. . .	. . .	780	1435	780	1435	. . .	0.05-0.13	**0.002-0.005**
BAG-SA	72	27.8	. . .	. . .	. . .	. . .	0.2 LI	765	1410	765	1410	89[C]	0.05-0.13	**0.002-0.005**
BAG-19	92.5	7.3	. . .	. . .	. . .	. . .	0.2 LI	780	1435	890	1635	88[C]	0.05-0.03	**0.002-0.005**
BAU-4	**. . .**	**. . .**	**. . .**	**. . .**	**. . .**	**18**	**82 AU**	**950**	**1740**	**950**	**1740**	**6**	**0.05-0.13**	**0.002-0.005**

(A) RATIO OF THE RESISTIVITY OF THE MATERIAL AT 20 °C (68 °F) TO THAT OF IACS, EXPRESSED AS A PERCENTAGE AND CALCULATED ON A VOLUME BASIS.

(B) SPECIAL FILLER METAL USED IN BRAZING NICKEL SILVER KNIFE HANDLES.

(C) CONDUCTIVITY OF FILLER METAL AFTER VOLATILIZATION OF LITHIUM IN BRAZING

The most widely used silver alloy is BAg-1, which has a solidus temperature of 607 °C (1125 °F) and a liquidus temperature of 618 °C (1145 °F). It is generally recognized as being the lowest-melting-point silver brazing alloy.

Other widely used filler metals are the RB-CuZn, BCuP, and BAu series. The copper-zinc (RBCuZn) filler metals have relatively high liquidus temperatures and are anodic to copper, leading to lower corrosion resistance. Zinc-containing filler metals sometimes lose this element or form voids if overheating is allowed to occur.

The copper-phosphorus (BCuP) filler metals are self-fluxing when used to braze copper. Fluxes may be necessary when joining other copper alloys. The high-phosphorus filler metals are not resistant to sulfur-containing atmospheres. Copper-phosphorus and copper-silver-phosphorus brazing filler metals are recommended only for copper and copper alloys without nickel, because brittle phosphide can form when nickel is present.

Silver alloy (BAg) filler metals can join all brazeable coppers and copper alloys, as well as many dissimilar combinations. The lower-melting-point alloys are good for joining brass. There is a trend toward avoiding filler metals that contain cadmium, because of its toxicity. Cadmium-bearing filler metals must not be used for food equipment. Lithium-containing filler metals that are joined in protective atmospheres are self-fluxing.

Gold (BAu) alloys are high-cost filler metals that are used in specialized applications, such as vacuum and electronic products. Although these filler metals can join copper alloys, they are generally not used because of their cost. The main application is in situations where low vapor pressure is important.

Brazing Fluxes

Four primary categories of fluxes are used to braze coppers and copper alloys. There are no standard compositions and fluxes are classified by type only.

Type FB3-A is the general-purpose, low-temperature flux used with all coppers and copper alloys, except those with high levels of aluminum.

Types FB3-C and FB3-D have higher active temperature ranges, respectively, up to 1205 °C (2200 °F). These fluxes can be used with any filler metal that is appropriate from Table 1. Other fluxes are classified by liquid, powder, and slurry forms, according to application.

Type FB4-A flux is specifically designed for aluminum-containing copper alloys and has a wide range of activity from 595 to 879 °C (1100 to 1600 °F).

The AWS brazing flux classifications for coppers and copper alloys are given in Table 2. Major ingredients, filler metal type for which the flux is suitable, activity temperature range, application process, and recommended base metals are also given in Table 2.

TABLE 2 BRAZING FLUXES

CLASSIFICATION	FORM	FILLER METAL TYPE	TYPICAL INGREDIENTS	APPLICATION	ACTIVITY TEMPERATURE RANGE		RECOMMENDED BASE METALS
					°C	°F	
FB3-A	PASTE	BAG AND BCUP	BORATES, FLUORIDES	GENERAL-PURPOSE FLUX FOR MOST FERROUS AND NONFERROUS ALLOYS. (NOTABLE EXCEPTION ALUMINUM BRONZE, ETC. SEE FLUX 4-A)	565-870	1050-1600	**ALL BRAZEABLE FERROUS AND NONFERROUS METAL, EXCEPT THOSE WITH ALUMINUM OR MAGNESIUM AS A CONSTITUENT. ALSO USED TO BRAZE CARBIDES**
FB3-C	PASTE	BAG AND BCUP	BORATES, FLUORIDES, BORON	SIMILAR TO 3-A, BUT WITH CAPABILITY FOR EXTENDED HEATING TIMES OR TEMPERATURE THROUGH USE OF A DEOXIDIZING ADDITIVE	565-925	1050-1700	**ALL BRAZEABLE FERROUS AND NONFERROUS METAL, EXCEPT THOSE WITH ALUMINUM OR MAGNESIUM AS A CONSTITUENT. ALSO USED TO BRAZE CARBIDES**
FB3-D	PASTE	BAG, BCU, BNI, BAU, AND RBCUZN	BORATES, FLUORIDES	SIMILAR TO 3-C, BUT WITH A HIGHER ACTIVE-TEMPERATURE RANGE	760-1205	1400-2200	**ALL BRAZEABLE FERROUS AND NONFERROUS METAL, EXCEPT THOSE WITH ALUMINUM OR MAGNESIUM AS A CONSTITUENT. ALSO USED TO BRAZE CARBIDES**
FB3-E	LIQUID	BAG AND BCUP	BORATES, FLUORIDES	LOW-ACTIVITY LIQUID FLUX USED IN BRAZING JEWELRY OR TO AUGMENT FURNACE BRAZING ATMOSPHERES	565-870	1050-1600	**ALL BRAZEABLE FERROUS AND NONFERROUS METAL, EXCEPT THOSE WITH ALUMINUM OR MAGNESIUM AS A CONSTITUENT. ALSO USED TO BRAZE CARBIDES**
FB3-F	POWDER	BAG AND BCUP	BORATES, FLUORIDES	SIMILAR TO 3-A IN A POWDER FORM	650-870	1200-1600	**ALL BRAZEABLE FERROUS AND NONFERROUS METAL, EXCEPT THOSE WITH ALUMINUM OR MAGNESIUM AS A CONSTITUENT. ALSO USED TO BRAZE CARBIDES**
FB3-G	SLURRY	BAG AND BCUP	BORATES, FLUORIDES	SIMILAR TO 3-A IN A SLURRY FORM	565-870	1050-1600	**ALL BRAZEABLE FERROUS AND NONFERROUS METAL, EXCEPT THOSE WITH ALUMINUM OR MAGNESIUM AS A CONSTITUENT. ALSO USED TO BRAZE CARBIDES**
FB3-H	SLURRY	BAG AND BCUP	BORATES, FLUORIDES, BORON	SIMILAR TO 3-C IN A SLURRY FORM	565-925	1050-1700	**ALL BRAZEABLE FERROUS AND NONFERROUS METAL, EXCEPT THOSE WITH ALUMINUM OR MAGNESIUM AS A CONSTITUENT. ALSO USED TO BRAZE CARBIDES**
FB3-I	SLURRY	BAG, BCU,	BORATES,	SIMILAR TO 3-D IN A	760-	1400-	**ALL BRAZEABLE FERROUS AND**

		BNI, BAU, AND RBCUZN	FLUORIDES	SLURRY FORM	1205	2200	**NONFERROUS METAL, EXCEPT THOSE WITH ALUMINUM OR MAGNESIUM AS A CONSTITUENT. ALSO USED TO BRAZE CARBIDES**
FB3-J	POWDER	BAG, BCU, BNI, BAU, AND RBCUZN	BORATES, FLUORIDES	SIMILAR TO 3-D IN A SLURRY FORM	760-1205	1400-2200	**ALL BRAZEABLE FERROUS AND NONFERROUS METAL, EXCEPT THOSE WITH ALUMINUM OR MAGNESIUM AS A CONSTITUENT. ALSO USED TO BRAZE CARBIDES**
FB3-K	LIQUID	BAG, BCUP, AND RBCUZN	BORATES	EXCLUSIVELY USED IN TORCH BRAZING BY PASSING FUEL GAS THROUGH A CONTAINER OF FLUX. FLUX APPLIED BY THE FLAME	760-1205	1400-2200	**ALL BRAZEABLE FERROUS AND NONFERROUS METAL, EXCEPT THOSE WITH ALUMINUM OR MAGNESIUM AS A CONSTITUENT. ALSO USED TO BRAZE CARBIDES**
FB4-A	**PASTE**	**BAG AND BCUP**	**CHLORIDES, FLUORIDES, BORATES**	**GENERAL-PURPOSE FLUX FOR MANY ALLOYS CONTAINING METALS THAT FORM REFRACTORY OXIDES**	**595-870**	**1100-1600**	**BRAZEABLE BASE METALS CONTAINING UP TO 9% AL (ALUMINUM BRASS, ALUMINUM BRONZE, MONEL K500). MAY ALSO HAVE APPLICATION WHEN MINOR AMOUNTS OF TITANIUM OR OTHER METALS ARE PRESENT,WHICH FORM REFRACTORY OXIDES**

Note: The selection of a flux designation for a specific type of work may be based on the filler metal type and the description above, but the information here is generally not adequate for flux selection.

The highest-temperature fluxes are types FB3-I, FB3-J, and FB3-K, which work at temperatures from 760 to 1205 °C (1400 to 2200 °F). These are generally used with the RBCuZn filler metals, with long and active conditions at temperature, although they can be used with all other brazing filler metals for copper alloys.

Joint Clearance and Design

Joint clearances are primarily related to the brazing filler metals being used and their capillary attraction. If the gap is too small, then the brazing filler metal will not flow into the joint. Typical joint clearances are identified in Table 1.

Clearance can also influence the mechanical strength of the brazed joints. Allowances should be made in joint design for relative expansion of the parts at the brazing temperature, especially where dissimilar metals are involved. Penetration of the brazing filler metal through a joint to the opposite side of placement can be an effective measure of brazing filler metal flow, and a preferable joint design allows this observation to be made. Generally, braze joints should be designed for an effective joint area of 80%, in order to allow for voids.

In the case of a lap joint, the joint length should be, at a minimum, three times the thickness of the thinnest component being joined.

Brazing Processes

The selection of the brazing process is as important as the selection of the brazing filler metal. In fact, one often depends on the other. When a specific process is required, the range of allowable filler metals may be restricted. The number of parts to be made and the production rates desired also influence brazing process selection. Another consideration is the materials to be joined, because brazing may affect their mechanical properties. All parts for brazing must be cleaned prior to the brazing operation.

Brazing can be carried out with a flux or in an atmosphere. Several different atmospheres are appropriate for copper and copper-alloy brazing. AWS atmosphere types, as well as approximate compositions, filler metals, and braze metal combinations, are described in Table 3. Note that some base metals require a low dew point, in addition to the protective atmospheres.

TABLE 3 ATMOSPHERES FOR BRAZING COPPER AND COPPER ALLOYS

AWS BRAZING ATMOSPHERE TYPE NO.	**SOURCE**	**MAXIMUM DEW POINT INCOMING GAS**	**COMPOSITION OF ATMOSPHERE, %**				**FILLER METALS**	**BASE METALS**	REMARKS
			H_2	**N_2**	**CO**	**CO_2**			
1	COMBUSTED FUEL GAS (LOW HYDROGEN)	ROOM TEMPERATURE	5-1	87	5-1	11-12	BAG[A], BCUP, RBCUZN[A]	COPPER, BRASS[A]	**REFERRED TO COMMONLY AS EXOTHERMIC GENERATED ATMOSPHERES**
2	COMBUSTED FUEL GAS (DECARBURIZING)	ROOM TEMPERATURE	14-15	70-71	9-10	5-6	BCU, BAG[A], RBCUZN, BCUP	COPPER[B], BRASS[A], LOW NICKEL, MONEL, MEDIUM-CARBON STEEL[C]	**DECARBURIZES REFERRED TO COMMONLY AS ENDOTHERMIC GENERATED ATMOSPHERES**
3	COMBUSTED FUEL GAS,DRIED	-40 °C (-40 °F)	15-16	73-75	10-11		SAME AS 2	SAME AS 2 PLUS MEDIUM- AND HIGH-CARBON STEELS, MONEL, NICKEL ALLOYS	**REFERRED TO COMMONLY AS ENDOTHERMIC GENERATED ATMOSPHERES**
4	COMBUSTED FUEL GAS, DRIED (DECARBURIZING)	-40 °C (-40 °F)	38-40	41-45	17-19		SAME AS 2	SAME AS 2 PLUS MEDIUM- AND HIGH-CARBON STEELS	**CARBURIZES**
5	DISSOCIATED AMMONIA	-54 °C (-65 °F)	75	25	. . .	. . .	BAG[A], BCUP, RBCUZN[A], BCU, BNI	SAME AS FOR 1, 2, 3, 4 PLUS ALLOYS CONTAINING CHROMIUM	
6A	CRYOGENIC OR PURIFIED $N_2 + H_2$	-68 °C (-90 °F)	1-30	70-99	. . .	. . .	SAME AS 5	SAME AS 3	
6B	CRYOGENIC OR PURIFIED $N_2 + H_2$ + CO	-29 °C (-20 °F)	2-20	70-99	1-10	. . .	SAME AS 5	SAME AS 4	

6C	CRYOGENIC OR PURIFIED N_2	-68 °C (-90 °F)	. . .	100	. . .	. . .	SAME AS 5	SAME AS 3	
7	DEOXYGENATED AND DRIED HYDROGEN	-59 °C (-75 °F)	100	. . .	. . .	. . .	SAME AS 5	SAME AS 5 PLUS COBALT, CHROMIUM, TUNGSTEN ALLOYS AND CARBIDES(D)	
8	HEATED VOLATILE MATERIALS	INORGANIC VAPORS(ZINC, VOLATILE FLUORIDES)	. . .	. . .	. . .	. . .	BAG	BRASSES	**SPECIAL PURPOSE. MAY BE USED IN CONJUNCTION WITH 1 THROUGH 5 TO AVOID USE OF FLUX**
9	PURIFIED INERT GAS	INERT GAS (HELIUM,ARGON , ETC.)	. . .	. . .	. . .	. . .	SAME AS 5	SAME AS 5 PLUS TITANIUM,ZIRCONIUM , HAFNIUM	**SPECIAL PURPOSE. PARTS MUST BE VERY CLEAN AND ATMOSPHERE MUST BE PURE**
9A	**PURIFIED INERT GAS + H_2**	**INERT GAS (HELIUM, ARGON, ETC.)**	**1-10**	**. . .**	**. . .**	**. . .**			

(A) FLUX REQUIRED IN ADDITION TO ATMOSPHERE WHEN ALLOYS CONTAINING VOLATILE COMPONENTS ARE USED.

(B) COPPER SHOULD BE FULLY DEOXIDIZED OR OXYGEN-FREE.

(C) HEATING TIME SHOULD BE MINIMIZED TO AVOID OBJECTIONABLE DECARBURIZATION.

(D) FLUX MUST BE USED IN ADDITION TO THE ATMOSPHERE IF APPRECIABLE QUANTITIES OF ALUMINUM, TITANIUM, SILICON. OR BERYLLIUM ARE PRESENT.

Furnace brazing has, as its primary advantage, the ability to handle mass production. However, a small furnace can be used for a wide variety of parts, materials, and filler metals. Furnaces can operate on either a batch or continuous basis. Furnaces can be mesh belt conveyor, batch, or pusher (where parts are loaded on trays) systems. The objective is to achieve minimum-cost operation for the particular application. Another advantage is that a number of joints can be brazed simultaneously in a furnace.

Copper and copper alloys are often furnace brazed on a conveyor or mesh belt system. This allows the use of protective atmospheres that can be either exothermic or endothermic. The conveyor furnace also allows for controlled heating and cooling rates. Separate belts are sometimes used for each zone to control these rates. The metallurgy of the alloys to be joined must be considered.

Brazing furnaces can be expensive, especially for mass-production operations with protective atmospheres, as well as preheating and cooling zones. Although electrical furnaces cost more to run, gas furnaces usually require muffles or linings that must be periodically replaced, which raises the overall expense and narrows the cost differential.

The brazing furnace must be designed to handle the desired temperature and mass load. Furnace linings are used when fluxes are necessary, even in electrically heated units, because flux can corrode the heating elements. Parts that can be self-fluxed and joined in a protective atmosphere avoid this potential flux problem.

Copper and copper alloys must not be exposed to gases containing sulfur. Leaks into the lining from gas firing can be a problem. Brasses are not generally furnace brazed.

The operation of a brazing furnace depends on the filler metal, the melting temperature, and the characteristics of the copper alloys to be joined. It is usually desirable to braze at approximately 28 °C (50 °F) higher than the liquidus of the filler metal. Most brazing filler metals can be used, except those that have large amounts of zinc and are subject to volatilization.

A dry hydrogen atmosphere can be used for some brazing filler-metal and base-metal combinations. However, as noted earlier, the hydrogen atmosphere must be completely avoided when oxygen-containing copper metal is used, because it would embrittle the copper.

An example of a furnace braze application without a protective atmosphere is the contact arm assembly shown in Fig. 1, which was joined with BCuP-5 filler metal.

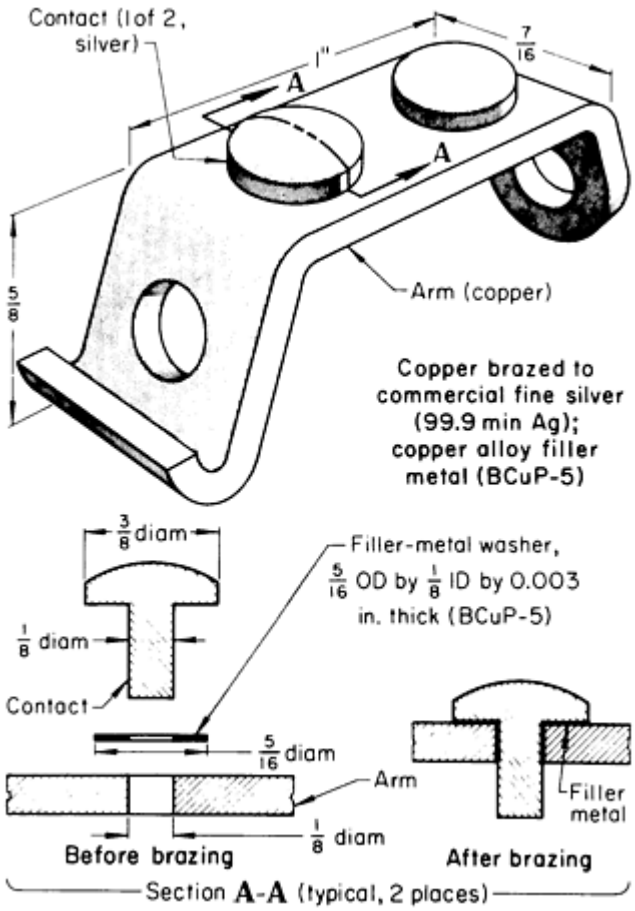

FIG. 1 FURNACE BRAZED CONTACT ARM ASSEMBLY, BRAZED WITHOUT PROTECTIVE ATMOSPHERE, 42 °C (75 °F) BELOW THE LIQUIDUS OF THE FILLER METAL

Components to be furnace brazed are preassembled with the filler metal preplaced for brazing. Preferably, the parts should be self-jigging. External jigs and fixtures can be used when absolutely necessary, but add extra capital and operating expense, because the parts have to be assembled in the jigs and the jigs themselves have a finite life. Fully enclosed parts must be vented to permit the escape of trapped air. Failure to do so can be dangerous.

Torch brazing of copper and copper alloys is used on many components and in numerous industrial applications. Examples are radiators, condensers, refrigerators, construction piping, motors, electrical equipment, and others. Equipment costs are low. The braze operator must be skilled in adjusting the heating flame and directing energy to the part to be joined. Torches can be extremely small, for electronic applications, or very large, for heavy fabrications and castings. Production capacity varies from one part to mass-production lots.

Tough-pitch coppers require reducing atmospheres because of hydrogen embrittlement. Brass can lose zinc by volatilization and must not be overheated or held too long at brazing temperature. Alloys with refractory elements require flux and reducing flames. Some copper alloys, such as phosphor bronze, crack if heated too rapidly.

Filler metals for torch brazing were described in Table 1. The filler material can be in wire, powder, or paste form. The application can be manual or automatic.

Examples of torch brazing applications are return bends in heat exchangers, which are usually automatically torch brazed; fin assemblies, which are usually manually torch brazed; instrumentation tubes; oil coolers; and large electrical parts.

A common example is a return bend joint 0made with alloy C12000, which is a phosphorus-deoxidized copper. A 9.5 mm ($\frac{3}{8}$ in.) diameter tube with a 0.5 mm (0.02 in.) wall thickness is typical. Tube ends of the heat exchanger are expanded to

allow insertion of the return bend. A clearance of 0.10 to 0.23 mm (0.004 to 0.009 in.) is used to provide a pressure-tight joint. Each leg of the rerum bend is fitted with a 0.75 mm (0.03 in.) diameter BCuP-5 filler wire. The joint is self-fluxing and multiple joints are passed through a series of torch flames to quickly make the joint in approximately 5 s.

Another example is an eight-station turntable for the automatic torch brazing of instrument assemblies (Fig. 2). These components are usually small and are joined at multiple stations by indexing the table. This system uses unskilled operators and can achieve high production rates. The brazing filler metal can be in flux-paste form or a wire feeding unit can be used in conjunction with separate fluxing.

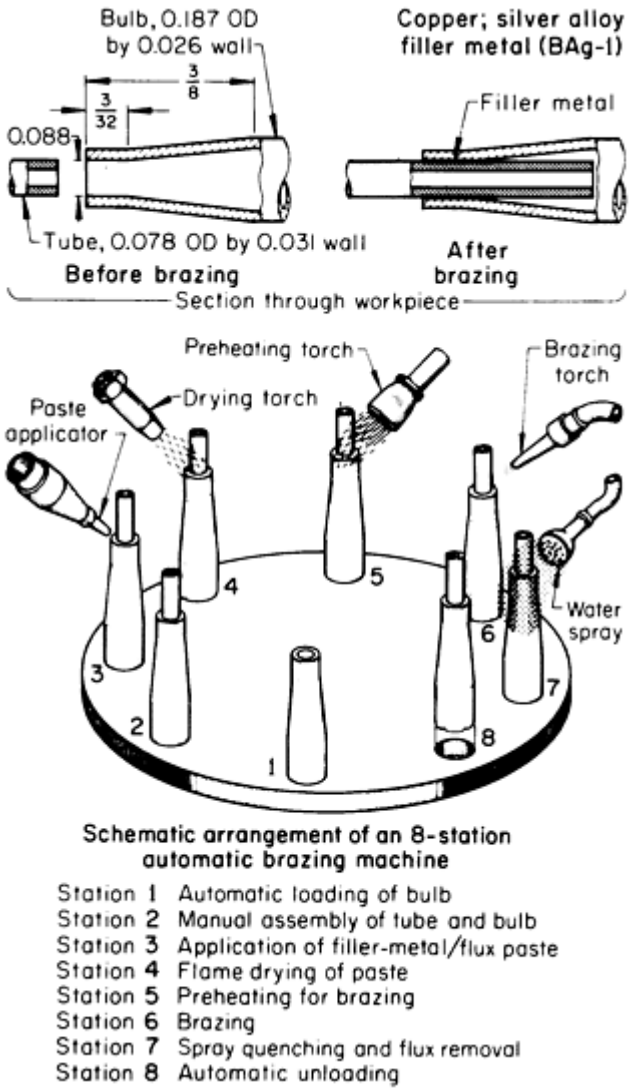

Schematic arrangement of an 8-station automatic brazing machine

Station 1 Automatic loading of bulb
Station 2 Manual assembly of tube and bulb
Station 3 Application of filler-metal/flux paste
Station 4 Flame drying of paste
Station 5 Preheating for brazing
Station 6 Brazing
Station 7 Spray quenching and flux removal
Station 8 Automatic unloading

FIG. 2 BULB AND TUBE ASSEMBLY, BRAZED BY MECHANICALLY HELD TORCHES ON AN EIGHT-STATION TURNTABLE

Induction brazing is less efficient with copper alloys than with other metals. However, this process is widely used because of its high-production capability, especially in situations where flames cannot be tolerated and atmosphere protection is an alternative to fluxing. Induction brazing usually minimizes the possible warping of parts. However, the initial costs of the induction heating equipment is high. The low efficiency of the process also demands relatively high power requirements.

Inductor design is similar to that needed for other metals. The objective is controlled heat input and distribution. Single- or multiple-turn inductors are utilized, sometimes in conjunction with concentrators, to focus heat in desirable locations.

Brazing filler metals for induction heating are usually the silver-containing alloys and the copper-phosphorus and copper-phosphorus-silver alloys.

An advantage of induction brazing is exemplified by the chromium-copper (C18200) post shown in Fig. 3. The heating step in the brazing process is a critical factor in obtaining optimum mechanical properties, because precipitation hardening can occur with improper heating. The brazing of a tungsten-silver contact required the use of a nickel-containing silver alloy, BAg3, to join with chromium-copper. Induction brazing is the best option for retaining material properties.

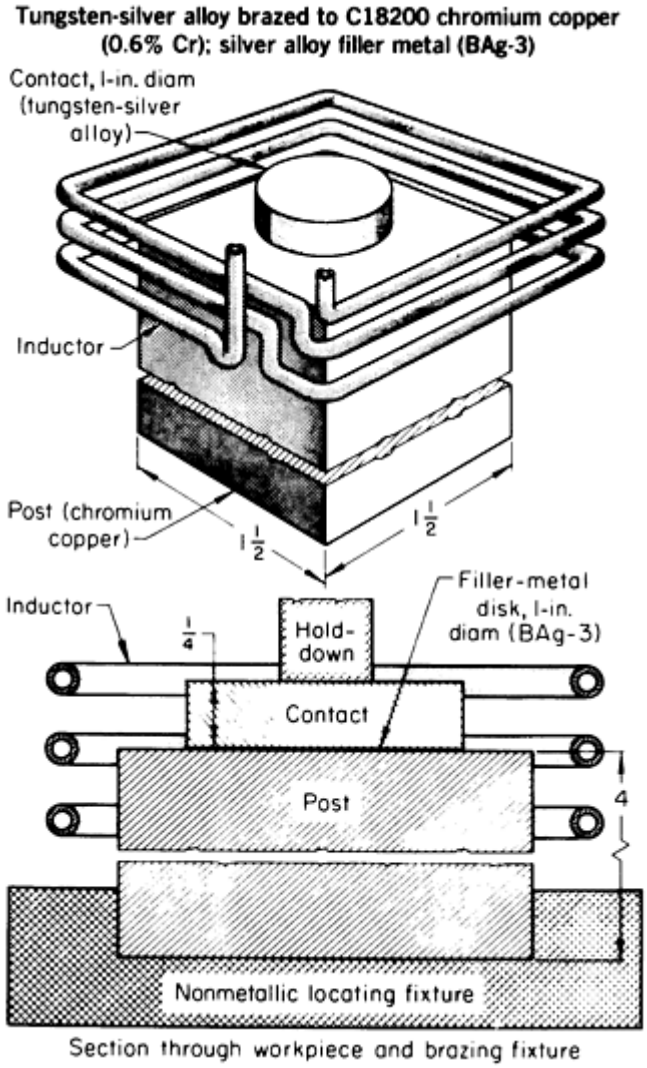

FIG. 3 TUNGSTEN-SILVER ALLOY CONTACT IN POSITION FOR INDUCTION BRAZING TO C18200 CHROMIUM-COPPER (0.6% CR) POST; BAG-3 SILVER ALLOY FILLER METAL

Another example is the use of multiple-station inductors in the brazing of armatures for motors. A preformed BCuP-5 filler metal is placed at the desired joint area and the inductor is allowed to bring the assembly to temperature quickly without flux.

Resistance brazing is used for small parts, such as terminals, fasteners, and attachments. The filler metal, which is usually preplaced, is often BCuP-5, because it can be used without flux. However, most brazing filler metals that contain silver have been used. Heat generation occurs by resistance through the assembly, using a standard resistance welding machine. A second heating method is to use graphite blocks as the contact, which spreads the heat over a larger area. This method is widely used in the electronics industry and for joining high-conductivity coppers and alloys. Brazing times are very short at 10 to 20 Hz with very high current inputs. A small quantity of hydrogen can be used for oxidation protection, except when joining tough-pitch coppers.

Portable resistance welding machines are used in the manufacture of electrical equipment, transformers, bus bars, and other components. Large areas can be joined by making a series of spot brazes.

Salt-bath dip brazing of copper and copper alloys is a less-popular brazing process. The procedure uses a molten neutral salt at the brazing temperature. The brazing filler metal is preplaced and the molten salt is used to activate joining. The procedure is useful for unusually shaped parts or those with multiple joints, such as heat exchangers. Applications include waveguides, which allow simultaneous brazing of all joints in a single immersion. A cast bronze alloy (C22000), for example, can be joined to a thin-walled tube to close tolerances without warpage. Self-jigging of parts is preferable during the assembly process, before the parts are mounted into the external jig used in the dip braze. External jigs must allow for expansion of the parts during brazing. A disadvantage of this process is the need to remove all residual salts after brazing.

Brazing of Copper, Copper Alloys, and Precious Metals

Roy E. Beal, Amalgamated Technologies, Inc. Rodger E. Cook, The Wilkinson Company

---

Precious Metals

Throughout history, precious metals have been used as adornments and jewelry. Even today, the use of gold in jewelry is the major source of demand for fabricated gold. Brazing is routinely employed in the manufacture of jewelry to produce joints that match in color and surface condition to the base materials. Biocompatibility and relative ease of workability have also historically placed precious metals in the fields of dentistry and medicine.

Like copper, precious metals exhibit good thermal and electrical conductivity, in addition to superior corrosion resistance--required traits for materials used for high-reliability electrical contacts.

Material Composition

Jewelry golds are usually yellow or white in color. The term "karat" refers to the fineness or percentage of gold in the alloy, with 24 karat (k) being pure gold. Diluting gold to 18 k would then mean that the resulting alloy is 75% Au (18 parts gold, plus six parts of other metals). Yellow golds are generally alloys containing gold, copper, silver, and zinc. White golds are lightened by the substitution of nickel for some of the copper in the alloy.

Dental materials may contain any of the precious metals in almost any combination. It is not unusual to find a dental casting material that is composed of gold, silver, platinum, palladium, iridium, and/or other precious or nonprecious metals to achieve special performance characteristics (for example, matched coefficient of thermal expansion with dental porcelain).

Precious-metal-base electrical and electronic materials are found in wide variety. Many of the original precious metal contact materials were derived from existing dental and jewelry alloys. Silver graphite, silver nickel, and silver metal oxides (for example, Ag-CdO) are common switch and relay materials fabricated by powder metallurgy or the oxidation of a wrought alloy. In many cases, these silver contact materials are provided with a silver backing to facilitate brazing. Parts that are not silver backed must be treated to provide a suitable surface for brazing. Silver graphite contacts can be air fired to remove surface carbon. Silver metal oxide parts can be chemically treated to remove surface nonmetallics. Additional surface treatment, plating, or coining can then be employed. Another very common silver contact alloy is coin silver (90Ag-10Cu).

Sterling silver (92.SAg-7.5Cu) is well-known for its application in jewelry, flatware, and decorative household serving utensils.

The platinum-group metals are platinum, palladium, iridium, rhodium, ruthenium, and osmium. With the exception of osmium, pure and alloyed platinum-group metals have a wide range of applications including jewelry, thermocouples, glass melting vessels and tools, labware, medical devices, and catalysts.

Precious metal plated or clad materials can be brazed, but they require process controls sufficient to prevent excessive diffusion or blistering of the plating or cladding.

Filler Metals

The fields of jewelry and dentistry each have selections of brazing filler metals that satisfy the specific demands of their disciplines. An extremely wide variety of gold jewelry filler metals is available. One important consideration in the selection of filler metals for gold jewelry is that the filler metal does not reduce the gold content of the finished brazement. Table 4 gives a partial list of gold filler metals for jewelry applications.

TABLE 4 SELECTED FILLER METALS USED IN GOLD JEWELRY BRAZING APPLICATIONS

COMPOSITION, %							**SOLIDUS**		LIQUIDUS	
Au	**Ag**	**Cu**	**Zn**	**Cd**	**Sn**	**Ni**	**°C**	**°F**	**°C**	°F
80.0[A]	. . .	. . .	8.0	. . .	. . .	12.0	782	1440	871	**1600**
75.0	12.0	8.0	. . .	5.0	. . .	. . .	826	1519	887	**1629**
75.0	9.0	6.0	. . .	10.0	. . .	. . .	776	1429	843	**1549**
75.0	9.0	6.0	10.0	. . .	. . .	. . .	730	1346	783	**1441**
75.0	2.8	11.2	9.0	2.0	. . .	. . .	747	1377	788	**1450**
75.0	. . .	15.0	1.8	8.2	. . .	. . .	793	1459	822	**1512**
66.6[A]	10.0	6.4	12.0	. . .	. . .	5.0	718	1324	810	**1490**
66.6	15.0	15.0	3.4	. . .	. . .	. . .	796	1465	826	**1519**
58.5	25.0	12.5	. . .	4.0	. . .	. . .	788	1450	840	**1544**
58.5	10.3	24.2	. . .	7.0	. . .	. . .	792	1458	831	**1528**
58.5	8.8	22.7	. . .	10.0	. . .	. . .	751	1384	780	**1436**
58.5	11.8	25.7	4.0	. . .	. . .	. . .	816	1501	854	**1569**
58.5	25.7	11.8	4.0	. . .	. . .	. . .	786	1447	818	**1504**
58.5	24.2	10.3	7.0	. . .	. . .	. . .	765	1409	808	**1486**
58.5	4.9	25.6	2.0	9.0	. . .	. . .	738	1360	760	**1400**
58.5	8.0	22.0	2.1	9.4	. . .	. . .	744	1371	776	**1429**
58.3	20.8	19.0	1.9	. . .	. . .	. . .	793	1459	830	**1526**
58.3	18.0	12.0	11.7	. . .	. . .	. . .	720	1328	754	**1389**
58.3[A]	15.0	5.7	15.0	. . .	. . .	6.0	. . .	. . .	. . .	**. . .**
50.0[A]	25.0	10.0	9.0	. . .	. . .	6.0	. . .	. . .	. . .	**. . .**
50.0	30.5	17.5	2.0	. . .	. . .	. . .	775	1427	806	**1483**
41.7	32.0	16.3	10.0	. . .	. . .	. . .	724	1335	749	**1380**
41.7[B]	24.0	16.3	9.0	9.0	. . .	. . .	. . .	. . .	. . .	**. . .**
41.7	35.0	21.9	1.4	. . .	. . .	. . .	. . .	. . .	. . .	**. . .**
33.3	30.0	16.7	. . .	0.0	. . .	. . .	635	1175	709	**1303**
33.3	30.0	16.7	20.0	. . .	. . .	. . .	695	1283	704	**1299**
33.3	40.5	17.0	6.6	2.6	. . .	. . .	722	1332	749	**1380**
33.3	1.8	49.4	2.3	10.2	3.0	. . .	689	1272	776	**1429**
33.3	31.0	28.0	7.7	. . .	. . .	. . .	737	1359	808	**1486**
33.3[A]	42.0	10.0	9.7	. . .	. . .	5.0	738	1360	807	**1485**
25.0	35.0	20.0	10.0	10.0	. . .	. . .	. . .	. . .	. . .	**. . .**
25.0[A]	**58.0**	**. . .**	**17.0**	**. . .**	**. . .**	**. . .**	**. . .**	**. . .**	**. . .**	**. . .**

Source: Ref 1

(A) WHITE GOLD.

(B) GREEN GOLD.

Platinum jewelry can be brazed with binary alloys of gold-platinum, platinum-silver, or palladium-silver, or multiple precious metal alloys (some of which contain copper).

Silver jewelry is generally brazed with silver-base filler metals that contain copper and zinc (and in some cases, include additions of tin, nickel, or cadmium). However, the elimination of cadmium is becoming more prevalent due to stringent Occupational Safety and Health Administration (OSHA) regulations.

There are some proprietary variations in the compositions of brazing filler metals for dentistry, although they are usually composed of gold, silver, copper, zinc, and tin. Table 5 gives typical dental gold filler metals with physical properties.

TABLE 5 COMPOSITION AND PHYSICAL PROPERTIES OF SELECT GOLD-BASE BRAZING FILLER METALS USED IN DENTAL APPLICATIONS

BRAZING DESIGNATION	COMPOSITION, %					MELTING RANGE		HEAT TREATMENT	PROPORTIONAL LIMIT		TENSILE STRENGTH		LONGATION, %
	AU	AG	CU	ZN	SN	°C	°F		MPA	KSI	MPA	KSI	
A	65.4	15.4	12.4	3.9	3.1	745-785	1375-1445	SOFTENED	186	27	293	42.5	**14**
								HARDENED	379	55	434	63	**1**
B	66.1	12.4	16.4	3.4	2.0	750-805	1385-1480	SOFTENED	203	29.5	307	44.5	**12**
								HARDENED	534	77.5	576	83.5	**<1**
C	65.0	16.3	13.1	3.9	1.7	765-800	1410-1470	SOFTENED	207	30	303	44	**9**
								HARDENED	531	77	634	92	**< 1**
D	72.9	12.1	10.0	3.0	2.0	755-835	1390-1535	SOFTENED	165	24	248	36	**7**
								HARDENED	424	61.5	483	70	**< 1**
E[(A)]	**80.9**	**8.1**	**6.8**	**2.1**	**2.0**	**745-870**	**1375-1595**	**SOFTENED**	**141**	**20.5**	**259**	**37.5**	**18**

Source: Ref 2

(A) NOT APPRECIABLY AFFECTED BY AGE HARDENING.

Filler metals for industrial applications of precious metals usually come from the American Welding Society (AWS) BAu and BAg groups. Pure gold and gold-base alloys can be brazed with materials from the BAu or BAg metals. Pure silver and silver-base alloys can be brazed with the BAg and, in some cases, the BCuP (see Fig. 1) filler metals. Platinum and palladium are brazeable with pure gold (which melts at 1063 °C, or 1945 °F) as a filler or by using one of the platinum jewelry filler metals.

Fluxes and Atmospheres

Generally, fluxes and atmospheres suitable for copper brazing will be sufficient for applications joining precious metals because precious metals are oxidation resistant. The user can choose a flux or atmosphere that corresponds to the type of filler metal used, or in the case of dissimilar metal brazing to precious metals, a flux or atmosphere that will protect the nonprecious base material.

Joint Clearance and Configuration

The brazing of precious metals may be achieved by following the criteria established for joint clearance and design for copper brazing (see the section "Copper and Copper Alloys" in this article).

Brazing Processes

Precious metals can be joined using furnace brazing, torch brazing, induction brazing, and resistance brazing processes.

Furnace Brazing. In the production of crown and bridge work, a dental laboratory technician may have to join a part that has been partially porcelain coated. The technician may in that case employ the use of a vacuum porcelain firing furnace to perform the brazing operation on the exposed metal surfaces. High-volume industrial applications (for example, electrical contact manufacture) may call for the use of furnace brazing.

Torch Brazing. In the dental laboratory and at the jeweler's bench, the most widely used process for brazing is manual torch brazing. Dental lab technicians frequently torch braze one-of-a-kind configurations that have been fixtured by embedding the parts into high-temperature-resistant plaster. Automated torch brazing has been applied to high-volume jewelry applications, such as chainmaking. Industrial precious metal users employ both manual and automated torch brazing.

Induction Brazing. Precious metal parts brazed to dissimilar metals (for example, the brazing of a contact to a holder), sometimes require the localized heating attainable by induction heating (Fig. 3). The same type of efficiency deficit encountered when induction brazing is used to braze copper is also present when the process is applied to precious metals (see the section "Copper and Copper Alloys" in this article).

Resistance Brazing. Because copper and precious metals are highly conductive, the process of resistance brazing of precious metals is applicable, but also limited by short times and high current outputs.

References cited in this section

1. *PRECIOUS METALS SCIENCE AND TECHNOLOGY,* INTERNATIONAL PRECIOUS METALS INSTITUTE, 1991, P 653
2. R.W. PHILLIPS, *SKINNER'S SCIENCE OF DENTAL MATERIALS,* 8TH ED., W.B. SAUNDERS COMPANY, 1982

Brazing of Copper, Copper Alloys, and Precious Metals

Roy E. Beal, Amalgamated Technologies, Inc. Rodger E. Cook, The Wilkinson Company

References

1. *PRECIOUS METALS SCIENCE AND TECHNOLOGY,* INTERNATIONAL PRECIOUS METALS INSTITUTE, 1991, P 653
2. R.W. PHILLIPS, *SKINNER'S SCIENCE OF DENTAL MATERIALS,* 8TH ED., W.B. SAUNDERS COMPANY, 1982

Brazing of Aluminum Alloys

E.B. Gempler

Introduction

ALUMINUM is a commonly used base material for brazing. It is easily fabricated by most manufacturing methods, such as machining, forming, and stamping. Although most brazing processes are applicable, the use of aluminum requires more attention. It is different from most metals in two ways: it quickly reforms its tenacious oxide coating whenever a reactive form of oxygen is present, such as air or water, and it is always brazed at temperatures close to its melting point. The latter factor compromises strength (in terms of holding shape during brazing) and tends to increase the rapidity in which the brazing alloy reacts with the base metal. The net result is that cycle times are critical and fixturing forces must be controlled.

Brazing of Aluminum Alloys

E.B. Gempler

Base Metals

The non-heat-treatable wrought alloys typically used as base metals are listed in Table 1. Those that are most successfully brazed are the l*xxx* and 3*xxx* series and the low-magnesium members of the 5*xxx* series.

TABLE 1 MELTING RANGES AND BRAZEABILITY OF SOME COMMON ALUMINUM ALLOYS

ALLOY	MELTING RANGE		BRAZEABILITY[A]
	°C	°F	
NON-HEAT-TREATABLE WROUGHT ALLOYS			
1350	646-657	1195-1215	**A**
1100	643-657	1190-1215	**A**
3003[B]	643-654	1190-1210	**A**
3004	629-652	1165-1205	**B**
5005	632-652	1170-1205	**B**
5050	627-652	1160-1205	**B**
5052	593-649	1100-1200	**C**
HEAT-TREATABLE WROUGHT ALLOYS			
6053	593-652	1100-1205	**A**
6061	593-649	1100-1200	**A**
6063	616-654	1140-1210	**A**
6951[C]	616-654	1140-1210	**A**
7005	607-649	1125-1200	**B**
CASTING ALLOYS[D]			
443.0	574-632	1065-1170	**B**
356.0	557-613	1035-1135	**B**

710.0	596-646	1105-1195	**B**
711.0	**604-643**	**1120-1190**	**A**

(A) A, GENERALLY BRAZEABLE BY ALL COMMERCIAL PROCEDURES; B, BRAZEABLE WITH SPECIAL TECHNIQUES OR IN SPECIFIC APPLICATIONS THAT JUSTIFY PRELIMINARY TRIALS OR TESTING TO DEVELOP THE PROCEDURE AND TO CHECK THE PERFORMANCE OF BRAZED JOINTS; C, LIMITED BRAZEABILITY.

(B) USED BOTH PLAIN AND AS THE CORE OF BRAZING SHEET.

(C) USED ONLY AS THE CORE OF BRAZING SHEET.

(D) SAND AND PERMANENT MOLD CASTINGS ONLY

The commonly brazed heat-treatable wrought alloys are the 6*xxx* series. Because the 2*xxx* and 7*xxx* series of aluminum alloys have melting points that are too low, they are not normally brazeable. Exceptions are the 7072 alloy, which is used for cladding material only, and 7005 alloy. Alloys with a solidus temperature above 595 °C (1100 °F) are readily brazed using the aluminum-silicon filler metals.

There are several brazeable cast aluminum alloys, which are listed in Table 1 along with their melting range and degree of brazeability. The most readily brazeable are those with the higher solidus temperatures, such as the 710 and 711 alloys.

Filler Metals

Alloys used in flux brazing usually contain between 7 and 12% silicon-balanced aluminum, and tramp metals are controlled to levels below 0.2%.

Alloys employed in fluxless brazing use higher percentages of silicon (>9%) and have varying additions of magnesium to enhance oxide film modification to promote wetting, as well as reduce the partial pressures of oxygen beating gases in the chamber. These alloys are primarily found in clad form. Some are semiproprietary to processes used in the automotive heat-exchanger industry. The vacuum (fluxless) alloys, BAlSi-6 through -11, are identified in Table 2. The alloys BAlSi-3 through -5 also can be used with the fluxless process if modifications related to magnesium are made, either in the base metal or as an addition to the furnace.

TABLE 2 COMPOSITIONS AND SOLIDUS, LIQUIDUS, AND BRAZING TEMPERATURE RANGES OF BRAZING FILLER METALS FOR USE ON ALUMINUM ALLOYS

AWS CLASSIFICATION	**COMPOSITION[A], %**						TEMPERATURE					
							SOLIDUS		**LIQUIDUS**		BRAZING	
	Si	**Cu**	**Mg**	**Zn**	**Mn**	**Fe**	**°C**	**°F**	**°C**	**°F**	**°C**	°F
BALSI-2	6.8-8.2	0.25	. . .	0.20	0.10	0.8	577	1070	613	1135	599-621	**1110-1150**
BALSI-3[B]	9.3-10.7	3.3-4.7	0.15	0.20	0.15	0.8	521	970	585	1085	571-604	**1060-1120**
BALSI-4	11.0-13.0	0.30	0.10	0.20	0.15	0.8	577	1070	582	1080	582-604	**1080-1120**
BALSI-5[C]	9.0-11.0	0.30	0.05	0.10	0.05	0.8	577	1070	591	1095	588-604	**1090-1120**
BALSI-6[D]	6.8-8.2	0.25	2.0-3.0	0.20	0.10	0.8	559	1038	607	1125	599-621	**1110-1150**

BALSI-7[(D)]	9.0-11.0	0.25	1.0-2.0	0.20	0.10	0.8	559	1038	596	1105	588-604	**1090-1120**
BALSI-8[(D)]	11.0-13.0	0.25	1.0-2.0	0.20	0.10	0.8	559	1038	579	1075	582-604	**1080-1120**
BALSI-9[(D)]	11.0-13.0	0.25	0.10-0.5	0.20	0.10	0.8	562	1044	582	1080	582-604	**1080-1120**
BALSI-10[(D)]	10.0-12.0	0.25	2.0-3.0	0.20	0.10	0.8	559	1038	582	1080	582-604	**1080-1200**
BALSI-11[(D)(E)]	**9.0-11.0**	**0.25**	**1.0-2.0**	**0.20**	**0.10**	**0.8**	**559**	**1038**	**596**	**1105**	**582-604**	**1080-1120**

(A) PRINCIPAL ALLOYING ELEMENTS.
(B) CONTAINS 0.15% CR.
(C) CONTAINS 0.20% TI.
(D) SOLIDUS AND LIQUIDUS TEMPERATURE RANGES VARY WHEN USED IN VACUUM.
(E) CONTAINS 0.02-0.20% BI

The ranges of brazing temperatures of both aluminum alloy base and filler metals are shown in Fig. 1.

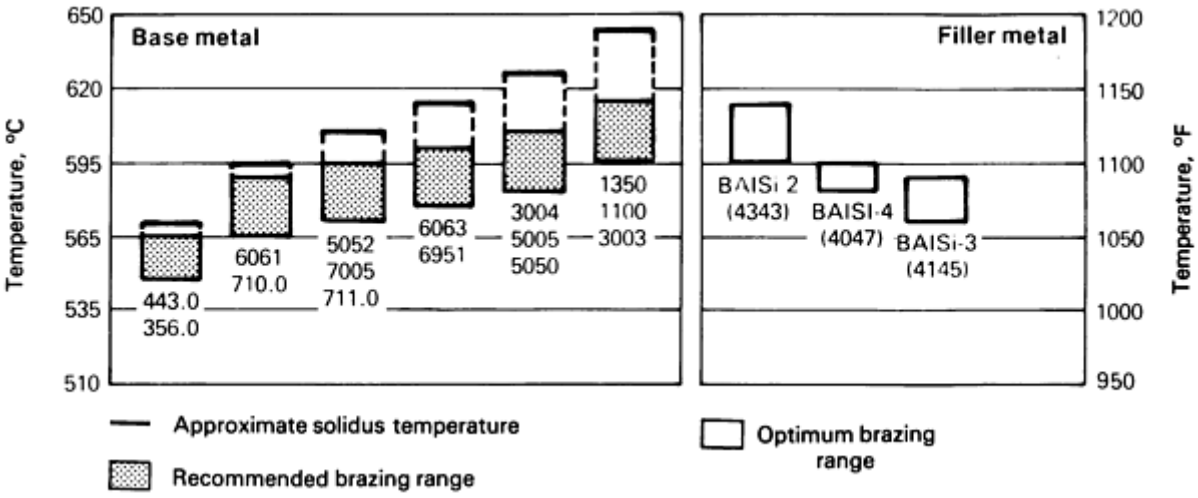

FIG. 1 COMPARISON OF BRAZING TEMPERATURE RANGES OF ALUMINUM ALLOY BASE METALS AND ALUMINUM ALLOY BRAZING FILLER METALS

Non-clad forms of brazing alloys are usually shim or wire stock and are limited to AA4047. Some paste forms are also available from powdered alloy and flux or from powdered alloy and binder for either flux or fluxless processes. These materials are available in the United States from only a few vendors.

Brazing of Aluminum Alloys

E.B. Gempler

Brazing Sheet

Brazing sheet is usually made by roll bonding the filler metal to the base metal. It can be single clad (on one side only) or double clad, and is an extremely useful way to apply filler metal.

Brazing sheet is advantageously used in the assembly of high-production items, such as heat exchangers and other complex assemblies, because the filler metal is already in place, thus avoiding an extra step that would slow down the assembly operation. Brazing sheet is an excellent aid in assemblies where many joints need to be brazed simultaneously.

Fluxes

Brazing that is performed in air or other oxygen-containing atmospheres requires the use of a chemical flux. These fluxes, whether used in torch, furnace, or dip brazing, or in braze pastes, usually contain chlorides and/or fluorides, the fumes of which are hazardous to the operator if inhaled. Flux fumes must be exhausted, not only for health reasons, but because they are highly corrosive to most metals.

Fluxes act as deoxidizers and prevent reoxidation by coating the surfaces. They are used to aid the wetting and flow of the filler metal on deoxidized and clean aluminum.

There are four generic types of fluxes in two basic formulas: chloride active and fluoride active. Chloride-active fluxes consist of either a straight chloride flux or a chloride flux modified with zinc. Fluoride-active fluxes consist of either a straight fluoride or a modified fluoride that produces an inert film over the brazed parts after brazing. In both cases, the modification is intended to reduce corrosion in postbrazed products.

In torch brazing, fluxes can be applied dry or mixed with either alcohol or water and painted, or sprayed, or they can be applied by dipping the joining parts. A suitable flux for torch or furnace brazing must:

- BEGIN TO MELT AT A TEMPERATURE LOW ENOUGH TO MINIMIZE OXIDATION OF THE PARTS
- BE ESSENTIALLY MOLTEN AT THE TIME THE FILLER METAL MELTS
- FLOW OVER THE JOINT AND FILLER METAL TO SHIELD THEM FROM OXIDIZING GASES
- PENETRATE OXIDE FILMS
- LOWER THE SURFACE TENSION TO ENCOURAGE WETTING
- REMAIN LIQUID UNTIL THE FILLER METAL HAS MELTED
- BE RELATIVELY EASY TO REMOVE AFTER BRAZING IS COMPLETE

Fluxes for dip brazing are less active than those used for torch or furnace brazing, because parts to be brazed are totally immersed in the molten flux. Therefore, oxygen cannot reach the surface of the parts to reform oxides. In dip brazing, the flux acts as a heat transfer medium, in addition to its fluxing action, to bring the aluminum parts to final temperature for brazing.

Powdered fluxes are mixed with liquids and powders to form pastes. Pastes can be mixed in the brazing operation or they can be bought premixed from several suppliers.

Brazing of Aluminum Alloys

E.B. Gempler

Joint Designs

Assemblies to be brazed can be designed with many types of joints. When joints are designed to permit the application of flux, provisions must be made to ensure the displacement of flux and accompanying gases and to allow the flow of filler metal into the joint.

Lap joints can be used to achieve joint strength that is equal to the strength of the base metal. Lap joints that require a long flow path for the filler metal should be designed for flow in one direction only, to prevent the entrapment of potentially corrosive flux. Scarf and butt joints usually are not as strong as the base metal, but they can be designed to give satisfactory performance. (It should be noted that scarf and butt joints are weaker than lap joints because their mating area is less than that of lap joints.) For fluxless brazing, line contact is desirable and zero clearance is preferred. Certain brazing alloys (for example, the BNi series) can approach the strength of the parent metal if homogenized for a long period of time to provide grain size and microstructure characteristics similar to those of the parent metal.

In flux brazing, joint clearances must be sufficient to prevent premature solidification of the filler metal in small capillary spaces that are caused by the mutual solubility of the base metal and filler metal. These spaces can entrap flux and cause porosity. Clearances that range from 0.05 to 0.10 mm (0.002 to 0.004 in.) can suffice for narrow laps when preplaced filler metal is used. Wider laps may require clearances up to 0.25 mm (0.010 in.). With brazing sheet, line contact is desirable. Clearances should not exceed 0.076 mm (0.003 in.).

Preblaze Cleaning

Non-heat-treatable alloys usually can be cleaned by degreasing. However, this cleaning method is being replaced by solvent cleaning using special water-base products, because of environmental requirements. Chemical deoxidation may be required for components that have been severely worked, such as in spinning, drawing, or extrusion processes.

For heat-treatable alloys, chemical cleaning is necessary to reduce the tenacious oxide films, which tend to be thicker, because of thermal processing methods such as solution heat treatment. Aluminum-silicon alloys often require a special nitric-hydrofluoric acid mix to remove the excess silicon smut that is not removed by alkaline (5% NaOH) or nitric-acid solutions alone. If necessary, stainless steel wire brushes, steel wool, or abrasive cloth can be used to achieve abrasive cleaning.

Thin, high-silicon-content braze foil should only be degreased to prevent the loss of available filler metal that is needed at the braze joint.

Brazing of Aluminum Alloys

E.B. Gempler

Assembly

In flux brazing, self-fixturing is an excellent assembly method. It may be accomplished through the use of tabs, rivets, screws, or tack welds. Self-fixturing is cost-effective, quick, and lends itself to many different types of assemblies. Care must be exercised when choosing fastener or tack weld alloys with solidus temperatures that are higher than the brazing process temperature.

Spring-loaded fixtures can be useful, especially for high-production and complicated assemblies. These fixtures are excellent for stacked assemblies, such as plate-fin heat exchangers. When adjusted properly, spring-loaded fixtures can prevent the crushing of assemblies that often is due to thermal expansion and aluminum softening during heating.

Both coil springs and strap springs are used. Strap springs are less costly to use, but typically do not have the inherent resiliency of coil springs. Coil springs are more expensive than strap springs, but coil springs offer variations in coil

diameter, coil thickness, stiffness, initial pressure, and the number of coils used that cannot be obtained with strap springs. Strap springs vary in width and thickness and are tightly bound around the fixture. When heated, strap springs tend to stretch and do not return to their original setting, thus losing stiffness and producing an effective loss in resiliency.

Weighted fixtures are often used on low-production runs and in cases where variations in shape and size preclude the use of more-expensive fixture types.

It is often necessary to apply stop-offs to parts of the assembly to be brazed in order to prevent filler metal from flowing onto certain areas. Stop-offs can consist of refractory oxides, graphites, or any number of commercial compounds readily available from welding and brazing suppliers. Furnace and dip brazing operations often use stop-offs to prevent fixtures and jigs from being brazed to the work. Stop-offs for fluxless brazing are usually refractory oxides sprayed on the jigs or fixtures. Stop-offs also can be formed on the fixtures by heating at a high temperature in an atmosphere.

Dip Brazing

Dip brazing is done by immersing the brazing assembly and fixture into a molten bath of flux. The flux acts as both a heating mechanism to bring the parts to temperature, as well as a deoxidizer. Prior to immersion, the part and fixture must be preheated to remove moisture and prevent solidification of the flux during immersion. Preheating is done in a hot-air furnace at approximately 540 °C (1000 °F) for about 0.5 h. Duration of the preheat cycle varies with the complexity of the brazement, its size, and the size of the fixture. Nevertheless, even with small waveguide components and thin box brazements that require a decreased preheat time, using a preheat cycle time of 0.5 h is still recommended. Moisture removal is necessary to prevent steam explosions when the part is lowered into the bath. Steam explosions can be very hazardous to the operator.

Initial temperatures are determined by attaching a thermocouple to the aluminum assembly. Time and temperature readings are taken and used for subsequent parts as a mechanism to control the braze quality.

Adequate salt drainage is necessary for several reasons. Salt must be removed to prevent trapping and the possible corrosion of the parts. Adequate drainage is necessary to allow filler metal solidification. Retention of excess salt in the assembly depletes the level of the molten salt in the dip pot, necessitating more-frequent additions of dry flux to the bath and resulting in higher costs.

The bulk of the salt is removed by immersing the fixture and brazement in a bath of boiling water. Then, the brazement is separated from the fixture and put through a series of water baths to remove more salt. Final baths, which use distilled water, are changed at intervals until chemical tests show an acceptable limit of salt in the clear runoff water. Concurrently, the fixtures are further boiled and then blasted with water to remove any residual salt.

The molten flux bath is regularly dehydrated by immersing clean sheets of 1100 or 3003 series aluminum to remove water, oxides, and other contaminants for an amount of time that varies from bath to bath. The sheets must be cleaned and dried to maintain their effectiveness. They can be used repeatedly.

Furnace Brazing

Standard fluxes must be used in furnace brazing because of the oxide atmospheres. Flux can be applied by brushing, dipping, or spraying. Furnace brazing is used for large loads that require good temperature control. Stop-offs are often used on parts and fixtures to inhibit the flow of molten filler metal to certain areas and to prevent brazing to the fixtures.

Special fluxes can be used with special furnaces that have reduced-oxygen atmospheres. One such flux is NOCOLOK, which has modest cleaning and fluxing ability and requires well-cleaned parts. During the brazing process, the chamber is filled with flowing dry nitrogen. At the completion of brazing, the parts are coated with an inert residue from the flux. The parts do not require postbraze cleaning to remove the flux residue.

The temperature accuracy requirement for these aluminum brazing furnaces is usually ±5.5 °C (±10 °F). However, ±3 °C (±5 °F) is preferred, especially where critical components are being brazed.

Torch Brazing

Torch brazing is used in either manual or automatic fabrication, as well as in repair operations. Torch brazing ranges from simple tube-to-tube joints to more-complex and mechanized assemblies. Torch brazing is similar to oxyfuel gas welding in that the heat to effect the joint is applied locally. Oxyacetylene, oxyhydrogen, and oxy-natural gas are used in commercial torch brazing applications. Close temperature control is needed when using the typical BAlSi-3 and BAlSi-4 filler metals.

Because aluminum shows no change in color when hot, it is difficult to know when parts approach the brazing temperature. Fluxes that melt at a slightly lower temperature than the filler metal can serve as a temperature indicator. Joint areas are pointed with a slurry of brazing flux. A soft, slightly reducing flame is played over the entire area. Filler metal can be either preplaced or force fed. After brazing, residual flux chloride must be removed.

Brazing of Aluminum Alloys

E.B. Gempler

Flux Removal Techniques

Whether a flux is used in torch brazing, furnace brazing, or dip brazing processes, it must be removed to prevent entrapment and the possibility of subsequent corrosion effects in the presence of moisture. Flux removal from dip-brazed assemblies was discussed in the dip brazing section of this article.

All fluoride fluxes are not safe to leave on the workpiece. If the flux residue remains in the inert form (for example, cryolite in the NOCOLOK process), it is considered to be an acceptable condition. However, under no circumstances should fluoride that can ionize remain on the surface because it can cause subsequent corrosion problems.

As much flux as possible should be removed by immersing torch-brazed and furnace-brazed parts in a bath of boiling water just after the filler metal has solidified. Scrubbing with a fiber brush in boiling water removes most of the flux. Pressure spray washers are often effective in opening passages that are plugged by flux. Agitation and turbulence, as well as ultrasound, help to remove flux from tight spaces. Acids (HNO_3, HNO_3-HF), as well as chromates, are often used in the final rinse water. Because of disposal problems, many companies avoid using chromates as corrosion inhibitors.

Testing for complete flux removal is done by monitoring the presence of chlorides in the final rinse water. An acidified solution of 5% silver nitrate is used to check the final rinse water for clarity. If white chloride residues cloud the water, then salt is still present. After several tests on subsequent rinses, the salt is considered removed if the water remains clear. Although this is a simple test, it is quite accurate.

Fluxless Vacuum Brazing

The main advantage of fluxless vacuum brazing is that no flux removal is necessary. If assemblies have been made using non-heat-treatable alloys, then they are ready for the next operation. If heat-treatable alloys are brazed, then a subsequent heat treatment will be necessary to reach the strengths required.

The required equipment is a vacuum furnace that can reach a vacuum of 133×10^{-5} Pa (10^{-5} torr) or lower, is leak tight, and is able to obtain temperature accuracy of ±3 °C (±5 °F) on the load being brazed.

Fluxless brazing is ideal for braze sheets where no flux is required and assemblies can easily be stacked and fixtured. Magnesium in some form is usually required to expedite the break-up of surface oxides and to facilitate the wetting mechanism. Magnesium is supplied by several techniques. It can be an integral part of the filler metal or base metal or it can be a part of other alloys used in the assemblies, such as the 5*xxx* series of aluminum-magnesium alloys. It can also be supplied in the form of chips or prealloyed aluminum-magnesium ingots.

Vacuum furnaces must be cleaned periodically to remove magnesium and magnesium oxide that condenses on the cold walls of the furnace and other appendages to those walls. These residues may, in time, short some of the electrodes and tend to be hygroscopic to water. Water is a contaminant that is very difficult to remove in vacuum.

Brazing of Aluminum Alloys

E.B. Gempler

Postbraze Heat Treatment

Dip-brazed heat-treatable assemblies can be spray quenched or immersion quenched after most of the salt has been drained and while the parts still remain at about 480 °C (900 °F). This puts the parts into a solution-heat-treated stage for subsequent precipitation hardening.

Heat-treatable assemblies usually are in the annealed or soft condition after furnace, torch, or fluxless brazing. Clean assemblies are usually heated at temperatures ranging from 480 to 515 °C (900 to 960 °F) for a period of time that allows the magnesium silicates to go into solid solution prior to quenching. The quenched parts are then aged for a period of time that allows precipitation hardening to take effect. The amount of time depends on the alloy system and on whether the parts are made from wrought or cast alloys. A typical precipitation heat treatment for 6061 shapes and tube is 160 °C (320 °F) for 16 to 20 h.

Brazing of Aluminum Alloys

E.B. Gempler

Safety Precautions

Exhaust fumes must be removed from the immediate vicinity of the operators. Suitable masks should be worn to prevent inhalation of these fumes.

Precautions are necessary when dip brazing. Operators must wear suitable burn-and heat-resistant coverings to protect themselves from splashes or burns and from inhaling flux fumes. As with all flux-type operations, fume exhaust is a necessity.

Lowering and removal of the parts and fixtures must be done at a rate that minimizes spatter from the molten bath. Parts to be brazed (including fixtures) must be preheated to prevent steam explosions as the part is lowered into the bath. Preheating also prevents the lower-temperature fixture and aluminum assembly from freezing out the molten salt as it is immersed.

The temperature of aluminum can be very deceptive, because this material does not turn red or glow when it is hot, like steel does. Precautions must be taken to prevent burns.

The cleaning of vacuum furnaces has already been discussed. When removing magnesium and magnesium oxides, nonsparking scraping tools should be used to prevent sparks that can ignite magnesium. Dust should be swept frequently into a metal container and removed from the vicinity of the furnace to prevent fires. The cleaning operators must work with adequate ventilation. Masks must also be used by the operators. The cleaning must be done by more than one operator as a precaution against accidents. Several buckets of appropriate materials, such as sand, as well as fire extinguishers, should be available at all times to douse potential fires.

Brazing of Refractory and Reactive Metals

Roy I. Batista, TRW, Inc.

Introduction

REFRACTORY METALS are metals that have melting points that are either higher than those of iron, nickel, and cobalt or exceed 2000 °C (3630 °F). Molybdenum, tungsten, niobium, and tantalum are the refractory metals discussed in this article. Reactive metals, which include titanium, zirconium, and beryllium, have in common the ability to form stable oxides at elevated temperatures. These diverse groups of metals have a wide range of mechanical and physical properties (Table 1).

TABLE 1 SELECTED PHYSICAL PROPERTIES OF REACTIVE AND REFRACTORY METALS

METAL	LIQUIDUS TEMPERATURE		SOLIDUS TEMPERATURE		ANNEALING TEMPERATURE		COEFFICIENT OF THERMAL EXPANSION, 10^{-6}/K	CRITICAL TEMPERATURE	
	°C	°F	°C	°F	°C	°F		°C	°F
MOLYBDENUM	2610	4730	2610	4730	1200	2192	4.9	RT[A]	**RT[A]**
MO-0.5TI	2610	4730	2610	4730	1450	2642	4.9	. . .	**. . .**
MO-0.5TI-0.008ZR	2620	4748	. . .	. . .	1550	2822	4.9	. . .	**. . .**
MO-50RE	2550	4622	2480	4496	1500	2732	6.3	. . .	**. . .**
TUNGSTEN	3410	6170	3410	6170	1300	2372	4.3	300[A]	**572[A]**
W-25RE	3100	5612	. . .	. . .	1500	2732	6.7	RT[A]	**RT[A]**
NIOBIUM	2468	4474	2468	4474	1150	2102	7.2	<-100[A]	**<-148[A]**
NB-10HF	2350	4262	. . .	. . .	1300	2372	8.1	. . .	**. . .**
NB-28TA-10W-1ZR	2590	4694	. . .	. . .	1370	2498	9	. . .	**. . .**
NB-10TA-10W	2600	4712	. . .	. . .	1400	2552	14	. . .	**. . .**
TANTALUM	2996	5425	. . .	. . .	1300	2372	6.6	<-200[A]	**<-328[A]**
TA-10W	3035	5495	. . .	. . .	1550	2822	6.7	. . .	**. . .**
TA-8W-2HF	3000	5432	. . .	. . .	1650	3002	6.5	. . .	**. . .**
TITANIUM 99+ TI[B]	1671	3040	1671	3040	700	1292	9.2	950[C]	**1742[C]**
TI-5AL-2.5SN (ALPHA)	1677	3050	. . .	. . .	820	1508	9.5	1040[C]	**1904[C]**
TI-8AL-1MO-IV	1650	3002	. . .	. . .	790	1454	9	1040[C]	**1904[C]**

(NEAR ALPHA)									
TI-6AL-2NB-1TA (NEAR ALPHA)	1650	3002	. . .	. . .	900	1652	9	1110[C]	**2030[C]**
TI-6AL-4V (ALPHA-BETA)	1660	3020	1615	2939	790	1454	9.1	990[C]	**1814[C]**
TI-6AL-6V-2SN (ALPHA-BETA)	1649	3000	1627	2961	800	1472	9	946[C]	**1735[C]**
TI-3AL-8V-6CR-4ZR-4MO (BETA)	1650	3002	1555	2831	800	1472	8.4	795[C]	**1463[C]**
ZIRCONIUM	1845	3353	1845	3353	. . .	. . .	5.8	865[C]	**1589[C]**
ZR-1.5SN-0.2FE-0.1CR	1845	3353	1845	3353	. . .	. . .	5.5	>865[C]	**>1589[C]**
BERYLLIUM	1285	2345	1285	2345	730	1346	11.4	. . .	**. . .**
BE-38AL	**660**	**1220**	**. . .**	**. . .**	**. . .**	**. . .**	**13.9**	**. . .**	**. . .**

RT, room temperature.

(A) DBTT OF ANNEALED MATERIAL.

(B) SIMILAR ALLOYS WITH VARYING INTERSTITIAL COMPOSITIONS.

(C) BETA TRANSUS

A vacuum atmosphere is suitable for brazing all of the refractory and reactive metals. Tungsten and molybdenum also can be brazed in reducing atmospheres and, in some applications, in air using a flux. The use of flux in the brazing of beryllium has been routine, but the preferred vacuum techniques are being developed. Inert gases with properly controlled purity are also useful atmospheres for the brazing of both refractory and reactive metals.

This article describes brazing filler metal selection and brazing procedures for each of these metals. The importance of fabricating samples to design requirements and then testing to the degree necessary to validate brazing procedures cannot be overemphasized. These materials do not have the data base that exists for alloys based on copper, iron, or nickel, and contradictions exist in the literature. Because specific details on brazing equipment, such as vacuum levels, type of vacuum equipment, quality of inert gases, and brazing cycles, are not reported in most of the development work on the refractory and reactive metals, verification is needed for specific braze designs.

The selection of filler metals presents a problem, because many recommendations are for materials that are not readily available. However, an attempt was made in this article to provide selections from commercially available compositions. Although these commercial alloys may not be optimal in all applications, they should be evaluated first to assess their suitability for specific designs. Consult the selected references at the end of this article for specific information on nonstandard brazing filler metals.

Brazing of Refractory and Reactive Metals

Roy I. Batista, TRW, Inc.

Refractory Metals

The four refractory metals that have the most commercial significance are molybdenum, tungsten, niobium, and tantalum. The brazing of these alloys is a complex subject, because their high melting points and specific mechanical, physical, and chemical properties have highly diverse applications, and the brazing procedures required by each application can be quite distinct. Molybdenum is used in high-temperature structures and electronic devices. Tungsten is most commonly associated with filaments, heating elements, and welding electrodes. Niobium is widely used in spacecraft propulsion systems and applications that require its corrosion resistance. The largest use of tantalum is for capacitors, followed by chemical processing equipment.

Ductile-to-Brittle Transition Temperature (DBTT)

DBTT is a metallurgical consideration that greatly influences the selection of brazing filler metals and the brazing environment. Tantalum and niobium are Group V metals and have a high solubility of interstitial elements and a low DBTT. Conversely, tungsten and molybdenum are Group VI metals and have a lower solubility for interstitial elements, but a high DBTT. Tungsten and molybdenum are specifically processed and alloyed to lower the DBTT. For both tungsten and molybdenum, a warm-worked structure has a lower DBTT than a recrystallized structure, and alloys have been developed to retard annealing. Annealed molybdenum has a DBTT that is near room temperature, whereas annealed tungsten may be brittle at temperatures below 315 °C (600 °F). Tantalum does not appear to have a ductile-to-brittle transition, and the DBTT of niobium can be as low as -200 °C (-330 °F).

Gas Reactions

The refractory metals are all sensitive to the absorption of, or reaction to, oxygen. Niobium and tantalum begin oxidizing at 200 and 400 °C (390 and 750 °F), respectively. Below 1370 °C (2500 °F), the oxides are nonvolatile, but the ductility of the parent metals is reduced, because of the absorption of oxygen.

Molybdenum starts to oxidize at about 500 °C (930 °F). At temperatures over 778 °C (1430 °F), which is the eutectic temperature of MoO_2-MoO, oxides become particularly volatile and the oxidation rate accelerates rapidly. Tungsten oxidizes rapidly at temperatures over 500 °C (930 °F), but not as rapidly as molybdenum. In general, oxygen absorption is not as much of a problem with tungsten and molybdenum as it is with tantalum and niobium.

Hydrogen exposure presents no problems to the use of molybdenum and tungsten. However, both tantalum and niobium will absorb hydrogen and form hydrides at moderate temperatures. The results can range from a loss of ductility at low concentrations to complete destruction, depending on time and hydrogen concentration. If it is not heavily contaminated, then hydrogen can be removed from tantalum and niobium by a high-temperature vacuum anneal.

Alloy Availability

Although there has been considerable development of the refractory metal alloys, their commercial availability in small quantities can be erratic. The alloys that are most common are identified in Table 1. Generally, tantalum, niobium, and their alloys are usually procured and used in the annealed condition. Tungsten and molybdenum are often used in the stress-relieved condition, because of higher strength and a lower DBTT. TZM is the most common alloy of molybdenum, and both molybdenum and tungsten are alloyed with rhenium to increase strength and ductility and to lower the DBTT. Molybdenum and tungsten may both contain dopants, such as potassium, to reduce grain growth at high temperatures, particularly in filament applications.

Brazing Filler Metal Selection

The wide range of applications and the high melting points of the refractory metals mean that a wide range of brazing alloys are available, but this also makes the selection process more complex. Alloys have been specifically developed for high-temperature, low-temperature, high-strength, or corrosion-resistant applications.

The higher the brazing temperature and the service temperature, the more difficult it becomes to select a brazing filler alloy. As temperature increases, adverse metallurgical reactions, erosion, and fixturing concerns are amplified. For example, nickel-containing alloys have resulted in brittle joints in both tungsten and molybdenum brazing, because of intermetallic formation. This brittleness can be minimized by short brazing cycles.

The refractory metals are not difficult to join. The objective of the selection process is to select an alloy that will provide the right combination of properties in service, such as high temperature, mechanical properties, or corrosion resistance.

Filler Metals for Brazing of Molybdenum. The commercially available alloys based on silver, gold, or palladium have all been evaluated for refractory metal brazing. In Ref 1, the 19 filler metals considered for molybdenum and the 32 considered for TZM are ranked on a wettability index. It was found that TZM was less-readily brazed than molybdenum, because of titanium oxide formation on its surface. As expected, higher brazing temperatures promoted wettability. Table 2 lists commercially available brazing filler alloys, as well as those alloys that may have special applications, but may not be commercially available.

TABLE 2 BRAZING FILLER METALS FOR REFRACTORY METAL BRAZING

BRAZING ALLOYS	LIQUIDUS TEMPERATURE		SOLIDUS TEMPERATURE		COMMENTS
	°C	°F	°C	°F	
COMMON BASE METALS					
25CR-20NI-FE	1454	2650	. . .	. . .	**25-20 STAINLESS STEEL**
55CO-20NI-15W-10NI	1427	2600	. . .	. . .	**L-605 COBALT ALLOY**
18CR-8NI-FE	1427	2600	. . .	. . .	**STAINLESS STEEL**
54CO-27CR-6MO-5NI	1400	2550	. . .	. . .	**ALLOY 21**
80NI-14CR-6FE	1393	2539	. . .	. . .	**INCONEL**
67NI-33CU	1349	2460	. . .	. . .	**MONEL**
COMMERCIALLY AVAILABLE SILVER-BASE BRAZING ALLOYS					
75AG-20PD-5MN	1072	1962	1008	1846	
AG	961	1762	961	1762	
54AG-21.3CU-24.7PD	950	1742	900	1652	**VARIOUS AG-CU-PD ALLOYS ARE AVAILABLE WITH DECREASING MELTING POINTS**
72AG-28CU	780	1436	780	1436	
82AG-9GA-9PD	880	1616	845	1553	
71.5AG-28.1CU-0.75NI	795	1463	780	1436	
54AG-42CU-2NI	893	1639	771	1420	
68AG-27CU-10SN	760	1400	743	1369	
COMMERCIALLY AVAILABLE GOLD-BASE BRAZING ALLOYS					
92AU-8PD	1240	2264	1200	2192	
50AU-25PD-25NI	1121	2050	1102	2016	**NUMEROUS AU-PD-NI COMPOSITIONS ARE AVAILABLE WITH DECREASING MELTING POINTS**
73.8AU-26.2NI	1010	1850	990	1814	
50AU-50CU	970	1778	955	1751	
82AU-18NI	950	1742	950	1742	
PURE METAL BRAZING FILLER METALS					
RE	3186	5767	. . .	. . .	**TUNGSTEN BRAZING, REMELT 2830 °C (5126 °F)WITHOUT DIFFUSION TREATMENT**
TA	3020	5468	. . .	. . .	**TUNGSTEN APPLICATIONS**
NB	2471	4480	. . .	. . .	**TUNGSTEN APPLICATIONS**
RU	2254	4089	. . .	. . .	**TUNGSTEN APPLICATIONS**
RH	1963	3565	. . .	. . .	**TUNGSTEN APPLICATIONS**
PT	1768	3214	. . .	. . .	**MOLYBDENUM AND TUNGSTEN APPLICATIONS**
PD	1552	2826	. . .	. . .	**MOLYBDENUM AND TUNGSTEN APPLICATIONS**
OTHER COMMERCIALLY AVAILABLE BRAZING ALLOYS					
80MO-20RU	2275	4127	2125	3857	**MOLYBDENUM AND TUNGSTEN APPLICATIONS**
60PT-20RH	1990	3614	1950	3542	**MOLYBDENUM AND TUNGSTEN APPLICATIONS**
75PT-20PD-5AU	1695	3083	1645	2993	**MOLYBDENUM AND TUNGSTEN APPLICATIONS**
65PD-35CO	1220	2228	1220	2228	**MOLYBDENUM AND TUNGSTEN APPLICATIONS**
OTHER BRAZING ALLOYS (NOT COMMERCIALLY AVAILABLE, SPECIAL ORDER REQUIRED)					
W-50MO-3RE	2900[A]	5252[A]	. . .	. . .	
MO-50S	2600[A]	4712[A]	. . .	. . .	
W-250S	2600[A]	4712[A]	. . .	. . .	
V-50MO	2257[A]	4095[A]	. . .	. . .	
TI-25CR-21V	1482[A]	2700[A]	. . .	. . .	**REMELT 1921 °C (3490 °F)**
84NI-16TI	1288[A]	2350[A]	. . .	. . .	**HIGH STRENGTH AT 1000 °C (1830 °F)**
FE-15MO-4C-1B	1200[A]	2192[A]	. . .	. . .	**CORROSION RESISTANT IN LIQUID BISMUTH AND SODIUM**
52NB-48NI	1190[A]	2174[A]	. . .	. . .	**HIGH STRENGTH AT 1000 °C (1830 °F)**
AG-30PD	1148[A]	2098[A]	. . .	. . .	**MINIMUM EROSION OF MOLYBDENUM**
TI-25CR-3BE	1110	2030	993	1819	**REMELT 1600 °C (2912 °F) AFTER DIFFUSION**

					TREATMENT
PT-B	**1100[(A)]**	**2012[(A)]**	**. . .**	**. . .**	**BORON CONTENT 1-4.5%; REMELT TO 2100 °C (3812 °F) AFTER DIFFUSION**

(A) BRAZING RANGE

Examples of special-purpose brazing include the joining of thin foils, such as the honeycomb structure in which the alloy Ag-30Pd alloy was used. At a brazing temperature of 1160 °C (2120 °F), 0.025 mm (0.001 in.) molybdenum foils were joined without excess erosion. In a high-temperature application, a brazed Ti-25Cr-21V alloy (solidus temperature of 1160 °C, or 2120 °F) had a remelt temperature of 1600 °C (2910 °F) after a 16 h postbraze diffusion cycle at the solidus temperature. The other recommended alloy systems for high-temperature performance include Ti-48Zr-4Be (brazing temperature of 986 °C, or 1810 °F), Ti-25Cr-21V (brazing temperature of 1482 °C, or 2700 °F), and Ti-28Zr-8Ge (brazing temperature of 1327 °C, or 2420 °F). The TiCrV composition has. a high remelt temperature of 1920 °C (3490 °F) (Ref 2). The high remelt temperatures of the chromium-containing alloys may be a result of the volatilization of the chromium during brazing. Therefore, a vacuum environment may be required to achieve these remelt temperatures.

Other high-temperature brazing filler alloys are Ti-65V (brazing temperature of 1700 °C, or 3090 °F) and V-50Mo (brazing temperature of 2257 °C, or 4095 °F). After postbraze diffusion treatment, shear test specimens failed in the parent metal when tested at 1400 °C (2550 °F). Additions of base-metal powder to the brazing filler alloy were necessary to prevent Kirkendall void formation (Ref 3).

A Mo-20Ru brazing filler was used to braze a doped Mo-3Re filament to a tungsten post. Because of a requirement to minimize any recrystallization of the filament, a laser welder working in an argon atmosphere was used to heat the assembly. Excellent wetting of both the molybdenum and tungsten was achieved without recrystallization of the filament adjacent to the braze (Ref 4).

When using brazing alloy powders, the addition of elemental powders to act as a "diffusion sink" is an effective method of raising remelt temperatures. The diffusion sink material will either shorten the diffusion time to achieve a high remelt temperature or it may form higher-melting-point compounds within the brazed joint. An example of a diffusion sink combination is Ti-25Cr-13Ni alloy combined with molybdenum powder that brazes at 1260 °C (2300 °F), but remelts at 1710 °C (3110 °F).

Filler Metals for Brazing of Tungsten. The brazing filler alloys that are appropriate for use with molybdenum are generally well suited for use with tungsten. In addition, there has been development work for specific tungsten applications. Platinum-boron alloys containing from 1 to 4.5% boron were brazed at about 1100 °C (2010 °F), both with and without tungsten powder additions. Remelt temperatures of 2100 °C (3810 °F) were obtained. The use of a diffusion sink (tungsten powder) was not necessary when gaps were below 0.038 mm (0.0015 in.). The addition of a halide salt, NaF or KHF_2, reduced the possibility of W_2B compound formation, thus raising the remelt temperature to about 2300 °C (4170 °F) (Ref 5).

Three alloys were evaluated for use at temperatures up to 2500 °C (4530 °F): W-25Os (melting temperature of 2600 °C, or 4710 °F), W-50Mo (melting temperature of 2900 °C, or 5250 °F), and Mo-5Os (melting temperature of 2600 °C, or 4710 °F). At 2200 °C (3990 °F), base-metal strength values were reported (Ref 6).

The number of alloys evaluated for use with both tungsten and molybdenum is extensive. A review of the selected references is recommended if nonstandard alloys are indicated for a specific application.

Filler Metals for Brazing of Niobium. Niobium may be selected for its corrosion resistance in chemical and nuclear applications or for its low density and high melting point in aerospace structural and propulsion applications. The welding of niobium does not present the brittleness problems associated with tungsten and molybdenum. However, brazing must be considered when welding is inappropriate.

Although commercial brazing alloys based on silver, gold, and nickel will wet niobium, brittleness is often noted with their use. In addition, their low melting points make them unusable for many applications. The active-metal modifications (titanium additions) of the silver-copper and gold-nickel alloys may be useful for niobium joining, particularly if residual oxide on the surface presents a wetting problem.

A series of Ta-V-Nb and Ta-V-Ti alloys is compatible with niobium and will resist liquid sodium. They can be brazed at temperatures ranging from 1760 to 1925 °C (3200 to 3500 °F), and have shear strength values that range from 140 to 205 MPa (20 to 30 ksi). The alloy Nb-1Zr, when brazed with Ti-28V-4Be, was resistant to potassium vapor and liquid exposed for 1000 h at 815 °C (1500 °F). Honeycomb structures of Nb alloys were evaluated using Pd-30Cu and Ti-11Cr-13V-3Al brazing filler alloys. There was some erosion with the palladium alloy, but the titanium-base alloy produced joints with high ductility and minimum base-metal erosion.

Two diffusion-enhanced approaches have been explored to produce higher-temperature properties in niobium brazes. One method adds base-metal powder to the brazing alloy, that is, niobium powder added to a Ti-33Cr alloy brazed at 1485 °C (2705 °F). Another approach, which depends on diffusion between the braze and parent material, is niobium brazed with a Ti-30V-4Be alloy that was brazed at 1315 °C (2400 °F). Postdiffusion of the Ti-33Cr alloy raised the remelt temperature by over 300 °C (540 °F), with corresponding increases to high-temperature strength. The Ti-Cr-V alloy had about the same remelt temperature, but its strength was lower.

A 316L stainless steel sleeve was brazed to the inner diameter of a Nb-10Hf rocket engine thrust chamber using 82Au-18Ni filler metal. The joint failed shortly after removal from the vacuum furnace, because of residual stresses resulting from the difference in thermal expansion. The joint was redesigned so that the 316L material was the outer member. This configuration was successfully brazed and the engine was flight qualified (Ref 4). This example emphasizes the need to consider the thermal expansion of the brazement pieceparts to prevent failure after brazing. It was fortunate that the assembly failed shortly after brazing. The residual stresses in a mismatched joint could just as easily cause failure weeks or months after brazing.

Filler Metals for Brazing of Tantalum. The brazing of tantalum is not as well documented as the brazing of tungsten and molybdenum. This situation may exist because, like niobium, it is an easily weldable material without the brittleness problem encountered with welded tungsten and molybdenum. Many of the brazing filler alloys presented for tungsten and molybdenum, as well as all of the recommendations made for niobium, can be considered for use with tantalum.

The diffusion-sink titanium powder and a Ti-30V brazing filler alloy (braze temperature of 1760 °C, or 3200 °F) produced a remelt temperature of 2100 °C (3810 °F). A similar approach with a 33Zr-34Ti-33V (brazing temperature of 1427 °C, or 2600 °F) resulted in a remelt temperature of 1650 °C (3000 °F). Other approaches using hafnium-base alloys have been considered. These include Hf-7Mo, Hf-40Ta, and Hf-19Ta-2.5Mo.

References cited in this section

1. M.M. MCDONALD, *ET AL.*, THE WETTABILITY OF BRAZING ALLOYS ON MOLYBDENUM AND TZM, *WELD. J. SUPPL.*, OCT 1988
2. G.M. SLAUGHTER *ET AL.*, WELDING AND BRAZING OF ADVANCED REFRACTORY ALLOYS, *SPACE SHUTTLE MATERIALS PROCEEDINGS*, SAMPE, OCT 1971
3. L.B. LUNBERG *ET AL.*, BRAZING OF MOLYBDENUM AND TUNGSTEN FOR HIGH-TEMPERATURE SERVICE, *WELD. RES. SUPPL.*, OCT 1978
4. R.I. BATISTA, TRW, INC., UNPUBLISHED NOTES
5. C.W. HAYNES, "DEVELOPMENT OF LOW TEMPERATURE BRAZING OF TUNGSTEN FOR HIGH TEMPERATURE SERVICE," REPORT R>D>R 1249-1/DTIC AD 260580, DEFENSE TECHNOLOGY INFORMATION CENTER, MAY 1962
6. T.J. MOORE *ET AL.*, "BRAZING TUNGSTEN FOR HIGH TEMPERATURE NUCLEAR SERVICE IN HYDROGEN," REPORT TN D-3944, NASA, MAY 1967

Reactive Metals

Of the reactive metals, titanium and its alloys are the most likely to be fabricated outside of a specialized facility. It is a structural material that finds varied uses, ranging from aircraft to body implants. The use of zirconium is most common in nuclear applications. Beryllium has many specific aerospace applications, because of its low density and high modulus values, but is most commonly utilized in its pure form, in x-ray window applications. Only beryllium and titanium have useful properties after exposure to elevated temperatures in an oxidizing atmosphere.

Titanium Alloys

Titanium is the most commercially available material among both reactive and refractory metals, in terms of its number of alloys, available product forms, and metallurgical complexity. These factors all impact brazing recommendations.

Because of the cost of titanium, its use is usually confined to those applications that take advantage of its specific properties, such as high strength-to-weight ratio, corrosion resistance, and high-temperature strength. Aerospace applications include airframe and engine components for both aircraft and spacecraft. Applications that require its corrosion resistance include chemical/petrochemical processing, marine exposure, and medical uses, such as instruments and implants. There are also emerging applications in the automotive and consumer products industries.

Titanium alloys are available in commercially pure and alloy compositions. They are generally categorized into four groups, depending on the principal phases present in the microstructure:

- COMMERCIALLY PURE (CP) ALLOYS (HEXAGONAL CLOSE-PACKED, OR HCP)
- ALPHA ALLOYS (HCP)
- ALPHA-BETA ALLOYS
- BETA ALLOYS (BODY-CENTERED CUBIC, OR BCC)

In pure titanium, the transformation (beta transus) occurs at 888 °C (1630 °F). By alloying, the alpha phase can be stabilized to increase the beta transus. Other alloy compositions may stabilize the beta phase or result in a two-phase alpha-beta structure. These various structures have a marked effect on mechanical properties and their response to heat treatment.

Commercially Pure and Alpha Alloys. The alpha-stable compositions are the CP grades and those alloyed with alpha stabilizers. The variations in strength of the CP grades depend on purity, particularly in terms of oxygen, nitrogen, hydrogen, silicon, and iron. The control of oxygen and iron is specified in order to control strength. The other interstitials are minimized to avoid embrittlement. As a class, the CP alloys are usually specified for applications requiring corrosion resistance, but they have mechanical properties that are useful for structural applications. The Ti-0.2Pd and Ti-0.3Mo-0.8Ni grades are also considered to be CP grades and are specified for more-corrosion-resistant applications. These alloys are generally used in the annealed condition and cannot be strengthened by heat treatment.

Alpha alloys are stabilized with aluminum and tin/zirconium. These alloys have both high-temperature and cryogenic applications. Their creep strengths are higher than those of the alpha-beta and beta compositions. The extra-low-interstitial (ELI) grades are specified for severe applications. The alpha alloys also have good weldability, but poor forging properties and an inability to be strengthened by heat treatment.

Near-beta alloys, which contain small amounts of beta stabilizers, are included with the alpha alloys. They have enhanced creep strength and elevated-temperature properties.

Alpha-beta alloys contain both alpha and beta stabilizers. The beta stabilizers are generally vanadium, molybdenum, and manganese. Titanium 6Al-4V, a classic example of an alpha-beta alloy, represents over 40% of the titanium produced.

Although these alloys can be strengthened by heat treatment, some of them, including Ti-6Al-4V, are used in the annealed condition. The heat treatment consists of quenching from the solution heat-treating temperature, followed by aging (solution-treated and aged, or STA, condition). The phases that are present after quenching vary with the alloy, the solution temperature, the cooling rate, and the cross-section size, but a beta phase will always be retained. Aging decomposes the retained beta as a fine alpha structure in the retained beta matrix and, accordingly, strengthens the alloy. Aging temperatures are between 425 and 650 °C (795 and 1200 °F). The equiaxed annealed structure has higher ductility

and better low-cycle fatigue properties than the STA condition. An acicular structure results from the STA heat treatment and has higher creep resistance, higher fracture toughness, and higher stress-corrosion resistance than the annealed condition.

The beta alloys have high concentrations of beta stabilizers that slow the transformation from the beta to the alpha phase. After normal processing, the structure is nearly all beta. The beta phase partially transforms into a finely dispersed alpha structure while aging at temperatures from 450 to 650 °C (840 to 1200 °F). When these alloys are in the beta phase and are solution heat treated, their ductility is excellent and their abilities to be forged and formed are superior to those of the alpha-beta alloys. After aging, the beta alloys are generally stronger and have higher fracture toughness values than the alpha-beta alloys, but they have lower creep resistance and ductility.

Applications that utilize the high formability and strength of beta alloys include complex aerospace structures and fasteners. The compositions and physical properties of selected titanium alloys are shown in Table 1.

Restrictive Titanium Brazing Attributes. Because of the variety of titanium alloys and corollary heat treatments, there are brazing limitations that can avoid possible compromise of the mechanical properties after brazing. To maintain properties, the brazing alloys must be selected to ensure that the brazing temperature will be within the recommended heat treatments of the alloys being brazed. Commercially pure and alpha alloys should be brazed below the beta transus to prevent a coarse structure that reduces ductility. Although alpha-beta alloys are usually solution treated below the beta transus, the beta transus can be exceeded in order to obtain specific high-temperature properties. Brazing temperatures higher than those specified for beta alloys can result in grain coarsening and a loss in ductility.

For any titanium brazement, it is recommended that the design requirements for strength and ductility be reviewed to confirm the suitability of the selected alloy and of using a brazed approach. Certain combinations that require high-temperature brazing and/or quenching may not be acceptable. For example, the brazing of honeycomb sandwich, or any thin-sheet metal structure, is not practical with an alloy that requires quenching for the required properties. When possible, the brazing filler alloy should be selected to coincide with a standard heat treatment, such as an annealing or a solution heat-treating temperature.

Brazing filler metal selection should occur within the restraints noted above and with consideration to the environment to which the brazement will be exposed. Of particular concern is the possibility of galvanic corrosion. Although it is a reactive metal, oxidized titanium is noble to many structural alloys. In critical applications, braze samples should be exposed to the end-use environments to ensure that there is not preferential corrosion of the brazing filler alloy.

A review of titanium brazing literature reveals a considerable body of work that includes many compositions that would not be commercially available. Considerable effort was expended on silver, both pure and alloyed, with various combinations of lithium, copper, manganese, cadmium, and tin. Pure silver appears preferable to most of the silver alloys. The Ag-Cu-Li alloys were successful if the brazing cycles were short to prevent excessive erosion of the base metal and to minimize the formation of the brittle Cu-Ti intermetallic.

Aluminum alloys, including 3003 and 4043, are also available, if their lower melting points are acceptable. Pure aluminum (99.9%) forms a thicker intermetallic zone than the preferred alloys, because the alloy additions, particularly silicon, reduce intermetallic formation.

A 82Al-9Pd-9Ga alloy is commercially available. It easily wets titanium and has good strength and corrosion resistance. Base-metal erosion is minimal when short brazing cycles and minimum brazing temperatures are used.

A Ga-Pd-Ag brazing filler alloy was used on two structural joints on the Mars Viking landing instrument. One application was a triangular truss structure consisting of a socket comer fitting and three tubular legs. A cold-wall vacuum furnace was used in combination with a short brazing cycle, about 5 min at temperature. After brazing, the part did not meet dimensional tolerances because of an improperly machined fixture. The brazement was separated by immersion in HNO_3 until the brazing filler metal was dissolved. There was essentially no attack of the titanium by the molten filler and the assembly was rebrazed on modified fixtures. Because of the required close tolerances of the part, the fixtures were made of titanium to avoid potential problems with thermal expansion differences.

The second Viking application was a titanium thermal standoff that was brazed to 304L stainless steel. The stainless steel was electrolytically plated with nickel and the part was brazed in a cold-wall vacuum furnace. Although wetting of the stainless steel by the Ga-Pd-Ag filler was not satisfactory, the nickel plating was easily wet by the filler.

The Pd-Cu-Ag series of alloys is also reported to have superior wetting characteristics on titanium, but its use would be limited by a high copper content. Ti-Ni-Cu alloys are available in several compositions and are increasingly employed for titanium brazing. Commercially available titanium brazing alloys are identified in Table 3.

TABLE 3 BRAZING FILLER METALS FOR REACTIVE METAL BRAZING

BRAZING ALLOYS	**LIQUIDUS TEMPERATURE**		**SOLIDUS TEMPERATURE**		APPLICATIONS
	°C	**°F**	**°C**	**°F**	
AL-0.12CU-1.2MN (3003)	649	1200	638	1180	**BERYLLIUM, LOW-STRENGTH TITANIUM APPLICATIONS**
AL-5.2SI (4043)	632	1170	574	1065	**BERYLLIUM, LOW-STRENGTH TITANIUM APPLICATIONS**
AG-30CU-10SN	718	1324	602	1116	**BERYLLIUM**
AG-28CU-0.2LI	779	1434	779	1434	**BERYLLIUM, HIGH-TEMPERATURE APPLICATIONS**
AG-5AL	810	1490	780	1436	**TITANIUM ZIRCONIUM**
TI-20ZR-20CU-20NI	848	1558	842	1548	**TITANIUM ZIRCONIUM**
TI-15NI-15CU	850	1562	830	1526	**TITANIUM ZIRCONIUM**
AG-26.7CU-4.5TI	850	1562	830	1526	**TITANIUM ZIRCONIUM**
AG-9PD-9GA	880	1616	845	1553	**TITANIUM ZIRCONIUM**
TI-15CU-15NI	932	1710	902	1656	**TITANIUM ZIRCONIUM; ALTERNATE CHEMISTRY WITH LOWER MELTING POINTS AVAILABLE**
AG-21.3CU-24.7PD	950	1742	900	1652	**TITANIUM, ZIRCONIUM; ALTERNATE CHEMISTRY WITH LOWER MELTING POINTS AVAILABLE**
ZR-8CR-8NI	950(A)	1742(A)	. . .	. . .	**ZIRCONIUM, NOT A COMMERCIAL ALLOY**
ZR-5BE	990(A)	1814(A)	. . .	. . .	**ZIRCONIUM, NOT A COMMERCIAL ALLOY**
TI-48ZR-4BE	**985(A)**	**1805(A)**	**. . .**	**. . .**	**TITANIUM, ZIRCONIUM, NOT A COMMERCIAL ALLOY**

(A) BRAZING TEMPERATURE

Of the noncommercial alloys, there has been success with Ti-Zr-Be and Ag-Al-Mn alloys. The beryllium additions have potential health considerations and the section of this article that addresses beryllium should be reviewed before its use is considered.

For all but the most-benign applications, the selection of titanium filler alloys and brazing cycles should be supported by braze samples that simulate the fabrication and design requirements.

Zirconium Alloys

Zirconium is available in most common mill products, such as sheet, strip, bar, plate, and billet. It can be forged and extruded. Commercially pure material and alloys that contain tin or niobium are available. The commercial grades may contain up to 4.5% hafnium, a neutron absorber, which prohibits their use in nuclear applications. The successful use of zirconium as a nuclear material is due to its low thermal neutron cross section, good mechanical properties, and excellent hot-water and steam corrosion resistance. Its high corrosion resistance to both organic and inorganic acids and its immunity to attack by alkalies has led to applications in the petrochemical and food processing industries.

Pure zirconium is hexagonal close-packed (alpha phase) at room temperature. It transforms to body-centered cubic at about 870 °C (1600 °F). The commercially pure grades and the tin-containing alloys are alpha structures at room temperature. Niobium is a beta stabilizer, and its addition to zirconium results in an alpha-beta structure at room temperature with a beta transus at 854 °C (1570 °F).

During primary fabrication, zirconium alloys are worked in the beta region. This is followed by a solution heat treatment in the beta region, at approximately 1065 °C (1950 °F), and a water quench. Further processing is performed in the alpha region to preserve the interstitial distribution established by solution heat treatment. The retention of fine disbursement of interstitials is critical to the corrosion resistance of the zirconium. Subsequent heating near or over the beta transus will redistribute the intermetallics, with a resulting loss in corrosion resistance and mechanical properties.

The composition and physical properties of zirconium alloys are shown in Table 1.

Brazing Filler Metal Selection. The narrow commercial use of zirconium has limited the development of brazing alloys. Basic joints have utilized alloys of copper, silver, and phosphorus, but such a joint would not have the corrosion resistance of the parent material. The major effort in the area of zirconium brazing has centered on nuclear applications that require high strength, high temperature, and hot-water corrosion resistance.

The wetting of zirconium alloys is not a particular problem, but the brazing filler metal selection is critical, because of the demanding corrosion resistance of most zirconium applications, and testing in the proposed use environment is compulsory.

Brazing filler alloys that have demonstrated acceptable pressurized hot-water corrosion properties after 1450 h at 360 °C (680 °F) include Zr-5Be, Cu-20Pd-3In, and Ni-20Pd-10Si. Zircaloy brazed with Zr-50Ag or Zr-29Mn filler alloy has shown acceptable corrosion rates and mechanical properties after testing in pressurized hot water at 315 °C (600 °F) for nearly 3000 h.

Brazed zirconium components are predominantly used in nuclear applications, particularly fuel rods. One example is the brazing of Zr-1.5Sn alloy tube cap assemblies using Zr-5Be alloy. Another example was the brazing of Zr-1.5Sn alloy to molybdenum using a 48Ti-48Zr-4Be brazing filler metal. The 48Ti-48Zr-4Be alloy has also been effective in joining zirconium to alumina. Note that the beryllium content of these fillers limits their use to facilities that have the proper beryllium control procedures.

The filler metals shown in Table 3 for use with titanium are acceptable for use with zirconium.

Beryllium Alloys

Virtually all beryllium mill forms are based on powder metallurgy techniques. Ingot sheet from cast material has limited availability. Large blocks of beryllium that approach 1270 mm (50 in.) in diameter and 2995 kg (6600 lb) are produced by the vacuum hot pressing of beryllium powder. Because the beryllium is very active, the powder is oxidized. The resulting pressing contains a significant oxide content. It is partially through the control of this oxide that the final properties of the beryllium are achieved. Them are structural, optical, and instrument grades of beryllium to permit design optimization. Other forms of beryllium sheet, plate, or extrusions are fabricated from the block material.

Beryllium has a low density, 2.7 g/cm^3, and a high modulus of elasticity, 295 GPa (43 × 10^6 psi). It is this high specific stiffness that compels the use of beryllium for aerospace applications. Nuclear applications provide another large market for beryllium.

The design of beryllium hardware is not without problems. The high stiffness and low ductility values of the material may result in failures if proper design requirements are not followed. The elongation values of beryllium mill products range from 1 to 3% for block forms, 5 to 10% for plate and extrusions, and 20% for sheet. These elongations are for the longitudinal direction; wrought beryllium is very anisotropic. Transverse properties are significantly lower. Thus, the uniaxial tensile properties will not indicate how beryllium will perform under complex stress conditions.

The aluminum-beryllium alloy system has had considerable attention in an effort to increase ductility with some loss in stiffness. Lockalloy, a 38% aluminum alloy originally developed around 1961, has a ductility and weldability advantage, compared with unalloyed beryllium, but its applications were limited because of its lower stiffness. The Al-Be system is again becoming available in several compositions. Because the two metals are mutually immiscible, the alloys are

processed to produce a fine structure of aluminum and beryllium. Beryllium alloy compositions and physical properties are shown in Table 1.

Although beryllium has a hexagonal close-packed structure, it is unlike titanium and zirconium in that it does not undergo a phase change at elevated temperatures. Wrought products must be worked hot, at temperatures from 800 to 1000 °C (1470 to 1830 °F). The temperatures used during processing are adjusted to prevent recrystallization, and the strength of these products rises significantly with increasing warm work.

The annealing temperature varies with the amount of work, but is reported to be between 725 and 900 °C (1340 and 1650 °F). The mechanical properties are reduced by recrystallization and grain coarsening if the material is heated too much, but there are no thermal strengthening treatments for beryllium.

The brazing of beryllium is well established, partly because of the difficulties of other joining methods. Because of a brittle, coarse-grained structure, the properties of welded joints have low strength and ductility, and an increase in the DBTT. Although mechanical fasteners, such as bolts and rivets, are used, careful design is required to prevent cracking during assembly and use. The Al-Be alloys are ductile and can be welded.

Brazing Filler Metal Selection. Brazing filler alloys for beryllium are primarily selected from the zinc, aluminum, and silver alloys. The advantages of zinc are that no reactions with the beryllium occur, the brazing temperatures are low to prevent recrystallization, and adequate strengths are obtained. Strength decreases rapidly with elevated temperatures. Aluminum systems are the most widely used brazing filler alloys. They have the same advantages as zinc, but higher strength values at both room temperature and elevated temperatures. The silver systems provide higher joint strengths at elevated temperatures, but at some sacrifice to parent metal strength because of recrystallization.

The wettability of beryllium with any brazing filler metal is difficult, and the preplacement of aluminum fillers is recommended. With close-tolerance joints, capillary flow is possible with the silver alloys, but not always predictable. Although fluxless brazing is possible, the use of proprietary fluxes is common. With flux, joint tolerances are less critical, and wetting of the base metal is more predictable. However, the potential corrosion problems from residual flux must be considered in the design and postbraze cleaning of the brazed component.

Aluminum-silicon alloys are the most common aluminum-base filler metals, although pure aluminum is also recommended. Shear strength values that exceed 62 MPa (9 ksi) have been reported, and useful strengths are possible at 175 °C (345 °F). Silver brazing was an early development in the beryllium joining process and is still recommended for joints that require high-temperature strength. The 60Ag-30Cu-10Sn, Ag-7Cu-0.2Li and pure silver have both been used with success. The shear strength of silver-brazed beryllium strongly depends on the braze cycle, and strength values between 140 and 275 MPa (20 and 40 ksi) have been reported. Lower brazing temperatures and short brazing cycles favor higher strengths. Copper, silver, and copper/silver filler metals were evaluated using low pressure (2.1 MPa, or 300 psi) and extended braze cycles (up to 8 h) to evaluate joints for high-temperature operation. With this braze/ diffusion approach, shear-strength values of 140 MPa (20 ksi) were obtained in the temperature range from 540 to 650 °C (1000 to 1200 °F).

The brazing of aluminum-beryllium alloys would be similar to that of beryllium, but the brazing filler selection must be based on the melting point of the aluminum-base material and would be limited to the zinc and aluminum-silicon alloys.

Health and safety rules must be thoroughly understood before conducting brazing operations that involve beryllium. Breathing of beryllium oxide has caused a loss of lung capacity in a manner similar to coal dust. Beryllium particles that enter open wounds have caused chronic ulcerations. Any beryllium process that can generate dust must be controlled. In machining operations, this is usually accomplished by using vacuum cleaners with output filtration that precludes the exhaust of any beryllium particles. Any etching, fluxing, or other treatments that may leave a beryllium dust residue after drying also must be controlled. Approved procedures must be used to dispose of chips, scrap material, and solutions.

Beryllium handling guidelines can be found in the Code of Federal Regulations, Title 29, Part 1910. The Office of Safety and Health Administration (OSHA) has established limits of atmospheric contamination at 2 $\mu g/m^3$ averaged over an 8 h day. The Environmental Protection Agency (EPA) has established 10 g/day as the maximum beryllium emission into the atmosphere. The time and cost of meeting safety requirements may be prohibitive for random beryllium brazing operations.

The handling of bulk beryllium poses minimal safety issues. Elevated-temperature heating below 780 °C (1435 °F) does not produce volatile or nonadherent oxides. Brazing can be accomplished with standard equipment if the surfaces to be brazed are plated to permit wetting of the filler metals and if no flux is used. Either vacuum or inert gas atmospheres would be suitable for fluxless brazing, and no postprocess cleaning would be required. Although the preceding procedure should safely permit beryllium use under normal conditions, appropriate approvals must be obtained.

Roy I. Batista, TRW, Inc.

Brazing Procedures

The joint designs that are valid for brazing the more-common metals, such as stainless steel or copper, are equally suitable for the reactive and refractory metals. At brazing temperatures, joint clearances should be between 0.013 and 0.050 mm (0.0005 and 0.002 in.) when using fillers that have good capillary flow. As happens with other metals, increased porosity and lower strength result from excessive joint clearances. Filler metals that have minimal wettability with the base metal should be preplaced in the braze joint and, when possible, a small load should be applied to the joint to accommodate some of the gap at the brazing temperature.

Because of the low thermal expansion of this group of metals, the calculation of the gap at the brazing temperature is of particular concern when brazing dissimilar metals that have great differences in thermal expansion. In tubular joints, the high-expansion material should be on the outside, so that the joint is in compression upon cooling. If these joints must be thermally cycled, then thermal fatigue failure can be a likely result. Therefore, such applications should not be brazed. For example, shear specimens of Mo-50Re brazed to L-605 with 82Au-18Ni failed after 20 to 30 cycles after cycling to 700 °C (1290 °F).

Fixturing. Whenever possible, the design should incorporate provisions for self-fixturing. Fixturing becomes more difficult with increasing braze temperatures. Two techniques that could avoid the use of hard tooling are alignment pins and tack welding, if satisfactory equipment is available in the latter case.

The need to fixture refractory metal brazements is required, just as it is for the brazing of any metal. However, it is complicated for refractory metals, because of their low thermal expansion values. The expense of fabricating fixtures from refractory metals is probably prohibitive for small-volume jobs. At lower temperatures, steel tools with springs or flexures that are made from stainless steel, superalloys, or molybdenum can be used to control the position of the brazements. Higher-temperature brazing requires that the tools be made from refractory materials, metals, or ceramics.

Because very clean atmospheres are usually recommended for brazing the reactive and refractory metals, the fixture is likely to join to the brazement if stop-off materials are not provided. Oxide slurries are suitable, as are more-permanent solutions, such as ceramic pads or flame-sprayed coatings. Because of the reactivity of this group of metals, any stop-off materials should be high in purity and nonreactive with the brazement. Zirconium oxide may not be suitable in contact with zirconium alloys at high temperature.

Surface preparation techniques include prebraze cleaning, surface plating, or other measures that improve the brazeability of the design or accommodate less-than-ideal brazing conditions.

The direct brazing of reactive and refractory metal surfaces, as discussed in this article, is based on the assumption that the filler metals would wet these surfaces. Another approach is to plate the surfaces with a metal, such as nickel, and then to consider the braze as a nickel joint, rather than a refractory or reactive metal. Although the use of platings has value, it also has disadvantages, because platings can peel or blister and because they are not suitable for refractory metal brazed assemblies that must operate at high temperatures.

Beryllium forms the most refractory oxide in this group of metals and is the most difficult to braze. Techniques such as electroplating or vacuum depositing coatings such as nickel, copper, or titanium have been used to enhance wettability. When powdered brazing filler alloys are used, additions of titanium hydride have been made. During brazing, the hydride decomposes and plates the beryllium surfaces with titanium.

Because of the reactivity of the reactive and refractory metals, prebraze cleaning is more important than it is when iron-, nickel-, or copper-base alloys are used. The sequence below is one of many that can be used:

- *ALKALINE CLEAN*, WHICH CAN BE PRECEDED BY SOLVENT CLEANING, AS REQUIRED BY THE SURFACE CONTAMINANTS
- *WATER RINSE*, PREFERABLY WITH DEIONIZED WATER
- *ACID PICKLE*. FOR TITANIUM, ZIRCONIUM, AND BERYLLIUM, USE 30 TO 40% HNO_3 WITH 1 TO 5% HYDROFLUORIC ACID, FOR 1 TO 5 RAIN AT 60 °C (140 °F). FOR NIOBIUM, TANTALUM, TUNGSTEN, AND MOLYBDENUM, USE 40 TO 70% HNO_3 WITH 10 TO 30% HYDROFLUORIC ACID. THE HIGHER CONCENTRATIONS ARE MORE SUITABLE FOR TANTALUM AND NIOBIUM; USE AT 55 TO 65 °C (130 TO 150 °F).
- *HOT-WATER RINSE*, PREFERABLY WITH DEIONIZED WATER
- *DRY AND PACKAGE* TO PREVENT CONTAMINATION BEFORE BRAZING

Parts should be brazed as soon as possible after brazing to minimize oxide formation. All cleaning of titanium must exclude any chlorinated solutions and menthol alcohol. Titanium is prone to stress-corrosion cracking when exposed to these solutions.

Brazing of Refractory and Reactive Metals

Roy I. Batista, TRW, Inc.

Brazing Equipment

Strict control of the brazing atmosphere is mandatory for the successful brazing of the reactive and refractory metals. The use of marginal atmospheres will, at a minimum, reduce the quality of reactive metal brazements and can potentially destroy the refractory metals, because of oxidation.

A cold-wall, high-vacuum furnace is highly recommended for the brazing of reactive and refractory metals. At brazing temperatures, a vacuum of 0.013 Pa (10^{-4} torr) can be considered a minimum level, and the leak rate of the furnace should be less than 1 μm/h (40 μin./h). Refractory metal heating elements are preferred to those of carbon in order to minimize potential contamination. The use of a cryogenic cold trap in diffusion-pumped equipment is also highly desirable.

The potential contamination problems associated with the use of hot-wall vacuum furnaces make their use questionable for high-quality work.

Induction brazing is a preferred process when the size and design of the hardware permits its use. However, the control of the brazing atmosphere is still critical. Vacuum induction, at a level of 0.013 Pa (10^{-4} torr), is acceptable, as are inert gases such as argon. Bottled inert gases are often not as clean as labeled, and a gettering system is recommended to minimize residual water and oxygen. A stainless steel tube filled with zirconium or titanium turnings and operating at about 800 °C (1470 °F) will reduce water to a few parts per million. A liquid-argon source minimizes gas contamination problems.

Tungsten and molybdenum can also be furnace or induction brazed in a hydrogen atmosphere, if the filler metal is compatible with hydrogen. The hydrogen dew point should be below -50 °C (-60 °F).

It is recommended, when furnace or induction brazing, that the equipment be cycled to a temperature higher than the braze temperature before actual brazements are made. This technique will completely heat the equipment and minimize outgassing problems during the subsequent brazing operation. If the recommended brazing equipment is not available, then successful brazing may be possible by protecting the brazement with metal foil, such as tantalum, which reacts with water vapor and oxygen and thereby offers some protection to the brazement. To check this approach or to check any brazing equipment, a piece of tantalum foil can be processed through the braze cycle and then checked for foil ductility. A more-sensitive test would be to metallographically examine the foil for contamination or to run a carbon and gas analysis on the sample and compare it to the starting material.

Although torch brazing with fluxes has been used to join reactive and refractory metals, the likely contamination of the base metal and future corrosion problems associated with residual flux should discourage this approach. Heliarc torch brazing has been performed within a dry box using inert gas atmospheres that are purified, as for induction brazing. The heating of components in an electron-beam welder also can be useful when permitted by the component configuration.

The use of flux, with one exception, is not recommended. The exception is the brazing of beryllium, especially with the zinc- and aluminum-base filler metals. The beryllium oxide will prohibit wetting by these fillers without the use of flux.

Whatever braze equipment is used, the lowest temperature for the shortest amount of time that will achieve the desired joint properties should be used as a technique to reduce contamination and erosion in the base metal.

References

1. M.M. MCDONALD, *ET AL.*, THE WETTABILITY OF BRAZING ALLOYS ON MOLYBDENUM AND TZM, *WELD. J. SUPPL.*, OCT 1988
2. G.M. SLAUGHTER *ET AL.*, WELDING AND BRAZING OF ADVANCED REFRACTORY ALLOYS, *SPACE SHUTTLE MATERIALS PROCEEDINGS*, SAMPE, OCT 1971
3. L.B. LUNBERG *ET AL.*, BRAZING OF MOLYBDENUM AND TUNGSTEN FOR HIGH-TEMPERATURE SERVICE, *WELD. RES. SUPPL.*, OCT 1978
4. R.I. BATISTA, TRW, INC., UNPUBLISHED NOTES
5. C.W. HAYNES, "DEVELOPMENT OF LOW TEMPERATURE BRAZING OF TUNGSTEN FOR HIGH TEMPERATURE SERVICE," REPORT R>D>R 1249-1/DTIC AD 260580, DEFENSE TECHNOLOGY INFORMATION CENTER, MAY 1962
6. T.J. MOORE *ET AL.*, "BRAZING TUNGSTEN FOR HIGH TEMPERATURE NUCLEAR SERVICE IN HYDROGEN," REPORT TN D-3944, NASA, MAY 1967

Brazing of Refractory and Reactive Metals

Roy I. Batista, TRW, Inc.

Selected References

- N.C. COLE AND G.M. SLAUGHTER, DEVELOPMENT OF BRAZING FILLER METALS FOR MOLYBDENUM, *NUCL. TECHNOL.*, VOL 26, JUNE 1975
- G.D. CREMER, J.R. WOODWARD, AND L.A. GRANT, BERYLLIUM BRAZING TECHNOLOGY, *SAE TRANS.*, VOL 76, SECT. 24, SAE REPRINT 670805, REPRINTED 1985
- A.H. DONOVAN, "BRAZE ALLOY DEVELOPMENT FOR ZIRCALOY," REPORT WHC-SA-0317-FP, WESTINGHOUSE HANFORD COMPANY, MAY 1988
- A.H. FREEDMAN *ET AL.*, "TANTALUM AND MOLYBDENUM BRAZING TECHNIQUES," TECHNICAL REPORT ML-TDR-64-270 PART II, AIR FORCE MATERIALS LABORATORY, SEPT 1964
- M. GARIN AND L.A. GRANT, "DESIGN AND FABRICATION OF BRAZED BERYLLIUM ASSEMBLIES," PAPER 83-0868-CP, 24TH ANNUAL AIAA SDM CONFERENCE, MAY 1983
- W.E. LUNBLAD, "INVESTIGATION OF WELDING AND BRAZING OF MOLYBDENUM AND TZM ALLOY TUBES," REPORT SRI-MME-91-097-7244, SOUTHERN RESEARCH INSTITUTE, FEB 1991

- A. ONZAWA *ET AL.*, BRAZING OF TITANIUM USING LOW MELTING POINT TI-BASED FILLER METALS, *WELD. RES. SUPPL.*, DEC 1990
- L.H. STONE *ET AL.*, RECRYSTALLIZATION BEHAVIOR AND BRAZING OF THE TZM MOLYBDENUM ALLOY, *WELD. RES. SUPPL.*, JULY 1967
- Y. SUEZAWA, BRAZING CHARACTERISTICS OF ZIRCONIUM AND SILVER FILLER METALS TO 304L STAINLESS SINTERED STEEL, *BRAZING SOLDERING*, NO. 6, SPRING 1984
- T. TAKEMOTO *ET AL.*, STRENGTH OF TITANIUM JOINTS BRAZED WITH ALUMINUM FILLER METALS, *TRANS. JWRI*, VOL 19, WELDING RESEARCH INSTITUTE OF OSAKA UNIVERSITY, NOV 1990
- T. TAKEMOTO AND I. OKAMOTO, INTERMETALLIC COMPOUNDS FORMED DURING BRAZING OF TITANIUM WITH ALUMINUM FILLER METALS, *J. MATER. SCI.*, APRIL 1988
- M.L. TORTI AND R.W. DOUGLASS, "BRAZING OF TANTALUM AND ITS ALLOYS," REFRACTORY METALS AND ALLOYS III APPLIED PROCESS CONFERENCE, AIME, 1963
- W.R. YOUNG, "ALLOY SYSTEMS FOR BRAZING OF COLUMBIUM AND TUNGSTEN," REFRACTORY METALS AND ALLOYS III APPLIED PROCESS CONFERENCE, AIME, 1963

Brazing of Ceramic and Ceramic-to-Metal Joints

A.J. Moorhead and W.H. Elliott, Jr., Oak Ridge National Laboratory H.-E. Kim, Seoul National University

Introduction

THIS ARTICLE is intended to assist in the development of procedures for the brazing of ceramic-to-ceramic or ceramic-to-metal joints for service under one or more of the following conditions: elevated temperatures, mechanical or thermal stresses, or corrosive atmospheres. Also described in this article are those factors that must be considered when preparing a procedure for the brazing of graphitic materials. However, because the interest in joining graphite is not nearly as intense at this time as the interest in joining ceramics, the former topic will be given less attention.

There is worldwide interest in using ceramic materials for applications not previously considered, that is, engineering applications. In these proposed or actual applications, ceramic-to-ceramic or ceramic-to-metal joints must be compatible with elevated temperatures and environments that are either oxidizing or corrosive, and they must have significant mechanical properties, including strength and fracture toughness. In addition, the joints must have demonstrable thermal stability at the temperatures of interest.

Material scientists and engineers now have an increased awareness of the critical nature of joints, their microstructural complexity, and the possibilities for joining a given set of components for a specific application. It should be noted that the uses for ceramic materials are changing rapidly, with a major emphasis on structural applications. Furthermore, these materials are becoming more complex, in terms of being strengthened and toughened by transformation processes, the addition of other ceramic or metallic materials, or the development of performance-enhancing microstructures made possible by processing. The successful use of advanced ceramic materials requires the development of equally advanced joining materials and technology.

Although advanced or fine ceramics also include the electronic ceramics, such as those used as substrates and encapsulants, ionic conductors, piezoelectric devices, and high-critical-temperature superconductors, this category of materials and the related joining technology is outside the scope of this article.

A primary impetus behind the emphasis on structural ceramics is the desire for improved efficiency and increased component life in various internal-combustion engines. For example, recent reviews of current research on ceramic joining technology in Europe, the United States, and Japan (Ref 1, 2, 3) strongly emphasize the research and development efforts that are aimed at utilizing structural ceramics in advanced heat engines.

Ceramic components are either being considered or actually used in a wide range of applications in experimental and commercial automotive applications. These applications include:

- VARIOUS WEAR-REDUCING PARTS IN CONVENTIONAL GASOLINE OR DIESEL ENGINES (REF 4)
- IN-CYLINDER COMPONENTS FOR LOW-HEAT-REJECTION DIESEL ENGINES (REF 1)
- SMALL CERAMIC TURBINE ROTORS THAT CAN REACH 900 °C (1650 °F) AND ARE SUBJECT TO A COMBINED CENTRIFUGAL AND THERMAL STRESS OF 200 MPA (29 KSI) IN TURBOCHARGERS FOR CONVENTIONAL GASOLINE ENGINES (REF 5) OR LARGER ROTORS THAT ARE EXPOSED TO EVEN MORE SEVERE TEMPERATURE AND STRESS CONDITIONS IN RELATIVELY SMALL, HIGH-EFFICIENCY, ADVANCED GAS TURBINE ENGINES (REF 6, 7, 8)

Many of these applications require ceramic-to-ceramic or ceramic-to-metal joints.

A second major impetus, at least in the United States, is the development of ceramic heat exchangers to recover the waste heat that is traditionally lost in the high-temperature, corrosive exhausts of industrial furnaces (Ref 9, 10). It should be obvious that much of the present interest in using ceramics for high-temperature structural applications is based on the worldwide desire to reduce the use of fossil fuels through energy conservation.

Carbon and graphite are widely used as electrodes in metallurgical applications and as moderator materials in nuclear applications. Specialized uses include rocket nozzles, guide vanes, nose cones, electric motor brushes and switches, bushings and bearings, high-temperature heat exchangers, and plumbing, as well as heart valves, synthetic teeth posts, air-frame composites, and high-performance brake linings. An antenna used for heating the plasma in a fusion reactor experiment, a recent example of a successful application, is discussed later in this article.

It is important to note that in the very early stages of brazing procedure development, there must be a clear understanding of the type of ceramic or graphite involved, how it differs from the more-familiar metallic materials, and whether the ceramic or graphite is to be attached to the same material, a similar material, or a metal. Such an understanding will facilitate the selection of a brazing filler material, the selection and use of a transition material in ceramic-to-metal joints, and the selection of a thermal cycle that is compatible with the heat-treatment response of the materials to be joined. Therefore, the following two sections describe ceramics and graphites, respectively, in terms of how they are made and how they differ from metals. These sections are followed by a discussion of procedure development and the available brazing processes, as well as a brief description of factors that are important to ceramic-to-metal joints.

References

1. D.A. PARKER, TECHNOLOGICAL REQUIREMENTS FOR DESIGNING INTERFACES FOR MECHANICAL AND THERMAL APPLICATIONS, *DESIGNING INTERFACES FOR TECHNOLOGICAL APPLICATIONS: CERAMIC-CERAMIC, CERAMIC-METAL JOINING,* S.D. PETEVES, ED., ELSEVIER, 1989, P 3-32
2. R.E. LOEHMAN, CERAMIC JOINING IN THE U.S., *DESIGNING INTERFACES FOR TECHNOLOGICAL APPLICATIONS: CERAMIC-CERAMIC, CERAMIC-METAL JOINING,* S.D PETEVES, ED., ELSEVIER, 1989, P 235-245
3. T. SUGA, CURRENT RESEARCH AND FUTURE OUTLOOK IN JAPAN, *DESIGNING INTERFACES FOR TECHNOLOGICAL APPLICATIONS: CERAMIC-CERAMIC, CERAMIC-METAL JOINING,* S.D. PETEVES, ED., ELSEVIER, 1989, P 247-263
4. L.M. SHEPPARD, AUTOMOTIVE PERFORMANCE ACCELERATES WITH CERAMICS, *AM. CERAM. SOC. BULL.,* VOL 69 (NO. 6), 1990, P 1012-1021
5. K. MATOBA, K. KATAYAMA, M. KAWAMURA, AND T. MIZUNO, THE DEVELOPMENT OF SECOND GENERATION CERAMIC TURBOCHARGER ROTOR--FURTHER IMPROVEMENTS IN RELIABILITY, *AUTOMOTIVE CERAMICS-RECENT DEVELOPMENTS,* SAE P-207, SAE, 1988, P 37-46
6. S. ISHIWATA, AUTOMOTIVE CERAMIC GAS TURBINE R & D IN JAPAN, *PROC. 27TH AUTOMOTIVE TECHNOLOGY DEVELOPMENT CONTRACTORS COORDINATION MEETING,* SAE P-

230, SAE, 1990, P 287-292

7. H.E. HELMS, P.J. HALEY, L.E. GROSECLOSE, S.J. HILPISCH, AND A.H. BELL, ADVANCED TURBINE TECHNOLOGY APPLICATIONS PROJECT, *PROC. 27TH AUTOMOTIVE TECHNOLOGY DEVELOPMENT CONTRACTORS COORDINATION MEETING,* SAE P-230, SAE, 1990, P 293-301
8. J.R. KIDWELL, L.J. LINDBERG, AND R.E. MOREY, ATTAP/AGT101--YEARS PROGRESS IN CERAMIC TECHNOLOGY DEVELOPMENT, *PROC. 27TH AUTOMOTIVE TECHNOLOGY DEVELOPMENT CONTRACTORS COORDINATION MEETING,* SAE P-230, SAE, 1990, P 327-334
9. B.D. FOSTER AND J.B. PATTON, ED., *CERAMICS IN HEAT EXCHANGERS,* VOL 14, *PROC. THREE SYMPOSIA ON HEAT EXCHANGERS,* AMERICAN CERAMIC SOCIETY, 1984-1985
10. A.J. HAYES, W.W. LIANG, S.L. RICHLEN, AND E.S. TABB, ED., *INDUSTRIAL HEAT EXCHANGERS, PROC. 1985 EXPOSITION AND SYMPOSIUM ON INDUSTRIAL HEAT EXCHANGER TECHNOLOGY,* AMERICAN SOCIETY FOR METALS, 1985

Brazing of Ceramic and Ceramic-to-Metal Joints

A.J. Moorhead and W.H. Elliott, Jr., Oak Ridge National Laboratory H.-E. Kim, Seoul National University

Ceramic Materials

Structural ceramics can be categorized as either monolithic materials or ceramic-matrix composites. The monolithic materials include the aluminas, mullites, silicon carbides, silicon nitrides, and Sialons. The ceramic-matrix composites can be subcategorized as those containing a random dispersion of particles or whiskers that am intended to improve fracture toughness and those containing semicontinuous fibers that are intended to carry the load during matrix-microcracking in a service-overload condition (Ref 11). Examples of oxide-matrix composites toughened by the dispersion of a second phase or material include the transformation-toughened zirconias (TTZ) (Ref 12), zirconia-toughened aluminas (Ref 13), and silicon carbide whisker-reinforced alumina and mullite (Ref 14). Examples of continuous fiber-reinforced composites include silicon carbide fiber-reinforced glass-ceramic composites (Ref 15); glass or glass-ceramic matrices reinforced with silicon carbide, alumina, or other fibers (Ref 16); and continuous and discontinuous fiber-reinforced oxide-matrix composites in which the matrix is formed from the hydrothermal decomposition of metal-organic precursors (Ref 17).

Materials that develop a microstructure that mimics the geometry and function of second-phase additions in ceramic-matrix composites represent a recent innovation. A principal example of these so-called self-reinforced ceramics is silicon nitride, in which a beneficial acicular microstructure is developed through the combined effects of chemical composition and thermal treatment (Ref 18, 19).

Generally, structural ceramics have lower coefficients of thermal expansion (CTE) than those of metals. For example, the CTE of silicon carbide ranges from 4 to 5×10^{-6}/K and that of silicon nitride ranges from 3 to $3.5 \times l0^{-6}$/K. Of the metals, tungsten has the lowest CTE of 4.5×10^{-6}/K, but it is generally not considered to be a structural metal, because it is brittle and subject to oxidation at low temperatures. Although differences in CTE values can introduce damaging thermal stresses, even in ceramic-to-ceramic joints brazed with metals or glasses, there are significantly greater potential risks associated with ceramic-to-metal joints. Although a thin metal or glass layer at the joint may be able to yield or even fail in a noncatastrophic manner, thereby reducing damaging residual stresses, such reductions may be precluded by the material, size, and geometry of a metallic component.

The general statement that structural ceramics have lower CTEs than structural metals does not apply to the TTZ ceramics, which have CTE values that range from approximately 8 to 11×10^{-6}/K. Such relatively high thermal-expansion behavior is similar to that of structural metals, including some cast irons and ferritic and martensitic stainless steels, as well as low-expansion superalloys, such as Incoloy 909. A potentially close CTE match improves the likelihood of success when zirconia ceramics are attached to metals. The damaging residual stresses associated with other ceramic-metal combinations that have significant CTE differences can be avoided by either designing the joint to always be subjected to compressive stresses or introducing one or more interlayers or graded joints between the ceramic and the metal. Such techniques for accommodating CTE differences will be discussed below.

Another important consideration when dealing with ceramics is that they are brittle and, therefore, less tolerant of tensile loads, stress intensifiers, and thermal shock than are most metals. For example, even advanced ceramic-matrix composites have fracture toughness values ranging from only 8 MPa $\sqrt{m}$ (7.3 ksi $\sqrt{in}$) for silicon carbide whisker-reinforced alumina to 14 MPa $\sqrt{m}$ (12.7 ksi $\sqrt{in}$) for some TTZ. These values are less than those of cast aluminum alloys or cast irons. Finally, because the structural ceramics tend to have greater thermo-dynamic stability than metals, it is difficult to form in ceramic joints strong chemical bonds that enhance adhesion. As will be seen in the section "Processing" in this article, this stability can be overcome by adding active elements to brazing filler metals, or by coating the ceramic surface with an active element prior to brazing with a conventional filler method.

Processing. In general, three processing routes prevail in the fabrication of high-performance ceramics. In the sintering process, powder particles in a "green" body coalesce in order to effect densification. Sintering can be accomplished in some materials either with or without pressure. However, a totally solid-state process that does not use sintering aids is unusual. The role of the sintering aids varies from material to material. Generally, these aids promote densification by modifying the diffusional process. In some systems, the sintering aid remains as a solid throughout the process. However, in the case of the silicon nitrides and Sialons, material is transported through a liquid phase (not by surface diffusion) that is formed by the reaction of metal-oxide sintering aids and the silicon dioxide that coats each of the silicon nitride grains. In most cases, at least some residue of the sintering aid remains at the grain boundaries after the ceramic densities. This residue, which in many cases is a glass, can significantly affect the joining process.

Reaction sintering and reaction bonding are two special processes that have been developed for fabricating silicon carbide or silicon nitride ceramics without the large volume decrease associated with conventional sintering. Reaction-bonded silicon nitride is fabricated by the nitridation of a compact of silicon powder that has been formed into the desired shape by a process such as isostatic pressing, slip casting, or injection molding. Reaction-sintered silicon carbide is fabricated by exposing a compact of silicon carbide powder and carbon to molten or vapor-phase silicon, which reacts with the carbon to form *in situ* silicon carbide that bonds the original silicon carbide particles together. Reaction-sintered silicon nitride has superior creep resistance, because it is densified without sintering aids. However, it retains about 15% open porosity, which can wick a brazing filler material away from the joint area. Reaction-sintered silicon carbide can have significant amounts of unreacted metallic silicon that can affect joining by reacting with the active element (such as titanium) in the filler metal. Such reactions reduce the amount of active element available to react with the silicon carbide, thus reducing wetting tendencies and resulting in the formation of excessive amounts of embrittling titanium silicides in the joint.

Table 1 identities some structural ceramic materials and the properties that are important to the joining process. It should he noted that most of these materials are still in the development stage, having been manufactured only since the late 1970s. Any tabulation of properties serves only as a general guideline and not as engineering data. The mechanical properties of ceramics heavily depend on specimen preparation and size, as well as the type of test being conducted. These factors can also explain why there is so much variation among data compilations. It is important to note that the type of test and the specimen geometry used to characterize the strength or toughness of a brazement also can have a very significant effect on the measured property values. These effects are discussed more extensively in Ref 28.

TABLE 1 SELECTED PROPERTIES OF VARIOUS CLASSES OF STRUCTURAL CERAMICS

	FLEXURAL STRENGTH		**FRACTURE TOUGHNESS**		**COEFFICIENT OF THERMAL EXPANSION, 10^{-6}/K**	**THERMAL CONDUCTIVITY**		REF
	MPA	**KSI**	**MPA $\sqrt{m}$**	**KSI $\sqrt{in}$**		**W/M · K**	**BTU/FT · H · °F**	
ALUMINA (AL_2O_3)	200-600	30-90	3-4	2.7-3.6	7-9	15-40	8.7-23.2	**20, 21, 22, 23, 24**
PSZ (CAO, MGO)	600-1000	90-145	8-16	7.3-14.5	10	2.2	1.3	**25**
TZP (Y_2O_3, CEO_2)	800-2000	115-290	7-8	6.4-7.3	10	2.2	1.3	**21, 22, 23, 25**
ALUMINA-ZIRCONIA ($AL_2O_3 \cdot ZRO_2$)	1500-2000	220-290	8-13	7.3-11.8	. . .	. . .	. . .	**21, 22, 25, 26**
$3AL_2O_3 \cdot 2SIO_2$	200	30	2	1.8	5.3	3.5	2.0	**20, 21, 23, 27**
$2MGO_2 \cdot 2AL_2O_3 \cdot 5SIO_2$	150	20	1-2	0.9-	2	3	1.7	**20, 23**

				1.8				
SILICON CARBIDE WHISKER-REINFORCED ALUMINA ($AL_2O_3 \cdot SIC_W$)	500-800	70-115	6-10	5.5-9.1	6	$30^{(A)}$	$17^{(A)}$	**22, 89**
SILICON CARBIDE (SIC)	300-600	45-90	3-5	2.7-4.6	4.5	$85^{(A)}$	$49^{(A)}$	**22, 90**
SILICON NITRIDE (SI_3N)	**200-1200**	**30-175**	**4-10**	**3.6-9.1**	**3.6**	**$17^{(A)}$**	**$10^{(A)}$**	**22, 90**

(A) AT ROOM TEMPERATURE

It is also important to note that alumina, silicon carbide, and other materials that are often considered to be single-component materials are, in fact, families of materials that may respond very differently to the conditions imposed in a joining procedure. For example, there are a wide variety of high-alumina ceramics ranging in aluminum oxide content from 79 wt% (alumina-mullite) (Ref 29) to 99.9 wt% (Ref 30, 31). Because these materials readily densify without pressure, they are almost invariably fabricated by pressureless sintering. The aluminas not only vary widely in chemical composition (and, thus, in the amounts and composition of grain-boundary phases), but also in grain size and porosity. The various high-alumina ceramics can, therefore, be expected to respond very differently during joining or service. Differences during joining might include the formation of different interfacial reaction products, depending on chemical composition of the ceramic, or the wicking of filler metal away from a brazed interface, in the case of a porous ceramic or graphite body.

The materials that are sometimes referred to individually as silicon nitride or silicon carbide also are families of materials, in actuality. Again, the compatibility of these materials with a filler metal or glass and the responses of these materials to the brazing process may vary widely, because of differences in sintering aids, processing techniques, degree of densification, and microstructural features (such as the acicular grains in the self-reinforced silicon nitrides). Thus, as a brazing procedure is being developed, it is very important that the actual ceramic be used in all wetting, adherence, and strength or toughness studies.

References cited in this section

11. M.H. LEWIS, CERAMICS TO BE JOINED 10 YEARS FROM NOW, *DESIGNING INTERFACES FOR TECHNOLOGICAL APPLICATIONS: CERAMIC-CERAMIC, CERAMIC-METAL JOINING,* S.D. PETEVES, ED., ELSEVIER, 1989, P 271-290
12. P.F. BECHER AND M.K. FERBER, MECHANICAL BEHAVIOUR OF MGO-PARTIALLY STABILIZED ZRO_2 CERAMICS AT ELEVATED TEMPERATURES, *J. MATER. SCI.,* VOL 22, 1987, P 973-980
13. M. RÜHLE AND N. CLAUSSEN, TRANSFORMATION AND MICROCRACK TOUGHENING AS COMPLEMENTARY PROCESSES IN ZRO_2-TOUGHENED AL_2O_3, *J. AM. CERAM. SOC.,* VOL 69 (NO. 3), 1986, P 195-197
14. P.F. BECHER AND T.N. TIEGS, TEMPERATURE DEPENDENCE OF STRENGTHENING BY WHISKER REINFORCEMENT: SIC WHISKER-REINFORCED ALUMINA IN AIR, *ADV. CERAM. MATER.,* VOL 3 (NO. 2), 1988, P 148-153
15. K.M. PREWO, TENSION AND FLEXURAL STRENGTH OF SILICON CARBIDE FIBRE-REINFORCED GLASS CERAMICS, *J. MATER. SCI.,* VOL 21, 1986, P 3590-3600
16. J.J. BRENNAN, GLASS AND GLASS-CERAMIC MATRIX COMPOSITES, *FIBER REINFORCED CERAMIC COMPOSITES,* K.S. MAZDIYASNI, ED., NOYES PUBLICATIONS, 1990, P 222-259
17. T. MAH *ET AL.,* CERAMIC FIBER REINFORCED METAL-ORGANIC PRECURSOR MATRIX COMPOSITES, *FIBER REINFORCED CERAMIC COMPOSITES,* K.S. MAZDIYASNI, ED., NOYES PUBLICATIONS, 1990, P 278-310
18. C.W. LI AND J. YAMANIS, SUPER-TOUGH SILICON NITRIDE WITH *R*-CURVE BEHAVIOR, *CERAM. ENG. SCI. PROC.,* VOL 10 (NO. 7-8), 1989, P 632-645
19. T. KAWASHIMA, H. OKAMOTO, H. YAMAMOTO, AND A. KITAMURA, GRAIN SIZE DEPENDENCE OF THE FRACTURE TOUGHNESS OF SILICON NITRIDE CERAMICS, *J. CERAM.*

SOC. JAPAN, INT. ED., VOL 99 (NO. 4), 1991, P 1-4

20. W.D. KINGERY, H.K. BOWEN, AND D.R. UHLMANN, *INTRODUCTION TO CERAMICS,* WILEY, 1976
21. R.W. RICE, CERAMIC COMPOSITES: FUTURE NEEDS AND OPPORTUNITIES, *FIBER REINFORCED CERAMIC COMPOSITES,* K.S. MAZDIYASNI, ED., NOYES PUBLICATIONS, 1990, P 451-495
22. P.F. BECHER, MICROSTRUCTURAL DESIGN OF TOUGHENED CERAMICS, *J. AM. CERAM. SOC.,* VOL 74 (NO. 2), 1991, P 255-269
23. "MATERIAL PROPERTIES DATA SHEET," COORS CERAMICS COMPANY
24. P. CHANTIDUL, S.J. BENNISON, AND B.R. LAWN, ROLE OF GRAIN SIZE IN THE STRENGTH AND *R*-CURVE PROPERTIES OF ALUMINA, *J. AM. CERAM. SOC.,* VOL 78 (NO. 8), 1991, P 2419-2427
25. S. SOMIYA, N. YAMAMOTO, AND H.H. YANAGIDA, ED., *SCIENCE AND TECHNOLOGY OF ZIRCONIA III,* AMERICAN CERAMIC SOCIETY, 1988
26. D. SHIN, K.K. ORR, AND H. SCHUBERT, MICROSTRUCTURE-MECHANICAL PROPERTY RELATIONSHIPS IN HOT ISOSTATICALLY PRESSED ALUMINA AND ZIRCONIA-TOUGHENED ALUMINA, *J. AM. CERAM. SOC.,* VOL 73 (NO. 5), 1990, P 1181-1188
27. H. SCHNEIDER AND E. EBERHARD, THERMAL EXPANSION OF MULLITE, *J. AM. CERAM. SOC.,* VOL 73 (NO. 7), 1990, P 2073-2076
28. A.J. MOORHEAD AND H.-E. KIM, JOINING OXIDE CERAMICS, *CERAMICS AND GLASSES,* VOL 4, *ENGINEERED MATERIALS HANDBOOK,* ASM INTERNATIONAL, 1991, P 511-531
29. J.B. WACHTMAN, JR. AND R.A. HABER, ADVANCED CERAMICS INVOLVING ALUMINA, *ALUMINA CHEMICALS: SCIENCE AND TECHNOLOGY HANDBOOK,* L.D. HART, ED., AMERICAN CERAMIC SOCIETY, 1990, P 329-335
30. "MECHANICAL AND INDUSTRIAL CERAMICS," CAT/2T8505TKU/3000E, KYOCERA CORPORATION
31. "COORS CERAMICS--MATERIALS FOR TOUGH JOBS," BULLETIN NO. 953, COORS PORCELAIN COMPANY

89. P.H. MCCLUSKEY, R.K. WILLIAMS, R.S. GRAVES, AND T.N. TIEGS, THERMAL DIFFUSIVITY AND CONDUCTIVITY OF ALUMINA-SILICON CARBIDE COMPOSITES, *J. AM. CERAM. SOC.,* VOL 73 (NO. 2), 1990, P 461-464
90. J.B. WACHTMAN, JR., ED., *STRUCTURAL CERAMICS, TREATISE ON MATERIALS SCIENCE AND TECHNOLOGY,* VOL 29, ACADEMIC PRESS, 1989

Brazing of Ceramic and Ceramic-to-Metal Joints

A.J. Moorhead and W.H. Elliott, Jr., Oak Ridge National Laboratory H.-E. Kim, Seoul National University

---

Graphitic Materials

Carbon, graphite, and composites based on these materials are somewhat similar to structural ceramics and ceramic-matrix composites, but they are different enough to require a separate discussion. Although both material types have high melting points and relatively low CTE values, structural ceramics are compatible with oxidizing environments, whereas the carbon-based materials typically begin oxidizing at temperatures ranging from 400 to 650 °C (750 to 1200 °F), depending on the perfection of the carbon structure and its purity.

In addition, many structural ceramics have little or no open porosity, whereas many carbon materials have significant amounts of open porosity. Such porosity complicates the brazing process by wicking filler materials away from a joint. On the other hand, carbon materials have higher thermal conductivity values and, in tandem with their low CTE values,

are much less sensitive to thermal shock. Finally, the carbon materials are also more creep resistant than structural ceramics.

Carbon materials vary widely in degree of crystallinity and crystal orientation and in the size, quantity, and distribution of porosity in the microstructure. These factors strongly depend on the precursor materials and on processing and, in turn, govern the physical and mechanical properties of these products. This potential for variation in properties can be advantageous, because properties that are significant from a brazing standpoint (such as CTE) can be readily modified by processing. For example, CTE values can be varied from essentially zero in the fiber direction in fiber-reinforced composites to 8×10^{-6}/K for isostatically molded isotropic graphites.

Carbons and graphites can be manufactured by several processes that yield materials with a wide range of crystalline perfection and properties. In the most widely used process, polycrystalline graphites are made from natural pitch sources or from cokes produced from the residue that remains from petroleum after all volatile materials have been removed. The coke product is broken up and then calcined at temperatures ranging from 900 to 1400 °C (1650 to 2550 °F) to further reduce the volatile content and create a filler coke that will not shrink excessively during subsequent heat treatments.

The calcined coke is crushed, milled, and sized through screens into various fractions. The size of the particles in the coarse fraction may exceed 1 mm (0.04 in.) in large bodies and may be as small as 0.1 mm (0.004 in.) in smaller blocks, depending on the desired properties. The shape and properties of the crushed coke particles primarily depend on the coke source. Some cokes naturally break up into highly anisotropic particles with platelike or needlelike shapes, whereas others produce rounder isotropic particles.

The size fractions are mixed according to the properties that are desired in the final material, and then blended with a hot coal-tar pitch. The pitch creates a plastic mix that can be shaped by extrusion or molding. The shape of particles is important, because forming processes tend to preferentially align the anisotropic particles. Particles that are aligned in this manner as the result of extrusion or molding processes produce bodies with highly anisotropic properties.

The formed body is typically baked in large gas-fired floor furnaces to pyrolize the binder pitch at temperatures ranging from 800 to 900 °C (1470 to 1650 °F). During baking, the binder experiences a weight loss of approximately 50 to 60% and a volume loss that is even greater. The effect is a reduction in overall density and subsequently increased porosity. Density can be increased by rebaking after impregnation with low-melting-point, high-viscosity pitches. Special impregnants, such as thermosetting resins or mixtures of resins and pitches, can be used to control porosity. Final graphitization of carbon bodies is achieved at temperatures ranging from 2300 to 3000 °C (4170 to 5430 °F) in an electric furnace similar to those used to produce silicon-carbide grains.

Carbon-carbon composites consist of carbon or graphite fibers in a carbon or graphite matrix. The fibers have been made into yarns that are then woven into either two-dimensional fabrics or three-dimensional bodies of the desired shape. These preforms are then combined with a matrix to form a composite by either of two processes: liquid impregnation or chemical-vapor infiltration (CVI) (Ref 32). In the former, a preform is impregnated with liquid phenolic resin or pitch, baked to reduce porosity, and graphitized. The process of impregnation under pressure, carbonization, and high-temperature heat treatment is typically repeated five or more times in order to produce a composite that has a higher density and a stronger matrix.

In the CVI process, gaseous hydrocarbons, such as methane, are used to deposit an internal carbon matrix within a carbon-fiber preform. Several specialized procedures have been developed to overcome a major problem with the CVI process, which involves achieving a uniform deposition of the carbon matrix throughout a thick preform.

The carbon-carbon composite bodies that result from either process generally have very high tensile strength values, as well as low CTE values, which provide excellent resistance to thermal shock or stresses. However, these materials tend to be anisotropic, and their mechanical strength is much lower in directions that are not reinforced with fibers, such as between plies in two-dimensional bodies. In addition, for applications in which oxidation resistance of the composite is a concern, the materials are given a primary oxygen barrier consisting of an external coating of a ceramic, such as silicon carbide or silicon nitride, and internal inhibitors, such as compounds of boron, titanium, and silicon. At high temperatures, the latter materials form glassy oxide phases within the composite, which seal any CTE mismatch-induced cracks that form in the coating and restrict passage of oxygen through the porous matrix.

Of course, such oxidation-protection methods can significantly affect the brazing of these materials. One consideration, for example, would be whether the external coating is applied before or after brazing, because the coatings are applied at

temperatures from 1000 to 1400 °C (1830 to 2550 °F), depending on the process. The glass-forming inhibitors may also affect wetting and/or adherence of a brazing filler metal.

Reference cited in this section

32. R.F. DIEFENDORF, CONTINUOUS CARBON FIBER REINFORCED CARBON MATRIX COMPOSITES, *COMPOSITES,* VOL 1, *ENGINEERED MATERIALS HANDBOOK,* ASM INTERNATIONAL, 1987, P 911-914

Brazing of Ceramic and Ceramic-to-Metal Joints

A.J. Moorhead and W.H. Elliott, Jr., Oak Ridge National Laboratory H.-E. Kim, Seoul National University

Procedure Development

Although ceramic joining technology has been highly developed since the 1940s, most of the effort has been directed toward the development of materials and techniques for applications involving "low" temperatures and low structural stress requirements. The technology of joining ceramics for use at elevated temperatures, at high stress levels, and in dirty environments is less well developed. By the careful selection of location or through judicious design, a joint in such applications may not be required to withstand the full intensity of the various service conditions. However, it is highly desirable that a ceramic-to-ceramic or ceramic-to-metal joint be capable of operation at near-peak conditions.

Wetting and adherence are the principal requirements for brazing. However, most ceramic and graphitic materials are inherently difficult to wet using the more-common filler metals. Most filler metals simply ball up when melted in contact with a structural ceramic or graphite. This problem can be overcome by either coating the ceramic surface with a suitable metal layer prior to brazing (indirect brazing) or using specially formulated filler metals that wet and adhere directly to an untreated ceramic surface (direct brazing).

Indirect Brazing. In this technique, the ceramic is first coated in the joint area with a material that can be wetted by a filler metal that will not wet the untreated surface. Coating techniques include sputtering (Ref 33, 34, 35, 36), vapor plating (Ref 37, 38, 39), and thermal decomposition of a metal-containing compound (Ref 40). The coating is usually, but not always, a metal. For instance, Hammond and Slaughter (Ref 41) re-acted chromium vapor with the surface of a graphite body to form a coating of chromium carbide. For graphite coated in this manner and then brazed with pure copper, the shear strength at room temperature and at 700 °C (1290 °F) was 140 MPa (5.8 ksi). Failure occurred at the chromium carbide and carbon interface.

The most widely used brazing technique for joining alumina ceramics is the molybdenum-manganese (Mo-Mn) process, in which a slurry consisting of powders of molybdenum and/or molybdenum trioxide (or tungsten/tungsten tri-oxide), manganese or manganese dioxide, and various glass-forming compounds is applied to the ceramic in the form of a paint. The coated ceramic is fired in a wet hydrogen atmosphere at a temperature of approximately 1500 °C (2730 °F). During firing, glassy material from the ceramic migrates into the molybdenum (or tungsten) powder layer, bonding it to the ceramic surface. Because the process depends on this glass migration out of the ceramic, it is also dependent on such factors as amount and viscosity of the glassy phases, ratio of grain size in the ceramic to the pore size in the molybdenum powder, and processing temperature and atmosphere. The molybdenum-manganese process is a well-developed commercial process that was thoroughly reviewed in a series of papers by Twentyman (Ref 42, 43, 44).

An example of using physical vapor deposition for coating is described by Santella (Ref 39), who coated cold isostatic pressed and sintered silicon nitride with a 1.0 μm (0.04 μin.) thick layer of titanium using vacuum evaporation, and then brazed the silicon nitride to itself and metals with standard (nonactive) filler metals. The room-temperature flexural strengths of some of the silicon nitride-silicon nitride brazements were comparable to that of the silicon nitride itself (Fig. 1). By depositing the titanium using vapor plating, Santella produced strong joints and overcame a problem that arose in earlier work.

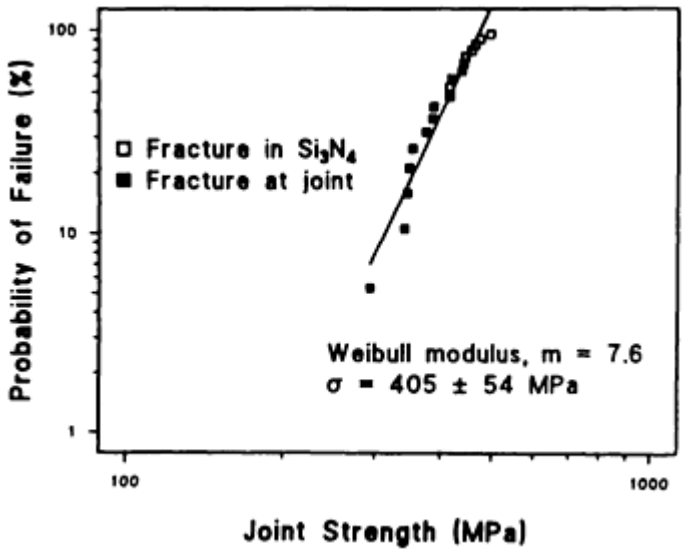

FIG. 1 FOUR-POINT FLEXURAL STRENGTH OF TITANIUM-VAPOR-COATED SILICON NITRIDE BRAZED TO ITSELF AT 1130 °C (2065 °F) WITH A AU-25NI-25PD, WT%, FILLER METAL. SOURCE: REF 39

In that earlier work (Ref 34), partially stabilized zirconia (PSZ) was coated by sputtering titanium and then brazed at 750 °C (1380 °F), either to nodular cast iron or to titanium with a commercial silver-copper-tin filler metal. Room-temperature shear strengths of both the PSZ/nodular cast iron and PSZ/titanium joints were about 140 MPa (20 ksi). However, at 400 °C (750 °F), the shear strength of the PSZ/ nodular cast iron brazement was only 28 MPa (4 ksi). Santella found that titanium coatings deposited by sputtering contain microporosity (apparently from trapped plasma gas) that coagulates during brazing and adversely affects high-temperature mechanical properties. Physical deposition of titanium by evaporation in a vacuum solved this problem.

Kohno *et al.* (Ref 45) coated silicon nitride by brazing at 1200 °C (2190 °F) with iron-nickel-chromium "paints" that contained silicon and carbon as melting-point depressants. They determined the adherence of the coatings by brazing the ceramic to itself at 1200 °C (2190 °F) with the paints themselves, and they achieved four-point bend strengths ranging from 125 to 200 MPa (18 to 29 ksi), depending on paint composition. However, the strength of similarly coated silicon nitride brazed to Kovar at 830 °C (1525 °F) with a silver-copper filler metal was only 50 MPa (7 ksi), apparently the result of damaging residual stresses.

Dunn *et al.* (Ref 46) studied the effects on mechanical properties of three silicon nitrides of various coatings applied by electron-beam evaporation. Polished bars were coated with hafnium, titanium, tantalum, or zirconium prior to being subjected to a thermal cycle simulating a brazing process (10 min at 980 °C, or 1795 °F, in vacuum) and then tested in four-point bending. The investigators found that zirconium and hafnium coatings did minimal damage to the silicon nitride. Titanium was found to be the coating most damaging to SNW-1000 (Si_3N_4-$13Y_2O_3$-$2Al_2O_3$), and it was even more severely damaging to AY6 (Si_3N_4-$6Y_2O_3$-$2Al_2O_3$). Interestingly, the effect of any of the coatings on PY6 material, which contains 6 wt% yttrium oxide, but no aluminum oxide, was minimal, which suggests a role for aluminum oxide in the property degradation of silicon nitride by active metal coatings. When silicon carbide was coated, heated, and tested in the same way, it was found that the hafnium coating was the most damaging.

Direct Brazing of Ceramics With Metallic Filler Metals. As mentioned above, most brazing filler metals will not wet structural ceramics and graphitic materials. Standard filler metals used to braze metals simply form a ball when melted in contact with a structural ceramic or graphite. This is due to the fact that the ceramic surface has very low surface energy, which means that there is no thermodynamic driving force for interface formation (wetting), as would be the case if a high surface energy surface were being wetted. However, for a number of years, it has been known that special alloying additions to conventional filler metals, such as the silver-copper eutectic composition, can promote wetting of and adherence to structural ceramics and graphite. The wetting of an untreated ceramic by a molten metal and the adhesion in such a system increases with the growing affinity of the metal constituents for the elements constituting the solid phase (Ref 47). Thus, the addition of chemically oxygen-active metals, such as titanium, zirconium, hafnium, aluminum, silicon, manganese, or lithium, should enhance both the wetting of and adherence to oxide ceramics, without the need for coating

the ceramic surface. In the same way, the wetting of and adherence to nonoxide ceramics, such as silicon carbide and silicon nitride, are aided by filler metals containing elements that strongly interact with silicon, carbon, or nitrogen. Whether the ceramic is an oxide, carbide, or nitride, the active metal reacts with the ceramic surface, forming an interfacial layer that can be wetted by the bulk of the filler metal.

Titanium is the most extensively studied and widely used active element added to filler metals formulated to directly braze structural ceramics and graphite (Ref 48, 49, 50, 51, 52). In the case of oxide ceramics brazed with titanium-containing filler metals, the critical interfacial reaction product is either titanium monoxide or dititanium trioxide, with appreciably higher adhesion resulting when titanium monoxide is formed (Ref 53). Titanium additions to filler metals have also been shown to enhance wetting of and adherence to silicon carbide (Ref 54), silicon nitride (Ref 55), and Sialon (Ref 56). The reaction products of the wetting process in the latter cases are titanium silicides, titanium carbides, and titanium nitride.

In recent years, there has been significant research in the use of another active element, aluminum, as a brazing material in joining silicon nitride and silicon carbide. In the case of silicon nitride, the reaction product after brazing with aluminum at 800 °C (1470 °F) was identified as a 500 nm (20 μin.) thick dual layer consisting of a fine-particle layer of β'-Sialon attached to the silicon nitride and an amorphous aluminum oxide layer (Ref 57, 58). The interfacial reaction product observed when silicon carbide is brazed with aluminum filler metal has been identified as aluminum carbide (Ref 59).

Some of the commercially available filler metals that have been developed for direct brazing of structural ceramics are shown in Table 2. Note that numerous active filler metals have been developed and, in many cases, patented, but only relatively few are commercially available. Generally, these filler metals consist of two types: those that have a relatively high active element content and will wet and flow on structural ceramics and graphite, and those that represent a new generation of materials that have a lower active element content and will wet and strongly bond to these ceramics, but only flow onto the ceramic surface very slowly, if at all (Ref 61). Therefore, filler metals in the latter category are preplaced between the mating components, rather than relying on capillary attraction to draw them into the joint. The filler metals with a high active element content are manufactured in the form of composites (such as a titanium core inside a sheath of silver-copper eutectic), because such high titanium contents form brittle and, therefore, unfabricable structures.

TABLE 2 SELECTED COMMERCIALLY AVAILABLE ACTIVE BRAZING FILLER METALS

ALLOY SYSTEM	CHEMICAL COMPOSITION, WT%	SOLIDUS TEMPERATURE		LIQUIDUS TEMPERATURE		BRAZING TEMPERATURE RANGE		MANUFACTURER
		°C	°F	°C	°F	°C	°F	
AUNITI	96.4AU-3NI-06TI	1003	1837	1030	1886	1025-1030	1880-1886	(A)
CUALSITI	92.75CU-2AL-3SI-2.25TI	958	1756	1024	1875	1025-1050	1880-1920	(A)
AGCUALTI	92.75AG-5CU-1AL-1.25TI	860	1580	912	1674	900-950	1650-1740	(A)
AGCUTI	63AG-35.2CU-1.75TI	780	1436	815	1499	830-850	1525-1560	(A)
AGCUSNTI	63AG-34.2CU- 1SN-1.75TI	775	1427	806	1483	810-860	1490-1580	(A)
AGCUINTI	59AG-27.2CU-12.5IN-1.25TI	605	1121	715	1320	700-750	1290-1380	(A)
TICUNI	70TI-15CU-15NI	910	1670	960	1760	960-1000	1760-1830	(A)
TICUAG	68.8AG-26.7CU-4.5TI	830	1526	850	1560	810-900	1490-1650	(A)
AGTI	96AG-4TI	970	1778	970	1778	1000-1050	1830-1920	(B)
AGCUTI	64AG-34.5CU-1.5TI	770	1418	810	1490	850-950	1560-1740	(B)
AGCUTI	70.5AG-26.5CU-3TI	780	1436	805	1481	850-950	1560-1740	(B)

AGCULNTI	72.5AG-19.5CU-5IN-3TI	730	1346	760	1400	850-950	1560-1740	(B)
PBINTI	92PB-4IN-4TI	320	608	325	617	850-950	1560-1740	(B)
SNAGTI	86SN-10AG-4TI	221	430	300	572	850-950	1560-1740	(B)
AGCUINTI	61.5AG-24CU-14.5IN + (TI)	620	1148	710	1310	~845	~1555	(C)
AGCUNITI	71.5AG-28CU-0.5NI + (TI)	780	1436	795	1463	~927	~1700	(C)
AGCUNITI	**56AG-42CU-2IN + (TI)**	**770**	**1418**	**895**	**1643**	**954**	**~1750**	(C)

Source: Ref 60

(A) GTE WESGO.

(B) DEGUSSA AG.

(C) LUCAS-MILHAUPT.

Direct Brazing With Nonmetallic Glasses. Numerous studies have been conducted to develop materials and techniques for joining structural ceramics, including alumina (Ref 62), PSZ (Ref 63), silicon nitride (Ref 64, 65, 66, 67, 68), and Sialon (Ref 69, 70) by brazing with nonmetallic glasses used as filler materials. The rationale for this approach is that many ceramics have amorphous phases remaining at the grain boundaries after the sintering process. Therefore, they would be expected to be wet by and compatible with similar glassy materials introduced at the joint. Glass viscosity and flow properties can be controlled over a wide range of temperatures. However, glasses have much lower toughness values than even monolithic ceramics, as well as low Young's modulus values, and are susceptible to stress corrosion (slow crack growth). As will be described below, some of the glasses, even those formulated to match the grain-boundary composition, have significantly different CTE values from that of the ceramic, which causes high residual stresses and cracking in the joint.

Generally, powdered glass in a slurry with a binder is applied to one or both of the mating components of a joint that is heated until the glass melts and reacts with the ceramic. In a variation of the process (Ref 66), the surface of one of the components was first coated with molten glass, and this glazed surface was ground to precisely control the thickness of the joining material. In another variation (Ref 64), aluminum foil was placed in a silicon nitride joint, along with sources of alumina and silicon dioxide, such as powders or oxidation layers on the aluminum and silicon nitride. The joints so produced had three-point bending strengths ranging from 35 to 210 MPa (5 to 30 ksi) at both room temperature and 1200 °C (2190 °F). In contrast to diffusion welding with high pressures applied to the joint area, brazing with glasses and metals uses relatively low pressures ranging from that provided by the weight of one of the parts being joined to 14 MPa (2 ksi) (Ref 63). Typical atmospheres are air (when joining oxides) and nitrogen (when joining silicon nitride).

The most extensive studies on brazing with glasses have been those on silicon nitride. The glasses include those similar to that which is found at the grain boundaries of a hot-pressed silicon nitride ($55SiO_2$-$35MgO$-$10Al_2O_3$) (Ref 66, 68, 69) and a very different CaO-TiO_2-SiO_2 (CTS) glass ($35CaO$-$25TiO_2$-$40SiO_2$) (Ref 67). Baik (Ref 65) stated that there are three potential problems when joining silicon nitride by brazing with glasses:

- A REACTION BETWEEN THE GLASS AND SILICON NITRIDE FORMS ACICULAR SILICON OXYNITRIDE CRYSTALS THAT PREVENT THE FORMATION OF A MICROSTRUCTURE TYPICAL OF A GRAIN BOUNDARY
- CTE MISMATCHES CAUSE CRACKING IN THE GLASS
- POROSITY FORMS IN THE GLASS LAYER DURING BRAZING OR UPON SUBSEQUENT HEATING TO ELEVATED TEMPERATURES

Such behavior was observed by Johnson and Rowcliff (Ref 66), who reported excellent strength (maximum of 400 MPa, or 58 ksi, within the optimum bonding conditions of 30 to 60 min and 1575 to 1650 °C, or 2870 to 3000 °F) in joints brazed with the composition similar to that found in the grain boundaries. However, significant cracking and porosity occurred in the joints. The cracking was attributed to differences in CTE, whereas the porosity was thought to result either

from the vaporization of silicon monoxide and magnesium or from the volume change associated with the formation of silicon oxynitride crystals.

Iwamoto (Ref 67) minimized the cracking problem by using a CTS glass that had a CTE value less than that of the silicon nitride and by mixing silicon nitride powder with the glass powder. At room temperature, the resulting joints had four-point bending strengths ranging from 235 MPa (34 ksi) with no silicon nitride powder in the glass to 272 MPa (44 ksi) with glass containing 30 wt% silicon nitride powder.

Baik (Ref 65) alleviated the porosity problem that he attributed to the decomposition of the silicon nitride to silicon and nitrogen by adding elemental silicon to a magnesium-silicon-oxynitride glass to increase the silicon activity and, thereby, retard the formation of nitrogen gas.

Neilson (Ref 69) and Coon (Ref 70) used glasses in the yttrium-silicon-aluminum-oxynitride system to bond a sintered Sialon at 1600 and 1725 °C (2910 and 3140 °F) under an applied load of 0.63 N (0.14 lbf) and nitrogen gas pressures of 138 and 207 MPa (20 and 30 ksi), respectively. Joint fracture toughness values (approximately 4.5 MPa$\sqrt{m}$, or 4 ksi$\sqrt{\text{in.}}$) and four-point flexure strengths (approximately 450 MPa, or 65 ksi) at temperatures to 1000 °C (1830 °F) were equal to that of the Sialon. At temperatures greater than 1000 °C (1830 °F), the strength of the joints made at 1600 °C (2910 °F), which contained significant amounts of glass (glass-filled joint), decreased rapidly until at 1100 °C (2010 °F) it was only 25 MPa (4 ksi). However, the joints produced at 1725 °C (3140 °F) (closed joint with little retained glass) had strengths of 200 MPa (29 ksi) at 1250 °C (2280 °F).

In addition to the above-mentioned study on the joining of silicon nitride, a CTS glass was also investigated for joining a magnesia-PSZ ceramic (Ref 63). The use of this type of glass was chosen because the system has several eutectic compositions with melting temperatures below the 1400 to 1500 °C (2550 to 2730 °F) annealing range of the ceramic. Therefore, the brazing step could be combined with the annealing treatment of this material. An applied pressure of 14 MPa (2 ksi) was used to distribute the molten glass through the joint. Unfortunately, the differences in the CTE values of the materials resulted in extensive cracking through the glass and interface when the joint area was large (20 cm^2, or 3 $in.^2$). Based on the work of Iwamoto (Ref 67), the CTE of the interlayer was made closer to that of the PSZ by adding 30 wt% zirconium oxide to the CTS interlayer powder. Using a thinner layer of the modified powder and a longer pressing time at 1420 °C (2590 °F), joints that had average four-point bending strengths of 66 MPa (10 ksi) were produced.

Several glass compositions were investigated for joining alumina ceramics (Ref 62). This work differed from that of the preceding studies in that one of the goals of these researchers was to initiate and control crystallization of the glass in the joint to increase fracture toughness and resistance to stress corrosion. Zirconium oxide powder was added to a magnesium aluminum silicate glass as a nucleating agent. Unfortunately, spontaneous crystallization occurred at the glass-alumina interface, limiting the desired degree of control over crystallization and resulting in large voids at the interface. Accordingly, the fracture toughness of the joint was only 1.8 MPa$\sqrt{m}$ (1.6 ksi$\sqrt{in}$) versus a value of about 4 MPa$\sqrt{m}$ (3.6 ksi$\sqrt{in}$) for the alumina (no joint strength data reported). The most successful joints (fracture toughness of 2.3 MPa$\sqrt{m}$, or 2.1 ksi$\sqrt{in}$) resulted when the alumina was joined at 1500 °C (2730 °F) with a mixture of 50 wt% talc (hydrated magnesium silicate) and 50% aluminum oxide. However, these joints contained a substantial number of pores that degraded the mechanical integrity of the joints. The authors suggested that the pores were caused by the evolution of adsorbed gases from the alumina body and, therefore, would be difficult to eliminate.

Alternate Brazing Techniques. Although brazing is typically accomplished through melting of a metallic alloy or glass-forming compound placed in the joint area, there are some other viable techniques for generating a liquid at an interface to effect a brazement. The most common of these, generally referred to as "eutectic brazing," relies on the reaction at the interface of an insert material or of the metallic member of a ceramic-metal joint with either the ceramic, another metal, or even a gaseous component of the atmosphere. Such reaction is based on the presence of a low-melting region (typically a eutectic reaction) of the respective phase diagram, and hence comes the name of the process.

The most widely studied of the eutectic brazing processes, known as gas-metal eutectic brazing, is based on the formation of a liquid skin on the metallic member as a result of reaction with the atmosphere (Ref 71, 72, 73). According to Burgess *et al.* (Ref 71), the idea is to form a liquid skin on a metal surface, with the requirement that the liquid wets both the ceramic and metal components being joined and forms a strong bond on cooling. Ideal for use as the liquid skin material are eutectics formed by the reaction of the brazing atmosphere with the metal component itself. Such a eutectic exists between copper and oxygen at 0.39 wt% oxygen. The melting point of this eutectic, 1065 °C (1950 °F), is sufficiently below the melting point of pure copper, 1083 °C (1980 °F), so that by careful temperature control an oxide ceramic can

be brazed to a copper component using this liquid. According to Yoshino (Ref 72) this technique is used in the electronics industry to manufacture copper-bonded alumina substrates for power semiconductor applications. Generally the copper is preoxidized prior to the joining operation, but Okamoto and coworkers (Ref 73)joined alumina to mild steel by simply using a copper filler metal foil in a slightly oxidizing atmosphere at 1200 °C (2190 °F). In addition to the copper-oxygen system, Burgess suggests that other beneficial metal-gas eutectics for joining might be iron-oxygen, nickel-oxygen, and cobalt-oxygen and even silver-phosphorus, nickel-phosphorus, copper-phosphorus, or molybdenum-silicon, and aluminum-silicon. The latter two types would be achieved by having small amounts of a phosphorus or silicon bearing compound (such as phosphine or silane) in the atmosphere.

A metal-metal eutectic was used by Naka and Okamoto (Ref 74) to braze an alumina (99.6 wt% Al_2O_3) to type 304 stainless steel. Titanium foil, which melts at 1670 °C (3040 °F), was placed between the two base materials and heated to 1400 °C (2550 °F) in vacuum of 0.13 mPa (1×10^{-6} mm Hg). The investigators suggest that the bond was made by the eutectic in the titanium-iron system at 68 at.% Ti at 1085 °C (1985 °F).

A recent and possibly very significant variation of the eutectic brazing process is one termed "partial transient liquid-phase" joining (Ref 75, 76). This process is based on the well-known transient liquid-phase bonding of nickel-base and cobalt-base superalloys (Ref 77). In this earlier work, a melting point depressant such as boron was added to a brazing filler metal and subsequently diffused into the base metals during brazing. Removal of the boron from the braze joint rids the brazement of embrittling compounds and results in a higher remelt temperature.

In the recent modifications of this process for joining of ceramics, three layers of metal are preplaced in the joint, with the outer two layers much thicker than the center layer. When the composite is heated, a thin film of low-melting-point liquid forms at the interfaces to make the braze, but the center layer is not totally consumed. Further holding at temperature results in diffusion of the liquid layer into the center layer, resulting in a more heat-resistant joint. The new process is termed "partial" transient liquid-phase joining because the transient liquid phase is formed only near the interface and the metal layer is not fully homogenized. One example of this process, cited by Iino (Ref 75), uses a thin layer of titanium on either side of a much thicker layer of nickel. According to the nickel-titanium phase diagram, when a nickel-titanium bilayer is heated at 1050 °C (1920 °F), a liquid phase occurs in the composition range of 60 to 75 wt% Ti. Because the titanium layer is much thinner than the nickel layer the liquid layer forms, the braze is made and then the liquid disappears as the titanium diffuses into the nickel and the local concentration of titanium falls below the liquidus line (below 60 wt%). If, by further diffusion, the titanium content falls below 30 wt%, the remelt temperature would be 1304 °C (2380 °F).

Shalz and coworkers (Ref 76) are considering a number of other possible material combinations for joining of ceramics such as alumina. Their work to date has included tri-layer compositions of copper/platinum/copper, copper/nickel/copper, copper/niobium/copper, and tin/ niobium/tin for joining alumina to alumina. The results of high-temperature postbonding anneals suggest that copper/platinum/copper and copper/ niobium/copper bonded alumina assemblies may be suitable for use at elevated temperatures in oxidizing and nonoxidizing environments, respectively.

Surface Preparation. Whether the filler material is a metal or glass, one of the initial decisions that must be made in brazing procedure development is the technique for preparing the ceramic surface. Although an as-fired surface is sometimes suitable for brazing, at least some machining is usually required to provide the contact surfaces necessary for joining. Because the machining of ceramic surfaces must generally be done by grinding with diamond-abrasive wheels, which is an inherently slow and costly process, surface preparation should be minimized. A surface preparation technique that is economically feasible, provides adequate surface finish and tolerances, and causes minimal damage to the ceramic is optimal. Unfortunately, ceramic machining itself is currently experiencing significant development, and it is not possible to recommend a set of grinding conditions (wheel grit, feeds, speeds, and such) that efficiently removes ceramic material while minimizing surface damage. However, enough information is available to state that the effect of a given preparation procedure on the ceramic is very material specific, even within a given family of ceramics.

For example, in working with an alumina ceramic containing 97.6% Al_2O_3, Mizuhara and Mally (Ref 50) found that grinding damage could be negated by retiring the ground parts at 1650 °C (3000 °F). Such a firing step, which apparently healed surface flaws induced during grinding, resulted in much higher peel strengths in Kovar/refired alumina joints brazed with silver-40 at.% copper plus titanium than in similar joints between Kovar and as-fired, ground, or ground/lapped alumina. However, a heat treatment of a higher-purity alumina (containing 99.5% Al_2O_3) after grinding did not have the same effect. Joints made with resintered samples of this alumina were much stronger than those made with ground material, but not as strong as those made with unground or ground/lapped alumina. It is assumed that the amount of glassy phase in the 99.5% alumina was insufficient to heal or blunt many of the grinding defects under the heat-treatment conditions used.

In the experience of the authors, a very different response to surface preparation has been observed among materials. For example, as shown in Fig. 2, it was found that the three-point bend strength of high-purity alumina (McDanel AD-998) ceramic-to-ceramic joints brazed in vacuum for 5 min at 800 °C (1470 °F) with an experimental filler metal were essentially the same, whether the joining surfaces were ground with a 180-grit diamond abrasive wheel or ground and then polished with 6 μm (240 μin.) and 3 μm (120 μin.) grit diamond pastes.

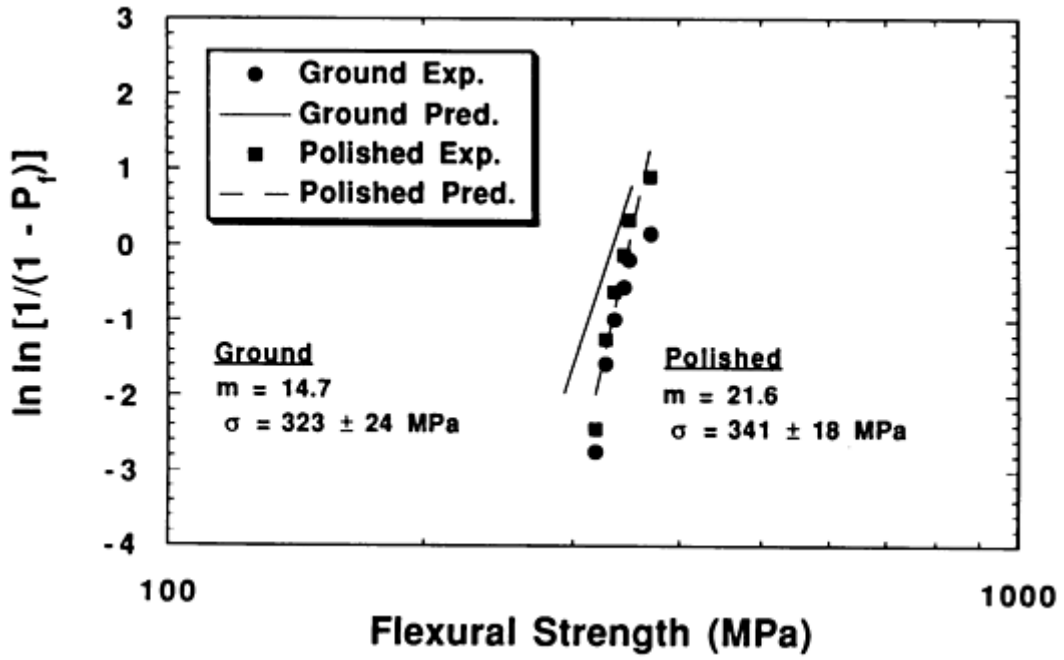

FIG. 2 EFFECT OF POLISHING INTERFACIAL AREA ON STRENGTH OF CU-41AG-3.5SN-7TI, AT.%, BRAZEMENT IN MCDANEL AD-998 ALUMINA

On the other hand, polishing the mating surfaces of coupons of silicon carbide whisker-rein-forced alumina prior to brazing led to significantly higher joint strengths, as shown in Fig. 3.

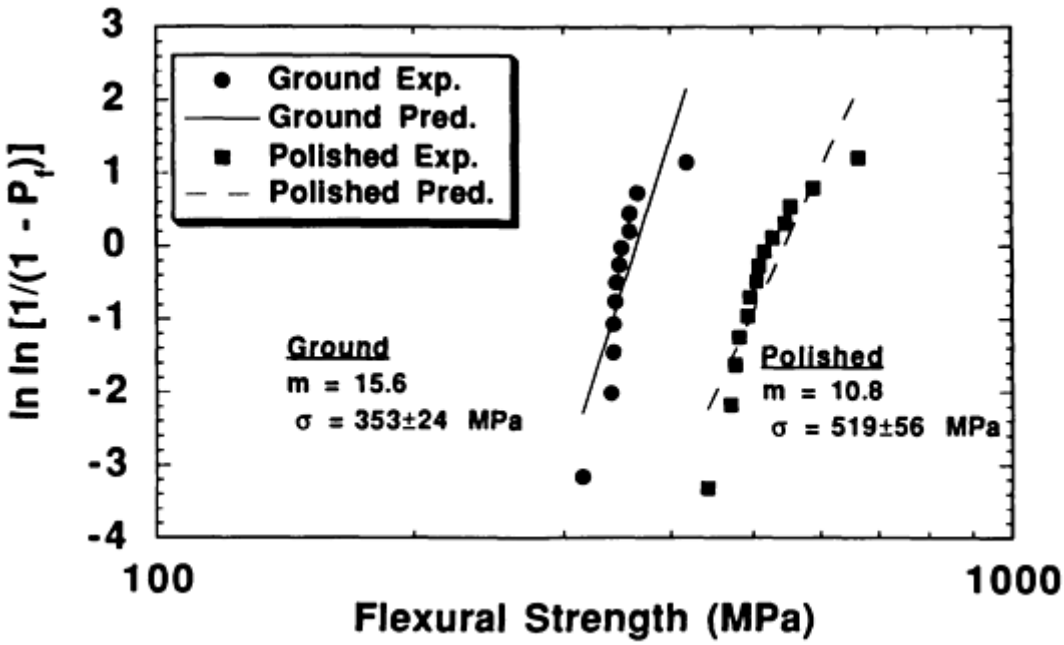

FIG. 3 EFFECT OF POLISHING INTERFACIAL AREA ON STRENGTH OF CU-41AG-3.5SN-7TI, AT.%, BRAZEMENT

IN SILICON CARBIDE WHISKER-REINFORCED ALUMINA

Examination of typically prepared coupons of both materials by scanning electron microscopy revealed that the morphologies of the ground surfaces were very different. As shown in Fig. 4(a), the ground alumina surface exhibited predominantly intergranular fracture, although some transgranular fracture was also evident, such as the grain just left of center. However, the most notable features in the alumina microstructure were the many cracks that appear to be both intergranular and transgranular. The microstructure of the ground composite (Fig. 5a) exhibited the general striations typically of grinding, with linear regions of predominantly transgranular fracture separated by areas with a "smeared" appearance suggesting plastic flow. Although the concept of plastic flow in an inherently brittle ceramic may seem incongruous, this behavior has been widely observed in machined ceramic surfaces. Despite the fact that the grain size in the alumina was much larger than that of the silicon carbide whisker-reinforced alumina material, the polished microstructures were somewhat similar (Fig. 4b, 5b), with both materials showing evidence of porosity and grain pullouts.

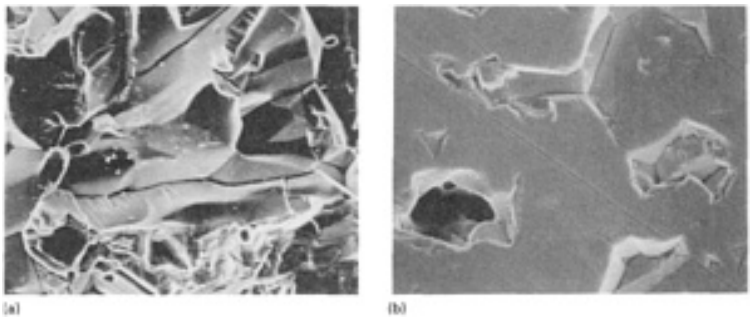

FIG. 4 SCANNING ELECTRON MICROGRAPHS OF SURFACE OF MCDANEL AD-998 ALUMINA AS PREPARED FOR JOINING. (A) GROUND, ROOT MEAN SQUARE (RMS) ROUGHNESS, R_Q, OF 0.63 μM (25 μIN.). (B) GROUND/POLISHED, R_Q OF 0.15 μM (6 μIN.). 3000×

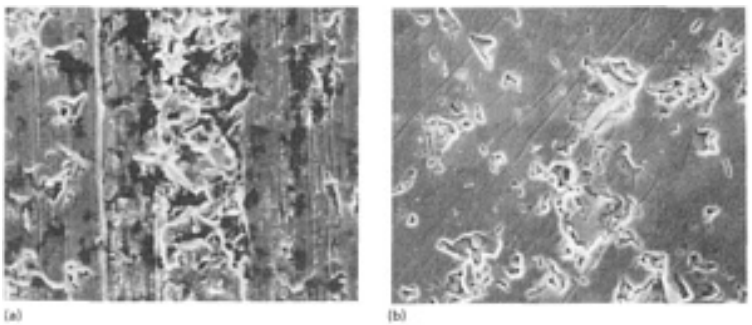

FIG. 5 TOPOGRAPHY OF SILICON CARBIDE WHISKER-REINFORCED ALUMINA SURFACES TO BE JOINED. (A) GROUND, R_Q OF 0.35 μM (14 μIN.). (B) GROUND/POLISHED, R_Q OF 0.04 μM (1.6 μIN.). 3000×

However, when the edges of the coupons were examined by scanning acoustic microscopy at 50 MHz before and after polishing, very significant differences were observed. Although the polishing of the composite material reduced the defect population, the procedure actually induced new subsurface defects in the alumina. A different set of grinding/polishing conditions might not produce the same results, but the importance of surface preparation on brazement strength should be obvious.

The brazing parameters themselves, that is, temperature, time at temperature (actually, the entire thermal cycle) and atmosphere, play a major role in the properties of a brazement and, therefore, are of critical importance in procedure development. Because strong bonds depend on chemical reactions at the ceramic/filler metal interface, one might assume that the strongest joints result from the highest temperatures and longest times. In many cases, it has been experimentally found that increasing a given parameter does, in fact, increase joint strength. However, this is true only up to a point. The

authors and other researchers have found that joint strengths tend to reach a maximum as temperature and/or time are increased and then decrease with further increases, as illustrated in Fig. 6.

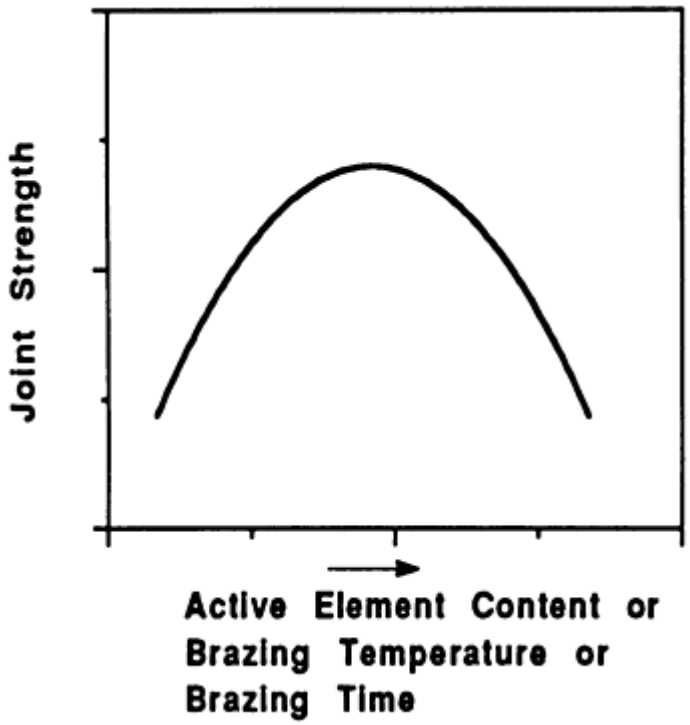

FIG. 6 RELATIONSHIP BETWEEN STRENGTH OF ACTIVE METAL BRAZEMENTS AND PRIMARY VARIABLES

For example, Kim and coworkers (Ref 78) observed this behavior when brazing a pressureless sintered silicon nitride with a series of copper-titanium filler metals. They found that the shear strengths of silicon nitride-silicon nitride joints were more affected by the morphology and thickness of the interfacial reaction layer than by wettability. As the titanium content of the binary filler alloys was increased, the equilibrium contact angle continually decreased, indicating improved wetting. As shown in Fig. 7, shear strength rapidly increased up to a relatively low titanium content of 5 wt% and then much more slowly afterwards. However, as shown in Fig. 8, the shear strengths initially increased and then decreased with further increases as temperature and time evidently exceeded optimum conditions. They attributed this behavior to excessive growth of the reaction layer, accompanied by the development of flaws in that layer.

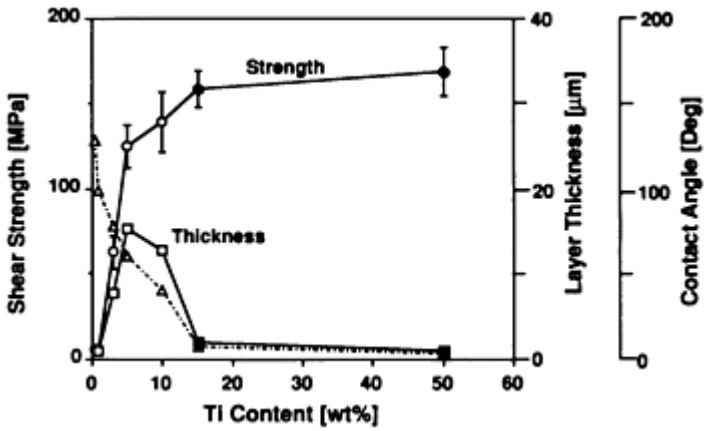

FIG. 7 EFFECT OF ACTIVE METAL CONTENT ON SHEAR STRENGTH, INTERFACIAL REACTION LAYER THICKNESS, AND WETTING ANGLE WHEN SILICON NITRIDE IS BRAZED WITH COPPER-TITANIUM FILLER METALS. OPEN DATA POINTS MEASURED AT 1100 °C (2010 °F), 1800 S; SOLID DATA POINTS MEASURED AT

1020 °C (1870 °F), 1800 S. SOURCE: REF 78

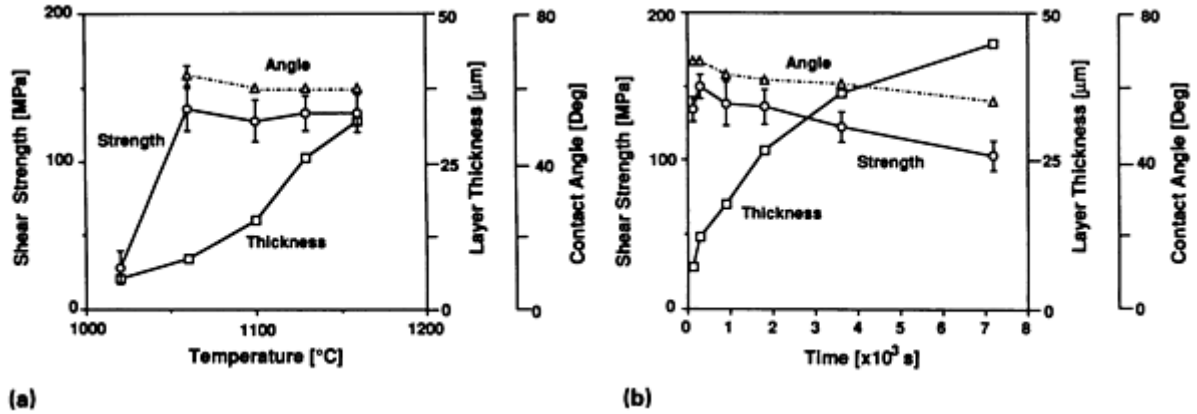

FIG. 8 EFFECT OF (A) BRAZING TEMPERATURE AND (B) HOLDING TIME AT TEMPERATURE ON SHEAR STRENGTH, CONTACT ANGLE, AND REACTION LAYER THICKNESS OF SILICON NITRIDE-SILICON NITRIDE JOINTS BRAZED WITH 95CU-5TI FILLER METAL. THE HOLDING TIME FOR THE BRAZEMENT OF (A) WAS 1800 S; THE SAMPLES FOR (B) WERE BRAZED AT 1130 °C (2070 °F). SOURCE: REF 78

The atmosphere used when brazing with active filler metals is also an important variable. Generally, a vacuum in the range of approximately 6 mPa (5×10^{-5} mm Hg) is used, but the literature of some manufacturers states that these filler metals can also be brazed in inert atmospheres, but of unspecified purity. Published reports have compared the strength of joints brazed in vacuum versus those brazed in inert gas, but little has been published on the effect of the actual magnitude of oxygen partial pressure on brazement wetting or adherence.

To facilitate an understanding of the effect of oxygen in the brazing atmosphere, the authors recently conducted a study that included PO_2 as one of the variables. A statistically designed experiment was conducted in order to objectively evaluate the role of certain parameters in the brazing of ceramic materials. An L9 orthogonal array and the Taguchi methodology were employed to examine four parameters at three levels on five different ceramic materials. The use of statistics in designing the experiment reduced the necessary number of brazing runs (for the five materials) from 320 to 45, while producing the same results. Each brazing run produced from six to twelve bend bars for testing. Therefore, the results were based on the average bend bar strength for each material and condition, or approximately 400 data points.

The materials were two aluminas (Coors AD-85, 85% Al_2O_3, and McDanel AD-998, 99.8% Al_2O_3), a silicon carbide whisker-reinforced alumina composite (Cercom PAD-AS30W), a sintered α-silicon carbide (Carborundum Hexoloy SA), and a sintered silicon nitride (GTE SNW-1000) that contained 13 wt% yttrium oxide (Y_2O_3) and 3 wt% Al_2O_3 as sintering aids. Material from a single lot of a commercially available brazing foil (GTE Wesgo's Cusil ABA, Ag-35Cu-2.0Ti, wt%) was used to join coupons of each ceramic material. The manufacturer recommends that this filler metal be brazed at temperatures ranging from 830 to 850 °C (1525 to 1560 °F), with a time at temperature of 3 to 10 min.

The mating edge of each coupon to be joined was prepared by one of three techniques: (1) Coarse grinding with a 180-grit diamond-impregnated grinding wheel; (2) Coarse grinding as in technique 1, followed by fine grinding with a 320-grit diamond wheel; or (3) Polishing the edges of some fine-ground coupons on a vibratory polisher using 6 μm (240 μin.) and 3 μm (120 μin.) grit diamond pastes. All of the grinding parameters, feeds, and speeds were held constant for coupons.

The brazing environments were flowing gases consisting of approximately 10, 100, and 1000 parts per million of oxygen in argon. The purity of the bottled argon was reduced to 10 ppm or less for each run by passing the gas through a commercial oxygen absorber. For the 100 and 1000 ppm runs, the $P\ O_2$ in the argon was controlled by mixing the purified argon with oxygen, and then measured with an oxygen analyzer with sensors located at the inlet and exit of the furnace tube.

The coupons were joined in a butt configuration in a silicon carbide fixture shown schematically in Fig. 9. The filler-metal foil was placed in the joint along with small, 38 μm (1.5 mil) thick tantalum shims on either end to prevent the joint

from closing completely under the slight end loading provided by 250 μm (0.01 in.) thick molybdenum sheet "springs." Both the shims and filler metal were held in place during assembly by small drops of a Nicrobraz cement.

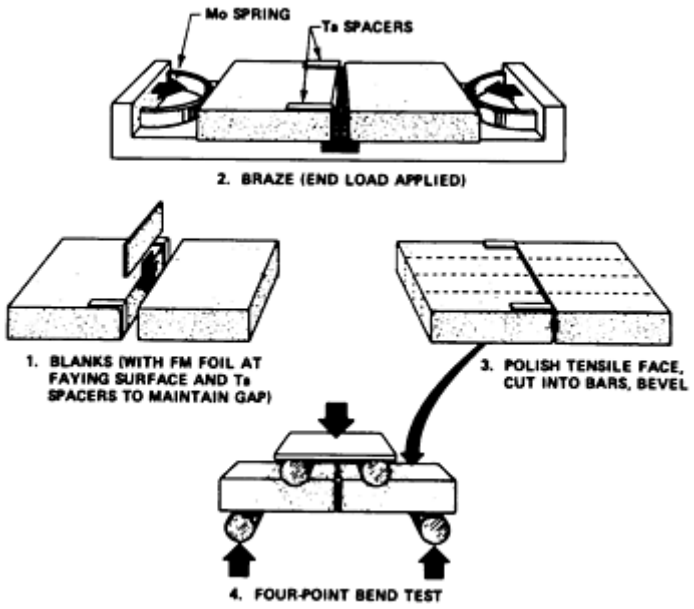

FIG. 9 SEQUENCE OF OPERATIONS FOR FABRICATING BRAZED FLEXURAL BARS FOR THREE- OR FOUR-POINT BENDING TESTS

It is important to note that because the filler metal was confined between the ceramic coupons, the authors do not know what the $P\,O_2$ actually was within that space. The filler metal that exuded from the joint during brazing was oxidized gray or black, but beneath the oxide layer, the filler metal was still bright and shiny. This observation was not surprising, because in a previous study on oxidation of titanium-containing brazing filler metals (Ref 79), the authors found that the oxidation followed a simple parabolic rate law. Such behavior is indicative of the formation of a nonporous, coherent oxide film acting as a physical barrier to restrict further oxidation. Although an arrangement that has the filler metal placed within the confines of the mating surfaces may not be typical for all brazements, the authors think it is typical for active-metal brazements made with filler metals containing relatively low amounts of the active species. The ability of these materials to flow through a capillary joint is restricted by their low titanium content, which requires that they be preplaced within the joint.

Brazing of the nine sets of coupons of each material was done in a resistance-heated, alumina-tube furnace. The brazing cycle consisted of heating to a brazing temperature of 800 °C (1470 °F), 850 °C (1560 °F), or 900 °C (1650 °F) in about 15 min, holding at that temperature for 6, 12, or 18 min, and then cooling to room temperature in about 90 min. After brazing, the coupons were attached to steel backing bars and ground on both faces using a 180-grit diamond-abrasive wheel with the grinding direction perpendicular to the braze joint. The ground blanks were polished (on what would become the tensile surface of the flexure bars) with 6 μm (240 μin.) and 3 μm (120 μin.) diamond pastes on a vibratory polishing machine. The polished brazed coupons were then sliced in a series of parallel cuts (Fig. 10) to produce 3 by 4 by 25 mm (0.12 by 0.16 by 1 in.) flexure bars with the brazed joint across the center of the bars. The long edges of the tensile face of each sample were beveled on a 6 μm (240 μin.) grit diamond lap. Each brazing run produced from six to twelve bend bars for testing. Testing was in four-point bending, with spans of 6.35 and 19.05 mm (0.25 and 0.75 in.) and a crosshead speed of 0.08 mm/s (3 mils/s).

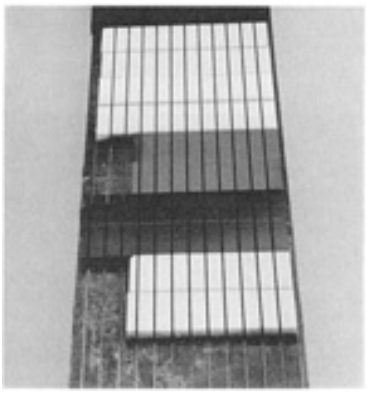

FIG. 10 POLISHED BRAZED COUPONS AFTER BEING SLICED IN A SERIES OF PARALLEL CUTS TO PRODUCE BARS FOR FLEXURAL STRENGTH TESTING

The results were very interesting and somewhat surprising. For example, very weak joints were produced in the sintered α-silicon carbide under many of the experimental conditions. In fact, the flexure bars from four of the nine brazements in this material failed after slicing. Because we have been able to prepare and test a number of bars with strengths of 20 MPa (3 ksi), we may assume that the failed bars had strengths less than that. As far as the effect of atmosphere is concerned, it was found that strong brazements could be produced in any of the materials, even when the oxygen partial pressure during brazing was 1000 ppm.

Figure 11 shows the ratios of the joint strength to ceramic strength for four of the materials. This figure illustrates that strong joints, with almost 50% of the bending strength of the respective ceramic, can be produced in each material, even in a relatively impure atmosphere. In order to make the comparisons valid, the strengths of the joints made with coarse-ground coupons brazed at 900 °C (1650 °F) for 12 min in an argon-1000 ppm O_2 atmosphere were used to calculate the ratios, not the maximum joint strength achieved for a given material. These were the conditions that produced the strongest brazement in the silicon carbide material, 256 ± 42 MPa (37 ± 6 ksi). The set of parameters, out of the nine sets of experimental conditions evaluated, that yielded the highest average joint strength for each material are given in Table 3. Interestingly, although these results may have been skewed by the failure of half of the silicon carbide brazements during bar fabrication, the recommended conditions (after statistical analysis of the results) that were predicted to produce optimum strength in the silicon carbide brazements were: 900 °C (1650 °F), 12 min, a coarse-ground finish, and 1000 ppm oxygen. In fact, two brazements in this material that were made in a vacuum of 4×10^{-3} Pa (3×10^{-5} mm Hg), which would be considered the "normal" atmosphere for active-metal brazing, for 6 min at 800 and 850 °C (1470 and 1560 °F), respectively, failed during flexure bar preparation.

TABLE 3 CONDITIONS FOUND TO PRODUCE THE HIGHEST AVERAGE JOINT STRENGTH WHEN BRAZING EACH OF FIVE STRUCTURAL CERAMICS WITH CUSIL-ABA IN AR-O_2 ATMOSPHERES

	TEMPERATURE, °C (°F)			**TIME, MIN**			**AR-*P* O_2, PPM**			JOINT FINISH
	800 (1470)	**850 (1560)**	**900 (1650)**	**6**	**12**	**18**	**10**	**100**	**1000**	
AD-85 ALUMINA (228 ± 42 MPA, OR 33 ± 6 KSI)	. . .	. . .	X	X	. . .	. . .	. . .	X	. . .	**POLISHED**
AD-998 ALUMINA (317 ± 16 MPA, OR 46 ± 2.5 KSI)	X	. . .	. . .	. . .	. . .	X	. . .	. . .	X	**POLISHED**
SILICON CARBIDE WHISKER-REINFORCED ALUMINA (445 ± 37 MPA, OR 65 ± 5.5 KSI)	. . .	. . .	X	X	. . .	. . .	. . .	X	. . .	**POLISHED**
α-SILICON CARBIDE (256 ± 42 MPA, OR 37 ± 6 KSI)	. . .	. . .	X	. . .	X	. . .	. . .	. . .	X	**COARSE**
SILICON NITRIDE (512 ± 74 MPA, OR 74 ± 11 KSI)	**X**	**. . .**	**. . .**	**. . .**	**. . .**	**X**	**. . .**	**. . .**	**X**	**POLISHED**

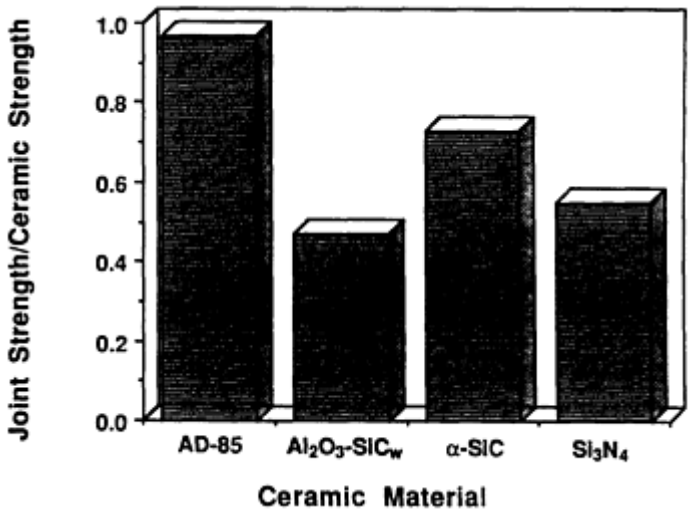

FIG. 11 RATIO OF JOINT STRENGTH TO CERAMIC STRENGTH FOR FOUR CERAMICS BRAZED WITH AG-35CU-2TI, WT%, FILLER METAL FOR 12 MIN AT 900 °C (1650 °F) IN AN AR-1000 PPM O_2 ATMOSPHERE

The statistical analysis also recommended the highest level of oxygen included in the experimental plan (1000 ppm), rather than 10 ppm, as one would anticipate, in the parameters *projected* to produce the highest strengths in brazements with this filler metal (Ag-35Cu-2.0Ti, wt%) in the AD-998 alumina and silicon nitride materials. The only material for which 10 ppm oxygen was recommended was the silicon carbide whisker-reinforced alumina composite. The necessary confirmatory braze runs have not been conducted, as of mid-1993, to determine whether even higher strengths are produced in the silicon carbide whisker-reinforced alumina and silicon nitride materials. The strengths of the alumina materials have already been exceeded by the strengths of the brazements made under several conditions.

However, the authors have conducted an interesting side study (outside the test matrix) that should provide some guidance to someone preparing a brazing procedure at this time. Coupons of the SNW-1000 silicon nitride ceramic were brazed as had been done before, but in a vacuum of 3 mPa (2×10^{-5} mm Hg), to determine whether that atmosphere had a significant effect on brazement strength. Very little differences in brazement strengths were observed. For example, the average strengths of the joints made with brazing conditions of 850 °C (1560 °F), 6 min, and a fine-ground joint surface were 505 ± 74 MPa (73.2 ± 10.5 ksi) and 496 ± 59 MPa (71.9 ± 8.5 ksi) for an atmosphere of vacuum and argon-1000 ppm O_2, respectively. These results suggest that atmosphere purity is not as critical as one might assume when brazing silicon nitride with an active filler metal (at least when the filler metal is preplaced in the joints).

References cited in this section

33. R.L. BRONNES, R.C. HUGHES, AND R.C. SWEET, CERAMIC-TO-METAL BONDING WITH SPUTTERING AS A METALLIZATION TECHNIQUE, *PHILIPS TECH. REV.*, VOL 35, 1975, P 209-211
34. J.P. HAMMOND, S.A. DAVID, AND M.L. SANTELLA, BRAZING CERAMIC OXIDES TO METALS AT LOW TEMPERATURES, *WELD. J.*, VOL 7, 1988, P 227-S TO 232-S
35. P.O. JARVINEN, "NOVEL CERAMIC RECEIVER FOR SOLAR BRAYTON SYSTEMS," CONF-790305-7, MIT LINCOLN LABORATORY, 1979
36. F. HEIM AND H.L. MCDOWELL, "METHOD OF METALLIZING A CERAMIC SUBSTRATE," U.S. PATENT 4,342,632, AUGUST 3, 1982
37. S. WEISS AND C.M. ADAMS, JR., THE PROMOTION OF WETTING AND BRAZING, *WELD. J. SUPPL.*, VOL 46, 1967, P 49S-57S
38. E.F. BRUSH AND C.M. ADAMS, VAPOR COATED SURFACES FOR BRAZING CERAMICS, *WELD. J.*, VOL 47 (NO. 3), 1968, P 106-S TO 114-S

39. M.L. SANTELLA, BRAZING OF TITANIUM-VAPOR-COATED SILICON NITRIDE, *ADV. CERAM. MATER.*, VOL 3 (NO. 5), 1988, P 457-462
40. M.J. RAMSEY AND M.H. LEWIS, INTERFACIAL REACTION MECHANISMS IN SYALON CERAMIC BONDING, *MATER. SCI. ENG.*, VOL 71, 1985, P 113-122
41. J.P. HAMMOND AND G.M. SLAUGHTER, BONDING GRAPHITE TO METALS WITH TRANSITION PIECES, *WELD. J.*, VOL 50 (NO. 1), 1971, P 33-40
42. M.E. TWENTYMAN, PART 1. THE MECHANISM OF GLASS MIGRATION IN THE PRODUCTION OF METAL-CERAMIC SEALS, *J. MATER. SCI.*, VOL 10, 1975, P 765-776
43. M.E. TWENTYMAN AND P. POPPER, PART 2. THE EFFECT OF EXPERIMENTAL VARIABLES ON THE STRUCTURE OF SEALS TO DEBASED ALUMINAS, *J. MATER. SCI.*, VOL 10, 1975, P 777-790
44. M.E. TWENTYMAN AND P. POPPER, PART 3. THE USE OF METALLIZING PAINTS CONTAINING GLASS OR OTHER INORGANIC BONDING AGENTS, *J. MATER. SCI.*, VOL 10, 1975, P 791-798
45. A. KOHNO *ET AL.*, METALLIZING OF NON-OXIDE CERAMICS, *SPECIAL CERAMICS 8, BR. CERAM. PROC.*, NO. 37, S.P. HOWLETT AND D. TAYLOR, ED., OCT 1986, P 125-130
46. E.M. DUNN *ET AL.*, ANALYTICAL AND EXPERIMENTAL EVALUATION OF JOINING SILICON NITRIDE TO METAL AND SILICON CARBIDE TO METAL, *PROC. 26TH AUTOMOTIVE TECHNOLOGY DEVELOPMENT CONTRACTORS COORDINATION MEETING*, SAE P-219, SAE, 1988, P 165-171
47. YU.V. NAIDICH, THE WETTABILITY OF SOLIDS BY LIQUID METALS, *PROGRESS IN SURFACE AND MEMBRANE SCIENCE*, VOL 14, INSTITUTE OF MATERIAL PROBLEMS, ACADEMY OF SCIENCES, UKRAINIAN S.S.R., 1981, P 333-484
48. M.G. NICHOLAS, ACTIVE METAL BRAZING, *BR. CERAM. TRANS. J.*, VOL 85, 1986, P 144-146
49. M.G. NICHOLAS, T.M. VALENTINE, AND M.J. WAITE, THE WETTING OF ALUMINA BY COPPER ALLOYED WITH TITANIUM AND OTHER ELEMENTS, *J. MATER. SCI.*, VOL 15, 1980, P 2197-2220
50. H. MIZUHARA AND K. MALLY, CERAMIC-TO-METAL JOINING WITH ACTIVE BRAZING FILLER METAL, *WELD. J.*, VOL 64 (NO. 10), 1985, P 27-32
51. A.J. MOORHEAD AND H. KEATING, DIRECT BRAZING OF CERAMICS FOR ADVANCED HEAVY-DUTY DIESELS, *WELD. J.*, VOL 65 (NO. 10), 1986, P 17-31
52. M.G. NICHOLAS, PROMOTING THE WETTING AND BRAZING OF CERAMICS, *STRUCT. CERAM. JOINING II*, CERAMIC TRANSACTIONS, VOL 35, A.J. MOORHEAD, R.E. LOEHMAN, AND S.M. JOHNSON, ED., AMERICAN CERAMIC SOCIETY, 1993
53. YU.V. NAIDICH AND V.S. ZHURAVLEV, ADHESION, WETTABILITY AND REACTION OF TITANIUM-CONTAINING MELTS WITH HIGH-MELTING OXIDES, TRANSLATED FROM *OGNEUPORY*, VOL 1, 1974, P 50-55
54. T. ISEKI, H. MATSUZAKI, AND J.K. BOADI, BRAZING OF SILICON CARBIDE TO STAINLESS STEEL, *AM. CERAM. SOC. BULL.*, VOL 64 (NO. 2), 1985, P 322-324
55. R.E. LOEHMAN AND A.P. TOMSIA, *AM. CERAM. SOC. BULL.*, VOL 67 (NO. 2), 1988, P 375
56. M.J. RAMSEY AND M.H. LEWIS, *MATER. SCI. ENG.*, VOL 71, 1985, P 113-122
57. T. ISEKI, H. MATSUZAKI, AND J.K. BOADI, BRAZING OF SILICON CARBIDE TO STAINLESS STEEL, *AM. CERAM. SOC. BULL.*, VOL 64 (NO. 2), 1985, P 322-324
58. M. NAKA *ET AL.*, JOINING OF SILICON NITRIDE WITH AL-CU ALLOYS, *J. MATER. SCI.*, VOL 22, 1987, P 4417-4421
59. T. ISEKI *ET AL.*, *CERAMIC SURFACES AND SURFACE TREATMENTS, BR. CERAM. PROC.*, NO. 34, R. MORRELL AND M.G. NICHOLAS, ED., AUGUST 1984, P 241-248
60. H. MIZUHARA AND T. OYAMA, CERAMIC-METAL SEALS, *CERAMICS AND GLASSES*, VOL 4, *ENGINEERED MATERIALS HANDBOOK*, ASM INTERNATIONAL, 1991, P 502-510
61. M.G. NICHOLAS, PROMOTING THE WETTING AND BRAZING OF CERAMICS, *STRUCT. CERAM.*

JOINING II, CERAMIC TRANSACTIONS, VOL 35, A.J. MOORHEAD, R.E. LOEHMAN, AND S.M. JOHNSON, ED., AMERICAN CERAMIC SOCIETY, 1993

62. W.A. ZDANIEWSKI *ET AL.,* CRYSTALLIZATION TOUGHENING OF CERAMIC ADHESIVES FOR JOINING ALUMINA, *ADV. CERAM. MATER.,* VOL 2 (NO. 3A), 1987, P 204-208
63. S.L. SWARTZ *ET AL.,* JOINING OF ZIRCONIA CERAMICS WITH A CAO-TIO_2-SIO_2 INTERLAYER, *PROC. 26TH AUTOMOTIVE TECHNOLOGY DEVELOPMENT CONTRACTORS COORDINATION MEETING,* P-219, SAE, 1988, P 149-154
64. M.E. MILBERG *ET AL.,* THE NATURE OF SIALON JOINTS BETWEEN SILICON NITRIDE BASED BODIES, *J. MATER. SCI.,* VOL 22, 1987, P 2560-2568
65. S. BAIK AND R. RAJ, LIQUID-PHASE BONDING OF SILICON NITRIDE CERAMICS, *J. AM. CERAM. SOC.,* VOL 70 (NO. 5), 1987, P C105-C107
66. S.M. JOHNSON AND D.J. ROWCLIFFE, MECHANICAL PROPERTIES OF JOINED SILICON NITRIDE, *J. AM. CERAM. SOC.,* VOL 68 (NO. 9), 1985, P 468-472
67. N. IWAMOTO *ET AL.,* JOINING OF SILICON NITRIDE CERAMICS WITH CAO-TIO_2-SIO_2 GLASS SOLDER, *CERAMIC MATERIALS AND COMPONENTS FOR ENGINES, PROC. 2ND INT. SYMPOSIUM,* W. BUNK AND H. HAUSNER, ED., DEUTSCHE KERAMISCHE GESELLSCHAFT E.V., 1986, P 467-474
68. M.L. MECARTNEY *ET AL.,* SILICON NITRIDE JOINING, *J. AM. CERAM. SOC.,* VOL 68 (NO. 9), 1985, P 472-478
69. M. NEILSON, JR. AND D.N. COON, STRENGTH OF SILICON NITRIDE-SILICON NITRIDE JOINTS BONDED WITH OXYNITRIDE GLASS, *CERAM. ENG. SCI. PROC.,* VOL 10 (NO. 11-12), 1989, P 1893-1907
70. D.N. COON, R.L. TALLMAN, AND R.M. NEILSON, JR., HOT ISOSTATICALLY PRESSED SI_3N_4-SI_3N_4 JOINTS BONDED WITH OXYNITRIDE GLASS, *ADV. CERAM. MATER.,* VOL 3 (NO. 2), 1988, P 154-158
71. J.F. BURGESS, C.A. NEUGEBAUER, AND G. FLANAGAN, THE DIRECT BONDING OF METALS TO CERAMICS BY THE GAS-METAL EUTECTIC METHOD, *J. ELECTROCHEM. SOC.,* VOL 122 (NO. 5), 1975, P 688-690
72. Y. YOSHINO, ROLE OF OXYGEN IN BONDING COPPER TO ALUMINA, *J. AM. CERAM. SOC.,* VOL 72 (NO. 8), 1989, P 1322-1327
73. I. OKAMOTO, M. NAKA, K. ASAMI, AND K. HASHIMOTO, FORMATION OF HERCYNITE ($FEAL_2O_4$) AT INTERFACE OF AL_2O_3/STEEL JOINT, *TRANS. JWRI,* VOL 11 (NO. 1), 1982, P 131-133
74. M. NAKA AND I. OKAMOTO, JOINING OF AL_2O_3 TO SUS 304 WITH TI FOIL, *TRANS. JWRI,* VOL 15 (NO. 1), 1986, P 157-158
75. Y. IINO, PARTIAL TRANSIENT LIQUID-PHASE METALS LAYER TECHNIQUE OF CERAMIC-METAL BONDING, *J. MATER. SCI. LETT.,* VOL 10 (NO. 2), 1991, P 104-106
76. M.L. SHALZ, B.J. DALGLEISH, A.P. TOMSIA, AND A.M. GLAESER, NEW APPROACHES TO JOINING CERAMICS FOR HIGH-TEMPERATURE APPLICATIONS, *STRUCTURAL CERAM. JOINING II,* CERAMIC TRANSACTIONS, VOL 35, A.J. MOORHEAD, R.E. LOEHMAN, AND S.M. JOHNSON, ED., AMERICAN CERAMIC SOCIETY, 1993
77. D.S. DUVALL, W.A. OWCZARSKI, AND D.F. PAULONIS, TLP BONDING: A NEW METHOD FOR JOINING HEAT RESISTANT ALLOYS, *WELD. J.,* VOL 53 (NO. 4), 1974, P 203-214
78. D.H. KIM, S.H. HWANG, AND S.S. CHUN, THE WETTING, REACTION AND BONDING OF SILICON NITRIDE BY CU-TI ALLOYS, *J. MATER. SCI.,* VOL 26 (NO. 12), JUNE 1991, P 3223-3234
79. A.J. MOORHEAD AND H.-E. KIM, OXIDATION BEHAVIOUR OF TITANIUM-CONTAINING BRAZING FILLER METALS, *J. MATER. SCI.,* VOL 26, 1991, P 4067-4075

A.J. Moorhead and W.H. Elliott, Jr., Oak Ridge National Laboratory H.-E. Kim, Seoul National University

Ceramic-to-Metal Joints

In addition to the factors considered above for ceramic-to-ceramic joints, there are specific factors that must be considered when developing a procedure for brazing ceramic-to-metal joints. One is that a thermal cycle must be chosen that does not degrade the properties of the materials being joined. Thermal exposure may be a problem for some structural ceramics, such as the magnesia-PSZ, the strength and toughness of which tend to be altered by exposure to temperatures of 1000 °C (1830 °F) and higher for only a few hours (Ref 80). However, most structural ceramics are thermally stable at temperatures typical of those used for brazing with active filler metals (see Table 2) or glasses. The problem, which has been deemed "thermal compatibility" by Pejryd (Ref 81), is generally more severe for the metallic member of a ceramic-to-metal joint. For example, he has shown (Fig. 12) that even a very modest thermal cycle can have a major effect on the mechanical properties of low-expansion superalloy Incoloy 909, which is often considered in the literature as a likely candidate metal in ceramic-to-metal joints. Such thermal behavior tendencies must be taken into account both during material selection and procedure development.

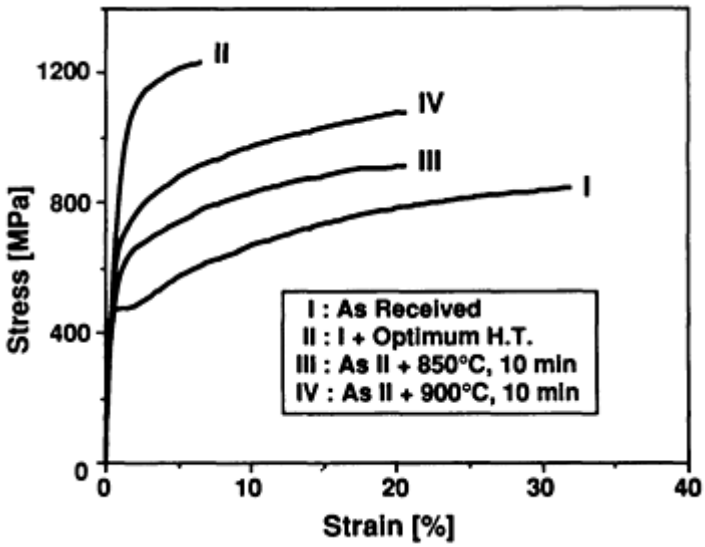

FIG. 12 TENSILE TEST CURVES FOR INCOLOY 909 SUBJECTED TO DIFFERENT BRAZING HEAT-TREATMENT CYCLES. SOURCE: REF 81

Another critical factor is the CTE mismatch of the materials. Differences in expansion behavior can generate significant thermal residual stresses in a ceramic-to-metal brazement, resulting in distortion and even failure during cooldown from the brazing temperature, as shown in Fig. 13.

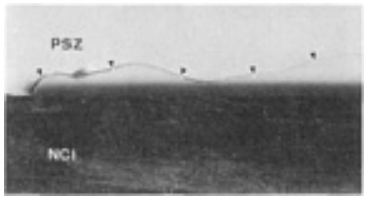

FIG. 13 FAILURE IN THE CERAMIC SIDE OF A CERAMIC-TO METAL BRAZEMENT RESULTING FROM A MISMATCH IN COEFFICIENTS OF THERMAL EXPANSION BETWEEN THE CERAMIC (MAGNESIA-PSZ) AND THE

METAL (NODULAR CAST IRON)

In this example, 2.5 by 4.5 by 26 mm (0.1 by 0.2 by 1 in.) coupons of nodular cast iron and magnesia-PSZ were joined along their long edges using an active filler metal. Upon cooling from the brazing temperature, failure occurred in the ceramic parallel to the interface. These materials are considered to have similar CTE values and had been successfully joined before. However, when thermal expansion data were taken for this particular piece of ceramic, an anomalous and large hysteresis loop was found, indicating that the material had been improperly heat treated during its manufacture, resulting in a different phase composition (and expansion behavior) than expected.

The obvious solution to the problem of CTE mismatch among the members of a ceramic-to-metal joint and the resulting damaging residual stresses is to select an alternate material for either the ceramic or the metallic member. When this cannot be done because of service requirements, or when the thermal expansion is still too great, there are several other alternatives. One is to design the joint such that the ceramic member and joint interfacial region are always in compression. Another is to use ductile metal, which elastically and plastically deforms, to relieve the residual stresses generated during cooldown (or thermal cycling during service), thereby avoiding joint failure. Both of these techniques are widely used by the commercial ceramic/metal or glass/metal seal industry (Ref 60, 82). A third option is to introduce one or more materials between the metal and ceramic components. These materials will serve as a transition between the properties of the two structural materials. The transition material can be one or more discrete layers of monolithic materials (Ref 83, 84, 85) or composite layers that can comprise varying proportions of the materials being joined (Ref 41, 86, 87).

The concept of monolithic transition layers, their compositions (and, thus, properties such as thermal expansion, modulus of elasticity, yield strength, and others), and the optimum thicknesses required are complex subjects. Readers are referred to the references cited above for the details of this approach.

The use of a series of composite layers (with a stepwise transition from one material to the next or a linear gradation in material composition) that are subsequently inserted in the braze joint area is not new. It has been applied successfully, as evidenced by the work of Hammond and Slaughter (Ref 41), who used a series of tungsten-nickel-iron inserts to braze graphite to a nickel-base alloy. In one example, seven transition inserts were used with compositions that varied from 97.5 wt% W and 2.5 wt% of 7Ni/3Fe, adjacent to the graphite, to 40 wt% W and 60 wt% of 7Ni/3Fe, in contact with the nickel alloy. The surface of the graphite was metallized with chromium carbide, and the entire assembly was brazed with pure copper as the filler material.

However, there are numerous cases in which this approach has led to failure. The recent work of Rabin and Heaps (Ref 80) provides a new understanding of how the geometry and micro-structure of the composite transition layer(s) affects the stress distributions in the materials. Using finite-element modeling of alumina-nickel functionally gradient materials, followed by experimental studies, they showed that it is desirable to have a continuous metal phase (high plasticity, low elastic modulus) in each of the transition pieces to best relieve the thermal residual stresses. From a practical standpoint, they were able to accomplish this by using different particle sizes of the alumina and nickel in the compacts. Thus, for the alumina, alumina-20% nickel, and alumina-40% nickel layers, they used 0.5 μm (20 μin.) doped aluminum oxide and 15 to 20 μm (600 to 800 μin.) nickel powders. For the nickel, 60% nickel, and 80% nickel layers, they used 22 μm (880 μin.) doped aluminum oxide and 3 to 7 μm (120 and 280 μin.) nickel powders. The "dopants" in this study were small amounts of manganese and titanium used as sintering aids.

Direct Brazing of Graphitic Materials. Most of the factors that are a concern when brazing ceramics to themselves or to metals are also valid when brazing the various graphites. Two major differences should be considered when these materials are to be joined. The first, which may be overcome through careful material selection, is the fact that the graphites generally tend either to be more porous than the structural ceramics or, if of similar bulk porosity, to have a much finer network of porosity. The effect of such fine porosity can be to draw the filler metal away from the interface, leaving insufficient metal to join the bodies (Ref 88). This effect is readily seen in the micrograph of Fig. 14(a), which shows extensive penetration of a porous graphite when brazed with GTE Wesgo's Ticuni (Ti-15Cu-15Ni, wt%) filler metal. Penetration of the graphite ranged in depth from 200 to 890 μm (0.008 to 0.035 in.) across the metallographic specimen. The solution to this problem was to use a graphite of much greater POCO AXF-5Q density (Fig. 14b), thereby minimizing the loss of filler metal into the component, resulting in the sound braze joint shown in Fig. 14(b).

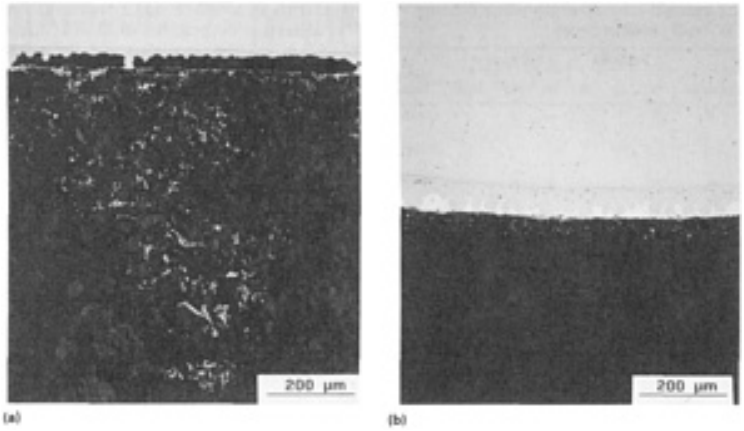

FIG. 14 EFFECT OF POROSITY ON ACTIVE METAL BRAZEMENTS OF GRAPHITE. (A) POROUS GRAPHITE HAS DRAWN THE MOLTEN FILLER METAL FROM THE JOINT, LEAVING A LARGE VOID. (B) MORE HIGHLY DENSE GRAPHITE HAS LEFT MOST OF THE FILLER METAL IN THE JOINT, RESULTING IN A SOUND BRAZEMENT. SOURCE: REF 88

The second major concern when brazing graphites is the stronger tendency for impurities, such as oxygen or water, to be either adsorbed on the surface or absorbed in the bulk of the material. Moisture retention always occurs to some extent, with levels as high as 0.25 wt%. This problem was overcome in one case (Ref 81) by cleaning and baking the graphite components in vacuum for 2 h at 1000 °C (1830 °F) prior to assembly, and then baking the subassemblies themselves (650 °C, or 1200 °F, for 10 min, followed by an overnight evacuation) as part of the brazing cycle.

References cited in this section

41. J.P. HAMMOND AND G.M. SLAUGHTER, BONDING GRAPHITE TO METALS WITH TRANSITION PIECES, *WELD. J.*, VOL 50 (NO. 1), 1971, P 33-40
60. H. MIZUHARA AND T. OYAMA, CERAMIC-METAL SEALS, *CERAMICS AND GLASSES,* VOL 4, *ENGINEERED MATERIALS HANDBOOK,* ASM INTERNATIONAL, 1991, P 502-510
80. D.J. GREEN, R.H.J. HANNINK, AND M.V. SWAIN, *TRANSFORMATION TOUGHENING OF CERAMICS,* CRC PRESS, 1989, P 115-121
81. L. PEJRYD, METAL CERAMIC JOINING FOR HIGH TEMPERATURE APPLICATIONS, *4TH INT. SYMPOSIUM ON CERAMIC MATERIALS AND COMPONENTS FOR ENGINES,* R. CARLSSON, T. JOHANSSON, AND L. KAHLMAN, ED., ELSEVIER APPLIED SCIENCE, 1992, P 50-66
82. E.K. BEAUCHAMP AND S.N. BURCHETT, TECHNIQUES OF SEAL DESIGN, *CERAMICS AND GLASSES,* VOL 4, *ENGINEERED MATERIALS HANDBOOK,* ASM INTERNATIONAL, 1991, P 532-541
83. M.G. NICHOLAS AND R.M. CRISPIN, DIFFUSION BONDING STAINLESS STEEL TO ALUMINA USING ALUMINUM INTERLAYERS, *J. MATER. SCI.,* VOL 17, 1982, P 3347-3360
84. K. SUGANUMA, T. OKAMOTO, AND M. KOIZUMI, EFFECT OF INTERLAYERS IN CERAMIC-METAL JOINTS WITH THERMAL EXPANSION MISMATCHES, *J. AM. CERAM. SOC.,* VOL 67 (NO. 12), 1984, P C256-C257
85. A.-P. XIAN AND Z.-Y. SI, INTERLAYER DESIGN FOR JOINING PRESSURELESS SINTERED SIALON CERAMIC AND 40CR STEEL BRAZING WITH $AG_{57}CU_{38}TI_5$ FILLER METAL, *J. MATER. SCI.,* VOL 27, 1992, P 1560-1566
86. K. SUGANUMA, T. OKAMOTO, M. SHIMADA, AND M. KOIZUMI, NEW METHOD FOR SOLID-STATE BONDING BETWEEN CERAMICS AND METALS, *J. AM. CERAM. SOC.,* 1983, P C117-C118
87. B.H. RABIN AND R.J. HEAPS, POWDER PROCESSING OF NI-AL_2O_3 FGM, TO BE PUBLISHED IN *CERAMIC TRANSACTIONS, PROC. 2ND INT. SYMPOSIUM ON FUNCTIONALLY GRADIENT*

MATERIALS, AMERICAN CERAMIC SOCIETY, 1993

88. J.F. KING *ET AL.*, MATERIALS TESTS AND ANALYSES OF FARADAY SHIELD TUBES FOR ICRF ANTENNAS, *FUSION TECHNOL.*, VOL 15 (NO. 2B), 1989, P 1093-1096

Brazing of Ceramic and Ceramic-to-Metal Joints

A.J. Moorhead and W.H. Elliott, Jr., Oak Ridge National Laboratory H.-E. Kim, Seoul National University

References

1. D.A. PARKER, TECHNOLOGICAL REQUIREMENTS FOR DESIGNING INTERFACES FOR MECHANICAL AND THERMAL APPLICATIONS, *DESIGNING INTERFACES FOR TECHNOLOGICAL APPLICATIONS: CERAMIC-CERAMIC, CERAMIC-METAL JOINING,* S.D. PETEVES, ED., ELSEVIER, 1989, P 3-32
2. R.E. LOEHMAN, CERAMIC JOINING IN THE U.S., *DESIGNING INTERFACES FOR TECHNOLOGICAL APPLICATIONS: CERAMIC-CERAMIC, CERAMIC-METAL JOINING,* S.D PETEVES, ED., ELSEVIER, 1989, P 235-245
3. T. SUGA, CURRENT RESEARCH AND FUTURE OUTLOOK IN JAPAN, *DESIGNING INTERFACES FOR TECHNOLOGICAL APPLICATIONS: CERAMIC-CERAMIC, CERAMIC-METAL JOINING,* S.D. PETEVES, ED., ELSEVIER, 1989, P 247-263
4. L.M. SHEPPARD, AUTOMOTIVE PERFORMANCE ACCELERATES WITH CERAMICS, *AM. CERAM. SOC. BULL.,* VOL 69 (NO. 6), 1990, P 1012-1021
5. K. MATOBA, K. KATAYAMA, M. KAWAMURA, AND T. MIZUNO, THE DEVELOPMENT OF SECOND GENERATION CERAMIC TURBOCHARGER ROTOR--FURTHER IMPROVEMENTS IN RELIABILITY, *AUTOMOTIVE CERAMICS-RECENT DEVELOPMENTS,* SAE P-207, SAE, 1988, P 37-46
6. S. ISHIWATA, AUTOMOTIVE CERAMIC GAS TURBINE R & D IN JAPAN, *PROC. 27TH AUTOMOTIVE TECHNOLOGY DEVELOPMENT CONTRACTORS COORDINATION MEETING,* SAE P-230, SAE, 1990, P 287-292
7. H.E. HELMS, P.J. HALEY, L.E. GROSECLOSE, S.J. HILPISCH, AND A.H. BELL, ADVANCED TURBINE TECHNOLOGY APPLICATIONS PROJECT, *PROC. 27TH AUTOMOTIVE TECHNOLOGY DEVELOPMENT CONTRACTORS COORDINATION MEETING,* SAE P-230, SAE, 1990, P 293-301
8. J.R. KIDWELL, L.J. LINDBERG, AND R.E. MOREY, ATTAP/AGT101--YEARS PROGRESS IN CERAMIC TECHNOLOGY DEVELOPMENT, *PROC. 27TH AUTOMOTIVE TECHNOLOGY DEVELOPMENT CONTRACTORS COORDINATION MEETING,* SAE P-230, SAE, 1990, P 327-334
9. B.D. FOSTER AND J.B. PATTON, ED., *CERAMICS IN HEAT EXCHANGERS,* VOL 14, *PROC. THREE SYMPOSIA ON HEAT EXCHANGERS,* AMERICAN CERAMIC SOCIETY, 1984-1985
10. A.J. HAYES, W.W. LIANG, S.L. RICHLEN, AND E.S. TABB, ED., *INDUSTRIAL HEAT EXCHANGERS, PROC. 1985 EXPOSITION AND SYMPOSIUM ON INDUSTRIAL HEAT EXCHANGER TECHNOLOGY,* AMERICAN SOCIETY FOR METALS, 1985
11. M.H. LEWIS, CERAMICS TO BE JOINED 10 YEARS FROM NOW, *DESIGNING INTERFACES FOR TECHNOLOGICAL APPLICATIONS: CERAMIC-CERAMIC, CERAMIC-METAL JOINING,* S.D. PETEVES, ED., ELSEVIER, 1989, P 271-290
12. P.F. BECHER AND M.K. FERBER, MECHANICAL BEHAVIOUR OF MGO-PARTIALLY STABILIZED ZRO_2 CERAMICS AT ELEVATED TEMPERATURES, *J. MATER. SCI.,* VOL 22, 1987, P 973-980
13. M. RÜHLE AND N. CLAUSSEN, TRANSFORMATION AND MICROCRACK TOUGHENING AS COMPLEMENTARY PROCESSES IN ZRO_2-TOUGHENED AL_2O_3, *J. AM. CERAM. SOC.,* VOL 69 (NO. 3), 1986, P 195-197

14. P.F. BECHER AND T.N. TIEGS, TEMPERATURE DEPENDENCE OF STRENGTHENING BY WHISKER REINFORCEMENT: SIC WHISKER-REINFORCED ALUMINA IN AIR, *ADV. CERAM. MATER.,* VOL 3 (NO. 2), 1988, P 148-153
15. K.M. PREWO, TENSION AND FLEXURAL STRENGTH OF SILICON CARBIDE FIBRE-REINFORCED GLASS CERAMICS, *J. MATER. SCI.,* VOL 21, 1986, P 3590-3600
16. J.J. BRENNAN, GLASS AND GLASS-CERAMIC MATRIX COMPOSITES, *FIBER REINFORCED CERAMIC COMPOSITES,* K.S. MAZDIYASNI, ED., NOYES PUBLICATIONS, 1990, P 222-259
17. T. MAH *ET AL.,* CERAMIC FIBER REINFORCED METAL-ORGANIC PRECURSOR MATRIX COMPOSITES, *FIBER REINFORCED CERAMIC COMPOSITES,* K.S. MAZDIYASNI, ED., NOYES PUBLICATIONS, 1990, P 278-310
18. C.W. LI AND J. YAMANIS, SUPER-TOUGH SILICON NITRIDE WITH *R*-CURVE BEHAVIOR, *CERAM. ENG. SCI. PROC.,* VOL 10 (NO. 7-8), 1989, P 632-645
19. T. KAWASHIMA, H. OKAMOTO, H. YAMAMOTO, AND A. KITAMURA, GRAIN SIZE DEPENDENCE OF THE FRACTURE TOUGHNESS OF SILICON NITRIDE CERAMICS, *J. CERAM. SOC. JAPAN,* INT. ED., VOL 99 (NO. 4), 1991, P 1-4
20. W.D. KINGERY, H.K. BOWEN, AND D.R. UHLMANN, *INTRODUCTION TO CERAMICS,* WILEY, 1976
21. R.W. RICE, CERAMIC COMPOSITES: FUTURE NEEDS AND OPPORTUNITIES, *FIBER REINFORCED CERAMIC COMPOSITES,* K.S. MAZDIYASNI, ED., NOYES PUBLICATIONS, 1990, P 451-495
22. P.F. BECHER, MICROSTRUCTURAL DESIGN OF TOUGHENED CERAMICS, *J. AM. CERAM. SOC.,* VOL 74 (NO. 2), 1991, P 255-269
23. "MATERIAL PROPERTIES DATA SHEET," COORS CERAMICS COMPANY
24. P. CHANTIDUL, S.J. BENNISON, AND B.R. LAWN, ROLE OF GRAIN SIZE IN THE STRENGTH AND *R*-CURVE PROPERTIES OF ALUMINA, *J. AM. CERAM. SOC.,* VOL 78 (NO. 8), 1991, P 2419-2427
25. S. SOMIYA, N. YAMAMOTO, AND H.H. YANAGIDA, ED., *SCIENCE AND TECHNOLOGY OF ZIRCONIA III,* AMERICAN CERAMIC SOCIETY, 1988
26. D. SHIN, K.K. ORR, AND H. SCHUBERT, MICROSTRUCTURE-MECHANICAL PROPERTY RELATIONSHIPS IN HOT ISOSTATICALLY PRESSED ALUMINA AND ZIRCONIA-TOUGHENED ALUMINA, *J. AM. CERAM. SOC.,* VOL 73 (NO. 5), 1990, P 1181-1188
27. H. SCHNEIDER AND E. EBERHARD, THERMAL EXPANSION OF MULLITE, *J. AM. CERAM. SOC.,* VOL 73 (NO. 7), 1990, P 2073-2076
28. A.J. MOORHEAD AND H.-E. KIM, JOINING OXIDE CERAMICS, *CERAMICS AND GLASSES,* VOL 4, *ENGINEERED MATERIALS HANDBOOK,* ASM INTERNATIONAL, 1991, P 511-531
29. J.B. WACHTMAN, JR. AND R.A. HABER, ADVANCED CERAMICS INVOLVING ALUMINA, *ALUMINA CHEMICALS: SCIENCE AND TECHNOLOGY HANDBOOK,* L.D. HART, ED., AMERICAN CERAMIC SOCIETY, 1990, P 329-335
30. "MECHANICAL AND INDUSTRIAL CERAMICS," CAT/2T8505TKU/3000E, KYOCERA CORPORATION
31. "COORS CERAMICS--MATERIALS FOR TOUGH JOBS," BULLETIN NO. 953, COORS PORCELAIN COMPANY
32. R.F. DIEFENDORF, CONTINUOUS CARBON FIBER REINFORCED CARBON MATRIX COMPOSITES, *COMPOSITES,* VOL 1, *ENGINEERED MATERIALS HANDBOOK,* ASM INTERNATIONAL, 1987, P 911-914
33. R.L. BRONNES, R.C. HUGHES, AND R.C. SWEET, CERAMIC-TO-METAL BONDING WITH SPUTTERING AS A METALLIZATION TECHNIQUE, *PHILIPS TECH. REV.,* VOL 35, 1975, P 209-211
34. J.P. HAMMOND, S.A. DAVID, AND M.L. SANTELLA, BRAZING CERAMIC OXIDES TO METALS AT LOW TEMPERATURES, *WELD. J.,* VOL 7, 1988, P 227-S TO 232-S

35. P.O. JARVINEN, "NOVEL CERAMIC RECEIVER FOR SOLAR BRAYTON SYSTEMS," CONF-790305-7, MIT LINCOLN LABORATORY, 1979
36. F. HEIM AND H.L. MCDOWELL, "METHOD OF METALLIZING A CERAMIC SUBSTRATE," U.S. PATENT 4,342,632, AUGUST 3, 1982
37. S. WEISS AND C.M. ADAMS, JR., THE PROMOTION OF WETTING AND BRAZING, *WELD. J. SUPPL.*, VOL 46, 1967, P 49S-57S
38. E.F. BRUSH AND C.M. ADAMS, VAPOR COATED SURFACES FOR BRAZING CERAMICS, *WELD. J.*, VOL 47 (NO. 3), 1968, P 106-S TO 114-S
39. M.L. SANTELLA, BRAZING OF TITANIUM-VAPOR-COATED SILICON NITRIDE, *ADV. CERAM. MATER.*, VOL 3 (NO. 5), 1988, P 457-462
40. M.J. RAMSEY AND M.H. LEWIS, INTERFACIAL REACTION MECHANISMS IN SYALON CERAMIC BONDING, *MATER. SCI. ENG.*, VOL 71, 1985, P 113-122
41. J.P. HAMMOND AND G.M. SLAUGHTER, BONDING GRAPHITE TO METALS WITH TRANSITION PIECES, *WELD. J.*, VOL 50 (NO. 1), 1971, P 33-40
42. M.E. TWENTYMAN, PART 1. THE MECHANISM OF GLASS MIGRATION IN THE PRODUCTION OF METAL-CERAMIC SEALS, *J. MATER. SCI.*, VOL 10, 1975, P 765-776
43. M.E. TWENTYMAN AND P. POPPER, PART 2. THE EFFECT OF EXPERIMENTAL VARIABLES ON THE STRUCTURE OF SEALS TO DEBASED ALUMINAS, *J. MATER. SCI.*, VOL 10, 1975, P 777-790
44. M.E. TWENTYMAN AND P. POPPER, PART 3. THE USE OF METALLIZING PAINTS CONTAINING GLASS OR OTHER INORGANIC BONDING AGENTS, *J. MATER. SCI.*, VOL 10, 1975, P 791-798
45. A. KOHNO *ET AL.*, METALLIZING OF NON-OXIDE CERAMICS, *SPECIAL CERAMICS 8, BR. CERAM. PROC.*, NO. 37, S.P. HOWLETT AND D. TAYLOR, ED., OCT 1986, P 125-130
46. E.M. DUNN *ET AL.*, ANALYTICAL AND EXPERIMENTAL EVALUATION OF JOINING SILICON NITRIDE TO METAL AND SILICON CARBIDE TO METAL, *PROC. 26TH AUTOMOTIVE TECHNOLOGY DEVELOPMENT CONTRACTORS COORDINATION MEETING*, SAE P-219, SAE, 1988, P 165-171
47. YU.V. NAIDICH, THE WETTABILITY OF SOLIDS BY LIQUID METALS, *PROGRESS IN SURFACE AND MEMBRANE SCIENCE*, VOL 14, INSTITUTE OF MATERIAL PROBLEMS, ACADEMY OF SCIENCES, UKRAINIAN S.S.R., 1981, P 333-484
48. M.G. NICHOLAS, ACTIVE METAL BRAZING, *BR. CERAM. TRANS. J.*, VOL 85, 1986, P 144-146
49. M.G. NICHOLAS, T.M. VALENTINE, AND M.J. WAITE, THE WETTING OF ALUMINA BY COPPER ALLOYED WITH TITANIUM AND OTHER ELEMENTS, *J. MATER. SCI.*, VOL 15, 1980, P 2197-2220
50. H. MIZUHARA AND K. MALLY, CERAMIC-TO-METAL JOINING WITH ACTIVE BRAZING FILLER METAL, *WELD. J.*, VOL 64 (NO. 10), 1985, P 27-32
51. A.J. MOORHEAD AND H. KEATING, DIRECT BRAZING OF CERAMICS FOR ADVANCED HEAVY-DUTY DIESELS, *WELD. J.*, VOL 65 (NO. 10), 1986, P 17-31
52. M.G. NICHOLAS, PROMOTING THE WETTING AND BRAZING OF CERAMICS, *STRUCT. CERAM. JOINING II*, CERAMIC TRANSACTIONS, VOL 35, A.J. MOORHEAD, R.E. LOEHMAN, AND S.M. JOHNSON, ED., AMERICAN CERAMIC SOCIETY, 1993
53. YU.V. NAIDICH AND V.S. ZHURAVLEV, ADHESION, WETTABILITY AND REACTION OF TITANIUM-CONTAINING MELTS WITH HIGH-MELTING OXIDES, TRANSLATED FROM *OGNEUPORY*, VOL 1, 1974, P 50-55
54. T. ISEKI, H. MATSUZAKI, AND J.K. BOADI, BRAZING OF SILICON CARBIDE TO STAINLESS STEEL, *AM. CERAM. SOC. BULL.*, VOL 64 (NO. 2), 1985, P 322-324
55. R.E. LOEHMAN AND A.P. TOMSIA, *AM. CERAM. SOC. BULL.*, VOL 67 (NO. 2), 1988, P 375
56. M.J. RAMSEY AND M.H. LEWIS, *MATER. SCI. ENG.*, VOL 71, 1985, P 113-122
57. T. ISEKI, H. MATSUZAKI, AND J.K. BOADI, BRAZING OF SILICON CARBIDE TO STAINLESS

STEEL, *AM. CERAM. SOC. BULL.*, VOL 64 (NO. 2), 1985, P 322-324

58. M. NAKA *ET AL.*, JOINING OF SILICON NITRIDE WITH AL-CU ALLOYS, *J. MATER. SCI.*, VOL 22, 1987, P 4417-4421
59. T. ISEKI *ET AL., CERAMIC SURFACES AND SURFACE TREATMENTS, BR. CERAM. PROC.*, NO. 34, R. MORRELL AND M.G. NICHOLAS, ED., AUGUST 1984, P 241-248
60. H. MIZUHARA AND T. OYAMA, CERAMIC-METAL SEALS, *CERAMICS AND GLASSES*, VOL 4, *ENGINEERED MATERIALS HANDBOOK*, ASM INTERNATIONAL, 1991, P 502-510
61. M.G. NICHOLAS, PROMOTING THE WETTING AND BRAZING OF CERAMICS, *STRUCT. CERAM. JOINING II*, CERAMIC TRANSACTIONS, VOL 35, A.J. MOORHEAD, R.E. LOEHMAN, AND S.M. JOHNSON, ED., AMERICAN CERAMIC SOCIETY, 1993
62. W.A. ZDANIEWSKI *ET AL.*, CRYSTALLIZATION TOUGHENING OF CERAMIC ADHESIVES FOR JOINING ALUMINA, *ADV. CERAM. MATER.*, VOL 2 (NO. 3A), 1987, P 204-208
63. S.L. SWARTZ *ET AL.*, JOINING OF ZIRCONIA CERAMICS WITH A CAO-TIO_2-SIO_2 INTERLAYER, *PROC. 26TH AUTOMOTIVE TECHNOLOGY DEVELOPMENT CONTRACTORS COORDINATION MEETING*, P-219, SAE, 1988, P 149-154
64. M.E. MILBERG *ET AL.*, THE NATURE OF SIALON JOINTS BETWEEN SILICON NITRIDE BASED BODIES, *J. MATER. SCI.*, VOL 22, 1987, P 2560-2568
65. S. BAIK AND R. RAJ, LIQUID-PHASE BONDING OF SILICON NITRIDE CERAMICS, *J. AM. CERAM. SOC.*, VOL 70 (NO. 5), 1987, P C105-C107
66. S.M. JOHNSON AND D.J. ROWCLIFFE, MECHANICAL PROPERTIES OF JOINED SILICON NITRIDE, *J. AM. CERAM. SOC.*, VOL 68 (NO. 9), 1985, P 468-472
67. N. IWAMOTO *ET AL.*, JOINING OF SILICON NITRIDE CERAMICS WITH CAO-TIO_2-SIO_2 GLASS SOLDER, *CERAMIC MATERIALS AND COMPONENTS FOR ENGINES, PROC. 2ND INT. SYMPOSIUM*, W. BUNK AND H. HAUSNER, ED., DEUTSCHE KERAMISCHE GESELLSCHAFT E.V., 1986, P 467-474
68. M.L. MECARTNEY *ET AL.*, SILICON NITRIDE JOINING, *J. AM. CERAM. SOC.*, VOL 68 (NO. 9), 1985, P 472-478
69. M. NEILSON, JR. AND D.N. COON, STRENGTH OF SILICON NITRIDE-SILICON NITRIDE JOINTS BONDED WITH OXYNITRIDE GLASS, *CERAM. ENG. SCI. PROC.*, VOL 10 (NO. 11-12), 1989, P 1893-1907
70. D.N. COON, R.L. TALLMAN, AND R.M. NEILSON, JR., HOT ISOSTATICALLY PRESSED SI_3N_4-SI_3N_4 JOINTS BONDED WITH OXYNITRIDE GLASS, *ADV. CERAM. MATER.*, VOL 3 (NO. 2), 1988, P 154-158
71. J.F. BURGESS, C.A. NEUGEBAUER, AND G. FLANAGAN, THE DIRECT BONDING OF METALS TO CERAMICS BY THE GAS-METAL EUTECTIC METHOD, *J. ELECTROCHEM. SOC.*, VOL 122 (NO. 5), 1975, P 688-690
72. Y. YOSHINO, ROLE OF OXYGEN IN BONDING COPPER TO ALUMINA, *J. AM. CERAM. SOC.*, VOL 72 (NO. 8), 1989, P 1322-1327
73. I. OKAMOTO, M. NAKA, K. ASAMI, AND K. HASHIMOTO, FORMATION OF HERCYNITE ($FEAL_2O_4$) AT INTERFACE OF AL_2O_3/STEEL JOINT, *TRANS. JWRI*, VOL 11 (NO. 1), 1982, P 131-133
74. M. NAKA AND I. OKAMOTO, JOINING OF AL_2O_3 TO SUS 304 WITH TI FOIL, *TRANS. JWRI*, VOL 15 (NO. 1), 1986, P 157-158
75. Y. IINO, PARTIAL TRANSIENT LIQUID-PHASE METALS LAYER TECHNIQUE OF CERAMIC-METAL BONDING, *J. MATER. SCI. LETT.*, VOL 10 (NO. 2), 1991, P 104-106
76. M.L. SHALZ, B.J. DALGLEISH, A.P. TOMSIA, AND A.M. GLAESER, NEW APPROACHES TO JOINING CERAMICS FOR HIGH-TEMPERATURE APPLICATIONS, *STRUCTURAL CERAM. JOINING II*, CERAMIC TRANSACTIONS, VOL 35, A.J. MOORHEAD, R.E. LOEHMAN, AND S.M. JOHNSON, ED., AMERICAN CERAMIC SOCIETY, 1993
77. D.S. DUVALL, W.A. OWCZARSKI, AND D.F. PAULONIS, TLP BONDING: A NEW METHOD FOR JOINING HEAT RESISTANT ALLOYS, *WELD. J.*, VOL 53 (NO. 4), 1974, P 203-214

78. D.H. KIM, S.H. HWANG, AND S.S. CHUN, THE WETTING, REACTION AND BONDING OF SILICON NITRIDE BY CU-TI ALLOYS, *J. MATER. SCI.*, VOL 26 (NO. 12), JUNE 1991, P 3223-3234
79. A.J. MOORHEAD AND H.-E. KIM, OXIDATION BEHAVIOUR OF TITANIUM-CONTAINING BRAZING FILLER METALS, *J. MATER. SCI.*, VOL 26, 1991, P 4067-4075
80. D.J. GREEN, R.H.J. HANNINK, AND M.V. SWAIN, *TRANSFORMATION TOUGHENING OF CERAMICS*, CRC PRESS, 1989, P 115-121
81. L. PEJRYD, METAL CERAMIC JOINING FOR HIGH TEMPERATURE APPLICATIONS, *4TH INT. SYMPOSIUM ON CERAMIC MATERIALS AND COMPONENTS FOR ENGINES*, R. CARLSSON, T. JOHANSSON, AND L. KAHLMAN, ED., ELSEVIER APPLIED SCIENCE, 1992, P 50-66
82. E.K. BEAUCHAMP AND S.N. BURCHETT, TECHNIQUES OF SEAL DESIGN, *CERAMICS AND GLASSES*, VOL 4, *ENGINEERED MATERIALS HANDBOOK*, ASM INTERNATIONAL, 1991, P 532-541
83. M.G. NICHOLAS AND R.M. CRISPIN, DIFFUSION BONDING STAINLESS STEEL TO ALUMINA USING ALUMINUM INTERLAYERS, *J. MATER. SCI.*, VOL 17, 1982, P 3347-3360
84. K. SUGANUMA, T. OKAMOTO, AND M. KOIZUMI, EFFECT OF INTERLAYERS IN CERAMIC-METAL JOINTS WITH THERMAL EXPANSION MISMATCHES, *J. AM. CERAM. SOC.*, VOL 67 (NO. 12), 1984, P C256-C257
85. A.-P. XIAN AND Z.-Y. SI, INTERLAYER DESIGN FOR JOINING PRESSURELESS SINTERED SIALON CERAMIC AND 40CR STEEL BRAZING WITH $AG_{57}CU_{38}TI_5$ FILLER METAL, *J. MATER. SCI.*, VOL 27, 1992, P 1560-1566
86. K. SUGANUMA, T. OKAMOTO, M. SHIMADA, AND M. KOIZUMI, NEW METHOD FOR SOLID-STATE BONDING BETWEEN CERAMICS AND METALS, *J. AM. CERAM. SOC.*, 1983, P C117-C118
87. B.H. RABIN AND R.J. HEAPS, POWDER PROCESSING OF NI-AL_2O_3 FGM, TO BE PUBLISHED IN *CERAMIC TRANSACTIONS, PROC. 2ND INT. SYMPOSIUM ON FUNCTIONALLY GRADIENT MATERIALS*, AMERICAN CERAMIC SOCIETY, 1993
88. J.F. KING *ET AL.*, MATERIALS TESTS AND ANALYSES OF FARADAY SHIELD TUBES FOR ICRF ANTENNAS, *FUSION TECHNOL.*, VOL 15 (NO. 2B), 1989, P 1093-1096
89. P.H. MCCLUSKEY, R.K. WILLIAMS, R.S. GRAVES, AND T.N. TIEGS, THERMAL DIFFUSIVITY AND CONDUCTIVITY OF ALUMINA-SILICON CARBIDE COMPOSITES, *J. AM. CERAM. SOC.*, VOL 73 (NO. 2), 1990, P 461-464
90. J.B. WACHTMAN, JR., ED., *STRUCTURAL CERAMICS, TREATISE ON MATERIALS SCIENCE AND TECHNOLOGY*, VOL 29, ACADEMIC PRESS, 1989

Brazing of Ceramic and Ceramic-to-Metal Joints

A.J. Moorhead and W.H. Elliott, Jr., Oak Ridge National Laboratory H.-E. Kim, Seoul National University

Selected References

• *CERAMICS AND GLASSES*, VOL 4, *ENGINEERED MATERIALS HANDBOOK*, ASM INTERNATIONAL, 1991

Application of Clad Brazing Materials

Michael Karavolis, Sunil Jha, and James Forster, Texas Instruments, Inc.; Kris Meekins, Long Manufacturing Ltd.

Introduction

BRAZING, which is one of the most versatile joining techniques, is the preferred method for making a large number of joints in an assembly. The manufacture of heat exchangers, for example, requires the creation of leak-free joints between specific points and along contact surfaces and seams. The fabrication of high-density heat exchangers, which have a large heat transfer area and a compact size, is best accomplished by brazing (Fig. 1).

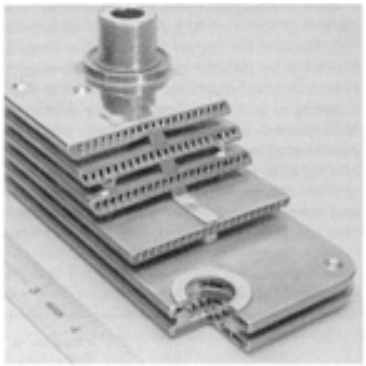

FIG. 1 AUTOMOTIVE ENGINE OIL COOLER MANUFACTURED WITH CLAD BRAZING MATERIALS

In a typical heat-exchanger assembly operation, the components are formed, cleaned, assembled, and fixtured prior to furnace brazing. During the assembly process, the brazing filler metal, which is often in the form of a wire, foil, paste, or powder sheet, is inserted at the appropriate locations. To simplify the assembly operation, the brazing filler metal can be clad to the materials to be brazed, as in aluminum-clad brazing sheet, where the brazing alloy is hot roll bonded to the aluminum alloy sheet (Ref 1). When the brazing filler metal is an integral part of the sheet or strip, the material is called a clad brazing material, because it can be brazed without the need for additional filler metal; that is, the brazing filler metal is already attached to the base material.

Although hot roll bonding is cited in the aluminum-clad brazing sheet example, many combinations of clad brazing materials are manufactured by cold roll bonding, a process that does not involve the explicit heating of the materials prior to the bonding operation. This material system is an economical solution for the fabrication of many high-volume, furnace-brazed products.

Additional information about the process involved in brazing with these materials is available in the article "Brazing With Clad Brazing Materials" in this Volume.

Acknowledgements

The authors thank the many people at Texas Instruments, Inc. who have been involved in the development and production of clad metals. In particular, we thank Jim Matthews, Jerry Johnson, Dick Delagi, and Russ Miller for their continued enthusiastic support and encouragement.

Reference

1. R. BROWN, ALUMINUM ALLOY LAMINATES: AL-CLAD AND CLAD ALUMINUM ALLOY PRODUCTS, *COMPOSITE ENGINEERING LAMINATES,* A.G.H. DIETZ, ED., MIT PRESS, 1969, P 227-239

Michael Karavolis, Sunil Jha, and James Forster, Texas Instruments, Inc.; Kris Meekins, Long Manufacturing Ltd.

Material Selection

The design of heat exchangers for automotive applications varies widely, as does the manufacturing method. The selection of the base metal and brazing filler metal used in a specific heat exchanger depends on several factors, the most important of which are the performance and cooling requirements of the unit. Typical design parameters include space allotted for the heat exchanger, maximum weight of the unit, burst-pressure resistance, cooling capacity, pressure drop, life expectancy, and cost. These factors, among others, influence the size, type, and number of brazed joints in the heat exchanger, and all must be considered.

The materials chosen for a particular heat-exchanger application can vary greatly. In terms of the performance requirements that typically represent the starting point in base metal and brazing filler metal selection, the major concerns are durability and corrosion resistance. Although the need for compatibility with hot and cold fluids is obvious, consideration must also be given to the other materials that the heat exchanger may contact, in order to avoid premature failure that is due to corrosion by galvanic coupling. Some under-the-hood automotive heat exchangers may be exposed to the environment, whereas those that are contained within the engine block are exposed to a totally different environment and temperature range.

Other design considerations include:

- TOTAL NUMBER AND TYPES OF JOINTS
- APPLICATION OF ADDITIONAL CONNECTORS ON THE EXTERIOR OF THE UNIT
- APPLICATION OF A GREATER AMOUNT OF BRAZING FILLER METAL IN CERTAIN AREAS THAN IN THE REST OF THE LOCATIONS TO BE BRAZED
- FIXTURING METHODS NEEDED TO ENSURE PROPER JOINT CONTACT AT THE BRAZING TEMPERATURE DURING THE BRAZING CYCLE

Many engine oil coolers are currently made from stainless steel and use copper as the brazing filler metal. This base metal and filler metal combination is also available as a clad brazing material, where a copper brazing filler metal is clad to a stainless steel base material. Although the AISI 300 and 400 series of stainless steels have been the most widely used materials, low-carbon steels are being used in applications with less-strict corrosion-resistance and strength requirements.

Precautions that must be exercised during the brazing cycle, when using clad brazing materials, are identical to those that must be used when brazing the monolithic metals. For example, low-carbon versions of the 300 series of stainless steels are recommended to reduce the potential for sensitization during cooling from the brazing temperature. An excessively slow cooling rate should be avoided, because it can result in carbide precipitation in the grain boundaries of the stainless steel base material.

For a similar reason, a stabilized grade of 400 stainless steel is recommended to avoid the embrittlement phenomenon that also can result from improper cooling down from the brazing temperature. Typically, low levels of titanium, niobium, or a combination of the two, provide sufficient protection against embrittlement by minimizing the migration of carbon and any dissolved gases, without seriously reducing the wettability of the stainless steel. The niobium grades should be preferred because they are easy to braze, when compared to titanium-stabilized grades.

The copper brazing filler metal that is typically used in these applications conforms to the American Welding Society (AWS) filler-metal specification AWS A5.B, Class BCu-1. Past processing experience has shown that this type of filler metal performs very well in brazed heat exchangers that utilize both AISI 300 and 400 series stainless steels as base materials.

Application of Clad Brazing Materials

Michael Karavolis, Sunil Jha, and James Forster, Texas Instruments, Inc.; Kris Meekins, Long Manufacturing Ltd.

Fabrication of Clad Brazing Materials

The clad brazing materials described here are metals that are metallurgically joined by cold roll bonding. The technology and science of roll bonding and solid-phase welding have been described in detail elsewhere (Ref 2, 3, 4), but are summarized below.

As shown in Fig. 2, the process involves three basic steps:

- CLEANING OF THE MATING SURFACES BY CHEMICAL AND/OR MECHANICAL MEANS TO REMOVE DIRT, LUBRICANTS, SURFACE OXIDES, AND ANY OTHER CONTAMINANTS
- JOINING OF THE MATERIALS IN A BONDING MILL BY ROLLING THEM TOGETHER WITH A THICKNESS REDUCTION THAT RANGES FROM 50 TO 80% IN A SINGLE PASS, IMMEDIATELY AFTER WHICH, THE MATERIALS HAVE AN INCIPIENT, OR GREEN, BOND CREATED BY THE MASSIVE COLD REDUCTION
- SINTERING, A HEAT TREATMENT DURING WHICH THE BOND AT THE INTERFACE IS COMPLETED. DIFFUSION OCCURS AT THE ATOMIC LEVEL ALONG THE INTERFACE AND RESULTS IN A METALLURGICAL BOND THAT IS DUE TO A SHARING OF ATOMS BETWEEN THE MATERIALS. THE RESULTING BOND CAN EXCEED THE STRENGTH OF EITHER OF THE PARENT MATERIALS

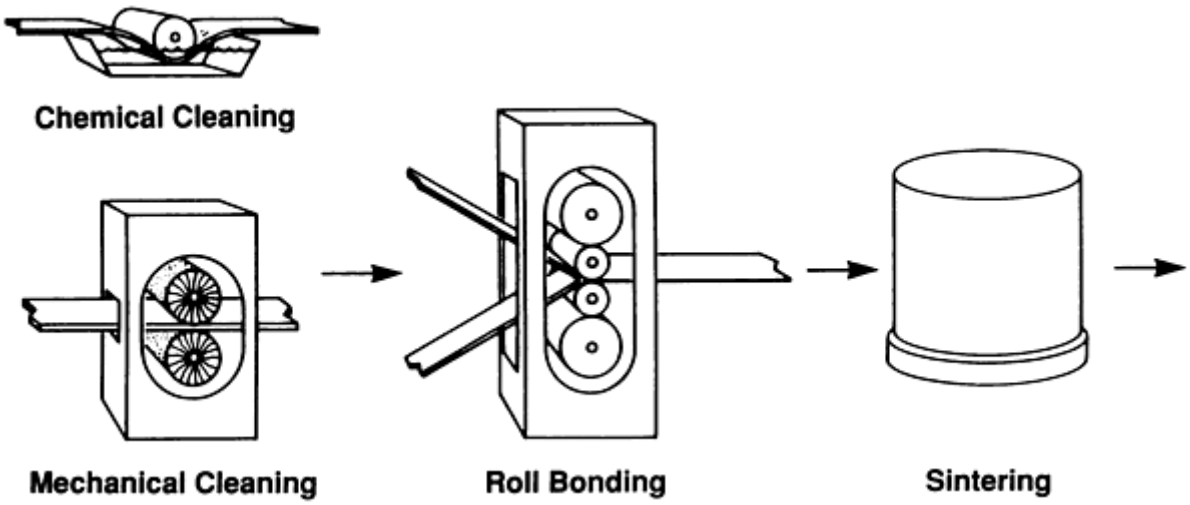

FIG. 2 PROCESS STEPS IN COLD ROLL BONDING

Upon completion of this three-step process, the resultant clad material can be treated in the same way as any other conventional monolithic metal. The clad material can be worked by any of the traditional processing methods for strip metals. Rolling, annealing, pickling, and slitting are typically performed to produce the finished strip to specific customer requirements, so that the material can be roll formed, stamped, or drawn into the required part.

Clad metals are defined by the materials that are present and the volume or thickness ratio of each layer. For example, a copper-clad stainless steel whose total thickness of 0.51 mm (0.020 in.) comprises 0.025 mm (0.001 in.) of copper, 0.46 mm (0.018 in.) of 301 stainless steel, and 0.025 mm (0.001 in.) of copper would be described as 5Cu/90/301SS/5Cu.

The thickness ratio can be determined by a number of techniques, including metallographic examination. A weigh/strip/weigh procedure can be used, where the material is weighed, the cladding is stripped by dissolving it in an appropriate solution such as an acid, and then the sample is weighed again. Another procedure utilizes the magnetic properties of the clad material. The volume ratio that is created during the roll-bonding operation remains through all subsequent finishing operations, including rolling. If appropriate starting material thicknesses and processing conditions are selected, then clad metals can be produced in an infinite number of layer ratios. It should be noted that it is not necessary that the cladding thickness be uniform on both sides of the core material, nor that the core material be clad on both sides. Nonsymmetrical material systems, as well as two-layer material systems, such as thermostat hi-metal, can also be produced. Figure 3 shows the cross section of a Cu/1008AK steel/Cu clad brazing material with a ratio of 5/90/5.

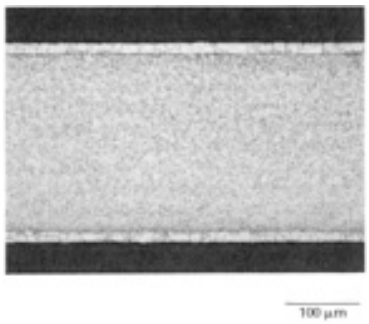

FIG. 3 PHOTOMICROGRAPH OF CU122/1008AK STEEL/CU122 CLAD BRAZING MATERIAL IN 5/90/5 RATIO, NO. 4 TEMPER

The amount of copper cladding is determined by the specific application and by the unit to be brazed. In areas where several hundred brazed joints can be made simultaneously, such as when a plate is joined to turbulator stock, a thicker copper layer (0.05 to 0.1 mm, or 0.002 to 0.004 in.) may be needed. In areas where only one or several joints are to be made, such as a can-to-lid or a plate-to-plate joint, a thinner copper layer (0.025 to 0.05 mm, or 0.001 to 0.002 in.) can be used. For applications in which a different number or different types of joints must be made on either side of a plate, different amounts of copper brazing filler metal can be clad on either side of the base metal. Nonsymmetrical layer ratio materials, such as 5/85/10 or 5/75/20, can be produced when needed.

References cited in this section

2. G. DURST, A NEW DEVELOPMENT IN METAL CLADDING, *J. MET.,* MARCH 1956
3. R.F. TYLECOTE, *THE SOLID PHASE WELDING OF METALS,* ST. MARTINS PRESS, 1968
4. R. DELAGI, DESIGNING WITH CLAD METALS, *MACH. DES.,* NOV 1980

Application of Clad Brazing Materials

Michael Karavolis, Sunil Jha, and James Forster, Texas Instruments, Inc.; Kris Meekins, Long Manufacturing Ltd.

Stamping, Cleaning, and Assembly

Clad metals should be considered to have the same forming characteristics as the core material. For example, a copper-clad 304L stainless steel system will have approximately the same ductility as the unclad 304L stainless steel. In some instances, the formability of the clad is better than that of the monolithic metal core because the copper on the surface of the stainless steel acts as a lubricant in the forming tool. The typical tensile properties of several copper-clad stainless steel clad brazing materials are shown in Tables 1 and 2.

TABLE 1 TWO-LAYER COPPER-CLAD BRAZING SYSTEMS

MATERIAL SYSTEM	LAYER THICKNESS RATIO	TENSILE STRENGTH		0.2% YIELD STRENGTH		ELONGATION IN 50 MM (2 IN.), %
		MPA	KSI	MPA	KSI	
C122/304LSS	6/94	590	86	255	37	**55**
	13.5/86.5	650	94	300	43	**55**
C122/409SS	**15/85**	**400**	**58**	**215**	**31**	**36**

TABLE 2 THREE-LAYER COPPER-CLAD BRAZING SYSTEMS

MATERIAL SYSTEM	VOLUME RATIO	TENSILE STRENGTH		0.2% YIELD STRENGTH		ELONGATION IN 50 MM (2 IN.),%
		MPA	KSI	MPA	KSI	
C122/304LSS/C122	10/80/10	600	87	310	45	**55**
	13/74/13	575	83	290	42	**53**
	32/34/32	380	55	170	25	**48**
C122/409SS/C122	10/80/10	385	56	205	30	**37**
	15/80/5	385	56	205	30	**37**
C122/1008AK/C122	**10/80/10**	**295**	**43**	**215**	**31**	**39**

Notes: All properties shown are typical values for annealed materials, except for Cu122/1008AK/Cu122, which is in the No. 4 temper. Recommended brazing temperature for CDA-122 (AWS A5.8, Class B Cu-1) copper brazing filler metal is 1095 to 1150 °C (2000 to 2100 °F). Brazing atmosphere should be appropriate for the unclad core material.

The tooling that is used for stamping parts from clad metals can be the same as that used to make the monolithic metal core. Because the brazing filler metal is an integral part of the core material, additional stamping and forming operations associated with the production of the shim material are eliminated.

The parts must be cleaned after stamping, prior to assembly. The procedure for the clad metal parts should be similar to that used for cleaning the brazing filler metal shims or preforms. Copper-clad materials should be cleaned by a procedure that is appropriate for copper pans. Because the copper cladding is metallurgically bonded to the stainless steel core, wetting by the copper is ensured, as shown in Fig. 4, and the cleaning of any stainless steel parts is eliminated.

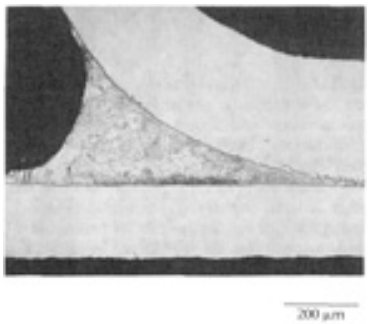

FIG. 4 PHOTOMICROGRAPH OF A TYPICAL BRAZED JOINT THAT WAS FORMED USING A CLAD BRAZING MATERIAL

As with any copper part, care must be taken to prevent oxidation during assembly prior to brazing. Because the copper brazing filler metal is bonded to the stainless steel, the number of pans to be assembled is significantly reduced and any handling of the thin, delicate brazing shim stock is eliminated. Unlike preform shims, which are usually used as flat, two-dimensional inserts, the brazing filler metal on the clad brazing material follows the complex surface topography that was stamped into the base material. Two examples are shown in Fig. 5 and 6. The former depicts a typical plate-type heat exchanger made from a clad brazing material, whereas the latter shows typical contoured joints that can be made easily with clad brazing materials.

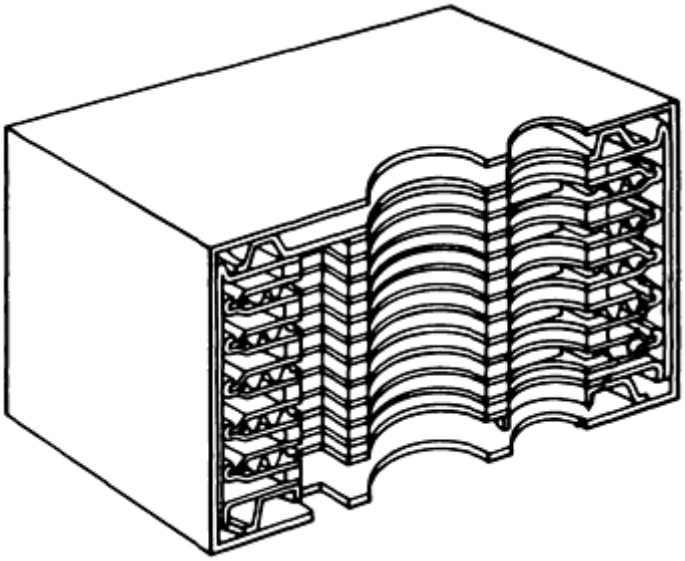

FIG. 5 CUTAWAY VIEW OF A TYPICAL PLATE-TYPE HEAT EXCHANGER

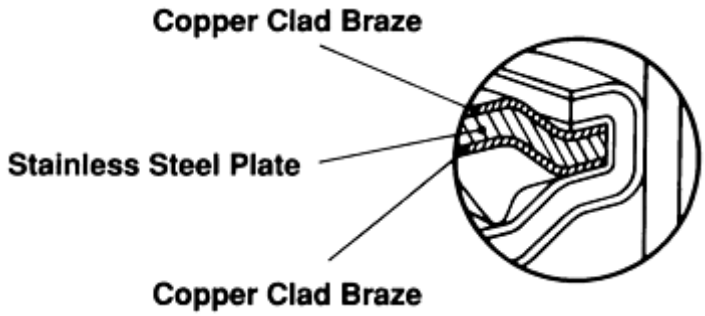

FIG. 6 CONTOURED JOINTS THAT CAN BE MADE EASILY WITH CLAD BRAZING MATERIALS

One design benefit of using clad brazing materials is a reduction of the clearance between the parts, because no allowance needs to be made for the insertion of thick shims, wires, or preforms.

Another benefit is that less copper brazing filler metal can be used, because the concerns associated with the handling of shim material have been eliminated. The thinner copper coating thickness, which typically ranges from 0.025 to 0.075 mm (0.001 to 0.003 in.), results in less shrinkage during brazing and is less likely to cause large brazing fillets. Consequently, the possibility that excess brazing filler metal will clog small passageways is greatly reduced. The typical joint shown in Fig. 7 illustrates the small-geometry passages that can be achieved and the capillary action of the brazing filler metal as it forms the fillets at the joints.

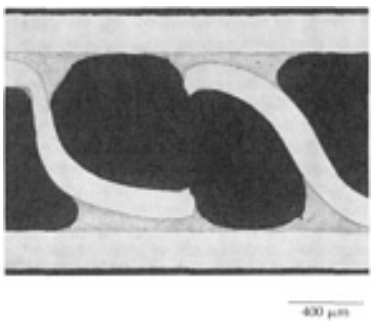

FIG. 7 PHOTOMICROGRAPH OF A PASSAGEWAY IN A HEAT EXCHANGER FABRICATED USING COPPER-CLAD STAINLESS STEEL CLAD BRAZING MATERIAL

Yet another benefit of using clad metals is that once the parts are assembled and fixtured, the brazing filler metal will not shift, move, or fall out as a result of the movement of fixtured assemblies prior to or during the brazing cycle.

Brazing Parameters

Brazing in a vacuum furnace is recommended for clad brazing materials, although the use of a protective gas atmosphere is also possible. Because stainless steel is typically used as the core material of heat exchangers, and because dissociation of the chromium oxide on the surface is essential, vacuum is the preferred brazing atmosphere. In many ways, vacuum furnace brazing with clad metals is similar to the vacuum brazing of stainless steel plates with copper shims. However, there are key differences. Furnace pressures from 0.0015 to 13.5 Pa (10^{-5} to 10^{-1} torr) are typical of the vacuum requirements for brazing with a stainless steel cored clad brazing material (Ref 5). The specific stainless steel alloy will determine the vacuum pressure that is required. No fluxes are needed, and the brazing operation can be considered to be a "clean" process.

Because the brazing filler metal is a pure, deoxidized copper, no additional time is needed to allow any binders to burn off or to outgas during the preheat stage. The heating rate is limited by the need to ensure a uniform temperature throughout the furnace load. Because the clad filler metal is metallurgically bonded to the core material, the wetting and rapid flow of the filler material is ensured. For these reasons, production costs can be lowered by reducing the total cycle time. Temperature control of ±5 °C (± 10 °F) is desired to ensure the proper flow of the brazing filler metal and to limit any filler metal-base metal penetration.

A fast cooling rate will help minimize any filler metal-base metal reactions, as well as production costs. Fast cooling rates are preferred for 300 series stainless steels, whereas slow cooling rates are preferred for the 400 series. The use of low-carbon 300 series and stabilized 400 series stainless steels, as described earlier, should result in a uniform, nonsensitized, non-embrittled core material.

Reference cited in this section

5. *BRAZING MANUAL*, 3RD ED., AWS, 1976, P 66

Application of Clad Brazing Materials

Michael Karavolis, Sunil Jha, and James Forster, Texas Instruments, Inc.; Kris Meekins, Long Manufacturing Ltd.

References

1. R. BROWN, ALUMINUM ALLOY LAMINATES: AL-CLAD AND CLAD ALUMINUM ALLOY PRODUCTS, *COMPOSITE ENGINEERING LAMINATES,* A.G.H. DIETZ, ED., MIT PRESS, 1969, P 227-239
2. G. DURST, A NEW DEVELOPMENT IN METAL CLADDING, *J. MET.,* MARCH 1956
3. R.F. TYLECOTE, *THE SOLID PHASE WELDING OF METALS,* ST. MARTINS PRESS, 1968

4. R. DELAGI, DESIGNING WITH CLAD METALS, *MACH. DES.*, NOV 1980
5. *BRAZING MANUAL*, 3RD ED., AWS, 1976, P 66

General Soldering

Paul T. Vianco, Sandia National Laboratories

Introduction

SOLDERING TECHNOLOGY has been used in applications that range from the packaging of integrated circuit chips to the fabrication of industrial heat exchangers. Consequently, soldering applications are informally categorized as being either structural or electronic in nature. Regardless of these categories, soldering technology depends on certain underlying fundamental parameters and the issues associated with each. This article provides information about these topics:

- *SOLDER ALLOY.* A VARIETY OF ALLOYS AND THEIR PROPERTIES ARE DESCRIBED IN TERMS OF THE SELECTION PROCESS.
- *SUBSTRATE MATERIAL.* ALTHOUGH THE SELECTION OF THE SUBSTRATE BASE MATERIAL IS GENERALLY DETERMINED BY CRITERIA OTHER THAN THE JOINING TECHNIQUE, COATINGS CAN BE USED TO ENHANCE SOLDERABILITY.
- *FLUX.* FLUX SELECTION IS PRIMARILY BASED ON PROMOTING ADEQUATE WETTABILITY BY THE SOLDER. HOWEVER, THE NEED FOR POSTASSEMBLY CLEANING PROCEDURES MUST BE ADDRESSED WHEN THE CORROSIVITY OF THE FLUX RESIDUES JEOPARDIZES THE RELIABILITY REQUIRED OF THE WORKPIECE DURING SERVICE.
- *COMBINED SUBSTRATE, SOLDER, AND FLUX PROPERTIES.* THE COMBINATION OF PROPERTIES MUST BE CONSIDERED IN ORDER TO ESTABLISH THE JOINT DESIGN AND MANUFACTURING PROCEDURES THAT ARE NECESSARY TO SUCCESSFULLY CONSTRUCT THE WORKPIECE.

Each of these parameters is fully explored in this article, using examples of both structural and electronic applications. The article "Soldering in Electronic Applications" explores the latter topic in further detail.

Acknowledgements

This work was performed at Sandia National Laboratories and was supported by the U.S. Department of Energy under contract DE-AC04-76DP00789.

General Soldering

Paul T. Vianco, Sandia National Laboratories

Solder (Filler-Metal) Alloys

The primary criterion used to select a solder is its melting properties. Alloy selection is also determined by the heat sensitivity of the substrate material, the temperature conditions that are expected during service, and the pasty range of the alloy. The melting characteristics of solders are expressed as the solidus and the liquidus temperatures for the alloy. Solders composed of one metallic element, such as tin or indium, have a single melting temperature. Alloys with a eutectic composition have liquidus and solidus temperatures, but they are coincident, and the temperature value is referred to as the "eutectic temperature." The temperature spread between the solidus and liquidus temperatures define the pasty range of the alloy. Solders are commercially available with liquidus temperatures that are as low as 11 °C (51 °F), for the

ternary gallium-indium-tin alloy, to as high as 425 °C (795 °F), for the germanium-aluminum solder. Metal alloys with melting temperatures that exceed 450 °C (812 °F) are categorized as brazing filler metals. The pasty region can range from only a few degrees to nearly 100 °C (180 °F).

Other attributes of the solder include mechanical properties, such as strength and creep resistance; physical properties, such as thermal expansion or thermal conductivity; corrosion resistance; and cost. Because the solder provides a means of fastening two substrates together, its mechanical properties are of great importance. Besides their monotonic strength (tensile and shear) to resist overload stresses, solders must possess sufficient creep strength under sustained loads. This factor is particularly critical, because typical service environments (including room temperature) are actually high-temperature applications, relative to the low melting temperatures of the alloy. The resistance of the solder to fatigue deformation is important to both structural and electronic applications. The coefficient of thermal expansion (CTE) mismatch between the solder and substrate(s) can directly affect the long-term integrity of the solder joint. Thermal conductivity is important for joints that must meet heat-transfer specifications. Corrosion must be considered at all stages of solder joint design, because solder joints have dissimilar metals in intimate contact. Many solders are microstructurally heterogeneous and have other corrosion concerns.

Specifications and standards have established requirements for certain solder alloys in terms of composition limits, impurity levels, and a nomenclature for referencing particular compositions. In the United States, the specifications of solder alloy compositions are found in ASTM B 32 (Ref 1) and Federal Specification QQ-S-571E (Ref 2). Users in the European community prefer the International Organization for Standardization (ISO) specification (draft form) ISO/DIS 9453 (Ref 3). Candidate alloys must be submitted to the particular governing organization for consideration and acceptance as a "specified composition." It should be noted that the commercial availability of a solder material does not necessarily imply that it is included in these and other federal, military, or industrial standards and specifications. In the case of nonstandardized compositions, the user should insist that the vendors certify the composition (including impurities) of their products. Many government and military projects contractually require that the supplier or manufacturer used specified solder compositions in their products.

Although the U.S. standards are generally recognized by foreign industries, the expansion of trade with overseas companies will require that U.S. producers and manufacturers gain an increased familiarity with international standards.

The physical and mechanical properties of bulk solders and solder joints are discussed below. When designing a product, solder joint data are preferred to bulk solder properties. Generally, the use of bulk strength data will underestimate the loading capacity of the joint; that is, calculations will typically be conservative. Although they are not always available, the solder joint properties should include the joint thickness and the testing rate used to obtain the values. Solder selection is also guided by cost. The 1992 prices of metals commonly used in solder alloys are shown in Table 1.

TABLE 1 PRICES OF METALS COMMONLY USED IN SOLDERS

METAL	**$/KG**	$/LB
IN	242.50	**110.00**
AG	132.30	**60.00**
BI	6.60	**3.00**
SN	4.85	**2.20**
CU	2.90	**1.30**
SB	2.00	**0.90**
PB	**0.80**	**0.35**

Prices shown are from 1992.

Source: Ref 4

Tin-lead, tin-lead-antimony, tin-lead-silver, and lead-silver solder compositions, per ASTM B 32, are listed in Table 2. The values are similar in the QQ-S-571E specification. The ISO/DIS 9453 guidelines are given in Table 3. Antimony may be found in solders for any one of three reasons: as an impurity, that is, not intentionally added to the material; as a minor addition of 0.25 wt%, minimum, to try to prevent the formation of the low-temperature allotrope of tin (α of tin at 13.2 °C, or 55.8 °F); and as a principal component, representing 1 to 5 wt%, to improve monotonic and

creep strength of the solder. The levels of added antimony should be less than 7 wt% of the tin component of the solder (the solubility limit of antimony in tin) in order to prevent the formation of tin-antimony intermetallic compounds, which can severely impact the fluidity of the molten solder or reduce the ductility of the solidified joint. The ASTM designation for antimony levels in the solders are: Class A (alloys with tin content greater than 35 wt%), maximum of 0.12 wt%; Class B, 0.2 to 0.5 wt%; and Class C (tin content, 20 to 40 wt%), maximum of 6 wt% (Ref 5).

TABLE 2 ASTM B 32 SPECIFICATION FOR TIN-LEAD, TIN-LEAD-ANTIMONY, TIN-LEAD-SILVER, AND LEAD-SILVER SOLDERS

ALLOY GRADE	**COMPOSITION, %**[A]											MELTING RANGE[B]			
												SOLIDUS		LIQUIDUS	
	Sn	**Pb**	**Sb**	**Ag**	**Cu**	**Cd**	**Al**	**Bi**	**As**	**Fe**	**Zn**	**°C**	**°F**	**°C**	°F
SN70	69.5-71.5	BAL	0.50	0.015	0.08	0.001	0.005	0.25	0.03	0.02	0.005	183	361	193	**377**
SN63	62.5-63.5	BAL	0.50	0.015	0.08	0.001	0.005	0.25	0.03	0.02	0.005	183	361	183	**361**
SN62	61.5-62.5	BAL	0.50	1.75-2.25	0.08	0.001	0.005	0.25	0.03	0.02	0.005	179	354	189	**372**
SN60	59.5-61.5	BAL	0.50	0.015	0.08	0.001	0.005	0.25	0.03	0.02	0.005	183	361	190	**374**
SN50	49.5-51.5	BAL	0.50	0.015	0.08	0.001	0.005	0.25	0.025	0.02	0.005	183	361	216	**421**
SN45	44.5-46.5	BAL	0.50	0.015	0.08	0.001	0.005	0.25	0.025	0.02	0.005	183	361	227	**441**
SN40A	39.5-41.5	BAL	0.50	0.015	0.08	0.001	0.005	0.25	0.02	0.02	0.005	183	361	238	**460**
SN40B	39.5-41.5	BAL	1.8-2.4	0.015	0.08	0.001	0.005	0.25	0.02	0.02	0.005	185	365	231	**448**
SN35A	34.5-36.5	BAL	0.50	0.015	0.08	0.001	0.005	0.25	0.02	0.02	0.005	183	361	247	**447**
SN35B	34.5-36.5	BAL	1.6-2.0	0.015	0.08	0.001	0.005	0.25	0.02	0.02	0.005	185	365	243	**470**
SN30A	29.5-31.5	BAL	0.50	0.015	0.08	0.001	0.005	0.25	0.02	0.02	0.005	183	361	255	**491**
SN30B	29.5-31.5	BAL	1.4-1.8	0.015	0.08	0.001	0.005	0.25	0.02	0.02	0.005	185	365	250	**482**
SN25A	24.5-26.5	BAL	0.50	0.015	0.08	0.001	0.005	0.25	0.02	0.02	0.005	183	361	266	**511**
SN25B	24.5-26.5	BAL	1.1-1.5	0.015	0.08	0.001	0.005	0.25	0.02	0.02	0.005	185	365	263	**504**
SN20A	19.5-21.5	BAL	0.50	0.015	0.08	0.001	0.005	0.25	0.02	0.02	0.005	183	361	277	**531**
SN20B	19.5-21.5	BAL	0.8-1.2	0.015	0.08	0.001	0.005	0.25	0.02	0.02	0.005	184	363	270	**517**
SN15	14.5-16.5	BAL	0.50	0.015	0.08	0.001	0.005	0.25	0.02	0.02	0.005	225	437	290	**554**
SN10A	9.0-11.0	BAL	0.50	0.015	0.08	0.001	0.005	0.25	0.02	0.02	0.005	268	514	302	**576**
SN10B	9.0-11.0	BAL	0.20	1.7-2.4	0.08	0.001	0.005	0.03	0.02	0.02	0.005	268	514	299	**570**
SN5	4.5-5.5	BAL	0.50	0.015	0.08	0.001	0.005	0.25	0.02	0.02	0.005	308	586	312	**594**
SN2	1.5-2.5	BAL	0.50	0.015	0.08	0.001	0.005	0.25	0.02	0.02	0.005	316	601	322	**611**
AG1.5	0.75-1.25	BAL	0.40	1.3-1.7	0.30	0.001	0.005	0.25	0.02	0.02	0.005	309	588	309	**588**
AG2.5	0.25	BAL	0.40	2.3-2.7	0.30	0.001	0.005	0.25	0.02	0.02	0.005	304	580	304	**580**
AG5.5	**0.25**	**BAL**	**0.40**	**5.0-6.0**	**0.30**	**0.001**	**0.005**	**0.25**	**0.02**	**0.02**	**0.005**	**304**	**580**	**380**	**716**

(A) LIMITS ARE MAXIMUM PERCENTAGES, UNLESS SHOWN AS A RANGE OR STATED OTHERWISE. FOR PURPOSES OF DETERMINING CONFORMANCE TO THESE LIMITS, AN OBSERVED VALUE OR CALCULATED VALUE OBTAINED FROM ANALYSIS SHALL BE ROUNDED TO THE NEAREST UNIT IN THE LAST RIGHT-HAND PLACE OF FIGURES USED IN EXPRESSING THE SPECIFIED LIMIT, IN ACCORDANCE WITH THE ROUNDING METHOD OF ASTM RECOMMENDED PRACTICE E 29.

(B) TEMPERATURES GIVEN ARE APPROXIMATIONS AND ARE FOR INFORMATION ONLY.

TABLE 3 ISO/DIS 9453 SPECIFICATION FOR TIN-LEAD, TIN-LEAD-ANTIMONY, TIN-LEAD-SILVER, AND LEAD-SILVER SOLDERS

ALLOY NO.	ALLOY DESIGNATION	MELTING OR SOLIDUS/LIQUIDUS TEMPERATURE (A)		CHEMICAL COMPOSITION, %(B)											SUM OF ALL IMPURITIES EXCEPT SB, BI, AND CU
		°C	°F	Sn	Pb	Sb	Cd	Zn	Al	Bi	As	Fe	Cu	Ag	
TIN-LEAD ALLOYS															
1	S-SN63PB37	183	360	62.5-63.5	BAL	0.12	0.002	0.001	0.001	0.10	0.03	0.02	0.05	...	**0.08**
1A	E-SN63PB37	183	360	62.5-63.5	BAL	0.05	0.002	0.001	0.001	0.05	0.03	0.02	0.05	...	**0.08**
2	S-SN60PB40	183-190	360-375	59.5-60.5	BAL	0.12	0.002	0.001	0.001	0.10	0.03	0.01	0.05	...	**0.08**
2A	E-SN60PB40	183-190	360-375	59.5-60.5	BAL	0.05	0.002	0.001	0.001	0.05	0.03	0.02	0.05	...	**0.08**
3	S-PB50SN50	183-215	360-420	49.5-50.5	BAL	0.12	0.002	0.001	0.001	0.10	0.03	0.02	0.05	...	**0.08**
3A	E-PB50SN50	183-215	360-420	49.5-50.5	BAL	0.05	0.002	0.001	0.001	0.05	0.03	0.02	0.05	...	**0.08**
4	S-PB55SN45	183-226	360-440	44.5-45.5	BAL	0.50	0.005	0.001	0.001	0.25	0.03	0.02	0.08	...	**0.08**
5	S-PB60SN40	183-235	360-455	39.5-40.5	BAL	0.50	0.005	0.001	0.001	0.25	0.03	0.02	0.08	...	**0.08**
6	S-PB65SN35	183-245	360-470	34.5-35.5	BAL	0.50	0.005	0.001	0.001	0.25	0.03	0.02	0.08	...	**0.08**
7	S-PB70SN30	183-255	360-490	29.5-30.5	BAL	0.50	0.005	0.001	0.001	0.25	0.03	0.03	0.08	...	**0.08**
8	S-PB90SN10	268-302	515-575	9.5-10.5	BAL	0.50	0.005	0.001	0.001	0.25	0.03	0.02	0.08	...	**0.08**
9	S-PB92SN8	280-305	535-580	7.5-8.5	BAL	0.50	0.005	0.001	0.001	0.25	0.03	0.02	0.08	...	**0.08**
10	S-PB98SN2	320-325	610-620	1.5-2.5	BAL	0.12	0.002	0.001	0.001	0.10	0.03	0.02	0.05	...	**0.08**
TIN-LEAD ALLOYS WITH ANTIMONY															
11	S-SN63PB37SB	183	360	62.5-63.	BAL	0.12-0.5	0.002	0.001	0.001	0.10	0.03	0.02	0.05	...	**0.08**

				5		0									
12	S-SN60PB40SB	183-190	360-375	59.5-60.5	BAL	0.12-0.50	0.002	0.001	0.001	0.10	0.03	0.02	0.05	. . .	**0.08**
13	S-PB50SN50SB	183-216	360-420	49.5-50.5	BAL	0.12-0.50	0.002	0.001	0.001	0.10	0.03	0.02	0.05	. . .	**0.08**
14	S-PB58SN40SB2	185-231	365-450	39.5-40.5	BAL	2.0-2.4	0.005	0.001	0.001	0.25	0.03	0.02	0.08	. . .	**0.08**
15	S-PB69SN30SB1	185-250	360-480	29.5-30.5	BAL	0.5-1.8	0.005	0.001	0.001	0.25	0.03	0.02	0.08	. . .	**0.08**
16	S-PB74SN25SB1	185-263	360-505	24.5-25.5	BAL	0.5-2.0	0.005	0.001	0.001	0.25	0.03	0.02	0.08	. . .	**0.08**
17	S-PB78SN20SB2	185-270	365-520	19.5-20.5	BAL	0.5-3.0	0.005	0.001	0.001	0.25	0.03	0.02	0.08	. . .	**0.08**
LEAD-SILVER AND LEAD-TIN-SILVER ALLOYS															
32	S-PB98AG2	304-305	580-581	0.25	BAL	0.10	0.002	0.001	0.001	0.10	0.03	0.02	0.05	2.0-3.0	**0.2**
33	S-PB95AG5	304-365	580-690	0.25	BAL	0.10	0.002	0.001	0.001	0.10	0.03	0.02	0.05	4.5-6.0	**0.2**
34	**S-PB93SN5AG2**	**296-301**	**560-570**	**4.8-5.2**	**BAL**	**0.10**	**0.002**	**0.001**	**0.001**	**0.10**	**0.03**	**0.02**	**0.05**	**1.2-1.8**	**0.2**

Source: Ref 3

(A) TEMPERATURES GIVEN ARE FOR INFORMATION PURPOSES AND ARE NOT SPECIFIED REQUIREMENTS FOR THE ALLOYS.

(B) ALL SINGLE FIGURE LIMITS ARE MAXIMUM PERCENTAGES.

The thick, tenacious oxide of lead and the corrosion product layers that form on tin limit the extent of general corrosion to tin-lead solders. However, the lead-rich phase is particularly susceptible to corrosion in the presence of chloride ions, water, or carbon dioxide (from the atmosphere). The reaction by-product from the latter two is a white powder, identified as lead carbonate (Ref 6). The poor adhesion of lead carbonate to the lead causes it to drop away (known as "spalling"), exposing new metal to corrosion, until the solder film becomes a skeleton of tin-rich crystals.

The high-lead solders, which have a 5 to 20 wt% Sn content, are used extensively in micro-electronics packaging (flipchip or C^4 technology) or in high-temperature applications. Other applications include radiator assembly and automobile body repair, which utilize torch heating techniques. A drop in the liquidus temperature is obtained when tin content increases from 20 to 30 wt%. The 5 to 20 wt% Sn alloys have a wider pasty range that provides greater workability, whereas the higher tin content improves the wetting and flow of the solder. On the other hand, increased concentrations of tin also raise the price of the solder.

The most widely used solders are the eutectic 63Sn-37Pb and the near-eutectic alloys, 60Sn-40Pb and 50Sn-50Pb. These solders are used in electronics and structural applications, such as the assembly of conduit for nonpotable water, industrial fluids, compressed gas products, and vacuum assemblies. The narrow pasty range of these alloys limits their workability

prior to solidification. The largest use of the eutectic and near-eutectic solder is in the assembly of circuit boards for electronic products.

The alloys with higher tin contents of 65 to 100 wt% have more limited applications, because the melting temperatures and pasty range needed for structural applications can be provided by the less-expensive lead-rich compositions. However, the tin-rich alloys have improved wettability for hard-to-solder substrates.

The physical and mechanical properties of bulk tin-lead solders are given in Tables 4, 5, 6, 7, 8, and 9. The room-temperature physical properties of the tin-lead solders, ranked by tin content, are listed in Table 4. The CTE decreases with increasing tin content, whereas both thermal and electrical conductivities rise with tin content. Surface tension and viscosity data, which are indicative of capillary filling in holes and gaps by the solders, are listed in Table 5. The addition of flux will tend to *lower* the surface tension of the molten solder.

TABLE 4 PHYSICAL PROPERTIES OF TIN-LEAD SOLDERS

TIN CONTENT, WT%	**DENSITY, G/CM^3**	**ELECTRICAL CONDUCTIVITY OF COPPER, %IACS$^{(A)}$**	**THERMAL CONDUCTIVITY**		COEFFICIENT OF LINEAR THERMAL EXPANSION, 10^{-6}/K
			W/M · K	**BTU · IN./S · FT^2 · °F**	
0	11.34	7.9	34.8	0.067	**29.3**
5	10.80	8.1	35.3	0.068	**28.4**
10	10.50	8.2	35.8	0.069	**27.9**
20	10.04	8.7	37.4	0.072	**26.5**
30	9.66	9.3	40.5	0.078	**25.6**
40	9.28	10.1	43.6	0.084	**24.7**
50	8.90	10.9	46.7	0.090	**23.6**
60	8.52	11.5	49.8	0.096	**21.6**
63	8.34	11.8	50.9	0.098	**21.2**
70	8.17	12.5	. . .	. . .	**20.7**
100	**7.29**	**15.6**	**73.2**	**0.141**	**23.5**

(A) IACS, INTERNATIONAL ANNEALED COPPER STANDARD

TABLE 5 SURFACE TENSION AND VISCOSITY OF TIN-LEAD SOLDERS

TIN CONTENT, WT%	**TEMPERATURE**		**SURFACE TENSION**		VISCOSITY	
	°C	**°F**	**10^3 N/M**	**LBF/FT**	**PA · S**	LB · S/FT^2
100	260	500	548	0.0378	42.3$^{(A)}$	**0.884$^{(A)}$**
80	280	536	514	0.0354	44.4	**0.928**
63	280	536	490	0.0338	45.6	**0.952**
50	280	536	476	0.0328	50.7	**1.058**
42	280	536	474	0.0327	53.0	**1.107**
30	280	536	470	0.0324	56.7	**1.184**
20	280	536	467	0.0322	62.9	**1.314**
0	**390**	**734**	**439**	**0.0302**	**56.5**	**1.179**

Source: Ref 7

(A) COMPUTED ESTIMATE AT 260 °C (500 °F) FROM DATA AT 232 °C (450 °F) AND 351 °C (665 °F).

TABLE 6 MECHANICAL PROPERTIES OF TIN-LEAD SOLDERS

TIN CONTENT, WT%	**TENSILE STRENGTH**		**SHEAR STRENGTH**		**ELONGATION, %**	**MODULUS OF ELASTICITY**		**HARDNESS, HB**	**IZOD IMPACT STRENGTH**		STRESS TO PRODUCE A CREEP STRAIN RATE OF 10^{-4}/DAY	
	MPA	**KSI**	**MPA**	**KSI**		**GPA**	**10^6 PSI**		**J**	**FT · LBF**	**MPA**	KSI
0	12	1.8	12	1.8	55	18	2.61	4	8.1	6	1.7	**0.250**
5	28	4.0	14	2.1	45			8	9.5	7	1.4	**0.200**
10	30	4.4	17	2.4	30	19	2.76	I0	11	8	. . .	**. . .**
20	33	4.8	21	3.0	20	20	2.90	11	15	11	. . .	**. . .**
30	34	5.0	28	4.0	18	21	3.05	12	16	12	0.80	**0.115**
40	37	5.4	32	4.6	25	23	3.34	12	19	14	. . .	**. . .**
50	41	6.0	36	5.2	35	. . .	. . .	14	20	15	0.86	**0.125**
60	52	7.6	39	5.6	40	30	4.35	16	20	15	. . .	**. . .**
63	54	7.8	37	5.4	37	. . .	. . .	17	20	15	2.3	**0.335**
70	**54**	**7.8**	**36**	**5.2**	**30**	**35**	**5.08**	**17**	**19**	**14**	**. . .**	**. . .**

TABLE 7 MECHANICAL PROPERTIES OF TIN-LEAD SOLDERS AT CRYOGENIC TEMPERATURES

TIN CONTENT, WT%	**TENSILE STRENGTH**		**SHEAR STRENGTH**		ELONGATION, %
	MPA	**KSI**	**MPA**	**KSI**	
TESTED AT -73 °C (-100 °F)					
10	43	5.9	31	4.5	**34**
20	48	7.0	37	5.3	**32**
40	48	6.9	40	5.8	**43**
60	59	8.5	54	7.9	**48**
TESTED AT -196 °C (-320 °F)					
10	59	8.6	43	6.3	**27**
20	85	12.0	58	8.4	**30**
40	87	13.0	77	11.0	**30**
60	**130**	**19.9**	**110**	**16.0**	**10**

Source: Ref 9

TABLE 8 MECHANICAL PROPERTIES OF TIN-LEAD-ANTIMONY SOLDERS

COMPOSITION, WT%			**TENSILE STRENGTH**		**SHEAR STRENGTH**		**IZOD IMPACT STRENGTH**		**ELONGATION, %**	STRESS FOR CREEP STRAIN RATE OF 10^{-3}/DAY	
SN	**PB**	**SB**	**MPA**	**KSI**	**MPA**	**KSI**	**J**	**FT · LBF**		**MPA**	KSI
30	69	1.0	46	6.6	30	4.4	15.3	11.3	21	2.0	**0.30**
40	57.5	2.5	49	7.1	37	5.3	14.1	10.4	34	2.9	**0.42**
50	47	3.0	52	7.5	42	6.1	15.0	11.1	29	3.3	**0.48**
60	**36.4**	**3.6**	**61**	**8.8**	**42**	**6.1**	**16.0**	**11.5**	**18**	**3.3**	**0.48**

TABLE 9 CREEP LIFE DATA FOR BULK TIN-LEAD AND TIN-LEAD-ANTIMONY SOLDERS

COMPOSITION, WT%			STRESS AT INDICATED TEMPERATURE					
			AT 20 °C (68 °F)		**AT 100 °C (212 °F)**		AT 149 °C (300 °F)	
SN	**PB**	**SB**	**MPA**	**KSI**	**MPA**	**KSI**	**MPA**	KSI
FOR CREEP LIFE OF 1000 H								
10	90	. . .	35.0	5.08	1.10	0.159	. . .	**. . .**
40	58	2	49.0	7.11	5.90	0.856	. . .	**. . .**
40	60	. . .	21.0	3.05	4.20	0.609	. . .	**. . .**
60	40	. . .	29.0	4.21	4.50	0.653	. . .	**. . .**
FOR CREEP LIFE OF 10 YEARS								
5	95	. . .	3.4	0.50	1.7	0.250	1.0	**0.150**
10	90	. . .	3.2	0.47	1.4	0.20	0.69	**0.100**
20	80	. . .	2.5	0.36	0.83	0.12	0.34	**0.05**
30	70	. . .	2.1	0.30	0.62	0.09	0.21	**0.03**
40	60	. . .	1.8	0.26	0.52	0.075	0.21	**0.03**
50	50	. . .	1.7	0.25	0.52	0.075	0.21	**0.03**
60	**40**	**. . .**	**1.7**	**0.25**	**0.52**	**0.075**	**0.21**	**0.03**

The mechanical properties of the tin-lead alloys are listed in Table 6. The tensile strength values were obtained at a strain rate of 0.5/min. The tensile and shear strength values of solders are very sensitive to the rate of testing, and they typically decrease with decreasing test rate. In fact, the percent decrease in strength is significantly *larger* at the elevated temperatures.

The room-temperature strength properties are a function of the time period between alloy solidification and testing. Annealing of the test sample (at room or higher temperatures) should be performed to stabilize the microstructure to ensure consistent, reproducible data. Tensile strength data of 63Sn-37Pb suggest that stability is reached by room-temperature aging for 60 days (Ref 8). Recommended high-temperature-aging treatments to accelerate stabilization have not been specified. The use of high-temperature annealing should be accompanied by microstructural evaluations to ensure that the aging mechanism is similar to that which exists at room temperature.

Strength data for the tin-lead alloys at cryogenic temperatures of -73 °C (-100 °F) and -196 °C (-320 °F) are included in Table 7. It is important to note that alloy ductility drops sharply at the lower temperatures. The Brinell hardness values of the tin-lead solders as a function of composition are given in Ref 9.

The mechanical properties of the tin-lead-antimony solders are listed in Table 8. Antimony additions of 2 to 4 wt% increase both the tensile and shear strengths and the creep resistance of the tin-lead alloys. Similar behavior is recorded with the addition of 1 to 3 wt% Ag, as occurs with the Sn62 (ASTM B 32) alloy. Impact strength is not significantly altered by antimony additions. Ductility varies with antimony content, reaching a maximum at approximately 2.5 wt% Sb.

Testing temperatures affect mechanical properties significantly. General trends can be obtained from the tensile strength and ductility data shown in Fig. 1 for 60Sn-40Pb and 90Pb-10Sn solders. Strength decreases and ductility increases as the test temperature increases. The tensile strength trend is not monotonic for the 60Sn-40Pb and 90Pb-10Sn solders. At approximately -129 °C (-200 °F), strength reaches a maximum.

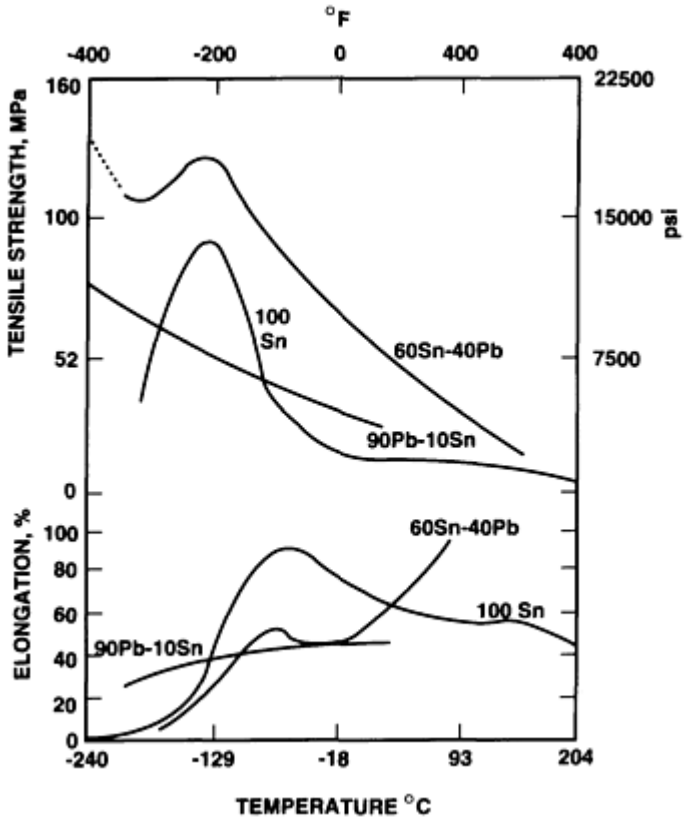

FIG. 1 TENSILE PROPERTIES OF BULK SOLDERS AS A FUNCTION OF TESTING TEMPERATURE

Table 9 gives the maximum creep stress values required to yield a life of 1000 h at temperatures of 20 °C (68 °F) and 100 °C (212 °F), as well as the maximum stress levels for the 10-year life of bulk tin-lead solders, as a function of tin content.

These data indicate that for a constant creep life, the stress value must decrease as the tin content increases. The addition of antimony improves the creep strength.

The fatigue life of bulk 60Sn-40Pb solder is shown in Fig. 2, whereas that of bulk 60Sn-40Pb solder as a function of testing rate is depicted in Fig. 3.

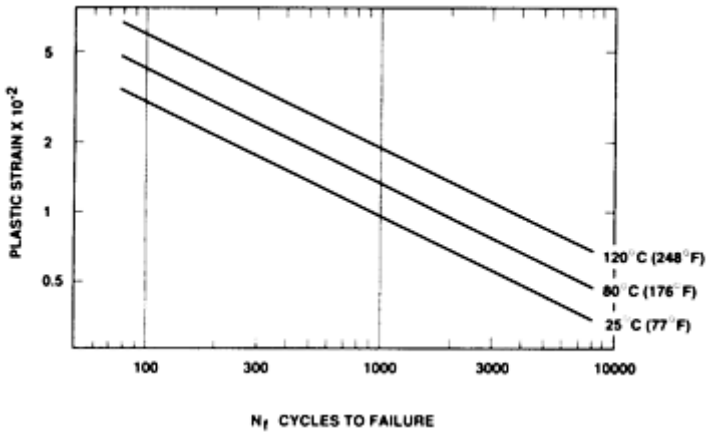

FIG. 2 ISOTHERMAL FATIGUE LIFE (PLASTIC STRAIN DEPENDENCE) OF BULK 60SN-40PB SOLDER. SOURCE: REF 10

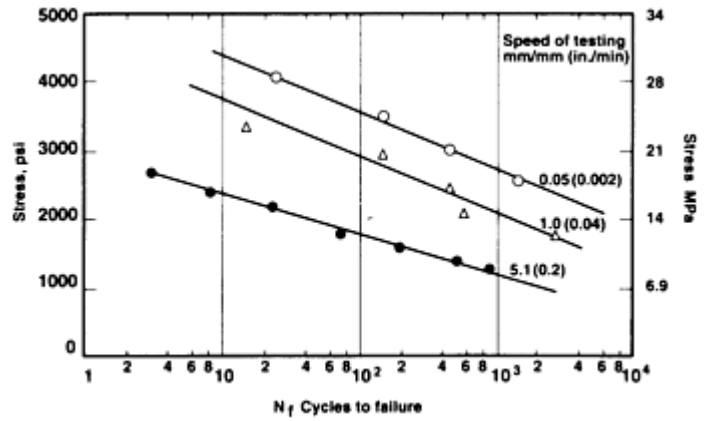

FIG. 3 ROOM-TEMPERATURE FATIGUE LIFE (STRESS DEPENDENCE) OF BULK 60SN-40PB SOLDER

The tin-lead-antimony solders demonstrate room-temperature aging of the microstructure and corresponding changes in the mechanical properties (Ref 11). Tensile strength data for the 60Sn-40Pb alloy following room-temperature aging are shown in Fig. 4. Strength and hardness do not decrease monotonically with time for alloys that have >3 wt% Sb. As shown in Fig. 5, a maximum in hardness is observed in the data for 47Sn-47Pb-6Sb.

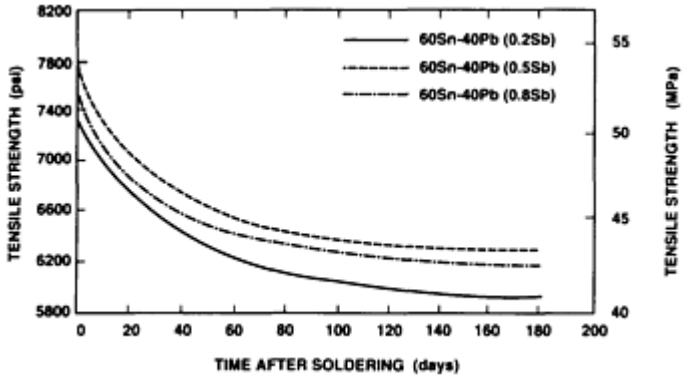

FIG. 4 TENSILE STRENGTH OF 60SN-40PB SOLDER AFTER ROOM-TEMPERATURE AGING. SOURCE: REF 8

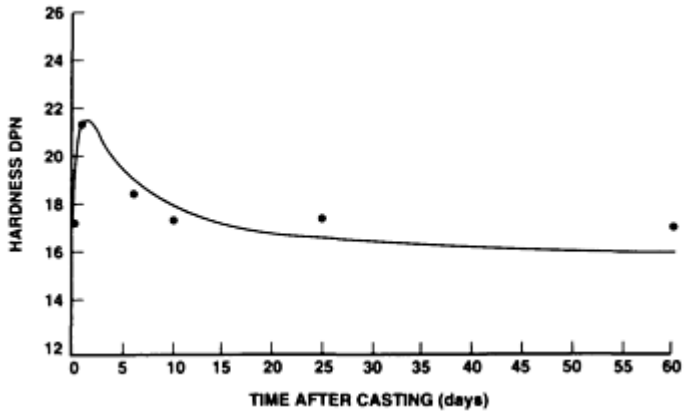

FIG. 5 HARDNESS OF 47SN-47PB-6SB SOLDER AFTER ROOM-TEMPERATURE AGING. SOURCE: REF 8

The effect of joint thickness on shear strength of copper substrates and 56Sn-44Pb solder is shown in Fig. 6. Typically, the maximum strength of solder joints is achieved with a thickness that ranges from 0.076 to 0.18 mm (3 to 7 mils).

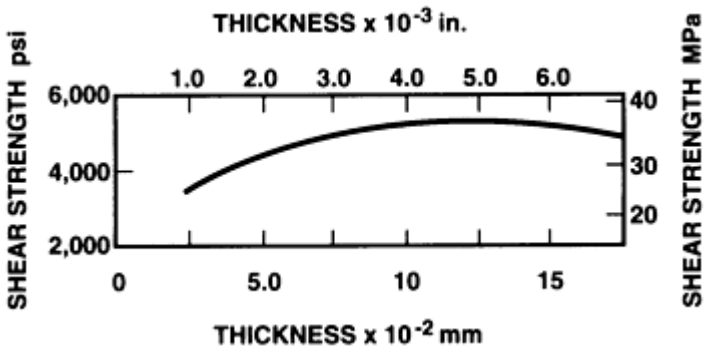

FIG. 6 SHEAR STRENGTH OF COPPER/56SN-44PB/COPPER SOLDER JOINTS AS A FUNCTION OF JOINT THICKNESS. SOURCE: REF 12

The primary sample geometries for the mechanical testing of solder joints are shown in Fig. 7. The appropriate ASTM test specifications for each configuration are D 1002, for the single-lap shear test; D 3528, for the double-lap shear test; F 1044, for the ring-in-plug test; D 897, for the tensile strength of joints; and D 1876, for the T-peel test. The sample

geometries test the joints in shear, the predominant loading mode for soldered joints. These test methods, along with those for measuring the creep and fatigue of adhesive joints, are listed in Table 10. The ring-in-plug test can be used for shear testing by tension (pulling the plug out of the ring) and by torsion (twisting).

TABLE 10 TEST METHODS FOR ADHESIVE JOINT MECHANICAL PROPERTIES

ASTM DESIGNATION(A)	DESCRIPTION
D 897-78	**STANDARD TEST METHOD FOR TENSILE PROPERTIES OF ADHESIVE BONDS**
D 1002-72	**STANDARD TEST METHOD FOR STRENGTH PROPERTIES OF ADHESIVES IN SHEAR BY TENSION LOADING (SINGLE-LAP SHEAR)**
D 1876-72	**STANDARD TEST METHOD FOR PEEL RESISTANCE OF ADHESIVES T-PEEL TEST**
D 3528-76	**STANDARD TEST METHOD FOR STRENGTH PROPERTIES OF DOUBLE-LAP SHEAR ADHESIVE JOINTS BY TENSION LOADING**
F 1044-87	**STANDARD TEST METHOD FOR SHEAR TESTING OF POROUS METAL COATING (RING-IN-PLUG)**
D 2294-69	**STANDARD TEST METHOD FOR CREEP PROPERTIES OF ADHESIVES IN SHEAR BY TENSION LOADING**
D 3166-73	**STANDARD TEST METHOD FOR FATIGUE PROPERTIES OF ADHESIVES IN SHEAR BY TENSION LOADING**
E 8-89	**STANDARD TEST METHOD FOR TENSION TESTING OF METALLIC MATERIALS (BULK MATERIAL)**
E 143-87	**STANDARD TEST METHOD FOR SHEAR MODULUS AT ROOM TEMPERATURE**

(A) PER VOL 15.06, *ANNUAL BOOK OF ASTM STANDARDS*, 1990

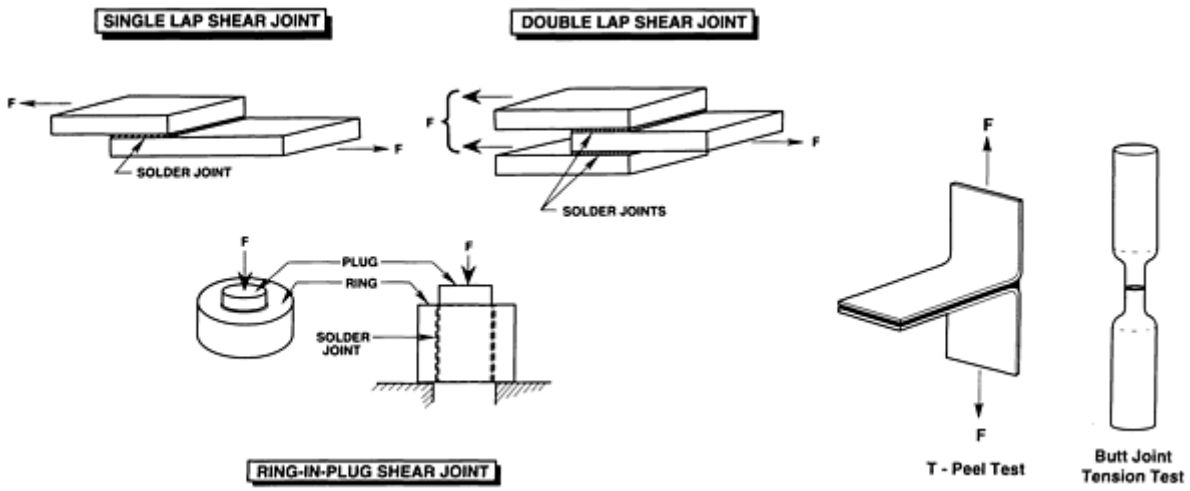

FIG. 7 MECHANICAL TEST SAMPLE GEOMETRIES

Additional properties that are specific to the eutectic 63Sn-37Pb and near-eutectic 60Sn-40Pb solders are provided below. The properties of either group of these solders can be approximated with those of the other. The physical properties of 60Sn-40Pb are listed in Table 11, whereas creep-rapture data are given in Table 12.

TABLE 11 PHYSICAL PROPERTIES OF 60SN-40PB SOLDER

PROPERTY	VALUE
SOLIDUS TEMPERATURE, °C (°F)	**183 (361)**
LIQUIDUS TEMPERATURE, °C (°F)	**188 (370)**
DENSITY, G/CM^3	**8.52**

TEMPERATURE DEPENDENCE OF DENSITY, °C/(G/CM^3)	**9.079 ± (9.708 × 10^4)**
SPECIFIC HEAT CAPACITY, J/KG · K	**150**
LATENT HEAT OF FUSION, J/KG × 10^3 (BTU/LB)	**37 (16)**
POISSON'S RATIO AT 25 °C (77 °F)[(A)]	**0.4**

Source: Ref 13

(A) FOR 63SN-37PB

TABLE 12 CREEP-RUPTURE STRENGTH OF 60SN-40PB SOLDER

TEMPERATURE		**STRESS**		LIFE, H
°C	**°F**	**MPA**	**KSI**	
20	68	2.0	0.29	**2750**
		2.9	0.42	**670**
		3.9	0.57	**270**
		4.9	0.71	**180**
		5.9	0.86	**60**
		6.9	1.0	**70**
		8.8	1.3	**30**
100	212	0.2	0.029	**2860 ± 1710**
		0.8	0.120	**210 ± 40**
		1.0	0.150	**100 ± 50**
		1.2	**0.170**	**70 ± 70**

Source: Ref 13

The temperature dependence of the tensile strength, yield strength, and ductility of bulk 63Sn-37Pb solder at a test rate of 1.3 mm/min (0.05 in./min) is shown in Fig. 8; the temperature dependence of the tensile modulus and Poisson's ratio is shown in Fig. 9. These properties are particularly useful for finite-element modeling of solder joint residual stresses.

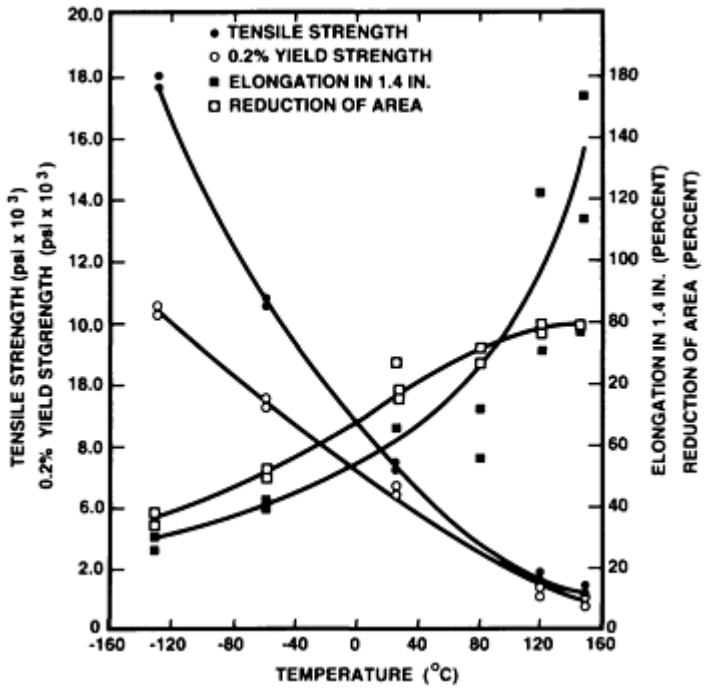

FIG. 8 TEMPERATURE DEPENDENCE OF TENSILE STRENGTH, YIELD STRENGTH, AND DUCTILITY OF 63SN-37PB

SOLDER. SOURCE: REF 14

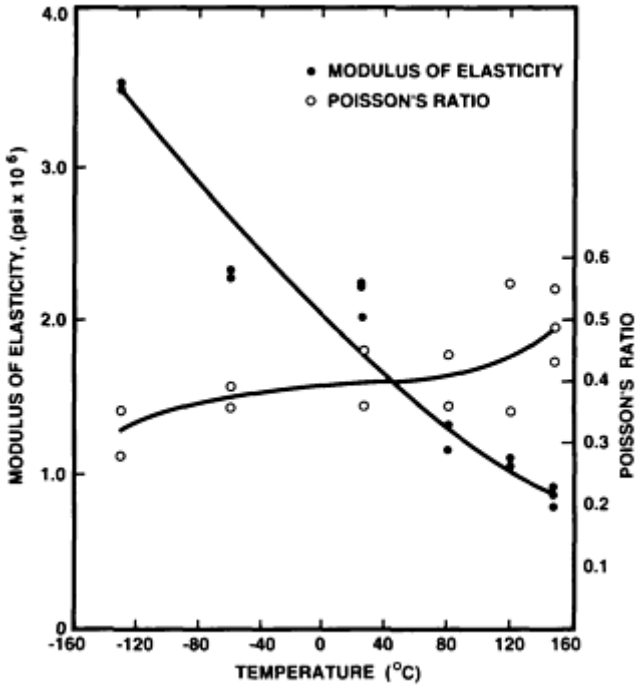

FIG. 9 TEMPERATURE DEPENDENCE OF TENSILE MODULUS AND POISSON'S RATIO OF 63SN-37PB SOLDER. SOURCE: REF 14

The room-temperature shear strength (copper ring-in-plug and single-overlap shear) of 60Sn-40Pb solder joints, as well as data from tests performed at elevated temperatures, are shown in Table 13. The single-lap joint gap thickness was 0.13 mm (0.005 in.). Thermal aging of the solder joints decreases the joint shear strength, and the effect on room-temperature data becomes much greater at higher strain rates (Ref 13).

TABLE 13 ROOM-TEMPERATURE AND ELEVATED-TEMPERATURE SHEAR STRENGTHS OF 60SN-40PB SOLDER

TEST SPEED		SHEAR STRENGTH					
		AT 20 °C (68 °F)		**AT 100 °C (212 °F)**		AT 150 °C (302 °F)	
mm/min	**in./min**	**MPA**	**KSI**	**MPA**	**KSI**	**MPA**	KSI
RING-IN-PLUG TEST							
50	2.0	49.7 ± 7.4	7.21 ± 1.07	33.3	4.83	. . .	**. . .**
20	0.8	47.8 ± 5.3	6.94 ± 0.77	31.2	4.53	23.4 ± 0.2	**3.40 ± 0.03**
5	0.2	41.9 ± 1.3	6.08 ± 0.19	25.5	3.70	18.1	**2.63**
1	0.04	33.6 ± 5.1	4.88 ± 0.74	21.6	3.13	9.7 ± 0.9	**1.41 ± 0.13**
0.2	0.008	26.1 ± 0.5	3.79 ± 0.07	15.7	2.28	4.7	**0.068**
0.05	0.002	21.3 ± 1.4	3.09 ± 0.20	12.2	1.77	4.2 ± 0.3	**0.061 ± 0.04**
SINGLE-LAP TEST[A]							
50	2.0	35.4	5.14	. . .	. . .	. . .	**. . .**
20	0.8	37.1	5.38	. . .	. . .	. . .	**. . .**
5	0.2	32.2	4.67	. . .	. . .	. . .	**. . .**
1	0.04	30.1	4.37	. . .	. . .	. . .	**. . .**
0.2	0.08	26.2	3.80	. . .	. . .	. . .	**. . .**
0.05	**0.002**	**23.2**	**3.37**	**. . .**	**. . .**	**. . .**	**. . .**

Source: Ref 13

(A) OVERALL AREA. 48-51 MM^2 (0.07-0.08 $IN.^2$).

Fatigue life data expressed as cycles to failure for a given load stress are presented in Fig. 3. Fatigue resistance can also be expressed as a function of the applied strain. Lap shear fatigue data from a variety of applied strain levels are shown in Fig. 10. Increasing the temperature above 20 °C (68 °F) generally decreases the number of cycles to failure. Isothermal fatigue life is also reduced by decreasing the frequency of cycles. The frequency effect is negligible for strains that exceed 4% and frequencies that exceed 0.01 Hz (Ref 16).

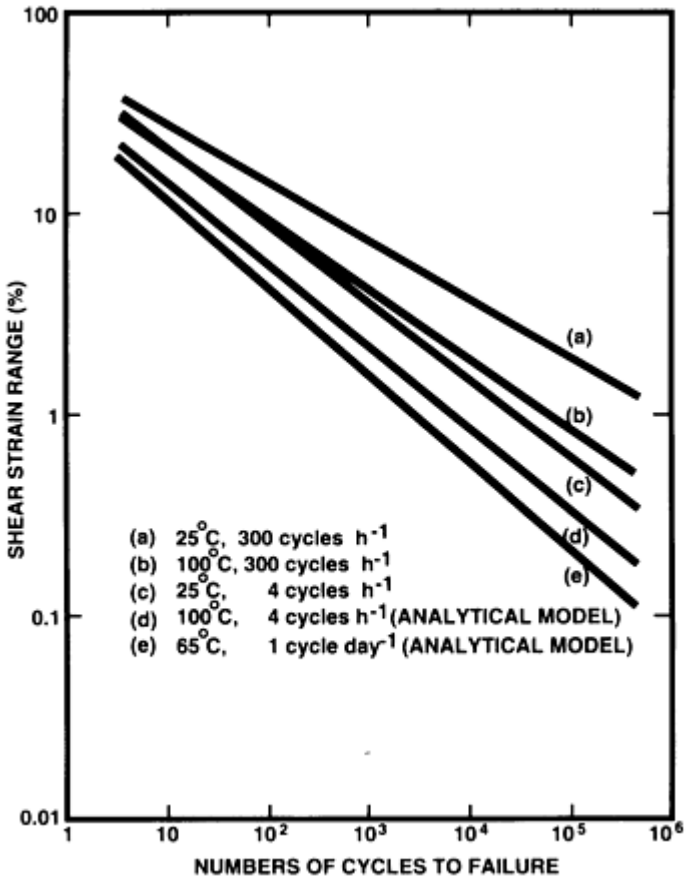

FIG. 10 FATIGUE LIFE OF 60SN-40PB SOLDER AS FUNCTION OF APPLIED STRAIN AMPLITUDE. SOURCE: REF 15

Resistance to creep diminishes as the temperature increases. Creep-rupture data at three temperatures are shown in Table 14.

TABLE 14 CREEP-RUPTURE DATA FOR 60SN-40PB COPPER RING-IN-PLUG JOINTS

STRESS		LIFE, H
MPA	**KSI**	
AT 20 °C (68 °F)		
3.4	0.49	**1050**
3.9	0.57	**610 ± 320**
4.9	0.71	**480**
5.9	0.86	**220**

7.8	1.13	**70**
AT 100 °C (212 °F)		
0.9	0.13	**2060**
1.1	0.16	**490**
1.3	0.19	**270**
1.5	0.22	**270**
1.7	0.25	**60**
AT 150 °C (302 °F)		
0.6	0.09	**130 ± 70**
1.0	0.15	**11 ± 8**
1.5	0.22	**5**
2.4	**0.35**	**0.4**

Source: Ref 13

Tin-Antimony and Tin-Antimony-Silver Solders. Tin-antimony solder compositions, as defined by three standards, are given in Tables 15, 16, and 17. The 95Sn-5Sb solder is used for most applications and is the only composition included in the tables.

TABLE 15 TIN-ANTIMONY SOLDER COMPOSITIONS PER ASTM B 32

ALLOY GRADE	COMPOSITION, %[A]											MELTING RANGE[B]			
												SOLIDUS		LIQUIDUS	
	Sn	Pb	Sb	Ag	Cu	Cd	Al	Bi	As	Fe	Zn	°C	°F	°C	°F
SB5	94.0 MIN	0.20	4.5-5.5	0.015	0.08	0.03	0.005	0.15	0.05	0.04	0.005	233	450	240	**464**
HA[C]	**BAL**	**0.10**	**0.5-4.0**	**0.1-3.0**	**0.1-2.0**	**0.005**	**0.005**	**0.15**	**0.05**	**0.02**	**0.5-4.0**	**216**	**420**	**227**	**440**

(A) LIMITS ARE % MAX, UNLESS SHOWN AS A RANGE OR STATED OTHERWISE. FOR PURPOSES OF DETERMINING CONFORMANCE TO THESE LIMITS, AN OBSERVED VALUE OR CALCULATED VALUE OBTAINED FROM ANALYSIS SHALL BE ROUNDED TO THE NEAREST UNIT IN THE LAST RIGHT-HAND PLACE OF FIGURES USED IN EXPRESSING THE SPECIFIED LIMIT, IN ACCORDANCE WITH THE ROUNDING METHOD OF PRACTICE E 29.

(B) TEMPERATURES GIVEN ARE APPROXIMATIONS AND FOR INFORMATION ONLY.

(C) DESIGNATION FOR SN-SB-AG-CU ALLOY COMPOSITION.

TABLE 16 TIN-ANTIMONY SOLDER COMPOSITION PER FEDERAL SPECIFICATION QQ-S-571E

ALLOY	COMPOSITION, %												APPROXIMATE MELTING RANGE[A]			
													SOLIDUS		LIQUIDUS	
	Sn	Pb	Sb	Bi max	Ag	Cu max	Fe max	Zn max	Al max	As max	Cd max	TOTAL OF ALL OTHERS MAX	°C	°F	°C	°F
SB5	**94.0 MIN**	**0.20 MAX**	**4.0-6.0**	**. . .**	**. . .**	**0.08**	**0.08**	**0.03**	**0.03**	**0.05**	**0.03**	**0.03**	**235**	**455**	**240**	**465**

(A) FOR INFORMATION ONLY

TABLE 17 TIN-ANTIMONY SOLDER COMPOSITION PER ISO/DIS 9453

ALL	ALLOY	MELTING	CHEMICAL COMPOSITION, %

OY NO.	DESIGNATION	OR SOLIDUS/ LIQUIDUS TEMPERATURE														
		°C	°F	Sn	Pb	Sb	Bi	Cd	Cu	In	Ag	Al	As	Fe	Zn	SUM OF ALL IMPURITIES
18	**S-SN95SB5**	**230-240**	**445-465**	**BAL**	**0.10**	**4.5-5.5**	**0.10**	**0.002**	**0.10**	**0.05**	**0.05**	**0.001**	**0.03**	**0.02**	**0.001**	**0.2**

Selected properties of the 95Sn-5Sb alloy are:

DENSITY, G/CM^3	**7.25**
HARDNESS, HB	**15**
ELECTRICAL CONDUCTIVITY, %IACS(A)	**12**
YOUNG'S MODULUS, GPA (10^6 PSI)	**49.99 (7.255)**

Source: Ref 8

(A) IACS, INTERNATIONAL ANNEALED COPPER STANDARD.

Alloys with 1 to 5 wt% Sb are commercially available. Antimony remains in solid solution in tin at levels up to 6 or 7 wt%. Higher amounts cause the precipitation of tin-antimony intermetallic crystals.

The tin-antimony-silver solder is certified in the ASTM specification. The silver improves the spreading of the solder, lowers the solidus and liquidus temperature, and extends the alloy pasty range. Tin-antimony solders exhibit excellent monotonic and creep strength levels for applications with high structural loads and elevated-temperature service, as well as in food handling equipment and potable water conduit and containers. Antimony additions above 0.3 wt% will deteriorate wetting and spreading. Solders with more than 0.2 to 0.5 wt% Sb can become embrittled when joined to aluminum, zinc, or zinc-coated parts because of the formation of aluminum-antimony and zinc-antimony intermetallic phases.

The room-temperature physical and mechanical properties of 95Sn-5Sb alloy are given in Table 18. The sensitivity of the room-temperature bulk tensile strength and copper ring-in-plug shear strength to testing rate (Table 19) is less than that for the tin-lead alloys. The tensile strength and elongation of tin-antimony solders also exhibit a smaller sensitivity to temperature (Fig. 11).

TABLE 18 PHYSICAL AND MECHANICAL PROPERTIES OF BULK 95SN-5SB SOLDER

PROPERTY	VALUE
DENSITY, G/CM^3	**7.25**
ELASTIC MODULUS, GPA (10^6 PSI)	**50 (7.26)**
ELONGATION, %	**38**
HARDNESS, HB	**15**
ELECTRICAL CONDUCTIVITY, %IACS	**11.9**
COEFFICIENT OF THERMAL EXPANSION, 10^{-6}/K	**27**

TABLE 19 TENSILE STRENGTH OF BULK 95SN-5SB COPPER RING-IN-PLUG JOINTS VERSUS TEST

SPEED

TENSILE STRENGTH[A]				TEST SPEED		SHEAR STRENGTH[B]			
AT 20 °C (68 °F)		AT 100 ° (212 °F)				AT 20 °C (68 °F)		AT 100 °C (212 °F)	
MPA	KSI	MPA	KSI	MM/MIN	IN./MIN	MPA	KSI	MPA	KSI
47.5	6.89	30.4	4.41	50.00	2.0	53.9	7.82	28.3	**4.11**
46.5	6.75	28.6	4.15	20.00	0.8	48.0	6.97	29.0	**4.21**
42.6	6.18	25.7	3.73	5.00	0.2	44.6	6.47	23.5	**3.41**
36.3	5.27	22.8 ± 2.6[C]	3.31 ± 0.38[C]	1.00	0.04	37.2	5.40	21.1	**3.06**
26.0	3.77	24.2	3.51	0.20	0.008	31.4	4.56	18.8	**2.73**
30.0	**4.35**	**19.9**	**2.89**	**0.05**	**0.002**	**27.4**	**3.98**	**13.2**	**1.92**

Source: Ref 13

(A) OF BULK MATERIAL.

(B) OF COPPER RING-IN-PLUG.

(C) PLUS OR MINUS ONE STANDARD DEVIATION, $N = 2$.

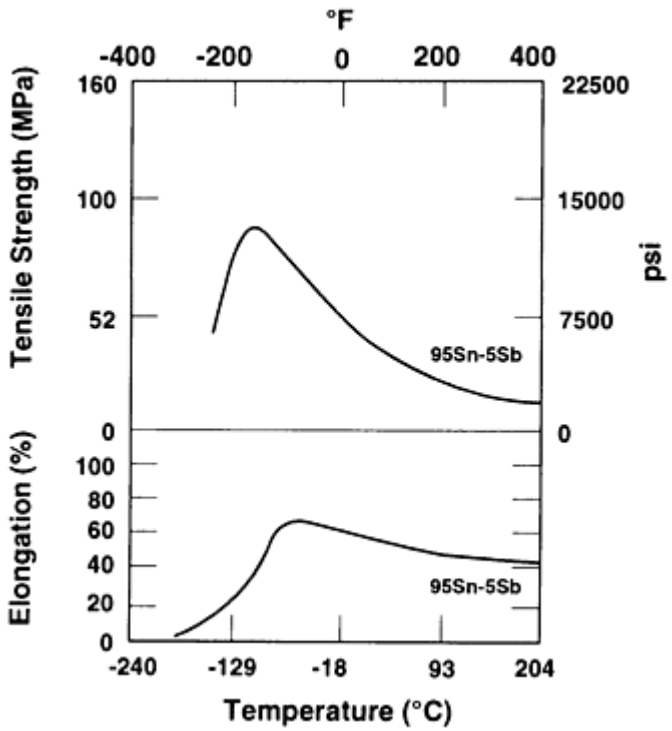

FIG. 11 TEMPERATURE SENSITIVITY OF TENSILE STRENGTH AND ELONGATION OF 95SN-5SB SOLDER

Bulk creep properties are illustrated in stress-rupture data in Table 20. Copper ring-in-plug creep-rupture data are shown in Table 21. Fatigue resistance is demonstrated by the results in Table 22 for cyclic compression/tension (zero mean stress). Both creep and fatigue properties of 95Sn-5Sb are superior to those of 60Sn-40Pb solder. The improved fatigue resistance is noted by the stress required to cause failure at 1000 cycles at a testing rate of 0.2 mm/min (0.008 in./min). The failure stresses at 20 °C (68 °F) are 21 MPa (3.05 ksi) for 95Sn-5Sb and 17 MPa (2.47 ksi) for 60Sn-40Pb.

TABLE 20 CREEP-RUPTURE DATA FOR BULK 95SN-5SB SOLDER

STRESS		LIFE, H
MPA	KSI	
AT 20 °C (68 °F)		

17.0	2.47	**497**
19.6	2.84	**10574**
20.6	2.99	**493**
20.7	3.00	**>4000**
21.6	3.13	**183**
22.5	3.27	**0.1**
AT 100 °C (212 °F)		
0.6	0.03	**>2770**
1.1	0.16	**>2090**
2.3	0.33	**>2030**
3.4	0.49	**>2020**
4.5	0.65	**>1870**
6.8	0.99	**4750**
9.0	**1.31**	**1050 ± 380[A]**

Source: Ref 13

(A) PLUS OR MINUS ONE STANDARD DEVIATION, 2 SAMPLES.

TABLE 21 CREEP STRENGTH OF 95SN-5SB COPPER RING-IN-PLUG JOINTS

STRESS		LIFE, H
MPA	**KSI**	
AT 20 °C (68 °F)		
8.8	1.28	**2130**
9.8	1.42	**>2300**
11.8	1.71	**580**
12.7	1.84	**22 ± 19**
13.7	1.99	**15**
14.7	2.13	**18 ± 12**
AT 100 °C (212 °F)		
2.9	0.42	**>3000**
3.9	0.57	**350**
4.9	0.71	**210**
6.4	0.93	**55**
7.3	1.06	**32**
8.0	**1.16**	**15**

Source: Ref 13

TABLE 22 FATIGUE STRENGTH VERSUS TESTING RATE OF 95SN-5SB COPPER RING-IN-PLUG JOINTS

STRESS		LIFE, CYCLES TO FAILURE[A]
MPA	**KSI**	
AT 20 °C (68 °F)		
20.6	2.99	**1200**
22.5	3.27	**43**
24.5	3.56	**1**
AT 100 °C (212 °F)		
13.7	1.99	**1800**
14.2	2.06	**15 ± 16[B]**

15.7	**2.28**	**1**

Source: Ref 13

(A) CYCLIC COMPRESSION/TENSION; MEAN STRESS = 0; SPEED, 0.2 MM/MIN (0.008 IN./MIN).

(B) PLUS OR MINUS ONE STANDARD DEVIATION, 2 SAMPLES.

Tin-silver solders include the tin-silver and tin-copper-silver compositions. The alloy compositions are listed in Tables 23, 24, and 25. ASTM B 32 recognizes the Sn96 solder as that composition which has a silver content of 3.4 to 3.8 wt%. The "same" alloy specified by QQ-S-571E has a composition of 3.6 to 4.4 wt% Ag. The ASTM document includes specifications for two additional tin-silver solders: Sn95, with 4.4 to 4.8 wt% Ag, and Sn94, with 5.4 to 5.8 wt% Ag. The tin-copper-silver alloy "E" included in ASTM B 32 contains 0.25 to 0.75 wt% Ag and 3.0 to 5.0 wt% Cu. Silver improves strength and spreading and lowers the melting temperature, when compared with pure tin. The addition of copper in the "E" alloy further improves its strength. Both the tin-silver (primarily, the eutectic 96.5Sn-3.5Ag) and the tin-copper-silver solders are used extensively in plumbing applications for potable water and in food handling equipment, where the use of lead-containing joints is restricted. Tin-silver alloys also form the high-temperature step of step-soldering processes with tin-lead alloys.

TABLE 23 TIN-SILVER SOLDER COMPOSITION PER ASTM B 32

ALLOY GRADE	**COMPOSITION, %**[A]											MELTING RANGE[B]			
												SOLIDUS		LIQUIDUS	
	Sn	**Pb**	**Sb**	**Ag**	**Cu**	**Cd**	**Al**	**Bi**	**As**	**Fe**	**Zn**	**°C**	**°F**	**°C**	°F
SN96	BAL	0.10	0.12 MAX	3.4-3.8	0.08	0.005	0.005	0.15	0.01 MAX	0.02	0.005	221	430	221	**430**
SN95	BAL	0.10	0.12	4.4-4.8	0.08	0.005	0.005	0.15	0.01	0.02	0.005	221	430	245	**473**
SN94	BAL	0.10	0.12	5.4-5.8	0.08	0.005	0.005	0.15	0.01	0.02	0.005	221	430	280	**536**
E[C]	**BAL**	**0.10**	**0.05**	**0.25-0.75**	**3.0-5.0**	**0.005**	**0.005**	**0.02**	**0.05**	**0.02**	**0.005**	**225**	**440**	**349**	**660**

Note: Data in table represent solder alloys containing >0.2% Pb.

(A) APPLICABLE ONLY TO COMPOSITION 60-40 IN THE FORM OF FLUX-CORE WIRE OR SOLDER PASTE.

(B) APPLICABLE ONLY TO COMPOSITION 60-40 IN THE FORM OF FLUX-CORE WIRE.

(C) APPLICABLE ONLY TO FLUX-CORE WIRE AND SOLDER PASTE.

TABLE 24 TIN-SILVER SOLDER COMPOSITION PER FEDERAL SPECIFICATION QQ-S-571E

ALLOY	**COMPOSITION, %**							APPROXIMATE MELTING RANGE[A]			
								SOLIDUS		LIQUIDUS	
	Sn	**Pb max**	**Ag**	**Cu max**	**Zn max**	**As max**	**Cd max**	**°C**	**°F**	**°C**	°F
SN96	**BAL**	**0.10**	**3.6-4.4**	**0.20**	**0.005**	**0.05**	**0.005**	**221**	**430**	**221**	**430**

(A) FOR INFORMATION ONLY

TABLE 25 TIN-SILVER SOLDER COMPOSITION PER ISO/DIS 9453

ALLOY NO.	**ALLOY DESIGNATION**	**MELTING OR SOLIDUS/ LIQUIDUS TEMPERATURE**		**CHEMICAL COMPOSITION, %**												SUM OF ALL IMPURITIES
		°C	**°F**	**Sn**	**Pb**	**Sb**	**Bi**	**Cd**	**Cn**	**In**	**Ag**	**Al**	**As**	**Fe**	**Zn**	
28	S-SN96AG4	221	430	BAL	0.10	0.10	0.10	0.002	0.05	0.05	3.5-	0.001	0.03	0.02	0.001	**0.2**

											4.0					
29	**S-SN97AG3**	**221-230**	**430-445**	**BAL**	**0.10**	**0.10**	**0.10**	**0.005**	**0.10**	**0.05**	**3.0-3.5**	**0.001**	**0.03**	**0.02**	**0.001**	**0.2**

Selected physical properties of the 96.5Sn-3.5Ag alloy are:

DENSITY, G/CM^3	**7.36**
HARDNESS, HB	**14.8**
ELECTRICAL CONDUCTIVITY, %IACS	**14**

IACS, International Annealed Copper Standard

The bulk tensile strength and copper ring-in-plug joint shear strength of this alloy, as a function of testing rate and temperature, are shown in Table 26.

TABLE 26 BULK TENSILE STRENGTH AND COPPER RING-IN-PLUG SHEAR STRENGTH OF 96.5SN-3.5AG SOLDER

TENSILE STRENGTH(A)				**TEST SPEED**		SHEAR STRENGTH(B)			
AT 20 °C (68 °F)		**AT 100 °C (212 °F)**				**AT 20 °C (68 °F)**		AT 100 °C (212 °F)	
MPA	**KSI**	**MPA**	**KSI**	**MM/MIN**	**IN./MIN**	**MPA**	**KSI**	**MPA**	KSI
51.2	7.43	36.7	5.33	50.00	2.0	55.9	8.11	31.8	**4.62**
56.8	8.24	31.4	4.56	20.00	0.8	50.0	7.26	29.9	**4.34**
43.7	6.34	30.4	4.41	5.00	0.2	44.6	6.47	. . .	**. . .**
44.1	6.40	28.0	4.06	1.00	0.04	37.7	5.47	22.5	**3.27**
41.9	6.08	26.6	3.86	0.20	0.008	28.9	4.19	18.1	**2.63**
36.3	**5.27**	**24.3**	**3.51**	**0.05**	**0.002**	**28.4**	**4.12**	**17.6**	**2.55**

Source: Ref 13

(A) OF BULK MATERIAL.

(B) OF COPPER RING-IN-PLUG.

Creep-rupture stress data on the bulk solder and copper ring-in-plug shear tests are shown in Fig. 12 and 13. Room-temperature fatigue life data (copper ring-in-plug), as a function of test rate, are shown in Table 27 for zero mean stress tension-compression loading.

TABLE 27 COPPER RING-IN-PLUG SHEAR JOINT FATIGUE TESTS FOR 96.5SN-3.5AG SOLDER

STRESS		LIFE, CYCLES TO FAILURE
MPA	**KSI**	
TEST RATE, 0.5 MM/MIN (0.02 IN./MIN)		
21.6	3.13	**3024**
25.4	3.69	**273**
29.4	4.27	**17**
TEST RATE, 2.0 MM/MIN (0.08 IN./MIN)		
19.6	2.84	**2600**

23.5	3.41	**262**
27.4	**3.98**	**119**

Zero mean stress data.

Source: Ref 13

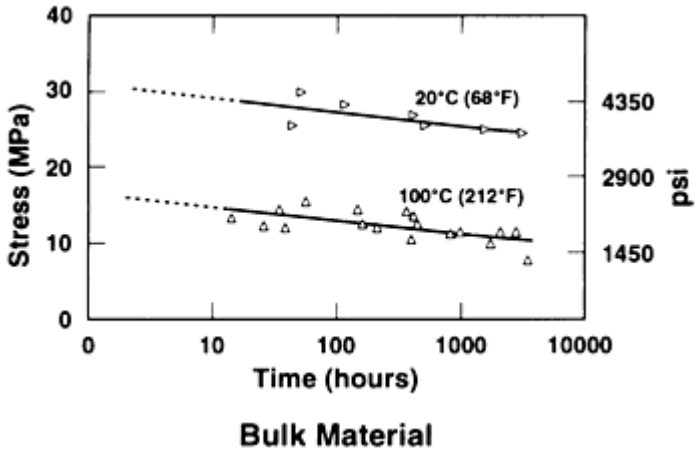

FIG. 12 BULK CREEP-RUPTURE TESTS OF 96.5S-3.5AG. SOURCE: REF 13

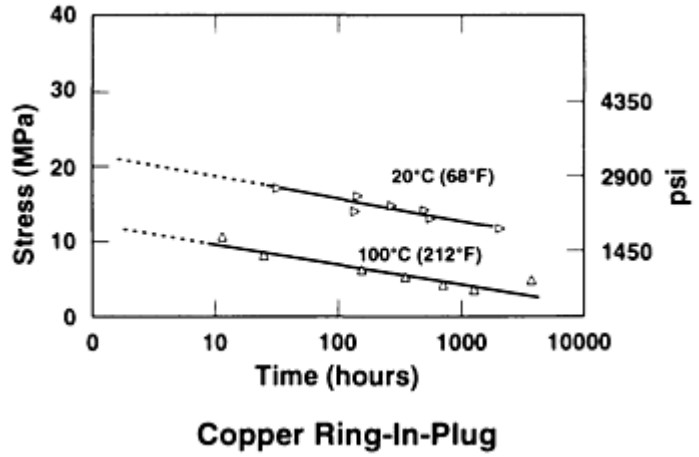

FIG. 13 COPPER RING-IN-PLUG SHEAR CREEP TESTS OF 96.5SN-3.5AG SOLDER. SOURCE: REF 13

Tin-zinc and zinc-aluminum solders are used primarily in joints composed of aluminum-base metals in order to limit galvanic corrosion (Table 28). The eutectic tin-zinc composition, 91Sn-9Zn, has a melting temperature of 199 °C (390 °F), which makes it suitable for low-temperature applications that traditionally use the tin-lead solders. However, oxidation of the zinc constituent of the solder causes excessive dross formation and sluggish spreading when processed in air. As a precaution, the potential for galvanic corrosion between the zinc constituent of the solder and the base metal(s) should be thoroughly investigated prior to its use.

TABLE 28 PHYSICAL PROPERTIES OF TIN-ZINC AND ZINC-ALUMINUM SOLDERS

ALLOY	**DENSITY, G/CM^3**	EUTECTIC TEMPERATURE	
		°C	°F
91SN-9ZN	7.27	199	**390**

95ZN-5AL	**6.60**	**382**	**720**

Zinc-aluminum solders were also developed for aluminum soldering. The eutectic 95Zn-5Al has a melting temperature of 382 °C (720 °F) and is used in tube joining for heat-exchanger applications. Solder joint mechanical properties have been measured in ultrasonic soldering studies (Ref 17). These alloys are not included in the ASTM, ISO, or QQ-S-571E specifications.

Indium-containing solders are used for joining temperature-sensitive substrates or as the low-temperature step in multiple ("step") soldering processes to prevent reflow of the pre-existing solder joints (typically, tin-lead eutectic). Good plasticity at cryogenic temperatures make these alloys suitable for applications such as space vehicles and satellites. Selected properties of these solders are listed in Table 29.

TABLE 29 PROPERTIES OF INDIUM-CONTAINING SOLDERS

ALLOY	TEMPERATURE				HARDNESS, HB	TENSILE STRENGTH		ELONGATION, %	ELECTRICAL CONDUCTIVITY %IACS	COEFFICIENT OF THERMAL EXPANSION, 10^{-6}/K
	SOLIDUS		LIQUIDUS							
	°C	°F	°C	°F		MPA	KSI			
44IN-42SN-14CD	58	136	58	136	. . .	. . .	. . .	. . .	. . .	**24**
50IN-50SN	117	243	125	257	4.94	11.8	1.72	83	11.7	**20**
52IN-48SN	118	244	118	244	. . .	11.8	1.72	. . .	11.7	**20**
90IN-10AG	141	286	238	460	2.68	11.4	1.65	61	22.1	**. . .**
97IN-3AG	143	289	143	289	. . .	5.5	0.80	. . .	23.0	**22**
100IN	157	315	157	315	(A)	3.5	0.52	41	24.0	**29**
50IN-50PB	**180**	**356**	**209**	**408**	**9.60**	**32.1**	**0.47**	**55**	**6.0**	**27**

Source: Indium Corporation of America

(A) TOO SOFT TO MEASURE.

Indium is frequently added to tin-lead solders as a ternary addition in order to depress the melting temperature (for example, 40Sn-40Pb-20In and 70Sn-18Pb-12In). Indium also improves ductility and oxidation resistance. Indium-containing alloys have poor corrosion resistance in the presence of halide ions, such as those used for some activators in flux chemistries. The alloys 52In-48Sn and 97In-3Ag easily wet glass, fused silica, and other ceramics for glass-to-metal or glass-to-glass joints. These alloys also have very low vapor pressure, which makes them ideal for vacuum applications. The 501n-50Pb alloy is used in electronic applications to limit the scavenging of precious-metal substrates or coatings, which occurs very rapidly with tin-base solders. The indium-containing solder compositions are not certified by ASTM B 32 or QQ-S-571E. However, the latter document does give nominal compositions and melting temperatures. ISO/DIS 9453 does certify the composition of the 50In-50Sn alloy. The high cost of indium has limited the general use of these solders.

Low-melting fusible alloy solders, which contain bismuth, are used for soldering processes that involve temperature-sensitive substrates or devices, as well as the low-temperature part of step soldering procedures. Their ability to melt at low temperatures makes these materials ideal for thermal fuses. Compositions, mechanical, and selected physical properties are listed in Table 30.

TABLE 30 PHYSICAL AND MECHANICAL PROPERTIES OF FUSIBLE ALLOYS

ALLOY[A]	TEMPERATURE				TENSILE STRENGTH		COEFFICIENT OF THERMAL EXPANSION, 10^{-6}/K
	SOLIDUS		LIQUIDUS				
	°C	°F	°C	°F	MPA	KSI	
44.7BI-22.6PB-8.3SN-5.3CD-19.1IN	47	117	47	117	. . .	. . .	**. . .**
49BI-21IN-18PB-12SN	58	136	58	136	43.4	6.30	**12.8**
50BI-25PB-12.5SN-12.5CD	68	154	73	163	27.8	4.04	**. . .**
55.5BI-44.5PB	124	255	124	255	. . .	. . .	**. . .**
58BI-42SN	**138**	**281**	**138**	**281**	**54.9**	**7.98**	**13.8**

Source: Ref 13

(A) EXTENDED LIST AVAILABLE IN REF 6 (P 110).

Excessive oxidation of bismuth promotes dross formation and can limit spreading for soldering processes conducted in air. The eutectic 58Bi-42Sn alloy has found some applications in electronic assemblies. Bulk properties and copper ring-in-plug shear strength, creep, and fatigue data are listed in Table 31.

TABLE 31 MECHANICAL TEST DATA FOR 58BI-42SN SOLDER

SHEAR STRENGTH				TEST SPEED	
AT 20 °C (68 °F)		AT 100 °C (212 °F)			
MPA	KSI	MPA	KSI	MM/MIN	IN./MIN
57.4	8.33	18.5	2.69	20.0	**0.8**
63.6	9.23	17.1	2.48	10.0	**0.4**
50.0	7.26	19.5	2.83	1.0	**0.04**
36.0	**5.22**	**11.3**	**1.64**	**0.1**	**0.004**

RUPTURE STRESS		LIFE, H
MPA	KSI	
AT 20 °C (68 °F)		
3.0	0.44	**1110**
5.0	0.73	**450**
7.0	1.02	**150**
AT 100 °C (212 °F)		
1.0	0.15	**360 ± 20[A]**
1.5	0.22	**90 ± 40[B]**
3.0	**0.44**	**30**

MAXIMUM STRESS		FATIGUE LIFE, CYCLES
MPA	KSI	
AT 20 °C (68 °F)		
9.8	1.42	**5200**
15.0	2.18	**32**
25.0	3.63	**1580**
AT 100 °C (212 °F)		
6.0	0.87	**15,400**
10.0	1.45	**420**
12.0	**1.74**	**7**

Source: Ref 13

(A) SAMPLE SIZE, $N = 3$.

(B) SAMPLE SIZE, $N = 5$.

The ISO/DIS 9453 specification sets guidelines on the composition of 60Sn-38Pb-2Bi, 49Pb-48Sn-3Bi, and 57Bi-43Sn alloys. Alloys with greater than 47 wt% Bi exhibit varying degrees of expansion upon cooling after solidification, because of changes to the lattice structure of the alloys (Ref 18). Dimensional changes to the alloy also take place during room-temperature aging. Whether the dimensional change is due to contraction, expansion, or both, and the magnitude of this change, depends on the composition. These alloys can be used to eliminate solder-joint cracking during the cooling of two substrates that have vastly different degrees of thermal contraction.

Precious-metal solders include the gold-tin, gold-germanium, and gold-silicon compositions. Selected physical and mechanical properties are listed in Table 32. The high concentration of gold causes the alloys to be very expensive.

TABLE 32 PHYSICAL AND MECHANICAL PROPERTIES OF SELECTED GOLD-BASE SOLDERS

ALLOY	EUTECTIC MELTING POINT		YOUNG'S MODULUS				ULTIMATE TENSILE STRENGTH				COEFFICIENT OF THERMAL EXPANSION, 10^{-6}/K
			AT 23 °C (73 °F)		AT 150 °C (302 °F)		AT 23 °C (73 °F)		AT 150 °C (302 °F)		
	°C	°F	GPA	10^6 PSI	GPA	10^6 PSI	MPA	KSI	MPA	KSI	
80AU-20SN	280	536	59.2	8.6	35.8	5.2	275	39.9	205	29.8	**15.9**
80AU-12GE	356	673	69.3	10.1	62.7	9.1	185	26.9	175	25.4	**13.4**
97AU-3SI	**363**	**685**	**83.0**	**12.0**	**83.0**	**12.0**	**255**	**37.0**	**225**	**32.7**	**12.3**

Source: Ref 19

These solders are used for attaching integrated circuit chips to packages. They are also used in the construction and hermetic sealing of packages that house delicate sensors and instrumentation. Their high melting temperature also allows them to be used in the step-soldering process with conventional tin-lead and lead-indium solders.

An attribute of their precious-metal content is that the gold-tin, gold-germanium, and gold-silicon alloys exhibit excellent solderability without the need for a flux (including short-duration processes in air) when soldering gold-coated parts. However, spreading is limited by the high surface tension of the alloys, particularly in the absence of the flux. Mechanical pressure is frequently used to assist spreading of the molten solder in the joint. Gold, tin, germanium, and silicon can be thermally evaporated, making them suitable for thin-film soldering processes, such as the assembly of microsensors (Ref 20). Ultimate tensile strength and yield strength data are given in Fig. 14, which shows that the values far exceed those of the tin-lead alloys. Conversely, these solders show very low ductility (4 to 5%) at room temperature. The composition of the precious-metal solders are not described by the ASTM, QQ-S-571E, or ISO specifications.

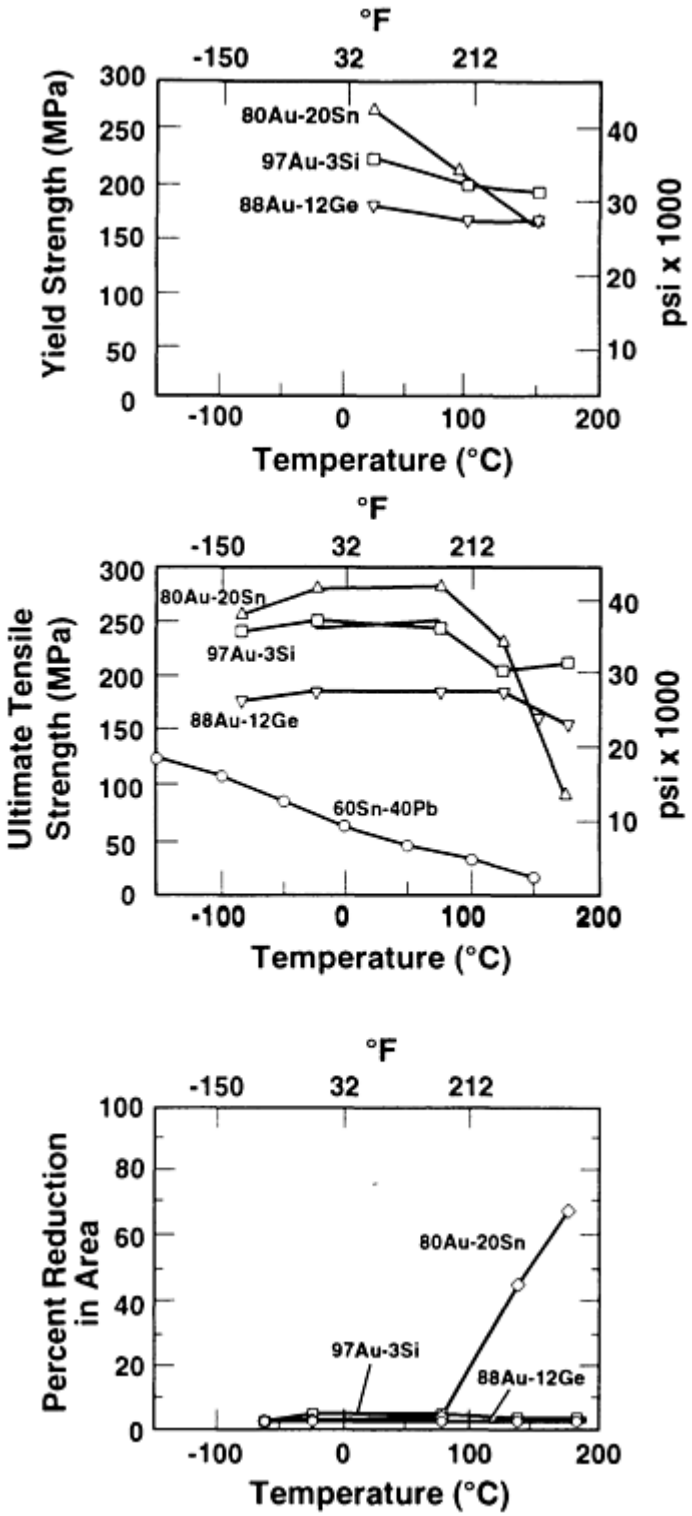

FIG. 14 TENSILE STRENGTH AND YIELD STRENGTH OF THE HIGH-MELTING-POINT PRECIOUS-METAL SOLDERS. SOURCE: REF 19

Cadmium-containing solders include special low-temperature alloys, such as 44In-42Sn-14Cd, which has a eutectic temperature of 93 °C (200 °F), as well as higher-temperature solders, such as the alloy 82.6Cd-17.4Zn, which has a eutectic temperature of 266 °C (511 °F). The corrosion protection offered by the cadmium permits these alloys to be used on aluminum or in corrosive service environments. The relatively high vapor pressure of cadmium precludes the use of cadmium-bearing solders in vacuum equipment. Generally, the use of cadmium-bearing solders is declining because of the health hazards associated with cadmium, particularly in terms of the vapors released during the soldering process. In fact, cadmium-bearing solders are now prohibited in numerous applications.

Available Solder-Metal Forms. In addition to alloy chemistry, the form of solder stock is also described by the ASTM, ISO, and QQ-S-571E specifications. Based on ASTM B 32, these forms include pig, 9.1 to 45 kg (20 to 100 lb); ingot, 1.4 to 4.5 kg (3 to 10 lb); bar, 0.22 to 0.91 kg (0.5 to 2.0 lb); and foil, sheet, or ribbon, which have various widths and thicknesses that are typically greater than 0.025 mm (0.001 in.). Solders that are contained in creams or pastes are specified according to solder powder size, metal content, flux, and viscosity. Solder wire without flux is specified by the wire diameter, which ranges from 0.25 to 6.35 mm (0.010 to 0.250 in.). Flux-cored wire must include flux type and quantity (percentage). Solder sheet may be cut or punched into particular shapes, and the stock is then referred to as a preform. The standard specifications also designate testing procedures to certify the composition and properties (flux activity of cored wire, viscosity of pastes, dimensions of wire and sheet, and so on) for the particular solder or solder-containing material.

References cited in this section

1. "STANDARD SPECIFICATION FOR SOLDER METAL," B 32, *ANNUAL BOOK OF ASTM STANDARDS*, ASTM
2. "SOLDER, TIN ALLOY: TIN-LEAD ALLOY; AND LEAD ALLOY," FEDERAL SPECIFICATION QQ-S-571E, SUPERINTENDENT OF DOCUMENTS, U.S. GOVERNMENT PRINTING OFFICE, WASHINGTON, DC
3. "SOFT SOLDER ALLOYS--CHEMICAL COMPOSITIONS AND FORMS," ISO/DIS 9453, INTERNATIONAL ORGANIZATION FOR STANDARDIZATION, THE HAGUE, NETHERLANDS
4. AMERICAN METALS MARKET, FAIRCHILD PUBLICATIONS, 17 JAN 1992
5. *SOLDERING MANUAL*, AWS, 1977, P 5
6. H. MANKO, *SOLDERS AND SOLDERING*, MCGRAW-HILL, 1979, P 14
7. H. MANKO, *SOLDERS AND SOLDERING*, MCGRAW-HILL, 1979, P 82
8. B. LAMPE, ROOM TEMPERATURE AGING PROPERTIES OF SOME SOLDER ALLOYS, *WELD. J., RES. SUPPL.*, OCT 1976, P 330S
9. SOLDERING MANUAL, AWS, 1977, P 5
10. R. KLEIN-WASSINK, *SOLDERING IN ELECTRONICS*, ELECTROCHEMICAL PUB. LTD., AYR, SCOTLAND, 1989, P 189
11. H. MANKO, *SOLDERS AND SOLDERING*, MCGRAW-HILL, 1979, P 89
12. S. NIGHTINGALE *ET AL.*, TIN SOLDERS, BRITISH NONFERROUS METALS RESEARCH ASSOCIATION, VOL 1, 1942
13. "SOLDER ALLOY DATA, MECHANICAL PROPERTIES OF SOLDERS AND SOLDERED JOINTS," PUBLICATION 656, INTERNATIONAL TIN RESEARCH INSTITUTE, UNITED KINGDOM, 1986
14. *DEVELOPMENT OF HIGHLY RELIABLE SOLDER JOINTS FOR PRINTED CIRCUIT BOARDS*, WESTINGHOUSE DEFENSE AND SPACE CENTER, 1968, P 4-55 TO 4-57
15. R. WILD, FATIGUE PROPERTIES OF SOLDER JOINTS, *WELD. RES. J.*, VOL 15, 1972, P 521S
16. H. SOLOMON, "FATIGUE OF 60/40 SOLDER," REPORT 86CRD024, GENERAL ELECTRIC CO., MAY 1986
17. J. JONES AND J. THOMAS, "ULTRASONIC SOLDERING OF ALUMINUM," RESEARCH REPORT 55-24, FRANKFORD ARSENAL, DEPARTMENT OF THE ARMY, PHILADELPHIA, FEB 1955
18. H. MANKO, *SOLDERS AND SOLDERING*, MCGRAW-HILL, 1979, P 112-115
19. D. OLSEN AND H. BERG, PROPERTIES OF DIE BOND ALLOYS RELATING TO THERMAL FATIGUE, *IEEE TRANS.*, CHMT-2, 1979, P 257
20. P. VIANCO AND J. REJENT, "SOLDER BOND APPLICATIONS IN A PIEZOELECTRIC SENSOR ASSEMBLY," *45TH ANNUAL FREQ. CONTROL SYMP.* (LOS ANGELES, CA), MAY 1991, P 266

Paul T. Vianco, Sandia National Laboratories

Substrate Materials

A substrate is solderable if a metallurgical bond can be formed between the molten solder alloy and the substrate surface. Solderability deteriorates with the presence of organic contaminants and surface oxide layers that restrict the metallurgical reaction. Organic films and heavy oxide layers must be removed by precleaning procedures prior to soldering. Most fluxes are capable of removing only relatively light oxide (or tarnish) films. The tenacity of an oxide film is determined by its intrinsic chemical nature (including adhesion to the base metal) and its thickness.

Table 33 gives a qualitative ordering of solderability for several categories of materials. Generally, the noble metals (for example, gold and silver) are readily solderable, because of limited oxide formation and strong reactivity with the solder. The materials that are most difficult to solder are ceramics and refractory metals, which require metal coatings to promote solder wetting.

TABLE 33 SOLDERABILITY ASSESSMENT OF SELECTED MATERIALS

GOOD	**FAIR**	**MODERATE**	**DIFFICULT**	PRACTICALLY IMPOSSIBLE
GOLD	BRONZE	KOVAR	ALUMINUM-BRONZE	**CHROMIUM**
TIN-LEAD	BRASS	NICKEL-IRON	ALLOYED STEEL	**MAGNESIUM**
TIN	MONEL	NICKEL	ALUMINUM	**MOLYBDENUM**
SILVER	NICKEL-SILVER	STEEL		**TUNGSTEN**
PALLADIUM		ZINC		**BERYLLIUM**
COPPER				

Source: Ref 21

The solderability of marginal materials (nickel, beryllium-copper, steels, or heavily tarnished copper) can be improved by the use of stronger fluxes. However, the highly corrosive nature of the residues typically require postsolder process cleaning steps.

Preassembly Cleaning Procedures. Organic contaminants need to be removed by organic solvents or by semiaqueous or aqueous cleaning solutions. The list of frequently used organic solvents has changed, because the use of chlorofluorocarbon-base materials has been restricted by environmental laws and codes. Substitute materials include acetone, isopropyl alcohol, terpenes, alkaline detergent solutions (for example, 1 to 3% trisodium phosphate with surfactants), and newer semiaqueous compounds. Contamination removal by solvents can be assisted by vapor degreasing, although toxicity to workers and the potential fire hazard generated by fumes or aerosols must be adequately assessed.

Agitated baths and ultrasonics also can improve the cleaning capabilities of organic, semiaqueous, and aqueous cleaning material. However, possible damage to parts by sonic energy must always be assessed before using ultrasonic cleaning processes. The use of soft or distilled water is recommended for aqueous and semiaqueous solutions in order to limit residue formation. Regardless of the cleaning system, all cleaning solution residues must be thoroughly removed from the workpiece prior to storage or processing in order to prevent the formation of stubborn surface films.

Degreasing requirements can be significantly reduced through preventive measures, such as the use of gloves by workers handling parts, enclosing parts in bags or containers, and providing storage facilities that do not contain detrimental

materials or airborne particulates. Solderable surfaces should not contact silicon-base materials, because their residues (particularly silicone oils) are extremely difficult to remove and nearly always cause a significant deterioration in substrate solderability.

The removal of heavy oxide layers from metal surfaces is performed by chemical (or acid) cleaning when the chemical action of the flux is incapable of removing the oxide layer during the soldering process. Prior to acid cleaning, the surface must be completely cleaned of organic contaminants, to ensure the effectiveness of the cleaning process. Water-base solutions typically do not penetrate organic films. Surface layers other than oxides, such as sulfides, hydrides, or chlorides, may require specialized cleaning solutions. For increasingly thicker layers, whether an oxide film or another type of surface contaminant, longer cleaning periods or more aggressive chemicals are required for the removal process. However, either approach increases the chance of damage to the substrate.

Table 34 identifies some general solutions used to clean metal surfaces. Inhibitors are typically added to commercially available acid solutions to prevent pitting. Distilled or deionized water should be used in solutions to prevent unwanted deposits and residual films after cleaning. Electropolishing processes can also be used to remove metal-oxide layers (Ref 23). In such procedures, the substrate forms the anode.

TABLE 34 CLEANING SOLUTIONS FOR SUBSTRATE MATERIALS

MATERIAL	**SOLUTION**	COMMENTS
IRON, STEELS, ALUMINUM	HCL (25%):3H_2O TO HCL (25%):9H_2O	**30 TO 38 °C (85 TO 100 °F), 10 TO 45 MIN; TIME DEPENDS ON SCALE THICKNESS**
STEELS	H_2SO_2 (77%):19H_2O TO H_2SO_2 (77%):9H_2O	**70-82 °C (160 TO 180 °F), 30 TO 120 S FOR LIGHT TARNISH, 15 MIN FOR HEAVY SCALE; BLACK SMUT IS WATER RINSED FOR COPPER ALLOYS, ADD 1 WT% SODIUM DICHROMATE OR 2 VOL% NITRIC ACID**
NICKEL ALLOYS	0.5HF:4HNO_3 (70%):8H_20	
STAINLESS STEELS	1. H_3PO_4 (100%):9H_2O TO 2H_3PO_4 (100%):3H_20	**CAUTION: HYDROFLUORIC ACID IS EXTREMELY CORROSIVE; AVOID ALL SKIN CONTACT**
	2. 2H_2SO_4 (77%):HCL (25%):8H_2O	
	3. 2HNO_3 (70%):3HF:5H_2O	
COPPER, COPPER ALLOYS	(SEE "STEELS" ABOVE)	**25 °C (75 °F); 2 TO 5 MIN FOR MODERATE OXIDES**
	2HNO_3 (70%):17H_2O TO 2HNO_3 (70%):4H_2O	
BRASS	0.015 HCL (25%):4HNO_3 (70%):8H_2SO_4 (77%):H_2O	
BERYLLIUM-COPPER (THREE STEPS)	FIRST STEP--H_2SO_4 (77%):3H_2O	**FIRST STEP, 75 °C (165 °F)**
	SECOND STEP--H_2O:RINSE	**THIRD STEP, 25 °C (75 °F)**
	THIRD STEP--HNO_3 (70%):2H_2O	
ALUMINUM, HIGH-SILICON ALLOYS, CAST IRON	**HF:H_2SO_4 (77%):18H_2O**	**25 °C (75 °F); 2 TO 5 MIN FOR MODERATE OXIDES**

Source: Ref 22

Whether a chemical etch or an electropolishing procedure is used, the corrosive solutions must be thoroughly rinsed from the surfaces to prevent staining or latent corrosion. These artifacts may also deteriorate solderability in follow-up processing steps. Rinses with distilled water, followed by an alcohol rinse to remove the water, is a typical sequence. Workpieces should not be dried with unfiltered or undried "house" compressed air, because oil and water droplets from

the air line will quickly contaminate the surface. Once cleaned, the surface should be soldered as soon as possible to limit reoxidation, or measures should be taken to protect surfaces from further contamination.

Mechanical abrasion can be used to remove excessively thick oxide films. Techniques include using sandpaper, steel wool, or metal files, or blasting with particulates. However, solderability can be quickly degraded by abrasive media that become embedded in the substrate surface and are not readily wetted by the molten solder. Procedures that use abrasive particles (blasting or sandpaper) or steel wool should be followed by a chemical etching treatment to remove the layer of surface material containing the foreign particles. Metal files are used to prepare the surfaces of larger, more-rugged substrates, such as pipes and fittings, and they should be cleaned of contaminant materials prior to use.

Coatings. Metals and alloys that are difficult to solder (aluminum, chromium-nickel steels, cast irons, and others) may lose their solderability too quickly after precleaning and become unprocessible. In these instances, coatings can be applied to protect the base metal prior to final assembly. Methods of application include electroplating, electroless plating, evaporation, chemical vapor deposition, or dipping in a molten metal bath. Table 35 identifies 100Sn and tin-lead solder coatings that are used to protect base-metal solderability. These protective coatings can be electroplated on the surface or they can be applied by dipping the substrate into a hot solder or tin bath. Substrates with electroplated films can be heated above the melting temperature of the coating to "fuse" it, which provides an improved seal against air and contaminants, similar to the protection obtained with hot-dipped tin or solder coatings. Electroless tin processes, including "immersion" platings, are also used.

TABLE 35 TIN AND SOLDER COATINGS TO PRESERVE BASE-METAL SOLDERABILITY

COATING	**THICKNESS**		COMMENTS
	µM	**µIN.**	
ELECTROPLATED 100SN	7.6-13	300-500	**CONCERN FOR WHISKER GROWTH WITH MOISTURE AND RESIDUAL STRESSES; RECOMMENDED FUSING**
ELECTROPLATED 100SN, FUSED	2.5-13	100-500	**MELTING POINT OF TIN, 232 °C (450 °F)**
ELECTROPLATED SN-PB	7.6-23	300-900	**AVAILABLE COMPOSITIONS: 63SN-37PB, 95PB-5SN, ETC.; PLATING COMPOSITION MAY DEVIATE FROM NOMINAL VALUES**
ELECTROPLATED SN-PB, FUSED	2.5-13	100-500	**MELTING POINTS: 63SN-37PB, 183 °C (361 °F); 95PB-5SN, 314 °C (597 °F)**
HOT-DIPPED 100SN OR SN-PB (63SN-37PB)	>5.1	>200	**UNIFORM COVERAGE REQUIRED**
ELECTROLESS ("IMMERSION") 100SN	**~1.5**	**~60**	**PROTECTION SENSITIVE TO DEPOSITION PROCESS DETAILS; QUALIFICATION TESTS RECOMMENDED**

Source: Ref 24

For metals such as aluminum and magnesium, which simply cannot be kept solderable, or for ceramics that are intrinsically unsolderable, a metal layer is deposited on the substrate. The solder more readily wets this layer, which is often referred as to the "solderable" layer. These films must be adequately thick to avoid being consumed by the metallurgical reaction with the solder, and they must exhibit adequate adhesion to the base material. In some instances, an "adhesive" layer may be deposited between the base material and the solderable layer. A "protective" layer can also be deposited onto the solderable coating in order to prevent excessive oxidation or contamination. This protective layer is then consumed by the solder. Table 36 lists the coating materials and processing steps used for substrates that are commonly involved in solder processing.

TABLE 36 SOLDERABLE AND PROTECTIVE FINISHES FOR COMMON SUBSTRATE MATERIALS

SUBSTRATE	SOLDERABLE LAYER	SOLDERABLE LAYER THICKNESS		PROTECTIVE LAYER	PROTECTIVE LAYER THICKNESS		COMMENTS
		µM	µIN.		µM	µIN.	
COPPER	ELECTROPLATED NICKEL[A]	1.5-3.8	60-150	ELECTROPLATED GOLD[B]	1.3-2.5	50-100	. . .
COPPER ALLOYS WITH ZINC	ELECTROPLATED COPPER	2.5[C]	100[C]	. . .	. . .	. . .	**12 µM (5000 µIN.) FOR ELEVATED-TEMPERATURE SERVICE**
NICKEL AND NICKEL ALLOYS	ELECTROPLATED NICKEL[A]	1.5-3.8	60-150	ELECTROPLATED GOLD[B]	1.3-2.5	50-100	. . .
	ELECTROPLATED SILVER	3.8-8.9	150-350	. . .	. . .	. . .	**SMALL SOLDERABILITY LOSS THAT IS DUE TO SILVER TARNISH**
	ELECTROPLATED COPPER	3.8-7.6	150-300	. . .	. . .	. . .	. . .
ALUMINUM AND ALUMINUM ALLOYS[D]	ELECTROPLATED COPPER (ZINCATE UNDERCOAT)	3.8-25	300-1000	. . .	. . .	. . .	**ANODIC FINISH (CD OR ZN) RECOMMENDED TO PREVENT CORROSION BETWEEN ALUMINUM AND COPPER OR NICKEL**
	ELECTROPLATED NICKEL (ZINCATE UNDERCOAT)[A]	1.3-3.8	50-150	ELECTROPLATED GOLD[B]	1.3-2.5	50-100	. . .
IRON,IRON-BASE ALLOYS (ALLOY 42, ALLOY 52, KOVAR), LOW-CARBON STEELS, AND STAINLESS STEELS	ELECTROPLATED NICKEL[A]	1.3-3.8	50-150	ELECTROPLATED GOLD[B]	1.3-2.5	50-100	**FOR COATED STEELS, USE RECOMMENDED SOLDERABLE AND PROTECTION FINISHES FOR THE PARTICULAR COATING MATERIAL**
	ELECTROPLATED SILVER	3.8-8.9	150-350	. . .	. . .	. . .	. . .
	ELECTROPLATED PALLADIUM-NICKEL	1.3-3.5	50-150	. . .	. . .	. . .	. . .
CAST IRON[D]	ELECTROPLATED IRON	1.3-3.8	50-150	. . .	. . .	. . .	**EXTENDED THICKNESS TO 2.5 TO 7.6 µM (100 TO 300 µIN.) FOR IMPROVED COVERAGE**
CERAMICS ($A1_2O_3$, BEO, SIO_2, SI_3N_4, ETC.)[D]	PRECIOUS METAL THICK FILMS	10-20	100-800	ELECTROPLATED GOLD[B]	2.0-2.5	80-100	**CERAMIC SURFACE ROUGHNESS AND THICK-FILM POROSITY MAY REQUIRE THICKER GOLD DEPOSITS**
	REFRACTORY THICK FILMS	10-20	100-800	. . .	. . .	. . .	. . .
	MAY INCLUDE NICKEL	**1.0-9.0**	**40-350**	. . .	. . .	. . .	. . .

	(SOLDERABLE OR BARRIER LAYER BARRIER LAYER)						

(A) THICKER LAYERS OF 2.5 TO 7.6 μM (100 TO 300 μIN.) PERMITTED FOR IMPROVED COVERAGE; ELECTROLESS NICKEL, 1.3 TO 3.0 μM (50 TO 120 μIN.) OR 2.5 TO 5.1 μM (100 TO 200 μIN.) PERMITTED ON NONFLEXIBLE SUBSTRATES; LAYER ADHESION AND SOLDERABILITY REQUIRE CLOSE MONITORING.

(B) THICKER LAYERS OF 2.5 TO 7.5 μM (100 TO 300 μIN.) PERMITTED FOR SOLDERABLE LAYER PROTECTION; HOWEVER, THINNER LAYERS ARE RECOMMENDED AND SOLDER JOINTS SHOULD BE MONITORED FOR EMBRITTLEMENT.

(C) MINIMUM.

(D) NOT CONTAINED IN MIL-STD-1276D

Gold plating layers should be removed by hot-solder dipping twice in a bath of molten solder if the calculated gold content of the solder joint will exceed 3 to 4 wt%, in order to prevent solder-joint embrittlement by gold-tin intermetallic formation. Electroplated gold layers should be pure gold, preferably type III, 99.9% pure, and grade A, according to MIL-G-45204C. Gold coatings alloyed with cobalt, nickel, or both (termed "hard gold"), which are used for wear resistance, are difficult to solder, because of oxidation of the cobalt or nickel component. Only matte finishes should be specified for soldering applications. "Bright" platings require organic additives in the bath, which then become entrapped in the gold coating and subsequently volatilize during soldering. This creates voids in the joints and poor wetting properties.

References cited in this section

21. R. KLEIN-WASSINK, *SOLDERING IN ELECTRONICS,* ELECTROCHEMICAL PUB. LTD., AYR, SCOTLAND, 1989, P 189
22. *SOLDERING MANUAL,* AWS, 1977, P 35-39
23. P. VIANCO *ET AL.,* SOLDERABILITY TESTING OF KOVAR WITH 60SN-40PB SOLDER AND ORGANIC FLUXES, *WELD. J. RES. SUPPL.,* JUNE 1990, P 230S
24. *BRAZING HANDBOOK,* AWS, 1991, P 267-276

General Soldering

Paul T. Vianco, Sandia National Laboratories

Fluxes

The major role of the flux is the removal of thin tarnish layers during the initial stages of the soldering process, thereby permitting the molten solder to react with the substrate and to spread. Fluxes do not effectively displace organic contaminants, so the substrate underneath such films will remain untouched by the flux and will therefore be unsolderable. A degreasing step should precede flux application. Even the strongest fluxes cannot remove thick oxides or heavy scales, so a mechanical or chemical precleaning procedure may be required.

The flux has two additional functions. One is that it lowers the surface tension of the solder, allowing it to more readily fill gaps and holes by capillary action. The other function is that the flux coating protects the metal surface from reoxidation during the heating steps just prior to soldering.

Fluxes contain three principal ingredients: an active chemical compound, such as a halide, for oxide removal; wetting agents to improve surface coverage; and a vehicle to dilute and mix the cleaning compound and wetting agents together. The vehicle, which is removed by evaporation during the soldering process, is typically water, isopropyl alcohol, glycerin, glycol (for liquid fluxes), or petroleum jelly (for flux pastes or creams). Fluxes are characterized by their cleaning agent

and are assigned to one of these categories of increasing activity: rosin-base fluxes, organic-acid fluxes (also called "intermediate" or "water-soluble" fluxes), and inorganic-acid fluxes.

Flux specifications are most numerous for the rosin-base materials, because of the criticality of their properties in the assembly of electronic products. Sample specifications include military standards MIL-F-14256E and MIL-STD-2000; federal specification QQ-S-571 E; and the industry standards ASTM D 509, IPC-S-815A, and IPC-TM-650 (test methods). Fluxes are tested for bulk corrosivity (copper mirror test), concentrations of Cl^- and F^- (halide content), and solids content. Tests of residues left by the flux on the substrate (typically a printed wiring board) include surface insulation resistance, and ionic residues. The ISO/DIS 9454-1 document includes organic- and inorganic-acid flux specifications and test procedures (ISO/DIS 9455-X, where X = 1, 2, . . ., 14), in addition to rosin-base flux specifications.

The removal of flux residues depends on the specific application, as well as the potential corrosivity of the residues left behind. If residues are specified for removal, then the workpiece should be cleaned as soon as possible after processing. Rosin residues become particularly difficult to remove with time.

Rosin-base fluxes contain "water-white" rosin, a distillation product from pine tree sap. When used alone, rosin-base fluxes are referred to as a "nonactivated," or type R, grade. Rosin is solid, noncorrosive, and insulating at room temperature. Heating causes it to liquefy and become slightly chemically active, because of its abietic and pimaric acid components. The rosin is typically dissolved in an organic vehicle, such as isopropyl alcohol, to form the liquid solution.

The addition of an activator to rosin fluxes increases their chemical activity. Activators can be organic halogenated compounds, such as amine hydrohalides that contain chloride, fluoride, or bromide ion groups or "halide-free" activators, such as oleic, stearic, or lactic acids. Halide-free fluxes are recommended for materials that are sensitive to stress-corrosion cracking. The concentration of activators, which defines the corrosivity of the flux, determines the flux category as being one of the following: rosin-base, mildly activated (RMA), fully activated (RA), and superactivated (SA). Generally, rosin-base fluxes have poor high-temperature stability; that is, the fluxes degrade rapidly after excessive exposure to elevated temperatures (for example, >25 s at 260 °C, or 500 °F).

R-type fluxes are used on electronic assemblies, where the benign residues are left on the soldered assembly. However, the substrate(s) must have excellent solderability, because the weak activity of these fluxes offers a very small window of variability for oxide thicknesses. R-type fluxes are effective on lightly tarnished copper surfaces and on precious-metal substrates, as well as on tin- and solder-coated base metals. Residues can be removed by nonpolar solvents, organic solvents (isopropyl alcohol, 1,1,1-trichloroethane), semi-aqueous solutions (terpenes), and aqueous baths or detergent solutions.

The residues left by R-type fluxes can be reduced by dilution with an organic solvent (for example, isopropyl alcohol). Such fluxes are termed "low solids" because the solids, which are responsible for the residues, are significantly reduced so that cleaning steps are not required. These fluxes are also referred to as "no-clean;" however, the term "no-clean" covers a much wider range of flux formulations that must simply comply with residue corrosivity, irrespective of the solids content.

The increased activity of the RMA fluxes improves solder wetting on more heavily tarnished copper substrates. Residues are relatively benign and only require removal when the fluxes are used on high-reliability electronic systems (for example, in military applications) or when the fluxes contain potentially harmful halide activators. Residue cleaning is a two-step process. The first step requires the use of organic solvents to remove the nonpolar rosin, and in the second step, a polar solvent (water or polar alcohols) is used to rinse away activator residues. Aqueous and semi-aqueous products can perform both functions.

The greater corrosivity of RA and SA fluxes is due, primarily, to higher levels of the activators that are used in RMA fluxes. These fluxes are used on base metals such as nickel (and nickel plate), lightly tarnished low-carbon steels, copper, iron-base alloys, and copper-base alloys (brasses, bronzes, and beryllium copper). Residues of the RA and SA fluxes must be removed to prevent the corrosion of the substrate later in service. Cleaning procedures similar to those identified for RMA fluxes are used. Cleanliness testing for ionic residues should be implemented to verify the adequate removal of flux deposits, particularly for the stronger fluxes.

Organic-acid fluxes have a chemical activity range that varies from the levels associated with RMA fluxes to those that exceed the activity of RA fluxes. These fluxes contain one or more organic acids, such as lactic, oleic, or stearic acid.

Chemical activity can be enhanced by adding organic halogen compounds (amine hydrohalide, which may contain chloride and bromide derivatives) or nonhalogenated substances, such as one of the amines or amides (urea or thylene diamine). Typical vehicles include water, isopropyl alcohol, polyglycols, or petroleum jelly for pastes.

The organic-acid fluxes are used in many electronic applications involving machine processes and hand assembly, as well as the hot tin or solder dipping of nickel and iron-base alloy leads and devices. These fluxes are also used on structural applications with copper and copper alloy workpieces that have light to moderate tarnishes.

Whether the fluxes are used in structural or electronic applications, their residues should be removed. The water-soluble residues are typically removed by rinsing with water or a polar organic solvent. The organic acid fluxes have better high-temperature stability, when compared with the rosin-base materials, which makes them good candidates for solders with melting temperatures that exceed 200 °C (363 °F).

Inorganic-acid fluxes have the highest levels of chemical activity. There are two categories of these fluxes:

- PURE ACIDS, SUCH AS HYDROCHLORIC, HYDROFLUORIC, OR PHOSPHORIC ACIDS, WHICH HAVE SURFACTANTS ADDED TO ENHANCE COVERAGE.
- INORGANIC SALT MIXTURES OR SOLUTIONS, WHICH MAY ALSO CONTAIN SURFACTANTS.

The pure acids are very strong and are capable of removing heavy oxide layers and scales. However, they offer the clean surface limited protection from reoxidation during the soldering process. Binary inorganic salt "alloys" are formed from the combination of zinc chloride ($ZnCl_2$), ammonium chloride (NH_4Cl), stannous chloride ($SnCl_2$), or sodium chloride (NaCl) components. The inorganic salt combinations form simple eutectics with minimum temperatures near the melting point of solders. (The melting temperature of the single salts are too high for them to flow at typical soldering temperatures.) For example, the NH_4Cl:3 ($ZnCl_2$) eutectic composition has a eutectic temperature (T_e) of 177 °C (351 °F). Other eutectic salt combinations include: $SnCl_2$-CuCl, T_e = 170 °C (338 °F); AgCl-CuCl, T_e = 260 °C (500 °F); and CuCl-$ZnCl_2$, T_e = 230 °C (446 °F).

Proper flux selection is based on the salt mixture having a melting temperature that is less than that of the solder. The molten salt reduces the surface oxides and coats the base metal to prevent reoxidation during the soldering process. Flux activity is further increased by dissolving the flux in a water vehicle. The salts break down to release Cl^- ions, which combine with water to form a hydrochloric acid (HCl) "activator." The fluxes, particularly the water solutions, may contain surfactants to assist the complete coverage of the joint area. A paste form of the flux uses petroleum jelly as the vehicle.

The inorganic-acid fluxes are limited to structural applications, such as plumbing or mechanical assemblies. Their corrosive activity is unacceptable for electronic devices or substrates, or for their assembly. These fluxes are effective on nickel and nickel alloys, stainless steels, chromium, and heavily tarnished copper and copper alloys. The inorganic fluxes are very stable at high temperatures. The flux residues and the fluxes themselves are extremely corrosive and must be thoroughly removed after processing.

It should be noted that chloride-containing residues and small amounts of water are particularly damaging to aluminum and aluminum alloys, because of the potential for stress-corrosion cracking. Residues are removed with hot-water rinses and follow-up polar-solvent rinses. Neutralizing solutions (mild caustics) can be used on nonsensitive substrates. A list of selected inorganic flux solutions for particular base metals is provided in Table 37.

TABLE 37 TYPICAL INORGANIC FLUXES FOR SELECTED BASE METALS

FOR STAINLESS STEEL AND GALVANIZED IRON	
ZINC CHLORIDE, ML (OZ)	**2510 (85)**
AMMONIUM CHLORIDE, ML (OZ)	**190 (6.5)**
STANNOUS CHLORIDE, ML (OZ)	**270 (9)**
HYDROCHLORIC ACID, ML (OZ)	**60 (2)**
WETTING AGENT (OPTIONAL), WT%	**0.1**
WATER[(A)]	
FOR STAINLESS STEEL	
ZINC CHLORIDE, ML (OZ)	**1420 (48)**
AMMONIUM CHLORIDE, ML (OZ)	**150 (5)**
HYDROCHLORIC ACID, ML (OZ)	**90 (3)**
WETTING AGENT (OPTIONAL), WT%	**0.1**
WATER[(A)]	
FOR MONEL	
ZINC CHLORIDE, ML (OZ)	**470 (16)**
AMMONIUM CHLORIDE, ML (OZ)	**470 (16)**
GLYCERIN, ML (OZ)	**470 (16)**
WATER, L (GAL)	**0.5 (0.125)**
FOR HIGH-TENSILE-STRENGTH MANGANESE, BRONZE, COPPER, OR BRASS	
ORTHOPHOSPHORIC ACID (85%), ML (OZ)	**1000 (34)**
WATER, ML (OZ)	**470 (16)**
FOR CAST IRON	
ZINC CHLORIDE, ML (OZ)	**950 (32)**
AMMONIUM CHLORIDE, ML (OZ)	**120 (4)**
SODIUM CHLORIDE, ML (OZ)	**240 (8)**
HYDROCHLORIC ACID, ML (OZ)	**240 (8)**
WATER[(A)]	
FOR CAST IRON	
ZINC CHLORIDE, ML (OZ)	**1180 (40)**
AMMONIUM CHLORIDE, ML (OZ)	**120 (4)**
HYDROFLUORIC ACID, ML (OZ)	**40 (1.25)**
WATER[(A)]	
PASTE FLUX FOR SOLDERING ALUMINUM	
STANNOUS CHLORIDE, ML (OZ)	**2450 (83)**
ZINC DIHYDRAZINIUM CHLORIDE, ML (OZ)	**210 (7)**
HYDRAZINE HYDROBROMIDE, ML (OZ)	**295 (10)**
WATER, ML (OZ)	**295 (10)**
FOR SOLDERING ALUMINUM	
CADMIUM FLUOBORIDE, ML (OZ)	**150 (5)**
ZINC FLUOBORIDE, ML (OZ)	**150 (5)**
FLUOBORIC ACID, ML (OZ)	**180 (6)**
DIETHANOL AMINE, ML (OZ)	**590 (20)**
DIETHANOL DIAMINE, ML (OZ)	**120 (4)**
DIETHANOL TRIAMINE, ML (OZ)	**295 (10)**
POTASSIUM CHLORIDE, ML (OZ)	**1330 (45)**
SODIUM CHLORIDE, ML (OZ)	**890 (30)**
LITHIUM CHLORIDE, ML (OZ)	**440 (15)**
POTASSIUM FLUORIDE, ML (OZ)	**210 (7)**

SODIUM PYROPHOSPHATE, ML (OZ)	**90 (3)**
TRIETHANOLAMINE, ML (OZ)	**740 (25)**
FLUOBORIC ACID, ML (OZ)	**90 (3)**
CADMIUM FLUOBORATE, ML (OZ)	**60 (2)**
STANNOUS CHLORIDE, ML (OZ)	**1300 (44)**
AMMONIUM CHLORIDE, ML (OZ)	**150 (5)**
SODIUM FLUORIDE, ML (OZ)	**30 (1)**
ZINC CHLORIDE, ML (OZ)	**1300 (44)**
AMMONIUM CHLORIDE, ML (OZ)	**150 (5)**
SODIUM FLUORIDE, ML (OZ)	**30 (1)**

(A) TO MAKE 3.8 L (1 GAL)

General Soldering

Paul T. Vianco, Sandia National Laboratories

Solder Joint Assembly

The configuration of a solder joint must have two basic attributes: It must meet the service requirements of the assembly, and it must be manufacturable to those requirements. Specifications and guidelines for the design of structural solder joints (for example, conduit) are limited, when compared with those used in electronic applications. Some British and European standards have been established, but few exist in the United States. Because standard joint design guidelines are not available, performance data are not well documented. However, the brazing community has several sets of standards that pertain to structural brazed joints (Ref 24). These specifications, which were established by the American Society of Mechanical Engineers (ASME), American National Standards Institute (ANSI), American Welding Society (AWS), and the Society of Automotive Engineers (SAE), cover joint construction, strength tests, and safety issues. Although these specific documents were developed for brazements, they can provide general guidelines for applying similar tests and criteria on solder joints. Under the circumstances, conservative design practices and inspection and test protocols that certify process quality have substituted for insufficient data. Additional information is available in the article "Evaluation and Quality Control of Soldered Joints" in this Volume.

Design for Service Requirements. Solder joint service conditions are typically represented by either electronic interconnect applications or structural applications. The former are described in the article "Soldering in Electronic Applications." Structural applications, which are described below, range from the assembly of small housings and containers to plumbing for fluid or gas conduit. Typical service requirements for structural joints include the support of mechanical loads (both high-temperature and cryogenic conditions), hermetic sealing for vacuum applications, and leak-tight joints for positive-pressure conduits and containers.

Several common structural solder joint configurations are shown in Fig. 15. It is recommended that solder joints be loaded in shear. Tensile loads should be avoided, because a slight deviation in the loading direction can place the joint in a peel-type fracture mode, which typically causes premature failure of the assembly. Lap-shear joints should have an overlap of approximately one-third of the base-metal thickness (Ref 25). Lap joints retain their strength over a range of gap thicknesses. However, the gap thicknesses of a single joint should be uniform for consistent capillary filling by the molten solder.

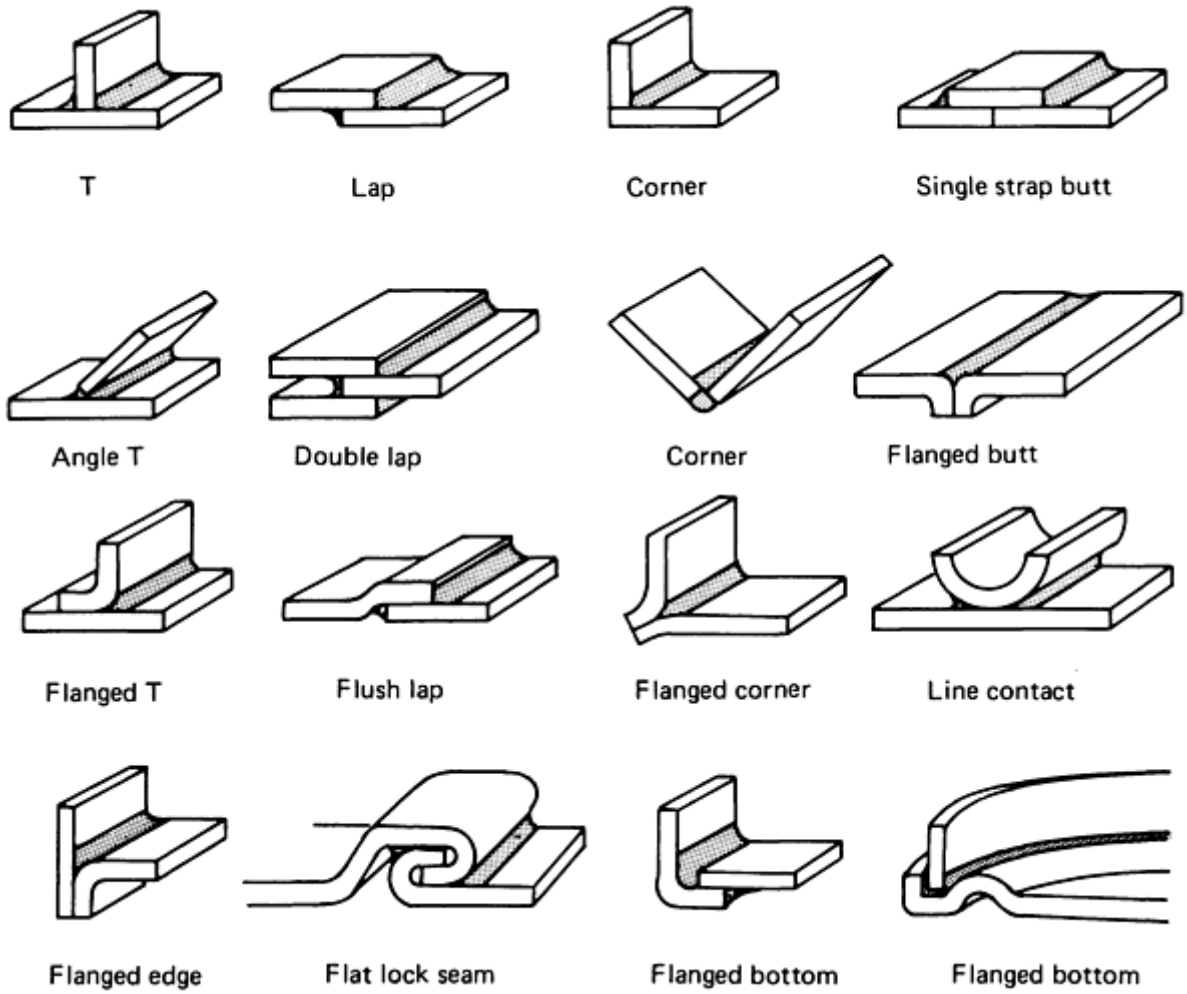

FIG. 15 COMMON STRUCTURAL SOLDER JOINTS

One of the first of the design criteria that pertains to the selection of a suitable solder is melting temperature, specifically the solidus and liquidus points. The solidus temperature is determined directly by the service conditions of the final assembly. Of course, the service temperature should never exceed the solidus point. However, how close the service temperature should be allowed to approach the solidus temperature depends on the level of monotonic or creep deformation and the fatigue life acceptable for the particular application. Tables of appropriate data either should be referred to or the necessary experiments performed.

A suitable liquidus temperature is primarily determined by the temperature sensitivity of the substrate materials during the soldering process. The molten solder working temperature should be approximately 25 to 50 °C (45 to 90 °F) greater than the liquidus temperature. A secondary factor in the selection of the liquidus and solidus temperatures is the desired pasty range for solder workability prior to solidification. Finally, multiple soldering processes require the solidus temperature of the first (high-temperature) soldering step to exceed the liquidus point by 30 to 50 °C (55 to 90 °F) of the second (low-temperature) step.

The mechanical properties of the solder must be considered in terms of the particular application. For example, the monotonic and creep strengths (shear or tensile) must be appropriate for the particular loading conditions and temperature environments to which the joint is subjected. Fatigue resistance is important for joints subjected to time-varying loads. Although such loads may be well below the ultimate monotonic or creep strength limits of the solder, they can result in significant cracking of the solder layer in a joint.

The size of the substrates and the thermal conductivity of the material from which they are constructed affect the joining process. A disparity of mass between the two substrates will result in the larger part heating up more slowly than the smaller one. Insufficient heat can result in a cold joint (that is, an absence of capillary flow and/or poor fillet formation

caused by premature solder solidification). Conversely, overheating the smaller workpiece may cause undesirable changes to the mechanical and physical properties of the base material. Similarly, two substrates with vastly different thermal conductivities (for example, stainless steel and aluminum) are difficult to uniformly heat, particularly in localized heating processes, such as soldering with an iron or torch.

When designing joints of dissimilar materials, the coefficient of thermal expansion (CTE) differences must be considered because sufficient stresses can build within the joint to cause catastrophic failure, particularly if the substrates are brittle. Time variations in environmental temperatures cause fatigue deformation to accumulate in the solder, thereby weakening the mechanical strength of the joint. An example of the method used to estimate the fatigue life of a 60Sn-40Pb solder joint can be made by calculations based on empirical data, as shown below. Unfortunately, data to support similar computations with other solders have not been compiled.

Laboratory tests of the isothermal fatigue life of 60Sn-40Pb over the temperature range from -50 to 125 °C (-58 to 257 °F) were used to develop the following equation for the fatigue life, N_f (Ref 16):

$$N_f = \left(\frac{1.14}{\Delta g_p} \right)^{1.96}$$

where N_f is the number of cycles to failure (50% load drop for equivalent strain) and $\Delta\gamma_p$ is the plastic strain level in the joint. A conservative estimate of $\Delta\gamma_p$ is made by using the total strain, $\Delta\gamma_t$, determined by:

$$\Delta g_t = \frac{(a_1 - a_2)\Delta TL}{t}$$

where α_i is the CTE of the two substrates (i = 1, 2), $\Delta T$is the temperature difference, L is the maximum dimension of the joint, and t is the joint thickness. The parameters and joint configuration are illustrated in Fig. 16. Solder fatigue cracks may be visible in the solder fillets, typically where L is a maximum.

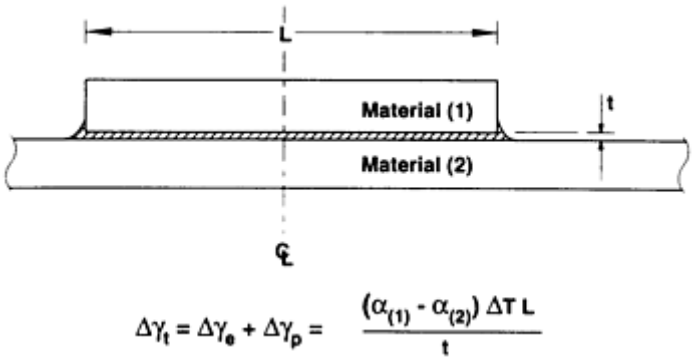

FIG. 16 PARAMETERS FOR THE CALCULATION OF TOTAL THERMAL MISMATCH STRAIN IN A GENERIC SOLDER JOINT CONFIGURATION. *T*, JOINT THICKNESS; *L*, MAXIMUM JOINT DIMENSION BETWEEN THE TWO SUBSTRATES

Thermal expansion mismatch between workpieces affects joint clearances during the soldering process. Consider the enclosed geometry tube-in-socket joint in Fig. 17. When the CTE of the outer part is larger than that of the inner part, the gap will increase with heating. An excessive gap will result in voids in the joint that are caused by an insufficient solder supply and/or poor capillary action. A sample calculation follows:

- INNER PART AT 20 °C (68 °F), COPPER; CTE (α_1), 17.0 × 10^{-6}/K; OUTER DIAMETER, 74.7 MM (2.94 IN.)
- OUTER PART AT 20 °C (68 °F), ALUMINUM; CTE (α_0), 23.5 × 10^{-6}/K; INNER DIAMETER, 75.0

MM (2.95 IN.)
- GAP AT 20 °C (68 °F), 0.15 MM (0.006 IN.)

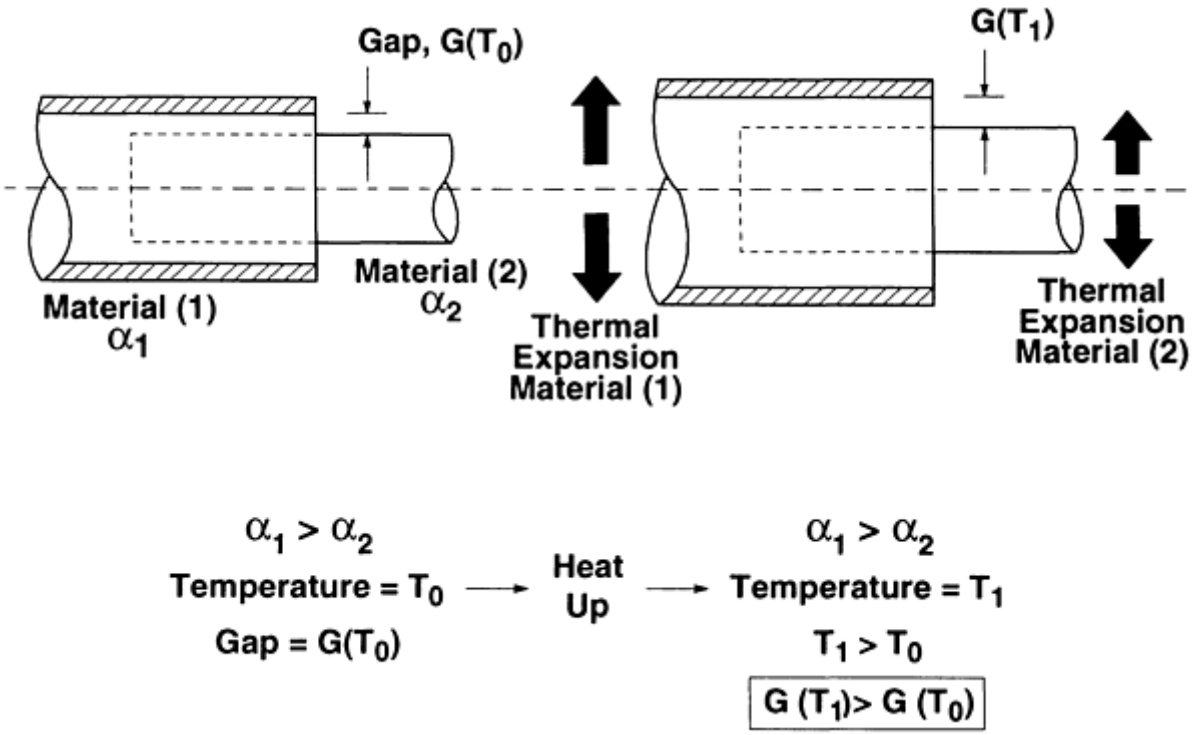

FIG. 17 EFFECTS OF HEATING ON THE JOINT GAP BETWEEN DISSIMILAR METALS

At 250 °C (482 °F), the new dimension, L_f, of the parts (the outer diameter of the aluminum and the inner diameter of the copper) are calculated by:

$$L_F = L_O + L_O \alpha \Delta T$$

where L_o is the dimension at 20 °C (68 °F), αis the CTE of the material, and ΔT is the temperature difference (T_f - T_o).

- T_F = 250 °C (482 °F), SO THAT ΔT = 230 °C (414 °F)
- INNER PART AT 250 °C (482 °F), COPPER; OUTER DIAMETER, 75.0 MM (2.95 IN.)
- OUTER PART AT 250 °C (482 °F), ALUMINUM; INNER DIAMETER, 75.4 MM (2.97 IN.)
- GAP AT 250 °C (482 °F), 0.2 MM (0.008 IN.)

In this example, the solder joint gap grew by 0.05 mm (0.002 in.). This computation can be applied to any geometry in which L_o is the dimension of the respective parts.

Conversely, an inner part with a CTE that is greater than that of the outer section will cause the gap to decrease with heating, causing voids and poor solder filling resulting from the inability of flux volatiles to escape from the joint.

Finally, consideration must be given to material compatibility. The first concern is that the substrate materials are not damaged by chemicals or the mechanical procedures used to preclean surfaces. Damage includes excessive metal removal, stress-corrosion cracking, or the deposition of hard-to-remove residues. Secondly, the corrosion potential of joining dissimilar metals, including the two base metals as well as the solder/base metal couples, must be adequately assessed. In the case of conduit for liquids or gases, the role of the carried medium, as an electrolyte in the corrosion of the joint, must also be considered. In many cases, references to the electromotive series or fundamental chemistry

textbooks (Ref 26) can provide corrosion information for a preliminary assessment. Finally, the assembled product must be compatible with the chemicals and processes used to remove flux residues after soldering.

Design for Processing Requirements. It is assumed that the substrates have adequate solderability for the selected solder alloy. Two processes must occur during product assembly to ensure an adequate joint: The solder must fill the gap area and flux volatiles and liquids must be ejected from the joint. Some general guidelines at the design stage will facilitate these processes.

First, the joint gaps should be in the range from 0.076 to 0.18 mm (0.003 to 0.007 in.). Workpiece design must also account for changes in gap dimensions caused by the heating/cooling of dissimilar substrates, surface roughness, plate flatness, eccentricity of circular-section workpieces, and consumption of the base metal or substrate coatings by the molten solder. Smaller gaps restrict solder flow and hinder the removal of flux volatiles, whereas larger gaps diminish the capillary effect required by the molten solder to fill the joint.

Second, the preferred gap geometry is a straight path opened to the atmosphere at two locations. One opening is used to supply flux and solder to the joint, while the other serves to vent flux volatiles and gases as the molten solder fills the gap. "Blind" gaps (or blind holes), which do not allow a vent path, should be avoided. A vent hole can be added and later filled in with a lower-melting-temperature solder if the design permits. Another rule of thumb is that solder has difficulty in "turning corners." Therefore, straight paths are preferred over sharp comers in the joint.

Third, ready access to the joint by a reservoir of solder containing an adequate quantity to fill the gap and to form the fillet must be provided. Inadequately filled gaps can be caused by an insufficient supply of solder to the joint. Poorly formed solder fillets reduce the monotonic strength, fatigue life, and creep strength of the joints, as well as limit the solderability assessment.

Fourth, solder joints that use preforms are always susceptible to void formation. Because the joint does not fill by capillary action, volatiles and gases have an increased likelihood of being trapped within the gap. Such joints must also be carefully assessed for corrosion potential by retained flux residues in those voids.

Fifth, the metallurgical reaction between the substrate and the solder during wetting necessarily consumes some of the substrate to form the reaction layer (typically, an intermetallic compound) at the interface. The dissolution of substrate material must be accounted for when soldering to very thin foils or coatings. The rate of dissolution will depend on substrate geometry (round or cylindrical sections dissolve slightly faster than flat plates), substrate composition, and the composition and volume of solder (flowing baths will remove more substrate metal than static baths). The temperature of the solder and the time of immersion (an increase of both raise the rate of substrate dissolution), are also factors. Dissolution data from unspecified geometries are determined from Fig. 18 and 19.

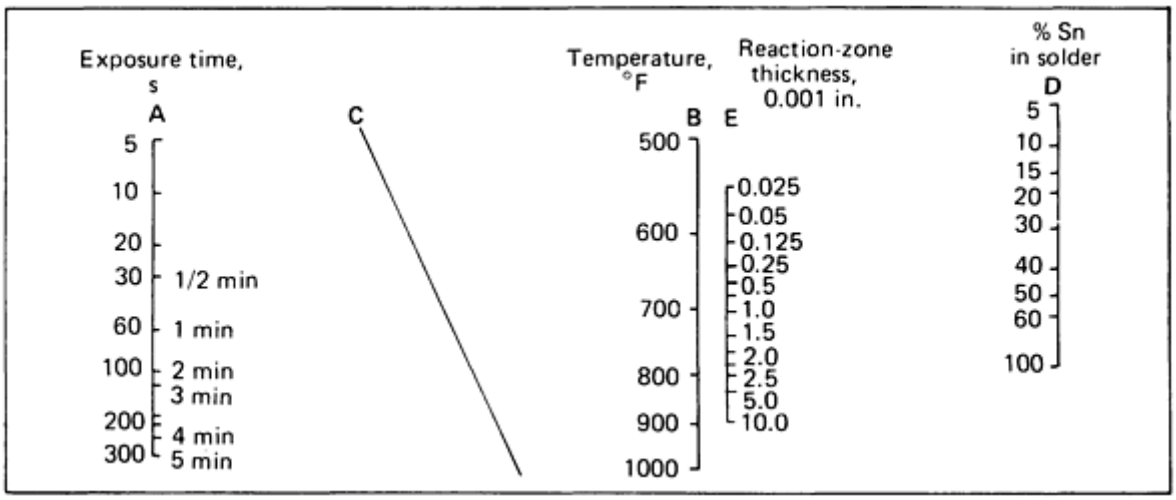

FIG. 18 NOMOGRAPH TO DETERMINE THE TIN-LEAD SOLDER REACTION ZONE THICKNESS FOR THE COPPER ALLOYS C10200 AND C26000 ALLOYS UNDER STATIC INFINITE-VOLUME CONDITIONS. SELECT THE EXPOSURE CONDITIONS ON SCALES A AND B. WITH A STRAIGHT EDGE BETWEEN THE CONDITIONS, FIND THE INTERSECTION WITH BASE LINE C. USING A STRAIGHT EDGE, CONNECT THIS POINT ON LINE C WITH THE

TIN CONTENT OF THE SOLDER ON SCALE D. READ THE REACTION-ZONE THICKNESS ON SCALE E. THE NOMOGRAPH CAN ALSO BE USED IN REVERSED SEQUENCE TO SELECT OPERATING CONDITIONS, GIVEN A PERMISSIBLE REACTION ZONE THICKNESS AND SOLDER COMPOSITION.

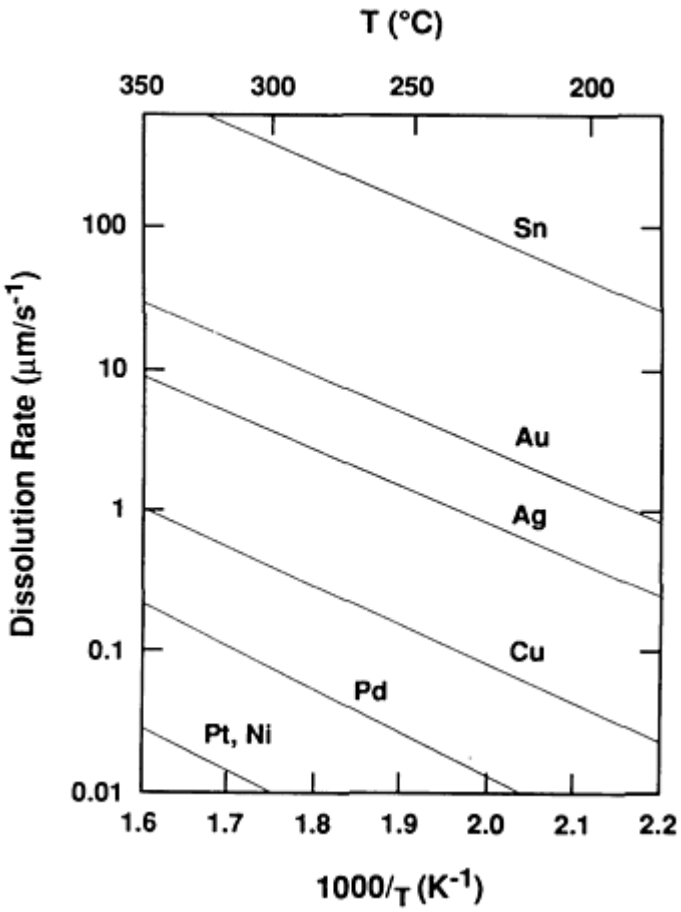

FIG. 19 METAL DISSOLUTION RATES FOR ELEMENTAL METALS AS A FUNCTION OF TEMPERATURE. SOURCE: REF 27

Intermetallic compounds represent the metallurgical reaction product between the solder and the substrate material. The compound formulations for common base metals and coatings with tin-bearing solders are:

- *COPPER:* CU_6SN_5 AND CU_3SN
- *NICKEL:* NI_3SN_4
- *GOLD:* $AUSN_4$ AND $AUSN_2$
- *IRON:* $FESN_2$
- *SILVER:* AG_3SN

These layers form when the solder is molten, as well as after solidification, by means of solid-state diffusion during storage or service at elevated temperature. In the solid state, the thickness is a function of the temperature and the time. Although intermetallic compounds are a necessary part of solder wetting, excessively thick layers can be detrimental to joint integrity or follow-up processing. Specifically, the brittle nature of intermetallic compounds can jeopardize the mechanical and fatigue strength of the joint, particularly at high loading rates, such as those that occur under impact or vibration conditions. Another detriment is that the solid-state growth of the layers consumes both the solder film and the base metal. Complete consumption of the tin or solder coating exposes the intermetallic surface to oxidation, making it very difficult to solder coat, even when using the strongest fluxes. The solid-state growth kinetics of several solders that were hot dip coated on copper are shown in Fig. 20. The typical as-soldered thickness of intermetallic compounds of

60Sn-40Pb on copper and nickel are 1 to 2 μm (39 μin.) and 0.5 μm (20 μin.), respectively. The layers grow very slowly at room temperature.

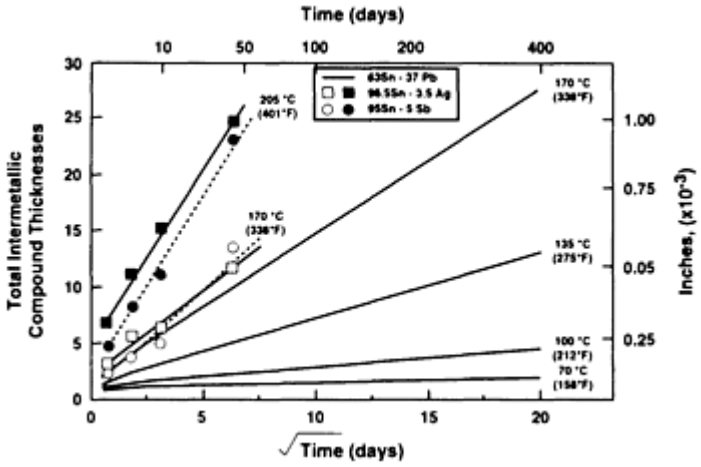

FIG. 20 SOLID-STATE INTERMETALLIC GROWTH KINETICS FOR HOT-DIPPED SOLDER COATINGS ON COPPER. SOURCE: SANDIA NATIONAL LABORATORIES

Joint design must include postassembly cleaning requirements. Materials compatibility between the cleaning agents and the workpiece, as well as the geometry of the workpiece, are important factors. Reentrant comers or hidden gaps and passages can entrap flux residues and prevent the flow of clean solvents into the areas.

The use of the high-temperature, precious-metal solders 80Au-20Sn or 88Au-12Ge on precious-metal substrates and coatings does not require a flux to remove the very limited oxide layers. The melting points of these solders preclude the use of rosin-base fluxes, because of significant high-temperature degradation. Other fluxes may also experience some degradation. The absence of a flux causes the surface tension of the solder to remain high, impeding capillary flow by the molten alloy. Therefore, the solders are typically introduced into the joint as preforms. Mechanical pressure on the joint is used to assist the spreading of the solder throughout the gap. Small quantities of oxide particles in the solder arise from the non-precious-metal component. Random spreading of the solder causes the joint to have a higher number of voids than is observed in a joint filled by capillary action.

Maintaining the position of the substrates during solder wetting is necessary for successful joint formation. Special fixturing can be designed to hold the workpieces for critical applications. Another approach is to design the joint itself to be self-jigging, in order to maintain the proper gaps and clearances during soldering (Fig. 21).

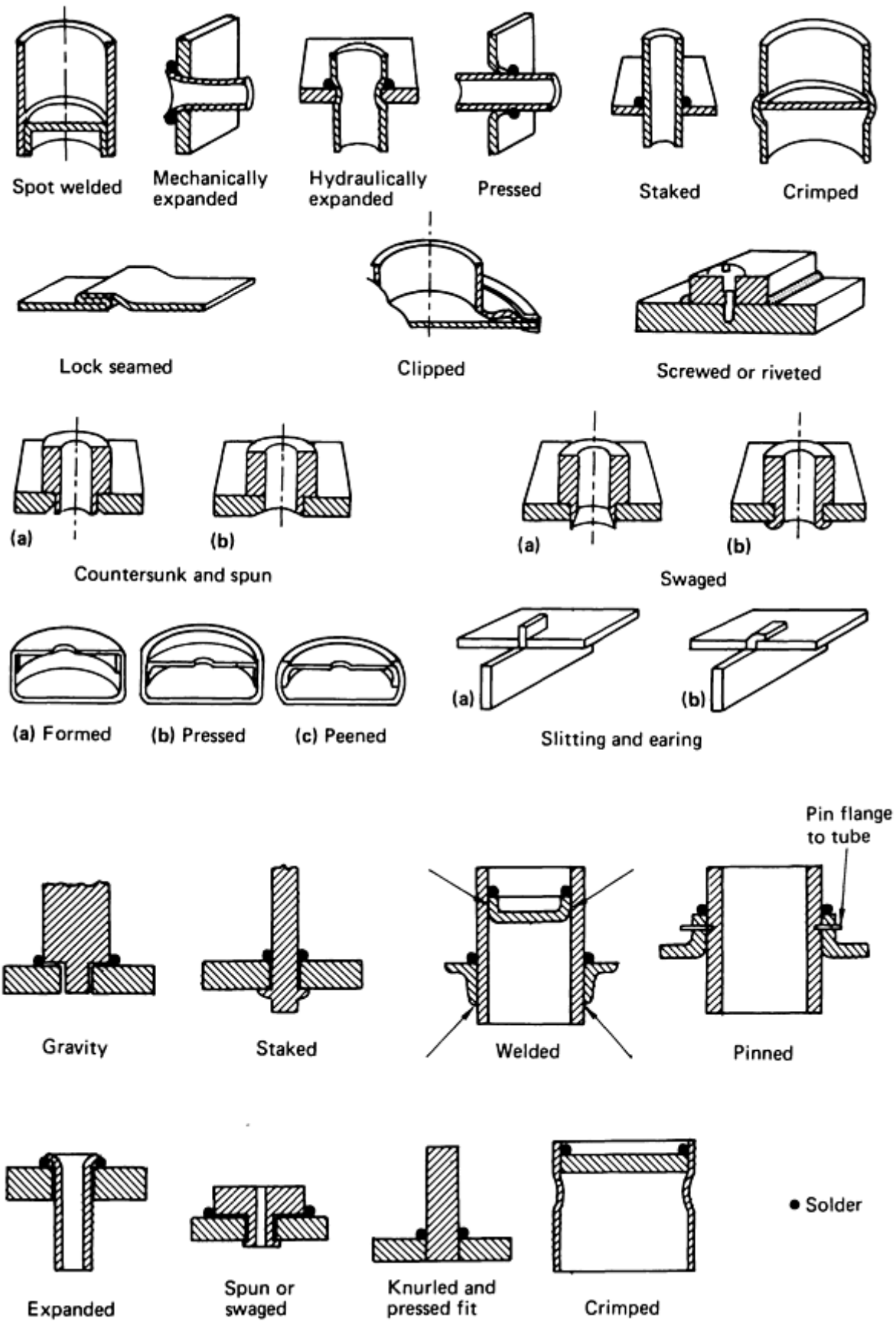

FIG. 21 SELF-JIGGING JOINT CONFIGURATIONS

Design for Inspection Requirements. The inspection techniques selected to qualify a solder joint will have particular requirements in terms of joint configuration. Visual inspection is typically used to determine whether the solder has flowed within the gap and on the external surfaces (fillets). For blind holes or gaps, witness holes can be drilled into the substrate(s). During soldering, the solder fills the witness hole to the outside surface, indicating to the operator that the solder has indeed filled the gap. Although they are not always practical, unobstructed views of the solder joint gap at the external surface vastly improve the visual inspection of the joint.

References cited in this section

16. H. SOLOMON, "FATIGUE OF 60/40 SOLDER," REPORT 86CRD024, GENERAL ELECTRIC CO., MAY 1986
24. *BRAZING HANDBOOK*, AWS, 1991, P 267-276
25. C. THWAITES, *CAPILLARY JOINING*, WILEY AND SONS, UNITED KINGDOM, 1982, P 52
26. J. SCULLY, *THE FUNDAMENTALS OF CORROSION*, 2ND ED., PERGAMON PRESS, INC., 1975
27. C. LEA, A SCIENTIFIC GUIDE TO *SURFACE-MOUNT TECHNOLOGY*, ELECTROCHEM. PUBL., LTD., 1988

General Soldering

Paul T. Vianco, Sandia National Laboratories

Soldering Techniques

The numerous soldering processes have the common goal of providing heat energy to the joint area in the presence of the flux and solder alloy. The heat energy (and subsequent temperature rise) must support activation of the flux cleaning activities, heating of the substrate, and melting of the solder alloy to permit wetting and joint formation. Too little heat limits solder wetting, whereas excessive heat chemically degrades the flux (which loses activity and deposits hard-to-remove residues), reoxidizes the substrate surface prior to completion of solder wetting, or causes heat damage to the substrate.

Heating techniques can be categorized as global processes, in which the entire substrate reaches the soldering temperature, and local techniques, in which only the immediate joint area is heated. Examples of global techniques include vapor-phase (condensation) reflow, furnace (infrared or convection) reflow, wave soldering, ultrasonic soldering (bath), as well as dip (including hot-air leveling) and drag soldering. Local heating techniques include the soldering iron (heat and heat plus ultrasonics), torch, hot gas reflow, focused infrared soldering, induction soldering, and laser soldering. Operator interaction depends on the particular process. For example, the entire process can be fully automated, as in furnace systems or specialized equipment used in electronic circuit board assembly. Nevertheless, operators must establish the proper zone temperatures, conveyor belt speeds, and heating rates. Thermocouple profiling of a prototype workpiece is essential to verifying that the proper thermal conditions will be achieved. Manual soldering, such as with the iron or torch, requires greater operator interaction and skill.

Control of the full sequence of heating, fluxing, and applying the filler metal is particularly critical in manual solder processes (whether iron, induction, torch, or hot-gas processes), because they are usually performed in air. Competing factors that occur during substrate heating are:

- NEED FOR AN INCREASE IN SUBSTRATE TEMPERATURE TO MAINTAIN THE MOLTEN STATE OF THE SOLDER
- ACTIVATION OF THE FLUX OXIDE REMOVAL PROCESS (OR PROCESSES)
- ACCELERATED OXIDATION OF THE SUBSTRATE SURFACE
- DEGRADATION OF SOME FLUX COATINGS

Circuit board soldering and structural applications are described below as general examples.

Circuit Board Soldering. First, flux is applied to the leads and circuit board, unless flux-cored soldering wire is used, in which case this step is omitted. The coated area should extend beyond the immediate joint to ensure adequate wetting by the solder. Next, the soldering iron is made to contact the lead (never the circuit board land), and the solder wire is fed so that it contacts the opposite side of the lead. Melting of the solder indicates that the lead has reached temperature. The wire, followed by the iron tip, is then removed from the joint area upon formation of the joint fillet.

Structural Applications. The larger thermal mass of typical workpieces requires preheating in order to bring the joint area to the working temperature. Then, the flux is applied to fully cover the hot surface. The joint is further heated and the filler metal is applied to the joint surfaces. Most inorganic and organic fluxes can tolerate the high temperatures required to supply heat to larger members. The rosin-base fluxes can quickly degrade, as indicated by the formation of thick, blackened residues on the surface. Heat and solder are removed when an adequate fillet forms at the joint opening, in order to ensure complete filling of the joint gap.

The hot dip coating of parts can be performed by ultrasonic activation, without using a flux. Ultrasonic energy is coupled to the sample through the solder bath (Fig. 22). Optimum coupling is a function of the sample geometry, power level, and workpiece-horn separation. Oxide removal does not occur through simple line-of-sight erosion by the horn (Ref 28). Rather, the oxide is disrupted by the ultrasonic energy that is transferred from the horn into the substrate. Therefore, hidden surfaces can also be coated by the solder. Hot-dipped coatings can be applied to large workpieces or to leads on small electronic devices. In the latter case, care should be taken to ensure that internal connections are not damaged by the ultrasonic energy. This technology has been used to assemble tube-socket joints on heat-exchanger equipment (Ref 29).

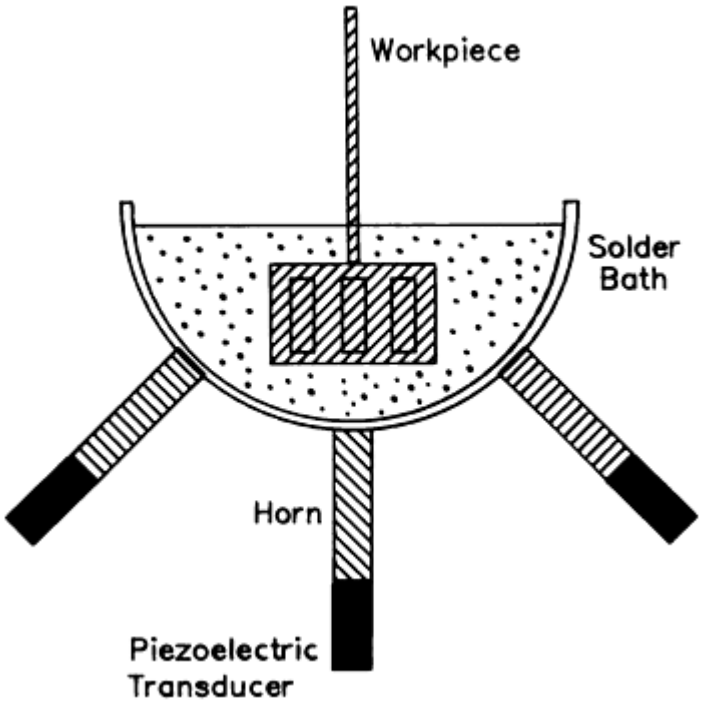

FIG. 22 ULTRASONIC SOLDERING BATH EQUIPMENT

An important component of the solder assembly process is the fixturing that is used to support the workpieces being assembled. Fixturing details are most critical for global heating processes in which the fixture will also be raised to the soldering temperature. The purpose of fixturing is to either anchor the two substrates to prevent movement while the solder is in the molten state or permit the controlled displacement of the substrates to establish specific joint gaps not achieved with the solder preform in the solid state. Lubricants include high-temperature petroleum products or solid lubricants (MoS_2 and graphite). Preloads on the workpieces are provided by springs (coil or Belleville configurations). The joint gap can be established by spacers between the workpieces or particles within the joint itself (Fig. 23). The spacer materials should not cause undesirable reactions with the solder or jeopardize the strength capacity of the joint.

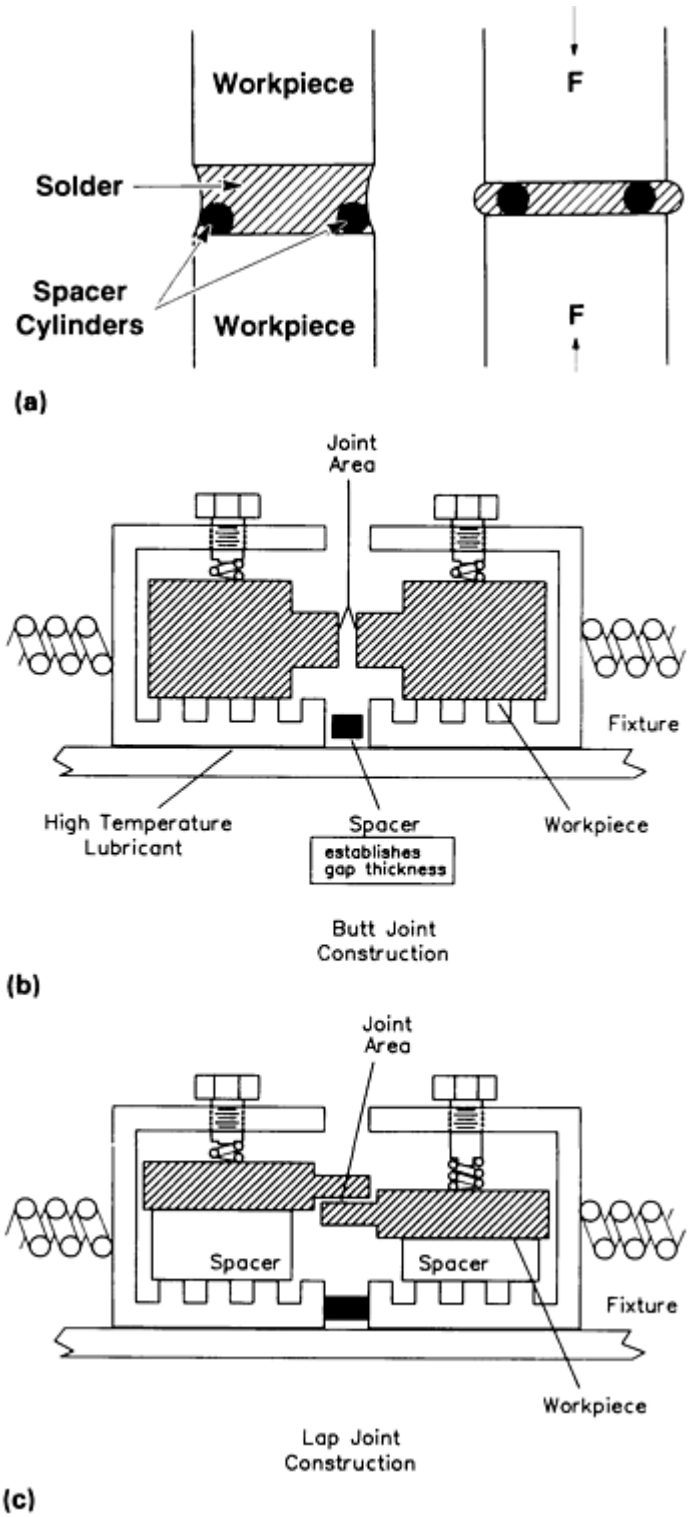

FIG. 23 TECHNIQUES TO MAINTAIN JOINT GAPS. (A) BUTT JOINT WITH SPACERS IN THE SOLDER. (B) BUTT JOINT WITH SPACER IN THE FIXTURE. (C) LAP JOINT CONSTRUCTION

Fixture materials should be carefully assessed. Although high vapor pressures generated by fixture metals is not of concern at the relatively low temperatures used in soldering, factors such as thermal expansion and fixture size should be considered. For example, a CTE mismatch between the workpiece and the fixture materials, with improperly designed dimensions, can cause the joint gap to grow or close at soldering temperatures. Fixtures with large thermal mass will lengthen the heating and cooling times for the workpiece, leading to possible flux degradation, base metal or coating erosion, and longer production time. Preferred fixturing materials include oxide ceramics (alumina, beryllia, or mullite), refractory metals (molybdenum, tungsten, or tantalum), and well-oxidized steels (low-carbon and stainless steels). These

materials will generally not be wetted by solder (and flux) spillage and can accommodate the elevated temperatures. Fixtures made of machined metals, such as aluminum, copper alloys, or steels, should be annealed in order to relieve any residual stresses that arise from the stock material or machining operations. These internal stresses may cause misalignment of the workpieces or the binding of moving parts, caused by warpage generated at soldering temperatures. Preoxidized surfaces will prevent inadvertent wetting by the solder.

Fixtures should be cleaned of organic residues to limit their outgassing in vacuum furnaces, prevent deposition of the contaminants onto the solderable surfaces, and limit spatter by their volatilization at soldering temperatures. Materials that contain or are coated with cadmium or zinc should not be used, because their high vapor pressures (even at soldering temperatures) may cause them to contaminate the joint area, as well as to poison vacuum and inert-atmosphere furnace systems.

The workpiece temperature should be monitored, at least in the prototype stages of process development, in order to document temperature conditions. In furnace operations, it is preferred that the controlling thermocouple contact the substrates to confirm the desired temperature profile at the joint area. The relatively low temperatures of soldering allow the use of inexpensive thermocouples, such as types J, T, and K, for many furnace cycles. The thermocouples should not interfere with the fixtures or the filling of the joint.

An undesirable spread of the molten solder on the substrate surface can be prevented by a number of "solder-stop" products. High-temperature tapes, which are popular in the electronics industry to prevent solder wetting of areas on printed circuit boards, are suited for many structural applications. Another product is a slurry made from powders that are mixed with water or alcohol and painted on the surface areas that are to be free of solder. The vehicle evaporates, leaving a coating that prevents spreading by the solder.

Detailed descriptions of the individual soldering processes, equipment, and applications are provided in the Section "Solid-State Welding, Brazing, and Soldering Processes" in this Volume.

References cited in this section

28. P. VIANCO AND F. HOSKING, *ANALYSIS OF ULTRASONIC TINNING*, NEPCON WEST, FEB 1992, P 1718
29. J. SCHUSTER AND R. CHILKO, ULTRASONIC SOLDERING OF ALUMINUM HEAT EXCHANGERS, *WELD. J.*, OCT 1975, P 711

General Soldering

Paul T. Vianco, Sandia National Laboratories

Postassembly Cleaning Procedures

After the soldering operation, the workpiece is cleaned, primarily to remove flux residues that can cause corrosion of the part while in storage or during service. Other cleaning procedures include the removal of solder-stop materials, as well as stray solder particles, which can interfere with mechanical or electrical performance of the assembly. Flux residues should be removed as soon as possible after the soldering process, because their ability to be removed decreases with time, whereas their tenacity and potential for corrosive damage increase with time.

Cleaning fluids and solvents to be used are determined by the particular flux residues. Guidelines are presented in the section "Fluxes" in this article. The selection of organic solvents is rapidly changing as chlorofluorocarbon materials are phased out by environmental regulations and new materials (and processes) become qualified as replacements.

Some general practices must be considered when establishing cleaning procedures. First, assess the compatibility of substrate materials and filler metals with the cleaning solutions. Organic solvents are benign toward metal surfaces. Alkaline solutions used to neutralize strongly acidic fluxes can affect some base-metal finishes (for example, copper

alloys, iron alloys, and some steels). When in doubt, samples of the substrate should be exposed to the cleaning agent prior to use on final assemblies.

Second, determine whether the cleaning solutions leave undesirable residues. Mineral deposits from tap water can corrode or stain substrate surfaces (especially in the continued presence of water vapor). Tap-water rinses should be followed with rinses in either deionized or distilled water. All traces of water can be removed by a final alcohol rinse. Isopropyl alcohol is generally used. Denatured alcohol and acetone should be avoided, because they also can leave residues.

Third, the drying of solvent or other cleaning-solution residues should utilize dry, clean gas, such as bottled or cryogenic nitrogen gas. Compressed "house" air may contain water particles or compressor oils that can quickly recontaminate the workpiece.

Fourth, limit the contact of the assembly with oily rags and fingerprints. Many instances of cosmetic staining or pitting of the workpiece surface have been traced to fingerprints.

Fifth, test for the effectiveness of postcleaning operations. Unlike the well-specified procedures used by the electronics industry, such procedures are not well standardized for structural applications. Temperature-humidity chambers can be used to assess the propensity for corrosion on the workpiece (a destructive test).

Cleaning effectiveness can be enhanced by thermal and mechanical assistance. Cleaning solvents and solutions have higher solubility for residues at elevated temperatures. Caution should be observed when heating solutions because of the generation of vapors that can result in health or fire hazards. The use of solvent vapors at their boiling point in vapor degreasers can remove residues from remote locations on the workpiece. However, the solvents that have been popular for vapor degreasing are being restricted from use by environmental statutes.

Mechanical agitation of cleaning solutions is obtained by ultrasonic activation, high-energy sprays, and manual scouring procedures. Ultrasonics are very effective for loosening residues, particularly in hidden locations. Although generally safe for the cleaning of structural members, care must be exercised when using ultrasonics on electronic assemblies because of the possible damage to internal connections. The use of sprays or jets to force the cleaning solution into crevices and hidden areas of the workpiece can increase cleaning efficiency. Batch and in-line equipment based on spray and jet technology is currently available. Because the cleaning material passes through a jet, aerosols and mists are generated, which may create an explosion hazard.

Manual scouring can remove residues on exposed surfaces only. Cleaning with sandpaper or vapor blasting metal surfaces with abrasive particles should be avoided in the postprocess cleaning steps for three reasons: First, the base-metal oxide layer protects the surface from corrosion or excessive oxidation later in service. For example, stainless steels are particularly susceptible to corrosion attack after abrasive treatments, particularly those that use steel wool or a steel brush. Second, solders are generally much softer than the base metals. Therefore, inadvertent damage can be easily done to the joint fillets, possibly jeopardizing monotonic strength and fatigue resistance. Third, abrasive grit particles can become embedded in the substrate and, particularly, in the softer solder. Dislodged particles can damage mechanical actuators that are part of the soldered assembly. The abrasive particles can also deteriorate surface solderability of the workpiece during subsequent assembly, repair, or rework procedures. Damage occurs readily to circuit boards (solder masks, coatings, and the laminate itself) by abrasive particles.

Finally, storage of the parts must be considered. The extent of storage control depends on factors such as the type of assembly and its service requirements, the cost of rework, repair or scrapping of damaged parts, and the environment of the factory. Acute contamination or corrosion of finished parts can be prevented by their enclosure in bags. Popular containers are polyethylene plastic bags, which can provide short-term storage (<1 year) when properly sealed. Solderability may deteriorate for longer storage times because of the outgassing of polymer components contained in the plastic. Only new bags should be considered for the storage of solderable parts because contamination of the bag interior from previous usage may deteriorate solderability. Plastic bag material should be a minimum 0.1 mm (0.004 in.) thick. The bags can be filled with an inert gas (nitrogen) to further limit oxidation of solderable surfaces. Paper bags should be considered only for the transport of devices because their inability to be sealed from the environment, as well as contamination of solderable surfaces by chemicals in the paper, limit their appropriateness as storage containers. Metal foils can be used as storage media, although greater effort is required to seal the material. The use of desiccants that comply with MIL-D-3464E, "Desiccants, Activated, Bagged, Packaging Use and Static Dehumidification," is acceptable.

More elaborate and expensive storage measures include the construction of special facilities that control temperature, humidity, and air-particulate counts. The prevention of mechanical damage that results from the movement of inventory must also be addressed. Storage conditions are of particular concern for electronic devices and circuit boards in which solderability loss can severely hinder subsequent automated assembly processes.

Paul T. Vianco, Sandia National Laboratories

Postassembly Cleaning Procedures

After the soldering operation, the workpiece is cleaned, primarily to remove flux residues that can cause corrosion of the part while in storage or during service. Other cleaning procedures include the removal of solder-stop materials, as well as stray solder particles, which can interfere with mechanical or electrical performance of the assembly. Flux residues should be removed as soon as possible after the soldering process, because their ability to be removed decreases with time, whereas their tenacity and potential for corrosive damage increase with time.

Cleaning fluids and solvents to be used are determined by the particular flux residues. Guidelines are presented in the section "Fluxes" in this article. The selection of organic solvents is rapidly changing as chlorofluorocarbon materials are phased out by environmental regulations and new materials (and processes) become qualified as replacements.

Some general practices must be considered when establishing cleaning procedures. First, assess the compatibility of substrate materials and filler metals with the cleaning solutions. Organic solvents are benign toward metal surfaces. Alkaline solutions used to neutralize strongly acidic fluxes can affect some base-metal finishes (for example, copper alloys, iron alloys, and some steels). When in doubt, samples of the substrate should be exposed to the cleaning agent prior to use on final assemblies.

Second, determine whether the cleaning solutions leave undesirable residues. Mineral deposits from tap water can corrode or stain substrate surfaces (especially in the continued presence of water vapor). Tap-water rinses should be followed with rinses in either deionized or distilled water. All traces of water can be removed by a final alcohol rinse. Isopropyl alcohol is generally used. Denatured alcohol and acetone should be avoided, because they also can leave residues.

Third, the drying of solvent or other cleaning-solution residues should utilize dry, clean gas, such as bottled or cryogenic nitrogen gas. Compressed "house" air may contain water particles or compressor oils that can quickly recontaminate the workpiece.

Fourth, limit the contact of the assembly with oily rags and fingerprints. Many instances of cosmetic staining or pitting of the workpiece surface have been traced to fingerprints.

Fifth, test for the effectiveness of postcleaning operations. Unlike the well-specified procedures used by the electronics industry, such procedures are not well standardized for structural applications. Temperature-humidity chambers can be used to assess the propensity for corrosion on the workpiece (a destructive test).

Cleaning effectiveness can be enhanced by thermal and mechanical assistance. Cleaning solvents and solutions have higher solubility for residues at elevated temperatures. Caution should be observed when heating solutions because of the generation of vapors that can result in health or fire hazards. The use of solvent vapors at their boiling point in vapor degreasers can remove residues from remote locations on the workpiece. However, the solvents that have been popular for vapor degreasing are being restricted from use by environmental statutes.

Mechanical agitation of cleaning solutions is obtained by ultrasonic activation, high-energy sprays, and manual scouring procedures. Ultrasonics are very effective for loosening residues, particularly in hidden locations. Although generally safe for the cleaning of structural members, care must be exercised when using ultrasonics on electronic assemblies because of the possible damage to internal connections. The use of sprays or jets to force the cleaning solution into crevices and hidden areas of the workpiece can increase cleaning efficiency. Batch and in-line equipment based on spray and jet technology is currently available. Because the cleaning material passes through a jet, aerosols and mists are generated, which may create an explosion hazard.

Manual scouring can remove residues on exposed surfaces only. Cleaning with sandpaper or vapor blasting metal surfaces with abrasive particles should be avoided in the postprocess cleaning steps for three reasons: First, the base-metal oxide layer protects the surface from corrosion or excessive oxidation later in service. For example, stainless steels are particularly susceptible to corrosion attack after abrasive treatments, particularly those that use steel wool or a steel brush. Second, solders are generally much softer than the base metals. Therefore, inadvertent damage can be easily done to the joint fillets, possibly jeopardizing monotonic strength and fatigue resistance. Third, abrasive grit particles can become embedded in the substrate and, particularly, in the softer solder. Dislodged particles can damage mechanical actuators that are part of the soldered assembly. The abrasive particles can also deteriorate surface solderability of the workpiece during subsequent assembly, repair, or rework procedures. Damage occurs readily to circuit boards (solder masks, coatings, and the laminate itself) by abrasive particles.

Finally, storage of the parts must be considered. The extent of storage control depends on factors such as the type of assembly and its service requirements, the cost of rework, repair or scrapping of damaged parts, and the environment of the factory. Acute contamination or corrosion of finished parts can be prevented by their enclosure in bags. Popular containers are polyethylene plastic bags, which can provide short-term storage (<1 year) when properly sealed. Solderability may deteriorate for longer storage times because of the outgassing of polymer components contained in the plastic. Only new bags should be considered for the storage of solderable parts because contamination of the bag interior from previous usage may deteriorate solderability. Plastic bag material should be a minimum 0.1 mm (0.004 in.) thick. The bags can be filled with an inert gas (nitrogen) to further limit oxidation of solderable surfaces. Paper bags should be considered only for the transport of devices because their inability to be sealed from the environment, as well as contamination of solderable surfaces by chemicals in the paper, limit their appropriateness as storage containers. Metal foils can be used as storage media, although greater effort is required to seal the material. The use of desiccants that comply with MIL-D-3464E, "Desiccants, Activated, Bagged, Packaging Use and Static Dehumidification," is acceptable.

More elaborate and expensive storage measures include the construction of special facilities that control temperature, humidity, and air-particulate counts. The prevention of mechanical damage that results from the movement of inventory must also be addressed. Storage conditions are of particular concern for electronic devices and circuit boards in which solderability loss can severely hinder subsequent automated assembly processes.

General Soldering

Paul T. Vianco, Sandia National Laboratories

Inspection

Because inspection necessarily implies a determination of defects in the workpiece, the type and number of defects that jeopardize the service requirements of the product should be documented. The search for, and rework of, noncritical defects (such as unnecessary cosmetic attributes) simply increases product cost, the amount of scrapped product, as well as the likelihood of heat damage to the substrates. Defects and their acceptance limits should be defined in conjunction with the design engineer, who understands service requirements and codes, and the manufacturing engineer, who understands the process limitations. Several defect types and testing procedures are summarized below. The defects include:

- *INCOMPLETE FILLING OF THE JOINT,* CAUSED BY POOR SOLDERABILITY (NONWETTING OR DEWETTING), AN INADEQUATE QUANTITY OF FILLER METAL, LOW REFLOW TEMPERATURE, FLUX ENTRAPMENT (HOLES AND VOIDS), OR POOR JOINT DESIGN (REENTRANT CORNERS OR BLIND HOLES THAT PREVENT THE ESCAPE OF GASES)
- *POOR FILLET GEOMETRY,* CAUSED BY POOR SOLDERABILITY OF THE BASE METALS, AN INADEQUATE SUPPLY OF FILLER METAL FOR THE GIVEN JOINT GEOMETRY, OR INSUFFICIENT COVERAGE OF THE SURFACES BY THE FLUX COATING
- *CRACKS IN THE SOLDER FILLET,* WHICH SIGNIFY PART MOVEMENT DURING THE SOLIDIFICATION PROCESS, SOLIDIFICATION SHRINKAGE OF THE SOLDER METAL, OR, IN THE WORST CASE, A MAJOR FLAW IN THE JOINT DESIGN IN WHICH RESIDUAL STRESSES (FOR EXAMPLE, CTE MISMATCH) OVERLOAD THE SOLDER JOINT. THE LATTER CONDITION CAN CAUSE CRACKS IN THE SUBSTRATES, PARTICULARLY IN

BRITTLE MATERIALS, SUCH AS CERAMICS OR REFRACTORY METALS

- *GRAINY OR VERY DULL FILLET SURFACES,* WHICH INDICATE EXCESSIVE SOLDER CONTAMINATION, SUCH AS THAT ARISING FROM THE DISSOLUTION OF THE BASE-METAL MATERIALS AND SURFACE COATINGS, INADEQUATE HEATING OF THE SUBSTRATES, OR SUBSTRATE MOVEMENT DURING SOLIDIFICATION. (HOWEVER, SOME SOLDERS NORMALLY EXHIBIT A DULL FINISH UPON SOLIDIFICATION. SLOW COOLING, ESPECIALLY IN VAPOR-PHASE SOLDERING, CREATES DULL JOINTS)
- *FLUX RESIDUES,* WHICH SUGGEST INADEQUATE CLEANING PROCEDURES OR THE OVERHEATING OF THE FLUX TO PRODUCE VERY TENACIOUS RESIDUES. LARGER PARTICLES MAY BE EMBEDDED IN THE SOLDER FILLET.
- *DISCOLORATION IN THE BASE METAL,* WHICH SIGNIFIES EXCESSIVE HEAT EXPOSURE

Nondestructive inspection techniques range from visual assessment to elaborate tests involving complex equipment and procedures. The principal nondestructive testing methods are discussed below.

Visual inspection is the most widely used technique. Pictorial guides help the inspector qualify the particular joint configuration. Because the inspector can only infer joint quality from external observations, some destructive assessments should accompany the visual evaluations on early prototypes to correlate with subsequent inspector observations on the actual product. Low-power microscopes (<70×) are used.

Radiographic (x-ray) and ultrasonic inspection are used to visualize the interior sections of the joint. X-ray radiographs are used to detect mass differences in the joint, which indicate areas that are absent of solder, such as gas voids or entrapped flux. Ultrasonic techniques detect discontinuities in the path between the receiver and the transmitter (transmission mode) or in the reflected path (reflection mode). Besides unfilled sections of the gaps, this process also detects discontinuities such as poor bonding or cracks.

Infrared (thermal transfer) imaging is based on the transfer of heat across the joint gap. Voids and, to a lesser extent, cracks, have a lower thermal conductivity than the continuous base metal-solder-base metal path. The decreased thermal conduction of these defects is imaged by an infrared-sensitive camera that views the opposite side of a heated substrate. This technique has relatively poor resolution because of lateral heat conduction within the materials.

Proof testing involves subjecting the solder joint to a mechanical load that exceeds the service design load. The joint is then inspected for damage using nondestructive techniques. In the prototype phase of process development, this procedure may be considered "destructive."

Pressure and vacuum testing represent other nondestructive techniques. In pressure testing, which is detailed in the ASME Boiler and Pressure Vessel Code, a positive pressure is applied to conduit joints or soldered vessels. The joint is either coated with a soapy solution or submerged in a water bath before being pressurized. Leaks are identified by the formation of bubbles on the workpiece surface. Air can be replaced by helium or a halogen gas, and special detection equipment can be used to locate leaks in the joints. Vacuum checks of conduit also require special equipment to detect the leakage of trace gases, such as helium, into the conduit or vessel. Mass spectrometers can be used to detect and identify the passage of other gas species into the vacuum. The detector monitors the inside of the conduit (vacuum environment) while the gas is passed along the exterior walls.

Fluorescent dye penetration involves the introduction of a fluorescent dye to one side of the joint. The opposite side is then inspected for dye leakage, which would indicate a continuous path of cracks or voids.

Destructive testing techniques include all types of mechanical testing techniques as well as metallographic sectioning for microstructural examination.

Mechanical testing involves numerous techniques that have been standardized to examine tensile, shear, peel, impact, and torsion strengths, as well as the fatigue life of adhesive joints (Table 10). The various strength measurements can be extended to quantify defects in the joints, such as voids or cracks that cannot support a load, or a microstructural modification to the solder metal, which changes its strength. Inspection of the fracture surface provides critical information on the failure mechanism, as well as data on void content and nonwetting that are caused by poor solderability.

Additional information is available in the article "Evaluation and Quality Control of Soldered Joints" in this Volume.

General Soldering

Paul T. Vianco, Sandia National Laboratories

Environmental, Safety, and Health Issues

Both the materials and processes used in soldering present some general, as well as unique, environmental, safety, and health considerations. There is an increased awareness of the environmental damage caused by manufacturing processes. Applicable rules and regulations can be set by local, state, and federal legislation, as well as regulations developed through the Environmental Protection Agency (EPA). The environmental concerns that relate to soldering operations include:

- RELEASE OF CLEANING SOLVENTS AND SOLUTIONS INTO THE LIQUID WASTE STREAM
- VENTING OF SOLVENT FUMES INTO THE ATMOSPHERE
- DISPOSAL OF HEAVY-METAL SOLID WASTES, SUCH AS SOLDER DROSS AND SCRAP MATERIAL

Rules and regulations that govern worker safety are established by local, state, and federal employment statutes. The federal agency responsible for worker safety is the Occupational Safety and Health Administration (OSHA). Industrial organizations, such as the National Fire Protection Agency, the Underwriters Laboratory, and many insurance companies, have developed excellent safety guidelines for industrial practices. Some safety concerns in soldering operations include:

- BURNS FROM MOLTEN METAL AND ELEVATED-TEMPERATURE PROCESSING EQUIPMENT
- BURNS FROM THE IGNITION OF FLAMMABLE SOLVENTS USED IN CLEANING PROCESSES OR AS FLUX VEHICLES
- CHEMICAL BURNS FROM CORROSIVE ACIDS IN CLEANING SOLUTIONS AND FLUXES, THE LATTER OF WHICH INCLUDES SPATTER DURING SOME SOLDER PROCESSES
- CHEMICAL BURNS FROM ALKALINE MATERIALS USED IN POSTASSEMBLY CLEANING

An extensive effort has been made to identify and control the worker health risks of industrial soldering operations. Unlike safety issues, which tend to address acute dangers, health concerns can manifest themselves in accumulated toxicity to the worker which may not be identified for months or years. Besides the legislative bodies, regulations are also set by agencies such as OSHA, EPA, and the U.S. Mine Safety and Health Administration (MSHA). In addition, various guidelines are provided by organizations such as the Food and Drug Administration (FDA) and the National Institutes of Health--National Cancer Institute. Some of the health issues associated with soldering operations are:

- EXPOSURE TO ORGANIC SOLVENT FUMES (ACETONE, ALCOHOLS) IN FLUXES AND CLEANING COMPOUNDS OR THEIR HEAT-GENERATED BY-PRODUCTS (FOR EXAMPLE, ALDEHYDES FROM ROSIN-BASE FLUXES)
- ILLNESS FROM THE INHALATION OF ACID OR ALKALINE FUMES USED IN CLEANING SOLUTIONS
- HEAVY-METAL TOXICITY FROM MOLTEN SOLDER FUMES, BASE-METAL COATINGS, AND FROM THE BASE METALS THEMSELVES (AIRBORNE PARTICLES OF BERYLLIUM, CHROMIUM STEELS, AND SUCH)

Exposure to toxins occurs through skin absorption, ingestion, or inhalation. The use of protective clothing and face protection, as well as the practice of good hygiene habits, will prevent the absorption and ingestion, respectively, of toxic

materials. Because the most likely source of accidental exposure is inhalation, some guidelines and exposure limits are described below for materials and processes used in soldering operations. Air-sampling procedures have been established and should be used to certify compliance with these specifications. The exposure limits provide some insight into the relative hazard presented by each of the listed materials. It is important to note that regulations and exposure limits can change frequently as data are accumulated by the appropriate agencies. Therefore, it is recommended that the reader consult the necessary documents or agency representative to ensure compliance with the most recent guidelines.

The exposure limits are expressed as the time-weighted average (TWA), which is equivalent to the threshold limit value (TLV) established by the American Conference of Governmental Industrial Hygienists (ACGIH). The TWA limits were also accepted by OSHA in 1972 as the legal permissible exposure limits (PEL). The TWA value represents the time-averaged airborne concentration of the material over an 8-h period, which is assumed to be the exposure period per day.

Fluxes and Cleaning Agents. The primary concern when using rosin-base fluxes are the thermal breakdown products generated upon their exposure to the molten solder temperature. These reaction products are primarily the aliphatic aldehydes, typically measured by the equivalent formaldehyde concentration (Ref 30). The adopted TWAs for these substances, together with values for organic solvents used as flux vehicles or cleaning agents, are listed in Table 38. No limits are available for the typical constituents of organic acid fluxes (lactic acid, benzoic acid, or glutamic acid) or any suspected thermal breakdown products. The exposure levels of fumes from the inorganic acids, whether used as the flux or precleaning material, and from sodium hydroxide (neutralizing agent) are listed in Table 39. New regulations and exposure limits change as new data become available. The reader should remain aware of updates to these guidelines for current practices.

TABLE 38 TWA LIMITS FOR ORGANIC SUBSTANCES USED IN SOLDER PROCESSING

MATERIAL	**TWA STANDARD, MG/M^3**	COMMENTS
FORMALDEHYDE (AS A ROSIN PYROLYSIS PRODUCT)	0.1	**REPRESENTATIVE OF ROSIN FLUX BY-PRODUCTS FROM HEAT EXPOSURE**
LSOPROPYL ALCOHOL	980	**SKIN EXPOSURE(A)**
ETHYL ALCOHOL	1900	
METHYL ALCOHOL	260	**SKIN EXPOSURE**
METHYL CHLORIDE	105	**LEVEL OF INTENDED CHANGE AS OF 1981**
METHYLENE CHLORIDE (DICHLOROMETHANE)	360	**LEVEL OF INTENDED CHANGE AS OF 1981**
CARBON TETRACHLORIDE	30	**SKIN EXPOSURE; SUSPECTED CARCINOGEN. LEVEL OF INTENDED CHANGE AS OF 1981**
BENZENE	30	
ACETONE	1780	**LEVEL OF INTENDED CHANGE AS OF 1981**
ETHYLENE GLYCOL	**10(B)**	**PARTICULATE**

Source: Ref 30

(A) INDICATES THAT A CUTANEOUS ROUTE (MUCOUS MEMBRANES, EYES, ETC.) CAN ALSO CONTRIBUTE TO OVERALL EXPOSURE.

(B) VAPOR, 125 MG/M^3.

TABLE 39 TWA LIMITS FOR INORGANIC ACIDS AND ALKALINES

MATERIAL	TWA STANDARD, MG/MM^3
HYDROCHLORIC ACID (HCL)	**7**
SULFURIC ACID (H_2SO_4)	**1**
NITRIC ACID (HNO_3)	**5**
HYDROFLUORIC ACID (HF)	**2.5**
PHOSPHORIC ACID (H_3PO_4)	**1**
SODIUM HYDROXIDE (NAOH)	**2**

ZINC CHLORIDE ($ZNCL_2$)	**1**
AMMONIUM CHLORIDE (NH_4CL)	**10**

Source: Ref 30

Solder and Base-Metal Constituents. The acute and chronic side effects of human exposure to metals are becoming better understood by the medical community. Toxicity hazards associated with the so-called "heavy" metals (lead, cadmium, antimony, tin, and others) used in the soldering processes are of particular concern to the health and regulatory agencies. Two mechanisms are responsible for airborne particulates: evaporation of metals by heat energy, which is applied to the molten solder or substrate, and mechanical agitation, which releases dust or abrasive particles.

Molten solder is generally used at temperatures well below the boiling point of either the solder or the substrate material. Exceptions are workpieces constructed with high vapor pressure metals or coatings, such as cadmium or zinc, or solders that contain these elements. Molten solders, like other liquids, release greater amounts of metal vapors as their temperature increases toward their vaporization point. Manual soldering processes, which exhibit the least degree of temperature control, are most susceptible to overheating of the solder and are therefore most likely to increase levels of toxic fumes in the atmosphere. Unfortunately, such processes also require the operator to be in close proximity to the workpiece. Therefore, proper ventilation must be maintained in the work area to minimize worker exposure.

Mechanical agitation of the molten solder for prolonged processing times, during which the solder is liquid, can accelerate the release of metal fumes. Airborne metal fumes and particulates are also caused by the agitation of solder dross and through abrasion of the solid metals. The dross that forms on the surface of solder baths can be a source of airborne particulates of tin, lead, or antimony, for example, when it is removed for disposal. Base-metal particles are generated by the use of abrasive precleaning techniques, such as grit or sand-blasting techniques. Base-metal particles and solder particles can also be generated when similar techniques are used to remove residues from the finished joints.

Table 40 gives the TWA values of metals that are used in solders or that compose substrate materials. Particulates of lead, cadmium, indium, platinum, silver, and chromium VI compounds are particularly hazardous, whereas those of zinc, copper, tin, and aluminum are relatively benign. Data are not available for bismuth and gold, a commonly used finish layer.

TABLE 40 TWA LIMITS FOR METAL PARTICULATES

MATERIAL	**TWA STANDARD, MG/M^3**	COMMENTS
LEAD	0.05	**FUMES AND DUST; ACTION LEVEL, 0.03**
TIN	10	**TIN OXIDE AS TIN, NUISANCE; FOR PARTICULATE, AUTOMATIC LEVEL SET AT 10 $MG/M^{3(A)}$**
ANTIMONY	0.5	**INCLUDES ALL COMPOUNDS**
SILVER	0.1	**METAL DUST AND FUMES$^{(B)}$**
INDIUM	0.1	**INDIUM AND COMPOUNDS**
BISMUTH	NONE AVAILABLE	**. . .**
ZINC	5	**ZINC OXIDE FUMES**
CADMIUM	0.05	**SUSPECTED CARCINOGEN**
GOLD	NONE AVAILABLE	**. . .**
PLATINUM	0.002	**. . .**
COPPER	1	**DUST AND MIST**
ALUMINUM	10	**OXIDE, NUISANCE PARTICULATE**
NICKEL	$1^{(C)}$	**METAL**
IRON	5	**IRON OXIDE FUMES**

CHROMIUM	**0.5**	**SOLUBLE CHROMIC OR CHROMOUS SALTS, METALS[D]**

Source: Ref 30

(A) LEVEL OF INTENDED CHANGE AS OF 1981, 2 MG/M^3.

(B) SOLUBLE COMPOUNDS, 0.01,

(C) SOLUBLE COMPOUNDS, 0.1.

(D) CR VI COMPOUNDS, CHROMATES, 0.05 MG/M^3.

Lead regulations governing airborne lead concentrations in the workplace are very complex. The maximum airborne concentration (TWA) is 0.05 mg/m^3. However, an "action level" was established at 0.03 mg/m^3, above which a list of measures identified by OSHA regulations must be carried out. Below the action level, employees need only be monitored for lead exposure and receive adequate job training to minimize potential hazards.

Data were accumulated in the late 1970s that measured the blood lead levels of workers performing various soldering operations, as well as the airborne lead concentration of a number of soldering processes. Table 41 shows the blood lead levels of eight persons from a group of 37 who performed one of the tasks under the "job description." No significant difference was observed between these values (mean of the entire group of 37 was 11.7 µg/100 mL) and the blood lead level in the normal population with no occupational exposure to lead (10 to 30 µg/100 mL).

TABLE 41 BLOOD LEAD LEVELS IN WORKERS PERFORMING VARIOUS SOLDERING OPERATIONS

EMPLOYEE	**BLOOD LEAD LEVEL, µG/100 ML**	JOB DESCRIPTION
1	15	**MASS SOLDERING**
2	14	**HAND IRON SOLDERING**
3	14	**HAND IRON SOLDERING**
4	14	**HAND IRON SOLDERING**
5	13	**OCCASIONAL HAND SOLDERING**
6	11	**LAYOUT OPERATOR**
7	17	**MASS SOLDERING**
37	**19**	**MASS SOLDERING**

Note: Mean blood level for 37 employees: 11.7 µg/100 mL.

(A) VALUES CITED ARE TYPICAL FOR ALL 37 EMPLOYEES.

Airborne levels for several soldering operations and industries are shown in Table 42. None of the examples matched the maximum level of 0.05 mg/m^3. However, radiator manufacturing and repair typically exceeded the "action" level of 0.03 mg/m^3. This study emphasized that adequate ventilation of the work area was the most effective means to minimize airborne concentrations.

TABLE 42 AIRBORNE LEAD CONCENTRATIONS FOR SEVERAL SOLDERING OPERATIONS

TYPE OF SOLDERING	TYPICAL AIRBORNE LEAD CONCENTRATIONS[A], MG/M^3
AUTOMATIC WAVE	
ELECTRONICS ASSEMBLY	**0.010**
MANUAL GUN AND IRON	

ELECTRONICS AND ELECTROMECHANICAL ASSEMBLY	**0.010**
RADIATOR MANUFACTURE AND REPAIR	**0.028**
OPEN DIP POT TINNING	
ELECTRONICS, ELECTROMECHANICAL ASSEMBLY, AND TOOL AND DIE REPAIR	**0.004**
RADIATOR MANUFACTURE AND REPAIR	**0.046**
OPEN-FLAME JOINING	
ARTS AND CRAFTS	**0.015**
RADIATOR MANUFACTURE AND REPAIR	**0.038**

(A) MEAN

Reference cited in this section

30. *PRUDENT PRACTICES FOR HANDLING HAZARDOUS CHEMICALS IN LABORATORIES,* NATIONAL ACADEMY PRESS, 1981, P 257-276

General Soldering

Paul T. Vianco, Sandia National Laboratories

References

1. "STANDARD SPECIFICATION FOR SOLDER METAL," B 32, *ANNUAL BOOK OF ASTM STANDARDS,* ASTM
2. "SOLDER, TIN ALLOY: TIN-LEAD ALLOY; AND LEAD ALLOY," FEDERAL SPECIFICATION QQ-S-571E, SUPERINTENDENT OF DOCUMENTS, U.S. GOVERNMENT PRINTING OFFICE, WASHINGTON, DC
3. "SOFT SOLDER ALLOYS--CHEMICAL COMPOSITIONS AND FORMS," ISO/DIS 9453, INTERNATIONAL ORGANIZATION FOR STANDARDIZATION, THE HAGUE, NETHERLANDS
4. AMERICAN METALS MARKET, FAIRCHILD PUBLICATIONS, 17 JAN 1992
5. *SOLDERING MANUAL,* AWS, 1977, P 5
6. H. MANKO, *SOLDERS AND SOLDERING,* MCGRAW-HILL, 1979, P 14
7. H. MANKO, *SOLDERS AND SOLDERING,* MCGRAW-HILL, 1979, P 82
8. B. LAMPE, ROOM TEMPERATURE AGING PROPERTIES OF SOME SOLDER ALLOYS, *WELD. J., RES. SUPPL.,* OCT 1976, P 330S
9. SOLDERING MANUAL, AWS, 1977, P 5
10. R. KLEIN-WASSINK, *SOLDERING IN ELECTRONICS,* ELECTROCHEMICAL PUB. LTD., AYR, SCOTLAND, 1989, P 189
11. H. MANKO, *SOLDERS AND SOLDERING,* MCGRAW-HILL, 1979, P 89
12. S. NIGHTINGALE *ET AL.,* TIN SOLDERS, BRITISH NONFERROUS METALS RESEARCH ASSOCIATION, VOL 1, 1942
13. "SOLDER ALLOY DATA, MECHANICAL PROPERTIES OF SOLDERS AND SOLDERED JOINTS," PUBLICATION 656, INTERNATIONAL TIN RESEARCH INSTITUTE, UNITED KINGDOM, 1986
14. *DEVELOPMENT OF HIGHLY RELIABLE SOLDER JOINTS FOR PRINTED CIRCUIT BOARDS,* WESTINGHOUSE DEFENSE AND SPACE CENTER, 1968, P 4-55 TO 4-57
15. R. WILD, FATIGUE PROPERTIES OF SOLDER JOINTS, *WELD. RES. J.,* VOL 15, 1972, P 521S
16. H. SOLOMON, "FATIGUE OF 60/40 SOLDER," REPORT 86CRD024, GENERAL ELECTRIC CO.,

MAY 1986

17. J. JONES AND J. THOMAS, "ULTRASONIC SOLDERING OF ALUMINUM," RESEARCH REPORT 55-24, FRANKFORD ARSENAL, DEPARTMENT OF THE ARMY, PHILADELPHIA, FEB 1955
18. H. MANKO, *SOLDERS AND SOLDERING,* MCGRAW-HILL, 1979, P 112-115
19. D. OLSEN AND H. BERG, PROPERTIES OF DIE BOND ALLOYS RELATING TO THERMAL FATIGUE, *IEEE TRANS.,* CHMT-2, 1979, P 257
20. P. VIANCO AND J. REJENT, "SOLDER BOND APPLICATIONS IN A PIEZOELECTRIC SENSOR ASSEMBLY," *45TH ANNUAL FREQ. CONTROL SYMP.* (LOS ANGELES, CA), MAY 1991, P 266
21. R. KLEIN-WASSINK, *SOLDERING IN ELECTRONICS,* ELECTROCHEMICAL PUB. LTD., AYR, SCOTLAND, 1989, P 189
22. *SOLDERING MANUAL,* AWS, 1977, P 35-39
23. P. VIANCO *ET AL.,* SOLDERABILITY TESTING OF KOVAR WITH 60SN-40PB SOLDER AND ORGANIC FLUXES, *WELD. J. RES. SUPPL.,* JUNE 1990, P 230S
24. *BRAZING HANDBOOK,* AWS, 1991, P 267-276
25. C. THWAITES, *CAPILLARY JOINING,* WILEY AND SONS, UNITED KINGDOM, 1982, P 52
26. J. SCULLY, *THE FUNDAMENTALS OF CORROSION,* 2ND ED., PERGAMON PRESS, INC., 1975
27. C. LEA, A SCIENTIFIC GUIDE TO *SURFACE-MOUNT TECHNOLOGY,* ELECTROCHEM. PUBL., LTD., 1988
28. P. VIANCO AND F. HOSKING, *ANALYSIS OF ULTRASONIC TINNING,* NEPCON WEST, FEB 1992, P 1718
29. J. SCHUSTER AND R. CHILKO, ULTRASONIC SOLDERING OF ALUMINUM HEAT EXCHANGERS, *WELD. J.,* OCT 1975, P 711
30. *PRUDENT PRACTICES FOR HANDLING HAZARDOUS CHEMICALS IN LABORATORIES,* NATIONAL ACADEMY PRESS, 1981, P 257-276

Soldering in Electronic Applications

Paul T. Vianco, Sandia National Laboratories

Introduction

SOLDERING represents the primary method of attaching electronic components, such as resistors, capacitors, or packaged integrated circuits, to either printed wiring boards (PWBs) or the ceramic substrates used for hybrid microcircuits.

Electronic miniaturization has fostered change in soldering technology as applied to electronic products. The increased functionality of electronic devices has placed a greater emphasis on solder joint integrity, not only in terms of increased reliability, but also with respect to limiting the cost of scrap product, inspection, or the repair of defective solder joints (especially on fine-pitch packages). The minimization of solder joint defects in electronic products depends on proper PWB design (for example, bonding pad geometries, conductor line layout, and laminate material), device packages (lead pitches and configurations or termination materials and finishes), and board assembly (flux and solder selection, process parameters and control, and cleaning).

This article discusses the categories that are most important to successful electronic soldering:

- SOLDERS AND FLUXES
- BASE MATERIALS AND FINISHES
- SOLDER JOINT DESIGN
- SOLDERABILITY TESTING

Additional information about the soldering processes discussed in this article can be found in the Section "Solid-State Welding, Brazing, and Soldering Processes" in this Volume.

Soldering in Electronic Applications

Paul T. Vianco, Sandia National Laboratories

Solders and Fluxes

Solders. The most commonly used solder alloys in electronics manufacturing are summarized in Table 1. Typical soldering temperatures in manufacturing operations are from 30 to 50 °C (55 to 90 °F) above the liquidus temperature to ensure adequate flow of the solder and proper heating of the substrate. The solder can be delivered to the joint area using numerous techniques. For example, the entire substrate can be placed in contact with the surface of a large molten solder bath, permitting the solder to either wet lands or fill holes. Solder wire can be directly heated at the joint by hand processes that use hot irons, gas jets, and other instruments. Preforms or solder paste can be placed at the joint area, and the substrate is either directly or indirectly heated, such as by an infrared (IR) furnace, causing the solder to melt and form the joint. Although solder pastes are often used in manual assembly or rework operations, their properties have been developed primarily for full-scale assembly processes.

TABLE 1 COMMONLY USED SOLDERS IN ELECTRONIC ASSEMBLIES

SOLDER ALLOY, WT%	SOLIDUS/LIQUIDUS TEMPERATURES	
	°C	°F
521N-48SN	118/118	244/244
50IN-50SN	118/125	244/257

58BI-42SN	138/138	281/281
43SN-43PB-14BI	143/163	289/325
97IN-3AG	143/143	289/289
70SN-18PB-12IN	162/162	324/324
63SN-37PB	183/183	361/361
60SN-40PB	183/190	361/374
62.5SN-36.1PB-1.4AG	170/179	354/354
50PB-501N	180/209	356/408
60PB-40IN	195/225	383/437
96.5SN-3.5AG	221/221	430/430
95SN-5PB	233/240	451/464
97.5PB-1.5AG-1.0SN	304/309	588/588
90PB-10SN	268/299	514/570
95PB-5SN	270/312	518/594

Tin-Base Tin-Lead Solders. Pure tin, which has a melting temperature of 232 °C (450 °F), readily wets the substrate materials typically found in electronics applications. In fact, it is the tin component of electronic solders that forms the metallurgical bond with those materials. However, pure tin is not used for PWB assembly, because of its higher melting point, increased cost, and reduced flow, when compared with tin-lead alloys. Tin plate is sometimes used as a protective finish on device leads and terminations, although a solder dip coating is the preferred finish.

Tin-base tin-lead solders represent the most widely used solders for electronic assembly: eutectic 63Sn-37Pb, near-eutectic 60Sn-40Pb, and the eutectic 62.5Sn-36.1Pb-l.4Ag alloys. The solidus-to-liquidus (mushy zone) temperature range of 60Sn-40Pb makes this alloy preferable to the eutectic composition when used with some leaded surface-mount devices in order to prevent solder wicking (Ref 1) or to facilitate the filling of large holes and vias on PWBs. The silver content of 62.5Sn-36.1Pb-1.4Ag reduces the dissolution of silver coatings, such as electroplated finishes on base metals, or the silver conductor used in thick-film terminations on either surface-mount packages or in hybrid microcircuit thick-film networks. The tin-lead with silver composition will improve creep-rupture strengths and will slightly reduce reactions when soldering to silver or copper. These solders typically contain 0.25% Sb to prevent the formation of the low-temperature allotrope of tin ("tin pest") at 13.2 °C (56 °F).

Lead-base tin-lead alloys are not used in general PWB assembly, because they have poor flow and their melting temperatures are incompatible with PWB materials. These alloys can be applied to surfaces such as electroplated finishes, evaporated thin films, or hot dip coatings. They have excellent fatigue and creep properties. The alloys 95Pb-5Sn and 90Pb-10Sn are used in the controlled collapse chip component (C^4) attachment of silicon chips to package frames (Ref 2). Their elevated melting temperatures prevent reflow of the C^4 joints during subsequent joining of the unit to the PWB with eutectic tin-lead solder (step soldering).

Tin-Silver Alloys. The eutectic composition, 96.5Sn-3.5Ag, is generally used, although alloy compositions are available with silver contents of up to 5%. These alloys are used at the high-temperature attachment stage of step soldering processes with eutectic tin-lead solders. The tin-silver solders exhibit excellent wetting, strength, and fatigue properties that are generally superior to those of the tin-lead eutectic solder (Ref 3). No significant silver migration has been observed in solder joints fabricated with 96Sn-4Ag alloy (Ref 4). The combination of tin and silver forms Sn-Ag intermetallic compounds that are stable and are insensitive to electromigration reactions.

Tin-Antimony Alloys. The 95Sn-5Sb alloy is used at the high-temperature attachment portion of step soldering processes with tin-lead eutectic alloy. This solder type has excellent creep strength and wettability, comparable to the tin-silver solders. Localized heating methods (soldering iron, laser, and others) are preferred for applications that utilize this alloy because the high heat input required to melt the solder may damage some PWB substrates or heat-sensitive devices.

Indium-Tin Alloys. The eutectic and near-eutectic indium-tin solders (52In-48Sn and 50In-50Sn, respectively) are low-melting-point alloys used in the solder attachment of heat-sensitive devices or in the soldering steps that follow the use of tin-lead alloys. Because most electronic fluxes are unable to activate at lower working temperatures, there can be some wetting difficulties when indium-tin alloys are used. Indium-base alloys can wet several ceramic materials, including quartz, and some glasses. However, they can be susceptible to corrosion damage, and have poor mechanical properties, especially in creep. Although the relatively high cost of indium metal has discouraged more-extensive use of these

solders, the cost per device is not excessive, and indium-base alloys are finding increased usage where their properties are advantageous, such as in cryogenic applications.

Bismuth-containing alloys are also referred to as "fusible" solders. They are used on heat-sensitive devices or in step soldering processes. Upon solidification, bismuth-containing alloys exhibit either limited contraction or expansion, as in the case of solders with more than 47 wt% Bi (Ref 5). These alloys are prone to moderate oxidation in both the liquid and solid states, and they exhibit some difficulty in wetting because of limited flux activity at the lower working temperatures. These alloys have good mechanical properties and are used very successfully in a number of electronic applications.

Lead-indium alloys are used when soldering to precious-metal (gold, silver, platinum, palladium, or their alloys) substrates or coatings and when attaching components to hybrid thick-film networks. These solders have a lower rate of metal dissolution (and subsequent intermetallic compound formation), when compared with tin-containing alloys. Wettability is slightly poorer than that of the tin-lead solders. The lead-indium solders are also used in C^4 technology (Ref 6). Because of the relatively high cost of indium, these alloys are used on a limited basis. They are also susceptible to corrosion and interface voiding reactions (with high thermal gradients). However, they have excellent fatigue properties.

Solder Impurities. Solder alloys are available in reclaimed or virgin grades, and their purity is established by government, military, and industrial specifications. Excessive contaminant levels are detrimental to the quality of solder joints made by full-scale assembly equipment. Such processes, which use large baths as the solder source (wave, drag, or dip soldering), are particularly prone to impurity buildup from the dissolution of PWB and lead finishes (for example, copper, gold, or cadmium) or metals from the fixturing and soldering processes (aluminum or iron).

Table 2 provides contaminant limits for tin-lead solder material procurement (per federal specification QQ-S-571-E) and for tin-lead solder baths (per IPC-S-815A) that are for hot-dip coatings or PWB assembly. Amendment 6 to the QQ-571-E specification indicates a reduction in the maximum antimony content of powdered material to 0.120% in the upcoming QQ-571-F edition. The complete list of impurities is found in Amendment 6 of the QQ-571-E specification.

TABLE 2 RECOMMENDED IMPURITY LIMITS OF SOLDERS AT TIME OF PROCUREMENT AND IN OPERATIONAL TIN-LEAD BATHS

CONTAMINANT	**MAXIMUM CONCENTRATION IN VIRGIN SOLDER, %(A)**	MAXIMUM CONCENTRATION IN SOLDER BATH, %(B)
COPPER	0.08	**0.75/0.30**
GOLD	. . .	**0.50/0.20**
CADMIUM	. . .	**0.10/0.005**
ZINC	0.005	**0.008/0.005**
ALUMINUM	0.005	**0.008/0.006**
ANTIMONY	0.2-0.5	**0.50/0.50**
IRON	0.02	**0.02/0.02**
ARSENIC	0.03	**0.03/0.03**
BISMUTH	0.25	**0.25/0.25**
SILVER	. . .	**0.75/0.10**
NICKEL	**. . .**	**0.025/0.01**

(A) PER QQ-S-571-E.

(B) PER IPC-S-815A

To prevent contamination, the recommended materials for solder pots are stainless steel or cast iron. Although solder dross in solder baths is not an impurity, excessive levels can impede the proper formation of solder joints. Organic contaminants from fluxes, soldering oils, and PWB residues can be picked up by solder joints on the printed boards. These materials polymerize under prolonged exposure to the solder temperatures and become difficult to remove using conventional cleaning measures. Ionic species remaining from flux residues can cause corrosion on assembled solder joints or leakage currents between conductors.

Solder paste is used primarily in PWB assembly based on surface-mount technology. Processes such as vapor-phase (condensation) and infrared (IR) furnace reflow are well suited to solder paste use. Solder paste is a mixture of solder particles with a binder composed of flux, rheological components (such as thickeners), and a solvent material. Solder particle shape, size distribution, and concentration, along with binder properties, determine the flow properties of the paste.

As shown in Fig. 1, the paste is deposited by screen printing, stencil printing, or bulk dispensing techniques. Paste properties (whether applied using screen or stencil) affect the number and kinds of defects observed on the finished solder joint. Printed circuit boards (PCBs) with 1.25 mm (50 mil) pitch require 0.20 to 0.25 mm (0.008 to 0.010 in.) of paste thickness, whereas fine-pitch PCBs (630 μm, or 25 mils, or less) typically use 0.08 to 0.20 mm (0.003 to 0.008 in.) of paste.

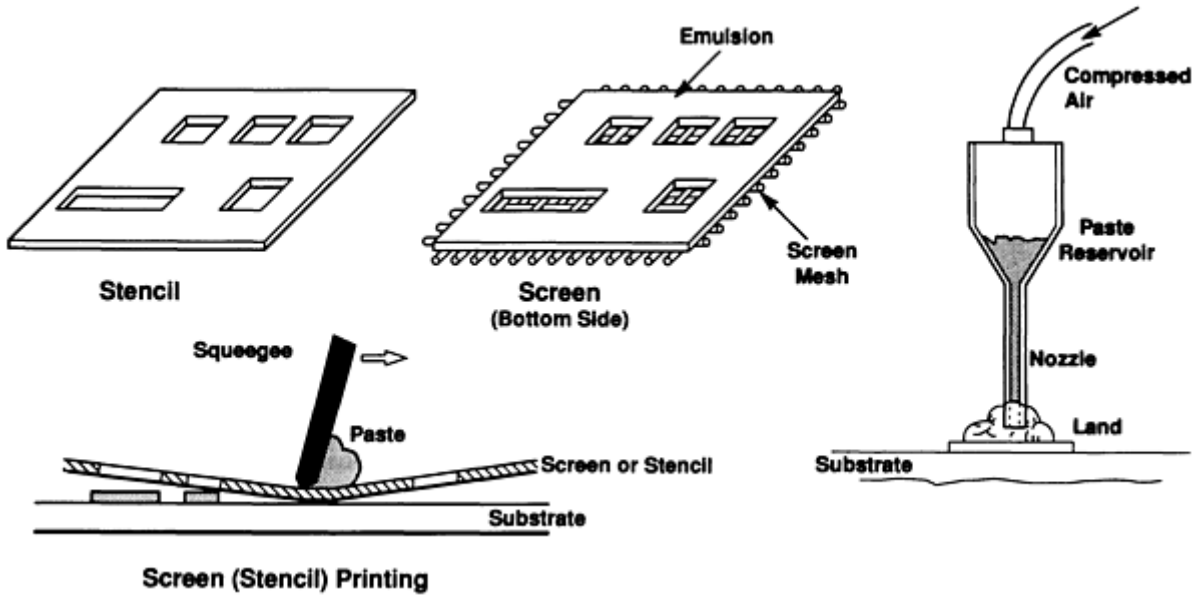

FIG. 1 STENCIL PRINTING, SCREEN PRINTING, AND BULK DISPENSING OF SOLDER PASTE

Printability can be affected by the distribution of the solder particles, metal content, slump, and viscosity of the paste. For example, smaller solder particles pass more easily through stencil or screen openings. However, the higher oxide content of the smaller particles (larger surface-to-volume ratio) creates a greater number of post-assembly solder balls, which are small spheres of solder that fail to coagulate with the larger solder mass in the joint (Fig. 2). Solder balls that are not removed by the cleaning process can cause short circuits during device electrical operation.

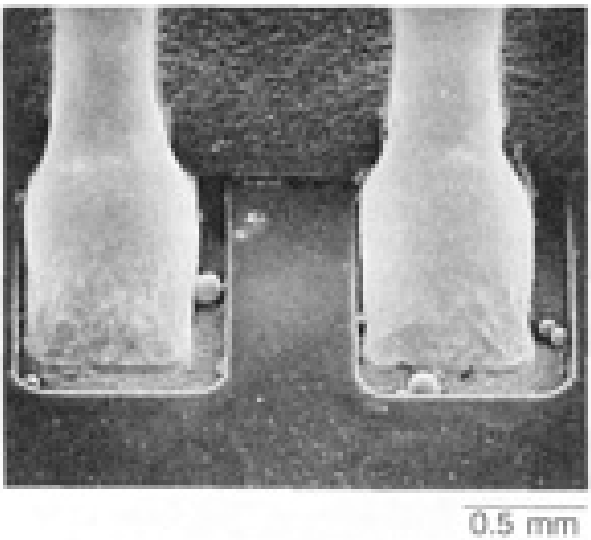

FIG. 2 SCANNING ELECTRON MICROGRAPH OF SOLDER BALLS ON A LEADLESS CERAMIC CHIP CARRIER SOLDER JOINT. COURTESY OF SANDIA NATIONAL LABORATORIES

Metal content refers to the mass percentage of the paste, that is, the solder component. Slump is a measure of the tendency of the paste to spread away from the deposited configuration prior to reflow. Excessive slump causes the deposits to contact one another (Fig. 3a), resulting in solder joint bridges (Fig. 3d), which can short circuit electrical signals (Ref 7).

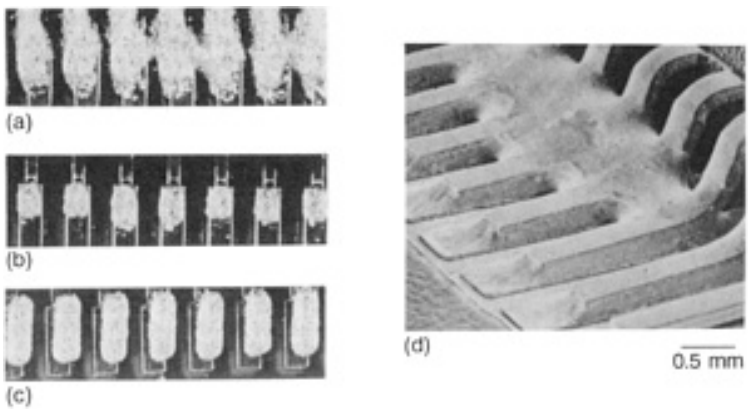

FIG. 3 DEFECTS OF SOLDER PASTE DEPOSITS. (A) APPEARANCE OF PASTE WITH POOR SLUMP (OPTICAL MICROSCOPY). (B) SKIPS IN PASTE DEPOSITS (OPTICAL MICROSCOPY). (C) PASTE DEPOSIT/LAND MISREGISTRATION (OPTICAL MICROSCOPY). (D) SOLDER BRIDGES (SEM). SOURCE: REF 1, 7

Viscosity determines the fluidity of the paste. When viscosity is too high, the paste will not pass through the screen or stencil, and will cause skips (Fig. 3b). When viscosity is too low, the paste will run out under the screen or stencil and will deteriorate the slump properties. Tackiness refers to the ability of the paste to hold devices onto the board prior to the reflow cycle. Paste with poor tackiness causes components to become displaced or to fall from the board during handling prior to reflow, resulting in part misalignment after assembly.

Test procedures that have been developed to quantify solder ball formation, slump, tackiness, and viscosity are identified in IPC-SP-819, "General Requirements and Test Methods for Electronic Grade Solder Paste."

Solder pastes deteriorate with storage time, which increases viscosity. The addition of thinners will reduce viscosity. Solder particles can further oxidize, leading to increased solder ball formation during reflow. Pastes that contain indium

deteriorate more quickly than those based on other alloys. The shelf life of solder pastes can be extended by storage under refrigerated (not freezing) conditions, where the paste surface is sealed from the atmosphere. Manufacturer recommendations should be strictly followed.

Process factors that affect the quality of the printed deposit are:

- STENCIL OR SCREEN THICKNESS
- DAMAGE AND WEAR TO THE STENCIL OR SCREEN
- SQUEEGEE STIFFNESS AND PRESSURE
- SNAP-OFF DISTANCE
- DRYING CONDITIONS FOLLOWING DISPENSING
- STENCIL (SCREEN) SUBSTRATE REGISTRATION (FIG. 3C)
- PRESSURE AND ORIFICE SIZE ON BULK DISPENSING EQUIPMENT

Table 3 provides typical solder paste properties for the noted delivery techniques (Ref 8, 9).

TABLE 3 GENERAL SOLDER PASTE PARAMETERS FOR DISPENSING TECHNIQUES

DISPENSING TECHNIQUE	**PARTICLE DIAMETER**		**METAL CONTENT, %**	VISCOSITY, PA · S[(A)]
	µM	**µIN.**		
SCREEN PRINTING (-80 MESH SCREEN)	45-75	1800-3000	85	**250-550**
STENCIL PRINTING	45-75	1800-3000	85-90	**400-800**
BULK	**30-75**	**1200-1800**	**80-85**	**100-400**

(A) 1 PA · S = 1 KCPS

Fluxes. The role of fluxes in electronic soldering is to reduce thin tarnish layers on the substrates and solder, lower the surface tension of the solder to improve capillary flow and optimize fillet geometries, and protect the substrate surfaces from reoxidation during preheat prior to reflow. Electronic-grade fluxes for assembly processes can effectively remove only light oxide layers. Precleaning steps with chemical etchants should be used to remove heavy oxide films and scales prior to assembly. Surface oxide removal by the flux is inhibited by organic films that can be present on the surface. Therefore, surfaces must be degreased prior to application of the flux coating. In electronics applications, the least chemically active flux that satisfies production yields is preferred in order to minimize potential corrosion from unremoved residues.

Fluxes are applied to the PWB by spraying, immersing the board into a bath of flux, passing it through a flux wave, or coating it with a flux foam. The condition of the flux, which changes with use because of solvent evaporation and contamination buildup, is typically monitored by tracking its density. Density can also be used to indicate the viscosity of fluxes used in foaming applications, which in turn determines the ability of the flux to form a foam. Manufacturer recommendations should always be strictly followed because formulation variations are often proprietary.

Safety and health concerns should be considered in flux usage. Alcohol is a widely used solvent in fluxes, which makes the baths and vapors flammable. Fluxes, like corrosives, can cause acute and chronic irritation to the respiratory tract and skin. Because rosin-base fluxes break down at soldering temperatures to produce fumes of compounds from the aldehyde family, adequate ventilation of the work area is required.

Flux use must address three materials compatibility issues. First, the potential for damage to device packages (header material, glass-to-metal seals, and such), base materials, and plated surfaces prior to assembly will increase with more-active fluxes. Second, postassembly corrosion may arise from flux residues with high ionic contents, necessitating their removal by post-assembly cleaning measures. Third, the cleaning agents and processes used to remove flux residues must be compatible with the devices, substrates, and environmental regulations. Organic solvents, such as 1,1,1-trichloroethane and Freon, are very effective in removing rosin-base flux residues. However, these hazardous materials are being restricted from use due to potential environmental damage. Although aqueous and semiaqueous cleaning systems based

on water, polar alcohols, and terpenes can be very effective, their compatibility with all electronic materials has not been fully characterized. It should be noted that ultrasonic cleaning processes may damage active and passive devices. Therefore, the compatibility of this technique with assemblies must be verified prior to its implementation. Designers and process engineers must address these concerns at the early stages of process development to prevent costly production errors.

The most critical aspect of PWB cleanliness is ionic residues from the fluxes. When combined with atmospheric moisture, these residues can generate "structural" corrosion between the dissimilar metals found in the solder joint. The residues can also create metal whiskers by the electromigration of metal ions between lands or conductor lines at different voltage potentials, causing leakage currents that disrupt electrical performance. Ionic flux residues on PWBs are measured by the extraction method, in which the residues are rinsed into a bath, the resistivity of which is converted into the equivalent amount of ionics removed from the board (expressed as μg NaCl/cm^2 of board surface).

The potential for leakage currents, which are a function of substrate material, moisture, and the ionic content of the flux residues, is assessed by the surface insulation resistance (SIR) test. A conductive comb pattern is constructed on the test board. A voltage difference is applied between adjacent legs and the resistance breakdown is monitored under different temperature-humidity-time conditions. Ionic residue and SIR tests are recommended in the process development stages of soldered assemblies. Several industrial, military, and federal specifications that quantify flux activity and PWB cleaning procedures and criteria for electronic applications have been established (Table 4).

TABLE 4 FLUX ACTIVITY TESTS AND WIRING BOARD CLEANLINESS GUIDELINES

SPECIFICATION	SUBJECT
IPC-TM-650, TEST METHODS MANUAL	**TESTS FOR CORROSIVITY OF FLUXES AND FLUX RESIDUES:** **COPPER MIRROR TEST** **SILVER CHROMATIC TEST** **FLUX SOLID DETERMINATION** **HALIDE CONTENT TEST** **CORROSION TEST** **FLUX CORROSIVITY ASSESSMENT** **MOISTURE TEST** **INSULATION RESISTANCE TEST** **DETERMINES LEAKAGE CURRENTS ON SUBSTRATE USING IPC-B-25 TEST VEHICLE**
IPC-S-815A, GENERAL REQUIREMENTS FOR SOLDERING ELECTRONIC INTERCONNECTIONS	**IONIC CONTAMINATION RESIDUE TEST (MEASURES IONIC RESIDUES ON THE ASSEMBLY; USED WITH IPC-TP-207 IF AUTOMATED TEST EQUIPMENT IS SPECIFIED)**
	ROSIN FLUX REMOVAL TEST (MEASURES THE EFFECTIVENESS OF CLEANING PROCESS TO REMOVE FLUX RESIDUES)
MIL-F-14256 E, FLUX, SOLDERING, LIQUID (ROSIN-BASE)	**TEST OF ROSIN-BASE FLUX CORROSIVITY AND SURFACE INSULATION RESISTANCE**
MIL-STD-2000 A, STANDARD REQUIREMENTS FOR SOLDERED ELECTRICAL AND ELECTRONIC ASSEMBLIES	**DETAILS IONIC CONTAMINATION (EXTRACTION) TEST PROCEDURES AND ACCEPTABILITY CRITERIA**

Rosin-base fluxes, which are based on the distilled products of pine saps, are the most widely used fluxes for electronics assemblies. Pure rosin (termed "water-white" rosin, after the test method for purity) is designated by the letter R. Because the R flux is a very weak acid, its residues are not corrosive in most applications. The activity of the rosin-base fluxes is strengthened by the addition of activators. Such fluxes are designated as mildly activated (RMA), fully activated (RA), and superactivated (RSA) (Ref 10).

RMA flux residues must be removed from most products designated for high-reliability applications. RA flux residues should be removed from all PWBs, except those used in low-end commercial electronic products. RSA fluxes are extremely corrosive, and their residues must by thoroughly removed from all products.

Activators are typically halide ions (Cl^-, F^-, and Br^-), which increase the activity of the rosin-base flux. However, "halide-free" activated fluxes are available and will lessen the corrosion potential of flux residues. Visible residues are tan or white in appearance (Ref 11). Black residues indicate that the flux has been exposed to excessive heat, and they are consequentially very difficult to remove. Ionic residue determination and SIR tests are strongly recommended for flux activities that exceed those of RMA materials.

No-Clean or Low-Solids Fluxes. Flux formulations for which the residues do not pose a corrosion concern after soldering--and thus do not need to be removed--are called "no-clean" fluxes. The fluxing activity of these materials can approach that of traditional RMA fluxes (Ref 12). A second approach to eliminating the need for postprocess cleaning is to use a "low-solids" flux, that is, a flux with limited solids content. (Solids form the residue after soldering.) However, low-solids fluxes have reduced oxide removal potential. Therefore, substrate tarnishes and contamination, flux density, and process conditions (inert atmospheres may be necessary) must be more tightly controlled to ensure consistent solderability.

Organic acid (OA) fluxes , which are also called water-soluble or intermediate fluxes, are water- or alcohol-base and have chemical activities greater than the rosin-base materials. OA fluxes improve the solderability of metals such as iron- or nickel-base alloys. Residues must be removed from the product using aqueous or semiaqueous cleaning methods. Flux activity can be provided by halide-containing compounds. The fluxes are also available in halide-free forms. Although they are more heat resistant than the rosin-base fluxes, the OA fluxes will char, producing hard-to-remove brown or black deposits. Ionic residue determination and SIR tests are strongly recommended for prototype development and lot sampling in assembly production to ensure adequate flux residue removal.

Inorganic acid (IA) fluxes either contain extremely corrosive acids (hydrochloric acid, phosphoric acid, and others) or are composed of metal chloride salts that form hydrochloric acid in the presence of water. Surfactants or wetting agents are also added. The residues are highly corrosive. These fluxes can be used for hot solder dipping of iron-base alloy or nickel leads, provided that adequate cleaning measures are taken to remove residues. These fluxes are not used in PWB assembly operations.

References cited in this section

1. R. PRASAD, *SURFACE MOUNT TECHNOLOGY, PRINCIPLE AND PRACTICE,* VAN NOSTRAND-RHEINHOLD, 1989, P 363
2. V. MARCOTTE, C^4 FLIP CHIP JOINING, *THE METAL SCIENCE OF JOINING*, M. CIESLAK *ET AL.*, ED., TMS, 1992, P 315
3. C. LEA, A SCIENTIFIC GUIDE TO SURFACE MOUNT TECHNOLOGY, ELECTROCHEM. PUB., LTD, 1988, P 169
4. R. GEHMAN, DENDRITIC GROWTH EVALUATION OF SOLDERED THICK FILMS, *INT. J. HYBRID MICROELEC.*, VOL 6, 1983, P 239
5. H. MANKO, *SOLDERS AND SOLDERING*, MCGRAW-HILL, 1979, P 112
6. L. GOLDMANN *ET AL.*, LEAD-INDIUM FOR CONTROLLED-COLLAPSE CHIP JOINING, *PROC. 27TH ELECTRON. COMP. CONF.*, 1977, P 25
7. R. KLEIN-WASSINK, *SOLDERING IN ELECTRONICS*, 2ND ED., ELECTROCHEM. PUB., LTD, 1989, P 548
8. R. KLEIN-WASSINK, *SOLDERING IN ELECTRONICS*, 2ND ED., ELECTROCHEM. PUB., LTD, 1989, P 557
9. J. LEE, SOLDER PASTE DISPENSING MATERIALS AND REQUIREMENTS, *ELECTRON. PACK. AND PROD.*, NOV 1990, P 22
10. H. MANKO, *SOLDERING HANDBOOK FOR PRINTED CIRCUITS AND SURFACE MOUNTING*, VAN NOSTRAND-RHEINHOLD, 1986, P 286

11. D. LOVERING, ROSIN ACIDS REACT TO FORM TAN RESIDUES, *ELECTRON. PACK. AND PROD.,* FEB 1985, P 232
12. D. KOCKA, NO-CLEAN FLUXES ARE A VIABLE ALTERNATIVE TO CFC CLEANING, *ELECTRON. PACK. AND PROD.,* JUNE 1990, P 95

Paul T. Vianco, Sandia National Laboratories

Base Materials, Finishes, and Storage/Corrosion Issues

The substrate can be characterized by the nature of the base material and the surface finish. The base materials of device leads are typically copper or one of the iron-base, low-expansion alloys. Leadless surface-mount devices have ceramic oxide base materials. Copper foil is used as the base material of PWB conductor lines and lands (bonding pads).

The surface layer of a substrate comprises the so-called *solderable layer* to which the molten solder metallurgically reacts and, frequently, an additional coating or *protective layer* to prevent the formation of excessive oxidation and/or contamination by organic films on the solderable layer. This solderable surface can be either the base material surface itself or a coating deposited by electroplating, electroless plating, evaporation, pretinning (solder dip coating), sputtering, or chemical vapor deposition (CVD). The protective layer is typically an electroplated film that is entirely consumed by the solder during wetting. It is primarily the condition of the surface of the solderable layer (base material or a separate coating) on the component lead, termination, and PWB lands that accounts for joint solderability during assembly. Base material bulk properties, such as thermal conductivity or heat capacity, indirectly affect solderability, particularly the time-dependent wetting performance.

Coatings that serve as the solderable layer must be sufficiently thick to ensure that:

- THE COATING COMPLETELY COVERS THE BASE MATERIAL SURFACE
- THE LAYER IS NOT DISSOLVED BY THE LIQUID SOLDER
- THE LAYER IS NOT CONSUMED BY SOLID-STATE GROWTH OF INTERMETALLIC COMPOUNDS WITH THE SOLDER

On the other hand, excessive thickness can lead to residual stresses that cause delamination of the coating and the entrapment of organic plating compounds and gases that in turn cause the deterioration of solderability. Coatings used as solderable surfaces are typically the elemental metals, that is, nickel or copper. Multi-elemental thick-film layers are used as solderable surfaces on ceramic substrates (for example, conductor networks for hybrid microcircuits or terminations on discrete leadless ceramic devices or chip carriers).

The protective layer must be of sufficient thickness to protect the wettability of the surface of the solderable layer. Nickel that has been coated by a protective coating can be wet by the molten solder using the rosin-base fluxes. An unprotected nickel film requires much more active fluxes to promote solder wetting. Because the protective coating is absorbed into the solder, its thickness must be limited to prevent excessive contamination of the solder, thereby affecting its physical and mechanical properties.

Protective layers are often made from precious metals, the most popular of which is gold. It is imperative that gold coatings be removed by hot solder dipping the leads twice in flowing or nonflowing solder baths prior to assembly in order to prevent solder joint embrittlement (MIL-STD-1276D). However, *three* immersions in solder at 250 °C (480 °F) are recommended to ensure the complete removal of all thicknesses of gold from beam-leaded, surface-mount devices (Ref 13). Additional information is provided in the section "Precious Metal and Alloy Base Materials" of this article.

Other protective layers include electroplated tin (the production of which is termed tin plating) and electroplated tin-lead solder (for example, 60Sn-40Pb). The tin and tin-lead solder platings can be heated above their respective melting temperatures of 232 °C (450 °F) and 183 °C (361 °F) to remove pores or gaps. These layers are then referred to as ***fused***

tin or *fused* tin-lead coatings, respectively. A protective layer of tin or tin-lead solder can also be added by applying flux to the solderable surface and immersing it into a molten bath of tin or tin-lead solder. These finishes are referred to as hot-dipped tin or hot-dipped solder layers, respectively.

Organic coatings, such as benzotriazole and imidazole, are used as protective finishes on solderable surfaces. They are popular for protecting bare copper surfaces on PWBs during storage prior to soldering.

Coating materials and their preferred thicknesses for solderable and protective finishes are specified by MIL-STD-1276D and MIL-M-3851OH. Examples are described below according to the base materials used most frequently in electronics applications. In general, properly prepared and protected solderable surfaces (base material or deposited layer) can be readily wetted by the solders listed in Table 1 using standard electronic fluxes and assembly practices.

Copper Alloys. Copper is used in electronic applications as wire leads (individual or as frames) on through-hole components, electroless/electroplated layers in PWB holes, or thin foil in the construction of lines and lands on PWB surfaces. In some PWB fabrication processes, copper foil surfaces can be built up with electroless and electroplated copper, as well. The thickness of copper layers that coat PWB through-holes is approximately 0.025 to 0.076 mm (0.001 to 0.003 in.). Typical foil thicknesses for PWB surface patterns range from 0.018 to 0.071 mm (0.0007 to 0.0028 in.). The most common thicknesses are termed 0.5 oz copper (0.018 mm, or 0.0007 in.), 1 oz copper (0.036 mm, or 0.0014 in.), and 2 oz copper (0.071 mm, or 0.0028 in.).

Copper is readily wetted by tin-lead solder using rosin-base fluxes, provided that the surface is not heavily oxidized. Oxide removal is performed by immersion in dilute hydrochloric acid or sulfuric acid solutions or another type of mixture. Compositions of acid solutions used for oxide removal are given in the article "General Soldering" in this Volume. Protective finishes for copper and copper alloys include layers of electroplated silver of a thickness from 3.8 to 8.9 μm (150 to 350 μin.), electroplated tin (7.6 to 13 μm, or 300 to 500 μin.), and electroplated tin-lead (7.6 to 23 μm, or 300 to 900 μin.). The latter two layers can be fused; the preferred thicknesses range from 2.5 to 13 μm (100 to 500 μin.). The silver coating is usually covered by a tarnish layer caused by a reaction with sulfur in the air. The resulting sulfide film causes the solderability to deteriorate with time of exposure. Silver coatings need to be removed just like the gold coatings to prevent embrittlement of the solder joint by silver-tin intermetallic formation.

A hot-dipped tin-lead finish (5.1 μm, or 200 μin., minimum) is most often specified for copper-base metal. A solid-state reaction takes place between copper and tin (or the tin component of solders) to form a layer of intermetallic compounds, Cu_3Sn and Cu_6Sn_5, at the solder-copper interface. The thickness of the intermetallic layer increases as exposure temperature and time increase. The total intermetallic layer thickness (Cu_3Sn + Cu_6Sn_5) as a function of time and temperature is shown in Fig. 4(a) for electroplated tin, Fig. 4(b) for electroplated tin-lead coatings, and Fig. 4(c) for hot-dipped tin-lead coatings. Growth kinetics at room temperature are illustrated in Fig. 4(d) (Ref 14, 15).

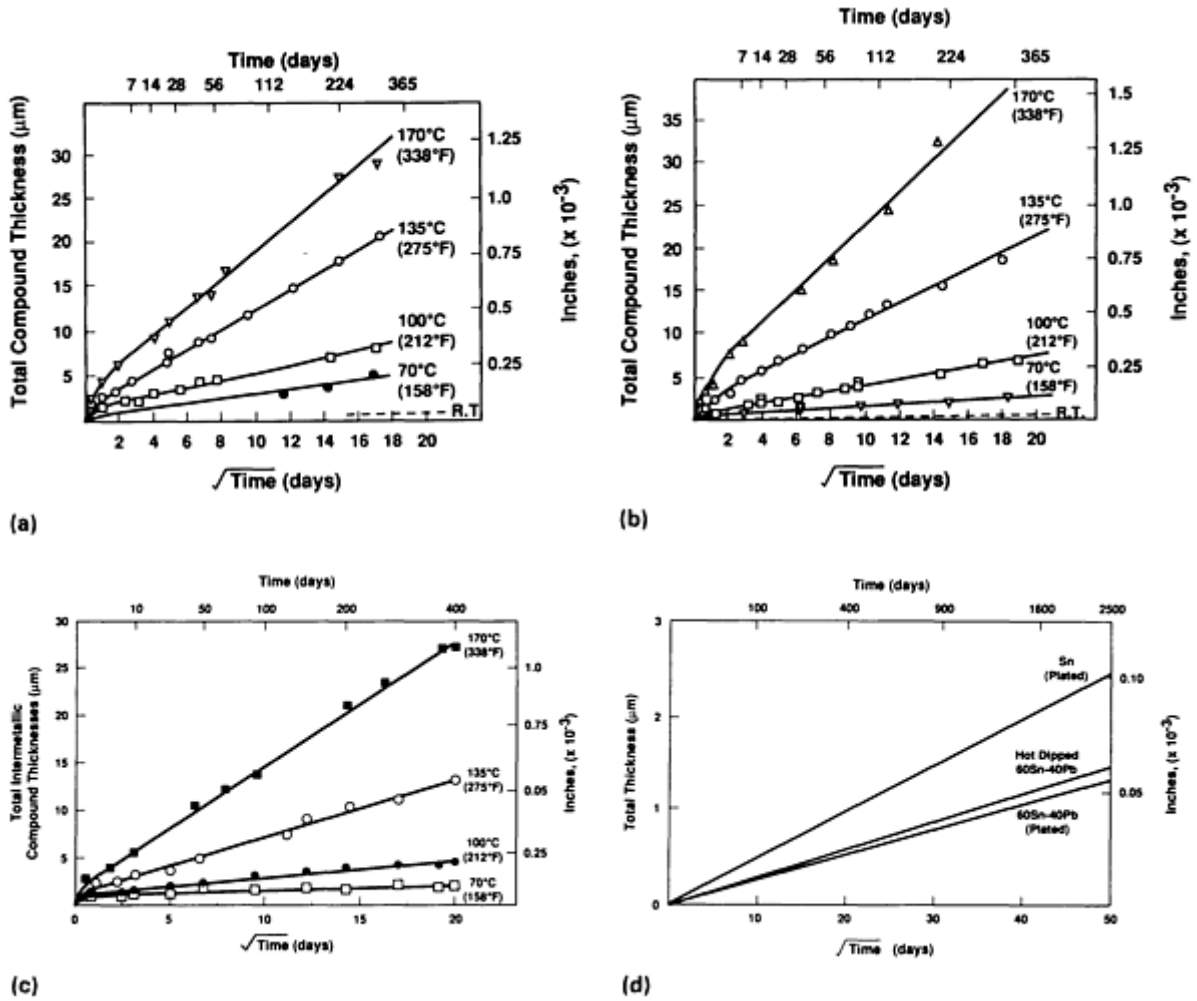

FIG. 4 COPPER-TIN INTERMETALLIC LAYER (CU_6SN_5 + CU_3SN) GROWTH KINETICS. (A) FOR ELECTROPLATED TIN COATING. (B) FOR ELECTROPLATED 60SN-40PB COATING. (C) FOR HOT-DIPPED 63SN-37PB COATING. (D) FOR TIN-LEAD COATINGS AT ROOM TEMPERATURE. SOURCE: INTERNATIONAL TIN RESEARCH INSTITUTE AND SANDIA NATIONAL LABORATORIES

Intermetallic layers have low ductility and, depending on their thickness, can affect the mechanical integrity of the solder joint (Fig. 5). In addition, the solid-state growth of the intermetallic film may consume very thin layers of tin or tin-lead alloy. The exposed intermetallic layer of Cu_6Sn_5 can readily oxidize and is difficult to wet with molten solder. Parts stored for over 1 or 2 years or those that will experience elevated temperatures (as in testing requirements) should be covered by a solderable layer of electroplated nickel (1.5 to 3.8 μm, or 60 to 150 μin.), followed by one of the above protective finishes. This coating structure will prevent the excessive formation of copper-tin intermetallic compounds at the solder-substrate interface, which may consume the tin or tin-lead protective finish and cause subsequent solderability to deteriorate.

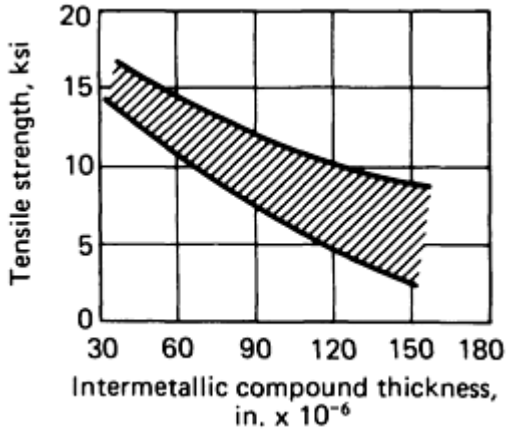

FIG. 5 EFFECT OF INTERMETALLIC COMPOUND THICKNESS ON ROOM-TEMPERATURE TENSILE STRENGTH OF SOLDER JOINTS (COPPER/COPPER BASE METALS)

Copper lines and lands on PWBs are protected with a hot-dipped solder coating that is generally applied by the hot-air leveling technique. The bare copper can also be protected with an organic inhibitor. Alloys of copper, including brasses, bronzes, copper-iron-zinc, copper-iron-tin, and copper-zinc-aluminum-cobalt, should be plated with a solderable layer (and protective coating) to overcome difficult-to-remove oxides or to act as a barrier against the diffusion of base metal constituents (for example, zinc) into the solder. Finishes include either a minimum 2.5 μm (100 μin.) of copper or a nickel layer with one of the protective coatings (described above).

Beryllium copper forms a tenacious oxide. Solder wetting with the use of activated rosin-base fluxes requires that the surface oxide be reduced by etching with strong acids. The soldering operation should immediately follow surface preparation steps to prevent reoxidation. Beryllium copper with very thin oxides can be wetted by solder if inorganic acid fluxes are used. However, a thorough cleaning of residues is required. The inorganic acid fluxes are used only to apply a protective layer of hot-dipped tin-lead solder. They are not recommended for PWB assembly.

Nickel and nickel-base alloys are used as the base metals on package leads. However, the most common electronics application is electroplated pure nickel used as the solderable coating on nickel-and iron-base lead materials that cannot be subjected to the cleaning measures and aggressive fluxes required to promote solderability. Nickel and its alloys are difficult to wet, because of the formation of a thin, tenacious oxide layer. Substrates must be chemically etched with aggressive solutions. The soldering operation or the application of a protective layer must immediately follow the etching treatment in order to minimize reoxidation of the surface. Freshly deoxidized leads made with nickel or nickel-containing alloys, or those that are electroplated with a solderable layer of nickel (1.3 to 3.8 μm, or 50 to 150 μin.), require one of the following protective layers prior to assembly on the PWB:

- ELECTROPLATED (MATTE) TIN (7.6 TO 13 μM, OR 300 TO 500 μIN.)
- ELECTROPLATED TIN-LEAD COATING (7.6 TO 23 μM, OR 300 TO 900 μIN.)
- HOT-DIPPED SOLDER COATING (5.1 μM, OR 200 μIN.)

The electroplated layers can be fused. The hot-dipped solder coating step may require the use of more-aggressive fluxes (organic acid or inorganic acid fluxes) to achieve a satisfactory finish. These fluxes must be compatible with the device package construction and their residues must be thoroughly removed after coating. It is very important that hot-dipped solder (or tin) layers on device leads and terminations contain neither "lumps" nor icicles, because these defects can interfere with the automated placement of components on the PWB, particularly with the use of fine-pitch devices. However, a properly applied hot solder dipped lead finish is superior to most tin or tin-lead plated surfaces.

The nickel solderable coating is protected by a finish of electroplated gold, particularly if the base metal is subject to temperatures that exceed the melting points of tin or tin-lead finishes prior to assembly. The MIL-G-45204C thickness recommendation for solderability is from 1.3 to 2.5 μm (50 to 100 μin.). However, general specification of gold thickness (MIL-STD-1276 D) can be as high as 2.5 to 7.6 μm (100 to 300 μin.) so that complete removal for soldering should be

verified if the thinner layers do not offer adequate protection. The previously described procedure regarding the removal of gold coatings pertains. Details are provided in the section "Precious Metal and Alloy Base Materials" in this article.

A less-expensive silver coating (3.9 to 8.9 μm, or 150 to 350 μin.) can also be used. However, silver tarnishes upon atmospheric exposure, causing a deterioration to solderability. As already mentioned, silver coatings need to be removed, just like gold coatings are.

Electroplated copper (3.8 to 7.6 μm, or 150 to 300 μin.), followed by one of the tin or tin-lead protective finishes, can also provide excellent solderability to nickel and nickel-alloy base metals. Although nickel forms an intermetallic compound layer with tin (primarily, Ni_3Sn_4), its growth rate is much slower than that of copper and tin. Therefore, it does not significantly affect the mechanical properties of solder joints in electronic assemblies. An ultrasonically activated solder pot can be used to apply a hot-dipped solder (or tin) coating to the lead without the use of aggressive fluxes. The ultrasonic energy disrupts the oxide layer, thereby allowing the solder to wet without the use of aggressive fluxes. Ultrasonics should not be used on devices that can be damaged by the ultrasonic energy.

Aluminum and its alloys are used as connector housings that attach cables to PWBs or other cable assemblies. A "strap" or lead is soldered to the housing to provide an electrical ground.

Aluminum alloys are difficult to wet, because of a tenacious surface oxide. Although aggressive fluxes, such as the inorganic acids, are required to promote solderability, they leave behind extremely corrosive residues that must be thoroughly removed to prevent corrosion in service.

Another issue when solder joining aluminum is galvanic corrosion between aluminum and a dissimilar substrate (for example, copper or nickel) or between aluminum and solder constituents (for example, tin). Solder alloys, such as 80Sn-20Zn (T_1 = 270 °C, or 518 °F; T_s = 198 °C, or 388 °F) and 95Zn-5Al (382 °C, or 720 °F), were developed for compatibility with aluminum. However, their high melting points require localized heating techniques and prohibit joining to organic materials or hybrid thick-film networks. The high thermal conductivity of aluminum alloys requires large heat input into the substrate to promote wetting.

Although solderable and protective finishes were not cited by the specifications noted above, adequate solderability can be obtained with coatings of electroplated nickel or copper to thicknesses of 1.3 to 3.8 μm (50 to 150 μin.) and 7.6 to 25 μm (300 to 1000 μin.), respectively. A zincate coating is applied to the aluminum prior to the nickel or copper finishes to promote adhesion. Once the soldering operation has been performed, it is recommended that the exposed nickel or copper layer be coated with an anodic finish (for example, cadmium or zinc) to reduce the potential for a corrosion couple with aluminum. Ultrasonic activation of the solder pot provides a means of depositing a hot solder or tin-dipped finish to aluminum substrates without a flux.

Iron-base alloys constitute the base materials for leads on a number of through-hole and surface-mount device packages. These alloys include Kovar, 29Ni-17Co-0.2Mn-balance Fe; alloy 52, 0.5Mn-0.25Si-50.5ONi-balance Fe; and alloy 42, 0.5Mn-O.25Si-5.5Cr-42Ni-balance Fe. Solder wetting of the iron-base alloys requires the removal of a thick, tenacious surface oxide by such procedures as the use of etchants and chemical brighteners or aggressive electropolishing treatments (Ref 16).

The hot-dipped solder coating may require the use of more-aggressive fluxes (organic acid or inorganic acid fluxes) to achieve a satisfactory finish. These fluxes must be compatible with the device package materials and their residues must be thoroughly removed after coating. Surfaces must be protected from reoxidation after surface preparation, typically by a hot-dipped tin or solder coating.

However, the most common technique to achieve solder wetting of these materials is the use of combined solderable and protective layers. The most frequent approach is to electroplate device leads with a solderable layer of nickel (1.3 to 3.8 μm, or 50 to 150 μin.), followed by a protective layer of electroplated (matte) tin (7.6 to 13 μm, or 300 to 500 μin.), electroplated tin-lead coating (7.6 to 23 μm, or 300 to 900 μin.), or hot-dipped solder coating (5.1 μm, or 200 μin., minimum). The electroplated layers can be fused. Silver (3.9 to 8.9 μm, or 150 to 350 μin.) can also be used as a protective finish. As previously mentioned, hot-dipped solder (or tin) finishes on package leads should not contain "lumps" or icicles, because they can interfere with the automated placement of components on the PWB.

The nickel solderable coating can be protected by a finish of electroplated gold, particularly if the base metal is subject to temperatures that exceed the melting points of tin or tin-lead prior to assembly. The recommended thickness for soldering

operations ranges from 1.3 to 2.5 μm (50 to 100 μin.), per MIL-G-45204C. Gold coatings must be removed in the manner previously described. Details are provided in the section "Precious Metal and Alloy Base Materials" in this article.

Alternative solderable coatings include electroless nickel (1.3 to 3.0 μm, or 50 to 120 μin.), palladium-nickel (1.3 to 2.5 μm, or 50 to 100 μin.), or copper (3.8 to 7.6 μm, or 150 to 300 μin.). Electroless nickel is not recommended for flexible or semirigid leads or substrates exposed to high-temperature testing procedures prior to PWB assembly. Phosphorus from the plating bath may become entrapped in the layer, resulting in film embrittlement or poor solderability because of its diffusion to the nickel surface at elevated temperatures. A palladium-nickel coating does not require a protective finish because the palladium component imparts oxidation resistance to the alloy coating. The electroless nickel and electroplated copper coatings require one of the protective finishes noted above.

Precious Metal and Alloy Base Materials. Excellent solderability of precious metals (gold, silver, palladium, platinum, and others) is achieved with tin-and indium-base solders, because of a strong metallurgical reaction at the solder/base metal interface. This metallurgical reaction results in the formation of intermetallic compounds at the interface. Their growth can take place when the solder is in either the liquid or solid state. In either case, intermetallic compound growth can quickly consume wires, leads, or the entire thick-film layer.

The dissolution rates of several precious metals in molten 60Sn-40Pb solder are shown in Fig. 6 (Ref 17). The excessive concentration of intermetallic compounds severely embrittles bulk tin-lead solder. In addition, thick intermetallic layers at the solder/base metal interface can drastically decrease solder joint ductility. Gold contents of 6 wt% decrease the ductility (reduction-in-area) by 50% (Ref 18); these data indicate that gold embrittlement is generally avoided in tin-lead solders by maintaining gold contamination to the joint at a level less than 4 wt%. (Some segments of the electronics industry have specified maximum gold contents of 1 wt%.)

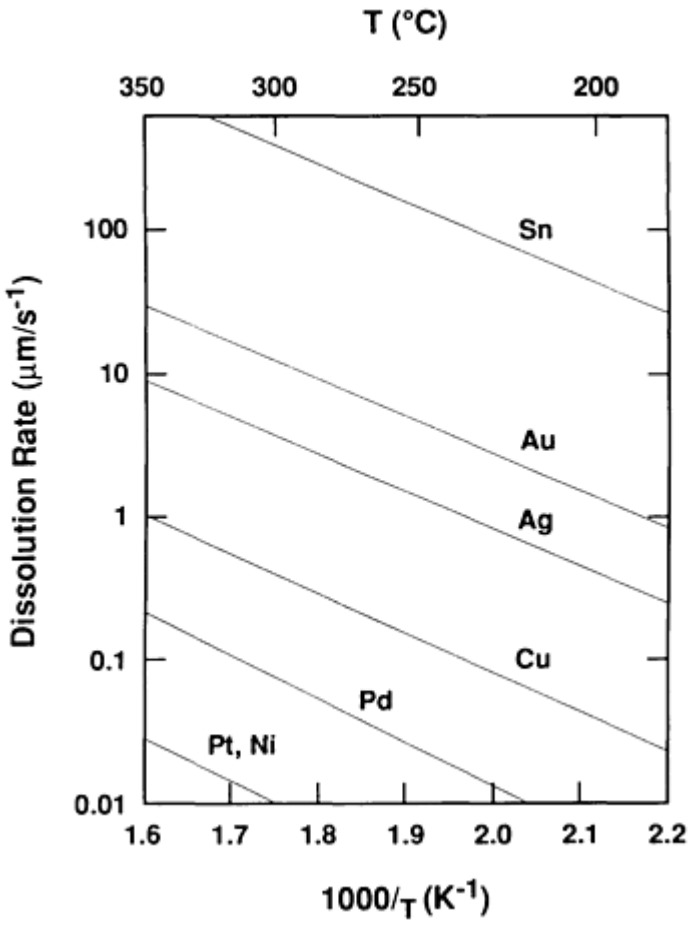

FIG. 6 DISSOLUTION RATES OF VARIOUS METALS IN MOLTEN 60SN-40PB SOLDER. SOURCE: REF 3

Silver wires or silver coatings on other metals have been used in place of gold to reduce cost. Silver has a lower dissolution rate in tin-lead solders than gold. The rate can be further diminished by adding from 1 to 2 wt% silver to the solder. However, silver rapidly tarnishes from airborne sulfur pollution, causing the surface to tarnish rapidly and lose solderability. The dissolution of precious metals is significantly less when lead-indium solders are used.

Wetting of precious metal base materials is assisted by the limited oxide layer that forms on them, which sometimes allows wetting by solders without the use of a flux. Wires or ribbons are used as jumper leads on PWBs by virtue of their low resistance. Pastes that contain precious metals or their alloys as the conductive component are used as thick-film networks for hybrid microcircuitry.

Ceramic materials used for electronic packages and substrates include alumina (Al_2O_3), beryllia (BeO), and silica (SiO_2), as well as several of the engineered ceramics, such as silicon nitride (Si_3N_4). Solders do not readily wet ceramic-base materials, because of the low surface energy of the substrate and the absence of a solder-ceramic metallurgical reaction.

Solderable surfaces are provided by thick-film metallization inks. These inks contain a powder of electrically conductive metals or alloys (for example, copper, nickel, gold-palladium-platinum, platinum-silver, platinum-gold, and others), an oxide powder and glass binder that bond the conductive component to the substrate by a high-temperature firing process, and an organic carrier comprising resin and solvents to give the ink "body" for printability on the substrate. The thick films have excellent solderability, because of their noble metal content. However, the 10 to 20 μm (100 to 800 μin.) thick film can be consumed by intermetallic formation with the tin component of the liquid solder, as well as through solid-state reaction at the solder-film interface of the solidified joint. The use of lead-indium solders greatly reduces the growth of intermetallic compounds. Copper and nickel thick films are not as quickly consumed by the tin-base solders and are less costly. However, these coatings must be protected from excessive oxidation during firing, solder processing, and contaminated atmospheres during storage.

Other thick-film systems are based on moly-manganese and refractory metals (Ref 19). The moly-manganese process uses an ink of molybdenum and manganese that is printed onto the selected location(s) and fired to bond the film to the ceramic. Next, a layer of copper or nickel is electroplated onto the moly-manganese film to form the solderable coating. Then, a protective layer of electroplated gold is added. Alternatively, some refractory metal thick-film systems use molybdenum or tungsten as the ceramic binder. Gold is electroplated onto the refractory metal binder. The resulting metallized layer is heated to partially consume the gold as gold-molybdenum or gold-tungsten alloy at the interface. The alloys form the solderable surface while the remaining gold serves as the protective finish. Electroplated nickel can be used to create the solderable surface in place of gold-molybdenum or gold-tungsten.

Storage. The base material or surface finish solderability is strongly affected by storage conditions (time, temperature, humidity, gases, and packing materials) and the integrity of the protective coating. Recommended electroplated and hot-dipped solder finishes that pass specified solderability tests are considered to preserve solderability for 1 to 2 years under typical industrial environments (Ref 20, 21). Longer periods may require special storage conditions, such as inert atmospheres in containers, controlled temperature and humidity levels, or additional solderability testing prior to assembly. Plasticizers and silicon-base mold releases in plastic containers, as well as sulfur compounds in paper products and factory atmospheres, can degrade solderability. Inventory control practices, including "first in, first out" and "just-in-time," can prevent solderability deterioration caused by excessive storage periods.

Corrosion. Solder alloys have necessarily dissimilar compositions, when compared with the base materials that they join together. Therefore, solder joints have a potential for corrosion activity. Water vapor from the atmosphere can provide the electrolyte medium, particularly given that most PWB laminates (and ceramic materials) are hygroscopic to varying degrees.

Sources of ionic species to form the electrolyte medium are flux residues, processing chemicals that remain in the PWB (laminate), or external contamination by handling or service environments. The electromotive series provides a preliminary estimate of corrosion "potential" for the metal systems in the joint. However, the series cannot describe the kinetics (rate) of corrosion.

Assembly processes for high-reliability electronics or those systems destined for harsh service conditions (for example, saltwater spray or high-humidity locations) must be thoroughly assessed for corrosion potential. Issues include: the compatibility of the solder and base material, the activity of the flux and the need for its residue removal after assembly,

and the use of either conformal (organic) coatings to exclude atmospheric moisture or coatings with metal finishes (zinc or cadmium electroplating) to act as sacrificial anodes.

References cited in this section

3. C. LEA, A SCIENTIFIC GUIDE TO SURFACE MOUNT TECHNOLOGY, ELECTROCHEM. PUB., LTD, 1988, P 169
13. P. VIANCO AND J. DAL PORTO, "EMBRITTLEMENT OF SURFACE MOUNT TRANSISTOR SOLDER JOINTS INVOLVING PRETINNED LEADS," INTERNATIONAL BRAZING AND SOLDERING CONFERENCE (DETROIT, MI), AWS, 1991
14. D. UNSWORTH AND C. MACKAY, A PRELIMINARY REPORT ON GROWTH OF COMPOUND LAYERS ON VARIOUS METAL BASES PLATED WITH TIN AND ITS ALLOYS, *TRANS. INST. MET.*, VOL 51, 1973, P 85
15. P. KAY AND C. MACKAY, THE GROWTH OF INTERMETALLIC COMPOUNDS ON COMMON BASIS MATERIALS COATED WITH TIN AND TIN-LEAD ALLOYS, *TRANS. INST. MET.*, VOL 54, 1976, P 68
16. P. VIANCO *ET AL.*, SOLDERABILITY TESTING OF KOVAR WITH 60SN-40PB SOLDER AND ORGANIC FLUXES, *WELD. J.*, JUNE 1990, P 230-S
17. C. LEA, *A SCIENTIFIC GUIDE TO SURFACE MOUNT TECHNOLOGY*, ELECTROCHEM. PUB., LTD, 1988, P 167
18. M. BESTER, METALLURGICAL ASPECTS OF SOLDERING GOLD OR GOLD PLATING, *PROC. INTERNEPCON*, 1968, P 221
19. P. HOLMES AND R. LOASBY, *HANDBOOK OF THICK FILM TECHNOLOGY*, ELECTROCHEM. PUB., LTD., 1976, P 192
20. R. WILD, COMPONENT LEAD SOLDERABILITY VS. ARTIFICIAL AGEING II, *PROC. 1 L TH ELECT. MFG. SEMINAR* (CHINA LAKE, CA), NAVAL WEAPONS CENTER, 1987, P 289
21. R. EDINGTON AND L. CONRAD-LOWANE, AGING ENVIRONMENTS AND THEIR EFFECTS ON SOLDERABILITY, *PROC. 12TH ELECTRON. MFG. SEMINAR* (CHINA LAKE, CA), NAVAL WEAPONS CENTER, 1988, P 31

Soldering in Electronic Applications

Paul T. Vianco, Sandia National Laboratories

Solder Joint Design

Solder joint performance depends on the package size of a device, the materials and layout of the PWB (or hybrid substrate), and the manufacturing processes used to assemble the PWB. Hardware package configurations and PWB layout guidelines have been established by several industrial standards organizations, such as the Electronics Industry Association (EIA), Institute for Interconnection and Packaging Electronic Circuits (IPC), American National Standards Institute (ANSI), and the Joint Electronic Devices Engineering Council (JEDEC). General solder joint configuration and performance recommendations are discussed below for through-hole technology, surface-mount technology, mixed technology (through-hole plus surface mount), and connector technology. Table 5 lists the numerous guidelines that provide details on these topics. (A list of industrial specifications can be obtained from IPC, 7380 N. Lincoln Ave., Lincolnwood, IL, 60646-1705; federal and military specifications are available from the Standardization Documents Order Desk, Building 4D, 700 Robbins Ave., Philadelphia, PA, 19111-5094.)

TABLE 5 GUIDELINES AND SPECIFICATIONS FOR SOLDER JOINT DESIGN

IPC-D-300G, PRINTED BOARD DIMENSIONS AND TOLERANCES
IPC-SM-782, SURFACE MOUNT LAND PATTERNS (CONFIGURATIONS AND DESIGN RULES)
IPC-S-815A, GENERAL REQUIREMENTS FOR SOLDERING ELECTRONIC INTERCONNECTIONS
IPC-SM-780, COMPONENT PACKAGING AND INTERCONNECTING WITH EMPHASIS ON SURFACE MOUNTING
IPC-D-275, DESIGN STANDARD FOR RIGID PRINTED BOARDS AND RIGID PRINTED BOARD ASSEMBLIES
IPC-D-322, GUIDELINES FOR SELECTING PRINTED WIRING BOARD SIZES USING STANDARD PANELS
IPC-MC-324, PERFORMANCE SPECIFICATION FOR METAL CORE BOARDS
IPC-D-330, DESIGN GUIDE
IPC-PD-325, ELECTRONIC PACKAGING HANDBOOK
IPC-CM-770, PRINTED BOARD COMPONENT MOUNTING
IPC-D-279, DESIGN GUIDELINES FOR RELIABLE SURFACE MOUNT TECHNOLOGY
IPC-SM-785, GUIDELINES FOR ACCELERATED RELIABILITY TESTING OF SURFACE MOUNT SOLDER ATTACHMENTS
IPC-S-816, SMT PROCESS GUIDELINE AND CHECKLIST
J-STD-001, REQUIREMENTS FOR SOLDERED ELECTRICAL AND ELECTRONIC ASSEMBLIES
J-STD-002, SOLDERABILITY TESTS FOR COMPONENT LEADS, TERMINATIONS, LUGS, TERMINALS AND WIRES
J-STD-003, SOLDERABILITY TESTS FOR PRINTED BOARDS
MIL-C-55302, CONNECTORS, PRINTED CIRCUIT SUBASSEMBLY, AND ACCESSORIES

An assessment of solder joint performance requires knowledge of several physical and mechanical properties of the solder alloy, package, and substrate materials. Strength calculations based on bulk solder properties typically provide a conservative estimate of solder joint performance (Ref 22); more accurate predictions are made from solder joint properties. The properties of those materials commonly used in electronics packaging and substrates are summarized in Table 6.

TABLE 6 SELECTED PROPERTIES FOR ELECTRONIC ASSEMBLY MATERIALS

MATERIAL	**GLASS TRANSITION TEMPERATURE**		**PLANAR COEFFICIENT OF THERMAL EXPANSION(A), 10^{-6}/K**	**THERMAL CONDUCTIVITY**		PLANAR TENSILE MODULUS	
	°C	**°F**		**W/M · K**	**10^{-4} BTU/FT · S · °F**	**GPA**	10^6 PSI
PRINTED BOARD SUBSTRATES							
EPOXY FIBERGLASS	125	257	13-18	0.16	0.26	17	**2.5**
POLYIMIDE FIBERGLASS	250	482	12-16	0.35	0.56	19	**2.8**
EPOXY-ARAMID FIBER	125	257	6-8	0.12	0.19	30	**4.4**
POLYIMIDE-ARAMID FIBER	250	482	3-7	0.15	0.24	28	**4.0**
POLYIMIDE QUARTZ	250	482	6-8	0.30	0.48	. . .	**. . .**
FIBERGLASS-TEFLON	75	167	20	0.26	0.42	1.4	**0.2**
CERAMICS							
ALUMINA, 86%	. . .	. . .	6.0	20	32	300	**44**
BERYLLIA, 99.5%	. . .	. . .	6.4	200	320	350	**51**
SILICON	. . .	. . .	2.3	150	240	115	**17**
METALS							
COPPER	. . .	. . .	17.0	370	590	130	**19**

NICKEL	. . .	. . .	13.0	89	140	220	**32**
ALUMINUM	. . .	. . .	24.0	230	370	70	**10**
BRASS, 33 WT% ZN	. . .	. . .	20.0	120	190	112	**16**
BRONZE, 5 WT% SN	. . .	. . .	18.0	75	120	121	**18**
LOW-CARBON STEEL	. . .	. . .	12.0	58	93	210	**30**
STAINLESS STEEL, 18-8	. . .	. . .	15.0	16	26	210	**30**
KOVAR	. . .	. . .	5.2	17	27	210	**30**
60SN-40PB SOLDER	**. . .**	**. . .**	**25.0**	**51**	**82**	**32**	**4.6**

Source: Ref 1

(A) THERMAL EXPANSION OF CIRCUIT BOARD SUBSTRATES IN THE *Z* (THICKNESS) DIMENSION CAN BE AN ORDER OF MAGNITUDE GREATER THAN IN THE *XY* (PLANAR) DIMENSIONS.

Organic materials used in PWB laminates soften significantly at temperatures that exceed their glass transition point. Time periods at temperatures greater than the transition value should be minimized to prevent permanent warpage or twist to the PWB, which can cause debonded lands and conductor lines or fractured joints and packages due to misfit in cabinet frames.

Coefficients of thermal expansion (CTE) are required to assess the thermal fatigue resistance of solder joints, a principal source of failure for leadless surface-mount components. The CTEs of PWB laminates are specified for the in-plane dimensions. It is important to note that the through-thickness CTEs of PWB laminates can be as much as an order of magnitude larger than the in-plane values. Because PWB CTEs are very sensitive to the resin content, resin type, and fiber weave of the laminate, precise values should be obtained by measuring them directly, rather than relying on generic information from the manufacturer.

Thermal conductivity is important in solder joint design for high-power applications.

Excessive moisture retention by the PWB (organic laminate or ceramic) can lead to voids in solder joints that are due to water vapor formed at soldering temperatures or it can cause movement of surface-mount parts during reflow that results in misaligned packages on the assembly.

Through-hole technology typically refers to the use of leaded device packages. The leads are inserted into holes in the PWB and are soldered in place. Several package/lead configurations are shown in Fig. 7. Device leads are typically copper or one of the iron-base alloys (typically coated with a solderable layer). These lead-base materials have a protective finish of tin-lead alloy (plated, plated and fused, or hot dipped) to facilitate solder wetting during assembly on the PWB. Although the coatings can accommodate lead-forming operations, such practices should not be performed on leads with an electroless nickel solderable layer.

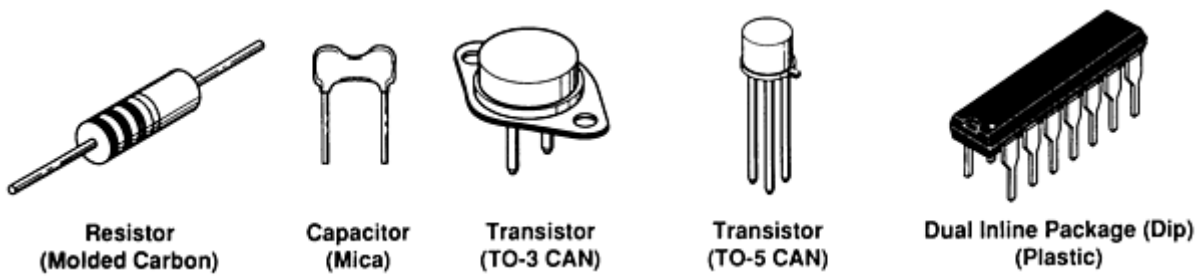

FIG. 7 PACKAGE AND LEAD CONFIGURATIONS FOR THROUGH-HOLE DEVICES

Substrates for through-hole technology include organic laminates, metal-clad substrates, and ceramics for hybrid microcircuits. Ceramic substrates are discussed below in the section on surface-mount technology. Through-hole PWBs are categorized as:

- SINGLE-SIDED, WITH CIRCUITRY ON ONE SURFACE ONLY
- DOUBLE-SIDED, WITH CIRCUITRY PLACED ON BOTH SURFACES
- MULTILAYER, WITH CIRCUIT LAYERS ON BOTH EXTERNAL SURFACES AS WELL AS CONDUCTIVE PATHS WITHIN THE LAMINATE

The solder joint configuration for each case is shown in Fig. 8. Lands (and conductor lines) are constructed of copper foil bonded to the laminate; the foil thicknesses are typically 0.017 mm (0.0007 in.), 0.035 mm (0.0014 in.), or 0.071 mm (0.0028 in.) and are designated as 0.5 oz, 1 oz, and 2 oz, respectively. The surfaces of lands (and lines) can be built up with a combination of electroless and electroplated copper to a thickness that ranges from 0.013 to 0.076 mm (0.0005 to 0.0030 in.) to satisfy final thickness requirements and enhance solderability.

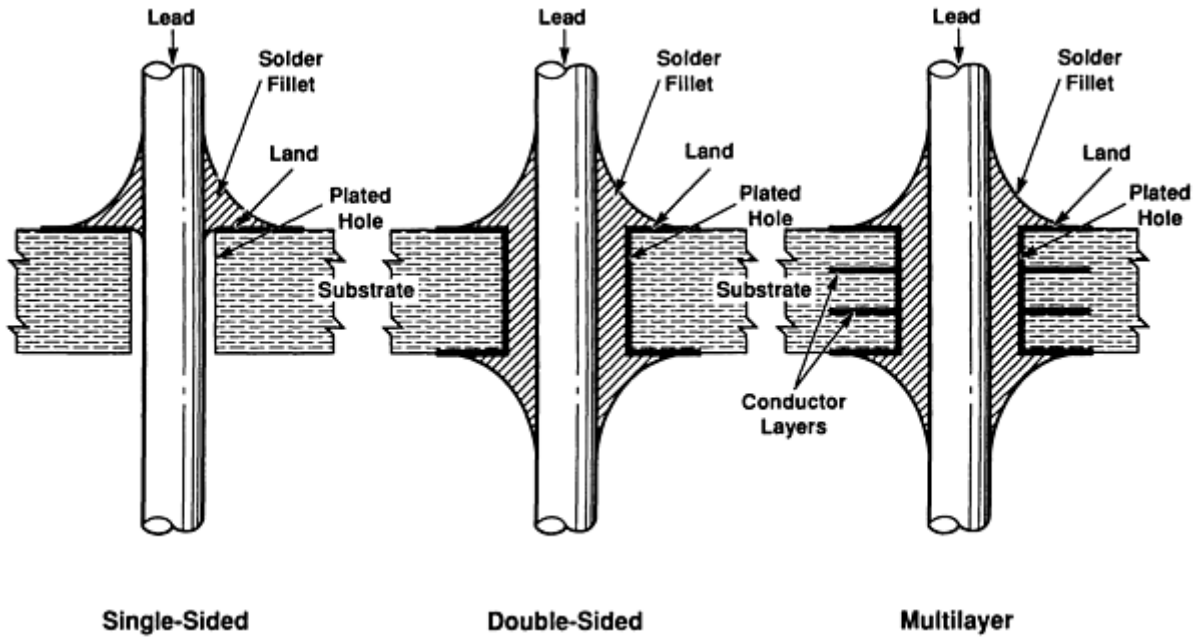

FIG. 8 SINGLE-SIDED, DOUBLE-SIDED, AND MULTILAYER SOLDER JOINT CONFIGURATIONS FOR THROUGH-HOLE TECHNOLOGY

Although the role of holes on single-sided circuitry is to mechanically secure the electronic devices, holes on double-sided and multilayer boards have an expanded role of providing electrical signal conduction between the two surfaces and internal layers. Holes used for interlayer signal transmission, but without a device lead, are termed "vias." The hole walls are deposited with copper to establish electrical conductivity and promote solder flow. The walls are coated with from 0.0003 to 0.0025 mm (0.0001 to 0.0001 in.) of electroless copper, followed by 0.025 to 0.076 mm (0.001 to 0.003 in.) of electroplated copper (Ref 23).

General guidelines for hole design are provided in Fig. 9. The hole size specified for a lead or wire should permit a gap of 0.15 to 0.20 mm (0.006 to 0.008 in.) to optimize the strength and capillary flow of the solder. Smaller gaps cause interference between the lead and hole, which can either damage the plating layer during insertion or generate voids caused by incomplete venting of flux gases produced during soldering. The recommended lead protrusion from the board underside is from 0.8 to 2.0 mm (0.03 to 0.07 in.). Values are kept small in order to minimize solder drainage from the fillet. The hole bonding land, or pad, should be round, and the outer diameter should be approximately three times the wire diameter. The annular width of the land should allow a lead height-to-pad width ratio of 1:1 for adequate fillet formation.

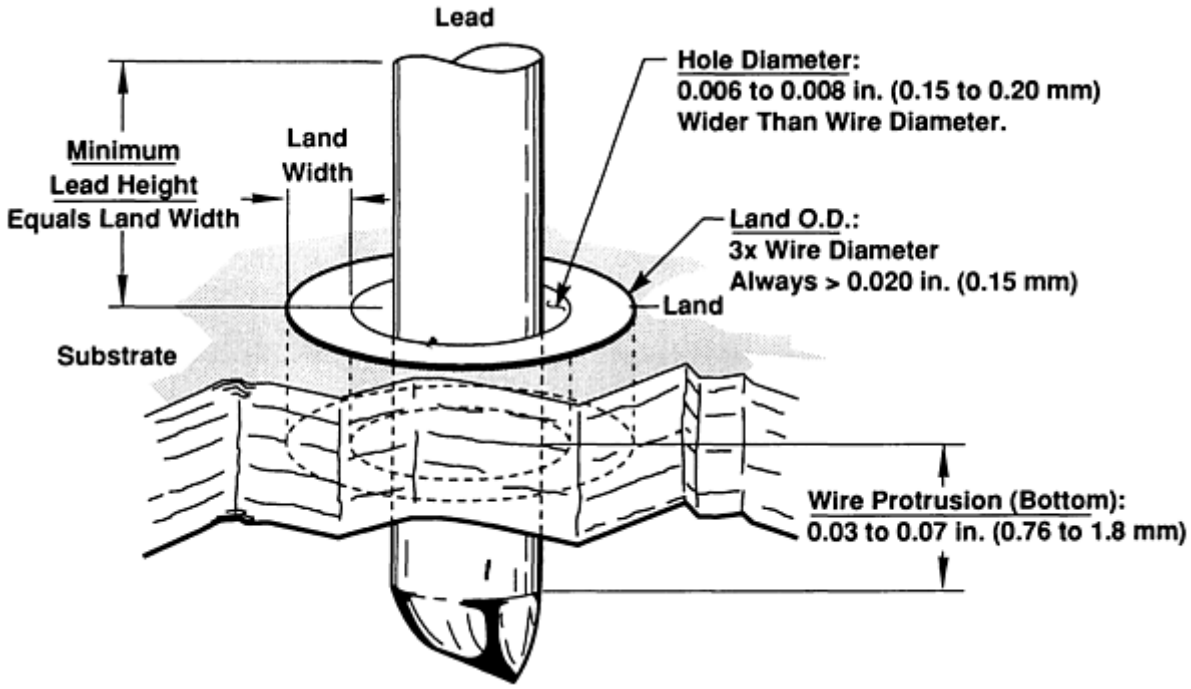

FIG. 9 GENERAL GUIDELINES FOR LEAD AND SUBSTRATE GEOMETRIES USED IN THROUGH-HOLE TECHNOLOGY

Loss of electrical continuity in the through-hole can arise from cracking (termed barrel cracking) of the hole plating layer because of the large CTE in the thickness dimension of the laminate (nearly a factor of 10 higher than in the laminate plane). This phenomena is particularly severe for via holes with large aspect ratios (the board thickness/hole diameter). Aspect ratios should be kept to a value smaller than 3 to ensure adequate reliability by typical assembly processes (Ref 24). The use of holes with larger aspect ratios requires additional attention to reliability.

Calculations have shown that the mechanical strength of the through-hole joint is limited primarily by PWB properties, specifically, the peel strength of the copper foil/laminate bond and the adhesion between the plating layer of the hole and the laminate (Ref 25). Similarly, the bond strength between the thick-film network and the ceramic substrate limits the strength of solder joints on hybrid microcircuits. Mechanical integrity can be lost through thermal fatigue. However, CTE mismatch between the device package and the PWB is not a principal source of thermal fatigue damage to through-hole solder joints, because the leads take up much of the displacement difference. Rather, thermal fatigue arises primarily from the difference between the lead CTE (for example, copper, at 9.4×10^{-6}/K, or 5.2×10^{-6}/°F) and the through-thickness thermal expansion value of PWB laminate (as much as 175×10^{-6}/K, or 98×10^{-6}/°F). Fatigue damage (Fig. 10) in through-hole solder joints is lessened by the CTE of the solder (25×10^{-6}/K, or 14×10^{-6}/°F), which is between those of the lead and PWB materials, as well as through proper assembly practices such as the incorporation of strain relief bends or loops placed in leads.

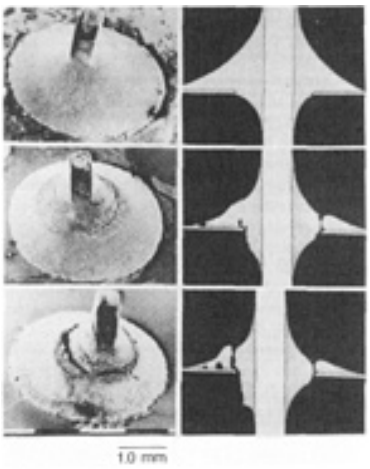

FIG. 10 PROGRESSION OF FATIGUE DAMAGE IN A THROUGH-HOLE SOLDER JOINT (OPTICAL MICROSCOPY AND SEM). SOURCE: REF 7

Plated-through holes are soldered from one side. Multilayer boards are more difficult to solder, because the interior conductor lines act as additional heat sinks that inhibit board heating. Solder assembly techniques for through-hole PWBs include hand soldering and larger-scale, automated processes such as dip, drag, or wave soldering. Solder pot working temperatures for the latter processes range from 240 to 260 °C (464 to 500 °F) for 63Sn-37Pb and 60Sn-40Pb solders. A good rule of thumb is to limit contact between the assembly and the molten solder to 3 to 10 s to minimize damage to the laminate and flux charring.

Heat damage to the attached device, neighboring components, and the substrate material must be considered when reworking through-hole solder joints. When a part is intended to be removed after assembly, it can be attached by hand soldering techniques with one of the lower melting temperature solders (Table 1). This technique is generally reserved for prototype assemblies; military and most commercial products specifications do not allow this operation.

Conformal coatings must be removed prior to reheating a solder joint. Clinched leads, that is, leads that are bent slightly on the opposite surface of the board to provide mechanical rigidity during assembly, hinder the removal of components. Generally, heat inputs will be greater when reworking a joint because the solder, lead, and land must be heated, which increases the likelihood of damage to the land/substrate bond or to the device. Cleanliness specifications must be followed after reworking to prevent functional failures caused by corrosion from flux residues.

The reliability of double-sided and multilayer circuit boards depends strongly on the plating quality of the hole walls. Water vapor and contaminants from the plating solutions can become entrapped in the deposited film. Plating layers should be free of embrittling contaminants that make them unable to adapt to board thermal expansion. The coating must have adequate thickness (and uniformity) so as not to be totally consumed by the metallurgical reaction with the solder. Contaminant materials vaporize at the soldering temperatures, causing cracks in the plating layer. Although plating cracks and voids, or delamination, do not necessarily jeopardize joint strength, they can interrupt electrical continuity between layers and surfaces.

A plated-through hole that is coated with a hot-dipped or plated-and-fused solder layer will have a very thin film of solder around its edge upon reflow. This phenomenon is a consequence of the surface physics of molten liquids. The limited protection offered by the thin solder film can cause nonwetting of the hole edge during assembly, in which case the joint is said to have a "weak knee." The effects of a weak knee on joint reliability are largely cosmetic for plated-through holes.

The traditional solders used in through-hole technology have been the tin-lead alloys. The solders with higher melting temperatures, such as tin-silver, tin-antimony, and lead-base tin-lead solders, have also been used in through-hole PWB systems designed for elevated-temperature service applications or step soldering processes. However, these solders are limited to specialized soldering assembly or those processes in which heat application is localized to the joint (for example, hot-air, hot-bar, fiber-optic infrared, or laser techniques), away from the electronic component. The higher heat inputs require that heat sinks be used on heat-sensitive devices. In addition, the higher reflow temperatures may

decompose the typical rosin-base fluxes. Synthetic-activated (SA) fluxes, which have activities comparable to those of RMA fluxes and water-soluble fluxes, can withstand the higher-temperature operations.

Surface-mount technology utilizes several types of assembly techniques. The technology generally refers to products that use conventional PWB assemblies, which include organic laminates, clad-metal substrates, as well as ceramic substrates for hybrid microcircuits. Although the architecture differs between organic laminates and hybrid substrates, the package configurations for electronic devices is similar. Surface-mount technology also includes chip (silicon)-on-board technologies (such as tape automated bonding, TAB), controlled collapse chip connection (C^4), or flip chip.

PWB Assemblies (Organic Laminate and Ceramic). Denser board populations and adaptability to fully automated assembly processes have increased the popularity of surface-mount technology. Figure 11 shows several leaded and leadless surface-mount packages. Lands on surface-mount PWBs are constructed with the same conduction layer material specifications used on boards with through-hole components:

- LAND THICKNESSES (COPPER) ARE BETWEEN 0.018 AND 0.071 MM (0.0007 AND 0.0028 IN.).
- PROTECTIVE FINISHES ON PWBS INCLUDE HOT-DIPPED SOLDER WITH HOT-AIR LEVELING OR ORGANIC COATINGS (INHIBITORS) ON BARE COPPER.
- THE CONTROL OF SOLDER THICKNESS ON HOT-AIR LEVELED LANDS IS CRITICAL WITH SURFACE-MOUNT PWBS.
- EXCESSIVE SOLDER QUANTITIES WILL INTERFERE WITH PART ALIGNMENT DURING PLACEMENT, DAMAGE FINE LEADS DURING AUTOMATED SETUP OF COMPONENTS ON THE BOARD, AND INCREASE THE LIKELIHOOD OF NONSYMMETRIC FILLETS ON DEVICES.
- NONSYMMETRIC FILLETS CAN LEAD TO MISALIGNMENT ("TOMBSTONING") OF DEVICES DURING AUTOMATED SOLDERING PROCESSES.

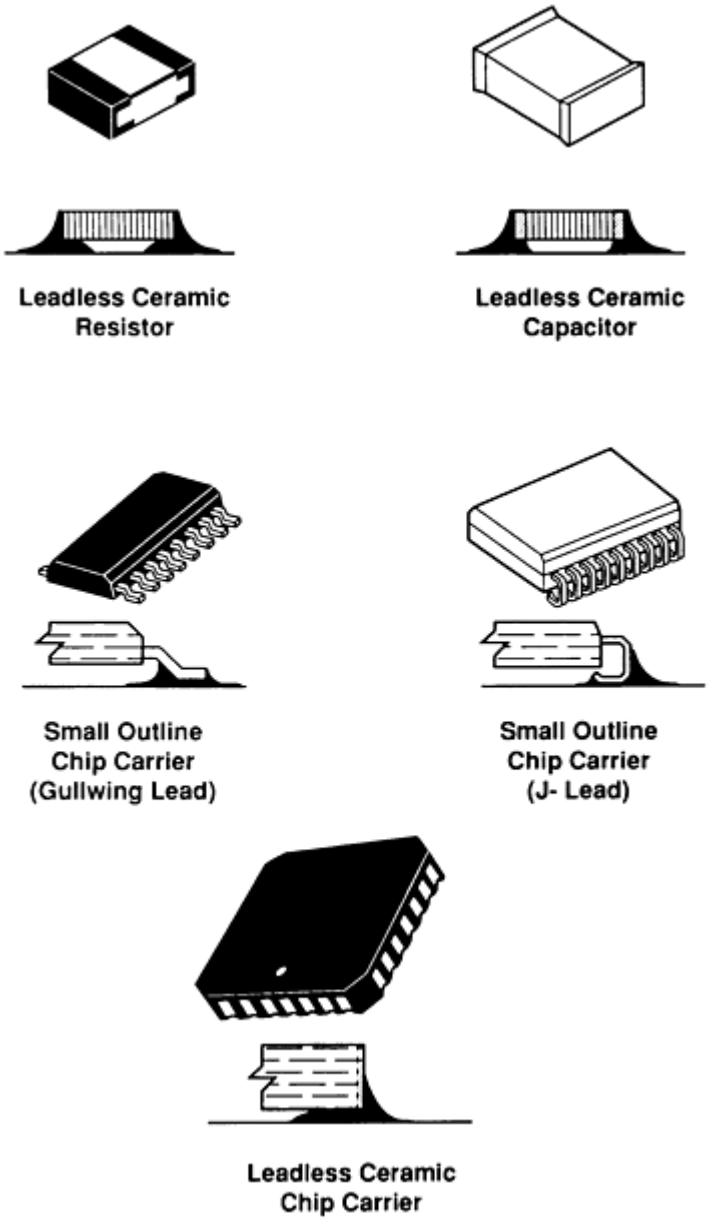

FIG. 11 PACKAGE AND LEAD CONFIGURATION OF SURFACE-MOUNT DEVICES, INCLUDING SOLDER JOINT PROFILES

A variety of land geometries are used in order to accommodate the range of package input/output (I/O) configurations. Holes, or vias, may be required on the PWB to permit signal transmission between the two external surfaces or between internal conductors of multilayer boards. In some cases, through-hole components are also found on the same PWBs. These assemblies are known as mixed technology. The quality of the plating layer in the hole is critical to system reliability, whether in vias for signal transmission or component holes for mixed technology applications.

Conductor lines and lands on ceramic boards are composed of one of the thick-film inks. The pattern is screen printed into the circuit configuration and fired to promote adhesion. Lines are usually formed from a single printed layer, with a thickness of approximately 0.01 mm (400 μin.). Lands to which soldering will take place may receive a second printing (double-printed), which improves solder joint reliability by reducing porosity in the film and limiting the dissolution of the conductive layer that is due to the formation of intermetallics between the solder and the precious metal. Double-printed layers are typically from 0.02 to 0.025 mm (0.0008 to 0.0010 in.) thick, depending on the porosity of the first layer.

Leadless surface-mount resistors and capacitors use terminations to form the solder interconnect. Terminations are regions on the package surface that are coated with a solderable layer to promote wetting by the solder. Leadless chip resistors and capacitors have a silver-bearing thick-film ink that is fired onto areas of the ceramic substrate; these areas are connected to the active electrical elements. Dissolution, or scavenging, of the thick film is reduced by adding more than 35% Pd to its composition (Ref 26). More commonly, the thick film is coated with a solderable nickel or copper finish to prevent the scavenging of silver by the solder. Candidate protective layers for the solderable finishes include electroplated tin or tin-lead and hot-dipped tin-lead solder.

Leadless ceramic packages for integrated circuits have multiple I/O terminations composed of metallized grooves on the package sides (castellation) and a metallized bonding area on the bottom of the package (blind lap joint). The metallized surfaces have a refractory layer (tungsten or molybdenum) that provides the electrical feedthrough to the interior. The refractory layer is then coated with a nickel solderable layer (1.3 to 8.9 μm, or 50 to 150 μin.). A protective layer of gold (1.3 to 2.5 μm, or 50 to 100 μin.) coats the nickel. The gold finish is removed by a hot-dipped solder coating step to prevent gold embrittlement of the solder joints. Gold embrittlement is of particular concern in surface-mount solder joints, because the limited amount of solder required to form the small joints can easily exceed the 4 wt% maximum Au content observed to degrade solder properties. Lower potential gold contents are preferred as a safety factor.

Leaded packages for surface-mount assembly have conductors fabricated from copper or one of the iron-base alloys and formed into the appropriate configuration (J-lead, gullwing, and others). A solderable layer of electroplated or electroless nickel, followed by a protective coating of electroplated gold, is deposited onto the iron-base alloy leads, per the recommended thicknesses (see the section "Base Materials, Finishes, and Storage/Corrosion Issues" in this article). The leads are hot dipped in tin-lead solder to remove the gold coating prior to assembly or to protect the copper solderable finish; however, tin or tin-lead electroplated coatings are preferred with fine-pitched leads and packages to eliminate the "crown" of solder on the lead. This crown causes the lead to deform and slide off of the similar crown of solder on the land when the part is placed on the PWB, causing component misalignment, solder joint distortion, or electrical failure.

The predominant solders used in surface-mount PWBs have been the tin-lead alloys. The tin-lead-silver solder (62.5Sn-36.1Pb-1.4Ag) has improved flow and a slightly improved isothermal fatigue life (for service conditions with limited temperature variations), when compared with the eutectic tin-lead alloy. The silver component of this solder improves creep strength. Silver-bearing solders also restrict the scavenging of silver from silver-bearing thick-film terminations on leadless ceramic devices that do not have a solderable (barrier) coating. A noneutectic tin-lead-silver alloy formed by the addition of 2% Ag, or the use of 60Sn-40Pb solder, will reduce the occurrence of solder wicking on leaded devices. Solder wicking is a phenomenon on leaded devices whereby the entire quantity of molten solder is drawn away from the pad to the lead because the lead heats up faster than the pad. This problem is particular to the vapor-phase reflow process and is compounded by leads that are noncoplanar with one another.

The noneutectic solders melt more slowly than eutectic alloys because they melt over a temperature range. This allows the lead and bonding pad surfaces to reach the same temperature, so that solder will simultaneously wet both surfaces. A longer melting sequence of the noneutectic alloys also decreases the incidence of "drawbridging," or "tombstoning," on leadless chip components (Fig. 12). A cause of drawbridging is the nonsimultaneous melting of the solder at the two terminations, causing the component to be drawn toward the molten joint by the surface tension of the solder. Other factors in drawbridging are paste tackiness, paste quantity, part location, and land design.

FIG. 12 DRAWBRIDGING OF A LEADLESS CERAMIC CHIP RESISTOR (OPTICAL MACROSCOPY). COURTESY OF SANDIA NATIONAL LABORATORIES

Other solders used for surface mounting include lead-indium alloys, which are used in hybrid microcircuit systems. The lead-indium solders limit the leaching of precious metals from thick-film networks and finishes on devices, and reduce the formation of brittle intermetallic compounds that jeopardize solder joint integrity. In addition, these alloys are more ductile than the tin-lead solders, thereby limiting the loads on the more-fragile thick-film/substrate ceramic bond. The low-temperature ductility of these solders provides a niche for them in cryogenic applications (for example, space vehicle electronics).

The low-melting-temperature tin-bismuth solders are used on PWBs with heat-sensitive devices or with those components that have to be removed and replaced on the board one or more times to satisfy testing or operational modes.

The high tin-silver solders are well suited for surface-mount assemblies because of their improved fatigue properties as compared to those of the tin-lead alloys. Their higher melting temperatures (96.5Sn-3.5Ag eutectic, 221 °C, or 430 °F) increase the service temperature window of assemblies, as well. It is critical that the finishes on substrate lands and device leads or terminations be compatible with the solder alloy. The mixture of different metals, which is due to nonsimilar pastes and finishes, can produce lower-melting-temperature phases that can deteriorate the physical and mechanical properties of the solder joints. For example, mixing bismuth-containing solders and lead finishes with tin-lead solder causes a low-melting-temperature tin-lead-bismuth phase that melts at 96 °C (205 °F).

The use of alternative solders implies solder joint cosmetics that are different from those of the tin-lead alloys. Cosmetics should not be relied upon to judge service performance. Typically, the tin-bismuth, lead-indium, and tin-silver solders have a grainy solder fillet. The fillets of lead-indium and tin-silver will be less concave than those of tin-lead, because of their higher surface tensions.

Typical fluxes used for surface-mount assembly are the rosin-base materials, usually the RMA forms. Water-soluble fluxes (organic acids) are being used increasingly in electronics, because of the variety of aqueous cleaning processes available to remove their residues. Although flux residue removal is determined by the reliability required of the assembly and flux activity, surface-mount technology requires additional attention to cleaning requirements and procedures. The high density of devices places conductors closer together, so that ionic residues are more likely to cause electrical shorts by the electromigration mechanism. In addition, flux residues can be easily entrapped in the 0.05 to 0.013 mm (0.002 to 0.005 in.) gap between the package and the substrate.

Surface-mount PWBs are manufactured by mass production techniques, such as vapor-phase reflow, heating in IR furnaces, or wave soldering. These processes, and numerous others, are described in separate articles in the Section "Joining Processes" in this Volume. Briefly, a typical assembly sequence for reflow techniques (that is, using vapor-phase or furnace processes) involves:

- DEPOSITING SOLDER PASTE ON THE SUBSTRATE LANDS BY EITHER SCREEN PRINTING, STENCIL PRINTING, OR BULK DISPENSING TECHNIQUES
- BAKING THE PASTE TO DRIVE OFF VOLATILES
- PLACING THE ELECTRONIC COMPONENTS ON THE PASTE DEPOSITS, OVER THE LANDS (MANUALLY OR WITH ROBOTICS)
- REFLOWING THE SOLDER
- CLEANING THE BOARDS OF FLUX RESIDUES, IF NECESSARY

The use of alternate solder alloys depends on their availability in paste form (with the optimum flux and flow properties). Preforms or wires of nontypical solders are more readily available. For vapor-phase reflow, working fluids that would accommodate solders with higher melting temperatures than tin-lead alloys may have limited availability. Infrared heating is more versatile in this regard. Damage to heat-sensitive components must be considered when higher-melting-temperature solders are used. Wave soldering utilizes a solder bath, which requires that an ingot form of the solder be available in order to fill the pot. Surface-mount parts are typically secured to the PWB with epoxies prior to being passed through the wave.

Some surface-mount PWBs are hand soldered. This technique is reserved for larger-pitch assemblies and runs of small quantities or for very high reliability electronic systems. It is also used as a means of repair and rework. For component placement, the conventional soldering iron tip has been replaced by hot bars or rectangles that conform to the various I/O configuration of surface-mount packages in order to simultaneously melt the solder in all joints. Heating rates should be

minimized on chip capacitors and resistors to prevent cracking of the ceramic chip or thick-film termination. Total heat input from the iron must not damage the land/substrate bond. An intermetallic layer formed between the copper land and molten tin-lead solder generally is not sufficient to restrict rework operations. However, solder removal that exposes the intermetallic layer to atmospheric oxidation can deteriorate solderability. Hand soldering processes may improve solder joint fatigue life by resulting in a finer solder microstructure, because of the fast cooling rate of joints after reflow (Ref 27). However, the fine microstructure coarsens with time and temperature, causing the strength advantage to be lost.

Solder joints for surface-mount technology fulfill electrical and mechanical attachment requirements. Adequate joint configurations have more than sufficient bonding strength to secure the device to the board. Shear tests (load application parallel to the board surface) are typically performed on leadless chip resistors and capacitors or on leadless ceramic packages to quantify the joint strength. Shear loads of chip resistors on polyimide-quartz PWBs are shown in Table 7 for as-fabricated, thermally cycled, and thermally shocked units (Ref 28). Leaded packages are more often tested in tension, that is, the load is applied perpendicular to the PWB surface.

TABLE 7 SHEAR STRENGTH OF SURFACE-MOUNT LEADLESS CERAMIC CHIP RESISTOR

TEST IDENTIFICATION	SHEAR STRENGTH	
	N	LBF
AS FABRICATED	84 ± 8	**19.0 ± 1.7**
300 THERMAL CYCLES	72 ± 6	**16.2 + 1.3**
100 THERMAL SHOCK CYCLES	**97 ± 4**	**21.9 ± 1.0**

Resistor dimensions, 2.67 × 1.27 × 0.457 mm (0.105 × 0.050 × 0.0018 in.); termination width, 0.25 mm (0.010 in.); thermal cycle, -55 to 125 °C (-67 to 257 °F), 120 min hold period, 6 °C/min (11 °F/min) ramp; thermal shock, -55 to 125 °C (-67 to 257 °F), 10 min hold period, liquid-to-liquid transfer; displacement rate, l0 mm/min (0.41 in./min).

Source: Sandia National Laboratories

A particular concern with surface-mount solder joints is thermal fatigue damage caused by the coefficient of thermal expansion (CTE) mismatch between the PWB laminate and the device package. Figure 13 shows scanning electron micrographs (SEM) of fatigue cracks on several different device packages. Thermal fatigue damage is of greater concern on leadless packages than on leaded configurations, because the latter can accommodate some of the displacement mismatch through the leads. For leadless packages (resistors, capacitors, or chip carriers), cracks begin under the package, as shown in Fig. 13(e), and grow toward the outer surface. Thus, cracks are well established prior to being visually detected on the fillet surface.

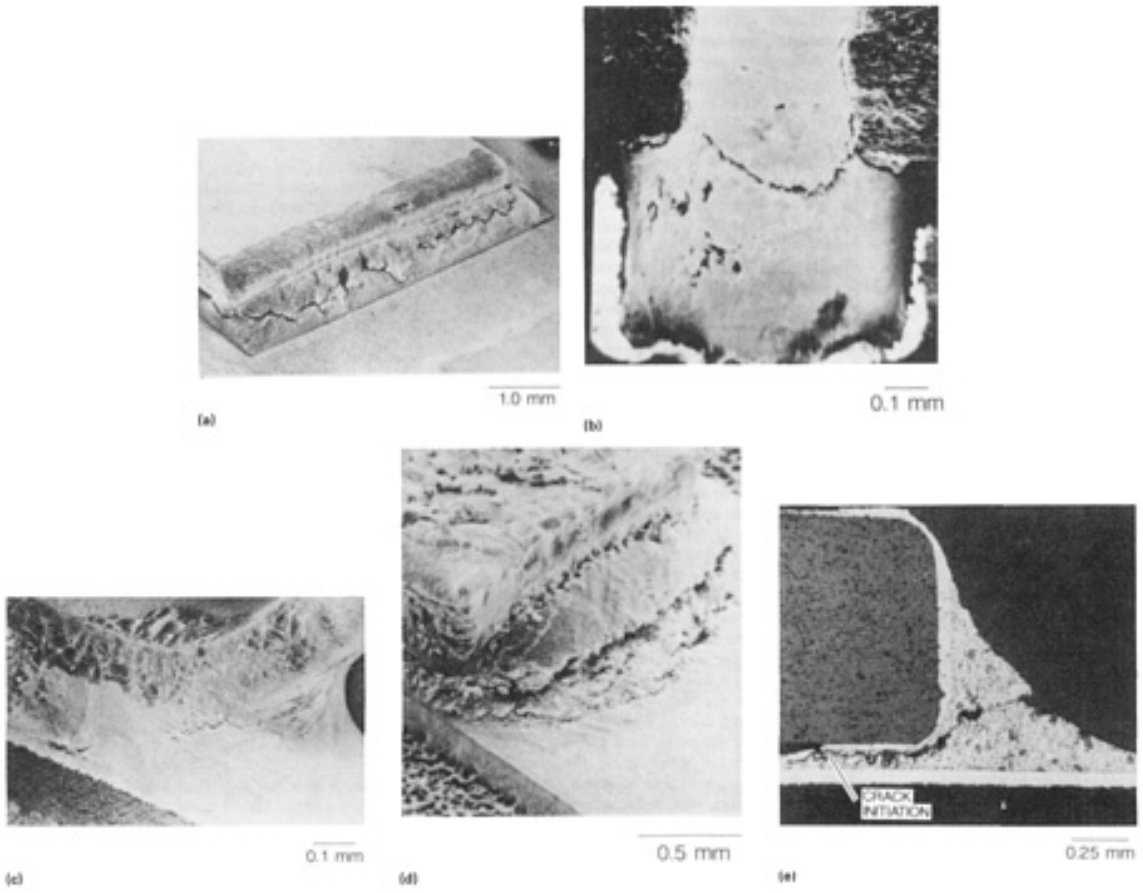

FIG. 13 FATIGUE CRACKS IN SURFACE-MOUNT SOLDER JOINTS. (A) LEADLESS CAPACITOR. (B) LEADLESS CERAMIC CHIP CARRIER. (C) J-LEADED PACKAGE. (D) GULLWING LEADED PACKAGE (SEM). (E) CRACKING IN A LEADLESS CERAMIC CHIP RESISTOR SOLDER FILLET. SOURCE: REF 7

Fatigue deformation that occurs under variable temperature conditions greatly complicates the prediction of solder joint failures. However, the thermal fatigue life of surface-mount solder joints can be estimated from isothermal fatigue test data when the microstructural damage is not strongly temperature dependent. Isothermal fatigue tests on surface-mount and leadless ceramic chip carrier 60Sn-40Pb solder joints at 35 °C (95 °F) and 125 °C (257 °F) show similar behavior. Tests at -55 °C (-67 °F) suggest a longer fatigue life, when compared with data from the higher-temperature tests (Ref 29). Therefore, isothermal fatigue test data on 60Sn-40Pb, taken at 35 °C (95 °F), can be used to estimate thermal fatigue performance over the temperature range from -25 to 125 °C (-77 to 257 °F).

The thermal fatigue life for eutectic and near-eutectic tin-lead solders can be predicted with the aid of Fig. 14. The configuration of the solder joint being tested (leadless ceramic chip resistor) is shown in Fig. 14(a). Let α_1 and α_2 be the CTEs of the package and PWB, respectively. ΔT is the absolute temperature range. The extension (or contraction) difference between the package and PWBs, Δx, is given as:

$$\Delta X = (\alpha_1 - \alpha_2)\, \Delta T L \qquad \textbf{(EQ 1)}$$

where L is the maximum separation between the solder joints, given the conservative assumption that all damage occurs to one joint.

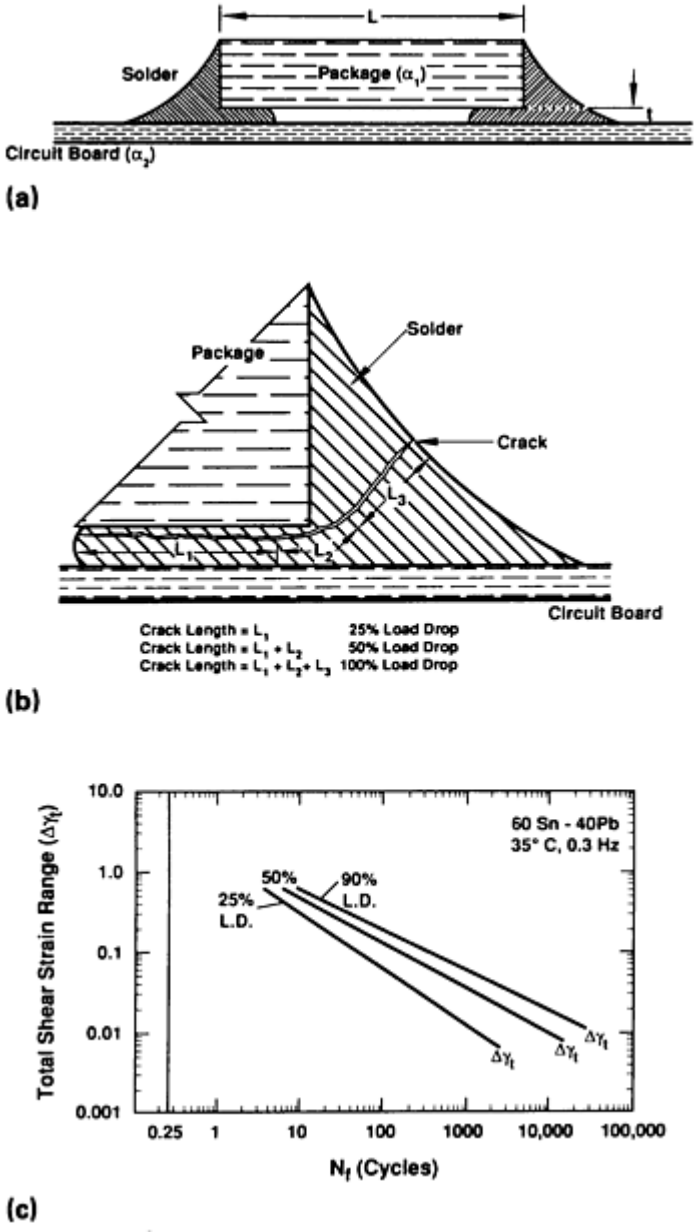

FIG. 14 ISOTHERMAL FATIGUE LIFE CALCULATION FOR THERMAL FATIGUE RESISTANCE APPROXIMATION. (A) PACKAGE/SOLDER JOINT GEOMETRY. L IS THE PACKAGE SIZE (DISTANCE BETWEEN SOLDER JOINTS), α_1 IS THE THERMAL EXPANSION COEFFICIENT, AND T IS THE SOLDER JOINT GAP. (B) FATIGUE LIFE VERSUS TOTAL SHEAR STRAIN RANGE PER LOAD DROP CRITERIA. (C) FATIGUE CRACK GROWTH CORRESPONDING TO PERCENT LOAD DROP CRITERIA FOR FATIGUE LIFE. SOURCE: REF 29, 30, AND 31

Equipartition of strain between the two joints requires the use of (L/2) in place of L. The total shear strain rate, $\Delta\gamma_t$, is:

$$\Delta g_t = \frac{\Delta x}{t} \qquad \textbf{(EQ 2)}$$

where t is the solder joint gap. For the crack extension (and associated load drop) depicted in Fig. 14(b), the value of $\Delta\gamma_t$ is found on the ordinate of Fig. 14(c), and the number of cycles to failure, N_f, is determined for each of the three failure criteria. The computed fatigue life is an approximation, that is, its accuracy is an order of magnitude. An in-depth treatment of the solder joint reliability issue is provided in Ref 32.

The data presented in Fig. 14(c) pertain to a cycle period of 3.3 s and are suitable for calculations of cycle times up to 1000 s (Ref 31). Periods in excess of 10,000 s/cycle cause the analysis described above to *overestimate* the fatigue life by nearly an order of magnitude.

Thermal fatigue life can be lengthened by matching the CTE of the substrate to that of the package material (note Table 6). Fatigue resistance is improved by increasing the standoff distance between the component and the substrate (that is, increase the value of *t*). Other techniques include the use of nonmelting balls in the solder paste or protrusions on the bonding surface of the package, both of which act as spacers to control the gap. In addition, it has been shown that fatigue life increases as the solder joint cooling rate is increased (Ref 33). The cooling rate can be controlled on automated assembly equipment such as IR furnaces and some vapor-phase units. However, thermal shock to the electronic devices and the substrate must be considered when increasing the cooling rate. Fast cooling rates are an inherent feature of localized heating techniques, such as hand soldering with an iron, hot gas or hot bar techniques, and laser soldering. However, room-temperature aging of the solder may counteract any fatigue life improvement.

Tape automated bonding (TAB) refers to bonding the silicon integrated circuit (IC) chip to a metal lead frame that, in turn, is soldered to the PWB. This technique is shown in Fig. 15. The Au_xSn_{1-x} solder inner lead bond, which attaches the silicon chip to the lead frame, is formed by the intermixing of gold and tin diffusing from corresponding metallizations deposited on the chip and lead, respectively, under elevated temperature and pressure. The outer lead bond, which attaches the silicon chip plus lead frame to the circuit substrate, is a tin-lead solder joint formed by one of the conventional assembly processes. A lead exists for each of the I/Os on the silicon chip. The thermal fatigue of solder joints is reduced by the lead, which takes up the thermal strain mismatch between the silicon IC and the substrate. Additional compliance is added to the lead by jogs or bends in the geometry.

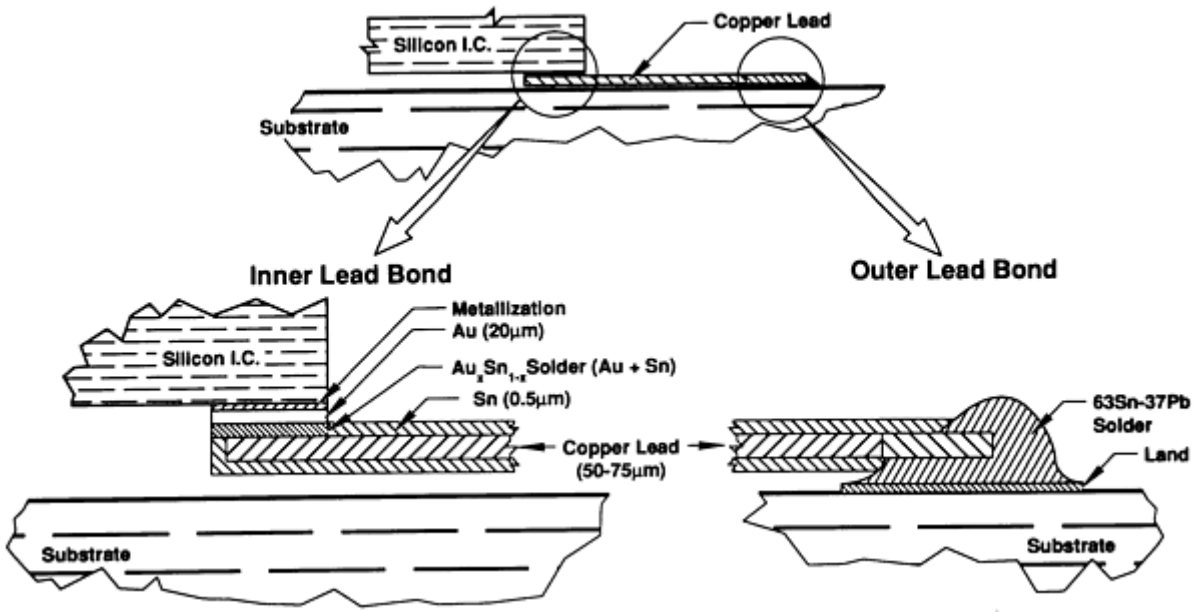

FIG. 15 TAPE AUTOMATED BONDING OF A SILICON CHIP TO THE SUBSTRATE

Controlled collapse chip connection (C^4) describes the process whereby the silicon IC chip is bonded directly to a ceramic substrate by small solder bumps that also serve as the signal I/O path (Fig. 16). This technique is widely used in computer assembly technology. The solderable surface on the silicon is a vacuum-deposited copper layer. A vacuum-deposited chromium film promotes adhesion of the copper to the SiO_2 layer. A gold layer (also vacuum-deposited) is the final protective finish. The ceramic substrate can be single-layered or multilayered.

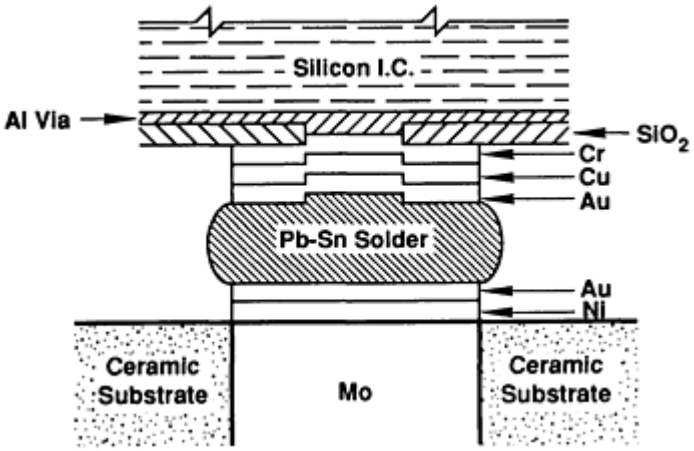

FIG. 16 SOLDER "BUMP" JOINT USED IN CONTROLLED COLLAPSE CHIP CONNECTION

When working with solder bumps to molybdenum vias, the molybdenum is coated with vacuum-deposited nickel and gold films, where nickel is the solderable surface and gold is the protective finish. The solder can be one of the lead-rich, tin-lead alloys (90Pb-10Sn or 95Pb-5Sn) or a lead-indium alloy (50In-50Pb). The lead-tin alloys are suited for assemblies that will later be processed with eutectic tin-lead soldering. The solder films are vacuum deposited onto the silicon chip in thicknesses ranging from 0.100 to 0.123 mm (0.004 to 0.005 in.). The units are passed through a belt furnace under a protective atmosphere to melt the solder.

The solder joints of C^4 interconnects must accommodate the thermal strain mismatch between the silicon IC and the substrate. Fatigue damage is reduced by maximizing and controlling uniformity of the silicon IC chip standoff distance above the substrate (hence the term, controlled collapse), limitation of the chip size, and the use of substrates with CTEs similar to that of silicon.

Connector Technology. In the signal analysis of an electronic product, the backplane forms the hub through which PWBs "talk" with one another and receive electrical power to operate devices mounted on them. As a result, the physical requirements placed on the backplane construction cause it to be a unique PWB. The backplane must mechanically support numerous PWBs and connector-cable assemblies that are frequently removed and reinserted in addition to heavier devices such as large capacitors or transformers. Therefore, the backplane is typically much thicker (2.4 to 3.2 mm, or 0.093 to 0.125 in.) than conventional PWBs (Ref 34). As the hub of electrical signal transmission, the backplane is often multilayered with thick conductor lines (0.071 to 2.8 mm, or 0.0028 to 0.11 in.), depending on the power transmission requirements of the system. Connector pins may be soldered on the substrate using preforms and vapor-phase assembly or manual processes. The thicker laminate and conductors as well as the multilayer construction can be a formidable heat sink to soldering processes in addition to being susceptible to warpage by overheating or inadequate support. Connector pins may also be press fit onto the substrate.

Signal transmission between devices that are not electrically connected via the PWB, between PWBs themselves, or between PWBs and the backplane, require the use of wires, cables, and connectors. Connectors are manufactured using attachment modes of soldering or a combination of soldering and mechanical fastening techniques. Examples of various connector techniques and design guidelines are shown in Fig. 17. The solder joints in connectors must be mechanically robust to accommodate loads caused by rigid, unyielding cables, as well as their frequent disconnection and reinstallation.

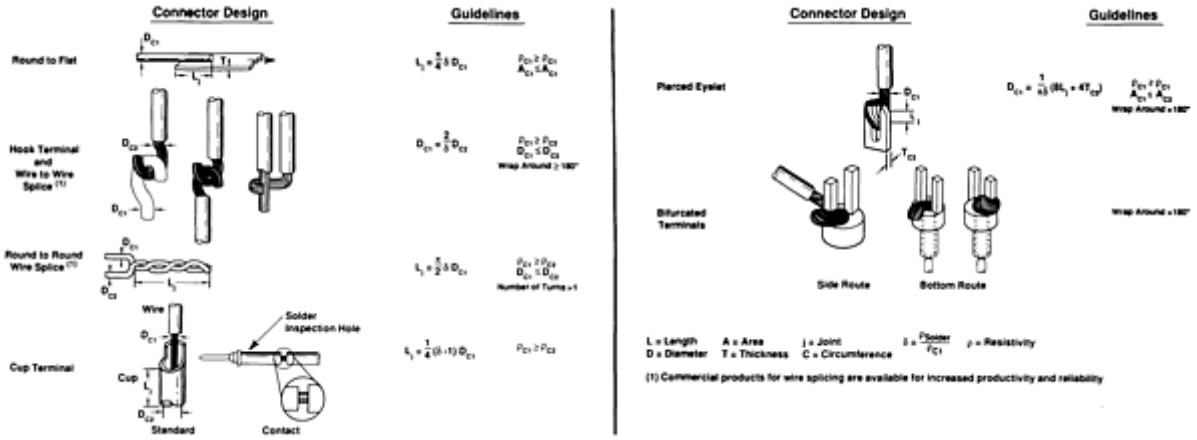

FIG. 17 CONNECTOR METHODOLOGIES

Base materials for connectors, wires, and cable conductors include copper alloys (for example, oxygen-free, high-conductivity copper and electrolytic pitch-grade copper, brass, beryllium copper, and others), iron-base alloys (Kovar, stainless steel, and others), and aluminum alloys. Preparation of the base metal and selection of solderable and protective finishes for solder attachment are described in the section "Base Materials, Finishes, and Storage/Corrosion Issues" in this article. Because connector assemblies typically use larger quantities of solder to form the joint, the electroplated gold that serves as the protective layer may not have to be removed by a hot-dipped solder coating prior to assembly. The solder joint may have a frosty appearance, because of the dissolved gold in the solder. However, a hot-dipped coating should be applied if the thickness of gold electroplating and the estimated quantity of solder used in the joint indicate a dissolved gold content in the solder that will potentially exceed the 4 wt% limit, which causes embrittlement in tin-lead solder joints.

Pins, which are part of a plug-and-socket connection, can be gold plated with so-called "hard coatings," that is, the gold electroplate contains approximately 0.3 wt% cobalt or nickel to improve abrasion resistance during removal and installation cycles of the connector. However, the cobalt or nickel additions can cause the solderability of the pin to be poor.

Silver coatings are preferred on some connector parts in order to lower contact resistance. Unfortunately, silver is tarnished by the formation of sulfides from airborne sulfur compounds, which also deteriorate solderability. For grounding applications, soldering processes to aluminum connector housings should be followed with an electroplated coating of zinc or cadmium to guarantee adequate corrosion resistance.

Solders used in connector assemblies are generally tin-lead alloys. Additional strength, particularly for products exposed to elevated temperatures or mechanical loads, is obtained with the tin-silver and tin-antimony solders. The higher melting temperatures, coupled with the generally massive structure of connectors (when compared with electrical components), requires greater heat input into the assembly for proper joint fabrication. Joining can be facilitated by first hot dipping the mating substrates in the particular solder prior to final assembly. The use of preforms can facilitate the introduction of solder into joints, particularly those of very small assemblies.

The preferred fluxes for connectors are the rosin-base materials. Residues from pure rosin need not be removed. Mildly activated (RMA) flux residues are removed for high-reliability applications. Residues of more-active fluxes (RA, SA, or water soluble) must be removed. Hand soldering with low-solids fluxes in air can give inconsistent solderability because only very thin layers of tarnish can be removed by the flux. The higher heat inputs required for connector structures can degrade rosin-base fluxes, necessitating the use of water-soluble and synthetic fluxes that will tolerate the higher working temperatures. In either case, the residues must be removed, because they are corrosive.

Connectors are typically assembled by localized heating, such as by soldering iron, hot gas jet, or hot bar techniques. The use of automated assembly processes that exploit vapor-phase reflow or IR furnaces is prohibited in order to prevent the exposure of heat-sensitive structural materials in the connector to elevated temperatures. Moreover, the generally cumbersome assemblies are not well suited for batch or continuous processes.

References cited in this section

1. R. PRASAD, *SURFACE MOUNT TECHNOLOGY, PRINCIPLE AND PRACTICE,* VAN NOSTRAND-RHEINHOLD, 1989, P 363
7. R. KLEIN-WASSINK, *SOLDERING IN ELECTRONICS,* 2ND ED., ELECTROCHEM. PUB., LTD, 1989, P 548
22. H. MANKO, *SOLDERS AND SOLDERING,* MCGRAW-HILL, 1979, P 96
23. R. BAHN, PLATING, *PRINTED CIRCUIT HANDBOOK,* C. COOMBS, ED., MCGRAW-HILL, 1979, P 7-1
24. R. PRASAD, *SURFACE MOUNT TECHNOLOGY, PRINCIPLE AND PRACTICE,* VAN NOSTRAND-RHEINHOLD, 1989, P 158
25. H. MANKO, *SOLDERING HANDBOOK FOR PRINTED CIRCUITS AND SURFACE MOUNTING,* VAN NOSTRAND-RHEINHOLD, 1986, P 23
26. R. KLEIN-WASSINK, NOTES ON THE EFFECTS OF METALLIZATION OF SURFACE MOUNTED COMPONENTS ON SOLDERING, *HYBRID MICROCIR.,* MAY 1987, P 89
27. R. WILD, SOME FACTORS AFFECTING LEADLESS CHIP CARRIER SOLDER JOINT FATIGUE LIFE, *PROC. 12TH ELECTRON. MFG. SEMINAR* (CHINA LAKE, CA), NAVAL WEAPONS CENTER, 1988, P 275
28. P. VIANCO AND J. DAL PORTO, AN EVALUATION OF THE BLIND LAP JOINT FOR THE SURFACE MOUNT ATTACHMENT OF CHIP COMPONENTS, *PROC. SURF. MOUNT INTER.,* TO BE PUBLISHED, 1992
29. H. SOLOMON, "INFLUENCE OF TEMPERATURE ON THE LOW CYCLE FATIGUE OF SURFACE MOUNTED CHIP CARRIER/PRINTED WIRING BOARD JOINTS," TECHNICAL INFORMATION SERIES, GENERAL ELECTRIC CRD, 1987
30. H. SOLOMON *ET AL.,* "PREDICTION OF SOLDER JOINT FATIGUE LIFE," TECHNICAL INFORMATION SERIES, GENERAL ELECTRIC CRD, 1988
31. H. SOLOMON, "FATIGUE OF 60/40 SOLDER," TECHNICAL INFORMATION SERIES, GENERAL ELECTRIC CRD, 1986
32. W. ENGELMAIER, PERFORMANCE CONSIDERATIONS: THERMAL-MECHANICAL EFFECTS, *PACKAGING,* VOL 1, *ELECTRONIC MATERIALS HANDBOOK,* ASM, 1989
33. D. KINSER *ET AL.,* RELIABILITY OF SOLDERED JOINTS IN THERMAL CYCLING ENVIRONMENTS, *PROC. NEPCON,* MAY 1976, P 61
34. P. VIANCO, AN OVERVIEW OF THE MENISCOMETER/WETTING BALANCE TECHNIQUE FOR WETTABILITY MEASUREMENTS, *THE METAL SCIENCE OF JOINING,* M. CIESLAK *ET AL.,* ED., TMS, 1992, P 265

Paul T. Vianco, Sandia National Laboratories

Solderability Testing in Electronics Applications

The formation of a solder joint that provides the necessary mechanical, electrical, and thermal properties for the particular device requires that all joint surfaces be wettable by the molten solder and that, upon solidification, a uniform solder film is retained. Solderability must be tightly controlled. Increased device functionality has placed greater demands on the performance of *each* solder joint. Full-scale manufacturing processes of PWBs, which can contain thousands of solder joints, make inspection and rework economically unfeasible.

The purpose of solderability testing is to quantitatively assess the wetting performance of component leads or terminations, as well as lands and holes of substrates, to ensure proper wetting performance by the solder at the time of PWB assembly. The goal is to prevent the expensive repair of solder joint defects on the assembled hardware and the operational failure of the device or entire electronic system. Solderability testing is typically performed on a lot sample with acceptance or rejection criteria that are based on the tested attribute(s).

Solderability tests, as well as lot sampling procedures and acceptance/rejection statistics, are specified by military and industrial specifications. Those specifications that control test procedures and acceptability criteria are listed in Table 8. The two predominant solderability tests are the dip-and-look evaluation and the wetting balance test.

TABLE 8 GUIDELINES AND SPECIFICATIONS FOR SOLDERABILITY TESTING OF ELECTRONICS APPLICATIONS

DOCUMENT	SUMMARY DESCRIPTION
MIL-STD-202F, METHOD 208F, SOLDERABILITY	**STRAND AND SOLID WIRES, LUGS, TABS, HOOK LEADS, AND SO ON, EVALUATED DIP-AND-LOOK TEST; INCLUDES STEAM AGING PROCEDURES**
MIL-STD-750C, METHOD 2026.5, SOLDERABILITY	**ELECTRONIC DEVICES EVALUATED BY DIP-AND-LOOK TEST PER MIL-STD-202F**
MIL-STD-883C, METHOD 2022.2, WETTING BALANCE SOLDERABILITY	**RIBBON LEADS EVALUATED BY THE WETTING BALANCE TEST; INCLUDES STEAM AGING PROCEDURES**
MIL-P-55110, GENERAL SPECIFICATION FOR PRINTED WIRING BOARDS	**INCLUDES SOLDERABILITY EVALUATION FOR RIGID PRINTED WIRING BOARDS**
MIL-P-50884C, PRINTED WIRING, FLEXIBLE AND RIGID-FLEX	**SOLDERABILITY EVALUATION OF FLEXIBLE AND RIGID-FLEX PRINTED WIRING BOARDS**
MIL-STD-883C, METHOD 5005.11, QUALIFICATION AND QUALITY CONFORMANCE PROCEDURES	**QUALITY CONFORMANCE AND CRITERIA FOR INSPECTION OF MICROELECTRONICS COMPONENTS USING INSPECTION TESTS (INCLUDING SOLDERABILITY TESTS)**
M1L-STD-150D, SAMPLING PROCEDURES AND TABLES FOR INSPECTION BY ATTRIBUTES	**SAMPLING PROCEDURES AND STATISTICS FOR ACCEPTANCE/REJECTION OF PARTS INSPECTED BY ATTRIBUTES (FOR EXAMPLE, SOLDERABILITY TESTING)**
MIL-STD-2000A, STANDARD REQUIREMENTS FOR SOLDERED ELECTRICAL AND ELECTRONIC ASSEMBLIES	**SPECIFIES SOLDERABILITY TESTS PER MIL-STD-202 AND CRITERIA FOR MAINTAINING SOLDERABILITY**
IPC-TM-650, TEST METHODS MANUAL	**SOLDERABILITY OF PRINTED WIRING BOARDS AND DIP-AND-LOOK PROCEDURE, AS WELL AS WAVE SOLDERING EVALUATION**
IPC-S-804, SOLDERABILITY TEST METHODS FOR PRINTED WIRING BOARDS	**SOLDERABILITY OF PRINTED WIRING BOARDS; EDGE DIP TEST ROTARY DIP TEST, WAVE SOLDERING TEST, THROUGH-HOLE SOLDER RISE TIME TEST; DIP-AND-LOOK TESTS**
IPC-S-805, SOLDERABILITY TESTS FOR COMPONENT LEADS AND TERMINATIONS	**SOLDERABILITY TESTS: DIP-AND-LOOK, WETTING BALANCE, AND GLOBULE TEST FOR COMPONENT LEADS AND TERMINATIONS; INCLUDES STEAM AGING PROCEDURES**
IPC-AJ-820, ASSEMBLY-JOINING HANDBOOK	**NO. 8.2.3, PROCEDURES FOR ACCELERATED AGING (IN CONJUNCTION WITH SOLDERABILITY TESTING)**
IPC-A-600C, GUIDELINES FOR	**INSPECTION CRITERIA FOR QUALITY ASSURANCE**

The dip-and-look test (for example, MIL-STD-883D, Method 2003.7) assesses the uniformity of the solder film that remains on a lead or termination after immersion in a solder pot. Shown in Fig. 18 are optical micrographs of samples demonstrating the three primary categories of wettability.

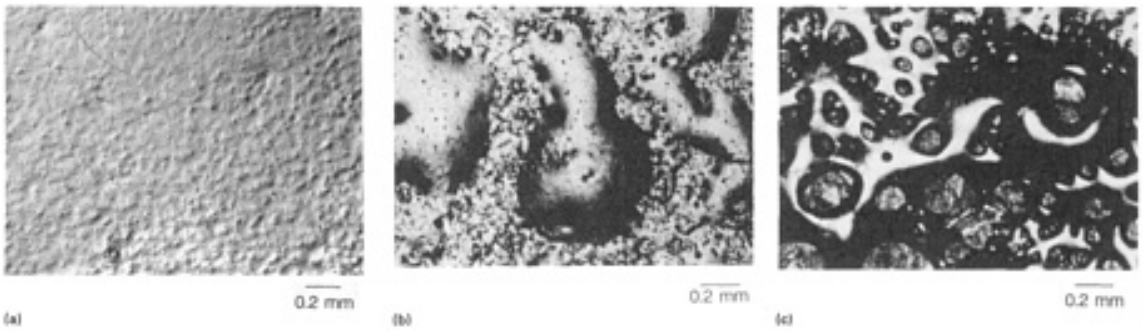

FIG. 18 OPTICAL MICROGRAPHS OF 60SN-40PB SOLDER ON SAMPLE SURFACES. (A) WETTING. (B) DEWETTING. (C) NONWETTING. SOURCE: SANDIA NATIONAL LABORATORIES

A less-subjective test is the wetting balance test (for example, MIL-STD-883C, Method 2022.2), in which a representative sample is attached to a force balance. The meniscus formed on the lead or termination causes a weight increase, which is detected by the balance. The typical wetting curve (force versus time) is shown in Fig. 19. The acceptability criteria of this test (by MIL-STD-883c), are the time for the trace to cross the zero line after the initial dip and the time required for the wetting force to reach two-thirds of its maximum. These parameters are also shown in Fig. 19. Variations to the wetting balance test procedure have been implemented to accommodate the wetting of terminations on leadless surface-mount devices. The wetting balance test should be accompanied by the dip-and-look procedure to verify the quality of the solder film. The wetting balance will *not* always detect dewetting of a solder film (Ref 34).

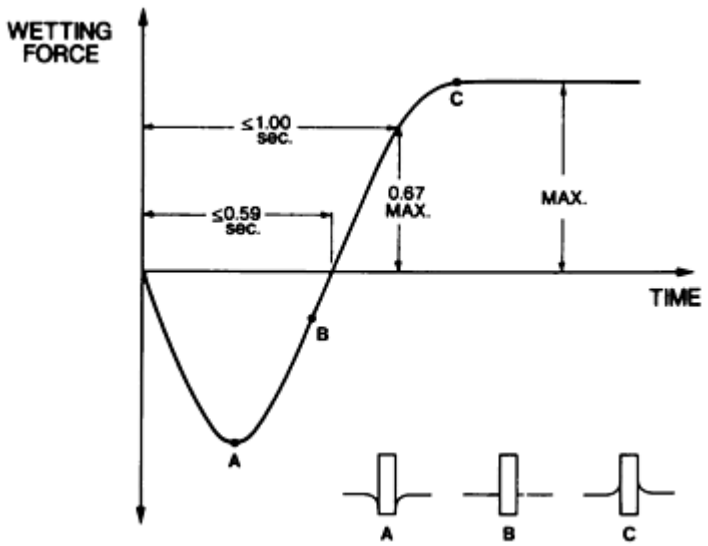

FIG. 19 WETTING BALANCE TRACE FOR SOLDERABILITY TESTS AND ACCEPTANCE CRITERIA PER MIL-STD-883C

Solderability tests for PWBs are typically dip-and-look tests, such as those specified in IPC-S-804 (J-STD-003) or the military specifications MIL-P-55110 and MIL-P-50804. Another test is the globule test, which measures the time for a solder globule to surround a horizontal wire or fill a hole (IPC-S-805).

The solderability of devices (and PWBs) deteriorates with time in storage. The tests noted above ensure adequate solderability within 120 days of the evaluation (MIL-STD-2000A). For longer periods, the steam aging treatment was instituted for the purpose of screening, on a lot sample basis, the leads, terminations, and other elements that would not be likely to retain adequate solderability under typical storage conditions prior to assembly. Steam aging (8.0 ± 0.5 h), followed by a successful solderability test, will indicate surfaces that can maintain adequate solderability for two years of "typical" storage conditions prior to use at the assembly level (MIL-STD-2000). Preferred storage conditions (see MIL-STD-2000; atmosphere, temperature, and humidity) can extend the storage time to 3 y. Parts that have exceeded the recommended storage life are considered to have questionable solderability and should be retested prior to use in an assembled product.

Reference cited in this section

34. P. VIANCO, AN OVERVIEW OF THE MENISCOMETER/WETTING BALANCE TECHNIQUE FOR WETTABILITY MEASUREMENTS, *THE METAL SCIENCE OF JOINING*, M. CIESLAK *ET AL.*, ED., TMS, 1992, P 265

Paul T. Vianco, Sandia National Laboratories

References

1. R. PRASAD, *SURFACE MOUNT TECHNOLOGY, PRINCIPLE AND PRACTICE,* VAN NOSTRAND-RHEINHOLD, 1989, P 363
2. V. MARCOTTE, C^4 FLIP CHIP JOINING, *THE METAL SCIENCE OF JOINING*, M. CIESLAK *ET AL.*, ED., TMS, 1992, P 315
3. C. LEA, A SCIENTIFIC GUIDE TO SURFACE MOUNT TECHNOLOGY, ELECTROCHEM. PUB., LTD, 1988, P 169
4. R. GEHMAN, DENDRITIC GROWTH EVALUATION OF SOLDERED THICK FILMS, *INT. J. HYBRID MICROELEC.*, VOL 6, 1983, P 239
5. H. MANKO, *SOLDERS AND SOLDERING,* MCGRAW-HILL, 1979, P 112
6. L. GOLDMANN *ET AL.*, LEAD-INDIUM FOR CONTROLLED-COLLAPSE CHIP JOINING, *PROC. 27TH ELECTRON. COMP. CONF.*, 1977, P 25
7. R. KLEIN-WASSINK, *SOLDERING IN ELECTRONICS,* 2ND ED., ELECTROCHEM. PUB., LTD, 1989, P 548
8. R. KLEIN-WASSINK, *SOLDERING IN ELECTRONICS,* 2ND ED., ELECTROCHEM. PUB., LTD, 1989, P 557
9. J. LEE, SOLDER PASTE DISPENSING MATERIALS AND REQUIREMENTS, *ELECTRON. PACK. AND PROD.*, NOV 1990, P 22
10. H. MANKO, *SOLDERING HANDBOOK FOR PRINTED CIRCUITS AND SURFACE MOUNTING,* VAN NOSTRAND-RHEINHOLD, 1986, P 286
11. D. LOVERING, ROSIN ACIDS REACT TO FORM TAN RESIDUES, *ELECTRON. PACK. AND PROD.*, FEB 1985, P 232
12. D. KOCKA, NO-CLEAN FLUXES ARE A VIABLE ALTERNATIVE TO CFC CLEANING, *ELECTRON. PACK. AND PROD.*, JUNE 1990, P 95

13. P. VIANCO AND J. DAL PORTO, "EMBRITTLEMENT OF SURFACE MOUNT TRANSISTOR SOLDER JOINTS INVOLVING PRETINNED LEADS," INTERNATIONAL BRAZING AND SOLDERING CONFERENCE (DETROIT, MI), AWS, 1991
14. D. UNSWORTH AND C. MACKAY, A PRELIMINARY REPORT ON GROWTH OF COMPOUND LAYERS ON VARIOUS METAL BASES PLATED WITH TIN AND ITS ALLOYS, *TRANS. INST. MET.,* VOL 51, 1973, P 85
15. P. KAY AND C. MACKAY, THE GROWTH OF INTERMETALLIC COMPOUNDS ON COMMON BASIS MATERIALS COATED WITH TIN AND TIN-LEAD ALLOYS, *TRANS. INST. MET.,* VOL 54, 1976, P 68
16. P. VIANCO *ET AL.,* SOLDERABILITY TESTING OF KOVAR WITH 60SN-40PB SOLDER AND ORGANIC FLUXES, *WELD. J.,* JUNE 1990, P 230-S
17. C. LEA, *A SCIENTIFIC GUIDE TO SURFACE MOUNT TECHNOLOGY,* ELECTROCHEM. PUB., LTD, 1988, P 167
18. M. BESTER, METALLURGICAL ASPECTS OF SOLDERING GOLD OR GOLD PLATING, *PROC. INTERNEPCON,* 1968, P 221
19. P. HOLMES AND R. LOASBY, *HANDBOOK OF THICK FILM TECHNOLOGY,* ELECTROCHEM. PUB., LTD., 1976, P 192
20. R. WILD, COMPONENT LEAD SOLDERABILITY VS. ARTIFICIAL AGEING II, *PROC. 1 L TH ELECT. MFG. SEMINAR* (CHINA LAKE, CA), NAVAL WEAPONS CENTER, 1987, P 289
21. R. EDINGTON AND L. CONRAD-LOWANE, AGING ENVIRONMENTS AND THEIR EFFECTS ON SOLDERABILITY, *PROC. 12TH ELECTRON. MFG. SEMINAR* (CHINA LAKE, CA), NAVAL WEAPONS CENTER, 1988, P 31
22. H. MANKO, *SOLDERS AND SOLDERING,* MCGRAW-HILL, 1979, P 96
23. R. BAHN, PLATING, *PRINTED CIRCUIT HANDBOOK,* C. COOMBS, ED., MCGRAW-HILL, 1979, P 7-1
24. R. PRASAD, *SURFACE MOUNT TECHNOLOGY, PRINCIPLE AND PRACTICE,* VAN NOSTRAND-RHEINHOLD, 1989, P 158
25. H. MANKO, *SOLDERING HANDBOOK FOR PRINTED CIRCUITS AND SURFACE MOUNTING,* VAN NOSTRAND-RHEINHOLD, 1986, P 23
26. R. KLEIN-WASSINK, NOTES ON THE EFFECTS OF METALLIZATION OF SURFACE MOUNTED COMPONENTS ON SOLDERING, *HYBRID MICROCIR.,* MAY 1987, P 89
27. R. WILD, SOME FACTORS AFFECTING LEADLESS CHIP CARRIER SOLDER JOINT FATIGUE LIFE, *PROC. 12TH ELECTRON. MFG. SEMINAR* (CHINA LAKE, CA), NAVAL WEAPONS CENTER, 1988, P 275
28. P. VIANCO AND J. DAL PORTO, AN EVALUATION OF THE BLIND LAP JOINT FOR THE SURFACE MOUNT ATTACHMENT OF CHIP COMPONENTS, *PROC. SURF. MOUNT INTER.,* TO BE PUBLISHED, 1992
29. H. SOLOMON, "INFLUENCE OF TEMPERATURE ON THE LOW CYCLE FATIGUE OF SURFACE MOUNTED CHIP CARRIER/PRINTED WIRING BOARD JOINTS," TECHNICAL INFORMATION SERIES, GENERAL ELECTRIC CRD, 1987
30. H. SOLOMON *ET AL.,* "PREDICTION OF SOLDER JOINT FATIGUE LIFE," TECHNICAL INFORMATION SERIES, GENERAL ELECTRIC CRD, 1988
31. H. SOLOMON, "FATIGUE OF 60/40 SOLDER," TECHNICAL INFORMATION SERIES, GENERAL ELECTRIC CRD, 1986
32. W. ENGELMAIER, PERFORMANCE CONSIDERATIONS: THERMAL-MECHANICAL EFFECTS, *PACKAGING,* VOL 1, *ELECTRONIC MATERIALS HANDBOOK,* ASM, 1989
33. D. KINSER *ET AL.,* RELIABILITY OF SOLDERED JOINTS IN THERMAL CYCLING ENVIRONMENTS, *PROC. NEPCON,* MAY 1976, P 61
34. P. VIANCO, AN OVERVIEW OF THE MENISCOMETER/WETTING BALANCE TECHNIQUE FOR WETTABILITY MEASUREMENTS, *THE METAL SCIENCE OF JOINING,* M. CIESLAK *ET AL.,* ED.,

TMS, 1992, P 265
35. F. KEAR, *PRINTED CIRCUIT ASSEMBLY MANUFACTURING,* MARCEL DEKKER, 1987, P 8-22

Introduction to Special Welding and Joining Topics

Hendrikus H. Vanderveldt, American Welding Society

Introduction

WELDING, BRAZING, AND SOLDERING are pervasive in our industrialized society, and it should come as no surprise that there are many unique aspects related to these.joining technologies that are not covered within the more traditional topic organization in the remainder of this Volume. It is the purpose of this "catchall" Section to provide coverage of some important topics that do not fit neatly in other sections of the book. However, no handbook--no matter how comprehensive--can exhaustively cover all subjects related to joining technology. This Section seeks to provide information about some of the more common, albeit unique, areas of interest and concern to the joining community. The articles that make up this Section provide overviews of these areas, point the reader towards more extensive literature, and help to identify additional areas of investigation.

The Section opens with an article on thermal spray coatings. The application of thermal spray aluminum and zinc coatings has seen a significant increase in the United States during recent years. The corrosion protection provided by these coatings can be as much as an order of magnitude greater than that obtained with traditional coating approaches. In addition, thermal spray coatings can be used to increase wear and abrasion resistance of in-service equipment and to repair and upgrade industrial components.

Introduction to Special Welding and Joining Topics

Hendrikus H. Vanderveldt, American Welding Society

Extreme Welding Environments

The next few articles in the Section provide information about extreme welding environments and service conditions. The construction of ships and offshore structures makes use of many of the same joining technologies used in shore-based construction industries, but also has its own set of unique requirements related to construction materials, fabrication environment, joining techniques, and so on. The article on underwater welding in this Section details some of the requirements involved during the original construction phase or later in-place repairs of large maritime structures; in addition, reference material is provided to point the reader to other sources of information.

Application of materials in cryogenic service (where temperatures can be as low as 4 K) provides opportunities to exploit special material properties associated with such low temperatures (superconductivity, for example). However, these opportunities must be weighed against some potential high penalties, such as the loss of structural properties exhibited at cryogenic operating temperatures. These problems can be significantly amplified in the joints produced for components intended for cryogenic service. The article "Welding for Cryogenic Service" discusses the impact of extremely low temperatures on the performance of welded structures.

The existence of long-term manned facilities in space is coming closer and closer to reality. Hence, the need to build structures or do repairs in space must be addressed. To date, very limited amount of work has been done to prepare ourselves for that day. The article "Welding in Space and Low-Gravity Environments" seeks to address what has been done and provide some guidance for future development efforts.

This Section also addresses the joining of nonmetallic and special-purpose materials. Although metals are generally the structural materials of choice, it is evident that increasing use is being made of plastics and composites in applications that include automotive parts and aerospace components, among many others. These materials are used because they exhibit high strength to weight and high stiffness, are producible as to properties, and have demonstrated reliability.

Experience related to joining of metals does not directly translate to joining of composite materials. The article "Joining of Organic-Matrix Composites" in this Section provides an extensive overview of this important topic as well as supplemental references to other sources of information. "Composite-to-Metal Joining" addresses the key factors involved in joining these dissimilar materials to one another.

The joining of plastics is generally accomplished by adhesive bonding or mechanical fastening. However, thermoplastic resins can be molded through the application of heat, and they can also be fusion welded. Various means of accomplishing such welding are discussed in the article "Welding of Plastics" in this Section.

Oxide-dispersion-strengthened materials provide high creep strength at very high temperatures and thus are used for applications such as gas turbine engines, high-temperature processing components, and so on. However, significant difficulties can be encountered in the processing of the oxide dispersions of these alloys. These can result in subsequent welding problems, such as porosity in the weldment and potentially in the adjacent heat-affected zone. The current state of the art in this area is high-lighted in the article "Joining of Oxide-Dispersion-Strengthened Materials" references are provided for further evaluation of this technology.

Computer technology has advanced to the stage where its application to welding and joining can make a major impact on the technical quality and cost of weldments, and this technology has the potential to revolutionize the entire joining manufacturing industry. The advent of personal desktop computer systems with high computational speed; the ability to model very complex parametric interrelationships without the need for exact theoretical understanding of those relationships; and the availability of comprehensive data base systems, computer-based engineering worksheets, and so on, all allow the modern manufacturing engineer to accomplish complex welding and joining tasks using minimal time and effort. The article "Intelligent Automation for Joining Technology" provides a general overview of this subject and detailed information about one particular development effort in this area. Related information is contained in the Section "Modeling of Joining Processes" in this Volume.

This Section concludes with an article on corrosion of weldments. Corrosion is a particularly difficult fabrication problem because it often appears only after significant in-service time has elapsed. A thorough understanding of corrosion phenomena can provide the designer of weldments with insight towards its avoidance. Additional information on this topic is available in *Corrosion,* Volume 13 of the *ASM Handbook.*

Thermal Spray Coatings

Herbert Herman, State University of New York, Robert A. Sulit, Sulit Engineering

Introduction

THERMAL SPRAY COATINGS (TSCs) are surface coatings engineered to provide wear-, erosion-, abrasion-, and corrosion-resistant coatings for original equipment manufacture and for the repair and upgrading of in-service equipment. In general, TSCs can be applied to a range of substrate materials, including metals, ceramics, plastics, and polymer composites. Thermal spray technology evolved and developed within the welding field because of similarities in the electrical and combustion equipment and the feedstock materials used in thermal spray with those used in welding and brazing. Accordingly, thermal spraying is classified as an allied welding process.

This article presents a general overview of the five thermal spray processes and the specific flame and arc spray processes used to preserve large steel components and structures. Also included are a TSC selection guide and an industrial process procedure guide for applying aluminum and zinc TSCs onto steel. Additional information on thermal spray processes is available in the article "Hardfacing, Weld Cladding, and Dissimilar Metal Joining" in this Volume.

Thermal spraying processes deposit finely divided metallic or nonmetallic feedstock surfing materials (wire, cored wires, ceramic rods, and powders) are heated to their plastic or molten state by combustion (flame, high-velocity oxygen fuel, and detonation) and by electric (arc and plasma) processes. The materials in their plastic or molten state are accelerated toward the substrate. The particles or droplets strike the surface, flatten, and form thin platelets (splats) that conform, adhere, and interlock with the roughened surface irregularities and with each other. As the sprayed particles impinge on the substrate, they cool and build up, particle by particle, into a lamellar-structured coating on the substrate. In general,

the substrate temperature can be kept at 200 °C (390 °F) or below to prevent metallurgical changes in the substrate material.

The properties of the TSC depend on such factors as its porosity, the cohesion between particles, adhesion to the substrate (including interface integrity), and the chemistry of the coating material. The particles bond to the substrate mechanically (the primary mechanism), metallurgically, or chemically. Particle impact velocity, particle size, substrate roughness, particle temperature, and substrate temperature influence bond strength. Figure 1 shows the lamellar structure of particle splats, oxide inclusions, and unmelted particles in a typical TSC cross section.

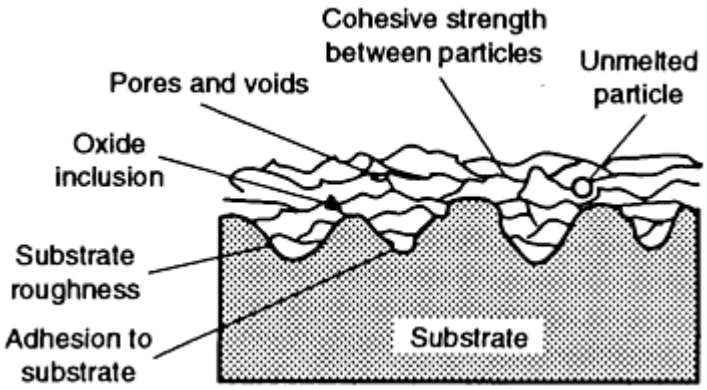

FIG. 1 SCHEMATIC SHOWING CROSS-SECTIONAL VIEW OF TSC LAMELLAR COMPONENTS THAT AFFECT COATING INTEGRITY

Aluminum and zinc TSCs have a long history of corrosion protection in structural steel work:

- BUILDINGS
- BRIDGES
- TOWERS
- RADIO AND TV ANTENNA MASTS
- STEEL GANTRY STRUCTURES
- HIGH-POWER SEARCH RADAR AERIALS
- OVERHEAD WALKWAYS
- RAILROAD OVERHEAD LINE SUPPORT COLUMNS
- ELECTRIFICATION MASTS
- TOWER CRANES
- TRAFFIC ISLAND POSTS
- STREET AND BRIDGE RAILINGS

On a smaller scale, aluminum-zinc TSCs have been successfully used to protect lawn furniture in corrosive seacoast environments.

Thermal Spray Coatings

Herbert Herman, State University of New York, Robert A. Sulit, Sulit Engineering

---

Thermal Spray Coating Processes

Thermal spray processes differ in the feedstock materials used, the method of heating applied, and the method of propelling the material toward the substrate. The primary TSC feedstock materials can be classified as powder, wire,

cored wire, and ceramic rod. Thermal spray processes can be categorized into two basic groups (combustion or electrical) according to the method of heat generation (Table 1).

TABLE 1 CLASSIFICATION OF THERMAL SPRAY PROCESSES RELATIVE TO METHOD OF HEAT GENERATION AND FEEDSTOCK FORM

FEEDSTOCK FORM	THERMAL SPRAY PROCESS[A]					
	COMBUSTION			ELECTRICAL		
				ARC	PLASMA	
	FLAME	**HVOF[B]**	**DETONATION**		**DIRECT CURRENT**	COUPLED INDUCTION
POWDER	X	X	X	. . .	X	**X**
WIRE	X	. . .	. . .	X	. . .	**. . .**
CORED WIRE	X	. . .	. . .	X	. . .	**. . .**
CERAMIC ROD	**X**	**. . .**	**. . .**	**. . .**	**. . .**	**. . .**

(A) X, APPLICABLE.

(B) HIGH-VELOCITY OXYFUEL

Table 2 gives typical characteristics of these thermal spray processes. The combustion flame and the electric arc processes are the main ones used for preserving steel. Recommended feedstock requirements, area coverage, and spray rates for flame and arc spraying are given in the section "Typical Process Parameters" in this article.

TABLE 2 TYPICAL PARAMETERS OF SELECTED TSC PROCESSES

PROCESS	**FEEDSTOCK**	**OPERATION**	**GAS FLOW**		**FLAME OR ARC TEMPERATURE**		**PARTICLE IMPACT VELOCITY**		SPRAY RATES	
			M^3/H	**FT^3/H**	**°C**	**°F**	**M/S**	**FT/S**	**KG/H**	LB/H
GROUP I (COMBUSTION)										
SUBSONIC	FLAME POWDER	POWDER FEEDSTOCK FED INTO OXYFUEL FLAME	10	350	2200	3990	30	100	$\frac{1}{2}$ - 10	**1.1-22**
	FLAME WIRE, ROD, AND CORD	FEEDSTOCK FED INTO OXYFUEL FLAME	70	2500	2800	5070	180	590	$\frac{1}{2}$ - 10	**1.1-22**
SUPERSONIC	HIGH-VELOCITY OXYGEN FUEL POWDER	POWDER FED INTO SUPERSONIC VELOCITY COMBUSTION FLAME	110	3900	2600	4710	900	2950	2-15	**4.4-33**
	DETONATION GUN	POWDER AND EXPLOSIVE GAS CYCLICALLY FED EXPLOSION	. . .	. . .	2600	4710	900	2950	. . .	**. . .**

		CHAMBER								
GROUP II (ELECTRICAL)										
ARC	WIRE	TWO CONSUMABLE ELECTRODES FED INTO ATOMIZING AIR/GAS STREAM	70	2500	5000	9300	240	790	2[A]	**4.4[B]**
PLASMA	**POWDER**	**POWDER FED INTO PLASMA TORCH WITH TEMPERATURES TO 8300 °F (15,000 °F)**	**4**	**140**	**5000**	**9300**	**240**	**790**	**0.1[A]**	**0.22[B]**

(A) KG/H/KW.

(B) LB/H/KW

Flame spraying is the simplest and most versatile process. All five feedstock forms can be sprayed with subsonic flame sp and most versatile process. All five feedstock forms can be sprayed with subsonic flame spray. The feed material is melted by an oxyfuel gas flame. In flame powder spraying (Fig. 2), powder particles are heated to 2200 °C (3990 °F), and impact the substrate at 30 m/s (100 ft/s). In flame wire spraying (Fig. 3), melted and vaporized wire particles are heated to 2800 °C (5070 °F), and impact the substrate at 180 m/s (590 ft/s). The higher gas flow used in flame wire spraying gives the droplets greater impact energy. The impact particle velocity in flame powder spraying is the lowest, resulting in reduced adhesion and increased porosity relative to the other thermal spray processes. Spray rates are usually in the range of 0.5 to 10 kg/h (1.1 to 22 lb/h) for both flame wire and flame powder spraying.

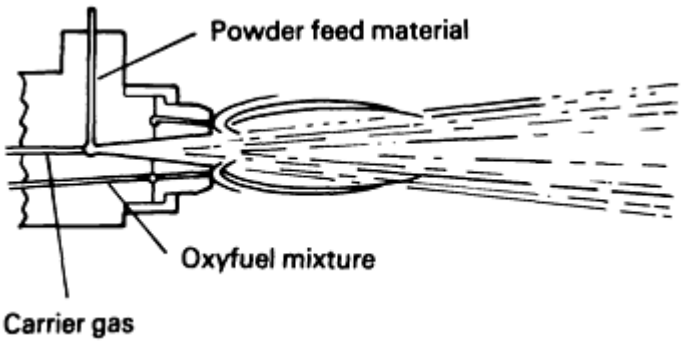

FIG. 2 CROSS-SECTIONAL VIEW OF A FLAME POWDER SPRAYING SYSTEM SHOWING POWDER FEED MATERIAL BEING TRANSPORTED BY THE CARRIER GAS AND THEN MELTED BY THE OXYFUEL MIXTURE

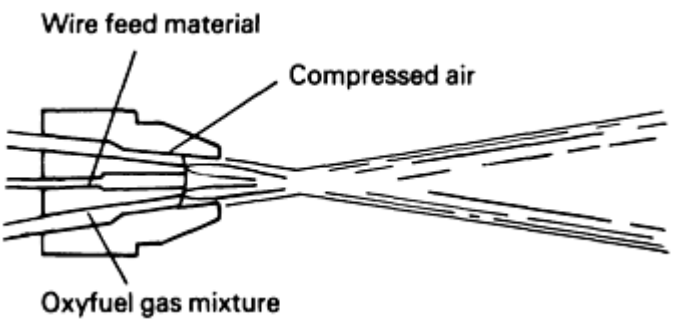

FIG. 3 ATOMIZATION OF WIRE FEEDSTOCK FROM THE NOZZLE OF A FLAME WIRE SPRAYING GUN

Detonation Gun. In the detonation gun (D-gun) process, oxygen and fuel gases are mixed with powder and cyclically injected into a constricted shotgunlike barrel and ignited. A spark ignites the mixture, producing a supersonic detonation wave that heats the powder particles to 2600 °C (4710 °F) and propels them at 900 m/s (2950 ft/s) onto the substrate.

The HVOF gun (Fig. 4) operates continuously and uses higher oxidant and fuel gas pressures, resulting in higher particle impact velocities, thus producing extremely dense, well-bonded TSCs.

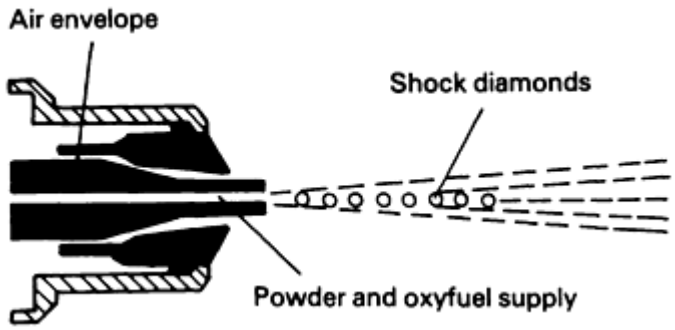

FIG. 4 CROSS-SECTIONAL VIEW SHOWING THE OUTPUT OF AN HVOF SPRAYING SYSTEM

Detonation Gun Versus HVOF Gun. High-velocity oxyfuel equipment is portable and can be transported to the job site, while the detonation gun equipment must be operated in fixed facilities. The HVOF gun can spray powder feedstock materials at the rate of 2 to 15 kg/h (4.4 to 33 lb/h).

Arc Spraying. Two oppositely charged consumable wires are fed into the gun (Fig. 5). Where they emerge from the nozzle, at their point of intersection, an arc is formed, melting the wire at 5000 °C (9030 °F). The molten metal is atomized and propelled by an air or gas stream, impacting the substrate at 240 m/s (785 ft/s). Metal and alloy wires and powders in metallic sheaths (cored wire) can be sprayed at rates of over 25 kg/h (55 lb/h).

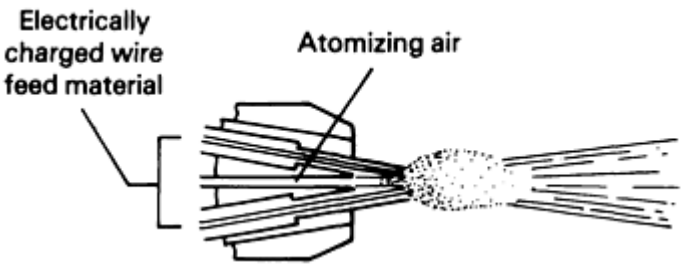

FIG. 5 SPRAY PATTERN GENERATED BY TWO ELECTRICALLY CHARGED WIRES MELTED AT THE NOZZLE OF AN ARC SPRAYING GUN

Plasma spraying uses a nontransferred arc gun to create the plasma jet that melts and propels the powder to the substrate (Fig. 6). The nontransferred plasma arc is contained in the gun. The arc is maintained between a thoriated tungsten cathode and a constricting nozzle anode (copper). An inert or reducing gas under pressure enters the annular space between the anode and the cathode, where it becomes partially ionized. The gas emerges from the nozzle as a high-temperature (up to 17,000 °C, or 30,600 °F) high-velocity jet. Powder feedstock material is injected into the hot gas stream, where it melts or softens, then impacts the substrate at 250 m/s (790 ft/s). Spray rates are 0.1 kg/h/kW (0.2 lb/h/kW). The usual power supplies range from 15 to 80 kW. Higher-power plasma guns, operating up to 200 kW can, in principle, spray ceramics at 25 to 50 kg/h (55 to 110 lb/h) and metals at an even higher rate.

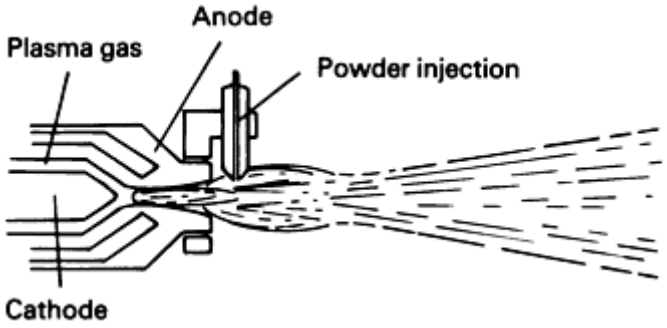

FIG. 6 SCHEMATIC OF A PLASMA ARC POWDER SPRAY SYSTEM SHOWING ROUTING OF PLASMA GAS AND POWDER MATERIAL AT THE OUTPUT NOZZLE

Thermal Spray Coatings

Herbert Herman, State University of New York, Robert A. Sulit, Sulit Engineering

Selection of TSCs to Preserve Integrity of Steels

Thermal spray coatings are extensively used for the corrosion protection of steel and iron in a wide range of environments. The long-term effectiveness (over 20 years) in rural, industrial, and marine environments is well documented. The corrosion tests carried out by the American Welding Society (Ref 1) and the 34-year marine-atmosphere performance report of the LaQue Center for Corrosion Technology (Ref 2) confirm the effectiveness of flame-sprayed aluminum and zinc coatings over long periods of time in a wide range of hostile environments. The British Standards Institution code of practice for the corrosion protection of steel specifies that only TSCs are able to give more than 20 years of protection before maintenance is necessary in the 19 industrial and marine environments considered. Only sealed, sprayed aluminum or zinc gives such protection in seawater immersion or splash zones (Ref 3). The Canadian Standards Association tabulates the life expectancy at more than 40 years for aluminum and zinc TSCs in various exposure environments (Ref 4).

The selection of a TSC depends on the service environment, the desired service life, operating duty cycle, and the maintenance and repair support to be provided during the life cycle. Tables 3 and 4 give current service life information for aluminum and zinc TSCs in various service environments. Figures 7 and 8 plot the required thickness specifications given in Tables 3 and 4, respectively. The service life estimates for 85/15 wt% Zn/Al alloy and the 90/10 vol% aluminum metal-matrix composites (MMCs) TSCs introduced in the late 1970s and 1980s, respectively, are based on accelerated laboratory tests and service applications through 1992. In a marine environment, powder TSC with higher aluminum content exhibits improved corrosion resistance (Ref 2). Where resistance to wear, abrasion, or both, is required in addition to corrosion protection, 90/10-MMC TSCs should be considered. The 90/10 MMC wire is composed of 90 vol% Al + 10 vol% Al_2O_3 (8 to 10 μm, or 320 to 400 μin., diameter).

TABLE 3 SERVICE LIFE ESTIMATES OF 85/15 ZN/AL TSCS IN SELECTED CORROSIVE ENVIRONMENTS

TYPE OF EXPOSURE	COATING THICKNESS REQUIRED FOR INDICATED SERVICE LIFE							
	5-10 YEARS		**10-20 YEARS**		**20-40 YEARS**		>40 YEARS	
	μm	**in.**	**μm**	**in.**	**μm**	**in.**	**μm**	in.
RURAL ATMOSPHERE	. . .	. . .	75-125	0.003-0.005	125-175	0.005-0.007	250-300	**0.010-0.012**
INDUSTRIAL ATMOSPHERE	. . .	. . .	150-200	0.006-0.008	300-375	0.012-0.015	350-400	**0.014-0.016**

MARINE ATMOSPHERE	. . .	. . .	250-300	0.010-0.012	300-375	0.012-0.015	350-400	**0.014-0.016**
FRESHWATER IMMERSION	150-200	0.006-0.008	250-350	0.010-0.014	300-375	0.012-0.015	. . .	**. . .**
SALTWATER IMMERSION	**250-300**	**0.010-0.012**	**350-400**	**0.014-0.016**	**. . .**	**. . .**	**. . .**	**. . .**

TABLE 4 SERVICE LIFE ESTIMATES OF ALUMINUM AND 90/10 ALUMINUM METAL-MATRIX COMPOSITE TSCS

TYPE OF EXPOSURE	COATING THICKNESS REQUIRED FOR INDICATED SERVICE LIFE(A)							
	5-10 YEARS		**10-20 YEARS**		**20-40 YEARS**		>40 YEARS	
	µm	**in.**	**µm**	**in.**	**µm**	**in.**	**µm**	in.
RURAL ATMOSPHERE	. . .	. . .	. . .	. . .	150-200	0.006-0.008	. . .	**. . .**
INDUSTRIAL ATMOSPHERE	. . .	. . .	150-200	0.006-0.008	250-300	0.010-0.012	250-375	**0.010-0.015**
MARINE ATMOSPHERE	150-200	0.006-0.008	200-250	0.008-0.010	250-300	0.010-0.012	250-375	**0.010-0.015**
FRESHWATER IMMERSION	150-200	0.006-0.008	200-250	0.008-0.010	250-300	0.010-0.012	. . .	**. . .**
SALTWATER IMMERSION	200-250	0.008-0.010	250-300	0.010-0.012	300-350	0.012-0.014	. . .	**. . .**
HIGH-TEMPERATURE (100-540 °C, OR 210-1000 °F)	150-200	0.006-0.008	200-250	0.008-0.010	250-300	0.010-0.012	. . .	**. . .**
WEAR, ABRASION, EROSION, AND IMPACT (90/10 MMC PREFERRED)	**150-200**	**0.006-0.008**	**250-300**	**0.010-0.012**	**. . .**	**. . .**	**. . .**	**. . .**

(A) WITH EXCEPTION OF WEAR, ABRASION, EROSION, AND IMPACT PROPERTIES,DATA FOR ALUMINUM AND 90/10 ALUMINUM MMC TSC ARE IDENTICAL.

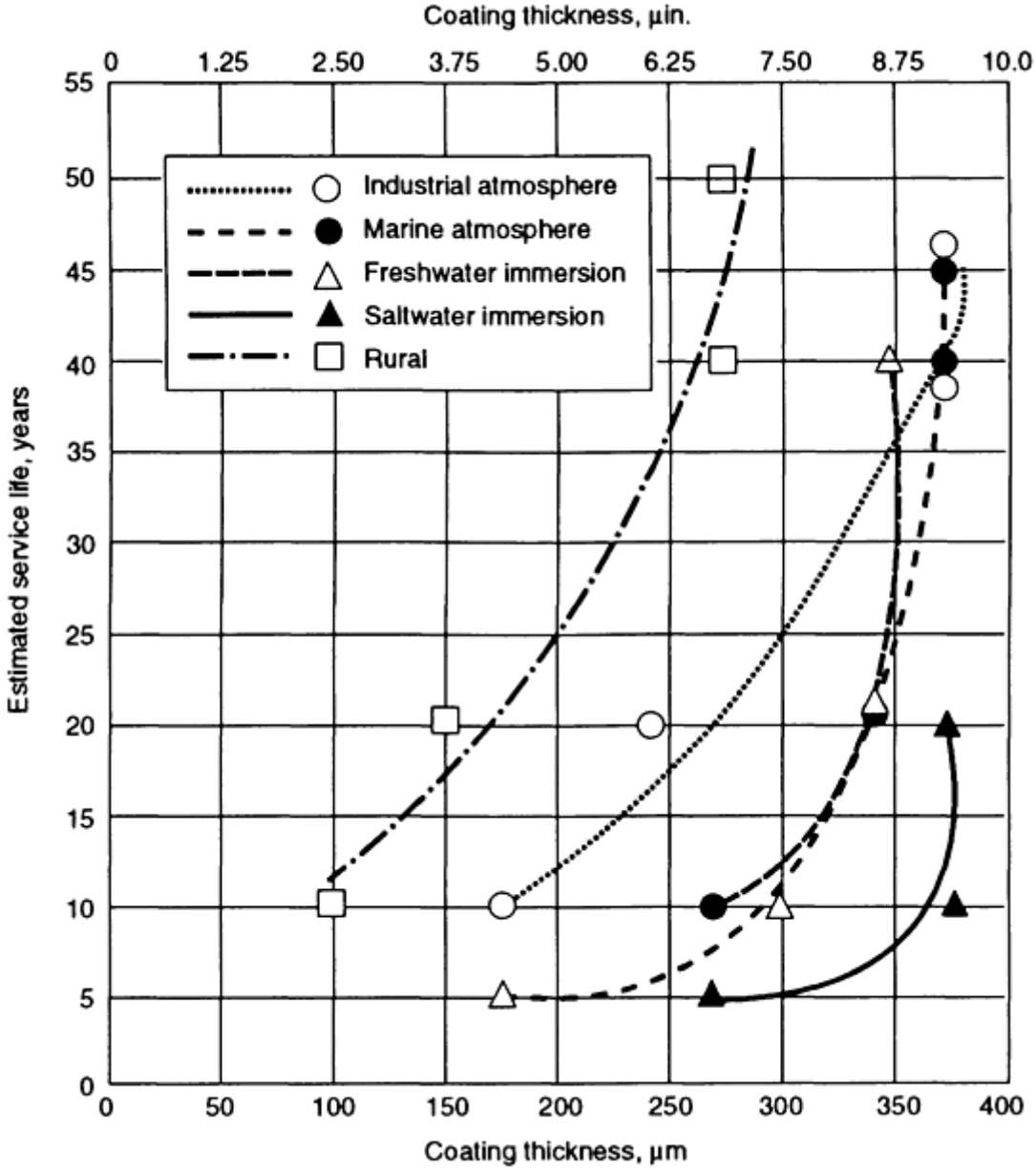

FIG. 7 PLOT OF SERVICE LIFE VERSUS COATING THICKNESS AS A FUNCTION OF SELECTED ENVIRONMENTS FOR AN 85/15 ZN/AL ALLOY WITH A TSC

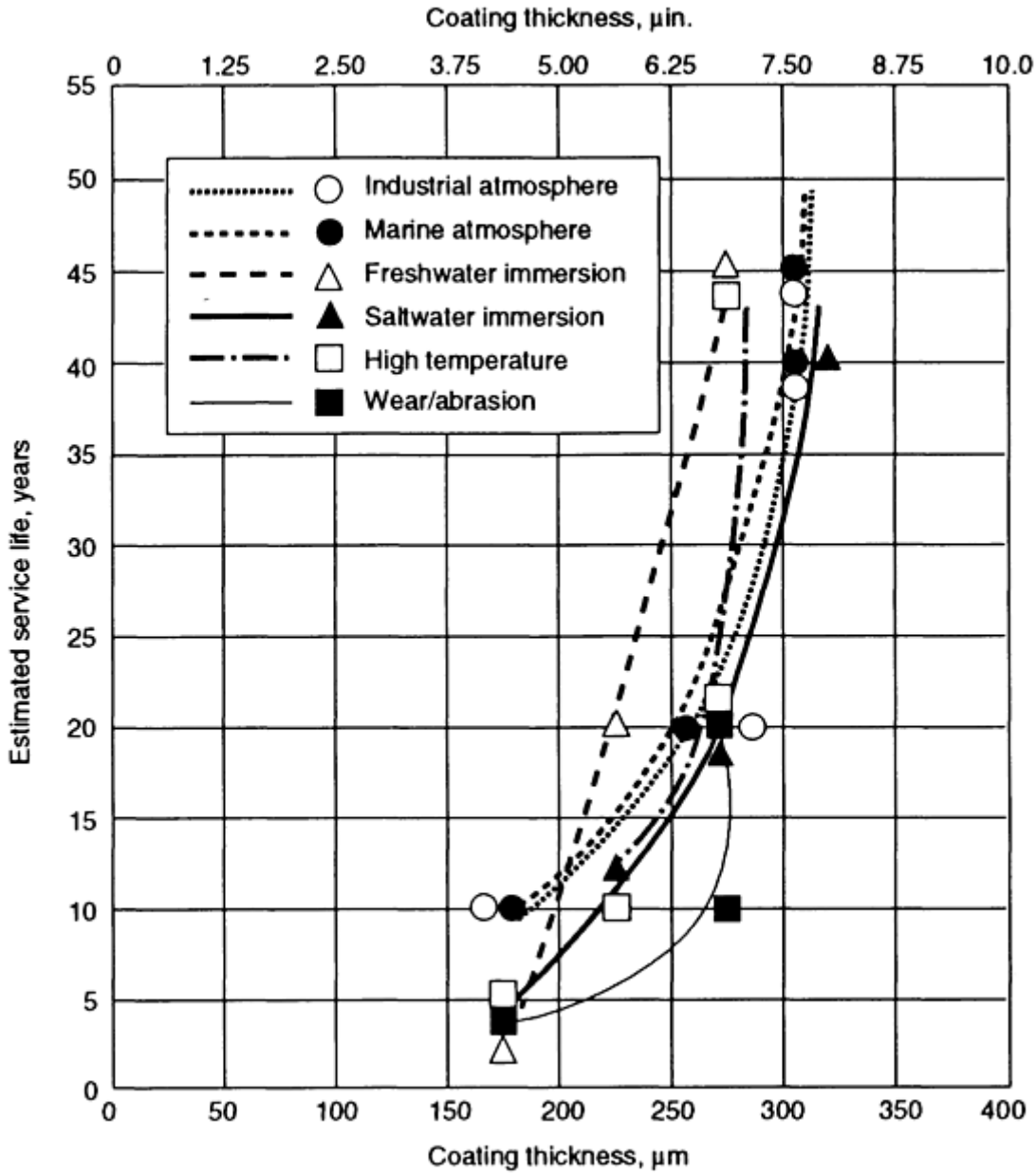

FIG. 8 PLOT OF SERVICE LIFE VERSUS COATING THICKNESS AS A FUNCTION OF SELECTED ENVIRONMENTS FOR A 90/10 ALUMINUM METAL-MATRIX COMPOSITE WITH A TSC

Galvanic Properties. Aluminum and zinc and their alloys and composites provide broad atmospheric protection. Aluminum and zinc are anodic to steel and protect the ferrous substrate in electrolytic solutions. When applied in a nonthrough porosity thickness, they provide both barrier and cathodic protection. When cut through to the steel or when applied too thinly to role out through porosity, these TSCs provide galvanic protection to the steel. Aluminum corrodes less rapidly than zinc in highly acidic conditions, while zinc performs better in alkaline conditions. Aluminum TSCs immediately oxidize to form a loosely adherent Al_2O_3 protective film (as compared to the tightly adherent protective film on stainless steels) that prevent further oxidation. Thus, there is no advantage to applying aluminum TSCs greater than the non-through-porosity thickness of 150 to 200 µm (0.006 to 0.008 in.) unless wear or abrasion resistance is also required in addition to corrosion resistance. Aluminum TSCs have greater wear, abrasion, and erosion resistance than zinc TSCs.

Zinc alloyed with aluminum forms an effective corrosion-resistant coating, combining the attributes of both elements. The greater electrochemical activity of zinc provides greater galvanic protection than aluminum. Aluminum, with its lower electrochemical activity and a loosely adherent aluminum oxide film, provides long-term protection even through porous coatings and gives better wear, abrasion, and erosion resistance than zinc TSCs.

Aluminum and aluminum composite TSCs can be used where the temperature is greater than 200 °C (390 °F). Aluminum composite TSCs are used when wear, abrasion, and erosion resistance are required beyond that provided by aluminum and zinc TSCs.

Thermite Sparking Hazard (Ref 5, 6). Thermite sparking is caused by the reaction of rusted steel and aluminum (in the form of a finely divided smear) when this combustible mix is ignited by an impact. Aluminum smears may be generated on rusting steel by striking or dragging steel components and tools over bare aluminum surfaces or vice versa. Bare aluminum and bare aluminum TSCs should be avoided whenever there is a thermite sparking hazard. Situations where bare aluminum or bare aluminum TSCs and rusted steel will be near a combustion or explosion source can occur on a regular basis and should be avoided. There appears to be little risk of thermite sparking as a result of the impact of rusted steel on a sealed or painted aluminum, aluminum alloy, or aluminum composite TSC surface.

Porosity is an inherent feature of TSCs. When applied to nonthrough porosity thickness (nominally about 175 μm, or 0.007 in.) for flame-sprayed aluminum and 90/10 MMC, these TSCs will protect the substrate steel. When applied to a less than nonthrough porosity thickness, the TSC will retard substrate corrosion because of galvanic protection. The porosity of the TSC is a function of the feedstock material, the application method, and the spray parameters.

Role of Sealants and Topcoats. Thermal spray coatings are applied in a single application. They emit no volatile organic compounds, need no drying time, and provide galvanic protection to exposed steel substrates. The natural surface texture of TSCs provides an excellent base for paint and thermoplastic or thermosetting powder sealers as well as paint and powder-coating topcoats.

It is preferable to seal TSCs. The sealer fills the pores of the TSC, smooths the sprayed surface, and improves appearance and service life. Sealers also simplify maintenance, which is generally only the reapplication of the sealer. Sealers should be applied immediately after applying the TSC.

TSC paint sealers should have low viscosity to flow and should be absorbed into the natural pores of the TSC. The pigment particle size of colored paint sealers must be small enough to freely flow into the pores of the TSC, nominally a 5 fineness grind per ASTM D 1210. Thermoplastic and thermosetting powder sealers have fine particles but should be electrostatically applied to maximize penetration into the pores of the TSC. Furthermore, thermal sprayed components must be sufficiently heated to maximize outgassing of the pores prior to electrostatic application of the powder coating.

Thermal spray coatings should be topcoated only when:

- THE ENVIRONMENT IS VERY ACID OR VERY ALKALINE (THAT IS, WHEN THE PH IS OUTSIDE THE RANGE OF 5 TO 12 FOR ZINC TSCS, OR 4 TO 9 FOR ALUMINUM AND 90/10 MMC TSCS).
- THE METAL IS SUBJECT TO DIRECT ATTACK BY SPECIFIC CHEMICALS.
- THE REQUIRED DECORATIVE FINISH CAN BE OBTAINED ONLY WITH PAINT.
- ADDITIONAL WEAR, ABRASION, AND EROSION RESISTANCE ARE REQUIRED.

One or two coats of paint may be sufficient except in abnormally aggressive environments. Sealed TSCs are preferable to painted TSCs. Paints usually have a longer life on TSCs than on bare steel, because the TSC reduces or prevents rusting and pitting of the steel.

Zinc TSCs complement hot-dip galvanizing and should be considered when fabricated goods are excessively large or cannot be hot-dip galvanized. Zinc TSCs should also be considered for repairing galvanized coatings damaged during fabrication (for example, welding and cutting) and for maintenance recoating.

Zinc spraying can restore corrosion protection to areas where galvanizing is inadvertently removed during fabrication and assembly. This can occur on the threaded end of electrical conduits or along the welded seams inside galvanized barrels and drums. Zinc spray is particularly advantageous in such cases because it ensures the uniformity and reproducibility of the galvanized coating thickness.

Wellhead valve assemblies for offshore use have been coated for salt atmosphere protection since the 1950s. Aluminum TSCs have been used for flare stacks. Aluminum and zinc TSCs have been used for the external protection of oil and

propane gas storage tanks. The interiors of steel coal rail cars have been sprayed with aluminum for sulfuric acid corrosion protection and with aluminum composite for both corrosion and abrasion protection. The exteriors have been sprayed with zinc for atmospheric-corrosion protection. Thermal spray coatings have been used to protect pipelines against many environments. Pile couplings, valves, manhole covers, industrial gas bottles, and other small industrial items are candidates for protection by TSCs.

Zinc TSCs are used to protect potable water pipelines and storage tanks (Ref 7). Aluminum and zinc TSCs are used in sluice and canal lock gates in irrigation systems and in shipping canal lock gates. Once coated, these components require virtually no maintenance for decades.

Sealed zinc coatings improve the resistance of steel bridgework and railings to marine corrosion and deicing salts. Rebars in reinforced concrete can be zinc sprayed to retard corrosion. Reinforced concrete bridges and highways, especially those in marine and freezing environments where deicing salts are used, commonly suffer from chloride intrusion into the concrete, leading to rebar corrosion and concrete spalling. Zinc TSCs are sometimes used for rebar protection before concrete is poured. Zinc TSCs are sprayed directly onto bridge concrete substructures to provide a cathodic-protection coating or to serve as secondary anodes connected to an impressed-current cathodic-protection system.

In marine applications, the structural areas and components of ships are preserved with aluminum and zinc TSCs. The U.S. Navy routinely uses aluminum TSCs in new ship construction, in the maintenance of ship structures, and for a wide range of shipboard components, especially those in topside and wet spaces. The British, Australian, and New Zealand Navies use a duplex zinc (base) and aluminum (top) TSC system. Commercial ships and barges have used TSCs to preserve ship superstructures and various topside and interior components.

Sealed TSCs have a longer service life than unsealed TSCs, are easier to clean and maintain, and provide both barrier and galvanic protection. Sealer paints and powder coatings must be chemically compatible with the TSC material, the service environment, and the intermediate/topcoat paint. Sealers must be suitably thinned and have a fine pigment grind to effectively penetrate the TSC. As indicated above, sealed TSCs are preferable to painted TSCs. Descriptions and specifications of sealer and intermediate/topcoat paints are given in Ref 3 and 8.

Future Outlook. The suitability of a particular paint or thermoplastic/thermosetting powder (applied electrostatically or by thermal spray) must be evaluated when the coating is designed and specified. Such an evaluation is necessary in order to get the sealer/topcoat paint or powder system that best meets the service and life cycle cost (LCC) requirements compliant with the evolving environmental and safety regulations. Specific paint or powder systems can be ranked and validated with accelerated exposure tests simulating the service environment and duty cycle. The penetrability of the sealer into the TSC can be validated by metallographic analysis and the service life ranked by accelerated weathering tests.

Thermal spray coatings are supplementing and replacing paint coating systems because of their predictable service life, increased effectiveness, and lower life cycle costs. The LCC includes the initial installation cost plus the repair and maintenance costs incurred during the service life of the coating system. The installation cost of TSC systems may range up to one and one-half times that of high-performance paint systems, but the LCCs could be less than three-fourths the paint system LCC. Comparative TSC and painting system LCC may be estimated with the economic models in Ref 3 and 8.

References cited in this section

1. "CORROSION TESTS OF FLAME-SPRAYED COATED STEEL, 19-YEAR REPORT," C2.14-74, AMERICAN WELDING SOCIETY, 1974
2. R.M. KAIN AND E.A. BAKER, MARINE ATMOSPHERIC CORROSION MUSEUM REPORT ON THE PERFORMANCE OF THERMAL SPRAY COATINGS ON STEEL, *TESTING OF METALLIC AND INORGANIC COATINGS,* STP 947, AMERICAN SOCIETY FOR TESTING AND MATERIALS, 1987
3. "CODE OF PRACTICE FOR PROTECTIVE COATING OF IRON AND STEEL STRUCTURES AGAINST CORROSION," BS 5493, BRITISH STANDARDS INSTITUTION, 1977; AVAILABLE FROM THE AMERICAN NATIONAL STANDARDS INSTITUTE
4. "SPRAYED METAL COATINGS FOR ATMOSPHERIC CORROSION PROTECTION," G 189-1966,

CANADIAN STANDARDS ASSOCIATION, 1966; REAFFIRMED 1980
5. ROSENBURGH *ET AL., ALUMINUM OFFSHORE--SAFETY ANALYSIS,* PUBLICATION 85-3208, VERITEC, 1985
6. THERMITE SPARKING, *ALUMINUM DESIGN GUIDE,* VOL 2, *DESIGN GUIDE ON THE USE OF ALUMINUM IN OFFSHORE STRUCTURES,* WIMPEY OFFSHORE, LONDON, SECTION 4.5
7. "PAINTING WATER STORAGE TANKS," ANSI/AWS D102-78, AMERICAN WELDING SOCIETY, 1978
8. *STEEL STRUCTURES PAINTING MANUAL,* STEEL STRUCTURES PAINTING COUNCIL

Thermal Spray Coatings

Herbert Herman, State University of New York, Robert A. Sulit, Sulit Engineering

---

Industrial Process Instruction for Applying TSCs on Steel

An industrial process instruction is an engineering procedure detailing the necessary equipment, consumables, method (step-by-step procedure), trained/certified personnel, and records required to accomplish the objective of that process with the requisite quality control, safety, and environmental compliance in a timely and cost-effective manner. The scope of an industrial process instruction for applying TSCs on steel should include (Ref 9):

- *DEFINITION* OF TERMS UNIQUE AND CRITICAL TO THE SAFE AND SUCCESSFUL ACCOMPLISHMENT OF THE PROCESS
- *SAFETY AND ENVIRONMENTAL COMPLIANCE* REQUIRED FOR OPERATOR, OBSERVERS, AND PASSERSBY. FOR THERMAL SPRAYING, AIRBORNE ALUMINUM AND ZINC DUST COULD BE AN EXPLOSIVE HAZARD IF NOT PROPERLY HANDLED. ALUMINUM AND ZINC FUMES PRODUCED IN THERMAL SPRAYING AND IN BLASTING DEBRIS FROM SURFACE PREPARATION, ESPECIALLY IF THERE WAS OLD LEAD-BEATING PAINT, REQUIRE PERSONNEL PROTECTION, CONTAINMENT, AND THE REQUISITE WASTE DISPOSAL
- *JOB AND CONTRACT DESCRIPTION* DETAILING THE FOLLOWING: THE THERMAL SPRAY WORK AREA BOUNDARY; WHAT IS AND WHAT IS NOT TO BE THERMAL SPRAYED; THE THERMAL SPRAY FEEDSTOCK AND TSC THICKNESSES; SEALING/TOPCOATING MATERIALS; AND THE INSPECTION AND ACCEPTANCE REQUIREMENTS
- *MATERIALS* REQUIRED, INCLUDING THERMAL SPRAY FEEDSTOCK (BASED ON THE NOMINAL AREA COVERAGE AND SPRAY RATES FOR THE SPECIFIED PROCESS EQUIPMENT), ABRASIVE BLASTING MEDIA FOR ROUGH AND FINAL ANCHOR-TOOTH BLASTING, SEALER AND TOPCOATING PAINTS OR THERMOPLASTIC/THERMOSETTING POWDER COATINGS, QUALITY CONTROL CONSUMABLES, AND ENERGY REQUIREMENTS (FUEL GASES, INERT GASES, AND OXYGEN)
- *EQUIPMENT FOR SURFACE PREPARATION AND THERMAL SPRAYING* TO INCLUDE SPRAY GUN QUALIFICATIONS, AIR COMPRESSOR, AND AIR DRYERS
- *QUALITY CONTROL EQUIPMENT* TO DETERMINE THE ACCEPTABILITY OF SURFACE PREPARATION (WHITE AND NEAR-WHITE METAL FINISH, BLASTING MEDIA CLEANLINESS, AND ANCHOR-TOOTH DEPTH) AND TSC APPLICATION (SUBSTRATE TEMPERATURE, AIR TEMPERATURE, DEW POINT AND HUMIDITY, TSC THICKNESS, AND TSC BEND TEST)
- *APPLICATION PROCESS:* SURFACE PREPARATION (INCLUDES NEW STEEL, OLD STEEL, MASKING, DEGREASING, AND SURFACE PROFILE WITH QUALITY CONTROL CHECK POINTS; POST BLASTING SUBSTRATE CONDITION AND THERMAL SPRAYING PERIOD; THERMAL SPRAYING (INCLUDES EQUIPMENT SETUP AND BEND TEST; PLANNING AND EXECUTING THERMAL SPRAY SEQUENCE AND CONTROLLING OVERSPRAY WITH TWO QUALITY CONTROL POINTS)

- *PROCEDURES* FOR SPRAYING EDGES OF MATERIALS OR INTO CAVITIES (THAT IS, HOLES)
- *SEALING AND TOPCOATING* WITH QUALITY CONTROL CONTROL CHECK POINTS
- *MAINTENANCE AND REPAIR OF TSCS* BASED ON DEGREE OF DAMAGE AND WEAR AS RELATED TO EXPOSURE OF THE UNDERLYING COATING OR SUBSTRATE STEEL AND THE SIZE OF THE DEGRADED AREA
- *DEBRIS* CONTAINMENT AND CONTROL
- *RECORDS,* INCLUDING A JOB CONTROL RECORD SUMMARIZING THE TSC JOB REQUIREMENTS, OPERATOR QUALIFICATIONS, AND A CHECK LIST OF THE NINE QUALITY CONTROL CHECK POINTS
- *OPERATOR TEST AND QUALIFICATIONS* PER ANSI/AWS C2.16-92 ("GUIDE FOR THERMAL-SPRAY OPERATOR QUALIFICATION")

Reference cited in this section

9. "GUIDE FOR THE PROTECTION OF STEEL WITH THERMAL SPRAY COATINGS OF ALUMINUM AND ZINC AND THEIR ALLOYS AND COMPOSITES," ANSI/AWS C2.18-X, AMERICAN WELDING SOCIETY, IN PREPARATION

Thermal Spray Coatings

Herbert Herman, State University of New York, Robert A. Sulit, Sulit Engineering

Typical Process Parameters (Ref 9)

Table 5 gives the nominal thermal spray deposit efficiency and feedstock material required per unit area or unit thickness for representative materials sprayed onto a flat plate. Deposit efficiency is the percentage by weight of sprayed materials adhering to a large flat plate. Table 6 gives the typical spray rates and area coverage for flame and arc spraying on a flat plate. Additional feedstock will be required to spray complex geometrical shapes. Specific values vary with the shop or field job site, thermal spray equipment, spray parameters, process used, and the geometrical shape of the components being sprayed. The data in Tables 5 and 6 are technical data supplied by various equipment manufacturers and are given for comparison purposes and relative ranking; they are not intended for cost estimating.

TABLE 5 DEPOSITION RATES FOR SELECTED FEEDSTOCK USED IN FLAME AND ARC TSC APPLICATIONS

PARAMETER	FEEDSTOCK MATERIAL					
	WIRE				POWDER	
	Al	**Zn**	**85/15 Zn/Al**	**90/10 AL MMC**	**Al**	Zn
FLAME SPRAY						
DEPOSIT EFFICIENCY(A), %	80-85	65-70	80-85	80-85	90	**85**
MATERIAL REQUIRED, KG/M^2/μM	0.0024-0.0026	0.0098-0.0105	0.0066-0.0070	0.0024-0.0026	0.0027	**0.0076**
ARC SPRAY						
DEPOSIT EFFICIENCY(A), %	75-80	65-70	72-78	75-80	(B)	**(B)**
MATERIAL REQUIRED, KG/M^2/μM	**0.0029-0.0031**	**0.009-0.010**	**0.0089-0.0096**	**0.0029-0.0031**	**(B)**	**(B)**

(A) DATA FOR FLAT PLATE.

(B) NOT APPLICABLE

TABLE 6 TYPICAL DEPOSITION RATES (SPRAY RATE AND AREA COVERAGE) FOR FLAME SPRAYING AND ARC SPRAYING WITH SELECTED FEEDSTOCK ON A FLAT PLATE

APPLICATION METHOD	DEPOSITION RATES PER INDICATED FEEDSTOCK							
	AL		**ZN**		**85/15 ZN/AL**		90/10 AL MMC	
	SPRAY RATE, KG/H	**COVERAGE, M^2/H/µM**	**SPRAY RATE, KG/H**	**COVERAGE, M^2/H/µM**	**SPRAY RATE, KG/H**	**COVERAGE, M^2/H/µM**	**SPRAY RATE, KG/H**	COVERAGE, M^2/H/µM
FLAME SPRAYING								
WITH WIRE DIAMETER: 2.38 MM (0.0937 IN.)	2.5	1.44	9.1	2.05	8.2	1.96	2.5	**1.44**
WITH WIRE DIAMETER: 3.18 MM (0.125 IN.)	5.4	3.18	20	3.33	18	3.33	5.4	**3.18**
WITH WIRE DIAMETER: 4.76 MM (0.187 IN.)	7.3	4.22	30	4.81	26	4.81	7.3	**4.22**
WITH POWDER	6.8	100	14	80	. . .	. . .	. . .	**. . .**
ARC SPRAYING (PER 100 A)	**2.7**	**1.39**	**12**	**2.85**	**10**	**2.66**	**2.7**	**1.39**

Thermal spray coating applicators should develop their own shop and field deposit-efficiency data and production planning factors for their specific equipment and their method of operation. Past production records should provide a good information base for job cost estimating, production scheduling, and cost control.

Reference cited in this section

9. "GUIDE FOR THE PROTECTION OF STEEL WITH THERMAL SPRAY COATINGS OF ALUMINUM AND ZINC AND THEIR ALLOYS AND COMPOSITES," ANSI/AWS C2.18-X, AMERICAN WELDING SOCIETY, IN PREPARATION

Thermal Spray Coatings

Herbert Herman, State University of New York, Robert A. Sulit, Sulit Engineering

References

1. "CORROSION TESTS OF FLAME-SPRAYED COATED STEEL, 19-YEAR REPORT," C2.14-74, AMERICAN WELDING SOCIETY, 1974
2. R.M. KAIN AND E.A. BAKER, MARINE ATMOSPHERIC CORROSION MUSEUM REPORT ON THE PERFORMANCE OF THERMAL SPRAY COATINGS ON STEEL, *TESTING OF METALLIC AND INORGANIC COATINGS,* STP 947, AMERICAN SOCIETY FOR TESTING AND MATERIALS, 1987
3. "CODE OF PRACTICE FOR PROTECTIVE COATING OF IRON AND STEEL STRUCTURES AGAINST CORROSION," BS 5493, BRITISH STANDARDS INSTITUTION, 1977; AVAILABLE FROM THE AMERICAN NATIONAL STANDARDS INSTITUTE

4. "SPRAYED METAL COATINGS FOR ATMOSPHERIC CORROSION PROTECTION," G 189-1966, CANADIAN STANDARDS ASSOCIATION, 1966; REAFFIRMED 1980
5. ROSENBURGH *ET AL., ALUMINUM OFFSHORE--SAFETY ANALYSIS,* PUBLICATION 85-3208, VERITEC, 1985
6. THERMITE SPARKING, *ALUMINUM DESIGN GUIDE,* VOL 2, *DESIGN GUIDE ON THE USE OF ALUMINUM IN OFFSHORE STRUCTURES,* WIMPEY OFFSHORE, LONDON, SECTION 4.5
7. "PAINTING WATER STORAGE TANKS," ANSI/AWS D102-78, AMERICAN WELDING SOCIETY, 1978
8. *STEEL STRUCTURES PAINTING MANUAL,* STEEL STRUCTURES PAINTING COUNCIL
9. "GUIDE FOR THE PROTECTION OF STEEL WITH THERMAL SPRAY COATINGS OF ALUMINUM AND ZINC AND THEIR ALLOYS AND COMPOSITES," ANSI/AWS C2.18-X, AMERICAN WELDING SOCIETY, IN PREPARATION

Underwater Welding

S. Liu and D.L. Olson, Colorado School of Mines, S. Ibarra, Amoco Corporation Research

Introduction

UNDERWATER ARC WELDING is performed in either the wet environment or in a protective habitat (Ref 1). Although both environments experience increased pressure with depth (0.1 MPa, or 1 bar, for each 10 m, or 33 ft, increase in depth), the wet environment also significantly alters the cooling rate during welding, which affects the nature of the weld-metal phase transformation. Whereas shielded metal arc welding (SMAW) for surface welding has a time to cool from 800 to 500 °C (1470 to 930 °F), $\Delta t_{8/5}$, in the range of 8 to 16 s, a typical wet-welding procedure reportedly has $\Delta t_{8/5}$ values between 1 and 6 s, depending on heat input (0.8 to 3.6 kJ/mm) and plate thickness (Ref 2, 3, 4). The greater cooling rate produces significant amounts of heat-affected zone (HAZ) martensite in nearly all low-carbon steels. As the carbon equivalent (CE) of these steels approaches a value of 0.40 wt%, the fusion-line hardness usually exceeds 400 on the Vickers scale (98 N, or 10 kgf), where

$$CE = \%C + \frac{\%Mn}{6} + \frac{\%(Cr + Mo + V)}{5} + \frac{\%(Ni + Cu)}{15} \qquad \textbf{(EQ 1)}$$

As the martensite content increases in the coarse-grained HAZ, the susceptibility to hydrogen cracking becomes a measurable concern.

When underwater arc welding is conducted directly in the water, the SMAW process is usually used, although more recently flux-cored arc welding (FCAW) has been used, as well. Wet underwater welding has been demonstrated to be an acceptable repair technique at depths of 100 m (330 ft). However, wet welds have been made on carbon steel structures at depths as low as 200 m (660 ft).

Welding that is performed in a dry, but high-pressure (hyperbaric) environment requires the construction of a chamber around the weld zone to create the dry habitat. The cost of hyperbaric welding is therefore much higher than that of wet welding. The setting up and tearing down of equipment can be very expensive in a deep-sea environment. Additionally, hyperbaric welding exhibits low mobility. Each fabrication situation often requires a customized setup. The gas-metal arc welding (GMAW) and gas-tungsten arc welding (GTAW) processes can both be used in hyperbaric welding, unlike wet welding.

Despite differences in process characteristics, the influences of water depth (pressure) on arc behavior are similar for both wet welding and hyperbaric welding (Ref 5, 6, 7). The specific technological features of each of these processes are provided in Ref 1. This article discusses the metallurgical aspects of the underwater welds.

References

1. C.L. TSAI AND K. MASUBUCHI, INTERPRETIVE REPORT ON UNDERWATER WELDING, *WELD. RES. COUNC. BULL.*, VOL 224, 1977, P 1-37
2. N. CHRISTENSEN, THE METALLURGY OF UNDERWATER WELDING, *UNDERWATER WELDING*, PERGAMON PRESS, 1983, P 71-79
3. A. HAUSI AND Y. SUGA, ON COOLING OF UNDERWATER WELDS, *TRANS. JPN. WELD. SOC.*, VOL 2 (NO. 1), 1980
4. C.L. TSAI AND K. MASUBUCHI, MECHANISMS OF RAPID COOLING IN UNDERWATER WELDING, *APPL. OCEAN RES.*, VOL 1 (NO. 2), 1979, P 99-110
5. C.E. GRUBBS AND O.W. SETH, "MULTIPASS ALL POSITION WET WELDING, A NEW UNDERWATER TOOL," OFFSHORE TECHNOLOGY CONFERENCE, OTC 1620 (HOUSTON), 1972
6. K. MASUBUCHI, UNDERWATER FACTORS AFFECTING WELDING METALLURGY, *PROC. CONF. UNDERWATER WELDING OF OFFSHORE PLATFORMS AND PIPELINES*, AWS, 1980, P 81-98
7. N.M. MADATOR, INFLUENCE OF THE PARAMETERS OF THE UNDERWATER WELDING PROCESS ON THE INTENSITY OF METALLURGICAL REACTIONS, *WELD. RES. ABROAD*, VOL 3, 1972, P 63

S. Liu and D.L. Olson, Colorado School of Mines, S. Ibarra, Amoco Corporation Research

Underwater Welding Pyrometallurgy

The pyrochemical behavior of underwater welds (both hyperbaric and wet) is reported (Ref 2, 8, 9, 10, 11) to be a function of depth (pressure) down to 300 m (990 ft). The variation of weld-metal manganese content as a function of depth is shown in Fig. 1. There is a sharp decrease in manganese content from 0.6 wt% for the surface weld to 0.25 wt% for the weld made at 30 m (90 ft). This decrease in weld-metal manganese content can be directly correlated to the rapid increase in weld-metal oxygen content for the same range of depth, as seen in Fig. 2. This observation suggests that manganese recovery in the weld pool is controlled by oxidation. Similar behavior was found for weld-metal silicon (Fig. 1). It is expected that all oxide-forming elements would react in this manner to an increase in oxygen.

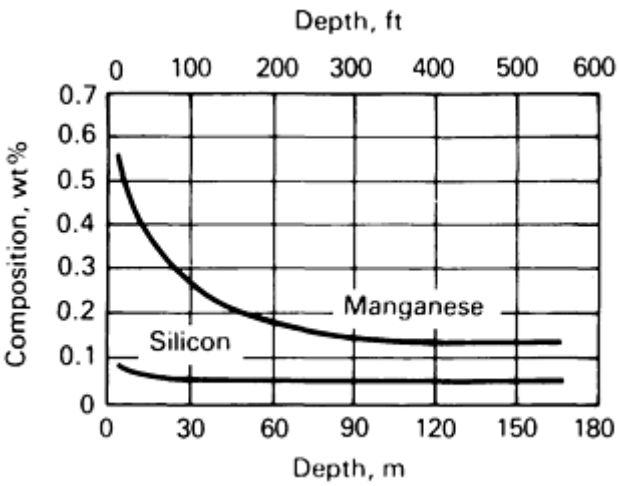

FIG. 1 WET UNDERWATER WELD-METAL MANGANESE AND SILICON AS A FUNCTION OF DEPTH. SOURCE: REF 11

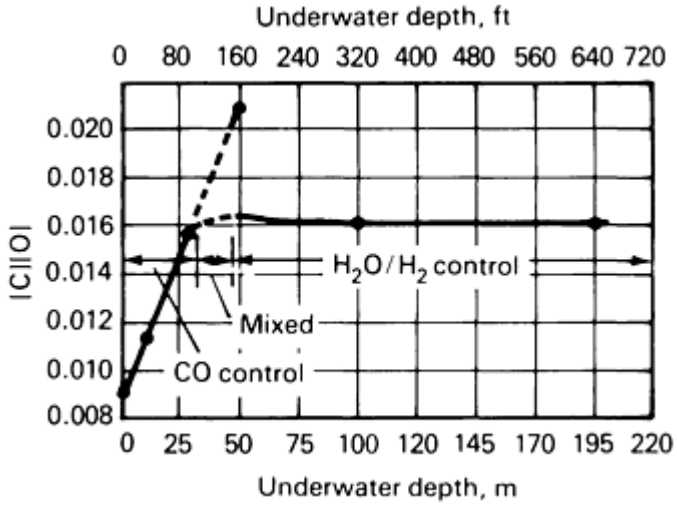

FIG. 2 PRODUCT OF WELD-METAL CARBON AND OXYGEN CONTENT AS A FUNCTION OF UNDERWATER DEPTH FOR WELD METAL PRODUCED WITH TREATED E6013 SMAW ELECTRODE. SOURCE: REF 11

The weld-metal carbon content, on the other hand, was found to increase significantly from the weld made at the surface to the welds made at 50 m (165 ft), as shown in Fig. 1. A linear relationship between the [C][O] product and the total pressure, *P*, or depth, has been found for both wet and hyperbaric SMAW processes, which suggests that the carbon monoxide reaction is a controlling mechanism. This behavior was observed for the hyperbaric SMAW process at depths equivalent to 300 m (990 ft). The carbon monoxide is a product of the decomposition of the calcium or magnesium carbonate that exists in the SMAW electrode coating to provide a working and protective welding plasma and cover. The resulting increases in weld-metal oxygen and carbon contents cause concern as to the use of a flux coating that contains carbonates for hyperbaric welding. Carbon pickup in the weld metal results in an increase in cracking susceptibility. Ferrosilicon additions to the flux did reduce weld-metal oxygen, but not sufficiently to alleviate this problem.

The carbon monoxide reaction was also found (Ref 10, 11) to be a controlling mechanism in wet underwater welding. The product of carbon and oxygen content, [C][O], for wet underwater welds was also plotted as a function of depth (pressure) in Fig. 2, which demonstrated an excellent linear correlation for the weld-metal carbon and oxygen product results down to 50 m (165 ft). This observation suggests that the carbon monoxide reaction controls the oxygen content down to 50 m (165 ft), and that the oxygencontent, in turn, controls the oxidation of manganese and silicon and, thus, the weld-metal contents of these elements. The actual depth to which the carbon monoxide reaction is a controlling factor is a function of the specific electrode composition.

In Fig. 2, the weld-metal oxygen and carbon contents become fairly constant between 50 and 100 m (165 and 330 ft). The weld-metal manganese and silicon contents are also fairly constant within this same range. These observations suggest that oxygen content still controls the weld-metal manganese and silicon contents, but that carbon monoxide formation is not the controlling reaction at depths greater than 50 m (165 ft).

The compositional results for depths greater than 50 m (165 ft) suggest that the H_2O decomposition reaction may be the controlling mechanism. At temperatures above 1000 °C (1830 °F), water vapor begins to dissociate into hydrogen and oxygen and dynamic equilibrium takes place (Ref 10, 11). For this reaction the weld-metal oxygen content is not a function of pressure (depth) and the [C][O] product will also remain constant. The diameter of the arc plasma column decreases with increasing pressure (depth). Thus, at depths greater than 50 m (165 ft), the water reaction becomes more dominant and the [C][O] product becomes less important and insensitive to depth, as seen in Fig. 2.

Another indication that hydrogen is more abundant in and involved with the rate-control chemistry is evident when considering arc stability, which decreases in extreme depth. In Fig. 3, the operating parameter space for underwater welding is shown to decrease with depth. This behavior can be explained by the high ionization potential for hydrogen, which makes it more difficult to sustain the welding arc.

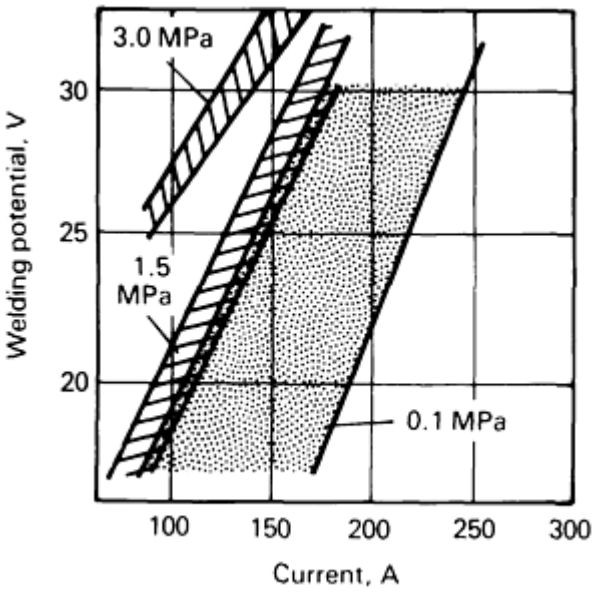

FIG. 3 REGIONS IN WELDING PARAMETER SPACE FOR SUCCESSFUL HIGH-PRESSURE WELDING AS A FUNCTION OF PRESSURE, OR DEPTH. NOTE THAT THE ACCEPTABLE WELDING PARAMETER SPACE REDUCES WITH PRESSURE, OR DEPTH. SOURCE: REF 11

References cited in this section

2. N. CHRISTENSEN, THE METALLURGY OF UNDERWATER WELDING, *UNDERWATER WELDING,* PERGAMON PRESS, 1983, P 71-79
8. O. GRONG, D.L. OLSON, AND N. CHRISTENSEN, ON THE CARBON OXIDATION IN HYPERBARIC MMA WELDING, *MET. CONSTR.,* VOL 17 (NO. 12), 1985, P 810R-814R
9. D.L. OLSON AND S. IBARRA, UNDERWATER WELDING METALLURGY, *PROC. FIRST OMAE SPECIALTY SYMPOSIUM ON OFFSHORE AND ARCTIC FRONTIERS,* ASME, 1986, P 439-447
10. S. IBARRA, C.E. GRUBBS, AND D.L. OLSON, FUNDAMENTAL APPROACHES TO UNDERWATER WELDING METALLURGY, *J. MET.,* VOL 40 (NO.12), 1988, P 8-10
11. S. IBARRA AND D.L. OLSON, WET UNDERWATER STEEL WELDING, *FERROUS ALLOY WELDMENTS,* VOL 69-70, *KEY ENG. MATERIALS,* TRANS TECH PUBLICATIONS, ZURICH, 1992, P 329-378

S. Liu and D.L. Olson, Colorado School of Mines, S. Ibarra, Amoco Corporation Research

Microstructural Development of Underwater Welds

Three types of ferrite are associated with low-carbon steel weld metal: grain-boundary ferrite (GBF), Widmanstätten, or sideplate, ferrite (SPF), and acicular ferrite (AF). Prior austenite grain boundaries can promote the formation of GBF and represent the sites for the nucleation of SPF, which protrudes from the grain boundaries into the prior austenite grains. Acicular ferrite is intragranular and has a much finer basket-weave structure. Other microconstituents, such as pearlite, cementite, and martensite, can also result. At faster cooling rates, the formation of bainite or ferrite with aligned carbide (AC) and martensite is possible. It is recognized that acicular ferrite is the microstructural constituent that gives a high resistance to cleavage fracture.

A typical wet (underwater) weld-metal microstructure, as a function of depth, is illustrated in Fig. 4. At shallow depths, the weld metal is primarily grain-boundary ferrite, with 10 to 20% aligned carbide. With increasing depths, the relative amount of grain-boundary ferrite decreases to about 50%, with increasing amounts of aligned carbide and sideplate ferrite. The major changes in microstructure occur in the first 50 m (165 ft) of depth. At depths greater than 50 m (165 ft), the weld-metal composition and microstructure remain fairly constant. This observation is also consistent with the constant weld-metal oxygen content described previously, which suggests a constant oxidation rate.

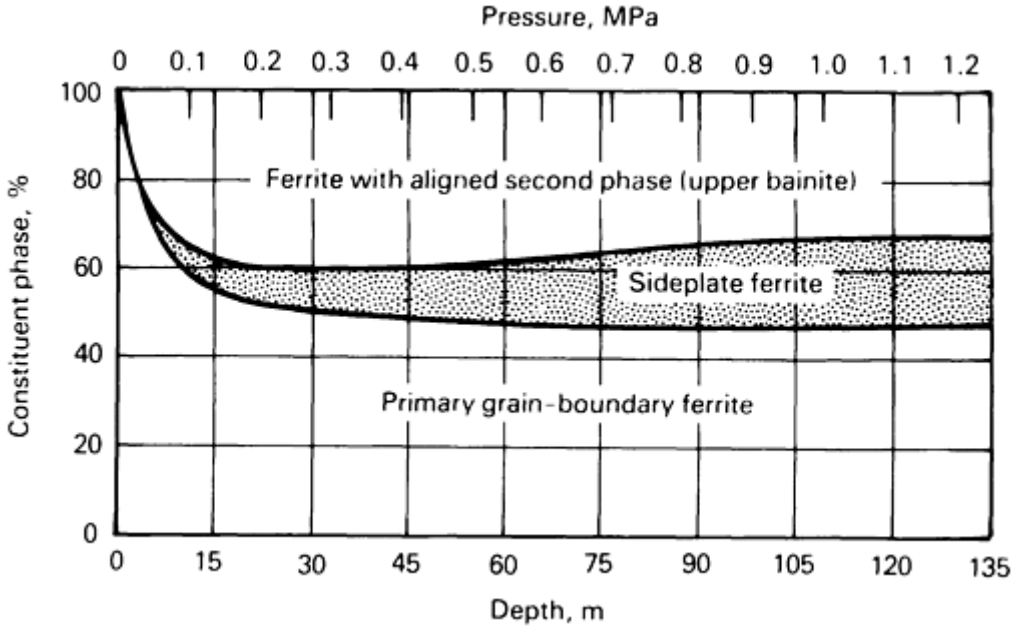

FIG. 4 PERCENTAGE OF WELD-METAL MICROSTRUCTURAL CONSTITUENTS FOR WET UNDERWATER WELDS AS A FUNCTION OF WATER DEPTH

The formation of acicular ferrite, instead of the significant sideplate ferrite content, is highly desirable in order to improve toughness. Acicular ferrite formation in underwater welds is possible, but only with specific weld-metal alloying additions, such as titanium or boron and with the proper weld-metal oxygen and manganese contents.

A diagram of weld-metal oxygen content versus effective weld-metal manganese content (Mn + 6C) has been used (Ref 8, 9, 10) to conceptually assist in selecting compositional modifications for the consumables of wet underwater welding, as shown in Fig. 5. Figure 5 represents a particular case in which deposits of an underwater wet E6013 electrode were constructed on the basis of microstructural and compositional analysis. This particular diagram represents the cooling rate typically found in wet welding.

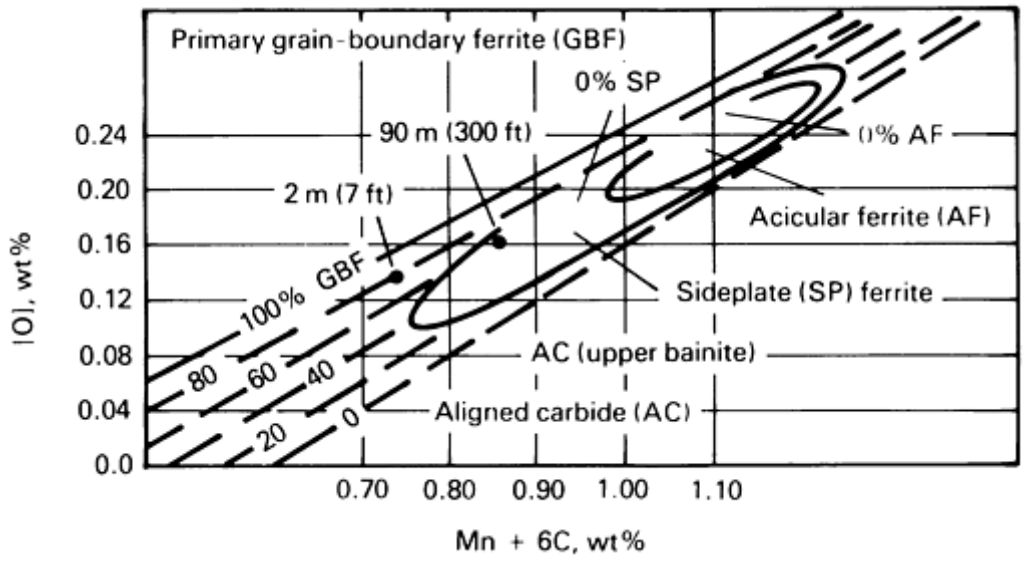

FIG. 5 SUGGESTED COMPOSITIONAL DIAGRAM FOR PREDICTION OF WELD-METAL MICROSTRUCTURE FOR WET UNDERWATER WELDS

References cited in this section

8. O. GRONG, D.L. OLSON, AND N. CHRISTENSEN, ON THE CARBON OXIDATION IN HYPERBARIC MMA WELDING, *MET. CONSTR.*, VOL 17 (NO. 12), 1985, P 810R-814R
9. D.L. OLSON AND S. IBARRA, UNDERWATER WELDING METALLURGY, *PROC. FIRST OMAE SPECIALTY SYMPOSIUM ON OFFSHORE AND ARCTIC FRONTIERS*, ASME, 1986, P 439-447
10. S. IBARRA, C.E. GRUBBS, AND D.L. OLSON, FUNDAMENTAL APPROACHES TO UNDERWATER WELDING METALLURGY, *J. MET.*, VOL 40 (NO.12), 1988, P 8-10

S. Liu and D.L. Olson, Colorado School of Mines, S. Ibarra, Amoco Corporation Research

Hydrogen Mitigation

Because moisture drastically increases the availability of hydrogen, the wet underwater welding of higher-strength steels is very susceptible to hydrogen cracking (Ref 12). Even during hyperbaric welding, after water has been removed from the chamber, the partial pressure of moisture is still high, causing the same effects as in wet welding.

The HAZ cracking that results from the wet welding of higher-strength steels is due to three necessary factors: hydrogen from the weld pool, microstructures that develop in the HAZ, and stress levels that develop in the weld joint. Hydrogen cracking can be reduced or managed by:

- USING CONSUMABLES THAT CAN HOLD A HIGH CONCENTRATION OF HYDROGEN IN MOLTEN WELD POOLS, AS WELL AS IN THE SOLIDIFIED WELD BEAD
- ALTERING THE FLUX COATINGS TO INTRODUCE ALTERNATE GASES IN THE WELDING PLASMA, THEREBY REDUCING THE HYDROGEN CONTENT
- SELECTING THE WELDING PARAMETERS THAT MINIMIZE WELD POOL HYDROGEN PICKUP

- DESIGNING THE WELD FOR MINIMUM STRESS

The use of ferritic-based weld deposits will cause the rejection of large amounts of hydrogen from the weld solidification. The hydrogen will go into the fully martensitic HAZ and will promote underbead cracking. A method that partially alleviates hydrogen susceptibility is to use an austenitic weld deposit that has a much larger solubility for hydrogen and, thus, a smaller tendency to transport hydrogen to the HAZ (Ref 13).

However, the use of an austenitic stainless steel consumable results in a deposit with a high coefficient of thermal expansion (CTE), relative to ferritic-based metal, as well as higher residual stresses and an increasing tendency for cracking. A solution to this problem, which is a compromise between high solubility for hydrogen and CTE mismatch, is to use high-nickel-content weld deposits, because nickel-base alloys have approximately the same CTE as ferritic steel and are capable of managing a large hydrogen content.

Although the nickel weld-metal deposit is virtually immune to the restraint cracking that was noted in the austenitic stainless steel welds, the use of nickel-base electrodes is restricted by their depth sensitivity. Although these electrodes are successful in preventing hydrogen cracking in the HAZ, the resulting welds can be porous and, in some cases, susceptible to embrittlement. Nickel-base welds at a depth of 30 m (100 ft) exhibited excessive porosity that was due to a lack of necessary heat input at this depth. These nickel-base wet-weld deposits have been successful only down to depths of 10 m (35 ft) when the SMAW process is used. Welding at greater depths, when using nickel-base electrodes, requires a higher level of heat input.

To reduce the influence of the plasma hydrogen content, other gases need to be introduced into the arc. Increasing the carbonate content of welding flux has been shown to increase the carbon monoxide content in the arc and, thus, to reduce the hydrogen content (Ref 14, 15). Carbonates (Ref 15) also increase the degree of oxidation of the deposited metal, which decreases weld-metal hydrogen content. The decomposition of carbonates results in higher oxygen and lower hydrogen contents.

The use of carbonates to reduce the plasma hydrogen content may not be as attractive when considering all the effects, because carbonates also promote weld-metal carbon and oxygen pickup with increasing pressure. Carbon has also been reported to reduce the hydrogen solubility in ferrite and to increase the hydrogen solubility in austenite. Thus, increasing carbon content will cause greater potential hydrogen supersaturation with the decomposition of austenite, thus reducing the favorable hydrogen reduction effects in the arc. This problem could limit the use of increased carbonate content to the shallower depths.

The influence of welding parameters on the underwater welding process and on the associated metallurgical reactions has been studied. The diffusible hydrogen content increases with increasing voltage, but decreases with increasing welding current. These results suggest that welding with lower potential and higher current will promote a significant reduction in the weld-metal diffusible hydrogen content (Ref 16). The diffusible hydrogen content in wet underwater welds decreases with increasing heat input for both SMAW and FCAW processes (Ref 17, 18).

The third factor that influences hydrogen cracking is the applied and residual stress states. The applied stress can be reduced by improving the fit-up on the weld joint to be used in the repair. In the underwater wet welding repair of platforms, scalloped sleeves are frequently fillet welded over the damaged area. Careful fabrication of the scalloped sleeve will result in improved fit-up and, thus, reduced stresses. The applied stress on a weldment can also be improved by using a larger weld-metal deposit. This practice will result in a larger HAZ, with a smaller applied stress.

The residual stresses are more difficult to manage in an environment that is not easily accessible to postweld heat treatment. Welding practices that can reduce residual stresses include:

- THE USE OF SMALL WELD DEPOSITS
- THE USE OF CONSUMABLES WITH CTES THAT ARE COMPATIBLE TO THAT OF THE BASE MATERIALS
- THE SELECTION OF EDGE PREPARATIONS THAT REDUCE THE SIZE OF THE TOTAL WELD DEPOSIT

The cross-sectional area of the total weld deposit is directly related to a shrinkage tendency. In designing an underwater weld joint, the concerns for applied stress and for residual stress must be balanced, because a different weld size is required in each case.

Temper Bead Practice. To further reduce stress and, thus, hydrogen cracking, the thermal experience(s) of the wet welding practice must be considered (Ref 8, 19). Although it is difficult to perform any significant preheat treatment procedures on the base material in wet, heavy-section welding, a temper bead practice that reduces the near-fusion-line hardness and cracking tendency has been perfected. A typical temper bead practice involves a weld deposition that is laid down over a previous weld deposit that has a less-susceptible cracking tendency than that of the base metal (Ref 20). As shown in Fig. 6, the second deposition, or temper bead, must be carefully located relative to the previous bead fusion line, such that its thermal experience tempers the near-fusion-line HAZ of the base material, which has a cracking-susceptible carbon equivalent (Ref 20).

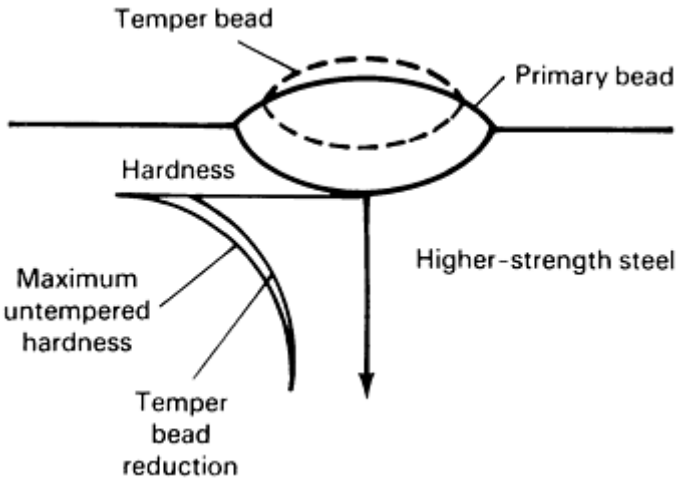

FIG. 6 USE OF TEMPER BEAD PRACTICE TO REDUCE HAZ HARDNESS AND SUSCEPTIBILITY FOR UNDERBEAD CRACKING. SOURCE: REF 11

There is evidence that temper weld beads can influence the properties of wet underwater welds. In the weld metal, Charpy V-notch toughness improved with an increasing number of weld passes (Ref 17, 18). This technique will reduce residual stresses, as well as hardness, and represents the optimum practice to wet weld the higher-CE steels. Another advantage to the temper bead practice is that while the temper bead is in the high-temperature austenitic condition, it is a favorable reservoir for hydrogen and, thus, it extracts some of the hydrogen from the more-crack-susceptible HAZ.

Welding consumables that generate chemical heat have been investigated as an additional heat source during underwater welding (Ref 8). Samples from a platform steel with a CE of 0.40 wt% were welded in a 10 m (35 ft) tank. A heat-generating thermit electrode weld was used after each pass to postweld heat treat the HAZ. Thermit-type reactions during arc welding have been used to improve the underwater temper bead practice in order to reduce the hydrogen cracking susceptibility of the HAZ.

References cited in this section

8. O. GRONG, D.L. OLSON, AND N. CHRISTENSEN, ON THE CARBON OXIDATION IN HYPERBARIC MMA WELDING, *MET. CONSTR.*, VOL 17 (NO. 12), 1985, P 810R-814R
11. S. IBARRA AND D.L. OLSON, WET UNDERWATER STEEL WELDING, *FERROUS ALLOY WELDMENTS*, VOL 69-70, *KEY ENG. MATERIALS*, TRANS TECH PUBLICATIONS, ZURICH, 1992, P 329-378
12. O. OZAKI, J. NAIMAN, AND K. MASUBUCHI, A STUDY OF HYDROGEN CRACKING IN UNDERWATER STEEL WELDS, *WELD. J.*, VOL 56 (NO. 8), 1977, P 231S-237S

13. W.A. STALKER, P.H.M. HART, AND G.R. SALTER, "AN ASSESSMENT OF SHIELDED METAL ARC ELECTRODES FOR THE UNDERWATER WELDING OF CARBON MANGANESE STRUCTURAL STEELS," OFFSHORE TECHNOLOGY CONFERENCE, OTC REPORT 2301 (HOUSTON), 1975
14. B. CHEW, PREDICTION OF WELD METAL HYDROGEN LEVELS OBTAINED UNDER TEST CONDITIONS, *WELD. J.,* VOL 52, 1973, P 386S-391S
15. L.I. SOROKIN AND Z.A. SIDLIN, THE EFFECT OF ALLOYING ELEMENTS AND OF MARBLE IN AN ELECTRODE COATING ON THE SUSCEPTIBILITY OF A DEPOSITED NICKEL CHROME METAL TO PORE FORMATION, *SVAR. PROIZVOD.,* NO. 11, 1974, P 7-9
16. V.Y. KONONENKO, EFFECT OF WATER SALINITY AND MECHANIZED UNDERWATER WELDING PARAMETERS ON HYDROGEN AND OXYGEN CONTENT OF WELD METAL, *WELDING UNDER EXTREME CONDITIONS,* PERGAMON PRESS, 1989, P 113-118
17. H. HOFFMEISTER AND K. KUSTER, PROCESS VARIABLES AND PROPERTIES OF UNDERWATER WET SHIELDED METAL ARC LABORATORY WELDS, *UNDERWATER WELDING,* PERGAMON PRESS, 1983, P 115-125
18. K. HOFFMEISTER AND K. KUSTER, PROCESS VARIABLES AND PROPERTIES OF WET UNDERWATER GAS METAL ARC LABORATORY AND SEA WELDS OF MEDIUM STRENGTH STEELS, *UNDERWATER WELDING*, PERGAMON PRESS, 1983, P 239-246
19. A. MATSUNAWA, H. TAKEMATA, AND I. OKAMOTO, ANALYSIS OF TEMPERATURE FIELD WITH EQUIRADIAL COOLING BOUNDARY AROUND MOVING HEAT SOURCES--HEAT CONDUCTION ANALYSIS FOR ESTIMATION OF THERMAL HYSTERESIS DURING UNDERWATER WELDING, *TRANS. JWRI,* VOL 9 (NO. 1), 1980, P 11-18
20. K. OLSEN, D.L. OLSON, AND N. CHRISTENSEN, WELD BEAD TEMPERING OF HEAT AFFECTED ZONE, *SCAND. J. METALL.,* VOL 11, 1982, P 163-168

S. Liu and D.L. Olson, Colorado School of Mines, S. Ibarra, Amoco Corporation Research

Weld-Metal Porosity

Weld-metal porosity is a major concern in underwater welds. The amount of porosity determines whether a wet weld will meet the type A, B, or C weld specification (ANSI/AWS D3.6-83 specification). Pore formation results from entrapment, supersaturation of dissolved gas, or gas-producing chemical reactions. The nature and amount of weld-metal porosity involves at least four competing time-dependent processes (Ref 21): the nucleation, growth, transport, and coalescence of pores. The physical requirement for pore formation is that the sum of the partial pressure, P_g, of soluble gases must exceed the sum of the following pressure terms:

$$P_G > P_A + P_H + P_B \qquad \textbf{(EQ 2)}$$

where P_a is the atmosphere pressure, P_h is the hydrostatic pressure, and P_b is the pressure increase that is due to the curvature of the pore. For underwater welding, P_h is the controlling term, because it is directly related to depth.

The effect of water pressure on the formation of porosity in underwater gravity welding with electrodes of the ilmenite type, high titanium oxide type, and iron powder/iron oxide type and with SM41 steel base metals has been reported (Ref 22). The amount of porosity increased with water pressure (depth) (Fig. 7). The pore shape changed from spherical to long and narrow with increasing pressure, which indicates a change of the pore-formation mechanism. In wet underwater welds, the pores contained approximately 96 vol% H_2, 0.4 vol% CO, and 0.06 vol% CO_2. Other bubble compositions (Ref 6, 23) of 62 to 82% H_2, 11 to 24% CO, and 4 to 6% CO_2 have been reported (Ref 24). More-specific data on a rutile iron powder (E7014) electrode are 45% H_2, 43% CO, 8% CO_2, and 4% other. The variation in bubble composition indicates the broad nature of the chemical processes associated with wet underwater welding and is most likely due to variations in electrode covering compositions, energy input, and water depth.

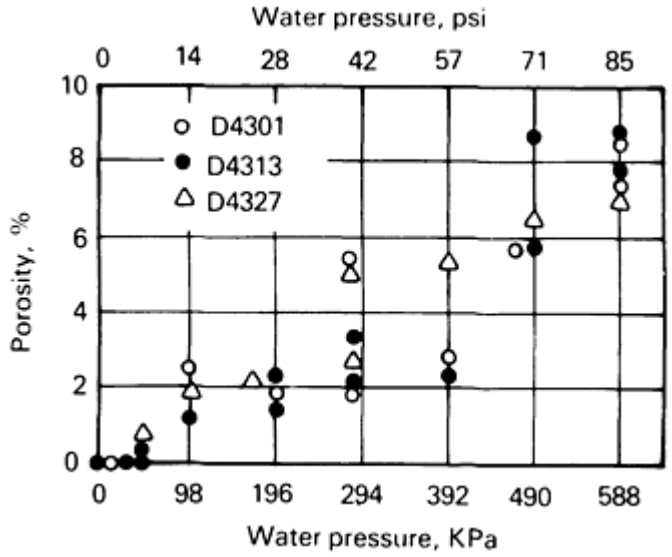

FIG. 7 EFFECT OF WATER PRESSURE ON POROSITY. SOURCE: REF 22

Two possible methods of reducing weld-metal porosity with depth, in the case of wet welding, are to add to the weld pool specific elements that getter the hydrogen by forming hydrides and to alter the welding parameters to reduce pore formation. At increasing travel speeds, the number of pores per volume of weld deposit goes through a maximum. A relationship between the product of travel speed (*S*) and bead area (*A*) and the amount of gas absorbed per unit volume of weld metal exists (Ref 25). This relationship suggests that for decreasing values of the product (*SA*), the gas absorbed per unit volume of weld metal increases for the same gas partial pressure. With small beads and a slow welding speed, the amount of gas absorbed per unit volume of weld metal is high. The faster freezing rate of the smaller, short-circuiting arc weld allows less time for gas desorption and causes more gas bubbles to be trapped before floating to the surface of the weld pool. This relationship holds significance for many of the practices used in wet underwater welding, which produce small weld deposits. In underwater welding, the relationship between porosity and welding current is strongly influenced by the type of moisture resistance coating on the electrode. The amount of gas pickup increases as the arc was lengthened (Ref 21). In general, the hydrogen absorption and, therefore, porosity levels in welding can be minimized by using a low current with direct current electrode positive (DCEP), a high current with direct current electrode negative (DCEN), a short arc, and a fast travel speed.

References cited in this section

6. K. MASUBUCHI, UNDERWATER FACTORS AFFECTING WELDING METALLURGY, *PROC. CONF. UNDERWATER WELDING OF OFFSHORE PLATFORMS AND PIPELINES,* AWS, 1980, P 81-98
21. R.E. TREVISAN, D.D. SCHWEMMER, AND D.L. OLSON, THE FUNDAMENTALS OF WELD METAL PORE FORMATION, *WELDING: THEORY AND PRACTICE,* D.L. OLSON, R.D. DIXON, AND A.L. LIBY, ED., ELSEVIER SCIENCE B.V., 1990
22. Y. SUGA AND H. ATSUSHI, "ON THE FORMATION OF POROSITY IN UNDERWATER WELD METAL (THE 1ST REPORT)--EFFECT OF WATER PRESSURE ON FORMATION OF POROSITY," IIW DOC. IX-1388-86, AMERICAN COUNCIL, AWS, 1986
23. N.M. MALATOR, THE PROPERTIES OF THE BUBBLES OF STEAM AND GAS AROUND THE ARC IN UNDERWATER WELDING, *AUTOMAT. WELD.,* VOL 18 (NO. 12), 1965, P 25-29
24. E.A. SILVA, GAS PRODUCTION AND TURBIDITY DURING UNDERWATER SHIELDED METAL-ARC WELDING WITH IRON POWDER ELECTRODES, *NAV. ENG. J.,* VOL 12, 1971
25. G.R. SALTER AND D.R. MILNER, GAS METAL REACTIONS IN ARC WELDING, *BRIT. WELD. J.,* VOL 33, 1965

S. Liu and D.L. Olson, Colorado School of Mines, S. Ibarra, Amoco Corporation Research

Fatigue as a Function of Porosity

The designers of offshore structures are usually concerned with the initiation and growth of fatigue cracks in fracture-critical members, because of noted decreases in fracture toughness, as well as the presence of varying amounts of porosity. Cyclic fatigue stresses will develop with any natural sea movement and will increase during storms.

Drilling the tip of a fatigue crack is a common field technique that is used to prevent further crack growth. In the same manner, the presence of porosity in weldments can be beneficial, because the pores act as pinning sites for fatigue cracks and can either retard or stop their growth. In particular, the presence of some amount of porosity retarded fatigue crack growth at low stress in surface habitat and wet underwater welds (Ref 26) (Fig. 8). The low-porosity dry habitat weld was shown to contain approximately 3% porosity on the fatigue fracture surface, whereas the high-porosity wet underwater weld contained approximately 12% porosity on the fatigue fracture surface.

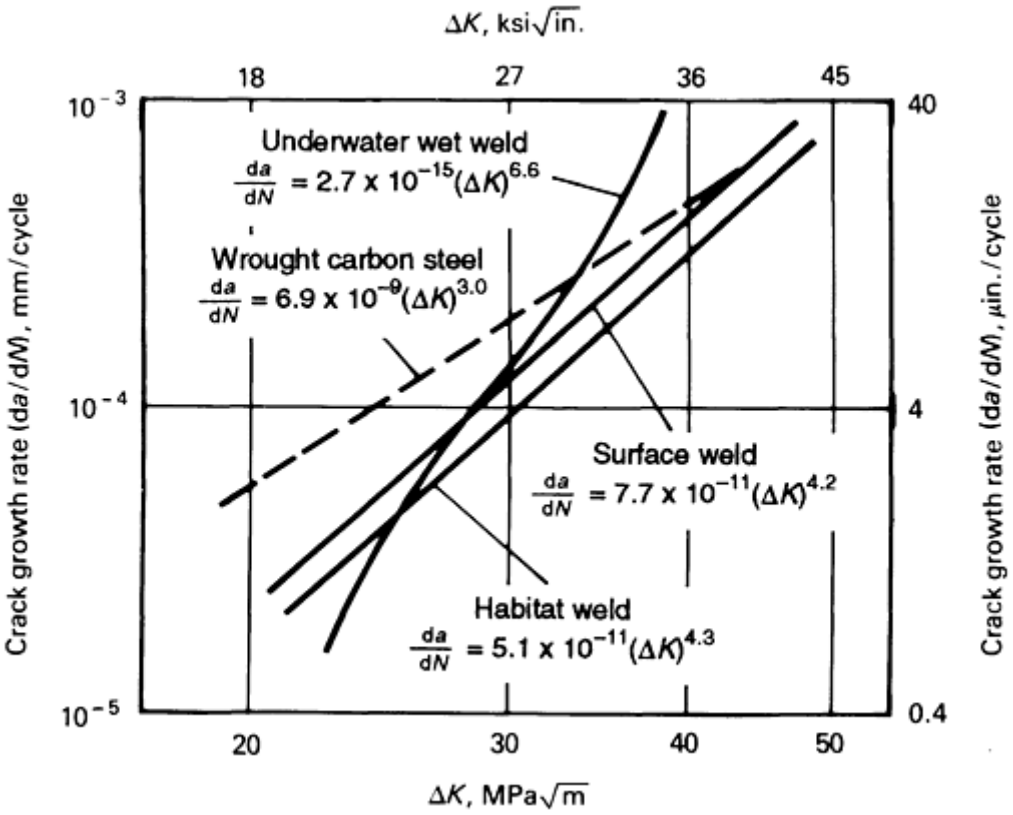

FIG. 8 COMPARISON OF EFFECTS OF POROSITY AND FREQUENCY ON THE FATIGUE CRACK GROWTH BEHAVIOR OF WELDS TESTED IN SEAWATER. SOURCE: REF 26

In comparison to normal wrought ferrite-pearlite steels, all experimental underwater welds exhibited lower growth rates for low values of ΔK, where ΔK is the cyclic variation in the stress intensity factor, K. However, the wet welds tended to have a higher fatigue crack growth rate than the wrought alloys at high values of ΔK, particularly in wet welds.

At low ΔK values, the wet underwater welds have the most fatigue crack growth resistance. The large number of pores act as pinning sites for the advancing fatigue crack front. Increased porosity in a weldment yielded lower fatigue crack growth at low ΔK values.

At high ΔK values, the crack growth rate is much greater for the higher-porosity content. At higher stress levels, the mechanical behavior of the sample is more like that experienced in a tensile test. The high numbers of pores act to reduce the cross-sectional area and, thus, allow the cracks to propagate at a high rate. The use of wet weld repairs in areas of high cyclic stress should be accompanied by caution and a load-reducing joint design.

Reference cited in this section

26. D.K. MATLOCK, G.R. EDWARDS, D.L. OLSON, AND J. IBARRA, AN EVALUATION OF THE FATIGUE BEHAVIOR IN SURFACE, HABITAT, AND UNDERWATER WET WELDS, *UNDERWATER WELDING*, PERGAMON PRESS, 1983, P 303-310

S. Liu and D.L. Olson, Colorado School of Mines, S. Ibarra, Amoco Corporation Research

Heat Sources

With increasing depth and, thus, pressure, the welding parameter space for sustaining a welding arc becomes more restricted. This effect necessitates a more careful selection of the welding voltage (gap) and current for a given size and type of welding electrode. The decreasing welding parameter space also reflects a shift of current to lower values and voltage to higher values (see Fig. 3), which changes the nature of the heat input. Electrode coating thickness can also influence the arc characteristics (Ref 16). Figure 9 illustrates that increasing coating thickness also raises the arc characteristic curves.

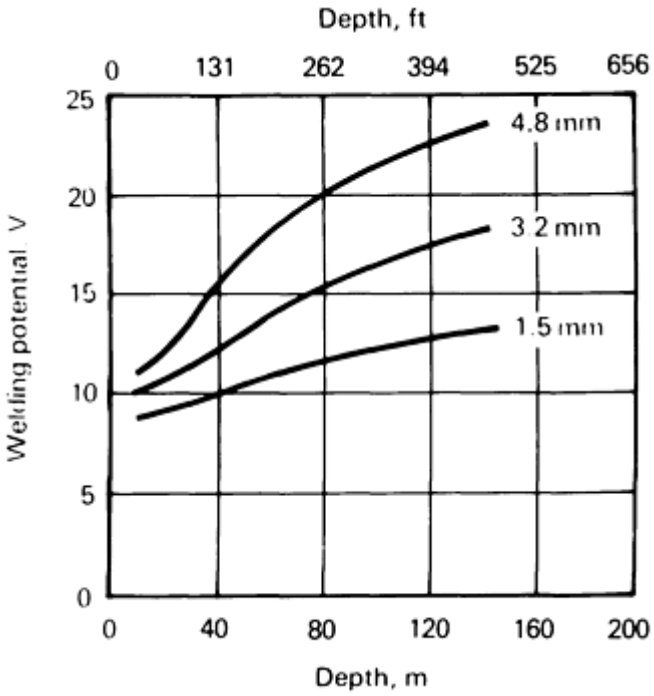

FIG. 9 EFFECTS OF DEPTH ON ARC VOLTAGE FOR THREE DIFFERENT GTAW ELECTRODE DIAMETERS. SOURCE: REF 29

With an increase in the welding depth, the duration and frequency of short circuits and arc extinctions were reported to grow significantly (Ref 28), and the process stability deteriorated. The observed rise of welding current is associated with the increase in the number of short circuits. The addition of rare earth metals into the charge of rutile-base flux-cored wire

provides considerable improvement in arc stability and reduces arc downtime (arc extinctions and short circuits) by nearly two times. The more-stable arc burning that occurs when welding with the rare earth metal-containing wire allows its use in any spatial position and within the depth ranges investigated.

An approach that separates the wet conditions from the weld pool has been demonstrated, in which a welding torch that produces a local gas cavity by controlling the fluid flow in the environment of the weld is utilized (Ref 29). This method hinders the water invasion by the momentum of the fluid jet and by the smooth exhausting of cavity gases by flow entrapment. The process allows near-surface welding conditions to exist and permits the flexibility of wet welding practices while achieving weld quality that is similar to dry-environment underwater welding.

References cited in this section

16. V.Y. KONONENKO, EFFECT OF WATER SALINITY AND MECHANIZED UNDERWATER WELDING PARAMETERS ON HYDROGEN AND OXYGEN CONTENT OF WELD METAL, *WELDING UNDER EXTREME CONDITIONS*, PERGAMON PRESS, 1989, P 113-118
28. I.K. POKHODNYA, V.N. GORPENYUK, V.YA. KONONENKO, V.E. PONOMAREV, AND S.YU. MAKSIMOV, SOME PECULIARITIES OF ARC BURNING AND METAL TRANSFER IN WET UNDERWATER SELF-SHIELDING FLUX-CORED WIRE WELDING, *WELDING UNDER EXTREME CONDITIONS*, PERGAMON PRESS, 1989, P 151
29. S. FUKUSHIMA, T. FUKUSHIMA, AND J. KINUGAWA, UNDERWATER WET PLASMA WELDING IN PRESSURIZED WATER, *TRANS. MET. INST. MET.*, VOL 19 (NO. 3), 1977, P 133-151

Underwater Welding

S. Liu and D.L. Olson, Colorado School of Mines, S. Ibarra, Amoco Corporation Research

Practical Applications for Underwater Welding

Underwater welding techniques are used primarily for the repair of offshore platforms, particularly after the normal 5 year inspection period. However, these techniques have also been very useful during the installation of new offshore structures and undersea pipelines, the installation of hot taps, the repair of dock and harbor facilities, the modification of and addition to underwater structures, and the repair of nuclear facilities.

Examples of maintenance and repair applications are described below.

Offshore Structures. Underwater welding techniques are used to repair damages caused by corrosion or by fatigue cracking, and to repair members that have been damaged by ship impact. The repair or replacement of structural members damaged during installation by objects that have fallen overboard or by other accidents have also been reported. The underwater wet welding repair of these structures requires that the carbon equivalent of the steel be below 0.40 wt% (as calculated using the International Institute of Welding formula) to prevent hydrogen cracking. For steels with high carbon equivalents, the use of multiple temper bead techniques is required in order to reduce the hardness in the HAZ and eliminate the presence of hydrogen.

Undersea Pipelines. The repair or replacement of undersea pipelines is usually conducted in a hyperbaric dry chamber. Although sleeve repairs using wet welds have been tested successfully, their use has not been reported to date. Hyperbaric chambers are used regularly for underwater tie-ins and for repairs of defects.

Harbor Facilities. Corrosion and collision damage to sheet and pilings have been repaired. The repair and replacement of tubular dock braces, dock supports, and tanker moorings have also been reported.

Floating Vessels. Permanent and temporary repairs to holes in ship and barge hulls have been conducted. The hulls and pontoons of semisubmersible drill ships have also been repaired.

Nuclear Power Plants. The wet welding of nuclear power plant components is usually conducted with austenitic stainless steel electrodes in order to match the austenitic base metal used in the construction of these power plants. Damaged reactor internal components and leaks in pool liners are the usual types of repairs.

Specifications. The first underwater welding specification, known as ANSI/AWS D3.6, "Specification for Underwater Welding," was published in 1983 by the American Welding Society. This specification provides comprehensive information that enables engineers to select the welding method (wet or dry) that meets the established fitness-for-purpose requirements. The specification also provides a means for the engineer to make critical decisions in structural fabrication when underwater welding techniques are used. It is also a performance specification that is intended to assist the purchaser in specifying and obtaining the desired mechanical properties when using underwater welding techniques. The specification also allows contractors to prepare estimates and quotations for each project with a clear understanding of what is required. The original specification has been revised and reissued several times.

The AWS D3.6 specification defines four weld types, or classes. Each weld type has a specific set of quality requirements that must be verified during procedure qualification. The type of weld selected for a specific application is determined by the user.

Type A welds are represented by a set of requirements that produces an underwater weld comparable to a surface weld. Underwater welds that meet these requirements are usually hyperbaric (dry) welds.

Type B welds are usually reserved for wet underwater welds. They are intended for less-critical applications where reduced ductility and increased porosity can be tolerated. Typical applications include scallop sleeves on offshore structures.

Type C welds satisfy lesser requirements than type B welds and are intended for applications where load-beating function is not a primary consideration.

Type O welds usually meet the requirements of surface dry welds, as well as those of other codes and specifications.

Other underwater welding documents are developed by agencies such as the International Institute of Welding (IIW Doc SCUW 124-90), the American Society of Mechanical Engineers (ASME Section X/IWA 4550 for Underwater Welding of Nuclear Vessels), and the Norwegian agency Det Norske Veritas (DNV) (Document RP3604, Recommended Practices for Underwater Welding).

Underwater Welding

S. Liu and D.L. Olson, Colorado School of Mines, S. Ibarra, Amoco Corporation Research

---

References

1. C.L. TSAI AND K. MASUBUCHI, INTERPRETIVE REPORT ON UNDERWATER WELDING, *WELD. RES. COUNC. BULL.*, VOL 224, 1977, P 1-37
2. N. CHRISTENSEN, THE METALLURGY OF UNDERWATER WELDING, *UNDERWATER WELDING,* PERGAMON PRESS, 1983, P 71-79
3. A. HAUSI AND Y. SUGA, ON COOLING OF UNDERWATER WELDS, *TRANS. JPN. WELD. SOC.*, VOL 2 (NO. 1), 1980
4. C.L. TSAI AND K. MASUBUCHI, MECHANISMS OF RAPID COOLING IN UNDERWATER WELDING, *APPL. OCEAN RES.*, VOL 1 (NO. 2), 1979, P 99-110
5. C.E. GRUBBS AND O.W. SETH, "MULTIPASS ALL POSITION WET WELDING, A NEW UNDERWATER TOOL," OFFSHORE TECHNOLOGY CONFERENCE, OTC 1620 (HOUSTON), 1972
6. K. MASUBUCHI, UNDERWATER FACTORS AFFECTING WELDING METALLURGY, *PROC. CONF. UNDERWATER WELDING OF OFFSHORE PLATFORMS AND PIPELINES,* AWS, 1980, P 81-98

7. N.M. MADATOR, INFLUENCE OF THE PARAMETERS OF THE UNDERWATER WELDING PROCESS ON THE INTENSITY OF METALLURGICAL REACTIONS, *WELD. RES. ABROAD,* VOL 3, 1972, P 63
8. O. GRONG, D.L. OLSON, AND N. CHRISTENSEN, ON THE CARBON OXIDATION IN HYPERBARIC MMA WELDING, *MET. CONSTR.,* VOL 17 (NO. 12), 1985, P 810R-814R
9. D.L. OLSON AND S. IBARRA, UNDERWATER WELDING METALLURGY, *PROC. FIRST OMAE SPECIALTY SYMPOSIUM ON OFFSHORE AND ARCTIC FRONTIERS,* ASME, 1986, P 439-447
10. S. IBARRA, C.E. GRUBBS, AND D.L. OLSON, FUNDAMENTAL APPROACHES TO UNDERWATER WELDING METALLURGY, *J. MET.,* VOL 40 (NO.12), 1988, P 8-10
11. S. IBARRA AND D.L. OLSON, WET UNDERWATER STEEL WELDING, *FERROUS ALLOY WELDMENTS,* VOL 69-70, *KEY ENG. MATERIALS,* TRANS TECH PUBLICATIONS, ZURICH, 1992, P 329-378
12. O. OZAKI, J. NAIMAN, AND K. MASUBUCHI, A STUDY OF HYDROGEN CRACKING IN UNDERWATER STEEL WELDS, *WELD. J.,* VOL 56 (NO. 8), 1977, P 231S-237S
13. W.A. STALKER, P.H.M. HART, AND G.R. SALTER, "AN ASSESSMENT OF SHIELDED METAL ARC ELECTRODES FOR THE UNDERWATER WELDING OF CARBON MANGANESE STRUCTURAL STEELS," OFFSHORE TECHNOLOGY CONFERENCE, OTC REPORT 2301 (HOUSTON), 1975
14. B. CHEW, PREDICTION OF WELD METAL HYDROGEN LEVELS OBTAINED UNDER TEST CONDITIONS, *WELD. J.,* VOL 52, 1973, P 386S-391S
15. L.I. SOROKIN AND Z.A. SIDLIN, THE EFFECT OF ALLOYING ELEMENTS AND OF MARBLE IN AN ELECTRODE COATING ON THE SUSCEPTIBILITY OF A DEPOSITED NICKEL CHROME METAL TO PORE FORMATION, *SVAR. PROIZVOD.,* NO. 11, 1974, P 7-9
16. V.Y. KONONENKO, EFFECT OF WATER SALINITY AND MECHANIZED UNDERWATER WELDING PARAMETERS ON HYDROGEN AND OXYGEN CONTENT OF WELD METAL, *WELDING UNDER EXTREME CONDITIONS,* PERGAMON PRESS, 1989, P 113-118
17. H. HOFFMEISTER AND K. KUSTER, PROCESS VARIABLES AND PROPERTIES OF UNDERWATER WET SHIELDED METAL ARC LABORATORY WELDS, *UNDERWATER WELDING,* PERGAMON PRESS, 1983, P 115-125
18. K. HOFFMEISTER AND K. KUSTER, PROCESS VARIABLES AND PROPERTIES OF WET UNDERWATER GAS METAL ARC LABORATORY AND SEA WELDS OF MEDIUM STRENGTH STEELS, *UNDERWATER WELDING,* PERGAMON PRESS, 1983, P 239-246
19. A. MATSUNAWA, H. TAKEMATA, AND I. OKAMOTO, ANALYSIS OF TEMPERATURE FIELD WITH EQUIRADIAL COOLING BOUNDARY AROUND MOVING HEAT SOURCES--HEAT CONDUCTION ANALYSIS FOR ESTIMATION OF THERMAL HYSTERESIS DURING UNDERWATER WELDING, *TRANS. JWRI,* VOL 9 (NO. 1), 1980, P 11-18
20. K. OLSEN, D.L. OLSON, AND N. CHRISTENSEN, WELD BEAD TEMPERING OF HEAT AFFECTED ZONE, *SCAND. J. METALL.,* VOL 11, 1982, P 163-168
21. R.E. TREVISAN, D.D. SCHWEMMER, AND D.L. OLSON, THE FUNDAMENTALS OF WELD METAL PORE FORMATION, *WELDING: THEORY AND PRACTICE,* D.L. OLSON, R.D. DIXON, AND A.L. LIBY, ED., ELSEVIER SCIENCE B.V., 1990
22. Y. SUGA AND H. ATSUSHI, "ON THE FORMATION OF POROSITY IN UNDERWATER WELD METAL (THE 1ST REPORT)--EFFECT OF WATER PRESSURE ON FORMATION OF POROSITY," IIW DOC. IX-1388-86, AMERICAN COUNCIL, AWS, 1986
23. N.M. MALATOR, THE PROPERTIES OF THE BUBBLES OF STEAM AND GAS AROUND THE ARC IN UNDERWATER WELDING, *AUTOMAT. WELD.,* VOL 18 (NO. 12), 1965, P 25-29
24. E.A. SILVA, GAS PRODUCTION AND TURBIDITY DURING UNDERWATER SHIELDED METAL-ARC WELDING WITH IRON POWDER ELECTRODES, *NAV. ENG. J.,* VOL 12, 1971
25. G.R. SALTER AND D.R. MILNER, GAS METAL REACTIONS IN ARC WELDING, *BRIT. WELD. J.,* VOL 33, 1965

26. D.K. MATLOCK, G.R. EDWARDS, D.L. OLSON, AND J. IBARRA, AN EVALUATION OF THE FATIGUE BEHAVIOR IN SURFACE, HABITAT, AND UNDERWATER WET WELDS, *UNDERWATER WELDING,* PERGAMON PRESS, 1983, P 303-310
27. G. EDWARDS, C.J. ALLUM, B.E. PINFOLD, AND J.H. NIXON, THE EFFECT OF PRESSURE ON THE TUNGSTEN ARGON WELDING ARC, *PROC. CONF. PHYSICS AND WELD POOL BEHAVIOR,* WELDING INSTITUTE, 1979, P 101-107
28. I.K. POKHODNYA, V.N. GORPENYUK, V.YA. KONONENKO, V.E. PONOMAREV, AND S.YU. MAKSIMOV, SOME PECULIARITIES OF ARC BURNING AND METAL TRANSFER IN WET UNDERWATER SELF-SHIELDING FLUX-CORED WIRE WELDING, *WELDING UNDER EXTREME CONDITIONS,* PERGAMON PRESS, 1989, P 151
29. S. FUKUSHIMA, T. FUKUSHIMA, AND J. KINUGAWA, UNDERWATER WET PLASMA WELDING IN PRESSURIZED WATER, *TRANS. MET. INST. MET.,* VOL 19 (NO. 3), 1977, P 133-151

Welding for Cryogenic Service

T.A. Siewert and C.N. McCowan, National Institute of Standards and Technology

Introduction

CRYOGENIC TEMPERATURES cause many structural alloys to become brittle, which is an unacceptable condition in most structural applications. Therefore, structures built for service at low temperatures are typically made from alloys that maintain some ductility at the service temperatures. Cryogenic alloys include 9Ni steels, austenitic stainless steels, manganese stainless steels, maraging steels, titanium, aluminum, and nickel alloys. The choice of weld-metal alloy may depend solely on the strength of the alloy at a given temperature or on a combination of strength, toughness, fatigue resistance, thermal conductivity, magnetic permeability, and other considerations.

Wrought or cast alloy structural members are usually joined using filler materials with compositions that are similar, but not identical, to the parent material. The weld composition is optimized to compensate for the inherent differences in the properties of weld and parent material that are due to grain structure, inclusion content, and cooling rate differences. The goal is to match, as closely as possible, the mechanical and physical properties of the weld and parent material. When nonmatching weld compositions are most appropriate, differences between the welds and parent material in terms of thermal contraction, corrosion, and other factors must be considered. This article discusses these differences and explains how they affect the choice of the weld filler metal.

Welding for Cryogenic Service

T.A. Siewert and C.N. McCowan, National Institute of Standards and Technology

Effects of Cryogenic Service on Properties

Strength. As the temperature drops below room temperature, some cryogenic alloys strengthen appreciably. Unless some other property degrades and offsets this effect, such strengthening is very beneficial in reducing the required weight and thickness of structural members that are designed on the basis of load. Figure 1 shows this strengthening effect for several alloy systems, using data that are representative of both base and weld metal. Unfortunately, not all alloys strengthen at the same rate. Therefore, a comparison of the strengths at one temperature cannot be used to predict the relative strengths at a different temperature. Most literature data are for certain convenient test temperatures (4 K, 77 K, and 298 K). Data for intermediate temperatures indicate that strength is a smoothly varying function of temperature, whereas data for the three common test temperatures can be linked with curved lines. Because the behavior is very predictable, this discussion concentrates on the extreme temperature, 4 K, where the effects are most pronounced. Behavior at 77 K can be estimated by interpolation.

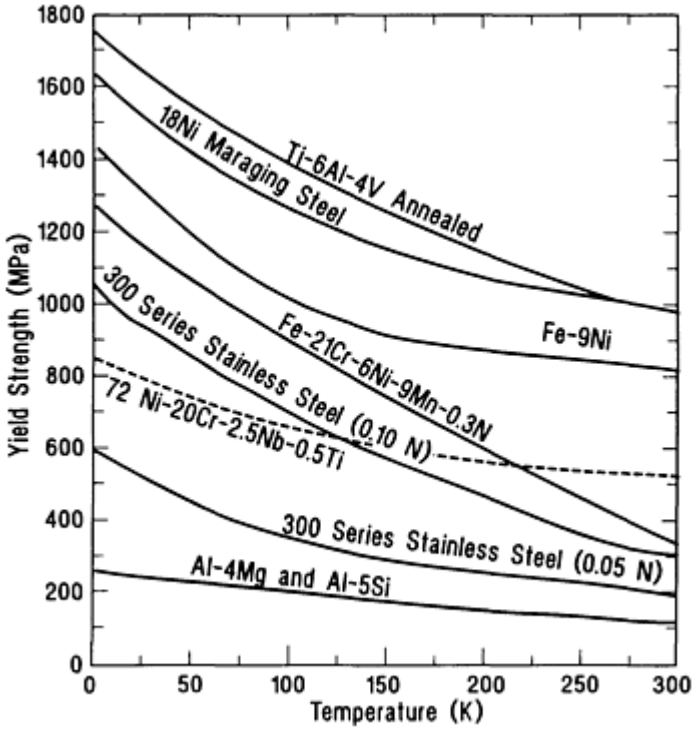

FIG. 1 YIELD STRENGTH VERSUS TEMPERATURE (4 TO 300 K) FOR VARIOUS BASE METALS AND WELD METALS THAT HAVE BEEN STUDIED FOR CRYOGENIC APPLICATIONS

As shown in Fig. 1, some alloys can reach very high yield strengths (well above 1000 MPa, or 140 ksi) at 4 K. Others, such as aluminum alloys, start from moderate or low strengths and respond mildly to a lowering of temperature (Ref 1, 2). Nine-percent nickel (Fe-9Ni) starts with a strength that is high at room temperature and rises from that point (Ref 1, 2). High-manganese steels, such as Fe-22Mn, and 21Cr-6Ni-9Mn stainless steel at 4 K approach the ultra-high-strength levels of 9Ni steel, maraging steel, and titanium (Ref 3, 4).

The austenitic (300 series) stainless steels offer medium strength at room temperature, but strengthen with decreasing temperature at a rate dependent on the nitrogen content of the alloy. As shown in Fig. 1, the strengthening of these alloys is a strong function of their nitrogen content: the trend line for the alloys with a higher nitrogen content shows much greater strengthening than the trend line for the alloys with a lower nitrogen content (Ref 5).

The maximum strength that can be reached is a function of the solubility limit of nitrogen in the stainless steel. This limit, in turn, is a function of composition and other factors. To control strength values, the nitrogen content of the weld must be carefully controlled, or else two effects can occur: pores may form in the weld during solidification (as the supersaturated liquid weld metal rejects nitrogen) or the weld pool may lose nitrogen through evaporation, weakening the weld. It should be noted that the strength of 21Cr-6Ni-9Mn is much higher than that of other austenitic steels because its nitrogen content is near 0.3 wt%. This higher level of strength is made possible by the improved nitrogen solubility in an alloy with a higher manganese content.

Equation 1 was developed to predict the strength of welds in austenitic stainless steel at a temperature of 4 K:

$$\sigma_Y(\text{MPA}) = 180 + 3200\ \text{N} + 33\ \text{Mo} + 32\ \text{Mn} + 13\ \text{Ni} \qquad \textbf{(EQ 1)}$$

where the elemental symbols represent their concentration in wt% (Ref 5). Equation 1 shows which elements have the greatest effect on strength and is very similar, in terms of elements and their coefficients, to an equation developed to predict the strength of austenitic stainless steel wrought material (Ref 6). Thus, it can be concluded that:

- AUSTENITIC WELD STRENGTH CAN BE ADJUSTED BY CHANGING THE COMPOSITION TO MEET THE NEEDS OF THE APPLICATION.
- WELD STRENGTH IS DETERMINED BY THE SAME FACTORS AS THOSE THAT DETERMINE THE BASE METAL STRENGTH.
- MATCHING THE COMPOSITION OF THE WELD TO THAT OF THE WROUGHT MATERIAL WILL RESULT IN NEARLY EQUIVALENT STRENGTHS.

Fracture Toughness at 4 K. Because many cryogenic structures are subject to fracture and other failure mechanisms, most designs must consider toughness, as well as strength. Unfortunately, toughness often degrades as the strength is increased or as the temperature decreases.

Figure 2 shows data for strength and fracture toughness at 4 K for some alloys that have been either proposed or actually used in cryogenic applications. The plotting of yield strength versus fracture toughness, K_{Ic}, provides an easy way to evaluate alloys, because these mechanical properties are common design criteria. A trend band or border was drawn around the data when warranted by the quantity of data. For some alloys, the data were so sparse that individual data points were plotted. Although most of these data are for base-metal alloys, data for selected welds are included to show that base-metal properties for important cryogenic alloys can be met or exceeded for high-toughness, fracture-critical applications.

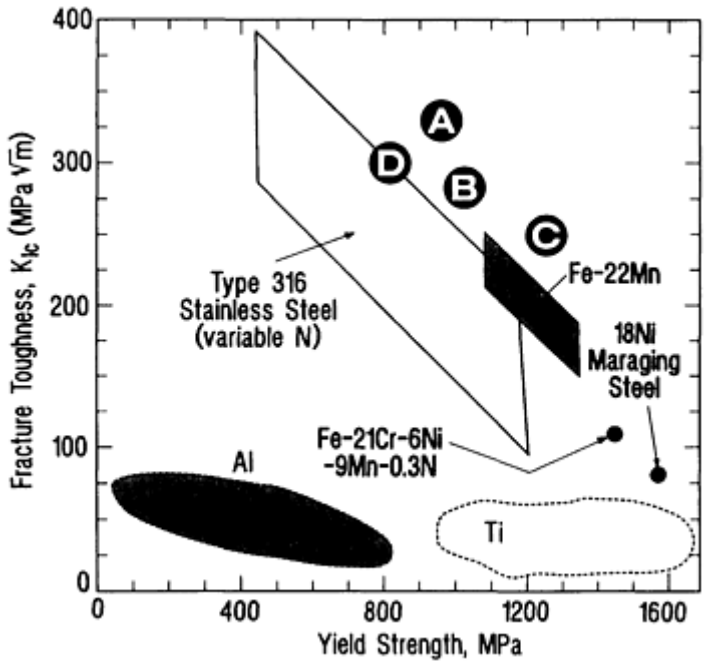

FIG. 2 YIELD STRENGTH VERSUS FRACTURE TOUGHNESS FOR VARIOUS BASE METAL ALLOYS AND SELECTED WELDS AT 4 K

Data for a Ti-6Al-4V alloy and an electron-beam (EB) weld showed an abrupt decrease in toughness at test temperatures below 125 K; toughness was lowest at the boundary between the heat-affected zone (HAZ) and the fusion zone of the weld (Ref 7). These data are grouped in the lower right corner of Fig. 2. Generally, titanium alloys and other ultrahigh-strength alloys, such as 18Ni maraging steel or 9Ni steel, exhibit low toughness at 4 K (as might be expected of an alloy with very high strength). Therefore, these alloys are most commonly used for compression loading or other applications where their limited ductility is acceptable (Ref 8, 9, 10). The 18Ni maraging steel and the titanium alloy do not show a transition from ductile to brittle fracture at low temperatures, as do 9Ni and other lower-nickel-content steels (Ref 1, 2, 9). No data for weld toughness were found for 18Ni maraging steels at 4 K.

Data for aluminum alloys and some welds are also included in Fig. 2 (Ref 11, 12). These data represent traditional aluminum alloys, as well as some of the new aluminum-lithium alloys. The zones indicated in Fig. 2 for the aluminum

and titanium alloys are intended to loosely identify mechanical property regions for the alloys, rather than to define limits for design purposes.

At a temperature of 4 K, considerable data exist for type 316L stainless steel wrought alloy (a common cryogenic structural material). Therefore, Fig. 2 includes a trend band for yield strength versus toughness (Ref 6). This alloy has a good balance of strength and toughness, and has found application as the structural case for large superconducting magnets. As its strength increases (through additions of nitrogen), its toughness decreases. This variation in strength with nitrogen content was shown in Fig. 1 as curves for two different nitrogen contents, whereas Fig. 2 shows the effect in terms of toughness as a function of strength at constant temperature. This trend shows the interrelationships between properties that must be considered by structural designers.

Although the trend line for the matching-composition electrodes is not included in Fig. 2, it extends over the same strength range, but at only 50 to 70% of the toughness of the base metal (Ref 4). This lower toughness for welding electrodes of matching composition has driven the search for electrodes of different compositions that can match the properties of these base metals. Two fully austenitic stainless steel weld compositions (shown as A and B in Fig. 2 and described in more detail in Table 1) have been proposed for joining AISI 316LN stainless steel (Ref 13, 14, 15).

TABLE 1 COMPOSITIONS FOR THE FOUR WELDS (A THROUGH D) INCLUDED IN FIG. 2

WELD	COMPOSITION, %								PROCESS
	FE	CR	NI	MN	N	C	S	P	
A	BAL	13	5	22	0.21	0.04	0.004	0.013	**EBW**
B	BAL	20	25	1.6	0.16	0.01	0.001	0.010	**GMAW**
C	BAL	18.1	20.4	5.4	0.16	0.03	0.007	0.006	**GMAW**
D	**1**	**20**	**BAL**	**3**	**. . .**	**0.02**	**. . .**	**. . .**	**GTAW**

Two other iron-base alloys, Fe-22Mn and 21Cr-6Ni-9Mn, have been used in structures that require high strength and toughness at 4 K. Figure 2 includes a trend line for a high-manganese alloy, Fe-22Mn, which is one of several iron-manganese alloys that have been developed since the early 1980s (Ref 3, 16). Its particular advantage is an ability to attain a strength higher than that of type 316 stainless steel. A matching-composition weld, shown as C in Fig. 2, was produced by electron-beam welding (EBW) (Ref 17). The strength of the weld was approximately 5% lower than that of the parent plate material, presumably because of the loss of nitrogen in the welding process. However, the fracture toughness of the weld exceeded the toughness of the plate material. Matching-composition welds have also been made using shielded metal arc welding (SMAW), gas-metal arc welding (GMAW), gas-tungsten arc welding (GTAW), and submerged arc welding (SAW) processes. The toughness of the welds produced by these other processes is lower than that of the EB weld, because their inclusion contents are higher (Ref 16).

Another common cryogenic alloy is 21Cr-6Ni-9Mn, for which one value is included in Fig. 2 (Ref 2). A trend band has not been developed, but the data would be expected to have a similar trend to those of Fe-22Mn and 316LN (but extending to a higher strength than that of 316LN, because the 21Cr-6Ni-9Mn can contain up to 0.4 wt% N). A nickel-base weld composition (weld D in Fig. 2) has been proposed for 21Cr-6Ni-9Mn. Although this nickel-base weld undermatches the strength, it overmatches the toughness. Thus, welds can be made in locations of lower stress, which permits the use of this high-strength alloy in the construction of structures.

Table 1 lists the compositions of the four welds included in Fig. 2. It shows that these welds (other than the Fe-22Mn composition) have more nickel than the iron-base alloys that they join. These weld composition data represent the best combinations of strength and toughness reported for the alloys. Because the matching-composition welds tend to have lower toughness than the parent plate, these nonmatching compositions are being considered for fracture-critical welds. Subsequent sections in this article describe how thermal expansion and other characteristics of the nonmatching compositions might affect the suitability of these alloys in particular applications.

Another common cryogenic temperature is 77 K, the normal boiling temperature of liquid nitrogen. Because toughness is higher at 77 K than at 4 K, higher-strength alloys can be considered for fracture-critical applications. Like other iron-base alloys that show a significant improvement in toughness with increasing temperature, Fe-21Cr-6Ni-9Mn is more suited for use at 77 K, where its high strength is an attractive option, when compared with that of 316LN alloy. For example, Fe-

21Cr-6Ni-9Mn base metal drops in strength from a level near 1450 MPa (210 ksi) at 4 K to near 1150 MPa (165 ksi) at 77 K, which is still a very respectable level of strength.

Charpy V-Notch Impact Energy at 77 K. Although not as useful in fitness-for-service calculations as K_{Ic} fracture toughness, the Charpy V-notch (CVN) test is a low-cost way to measure the resistance of an alloy to fracture. A literature search found that most data on fracture resistance at 77 K were reported as CVN data. In Fig. 3, CVN absorbed-energy data at 77 K are plotted versus the yield strength for a number of weld metals. The trends reiterate the effects of strength and nickel content on CVN toughness. Because many structural designs specify a minimum of 30 or 40 J (22 to 30 ft · lbf), numerous weld compositions can be considered at this temperature, including compositions that match that of the base plate.

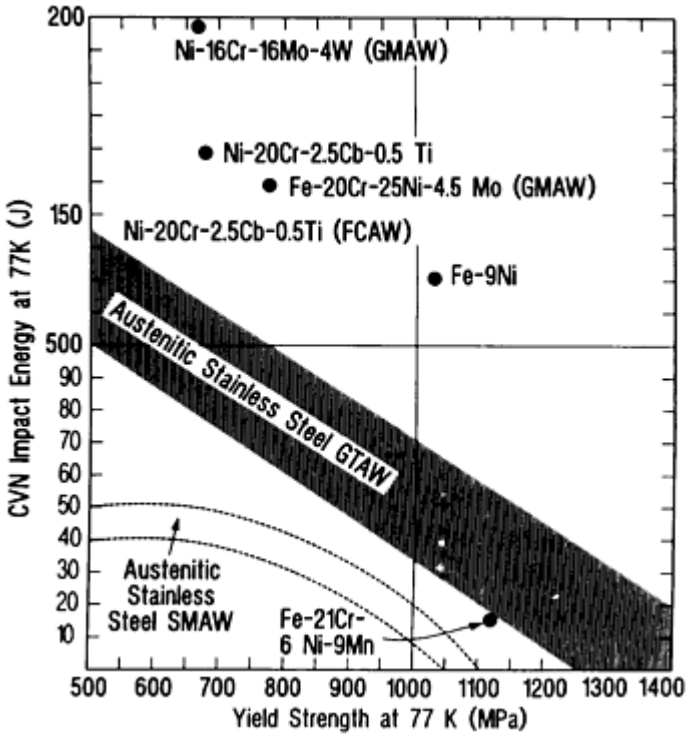

FIG. 3 CHARPY V-NOTCH ABSORBED ENERGY VERSUS STRENGTH FOR VARIOUS WELD METALS AT 77 K

In the lower right quadrant of Fig. 3 is a data point for a matching-composition weld for the Fe-21Cr-6Ni-9Mn steel (Ref 18). The low absorbedenergy indicates that the nickel-base undermatching weld compositions should be considered for applications with this composition at 77 K (Ref 19). Nickel-base weld compositions are also used for welding the Fe-9Ni alloy included in Fig. 3 (Ref 10).

For the austenitic (300 series) stainless steels, there are two trend bands. The lower band is for welds produced by the SMAW process, whereas the upper is for welds produced by the GTAW process. The difference is attributed to weld inclusions, as discussed in the next section of this article. Above the GTAW trend band are the four special weld compositions identified in Table 1. These higher absorbed energy levels are comparable to the level that type 316LN plate would develop at this temperature.

Equation 2 was developed to predict the absorbed energy at 77 K for the welds in austenitic stainless steel:

$$CVN(J) = 19 - 1.4\,FN - 890\,C^2 + 1.4\,NI \qquad \textbf{(EQ 2)}$$

where the elemental symbols represent the composition in wt%, and FN is a measure of the delta ferrite content (calculated by the Schaeffler diagram coefficients and allowed to be negative) in the weld (Ref 20).

This equation was not developed for weld compositions strengthened by nitrogen. Therefore, carbon represents the principal strengthening element. If carbon is considered as a generic strengthening term (combined effects of carbon, nitrogen, manganese, molybdenum, and others), then Eq 2 shows that increased strength and ferrite content lower the CVN toughness, and that nickel increases toughness. The effects of these factors on toughness are generally accepted to be true for stainless steel weld and base material. Because an increase in nickel content also decreases the ferrite content, nickel additions improve the toughness via two terms in Eq 2. This information on the effect of nickel confirms the reasons for the better toughness of the four nonmatching compositions (Ref 13, 14, 15, 17).

Inclusion Content. In austenitic stainless steels and manganese stainless steels, the fracture modes of both base metals and welds are usually quite ductile, and fracture originates at inclusions in the microstructure. A minor difference between the fracture surfaces of the base metal and weld metal is that those of the welds have a finer ductile dimple spacing. This finer spacing has been attributed to the higher inclusion content of the welds and explains why the welds are less tough than those of the matching-composition wrought material (Ref 21, 22, 23).

Figure 4 shows normalized toughness data versus inclusion spacings for both wrought materials and welds (Ref 21, 24). The vertical axis is known as a quality index, and it allows alloys with different strengths and nickel contents to be compared on a scale that has fracture toughness in the numerator (higher values are better). The similarity of the trend line for both sets of data supports the need to reduce the inclusion content of welds that require a higher fracture toughness. Most of the welds in Fig. 2 were produced using welding processes and procedures that minimize the inclusion content. The exceptions here are the nickel-alloy welds and the very high nickel content (greater than 20 wt%) stainless steel welds. Preliminary data indicate that the toughness of these compositions is less sensitive to inclusion content. Therefore, these materials could be more appropriate for welding at higher deposition rates.

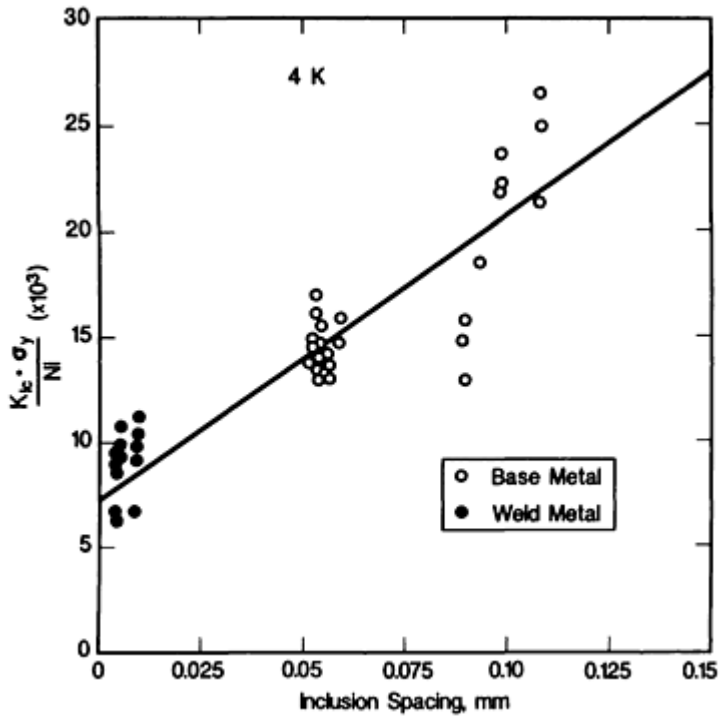

FIG. 4 NORMALIZED TOUGHNESS DATA (QUALITY INDEX) VERSUS INCLUSION SPACING FOR TYPE 316LN BASE METALS AND WELDS, SHOWING HOW THE WELD DATA FOLLOW THE SAME TREND AS THE BASE METAL, BUT A SMALLER INCLUSION SPACING RESULTS IN LOWER TOUGHNESS FOR THE WELDS

Fatigue Strength. Few data are available for the fatigue strength of cryogenic welds. However, the data that are available suggest that fatigue strength could limit the structural life in high-cycle applications. Table 2 lists data from a study that used the GTAW process to join a number of different materials (Ref 25). The data show that fatigue strength does not necessarily increase as temperatures decrease from 295 to 4 K. Expected yield strength data, extracted from Fig. 1, have been added for comparison.

TABLE 2 FATIGUE STRENGTH FOR GAS-TUNGSTEN ARC WELDS AT 4×10^4 CYCLES

SPECIMEN	ESTIMATED FATIGUE STRENGTH				YIELD STRENGTH AT 4 K	
	AT 295 K		AT 4 K			
	MPA	KSI	MPA	KSI	MPA	KSI
21CR-6NI-9MN TO 304L	380	55	360	52	1050	**150**
21CR-6NI-9MN TO 316L	420	60	390	57	1100	**160**
21CR-6NI-9MN BASE METAL	**370**	**54**	**290**	**42**	**1200**	**175**

The coefficient of thermal expansion (CTE) can have an important bearing on structural integrity. If the weld metal has a CTE that is very different from that of the base metal, cooling from room temperature to cryogenic temperature can introduce substantial stresses. These stresses can add to the residual stresses that exist around any weld and can permit the plastic deformation of the structure. Repeated thermal cycles could lead to work hardening of the microstructure or to fatigue failure, in the most severe cases. Other physical properties that are often important in cryogenic structures are phase stability and magnetic permeability.

References cited in this section

1. MECHANICAL, THERMAL, ELECTRICAL, AND MAGNETIC PROPERTIES OF STRUCTURAL MATERIALS, *HANDBOOK ON MATERIALS FOR SUPERCONDUCTING MACHINERY*, 1ST ED., MCIC-HB-04, METALS AND CERAMICS INFORMATION CENTER, BATTELLE COLUMBUS LABORATORIES, JAN 1977
2. "MATERIALS FOR SUPERCONDUCTING MAGNET SYSTEMS: MECHANICAL AND PHYSICAL PROPERTIES DATA AT LOW TEMPERATURES," BELFOUR STULEN DIVISION, TRAVERSE CITY, MI, 1979
3. T. HORIUCHI, R. OGAWA, AND M. SHIMADA, CRYOGENIC FE-MN AUSTENITIC STEELS, *ADV. CRYOGENIC ENG. (MATER.)*, VOL 32, 1985
4. R.L. TOBLER, T.A. SIEWERT, AND H.I. MCHENRY, STRENGTH-TOUGHNESS RELATIONSHIP OF AUSTENITIC STAINLESS STEEL WELDS AT 4 K, *CRYOGENICS*, VOL 26, 1986
5. C.N. MCCOWAN AND T.A. SIEWERT, INFLUENCE OF MOLYBDENUM ON THE STRENGTH AND TOUGHNESS OF STAINLESS STEEL WELDS FOR CRYOGENIC SERVICE, "MATERIALS STUDIES FOR MAGNETIC FUSION ENERGY APPLICATIONS AT LOW TEMPERATURES--X," NBSIR 87-3067, NATIONAL BUREAU OF STANDARDS, 1987
6. N.J. SIMON AND R.P. REED, STRENGTH AND TOUGHNESS OF AISI 304 AND 316 AT 4 K, "MATERIALS STUDIES FOR MAGNETIC FUSION ENERGY APPLICATIONS AT LOW TEMPERATURES--X," NBSIR 86-3050, NATIONAL BUREAU OF STANDARDS, 1986
7. R.L. TOBLER, *LOW TEMPERATURE FRACTURE BEHAVIOR OF A TI-6AL-4V ALLOY AND ITS ELECTRON BEAM WELDS*, STP 651, ASTM, 1978
8. R.L. TOBLER, R.P. REED, AND R.E. SCHRAMM, CRYOGENIC TENSILE, FATIGUE, AND FRACTURE PARAMETERS FOR A SOLUTION-ANNEALED 18 PERCENT NICKEL MARAGING STEEL, *J. ENG. MATER. TECHNOL.*, VOL 100, APRIL 1978, P 189-194
9. J.A. WAGNER, CORRELATION OF MECHANICAL PROPERTIES WITH METALLURGICAL STRUCTURE FOR 18NI 200 GRADE MARAGING STEEL AT ROOM AND CRYOGENIC TEMPERATURES, *CRYOGENICS*, VOL 31, SEPT 1991
10. R.D. STOUT AND S.J. WIERSMA, FRACTURE TOUGHNESS OF MODERN 9% NICKEL CRYOGENIC STEELS, *ADV. CRYOGENIC ENG. (MATER.)*, VOL 32, 1985
11. J. GLAZER, S.L. VERASCONI, E.N.C. DALDER, W. YU, R.A. EMIGH, R.O. RICHIE, AND J.W. MORRIS, JR., CRYOGENIC MECHANICAL PROPERTIES OF AL-CU-LI-ZR ALLOY 2090, *ADV. CRYOGENIC ENG. (MATER.)*, VOL 32, 1985

12. R.P. REED, P.T. PURTSCHER, N.J. SIMON, J.D. MCCOLSKEY, R.P. WALSH, J.R. BERGER, E.S. DREXLER, AND R.L. SANTOYO, "ALUMINUM ALLOYS FOR ALS CRYOGENIC TANKS: COMPARATIVE MEASUREMENTS OF CRYOGENIC MECHANICAL PROPERTIES OF AL-LI ALLOYS AND ALLOY 2219," REPORT PL-TR--91-3073, PHILLIPS LABORATORY, PROPULSION DIRECTORATE, AIR FORCE SYSTEMS COMMAND, EDWARDS AIR FORCE BASE, 1991
13. C.N. MCCOWAN, T.A. SIEWERT, AND R.L. TOBLER, TENSILE AND FRACTURE PROPERTIES OF AN FE-18CR-20NI-5MN-0.16N FULLY AUSTENITIC WELD METAL AT 4 K, *J. ENG. MATER. TECHNOL.*, VOL 108, 1986
14. T.A. SIEWERT AND C.N. MCCOWAN, THE FRACTURE TOUGHNESS OF 25CR-22NI-4MN-2MO STAINLESS STEEL WELDS AT 4 K, "MATERIALS STUDIES FOR MAGNETIC FUSION ENERGY APPLICATIONS AT LOW TEMPERATURES--XII," NISTIR 3931, NATIONAL INSTITUTE OF STANDARDS AND TECHNOLOGY, 1990
15. A.O. KLUKEN, C.N. MCCOWAN, AND T.A. SIEWERT, EFFECT OF INCLUSION VOLUME FRACTION AND SIZE DISTRIBUTION ON THE CRYOGENIC TOUGHNESS OF AUSTENITIC STAINLESS STEEL WELD METALS, SUBMITTED FOR PUBLICATION IN *MICROSTRUCTURAL SCIENCE,* VOL 19, ASM INTERNATIONAL/INTERNATIONAL METALLOGRAPHIC SOCIETY, 1993
16. Y.W. CHENG, H.I. MCHENRY, P.N. LI, T. INOUE, AND T. OGAWA, FRACTURE TOUGHNESS OF 25MN AUSTENITIC STEEL WELDMENTS AT 4 K, *ADV. CRYOGENIC ENG. (MATER.),* VOL 30, 1983
17. S. TONE, M. HIROMATSU, J. NUMATA, T. HORIUCHI, H. NAKAJIMA, AND S. SHIMAMOTO, CRYOGENIC PROPERTIES OF ELECTRON-BEAM WELDED JOINTS IN A 22MN-13CR-5NI-0.22N AUSTENITIC STAINLESS STEEL, *ADV. CRYOGENIC ENG. (MATER.),* VOL 32, 1985
18. R.H. ESPY, WELDABILITY OF 21-6-9 STAINLESS STEEL (ARMCO NITRONIC STAINLESS STEEL), "MATERIALS STUDIES FOR MAGNETIC FUSION ENERGY APPLICATIONS AT LOW TEMPERATURES--I, " NBSIR 78-884, NATIONAL INSTITUTE OF STANDARDS AND TECHNOLOGY, 1978
19. D.J. ALEXANDER AND G.M. GOODWIN, THICK-SECTION WELDMENTS IN 21-6-9 AND 316LN STAINLESS STEEL FOR FUSION ENERGY APPLICATIONS, SUBMITTED TO *J. NUCL. MATER.*, 1992
20. T.A. SIEWERT, PREDICTING THE TOUGHNESS OF SMA AUSTENITIC STAINLESS STEEL WELDS AT 77 K, *WELD. J.*, VOL 65, 1986
21. C.N. MCCOWAN AND T.A. SIEWERT, FRACTURE TOUGHNESS OF 316L STAINLESS STEEL WELDS WITH VARYING INCLUSION CONTENTS AT 4 K, *ADV. CRYOGENIC ENG. (MATER.),* VOL 34, 1989
22. J.H. KIM, B.W. OH, J.G. YOUN, G.-W. BAHNG, AND H.-M. LEE, EFFECT OF OXYGEN CONTENT ON CRYOGENIC TOUGHNESS OF AUSTENITIC STAINLESS STEEL WELD METAL, *ADV. CRYOGENIC ENG. (MATER.),* VOL 34, 1989
23. N. YAMAGAMI, Y. KOHSAKA, AND C. OUCHI, MECHANICAL PROPERTIES OF WELDED JOINTS IN MN-CR AND NI-CR STAINLESS STEELS AT 4 K, *ADV. CRYOGENIC ENG. (MATER.),* VOL 34, 1989
24. C.N. MCCOWAN AND T.A. SIEWERT, INCLUSIONS AND FRACTURE TOUGHNESS IN STAINLESS STEEL WELDS AT 4 K, "MATERIALS STUDIES FOR MAGNETIC FUSION ENERGY APPLICATIONS AT LOW TEMPERATURES--XI," NBSIR 88-3082, NATIONAL INSTITUTE OF STANDARDS AND TECHNOLOGY, 1988
25. T.A. SIEWERT, C.N. MCCOWAN, AND D.P. VIGLIOTTI, CRYOGENIC MATERIAL PROPERTIES OF STAINLESS STEEL TUBE-TO-FLANGE WELDS, *CRYOGENICS,* VOL 30, 1990

References

1. MECHANICAL, THERMAL, ELECTRICAL, AND MAGNETIC PROPERTIES OF STRUCTURAL MATERIALS, *HANDBOOK ON MATERIALS FOR SUPERCONDUCTING MACHINERY*, 1ST ED., MCIC-HB-04, METALS AND CERAMICS INFORMATION CENTER, BATTELLE COLUMBUS LABORATORIES, JAN 1977
2. "MATERIALS FOR SUPERCONDUCTING MAGNET SYSTEMS: MECHANICAL AND PHYSICAL PROPERTIES DATA AT LOW TEMPERATURES," BELFOUR STULEN DIVISION, TRAVERSE CITY, MI, 1979
3. T. HORIUCHI, R. OGAWA, AND M. SHIMADA, CRYOGENIC FE-MN AUSTENITIC STEELS, *ADV. CRYOGENIC ENG. (MATER.)*, VOL 32, 1985
4. R.L. TOBLER, T.A. SIEWERT, AND H.I. MCHENRY, STRENGTH-TOUGHNESS RELATIONSHIP OF AUSTENITIC STAINLESS STEEL WELDS AT 4 K, *CRYOGENICS*, VOL 26, 1986
5. C.N. MCCOWAN AND T.A. SIEWERT, INFLUENCE OF MOLYBDENUM ON THE STRENGTH AND TOUGHNESS OF STAINLESS STEEL WELDS FOR CRYOGENIC SERVICE, "MATERIALS STUDIES FOR MAGNETIC FUSION ENERGY APPLICATIONS AT LOW TEMPERATURES--X," NBSIR 87-3067, NATIONAL BUREAU OF STANDARDS, 1987
6. N.J. SIMON AND R.P. REED, STRENGTH AND TOUGHNESS OF AISI 304 AND 316 AT 4 K, "MATERIALS STUDIES FOR MAGNETIC FUSION ENERGY APPLICATIONS AT LOW TEMPERATURES--X," NBSIR 86-3050, NATIONAL BUREAU OF STANDARDS, 1986
7. R.L. TOBLER, *LOW TEMPERATURE FRACTURE BEHAVIOR OF A TI-6AL-4V ALLOY AND ITS ELECTRON BEAM WELDS*, STP 651, ASTM, 1978
8. R.L. TOBLER, R.P. REED, AND R.E. SCHRAMM, CRYOGENIC TENSILE, FATIGUE, AND FRACTURE PARAMETERS FOR A SOLUTION-ANNEALED 18 PERCENT NICKEL MARAGING STEEL, *J. ENG. MATER. TECHNOL.*, VOL 100, APRIL 1978, P 189-194
9. J.A. WAGNER, CORRELATION OF MECHANICAL PROPERTIES WITH METALLURGICAL STRUCTURE FOR 18NI 200 GRADE MARAGING STEEL AT ROOM AND CRYOGENIC TEMPERATURES, *CRYOGENICS*, VOL 31, SEPT 1991
10. R.D. STOUT AND S.J. WIERSMA, FRACTURE TOUGHNESS OF MODERN 9% NICKEL CRYOGENIC STEELS, *ADV. CRYOGENIC ENG. (MATER.)*, VOL 32, 1985
11. J. GLAZER, S.L. VERASCONI, E.N.C. DALDER, W. YU, R.A. EMIGH, R.O. RICHIE, AND J.W. MORRIS, JR., CRYOGENIC MECHANICAL PROPERTIES OF AL-CU-LI-ZR ALLOY 2090, *ADV. CRYOGENIC ENG. (MATER.)*, VOL 32, 1985
12. R.P. REED, P.T. PURTSCHER, N.J. SIMON, J.D. MCCOLSKEY, R.P. WALSH, J.R. BERGER, E.S. DREXLER, AND R.L. SANTOYO, "ALUMINUM ALLOYS FOR ALS CRYOGENIC TANKS: COMPARATIVE MEASUREMENTS OF CRYOGENIC MECHANICAL PROPERTIES OF AL-LI ALLOYS AND ALLOY 2219," REPORT PL-TR--91-3073, PHILLIPS LABORATORY, PROPULSION DIRECTORATE, AIR FORCE SYSTEMS COMMAND, EDWARDS AIR FORCE BASE, 1991
13. C.N. MCCOWAN, T.A. SIEWERT, AND R.L. TOBLER, TENSILE AND FRACTURE PROPERTIES OF AN FE-18CR-20NI-5MN-0.16N FULLY AUSTENITIC WELD METAL AT 4 K, *J. ENG. MATER. TECHNOL.*, VOL 108, 1986
14. T.A. SIEWERT AND C.N. MCCOWAN, THE FRACTURE TOUGHNESS OF 25CR-22NI-4MN-2MO STAINLESS STEEL WELDS AT 4 K, "MATERIALS STUDIES FOR MAGNETIC FUSION ENERGY APPLICATIONS AT LOW TEMPERATURES--XII," NISTIR 3931, NATIONAL INSTITUTE OF STANDARDS AND TECHNOLOGY, 1990
15. A.O. KLUKEN, C.N. MCCOWAN, AND T.A. SIEWERT, EFFECT OF INCLUSION VOLUME FRACTION AND SIZE DISTRIBUTION ON THE CRYOGENIC TOUGHNESS OF AUSTENITIC

STAINLESS STEEL WELD METALS, SUBMITTED FOR PUBLICATION IN *MICROSTRUCTURAL SCIENCE,* VOL 19, ASM INTERNATIONAL/INTERNATIONAL METALLOGRAPHIC SOCIETY, 1993

16. Y.W. CHENG, H.I. MCHENRY, P.N. LI, T. INOUE, AND T. OGAWA, FRACTURE TOUGHNESS OF 25MN AUSTENITIC STEEL WELDMENTS AT 4 K, *ADV. CRYOGENIC ENG. (MATER.),* VOL 30, 1983
17. S. TONE, M. HIROMATSU, J. NUMATA, T. HORIUCHI, H. NAKAJIMA, AND S. SHIMAMOTO, CRYOGENIC PROPERTIES OF ELECTRON-BEAM WELDED JOINTS IN A 22MN-13CR-5NI-0.22N AUSTENITIC STAINLESS STEEL, *ADV. CRYOGENIC ENG. (MATER.),* VOL 32, 1985
18. R.H. ESPY, WELDABILITY OF 21-6-9 STAINLESS STEEL (ARMCO NITRONIC STAINLESS STEEL), "MATERIALS STUDIES FOR MAGNETIC FUSION ENERGY APPLICATIONS AT LOW TEMPERATURES--I, " NBSIR 78-884, NATIONAL INSTITUTE OF STANDARDS AND TECHNOLOGY, 1978
19. D.J. ALEXANDER AND G.M. GOODWIN, THICK-SECTION WELDMENTS IN 21-6-9 AND 316LN STAINLESS STEEL FOR FUSION ENERGY APPLICATIONS, SUBMITTED TO *J. NUCL. MATER.,* 1992
20. T.A. SIEWERT, PREDICTING THE TOUGHNESS OF SMA AUSTENITIC STAINLESS STEEL WELDS AT 77 K, *WELD. J.,* VOL 65, 1986
21. C.N. MCCOWAN AND T.A. SIEWERT, FRACTURE TOUGHNESS OF 316L STAINLESS STEEL WELDS WITH VARYING INCLUSION CONTENTS AT 4 K, *ADV. CRYOGENIC ENG. (MATER.),* VOL 34, 1989
22. J.H. KIM, B.W. OH, J.G. YOUN, G.-W. BAHNG, AND H.-M. LEE, EFFECT OF OXYGEN CONTENT ON CRYOGENIC TOUGHNESS OF AUSTENITIC STAINLESS STEEL WELD METAL, *ADV. CRYOGENIC ENG. (MATER.),* VOL 34, 1989
23. N. YAMAGAMI, Y. KOHSAKA, AND C. OUCHI, MECHANICAL PROPERTIES OF WELDED JOINTS IN MN-CR AND NI-CR STAINLESS STEELS AT 4 K, *ADV. CRYOGENIC ENG. (MATER.),* VOL 34, 1989
24. C.N. MCCOWAN AND T.A. SIEWERT, INCLUSIONS AND FRACTURE TOUGHNESS IN STAINLESS STEEL WELDS AT 4 K, "MATERIALS STUDIES FOR MAGNETIC FUSION ENERGY APPLICATIONS AT LOW TEMPERATURES--XI," NBSIR 88-3082, NATIONAL INSTITUTE OF STANDARDS AND TECHNOLOGY, 1988
25. T.A. SIEWERT, C.N. MCCOWAN, AND D.P. VIGLIOTTI, CRYOGENIC MATERIAL PROPERTIES OF STAINLESS STEEL TUBE-TO-FLANGE WELDS, *CRYOGENICS,* VOL 30, 1990

Welding for Cryogenic Service

T.A. Siewert and C.N. McCowan, National Institute of Standards and Technology

---

Selected References

- T. OGAWA AND T. KOSEKI, WELDABILITY OF NEWLY DEVELOPED AUSTENITIC ALLOYS FOR CRYOGENIC SERVICE: PART 2--HIGH-NITROGEN STAINLESS WELD METAL, *WELD. J.,* NOV 1987
- R.P. REED, AUSTENITIC STAINLESS STEELS WITH EMPHASIS ON STRENGTHENING AT LOW TEMPERATURES, *ALLOYING,* J.L. WALTER, M.R. JACKSON, AND C.T. SIMS, ED., ASM INTERNATIONAL, 1988
- R.L. TOBLER, R.P. MIKESELL, AND R.P. REED, *CRYOGENIC EFFECTS ON THE FRACTURE MECHANICS PARAMETERS OF FERRITIC NICKEL ALLOY STEELS,* STP 677, ASTM, 1979
- K.A. YUSHCHENKO, PROGRESS IN CRYOSTRUCTURAL MATERIALS AND THEIR WELDING IN

THE USSR, *ADV. CRYOGENIC ENG. (MATER.)*, VOL 30, 1983

Welding in Space and Low-Gravity Environments

Milo Nance, Martin Marietta Corporation; Jerald E. Jones, Colorado School of Mines

Introduction

WELDING AS AN ASSEMBLY PROCESS has become increasingly more attractive to designers of space structures for the same reasons welding is popular on earth. Welding applications in space are similar to those on earth in that they both involve the need to assemble structural components that will exhibit sufficient strength, endurance, and reliability during their service lives. In addition, ease of repair of welded structures is another consideration that makes various welding methods viable for space applications. Typical space welding applications generally fall into three categories:

- ON-ORBIT CONSTRUCTION OF LARGE STRUCTURES
- REPAIR WELDING ON-ORBIT AND FOR EXPLORATION FLIGHTS BEYOND THE VICINITY OF THE EARTH
- WELDING AND REPAIR OF STRUCTURES ON A LUNAR BASE

This article will review a variety of applications for welding in space and low-gravity environments, describe the unique aspects of the space environment, compare applicable welding processes, and examine the metallurgy of low-gravity welds. In addition, steps that must be taken to ensure the continued development of welding technology in space are discussed.

Welding in Space and Low-Gravity Environments

Milo Nance, Martin Marietta Corporation; Jerald E. Jones, Colorado School of Mines

Examples of Application

Welded joints have the potential to reduce the cost of fabrication and repair on-orbit. For example, large mechanical joints are planned for use on the U.S. Space Station Freedom. Each of these joints weighs approximately 1.36 kg (3 lb). When one considers that the cost for low earth orbit missions is several thousand dollars per pound of payload, it is easy to see how the replacement of these joints with a welded design would save significant amounts of weight and offer the potential to save large amounts of capital.

There are other applications for welding technology in space. These involve the modification and repair of structures and components in orbit. It has been suggested that structural material could be scavenged for reuse in orbit. An example of this is the Space Shuttle external tank (Fig. 1). On each shuttle mission the external tank is brought nearly into orbit. With minimal loss of payload capability, these tanks could be brought into orbit allowing the use of the tank structure for experimental platforms or for raw stock material. Cutting and joining technologies could enable the reuse of this valuable resource.

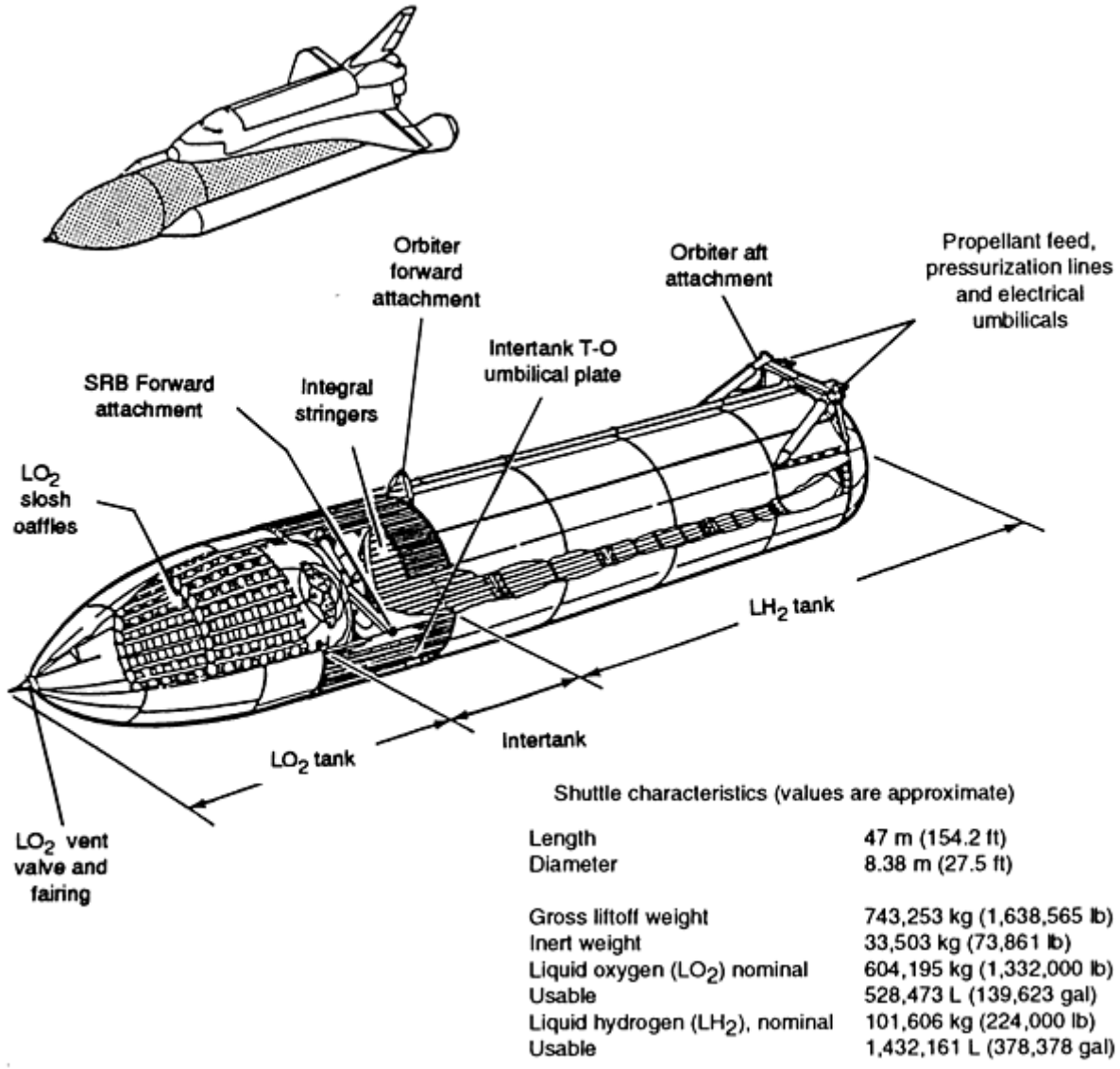

FIG. 1 SPACE SHUTTLE EXTERNAL FUEL TANK

Another application is the repair of major structures. Damage to space structures can result from many causes, including accidental misuse. However, one common cause of damage is "space debris," or miscellaneous small and large pieces of disintegrated satellites, material jettisoned from spacecraft, and other miscellaneous material. This debris is travelling at very high speeds, and may not be in the same orbital path and direction as a spacecraft. A resulting high-speed collision, even with a small piece of material, can cause significant damage. The amount of space debris in low earth orbit is increasing. Figure 2 shows the increase in concentration of debris in orbit from data collected by the Long Duration Exposure Facility (LDEF). The Space Shuttle has already been hit by at least one particle of debris, resulting in a damaged windshield, and there is speculation of impact damage to satellites.

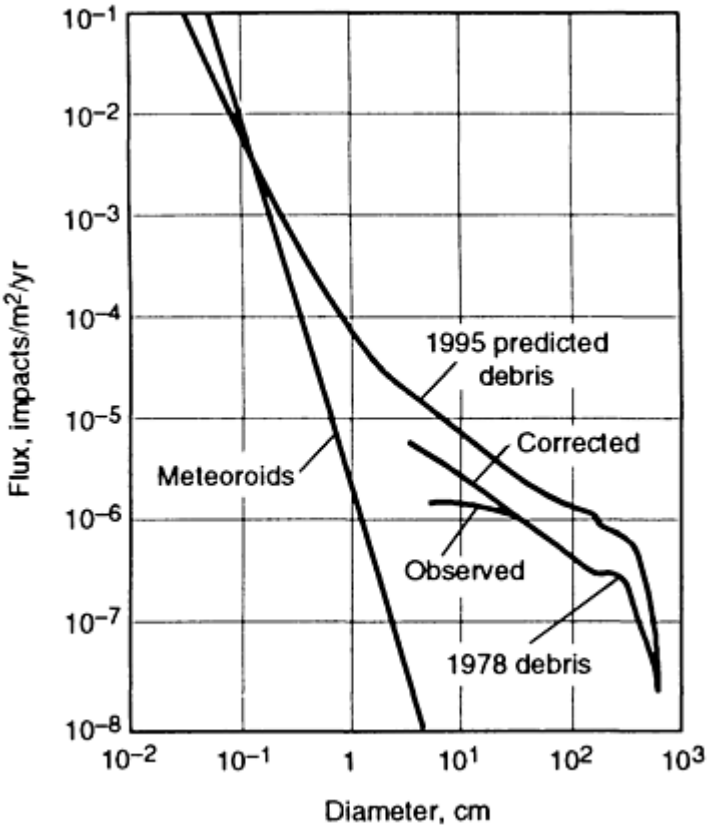

FIG. 2 DIAGRAM SHOWING THE INCREASE IN THE CONCENTRATION OF "SPACE DEBRIS" ENCOUNTERED IN ORBIT. COURTESY OF D.J. KESSLER, NASA JOHNSON SPACE CENTER

On-orbit repair of high-value, long-duration space-based assets has proven to be more effective than to return them to earth. On-orbit welding is a logical technology to assist in the repair of systems such as a space station. In other cases, such as a manned mission to Mars or the vicinity of the moon, it is impractical or impossible to return damaged structures to earth. The Soviet space program already has used welding to repair Soyuz space station tubing.

If a lunar base is established, structures will need to be economically constructed. Welding offers the potential for fast and cost-effective fabrication. In addition, repair of structures and equipment damaged by use and/or meteor collision will be necessary. Lunar dust contains many abrasive components, and wear of equipment will be inevitable. The cost of equipment replacement will probably be prohibitive, while repair by weld hardfacing and surfacing is a very cost-effective technology that is employed in earth-based applications subjected to wear. See the article "Hardfacing, Weld Cladding, and Dissimilar Metal Joining" in this Volume.

Both the United States and the former Soviet Union have carried out welding experiments in space. The United States used Skylab to weld 2219-T87 aluminum alloy, type 304 stainless steel, and pure tantalum samples. The Soviet program used the Soyuz to perform its experiments and still has its space welding technology available. Both efforts involved electron-beam welding. The findings from these experiments are discussed later.

Welding in Space and Low-Gravity Environments

Milo Nance, Martin Marietta Corporation; Jerald E. Jones, Colorado School of Mines

---

Space Welding Environment

Space presents a unique welding environment and many technological challenges. The most obvious and dramatic factors are microgravity and high vacuum. Microgravity in earth orbit occurs due to the centrifugal force of the orbiting craft that counters the effects of gravity, making the spacecraft and all orbiting objects, including those within the spacecraft, in continual free fall until a force acts upon them. Typical gravitation accelerations are on the order of 10^{-6} G (acceleration due to gravity).

High vacuum is present around the spacecraft. Typical levels in low earth orbit are 1×10^{-4} to 1×10^{-16} Pa. This vacuum aids some welding processes, such as electron beam. Since virtually no atmosphere is present, there is no attenuation caused by scatter of the electron beam. In addition, for all welding processes there is no need to protect the metal from oxidation or other atmospheric contaminants with a vacuum chamber, flux, or an inert gas atmosphere.

The space environment also offers several technological challenges. One of the problems is the lack of a high-capacity electrical power supply. Electrical power generation is currently produced by one of three methods: batteries, fuel cells (power generation from the combination of oxygen and hydrogen to form water), and direct solar conversion. All three of these methods produce a relative small amount of power compared to the requirements of the typical earth-based welding system. Typically, power is limited to 4.5 kW for a period of a few minutes on board the Space Shuttle. This power constraint will be present for the foreseeable future. Larger-capacity generation systems based on thermal-nuclear generators are being developed, but have not yet been used in service with manned spacecraft.

A second problem is the lack of nondestructive testing methods qualified for space use. Many of the traditional methods of inspection will not operate well in a space environment. For example, there is no method of dye penetrant inspection developed to date that can be applied in a vacuum. Methods such as radiography and eddy current inspection may be feasible, but no space-qualified equipment has yet been developed. Even if such equipment was available, the competition for weight and volume onboard a spacecraft might prevent its usage.

The application of intelligent automation techniques that allow the production of high-quality welds with a high degree of reliability appears to be the most attractive alternative with regard to the available space and weight limitations (see the discussion of the future of space welding later in this article). In order to produce such welds, a clear and precise knowledge of the mechanisms involved in space welding must be developed as well as the equipment necessary to carry out such welds. There have been several advances made in the necessary sensor and control technologies for earth-based welding that can be used in space welding.

Welding in Space and Low-Gravity Environments

Milo Nance, Martin Marietta Corporation; Jerald E. Jones, Colorado School of Mines

Welding Processes

The space environment has constraints that limit the application of certain conventional welding processes. For example, submerged arc welding (SAW) generally depends on gravity to feed the granulated flux and hold it in place on the weld; this is not possible in low-gravity environments. The space environment also affects some of the basic physical processes involved in welding, making welding processes operate differently in space than in earth-based environments. In addition, the weight limitations of orbital payloads on spacecraft will impose constraints on the processes that can be feasibly used in space.

The three processes that appear to have good potential for space application are electron-beam welding (EBW), laser-beam welding (LBW), and gas-tungsten arc welding (GTAW). All three processes are often used for autogenous welding, thereby eliminating the need for transport of high-weight consumables. These processes are also amenable to welding in vacuum (with certain modifications to the GTAW process as discussed below). Also, all of these processes have relatively low power requirements when used for thin-section materials typical of spacecraft and space structures, making these processes most useful in space, where all utilities, including electricity, are limited.

Electron-Beam Welding (EBW)

The EBW process consists of an electron-beam gun that generates a high-energy stream of electrons. When directed through a series of focusing electromagnets, this high-energy stream has sufficient power density to melt metals. The

EBW process is described in detail in the articles "Electron-Beam Welding" and "Procedure Development and Practice Considerations for Electron-Beam Welding" in this Volume. In earth-based environments, EBW generally requires a vacuum since the electrons scatter in a gas atmosphere. In space, however, the natural vacuum environment is ideally suited for the EBW process.

Both the United States and the former Soviet Union have experimented with EBW and melting in space. The M512 metals melting experiments using an electron-beam gun, which were conducted by the United States in the Skylab in 1972, are described later in this article. In this case, the operations were performed in a vacuum chamber that was inside the spacecraft, but vented to the outside. At the time of the experiments, there was some concern as to the quality of the vacuum achievable. Often, certain gases and liquids are jettisoned from spacecraft that remain in the environment in the local vicinity of the vehicle and can produce contamination of the vacuum.

Advantages. The electron-beam gun is, perhaps, the most efficient of the processes proposed for on-orbit welding. Due to the power limitations of spacecraft, this process is the most capable for welding of thicker-section materials. For autogenous welding, no consumables are required, thereby eliminating the cost of including them in the spacecraft payload.

Limitations. The impingement of electrons onto a metal surface causes the emission of x-rays. The former Soviet Union experimented with a manual electron-beam welding gun for space application. However, x-ray shielding capacity is proportional to the mass of the shield; therefore, shielding of workers may be difficult due to the high cost of payload weight on spacecraft. Automated or robotic welding may be recommended due to the radiation exposure to workers, particularly for extended periods of welding activity.

Safety Considerations. Grounding of the part to be welded is very important. Without proper grounding, the part being welded will acquire a net negative charge from the absorbed electrons. This will cause the beam to be deflected and the weld will not form properly. In addition, if the part becomes charged, then it will discharge to anything that it comes in contact with. Such a discharge could be very dangerous for a worker, or could damage electronic equipment such as computers or communications equipment onboard the spacecraft. Although the inherent repulsion of the like-charged electrons will cause beam spread, the beam will remain a fairly concentrated heat source for some distance from the electron-beam gun. Care will be required, both for manual as well as automatic or robotic welds, to ensure that the gun is not activated except when directed at properly prepared components to be welded. Significant damage could occur to workers, to component parts, or to the spacecraft itself if the gun were activated when directed improperly.

Laser-Beam Welding

The LBW process consists of a laser and a series of lenses or mirrors that direct and focus the beam at the component to be welded. The process is described in detail in the articles "Laser-Beam Welding" and "Procedure Development and Practice Considerations for Laser-Beam Welding" in this Volume. While the LBW process, unlike the EBW process, does not require a vacuum, the inherent vacuum environment in space will help to prevent oxidation and other contamination of the weld. There are two types of lasers used for welding, gas (CO_2) and solid state (Nd:YAG). While the solid-state lasers are relatively low power, this power level is adequate for thin-section components that are likely to be welded in space.

Advantages. As with EBW, the LBW process provides a concentrated heat source that can quickly melt through thin materials without heating large sections of the workpiece. Thus, the necessary power is less than that required for many other processes. However, the laser system is inherently inefficient in the conversion of energy so the input power requirements will be much greater than for an equivalent output heating capacity when compared to EBW. Also, for autogenous welding, no consumables are necessary for LBW, so the payload cost will be low. In addition, the LBW process, unlike EBW, can be used to weld electrically nonconducting materials, including ceramics, glasses, and polymers.

Limitations. The inefficiency of the laser system is due to a significant amount of heat generated in the lasing process itself. This heat will need to be dissipated through the spacecraft radiators or using separate radiators for the laser system. Because heat radiation from low-temperature systems is fairly slow, this may require large radiators to be installed for the laser system; thus the cost and payload weight of the system is increased. Secondly, due to the power input and heat dissipation requirements, it is difficult to produce a laser system for portable application. Recent work with Nd:YAG lasers and fiber optics has resulted in optical fiber delivery of the laser beam at a location remote to the laser system.

However, the laser system generally should be approximately 10 to 30 m (30 to 100 ft) from the LBW torch. Also, great care must be taken to avoid any damage to the cable containing the optical fiber.

Safety Considerations. A laser beam will not spread and dissipate with distance as will an electron beam. Consequently, a misdirected laser beam has the potential to cause damage, even over large distances to workers, components, and to the spacecraft. The laser light itself is dangerous to workers if reflected into the eyes. Proper shielding for persons working around laser welding equipment is necessary.

Gas-Tungsten Arc Welding

The GTAW process consists of a tungsten electrode connected to one lead of a power source, the other lead of which is connected to the workpiece. When the power supply is activated, current flows to the tungsten electrode through an arc plasma to the workpiece, and returns to the power supply to complete the circuit. The arc plasma is the primary source of heat as electrons move from the metal surface, are accelerated through the plasma column, and impinge on the metal surface at the opposite side of the arc. This welding process is described in the article "Gas-Tungsten Arc Welding" in this Volume.

The arc plasma consists of a superheated gas of ions and electrons. To shield the weld from atmospheric contaminants and to provide a stable plasma, inert gas is used. Typically argon, helium, or a mixture of these is chosen for GTAW. Because of the vacuum in the space welding environment, it is not necessary to shield the weld from contaminants; however, a small amount of gaseous material is necessary to sustain a stable arc plasma. The GTAW torch to be used for space welding will be modified from the torch used for earth-based welding. Through the use of a hollow tungsten electrode, the small amount of gas needed to sustain the arc plasma can be provided. A non-reactive gas or gas mixture will be necessary to avoid contamination of the weld. This modified GTAW process is similar to the earth-based PAW process.

Advantages. The equipment used for GTAW is simpler and much less expensive to produce and maintain in comparison to EBW and LBW. Secondly, the arc plasma only exists as a part of the overall welding power circuit, therefore it is nearly impossible to direct the GTAW arc toward a component, worker, or spacecraft that is not connected to this power circuit. Thirdly, as the length of the plasma increases, the voltage required to initiate and maintain the arc increases. By limiting the available voltage in the welding power circuit, the distance that the arc can strike is limited, and the possible damage resulting from a misdirected arc is limited to near-vicinity (25 to 50 mm, or 1 to 2 in.) objects.

Limitations. The GTAW arc plasma requires a constant flow of gas. This gas supply, in the form of fairly heavy compressed gas cylinders, adds to the cost and weight of the spacecraft payload. In addition, this supply will need to be constantly replenished as welding progresses. If resupply is not available, the process will not be available for use. With both LBW and EBW, the welding process would always be available regardless of a resupplied source of welding gas.

The arc plasma is a much less concentrated heat source in comparison to EBW and LBW. This results in the need for a higher power feed from the spacecraft to produce a weld in the same thickness material.

Safety Considerations. The primary concern with arc welding is grounding and insulation for workers. Should the worker become part of the welding circuit, the power supply will generally be capable of delivering several kilowatts through the worker at a current level that can cause permanent disability and/or death. Secondly, in order to ionize the inert gas plasma and initiate the arc, a high voltage is usually applied. This is accomplished through the use of a high voltage pulse, or a superimposed high-frequency high-peak voltage signal. Either of these generates a significant amount of electromagnetic interference (EMI) radiation, which can result in damage or shutdown of such equipment as computers and other advanced electronics onboard the spacecraft.

Other Joining Processes

With a few exceptions (for example, SAW), virtually all welding processes could be used in space. The EBW, LBW, and GTAW generally have been based on weight limitations or on the inherent aspects of the space environment (for example, vacuum for EBW). The materials likely to be found in space that would be welded are typically welded with EBW, LBW, or GTAW in the earth-based environment. These include aluminum and titanium and their alloys. In addition, these processes are well understood, commonly used, and very controllable for thin-section aerospace applications.

Another process that takes advantage of the space environment is solar heat welding. Solar radiation in space is unshielded by the atmosphere. A spacecraft in low earth orbit typically receives 1.4 kW/m^2 (0.13 kW/ft^2) in daylight conditions. This energy can be taken advantage of by focusing the solar radiation on the workpiece through the use of a large collecting mirror and focusing lenses. Because the optics of the mirror need not be perfect, the cost would be reasonable and the system would not be a drain on the limited power capacity of the spacecraft.

Other joining processes that could be utilized include mechanical fastening, solid-state bonding, brazing, and adhesive bonding. However, each of these has inherent limitations that tend to make the three welding processes discussed above more attractive. For example, it may be difficult to use adhesives because they require curing by the application of heat and/or the use of hardening (curing) agents. As a result, adhesives may outgas and contaminate the local environment with volatile components. Mechanical fastening has been used extensively for some joining applications in space. However, mechanical fastening is generally not capable of producing pressurized seals, and mechanically fastened joints are more susceptible to external mechanical damage than are welds.

Milo Nance, Martin Marietta Corporation; Jerald E. Jones, Colorado School of Mines

Metallurgy of Low-Gravity Welds

Influences of Microgravity. The microgravity environment that exists in space applications can have significant effect on the metallurgy of welds. Two important effects on the microstructure of a weld are cooling and fluid flow within the weld pool. In addition, certain other effects can be evident, including the deformation of the weld pool that occurs due to absence of gravity in the space environment. In the latter case, large weld pools in through-penetration or out-of-position welds will not droop or run, but instead their shape will be determined by surface energy and other forces.

Both the cooling rate and the liquid pool stirring behavior are influenced by gravity in earth-based welds. In space, the cooling rate will be different because convective flow is completely suppressed, and this affects the stirring forces in the pool. The principal heat loss from a weld is conduction into the surrounding solid metal. Because there is a significant temperature difference between the weld pool and its surroundings during the time the weld pool is at an elevated temperature, radiative cooling is also important. Generally, convective cooling from the weld surface is only a secondary cooling mechanism until the weld has dropped to a temperature at which little other cooling is occurring and further metallurgical transformation is unlikely to occur.

Both the conduction of heat into the surrounding metal and the radiation of heat from the weld pool are directly affected by the local surface temperatures of the weld pool. This includes the exposed surfaces as well as the interface between the liquid pool and the solid base metal. The conductive heat flow is governed by:

$$\boldsymbol{Q} = K \nabla \boldsymbol{T}$$

where ∇T is the temperature difference vector between the liquid metal and the solid metal at the interface and $\boldsymbol{q}$ is the heat flux vector. This same equation governs the loss of heat by convection from the exposed surface of the weld. However, the value of k is significantly less for heat flow across an interface into a gaseous medium than into a solid metal medium, and the k value for the convective heat transfer in a gas is much less still.

The equation for radiative heat flow is:

$$\boldsymbol{Q} = E\sigma(\nabla \boldsymbol{T})^4$$

where e is the emissivity of the emitting surface and σ is the Steffan-Boltzmann constant. Because the ∇T term is raised to the fourth power when the temperature difference vector is large, radiation heat transfer is a significant heat loss mechanism for the weld. It should be noted that the radiation of heat from the weld as well as the weld heat source may cause surrounding surfaces to heat, particularly if the weld is made in a vacuum such as outside the spacecraft

environment. The result might be damage to exposed components that are heat sensitive if appropriate shielding is not provided.

If convective pool stirring is suppressed, the temperature difference at the liquid-solid interface decreases. The liquid at that surface cools by conduction and the flow of hot liquid from the center of the pool is reduced. The result is a reduced cooling rate for the weld. This reduced cooling rate should tend to cause the grain size in the weld to increase. The opposite effect has, however, been observed and reported by investigators of space-based weld experiments.

The absence of gravitational forces also suppresses any buoyancy effects. Because of buoyancy forces, small particles of contaminants in earth-based welds will tend to either float to the weld surface or sink to the weld bottom depending on their density relative to the weld pool liquid. Surface energy effects may cause these particles to accumulate near surfaces. In low-gravity environments, it would be expected that these particles would remain suspended in the liquid pool as it solidifies. If these particles are good nucleants for metallurgical transformations in the weld metal, those transformations would tend to be enhanced. The result would be a difference in the microstructure between earth-based and space-based welds.

Differences between the distribution of inclusion particles in earth-based versus space-based welds has been observed. The effects of buoyancy and of cooling rate on actual welds were examined based on experiments conducted on Skylab in June of 1972. Some of those effects are discussed below.

Russian Welding Program. Space welding has long been a priority for the space program of the former Soviet Union. In 1969 Soyuz-6 performed the first welds in space on AMG6 and DM-20 aluminum alloys using the Vulkan apparatus. This work was carried on by the E.O. Paton Welding Institute of the Ukraine SSR Academy of Sciences. This work was conducted to develop methods of space repair and construction. Soon thereafter, the United States performed space welding experiments onboard the first manned Skylab Mission in June of 1973. Russian welding efforts have continued, and a portable EBW system has been developed. This hand-held EBW system is currently available for use on aircraft on the Mir space station.

United States M512 Experiments. The M551 EBW experiment was conducted in 1973 by astronaut Pete Conrad inside the multiple docking adapter of Skylab. Figures 3 and 4 show the Skylab spacecraft and the M512 material melting apparatus, respectively. The objectives of the M551 experiment, as described by McKannan and Poorman (Ref 1), were to demonstrate the feasibility of EBW in space and to investigate the differences caused by microgravity. The three materials tested included 2219T87 aluminum alloy, 304 type stainless steel, and tantalum. The aluminum and stainless steel alloys were chosen due to their commonality of use for aerospace applications; the tantalum was chosen as a nearly pure material with no complex phase transformations that would provide information on grain size and other physical and mechanical influences by microgravity. The density, melting point, thermal conductivity, and composition of these base metals are listed in Table 1. In this experiment, an electron beam was used to cut and also produce a weld bead on a 165 mm (6.5 in.) diam rotating disk that varied in thickness from 0.64 to 6.4 mm (0.025 to 0.250 in.) for the stainless steel and aluminum, and from 0.43 to 1.57 mm (0.017 to 0.062 in.) for the tantalum. Finally, the beam was directed at a stationary point on the disk to make a single dwell weld and tO produce a large molten pool. The electron-beam gun was held a constant distance of 38 mm (1.5 in.) with beam adjusted to 80 mA (70 mA for the tantalum sample) and 20 kV. These samples were then compared to samples welded with a duplicate earthbound apparatus using the same welding parameters. All the samples from this experiment were examined in depth at the Battelle Memorial Institute (Ref 2) and at NASA laboratories. In addition, several other organizations received samples for testing and evaluation.

TABLE 1 PROPERTIES AND COMPOSITIONS OF BASE METALS STUDIED IN THE M512 MELTING EXPERIMENTS

ALLOY	**DENSITY, G/CM^3**	**MELTING POINT**		**THERMAL CONDUCTIVITY**		COMPOSITION, WT%															
		°C	**°F**	**W/M · K**	**CAL/CM · S · °C**	**Al**	**C**	**Nb**	**Cr**	**Cu**	**Fe**	**Mg**	**Mn**	**Mo**	**Ni**	**P**	**S**	**Si**	**Ta**	**Ti**	Zn
2219-T87 ALUMINUM	2.83	638	1180	251	0.6	BAL	. . .	. . .	. . .	6.2	0.25	0.02	0.3	. . .	. . .	. . .	. . .	0.15	. . .	0.15	**0.10**
TYPE 304 STAINLESS STEEL	8.03	1442	2628	159	0.38	. . .	0.05	. . .	19.0	0.5	BAL	. . .	1.5	0.5	8.5	0.04	0.03	0.75	. . .	. . .	**. . .**
TANTALUM	**16.6**	**2996**	**5425**	**54.4**	**0.13**	**. . .**	**. . .**	**0.1**	**. . .**	**. . .**	**. . .**	**. . .**	**. . .**	**. . .**	**. . .**	**. . .**	**. . .**	**. . .**	**BAL**	**. . .**	**. . .**

FIG. 3 PHOTOGRAPH OF SKYLAB, WHICH HOUSED THE M512 METALS MELTING EXPERIMENT

FIG. 4 PHOTOGRAPH OF THE M512 MELTING APPARATUS TAKEN AT THE AIR AND SPACE MUSEUM IN WASHINGTON D.C.

The metallurgical study concluded that electron-beam space welding was feasible. However, distinct changes in weld morphology and metallurgy were found. These are reported in Table 2.

TABLE 2 DIFFERENCES IN SPACED-BASED (SKYLAB) AND EARTH-BASED WELD SAMPLES

MATERIAL	CHARACTERISTICS OF SKYLAB SAMPLE
2219-T87 ALUMINUM	**INCREASED OXIDE ON BACK SIDE OF WELD** **GRAIN REFINEMENT IN WELD** **REDUCTION IN SURFACE RIPPLE, BEADING, AND SPATTER** **INCREASED NUGGET SYMMETRY**
304 STAINLESS STEEL	**GRAIN AND SUBGRAIN REFINEMENT** **DECREASED BANDING** **DECREASED WELD POOL SAG** **REDUCTION IN SURFACE RIPPLE, BEADING, AND SPATTER** **INCREASED NUGGET SYMMETRY**
TANTALUM	**GRAIN REFINEMENT** **DECREASED WELD POOL SAG** **INCREASED NUGGET SYMMETRY**

A subsequent investigation by Nance and Jones at the Colorado School of Mines has shown that both the grain size and the inclusion distribution were affected by the microgravity environment. This study concentrated on the tantalum material. It had been previously hypothesized that the grain size of the weld made in space would be larger due to the reduced cooling rate of the liquid pool. This hypothesis was contradicted by the observation of a 23% reduction in grain size observed in the Skylab tantalum welds in comparison to the earth-based welds. Figures 5(a) and 5(b) compare the grain size of the earth-based and Skylab tantalum welds. A similar grain size reduction was also noted in the aluminum and stainless steel alloys. The mechanism for grain size refinement in these alloys is complex, and it is difficult to draw

direct conclusions. For the pure tantalum samples, there were no solid-state transformations; however, the grain size change may be attributable to an inoculant nucleation mechanism.

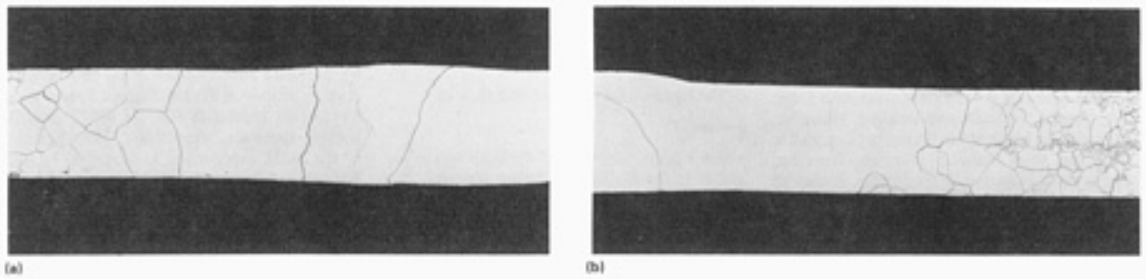

FIG. 5 COMPARISON OF (A) GROUND-BASED AND (B) SKYLAB-BASED WELDS IN PURE TANTALUM SAMPLES. NOTE THE LARGER GRAIN SIZE IN THE GROUND-BASED WELD. SOURCE: REF 2

Utilizing scanning electron microscopy (SEM) with energy dispersive x-ray analysis and scanning Auger spectroscopy (SAS), it was determined that oxide inclusions were well distributed throughout the Skylab welds. In the earth-based welds, these oxide particles, possibly due to the influence of gravity-induced buoyant forces, had floated to the top surface of the weld pool. Figure 6(a) is a SEM micrograph of the Skylab tantalum weld. There is a large carbide particle near the center of the SEM photomicrograph, as confirmed by the SAS carbon map shown in Fig. 6(b). Figure 6(c) is the SAS oxygen map, showing only a small accumulation of oxide particles near the surface of the weld, with a well-distributed oxide particle dispersion in the center of the weld. The earth-based weld showed virtually no oxide particles in the middle of the weld and a very heavy accumulation of oxides at the weld surface.

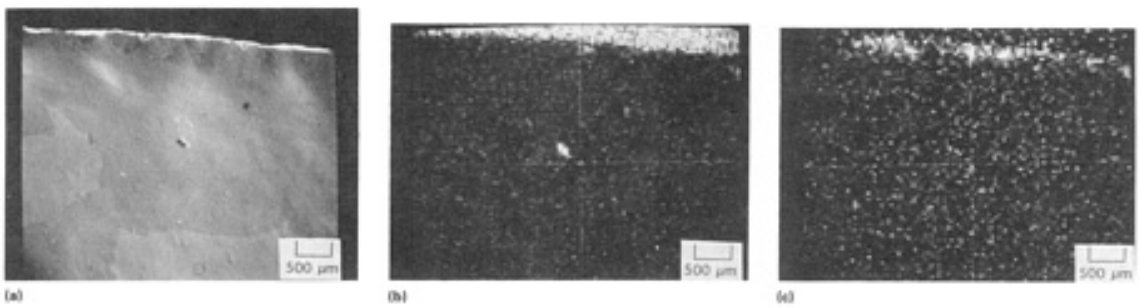

FIG. 6 MATERIALS CHARACTERIZATION TECHNIQUES FOR EXAMINING A TANTALUM WELD CARRIED OUT IN SKYLAB. (A) SEM MICROGRAPH SHOWING A LARGE CARBIDE PARTICLE NEAR THE CENTER OF THE SAMPLE. (B) SCANNING AUGER SPECTROSCOPIC CARBON MAP SHOWING A LARGE CARBIDE PARTICLE NEAR THE CENTER OF THE SAMPLE. (C) SCANNING AUGER SPECTROSCOPIC OXYGEN MAP SHOWING ONLY A SMALL ACCUMULATION OF OXIDE PARTICLES NEAR THE SURFACE OF THE WELD WITH A WELL-DISTRIBUTED OXIDE PARTICLE DISPERSION IN THE CENTER OF THE WELD

References cited in this section

1. E.C. MCKANNAN AND R.M. POORMAN, PAPER 35812, GEORGE C. MARSHALL SPACE FLIGHT CENTER, ALABAMA, 1974, P 20
2. R.E. MONROE, "CHARACTERIZATION OF METALS MELTING RISKS: SKYLAB EXPERIMENT M551," NASA CONTRACTOR REPORT, BATTELLE MEMORIAL INSTITUTE, COLUMBUS, OHIO, 4 DEC 1973, P 109

Milo Nance, Martin Marietta Corporation; Jerald E. Jones, Colorado School of Mines

Future of Space Welding

The most important space-based welding application for long-duration manned spacecraft is repair welding. This technology offers the possibility of decreasing assembly time and decreasing the weight and cost of space structures. However, before welding technology can become commonplace in space, several steps must be taken. These involve the development of processes and controls that allow highly reliable welds to be performed in space. These steps include:

- DEVELOPMENT OF EQUIPMENT THAT HAS SUFFICIENT SENSOR TECHNOLOGY TO REPORT IN REAL TIME THE QUALITY OF WELDS AND TO FACILITATE REAL-TIME PROCESS CONTROL AND CORRECTION OF WELDS IN PROGRESS
- CHARACTERIZATION OF THE DIFFERENCES IN SPACE-BASED WELDS AND EQUIVALENT EARTH-BASED WELDS TO PROVIDE A BASIS FOR MODELING AND UNDERSTANDING OF THE DIFFERENCES IN THESE WELDS
- PROCESS DEVELOPMENT FOR WELDS CONDUCTED IN SPACE

If these three actions are taken, welding can potentially become the preferred method of joining metallic components in space and an important method for the long-term maintenance of structures, including large space-borne structures that are independent of earth.

The Need for Automation. Earth-based welding is a difficult task and requires both significant skill as well as time-consuming and tedious effort. If performed manually, space welding will be, at best, a very difficult task. The problems with space welding are compounded if the welding is to be done outside the spacecraft environment. Extra-vehicular activity (EVA) requires large numbers of ground personnel and considerable time and preparation by the mission specialist. In order for spacecraft crews to have the skill level required to make critical welds, considerable time and additional effort would have to be expended. Such training would be very expensive. Computer intelligent autonomous or semi-autonomous welding systems will probably be the most cost-effective means for space welding, particularly for EVA welding.

Intelligent Engineering/Planning Systems. Recently developed systems have demonstrated the possibility of coupling extensive databases with artificial-intelligence-based software to produce "intelligent" engineering and planning software that can make many routine engineering decisions for welding applications and guide a human user to optimum decisions for welding. These systems utilize expert system and neural network technology to provide accurate weld process models and engineering decision-making capability. This subject is addressed for earth-based welding applications in the article "Intelligent Automation for Joining Technology" in this Volume.

Intelligent engineering and planning workstations that are electronically coupled to automatic welding machines will substantially reduce the need for time-consuming work by mission specialists. The planning and development of welding schedules and procedures can be accomplished in a matter of a few minutes on a computer terminal rather than hours of work by hand. By having a complete set of databases and most of the routine engineering completed by the computer, the human user will need only to answer a few questions about the application, and the system will produce a complete welding plan and weld schedule that can be downloaded directly to the automated welding system. Such systems will offer considerable cost savings and manhour reduction while at the same time providing a carefully optimized welding plan and procedure.

Welding in Space and Low-Gravity Environments

Milo Nance, Martin Marietta Corporation; Jerald E. Jones, Colorado School of Mines

References

1. E.C. MCKANNAN AND R.M. POORMAN, PAPER 35812, GEORGE C. MARSHALL SPACE FLIGHT CENTER, ALABAMA, 1974, P 20
2. R.E. MONROE, "CHARACTERIZATION OF METALS MELTING RISKS: SKYLAB EXPERIMENT M551," NASA CONTRACTOR REPORT, BATTELLE MEMORIAL INSTITUTE, COLUMBUS, OHIO, 4 DEC 1973, P 109

Joining of Organic-Matrix Composites

L.J. Hart-Smith, McDonnell Douglas Aerospace

Introduction

SUCCESSFUL ADHESIVE BONDING of organic-matrix composites is dependent on the nature of the adherend surfaces. Factors that influence the integrity and durability of composite-to-composite bonds include wetting of the adherend, cleanliness of the substrate, chemical and physical properties of the adherends, and joint design. In this article, major emphasis is placed on the critical importance of proper surface preparation; both thermoset and thermoplastic composites are covered. The techniques used to analyze and design adhesively bonded composite joints are described in a companion article (Ref 1). Additional information can also be found in *Adhesives and Sealants,* Volume 3 of the *Engineered Materials Handbook* published by ASM International.

Reference

1. L.J. HART-SMITH, JOINTS, *COMPOSITES,* VOL 1, *ENGINEERED MATERIALS HANDBOOK*, T.J. REINHART, ED., ASM INTERNATIONAL, 1987, P 479-495

Joining of Organic-Matrix Composites

L.J. Hart-Smith, McDonnell Douglas Aerospace

Common Problems Encountered

The Importance of Proper Processing. It is well known that the adhesive bonding of metal structures requires strict adherence to the process specifications if the glue is to remain stuck for a long service life. It is also apparent that not all approved specifications are adequate. The Primary Adhesively Bonded Structures Technology (PABST) program (Ref 2) was conducted to demonstrate the tremendous benefits to metallic aircraft structures from good adhesive bonding, to associate previous problems in service with processing techniques that should be discontinued, and to validate the use of phosphoric acid anodizing with a corrosion-inhibiting primer as a reliable technique--as durable as the British chromic acid anodizing with Redux adhesive, and easier to use.

Only when the adhesive is stuck securely to the adherends is it possible to develop a bond strength that can be relied upon. Only then is it possible to use rational design procedures in which the joint can be designed for the bond to never fail, or if it does fail, for the failure to be characterized by cohesive failure of the adhesive layer itself. The interfacial failures associated with improper or inadequate processing are both unpredictable and variable--so variable, in fact, that

neither the strength nor fatigue life can be established. This poor processing is the source of the so-called "weak bonds" that are discovered only after the structure has fallen apart.

Industrial experience with bonding of both metals and composites has shown that it is very easy to fabricate defective bonds that are strong enough to pass all initial inspections, but that have only a small fraction of the strength to be expected from properly processed bonds. Techniques for creating suitable surface preparations must be followed to achieve the normal situation in which the bonds are so much stronger than the thin members they join that all failures will occur outside the joint. The necessary steps are not difficult, but are often omitted because of a failure to appreciate the need for them.

Unfortunately, the importance of surface preparation for the adhesive bonding of fibrous composites is not widely acknowledged. Robert Schliekelmann, the pioneer of Redux bonding at Fokker, was sufficiently concerned about this oversight to make a plea for more attention to this issue (Ref 3). Hart-Smith and co-workers at Douglas Aircraft Company prepared a document on surface preparation of fibrous composites to help the airlines until repair manuals were completed (Ref 4). When this document was reprinted in the Canadair house journal (Ref 5), every experiment had to be repeated to create new photographs and every phenomenon was duplicated in order to verify that the problems discussed in the Douglas Aircraft article really existed.

A similar concern was expressed in England, where Parker and Waghorn (Ref 6) reported on a far more comprehensive test program on the effects of surface preparations on adhesive bond strength for carbon-epoxy laminates. They also concluded that composite surfaces must be abraded to achieve strong adhesive-bonded joints. Pocius and Wenz (Ref 7) advocated the use of Scotchbrite pads with embedded abrasive particles as an effective and reliable surface preparation technique for achieving good composite bonds (Ref 7). The form of Scotchbrite giving the best results is of the consistency now used widely in floor-scrubbing pads, which is a little finer than that used in rotary discs for stripping rust from automobiles before repainting.

Sources of Defective Bonds. A major source of defective bonding of composite adherends is the omission of a thorough mechanical abrasion of the surface, either by a low-powered grit-blast machine or thorough sanding, following the removal of a peel ply from the surface of the laminate. Grit blasting is shown to lead to the best thermoset bonds, which are enhanced by the use of an adhesive film cured on the surfaces of the part as it is made. Although peel plies can protect against gross contamination, they do not create a surface that is easily wetted by adhesives. Despite the cautions about the many wrong ways to make bonded joints, correct processing is neither difficult nor expensive and results in strong durable structures.

Most, if not all, peel-ply surfaces are inadequate for adhesive bonding. This is a contentious issue because many bonded composite structures are so thin that the laminate or honey-comb core fails first during testing, even when the bond is less than 10% effective. However, that is often not the case in service. It has sometimes been found that when a part damaged in service is disassembled to provide access to abrade the surfaces for a bonded or co-cured repair, it is relatively easy to break the bonds apart without delaminating much of the composite. In such a case, all of the original bond area that was neither detected as defective during initial inspection, nor delaminated as the doublers and stiffeners were removed from the skin, should be regarded as weak (defective) bonds that could not be detected by ultrasonic inspection. This fraction of the bond area may be as high as 90% of the total if the original bonding had not been processed correctly. This condition is usually associated with virtually all of the adhesive on one surface or the other, when assessed locally, although the surface to which the adhesive adhered may vary throughout the total bond area. The local areas in which there was no adhesion are typically quite large and cannot be mistaken for porosity.

It is extremely rare to see half the bond completely covering each surface after disassembly; the cohesive strength of the adhesive layer, if it has been processed correctly, is usually so much greater than that of the adherends that trying to pry good bonds apart will result in delaminating the composite, not the adhesive layer. As a point of reference for the tremendous peel strength of most modern adhesives, attempts to salvage machined metal fittings from completed test panels for reuse on later panels in the PABST bonded metal fuselage program were largely fruitless, even when the structure was struck with sledge hammers and cold chisels after chilling the panels with liquid nitrogen. (Some older adhesives have so little peel strength at low temperature that it used to be possible to disassemble bonded metal structures by giving them a sharp rap after chilling them with dry ice.) It would seem to make more sense to heat bonded composite structures above the glass transition temperature for the adhesive, but below that of the parent laminate to facilitate safe disassembly. The disadvantage here would be that the working environment of some 120 °C (250 °F) would be rather unpleasant, unless it could be confined to the immediate vicinity of the area of prying by using a jet of hot air.

There is no history of bonds that were truly good at the time of manufacture deteriorating in service. There have, however, been numerous instances in which the interface of a metal bonded structure has corroded in service because it had not been properly prepared in the first place and was just sound enough to pass the initial inspection. Although poor composite bonds deteriorate by mechanisms other than corrosion, they share with poor metal bonding the characteristic that their short-term static strength is sufficient to conceal their deficiencies. Weak bonds have been notoriously difficult to detect prior to failure when only the parts have been examined; however, they are easy to identify after failure and can be recognized reliably from a straightforward reading of the process monitoring records and an on-site survey of the procedures followed (and ignored) during manufacture. The process monitoring records should always take precedence over successful test coupon results, even when it means rejecting and rebuilding (not reworking) complete assemblies.

The reason for the difficulty in bonding of polymer composites is that it is difficult to create strong chemical bonds between the adhesive and a cured (and therefore largely fully crosslinked) polymer matrix. The cured surface needs to be activated and, even then, chemical bonds may be degraded by absorbed water (Ref 8). The most durable bond strengths rely upon mechanical interlocking of the adhesive and the thermoset composite surface, just as with the primer and porous anodized surface on metal adherends. If the surface is not adequately roughened, the glue will not stick, even if the surface is not contaminated. The most common contaminants are industrial-grade cleaning solvents and coupling fluids for ultrasonic inspections. These are particularly difficult to remove from delaminations and areas of porosity. Failure to remove them completely results in a bond with inadequate adhesion to the adherend, just as is the case with a metal-bond surface that had been contaminated before the primer was applied.

Effects of Absorbed Moisture. Water is the most widespread and troublesome source of defective bonded joints and repairs in composite structures. It may be absorbed by the basic composite material before it is ever cured. If it is not removed by drying prior to curing or by venting during cure, it will result in porosity as well as harmful changes in the chemical structure of the polymer. Water may also be absorbed by uncured adhesive films that have been improperly stored or that have not thawed out before being unwrapped after removal from the freezer or that have been subjected to an extended layup time in a humid work environment. Adhesives vary in susceptibility to this problem, but most have a far greater affinity for water than do epoxy prepregs. The consequences are much the same, and just as detrimental. Water may also be absorbed within cured laminates that are to be secondarily bonded either during initial manufacture or as part of an in-service repair. If this water is not removed by slow drying prior to bonding, the water will react adversely with the adhesive and result in defective bonds. Cured epoxies have very low diffusion coefficients, so water is not absorbed very rapidly. However, they cannot be dried rapidly for the same reason.

A systematic series of tests to differentiate between the effects of different kinds of prebond moisture has not been carried out to date. However, a weak, porous adhesive that crumbles easily into powder when the fractured surface is handled after the adhesive layer has been exposed, but that has stuck to the adherends, can be associated with too much moisture absorbed by the adhesive before cure. A perfectly sound solid adhesive film that simply did not stick is more likely to be caused by precured laminates to be bonded that were not dried or by condensate on the surface of an otherwise dry adhesive film that was unwrapped too soon after removal from storage in the freezer. However, some film adhesives left out for several days in a humid layup area can absorb so much water that they will not stick even if they are not visibly covered by condensate during layup. Even then, there is a chance that the strength of the fillets at the edges of the bonds will be sufficient to disguise the weakness by preventing the parts from falling apart after completion of the cure.

Labor and Myhre (Ref 9) found that if they did not dry the parent laminate first, they could not attach even a single 0.13 mm (0.005 in.) thick carbon-epoxy tape without serrating the ends with pinking shears. With square-cut ends, the single layer would rapidly delaminate under fatigue loads of only about 25% of design limit load. Obviously, however, such weak bonds would have passed all nondestructive inspections at the time the repair was executed. The only way of knowing that the bond would have failed had it been placed in service was recognition that water definitely was present during the cure of the adhesive--water that was added deliberately to make the coupons representative of structures in service that were being quickly repaired without first being dried out slowly and carefully. In extreme cases, with a rapid temperature rise during bonding, the parent laminate may even split apart because of the steam generated by the water that was unable to escape fast enough. Figure 1 shows the dramatic reduction in the hot-wet strength of adhesively bonded joints caused by as little as 0.25% absorbed moisture in the composite laminates before bonding. Less than 20% of the room-temperature strengths were retained. Figure 2 shows equally dramatic losses in the fatigue life under slow-cycle testing of bonded aluminum joints as a function of different levels of prebond moisture in the adhesive film prior to bonding.

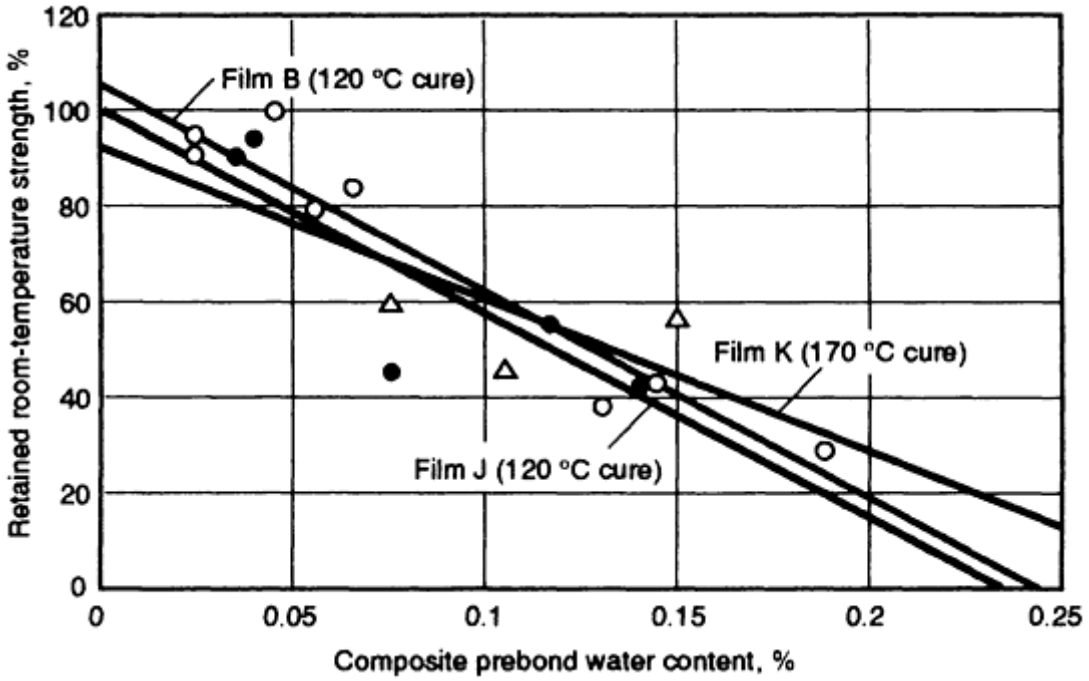

FIG. 1 EFFECT OF MOISTURE CONTENT ON THE HOT-WET BOND STRENGTH OF CARBON-EPOXY COMPOSITES. SOURCE: REF 10

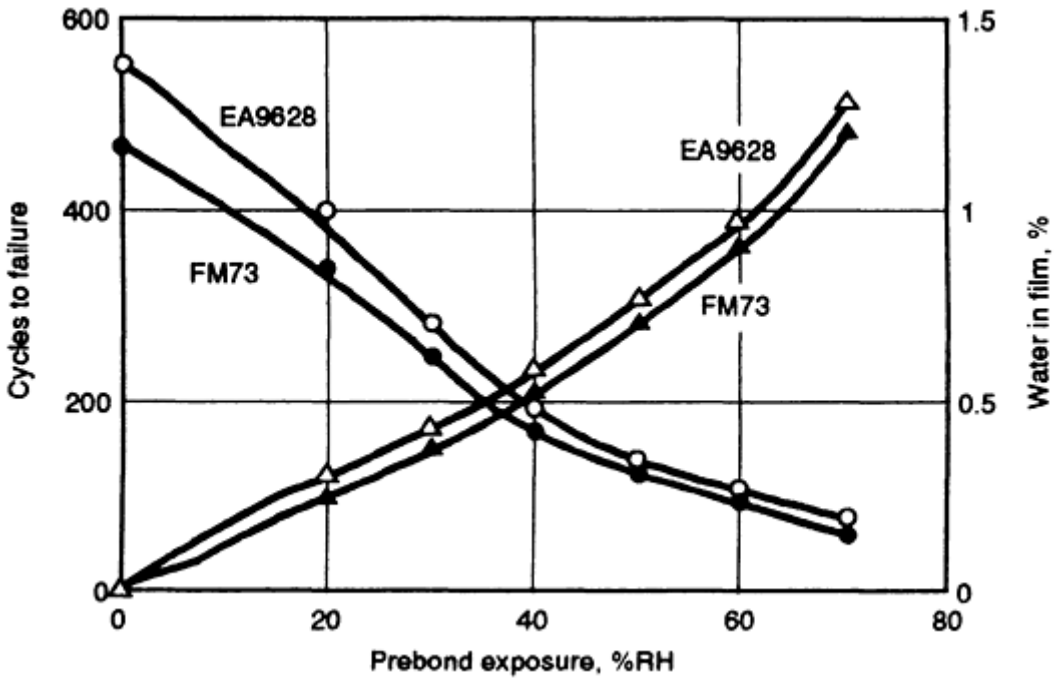

FIG. 2 EFFECT OF PREBOND MOISTURE ON FATIGUE STRENGTH OF ADHESIVELY BONDED ALUMINUM JOINTS. FILMS WERE PRECONDITIONED FOR 10 DAYS AT ROOM TEMPERATURE. RAAB SPECIFICATIONS, 10.3 MPA (1500 PSI), 4 CYCLES/H, 60 °C (140 °F), 100% RELATIVE HUMIDITY (RH). SOURCE: REF 11

Although the evidence is not yet absolutely conclusive, the epoxy resins may be more tolerant of absorbed moisture than is generally acknowledged if moisture can easily be driven off early in the cure cycle. However, if there are no vents to allow the steam (or solvents) to escape, as is often the case with no-bleed cure cycles, moisture cannot be driven off. There is conclusive evidence that the combination of the presence of moisture and a closed cure environment is

disastrous. However, there have been some instances with metal-bonded structures when water was known to be present in the uncured adhesive, yet the bonds appear to have been good (per service). In each case, the bonding tool permitted easy egress of the steam generated during cure. Companion panels manufactured with a different bonding tool that trapped the moisture in the adhesive from the very same rolls, passed all ultrasonic inspections but were found to be unbonded during assembly.

A similar problem arose with the two-stage bonding of a composite spoiler. Although water was present in some form during both bonds, there was adequate venting for the steam to escape while the first skin was bonded to an oversize block of honeycomb core, to stabilize it for subsequent machining of the aerodynamic profile (it is not known if the water was absorbed in the uncured adhesive film, if the Nomex honeycomb core had not been dried properly, or if the precured laminates had not been dried properly). This first bond was so strong as to give no warning of the problems to follow. When the second skin was bonded to the other side of the core, the water was trapped and the second bond had only a small fraction of the strength exhibited by the first bond. When tested, the second bond failed prematurely; it looked porous and weak, with poor filleting at the cell walls, while the first bond showed good filleting, as if the water had never been present.

The above examples are included not as an invitation to disregard the concerns about moisture present during the cure, but as encouragement to pursue this subject further to see if there are any consistently reliable alternatives to careful drying prior to bonding, which is obviously time consuming and costly. It is also intended to emphasize the need for venting during cure. There are other known instances in which simple thin laminates have suffered locally from very wavy fibers caused by the lack of an escape path for bubbles of gas created from the solvent used during the process of impregnating the fibers with resin. The bubbles lifted the fibers off the tool surface, pulling the ends in toward the bubbles. Eventually, the bubbles burst, causing the fibers to wrinkle as they were flattened out. There was no mechanism to push the fibers back to where they had been.

Difficulties in Detecting Defective Bonds. The most difficult aspect of defective bonds caused by prebond moisture or inadequate surface preparation is that the condition cannot be detected by ultrasonic inspection. It must be avoided by adherence to the correct procedures--which may differ from those specified--during processing because the weak bonds resulting from such errors cannot be repaired, even if they are detected before they fail. The parts must be disassembled, the surfaces cleaned and prepared again and the entire bonding cycle repeated. In general, it is easy to rework improperly manufactured mechanically fastened metallic structures and to restore 100% of the design strength. That is not true for either adhesively bonded metal or composite structures; the rework is difficult and the strength recovered far less than complete. This is why it is so important to do the job properly in the first place.

The cost of accepting defective parts is compounded as the original panels are embedded ever more deeply in the structural assemblies. It is bad enough when the defects are unrecognized because the end-item inspections are ineffective; inspection can exclude a few very bad parts, but cannot ensure the integrity of the great majority of assemblies. It is worse when parts are recognized as defective from a visual inspection, but are accepted anyway on the basis of coupon tests or ultrasonic inspections.

Bonding of Thermoplastic Composites. Thermoplastics are far more difficult to bond than are thermoset composites, but good results have been achieved by chemically etching the surface prior to bonding. The most promising approach for joining thermoplastic composites appears to be fusion bonding, using a compatible surface layer of plastic that melts at a lower temperature than that needed to melt the parent matrix. The ability of typical modified epoxy adhesives to bond chemically to the thermoplastic matrix is even less than for thermoset composites. Also, the thermoplastic surface is so resilient that it is very difficult to abrade sufficiently without breaking too many surface fibers in the process of creating the roughened bond surface. The best bonds made with layers of thermoset adhesives between thermoplastic adherends seem to have a strength of only about 80% of that of the best bonds using the same adhesive between thermoset adherends. One must conclude, therefore, that this loss of strength results from an interfacial bond strength that is weaker than the intrinsic cohesive strength of the adhesive layer. It follows, therefore, that the strength to be attained would be highly variable, as would the service life. Far better success has been achieved by chemically changing the surface to be bonded by oxidation using hot gases, by cold gas plasma treatment, or by corona discharge. The surface energy is increased by each of these techniques, permitting better wetting by the adhesive. However, these processes are rather slow if a large area has to be covered.

Success in bonding thermoplastics has also been achieved by fusion, or welding. The best success has been achieved when the original thermoplastic laminates have been fused together with a special surface layer of a different polymer that can be melted at a lower temperature than is needed to melt the base laminates. Direct fusion of thermoplastic laminates often results in considerable distortion, even if a structurally sound bond is achieved. Even making thermoplastic

composites using focused local heat to fuse each ply to the substrate has proved to be a slow process that is not well suited to large panels.

Similarly, it is common practice in making thermoset composite aircraft panels to include a surfacing layer of film adhesive co-cured with the parent matrix to both facilitate getting the paint to adhere and to provide a tough gel coat to compensate for the excessively dry surface plies in normal composite laminates. (The weight of this surfacing layer is less than that of the glazing that would otherwise need to be applied, by hand, to avoid pinhole porosity and an unacceptable paint finish.) Curiously, less use is made of this concept for preparing surfaces to be bonded, although an Australian firm has reported great success with it (Ref 12).

References cited in this section

2. E.W. THRALL, JR. AND R.W. SHANNON, ED., *ADHESIVE BONDING OF ALUMINUM ALLOYS*, MARCEL DEKKER, 1985
3. R.J. SCHLIEKELMANN, ADHESIVE BONDING AND COMPOSITES, *PROGRESS IN SCIENCE AND ENGINEERING OF COMPOSITES*, VOL 1, PROC. 4TH INT. CONF. COMPOSITE MATERIALS (TOKYO), 22-28 OCT 1982, JAPAN SOCIETY FOR COMPOSITE MATERIALS AND THE METALLURGICAL SOCIETY (TMS) OF AIME, T. HAYASHI, K. KAWATA, AND S. UMEKAWA, ED., NORTH-HOLLAND, AMSTERDAM, 1982, P 53-78
4. L.J. HART-SMITH, R.W. OCHSNER, AND R.L. RADECKY, SURFACE PREPARATION OF FIBROUS COMPOSITES FOR ADHESIVE BONDING OR PAINTING, *DOUGLAS SERVICE MAGAZINE*, FIRST QUARTER 1984, P 12-22
5. L.J. HART-SMITH, R.W. OCHSNER, AND R.L. RADECKY, SURFACE PREPARATION OF FIBROUS COMPOSITES FOR ADHESIVE BONDING OR PAINTING, *CANADAIR SERVICE NEWS*, VOL 14 (NO. 2), SUMMER 1985, P 2-8
6. B.M. PARKER AND R.M. WAGHORNE, SURFACE PRETREATMENT OF CARBON FIBRE-REINFORCED COMPOSITES FOR ADHESIVE BONDING, *COMPOSITES*, VOL 13, JULY 1982, P 280-288
7. A.V. POCIUS AND R.P. WENZ, MECHANICAL SURFACE PREPARATION OF GRAPHITE-EPOXY COMPOSITE FOR ADHESIVE BONDING, *SAMPE J.*, SEPT/OCT 1985, P 50-58
8. A.J. KINLOCH AND G.K.A. KODOKIAN, "THE ADHESIVE BONDING OF THERMOPLASTIC COMPOSITES," EUROPEAN RESEARCH OFFICE OF THE U.S. ARMY, CONTRACT DAJA 45-86-C-0037, FOURTH PERIODIC REPORT, IMPERIAL COLLEGE, LONDON, AUG-DEC, 1987
9. J.D. LABOR AND S.H. MYHRE, "LARGE AREA COMPOSITE STRUCTURE REPAIR," NORTHROP AIRCRAFT CORPORATION, USAF TECHNICAL REPORT AFFDL-TR-79-3040, MARCH 1979
10. B.M. PARKER, THE EFFECT OF COMPOSITE PREBOND MOISTURE ON ADHESIVE-BONDED CFRP-CFRP JOINTS, *COMPOSITES*, VOL 14, JULY 1983, P 226-232
11. E.W. THRALL, JR., PROSPECTS FOR BONDING PRIMARY AIRCRAFT STRUCTURES IN THE 80'S, *25TH NATIONAL SAMPE SYMPOSIUM*, VOL 25, SOCIETY FOR THE ADVANCEMENT OF MATERIAL AND PROCESS ENGINEERING, 6-8 MAY 1980, P 716-727
12. I. MCARTHUR, HAWKER DEHAVILLAND, BANKSTOWN, AUSTRALIA, PRIVATE COMMUNICATION, 1992

Examples of Good and Bad Adhesive Bonds

Properly Processed Bonds. Figure 3 shows the magnified fractured surface of a properly processed adhesive bond, with continuous coverage of the adherend. With composite adherends, this condition can occur only in test coupons deliberately designed with so little bond area that the bond will fail by shear. It is also necessary to suppress the generation of peel stresses at the ends of the overlap, by keeping the tip thickness of the adherends low. Properly designed structural joints will always fail outside the bond area, and while a coupon test based on such a joint can confirm the adequacy of the design, it cannot confirm that the processing was done properly because there is no fractured bond line to inspect. In properly designed bonded joints, the integrated shear strength of the bond should exceed the load needed to fail the adherends. It is almost impossible not to satisfy this condition for thin adherends, even for improperly processed bonded joints that will fail in service, but are strong enough to pass all the initial inspections. However, for thick adherends, it becomes necessary to use stepped-lap joints to prevent the bond from becoming a weak-link fuse.

FIG. 3 COHESIVE FRACTURE SURFACE IN A PROPERLY PROCESSED COMPOSITE-TO-COMPOSITE ADHESIVE BOND. VISIBLE FIBERS ARE THE RANDOM MAT CARRIER IN THE ADHESIVE FILM. 68×

Adhesion Failures. * Figure 4 shows a typical adhesion failure in which the adhesive almost totally failed to adhere to one of the adherends because the surface had not been adequately roughened. Although this photomicrograph is of the surface of the adhesive, not the composite, it clearly shows the imprint of the peel-ply woven surface to which it had not bonded over most of the surface. The comparison between the two modes of failure is dramatic. This failure of the adhesive to bond to a surface arises frequently when an attempt is made to bond directly to the surface that remains after removal of a peel ply, but it also occurs when one tries to bond directly to the other surface of the laminate, which is usually contaminated by release agents used to prevent the part from sticking permanently to the layup tool.

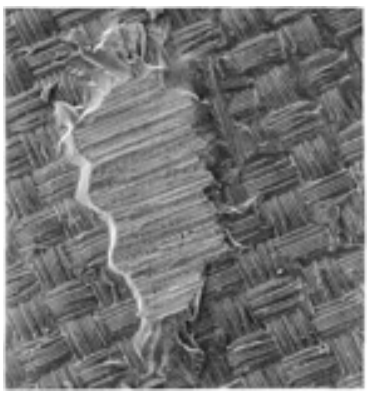

FIG. 4 ADHESION FAILURE SHOWING IMPRINT OF THE PEEL PLY AND FAILURE TO BOND OVER MOST OF THE SURFACE. A SMALL PIECE OF RESIN ADHERED AND IS IDENTIFIED BY THE IMPRINT OF THE FIBERS. 27×

In a different kind of adhesion failure, the adhesive does not remain in one continuous disbonded layer, but remains attached to one of the adherend surfaces in discrete full-thickness fragments. The underlying shiny peel-ply surface is clearly evident in the holes in the adhesive on both surfaces. Roughly half the adhesive is attached to each surface, but

only weakly. This kind of fracture has been observed in uncontaminated bond surfaces that had not been mechanically abraded to make the glue stick. It is the author's belief that this condition, in contrast to that shown in Fig. 4, can occur only in conjunction with small amounts of moisture trapped in the adhesive as it cures. Given that the interfacial bond is uniformly poor, it seems inconceivable that it could have been strong enough to tear a properly cured adhesive film from side to side. However, it is well known that a weak powdery bond results if the adhesive is cured in the presence of moisture. This moisture can either be absorbed by the adhesive film, through improper storage and handling, or by the laminate during service (with even more absorbed moisture, some adhesives will not stick at all). Actually, even the time involved between detail manufacturing and assembly can be sufficient to permit the absorption of sufficient moisture to create a weak powdery adhesive bond, even if the bond surfaces had been properly prepared by thorough abrasion. The laminates need to be stored in sealed containers until bonded or in a dehumidified air-conditioned room.

Inspection Methods. None of the structural deficiencies associated with weak or improperly cured adhesive bonds are detected by conventional ultrasonic nondestructive inspection (NDI), and it is most improbable that they could be detected prior to a gap being opened up by mechanical failure in service. Although the fillets at the ends of the bond overlap will be visibly porous for adhesives cured with trapped prebond moisture, it is usually only the hot-wet lap-shear tests that fail to meet the specified strengths. Consequently, the customary room-temperature tests that follow would not have caught this condition had it been on a real part. Figure 5 shows why visual inspections of adhesive bonds can be more informative and reliable than conventional ultrasonic NDI. More reliable results can be obtained from a visual inspection of the fillet than from either ultrasonic inspections or a defined "adequate" lap-shear test result on a coupon with abnormal fillets. Ironically, the ultrasonic signals are unreliable in the immediate vicinity of the edges of panels--which are the only locations where any significant load is transferred through bonded joints.

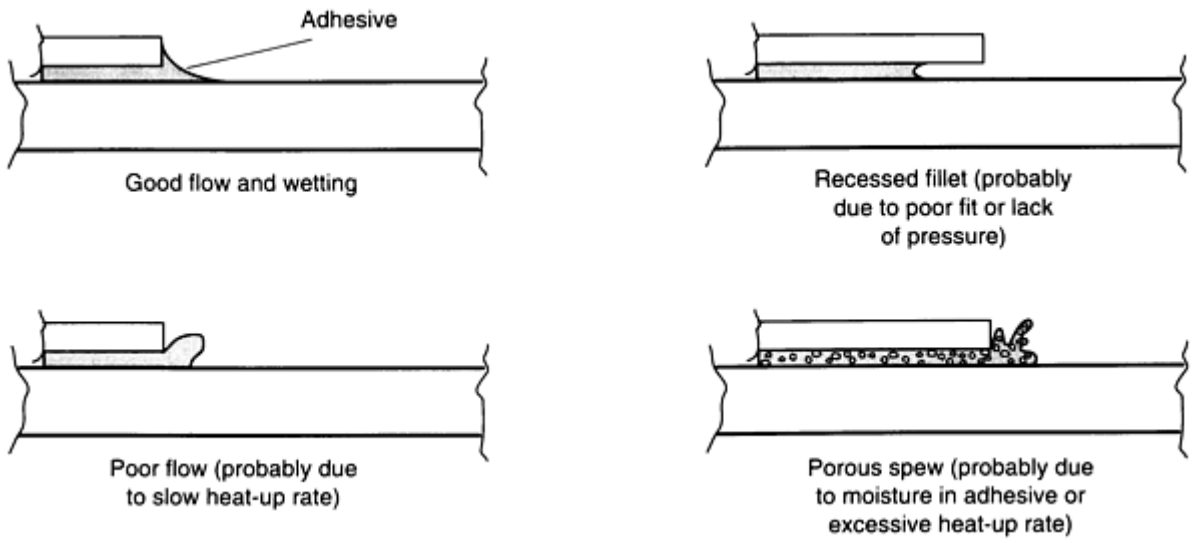

FIG. 5 EXAMPLES OF GOOD AND BAD ADHESIVE FILLETS

Note cited in this section

* *IT IS A COMMON MALPRACTICE TO USE THE WORDS "ADHESIVE FAILURES" EXCLUSIVELY TO DESCRIBE ONLY THOSE SITUATIONS IN WHICH THE ADHESIVE ITSELF HAS *NOT* FAILED, BECAUSE ADHESION IS A NOUN AND NOT AN ADJECTIVE. ACTUAL FRACTURE OF THE ADHESIVE ITSELF IS DESCRIBED AS A COHESIVE FAILURE. THE FORMER FAILURE OCCURS WHEN THE GLUE HAS NOT ADHERED TO ONE OR BOTH ADHERENDS. THE CURRENT MEANING ASCRIBED TO ADHESIVE FAILURES IS THUS VERY MISLEADING, EVEN IF IT IS GRAMMATICALLY CORRECT. IN THIS ARTICLE, THE WORD ADHESION IN PLACE OF ADHESIVE WILL BE USED IN THIS CONTEXT.

Surface Preparation for Thermoset Composite Adherends

While not always used in production, light grit blasting, thorough sanding, or some other form of mechanical abrasion are the best surface preparations for both adhesive bonding and painting of thermoset composites. This is confirmed by the test results shown in Fig. 6. As shown in this figure, the best example of sanding was as good as the grit-blasted coupons, but all other treatments were markedly inferior.

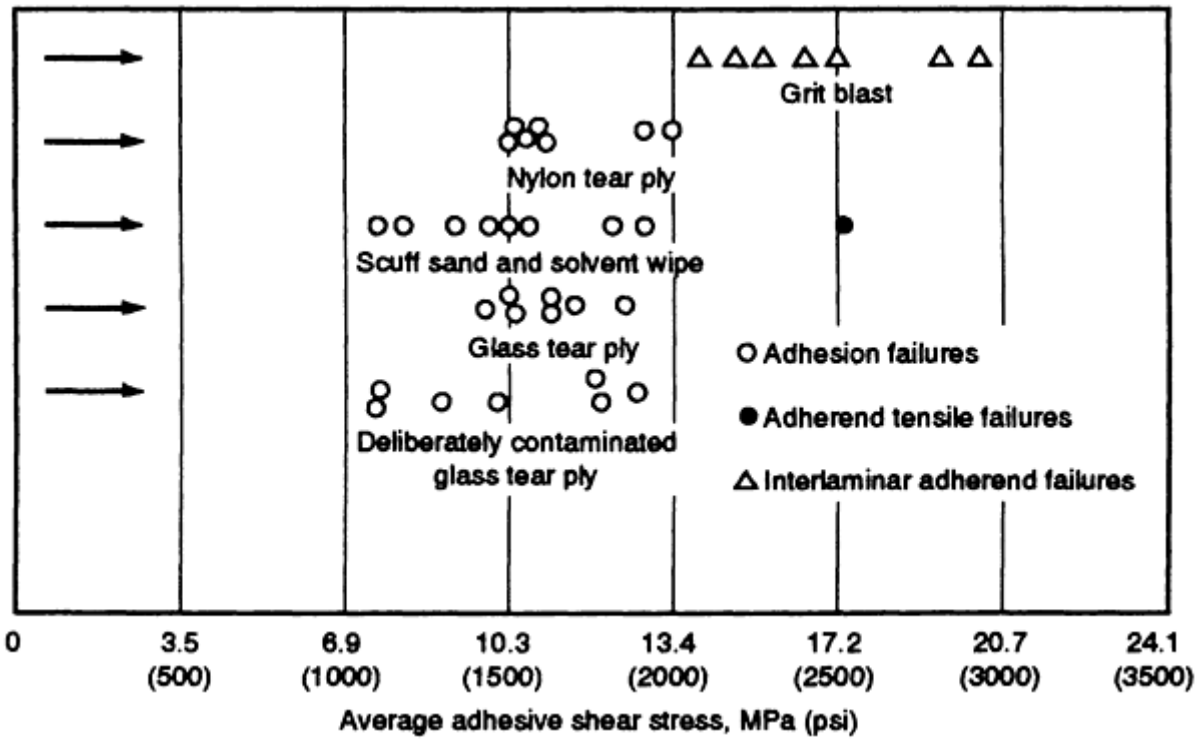

FIG. 6 EFFECT OF SURFACE PREPARATION ON THE STRENGTH OF DOUBLE-LAP GRAPHITE/EPOXY-TO-ALUMINUM ADHESIVE JOINTS (13 MM, OR $\frac{1}{2}$ IN., OVERLAP)

Peel-Ply Surfaces. While it is extremely difficult to ensure that a peel-ply surface will be satisfactory before the peel ply is removed, it is quite easy to evaluate the surface after removal in time to prevent bonding to an unsatisfactory surface. Figure 7 shows a magnification of the imprint of a nylon peel ply that had supposedly been corona treated to enhance its adhesion to the resin matrix to create a fresh fractured surface over the entire bond. Yet it is quite clear that, at the microscopic level, the surface is absolutely slick. The groove left by every fiber in the peel ply is clearly shown. The matrix is fractured over only an extremely small fraction of the surface, as shown in the higher magnification view of the same surface in Fig. 8. The adhesive will stick only to the fractured surface, not the obviously ultraslick surface so clearly evident in most of Fig. 8. The adhesive could bond to barely 10% of this surface and will not stick anywhere else. A reliable peel ply would leave an imprint so rough at the microscopic level that the weave of the peel ply so prominent in Fig. 7 would never be seen.

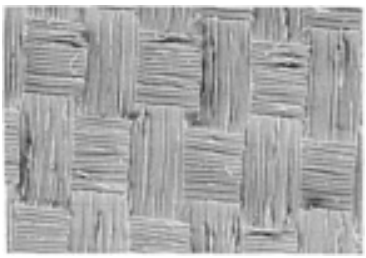

FIG. 7 IMPRINT OF A NYLON PEEL PLY LEFT AFTER REMOVAL FROM COMPOSITE LAMINATE. 58×

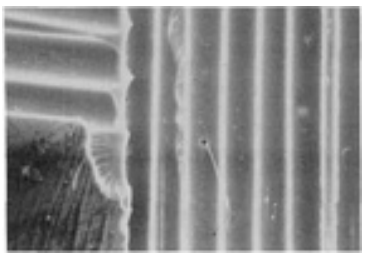

FIG. 8 IMPRINT OF A PEEL PLY SHOWING EXTREMELY SMALL FRACTION OF SURFACE COVERED BY FRACTURED RESIN MATRIX TO WHICH THE ADHESIVE COULD BOND. 580×

Figure 9 shows the imprint left by a different peel ply, that was believed to be producing satisfactory bonds, or at least much stronger bonds than had been achieved using another peel ply that left a surface like that shown in Fig. 7. There is clearly far less imprint visible in Fig. 9 than in Fig. 7, and far more fractured surface resin. Even so, one would be relying on good adhesion to no more than about 30% of the total area. Also, the surface in Fig. 9 is so rough as to be likely to trap pockets of air between the adhesive and the substrate. Fortunately, unless they coalesced, these air pockets would prevent contact only between the glue and those parts of the laminate to which it would not stick anyway.

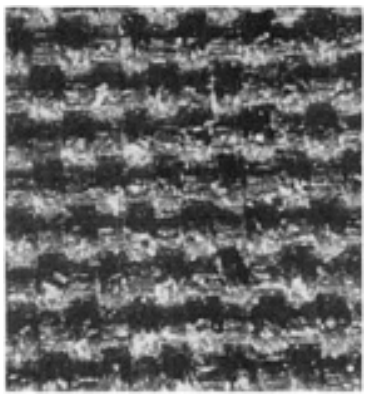

FIG. 9 IMPRINT OF A BETTER PEEL PLY ON A COMPOSITE SURFACE SHOWING A FAR GREATER FRACTION OF FRACTURED RESIN OF THE SURFACE. 34×

The real purpose of peel plies is to protect against gross contamination, which is removed as the peel ply is lifted off. Its removal must be followed by grit blasting or by sanding so thorough that all traces of the imprint from the peel ply have been removed. Figure 10 shows a scanning electron micrograph of a carbon-epoxy composite thoroughly sanded with 120 grit abrasive. There is no similarity with either Fig. 7 or Fig. 9. However, if the abrasion is so severe as to expose bare fibers, from which the surface treatment (coating) has been removed everywhere by sanding, the bond will be even

weaker. The solution to this problem is a resin-rich surface layer, like a conventional gel coat applied to simple fiberglass composite components before they are painted.

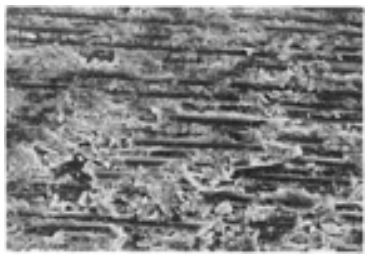

FIG. 10 SURFACE OF A CARBON-EPOXY COMPOSITE AFTER 120 GRIT ABRASIVE SURFACE PREPARATION. NOTE EXPOSED FIBERS AND SMALL AMOUNT OF DAMAGED FIBERS. 415×

Peel plies are either coated with release agents so that they will not delaminate the composite they are meant to protect or are so slick that the surface is like a mirror at the microscopic level. In either case, the glue cannot stick, except at the small nodules of fractured laminating resin in between the bundles of fibers in the weave of the peel ply. This increment of strength is often sufficient to bond successfully honeycomb cores in sandwich construction. Providing that all the remainder of the processing is done properly, even this limited bond strength is often enough to break the core away from the faces. In addition, this bond strength seems always to be enough to pass any ultrasonic NDI tests, even for faying-surface bonds. Another reason for thorough abrasion after removal of a peel ply is that the polymer molecules formed adjacent to the peel ply (or released tool surface) are oriented in such a way as to make them very difficult to be wetted by the adhesive. A stronger bond is possible in the more randomly oriented interior molecules.

Alternatives to Peel-Ply Surfaces. An alternative technique used to some extent in both Europe and North America is to not use a peel ply as such, but to add an extra layer of preimpregnated fine-weave aramid cloth to both surfaces of the composite laminate, using the same resin as for the primary laminate. This achieves two things. First, it avoids the acutely resin-starved surfaces left as the conventional dry peel plies absorb resin from the base laminate; second, it ensures a completely roughened surface to which to bond, without any trace of release agent from the caul plate.

Tests using fiberglass tear plies that were not intended to separate cleanly, but to remove a little resin from the entire surface, failed because the glass fibers were too brittle and broke repeatedly. The surface was contaminated, and possibly damaged as well, whenever razor blades were used to strip off the surface ply. Obviously, if the tear ply sticks too well, it will not come off alone, but will probably take one or two top plies from the laminate as well. This has been known to occur during the removal of metallic fittings from composite structures that had been installed with a layer of rubber-base sealant between the faying surfaces to prevent galvanic corrosion.

Grit Blasting. The objections to grit blasting are easier to recognize, even though they are not all valid. Grit blasting can create dust--black dust from carbon-epoxy laminates is perceived as a greater health hazard than white dust from fiberglass-polyester laminates. Also, it relies to some extent on operator skill, and if the only available grit-blasting machine must be borrowed from a nearby foundry where it is normally used to clean sand castings, it will be so powerful that it is easy to burn right through a laminate in a matter of seconds. Both of these objections can be overcome, as they were on the Lear Fan all-composite aircraft, by buying an inexpensive low-pressure machine in which the nozzle is surrounded by a ring of vacuum ports, which are themselves surrounded by a circular comb of soft bristles like those on domestic vacuum cleaners. It took only two to three days to properly train someone with no prior mechanical skills to operate such a machine. The bristles held the nozzle a fixed distance away from the work. An adequately blasted surface had a dull matt texture, which contrasted strongly against the shiny black unblasted areas nearby. The pressure was only 140 kPa (20 psi) instead of 700 kPa (100 psi), so it would take such a long time of holding the nozzle in one place to damage the composite surface that it would be obvious that something was wrong long before any damage actually occurred. The grit-blast machine was used in a room that was depressurized slightly with respect to the rest of the factory, but there was no need for protective clothing or respiratory masks. A fixed machine with many nozzles under which the parts pass on a roller table has also been developed. The nozzles may someday be computer controlled.

Currently, there are many forms of grit available, some of which are recyclable. Aluminum oxide (Al_2O_3) has been used traditionally, but is sufficiently expensive that recirculation of the used grit must be considered. It would seem that the use

of recirculated abrasives can be permitted on an otherwise uncontaminated peel-ply surface. However, so much release agent is transferred from caul plates to the adherend surface that no recirculation can be permitted on that kind of surface. Examples of inexpensive media are plastic beads, which can be separated from the debris by floatation in a water tank, biodegradable corn husks, and a number of powders, such as sodium bicarbonate, which can be recovered from aqueous solutions. Since chemical paint stripping is being outlawed, there is considerable pressure to come up with safe replacements. Grit blasting is certainly preferable to the use of jets of hot air, which have been observed to burn as many as two surface plies to the bare fibers in several places on thin-skinned fibrous composite parts.

Perhaps the most compelling argument in favor of using grit blasting is that none of the more widely used techniques for initial production can ever be used for repairs, whether by an airline during service or by the original manufacturer because of damage during manufacture. For example, a peel-ply surface cannot be recreated on a previously cured laminate--one is forced to abrade it.

Joining of Organic-Matrix Composites

L.J. Hart-Smith, McDonnell Douglas Aerospace

The Water-Break Test

The water-break test has long been a standard technique for verifying the adequacy of surface preparation for metal bonding. It can also be used for composite surfaces, as described in Ref 4. This is clear from Fig. 11, which compares the even wetting of a properly grit-blasted surface with the repelling of water on an untreated surface contaminated by the release agent on the lay-up tool. Although the water is on the surface for only a small time, and very little is absorbed into the laminate, some adhesives are so moisture-sensitive that it is necessary to dry even that moisture out before bonding. It would seem to make more sense to prime the composite surface after grit blasting so that it could be recleaned using solvents, than to use the water-break test on a surface known to have been prepared properly immediately beforehand. The benefit from the water-break test comes from confirming that a previously prepared panel has not been contaminated during storage.

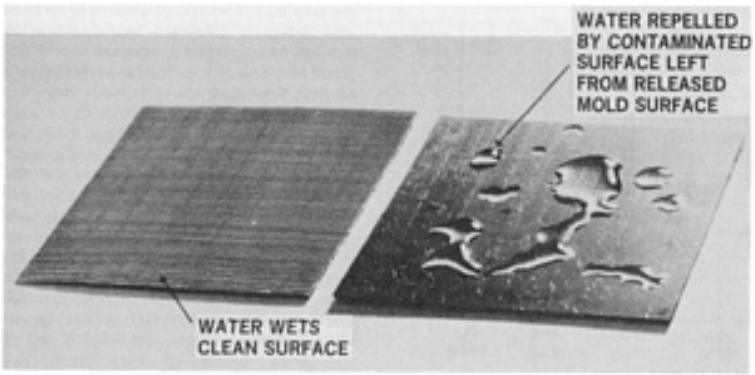

FIG. 11 COMPARATIVE WATER-BREAK TEST RESULTS. LEFT: PROPER PREPARATION. RIGHT: IMPROPER PREPARATION. COURTESY OF CANADAIR

Experience gained since the preparation of Ref 4 indicates that water-break tests are inappropriate for surfaces that have not been abraded. If water is applied to the surface left by removing a peel ply, the water will bridge between the small areas of fractured resin matrix and totally mask the unwettability of the majority of the surface. The test is ineffective in this case. Worse, it falsely creates the illusion that the surface has been prepared adequately for bonding, as well as the opportunity for someone to shift the blame for a poor bond from failure to dry out water absorbed from other sources to the microscopic traces of water left by the water-break test. Such traces are easily removed by a moderately hot air gun because the water is not on the surface long enough to permit significant absorption.

Matienzo *et al.* (Ref 13) indicate that lightly sanding the surface created by curing a laminate directly against a tool surface coated with mold release can be good enough to pass the water-break test, yet such surfaces cause bonds weaker than those achieved by untreated peel-ply surfaces. This indicates that even more emphasis must be placed on the thorough sanding or abrasion of the surface to be bonded and less on any subsequent verification. Unfortunately, their test data do not include baseline tests on anodized aluminum adherends against which the composite bonds could be assessed. One of their prime conclusions was that the simple removal of peel plies gave stronger bonds than were achieved with light sanding. However, it is significant that according to their test data, even higher average strengths were attained by deliberately contaminating one of the two peel plies by spraying it with mold release before the panel was cured. It should be pointed out that mold-release agents will stick like glue if they are not baked before a part is cured on the surface. This "contaminated" peel ply gave such better results than the uncontaminated peel ply that it is clear that the untreated peel-ply surfaces were capable of considerable improvement. Even a peel ply that showed no sign of silicon transfer gave slightly weaker average results than the spray-contaminated peel ply, although the highest individual strength was attained with the silicon-free peel ply. This peel ply was also effective in isolating the laminate from the silicon introduced from the mold release. However, as noted in their work, the use of peel plies on both sides of the part would not be applicable to compound-curved panels or to tool surfaces very much larger than available pieces of peel ply, which could not be lapped without unacceptable mark-off on the outside of the finished part. While even the highest strengths reported in Ref 13 are only about half what one might expect from a grit-blasted surface, the very low strengths they show from either gross contamination or from failure to make any attempt to remove the mold release indicate an irrefutable need for proper surface preparation for bonding polymer composites.

The change of surface texture between thoroughly abraded and bare surfaces is so great that, even though the water-break test works reliably, it is not always necessary. A visual inspection, which is capable of distinguishing between thorough and light sanding with the use of a magnifying glass, should suffice. This justification for omitting the water-break test is particularly relevant whenever the adhesive bonding follows immediately after the surface preparation and there is no opportunity for contamination. On the other hand, a drying cycle to remove water applied during the water-break test would also remove absorbed water from near the surface of the part. The omission of a compulsory drying cycle would demand great care in ensuring that the parts to be bonded had not absorbed water since their manufacture, even if they had been protected against the more widely recognized contaminants.

The water-break test would still seem to be very valuable for repairs to structures contaminated by chemicals absorbed during service or by coupling fluid for ultrasonic NDI of a porous or delaminated panel. It has already been shown to be effective in proving that most cleaning solvents applied to an unprimed surface actually contaminate the surface and need to be removed by water-soluble solvents such as alcohol. This issue is discussed in Ref 4, which includes photographs of the beach marks left as the solvent evaporates.

Experience with using the water-break test has revealed that the application of the least amount of water possible is preferable because a thick film of water can bridge a small local area of contamination and conceal a defect such as a thumb print. One needs to watch the film as it evaporates. A slow uniform drying out simultaneously over the entire surface is an indication of satisfactory surface preparation. If, on the other hand, a discrete dry area suddenly appears at some point during the evaporation, that is an indication of contamination.

References cited in this section

4. L.J. HART-SMITH, R.W. OCHSNER, AND R.L. RADECKY, SURFACE PREPARATION OF FIBROUS COMPOSITES FOR ADHESIVE BONDING OR PAINTING, *DOUGLAS SERVICE MAGAZINE,* FIRST QUARTER 1984, P 12-22
13. L.J. MATIENZO, J.D. VENABLES, J.D. FUDGE, AND J.J. VELTEN, SURFACE PREPARATION OF BONDING ADVANCED COMPOSITES, PART 1; EFFECT OF PEEL PLY MATERIALS AND MOLD RELEASE AGENTS ON BOND STRENGTH, *30TH NATIONAL SAMPE SYMPOSIUM,* SOCIETY FOR THE ADVANCEMENT OF MATERIAL AND PROCESS ENGINEERING, 19-21 MARCH 1985, P 302-314

L.J. Hart-Smith, McDonnell Douglas Aerospace

Control of the Bonding Process for Thermoset Adhesives

The chemistry of creating a properly cross-linked adhesive bond is well understood by a large number of materials and process engineers. However, far fewer people who actually control autoclaves are knowledgeable of adhesive chemistry or have real-time access to such information. With the help of a polymer chemistry expert, an experienced process engineer can identify the cause of a problem and modify a cure cycle in progress to save a part that would otherwise need to be scrapped. Some of the more important process variables that need to be understood and controlled are outlined below.

Effects of Temperature Variations on Bond Strength. Some aspects of the process specification are almost so self-evident that their significance is underestimated. It is obvious that if an adhesive is heated up too slowly, it will not wet the surface to be bonded. The adhesive may eventually cure, but there will be a dry bond. Therefore, the process specifications include minimum heat-up rates. These vary with the adhesive, but are on the order of 3 °C (5 °F) per minute. Likewise, an adhesive can be made to boil if heated up very much faster, so there must be maximum heat-up rates and maximum temperatures as well. These limits present no problem when making a small, uniformly thick test panel. The problems arise when a large, complex assembly of variable thickness is either cured or bonded on a large tool having a variable heat sink. It then becomes very easy for some parts of the structure to be heated up too slowly while other parts are on the verge of being burned. For all but the simplest of parts, a proof-of-tool demonstrator should be carried out to ensure that the assembly can be properly cured the first time. It makes sense to save on the cost of this operation by using cheaper fibers with the same resin.

One solution for the problem of a large range in temperature within the composite part or assembly, once a cure is already in progress, is to put constant-temperature dwells in the cure cycle to give the various segments of the part time to equilibrate. This is best done early in the cure cycle, before any of the adhesive (or resin matrix) has gelled. Thus, in addition to maximum and minimum heat-up rates, there is a need for a maximum variation between high and low temperatures--measured on the part, not on the tool, even if that takes more time than it does to hook up a permanently wired thermocouple. In some cases, multiple dwells may be needed. There is a limit, however, since an excessive number of dwells will cause the adhesive to gel before it has a chance to wet the surface needing to be bonded.

Once such a problem is detected, blankets can be added for subsequently made parts to shield the hot spots and local heaters added to overcome the colder areas. It is not acceptable to simply disconnect the thermocouples giving the highest and lowest readings in subsequent cure cycles. It is better still to thermally isolate large heat sinks from the rest of the tool if this can be done without causing distortion of the part. A simple but effective solution to some such problems is to thermally isolate the tool from the bed of the autoclave and, wherever possible, to thermally isolate the tool surface contacting the part or assembly from the supporting structure. Other than the possibility of tool distortion, which may or may not adversely affect the product, no harm will come to the composite part or bonded assembly if it is heated correctly and only the tool support structure lags behind.

Most tools are made from metal because hand layed-up plastic tools tend to have internal voids that collapse and need patching. However, the metal tools expand and contract more than composite parts. A solution to this problem is to use autoclave-cured composite members to hold composite parts in the work station during a bond cycle. The composite holding frame is supported by the basic metal tool, but it is held at only one point and permitted to slide freely as the size of the metal tool changes. This enables linear dimensions to be held and avoids the problem of crushing the composite parts as the tool contracts during cool down. It also thermally isolates composite parts from the metal tools.

The problem of tools having excessive heat sinks arises because tool designers are used to extremely rigid tools rather than tools that are barely able to maintain their shape, but so simple and compact as to permit many of them to be loaded into a single autoclave cycle. For thin, flexible skins, it makes more sense to rack several caul plates in a single holding fixture than to make one massive lay-up and cure tool per part. The productivity of the autoclave is enhanced this way as well. While the caul plates may distort out-of-plane, they will retain their in-plane dimensions, and only light pressure will be needed to restore the profile of the parts as they are bonded into assemblies. For example, 9 m (30 ft) long Lear Fan unstiffened fuselage skin panels, which were mildly compound curved, were rolled up like giant cigars to stiffen

them for safer as well as easier handling as they were transported from the autoclave to the assembly room. The more common flat panels flex even more easily. Obviously, the entire shape must be well defined for the final bonding operation since the assembly will be too rigid to match the surrounding structure if it is made to the wrong shape. However, the bond cure cycle is typically 25 to 40 °C (50 to 100 °F) lower in peak temperature than the cure cycle for detail composite parts, so the problems of variable temperatures are diminished.

Effects of Prebond Moisture on the Strength of Bonded Joints. Another widespread problem is the need for the removal of volatiles before the start of cure and throughout its duration. Some manufacturers of composite and bonded structures want materials that are so tolerant of abusive cure cycles that it is permissible to: (1) apply full pressure from the start of the cure, flipping one switch for the heaters (with no automatic control system); and (2) to come back once during the cure at a preestablished time to cut back on the heat when the peak temperature has been attained and once more to switch the heat off when the cure is complete, preferably quickly enough not to need the services of a second shift of workers. Material development engineers have failed to create such forgiving materials, even though some process specifications permit parts to be made this way, so there are opportunities for using closed-loop control systems. Such systems, however, require experts to anticipate what should happen, what might happen, and what must not be permitted to happen--along with corrective responses.

The reliability of manufacture will be increased by demanding that all materials and parts be dried thoroughly immediately before each cure cycle. This refers also to Nomex honeycomb cores, which are known to have a great affinity for water and to absorb it rapidly if left in a humid environment. Wet cores result in weak glue fillets at honeycomb cell walls (Fig. 12). Such a goal of thorough drying exceeds the current practice at many composite manufacturing facilities today, whether or not the up-front savings exceed the consequently higher down-stream costs. But even if thorough drying were the norm, bagging procedures that permitted small amounts of moisture to be removed harmlessly during cure would also be desirable. The initial manufacturer also needs to be aware of the very high costs (to the consumer and/or the manufacturer) whenever a composite part or assembly is manufactured with sufficient trapped moisture to create an inferior part of unreliable service strength, but sufficient initial strength to be accepted after normal ultrasonic inspection. Under the prevailing circumstances, the original manufacturer is exposed to the consequences of improper processing only when there is sufficient residual strength in a rejected bonded panel to make it virtually impossible to disassemble the pieces for rebonding without destroying them by delaminations in the process.

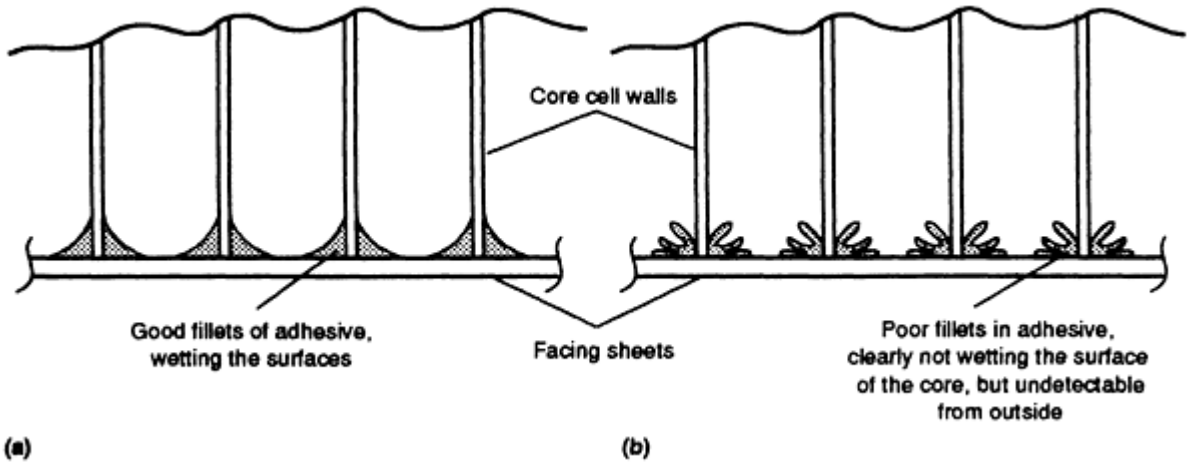

FIG. 12 EFFECT OF NOT PREDRYING ORGANIC HONEYCOMB CORES. (A) DRIED CORE. (B) UNDRIED CORE

Adhesives vary in their susceptibility to problems caused by moisture absorption. The first generation of modified epoxy adhesives introduced in the 1960s were discredited because of corrosion problems with bonded metal structures. These adhesives had a high permeability for moisture absorption after cure. This led to corrosion of the metal surfaces, which were usually only etched, not anodized, and were not protected by a corrosion-inhibiting primer. Ironically, these same adhesives have been used successfully with composite adherends that cannot corrode, but they have suffered limited application because of their bad reputation earned in a totally unrelated context. Actually, it was proved more than 20 years ago that the primary cause of such problems was inadequate surface preparation. However, other contemporary adhesives, cured at higher temperatures, lasted longer on the same poor surfaces and were then used in their place.

The second generation of modified epoxy adhesives, introduced in the late 1970s, were specially formulated to impede moisture migration and were used in combination with a phenolic-based primer baked on an aluminum alloy surface anodized with phosphoric acid. Their durability was established during the PABST program, and they have performed well in metal bonded structures. However, this class of adhesives has a great affinity for moisture in the uncured state. One of the first developed was so sensitive that it was withdrawn from sale. Other adhesives in this class are now associated with numerous problems with bonding composite laminates together and with the co-cure and bonding of composite patches. The problem, which was exposed and evaluated during the PABST program, occurs only when the adhesive is allowed to absorb moisture before bonding or when making sandwich panels with wet foam or Nomex honeycomb cores. The adhesive film can be restored by drying before use, but the best solution is to avoid the problem by limiting the exposure to humid environments or by regulating the atmosphere in the lay-up room.

It is vital that adhesives be stored in relatively small rolls so that the supply of material for an excessive lay-up period is not exposed to the atmosphere. They should be removed from frozen storage the day before they are to be used and allowed to thaw out overnight while still sealed, to prevent condensate from forming on the adhesive. If they do absorb moisture, they should be dried before further use. It is better to close down production for a day than to take a roll of adhesive straight out of the freezer, unwrap it, and start using it immediately while it is covered with condensate.

Laboratory experiments performed to prove that trapped moisture could actually prevent the adhesive from sticking, not merely degrade its properties, required fairly large blister panels to replicate the effect. It was shown that 150 mm (6 in.) square panels that were sealed around the edges would show the effect, but that smaller ones would not. It follows, therefore, that the conventional half-square-inch lap-shear test coupons used as travellers while parts are made cannot possibly expose this condition. If the adhesive has been exposed to high humidity and temperature for even the normal duration of a lay-up operation, or covered with condensate because it was unsealed before it had thawed out, the weak bonds will almost certainly be in the structure. If left out for an entire week, them is a good chance that the pieces will fall apart as they are removed from the bonding tool.

What is far worse than the above scenario is a degraded adhesive bond with sufficient residual strength that it does fall apart. There is then no way of characterizing the strength or the time taken for the bonds to fail in service. They will pass all ultrasonic inspections, unless there was so much trapped water that large blisters occurred during cure.

Better composite parts can be made more cheaply if the manufacturer starts with a slow vacuum-consolidation cycle, usually overnight, not in an autoclave, but possibly in a low-temperature oven or under an insulating styrofoam shelter. This enables trapped air bubbles to escape, solvents to be driven off, and some moisture to be expelled. Failure to do this, or the equivalent step of thoroughly drying detail parts to be bonded, as well as the adhesive itself if it is suspected of absorbing moisture, guarantees that all of these ingredients will be trapped inside the part once the autoclave pressure is applied. Full vacuum would be applied inside the bag until slightly short of the minimum viscosity point for the resin matrix, or until no further volatiles could be detected in the vent, if that occurred sooner. Most resins will boil if cured under high vacuum, so the bag needs to be vented to the atmosphere once the vent is no longer useful. The cure can then proceed, with the autoclave gage pressure holding the laminate down and the resin in the bag being subjected to the atmospheric pressure. After gelation, the pressure felt by the rosin will increase progressively toward that experienced inside the autoclave.

Partial-Vacuum Cures. A minor variation of the scheme above can eliminate the need for autoclaves, when curing simple parts that need little pressure to hold the laminates against the tool surface. After an unusually thorough consolidation cycle, the cure would start with a full vacuum inside the bag, using only an oven as a heat source. Once the point of minimum viscosity was reached, a regulated pressure of between one-third and two-thirds of an atmosphere would be maintained inside the bag, with the remaining differential pressure holding the laminate onto the tool. Many, but not all, resins should be capable of being cured this way. Phenolics, which generate steam during cure, are the most obvious exception.

There are new adhesives and resins being developed that will tolerate curing under full vacuum throughout the entire cycle, but the approach outlined above would produce better laminates and bonds even with such materials. It would also eliminate the need for an autoclave for many more resins and adhesives than a requirement for full vacuum would permit. It is a technique worthy of further study, particularly for repairs to thin composite sections. In-house assessments of both new and old adhesives at Douglas Aircraft have shown that the partial-vacuum cure achieves bond strengths almost as great as those produced by full autoclave pressure, and far better than those achieved under a full-vacuum cure of the same adhesive. This is true of adhesives specially developed for vacuum-bag curing as well as those formulated for autoclave cures and known to be totally unsatisfactory if cured under full vacuum. It is likely that the need for more heat

to maintain the heat-up rate on thicker panels, or with large tools that have not been thermally isolated from the work, would favor the use of an autoclave because the thermal conductivity of air increases as it is compressed.

Susman (Ref 14) has described the benefits of the dwell cycle for autoclave cures. Maintaining full vacuum while holding the temperature for about an hour at some 55 °C (100 °F) below the cure temperature permitted such a thorough removal of volatiles that the interlaminar shear strengths were doubled with respect to traditional cures. The worst laminates were made by the so-called straight-up cure, in which both full heat and full autoclave pressure were applied at the start of cure to minimize the cycle time.

Reference cited in this section

14. S.E. SUSMAN, THE DWELL CYCLE: A COST SAVINGS ROUTE TO QUALITY COMPOSITES, *25TH NATIONAL SAMPE SYMPOSIUM*, SOCIETY FOR THE ADVANCEMENT OF MATERIAL AND PROCESS ENGINEERING, 6-8 MAY 1980, P 251-258

Joining of Organic-Matrix Composites

L.J. Hart-Smith, McDonnell Douglas Aerospace

Bonding of Thermoplastic Composite Panels

Three different approaches have been evaluated for bonding thermoplastic composite components together. Adhesive bonding has been used, much as for thermoset composites, but needing different surface preparations. Fusing the panels together with or without an interlayer has also been used. This technique is of interest to engineers because it suggests that repairs could be performed far more easily than is possible with thermoset composites. However, there is the obvious disadvantage that it is difficult to melt such a localized area of resin without distorting the rest of the structure. Perhaps the most promising approach is that of coating the surfaces to be bonded with a different thermoplastic, which melts at a lower temperature than that in the basic laminate. Fusion bonding is then possible at a temperature low enough not to distort the part itself.

Bonding with Thermoset Adhesives. The reluctance of liquid polymers to wet solid thermoplastics is even greater than for thermosets. Having the surfaces free from contamination is but one of many criteria that must be met for one material to stick to another. Having the right surface energies is equally critical. An uncured resin or adhesive will typically not wet a cured surface having a far lower surface tension, as is achieved with release coatings. It is much more likely to adhere to a surface of far higher surface energy, as can be created by oxidation via corona treatment. Figure 13 shows how little corona energy is needed to almost double the surface energy of polyether ether ketone (PEEK). However, testing also showed that far more corona energy was needed to ensure a cohesive rather than interfacial failure (Ref 8). This supports the assessment that even after surface contaminants have been removed, there are still polymer layers of low surface energy between the bulk matrix and the surface created by curing against an inert tool surface. Much the same problem exists when trying to epoxy bond injection-molded thermoplastic inserts into honey-comb sandwich panels. The glue will not stick unless the initially inert plastic surface has been activated to form a chemical bond or etched to permit a mechanical bond.

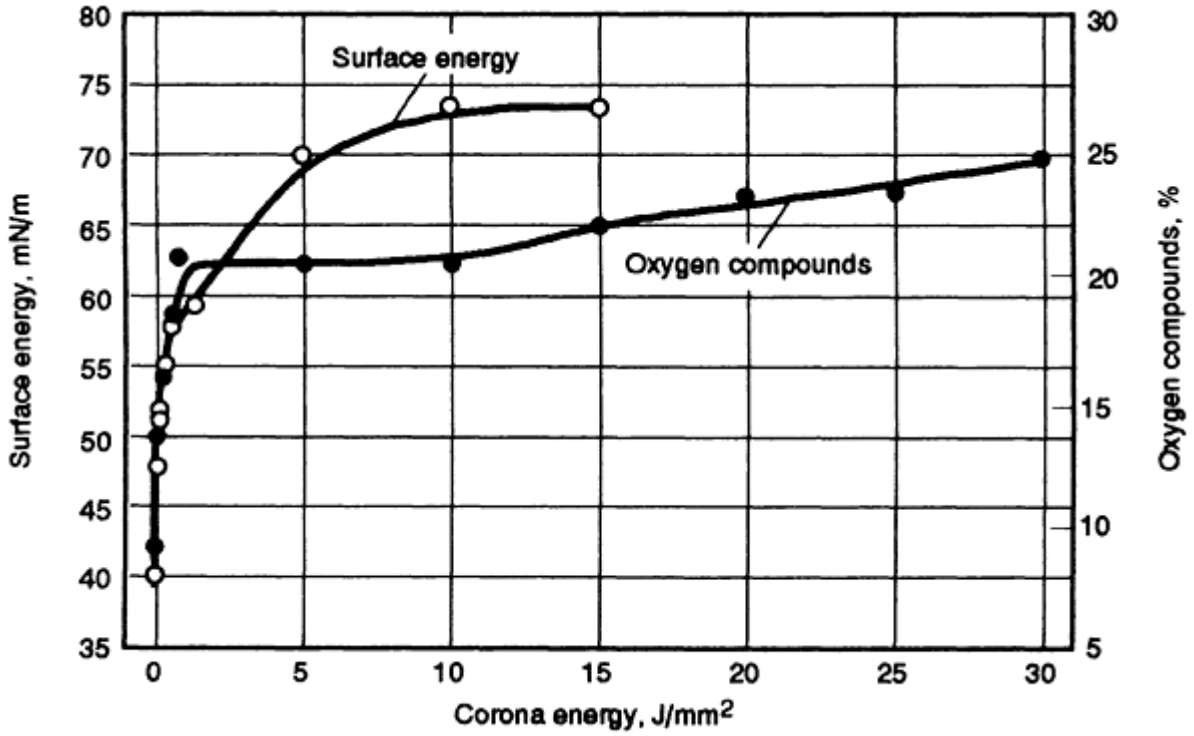

FIG. 13 EFFECT OF CORONA TREATMENT ON THE SURFACE ENERGY OF PEEK. SOURCE: REF 8

Wu *et al.* (Ref 15) describe the adhesive bonding of thermoplastic composites using several adhesives and a variety of surface treatments. Figure 14 shows results from their study. It is clear from Fig. 14 that weak interfacial failures are the inevitable result of failure to appreciate the need for proper surface treatment, for both the hot-bond epoxy FM-300 film adhesive and the BMI film adhesive EA-9673. Cohesive failures within the bond layer were achieved only for the chromic-sulfuric acid etch and plasma treatments. Significantly, these are the highest strengths obtained. While the highest average shear strengths are slightly less than one would expect on anodized aluminum coupons, they are credible for fibrous composite adherends having a quasi-isotropic fiber pattern and a slightly lower modulus. Higher strengths should have been obtained on unidirectional test coupons.

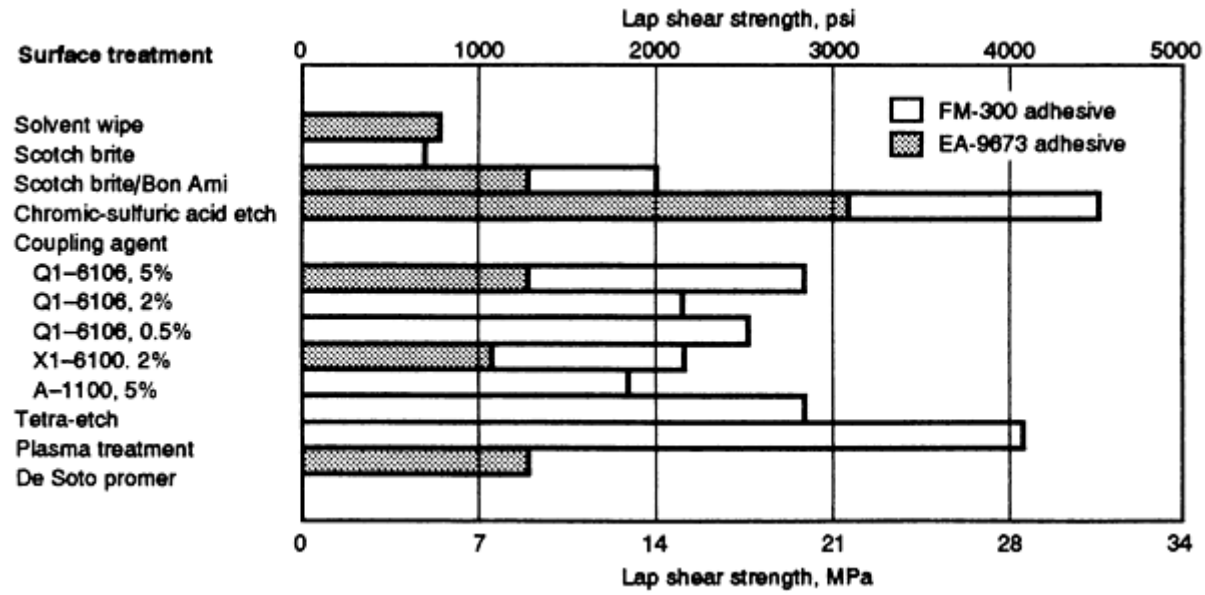

FIG. 14 EFFECT OF SURFACE TREATMENT ON THE LAP SHEAR STRENGTH OF AS4-APC-2 LAMINATE. SOURCE:

Other researchers have also reported success with plasma treatment, with various gaseous environments. While the technique is effective, and probably quite practical for small parts, the need to enclose the composite part in an evacuated chamber during the surface preparation would seem to render it impractical for very large components. On the other hand, the reliability of this process in comparison with others is of paramount concern. The acid etching would require a large tank, in any event, and the corona-discharge technique would require electrodes tailored for each part to achieve uniform treatment over the area if the thickness varied or if the part were contoured. The capital cost of the equipment for carrying out the process correctly is a small fraction of the cost of scrapping one or two large composite assemblies because the surfaces had not been prepared properly while there was access to the individual panels.

Figure 15 makes it clear that mere abrasive cleaning of thermoplastic adherends is unsatisfactory, no matter what thermoset adhesive is used, while the chromic-sulfuric acid etch is effective with all the adhesives tested. In other tests, Wu and co-workers found that extended etching did not increase the joint strength; worse, it pitted and degraded the surface. They also established by preliminary testing that them is a need to consider the environmental durability of bonds to thermoplastic adherends, just as them is with thermoset adherends.

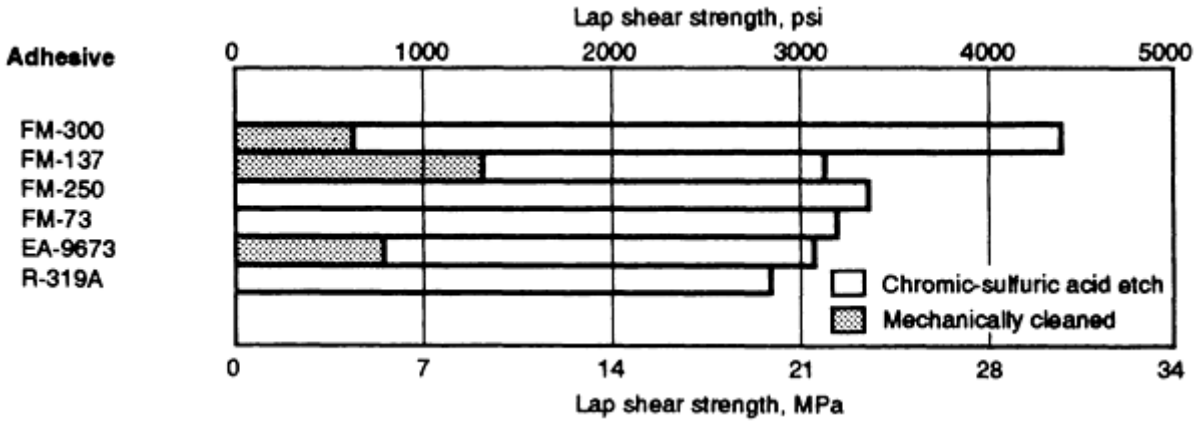

FIG. 15 EFFECT OF ABRASIVE CLEANING AND ACID ETCHING ON THE LAP SHEAR STRENGTH OF AS4/APC-2 LAMINATES. SOURCE: REF 15

Fusion Bonding of Thermoplastic Composites. Wu and co-workers also included some welded thermoplastic joints in their study (Ref 15). Lap-shear coupons that were bonded by ultrasonic welding exhibited good strengths for this process, whether the surface had been acid etched or merely abraded (Fig. 16). However, the procedure was not considered practical for large structures. Wu and co-workers examined such techniques as resistance welding, induction welding, laser welding, hot plate welding, and ultrasonic welding. It was determined that the high carbon-fiber content in the thermoplastic matrix and the high thermal and electrical conductivities of the fibers impose a tremendous amount of difficulty on fusion bonding processing. Uneven heating throughout the bonded area and delamination and distortion of the composite materials must be overcome with fusion bonding methods. In addition, such welding methods will change the crystalline structure of the resin because the remelting would be followed by cooling at a different rate from that experienced when the laminate was originally made.

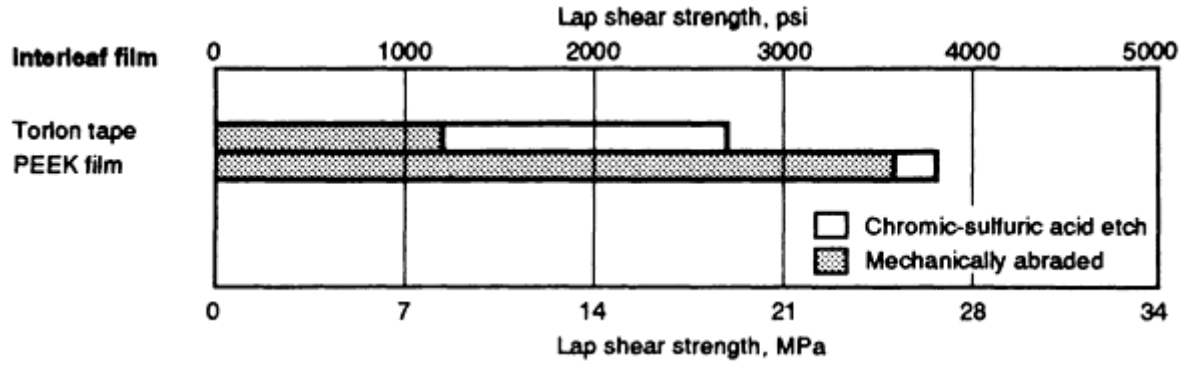

FIG. 16 EFFECT OF ABRASIVE CLEANING AND ACID ETCHING ON FUSION-BONDED AS4-APC-2 LAMINATES. TEST COUPONS WERE JOINED BY ULTRASONIC WELDING. SOURCE: REF 15

Fusion Bonding Using the Dual Resin Approach. The problems cited above can be avoided by using an interlayer that melts at a lower temperature than the parent thermoplastic matrix, but which is miscible with it. Several studies have been made using polyetherimide (PEI) to join PEEK laminates. Zelenak and Radford (Ref 16) cite success with a process in which a PEI film was melted onto the surface of APC2/PEEK tubes prior to joining. The PEI flowed into the PEEK parent, becoming a part of the parent material. This process occurred at the 320 °C (610 °F) processing temperature for the PEEK. To form the actual joint, another film of PEI was placed between the pieces to be joined as a filler. The joint was made under light pressure at a temperature of 300 °C (570 °F). This temperature is substantially above the glass transition temperature of PEI, which is 210 °C (410 °F), but below the melting temperature of PEEK (334 °C, or 633 °F). At this temperature the joint was formed by the PEI film bonding with the PEI in the parent material, which was intimately mixed with the PEEK material.

Unfortunately, the testing was marred by the limited strength of the structure outside the joint which, while it may have been able to carry the design loads, was not strong enough to fail either the laminate adjacent to the joint or the bond itself, except for two premature failures. Consequently, the absolute strengths of the joints were not established. However, in other regards, the use of PEI/PEEK as a miscible combination for bonding of structural PEEK matrix composites gives excellent joint performance with minimal susceptibility to surface contamination during bonding. While there remains the question of resistance to the environment, various chemicals, and age, this method is most promising. It would obviously be feasible to use the same technique to either repair damage in service or to add additional bonds as requirements changed, provided that the entire surface of the parts had been coated with PEI when the details were initially made.

Yoon and McGrath (Ref 17) have reported on bonding PEEK laminates with polyimide thermoplastic adhesive films. Their work is similar to that above in terms of processing at temperatures insufficient to melt the PEEK, but it differed significantly in that they bonded directly to the PEEK laminate. The absence of a compatible surface layer caused them to investigate the effectiveness of different surface treatments. They were able to make very good bonds without adhesive at 360 °C (680 °F), developing shear strengths of 47 MPa (6800 psi), which are not surprising given that their adherends were 24-ply thick unidirectional carbon-fiber reinforced laminates. However, they concluded that this temperature could not be used due to severe deformation. Their joints that fused together at 340 and 350 °C (645 and 660 °F) attained less than 20% of the highest strengths reached with adhesive films fused to treated surfaces that had been promptly primed with a solution of the adhesive to protect the surface. It was concluded that the highest practical temperature for the PEEK-graphite composite adhesion was around 340 °C (645 °F); however, high pressure was also required. Simple fusion of thermoplastic laminates does not seem to be a productive avenue at the present time.

It should be pointed out, however, that the work of Yoon and McGrath in activating the surface prior to bonding with thermoplastic adhesive closely parallels what was reported earlier for bonding with thermoset adhesives. Grit blasting showed a distinct improvement but clearly failed to enable the true material strengths to be exploited. The various gas plasma treatments were effective in producing cohesive failures, and the combinations of grit blasting and gas plasma treatments were better still, reaching nearly 41 MPa (6000 psi) and coming close to the strengths attained by fusion at 360 °C (680 °F).

Of the successful techniques described above, only one is applicable for joining large components. Fusion welding at a reduced temperature, made possible because the thermoplastic parts have been coated during fabrication with a miscible

plastic that melts at a lower temperature than does the base matrix, should enable full use to be made of the strength of the parent laminates. The plasma treatment and corona-discharge techniques are reliable for small parts. The other techniques for developing high strengths are nevertheless invaluable as a warning of how weak the structures will be if no attention is paid to the need for proper surface preparation. They establish the target that should be obtained by any method used in practice.

Solvent Bonding of Amorphous Thermoplastics. The difficulties cited above, when bonding aircraft-grade fiber-reinforced thermoplastic composites, apply specifically to crystalline thermoplastics. Amorphous thermoplastics have not been used widely for such structures because of their lower resistance to common solvents. However, this greater susceptibility to solvents can become an advantage for adhesive bonding. The extreme case of assembling polystyrene plastic model aircraft kits by local application of styrene monomer cement or methyl ethyl ketone solvent is well known. Solvent bonding of nonstructural thermoplastics is quite common in other industries. The same effect can also be used to enhance the bonding of amorphous thermoplastics by epoxy-type adhesives. Such adhesives do not normally bond well to these plastics. However, wiping the surfaces with a suitable solvent and bonding the parts together before the thermoplastic has time to revert to an inert state can produce adhesive bonds strong enough to tear honeycomb cores apart; that is, strength similar to good metal-bond structures. This has been demonstrated by the Ten Cate organization for their continuous-fiber-reinforced PEI thermoplastic bonded with 120 °C (250 °F) cured modified epoxy adhesives. They even advocate the direct use of solvent bonding for cosmetic repairs of local damage to such structures. This technique is no panacea, however, because some thermoplastics will craze after being subjected to the wrong solvent. Nevertheless, under suitable circumstances, solvent bonding or solvent-enhanced bonding can be a very useful technique.

References cited in this section

8. A.J. KINLOCH AND G.K.A. KODOKIAN, "THE ADHESIVE BONDING OF THERMOPLASTIC COMPOSITES," EUROPEAN RESEARCH OFFICE OF THE U.S. ARMY, CONTRACT DAJA 45-86-C-0037, FOURTH PERIODIC REPORT, IMPERIAL COLLEGE, LONDON, AUG-DEC, 1987
15. S-I.Y. WU, A.M. SCHULER, AND D.V. KEANE, ADHESIVE BONDING OF THERMOPLASTIC COMPOSITES, 1. THE EFFECT OF SURFACE TREATMENT ON ADHESIVE BONDING, *19TH INT. SAMPE TECH. CONF.*, SOCIETY FOR THE ADVANCEMENT OF MATERIAL AND PROCESS ENGINEERING, 13-15 OCT 1987, P 277-290
16. S. ZELENAK, D.W. RADFORD AND M.W. DEAN, THE PERFORMANCE OF CARBON FIBER REINFORCED PEEK SUBASSEMBLIES JOINED USING A DUAL RESIN BONDING APPROACH, *37TH INTERNATIONAL SAMPE SYMPOSIUM,* SOCIETY FOR THE ADVANCEMENT OF MATERIAL AND PROCESS ENGINEERING, 9-12 MARCH 1992, P 1346-1356
17. T-H. YOON AND J.E. MCGRATH, ADHESION STUDY OF PEEK/GRAPHITE COMPOSITES, *36TH INTERNATIONAL SAMPE SYMPOSIUM,* SOCIETY FOR THE ADVANCEMENT OF MATERIAL AND PROCESS ENGINEERING, 15-18 APRIL 1991, P 428-436

Joining of Organic-Matrix Composites

L.J. Hart-Smith, McDonnell Douglas Aerospace

References

1. L.J. HART-SMITH, JOINTS, *COMPOSITES,* VOL 1, *ENGINEERED MATERIALS HANDBOOK,* T.J. REINHART, ED., ASM INTERNATIONAL, 1987, P 479-495
2. E.W. THRALL, JR. AND R.W. SHANNON, ED., *ADHESIVE BONDING OF ALUMINUM ALLOYS,* MARCEL DEKKER, 1985
3. R.J. SCHLIEKELMANN, ADHESIVE BONDING AND COMPOSITES, *PROGRESS IN SCIENCE AND ENGINEERING OF COMPOSITES,* VOL 1, PROC. 4TH INT. CONF. COMPOSITE MATERIALS (TOKYO), 22-28 OCT 1982, JAPAN SOCIETY FOR COMPOSITE MATERIALS AND THE

METALLURGICAL SOCIETY (TMS) OF AIME, T. HAYASHI, K. KAWATA, AND S. UMEKAWA, ED., NORTH-HOLLAND, AMSTERDAM, 1982, P 53-78

4. L.J. HART-SMITH, R.W. OCHSNER, AND R.L. RADECKY, SURFACE PREPARATION OF FIBROUS COMPOSITES FOR ADHESIVE BONDING OR PAINTING, *DOUGLAS SERVICE MAGAZINE,* FIRST QUARTER 1984, P 12-22
5. L.J. HART-SMITH, R.W. OCHSNER, AND R.L. RADECKY, SURFACE PREPARATION OF FIBROUS COMPOSITES FOR ADHESIVE BONDING OR PAINTING, *CANADAIR SERVICE NEWS,* VOL 14 (NO. 2), SUMMER 1985, P 2-8
6. B.M. PARKER AND R.M. WAGHORNE, SURFACE PRETREATMENT OF CARBON FIBRE-REINFORCED COMPOSITES FOR ADHESIVE BONDING, *COMPOSITES,* VOL 13, JULY 1982, P 280-288
7. A.V. POCIUS AND R.P. WENZ, MECHANICAL SURFACE PREPARATION OF GRAPHITE-EPOXY COMPOSITE FOR ADHESIVE BONDING, *SAMPE J.,* SEPT/OCT 1985, P 50-58
8. A.J. KINLOCH AND G.K.A. KODOKIAN, "THE ADHESIVE BONDING OF THERMOPLASTIC COMPOSITES," EUROPEAN RESEARCH OFFICE OF THE U.S. ARMY, CONTRACT DAJA 45-86-C-0037, FOURTH PERIODIC REPORT, IMPERIAL COLLEGE, LONDON, AUG-DEC, 1987
9. J.D. LABOR AND S.H. MYHRE, "LARGE AREA COMPOSITE STRUCTURE REPAIR," NORTHROP AIRCRAFT CORPORATION, USAF TECHNICAL REPORT AFFDL-TR-79-3040, MARCH 1979
10. B.M. PARKER, THE EFFECT OF COMPOSITE PREBOND MOISTURE ON ADHESIVE-BONDED CFRP-CFRP JOINTS, *COMPOSITES,* VOL 14, JULY 1983, P 226-232
11. E.W. THRALL, JR., PROSPECTS FOR BONDING PRIMARY AIRCRAFT STRUCTURES IN THE 80'S, *25TH NATIONAL SAMPE SYMPOSIUM,* VOL 25, SOCIETY FOR THE ADVANCEMENT OF MATERIAL AND PROCESS ENGINEERING, 6-8 MAY 1980, P 716-727
12. I. MCARTHUR, HAWKER DEHAVILLAND, BANKSTOWN, AUSTRALIA, PRIVATE COMMUNICATION, 1992
13. L.J. MATIENZO, J.D. VENABLES, J.D. FUDGE, AND J.J. VELTEN, SURFACE PREPARATION OF BONDING ADVANCED COMPOSITES, PART 1; EFFECT OF PEEL PLY MATERIALS AND MOLD RELEASE AGENTS ON BOND STRENGTH, *30TH NATIONAL SAMPE SYMPOSIUM,* SOCIETY FOR THE ADVANCEMENT OF MATERIAL AND PROCESS ENGINEERING, 19-21 MARCH 1985, P 302-314
14. S.E. SUSMAN, THE DWELL CYCLE: A COST SAVINGS ROUTE TO QUALITY COMPOSITES, *25TH NATIONAL SAMPE SYMPOSIUM,* SOCIETY FOR THE ADVANCEMENT OF MATERIAL AND PROCESS ENGINEERING, 6-8 MAY 1980, P 251-258
15. S-I.Y. WU, A.M. SCHULER, AND D.V. KEANE, ADHESIVE BONDING OF THERMOPLASTIC COMPOSITES, 1. THE EFFECT OF SURFACE TREATMENT ON ADHESIVE BONDING, *19TH INT. SAMPE TECH. CONF.,* SOCIETY FOR THE ADVANCEMENT OF MATERIAL AND PROCESS ENGINEERING, 13-15 OCT 1987, P 277-290
16. S. ZELENAK, D.W. RADFORD AND M.W. DEAN, THE PERFORMANCE OF CARBON FIBER REINFORCED PEEK SUBASSEMBLIES JOINED USING A DUAL RESIN BONDING APPROACH, *37TH INTERNATIONAL SAMPE SYMPOSIUM,* SOCIETY FOR THE ADVANCEMENT OF MATERIAL AND PROCESS ENGINEERING, 9-12 MARCH 1992, P 1346-1356
17. T-H. YOON AND J.E. MCGRATH, ADHESION STUDY OF PEEK/GRAPHITE COMPOSITES, *36TH INTERNATIONAL SAMPE SYMPOSIUM,* SOCIETY FOR THE ADVANCEMENT OF MATERIAL AND PROCESS ENGINEERING, 15-18 APRIL 1991, P 428-436

Joining of Oxide-Dispersion-Strengthened Materials

David O'Donnell, Inco Alloys International Inc.

Introduction

OXIDE - DISPERSION - STRENGTHENED (ODS) MATERIALS utilize an extremely fine oxide dispersion for strengthening, such as yttria (Y_2O_3) or alumina (Al_2O_3). The majority of ODS alloys are produced by mechanical means, often referred to as mechanical alloying (MA), where elemental or alloyed powders are ball milled, or attrited. This mechanical working of different powders between large shot will cold weld particles and break them apart until a fine interlayered structure is produced. The powder is typically consolidated and homogenized by hot isostatic pressing or hot extrusion. Further consolidation is typically performed, producing a final product that is more than 99% dense (Ref 1, 2). The compositions of selected ODS alloys are given in Table 1.

TABLE 1 COMPOSITION OF SELECTED ODS ALLOYS

ODS ALLOY	COMPOSITIONS, %								TYPICAL APPLICATIONS
	Cr	Ni	Fe	Ti	Al	C	Y_2O_3	OTHER	
MA 956	20.0	. . .	74.0	0.5	4.5	. . .	0.5	. . .	**COMBUSTOR COMPONENTS**
PM 2000	20.0	. . .	73.0	0.5	5.5	. . .	0.5	. . .	**. . .**
MA 754	20.0	78.0	1.0	0.5	0.3	0.05	0.6	. . .	**TURBINE VANES, NOZZLES**
PM 1000	20.0	79.0	. . .	0.5	0.3	. . .	0.6	. . .	**. . .**
MA 758	30.0	68.0	1.0	0.5	0.3	. . .	0.6	. . .	**GLASS EQUIPMENT**
MA 6000	15.0	69.0	. . .	2.5	4.5	0.05	1.1	4.0 W; 2.0 MO; 2.0 TA; 0.01 B; 0.15 ZR	**TURBINE BLADES**
PM 3030	17.0	68.2	. . .	. . .	6.0	<0.05	1.1	3.5 W; 2.0 MO; 2.0 TA; 0.01 B; 0.15 ZR	**. . .**
AL-905XL	. . .	. . .	. . .	. . .	93.2	1.1	. . .	4.0 MG; 1.3 LI; 0.4 O_2	**AIRFRAME COMPONENTS**
AL-9052	**. . .**	**. . .**	**. . .**	**. . .**	**94.5**	**1.1**	**. . .**	**4.0 MG; 0.4 O_2**	**MARINE CORROSION**

MA, mechanically alloyed; PM, powdered metal

A typical dispersoid diameter of Incoloy alloy MA 956, for example, is on the order of 30 nm (1.2×10^{-6} in.), which is too small for observation using optical metallographic techniques (Ref 3). The dispersion of stable oxides provides exceptional creep-rupture strength at temperatures above 980 °C (1800 °F) because carbides and many secondary phases used for strengthening conventional wrought alloys go into solution. The level of creep strength achieved at very high temperatures in ODS alloys has not been matched by similar wrought or cast alloys.

The processing techniques employed in the production of ODS alloys produce some entrapped gases, which tend to create porosity during fusion welding. Porosity can form either within the bulk of the fusion zone or near the fusion boundary, as a very fine porosity interface. This tendency is generally most severe in aluminum alloys and least evident in nickel-base alloys. The porosity tendency in iron-base alloys is between that of aluminum- and nickel-base alloys. The level of porosity that results from the fusion welding of aluminum ODS alloys is such that they are not generally considered to be fusion weldable.

Most ODS applications involve high temperatures and, possibly, corrosive environments. The first commercial applications were aircraft gas-turbine engines, followed by industrial engines. Vane airfoils are typically furnace brazed to platforms, both of which can be made from ODS alloys. Combustor parts can be riveted, resistance welded, or brazed. Some ODS alloys are being used to a significant extent in various components of molten glass handling equipment. Heat-treatment baskets, trays, shields, and furnace skid rails are also becoming common applications.

References

1. L.R. CURWICK, THE MECHANICAL ALLOYING PROCESS: POWDER TO MILL PRODUCT, *FRONTIERS OF HIGH TEMPERATURE ALLOYS I, PROC. 1ST INT. CONF. ON OXIDE DISPERSION STRENGTHENED ALLOYS BY MECHANICAL ALLOYING,* J.S. BENJAMIN, ED., INCO ALLOYS INTERNATIONAL, 1981, P 3-10

2. G.A. HACK, FUNDAMENTALS OF MECHANICAL ALLOYING, *FRONTIERS OF HIGH TEMPERATURE ALLOYS II, PROC. 2ND INT. CONF. ON OXIDE DISPERSION STRENGTHENED ALLOYS BY MECHANICAL ALLOYING,* J.S. BENJAMIN AND R.C. BENN, ED., INCO ALLOYS INTERNATIONAL, 1983, P 3-18
3. R. PETKOVIC-LUTON, D.J. SROLOVITZ, AND M.J. LUTON, MICROSTRUCTURAL ASPECTS OF CREEP IN OXIDE DISPERSION STRENGTHENED ALLOYS, *FRONTIERS OF HIGH TEMPERATURE ALLOYS II, PROC. 2ND INT. CONF. ON OXIDE DISPERSION STRENGTHENED ALLOYS BY MECHANICAL ALLOYING,* J.S. BENJAMIN AND R.C. BENN, ED., INCO ALLOYS INTERNATIONAL, 1983, P 73-97

Joining of Oxide-Dispersion-Strengthened Materials

David O'Donnell, Inco Alloys International Inc.

Design Strategy

The high-temperature creep strength obtained from a cast weld structure, using ODS alloys, is generally comparable to that obtained with conventional wrought alloys and does not exhibit the same exceptional high-temperature creep strength of unwelded ODS materials. The stable oxides, or dispersoids, that are used in the ODS alloy systems have essentially no equilibrium solubility in the liquid phase. If melting occurs, then the dispersoids rapidly agglomerate, and buoyancy floats the oxide to an upper surface, if possible. In fusion welds, this results in the loss of the primary means of high-temperature strengthening. Agglomerated semicontinuous dispersoids in the partially melted zones of fusion welds are also suspected as contributing to early weld-service failures.

A number of successful strategies have been employed in joining ODS alloys. Conventional fusion welds or brazes are often placed in cooler locations in order to retain acceptable strength levels. A design is often altered so that conventional fusion welds are not the principal load-carrying members, but are attachments instead. Solid-state joining techniques can often be used, but the resulting grain structure must also be considered.

Grain Structure. At very high temperatures, grain boundaries become the weak link, so to speak, and fracture becomes intergranular. In order to minimize such a grain boundary strength limitation, ODS alloys are produced with a macro grain size, where the grain boundary area normal to the principal stresses are minimized without incurring the difficulties inherent in producing single crystals. This elongated grain structure is often referred to as a high grain aspect ratio (GAR). Welds or joints that significantly interrupt this large interlocked grain structure will fail prematurely at extreme temperatures, even if they are produced by solid-state means. A friction weld in a rod, where there is a straight grain boundary interface through the thickness and normal to the principal stresses, typically will not perform significantly better than a conventional fusion weld in which a similar structure is produced. The large, interlocking grain structure in such materials is a key attribute for good performance at extreme temperatures.

Because of grain-structure considerations, it is often preferable to use resistance welds, braze welds, or both in a lap joint, rather than a butt joint, where there is invariably a through-thickness noninterlocked grain structure normal to the principal stresses across the joint. When lap welds are used, double-lap joints outperform single-lap joints, which fail by peeling at lower stresses.

Postweld recrystallization anneals have been used with all types of welds to grow grains across the welds to the greatest extent possible. The best structural and strength results are generally obtained by joining base metals in a fine, unrecrystallized condition and by performing a grain-coarsening recrystallization anneal after welding. However, a postweld recrystallization anneal typically improves properties only in narrow joints, such as those commonly produced by electron-beam, diffusion, resistance, and friction welding techniques. Creep-rupture properties from wide-gap joints, such as those produced in gas-metal or gas-tungsten-arc welds can be reduced by such an anneal. This anneal is typically 1316 °C (2400 °F) for 1 h, when MA 754 and MA 956 alloys are used. The fine-grain approach, if adopted, requires coordination with materials suppliers, because most ODS alloys are typically supplied in the coarse-grained, recrystallized condition. However, some measure of improved properties may be obtained in narrow joints through postweld recrystallization, even where the base metal was joined in the coarse-grained condition. Table 2 provides transverse property data on selected alloys used in each of the welding processes discussed later in this article.

TABLE 2 WELD TRANSVERSE PROPERTIES OF SELECTED ODS ALLOYS

ODS ALLOYS	CONDITION[A]	WELDING PROCESS[B]	JOINT TYPE	FILLER METAL	POSTWELD HEAT TREATMENT[C]		TEST TEMPERATURE		STRESS[D]		LIFE[E], H	LONGITUDINAL BASE-METAL STRENGTH, APPROXIMATE %	COMMENT
					°C	°F	°C	°F	MPA	KSI			
MA 956	FG	FRW	BUTT	. . .	1315	2400	982	1800	77.9	11.3	HTT	75	. . .
	CG	FRW	BUTT	. . .	1315	2400	982	1800	6.9	1.0	24.0	8	. . .
	FG	FRW	BUTT	. . .	1315	2400	982	1800	6.9/13.8	1.0/2.0	13.0	17	. . .
MA 758	CG	GMAW	BUTT	52	. . .	. . .	1093	2000	13.8	2.0	40.4	11	. . .
	CG	GMAW	BUTT	52	. . .	. . .	1093	2000	6.9	1.0	1601	8	. . .
	CG	GMAW	BUTT	52	1315	2400	1093	2000	13.8	2.0	16.5	10	. . .
	CG	GMAW	BUTT	52	1315	2400	1093	2000	6.9	1.0	259.9	7	. . .
MA 956	CG	EBW	BUTT	. . .	. . .	. . .	982	1800	13.8	2.0	5.4	15	**90° BUTT**
	CG	EBW	BUTT	. . .	. . .	. . .	982	1800	27.6	4.0	38	33	**5° BUTT**
	CG	EBW	SINGLE LAP	. . .	. . .	. . .	1093	2000	13.8	2.0	710	25	**DOUBLE WELD**
	CG	EXW	SINGLE LAP	. . .	1100[F]	2012[F]	1100	2012	18/28/38	2.6/4.1/5.5	14.0	58	**STRESS IS BASE METAL**
	FG	EXW	SINGLE LAP	. . .	1315	2400	1100	2012	18/28/38	2.6/4.1/5.5	8.0	56	**STRESS IS BASE METAL**
	CG	EXW	SINGLE LAP	. . .	. . .	. . .	1100	2012	18	2.6	2.0	25	**STRESS IS BASE METAL**
	FG	RSW	DOUBLE LAP	. . .	[G]	[G]	1093	2000	37.9	5.5	HTT	42	**SINGLE-SPOT STRESS**
	FG	**RSW**	**DOUBLE LAP**	**. . .**	[G]	[G]	**982**	**1800**	**44.1[H]**	**6.4[H]**	**HTT**	**43**	**SINGLE-SPOT STRESS**

(A) FG, FINE GRAIN; CG, COARSE GRAIN.

(B) FRW, FRICTION WELDING; GMAW, GAS-METAL ARC WELDING; EBW, ELECTRON-BEAM WELDING; EXW, EXPLOSION WELDING; RSW, RESISTANCE SPOT WELDING.

(C) 1 H, EXCEPT WHERE NOTED.

(D) STEP LOADING OF STRESS DENOTED BY "/." STRESS WAS INCREASED EVERY 24 H UNTIL FAILURE.

(E) HTT, HIGH-TEMPERATURE TENSILE TEST.

(F) 10 H.

(G) 1204 °C (2200 °F) FOR 24 H PLUS 1315 °C (2400 °F) FOR 1 H.
(H) ATTACHMENT PIN SHEARED THROUGH SHEET

Other attributes of ODS alloys, relative to welding, are typical of their respective alloy groups. For example, ferritic ODS alloys will exhibit a ductile-to-brittle transition temperature (DBTT), and, because of their high alloy content, will have a marked sensitivity to delayed hydrogen cracking.

Iron-Base ODS Alloys

The alloy MA 956 utilizes a coarse, high-aspect grain structure as part of its high-temperature strengthening ability. This structure is achieved through processing and a final recrystallization anneal of 1316 °C (2400 °F) before service. The alloy has a high melting point of 1480 °C (2700 °F), and is often used in service at 1093 °C (2000 °F) and above. The alloy is quite ductile above its DBTT, which is near room temperature. All strain-forming operations, such as bend tests, friction welding, and explosion welding, should be performed after heating to 100 °C (212 °F) or higher. Below the DBTT, the alloy can be notch brittle. The MA 956 alloy undergoes no solid-state phase transformations between melting and cryogenic temperatures, and it cannot be quench hardened.

Iron-base ODS alloys are generally very sensitive to delayed weld zone and heat-affected zone (HAZ) hydrogen cracking. Good low-hydrogen welding practice should be followed for all fusion-welding processes, and only low-hydrogen fusion welding processes are recommended. For this reason, shielded metal arc welding or other flux-bearing welding processes are generally not recommended. Delayed cracking has been observed, even in heavy resistance welds, when no precautions were taken.

Fusion welding should utilize low-hydrogen practices, on the assumption that enough hydrogen will be present to cause cracking, and should incorporate preheating, minimum interpass temperatures, and a postweld hydrogen diffusion treatment prior to cooling in order to prevent cracking. Preheating and use of minimum interpass temperatures ranging from 149 to 204 °C (300 to 400 °F) have generally prevented cracking during welding. A postweld diffusion treatment before cooling at 300 °C (572 °F) for 10 h, or 400 °C (752 °F) for 6 h, has been effective in removing hydrogen in section thicknesses less than 11 mm (0.4 in.) thick. More information on hydrogen diffusion treatments for various thicknesses and temperatures is provided in Ref 4. The unique aspects of the different welding processes are described in the section "Welding Processes" in this article.

Reference cited in this section

4. F.R. COE, *WELDING STEELS WITHOUT HYDROGEN CRACKING,* THE WELDING INSTITUTE, 1973

Joining of Oxide-Dispersion-Strengthened Materials

David O'Donnell, Inco Alloys International Inc.

Nickel-Base ODS Alloys

Most of the nickel-base ODS alloys use a high GAR, but some are also highly textured to provide the best resistance to thermal fatigue. This structure is achieved in MA 754 through processing and a final recrystallization anneal of 1316 °C (2400 °F) before service. In MA 6000, zone annealing is used for an optimum longitudinal GAR.

The alloy MA 758 has been used increasingly in handling equipment for molten glass; such equipment is exposed to high temperatures, stress, and corrosive glasses. Welds have been made, primarily for attachment purposes, using the gas-metal arc, gas-tungsten arc, and shielded metal arc welding processes. Filler consumables that contain 30% Cr, such as Inconel filler metal 52 or Inconel welding electrode 152, are needed to provide corrosion resistance to most molten glasses.

The alloy MA 6000, an advanced gas-turbine blade material that utilizes both oxide-dispersion and γ' strengthening, is not typically fusion welded. Its aluminum content may make it susceptible to strain-age cracking, which can occur in fast precipitation-hardening alloys where significant residual stresses are present. These stresses can be caused by cold working or welding. If the piece is not heated rapidly to annealing temperatures after welding, then it may age fast enough for the locked-in stresses to exceed the rupture strength, at which point cracking will occur. Furnace brazing and diffusion welding should be performed after plating the joint area with a thin layer of nickel to prevent the oxidation of aluminum, which could cause incomplete bonding.

The alloy MA 754 is primarily a turbine vane material that is used for its exceptional combination of creep-rupture strength and thermal-fatigue resistance. Most applications involve vacuum furnace brazing to similar and dissimilar alloys, in situations where the joint is located in relatively cool locations or is subjected to reduced stresses (Fig. 1).

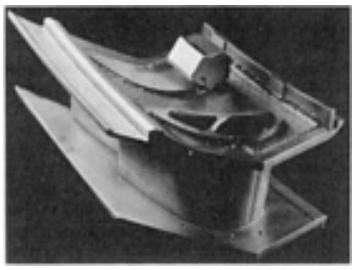

FIG. 1 FURNACE BRAZED MA 754 GAS TURBINE VANE

Joining of Oxide-Dispersion-Strengthened Materials

David O'Donnell, Inco Alloys International Inc.

Welding Processes

Gas-tungsten arc welding of ODS alloys is typically carried out using minimal welding current and techniques that are designed to minimize melting of the alloys. When welding alloys with a significant aluminum content, such as MA 956, there is a high propensity for an aluminum-rich light gray oxide film to form on the weld-bead surface. The dispersoid from the melted base metal also floats to the weld-bead surface. These oxides should be removed by light abrasive techniques before subsequent weld beads are deposited, in order to prevent incomplete-fusion defects or oxide inclusions. Balanced-wave alternating current is generally not recommended, because the reverse current (electrode positive) part of the cycle attempts to "cathodically clean" the dispersoid oxides from the bulk of the base metal by arcing into the base metal. Power supplies for which the reverse-polarity cycle time can be minimized have been used with some success, producing only a weld-bead surface cleaning. Figures 2 and 3 show MA 956 products that have been gas-tungsten arc welded using different filler metals.

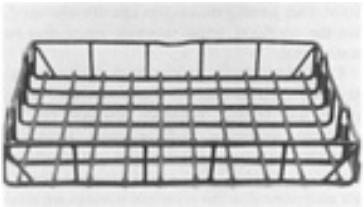

FIG. 2 GAS-TUNGSTEN ARC WELDED MA 956 HEAT TREAT BASKET. INCONEL 617 FILLER METAL WAS USED.

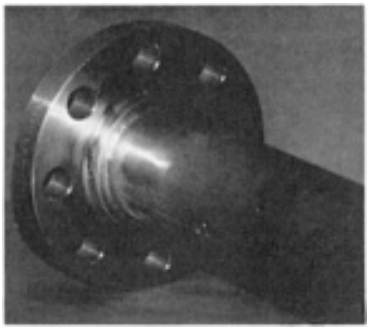

FIG. 3 MA 956 PIPE GAS-TUNGSTEN ARC WELDED TO A 304 STAINLESS STEEL FLANGE. 308 STAINLESS STEEL FILLER METAL WAS USED.

Because joint properties are representative of conventional wrought alloys, attempts should be made to either design welds as attachments that are subjected to reduced stresses or place the welds in cooler locations where they can withstand the stress. Table 3 lists typical filler-metal alloys for the ODS alloys discussed in this article.

TABLE 3 SELECTED WELDING CONSUMABLES FOR ODS ALLOYS

ODS ALLOY	**FILLER METAL**	**SHIELDED METAL ARC WELDING ELECTRODE**	BRAZING ALLOY
MA 956	BRIGHTRAY ALLOY ICA	. . .	**B93[(A)], AM 788[(B)], TD6[(C)]**
MA 754	INCONEL 617	. . .	**B93, AM 788, TD6**
MA 758	**INCONEL 52**	**INCONEL WELDING ELECTRODE 152**	

(A) GENERAL ELECTRIC ALLOY B50TF108, AVAILABLE IN POWDER FORM FROM ALLOY METALS, INC. COMPOSITION: 14% CR, 9.5% CO, 4.9% TI, 4% W, 4% MO, 3% AL, 4.5% SI, 0.7% B, BALANCE NI.

(B) AVAILABLE IN POWDER FORM FROM ALLOY METALS, INC. COMPOSITION: 22% CR, 21% NI, 14% W, 2% B, 0.03% LA, BALANCE CO.

(C) GENERAL ELECTRIC ALLOY B5DTF83, AVAILABLE IN POWDER FORM. COMPOSITION: 16% CR, 17% MO, 5% W, 5% SI, 1% AL, BALANCE NI

Gas-metal arc welding of ODS alloys is typically implemented with pulsed or synergic power sources and low-to-average current settings to minimize the melting of the base metals. This typically amounts to an average welding current of 60 to 180 A, depending on the section thickness of the joint.

Electron-beam and laser-beam welding have been used to join MA 956, and the best results have been obtained in lap joints where the beam is oriented as close to parallel to the joint as possible. In butt joints, the best results can be obtained by inclining the joint and beam as much as possible from 90°. This will reduce the load per unit area on the weld fusion-boundary and centerline grain structure (Ref 5, 6). At the same time, melting should be minimized and the beam should be projected vertically to help prevent incomplete-fusion defects from dispersoid entrapment. Because MA 956 is magnetic, it should be demagnetized before electron-beam welding to prevent unwanted beam deflection.

Resistance welding of ODS alloys is typically implemented with parameters designed to minimize the thickness of the weld nugget and solidification time (high current, tip pressure, and minimum weld time). The typical lap joint produces a favorable grain orientation relative to the weld and principal stress, and the process is fast and repeatable. The overlap and number of spots are controlled to develop the required joint properties. Delayed hydrogen cracking can occur in iron-base

ODS alloys, particularly in thicker restrained pieces if preheat, minimum interpass temperatures, and postweld diffusion treatments are not employed.

Dedicated efforts to minimize melting or the thickness of the weld nugget have succeeded in producing solid-state, or very-near-solid-state, resistance welds. The commercial practicality and benefits of these techniques still need to be better defined.

Furnace brazing of ODS alloys has been extensively used by the aircraft industry. Iron- and nickel-base ODS alloys containing significant aluminum or titanium are typically plated with a very thin barrier of nickel to prevent oxidation of these elements during the brazing cycle. If oxidation occurs, then the flow of the brazing filler metals is inhibited. Brazing filler metals that are rich in silicon and lean in boron are preferred to avoid erosion of the ODS base metals during the brazing cycle. If significant erosion occurs, then dispersoids can form oxide inclusions or incomplete-fusion defects within the joint. For best results, joint gaps should be as narrow as possible without hampering filler-metal flow. Typical properties are shown in Table 4. Attempts to improve properties have utilized special techniques, such as diffusion brazing, transient liquid-phase bonding, and pressure brazing.

TABLE 4 FURNACE-BRAZED WELD PROPERTIES

ODS ALLOY	JOINT TYPE	FILLER METAL	TEST TEMPERATURE		STRESS(A)		LIFE, H	LONGITUDINAL BASE-METAL STRENGTH, APPROXIMATE %	COMMENT
			°C	°F	MPA	KSI			
MA 754	DOUBLE LAP	B93	982	1800	110	16	392	85	**SHEARED BRAZE**
	DOUBLE LAP	AM 788	982	1800	110	16	168	84	**SHEARED BRAZE AND BASE METAL**
	DOUBLE LAP	AM 788	1093	2000	41.4	6	178	40	**SHEARED BRAZE**
	DOUBLE LAP	TD6	1093	2000	56.2	8	105.5	53	**SHEARED BRAZE**
MA 956	SINGLE LAP (8*T*)	B93	982	1800	41.4	6	89.4	30	**SHEARED BRAZE**
	SINGLE LAP (8*T*)	**AM 788**	**982**	**1800**	**48.3**	**7**	**23.5**	**58**	**SHEARED BRAZE**

(A) STRESSES ARE BELIEVED TO BE BASED ON BASE METAL.

Although it has not yet been confirmed, the aluminum-base ODS alloys AL-905XL and AL-9052 should vacuum furnace braze well, by virtue of their magnesium content.

Friction welding is capable of creating sound solid-state joints in ODS alloys. The plastic deformation and flow at the bond interface typically produce a relatively straight grain-boundary interface through-thickness after annealing. This relatively flat grain-boundary interface normal to the principal stresses is undesirable, and it produces properties that are no better than most fusion processes. The best results have been obtained by welding fine-grained unrecrystallized rod and then performing a postweld recrystallization anneal.

Explosion welding generally creates a favorable grain structure by virtue of the lap joints used. In a limited study in which MA 956 was joined, the best results were obtained by bonding coarse-grained material and giving it a postweld diffusion treatment of 1100 °C (2012 °F) for 10 h.

References cited in this section

5. T.J. KELLY, JOINING MECHANICAL ALLOYS FOR FABRICATION, *FRONTIERS OF HIGH TEMPERATURE ALLOYS II, PROC. 2ND INT. CONF. ON OXIDE DISPERSION STRENGTHENED ALLOYS BY MECHANICAL ALLOYING,* J.S. BENJAMIN AND R.C. BENN, ED., INCO ALLOYS

INTERNATIONAL, 1983, P 129-148

6. H.D. HEDRICH, H.G. MAYER, G. HAUFLER, M. KOPH, AND N. REHEIS, "JOINING OF ODS-SUPERALLOYS," ASME 91-GT-411, THE INTERNATIONAL GAS TURBINE AND AEROENGINE CONGRESS AND EXPOSITION (ORLANDO, FL), AMERICAN SOCIETY OF MECHANICAL ENGINEERS, JUNE 1991

Joining of Oxide-Dispersion-Strengthened Materials

David O'Donnell, Inco Alloys International Inc.

References

1. L.R. CURWICK, THE MECHANICAL ALLOYING PROCESS: POWDER TO MILL PRODUCT, *FRONTIERS OF HIGH TEMPERATURE ALLOYS I, PROC. 1ST INT. CONF. ON OXIDE DISPERSION STRENGTHENED ALLOYS BY MECHANICAL ALLOYING,* J.S. BENJAMIN, ED., INCO ALLOYS INTERNATIONAL, 1981, P 3-10
2. G.A. HACK, FUNDAMENTALS OF MECHANICAL ALLOYING, *FRONTIERS OF HIGH TEMPERATURE ALLOYS II, PROC. 2ND INT. CONF. ON OXIDE DISPERSION STRENGTHENED ALLOYS BY MECHANICAL ALLOYING,* J.S. BENJAMIN AND R.C. BENN, ED., INCO ALLOYS INTERNATIONAL, 1983, P 3-18
3. R. PETKOVIC-LUTON, D.J. SROLOVITZ, AND M.J. LUTON, MICROSTRUCTURAL ASPECTS OF CREEP IN OXIDE DISPERSION STRENGTHENED ALLOYS, *FRONTIERS OF HIGH TEMPERATURE ALLOYS II, PROC. 2ND INT. CONF. ON OXIDE DISPERSION STRENGTHENED ALLOYS BY MECHANICAL ALLOYING,* J.S. BENJAMIN AND R.C. BENN, ED., INCO ALLOYS INTERNATIONAL, 1983, P 73-97
4. F.R. COE, *WELDING STEELS WITHOUT HYDROGEN CRACKING,* THE WELDING INSTITUTE, 1973
5. T.J. KELLY, JOINING MECHANICAL ALLOYS FOR FABRICATION, *FRONTIERS OF HIGH TEMPERATURE ALLOYS II, PROC. 2ND INT. CONF. ON OXIDE DISPERSION STRENGTHENED ALLOYS BY MECHANICAL ALLOYING,* J.S. BENJAMIN AND R.C. BENN, ED., INCO ALLOYS INTERNATIONAL, 1983, P 129-148
6. H.D. HEDRICH, H.G. MAYER, G. HAUFLER, M. KOPH, AND N. REHEIS, "JOINING OF ODS-SUPERALLOYS," ASME 91-GT-411, THE INTERNATIONAL GAS TURBINE AND AEROENGINE CONGRESS AND EXPOSITION (ORLANDO, FL), AMERICAN SOCIETY OF MECHANICAL ENGINEERS, JUNE 1991

Composite-to-Metal Joining

Raymond E. Bohlmann, McDonnell Douglas Aerospace-East

Introduction

SELECTING THE BEST METHODS and practices for joining composites to metals is highly dependent on the particular combination of composite and metal materials being joined and the design details and/or requirements of the joint. For example, if a carbon-epoxy laminate must be joined to an all-metal fitting through an adhesive bondline that should perform well in a hot-wet environment, aluminum would be a poor choice. To develop the hot-wet strength, the adhesive must be cured at elevated temperature. Because of the high coefficient of thermal expansion (CTE) of the aluminum and a low CTE for the carbon-epoxy composite, significant fabrication thermal stresses can occur in the adhesive bondline at room temperature after the elevated-temperature cure. These fabrication thermal stresses, which are at a maximum at the ends of the joint, can be sufficient to cause the adhesive to fail before any mechanical loads are applied. Also, the carbon-epoxy and aluminum combination is susceptible to galvanic corrosion. Titanium would be a better material selection for

the metal adherend--both for minimizing thermal stresses (CTE of titanium is less than one-half that of the aluminum) and for minimizing corrosion.

This article will discuss material combinations, design details, and fabrication processes that should be considered when joining resin-matrix composites to metals. Resin-matrix composites, also referred to as organic-matrix composites, can be divided into thermoset composites (resin chemical reaction during 120 to 175 °C, or 250 to 350 °F cure) and thermoplastic composites (resin melt fuse between 315 and 400 °C, or 600 and 750 °F). Thermoset composites can be joined to metals by adhesive bonding, whereas thermoplastic composites can be joined by adhesive bonding or through the use of a melt-fuse interface (amorphous bond). Themoplastics can be further divided into semicrystalline and amorphous materials. A semicrystalline thermoplastic material has a low moisture saturation level (0.25%) as compared to an amorphous thermoplastic (0.6%) and a typical thermoset (1.6%). Composite hot-wet properties and bonded-joint shear strengths (adhesive or amorphous bond) are reduced by the degree of absorbed moisture and the joining materials should be selected to minimize this effect.

Composite-to-Metal Joining

Raymond E. Bohlmann, McDonnell Douglas Aerospace-East

Bonded Joints

Design Issues. The analysis of adhesively bonded joints has advanced to the stage where it can legitimately be called a science. Hart-Smith has added nonlinear adhesive behavior to the analysis and design of adhesive bonded joints in the form of an elastic-plastic adhesive model (Ref 1, 2, 3). In addition, a series of digital computer programs has been developed for the analysis of bolted and bonded joints of various geometries (Ref 4, 5). As was stated earlier, selecting the best methods and practices for joining composites to metals depends on the particular combination of materials being joined and the design details/requirements of the joint.

The effect of several important design variables will be illustrated by application of the A4EI STEPLAP analysis computer program (Ref 5). The capabilities of the A4EI program include:

- ELASTIC OR ELASTIC-PLASTIC STRESS DISTRIBUTIONS
- STEPPED-LAP ADHESIVELY BONDED SPLICES OR DOUBLERS
- CHECKS FOR ADHEREND OR ADHESIVE FAILURE
- ACCOUNTS FOR ADHEREND STIFFNESS IMBALANCE, ADHEREND THERMAL MISMATCH, VARIABLE ADHEREND THICKNESS AND STIFFNESS, NONUNIFORM BONDLINE THICKNESS AND ADHESIVE PROPERTIES, AND TENSION, COMPRESSION, AND SHEAR LOADING

The STEPLAP computer procedure is based on a closed-form analysis, which, through an iterative scheme, provides the complete internal stress distribution of a stepped-lap joint (Fig. 1). Two program-detectable failure modes are adherend axial failure and adhesive shear failure. The elastic-plastic methodology represents a major improvement in stepped-lap joint analysis because it accounts for all significant variables in one procedure. In particular, the analysis accounts for adherend stiffness imbalance, adherend thermal mismatch, step thicknesses, number of steps, and adhesive ductility (in terms of an elastic-plastic model). This analytic capability allows the user to quickly identify the critical or limiting detail of a stepped-lap joint configuration and make changes in the joint design to maximize the stepped-lap joint strength. To apply these analyses procedures to a design requires the availability of the adhesive shear stress-strain data (Fig. 2), which are obtained by conducting a thick adherend test on the adhesive (Fig. 3). For design-limit loads (operating loads), the recommended procedure is to limit the bondline shear strain to the elastic knee of the shear stress-strain curve to prevent adhesive failure during repeated fatigue loading.

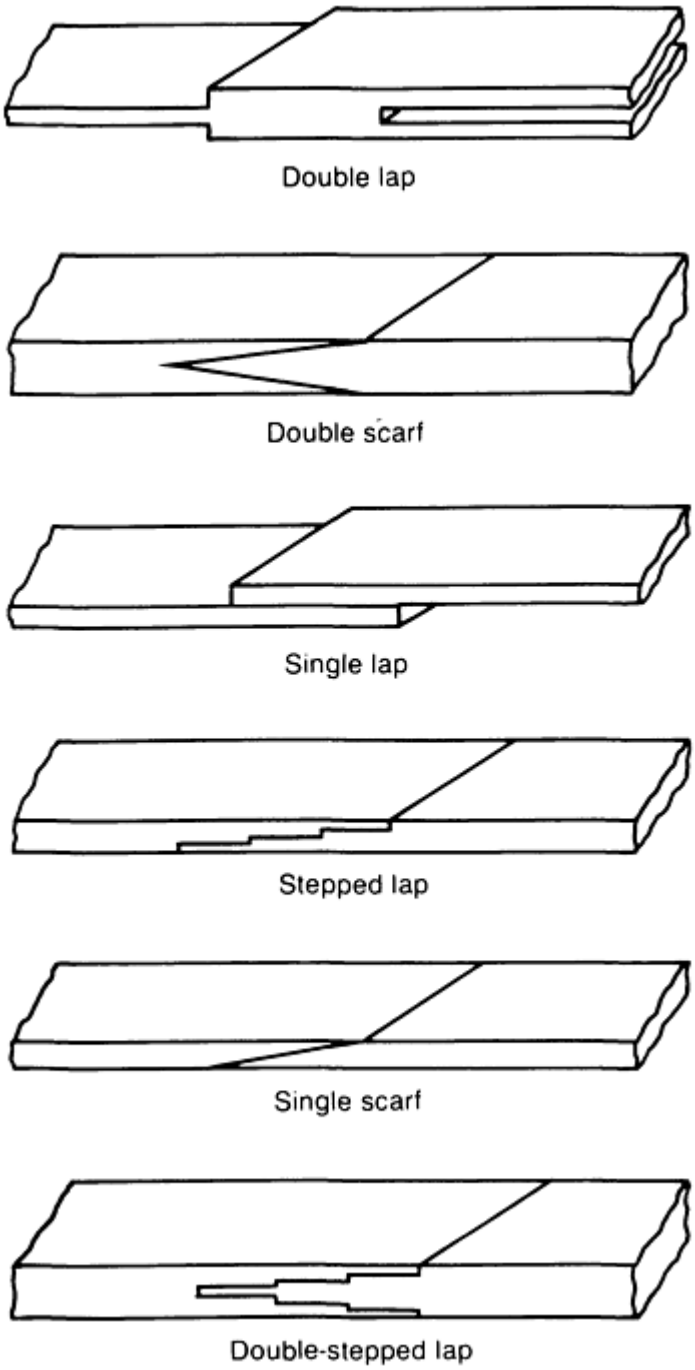

FIG. 1 JOINT DESIGNS USED FOR ADHESIVE BONDING

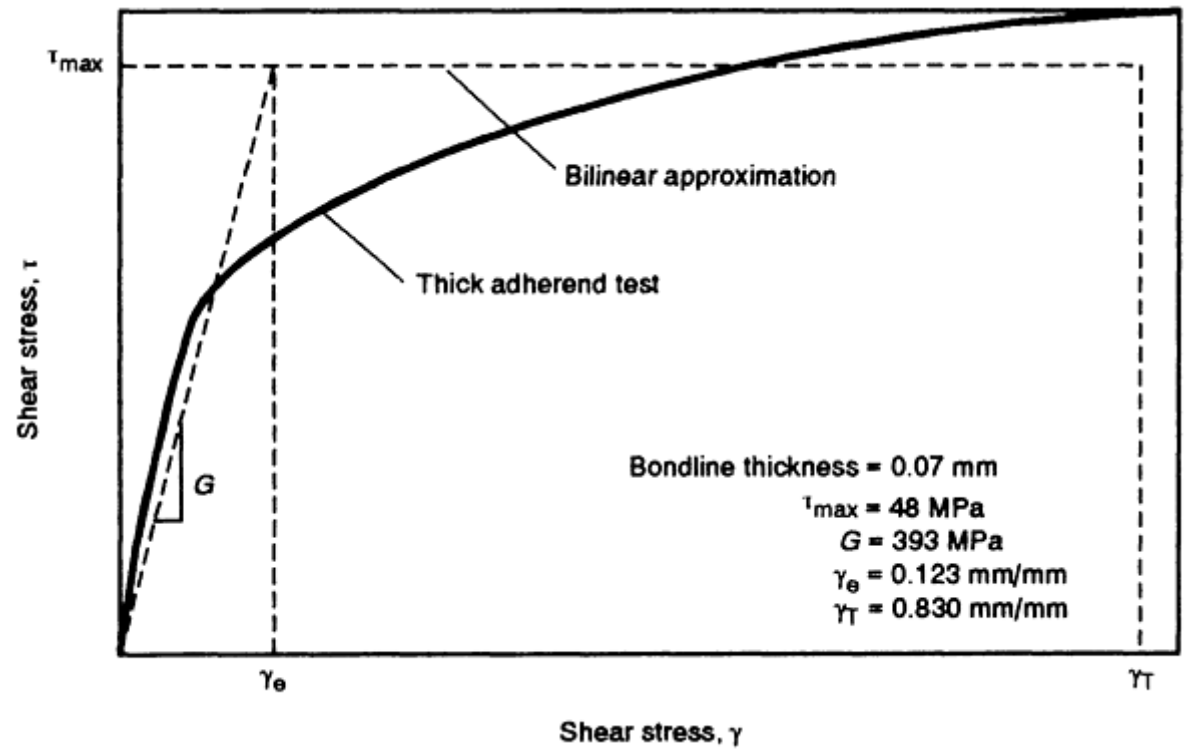

FIG. 2 STRESS-STRAIN CURVE DEVELOPED FROM A THICK ADHEREND (ROOM-TEMPERATURE/DRY) TEST USING FM300K ADHESIVE. *G*, SHEAR MODULUS; γ_E, ELASTIC STRAIN; γ_T, TOTAL STRAIN

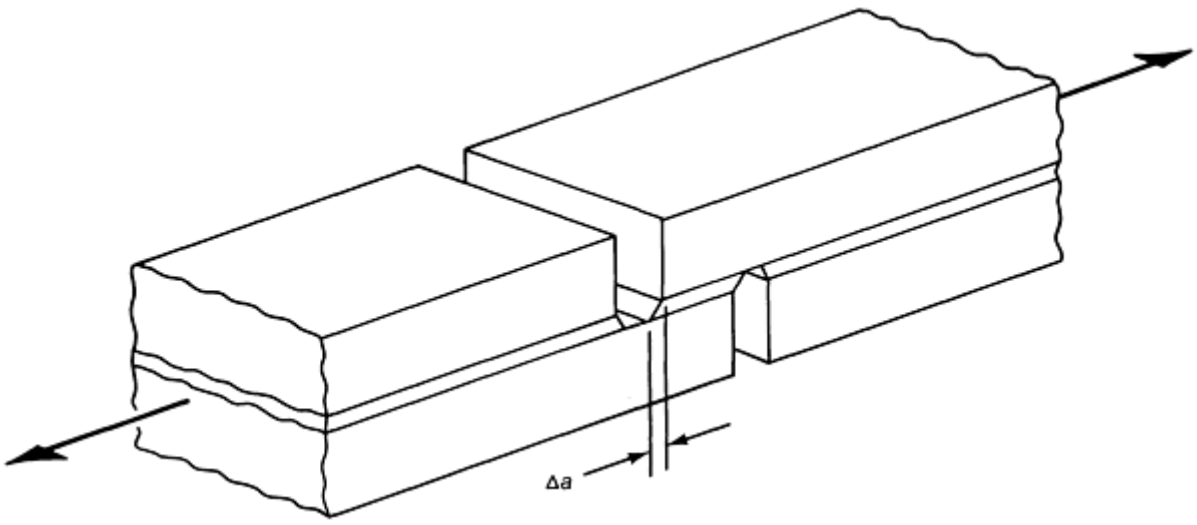

FIG. 3 THICK ADHEREND LAP-SHEAR SPECIMEN

The effect of adhesive bondline thickness on joint load capability is shown in Fig. 4 for a constant thickness composite-to-metal splice joint. The shear stress distributions along the bond length for two different bondline thicknesses were predicted by the computer program. The joint load capability is equivalent to the area under the curve. The curve for a bondline thickness of 0.13 mm (0.005 in.) has 60% more area under the curve and therefore can carry 60% more load than a 0.05 mm (0.002 in.) thickness. For a joint with an elastic distribution, the joint load-carrying capability increase is proportional to the square root of the bondline thickness increase. In this example, the joint load increased by $(0.005 \text{ in.}/0.002 \text{ in.})^{0.5}$, which is a 60% increase.

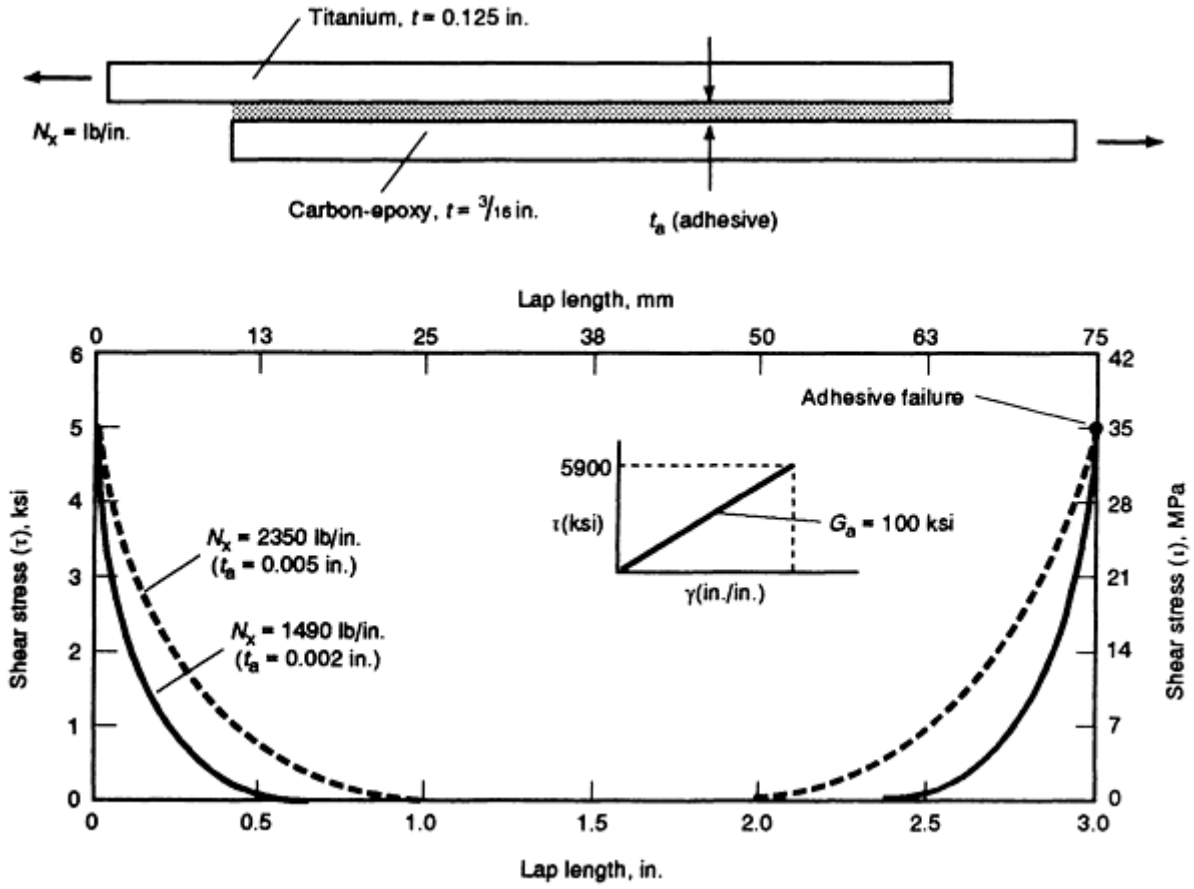

FIG. 4 THE EFFECT OF BONDLINE THICKNESS ON JOINT LOAD-CARRYING CAPABILITY. N_X, JOINT LOAD CAPABILITY; G_A, ADHESIVE SHEAR MODULUS; T_A, ADHESIVE THICKNESS; γ^{SU}, ADHESIVE PLASTIC SHEAR STRAIN (SU, SHEAR ULTIMATE). ORIGINAL SPECIMEN DIMENSIONS GIVEN IN INCHES

The benefits of tapering the adherend thickness are shown in Fig. 5. In the composite (carbon-epoxy)-to-titanium splice joint, two cases are compared using an elastic analysis. In the first case, both adherends are a constant thickness; in the second case, the titanium adherend is tapered as if the titanium is a repair patch that could be tapered prior to bonding. For the first case (adherend constant thickness), the shear stress in the adhesive is maximum on the right end of the joint. For the second case, tapering the thickness of the titanium patch on the right end of the joint reduces the maximum shear stresses in the adhesive, forcing the failure in the adhesive at the left end of the joint and increasing the joint load-carrying capability by 16%. The joint load capability can be further increased by tapering the carbon-epoxy laminate at the left end of the joint, which will further reduce the maximum shear stress in the adhesive. An additional benefit of tapering the ends is to reduce the peel stresses in the adhesive and the interlaminar tension in the laminate.

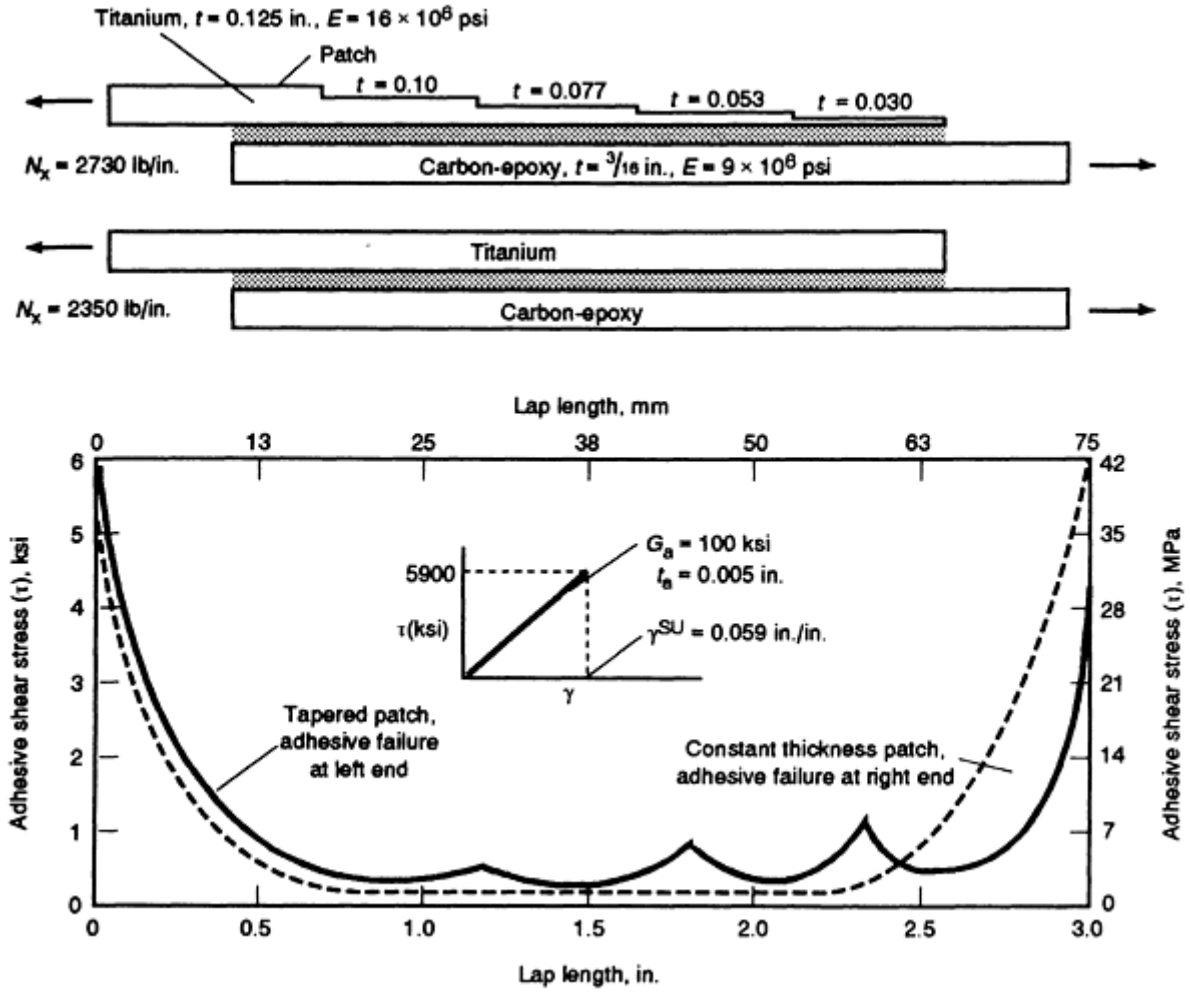

FIG. 5 THE EFFECT OF TAPERING THE ADHEREND THICKNESS ON JOINT LOAD-CARRYING CAPABILITY. SEE FIG. 4 FOR EXPLANATION OF SYMBOLS. ORIGINAL SPECIMEN DIMENSIONS GIVEN IN INCHES

Taking advantage of the adhesive plasticity will provide a significant increase in the area under the shear stress versus lap length curve and the resultant joint load capability (Fig. 6). The example shown in this figure is the same as the tapered-thickness titanium patch shown in Fig. 5 with the adhesive plasticity condition added. For the elastic case, the joint load capability is 49.5 kg/mm (2730 lb/in.). Increasing the adhesive shearing strain allowable from the elastic value of 0.059 mm/mm (in./in.) to the plastic value of 0.20 mm/mm (in./in.) increases the joint load to 118 kg/mm (6520 lb/in.) (a factor of 2.4). Increasing the adhesive plastic shear strain to 0.30 mm/mm (in./in.) further increases the joint load capability to 148 kg/mm (8140 lb/in.), which is a three-fold increase over the elastic condition. Adhesive plasticity will generally provide the added load-carrying capability needed between the operating loads (design limit) and the design ultimate loads when the operating loads (fatigue loading) are limited to the elastic knee in the adhesive shear stress-strain curve.

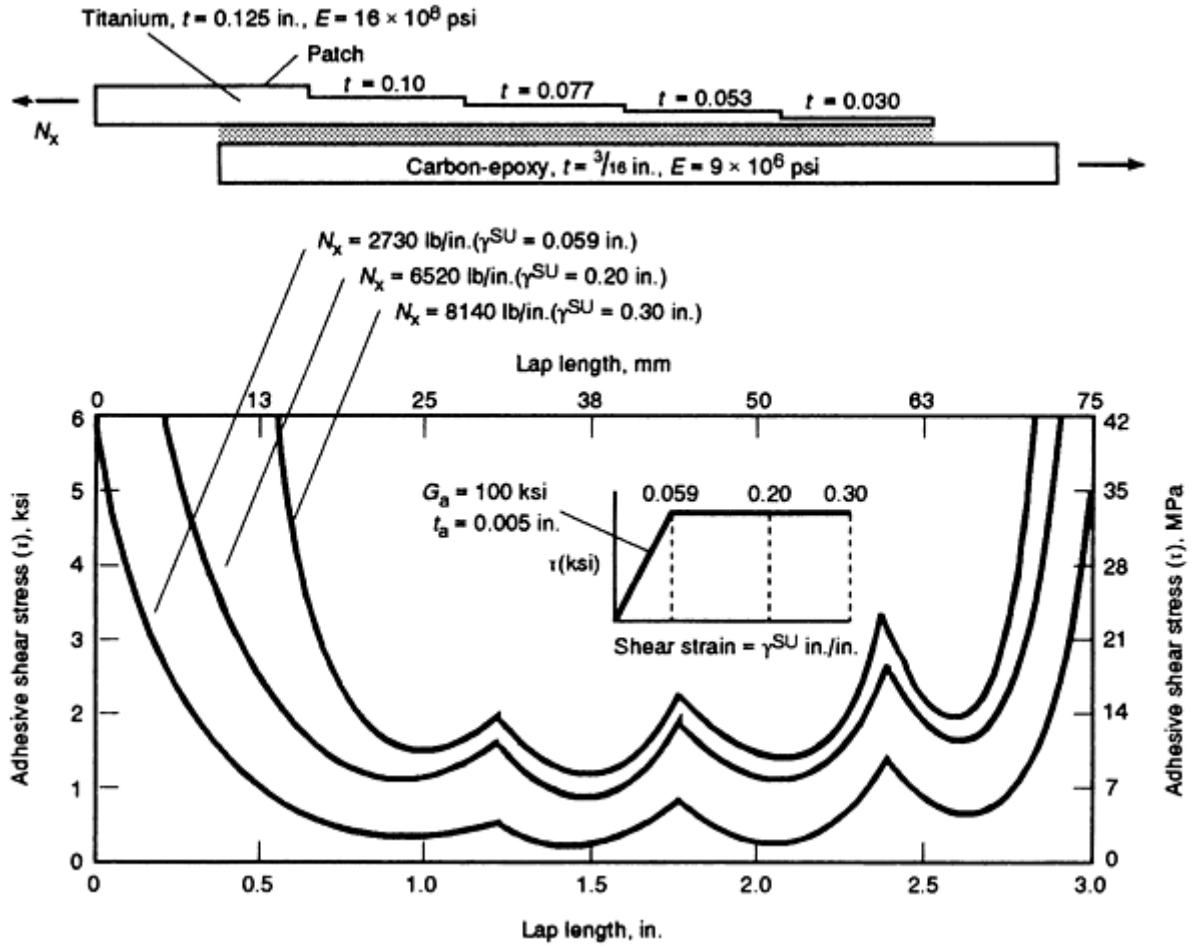

FIG. 6 THE EFFECT OF ADHESIVE PLASTICITY ON JOINT LOAD-CARRYING CAPABILITY. SEE FIG. 4 FOR EXPLANATION OF SYMBOLS. ORIGINAL SPECIMEN DIMENSIONS GIVEN IN INCHES

Thermoset Composites. (Carbon-epoxy)-to-titanium adhesively bonded splice joints are being utilized in aircraft primary structures. Joining carbon-epoxy to titanium using adhesive bonding has provided substantial weight savings. For these co-cured bonded joints, adhesive comparison testing led to the selection of FM300K, which is a film adhesive that contains an open-knit polyester carrier cloth to control bondline thickness. Figure 7 is a plot of the STEPLAP program output for typical joint analysis at room temperature. Joint configuration, ultimate loading, and adhesive strain are included. The adhesive strain plot illustrates the elastic trough on each step and the spike at each step end. Shear strains at the joint ends exceed the elastic strain of the bilinear FM300K stress-strain design curve (Fig. 4), and the shear stress plateaus at 39 MPa (5700 psi). For the room-temperature analysis, only a small length of the end steps is strained in the plastic range.

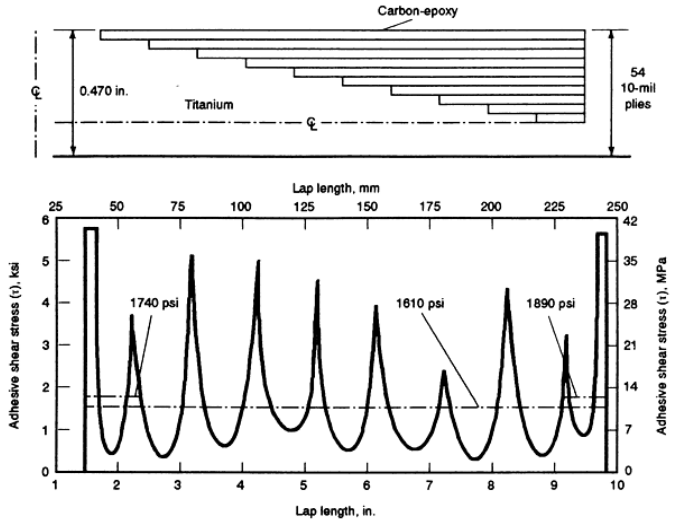

FIG. 7 ADHESIVE SHEAR STRESS DISTRIBUTION FOR AN ADHESIVELY BONDED STEPPED-LAP JOINT GENERATED USING THE STEPLAP COMPUTER PROGRAM

Thermoplastic Composites. AS4/APC-2 is one of the most frequently used and well characterized thermoplastic materials available. AS4/APC-2 is a semicrystalline material with excellent resistance to fluids (except fuel) and solvents and has low moisture absorption (AS4/APC-2 absorbs 0.25% moisture at 95% relative humidity). The two current methods used for bonding thermoplastics to metals or other composites are amorphous bonding and adhesive bonding. The primary joining technique used for thermoplastic semicrystalline adherends (such as AS4/APC-2) is to melt-fuse an amorphous thermoplastic film (Ultem) at the interface. This joining process (amorphous bonding) is accomplished by first adding a lower melt-fuse temperature resin onto the surface of the adherend to be subsequently joined (Fig. 8). Since the melting point of the amorphous film on the adherend surface and at the interface is about 300 °C (570 °F), the bonding does not affect the integrity of the AS4/APC-2 laminates, which are processed at 380 °C (720 °F). Amorphous bonded joints are structurally efficient and can produce room-temperature shear strengths in the 28 to 34 MPa (4000 to 5000 psi) range (Fig. 9). One limitation of amorphous joining is that the amorphous thermoplastic resin absorbs more water (1.3%) than semicrystalline thermoplastic composite laminates and the service temperature must be kept below 200 °C (390 °F) to prevent steam-pressure delamination damage of the joint (Fig. 10). A detailed explanation of the steam-pressure delamination phenomenon is described in Ref 6.

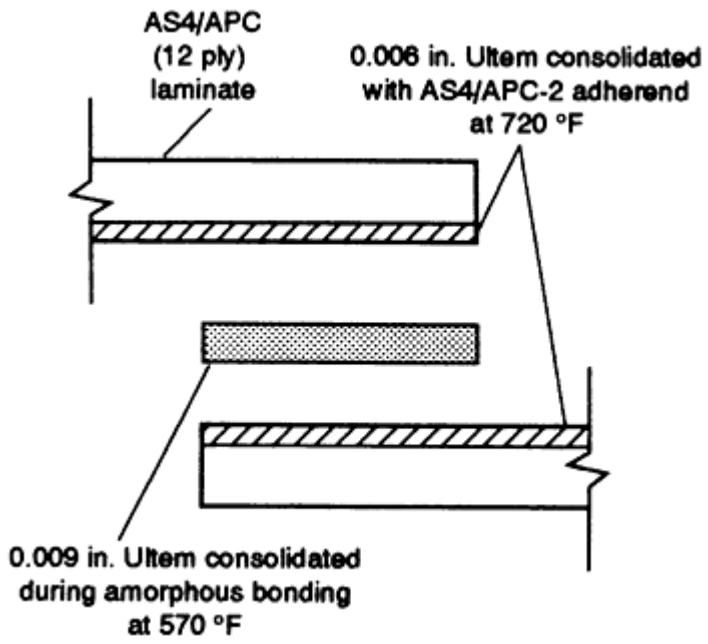

FIG. 8 SCHEMATIC OF THE AMORPHOUS BONDING PROCESS. ORIGINAL SPECIMEN DIMENSIONS GIVEN IN INCHES

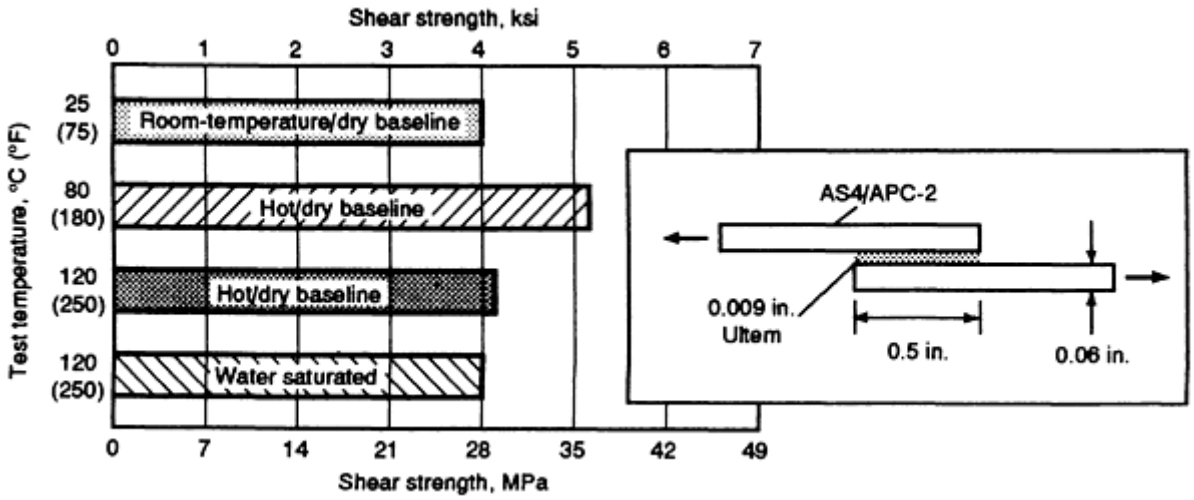

FIG. 9 SHEAR STRENGTHS OF SINGLE-LAP JOINTS PRODUCED BY AMORPHOUS BONDING

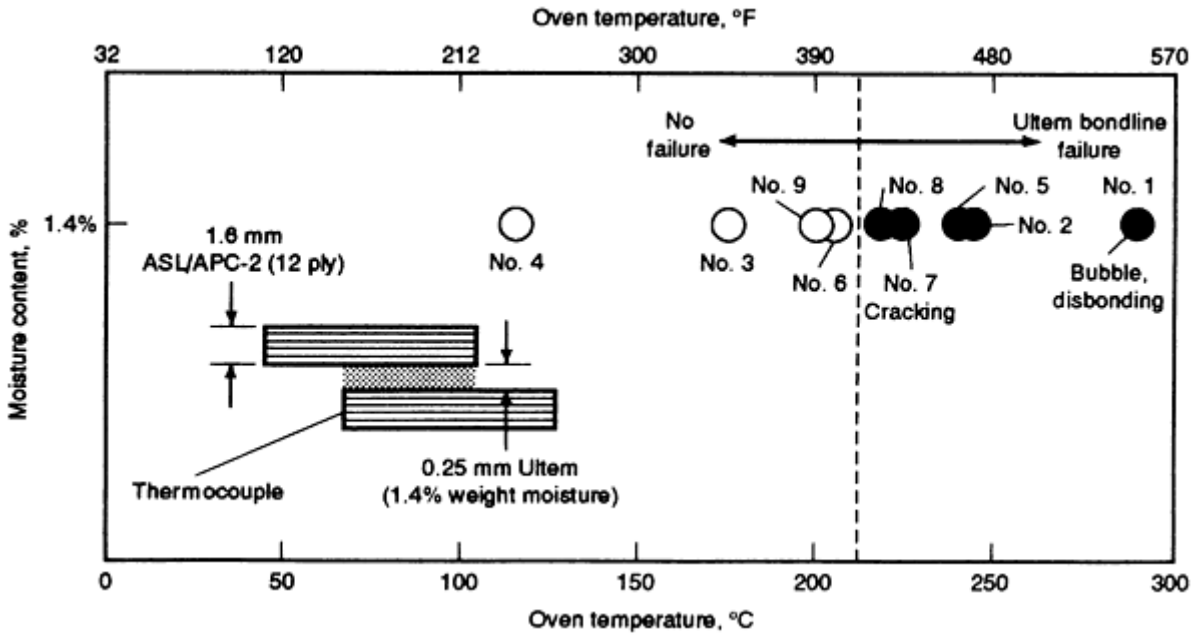

FIG. 10 THERMAL SHOCK (STEAM DELAMINATION) PROPERTIES FOR MOISTURE-SATURATED THERMOPLASTIC ADHERENDS JOINED BY AMORPHOUS BONDING WITH ULTEM. EACH CIRCLE REPRESENTS TESTING RESULTS OF ONE SPECIMEN. NUMBER INDICATES TESTING SEQUENCE.

Amorphous bonding of thermoplastics that requires an autoclave process (290 °C at ~700 kPa, or 550 °F at ~100 psi) is difficult to accomplish in a field-repair environment where minimal equipment is available. Therefore, adhesive bonding is a viable approach for attaching a metal or composite repair patch because the adhesive bond can be cured with a heating blanket (up to 175 °C, or 350 °F) and a vacuum bag. Epoxy adhesive systems do not bond as well to semicrystalline thermoplastics as to amorphous thermoplastics or thermoset composites. A test program was conducted to evaluate the benefit of adhesive bonding of an AS4/APC-2 thermoplastic with or without a layer of Ultem film. Two different adhesives were included in the evaluation --FM300 and FM73. The room-temperature dry test results indicated that the optimum combination was with the co-consolidated Ultem film and the FM73 adhesive. This combination

produced the highest lap shear strength (34 MPa, or 5000 psi), minimum test scatter, and a desirable cohesive failure mode. The quasi-isotropic AS4/APC-2 adherends used in the double-lap shear specimens (Fig. 1) were 2 mm (0.08 in.) thick. All adherends were surface treated by grit blasting followed by an isopropyl alcohol wipe and were bonded under vacuum bag pressure. The FM300 adhesive was processed at 150 °C (300 °F) for 4 h, and the FM73 adhesive was processed at 120 °C (250 °F) for 2 h. Prior to testing, all specimens were heated in a 95 °C (200 °F) oven until dry, stabilized weights were achieved.

Since previous shear strength tests of amorphous bonded thermoplastic joints showed that Ultem was sensitive to absorbed moisture, double-lap shear tests were conducted with and without Ultem for the FM73 adhesive at 25 °C (77 °F) and 60 °C (140 °F) in the dry condition and in the wet condition (95% relative humidity) at 60 °C (140 °F). The results summarized in Fig. 11 show that the moisture reduction factor is 28% at room temperature and 51% at 60 °C (140 °F) for the specimens with Ultem.

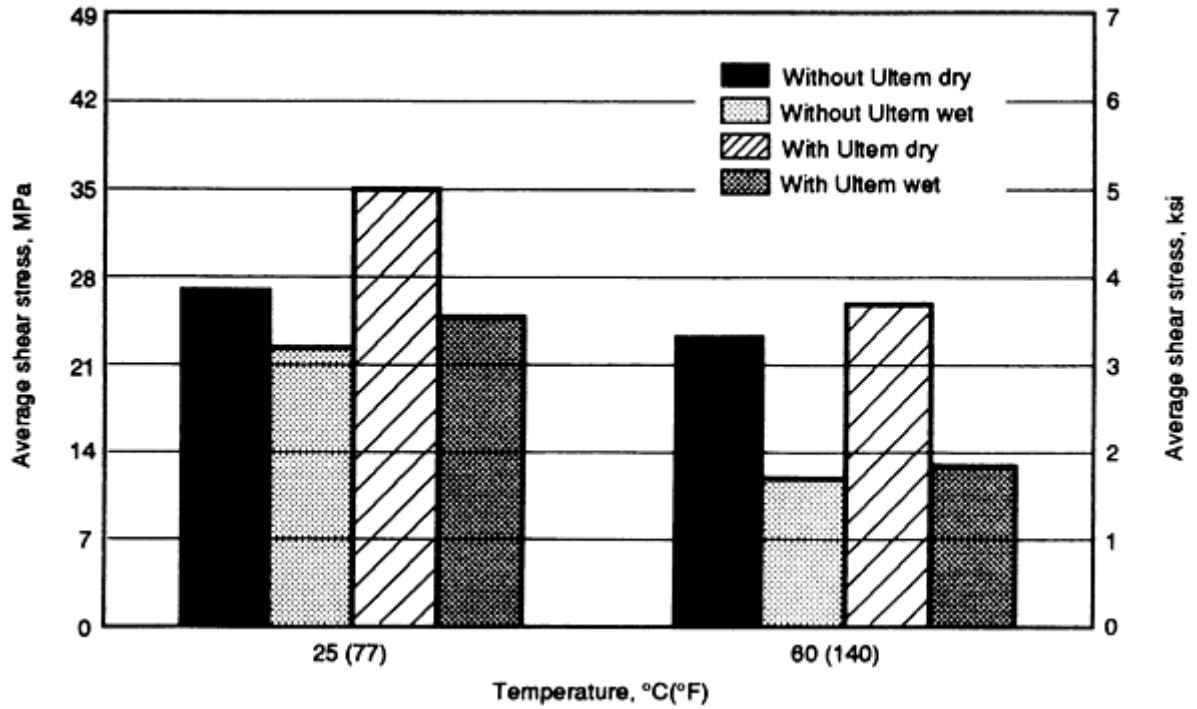

FIG. 11 EFFECTS OF MOISTURE CONTENT ON THE BOND STRENGTH OF AS4/APC-2 ADHERENDS JOINED BY AMORPHOUS BONDING WITH ULTEM

References cited in this section

1. L.J. HART-SMITH, "ANALYSIS AND DESIGN OF ADVANCED COMPOSITE BONDED JOINTS," DOUGLAS AIRCRAFT COMPANY, NASA CR-2218, JAN 1973, REPRINTED AUG 1974
2. L.J. HART-SMITH, DESIGN AND ANALYSIS OF ADHESIVE-BONDED JOINTS, PROC. *1ST AIR FORCE CONF. FIBROUS COMPOSITES IN FLIGHT VEHICLE DESIGN*, AFFDL-TR-72-130, AIR FORCE FLIGHT DYNAMICS LABORATORY, 1972, P 813-856
3. L.J. HART-SMITH, ADVANCES IN THE ANALYSIS AND DESIGN OF ADHESIVE-BONDED JOINTS IN COMPOSITE AEROSPACE STRUCTURES, *14TH NATIONAL SAMPE SYMP. AND EXHIBITION*, SOCIETY FOR THE ADVANCEMENT OF MATERIAL AND PROCESS ENGINEERING, APRIL 1974, P 722-737
4. L.J. HART-SMITH, BONDED-BOLTED COMPOSITE JOINTS, *J. AIRCRAFT*, VOL 22, 1985, P 993-1000
5. L.J. HART-SMITH, ADHESIVELY BONDED JOINTS FOR FIBROUS COMPOSITE STRUCTURES, *JOINING FIBRE-REINFORCED PLASTICS*, F.L. MATTHEWS, ED., ELSEVIER, 1987, P 271-311
6. H.J. KIM AND R.E. BOHLMANN, "THERMAL SHOCK TESTING OF WET THERMOPLASTIC

Composite-to-Metal Joining

Raymond E. Bohlmann, McDonnell Douglas Aerospace-East

Bolted Joints

A composite-to-metal bolted joint was studied as an alternative to the high-load transfer bonded stepped-lap joint discussed earlier (Ref 7). The titanium seven-fastener design shown in Fig. 12 is 380 mm (15 in.) in length (about twice the length of the bonded design) and is 30% heavier than the baseline adhesively bonded joint design. A fastener load-distribution curve is shown in Fig. 13. The test specimen was designed for a zero margin at 150% of design limit load (DLL); failure occurred at 173% DLL. The specimen failed as predicted at the end fastener hole (fastener No. 1) in the high bypass strain area of the carbon-epoxy laminate.

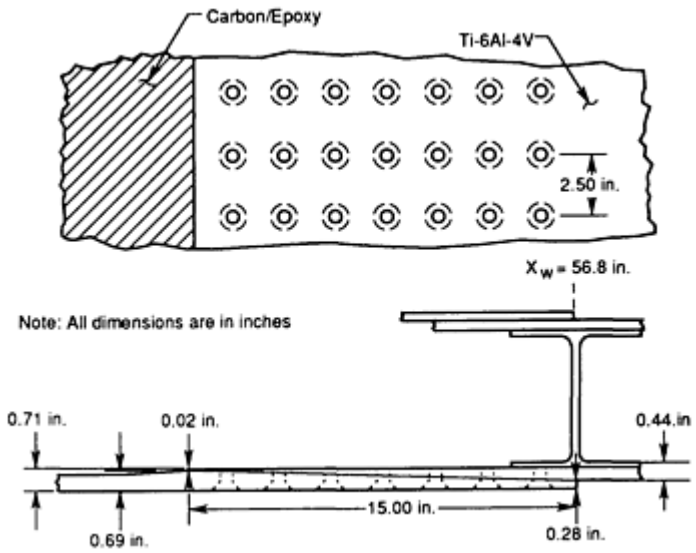

FIG. 12 COMPOSITE-TO-METAL BOLTED JOINT CONCEPT. ORIGINAL SPECIMEN DIMENSIONS GIVEN IN INCHES

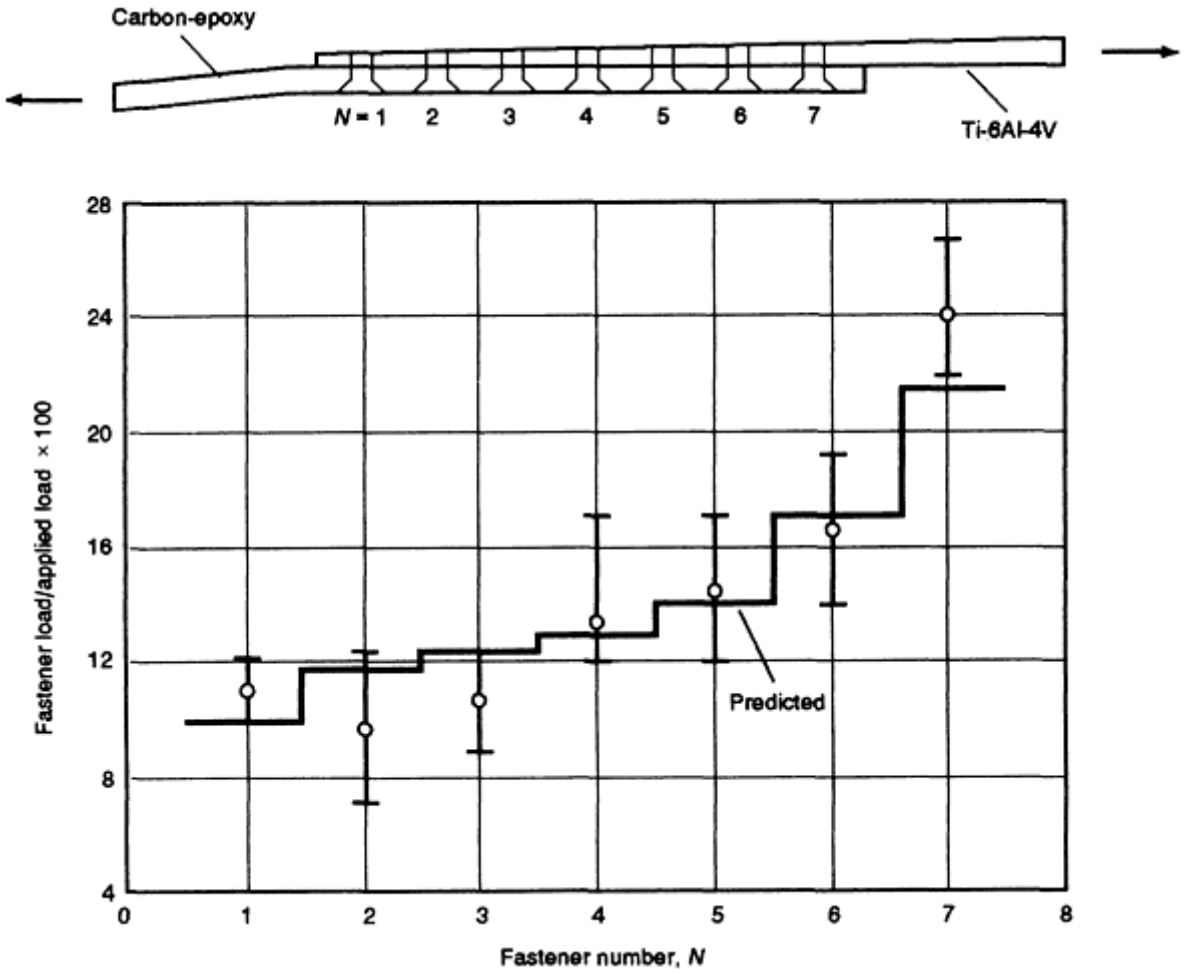

FIG. 13 CORRELATION BETWEEN PREDICTED RESPONSE AND ACTUAL TEST VALUES FOR BOLTED TITANIUM-TO-COMPOSITE (CARBON-EPOXY) JOINTS

Reference cited in this section

7. D.L. BUCHANAN AND S.P. GARBO, "DESIGN OF HIGHLY LOADED COMPOSITE JOINTS AND ATTACHMENTS FOR WING STRUCTURES," REPORT NADC-81194-80, NAVAL AIR DEVELOPMENT CENTER, AUGUST 1981

Composite-to-Metal Joining

Raymond E. Bohlmann, McDonnell Douglas Aerospace-East

Submersible Thick Composite-to-Metal Joint

The optimum composite-to-metal joining method for a thick (>25 mm, or 1.0 in.) composite compression-loaded submersible is a block compression joint (Fig. 14). The type of loading for a submersible structure is primarily hydrostatic pressure, which results in biaxial compression loading of 2:1 for cylinders and equal biaxial loading for spheres. Bolted joints are not recommended for submersible structures because they provide a path for a potential water leak. Submersibles made from composites for significant depth operation require thick composite walls that cannot be readily joined by adhesive bonding. Bonded joints are best suited for joining thin structures (<2.5 mm, or 0.10 in.) where peeling

stresses are acceptable. Resin-matrix composites have good in-plane properties (fibers are in-plane) but low interlaminar properties and are weak in resisting peel-type loads.

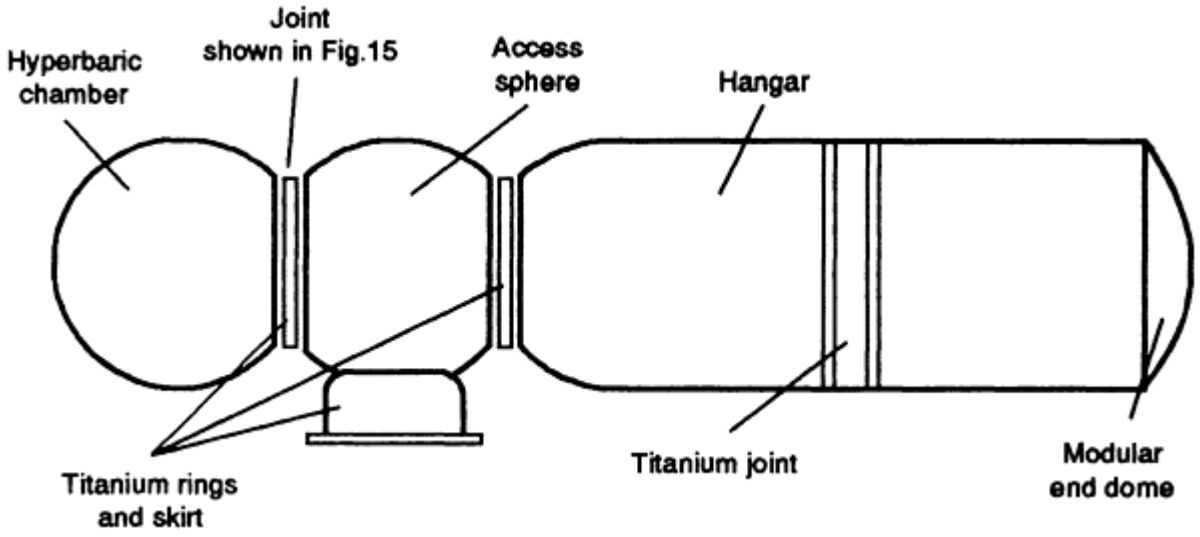

FIG. 14 SCHEMATIC OF THE MAN-RATED DEMONSTRATION ARTICLE (MRDA). SEE ALSO FIG. 15.

A Defense Advanced Research Projects Agency (DARPA) Man-Rated Demonstration Article (MRDA) is being developed (Ref 8). The MRDA is composed of a spherical hyperbaric chamber, a spherical access chamber, a cylindrical hangar section, and a modular end dome (Fig. 14). These components are joined to form a single structure; the joint assemblies used to join the composite spherical elements are made from titanium. The stress state in the regions where the titanium and composite material are in contact are very complex. Analysis of the joint region of the composite spheres indicates that small changes in manufacturing tolerances create significant strain concentrations in the composite spherical hyperbaric chamber. In this region, strains have been shown to be particularly high in the sphere at the point where it contacts the titanium joint. The joint region of concern is shown in Fig. 15.

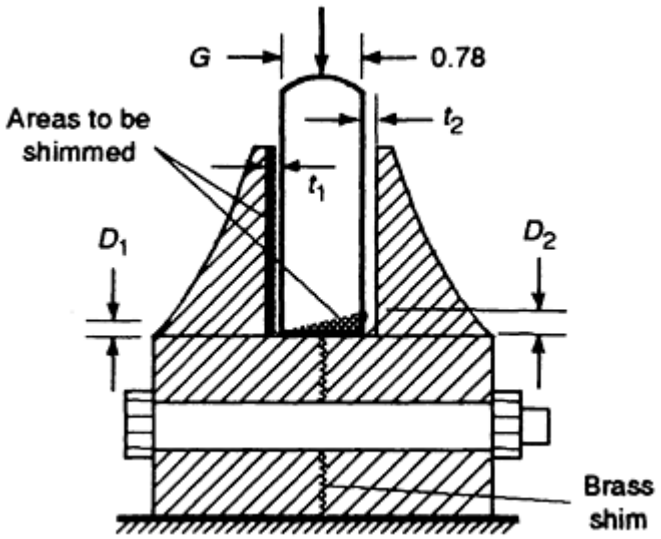

FIG. 15 CROSS-SECTIONAL VIEW OF THE MODULAR COMPOSITE SPHERE JOINT IN THE MRDA SHOWN IN FIG. 14

The tolerance variables considered in this investigation were the thickness of the fiberglass tabs and the perpendicularity between the composite sphere tabs and the composite sphere ends, as shown in the figure accompanying Table 1. Since the fiberglass tabs were to serve as sacrificial material to be machined for fit-up between the sphere and joint, two possible machining conditions were considered. The first condition was to have equal amounts of fiberglass (1.5 mm, or 0.060 in.) on each side of the composite sphere. The second condition was to have all machining performed on the inside of the sphere and resulting in full tab thickness on the outside of the sphere (~3 mm, or 0.12 in.) and essentially no tab material on the inside.

TABLE 1 TEST COUPON TOLERANCES USED TO STUDY COMPOSITE-TO-METAL JOINTS IN THE MRDA SHOWN IN FIG. 14

Original dimensions given in inches (1 in. = 25 mm)

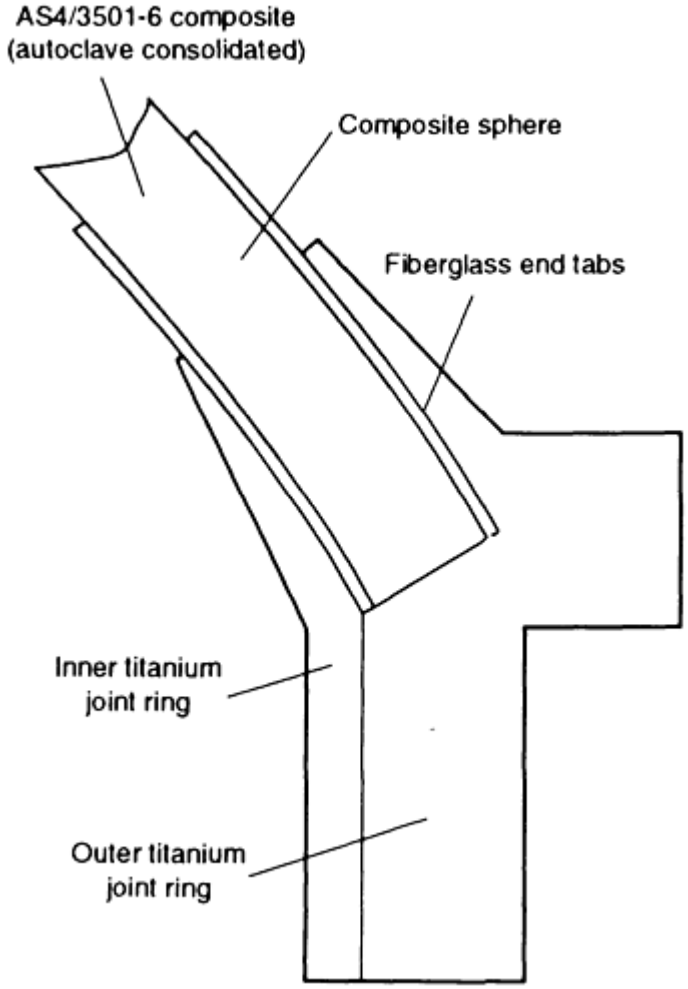

TEST CASE	EVALUATION OBJECTIVE	LATERAL GAP (G), IN.	LEFT-SIDE GAP (D_1), IN.	RIGHT-SIDE GAP (D_2), IN.	END TAB THICKNESS, IN.		END SHIM
					T_1	T_2	
1A,B	BASELINE, NOMINAL CASE	0	0	0	0.06	0.06	**NO**
2	MAXIMUM END TAB THICKNESS	0	0	0	0.02	0.12	**NO**
3	EFFECT OF END TAPER	0	0	0.020	0.06	0.06	**NO**
4	EFFECT OF SEVERE END TAPER	0	0	0.040	0.06	0.06	**NO**
5	LATERAL GAP/LIQUID SHIM	0.02	0	0	0.06	0.06	**NO**
6	LATERAL GAP/TAPER LIQUID SHIM	0.02	0	0.020	0.06	0.06	**NO**
7	END TAPER AND LIQUID SHIM	0	0.06	0.080	0.06	0.06	**YES**
8	END TAPER AND LIQUID SHIM	0	0	0.020	0.06	0.06	**YES**
9	**BASELINE, TEST-TO-FAILURE**	**0**	**0**	**0**	**0.06**	**0.06**	**NO**

For the second tolerance condition, out-of-perpendicularity between the sphere end and the joint, which may result from machining or fitup, occurs where the end of the sphere sits in the titanium joint. For the best condition, the entire end of the sphere would contact the joint with no clearance in the fit. Considering the spherical geometry and size of both components, there is the possibility of a clearance in this region rather than intimate contact. To simulate both tolerance conditions, a series of rectilinear coupons to be loaded in uniaxial compression were machined. Table 1 summarizes the test coupon tolerances.

The quasi-isotropic AS4/3501-6 unidirectional tape thermoset compression specimens 20 mm (0.78 in.) thick were autoclave consolidated and then tested. The results of the complete test program are summarized in Ref 8. Only two of the nine specimens tested will be discussed here. These include test case No. 3 (see Table 1), which featured a 0.5 mm (0.02 in.) end taper and test case No. 9, which is a no-gap baseline specimen. The design goal of these tests was to evaluate the assembly up to a gage section strain of 6700 microstrain.

The results of test case No. 3 with the 0.5 mm (0.02 in.) showed significant strain variation at the load introduction end and only minor strain differences in the gage region. After unloading the specimen, no damage was observed. The results of test case No. 9, the baseline with no end taper, showed that the gage section strains were 13,500 microstrain when failure occurred in the gage region. A failed test specimen from test case No. 9 is shown in Fig. 16. An encouraging result of this test is that the 13,500 microstrain is the same level obtained in testing thin-section composites, indicating that thick-section compression properties are not reduced.

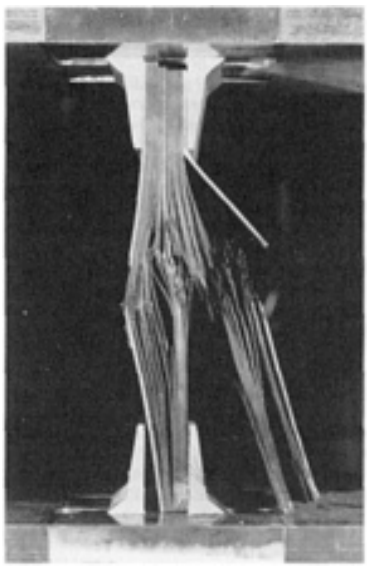

FIG. 16 PHOTOGRAPH OF A FAILED SPECIMEN FROM TEST CASE NO. 9 (SEE TABLE 1)

Reference cited in this section

8. E.T. CAMPONESCHI, R.E. BOHLMANN, J. HALL, AND T.T. CARR, "EFFECT OF ASSEMBLY ANOMALIES ON THE STRAIN RESPONSE OF COMPOSITES IN THE SPHERE JOINT REGION OF THE DARPA MAN RATED DEMONSTRATION ARTICLE," CDNSWC-SME-92/22, DEFENSE ADVANCED RESEARCH PROJECT AGENCY, ARLINGTON, VA, 4 MARCH 1992

Raymond E. Bohlmann, McDonnell Douglas Aerospace-East

References

1. L.J. HART-SMITH, "ANALYSIS AND DESIGN OF ADVANCED COMPOSITE BONDED JOINTS,"

DOUGLAS AIRCRAFT COMPANY, NASA CR-2218, JAN 1973, REPRINTED AUG 1974

2. L.J. HART-SMITH, DESIGN AND ANALYSIS OF ADHESIVE-BONDED JOINTS, PROC. *1ST AIR FORCE CONF. FIBROUS COMPOSITES IN FLIGHT VEHICLE DESIGN,* AFFDL-TR-72-130, AIR FORCE FLIGHT DYNAMICS LABORATORY, 1972, P 813-856
3. L.J. HART-SMITH, ADVANCES IN THE ANALYSIS AND DESIGN OF ADHESIVE-BONDED JOINTS IN COMPOSITE AEROSPACE STRUCTURES, *14TH NATIONAL SAMPE SYMP. AND EXHIBITION,* SOCIETY FOR THE ADVANCEMENT OF MATERIAL AND PROCESS ENGINEERING, APRIL 1974, P 722-737
4. L.J. HART-SMITH, BONDED-BOLTED COMPOSITE JOINTS, *J. AIRCRAFT,* VOL 22, 1985, P 993-1000
5. L.J. HART-SMITH, ADHESIVELY BONDED JOINTS FOR FIBROUS COMPOSITE STRUCTURES, *JOINING FIBRE-REINFORCED PLASTICS,* F.L. MATTHEWS, ED., ELSEVIER, 1987, P 271-311
6. H.J. KIM AND R.E. BOHLMANN, "THERMAL SHOCK TESTING OF WET THERMOPLASTIC LAMINATES," *37TH INT. SAMPE SYMP. EXHIBITION,* MARCH 1992
7. D.L. BUCHANAN AND S.P. GARBO, "DESIGN OF HIGHLY LOADED COMPOSITE JOINTS AND ATTACHMENTS FOR WING STRUCTURES," REPORT NADC-81194-80, NAVAL AIR DEVELOPMENT CENTER, AUGUST 1981
8. E.T. CAMPONESCHI, R.E. BOHLMANN, J. HALL, AND T.T. CARR, "EFFECT OF ASSEMBLY ANOMALIES ON THE STRAIN RESPONSE OF COMPOSITES IN THE SPHERE JOINT REGION OF THE DARPA MAN RATED DEMONSTRATION ARTICLE," CDNSWC-SME-92/22, DEFENSE ADVANCED RESEARCH PROJECT AGENCY, ARLINGTON, VA, 4 MARCH 1992

Welding of Plastics

Thomas H. North and Geetha Ramarathnam, University of Toronto

---

Introduction

POLYMERS AND POLYMERIC COMPOSITES are attractive because of their high strength-to-weight ratio, chemical inertness, and ability to be molded into complex shapes at relatively low cost. Polymers can be categorized as thermosets or thermoplastics.

In the case of thermoset resins, a chemical reaction occurs during processing and curing, that is, as a result of irreversible cross-linking reactions in the mold. Both molded thermoset and vulcanized elastomer components cannot be reshaped by means of heating, because degradation occurs. It follows that thermoset and vulcanized robber components can only be joined using adhesive bonding or mechanical fastening methods.

Thermoplastic resins, on the other hand, can be softened, as a result of the weakening of secondary van der Waals or hydrogen bonding forces between adjacent polymer chains. Therefore, thermoplastics can be remolded by the application of heat, and they can be fusion welded successfully.

Thermoplastics can be broadly divided into amorphous and crystalline resins, based on morphology, or structure. These materials are more attractive than thermosets because they:

- ARE CHEAPER
- ARE RECYCLABLE
- CAN BE JOINED USING FUSION WELDING
- HAVE GREATER DAMAGE TOLERANCE
- ARE EASY TO PROCESS
- HAVE GREATER IMPACT-RESISTANCE PROPERTIES

Table 1 lists the major thermoplastic resins. Filled thermoplastics are being increasingly used in semistructural applications. Fillers can reduce material cost, enhance mechanical properties, improve thermal properties, provide flame retardation, and so on.

TABLE 1 MAJOR CATEGORIES OF THERMOPLASTICS AND COMPOSITES

COMMODITY PLASTICS
POLYETHYLENE
POLYPROPYLENE
POLYVINYL CHLORIDE
POLYSTYRENE
ENGINEERING PLASTICS
ACETAL
ACRYLONITRILE-BUTADIENE-STYRENE
POLYMETHYL METHACRYLATE
POLYTETRAFLUOROETHYLENE
NYLON
POLYETHYLENE TEREPHTHALATE
POLYBUTYLENE TEREPHTHALATE
POLYPHENYLENE OXIDE
POLYCARBONATE
ADVANCED ENGINEERING PLASTICS
POLYETHERETHER KETONE
POLYETHERIMIDE
POLYETHER KETONE
POLYPHENYLENE SULFIDE
LIQUID-CRYSTAL POLYMER
POLYSULFONE
REINFORCED AND ADVANCED THERMOPLASTIC COMPOSITES
THERMOPLASTIC RESINS FILLED WITH SHORT, LONG, OR CONTINUOUS FIBERS OF GLASS, CARBON, OR ARAMID

Joining is generally the final step in any fabrication cycle. Some important review articles are represented by Ref 1, 2, 3, 4, 5, and 6. The effectiveness of the joining operation can have a large influence on the application of any polymer or composite material. A variety of polymer joining techniques are available. Figure 1 provides a classification of these different methods (Ref 4).

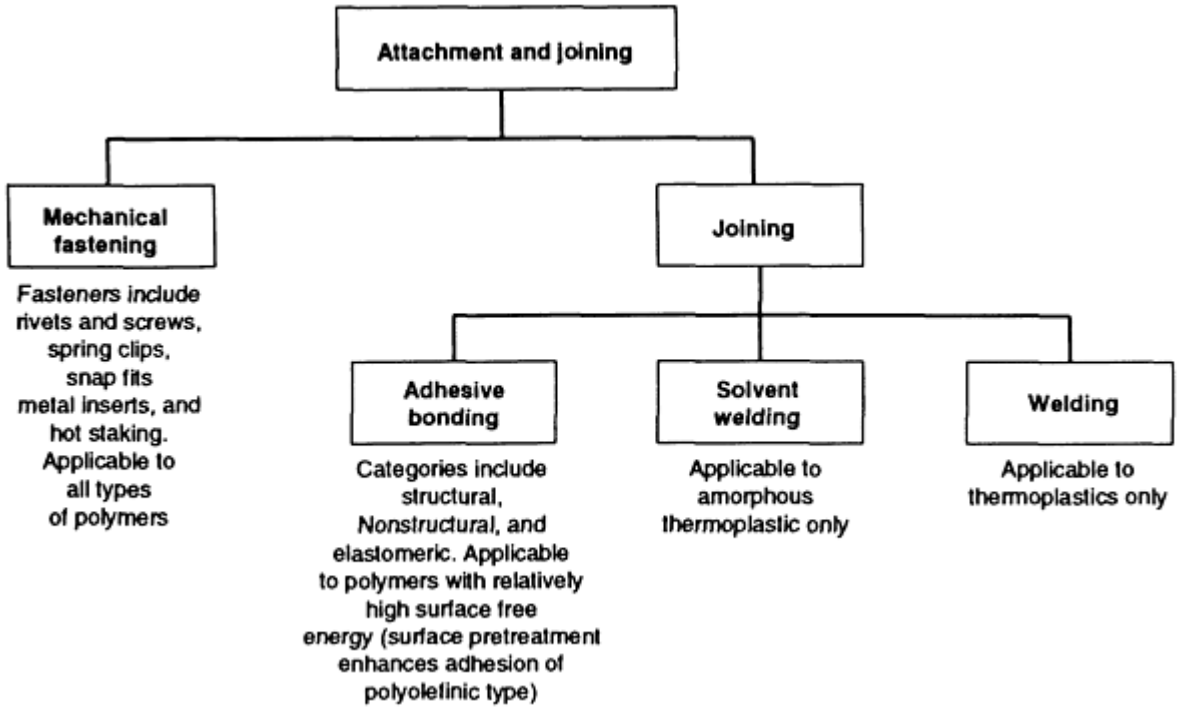

FIG. 1 CLASSIFICATION OF DIFFERENT JOINING METHODS. SOURCE: REF 4

Polymers are low-energy substrates, with surface free energies of less than approximately 50 mJ/m^2 (0.003 ft · lbf/ft^2) (Ref 7). The creation of a successful joint depends on four factors: the chemical nature of the polymer, the surface free energy, the surface topography, and contamination of the polymer surface by dust, oil, and grease. These factors markedly affect the effectiveness of the adhesive and solvent bonding methods. Fusion welding, however, is much more tolerant of aspects such as surface contamination and material variations from sample to sample.

Adhesives are thermoset-type polymers that are classified as structural, nonstructural, or elastomeric. Reference 7 provides additional details. Structural adhesives are generally used in load-bearing applications, in joints that have high strength-to-weight ratios. They are also used to improve resistance to both component fatigue and corrosion resistance. The principal disadvantages of adhesive bonding are that surface preparation is required prior to bonding, curing times can be long, the components cannot be disassembled following the joining operation, and health and/or safety hazards may be involved in their use. In spite of these problems, adhesive bonding is used extensively in numerous industries.

Mechanical fastening and adhesive bonding can be used to join both similar and dissimilar materials. For example, mechanical fastening is commonly used when joining a plastic to a metal (Ref 8), producing either permanent joints or connections that can be opened and sealed again. The advantages of this approach are that no surface treatment is required and disassembly of the components for inspection and repair is straightforward. The main limitations of this approach are increased weight, the presence of large stress concentrations around the fastener holes, and subsequent in-service corrosion problems (Ref 8). The typical applications of mechanical fastening are in the aerospace, automotive, and construction industry.

Polymeric materials that possess similar solubility parameters can be joined using solvent or fusion welding. Interdiffusion of polymer chains plays a major role in achieving intrinsic adhesion (Ref 9) and in promoting chain diffusion, either by applying a suitable solvent or by heating the polymer sample.

As mentioned previously, only thermoplastics can be joined using the fusion-welding process. The glass transition temperature, T_g, in amorphous polymers, and the melting temperature, T_m, in crystalline polymers must be exceeded so that the polymer chains can acquire sufficient mobility to interdiffuse. A variety of methods exist for welding thermoplastics and thermoplastic composites (Fig. 2). Thermal energy can be delivered externally via conduction, convection, and/or radiation methods, or internally via molecular friction caused by mechanical motion at the joint interface. In the case of external heating, the heat source is removed prior to the application of pressure, and longer

welding times are balanced by the greater tolerance to variations in material characteristics. Internal heating methods depend markedly on the material properties (Ref 10). Heating and pressure are applied simultaneously, and shorter welding times are generally involved during the joining process.

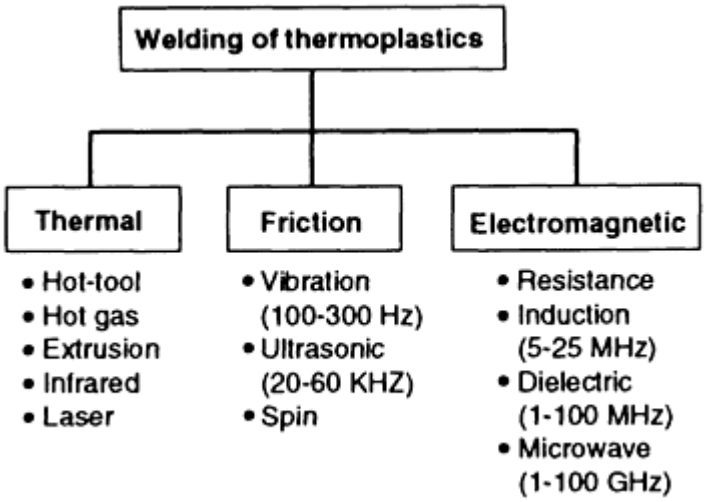

FIG. 2 CLASSIFICATION OF DIFFERENT WELDING METHODS FOR THERMOPLASTICS

Welding is accomplished in many stages. During the initial stage, the polymer-chain molecules become mobile and surface rearrangement occurs. This is followed by wetting and the diffusion of polymer chains across the interface. The final stage involves cooling and solidification. For linear random-coil chains, the mechanical energy required to separate the welded substrates, *G*, is given by the relation (Ref 11):

$$G = W(T,T,P,M) \qquad \textbf{(EQ 1)}$$

where *W* is the welding function to be determined, *t* is the time of contact, *T* is the temperature of welding, *P* is the pressure, and *M* is the molecular weight of the polymer.

In solvent welding, the application of a solvent at the bond line induces sufficient mobility for the polymer chains to interdiffuse (Ref 12, 13). Because the solvent must strongly plasticize the polymer surface, this joining technique is primarily applied to glassy amorphous thermoplastics, such as polycarbonate, acrylic, and polystyrene resins.

References

1. G. GEHARDSSON, THE WELDING OF PLASTICS, *WELD. REV.*, FEB 1983, P 17-22
2. M.N. WATSON, R.M. RIVETT, AND K.I. JOHNSON, "PLASTICS--AN INDUSTRIAL AND LITERATURE SURVEY OF JOINING TECHNIQUES," REPORT NO. 7846.01/85/471.3, THE WELDING INSTITUTE, ABINGTON, UK, 1986
3. H. POTENTE AND P. MICHEL, THE STATE OF THE ART DEVELOPMENT TRENDS IN THE WELDING OF PLASTICS, *PROC. 5TH ANNUAL NORTH AMERICAN WELDING RESEARCH CONFERENCE,* EWI AND AWS, 1989
4. V.K. STOKES, JOINING METHODS FOR PLASTICS AND PLASTIC COMPOSITES: AN OVERVIEW, *POLYM. ENG. SCI.*, VOL 29 (NO. 19), 1989, P 1310-1324
5. R.A. GRIMM, FUSION WELDING TECHNIQUES FOR PLASTICS, *WELD. J.*, MARCH 1990, P 23-28
6. G. MENGES, THE JOINING OF PLASTICS AND THEIR COMPOSITES, *PROC. LNT. CONF. ADVANCES IN JOINING NEWER STRUCTURAL MATERIALS*, IIW (MONTREAL), P 33-63

7. A.J. KINLOCH, *ADHESION AND ADHESIVES,* CHAPMAN AND HALL, 1987, P 101
8. D. CHANT, JOINING TECHNOLOGY FOR THERMOPLASTIC COMPOSITE STRUCTURES IN AEROSPACE APPLICATIONS, *PROC. INT. CONF. ADVANCES IN JOINING PLASTICS AND COMPOSITES,* THE WELDING INSTITUTE, CAMBRIDGE, 1991
9. S.S. VOYUTSKII, AUTOHESION AND ADHESION OF HIGH POLYMERS, WILEY INTERSCIENCE, 1963
10. A. BENATAR, MATERIAL CHARACTERISTICS FOR WELDING, *PROC. 5TH ANNUAL NORTH AMERICAN WELDING RESEARCH CONFERENCE,* EWI AND AWS, 1989
11. R.P. WOOL, B.-L. YUAN, AND O.J. MCGAREL, *POLYM. ENG. SCI.,* VOL 29 (NO. 19), 1989, P 1340-1367
12. W.V. TITOW, CHAPTER 12, *SOLVENT WELDING OF PLASTICS,* APPLIED SCIENCE PUBLISHERS, LONDON, P 181-196
13. M. LICATA AND E. HAAG, SOLVENT WELDING WITH POLYCARBONATE, *PROC. SPE 44TH ANTEC MEETING,* SOCIETY OF PLASTICS ENGINEERS, 1986, P 1092-1094

Welding of Plastics

Thomas H. North and Geetha Ramarathnam, University of Toronto

Fusion-Welding Techniques

The commonly available fusion-welding techniques will be described in terms of the basis of the joining method, the key joining parameters involved in the process operation, and the application areas of each joining method.

Hot-Tool Welding

Hot-tool welding occupies a central position among the different thermal fusion-welding techniques. This method can provide joint strength that is equal to that of the base material. The surfaces to be joined are brought to the melting or softening temperature by direct contact with a heated tool. Once the desired molten film thickness is produced, the heated tool is removed, the melted surfaces are brought together, and the joint is allowed to cool and consolidate under pressure. Typical welding times range from 10 s to 60 min, depending on the size of the component being joined.

The surfaces of the heated tool are usually coated with polytetrafluoroethylene (PTFE) to prevent the polymers from sticking to the platen. However, the PTFE coating generally restricts the maximum tool surface temperature to 260 °C (500 °F). Some research on heated-tool welding has involved hot-plate temperatures in excess of 350 °C (660 °F) for very short heating times (4 to 6 s). This thermal cycle has been made possible through the use of high-temperature aluminum-bronze heating elements (Ref 1).

The hot-tool welding process can be described by four phases (Fig. 3). During phase I, the surfaces of the material are brought in contact with the heated tool and are held under pressure. This pressure is maintained until a molten film appears. In phase II, the contact pressure between the heated tool and the substrate is reduced to increase the molten-film thickness. The rate of increase of melted-film thickness depends on the thermal conductivity of the polymer. Phase III is the change-over (removal of the hot tool) time, whereas phase IV is the joining and cooling under pressure. The amount of melted-polymer displacement from the weld zone is controllable. For example, computer-controlled machines will allow preselection of the pressure or displacement values that are applied during joining (Ref 15). In this connection, detailed mathematical analyses of the hot-tool welding process have already been carried out (Ref 15, 17).

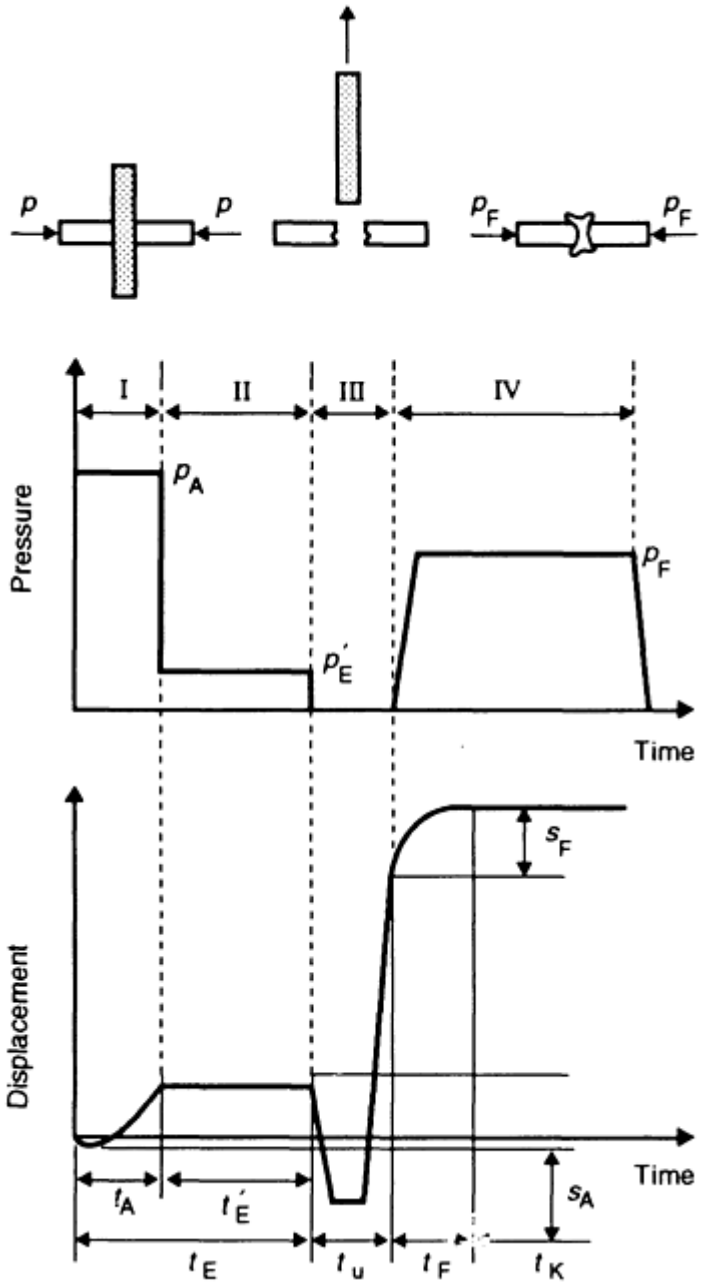

FIG. 3 PRESSURE-TIME AND DISPLACEMENT-TIME GRAPH SHOWING DIFFERENT PHASES OF HOT-TOOL WELDING PROCESS. P_A, P_E, AND P_F ARE MATCHING, HEATING, AND JOINING PRESSURES, RESPECTIVELY. T_E, T_U, T_F, AND T_K REPRESENT HEATING, CHANGE-OVER, JOINING, AND COOLING TIMES, RESPECTIVELY. S_F, REDUCTION IN LENGTH OF THE PART BEING JOINED; S_A, DISPLACEMENT PATH PRODUCED DURING TIME T_E. SOURCE: REF 16

The key joining parameters of hot-tool welding are:

- THE HEATED-TOOL TEMPERATURE, WHICH DEPENDS ON THE POLYMER BEING WELDED
- THE PRESSURE APPLIED AND THE DURATION OF PHASE I. (HOWEVER, HIGH PRESSURE DURING PHASE IV WILL PRODUCE TOO MUCH LATERAL FLOW AND POLYMER-CHAIN ORIENTATION IN THE COMPLETED JOINT, RESULTING IN ADVERSE MECHANICAL PROPERTY EFFECTS, AS DESCRIBED IN REF 15 AND 16)
- THE THERMAL CONDUCTIVITY AND SPECIFIC HEAT OF THE POLYMER AND THE SIZE

AND WALL THICKNESS OF THE PART BEING JOINED, WHICH ARE THE PARAMETERS THAT DETERMINE THE DURATION OF PHASE II

- THE TOOL TRANSFER, OR CHANGE-OVER, TIME, WHICH MUST BE MINIMIZED SO THAT COOLING OF THE MOLTEN LAYER DOES NOT OCCUR (TO AVOID INHIBITING POLYMER-CHAIN INTERDIFFUSION)

Applications. All thermoplastic materials can be joined using hot-tool welding. Components that have large, flat surface areas are commonly butt welded using this technique. It is also possible to join dissimilar materials through the use of two heated platens that are at different temperatures (Ref 14). The weldability factor, in this case, is the degree of compatibility.

Hot-tool welding can be readily automated. Portable equipment is primarily used for on-site weld repairs. Small amounts of joint misalignment prior to joining have negligible effects on the weld quality. Hot-tool welding is used in a variety of industrial applications. The automotive sector, for example, uses it to weld polypropylene (PP) copolymer cases for batteries and to weld rear-light casings of acrylonitrile-butadiene-styrene (ABS) joints to polymethyl methacrylate (PMMA) or polycarbonate (PC) lenses. Hot-tool welding is also employed when welding thermoplastic tanks and when joining large-diameter polyethylene (PE) pipeline to transport gas, water, and sewage wastes.

Hot-Gas Welding

A stream of hot air or gas (nitrogen, air, carbon dioxide, hydrogen, or oxygen) is directed toward the filler and the joint area using a torch (Ref 18). A filler rod or tape (of a similar composition to the polymer being joined) is gently pushed into the gap between the substrates (Fig. 4). A variety of nozzles are available for different applications, and either automated or manual welding can be carried out. During welding, the gas temperature can range from 200 to 600 °C (390 to 1110 °F), depending on the polymer being joined.

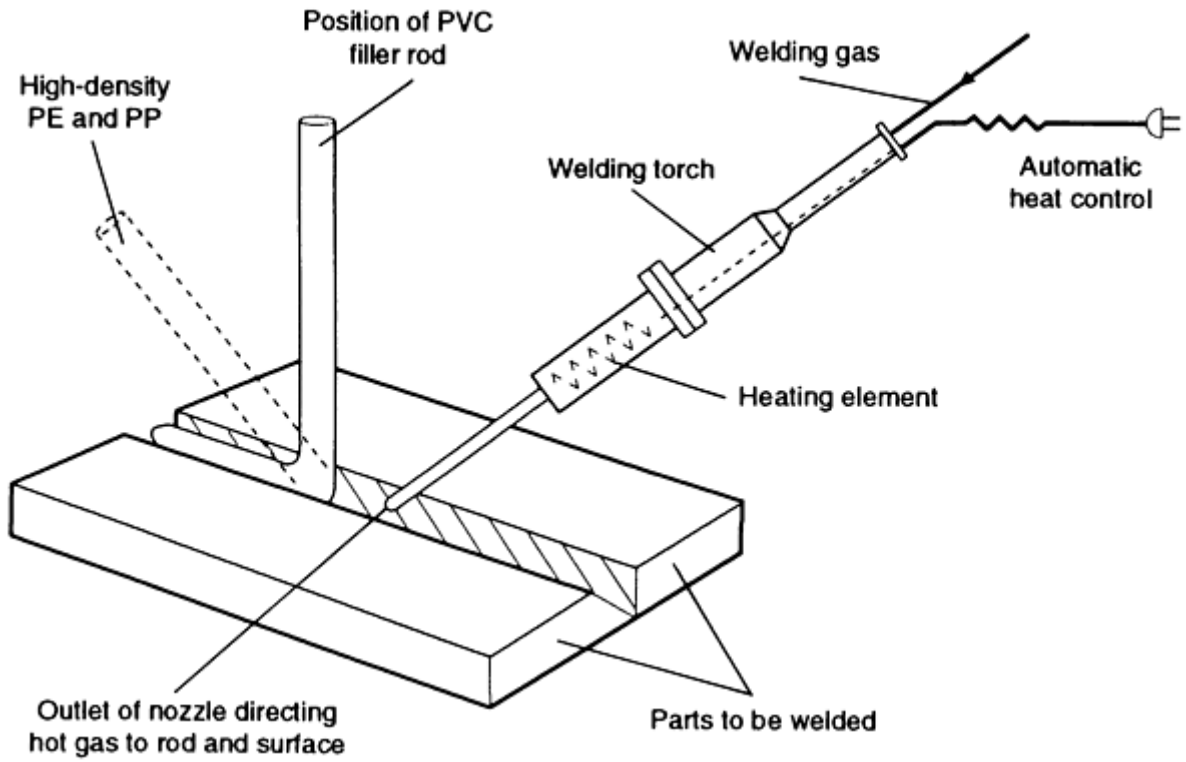

FIG. 4 SCHEMATIC OF HOT-GAS WELDING, SHOWING THE CORRECT POSITION OF TORCH AND FILLER ROD FOR DIFFERENT THERMOPLASTICS. SOURCE: REF 19

The key joining parameters of the hot-gas welding process are:

- GAS TEMPERATURE, WHICH DEPENDS ON THE TYPE OF POLYMER BEING JOINED, AND WHICH DETERMINES THE HEATING ELEMENT, NOZZLE DIMENSIONS, AND GAS/AIR FLOW RATES THAT ARE USED
- WELDING SPEED AND DOWNWARD PRESSURE OF THE WELDING ROD (MANUAL JOINING OPERATIONS)

Applications. The principal application areas involve the continuous welding of polyolefin tanks and containers, the welding of polyvinyl chloride (PVC), ABS, PE, and PP pipe sections, the sealing of packaging materials, and the field repair of PVC and other thermoplastic resins that are used in the construction and automotive industries. Hot-gas welding has a disadvantage in that the temperature of the hot gas/air is much higher than the melting point of the polymer being joined. Therefore, the process has poor energy efficiency, and degradation of the polymer substrate is possible unless care is taken. Polymers that oxidize at temperatures close to their melting points cannot be welded by this technique.

Extrusion Welding

Extrusion welding is similar to hot-gas welding. The weld area is heated using hot air, and plasticized filler material is extruded into V-shaped or lap seam joints under pressure by means of a welding shoe (Ref 20, 21). The preheating and welding-shoe assemblies are connected to the welding head, and the welding speed is kept constant by an automatic traversing unit that has adjustable motor speeds (Fig. 5).

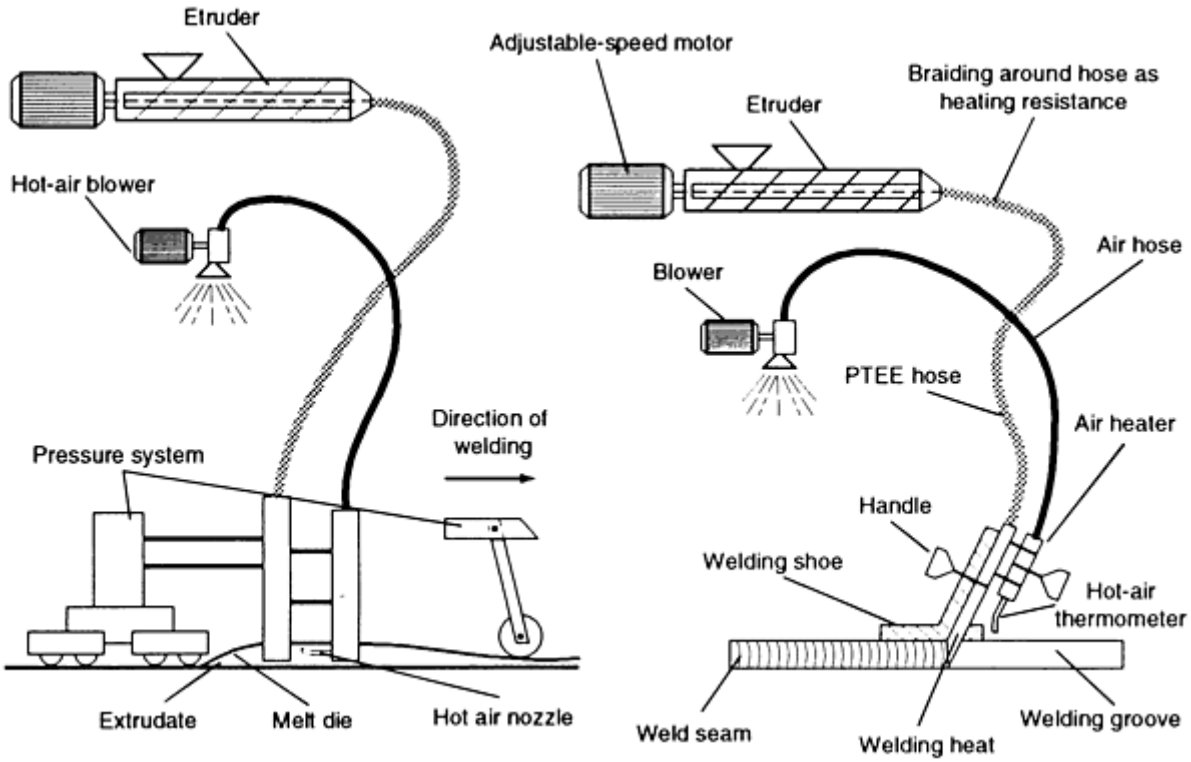

FIG. 5 SCHEMATIC OF VARIANTS OF EXTRUSION WELDING PROCESS. SOURCE: REF 20

The key joining parameters of this process are the:

- FEED ANGLE AND TEMPERATURE OF THE HOT GAS
- TEMPERATURE AND PRESSURE OF THE EXTRUDATE
- RELATION BETWEEN THE EXTRUDATE DELIVERY RATE AND THE WELDING SPEED
- HORIZONTAL AND VERTICAL FORCES APPLIED AT THE WELDING SHOE

- WELD LENGTH AND TIME REQUIRED TO COMPLETETHE JOINT

Applications. Extrusion welding is primarily used for producing long seams in thick-section polyolefin components. This joining technique is particularly useful when welding large container sections.

Focused Infrared Welding

This joining technique uses a quartz lamp and focuses the infrared (IR) radiation using highly polished, parabolic, elliptical reflectors. The focused IR method directs a precise, high-intensity reciprocating IR beam of a width that ranges from 1.5 to 3.0 mm (0.06 to 0.12 in.) onto the joint interface (Ref 22). A robotic fixture scans the IR beam back and forth over the two adherend surfaces, and when the joint line reaches the desired temperature, the heat source is removed and the substrates are forged together in a press. Sensors are mounted adjacent to the lamp fixture and are calibrated so that they selectively measure the adherend interface temperature only (Fig. 6).

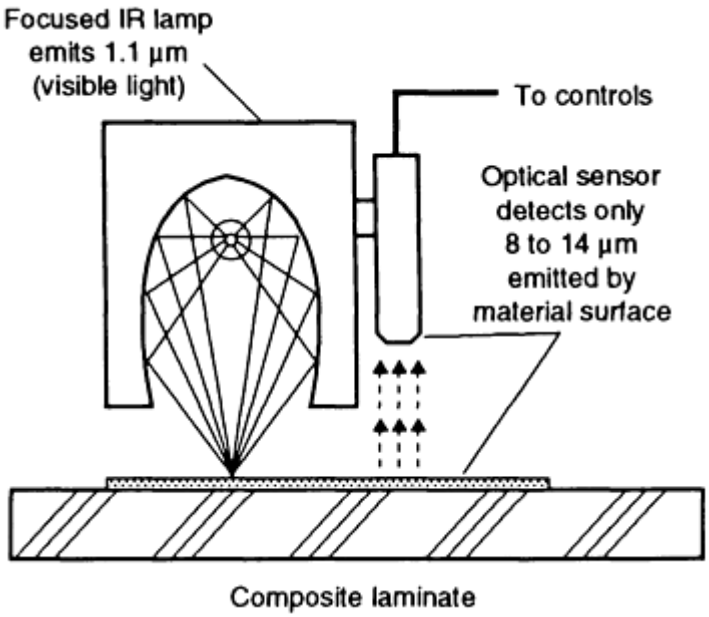

FIG. 6 SCHEMATIC OF FOCUSED IR LAMP AND OPTICAL SENSOR. SOURCE: REF 22

The welding of polyphenylene sulfide, using this IR technique, has been reported (Ref 23). Focused IR welding can be automated. Because this is a relatively new joining process, a detailed analysis of process operation has yet to be conducted.

The key joining parameters of this welding process are the:

- RADIATION DENSITY AND TIME OF IRRADIATION
- RADIATION ABSORPTION, REFLECTION, AND TRANSMISSION PROPERTIES OF THE POLYMER, WHICH DETERMINE THE RATE OF THE TEMPERATURE RISE IN THE IRRADIATED MATERIAL
- FLOW TEMPERATURE AND THERMAL CONDUCTIVITY OF THE IRRADIATED POLYMER
- RECIPROCATION RATE OF THE RADIATOR, WHICH DEPENDSON THE TYPE OF POLYMER BEING JOINED, AND ON THE PART SIZE
- RETRACTION RATE OF THE RADIATIVE HEAT SOURCE AND CLOSING SPEED OF THE PRESS (IN ORDER TO AVOID COOLING THE MELTED MATERIAL AT THE JOINT INTERFACE)

Applications. This technique can be used to join both simple and complex joint configurations when a noncontacting method of heating is essential. In addition, reinforced-fiber disruption can be minimized when advanced thermoplastic composites are joined.

Laser Welding

Limited information is available on laser welding. Carbon dioxide (CO_2) lasers induce excitation of the vibrational modes and, hence, heating of the irradiated organic material (Ref 24, 25). At low power input levels, satisfactory weld penetration can be achieved. The technique also provides high welding speeds and produces very small heat-affected zones (HAZ). Typical joining conditions involve an energy input of 100 W using a wavelength of 10.6 μm. The absorption of laser radiation depends on the relation:

$$I(Z) = I_0 \text{ EXP } (-\alpha Z) \qquad \textbf{(EQ 2)}$$

where z is the distance into the sample at which the laser intensity I (W/cm^2) is measured, I_0 is the laser intensity at the surface of the polymer sample (at $z = 0$), and α (1/cm) is the absorption coefficient. The laser power, P (watts) required for any given material to depth a (meters) can be derived using the relation (Ref 25):

$$p = \frac{vWa(\rho C_p T_m + \Delta H_m)}{0.484} \qquad \textbf{(EQ 3)}$$

where v is the welding speed (m/s), W is the weld width (m), ρ is the density of polymer (ks/m^3), C_p is the heat capacity (J/kg · °C), T_m is the melting temperature (°C), and ΔH_m is the latent heat of melting (J/m^3).

There is not much that has been published concerning the commercial application of this joining method.

References cited in this section

1. G. GEHARDSSON, THE WELDING OF PLASTICS, *WELD. REV.*, FEB 1983, P 17-22
14. K. GABLER AND H. POTENTE, WELDABILITY OF DISSIMILAR THERMOPLASTICS--EXPERIMENTS IN HEATED TOOL WELDING, *J. ADHES.*, VOL 11, 1980, P 145-163
15. H. POTENTE AND P. TAPPE, SCALE-UP LAWS IN HEATED TOOL BUTT WELDING OF HDPE AND PP, *POLYM. ENG. SCI.*, VOL 29 (NO. 23), 1989, P 1642-1648
16. H. POTENTE AND J. NATROP, COMPUTER AIDED OPTIMIZATION OF THE PARAMETERS OF HEATED TOOL BUTT WELDING, *POLYM. ENG. SCI.*, VOL 29 (NO. 23), 1989, P 1649-1654
17. A.J. POSLINSKI AND V.K. STOKES, ANALYSIS OF THE HOT-TOOL WELDING PROCESS, *PROC. SPE 50TH ANTEC MEETING*, 1992, SOCIETY OF PLASTICS ENGINEERS, P 1228-1233
18. H. GUMBLETON, HOT GAS WELDING OF THERMOPLASTICS--AN INTRODUCTION, *JOIN. MAT.*, VOL 5, 1989, P 215-218
19. "RECOMMENDED PRACTICES FOR JOINING PLASTIC PIPING," DOCUMENT XVI-322-78-E, IIW
20. P. MICHEL, "AN ANALYSIS OF THE EXTRUSION WELDING PROCESS," *POLYM. ENG. SCI.*, VOL 29 (NO. 19), 1989, P 1376-1382
21. M. GEHDE AND G.W. EHRENSTEIN, STRUCTURAL AND MECHANICAL PROPERTIES OF OPTIMIZED EXTRUSION WELDS, *POLYM. ENG. SCI.*, VOL 31 (NO. 7), 1991, P 495-501
22. H. SWARTZ AND J.L. SWARTZ, FOCUSSED INFRARED--A NEW JOINING TECHNOLOGY FOR HIGH PERFORMANCE THERMOPLASTICS AND COMPOSITE PARTS, *PROC. 5TH ANNUAL NORTH AMERICAN WELDING RESEARCH CONFERENCE*, EWI AND AWS, 1989
23. H. POTENTE, P. MICHEL, AND M. HEIL, INFRARED RADIATION WELDING: A METHOD FOR WELDING HIGH TEMPERATURE RESISTANT THERMOPLASTICS, *PROC. SPE 49TH ANTEC MEETING*, SOCIETY OF PLASTICS ENGINEERS, 1991, P 2502-2504

24. W.W. DULEY, IN *LASER PROCESSING AND ANALYSIS OF MATERIALS,* PLENUM PRESS, 1983
25. W.W. DULEY AND R.E. MUELLER, CO_2 LASER WELDING OF POLYMERS, *POLYM. ENG. SCI.*, VOL 32 (NO. 9), 1992, P 582-585

Thomas H. North and Geetha Ramarathnam, University of Toronto

Friction Welding

Frictional heating is important in the ultrasonic, vibration, and spin-welding methods. In ultrasonic welding, heat generation depends on the storage and loss moduli of the polymer. In the cases of vibration and spin welding, heat generation depends on the frictional coefficient of the polymer material, and on the storage and loss moduli values (Ref 10). As would be expected, joining processes that depend on direct heat generation at the bond line are more efficient in terms of energy utilization, and the heating and pressure cycles are applied simultaneously.

Vibration Welding

Samples are clamped together and vibrated using an oscillating motion under pressure (Fig. 7). Frictional heating is due to one solid being rubbed against the other, and to the shear heating of the melt. Vibratory motion is applied until the polymer melts at the bond line. Then, the motion is terminated and melted polymer at the joint interface is cooled under pressure.

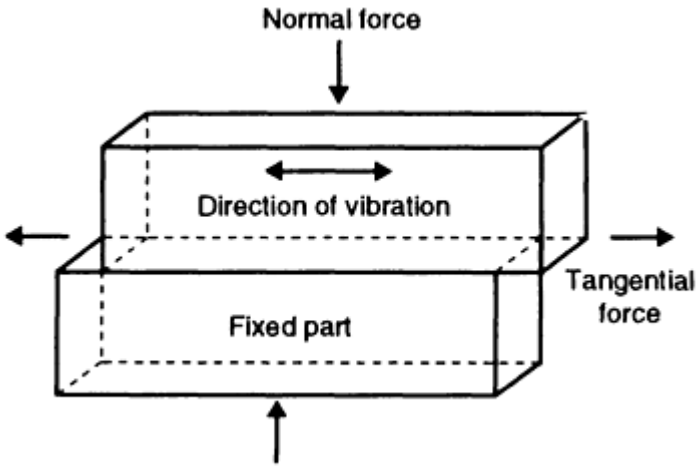

FIG. 7 SCHEMATIC OF VIBRATION WELDING PROCESS

Two types of vibration welding machines are available: linear machines, in which the center of motion lies outside of the molded part; and angular machines, in which the center of motion lies within the molded part (Ref 3). Linear vibration welding is more popular, because of its ability to weld long and narrow molded parts.

During welding, the samples are fixed to upper and lower platens, and the lower platen is kept fixed while the upper platen is vibrated using an electromagnetic or hydraulic drive system at frequencies ranging from 100 to 500 Hz. The vibrational amplitude ranges from 0.1 to 5.0 mm (0.004 to 0.2 in.), depending on the frequency used (Ref 26, 27).

The detailed features of the vibrational welding process have been studied, along with welding parameter optimization, by a number of investigators (Ref 28, 29, 30). It has been shown that the vibration welding process involves four distinct phases (Fig. 8). Phase I comprises the initial heating of the interface to the melting point as a result of coulomb friction. Phase II involves melting and unsteady material flow in the lateral direction. In phase III, melting and flow are at a steady

state, and weld penetration (the decrease in the melted zone width that is due to lateral flow) increases linearly with time. When the vibratory motion is terminated, weld penetration continues to increase until the material solidifies, which represents phase IV.

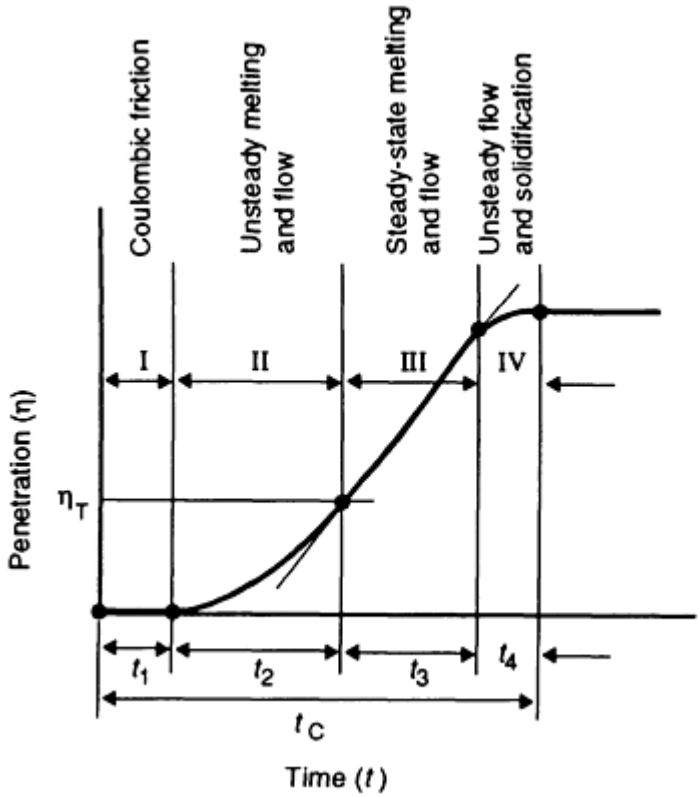

FIG. 8 SCHEMATIC OF PENETRATION-TIME GRAPH SHOWING THE FOUR PHASES OF VIBRATION WELDING PROCESS. SOURCE: REF 26

The key joining parameters of this process are the:

- AMPLITUDE, FREQUENCY, AND TIME OF VIBRATION APPLIED DURING WELDING
- PRESSURE APPLIED DURING THE JOINING OPERATION

It has been reported that the use of a process-controlled pressure profile (high pressures during phase I and lower applied pressures during the subsequent phases) will improve final joint mechanical properties and decrease the welding time, when compared with the time used in a constant weld pressure cycle (Ref 29).

Applications. The success of vibration welding lies in the fact that it can be used to join large parts and is limited by machine size. The joining process, which can be readily automated, can be applied to a variety of plastics, particularly semicrystalline polymers such as PP, PE, acetal, and nylon, which are difficult to weld using ultrasonic welding. Butt weld joints are the principal type of joint geometry that is used. The primary application areas are in the automotive, aeronautical, and household appliance sectors.

Spin Welding

Spin welding is ideally suited for joining cylindrical or circular parts. One half of the component is fixed, and the other half rotates at a prescribed angular velocity while pressure is applied (Fig. 9). Once a desired melted polymer thickness is achieved, the rotational motion is terminated and the parts are pressed together and cooled.

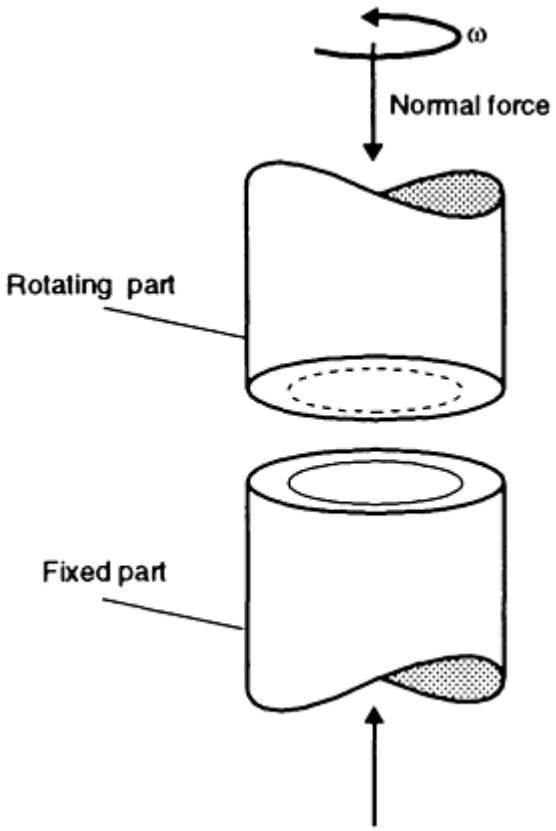

FIG. 9 SCHEMATIC OF SPIN WELDING PROCESS

Spin-welding machines can contain a range of sensors that indicate the rotational speed, axial pressure, weld penetration, velocity, and torque during the joining operation (Ref 31). The joining process can be described as having five distinct phases (Fig. 10). Solid (coulombic) friction, followed by friction and generation of wear particles, occurs during phases I and II. Phase III is the melting transition. Shearing of the melt produces further heat generation, and the weld penetration increases linearly with time in phase IV. Phase V involves cooling and consolidation of the joint under pressure.

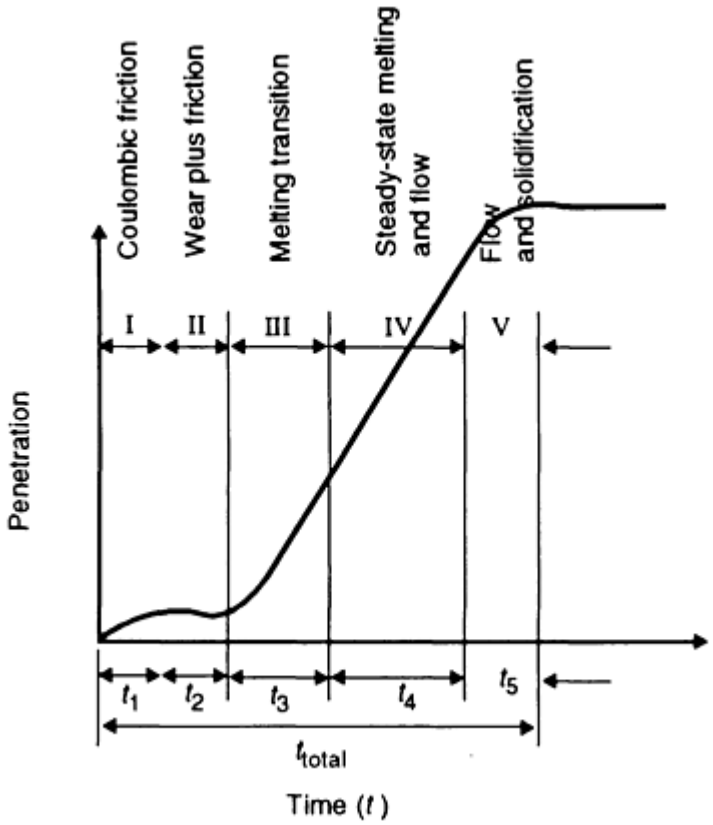

FIG. 10 PENETRATION-TIME GRAPH OF THE SPIN-WELDING PROCESS. SOURCE: REF 32

The key welding parameters are the:

- AXIAL FORCE APPLIED DURING THE WELDING OPERATION, WHICH DETERMINES THE ORIENTATION OF POLYMER CHAINS THAT DEVELOP IN THE COMPLETED JOINT AND MARKEDLY AFFECTS JOINT MECHANICAL PROPERTIES (REF 33)
- TIME REQUIRED TO COMPLETE THE WELDING OPERATION
- ROTATION SPEED EMPLOYED DURING SPIN WELDING

Applications. This inherently simple joining technique is capable of joining large-diameter sections, although it is applicable only to rotationally symmetric components. In the automotive sector, a typical application involves the joining of small, circular parts to large, blow-molded or injection-molded sections. Other automotive-related examples are the joining of ventilation fittings to blow-molded fuel tanks and the welding of gasoline filters and carburetor housings. Spin welding is also used in the manufacture of floats and aerosol bottles in the packaging industry.

Ultrasonic Welding

Ultrasonic welding is the most widely used polymer joining process. Numerous published papers describe the basic features of this joining technique. In this welding process, the sonotrode delivers low-amplitude (15 to 60 μm), high-frequency sinusoidal vibration in a direction perpendicular to the bond line. Although ultrasonic welding machine frequencies range from 10 to 50 kHz, the commonly available devices apply frequencies that are between 20 and 40 kHz.

Ultrasonic-welding machines generally comprise an actuator that contains the converter, booster, horn, and other pneumatic controls (Fig. 11). The ultrasonic vibrations are generated by exciting piezoelectric or magnetostrictive transducer crystals using electrical energy from a power supply. The transducer assembly is rigidly attached to a booster rod that increases or decreases the vibrational amplitude. Finally, the booster is connected to the sonotrode, which

transfers the vibratory motion to the workpiece. The converter, booster, and horn must be resonant at the operating frequency.

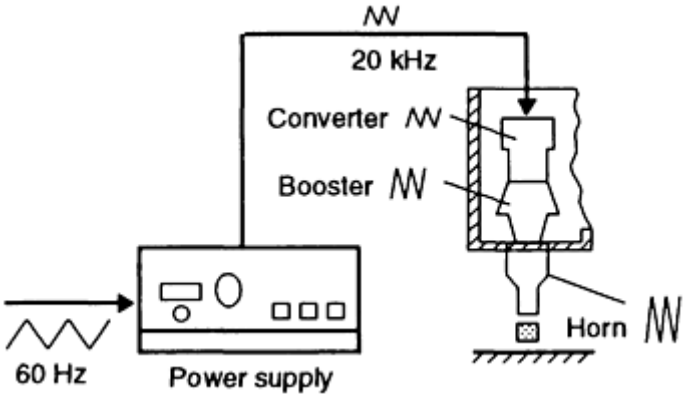

FIG. 11 SCHEMATIC OF ULTRASONIC-WELDING COMPONENTS

The weldability of any polymer depends on the damping capacity, or attenuation characteristics, and size of the component being joined. Depending on the distance between the sonotrode and the bond line, ultrasonic welding is classified as being either near-field (for distances under 6 mm, or 0.24 in.) or far-field (for distances over 6 mm, or 0.24 in.) welding.

It follows that the component geometry has a crucial influence on energy transmission, heat generation, and polymer melting at the joint interface. The transmission of ultrasonic vibrations through the workpiece sets up standing-wave patterns and regions of maximum and minimum displacements (Ref 34). The material fuses in regions of maximum strain or stress.

Amorphous thermoplastics are more readily weldable when an energy director is used. A triangular projection is molded onto one of the specimen surfaces, usually the one that contacts the sonotrode (Fig. 12a). Ultrasonic welds in semicrystalline resins are commonly produced using an interference, or shear joint, design (Fig. 12b). A novel technique that utilizes a tielayer at the interface has been developed recently (Fig. 12c) for use during the ultrasonic welding of flat contacting surfaces.

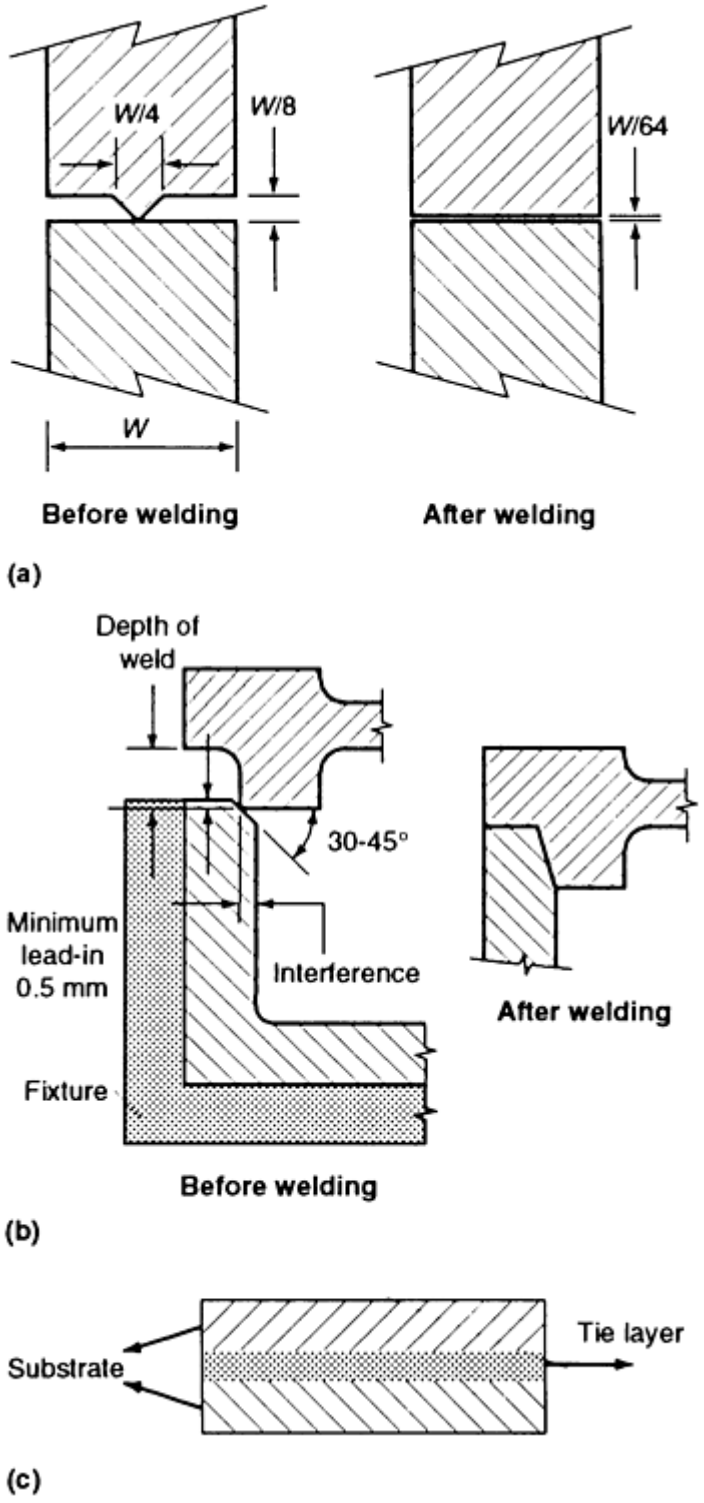

FIG. 12 SCHEMATIC OF ULTRASONIC CONFIGURATION. (A) ENERGY DIRECTOR DESIGN. (B) SHEAR JOINT DESIGN. (C) TIE-LAYER DESIGN. SOURCE: REF 35 AND 36

Energy generation and welding-parameter optimization during the ultrasonic welding of polystyrene (PS), a blend of PC and polybutylene terephthalate, and a composite of polyetherether ketone (PEEK) and graphite APC-2 have been analyzed in detail by different authors (Ref 37, 38, 39). The joining process comprises four distinct phases when tie layers are employed (Fig. 13). The rapid increase in temperature up to the polymer melting point results from frictional heating at surface asperities and, to a much lesser extent, viscoelastic dissipation. In phase II of the ultrasonic-welding process, bulk melting of the interface region predominantly results from viscoelastic energy dissipation. Further heating is due to viscous dissipation during phase III. In phase IV, the joint cools under pressure.

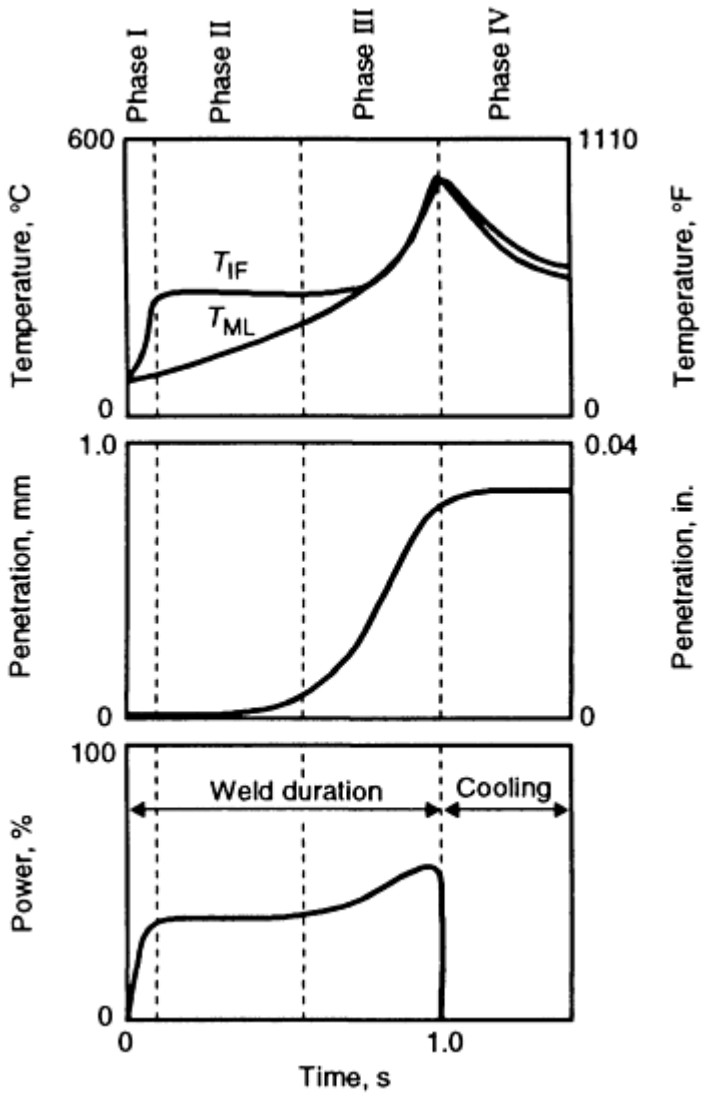

FIG. 13 TYPICAL PROCESS DATA TRACES-TIME GRAPH OF ULTRASONIC-WELDING PROCESS WHEN USING TIE LAYERS AT THE INTERFACE. SOURCE: REF 40

The weldability of a thermoplastic can be defined using the following relationships (Ref 3):

$$f = \int_{T1}^{T2} \frac{r\,c}{\left\{ E' \frac{\tan d}{2} + \frac{0.25}{p}\left[1 - \left(\frac{P}{P_x}\right)^{0,7}\right] v \right\}} dt \qquad \textbf{(EQ 4)}$$

$$\wedge = \pi \mathrm{TAN}\,\delta \qquad \textbf{(EQ 5)}$$

where f is the energy index, T_1 is the ambient temperature, T_2 is the softening point or crystalline melting point of the polymer, ρ is the density, c is the specific heat, E' is the real component of the complex elastic modulus, tan δ is the mechanical loss factor, P and P_x are the joining and critical joining pressure values, respectively, v is the coefficient of friction, and $\wedge$ is the logarithmic damping decrement. When the f value increases, more energy is required during the ultrasonic-welding process. When the logarithmic decrement factor $\wedge$ has a low value, more energy arrives at the joint interface. The f and $\wedge$ indexes are plotted in Fig. 14.

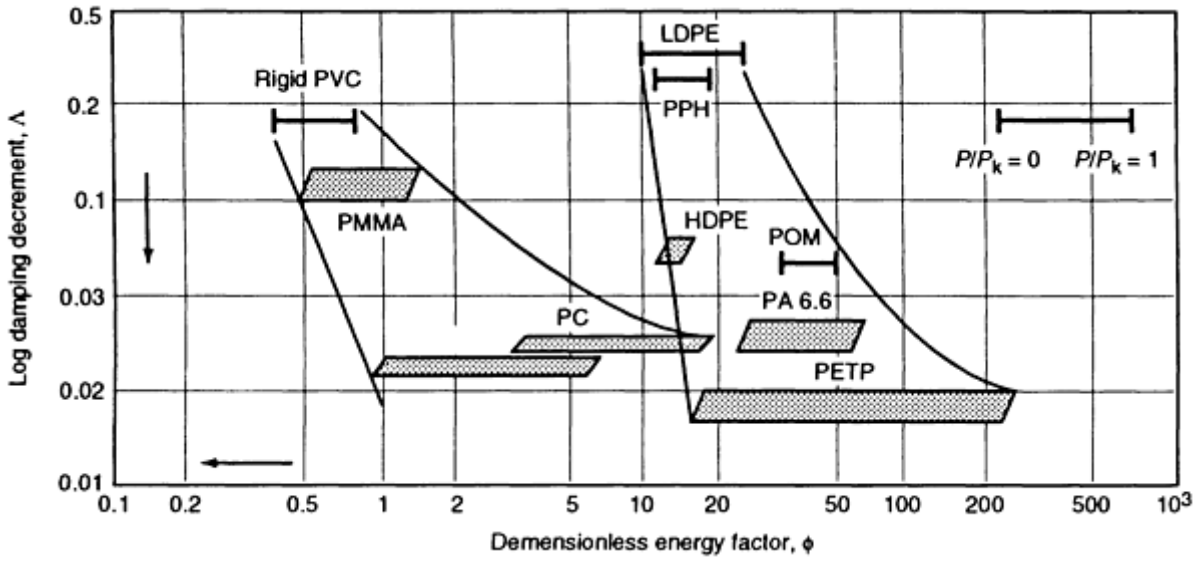

FIG. 14 DIAGRAM FOR ASSESSMENT OF WELDING CAPACITY OF THERMOPLASTICS. ARROW DIRECTION SHOWS INCREASE IN WELDABILITY BY THE INDIRECT METHOD. LDPE, LOW-DENSITY POLYETHYLENE; HDPE, HIGH-DENSITY POLYETHYLENE; PA, POLYAMIDE; POM, POLYOXYMETHYLENE. SOURCE: REF 34

The key joining parameters of ultrasonic welding are the:

- AMPLITUDE OF VIBRATION DURING JOINING
- PRESSURE APPLIED DURING THE WELDING OPERATION
- JOINT GEOMETRY WHEN WELDING AMORPHOUS AND SEMICRYSTALLINE POLYMERS
- WELDING TIME AND ENERGY APPLIED DURING THE WELDING PROCESS
- TRIGGER PRESSURE/FORCE RELATIONSHIP (THE PRESSURE AT WHICH ULTRASONIC VIBRATIONS ARE INITIATED)

Applications. The success of ultrasonic welding lies in the fact that the process is very fast (welding times are approximately 1 s), the equipment is compact, the process can be readily automated, and consistently acceptable weld quality can be produced. Ultrasonic welding is commonly used to join components in the automotive, toy, domestic appliance, and packaging industries. It is also the method of choice when welding many medical plastic components. The only limitation is that large parts cannot be welded using this method.

References cited in this section

3. H. POTENTE AND P. MICHEL, THE STATE OF THE ART DEVELOPMENT TRENDS IN THE WELDING OF PLASTICS, *PROC. 5TH ANNUAL NORTH AMERICAN WELDING RESEARCH CONFERENCE,* EWI AND AWS, 1989
10. A. BENATAR, MATERIAL CHARACTERISTICS FOR WELDING, *PROC. 5TH ANNUAL NORTH AMERICAN WELDING RESEARCH CONFERENCE,* EWI AND AWS, 1989
26. V.K. STOKES, VIBRATION WELDING OF THERMOPLASTICS, PART I, *POLYM. ENG. SCI.,* VOL 28, 1988, P 718-727
27. E. PECHA, D. CALINSKI, AND H. DIETER, PRODUCTION MACHINES AND TECHNICAL APPLICATION FOR HOT PLATE AND VIBRATION WELDING, *PROC. LNT. CONF. ADVANCES IN JOINING PLASTICS AND COMPOSITES,* THE WELDING INSTITUTE, CAMBRIDGE, 1991
28. V.K. STOKES, VIBRATION WELDING OF THERMOPLASTICS, PART II, *POLYM. ENG. SCI.,* VOL

28, 1988, P 727-739

29. H. POTENTE AND H. KAISER, PROCESS VARIANT OF VIBRATION WELDING WITH VARIABLE WELDING PRESSURE, *PROC. SPE 48TH ANTEC MEETING,* SOCIETY OF PLASTICS ENGINEERS, 1990, P 1762-1765
30. H. POTENTE AND M. UEBBING, COMPUTER AIDED LAYOUT OF THE VIBRATION WELDING PROCESS, *PROC. SPE 50TH ANTEC MEETING*, 1992, SOCIETY OF PLASTICS ENGINEERS, P 888
31. M. CAKMAK AND K. KEUCHEL, U.S. PATENT 4,998,663, MARCH 1991
32. K. KEUCHEL AND M. CAKMAK, SPIN WELDING OF POLYPROPYLENE: CHARACTERIZATION OF HEAT AFFECTED ZONE BY MICRO-BEAM WAXS TECHNIQUE, *PROC. SPE 49TH ANTEC MEETING*, SOCIETY OF PLASTICS ENGINEERS, 1991, P 2477-2481
33. H. RAJARAMAN AND M. CAKMAK, THE EFFECT OF GLASS FIBER FILLERS ON THE WELDING BEHAVIOR OF POLY P-PHENYLENE SULFIDE, *PROC. SPE 50TH ANTEC MEETING,* SOCIETY OF PLASTICS ENGINEERS, 1992, P 896-899
34. H. POTENTE, ULTRASONIC WELDING--PRINCIPLES AND THEORY, *MAT. DES.,* VOL 5, 1984
35. T.B. ZACH, J. LEW, T.H. NORTH, AND R.T. WOODHAMS, "JOINING OF HIGH STRENGTH ORIENTED POLYPROPYLENE USING ELECTROMAGNETIC INDUCTION BONDING AND ULTRASONIC WELDING, *MAT. SCI. TECH.,* VOL 5, 1989, P 281-287
36. J.S. WOLCOTT, DESIGNING PARTS FOR ULTRASONIC ASSEMBLY, *PROC. SPE 48TH ANTEC MEETING*, SOCIETY OF PLASTICS ENGINEERS, 1990, P 1829-1833
37. M.N. TOLUNAY, P.R. DAWSON, AND K.K. WANG, HEATING AND BONDING MECHANISMS IN ULTRASONIC WELDING OF THERMOPLASTICS, *POLYM. ENG. SCI.,* VOL 23, 1983, P 726-733
38. G. HABERNICHT AND J. RITTER, ENERGY CONVERSION IN THE ULTRASONIC WELDING OF THERMOPLASTICS, *KUNSTST. GER. PLAST.,* VOL 78, 1988, P 49-66
39. A. BENATAR AND T.G. GUTOWSKI, ULTRASONIC WELDING OF PEEK GRAPHITE APC-2 COMPOSITES, *POLYM. ENG. SCI.,* VOL 29 (NO. 23), 1989, P 1705-1721
40. N. TATEISHI, T.H. NORTH, AND R.T. WOODHAMS, ULTRASONIC WELDING USING TIE-LAYERS, PART I: ANALYSIS OF PROCESS OPERATION, *POLYM. ENG. SCI.,* VOL 32, 1992, P 600-611

Thomas H. North and Geetha Ramarathnam, University of Toronto

Electromagnetic Welding

The joining techniques described in this section include resistance, induction, dielectric, and microwave welding.

Resistance or Implant Welding

In this technique, a conducting wire or mesh is inserted at the interface between the parts being welded. This insert is resistively heated by the passage of electric current (Fig. 15a), which melts the thermoplastic surrounding the insert, forming a weld. It should be noted that the implant remains in the completed joint. Electrofusion is a technique whereby the two ends of the pipe to be welded are inserted into a fitting/collar/coupler, the inside of which constitutes the heating element (Ref 41, 42). The electric current that passes through the heating element promotes melting on the inside surface of the fitting. Figure 15(b) shows a typical rectangular cross section of an electrofusion weld.

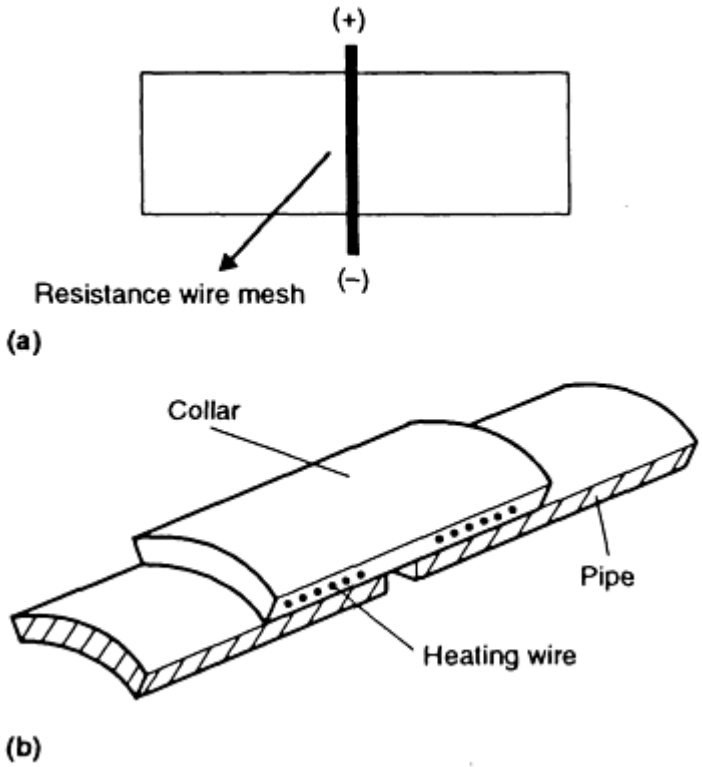

FIG. 15 (A) ELECTROFUSION (RESISTANCE) WELDING PROCESS. (B) ELECTROFUSION WELDING PROCESS. SOURCE: REF 42

The key joining parameters are the:

- APPLIED VOLTAGE AND APPLIED CURRENT, WHICH CAN BE AS HIGH AS 150 A
- CLAMPING PRESSURE DURING WELDING
- HEATING TIME
- AVOIDANCE OF CONTACTING SURFACE CONTAMINATION. BECAUSE MELT FLOW IS RESTRICTED DURING WELDING, IMPURITIES CAN BE TRAPPED AT THE JOINT INTERFACE, REDUCING THE STRENGTH OF THE WELD

Applications. The principal advantage of this joining method is that the equipment is relatively simple and portable. Therefore, it can be used in on-site repair situations. The primary application area for electrofusion welding is the joining of PE pipes with diameters less than 180 mm (7 in.), which are used for water transportation and natural gas distribution (Ref 42).

Induction Welding

In this joining method, a layer of electromagnetic material in the form of a tape or a thin sheet is placed at the joint interface. This insert material is heated using a high-frequency (2 to 10 MHz) inductive supply (Ref 43, 44). The electromagnetic tapes contain conductive and ferromagnetic particles. The particle size, type, and concentration depend on the application desired. The welding equipment comprises a high-frequency induction generator, a water-cooled copper working coil, and press fixtures, which hold the polymer component so that it can be heated and loaded.

Heating results from eddy currents that are induced in the thermoplastic tape containing the ferromagnetic particles (Fig. 16), and energy generation is proportional to I^2R. Heat generation during electromagnetic welding has been modeled, particularly for cross-ply carbon fiber thermoplastic composites (Ref 45, 46).

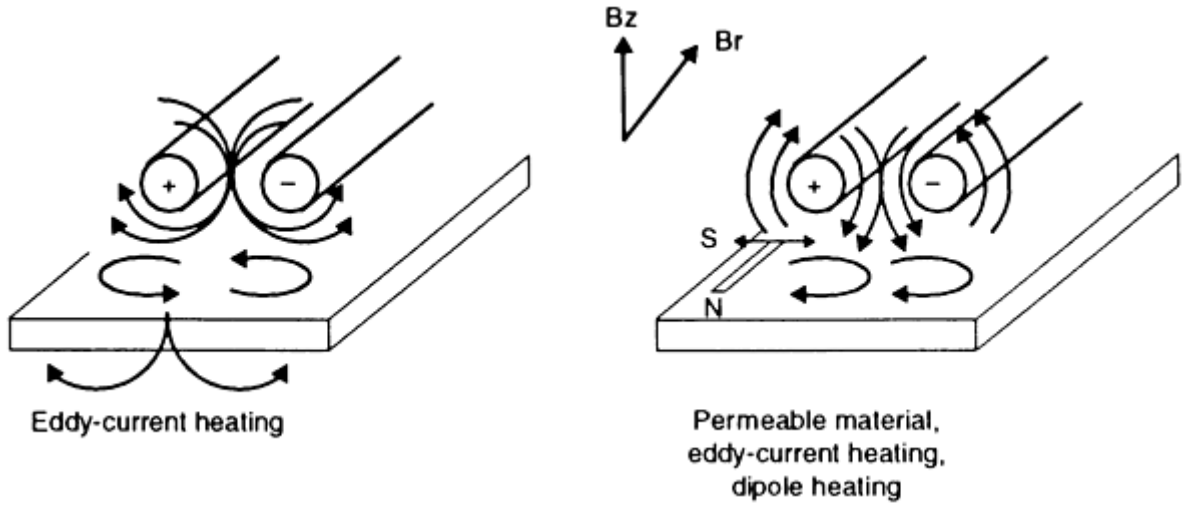

FIG. 16 INDUCTION-HEATING MECHANISM. SOURCE: REF 5

The key joining parameters of this technique are the:

- COIL DESIGN, WHICH MUST BE CAREFULLY TAILORED TO SUIT THE END USE AND TO PRODUCE A UNIFORM RADIO-FREQUENCY (RF) FIELD. A RANGE OF COIL DESIGNS (SINGLE TURN, MULTITURN, HELICAL, BENT HAIRPIN, AND SO ON) ARE ALL POSSIBLE
- FREQUENCY AND POWER OUTPUT OF THE INDUCTION GENERATOR
- PARTICLE SIZE AND TYPE OF FILLER USED IN ELECTROMAGNETIC TAPE MANUFACTURE
- DISTANCE BETWEEN THE INDUCTOR COILS AND THE BOND LINE

Applications. The principal advantage of this joining method is that it can handle components of complex geometry. The process is also suitable for joining filled thermoplastic materials. The primary applications are in the automotive, packaging, and appliance industries. In the medical field, electromagnetic induction welding has been employed for joining PC blood oxygenators and arterial filter components.

The principal disadvantages of this joining process are the high cost of the equipment, the recurring costs associated with the purchase of ferromagnetic-filled tapes, and the care that is required in the design and construction of the inductive heating coils.

Dielectric Welding

In dielectric welding, the joint interface is subjected to much higher RF electrical energy. The process utilizes these major components:

- A GENERATOR THAT PRODUCES A FREQUENCY RANGING FROM 13 TO 100 MHZ (27.12 MHZ IS TYPICAL) OF ELECTRICAL ENERGY AT AN OUTPUT OF 1 TO 25 KW
- A PRESS THAT CLAMPS THE SECTIONS TOGETHER DURING THE HEATING AND SUBSEQUENT COOLING CYCLES
- A BRASS ELECTRODE OR DIE THAT IS MOUNTED ON AN ALUMINUM PLATE, WHICH APPLIES THE ELECTRICAL ENERGY DIRECTLY TO THE PLASTIC (REF 47)

The key joining parameters of this process are the:

- DIELECTRIC LOSS FACTOR OF THE POLYMER OR THE PRESENCE OF A DIPOLE, BECAUSE A HIGH DIELECTRIC LOSS FACTOR INCREASES THE EFFECTIVENESS OF THE JOINING OPERATION
- THICKNESS OF THE MATERIAL BEING JOINED
- OUTPUT POWER AND FREQUENCY OF THE GENERATOR EMPLOYED DURING WELDING

Applications. Dielectric welding is a fast, efficient joining method for sealing thin polymer films and sheet materials. The equipment can be readily automated. However, the process can only be used on materials that have a high dielectric loss factor, such as rigid or flexible PVC, ABS, and thermoplastic polyurethane materials. The principal application area is in the packaging industry, where the process is used to join medical components, such as blood-pressure cuffs, medical bags, rainwear, pool liners, and so on.

The primary disadvantage of this joining technique is that the initial equipment cost is high.

Microwave Joining

This joining technique depends on the heat produced by microwave-frequency radiation. The parts being joined are held together under a slight pressure of 35 to 70 kPa (5 to 10 psi), and then the interface is irradiated by electromagnetic (EM) radiation using well-focused horn antennas. In order to absorb EM energy, the polymer must contain polar groups. To attain viable heating, either a nonconducting or a low-conductivity polymer may have to be doped with conducting polymer or, as an alternative, an adhesive film that contains polar and/or electron-withdrawing groups can be placed at the joint interface (Ref 48).

This joining method is relatively new and is still in the experimental stage. The experimental equipment (Ref 48) consists of a magnetron tube that generates the microwave energy, a ferrite isolator that shields the magnetron and promotes the efficient transmission of power with very little attenuation, a forward/reflected-power indicator that monitors the whole system while it is in operation, a tuner that can be adjusted to minimize the reflected power and aid in the maximum transfer of power from the source to the workpiece, a variable-coupling iris that optimizes and adjusts the power coupled to the load, and, finally, an applicator that concentrates the microwave power at the joint region.

The key joining parameters of this process are the:

- MICROWAVE PROPERTIES OF THE MATERIAL, SUCH AS PERMITTIVITY AND PERMEABILITY
- FREQUENCY AND ENERGY OF THE MICROWAVE SUPPLY

Applications. This welding technique is simple, fast, clean, and very efficient in terms of energy conversion. Consequently, short welding times are involved. Dissimilar materials can be joined, and the use of a microwave-absorbing adhesive will permit the repair of thermoset- or thermoplastic-based composite materials. This joining method can be very useful for in-situ repairs of structures, especially on space vehicles and other aircraft.

References cited in this section

5. R.A. GRIMM, FUSION WELDING TECHNIQUES FOR PLASTICS, *WELD. J.*, MARCH 1990, P 23-28
41. R.G. WILLIAMS, DEVELOPMENT OF A NOVEL ELECTROFUSION SYSTEM," *GAS ENGINEERING AND MANAGEMENT*, VOL 26, 1986, P 43-46
42. J.R. ATKINSON AND I.M. WARD, THE JOINING OF BIAXIALLY ORIENTED POLYETHYLENE PIPES, *POLYM. ENG. SCI.*, VOL 29 (NO. 23), 1989, P 1638-1641
43. SM. CHOOKAZIAN, BONDING PLASTICS BY INDUCTION HEATING, *SPE J.*, VOL 26, 1970, P 49-53
44. A. LEATHERMAN, INDUCTION BONDING FINDS A NICHE IN AN EVOLVING PLASTICS

INDUSTRY, *PLAST. ENG.*, VOL 4, 1981, P 27-29

45. S.P. MOLNAR, CHARACTERIZATION AND CONTROL OF INDUCTION FUSION BONDING OF THERMOPLASTIC COMPOSITE,*PROC. SPE 50TH ANTEC MEETING*, SOCIETY OF PLASTICS ENGINEERS, 1992, P 2102-2105
46. B.K. FINK, R.L. MCCULLOUGH, AND J.W. GILLESPIE JR., A LOCAL THEORY OF HEATING IN CROSS-PLY CARBON FIBER THERMOPLASTIC COMPOSITES BY MAGNETIC INDUCTION, *POLYM. ENG. SCI.*, VOL 32, 1992, P 357-369
47. C.J. GIANNANDREA, RADIO FREQUENCY SEALING, *MOD. PLAST.*, ENCYCLOPEDIA ISSUE, OCT 1990, P 386-388
48. V.K. VARADAN AND V.V. VARADAN, MICROWAVE JOINING AND REPAIR OF COMPOSITE MATERIALS, *POLYM. ENG. SCI.*, VOL 31, 1992, P 470-486

Thomas H. North and Geetha Ramarathnam, University of Toronto

Evaluation of Welds

Because polymers are being used increasingly for semistructural and load-bearing applications, the testing of the welded joints is important. The mechanical properties of welded plastics can be evaluated by performing standard destructive tests, such as tensile, peel, wedge, and four-point bending. Of particular interest is the development of short-term tests (Ref 49), where a hole is notched in the weld area (to create multiaxial stress). These short-term tests are for quality-assurance purposes only.

For long-term applications, creep tests are much more favored. The measurement of thermal and residual stress has been evaluated using the Moire interferometric method (Ref 50).

The microstructure of the weld zone can be examined using light microscopy, scanning electron microscopy (SEM), or x-ray techniques (Ref 32, 51, 52). The microstructural examination of bonded regions is important because it allows:

- MEASUREMENT OF THE WELD ZONE AND HEAT-AFFECTED ZONE DIMENSIONS AND THEIR UNIFORMITY ALONG THE WELD LINE
- EVALUATION OF THE DEVELOPMENT OF CRYSTALLINITY, ESPECIALLY THE TRANSCRYSTALLINE REGION
- EVALUATION OF THE CHAIN ORIENTATION, ESPECIALLY PARALLEL TO THE BOND-LINE REGION
- ESTIMATION OF THE FAILURE MODES OF MECHANICALLY TESTED WELD SECTIONS
- OPTIMIZATION OF WELDING CONDITIONS IN ORDER TO CONSISTENTLY PRODUCE JOINTS OF OPTIMUM STRENGTH

Nondestructive evaluation (NDE) techniques for the detection of flaws in metal joints are well established. However, in the case of plastic joints, much work is still required to optimize the application of NDE techniques (Ref 53).

References cited in this section

32. K. KEUCHEL AND M. CAKMAK, SPIN WELDING OF POLYPROPYLENE: CHARACTERIZATION OF HEAT AFFECTED ZONE BY MICRO-BEAM WAXS TECHNIQUE, *PROC. SPE 49TH ANTEC MEETING*, SOCIETY OF PLASTICS ENGINEERS, 1991, P 2477-2481
49. G. MENGES, E. SCHMACHTENBERG, AND R. KRAUSENBERGER, EIN SCHNELLER WEG ZUR

ERMITTLUNG DES LANGZEITVERHALTENS VON SCHWEIßNAHTEN, *DVS--BER.*, VOL 84, P 62-65

50. J.B. PARK AND A. BENATAR, MOIRE INTERFEROMETRY MEASUREMENT OF RESIDUAL STRAINS IN IMPLANT RESISTANCE WELDING, *PROC. SPE 50TH ANTEC MEETING*, SOCIETY OF PLASTICS ENGINEERS, 1992, P 353-358
51. L.C. SAWYER AND D.T. GRUBB, IN *POLYMER MICROSCOPY*, CHAPMAN AND HALL, 1987
52. M.J. DAY AND M.F. GITTOS, "THE APPLICATION OF LIGHT MICROSCOPY TO WELDED JOINTS IN THERMOPLASTICS," REPORT 390, THE WELDING INSTITUTE, 1989
53. G.R. EDWARDS, NONDESTRUCTIVE EVALUATION OF WELDS IN PLASTICS, *PROC. 5TH ANNUAL NORTH AMERICAN WELDING RESEARCH CONFERENCE*, EWI AND AWS, 1989

References

General Review Articles on Joining and Welding of Polymers:

1. G. GEHARDSSON, THE WELDING OF PLASTICS, *WELD. REV.*, FEB 1983, P 17-22
2. M.N. WATSON, R.M. RIVETT, AND K.I. JOHNSON, "PLASTICS--AN INDUSTRIAL AND LITERATURE SURVEY OF JOINING TECHNIQUES," REPORT NO. 7846.01/85/471.3, THE WELDING INSTITUTE, ABINGTON, UK, 1986
3. H. POTENTE AND P. MICHEL, THE STATE OF THE ART DEVELOPMENT TRENDS IN THE WELDING OF PLASTICS, *PROC. 5TH ANNUAL NORTH AMERICAN WELDING RESEARCH CONFERENCE*, EWI AND AWS, 1989
4. V.K. STOKES, JOINING METHODS FOR PLASTICS AND PLASTIC COMPOSITES: AN OVERVIEW, *POLYM. ENG. SCI.*, VOL 29 (NO. 19), 1989, P 1310-1324
5. R.A. GRIMM, FUSION WELDING TECHNIQUES FOR PLASTICS, *WELD. J.*, MARCH 1990, P 23-28
6. G. MENGES, THE JOINING OF PLASTICS AND THEIR COMPOSITES, *PROC. LNT. CONF. ADVANCES IN JOINING NEWER STRUCTURAL MATERIALS*, IIW (MONTREAL), P 33-63

Adhesive Bonding:

7. A.J. KINLOCH, *ADHESION AND ADHESIVES*, CHAPMAN AND HALL, 1987, P 101

Mechanical Fastening:

8. D. CHANT, JOINING TECHNOLOGY FOR THERMOPLASTIC COMPOSITE STRUCTURES IN AEROSPACE APPLICATIONS, *PROC. INT. CONF. ADVANCES IN JOINING PLASTICS AND COMPOSITES*, THE WELDING INSTITUTE, CAMBRIDGE, 1991

Welding Mechanisms and Weldability of Thermoplastics:

9. S.S. VOYUTSKII, AUTOHESION AND ADHESION OF HIGH POLYMERS, WILEY INTERSCIENCE, 1963
10. A. BENATAR, MATERIAL CHARACTERISTICS FOR WELDING, *PROC. 5TH ANNUAL NORTH AMERICAN WELDING RESEARCH CONFERENCE*, EWI AND AWS, 1989
11. R.P. WOOL, B.-L. YUAN, AND O.J. MCGAREL, *POLYM. ENG. SCI.*, VOL 29 (NO. 19), 1989, P 1340-1367

Solvent Welding:

12. W.V. TITOW, CHAPTER 12, *SOLVENT WELDING OF PLASTICS*, APPLIED SCIENCE PUBLISHERS, LONDON, P 181-196

13. M. LICATA AND E. HAAG, SOLVENT WELDING WITH POLYCARBONATE, *PROC. SPE 44TH ANTEC MEETING*, SOCIETY OF PLASTICS ENGINEERS, 1986, P 1092-1094

Heated-Tool Welding:

14. K. GABLER AND H. POTENTE, WELDABILITY OF DISSIMILAR THERMOPLASTICS--EXPERIMENTS IN HEATED TOOL WELDING, *J. ADHES.*, VOL 11, 1980, P 145-163
15. H. POTENTE AND P. TAPPE, SCALE-UP LAWS IN HEATED TOOL BUTT WELDING OF HDPE AND PP, *POLYM. ENG. SCI.*, VOL 29 (NO. 23), 1989, P 1642-1648
16. H. POTENTE AND J. NATROP, COMPUTER AIDED OPTIMIZATION OF THE PARAMETERS OF HEATED TOOL BUTT WELDING, *POLYM. ENG. SCI.*, VOL 29 (NO. 23), 1989, P 1649-1654
17. A.J. POSLINSKI AND V.K. STOKES, ANALYSIS OF THE HOT-TOOL WELDING PROCESS, *PROC. SPE 50TH ANTEC MEETING*, 1992, SOCIETY OF PLASTICS ENGINEERS, P 1228-1233

Hot-Gas Welding:

18. H. GUMBLETON, HOT GAS WELDING OF THERMOPLASTICS--AN INTRODUCTION, *JOIN. MAT.*, VOL 5, 1989, P 215-218
19. "RECOMMENDED PRACTICES FOR JOINING PLASTIC PIPING," DOCUMENT XVI-322-78-E, IIW

Extrusion Welding:

20. P. MICHEL, "AN ANALYSIS OF THE EXTRUSION WELDING PROCESS," *POLYM. ENG. SCI.*, VOL 29 (NO. 19), 1989, P 1376-1382
21. M. GEHDE AND G.W. EHRENSTEIN, STRUCTURAL AND MECHANICAL PROPERTIES OF OPTIMIZED EXTRUSION WELDS, *POLYM. ENG. SCI.*, VOL 31 (NO. 7), 1991, P 495-501

Infrared Welding:

22. H. SWARTZ AND J.L. SWARTZ, FOCUSSED INFRARED--A NEW JOINING TECHNOLOGY FOR HIGH PERFORMANCE THERMOPLASTICS AND COMPOSITE PARTS, *PROC. 5TH ANNUAL NORTH AMERICAN WELDING RESEARCH CONFERENCE*, EWI AND AWS, 1989
23. H. POTENTE, P. MICHEL, AND M. HEIL, INFRARED RADIATION WELDING: A METHOD FOR WELDING HIGH TEMPERATURE RESISTANT THERMOPLASTICS, *PROC. SPE 49TH ANTEC MEETING*, SOCIETY OF PLASTICS ENGINEERS, 1991, P 2502-2504

Laser Welding:

24. W.W. DULEY, IN *LASER PROCESSING AND ANALYSIS OF MATERIALS*, PLENUM PRESS, 1983
25. W.W. DULEY AND R.E. MUELLER, CO_2 LASER WELDING OF POLYMERS, *POLYM. ENG. SCI.*, VOL 32 (NO. 9), 1992, P 582-585

Vibration Welding:

26. V.K. STOKES, VIBRATION WELDING OF THERMOPLASTICS, PART I, *POLYM. ENG. SCI.*, VOL 28, 1988, P 718-727
27. E. PECHA, D. CALINSKI, AND H. DIETER, PRODUCTION MACHINES AND TECHNICAL APPLICATION FOR HOT PLATE AND VIBRATION WELDING, *PROC. LNT. CONF. ADVANCES IN JOINING PLASTICS AND COMPOSITES*, THE WELDING INSTITUTE, CAMBRIDGE, 1991
28. V.K. STOKES, VIBRATION WELDING OF THERMOPLASTICS, PART II, *POLYM. ENG. SCI.*, VOL 28, 1988, P 727-739
29. H. POTENTE AND H. KAISER, PROCESS VARIANT OF VIBRATION WELDING WITH VARIABLE WELDING PRESSURE, *PROC. SPE 48TH ANTEC MEETING*, SOCIETY OF PLASTICS ENGINEERS, 1990, P 1762-1765
30. H. POTENTE AND M. UEBBING, COMPUTER AIDED LAYOUT OF THE VIBRATION WELDING PROCESS, *PROC. SPE 50TH ANTEC MEETING*, 1992, SOCIETY OF PLASTICS ENGINEERS, P 888

Spin Welding:

31. M. CAKMAK AND K. KEUCHEL, U.S. PATENT 4,998,663, MARCH 1991
32. K. KEUCHEL AND M. CAKMAK, SPIN WELDING OF POLYPROPYLENE: CHARACTERIZATION OF HEAT AFFECTED ZONE BY MICRO-BEAM WAXS TECHNIQUE, *PROC. SPE 49TH ANTEC MEETING,* SOCIETY OF PLASTICS ENGINEERS, 1991, P 2477-2481
33. H. RAJARAMAN AND M. CAKMAK, THE EFFECT OF GLASS FIBER FILLERS ON THE WELDING BEHAVIOR OF POLY P-PHENYLENE SULFIDE, *PROC. SPE 50TH ANTEC MEETING,* SOCIETY OF PLASTICS ENGINEERS, 1992, P 896-899

Ultrasonic Welding:

34. H. POTENTE, ULTRASONIC WELDING--PRINCIPLES AND THEORY, *MAT. DES.,* VOL 5, 1984
35. T.B. ZACH, J. LEW, T.H. NORTH, AND R.T. WOODHAMS, "JOINING OF HIGH STRENGTH ORIENTED POLYPROPYLENE USING ELECTROMAGNETIC INDUCTION BONDING AND ULTRASONIC WELDING, *MAT. SCI. TECH.,* VOL 5, 1989, P 281-287
36. J.S. WOLCOTT, DESIGNING PARTS FOR ULTRASONIC ASSEMBLY, *PROC. SPE 48TH ANTEC MEETING,* SOCIETY OF PLASTICS ENGINEERS, 1990, P 1829-1833
37. M.N. TOLUNAY, P.R. DAWSON, AND K.K. WANG, HEATING AND BONDING MECHANISMS IN ULTRASONIC WELDING OF THERMOPLASTICS, *POLYM. ENG. SCI.,* VOL 23, 1983, P 726-733
38. G. HABERNICHT AND J. RITTER, ENERGY CONVERSION IN THE ULTRASONIC WELDING OF THERMOPLASTICS, *KUNSTST. GER. PLAST.,* VOL 78, 1988, P 49-66
39. A. BENATAR AND T.G. GUTOWSKI, ULTRASONIC WELDING OF PEEK GRAPHITE APC-2 COMPOSITES, *POLYM. ENG. SCI.,* VOL 29 (NO. 23), 1989, P 1705-1721
40. N. TATEISHI, T.H. NORTH, AND R.T. WOODHAMS, ULTRASONIC WELDING USING TIE-LAYERS, PART I: ANALYSIS OF PROCESS OPERATION, *POLYM. ENG. SCI.,* VOL 32, 1992, P 600-611

Electrofusion (Resistance) Welding:

41. R.G. WILLIAMS, DEVELOPMENT OF A NOVEL ELECTROFUSION SYSTEM," *GAS ENGINEERING AND MANAGEMENT,* VOL 26, 1986, P 43-46
42. J.R. ATKINSON AND I.M. WARD, THE JOINING OF BIAXIALLY ORIENTED POLYETHYLENE PIPES, *POLYM. ENG. SCI.,* VOL 29 (NO. 23), 1989, P 1638-1641

Electromagnetic Induction Welding:

43. SM. CHOOKAZIAN, BONDING PLASTICS BY INDUCTION HEATING, *SPE J.,* VOL 26, 1970, P 49-53
44. A. LEATHERMAN, INDUCTION BONDING FINDS A NICHE IN AN EVOLVING PLASTICS INDUSTRY, *PLAST. ENG.,* VOL 4, 1981, P 27-29
45. S.P. MOLNAR, CHARACTERIZATION AND CONTROL OF INDUCTION FUSION BONDING OF THERMOPLASTIC COMPOSITE,*PROC. SPE 50TH ANTEC MEETING,* SOCIETY OF PLASTICS ENGINEERS, 1992, P 2102-2105
46. B.K. FINK, R.L. MCCULLOUGH, AND J.W. GILLESPIE JR., A LOCAL THEORY OF HEATING IN CROSS-PLY CARBON FIBER THERMOPLASTIC COMPOSITES BY MAGNETIC INDUCTION, *POLYM. ENG. SCI.,* VOL 32, 1992, P 357-369

Dielectric or Radio-Frequency Welding:

47. C.J. GIANNANDREA, RADIO FREQUENCY SEALING, *MOD. PLAST.,* ENCYCLOPEDIA ISSUE, OCT 1990, P 386-388

Microwave Welding:

48. V.K. VARADAN AND V.V. VARADAN, MICROWAVE JOINING AND REPAIR OF COMPOSITE MATERIALS, *POLYM. ENG. SCI.,* VOL 31, 1992, P 470-486

Evaluation of Plastic Welds:

49. G. MENGES, E. SCHMACHTENBERG, AND R. KRAUSENBERGER, EIN SCHNELLER WEG ZUR

ERMITTLUNG DES LANGZEITVERHALTENS VON SCHWEIßNAHTEN, *DVS--BER.,* VOL 84, P 62-65

50. J.B. PARK AND A. BENATAR, MOIRE INTERFEROMETRY MEASUREMENT OF RESIDUAL STRAINS IN IMPLANT RESISTANCE WELDING, *PROC. SPE 50TH ANTEC MEETING,* SOCIETY OF PLASTICS ENGINEERS, 1992, P 353-358
51. L.C. SAWYER AND D.T. GRUBB, IN *POLYMER MICROSCOPY,* CHAPMAN AND HALL, 1987
52. M.J. DAY AND M.F. GITTOS, "THE APPLICATION OF LIGHT MICROSCOPY TO WELDED JOINTS IN THERMOPLASTICS," REPORT 390, THE WELDING INSTITUTE, 1989
53. G.R. EDWARDS, NONDESTRUCTIVE EVALUATION OF WELDS IN PLASTICS, *PROC. 5TH ANNUAL NORTH AMERICAN WELDING RESEARCH CONFERENCE,* EWI AND AWS, 1989

Intelligent Automation for Joining Technology

Xiaoshu Xu and Jerald E. Jones, American Welding Institute

Introduction

AS JOINING TECHNOLOGY IMPROVES, industry is incorporating more types of automatic joining equipment and is expending significant efforts to make automated equipment more efficient. One of the most important approaches being used is called "intelligent automation." This approach combines automatic joining equipment, the knowledge of human experts in terms of joining, and a modem computer technique known as artificial intelligence (AI).

Artificial intelligence traditionally covers several application areas. AI techniques that can be applied to the intelligent automation of joining include expert systems, intelligent data-base systems, image processing, signal analysis, fuzzy-logic systems, and artificial neural networks.

An intelligent automation system usually includes an off-line planning system and a real-time adaptive control system that are connected through a computer communications interface. In the off-line planning system, the user develops a plan, with computer assistance, for the specific joining application, such as designing the joint, determining the process control parameters, or planning the robot path. The plan is then sent to the real-time control system through the interface. The real-time controller, using this down-loaded plan, controls the operation of the equipment. During execution, several sensors monitor the process and feed back information to the real-time controller. Using the feedback information, the real-time adaptive controller will adjust the robot trajectory, process parameters, and other controllable variables to correct any run-time errors.

Intelligent automation systems that vary in complexity are being developed by several organizations, as of 1993. Less-complex systems should be released in the near future by welding robot vendors. Currently, an intelligent automation system for arc welding, called WELDEXCELL, is being developed for the U.S. Navy at the American Welding Institute (AWI).

A graphical overview of the WELDEXCELL system is shown in Fig. 1. This system, which is relatively complex, utilizes most of the intelligent system techniques. For this reason, and because the authors are very familiar with it, WELDEXCELL is used for the examples described in this article. Although the discussion concentrates on the application of intelligent automation to arc welding processes, the technique also can be used for other joining processes.

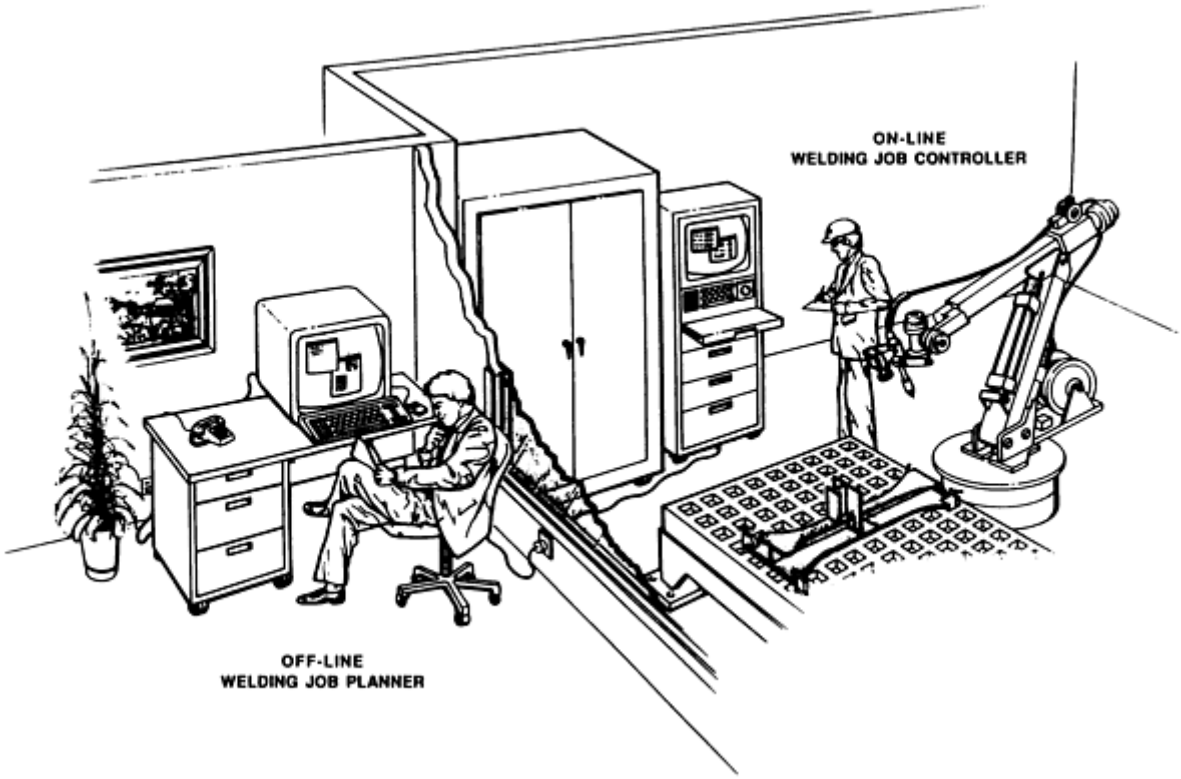

FIG. 1 INTELLIGENT AUTOMATED WELDING SYSTEM

Xiaoshu Xu and Jerald E. Jones, American Welding Institute

Off-Line Planning System

An intelligent off-line planning system comprises several modules. WELDEXCELL, for example, contains four: the parts designer, path planner, welding schedule developer, and system integrator (Fig. 2).

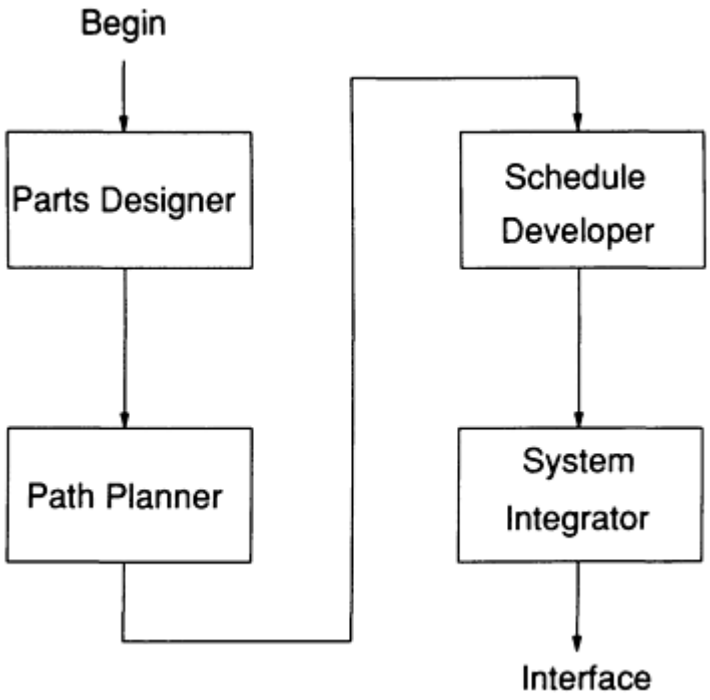

FIG. 2 SEQUENTIAL OPERATION OF AN OFF-LINE PLANNING SYSTEM

Parts Designer. The parts to be joined should first be drawn in a three-dimensional (3-D) computer-aided design (CAD) system. Many suitable commercial CAD systems are available. For a CAD system to be used in an off-line planning system, the required functions include:

- DRAWING FUNCTIONS THAT DRAW EITHER 3-D OR PSEUDO 3-D OBJECTS, INCLUDING LINES, CIRCLES, ARCS, POLYGONS, AND ELLIPSES
- EDIT FUNCTIONS THAT ERASE, MOVE, OR COPY DRAWN OBJECTS
- A FUNCTION THAT CHANGES THE COORDINATE SYSTEM, INCLUDING THE ORIGIN AND THE VIEW POINT (IMPORTANT FOR THE USER INTERFACE, AS WELL AS FOR LATER ROBOT GUIDANCE)
- OUTPUT DRAWING FILES IN ONE OF THE STANDARD VECTOR GRAPHICS REPRESENTATION FORMATS

In the WELDEXCELL system, the user superimposes the weld segments on a separate layer of the CAD part representation. A weld segment is a portion of a weld, and a series of one or more weld segments will produce a single weld on the part. It can be a single- or a multiple-pass weld. However, it has to satisfy the following two restrictions. First, the welding segment must contain a continuous trajectory, which can be a straight line, polyline, circle, arc, or spline in 3-D space. Second, the welding process, position, and all other non-real-time adjustable parameters, such as filler-metal diameter or type of shielding gas, must be kept constant during each weld pass when welding the defined segment.

In the parts designer module, the user is able to set any required welding restrictions for any welding segment. After the parts are designed and the weld segments are defined, they are stored by the CAD system in a vector-based format. This allows the later retrieval of any points that are located on the parts, especially the weld segments and associated restrictions.

- *THE PATH PLANNER* IS AN INTELLIGENT, OFF-LINE, WELD PLANNING SYSTEM COMPRISING TWO PARTS: PATH GENERATION AND ROBOT SIMULATION. FIRST, THE INITIAL ROBOT WELDING PATH IS DETERMINED. THIS PATH INCLUDES THE

TRAJECTORY OF THE ROBOT, AS WELL AS THE MOVEMENT OF A POSITIONING TABLE (IF APPLIED). THE PATH CONTAINS THREE MAJOR SECTIONS.

The start section represents the path from the home (or start) position of the robot to the beginning of the first weld segment.

The welding section, which is the most important section of the path plan, includes the path for each weld segment and the transition path between segments and between welding passes for each segment (in the case of a multiple-pass weld). Because the number of passes and the offset of each pass from the joint centerline for each segment are not known until the welding schedules are later developed, the initial path plan does not take multiple passes into consideration.

The end section represents the path from the end of the last weld segment back to the robot home position.

After the initial path is generated, it can then be sent electronically to the robot simulation model for execution. The simulation environment on the computer should include an animated robot and its environment. Objects that the robot could collide with, such as the welding torch, positioning table, parts to be welded, fixtures to secure the part, and others, should be included in the robot simulation environment (Fig. 3). The simulation will run through the designated path to ensure that no collision occurs between the robot arm and any environmental object and that the path is smooth and satisfies the requirements of the user. The simulation should provide a full 3-D or pseudo 3-D representation and should allow viewing from various positions. Them may be a system inside the simulation that can automatically correct or even optimize the robot trajectory to avoid any possible collision.

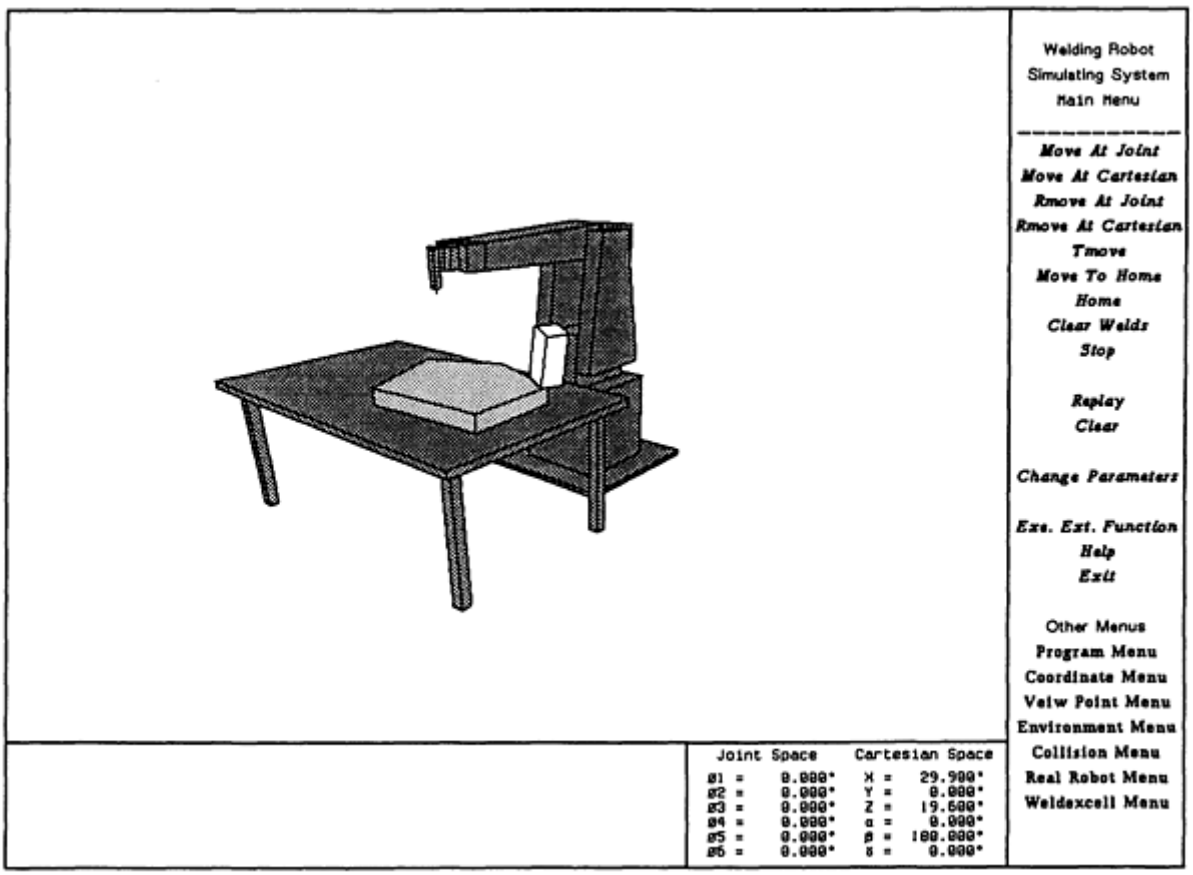

FIG. 3 PATH PLANNER AND ROBOT SIMULATOR IN THE WELDEXCELL SYSTEM

Based on the results of this simulation, either the system or the user can modify the path by using any extra degrees-of-freedom of the robot and/or by rotating the positioning table to adjust the trajectory. If necessary, the welding position can be changed for some weld segments. If the welding position has been restricted by the user, then input from the user is

needed to modify that portion of the path plan. This modified path can then be sent to the robot simulation to run again. Several iterations of this cycle may be required before a satisfactory path plan can be attained. Note that the path generated here is not complete. Multiple-pass welding segments have not been planned, nor has the velocity been set. Final path planning will occur in the system integrator module.

Schedule Developer. A welding schedule is developed for each individual welding segment. All welding variables, except for welding position (determined in the path planner module), are determined by the schedule developer (in combination with user input). These variables include welding process, number of welding passes, consumable type and size, welding current, voltage, wire feed rate, travel speed, shielding gas type and flow rate, required heat treatment, and others.

Several modules in the WELDEXCELL system are used to develop a welding schedule for each segment. These modules, called knowledge sources, will determine the individual variables. The knowledge sources include expert systems, neural networks, and CAD systems. A distributed data base system that contains several data bases is required to support these knowledge sources.

Data Base Systems. Several data bases should be available to the off-line planner. Data can be directly used by either the human user, to develop the welding schedule, or the intelligent off-line planner, in which case the data are available to the other knowledge sources. The data base system should include:

- A BASE-MATERIAL DATA BASE, WHICH STORES THE DESIGNATION AND THE CHEMICAL, THERMOPHYSICAL, AND MECHANICAL PROPERTIES OF THE BASE MATERIALS
- A FILLER-MATERIAL DATA BASE, WHICH STORES THE DESIGNATIONS, CHEMICAL PROPERTIES, AND MECHANICAL PROPERTIES OF THE FILLER MATERIALS
- A JOINT DATA BASE, WHICH STORES JOINT DESIGNS THAT ARE STANDARD (SUCH AS THOSE FROM THE AWS/ANSI STRUCTURAL WELDING CODE D 1.1) AND NONSTANDARD (USER), AS WELL AS DIMENSION INFORMATION, INCLUDING GRAPHICAL (CAD) REPRESENTATIONS
- A WELDING PROCEDURE SPECIFICATION (WPS) DATA BASE (REFER TO REF 1 FOR AN EXPLANATION OF WPS)
- A PROCEDURE QUALIFICATION RECORD (PQR) DATA BASE (REFER TO REF 1)
- A WELD-SCHEDULE DATA BASE, WHICH MAINTAINS THE WELD SCHEDULES ONCE THEY ARE DEVELOPED

An expert system consists of a "knowledge base," which stores information on a subject from a human expert, and an "inference engine," which contains a set of logic processes that is useful in applying the information in the knowledge base. The separation of the knowledge from the logic processes is one way in which expert systems differ from conventional software.

In the field of artificial intelligence, several methodologies have been developed for the representation of knowledge. Some of these have been used to develop computerized applications. Two of the methodologies, specifically "frames" and "production rules," have been successfully used to develop expert systems.

In this type of expert system, the knowledge of the human expert is stored in the production rules. These rules are written in the form of: if (A), then (C); where (A) is known as the antecedent and (C) is known as the consequent. For organizational purposes, and to aid in the application of the logic processes, the rules are then grouped together in a frame structure that is hierarchical in nature.

The expert system operates by selectively choosing rules that generate conclusions or formulate parts of answers to questions. This process is accomplished by the inference engine as the antecedent of a rule is shown to be true by either user input or data derived from a data base for a specific situation.

Sometimes, these rules are also associated with certainties. This gives the final result, or a set of results from an expert system operation, a certainty value. A detailed discussion of expert systems can be found in Ref 2 and 3. As the logic system applies specific rules to generate conclusions, those rules are "chained" together. If the system is designed to form a conclusion, then "backward" chaining is used (that is, working backward from a possible conclusion to show whether it is true or false). Forward chaining is applied if the purpose is to synthesize information, such as to generate a welding procedure.

In a schedule developer, the expert system usually includes such tasks as: select suitable filler-metal type and size, determine preheat and postweld heat-treatment schedule, determine welding parameters, and others.

The WELDEXCELL system, for example, contains several expert systems in the area of arc welding, which can be used in the off-line planning activity. Examples of these include:

- WELDSELECTOR: AN EXPERT SYSTEM TO HELP SELECT AN ELECTRODE (FILLER MATERIAL) AND ELECTRODE DIAMETER. THIS SYSTEM HAS A CERTAINTY-FACTOR-BASED, BACKWARD CHAINING, INFERENCE ENGINE AND GIVES A RANKED LIST OF ELECTRODES FOR A GIVEN APPLICATION. THIS WAS THE FIRST PERSONAL-COMPUTER-BASED EXPERT SYSTEM COMMERCIALLY AVAILABLE IN THE UNITED STATES.
- FERRITEPREDICTOR: AN EXPERT SYSTEM THAT PERFORMS THE FERRITE ANALYSIS FOR STAINLESS STEEL WELDING. FOUR CONSTITUTION DIAGRAMS CAN BE CONSULTED: SCHAEFFLER, DELONG, AND THE 1988 AND 1992 WELDING RESEARCH COUNCIL (WRC) DIAGRAMS. FIGURE 4(A) SHOWS THE GENERAL USER INTERFACE, WHEREAS FIG. 4(B) SHOWS THE WRC DIAGRAM ANALYSIS.
- WELDHEAT: AN EXPERT SYSTEM THAT DETERMINES THE PREHEAT, INTERPASS TEMPERATURE, AND POSTWELD HEAT TREATMENT. THE WELDHEAT EXPERT SYSTEM USES FOUR DIFFERENT METHODS: INTERNATIONAL INSTITUTE OF WELDING (IIW) CARBON EQUIVALENT, WRC PREHEAT AND POSTWELD HEAT TREATMENT TABLE (FROM REF 4), AND A MATHEMATICAL MODEL PREDICTION BASED ON THE WORK DONE BY N. YURIOKA AND M. OKUMURA (REF 5, 6, 7).
- WELDPROSPEC: A SYSTEM THAT INTELLIGENTLY SEARCHES THE PQR DATA BASE, BASED ON A SPECIFIED WELDING CODE, SUCH AS THE AWS/ANSI STRUCTURAL WELDING CODE D1.1. THE WELDPROSPEC SEARCHES THE PQR(S) IN THE PQR DATA BASE THAT CAN QUALIFY THE CURRENT WELD SCHEDULE. IF NECESSARY, WELDPROSPEC CAN CREATE A WPS FROM SELECTED PQR(S) TO SUPPORT THE CURRENT WELD SCHEDULE.

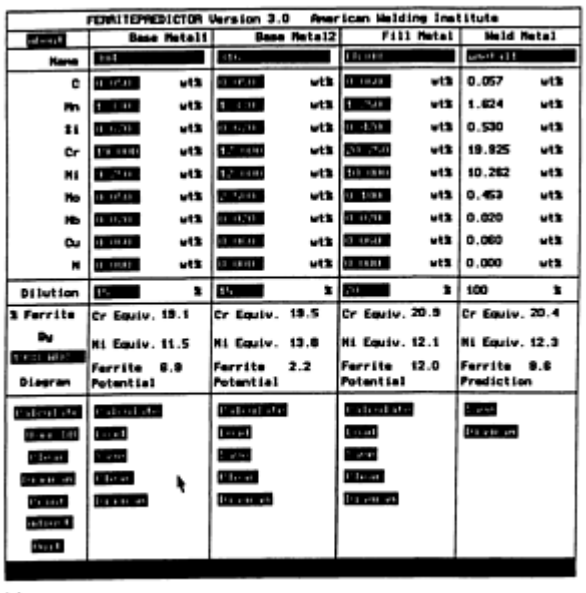

(a)

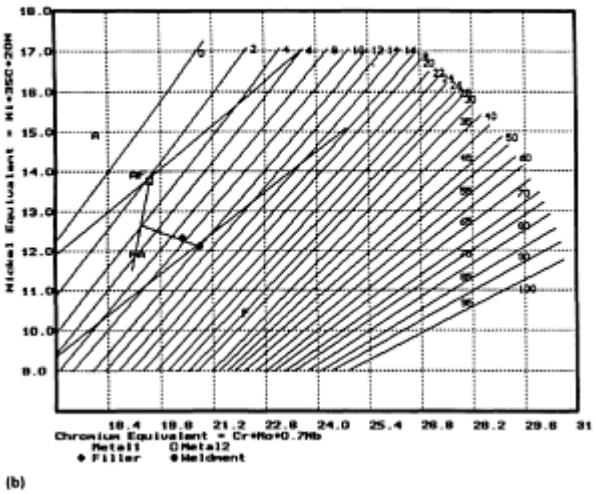

(b)

FIG. 4 EXAMPLES OF EXPERT SYSTEM SCREEN DISPLAYS. (A) USER INTERFACE OF THE FERRITEPREDICTOR EXPERT SYSTEM FOR STAINLESS STEEL FERRITE ANALYSIS. (B) A FERRITE ANALYSIS OF A DISSIMILAR METAL STAINLESS STEEL WELD (BASE METALS, 304 AND 316; FILLER METAL, ER308) USING THE 1988 WRC DIAGRAM IN THE FERRITEPREDICTOR EXPERT SYSTEM

A *neural network system* (NNS) is a computer hardware and software technique that simulates an interconnected network of biological neurons, similar to a portion of the human brain. A neural network can be trained with given patterns, called training sets. After the NNS "learns" from the training set, the network can retrieve these patterns and can make generalizations for patterns that are not included in the training set. Neural networks can be used in associative memory, object or pattern classification, process modeling and control, and signal processing. A detailed discussion of neural networks can be found in Ref 8 and 9.

The important NNSs contained in the WELDEXCELL off-line planner are WELDBEAD and HEATFLOW. WELDBEAD, a neural network model of the welding process, predicts bead geometry, such as the bead width, height, and penetration, for a given set of welding parameters and a specific joint configuration. Figure 5 shows the user interface for the WELDBEAD software. A more detailed discussion of the WELDBEAD system can be found in Ref 10.

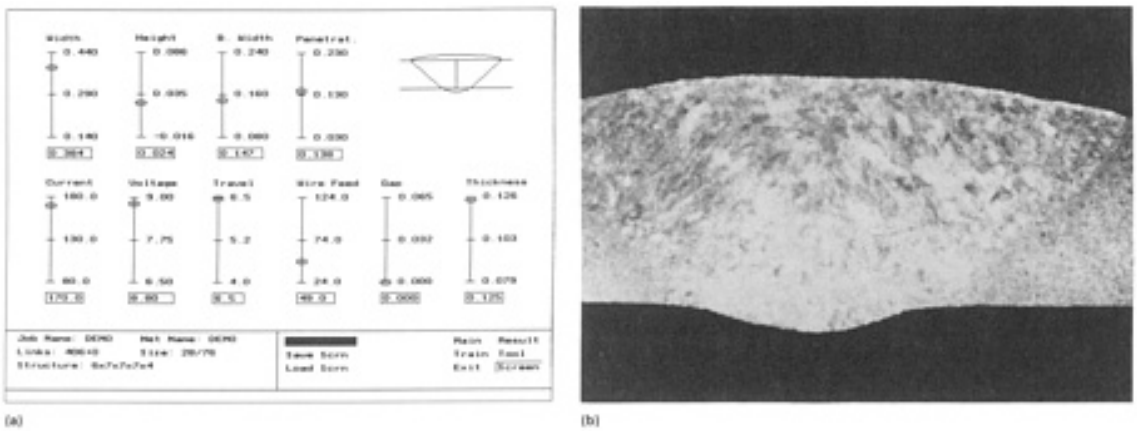

FIG. 5 NEURAL NETWORK SYSTEM FOR AUTOMATED WELDING. (A) USER INTERFACE OF WELDBEAD NEURAL NETWORK WELD MODEL FOR A GTAW WELD IN THIN-SECTION STAINLESS STEEL. (B) MACROGRAPH OF THE RESULTING TEST WELD CORRESPONDING TO THE PREDICTION BY THE WELDBEAD NEURAL NETWORK, SHOWN IN (A)

The HEATFLOW system is used to predict the temperature distribution in the weld. This neural network is a model of the heat flow during welding. When given the voltage, current, wire speed, and travel speed, it can predict the size and shape of the liquid weld pool, as well as provide a map of isothermal lines. This system produces information that is helpful in selecting the proper preheat and postweld heat treatment schedule. Figure 6 shows the WELDHEAT user interface. Reference 11 provides more information.

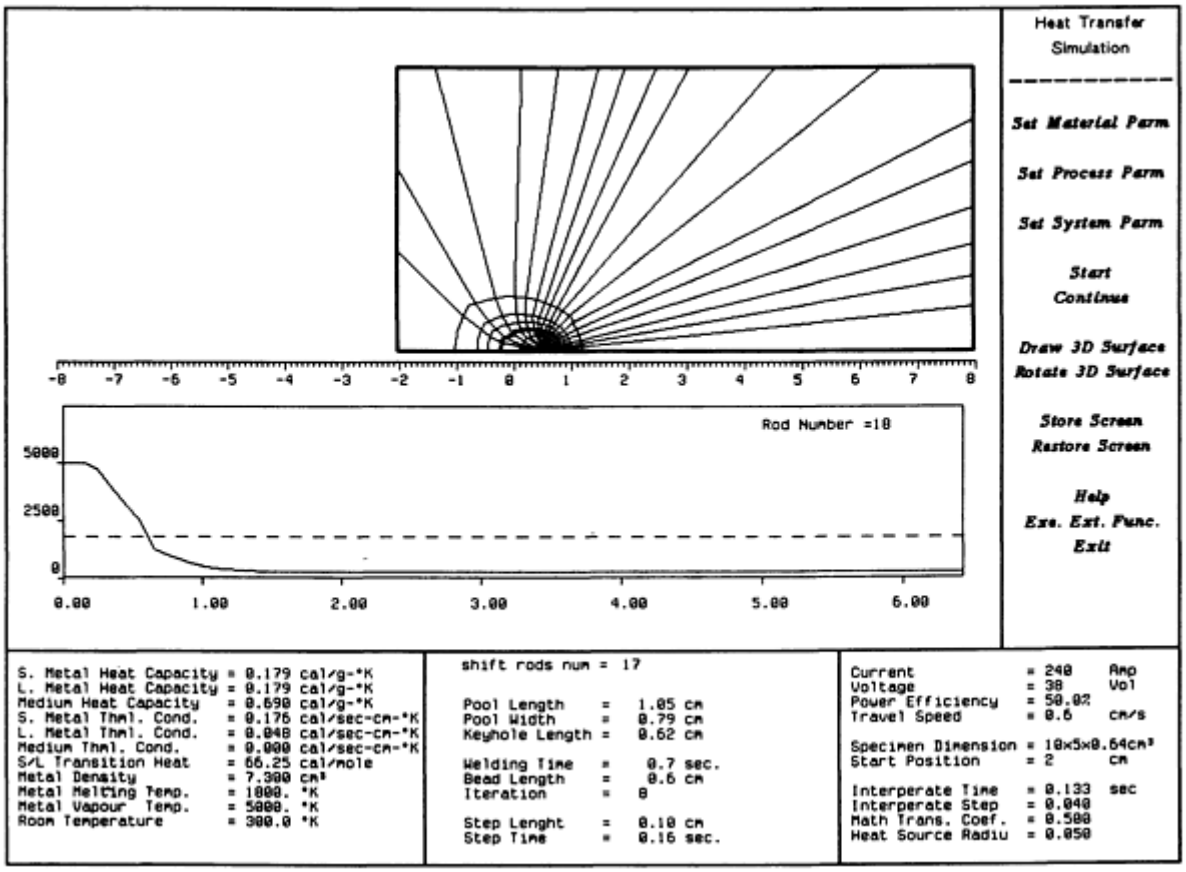

FIG. 6 WELDHEAT PROGRAM USER INTERFACE

In a complex computer software system, such as intelligent welding off-line planning, supervisory software is needed to coordinate the system. One type of supervisory system, known as a "blackboard," was first developed in the 1980s (Ref 12, 13). The computer blackboard architecture has proven to be an efficient system for controlling multiple-knowledge sources, including expert systems, data base systems, neural network systems, and human users. The blackboard integrates and organizes the actions of the various software systems. Often, a blackboard will have an expert system as the principal control element. As an example, the structure of the WELDEXCELL schedule developer is shown in Fig. 7 with the blackboard as the central controller.

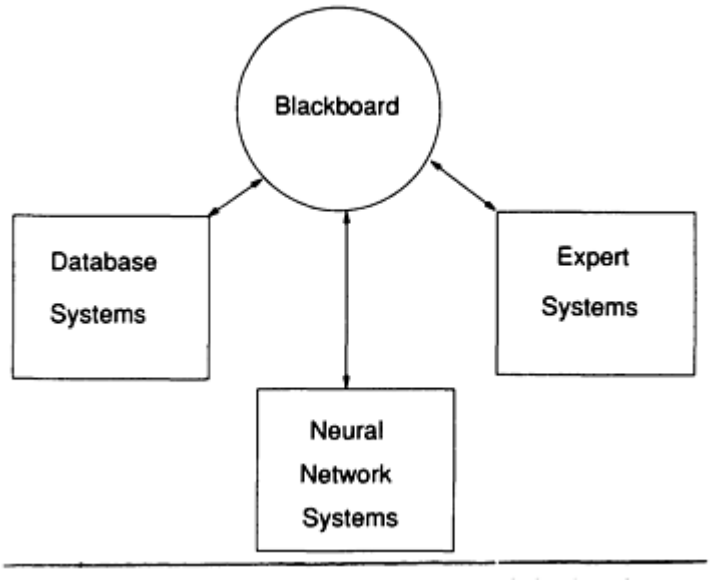

FIG. 7 OPERATION OF THE WELDING SCHEDULE DEVELOPER FROM THE WELDEXCELL SYSTEM

System Integrator. Once an initial weld path has been established and the welding schedule determined, the two separate sets of information must be integrated. Then, the automated welding system will be able to control the process and the torch motion simultaneously to produce a weld.

The first task of this module is to develop a complete robot path. Using the previously developed initial path, this module expands the welding portion to include all passes of a multiple-pass weld. Torch velocity is also assigned to each segment based on the travel speed specified in the schedule developer model. The final welding instruction (path and process control information) can then be sent to the robot simulation, where final modifications can be made by the human user, based on the performance of the simulation execution.

The other task of this module is to combine all of the information, such as pass number(s) and welding parameters, into a set of interface files. These interface files can then be sent to the real-time control system for execution.

References cited in this section

1. CHAPTER 14, *WELDING HANDBOOK,* 8TH ED., VOL 1, AWS, 1987
2. M.Y. DEMDERI, "EXPERT SYSTEM APPLICATION IN MATERIAL PROCESSING AND MANUFACTURING," FORD MOTOR COMPANY, OCT 1989
3. J. JONES, D. WHITE, X. XU, *ET AL.,* DEVELOPMENT OF AN OFF-LINE WELD PLANNING SYSTEM, *TEXAS INSTRUMENTS TECH. J.,* WINTER 1987, P 47-53
4. R.D. STOUT, *WELDABILITY OF STEELS,* 4TH ED., WELDING RESEARCH COUNCIL, 1987
5. H. SUZUKI, N. YURIOKA, AND M. OKUMURA, A NEW CRACKING PARAMETER FOR WELDED STEELS CONSIDERING LOCAL ACCUMULATION OF HYDROGEN, *WELD. WORLD,* VOL 21, 1983, P 2-15
6. H. SUZUKI AND N. YURIOKA, PREVENTION AGAINST COLD CRACKING BY THE HYDROGEN ACCUMULATION CRACKING PARAMETER PHA, *TRANS. JPN. WELD. SOC.,* VOL 14 (NO. 1), APRIL 1983, P 2-14
7. N. YURIOKA, M. OKUMURA, T. KASUYA, AND S. OHSHITA, *WELDING NOTE,* 2ND ED., NIPPON STEEL R&D LABORATORIES
8. D.E. RUMELHART, J.L. MCCLELLAND, AND THE PDP RESEARCH GROUP, *PARALLEL DISTRIBUTED PROCESSING,* MIT PRESS, 1988

9. C. LAU, ED., *NEURAL NETWORKS,* IEEE PRESS, 1992
10. A. ROCK, X. XU, AND J. JONES, "TYPICAL NEURAL NETWORK APPLICATIONS IN SIGNAL PROCESSING AND PROCESS MODELLING," PAPER NO. 256, CORROSION 92, NACE
11. X. XU AND J. JONES, "A COMPUTER MODEL OF HEAT FLOW IN ARC WELDING," PAPER PRESENTED AT 1991 AWS CONFERENCE (DETROIT, MI), AWS
12. H.P. NII, BLACKBOARD SYSTEMS: THE BLACKBOARD MODEL OF PROBLEMS SOLVING AND THE EVOLUTION OF BLACKBOARD ARCHITECTURES, *THE AI MAGAZINE,* SUMMER 1986, P 28-53
13. X. XU, J. JONES, *ET AL.,* INVESTIGATION OF A BLACKBOARD ARTIFICIAL INTELLIGENCE COMPUTER ARCHITECTURE FOR WELDING PROCEDURE SPECIFICATION AND STRUCTURE INTEGRITY ANALYSIS, PROC. *2ND INT. CONF. ON TRENDS IN WELDING RESEARCH,* ASM INTERNATIONAL 1990, P 985-989

Intelligent Automation for Joining Technology

Xiaoshu Xu and Jerald E. Jones, American Welding Institute

Interface Between Off-Line Planners and Real-Time Control Systems

The interface is the communication link between the off-line planner and the real-time control system. This interface is based on computer files, which include the:

- *JOB DESCRIPTION FILE* (*JDF*). THIS FILE CONTAINS THE NAMES OF THE OTHER FILES THAT ARE ASSOCIATED WITH A SPECIFIC WELD JOB.
- *PART SEGMENT FILE* (*PSF*). THIS FILE PROVIDES A DESCRIPTION OF EACH PART SEGMENT TO WELD.
- *JOB TASK FILE* (*JTF*). THIS FILE CONTAINS A SEQUENCE OF TASKS DESCRIBING THE EXECUTION SEQUENCE OF A WELD JOB.
- *WELD SET FILE* (*WSF*). THIS FILE CONTAINS ALL OF THE WELD SETS TO BE USED FOR THE JOB. (WELD SETS ARE DESCRIBED BELOW.)
- *WELD PASS FILE* (*WPF*). THIS FILE PROVIDES INFORMATION FOR CONTROLLING THE MOVEMENTS OF THE ROBOT ALONG EACH PASS.
- *ROB TRAJECTORY FILE* (*RTF*). THIS FILE DEFINES THE ROBOT TRAJECTORY AND POSITIONER MOVEMENT.
- *PART SETUP FILE* (*PSF*).THIS FILE CONTAINS INFORMATION FOR POSITIONING THE PART TO BE WELDED ON THE PART POSITION TABLE, AND FOR LOCATING THE PART RELATIVE TO THE WORLD COORDINATE FRAME OPERATOR.
- *JOB PICTURE FILE* (*JPF*). THIS FILE CONTAINS PIXEL-MAP IMAGES SHOWING THE CROSS-SECTIONAL VIEW OF ALL WELDED JOINTS.
- *JOB NOTES FILE* (*JNF*). THE JNF CONTAINS NOTES OR COMMENTS ABOUT THE WELDING PROCEDURE AND PROVIDES FOR COMMUNICATION BETWEEN THE ENGINEER AND THE WELDING SYSTEM OPERATOR.
- *JOB INTERMEDIATE FILE* (*JIF*). THIS FILE REFLECTS THE JOB STATE AND CONTAINS ANY CHANGES DETERMINED BY THE OPERATOR IN THE SETUP PROCEDURE.
- *JOB RESULTS FILE* (*JRF*). THIS FILE REFLECTS THE FINAL JOB STATE, AS IT WAS ACTUALLY EXECUTED.

This set of files has been proposed to the American Welding Society (AWS) A9 Committee as part of a standard (A9.3) for such interfaces.

The JDF, JTF, PSF, WSF, WPF, RTF, PSF, JPF, and JNF are generated by the off-line planner and sent to the real-time controller. The JIF and JRF store information retrieved during weld job execution from the real-time controller. These files are then sent back to the off-line planner in order to update it and to provide additional training examples for the neural network systems. Many automated welding systems that are computer controlled utilize a "weld set."

- THE FOLLOWING INFORMATION SHOULD HELP TO CLARIFY THE DESCRIPTION OF THE INTERFACE:
- *WELD SET.* A WELD SET IS A COLLECTION OF WELDING PARAMETERS THAT INCLUDES CURRENT, VOLTAGE, TRAVEL SPEED, WIRE FEED SPEED, AND WELDING TORCH ANGLE. WELD SETS ARE IDENTIFIED BY A DESIGNATOR SUCH AS A WELD SET NUMBER (WSN).
- *TRAJECTORY.* A TRAJECTORY IS A CONTINUOUS MOVEMENT OF THE ROBOT WITH THE FOLLOWING RESTRICTIONS: FIRST, A TRAJECTORY HAS EITHER ONE WELD PATH ASSOCIATED WITH IT OR NO PATH, AS IN THE CASE OF A TRANSITION FROM ONE WELD SEGMENT TO AN ADJACENT WELD SEGMENT. SECOND, A TRAJECTORY HAS ONE MOVE PATTERN. THE MOVE PATTERN CAN BE A 3-D STRAIGHT LINE, ARC, SPLINE, OR NONE. NONE, IN THIS CONTEXT, MEANS THAT NO SPECIFIC MOVE PATTERN IS REQUIRED. FOR ROBOTS OF THE PRESENT TIME, THE MOVING VELOCITY HAS TO BE CONSTANT. IT IS LIKELY THAT THIS WILL NOT BE TRUE OF FUTURE ROBOT SYSTEMS. A TRAJECTORY IS IDENTIFIED BY AN IDENTIFIER, SUCH AS A TRAJECTORY NUMBER. BASED ON THIS DEFINITION, EACH PASS IS ASSOCIATED WITH ONE UNIQUE TRAJECTORY.
- *WELD JOB.* A WELD JOB CAN HAVE SEVERAL WELD SCHEDULES. THIS MEANS THAT IN THE EXECUTION OF A WELD JOB, THE WELDING PARAMETERS IDENTIFIED ABOVE CAN BE VARIED. PARAMETERS THAT CANNOT BE ADJUSTED DURING WELDING, SUCH AS FILLER-METAL TYPE AND SIZE OR GAS TYPE AND FLOW RATE, REMAIN CONSTANT FOR ANY CONTINUOUS OPERATION. HOWEVER, THESE PARAMETERS MAY CHANGE FROM ONE PASS TO ANOTHER.

Intelligent Automation for Joining Technology

Xiaoshu Xu and Jerald E. Jones, American Welding Institute

Real-lime Intelligent Control System

The real-time controller for an intelligent automated welding system has several functions. First, it must control the motion of the welding torch. Second, the control of the welding process equipment must be coordinated with the location of the torch in the weld joint. Third, software and hardware are needed to process and interpret the signal data from one or more sensors. Fourth, the controller must have an adaptive process planning and control modification system for making adjustments to the control parameters based on the interpreted sensor data and process models. Finally, for process control and planning improvement, the real-time controller is a platform for the collection of data about the weld that can be up-loaded electronically to the off-line planning system.

Standards

In order for the real-time controller to communicate with the welding process systems and with the off-line planner, it is important that standards be established for the storage and communication of computerized welding information. The AWS A9 and D16 Committees are developing such standards, and the reader is referred to AWS/ANSI A9.1-92 and A9.2-92, as well as the soon to be published standards, such as AWS/ANSI A9.3 and A9.4, and ASTM E49 Committee standards.

Real-Time Control System

The real-time control system comprises six major modules:

- THE INTERFACE TO A JOB DATA FILE OR AN OFF-LINE PLANNER
- THE JOB INTERPRETER
- THE JOB EDITOR AND USER INTERFACE
- THE HARDWARE CONTROLLER OF THE WELDING CELL
- THE HARDWARE OF THE WELDING CELL AND THE ASSOCIATED SENSORS
- THE SENSOR DATA PROCESSOR

Figure 8 shows the structure of a typical real-time intelligent welding control system. Such a system generally consists of a stand-alone computer system and video display device that are built into a shop floor "hardened" cabinet. The cabinet also includes the necessary computing hardware (that is, backplane, processor boards, and other special-purpose electronics) for the real-time control of the welding cell hardware and sensor data input.

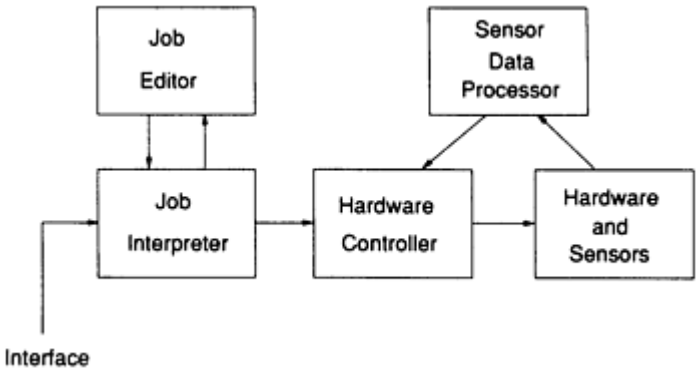

FIG. 8 TYPICAL REAL-TIME CONTROL SYSTEM

The interface module is capable of bidirectional data transfer between the real-time control system and external job data. The job data can reside in a simple data base, for example, on a central data storage device in a network. The interface may only need to download this data. Alternatively, the job data can be obtained by direct communication with the off-line planning system.

The job interpreter reads the interface files and generates the control information. The files that are sent from the interface are used to develop all of the "low-level" control-system parameter values, such as the trajectory for the robot controller and welding parameters for the welding power supply controller. This information is then sent electronically to the welding cell hardware controller subsystem. In addition, the control information is presented to a user interface video screen that the welding cell operator can access. The job interpreter translates the control parameters into data that can be understood by the operator.

The job editor provides an interface for the operator to modify the set points of the welding parameters and robot trajectory prior to the execution. An "intelligent" system will provide software that ensures that these modifications cannot exceed the given minimum and maximum limitations, as specified by the welding engineer or the applicable codes and specifications.

Hardware Controller. A controller is provided for each piece of controllable hardware, such as the robot, welding power supply, wire feed system, gas solenoid and pressure regulators, and others. These hardware controllers typically consist of a digital signal processing integrated circuit that is fast enough to provide control signals to the cell hardware components. These controllers receive information from a software system that interprets sensor data, combines the data with information from the job interpreter, and sends the corresponding commands to the hardware controllers to perform the proper task. Such software systems can be simple set-point or proportional-integral-differential (PID) control systems, or they can be very complex, adaptive, model-based control systems or fuzzy-logic-based control systems.

Basic software control systems attempt to control specific variables based on predefined set-point values. The simplest is an on/off type that turns either on or off, depending on the current value of a control parameter. For example,

if the voltage is less than the set-point value, then an on/off type controller would step up the voltage by the difference between the current value and the set-point value. A more complex controller, the PID type, would make an adjustment to the voltage, but would try not to "overshoot" the value by making small changes to the voltage that were "proportional" to the difference between the current value and the set-point value.

Intelligent adaptive software control systems change the values of one or more control parameters simultaneously, according to the desired "result" of the weld. That is, if a sensor indicated that the weld was not penetrating completely through a root pass, then an intelligent adaptive system would simultaneously change the values of the voltage, current, and travel speed to achieve the end result of increasing the weld penetration. These systems represent a significant improvement in the control capability of the welding process and will, in the future, offer the ability to improve quality and productivity while reducing costs and postweld inspection requirements.

Intelligent adaptive control depends on accurate models of the welding process and, in turn, good theoretical research and empirical results from adequate experimentation. One system design that appears to offer a good methodology for solving the intelligent adaptive control problem is the "hierarchical" architecture. In a hierarchical system, one or more control loops exercise supervisory control over the bottom-level process parameter control system (generally, a PID-type controller).

For example, there could be two supervisory control loops. A neural-network-based inner loop could make direct modifications to the weld control parameter set points for the PID controller. An expert-system-based outer loop would make longer-range control decisions, such as overall weld size for adaptive fill, or overall heat-input changes to account for large dimensional changes to the material being welded. The inner loop would take input from sensors, such as a penetration sensor, and make adjustments quickly to account for penetration variations. The outer loop would accept input from sensors, such as a laser scanner joint profiler, and make changes to the weld deposit size and shape inputs to the inner loop.

Welding Cell Hardware and Sensors. The welding cell includes a set of equipment designed to produce automated welds. This equipment consists of a welding torch manipulation system (for example, a robot), a fixturing and positioning system, a parts transport system, a welding power supply, welding consumable supply systems (wire feeder, flux feeder, gas control equipment, and others), control hardware as described above, fume/consumable removal systems (flux vacuum, fume extraction, and others), sensor systems, and other cell-servicing systems (for example, an automated torch cleaning system).

Robot System. The torch manipulation system must be capable of positioning the torch correctly for the welding operation, moving the torch along the weld in a smooth and controllable manner, operating at useful speeds for the welding operations, and positioning the torch for service (for automatic cleaning, for example). Because not all robot systems can move in continuous paths at the appropriate speeds for welding, the choice of robot hardware is important when setting up an automated welding manufacturing cell. Although a robot system is capable of traversing continuous paths at the appropriate speeds, the robot control software and programming language may not be amenable to welding. The software should be designed to easily produce continuous smooth-path motions, including automatic straight line, arc, and spline interpolation and speed control.

The range of motion of the robot should be considered. Its required motion can be very dependent on the motion capability of the welding part fixture and positioning system. The "operating window" of the robot can easily be obtained from its manufacturer and should be carefully examined to determine the suitability of the robot for the parts to be produced. Because robots can have extended lifetimes, all of the anticipated uses of the robot during its expected life should be considered.

The weight-carrying capacity of the robot and the influence of weight on robot accuracy and repeatability should also be considered. The manipulator must be able to lift the weight of the welding torch; the gas, water, and electrode supply tubes; the sensor systems; the flux supply system; and other equipment. As the weight on the robot end effector increases, the accuracy and repeatability of the robot may degrade.

Robot accuracy is a measure of the ability of the robot hardware and associated control system to position the robot at a specific location in 3-D space, given the coordinates of that position. Robot repeatability is the measure of the ability of the robot to return to the same position in space at a later time. Both of these values will affect the ability of the robot to repeatedly position the welding electrode and sensors in the correct positions for welding during the life of the system. These values can be obtained from the robot vendor. Often, these values are also affected by the speed of the robot, and

either the vendor or an independent testing laboratory can test the degradation of accuracy and repeatability under dynamic conditions. For welding purposes, it is important to obtain information about the dynamic response of the system, because robot accuracy and repeatability will change as the speed increases. Furthermore, during the welding process, the robot will always be moving (except in the case of spot resistance welds).

Fixturing and Positioning System. The parts to be welded must be held in position for welding. The robot is capable of being programmed to travel along a complex path and to position the welding torch in that preplanned path. However, the accuracy of that positioning not only depends on the robot system and its controller, but on the accuracy of the part location, as well. The positioning system must accurately locate the weld joint so that the robot can "find" the joint. It is difficult and often costly to have a sensor system (for example, a camera) that can locate the part for the robot. Therefore, it is advantageous to utilize a positioning system that can locate the part with sufficient accuracy and repeatability for the weld being made.

Often, it is advantageous to have a positioning system that can move the part to the robot operating window. Such positioners may have several "indexed" positions. An indexed positioner could have four positions: one for loading the part, one for inspecting the part to be welded, one for the welding operation, and one for postweld inspection.

Finally, moving positioners are capable of positioning the weld dynamically during the welding process. In this way, the weld can be maintained in the same welding position (for example, flat) throughout the welding operation. Flat welding often will provide greater weld quality and consistency. Consequently, positioners of this type represent a useful addition to an automated welding cell. Such a system, however, is much more complex than a simple indexed positioner. The motion of the robot and of the positioner must be coordinated. Generally, the positioner has a completely separate controller. Therefore, either the robot controller or a separate computer system must integrate the actions of the positioner with the robot.

Parts Transport System. The parts to be welded must be transported to and from the automated welding cell. Because of the expense of the cell, it should weld as many parts as possible per unit time. To accomplish this, parts need to be transported to and from the weld cell at rates and times that provide the most efficient operation. Thus, if an automated transport system is used, it should be electronically or mechanically coordinated to operate in conjunction with the robot cell positioner and welding operation cycle time.

Welding Power Supply. The choice of welding power supply is important to the success of an intelligent automated welding system. Because the adaptive control system will need to both change the welding parameters during the welding process and control the power supply, a communications link is essential. The power supply must be controllable by an external computer system through this communications link, and must allow modification of voltage and/or current set-point values during the welding process.

Most robots are operated by electric motors with sensitive controls. If the power supply emits high-frequency electromagnetic noise (for example, a high-frequency start or a pulsed-voltage start for gas-tungsten arc welding) or other types of electromagnetic noise, then the robot system may not be able to operate. This type of electronic noise can cause the robot computer to "crash." More serious damage to the robot or the cell controller can also result.

Welding Consumable Supply Systems. The intelligent automated welding cell requires equipment that can supply welding consumables to the welding operation. This includes devices such as a flux feeder, gas supplies, wire/electrode feed system, and others. Each of these components should have a digital (computer) or analog control communications link that can be accessed by the control system. These can be as simple as turning the gas flow on and off or as complex as fully computer controlled linear mass flow metering for accurate gas mixing and flow control. The systems selected should reflect the type of welding that needs to be performed and the necessary control communication links.

Control hardware, as described above, needs to be in a shop floor "hardened" cabinet that may require external cooling. The cabinet also should be shielded from any electromagnetic noise that is generated by the weld or any associated equipment.

Fume/Consumable Removal Systems. Many welding fume components are now recognized as being hazardous or noxious. Therefore, the welding fumes should be removed from the weld at a point that is as close to the weld as possible in order to minimize the volume of air that requires filtering. Fume extraction systems should be obtained and fitted so that they minimally interfere with the operation and motion of the robot and welding torch. For submerged arc welding, flux vacuum systems can provide flux recovery, and the reuse of used flux can provide some cost savings. In some cases,

the flux can easily be screened and reused. Because some specifications put limits on the number of times a flux can be recycled, a used-flux management system may need to be developed for the recovery system.

Sensor Systems. A wide variety of sensor systems can be employed in an intelligent automated welding cell. Types of sensors are described below.

Laser scanning sensors use reflected light information from a scanned laser stripe or region to provide data for weld seam guidance, dynamic calculation of the amount of fill required, and location of the part and weld joint for purposes of robot orientation.

A charge-coupled device (CCD) video camera provides information that can be used to determine weld pool size and shape, welding joint guidance (Fig. 9), and collision detection. The camera can be placed inside of a gas-tungsten arc welding (GTAW) torch in order to decrease the sensor package size and to obtain weld pool data. It can be combined with a laser stripe to provide joint geometry and fill information. In addition, a camera has been used to "look" at the back side of a weld and to determine, through measurements of total light intensity, the penetration or lack thereof by the liquid weld pool.

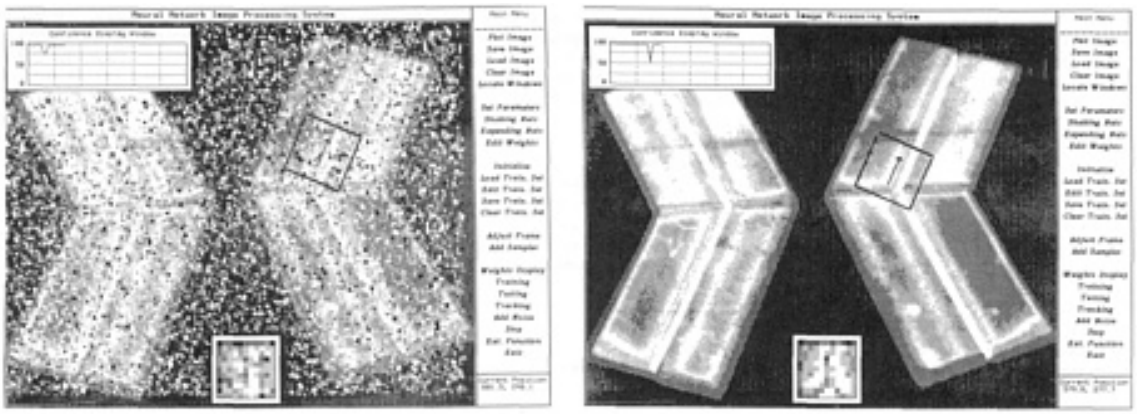

FIG. 9 NEURAL-NETWORK-BASED SEAM-TRACKING SYSTEM. (A) SYSTEM UTILIZING A CCD ARRAY CAMERA TRACKING A CLEAR IMAGE. (B) SYSTEM UTILIZING A CCD ARRAY CAMERA TRACKING AN IMAGE WITH SIMULATED SMOKE AND SPATTER FROM A FCAW PROCESS

Ultrasonic sensors, of both the contacting (piezoelectric crystal) and noncontacting (electromagnetic acoustic transducer) varieties, have been used in the laboratory to evaluate the penetration characteristics of the weld. Other uses also are being investigated.

Acoustic emission sensor data have been used in the laboratory and in limited production applications to determine the formation of welding discontinuities. This sensor has been reported to be able to detect cracking, incomplete fusion, inadequate penetration, and porosity formation.

Through-the-arc voltage/current sensors can detect voltage changes. In a weaving-type weld, the arc gap decreases as the sides of the joint are approached, causing a detectable change in voltage. This voltage change can be used to "guide" the robot along a weld seam in a prepared joint groove. This type of sensor can also determine the transfer modes for gas-metal arc welding and flux-cored arc welding (FCAW), as demonstrated in the laboratory. In addition, it can detect inadequate penetration defect formation through the use of advanced signal processing technology.

Airborne acoustics information (that is, the sound that the weld makes) has been used to diagnose the formation of defects and to determine metal-transfer modes. This type of sensor has been demonstrated in the laboratory. Through the use of multiple sensors and a triangulation algorithm, airborne acoustic data also have been used to locate the position of the welding torch in laboratory demonstrations.

An emission spectroscopic sensor has been developed by the U.S. Army and is patented for use in detecting hydrogen contamination of the welding arc plasma. This sensor can detect the presence of excessive amounts of hydrogen that cause cracking in higher-strength welds.

Infrared thermal area-type cameras have been used in the laboratory and in limited production applications to determine the shape and size of the weld pool and to provide some cooling rate data. A point-type camera also has been used, in conjunction with an AI-based heat-flow model, to determine thermal information and to control the cooling rate of welds.

A low-voltage "touch" sensor operates by energizing the electrode with a very low voltage, which enables the reasonably accurate detection of the electrode when it is brought in very close proximity to the part. This type of sensor also has been used to allow a GTAW electrode to be withdrawn an accurate and small distance from the part and then to energize the arc plasma. This eliminates the need for a high-frequency or high-voltage pulse starter for the automated GTAW process. Experimentally, such sensors are being developed to locate the joint or other locating positions on a part for robot spatial orientation.

An eddy current seam locator (probe) has been used in the laboratory and in limited production applications to scan the surface of a weld joint just ahead of the weld torch in order to "find" the weld seam and track the automated welding system along the joint. This is particularly useful for tracking square butt joints in shiny materials (for example, polished aluminum) that are tightly closed and not visible in CCD camera images.

Other cell services may be required in order to keep the welding equipment operational. For example, automated torch cleaning systems utilize rotating wire brushes or other devices to clean the spatter from GMAW and FCAW welding torches.

Automated welding cell utility services provide adequate power for the welding power supply and for the operation of other equipment; water as a coolant; welding gas; compressed air (for pneumatic devices on the robot or positioner); and network communication links to the computer-integrated manufacturing system.

Intelligent Automation for Joining Technology

Xiaoshu Xu and Jerald E. Jones, American Welding Institute

References

1. CHAPTER 14, *WELDING HANDBOOK,* 8TH ED., VOL 1, AWS, 1987
2. M.Y. DEMDERI, "EXPERT SYSTEM APPLICATION IN MATERIAL PROCESSING AND MANUFACTURING," FORD MOTOR COMPANY, OCT 1989
3. J. JONES, D. WHITE, X. XU, *ET AL.,* DEVELOPMENT OF AN OFF-LINE WELD PLANNING SYSTEM, *TEXAS INSTRUMENTS TECH. J.,* WINTER 1987, P 47-53
4. R.D. STOUT, *WELDABILITY OF STEELS,* 4TH ED., WELDING RESEARCH COUNCIL, 1987
5. H. SUZUKI, N. YURIOKA, AND M. OKUMURA, A NEW CRACKING PARAMETER FOR WELDED STEELS CONSIDERING LOCAL ACCUMULATION OF HYDROGEN, *WELD. WORLD,* VOL 21, 1983, P 2-15
6. H. SUZUKI AND N. YURIOKA, PREVENTION AGAINST COLD CRACKING BY THE HYDROGEN ACCUMULATION CRACKING PARAMETER PHA, *TRANS. JPN. WELD. SOC.,* VOL 14 (NO. 1), APRIL 1983, P 2-14
7. N. YURIOKA, M. OKUMURA, T. KASUYA, AND S. OHSHITA, *WELDING NOTE,* 2ND ED., NIPPON STEEL R&D LABORATORIES
8. D.E. RUMELHART, J.L. MCCLELLAND, AND THE PDP RESEARCH GROUP, *PARALLEL DISTRIBUTED PROCESSING,* MIT PRESS, 1988
9. C. LAU, ED., *NEURAL NETWORKS,* IEEE PRESS, 1992
10. A. ROCK, X. XU, AND J. JONES, "TYPICAL NEURAL NETWORK APPLICATIONS IN SIGNAL

PROCESSING AND PROCESS MODELLING," PAPER NO. 256, CORROSION 92, NACE

11. X. XU AND J. JONES, "A COMPUTER MODEL OF HEAT FLOW IN ARC WELDING," PAPER PRESENTED AT 1991 AWS CONFERENCE (DETROIT, MI), AWS
12. H.P. NII, BLACKBOARD SYSTEMS: THE BLACKBOARD MODEL OF PROBLEMS SOLVING AND THE EVOLUTION OF BLACKBOARD ARCHITECTURES, *THE AI MAGAZINE,* SUMMER 1986, P 28-53
13. X. XU, J. JONES, *ET AL.*, INVESTIGATION OF A BLACKBOARD ARTIFICIAL INTELLIGENCE COMPUTER ARCHITECTURE FOR WELDING PROCEDURE SPECIFICATION AND STRUCTURE INTEGRITY ANALYSIS, PROC. *2ND INT. CONF. ON TRENDS IN WELDING RESEARCH,* ASM INTERNATIONAL 1990, P 985-989

Corrosion of Weldments

A. Wahid, D.L. Olson, and D.K. Matlock, Colorado School of Mines; C.E. Cross, Martin Marietta Astronautics Group

Introduction

WELDMENTS exhibit special microstructural features that need to be recognized and understood in order to predict acceptable corrosion service life of welded structures (Ref 1). This article describes some of the general characteristics associated with the corrosion of weldments. The role of macrocompositional and microcompositional variations, a feature common to weldments, is emphasized in this article to bring out differences that need to be realized in comparing corrosion of weldments to that of wrought materials. A more extensive presentation, with data for specific alloys, is given in Volume 13 of the *ASM Handbook* (Ref 2).

Weldments inherently possess compositional and microstructural heterogeneities, which can be classified by dimensional scale. On the largest scale, a weldment consists of a transition from wrought base metal through a heat-affected zone and into solidified weld metal and includes five microstructurally distinct regions normally identified (Ref 3) as the fusion zone, the unmixed region, the partially melted region, the heat-affected zone, and the base metal. This microstructural transition is illustrated in Fig. 1. The unmixed region is part of the fusion zone, and the partially melted region is part of the heat-affected zone, as described below. Not all five zones are present in any given weldment. For example, autogenous (that is, no filler metal) welds do not have an unmixed zone.

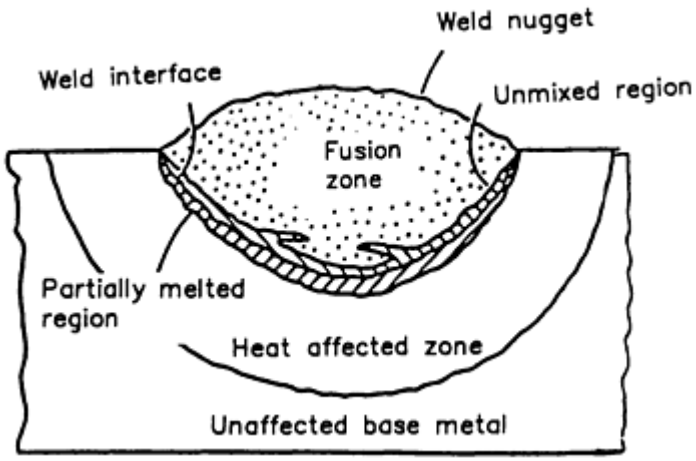

FIG. 1 SCHEMATIC SHOWING THE REGIONS OF A HETEROGENEOUS WELD. SOURCE: REF 3

The fusion zone is the result of melting which fuses the base metal and filler metal to produce a zone with a composition that is most often different from that of the base metal. This compositional difference produces a galvanic couple, which can influence the corrosion process in the vicinity of the weld. This dissimilar-metal couple can produce macroscopic galvanic corrosion.

The fusion zone itself offers a microscopic galvanic effect due to microstructural segregation resulting from solidification (Ref 4). The fusion zone also has a thin region adjacent to the fusion line, known as the unmixed (chilled) region, where the base metal is melted and then quickly solidified to produce a composition similar to the base metal (Ref 5). For example, when type 304 stainless steel is welded using a filler metal with high chromium-nickel content, steep concentration gradients of chromium and nickel are found in the fusion zone, whereas the unmixed zone has a composition similar to the base metal (Fig. 2).

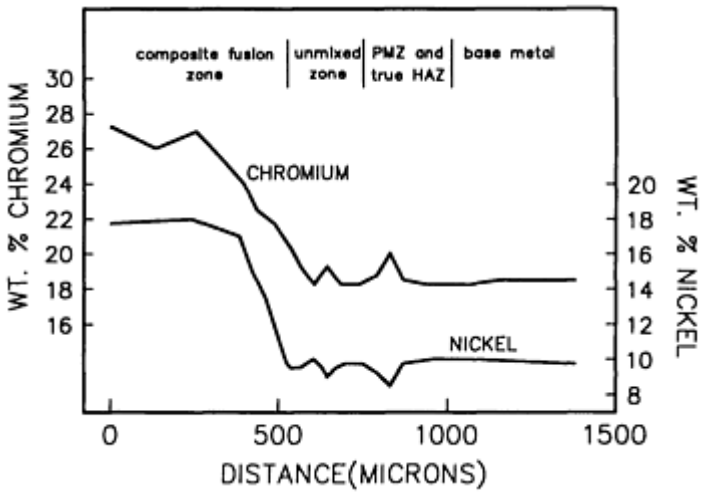

FIG. 2 CONCENTRATION PROFILE OF CHROMIUM AND NICKEL ACROSS THE WELD FUSION BOUNDARY REGION OF TYPE 304 STAINLESS STEEL. SOURCE: REF 5

Heal-Affected Zone. Every position in the heat-affected zone relative to the fusion line experiences a unique thermal experience during welding, in terms of both maximum temperature and cooling rate. Thus, each position has its own microstructural features and corrosion susceptibility.

The partially melted region is usually one or two grains into the heat-affected zone relative to the fusion line. It is characterized by grain boundary liquation, which may result in liquation cracking. These cracks, which are found in the grain boundaries one or two grains below the fusion line, have been identified as potential initiation sites for hydrogen-promoted underbead cracking in high-strength steel.

Microstructural Gradients. On a fine scale, microstructural gradients exist within the heat-affected zone due to different time-temperature cycles experienced by each element of material. Gradients on a similar scale exist within solidified multi-pass weld metal due to bead-to-bead variations in thermal experience. Compositional gradients on the scale of a few microns, referred to as microsegregation, exist within individual weld beads due to segregation of major and trace elements during solidification (Ref 4).

References

1. O.I. STEKLOV *ET AL.*, METHOD OF EVALUATING THE INFLUENCE OF NON-UNIFORMITY OF WELDED JOINT PROPERTIES ON CORROSION, *SVAR. PROIZ.*, VOL 19 (NO. 9), 1972, P 34-36
2. K.F. KRYSIAK *ET AL.*, *METALS HANDBOOK*, VOL 13, 9TH ED., ASM, 1987, P 344-367
3. W.F. SAVAGE, NEW INSIGHT INTO WELD CRACKING AND A NEW WAY OF LOOKING AT WELDS, *WELD. DES. ENG.*, DEC 1969
4. R.G. BUCHHEIT, JR., J.P. MORAN, AND G.E. STONER, LOCALIZED CORROSION BEHAVIOR OF ALLOY 2090--THE ROLE OF MICROSTRUCTURAL HETEROGENEITY, *CORROSION*, VOL 46 (NO. 8), 1990, P 610-617
5. W.A. BAESLACK III, J.C. LIPPOLD, AND W.F. SAVAGE, UNMIXED ZONE FORMATION IN AUSTENITIC STAINLESS STEEL WELDMENTS, *WELD. J.*, VOL 58 (NO. 6), 1979, P 168S-176S

A. Wahid, D.L. Olson, and D.K. Matlock, Colorado School of Mines; C.E. Cross, Martin Marietta Astronautics Group

Forms of Weld Corrosion

Weldments can experience all the classical forms of corrosion, but they are particularly susceptible to those affected by variations in microstructure and composition. Specifically, galvanic corrosion, pitting, stress corrosion, intergranular corrosion, and hydrogen cracking must be considered when designing welded structures.

Galvanic Couples. Although some alloys can be autogenously welded, filler metals are more commonly used. The use of filler metals with compositions different from the base material may produce an electrochemical potential difference that makes some regions of the weldment more active. For example, Fig. 3 depicts weld metal deposits that have different corrosion behavior from the base metal in three aluminum alloys (Ref 6).

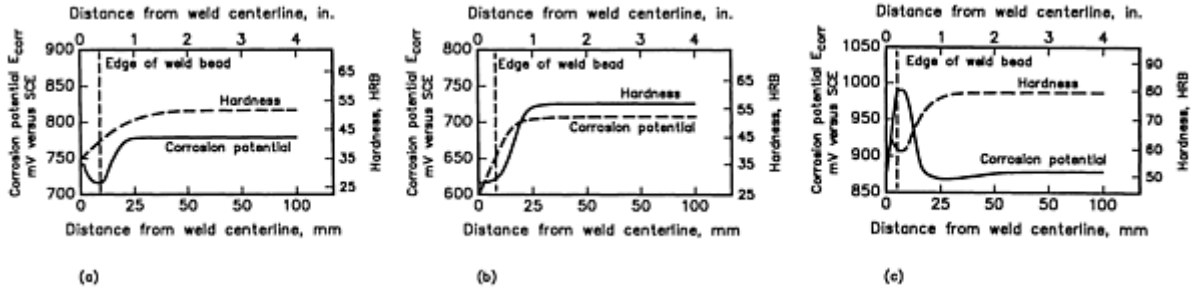

FIG. 3 EFFECT OF WELDING HEAT ON MICROSTRUCTURE, HARDNESS, AND CORROSION POTENTIAL OF THREE ALUMINUM ALLOY WELDED ASSEMBLIES. (A) ALLOY 5456-H321 BASE METAL WITH ALLOY 5556 FILLER. (B) ALLOY 2219-T87 BASE METAL WITH ALLOY 2319 FILLER. (C) ALLOY 7039-T651 BASE METAL WITH ALLOY 5183 FILLER. SOURCE; REF 6

For the majority of aluminum alloys, the weld metal and the heat-affected zone become more noble relative to the base metal, as demonstrated in Fig. 3(a) and 3(b) for a saltwater environment (Ref 6). Certain aluminum alloys, however, form narrow anodic regions in the heat-affected zone and are prone to localized attack. Alloys 7005 and 7039 are particularly susceptible to this problem (Fig. 3c).

There are a number of other common weld deposit/base metal combinations that are known to form galvanic couples. It is common practice to use austenitic stainless steel welding consumables for field repair of heavy machinery, particularly those fabricated from high-strength low-alloy steel. This practice leaves a cathodic stainless steel weld deposit in electrical contact with the steel. In the presence of corrosive environments, hydrogen is generated at the austenitic weld metal cathode, which is capable of maintaining a high hydrogen content without cracking. However, the cathodic behavior of the austenitic weld deposit may increase the susceptibility for stress-corrosion cracking in the heat-affected zone of the high-strength steel. A 40% thermal expansion mismatch between the austenitic stainless steel and ferritic base metal produces a significant residual stress field in the weldment; this residual stress field also contributes to cracking susceptibility. A similar, but more localized, behavior may explain the correlation between stress-corrosion cracking susceptibility and the presence of retained austenite in high-strength steel weld deposits.

Another common dissimilar metal combination involves the use of high-nickel alloys for weld repair of cast iron. Fe-55Ni welding electrodes are used to make weld deposits that can hold in solid solution many of the alloying elements common to cast iron. Furthermore, weld deposits made with Fe-55Ni welding consumables have an acceptable thermal expansion match to the cast iron. Because cast iron is anodic to the high-nickel weld deposit, corrosive attack occurs in the cast iron adjacent to the weld deposit. It is suggested that cast iron welds made with high-nickel deposits be coated (painted) to reduce the susceptibility to selective corrosion attack.

Plain carbon steel weldments can also exhibit galvanic attack. For example, the E6013 welding electrode is known to be highly anodic to A285 base metal in a seawater environment (Ref 7). It is important to select a suitable filler metal when an application involves a harsh environment.

Weld Decay of Stainless Steel. During welding of stainless steels, local sensitized zones (i.e., regions susceptible to corrosion) often develop. Sensitization is due to the formation of chromium carbide along grain boundaries, resulting in depletion of chromium in the region adjacent to the grain boundary (Ref 8, 9, 10, 11, 12, 13, 14). This chromium

depletion produces very localized galvanic cells (Fig. 4). If this depletion drops the chromium content below the necessary 12 wt% that is required to maintain a protective passive film, the region will become sensitized to corrosion, resulting in intergranular attack. This type of corrosion most often occurs in the heat-affected zone. Intergranular corrosion causes a loss of metal in a region that parallels the weld deposit (Fig. 5). This corrosion behavior is called weld decay (Ref 13).

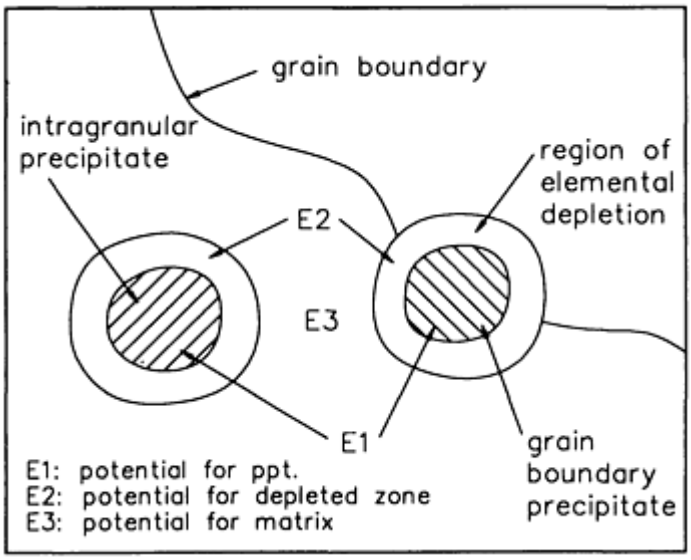

FIG. 4 DEPLETED REGIONS ADJACENT TO PRECIPITATES. THESE REGIONS CAUSE AN ELECTROCHEMICAL POTENTIAL (E) DIFFERENCE THAT CAN PROMOTE LOCALIZED CORROSION AT THE MICROSTRUCTURAL LEVEL.

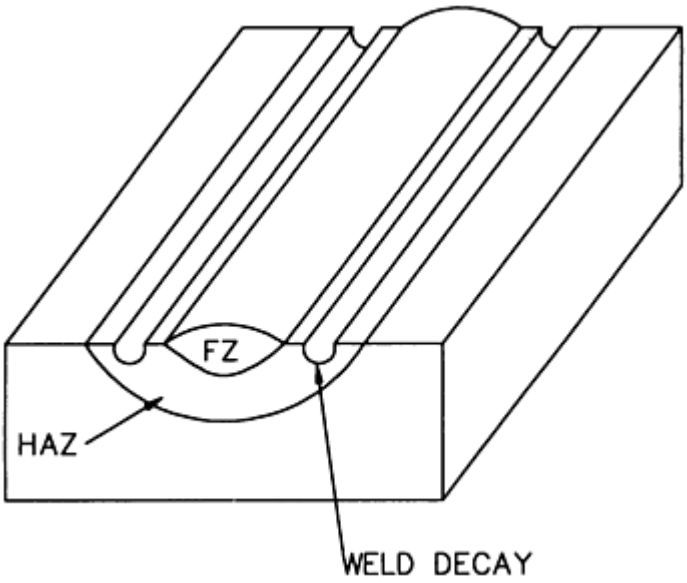

FIG. 5 INTERGRANULAR CORROSION (WELD DECAY) OF STAINLESS STEEL WELDMENTS. FZ, FUSION ZONE

The formation of sufficient chromium carbide to cause sensitization can be described by the C-shaped curves on the continuous cooling diagram illustrated in Fig. 6. The figure shows susceptibility to sensitization as a function of temperature, time, and carbon content (Ref 15). If the cooling rate is sufficiently great (curve A in Fig. 6), the cooling curve will not intersect the given C-shaped curve for chromium carbide and the stainless steel will not be sensitized. By decreasing the cooling rate, the cooling curve (curve B) eventually intersects the C-shape nucleation curve, indicating that sensitization may occur. At very low cooling rates, the formation of chromium carbide occurs at higher temperature and allows for more nucleation and growth, resulting in a more extensive chromium-depleted region.

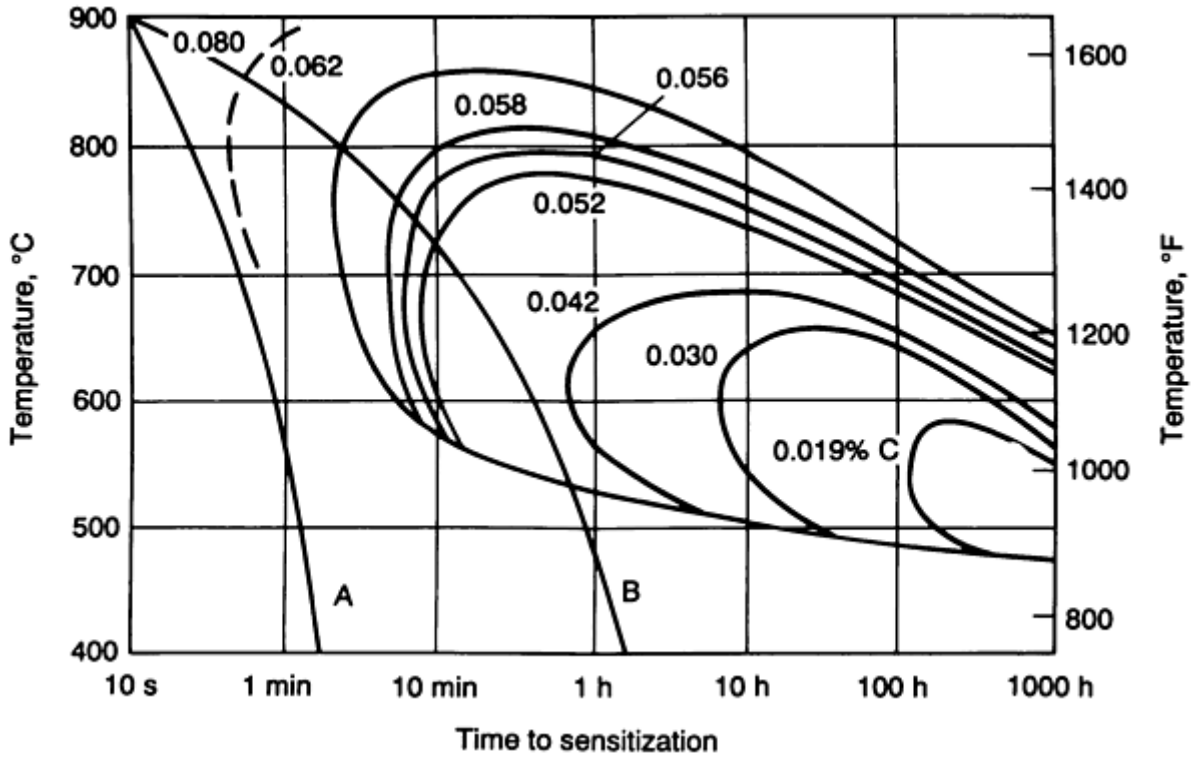

FIG. 6 TIME-TEMPERATURE-SENSITIZATION CURVES FOR TYPE 304 STAINLESS STEEL IN A MIXTURE OF $CUSO_4$ AND HSO_4 CONTAINING COPPER. SOURCE: REF 15. CURVES A AND B INDICATE HIGH AND MEDIUM COOLING RATES, RESPECTIVELY.

The minimum time required for sensitization as a function of carbon content in a typical stainless steel alloy is depicted in Fig. 7. Because the normal welding thermal cycle is completed in approximately two minutes, for this example the carbon content must not exceed 0.07 wt% to avoid sensitization. Notice that the carbide nucleation curves of Fig. 6 move down and to longer times with decreasing carbon content, making it more difficult to form carbides for a given cooling rate.

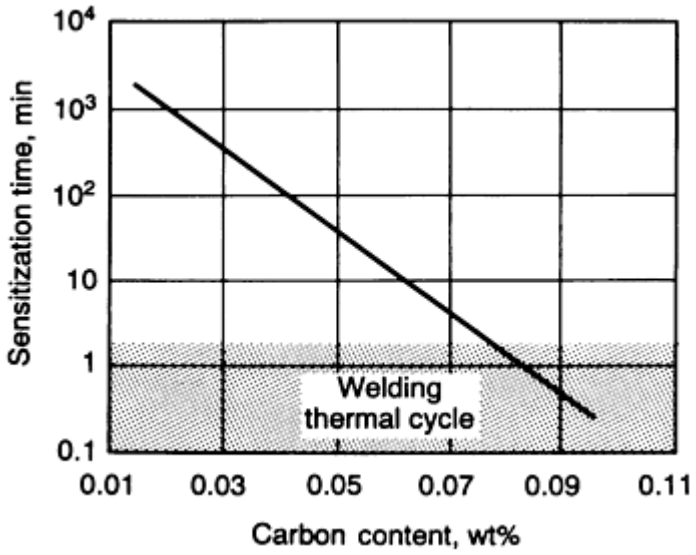

FIG. 7 MINIMUM SENSITIZATION TIME FROM A TIME-TEMPERATURE-SENSITIZATION DIAGRAM AS A FUNCTION OF CARBON CONTENT FOR A TYPICAL 300-SERIES STAINLESS STEEL ALLOY. SOURCE: REF 15

The control of stainless steel sensitization may be achieved by using:

- A POSTWELD HIGH-TEMPERATURE ANNEAL AND QUENCH TO REDISSOLVE THE CHROMIUM AT GRAIN BOUNDARIES, AND HINDER CHROMIUM CARBIDE FORMATION ON COOLING
- A LOW-CARBON GRADE OF STAINLESS STEEL (E.G., 304L OR 316L) TO AVOID CARBIDE FORMATION
- A STABILIZED GRADE OF STAINLESS STEEL CONTAINING TITANIUM (ALLOY 321) OR NIOBIUM (ALLOY 327), WHICH PREFERENTIALLY FORM CARBIDES AND LEAVE CHROMIUM IN SOLUTION. (THERE IS THE POSSIBILITY OF KNIFE-LINE ATTACK IN STABILIZED GRADES OF STAINLESS STEEL.)
- A HIGH-CHROMIUM ALLOY (E.G., ALLOY 310)

Role of Delta Ferrite in Stainless Steel Weld Deposits. Austenitic weld deposits are frequently used to join various ferrous alloys. It has been well established that it is necessary to have austenitic weld deposits solidify as primary ferrite, also known as a δ ferrite, if hot cracking is to be minimized (Ref 16, 17). The amount and form of ferrite in the weld metal can be controlled by selecting a filler metal with the appropriate chromium and nickel equivalent. A high chromium/nickel ratio favors primary ferrite formation, whereas a low ratio promotes primary austenite (Fig. 8). An optimum condition can be attained for ferrite contents between 3 and 8 vol% in the weld deposit. Ferrite contents above 3 vol% usually guarantee primary ferrite formation and thus reduce hot cracking susceptibility. However, ferrite above 10 vol% can degrade mechanical properties at low- or high-temperature service. At low temperatures, excess ferrite can promote crack paths when the temperature is below the ductile-brittle transition temperature. At high temperatures, continuous brittle sigma phase may form at the interface between the austenite and the ferrite. The ferrite content can be confirmed using magnetic measuring equipment (Ref 16, 17).

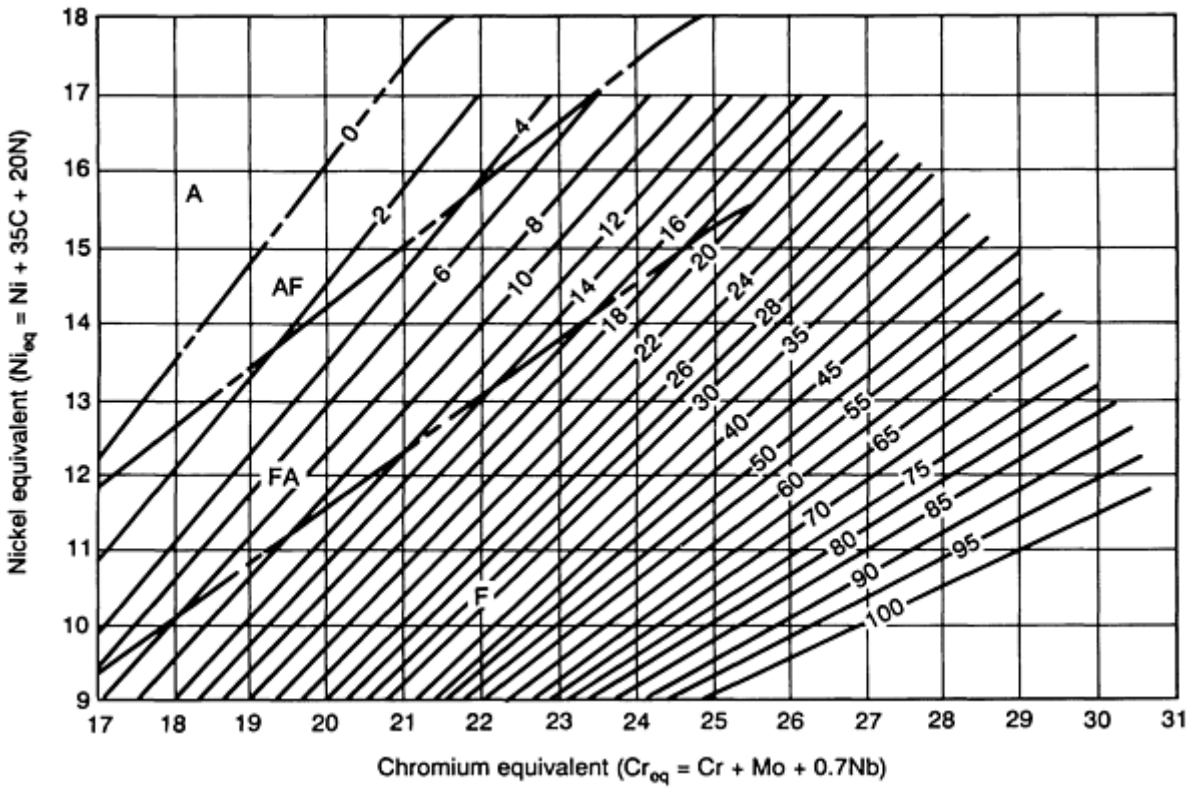

FIG. 8 WELDING RESEARCH COUNCIL (WRC-1988) DIAGRAM USED TO PREDICT WELD METAL FERRITE CONTENT. SOURCE: REF 18

Figure 8 can be used to predict the type of ferrite (primary or eutectic) and the ferrite content when a difference exists between the stainless steels being joined, such as when welding type 304 to type 310 stainless steel (Ref 18). This diagram shows the compositional range for the desirable primary solidification mode. The dotted lines on the diagram indicate the various transitions in the primary solidification phase. Because not all ferrite is primary ferrite (i.e., some is a phase component of a ferrite-austenite eutectic), this diagram can be used to ensure that ferrite is the first solid (primary) phase to form. This condition occurs when the weld deposit has a composition in the range labeled FA in Fig. 8. Because primary ferrite is the preferable microstructure, use of this diagram should reduce problems of hot cracking during welding. Also, the corrosion behavior of stainless steel weld deposits and castings is measurably different depending on whether the stainless steel has a microstructure generated with primary ferrite or primary austenite (Ref 19, 20, 21, 22, 23, 24, 25). Thus, knowledge of the weld metal ferrite content and form is necessary in order to be able to properly characterize and predict corrosion behavior.

Pitting is a form of localized attack caused by a breakdown in the thin passive oxide film that protects material from the corrosion process. Pits are commonly the result of a concentration cell established by a variation in solution composition that is in contact with the alloy material. Such compositional variations result when the solution at a surface irregularity is different from that of the bulk solution composition. Once a pit has formed, it acts as an anode supported by relatively large cathodic regions. Pitting has a delay time prior to nucleation and growth, and nucleation is very site-selective and microstructure-dependent. Pits are often initiated at specific microstructural features in the weld deposit (Ref 26). Pitting occurs when the material/solution combination achieves a potential that exceeds a critical value, known as the pitting potential. The tendency for a given alloy/solution combination to pit can often be characterized by critical potentials for pitting and repassivation determined by a cyclic potentiodynamic polarization technique.

Pits develop more readily in metallurgically heterogeneous materials. For example, when austenitic stainless steel is heated to temperatures where sensitization takes place (Ref 26, 27), the resulting chromium-depleted region is subject to pitting. Pits may also initiate at the austenite-ferrite interfaces in stainless steel weld metal.

Although weld metal has a higher probability of being locally attacked because of microsegregation in the dendritic structure, filler metals are now available that have better pitting resistance than their respective base metals; information about these filler metals can be obtained from consumable suppliers. However, even when the proper filler metal is used, pitting may still occur in the unmixed zone.

Duplex stainless steels, with ferrite contents in the range of 40 to 50 vol%, are often used to decrease the tendency of stress-corrosion cracking in chromium-nickel high-alloy steels. The welding practice for duplex stainless steels must be given special attention (Ref 20, 21, 22, 24, 25, 27) to avoid reduction in corrosion resistance. The combination of a low carbon content and a carefully specified nitrogen addition have been reported to improve resistance to pitting corrosion, stress-corrosion cracking, and intergranular corrosion in the as-welded condition. The low carbon content helps avoid sensitization, while the addition of nitrogen slows the precipitation kinetics associated with the segregation of chromium and molybdenum during the welding process (Ref 1). On rapid cooling from high temperature, nitrogen also has been reported to form deleterious precipitates (for example, Cr_2N) in the ferrite, thus reducing the corrosion resistance (Ref 28). Nitrogen also increases the formation of austenite in the heat-affected zone and weld metal during cooling. A minimum pitting corrosion rate is achieved at a ferrite content of about 50 vol%.

Stress-Corrosion Cracking. Weldments can be susceptible to stress-corrosion cracking under specific environmental conditions. This cracking requires the proper combination of corrosive media, susceptible microstructure, and tensile stress. Welds are often loaded in tension (due to residual stress) to a level approaching the yield strength of the base metal. A weld, with its various heterogeneous microstructural features, thus becomes an excellent candidate for stress-corrosion cracking.

Stress-corrosion cracks have an anodic crack tip and often leave apparent corrosion products along the fracture. Cracking is often characterized by crack branching and usually has a delay time prior to crack initiation, with initiation occurring at corrosion pits. Increasing the ferrite content in stainless steel weld metal reduces stress-corrosion cracking susceptibility. Approximately 50 vol% ferrite gives optimum stress-corrosion cracking resistance.

Welding parameters influence the amount and distribution of residual stress, because the extent of the stressed region and the amount of distortion are directly proportional to the size of the weld deposit; this deposit is directly related to the heat input. The thermal experience of welding is often very localized, resulting in strains that can cause distortion and residual stress. These residual stresses can be important in the initiation and propagation of environmentally assisted cracking. The use of small weld deposits reduces the stress and thus reduces the susceptibility of environmentally enhanced cracking.

It is known that postweld heat treatment can reduce stress-corrosion cracking by redistributing the localized load and by reducing the magnitude of the residual tensile stress available to induce corrosion cracking (Ref 29). In a recent study on a cast austenitic stainless steel, post-solidification heat treatments were also shown to modify the local composition gradients, significantly altering the susceptibility of the solidified microstructure to stress-corrosion cracking (Ref 30).

Hydrogen damage results from the combined actions of hydrogen and stress (Ref 31); the stress can be residual or applied. The weld pool in the liquid state has a much higher solubility for hydrogen than solid metal, and during solidification the hydrogen content becomes supersaturated in the weld pool as hydrogen attempts to transport from the weld deposit. While some of the hydrogen leaves the weldment, significant amounts transport through the fusion line and into the heat-affected zone.

The fusion line region also has the highest cooling rate, which may lead in some alloys to fracture-sensitive microstructures (e.g., martensite). The combination of high hydrogen content and brittle microstructures can produce cracking. The result is underbead cracking, characterized by delayed slow propagating cracks that travel adjacent to the fusion line in the heat-affected zone. The typical hydrogen crack travels one or two grains from the fusion line in the heat-affected zone.

Weld metal hydrogen cracking often takes the form of chevron cracks (Ref 32, 33, 34). Chevron crack formation and propagation are influenced by the combination of stress and orientation of the columnar grain boundaries. Chevron cracking occurs at high hydrogen content levels and appears to be inactive at low levels. This type of cracking appears to be sensitive to reheating during multi-pass deposition of welding beads. Chevron cracking is most likely found with flux-related welding processes.

Microbiologically Influenced Corrosion (MIC) is a phenomenon in which microorganisms play a role in the corrosion of metals. This role may be to initiate or accelerate the corrosion process. For example, water and some organic media may contain certain microorganisms that can produce a biofilm when exposed to a metal surface. The resulting nonuniform coverage may lead to a concentration cell and eventually initiate corrosion. In addition, the metabolic process of the microorganism can produce a localized acid environment that changes the corrosion behavior of the exposed metal by, for example, altering anodic and cathodic reactions, destroying protective films, or creating corrosive deposits (Ref 35).

In austenitic stainless steel weldments, the effects of MIC are usually observed as pitting on or adjacent to welds (Ref 36, 37). MIC attacks either γ or α phases, and chlorides am sometimes found in a pit, even when the water has extremely low chloride content. Pits are found in regions of the heat-affected zone at the fusion line, and in the base metal near the weld for reasons not well understood. Them is some evidence that MIC takes place along with stress-corrosion cracking in weldments of austenitic stainless steel. Welding design and plant operation can minimize MIC attack, mainly by preventing an acceptable environment for microorganisms.

Heat-Tint Oxide Formation. The welding process, especially with poor gas shielding, can produce a variation in the thickness of the passivating oxide. The variation in oxidation will result in a gradient in the degree of chromium depletion adjacent to a stainless steel weld. This behavior will cause some tendency for localized corrosion (Ref 1). An indication of this problem can be seen by the heat-tint oxide formation (Ref 38).

References cited in this section

1. O.I. STEKLOV *ET AL.*, METHOD OF EVALUATING THE INFLUENCE OF NON-UNIFORMITY OF WELDED JOINT PROPERTIES ON CORROSION, *SVAR. PROIZ.*, VOL 19 (NO. 9), 1972, P 34-36
6. J.E. HATCH, ED., *ALUMINUM: PROPERTIES AND PHYSICAL METALLURGY*, ASM, 1984, P 283
7. C.A. ARNOLD, "GALVANIC CORROSION MEASUREMENT OF WELDMENTS," PRESENTED AT NACE CORROSION/80, CHICAGO, MARCH 1980
8. M.W. MARSHALL, CORROSION CHARACTERISTICS OF TYPES 304 AND 304L WELDMENTS, *WELD. J.*, VOL 38 (NO. 6), 1959, P 247S-250S
9. M.E. CARRUTHERS, WELD CORROSION IN TYPE 316 AND 316L STAINLESS STEEL AND RELATED PROBLEMS, *WELD. J.*, VOL 38 (NO. 6), 1959, P 259S-267S
10. K.E. PINNOW AND A. MOSKOWITZ, CORROSION RESISTANCE OF STAINLESS STEEL

WELDMENTS, *WELD. J.*, VOL 49 (NO. 6), 1970, P 278-284S

11. T.J. MOORE, TIME-TEMPERATURE PARAMETERS AFFECTING CORROSION OF 18CR-8NI WELD METALS, *WELD. J.*, VOL 39 (NO. 5), 1960, P 199S-204S
12. J. HONEYCOMBE AND T.G. GOOCH, INTERGRANULAR ATTACK IN WELDED STRESS-CORROSION RESISTANT STAINLESS STEEL, *WELD. J.*, VOL 56 (NO. 11), 1977, P 339S-353S
13. T.G. GOOCH AND D.C. WILLINGHAM, WELD DECAY IN AISI 304 STAINLESS STEEL, *MET. CONST. BRIT. WELD. J.*, VOL 3 (NO. 10), 1971, P 366
14. T.G. GOOCH, CORROSION OF AISI TYPE 304 AUSTENITIC STAINLESS STEEL, *BRIT. WELD. J.*, VOL 15 (NO. 7), 1968, P 345
15. R.M. DAVIDSON, T. DEBOLD, AND M.J. JOHNSON, *METALS HANDBOOK*, VOL 13, 9TH ED., ASM INTERNATIONAL, 1987, P 551
16. D.J. KOTECKI, UNDERSTANDING DELTA FERRITE, *WELD. DES. FABR.*, VOL 63 (NO. 12), 1990, P 33-36
17. D.J. KOTECKI, FERRITE CONTROL IN DUPLEX STAINLESS STEEL WELD METAL, *WELD. J.*, VOL 65 (NO. 10), 1987, P 273S-278S
18. T.A. SIEWERT, C.N. MCCOWAN, AND D.L. OLSON, FERRITE NUMBER PREDICTION TO 100FN IN STAINLESS STEEL WELD METAL, *WELD. J.*, VOL 67 (NO. 12), 1988, P 289S-298S
19. W.A. BAESLACK III, D.J. DUQUETTE, AND W.F. SAVAGE, THE EFFECT OF FERRITE CONTENT ON STRESS CORROSION CRACKING IN DUPLEX STAINLESS STEEL WELD METALS AT ROOM TEMPERATURE, *CORROSION*, VOL 35 (NO. 2), 1979, P 45-54
20. W.A. BAESLACK III, D.J. DUQUETTE, AND W.F. SAVAGE, TECHNICAL NOTE: STRESS CORROSION CRACKING IN DUPLEX STAINLESS STEEL WELDMENTS, *WELD. J.*, VOL 57 (NO. 6), 1978, P 175S-177S
21. D.H. SHERMAN, D.J. DUQUETTE, AND W.F. SAVAGE, STRESS CORROSION CRACKING BEHAVIOR OF DUPLEX STAINLESS STEEL WELDMENTS IN BOILING $MGCL_2$, *CORROSION*, VOL 31 (NO. 10), 1975, P 376-380
22. T.G. GOOCH, WELDABILITY OF DUPLEX FERRITIC-AUSTENITIC STAINLESS STEELS, *DUPLEX STAINLESS STEELS*, ASM, 1983, P 573-602
23. A. BACKMAN AND B. LUNDQVIST, PROPERTIES OF A FULLY AUSTENITIC STAINLESS STEEL WELD METAL FOR SEVERE CORROSION ENVIRONMENTS, *WELD. J.*, VOL 56, 1977, P 23S-28S
24. H. MENENDEZ AND T.M. DEVINE, THE INFLUENCE OF MICROSTRUCTURE ON THE SENSITIZATION BEHAVIOR OF DUPLEX STAINLESS STEEL WELDS, *CORROSION*, VOL 46 (NO. 5), 1990, P 410-417
25. T. OGAWA AND T. KOSEKI, EFFECT OF COMPOSITION PROFILES ON METALLURGY AND CORROSION BEHAVIOR OF DUPLEX STAINLESS STEEL WELD METALS, *WELD. J.*, VOL 68 (NO. 5), 1989, P 181S-191S
26. A. GARNER, THE EFFECT OF AUTOGENEOUS WELDING ON CHLORIDE PITTING CORROSION IN AUSTENITIC STAINLESS STEELS, *CORROSION*, VOL 35 (NO. 3), 1979, P 108-114
27. T.A. DEBOLD, J.W. MARTIN, AND J.C. TVERBERG, DUPLEX STAINLESS OFFERS STRENGTH AND CORROSION RESISTANCE, *DUPLEX STAINLESS STEEL*, ASM, 1983, P 169-189
28. N. SRIDHAR AND J. KOLTS, EFFECTS OF NITROGEN ON THE SELECTIVE DISSOLUTION OF A DUPLEX STAINLESS STEEL, *CORROSION*, VOL 43 (NO. 11), 1987, P 646-651
29. K.N. KRISHNAN AND K.P. RAO, ROOM-TEMPERATURE STRESS CORROSION CRACKING RESISTANCE OF POST-WELD HEAT-TREATED AUSTENITIC WELD METALS, *CORROSION*, VOL 46 (NO. 9), 1990, P 734-742
30. G.L. BERRY, JR., D.L. OLSON, AND D.K. MATLOCK, INFLUENCE OF MICROCOMPOSITIONAL GRADIENTS ON STRESS CORROSION CRACK PROPAGATION, *MAT. ENG. SCI.*, VOL A148, 1991, P 1-6
31. B. CRAIG, HYDROGEN DAMAGE, *METALS HANDBOOK*, VOL 13, 9TH ED., ASM, 1987, P 163-164

32. R.A. FARRAR, THE NATURE OF CHEVRON CRACKING IN SUBMERGED ARC WELD METALS, *WELD. RES. LNT.*, VOL 7 (NO. 2), 1987, P 85-89
33. B.R. KEVILLE, AN INVESTIGATION TO DETERMINE THE MECHANISMS INVOLVED IN THE FORMATION AND PROPAGATION OF CHEVRON CRACKS IN SUBMERGED ARC WELDMENTS, *WELD. RES. LNT.*, VOL 6 (NO. 6), 1976, P 47-66
34. D.J. ALLEN, B. CHEW, AND P. HARRIS, THE FORMATION OF CHEVRON CRACKS IN SUBMERGED ARC WELD METAL, *WELD. J.*, VOL 61 (NO. 7), 1982, P 212S-221S
35. S.C. DEXTER, LOCALIZED BIOLOGICAL CORROSION, *METALS HANDBOOK*, VOL 13, 9TH ED., ASM, 1987, P 114-120
36. G.J. LICINA, *SOURCEBOOK OF MICROBIOLOGICALLY INFLUENCED CORROSION IN NUCLEAR POWER PLANTS*, NP5580, ELECTRIC POWER RESEARCH INSTITUTE, 1988
37. S.W. BORENSTEIN, "MICROBIOLOGICALLY INFLUENCED CORROSION FAILURES OF AUSTENITIC STAINLESS STEEL WELDS," PAPER 78, *CORROSION '88*, NACE, 1988
38. S. TURNER AND F.P.A. ROBINSON, THE EFFECT OF THE SURFACE OXIDES PRODUCED DURING WELDING ON THE CORROSION RESISTANCE OF STAINLESS STEELS, *CORROSION*, VOL 45 (NO. 9), 1989, P 710-716

A. Wahid, D.L. Olson, and D.K. Matlock, Colorado School of Mines; C.E. Cross, Martin Marietta Astronautics Group

Welding Practice to Minimize Corrosion

Several methods are available to minimize corrosion in weldments (Ref 39). The most important of these are discussed below.

Material and Welding Consumable Selection. Careful selection of materials and welding consumables can reduce the macro- and micro- compositional differences across the weldment and thus reduce the galvanic effects.

Surface Preparation. A properly selected cleaning process can reduce defects that are often sites for corrosive attack in aggressive environments. However, the cleaning process can also be a source of trouble. For example, any mechanically cleaned surface (i.e., cleaned by sand blasting or grinding) can leave impurities on the surface. The type of wire brush used can also be an important consideration (Ref 39). Stainless steel brushes are generally preferred because they do not form corrosion products capable of holding moisture.

Welding design should promote deposits that have relatively flat beads with low profiles and have minimal slag entrapment. A poor design can generate crevices that trap stagnant solutions, leading to pitting and crevice corrosion. Irregular weld deposit shapes can promote turbulent flow in a tubular product and result in erosion corrosion.

Welding Practice. Complete penetration is preferred to avoid underbead gaps. Slag should be removed after each pass with a power grinder or power chipping tool. If the welding method uses flux, the geometry of the joint must permit thorough flux removal, because many flux residues are hydrophilic and corrosive.

Weld Surface Finishing. The weld deposit should be inspected visually immediately after welding. Maximum corrosion resistance usually demands a smooth uniformly oxidized surface that is free from foreign particles and irregularities (Ref 37). Deposits normally vary in roughness and in degree of weld spatter, a concern that can be minimized by grinding. For smooth weld deposits, wire brushing may be sufficient. For stainless steel, however, brushing disturbs the existing passive film and may aggravate corrosive attack.

Surface Coating. When a variation in composition across the weld metal can cause localized attack, it may be desirable to use protective coatings. The coating needs to cover both the weldment and the parent metal and often requires special surface preparation.

Postweld Heat Treatment. A postweld heat treatment can be an effective way to reduce corrosion susceptibility. This improved corrosion resistance is accomplished through a reduction in residual stress gradients that influence stress-corrosion cracking growth. Postweld heat treatment can assist in the transport of hydrogen from the weldment and reduce susceptibility to hydrogen cracking. The treatment can also reduce compositional gradients (i.e., microsegregation) and corresponding microgalvanic cells.

Preheat and Interpass Temperature. The selection and use of proper preheat treatment and interpass temperature may prevent hydrogen cracking in carbon and low-alloy steel.

Passivation Treatment. A passivation treatment may increase the corrosion resistance of stainless steel welded components.

Avoidance of Forming Crevices. Slag that is still adhering to the weld deposit and defects such as lack of penetration and microfissures can result in crevices that can promote a localized concentration cell, resulting in crevice corrosion. Proper selection of welding consumables, proper welding practice, and thorough slag removal can alleviate this form of corrosion damage.

Removing Sources of Hydrogen. Through proper selection of welding consumables (that is, low-hydrogen shielded metal arc welding electrodes), proper drying of flux, and welding clean surfaces, the hydrogen pickup can be drastically reduced.

References cited in this section

37. S.W. BORENSTEIN, "MICROBIOLOGICALLY INFLUENCED CORROSION FAILURES OF AUSTENITIC STAINLESS STEEL WELDS," PAPER 78, *CORROSION '88*, NACE, 1988
39. F.C. BRAUTIGAM, WELDING PRACTICES THAT MINIMIZE CORROSION, *CHEM. ENG.*, 17 JAN 1977, P 145-147

A. Wahid, D.L. Olson, and D.K. Matlock, Colorado School of Mines; C.E. Cross, Martin Marietta Astronautics Group

References

1. O.I. STEKLOV *ET AL.*, METHOD OF EVALUATING THE INFLUENCE OF NON-UNIFORMITY OF WELDED JOINT PROPERTIES ON CORROSION, *SVAR. PROIZ.*, VOL 19 (NO. 9), 1972, P 34-36
2. K.F. KRYSIAK *ET AL.*, *METALS HANDBOOK*, VOL 13, 9TH ED., ASM, 1987, P 344-367
3. W.F. SAVAGE, NEW INSIGHT INTO WELD CRACKING AND A NEW WAY OF LOOKING AT WELDS, *WELD. DES. ENG.*, DEC 1969
4. R.G. BUCHHEIT, JR., J.P. MORAN, AND G.E. STONER, LOCALIZED CORROSION BEHAVIOR OF ALLOY 2090--THE ROLE OF MICROSTRUCTURAL HETEROGENEITY, *CORROSION*, VOL 46 (NO. 8), 1990, P 610-617
5. W.A. BAESLACK III, J.C. LIPPOLD, AND W.F. SAVAGE, UNMIXED ZONE FORMATION IN AUSTENITIC STAINLESS STEEL WELDMENTS, *WELD. J.*, VOL 58 (NO. 6), 1979, P 168S-176S
6. J.E. HATCH, ED., *ALUMINUM: PROPERTIES AND PHYSICAL METALLURGY*, ASM, 1984, P 283
7. C.A. ARNOLD, "GALVANIC CORROSION MEASUREMENT OF WELDMENTS," PRESENTED AT NACE CORROSION/80, CHICAGO, MARCH 1980
8. M.W. MARSHALL, CORROSION CHARACTERISTICS OF TYPES 304 AND 304L WELDMENTS, *WELD. J.*, VOL 38 (NO. 6), 1959, P 247S-250S
9. M.E. CARRUTHERS, WELD CORROSION IN TYPE 316 AND 316L STAINLESS STEEL AND

RELATED PROBLEMS, *WELD. J.*, VOL 38 (NO. 6), 1959, P 259S-267S

10. K.E. PINNOW AND A. MOSKOWITZ, CORROSION RESISTANCE OF STAINLESS STEEL WELDMENTS, *WELD. J.*, VOL 49 (NO. 6), 1970, P 278-284S
11. T.J. MOORE, TIME-TEMPERATURE PARAMETERS AFFECTING CORROSION OF 18CR-8NI WELD METALS, *WELD. J.*, VOL 39 (NO. 5), 1960, P 199S-204S
12. J. HONEYCOMBE AND T.G. GOOCH, INTERGRANULAR ATTACK IN WELDED STRESS-CORROSION RESISTANT STAINLESS STEEL, *WELD. J.*, VOL 56 (NO. 11), 1977, P 339S-353S
13. T.G. GOOCH AND D.C. WILLINGHAM, WELD DECAY IN AISI 304 STAINLESS STEEL, *MET. CONST. BRIT. WELD. J.*, VOL 3 (NO. 10), 1971, P 366
14. T.G. GOOCH, CORROSION OF AISI TYPE 304 AUSTENITIC STAINLESS STEEL, *BRIT. WELD. J.*, VOL 15 (NO. 7), 1968, P 345
15. R.M. DAVIDSON, T. DEBOLD, AND M.J. JOHNSON, *METALS HANDBOOK*, VOL 13, 9TH ED., ASM INTERNATIONAL, 1987, P 551
16. D.J. KOTECKI, UNDERSTANDING DELTA FERRITE, *WELD. DES. FABR.*, VOL 63 (NO. 12), 1990, P 33-36
17. D.J. KOTECKI, FERRITE CONTROL IN DUPLEX STAINLESS STEEL WELD METAL, *WELD. J.*, VOL 65 (NO. 10), 1987, P 273S-278S
18. T.A. SIEWERT, C.N. MCCOWAN, AND D.L. OLSON, FERRITE NUMBER PREDICTION TO 100FN IN STAINLESS STEEL WELD METAL, *WELD. J.*, VOL 67 (NO. 12), 1988, P 289S-298S
19. W.A. BAESLACK III, D.J. DUQUETTE, AND W.F. SAVAGE, THE EFFECT OF FERRITE CONTENT ON STRESS CORROSION CRACKING IN DUPLEX STAINLESS STEEL WELD METALS AT ROOM TEMPERATURE, *CORROSION*, VOL 35 (NO. 2), 1979, P 45-54
20. W.A. BAESLACK III, D.J. DUQUETTE, AND W.F. SAVAGE, TECHNICAL NOTE: STRESS CORROSION CRACKING IN DUPLEX STAINLESS STEEL WELDMENTS, *WELD. J.*, VOL 57 (NO. 6), 1978, P 175S-177S
21. D.H. SHERMAN, D.J. DUQUETTE, AND W.F. SAVAGE, STRESS CORROSION CRACKING BEHAVIOR OF DUPLEX STAINLESS STEEL WELDMENTS IN BOILING $MGCL_2$, *CORROSION*, VOL 31 (NO. 10), 1975, P 376-380
22. T.G. GOOCH, WELDABILITY OF DUPLEX FERRITIC-AUSTENITIC STAINLESS STEELS, *DUPLEX STAINLESS STEELS*, ASM, 1983, P 573-602
23. A. BACKMAN AND B. LUNDQVIST, PROPERTIES OF A FULLY AUSTENITIC STAINLESS STEEL WELD METAL FOR SEVERE CORROSION ENVIRONMENTS, *WELD. J.*, VOL 56, 1977, P 23S-28S
24. H. MENENDEZ AND T.M. DEVINE, THE INFLUENCE OF MICROSTRUCTURE ON THE SENSITIZATION BEHAVIOR OF DUPLEX STAINLESS STEEL WELDS, *CORROSION*, VOL 46 (NO. 5), 1990, P 410-417
25. T. OGAWA AND T. KOSEKI, EFFECT OF COMPOSITION PROFILES ON METALLURGY AND CORROSION BEHAVIOR OF DUPLEX STAINLESS STEEL WELD METALS, *WELD. J.*, VOL 68 (NO. 5), 1989, P 181S-191S
26. A. GARNER, THE EFFECT OF AUTOGENEOUS WELDING ON CHLORIDE PITTING CORROSION IN AUSTENITIC STAINLESS STEELS, *CORROSION*, VOL 35 (NO. 3), 1979, P 108-114
27. T.A. DEBOLD, J.W. MARTIN, AND J.C. TVERBERG, DUPLEX STAINLESS OFFERS STRENGTH AND CORROSION RESISTANCE, *DUPLEX STAINLESS STEEL*, ASM, 1983, P 169-189
28. N. SRIDHAR AND J. KOLTS, EFFECTS OF NITROGEN ON THE SELECTIVE DISSOLUTION OF A DUPLEX STAINLESS STEEL, *CORROSION*, VOL 43 (NO. 11), 1987, P 646-651
29. K.N. KRISHNAN AND K.P. RAO, ROOM-TEMPERATURE STRESS CORROSION CRACKING RESISTANCE OF POST-WELD HEAT-TREATED AUSTENITIC WELD METALS, *CORROSION*, VOL 46 (NO. 9), 1990, P 734-742
30. G.L. BERRY, JR., D.L. OLSON, AND D.K. MATLOCK, INFLUENCE OF MICROCOMPOSITIONAL GRADIENTS ON STRESS CORROSION CRACK PROPAGATION, *MAT. ENG. SCI.*, VOL A148, 1991, P 1-6

31. B. CRAIG, HYDROGEN DAMAGE, *METALS HANDBOOK*, VOL 13, 9TH ED., ASM, 1987, P 163-164
32. R.A. FARRAR, THE NATURE OF CHEVRON CRACKING IN SUBMERGED ARC WELD METALS, *WELD. RES. LNT.*, VOL 7 (NO. 2), 1987, P 85-89
33. B.R. KEVILLE, AN INVESTIGATION TO DETERMINE THE MECHANISMS INVOLVED IN THE FORMATION AND PROPAGATION OF CHEVRON CRACKS IN SUBMERGED ARC WELDMENTS, *WELD. RES. LNT.*, VOL 6 (NO. 6), 1976, P 47-66
34. D.J. ALLEN, B. CHEW, AND P. HARRIS, THE FORMATION OF CHEVRON CRACKS IN SUBMERGED ARC WELD METAL, *WELD. J.*, VOL 61 (NO. 7), 1982, P 212S-221S
35. S.C. DEXTER, LOCALIZED BIOLOGICAL CORROSION, *METALS HANDBOOK*, VOL 13, 9TH ED., ASM, 1987, P 114-120
36. G.J. LICINA, *SOURCEBOOK OF MICROBIOLOGICALLY INFLUENCED CORROSION IN NUCLEAR POWER PLANTS*, NP5580, ELECTRIC POWER RESEARCH INSTITUTE, 1988
37. S.W. BORENSTEIN, "MICROBIOLOGICALLY INFLUENCED CORROSION FAILURES OF AUSTENITIC STAINLESS STEEL WELDS," PAPER 78, *CORROSION '88*, NACE, 1988
38. S. TURNER AND F.P.A. ROBINSON, THE EFFECT OF THE SURFACE OXIDES PRODUCED DURING WELDING ON THE CORROSION RESISTANCE OF STAINLESS STEELS, *CORROSION*, VOL 45 (NO. 9), 1989, P 710-716
39. F.C. BRAUTIGAM, WELDING PRACTICES THAT MINIMIZE CORROSION, *CHEM. ENG.*, 17 JAN 1977, P 145-147

Overview of Weld Discontinuities

Introduction

DISCONTINUITIES are interruptions in the desirable physical structure of a weld. A discontinuity constituting a danger to the fitness-for-service of a weld is a defect. By definition, a defect is a condition that must be removed or corrected (Ref 1). The word "defect" should therefore be carefully used, because it implies that a weld is defective and requires corrective measures or rejection. Thus, repairs may be made unnecessarily and solely by implication, without a critical engineering assessment. Consequently, the engineering community now tends to use the word "discontinuity" or "flaw" instead of "defect."

The significance of a weld discontinuity should be viewed in the context of the fitness-for-service of the welded construction. Fitness-for-service is a concept of weld evaluation that seeks a balance among quality, reliability, and economy of welding procedure. Fitness-for-service is not a constant. It varies depending on the service requirements of a particular welded structure, as well as on the properties of the material involved. (See the article "Fitness-for-Service Assessment of Welded Structures" in this Section for more information.)

Neither construction materials nor engineered structures are free from imperfections. Welds and weld repairs are not exceptions. Weld acceptance standards are used when a discontinuity has been clearly located, identified, sized, its orientation determined, and its structural significance questioned. Critical engineering assessments of weld discontinuities are performed to define acceptable, harmless discontinuities in a structure that will not sacrifice weldment reliability. One of the major reasons for understanding the engineering meaning of weld discontinuities is to decrease the cost of welded structures by avoiding unnecessary repairs of harmless weld discontinuities (Ref 2). Welders, of course, must constantly be encouraged to make sound (perfect) welds independent of prevailing acceptance standards.

This article describes the types of weld discontinuities that are characteristic of the principal welding processes. In addition, information is provided about the common inspection methods used to detect these discontinuities. More detailed descriptions of these inspection methods can be found in the article "Inspection of Welded Joints" in this Section of the Handbook.

References

1. ASME BOILER AND PRESSURE VESSEL CODE, APPENDIX IV, DRAFT 1, 21 OCT 1981

2. L.W. SANDOR, THE MEANING OF WELD DISCONTINUITIES IN SHIPBUILDING, *PROC. 1ST NAT. CONF. FITNESS-FOR-SERVICE IN SHIPBUILDING* (BOULDER, CO), OCT 1980

Classification of Weld Discontinuities

Discontinuities may be divided into three broad classifications: design related, welding process related, and metallurgical. Design-related discontinuities include problems with design or structural details, choice of the wrong type of weld joint for a given application, or undesirable changes in cross section.

Process-related discontinuities include:

- *UNDERCUT:* A GROOVE MELTED INTO THE BASE METAL ADJACENT TO THE TOE OR ROOT OF A WELD AND LEFT UNFILLED BY WELD METAL
- *SLAG INCLUSIONS:* NONMETALLIC SOLID MATERIAL ENTRAPPED IN WELD METAL OR BETWEEN WELD METAL AND BASE METAL
- *POROSITY:* CAVITY-TYPE DISCONTINUITIES FORMED BY GAS ENTRAPMENT DURING SOLIDIFICATION
- *OVERLAP:* THE PROTRUSION OF WELD METAL BEYOND THE TOE, FACE, OR ROOT OF THE WELD
- *TUNGSTEN INCLUSIONS:* PARTICLES FROM TUNGSTEN ELECTRODES THAT RESULT FROM IMPROPER GAS-TUNGSTEN ARC WELDING PROCEDURES
- *BACKING PIECE LEFT ON:* FAILURE TO REMOVE MATERIAL PLACED AT THE ROOT OF A WELD JOINT TO SUPPORT MOLTEN WELD METAL
- *SHRINKAGE VOIDS:* CAVITY-TYPE DISCONTINUITIES NORMALLY FORMED BY SHRINKAGE DURING SOLIDIFICATION
- *OXIDE INCLUSIONS:* PARTICLES OF SURFACE OXIDES THAT HAVE NOT MELTED AND ARE MIXED INTO THE WELD METAL
- *LACK OF FUSION (LOF):* A CONDITION IN WHICH FUSION IS LESS THAN COMPLETE
- *LACK OF PENETRATION (LOP):* A CONDITION IN WHICH JOINT PENETRATION IS LESS THAN THAT SPECIFIED
- *CRATERS:* DEPRESSIONS AT THE TERMINATION OF A WELD BEAD OR IN THE MOLTEN WELD POOL
- *MELT-THROUGH:* A CONDITION RESULTING WHEN THE ARC MELTS THROUGH THE BOTTOM OF A JOINT WELDED FROM ONE SIDE
- *SPATTER:* METAL PARTICLES EXPELLED DURING WELDING THAT DO NOT FORM A PART OF THE WELD
- *ARC STRIKES (ARC BURNS):* DISCONTINUITIES CONSISTING OF ANY LOCALIZED REMELTED METAL, HEAT-AFFECTED METAL, OR CHANGE IN THE SURFACE PROFILE OF ANY PART OF A WELD OR BASE METAL RESULTING FROM AN ARC
- *UNDERFILL:* A DEPRESSION ON THE FACE OF THE WELD OR ROOT SURFACE EXTENDING BELOW THE SURFACE OF THE ADJACENT BASE METAL

Metallurgical discontinuities include:

- *CRACKS:* FRACTURE-TYPE DISCONTINUITIES CHARACTERIZED BY A SHARP TIP AND HIGH RATIO OF LENGTH AND WIDTH TO OPENING DISPLACEMENT
- *FISSURES:* SMALL CRACKLIKE DISCONTINUITIES WITH ONLY A SLIGHT SEPARATION (OPENING DISPLACEMENT) OF THE FRACTURE SURFACES
- *FISHEYE:* A DISCONTINUITY FOUND ON THE FRACTURE SURFACE OF A WELD IN STEEL THAT CONSISTS OF A SMALL PORE OR INCLUSION SURROUNDED BY A BRIGHT, ROUND AREA

- *SEGREGATION:* THE NONUNIFORM DISTRIBUTION OR CONCENTRATION OF IMPURITIES OR ALLOYING ELEMENTS THAT ARISES DURING THE SOLIDIFICATION OF THE WELD
- *LAMELLAR TEARING:* A TYPE OF CRACKING THAT OCCURS IN THE BASE METAL OR HEAT-AFFECTED ZONE (HAZ) OF RESTRAINED WELD JOINTS THAT IS THE RESULT OF INADEQUATE DUCTILITY IN THE THROUGH-THICKNESS DIRECTION OF STEEL PLATE

The observed occurrence of discontinuities and their relative amounts depend largely on the welding process used, the inspection method applied, the type of weld made, the joint design and fit-up obtained, the material utilized, and the working and environmental conditions. The most frequent weld discontinuities found during manufacture, ranked in order of decreasing occurrence on the basis of arc-welding processes are:

SHIELDED METAL ARE WELDING (SMAW)
SLAG INCLUSIONS
POROSITY
LOF/LOP
UNDERCUT
SUBMERGED ARE WELDING (SAW)
LOF/LOP
SLAG INCLUSIONS
POROSITY
FLUX-CORED ARC WELDING (FCAW)
SLAG INCLUSIONS
POROSITY
LOF/LOP
GAS-METAL ARC WELDING (GMAW)
POROSITY
LOF/LOP
GAS-TUNGSTEN ARC WELDING (GTAW)
POROSITY
TUNGSTEN INCLUSIONS

The commonly encountered inclusions-as well as cracking, the most serious of weld defects--will be discussed in this Section.

Gas porosity can occur on or just below the surface of a weld. Pores are characterized by a rounded or elongated teardrop shape with or without a sharp point. Pores can be uniformly distributed throughout the weld or isolated in small groups; they can also be concentrated at the root or toe of the weld. Porosity in welds is caused by gas entrapment in the molten metal, by too much moisture on the base or filler metal, or by improper cleaning of the joint during preparation for welding.

The type of porosity within a weld is usually designated by the amount and distribution of the pores. Some of the types are classified as follows:

- *UNIFORMLY SCATTERED POROSITY:* CHARACTERIZED BY PORES SCATTERED UNIFORMLY THROUGHOUT THE WELD (FIG. 1)
- *CLUSTER POROSITY:* CHARACTERIZED BY CLUSTERS OF PORES SEPARATED BY POROSITY-FREE AREAS (FIG. 1B)
- *LINEAR POROSITY:* CHARACTERIZED BY PORES THAT ARE LINEARLY DISTRIBUTED (FIG. 1C). LINEAR POROSITY GENERALLY OCCURS IN THE ROOT PASS AND IS ASSOCIATED

WITH INCOMPLETE JOINT PENETRATION

- *ELONGATED POROSITY:* CHARACTERIZED BY HIGHLY ELONGATED PORES INCLINED TO THE DIRECTION OF WELDING. ELONGATED POROSITY OCCURS IN A HERRINGBONE PATTERN (FIG. 1D)
- *WORMHOLE POROSITY:* CHARACTERIZED BY ELONGATED VOIDS WITH A DEFINITE WORMLIKE SHAPE AND TEXTURE (FIG. 2)

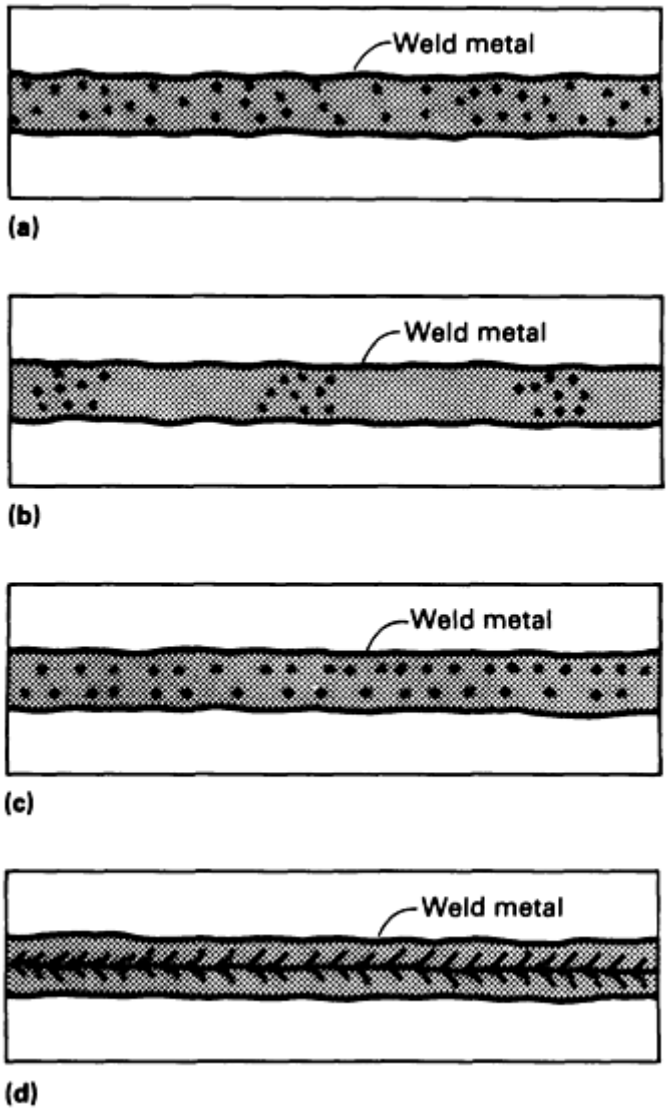

FIG. 1 TYPES OF GAS POROSITY COMMONLY FOUND IN WELD METAL. (A) UNIFORMLY SCATTERED POROSITY. (B) CLUSTER POROSITY. (C) LINEAR POROSITY. (D) ELONGATED POROSITY

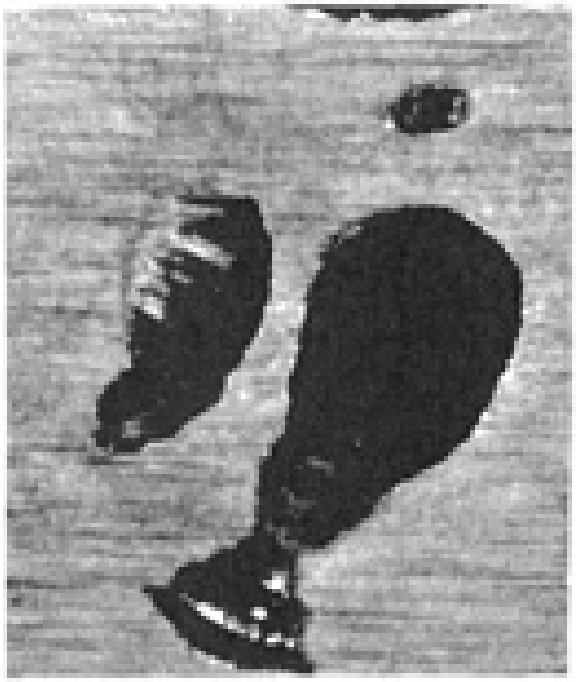

FIG. 2 WORMHOLE POROSITY IN A WELD BEAD. LONGITUDINAL CUT. 20×

Radiography is the most widely used nondestructive method for detecting subsurface gas porosity in weldments. The radiographic image of round porosity appears as round or oval spots with smooth edges, and elongated porosity appears as oval spots with the major axis sometimes several times longer than the minor axis. The radiographic image of wormhole porosity depends largely on the orientation of the elongated cavity with respect to the incident x-ray beam. The presence of top-surface or root reinforcement affects the sensitivity of inspection, and the presence of foreign material, such as loose scale, flux, or weld spatter, may interfere with the interpretation of results.

Ultrasonic inspection is capable of detecting subsurface porosity. However, it is not extensively used for this purpose except to inspect thick sections or inaccessible areas where radiographic sensitivity is limited. Surface finish and grain size affect the validity of the inspection results.

Eddy current inspection, like ultrasonic inspection, can be used for detecting subsurface porosity. Normally, eddy current inspection is confined to use on thin-wall welded pipe and tubing because eddy currents are relatively insensitive to flaws that do not extend to the surface or into the near-surface layer.

Magnetic particle inspection and liquid penetrant inspection are not suitable for detecting subsurface gas porosity. These methods are restricted to the detection of only those pores that are open to the surface.

Slag inclusions may occur when using welding processes that employ a slag covering for shielding purposes. (With other processes, the oxide present on the metal surface before welding may also become entrapped.) Slag inclusions can be found near the surface and in the root of a weld (Fig. 3a), between weld beads in multiple-pass welds (Fig. 3b), and at the side of a weld near the root (Fig. 3c).

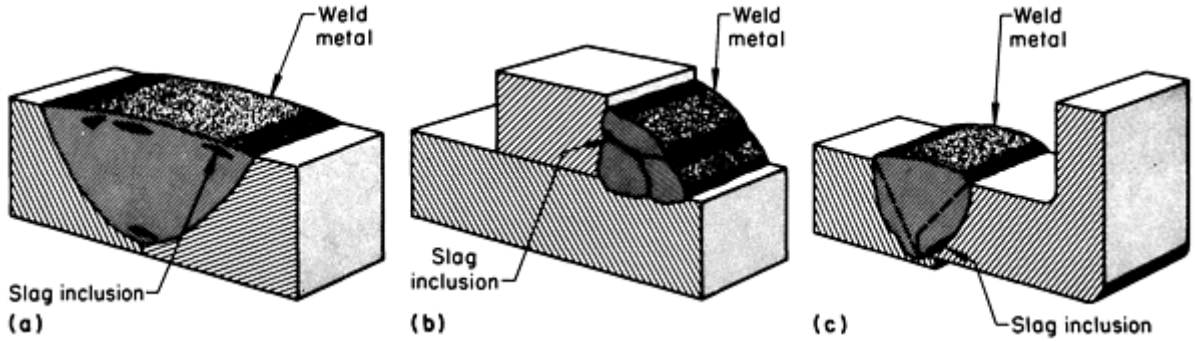

FIG. 3 SECTIONS SHOWING LOCATIONS OF SLAG INCLUSIONS IN WELD METAL. (A) NEAR THE SURFACE AND IN THE ROOT OF A SINGLE-PASS WELD. (B) BETWEEN WELD BEADS IN A MULTIPLE-PASS WELD. (C) AT THE SIDE OF A WELD NEAR THE ROOT

During welding, slag may spill ahead of the arc and subsequently be covered by the weld pool because of poor joint fit-up, incorrect electrode manipulation, or forward arc blow. Slag trapped in this manner is generally located near the root. Radical motions of the electrode, such as wide weaving, may also cause slag entrapment on the sides or near the top of the weld after the slag spills into a portion of the joint that has not been filled by the molten pool. Incomplete removal of the slag from the previous pass in multiple-pass welding is another common cause of entrapment. In multiple-pass welds, slag may be entrapped any number of places in the weld between passes. Slag inclusions are generally oriented along the direction of welding.

Three methods used for the detection of slag below the surface of single-pass or multiple-pass welds are magnetic particle, radiographic, and ultrasonic inspection. Depending on their size, shape, orientation, and proximity to the surface, slag inclusions can be detected by magnetic particle inspection with a dc power source, provided the material is ferromagnetic. Radiography can be used for any material, but is the most expensive of the three methods. Ultrasonic inspection can also be used for any material and is the most reliable and least expensive method. If the weld is machined to a flush contour, flaws as close as 0.8 mm ($\frac{1}{32}$ in.) to the surface can be detected with the straight-beam technique of ultrasonic inspection, provided the instrument has sufficient sensitivity and resolution. A 5 or 10 MHz dual-element transducer is normally used in this application. If the weld cannot be machined, near-surface sensitivity will be low because the initial pulse is excessively broadened by the rough as-welded surface. Unmachined welds can be readily inspected by direct-beam and reflected-beam techniques, using an angle-beam (shear-wave) transducer.

Tungsten inclusions are particles found in the weld metal from the nonconsumable tungsten electrode used in GTAW. These inclusions are the result of:

- EXCEEDING THE MAXIMUM CURRENT FOR A GIVEN ELECTRODE SIZE OR TYPE
- LETTING THE TIP OF THE ELECTRODE MAKE CONTACT WITH THE HOT TIP OF THE ELECTRODE
- USING AN EXCESSIVE ELECTRODE EXTENSION
- INADEQUATE GAS SHIELDING OR EXCESSIVE WIND DRAFTS, WHICH RESULT IN OXIDATION
- USING IMPROPER SHIELDING GASES SUCH AS ARGON-OXYGEN OR ARGON-CO2 MIXTURES, WHICH ARE USED FOR GMAW

Tungsten inclusions, which are not acceptable for high-quality work, can only be found by internal inspection techniques, particularly radiographic testing.

Lack of fusion and lack of penetration result from improper electrode manipulation and the use of incorrect welding conditions. Fusion refers to the degree to which the original base metal surfaces to be welded have been fused to the filler metal; penetration refers to the degree to which the base metal has been melted and resolidified to result in a deeper throat

that was present in the joint before welding. In effect, a joint can be completely fused but have incomplete root penetration to obtain the throat size specified. Based on these definitions, LOF discontinuities are located on the sidewalls of a joint, and LOP discontinuities are located near the root (Fig. 4). With some joint configurations, such as butt joints, the two terms can be used interchangeably. The causes of LOF include excessive travel speed, bridging, excessive electrode size, insufficient current, poor joint preparation, overly acute joint angle, improper electrode manipulation, and excessive arc blow. Lack of penetration may be the result of low welding current, excessive travel speed, improper electrode manipulation, or surface contaminants such as oxide, oil, or dirt that prevent full melting of the underlying metal.

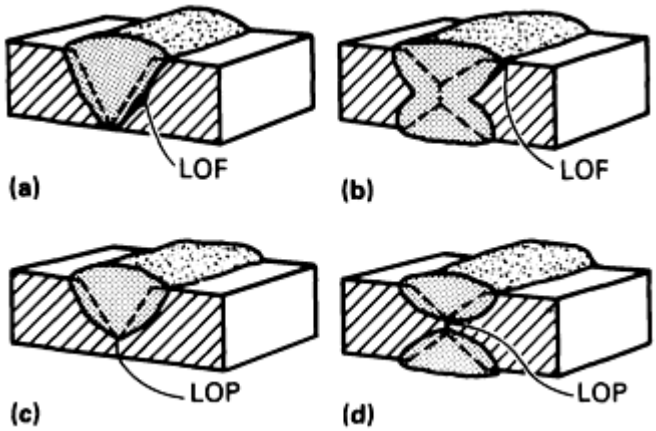

FIG. 4 LACK OF FUSION IN (A) A SINGLE-V-GROOVE WELD AND (B) DOUBLE-V-GROOVE WELD. LACK OF PENETRATION IN (C) A SINGLE-V-GROOVE WELD AND (D) A DOUBLE-V-GROOVE WELD

Radiographic methods may be unable to detect these discontinuities in certain cases, because of the small effect they have on x-ray absorption. As will be described later, however, lack of sidewall fusion is readily detected by radiography. Ultrasonically, both types of discontinuities often appear as severe, almost continuous, linear porosity because of the nature of the unbonded areas of the joint. Except in thin sheet or plate, these discontinuities may be too deep-lying to be detected by magnetic particle inspection.

Geometric weld discontinuities are those associated with imperfect shape or unacceptable weld contour. Undercut, underfill, overlap, excessive reinforcement, fillet shape, and melt-through, all of which were defined earlier, are included in this grouping. Geometric discontinuities are shown schematically in Fig. 5. Radiography is used most often to detect these flaws.

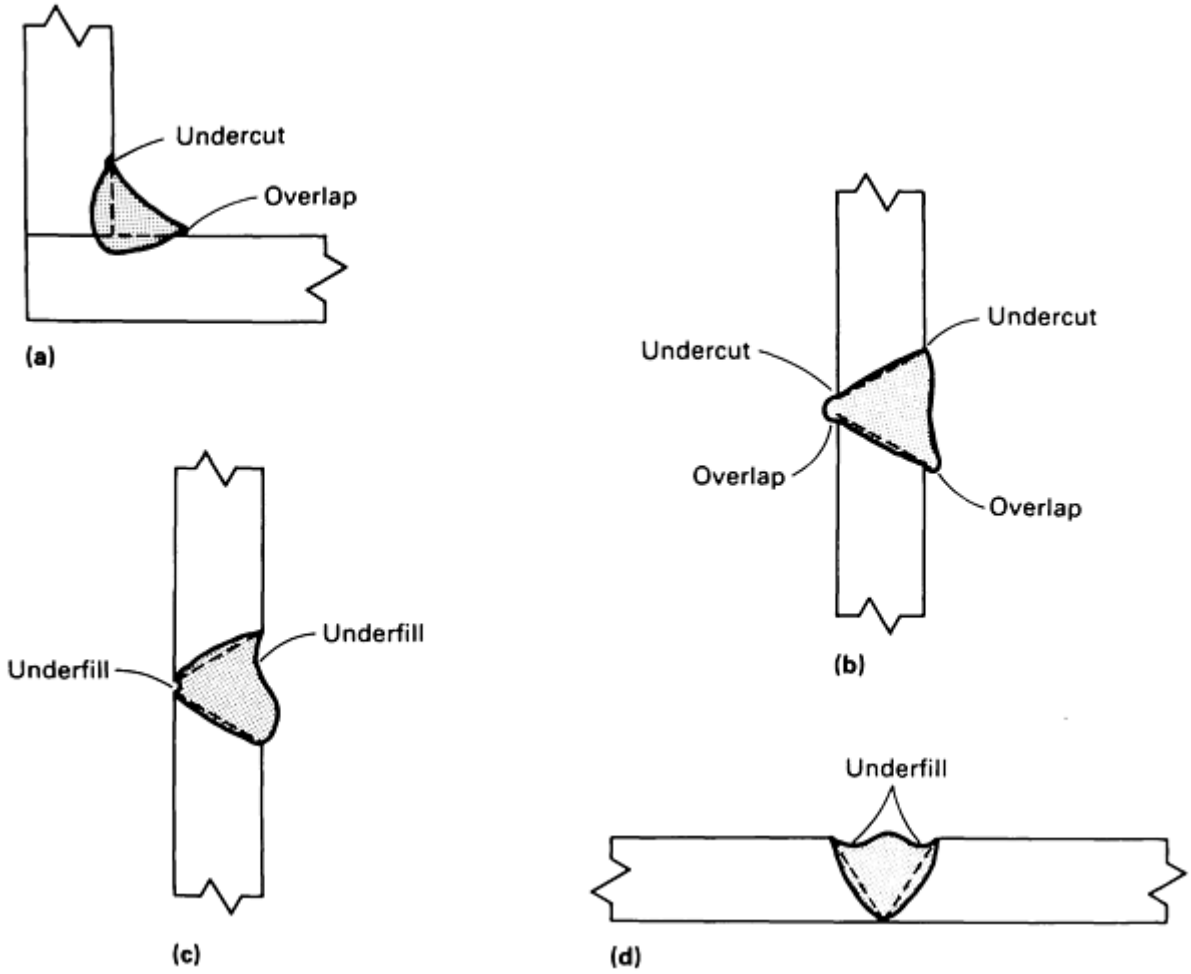

FIG. 5 WELD DISCONTINUITIES AFFECTING WELD SHAPE AND CONTOUR. (A) UNDERCUT AND OVERLAPPING IN A FILLET WELD. (B) UNDERCUT AND OVERLAPPING IN A GROOVE WELD. (C) AND (D) UNDERFILL IN GROOVE WELDS

Cracks can occur in a wide variety of shapes and types and can be located in numerous positions in and around a welded joint (Fig. 6). Cracks associated with welding can be categorized according to whether they originate in the weld itself or in the base metal. Four types commonly occur in the weld metal: transverse, longitudinal, crater, and hat cracks. Base metal cracks can be divided into seven categories: transverse cracks, underbead cracks, toe cracks, root cracks, lamellar tearing, delaminations, and fusion-line cracks.

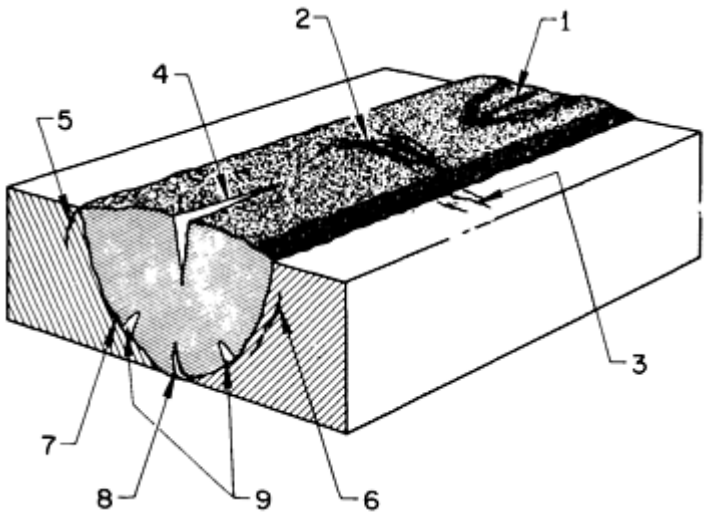

FIG. 6 IDENTIFICATION OF CRACKS ACCORDING TO LOCATION IN WELD AND BASE METAL. 1, CRATER CRACK IN WELD METAL; 2, TRANSVERSE CRACK IN WELD METAL; 3, TRANSVERSE CRACK IN HAZ;, 4, LONGITUDINAL CRACK IN WELD METAL; 5, TOE CRACK IN BASE METAL; 6, UNDERBEAD CRACK IN BASE METAL; 7, FUSION-LINE CRACK; 8, ROOT CRACK IN WELD METAL; 9, HAT CRACKS IN WELD METAL

Weld metal cracks and base metal cracks that extend to the surface can be detected by liquid penetrant and magnetic particle inspection. Magnetic particle inspection can also detect subsurface cracks, depending on their size, shape, and proximity to the surface. Although the orientation of a crack with respect to the direction of the radiation beam is the dominant factor in determining the ability of radiography to detect the crack, differences in composition between the base metal and the weld metal may create shadows to hide a crack that otherwise might be visible. Ultrasonic inspection is generally effective in detecting most cracks in the weld zone.

Transverse cracks in weld metal (No. 2, Fig. 6) are formed when the predominant contraction stresses are in the direction of the weld axis. They can be hot cracks, which separate intergranularly as the result of hot shortness or localized planar shrinkage, or they can be transgranular separations produced by stresses exceeding the strength of the material. Transverse cracks lie in a plane normal to the axis of the weld and are usually open to the surface. They usually extend across the entire face of the weld and sometimes propagate into the base metal.

Transverse cracks in base metal (No. 3, Fig. 6) occur on the surface in or near the HAZ. They are the result of the high residual stresses induced by thermal cycling during welding. High hardness, excessive restraint, and the presence of hydrogen promote their formation. Such cracks propagate into the weld or beyond the HAZ into the base metal as far as is needed to relieve the residual stresses.

Underbead cracks (No. 6, Fig. 6) are similar to transverse cracks in that they form in the HAZ because of high hardness, excessive restraint, and the presence of hydrogen. Their orientation follows the contour of the HAZ.

Longitudinal cracks (No. 4, Fig. 6) may exist in three forms, depending on their positions in the weld. Check cracks are open to the surface and extend only partway through the weld. Root cracks extend from the root to some point within the weld. Full centerline cracks may extend from the root to the face of the weld metal.

Check cracks are caused either by high contraction stresses in the final passes applied to a weld joint or by a hot-cracking mechanism.

Root cracks are the most common form of longitudinal weld metal crack because of the relatively small size of the root pass. If such cracks are not removed, they can propagate through the weld as subsequent passes are applied. This is the usual mechanism by which full centerline cracks are formed.

Centerline cracks may occur at either high or low temperatures. At low temperatures, cracking is generally the result of poor fit-up, overly rigid fit-up, or a small ratio of weld metal to base metal.

All three types of longitudinal cracks are usually oriented perpendicular to the weld face and run along the plane that bisects the welded joint. Seldom are they open at the edge of the joint face, because this requires a fillet weld with an extremely convex bead.

Crater cracks (No. 1, Fig. 6) are related to centerline cracks. As the name implies, crater cracks occur in the weld crater formed at the end of a welding pass. Generally, this type of crack is caused by failure to fill the crater before breaking the arc. When this happens, the outer edges of the crater cool rapidly, producing stresses sufficient to crack the interior of the crater. This type of crack may be oriented longitudinally or transversely or may occur as a number of intersecting cracks forming the shape of a star. Longitudinal crater cracks can propagate along the axis of the weld to form a centerline crack. In addition, such cracks may propagate upward through the weld if they are not removed before subsequent passes are applied.

Hat cracks (No. 9, Fig. 6) derive their name from the shape of the weld cross section with which they are usually associated. This type of weld flares out near the weld face, resembling an inverted top hat. Hat cracks are the result of excessive voltage or welding speed. The cracks are located about halfway up through the weld and extend into the weld metal from the fusion line of the joint.

Toe and root cracks (No. 5 and 8, Fig. 6) can occur at the notches present at notch locations in the weld when high residual stresses are present. Both toe and root cracks propagate through the brittle HAZ before they are arrested in more ductile regions of the base metal. Characteristically, they are oriented almost perpendicular to the base metal surface and run parallel to the weld axis.

Lamellar tearing is the phenomenon that occurs in T-joints that are fillet welded on both sides. This condition, which occurs in the base metal or HAZ of restrained weld joints, is characterized by a steplike crack parallel to the rolling plane. The crack originates internally because of tensile strains produced by the contraction of the weld metal and the surrounding HAZ during cooling. Figure 7 shows a typical condition.

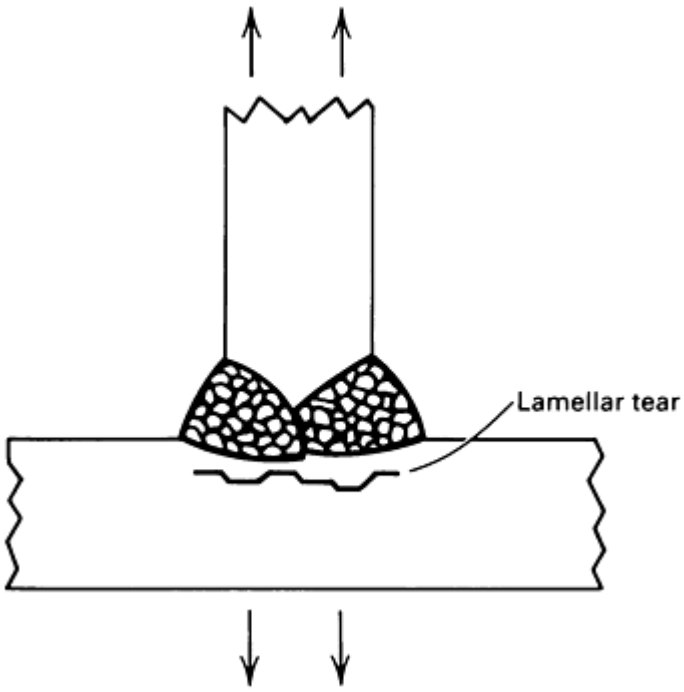

FIG. 7 LAMELLAR TEAR CAUSED BY THERMAL CONTRACTION STRAIN

Fusion-line cracks (No. 7, Fig. 6) can be classified as either weld metal cracks or base metal cracks because they occur along the fusion line between the two. There are no limitations as to where along the fusion line these cracks can occur or how far around the weld they can extend.

Discontinuities Associated With Specialized Welding Processes

The preceding section has dealt mainly with the discontinuities common to conventional arc-welding processes. In addition, there are certain more specialized welding methods that may have discontinuities unique to them. These methods include electron-beam, plasma arc, electroslag, friction, and resistance welding. In general, the types of discontinuities associated with these processes are the same as those associated with conventional arc welding; however, because of the nature of the processes and the joint configurations involved, such discontinuities may be oriented differently from those previously described, or they may present particular problems of location and evaluation.

Electron-Beam Welding

In electron-beam welding, as in all other welding processes, weld discontinuities can be divided into two major categories:

- THOSE THAT OCCUR AT, OR ARE OPEN TO, THE SURFACE
- THOSE THAT OCCUR BELOW THE SURFACE

Surface flaws include undercut, mismatch, underfill, reinforcement, cracks, missed seams, and LOP. Subsurface flaws include porosity, massive voids, bursts, cracks, missed seams, and LOP. Figure 8 shows poor welds containing these flaws, and a good weld with none of them.

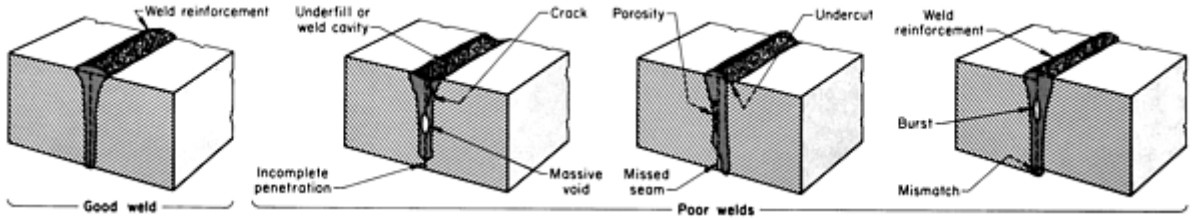

FIG. 8 ELECTRON-BEAM WELDS SHOWING FLAWS THAT CAN OCCUR IN POOR WELDS AND THE ABSENCE OF FLAWS IN A GOOD WELD WITH REINFORCEMENT

Surface discontinuities such as undercut, mismatch, reinforcement, and underfill are macroscopic discontinuities related to the contour of the weld bead or the joint. As such, they are readily detected visually or dimensionally. Surface discontinuities such as cracks are usually detected visually using liquid penetrant inspection or using magnetic particle inspection if the material is ferromagnetic.

When liquid penetrants are used to inspect a weld for surface discontinuities such as cracks, missed seams, and LOP, the surface to be inspected must be clean and the layers of metal smeared from machining or peened from grit- or sandblasting must be removed. Generally, some type of etching or pickling treatment works well, but the possibility of hydrogen pickup from the treatment must be considered.

Occasionally, special inspection procedures must be employed to detect some types of surface discontinuities in electron-beam welds. Missed seams and LOP are often difficult to detect because they are frequently associated with complex weld joints that prevent direct viewing of the affected surface.

Because of this difficulty, missed seams are often detected using a visual witness-line procedure in which equally spaced parallel lines are scribed on both sides of the unwelded joint at the crown and root surfaces. Missed seams, which result from misalignment of the electron beam with the joint such that the fusion zone fails to encompass the entire joint, are detected by observing the number of witness lines remaining on either side of the weld bead. By establishing the relationship between the width of the fusion zone and the spacing of the witness lines, reasonably accurate criteria for determining whether the joint has been contained within the weld path (and therefore whether missed seams are present) can be developed.

Lack-of-penetration discontinuities occur when the fusion zone fails to penetrate through the entire joint thickness, resulting in an unbonded area near the root of the joint. These discontinuities are best detected by etching the root surface and observing the macroscopic shape and width of the fusion zone for full and even penetration.

An alternative method for inspecting complete weld penetration is that of immersion pulse-echo ultrasonic testing. The planet gear carrier assembly shown in Fig. 9(a) consists of three decks (plates) and eight curved spacer sections. The assembly, which is made from SAE 15B22M boron-treated structural steel, is held together by 16 welds. Weld integrity is monitored by ultrasonic methods.

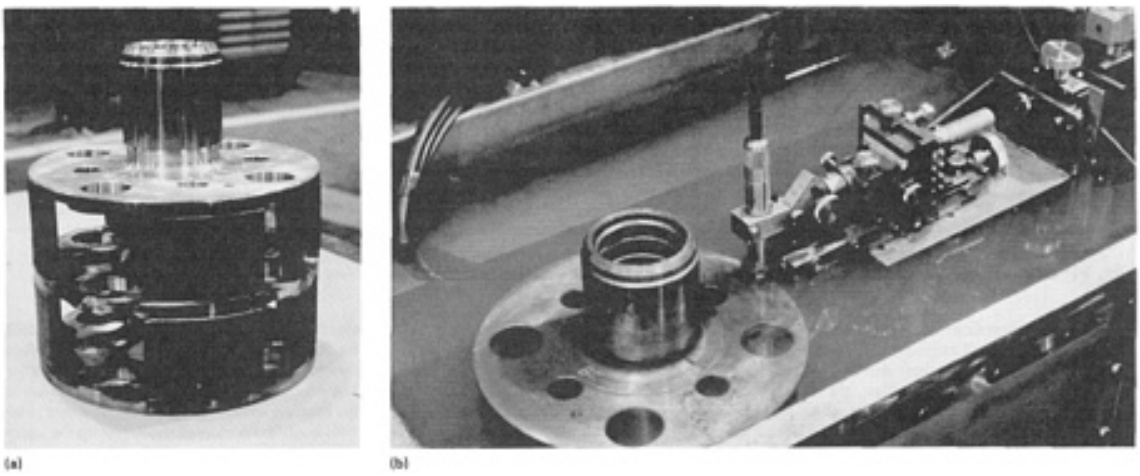

FIG. 9 PLANET GEAR CARRIER ASSEMBLY (A) SHOWING THE FOUR WELDS IN ONE STACK THAT CONNECT THE THREE DECKS. THE TOP AND TOP-CENTER WELDS ARE TESTED BY THE TOP ULTRASONIC TRANSDUCER, AND THE BOTTOM AND BOTTOM-CENTER WELDS ARE INSPECTED BY THE BOTTOM TRANSDUCER. (B) CLOSE-UP OF UPPER TRANSDUCER IN POSITION TO TEST THE WELDS. COURTESY OF CATERPILLAR, INC.

The parts are mounted on a turntable on a locating fixture so that the welds along the outside diameter are accessible. Two transducers, located above and below the assembly, are used. Figure 9(b) shows the upper transducer in position to test the welds. An overall view of the tank, turntable, controls, and reject/accept light panel is shown in Fig. 10. The use of such a system involves little downtime and enables a high quality level to be maintained. More information on ultrasonic test methods is presented later in this article.

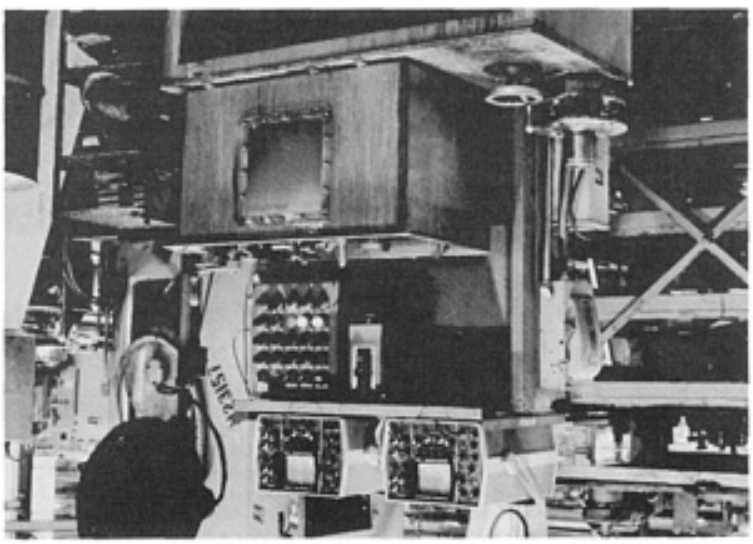

FIG. 10 OVERALL VIEW OF THE ULTRASONIC UNIT USED TO TEST THE ELECTRON-BEAM WELDED ASSEMBLY

SHOWN IN FIG. 9. COURTESY OF CATERPILLAR, INC.

Subsurface discontinuities in electron-beam welds are generally considerably more difficult to detect than surface discontinuities because observation is indirect. The two most reliable and widely used nondestructive inspection methods are radiography and ultrasonics.

Volume-type discontinuities such as porosity, voids, and bursts are detected by radiographic inspection, provided their cross sections presented to the radiating beam exceed 1 to 2% of the beam path in the metal. Discontinuities that present extremely thin cross sections to the beam path, such as cracks, missed seams, and LOP, are detectable with x-rays only if they are viewed from the end along their planar dimensions.

Ultrasonic inspection can detect most volume discontinuities as well as planar discontinuities. Planar discontinuities are best detected normal to the plane of the discontinuities, but missed seams and LOP often appear as continuous porosity when viewed looking down from the crown to the root of the weld in the plane of the discontinuity.

Because of the inherent dependence of both radiographic and ultrasonic inspection on the shape and orientation of flaws because each of the two methods can generally detect those flaws that the other misses, it is most advisable to complement one method with the other. Furthermore, to increase the likelihood of properly viewing a flaw, one of the methods should be employed in at least two (preferably perpendicular) directions.

Plasma Arc Welding

Discontinuities that occur in plasma arc welds include both surface and subsurface types, as shown in Fig. 11.

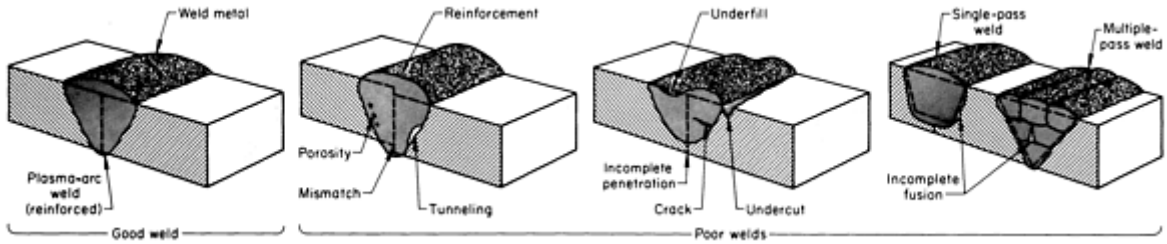

FIG. 11 PLASMA ARC WELDS SHOWING FLAWS THAT CAN OCCUR IN POOR WELDS AND THE ABSENCE OF FLAWS IN GOOD REINFORCED WELD

Surface discontinuities such as irregular reinforcement, underfill, undercut, and mismatch that are associated with weld bead contour and joint alignment are easily detected visually or dimensionally. Lack of penetration is also detected visually through the absence of a root bead. Weld cracks that are open to the surface are detected with liquid penetrants. Surface contamination, which results from insufficient shielding-gas coverage, is detected by the severe discoloration of the weld bead or adjacent HAZ.

Subsurface discontinuities are generally more prevalent in manual than in automatic plasma arc welding and are detected primarily by radiographic or ultrasonic inspection.

Porosity is by far the most commonly encountered discontinuity. Radiographic inspection is limited to detecting pores greater than approximately 1 to 2% of the joint thickness. Visibility is greater if both the crown and root beads are machined flush. Ultrasonic inspection can detect porosity if the joint is machined flush and joint thickness exceeds approximately 1.3 mm (0.050 in.).

Tunneling, as shown in Fig. 11, is a severe void along the boundary of the fusion zone and the HAZ. This discontinuity results from a combination of torch alignment and welding conditions (particularly travel speed). Tunneling is readily detectable by radiographic inspection.

Lack-of-fusion discontinuities occur in either single-pass or multiple-pass repair welds (Fig. 11). These discontinuities result from insufficient heat input to permit complete fusion of a particular weld bead to the part. Incomplete fusion can be detected by radiographic or ultrasonic inspection. Depending on the orientation of the discontinuity, one method may have an advantage over the other, so both should be used for optimum inspection.

Subsurface weld cracks, regardless of their cause, are detectable by radiographic and ultrasonic inspection.

Subsurface contamination in plasma arc welding results when copper from the torch nozzle is expelled into the weld. This is caused by excessive heat, usually produced in manual repair welding when the torch nozzle is placed too close to the weld, particularly in a groove. The resulting contamination, which may be detrimental, is undetectable by conventional nondestructive inspection methods. The only way of detecting copper contamination is by alerting the operator to watch for copper expulsion, which then must be machined off.

Electroslag Welding

Electroslag welding involves the use of copper dams over the open surfaces of a butt joint to hold the molten metal and the slag layer as the joint is built up vertically. Wire is fed into the slag layer continuously and is melted by the heat generated as current passes through the highly resistant slag layer.

Generally, electroslag welds are inspected with the same nondestructive examination methods as other heavy-section welds. With the exception of procedure qualification, all testing is nondestructive because of the sizes used. Techniques such as radiography and ultrasonic inspection are most often used, while visual, magnetic particle, and liquid penetrant testing are used also. Internal defects are generally more serious. Radiography and ultrasonic tests are the best methods for locating internal discontinuities.

Because of the nature of the process, LOF is rare. If fusion is achieved on external material edges, then fusion is generally complete throughout. Cracking may occur either in the weld or the HAZ. Porosity may either take the form of a rounded or a piped shape; the latter is often called wormhole porosity. Ultrasonic inspection is probably the quickest single method for inspecting any large weldment. If defects should occur, they appear as porosity or centerline cracking. Ultrasonic inspection is effective for locating either type of detect; however, only well-qualified personnel should set up the equipment and interpret the test results.

Electroslag welding results in large dendritic grain sizes because of the slow cooling rate. Inexperienced personnel often use high sensitivity and actually pick up the large coarse grains; when such welds are sectioned, usually no defects are present. Inspectors must learn to use low sensitivity to obtain good results when inspecting electroslag welds. Magnetic particle inspection is not a particularly good inspection method, because the areas examined by this technique are primarily surface or near surface. This is only a small percentage of the total weld; the only useful information is either checking the ends for craters, cracks, or centerline cracking or possibly for lack of edge fusion on the weld faces. Usually, a visual examination gives the same result unless the defect is subsurface. Visual examinations are only effective for surface defects, which are not common in this process.

Friction Welding

If impurities are properly dispelled during upsetting, friction or inertia welds are generally free of voids and inclusions. Incomplete center fusion can occur when flywheel speed is too low, when the amount of upset is insufficient, or when mating surfaces are concave. Tearing in the HAZ can be caused by low flywheel speed or excessive flywheel size. Cracks can occur when materials that are prone to hot shortness are joined. The penetration of a split between the extruded flash into the workpiece cross section is most prevalent during the welding of thin-wall tubing using improper conditions that do not allow for sufficient material upset.

The area where LOF generally occurs is at or near the center of the weld cross section. Because this is a subsurface discontinuity, detection is limited to radiographic or ultrasonic inspection; ultrasonic inspection is more practical. The longitudinal wave test (either manual-contact or immersion method) with beam propagation perpendicular to the area of LOF gives the most reliable results. This test can be performed as long as one end of the workpiece is accessible to the transducer.

Penetration of the split between the extruded flash on the outer surface of a tube is readily detected by liquid penetrant or magnetic particle inspection after the flash has been removed by machining. A split between the weld flash on the inner

surface of the tube can be detected by ultrasonic inspection using the angle-beam technique with manual contact of the transducer to the outside surface of the tube. The transducer contacts the tube so that the sound propagates along the longitudinal axis of the tube through the weldment.

Resistance Welding

Resistance welding encompasses spot, seam, and projection welding, each of which involves the joining of metals by passing current from one side of the joint to the other. The types of discontinuities found in resistance welds include porosity, LOF, and cracks. Porosity will generally be found on the centerline of the weld nugget. Lack of fusion may also be manifested as a centerline cavity. Either of these can be caused by overheating, inadequate pressure, premature release of pressure, or late application of pressure. Cracks may be induced by overheating, removal of pressure before weld quenching is completed, improper loading, poor joint fit-up, or expulsion of excess metal from the weld.

Weld Appearance. On the surface of a resistance spot welded assembly, the weld spot should be uniform in shape and relatively smooth, and it should be free of surface fusion, deep electrode indentations, electrode deposits, pits, cracks, sheet separation, abnormal discoloration around the weld, or other conditions indicating improper maintenance of electrodes or functioning of equipment. However, surface appearance is not always a good indicator of spot weld quality, because shunting and other causes of insufficient heating or incomplete penetration usually leave no visible effects on the workpiece.

The common practice for monitoring spot weld quality in manufacturing operations is the teardown method augmented with pry testing and visual inspection (Ref 3). In visual inspection, the operator uses the physical features of the weld surface, such as coloration, indentation, and smoothness, for assessing the quality of the weld. In pry testing, a wedge-shaped tool is inserted between the metal sheets next to the accessible welds, and a prying action is performed to see if the sheets will separate in the weld zone. The teardown method consists of physically tearing apart the welded members with hammers and chisels to determine the presence and size adequacy of fused metal nuggets at the spot weld site. The specifications require that the parent metal be torn and that the weld nugget remain intact. The destructiveness and/or inadequacy of these common inspection methods has long been recognized, and as a result, nondestructive methods have been extensively studied. The pulse-echo ultrasonic inspection of spot welds is now feasible.

Diffusion Welding

Diffusion welding (also known as diffusion bonding) is a metal joining process that requires the application of controlled pressures at elevated temperatures and usually a protective atmosphere to prevent oxidation. No melting and only limited macroscopic deformation or relative motion between the faying surfaces of the parts occur during bonding. As such, the principal mechanism for joint formation is solid-state diffusion. A diffusion aid (filler metal) may or may not be used. Diffusion welding has the advantage of producing a product finished to size, with joint efficiencies approaching 100%.

Discontinuities in Diffusion Welds. In the case of fusion welds, the detection of discontinuities less than 1 mm (0.04 in.) in size is not generally expected. In diffusion welding, in which no major lack of bonding occurs, individual discontinuities may be only micrometers in size. To understand how discontinuities form in diffusion-welded structures, it is first necessary to consider the principles of the process.

As illustrated in Fig. 12, metal surfaces have several general characteristics:

- ROUGHNESS
- AN OXIDIZED OR OTHERWISE CHEMICALLY REACTED AND ADHERENT LAYER
- OTHER RANDOMLY DISTRIBUTED SOLID OR LIQUID PRODUCTS SUCH AS OIL, GREASE, AND DIRT
- ADSORBED GAS, MOISTURE, OR BOTH

Because of these characteristics, two necessary conditions that must be met before a satisfactory diffusion weld can be made are:

- MECHANICAL INTIMACY OF METAL-TO-METAL CONTACT MUST BE ACHIEVED
- INTERFERING SURFACE CONTAMINANTS MUST BE DISRUPTED AND DISPERSED TO

PERMIT METALLIC BONDING TO OCCUR (SOLVENT CLEANING AND INERT GAS ATMOSPHERES CAN REDUCE OR ELIMINATE PROBLEMS ASSOCIATED WITH SURFACE CONTAMINATION AND OXIDE FORMATION, RESPECTIVELY)

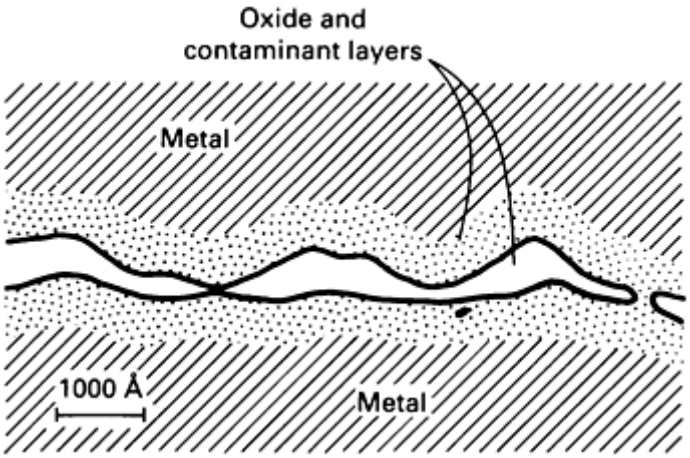

FIG. 12 CHARACTERISTICS OF A METAL SURFACE SHOWING ROUGHNESS AND CONTAMINANTS PRESENT. SOURCE: REF 7

For a given set of processing parameters, surface roughness is probably the most important variable influencing the quality of diffusion-welded joints. The size of the discontinuities (voids) is principally determined by the scale of roughness of the surfaces being bonded. The degree of surface roughness is dependent on the material and fabrication/machining technique used. It has been shown that bonding becomes easier with finer surface roughness prior to bonding. Figure 13 compares the surface roughness values produced by a variety of fabrication methods. More detailed information on surface roughness can be found in the article "Surface Finish and Surface Integrity" in *Machining,* Volume 16 of the *ASM Handbook.*

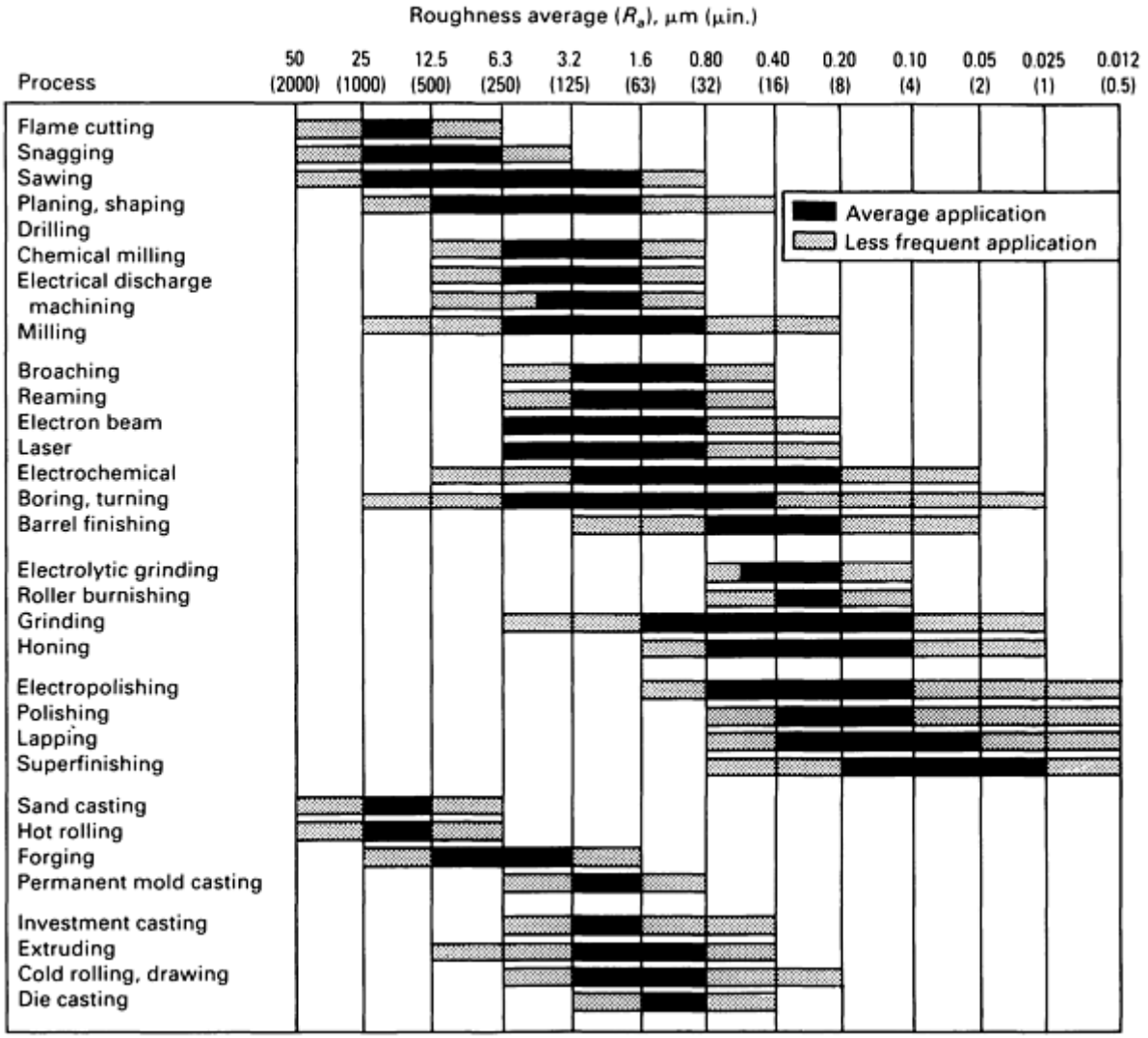

FIG. 13 SURFACE ROUGHNESS PRODUCED BY COMMON PRODUCTION METHODS. THE RANGES SHOWN ARE TYPICAL OF THE PROCESSES LISTED. HIGHER OR LOWER VALUES CAN BE OBTAINED UNDER SPECIAL CONDITIONS.

The mechanism of bond formation in diffusion welding is believed to be the deformation of the surface roughness in order to cause metal-to-metal contact at asperities, followed by the removal of interfacial voids and cracks by diffusional and creep processes. For conventional diffusion bonding without a diffusion aid, the three-stage mechanistic model shown in Fig. 14 describes bond formation. In the first stage, deformation of the contacting asperities occurs primarily by yielding and by creep deformation mechanisms to produce intimate contact over a large fraction of the interfacial area. At the end of this stage, the joint is essentially a grain boundary at the areas of contact with voids between these areas. During the second stage, diffusion becomes more important than deformation, and many of the voids disappear as the grain-boundary diffusion of atoms continues. Simultaneously, the interfacial grain boundary migrates to an equilibrium configuration away from the original plane of the joint, leaving many of the remaining voids within the grains. In the third stage, the remaining voids are eliminated by the volume diffusion of atoms to the void surface (equivalent to diffusion of vacancies away from the void). Successful completion of stage three is dependent on proper surface processing and joint processing.

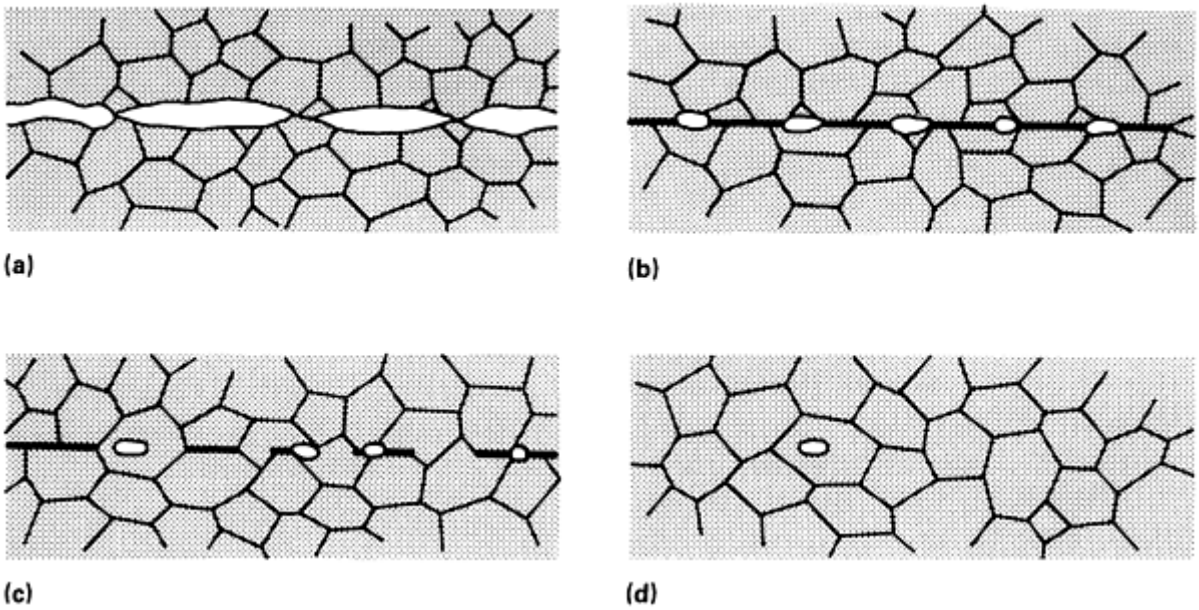

FIG. 14 THREE-STAGE MECHANISTIC MODEL OF DIFFUSION WELDING. (A) INITIAL ASPERITY CONTACT. (B) FIRST-STAGE DEFORMATION AND INTERFACIAL BOUNDARY FORMATION. (C) SECOND-STAGE GRAIN BOUNDARY MIGRATION AND PORE ELIMINATION. (D) THIRD-STAGE VOLUME DIFFUSION AND PORE ELIMINATION. SOURCE: REF 7

Successful nondestructive evaluation of diffusion-welded joints requires that the maximum size and distribution of discontinuities be determined. However, many conventional NDE methods and equipment are not adequate for discontinuity determination. Fluorescent penetrants provide excellent detection capability for lack of bonding as long as the interfacial crack breaks the surface. They are completely ineffective for defects that have no path to the surface.

Conventional film radiography is not suitable for detecting the extremely small defects involved in diffusion welding, but the use of x-ray microfocus techniques coupled with digital image enhancement offers an improvement in resolution. Discontinuities as small as 50 μm (0.002 in.) have been detected.

Conventional ultrasonic testing has some applications, although only significant lack of bonding or clusters of smaller defects can be reliably detected. High-resolution flaw detection involving frequencies approaching 100 MHz appears to have distinct advantages over conventional testing. Scanning acoustic microscopy also appears to offer excellent possibilities in diffusion bond inspection. Eddy current and thermal methods are relatively unsatisfactory for most applications.

References cited in this section

3. T.M. MANSOUR, ULTRASONIC INSPECTION OF SPOT WELDS IN THIN-GAGE STEEL, *MATER. EVAL.*, VOL 46 (NO. 5), APRIL 1988, P 650-658
7. DIFFUSION WELDING AND BRAZING, *WELDING HANDBOOK*, 7TH ED., AMERICAN WELDING SOCIETY, 1980, P 311-335

Overview of Weld Discontinuities

References

1. ASME BOILER AND PRESSURE VESSEL CODE, APPENDIX IV, DRAFT 1, 21 OCT 1981
2. L.W. SANDOR, THE MEANING OF WELD DISCONTINUITIES IN SHIPBUILDING, *PROC. 1ST NAT.*

CONF. FITNESS-FOR-SERVICE IN SHIPBUILDING (BOULDER, CO), OCT 1980

3. T.M. MANSOUR, ULTRASONIC INSPECTION OF SPOT WELDS IN THIN-GAGE STEEL, *MATER. EVAL.*, VOL 46 (NO. 5), APRIL 1988, P 650-658
4. P. KAPRANOS AND R. PRIESTNER, NDE OF DIFFUSION BONDS, *MET. MATER.*, VOL 3 (NO. 4), APRIL 1987, P 194-198
5. P.G. PARTRIDGE, "DIFFUSION BONDING OF METALS," ADVISORY GROUP FOR AEROSPACE RESEARCH AND DEVELOPMENT (NATO), AUG 1987, P 5.1-5.23
6. G. TOBER AND S. ELZE, "ULTRASONIC TESTING TECHNIQUES FOR DIFFUSION-BONDED TITANIUM COMPONENTS," ADVISORY GROUP FOR AEROSPACE RESEARCH AND DEVELOPMENT (NATO), JULY 1986, P 11.1-11.10
7. DIFFUSION WELDING AND BRAZING, *WELDING HANDBOOK*, 7TH ED., AMERICAN WELDING SOCIETY, 1980, P 311-335

Inspection of Welded Joints

G.R. Edwards, The Welding Institute

Introduction

WELDED JOINTS in any component or structure require thorough inspection. The role of nondestructive evaluation (NDE) in the inspection of welds is very important, and the technology has become highly developed as a result. This article describes the applications, methods, and limitations of NDE, and provides guidance as to method selection.

Nondestructive evaluation comprises a range of test methods for detecting discontinuities in a material, component, or structure, without causing damage. Therefore, the principal advantages of nondestructive tests, as opposed to alternative destructive proof tests, are that a 100% inspection can be performed at manufacture and that monitoring of the structure or component can continue while it is in service. The principal disadvantage of NDE is that the measurements obtained are only indirectly related to the presence and severity of the flaws, and much subjective interpretation is necessary.

Any discussion of NDE requires a clear definition of the term "defect." A defect is a discontinuity that creates a substantial risk of failure in a component or structure during its service life. Although the aim of NDE is to detect defects, it provides evidence of flaws, as well. The significance of these flaws and whether or not they are actually defects must then be determined. The development of NDE procedures often includes a collaboration between the NDE, engineering, and design functions to investigate the significance of defects.

There are five principal test methods: penetrant testing, magnetic-particle testing, eddy-current testing, radiographic testing, and ultrasonic testing. Although visual inspection is not strictly a test method, it does have an important role in NDE procedures and is often the only inspection method used. Acoustic emission (AE) testing and leak testing are described separately, because they are somewhat different in character and are not used as widely. There are other NDE methods that have been omitted, because they are very specialized.

Inspection of Welded Joints

G.R. Edwards, The Welding Institute

Applications

A useful distinction can be made between those NDE methods that are applied to welds during manufacturing and those that are applied to welds as part of plant and machinery maintenance. Although the same methods and techniques can be applied in both areas, there are important differences in inspection goals and, therefore, in test procedures.

In manufacturing, NDE is one of a series of quality-control techniques. The integration of these techniques into the manufacturing process is an important management subject. The first step is to decide at what stage or stages the NDE is to be carried out. Components that are brought in-house can be inspected prior to welding. An ultrasonic examination of a parent plate, for example, will show areas that contain laminations. Although these laminations may not be defects in themselves, lamellar tears could result where they occur near the weld in a specific orientation.

During the welding of thick sections, the magnetic-particle testing (MPT) of the root-pass and hot pass, in an attempt to find cracks before filling the weld groove, could save on repair costs. Using dry powder techniques, MPT can be carried out while surfaces are still hot.

Attempts have been made to incorporate NDE techniques with continuous monitoring of the weld process. Eddy-current testing, for example, has been used on small-bore induction-welded tube to provide feedback to control the welding process. However, total automation with real-time evaluation of test results is still not generally available, except in very simple applications, where results can be evaluated with simple go/no-go acceptance criteria.

Nondestructive evaluation is usually conducted at the end of a manufacturing process. In that capacity, it functions as part of the specification requirements and thus provides a safeguard against sending defective components or structures to customers. Unfortunately, conducting NDE after welding has been completed is not satisfactory. The necessity of repairs has given NDE a negative image in the manufacturing process. The early implementation of NDE in the process and the consequent actions to reduce repair rates is a more positive use.

NDE techniques have been used increasingly in plant and machinery maintenance, as a result of numerous industrial trends. The trend toward improved safety of operation, particularly in aircraft and nuclear power plants, is an obvious example. In times of economic recession, the operating life of a plant tends to be extended, and NDE has been utilized with increasing frequency. Environmental issues also have provided a stimulus to NDE activity. The inspection of storage tanks at refineries, where corrosion needs to be detected before leaks develop, is a good example.

As already noted, the performance capability required of NDE during the manufacturing process can be quite different from that needed during plant maintenance. Generally, the sizing accuracy is more important in maintenance, whereas the reliability of detection is more important in manufacturing. Because of the inherent unreliability of many techniques, a wide tolerance between critical defect size and flaw detection threshold is needed in manufacturing. However, the incorporation of fitness-for-purpose philosophies into quality control is having the effect of reducing this tolerance and placing greater emphasis on NDE sizing accuracy in all applications.

Inspection of Welded Joints

G.R. Edwards, The Welding Institute

NDE Methods

A variety of NDE methods are briefly described below, along with some of the operating problems that can be encountered. The limitations of NDE methods are further described in the section "NDE Performance" in this article.

Visual inspection, although not itself a test method, is the most common NDE method and, arguably, the most important. Indeed, a thorough visual examination is a prerequisite of successful NDE. Much can be inferred from the surface of the weld, including information about its internal condition, although a good weld surface does not necessarily indicate a defect-free weld.

Mechanical gages are available for measuring such dimensions as the height of the weld bead, the depth of the undercut, and the weld size (Fig. 1). When surfaces are not accessible, it may be possible to use boroscopes and flexible endoscopes to view the weld. Their use does require some familiarization, because they give a very flat field of view in which important features can be lost unless the surface is illuminated carefully.

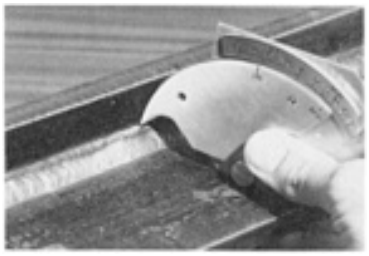

FIG. 1 WELD GAGE

Penetrant Testing. Penetrants provide a method of enhancing the visibility of flaws. A strongly colored, or fluorescent, liquid is applied liberally to the test surface and left to infiltrate surface-breaking cavities and cracks. The surface contact time is typically about 15 min. The excess liquid is then wiped from the surface, using some solvent, and a fine white developer powder is applied, usually as an aerosol in a volatile solvent. As the solvent evaporates, the penetrant liquid that is trapped in the flaws is drawn into the dry developer powder by a reverse-capillary action. For a cavity, this process may take no more than 1 s, but for a fine hairline crack, it may be necessary to wait more than 1 h for a visible indication.

The several penetrant types that exist can be distinguished on the basis of color, method of removal, and the form of the developer. Red penetrants, which are the most commonly used, require good daylight viewing conditions and a white background to improve contrast. Fluorescent penetrants are used when high sensitivity to fine flaws on relatively smooth surfaces is needed. They require black-light viewing conditions.

Solvent-removable red penerrants are the most convenient for site use. They can be provided in three aerosol cans of penetrant, cleaning fluid, and developer. Unfortunately, solvents are a health hazard and should be applied only in well-ventilated areas. A safer alternative is the water-washable penetrant.

When the geometry of the test piece is too complicated for an even coating to be applied using a spray, the developer can be applied directly as a dry powder. A dry powder is more suited to fluorescent penetrants, because it does not provide a white background, and the thickness of the coating reduces the blotting action and sensitivity, but improves image definition.

The compatibility of the penetrant with the test material must be considered. Residues of penetrant can be difficult to remove after the test. Traces of chlorine will corrode stainless steels and hydroxides will attack aluminum. The trace element content is provided by the manufacturer of the penetrant.

Although it is the most common NDE method, penetrant testing is widely misused. The test surfaces are often inadequately cleaned, the penetrant contact time with the surface is too short, or the excess penetrant is removed carelessly from flaws, as well as from the surface. In addition, because the method only detects flaws that are open to the surface, abrasive cleaning methods may peen over fine, surface-breaking cracks. This problem can arise when penetrants are used to chase fine hairline cracks or incomplete fusion with grinding.

Magnetic particle testing is the preferred method for detecting surface-breaking and, under certain circumstances, near-surface flaws in situations where a test material can be magnetized.

This method depends on the flaw disrupting the magnetic flux generated along the surface of the weld by a permanent magnet or electromagnets, or by electric-current-carrying electrodes and cables. Flux leakage from the surface creates magnetic poles, which attract the magnetic particles, creating a clearly visible image of the flaw. The method is particularly sensitive to the detection of cracks, where, like penetrants, the particles identify flaws with well-defined features. However, the flux leakage may be absent altogether, if the crack runs parallel with the magnetic field. It is therefore vital that the inspection surface be magnetized in two directions at right angles to each other.

Important considerations associated with MPT are the method of magnetization, the detecting medium, and the ways in which the field direction and strength can be measured. A very convenient method of magnetization is to use permanent magnets, which do not need a power source. Because the magnetic field is in a constant direction and does not alternate, it penetrates the surface to give some sensitivity to subsurface flaws. However, permanent magnets are difficult to

manipulate in confined spaces. If proper contact between the feet of the magnet and the test surface is not achieved, then the density of magnetic flux in the test piece is weakened, and the test sensitivity is reduced.

Electromagnets are easier to use and can generate magnetic fields with alternating current (ac) (Fig. 2). The skin effect caused by ac concentrates the flux at the surface, improving the sensitivity to surface-breaking flaws, particularly on contoured surfaces.

FIG. 2 MAGNETIC-PARTICLE TESTING OF A WELD WITH AN ELECTROMAGNET

Prod magnetization, in which electrodes carrying a high-amperage, low-voltage current are pressed onto the test surface to induce a distorted, circular magnetic field, provides the most controlled method of magnetization. Although the electrodes can be manipulated more easily into tight corners, they do have two major disadvantages, which can preclude their usefulness. First, the arc strikes that can occur at the prod contact points can damage the test surface. Second, the electrodes may require a two-man operation.

Cable magnetization is common in diver inspections of underwater node welds on oil platforms. The cables are wrapped around the pipe adjacent to the weld. The induced field, which is directed across the weld, is sensitive to longitudinal cracks only.

The fine particles that are applied to the magnetized surface to detect the flux-leakage fields must be highly magnetic. Materials commonly used are black iron and red or yellow iron oxides. The iron particles can be coated with a fluorescent material and viewed in black light. Before black particles are applied, the surface can be coated with a thin, white lacquer to improve contrast. Although the particles are typically sprayed on the surface as a suspension in water or solvent, they also can be applied as a dry powder. Dry powders can be used on hot surfaces or in cases where contamination is an issue.

To ensure that the magnetic flux is adequate, indicators such as the Berthold gage can be placed on the test surface. This type of indicator contains fine graticules of a highly magnetic material set in a nonmagnetic base. The graticules are made visible when the particles are applied and the magnetic field is of sufficient strength in a right-angled direction to the graticule. However, the indicators are influenced more by the tangential field across the test surface than by the magnetic field within the test piece. Therefore, as an indicator of test sensitivity, they should be treated with circumspection. It is possible to see defects, even when the indicator has been placed on a nonmagnetic material, where there is obviously no defect sensitivity at all.

The MPT process can leave residual fields that interfere with welding processes, Demagnetization can be achieved by slowly wiping the surface with an ac yoke.

Eddy-current testing techniques have been used widely in automated tube-testing systems and material sorting, as well as in the inspection of aircraft components and structures. For the testing of welds, there is a growing interest in using eddy-current testing as an alternative to MPT and penetrant testing, because the method is able to detect cracks beneath a thick layer of paint.

Like MPT, eddy-current testing relies on the flaw disrupting the energizing field, which is electrical, circular, and induced by a small coil carrying high-frequency alternating current. Therefore, the orientation of vertical planar flaws is not important, but the coil has to be scanned intensively over the test surface to ensure coverage. Laminar flaws are not detectable.

The method relies on detecting changes in the impedance of a coil that are caused by deflections in the eddy-current field around a flaw. The eddy-current field is affected by changes in material properties, surface geometry, edges, and many other factors that are unrelated to flaws. For this reason, the analysis of eddy-current test results can be difficult. The important components of the test equipment are the instrument, the probe containing the coil, and the calibration block containing slots or other artificial flaws.

Meter-reading instruments may be adequate for simple tests, but for more complex applications, such as weld testing, a cathode-ray tube with a vector point display is needed for analyzing the induced coil current (Fig. 3). The vector point provides information about the impedance of the coil. This is a complex quantity, which measures the amplitude and phase of the coil current. Certain directional movements in the vector point on the screen representing phase changes between coil current and voltage are associated with well-defined effects, such as lift-off effect (the up and down movement of the coil) and the edge effect (coil approaching an edge of the test piece). These can be distinguished from vector movements in other directions that are caused by cracks.

FIG. 3 EDDY-CURRENT TEST INSTRUMENT WITH VECTOR POINT DISPLAY

For weld testing, the coils are housed in pencil-like probes, which can be scanned along the weld cap. Coil arrangements can be varied to improve performance. Simple absolute coils, for example, are generally too noisy for testing welds. Alternative differential coil arrangements have been developed, which almost remove the lift-off noise completely as the probe scans the rough surface of the weld cap.

A measurement of crack depth is achieved by comparing the crack signal with the signal from a slot of known depth in a calibration block. This can be regarded only as a very approximate measure. It does not consider the crack width and inclination to the surface.

On the vector point display, the phase separation between lift-off and crack signals depends on the frequency of the coil current, as well as the coil design. The test frequency also determines the depth of penetration of the eddy-current field and, therefore, the sensitivity to subsurface flaws. At test frequencies below 1 kHz, the field can penetrate aluminum to a depth of several millimeters. However, for ferromagnetic materials, the overriding factor determining depth of penetration is the magnetic permeability, which restricts the eddy-current field to the surface unless it is removed by saturating the material with magnetism.

Radiographic testing, in the past, has formed the basis of weld inspection for internal flaws. However, it is an expensive method, and increasing restrictions on the use of ionizing radiation has led to a shift toward alternative ultrasonic testing techniques.

The radiographic technique uses radiation, either as x-rays or gamma rays, to penetrate the weld to create a latent image on radiographic film. The test piece absorbs radiation, but when flaws are present, less is absorbed than the amount

absorbed by the parent material, which produces a localized darkening of the film. If the radiation source is sufficiently far from the object, then the image of the flaw will be sharp. Cavities with a through thickness of the order of only 1% of wall thickness can be discerned.

Most radiography is carried out with x-rays from tubes that operate in a voltage range between 120 and 400 kV. Higher voltages can be achieved using special equipment. As the thickness of the test object increases, the amount of kilovolts also must increase to keep the exposure time down to 4 to 6 min, typically, to avoid shortening the tube service life. However, high voltages reduce the image quality.

Gamma rays are produced by the radioactive decay of isotopes and do not need an electric power supply. Therefore, they are used extensively in site work. Iridium 192 is the usual isotope choice. However, for thick sections (72 in.), Cesium 137 and Cobalt 60 provide higher energy, whereas for thin sections, Ytterbium 169 is suitable. Generally, the quality of gamma radiographs is not as good as that of x-radiographs.

The test results are viewed in a radiograph. The radiographic films are chosen to achieve optimum definition and contrast within practicable exposure times. Faster films are needed where sections are thick, but at the sacrifice of image definition. Speed can be increased by replacing lead-intensifying screens that are in contact with the film with fluorescent ones, but this will result in a loss of definition.

The radiographs are viewed as negatives. The highest contrast is attained at image densities of the order of 3.0 on a log scale and, therefore, the radiographs can only be viewed in high-intensity transmitted light. If the image can be viewed with the film held up in front of normal light bulbs, then the density is much too low.

As an alternative to film radiography, where it can take 20 min to develop a radiograph that can be viewed, radioscopy offers images in real time. The images are created on x-ray-sensitive screens that can be intensified and scanned with a camera for visual display. However, screen resolution and contrast are not as high as with film radiography.

Obviously, taking a conventional radiograph necessitates access to both sides of the object. Thus, there is a variety of techniques for inspecting pipe welds. For pipe diameters that exceed 750 mm (30 in.) and allow access to the center, panoramic techniques are the most efficient (Fig. 4). For smaller pipes that do not allow internal access, both film and source must be on the outside. Exposure times are increased because the radiation must penetrate two walls. Inspection rates are reduced further, because the pipe has to be covered in multiple exposures.

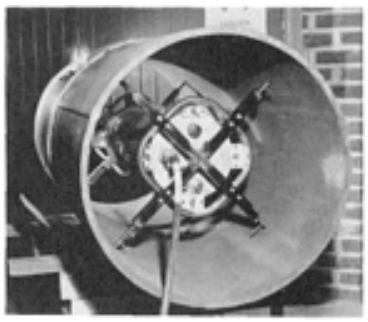

FIG. 4 RADIOGRAPHIC TESTING OF A PIPE WITH A PANORAMIC TECHNIQUE

If the pipe diameter is less than 75 mm (3 in.), then the number of exposures can be halved by putting the source at a sufficient distance away from the pipe to provide images of both the near and the far sides of the weld. The so-called double-wall, double-image technique is often used on welds in steam-generator pipes and condenser tubes.

Radiography can be used on welds in more complex geometries, such as nodes and T-joints, but only for detecting large volumetric flaws. Film cassettes that are double loaded with one fast and one slow film are used to accommodate the large variation in penetrated thickness across the weld.

The sensitivity of the radiograph is assessed using image quality indicators (IQIs), which can either be fine wires placed across the weld or plaques with small drilled holes placed adjacent to the weld. The dimension of the smallest visible hole

or wire in the radiograph is a measure of its sensitivity. These are described in greater detail in the section "Sensitivity" in this article.

Ultrasonic testing receives more attention in the literature than any other NDE method, because of its use in critical applications, such as in the nuclear industry, and because it requires the highest level of skill. Like sonar, the method relies on propagating pulses of sound through a medium and then picking up reflected echoes. However, because the sound is of an ultrasonic frequency, the pulses are propagated along a narrow beam in a fixed direction, typically at refraction angles of 0, 45, 60, or 70° from the probe placed on the surface. To achieve coverage, the beam must therefore be scanned in a tight raster fashion over the test surface.

The surface of the flaw will have an important effect on the echo. Planar specular reflectors will only reflect the sound back to the probe if they lie in a plane perpendicular to the beam. Therefore, the detection of incomplete fusion in the sidewall of groove welds will require the judicious selection of probe beam angles. On the other hand, the echo amplitude is independent of beam direction for spherical reflectors, such as pores.

In conventional ultrasonic testing, the information collected by manually scanning the probe up to the weld and, where the cap has been removed, across the weld, is displayed on a cathoderay oscilloscope in an A-scan display (Fig. 5). This provides information about the amplitude of the echo and the distance of the reflector from the probe. Interpretation of the A-scan requires a high level of skill. It does not provide a permanent record of the test, which is, perhaps, the most important disadvantage of ultrasonic testing. On the other hand, the A-scan does provide information about the nature, size, and location of the flaw, which is further described in the section "NDE Performance" in this article.

FIG. 5 ULTRASONIC EXAMINATION OF A NOZZLE WELD

The A-scan is viewed with the ultrasonic flaw-detector instrument, which has controls to adjust range, delay, and gain. Recently, instruments with digitally created A-scans have started to replace those based on analog. They are capable of making print-outs of the screen, but with some loss in resolution.

In addition to the beam angle mentioned above, probes can be selected according to ultrasound frequency, transducer diameter, and wave mode (shear or compression). Lower frequencies, such as 1 to 2.5 MHz, are used on thick sections.

An important aspect of ultrasonic testing is calibration. The time base of the A-scan must be calibrated for distance in millimeters or inches, and the amplitude of signals must be calibrated in dB, relative to some reference reflector. This is achieved using standard calibration blocks that are made from the same material as the test piece and contain reflectors at known distances and of known dimensions. To calibrate the amplitude of the A-scan, side-drilled holes are typically used in a range of distances. By observing the fall-off in signal amplitude with distance, the important distance-amplitude correction (DAC) can be applied to the A-scan.

Besides the flaw detector, probes, and calibration blocks, thick liquid couplants are needed to transmit the ultrasound from the probe into the test piece. The test surface has an important bearing on coupling efficiency. It should be smooth and free from loose debris. Although ultrasonic tests can be carried out on painted surfaces, the instrument gain should be increased to account for transfer losses.

One of the most common problems with ultrasonic testing is insufficient access for probe scanning. The width of scanning surfaces should be considered carefully at the weld design stage.

Other NDE methods also exist. Acoustic emission (AE) and leak testing are worth mentioning here because of their use in weld testing. Acoustic emissions are stress waves generated from crack growth and plastic deformation. Therefore, the weld has to be loaded. The emissions range in frequency from 20 to 1200 kHz and are picked up with piezoelectric transducers fixed to the structure in arrays that are from 1 to 6 m (3.3 to 19.7 ft) apart. The emissions generally occur in bursts and are of very low amplitude. The instruments are able to amplify the signals and filter out the high levels of associated noise, producing a record of emissions over time. The emissions are difficult to define, because of their wide amplitude and frequency range. Moreover, the response of the transducers has an overriding effect on the signals. In most conventional systems, the analysis of emissions is simplified to include the number of counts (emissions exceeding a threshold level), their amplitude, and the rise time of pulses.

Acoustic emission testing has three important applications in the welding field: the in-process monitoring of resistance welds, the detection of leaking welds in storage tanks, and the proof testing of welded pressure vessels.

In the first of these applications, the AE is produced by the thermal stresses created as the weld cools and solidifies. Each weld process has a particular AE signature, which can be monitored to indicate suboptimal performance.

Leaks that produce turbulent flow in the escaping fluid also produce stress waves. Therefore, AE provides a noninvasive method of detecting leaks in storage tanks. By taking triangulation measurements from points around the tank, the source can be located.

Perhaps the most effective use of AE is in the proof testing of pressure vessels. The AE process was originally developed for use with pressure tests of vessels in glass fiber reinforced plastic. In effect, it sensitizes the proof test, so that subcritical defects, which do not lead to failure in the test, but which may lead to subsequent failure, are revealed.

Most AE problems are associated with noise. Site testing requires quiet environmental conditions, without rain or wind. In addition, great care has to be taken when loading structures to avoid flaw propagation to critical levels. The past loading history of the structure affects its AE signature. For this reason, effective AE tests of pressure vessels can only take place with the initial pressure test. After the first loading, some information about flaws will be lost.

As already mentioned, leak testing can be carried out using AE methods. However, there are simpler methods that can be used in the field for inspecting welds. For example, penetrant testing can be adapted by applying the liquid to one surface and observing the development of flaws on the other.

The most common method of leak testing is the bubble test, in which a bubble-forming solution is sprayed onto the surface. To create the pressure difference across the weld, which is necessary to form the bubbles, the test area is either encased in a transparent vacuum box or a positive pressure is applied to the opposite side of the component.

For very small leaks, it is necessary to use tracer gases with specialized detection equipment and probes to locate the position of the leak. Gases of small molecular size, such as helium, are used for this purpose.

Inspection of Welded Joints

G.R. Edwards, The Welding Institute

Test Procedures

A very important aspect of NDE is the development of test procedures. These are control documents, which state how the test is to be performed and how the results are to be evaluated and recorded. Written by an NDE specialist, the procedure attempts to provide the test operator with information to ensure that the defects being sought are detected in a repeatable manner.

NDE procedures can be classified as either routine or special. The routine procedure is written in accordance with a specification or code. The special procedure is written to meet a particular requirement, which is not covered by a specification. Special procedures are more prevalent during in-service monitoring and may require validation trials on specimens that possess simulated defects.

A good procedure will be clear and concise, and it will provide adequate coverage within the constraints set by cost and time for inspection. The procedure will start with a title page that includes a reference number as part of a quality-assurance system. At times, the procedures may be amended, and the system must be able to cope with this. In addition to the name of the person who wrote the procedure, someone in authority, who must also print his or her name and sign and date the document, must approve the procedure. The next section of the procedure will list the precise details of the equipment to be used, listing alternatives, if possible.

The level of competence required of the test operators must also be defined. In situations where nationally accepted schemes, such as the American Society of Nondestructive Testing (ASNT), are mentioned, finding an equivalent scheme can be a problem. Attempts are being made to formalize agreements among national certification schemes.

The section of the procedure that is known as the technique comprises equipment setup and test operation. This is at the core of the procedure document and requires the most careful preparation. It is not uncommon to list several techniques within one procedure document, where each refers to a different type of weld in a structure, but is covered by the same equipment, personnel, calibration, evaluation, and recording requirements as the other techniques.

The methods used to evaluate the test results must be described carefully. They should consider the way in which the results are presented, that is, images or signals. It may be appropriate to evaluate the porosity visible in a radiographic image in terms of density as a percentage of area. However, with ultrasonic testing, the signals on the A-scan cannot be interpreted in this way.

The final section of the document deals with the recording of results. Written evidence is always required to document how the test was carried out, so that it can be repeated. Report forms must be designed carefully to include serial numbers of equipment, for example. Radiography is the only routine method that provides a permanent record of the test results. Although photographs can be taken of flaws found by penetrant and magnetic-particle testing, the results of eddy-current and ultrasonic tests are more difficult to record. The information about signal amplitude and position can be logged in a table and plotted onto diagrams of the weld, but it is the skill of the test operator that ultimately determines the quality of the report.

Inspection of Welded Joints

G.R. Edwards, The Welding Institute

Test-Operator Training

The training and certification of NDE operators receives a great deal of attention. The approach established by the American Society of Nondestructive Testing (ASNT) has been adopted by many national schemes, but with important differences. Broadly speaking, there are three levels of competence for each method. At Level I, the test operators have progressed from trainees to a stage at which they can conduct tests under supervision. At Level II, they are able to conduct tests independently, write test procedures, and generally provide the base manpower for NDE operations. At Level III are supervisors and managers responsible for the NDE function. They have a more general knowledge of NDE and quality control and are in a position to approve NDE procedure documents, for example. At each level, the technician will have passed a written examination and demonstrated practical proficiency in conducting tests.

The situation is complicated by the need to qualify test operators not only for the method, but for the application. Personnel involved in the inspection of groove welds in plate, for example, may not have received training for the inspection of groove welds in T-joints. This led the ASNT to establish schemes that were company specific. Each company establishes its own training and certification scheme according to the document SNT-TC-1A, "Recommended Practice for Qualification and Certification in NDT." This is subject to external audit.

European certification schemes such as PCN (United Kingdom), COFREND (France), and NORDTEST (Scandinavia) also have three levels of competence, but the approvals are conducted at independent test centers.

G.R. Edwards, The Welding Institute

NDE Performance

NDE detects and evaluates flaws indirectly by the way in which the flaw interrupts a magnetic field or reflects ultrasound, for example. Measuring the performance of NDE in carrying out this task is difficult, because of ambiguities in the interpretation of test results. Nondestructive evaluation is not an exact science.

The detection capability of the test is expressed in terms of its sensitivity, but the test may also provide information about the nature, size, and location of the flaw. These are all important attributes in determining whether or not a flaw is significant.

Nature of the Flaw. NDE methods can be segregated in terms of those that provide images of the flaw (visual inspection and penetrant, magnetic particle, and radiographic testing) and those that provide signals from the flaw (ultrasonic and eddy-current testing).

The nature of the flaw can be more easily assessed from images than from signals. However, interpreting images is not always straight-forward. Penetrant tests, for example, indicate flaws that are a result of a blotting action. This can have the effect of forming a line of rounded flaws from a linear flaw. Cleaning away the developer and closely examining the purported flaw with a magnifying glass is usually sufficient to assess ambiguity.

With MPT, the sharp change in contour that occurs at the weld toe produces a flux-leakage field that attracts magnetic particles. This indicates a flaw that can be mistaken for a toe crack. Generally, however, the flaw is weak and can be blown away from the surface. Grinding the weld toe to a favorable profile can improve accuracy.

Because radiographic testing provides a two-dimensional image of a three-dimensional object, images from the surface can be confused with those from internal flaws. Visual inspection may be necessary to distinguish an undercut from a slag inclusion, for example.

The identification of flaws from signals is severely limited. With eddy-current testing, an observation of vector displacements on the cathode-ray tube may distinguish surface from subsurface cracks, for example, but only after careful selection of the test frequency.

The signals displayed in the A-scan of an ultrasonic flaw detector provide more information, including distance and amplitude information collected as the probe scans the surface. These so-called echo dynamic patterns make it easier to characterize a flaw using an ultrasonic test than it is with an eddy-current test. Flaw characterization based on ultrasonic tests is currently a matter of much interest.

Flaw Size. After a flaw has been detected and its nature determined, the next step is to measure its dimensions. Measuring the length of a flaw is straightforward. However, the blotting effects of penetrants must be taken into account. Other problems can arise in radiography, where the full extent of a fine linear flaw can be seriously underestimated if its plane moves out of parallel with the radiation beam.

In an eddy-current or ultrasonic test, the length of probe movement between the indication end points is what is being measured. The definition of the end points can be a problem. The most common method employed in ultrasonic tests is the 6 dB drop sizing method, in which the probe is moved off the edge of the flaw to the point where the signal has dropped in amplitude by 6 dB or half its original amplitude. The axis of the sound beam is now half on and half off the flaw and can be taken as delineating the flaw edge. This can be done to an accuracy of ±5 mm (0.2 in.).

The width of a flaw also can be measured in an image, but it is generally too small to be measured by eddy-current or ultrasonic test methods.

After length, the next most important dimension in assessing the significance of a flaw is its height in the through-wall direction. Here, the performance of imaging methods is severely limited. Only qualitative assessments can be made from

the density of a defect indicated by penetrant, magnetic particle, or radiographic testing. On the other hand, eddy-current and ultrasonic tests do provide quantifiable information.

Comparisons with slots of known depth in a reference block serve to calibrate the vector displacements on an eddy-current instrument. Cracks to a depth of 3 mm (0.12 in.) can be measured with an accuracy of 0.5 mm (0.02 in.) in this way.

Ultrasonic tests can provide a measure of the through height of an internal flaw. There are four methods, the simplest of which involves comparing the amplitude of the echo signal from the flaw with the echo signal from a side-drilled or flat-bottomed hole. This can only be applied if the dimension is smaller than the width of the ultrasound beam (typically, 5 to 10 mm, or 0.2 to 0.4 in.). More importantly, when dealing with planar flaws, the orientation must be taken into account. If the plane of the flaw is more than 20° off perpendicular to the axis of the sound beam, then the echo will not be reflected back to the probe and it even may go undetected.

For small planar flaws with a height of more than 3 mm (0.12 in.), the preferred ultrasonic sizing method is the 20 dB drop method. This involves scanning the beam across the flaw and finding the 20 dB drop points. The beam path and probe positions at these points are plotted on a diagram of the weld using a cursor or overlay with the 20 dB beam profile to give the flaw edges. An accuracy of ±3 mm (0.12 in.) is achievable.

For planar flaws with large through-wall dimensions, such as cracks, the maximum-amplitude method involves plotting the facets of a flaw to indicate its orientation and dimension.

The location of the flaw in the through dimension of the weld is important in determining its significance. Flaws that are near a surface are more significant than flaws in the center of a weld. In a radiograph, this can only be inferred. Root flaws may appear in the center of the weld image, but may be confused with flaws that are near the weld cap. Only ultrasonic testing can provide definitive information about the through-wall location of a flaw. Indeed, it is often necessary to supplement radiographic tests with ultrasonic tests for this purpose.

Flaw location is, perhaps, the most reliable function of ultrasonic tests. To locate an echo signal, the time base of the A-scan must be accurately calibrated for distance. Variations in the velocity of ultrasound are not uncommon, but generally an accuracy to within 1 mm (0.04 in.) can be expected. The angle of the ultrasound beam and the probe index point must also be checked regularly with a calibration block. Shoe wear can lead to inaccuracies.

Finally, the position of the probe on the test surface at the point of maximum signal amplitude must be measured from the weld centerline, which should always be marked clearly on the test surface. However, the reliability of flaw location with ultrasonic testing depends on the skill of the operator. Carelessness can lead to errors, for example, in plotting the flaw on the wrong side of the weld.

Sensitivity. When dealing with images, sensitivity is expressed in terms of contrast and definition. When dealing with signals, it is the separation of signals from the background noise or signal/noise ratio.

The contrast and definition of penetrant testing and MPT can be enhanced by using fluorescent materials. Variations in contrast can be recognized more easily than with colored materials, and finer details in the flaw can be observed. However, on rough surfaces, background color can lead to a loss in sensitivity.

The contrast in a radiographic image is improved by decreasing the energy of the radiation and increasing the density of the image. In gamma radiography, the energy is fixed by the type of isotope, whereas in x-radiography, it can be varied with the tube voltage. The radiation from Iridium 192 has an x-ray equivalent in the 500 kV to 1 MeV range and, therefore, image quality is not as good as it is with x-rays in the usual 150 to 400 kV range. Ytterbium 169 has a much lower energy level, producing nearly x-ray image quality, but it suffers from a short half life and low output.

Although radiographic definition is also reduced by using higher-energy radiation, the most important factor that affects definition is the unsharpness, or penumbra, effect. This is caused by having a source, or x-ray focal spot, of finite size, typically 3 to 4 mm (0.12 to 0.16 in.). It is reduced by moving the object away to a distance of 0.5 to 1 m (1.6 to 3.3 ft) from the source, depending on object thickness, or by using special minifocused or microfocused x-ray tubes.

The contrast and definition of a radiograph can be assessed using a penetrameter or an image quality indicator (IQI). The size and type of penetrameter are specified by standards such as ASTM 747, "Method for Controlling Quality of

Radiographic Examination Using Wire Parameter." This instrument is placed near the weld or, in the case of a wire-type IQI, across the weld, on its source side at the time the radiograph is taken. The IQI comprises carefully dimensioned wires or steps with holes. By counting the number of wires or stepped holes that are visible on the radiograph, the sensitivity can be calculated as a percentage of wall thickness, or *T* value. If calculated as a percentage, then a value of 1 to 2% is normally acceptable. A higher percentage indicates a lower sensitivity.

Despite a high level of sensitivity, fine planar flaws can be missed if they are not oriented almost parallel with the radiation beam. Radiography is not effective at detecting incomplete side-wall fusion in metal-inert gas welds with a 30° chamfer angle, for example, unless the radiographic source is aligned with the angle, which requires multiple exposures.

In eddy-current testing, improving the signal/noise ratio is based on selecting appropriate coil configurations, test frequencies, and *y*/*x* potential ratios on the vector point display. A phase separation approaching 90° between the impedance vector caused by noise as the probe moves along the weld surface (lift-off) and the impedance vector from cracks can be achieved. Further reductions in noise can be made using signal filters, but the probe then has to be scanned at a constant speed.

The test frequency also affects the signal-to-noise separation in ultrasonic testing. As the frequency increases, the ultrasound attenuation rises, and the reduced ultrasound wavelength is scattered to produce more noise. Generally, the optimal frequencies for ultrasonic testing of welds in ferritic steels range from 4 to 5 MHz. The frequencies are higher for welds that are less than 10 mm (0.4 in.) thick, and lower for welds that are more than 50 mm (2 in.) thick. It should be noted, however, that some test procedures call for lower frequencies, because their flaw evaluation is based on echo amplitude only. At lower frequencies, beam spread is greater and, therefore, signal amplitude is less dependent on flaw orientation.

Inspection of Welded Joints

G.R. Edwards, The Welding Institute

Evaluation of Test Results

The evaluation of test results and the setting of accept/reject criteria for weld flaws are the subjects of much current debate. This is because of the empirical way in which the criteria were derived in the past. As new developments in defect assessment, such as fracture mechanics, set the trend toward more sophisticated methods of evaluating NDE results, the discrepancies in current practice become more apparent. This is particularly true of ultrasonic testing.

In general, the accept/reject criteria used in national standards draw a distinction between rounded and elongated flaws, as well as volumetric and planar ones. With NDE methods that produce an image of the flaw, this is a simple task. An elongated flaw is usually defined as one in which the length is more than three times the width.

Flaws rarely occur in isolation, and their distribution and proximity to each other are important characteristics. Porosity may be isolated, clustered, or aligned. If it is aligned, then it is more significant than if it were random, because there is likely to be incomplete fusion.

The NDE methods that produce signals from the flaw are the most difficult to evaluate. In ultrasonic tests, the simplest method of evaluation is to use echo amplitude and length criteria only. This can lead to planar flaws being undersized, if they are poorly oriented in the ultrasound beam. It is therefore important, in an ultrasonic test, to first characterize the flaw and, in particular, to distinguish planar flaws from volumetric ones. The identification of planar flaws such as cracks and incomplete fusion primarily depends on the skill of the test operator, who considers the signal location, shape, response to probe movement, and relative amplitude from different sides of the weld and with different probe beam angles.

Volumetric flaws, on the other hand, can be evaluated in terms of signal amplitude and length. In some specifications, for example, if the signal amplitude exceeds the DAC set-off 3 mm (0.12 in.) diameter holes, and the dB-drop length of the flaw exceeds the wall thickness of the weld, then the flaw is rejected as a defect.

The accept/reject criteria are usually set by a fabrication or manufacturing standard. In the past, these standards have been application specific. For example, ASME Section VIII has governed the manufacture of unfired pressure vessels. In the new European standards, however, the move is toward blanket quality levels, where each quality level defines the NDE procedures and defect accept/reject criteria and is selected according to the application.

Inspection of Welded Joints

G.R. Edwards, The Welding Institute

Selection of the NDE Method

The selection of the appropriate NDE method is influenced by a number of factors related to the test conditions. Those described here are not exclusive. There may be other constraints on selection, such as availability of trained personnel or costs. The methods shown in Tables 1, 2, and 3 are rated according to their applicability. This rating is not easily quantifiable, because it must account for the ease of test operation, its efficacy in finding flaws common to the application, and whether or not it is the only applicable NDE method.

TABLE 1 SELECTION OF NDE TECHNIQUE ON BASIS OF MATERIAL

A, most applicable; B, applicable; C, least applicable

MATERIAL	VISUAL	PENETRANTS	MPT	EDDY CURRENT	RADIOGRAPHIC TESTING	ULTRASONIC TESTING
BULK PLASTIC	A	B	. . .	. . .	A	**C**
GLASS FIBER REINFORCED PLASTIC	A	B	. . .	. . .	A	**C**
CARBON FIBER REINFORCED PLASTIC	B	C	. . .	C	A	**A**
LOW-CARBON STEEL	B	B	A	C	B	**A**
HIGH-ALLOY STEEL	B	B	C	B	B	**B**
ALUMINUM ALLOY	B	B	. . .	B	A	**B**
TITANIUM ALLOYS	B	B	. . .	B	A	**B**
DUPLEX STAINLESS STEEL	B	B	C	C	A	**B**
COPPER ALLOYS	**B**	**A**	**. . .**	**C**	**B**	**C**

TABLE 2 SELECTION OF NDE TECHNIQUE ON BASIS OF WELD GEOMETRY

A, most applicable; B, applicable; C, least applicable

GEOMETRY	VISUAL	PENETRANTS	MPT	EDDY CURRENT	RADIOGRAPHIC TESTING	ULTRASONIC TESTING
GROOVE PLATE/PIPE	B	B	B	C	A	**A**
T GROOVE	B	B	B	C	C	**A**
BRANCH GROOVE	B	B	C	C	C	**A**
NODE	B	B	B	B	C	**B**
T FILLET	A	B	A	C	C	**C**
BRANCH FILLET	A	B	A	C	C	**C**
LAP	A	B	A	C	B	**C**
<6 MM (<0.2 IN.)	A	B	A	B	B	**C**
6-15 MM (0.2-0.6 IN.)	B	B	B	C	A	**B**
16-50 MM (0.6-2 IN.)	C	C	C	C	B	**A**
>50 MM (>2 IN.)	C	C	C	C	B	**A**

ONE-SIDE ACCESS	C	C	C	C	. . .	**A**
BOTH-SIDE ACCESS	B	B	B	C	A	**A**
SINGLE V	C	C	C	C	B	**A**
DOUBLE V	**B**	**B**	**B**	**C**	**A**	**A**

TABLE 3 SELECTION OF NDE TECHNIQUE ON BASIS OF FLAW TYPE

A, most applicable; B, applicable; C, least applicable

FLAW	**VISUAL**	**PENETRANTS**	**MPT**	**EDDY CURRENT**	**RADIOGRAPHIC TESTING**	ULTRASONIC TESTING
MICROCRACKS	A	C	C	C	C	**C**
LONGITUDINAL CRACKS	C	B	B	B	A	**A**
TRANSVERSE CRACKS	C	B	B	B	A	**B**
RADIATING CRACKS	C	A	B	C	A	**B**
CRATER CRACKS	B	B	B	C	A	**C**
GROUP DISCONTINUOUS CRACKS	B	B	B	C	A	**C**
BRANCHING CRACKS	B	B	B	B	A	**C**
UNIFORMLY DISTRIBUTED POROSITY	C	B	C	C	A	**C**
LINEAR POROSITY	C	B	C	C	A	**C**
ELONGATED CAVITY	C	C	C	C	A	**B**
WORM HOLE	C	C	C	C	A	**C**
SURFACE PORE	B	A	B	C	B	**C**
SHRINKAGE CAVITY	A	B	B	C	B	**C**
INTERDENDRITIC SHRINKAGE	A	C	C	C	C	**C**
MICROSHRINKAGE	A	C	C	C	C	**C**
INTERDENDRITIC MICROSHRINKAGE	A	C	C	C	C	**C**
CRATER PIPE	B	A	B	C	B	**C**
SOLID INCLUSION	. . .	. . .	. . .	C	A	**B**
SLAG INCLUSION	. . .	. . .	. . .	C	A	**B**
FLUX INCLUSION	. . .	. . .	. . .	C	A	**B**
OXIDE INCLUSION	C	. . .	. . .	C	A	**B**
PUCKERING	. . .	. . .	. . .	. . .	A	**C**
METALLIC INCLUSION	. . .	. . .	. . .	. . .	A	**B**
INCOMPLETE SIDEWALL FUSION	C	B	B	C	B	**A**
INCOMPLETE INTERRUN FUSION	C	B	B	C	B	**A**
INCOMPLETE ROOT FUSION	C	B	B	C	A	**B**
INCOMPLETE PENETRATION	B	B	B	C	A	**B**
UNDERCUT	A	B	B	C	B	**C**
SHRINKAGE GROOVE	A	. . .	. . .	. . .	B	**C**
EXCESSIVE REINFORCEMENT	A	. . .	. . .	. . .	B	**C**

EXCESSIVE CONVEXITY	A	. . .	. . .	. . .	B	**C**
EXCESSIVE PENETRATION	A	. . .	. . .	. . .	B	**C**
BAD REINFORCEMENT ANGLE	A	. . .	. . .	. . .	. . .	**. . .**
OVERLAP	B	A	B	C	C	**C**
MISALIGNMENT	A	. . .	. . .	. . .	. . .	**C**
BURN THROUGH	A	B	C	C	B	**B**
INCOMPLETELY FILLED GROOVE	A	. . .	. . .	. . .	B	**C**
ASYMMETRICAL FILLET	A	. . .	. . .	. . .	. . .	**. . .**
IRREGULAR BEAD	A	. . .	. . .	. . .	B	**. . .**
ROOT CONCAVITY	A	. . .	. . .	. . .	B	**C**
POOR RESTART	A	. . .	. . .	. . .	B	**. . .**
MISCELLANEOUS DEFECTS (SPATTER, ETC.)	**A**	**C**	**C**	**. . .**	**B**	**. . .**

Source: ISO 6520

There are various techniques for applying each NDE method, some of which are more appropriate than others and might therefore alter the rating. It is often the case that two methods are complementary to each other. For example, radiographic testing will detect volumetric flaws and ultrasonic testing will detect planar ones. The method of selection discussed below is based on the material, weld geometry, and type of flaw.

Material. For NDE purposes, the material being tested can be categorized as shown in Table 1. First, a distinction is drawn between metal and nonmetal.

NDE methods are being increasingly applied to welds in thermoplastics, which can take the form of bulk plastics or composites with reinforcing fibers. Electrical and magnetic testing methods cannot be applied to bulk plastics, of course. Eddy-current techniques have been used on carbon fiber reinforced plastics, because of the conductive properties of the fibers. Penetrants also can be used, but care must be taken to ensure that solvents do not attack the plastic.

Radiographic techniques can be applied using low-kilovolt techniques, which are necessary because of the low absorption coefficient for x-rays of plastics. Typical values are between 10 and 25 kV. This can introduce problems such as cassette pick-up and air absorption.

Plastics are highly attenuative of ultrasound, and they will only propagate compressional waves to any distance. However, ultrasonic techniques have been used with some success for the inspection of hot-plate groove fusion welds in polyethylene pipe.

Metals can be subcategorized as being either magnetic or nonmagnetic, dense or light, and isotropic or anisotropic. Obviously, MPT cannot be used on nonferrous metals, but there are also many high-alloy steels that are too weakly magnetic to be magnetized. Other ferrous steels that are often used in the aerospace industry are ferromagnetic, but require stronger magnetizing fields to create adequate flux leakage from flaws. These also tend to have high magnetic retentivity and are difficult to demagnetize after the inspection.

The density and anisotropy in metals have the greatest effect on test sensitivity in radiographic and ultrasonic tests.

In general, radiation is absorbed more by dense materials, such as austenitic steel, than by less-dense materials, such as aluminum. Because higher-energy radiation is needed to penetrate the same thickness of material, it has the effect of decreasing image contrast and, therefore, test sensitivity. Anisotropy that is due to a large grain structure also results in radiation scattering and, sometimes, the appearance of diffraction mottling in the radiographs.

The velocity and attenuation of ultrasound is affected by changes in material composition or structure. This can be particularly apparent in aluminum welds and duplex stainless steel. In addition, large grain size can distort ultrasonic signals.

Eddy-current tests are particularly susceptible to interference from quite minor changes in the material. For example, the change in magnetic permeability at the heat-affected zone of a weld in low-carbon steel can create noise that obscures signals from toe cracks.

Weld geometry also has an important effect on test method selection. The factors that need to be considered include joint type and thickness, whether or not there is access to both sides, and, in the case of groove welds, the inclination of the weld groove faces (Table 2).

Visual inspection is applicable to all weld geometries, but is particularly applicable to fillet welds and welds in thin sections. Penetrant testing and MPT serve to enhance visual inspection.

Eddy-current testing is the least applicable of the test methods for weld inspection, but it is being used increasingly in underwater node inspection as an alternative to MPT. For thin-section welds in nonmagnetic materials, it has sufficient penetrating power to offer an alternative to ultrasonic testing.

Radiographic testing is of limited use in testing welds that have a complex geometry, as well as thick-section welds. Access to both sides of the weld is essential.

Ultrasonic testing does not suffer from as many geometric restrictions as radiographic testing, but the method is difficult to use on small fillet welds and thin sections, where A-scan interpretation is complicated by the numerous geometric echo signals.

Type of Flaw. Visual inspection is not applicable to internal flaws, but it is the only method that can be used with most geometric flaws (Table 3). Microflaws will only be visible with the aid of magnification.

Penetrant testing and MPT enhance visual inspection, but are particularly sensitive to surface-breaking cracks and incomplete fusion. Undercut and other shallow and open flaws usually give weak images, whereas overlap can be difficult to distinguish from the sharp change in contour at the weld toe. Eddy-current tests are very sensitive to planar flaws at the surface, but not to volumetric flaws.

There are very few flaws that cannot be detected by radiographic testing. Planar flaws must be oriented favorably in the radiation beam, and it can be difficult to distinguish surface from subsurface flaws, because of the two-dimensional nature of the image. The angular "cusp" shapes of an undercut can, for example, be indistinguishable from inclusions. In addition to magnification by way of microfocus radiographic techniques, microflaws need very high levels of contrast and definition in the radiograph, in order to be detected.

Ultrasonic testing is often regarded as being complementary to radiographic testing. Planar flaws need to be oriented in a perpendicular plane to the ultrasound beam, but because a range of beam angles can be utilized, ultrasonic testing is generally regarded as more sensitive to cracks and incomplete fusion than radiography. However, the characterization of different types of flaw, both planar and volumetric, is extremely difficult. Porosity produces low-amplitude echo signals that barely exceed the recording threshold levels in most procedures.

Inspection of Welded Joints

G.R. Edwards, The Welding Institute

Advanced Methods

As with all technologies, advances in NDE are being dominated by the introduction of computers. The emphasis has been on the acquisition and recording of data to aid the test operator and interpreter. In the future, it is likely that computers may complete the analysis and evaluation of test results, although the problems in interpreting the results of even the simplest NDE procedure should not be underestimated.

In radiographic testing, the replacement of films by real-time imaging systems has been aided by the introduction of image processing software that is able to improve the image quality to almost film-like levels.

In eddy-current testing, the characterization of different types of flaws by their effect on the impedance at mixed coil frequencies is a complex problem that is being tackled with neural network software.

The greatest advances have been made in ultrasonic testing. Digitally controlled flaw detectors make calibration more consistent and can provide print-outs of the A-scan display. With probe scanners, ultrasonic images can be created to provide a hard copy of test results. Digitized signals can be processed at much higher gain settings to reveal diffracted echoes in accurate flaw sizing.

Weld Procedure Qualification

Harvey R. Castner, Edison Welding Institute

Introduction

WELDING CODES AND STANDARDS usually require the qualification of welding procedures prior to being used in production to ensure that welds will meet the minimum quality and mechanical property requirements for the application. This article provides an overview of welding procedure qualification guidelines and test methods. The reader is referred to codes, standards, and specifications that govern the design and fabrication of welded structures for the procedure qualification details that are appropriate for the given application.

Some of the most widely recognized codes, standards, and specifications that cover welding procedure qualification include:

- SECTION IX OF THE AMERICAN SOCIETY OF MECHANICAL ENGINEERS (ASME) BOILER AND PRESSURE VESSEL CODE
- AMERICAN NATIONAL STANDARDS INSTITUTE/AMERICAN WELDING SOCIETY (ANSI/AWS) B2.1, STANDARD FOR WELDING PROCEDURE AND PERFORMANCE QUALIFICATION
- ANSI/AWS D1.1, STRUCTURAL WELDING CODE FOR STEEL
- ANSI/AWS D1.2, STRUCTURAL WELDING CODE FOR ALUMINUM
- ANSI/AWS D1.3, STRUCTURAL WELDING CODE FOR SHEET STEEL
- ANSI/AWS D1.5, BRIDGE WELDING CODE
- ANSI/AWS D1.4, STRUCTURAL WELDING CODE FOR REINFORCING STEEL
- MILITARY STANDARD 248, WELDING AND BRAZING PROCEDURE AND PERFORMANCE QUALIFICATION
- AMERICAN PETROLEUM INSTITUTE (API) 1104, STANDARD FOR WELDING PIPELINES AND RELATED FACILITIES
- INDUSTRIAL SPECIFICATIONS, SUCH AS ANSI/AWS D14.1, SPECIFICATION FOR WELDING INDUSTRIAL AND MILL CRANES AND OTHER MATERIAL HANDLING EQUIPMENT; ANSI/AWS D14.3, SPECIFICATION FOR WELDING EARTHMOVING AND CONSTRUCTION EQUIPMENT; ANSI/AWS D14.5, SPECIFICATION FOR WELDING OF PRESSES AND PRESS COMPONENTS; ANSI/AWS D14.6, SPECIFICATION FOR WELDING ROTATING ELEMENTS OF EQUIPMENT; AND ANSI/AWS D15.1, RAILROAD WELDING SPECIFICATION

Additional information about standards and specifications for particular welding applications is available in the Section "Material Requirements for Service Conditions" in this Volume.

Procedure qualification is an important part of any total weld quality management program, because it confirms that the welding procedure will meet the mechanical design requirements. Therefore, some form of welding procedure

qualification should be performed for all critical welding operations, regardless of whether the application is covered by a code or standard.

Purpose of Qualification and Responsibility for the Task

Fabricators, manufacturers, and contractors are responsible for the selection, definition, and control of the welding procedures they use. This control normally includes the preparation of detailed written instructions known as welding procedure specifications (WPS), and may include the qualification of both welding procedures and personnel. The purpose of qualifying a welding procedure is to demonstrate that the resulting welds will meet prescribed quality standards and have the requisite mechanical properties for the intended application. A sample WPS form is shown in the article "Welding of Carbon Steels" in this Volume.

Some codes allow the use of prequalified welding procedures, if they meet all of the requirements contained in the code. The use of prequalified procedures does not lessen the responsibility of the fabricator or contractor to ensure that the welding procedures are satisfactory for the application.

The qualification of welders, welding operators, and tack welders is another important part of weld quality control. The qualification of personnel demonstrates the ability to produce satisfactory welds when the prescribed welding procedure is used.

Procedure qualification involves examining the welds according to the specified welding procedure, testing specimens taken from these welds, and documenting the results on a procedure qualification record. The fabricator, manufacturer, or contractor must supervise and control the preparation of the qualification test welds. Many codes permit another organization to assist in the removal and assessment of test specimens. However, the contractor or fabricator is ultimately responsible for the procedure qualification tests, the results of these tests, and the control and application of the procedures in production. A single welding procedure qualification test may support a number of WPSs, or a single WPS may be supported by several procedure qualifications.

Weld Procedure Qualification

Harvey R. Castner, Edison Welding Institute

Types of Tests

Welding procedure qualification tests can be categorized as either standard or special tests. Standard tests include visual, metallurgical, and nondestructive examinations; chemical analysis; crack susceptibility tests; and tests to determine mechanical properties. The mechanical property tests can include tension, bend, and hardness tests, as well as tests to determine notch toughness.

Although the use of standard tests to qualify a WPS demonstrates the ability of the procedure to produce sound welds that meet the minimum required properties, these tests may not ensure that the welding procedure is suitable for all applications. Standard test plates are relatively small and are normally welded under laboratory, rather than production, conditions.

The fabricator, designer/owner, or operator of the welded structure or component may determine that additional special qualification tests are required in order to establish the acceptability of a welding procedure for the application and to ensure that the welded structure will meet the mechanical requirements. Special tests may involve welding mock-up or prototype structures and then subjecting these structures to static or dynamic tests, corrosion tests, high-temperature tests, macrosectioning, or other tests.

Standard Tests

Standard procedure qualification test weldments represent the type of weld and weld joint that are to be used in production. Groove welds in butt joints in plate and pipe are shown in Fig. 1 and 2, respectively. Two examples of fillet welds in T-joints are shown in Fig. 3. Fillet welds can also be deposited on lap, corner, or edge joints. A partial penetration weld in a T-joint is shown in Fig. 4, whereas a plug weld test specimen is shown in Fig. 5. The latter could be a slot weld as well, and a similar weldment could be used for spot welds.

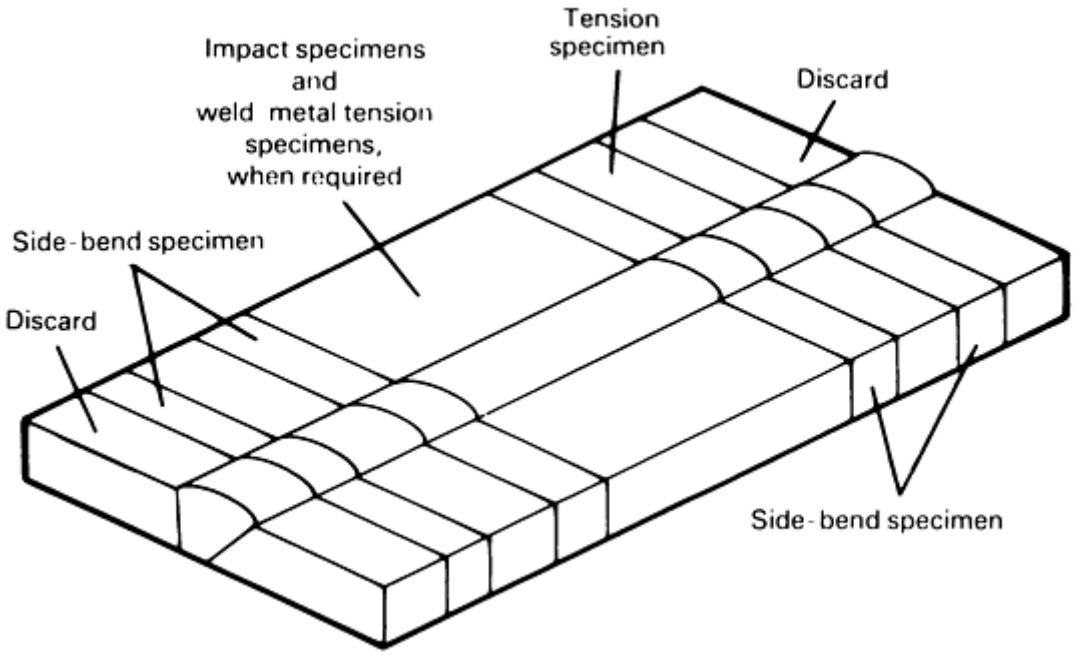

FIG. 1 TYPICAL LOCATION OF TEST SPECIMENS FROM GROOVE WELDS IN BUTT-JOINT TEST PLATE

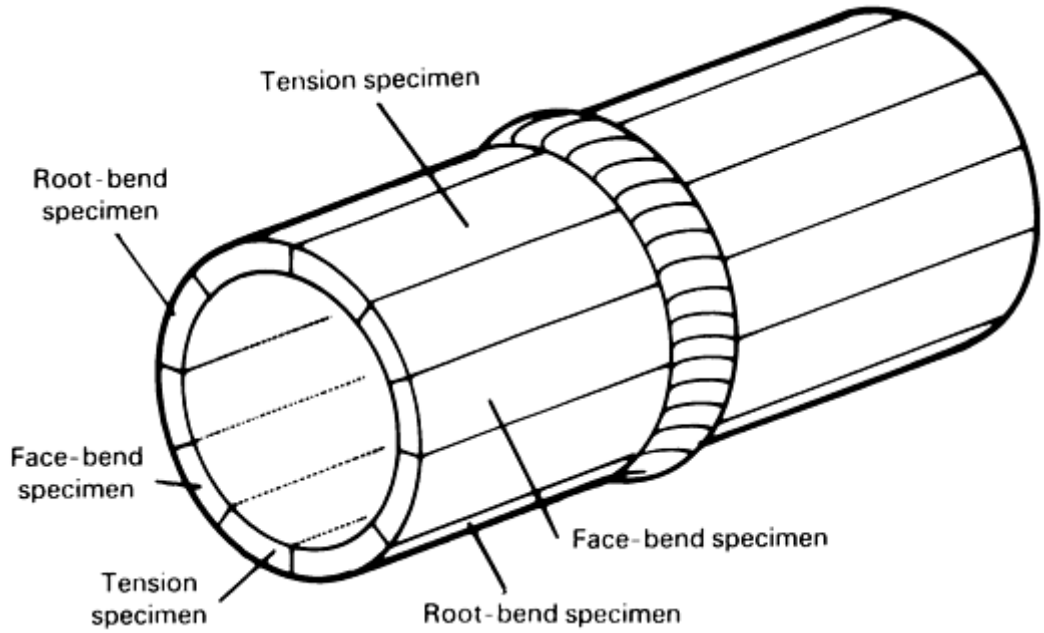

FIG. 2 TYPICAL LOCATION OF TEST SPECIMENS FROM GROOVE WELDS IN BUTT-JOINT PIPE TEST

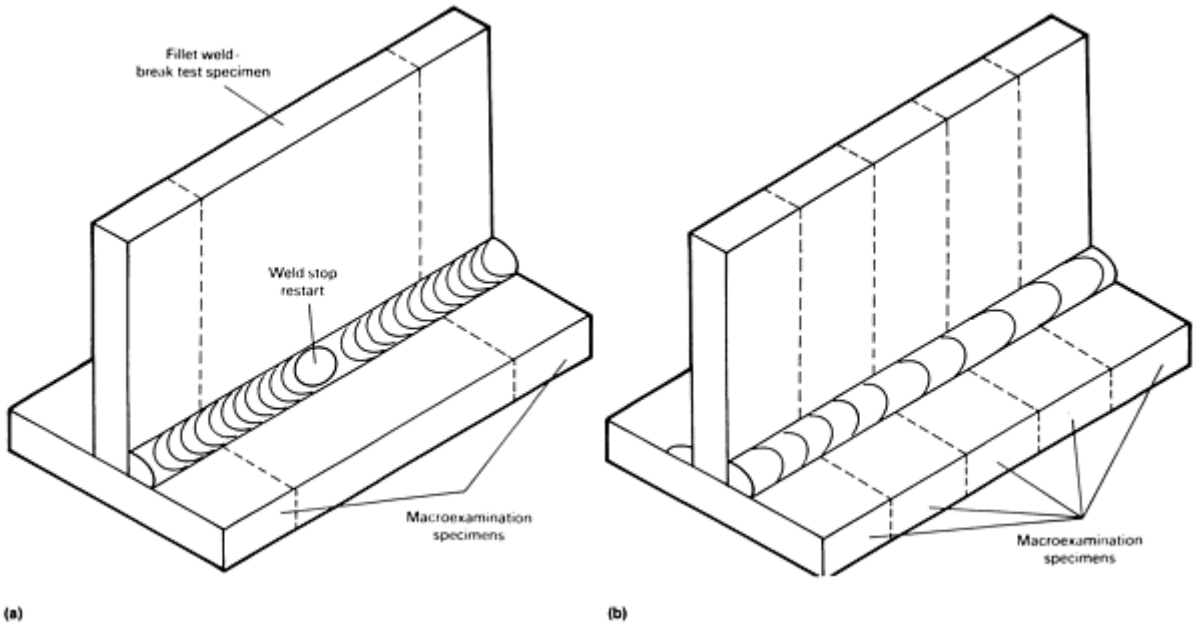

FIG. 3 TWO EXAMPLES OF T-JOINT WELDMENTS FOR FILLET WELD QUALIFICATION. (A) FILLET WELD ON ONE SIDE OF T-JOINT. (B) FILLET WELD ON BOTH SIDES OF T-JOINT

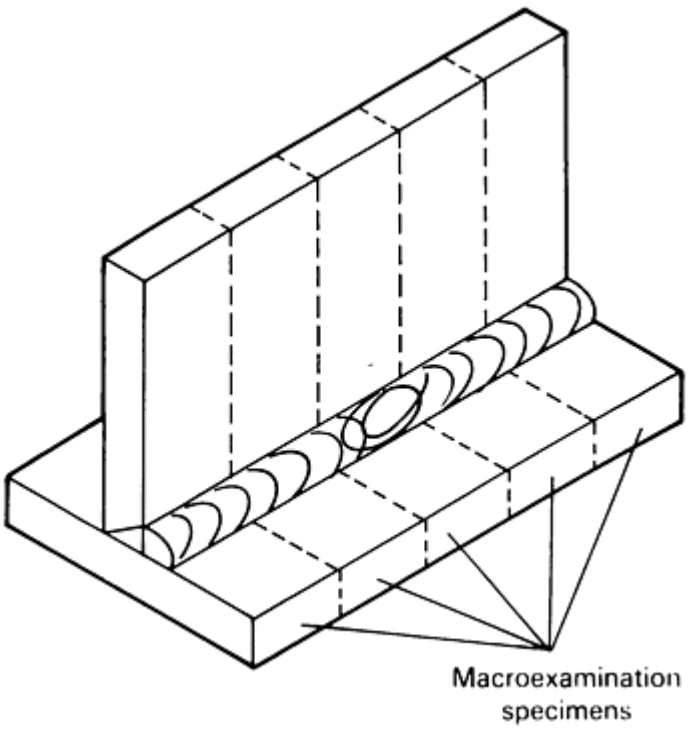

FIG. 4 PARTIAL-PENETRATION WELD SPECIMEN

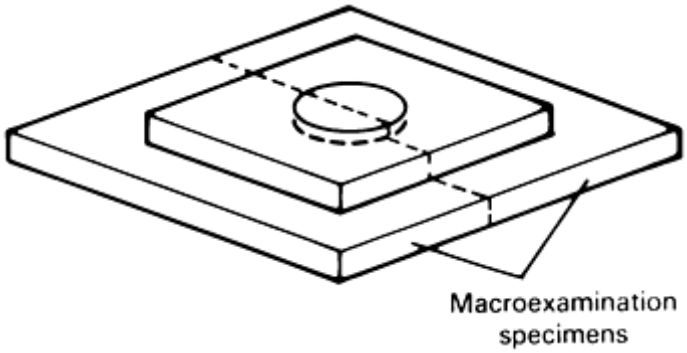

FIG. 5 PLUG WELDS QUALIFIED BY GROOVE WELD TEST

Resistance spot and seam welds are typically made on lap joints. Other weldments are appropriate for friction, laser-beam, electron-beam, and stud welding, or for surfacing weld deposits. The thickness of test weldments should be selected after considering the thickness of materials used in actual fabrications and the thickness limitations of the code or standard. The length and width of the test weldment should be sufficient to permit removal of the necessary test specimens.

The test weldment is prepared and welded using the methods that are detailed in the WPS. Standard test requirements vary, depending on the code or standard being used. However, it is common to examine the completed weldment by visual and nondestructive examination methods. It is also common to section the weldment and remove specimens for mechanical property tests or other examinations.

Tests for full-penetration groove welds include tension, bend, and toughness tests. It is also common to subject weldments to chemical analysis, hardness tests, and metallurgical examinations. Figures 1 and 2 indicate the location of tension and bend specimens in plate and pipe test weldments, respectively. Figure 6 shows the configuration of tension and bend specimens. The details of specimen size, orientation, removal, testing, and acceptance are provided in the welding codes and standards listed above, in ASTM test standards, or in ANSI/AWS B4.0.

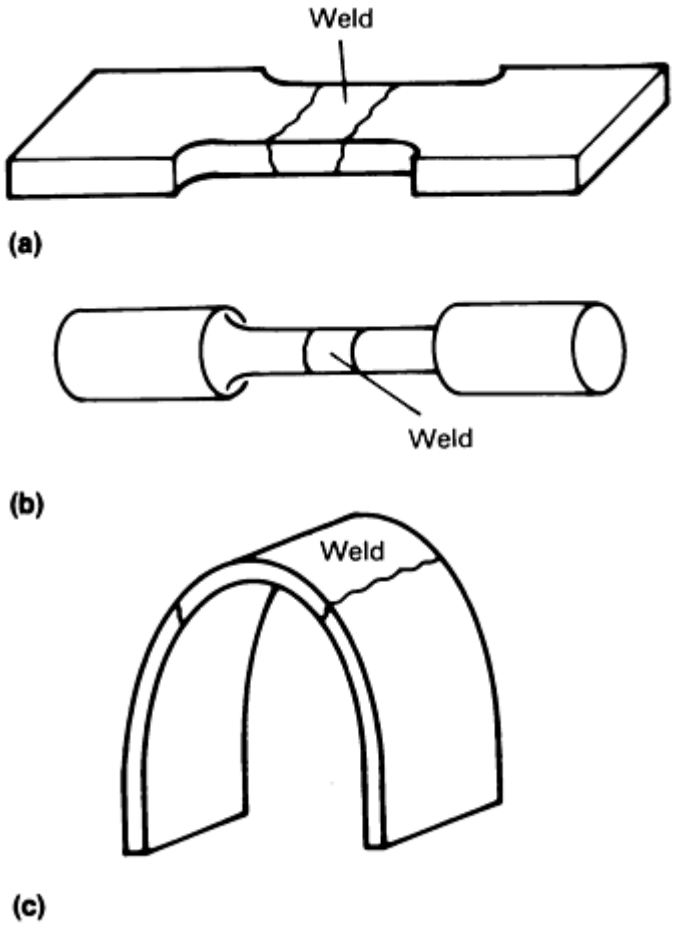

FIG. 6 TENSION AND BEND SPECIMENS FOR TESTING OF FULL-PENETRATION GROOVE WELDS. (A) REDUCED-SECTION TENSION SPECIMEN. (B) ROUND TENSION SPECIMEN. (C) BEND SPECIMEN

Transverse tension tests are performed on full-penetration groove welds to determine the tensile strength of the weld region. The specimens can be one of several configurations: full-section specimens, reduced-section specimens, or round specimens (see Fig. 6). Multiple tension specimens can be used for plates that are more than 25 mm (1 in.), as shown in Fig. 7, in order to test the entire thickness. The acceptance of the tension test results normally is based on a tensile strength that is either equal to or greater than the minimum specified tensile strength of the base metal being welded. If the weld metal has a lower specified strength than the base metal, then the tension test must exceed the specified minimum tensile strength of the weld metal. Some codes permit the strength of the tension specimen to be 5% below the specified minimum tensile strength of the base metal if the specimen breaks outside of the weld or fusion line. If all-weld-metal tension tests are required, then round specimens are typically removed from the center of the weld and oriented parallel to the weld axis.

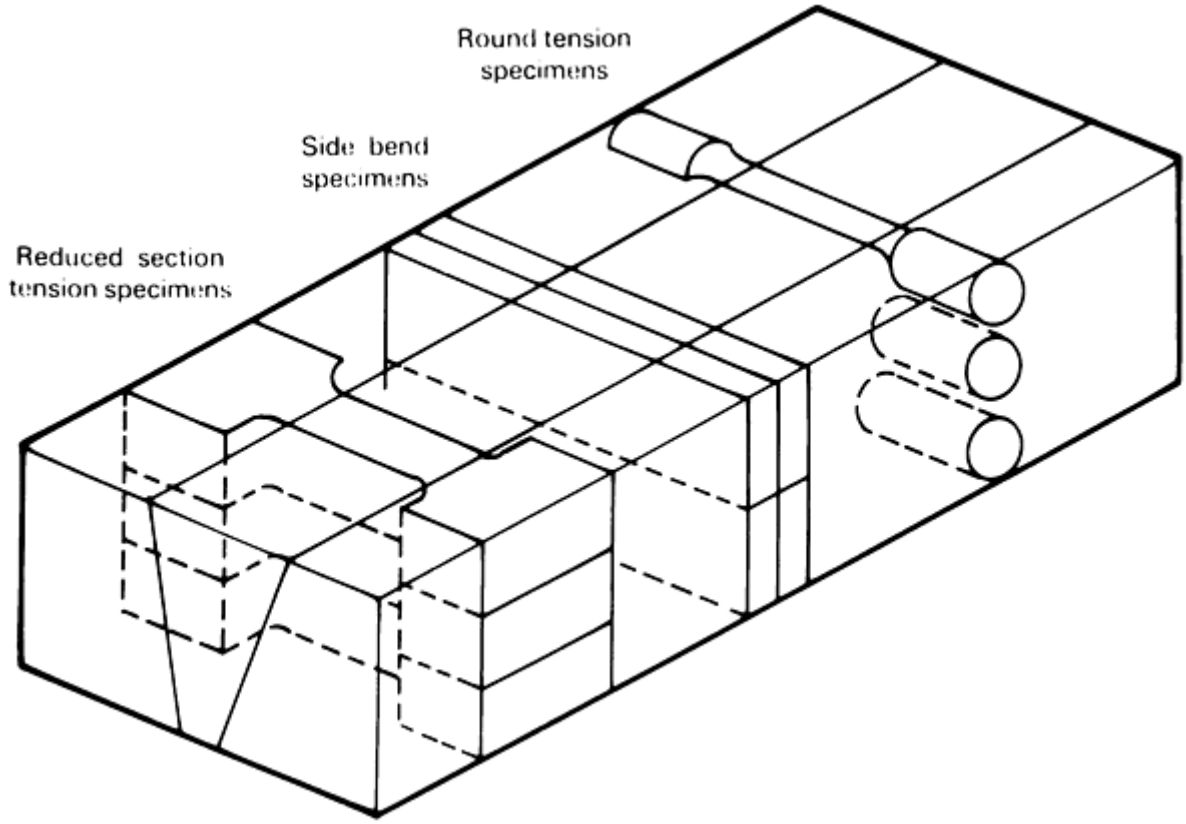

FIG. 7 REMOVAL OF MULTIPLE BEND AND TENSION SPECIMENS FROM THICK TEST PLATES

Bend tests are performed to verify the soundness and ductility of the weld and the heat-affected zone (HAZ), as shown in Fig. 6. Figures 1, 2 and 7 show bend specimens that are typically oriented transverse to the weld axis, with the center of the weld in the center of the specimen. Under some circumstances, longitudinal bends are removed with their length parallel to the axis of the weld. Longitudinal bend specimens are used for welds of dissimilar metal, where there is a large difference in bend properties between the two base metals or between the weld metal and the base metal.

The face of the weld (face-bend), the root of the weld (root-bend), or the cross section of the weld (side-bend) can be placed on the convex face of the bent specimen. Face-bend and root-bend specimens are typically specified for base-metal thicknesses of less than 9.5 mm (0.375 in.). Side-bend specimens are required for thicker test plates in order to test the entire weld cross section. Plates that are more than 38 mm (1.5 in.) thick may require multiple side-bend specimens to ensure that the entire weld thickness is tested (see Fig. 7).

Guided bend specimens are forced into a specified curvature (Fig. 6) by either applying a load to a plunger or forming the specimen around a fixed mandrel. The width and thickness of the specimen and the radius of the plunger or mandrel are designed to produce a minimum specified elongation (approximately 20%) in the outer surface of the specimen. It is important to follow the recommendations for specimen dimensions, because width and thickness influence test performance. The most common bend specimen is 9.5 mm (0.375 in.) thick and is formed around a 19.1 mm (0.75 in.) radius. However, codes specify larger radii for low-ductility base metals and for weld metals that are not capable of being bent to a small radius. Acceptable bend specimens must not fracture or have cracks or other open defects that exceed a specified maximum size (usually, 3.2 mm, or 0.125 in.) on their convex surface.

Notch Toughness Tests. Charpy V-notch impact tests are used to measure the toughness of weld metals and HAZs. Charpy V-notch specimens are usually removed from the weld metal and HAZ, with the notch oriented normal to the surface. One face of the V-notch specimen is located within 1.6 mm ($\frac{1}{16}$ in.) of the surface of the material. Thick materials require additional specimens at subsurface locations. The number of specimens, their location and orientation, and the test temperature are determined by the design requirements or material specifications. Acceptance criteria may be

a minimum specified absorbed energy in joules (ft · lbf), a minimum percentage of shear fracture appearance, or a minimum specified lateral expansion opposite the notch.

Drop-weight notch toughness tests are sometimes used to determine the minimum nil-ductility transition temperature for ferritic steel weld metal and HAZs. The assessment of toughness, in terms of the stress-intensity factor, *K*, the J integral, or crack tip opening displacement, may be required for some welding procedures. Codes and specifications describe how specimens can be removed from the weld metal and HAZs to permit the measurement of each of these fracture-toughness properties.

Tests for Fillet Welds, Partial-Penetration Groove Welds, and Spot and Plug Welds. The procedure qualification of fillet welds typically involves T-joint test weldments, like those shown in Fig. 3. Some codes and specifications permit lap joints, comer joints, or other joint configurations that represent the actual joint used in production.

Procedures for partial-penetration groove welds can be qualified by making test weldments that represent the joint used for the application. Figure 4 shows a T-joint test weldment for a partial-penetration groove weld. Figure 5 shows the configuration of the test weldment for the qualification of plug or slot welds.

Completed fillet, partial-penetration, and plug or slot weldments are usually examined visually and by nondestructive methods to ensure that they meet the acceptance requirements of the weld quality specification. These welds do not normally lend themselves to mechanical property testing, although tension-shear tests and weld-break tests can be conducted on them. The required mechanical properties must be determined from a standard groove weld test. Macrosections are removed to verify root penetration.

Figures 3 and 4 show how macroexamination specimens are removed from fillet or partial-penetration welds. Figure 5 illustrates how plug or slot welds are cut through their center to produce macroetch specimens. The faces of macroetch specimens are ground smooth, etched, and then examined. Acceptable welds must have:

- THE DESIGNATED WELD SIZE AND PROFILE
- FUSION TO THE ROOT OF THE JOINT
- NO CRACKS
- COMPLETE FUSION BETWEEN ADJACENT LAYERS OF WELD METAL, AS WELL AS BETWEEN WELD METAL AND BASE METAL

Shear tests can also be used to measure the strength of fillet, partial-penetration, plug, or slot welds. Usually, an acceptable shear strength is at least 60% of the minimum specified tensile strength of the base metal.

Weld-break or fracture tests may also be required for fillet and partial-penetration welds. These specimens are removed from the weld, as shown in Fig. 3, and loaded so that the root of the weld is in tension until the specimen fractures or bends flat upon itself. Acceptance of a fractured specimen is determined by examining the fractured surface for complete fusion, the required depth of penetration, and porosity and inclusion levels that do not exceed a specified maximum size. The specimen is also acceptable if it bends flat upon itself without fracturing.

Procedure qualification tests for arc and resistance spot welds include tension-shear, torsion, peel, and hardness tests, as well as macroexaminations. Tension, torsion, and peel test specimens are examined to determine the location of failure and the size and soundness of the weld nugget.

Tests For Stud Welds. The qualification of stud welding procedures can involve the macroexamination of cross sections, bend tests, tensile tests, or torsion tests. Sectioning and macroexamination can determine whether or not the welds and HAZs have the proper fusion and are free of cracks. Bend tests for stud welds involve bending the stud through a minimum angle, usually 15°, and then bending it back to the original position. An alternative test is to bend the studs by hammering them flat onto the test plate. The bent studs must be free of visible separation or fracture. Stud welds also are tested by applying torque or tension loads.

Tests For Weld Cladding and Surfacing. The qualification of weld cladding procedures involves chemical analysis of the deposit, macroexamination of cross sections, and bend tests. The qualification for hard-surfacing welding procedures can include hardness tests, in addition to chemical analysis of the deposit and macroexamination of cross sections.

Special Tests

Special tests for welding procedure qualification often utilize prototype structures or mock-up components that are fabricated per the specified welding procedure. These structures or components can then be subjected to loads that simulate the actual conditions encountered in service. Tests can include static or dynamic tensile loads, bending loads, fatigue loads, or impact loading. After load testing, the structure can also be tested destructively; welds can be sectioned and the cross sections examined for proper penetration, bead placement, profile, and so on. An example of this type of testing, for roll-over protection structures, is described in ANSI/AWS D14.3.

Weld Procedure Qualification

Harvey R. Castner, Edison Welding Institute

Limitations on Procedure Qualification

A new welding procedure must be qualified if it differs significantly from another procedure that has already been qualified. The application range of a welding procedure qualification is determined by placing limits on the welding variables specified in a welding procedure. Codes define these limiting variables as "essential variables," because the WPS must be requalified if the values are changed so that they exceed the specified limits.

Supplementary essential variables are the variables that affect notch toughness. Supplementary variables become essential variables when notch toughness tests are required.

Nonessential variables are the remaining variables that are contained in the WPS, but that can be changed without requiring requalification. An essential variable for one process may be nonessential for another process.

Although there are differences in how codes and standards define essential variables, the variables described below are considered to be essential by most codes and standards.

Welding Process. A change of welding process will require requalification, because the process has a significant effect on the mechanical properties and metallurgical structure of the weld.

Base Metal. Changing from one type of base metal to another can affect weldability, as well as the metallurgical and mechanical properties of the weld. For certain welding processes, changes in base metals also can cause differences in penetration and weld fusion characteristics. Therefore, significant changes in base-metal type, composition, heat treatment, or processing will require requalification.

Some codes require separate welding procedure qualifications for pipe and plate. Although a procedure qualification on pipe may also cover plate, a procedure qualification on plate might be restricted to the welding of large-diameter pipes. Base-metal thickness influences cooling rate and, therefore, metallurgical and mechanical properties. The composition of a metal may also change with thickness. Some codes require qualification on the exact thickness of metal that is to be used for production welds. Other codes require qualification on the thinnest and thickest metals that are used in production. Most codes permit qualification on one thickness of test specimen to cover a range of base-metal thicknesses.

Codes often group together those base metals that have similar weldability characteristics, metallurgical properties, chemical compositions, or mechanical properties. The grouping of base metals reduces the number of required qualifications by allowing the qualification of one of the materials in the group to qualify the other base metals in that group.

Filler Metal. Codes group filler metals and welding electrodes with similar chemical compositions and operating characteristics together. Grouping reduces the number of tests by allowing the qualification of one of the filler metals in

the group to also qualify the others in that group. Ferrous filler metals can be grouped by both chemical composition and usability. The addition or deletion of a consumable insert is an essential variable.

Position is not an essential variable for all codes and specifications, which may allow qualification in one position to cover qualification in another position. For example, qualification in the horizontal position may also qualify for the flat position.

Joint design is an essential variable for some codes, but not for others. Weld joint design should be an essential variable for processes in which joint changes affect metallurgical structures and weld properties. These processes include stud, laser-beam, electron-beam, and friction welding.

Electrical Characteristics. Variations in the type of welding current (alternating or direct, for arc welds) or in polarity normally require requalification. A small change in welding current or voltage does not typically require requalification. Many codes limit changes to ± 10% from the mean value, without necessitating requalification. The use of current pulsation and the pulse parameters may be essential variables. For example, beam current or beam power are essential variables for both laser- and electron-beam welding.

Shielding. The use and the composition of a shielding gas are essential variables for arc welding, friction welding, and laser-beam welding processes. An essential variable for electron-beam welding is the use of a vacuum.

Preheat and Interpass Temperatures. Significant changes in preheat or interpass temperatures will affect properties and, therefore, will require requalification. Codes and standards differ on the size of the change in temperature that is permitted. Some codes limit changes to a maximum of 14 °C (25 °F), whereas others permit an increase or decrease of up t 56 °C (100 °F) before requalification is required.

Postweld Heat Treatment. The use of postweld heat treatment, as well as changes in the postweld heat-treatment temperature or time at temperature, will require requalification.

Other variables that affect the soundness, metallurgical structure, or mechanical properties of the weld are essential variables. These variables depend on the welding process being used. Examples of other essential variables include:

- CHANGES IN MEAN TRAVEL SPEED OF MORE THAN 10%
- CHANGING FROM A STRINGER TO A WEAVE BEAD, OR CHANGING THE DIRECTION OF WELDING FOR VERTICAL ARC WELDING PROCEDURES
- CHANGES IN ELECTRODE COMPOSITION OR CONFIGURATION FOR RESISTANCE WELDING
- CHANGES IN FILAMENT TYPE, SIZE, OR SHAPE, AND IN GUN-TO-WORK DISTANCE FOR ELECTRON-BEAM WELDING
- CHANGES IN FOCAL LENGTH, FOCUS POSITION, OR SPOT SIZE FOR LASER-BEAM WELDING
- CHANGES IN ENERGY, APPLIED LOADS, OR THE AMOUNT OF UPSET FOR FRICTION WELDING

Weld Procedure Qualification

Harvey R. Castner, Edison Welding Institute

Limitations on Procedure Qualification

A new welding procedure must be qualified if it differs significantly from another procedure that has already been qualified. The application range of a welding procedure qualification is determined by placing limits on the welding variables specified in a welding procedure. Codes define these limiting variables as "essential variables," because the WPS must be requalified if the values are changed so that they exceed the specified limits.

Supplementary essential variables are the variables that affect notch toughness. Supplementary variables become essential variables when notch toughness tests are required.

Nonessential variables are the remaining variables that are contained in the WPS, but that can be changed without requiring requalification. An essential variable for one process may be nonessential for another process.

Although there are differences in how codes and standards define essential variables, the variables described below are considered to be essential by most codes and standards.

Welding Process. A change of welding process will require requalification, because the process has a significant effect on the mechanical properties and metallurgical structure of the weld.

Base Metal. Changing from one type of base metal to another can affect weldability, as well as the metallurgical and mechanical properties of the weld. For certain welding processes, changes in base metals also can cause differences in penetration and weld fusion characteristics. Therefore, significant changes in base-metal type, composition, heat treatment, or processing will require requalification.

Some codes require separate welding procedure qualifications for pipe and plate. Although a procedure qualification on pipe may also cover plate, a procedure qualification on plate might be restricted to the welding of large-diameter pipes. Base-metal thickness influences cooling rate and, therefore, metallurgical and mechanical properties. The composition of a metal may also change with thickness. Some codes require qualification on the exact thickness of metal that is to be used for production welds. Other codes require qualification on the thinnest and thickest metals that are used in production. Most codes permit qualification on one thickness of test specimen to cover a range of base-metal thicknesses.

Codes often group together those base metals that have similar weldability characteristics, metallurgical properties, chemical compositions, or mechanical properties. The grouping of base metals reduces the number of required qualifications by allowing the qualification of one of the materials in the group to qualify the other base metals in that group.

Filler Metal. Codes group filler metals and welding electrodes with similar chemical compositions and operating characteristics together. Grouping reduces the number of tests by allowing the qualification of one of the filler metals in the group to also qualify the others in that group. Ferrous filler metals can be grouped by both chemical composition and usability. The addition or deletion of a consumable insert is an essential variable.

Position is not an essential variable for all codes and specifications, which may allow qualification in one position to cover qualification in another position. For example, qualification in the horizontal position may also qualify for the flat position.

Joint design is an essential variable for some codes, but not for others. Weld joint design should be an essential variable for processes in which joint changes affect metallurgical structures and weld properties. These processes include stud, laser-beam, electron-beam, and friction welding.

Electrical Characteristics. Variations in the type of welding current (alternating or direct, for arc welds) or in polarity normally require requalification. A small change in welding current or voltage does not typically require requalification. Many codes limit changes to ± 10% from the mean value, without necessitating requalification. The use of current pulsation and the pulse parameters may be essential variables. For example, beam current or beam power are essential variables for both laser- and electron-beam welding.

Shielding. The use and the composition of a shielding gas are essential variables for arc welding, friction welding, and laser-beam welding processes. An essential variable for electron-beam welding is the use of a vacuum.

Preheat and Interpass Temperatures. Significant changes in preheat or interpass temperatures will affect properties and, therefore, will require requalification. Codes and standards differ on the size of the change in temperature that is permitted. Some codes limit changes to a maximum of 14 °C (25 °F), whereas others permit an increase or decrease of up t 56 °C (100 °F) before requalification is required.

Postweld Heat Treatment. The use of postweld heat treatment, as well as changes in the postweld heat-treatment temperature or time at temperature, will require requalification.

Other variables that affect the soundness, metallurgical structure, or mechanical properties of the weld are essential variables. These variables depend on the welding process being used. Examples of other essential variables include:

- CHANGES IN MEAN TRAVEL SPEED OF MORE THAN 10%
- CHANGING FROM A STRINGER TO A WEAVE BEAD, OR CHANGING THE DIRECTION OF WELDING FOR VERTICAL ARC WELDING PROCEDURES
- CHANGES IN ELECTRODE COMPOSITION OR CONFIGURATION FOR RESISTANCE WELDING
- CHANGES IN FILAMENT TYPE, SIZE, OR SHAPE, AND IN GUN-TO-WORK DISTANCE FOR ELECTRON-BEAM WELDING
- CHANGES IN FOCAL LENGTH, FOCUS POSITION, OR SPOT SIZE FOR LASER-BEAM WELDING
- CHANGES IN ENERGY, APPLIED LOADS, OR THE AMOUNT OF UPSET FOR FRICTION WELDING

Documentation of Procedure Qualification

Record keeping is an essential part of welding procedure qualification. The WPS defines the variables and methods to be used for welding. As noted earlier, a procedure qualification record is used to document the actual welding variables that are used for the procedure qualification test weldment, as well as the results of the tests. The manufacturer or contractor should have these records available for review by customers or authorized inspectors.

Weld Procedure Qualification

Harvey R. Castner, Edison Welding Institute

Selected References

• "STANDARD FOR WELDING PROCEDURE AND PERFORMANCE QUALIFICATION," ANSI/AWS B2.1, AWS
• "STANDARD METHODS FOR MECHANICAL TESTING OF WELDS," ANSI/AWS B4.0, AWS
• "STRUCTURAL WELDING CODE, STEEL," ANSI/ AWS D1.1, AWS
• "WELDING AND BRAZING PROCEDURE AND PERFORMANCE QUALIFICATION," MIL-STD 248, U.S. DEPARTMENT OF THE NAVY
• WELDING AND BRAZING QUALIFICATIONS, "BOILER AND PRESSURE VESSEL CODE," ANSI/ASME BPV-IX, ASME
• *WELDING HANDBOOK,* 8TH ED., VOL 1, AWS, 1987

Introduction

COMPLEX THERMAL STRESSES occur in parts during welding due to the localized application of heat. Residual stresses and distortion remain after welding is completed. Transient thermal stresses, residual stresses, and distortion sometimes cause cracking and mismatching of joints. High tensile residual stresses in areas near the weld can cause premature failures of welded structures under certain conditions. Distortion, especially out-of-plane distortion, and compressive residual stresses in the base plate can reduce the buckling strength of a structural member subjected to compressive loading. Correction of unacceptable distortion is costly and, in some cases, impossible. The subjects related to residual stresses, distortion, and their consequences are too broad to be discussed in depth in this article. Those who need more detailed information are advised to refer to the references, especially Ref 1, 2, 3.

References

1. K. MASUBUCHI, *ANALYSIS OF WELDED STRUCTURES--RESIDUAL STRESSES, DISTORTION, AND THEIR CONSEQUENCES,* PERGAMON PRESS, 1980
2. K. MASUBUCHI, RESIDUAL STRESSES AND DISTORTION, *METALS HANDBOOK,* 9TH ED., VOL 6, *WELDING, BRAZING, AND SOLDERING,* ASM, 1983, P 856-895
3. K. MASUBUCHI, O.W. BLODGETT, S. MATSUI, E.P. ROSS, AND C.L. TSAI, RESIDUAL STRESSES AND DISTORTION, *WELDING HANDBOOK,* 8TH ED., VOL 1, *WELDING TECHNOLOGY,* AWS, 1987

Residual Stresses and Distortion

Koichi Masubuchi, Massachusetts Institute of Technology

Formation of Residual Stresses and Distortion

Residual stresses, also referred to as internal stresses, initial stresses, inherent stresses, and locked-in stresses, are stresses that exist in a body after all external loads are removed. Residual stresses also occur when a body is subjected to nonuniform temperature changes; these stresses are called thermal stresses. The intensity of stress is usually expressed in load or force per unit area, such as newtons per square meter (N/m^2) or pascals (Pa), kilograms force per square millimeter (kg/mm^2), or pounds per square inch (psi).

Residual stresses in metal structures occur for many reasons during various manufacturing stages, including casting, rolling, bending, flame cutting, forging, machining, and grinding. Heat treatments at various stages also influence residual stresses. For example, quenching treatments produce residual stresses, while stress-relieving heat treatments may reduce such stresses. Areas in which residual stresses exist vary greatly--from microscopic areas to large sections of the metal structure. This article focuses primarily on macroscopic residual stresses. Residual stresses can be classified into two groups according to the mechanisms that produce them:

- STRESSES PRODUCED BY STRUCTURAL MISMATCH
- STRESSES PRODUCED BY AN UNEVEN DISTRIBUTION OF NONELASTIC STRAINS, INCLUDING PLASTIC AND THERMAL STRAINS

Thermal Stresses and Metal Movement During Welding

Because a weldment is locally heated by the welding heat source, the temperature distribution is not uniform and changes as welding progresses. During the welding thermal cycle, complex transient thermal stresses are produced in the weldment and the surrounding joint. The weldment also undergoes shrinkage and deformation during solidification and cooling.

Thermal Stresses During Welding. Figure 1 schematically shows changes in temperature and resulting stresses that occur during welding by examining a bead-on-plate weld of a thin plate made along the *x*-axis. The welding arc, which is moving at a speed *v*, is presently located at the origin, *O*, as shown in Fig. 1(a). The area where plastic deformation occurs during the welding thermal cycle is shown by the shaded area, *M-M '*, in Fig. 1(a). The region where the metal is molten is

indicated by the ellipse near *O*. The region outside the shaded area remains elastic throughout the entire welding thermal cycle.

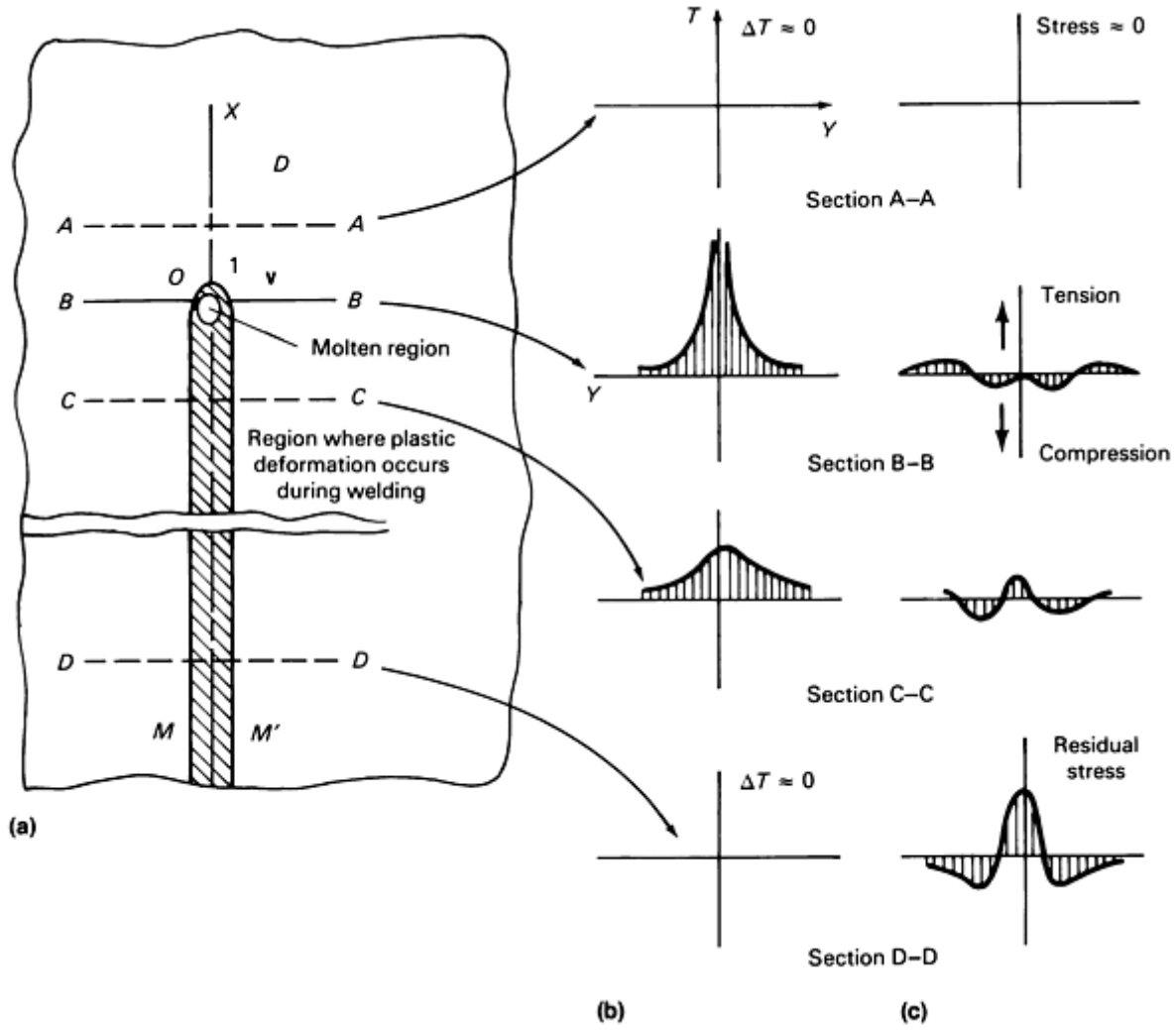

FIG. 1 SCHEMATIC REPRESENTATION OF CHANGES IN TEMPERATURE AND STRESSES DURING WELDING. (A) WELD. (B) TEMPERATURE CHANGE. (C) STRESS, σ_x. STRESS DISTRIBUTION IS SHOWN IN THE PLANE STRESS CONDITION. THEREFORE, STRESSES ARE REGARDED AS BEING UNIFORM IN THE THICKNESS DIRECTION. SOURCE: WELDING RESEARCH COUNCIL

Temperature gradients along several cross sections through the weld bead path are indicated in Fig. 1 (b). In the base metal ahead of the welding arc (denoted as section A-A), the slope of the temperature gradient due to welding ($\Delta T/\Delta Y$) is almost zero. However, along section B-B, which crosses the welding arc, the slope becomes very steep. Along section C-C, somewhat behind the welding arc, the slope becomes less steep. The slope of the temperature gradient due to welding once again approaches zero along section D-D, which is some distance behind the welding arc. Figure 1(c) shows the distribution of normal stress in the *x*-direction (σ_x) along the cross sections. Normal stress in the *y*-direction (σ_y) and shearing stress (t_{xy}) also exist in a two-dimensional stress field. In a three-dimensional stress field, six stress components exist: σ_x, σ_y, σ_z, t_{xy}, t_{yz}, and t_{zx}.

Figure 1(c) shows the distribution (along the *y*-axis) of normal stress in the *x*-direction (σ_x) due to welding (that is, thermal stress). Along section A-A, the stresses are almost zero. The stress distribution along section B-B is complicated. Beneath the welding arc, stresses are close to zero, because molten metal does not support shear loading. Moving away from the arc, stresses become compressive, because expansion of the metal surrounding the weld pool is restrained by the base metal. Because the temperatures of these areas are quite high, the yield stress of the material becomes quite low. In other words, a situation occurs in which stresses in these areas are as high as the yield stress of the base metal at corresponding temperatures. The magnitude of compressive stress passes through a maximum with increasing distance

from the weld or with decreasing temperature. However, stresses occurring in regions farther away from the welding arc are tensile in nature and balance with compressive stresses in areas near the weld pool.

Figure 1(b) shows that along section C-C the weld-metal and base-metal regions have cooled. As they shrink, tensile stresses are caused in regions in and adjacent to the weld (Fig. 1c). As the distance from the weld increases, stresses become compressive. High tensile stresses exist along section D-D in and adjacent to the weld. Compressive stresses are produced in areas away from the weld.

Equilibrium Condition of Residual Stresses. Because residual stresses exist without external forces, the resultant force and the resultant moment produced by the residual stresses must vanish on any plane section:

$$\int \sigma \cdot DA = 0 \qquad \textbf{(EQ 1)}$$

$$\int DM = 0 \qquad \textbf{(EQ 2)}$$

where *dA* is area and *dM* is the resultant moment. Residual stress data must be checked in any experiment to ensure that they satisfy the above condition.

Metal Movement During Welding. During welding, the weldment undergoes shrinkage and deformation. The transient deformation, or metal movement, is most evident when the weld line is away from the neutral axis of the weldment, causing a large amount of bending moment. Figure 2 schematically shows how a rectangular plate distorts when its longitudinal edge is heated by a welding arc or an oxyacetylene torch (for cutting, welding, or flame heating). Areas near the heat source, or the upper regions of the rectangular plate, are heated to higher temperatures and thus expand more than areas away from the heat source, or the lower regions of the plate. Therefore, the plate first deforms as shown by curve *AB*.

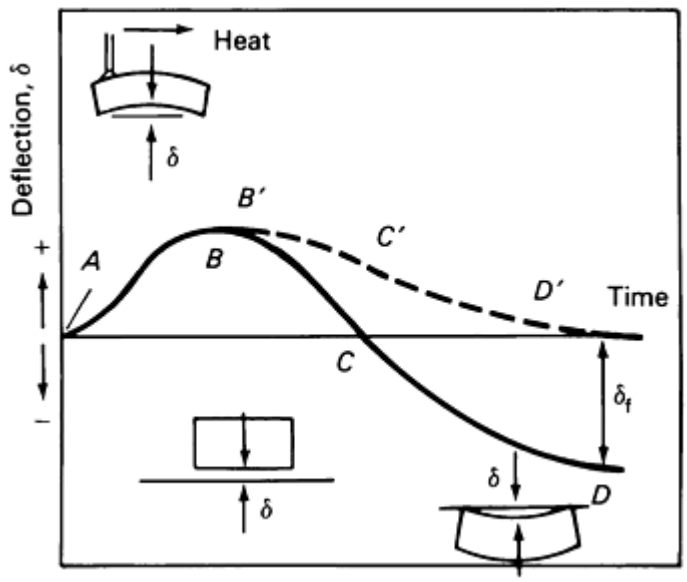

FIG. 2 CHANGES OF DEFLECTION AT THE CENTER OF THE LOWER EDGE OF A RECTANGULAR PLATE DUE TO HEATING BY A HEAT SOURCE MOVING ALONG THE UPPER EDGE AND SUBSEQUENT COOLING

If all the parts of the material remained completely elastic during the entire thermal cycle, thermal stresses produced during the heating and cooling cycle would disappear when the temperature returned to the initial temperature. Deformation of the plate during the welding process would be indicated by curve *AB'C'D'*, resulting in no deformation after the thermal cycle. However, in most practical materials, plastic strains are produced in areas heated to elevated temperatures, causing plastic upsetting. The thermal stresses do not disappear when the temperature returns to the initial temperature, causing residual stresses. Transient deformation of the plate during heating and cooling is shown by curve *ABCD*. After the plate cools to the initial temperature, final deformation in the amount δ_f remains, which also is called

distortion. The metal movement (that is, transient distortion or transient deformation) during welding and the distortion after welding is completed occur in opposite directions, generally with the same order of magnitude.

In summary, some basic characteristics of residual stresses and distortion are (Ref 4):

- THE METAL MOVEMENT DURING WELDING (EXPANSION) IS OPPOSITE TO THE DISTORTION THAT REMAINS AFTER WELDING.
- ALTHOUGH WELDING IS COMPLETED IN A SHORT PERIOD (IN A FEW MINUTES, FOR EXAMPLE), RESIDUAL STRESSES AND DISTORTION TAKE A RELATIVELY LONG TIME TO DEVELOP COMPLETELY (30 MIN TO 1H)
- BECAUSE MOST OF THE NONELASTIC STRAINS THAT CAUSE RESIDUAL STRESSES AND DISTORTIONS ARE PRODUCED DURING WELDING, NECESSARY ACTIONS MUST BE PERFORMED DURING WELDING TO EFFECTIVELY CONTROL AND REDUCE RESIDUAL STRESSES AND DISTORTION.

Analyses of Residual Stresses and Distortion in Weldments

Residual stresses and distortion in welded structures have been recognized and studied since the 1930s. Analyses of these subjects require complex computation; therefore, most early studies were primarily empirical or limited to the analysis of simple cases. With the advancement of modern computers and computational techniques (for example, the finite-element and finite-difference method), a renewed effort has been made in recent years to study residual stresses and related phenomena. Therefore, it is now possible using computer programs to simulate the transient thermal stresses and metal movement during welding as well as the residual stresses and distortion that remain after welding is completed (Ref 5, 6, 7, 8, 9). However, because these analysis methods are very complex, most are not practical for analyzing and controlling residual stresses and distortion in weldments.

References cited in this section

4. K. MASUBUCHI, RESEARCH ACTIVITIES EXAMINE RESIDUAL STRESSES AND DISTORTION IN WELDED STRUCTURES, *WELD. J.*, VOL 70 (NO. 12), 1991, P 41-47
5. L. TALL, RESIDUAL STRESSES IN WELDED PLATES--A THEORETICAL STUDY, *WELD. J.*, VOL 43 (NO. 1), 1991, P 10S-23S
6. H.D. HIBBIT AND P.V. MARCEL, "A NUMERICAL THERMOMECHANICAL MODEL FOR THE WELDING AND SUBSEQUENT LOADING OF A FABRICATED STRUCTURE," NSRDC CONTRACT NO. N00014-67-A-019-0006, TECH. REP. NO. 2, DEPARTMENT OF THE NAVY, MARCH 1972
7. T. MURAKI, J.J. BRYAN, AND K. MASUBUCHI, ANALYSIS OF THERMAL STRESSES AND METAL MOVEMENT DURING WELDING--PART I: ANALYTICAL STUDY; PART II: COMPARISON OF EXPERIMENTAL DATA AND ANALYTICAL RESULTS, *J. ENG. MATER. TECHNOL. (TRANS. ASME)*, 1975, P 81-84, 85-91
8. E.F. RYBICKI *ET AL.*, A FINITE-ELEMENT MODEL FOR RESIDUAL STRESSES AND DEFLECTION IN GIRTH-BUTT WELDED PIPES, *J. PRESSURE VESSEL TECHNOL. (TRANS. ASME)*, VOL 100, 1978, P 256-262
9. P.O. DEXTER AND D. PONT, "EVALUATION OF AVAILABLE WELDING SIMULATION SOFTWARE," PREPARED FOR EPRI UNDER RESEARCH PROJECT C102-3 BY SOUTHWEST RESEARCH INSTITUTE, MAY 1991

Koichi Masubuchi, Massachusetts Institute of Technology

Techniques for Measuring Residual Stresses

Many techniques have been used to measure residual stresses in metals (Ref 1, 10, 11). Table 1 lists most of the presently available measurement techniques and classifies them as follows:

- STRESS-RELAXATION TECHNIQUES
- X-RAY DIFFRACTION TECHNIQUES
- TECHNIQUES USING STRESS-SENSITIVE PROPERTIES
- CRACKING TECHNIQUES

TABLE 1 CLASSIFICATION OF TECHNIQUES FOR MEASURING RESIDUAL STRESS

A-1 STRESS RELAXATION TECHNIQUES USING ELECTRIC AND MECHANICAL STRAIN GAGES
PLATE
SECTIONING TECHNIQUE USING ELECTRIC RESISTANCE STRAIN GAGES
GUNNERT TECHNIQUE
MATHAR-SOETE DRILLING TECHNIQUE
STÄBLEIN SUCCESSIVE MILLING TECHNIQUE
SOLID CYLINDERS AND TUBES
HEYN-BAUER SUCCESSIVE MACHINING TECHNIQUE
MESNAGER-SACHS BORING-OUT TECHNIQUE
THREE-DIMENSIONAL SOLIDS
GUNNERT DRILLING TECHNIQUE
ROSENTHAL-NORTON SECTIONING TECHNIQUE
A-2 STRESS RELAXATION TECHNIQUES USING APPARATUS OTHER THAN ELECTRIC AND MECHANICAL STRAIN GAGES
GRID SYSTEM-DIVIDING TECHNIQUE
BRITTLE COATING-DRILLING TECHNIQUE
PHOTOELASTIC COATING-DRILLING TECHNIQUE
B X-RAY DIFFRACTION TECHNIQUES
X-RAY FILM TECHNIQUE
X-RAY DIFFRACTOMETER TECHNIQUE
C TECHNIQUES USING STRESS-SENSITIVE PROPERTIES
ULTRASONIC TECHNIQUES
POLARIZED ULTRASONIC WAVE TECHNIQUE
ULTRASONIC ATTENUATION TECHNIQUE
HARDNESS TECHNIQUES
D CRACKING TECHNIQUES
HYDROGEN-INDUCED CRACKING TECHNIQUE
STRESS-CORROSION CRACKING TECHNIQUE

Source: Ref 12

In the stress-relaxation technique, residual stress is determined by measuring the elastic-strain release that takes place when a specimen is cut into pieces or has a piece removed. In most cases, electric or mechanical gages are used for measuring this strain release (group A-1 in Table 1). A variety of such techniques exist (that is, there are many ways to section a specimen to determine residual stresses). Certain techniques are used to study stresses in a plate, while others are used for cylinders, tubes, or three-dimensional solids. Strain release caused by stress relaxation can also be determined by using grid systems, brittle coatings, or photoelastic coatings (group A-2 in Table 1). An inherent disadvantage of stress-relaxation techniques is that they are destructive (that is, the specimen must be partially or entirely sectioned). Nevertheless, the stress-relaxation techniques provide reliable quantitative data and are the most widely used method for measuring residual stresses in weldments.

In metals with crystalline structures, elastic strains can also be determined by using x-ray diffraction to measure the lattice parameter. Because the lattice parameter of a metal in the unstressed state is known or can be determined separately, elastic strain in the metal can be measured nondestructively without machining or drilling. Two methods are presently available: the x-ray film technique and the x-ray diffractometer technique. With x-ray diffraction, surface strains can be determined within a small area--for example, to a depth of 0.025 mm (0.001 in.) and a diameter of 0.0025 mm (0.0001 in.). Modern x-ray diffraction stress measurement instrumentation can provide one complete measurement in time scales as short as a fraction of a second, and typically less than 1 min. However, x-ray diffraction techniques have some disadvantages. They are time consuming, and they are not accurate, especially in situations where high temperatures have distorted the atomic structure of the material. Studies have recently been made using diffraction of neutrons, which can penetrate deeper into the metal than x-rays (Ref 13).

Attempts have been made to determine the residual stresses in metals by measuring their stress-sensitive properties. The following stress-measurement techniques have been proposed:

- ULTRASONIC TECHNIQUES, SUCH AS THE POLARIZED ULTRASONIC WAVE TECHNIQUE (WHICH MAKES USE OF STRESS-INDUCED CHANGES IN THE ANGLE OF POLARIZATION OF POLARIZED ULTRASONIC WAVES) AND THE ULTRASONIC ATTENUATION TECHNIQUE (WHICH MAKES USE OF STRESS-INDUCED CHANGES IN THE RATE OF ABSORPTION OF ULTRASONIC WAVES)
- HARDNESS TECHNIQUES, WHICH MAKE USE OF STRESS-INDUCED CHANGES IN HARDNESS

However, none of these techniques has been developed beyond the laboratory stage, and they have not been used successfully for the measurement of residual stresses in weldments.

Another technique developed for the study of residual stresses involves the close observation of cracks induced in the specimen by hydrogen embrittlement or stress-corrosion cracking (SCC). Cracking techniques are useful when studying residual stresses in complex structural models in which the distribution of residual stresses is complicated, but these techniques provide only qualitative, not quantitative, data.

References cited in this section

1. K. MASUBUCHI, *ANALYSIS OF WELDED STRUCTURES--RESIDUAL STRESSES, DISTORTION, AND THEIR CONSEQUENCES,* PERGAMON PRESS, 1980

10. R.G. TREUTING, J.J. LYNCH, H.B. WISHART, AND D.G. RICHARDS, *RESIDUAL STRESS MEASUREMENTS,* ASM, 1952
11. K. MASUBUCHI, "NONDESTRUCTIVE MEASUREMENT OF RESIDUAL STRESSES IN METALS AND METAL STRUCTURES," RSIC-410, REDSTONE SCIENTIFIC INFORMATION CENTER, REDSTONE ARSENAL, 1965
12. K. MASUBUCHI, RESIDUAL STRESSES AND DISTORTION, *WELDING HANDBOOK,* VOL 1, 7TH ED., AWS, 1976
13. R.R. HOSBONS, THE USE OF NEUTRON DIFFRACTION TO DETERMINE NONDESTRUCTIVELY THE RESIDUAL STRAIN AND TEXTURE IN WELDS, *RECENT TRENDS IN WELDING SCIENCE AND TECHNOLOGY,* ASM INTERNATIONAL, 1989, P 103-106

Koichi Masubuchi, Massachusetts Institute of Technology

Magnitude and Distribution of Residual Stresses in Weldments

A number of investigators have studied distributions of residual stresses in various types of weldments. Most of the data presented in this section relates to single welds as opposed to multipass welds. References 1, 2, and 3 present detailed information.

Residual Welding Stresses, Reaction Stresses, and Stress Distributions in a Groove Weld. As stated earlier, residual stresses can be classified as (1) stresses produced by structural mismatch or displacement and (2) stresses produced by uneven distribution of nonelastic strains. The same method of classification is applicable to residual stresses in weldments: (1) reaction stresses caused when the weldment is restrained externally and (2) residual stresses produced in an unrestrained weldment.

Figure 3 shows a typical distribution of residual stresses in a groove weld. The significant stresses are those parallel to the weld direction, designated σ_x, which are usually called the longitudinal stresses, and those transverse to σ_x, designated σ_y, which are called the transverse stresses. The distribution of the longitudinal stress is shown in Fig. 3(b). Near the weld, tensile stresses of high magnitude are produced. These taper off quickly and become compressive at a distance equal to several times the width of the weld metal. The stress distribution is characterized by two parameters:

- THE MAXIMUM STRESS AT THE WELD REGION, σ_M
- THE WIDTH OF THE TENSION ZONE OF RESIDUAL STRESS, B

The distribution of longitudinal residual stress, σ_x, can be approximated by:

$$s_x(y) = s_m\left[1-\left(\frac{y}{b}\right)^2\right]e^{-[1/2(y/b)^2]} \qquad \textbf{(EQ 3)}$$

Equation 3 satisfies the equilibrium conditions given in Eq 1 and 2.

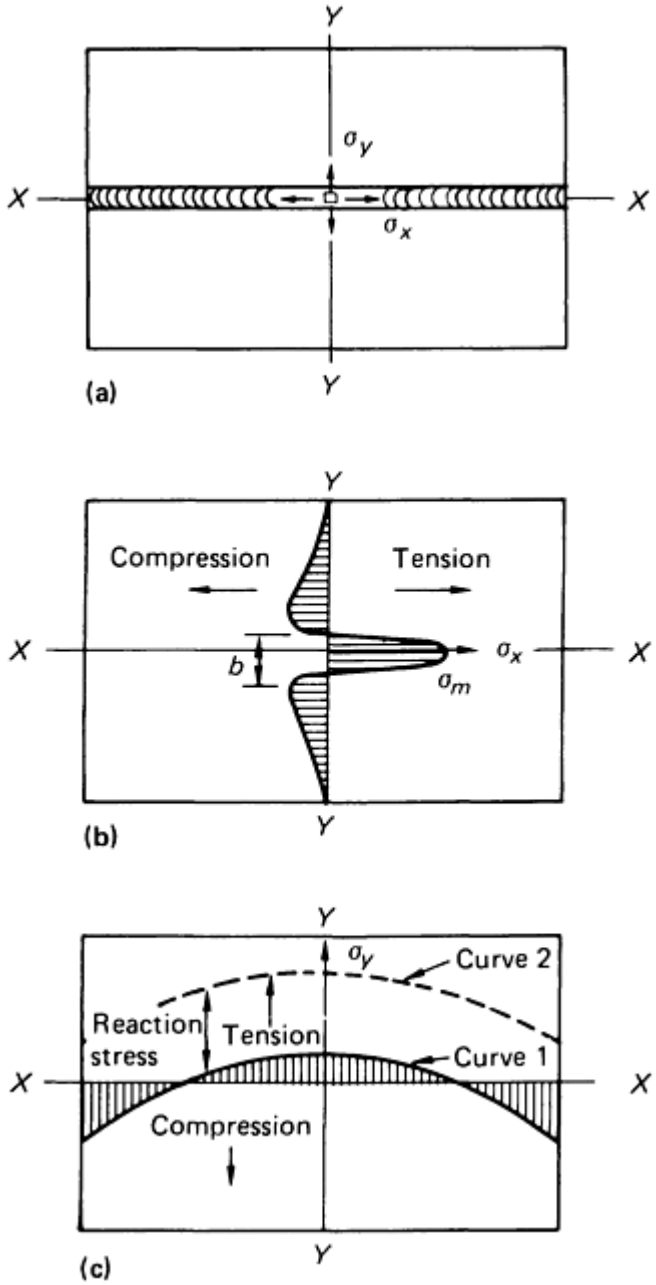

FIG. 3 TYPICAL DISTRIBUTIONS OF RESIDUAL STRESSES IN A GROOVE WELD. (A) GROOVE WELD. (B) DISTRIBUTION OF σ_x ALONG *YY*. (C) DISTRIBUTION OF σ_y ALONG *XX*. SOURCE: WELDING RESEARCH COUNCIL

Curve 1 of Fig. 3(c) shows the distribution of transverse stress,σ_y, along the length of the weld. In the center of the joint, tensile stresses of relatively low magnitude are produced. Compressive stresses are produced at the ends of the joint. If an external constraint is used to restrain the lateral contraction of the joint, approximately uniform tensile stresses along the weld are added, resulting in curve 2 of Fig. 3(c). However, an external constraint has little influence on the distribution of residual stress (σ_x).

Residual Stresses in a Plug Weld. Figure 4 shows the distribution of both the theoretical and experimental residual stresses in a circular plug weld (Ref 14). Tensile stresses, as high as the yield stress of the material, are produced in both radial and tangential directions in the weld and adjacent areas. In areas away from the weld, radial stresses (σ_r) are tensile, and tangential stresses ($\sigma\theta$) are compressive; both stresses decrease with increasing distance from the weld (*r*).

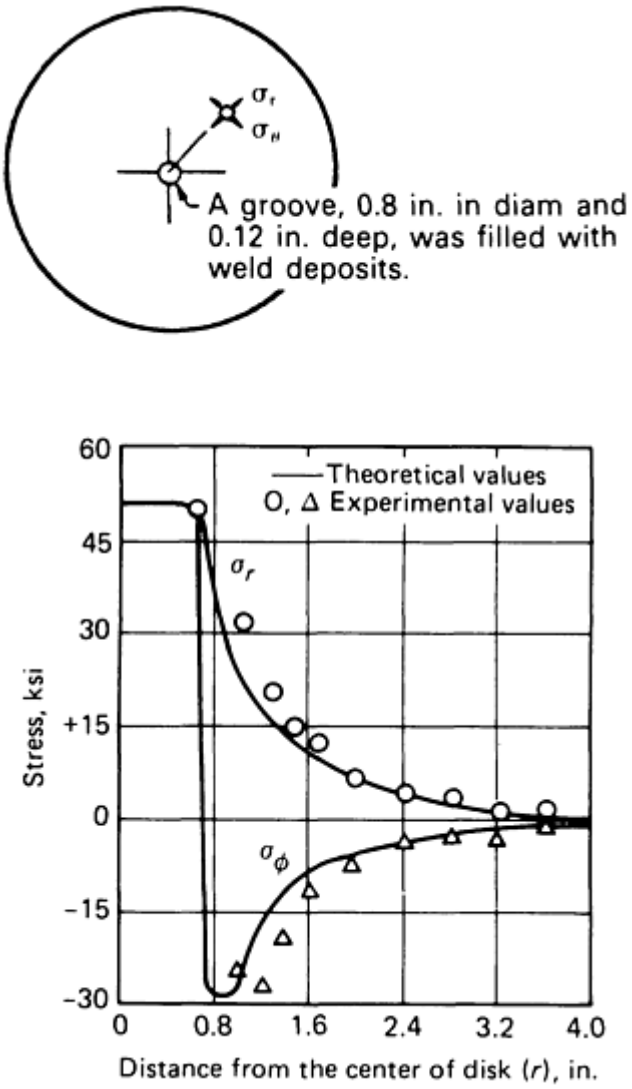

FIG. 4 THEORETICAL AND EXPERIMENTAL DISTRIBUTIONS OF RESIDUAL STRESSES IN A PLUG WELD

Residual Stresses in a Welded Shape and a Column. Figure 5 shows typical distributions of residual stresses and distortion in various welded shapes (Ref 15). As shown in section *xx* of Fig. 5(a), high tensile residual stresses are produced in areas near the weld, in the direction parallel to the weld line (axis). In the flange, longitudinal stresses are compressive (-) in areas away from the weld and tensile (+) in areas near the weld. Tensile stresses in areas near the upper edge of the web are caused by longitudinal bending distortion of the T-shape, which are caused by the longitudinal shrinkage of the weld. Angular distortion also is produced.

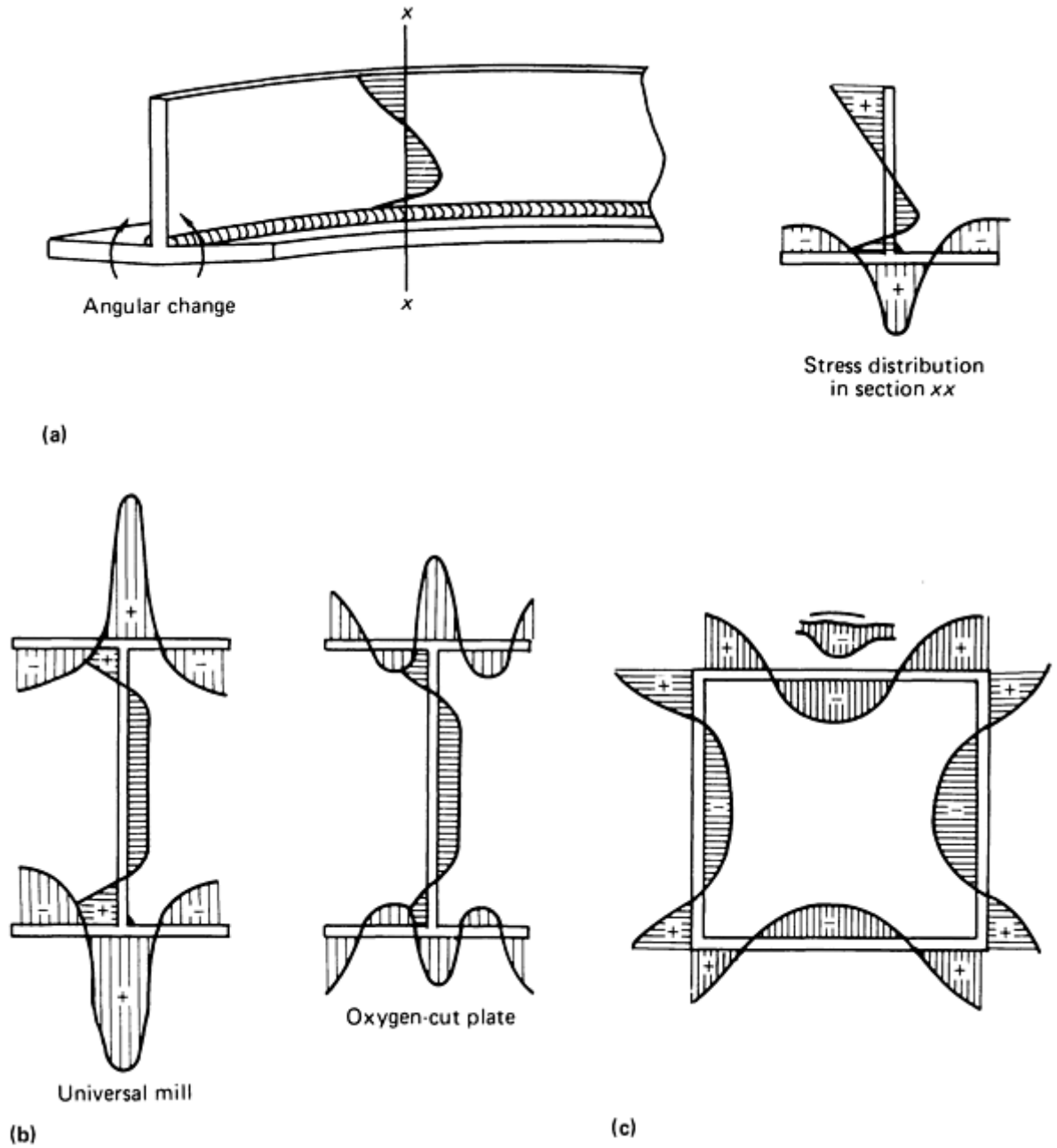

FIG. 5 TYPICAL RESIDUAL STRESSES IN WELDED SHAPES. (A) T-SHAPES. (B) H-SHAPES. (C) BOX SHAPES. COMPRESSIVE STRESS, -; TENSILE STRENGTH, +

Figures 5(b) and 5(c) show typical distributions of residual stress in H-shapes (I-beams) and in a welded box shape, respectively. Residual stresses are shown parallel to the weld line (axis); they are compressive in areas away from the welds and tensile in areas near the welds.

Residual Stresses in Weldments of Selected Materials. Distributions of residual stresses in welds in various metals are similar to those in low-carbon steel welds, discussed above. In most cases, the maximum residual stresses are as high as the yield stress of the material. One exception is ultrahigh-strength steels, such as 4130, D-6a, and H13 (Ref 1). For such steels, peak values of residual stresses in some areas can be as high as the yield stress (or even higher in the case of triaxiality); however, average values of residual stresses in the weld metal are considerably lower than the yield stress.

References cited in this section

1. K. MASUBUCHI, *ANALYSIS OF WELDED STRUCTURES--RESIDUAL STRESSES, DISTORTION, AND THEIR CONSEQUENCES,* PERGAMON PRESS, 1980
2. K. MASUBUCHI, RESIDUAL STRESSES AND DISTORTION, *METALS HANDBOOK,* 9TH ED., VOL 6, *WELDING, BRAZING, AND SOLDERING,* ASM, 1983, P 856-895
3. K. MASUBUCHI, O.W. BLODGETT, S. MATSUI, E.P. ROSS, AND C.L. TSAI, RESIDUAL STRESSES AND DISTORTION, *WELDING HANDBOOK,* 8TH ED., VOL 1, *WELDING TECHNOLOGY,* AWS, 1987

14. H. KIHARA, M. WATANABE, K. MASUBUCHI, AND K. SATOH, *RESEARCHES ON WELDING STRESSES AND SHRINKAGE DISTORTION IN JAPAN,* VOL 4, 60TH ANNIVERSARY SERIES OF THE SOCIETY OF NAVAL ARCHITECTS OF JAPAN, TOKYO, 1959
15. N.R. NAGARAJA RAO, F.R. ESATUAR, AND K. TALL, RESIDUAL STRESSES IN WELDED SHAPES, *WELD. J.,* VOL 39 (NO. 3), 1964, P 295-306S

Koichi Masubuchi, Massachusetts Institute of Technology

Distortion in Weldments

Distortions found in fabricating structures are caused by three fundamental dimensional changes:

- TRANSVERSE SHRINKAGE
- LONGITUDINAL SHRINKAGE PARALLEL TO THE WELD LINE
- ANGULAR DISTORTION AROUND THE WELD LINE

These dimensional changes are shown in Fig. 6.

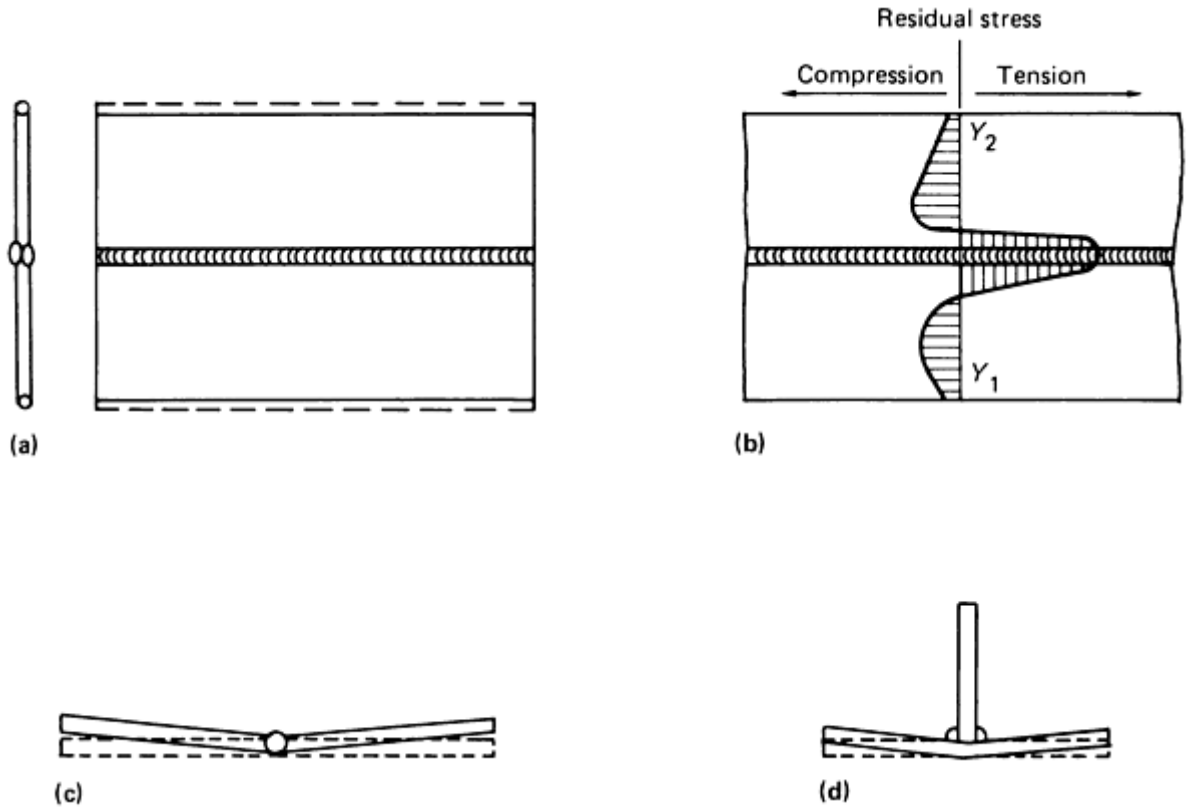

FIG. 6 DIMENSIONAL CHANGES OCCURRING IN WELDMENTS. (A) TRANSVERSE SHRINKAGE IN A GROOVE WELD. (B) LONGITUDINAL SHRINKAGE IN A GROOVE WELD. DISTRIBUTION OF LONGITUDINAL RESIDUAL STRESS, σ_x, IS ALSO SHOWN. (C) ANGULAR CHANGE IN A GROOVE WELD. (D) ANGULAR CHANGE IN A FILLET WELD. SOURCE: WELDING RESEARCH COUNCIL

The shrinkage and distortion that occur during fabrication of actual structures are far more complex than those shown in Fig. 6. For example, when longitudinal shrinkage occurs in a fillet joint, the joint bends longitudinally unless the weld line is located along the neutral axis of the joint. A common structural element is a stiffened panel structure in which longitudinal and transverse stiffeners are fillet welded to a flat plate. Angular changes that occur in the fillet welds cause out-of-plane distortion in the plate, resulting in a shape which looks like a "hungry horse." Presented below are brief discussions of:

- TRANSVERSE SHRINKAGE OF GROOVE WELDS
- ANGULAR DISTORTION OF GROOVE WELDS
- OUT-OF-PLANE DISTORTION CAUSED BY ANGULAR DISTORTION OF FILLET WELDS
- LONGITUDINAL DISTORTION OF BUILT-UP BEAMS
- BUCKLING DISTORTION

Transverse Shrinkage of Square Groove Welds. In Fig. 6(a), shrinkage is uniform along the weld; however, transverse shrinkage that occurs in a groove weld, especially in a long groove weld, is not uniform and is typically much more complex. The major factors causing nonuniform transverse shrinkage in a groove weld are rotational distortion and joint restraint. When two separate planes are joined progressively from one end to the other, the plate edges of the unwelded portion of the joint move, causing a rotational distortion. This can be understood from Fig. 2. The rotational distortion is affected by welding conditions and the location of tack welds. In many practical joints, the degree of joint restraint is not uniform along the weld. Because the amount of transverse shrinkage is less when the joint is more severely restrained, nonuniform distribution of the magnitude of restraint results in an uneven distribution of transverse shrinkage.

Mechanisms of Transverse Shrinkage. The most important finding of mathematical analyses of mechanisms of transverse shrinkage is that the major portion of the transverse shrinkage of a groove joint is caused by contraction of the

base plate adjacent to the weld. The base plate near the weld expands during welding. When the weld metal solidifies, the expanded base metal must shrink; this shrinkage accounts for the major part of transverse shrinkage. Shrinkage of the weld metal accounts for about 10% of the actual total shrinkage. Therefore, most formulas developed for computing transverse shrinkage of a square groove weld are composed of two parts:

- SHRINKAGE OF THE ADJACENT BASE PLATE
- SHRINKAGE OF THE WELD METAL

Transverse Shrinkage During Multipass Welding. Welding of a square groove joint in a thick plate commonly requires a number of passes. Figure 7(a) shows how transverse shrinkage increases during multipass welding of a groove joint in 19 mm ($\frac{3}{4}$ in.) thick low-carbon steel plates. Shrinkage is pronounced during the early weld passes, but diminishes during later passes because of the resistance to shrinkage that increases as the weld metal is increased. The effects of transverse shrinkage on various factors, including root opening, joint design, electrode diameter, and degree of restraint, have been studied extensively (Ref 1).

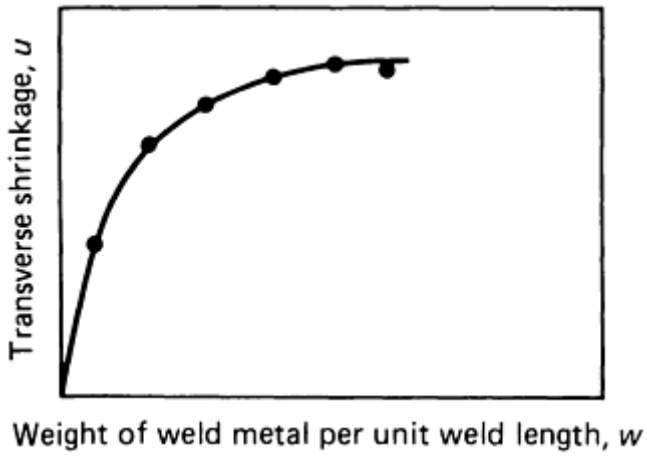

FIG. 7 INCREASE OF TRANSVERSE SHRINKAGE DURING MULTIPASS WELDING OF A GROOVE JOINT. SPECIMENS WERE 19 MM ($\frac{3}{4}$ IN.) THICK LOW-CARBON STEEL PLATES.

Transverse Shrinkage in a Square Groove Weld in Aluminum. As stated earlier, the major portion of transverse shrinkage of a square groove weld is caused by contraction of the base plate adjacent to the weld. Compared with steel, aluminum has a much higher heat conductivity and coefficient of thermal expansion; therefore, transverse shrinkage of an aluminum groove weld is approximately three times greater than that of a steel groove weld of similar dimensions (Ref 1). Because the value of thermal conductivity of aluminum is much greater than that of steel, heat generated by the welding arc dissipates faster in aluminum than in steel, resulting in a broader HAZ (Ref 2).

Angular Distortion of Groove Welds. In a groove weld, when transverse shrinkage is not uniform in the thickness direction, angular distortion often occurs. The angular change of a weld in a thick plate can be minimized by properly selecting the ratio of the size of the weld groove on the front surface to that of the back surface (Ref 1).

Out-of-Plane Distortion Caused by Angular Distortion in Fillet Welds. A stiffened panel composed of a flat plate with longitudinal and transverse stiffeners fillet welded to the plate is widely used for many structures. Angular changes that occur at fillet welds cause out-of-plane distortion of the flat plate (Ref 1). Figure 8 compares values of distortion at the panel center (δ_m) for steel and aluminum welded structures on the basis of the same fillet size (D_f) for selected plate thicknesses. Distortion in aluminum structures is less than in steel structures because the temperature distribution in the thickness direction is more uniform in an aluminum weld than in a steel weld (Ref 2).

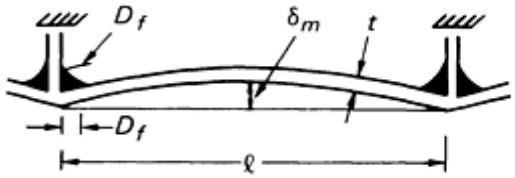
D_f
δ_m
t
D_f
ℓ

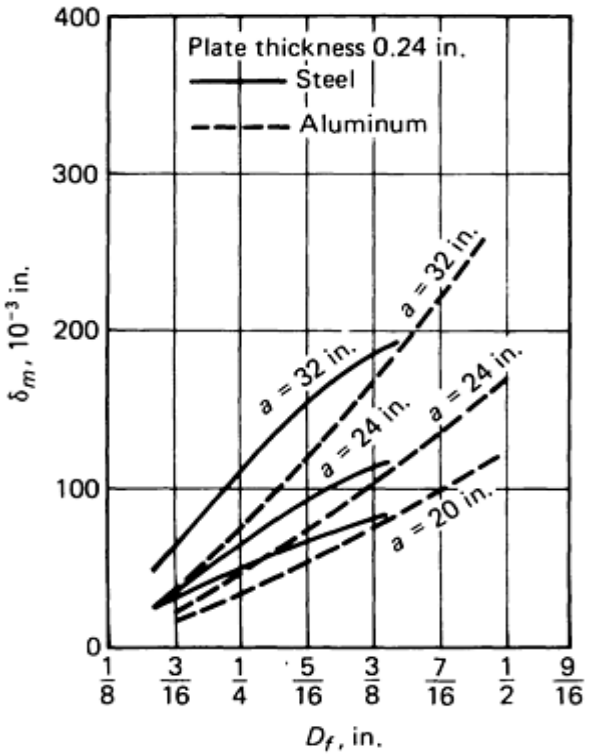
Plate thickness 0.24 in.
Steel
Aluminum
a = 32 in.
a = 32 in.
a = 24 in.
a = 24 in.
a = 20 in.
δ_m, 10^{-3} in.
400
300
200
100
0
$\frac{1}{8}$ $\frac{3}{16}$ $\frac{1}{4}$ $\frac{5}{16}$ $\frac{3}{8}$ $\frac{7}{16}$ $\frac{1}{2}$ $\frac{9}{16}$
D_f, in.

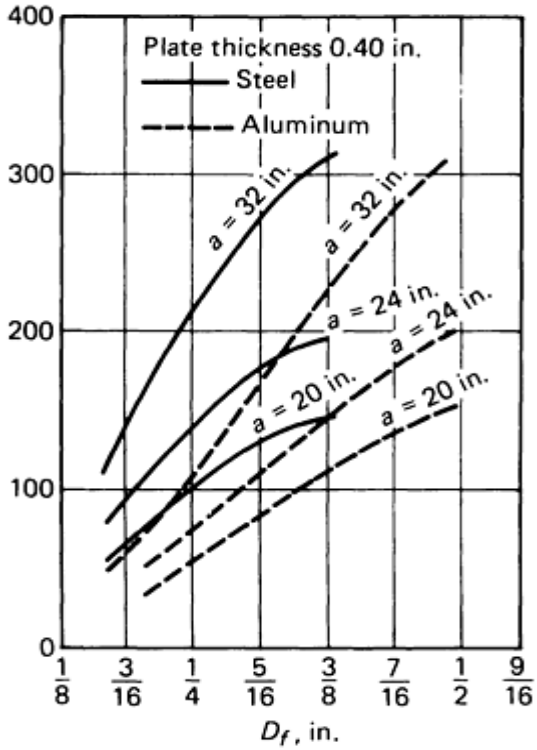
Plate thickness 0.40 in.
Steel
Aluminum
a = 32 in.
a = 32 in.
a = 24 in.
a = 24 in.
a = 20 in.
a = 20 in.
400
300
200
100
0
$\frac{1}{8}$ $\frac{3}{16}$ $\frac{1}{4}$ $\frac{5}{16}$ $\frac{3}{8}$ $\frac{7}{16}$ $\frac{1}{2}$ $\frac{9}{16}$
D_f, in.

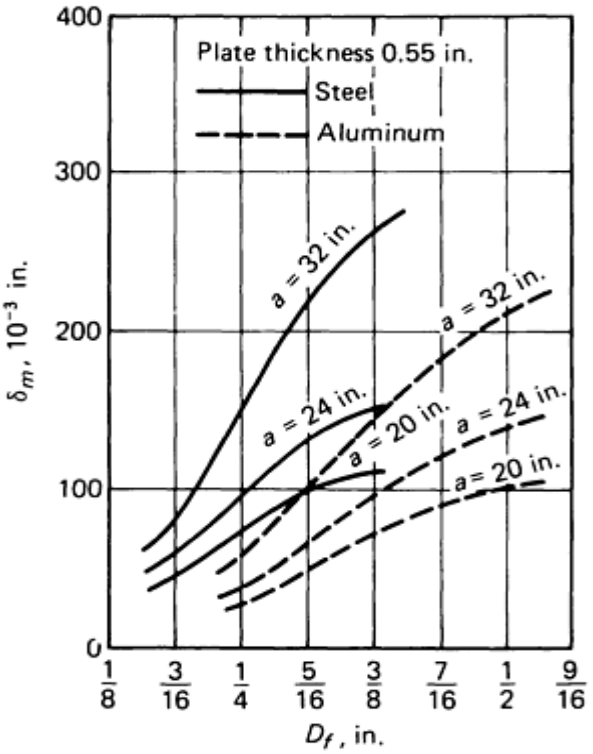
Plate thickness 0.55 in.
Steel
Aluminum
a = 32 in.
a = 32 in.
a = 24 in.
a = 20 in.
a = 24 in.
a = 20 in.
δ_m, 10^{-3} in.
400
300
200
100
0
$\frac{1}{8}$ $\frac{3}{16}$ $\frac{1}{4}$ $\frac{5}{16}$ $\frac{3}{8}$ $\frac{7}{16}$ $\frac{1}{2}$ $\frac{9}{16}$
D_f, in.

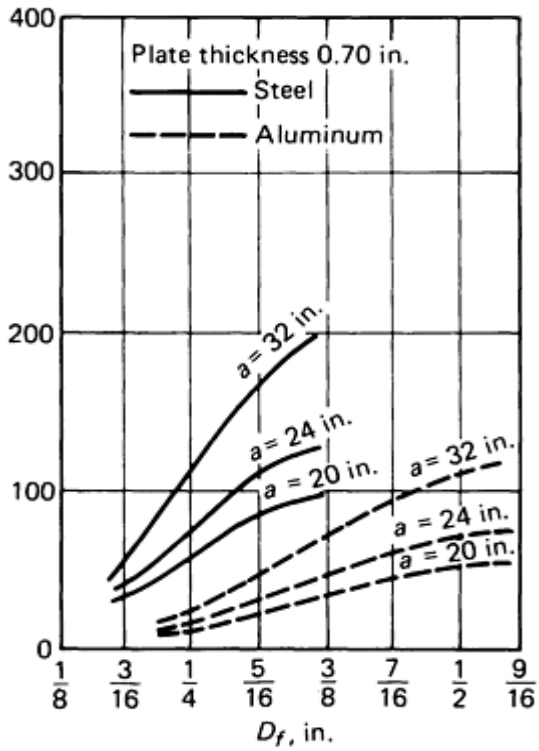
Plate thickness 0.70 in.
Steel
Aluminum
a = 32 in.
a = 24 in.
a = 20 in.
a = 32 in.
a = 24 in.
a = 20 in.
400
300
200
100
0
$\frac{1}{8}$ $\frac{3}{16}$ $\frac{1}{4}$ $\frac{5}{16}$ $\frac{3}{8}$ $\frac{7}{16}$ $\frac{1}{2}$ $\frac{9}{16}$
D_f, in.

FIG. 8 OUT-OF-PLANE DISTORTION (δ_M) AS A FUNCTION OF PLATE THICKNESS (T), SPAN LENGTH (L), AND THE SIZE OF THE FILLET WELD (D_F) FOR STEEL AND ALUMINUM. RELATION OF L TO A IN GRAPHS: $A = L$

Longitudinal Distortion of Built-up Beams. Figure 9 compares values of longitudinal distortion expressed in terms of the radius of curvature of built-up beams in steel and aluminum. In this instance, aluminum welds distorted less than steel welds, perhaps because the temperature distribution in the *z*-direction is more uniform in an aluminum weld than in a steel weld.

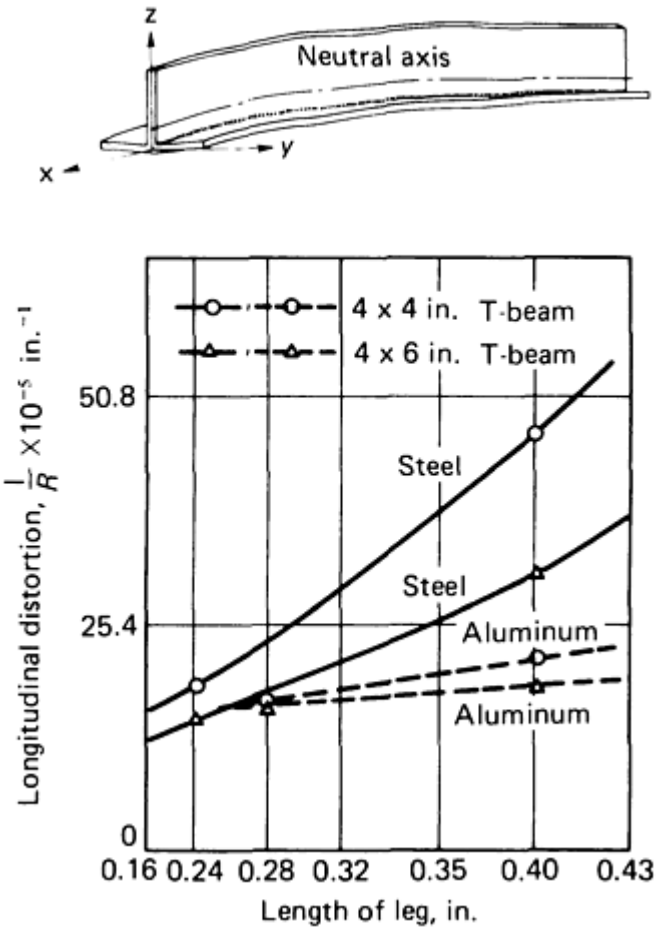

FIG. 9 RELATIONSHIP BETWEEN LENGTH OF LEG AND CURVATURE OF LONGITUDINAL DEFLECTION IN T-SECTION BEAM. SOURCE: REF 1, 16

Buckling Distortion. In any weldment, longitudinal residual stresses are compressive in areas away from the weld, as shown in Fig. 3. When the plate is thin, it may buckle due to these compressive residual stresses. Buckling distortion differs from bending distortion in that the amount of distortion in buckling is much greater. Also, there may be more than one stable deformed shape in buckling distortion. The most effective method for dealing with buckling distortion is prevention by proper selection of plate thickness, length of free span, and welding heat input.

When stiffeners are fillet welded to thin plate, the plate may buckle because of the compressive residual stresses that occur in the plate. Figure 10 shows relationships between distortion at the center of the panel and heat input for square panels 500 mm (20 in.) long made with plates 4.6 to 10 mm (0.18 to 0.4 in.) thick. For example, in the case of a 500 × 500 mm (20 × 20 in.) panel with a plate 6 mm (0.24 in.) thick, the plate deflection increases suddenly when the heat input exceeds approximately 3700 cal/cm^2. This indicates that the critical heat input is approximately 3700 cal/cm^2. When the plate is 4.6 mm (0.18 in.) thick, this critical heat input is only approximately 2000 cal/cm^2. The following formula can be used to determine the critical heat input, H_{cr}, above which excessive buckling distortion occurs:

$$H_{cr} = \frac{Q}{t^3} \quad b \geq \sim 4x10^5 cal/cm^3 \qquad \textbf{(EQ 4)}$$

where *b* is the length of the panel and *t* is the plate thickness, both in millimeters. The above parameter, H_{cr}, is also called the critical heat input index.

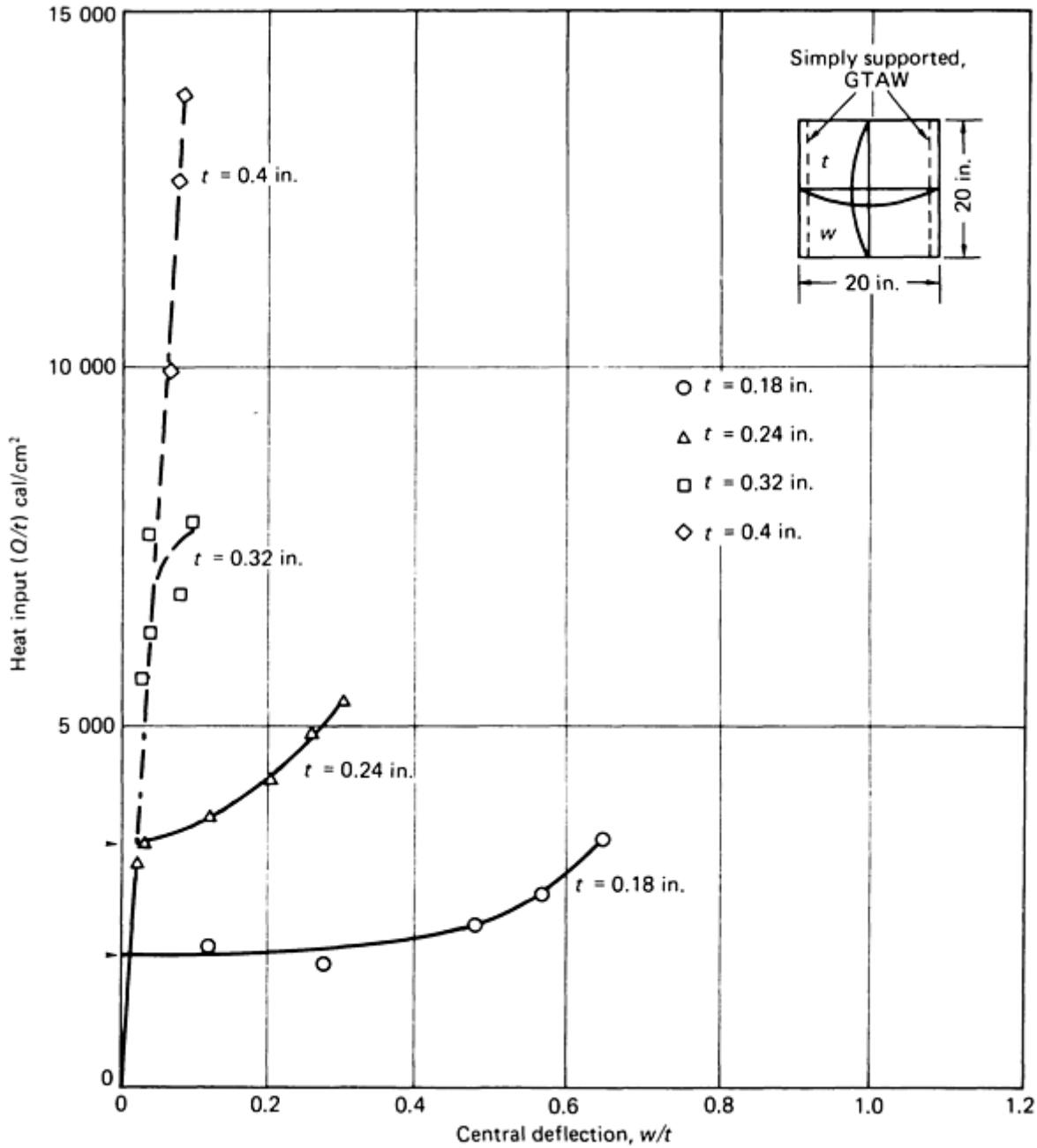

FIG. 10 PLOT OF HEAT INPUT VERSUS DEFLECTION FOR 500 × 500 MM (20 × 20 IN.) LOW-CARBON STEEL PANELS AS A FUNCTION OF PANEL THICKNESS

References cited in this section

1. K. MASUBUCHI, *ANALYSIS OF WELDED STRUCTURES--RESIDUAL STRESSES, DISTORTION, AND THEIR CONSEQUENCES,* PERGAMON PRESS, 1980
2. K. MASUBUCHI, RESIDUAL STRESSES AND DISTORTION, *METALS HANDBOOK,* 9TH ED., VOL

6, *WELDING, BRAZING, AND SOLDERING,* ASM, 1983, P 856-895

16. G. YAMAMOTO, "STUDY OF LONGITUDINAL DISTORTION OF WELDED BEAMS," M.S. THESIS, MASSACHUSETTS INSTITUTE OF TECHNOLOGY, MAY 1975

Thermal Treatments of Weldments

Thermal treatments are often necessary to maintain or restore the properties of base metal affected by the heat of welding. Thermal treatment may also affect the properties of the weld metal. The extent of changes in the properties of the base metal, weld metal, and heat-affected zone (HAZ) are determined by several factors, including the soaking temperature, time, cooling rate, and material thickness. Further detailed information is available in Ref 2 and 3.

Preheat is the most common thermal treatment applied to weldments. Proper use of preheat can minimize residual stresses and distortion that would normally occur during welding as a result of lower thermal gradients around the weld. Preheat also has the beneficial effect in steels of reducing the tendency for the formation of a HAZ and weld metal cracking.

Postweld Thermal Treatments. A properly executed postweld heat treatment results in uniform mechanical properties and reduced residual stresses. The effects of time at temperature and the stress-relieving temperature on residual stresses are shown in Fig. 14(a) and 14(b), respectively (Ref 3). When thick weldments require a postweld machining operation, a stress-relief treatment is usually necessary to achieve normal machining tolerance.

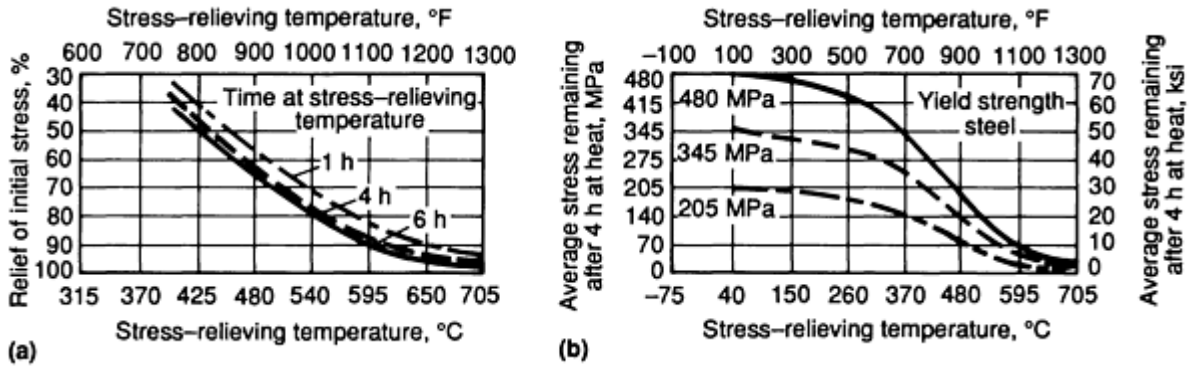

FIG. 14 EFFECT OF TEMPERATURE AND TIME ON STRESS RELIEF. TIME AND TEMPERATURE, 4 H

References cited in this section

2. K. MASUBUCHI, RESIDUAL STRESSES AND DISTORTION, *METALS HANDBOOK,* 9TH ED., VOL 6, *WELDING, BRAZING, AND SOLDERING,* ASM, 1983, P 856-895

3. K. MASUBUCHI, O.W. BLODGETT, S. MATSUI, E.P. ROSS, AND C.L. TSAI, RESIDUAL STRESSES AND DISTORTION, *WELDING HANDBOOK,* 8TH ED., VOL 1, *WELDING TECHNOLOGY,* AWS, 1987

References

1. K. MASUBUCHI, *ANALYSIS OF WELDED STRUCTURES--RESIDUAL STRESSES, DISTORTION, AND THEIR CONSEQUENCES,* PERGAMON PRESS, 1980
2. K. MASUBUCHI, RESIDUAL STRESSES AND DISTORTION, *METALS HANDBOOK,* 9TH ED., VOL 6, *WELDING, BRAZING, AND SOLDERING,* ASM, 1983, P 856-895
3. K. MASUBUCHI, O.W. BLODGETT, S. MATSUI, E.P. ROSS, AND C.L. TSAI, RESIDUAL STRESSES AND DISTORTION, *WELDING HANDBOOK,* 8TH ED., VOL 1, *WELDING TECHNOLOGY,* AWS, 1987
4. K. MASUBUCHI, RESEARCH ACTIVITIES EXAMINE RESIDUAL STRESSES AND DISTORTION IN WELDED STRUCTURES, *WELD. J.,* VOL 70 (NO. 12), 1991, P 41-47
5. L. TALL, RESIDUAL STRESSES IN WELDED PLATES--A THEORETICAL STUDY, *WELD. J.,* VOL 43 (NO. 1), 1991, P 10S-23S
6. H.D. HIBBIT AND P.V. MARCEL, "A NUMERICAL THERMOMECHANICAL MODEL FOR THE WELDING AND SUBSEQUENT LOADING OF A FABRICATED STRUCTURE," NSRDC CONTRACT NO. N00014-67-A-019-0006, TECH. REP. NO. 2, DEPARTMENT OF THE NAVY, MARCH 1972
7. T. MURAKI, J.J. BRYAN, AND K. MASUBUCHI, ANALYSIS OF THERMAL STRESSES AND METAL MOVEMENT DURING WELDING--PART I: ANALYTICAL STUDY; PART II: COMPARISON OF EXPERIMENTAL DATA AND ANALYTICAL RESULTS, *J. ENG. MATER. TECHNOL. (TRANS. ASME),* 1975, P 81-84, 85-91
8. E.F. RYBICKI *ET AL.,* A FINITE-ELEMENT MODEL FOR RESIDUAL STRESSES AND DEFLECTION IN GIRTH-BUTT WELDED PIPES, *J. PRESSURE VESSEL TECHNOL. (TRANS. ASME),* VOL 100, 1978, P 256-262
9. P.O. DEXTER AND D. PONT, "EVALUATION OF AVAILABLE WELDING SIMULATION SOFTWARE," PREPARED FOR EPRI UNDER RESEARCH PROJECT C102-3 BY SOUTHWEST RESEARCH INSTITUTE, MAY 1991
10. R.G. TREUTING, J.J. LYNCH, H.B. WISHART, AND D.G. RICHARDS, *RESIDUAL STRESS MEASUREMENTS,* ASM, 1952
11. K. MASUBUCHI, "NONDESTRUCTIVE MEASUREMENT OF RESIDUAL STRESSES IN METALS AND METAL STRUCTURES," RSIC-410, REDSTONE SCIENTIFIC INFORMATION CENTER, REDSTONE ARSENAL, 1965
12. K. MASUBUCHI, RESIDUAL STRESSES AND DISTORTION, *WELDING HANDBOOK,* VOL 1, 7TH ED., AWS, 1976
13. R.R. HOSBONS, THE USE OF NEUTRON DIFFRACTION TO DETERMINE NONDESTRUCTIVELY THE RESIDUAL STRAIN AND TEXTURE IN WELDS, *RECENT TRENDS IN WELDING SCIENCE AND TECHNOLOGY,* ASM INTERNATIONAL, 1989, P 103-106
14. H. KIHARA, M. WATANABE, K. MASUBUCHI, AND K. SATOH, *RESEARCHES ON WELDING STRESSES AND SHRINKAGE DISTORTION IN JAPAN,* VOL 4, 60TH ANNIVERSARY SERIES OF THE SOCIETY OF NAVAL ARCHITECTS OF JAPAN, TOKYO, 1959
15. N.R. NAGARAJA RAO, F.R. ESATUAR, AND K. TALL, RESIDUAL STRESSES IN WELDED SHAPES, *WELD. J.,* VOL 39 (NO. 3), 1964, P 295-306S
16. G. YAMAMOTO, "STUDY OF LONGITUDINAL DISTORTION OF WELDED BEAMS," M.S. THESIS, MASSACHUSETTS INSTITUTE OF TECHNOLOGY, MAY 1975
17. H. KIHARA AND K. MASUBUCHI, EFFECT OF RESIDUAL STRESS ON BRITTLE FRACTURE, *WELD. J.,* VOL 38 (NO. 4), 1959, P 159S-168S
18. W.J. HALL, H. KIHARA, W. SOETE, AND A.A. WELLS, *BRITTLE FRACTURE OF WELDED PLATES,* PRENTICE-HALL, 1967
19. H. KIHARA, K. MASUBUCHI, K. IIDA, AND H. OHBA, "EFFECT OF STRESS RELIEVING ON BRITTLE FRACTURE STRENGTH OF WELDED STEEL PLATE," DOCUMENT X-218-59,

INTERNATIONAL INSTITUTE OF WELDING, LONDON, 1959 (DISTRIBUTED IN U.S. BY AWS)
20. W.H. MUNSE, *FATIGUE OF WELDED STEEL STRUCTURES*, WELDING RESEARCH COUNCIL, 1964
21. T.R. GURNEY, *FATIGUE OF WELDED STRUCTURES*, 2ND ED., CAMBRIDGE UNIVERSITY PRESS, LONDON, 1979
22. *RESIDUAL STRESS EFFECTS IN FATIGUE*, STP 776, ASTM, 1982
23. A.S. TETELMAN AND A.J. MCEVILY, JR., *FRACTURE OF STRUCTURAL MATERIALS*, JOHN WILEY & SONS, 1967

Residual Stresses and Distortion

Koichi Masubuchi, Massachusetts Institute of Technology

Selected References

- O.W. BLODGETT, TYPES AND CAUSES OF DISTORTION IN WELDED STEEL AND CORRECTIVE MEASURES, *WELD. J.*, JULY 1960
- W.R. OSGOOD, *RESIDUAL STRESSES IN METALS AND METAL CONSTRUCTION*, REINHOLD PUBLISHING, 1954

Repair Welding

Vern Sutter, American Welding Institute; Robert J. Dybas, General Electric Company

Introduction

REPAIR AND MAINTENANCE of parts and components is a multibillion dollar industry. Repair welding can be carried out as a logical procedure that ensures the production of a usable and safe component or it can be approached haphazardly. The latter approach results in poor-quality workmanship and can lead to failed parts, large warranty claims, and dissatisfied customers.

It is to the advantage of the individual welder, job shop owner, end user, and others who depend on the weld repair industry to approach each repair with a thorough knowledge of component history in terms of:

- COMPONENT FUNCTION
- MATERIAL COMPOSITION
- COMPONENT SURFACE OR THROUGH HARDNESS
- PART ORIGINALLY CAST, FABRICATED, OR WELDED

Repair welding can fall into one of three general categories: repair of weld defects, repair of failed parts, and repair of worn parts. This article describes the repair of weld defects and structural failures. Welding buildup of worn parts is described in the article "Cladding, Hardfacing, and Dissimilar Metal Joining" in this Volume.

Requirements and repair techniques discussed in this article apply to arc and oxyfuel welding processes. Materials can be any that are usually joined successfully using arc or oxyfuel welding processes. Generally, the repair welding procedures will apply whether the structure is built under code construction specifications or not. Many construction codes require that a written procedure be prepared prior to any repair welding. Code or contractual requirements supersede any statements made in this article.

If the component to be repaired was originally a welded fabrication, then data and information on the original process are important to a successful repair. If access to this information is not practical, then an analysis of the base material, including previous weld deposits, becomes mandatory. If dimensions require close tolerances or if flatness is critical, then benchmarks that will aid the repair without causing excessive and expensive damage to the workpiece must be established.

Understanding the basics of each group of metals covered in this article helps to ensure a successful repair. All references and sources of information should be exhausted before any job commences. Excellent sources include filler-metal manufacturers and manufacturers of bar, plate, forgings, and castings. Either of these producers can supply key information on the weldability of the workpiece alloys.

Depending on the specific application, all of the common welding processes can be used for repair welding:

- SHIELDED METAL ARC WELDING (SMAW)
- GAS-METAL ARC WELDING (GMAW)
- GAS-TUNGSTEN ARC WELDING (GTAW)
- SUBMERGED ARC WELDING (SAW)
- PLASMA ARC WELDING (PAW)

For the highest-quality welds, the GTAW and PAW processes find the widest application. For long runs or when a large amount of weld metal must be deposited and mechanization is feasible, the SAW process or, to a lesser extent, the GMAW process, is utilized. For general repairs, the SMAW process still enjoys the widest range of applications for out-of-position welding and for short runs, especially when time is critical and when readily portable equipment is utilized. Electrodes are easily transported in sealed 4.5 kg (10 lb) containers.

In addition to the SMAW process, the GMAW process has been gaining wider support and utilization since the introduction of the flux-cored arc welding (FCAW) process, a core wire variation of solid-wire welding. The cored wires are manufactured in smaller diameters to make the wires suitable for out-of-position welding and, especially, for many field and construction applications.

Repair Welding

Vern Sutter, American Welding Institute; Robert J. Dybas, General Electric Company

---

Preliminary Assessment

Before attempting a repair, three factors must first be considered: material weldability, nature of the failure that prompted the repair, and involvement of any code requirements.

Base Metal Weldability

If the item to be repaired was not welded previously, then a special investigation may be necessary to determine weldability. Original documents and drawings are helpful in determining the specifications or description of the base metal. Some tests that can determine degree of weldability include the spark test, chemical analysis test, and simulated weld tests.

The spark test determines the approximate base metal chemistry for carbon steels. Full chemical analysis using drillings can accurately determine chemistry, but not necessarily the heat treatment history of the base metal. Simulated weld tests can determine some practical approaches to repair welding, but seldom give any absolute requirements. These tests require samples of some of the base metal from the workpiece to be repaired.

Nature of Failure

When designing and producing a successful repair, it is often necessary to assess the reasons that a repair is required. Failures can be grouped into four major categories:

- BASE-METAL DEFECTS
- BASE-METAL STRENGTH DEFICIENCIES
- FAILURES INTRODUCED DURING FABRICATION
- DEFECTS CAUSED BY ABRASION, CAVITATION, CORROSION, OR EROSION

Base-Metal Defects. During or subsequent to fabrication, defects in the base metal may be detected. Defects can include pits, stringers, slivers, and a variety of internal discontinuities, the latter of which may be discovered when sawing through the base metal or subjecting the base metal to nondestructive testing (NDT).

Base-Metal Strength Deficiencies. Weld repair alone may not adequately repair a structure that has been overloaded. Reduction of load and additional reinforcing may be necessary. The loading and member arrangement should be thoroughly investigated. Repair of a crack or other structural discontinuity may involve repairing the crack as a weld repair and adding reinforcing plates or members to the workpiece by welding.

Weld Failure if Fabricated. Repair may be required on weld joints that have failed structurally or have undergone nondestructive evaluation (NDE), but do not meet soundness criteria. In these cases, it is usually prudent to prepare the joint for rewelding with procedures similar to the original welding operations.

Defects Caused by Abrasion, Cavitation, Corrosion, and Erosion. Buildup of the workpiece to repair surface damage that is due to abrasion, cavitation, corrosion, or erosion can be carried out as a weld repair. These conditions may or may not be associated with an original weld. The same weldability problems associated with structural repairs are encountered with the defects induced by these conditions. The article "Cladding, Hardfacing, and Dissimilar Metal Joining" in this Volume addresses the conditions that produce these defects in much more detail.

Codes and Standards

Repairs may be governed by welding or construction standards. Some codes address repair welding requirements as a specific subject and others simply require welding qualification that would apply to both new and repair welding. Organizations such as the American Society of Mechanical Engineers (ASME), American Welding Society (AWS), American Petroleum Institute (API), and military standards (MIL-STD) publish their own codes. Owner or engineer approval of repair welding procedures may be required by contract specifications.

Repair Welding

Vern Sutter, American Welding Institute; Robert J. Dybas, General Electric Company

---

Welding Process Selection

When selecting a welding process for a specific application, several factors that affect productivity and weld quality must be balanced. Selection can be difficult because each process has a number of conflicting advantages and limitations in specific situations.

Productivity is usually not an important consideration on most repair jobs. Each process can be ranked in terms of its deposition rate in kilograms (pounds) of weld metal deposited per hour. However, there are other factors that must be considered, as a minimum, before selecting a welding process:

- BASE-METAL TYPE
- JOINT DESIGN AND THICKNESS
- WELDING POSITION
- ENVIRONMENTAL CONDITIONS

- EQUIPMENT AVAILABILITY

Base-Metal Type. Some processes are better suited for use with certain base materials. The maximum heat input must be limited on certain types of materials, such as heat-treated materials that have been quenched, tempered, and age hardened, as well as other heat-treated or cold-worked materials. Processes that derive their advantage from high productivity and high heat input may be unsuitable for these applications.

Joint Design and Thickness. As section thickness increases, welding productivity becomes more important, which should be reflected in the process selection. The length of the weld must also be considered, because a higher-productivity process may not realize this advantage, particularly if the operator must frequently stop the process in order to set up the next pass, as would be necessary with a small repair. Because some processes require more access to the joint root to avoid fusion defects, the selection of some processes may also require a joint design change.

Welding Position. The weld joint position is very important in terms of process selection, because many processes are limited to only a few positions. Whenever possible, the joint should be in the flat (1G) position, because the highest productivity and weld quality are attained when welding is accomplished in this position. Because most field repair work is done on large weldments that cannot be repositioned and because access to the joint is limited, the use of high-productivity processes and filler materials is also limited.

Environmental Conditions. Wind and rain are the two conditions that typically affect field welding. It takes very little wind to disturb the gas shield that is critical for high-quality GMAW and GTAW processes. This restricts their use outside of sheltered containments. The SMAW and FCAW processes can also be affected by wind, but to a lesser degree. Because no process ever tolerates direct exposure to rain, the proper placement of tarps, dams, or other temporary containments is in order.

Availability of Equipment. Most large welding shops have access to the welding equipment required for the processes discussed. However, there are occasions when new equipment must be evaluated to determine if its increased productivity or versatility would offset the capital expense of its initial cost and training.

A general comparison of the most commonly used processes relative to some of the factors discussed above is provided in Table 1. Although some of the ratings are very subjective, they do provide a general guideline for many applications.

TABLE 1 RATING OF SELECTED WELDING PROCESSES AS A FUNCTION OF WELD PARAMETERS AND CHARACTERISTICS

PARAMETER OR CHARACTERISTIC	PROCESS				
	SMAW	**GTAW**	**GMAW**	**FCAW**	SAW
WELD QUALITY	GOOD	EXCELLENT	EXCELLENT	GOOD	**EXCELLENT**
WELD DEPOSITION RATE	FAIR	POOR	GOOD	GOOD	**EXCELLENT**
FIELD WORK	EXCELLENT	POOR	FAIR	EXCELLENT	**POOR**
EQUIPMENT MAINTENANCE	LOW	LOW	MEDIUM	MEDIUM	**MEDIUM**
SMOKE/FUME EMISSION	HIGH	LOW	MEDIUM	HIGH	**VERY LOW**
HEAT INPUT CONTROL	EXCELLENT	POOR	GOOD	GOOD	**SATISFACTORY**
ARC VISIBILITY AND FILLER-METAL PLACEMENT	GOOD	EXCELLENT	SATISFACTORY	SATISFACTORY	**POOR**
VARIETY OF METALS WELDABLE	**EXCELLENT**	**EXCELLENT**	**GOOD**	**GOOD**	**FAIR**

Vern Sutter, American Welding Institute; Robert J. Dybas, General Electric Company

Base-Metal Preparation

Methods of preparing base metal for repair welding may vary, depending on the specific metal to be welded. Generally, all coatings in the vicinity of the repair weld should be removed. Coatings can cause defective welds and can become surface contaminants when heated to the temperatures required for welding.

Where cracks are to be excavated and the part rewelded, a welding groove should be prepared. Most base metals can be cut or grooved using air-carbon arc cutting (CAC-A). Table 2 shows some parameters for carbon arc cutting, whereas Fig. 1 shows a typical joint preparation using the CAC technique. It should be noted that the groove must be prepared in such a way as to allow adequate access to the root of the joint. This preparation is sometimes described as "canoe-shaped." Additional information on this cutting process is provided in the article "Air-Carbon Arc Cutting" in this Volume.

TABLE 2 RECOMMENDED CURRENT RANGE FOR SELECTED SIZES OF AC AND DC ELECTRODES USED FOR CARBON ARC GOUGING AND CUTTING IN AIR

ELECTRODE DIAMETER		CURRENT, A
MM	**IN.**	
DIRECT-CURRENT ELECTRODES (DCEP POLARITY)		
3.2	$\frac{1}{8}$	**30-60**
4.0	$\frac{5}{32}$	**90-150**
4.8	$\frac{3}{16}$	**200-250**
6.4	$\frac{1}{4}$	**300-400**
7.9	$\frac{5}{16}$	**350-450**
9.5	$\frac{3}{8}$	**450-600**
9.5[(A)]	$\frac{3}{8}$ (A)	**250-450**
13	$\frac{1}{2}$	**800-1000**
16	$\frac{5}{8}$	**1000-1250**
16[(A)]	$\frac{5}{8}$ (A)	**300-500**
19	$\frac{3}{4}$	**1250-1600**
25	1	**1600-2200**
ALTERNATING-CURRENT ELECTRODES		
4.8	$\frac{3}{16}$	**200-250**
6.4	$\frac{1}{4}$	**300-400**
7.9	$\frac{5}{16}$	**325-425**
9.5	$\frac{3}{8}$	**350-450**
13	$\frac{1}{2}$	**500-600**

(A) FLAT

FIG. 1 USE OF AIR-CARBON ARC CUTTING TO PRODUCE A GROOVE IN A PLATE. ELECTRODE HOLDER IS EQUIPPED WITH A JET OF COMPRESSED AIR IN LINE WITH THE ELECTRODE TO BLOW AWAY THE MOLTEN METAL.

Grooves can also be prepared by grinding. However, grinding particles left on a groove surface can cause problems, especially in nonferrous materials. The proper grinding wheels must be carefully selected. Carbon arc cutting usually leaves some undesirable by-product on the cut surfaces. A grinding operation following CAC is necessary to remove this layer.

Repair Welding

Vern Sutter, American Welding Institute; Robert J. Dybas, General Electric Company

Guidelines for Various Base Metals

Each group of base metals has specific general repair guidelines that must be followed to ensure successful weld repairs of both ferrous (carbon steels, cast irons, and stainless steels) and nonferrous (for example, titanium) base metals.

Low-Carbon Steel

The most commonly welded group of materials is that which has a carbon-manganese-iron base and is known as mild, or low-carbon, steel. They constitute the bulk of construction materials used today and are the common choice for equipment and fabricated component assemblies, because of their weldability.

Mild steels (up to 0.25% C) are readily weldable and, in cross sections of less than 50 mm (2 in.), usually do not require any preheat or postweld heat treatment. Hardened heat-affected zones (HAZ) are not a problem, and cracking is nonexistent when electrodes are used from fresh containers or electrode storage ovens and are dry. American Welding Society specification A5.1, "Carbon Steel Electrodes for Shielded Metal Arc Welding," covers the filler metals of choice for greater than 50% of all welding fabrication and repair work performed in the world. With the greater demand for higher-production deposition rates, continuous welding wire has grown in usage and application areas.

AWS specifications A5.17 ("Carbon Steel Electrodes and Fluxes for Submerged Arc Welding"), A5.18 ("Carbon Steel Filler Metals for Gas-Shielded Arc Welding"), and A5.20 ("Carbon Steel Electrodes for Flux-Cored Arc Welding") have gained wide support for automatic, semiautomatic, and mechanized welding processes.

Electrodes that are not suitably protected nor kept dry in an electrode storage oven can absorb moisture, which is released as hydrogen gas during the welding process. This hydrogen gas is entrapped in the solidifying weld metal, resulting in immediate or delayed cracking and expensive repairs. When abrasion, friction, or sliding wear is the reason for equipment downtime, either AWS specification A5.13 ("Solid Surfacing Welding Rods and Electrodes") or A5.21 ("Composite Surfacing Welding Rods and Electrodes") is the first choice in the selection process to deposit and build up a resistant

surface capable of withstanding the original wear phenomena in the most severe working environment. In addition, there are numerous electrodes of proprietary composition on the market that perform satisfactorily in service. These electrodes require evaluation and testing before being used.

Base-metal preparation usually consists of removing paint, mill scale, rust, or grease, because they contribute to porous welds. When making field repairs, especially in high-humidity areas, it is always a good practice to apply a preheat in the range from 120 to 150 °C (250 to 300 °F). Postweld heat treatment, though normally not required on mild steels, is sometimes used to ensure dimensional stability where close, flat tolerances are required.

Medium-Carbon Steels

Steels containing from 0.25 to 0.60% C and 0.25 to 1.65% Mn are classified as medium-carbon steels. Based on their base-metal mechanical properties, the electrodes in AWS specification A5.1 usually suffice in most applications.

The use of preheat, interpass temperature, and postweld heat treatment is always required to ensure fusion of the base metal and the weld metal, to prevent distortion, and to ensure dimensional stability of the finished product. Depending on chemical composition, the preheat temperature ranges from 120 to 205 °C (250 to 400 °F). Postweld heat treatment for this group of materials ranges from 595 to 620 °C ± 14 °C (1100 to 1150 °F ± 25 °F). The AWS electrode specifications listed for mild steels are suitable for repairing medium-carbon steels.

High-Carbon Steels

High-carbon steels have a carbon content ranging from 0.60 to 1.00% C. These metals require preheats in the range from 205 to 260 °C (400 to 500 °F), interpass temperatures from 205 to 290 °C (400 to 550 °F), and postweld heat treatments from 620 to 650 °C (1150 to 1200 °F).

Because of the higher carbon content of these steels, greater care must be exercised when welding and during subsequent heat treatment. The HAZ has a higher hardness and cooling must be controlled to preclude any chilling effects that could result in fusion line cracking.

For steels in the annealed or normalized condition, the welding electrodes listed for mild steels will suffice, based on mechanical properties. In the heat-treated condition (that is, higher strength levels), the repair may require stronger filler metal as provided by AWS specifications A5.5 ("Low Alloy Steel Covered Arc Welding Electrodes"), A5.23 (Low Alloy Steel Electrodes and Fluxes for Submerged Arc Welding"), A5.28 ("Low Alloy Steel Filler Metals for Gas-Shielded Arc Welding"), and A5.29 ("Low Alloy Steel Electrodes for Flux Cored Arc Welding").

Cast Irons

Cast irons are a family of high-carbon iron-base alloys containing from 2 to 4% C, 0.50 to 2% Si, and varying amounts of added manganese and chromium strengtheners, in addition to other elements that control graphite formation.

The most common members of this family are the gray cast irons (flake graphite) described in ASTM specification A 48. They are primarily carbon-manganese-silicon in content and no other elements are deliberately added. These materials have tensile strengths ranging from 140 to 415 MPa (20 to 60 ksi) with nil yield ductility and elongations less than 0.5%. Because of this characteristic, they are most difficult to weld and usually suffer from fusion line cracking, because of the presence of carbides formed by the flake graphite. If the broken area (cracked zone) can be placed in compression, then the chance of a successful repair is significantly improved.

Ductile cast irons, clearly identified by the presence of nodular graphite in their microstructure, are sometimes called nodular irons or spheroidal-graphite cast irons. ASTM A 536 grades 60-40-18 through 120-90-02 (designations indicate tensile strength in units of ksi, yield strength in ksi, and elongation in percent, respectively) have better ductility, which makes them more readily weldable by the higher-strength filler metals.

Malleable irons, described in specification ASTM A 47 (ferritic malleable iron castings), A 220 (pearlitic malleable irons), and A 602 (automotive malleable iron castings), are generally weldable and do not suffer the same problems that gray irons have.

The welding processes suitable for repair work are identified in AWS specification D11.2 ("Guide for Welding Iron Castings"):

- SHIELDED METAL ARC WELDING
- GAS-METAL ARC WELDING
- FLUX-CORED ARC WELDING
- GAS-TUNGSTEN ARC WELDING
- SUBMERGED ARC WELDING

The gas processes used for the repair of iron castings are oxyfuel welding (OFW) and braze welding, which utilizes specific filler metals of AWS specification A5.8 ("Filler Metals for Brazing"). The group of welding electrodes used for the arc welding of cast irons is described in AWS specification A5.15 ("Welding Electrodes and Rods for Cast Iron").

Stainless Steels

Stainless steel is a generic term encompassing three distinct families of iron-base alloys:

- AUSTENITIC STAINLESS STEELS
- FERRITIC STAINLESS STEELS
- MARTENSITIC STAINLESS STEELS

The rules for the repair welding of stainless steels will vary with the composition and physical characteristics of the material.

Austenitic stainless steels can be welded by the SMAW process, using electrodes listed in AWS specification A5.4 ("Stainless Steel Electrodes for Shielded Metal Arc Welding"). The GMAW, GTAW, FCAW, SAW, and PAW processes use electrodes listed in AWS specification A5.9 ("Bare Stainless Steel Welding Electrodes and Welding Rods"). SAW process fluxes of proprietary composition are available from manufacturers.

Austenitic stainless steels are usually not preheated and are readily weldable, but they must be clean and free from contamination to ensure weld-metal quality. The free-machining sulfurized grades and those containing selenium or phosphorus are generally not weldable. The titanium or niobium-plus-tantalum stabilized grades of types 318, 321, 347, and 348 have altered chemistries to prevent intergranular precipitation upon heating to a temperature-sensitizing range, such as occurs in welding. The selection of a suitable electrode is critical, and the steel manufacturer or electrode manufacturer should be consulted for the latest technology. Because of their lower thermal conductivity and higher electrical resistivity, stainless steel welds require from 20 to 30% less heat input to prevent weld cracking, loss of corrosion resistance, warping, and undesirable changes in mechanical properties.

The GMAW and GTAW processes use argon gas for a cool, stable arc and helium for a hotter, deeper-penetrating, but somewhat unstable arc. Table 3 lists various combinations of base metal and filler metal that are suitable for a variety of service conditions. This table is an excellent starting point for any repair.

TABLE 3 ELECTRODES OR WELDING RODS AS FILLER METALS FOR USE IN ARC WELDING OF STAINLESS STEELS

TYPE OF STEEL WELDED	**CONDITION OF WELDMENT FOR SERVICE[A]**	ELECTRODE OR WELDING ROD[B]
AUSTENITIC STEELS		
301, 302, 304, 305, 308[C]	1 OR 2	**308**
302B[D]	1	**309**
304L	1 OR 4	**347, 308L**
303, 303SE[E]	1 OR 2	**312**

309, 309S	1	**309**
310, 310S	1	**310**
316[F]	1 OR 2	**316**
316L[F]	1 OR 4	**318, 316L**
317[F]	1 OR 2	**317**
317L[F]	1 OR 4	**317CB**
318, 316CB[F]	1 OR 5	**318**
321[G]	1 OR 5	**347**
347[H]	1 OR 5	**347**
348[I]	1 OR 5	**347**
MARTENSITIC STEELS		
403, 410, 416, 416SE[J]	2 OR 3	**410**
403, 410[K]	1	**308, 309, 310**
416, 416SE[K]	1	**308, 309, 312**
420[L]	2 OR 3	**420**
431[L]	2 OR 3	**410**
431[M]	1	**308, 309, 310**
FERRITIC STEELS		
405[N]	2	**405CB, 430**
405,430[K]	1	**308, 309, 310**
430F, 430FSE[K]	1	**308, 309, 312**
430, 430F, 430FSE[O]	2	**430**
446	2	**446**
446[P]	**1**	**308, 309, 310**

Source: Ref 1

(A) 1, AS WELDED; 2, ANNEALED; 3, HARDENED AND STRESS RELIEVED; 4, STRESS RELIEVED; 5, STABILIZED AND STRESS RELIEVED.

(B) PREFIX E OR ER OMITTED.

(C) TYPE 308 WELD METAL IS ALSO REFERRED TO AS 18-8 AND 19-9 COMPOSITION. ACTUAL WELD ANALYSIS REQUIREMENTS ARE: 0.08% C MAX, 19.0% CR MIN, AND 9.0% NI MIN.

(D) TYPE 310 (1.50% SI MAX) MAY BE USED AS FILLER METAL, BUT THE PICKUP OF SILICON FROM THE BASE METAL MAY RESULT IN WELD HOT CRACKING.

(E) FREE-MACHINING BASE METAL WILL INCREASE THE PROBABILITY OF HOT CRACKING OF THE WELD METAL. TYPE 312 FILLER METAL PROVIDES WELD DEPOSITS THAT CONTAIN A LARGE AMOUNT OF FERRITE TO PREVENT HOT CRACKING.

(F) WELDS MADE WITH TYPES 316, 316L, 317, AND 317CB ELECTRODES OR WELDING RODS MAY OCCASIONALLY DISPLAY POOR CORROSION RESISTANCE IN THE AS-WELDED CONDITION. IN SUCH CASES, CORROSION RESISTANCE OF THE WELD METAL MAY BE RESTORED BY THE FOLLOWING HEAT TREATMENTS: FOR TYPES 316 ANE 317 BASE METAL, FULL ANNEAL AT 1065 TO 1120 °C (1950 TO 2050 °F); FOR TYPES 316L AND 317L BASE METAL, 870 °C (1600 °F) STRESS RELIEF; FOR TYPE 518 BASE METAL, 870 TO 900 °C (1600 TO 1650 °F) STABILIZING TREATMENT. WHERE POSTWELD HEAT TREATMENT IS NOT POSSIBLE, OTHER FILLER METALS MAY BE SPECIALLY SELECTED TO MEET THE REQUIREMENTS OF THE APPLICATION FOR CORROSION RESISTANCE.

(G) TYPE 321 COVERED ELECTRODES ARE NOT REGULARLY MANUFACTURED, BECAUSE TITANIUM IS NOT READILY RECOVERED DURING DEPOSITION.

(H) CAUTION IS NEEDED IN WELDING THICK SECTIONS, BECAUSE OF CRACKING PROBLEMS IN HEAT-AFFECTED ZONES.

(I) IN BASE METAL AND WELD METAL, FOR NUCLEAR SERVICE, TANTALUM IS RESTRICTED TO 0.10% MAX AND COBALT TO 0.20% MAX.

(J) ANNEALING SOFTENS AND IMPARTS DUCTILITY TO HEAT-AFFECTED ZONES AND WELD. WELD METAL RESPONDS TO HEAT TREATMENT IN A MANNER SIMILAR TO THE BASE METAL.

(K) THESE AUSTENITIC WELD METALS ARE SOFT AND DUCTILE IN AS-WELDED CONDITION, BUT THE HEAT-AFFECTED ZONE WILL HAVE LIMITED DUCTILITY.

(L) REQUIRES CAREFUL PREHEATING AND POSTWELD HEAT TREATMENT TO AVOID CRACKING.

(M) REQUIRES CAREFUL PREHEATING. SERVICE IN AS-WELDED CONDITION REQUIRES CONSIDERATION OF HARDENED HEAT-AFFECTED ZONES.

(N) ANNEALING INCREASES DUCTILITY OF HEAT-AFFECTED ZONES AND WELD METAL. TYPE 405 WELD METAL CONTAINS NIOBIUM, RATHER THAN ALUMINUM, TO REDUCE HARDENING.

(O) ANNEALING IS EMPLOYED TO INCREASE DUCTILITY OF THE WELDED JOINT.

(P) TYPE 308 FILLER METAL WILL NOT DISPLAY SCALING RESISTANCE EQUAL TO THAT OF THE BASE METAL. CONSIDERATION MUST BE GIVEN TO DIFFERENCES IN THE COEFFICIENTS OF THERMAL EXPANSION OF THE BASE METAL AND THE WELD METAL.

Ferritic stainless steels (types 446, 430, 405, and 409) are generally less weldable than the austenitic grades. Preheat temperatures ranging from 150 to 230 °C (300 to 450 °F) are necessary to prevent weld cracking, warping, and other serious repair problems. Postweld heat treatment ranging from 790 to 815 °C (1450 to 1500 °F) is necessary to transform a mixed structure to a wholly ferritic structure and to restore the mechanical properties and corrosion resistance that were seriously affected by the heat of welding. The filler metals in Table 3 apply to these grades of stainless steels, as well.

Martensitic stainless steels (types 403, 410, 414, 420, and the 440 series) are weldable with adequate preheat and interpass temperature control ranging from 205 to 315 °C (400 to 600 °F). To restore mechanical properties and reduce the hardened HAZ, a postweld heat treatment ranging from 650 to 675 °C (1200 to 1250 °F) is commonly used to restore properties and reduce internal welding stresses. Austenitic electrodes are used for minor repairs or when properties are not the prime consideration (see Table 3).

Precipitation-hardening stainless steels are divided into three groups on the dual basis of characteristic alloying additions, particularly the elements added to promote precipitation hardening (PH), and the matrix structures of the steels in the solution-annealed and aged condition. Differences among the steels have a direct bearing on the behavior of the steels in welding.

Martensitic Precipitation-Hardening Steels. These steels have a predominantly austenitic structure at the solution-annealing temperature of approximately 1040 to 1065 °C (1900 to 1950 °F), but they undergo an austenite-to-martensite transformation when cooled to room temperature. These steels can be readily welded. The welding procedures resemble those ordinarily used for the 300-series stainless steels, despite differences in composition and structure between the two classes.

The selection of filler metal depends on the properties required for the welded joint (Table 4). If strength comparable to that of the base metal is not required at the welded joint, then a tough 300-series stainless steel filler metal may be adequate. When a weld having mechanical properties comparable to those of the hardened base metal is desired, the filler metal must be of comparable composition, although slight modifications are permissible to obtain better weldability.

TABLE 4 RECOMMENDED FILLER METALS FOR WELDING PRECIPITATION-HARDENING STAINLESS STEELS

TYPE	**UNS DESIGNATION**	**COVERED ELECTRODES**	**BARE WELDING WIRE**	DISSIMILAR PH STAINLESS STEELS
MARTENSITIC				
17-4 PH	S17400	AMS 5827B (17-4 PH) OR E308	AMS 5826 (17-4 PH) OR ER308	**E309 OR ER309, E309CB OR ER309CB**
15-5 PH	S15500	AMS 5827B (17-4 PH) OR E308	AMS 5826 (17-4 PH) OR ER308	**E309 OR ER309, E309CB OR ER309CB**
SEMIAUSTENITIC				
17-7 PH	S17700	AMS 5827B (17-4 PH), E308, OR E309	AMS 5824A (17-7 PH)	**E310 OR ER310, ENICRFE-2, OR ERNICR-3**

PH 15-7 MO	S15700	E308 OR E309	AMS 5812C (PH 15-7 MO)	**E309 OR ER309, E310 OR ER310**
AM350	S35000	AMS 5775A (AM350)	AMS 5774B (AM 350)	**E308 OR ER308, E309 OR ER309**
AM355	**S35500**	**AMS 5781A (AM355)**	**AMS 5780A (AM 355)**	**E308 OR ER308, E309 OR ER309**

Source: Ref 2

Semiaustenitic Precipitation-Hardening Steels. Unlike martensitic PH steels, semiaustenitic PH steels are soft enough in the annealed condition to permit cold working. When cooled rapidly from the annealing temperature to room temperature, they retain their austenitic structure, which displays good toughness and ductility in cold-forming operations.

The semiaustenitic PH steels are normally welded in the annealed condition. The tough austenitic structure imparts welding characteristics similar to those of 300-series stainless steels. The semiaustenitic PH steels are not susceptible to cracking when welded after transformation to martensite, because the low-carbon martensite developed is not of high hardness or low ductility. Also, cold cracking does not occur in the base metal adjacent to the weld because the HAZ is austenitized during welding and remains substantially austenitic as the joint cools to room temperature.

The choice of filler metal depends largely on the weld properties desired. The filler metal can be an alloy of precipitation-hardening composition that is capable of developing mechanical properties comparable to those of the base metal (Table 4). If high strength is not required, then the filler metal can be a 300-series austenitic stainless steel. When these steels are welded in the annealed condition, certain microstructural relations are generally obtained as a result of relatively rapid heating and cooling at the joint:

- WELD METAL CONTAINS SMALL AMOUNTS OF FERRITE IN AN ESSENTIALLY AUSTENITIC MATRIX; HARDNESS IS APPROXIMATELY 90 HRB
- BASE METAL IMMEDIATELY ADJACENT TO THE WELD DISPLAYS HIGH-TEMPERATURE ANNEALED (AUSTENITIC) STRUCTURE; HARDNESS IS APPROXIMATELY 90 HRB
- BASE METAL IN THE NARROW ZONE JUST BEYOND THE ANNEALED ZONE NEXT TO THE WELD IS HARDENED SLIGHTLY; HARDNESS IS APPROXIMATELY 90 TO 98 HRB

Austenitic Precipitation-Hardened Steels. The alloy content of these steels is high enough to maintain an austenitic structure after annealing and after any aging or hardening treatment. Although the austenitic PH steels remain austenitic during all phases of forming, welding, and heat treatment, some contain alloying elements (for precipitation-hardening purposes) that greatly affect behavior in welding.

The austenitic PH stainless steels can be welded using the arc welding techniques applied when welding the austenitic stainless steels. The major difference is that these steels are usually heat treated after welding to achieve the required mechanical properties, which is usually unnecessary with austenitic PH stainless steels. Austenitic PH stainless steels can be welded with matched or dissimilar filler metals or without filler metals, as in the case of most stainless steels. There is a wide variety of hardenable filler metals available for these PH grades through the manufacturer of consumables. The most commonly used grade is the AWS A5.4 Class E630/AWS A5.9 Class ER630 alloy, the only one currently included in the AWS specifications. Its composition is shown in Table 5.

TABLE 5 COMPOSITION OF WELDING CONSUMABLES FOR PRECIPITATION-HARDENING STAINLESS STEELS

All data are maximum percentages.

AWS CLASSIFICATION	COMPOSITION, %									
	C	**Cr**	**Ni**	**Mo**	**Nb + Ta**	**Mn**	**Si**	**P**	**S**	Cu
E630[A], ER630[B]	**0.05**	**16.0-16.75**	**4.5-5.0**	**0.75**	**0.15-0.30**	**0.25-0.75**	**0.75**	**0.04**	**0.03**	**3.25-4.00**

Source: AWS A5.4, A5.9

(A) UNDILUTED WELD METAL COMPOSITION.

(B) CONSUMABLE COMPOSITION.

Duplex Stainless Steels (Ref 3, 4, 5). The physical and mechanical properties of duplex (ferritic-austenitic) stainless steels affect the welding process. Because of their better stress-corrosion cracking resistance and appreciably higher yield and tensile strengths, these steels are currently used as direct substitutes for austenitic stainless steels when service above about 260 to 315 °C (500 to 600 °F) is not required.

Because duplex stainless steels generally have a higher thermal conductivity and a lower coefficient of thermal expansion than austenitic stainless steels, they generally exhibit less distortion during welding than do austenitic stainless steels.

The general welding characteristics of the duplex alloy steels are very similar to those of austenitic stainless steels. They can be welded by any of the conventional arc welding processes (SMAW, GTAW, GMAW, PAW, and SAW). In addition, electron-beam and laser-beam welding are used, as well as resistance welding. Heat input should be low enough to minimize intergranular carbide precipitation. Surface cleanliness is a must when welding duplex stainless steels. It is necessary to eliminate any source of hydrogen in the welding operation. For the gas-shielded processes, particularly on pipe, argon-helium purge gas should be used.

Filler metal selection is critical. A filler metal with matching composition may result in a higher ferrite content than that of the base metal. Gooch (Ref 4) and others have shown that filler metals of duplex stainless steel with higher nickel and/or nitrogen are preferred. Weld metal cracking in duplex steels has rarely been identified. Because extensive austenite-to-ferfite and ferrite-to-austenite transformations occur in the HAZ, along with grain growth, the welding procedure must be carefully controlled. The extent of the above transformations greatly depends on the composition and the precise weld thermal cycle experienced by the HAZ during welding. Because of their high chromium level, these steels are prone to σ phase and 475 °C (885 °F) embrittlement. Though the weld thermal cycle is too short for σ-phase formation of 475 °C (885 °F) embrittlement to occur, care must be exercised in welding heavy-section steels of this type.

Titanium

Titanium is a reactive metal that requires special considerations before and during the welding cycle. The metal must be cleaned at least 50 mm (2 in.) beyond any gas shield. Abrasive blasting is an acceptable cleaning method. Chlorinated solvents (for example, trichloroethylene), should not be used for degreasing titanium alloys because the chlorine residues can result in intergranular cracking during subsequent heating operations.

Titanium alloys are most successfully welded in sealed chambers, although welding in air can be accomplished with a suitable trailing gas shield. Argon gas is the preferred gas for welding and is also used for welding in argon atmosphere chambers to protect the molten metal from oxidation.

The most commonly used process for repairing titanium components is GTAW, using AWS specification A5.12 Class EWTh2 and EWTh1 tungsten electrodes. Helium and argon-helium gas mixtures are also used when higher heat inputs are necessary for deeper penetration and when welding thicker sections. The GMAW process is also effectively applied on thicker parts (6.35 mm, or 0.25 in.) and large parts or when significant amounts of weld metal is to be deposited. Thirteen filler metals of pure and alloyed titanium are classified in AWS specification A5.16 ("Titanium and Titanium Alloy Welding Electrodes and Rods").

All grades of unalloyed titanium are welded in the annealed condition because annealing offsets the effect of cold working with its attendant loss of strength. Metastable beta alloys are welded in the annealed or solution-treated condition, where the welds are low in strength, but ductile. To obtain full strength, the weld is cold worked by peening or planishing and the weldment is solution treated and aged. Additional information can be found in the article "Welding of Titanium" in this Volume.

References cited in this section

1. G.E. LINNERT, WELDING CHARACTERISTICS OF STAINLESS STEELS, *MET. ENG. QUART.*, NOV 1967
2. *WELDING HANDBOOK*, VOL 4, *METALS AND THEIR WELDABILITY*, 7TH ED., AWS, 1982
3. H.B. CARY, *MODERN WELDING TECHNOLOGY*, 2ND ED., PRENTICE-HALL, 1989
4. T.G. GOOCH, WELDABILITY OF DUPLEX FERRITIC-AUSTENITIC STAINLESS STEELS, *DUPLEX STAINLESS STEELS*, R.A. LULA, ED., PROC. CONF. ON DUPLEX AUSTENITIC-FERRITIC STAINLESS STEELS, ASM, OCT 1982
5. S.A. DAVID, WELDING OF STAINLESS STEELS, *ENCYCLOPEDIA OF MATERIALS SCIENCE AND ENGINEERING*, VOL 7, M.B. BEVER, ED., THE MIT PRESS, P 5316-5320

Repair Welding

Vern Sutter, American Welding Institute; Robert J. Dybas, General Electric Company

References

1. G.E. LINNERT, WELDING CHARACTERISTICS OF STAINLESS STEELS, *MET. ENG. QUART.*, NOV 1967
2. *WELDING HANDBOOK*, VOL 4, *METALS AND THEIR WELDABILITY*, 7TH ED., AWS, 1982
3. H.B. CARY, *MODERN WELDING TECHNOLOGY*, 2ND ED., PRENTICE-HALL, 1989
4. T.G. GOOCH, WELDABILITY OF DUPLEX FERRITIC-AUSTENITIC STAINLESS STEELS, *DUPLEX STAINLESS STEELS*, R.A. LULA, ED., PROC. CONF. ON DUPLEX AUSTENITIC-FERRITIC STAINLESS STEELS, ASM, OCT 1982
5. S.A. DAVID, WELDING OF STAINLESS STEELS, *ENCYCLOPEDIA OF MATERIALS SCIENCE AND ENGINEERING*, VOL 7, M.B. BEVER, ED., THE MIT PRESS, P 5316-5320

Repair Welding

Vern Sutter, American Welding Institute; Robert J. Dybas, General Electric Company

Selected References

• M.J. DONACHIE, ED., *TITANIUM: A TECHNICAL GUIDE*, ASM INTERNATIONAL, 1988
• "RECOMMENDED PRACTICES FOR AIR CARBON ARC GOUGING AND CUTTING," ANSI/AWS C5.3-91, AMERICAN WELDING SOCIETY
• R.D. STOUT, *WELDABILITY OF STEELS*, 4TH ED., WELDING RESEARCH COUNCIL, 1987
• *WELD SURFACING AND HARDFACING*, THE WELDING INSTITUTE, CAMBRIDGE, U.K., 1980

Fitness-for-Service Assessment of Welded Structures

J.R. Gordon, Edison Welding Institute

Introduction

IT IS GENERALLY ACCEPTED THAT all welded structures enter service containing flaws that can range from volumetric discontinuities, such as porosity or slag inclusions, to planar defects, such as a lack of side-wall fusion or

hydrogen cracks. For this reason, most welding codes include clauses that cover the inspection of production welds and set acceptance standards for the discontinuities that may be found. Any flaws that are not acceptable are repaired.

The acceptance standards included in the majority of codes are based on good workmanship practices. Although this is a very useful basis, in some cases it can result in the repair of relatively harmless flaws, with the possibility that the repair weld (often made under more-demanding conditions than the production weld) will contain a more-serious flaw. Since the early 1980s, a number of fracture mechanics-based assessment procedures have been developed that enable the significance of weld discontinuities to be assessed on a "fitness-for-service" basis. Using this concept, a structure is considered to be fit for service if it can be operated safely throughout its design life. The adoption of fitness-for-service concepts in several codes has resulted in the development of more-rational flaw-acceptance criteria.

Fitness-for-service assessment procedures also can be used to assess the integrity, or remaining life, of components in service. Indeed, one of the most widespread uses of fitness-for-service concepts is the justification of life extension, which is a term that has often been misunderstood. The purpose of life-extension activities is not to continue the operation of a plant beyond its useful life but merely to ensure full utilization up to its useful life. The idea is to avoid premature retirement of plants and plant components, on the basis of the so-called design life, because actual useful lives can often exceed the design life.

Overview of Failure Modes. Depending on the operating environment and the nature of the applied loading, a structure can fail by a number of different modes, including:

- BRITTLE FRACTURE
- DUCTILE FRACTURE
- PLASTIC COLLAPSE
- FATIGUE
- CREEP
- CORROSION
- BUCKLING

These failure modes can be broken down into the following broad categories:

- FRACTURE
- FATIGUE
- ENVIRONMENTAL CRACKING
- HIGH-TEMPERATURE CREEP

Fracture includes the conventional static failure modes, such as brittle fracture, ductile fracture, plastic collapse, buckling, as well as dynamic fracture. Fatigue failure is caused by cyclic loading. Environmentally assisted cracking includes corrosion, stress-corrosion cracking, hydrogen-induced cracking, and other environmentally assisted failure modes. High-temperature creep includes creep rupture and creep crack growth. This article discusses each of these categories, as well as the benefits of a fitness-for-service approach.

Fitness-for-Service Assessment of Welded Structures

J.R. Gordon, Edison Welding Institute

Fracture

Of all the conventional failure modes, brittle fracture is undoubtedly the most spectacular and dangerous mode of fracture, frequently occurring with no prior warning and with the potential to produce devastating consequences. The notched-bar impact test was one of the earliest tests developed to study the fracture behavior of steel. The most widely used impact

test, as of the early 1990s, is the Charpy impact test, the results of which are most useful when presented as a plot of absorbed energy or percentage shear fracture against test temperature (Fig. 1).

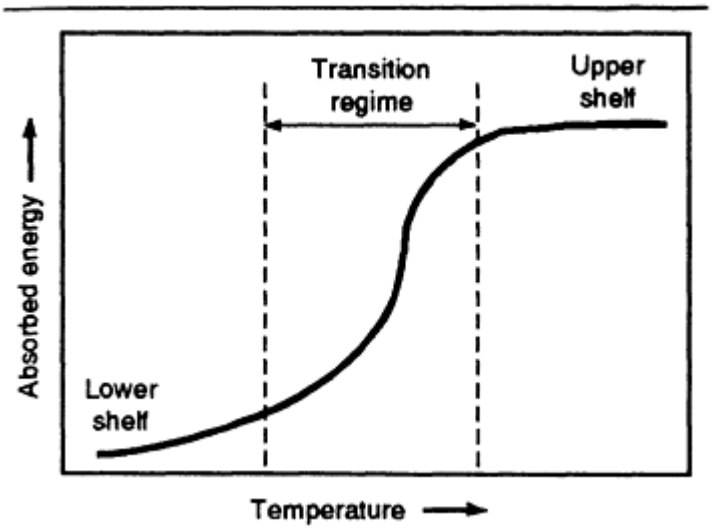

FIG. 1 TYPICAL CHARPY IMPACT ENERGY TRANSITION CURVE

In the case of ferritic steels, the subsequent results show fracture behavior that ranges from low-energy brittle fracture (lower shelf) to high-energy ductile fracture (upper shelf). Between these two modes of fracture, there is a transition regime, in which the fracture mode changes from brittle to ductile fracture as the temperature increases. In design, Charpy impact data are used to ensure that the material exhibits good toughness properties (that is, upper-transition or upper-shelf behavior) at the minimum operating temperature. Most design codes include Charpy impact toughness requirements to minimize the risk of structures failing by unstable fracture.

Although the Charpy impact test has received widespread acceptance, it has a number of drawbacks. First, unlike a tensile test, the results from notched-bar impact tests are highly dependent on specimen size. Larger specimens translate the transition curve to higher temperatures because of increased specimen constraint and sampling size.

Second, toughness is also a function of loading rate. In most structural applications, this rate is relatively low, whereas in a Charpy test, the specimen is subjected to impact loading. If Charpy specimens were tested under loading rates that were more representative of structural applications, then the transition curve could be translated to a lower temperature.

Third, Charpy specimens contain 2 mm (0.8 in.) deep V notches, which are relatively blunt. In comparison, structures can contain much sharper cracks, such as fatigue cracks. Increasing the notch acuity in a Charpy specimen would cause the transition curve to shift to a higher temperature.

Fracture comprises two phases: initiation and propagation. Initiation is defined as the first extension of an existing defect, whereas propagation is the continued extension thereafter. Which of these phases is the most important depends on the material and the structural application. Unfortunately, the Charpy impact test does not distinguish between these two phases; that is, it just provides an indication of the energy necessary to initiate and propagate a crack.

Thus, although the Charpy impact test is widely accepted by engineers and designers because it can indicate the "quality" of a material, its most-significant shortcoming is that the results cannot be used in any quantitative sense to assess the significance of flaws in a structure. Fracture mechanics can, to a certain extent, bridge the gap between the measurement of material properties and their application to design.

Fracture Mechanics Assessment Procedures. As shown in Fig. 2, fracture mechanics seeks to relate the three parameters that combine to control the fracture process. These parameters are: the size of the discontinuity, material toughness, and the applied stress.

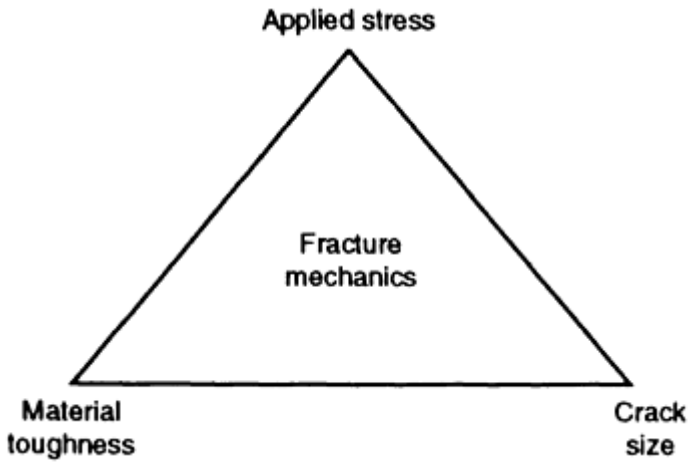

FIG. 2 ROLE OF FRACTURE MECHANICS

If any two of these three parameters are known, then it is possible, using the principles of fracture mechanics, to estimate the value of the third parameter that will elicit the failure of the structure. Alternatively, if all three parameters are known, then it is possible to predict whether or not the structure is fit for service, and, if it is, estimate the margin of safety.

Figure 3 summarizes the different loading paths that can result in the failure of a structure (assuming that fatigue, creep, and corrosion effects are not significant). The loading paths range from brittle fracture under nominally elastic loading (applied stresses well below yield) to plastic collapse (overload of remaining ligament). In cases where brittle fracture occurs at low applied stresses, the concept of linear-elastic fracture mechanics (LEFM) can be applied, that is, a stress-intensity factor, *K*, approach. At the other extreme, when the failure mechanism is plastic overload, then assessments should be performed using limit load or plastic-collapse analyses.

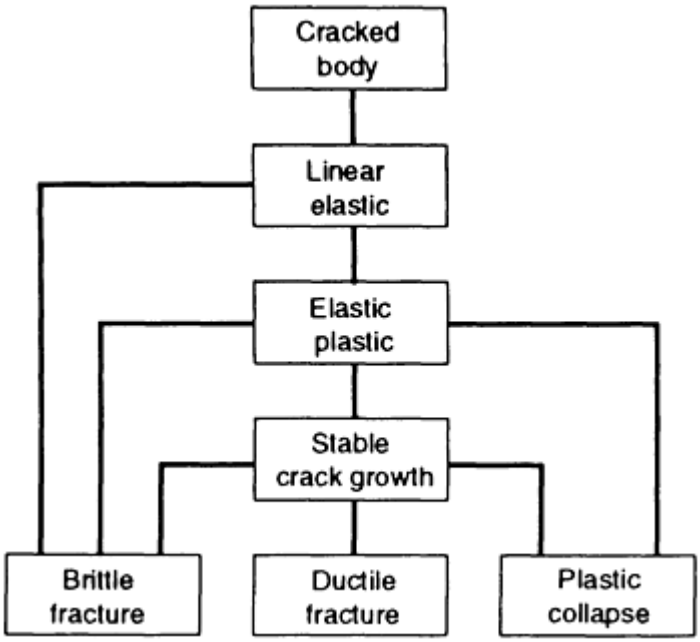

FIG. 3 SUMMARY OF LOADING PATHS TO FAILURE

Between these two extremes, elastic-plastic fracture mechanics (EPFM) methods can be applied to assess the integrity of structures. The two most common EPFM fracture-characterizing parameters are the crack-tip opening displacement (CTOD) and the J-integral, *J*. Fitness-for-service methodologies have been developed using both of these parameters.

A number of different fitness-for-service assessment methodologies for calculating allowable or critical flaw sizes are currently in use throughout the world, such as those cited in Ref 1, 2, 3, 4, 5.

Failure-Assessment Diagrams. The concept of performing fitness-for-service assessments using a failure-assessment diagram (FAD) was first proposed in 1975. These diagrams provide a convenient method of assessing the risk of failure by brittle fracture, ductile fracture, or plastic collapse, that is, all the loading/failure paths presented in Fig. 3. As a result, most of the widely used fracture assessment methodologies are now based on FADs. Although the exact form of the FADs in the different assessment procedures can vary, the basic concept of the FAD is identical; that is, the *y*-axis (K_r axis) of a FAD provides an indication of the resistance of the structure to brittle fracture, whereas the *x*-axis (S_r axis) assesses resistance to plastic collapse. The failure-assessment curve interpolates between these two limiting failure modes, as shown in Fig. 4.

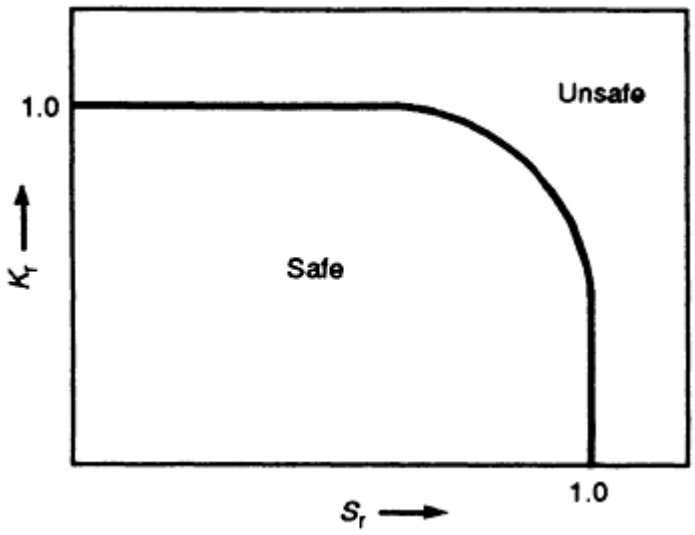

FIG. 4 BASIC CONCEPT OF FAILURE-ASSESSMENT DIAGRAM

To perform a structural integrity assessment, the user plots assessment points on the FAD. The location of each point is a function of the applied loading conditions, flaw size, material properties, and other factors.

Although the exact procedures for calculating assessment points can vary from procedure to procedure, the general procedure to determine an assessment point is as follows:

$$K_t = \frac{k_I}{k_{mat}} \qquad \textbf{(EQ 1)}$$

$$S_t = \frac{s}{s_{pc}} \qquad \textbf{(EQ 2)}$$

where K_I is the applied stress intensity for crack under consideration subjected to the primary and secondary loading conditions of interest; K_{mat} is the material toughness (for example, K_{Ic}); σis the applied primary stress; and σ_{pc} is the plastic collapse stress for the component under consideration.

It should be noted from the above equations that secondary stresses (for example, welding residual stresses or thermal stresses) are incorporated in the calculation of the K_r coordinate but are not included in the calculation of S_r because, by definition, secondary stresses are self-equilibrating and, as a result, cannot contribute to plastic collapse.

Although fracture assessment procedures have improved significantly in recent years due to the advances in fracture mechanics, there are still a number of issues, particularly with regard to performing fracture assessments of welded structures, that have not been fully resolved. It should be noted that the current fracture assessment procedures are

generally unsafe. The unresolved issues tend to make current predictions conservative. A better understanding of these complexities would merely make analyses of critical conditions more accurate.

The major unresolved issues with regard to applying fracture mechanics assessment procedures to welded structures are undoubtedly weld metal mismatch and welding residual stresses. When designing a welded structure, it is normal practice to specify welding consumables with a higher yield strength than the surrounding parent material to avoid the possibility of localized plastic straining in the weld metal. Conversely, there are a number of materials that can only be welded successfully with consumables that will give rise to undermatching welds. This is becoming more common with the increasing use of high-heat-affected zone (HAZ), and parent material cannot be taken into account in the currently available fracture assessment models, it is normal practice to assume the tensile properties of the material in which the defect is located (that is, if a crack is located in the weld metal, the assessment is performed assuming the tensile properties of the weld metal). In reality, the difference in tensile properties between the different weld regions will influence how plasticity develops at defects and, hence, the relationship between crack driving force and applied loading. This can lead to significant errors in a fracture assessment.

At present, the only method of performing an accurate fracture assessment of under or overmatched welded joints is to perform a detailed finite-element analysis to compute the applied crack driving force. This level of sophistication is clearly excessive in situations where assessments of simple welded components are required on a regular basis. Research is required to investigate the effect of weld metal mismatch on the accuracy of fracture prediction models. Results from such research will hopefully lead to the proposal of modifications to fracture assessment models to account for weld metal mismatch.

Another unresolved issue, which, again, is particularly relevant to welded structures, concerns the estimation (prediction) and incorporation of residual stresses (or secondary stresses) in fracture assessment models. The major problem is that there is no quick or convenient method of measuring or predicting the through-thickness variation of residual stresses in a welded joint. Consequently, in the absence of definitive measurements, it is common practice to assume that residual stresses in an as-welded structure are both tensile and yield strength in magnitude. Moreover, it is common practice to assume that the residual stresses are uniform across the section under consideration, despite the fact that the assumed residual stress distribution is not self-equilibrating. This, undoubtedly, leads to extremely conservative assessments, particularly when it is considered that the residual stress components frequently play a major role in an assessment. The other area of concern with regard to residual stresses is the relaxation of residual stresses with increasing primarily load (that is, mechanical stress relief). Although the latest version of PD 6493 includes a procedure for calculating the relaxation of secondary stresses with increasing primary load, there is concern that the method may still overestimate the subsequent residual stress levels.

If the assessment points lie within the area bounded by the axes of the failure-assessment diagram and the failure-assessment curve, then the structure is deemed to be safe. Alternatively, if the assessment points lie outside the FAD, then the structure is considered to be unsafe. This approach also can be used to determine the limiting flaw size by plotting a series of assessment points for different crack sizes. The limiting flaw size corresponds to the flaw size that results in the assessment locus intersecting the FAD, as shown in Fig. 5.

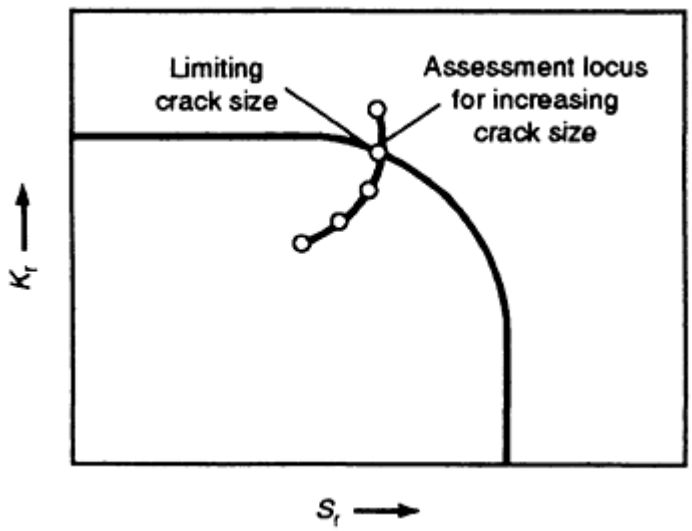

FIG. 5 ASSESSMENT PROCEDURE TO DETERMINE LIMITING CRACK SIZE

When performing fracture assessments, it is essential that the fracture-toughness values used in the assessment are representative of the material in which the crack is located (for example, parent material, weld metal, or heat-affected zone). Furthermore, the fracture-toughness values should be representative of the condition of the material or the welded joints in the structure. For example, if the material has suffered degradation, such as temper or hydrogen embrittlement, then tests should be performed on material/welded joints in the same condition. Finally, to ensure conservative assessments, the fracture-toughness tests should be performed at the minimum operating temperature of the structure.

Application of Fracture-Assessment Procedures. Fitness-for-service design philosophies can be applied to welded structures in several different ways. The most widely used approach is to develop relaxed flaw-acceptance criteria. These are typically derived by assuming a minimum toughness level that is incorporated in a weld procedure qualification. These relaxed flaw-acceptance criteria can result in significant economic savings and can accelerate construction schedules through a dramatic reduction in the number of repairs. Nevertheless, it should be emphasized that the adoption of fitness-for-service concepts should never be used to condone poor workmanship. The general quality of fabrication should remain constant, regardless of whether fitness-for-service concepts are applied.

Fitness-for-service concepts also can be used to develop inspection criteria, including sensitivity requirements. These concepts also can be used to demonstrate that flaws that may escape detection will not impair overall structural integrity, even under accident or overload conditions.

References cited in this section

1. "GUIDANCE ON SOME METHODS FOR THE DERIVATION OF ACCEPTANCE LEVELS FOR DEFECTS IN FUSION WELDED JOINTS," PD 6493, BRITISH STANDARDS INSTITUTION, 1991
2. F.M. BURDEKIN, "FINAL REPORT ON QUESTIONNAIRE ON THE USE OF FRACTURE MECHANICS METHODS FOR THE ASSESSMENT OF THE SIGNIFICANCE OF WELD DEFECTS," DOCUMENT X-1076-84, IIW, 1984
3. I. MILNE, R.A. AINSWORTH, A.R. DOWLING, AND A.T. STEWART, "ASSESSMENT OF THE INTEGRITY OF STRUCTURES CONTAINING DEFECTS," CEGB R/H/R6, REVISION 3, MAY 1986
4. V. KUMAR, M.D. GERMAN, AND C.F. HIH, "AN ENGINEERING APPROACH FOR ELASTIC-PLASTIC FRACTURE ANALYSIS," REPORT EPRI NP 1931, RESEARCH PROJECT 1237-1, GENERAL ELECTRIC COMPANY, JULY 1981
5. J.M. BLOOM, *VALIDATION OF A DEFORMATION PLASTICITY FAILURE ASSESSMENT DIAGRAM APPROACH TO FLAW EVALUATION*, STP 803, VOL II, ASTM, 1983, P 206

Fitness-for-Service Assessment of Welded Structures

J.R. Gordon, Edison Welding Institute

Fatigue Design

The fatigue life of a welded structure is almost invariably limited by the fatigue life of the weld details. As a result, the design stresses in welded structures that are subjected to cyclic loading are limited by the fatigue strength of the weld details. For this reason, extensive research has been undertaken in recent years to study the fatigue behavior of welded joints. This has culminated in a number of proposed methodologies to assess the fatigue behavior of different welded joint geometries. The most widely used procedure for assessing the fatigue performance of welded joints is the *S-N* curve approach.

In general, the fatigue life of a component is comprised of initiation and propagation phases. For smooth components, the crack-initiation period represents the bulk of the total fatigue life. This is particularly noticeable with high-fatigue applications, where the fatigue crack-initiation period may exceed 95% of the fatigue life. In the case of machined components, once a fatigue crack has grown to a detectable size, the component is virtually at the end of its useful life and would normally be withdrawn from service. In the case of welded joints, there is practically no crack-initiation period, because of the presence of weld-toe discontinuities, which behave as preexisting cracks. As a result, the bulk of the fatigue life of a welded joint can be attributed to fatigue-crack propagation.

The fatigue strength of unwelded components increases with material tensile strength. In the case of welded joints, however, the fatigue strength is relatively unaffected by material tensile strength, as shown in Fig. 6. This is because the bulk of the fatigue life of a welded joint is spent in the propagation phase and, although crack-propagation rates can change from one material to another, there is no consistent trend with regard to tensile strength. This indicates that the improved fatigue performance produced by increasing material tensile strength is limited primarily to the crack-initiation phase. As a result, increasing the material tensile strength will not improve the fatigue performance of welded joints.

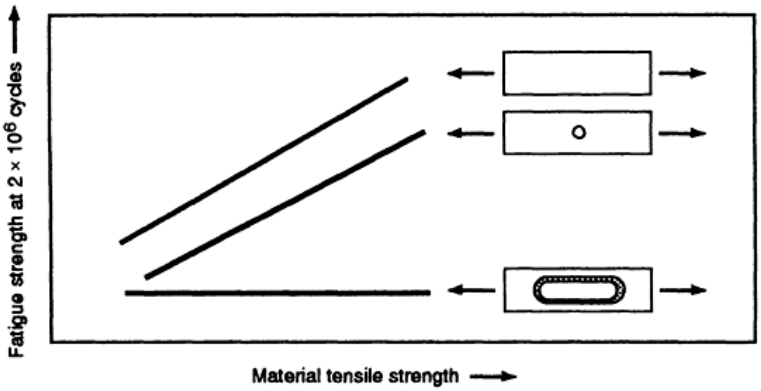

FIG. 6 EFFECT OF MATERIAL TENSILE STRENGTH OR THE FATIGUE STRENGTH OF WELDED AND UNWELDED SPECIMENS

The potential initiation sites at which fatigue cracks may develop in welded joints depends on the geometry of the joint details. Nevertheless, the most common initiation site, by far, is the weld toe. This is a particularly severe location, because of the geometric discontinuity that gives rise to a local stress concentration and the possible presence of undercutting and weld-toe intrusions (Ref 6, 7, 8, 9). The weld-toe intrusions that form as a result of the welding process are generally angular in nature and protrude below the plate surface. The precise origin of these discontinuities is not fully understood, although it has been suggested that they may be caused by slag or impurities in the steel.

Limited studies (Ref 6, 7, 8, 9) have indicated that the weld-toe discontinuities range in depth from 0.1 to 1.0 mm (0.004 to 0.04 in.). The depth of the weld-toe intrusions depends on a number of variables, including welding process, welding consumables, flux, and welding parameters. These studies have indicated that the average root radius of intrusions is from 2 to 3 μm (80 to 120 μin.), although root radii of less than 1 μm (40 μin.) have been recorded. In addition to the local stress concentration and the presence of sharp weld-toe discontinuities, the weld-toe region is also subjected to tensile residual stresses that form as a result of the thermal cycle associated with welding. Thus, the weld toe is a location of high local stress with preexisting crack-like discontinuities and large tensile residual stresses, which means that it is a prime source for fatigue cracks.

For this reason, the fatigue performance of welded joints is generally much lower than the fatigue performance of unwelded components, even if they contain stress concentrations (Fig. 7).

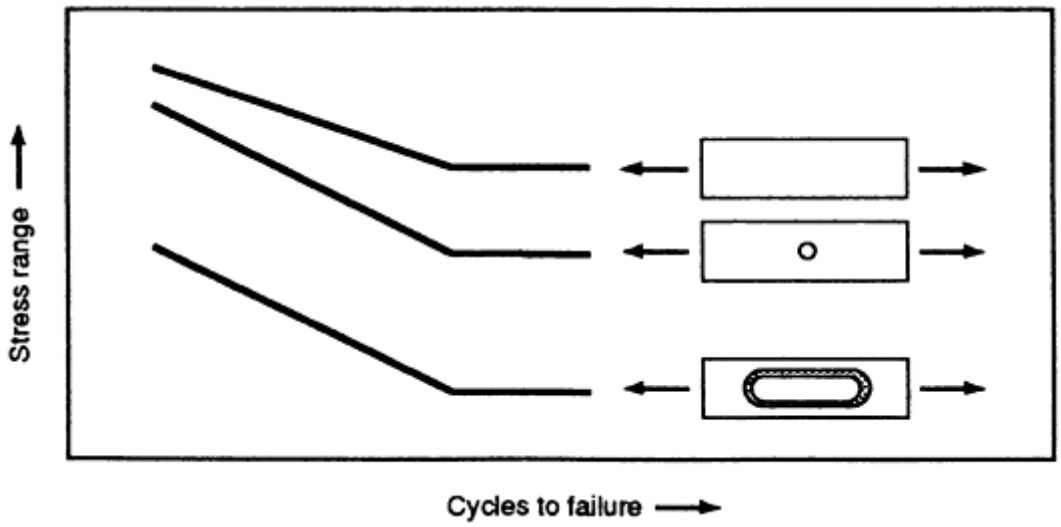

FIG. 7 RELATIVE FATIGUE BEHAVIOR OF WELDED JOINTS AND UNWELDED COMPONENT (WITH AND WITHOUT STRESS CONCENTRATORS)

The *S-N* curve approach is probably the most widely used method of assessing the fatigue performance of welded structures. The fatigue design rules proposed by Gurney in 1976 (Ref 10) provide a framework to assess the fatigue behavior of welded joints. Based on the results of an extensive welded joint fatigue test program, a series of *S-N* curves that incorporate a wide range of welded joint details was developed. Similar design approaches have now been included in many national and international codes and standards (Ref 11, 12, 13, 14). In a typical set of fatigue design curves (Fig. 8), the different classifications correspond to different welded joint geometries.

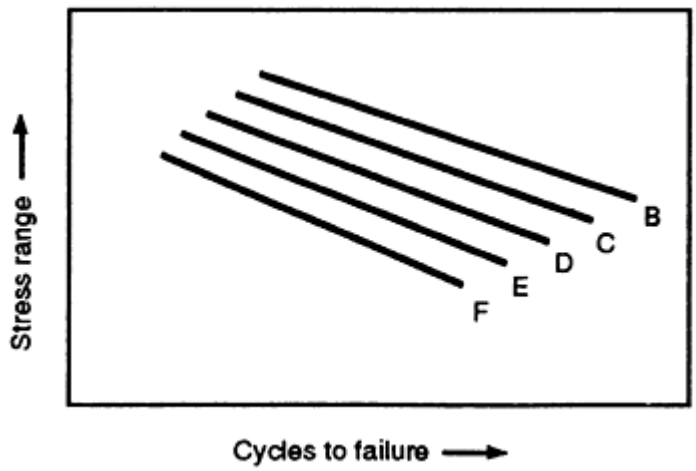

FIG. 8 SCHEMATIC OVERVIEW OF TYPICAL FATIGUE DESIGN RULES

Although the exact classification system can vary from code to code, the general approach is consistent. Most codes adopt a weld joint classification system that uses letters to denote different classes. In the original fatigue design rules proposed by Gurney, the following nine weld joint classifications were adopted: A, B, C, D, E, F, F2, G, and W; where class A is the parent material *S-N* curve obtained from uniform, machined, and polished specimens; class W is the welded joint *S-N* curve based on nominal shear stress on the minimum weld throat area; and classes B through G are the welded joint *S-N* curves for joints of decreasing fatigue performance.

S-N curves are used in design either to determine the maximum allowable cyclic stress for a given fatigue design life or to estimate design life for a given set of operating conditions.

Fracture-Mechanics Assessment Procedures. As already mentioned, the majority of the fatigue life of a welded joint is spent in the crack-propagation phase. Consequently, the analysis of fatigue cracking in welded joints is well suited to fracture mechanics, which can be used to predict the fatigue strength of nominally sound welds by considering the propagation of a fatigue crack from the inherent discontinuities that exist at the weld toe and the weld root. Fracture mechanics also can be used to predict the life of a joint with a weld discontinuity. The most widely accepted fatigue crack growth relationship is the Paris law (Ref 15), which can be expressed as:

$$\frac{da}{dN} = C(\Delta K)^m \qquad \textbf{(EQ 3)}$$

where ΔK is the applied stress-intensity factor range, a is the crack size, N is the number of cycles, and C and m are constants that depend on the material and environment.

Maddox (Ref 16) has carried out a series of fatigue crack propagation tests on various parent steels, weld metals, and heat-affected zone (HAZ) microstructures. He found that there was no significant variation in crack-propagation rates among any of the materials tested. The upper-bound crack-growth rate constants for ferritic steels operating in nonaggressive environments are given by:

$$C = 3.0 \times 10^{-13} \text{ AND } M = 3.0 \qquad \textbf{(EQ 4)}$$

For structural ferritic steels operating in marine environments up to 20 °C (68 °F), the following crack-growth constants can be used:

$$C = 2.3 \times 10^{-13} \text{ AND } M = 3.0 \qquad \textbf{(EQ 5)}$$

For design purposes, it is sometimes necessary to estimate the limiting flaw size that will not extend by fatigue during service. The limiting crack size, below which fatigue crack growth will not occur, can be calculated using fatigue-threshold concepts. The following threshold stress-intensity factor ranges have been proposed for carbon and carbon-manganese steels operating in air or seawater environments (Ref 1, 2):

$$\Delta K_0 = 5.44 - 6.85R \text{ MPA } \sqrt{m} \text{ FOR } 0 \le R \le 0.5$$
$$K_0 = 63 \text{ N}\sqrt{mm} \text{ FOR } 0.5 \le R \qquad \textbf{(EQ 6)}$$

where R is the stress ratio (that is, minimum stress divided by maximum stress). It should be noted that welding residual stresses must be taken into account when calculating the stress ratio. Using the above expressions, it is possible to calculate the limiting flaw size that will not extend by fatigue during service.

Fracture mechanics-based fatigue-assessment procedures can also be used to define inspection criteria and, in particular, inspection intervals. This is achieved by assuming the maximum flaw size that may escape detection and by specifying a critical crack size that should be detected to avoid unnecessary damage to the structure or the risk of failure. Using fracture mechanics-based fatigue crack growth procedures, the user can determine the number of cycles (or time) needed for the crack to extend from the initial size to the critical size.

The time for the crack to extend from its initial size to the critical size represents the maximum inspection interval (that is, if an inspection is not performed during this period, the structure could conceivably fail without any obvious warning). To guard against premature failure, it is normal practice to set inspection intervals that are considerably less than the maximum inspection interval. This will enable the operator to determine if cracks have initiated or extended during service before they have the potential of reaching a critical size.

After inspecting the component and sizing any defects/cracks that are present, the operator can determine a new maximum inspection interval for the component by calculating the time needed for the current cracks to extend to a critical size. Using this approach, an operator may specify decreasing inspection intervals for a component that is experiencing in-service cracking. Another reason for specifying inspection intervals that are considerably less than the

maximum inspection interval is that it provides the operator with an opportunity to evaluate the validity of the assessment and the initial assumptions.

References cited in this section

1. "GUIDANCE ON SOME METHODS FOR THE DERIVATION OF ACCEPTANCE LEVELS FOR DEFECTS IN FUSION WELDED JOINTS," PD 6493, BRITISH STANDARDS INSTITUTION, 1991
2. F.M. BURDEKIN, "FINAL REPORT ON QUESTIONNAIRE ON THE USE OF FRACTURE MECHANICS METHODS FOR THE ASSESSMENT OF THE SIGNIFICANCE OF WELD DEFECTS," DOCUMENT X-1076-84, IIW, 1984
6. E.J. SIGNES, R.G. BAKER, J.D. HARRISON, AND F.M. BURDEKIN, FACTORS AFFECTING THE FATIGUE STRENGTH OF WELDED HIGH STRENGTH STEELS, *BR. WELD. J.*, VOL 14 (NO. 3), 1967, P 108-116
7. S. BERGE, O.I. EIDE, AND E.T. MOE, FATIGUE CRACK INITIATION IN WELDMENTS OF A CARBON-MANGANESE STEEL, *PROC. EUROPEAN OFFSHORE STEELS RESEARCH SEMINAR,* (CAMBRIDGE, U.K.), PAPER 6, 1978
8. F.C. SMITH AND R.A. SMITH, DEFECTS AND CRACK SHAPE DEVELOPMENT IN FILLET WELDED JOINTS, *FATIGUE FRACT. ENG. MATER. STRUCT.,* VOL 5 (NO. 2), 1982, P 151-165
9. F. WATKINSON, P.H. BODGER, AND J.D. HARRISON, THE FATIGUE STRENGTH OF WELDED JOINTS IN HIGH STRENGTH STEELS AND METHODS FOR ITS IMPROVEMENT, *PROC. LNT. CONF. FATIGUE OF WELDED STRUCTURES,* THE WELDING INSTITUTE, 1971
10. T.R. GURNEY, FATIGUE DESIGN RULES FOR WELDED JOINTS, *WELD. INST. RES. BULL.,* VOL 17, MAY 1976, P 115-124
11. "SPECIFICATION FOR STEEL, CONCRETE AND COMPOSITE BRIDGES--CODE OF PRACTICE FOR FATIGUE," B5 5400, PART 10, BRITISH STANDARDS INSTITUTION, 1980
12. "SPECIFICATION FOR UNFIRED FUSION WELDED PRESSURE VESSELS--ENQUIRY CASE NO. 79," BS 5500 1988, BRITISH STANDARDS INSTITUTION
13. AWS STRUCTURAL WELDING CODE D1-1, 1992
14. AASHTO STANDARD SPECIFICATION FOR HIGHWAY BRIDGES, 13TH ED., 1983
15. P.C. PARIS AND F. ERDOGAN, A CRITICAL ANALYSIS OF CRACK PROPAGATION LAWS, *J. BASIS ENG.,* VOL 85, 1960, P 528-534
16. S.J. MADDOX, *WELD. RES. LNT.,* VOL 4 (NO. 1), 1974, P 36-60

Introduction

THE HEAT THAT IS SUPPLIED TO THE WORKPIECE, which then is transferred within the workpiece to produce melting, forms the basis of every welding process. The heat-transfer process, or thermal cycle, in the weldment has many consequences, including the complex metallurgical changes that take place in the fusion zone, where the metal is liquified and subsequently solidified, and in the adjacent heat-affected zone, where material is heated to temperatures that are below the melting point, but are sufficiently high to produce changes in the microstructure and in mechanical properties.

The description of the input-energy source is basic to any numerical modeling formulation designed to predict the outcome of the welding process. Both the magnitude and distribution of the source are fundamental and unique to each joining process, and the resultant output of any numerical model is therefore affected by the initial description of the heat source. An understanding of both the physics and the mathematical simulation of these sources is essential for characterizing the heat source. This article briefly reviews the physical phenomena that influence the input-energy distribution and discusses several simplified and detailed heat-source models that have been used in the modeling of arc welding, high-energy-density welding, and resistance welding processes.

Characterization and Modeling of the Heat Source

S.S. Glickstein and E. Friedman, Westinghouse Electric Corporation

Simplified Modeling of the Heat Source

Analytical modeling of the welding heat source is generally complex, because of the nature of energy transfer to the workpiece, whether the source of that energy is an arc, a high-energy-density beam of electrons or laser light, or joule heating. For numerical modeling purposes, heat input to the weldment is usually applied as a distribution of surface flux, a distribution of heat generated internally, or a combination of both. Many analytical treatments, however, have sought to simplify the characterization of the heat source by assuming that the effective thermal energy supplied by the heat source is deposited in such a narrow band of material that it may be idealized mathematically as a point or a line source, depending on the geometry of the weldment (Ref 1). Heat input idealizations of this sort lend themselves to the derivation of closed-form welding temperature solutions and the avoidance of developing numerical finite-element or finite-difference models to calculate temperatures. These solutions are valid only for simple geometries and in regions removed from the fusion and heat-affected zones, where details of the distribution of heat input from the source and accurate representations of the thermal energy transferred from the weld bead to the rest of the weld joint are not important.

The fundamental simplified heat-source model is developed for a flat plate of infinite extent bounded by the planes $z = 0$ and $z = h$. Heat is input at a point that is either stationary or is moving at uniform speed, v, in the x direction on the surface $z = 0$, so that at any time, t, the point source is located at $x = vt$ (Fig. 1). If the end effects that result from the initiation or termination of the heat source or the finite dimensions of the weldment are neglected, then the resulting temperature distribution associated with the moving source is stationary with respect to a moving coordinate system, the origin of which coincides with the point of application of the heat source. This class of temperature response is termed "quasi-stationary."

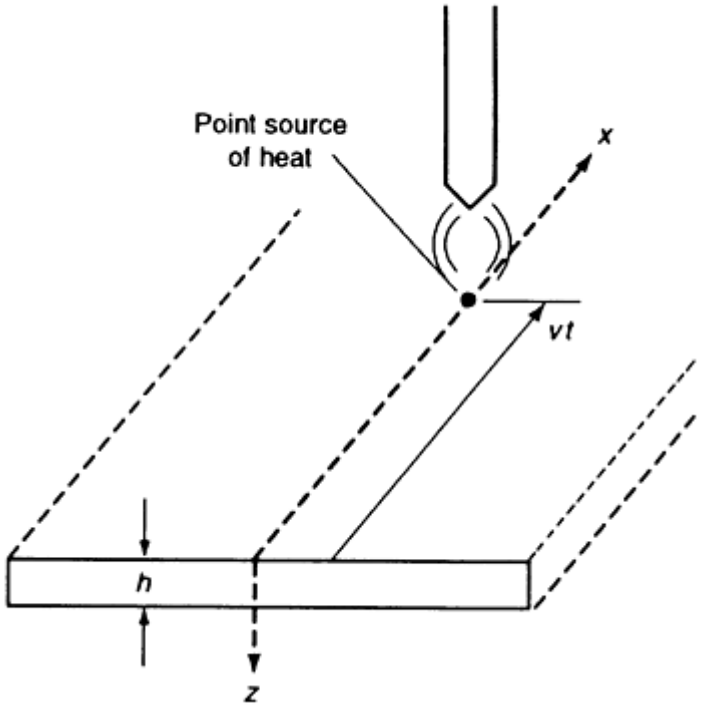

FIG. 1 MOVING POINT SOURCE IN INFINITE PLATE

In general, for either a stationary or a moving point source, heat is conducted through the plate without hindrance until the insulating effect of the ideally adiabatic surface at $z = h$ is felt. For a sufficiently thick plate, the temperature rise at $z = h$ is so small that the solution for an infinitely thick plate, which is associated with a single source of heat, is applicable. For a moderately thick plate, the temperature rise at $z = h$ from the infinitely thick plate point source solution is large enough to result in nonzero heat flow at $z = h$. An image source of the same strength applied at $z = 2h$ ensures that the surface $z = h$ is adiabatic. However, the image source produces nonzero heat flow at $z = 0$, and another image source applied at $z = -2h$ is now required to satisfy conditions at $z = 0$.

Carrying this imposition of image point sources of heat along ad infinitum (Fig. 2), an infinite distribution of image sources superposed with the original source at $z = 0$ yields the desired adiabatic conditions at both the $z = 0$ and $z = h$ surfaces. The temperature solution for this series of image sources is in the form of an infinite series (Ref 2), which converges more rapidly for thicker plates. The solution for the moderately thick plate applies to thin plates as well, but convergence of the infinite series would be extremely slow. As an alternative, the heat source can be applied as a line source distributed uniformly through the thickness (Ref 3). This approach eliminates any variation of the temperature distribution through the thickness, and is often used to model high-energy-density welding processes that result in the formation of a keyhole, as will be discussed later.

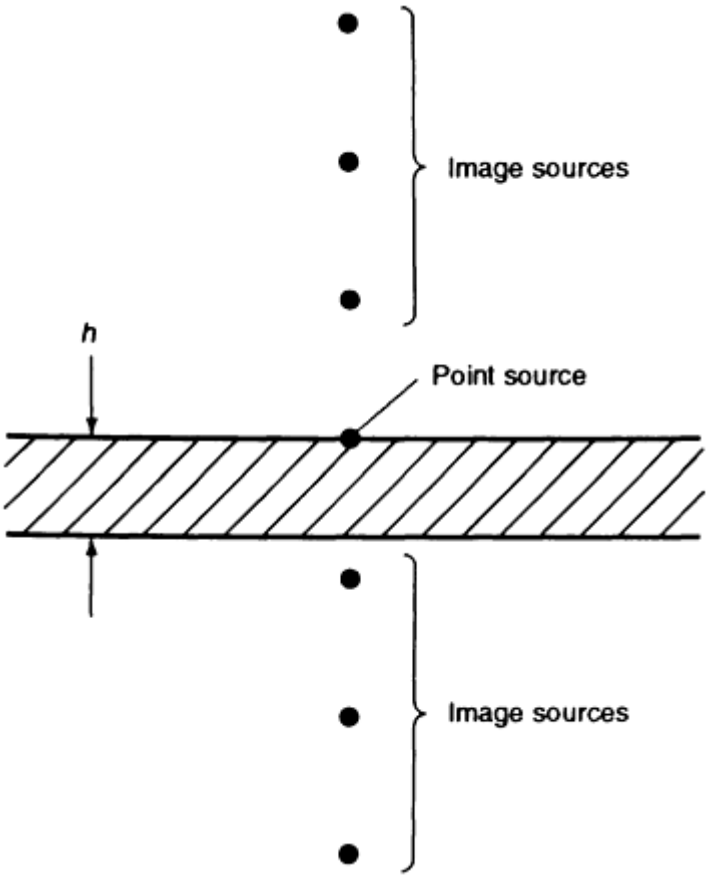

FIG. 2 SUPERPOSITION OF IMAGE SOURCES IN FINITE-THICKNESS PLATE

Offshoots of these cases also have been developed. These include considerations of plates of finite width, in which case sets of image sources are needed to ensure adiabatic conditions at the edges (Ref 4); line sources of heat traveling on a circular path (Ref 5); and conditions that simulate either initiation or termination of the heat source (Ref 6). Variations of the moving point source approach have been employed (Ref 7) to calculate the temperatures needed for weld-induced residual stress calculations in piping.

References cited in this section

1. P.S. MYERS, O.A. UYEHARA, AND G.L. BORMAN, FUNDAMENTALS OF HEAT FLOW IN WELDING, *WELD. RES. COUNC. BULL.,* NO. 123, JULY 1967
2. H.S. CARSLAW AND J.C. JAEGER, *CONDUCTION OF HEAT IN SOLIDS,* CLARENDON PRESS, LONDON, 1959
3. D. ROSENTHAL AND R. SCHMERBER, THERMAL STUDY OF ARC WELDING, *WELD J. RES. SUPPL.,* VOL 17 (NO. 4), 1938, P 2S-8S
4. D. ROSENTHAL, THE THEORY OF MOVING SOURCES OF HEAT AND ITS APPLICATION TO METAL TREATMENTS, *TRANS. ASME.,* VOL 68, 1946, P 849-866
5. W. SOEDEL AND R. COHEN, ARC-WELDING TEMPERATURES IN A CIRCULAR DISK STRUCTURE, *WELD. J. RES. SUPPL.,* VOL 49 (NO. 7), 1970, P 337S-340S
6. T. NAKA AND K. MASUBUCHI, TEMPERATURE DISTRIBUTION OF WELDED PLATES, *J. JPN. WELD. SOC.,* VOL 16 (NO. 7 AND 12), 1947, P 281-290 (PART 1) AND P 374-378 (PART II)
7. E.F. RYBICKI *ET AL.,* A FINITE-ELEMENT MODEL FOR RESIDUAL STRESSES AND DEFLECTIONS IN GIRTH-BUTT WELDED PIPES, *J. PRESSURE VESSEL TECHNOL. (TRANS. ASME),*

VOL 100, AUG 1978, P 256-262

Characterization and Modeling of the Heat Source

S.S. Glickstein and E. Friedman, Westinghouse Electric Corporation

Arc Welding

Gas-tungsten arc welding (GTAW) is the most frequently modeled arc-welding process in which the heat source is a nonconsumable electrode. In the direct current electrode negative GTAW process, the pieces of material are joined together by energy that is transferred to the workpiece by four primary mechanisms (Ref 8):

- KINETIC ENERGY OF THE ELECTRONS THAT CONSTITUTE THE ARC CURRENT
- HEAT OF CONDENSATION OF THE ELECTRONS (WORK FUNCTION) PENETRATING THE SOLID WORK SURFACE
- RADIATION FROM THE ARC
- THERMAL CONDUCTION FROM THE ARC PLASMA TO THE WORKPIECE

The first two mechanisms constitute the major source of energy to the weldment (Ref 9).

Because of the complicated nature in which energy is transferred from the arc, heat input to the weldment can be modeled by one of the point- or line-source approaches discussed in the preceding section of this article. If none of these treatments is appropriate for the particular application, then a more realistic approach is to input the energy by a distribution of surface flux, a distribution of heat generated internally, or a combination of the two. If an internal heat distribution is confined to a thin layer of material adjacent to the heated surface, then the choice of heat-input model is immaterial (Ref 10). The magnitude of heat input to the workpiece is expressed simply as the product of what has traditionally been defined as the arc power (that is, the product of the voltage drop across the arc and the arc current) and a factor called the arc efficiency, which accounts for energy losses from the arc.

Estimates of arc efficiency can be made by correlating computed temperatures with thermocouple readings from test welds, making calorimeter measurements for a specific set of welding conditions, or utilizing some other observable response to the welding thermal cycle. Because the voltage used is usually determined from measurements at some point within the power supply, estimates need to be made to account for losses within the electrode and other parts of the system (Ref 11). Changes in welding process variables, such as shielding gas, electrode configuration, arc gap, and minor element additions to the arc, all affect arc efficiency, as does the material that is being welded.

The magnitude of heat applied to the weldment surface is usually not known with great accuracy, and the distribution of the heat input is even more uncertain. Input-energy distribution depends on factors related to the electrode and the physics of the arc, as well as on the interaction of the arc with the molten weld pool. For example, the arc characteristics and the depth-to-width ratio of the weld puddle will change as the vertex angle of the conical tip of the electrode is altered (Fig. 3). As the arc becomes more constricted, the heat source becomes more concentrated, thus increasing weld penetration. Changes in heat-source distribution (that is, input current) will affect the electromagnetic forces in both the arc and the weld puddle, resulting in changes in weld-puddle motion, which can promote alterations in convection heat transfer within the weld puddle. Shielding gas composition and minor alloying elements also can influence the distribution of input energy.

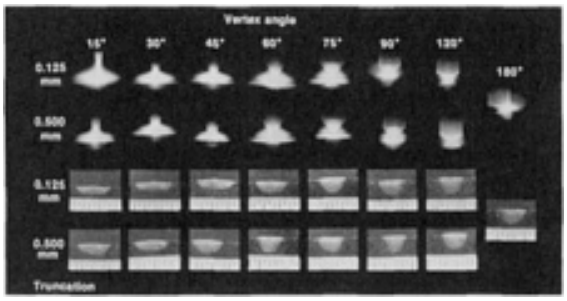

FIG. 3 ARC SHAPE AND WELD-BEAD GEOMETRY AS A FUNCTION OF ELECTRODE TIP ANGLE IN A PURE ARGON SHIELD FOR 2.38 MM (0.10 IN.) DIAMETER ELECTRODES TRUNCATED TO 0.125 AND 0.500 MM (0.005 AND 0.2 IN.); ARC GAP, 1 MM (0.04 IN.). SOURCE: REF 12

When welding at low currents and high voltages, the perturbation of the weld-puddle surface may be considered to have a small effect on the heat-input distribution, and a model that considers heat to be applied as a surface flux is usually satisfactory. However, as the current increases (particularly when the arc voltage is small, indicating a short electrode-to-work surface distance), the arc jet can depress the weld-puddle surface and affect the configuration of the distribution on the surface of the weldment (Fig. 4). The effects of depressing the weld puddle can be accommodated empirically by postulating some or all of the heat from the arc to be deposited internally. However, the specification of an internal heat-generation distribution is more complex than that of a surface flux.

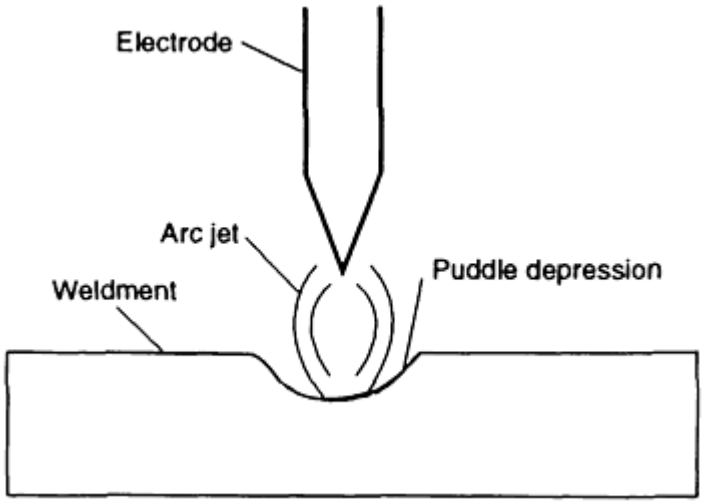

FIG. 4 EFFECT OF ARC JET ON DEPRESSION OF WELD POOL

For models in which heat from the welding arc is postulated to be deposited on the surface of the weldment, the input energy is often assumed to be a radially symmetric, normally distributed surface flux at any instant in time (Ref 13). The incident heat flux, *q,* can be expressed conveniently as an exponential, or Gaussian, function such that:

$$Q\,(R) = (3Q/\pi R'^2)\ \mathrm{EXP}[-\,3(R/R')^2] \qquad \textbf{(EQ 1)}$$

where Q is the magnitude of the heat input per unit time, r is the distance from the center of the heat source to the surface, and r' is a characteristic radial dimensional distribution parameter that defines the region in which 95% of the heat flux is deposited. In the limit as $r' \rightarrow 0$, the heat input becomes a point source of strength Q on the surface. The applicability of point sources to characterize energy input for laser-beam welding processes will be explored later in this article.

Equation 1 describes the heat-input distribution from a stationary arc. Only the magnitude of the heat input, the distribution parameter, and the duration of heating are necessary to fully characterize the input energy. Figure 5 shows typical variations of the weld bead depth and width for stationary spot welds on 6.5 mm (0.25 in.) thick plates with both the distribution parameter, *r*', and the duration of heating, *t**.

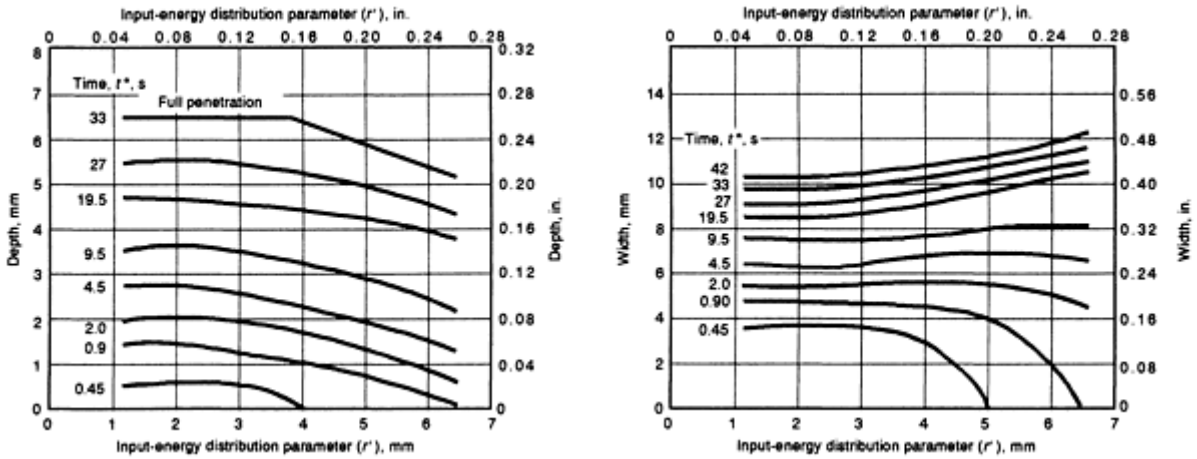

FIG. 5 WELD-BEAD DIMENSIONS FOR DIFFERENT DURATIONS OF HEATING, *T, AND INPUT-ENERGY DISTRIBUTION PARAMETER, *R*'. Q_O = 1060 W. SOURCE: REF 10**

Other forms of the heat-input distribution also can be used. These include ramp, or triangular, distributions; uniform heat-input distributions over finite areas (for example, the area of the weld puddle surface); or combinations of the two (that is, trapezoidal distributions).

The axisymmetric characterization of heat input for stationary arcs enables temperatures in the weldment to be calculated using axisymmetric thermal analysis methods, if the weldment geometry justifies such an analysis. On the other hand, if the heat source is moving, then the resultant flow of heat is three-dimensional, that is, temperature gradients develop through the thickness of the weldment, as well as in directions parallel to and transverse to the welding direction. If the weldment geometry is regular (for example, flat plate), then the heat source from the arc is moving at a constant, sufficiently high speed, *v*, and if end effects such as the starting and stopping of the arc are neglected, then transient two-dimensional thermal analyses at cross sections normal to the welding direction may be satisfactory (Ref 14). The heat input at a section transverse to the direction of arc travel is given by:

$$Q\,(X,T) = (3Q/\pi R'^2)\ \mathrm{EXP}[-3(X/R')^2]\ \mathrm{EXP}[-3(VT/R')^2] \qquad \textbf{(EQ 2)}$$

where *x* is the distance from the centerline of the weld and *t* is the time measured from the moment the center of the heat source passes over the weld section being analyzed. The three heat-input parameters characterizing a moving arc (*Q*,*r*',*v*) are embodied in this formulation. The inverse of the speed of a moving arc is akin to the duration, *t**, of a stationary arc, because a moving arc supplies a heat input, *Q*/*v*, per unit length of weld, whereas a stationary arc provides a total amount of heat, *Qt**, to the weldment.

For models in which heat is deposited internally, rather than as a surface flux, the input energy can be assumed to be deposited within a spheroidal or ellipsoidal region that is similar in shape to the weld puddle. As described by Ref 15, the heat input can be taken to vary exponentially as a Gaussian distribution in all directions within the ellipsoid. Thus, the energy-input distribution is completely specified by the dimensions of the ellipsoid. More elaborate models can be formulated by prescribing either double-ellipsoid heat-input regions that better match weld-puddle shape or conical regions of internal energy deposition. Regardless of the methodology chosen to characterize the distribution of the heat input, the geometric parameters of the distribution should be established, at this stage of computer-modeling development, by correlating calculated thermal-response characteristics, such as the weld bead and heat-affected zone dimensions, with measured values.

Gas-metal arc welding (GMAW) modeling is more complex than that of the GTAW process, because of the need to consider thermal energy that is transferred to the workpiece not only by mechanisms similar to those associated with the GTAW process, but, more importantly, by heat contained in the molten metal drops that are transferred as filler metal from the consumable electrode wire to the workpiece. Refer to Ref 16 for additional details. Because the GMAW process utilizes direct current electrode positive, the heat associated with the kinetic energy of the electrons and the heat of condensation is now input to the electrode. The energy previously input to the weldment is replaced by the energy of positively charged ions, which contribute a much smaller amount of heat to the weldment.

In addition, the radiation and conduction via the arc plasma make minor contributions to the heat input to the weldment. The more-important source of heat is derived from the mass of molten material and is related directly to both the temperature and the melting rate of the electrode wire. The melting rate of the electrode is governed primarily by joule heating and by arc heating similar to that of the GTAW process. The transfer of material to the workpiece can be globular, such that the metal is deposited in droplets, the diameters of which are greater than that of the electrode, or in a spray, in which mass is transferred to the weld puddle as droplets with diameters that are smaller than that of the electrode.

The thermal energy applied to the workpiece therefore consists of two sources: the arc-energy distribution generated at the cathode area (workpiece) and the thermal energy of the metal drops transferred from the filler wire. The arc input energy has a significant effect on the width of the weld puddle and, thus, of the solidified weld bead, whereas the energy in the molten metal contributes significantly to the melting of the workpiece (Ref 17). Furthermore, the impingement of the metal drops on the puddle significantly affects the depth of penetration (Ref 18), because the impact of each drop causes a distinct indentation in the weld puddle, especially at high currents.

Modeling of the heat input from the GMAW process should generally include the effects of heat input from the filler-metal droplets, the addition of new weld material from the filler wire, and, in many cases, the significant indentation of the weld-puddle surface, as well as a spatially distributed heat flux on the surface to represent radiation energy from the arc and positive ion impingement. Accurate representations of these phenomena are so complex that alternate treatments are essential. In Ref 19, the heat input from the GMAW process was modeled as a Gaussian distribution and accounted for the energy necessary to melt the electrode wire. In Ref 20, a model in which heat is input partly in the weld puddle and partly as a surface flux was developed. A more common approach is to model the addition of filler metal by "creating" new metal in an analytical model.

In finite-element treatments, for example, new metal is simulated by adding sets of elements to the model. For three-dimensional models, these elements can be introduced in distinct increments of time, whereas for a two-dimensional analysis of a cross section normal to the welding direction, a set of elements corresponding to a weld bead cross section can be created. More recently, the contour outlining the weld bead has been determined experimentally and then used as the starting boundary condition for the thermal modeling of welds. As an example, the boundary condition can be a time-dependent temperature that may reach or exceed the melting temperature of the material.

Other Arc-Welding Processes. Shielded metal arc welding (SMAW), submerged arc welding (SAW), and flux-cored arc welding (FCAW) are other processes in which energy is transferred to the workpiece both from the arc and from an overheated consumable electrode. The previously outlined semiempirical methodology for simulating the heat input for the GMAW process also appears to be well suited for the flux welding processes, although the introduction of a slag layer, whether it develops from the melting and solidification of electrode-covering material or from a flux feeding tube, presents another factor to be considered when calculating weld-induced temperatures.

References cited in this section

8. P.A. SCHOECK, AN INVESTIGATION OF THE ANODE ENERGY BALANCE OF HIGH INTENSITY ARCS IN ARGON, *MODERN DEVELOPMENTS IN HEAT TRANSFER,* ACADEMIC PRESS, 1963, P 353-400
9. M.B.C. QUIGLEY, P.H. RICHARDS, D.T. SWIFT-HOOK, AND A.E.F. GICK, HEAT FLOW TO THE WORKPIECE FROM A TIG WELDING ARC, *J. PHYS. D: APPL. PHYS.,* VOL 6, DEC 1973, P 2250-2259
10. E. FRIEDMAN AND S.S. GLICKSTEIN, AN INVESTIGATION OF THE THERMAL RESPONSE OF STATIONARY GAS TUNGSTEN-ARC WELDS, *WELD. J. RES. SUPPL.,* VOL 55 (NO. 12), DEC 1976, P 408S-420S

11. R.A. CHIHOSKI, THE RATIONING OF POWER BETWEEN THE GAS TUNGSTEN ARC AND ELECTRODE, *WELD. J. RES. SUPPL.,* VOL 49 (NO. 2), FEB 1970, P 69S-82S
12. J.F. KEY, ANODE/CATHODE GEOMETRY AND SHIELDING GAS INTERRELATIONSHIPS IN GTAW, *WELD. J. RES. SUPPL.,* DEC 1980, P 364-S
13. V. PAVELIC, R. TANBAKUCHI, O.A. UYEHARA, AND P.S. MYERS, EXPERIMENTAL AND COMPUTED TEMPERATURE HISTORIES IN GAS TUNGSTEN-ARC WELDING OF THIN PLATES, *WELD. J. RES. SUPPL.,* VOL 48 (NO. 7), 1969, P 295S-305S
14. E. FRIEDMAN, THERMOMECHANICAL ANALYSIS OF THE WELDING PROCESS USING THE FINITE ELEMENT METHOD, *J. PRESSURE VESSEL TECHNOL. (TRANS. ASME),* VOL 97, AUG 1975, P 206-213
15. J. GOLDAK *ET AL.,* COMPUTER MODELING OF HEAT FLOW IN WELDS, *METALL. TRANS. B,* VOL 17, SEPT 1986, P 587-600
16. J.H. WASZINK AND G.J.P.M. VAN DEN HEUVAL, HEAT GENERATION AND HEAT FLOW IN THE FILLER METAL IN GMA WELDING, *WELD. J. RES. SUPPL.,* VOL 61, AUG 1982, P 269S-282S
17. W.G. ESSERS AND R. WALTER, HEAT TRANSFER AND PENETRATION MECHANISMS WITH GMA AND PLASMA-GMA WELDING, *WELD. J. RES. SUPPL.,* VOL 60, FEB 1981, P 37S-42S
18. K.C. TSAO AND C.S. WU, FLUID FLOW AND HEAT TRANSFER IN GMA WELD POOLS, *WELD. J. RES. SUPPL.,* VOL 67, MAR 1988, P 70S-75S
19. P. TEKRIWAL AND J. MAZUMDER, FINITE ELEMENT ANALYSIS OF THREE-DIMENSIONAL TRANSIENT HEAT TRANSFER IN GMA WELDING, *WELD. J. RES. SUPPL.,* VOL 67 (NO. 7), 1988, P 150S-156S
20. B.L. JOSEFSON, RESIDUAL STRESSES AND THEIR REDISTRIBUTION DURING ANNEALING OF A GIRTH-BUTT WELDED THIN-WALLED PIPE, *J. PRESSURE VESSEL TECHNOL. (TRANS. ASME),* VOL 104, AUG 1982, P 245-250

Characterization and Modeling of the Heat Source

S.S. Glickstein and E. Friedman, Westinghouse Electric Corporation

High-Energy-Density Welding

In modeling the heat source for high-energy-density welding, one first needs to determine the type of welding process being formulated. Depending on the weld parameters, high-energy-density welding can simulate either a conduction-mode weld process or a keyhole weld process. If a strict conduction-mode weld process is being modeled, then the energy density will be low enough to prevent intense vaporization of the material. All of the energy of the beam is deposited directly on the surface of the weldment as a heat flux, similar to that discussed in terms of the GTAW process. The major difference between this mode of welding and that of arc welding is in the magnitude and distribution of the heat source. In laser-beam welding, the input-energy distribution is very dependent on the operational mode of the laser system.

Figure 6 shows several shapes of the source distribution that can be present at any one time. The fundamental transverse electromagnetic mode, TEM_{00} (a Gaussian distribution), is often selected as the heat-input description for conduction welding. It is also assumed to be the source distribution for electron-beam welding. The exact determination of the Gaussian width parameter, r', depends on the optics of the laser-or electron-beam welding system. In many cases, a point source on the surface is an excellent approximation. In laser-beam welding, if the energy is delivered via a fiber-optic system, then the output source distribution is often described as a truncated Gaussian source distribution of specified width. However, the beam exiting a fiber-optic system has been examined (Ref 21), and the output-energy distribution is reported to depend on the incident angle of the beam into the fiber. A variety of output configurations can be obtained as a function of the angle.

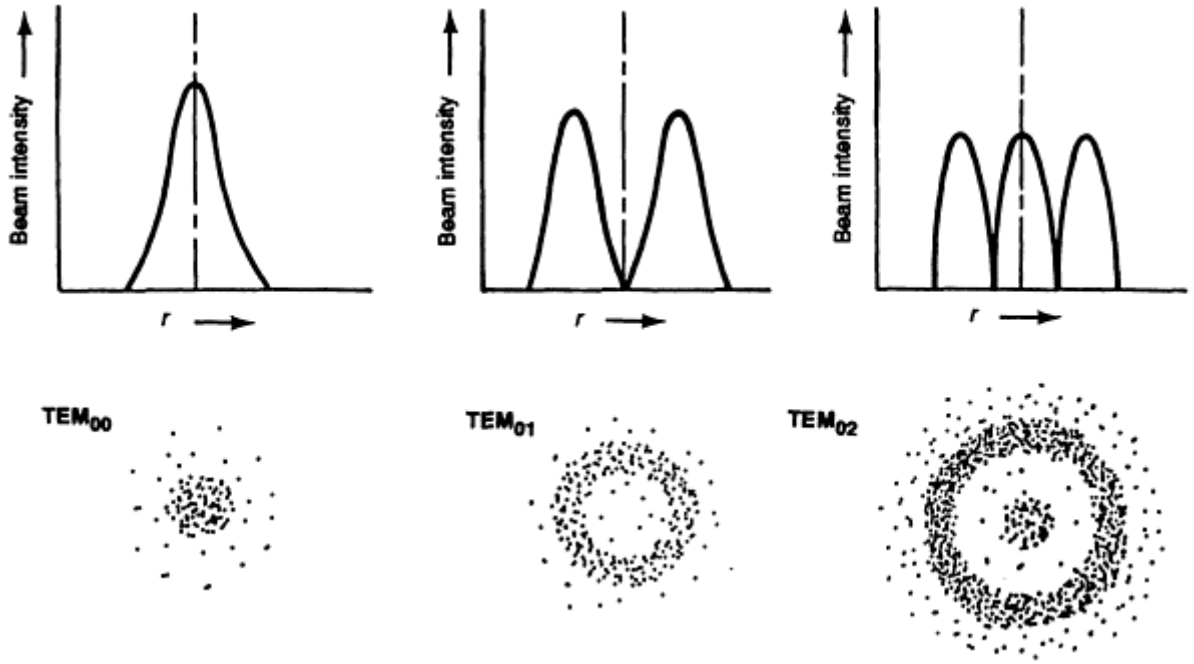

FIG. 6 APPEARANCE OF LASER BEAM FOR THREE DIFFERENT TRANSVERSE ELECTROMAGNETIC MODES (TEM). HORIZONTAL AXIS SHOWS INCREASING DISTANCE FROM THE CENTER OF THE HEAT SOURCE TO THE SURFACE.

Some laser systems, such as the multikilowatt carbon-dioxide laser, operate with the TEM_{01} as the dominant mode. This donut shape (Fig. 6) has been used very effectively for specific welding operations. Other laser systems may display a combination of these modes (for example, TEM_{02}), as well as higher-order modes. Beam analyzers are currently being employed to measure the precise distribution of the laser input energy to the weldment.

If a keyhole mode of welding is being formulated, then modeling of the input-energy distribution is complicated. Several different formulations have been discussed in the literature. In the keyhole mode, the energy density is sufficiently high to cause material ablation near the center of the beam, resulting in beam penetration further into the weldment. A hole created in the maternal is maintained by equilibrium between vapor pressure in the keyhole, surface tension, and hydrodynamic pressure in the surrounding melt. The exact distribution of energy deposited in the hole is complicated and depends on the scattering and absorption of the beam through the weldment, as well as on the focal parameters of the system. Several different models have been used to simulate these conditions.

The simplest model for the keyhole mode of welding is that of a moving line source through the weldment (Ref 22). The appropriate solution of the heat equation was obtained by Rosenthal (Ref 23). The model does not describe the typically observed semicircular part of the weld cross section at the top, because it corresponds to a liquid region, the size of which does not vary through the thickness of the workpiece. This simple model has been found to be very useful, however, in providing relations between such quantities as the power absorbed and the width of the weld.

A thermal analysis of the laser process has been derived for a Gaussian source moving at a constant velocity over a large range of conditions, from simple heat treating to deep-penetration welding (Ref 24). To obtain a more realistic weld shape, the simple line-source approach was modified (Ref 25) by adding a point source close to the surface of the workpiece to the line source distributed uniformly through the thickness. The line-source models uniform absorption of heat by the workpiece with depth, whereas the point source corresponds to a much more concentrated region of absorption in the vicinity of the laser focus, which contrasts with the absorption from multiple reflections that occur in the main part of the keyhole. The temperature distribution from this combined-source model yields a vertical weld seam shape that reflects the general shape of that found from experimental investigations (Fig. 7).

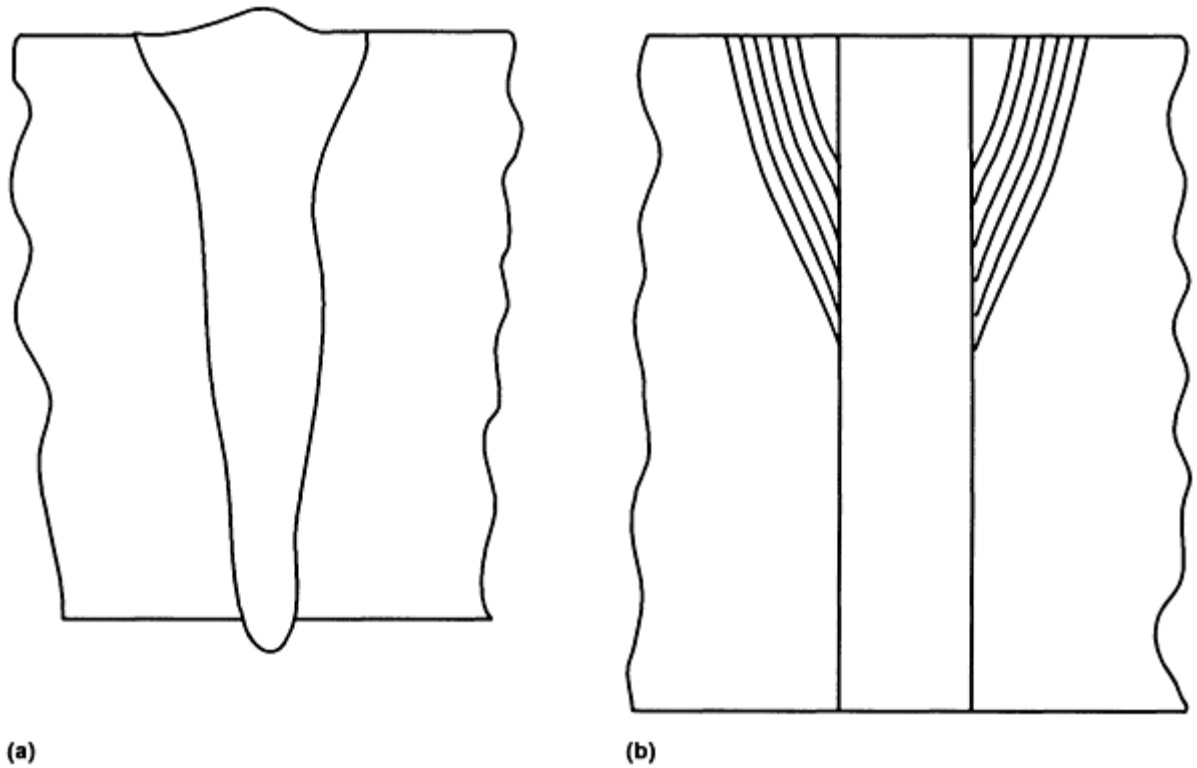

FIG. 7 OUTLINES OF CROSS SECTIONS OF (A) EXPERIMENTAL AND (B) CALCULATED KEYHOLE WELDS. CALCULATED RESULTS SHOWN FOR SEVERAL DIFFERENT POINT SOURCES ADDED TO THE LINE SOURCE. SOURCE: REF 25

A simple description of the input energy avoids the problem of defining the exact nature of the energy-transfer process in the keyhole itself. A more sophisticated model is necessary to characterize this effect. The attenuation of the laser beam in the vertical direction has been accounted for (Ref 26) by calculating the temperature at a depth, *d*, below the surface. If the temperature at depth, *d*, exceeds the boiling point of the material, then point *d* is deemed to be transparent. The incident power is then applied at a point below it, after suffering some absorption. This sequence continues through the substrate. The transparent grid points keep their high temperatures as if the keyhole were filled with a hot plasma.

This brief overview of several of the approaches used to model the high-energy-density welding process points out the difficulty in defining a unique methodology. Experimental data must be used for specific welding conditions to establish the overall approach, as well as the magnitude and distribution of the input source energy.

References cited in this section

21. Y. LIU AND K.H. LEONG, LASER BEAM DIAGNOSTICS FOR KILOWATT POWER PULSED YAG LASER, *PROC. LASER MATERIALS PROCESSING*, INTERNATIONAL CONGRESS ON APPLICATION OF LASERS AND ELECTRO-OPTICS '92, VOL 72, LASER INSTITUTE OF AMERICA, 1992
22. D.T. SWIFT-HOOK AND A.E.F. GICK, PENETRATION WELDING WITH LASERS--ANALYTICAL STUDY INDICATES THAT PRESENT LASER BEAM WELDING CAPABILITIES MAY BE EXTENDED TENFOLD, *WELD. J. RES. SUPPL.*, VOL 52, 1973, P 492S-499S
23. D. ROSENTHAL, MATHEMATICAL THEORY OF HEAT DISTRIBUTION DURING WELDING AND CUTTING, *WELD. J. RES. SUPPL.*, VOL 20, 1941, P 220S-234S
24. H.E. CLINE AND T.R. ANTHONY, HEAT TREATING AND MELTING MATERIAL WITH A SCANNING LASER OR ELECTRON BEAM, *J. APPL. PHYS.*, VOL 48 (NO. 9), 1977, P 3895

25. W.M. STEEN, J. DOWDEN, M. DAVIS, AND P. KAPADIA, A POINT AND LINE SOURCE MODEL OF LASER KEYHOLE WELDING, *J. PHYS. D: APPL. PHYS.*, VOL 21, 1988, P 1255-1260
26. J. MAZUMDER AND W.M. STEEN, HEAT TRANSFER MODEL FOR CW LASER MATERIAL PROCESSING, *J. APPL. PHYS.*, VOL 51 (NO. 2), 1980, P 941

Characterization and Modeling of the Heat Source

S.S. Glickstein and E. Friedman, Westinghouse Electric Corporation

Resistance Spot Welding

The electrical resistance spot welding process for joining two materials at their common interface involves a complicated interaction of electrical, thermal, mechanical, metallurgical, and surface phenomena. Figure 8, a simplified representation of the process, shows some essential features for producing a weld.

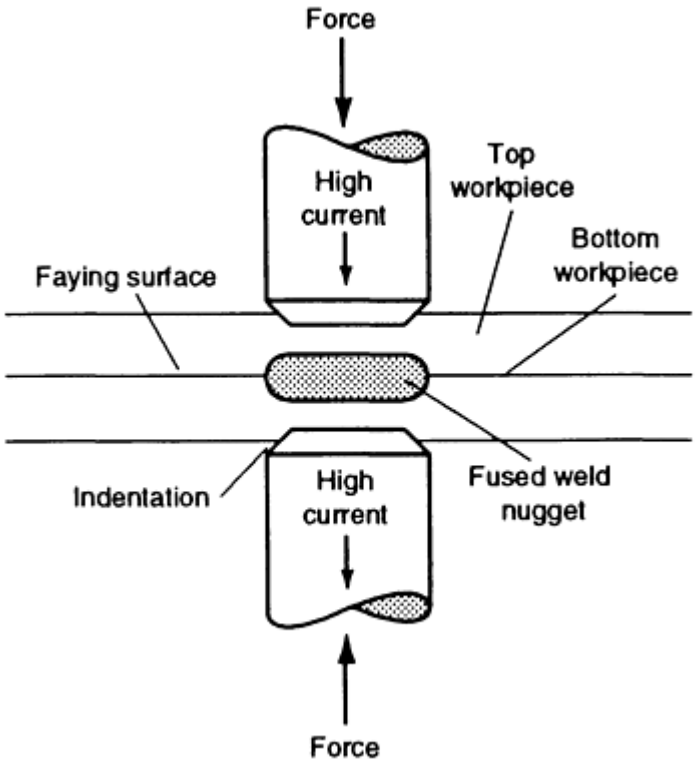

FIG. 8 RESISTANCE SPOT WELDING PROCESS

In this welding process, the faying surfaces of two or more workpieces are fused and joined at a spot by electric current flowing through the weldment (joule heating). The weldment is actually held together by the compressive force exerted by the electrodes. Because the input energy in this weld process is due to joule heating, the spatial distribution of the current and the electrical resistance within the workpiece must be determined when modeling the heat source. Most importantly, the contact resistance at the surfaces of both the electrode and the work-piece, as well as the interfaces of the work-pieces, must be established. The electrical contact resistance depends on the surface condition of the material, its hardness, the degree of oxidation, the amount and kind of impurities, as well as the apparent pressure at the surfaces and the temperature. The fact that these quantities are time dependent is another complication, because the joule heat source must be considered as a time-dependent parameter.

A detailed description of the process is presented in the article "Resistance Spot Welding" in this Volume. Literature reviews of the resistance spot welding process simulation are provided in Ref 27 and 28. The brief overview provided below of some important findings in the literature on resistance welding highlights several points that need to be considered when developing a model of the heat source.

In 1958, experimental and analytical investigations of the resistance spot welding process were performed (Ref 29). The researchers reported current-density singularities at the outer rim of the contact area from theory and correlated this phenomenon with experimental results that showed heat concentration at the periphery. They concluded that the bulk of the material near the contact region was not heated appreciably by the flow of current through it, but was heated indirectly by conduction from the peripheral region of the contact area. However, further study indicated that the contact area plays a major role only in the early stages of heat production and becomes less influential in later stages of weld-nugget formation. This fact reinforces the earlier remarks that the modeling of the heat source must consider not only the spatial distribution of the heat source, but its time dependence.

Further reinforcing this idea, it was found (Ref 30) that in the beginning of the welding process, most of the voltage drop occurred at the interface between the electrode and the weldment and in the interface of the two workpieces (21% and 66%, respectively). The researchers determined that after six cycles from the instant that weldment fusion begins, most of the voltage drop takes place in the base metal (87%). This occurs because the interfacial resistance decreases as the temperature rises, which is due to melting at the interface, and because the resistivity of the base metal increases with increased temperature.

Complicating the modeling process is the unknown, but very important, contact diameter at the faying surface. This parameter depends on the geometry of the electrodes, the surface conditions, and, most importantly, the mechanical load applied by the electrode. Recent work (Ref 28) in modeling this process uses the diameter of the electrode face as the contact diameter between the electrode and the workpiece, but a slightly larger diameter is used to represent the contact diameter at the interface of the work-pieces. Figures 9 and 10 show the current density and joule heating as functions of the nondimensional radius R/R_c, where R_c is the assumed contact radius.

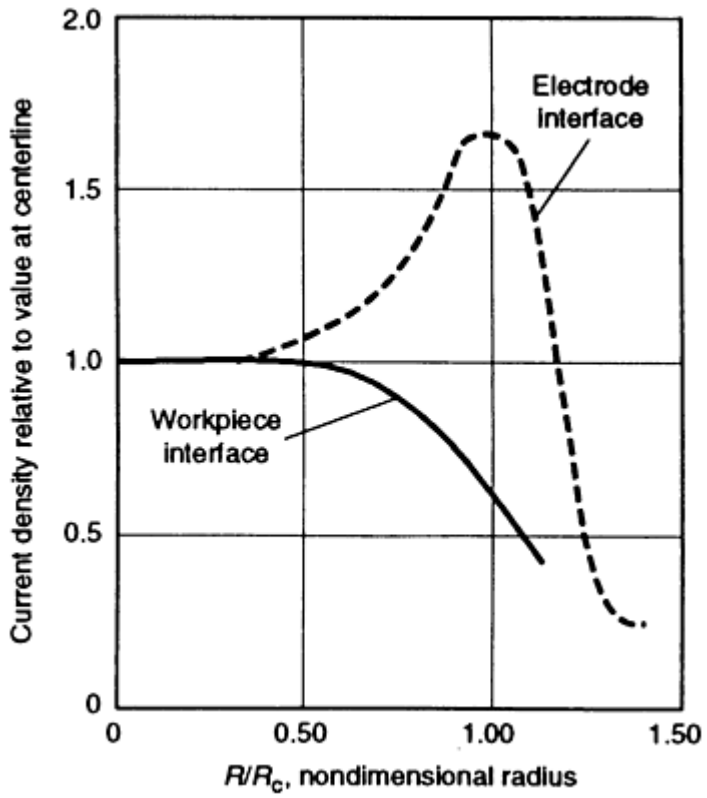

FIG. 9 CURRENT DENSITY RATIO VERSUS NONDIMENSIONAL RADIUS. TIME, 2 CYCLES; R_C, RADIUS OF CONTACT. SOURCE: REF 27

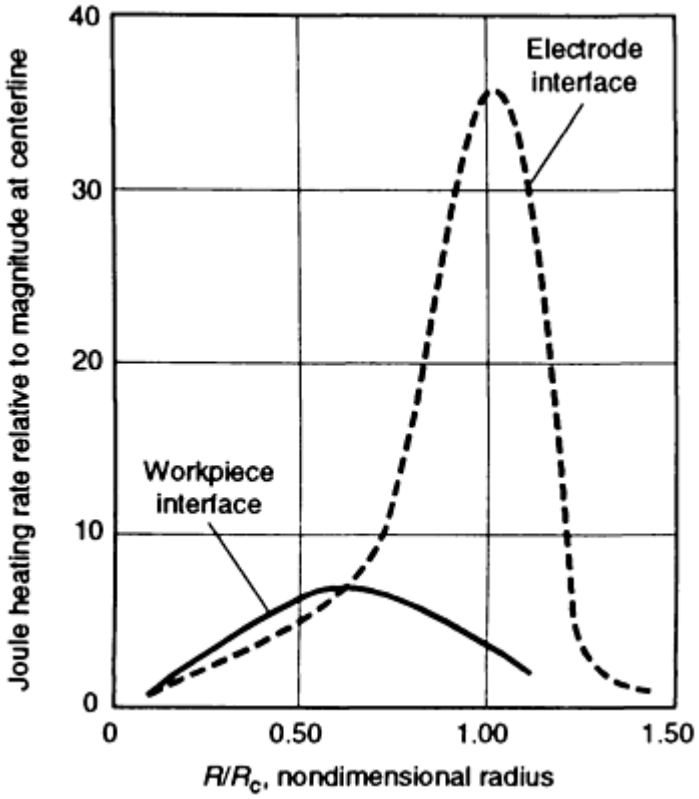

FIG. 10 JOULE HEATING RATE RATIO VERSUS NONDIMENSIONAL RADIUS. TIME, 2 CYCLES; R_C, RADIUS OF CONTACT. SOURCE: REF 27

The authors of both Ref 27 and 28 stress the importance of developing a thermomechanical coupling model that will account for changes in resistance and current distributions during the welding process. This article has tried to point out that the input description of the heat source for resistance welding is extremely complicated. It depends on the electrode geometry, the weldment material, and the weldment surface condition, as well as the weld parameters (including the mechanical forces on the electrode) that must be considered as being time dependent.

References cited in this section

27. H.A. NIED, THE FINITE ELEMENT MODELING OF THE RESISTANCE SPOT WELDING PROCESS, *WELD. J. RES. SUPPL.*, APRIL 1984, P 123-S
28. C.L. TSAI, O.A. JAMMAL, J.C. PAPRITAN, AND D.W. DICKINSON, MODELING OF RESISTANCE SPOT WELD NUGGET GROWTH, *WELD. J. RES. SUPPL.*, FEB 1992, P 47-S
29. J.A. GREENWOOD AND J.B.P. WILLIAMSON, ELECTRICAL CONDUCTION IN SOLIDS--II. THEORY OF TEMPERATURE-DEPENDENT CONDUCTORS, *PROC. ROYAL SOC. LONDON*, VOL 246, 1958, P 13-31
30. H.S. CHO AND Y.J. CHO, A STUDY OF THE THERMAL BEHAVIOR IN RESISTANCE SPOT WELDING, *WELD J. RES. SUPPL.*, JUNE 1989, P 236-S TO 244-S

Characterization and Modeling of the Heat Source

S.S. Glickstein and E. Friedman, Westinghouse Electric Corporation

References

1. P.S. MYERS, O.A. UYEHARA, AND G.L. BORMAN, FUNDAMENTALS OF HEAT FLOW IN WELDING, *WELD. RES. COUNC. BULL.,* NO. 123, JULY 1967
2. H.S. CARSLAW AND J.C. JAEGER, *CONDUCTION OF HEAT IN SOLIDS,* CLARENDON PRESS, LONDON, 1959
3. D. ROSENTHAL AND R. SCHMERBER, THERMAL STUDY OF ARC WELDING, *WELD J. RES. SUPPL.,* VOL 17 (NO. 4), 1938, P 2S-8S
4. D. ROSENTHAL, THE THEORY OF MOVING SOURCES OF HEAT AND ITS APPLICATION TO METAL TREATMENTS, *TRANS. ASME.,* VOL 68, 1946, P 849-866
5. W. SOEDEL AND R. COHEN, ARC-WELDING TEMPERATURES IN A CIRCULAR DISK STRUCTURE, *WELD. J. RES. SUPPL.,* VOL 49 (NO. 7), 1970, P 337S-340S
6. T. NAKA AND K. MASUBUCHI, TEMPERATURE DISTRIBUTION OF WELDED PLATES, *J. JPN. WELD. SOC.,* VOL 16 (NO. 7 AND 12), 1947, P 281-290 (PART 1) AND P 374-378 (PART II)
7. E.F. RYBICKI *ET AL.,* A FINITE-ELEMENT MODEL FOR RESIDUAL STRESSES AND DEFLECTIONS IN GIRTH-BUTT WELDED PIPES, *J. PRESSURE VESSEL TECHNOL. (TRANS. ASME),* VOL 100, AUG 1978, P 256-262
8. P.A. SCHOECK, AN INVESTIGATION OF THE ANODE ENERGY BALANCE OF HIGH INTENSITY ARCS IN ARGON, *MODERN DEVELOPMENTS IN HEAT TRANSFER,* ACADEMIC PRESS, 1963, P 353-400
9. M.B.C. QUIGLEY, P.H. RICHARDS, D.T. SWIFT-HOOK, AND A.E.F. GICK, HEAT FLOW TO THE WORKPIECE FROM A TIG WELDING ARC, *J. PHYS. D: APPL. PHYS.,* VOL 6, DEC 1973, P 2250-2259
10. E. FRIEDMAN AND S.S. GLICKSTEIN, AN INVESTIGATION OF THE THERMAL RESPONSE OF STATIONARY GAS TUNGSTEN-ARC WELDS, *WELD. J. RES. SUPPL.,* VOL 55 (NO. 12), DEC 1976, P 408S-420S
11. R.A. CHIHOSKI, THE RATIONING OF POWER BETWEEN THE GAS TUNGSTEN ARC AND ELECTRODE, *WELD. J. RES. SUPPL.,* VOL 49 (NO. 2), FEB 1970, P 69S-82S
12. J.F. KEY, ANODE/CATHODE GEOMETRY AND SHIELDING GAS INTERRELATIONSHIPS IN GTAW, *WELD. J. RES. SUPPL.,* DEC 1980, P 364-S
13. V. PAVELIC, R. TANBAKUCHI, O.A. UYEHARA, AND P.S. MYERS, EXPERIMENTAL AND COMPUTED TEMPERATURE HISTORIES IN GAS TUNGSTEN-ARC WELDING OF THIN PLATES, *WELD. J. RES. SUPPL.,* VOL 48 (NO. 7), 1969, P 295S-305S
14. E. FRIEDMAN, THERMOMECHANICAL ANALYSIS OF THE WELDING PROCESS USING THE FINITE ELEMENT METHOD, *J. PRESSURE VESSEL TECHNOL. (TRANS. ASME),* VOL 97, AUG 1975, P 206-213
15. J. GOLDAK *ET AL.,* COMPUTER MODELING OF HEAT FLOW IN WELDS, *METALL. TRANS. B,* VOL 17, SEPT 1986, P 587-600
16. J.H. WASZINK AND G.J.P.M. VAN DEN HEUVAL, HEAT GENERATION AND HEAT FLOW IN THE FILLER METAL IN GMA WELDING, *WELD. J. RES. SUPPL.,* VOL 61, AUG 1982, P 269S-282S
17. W.G. ESSERS AND R. WALTER, HEAT TRANSFER AND PENETRATION MECHANISMS WITH GMA AND PLASMA-GMA WELDING, *WELD. J. RES. SUPPL.,* VOL 60, FEB 1981, P 37S-42S
18. K.C. TSAO AND C.S. WU, FLUID FLOW AND HEAT TRANSFER IN GMA WELD POOLS, *WELD. J. RES. SUPPL.,* VOL 67, MAR 1988, P 70S-75S
19. P. TEKRIWAL AND J. MAZUMDER, FINITE ELEMENT ANALYSIS OF THREE-DIMENSIONAL TRANSIENT HEAT TRANSFER IN GMA WELDING, *WELD. J. RES. SUPPL.,* VOL 67 (NO. 7), 1988, P 150S-156S
20. B.L. JOSEFSON, RESIDUAL STRESSES AND THEIR REDISTRIBUTION DURING ANNEALING OF A GIRTH-BUTT WELDED THIN-WALLED PIPE, *J. PRESSURE VESSEL TECHNOL. (TRANS. ASME),* VOL 104, AUG 1982, P 245-250
21. Y. LIU AND K.H. LEONG, LASER BEAM DIAGNOSTICS FOR KILOWATT POWER PULSED YAG LASER, *PROC. LASER MATERIALS PROCESSING,* INTERNATIONAL CONGRESS ON

APPLICATION OF LASERS AND ELECTRO-OPTICS '92, VOL 72, LASER INSTITUTE OF AMERICA, 1992

22. D.T. SWIFT-HOOK AND A.E.F. GICK, PENETRATION WELDING WITH LASERS--ANALYTICAL STUDY INDICATES THAT PRESENT LASER BEAM WELDING CAPABILITIES MAY BE EXTENDED TENFOLD, *WELD. J. RES. SUPPL.,* VOL 52, 1973, P 492S-499S
23. D. ROSENTHAL, MATHEMATICAL THEORY OF HEAT DISTRIBUTION DURING WELDING AND CUTTING, *WELD. J. RES. SUPPL.,* VOL 20, 1941, P 220S-234S
24. H.E. CLINE AND T.R. ANTHONY, HEAT TREATING AND MELTING MATERIAL WITH A SCANNING LASER OR ELECTRON BEAM, *J. APPL. PHYS.,* VOL 48 (NO. 9), 1977, P 3895
25. W.M. STEEN, J. DOWDEN, M. DAVIS, AND P. KAPADIA, A POINT AND LINE SOURCE MODEL OF LASER KEYHOLE WELDING, *J. PHYS. D: APPL. PHYS.,* VOL 21, 1988, P 1255-1260
26. J. MAZUMDER AND W.M. STEEN, HEAT TRANSFER MODEL FOR CW LASER MATERIAL PROCESSING, *J. APPL. PHYS.,* VOL 51 (NO. 2), 1980, P 941
27. H.A. NIED, THE FINITE ELEMENT MODELING OF THE RESISTANCE SPOT WELDING PROCESS, *WELD. J. RES. SUPPL.,* APRIL 1984, P 123-S
28. C.L. TSAI, O.A. JAMMAL, J.C. PAPRITAN, AND D.W. DICKINSON, MODELING OF RESISTANCE SPOT WELD NUGGET GROWTH, *WELD. J. RES. SUPPL.,* FEB 1992, P 47-S
29. J.A. GREENWOOD AND J.B.P. WILLIAMSON, ELECTRICAL CONDUCTION IN SOLIDS--II. THEORY OF TEMPERATURE-DEPENDENT CONDUCTORS, *PROC. ROYAL SOC. LONDON,* VOL 246, 1958, P 13-31
30. H.S. CHO AND Y.J. CHO, A STUDY OF THE THERMAL BEHAVIOR IN RESISTANCE SPOT WELDING, *WELD J. RES. SUPPL.,* JUNE 1989, P 236-S TO 244-S

Validation Strategies for Heat-Affected Zone and Fluid-Flow Calculations

J. Mazumder, University of Illinois at Urbana-Champaign

Introduction

FUSION WELDING PROCESSES involve all four phase changes: solid-solid state, solid-liquid, liquid-vapor, and vapor-plasma. Attempts to model the associated heat transport and related phenomena have been ongoing for more than half a century. The temperature history and the peak temperature determine the nature and extent of the phase change. One of the earlier analytical models for heat conduction in welding developed by Rosenthal (Ref 1) is still being used by many welding practitioners to estimate the heat-affected zone (HAZ). Although the existence of convection and its effect on molten weld pools were first reported in mid-1950s (Ref 2, 3), major modeling efforts on convection in welding started after the work reported by Heiple and Roper (Ref 4) on the effect of surface-tension-driven flow in the weld pool. During the past decade, several research groups developed two- and three-dimensional models for convection in the weld pool (Ref 5, 6, 7, 8, 9, 10, 11, 12, 13, 14, 15). Of course, these convection models also predict the thermal history of the weld. Another effect of thermal history is the generation of residual stress and strain due to thermal expansion and solid-state phase transformation. Due to the importance of residual stress on the mechanical performance of welded joints, several groups also became involved in modeling the stress/strain history of welds (Ref 16, 17, 18, 19, 20, 21, 22, 23, 24, 25, 26, 27, 28, 29, 30, 31, 32, 33, 34, 35).

Each model has its own sets of assumptions. Validation of a model requires careful experiments to satisfy the underlying assumptions for that particular model. For example, Rosenthal's two-dimensional model is only valid for thin-plate welding and temperature prediction (Ref 1). Prediction for the center of the heat source for his three-dimensional model is erroneous because the assumption of a point heat source will lead to infinitely high temperatures, which is physically impossible. Also, lack of physics such as latent heat of fusion, radiative and convective heat loss, convection in the weld pool, and vaporization heat loss will lead to significant error in the melt pool prediction. Therefore, the only reasonable strategy for validation of such an analytical model will be temperature measurement at the HAZ, preferably away from the liquid-solid interface.

In designing experiments for validation of any analytical or numerical models for thermal, momentum, or stress history, one should clearly be aware of the model assumptions and boundary conditions. In this article, some important techniques to validate temperature, momentum, and stress history observed in welded materials will be discussed.

References

1. D. ROSENTHAL, *WELD. J.,* VOL 20, 1941, P 220S-225S
2. P.T. HOULDCROFT, *BR. WELD. J.,* VOL 1, 1954, P 468
3. W.J. PUMPHREY, *BR. WELD. J.,* VOL 2, 1955, P 92
4. C.R. HEIPLE AND J.R. ROPER, *WELD. J.,* VOL 61, 1982, P 973-1025
5. J. MAZUMDER AND A. KAR, *THERMOMECHANICAL ASPECTS OF MANUFACTURING AND MATERIALS PROCESSING,* R.K. SHAH *ET AL.,* ED., HEMISPHERE PUBLISHING, P 283-304
6. J. MAZUMDER, *OPT. ENG.,* VOL 30 (NO. 8), 1992, P 1208-1219
7. A. PAUL AND T. DEBROY, *METALL. TRANS. B,* VOL 19, 1988, P 851-858
8. N. PIRCH, E.W. KREUTZ, L. MOLLER, A. GASSER, AND K. WISSENBACH, *PROC. 3RD EUROPEAN CONF. ON LASER TREATMENT OF MATERIALS, ECLAT '90,* VOL 1, ERLANGEN, GERMANY, 17-19 SEPT 1990, SPRECHSAAL PUBLISHING GROUP
9. R.L. ZEHR, "THERMOCAPILLARY CONVECTION IN LASER MELTED POOL DURING MATERIALS PROCESSING," PH.D. THESIS, UNIVERSITY OF ILLINOIS AT URBANA-CHAMPAIGN, 1991
10. C.L. CHAN, R. ZEHR, J. MAZUMDER, AND M.M. CHEN, *PROC. 3RD ENGINEERING FOUNDATION CONF. ON MODELING AND CONTROL CASTING AND WELDING PROCESSES,* S. KOU AND R. MEHRABIAN, ED., TMS-AIME, 1986, P 229-246
11. M.C. TSAI AND S. KOU, *INT. J. NUMER. METHODS FLUIDS,* VOL 9 (NO. 12), DEC 1989, P 1503-1516
12. M.C. TSAI AND S. KOU, *NUMER. HEAT TRANSFER A: APPLICATIONS,* VOL 17 (NO. 1), 1990, P 73-89
13. T. ZACHARIA, A.H. ERASLAN, AND D.K. AIDUN, *WELD. J.,* VOL 67 (NO. 3), MARCH 1988, P 53S-62S
14. T. ZACHARIA, A.H. ERASLAN, AND D.K. AIDUN, *WELD. J.,* VOL 67 (NO. 1), JAN 1988, P 18S-27S
15. R.T.C. CHOO, J. SZEKELY, AND R.C. WESTHOFF, *WELD. J.,* VOL 69 (NO. 9), SEPT 1990, P 346S-361S
16. L. KARLSSON, CHAPTER 5, *THERMAL STRESSES I,* R.B. HETNARSKI, ED., NORTH-HOLLAND, 1986, P 299-389
17. J. GOLDAK, *RECENT TRENDS IN WELDING SCIENCE AND TECHNOLOGY,* S.A. DAVID AND J.M. VITEK, ED., ASM INTERNATIONAL, 1989, P 71-82
18. H.D. HIBBIT AND P.V. MARCAL, *COMPUTERS AND STRUCTURES,* VOL 3 (NO. 5), SEPT 1973, P 1145-1174
19. E. FRIEDMAN, *J. PRESSURE VESSEL TECHNOL. (TRANS. ASME),* VOL 97 (NO. 3), AUG 1975, P 206-213
20. B.A.B. ANDERSSON, *ENG. MATER. TECHNOL. (TRANS ASME),* VOL 100, OCT 1978, P 345-362
21. E.F. RYBICKI, D.W. SCHMUESER, R.W. STONESIFER, J.J. GROOM, AND H.W. MISHLER, *J. PRESSURE VESSEL TECHNOL. (TRANS ASME),* VOL 100, AUG 1978, P 256-262
22. E.F. RYBICKI AND R.B. STONESIFER, *J. PRESSURE VESSEL TECHNOL. (TRANS. ASME),* VOL 101, MAY 1979, P 149-154
23. Y. UEDA AND K. NAKACHO, *TRANS. JWRI,* VOL 9 (NO. 1), 1980, P 107-114
24. D.H. ALLEN AND W.E. HAISLER, *COMPUTERS AND STRUCTURES,* VOL 13, 1981, P 129-135
25. J.H. ARGYRIS, J. SZIMMAT, AND K.J. WILLIAM, *COMPUTER METHODS IN APPLIED*

MECHANICS AND ENGINEERING, VOL 33, 1982, P 635-666

26. B. ANDERSSON AND L. KARLSSON, *J. THERM. STRESSES,* VOL 4, 1981, P 491-500
27. B. PATEL, "THERMO-ELASTO-PLASTIC FINITE ELEMENT FORMULATION FOR DEFORMATION AND RESIDUAL STRESSES DUE TO WELDS," PH.D. THESIS, CARLETON UNIVERSITY, OTTAWA, ONTARIO, CANADA, APRIL 1985
28. K.W. MAHIN, S. MACEWEN, W.S. WINTERS, W. MASON, M. KANOUFF, AND E.A. FUCHS, *MODELING AND CONTROL OF CASTING AND WELDING PROCESSES IV,* PROC. INT. CONF. ON MODELING OF CASTING AND WELDING PROCESSES IV, A.F. GIAMEI AND G.J. ABBASCHIAN, ED., ENGINEERING FOUNDATION AND TMS/AIME, APRIL 1988, P 339-350
29. J. GOLDAK, A. ODDY, M. MCDILL, A. CHAKRAVARTI, M. BIBBY, AND R. HOUSE, *ADVANCES IN WELDING SCIENCE AND TECHNOLOGY,* S.A. DAVID, ED., ASM INTERNATIONAL, 1986, P 523-527
30. P. TEKRIWAL AND J. MAZUMDER, *ADVANCES IN WELDING SCIENCE AND TECHNOLOGY,* S.A. DAVID, ED., ASM INTERNATIONAL, 1986, P 71-80
31. R.I. KARLSSON AND B.L. JOSEFSON, *J. PRESSURE VESSEL TECHNOL. (TRANS. ASME),* VOL 112, FEB 1990, P 76-84
32. C.K. LEUNG, "STUDY OF FINITE ELEMENT MODELING OF MULTIPASS WELDS," PH.D. THESIS, UNIVERSITY OF WATERLOO, WATERLOO, ONTARIO, CANADA, 1986
33. S.Z. NEWMAN, "FEM MODEL OF 3D TRANSIENT TEMPERATURE AND STRESS FIELDS IN WELDED PLATES," PH.D. THESIS, CARNEGIE MELLON UNIVERSITY, PITTSBURGH, PA, APRIL 1986
34. P. TEKRIWAL, "THREE-DIMENSIONAL TRANSIENT THERMO-ELASTO-PLASTIC MODELING OF GAS METAL ARC WELDING USING THE FINITE ELEMENT METHOD," PH.D. THESIS, UNIVERSITY OF ILLINOIS AT URBANA-CHAMPAIGN, URBANA, IL, AUGUST 1989
35. P. TEKRIWAL AND J. MAZUMDER, *TRANS. ASME,* VOL 113, JULY 1991, P 336-343

Validation Strategies for Heat-Affected Zone and Fluid-Flow Calculations

J. Mazumder, University of Illinois at Urbana-Champaign

Validation of Fluid-Flow Calculation

Convection is the single most important factor influencing the geometry of the weld pool including pool shape, aspect ratio, and surface ripples, and can result in defects such as variable penetration, porosity, and lack of fusion. Convection is also primarily responsible for mixing and, as a result, also affects the composition of the weld pool.

Recently, the sophistication of fluid-flow modeling has reached a stage where most of the important physics are considered. Buoyancy, surface tension, and electromagnetic forces are the three driving forces for convection. Electromagnetic force is important for arc welding. Initial work by Orepar, Eager, and Szekely (Ref 36) showed that even for arc welding, surface-tension-driven flow is dominant until the current level is very high (exceeding 250 A). Recently, several authors published models for thermocapillary flow (surface-tension-driven flow) for welding (Ref 6, 7, 8, 9, 10, 11, 12, 13, 14, 15). For validation of fluid-flow models, free surface models are the best candidates since they incorporate the most physics of the welding process. However, until recently, measurement of free surface deformation was difficult to perform. A new technique utilizing the specular reflection of a 488 nm argon-ion laser beam from the melt pool is employed to measure the free surface deformation (Ref 37, 38). Another challenge for validation of the fluid flow model is the measurement of liquid-metal velocity during welding. Temperature measurement techniques for the weld pool were recently reviewed by Kraus (Ref 39). Important techniques for the measurement of free surface deformation, fluid velocity, and pool temperature are discussed below.

References cited in this section

6. J. MAZUMDER, *OPT. ENG.*, VOL 30 (NO. 8), 1992, P 1208-1219
7. A. PAUL AND T. DEBROY, *METALL. TRANS. B*, VOL 19, 1988, P 851-858
8. N. PIRCH, E.W. KREUTZ, L. MOLLER, A. GASSER, AND K. WISSENBACH, *PROC. 3RD EUROPEAN CONF. ON LASER TREATMENT OF MATERIALS, ECLAT '90*, VOL 1, ERLANGEN, GERMANY, 17-19 SEPT 1990, SPRECHSAAL PUBLISHING GROUP
9. R.L. ZEHR, "THERMOCAPILLARY CONVECTION IN LASER MELTED POOL DURING MATERIALS PROCESSING," PH.D. THESIS, UNIVERSITY OF ILLINOIS AT URBANA-CHAMPAIGN, 1991
10. C.L. CHAN, R. ZEHR, J. MAZUMDER, AND M.M. CHEN, *PROC. 3RD ENGINEERING FOUNDATION CONF. ON MODELING AND CONTROL CASTING AND WELDING PROCESSES*, S. KOU AND R. MEHRABIAN, ED., TMS-AIME, 1986, P 229-246
11. M.C. TSAI AND S. KOU, *INT. J. NUMER. METHODS FLUIDS*, VOL 9 (NO. 12), DEC 1989, P 1503-1516
12. M.C. TSAI AND S. KOU, *NUMER. HEAT TRANSFER A: APPLICATIONS*, VOL 17 (NO. 1), 1990, P 73-89
13. T. ZACHARIA, A.H. ERASLAN, AND D.K. AIDUN, *WELD. J.*, VOL 67 (NO. 3), MARCH 1988, P 53S-62S
14. T. ZACHARIA, A.H. ERASLAN, AND D.K. AIDUN, *WELD. J.*, VOL 67 (NO. 1), JAN 1988, P 18S-27S
15. R.T.C. CHOO, J. SZEKELY, AND R.C. WESTHOFF, *WELD. J.*, VOL 69 (NO. 9), SEPT 1990, P 346S-361S
36. G.M. OREPAR, T.W. EAGER, AND J. SZEKELY, *WELD. J.*, VOL 63, 1983, P 307S
37. J. MAZUMDER AND D. VOELKEL, *PROCEEDINGS OF LAMP '92*, A. MATSUNAWA AND KATAYAMA, ED., HIGH TEMPERATURE SOCIETY OF JAPAN, JUNE 1992, P 373-380
38. J. MAZUMDER AND D. VOELKEL, U.S. PATENT APPLICATION 08/004763, JAN 1993
39. H.G. KRAUS, *MODELING AND CONTROL OF CASTING AND WELDING PROCESSES IV*, PROC. CONF., A.F. GIAMEI AND G.J. ABBASCHIAN, ED., TMS-AIME, 1988, P 205-212

Validation Strategies for Heat-Affected Zone and Fluid-Flow Calculations

J. Mazumder, University of Illinois at Urbana-Champaign

Measurement of Free Surface Deformation

Measurement of free surface deformation during welding is extremely complicated due to melt pool characteristics such as the specular pool surface, the wide range of deformation slopes possible, vaporization of metal from the pool surface, shielding gas, radiation of many wavelengths from the hot surface and plasma, small pool size, high temperature, and the incoming processing beam. Various optical techniques have been considered, but were found inadequate for characterizing the aforementioned characteristics (Ref 40). Since none of the classic methods were appropriate, a new technique was developed based on the specularity and steepness of the surface of the weld pool.

The fundamental step of this method is to reflect light off of a specular surface and measure the slope of the surface where the reflection is observed. This slope is measured indirectly by measuring the difference between the angles of the incident light when it reflects into a camera at a location on a flat surface and the corresponding location of the melt pool. If the angle of incidence is varied over a large enough range, each portion of the pool will at some time reflect the incident light into the camera, thereby revealing its slope. This will result in a known slope for every portion of the melt pool surface. If the slope between the areas of interest and the edge of the pool is known, it can be integrated to obtain the surface elevation. This is the basic idea behind the melt pool surface contour measurement method (Ref 38, 40). Figure 1 shows a schematic of the surface contour measurement system.

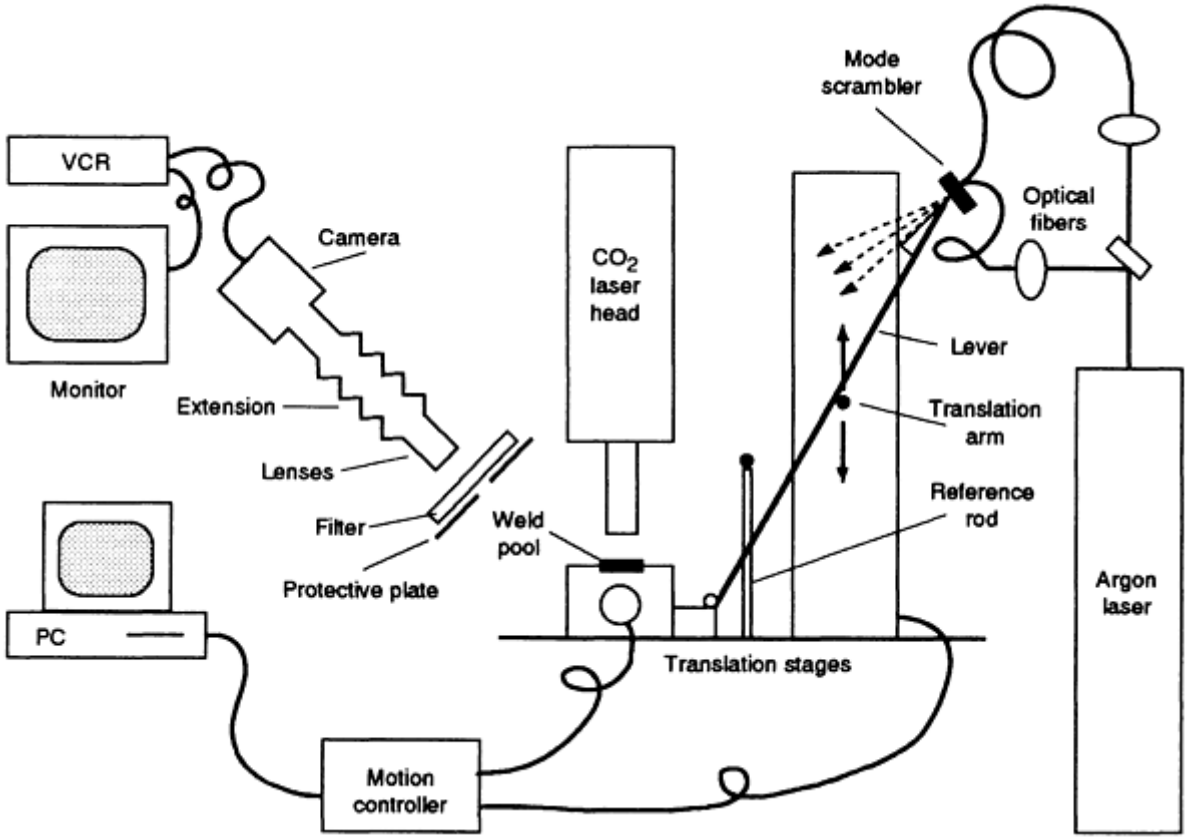

FIG. 1 SCHEMATIC OF THE SPECULAR SURFACE CONTOUR MEASUREMENT SYSTEM

Figure 2 shows a typical laser weld pool free surface measured by the "reflective topography" technique described above. This technique has shown the capability of measuring all types of free surface shapes including convex, concave (Ref 37), and complicated shapes with a lip as shown in Fig. 2.

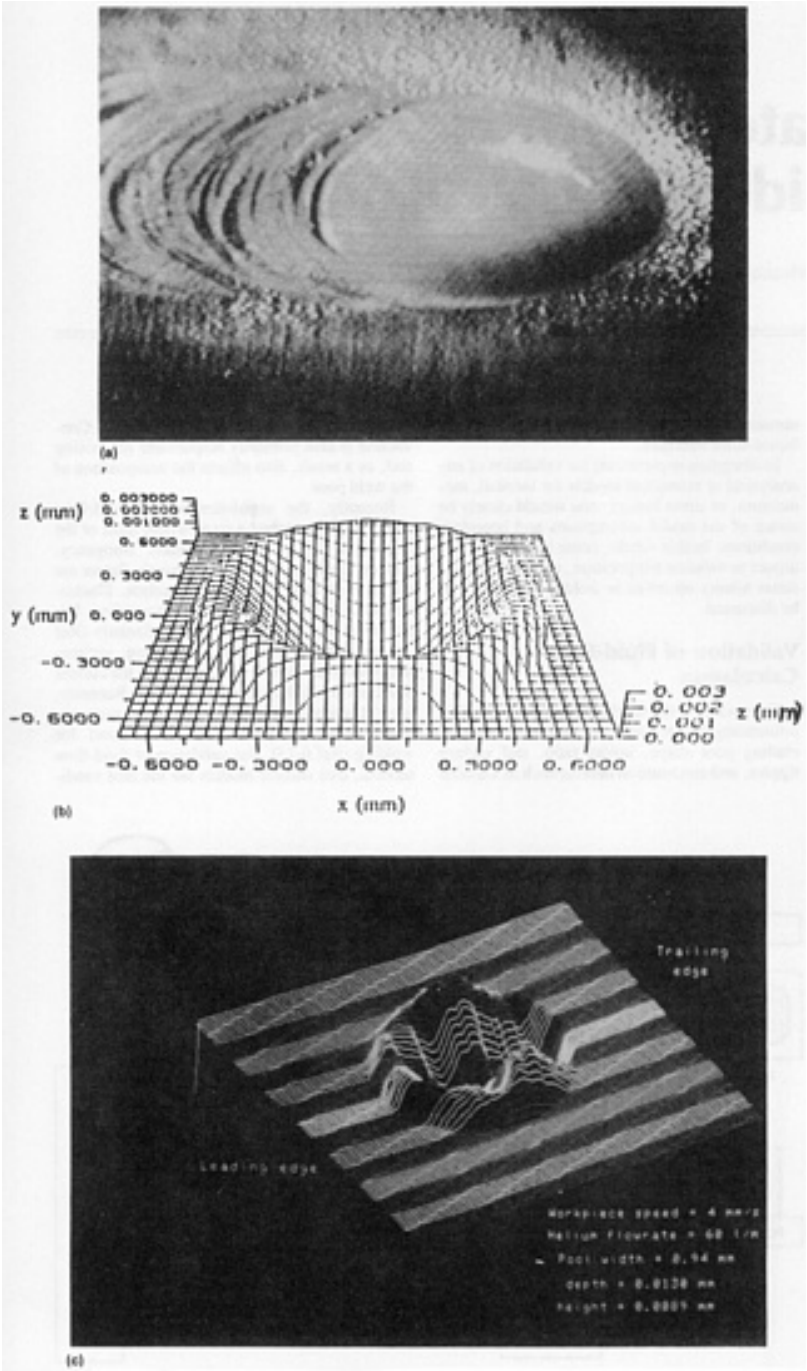

FIG. 2 LASER WELD POOL FREE SURFACE MEASURED BY THE REFLECTIVE TOPOGRAPHY TECHNIQUE. (A) VISUALIZED PICTURE. (B) PREDICTED MODEL. (C) REFLECTIVE TOPOGRAPHY IMAGE

There are several uncertainties in the modeling of free surface deformation of the weld pool. Most common for weld modeling is the paucity of temperature-dependent thermophysical property data. For the free surface deformation problem in particular, the nature of the surface tension gradient as a function of temperature and composition is poorly understood, and very little data are available. Presently, a linear dependence on temperature is assumed by most researchers. Recently, experimental measurements carried out by Sahoo *et al.* (Ref 41) and McNallan *et al.* (Ref 42), indicate a nonlinear relationship which may affect the free surface contour significantly. Also, there is controversy over the role of plasma, which is often present in welding, on the surface tension characteristics. The effect of vaporization on the pressure boundary condition also needs attention. Although significant progress has been made in modeling the melt pool free surface, there is considerable controversy over the basic assumptions for process phenomena and the physics of the process.

Various researchers have used metallographic techniques to measure the weld pool aspect ratio for the solidified weld and compared that with modeling data for model validation. This technique provides a qualitative validation of the overall model. However, comparison of the surface contour measurement of the solidified weld pool using a stylus profilometer with that of the liquid metal free surface measured by the reflective topographic technique reveal that the assumption of similar liquid and resolidified surface contours, which is sometimes suggested because the pool is expected to resolidify quickly, is not an accurate assumption for model validation (Ref 37). Therefore, for more accurate validation of the physics of the model, reflective topography accompanied with velocity measurement by x-ray radiography is more desirable.

References cited in this section

37. J. MAZUMDER AND D. VOELKEL, *PROCEEDINGS OF LAMP '92*, A. MATSUNAWA AND KATAYAMA, ED., HIGH TEMPERATURE SOCIETY OF JAPAN, JUNE 1992, P 373-380
38. J. MAZUMDER AND D. VOELKEL, U.S. PATENT APPLICATION 08/004763, JAN 1993
40. D. VOELKEL, "LASER WELD POOL OPTICAL DIAGNOSTICS: TOPOGRAPHY AND VISUALIZATION USED FOR SURFACE CONTOUR ANALYSIS AND PROCESS MONITORING," PH.D. THESIS, UNIVERSITY OF ILLINOIS AT URBANA-CHAMPAIGN, URBANA, IL, JAN 1992
41. P. SAHOO, T. DEBROY, AND M.J. MCNALLAN, *METALL. TRANS. B*, VOL 19, 1988, P 484-491
42. M.J. MCNALLAN AND T. DEBROY, *METALL. TRANS. B*, VOL 22, 1991, P 557-560

J. Mazumder, University of Illinois at Urbana-Champaign

Velocity Measurement

Heiple and Roper (Ref 4) used a high-speed movie to track the flow of Al_2O_3 particles on the weld pool surface to measure surface velocity. To validate the nature and velocity of the recirculating flow at the weld pool, x-ray radiography must be utilized. A schematic diagram of the experimental arrangement used by Mazumder *et al.* (Ref 43) is shown in Fig. 3. The substrate material used for this arc welding experiment is aluminum. Tungsten particles are used as tracers to provide contrast. A microfocused x-ray beam is directed through the test sections and an image intensifier is located on the back of the sample to receive the image. This image is processed and stored on videotape. Because of the density difference between aluminum and tungsten, the tungsten particles can be traced as they travel with the moving molten aluminum. Because the frame speed of the television camera is known, the relative position of the tungsten particles will provide the velocity of the weld pool, assuming the particles flow with the same velocity as the liquid metal (Ref 43).

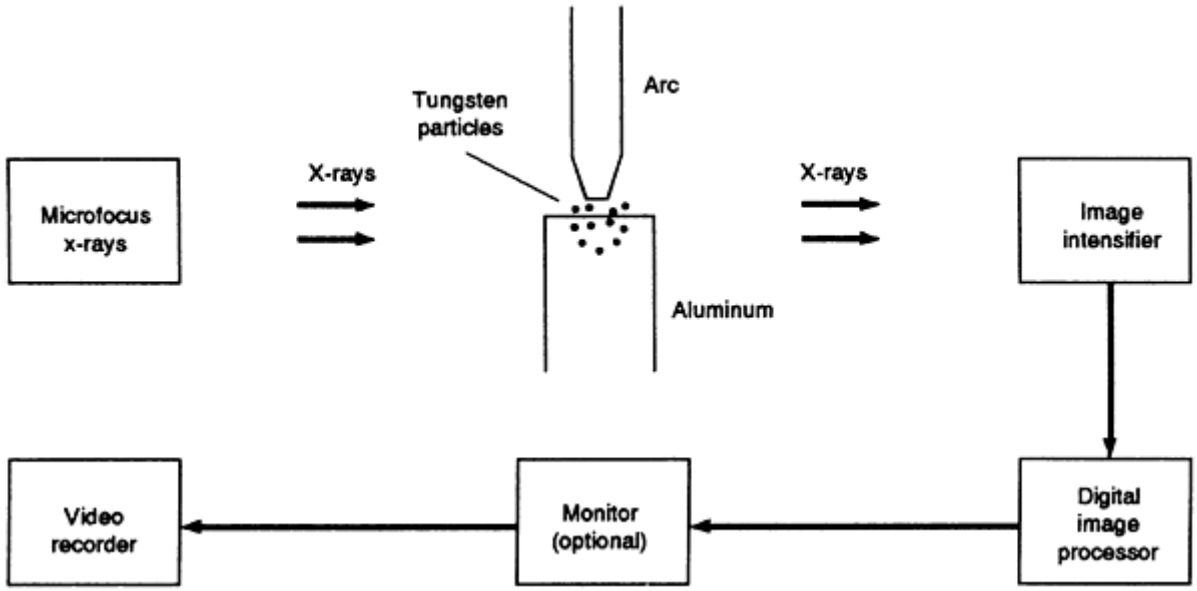

FIG. 3 SCHEMATIC OF THE X-RAY RADIOGRAPHY SYSTEM USED FOR MEASURING WELD POOL SURFACE VELOCITY

References cited in this section

4. C.R. HEIPLE AND J.R. ROPER, *WELD. J.*, VOL 61, 1982, P 973-1025

43. J. MAZUMDER, M.M. CHEN, C.L. CHAN, R. ZEHR, AND D. VOELKEL, *PROC. ECLAT '90,* H. BERGMANN, ED., SPRECHSAAL PUBLISHING GROUP, COBURG, GERMANY, 1990, P 37-53

Validation Strategies for Heat-Affected Zone and Fluid-Flow Calculations

J. Mazumder, University of Illinois at Urbana-Champaign

Temperature Measurement

Thermocouples. Temperature measurement for model validation is probably the most mature arena for model validation. An excellent review of the field has been published by Kraus (Ref 39). Most of the earlier work for temperature measurement for welding was with thermocouples. Sundell *et al.* (Ref 44) used tungsten-rhenium thermocouples to measure the temperature for low-alloy steel, type 316L stainless steel, and Inconel 718 weld pools created during gas-tungsten] arc welding (GTAW). Thermocouples were inserted from the underside of the work-piece in holes drilled to within 0.38 mm (0.015 in.) from the surface in order to measure weld pool surface temperatures. Some thermocouples were found to protrude beyond the free surface due to the weld pool surface deformation. Draw-backs for thermocouple measurements are the several-millisecond time constant for temperature measurement and weld pool temperature and flow field perturbations. However, the response time constant can be reduced by 3 to 4 times using the procedure reported by Dantzig (Ref 45), which entails calibration of the thermocouple and signal conditioning.

Thermography. Infrared (IR) thermographic cameras are now commercially available. A number of research groups have used them for weld pool temperature measurement (Ref 46, 47, 48, 49, 50, 51). Thermographic cameras can be used for high-resolution measurements of relative emissive power of the weld pools, but lack of emissivity data prevents their use for accurate absolute temperature measurement (Ref 39). Lukens and Morris (Ref 49) correlated the IR emission intensity measurements with temperatures measured by thermocouples embedded 2 mm (0.08 in.) below the surface. Although this provides some idea about the average temperature of the weld pool, it fails to validate the surface temperature observed by the thermographic camera. However, this technique can be applied for weld control and monitoring of weld cooling rate (Ref 49).

Narrow-band IR pyrometry was used for weld pool temperature measurement by Schaver *et al.* (Ref 52) for translating electron-beam welds, and Giedt *et al.* (Ref 53) for stationary welds. They used a 1.4 μm wavelength, and spectral emissivity was measured at the gas-tungsten arc at the melting point of the metals welded.

Hunter, Allemand, and Eager (Ref 54, 55) developed techniques for temperature measurement using multiwavelength pyrometry to alleviate the emissivity variation problem. However, so far the only proof of the concept was demonstrated using a heated platinum substrate. This could be a valuable tool for surface temperature measurement. Spatial resolution of 100 μm with 5% accuracy in temperature measurements above 1100 K is possible in this technique. They reported measurement of spectral radiance at approximately 200 wavelengths in a range of 0.6 to 0.8 μm. In real life, measurement of 5 or 6 wavelengths is adequate.

Optical Spectral Radiometric/Laser Reflectance (OSRLR). Kraus (Ref 56, 57) developed the OSRLR technique for high-resolution weld pool surface temperature measurements. This technique combines high-speed-film radiographic measurements of weld pool spectral directional thermal emissive power with spectral directional emissivity measurements to enable temperature calculation up to a point (Ref 39). However, this method requires knowledge of the weld pool free surface topology as well as an oxide-free weld pool surface because the surface has to reflect a focused laser beam. High resolution with spot sizes up to 60 μm have been achieved using this technique. Figure 4 shows the experimental setup for measurement of spectral directional emissivity in the weld pool. The details of the application of this technique for weld pool surface temperature measurements using OSRLR for gas-tungsten arc welds in types 304 and 316 stainless steels and AISI 8630 alloy steel are provided in Ref 58. Similar temperature measurements based on laser line reflection were also applied by Fuchs *et al.* (Ref 51) for weld pool surface temperature measurement of gas-metal arc welds.

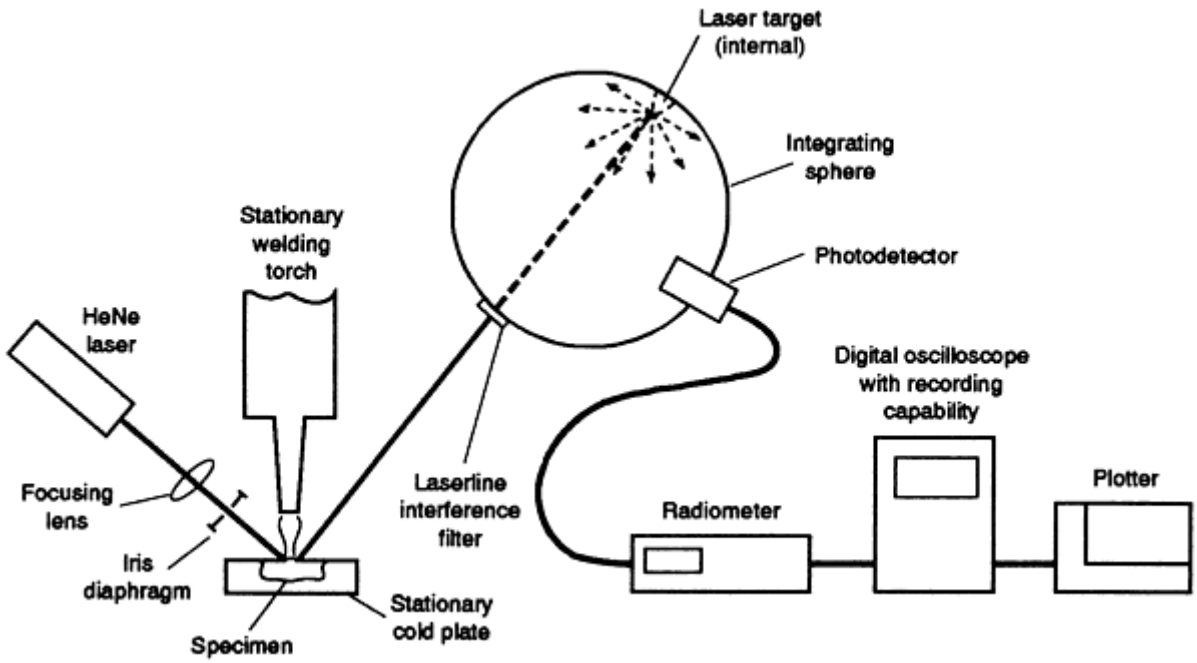

FIG. 4 SCHEMATIC OF THE SETUP USED FOR MEASURING SPECTRAL DIRECTIONAL EMISSIVITY IN THE WELD POOL

References cited in this section

39. H.G. KRAUS, *MODELING AND CONTROL OF CASTING AND WELDING PROCESSES IV*, PROC. CONF., A.F. GIAMEI AND G.J. ABBASCHIAN, ED., TMS-AIME, 1988, P 205-212
44. R.E. SUNDELL *ET AL.*, REPORT NO. 86SRD013 SUBMITTED TO THE NATIONAL SCIENCE FOUNDATION, GENERAL ELECTRIC COMPANY, SCHENECTADY, NY, 1986
45. J.A. DANTZIG, *REV. SCI. INSTRUM.*, VOL 56 (NO. 5), 1984, P 723-725
46. R.E. SAMPSON, G. SUITS, AND C.B. ARNOLD, REPORT NO. 176200-1-F, ENVIRONMENTAL

RESEARCH INSTITUTE OF MICHIGAN, MARCH 1985

47. B.A. CHIN, J.S. GOODLING, AND N.H. MADSEN, *ROBOTICS TODAY,* VOL 5 (NO. 1), 1983, P 85-87
48. M.A. KHAN, N.H. MADSEN, J.S. GOODLING, AND B.A. CHIN, *OPT. ENG.,* VOL 25 (NO. 6), 1986, P 799-805
49. W.E. LUKENS AND R.A. MORRIS, *WELD. J.,* VOL 61 (NO. 1), 1982, P 27-33
50. J.P. BOILLOT, P. CIELO, G. BEGIN, C. MICHEL, M. LESSARD, P. FAFARD, AND D. VILLEMURE, *WELD. J.,* VOL 64 (NO. 7), 1985, P 209S-217S
51. E.A. FUCHS, K.W. MAHIN, A.R. ORTEGA, L.A. BERTRAM, D.R. WILLIAMS, AND A.R. POMPLUN, *THERMOSENSE XIII,* SOCIETY OF PHOTO-OPTICAL INSTRUMENTATION ENGINEERS (SPIE), VOL 1467, 1991, P 136-149
52. D.A. SCHAUER, W.H. GIEDT, AND S.M. SHINTAKU, *WELD. J.,* VOL 57 (NO. 5), 1978, P 127S-133S
53. W.H. GEIDT, X.-C. WEI, AND S.-R. WEI, *WELD. J.,* VOL 63 (NO. 12), 1984, P 376S-383S
54. G.B. HUNTER, C.D. ALLEMAND, AND T.W. EAGER, *OPT. ENG.,* VOL 24 (NO. 6), 1985, P 1081-1085
55. G.B. HUNTER, C.D. ALLEMAND, AND T.W. EAGER, *OPT. ENG.,* VOL 25 (NO. 11), 1986, P 1222-1231
56. H.G. KRAUS, *OPT. LETT.,* VOL 11 (NO. 12), 1986, P 773-775
57. H.G. KRAUS, *OPT. ENG.,* VOL 26 (NO. 12), 1987, P 1183-1190
58. H.G. KRAUS, *WELD. J.,* VOL 68, JULY 1989, P 269S-279S

Validation Strategies for Heat-Affected Zone and Fluid-Flow Calculations

J. Mazumder, University of Illinois at Urbana-Champaign

Model Validation and Boundary Condition

The importance of matching the boundary condition during the experimental measurement for model validation cannot be overemphasized. One of the concepts employs various measurement techniques at different parts of the weld pool to define the boundary conditions as tightly as possible (Ref 51). Another approach uses a cold plate, as shown in Fig. 5, which was specially designed to hold the specimens in order to achieve symmetry of temperature and electromagnetic boundary conditions.

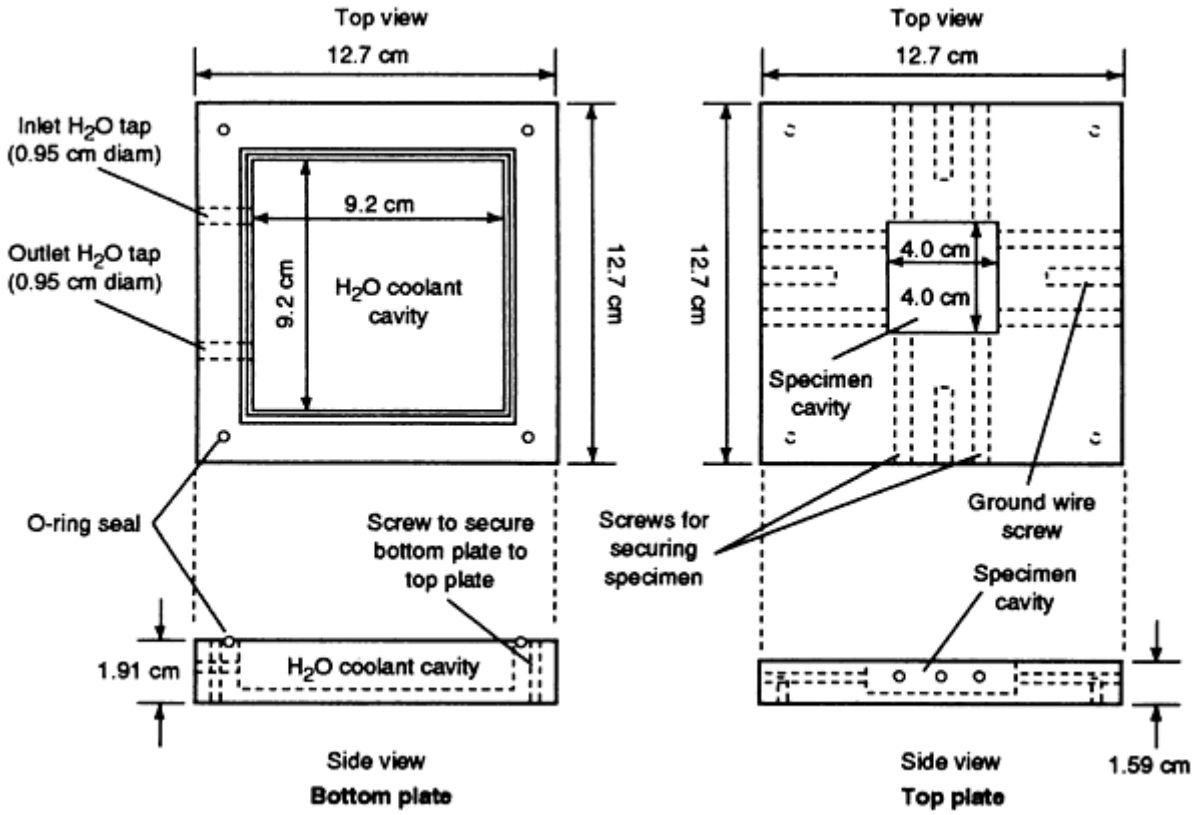

FIG. 5 SCHEMATIC OF THE COLD PLATE USED FOR SECURING SPECIMENS IN ORDER TO ACHIEVE SYMMETRY OF TEMPERATURE AND ELECTROMAGNETIC BOUNDARY CONDITIONS DURING MODEL VALIDATION

Reference cited in this section

51. E.A. FUCHS, K.W. MAHIN, A.R. ORTEGA, L.A. BERTRAM, D.R. WILLIAMS, AND A.R. POMPLUN, *THERMOSENSE XIII*, SOCIETY OF PHOTO-OPTICAL INSTRUMENTATION ENGINEERS (SPIE), VOL 1467, 1991, P 136-149

Validation Strategies for Heat-Affected Zone and Fluid-Flow Calculations

J. Mazumder, University of Illinois at Urbana-Champaign

Validation of Residual Strain Calculation

Residual strains for weld HAZs are often measured by strain gages (Ref 35). Nonobtrusive techniques such as interferometry are also employed by some researchers (Ref 59, 60). For postweld residual strain measurements, x-ray diffraction is the most popular. Recently, neutron scattering techniques have been employed by some groups (Ref 61, 62). From the strain measurement data, stress data can be calculated provided modulus data for the particular material at the temperature range of interest are available.

Strain gages are essentially Wheatstone bridges that use the change of electrical resistance of a wire under strain to measure pressure. Strain gages generally consist of an array of four metal thin-film resistors. When they are deformed due to strain, the difference of output voltage is the measure of strain. Output voltages are generally very small; for example, 3 mv per volt of excitation for full-scale deformation with accuracies ranging from 1% to 0.1% (Ref 63). Therefore, one needs an amplifier to either plot the data on a chart recorder or to send it to the input/output board of a computer. Strain gages are generally mounted on the weld specimen with bonding agents (adhesives). Because both bonding agents and

strain gages are very sensitive to high temperatures, strain measurement is limited to a region substantially outside the immediate vicinity of the HAZ.

Interferometry. All interferometric techniques are based on the interference of two coherent light wave trains. Masubuchi *et al.* (Ref 59) measured out-of-plane displacement using laser interferometer. Chavez *et al.* (Ref 60) used Moire interferometry to obtain full-field strain data across welds in stainless steel plates with Ferralium or nickel filler. Moire interferometry provides full-field surface displacement data with displacement resolution on the order of 1 μm. Holographic interferometric techniques can provide a higher resolution, whereas the Moire technique can be used in situations involving large strain variations such as occur during welding. Norvell (Ref 64) found strain variation for a 1 °C (1.8 °F) change in temperature can be measured by holographic interferometry; thus this method is too sensitive for welding. On the other hand, Moire interferometry is much more forgiving. Another interferometric technique called shearography seems to be more promising because the interference pattern is created simply by shearing the image by placing an optical wedge in front of the camera (Ref 65). Although Fourier transformation is required to deduce the strain data, unlike other interferometric techniques, shearography provides a strain field directly and minimizes data reduction.

X-Ray and Neutron Diffraction Methods. Both x-ray and neutron diffraction follow Bragg's law:

$$\lambda = 2D_{HKL} \text{ SIN } \theta_{HKL}$$

where λ is the wavelength, d_{hkl} is interplanar spacing of the plane ***hkl,*** and θ_{hkl} is the scattering angle.

An advantage of neutron diffraction is that it can penetrate to much greater depths. For example, a penetration depth in excess of 16 mm (0.63 in.) was observed for steel (Ref 61). For an x-ray, one needs to section off a specimen layer by layer, assuming that machining or chemical etching will not introduce any additional strain. This increased penetration depth is due to the extremely small wavelength (~0.165 nm) for neutrons. Root *et al.* (Ref 62) have determined the longitudinal, normal, and transverse strain components at 1.5 mm (0.06 in.) from inside the bottom surface of a multipass ferritic weldment. However, the major draw-back is that one needs a nuclear reactor for the neutron source. Penetration depth provides a unique opportunity to compose the prediction from three-dimensional models.

References cited in this section

35. P. TEKRIWAL AND J. MAZUMDER, *TRANS. ASME,* VOL 113, JULY 1991, P 336-343
59. K. MASUBUCHI, A. DEBICCARI, AND W.J.C. COOK, *ADVANCES IN WELDING SCIENCE AND TECHNOLOGY,* S.A. DAVID, ED., ASM INTERNATIONAL, 1986, P 529-532
60. S.A. CHAVEZ, V.A. DEASON, AND J.S. EPSTEIN, *ADVANCES IN WELDING SCIENCE AND TECHNOLOGY,* S.A. DAVID, ED., ASM INTERNATIONAL, 1986, P 533-537
61. K.W. MAHIN, W.S. WINTERS, T.M. HOLDEN, AND R.R. HOSBONS, *MODELING OF CASTING, WELDING AND ADVANCED SOLIDIFICATION PROCESSES V,* M. RAPPAZ, M.R. ÖZGÜ, AND K.W. MAHIN, ED., TMS-AIME, 1990, P 265-272
62. J.H. ROOT, T.M. HOLDEN, J. SCHÖDER, S. SPOONER, C.A. HUBBARD, T.A. DODSON, AND S.A. DAVID, *ADVANCES IN WELDING SCIENCE AND TECHNOLOGY,* S.A. DAVID AND J. VITEK, ED., ASM INTERNATIONAL, 1992, P 99-104
63. P. HOROWITZ AND W. HILL, *THE ART OF ELECTRONICS,* CAMBRIDGE UNIVERSITY PRESS, CAMBRIDGE, U.K., 1980
64. W. NORVELL, "THE STUDY OF MECHANICAL AND THERMAL DEFORMATION USING MULTI-DIMENSIONAL OPTICAL NON-DESTRUCTIVE TESTING METHOD," MASTERS THESIS, UNIVERSITY OF ILLINOIS AT URBANA-CHAMPAIGN, 1987
65. Y.Y. HUNG, *OPT. ENG.,* VOL 21 (NO. 3), 1982, P 391-395

References

1. D. ROSENTHAL, *WELD. J.*, VOL 20, 1941, P 220S-225S
2. P.T. HOULDCROFT, *BR. WELD. J.*, VOL 1, 1954, P 468
3. W.J. PUMPHREY, *BR. WELD. J.*, VOL 2, 1955, P 92
4. C.R. HEIPLE AND J.R. ROPER, *WELD. J.*, VOL 61, 1982, P 973-1025
5. J. MAZUMDER AND A. KAR, *THERMOMECHANICAL ASPECTS OF MANUFACTURING AND MATERIALS PROCESSING*, R.K. SHAH *ET AL.*, ED., HEMISPHERE PUBLISHING, P 283-304
6. J. MAZUMDER, *OPT. ENG.*, VOL 30 (NO. 8), 1992, P 1208-1219
7. A. PAUL AND T. DEBROY, *METALL. TRANS. B*, VOL 19, 1988, P 851-858
8. N. PIRCH, E.W. KREUTZ, L. MOLLER, A. GASSER, AND K. WISSENBACH, *PROC. 3RD EUROPEAN CONF. ON LASER TREATMENT OF MATERIALS, ECLAT '90*, VOL 1, ERLANGEN, GERMANY, 17-19 SEPT 1990, SPRECHSAAL PUBLISHING GROUP
9. R.L. ZEHR, "THERMOCAPILLARY CONVECTION IN LASER MELTED POOL DURING MATERIALS PROCESSING," PH.D. THESIS, UNIVERSITY OF ILLINOIS AT URBANA-CHAMPAIGN, 1991
10. C.L. CHAN, R. ZEHR, J. MAZUMDER, AND M.M. CHEN, *PROC. 3RD ENGINEERING FOUNDATION CONF. ON MODELING AND CONTROL CASTING AND WELDING PROCESSES*, S. KOU AND R. MEHRABIAN, ED., TMS-AIME, 1986, P 229-246
11. M.C. TSAI AND S. KOU, *INT. J. NUMER. METHODS FLUIDS*, VOL 9 (NO. 12), DEC 1989, P 1503-1516
12. M.C. TSAI AND S. KOU, *NUMER. HEAT TRANSFER A: APPLICATIONS*, VOL 17 (NO. 1), 1990, P 73-89
13. T. ZACHARIA, A.H. ERASLAN, AND D.K. AIDUN, *WELD. J.*, VOL 67 (NO. 3), MARCH 1988, P 53S-62S
14. T. ZACHARIA, A.H. ERASLAN, AND D.K. AIDUN, *WELD. J.*, VOL 67 (NO. 1), JAN 1988, P 18S-27S
15. R.T.C. CHOO, J. SZEKELY, AND R.C. WESTHOFF, *WELD. J.*, VOL 69 (NO. 9), SEPT 1990, P 346S-361S
16. L. KARLSSON, CHAPTER 5, *THERMAL STRESSES I*, R.B. HETNARSKI, ED., NORTH-HOLLAND, 1986, P 299-389
17. J. GOLDAK, *RECENT TRENDS IN WELDING SCIENCE AND TECHNOLOGY*, S.A. DAVID AND J.M. VITEK, ED., ASM INTERNATIONAL, 1989, P 71-82
18. H.D. HIBBIT AND P.V. MARCAL, *COMPUTERS AND STRUCTURES*, VOL 3 (NO. 5), SEPT 1973, P 1145-1174
19. E. FRIEDMAN, *J. PRESSURE VESSEL TECHNOL. (TRANS. ASME)*, VOL 97 (NO. 3), AUG 1975, P 206-213
20. B.A.B. ANDERSSON, *ENG. MATER. TECHNOL. (TRANS ASME)*, VOL 100, OCT 1978, P 345-362
21. E.F. RYBICKI, D.W. SCHMUESER, R.W. STONESIFER, J.J. GROOM, AND H.W. MISHLER, *J. PRESSURE VESSEL TECHNOL. (TRANS ASME)*, VOL 100, AUG 1978, P 256-262
22. E.F. RYBICKI AND R.B. STONESIFER, *J. PRESSURE VESSEL TECHNOL. (TRANS. ASME)*, VOL 101, MAY 1979, P 149-154
23. Y. UEDA AND K. NAKACHO, *TRANS. JWRI*, VOL 9 (NO. 1), 1980, P 107-114
24. D.H. ALLEN AND W.E. HAISLER, *COMPUTERS AND STRUCTURES*, VOL 13, 1981, P 129-135
25. J.H. ARGYRIS, J. SZIMMAT, AND K.J. WILLIAM, *COMPUTER METHODS IN APPLIED MECHANICS AND ENGINEERING*, VOL 33, 1982, P 635-666

26. B. ANDERSSON AND L. KARLSSON, *J. THERM. STRESSES,* VOL 4, 1981, P 491-500
27. B. PATEL, "THERMO-ELASTO-PLASTIC FINITE ELEMENT FORMULATION FOR DEFORMATION AND RESIDUAL STRESSES DUE TO WELDS," PH.D. THESIS, CARLETON UNIVERSITY, OTTAWA, ONTARIO, CANADA, APRIL 1985
28. K.W. MAHIN, S. MACEWEN, W.S. WINTERS, W. MASON, M. KANOUFF, AND E.A. FUCHS, *MODELING AND CONTROL OF CASTING AND WELDING PROCESSES IV,* PROC. INT. CONF. ON MODELING OF CASTING AND WELDING PROCESSES IV, A.F. GIAMEI AND G.J. ABBASCHIAN, ED., ENGINEERING FOUNDATION AND TMS/AIME, APRIL 1988, P 339-350
29. J. GOLDAK, A. ODDY, M. MCDILL, A. CHAKRAVARTI, M. BIBBY, AND R. HOUSE, *ADVANCES IN WELDING SCIENCE AND TECHNOLOGY,* S.A. DAVID, ED., ASM INTERNATIONAL, 1986, P 523-527
30. P. TEKRIWAL AND J. MAZUMDER, *ADVANCES IN WELDING SCIENCE AND TECHNOLOGY,* S.A. DAVID, ED., ASM INTERNATIONAL, 1986, P 71-80
31. R.I. KARLSSON AND B.L. JOSEFSON, *J. PRESSURE VESSEL TECHNOL. (TRANS. ASME),* VOL 112, FEB 1990, P 76-84
32. C.K. LEUNG, "STUDY OF FINITE ELEMENT MODELING OF MULTIPASS WELDS," PH.D. THESIS, UNIVERSITY OF WATERLOO, WATERLOO, ONTARIO, CANADA, 1986
33. S.Z. NEWMAN, "FEM MODEL OF 3D TRANSIENT TEMPERATURE AND STRESS FIELDS IN WELDED PLATES," PH.D. THESIS, CARNEGIE MELLON UNIVERSITY, PITTSBURGH, PA, APRIL 1986
34. P. TEKRIWAL, "THREE-DIMENSIONAL TRANSIENT THERMO-ELASTO-PLASTIC MODELING OF GAS METAL ARC WELDING USING THE FINITE ELEMENT METHOD," PH.D. THESIS, UNIVERSITY OF ILLINOIS AT URBANA-CHAMPAIGN, URBANA, IL, AUGUST 1989
35. P. TEKRIWAL AND J. MAZUMDER, *TRANS. ASME,* VOL 113, JULY 1991, P 336-343
36. G.M. OREPAR, T.W. EAGER, AND J. SZEKELY, *WELD. J.,* VOL 63, 1983, P 307S
37. J. MAZUMDER AND D. VOELKEL, *PROCEEDINGS OF LAMP '92,* A. MATSUNAWA AND KATAYAMA, ED., HIGH TEMPERATURE SOCIETY OF JAPAN, JUNE 1992, P 373-380
38. J. MAZUMDER AND D. VOELKEL, U.S. PATENT APPLICATION 08/004763, JAN 1993
39. H.G. KRAUS, *MODELING AND CONTROL OF CASTING AND WELDING PROCESSES IV,* PROC. CONF., A.F. GIAMEI AND G.J. ABBASCHIAN, ED., TMS-AIME, 1988, P 205-212
40. D. VOELKEL, "LASER WELD POOL OPTICAL DIAGNOSTICS: TOPOGRAPHY AND VISUALIZATION USED FOR SURFACE CONTOUR ANALYSIS AND PROCESS MONITORING," PH.D. THESIS, UNIVERSITY OF ILLINOIS AT URBANA-CHAMPAIGN, URBANA, IL, JAN 1992
41. P. SAHOO, T. DEBROY, AND M.J. MCNALLAN, *METALL. TRANS. B,* VOL 19, 1988, P 484-491
42. M.J. MCNALLAN AND T. DEBROY, *METALL. TRANS. B,* VOL 22, 1991, P 557-560
43. J. MAZUMDER, M.M. CHEN, C.L. CHAN, R. ZEHR, AND D. VOELKEL, *PROC. ECLAT '90,* H. BERGMANN, ED., SPRECHSAAL PUBLISHING GROUP, COBURG, GERMANY, 1990, P 37-53
44. R.E. SUNDELL *ET AL.,* REPORT NO. 86SRD013 SUBMITTED TO THE NATIONAL SCIENCE FOUNDATION, GENERAL ELECTRIC COMPANY, SCHENECTADY, NY, 1986
45. J.A. DANTZIG, *REV. SCI. INSTRUM.,* VOL 56 (NO. 5), 1984, P 723-725
46. R.E. SAMPSON, G. SUITS, AND C.B. ARNOLD, REPORT NO. 176200-1-F, ENVIRONMENTAL RESEARCH INSTITUTE OF MICHIGAN, MARCH 1985
47. B.A. CHIN, J.S. GOODLING, AND N.H. MADSEN, *ROBOTICS TODAY,* VOL 5 (NO. 1), 1983, P 85-87
48. M.A. KHAN, N.H. MADSEN, J.S. GOODLING, AND B.A. CHIN, *OPT. ENG.,* VOL 25 (NO. 6), 1986, P 799-805
49. W.E. LUKENS AND R.A. MORRIS, *WELD. J.,* VOL 61 (NO. 1), 1982, P 27-33
50. J.P. BOILLOT, P. CIELO, G. BEGIN, C. MICHEL, M. LESSARD, P. FAFARD, AND D. VILLEMURE, *WELD. J.,* VOL 64 (NO. 7), 1985, P 209S-217S
51. E.A. FUCHS, K.W. MAHIN, A.R. ORTEGA, L.A. BERTRAM, D.R. WILLIAMS, AND A.R.

POMPLUN, *THERMOSENSE XIII*, SOCIETY OF PHOTO-OPTICAL INSTRUMENTATION ENGINEERS (SPIE), VOL 1467, 1991, P 136-149

52. D.A. SCHAUER, W.H. GIEDT, AND S.M. SHINTAKU, *WELD. J.*, VOL 57 (NO. 5), 1978, P 127S-133S
53. W.H. GEIDT, X.-C. WEI, AND S.-R. WEI, *WELD. J.*, VOL 63 (NO. 12), 1984, P 376S-383S
54. G.B. HUNTER, C.D. ALLEMAND, AND T.W. EAGER, *OPT. ENG.*, VOL 24 (NO. 6), 1985, P 1081-1085
55. G.B. HUNTER, C.D. ALLEMAND, AND T.W. EAGER, *OPT. ENG.*, VOL 25 (NO. 11), 1986, P 1222-1231
56. H.G. KRAUS, *OPT. LETT.*, VOL 11 (NO. 12), 1986, P 773-775
57. H.G. KRAUS, *OPT. ENG.*, VOL 26 (NO. 12), 1987, P 1183-1190
58. H.G. KRAUS, *WELD. J.*, VOL 68, JULY 1989, P 269S-279S
59. K. MASUBUCHI, A. DEBICCARI, AND W.J.C. COOK, *ADVANCES IN WELDING SCIENCE AND TECHNOLOGY*, S.A. DAVID, ED., ASM INTERNATIONAL, 1986, P 529-532
60. S.A. CHAVEZ, V.A. DEASON, AND J.S. EPSTEIN, *ADVANCES IN WELDING SCIENCE AND TECHNOLOGY*, S.A. DAVID, ED., ASM INTERNATIONAL, 1986, P 533-537
61. K.W. MAHIN, W.S. WINTERS, T.M. HOLDEN, AND R.R. HOSBONS, *MODELING OF CASTING, WELDING AND ADVANCED SOLIDIFICATION PROCESSES V*, M. RAPPAZ, M.R. ÖZGÜ, AND K.W. MAHIN, ED., TMS-AIME, 1990, P 265-272
62. J.H. ROOT, T.M. HOLDEN, J. SCHÖDER, S. SPOONER, C.A. HUBBARD, T.A. DODSON, AND S.A. DAVID, *ADVANCES IN WELDING SCIENCE AND TECHNOLOGY*, S.A. DAVID AND J. VITEK, ED., ASM INTERNATIONAL, 1992, P 99-104
63. P. HOROWITZ AND W. HILL, *THE ART OF ELECTRONICS*, CAMBRIDGE UNIVERSITY PRESS, CAMBRIDGE, U.K., 1980
64. W. NORVELL, "THE STUDY OF MECHANICAL AND THERMAL DEFORMATION USING MULTI-DIMENSIONAL OPTICAL NON-DESTRUCTIVE TESTING METHOD," MASTERS THESIS, UNIVERSITY OF ILLINOIS AT URBANA-CHAMPAIGN, 1987
65. Y.Y. HUNG, *OPT. ENG.*, VOL 21 (NO. 3), 1982, P 391-395

Oxyfuel Gas Cutting

Introduction

OXYFUEL GAS CUTTING (OFC) includes a group of cutting processes that use controlled chemical reactions to remove preheated metal by rapid oxidation in a stream of pure oxygen. A fuel gas/oxygen flame heats the workpiece to ignition temperature, and a stream of pure oxygen feeds the cutting (oxidizing) action. The OFC process, which is also referred to as burning or flame cutting, can cut carbon and low-alloy plate of virtually any thickness. Castings more than 760 mm (30 in.) thick commonly are cut by OFC processes. With oxidation-resistant materials, such as stainless steels, either a chemical flux or metal powder is added to the oxygen stream to promote the exothermic reaction.

The simplest oxyfuel gas cutting equipment consists of two cylinders (one for oxygen and one for the fuel gas), gas flow regulators and gages, gas supply hoses, and a cutting torch with a set of exchangeable cutting tips. Such manually operated equipment is portable and inexpensive. Cutting machines, employing one or several cutting torches guided by solid template pantographs, optical line tracers, numerical controls, or computers, improve production rates and provide superior cut quality. Machine cutting is important for profile cutting--the cutting of regular and irregular shapes from flat stock.

Acknowledgements

This article was adapted from "Thermal Cutting" in *Welding, Brazing, and Soldering*, Volume 6 of the 9th edition of *Metals Handbook*. The author of the original article is Rosalie Brosilow of Penton Publishing. Special thanks are due to Lance Soisson of Welding Consultants Inc. for his help in adapting the article for this volume.

Principles of Operation

Oxyfuel gas cutting begins by heating a small area on the surface of the metal to the ignition temperature of 760 to 870 °C (1400 to 1600 °F) with an oxyfuel gas flame. Upon reaching this temperature, the surface of the metal will appear bright red. A cutting oxygen stream is then directed at the preheated spot, causing rapid oxidation of the heated metal and generating large amounts of heat. This heat supports continued oxidation of the metal as the cut progresses. Combusted gas and the pressurized oxygen jet flush the molten oxide away, exposing fresh surfaces for cutting. The metal in the path of the oxygen jet burns. The cut progresses, making a narrow slot, or kerf, through the metal.

To start a cut at the edge of a plate, the edge of the preheat flame is placed just over the edge to heat the material. When the plate heats to red, the cutting oxygen is turned on, and the torch moves over the plate to start the cut.

During cutting, oxygen and fuel gas flow through separate lines to the cutting torch at pressures controlled by pressure regulators, adjusted by the operator. The cutting torch contains ducts, a mixing chamber, and valves to supply an oxyfuel gas mixture of the proper ratio for preheat and a pure oxygen stream for cutting to the torch tip. By adjusting the control valves on the torch handle or at the cutting machine controller, the operator sets the precise oxyfuel gas mixture desired. Depressing the cutting oxygen lever on the torch during manual operation initiates the cutting oxygen flow. For machine cutting, oxygen is normally controlled by the operator at a remote station or by numerical control. Cutting tips have a single cutting oxygen orifice centered within a ring of smaller oxyfuel gas exit ports. The operator changes the cutting capacity of the torch by changing the cutting tip size and by resetting pressure regulators and control valves. Because different fuel gases have different combustion and flow characteristics, the construction of cutting tips, and sometimes of mixing chambers, varies according to the type of gas.

Oxyfuel gas flames initiate the oxidation action and sustain the reaction by continuously heating the metal at the line of the cut. The flame also removes scale and dirt that may impede or distort the cut.

The rate of heat transfer in the workpiece influences the heat balance for cutting. As the thickness of the metal to be cut increases, more heat is needed to keep the metal at its ignition temperature. Increasing the preheat gas flow and reducing the cutting speed maintains the necessary heat balance.

Oxygen flow also must increase as the thickness of the metal to be cut increases. The jet of cutting oxygen must have sufficient volume and velocity to penetrate the depth of the cut and still maintain its shape and effective oxygen content.

Quality of Cut. Oxyfuel gas cutting operations combine more than 20 variables. Suppliers of cutting equipment provide tables that give approximate gas pressures for various sizes and styles of cutting torches and tips and recommended cutting speeds; these variables are operator controlled. Other variables include type and condition (scale, oil, dirt, flatness) of material, thickness of cut, type of fuel gas, and quality and angle of cut.

Where dimensional accuracy and squareness of the cut edge are important, the operator must adjust the process to minimize the kerf, the width of metal removed by cutting, and to increase smoothness of the cut edge. Careful balancing of all cutting variables helps attain a narrow kerf and smooth edge. The thicker the work material, the greater the oxygen volume required and therefore, the wider the cutting nozzle and kerf.

Process Capabilities

Oxyfuel gas cutting processes are used primarily for severing carbon and low-alloy steels. Other iron-base alloys and some nonferrous metals can be oxyfuel gas cut, although process modification may be required, and cut quality may not be as high as is obtained in cutting the more widely used grades of steel. High-alloy steels, stainless steels, cast iron, and nickel alloys do not readily oxidize and therefore do not provide enough heat for a continuous reaction. As the carbon and alloy contents of the steel to be cut increase, preheating or postheating, or both, often are necessary to overcome the effect of the heat cycle, particularly the quench effect of cooling.

Some of the high-alloy steels, such as stainless steel, and cast iron can be cut successfully by injecting metal powder (usually iron) or a chemical additive into the oxygen jet. The metal powder supplies combustion heat and breaks up oxide films. Chemical additives combine with oxides to form lower temperature melting products that flush away.

Applications. Large-scale applications of oxyfuel cutting are found in shipbuilding, structural fabrication, manufacture of earthmoving equipment, machinery construction, and in the fabrication of pressure vessels and storage tanks. Many machine structures, originally made from forgings and castings, can be made at less cost by redesigning them for OFC and welding with the advantages of quick delivery of plate material from steel suppliers, low cost of oxyfuel gas cutting equipment, and flexibility of design.

Structural shapes, pipe, rod, and similar materials can be cut to length for construction or cut up in scrap and salvage operations. In steel mills and foundries, projections such as caps, gates, and risers can be severed from billets and castings. Mechanical fasteners can be quickly cut for disassembly using OFC. Holes can be made in steel components by piercing and cutting. Machine OFC is used to cut steel plate to size, to cut various shapes from plate, and to prepare plate edges (bevel cutting) for welding.

Gears, sprockets, handwheels, clevises and frames, and tools such as wrenches can be cut out by oxyfuel gas torches. Often, these oxyfuel cut products can be used without further finishing. However, when cutting medium- or high-carbon steel or other metal that hardens by rapid cooling, the hardening effect must be considered, especially if the workpiece is to be subsequently machined.

Thickness Limits. Gas can cut steels less than 3.2 mm ($\frac{1}{8}$ in.) thick to over 1525 mm (60 in.) thick, though some sacrifice in quality occurs near both ends of this range. With very thin material, operators may have some difficulty in keeping heat input low to avoid melting the kerf edges and to minimize distortion. Steel under 6.4 mm ($\frac{1}{4}$ in.) thick often is stacked for cutting of several parts in a single torch pass.

There are a number of advantages and disadvantages when OFC is compared to other cutting operations such as arc cutting, milling, shearing, or sawing. The advantages of OFC are:

- METAL CAN BE CUT FASTER BY OFC. SETUP IS GENERALLY SIMPLER AND FASTER THAN FOR MACHINING AND ABOUT EQUAL TO THAT OF MECHANICAL SEVERING (SAWING AND SHEARING).
- OXYFUEL GAS CUTTING PATTERNS ARE NOT CONFINED TO STRAIGHT LINES AS IN SAWING AND SHEARING, OR TO FIXED PATTERNS AS IN DIE CUTTING PROCESSES. CUTTING DIRECTION CAN BE CHANGED RAPIDLY ON A SMALL RADIUS DURING OPERATION.
- MANUAL OFC EQUIPMENT COSTS ARE LOW COMPARED TO MACHINE TOOLS. SUCH EQUIPMENT IS PORTABLE AND SELF-CONTAINED, REQUIRING NO OUTSIDE POWER AND WELL SUITED FOR FIELD USE.
- WHEN PROPERTIES AND DIMENSIONAL ACCURACY OF GAS CUT PLATE ARE ACCEPTABLE, OFC CAN REPLACE COSTLY MACHINING OPERATIONS. IT OFFERS REDUCED LABOR AND OVERHEAD COSTS, REDUCED MATERIAL COSTS, REDUCED TOOLING COSTS, AND FASTER DELIVERY.
- WITH ADVANCED MACHINERY, OFC LENDS ITSELF TO HIGH-VOLUME PARTS PRODUCTION.
- LARGE PLATES CAN BE CUT QUICKLY IN PLACE BY MOVING THE GAS TORCH RATHER THAN THE PLATE.
- TWO OR MORE PIECES CAN BE CUT SIMULTANEOUSLY USING STACK CUTTING METHODS AND MULTIPLE-TORCH CUTTING MACHINES.

The limitations of the OFC process include:

- DIMENSIONAL TOLERANCES ARE POORER THAN FOR MACHINING AND SHEARING.
- BECAUSE OFC RELIES ON OXIDATION OF IRON, IT IS LIMITED TO CUTTING STEELS AND CAST IRON.
- HEAT GENERATED BY OFC CAN DEGRADE THE METALLURGICAL PROPERTIES OF THE WORK MATERIAL ADJACENT TO THE CUT EDGES. HARDENABLE STEELS MAY REQUIRE PREHEAT AND/OR POSTHEAT TO CONTROL MICROSTRUCTURE AND MECHANICAL PROPERTIES.
- PREHEAT FLAMES AND THE EXPELLED RED HOT SLAG POSE A FIRE HAZARD TO PLANT AND PERSONNEL.

Oxygen consumption and flow rates vary depending on whether economy, speed, or accuracy of cut is desired. For average straight-line cutting of low-carbon steel, consumption of cutting oxygen per pound of metal removed varies with thickness of the metal and is lowest at a thickness of 100 to 125 mm (4 to 5 in.).

By assuming that for every unit mass of iron oxidized an equal mass of iron melts, one can calculate the amount of heat generated by the cutting reaction--heat emitted is 6680 kJ/kg (2870 Btu/lb) of iron oxidized. Melting of 0.5 kg (1 lb) of iron takes 715 kJ (680 Btu), based on a melting point of 1540 °C (2800 °F), 0.8 kJ/kg · K (0.2 Btu/lb · °F) as the specific heat, and 272 kJ/kg (117 Btu/lb) as the heat of fusion. Only a small amount of the heat melts the iron; most of it, about 4900 kJ/kg (2100 Btu/lb), goes into the reaction. Some of this superheats the molten metal, some soaks into the workpiece, and some leaves by radiation and convection. Most of it leaves with the slag and hot exhaust gases.

As cutting oxygen flows down through the cut, the quantity available for reaction decreases. If the flow of oxygen is large and well collimated, the rate of cutting through the depth of the cut is approximately constant. The cutting face remains vertical if the oxygen is in excess and if cutting speed is not excessive.

If oxygen flow is insufficient, or cutting speed too high, the lower portions of the cut react more slowly, and the cutting face curves behind the torch. The horizontal distance between point of entry and exit is called drag (see Fig. 1).

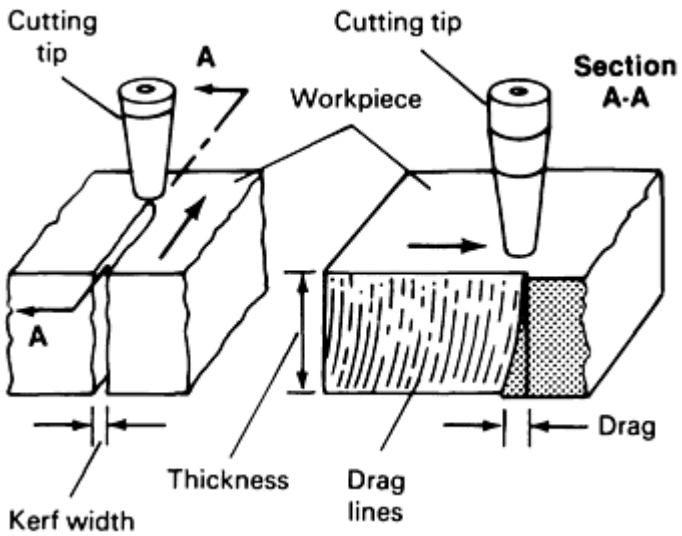

FIG. 1 SCHEMATIC CROSS SECTION OF WORK METAL DURING OFC SHOWING DRAG ON CUTTING FACE

Drag influences edge quality. Optimum edge quality results from zero drag--the oxygen stream enters and leaves the cut in a straight line along the cutting tip axis. This is called a "drop-cut," designating a clean, fully severed edge. Increasing cutting speed or reducing oxygen flow makes less oxygen available at the bottom of the cut, causing the bottom of the cut to "drag" behind the top of the cut. A drag of 20% means that the bottom of the cut edge lags the top surface by 20% of the material thickness. Drag lines appear as curved ripples on the cut edge. For fast, rough cuts, some drag is acceptable.

Drag is a rough measure of cut quality and of economy in oxygen consumption. In metal thicknesses up to 50 to 75 mm (2 or 3 in.), 10 to 15% drag indicates good quality of cut and economy. The key to quality cuts is control of heat input. Higher quality demands less drag; more drag indicates poorer quality and low oxygen consumption. Excessive drag may lead to incomplete cutting.

In very thin sections, drag has little significance. In very thick sections, the goal is to avoid excessive drag.

Preheating may consist of merely warming a cold workpiece with a torch or may require furnace heating of the work beyond 540 °C (1000 °F). For some alloy steels, preheat temperatures are 205 to 315 °C (400 to 600 °F). Carbon steel billets and other sections occasionally are cut at 870 °C (1600 °F) and higher.

In OFC, preheating is accomplished by means of the oxyfuel gas flame, which surrounds the cutting oxygen stream. At cut initiation, the preheat flame, the result of oxygen and fuel gas combustion, brings a small amount of material to ignition temperature so that combustion can proceed. After cutting begins, the preheat flame merely adds heat to compensate for heat lost by convection and radiation or through gas exhausted during cutting. The flame also helps to remove or burn off scale and dirt on the plate surface; the hot combusted gases protect the stream of cutting oxygen from the atmosphere.

Preheating may also be applied over a broader area of the work. It may include soaking the entire workpiece in a furnace to bring it up to 95 to 205 °C (200 to 400 °F), or a simple overall warm-up with a torch to bring cold plate to room temperature. A preheat improves cutting speed significantly, allowing faster torch travel for greater productivity and reduced consumption of fuel gas. Broader preheat smooths the temperature gradient between the base metal and the cut edge, possibly reducing thermal stress and minimizing hardening effects in some steels.

Properties of Fuel Gases

Each cutting job entails a different type or volume of work to be completed. Consequently, the best gas for all cutting in a fabricating plant is found through experimentation. Evaluating a gas for a single job requires a test run that monitors fuel gas and oxygen flow rate, labor costs, overhead, and the amount of work performed. If plant production varies from week to week, gas performance should be measured over a long enough period to achieve an accurate cost analysis. Any of the fuel gases may perform well over a range of flow rates. When comparing gases, performance should be rated at the lowest flow rate that gives acceptable results for each gas.

Gas manufacturers provide comprehensive data on flame temperature, heat of combustion, oxygen-to-gas consumption ratio, heat transfer, and heat distribution in the flame. Gas properties can be rated on a weight or volume basis. Flow rates, for example, commonly are given in terms of volume. Gas may be sold, however, by weight or by volume, and specifications may state properties in terms of one or the other to make the product seem as attractive as possible. For example, acetylene occupies more volume per pound than does propane. Consequently, cost based on weight makes propane liquid seem inexpensive. Cost based on volume makes the lighter fuels, such as acetylene, seem less costly. The user must understand these ratings and comparisons.

Heat Distribution in the Flame. Combustion of fuel gas produces the preheat flame, which initiates cutting action and helps sustain the operation. These flames heat the surface of the work to ignition temperature to (1) initiate cutting, (2) descale and clean the work surface, (3) supply heat to the work and the cutting oxygen stream to maintain the heat needed for continuous cutting, and (4) shield the cutting oxygen stream from surrounding air. Preheat gases consist of hydrocarbons, which produce water vapor and carbon dioxide as products of chain reactions. These reactions occur in cones within the flame, usually visible as an inner and outer flame. A gas whose inner flame has a high temperature and high heat release provides the most concentrated heat. These gases are superior for fast starts in flame cutting of high-alloy steels that are difficult to cut.

When low heat release is accompanied by high flame temperature, even though it is above the melting point of steel, heat is diffused and gives slow starts in flame cutting. Gases, such as natural gas, that release most of their heat in the outer flame are well suited to heating and heavy cutting. Heat distribution is a good indication of the potential performance of a particular gas.

Acetylene

Acetylene is the most widely used cutting gas. It burns hotter than any of the other common fuel gases, making it indispensable for certain jobs. The volume of oxygen consumed per volume of acetylene is $2\frac{1}{2}$. Combustion occurs in stages. In the small inner cone at the tip of the torch, acetylene burns with feed-line oxygen. This reaction gives off a blistering amount of heat; the tip of the inner cone is the hottest part. Burning continues in the outer envelope of the flame, in a cooler, blue-colored region.

Most oxygen for this reaction comes from the air surrounding the flame. Of the $2\frac{1}{2}$ parts of oxygen needed for acetylene to burn completely, about $1\frac{1}{2}$ comes from the air and 1 part from line oxygen. A neutral flame, recommended for manual cutting, consumes equal volumes of line oxygen and acetylene. In practice, operators may raise the line oxygen ratio to $1\frac{1}{2}$, a proportion that produces an oxidizing flame. The inner cone contracts and becomes sharply defined. This is the hottest flame attainable with acetylene or with any other raw fuel gas. The triple bond in acetylene makes it the hottest burning gas. In cutting of steel, operators should adjust the acetylene-to-oxygen ratio to produce a neutral flame, even though it is below the highest possible temperature. A neutral flame minimizes oxidation and carburization of the base metal. Users sometimes use the hotter oxidizing flame for piercing at the start of a cut.

Acetylene is unstable at room temperature and moderate pressure and can explode under a blow even without the presence of air or oxygen. For safe storage and handling, it is dissolved in acetone. A typical cylinder is filled with heavy porous clay, which holds the acetone. Acetylene, forced into the cylinder, saturates the acetone. When the cylinder valve opens, acetylene vaporizes above the acetone solution. The regulator limits outlet pressure to 105 kPa gage pressure (15 psig) or less.

Cylinders for acetylene should be handled with care. Safety requires them to be placed upright to prevent acetone solvent from entering the regulator. The ratio of line oxygen consumption to acetylene consumption is lower than that for the other fuel gases. Acetylene uses less oxygen at its maximum flame temperature, so that handling of oxygen cylinders may be reduced, thus offsetting the inconvenience of the acetylene cylinder.

Cost of acetylene as a fuel gas changes with consumption. Large-volume users of acetylene often install bulk trailers that hook up to manifold piping systems. When volume justifies, users may install acetylene-generating plants, thus reducing handling costs.

Heat content of acetylene (kJ/m^3, or Btu/ft^3) is lower than all gases except natural gas. Although acetylene burns at a high temperature, it has to burn at higher flow rates than other gases to deliver the same amount of heat. Acetylene releases heat rapidly in a small, concentrated area. Acetylene is a poor choice for cutting a large block of metal because of high fuel cost and the need for large volumes of the fuel to obtain required total heat. To concentrate heat on a limited area, as in cutting thin plate, acetylene is a good choice. It burns faster than other gases, and it burns close to the torch tip. Heat energy concentrates at the tip of the tiny cone.

Acetylene gives a narrow heat-affected zone (HAZ) and possibly less distortion (depending on the volume and shape of the work) than a wider spreading heat. It is particularly well suited to fast cutting of plate under 13 mm ($\frac{1}{2}$ in.) thick. The hot flame cuts through heavy mill scale or rust and can make a bevel quickly with good edge quality. Acetylene facilitates short, stop-and-start cutting jobs, such as cutting structural members and reinforcing bars, because of its short preheat time. For stack cutting and for cutting heavy sections--operations requiring large heat input into a deep kerf--acetylene does not perform as well as other gases. This type of work calls for a fuel gas with high heat output in the secondary flame, such as propane or methylacetylene-propadiene-stabilized (MPS or MAPP) gas.

However, manual cutting is cooler with acetylene than with other gases; less heat rises into the operator's face. It is one of the most versatile and convenient fuels for shops that perform a wide range of fuel gas operations and for shops that cannot justify handling more than one gas. Data for both machine and manual oxyacetylene cutting (OFC-A) of carbon steel plate of varying thickness are given in Tables 1 and 2.

TABLE 1 RECOMMENDED PARAMETERS FOR MANUAL OFC-A OF CARBON STEELS

PLATE THICKNESS		DIAMETER OF CUTTING ORIFICE[A]		OXYGEN PRESSURE[A]		CUTTING SPEED[A][B]		GAS CONSUMPTION					
								OXYGEN			ACETYLENE[C]		
mm	in.	mm	in.	kpa	psi	mm/min	in./min	m^3/h	ft^3/h	ft^3/linear ft	m^3/h	ft^3/h	ft^3/linear ft
3.2	$\frac{1}{8}$	0.965-1.016	0.0380-0.0400	103-159	15-23	510-760	20-30	1.3-1.6	45-55	0.37-0.45	0.20-0.25	7-9	0.06-0.07
6.4	$\frac{1}{4}$	0.965-1.511	0.0380-0.0595	76-96	11-20	405-660	16-26	1.4-2.6	50-93	0.63-0.72	0.25-0.31	9-11	0.08-0.11
9.5	$\frac{3}{8}$	0.965-1.511	0.0380-0.0595	117-173	17-25	380-610	15-24	1.7-3.26	60-115	0.80-0.96	0.28-0.34	10-12	0.10-0.13
13	$\frac{1}{2}$	1.181-1.511	0.0465-0.0595	138-207	20-30	305-560	12-22	1.9-3.54	66-125	1.10-1.14	0.28-0.37	10-13	0.12-0.17
19	$\frac{3}{4}$	1.181-1.511	0.0465-0.0595	165-241	24-35	305-510	12-20	3.31-4.04	117-143	1.43-1.95	0.34-0.42	12-15	0.15-0.20
25	1	1.181-1.511	0.0465-0.0595	193-276	28-40	230-460	9-18	3.7-4.5	130-160	1.78-2.89	0.37-0.45	13-16	0.18-0.29
38	$1\frac{1}{2}$	1.511-2.057	0.0595-0.0810	241-331	35-48	150-355	6-14	4.05-5.04	143-178	1.96-3.18	0.42-0.51	15-18	0.21-0.33
50	2	1.702-2.057	0.0670-0.0810	152-345	22-50	150-330	6-13	5.23-6.54	185-231	3.55-6.16	0.45-0.57	16-20	0.31-0.53
75	3	1.702-2.057	0.0670-0.0810	228-379	33-55	100-255	4-10	6.8-8.2	240-290	5.80-12.00	0.54-0.65	19-23	0.46-0.95
100	4	2.057-2.184	0.0810-0.0860	290-414	42-60	100-205	4-8	8.29-10.9	293-388	9.70-14.64	0.59-0.74	21-26	0.65-1.05
125	5	2.057-2.184	0.0810-0.0860	365-483	53-70	90-165	3.5-6.4	9.82-12.4	347-437	13.66-19.83	0.68-0.82	24-29	0.91-1.37
150	6	2.489-2.577	0.0980-0.0995	310-552	45-80	76-137	3.0-5.4	11.3-16.1	400-567	21.00-26.70	0.76-0.91	27-32	1.19-1.80
205	8	2.527	0.0995	414-531	60-77	66-107	2.6-4.2	14.3-17.4	505-615	29.30-38.84	0.892-1.09	31.5-38.5	1.83-2.42
255	10	2.527	0.0995	517-662	75-96	48-81	1.9-3.2	17.3-21.2	610-750	46.90-64.20	1.04-1.28	36.9-45.1	2.57-3.84
305	12	3.048	0.1200	476-593	69-86	36-66	1.4-2.6	20.4-24.9	720-880	67.70-103.00	1.20-1.46	42.3-51.7	3.98-6.05

(A) VALUES DO NOT NECESSARILY VARY IN EXACT PROPORTION TO PLATE THICKNESS, BECAUSE STRAIGHT-LINE RELATIONS DO NOT EXIST AMONG PRESSURE, SPEED, AND ORIFICE SIZES.

(B) LOWEST SPEEDS AND HIGHEST GAS CONSUMPTIONS ARE FOR INEXPERIENCED OPERATORS, SHORT CUTS, DIRTY OR NONUNIFORM MATERIAL. HIGHEST SPEEDS AND LOWEST GAS CONSUMPTIONS ARE FOR EXPERIENCED OPERATORS, LONG CUTS, CLEAN AND UNIFORM MATERIAL.

(C) PRESSURE OF ACETYLENE FOR THE PREHEATING FLAMES IS MORE A FUNCTION OF TORCH DESIGN THAN OF THE THICKNESS OF THE PART BEING CUT. FOR ACETYLENE PRESSURE DATA, SEE CHARTS FROM MANUFACTURERS OF APPARATUS.

TABLE 2 RECOMMENDED PARAMETERS FOR MACHINE OFC-A OF CARBON STEELS

PLATE THICKNESS		DIAMETER OF CUTTING ORIFICE[A]		OXYGEN PRESSURE[A]		CUTTING SPEED[B]		GAS CONSUMPTION					
								OXYGEN			ACETYLENE[C]		
mm	in.	mm	in.	kpa	psi	mm/min	in./min	m^3/h	ft^3/h	ft^3/linear ft	m^3/h	ft^3/h	ft^3/linear ft
3.2	$\frac{1}{8}$	0.635-1.016	0.0250-0.0400	103-159	15-23	560-815	22-32	1.13-1.56	40-55	0.34-0.36	0.20-0.25	7-9	0.054).06
6.4	$\frac{1}{4}$	0.787-1.511	0.0310-0.0595	76-241	11-35	510-710	20-28	1.27-2.63	45-93	0.34-0.66	0.23-0.31	8-11	0.07-0.08
9.5	$\frac{3}{8}$	0.787-1.511	0.0310-0.0595	117-276	17-40	485-660	19-26	2.32-3.26	82-115	0.86-0.89	0.25-0.34	9-12	0.08-0.09
13	$\frac{1}{2}$	0.787-1.511	0.0310-0.0595	138-379	20-55	430-610	17-24	2.97-3.54	105-125	1.04-1.24	0.28-0.37	10-13	0.11-0.12
19	$\frac{3}{4}$	0.965-1.511	0.0380-0.0595	165-345	24-50	380-560	15-22	3.31-4.50	117-159	1.45-1.56	0.34-0.42	12-15	0.14-0.16
25	1	1.181-1.511	0.0465-0.0595	193-379	28-55	355-485	14-19	3.68-4.93	130-174	1.83-1.86	0.37-0.45	13-16	0.17-0.19
38	$1\frac{1}{2}$	1.702-2.057	0.0670-0.0810	172-379	25-55	305-380	12-15	5.24-6.79	185-240	3.20	0.40-0.51	14-18	0.23-0.24
50	2	1.702-2.057	0.0670-0.0810	152-415	22-60	255-355	10-14	5.24-7.36	185-260	3.70-3.72	0.45-0.57	16-20	0.29-0.32
75	3	2.057-2.184	0.0810-0.0860	228-345	33-50	205-280	8-11	6.79-9.40	240-332	6.00-6.04	0.51-0.65	18-23	0.42-0.45
100	4	2.057-2.184	0.0810-0.0860	290-415	42-60	165-230	6.5-9	8.29-10.9	293-384	8.53-9.02	0.59-0.74	21-26	0.58-0.65
125	5	2.057-2.184	0.0810-0.0860	365-448	53-65	140-190	5.5-7.5	9.82-11.6	347-411	10.97-12.62	0.65-0.82	23-29	0.77-0.84
150	6	2.489-2.527	0.0980-0.0995	310-448	45-65	115-165	4.5-6.5	11.3-13.9	400-490	15.10-17.78	0.74-0.91	26-32	0.98-1.16
205	8	2.489-2.527	0.0980-0.0995	415-620	60-90	94-124	3.7-4.9	14.3-17.7	505-625	25.52-27.30	0.88-1.10	31-39	1.59-1.68
255	10	2.527-2.794	0.0995-0.1100	517-620	75-90	74-102	2.9-4.0	17.3-21.2	610-750	37.50-42.10	1.05-1.27	37-45	2.25-2.55
305	12	2.794-3.048	0.1100-0.1200	476-724	69-105	61-89	2.4-3.5	20.4-24.9	720-880	49.70-60.00	1.19-1.47	42-52	2.97-3.50

(A) VALUES DO NOT NECESSARILY VARY IN EXACT PROPORTION TO PLATE THICKNESS, BECAUSE STRAIGHT LINE RELATIONS DO NOT EXIST AMONG PRESSURE, SPEED, AND ORIFICE SIZES.

(B) LOWEST SPEEDS AND HIGHEST GAS CONSUMPTIONS ARE FOR INEXPERIENCED OPERATORS, SHORT CUTS, DIRTY OR NONUNIFORM MATERIAL. HIGHEST SPEEDS AND LOWEST GAS CONSUMPTIONS ARE FOR EXPERIENCED OPERATORS, LONG CUTS, CLEAN AND UNIFORM MATERIAL.

(C) PRESSURE OF ACETYLENE FOR THE PREHEATING FLAMES IS MORE A FUNCTION OF TORCH DESIGN THAN OF THE THICKNESS OF THE PART BEING CUT. FOR ACETYLENE PRESSURE DATA. SEE CHARTS FROM MANUFACTURERS OF APPARATUS.

Natural Gas

The composition of natural gas varies, depending on its composition at the well, but its main component is methane (CH_4). One volume of methane requires two volumes of oxygen. The combustion ratio is 2 to 1.

Although available in pressurized cylinders, natural gas usually is supplied through low-pressure lines from a local utility. Torchmakers overcome low line pressure through torch design. A siphon stream in the mixing chamber pulls the gas in at the required rate for complete combustion. Torches operate at pressures as low as 2 kPa (4 ozf/in.^{2}) gage line pressure.

A natural gas flame is more diffuse than an acetylene flame--heat intensity is lower, and adjustment for reducing (carburizing), neutral, and oxidizing flames is less clearly defined. Preheating time is longer.

Because heat content is low and heat emission is diffuse, natural gas cannot be used to weld steel. Consequently, if cutting and welding must be performed with a single fuel gas, natural gas cannot be used.

Despite these disadvantages, use of natural gas for cutting has increased. It is the lowest cost commercial fuel gas and, with careful torch adjustment, produces excellent cuts in light- to heavy-gage material. Data for manual oxynatural gas straight-line cutting of carbon steel plate of varying thickness are given in Table 3. Table 4 gives data for oxynatural gas shape cutting of carbon steel plate. Table 5 gives data for machine oxynatural gas drop cutting of shapes from thick carbon steel plate.

TABLE 3 RECOMMENDED PARAMETERS FOR MANUAL OXYNATURAL GAS STRAIGHT-LINE CUTTING OF CARBON STEELS

PLATE THICKNESS		DIAMETER OF CUTTING ORIFICE[A]		OXYGEN PRESSURE		MINIMUM NATURAL GAS PRESSURE		CUTTING SPEED[B]		APPROXIMATE GAS CONSUMPTION			
										OXYGEN		NATURAL GAS	
mm	in.	mm	in.	kpa	psi	kpa	psi	mm/min	in./min	m^3/h	ft^3/h	m^3/h	ft^3/h
3.2	1/8	1.17	0,046	103	15	21	3	510-710	20-28	0.71	25	0.23	8
6.4	1/4	1.17	0.046	124	18	21	3	455-710	18-28	0.99	35	0.28	10
9.5	3/8	1.17	0.046	138	20	21	3	405-510	16-20	1.27	45	0.40	14
13	1/2	1.50	0.059	207	30	21	3	330-430	13-17	1.42	50	0.51	18
19	3/4	1.50	0.059	241	35	21	3	255-380	10-15	2.12	75	0.57	20
25	1	1.50	0.059	275	40	21	3	230-330	9-13	2.83	100	0.68	24
38	1 1/2	1.70	0.067	275	40	21	3	180-305	7-12	4.10	145	0.74	26
50	2	1.70	0.067	310	45	21	3	150-255	6-10	5.38	190	0.79	28
64	2 1/2	1.70	0.067	345	50	21	3	150-230	6-9	6.94	245	0.85	30
75	3	2.36	0.093	345	50	21	3	125-205	5-8	7.64	270	0.91	32
100	4	2.36	0.093	379	55	21	3	125-180	5-7	9.06	320	1.02	36
125	5	2.36	0.093	414	60	21	3	100-	4-6	11.3	400	1.13	40

								150					
150	6	2.79	0.110	414	60	21	3	100-150	4-6	13.3	470	1.36	48
180	7	2.79	0.110	483	70	21	3	75-125	3-5	14.7	520	1.47	52
205	8	2.79	0.110	552	80	21	3	75-100	3-4	16.4	580	1.59	56
255	10	2.79	0.110	620	90	21	3	75-100	3-4	24.1	850	1.70	60
305	12	2.79	0.110	690	100	21	3	50-75	2-3	28.3	1000	1.81	64

(A) USING INJECTOR-TYPE TORCH AND TWO-PIECE TIPS.

(B) VARIATIONS IN CUTTING SPEEDS MAY BE CAUSED BY MILL SCALE ON PLATE, VARIATION IN OXYGEN PURITY, FLAME ADJUSTMENT, CONDITION OF EQUIPMENT, IMPURITIES IN STEEL, AND VARIATION IN HEAT CONTENT OF NATURAL GAS.

TABLE 4 RECOMMENDED PARAMETERS FOR MACHINE OXYNATURAL GAS SHAPE CUTTING OF CARBON STEELS

PLATE THICKNESS		DIAMETER OF CUTTING ORIFICE[A]		HIGH PREHEAT				LOW PREHEAT				NATURAL GAS		CUTTING SPEED[B]		WIDTH OF KERF (APPROX)	
				OXYGEN		NATURAL GAS		OXYGEN		NATURAL GAS							
mm	in.	mm	in.	kpa	psi	kpa	psi	kpa	psi	pa	ozf/in.^{2}	kpa	psi	mm/min	in./min	mm	in.
6.4	$\frac{1}{4}$	0.91	0.036	193	28	21	3	48-83	7-12	430	1	482-517	70-75	455-710	18-28	2.0	0.08
9.5	$\frac{3}{8}$	0.94	0.037	193	28	21	3	48-83	7-12	430	1	482-551	70-80	455-660	18-26	2.0	0.08
13	$\frac{1}{2}$	0.99	0.039	234	34	21	3	48-83	7-12	430	1	517-551	75-80	405-610	16-24	2.3	0.09
16	$\frac{5}{8}$	0.99	0.039	234	34	21	3	48-83	7-12	430	1	517-551	75-80	405-585	16-23	2.3	0.09
19	$\frac{3}{4}$	1.17	0.046	317	46	21	3	55-83	8-12	430	1	551-586	80-85	405-560	16-22	2.5	0.10
25	1	1.17	0.046	331	48	21	3	55-83	8-12	430	1	551-586	80-85	355-510	14-20	2.5	0.10
32	$1\frac{1}{4}$	1.37	0.054	303	44	21	3	55-83	8-12	430	1	551-586	80-85	355-560	14-18	3.0	0.12
38	$1\frac{1}{2}$	1.37	0.054	303	44	21	3	55-83	8-12	430	1	620-655	90-95	330-455	13-18	3.0	0.12
44	$1\frac{3}{4}$	1.37	0.054	310	45	21	3	55-83	8-12	430	1	620-655	90-95	305-430	12-17	3.0	0.12
50	2	1.37	0.054	310	45	21	3	55-83	8-12	430	1	690	100	255-380	10-15	3.0	0.12
57	$2\frac{1}{4}$	1.40	0.055	317	46	21	3	55-83	8-12	430	1	690	100	230-380	9-15	3.3	0.13
64	$2\frac{1}{2}$	1.40	0.055	317	46	21	3	55-83	8-12	430	1	690	100	205-355	8-14	3.3	0.13
70	$2\frac{3}{4}$	1.70	0.067	317	46	21	3	55-83	8-12	430	1	690	100	205-330	8-13	3.6	0.14
75	3	1.70	0.067	317	46	21	3	55-83	8-12	430	1	690	100	180-330	7-13	3.6	0.14
89	$3\frac{1}{2}$	1.85	0.073	345	50	21	3	69-97	10-14	430	1	724	105	150-305	6-12	3.8	0.15
100	4	1.85	0.073	345	50	21	3	69-	10-	430	1	758	110	150-280	6-11	3.8	0.15

								97	14								
114	$4\frac{1}{2}$	2.08	0.082	345	50	21	3	69-97	10-14	430	1	758	110	125-255	5-10	4.3	0.17
125	5	2.08	0.082	345	50	21	3	69-97	10-14	430	1	793	115	125-255	5-10	4.3	0.17
140	$5\frac{1}{2}$	2.44	0.096	345	50	21	3	69-97	10-14	430	1	793	115	125-230	5-9	4.6	0.18
150	6	2.44	0.096	345	50	21	3	69-97	10-14	430	1	827	120	125-230	5-9	4.6	0.18
165	$6\frac{1}{2}$	2.44	0.096	345	50	21	3	69-97	10-14	430	1	827	120	100-205	4-8	4.6	0.18
190	$7\frac{1}{2}$	2.44	0.096	345	50	21	3	69-97	10-14	430	1	827	120	100-205	4-8	4.6	0.18
205	8	2.44	0.096	345	50	21	3	69-97	10-14	430	1	827	120	75-180	3-7	4.6	0.18

(A) TWO-PIECE TIPS FOR HIGH-SPEED MACHINE CUTTING.

(B) VARIATIONS IN CUTTING SPEED MAY BE CAUSED BY MILL SCALE ON PLATE, VARIATION IN OXYGEN PURITY, FLAME ADJUSTMENT, CONDITION OF EQUIPMENT, IMPURITIES IN STEEL, AND VARIATION IN HEAT CONTENT OF NATURAL GAS.

TABLE 5 TYPICAL PARAMETERS FOR MACHINE OXYNATURAL GAS DROP CUTTING OF SHAPES FROM LOW-CARBON STEEL PLATE 255 TO 545 MM (10 TO $21\frac{1}{2}$ IN.) THICK

Torch constructed with two-piece recessed tips that have milled preheat flutes (heavy preheat) and straight-bore cutting-oxygen orifices

PLATE THICKNESS		CUTTING ORIFICE DIAMETER		PREHEAT				CUTTING OXYGEN(A)		CUTTING SPEED		CUTTING OXYGEN	
				OXYGEN		NATURAL GAS							
mm	in.	mm	in.	kpa	psi	kpa	psi	kpa	psi	mm/min	in./min	m^3/h	ft^3/h
255	10	6.35	0.250	240-310	35-45	34	5	186	27	82.6	3.25	39.6	1400
325	$12\frac{3}{4}$	7.14	0.281	240-310	35-45	34	5	193	28	82.6	3.25	49.5	1750
395	$15\frac{1}{2}$	7.14	0.281	240-310	35-45	34	5	207	30	76.2	3.0	53.8	1900
455	18	7.92	0.312	240-310	35-45	34	5	193	28	108	4.25	63.6	2245

535	21	7.92	0.312	240-310	35-45	34	5	193	28	76.2	3.0	63.6	2245
545	$21\frac{1}{2}$	7.92	0.312	240-310	35-45	34	5	207	30	95.3	3.75	67.0	2365

(A) PRESSURE MEASURED AT TORCH INLET

Methylacetylene-Propadiene-Stabilized Gas

The common trade name of methylacetylene-propadiene-stabilized gas is MAPP gas. Methylacetylene-propadiene-stabilized mixtures are by-products of the manufacture of chemicals such as ethylene. These mixtures combine the qualities of an acetylene flame with a more even heat distribution in a fuel that is less prone to explosion and less costly than acetylene. It is supplied as a liquid, in large tanks or in portable cylinders.

Methylacetylene-propadiene-stabilized gases contain a mixture of several hydrocarbons, including propadiene (allene), propane, butane, butadiene, and methylacetylene. Methylacetylene, like acetylene, is a high-energy triple-bond compound. It is unstable, but other compounds in the mixture dilute it sufficiently to enable safe handling.

Compositions of MPS mixtures are proprietary and may vary; consequently, an exact combustion equation cannot be specified. The mixture bums hotter than propane or propylene. It also affords a high release of heat energy in the primary flame cone, characteristic of acetylene. The outer flame gives relatively high heat release, similar to propane and propylene. The overall heat distribution in the flame is the most even of any of the other gases. The inner cone releases 19.3 MJ/m^3 (517 Btu/ft^3), and the outer flame releases 70.37 MJ/m^3 (1889 Btu/ft^3). The coupling distance is therefore less exacting than for acetylene. The best coupling distance for MPS fuel places the outer cone on the plate; however, a shorter coupling distance also delivers considerable heat.

The neutral MPS gas-oxygen flame generates 89.62 MJ/m^3 (2406 Btu/ft^3) with a 2925 °C (5300 °F) flame with a ratio of 3.5 to 4 parts oxygen to 1 part fuel. Values vary with the composition of the gas. The carburizing flame, 2.2 parts or less oxygen to 1 part fuel, can weld alloys, such as aluminum, which oxidize readily. A neutral flame, with a ratio of 2.3 parts line oxygen to 1 part fuel gas, can weld steel. At 2.8 line oxygen ratio, the flame becomes oxidizing, unsuitable for welding. Methylacetylene-propadiene-stabilized gas produces its hottest flame at 3.3 line oxygen-to-gas ratio.

In comparing the cost of MPS gas with the cost of acetylene, differences in cylinder yield and consumption rate must be considered. A 54 kg (120 lb) cylinder of MPS gas yields 17.5 m^3 (620 ft^3) of gas; a 115 kg (240 lb) cylinder of acetylene yields only 7.4 m^3 (260 ft^3) of gas. In addition, acetylene bums faster. Thus, storage, transportation, and time and labor for changing cylinders become important cost factors.

Methylacetylene-propadiene-stabilized gas competes with acetylene for almost every job that uses fuel gas. Its most unusual use perhaps is in deep water cutting. Because acetylene outlet pressure is limited to 105 kPa gage pressure (15 psig), it cannot be used below 9 m (30 ft) of water. The Navy and several shipyards use MPS gas for underwater work. Table 6 provides data for oxy/MPS gas cutting of carbon steel plate.

TABLE 6 RECOMMENDED PARAMETERS FOR OXY/MPS GAS CUTTING OF CARBON STEELS

PLATE THICKNESS		CUTTING TIP NO.[A]	CUTTING SPEED		OXYGEN								MPS GAS					
					CUTTING PRESSURE[B]		CUTTING RATE OF FLOW		PREHEAT PRESSURE		PREHEAT RATE OF FLOW		CUTTING PRESSURE		CUTTING RATE OF FLOW		KERF WIDTH	
mm	in.		mm/min	in./min	kpa	psi	m^3/h	ft^3/h	kpa	psi	m^3/h	ft^3/h	kpa	psi	m^3/h	ft^3/h	mm	in.
CUTTING WITH STANDARD-PRESSURE TIPS																		
3.2	$\frac{1}{8}$	75	760-915	30-36	275 345	40-50	0.344).42	12-15	35-70	5-10	0.20-0.71	7-25	14-70	2-10	0.06-0,28	2-10	0,64	0.025
4.7	$\frac{3}{16}$	72	660-815	26-32	275-345	40-50	0.57-0.85	20-30	35-70	5-10	0.20-0.71	7-25	14-70	2-10	0.06-0.28	2-10	0.76	0.03
6.4	$\frac{1}{4}$	68	610-760	24-30	275-345	40-50	0.85-1.13	30-40	35-70	5-10	0.20-0.71	7-25	14-70	2-10	0.06-0.28	2-10	1.02	0.04
13	$\frac{1}{2}$	61	560-710	22-28	275-345	40-50	1.56-1.84	55-65	35-70	5-10	0.34-0,71	12-25	14-70	2-10	0.14-0.28	5-10	1.27	0.05
19	$\frac{3}{4}$	56	405-560	16-22	275-345	40-50	1.70-2.12	60-75	35-70	5-10	0.34-0.71	12-25	14-70	2-10	0.14-0.28	5-10	1.52	0.06
25	1	56	355-510	14-20	275-345	40-50	1.70-2.12	60-75	35-70	5-10	0.34-0.71	12-25	14-70	2-10	0.14-0.28	5-10	1.52	0.06
32	$1\frac{1}{4}$	54	330-430	13-17	345-415	50-60	2.97-3.40	105-120	70-140	10-20	0.57-0.99	20-35	14-70	2-10	0.23-0.42	8-15	2.03	0.08
38	$1\frac{1}{2}$	54	305-405	12-16	345-415	50-60	2.97-3.40	105-120	70-140	10-20	0.57-0.99	20-35	14-70	2-10	0.23-0.42	8-15	2.03	0.08
50	2	52	255-355	10-14	345-415	50-60	4.10-5.38	145-190	70-140	10-20	0.57-0.99	20-35	14-70	2-10	0.23-0.42	8-15	2.29	0.09
64	$2\frac{1}{2}$	48	230-330	9-13	345-415	50-60	5.95-7.50	210-265	70-205	10-30	0.57-1.42	20-50	41-70	6-10	0.23-0.57	8-20	2.54	0.10
75	3	48	205-330	8-13	345-415	50-60	5.95-7.50	210-265	70-205	10-30	0.57-1.42	20-50	41-70	6-10	0.23-0.57	8-20	2.54	0.10
100	4	46	180-305	7-12	415-485	60-70	8.21-9.34	290-330	70-205	10-30	0.71-1.42	25-50	41-70	6-10	0.28-0.57	10-20	3.81	0.15
125	5	46	150-255	6-10	485-550	70-80	9.34-11.46	330-405	70-205	10-30	0.71-1.42	25-50	41-70	6-10	0.28-0.57	10-20	3.81	0.15
150	6	42	125-205	5-8	415-485	60-70	10.62-13.31	375-470	70-205	10-30	0.71-1.42	25-50	41-105	6-15	0.28-0.57	10-20	4.06	0.16
205	8	35	100-	4-7	415-	60-	13.73-	485-	205-	30-	1.13-	40-	70-	10-	0.57-	20-	4.83	0.19

			180		485	70	16.70	590	345	50	2.83	100	105	15	1.27	45		
255	10	30	75-150	3-6	275-485	40-70	14.16-17.69	500-625	205-345	30--50	1.13-2.83	40-100	70-105	10-15	0.57-1.27	20-45	5.08	0.20
305	12	30	75-125	3-5	345-585	50-85	18.26-24.49	645-865	205-345	30-50	1.70-4.25	60-150	70-105	10-15	0.85-1.70	30-60	5.33	0.21
CUTTING WITH HIGH-SPEED TIPS																		
3.2	$\frac{1}{8}$	75	815-965	32-38	415-485	60-70	0.57-0.71	20-25	35-70	5-10	0.20-0.71	7-25	14-70	2-10	0.08-0.28	3-10	0.64	0.025
4.7	$\frac{1}{16}$	72	710-815	28-32	485-550	70-80	0.85-1.13	30-40	35-70	5-10	0.20-0.71	7-25	14-70	2-10	0.08-0.28	3-10	0.76	0.03
6.4	$\frac{1}{4}$	68	660-815	26-32	485-550	70-80	1.56-1.84	55-65	35-70	5-10	0.20-0.71	7-25	14-70	2-10	0.08-0.28	3-10	1.27	0.05
13	$\frac{1}{2}$	61	610-760	24-30	550-620	80-90	2.12-2.70	75-95	35-70	5-10	0.34-0.71	12-25	14-70	2-10	0.14-0.28	5-10	1.52	0.06
19	$\frac{3}{4}$	56	510-660	20-26	550-620	80-90	3.26-3.68	115-130	35-70	5-10	0.34-0.71	12-25	14-70	2-10	0.14-0.28	5-10	1.78	0.07
25	1	56	455-610	18-24	550-620	80-90	3.26-3.68	115-130	35-70	5-10	0.34-0.71	12-25	14-70	2-10	0.14-0.28	5-10	1.78	0.07
32	$1\frac{1}{4}$	54	405-510	16-20	485-550	70-80	4.39-4.81	155-170	70-140	10-20	0.57-0.99	20-35	14-70	2-10	0.23-0.42	8-15	2.03	0.08
38	$1\frac{1}{2}$	54	380-485	15-19	550-620	80-90	4.81-5.10	170-180	70-140	10-20	0.57-0.99	20-35	14-70	2-10	0.23-0.42	8-15	2.03	0.08
50	2	52	355-455	14-18	550-620	80-90	6.09-7.22	215-255	70-140	10-20	0.57-0.99	20-35	14-70	2-10	0.23-0.42	8-15	2.29	0.09
64	$2\frac{1}{2}$	52	305-430	12-17	550-620	80-90	6.09-7.22	215-255	70-140	10-20	0.57-0.99	20-35	14-70	2-10	0.23-0.42	8-15	2.29	0.09
75	3	48	255-380	10-15	550-620	80-90	9.48-11.32	335-400	70-140	10-20	0.57-0.99	20-35	41-70	6-10	0.28-0.42	10-15	2.54	0.10
100	4	46	230-355	9-14	550-620	80-90	10.61-12.03	375-425	70-140	10-20	0.57-0.99	20-35	41-70	6-10	0.28-0.42	10-15	3.05	0.12

Note: All recommendations are for straight-line cutting with a three-hose torch perpendicular to work.

(A) ALL TIPS ARE OF DESIGN RECOMMENDED BY THE SUPPLIER.

(B) PRESSURE OF CUTTING OXYGEN MEASURED AT THE TORCH.

Effect of Oxyfuel Cutting on Base Metal

During cutting of steel, the temperature of a narrow zone adjacent to the cut face is raised considerably above the transformation range. As the cut progresses, the steel cools through this range. Cooling rate depends on the heat conductivity and the mass of the surrounding material, on loss of heat by radiation and convection, and on speed of cutting. When steel is at room temperature, the rate of cooling at the cut is sufficient to produce a quenching effect on the cut edges, particularly in heavier cuts in large masses of cold metal. Depending on the amount of carbon and alloying elements present, and on the rate of cooling, pearlitic steel transforms into structures ranging from spheroidized carbides in ferrite to harder constituents. The HAZ may be 0.8 to 6.4 mm ($\frac{1}{32}$ to $\frac{1}{4}$ in.) deep for steels 9.5 to 150 mm ($\frac{3}{8}$ to 6 in.) thick. Approximate depths of the HAZ in oxyfuel gas cut carbon steels are given in Table 7. Some increase in hardness usually occurs at the outer margin of the HAZ of nearly all steels.

TABLE 7 APPROXIMATE DEPTHS OF HAZ IN OXYGEN CUT CARBON STEELS

PLATE THICKNESS		HAZ DEPTH	
MM	IN.	MM	IN.
LOW-CARBON STEELS			
<13	$<\frac{1}{2}$	<0.8	$<\frac{1}{32}$
13	$\frac{1}{2}$	0.8	$\frac{1}{32}$
150	6	3.2	$\frac{1}{8}$
HIGH-CARBON STEELS			
<13	$<\frac{1}{2}$	<0.8	$<\frac{1}{32}$
13	$\frac{1}{2}$	0.8-1.6	$\frac{1}{32}$-$\frac{1}{16}$
150	6	3.2-6.4	$\frac{1}{8}$-$\frac{1}{4}$

Note: The depth of the fully hardened zone is considerably less than the depth of the HAZ. For most applications of gas cutting, the affected metal does not have to be removed.

Low-Carbon Steel. For steels containing 0.25% C or less cut at room temperature, the hardening effect usually is negligible, though at the upper carbon limit it may be significant if subsequent machining is required. Short of preheating or annealing the workpiece, hardening may be lessened by ensuring that (1) the cutting flame is neutral to slightly oxidizing, (2) the flame is burning cleanly, and (3) that the inner cones of the flame are at the correct height. By increasing the machining allowance slightly, the first cut usually can be made deep enough to penetrate below the hardened zone in most steels. Mechanical properties of low-carbon steels generally are not adversely affected by OFC. Typical data for OFC of low-carbon steel plate are given in Tables 1, 2, 3, 4, 5, and 6.

Medium-Carbon Steels. Steels having carbon contents of 0.25 to 0.45% are affected only slightly by hardening caused by OFC. Up to 0.30% C, steels with very low alloy content show some hardening of the cut edges, but generally not enough to cause cracking. Over 0.35% C, preheating to 260 to 315 °C (500 to 600 °F) is needed to avoid cracking. All medium-carbon steels should be preheated if the gas cut edges are to be machined.

High-Carbon and Alloy Steels. Oxyfuel gas cutting of steels containing over 0.45% C and of hardenable alloy steels at room temperature may produce a thin layer of hard, brittle material on the cut surface that may crack from the stress of cooling. Preheating and annealing may alleviate hardening and the formation of residual stress.

Preheating to 260 to 315 °C (500 to 600 °F) is sufficient for high-carbon steels; alloy steels may require preheating as high as 540 °C (1000 °F). Preheat temperature should be maintained during cutting. Thick preheated sections should be cut as soon as possible after the piece has been withdrawn from the furnace.

Local preheating heats the volume of the workpiece enclosing the HAZ of the cut. If the volume of material to be heated is small, the flame of a cutting. torch can be used for preheating. When the workpiece is thick and broad, a special heating torch may be necessary. Workpieces must be heated uniformly through the section to be cut, without excessive temperature gradient.

Distortion, which is the result of heating by the gas flame, can cause considerable damage during (1) cutting of thin plate (less than 7.9 mm, or $\frac{5}{16}$ in., thick), (2) cutting of long narrow widths, (3) close-tolerance profile cutting, and (4) cutting of plates that contain high residual stresses. The heat may release some of the restraint to locked-in stress, or may add new stress. In either case, deformation (warpage) may occur, thus causing inaccurate finished cuts. Plates in the annealed condition have little or no residual stress.

Deformation. In cuts made from large plates, the cutting thermal cycle changes the shape of narrow sections and leaves residual stress in the large section (see Fig. 2). The temperature gradient near the cut is steep, ranging from melting point at the cut to room temperature a short distance from it. Plate does not return to its original shape unless the entire plate is uniformly heated and cooled.

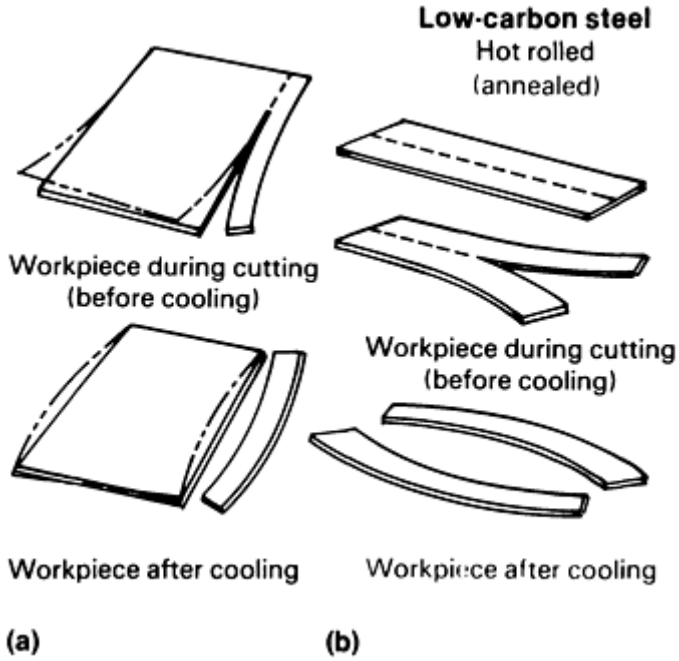

FIG. 2 EFFECTS OF OFC THERMAL CYCLE ON SHAPE OF SECTIONS. (A) PLATE WITH LARGE RESTRAINT ON ONE SIDE OF KERF, LITTLE RESTRAINT ON THE OTHER SIDE. PHANTOM LINES INDICATE DIRECTION OF RESIDUAL STRESS THAT WOULD CAUSE DEFORMATION EXCEPT FOR RESTRAINT. (B) PLATE WITH LITTLE RESTRAINT ON EITHER SIDE

As the metal heats, it expands and its yield strength decreases; the weakened heated material is compressed by the surrounding cooler, stronger metal. The hotter metal continues to expand elastically in all directions until its compressive yield strength is reached, at which point it yields plastically in directions not under restraint. The portion of this upset metal above 870 °C (1600 °F) is virtually stress-free; the remainder is under compressive stress that is equal to its yield strength. Metal that expands but does not upset is under compressive strength below yield. The net stress on the heated side of the neutral axis causes bowing of a narrow plate during cutting, as shown in Fig. 2.

As the heated metal begins to cool, it contracts, and its strength increases. First, the contraction reduces the compressire stress in the still-expanded metal. When the compressive stress reaches zero and the plate regains its original shape,

previously upset metal also has regained strength. This metal is now in tension as it cools, and its tensile yield strength increases. Tension increases until the metal reaches room temperature. Residual tensile stress in the cooling side of the neutral axis causes the bowing of narrow plates after cooling (see Fig. 2). Controlled upsetting is the basis of flame straightening.

Control of Distortion. Preheating the workpiece can reduce distortion by reducing differential expansion, thereby decreasing stress gradients. Careful planning of the cutting sequence also may help. For example, when trimming opposite sides of a plate, both sides should be cut in the same direction at the same time. When cutting rings, the inside diameter should be cut first; the remaining plate restrains the material for the outside-diameter cut. In general, the larger portion of material should be used to retain a shape for as long as possible; the cutting sequence should be balanced to maintain even heat input and resultant residual stresses about the neutral axis of plate or part.

Oxyfuel Gas Cutting

Equipment

Commercial gases usually are stored in high-pressure cylinders. Natural gas--primarily methane--is supplied by pipeline from gas wells. The user taps into local gas lines. Acetylene, dissolved in acetone, is available in clay-filled cylinders. High-volume users often have acetylene generators on site. For heavy consumption or where many welding and cutting stations use fuel gas, banks of gas cylinders are maintained at a central location in the plant, and the gas is manifolded and piped to the point of use.

Manual gas cutting equipment consists of gas regulators, gas hoses, cutting torches, cutting tips, and multipurpose wrenches. Auxiliary equipment may include a hand truck, tip cleaners, torch ignitors, and protective goggles. Machine cutting equipment varies from simple rail-mounted "bug" carriages to large bridge-mounted torches that are driven by computer-directed drives.

Gas regulators reduce gas pressure and moderate gas flow rate between the source of gas and its entry into the cutting torch to deliver gas to the cutting apparatus at the required operating pressure. Gas enters the regulating device at a wide range of pressures. Gas flows through the regulator and is delivered to the hose-torch-tip system at the operating pressure, which is preset by manual adjustment at the regulator and at the torch. When pressure at the regulator drops below the preset pressure, regulator valves open to restore pressure to the required level. During cutting, the regulator maintains pressure within a narrow range of the pressure setting.

Regulators should be selected for use with specific types of gas and for specific pressure ranges. Portable oxyacetylene equipment requires an oxygen regulator on the oxygen cylinder and an acetylene regulator on the acetylene cylinder, which are not interchangeable.

High-low regulators conserve preheat oxygen when natural gas or liquefied petroleum gas (LPG) is the preheat fuel used in OFC. These gases require a longer time to start a cut than acetylene or MPS. High-low regulators reduce preheat flow to a predetermined level when the flow of cutting oxygen is initiated. When the regulator switches from high to low, preheat cut-back may range from 75 to 25% as plate thicknesses increase from 9.5 to 205 mm ($\frac{3}{8}$ to 8 in.). High-low regulators are used for manual and automatic cutting with natural gas and with LPG.

Hose. Flexible hose, usually 3.2 to 13 mm ($\frac{1}{8}$ to $\frac{1}{2}$ in.) in diameter, rated at 1.4 MPa gage pressure (200 psig) maximum, carries gas from the regulator to the cutting torch. Oxygen hoses are green; the fittings have right-hand threads. Fuel gas hoses are red; the fittings have left-hand threads and a groove cut around the fittings. For heavy cutting, two oxygen hoses may be necessary--one for preheat and one for cutting oxygen. Multi-torch cutting machines often have three-hose torches.

Cutting torches, such as the one shown in Fig. 3, control the mixture and flow of preheat oxygen and fuel gas and the flow of cutting oxygen. The curing torch discharges these gases through a cutting tip at the proper velocity and flow rate. Pressure of the gases at the torch inlets, as well as size and design of the cutting tip, limits these functions, which are operator controlled.

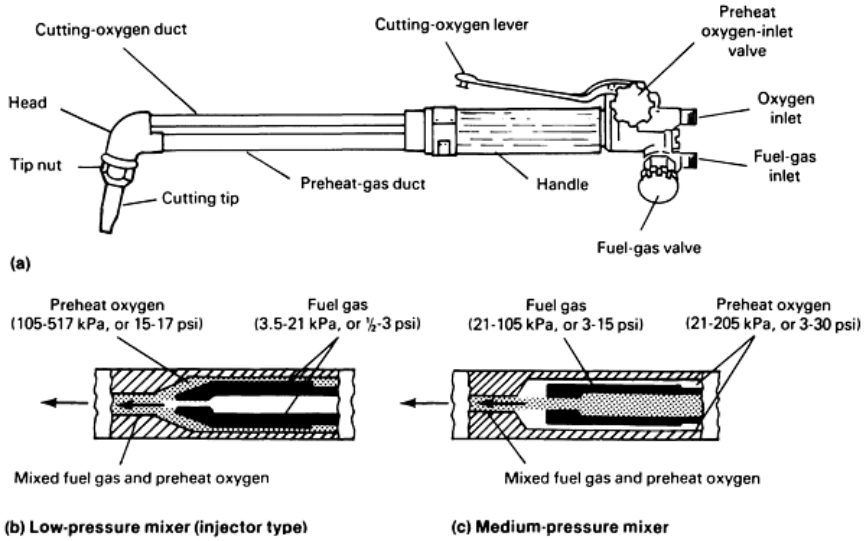

FIG. 3 TYPICAL MANUAL CUTTING TORCH IN WHICH PREHEAT GASES ARE MIXED BEFORE ENTERING TORCH HEAD. (B) AND (C) SECTIONS THROUGH PREHEAT GAS DUCT SHOWING TWO TYPES OF MIXERS COMMONLY USED WITH THE TORCH SHOWN. AFTER THE WORKPIECE IS SUFFICIENTLY PREHEATED, THE OPERATOR DEPRESSES THE LEVER TO START THE FLOW OF CUTTING OXYGEN. VALVES CONTROL THE FLOW OF OXYGEN AND FUEL GAS TO ACHIEVE REQUIRED FLOW AND MIXTURE AT THE CUTTING TIP.

Oxygen inlet control valves and fuel gas inlet control valves permit operator adjustment of gas flow. Fuel gas flows through a duct and mixes with the preheat oxygen; the mixed gases then flow to the preheating flame orifices in the cutting tip. The oxygen flow is divided--a portion of the flow mixes with the fuel gas, and the remainder flows through the cutting oxygen orifice in the cutting tip. A lever-actuated valve on the manual torch starts the flow of cutting oxygen; machine cutting starts the oxygen from a panel control.

Fuel gases supplied at low pressure, such as natural gas tapped from a city line, require an injector-mixer (Fig. 3b) to increase fuel gas flow above normal operating pressures. Optimum torch performance relies on proper matching of the mixer to the available fuel gas pressure.

Cutting tips are precision-machined nozzles, produced in a range of sizes and types. Figure 4(a) shows a single-piece acetylene cutting tip. A two-piece tip used for natural gas (methane) or LPG is shown in Fig. 4(b). A tip nut holds the tip in the torch. For a given type of cutting tip, the diameters of the central hole, the cutting oxygen orifice, and the preheat ports increase with the thickness of the metal to be cut. Cutting tip selection should match the fuel gas: hole diameters must be balanced to ensure an adequate preheat-to-cutting oxygen ratio. Preheat gas flows through ports that surround the cutting oxygen orifice. Smoothness of bore and accuracy of size and shape of the oxygen orifice are important to efficiency. Worn, dirty bores reduce cut quality by causing turbulence in the cutting oxygen stream.

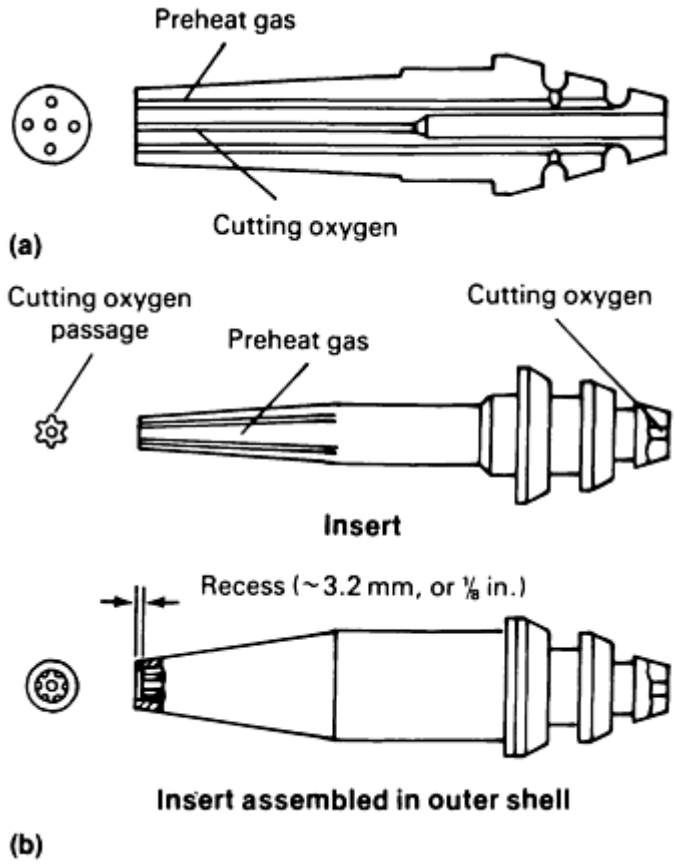

FIG. 4 TYPES OF CUTTING TIPS. (A) SINGLE-PIECE ACETYLENE CUTTING TIP. (B) TWO-PIECE TIP FOR NATURAL GAS OR LPG. FUEL GAS AND PREHEAT OXYGEN MIX IN TIP. RECESSED BORE HELPS PROMOTE LAMINAR FLOW OF GAS.

The size of the cutting tip orifice determines the rate of flow and velocity of the preheat gases and cutting oxygen. Flow to the cutting tip can be varied by adjustment at the torch inlet valve or at the regulator, or both.

Increasing cutting oxygen flow solely by increasing the oxygen pressure results in turbulence and reduces cutting efficiency. Turbulence in the cutting oxygen causes wide kerfs, slows cutting, increases oxygen consumption, and lowers quality of cut. Consequently, larger cutting tips are required for making heavier cuts.

Standard tips, as shown in Fig. 5(a), have a straight-bore oxygen port. Oxygen pressures range from 205 to 415 kPa (30 to 60 psi) and are used for manual cutting. High-speed tips, or divergent cutting tips (Fig. 5b), use a converging, diverging orifice to achieve high gas velocities. The oxygen orifice flares outward. High-speed tips operate at cutting oxygen pressures of about 670 kPa (100 psi) and provide cutting jets of supersonic velocity. These tips are precision made and are more costly than straight-drilled tips, but they produce superior results--improved edge quality and cutting speeds 20% higher than standard tips. Best suited to machine cutting, high-speed tips produce superior cuts in plate up to about 150 mm (6 in.) thick. Above this thickness, advantages of their use decrease; they are not recommended for cutting metal more than 255 mm (10 in.) thick.

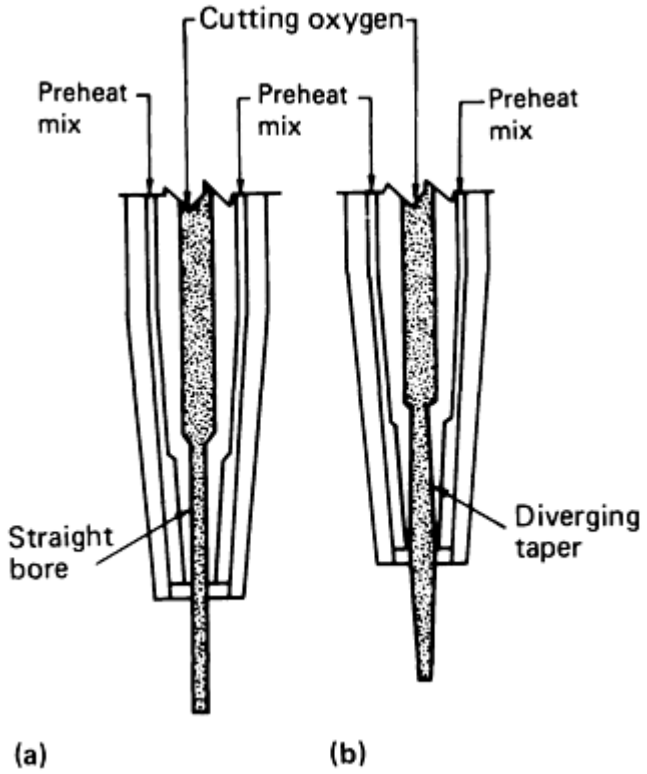

FIG. 5 OXYFUEL CUTTING TIPS. (A) STANDARD CUTTING TIP WITH STRAIGHT-BORE OXYGEN ORIFICE. (B) HIGH-SPEED CUTTING TIP WITH DIVERGENT-BORE OXYGEN ORIFICE

Equipment Selection Factors. Natural gas and liquefied petroleum gases operate most efficiently with high-low gas regulators, injector-type cutting torches, and two-piece, divergent, recessed cutting tips. Acetylene cutting is most efficient with divergent single-piece tips. If acetylene is supplied by low-pressure generators, an injector-type torch is best suited to most cutting applications.

Two-piece, divergent cutting tips are best suited for use with MPS gas; the tip recess should be less than for use of natural gas or propane. Injector-type torches and high-low regulators are not required with MPS gas.

Starting the Cut

To start a cut at the outer edge of the workpiece, the operator should place the cutting torch so that the ends of the inner cones in the preheating flame just clear the work metal. When a spot of metal at the top of the edge is heated to bright red, the stream of cutting oxygen is turned on. The reactions form a slot in the plate edge, and the torch can move along the desired line of cut. Piercing starts are necessary to cut holes, slots, and shapes.

In manual piercing, the spot should be heated to bright red. Then the torch should be raised to 13 mm ($\frac{1}{2}$ in.) above the normal cutting distance, and cutting oxygen should be turned on slowly. As soon as the metal is penetrated, the torch is lowered to cutting height and cutting action is started.

Machine torch piercing is similar to manual operations, except that torch travel begins after the cutting oxygen is slowly turned on and the flame starts to eject molten slag. Initial piercing action does not completely penetrate the plate, so that the completed pierce covers a short distance (depending on plate thickness) and forms a sloping trough with molten slag ejected from the torch. Length of the lead-in should be increased for heavy plate.

Light Cutting

Light cutting (material less than 9.5 mm, or $\frac{3}{8}$ in., thick) requires extra care in tip selection, tip cleanliness, and control of gas pressure. Quality of cut when oxyfuel gas cutting steel thinner than 3.2 mm ($\frac{1}{8}$ in.) is virtually impossible to control. Wide, uneven kerf, ragged edge, and distortion result from heat buildup.

For straight or large-radius cuts in thicknesses 3.2 mm ($\frac{1}{8}$ in.) and over, angling the cutting torch forward increases the distance through the cut and may help to deflect some of the heat input. When cutting shapes, however, the torch must be vertical.

One of the most important techniques for cutting of thin sections is stack cutting (see the section of this article on stack cutting for more detailed information on this process). This technique avoids the difficulties inherent in light cutting and also increases production. Sections stacked for cutting must be flat and tightly clamped together.

Oxyfuel Gas Cutting

Medium Cutting

In cutting plate 9.5 to 255 mm ($\frac{3}{8}$ to 10 in.) thick, OFC achieves its highest efficiency and produces the most satisfactory cuts. Conditions for medium cutting of carbon steel plate using a variety of oxyfuel combinations are presented in Tables 1, 2, 3, 4, 5, and 6. Commercial cuts must meet these requirements:

- DRAG IS SHORT, MARKINGS ON THE FACE OF THE CUT APPROACH VERTICAL.
- SIDE OF THE CUT IS SMOOTH, NOT FLUTED, GROOVED, OR RAGGED.
- SLAG SHOULD NOT ADHERE TO THE BOTTOM OF THE CUT.
- UPPER AND LOWER EDGES SHOULD BE SHARP.
- COST IS MODERATE.

The following variables require adjustment to obtain satisfactory commercial cuts:

- SUITABLE CUTTING TIP, WITH CUTTING ORIFICE OF CORRECT TYPE AND SIZE, AND PROPER DEGREE OF PREHEAT
- SUITABLE OXYGEN AND FUEL GAS PRESSURES
- CORRECT CUTTING SPEED
- UNIFORM TORCH MOVEMENT
- CLEAN, SMOOTH-BORE CUTTING ORIFICE AND PREHEAT HOLES
- HIGH-PURITY OXYGEN
- PROPER ANGLE OF THE CUTTING JET IN RELATION TO THE UPPER EDGE OF THE CUT

Surface finish for gas cut production parts is compared with sample cuts. One such group of machine cut samples is shown in Fig. 6. Sample A represents high quality, with drag varying about 2 to 7%. Samples B, C, D, and E show typical defects resulting from improper cutting speed or torch settings. The American Welding Society (AWS) provides standard plastic samples of cut edges.

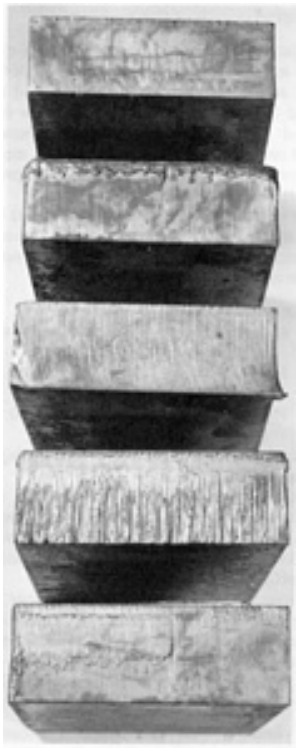

TORCH SETTINGS FOR BAR A[(A)]	
PREHEAT OXYGEN PRESSURE:	
HIGH (EDGE STARTING)	310 KPA (45 PSI)
LOW (CUTTING)	55-83 KPA (8-12 PSI)
PREHEAT NATURAL GAS PRESSURE:	
HIGH (EDGE CUTTING)	21 KPA (3 PSI)
LOW (CUTTING)	UNDER 430 PA (1 OZ/IN.^{2})
CUTTING OXYGEN PRESSURE	670 KPA (100 PSI)
CUTTING SPEED	255-380 MM/MIN (10-15 IN./MIN)

(A) SETTINGS FOR BARS B, C, D, AND E WERE VARIED AS NOTED IN THE LEGEND ABOVE. ALL BARS WERE CUT WITH TWO-PIECE DIVERGENT-NOZZLE (HIGH-SPEED) TIPS WITH 1.37 MM (0.054 IN.) DIAM CUTTING OXYGEN ORIFICE. ALL CUTTING WAS DONE WITH LOW PREHEAT SETTINGS, EXCEPT FOR BAR B, WHICH WAS CUT WITH BOTH PREHEAT

FIG. 6 COMPARISON OF SURFACE FINISH OF GAS CUT SPECIMENS. (A) PROPER SPEED, PREHEAT, AND CUTTING-OXYGEN PRESSURE. NOTE CLEAN FACE AND NEARLY STRAIGHT DRAG LINES. (B) PROPER SPEED AND CUTTING-OXYGEN PRESSURE, TOO MUCH PREHEAT. NOTE EXCESSIVE SLAG AND ROUNDING OF TOP EDGE. (C) PROPER PREHEAT AND CUTTING-OXYGEN PRESSURE, BUT TOO MUCH SPEED. NOTE INCREASE IN DRAG AND UNCUT CORNER AT LOWER LEFT. (D) PROPER SPEED AND PREHEAT, BUT TOO MUCH CUTTING-OXYGEN PRESSURE. SURFACE IS ROUGH AND TOP EDGE IS MELTED. (E) PROPER PREHEAT AND CUTTING-OXYGEN PRESSURE, BUT SPEED TOO LOW. BURNED SLAG ADHERES TO CUT SURFACE.

Tip Design. General-purpose cylindrical-bore tips operate best with cutting oxygen pressures of 205 to 415 kPa (30 to 60 psi); a pressure of 275 kPa (40 psi) is a good initial setting. Divergent-orifice tips operating with cutting oxygen pressures of about 690 kPa (100 psi), with variations of ± 140 kPa (±20 psi) may provide better results. Because tip size controls kerf width, a smaller tip should be used for a narrower kerf; the part may not drop free, and slower speed must be used. Larger-than-normal tips may be used when the metal is covered with thick scale.

Cutting Speed. Within recommended speed ranges, slow cutting produces the best results; higher speeds are used for maximum output. Optimum cutting speed may be determined by observing the material that is expelled from the underside of the workpiece. When speed is too slow, the cutting stream forms slag drippings. At excessive speed, a stream trails at a sharp angle to the bottom of the workpiece. Highest quality cutting occurs when a single, continuous stream is expelled from the underside for about 6.4 mm ($\frac{1}{4}$ in.), then breaks into a uniform spray. This condition is accompanied by a sound similar to that of canvas ripping.

Preheat. Less preheat is needed to continue a cut than to start it. When optimum quality is desired, the amount of preheat should be reduced after starting the cut. Commercially available devices automatically reduce preheat after cutting begins.

In thicknesses up to 50 mm (2 in.), excessive preheat may cause the top corner to melt and roll over. Insufficient preheat results in loss of cut. Correct preheat provides a continuous reaction with a sharp, clean top edge of the cut.

Kerf compensation, or the allowance of half the kerf width on the outline of the template, is the amount added for outside cuts and subtracted for inside cuts. In straight-line cutting or in following a layout, the operator may compensate for this measurement; in machine cutting, kerf compensation should be incorporated in the template. Many automatic machines incorporate kerf compensation in their controllers.

Machine Accuracy. When a machine is properly maintained, the guidance system controls accuracy. Mechanical followers are very accurate when properly adjusted. Compensation for the diameter of the follower wheel or spindle must be made in the same manner as for kerf width when making a template.

Kerf angle, the small deviation of the kerf wall from a right angle, may be caused by failure to set the torch perpendicular to the work. It may also be the result of widening of the cutting oxygen stream. In the latter case, the width of the kerf increases from the top to the bottom of the cut; this may be corrected in straight cutting by angling the torch slightly to make one wall of the kerf perpendicular. In shape cutting, where this cannot be done, kerf angle can be corrected by slightly reducing cutting oxygen pressure.

Plate movement may be vertical, caused by warp, or lateral, caused by planar expansion and contraction of the part. Vertical movement requires either manual or automatic control of torch height. A very slight allowance can be made in the initial setting of the tip-to-work distance. Lateral movement can be controlled by fixing the part to be cut on the plate support, wedging the cut within the stock plate, or allowing only a small amount of scrap trim around the part so that the scrap will move instead of the workpiece.

Heavy Cutting

Cutting of metal 255 mm (10 in.) or more in thickness requires attention to gas flow, preheat flame setting, drag, and starting technique. Standard cutting torches may be used to cut steel up to 455 to 510 mm (18 to 20 in.) thick; heavy-duty torches are necessary for sections up to 1525 mm (60 in.) thick.

Gas Flow Requirements. Heavy cutting requires a uniform supply of high-purity oxygen and fuel gas at constant pressure, and an adequate volume of cutting oxygen. Torches should have three hoses--one for the cutting oxygen, one for the preheat oxygen, and one for the fuel gas. This allows setting of proper pressures independently for preheating and cutting. Cutting oxygen hose should be at least 13 mm ($\frac{1}{2}$ in.) in diameter to ensure an adequate volume of oxygen at low pressure settings. Regulators should be used that are capable of providing the large volumes of gas required. Cutting oxygen flow requirements (ft^3/h) vary from 80 to 120 times (80*t* to 120*t*) the thickness to be cut measured in inches. Cutting oxygen consumption for shape cutting approaches 120*t* or higher; for straight-line cutting, it is between 80*t* and 100*t*. Pressures are 140 to 415 kPa (20 to 60 psi) at the torch.

Preheating. In heavy cutting, the preheat flame must extend almost to the bottom of the thickness to be cut to avoid excessive drag. If the cutting torch cannot deliver enough heat, an extra torch may be needed, or the workpiece may be furnace heated. A temperature boost of 95 to 150 °C (200 to 300 °F) assists cutting action considerably. Tip height above the work is important; if the tip is too close, excessive melting and rounding of the top edge occur. If too high, preheat will be insufficient and cutting will be slowed. Generally, 25 to 50 mm (1 to 2 in.) of separation is satisfactory.

The starting edge should be thoroughly preheated, with the preheated zone extending far down the face as shown in Fig. 7(a). As soon as the metal begins to melt, the flow of cutting oxygen and the cutting motion should proceed simultaneously, cutting at normal speed. The cut should progress down the face at a constant rate until it breaks through the bottom. Drag will be long at first, but it will shorten as soon as the cut is confined. Too slow a speed causes a shelf part way through the cut edge (Fig. 7e). Too high a speed results in incomplete penetration or in extremely long drag, as shown in Fig. 7(f).

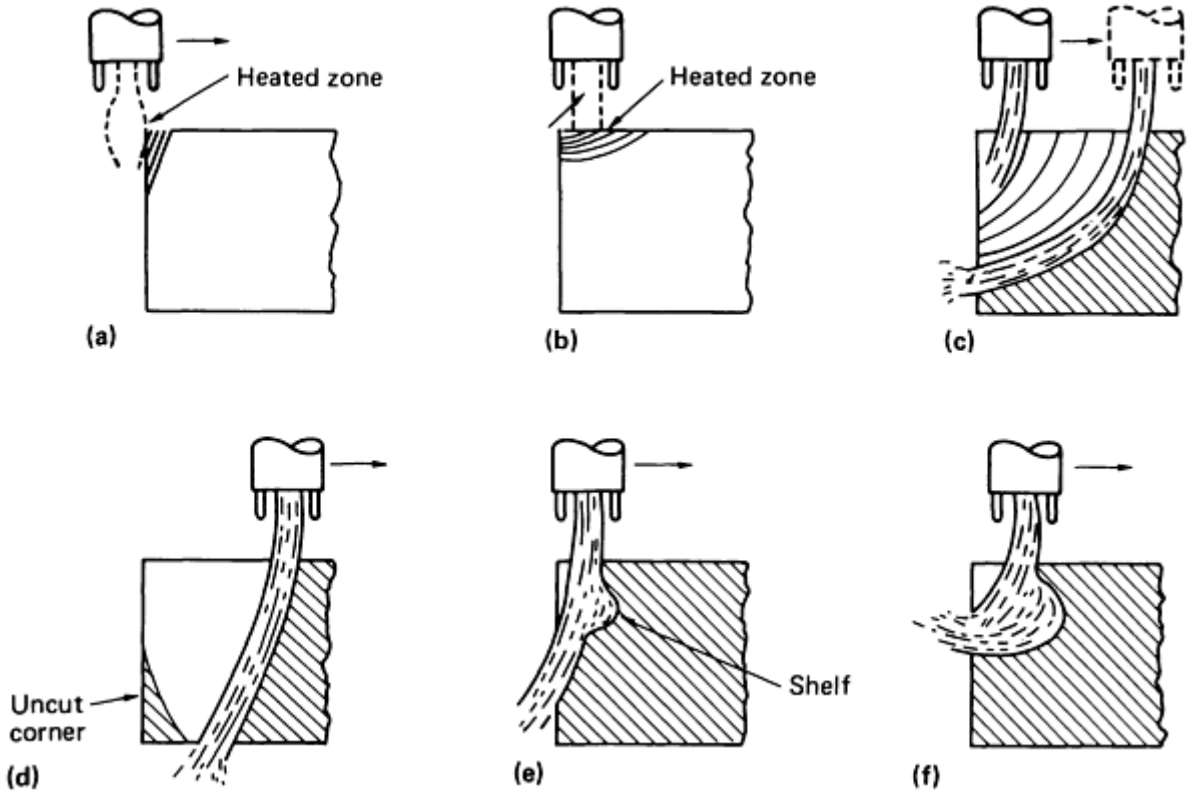

FIG. 7 PROPER AND IMPROPER TECHNIQUES FOR HEAVY CUTTING. (A) PROPER TORCH POSITION; PREHEAT IS PRIMARILY ON STARTING FACE. (B) IMPROPER START; OXYGEN STREAM IS TOO FAR ONTO WORK, WHICH RESULTS IN ACTION OF CUT AS SHOWN IN (C) AND IN UNCUT CORNER AS SHOWN IN (D). (E) EXCESSIVE OXYGEN PRESSURE OR ACTION OF CUT AT TOO LOW A SPEED. (F) INSUFFICIENT OXYGEN PRESSURE OR ACTION OF CUT AT TOO HIGH A SPEED

Drag. To successfully complete the cut (drop cutting), minimum drag conditions must exist, as shown in Fig. 8(a). Too much drag leaves an uncut corner at the end of the cut (Fig. 8b and c). Angled cutting may be used in straight-line work to counter drag (Fig. 8d and e), but for shape cutting, the torch must be perpendicular to the work.

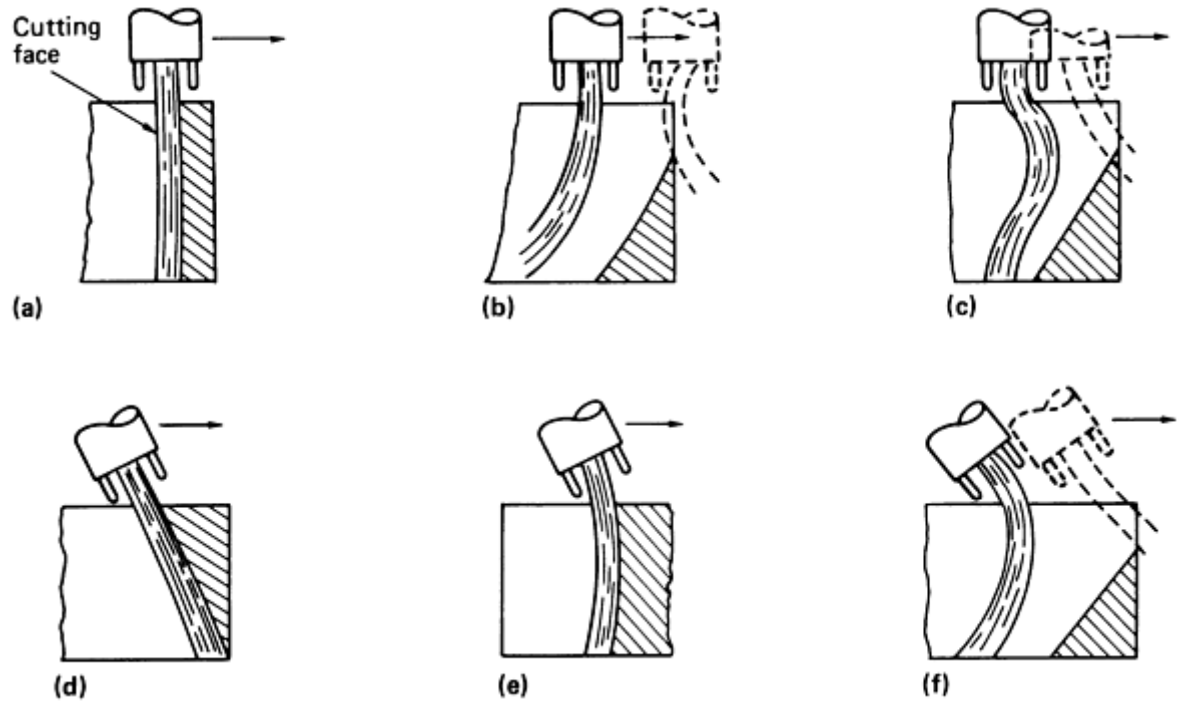

FIG. 8 PROPER AND IMPROPER TECHNIQUES FOR A HEAVY CUT. (A) MINIMUM DRAG (TYPICAL AT BALANCED CONDITIONS) PERMITS FLAME TO BREAK THROUGH CUTTING FACE UNIFORMLY AT ALL POINTS. (B) EXCESSIVE DRAG, TYPICALLY CAUSED BY INSUFFICIENT OXYGEN OR EXCESSIVE SPEED, RESULTS IN UNDERCUT. (C) FORWARD DRAG RESULTING FROM EXCESSIVE OXYGEN PRESSURE OR TOO LITTLE SPEED. (D) AND (E) FORWARD ANGLING OF TORCH TO MINIMIZE DRAG AND THUS AVOID AN UNCUT CORNER. (F) EXCESSIVE FORWARD ANGLING OF TORCH, RESULTING IN UNDERCUT

Starting. Extra care is needed in starting a heavy cut to avoid leaving an uncut corner or pocketing the flame in the lower portion of the cut. Starting sometimes is facilitated by first undercutting the forward edge of the material with a hand torch.

Cutting of Bars and Structural Shapes

To cut round steel bars, gas pressure should be adjusted for the maximum thickness (diameter), and the cut should be started at the outside. As the cut progresses, the torch should be raised and lowered to follow the circumference. The bar should be nicked with a chisel to make a burr at the point where the cut is to begin. Oxyfuel gas cutting of round bars is usually manual, so that the cut surface is rough. The chief advantage of OFC over sawing is that the torch can be brought to the work. The same advantage applies to OFC of various structural shapes.

Close-Tolerance Cutting

Shapes can be oxyfuel gas cut to tolerances of 0.8 mm ($\frac{1}{32}$ in.) in plate up to 64 mm ($2\frac{1}{2}$ in.) thick with multi-torch pantograph or coordinate-drive machines. Conditions must be optimum:

- OPERATORS MUST BE WELL TRAINED AND EXPERIENCED.
- MACHINES MUST BE PROPERLY ADJUSTED SO THAT THEY CAN TRACE AND RETRACE A PATTERN WITH ACCURACY OF ±0.13 MM (±0.005 IN.) IN A GIVEN DIRECTION.
- WORKPIECE MUST BE FLAT AND FREE OF DIRT, SCALE, GREASE, AND OIL.

- WORKPIECE SHOULD BE SUPPORTED OR RESTRAINED TO PREVENT MOVEMENT OF THE SHAPE DURING CUTTING.
- CUTTING TIP MUST BE CLEAN (SELECTED FOR HIGH-QUALITY, NARROW-KERF CUTTING).
- CUTTING SPEED AND GAS PRESSURES SHOULD BE TUNED TO SPECIFIC PRODUCTION CONDITIONS.

Optical tracing devices can follow an ink line 0.64 mm (0.025 in.) wide on paper. If cutting speed does not exceed 760 mm/min (30 in./ min), a template with an outside corner radius of 2.4 mm ($\frac{3}{32}$ in.) will produce a sharp corner. A 2.4 mm ($\frac{3}{32}$ in.) inside radius on the template produces a somewhat larger radius in the workpiece, depending on thickness and cutting tip. Numerical control tracing, whether punched tape or computer assisted, offers the greatest accuracy. Inaccuracies introduced by distortion of templates are avoided, and electronic directions are more exacting than those generated by mechanical cutting machines, which set limits on cutting speed.

Oxyfuel Gas Cutting

Safety*

The hazards of combustion or possible explosion associated with the gases used in OFC, as well as the presence of toxic gases and dust, make it necessary for the user to follow established safety precautions. The three areas of most concern, dealt with in this section, are protective clothing, handling and storage of gas cylinders, and the working environment.

Protective Clothing. Size, nature, and location of the work to be cut dictate the necessary protective clothing. The operator may require some or all of the following:

- TINTED GOGGLES OR FACE SHIELD:

- LIGHT CUTTING, UP TO 25 MM (1 IN.)--SHADE NO. 3 OR 4
- MEDIUM CUTTING, 25 TO 150 MM (1 TO 6 IN.)--SHADE NO. 4 OR 5
- HEAVY CUTTING, THICKER THAN 150 MM (6 IN.)--SHADE NO. 5 OR 6

- HARD HAT AND SOMETIMES A CLOSE-FITTING HAT BENEATH
- SAFETY GLASSES
- FLAME-RESISTANT JACKET, COAT, HOOD, APRON; WEAR WOOLEN CLOTHING, NOT COTTON OR SYNTHETIC FIBER; KEEP SLEEVES AND COLLARS BUTTONED, NO CUFFS; BUTTON-DOWN POCKETS
- PROTECTIVE GLOVES, WRISTLETS, LEGGINGS, AND SPATS. WHEN CUTTING PLATED OR COATED STOCK, RESPIRATORY PROTECTION SHOULD BE USED IF NECESSARY
- CLOTHING SHOULD BE FREE OF GREASE AND OIL, AND FREE OF RAGGED EDGES

Cylinders. Fuel gas cylinders should be placed in a location where they cannot be knocked over. Cylinders should be kept upright with valve ends up to avoid hazardous liquid withdrawal; the protective caps should never be removed except when the cylinders are connected for use. Cylinders should never be exposed to high heat or open flame, which could cause them to explode.

Cylinders should not be placed where they might complete an electric circuit, such as against a welding bench. They should not be used as an electrical ground or as a surface on which to strike an arc.

Damage to cylinders by impact should be avoided. Regulators should be removed before cylinders are moved, except on portable outfits. Slings or magnets should not be used as supports or rollers.

Damaged or defective cylinders should be removed from service immediately, tagged with a statement of the problem, and returned to the supplier. Leaking cylinders should be transported to an isolated location outdoors, the supplier notified, and his instructions for disposal followed.

No attempt should be made to fill a small cylinder from a large one. Filling requires special equipment and training.

Before storing, valves should be closed and caps replaced on empty or unused cylinders. Empty cylinders should be marked accordingly and kept separate from filled ones. Unused oxygen or fuel gas should not be drained from cylinders, and oxygen cylinders should be kept away from fuel gas cylinders.

Working Environment. Torches should not be used around chlorinated solvent vapors; heat forms phosgene and other corrosive, toxic products from them. Adequate ventilation must be provided, especially when alloys containing lead, cadmium, zinc, mercury, beryllium, or other toxic elements are being cut. A flame should not be used in a closed vessel or pipeline that has held flammable or explosive material, such as gasoline. Adequate ventilation should also be provided when work is being performed in a confined area. Under such conditions, the person doing the cutting should have an assistant in case trouble occurs.

Fire prevention warnings in "Safety in Welding and Cutting" (ANSI/AWS 249.1), which have legal status as Occupational Safety and Health Administration (OSHA) regulations, should be heeded. Workers should know the locations and operating procedures of the nearest fire extinguishers.

If cutting is to be done over concrete, it should be protected with metal or another suitable material; concrete spalls explosively when overheated. Hoses should be protected from sparks, hot slag, hot objects, sharp edges, and open flame.

Additional information is available in the article "Safe Practices" in this volume.

Note cited in this section

* *FROM WELDING ENGINEERING DATA SHEET NO. 491, "SAFETY CHECKLIST FOR OXYFUEL GAS CUTTING."

Plasma Arc Cutting

Chuck Landry, Thermal Dynamics Corporation

Introduction

PLASMA ARC CUTTING (PAC) is an erosion process that utilizes a constricted arc in the form of a high-velocity jet of ionized (electrically conductive) gas to melt and sever metal in a narrow, localized area.

Process Description. In the PAC process, a cool and inert gas, such as compressed air, is forced under pressure through a small orifice in the front of the cutting torch. This torch is connected by leads to a direct-current (dc) power supply. In the torch, a portion of the inert gas is changed into a plasma (ionized gas) by heat created by the discharge of a high-voltage arc from the power supply. This arc is created between an electrode (dc negative) in the torch and the tip (nozzle) of the torch through which the gas flows.

When a small amount of dc from the power supply is imposed on this high-voltage arc, it achieves a pilot arc that extends approximately 13 mm ($\frac{1}{2}$ in.), as a plasma jet from the tip orifice. This pilot arc acts as a path that establishes the main cutting arc to the workpiece. When the pilot arc is brought in contact with the metal workpiece, which is connected to the positive side of the dc power supply, the transferred (main) arc occurs and the pilot arc is shut off. The cutting torch is

then usually operated with a standoff, that is, the distance between torch and workpiece, of approximately 3 to 10 mm ($\frac{1}{8}$ to $\frac{3}{8}$ in.).

However, in some applications, the torch tip can actually be dragged along the workpiece. The transferred plasma arc heats the metal by the combined effects of the electric arc from the power supply, the high-temperature plasma created by constriction of the arc by the orifice, and the reassociation of the gas molecules at the workpiece. The molten metal is blown out of the cut, or kerf, by the high-velocity, well-columnated plasma jet, resulting in fast, clean cuts.

Plasma Arc Cutting

Chuck Landry, Thermal Dynamics Corporation

Equipment

The required equipment for the PAC process comprises:

- A TORCH DESIGNED FOR EITHER MANUAL OR MECHANIZED OPERATION
- TORCH LEADS THAT CARRY THE ELECTRIC POWER, GAS, AND COOLANT TO THE TORCH
- A COOLANT SYSTEM FOR THE TORCH
- A POWER SUPPLY THAT PROVIDES THE PROPER CURRENT AND VOLTAGE FOR THE PLASMA ARC
- A MANIFOLD SYSTEM FOR COMBINING POWER, GAS, AND COOLANT FOR CONNECTION TO THE TORCH
- A CONTROL SYSTEM THAT CONSISTS OF SWITCHES, GAGES, DIALS, METERS, AND OTHER CONTROLS FOR OPERATING THE PAC SYSTEM AND THE GAS SUPPLY

In its simplest form, a PAC system includes a gas-cooled torch with leads that connect to a power supply.

All PAC torches possess the same basic components (Fig. 1). The tip, or nozzle, of the torch contains the orifice that constricts the arc. The diameter of the orifice, which ranges from 1 to 6.4 mm (0.038 to 0.250 in.), determines the maximum cutting current that can be used with that tip. The larger the orifice, the more current that can be forced through it.

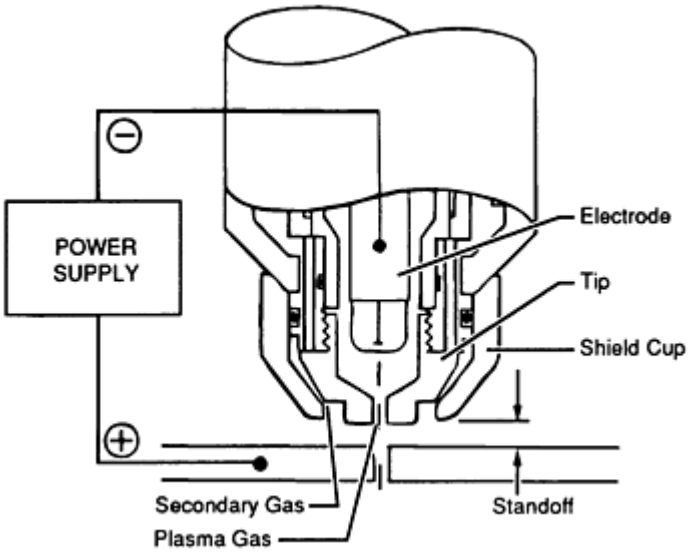

FIG. 1 TYPICAL PAC TORCH

Tips are designed so that the orifice provides maximum arc constriction. If a tip orifice is overpowered, then it will become gouged or washed out, resulting in a change of arc characteristics and in the deterioration of cut quality and cutting speed. To attain optimal cutting conditions, tips are used at or very near their maximum cutting rating. Torch tips are either water cooled, through internal passages connected to a closed-loop coolant system, or indirectly cooled, by good thermal contact with other torch parts that are either water or gas cooled.

The electrode, or cathode, in a PAC torch is the surface from which the plasma arc is generated. This electrode is in electrical contact with the negative potential in the power supply. Both electrode material and design are quite varied. For most applications that use nitrogen or argon-hydrogen as the plasma gas, a 2% thoriated tungsten is used as the electrode. Hafnium and zirconium are commonly used as electrode materials for both air and oxygen plasma cutting.

In terms of its construction, the electrode can be solid, such as a rod of tungsten or a tungsten element held in a solid-copper holder, or it can be hollow and have two pieces (copper and the electrode element) that allow direct water or gas cooling. Because proper cooling will promote both tip and electrode life, PAC torches designed for cutting above 150 A are usually water cooled.

In the area between the electrode and the tip orifice, which is called the plenum, the initial ionization or plasma formation takes place. The plasma gas enters the plenum in either a straight (laminar) flow pattern or a tangentially swirling pattern. Although torch design depends on several factors, pointed electrodes usually utilize laminar flow patterns, whereas flat or blunt-ended electrodes utilize a swirling gas to keep the arc attachment point moving around the center of the electrode. The swirl is most commonly imparted on the gas by a gas distributor, or swirl ring, that is located near the end of the electrode.

Other parts that are common to most PAC torches include internal ceramic or high-temperature plastic insulators for electrical insulation, collets or other mechanisms for retaining the electrode, and shield cups to insulate the front end of the torch from the workpiece.

Leads. The PAC torch is connected to the other system components by means of a leads package that consists of hoses, fittings, and wires. The leads supply the electric power, gases, and cooling medium to the torch. Lead lengths vary from 3 to 68 m (10 to 225 ft), depending on the application. Simple extension kits can be used to join leads packages together for increased length.

Cooling of PAC torches that operate at less than 150 A can be simply accomplished by properly channeling the gases used in torch operation. High-powered systems require a water-based coolant system, which consists of a reservoir, pump, and heat-exchanger assembly. Because this type of coolant is often in contact with both negative and positive electric potentials within the torch, it is important to use a deionized (nonconductive) coolant.

The power supply for a PAC system must have a dc output with the negative side connected to the electrode in the torch and the positive side connected to the workpiece. Systems that include a pilot arc also have a positive connection, limited in current through a resistor, to the tip in the torch. Power supplies are usually of a constant-current, dropping volt-amp curve design, and they have higher open-circuit voltages (up to 400 V) than those found in common welding power supplies, in order to accommodate the high operating voltage (90 to 200 V) of the torches. The amperage output of power supplies can be designed to have one fixed level, or several switchable fixed settings, or an infinitely adjustable output by means of a control potentiometer.

The manifold assembly combines the dc power, gas, coolant, and high-voltage starting circuitry and provides it to the cutting torch via the leads package.

Controls for starting and stopping the cutting operation, selecting the proper amperage output, adjusting gas flows, and regulating other system functions can be located on the manifold box, on the power supply, or in a dedicated control cabinet for convenient mounting near an operator station.

All-in-one packaged PAC systems that combine the coolant system, power supply, manifold assembly, and controls in one unit are available. These systems offer improved portability, simplicity of operation, and reduced costs.

Optional equipment for manual PAC systems includes drag-type shield cups with protrusions, or feet, that enable direct contact with the workpiece to allow the operator to maintain a constant standoff. Wheels that can be attached to the torch for manual guidance, as well as circle-cutting attachments that include an adjustable radius rod to allow the cutting of various-sized holes, are also available.

Optional equipment for mechanized PAC systems includes torch-standoff controls that automatically find and maintain the proper standoff for the cutting operation. Water-shrouded systems are also available. When used in conjunction with water tables, these systems provide a blanket of water around the front of the torch during the cut, in order to minimize smoke, fumes, noise, and arc glare.

Plasma Arc Cutting

Chuck Landry, Thermal Dynamics Corporation

Gases

The plasma or secondary shielding gases that are used in PAC systems are inert, and they are usually supplied from high-pressure cylinders, bulk tanks, or air compressors. Pressure regulators are adjusted to provide from 140 to 560 kPa (20 to 80 psi) of gas, depending on system requirements.

If water is used in place of a secondary gas, then it is usually supplied from a filtered, in-plant water system at a flow rate of 0.63 to 1.9 L/min (10 to 30 gal/h), again, depending on system requirements.

The purity of plasma gases is usually of a welding grade or higher. The plasma gas can be compressed air, which is inexpensive and provides fast, clean, high-quality cuts on carbon steels, but a relatively short electrode life, because of the rapid oxidation that occurs at high temperatures. If purity from an in-plant compressor is a problem, then either charcoal filters that remove oil vapors and moisture traps or dryers can be added into the line. As an alternative, clean, dry, compressed air can be obtained in cylinder form.

Another choice is nitrogen, which is relatively inexpensive and provides good-quality cuts on stainless steels and aluminum. It also provides good electrode life.

Argon-hydrogen, which is usually supplied in a 65 or 70% Ar and a 35 or 30% H mixture, operates at a higher temperature. It can reduce the quantity of smoke and fumes created during the cutting operation and provide a higher-quality surface finish on aluminum and stainless steels that are more than 12 mm (0.5 in.) thick. However, argon-hydrogen is usually from two to three times more expensive than nitrogen. In addition, it is not as readily available and requires more-critical adjustment of the operating parameters.

Oxygen plasma provides the same benefits as air plasma when cutting carbon steels. Because of the absence of nitrogen, it can minimize the amount of nitrides in the cut surface, thereby enabling better-quality welds on "as-cut" pieces that have not undergone additional finishing operations. Like air plasma, oxygen causes more-rapid electrode erosion than does nitrogen or argon-hydrogen plasma.

Operating Sequence

A routine check of the PAC system before power is applied involves examining the torch to ensure proper assembly, verifying adequate coolant and gas supplies, and inspecting all components of the system to verify that they are in order.

The disconnect switch can then be turned on, which applies power to the system. Gas supplies should be turned on and adjusted according to the recommended pressure or flow. The plasma gas should be allowed to purge for an additional 2 to 3 min in order to eliminate any traces of moisture that accumulated within the plasma lines. This moisture is usually the result of condensation that forms when the system is off for prolonged periods of time.

The "start-cut" signal can be supplied by either an operator who simply pushes a start button on a mechanized control station to energize the switch on a manually operated torch or by a computer-generated signal on a fully automated system. The start-cut signal will cause the main contactor in the power supply to energize and initiate a gas prepurge. The prepurge ensures that gas is at the torch before an arc is struck and can last from 2 to 10 s if extra-long torch leads are used. At the end of the prepurge, the high-frequency arc and pilot arc circuits are energized, establishing the pilot arc at the torch. The pilot arc duration can be controlled by a timing circuit, limiting it to approximately 5 s, or it can be continuous, thereby shutting off only after an actual cut is established. Some PAC systems include circuitry for an automatic restart pilot, which enables automatic cycling between the pilot and cut modes as long as the start signal is present. This type of operation is valuable when cutting expanded metal, grating, or other material with an interrupted cut line.

The cutting arc will begin as soon as the torch and pilot arc are brought close enough to the workpiece (usually, 13 to 25 mm, or $\frac{1}{2}$ to 1 in.) to allow main arc transfer. However, some systems do not use a pilot arc to start the torch. Rather, they only use high frequency, and require that the torch be placed within 1 mm (0.038 in.) to establish a cutting arc. The cutting action will continue as long as there is metal to which the arc can transfer. If the cutting speed is too fast, then the arc will not fully penetrate the metal, and an incomplete cut or gouge will occur. If the cutting speed is too slow, then the kerf will widen as available metal is blown away and, eventually, the arc will be extinguished.

When the "start signal" is removed, or when a stop signal is provided, the cutting arc or pilot arc will shut off and the system will enter a postpurge mode, which is a continuation of plasma gas flow for 2 to 40 s to ensure that the electrode cools in a good atmosphere and to remove any residual heat within the torch.

The system is then ready for the next start signal to begin the cutting sequence again. Some systems include circuitry that allows immediate starting of the pilot or cutting sequence at any time during the postpurge.

For manual operation, the torch is usually held with two hands to provide optimum comfort and speed control. An exception to this rule occurs when small, lightweight torches are used in conjunction with templates or a straight edge that requires one hand to be used for positioning while the other hand operates the torch.

There are two means of starting the cut in manual PAC systems: edge starts and pierce starts. For edge starting, the torch tip is usually placed directly over the edge of the workpiece. Resting the torch at the start position ensures that the cut will begin at the proper location. The torch switch is pressed and the torch is moved along the cut line as soon as the arc is established.

Piercing is best accomplished by slightly angling the torch over the starting point so that the molten metal is directed away from the torch. After starling the arc, the torch is moved to the vertical position and the cut proceeds along the cut

line. This technique prevents molten metal from blowing back at the torch and causing damage. Thicker metals may require that the torch be left stationary over the start point for a few seconds to ensure full arc penetration. Because a pierce will sometimes result in a blow hole that is larger than the normal kerf width, it is good practice to start the pierce off the cut line in the scrap piece to eliminate discontinuities in the cut surface of a good piece.

In mechanized applications, edge starts are accomplished by lining the torch up with the cut line. Pierce starts cannot be done in the same way as they are in manual cutting, because the torch cannot be conveniently angled and then brought back to a vertical position. Best results are achieved with a slow-moving pierce, in which the torch motion begins when the arc is struck. This allows the molten metal to flow back along the cut line until full penetration is achieved. Some allowance should be made for the start of a moving pierce to ensure that the entire piece is cut out.

A third means of starting the arc in mechanized applications is the running-edge start. In this mode, the torch is positioned off the workpiece, the pilot arc is established, and then the torch is put in motion. The cutting arc is established as soon as the pilot hits the edge of the work.

For either manual or mechanized operation, the best cut quality is usually achieved with a torch standoff of 3 to 10 mm ($\frac{1}{8}$ to $\frac{1}{2}$ in.). Thinner metals, under 3 mm ($\frac{1}{8}$ in.) thick, require a closer standoff. At low power levels (below 40 A), good-quality cuts can be obtained by dragging the torch tip in contact with the work.

The proper cutting speed for achieving the best quality is determined by the angle that the arc makes with a vertical plane as it exits the workpiece (Fig. 2). The optimal speed for air cutting is usually achieved when the arc is vertical (0°). Nitrogen and argon-hydrogen cuts are optimized by adjusting speed to obtain a 5 to 10° trailing arc. The best oxygen cuts are made using a speed that provides a slight (1 to 2°) leading arc. The PAC torch should always be kept square with the workpiece to provide maximum arc penetration and to obtain consistent quality when contour cutting.

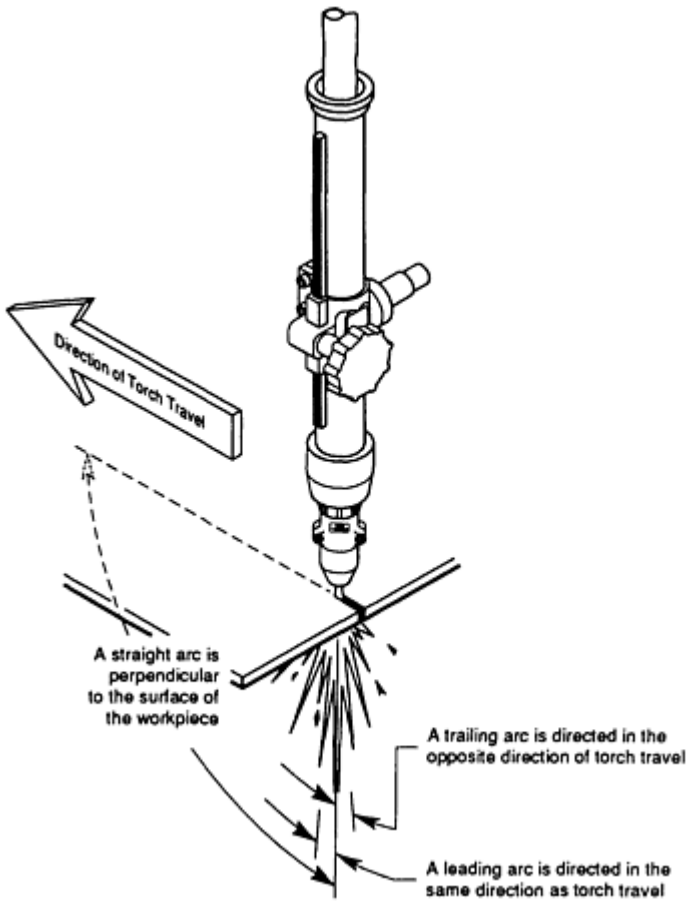

FIG. 2 ARC CHARACTERISTICS OF PAC TORCH

Chuck Landry, Thermal Dynamics Corporation

Process Considerations

Process Variations. The major difference between a conventional PAC process, which utilizes the basic system components described earlier, and other process variations is that the conventional PAC torch uses only a single gas, and the orifice in its tip represents the only gas exit. Because these torches do not incorporate any secondary gas, they must be liquid cooled.

Gas-shielded plasma arc cutting utilizes the traditional plasma gases plus a secondary gas that forms a shield around the plasma arc. The torch design provides special passages for this secondary gas. The functions of the secondary gas are to:

- ASSIST THE PLASMA IN BLOWING AWAY MOLTEN METAL
- ENABLE FASTER AND CLEANER CUTS
- PROVIDE BETTER COOLING OF THE TORCH FRONT END
- REDUCE ACCUMULATION OF METAL SPATTER ON THE TORCH
- REDUCE TOP-EDGE ROUNDING OF THE WORKPIECE
- PERMIT EASIER PIERCING
- MINIMIZE DOUBLE ARCING

In gas-cooled, rather than liquid-cooled, torches, it is the secondary gas that provides the cooling action. The choice of secondary gas can also affect cut quality, cutting speed, and the amount of smoke and fumes produced during the PAC process.

Water-shielded plasma arc cutting is a variation of the gas-shielded process that is only used in mechanized applications. The water, which can be provided from standard plant water systems at a rate of 0.63 to 0.95 L/min (10 to 15 gal/h), is substituted for the secondary gas in torches designed for this type of operation. Using a water shield, rather than a gas shield, is less expensive, because water is virtually free. It also results in reduced top-edge rounding, a reduced amount of smoke and fumes, and a clean, shiny, cut surface.

Water-injection plasma arc cutting is similar to the water-shielded process, except that the water is forced into the plasma stream, at approximately 1.26 L/min (20 gal/h), just after the arc exits the tip orifice and just before it leaves the ceramic piece on the front end of the torch (Fig. 3). The impinging water increases the constriction and density of the plasma arc, resulting in improved cut squareness and increased cutting speed. Because of the entry of water at the tip orifice in a water-injection torch, the quality of water is more critical than that used in water-shielded cutting. A plant water system that has high levels of dissolved minerals may require water softeners in conjunction with the system in order to avoid rapid deterioration of part lifetimes. Water-injection cutting is only used in mechanized setups.

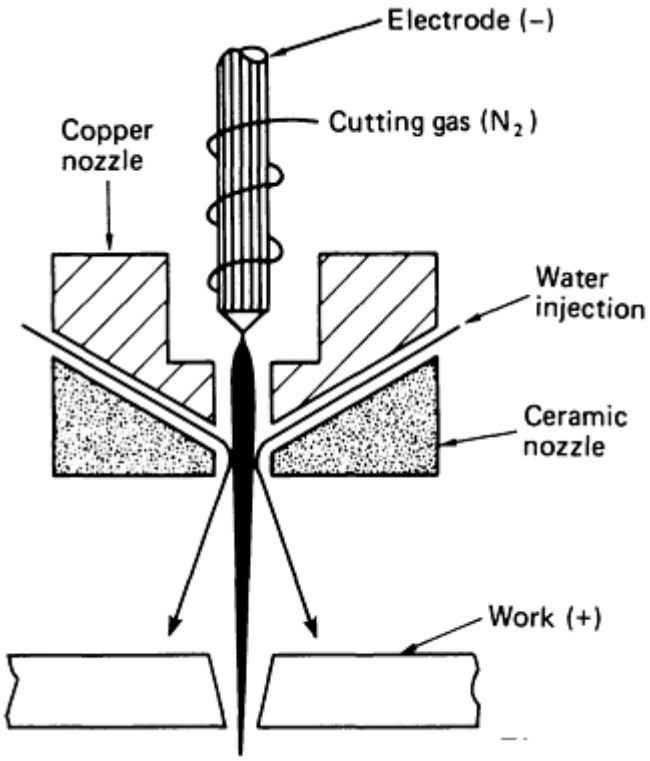

FIG. 3 WATER-INJECTION PAC TORCH

Process Capabilities. Plasma arc cutting is unique in its ability to make fast, clean cuts on both ferrous and nonferrous metals. When compared with the oxyfuel cutting of ferrous metals, the major advantage of this process it its speed, which can be from 4 to 5 times greater than the speed of oxyfuel cutting. For example, when cutting 6 mm ($\frac{1}{4}$ in.) carbon steel with an oxyfuel process, a speed of 0.68 m/min (27 in./min) is used, but when using a 150 A PAC system with air plasma, the speed goes up to 3.81 m/min (150 in./min) (Fig. 4). Because labor and overhead represent the primary costs of operating a mechanized cutting system, reducing the time to cut a part will, in turn, reduce the cost of the part itself. The five-fold increase in cutting speed of the PAC process, versus that of the oxyfuel process on carbon steel, will translate to a part cost of only one-fifth that achieved with the oxyfuel process.

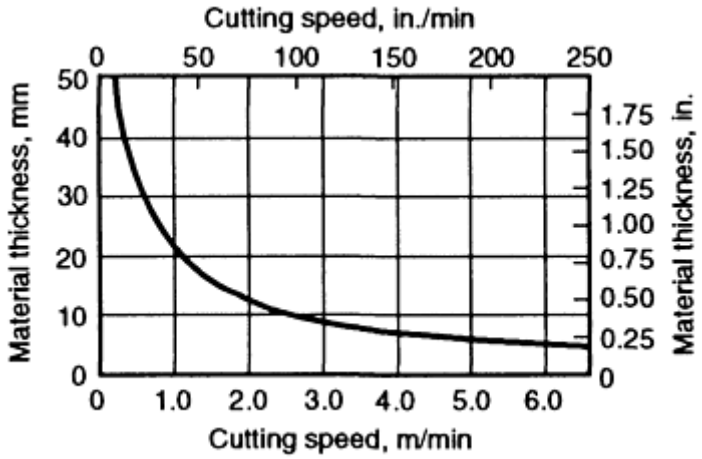

FIG. 4 CUTTING SPEEDS VERSUS MILD STEEL THICKNESS (150 A, AIR PLASMA)

Because the speed of the PAC process, like that of the oxyfuel process, is dependent on metal thickness, increasing thickness will diminish the speed advantage. Therefore, other factors that favor the PAC process have to be determined when comparing it with the oxyfuel process for cutting carbon steel that is more than 50 mm (2 in.) thick.

Another advantage of the PAC process, versus the oxyfuel process, is its ability to cut carbon steel with virtually no distortion, because of the fast travel speed and narrow, localized heating of the metal. This same high-speed localized heating results in a much narrower heat-affected zone (HAZ), that is, the depth of metallurgical change from the cut surface, than that of the oxyfuel process. Typical HAZs of up to 1.78 mm (0.070 in.) from oxyfuel cuts on carbon steel have been measured, whereas the PAC process produces HAZs of only 0.51 mm (0.020 in.). The HAZ will have an effect on the overall strength, corrosion resistance, and susceptibility to surface cracking of the cut part. If the application is such that the cut part must undergo machining to remove the HAZ, then the depth of machining required is much less with the PAC process.

Normally, PAC surfaces do not require any additional finishing operations before they are welded, although this usually depends on the final application and the codes to which the cut part being welded must conform.

The PAC process has the ability to make both edge starts and pierce starts without a preheat, as is required for oxyfuel cutting. This advantage becomes quite dramatic when the application calls for interrupted cuts, such as on grating or expanded metal.

These same capabilities apply to the cutting of stainless steel and aluminum. No preheat is required, and there is no distortion of the cut part. For plasma arc cuts on stainless steel and aluminum, respectively, the HAZ has been measured at 0.25 and 2.03 mm (0.010 and 0.080 in.).

Process Mechanization. Plasma arc cutting can be mechanized in several ways, the simplest of which takes the form of portable carriages or tractors. These devices can travel along a track to achieve straight-line cutting or along an arc guided either by a radius rod or by hand to cut curves. Although tractors are primarily used for simple cut-off, squaring, and trimming operations, they are also used as parts of large fixtures for cutting cast and rolled metals.

Pattern/follower wheel-shaped cutting machines or pantographs are used for the plasma arc cutting of relatively small, simple shapes. A scale model of the desired piece is held and traced by a follower that is connected, through a series of arms, to the torch, which cuts either an identical or a larger-scale part.

Optical tracing or electric-eye machines are used to trace part shapes that are in the form of templates or, more commonly, in the form of line drawings that are the same scale as the desired part. A mechanized PAC setup that uses optical tracing is shown in Fig. 5. The speed of an optical tracing machine is limited by the capability of the electric eye to follow a line. Low-speed machines that operate at speeds up to 1.52 m/min (60 in./min), which were originally designed for use with oxyfuel torches, are compatible with lower-amperage PAC systems. New high-speed machines, with speeds of up to 12.7 m/min (500 in./min), have been developed for operation with high-amperage plasma cutting systems.

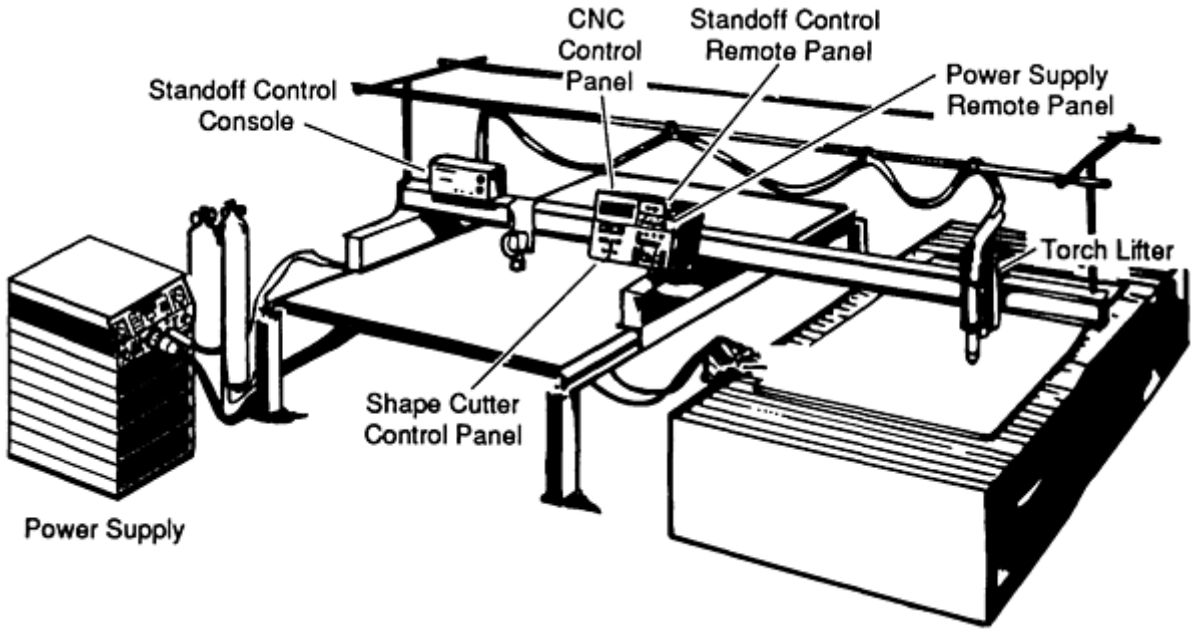

FIG. 5 MECHANIZED PAC SYSTEM THAT USES OPTICAL TRACING OF PART SHAPES

Computer numerical control (CNC) shape-cutting machines with speeds of up to 25.4 m/min (1000 in./min) represent the state of the art in automated cutting. CNC machines are much more reliable, have greater capabilities, and are lower priced than their numerical (tape) control machine predecessors, which are now considered obsolete. CNC machines can be connected directly into the central processor (direct numerical control) of a plant for complete integration of product design, material requirements, work in process, and other functions. Because the evolution of CNC machines paralleled that of mechanized PAC systems, their combination represents the highest level of productivity available in metal cutting today.

Automated material handling systems are sometimes used to keep up with the speed of CNC PAC systems. Typical systems utilize a raw material loading station, a cutting station, and a finished parts station. While the cutting operation is taking place, the operator is loading raw material and unloading finished parts. Upon completion of the cutting sequence, a conveyor moves the finished parts off the cutting area as it moves raw material onto the cut station. The operator signals the start-cut sequence and the cycle is repeated.

Robots are being used in increasing numbers for PAC operations involving the contour cutting of pipe and vessels, the removal of sprues and risers from castings, and the cutting of shapes in various planes of cast or formed parts. Material handling is also a great concern in robotics applications. Multiple work stations are the rule, because they allow an operator or another robot to load unfinished work and remove finished parts while the cutting operation is ongoing.

Cut Quality. Besides the HAZ, which was discussed above, several other factors (Fig. 6) that also must be considered in determining the quality of a plasma arc cut are the:

- CUT ANGLE
- DROSS
- SURFACE FINISH
- TOP-EDGE SQUARENESS
- KERF WIDTH

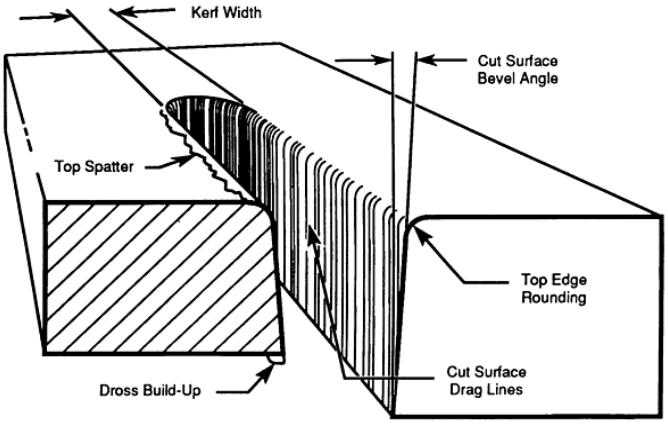

FIG. 6 CHARACTERISTICS OF A PLASMA ARC CUT

Cut Angle. Plasma arc cutting will usually result in an angle on the cut surface of approximately 1 to 3° on the "good" side and 3 to 8° on the "bad" side, when using torches that swirl the plasma. With laminar-flow torches, the angle on both sides is usually about 4 to 8°. These angles are most noticeable in mechanized applications where the torch is square to the workpiece. The good and bad sides of the cut are determined by torch travel direction and plasma gas swirl. With a clockwise gas swirl, the good side of the cut will be on the right with respect to torch motion. Therefore, in the cutting of a ring or flange in which the minimum angle is desired on both the inside and outside diameters, the outside would be cut in the clockwise direction, while the inside would be cut counterclockwise (Fig. 7). This change in angle from good side to bad side of the cut is the result of the arc attachment point on the cut surface and the release of energy on the good side before contact with the bad side occurs.

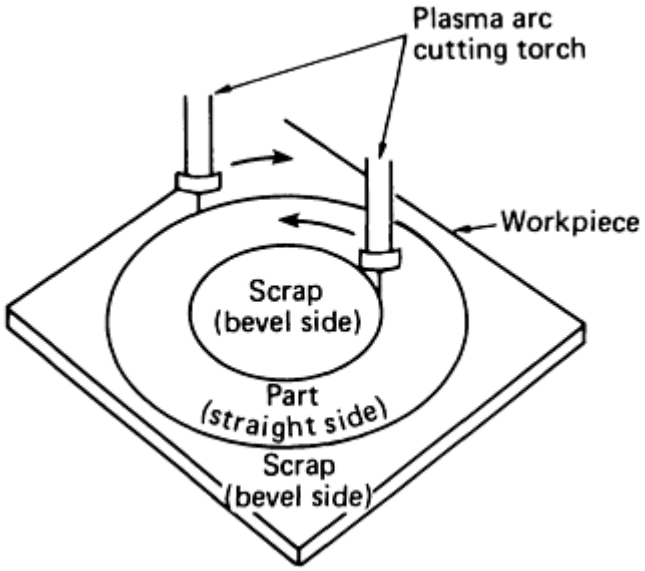

FIG. 7 PAC TORCH DIRECTION THAT ACHIEVES BEST QUALITY

Changing an internal torch part, such as the electrode or gas distributor, can enable those plasma cutting torches that create a gas swirl to change from a clockwise to a counterclockwise swirl direction. This then enables mirror-image cutting when using two torches in a mechanized setup, such as in strip-cutting applications.

Dross is the resolidified metal that adheres to the bottom edge of the plasma cut. The concentration of dross will be heavier on the bad side of the cut. The amount of dross that forms is a result of the type of metal being cut, the cutting speed, and the arc current. Dross can be formed from either too high or too low a cutting speed, but there is a "window"

between these two extremes in which dross-free cuts can usually be achieved. The dross-free range is greater on stainless steel and aluminum than it is on carbon steel and copper alloys. If dross-free cuts cannot be achieved, then a minimum amount of low-speed dross is more desirable, because it is more easily removed than the high-speed variety.

Surface Finish. The cut surface from the plasma arc process is normally rougher than that achieved by oxyfuel cutting on carbon steels, and it is definitely more rough than most machining processes. In most metals, this roughness usually appears as a ripple along the cut surface. This is partly due to the output waveform of the dc power supply (the smoother the output, the smoother the cut), but it is also determined to an extent by the gases used and the torch design. Water-shielded and water-injection plasma arc cutting provide much smoother cuts than do gas-shielded or conventional plasma techniques. The use of argon-hydrogen as a plasma or a shielding gas will result in smoother cut surfaces on most metals than when using nitrogen plasma or any other gas shield.

Top-Edge Squareness. Most metals experience some top-edge rounding when the PAC process is applied. Top-edge rounding is more pronounced on the thinner metals. This rounding is due to a higher heat concentration at the top of the cut, and can be minimized by using a gas-shielded PAC process. It can be even better controlled when water-shielded or water-injection plasma arc cutting is used.

The kerf width obtained by plasma arc cutting will be greater than that achieved by oxyfuel cutting on carbon steel, but not as great as that obtained by other processes, such as abrasive cutting or arc gouging. The rule of thumb for estimating the kerf in plasma arc cutting is that its width will be approximately 1.5 to 2 times the tip orifice diameter.

Plasma Arc Cutting

Chuck Landry, Thermal Dynamics Corporation

Applications

Plasma arc cutting is used in a variety of industries. End users of smaller systems with output capabilities of 100 A or less include:

- SMALL JOB SHOPS THAT MUST FABRICATE SPECIALTY AND SUBCONTRACTED ITEMS FROM STAINLESS STEEL, ALUMINUM, BRASS, COPPER, CARBON STEEL, GALVANIZED METAL, AND OTHER METALS
- MANUFACTURERS AND INSTALLERS OF DUCTWORK FOR HEATING, VENTILATING, AND AIR CONDITIONING, WHO MUST CUT GALVANIZED METALS
- MANUFACTURERS OF FOOD PROCESSING AND INSTITUTIONAL KITCHEN EQUIPMENT, WHO MUST CUT STAINLESS STEELS
- AUTOMOBILE MANUFACTURERS, AUTO BODY REPAIR SHOPS, AND DISMANTLERS, WHO MUST CUT HIGH-STRENGTH STEELS USED IN UNIBODY CONSTRUCTION
- MANUFACTURERS AND REBUILDERS OF OVER-THE-ROAD LIQUID TRANSPORT TRAILERS USED TO HAUL PETROLEUM, CHEMICALS, MILK, AND FERTILIZERS, WHO MUST CUT STAINLESS STEELS AND ALUMINUM
- CONTRACTORS AND MAINTENANCE DEPARTMENTS THAT ERECT AND MAINTAIN ALL KINDS OF PLANTS, INCLUDING FOOD PROCESSING, PETROLEUM, CHEMICAL, PULP AND PAPER MILLS, POWER PLANTS, AND MINING OPERATIONS

The end users of PAC systems with an output greater than 100 A include:

- LARGE SHOPS THAT FABRICATE SPECIALTY AND SUBCONTRACTED PARTS FROM VIRTUALLY ANY METAL
- STEEL WAREHOUSES AND SERVICE CENTERS THAT SIZE AND SHAPE-CUT BOTH FERROUS AND NONFERROUS METALS, AS WELL AS THOSE THAT SIZE SCRAP

- PIPE FABRICATORS AND PIPING CONTRACTORS, WHO MUST SIZE, BEVEL, AND MAKE INTERSECTION CUT-OUTS ON CARBON AND STAINLESS STEEL PIPE
- STRUCTURAL FABRICATORS, WHO MUST PERFORM HIGH-SPEED SLITTING OF H AND I BEAMS AND THE SIZING AND SLITTING OF PLATE
- MANUFACTURERS OF SHIPS, BARGES, AND OFF-SHORE RIG PLATFORMS, WHO MUST PERFORM PLATE SIZING, PIPE CUTOFF, BULKHEAD FABRICATION, AND PROPELLER TRIMMING
- ALUMINUM, STEEL, AND COPPER MILLS THAT SIZE AND STRIP ROLLED PLATE AND SHEET, OR THAT SIZE SCRAP, OR THAT PERFORM PLANT EQUIPMENT MAINTENANCE
- SCRAP YARDS THAT PERFORM HIGH-SPEED SIZING OF STAINLESS STEEL, COPPER, BRASS, ALUMINUM, AND OTHER METALS

Plasma Arc Cutting

Chuck Landry, Thermal Dynamics Corporation

Safety

Operators of PAC equipment should be aware of seven areas of potential hazards that are associated with the process. The proper operation of the equipment and adherence to certain precautions will minimize the risks involved.

Gases and Fumes. Potentially hazardous gases associated with the PAC process include ozone, nitrogen dioxide, and phosgene (caused by the breakdown of chlorinated solvents in ultraviolet light). Metal fumes vary with the composition of the metal being cut. Fumes of beryllium, cadmium, cobalt, copper, lead, mercury, silver, vanadium, and several other elements may be hazardous to individuals in the PAC area. Various limits imposed on the levels of gases and fumes in the work area are listed in a handbook published by the Occupational Safety and Health Administration (OSHA) and in the American Welding Society document A6.3-69, "Recommended Safe Practices for Plasma Arc Cutting."

Gases and fumes created by the PAC process can be effectively controlled by properly installed ventilation systems in the work area. Water tables that are used either alone, for surface or underwater cutting, or in conjunction with water-shrouded systems can effectively reduce gases and fumes. Respirators can be used when ventilation systems and water tables are impractical. Chlorinated solvents and other sources of phosgene gas should be removed from the PAC work area.

Noise. The high level of noise associated with some PAC operations (usually, high power) can lead to hearing damage. Maximum exposure times to various noise levels are printed in the OSHA handbook. The operator and any other personnel within the vicinity of the PAC operation should wear proper ear protection. Underwater cutting and the use of water-shrouded systems are effective means for reducing noise levels.

Radiant Energy. The ultraviolet infrared and visible light from the plasma arc can lead to injury of the eyes and skin. Operators and anyone else in the vicinity of the PAC operation should be protected by proper clothing that covers all skin and by welding helmets or shields that contain the proper shaded lens. For high-powered operations, the use of a number 10 (or greater) shaded lens may be required by the operator. If the intensity of the PAC process causes eye discomfort to the operator, a lens with a darker shade should be utilized.

Electric Shock. Both the input power to and the output from a PAC system is sufficient to be hazardous if an individual receives a shock from the system. Output voltages in the PAC process usually range from 100 to 200 V dc; typical welding processes run at 20 to 40 V dc. All equipment should be installed and maintained according to the USA Standard National Electrical Code and any local standards. All components of a PAC system should be properly earth grounded. System power should be shut off at a wall disconnect before the torch or any other system component is serviced. Any cracked insulators, power leads, or exposed live parts should be corrected immediately. Operators of PAC systems should be insulated from the workpiece and ground, and those who work in wet or damp areas should take precautions to ensure adequate protection from electric shock.

Fire. The sparks and the hot molten metal that is blown out of the cut can cause fires. Sparks that result from piercing can travel a considerable distance. All combustibles should be removed from the work area, and a fire extinguisher should be located in the vicinity. Because the pilot arc from a PAC torch is very hot, extra care should be taken to prevent it from contacting clothing and other flammable materials.

Compressed Gas Cylinders. High-pressure gas cylinders, which are often used to supply PAC systems, can be hazardous if they are not treated properly. Proper handling requires that valve covers always be in place when transporting cylinders, and that cylinders be secured to stationary objects by chains or lashing straps to prevent them from falling over.

Explosions. When hydrogen is used as a plasma or secondary gas, in conjunction with argon, extra care should be taken, because it is highly explosive. In some instances, explosions of hydrogen gas can occur even if hydrogen is not supplied as a portion of the plasma or secondary gas. This is because hydrogen can form when some metals, particularly aluminum, are being cut over a water table, by a reaction between the metal and the water, and by the dissociation of water that is due to the plasma arc. During the cutting operation, the plasma arc can ignite this hydrogen, which will explode if it is confined. Adequate ventilation of these hydrogen pockets is necessary for the safe operation of PAC systems. The water in the water table should not be any deeper than 50.8 mm (2 in.) below the bottom of the metal workpiece support bars. A blower system should be used to flush out all hydrogen from beneath the workpiece.

Air-Carbon Arc Cutting

Robert L. Strohl, Tweco Arcair

Introduction

AIR-CARBON ARC CUTTING (CAC-A) removes metal physically, rather than chemically, as in the oxyfuel cutting process. Gouging, or cutting, occurs when the intense heat of the arc between the carbon electrode and the workpiece melts part of the workpiece. Air simultaneously passes through the arc quickly enough to blow the molten material away. Because this process does not require oxidation to maintain the cut, it can gouge metals that the oxyfuel cutting process cannot. The metal re- moval rate depends on the melting rate and efficiency of the air jet in removing the molten metal. The air must lift the molten metal clear of the arc before the metal solidifies.

Applications. Industry has enthusiastically adopted CAC-A gouging for numerous applications, such as metal fabrication and casting finishing, chemical and petroleum technology, construction, mining, and general repair and maintenance.

The process is used throughout the world to create consistent grooves requiring little or no additional cleaning, on square-butt plate seams to prepare them for welding. The process can then be used to backgouge the seam to sound metal to ensure 100% penetration of the welded joint. If a problem arises during the welding process and an area of the weld does not meet specifications, then the process can be used to remove the defective area without damaging or detrimentally affecting the base metal.

The CAC-A process is also used in foundries to remove fins and risers from castings. It can then be used to smooth areas that contact the surface to prepare the casting for shipment. The process is flexible, efficient, and cost effective to use on numerous metals, such as carbon steel, stainless steel, and other ferrous alloys; gray, malleable, and ductile iron; aluminum; nickel; copper alloys; and other nonferrous metals.

Air-Carbon Arc Cutting

Robert L. Strohl, Tweco Arcair

Principles of Operation

Like electric arc welding, the CAC-A process requires an arc of intense heat to develop a molten pool on the workpiece. Compressed air then blows away this molten metal. The process requires a welding power source, an air compressor, a carbon electrode, and a gouging torch. Figure 1 shows how the components are typically arranged.

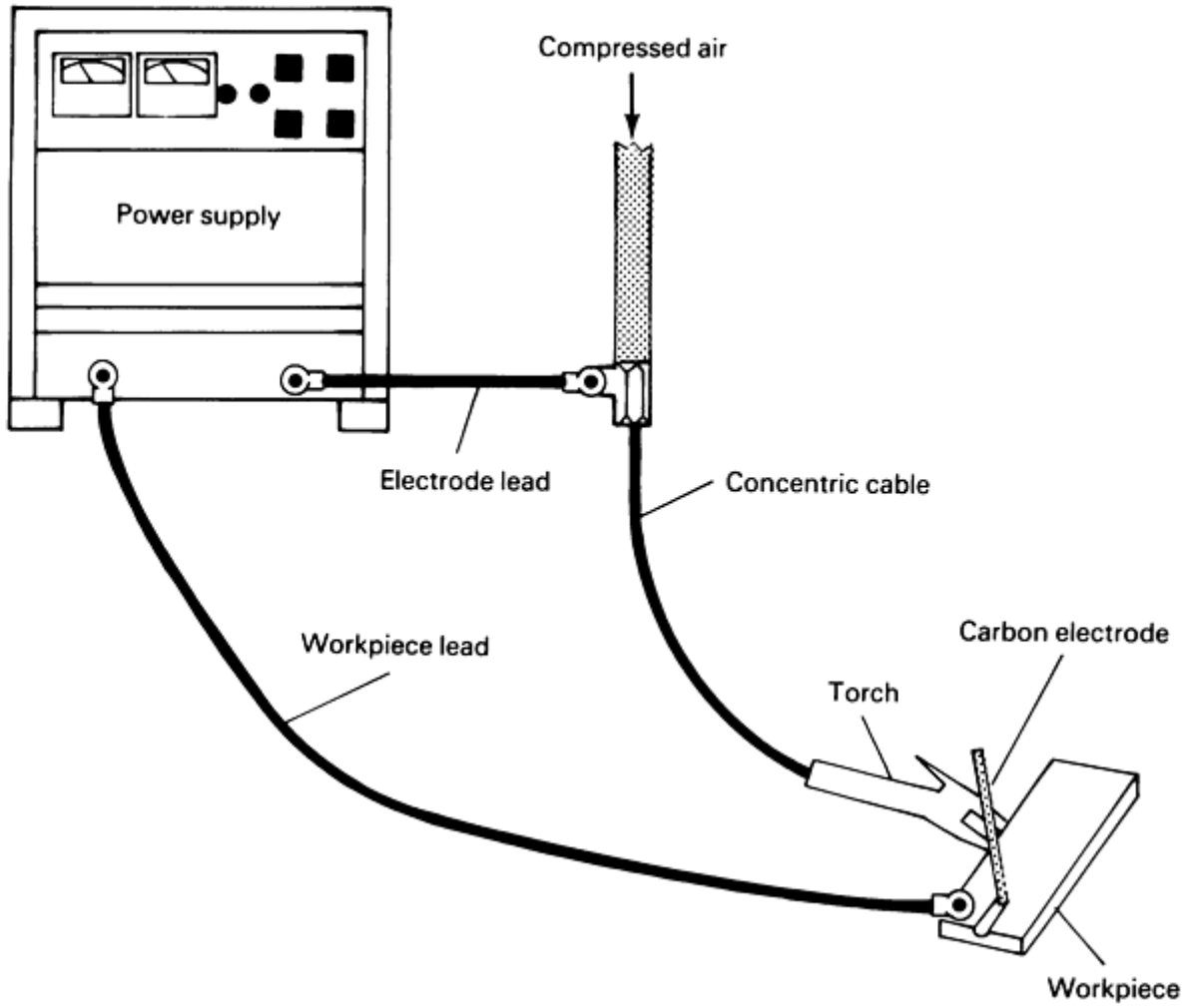

FIG. 1 ARRANGEMENT OF COMPONENTS USED IN THE CAC-A PROCESS

Cuts or gouges should be made only in the direction of the air flow. The electrode angle will vary, depending on the application. The cutter should maintain the correct arc length to enable air to remove molten metal (Fig. 2).

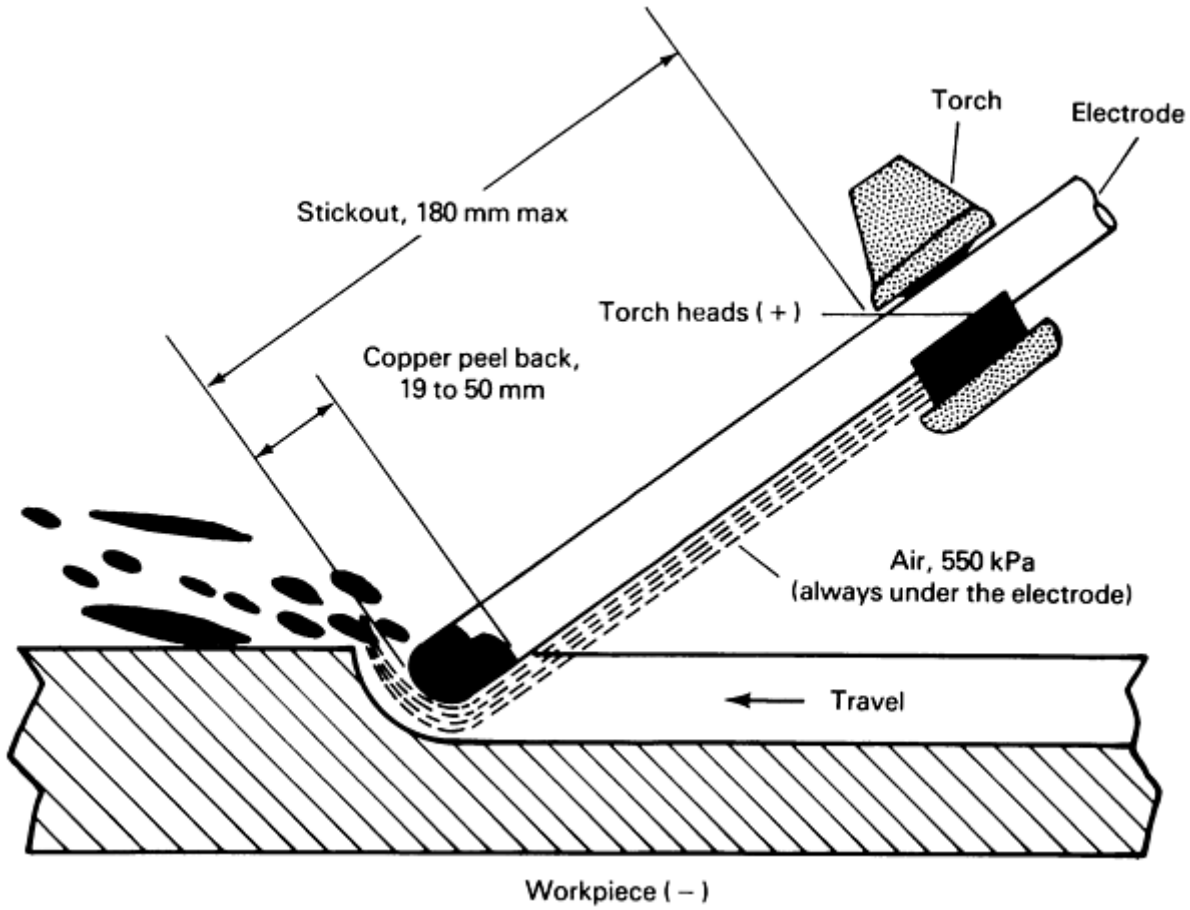

FIG. 2 PRINCIPLES OF CAC-A CUTTING

Power Sources. Single-phase machines with low open-circuit voltage may not work for CAC-A gouging. However, any three-phase welding power source of sufficient capacity can be used. The open-circuit voltage should be higher than the required arc voltage to allow for voltage drop in the circuit. Because the arc voltage typically ranges from a low of 35 to a high of 56 V, the open-circuit voltage should be at least 60 V. The actual arc voltage used in the process is governed by arc length and the type of gouging.

Direct current, electrode positive (reverse polarity, DCEP) is used with the process, except in special applications discussed later. The electrode should extend, at most, 178 mm (7 in.) from the gouging torch, with the air jet between the electrode and workpiece. A minimum extension of 50 mm (2 in.) should be used. Damage of the torch parts will occur if the electrode sticks out less than 50 mm (2 in.).

Compressed Air. Ordinary compressed air should be used for CAC-A gouging. Normal pressures range from 550 to 690 kPa (80 to 100 psi) at the torch. Higher pressures can be used, but they do not remove metal more efficiently. A pressure of 415 kPa (60 psi) should be used with the light-duty manual torch. This low level of pressure should not be used with general-duty torches.

Regardless of the pressure used with manual torches, the air hose supplying the cable assembly that is connected to the torch body should have an inside diameter (ID) of at least 6.4 mm ($\frac{3}{8}$ in.). Mechanized torches with automatic arc length control should have an air-supply hose with minimum ID of 12 mm ($\frac{1}{2}$ in.). Attention should be given to the field connections to ensure that this minimum is maintained without severely restricting the air-flow volume. Table 1 gives the consumption rates of compressed air for manual and mechanized torches, as well as compressor power rating for intermittent and continuous use. The compressor receiver tank must be large enough to accommodate the compressor rating.

TABLE 1 RECOMMENDED MINIMUM AIR SUPPLY REQUIREMENTS FOR AIR-CARBON ARC CUTTING

TYPE OF TORCH	AIR PRESSURE[A]		AIR CONSUMPTION		RECOMMENDED COMPRESSOR RATING				ASME RECEIVER SIZE	
					INTERMITTENT USE		CONTINUOUS USE			
	kpa	psi	l/min	ft^3/min	kw	hp	kw	hp	l	gal
LIGHT DUTY[B]	280	40	227	8	0.4	0.5	1.1	1.5	227	60
GENERAL DUTY[B]	550	80	708	25	3.7	5	5.6	7.5	303	80
MULTIPURPOSE[C]	550	80	934	33	5.6	7.5	7.5	10	303	80
AUTOMATIC[D]	414	60	1303	46	. . .	. . .	11.2	15	303	80

(A) PRESSURE WHILE TORCH IS IN OPERATION.
(B) ACCOMMODATES FLAT ELECTRODES.
(C) GENERALLY CONSIDERED TO BE A FOUNDRY TORCH.
(D) REQUIRES SOME KIND OF MECHANICAL MANIPULATION

Electrodes. The basic types of electrodes are described below.

Direct-current copper-coated electrodes are the most widely used type, because of their comparatively long electrode life, stable arc characteristics, and groove uniformity. These electrodes are made by mixing carbon and graphite with a binder. When this mixture is baked, it produces dense, homogeneous graphite electrodes of low electrical resistance. These electrodes are then coated with a controlled thickness of copper. The available diameters of these electrodes are 3.2 mm ($\frac{1}{8}$ in.), 4.0 mm ($\frac{5}{32}$ in.), 4.8 mm ($\frac{3}{16}$ in.), 6.4 mm ($\frac{1}{4}$ in.), 7.9 mm ($\frac{5}{16}$ in.), 9.5 mm ($\frac{3}{8}$ in.), 12.7 mm ($\frac{1}{2}$ in.), 15.9 mm ($\frac{5}{8}$ in.), and 19.1 mm ($\frac{3}{4}$ in.).

Jointed electrodes work without stub loss. They are furnished with a female socket and a matching male tang, and are available in diameters of 7.9 mm ($\frac{5}{16}$ in.), 9.5 mm ($\frac{3}{8}$ in.), 12.7 mm ($\frac{1}{2}$ in.), 15.9 mm ($\frac{5}{8}$ in.), 19.1 mm ($\frac{3}{4}$ in.), and 25.4 mm (1 in.). Jointed carbons are always used with the male tang pointing up (that is, away from the gouge). This ensures proper joint performance.

Flat, or rectangular, coated electrodes are available in dimensions of 4.0 × 9.5 mm ($\frac{5}{32} \times \frac{3}{8}$ in.) and 4.8 × 15.9 mm ($\frac{3}{16} \times \frac{5}{8}$ in.). These electrodes are used to make rectangular grooves and to remove weld reinforcements.

Direct-current electrodes are generally restricted to diameters of less than 9.5 mm ($\frac{3}{8}$ in.), and are therefore limited in use. During cutting, these electrodes erode more than the coated electrodes. They are manufactured in the same way as the coated electrodes, but without the copper coating. Plain electrodes are available in diameters of 4.0 mm ($\frac{5}{32}$ in.), 4.8 mm ($\frac{3}{16}$ in.), 6.4 mm ($\frac{1}{4}$ in.), 7.9 mm ($\frac{5}{16}$ in.), and 9.5 mm ($\frac{3}{8}$ in.).

Alternating-current (ac) coated electrodes are made from a mixture of carbon, graphite, and a special binder. Rare-earth materials are added to ensure arc stabilization when using alternating current. These electrodes, coated with copper, are available in diameters of 4.8 mm ($\frac{3}{16}$ in.), 6.4 mm ($\frac{1}{4}$ in.), and 9.5 mm ($\frac{3}{8}$ in.).

A manual gouging torch is shown in Fig. 3. The electrode is held in a swivel head that contains one or more air holes, so that the air jet stays aligned with the electrode, regardless of the angle of the electrode to the gouging torch. Torches

with two heads (that is, the air jet is on two sides of the electrode) or with a fixed angle between the electrode and the holder are better for certain applications, such as removing pads and risers from large castings (pad washing).

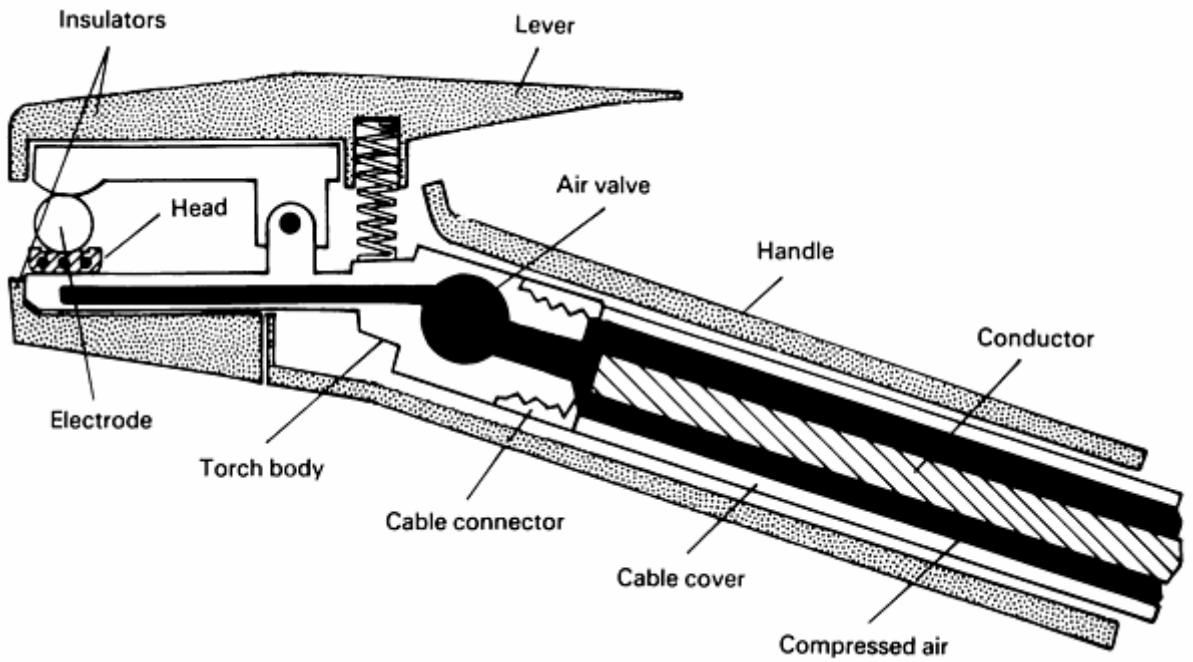

FIG. 3 CUTAWAY VIEW OF A MANUAL GOUGING TORCH WITH AIR FLOW ON BOTTOM OF ELECTRODE

Manual torches are usually air cooled. In high-current applications, water-cooled cable assemblies can be used with heavy-duty torches.

Control of Automatic Gouging Torches. There are two methods of controlling automatic CAC-A gouging torches. Either method can make grooves of consistent depth to a tolerance of ±0.64 mm (±0.025 in.). These automatic units are used to achieve high-quality gouges and to increase production (Fig. 4).

FIG. 4 AUTOMATIC GOUGING UNIT

The amperage-controlled method maintains the arc current by amperage signals through solid-state controls. This method controls the electrode feed speed, which maintains the preset amperage. It is run with constant-voltage power sources only.

A voltage-controlled method maintains arc length by voltage signals through solid-state electronic controls. This method controls the electrode feed speed, which maintains the preset voltage. It can run with constant-current power sources.

Robert L. Strohl, Tweco Arcair

Operating Techniques

Gouging with Manual Torches. As shown in Fig. 2, the electrode should be gripped so that a maximum of 178 mm (7 in.) extends from the torch. For aluminum, this extension should be 76.5 mm (3 in.). Table 2 shows suggested currents for the different electrode types and sizes.

TABLE 2 SUGGESTED CURRENT RANGES FOR VARIOUS ELECTRODE SIZES

ELECTRODE SIZE		MINIMUM AMPERAGE	MAXIMUM AMPERAGE
mm	in.		
3	$\frac{1}{8}$	60	90
4	$\frac{5}{32}$	90	150
5	$\frac{3}{16}$	200	250
6	$\frac{1}{4}$	300	400
8	$\frac{5}{16}$	350	450
10	$\frac{3}{8}$	450	600
13	$\frac{1}{2}$	800	1000
16	$\frac{5}{8}$	1000	1250
19	$\frac{3}{4}$	1250	1600
25	1	1600	2200

The air jet should be turned on before striking the arc, and the torch should be held as shown in Fig. 5. The electrode should slope back from the direction of travel, with the air jet behind the electrode. During gouging, the air jet sweeps beneath the electrode end and removes all molten metal. The arc can be struck by lightly touching the electrode to the workpiece. The electrode should not be drawn back once the arc is struck.

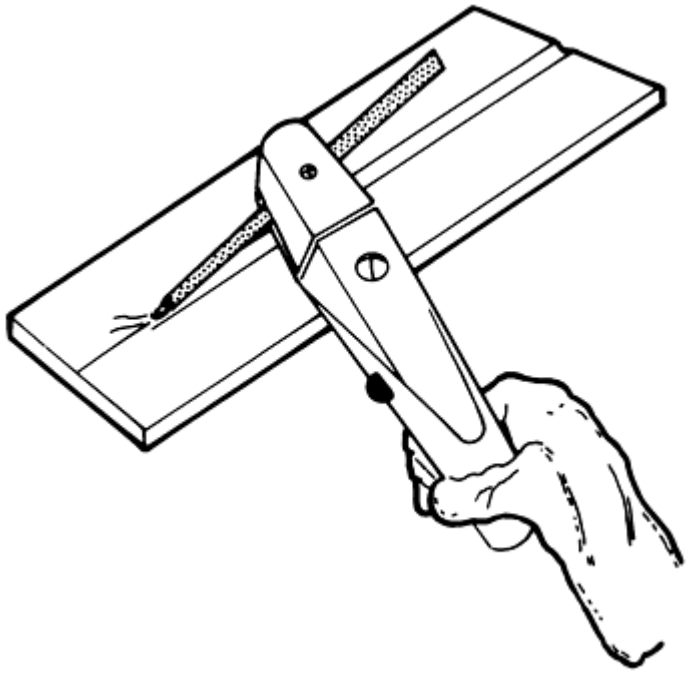

FIG. 5 FLAT GOUGING POSITION

Gouging is different from arc welding in that metal is removed, rather than deposited. A short arc should be maintained in the direction of cut by working fast enough to keep up with metal removal. Steadiness of movement controls the smoothness of the resulting cut.

Vertical gouging should be conducted downhill, permitting gravity to help remove the molten metal. Although vertical gouging can be accomplished uphill, it is difficult. Horizontal gouging can be done either to the right or to the left, but always with forehand gouging.

The air jet should always be positioned under the electrode. When gouging in the overhead position, the electrode and torch should be held to prevent molten metal from dripping on the glove of the operator. The depth of the groove is controlled by the travel speed. Grooves up to 25 mm (1 in.) deep can be made. However, the deeper the groove, the more experienced the operator needs to be. Slow travel speeds will produce a deep groove. Fast speeds will produce a shallow groove. The width of the groove is determined by the size of the electrode used. The groove is usually about 3.2 mm ($\frac{1}{8}$ in.) wider than the diameter of the electrode. A wider groove can be made with a small electrode that is oscillated in either a circular or weave motion. When gouging, a push angle that is 35° from the surface of the workpiece should be used for most applications. A steady rest will ensure a smoothly gouged surface, especially in the over-head position. Proper travel speed depends on electrode size, the base metal being used, amperage, and air pressure. The proper speed, which produces a smooth hissing sound, will result in a good gouge.

The severing technique is like gouging, except that the operator holds the electrode at a steeper angle that is between 70 and 80° to the workpiece surface. When cutting thick, nonferrousmetals, the electrode should be held perpendicular to the workpiece, with the air jet favoring the desired side. With the electrode in this position, the operator can sever the metal by moving the arc up and down using a sawing motion.

Washing. When using the CAC-A process to remove metal from large areas (for example, surfacing metal or riser pads on castings), the operator should position the electrode as shown in Fig. 6. The electrode should weave from side to side while it is being pushed forward at the depth desired. In the pad-washing operation, an angle that is 15 to 70° to the workpiece should be used. The 15° angle is used for light finishing passes, whereas steeper angles allow deeper rough gouging with greater ease.

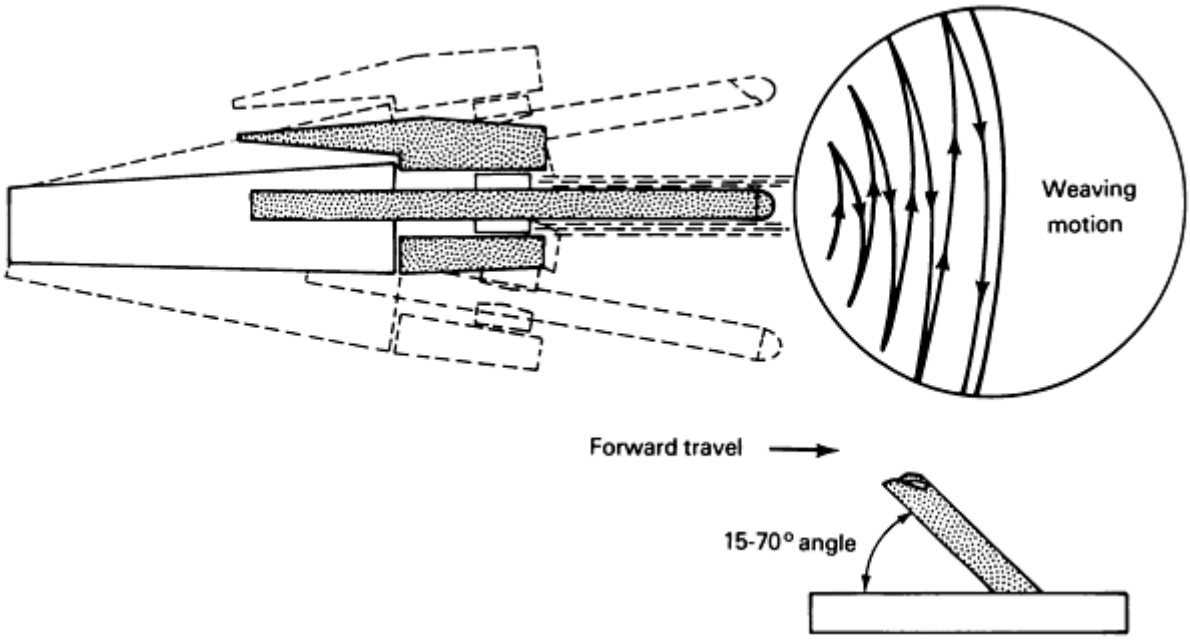

FIG. 6 PAD-WASHING TECHNIQUE. THE TORCH REMAINS PARALLEL TO THE WORKPIECE, AND A WEAVING MOTION IS USED FORWARD ACROSS THE WIDTH OF THE AREA BEING CLEANED. THE ELECTRODE-TO-WORKPIECE ANGLE SHOULD BE FROM 15 TO 70°. THE MORE SHALLOW THE ANGLE, THE SMOOTHER THE FINISH; THE 70° ANGLE IS USED MAINLY ON CAST IRON.

Gouging torches with fixed-angle heads that hold the electrode at the correct angle are well-suited for this application. When other types of torches are used, the air jet should be kept behind the electrode. Operator steadiness determines the smoothness of the surface produced.

Beveling. In one beveling method that is used for thick plates, the electrode should be held with a travel angle of 90° and a work angle that is equal to the bevel angle. The air jet should be positioned between the electrode and the workpiece. A second method, usually used for thin plates, requires that the torch be held parallel to the edge being beveled. Its position should equal the bevel angle. The air jet should be positioned between the electrode and the workpiece surface.

Air-Carbon Arc Cutting

Robert L. Strohl, Tweco Arcair

Equipment Selection

Gouging torches are selected for the specific application. They range from light-duty sizes appropriate for farm and body shop applications to extra-heavy-duty torches that are best suited to foundry applications.

General-purpose torches are available in four duty levels. Light-duty torches accept round electrodes that range from 3.2 to 6.5 mm ($\frac{1}{8}$ to $\frac{1}{4}$ in.) and 9.5 mm ($\frac{3}{8}$ in.) flat electrodes. Their maximum current level is 450 A. Medium-duty torches accept round electrodes that range from 3.97 to 9.5 mm ($\frac{5}{32}$ to $\frac{3}{8}$ in.) and 9.5 mm ($\frac{3}{8}$ in.) flat electrodes. Their maximum current level is 600 A. Heavy-duty torches accept round electrodes that range from 3.97 to 12.7 mm ($\frac{5}{32}$ to $\frac{1}{2}$ in.) and flat electrodes of 9.5 or 15.9 mm ($\frac{3}{8}$ or $\frac{5}{8}$ in.). Their maximum current level is 1000 A. Extra-heavy-duty

torches accept round electrodes that range from 3.97 to 15.9 mm ($\frac{5}{32}$ to $\frac{5}{8}$ in.) and flat electrodes of 9.5 or 15.9 mm ($\frac{3}{8}$ or $\frac{5}{8}$ in.). Their maximum current level is 1250 A.

Foundry heavy-duty torches are appropriate for general foundry work and heavy-duty fabrication. They are limited to 1600 A when used with air-cooled cables and 2000 A when used with water-cooled cables.

Automated gouging torches are used for edge preparations and backgouging, as well as high-quality and high-productivity applications. Jointed carbon electrodes ranging from 7.9 to 19.1 mm ($\frac{5}{16}$ to $\frac{3}{4}$ in.) are accepted.

Power Sources. Any three-phase welding power source with enough capacity can be used for the CAC-A gouging process if the open-circuit voltage is high enough to allow for a voltage drop in the circuit. Some constant-voltage power sources with drooping characteristics require a very high open-circuit voltage to run CAC-A gouging equipment. Mechanized gouging and other applications that require maximum arc time should utilize a power source with a 100% duty cycle for the required amperage.

A dc constant-current power source motor generator, rectifier, or resistor grid unit is preferred for use with all electrode sizes. A dc constant-voltage power source motor generator or rectifier is usable only for 7.9 mm ($\frac{5}{16}$ in.) diameter and larger electrodes. It may cause carbon deposits when used with small electrodes, and it is not suitable for automatic torches with voltage control only. An ac constant-current power source (transformer) is recommended for ac electrodes only. With ac/dc transformer rectifiers, the direct current should be supplied by a three-phase source, because single-phase sources give unsatisfactory arc characteristics. Alternating current output from ac/dc units is satisfactory, if ac electrodes are used.

Automatic systems are often used in modern fabrication facilities. These systems offer a high-quality, high-productivity alternative to manual gouging. Two types of systems can be considered. Both operate on a signal from the arc to control the gouging.

Dual-Signal System. Either constant-current or constant-voltage power supplies can be used with this type of automatic system. When the system uses constant current, the arc length is maintained through a voltage-signal system. A predetermined voltage setting is set on the system controller, which then advances or retracts the electrode through a stepping motor to maintain the arc length. With a constant-voltage power source, amperage sensing controls the feeding or retracting of the electrode to maintain the right arc current.

The single-signal system, like the dual-signal system, maintains arc length through voltage signal. However, it will not operate with an amperage signal. This type of system only operates with a constant-current power source.

Advantages. Automatic CAC-A systems ensure better productivity and quality. The systems can perform out-of-position gouging. They perform well when making long gouges in flat workpieces using a moving gouging apparatus and when making circular gouges in pipes and tanks using stationary gouging apparatus. They produce an even U-shaped groove and can control the depth of the groove to within ±0.64 mm (±0.025 in.). Table 3 shows typical operating information for U-shaped grooves.

TABLE 3 AUTOMATIC AIR-CARBON ARC U-SHAPED GROOVE OPERATING DATA[(A)]

ELECTRODE DIAMETER		DESIRE DEPTH		DC CURRENT, A	TRAVEL SPEED	
mm	in.	mm	in.		mm/min	in./min
7.9	$\frac{5}{16}$	3.2	$\frac{1}{8}$	400	1651	65
7.9	$\frac{5}{16}$	4.8	$\frac{3}{16}$	400	1143	45

7.9	5/16	6.4	1/4	450	914	36
7.9	5/16	7.9	5/16	450	838	33
7.9	5/16	11.1	7/16	450	572	22.5
9.5	3/8	3.2	1/8	500	1778	70
9.5	3/8	4.8	3/16	500	1118	44
9.5	3/8	6.4	1/4	500	889	35
9.5	3/8	9.5	3/8	500	508	20
9.5	3/8	14.3	9/16	500	445	17.5
12.7	1/2	3.2	1/8	850	2438	96
12.7	1/2	6.4	1/4	850	1448	57
12.7	1/2	9.5	3/8	850	889	35
12.7	1/2	12.7	1/2	850	610	24
12.7	1/2	19.1	3/4	850	445	17.5
15.9	5/8	6.4	1/4	1250	1829	72
15.9	5/8	9.5	3/8	1250	1219	48
15.9	5/8	12.7	1/2	1250	940	37
15.9	5/8	15.9	5/8	1250	762	30
15.9	5/8	23.8	15/16	1250	495	19.5
19.1	3/4	6.4	1/4	1400	1829	72
19.1	3/4	9.5	3/8	1400	1068	42
19.1	3/4	12.7	1/2	1400	865	34
19.1	3/4	15.9	5/8	1400	687	27
19.1	3/4	19.1	3/4	1400	560	22
19.1	3/4	28.6	1 1/8	1400	330	13

Note: If a groove depth greater than 1.5 times the diameter of the electrode being used is desired, then the groove should be made in two or more passes.

(A) BASED ON LABORATORY CONDITIONS; INFORMATION SHOULD BE USED AS A GUIDE

AND ADJUSTED FOR FIELD VARIANCE AS REQUIRED.

Vacuum gouging represents a new variation of gouging that was developed in the late 1980s. This process replaces the air jet that is used to evacuate the molten slag from the groove area with a high-volume vacuum that not only captures the slag and fume associated with the gouging process, but also reduces the noise level created when performing the gouging process.

The vacuum gouging process utilizes a specially designed nozzle that attaches to an automatic gouging head. By water cooling the nozzle and the attached vacuum hose, the slag and fume from the gouging process are pulled by the vacuum into a capture dram. The slag is knocked into the bottom of the catch tank, which is partially filled with water, and the fume is caught in a filter before the air is exhausted from the vacuum. Currently, this new vacuum system is limited to automated gouging operations on flat plate or pressure vessel circumferential seams.

Air-Carbon Arc Cutting

Robert L. Strohl, Tweco Arcair

Important Process Variables

Like any thermal-cutting process, the CAC-A process is sensitive to variables in operation. These variables can cause changes in the finished gouge that range from being undetectable to being unacceptable.

Electrode diameter and type are variables that determine the groove size, as well as productivity, groove quality, and metal-removal rates. The width of the groove will be about 3.2 mm ($\frac{1}{8}$ in.) wider than the diameter of the electrode. The choice of a proper electrode can be based on the size of the desired groove. Available power will dictate the outer limit. For example, a 13 mm ($\frac{1}{2}$ in.) wide, 6.4 mm ($\frac{1}{4}$ in.) deep groove that is 254 mm (10 in.) long could be made manually in two passes using a 6.4 mm ($\frac{1}{4}$ in.) diameter electrode, or in one pass using a 9.5 mm ($\frac{3}{8}$ in.) diameter electrode. In the first case, the best gouging rate would be 254 mm/min (10 in./min), divided by 2, or 125 mm/min(5 in./min). The travel speed of the second case (one pass) is 430 mm/min (17 in./min).

The 9.5 mm ($\frac{3}{8}$ in.) diameter electrode increases the gouging rate by 200%, which could offset the additional cost of the electrode. Automatic systems increase the productivity rate even further, through finite control of the arc voltage.

The gouging amperage is the melting force of the process. It is affected by electrode size. If the amperage were set too low for the electrode size, then the melting rate of the base metal would be inadequate and free-carbon deposits would occur. Although the base metal would melt, a setting that is too high would rapidly deteriorate the electrode while reducing the metal removed per electrode. Too high a setting can also substantially reduce torch life.

Voltage is the pressure, or arc force, that enables the current to flow across the arc gap. The CAC-A process often requires a higher voltage than do most welding processes. To ensure proper operation, a power source with a high enough open-circuit voltage to maintain a 28 V operating minimum should be used. Inadequate voltage can create a sputtering arc or it can prevent arc establishment, resulting in uneven grooves and, probably, free-carbon deposits that would require excessive grinding to remove.

Adequate air pressure and flow rate are required for the adequate removal of molten metal by the air jet. Air volume is as important as air pressure. Pressure is the speed of the air that moves the molten metal from the groove. If there is an inadequate volume of air to lift the molten material out of the groove, then it cannot be removed by the pressure or velocity. The result is excessive slag adhesion and unnecessary grinding to clean up the groove.

Travel speed affects the depth of the gouge and the quality of the groove. The faster the travel speed of an electrode, the shallower the gouge. A smaller electrode can be used if the travel speed is too fast for the comfort of the operator, or automatic gouging can be used. A groove that is too deep for the diameter of the electrode results in a poor-quality groove that requires much grinding.

The electrode push angle can vary some-what. When gouging manually, a steeper angle tends to give a more V-shaped groove. When gouging automatically, a steeper angle gives a slightly deeper groove at the same travel speed.

Base Metals. The gouging procedures that are recommended for specific base metals are:

- FOR CARBON STEEL AND LOW-ALLOY STEEL, SUCH AS ASTM A 514 AND A 517, USE DC ELECTRODES WITH DCEP. ALTHOUGH AC ELECTRODES WITH AN AC TRANSFORMER CAN BE USED, THEIR EFFICIENCY IS HALF THAT OF DC ELECTRODES.
- FOR STAINLESS STEEL, THE SAME GUIDELINES APPLY AS FOR CARBON STEEL.
- FOR CAST IRON, INCLUDING MALLEABLE AND DUCTILE (NODULAR) FORMS, USE 13 MM ($\frac{1}{2}$ IN.) DIAMETER OR LARGER ELECTRODES AT THE HIGHEST RATED AMPERAGE. SPECIAL TECHNIQUES ARE NEEDED WHEN GOUGING THESE METALS. THE PUSH ANGLE SHOULD BE AT LEAST 70° OFF THE WORKPIECE, AND THE DEPTH OF THE CUT SHOULD NOT EXCEED 13 MM ($\frac{1}{2}$ IN.) PER PASS.
- FOR COPPER ALLOYS (COPPER CONTENT $\leq$60%), USE DC ELECTRODES WITH DIRECT CURRENT ELECTRODE NEGATIVE (DCEN) AT THE MAXIMUM AMPERAGE RATING OF THE ELECTRODE.
- FOR COPPER ALLOYS (COPPER CONTENT >60% OR LARGE WORKPIECE), USE DC ELECTRODES WITH DCEN AT THE MAXIMUM AMPERAGE RATING OF THE ELECTRODE, OR USE AC ELECTRODES WITH ALTERNATING CURRENT.
- FOR ALUMINUM BRONZE AND ALUMINUM-NICKEL-BRONZE (SPECIAL NAVAL PROPELLER ALLOYS), USE DC ELECTRODES WITH DCEN.
- FOR NICKEL ALLOYS (NICKEL CONTENT >80% OF MASS), USE AC ELECTRODES WITH ALTERNATING CURRENT.
- FOR NICKEL ALLOYS (NICKEL CONTENT <80% OF MASS), USE DC ELECTRODES WITH DCEP.
- FOR MAGNESIUM ALLOYS, USE DC ELECTRODES WITH DCEP AND WIRE-BRUSH THE GROOVE BEFORE WELDING.
- FOR ALUMINUM ALLOYS, USE DC ELECTRODES WITH DCEP AND WIRE-BRASH THE GROOVE WITH STAINLESS BRUSHES BEFORE WELDING. ELECTRODE EXTENSION (LENGTH OF ELECTRODE BETWEEN TORCH AND WORK) SHOULD NOT EXCEED 76.2 MM (3 IN.). DIRECT-CURRENT ELECTRODES WITH DCEN CAN ALSO BE USED.
- FOR TITANIUM, ZIRCONIUM, HAFNIUM, AND THEIR ALLOYS, THERE ARE NO CURRENT PROCEDURES. IF THESE METALS ARE PREPARED FOR WELDING USING THE CAC-A PROCESS, THEN THE GROOVE SHOULD BE CLEANED BEFORE WELDING. THESE METALS CAN BE CUT FOR REMELTING. IN CASES WHERE PREHEAT IS REQUIRED FOR WELDING, A SIMILAR PREHEAT SHOULD BE USED FOR GOUGING.

Effects of the Cutting Process on Base Metals. Metallurgically, the base metal is not affected by the carbon particles being carried toward it from the electrode, because it remains solid and the atoms are very tightly packed. However, because the material being removed is molten, the atoms are loosely spread. This material, usually referred to as slag, easily absorbs the carbon particles.

If the CAC-A process is properly used, no surface carburization will occur. Due to the rapid quenching effect of the air used to remove the metal, the heat-affected zone (HAZ) will undergo hardening. The heat-affected zone for CAC-A is typically 2.5 mm (0.10 in.) or less in thickness. This HAZ hardening must be considered when a finish machining operation follows the gouging process, especially when working on high-carbon steels. Some materials (for example, nickel) will undergo surface cracking when gouged. These conditions should be considered when choosing the parameters for any required machining operations.

When the CAC-A process is used under improper conditions, this molten carburized metal may be left on the workpiece surface. Its color is a dull gray-black, in contrast to the bright blue of the properly made groove. Inadequate air flow may

leave small pools of carburized metal in the bottom of the groove. Irregular electrode travel, especially in a manual operation, may cause ripples in the groove wall that trap the carburized metal. Finally, an improper electrode push angle may cause small beads of carburized metal to remain on the edge of the groove.

Copper from copper-coated electrodes does not transfer to the cut surface in base metal, unless the process is improperly used.

Carburized metal can be removed from a cut surface by grinding, but the necessity to do so can be prevented by gouging properly in the right condition.

When compared with oxyfuel cutting, the CAC-A process requires less heat input. Therefore, a workpiece that is gouged or cut by the CAC-A process is less distorted. The machining of low-carbon and nonhardenable steel is not affected by the CAC-A process. However, when used on cast iron and high-carbon steels, this process may cause enough hardening to make the cut surface tough to machine. Still, because the hardened zone is shallow (approximately 0.15 mm, or 0.006 in.), a cutting tool can penetrate it to remove the hardened surface.

Air-Carbon Arc Cutting

Robert L. Strohl, Tweco Arcair

Safety and Health

Safe practices in welding and cutting processes are described in ANSI Z49.1, "Safety in Welding and Cutting," and ANSI Z49.2, "Fire Prevention in Use of Welding and Cutting Processes." The operators of the CAC-A process and their supervisors should adhere to the practices discussed in these documents.

Electrodes. An electrode that carries electric current will arc if it touches the workpiece or any grounded metal object. Proper handling of the torch and electrode will prevent accidental arcing. Electrodes should always be used within their proper amperage range in order to effectively remove metal and to avoid damage to the torch. Carbon electrodes should be kept dry. Damp electrodes should be baked for 10 h at 176 °C (300 °F). Wet electrodes may shatter.

Torches. Oxygen should never be used in an air carbon-arc torch. Neither the torch nor the electrode should ever be immersed in water. All electrical connections should be wrench tight before the torches are used.

Electrical Power. The CAC-A process uses electric energy from a welding power source. The same safety precautions should be used as when welding. An operator should never stand in water while using CAC-A equipment, and the torches and electrodes should never be cooled by water. To prevent accidental arcing, partially used electrodes should be removed from torches when work is interrupted.

Personal Protective Equipment and Clothing. A No. 12 shade-filter lens should be used for eye protection against arc radiation. When conducting heavy metal-removal operations with large electrodes, a No. 14 shade-filter lens or an equivalent combination of filter lenses provides the best protection. Flash goggles should be used, especially when two or more welders are working in the same area. Proper protective clothing must be worn to provide enough protection from the infrared and ultraviolet radiations of the arc. Leather aprons, sleeves, leggings, and so on should be used for out-of-position gouging or for heavy metal-removal operations with large electrodes. Ear protection is recommended when noise exceeds permissible levels.

Fire and Burn Hazards. The CAC-A process may cause fire. All flammable materials should be removed from the work area. Booths, metal screens, and other deflectors should be placed to catch the hot metal and particle spray ejected by the compressed air stream. Protective clothing should be used to prevent burns caused by contact with hot metal or electrodes. Out-of-position or heavy metal-removal operations require that many precautions be taken.

Ventilation Hazards. The fumes from the CAC-A process can be harmful. Ventilation and/or an exhaust around the arc is necessary. When using gouging torches, the operator should keep his head away from the fumes. Protective-breathing or air-circulation gear may be needed.

Additional information is available in the article "Safe Practices" in this Volume.

Mechanical Cutting for Weld Preparation

ASM Committee on Mechanical Cutting for Welding Preparation*

Introduction

OXYFUEL AND PLASMA CUTTING are the processes most commonly associated with preparing metals for welding; however, mechanical cutting methods are also widely used by the metal fabrication industry. The purpose of this article is to introduce the welding fabricator to some of the mechanical equipment used to shape or prepare metals for welding. The most prevalent equipment used for mechanical cutting includes shears, iron workers, nibblers, and band saws. Each has specific applications for which it is efficient and cost effective.

Acknowledgements

Some of the information in this article was drawn from the articles "Shearing of Plate and Flat Sheet" and "Shearing of Bars and Bar Sections" in *Forming and Forging,* Volume 14 of the *ASM Handbook,* and "Sawing" in *Machining,* Volume 16 of the *ASM Handbook.* Special thanks are due to the contributors to those articles.

Note

* LANCE R. SOISSON, *CHAIRMAN,* WELDING CONSULTANTS, INC.; CHRIS CABLE, FEIN POWER TOOLS, INC.; RICHARD S. CREMISIO, RESCORP INTERNATIONAL, INC.; CHUCK DVORAK AND JIM DVORAK, UNI-HYDRO, INC.; GERHARD LAEPPLE, C & E FEIN GMBH; AND JOHN R. WHALEN, CONTOUR SAWS, INC.

Mechanical Cutting for Weld Preparation

ASM Committee on Mechanical Cutting for Welding Preparation*

Shears

Shears are normally used to prepare large, relatively thin materials (≤ 25 mm, or 1 in., thick) by cutting them to final dimensions. When maintained and adjusted properly, shears provide a clean, straight edge preparation. For thin sections, the square butt edge preparation provided by shearing may be all that is required for the welding operation. As a role, material with a thickness of 10 mm ($\frac{3}{8}$ in.) or more will require further preparation; the straightness of the sheared edge is an excellent reference point for setting up other equipment. The two principal shearing variations are straight-knife shearing and rotary shearing. Because straight-knife shearing is more widely used for welding preparation, it will be the focus of this section.

In straight-knife shearing, the work metal is placed between a stationary lower knife and a movable upper knife. As the upper knife is forced down, the work metal is penetrated to a specific portion of its thickness. The unpenetrated portion then fractures, and the work metal separates (Fig. 1). The amount of penetration depends largely on the ductility and thickness of the work metal. The knife will penetrate 30 to 60% of the work metal thickness for low-carbon steel, depending on thickness (see the section "Capacity" in this article). The penetration will be greater for a more ductile metal such as copper. Conversely, the penetration will be less for metals that are harder than low-carbon steel.

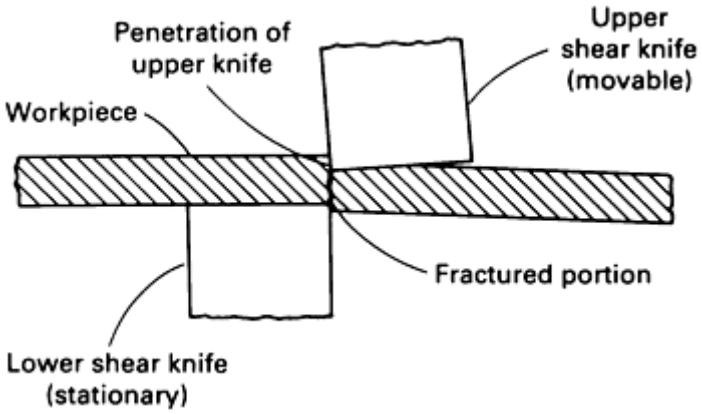

FIG. 1 SCHEMATIC SHOWING THE MECHANISM OF STRAIGHT-KNIFE SHEARING

A sheared edge is characterized by the smoothness of the penetrated portion and the relative roughness of the fractured portion. Sheared edges cannot compete with machined edges, but when knives are kept sharp and in proper adjustment, it is possible to obtain sheared edges that are acceptable for a wide range of applications. The quality of sheared edges generally improves as work metal thickness decreases.

Applicability. Straight-knife shearing is the most economical method of cutting straightsided blanks from stock no more than 50 mm (2 in.) thick. The process is also widely used for cutting sheet into blanks that will subsequently be formed or drawn. Because shear gaging can be set within ±0.13 mm (±0.005 in.), the shearing process is generally limited to ±0.4 mm ($\pm\frac{1}{64}$ in.) tolerances in 16 gage material. The tolerance range increases with thickness.

Straight-knife shearing is seldom used for shearing metal harder than about 30 HRC. When extremely soft, ductile metal (especially thin sheet) is sheared, the edges of the metal roll and large burrs result. As the hardness of the work metal increases, knife life decreases for shearing a given thickness of metal.

In general, it is practical to shear flat stock up to 38 mm ($1\frac{1}{2}$ in.) thick in a squaring shear. Squaring shears up to 9 m (30 ft) long are available (even longer shears have been built), and some types are equipped with a gap that permits shearing of work metal longer than the shear knife.

Machines for Straight-Knife Shearing

Punch presses and press brakes are sometimes used for shearing a few pieces or are used temporarily when more efficient equipment is not available. Production shearing, however, is usually done in machines that are designed for this operation.

Squaring shears are usually used for trimming and cutting sheet or plate to specific size (Fig. 2). Squaring shears (also called resquaring or guillotine shears) are available in a wide range of sizes and designs. Some types permit slitting by moving the work metal a predetermined amount in a direction parallel with the cutting edge of the knife after each stroke of the shear.

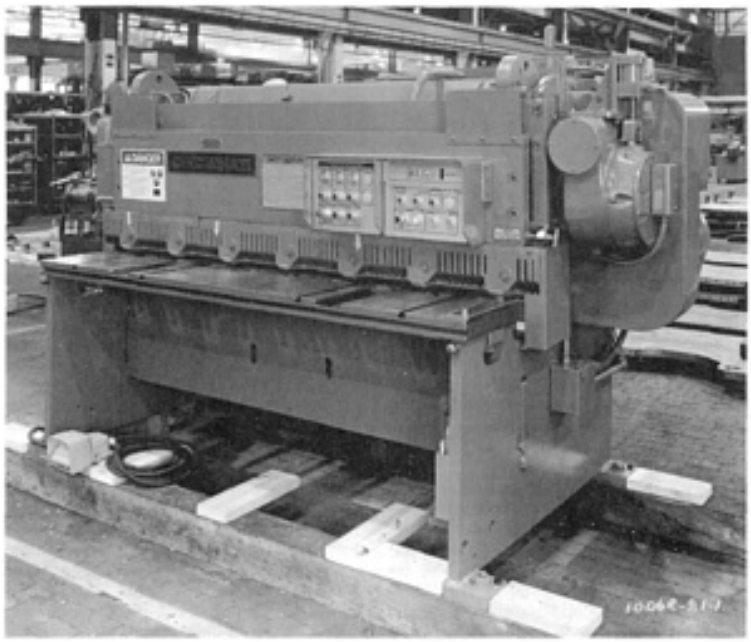

FIG. 2 TYPICAL SQUARING SHEAR. COURTESY OF CINCINNATI INC.

The sheet or plate is held rigid by hold-down devices while the upper knife moves down past the lower knife. Most sheet or plate is sheared by setting the upper knife at an angle. The position of one knife can be adjusted to maintain optimal clearance between the knives. Squaring shears can be actuated mechanically, hydraulically, or pneumatically.

Mechanical Shears. The power train of a mechanical shear consists of a motor, the flywheel, a worm shaft that is gear driven by a flywheel, a clutch that connects the worm gear drive to the driveshaft, and a ram actuated by the driveshaft through eccentrics and connecting links. Under most operating conditions, a mechanical shear can deliver more strokes per minute (spm) than a hydraulic shear. Some mechanical shears cycle as fast as 100 spm.

Another advantage of the mechanical shear is that, because of the energy stored in the flywheel, a smaller motor can be used for intermittent shearing. For example, a mechanical shear with a no-cutting or free-running speed of 65 spm can make approximately six full shearing strokes (maximum thickness and length of cut) per minute with a standard motor. However, when the same shear is cutting at full capacity in a rapid shear mode, a much larger motor is required. For such rapid cutting, there is not enough time between cuts for the smaller motor to restore the speed of the flywheel.

An additional advantage of the mechanical shear is that its moving knife travels faster than the moving knife of a hydraulic shear. In some cases, greater knife speed can decrease work metal twist, bow, and camber.

Hydraulic shears are actuated by a motordriven pump that forces oil into a cylinder against a piston; the movement of the piston energizes the ram holding the upper knife. A hydraulic shear can make longer strokes than a mechanical shear. In general, long shears and shears with low-carbon steel capacities above 12.7 mm ($\frac{1}{2}$ in.) are almost all hydraulic.

Hydraulic shears are designed with a fixed load capacity. This prevents the operator from shearing material that exceeds capacity and therefore saves costly damage to the machine structure. This is a basic advantage of hydraulic shears.

The total load that is experienced during the cut is related to the rake angle, sharpness of the knives, mechanical properties of the material, type of material, knife clearance, and the depth of the back piece. It is possible to stall the machine on a rated-capacity cut if the clearance is incorrect, the knife is dull, or the back piece is excessively deep. In this way, the hydraulic shear is protected from damage caused by overloading. A mechanical shear would not be constrained by an overload prevention system and would continue to cut under nearly all conditions.

Most mechanical shears are provided with enough horsepower to build up the flywheel speed after each cut, but not enough to allow the operator to run full-capacity cuts in a high-speed manner. Mechanical shears are rated in strokes per minute, not cuts per minute. Most shearing applications do not require high-speed cutting.

Hold-down pressure must be greater than the forces generated in cutting the work material. These forces depend on the knife clearance, rake angle, and depth of material back piece.

Greater knife clearance must be used to prevent the hydraulic shears from stalling when shearing large-area work, especially at or near maximum thickness capacity. For example, in cutting a 3 × 3 m (10 × 10 ft) plate into two equal parts, greater shearing force is required than for trimming a narrow strip from a 3 m (10 ft) long plate.

Capacity. Most shearing machines are rated according to the section size of low-carbon steel they can cut. The tensile strength of low-carbon steel sheet and plate is generally no higher than 520 MPa (75 ksi); the yield strength, no greater than 350 MPa (51 ksi). Shears frequently are rated in terms of their ability to cut low-carbon steel with a tensile strength of 414 MPa (60 ksi) and yield strength of 276 MPa (40 ksi). An allowance for normal over-tolerance material thickness is included in the capacity rating of the machine. The use of a machine for shearing other metals is primarily based on the relationship of the tensile strength and ductility of low-carbon steel to that of the metal to be sheared. Metals with a tensile strength greater than that of low-carbon steel almost always reduce the capacity of the machine. For example, the machine capacity for shearing high-strength low-alloy steels is reduced to about two-thirds to three-quarters of the rated capacity for low-carbon steel. Conversely, for shearing aluminum alloys, machine capacity can range from $1\frac{1}{4}$ to $1\frac{1}{2}$ times the rated capacity for low-carbon steel.

Table 1 compares the shearing capacities of various metals with those of low-carbon steel. The metal thicknesses given in Table 1 are based on the thickness of low-carbon steel that can be sheared with the same shearing capacity. For example, a specific force is required to shear 6.4 mm ($\frac{1}{4}$ in.) thick low-carbon steel. Table 1 shows that the same force can shear only a 4.8 mm ($\frac{3}{16}$ in.) thickness of type 302 stainless steel, but can shear a 9.5 mm ($\frac{3}{8}$ in.) thickness of aluminum.

TABLE 1 SHEARING CAPACITIES FOR VARIOUS METALS COMPARED TO THOSE FOR LOW-CARBON STEEL

THICKNESS OF LOW-CARBON STEEL[A]		THICKNESS THAN CAN SHEARED WITH SAME FORCE AS FOR LOW-CARBON STEEL					
		AISI TYPE 203 STAINLESS STEEL [B]		FULL-HARD STEEL STRIP		ALUMINUM ALLOYS	
mm	in.	mm	in.	mm	in.	mm	in.
1.52	0.060	0.91	0.036	1.22	0.048	1.90	0.075
1.90	0.075	1.22	0.048	1.52	0.060	3.05	0.120
3.05	0.120	1.52	0.060	1.90	0.075	3.40	0.134
3.40	0.134	1.90	0.075	2.67	0.105	4.8	$\frac{3}{16}$
4.8	$\frac{3}{16}$	3.40	0.134	3.9	$\frac{5}{32}$	5.6	$\frac{7}{32}$
6.4	$\frac{1}{4}$	4.8	$\frac{3}{16}$	4.8	$\frac{3}{16}$	6.4	$\frac{1}{4}$
7.9	$\frac{5}{16}$	5.6	$\frac{7}{32}$	5.6	$\frac{7}{32}$	9.5	$\frac{3}{8}$
9.5	$\frac{3}{8}$	6.4	$\frac{1}{4}$	6.4	$\frac{1}{4}$	11.1	$\frac{7}{16}$
11.1	$\frac{7}{16}$	7.9	$\frac{5}{16}$	7.9	$\frac{5}{16}$	12.7	$\frac{1}{2}$
12.7	$\frac{1}{2}$	9.5	$\frac{3}{8}$	9.5	$\frac{3}{8}$	15.9	$\frac{5}{8}$

15.9	$\frac{5}{8}$	11.1	$\frac{7}{16}$	11.1	$\frac{7}{16}$	19.0	$\frac{3}{4}$
19.0	$\frac{3}{4}$	12.7	$\frac{1}{2}$	12.7	$\frac{1}{2}$	25.4	1
22.2	$\frac{7}{8}$	15.9	$\frac{5}{8}$	15.9	$\frac{5}{8}$	31.8	$1\frac{1}{4}$
25.4	1	19.0	$\frac{3}{4}$	19.0	$\frac{3}{4}$	38.1	$1\frac{1}{2}$
31.8	$1\frac{1}{4}$	25.4	1	25.4	1	50.8	2

(A) ALSO APPLICABLE TO SOFT TO HALF-HARD STRIP STEEL, ALCLAD STEEL, AND COPPER AND COPPER ALLOYS.

(B) ALSO APPLIES TO MOST OTHER AUSTENITIC STAINLESS STEELS, NORMALIZED ALLOY STEELS SUCH AS 4130 OR 8630, ANNEALED HIGH-CARBON STEELS, AND ANNEALED TOOL STEELS

Ductility, measured by the elongation of the work metal, can also affect machine capacity. For example, annealed copper, because of its high elongation, requires as much shearing effort as low-carbon steel, even though copper has considerably lower tensile strength. Similarly, carbon steel with very low carbon (<0.1% C) and higher-than-normal elongation will reduce the capacity of a machine.

Accessory Equipment for Straight-Knife Shearing

Certain pieces of accessory equipment have been incorporated into most shear designs and are required for efficient and accurate straight-knife shearing.

Hold-downs (Fig. 2) are mechanical or hydraulic devices that hold the work metal firmly in position to prevent movement during shearing. The most efficient hold-down system is a series of independent units that securely clamps stock of varying thicknesses automatically and without adjustment.

The force on each hold-down foot must be substantial and can range from several hundred pounds on a machine for shearing sheet to several tons for shearing plate. Hold-downs must be timed automatically with the stroke of the ram so that they clamp the work metal securely before the knife makes contact and release their hold instantly after shearing is completed.

Back gages are adjustable stops that permit reproducibility of dimensions of sheared work-pieces in a production run. Most gages are controlled electrically. Push-button control provides a selection of fast traverse speeds and slow locating movements for accurate final positioning. The addition of a microcomputer (Fig. 3) permits gage positions to be quickly entered. An LED display enables the operator to confirm immediately the gage position entered, the current gage position, or the final gage location after positioning. Accurate gage screws, compensating nuts, precision slides and guides, and decimal indicators permit repeatable gage settings to an accuracy of 0.025 to 0.05 mm (0.001 to 0.002 in.).

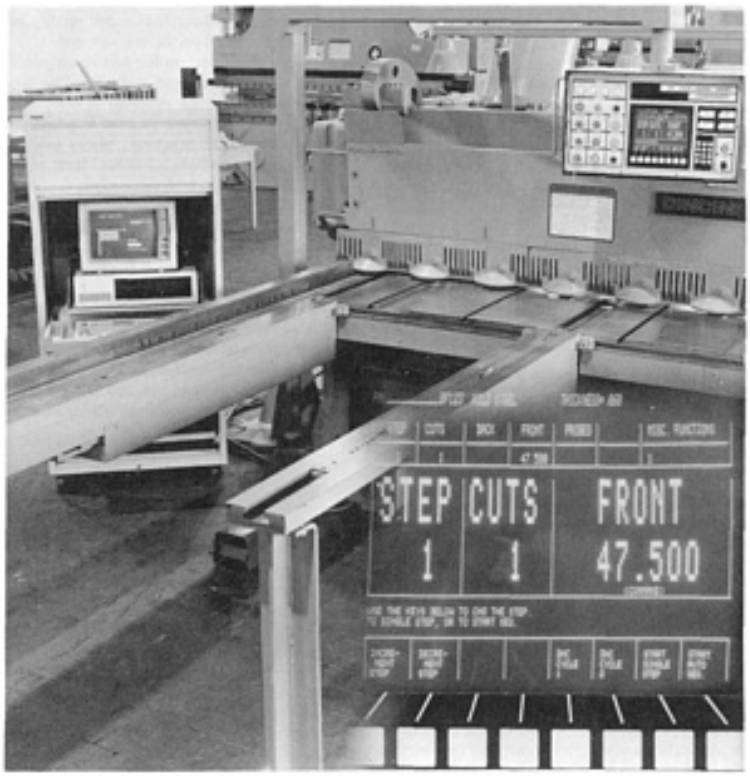

FIG. 3 MICROPROCESSOR-CONTROLLED SHEARING MACHINE WITH INSET (LOWER RIGHT) SHOWING LED DISPLAY. COURTESY OF CINCINNATI INC.

For thin sheet, magnetic overhead rollers eliminate sag and support the sheet for accurate gaging to a depth of 1.2 m (4 ft) into the shear. For rapid and accurate cutting, back gages are equipped with electronic sensors that automatically trip the shear only when the sheet is accurately positioned.

Pneumatic sheet supports are used to support ferrous and nonferrous thin sheet. Sheet support arms are designed to elevate into a horizontal position, flush with the shear table, permitting material to be supported in the correct position against the backgage stop. Blank inaccuracies due to unsupported and poorly positioned sheets are virtually eliminated.

Back gages are also equipped with retractable stops for shearing mill plate. With the stops out of the way, mill plate of almost any length can be fed into the shear and cut to the desired length. When stops are not used, the workpiece can be notched or scribed to indicate the cutoff position.

Front Gages. When gaging from the front of the machine, the operator locates the work metal by means of stops secured in the table or in the front support arms. Power operation of the front support arms allows the blank dimensions to be entered digitally using a microcomputer-based control. Front gaging is often done by means of a squaring arm.

Squaring arms (Fig. 4) are extensions attached to the entrance side of a shearing machine that are used to locate long sections of work metal in the proper position for shearing. Each arm is provided with a linear scale and with stops for accurate, consistent positioning of the work metal. Squaring arms are reversible to allow use of the shear at either end and to distribute the wear on the shear knives. Power operation can be added to the squaring arm for increasing blank accuracy and reducing setup time. This type of squaring arm prevents the arm from moving from side to side.

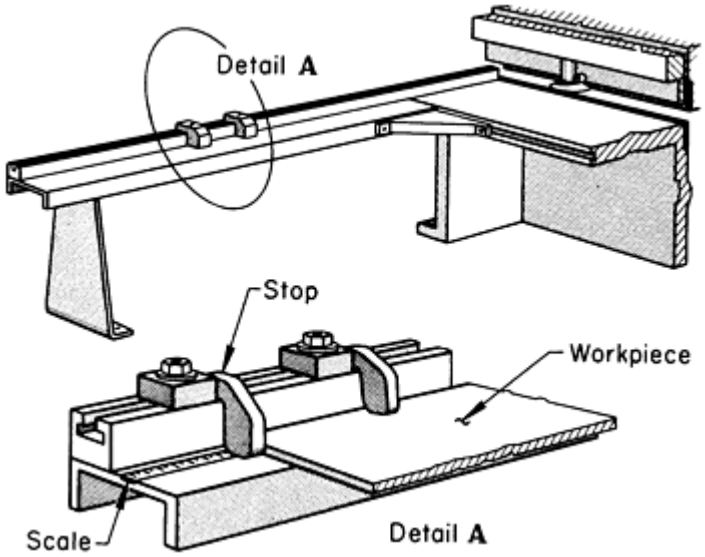

FIG. 4 SQUARING ARM ATTACHMENT FOR POSITIONING LONG PIECES IN A SHEARING MACHINE

Knife Rake

Rake is the slope of the angle formed by the cutting edges of the upper and lower knives (Fig. 2). It is usually expressed as the ratio of the amount of rise to a given linear measurement. For example, a rake of 21 mm/m ($\frac{1}{4}$ in./ft) means that the upper knife rises 21 mm for each meter ($\frac{1}{4}$ in. for each foot) of linear distance along the knives. Rakes below 21 mm/m ($\frac{1}{4}$ in./ft) are rarely used; a rake of 42 mm/m ($\frac{1}{2}$ in./ft) or higher is typical of many plate shears.

Rake is used to permit progressive shearing of the work metal along the length of the knife. This reduces the amount of force required and allows the use of a smaller machine than would be necessary if the cutting edges of the knives were parallel.

It is not possible, however, to calculate the required force for different work metal thicknesses based solely on change of rake, because knife penetration varies for different thicknesses. Even for low-carbon steel, the amount of knife penetration before fracture occurs can be as great as 60% of the work metal thickness for 3.43 mm (0.135 in.) thick stock and as little as 30% for 19 mm ($\frac{3}{4}$ in.) thick stock.

The primary disadvantage of using a high rake angle is that it increases the distortion of the work. Large rake angles can also cause slippage and therefore require high hold-down forces.

Knife Clearance

Excessive knife clearance causes the work metal to be wiped down between the knives during cutting and results in heavy burring or flanging of the work metal. The burrs and deformed metal are objectionable because of their interference with subsequent processing. A more serious consequence of excessive clearance is that it can cause the workpiece to be pulled between the knives, and this in turn causes overloading of the machine and may result in failure of machine components or shear knives.

When soft metals are sheared, insufficient clearance causes double (secondary) shearing, which appears as a burnished area at the top and bottom of a sheared edge with a rough area between the burnished edges. Because of the difference in action, greater tolerances are usually required when shearing plate than when shearing sheet--all other conditions being equal. Some mechanical shears are constructed to operate with a fixed clearance, and no adjustments are made for

variations in work metal composition or thickness. The knife clearance is set for the thinnest material to be sheared, and double shear is avoided if the range of thicknesses sheared is not too large.

Because of deflection, clearance at the center of the knife is usually set less than that at the ends. Knife clearance (except on machines using a fixed clearance) is generally increased as work metal thickness increases. For example, in one plant, a clearance of approximately 0.076 mm (0.003 in.) is used for squaring shears with a capacity of up to 6.4 mm ($\frac{1}{4}$ in.) thick low-carbon steel. To minimize knife deflection, clearance at the center of the knife is reduced to 0.051 mm (0.002 in.). Similarly, the clearance for shearing 6.4 to 25 mm ($\frac{1}{4}$ to 1 in.) thick low-carbon steel is 0.36 mm (0.014 in.) at each end of the knives and 0.30 mm (0.012 in.) at the center of 3 to 3.7 m (10 to 12 ft) long knives used in a mechanical shear.

Ram Speed in Straight-Knife Shearing

The speed of the ram (and, in turn, that of the knife) has a slight effect on results in the shearing of flat stock. Low linear speed produces a rough sheared surface. As speed is increased, a cleaner sheared surface is obtained. In general, speeds to 21 to 24 m/min (70 to 80 ft/min) can be used without difficulty when shearing annealed metals. Regardless of the speed used, adequate hold-down force is mandatory.

Accuracy in Straight-Knife Shearing

The dimensional accuracy obtained in shearing is influenced by the capacity and condition of the machine, condition of the knives, knife clearance, work metal thickness, and work metal condition. Expressed as total tolerance, sheets no thicker than approximately 3.43 mm (0.135 in.) can be cut to size within 0.25 mm (0.010 in.) and strips can be sheared to width at the same total tolerance. These tolerances apply to stock up to 3.7 m (12 ft) long that is essentially free from stress and is flat within commercial limits. Sheets that are not flat or that have residual stress, or both, cannot be sheared with the same accuracy.

Greater tolerances are required in shearing plate. A total tolerance of 0.5 to 1.0 mm (0.020 to 0.040 in.) can be maintained when plate is sheared in squaring shears. Dimensions can be held to tolerance of about ±1.6 mm ($\pm\frac{1}{16}$ in.) when shearing in alligator shears.

Safety

Shearing machines must be equipped with devices for protecting personnel from the hazards of shear knives, flywheels, gears, and other moving parts. The guards and safety devices used must be rigid enough to withstand damage from operating personnel moving heavy material into position.

The squaring shears used for sheet metal should have guards on all moving parts, including flywheels, hold-downs, and knives. The treadle, whether mechanical or electrical, should have a lock for supervisory control. Knife and hold-down guard openings should be large enough to provide visibility but small enough to keep the operator's fingers out of the danger area. Proper opening dimensions are outlined in ANSI standard B11.4 (latest edition).

The shears used for shearing plate are more difficult to safeguard because of the greater clearances needed under the hold-downs and upper knife to permit entry of the plate (especially when it is bowed or buckled). Guards on shears for plate should be of the type that raises only when the plate is inserted and then rests on the surface of the plate. When there is no workpiece in the machine, the guards rest within 6.4 mm ($\frac{1}{4}$ in.) of the surface of the table.

Shears should comply with the construction requirements of the Occupational Safety & Health Act and National Safety Standards such as ANSI B11.4. Additional safety information can be obtained from the loss prevention group of major insurance carders for Workman's Compensation and the National Safety Council. Safety regulations also cover the maximum noise level permitted from a shearing operation to prevent permanent impairment of hearing.

Mechanical Cutting for Weld Preparation

ASM Committee on Mechanical Cutting for Welding Preparation*

Iron Workers

Iron workers (heavy-duty shears) are used primarily for preparing structural shapes such as bars, angles, and T-bars. Like the shears used for plate and flat sheet, iron workers leave a square butt edge that may require further preparation for heavier sections before welding. The production shearing of bars and bar sections is usually done in machines with a throat opening designed for large, bulky workpieces. Guillotine and multipurpose (combination) machines are widely used for welding preparation. The multipurpose machines feature interchangeable punches and dies for shearing, punching, and coping. Squaring shears, normally used for sheet and plate, can also be used for cutting bar stock to length. Punch presses and press brakes can be provided with appropriate tooling for cutting operations.

Combination Machines

Combination machines are multipurpose machines used primarily in metal-fabricating shops where there is a constant need for shearing small quantities (often two or three pieces) of a variety of shapes and sizes from bars or bar sections. Some combination machines can also be used for punching, slotting, and notching.

Many combination machines incorporate several devices within the frame for performing different operations; therefore, a new setup is not required for each. A holder for an interchangeable punch and die is located in an area with a deep throat. This facilitates the punching of holes, slots, or notches in plates and bars, and in webs or legs of structural members.

A slide moving at 45° from vertical carries a blade for shearing angles. The support bed is on a swivel so that the ends of the angle section can be varied as desired from 45 to 90°. In two strokes of the machine, angles can be sheared to produce miter joints for subsequent welding (see the section "Cutting of Angles" in this article).

Combination machines can be used for cutting square and rectangular notches in the leg of an angle. These machines can be set up to cut a 90° V-shaped notch in angles that subsequently will be bent into frames. Other shapes, such as beams and channels, can be notched in a similar manner if the machine can accommodate the vertical height between the upper and lower legs of the workpiece. Provision is also made for shearing bars with guillotine-type blades or special blades (see the section "Conforming Blades" in this article).

Combination machines are available in capacities ranging from 110 to 890 kN (12 to 100 tonf). The 110 kN (12 tonf) machine can punch a 14 mm ($\frac{9}{16}$ in.) diam hole through a 6.4 mm ($\frac{1}{4}$ in.) thick section and can shear 75 × 75 × 6.4 mm (3 × 3 × $\frac{1}{4}$ in.) angles, 22 mm ($\frac{7}{8}$ in.) diam rounds, 19 mm ($\frac{3}{4}$ in.) squares, and 102 × 6.4 mm (4 × $\frac{1}{4}$ in.) flats. The 890 kN (100 tonf) machine can shear 152 × 152 × 16 mm (6 × 6 × $\frac{5}{8}$ in.) rounds, 50 mm (2 in.) squares, and 203 × 19 mm (8 × $\frac{3}{4}$ in.) flats.

Guillotine Machines

Guillotine iron-working machines are designed for cutting bars and bar sections to desired lengths from mill stock. They are extensively used throughout the fabricating industry. Two general types are available: open end (Fig. 5) and closed end. The machine illustrated in Fig. 5 is termed an open-end machine because it has a C-frame construction with one end open and unsupported. Open-end machines are either single end, for one operator, or double end, for two operators. On double-end machines, both ends can be right-hand or left-hand, or one end can be right-hand and the other end left-hand, depending on the type of cutting to be done. A closed-end guillotine machine, on the other hand, is basically the same as the one shown in Fig. 5 except that it has frame supports on both sides.

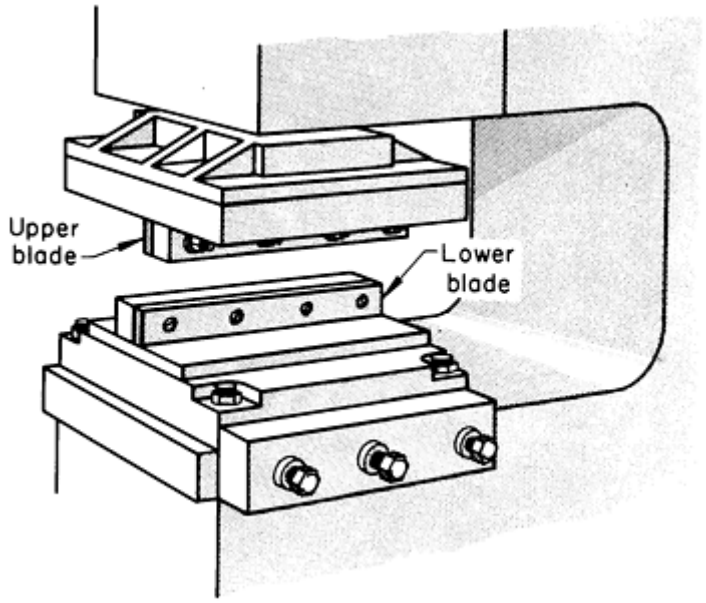

FIG. 5 OPEN-END GUILLOTINE IRON-WORKING MACHINE

An open-end machine has the advantage of giving the operator a clear view of the blades. However, because one end is open, a heavier frame and more floor space are required than for a closed-end machine of equal capacity.

Guillotine iron workers for bars and angles are available in capacities to 2700 kN (300 tonf). Either intermittent or continuous operation is possible. Guillotine iron workers can be equipped with simple straight blades (Fig. 5) or with two or more short blades having specific shapes.

Guillotine iron workers are actuated mechanically, hydraulically, or pneumatically. Hydraulic and pneumatic machines are lighter in weight for a specific shearing power, are more economical, and operate with less vibration than mechanical iron workers. Therefore, hydraulic or pneumatic machines up to 89 kN (10 tonf) capacity are completely portable, and units of 1800 to 2700 kN (200 to 300 tonf) capacity are semiportable (need not be solidly mounted in concrete).

Punching and Shearing Machines

Punching and shearing machines are deep-throat C-frame machines for the punching, shearing, notching, or coping of plates, bars, and structural sections. Shoes, into which punches, dies, and shear blades can readily be inserted, are mounted on the bed and ram.

The shoes either rest on the bed or are overhung; the overhanging type is designed so that structural shapes can be punched in both web and flange. The plain type of shoe is primarily used for plate work; however, plates can be worked with the overhanging shoes. Both types of die blocks are fitted with die sockets that hold dies of different inside diameters. The punch holder is adjustable to suit the location of the dies.

Fixturing

Fixturing is an important consideration in the shearing of bars. For safety and the proper functioning of open-end machines (Fig. 5) and many other iron-working machines, hold-down fixtures are essential. Guide pins are also helpful, especially when cutting with conforming blades.

Blade Design and Production Practice

Straight-edge blades can cut almost any bar or shape that is within the capacity of the machine. However, unacceptable distortion may result in some shapes of workpieces when they are sheared with blades that are not designed for cutting specific edges.

Conforming Blades. One method of minimizing distortion in cut bars employs two hardened blades mounted face-to-face, with identical holes through each blade. The holes should conform to the shape of the work metal and should be large enough to allow easy passage through the blades (Fig. 6a). One blade is movable vertically and one is stationary. Relatively little movement of the machine is required when blades of this type are used. In addition, because the blades completely encircle the work metal, hold-downs are not needed. However, these blades are usually limited for use on specially built or combination machines.

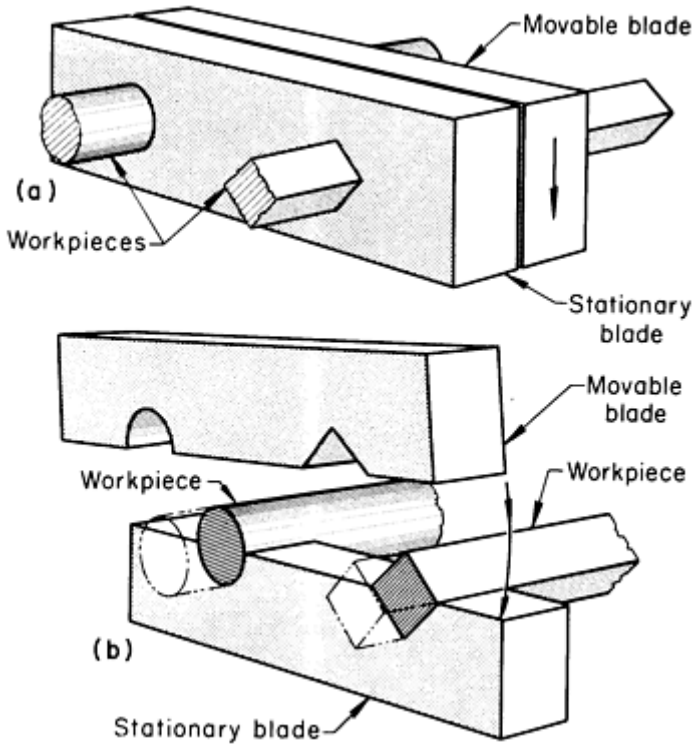

FIG. 6 TWO TYPES OF BLADES FOR THE CUTTING OF BARS

The cutting of round and square bars is more frequently done with the open-type blades illustrated in Fig. 6(b). Each blade is contoured to accommodate one-half the cross section of the work metal. The upper blade moves in a vertical direction, while the lower blade remains stationary. When using this technique, some type of hold-down is needed. Because of the stiffness of the work metal, the hold-down for bars should permit slight movement of the work metal in the axial direction to avoid double shearing. The hold-down can be a simple set screw (to permit adjustment) in a bracket or can be a more elaborate unit, such as a handwheel assembly utilizing an Acme thread.

For cutting square bars with any type of blade, the work metal should be placed so that the movement of the blade is across the diagonal of the square. With this technique the cutting force is applied to four sides instead of two, resulting in a smoother sheared surface. Cutting across the diagonal provides support on two sides of the square shape, which minimizes distortion and permits more than one size of bar stock to be cut in a given hole.

Best practice for cutting round bars is to use blades with holes for each size of stock to be cut. Blade holes appreciably larger than the stock size cause excessive distortion of the workpiece.

Cutting of angles is done either in a combination machine or by double cutting. In a combination machine--the more common method--two blades such as those shown in Fig. 7(a) are used. One blade, usually the one that is stationary, is L-shaped and is positioned as shown. The movable blade is square or rectangular and is mounted with its two cutting edges parallel to those of the stationary blade. Figure 7(a) also shows that the space between the blades in the loading position is the same shape as the workpiece.

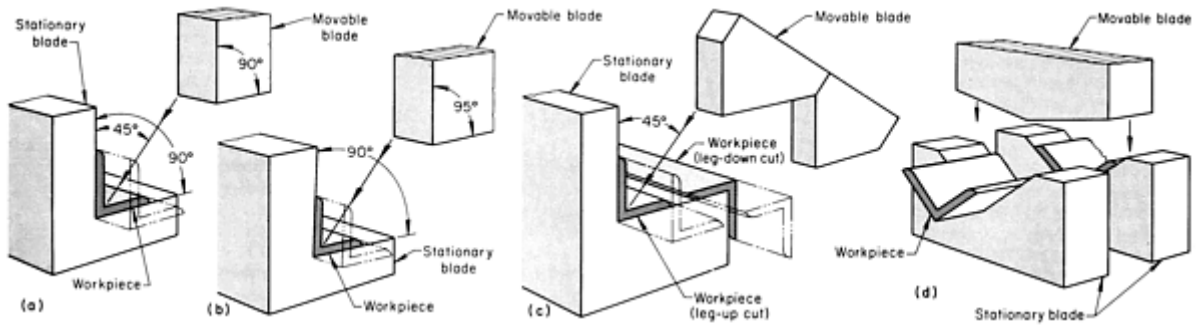

FIG. 7 FOUR TYPES OF BLADES FOR THE CUTTING OF ANGLE SECTIONS. (A) TO (C) CUTTING IN A COMBINATION MACHINE. (D) DOUBLE-CUTTING METHOD

The movable blade travels at 45° toward the stationary blade, and both blades contact the work metal uniformly. Shearing by this technique is essentially a blanking cut, and distortion of the workpiece is minimal. One disadvantage of the method is that all cutting occurs at once, resulting in a high shear load. This condition is not important when small angle sections are cut; however, for work metal larger than 102 × 102 × 13 mm (4 × 4 × $\frac{1}{2}$ in.), the movable blade should be provided with rake to prevent excessive loading.

To provide a rake angle between the movable and stationary blades, the included angle between the cutting edges of the upper or movable blade is increased to 95°, as shown in Fig. 7(b). Shearing begins at the extremity of each leg and progresses toward the root of the angle. The increase in the included angle of the movable blade results in some distortion of the drop-cut piece; the amount of distortion is about equal to the difference in angle between the movable and stationary blades (5° is normal). The part remaining on the table or stationary blade is not distorted.

Most combination cutting machines use a more versatile blade arrangement than those shown in Fig. 7(a) and 7(b). The setup shown in Fig. 7(c) is used to shear angle sections in both the leg-up and the leg-down positions. A swiveling table locates and holds the workpiece during shearing. With the swiveling table and two positions for the workpiece, the flanges can be easily mitered to any specific angle. For example, when cutting angle sections for a frame having the leg on the inside, the table would be set and locked at 45°. One end is mitered by placing the section in a leg-down position on the table and shearing off enough to make a clean cut. The other end is mitered by placing the section leg-up on the table and cutting to the proper length. The opposite positions are applicable when angle sections for a frame having the leg on the outside are being cut.

Cutting at a 45° angle reduces the capacity of the machine because a greater length of metal is cut at one time when a 90° cut is made. For example, a machine with a capacity of 203 × 203 × 32 mm (8 × 8 × $1\frac{1}{4}$ in.) when making a 90° cut has a capacity of only 203 × 203 × 25 mm (8 × 8 × 1 in.) when cutting at 45°.

Double cutting of angle sections, also called slugging, is used less frequently than cutting in a combination-type machine. This technique uses two stationary blades, spaced 13 mm ($\frac{1}{2}$ in.) apart, and one movable V-shaped blade arranged as shown in Fig. 7(d). The movable blade has a shallow V-shape that does not conform to the shape of the workpiece. Shearing starts at the extremity of each leg and progresses to the root of the angle, producing a 13 mm ($\frac{1}{2}$ in.) wide slug that is pushed out the bottom between the stationary blades.

In the double-cutting method, distortion occurs only in the slug, because the work metal is supported by the two stationary blades. There are two disadvantages of using the double-cutting method. First, increased power is required for making two cuts at the same time, and second, some metal is lost in the slug. The two stationary blades must be firmly supported to prevent their spreading during the cutting operation.

A similar tool can be used for cutting a channel section. The stationary blades should closely fit the contour of the channel section. Double cutting is adaptable to a guillotine machine, a combination machine, or a press.

Multiple Setups. Fabricating shops often must cut small quantities to a variety of shapes. To handle such work, many shops use a machine with a multiple setup. Without changing blades, the user can perform operations such as double cutting of angle sections, straight-blade cutting, cutting of round and square bars, and single cutting of L-sections. In this type of setup, all of the movable blades are attached to a single ram.

Mechanical Cutting for Weld Preparation

ASM Committee on Mechanical Cutting for Welding Preparation*

Iron Workers

Iron workers (heavy-duty shears) are used primarily for preparing structural shapes such as bars, angles, and T-bars. Like the shears used for plate and flat sheet, iron workers leave a square butt edge that may require further preparation for heavier sections before welding. The production shearing of bars and bar sections is usually done in machines with a throat opening designed for large, bulky workpieces. Guillotine and multipurpose (combination) machines are widely used for welding preparation. The multipurpose machines feature interchangeable punches and dies for shearing, punching, and coping. Squaring shears, normally used for sheet and plate, can also be used for cutting bar stock to length. Punch presses and press brakes can be provided with appropriate tooling for cutting operations.

Combination Machines

Combination machines are multipurpose machines used primarily in metal-fabricating shops where there is a constant need for shearing small quantities (often two or three pieces) of a variety of shapes and sizes from bars or bar sections. Some combination machines can also be used for punching, slotting, and notching.

Many combination machines incorporate several devices within the frame for performing different operations; therefore, a new setup is not required for each. A holder for an interchangeable punch and die is located in an area with a deep throat. This facilitates the punching of holes, slots, or notches in plates and bars, and in webs or legs of structural members.

A slide moving at 45° from vertical carries a blade for shearing angles. The support bed is on a swivel so that the ends of the angle section can be varied as desired from 45 to 90°. In two strokes of the machine, angles can be sheared to produce miter joints for subsequent welding (see the section "Cutting of Angles" in this article).

Combination machines can be used for cutting square and rectangular notches in the leg of an angle. These machines can be set up to cut a 90° V-shaped notch in angles that subsequently will be bent into frames. Other shapes, such as beams and channels, can be notched in a similar manner if the machine can accommodate the vertical height between the upper and lower legs of the workpiece. Provision is also made for shearing bars with guillotine-type blades or special blades (see the section "Conforming Blades" in this article).

Combination machines are available in capacities ranging from 110 to 890 kN (12 to 100 tonf). The 110 kN (12 tonf) machine can punch a 14 mm ($\frac{9}{16}$ in.) diam hole through a 6.4 mm ($\frac{1}{4}$ in.) thick section and can shear 75 × 75 × 6.4 mm (3 × 3 × $\frac{1}{4}$ in.) angles, 22 mm ($\frac{7}{8}$ in.) diam rounds, 19 mm ($\frac{3}{4}$ in.) squares, and 102 × 6.4 mm (4 × $\frac{1}{4}$ in.) flats. The 890 kN (100 tonf) machine can shear 152 × 152 × 16 mm (6 × 6 × $\frac{5}{8}$ in.) rounds, 50 mm (2 in.) squares, and 203 × 19 mm (8 × $\frac{3}{4}$ in.) flats.

Guillotine Machines

Guillotine iron-working machines are designed for cutting bars and bar sections to desired lengths from mill stock. They are extensively used throughout the fabricating industry. Two general types are available: open end (Fig. 5) and closed end. The machine illustrated in Fig. 5 is termed an open-end machine because it has a C-frame construction with one end open and unsupported. Open-end machines are either single end, for one operator, or double end, for two operators. On double-end machines, both ends can be right-hand or left-hand, or one end can be right-hand and the other end left-hand, depending on the type of cutting to be done. A closed-end guillotine machine, on the other hand, is basically the same as the one shown in Fig. 5 except that it has frame supports on both sides.

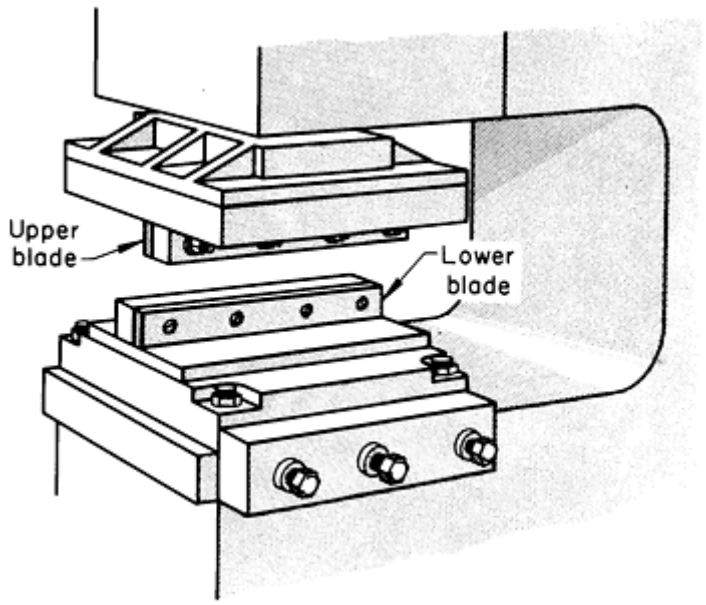

FIG. 5 OPEN-END GUILLOTINE IRON-WORKING MACHINE

An open-end machine has the advantage of giving the operator a clear view of the blades. However, because one end is open, a heavier frame and more floor space are required than for a closed-end machine of equal capacity.

Guillotine iron workers for bars and angles are available in capacities to 2700 kN (300 tonf). Either intermittent or continuous operation is possible. Guillotine iron workers can be equipped with simple straight blades (Fig. 5) or with two or more short blades having specific shapes.

Guillotine iron workers are actuated mechanically, hydraulically, or pneumatically. Hydraulic and pneumatic machines are lighter in weight for a specific shearing power, are more economical, and operate with less vibration than mechanical iron workers. Therefore, hydraulic or pneumatic machines up to 89 kN (10 tonf) capacity are completely portable, and units of 1800 to 2700 kN (200 to 300 tonf) capacity are semiportable (need not be solidly mounted in concrete).

Punching and Shearing Machines

Punching and shearing machines are deep-throat C-frame machines for the punching, shearing, notching, or coping of plates, bars, and structural sections. Shoes, into which punches, dies, and shear blades can readily be inserted, are mounted on the bed and ram.

The shoes either rest on the bed or are overhung; the overhanging type is designed so that structural shapes can be punched in both web and flange. The plain type of shoe is primarily used for plate work; however, plates can be worked with the overhanging shoes. Both types of die blocks are fitted with die sockets that hold dies of different inside diameters. The punch holder is adjustable to suit the location of the dies.

Fixturing

Fixturing is an important consideration in the shearing of bars. For safety and the proper functioning of open-end machines (Fig. 5) and many other iron-working machines, hold-down fixtures are essential. Guide pins are also helpful, especially when cutting with conforming blades.

Blade Design and Production Practice

Straight-edge blades can cut almost any bar or shape that is within the capacity of the machine. However, unacceptable distortion may result in some shapes of workpieces when they are sheared with blades that are not designed for cutting specific edges.

Conforming Blades. One method of minimizing distortion in cut bars employs two hardened blades mounted face-to-face, with identical holes through each blade. The holes should conform to the shape of the work metal and should be large enough to allow easy passage through the blades (Fig. 6a). One blade is movable vertically and one is stationary. Relatively little movement of the machine is required when blades of this type are used. In addition, because the blades completely encircle the work metal, hold-downs are not needed. However, these blades are usually limited for use on specially built or combination machines.

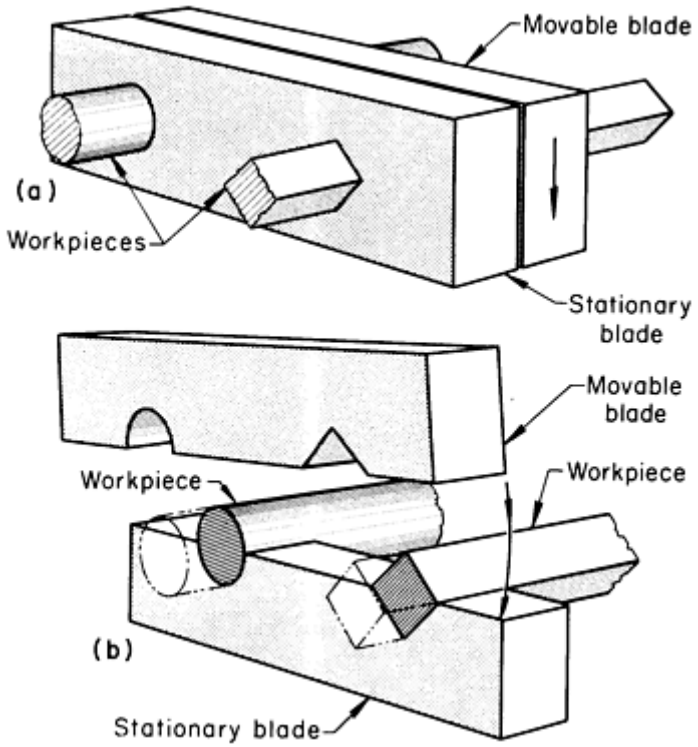

FIG. 6 TWO TYPES OF BLADES FOR THE CUTTING OF BARS

The cutting of round and square bars is more frequently done with the open-type blades illustrated in Fig. 6(b). Each blade is contoured to accommodate one-half the cross section of the work metal. The upper blade moves in a vertical direction, while the lower blade remains stationary. When using this technique, some type of hold-down is needed. Because of the stiffness of the work metal, the hold-down for bars should permit slight movement of the work metal in the axial direction to avoid double shearing. The hold-down can be a simple set screw (to permit adjustment) in a bracket or can be a more elaborate unit, such as a handwheel assembly utilizing an Acme thread.

For cutting square bars with any type of blade, the work metal should be placed so that the movement of the blade is across the diagonal of the square. With this technique the cutting force is applied to four sides instead of two, resulting in a smoother sheared surface. Cutting across the diagonal provides support on two sides of the square shape, which minimizes distortion and permits more than one size of bar stock to be cut in a given hole.

Best practice for cutting round bars is to use blades with holes for each size of stock to be cut. Blade holes appreciably larger than the stock size cause excessive distortion of the workpiece.

Cutting of angles is done either in a combination machine or by double cutting. In a combination machine--the more common method--two blades such as those shown in Fig. 7(a) are used. One blade, usually the one that is stationary, is L-shaped and is positioned as shown. The movable blade is square or rectangular and is mounted with its two cutting edges parallel to those of the stationary blade. Figure 7(a) also shows that the space between the blades in the loading position is the same shape as the workpiece.

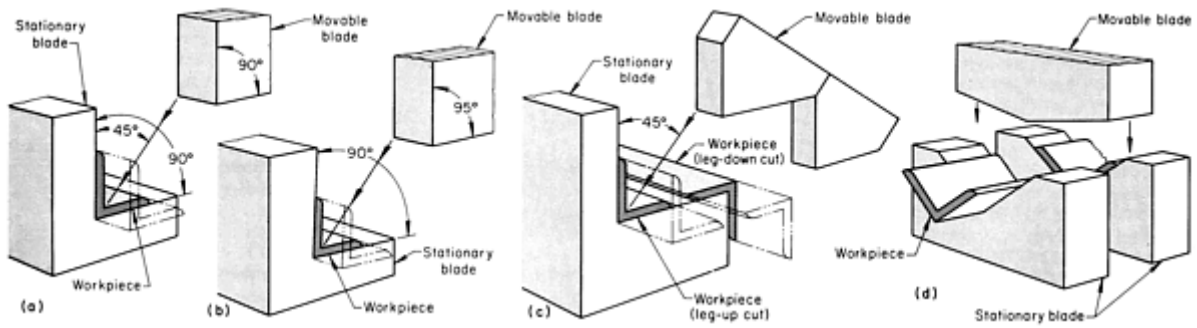

FIG. 7 FOUR TYPES OF BLADES FOR THE CUTTING OF ANGLE SECTIONS. (A) TO (C) CUTTING IN A COMBINATION MACHINE. (D) DOUBLE-CUTTING METHOD

The movable blade travels at 45° toward the stationary blade, and both blades contact the work metal uniformly. Shearing by this technique is essentially a blanking cut, and distortion of the workpiece is minimal. One disadvantage of the method is that all cutting occurs at once, resulting in a high shear load. This condition is not important when small angle sections are cut; however, for work metal larger than 102 × 102 × 13 mm (4 × 4 × $\frac{1}{2}$ in.), the movable blade should be provided with rake to prevent excessive loading.

To provide a rake angle between the movable and stationary blades, the included angle between the cutting edges of the upper or movable blade is increased to 95°, as shown in Fig. 7(b). Shearing begins at the extremity of each leg and progresses toward the root of the angle. The increase in the included angle of the movable blade results in some distortion of the drop-cut piece; the amount of distortion is about equal to the difference in angle between the movable and stationary blades (5° is normal). The part remaining on the table or stationary blade is not distorted.

Most combination cutting machines use a more versatile blade arrangement than those shown in Fig. 7(a) and 7(b). The setup shown in Fig. 7(c) is used to shear angle sections in both the leg-up and the leg-down positions. A swiveling table locates and holds the workpiece during shearing. With the swiveling table and two positions for the workpiece, the flanges can be easily mitered to any specific angle. For example, when cutting angle sections for a frame having the leg on the inside, the table would be set and locked at 45°. One end is mitered by placing the section in a leg-down position on the table and shearing off enough to make a clean cut. The other end is mitered by placing the section leg-up on the table and cutting to the proper length. The opposite positions are applicable when angle sections for a frame having the leg on the outside are being cut.

Cutting at a 45° angle reduces the capacity of the machine because a greater length of metal is cut at one time when a 90° cut is made. For example, a machine with a capacity of 203 × 203 × 32 mm (8 × 8 × $1\frac{1}{4}$ in.) when making a 90° cut has a capacity of only 203 × 203 × 25 mm (8 × 8 × 1 in.) when cutting at 45°.

Double cutting of angle sections, also called slugging, is used less frequently than cutting in a combination-type machine. This technique uses two stationary blades, spaced 13 mm ($\frac{1}{2}$ in.) apart, and one movable V-shaped blade arranged as shown in Fig. 7(d). The movable blade has a shallow V-shape that does not conform to the shape of the

workpiece. Shearing starts at the extremity of each leg and progresses to the root of the angle, producing a 13 mm ($\frac{1}{2}$ in.) wide slug that is pushed out the bottom between the stationary blades.

In the double-cutting method, distortion occurs only in the slug, because the work metal is supported by the two stationary blades. There are two disadvantages of using the double-cutting method. First, increased power is required for making two cuts at the same time, and second, some metal is lost in the slug. The two stationary blades must be firmly supported to prevent their spreading during the cutting operation.

A similar tool can be used for cutting a channel section. The stationary blades should closely fit the contour of the channel section. Double cutting is adaptable to a guillotine machine, a combination machine, or a press.

Multiple Setups. Fabricating shops often must cut small quantities to a variety of shapes. To handle such work, many shops use a machine with a multiple setup. Without changing blades, the user can perform operations such as double cutting of angle sections, straight-blade cutting, cutting of round and square bars, and single cutting of L-sections. In this type of setup, all of the movable blades are attached to a single ram.

Mechanical Cutting for Weld Preparation

ASM Committee on Mechanical Cutting for Welding Preparation*

Nibblers

Nibblers are power tools that "nibble" small pieces away from the material being worked. They range in size from hand-held machines to large floor-mounted equipment. Because the hand-held machines are portable, they are suitable for preparation of large parts on site, where thermal cutting may be impractical.

Nibblers can cut flat sheet of both ferrous and nonferrous metals, as well as of fiberglass and plastic. Corrugated and trapezoidal metal sheets can also be cut. Nibblers are frequently used to make edge preparations for welding of stainless steels and nonferrous metals. Unlike shears, which can curl or distort the separated pieces, nibblers remove material, creating a kerf or cutting slot; therefore, distortion of the sheet is eliminated.

Nibblers use a reciprocating punch and stationary die to accomplish the cutting process. During operation, the punch approaches and makes contact with the material being worked. The stroke of the punch compresses the material; the increased compression causes the material to deflect. As the shear point of the material is exceeded, the material is penetrated by the punch. The material then breaks (Fig. 8), and the break continues to widen until a cone-shaped chip is ejected. The punch is then withdrawn.

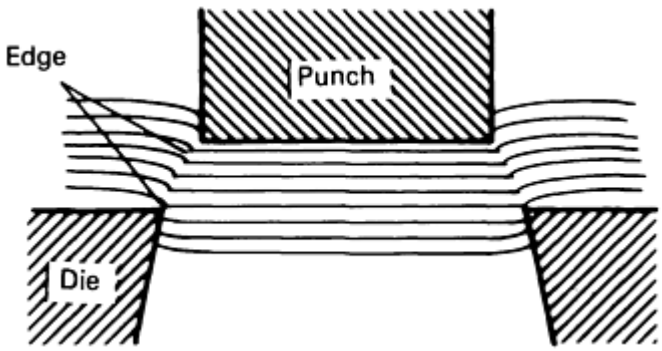

FIG. 8 SCHEMATIC OF NIBBLER CUTTING ACTION

The resulting edges are usually free of burrs. If burrs do occur, the gap between the punch and die is too wide (Fig. 9). On some equipment this gap can be varied.

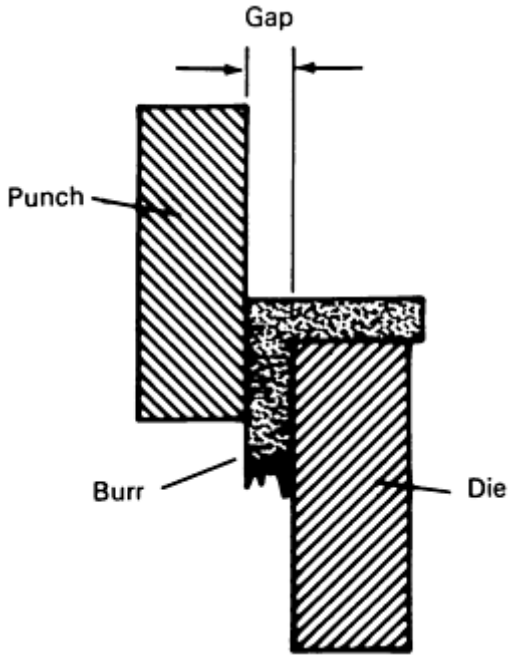

FIG. 9 SCHEMATIC OF NIBBLER SETUP WITH EXCESSIVE GAP BETWEEN THE PUNCH AND DIE, RESULTING IN THE FORMATION OF BURRS ON THE WORKPIECE

Because of their unique cutting action, nibblers do not need to be forced into the material. This so-called "natural feed" requires only light operator pressure. Also, the weight of the nibbler does not need to be supported solely by the operator: Once the nibbler has started cutting, the weight of the tool is supported by the sheet being worked. Nibblers are considered to be very safe to operate.

Some equipment is available with guide fences (similar to those used with circular saws), circle-cutting attachments, and template guides. Punches and dies on some nibblers can be resharpened; however, in many cases these parts are disposable. For optimum punch and die life, cutting oil should be used to lubricate the cutting process.

Mechanical Cutting for Weld Preparation

ASM Committee on Mechanical Cutting for Welding Preparation*

Band Saws

Band sawing is one method of cutting a workpiece to prepare it for further processing such as welding. The band saw machine, in its simplest form, consists of two wheels--one driven and one idle. The cutting tool is a welded continuous loop of flexible saw blade carried in one direction around the wheels and through the workpiece. This configuration permits full utilization of a cutting tool with hundreds of cutting edges, or teeth (Fig. 10). The band saw blade is thinner than other cutoff tools (typically 1.6 mm, or $\frac{1}{16}$ in. thick), which allows it to use less power and waste less material.

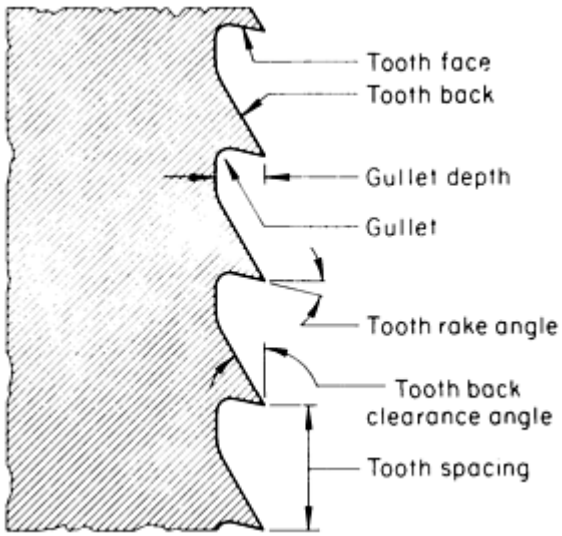

FIG. 10 SCHEMATIC SHOWING THE KEY ELEMENTS OF A BAND SAW BLADE CUTTING EDGE

Types of Machines

Band saw machines are either horizontal or vertical types; some are available as combination horizontal-vertical machines.

Contour band saws are vertical types that allow an operator to cut various contoured shapes by guiding the blade along a layout line. These machines can use very narrow bands for cutting small radii as well as wider bands for larger radii and straight cuts.

Cutoff band saws can be either horizontal or vertical. They cannot cut contours, but can make straight cuts very efficiently. Some machines can cut angles and compound miters in solids as well as structural shapes.

Band Saw Blade Selection

The two most widely used types of band saw blades available are carbon and bimetal.

Carbon steel blades are made from very high carbon tool steel and have either flexible backs or hard backs. The hard-back type has a heat-treated back for better strength and straighter cuts. Both types have hardened tooth tips for good wear resistance.

Carbon steel blades are most widely used for cutting of nonmetallic materials. However, they also do a satisfactory job when cutting low-carbon and low-alloy steels and perform well when cutting nonferrous alloys (for example, aluminum).

Bimetal blades are made with high-speed steel that is electron-beam welded to a lower-alloy backing steel. The result is a blade with the cutting properties of high-speed steel at the tooth tips and the flexibility and strength of a heat-treated alloy on the backing or carrier band. Bimetal blades should be used when cutting difficult-to-machine materials, and for high-production sawing. Bimetal blades will last longer than carbon blades, and they typically cut at ten times faster rates than those achieved with carbon blades.

Bimetal blades can be made with different grades of high-speed steels electron-beam welded to the tooth tips. The most popular grades used are M42 and Matrix II. Matrix II edges are best for cutting the lower-alloy materials and for cutting structural shapes or materials with varying cross sections. The higher hot hardness property of M42 is necessary when cutting difficult-to-machine alloys (for example, stainless steels and nickel alloys).

Table 2 gives the composition and physical properties of some welded-edge high-speed steel band saws.

TABLE 2 COMPOSITION AND PHYSICAL PROPERTIES OF SELECTED WELDED-EDGE HIGH-SPEED STEEL BAND SAW BLADES

PRODUCT	COMPOSITION, WT%								HEAT RESISTANCE		HARDNESS, HRC	
	C	Si	Mn	Cr	V	W	M	Co	°C	°F	TEETH	BODY
M2 HIGH-SPEED WELDED-EDGE BAND SAW	0.79-0.86	0.25	0.35	4.25	1.95	6.50	5.00	. . .	540	1000	64-66	40-47
MATRIX BAND SAW	0.70-0.78	0.30	0.25	4.25	1.00	1.00	5.00	8.00	590	1100	65-67	40-47
COBALT M42 BAND SAW	1.05-1.10	0.25	0.25	3.75	1.15	1.50	9.50	8.00	700	1300	67-69	40-47

Saw Width. The width of the saw blade along with its thickness determines the beam strength and thus its ability to cut straight and at high rates. Operators should always select the widest blade available in order to obtain the straightest cuts. For contour sawing, the widest blade that will cut the smallest radius should be selected.

The pitch of a saw blade is the number of teeth per 25 mm (1 in.). Selection of the correct pitch depends on the thickness of the material being cut. Thin materials require fine pitches, and thicker materials require coarser pitches. Blades are available in pitches as fine as 32 pitch and as coarse as 0.75 pitch. At least two teeth--and preferably three or more--should always be in contact with the piece being cut. It is especially important to observe this practice when cutting thin materials. A pitch that is too coarse will cause the teeth to rip out.

The selection of pitch often determines the success or failure of a particular cutting job. A pitch that is too coarse can cause the teeth to strip. A pitch that is too fine makes excessive feed pressure necessary, can cause binding in the cut, and will result in slow cutting or stripped teeth.

Variable-pitch blades are shapes designed to dampen resonance vibrations, especially when cutting structural shapes and workpieces with varying cross sections. The tooth spacing varies from tooth to tooth along an established length. This change in spacing cuts down on noise and vibration, resulting in quieter operation and smoother cuts.

Tooth Form. The choice of tooth form varies with each band saw blade manufacturer. Two basic forms are now most widely used: regular tooth and hook tooth (Fig. 11).

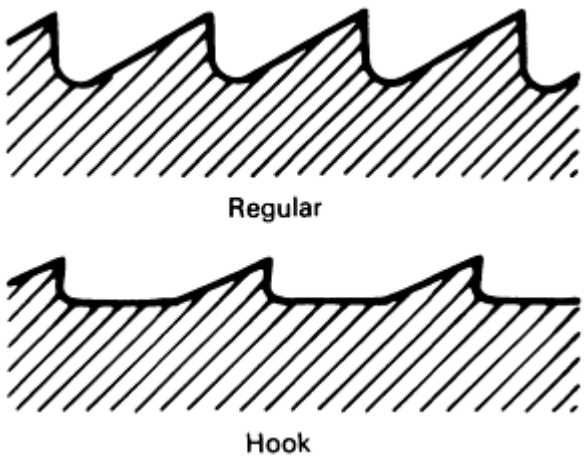

FIG. 11 BASIC TOOTH FORMS USED IN BAND SAW BLADES

The regular tooth form has deep gullets with smooth radii. The face angles vary from 0° rake to 15° positive rake. The neutral-rake blades work best for cutting structural shapes and thin materials, and for general-purpose low-volume cutting. The positive-rake blades use less feed pressure and cut more freely. This results in faster cutting rates and longer blade life, especially on heavy-duty band saws and at high production rates.

The hook tooth form is also a positive-rake blade, but the gullets are more shallow than those on the regular tooth form. The back angle is smaller than that on most regular tooth form blades. These factors combine to make a strong tooth that is capable of fast cutting speeds. The hook tooth form is especially suited for cutting of wide cross sections and for cutting of nonferrous materials such as aluminum.

Selection of Speeds and Cutting Rates

Table 3 lists the recommended speeds and cutting rates for many commonly sawed materials. The numbers are based on sawing of solid materials in the fully annealed condition. The data given should only be considered as a starting point; actual speeds and cutting rates will vary due to material variations and the type and condition of the saw that is used.

TABLE 3 SPEED AND CUTTING RATES FOR CUTOFF BAND SAWING WITH BIMETAL BLADES OF SELECTED FERROUS AND NONFERROUS METALS

WORK METAL	BAND SPEED[A]		CUTTING RATE[A]	
	m/min	sfm	$mm^2 \times 10^3$/min	$in.^2$/min
FERROUS METALS				
CARBON AND STEEL LOW-ALLOY STEELS				
1008-1013	100-84	325-275	9.0-6.4	14-10
1015-1035	106-90	350-300	9.7-7.1	15-11
1036-1064	68-58	225-190	5.8-4.5	9-7
1065-1095	52-44	170-145	5.2-3.9	8-6
1108-1132	106-84	350-275	9.7-7.7	15-12
1137-1151	80-68	260-225	6.4-5.2	10-8
1212-1213	106-90	350-300	9.7-7.7	15-12
1330-1345	65-58	210-190	5.2-3.9	8-6
4023-4047	80-70	260-230	5.2-3.9	8-6
4130-4140	75-67	250-220	5.8-4.5	9-7
4320-4340	70-55	230-180	4.5-3.2	7-5
4815-4820	58-53	190-175	3.9-2.9	6-4.5
5046	75-67	250-220	5.8-4.5	9-7
5140-5160	70-60	230-200	4.2-3.2	6.5-5
50100-52100	50-37	170-120	3.9-2.6	6-4
6118-6150	68-45	225-150	4.8-2.6	7.5-4
8615-8645	70-53	230-175	4.5-3.2	7-5
8720-8740	68-53	225-175	4.5-3.2	7-5
9310	53-45	175-150	2.6-1.9	4-3
TOOL STEELS				
W1	67-55	220-180	3.9-3.2	6-5
S2, S5	45-33	150-110	2.6-1.9	4-3
O1, O2	65-55	210-180	3.9-2.6	6-4
A2	60-52	200-170	2.6-1.9	4-3
D2, D3	37-27	120-90	1.9-1.3	3-2
D7	27-18	90-60	1.3-0.6	2-1
H12, H13, H21	58-49	190-160	3.2-2.6	5-4
T1, T2	40-30	130-100	2.3-1.3	3.5-2
T6, T8	30-21	100-70	1.6-0.6	2.5-1

T15	23-15	75-50	1.3-0.6	2-1
M1	45-37	150-120	3.2-1.9	5-3
M2, M3	33-24	110-80	2.6-1.3	4-2
M4, M10, M15	27-18	90-60	1.6-0.6	2.5-1
L6	55-49	180-160	3.9-2.6	6-4
STAINLESS STEELS				
201,202, 302, 304	37-24	120-80	2.6-1.3	4-2
303,303F	40-27	130-90	3.2-1.3	5-2
308, 309, 310, 330	24-18	80-60	1.3-0.6	2-1
314, 316, 317	23-15	75-50	1.3-0.6	2-1
321,347	37-27	120-90	2.6-1.3	4-2
410, 420, 420F	43-30	140-100	2.6-1.3	4-2
416, 430F	55-43	180-140	4.5-3.2	7-5
430, 446	27-18	90-60	2.6-1.9	4-3
440A, B, C	33-21	110-70	2.6-1.3	4-2
44OF, 443	40-30	130-100	2.6-1.3	4-2
17-7 PH, 17-4 PH	27-15	90-50	2.6-1.3	4-2
NONFERROUS METALS				
COPPER ALLOYS				
170, BERYLLIUM COPPER	84-60	275-200	5.2-3.9	8-6
	68-53	225-175	3.9-2.6	6-4
	43-27	140-90	1.9-1.3	3-2
510 PHOSPHOR BRONZE 5% A	90-75	300-250	6.4-5.2	10-8
	53-38	175-125	3.2-1.9	5-3
614, ALUMINUM BRONZE D	106-90	350-300	9.0-6.4	14-10
	53-38	175-125	3.2-1.9	5-3
656, HIGH-SILICON BRONZE	100-384	325-275	9.7-7.7	15-12
	53-38	175-125	3.9-1.9	6-3
675, MANGANESE BRONZE A	100-584	325-275	9.7-7.7	15-12
	60-45	200-150	3.9-2.6	6-4
NICKEL ALLOYS				
INCONEL	30-18	100-60	1.9-1.3	3-2
INCONEL X-750	24-18	80-60	1.0-0.3	1.5-0.5
MONEL 400	30-18	100-60	1.9-0.6	3-1
MONEL R-405	45-23	150-75	2.6-1.3	4-2
MONEL K-500	24-18	80-60	1.3-0.3	2-0.5
MONEL 501	30-18	100-60	1.9-0.6	3-1
HASTELLOY A	37-23	120-75	1.9-1.0	3-1.5
HASTELLOY B	30-23	100-75	1.6-0.6	2.5-1
HASTELLOY C	27-18	90-60	1.0-0.45	1.5-0.7
TITANIUM ALLOYS				
TI; TI-1.5FE-2.5CR	27-18	90-60	0.6-0.2	1-0.3
TI-4AL-4MN; TI-6AL-4V	33-21	110-70	1.3-3.9	2-6
TI-2FE-2CR-2MO	27-18	90-60	1.0-0.3	1.5-0.5

(A) BASED ON THE USE OF A 25 MM (1 IN.) WIDE HIGH-SPEED STEEL BAND, REGULAR TOOTH FORM (EXCEPT HOOK TOOTH FORM FOR METAL THICKER THAN ABOUT 250 MM, OR 10 IN.), RAKER SET, TO CUT SCALE-FREE, SOLID BAR STOCK UP TO 460 MM (18 IN.) THICK; BASED ON THE USE OF A CUTTING FLUID, EXCEPT FOR D2, D3, AND D7 TOOL STEELS, WHICH ARE CUT DRY

Table 3 only applies when using bimetal blades. Carbon steel blades cannot be run at the band speeds shown because the heat generated at these speeds will cause them to soften and fail immediately.

When cutting pipes, tubes, or structural shapes, it is necessary to compute slower cutting rates than those given in Table 3. The cutting rates should be modified as follows:

PART SIZE		PERCENTAGE OF SPEED SHOWN IN TABLE 3
MM	IN.	
<4.8	$< \frac{3}{16}$	40
4.8-9.5	$\frac{3}{16} - \frac{3}{8}$	50
9.5-16	$\frac{3}{8} - \frac{5}{8}$	60
>16	$> \frac{5}{8}$	70

Proper break-in is important to ensure optimum blade performance. When using a new blade, cutting at the full rate will cause fracturing of the very sharp tooth edges. Breaking in a new blade removes the ultrasharp edges and allows the blade to retain its cutting ability longer. A new blade can be broken in by running at the recommended band speed, but reducing the feed pressure for the initial cuts. When cutting work-hardening materials (for example, nickel alloys), it is important to use enough feed pressure to generate a chip and to prevent work hardening of the cut surface.

Knowledge of chip formation is helpful in finding the optimum speeds and cutting rates to use when band sawing. When a blade cuts, each tooth tip penetrates the workpiece and shears off a chip of material. Parameters such as band speed, feed, lubrication, and blade tip design all affect chip formation.

Visual examination of the chips can be used to determine proper speeds and cutting rates (Table 4). In general, the optimum conditions are present when the chips are curled and silver in color, indicating they were properly formed without excessive heat generation.

TABLE 4 VISUAL EXAMINATION OF CHIPS TO DETERMINE ADJUSTMENTS IN BAND SAW PARAMETERS THAT ARE REQUIRED TO OPTIMIZE MACHINABILITY

Source: "Operator's Guide and Application Guide," DoALL Co., 1990

Form	Color	Appearance or condition	Recommended parameter adjustment		
			Blade speed	Blade feed	Other
	Blue or brown	Thick and hard; thick and short	Decrease	Decrease	Check cutting fluid and mix
	Blue or brown	Thick and hard; brittle	Decrease	Decrease	Check cutting fluid and mix
	Silver or light straw	Thick and hard; springy (stiff)	Suitable	Decrease slightly	Check blade for proper pitch
	Silver	Thin and hard; springy (loose)	Increase	Decrease	Check blade for proper pitch
	Silver	Thin and curled (loose)	Suitable	Suitable	...
	Silver	Thin and straight; springy (loose)	Suitable	Increase	...
	Silver	Powdered	Decrease	Increase	...
	Silver	Thin and curled (very tight)	Suitable	Decrease	Use blade with coarser pitch

Source: "Operator's Guide and Applications Guide," DoALL Co., 1990

Safe Practices*

American Welding Society

Introduction

THIS ARTICLE covers the basic elements of safety general to all welding, cutting, and related processes. It includes safety procedures common to a variety of applications. However, it does not cover all safety aspects of every welding process; especially not those involving sophisticated technology. For this reason, those chapters in this Volume devoted to specific processes should also be referenced for additional important safety information.

Note

* THIS ARTICLE IS REPRINTED BY PERMISSION OF THE AMERICAN WELDING SOCIETY FROM THE *WELDING HANDBOOK*, 8TH EDITION, VOLUME 1, AMERICAN WELDING SOCIETY, 1987. IT WAS PREPARED BY THE AWS WELDING HANDBOOK SAFE PRACTICES CHAPTER COMMITTEE CONSISTING OF G.R. SPIES, *CHAIRMAN*, THE B.O.C. GROUP, LNC.; G.C. BARNES, ALLOY RODS COMPANY; K.L. BROWN, THE LINCOLN ELECTRIC COMPANY; W. BEISNER, HOBART BROTHERS COMPANY; O.J. FISHER, BABCOCK AND WILCOX COMPANY; W.S. HOWES, NEMA; C. PHILP, HANDY AND HARMAN COMPANY; UNDER THE DIRECTION OF AWS WELDING HANDBOOK COMMITTEE MEMBER A.F. MANZ, A.F. MANZ ASSOCIATES, AND AWS WELDING HANDBOOK COMMITTEE CHAIRMEN J.H. HANNAHS, MIDMARK CORPORATION, AND M.J. TOMSIC, PLASTRONICS INCORPORATED (AFFILIATIONS CIRCA 1987).

Safe Practices*

American Welding Society

General Welding Safety

Safety is an important consideration in all welding, cutting, and related work. No activity is satisfactorily completed if someone is injured. The hazards that may be encountered and the practices that will minimize personal injury and property damage are discussed here.

Management Support

The most important component of an effective safety and health program is management support and direction. Management must clearly state objectives and demonstrate its commitment to safety and health by consistent execution of safe practices.

Management must designate approved areas where welding and cutting operations may be carried on safely. When these operations must be done in other than designated areas, management must ensure that proper procedures to protect personnel and property are established and followed.

Management must be certain that only approved welding, cutting, and allied equipment is used. Such equipment includes torches, regulators, welding machines, electrode holders, and personal protective devices. Adequate supervision must be provided to ensure that all equipment is properly used and maintained.

Training

Thorough and effective training is a key aspect of a safety program. Adequate training is mandated under provisions of the U.S. Occupational Safety and Health Administration (OSHA), especially those of the Hazard Communication Standard (29 CFR 1910.1200). Welders and other equipment operators perform most safely when they are properly trained in the subject. (The term *welder* as used in this article is intended to include all welding and cutting personnel, brazers, and solderers.) Proper training includes instruction in the safe use of equipment and processes, and the safety rules that must be followed. Personnel need to know and understand the rules and the consequences of disobeying them. For example, welders must be trained to position themselves while welding or cutting so that their heads are not in the gases or fume plume. (Fume plume is the smokelike cloud containing minute solid particles arising directly from the area of melting metal. In distinction to a gas, fumes are metallic vapors that have condensed to solid and are often associated with a chemical reaction, such as oxidation.)

Before work begins, users must always read and understand the manufacturer's instructions on safe practices for the materials and equipment, and also the material safety data sheets.

Certain AWS specifications call for precautionary labels on consumables and equipment. These labels concerning the safe use of the products should be read and followed. A typical label is illustrated in Fig. 1.

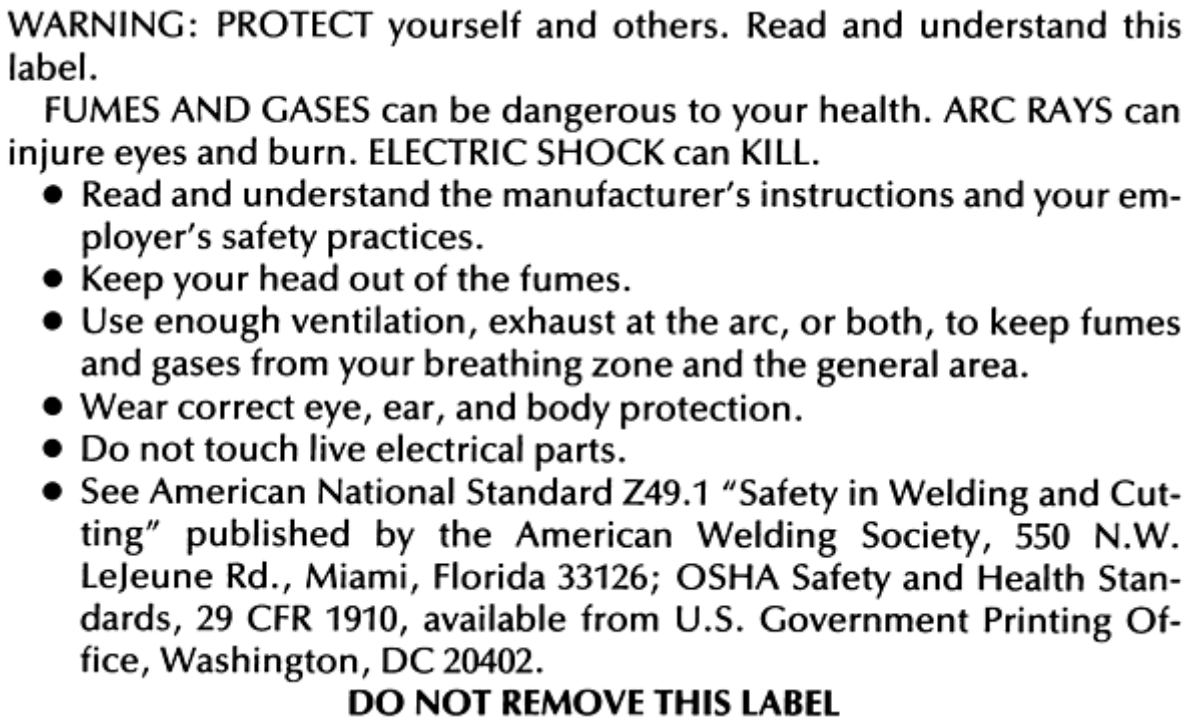

FIG. 1 MINIMUM WARNING FOR ARC WELDING PROCESSES AND EQUIPMENT

Manufacturers of welding consumables must provide on request a Material Safety Data Sheet (MSDS) that identifies those materials present in their products that have hazardous physical or health properties. The MSDS provides the OSHA permissible exposure limit, called the Threshold Limit Value (TLV), and any other exposure limit used or recommended by the manufacturer.

Employers that use consumables must make the applicable MSDS readily available to their employees, as well as train them to read and understand the contents. The MSDS contain important information about the ingredients contained in welding electrodes, rods, and fluxes, the composition of fumes that may be generated in their use, and means to be followed to protect the welder and others from hazards which might be involved.

Under OSHA Hazard Communication Standard 29 CFR 1910.1200, employers are responsible for the training of employees with respect to hazardous materials used in their workplace. Many welding consumables are included in the definition of hazardous materials according to this standard. Welding employers must comply with the communication and training requirements of this standard.

The proper use and maintenance of the equipment must also be taught. For example, defective or worn electrical insulation cannot be tolerated in arc welding or cutting, nor can defective or worn hoses be used in oxyfuel gas welding and cutting, brazing, or soldering. Proper training in equipment operation is fundamental to safe operation.

Persons must be trained to recognize safety hazards. If they are to work in an unfamiliar situation or environment, they must be thoroughly briefed on the potential hazards involved. For example, consider a person who must work in a confined space. If the ventilation is poor and an air-supplied helmet is required, the need and instructions for its proper use must be thoroughly explained to the employee. The consequences of improperly using the equipment must be covered. When employees believe that the safety precautions for a given task are not adequate, or not understood, they should question their supervisors before proceeding.

General Housekeeping

Good housekeeping is essential to avoid injuries. A welder's vision is often restricted by necessary eye protection. Persons passing a welding station must shield their eyes from the flame or arc radiation. The limited vision of the welder and passers-by make them vulnerable to tripping over objects on the floor. Therefore, welders and supervisors must always

make sure that the area is clear of tripping hazards. Management must lay out the production area so that gas hoses, cables, mechanical assemblies, and other equipment do not cross walkways or interfere with routine tasks.

When work is above ground or floor level, safety rails or lines must be provided to prevent falls as a result of restricted vision from eye protection devices. Safety lines and harnesses can be helpful to restrict workers to safe areas, and to catch them in case of a fall.

Unexpected events, such as fire and explosions, do occur in industrial environments. All escape routes must be identified and kept clear so that orderly, rapid, and safe evacuation of an area can take place. Storage of goods and equipment in evacuation routes should be avoided. If an evacuation route must be temporarily blocked, employees who would normally use that route must be trained to use an alternate route.

Protection in the General Area

Equipment, machines, cables, hoses, and other apparatus should always be placed so that they do not present a hazard to personnel in passageways, on ladders, or on stairways. Warning signs should be posted to designate welding areas and to specify that eye protection must be worn.

Protective Screens. Persons in areas adjacent to welding and cutting must be protected from radiant energy and hot spatter by (1) flame-resistant screens or shields, or (2) suitable eye and face protection and protective clothing. Appropriate radiation-protective, semitransparent materials are permissible.

Where operations permit, work stations should be separated by noncombustible screens or shields (Fig. 2). Booths and screens should permit circulation of air at floor level as well as above the screen.

FIG. 2 PROTECTIVE SCREENS BETWEEN WORK STATIONS

Wall Reflectivity. Where arc welding or cutting is regularly carried on adjacent to painted walls, the walls should be painted with a finish having a low reflectivity of ultraviolet radiation. Finishes formulated with certain pigments, such as titanium dioxide or zinc oxide, have low reflectivity to ultraviolet radiation. Color pigments may be added if they do not increase reflectivity. Pigments based on powdered or flaked metals are not recommended because they reflect ultraviolet radiation. Additional information is available in *Ultraviolet Reflectance of Paint,* published by the American Welding Society.

Public Demonstrations

Persons putting on public demonstrations involving observations of arc or oxyfuel gas welding or cutting processes are responsible for the safety of observers and the general public. Observers are not likely to have the necessary protective equipment to let them observe demonstrations safely. For exhibits involving observation of arc or oxyfuel gas welding and cutting processes, appropriate eye protection for both observers and passers-by is mandatory.

Fume exposure must be controlled by appropriate ventilation. Electric cables and hoses must be routed to avoid audience exposure to possible electric shock or tripping hazards. Protection must be provided against fires from fuels, combustibles, and overheated apparatus and wiring.

Fire extinguishers must be on hand in case of fire. Combustible materials must be removed from the area or shielded from flames, sparks, and molten metal.

Safety precautions at public events should be passive types, that is, they should not require the audience to take action to protect itself. For example, a protective, moveable transparent screen allows an audience to observe a welding operation with the screen in place. After welding is completed, the screen can be moved to allow the audience to observe the completed weld. Additional information is given in ANSI/AWS Z49.1, *Safety in Welding and Cutting.*

Fire

In most welding, cutting, and allied processes, a high-temperature heat source is present. Open flames, electric arcs, hot metal, sparks, and spatter are ready sources of ignition. Many fires are started by sparks, which can travel horizontally up to 10 m (35 ft) from their source and fall much greater distances. Sparks can pass through or lodge in cracks, holes, and other small openings in floors and walls.

The risk of fire is increased by combustibles in the work area, or by welding or cutting too close to combustibles that have not been shielded. Materials most commonly ignited are combustible floors, roofs, partitions, and building contents including trash, wood, paper, textiles, plastics, chemicals, and flammable liquids and gases. Outdoors, the most common combustibles are dry grass and brush.

The best protection against fire is to perform welding and cutting in specially designated areas or enclosures of noncombustible construction that are kept free of combustibles. Combustibles should always be removed from the work area or shielded from the operation.

Fuel for engine-driven equipment should be stored and used with care. Equipment manufacturer instructions should be followed because fuels and their vapors are combustible and can be explosive under some conditions.

Fuel gases, such as acetylene or propane, are other common flammables often found in cutting and welding areas. Special attention should be given to fuel gas cylinders, hoses, and apparatus to prevent gas leakage.

Combustibles that cannot be removed from the area should be covered with tight fitting, flame-resistant material. These include combustible walls and ceilings. Floors should be free of combustible materials for a radius of 10 m (35 ft) around the work area. All doorways, windows, cracks, and other openings should be covered with a flame-resistant material or, if possible, the work area should be enclosed with portable flame-resistant screens.

If welding or cutting is to be performed on or adjacent to a metal wall, ceiling, or partition, combustibles on the other side must be moved to a safe location. If this cannot be done, a fire watcher should be stationed where the combustibles are located. Heat from welding can be conducted through metal partitions and ignite combustibles on the opposite side. A thorough examination for evidence of fire should be made before leaving the work area. Fire inspection should be continued for at least 30 min after the operation is completed.

Welding or cutting should not be performed on material having a combustible coating or internal structure, as in walls or ceilings. Hot scrap or slag must not be placed in containers holding combustible materials. Suitable fire extinguishers should always be available nearby.

Welding, brazing, or cutting should not be performed on combustible floors or platforms that may readily be ignited by heat from the operation. Welders must be alert for traveling vapors of flammable liquids. Vapors are often heavier than air and can travel along floors and in depressions for distances of several hundred feet from where the flammable liquid is stored. Light vapors can travel along ceilings to adjacent rooms.

Hot Work Permit System

When welding, cutting, or similar hot working operations are to be performed in areas not normally assigned for such operations, a hot work permit system should be used. The purpose of the hot work permit system is to alert area supervisors to an extraordinary danger of fire that will exist at a particular time. The permit system should include a check list of safety precautions that includes an inspection for fire extinguishers, establishment of fire watches if necessary, search for flammable materials, and safety instructions for personnel in the area who are not involved in the hot work.

Explosion

Flammable gases, vapors, and dusts, when mixed with air or oxygen in certain proportions, present danger of explosion as well as fire. To prevent explosions, operators must avoid all sources of ignition. Welding, brazing, soldering, cutting, or operating equipment that can produce heat or sparks must not be done in atmospheres containing flammable gases, vapors, or dusts. Such flammables must be kept in leak-fight containers or be well removed from the work area. Heat or sparks may cause otherwise low-volatile materials to produce flammable vapors.

Hollow containers must be vented before applying heat. Heat must not be applied to a container that has held an unknown material, a combustible substance, or a substance that may form flammable vapors on heating. Additional information is given in AWS F4.1, *Recommended Safe Practices for the Preparation for Welding and Cutting of Containers and Piping That Have Held Hazardous Substances*, American Welding Society, latest edition. The container must first be thoroughly cleaned or filled with an inert gas. Heat should never be applied to a workpiece that is covered by an unknown substance, nor to a substance that may form flammable or toxic vapors on heating.

Adequate eye and body protection must be worn when operations involve a risk of explosion.

Burns

Burns of the eye or body are serious hazards of welding, brazing, soldering, and cutting. Eye, face, and body protection for the operator and others in the work area are required to prevent burns from ultraviolet and infrared radiation, sparks, and spatter.

Eye and Face Protection

Arc Welding and Cutting. Welding helmets or handshields containing appropriate filter lenses and cover plates must be used by welders and welding operators and nearby personnel when viewing an arc. Suggested shade numbers of filter plates for various welding, brazing, soldering, and thermal cutting operations are given in Table 1.

TABLE 1 SUGGESTED VIEWING FILTER PLATES

OPERATION	PLATE THICKNESS		WELDING CURRENT, A	LOWEST SHADE NO.	COMFORT SHADE NO.[A]
	mm	in.			
SHIELDED METAL ARC WELDING	. . .	. . .	<60	7	. . .
			60-160	7	10
			160-250	10	12
			250-550	11	14
GAS-METAL ARC AND FLUX-CORED ARC WELDING	. . .	. . .	<60	7	. . .
			60-160	10	11
			160-250	10	12
			250-500	10	14
GAS-TUNGSTEN ARC WELDING	. . .	. . .	<50	8	10
			50-150	8	12
			150-500	10	14
PLASMA ARC WELDING	. . .	. . .	<20	6	6-8
			20-100	8	10
			100-400	10	12
			400-800	11	14
OXYFUEL GAS WELDING (STEEL)[B]	3.2	$<\frac{1}{8}$	. . .	. . .	4, 5
	3.2-12.7	$\frac{1}{8}-\frac{1}{2}$	. . .	. . .	5, 6

	12.7	$>\frac{1}{2}$	. . .	. . .	6, 8
PLASMA ARC CUTTING[C]	. . .	. . .	<300	8	9
			300-400	9	12
			400-800	10	14
AIR-CARBON ARC CUTTING	. . .	. . .	<500	10	12
			500-1000	11	14
OXYFUEL GAS CUTTING (STEEL)[B]	25	<1	. . .	. . .	3, 4
	25-100	1-6	. . .	. . .	4, 5
	150	>6	. . .	. . .	5, 6
TORCH BRAZING	. . .	. . .	. . .	. . .	3, 4
TORCH SOLDERING	. . .	. . .	. . .	. . .	2

(A) TO SELECT THE BEST SHADE FOR THE APPLICATION, FIRST SELECT A DARK SHADE. IF IT IS DIFFICULT TO SEE THE OPERATION PROPERLY, SELECT SUCCESSFULLY LIGHTER SHADES UNTIL THE OPERATION IS SUFFICIENTLY VISIBLE FOR GOOD CONTROL. HOWEVER, DO NOT GO BELOW THE LOWEST RECOMMENDED NUMBER, WHERE GIVEN.

(B) WITH OXYFUEL GAS WELDING OR CUTTING, THE FLAME EMITS STRONG YELLOW LIGHT. A FILTER PLATE THAT ABSORBS YELLOW OR SODIUM WAVE LENGTHS OF VISIBLE LIGHT SHOULD BE USED FOR GOOD VISIBILITY.

(C) THE SUGGESTED FILTERS ARE FOR APPLICATIONS WHERE THE ARC IS CLEARLY VISIBLE. LIGHTER SHADES MAY BE USED WHERE THE ARC IS HIDDEN BY THE WORK OR SUBMERGED IN WATER.

Safety spectacles, goggles, or other suitable eye protection must also be worn during welding and cutting operations. Such devices must have full conforming side shields when there is danger of exposure to injurious rays or to flying particles from grinding or chipping operations. Spectacles or goggles may have clear or colored lenses, depending on the intensity of the radiation that may come from adjacent welding or cutting operations when the welding helmet is raised or removed. Number 2 filter lenses are recommended for general purpose protection.

Oxyfuel Gas Welding and Cutting, Submerged Arc Welding. Safety goggles with filter lenses (Table 1) and full conforming side shields must be worn while performing oxyfuel gas welding and cutting. During submerged arc welding, the arc is covered by flux and not readily visible; hence, an arc welding helmet is not needed. However, because the arc occasionally flashes through the flux burden, the operator should wear tinted safety glasses.

Torch Brazing and Soldering. Safety spectacles with or without side shields and with appropriate filter lenses are recommended for torch brazing and soldering. As with oxyfuel gas welding and cutting, a bright yellow flame may be visible during torch brazing. A filter similar to that used with those processes should be used for torch brazing.

Resistance, Induction, Salt-Bath, Dip, Infrared Welding, and Brazing. Operators and helpers engaged in these processes must wear safety spectacles, goggles, and a face shield to protect their eyes and face from spatter. Filter lenses are not necessary but may be used for comfort.

Standards for welding helmets, handshields, face shields, goggles, and spectacles are given in ANSI Z87.1, *Practices for Occupational and Educational Eye and Face Protection,* American National Standards Institute (latest edition).

Protective Clothing

Sturdy shoes or boots, and heavy clothing similar to that in Fig. 3 should be worn to protect the whole body from flying sparks, spatter, and radiation burns. Woolen clothing is preferable to cotton because it is not so readily ignited. Cotton clothing, if used, should be chemically treated to reduce its combustibility. Clothing treated with nondurable flame retardants must be retreated after each washing or cleaning. Clothing or shoes of synthetic or plastic materials which can melt and cause severe burns should not be worn. Outer clothing should be kept free of oil and grease, especially in an oxygen-rich atmosphere.

FIG. 3 TYPICAL PROTECTIVE CLOTHING FOR ARC WELDING

Cuffless pants and covered pockets are recommended to avoid spatter or spark entrapment. Pockets should be emptied of flammable or readily ignitable materials before welding because they may be ignited by sparks or weld spatter and result in severe burns. Pants should be worn outside of shoes. Protection of the hair with a cap is recommended, especially if a hair-piece is worn. Flammable hair preparations should not be used.

Durable gloves of leather or other suitable material should always be worn. Gloves not only protect the hands from burns and abrasion, but also provide insulation from electrical shock. A variety of special protective clothing is also available for welders. Aprons, leggings, suits, capes, sleeves, and caps, all of durable materials, should be worn when welding overhead or when special circumstances warrant additional protection of the body.

Sparks or hot spatter in the ears can be particularly painful and serious. Properly fitted, flame-resistant ear plugs should be worn whenever operations pose such risks.

Noise

Excessive noise, particularly continuous noise at high levels, can damage hearing. It may cause either temporary or permanent hearing loss. U.S. Department of Labor Occupational Safety and Health Administration regulations describe allowable noise exposure levels. Requirements of these regulations can be found in General Industry Standards, 29 CFR 1910.95.

In welding, cutting, and allied operations, noise may be generated by the process or the equipment, or both. Processes that tend to have high noise levels are air carbon arc and plasma arc cutting. Engine-driven generators sometimes emit a high noise level, as do some high-frequency and induction welding power sources.

Additional information is presented in *Arc Welding and Cutting Noise,* American Welding Society, 1979.

Machinery Guards

Welders and other workers must be protected from injury by machinery and equipment that they are operating or by other machinery operating in the work area. Moving components and drive belts must be covered by guards to prevent physical contact.

Because welding helmets and dark filter lenses restrict the visibility of welders, they may be even more susceptible than ordinary welders to injury from unseen, unguarded machinery. Therefore, special attention is required to this hazard.

When repairing machinery by welding or brazing, the power to the machinery must be disconnected, locked out, and tagged to prevent inadvertent operation and injury. Welders assigned to work on equipment with safety devices removed should fully understand the hazards involved and the steps to be taken to avoid injury. When the work is completed, the safety devices must be replaced. Rotating and automatic welding machines, fixtures, and welding robots must be equipped with appropriate guards or sensing devices to prevent operation when someone is in the danger area.

Pinch points on welding and other mechanical equipment can also result in serious injury. Examples of such equipment are resistance welding machines, robots, automatic arc welding machines, jigs, and fixtures. To avoid injury with such equipment, the machine should be equipped so that both of the operator's hands must be at safe locations when the machine is actuated. Otherwise, the pinch points must be suitably guarded mechanically. Metalworking equipment should not be located where a welder could accidently fall into or against it while welding. During maintenance of the equipment, pinch points should be blocked to prevent them from closing in case of equipment failure. In very hazardous situations, an observer should be stationed to prevent someone from turning the power on until the repair is completed.

Safe Practices*

American Welding Society

Fumes and Gases

Welders, welding operators, and other persons in the work area must be protected from overexposure to fumes and gases produced during welding, brazing, soldering, and cutting. Overexposure is exposure that is hazardous to health and exceeds the permissible limits specified by a government agency, such as the U.S. Department of Labor, Occupational Safety and Health Administration Regulations 29 CFR 1910.1000, or other recognized authority, such as the American Conference of Governmental Industrial Hygienists in its publications *Threshold Limit Values for Chemical Substances* and *Physical Agents in the Workroom Environment.* Persons with special health problems may have unusual sensitivity that requires even more stringent protection.

Fumes and gases are usually a greater concern in arc welding than in oxyfuel gas welding, cutting, or brazing because a welding arc may generate a larger volume of fume and gas, and greater varieties of materials are usually involved.

Protection from excess exposure is usually accomplished by ventilation. Where exposure would exceed permissible limits with available ventilation, respiratory protection must be used. Protection must be provided not only for the welding and cutting personnel but also for other persons in the area.

Arc Welding

Nature and Sources. Fumes and gases from arc welding and cutting cannot be classified simply. Their composition and quantity depend upon the base metal composition; the process and consumables used; coatings on the work, such as paint, galvanizing, or plating; contaminants in the atmosphere, such as halogenated hydrocarbon vapors from cleaning and degreasing activities; and other factors.

In welding and cutting, the composition of the fume usually differs from the composition of the electrode or consumables. Reasonably expected fume constituents from normal operations include products of volatilization, reaction, or oxidation of consumables, base metals, coatings, and atmospheric contaminants. Reasonably expected gaseous products include carbon monoxide, carbon dioxide, fluorides, nitrogen oxides, and ozone.

The quantity and chemical composition of air contaminants change substantially with the process and with a wide range of variables inherent in each process. During arc welding, the arc energy and temperature depend on the process as well as the welding variables. Therefore, fumes and gases are generated in varying degrees in different welding operations.

Welding fume is a product of vaporization, oxidation, and condensation of components in the consumable and, to some degree, the base metal. The electrode, rather than the base metal, is usually the major source of fume. However, significant fume constituents can originate from the base metal if it contains alloying elements or a coating that is volatile at elevated temperatures.

Various gases are generated during welding. Some are a product of the decomposition of fluxes and electrode coatings. Others are formed by the action of arc heat or ultraviolet radiation emitted by the arc on atmospheric constituents and contaminants. Potentially hazardous gases include carbon monoxide, oxides of nitrogen, ozone, and phosgene or other decomposition products of chlorinated hydrocarbons, such as phosgene.

Helium and argon, although chemically inert and nontoxic, are simple asphyxiants and could dilute the atmospheric oxygen concentration to potentially harmful low levels. Carbon dioxide (CO_2) and nitrogen can also cause asphyxiation.

Ozone may be generated by ultraviolet radiation from welding arcs. This is particularly true with gas shielded arcs, especially when argon is used. Photochemical reactions between ultraviolet radiation and chlorinated hydrocarbons result in the production of phosgene and other decomposition products.

The arc heat is responsible for the formation of oxides of nitrogen from atmospheric nitrogen. Hence, nitrogen oxides may be produced by a welding arc or other high-temperature heat sources. Thermal decomposition of carbon dioxide and inorganic carbonate compounds by an arc results in the formation of carbon monoxide. Levels can be significant when CO_2 is used as the shielding gas.

Reliable estimates of fume and gas composition cannot be made without considering the nature of the welding process and system being examined. For example, aluminum and titanium are normally welded in an atmosphere of argon or helium, or mixtures of the two gases. The arc creates relatively little fume but may emit an intense radiation that can produce ozone. Inert gas shielded arc welding of steels also creates a relatively low fume level.

Arc welding of steel in oxidizing environments, however, generates considerable fume and can produce carbon monoxide and oxides of nitrogen. The fumes generally consist of discrete particles of amorphous slags containing iron, manganese, silicon, and other metallic constituents, depending on the alloy system involved. Chromium and nickel compounds are found in fumes when stainless steels are arc welded.

Some covered and flux-cored electrodes are formulated with fluorides. The fumes associated with those electrodes can contain significantly more fluorides than oxides.

Factors Affecting Generation Rates. The rate of generation of fumes and gases during arc welding of steel depends on numerous variables. Among these are:

- WELDING CURRENT
- ARC VOLTAGE (ARC LENGTH)
- TYPE OF METAL TRANSFER OR WELDING PROCESS
- SHIELDING GAS

These variables are interdependent and can have a substantial effect on total fume generation.

Welding Current. In general, fume generation rate increases with increased welding current. The increase, however, varies with the process and electrode type. Certain covered, flux-cored, and solid-wire electrodes exhibit a nonproportional increase in fume generation rate with increasing current.

Studies have shown that fume generation rates with covered electrodes are proportional to the welding current raised to a power. The exponent is 2.24 for E6010 electrodes and 1.54 for E7018 electrodes. Similar trends were reported in other studies. Additional information is available in *Fumes and Gases in the Welding Environment,* American Welding Society, 1979.

Flux-cored and solid electrode fume generation rates are more complexly related to welding current. Welding current levels affect the type of metal droplet transfer. As a result, the fume generation rate can decrease with increasing current until some minimum is reached. Then, it will increase in a relatively proportional fashion.

An increase in current can increase ultraviolet radiation from the arc. Therefore, the generation of gases formed photochemically by this radiation, such as ozone, can be expected to increase as welding current is increased. Measurements of ozone concentration during gas-metal arc and gas-tungsten arc welding have shown such behavior.

Arc voltage and arc length are directly related. For a given arc length, there is a corresponding arc voltage, mostly dependent upon the type of electrode, welding process, and power supply. In general, increasing arc voltage (arc length) increases the fume generation rate for all open arc welding processes. The levels differ somewhat for each process or electrode type.

Type of Metal Transfer. When steel is joined with gas-metal arc welding using a solid-wire electrode, the mode of metal transfer depends upon the current and voltage. At low welding current and voltage, short-circuiting transfer takes

place; that is, droplets are deposited during short circuits between the electrode and molten weld pool. As the current or voltage is increased, metal transfer changes to globular type, where large globules of metal are projected across the arc into the weld pool. At high currents, transfer changes to a spray mode, where fine metal droplets are propelled rapidly across the arc. Fume generation rate appears to follow a transition also. It is relatively high during short-circuiting transfer because of arc turbulence. As the transition current is approached in an argon-rich shielding gas, the fume rate decreases and then increases again as spray transfer is achieved. In the spray region, the rate of fume generation is proportional to welding current.

For other welding processes, the type of metal transfer does not vary substantially with current or voltage. In these cases, fume generation follows the relationship for welding current changes.

Shielding Gas. When gas-metal arc welding or flux-cored arc welding with certain electrodes, shielding gas must be used. The type of shielding gas affects both the composition of the fume and its rate of generation. It also affects the kind of gases found in the welding environment. For example, the fume generation rate is higher with CO_2 shielding than with argon-rich shielding. The rate of fume formation with argon-oxygen or argon-CO_2 mixtures increases with the oxidizing potential of the mixture.

For welding processes where inert gas shielding is used, such as gas-tungsten arc or plasma arc welding, the fume generation rate varies with the type of gas or gas mixture. For example, there can be more fume with helium than with argon shielding.

By-product gases also vary with shielding gas composition. The rate of formation of ozone depends upon the wave lengths and intensity of the ultraviolet rays generated in the arc; ozone is more commonly found with argon-rich gases than with carbon dioxide. Oxides of nitrogen are present in the vicinity of any open arc process. Carbon monoxide is commonly found around CO_2 shielded arcs.

Welding Process. Studies of the relative fume generation rates of consumable electrode processes for welding on mild steel have shown definite trends. Considering the ratio of the weight of fumes generated per weight of metal deposited, covered electrodes and self-shielded fluxcored electrodes produce the most fume. Gas-shielded flux-cored electrodes produce less fume, and solid-wire electrodes produce an even smaller amount. The submerged arc welding process consistently produces the least fumes because the fume is captured in the flux and slag cover.

Consumables. With a specific process, the fume rate depends on the composition of the consumables. Some components of covered and flux-cored electrodes are designed to decompose and form protective gases during welding. Hence, they will generate relatively high fume levels.

Because the constituents of many covered and flux-cored electrodes are proprietary, the fume generation rates of electrodes of the same AWS classification produced by different manufacturers can differ substantially. The only reliable method for comparing filler metals is actual product testing to determine specific fume generation characteristics.

Oxyfuel Gas Welding and Cutting

The temperatures encountered in oxyfuel gas welding and cutting are lower than those found in electric arc processes. Consequently, the quantity of fumes generated is normally lower. The gases formed are reaction products of fuel gas combustion and of chemical reactions between the gases and the other materials present. The fumes generated are the reaction products of the base metals, coatings, filler metals, fluxes, and the gases being used. In oxyfuel gas cutting of steel, the fumes produced are largely oxides of iron.

Fume constituents of greater hazard may be expected when coatings such as galvanizing, paint primers, or cadmium plating are present. Gases of greatest concern include oxides of nitrogen, carbon monoxide, and carbon dioxide. Oxides of nitrogen may be present in especially large amounts when oxyfuel gas cutting stainless steels using either the chemical flux or the iron powder process.

Exposure Factors

Position of the Head. The single most important factor influencing exposure to fume is the position of the welder's head with respect to the fume plume. When the head is in such a position that the fume envelops the face or helmet,

exposure levels can be very high. Therefore, welders must be trained to keep their heads to one side of the fume plume. In some cases, the work can be positioned so the fume plume rises to one side.

Type of Ventilation. Ventilation has a significant influence on the amount of fumes in the work area and hence the welder's exposure. Ventilation may be local, where the fumes are extracted near the point of welding, or general, where the shop air is changed or filtered. The appropriate type will depend on the welding process, the material being welded, and other shop conditions. Adequate ventilation is necessary to keep the welder's exposure to fumes and gases within safe limits.

Shop Size. The size of the welding or cutting enclosure is important. It affects the background fume level. Fume exposure inside a tank, pressure vessel, or other confined space will certainly be higher than in a high-bay fabrication area.

The background fume level depends on the number and type of welding stations and the duty cycle for each station.

Design of Welding Helmet. The extent to which the helmet curves under the chin towards the chest affects the amount of fume exposure. Close-fitting helmets can be effective in reducing exposure.

Base Metal and Surface Condition. The type of base metal being welded influences both the constituents and the amount of fume generated. Surface contaminants or coatings may contribute significantly to the hazard potential of the fume. Paints containing lead and platings containing cadmium generate dangerous fumes during welding and cutting. Galvanized material evolves zinc fume.

Ventilation

The bulk of fume generated during welding and cutting consists of small particles that remain suspended in the atmosphere for a considerable time. As a result, fume concentration in a closed area can build up over time, as can the concentration of any gases evolved or used in the process. The particles eventually settle on the walls and floor, but the settling rate is low compared to the generation rate of the welding or cutting processes. Therefore, fume concentration must be controlled by ventilation.

Adequate ventilation is the key to control of fumes and gases in the welding environment. Natural, mechanical, or respirator ventilation must be provided for all welding, cutting, brazing, and related operations. The ventilation must ensure that concentrations of hazardous airborne contaminants are maintained below recommended levels. These levels must be no higher than the allowable levels specified by the U.S. Occupational Safety and Health Administration or other applicable authorities.

Many ventilation methods are available. They range from natural convection to localized devices, such as air-ventilated welding helmets. Examples of ventilation include:

- NATURAL VENTILATION
- GENERAL AREA MECHANICAL VENTILATION
- OVERHEAD EXHAUST HOODS
- PORTABLE LOCAL EXHAUST DEVICES
- DOWNDRAFT TABLES
- CROSSDRAFT TABLES
- EXTRACTORS BUILT INTO THE WELDING EQUIPMENT
- AIR-VENTILATED HELMETS

General Ventilation. In most cases, general ventilation is more effective in protecting personnel in adjacent areas than in protecting the welders themselves. Such ventilation may occur naturally outdoors, or when the shop doors and windows are open. It is acceptable when precautions are taken by the welder to keep his or her breathing zone away from the fume plume and when sampling of the atmosphere shows that concentrations of contaminants do not exceed permissible limits. Natural ventilation often meets these criteria when all of the following conditions are present:

- SPACE OF MORE THAN 283 M^3 (10,000 FT^3) PER WELDER IS PROVIDED.
- CEILING HEIGHT IS MORE THAN 5 M (16 FT).
- WELDING IS NOT DONE IN A CONFINED AREA.
- THE GENERAL WELDING AREA IS FREE OF PARTITIONS, BALCONIES, OR OTHER STRUCTURAL BARRIERS THAT SIGNIFICANTLY OBSTRUCT CROSS VENTILATION. (GENERAL AREA REFERS TO A BUILDING OR A ROOM IN A BUILDING, NOT A WELDING BOOTH OR SCREENED AREA THAT IS USED TO PROVIDE PROTECTION FROM WELDING RADIATION.)
- TOXIC MATERIALS WITH LOW PERMISSIBLE EXPOSURE LIMITS ARE NOT PRESENT AS DELIBERATE CONSTITUENTS. (THE EMPLOYER SHOULD REFER TO THE MATERIAL SAFETY DATA SHEET PROVIDED BY THE MATERIAL SUPPLIER.) WHEN NATURAL VENTILATION IS NOT SUFFICIENT, FANS MAY BE USED TO FORCE AND DIRECT THE REQUIRED AMOUNT OF AIR THROUGH A BUILDING OR WORK ROOM.

The effectiveness of general ventilation, natural or forced, depends on the design of the system. Work areas where fresh air is introduced and contaminated air is exhausted must be arranged so that the welding fumes and gases are carried away, not concentrated in dead zones. In some cases, the fresh air supply may be located so that incoming air provides the required protection for the welders as well as for personnel in the general area.

Air movement should always be from either side across the welder. This makes it easier for the welder to keep out of the plume and to keep fumes and gases from entering the welding helmet. Air should not blow toward the face or back of the welder because it may force the fume behind the helmet.

General mechanical ventilation may be a necessary supplement to local ventilation to maintain the background level of airborne contaminants within acceptable limits. Local ventilation is usually necessary to provide satisfactory health hazard control at the individual welding station.

Local Ventilation. General ventilation may control contamination levels in the broad area, but in many cases, it will not provide the local control needed to protect the welder. Local exhaust ventilation is usually the most effective way of providing protection at the local work station. It provides efficient and economical fume control and may be applied by one of the methods listed below.

A fixed open or enclosing hood consisting of a top and at least two sides can be placed to surround the welding or cutting operation. It must have sufficient air flow and velocity to keep contaminant levels at or below permissible limits. Additional information is available in *Industrial Ventilation: A Manual of Recommended Practice,* American Conference of Governmental Industrial Hygienists (latest edition).

A movable hood with a flexible duct can be positioned by the welder as close as practicable to the point of welding (Fig. 4). It should have sufficient air flow to produce a velocity of 30 m/min (100 ft/min) in the zone of welding.

FIG. 4 MOVABLE HOOD POSITIONED NEAR THE WELDING ARC

Air flow requirements range from 4 m^3/min (150 ft^3/min) when the hood is positioned at 100 to 150 mm (4 to 6 in.) from the weld, to 17 m^3/min (600 ft^3/min) at 250 to 300 mm (10 to 12 in.) from the weld. This is particularly applicable for bench work but may be used for any location, provided the hood is moved as required. An air velocity of 31 m/min (100 ft/min) will not disturb the torch gas shield during gas shielded arc welding, provided adequate gas flow rates are used. Higher air velocities may disturb the gas shield and render it less effective.

Crossdraft or Downdraft Table. A crossdraft table is a welding bench with the exhaust hood placed to draw air horizontally across the table. The welder should face in a direction perpendicular to the air flow so that the air flow is across his or her body. A downdraft table has a grill to support the work above an exhaust hood that draws the air downward and away from the welder's head.

Gun-mounted fume removal equipment extracts the fumes at the point of welding and results in an almost smokeless environment. The exhaust rate must be set so that it does not interfere with the shielding gas pattern provided by the welding process. The flux-cored arc welding process produces large quantities of fume, and virtually all of the fume can be collected using a gun-mounted fume removal device (Fig. 5).

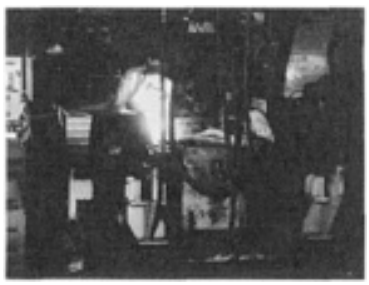

FIG. 5 REMOVAL OF FUME WITH A GUN-MOUNTED DEVICE

Where permissible, air cleaners that have high efficiencies in the collection of submicron particles may be used to recirculate a portion of ventilated air that would otherwise be exhausted. Some air cleaners do not remove gases. Therefore, the filtered air must be monitored to ensure that harmful gas concentrations do not exceed safe limits.

Water Table Used for Oxyfuel Gas and Plasma Arc Cutting Operations. This is a cutting table filled with water near or in contact with the bottom surface of the work. Much fume emerging from the cut is captured in the water.

Respiratory Protective Equipment. Where natural or mechanical ventilation is not adequate or where very toxic materials require a supplement to ventilation, respiratory protective equipment must be used. Airline respirators or face masks that give protection against all contaminants are generally preferred. Air-supplied welding helmets are also available commercially. Filter-type respirators, approved by the U.S. Bureau of Mines for metal fume, give adequate protection against particulate contaminants that are less toxic than lead, provided they are used and maintained correctly. Their general use is not recommended, however, because of the difficulty in ensuring proper use and maintenance. They will not protect against mercury vapor, carbon monoxide, or nitrogen dioxide. For these hazards an airline respirator, hose mask, or gas mask is required.

For additional information, refer to ANSI Z88.2, *Practices for Respiratory Protection,* American National Standards Institute (latest edition).

Special Ventilation Situations

Welding in Confined Spaces. Special consideration must be given to the safety and health of the welders and other workers in confined spaces. Gas cylinders must be located outside of the confined space to avoid possible contamination

of the space with leaking gases or volatiles. Welding power sources should also be located outside to reduce danger of engine exhaust and electric shock.

A means for removing persons quickly in case of emergency must be provided. Safety belts and lifelines, when used, should be attached to the worker's body in a manner that avoids the possibility of the person becoming jammed in the exit. A trained helper should be stationed outside the confined space with a preplanned rescue procedure to be put into effect in case of emergency.

In addition to keeping airborne contaminants in breathing atmospheres at or below recommended limits, ventilation in confined spaces must also (1) ensure adequate oxygen for life support (at least 19.5% by volume), (2) prevent accumulation of an oxygen-enriched atmosphere (i.e., not over 23.5% by volume), and (3) prevent accumulation of flammable mixtures. Asphyxiation can quickly result in unconsciousness and death without warning if oxygen is not present in sufficient concentration to support life. Air contains approximately 21% O by volume. A confined space must not be entered unless it is well ventilated, or the welder is properly trained to work in such spaces and is wearing an approved air-supplied breathing apparatus. (Approved air-supplied respirators or hose masks are those accepted by the U.S. Bureau of Mines or other recognized agency.) A similarly equipped second person must be present.

Confined spaces should be tested before entering for (1) toxic or flammable gases and vapors and (2) adequate or excess oxygen. The tests should be made with instruments approved by the U.S. Bureau of Mines. Heavier-than-air gases, such as argon, methylacetylene-propadiene, propane, and carbon dioxide, may accumulate in pits, tank bottoms, low areas, and near floors. Lighter-than-air gases, such as helium and hydrogen, may accumulate in tank tops, high areas, and near ceilings. The precautions for confined spaces also apply to those areas. If practical, a continuous monitoring system with audible alarms should be used for work in a confined space.

Oxygen-enriched atmospheres pose great danger to occupants of confined areas. They are especially hazardous at oxygen concentrations above 25%. Materials that burn normally in air may flare up violently in an oxygen-enriched atmosphere. Clothing may burn fiercely; oil or grease-soaked clothing or rags may catch fire spontaneously; paper may flare into flame. Very severe and fatal burns can result.

Protection in confined spaces must be provided not only for welders but also for other persons in the enclosure. Only clean, respirable air must be used for ventilation. Oxygen, other gases, or mixtures of gases must never be used for ventilation.

When welding, cutting, or related processes are performed in confined areas where adequate and proper ventilation cannot be provided and there is immediate danger to life and health, positive pressure self-contained breathing apparatus must be used. It must have an emergency air supply of at least five minutes duration in the event that the main source fails.

For further precautions, see ANSI Z117.1, *Safety Requirements for Working in Tanks and Other Confined Spaces* (latest edition).

Welding of Containers. Welding or cutting on the outside or inside of containers or vessels that have held dangerous substances presents special hazards. Flammable or toxic vapors may be present, or may be generated by the applied heat. The immediate area outside and inside the container should be cleared of all obstacles and hazardous materials. For more complete procedures, refer to AWS F4.1, *Recommended Safe Practices for the Preparation for Welding and Cutting of Containers and Piping That Have Held Hazardous Substances*, American Welding Society, latest edition. When repairing a container in place, entry of hazardous substances released from the floor or the soil beneath the container must be prevented. The required personal and fire protection equipment must be available, serviceable, and in position for immediate use.

When welding or cutting inside of vessels that have held dangerous materials, the precautions for confined spaces must also be observed.

Gases generated during welding should be discharged in a safe and environmentally acceptable manner in accordance with Government rules and regulations. Provisions must be made to prevent pressure buildup inside containers. Testing for gases, fumes, and vapors should be conducted periodically to ensure that recommended limits are maintained during welding.

An alternative method of providing safe welding of containers is to fill them with an inert medium such as water, inert gas, or sand. When using water, the level should be kept to within a few inches of the point where the welding is to be done. The space above the water should be vented to allow the heated air to escape. With inert gas, the responsible individual needs to know the percentage of inert gas that must be present in the tank to prevent fire or explosion, and how to safely produce and maintain a safe atmosphere during welding.

Highly Toxic Materials. Certain materials, which are sometimes present in consumables, base metals, coatings, or atmospheres for welding or cutting operations, have permissible exposure limits of 1.0 mg/m^3 (4.4×10^{-4} gr/ft^3) or less. Among such materials are the following metals and their compounds:

- ANTIMONY
- ARSENIC
- BARIUM
- BERYLLIUM
- CADMIUM
- CHROMIUM
- COBALT
- COPPER
- LEAD
- MANGANESE
- MERCURY
- NICKEL
- SELENIUM
- SILVER
- VANADIUM

Base metals and filler metals that may release some of these materials as fume during welding or cutting are given in Table 2.

TABLE 2 POSSIBLE TOXIC MATERIALS EVOLVED DURING WELDING OR THERMAL CUTTING

BASE OR FILLER METAL	**EVOLVED METALS OR THEIR COMPOUNDS**
CARBON AND LOW-ALLOY STEELS	CHROMIUM, MANGANESE, VANADIUM
STAINLESS STEELS	CHROMIUM, MANGANESE, NICKEL
MANGANESE STEELS AND HARDFACING MATERIALS	CHROMIUM, COBALT, MANGANESE, NICKEL, VANADIUM
HIGH-COPPER ALLOYS	BERYLLIUM, CHROMIUM, COPPER, LEAD, NICKEL
COATED OR PLATED STEEL OR COPPER	CADMIUM(A), CHROMIUM, COPPER, LEAD, NICKEL, SILVER

(A) WHEN CADMIUM IS A CONSTITUENT IN A FILLER METAL, A WARNING LABEL MUST BE AFFIXED TO THE CONTAINER OR COIL. REFER TO ANSI/ASC Z49.1, *SAFETY IN WELDING AND CUTTING,* AMERICAN NATIONAL STANDARDS INSTITUTE (LATEST EDITION).

Manufacturer's material safety data sheets should be consulted to determine if any of these highly toxic materials are present in welding filler metals and fluxes being used. Material safety data sheets should be requested from suppliers. However, welding filler metals and fluxes are not the only source of these materials. They may also be present in base metals, coatings, or other sources in the work area. Radioactive materials under Nuclear Regulatory Commission jurisdiction require special considerations.

When toxic materials are encountered as designated constituents in welding, brazing, or cutting operations, special ventilation precautions must be taken to ensure that the levels of these contaminants in the atmosphere are at or below the limits allowed for human exposure. All persons in the immediate vicinity of welding or cutting operations involving toxic materials must be similarly protected. Unless atmospheric tests under the most adverse conditions establish that exposure is within acceptable concentrations, the following precautions must be observed.

Confined Spaces. Whenever any toxic materials are encountered in confined space operations, local exhaust ventilation and respiratory protection must be used.

Indoors. When any toxic materials are encountered in indoor operations, local exhaust mechanical ventilation must be used. When beryllium is encountered, respiratory protection in addition to local exhaust ventilation is essential.

Outdoors. Whenever any toxic materials are encountered in outdoor operations, respiratory protection approved by the Mine Safety and Health Association (MSHA), the National Institute of Occupational Safety and Health (NIOSH), or other approving authority may be required.

Persons should not consume food in areas where fumes that contain materials with very low allowable exposure limits may be generated. They should also practice good personal hygiene, such as washing hands before touching food, to prevent ingestion of toxic contaminants.

Fluorine Compounds. Fumes and gases from fluorine compounds can be dangerous to health and can burn the eyes and skin on contact. Local mechanical ventilation or respiratory protection must be provided when welding, brazing, cutting, or soldering in confined spaces involving fluxes, coatings, or other material containing fluorine compounds.

When such processes are employed in open spaces, the need for local exhaust ventilation or respiratory protection will depend upon the circumstances. Such protection is not necessary when air samples taken in breathing zones indicate that all fluorides are within allowable limits. However, local exhaust ventilation is always desirable for fixed-location production welding and for all production welding of stainless steels when filler metals or fluxes containing fluorides are used.

Zinc. Fumes containing zinc compounds may produce symptoms of nausea, dizziness, or fever (sometimes called metal fume fever). Welding or cutting where zinc may be present in consumables, base metals, or coatings should be done as described for fluorine compounds.

Cleaning compounds often require special ventilation precautions because of their possible toxic or flammable properties. Manufacturers' instructions should be followed before welding or cutting is done with cleaned consumables or on cleaned base metal.

Chlorinated Hydrocarbons. Degreasing or cleaning operations involving chlorinated hydrocarbons must be so located that vapors from such operations do not enter the atmosphere surrounding molten weld metal or the welding arc. A reaction product having an objectionable, irritating odor, and containing highly toxic phosgene gas is produced when such vapors enter the atmosphere of arc welding operations. Low levels of exposure can produce feelings of nausea, dizziness, and weakness. High exposures may produce serious health impairment.

Cutting of stainless steel by oxyfuel gas, gas shielded arc, or plasma arc cutting should be done using local mechanical ventilation to remove the fumes generated. Fume from plasma arc cutting done under water is mostly captured in the water.

Measurement of Exposure

The American Conference of Governmental Industrial Hygienists (ACGIH) and the U.S. Department of Labor, Occupational Safety and Health Administration (OSHA) have established allowable limits of airborne contaminants. They are called threshold limit values (TLV) or permissible exposure limits (PEL).

The TLV is the concentration of an airborne substance to which most workers may be repeatedly exposed day after day, without adverse effect. In adapting these to the working environment, a threshold limit value-time weighted average (TLV-TWA) quantity is defined. TLV-TWA is the time-weighted average concentration for a normal 8 h workday or 40 h workweek to which nearly all workers may be repeatedly exposed without adverse effect. TLV-TWA values should be

used as guides in the control of health hazards and should not be interpreted as sharp lines between safe and dangerous concentrations.

TLVs are revised annually as necessary. They may or may not correspond to OSHA permissible limits (PEL) for the same materials. In many cases, current ACGIH values for welding materials are more stringent than OSHA levels.

The only way to ensure that airborne contaminant levels are within the allowable limits is to take air samples at the breathing zones of the personnel involved. An operator's actual on-the-job exposure to welding fume should be measured following the guidelines provided in ANSI/AWS F1.1, *Method for Sampling Airborne Particulates Generated by Welding and Allied Processes.* This document describes how to obtain an accurate breathing zone sample of welding fume for a particular welding operation. Both the amount of fume and the composition of the fume can be determined in a single test using this method. Multiple samples are recommended for increased accuracy. When a helmet is worn, the sample should be collected inside the helmet in the welder's breathing zone.

Safe Practices*

American Welding Society

Handling of Compressed Gases

Gas Cylinders and Containers

Gases used in welding and cutting operations are packaged in containers called cylinders. Only cylinders designed and maintained in accordance with U.S. Department of Transportation (DOT) specifications may be used in the United States. The use of other cylinders may be extremely dangerous and is illegal. Cylinders requiring periodic retest under DOT regulations may not be filled unless the retest is current.

Filling. Cylinders may be filled only with the permission of the owner. They should only be filled by recognized gas suppliers or those with the proper training and facilities to do so. Filling one cylinder from another is dangerous and should not be attempted by anyone not qualified to do so. Combustible or incompatible combinations of gases must never be mixed in cylinders.

Usage and Storage. Welding must not be performed on gas cylinders. Cylinders must not be allowed to become part of an electrical circuit because arcing may result. Cylinders containing shielding gases used in conjunction with arc welding must not be grounded. Electrode holders, welding torches, cables, hoses, and tools should not be stored on gas cylinders, which might cause arcing or interference with valve operation. Are-damaged gas cylinders may rupture and result in injury or death.

Cylinders must not be used as work rests or rollers. They should be protected from bumps, falls, falling objects, and weather, and they should not be dropped. Cylinders should not be kept in passageways where they might be struck by vehicles. They should be kept in areas where temperatures do not fall below -30 °C (-20 °F) nor exceed 55 °C (130 °F). Any of these exposures, misuses, or abuses could damage them to the extent that they might fail, with serious consequences.

Cylinders must not be hoisted using ordinary slings or chains. A proper cradle or cradle sling that securely retains the cylinder should be used. Electromagnets should not be used to handle cylinders.

Cylinders must always be secured by the user against falling during either use or storage. Acetylene and liquefied gas cylinders should always be stored and used in the upright position. Other cylinders are preferably stored and used in the upright position, but this is not essential in all circumstances.

Before using gas from a cylinder, the contents should be identified by the label thereon. Contents must never be identified by any other means such as cylinder color, banding, or shape. These may vary among manufacturers, geographical areas, or product lines and could be completely misleading. The label on the cylinder is the only proper notice of the contents. If a label is not on a cylinder, the contents should not be used and the cylinder should be returned to the supplier.

A valve protection cap is provided on many cylinders to protect the safety device and the cylinder valve. This cap should always be in place except when the cylinder is in use. The cylinder should never be lifted manually or by hoist by the valve protection cap. The threads that secure these valve protection caps are intended only for that purpose and may not be capable of supporting full cylinder weight. The caps should always be threaded completely onto the cylinders and hand tightened.

Gas cylinders and other containers must be stored in accordance with all state and local regulations and the appropriate standards of OSHA and the National Fire Protection Association (NFPA). Safe handling and storage procedures are discussed in the Compressed Gas Association's *Handbook of Compressed Gases.*

Withdrawal of Gas. Many gases in high-pressure cylinders are filled to pressures of 14 MPa (2000 psig) or more. Unless the equipment to be used with a gas is designed to operate at full cylinder pressure, an approved pressure-reducing regulator must be used to withdraw gas from a cylinder or manifold. Simple needle valves should never be used. A pressure-relief or safety valve, rated to function at less than the maximum allowable pressure of the welding equipment, should also be employed. The valve function is to prevent failure of the equipment at pressures in excess of working limits if the regulator should fail in service.

Valves on cylinders containing high-pressure gas, particularly oxygen, should always be opened slowly to avoid the high temperature of adiabatic recompression, which can occur if the valves are opened rapidly. In the case of oxygen, the heat can ignite the valve seat, which, in turn, may cause the metal to melt or burn. The cylinder valve outlet should point away from the operator and other persons when the valve is being opened to avoid injury should a fire occur.

Prior to the connection of a gas cylinder to a pressure regulator or a manifold, the valve outlet should be cleaned of dirt, moisture, and other foreign matter by first being wiped with a clean, oil-free cloth. Then the valve should be opened momentarily and closed immediately. This is known as "cracking the cylinder valve." Fuel gas cylinders must never be cracked near sources of ignition (i.e., sparks and flames), while the operator is smoking, or in confined spaces.

A regulator should be drained of gas pressure prior to being connected to a cylinder and also after the cylinder valve is closed upon shutdown of operation. The outlet threads on cylinder valves are standardized for specific gases so that only regulators or manifolds with similar threads can be attached. (Refer to ANSI/CGA V-l, *Compressed Gas Cylinder Valve Outlet and Inlet Connections,* Compressed Gas Association.) Standard valve thread connections for gases normally used for welding, brazing, and allied processes are given in Table 3.

TABLE 3 COMPRESSED GAS ASSOCIATION STANDARD AND ALTERNATE VALVE THREAD CONNECTIONS FOR COMPRESSED GAS CYLINDERS

GAS	CONNECTION NO.
ACETYLENE	510 OR 300
ARGON	580
BUTANE	510
CARBON DIOXIDE (CO_2)	320
HELIUM	580
HYDROGEN	350
METHYLACETYLENE-PROPADIENE (MPS)	510
NITROGEN	580 OR 555
OXYGEN	540
PROPANE	510
PROPYLENE	510

It is preferable not to open valves on low-pressure fuel gas cylinders more than one turn. This usually provides adequate flow and permits rapid closure of the cylinder valve in an emergency. High-pressure cylinder valves, on the other hand, usually must be opened fully to backseat the packing and prevent packing leaks during use.

The cylinder valve should be closed after each use of a cylinder and when an empty cylinder is to be returned to the supplier. This prevents loss of product through leaks that might develop and go undetected while the cylinder is

unattended and also avoids hazards that might be caused by leaks. It also prevents backflow of contaminants into the cylinder. It is advisable to return cylinders to the supplier with about 172 kPa (25 psi) of contents remaining. This prevents possible contamination by the atmosphere during shipment.

Pressure-Relief Devices. Only trained personnel should be allowed to adjust pressure-relief devices on cylinders. These devices are intended to provide protection in the event the cylinder is subjected to a hostile environment, usually fire or other source of heat. Such environments may raise the pressure within cylinders. To prevent cylinder pressures from exceeding safe limits, the safety devices are designed to relieve the contents.

Cryogenic Cylinders and Tanks

Cryogenic cylinders and tanks are used to store at very low temperatures those liquids that change to gases at normal conditions of temperature and pressure. So-called cryogenic liquids for commercial purposes include oxygen, nitrogen, and argon, although other gases may be handled as cryogenic liquids.

Cylinders and tanks for storing cryogenic liquids are usually double-walled vessels that are evacuated and insulated between the walls. They are designed to contain liquids at very low temperatures with a minimum of heat gain. Heat gain from the atmosphere causes evaporation of the product. Liquid containers hold a greater amount of product for a given volume than high-pressure gas cylinders. For safety, containers of liquid must be handled carefully. They must always be maintained in an upright position. Whenever they are moved, a cylinder handling truck designed for this purpose must be used. They should not be rolled on a bottom edge, as is often done with high-pressure cylinders.

Failure to properly handle these cylinders can result in rupture of either the inner or outer cylinder wall with consequent loss of vacuum and rapid rise of internal pressure. This will result in activation of the cylinder's protective devices and loss of the cylinder contents. The cylinder protection devices must never be tampered with nor deactivated. Overpressurization could result in explosive failure.

Damage to the internal walls or fittings of a cryogenic-liquid container is often evidenced by visible frosting on the exterior of the container. Whenever frosting appears on the exterior of a cryogenic-liquid container, personnel should be kept clear and the gas supplier notified. In general, people should stay clear of the container until the frost disappears. When the frost disappears it means that the contents have evaporated and any dangerous internal pressure has been relieved.

Although the contents of cryogenic-liquid containers are predominantly in liquid form at very low temperatures, the product withdrawn from these containers should be a gas at room temperature. The conversion takes place within a vaporizer system that evaporates the liquid and warms the gas to atmospheric temperature.

In some cases, the user may want to withdraw liquid from the container. When liquid is withdrawn, protective clothing should be worn to prevent bodily contact with the cold product. Loose-fitting insulated gloves and an adequate face shield are essential. Contact of liquid with the skin will cause burns similar to heat burns, and prolonged contact will cause severe frostbite. Injuries of this nature should be treated in the same manner as injuries from exposure to *low* temperatures.

Compared to their normal properties, the properties of many materials are drastically different at cryogenic liquid temperatures. Many metals, including carbon steel, and most elastomers, such as rubber, become extremely brittle. When cryogenic liquids are to be withdrawn from cylinders, all materials in the transfer line must have satisfactory properties at the low temperatures.

Liquid oxygen may react with explosive violence on contact with asphalt or similar bituminous materials. Therefore, liquid oxygen tanks must never be mounted on such surfaces and liquid oxygen must not be allowed to contact them. Liquid oxygen tanks must always be installed on concrete pads.

Regulators

A pressure-reducing regulator should always be used when withdrawing gas from gas cylinders for welding or cutting operations. Gas regulators should meet the requirements of E-4, *Standard for Gas Regulators for Welding and Cutting,* Compressed Gas Association, and other code regulations.

Pressure-reducing regulators must be used only for the gas and pressure given on the label. They should not be used with other gases, or at other pressures even though the cylinder valve outlet threads may be the same. The threaded connections to the regulator must not be forced. Improper fit of threads between a gas cylinder and regulator or between the regulator and hose indicates that an improper combination of devices is being used.

Use of adapters to change the cylinder connection thread is not recommended because of the danger of using an incorrect regulator or of contaminating the regulator. For example, gases that are oil-contaminated can deposit an oily film on the internal parts of the regulator. This film can contaminate oil-free gas or result in fire or explosion in the case of oxygen.

The threads and connection glands of regulators should be inspected before use for dirt or damage. If a hose or cylinder connection leaks, it should not be forced with excessive torque. Damaged regulators and components should be repaired by properly trained mechanics or returned to the manufacturer for repair.

A suitable valve or flowmeter should be used to control gas flow from a regulator. The internal pressure in a regulator should be drained before it is connected to or removed from a gas cylinder or manifold.

Manifolds

A manifold is used when gas is needed without interruption or at a higher delivery rate than can be supplied from a single cylinder. A manifold must be designed for the specific gas and operating pressure, and be leak tight. The manifold components should be approved for such purpose and used only for the gas and pressure for which they are approved. Oxygen and fuel gas manifolds must meet specific design and safety requirements. (Refer to ANSI/NFPA 51, *Oxygen-Fuel Gas Systems for Welding, Cutting, and Allied Processes,* National Fire Protection Association, latest edition, for information on manifold and piping systems.)

Piping and fittings for acetylene and methyl-acetylene-propadiene (MPS) manifolds must not be unalloyed copper or alloys containing 70% or more copper. These fuel gases react with copper under certain conditions to form unstable copper acetylide. This compound may detonate under shock or heat.

Manifolded piping systems must contain an appropriate over-pressure relief valve. Each fuel gas cylinder lead should incorporate a backflow check valve and a flash arrester. Backflow check valves must also be installed in each line at each station outlet where both fuel gas and oxygen are provided for a welding, cutting, or preheating torch.

Piping Systems. Unless it is known that a piping system is specifically designed and constructed to withstand the full cylinder pressure or tank pressure of the compressed gas source supplying it, the piping system must always be protected with safety pressure-relief devices sufficient to prevent development of pressure in the system beyond the capacity of the weakest element.

Such pressure-relief devices may be relief valves or bursting disks. A pressure-reducing regulator must never be solely relied upon to prevent overpressurization of the system. A pressure-relief device must be located in every section of the system which could be exposed to the full source supply pressure while isolated from other protective relief devices (such as by a closed valve).

Some pressure regulators have integral safety relief valves. These valves are designed for the protection of the regulator only and should not be relied upon to protect the downstream system.

In cryogenic piping systems, relief devices should be located in every section of the system where liquified gas may become trapped. Upon warming, such liquids vaporize to gas, and in a confined space, the gas pressure can increase dramatically.

Pressure-relief devices protecting fuel gas piping systems or other hazardous gas systems should be vented to safe locations.

Oxygen

Oxygen is nonflammable, but it supports the combustion of flammable materials. It can initiate combustion and vigorously accelerate it. Therefore, oxygen cylinders and liquid oxygen containers should not be stored in the vicinity of combustibles nor with cylinders of fuel gas. Oxygen should never be used as a substitute for compressed air. Pure oxygen

supports combustion more vigorously than air, which contains only 20% O. Therefore, the identification of oxygen and air should be differentiated.

Oil, grease, and combustible dusts may spontaneously ignite on contact with oxygen. Hence, all systems and apparatus for oxygen service must be kept free of any combustibles. Valves, piping, or system components that have not been expressly manufactured for oxygen service must be cleaned and approved for this service before use. (Refer to G4.1, *Cleaning Equipment for Oxygen Service,* Compressed Gas Association.)

Apparatus that has been manufactured expressly for oxygen service, and is usually so labeled, must be kept in the clean condition as originally received. Oxygen valves, regulators, and apparatus should never be lubricated with oil. If lubrication is required, the type of lubricant and the method of applying the lubricant should be specified in the manufacturer's literature. If it is not, then the device should be returned to the manufacturer or authorized representative for service.

Oxygen must never be used to power compressed air tools. These are almost always lubricated with oil. Similarly, oxygen must not be used to blow dirt from work and clothing because they are often contaminated with oil, or grease, or combustible dust.

Only clean clothing should be worn when working with oxygen systems. Oxygen must not be used to ventilate confined spaces. Severe bums may result from ignition of clothing or the hair in an oxygen-rich atmosphere.

Fuel Gases

Fuel gases commonly used in oxyfuel gas welding (OFW) and cutting (OFC) are acetylene, methylacetylene-propadiene (MPS), natural gas, propane, and propylene. Hydrogen is used in a few applications. Gasoline is sometimes used as a fuel for oxygen cutting. It vaporizes in the torch. These gases should always be referred to by name.

Acetylene in cylinders is dissolved in a solvent so that it can be safely stored under pressure. In the free state, acetylene should never be used at pressures over 15 psig (100 kPa) because it can dissociate with explosive violence at higher pressures.

Acetylene and MPS should never be used in contact with silver, mercury, or alloys containing 70% or more copper. These gases react with these metals to form unstable compounds that may detonate under shock or heat. Valves on fuel gas cylinders should never be opened to clean the valve outlet, especially not near possible sources of flame ignition or in confined spaces.

When fuel gases are used for a brazing furnace atmosphere, they must be burned or vented to a safe location. Prior to filling a furnace or retort with fuel gas, the equipment must first be purged with a nonflammable gas, such as nitrogen or argon, to prevent formation of an explosive air-fuel mixture.

Special attention must be given when using hydrogen. Flames of hydrogen may be difficult to see and parts of the body, clothes, or combustibles may come in contact with hydrogen flames.

Fuel Gas Fires. The best procedures for avoiding fire from a fuel gas or liquid is to keep it contained within the system, that is, to prevent leaks. All fuel systems should be checked carefully for leaks upon assembly and at frequent intervals thereafter. Fuel gas cylinders should be examined for leaks, especially at fuse plugs, safety devices, and valve packing. One common source of fire in welding and cutting is ignition of leaking fuel by flying sparks or spatter.

In the event of a fuel fire, one of the most effective means for controlling the fire is to shut off the fuel valve, if accessible. A fuel gas valve should not be opened beyond the point necessary to provide adequate flow. In this way it can be shut off quickly in an emergency. In most cases, this is less than one turn of the handle. If the immediate valve controlling the burning gas is inaccessible, another upstream valve may cut off the flow of gas.

Most fuel gases in cylinders are in liquid form or dissolved in liquids. Therefore, the cylinders should always be used in the upright position to prevent liquid surges into the system.

A fuel gas cylinder can develop a leak and sometimes result in a fire. In case of fire, the fire alarm should be sounded, and trained fire personnel should be summoned immediately. A small fire in the vicinity of a cylinder valve or a safety device

should be extinguished, if possible, by closing the valve or by the use of water, wet cloths, or fire extinguishers. If the leak cannot be stopped, the cylinder should be removed by trained fire personnel to a safe outdoor location, and the supplier notified. A warning sign should be posted, and no smoking or other ignition sources should be permitted in the area.

In the case of a large fire at a fuel gas cylinder, the fire alarm should be actuated, and all personnel should be evacuated from the area. The cylinder should be kept wet by fire personnel with a heavy stream of water to keep it cool. It is usually better to allow the fire to continue to burn and consume the issuing gas rather than attempt to extinguish the flame. If the fire is extinguished, there is danger that the escaping gas may reignite with explosive violence.

Shielding Gases

Argon, helium, nitrogen, and carbon dioxide (CO_2) are used for shielding with some welding processes. All, except carbon dioxide, are used as brazing atmospheres. They are odorless and colorless and can displace air needed for breathing.

Confined spaces filled with these gases must be well ventilated before personnel enter them. If there is any question, the space should be checked first for adequate oxygen concentration with an oxygen analyzer. If an analyzer is not available, an air-supplied respirator should be worn by anyone entering the space. Containers of these gases should not be placed in confined spaces, as discussed previously.

Safe Practices*

American Welding Society

Electrical Safety

Electric Shock

Electric shock can cause sudden death. Injuries and fatalities from electric shock in welding and cutting operations can occur if proper precautionary measures are not followed. Most welding and cutting operations employ some type of electrical equipment. For example, automatic oxyfuel gas cutting machines use electric motor drives, controls, and systems.

Some electrical accidents may not be avoidable, such as those caused by lightning. However, the majority are avoidable, including those caused by lack of proper training.

Shock Mechanism. Electric shock occurs when an electric current of sufficient magnitude to create an adverse effect passes through the body. The severity of the shock depends mainly on the amount of current, the duration of flow, the path of flow, and the state of health of the person. The current is caused to flow by the applied voltage. The amount of current depends upon the applied voltage and the resistance of the body path. The frequency of the current may also be a factor when alternating current is involved.

Shock currents greater than about 6 milliamperes (mA) are considered primary because they are capable of causing direct physiological harm. Steady state currents between 0.5 and 6 mA are considered secondary shock currents. Secondary shock currents are defined as those capable of causing involuntary muscular reactions without normally causing direct physiological harm. The 0.5 mA level is called the perception threshold because it is the point at which most people just begin to feel the tingle from the current. The level of current sensation varies with the weight of the individual and to some extent between men and women.

Shock Sources. Most electrical equipment can be shock hazards if improperly installed, used, or maintained. Shock can occur from lightning-induced voltage surges in power distribution systems. Even earth grounds can attain high potential relative to true ground during severe transient phenomena. Such circumstances, however, are rare.

In welding and cutting work, most electrical equipment is powered from ac sources of between 115 and 575 V, or by engine-driven generators. Most welding is done with less than 100 arc volts. (Fatalities have resulted with equipment

operating at less than 80 volts.) Some arc cutting methods operate at over 400 V, and electron-beam welding machines at up to about 150 kV. Most electric shock in the welding industry occurs as the result of accidental contact with bare or poorly insulated conductors operating at such voltages. Therefore, welders must take precautions against contacting bare elements in the welding circuit, as well as those in the primary circuits.

Electrical resistance is usually reduced in the presence of water or moisture. Electrical hazards are often more severe under such circumstances. When arc welding or cutting is to be done under damp or wet conditions including heavy perspiration, the welder must wear dry gloves and clothing in good condition to prevent electric shock. The welder should be protected from electrically conductive surfaces, including the earth, by rubber-soled shoes as a minimum and preferably by an insulating layer such as a rubber mat or dry wooden board. Similar precautions against accidental contact with bare conducting surfaces must be taken when the welder is required to work in a cramped kneeling, sitting, or lying position. Rings and jewelry should be removed before welding to decrease the possibility of electric shock.

Wearers of Pacemakers

The technology of heart pacemakers and the extent to which they are influenced by other electrical devices is constantly changing. It is impossible to make a general statement concerning the possible effects of welding operations on such devices. Wearers of pacemakers or other electronic equipment vital to life should check with the device manufacturer or their doctor to determine whether any hazard exists.

Equipment Selection

Electric shock hazards are minimized by proper equipment installation and maintenance, good operator practice, proper operator clothing and body protection, and the use of equipment designed for the job and situation. Equipment should meet applicable NEMA or ANSI standards, such as American National Standards Institute's ANSI/UL 551, *Safety Standard for Transformer Type Arc Welding Machines,* latest edition.

If a significant amount of welding and cutting work is to be done under electrically hazardous conditions, automatic machine controls that reduce the no-load (open circuit) voltage to a safe level are recommended. When special welding and cutting processes require open-circuit voltages higher than those specified in ANSI/NEMA publication EW-1, *Electrical Arc Welding Apparatus,* insulation and operating procedures that are adequate to protect the welder from these higher voltages must be provided.

Personnel Training

A good safety training program is essential. Employees must be fully instructed in electrical safety by a competent person before being allowed to commence operations. As a minimum, this training should include the points covered in ANSI/ASC Z49.1, *Safety in Welding and Cutting* (published by the American Welding Society). Persons should not be allowed to operate electrical equipment until they have been properly trained.

Equipment Installation

Equipment should be installed in a clean, dry area. When this is not possible, it should be adequately guarded from dirt and moisture. Installation must be done to the requirements of ANSI/NFPA 70, *National Electric Code,* and local codes. This includes necessary disconnects, fusing, and type of incoming power lines.

Terminals for welding leads and power cables must be shielded from accidental contact by personnel or by metal objects, such as vehicles and cranes. Connections between welding leads and power supplies may be guarded using (1) dead front construction and receptacles for plug connections, (2) terminals located in a recessed opening or under a non-removable hinged cover, (3) insulating sleeves, or (4) other equivalent mechanical means.

Grounding

The workpiece being welded and the frame or chassis of all electrically powered machines must be connected to a good electrical ground. Grounding can be done by locating the workpiece or machine on a grounded metal floor or platen, or by connecting it to a properly grounded building frame or other satisfactory ground. Chains, wire ropes, cranes, hoists, and elevators must not be used as grounding connectors nor to carry welding current.

The work lead is not the grounding lead. The work lead connects the work terminal on the power source to the workpiece. A separate lead is required to ground the workpiece or power source work terminal.

Care should be taken when connecting the grounding circuit. Otherwise, the welding current may flow through a connection intended only for grounding and may be of higher magnitude than the grounding conductor can safely carry. Special radio-frequency grounding may be necessary for arc welding machines equipped with high-frequency arc initiating devices. (See EW-1, *Electric Arc Welding Power Sources,* Section 10.5.6, National Electrical Manufacturers Association.)

Connections for portable control devices, such as push buttons to be carried by the operator, must not be connected to circuits with operating voltages above about 120 V. Exposed metal parts of portable control devices operating on circuits above 50 V must be grounded by a grounding conductor in the control cable. Controls using intrinsically safe voltages below 30 V are recommended.

Cables and Connections

Electrical connections must be tight and checked periodically for tightness. Magnetic work clamps must be free of adherent metal particles and spatter on contact surfaces. Coiled welding leads should be spread out before use to avoid overheating and damage to the insulation. Jobs alternately requiring long and short leads should be equipped with insulated cable connectors so that idle lengths can be disconnected when not needed.

Equipment, cables, fuses, plugs, and receptacles must be used within their current carrying and duty cycle capacities. Operation of apparatus above the current rating or the duty cycle results in overheating and rapid deterioration of insulation and other parts. Actual welding current may be higher than that shown by indicators on the welding machine if welding is done with short leads or low voltage, or both. High currents are likely with general-purpose welding machines when they are used with processes that use low arc voltage, such as gas-tungsten arc welding.

Welding leads should be the flexible type of cable designed especially for the rigors of welding service. Insulation on cables used with high voltages or high-frequency oscillators must provide adequate protection. The recommendations and precautions of the cable manufacturer should always be followed. Cable insulation must be kept in good condition, and cables repaired or replaced promptly when necessary.

Operations

Welders should not allow the metal parts of electrodes, electrode holders, or torches to touch their bare skin or any wet covering of the body. Dry gloves in good condition must always be worn. The insulation on electrode holders must be kept in good repair. Electrode holders should not be cooled by immersion in water. If water-cooled welding guns or holders are used, they should be free of water leaks and condensation that would adversely affect the welder's safety. Welders should not drape nor coil the welding leads around their bodies.

A welding circuit must be de-energized to avoid electric shock while the electrode, torch, or gun is being changed or adjusted. One exception concerns covered electrodes with shielded metal arc welding. When the circuit is energized, covered electrodes must be changed with dry welding gloves, not with bare hands. In any case, de-energization of the circuit is desirable for optimum safety even with covered electrodes.

When a welder has completed the work or has occasion to leave the work station for an appreciable time, the welding machine should be turned off. Similarly, when the machine is to be moved, the input power supply should be electrically disconnected at the source. When equipment is not in use, exposed electrodes should be removed from the holder to eliminate the danger of accidental electrical contact with persons or conducting objects. Also, welding guns of semi-automatic welding equipment should be placed so that the gun switch cannot be operated accidently.

Multiple Arc Welding Operations

There can be increased danger of electrical shock when several welders are welding on a large metal structure, such as a building frame or ship, and the structure is part of the return welding circuits. Proper electrical contact must exist at all joints in the structure. Sparking or heating at any point in the structure makes it unsuitable as a return circuit.

Where two or more welders are working on the same structure and one is likely to touch simultaneously the exposed parts of more than one electrode holder, the welding machines must be connected to minimize shock hazard. It is preferable that all dc welding machines be connected with the same polarity. A test lamp or voltmeter can be used to determine whether the polarities are matched. It is preferable to connect all single-phase ac welding machines to the same phase of the supply circuit with the same instantaneous polarity. These precautions minimize the potential difference between electrode holders.

In some cases, the preferable connections may not be possible. Welding may require the use of both dc polarities, or supply circuit limitations may require distribution of ac welding machines among the phases of the supply circuit. In such cases, the no-load voltage between electrode holders or welding guns may be twice the normal voltage. Because of the increased voltage, the welders and other area personnel must be instructed to avoid simultaneous contact with more than one electrode holder, welding gun, or installed electrode.

Modification and Maintenance

Only qualified personnel should perform equipment modification and maintenance. Commutators on rotating welding machines should be kept clean to prevent excessive arcing. Rectifier-type welding machines should be inspected frequently for accumulations of dust or lint that interfere with ventilation. Louvers and internal electrical coil ventilating ducts should be similarly inspected. It is good practice to occasionally blow out the welding machine with clean, dry compressed air at low pressure. Adequate safety precautions such as proper eye protection should be taken. Air filters in the ventilating systems of electrical components are not recommended unless provided by the manufacturer of the welding machine. The filters should be inspected as recommended by the manufacturer. The reduction of air flow resulting from the accumulation of dust on the air filter can subject internal components to an overheating condition and subsequent failure. Machines that have become wet should be thoroughly dried and properly retested before being used.

Prevention of Fires

Fires resulting from electric welding equipment are generally caused by overheating of electrical components, flying sparks or spatter from the welding or cutting operation, or mishandling of fuel in engine-driven equipment. Most precautions against electrical shock are also applicable to the prevention of fires caused by overheating of the equipment. Avoidance of fire from sparks and spatter was covered previously in this article.

The fuel systems of engine-driven equipment must be in good condition. Leaks must be repaired promptly. Engine-driven machines must be turned off before refueling, and any fuel spills should be wiped up and fumes allowed to dissipate before the engine is restarted. Otherwise, the ignition system, electrical controls, spark producing components, or engine heat may start a fire.

Safe Practices*

American Welding Society

Processes

The broad areas of welding safety that are applicable to most welding, cutting, brazing, or soldering processes have been addressed previously in this article. The precautions and procedures that are unique to the particular processes are discussed here. All applicable information must be considered to provide complete safety precautions and procedures for each process.

Oxyfuel Gas Welding and Cutting

Torches. Only approved welding and cutting torches should be used. Oxyfuel gas torches should meet the requirements of E-5, *Torch Standard for Welding and Cutting,* Compressed Gas Association, and appropriate government regulations. They should be kept in good working order and should be serviced at regular intervals by the manufacturer or qualified technicians. A torch must be used only with the fuel gas for which it is designed. The fuel gas and oxygen pressures should be those recommended by the torch manufacturer.

The procedures recommended by the manufacturer should be followed when lighting and extinguishing the torch. The torch should be lighted only with a friction lighter, pilot light, or similar ignition source. Matches or cigarette lighters should not be used.

Hoses. Hoses used should be only those specified for oxyfuel gas welding and cutting systems. Generally, these hoses are manufactured in accordance with *Specification 1P-7 for Rubber Welding Hose,* published by the Compressed Gas Association and the Rubber Manufacturer's Association. Fuel gas hose is usually red with left-hand threaded fittings. Green hose with right-hand threaded fittings is generally used for oxygen. Hose connections must comply with E-l, *Standard Connections for Regulators, Torches and Fitted Hose for Welding and Cutting Equipment*, Compressed Gas Association. Hoses should be free of oil and grease, and in good condition. When parallel lengths are strapped together for convenience, no more than 100 mm (4 in.) of any 300 mm (12 in.) section of hose should be covered.

Only proper ferrules and clamps should be used to secure hose to fittings. Long runs of hose should be avoided. Excess hose should be coiled to prevent kinks and tangles, but it should not be wrapped around cylinders or cylinder carts while in use.

Backfire and Flashback. A backfire during welding and cutting is a momentary retrogression of the flame back into the tip. It usually results in a momentary flame-out followed by reignition of the normal tip flame and is accompanied by a pop or bang, depending upon the size of the tip. In severe cases, the hot combustion products within the tip may be forced back into the torch and even the hoses. Occasionally (but especially with oxygen), such backfires ignite the inner liner of the hose and result in burn-through of the hose wall. Such backfires can cause injury. Furthermore, when the hose ruptures, the flow of gases into the area is continuous until the valve at the tank is closed.

A flashback is an occurrence initiated by a backfire where the flame continues to burn inside the equipment instead of being re-established at the tip. Flashbacks result in very rapid internal heating of the equipment and can quickly destroy it. A flashback is usually recognized by a whistling or squealing sound. The equipment will heat up rapidly and sparks may issue from the tip. The flashback should be extinguished by turning off the torch valves as quickly as possible. Different manufacturers may recommend shutting off either the fuel or oxygen first, but the most important concern is to get both valves closed quickly.

Backfires and flashbacks are not ordinarily a concern if the apparatus is operated in accordance with the manufacturer's instructions. Generally, they occur from allowing a tip to become overheated by flame backwash, forcing the tip into the work, or providing insufficient gas flow for the size of the tip. If frequent backfiring or flashbacks are experienced, the cause should be investigated. There is probably something wrong with the equipment or operation.

To prevent backfires and flashbacks, hose lines should be purged before lighting oxyfuel gas equipment. Purging flushes out any combustible oxygen-fuel or air-fuel gas mixtures in the hoses. It is done by first opening either the fuel or oxygen valve on the torch and allowing that gas to flow for several seconds to clear that hose of any possible gas mixtures. That valve is then closed, and the other valve is opened to allow the other gas to flow for a similar period of time. Purging should always be done before any welding or cutting tip is lighted. The purge stream must not be directed toward any flame or source of ignition. Torches should not be purged in confined spaces because of possible explosion of accumulated gases.

Hose Line Safety Devices. Reverse-flow check valves and flashback arresters for hose line service are available. These devices can prevent backflow of gases and flashbacks into hoses provided they are operating properly. They must be used strictly in accordance with the manufacturer's instructions and maintained regularly in accordance with the manufacturer's recommendations.

Shutdown Procedures. When oxyfuel gas operations are completed, the equipment should always be completely shut down and the gas pressures drained from the system. Cylinder supply valves must be closed. The equipment should not be left unattended until the shutdown has been completed.

Ventilated Storage. Oxyfuel gas cylinders or equipment connected to cylinders must always be stored in well-ventilated spaces and should not be stored in confined areas or unventilated cabinets. Even small gas leaks in confined spaces can result in explosive mixtures that might be ignited with disastrous results. For the same reason, oxygen gas cylinders should never be transported in enclosed vehicles, particularly not in closed vans or the trunks of automobiles.

Arc Welding and Cutting

The potential hazards of arc welding are fumes and gases, electric shock, infrared and ultraviolet radiation, burns, fire, explosion, and sometimes noise. These hazards have been described previously. Precautions to avoid injury or death from these hazards must be followed. The safety precautions for arc welding also apply to arc cutting.

Noise during arc cutting operations can be high. Prolonged exposure to high noise levels can lead to hearing damage. Where necessary, ear protection must be provided for the operator and others in the area.

Plasma arc cutting is a particularly noisy and a high fume generating process. Two common accessories are available for mechanized plasma arc cutting of plate to aid in fume and noise control. One accessory is a water table, which is simply a cutting table filled with water to the bottom surface of the plate or above the plate. In the latter case, cutting is done under water using a special torch to minimize noise and reduce radiation. The high-speed gases emerging from the plasma jet produce turbulence in the water. This action traps almost all of the fume particles in the water.

Another accessory is a water muffler to reduce noise. The muffler is a nozzle attached to a special torch body that produces a curtain of water around the front of the torch. It is always used in conjunction with a water table. The combination of a water curtain at the top of the plate and a water table contacting the bottom of the plate encloses the arc in a noise-reducing shield. The noise output is reduced by roughly 20 dB. This equipment should not be confused with cutting variations using water injection or water shielding.

Resistance Welding

The main hazards of resistance welding processes and equipment are:

- ELECTRIC SHOCK FROM CONTACT WITH HIGH-VOLTAGE TERMINALS OR COMPONENTS
- EJECTION OF SMALL PARTICLES OF MOLTEN METAL FROM THE WELD
- CRUSHING OF SOME PART OF THE BODY BETWEEN THE ELECTRODES OR OTHER MOVING COMPONENTS OF THE MACHINE

Guarding. Initiating devices on resistance welding equipment, such as push buttons and switches, must be positioned or guarded to prevent the operator from inadvertently activating them.

With some machines, the operator's hands can be expected to pass under the point of operation during loading and unloading. These machines must be effectively guarded by proximity-sensing devices, latches, blocks, barriers, dual hand controls, or similar accessories that prevent (1) the hands from passing under the point of operations or (2) the ram from moving while the hands are under the point of operation.

Static Safety Devices. Press, flash, and upset welding machines should have static safety devices to prevent movement of the platen or head during maintenance or setup for welding. Pins, blocks, and latches are examples of such devices.

Portable Welding Machines. The support system of suspended portable welding gun equipment, with the exception of the gun assembly, must be capable of withstanding the total mechanical shock load in the event of failure of any component of the system. Devices such as cables, chains, or clamps are considered satisfactory.

Guarding should be provided around the mounting and actuating mechanism of the movable arm of a portable welding gun if it can cause injury to the operator's hands. If suitable guarding cannot be achieved, the gun should have two handles and two operating switches that must be actuated to energize the machine.

Stop Buttons. One or more emergency stop buttons should be provided on all welding machines, with a minimum of one at each operator position.

Guards. Eye protection against expelled metal particles must be provided by a guard of suitable fire-resistant material or by the use of approved personal protective eye wear. For flash welding equipment, flash guards of suitable fire-resistant material must be provided to control flying sparks and molten metal.

Electrical Considerations. All external welds initiating control circuits should operate at a maximum of about 120 V for stationary equipment and about 36 V for portable equipment.

Resistance welding equipment containing high-voltage capacitors must have adequate electrical insulation and must be completely enclosed. All enclosure doors must be provided with suitable interlocks that are wired into the control circuit. The interlocks must effectively interrupt power and discharge all high-voltage capacitors when the door or panel is open. In addition, a manually operated switch or suitable positive device should be provided to ensure complete discharge of all high-voltage capacitors. The doors or panels must be kept locked except during maintenance.

The welding transformer secondary should be grounded by one of the following methods:

- PERMANENT GROUNDING OF THE WELDING SECONDARY CIRCUIT
- CONNECTION OF A GROUNDING REACTOR ACROSS THE SECONDARY WINDING WITH A REACTOR TAP TO GROUND

As an alternative on stationary machines, an isolation contactor may be used to open all of the primary lines.

The grounding of one side of the secondary windings on multiple spot welding machines can cause undesirable transient currents to flow between the transformers when they are connected to different primary phases or have different secondary voltages, or both. A similar condition can also exist with portable spot welding guns when several units are used to weld the same assembly or another one that is nearby. Such situations require use of a grounding reactor or isolation contactor.

Installation. All equipment should be installed in conformance with the ANSI/NFPA 70, *National Electric Code* (latest edition). The equipment should be installed by qualified personnel under the direction of a competent technical supervisor. Prior to production use, the equipment should be inspected by competent safety personnel to ensure that it is safe to operate.

Brazing and Soldering

Hazards encountered with brazing and soldering operations are similar to those associated with welding and cutting processes. Brazing and soldering operations may be done at temperatures where some elements in the filler metal will vaporize. Personnel and property must be protected against hot materials, gases, fumes, electrical shock, radiation, and chemicals.

It is essential that adequate ventilation be provided so that personnel do not inhale gases and fumes generated during brazing or soldering. Some filler metals and base metals contain toxic materials such as cadmium, beryllium, zinc, mercury, or lead that vaporize during brazing. Fluxes contain chemical compounds of fluorine, chlorine, and boron that are harmful if they are inhaled or contact the eyes or skin. Suitable ventilation to avoid these hazards was described previously.

Brazing Atmospheres. Flammable gases are sometimes used as atmospheres for furnace brazing operations. These include combusted fuel gas, hydrogen, and dissociated ammonia. Prior to introducing such atmospheres, the furnace or retort must be purged of air by safe procedures recommended by the furnace manufacturer.

Adequate area ventilation must be provided to exhaust and discharge to a safe place explosive or toxic gases that may emanate from furnace purging and brazing operations. Local environmental regulations should be consulted when designing the exhaust system.

Dip Brazing and Soldering. In dip brazing and soldering, the parts to be immersed in the bath must be completely dry. The presence of moisture on the parts will cause an instantaneous generation of steam that may expel the contents of the dip pot with explosive force and create a serious burn hazard. Predrying of the parts will prevent this problem. If supplementary flux is necessary, it must be adequately dried to remove not only moisture but also water of hydration to avoid explosion hazards.

Solder Flux. Some fluxes, such as the rosin, petrolatum, and reaction types, give off considerable smoke, the amount depending on the soldering temperature and the duration of heating. The American Conference of Governmental Industrial Hygienists has established a safe threshold limit value for decomposition products of rosin core solder of 0.1

mg/m^3 (4×10^{-5} gr/ft^3) aliphatic aldehydes, measured as formaldehyde. Suitable ventilation must be provided for soldering operations to meet this requirement.

Other fluxes give off fumes that are harmful if breathed in any but small quantities. Prolonged inhalation of halides and some of the newer organic fluxes should be avoided. The aniline type fluxes and some of the amines also evolve fumes that are harmful and can cause dermatitis. Fluorine in flux can be dangerous to health, cause burns, and be fatal if ingested. Thus, proper ventilation must be provided in the work area to remove fume from soldering operations.

High-Frequency Welding

High-frequency generators are electrical devices and require all usual safety precautions in handling and repairing such equipment. Voltages are in the range from 400 to 20,000 V and are lethal. These voltages may be either low or high frequency. Proper care and safety precautions should be taken while working on high-frequency generators and their control systems. Units must be equipped with safety interlocks on access doors and with automatic safety grounding devices to prevent operation of the equipment when access doors are open. The equipment should not be operated with panels or high-voltage covers removed nor with interlocks and grounding devices blocked. This equipment should not be confused with high-frequency arc stabilization equipment used in GTAW.

The output high-frequency primary leads should be encased in metal ducting and should not be operated in the open. Induction coils and contact systems should always be properly grounded for operator protection. High-frequency currents are more difficult to ground than low-frequency currents, and grounding lines must be kept short and direct to minimize inductive impedance. The magnetic field from the output system must not induce heat in adjacent metallic sections and cause fires or burns.

The injuries from high-frequency power, especially at the upper range of welding frequencies, tend to produce severe local surface tissue damage. However, they are not likely to be fatal because current flow is shallow.

High-frequency welding stations often emit a loud steady whine that can cause permanent hearing loss. Ear protection is essential under these circumstances.

Electron-Beam Welding

The primary hazards associated with electron-beam welding equipment are electric shock, x-radiation, fumes and gases, and damaging visible radiation. Precautionary measures must be taken at all times to ensure that proper protective procedures are always observed. AWS F2.1, *Recommended Safe Practices for Electron Beam Welding and Cutting* and ANSI/ASC Z49.1, *Safety in Welding and Cutting* (latest edition) give the general safety requirements that should be strictly adhered to at all times.

Electric Shock. Every electron-beam welding machine operates at voltages above 20 kV. These voltages can cause fatal injury, regardless of whether the machine is referred to as a low-voltage or a high-voltage machine. The manufacturers of electron-beam welding equipment, in meeting various regulatory requirements, produce machines that are well-insulated against high voltage. However, precautions should be exercised with all systems when high voltage is present. The manufacturer's instructions should be followed for operation and maintenance of the equipment.

X-rays. The x-rays generated by an electron-beam welding machine are produced when electrons, traveling at high velocity, collide with matter. The majority of x-rays are produced when the electron beam impinges upon the workpiece. Substantial amounts are also produced when the beam strikes gas molecules or metal vapor in the gun column and work chamber. Underwriters Laboratories and OSHA regulations have established firm rules for permissible x-ray exposure levels, and producers and users of equipment must observe these rules.

Generally, the steel walls of the chamber are adequate protection in systems up to 60 kV, assuming proper design. High-voltage machines utilize lead lining to block x-ray emission beyond the chamber walls. Leaded glass windows are employed in both high- and low-voltage electron-beam systems. Generally, the shielded vacuum chamber walls provide adequate protection for the operator.

In the case of nonvacuum systems, a radiation enclosure must be provided to ensure the safety of the operator and other persons in the area. Thick walls of high-density concrete or other similar material may be employed in place of lead, especially for large radiation enclosures on nonvacuum installations. In addition, special safety precautions should be

imposed to prevent personnel from accidently entering or being trapped inside the enclosure when equipment is in operation.

A complete x-ray radiation survey of the electron-beam equipment should always be made at the time of installation and at regular intervals thereafter. This should be done by personnel trained to make a proper radiation survey to ensure initial and continued compliance with all radiation regulations and standards applicable to the site where the equipment is installed.

Fumes and Gases. It is unlikely that the very small amount of air in a high-vacuum electron-beam chamber would be sufficient to produce ozone and oxides of nitrogen in harmful concentrations. However, nonvacuum and medium-vacuum electron-beam systems are capable of producing these by-products, as well as other types of airborne contaminants in concentrations above acceptable levels.

Adequate area ventilation must be employed to reduce concentrations of airborne contaminants around the equipment within permissible exposure limits. Proper exhausting techniques should be employed to maintain residual concentrations in the enclosure within those limits.

Visible Radiation. Direct viewing of intense radiation emitted by molten weld metal can be harmful to eyesight. Viewing of the welding operation should be done through a filter lens commonly used for arc welding.

Laser-Beam Welding and Cutting

The basic hazards associated with laser operation are:

- EYE DAMAGE FROM THE BEAM INCLUDING BURNS OF THE CORNEA OR RETINA, OR BOTH
- SKIN BURNS FROM THE BEAM
- RESPIRATORY SYSTEM DAMAGE FROM HAZARDOUS MATERIALS EVOLVED DURING OPERATION
- ELECTRICAL SHOCK
- CHEMICAL HAZARDS
- CONTACT WITH CRYOGENIC COOLANTS

Laser manufacturers are required to qualify their equipment with the U.S. Bureau of Radiological Health (BRH). Electrical components should be in compliance with NEMA standards. User action is governed by OSHA requirements. In all cases, American National Standard Z136.1, *Safe Use of Lasers* (latest edition), should be followed.

Eye Protection. Eye injury is readily caused by laser beams. With laser beams operating at visible or near infrared wavelengths, even a 5 mW beam can inflict retinal damage. Safety glasses are available that are substantially transparent to visible light but are opaque to specific laser beam outputs. Selective filters for ruby, Nd:YAG, and other laser systems are available. Glasses appropriate to the specific laser system must be used. At longer infrared wavelengths (such as that of a CO_2 laser), ordinarily transparent materials such as glass are opaque. Clear safety glasses with side shields may be used with these systems, and the only light reaching the eye will be from incandescence of the workpiece. Nevertheless, extreme brilliance can result if a plasma is generated at high power and, filter lenses should then be used for viewing the operation.

Burns. Laser burns can be deep and very slow to heal. Exposure must be avoided by appropriate enclosure of the beam or by methods that prevent beam operation unless the beam path is unobstructed. This is particularly important for nonvisible beams that provide no external evidence of their existence unless intercepted by a solid.

Electric Shock. High voltages as well as large capacitor storage devices are associated with lasers. Therefore, the possibility for lethal electrical shock is always present. Electrical system enclosures should have appropriate interlocks on all access doors and provisions for discharging capacitor banks before entry. The equipment should be appropriately grounded.

Fumes and Gases. Hazardous products may be generated from interaction of the beam and the workpiece. For example, plastic materials used for "burn patterns" to identify beam shape and distribution in high-power CO_2 laser systems can generate highly toxic vapors if irradiated in an oxygen-lean atmosphere.

In deep-penetration welding, fine metal fume can arise from the joint. Also, intense plasma generation can produce ozone. Consequently, adequate ventilation and exhaust provisions for laser work areas are necessary.

Friction Welding

Friction welding machines are similar to machine tool lathes in that one workpiece is rotated by a drive system. They are also similar to hydraulic presses in that one workpiece is forced against the other. Therefore, safe practices for lathes and power presses should be used as guides for the design and operation of friction welding machines.

Machines should be equipped with appropriate mechanical guards and shields as well as two-hand operating switches and electrical interlocks. These devices should be designed to prevent operation of the machine when the work area, rotating drive, and force system are accessible to the operator or others.

Operating personnel should wear appropriate eye protection and safety apparel commonly used with machine tool operations. In any case, applicable Occupational Safety and Health Administration (OSHA) standards should be strictly observed.

Explosion Welding

Explosives and explosive devices are a part of explosion welding. Such materials and devices are inherently dangerous, but there are safe methods for handling them. However, if the materials are misused, they can kill or injure, and destroy or damage property.

Explosive materials should be handled and used only by trained personnel who are experienced in that field. Handling and safety procedures must comply with all applicable federal, state, and local regulations. Federal jurisdiction on the sale, transport, storage, and use of explosives is through the U.S. Bureau of Alcohol, Tobacco, and Firearms; the Hazardous Materials Regulation Board of the U.S. Department of Transportation; the Occupational Safety and Health Administration; and the Environmental Protection Agency. Many states and local governments require a blasting license or permit, and some cities have special explosive requirements.

The Institute of Makers of Explosives provides educational publications to promote the safe handling, storage, and use of explosives. The National Fire Protection Association provides recommendations for safe manufacture, storage, handling, and use of explosives. (See ANSI/NFPA 495, *Manufacture, Transportation, Storage, and Use of Explosive Materials,* American National Standards Institute, latest edition.)

Ultrasonic Welding

With high-power ultrasonic equipment, high voltages are present in the frequency converter, the welding head, and the coaxial cable connecting these components. Consequently, the equipment should not be operated with the panel doors open or housing covers removed. Door interlocks are usually installed to prevent introduction of power to the equipment when the high-voltage circuitry is exposed. The cables are shielded fully and present no hazard when properly connected and maintained.

Because of hazards associated with application of clamping force, the operator should not place hands or arms in the vicinity of the welding tip when the equipment is energized. For manual operation, the equipment should be activated by dual palm buttons that meet the requirements of OSHA. Both buttons must be pressed simultaneously to actuate a weld cycle, and both must be released before the next cycle is initiated. For automated systems in which the weld cycle is sequenced with other operations, guards should be installed for operator protection. Such hazards can be further minimized by setting the welding stroke to the minimum that is compatible with workpiece clearance.

Thermite Welding

Thermite mix, in the crucible or on the workpieces, can lead to rapid formation of steam when the chemical reaction for thermite welding takes place. This may cause ejection of molten metal from the crucible. Therefore, the thermite mix

should be stored in a dry place, the crucible should be dry, and moisture should not be allowed to enter the system before or during welding.

The work area should be free of combustible materials that may be ignited by sparks or small particles of molten metal. The area should be well ventilated to avoid the buildup of fumes and gases from the reaction. Starting powders and rods should be protected against accidental ignition.

Personnel should wear appropriate protection against hot particles or sparks. This includes full face shields with filter lenses for eye protection and headgear. Safety boots are recommended to protect the feet from hot sparks. Clothing should not have pockets or cuffs that might catch hot particles.

Preheating should be done using the safety precautions applicable to oxyfuel gas equipment and operations.

Thermal Spraying

The potential hazards to the health and safety of personnel involved in thermal spraying operations and to persons in the immediate vicinity are:

- ELECTRICAL SHOCK
- FIRE
- FUMES AND GASES
- DUST
- ARC RADIATION
- NOISE

These hazards are not unique to thermal spraying methods. For example, flame spraying has hazards similar to those associated with the oxyfuel gas welding and cutting processes. Likewise, arc spraying and plasma spraying are similar in many respects to gas metal arc and plasma arc welding, respectively. Safe practices for these processes should be followed when thermal spraying with similar equipment. However, thermal spraying does generate dust and fumes to a greater degree. Additional information may be found in *Thermal Spraying: Practice, Theory, and Application,* American Welding Society, 1985.

Fire Prevention. Airborne finely divided solids, especially metal dusts, must be treated as explosives. To minimize danger from dust explosions, spray booths must have adequate ventilation.

A wet collector of the water-wash type is recommended to collect the spray dust. Bag or filter-type collectors are not recommended. Good housekeeping in the work area should be maintained to avoid accumulation of metal dusts, particularly on rafters, tops of booths, and in floor cracks.

Paper, wood, oily rags, and other combustibles in the spraying area can cause a fire and should be removed before the equipment is operated.

Protection of Personnel. The general requirements for the protection of thermal spray operators are the same as for welders.

Eye Protection. Helmets, hand shields, face shields, or goggles should be used to protect the eyes, face, and neck during all thermal spraying operations. Safety goggles should be worn at all times. Table 4 is a guide for the selection of the proper filter shade number for viewing a specific spraying operation.

TABLE 4 RECOMMENDED EYE FILTER PLATES FOR THERMAL SPRAYING OPERATIONS

OPERATION	FILTER SHADE NUMBERS
WIRE FLAME SPRAYING (EXCEPT MOLYBDENUM)	2 TO 4

WIRE FLAME SPRAYING OF MOLYBDENUM	3 TO 6
FLAME SPRAYING OF METAL POWDER	3 TO 6
FLAME SPRAYING OF EXOTHERMICS OR CERAMICS	4 TO 8
PLASMA AND ARC SPRAYING	9 TO 12
FUSING OPERATIONS	4 TO 6

Respiratory Protection. Most thermal spraying operations require that respiratory protective devices be used by the operator. The nature, type, and magnitude of the fume and gas exposure determine which respiratory protective device should be used. All devices selected for use should be of a type approved by the U.S. Bureau of Mines, National Institute for Occupational Safety and Health, or other approving authority for the purpose intended.

Ear Protection. Ear protectors or properly fitted soft rubber ear plugs should be worn to protect the operator from the high-intensity noise from the process. Federal, state, and local codes should be checked for noise protection requirements.

Protective Clothing. Appropriate protective clothing required for a thermal spraying operation will vary with the size, nature, and location of the work to be performed. When working in confined spaces, flame-resistant clothing and gauntlets should be worn. Clothing should be fastened tightly around the wrists and ankles to keep dusts from contacting the skin.

The intense ultraviolet radiation of plasma and electric arc spraying can cause skin burns through normal clothing. Protection against radiation during arc spraying is practically the same as that for normal arc welding at equivalent current levels.

Adhesive Bonding

Adequate safety precautions must be observed with adhesives. Corrosive materials, flammable liquids, and toxic substances are commonly used in adhesive bonding. Therefore, manufacturing operations should be carefully supervised to ensure that proper safety procedures, protective devices, and protective clothing are being used. All federal, state, and local regulations should be complied with, including OSHA Regulation 29CRF 1900.1000, *Air Contaminants.*

Flammable Materials. All flammable materials, such as solvents, should be stored in tightly sealed drums and issued in suitably labeled safety cans to prevent fires during storage and use. Solvents and flammable liquids should not be used in poorly ventilated, confined areas. When solvents are used in trays, safety lids should be provided. Flames, sparks, or spark-producing equipment must not be permitted in the area where flammable materials are being handled. Fire extinguishers should be readily available.

Toxic Materials. Severe allergic reactions can result from direct contact, inhalation, or ingestion of phenolics and epoxies as well as most catalysts and accelerators. The eyes or skin may become sensitized over a long period of time even though no signs of irritation are visible. Once workers are sensitized to a particular type of adhesive, they may no longer be able to work near it because of allergic reactions. Careless handling of adhesives by production workers may expose others to toxic materials if proper safety rules are not observed. For example, co-workers may touch tools, door knobs, light switches, or other objects contaminated by careless workers.

For the normal individual, proper handling methods that eliminate skin contact with an adhesive should be sufficient. It is mandatory that protective equipment, barrier creams, or both be used to avoid skin contact with certain types of formulations.

Factors to be considered in determining the extent of precautionary measures to be taken include:

- THE FREQUENCY AND DURATION OF EXPOSURE
- THE DEGREE OF HAZARD ASSOCIATED WITH A SPECIFIC ADHESIVE
- THE SOLVENT OR CURING AGENT USED
- THE TEMPERATURE AT WHICH THE OPERATIONS ARE PERFORMED
- THE POTENTIAL EVAPORATION SURFACE AREA EXPOSED AT THE WORK STATION

All these elements should be evaluated in terms of the individual operation.

Precautionary Procedures. A number of measures are recommended in the handling and use of adhesives and auxiliary materials.

Personal Hygiene. Personnel should be instructed in proper procedures to prevent skin contact with solvents, curing agents, and uncured base adhesives. Showers, wash bowls, mild soaps, clean towels, refatting creams, and protective equipment should be provided.

Curing agents should be removed from the hands with soap and water. Resins should be removed with soap and water, alcohol, or a suitable solvent. Any solvent should be used sparingly and be followed by washing with soap and water. In case of allergic reaction or burning, prompt medical aid should be obtained.

Work Area. Areas in which adhesives are handled should be separated from other operations. These areas should contain the following facilities in addition to the proper fire equipment:

- SINK WITH RUNNING WATER
- EYE SHOWER OR RINSE FOUNTAIN
- FIRST AID KIT
- VENTILATING FACILITIES

Ovens, presses, and other curing equipment should be individually vented to remove fume. Vent hoods should be provided at mixing and application stations.

Protective Devices. Plastic or rubber gloves should be worn at all times when working with potentially toxic adhesives. Contaminated gloves must not contact objects that others may touch with their bare hands. Those gloves should be discarded or cleaned using procedures that remove the particular adhesive. Cleaning may require solvents, soap and water, or both. Hands, arms, face, and neck should be coated with a commercial barrier ointment or cream. This type of material may provide short-term protection and facilitate removal of adhesive components by washing.

Full face shields should be worn for eye protection whenever the possibility of splashing exists, otherwise glasses or goggles should be worn. In case of irritation, the eyes should be immediately flushed with water and then promptly treated by a physician.

Protective clothing should be worn at all times by those who work with the adhesives. Shop coats, aprons, or coveralls may be suitable, and they should be cleaned before reuse.

Safe Practices*

American Welding Society

Selected References

- *ARC WELDING AND CUTTING NOISE,* AWS, 1979
- *ARC WELDING SAFELY,* AWS, 1988
- *ASM HANDBOOK,* VOL 4, *HEAT TREATING,* ASM INTERNATIONAL, 1991
- N.C. BALCHIN, *HEALTH AND SAFETY IN WELDING AND ALLIED PROCESSES,* 3RD ED., THE WELDING INSTITUTE, 1983
- L.O. BARTHOLD *ET AL.,* ELECTROSTATIC EFFECTS OF OVERHEAD TRANSMISSION LINES, PART I: HAZARDS AND EFFECTS, *IEEE TRANS. POWER APP. SYST.,* VOL PAS-91, 1972, P 422-444
- *CHARACTERIZATION OF ARC WELDING FUMES,* AWS, 1983

- *CUTTING AND WELDING PROCESSES,* ANSI/NFPA SIB-1977, AMERICAN NATIONAL STANDARDS INSTITUTE/NATIONAL FIRE PROTECTION ASSOCIATION, 1977
- C.F. DALZIEL, EFFECTS OF ELECTRIC CURRENT ON MAN, *ASEE J.,* JUNE 1973, P 18-23
- *EFFECTS OF WELDING ON HEALTH, I, II, III, AND IV,* AWS, 1979, 1981, 1983
- *THE FACTS ABOUT FUME,* THE WELDING INSTITUTE, 1976
- *FUMES AND GASES IN THE WELDING ENVIRONMENT,* AWS, 1979
- *HANDBOOK OF COMPRESSED GASES,* 2ND ED., COMPRESSED GAS ASSOCIATION, INC./VAN NOSTRAND REINHOLD, 1981
- *HANDLING ACETYLENE CYLINDERS IN FIRE SITUATIONS,* SB-4, COMPRESSED GAS ASSOCIATION, 1974
- *OXYFUEL GAS WELDING, CUTTING, AND HEATING SAFELY,* AWS
- *OXYGEN-FUEL GAS SYSTEMS FOR WELDING, CUTTING, AND APPLIED PROCESSES,* ANSI/NFPA S1-1983, AMERICAN NATIONAL STANDARDS INSTITUTE/NATIONAL FIRE PROTECTION ASSOCIATION, 1983
- *RECOMMENDED SAFE PRACTICES FOR ELECTRON BEAM WELDING AND CUTTING,* AWS F2.1-78, AWS, 1978
- *RECOMMENDED SAFE PRACTICES FOR THE PREPARATION FOR WELDING AND CUTTING OF CONTAINERS THAT HAVE HELD HAZARDOUS SUBSTANCES,* AWS F4.1-80, AWS, 1980
- *RECOMMENDED SAFE PRACTICES FOR THERMAL SPRAYING,* AWS C2.1-73, AWS, 1973
- *SAFE HANDLING OF COMPRESSED GASES IN CONTAINERS,* P-1, COMPRESSED GAS ASSOCIATION, 1974
- *SAFETY IN WELDING AND CUTTING,* ANSI/ASC Z49.1, AWS
- *ULTRAVIOLET REFLECTANCE OF PAINT,* AWS, 1976
- *THE WELDING ENVIRONMENT,* AWS, 1973
- *WELDING FUME CONTROL: A DEMONSTRATION PROJECT,* AWS, 1982
- *WELDING FUME CONTROL WITH MECHANICAL VENTILATION,* 2ND ED., FIREMAN'S FUND INSURANCE COMPANIES, 1981

Glossary of Terms*

American Welding Society Committee on Definitions and Symbols

THE COMMITTEE on Definitions and Symbols was formed by the American Welding Society to establish standard terms and symbols to aid in the communication of welding information. *Standard Welding Terms and Definitions,* ANSI/AWS A3.0, is the major product of work done by the Subcommittee on Definitions in support of this purpose. This glossary is a selection of terms and definitions from ANSI/AWS A3.0; the reader is referred to the latest edition of ANSI/AWS A3.0 for the most current and complete welding vocabulary, including illustrations and commentary.

The standard terms and definitions published here are those that should be used in both the oral and the written language of welding; however, their use is particularly important in the writing of standards (codes, specifications, recommended practices, methods, classifications, and guides) and all other documents concerning welding. Because ANSI/AWS A3.0, from which this glossary is extracted, is intended to be a comprehensive compilation of welding terminology, nonstandard terms used in the welding industry are also included. All terms are either standard or nonstandard, and nonstandard terms are labeled as such.

To make this glossary most useful, the terms are arranged in the conventional dictionary letter-by-letter alphabetical sequence. It is the policy of the American Welding Society to use only generic terms and definitions in this glossary. The numerous proprietary brand and trademark names commonly used to describe welding processes, equipment, and filler metals are not included.

It should be noted that the *ASM Handbook* editorial style for the hyphenation of certain terms deviates from that dictated by ANSI/AWS A3.0. The style shown in this glossary is the standard AWS usage.

- A
- ACTIVATED ROSIN FLUX
- A rosin-base flux containing an additive that increases wetting by the solder.
- ACTUAL THROAT
- The shortest distance between the weld root and the face of a fillet weld.
- ADHESIVE BONDING
- A materials joining process in which an adhesive is placed between the faying surfaces. The adhesive solidifies to produce an adhesive bond.
- AIR CARBON ARC CUTTING (AC-A)
- An arc cutting process that melts base metals by the heat of a carbon arc and removes the molten metal by a blast of air.
- ARC BLOW
- The deflection of an electric arc from its normal path because of magnetic forces.
- ARC BRAZING (AB)
- A brazing process that uses an arc to provide the heat. See carbon arc brazing .
- ARC CUTTING (AC)
- A group of cutting processes that melt the base metal with the heat of an arc between an electrode and the base metal.
- AIR CUTTING GUN (GAS METAL ARC CUTTING)
- A device used in semiautomatic, machine, and automatic arc cutting to transfer current, guide the consumable electrode, and direct the shielding gas.
- ARC FORCE
- The axial force developed by an arc plasma.
- ARC GOUGING
- An arc cutting process variation used to form a bevel or groove.
- ARC OXYGEN CUTTING
- A nonstandard term for oxygen arc cutting .
- ARC SEAM WELD
- A seam weld made by an arc welding process.
- ARC SPOT WELD
- A spot weld made by an arc welding process.
- ARC SPRAYING (ASP)
- A thermal spraying process using an arc between two consumable electrodes of surfacing materials as a heat source and a compressed gas to atomize and propel the surfacing material to the substrate.
- ARC STRIKE
- A discontinuity consisting of any localized remelted metal, heat-affected metal, or change in the surface profile of any part of a weld or base metal resulting from an arc.
- ARC WELDING (AW)
- A group of welding processes that produces coalescence of metals by heating them with an arc, with or without the application of pressure, and with or without the use of filler metal.
- ARC WELDING ELECTRODE
- A component of the welding circuit through which current is conducted and which terminates at the arc.
- ARC WELDING GUN
- A device used in semiautomatic, machine, and automatic arc welding to transfer current, guide the consumable electrode, and direct the shielding gas.
- AS-WELDED
- The condition of weld metal, welded joints, and weldments after welding, but prior to any subsequent thermal, mechanical, or chemical treatments.
- AUTOGENOUS WELD
- A fusion weld made without the addition of filler metal.
- AUTOMATIC WELDING
- Welding with equipment that performs the welding operation without adjustment of the controls by a welding operator. The equipment may or may not load and unload the workpieces. See also machine welding .

- B
- BACK BEAD
- A weld bead resulting from a back weld pass.
- BACKFIRE
- The momentary recession of the flame into the welding tip or cutting tip followed by immediate reappearance or complete extinction of the flame.
- BACK GOUGING
- The removal of weld metal and base metal from the other side of a partially welded joint to facilitate complete fusion and complete joint penetration upon subsequent welding from that side.
- BACKHAND WELDING
- A welding technique in which the welding torch or gun is directed opposite to the progress of welding.
- BACKING
- A material or device placed against the back side of the joint, or at both sides of a weld in electroslag and electrogas welding, to support and retain molten weld metal. The material may be partially fused or remain unfused during welding and may be either metal or nonmetal.
- BACKING BEAD
- A weld bead resulting from a backing pass.
- BACKING FILLER METAL
- A nonstandard term for consumable insert .
- BACKING PASS
- A weld pass made for a backing weld.
- BACKING RING
- Backing in the form of a ring, generally used in the welding of pipe.
- BACKING SHOE
- A nonconsumable backing device used in electroslag and electrogas welding.
- BACKING WELD
- Backing in the form of a weld.
- BACKSTEP SEQUENCE
- A longitudinal sequence in which weld passes are made in the direction opposite to the progress of welding.
- BACK WELD
- A weld made at the back of a single-groove weld.
- BALLING UP
- The formation of globules of molten brazing filler metal or flux due to lack of wetting of the base metal.
- BASE MATERIAL
- The material to be welded, brazed, soldered, or cut. See also base metal and substrate .
- BASE METAL
- The metal to be welded, brazed, soldered, or cut. See also base material and substrate .
- BEAD WELD
- A nonstandard term for surfacing weld .
- BEVEL
- An angular edge preparation.
- BEVEL ANGLE
- The angle formed between the prepared edge of a member and a plane perpendicular to the surface of the member.
- BEVEL GROOVE WELD
- A type of groove weld.
- BIT
- That part of the soldering iron, usually made of copper, that actually transfers heat (and sometimes solder) to the joint.
- BLACKSMITH WELDING
- A nonstandard term for forge welding .
- BLOCK SEQUENCE
- A combined longitudinal and cross-sectional sequence for a continuous multiple-pass weld in which separated increments are completely or partially welded before intervening increments are welded.
- BLOWHOLE
- A nonstandard term for porosity .

- BOND
- See bonding force , covalent bond , mechanical bond , and metallic bond .
- BOND COAT (THERMAL SPRAYING)
- A preliminary (or prime) coat of material that improves adherence of the subsequent spray deposit.
- BONDING FORCE
- The force that holds two atoms together. It results from a decrease in energy as two atoms are brought closer to one another.
- BOND LINE
- The cross section of the interface between thermal spray deposits and substrate, or between adhesive and adherend in an adhesive bonded joint.
- BOTTLE
- A nonstandard term for gas cylinder .
- BOXING
- The continuation of a fillet weld around a corner of a member as an extension of the principal weld.
- BRAZE
- A weld produced by heating an assembly to the brazing temperature using a filler metal having a liquidus above 450 °C (840 °F) and below the solidus of the base metal. The filler metal is distributed between the closely fitted faying surfaces of the joint by capillary action.
- BRAZE INTERFACE
- The interface between filler metal and base metal in a brazed joint.
- BRAZEMENT
- An assembly whose component parts are joined by brazing.
- BRAZER
- One who performs a manual or semiautomatic brazing operation.
- BRAZE WELDING
- A welding process variation in which a filler metal, having a liquidus above 450 °C (840 °F) and below the solidus of the base metal, is used. Unlike brazing, in braze welding the filler metal is not distributed in the joint by capillary action.
- BRAZING (B)
- A group of welding processes that produce coalescence of materials by heating them to the brazing temperature in the presence of a filler metal having a liquidus above 450 °C (840 °F) and below the solidus of the base metal. The filler metal is distributed between the closely fitted faying surfaces of the joint by capillary action.
- BRAZING ALLOY
- A nonstandard term for brazing filler metal .
- BRAZING FILLER METAL
- The metal that fills the capillary joint clearance and has a liquidus above 450 °C (840 °F) but below the solidus of the base metals.
- BRAZING OPERATOR
- One who operates machine or automatic brazing equipment.
- BRITTLE NUGGET
- A nonstandard term used to describe a faying plane failure in a resistance weld peel test.
- BRONZE WELDING
- A nonstandard term for braze welding .
- BUILDUP
- A surfacing variation in which surfacing metal is deposited to achieve the required dimensions. See also buttering .
- BURNER
- A nonstandard term for oxygen cutter .
- BURNING
- A nonstandard term for oxygen cutting .
- BURN THROUGH
- A nonstandard term for excessive melt through or a hole.
- BURN THROUGH WELD
- A nonstandard term for a seam weld or spot weld .
- BUTTERING

- A surfacing variation that deposits surfacing metal on one or more surfaces to provide metallurgically compatible weld metal for the subsequent completion of the weld. See also buildup .
- BUTT JOINT
- A joint between two members aligned approximately in the same plane.
- BUTTON
- That part of a weld, including all or part of the nugget, that tears out in the destructive testing of spot, seam, or projection welded specimens.
- BUTT WELD
- A nonstandard term for a weld in a butt joint.
- C
- CARBON ARC BRAZING (CAB)
- A brazing process that produces coalescence of metals by heating them with an electric arc between two carbon electrodes. The filler metal is distributed in the joint by capillary action.
- CARBON ARC CUTTING (CAC)
- An arc cutting process that severs base metals by melting them with the heat of an arc between a carbon electrode and the base metal.
- CARBON ARC WELDING (CAW)
- An arc welding process that produces coalescence of metals by heating them with an arc between a carbon electrode and the base metal. No shielding is used. Pressure and filler metal may or may not be used.
- CARBONIZING FLAME
- A nonstandard term for reducing flame .
- CAULK WELD
- A nonstandard term for seal weld .
- CHAIN INTERMITTENT WELD
- An intermittent weld on both sides of a joint in which the weld increments on one side are approximately opposite those on the other side.
- CHAMFER
- A nonstandard term for bevel .
- CHEMICAL FLUX CUTTING (FOC)
- An oxygen cutting process that severs base metals using a chemical flux to facilitate cutting.
- CHILL RING
- A nonstandard term for backing ring .
- CLAD BRAZING SHEET
- A metal sheet on which one or both sides are clad with brazing filler metal.
- COALESCENCE
- The growing together or growth into one body of the materials being welded.
- COATED ELECTRODE
- A nonstandard term for covered electrode .
- COATING DENSITY
- A nonstandard term for spray deposit density ratio .
- COEXTRUSION WELDING (CEW)
- A solid-state welding process that produces coalescence of the faying surfaces by heating and forcing base metals through an extrusion die.
- COLD CRACK
- A crack that develops after solidification is complete.
- COLD SOLDERED JOINT
- A joint with incomplete coalescence caused by insufficient application of heat to the base metal during soldering.
- COLD WELDING (CW)
- A solid-state welding process in which pressure is used at room temperature to produce coalescence of metals with substantial deformation at the weld. See also diffusion welding , forge welding , and hot pressure welding .
- COMPLETE FUSION
- Fusion which has occurred over the entire base metal surface intended for welding and between all adjoining weld beads.
- COMPLETE JOINT PENETRATION

- A penetration by weld metal for the full thickness of the base metal in a joint with a groove weld.
- COMPLETE PENETRATION
- A nonstandard term for complete joint penetration .
- CONCAVITY
- The maximum distance from the face of a concave fillet weld perpendicular to a line joining the weld toes.
- CONE
- The conical part of an oxyfuel gas flame next to the orifice of the tip.
- CONSTRICTED ARC (PLASMA ARC WELDING AND CUTTING)
- A plasma arc column that is shaped by a constricting nozzle orifice.
- CONSUMABLE INSERT
- Preplaced filler metal that is completely fused into the joint root and becomes part of the weld.
- CONTACT RESISTANCE (RESISTANCE WELDING)
- Resistance to the flow of electric current between two workpieces or an electrode and a workpiece.
- CONTACT TUBE
- A device that transfers current to a continuous electrode.
- CONVEXITY
- The maximum distance from the face of a convex fillet weld perpendicular to a line joining the weld toes.
- COPPER BRAZING
- A nonstandard term for brazing with a copper filler metal.
- CORED SOLDER
- A solder wire or bar containing flux as a core.
- CORNER-FLANGE WELD
- A flange weld with only one member flanged at the joint.
- CORNER JOINT
- A joint between two members located approximately at right angles to each other.
- CORONA (RESISTANCE WELDING)
- The area sometimes surrounding the nugget of a spot weld at the faying surface which provides a degree of solid-state welding.
- CO_2 WELDING
- A nonstandard term for gas metal arc welding .
- COVALENT BOND
- A primary bond arising from the reduction in energy associated with overlapping half-filled orbitals of two atoms.
- COVERED ELECTRODE
- A composite filler metal electrode consisting of a core of a bare electrode or metal-cored electrode to which a covering sufficient to provide a slag layer on the weld metal has been applied. The covering may contain materials providing such functions as shielding from the atmosphere, deoxidation, and arc stabilization and can serve as a source of metallic additions to the weld.
- CRACK
- A fracture type discontinuity characterized by a sharp tip and high ratio of length and width to opening displacement.
- CRATER
- A depression at the termination of a weld bead.
- CUTTING ATTACHMENT
- A device for converting an oxyfuel gas welding torch into an oxygen cutting torch.
- CUTTING BLOWPIPE
- A nonstandard term for cutting torch.
- CUTTING NOZZLE
- A nonstandard term for cutting tip .
- CUTTING TIP
- The part of an oxygen cutting torch from which the gases issue.
- CUTTING TORCH (ARC)
- A device used in air carbon arc cutting, gas tungsten arc cutting, and plasma arc cutting to control the position of the electrode, to transfer current, and to control the flow of gases.
- CUTTING TORCH (OXYFUEL GAS)

- A device used for directing the preheating flame produced by the controlled combustion of fuel gases and to direct and control the cutting oxygen.
- CYLINDER MANIFOLD
- A multiple header for interconnection of gas or fluid sources with distribution points.
- D
- DEFECT
- A discontinuity or discontinuities that by nature or accumulated effect (for example, total crack length) render a part or product unable to meet minimum applicable acceptance standards or specifications. This term designates rejectability. See also discontinuity and flaw .
- DEPOSIT (THERMAL SPRAYING)
- A nonstandard term for spray deposit .
- DEPOSITED METAL
- Filler metal that has been added during welding.
- DEPOSITION EFFICIENCY (ARC WELDING)
- The ratio of the weight of deposited metal to the net weight of filler metal consumed, exclusive of stubs.
- DEPOSITION EFFICIENCY (THERMAL SPRAYING)
- The ratio of the weight of spray deposit to the weight of the surfacing material sprayed, usually expressed in percent.
- DEPOSITION SEQUENCE
- A nonstandard term for weld pass sequence .
- DEPTH OF FUSION
- The distance that fusion extends into the base metal or previous pass from the surface melted during welding.
- DIFFUSION BONDING
- A nonstandard term for diffusion brazing and diffusion welding .
- DIFFUSION BRAZING (DFB)
- A brazing process that produces coalescence of metals by heating them to brazing temperature and by using a filler metal or an *in situ* liquid phase. The filler metal may be distributed by capillary action or may be placed or formed at the faying surfaces. The filler metal is diffused with the base metal to the extent that the joint properties have been changed to approach those of the base metal. Pressure may or may not be applied.
- DIFFUSION WELDING (DFW)
- A solid-state welding process that produces coalescence of the faying surfaces by the application of pressure at elevated temperature. The process does not involve macroscopic deformation, melting, or relative motion of the workpieces. A solid filler metal may or may not be inserted between the faying surfaces. See also cold welding , forge welding , and hot pressure welding .
- DILUTION
- The change in chemical composition of a welding filler metal caused by the admixture of the base metal or previous weld metal in the weld bead. It is measured by the percentage of base metal or previous weld metal in the weld bead.
- DIP BRAZING (DB)
- A brazing process using the heat furnished by a molten chemical or metal bath. When a molten chemical bath is used, the bath may act as a flux. When a molten metal bath is used, the bath provides the filler metal.
- DIP SOLDERING (DS)
- A soldering process using the heat furnished by a molten metal bath which provides the solder filler metal.
- DIRECT CURRENT ELECTRODE NEGATIVE (DCEN)
- The arrangement of direct current arc welding leads in which the workpiece is the positive pole and the electrode is the negative pole of the welding arc.
- DIRECT CURRENT ELECTRODE POSITIVE (DCEP)
- The arrangement of direct current arc welding leads in which the workpiece is the negative pole and the electrode is the positive pole of the welding arc.
- DIRECT CURRENT REVERSE POLARITY
- A nonstandard term for direct current electrode positive .
- DIRECT CURRENT STRAIGHT POLARITY
- A nonstandard term for direct current electrode negative .
- DISCONTINUITY

- An interruption of the typical structure of a weldment, such as a lack of homogeneity in the mechanical, metallurgical, or physical characteristics of the material or weldment. A discontinuity is not necessarily a defect. See also defect and flaw .
- DOUBLE-BEVEL-GROOVE WELD
- A type of groove weld.
- DOUBLE-FLARE-BEVEL-GROOVE WELD
- A weld in grooves formed by a member with a curved surface in contact with a planar member.
- DOUBLE-FLARE-V-GROOVE WELD
- A weld in grooves formed by two members with curved surfaces.
- DOUBLE-J-GROOVE WELD
- A type of groove weld.
- DOUBLE-SQUARE-GROOVE WELD
- A type of groove weld.
- DOUBLE-U-GROOVE WELD
- A type of groove weld.
- DOUBLE-V-GROOVE WELD
- A type of groove weld.
- DOUBLE-WELDED JOINT
- A fusion-welded joint that is welded from both sides.
- DOWNHAND
- A nonstandard term for flat position .
- DRAG (THERMAL CUTTING)
- The offset distance between the actual and straight line exit points of the gas stream or cutting beam measured on the exit surface of the material.
- E
- EDGE-FLANGE WELD
- A flange weld with two members flanged at the location of welding.
- EDGE JOINT
- A joint between the edges of two or more parallel or nearly parallel members.
- EDGE WELD
- A weld in an edge joint.
- EDGE WELD SIZE
- The weld metal thickness measured at the weld root.
- EFFECTIVE THROAT
- The minimum distance minus any convexity between the weld root and the face of a fillet weld.
- ELECTRIC ARC SPRAYING
- A nonstandard term for arc spraying .
- ELECTRIC BONDING
- A nonstandard term for surfacing by thermal spraying.
- ELECTRIC BRAZING
- A nonstandard term for arc brazing and resistance brazing .
- ELECTRODE
- See welding electrode .
- ELECTRODE EXTENSION
- For gas metal arc welding, flux cored arc welding, and submerged arc welding, the length of unmelted electrode extending beyond the end of the contact tube.
- ELECTRODE FORCE
- The force between the electrodes in making spot, seam, or projection welds by resistance welding.
- ELECTRODE HOLDER
- A device used for mechanically holding the electrode while conducting current to it.
- ELECTRODE INDENTATION (RESISTANCE WELDING)
- The depression formed on the surface of workpieces by electrodes.
- ELECTRODE LEAD
- The electrical conductor between the source of arc welding current and the electrode holder.
- ELECTROGAS WELDING (EGW)
- An arc welding process that produces coalescence of metals by heating them with an arc between a continuous filler metal electrode and the work. Molding shoes are used to confine the molten weld metal

for vertical position welding. The electrodes may be either flux cored or solid. Shielding may or may not be obtained from an externally supplied gas or mixture.

- ELECTRON BEAM CUTTING (EBC)
- A cutting process that uses the heat obtained from a concentrated beam composed primarily of high-velocity electrons which impinge upon the workpieces; it may or may not use an externally supplied gas.
- ELECTRON BEAM GUN
- A device for producing and accelerating electrons. Typical components include the emitter (also called the filament or cathode), which is heated to produce electrons via thermionic emission; a cup (also called the grid or grid cup); and the anode.
- ELECTRON BEAM WELDING (EBW)
- A welding process that produces coalescence of metals with the heat obtained from a concentrated beam composed primarily of high-velocity electrons impinging on the joint.
- ELECTROSLAG WELDING (ESW)
- A welding process that produces coalescence of metals with molten slag that melts the filler metal and the surfaces of the workpieces. The weld pool is shielded by this slag, which moves along the full cross section of the joint as welding progresses. The process is initiated by an arc that heats the slag. The arc is then extinguished by the conductive slag, which is kept molten by its resistance to electric current passing between the electrode and the workpieces.
- END RETURN
- A nonstandard term for boxing .
- EROSION (BRAZING)
- A condition caused by dissolution of the base metal by molten filler metal resulting in a reduction in the thickness of the base metal.
- EXPLOSION WELDING (EXW)
- A solid-state welding process that affects coalescence by high-velocity movement together with the workpieces produced by a controlled detonation.
- F
- FACE REINFORCEMENT
- Weld reinforcement at the side of the joint from which welding was done. See also root reinforcement .
- FAYING SURFACE
- That mating surface of a member that is in contact with or in close proximity to another member to which it is to be joined.
- FERRITE NUMBER
- An arbitrary, standardized value designating the ferrite content of an austenitic stainless steel weld metal. It should be used in place of percent ferrite or volume percent ferrite on a direct replacement basis.
- FILLER METAL
- The metal to be added in making a welded, brazed, or soldered joint. See also brazing filler metal , consumable insert , solder , welding electrode , welding rod , and welding wire .
- FILLER WIRE
- A nonstandard term for welding wire .
- FILLET WELD
- A weld of approximately triangular cross section joining two surfaces approximately at right angles to each other in a lap joint, T-joint, or corner joint.
- FILLET WELD BREAK TEST
- A test in which the specimen is loaded so that the weld root is in tension.
- FILLET WELD LEG
- The distance from the joint root to the toe of the fillet weld.
- FILLET WELD SIZE
- For equal leg fillet welds, the leg lengths of the largest isosceles right triangle that can be inscribed within the fillet weld cross section. For unequal leg fillets, the leg lengths of the largest right triangle that can be inscribed within the fillet weld cross section.
- FILLET WELD THROAT
- See actual throat , effective throat , and theoretical throat .
- FIRECRACKER WELDING
- A variation of the shielded metal arc welding process in which a length of covered electrode is placed along the joint in contact with the workpieces. During the welding operation, the stationary electrode is consumed as the arc travels the length of the electrode.
- FISHEYE

- A discontinuity found on the fracture surface of a weld in steel that consists of a small pore or inclusion surrounded by an approximately round, bright area.
- FLAME CUTTING
- A nonstandard term for oxygen cutting .
- FLAME PROPAGATION RATE
- The speed at which a flame travels through a mixture of gases.
- FLAME SPRAYING (FLSP)
- A thermal spraying process in which an oxyfuel gas flame is the source of heat for melting the surfacing material. Compressed gas may or may not be used for atomizing and propelling the surfacing material to the substrate.
- FLANGE WELD
- A weld made on the edges of two or more members to be joined, usually light gage metal, at least one of the members being flanged.
- FLANGE WELD SIZE
- The weld metal thickness measured at the weld root.
- FLARE-BEVEL-GROOVE WELD
- A weld in a groove formed by a member with a curved surface in contact with a planar member.
- FLARE-V-GROOVE WELD
- A weld in a groove formed by two members with curved surfaces.
- FLASH
- Material that is expelled from a flash weld prior to the upset portion of the welding cycle.
- FLASH BUTT WELDING
- A nonstandard term for flash welding .
- FLASH COAT
- A thin coating usually less than 0.05 mm (0.002 in.) in thickness.
- FLASH WELDING (FW)
- A resistance welding process that produces coalescence at the faying surfaces of a butt joint by a flashing action and by the application of pressure after heating is substantially completed. The flashing action, caused by the very high current densities at small contacts between the parts, forcibly expels the material from the joint as the parts are slowly moved together. The weld is completed by a rapid upsetting of the workpieces.
- FLAT POSITION
- The welding position used to weld from the upper side of the joint; the face of the weld is approximately horizontal.
- FLAW
- A near synonym for discontinuity but with an undesirable connotation. See also defect and discontinuity .
- FLOW BRIGHTENING (SOLDERING)
- Fusion of a metallic coating on a base metal.
- FLUX
- Material used to prevent, dissolve, or facilitate removal of oxides and other undesirable surface substances.
- FLUX CORED ARC WELDING (FCAW)
- An arc welding process that produces coalescence of metals by heating them with an arc between a continuous filler metal electrode and the work. Shielding is provided by a flux contained within the tubular electrode. Additional shielding may or may not be obtained from an externally supplied gas or gas mixture. See also flux cored electrode .
- FLUX CORED ELECTRODE
- A composite filler metal electrode consisting of a metal tube or other hollow configuration containing ingredients to provide such functions as shielding atmosphere, deoxidation, arc stabilization, and slag formation. Minor amounts of alloying materials may be included in the core. External shielding may or may not be used.
- FLUX COVER (METAL BATH DIP BRAZING AND DIP SOLDERING)
- A layer of molten flux over the molten filler metal bath.
- FLUX OXYGEN CUTTING
- A nonstandard term for chemical flux cutting .
- FOREHAND WELDING
- A welding technique in which the welding torch or gun is directed toward the progress of welding.

- FORGE WELDING (FOW)
- A solid-state welding process that produces coalescence of metals by heating them in air in a forge and by applying pressure or blows sufficient to cause permanent deformation at the interface. See also cold welding , diffusion welding , hot pressure welding , and roll welding .
- FRICTION WELDING (FRW)
- A solid-state welding process that produces coalescence of materials under compressive force contact of workpieces rotating or moving relative to one another to produce heat and plastically displace material from the faying surfaces.
- FURNACE BRAZING (FB)
- A brazing process in which the workpieces are placed in a furnace and heated to the brazing temperature.
- FURNACE SOLDERING (FS)
- A soldering process in which the workpieces are placed in a furnace and heated to the soldering temperature.
- FUSED SPRAY DEPOSIT (THERMAL SPRAYING)
- A self-fluxing spray deposit that is subsequently heated to coalescence within itself and with the substrate.
- FUSION
- The melting together of filler metal and base metal (substrate), or of base metal only, which results in coalescence. See also depth of fusion .
- FUSION FACE
- A surface of the base metal that will be melted during welding.
- FUSION WELDING
- Any welding process that uses fusion of the base metal to make the weld.
- FUSION ZONE
- The area of base metal melted as determined on the cross section of a weld.
- G
- GAP
- A nonstandard term for joint clearance and root opening .
- GAS BRAZING
- A nonstandard term for torch brazing .
- GAS CUTTER
- A nonstandard term for oxygen cutter .
- GAS CUTTING
- A nonstandard term for oxygen cutting .
- GAS CYLINDER
- A portable container used for transportation and storage of a compressed gas.
- GAS GOUGING
- A nonstandard term for oxygen gouging .
- GAS LASER
- A laser in which the lasing medium is a gas.
- GAS METAL ARC CUTTING (GMAC)
- An arc cutting process in which metals are severed by melting them with the heat of an arc between a continuous filler metal electrode and the workpiece. Shielding is obtained entirely from an externally supplied gas.
- GAS METAL ARC WELDING (GMAW)
- An arc welding process that produces coalescence of metals by heating them with an arc between a continuous filler metal electrode and the workpieces. Shielding is obtained entirely from an externally supplied gas.
- GAS POCKET
- A nonstandard term for porosity .
- GAS REGULATOR
- A device for controlling the delivery of gas at some substantially constant pressure.
- GAS SHIELDED ARC WELDING
- A general term used to describe flux cored arc welding (when gas shielding is employed), gas metal arc welding , and gas tungsten arc welding .
- GAS TORCH
- A nonstandard term for cutting torch and welding torch.

- GAS TUNGSTEN ARC CUTTING (GTAC)
- An arc cutting process in which metals are severed by melting them with an arc between a single tungsten electrode and the workpiece. Shielding is obtained from a gas.
- GAS TUNGSTEN ARC WELDING (GTAW)
- An arc welding process that produces coalescence of metals by heating them with an arc between a tungsten electrode (nonconsumable) and the workpieces. Shielding is obtained from a gas. Pressure may or may not be used, and filler metal may or may not be used.
- GAS WELDING
- A nonstandard term for oxyfuel gas welding .
- GLOBULAR TRANSFER (ARC WELDING)
- The transfer of molten metal in large drops from a consumable electrode across the arc. See also short circuiting transfer and spray transfer .
- GOUGING
- The forming of a bevel or groove by material removal. See also arc gouging , back gouging , and oxygen gouging .
- GROOVE ANGLE
- The total included angle of the groove between the workpieces.
- GROOVE FACE
- That surface of a joint member included in the groove.
- GROOVE RADIUS
- The radius used to form the shape of a J- or U-groove weld.
- GROOVE WELD
- A weld made in a groove between the workpieces.
- GROOVE WELD SIZE
- The joint penetration of a groove weld.
- GROOVE WELD THROAT
- A nonstandard term for groove weld size .
- GROUND CONNECTION
- An electrical connection of the welding machine frame to the earth for safety. See also workpiece connection and workpiece lead .
- GROUND LEAD
- A nonstandard term for workpiece lead .
- GUN
- See air cutting gun , arc welding gun , electron beam gun , resistance welding gun , soldering gun , and thermal spraying gun .
- H
- HAMMER WELDING
- A nonstandard term for cold welding and forge welding .
- HARD SOLDER
- A nonstandard term for silver-base brazing filler metals.
- HEAT AFFECTED ZONE
- That portion of the base metal that has not been melted, but whose mechanical properties or microstructure have been altered by the heat of welding, brazing, soldering, or cutting.
- HIGH FREQUENCY RESISTANCE WELDING
- A group of resistance welding process variations that uses high frequency welding current to concentrate the welding heat at the desired location.
- HORIZONTAL FIXED POSITION (PIPE WELDING)
- The position of a pipe joint in which the axis of the pipe is approximately horizontal, and the pipe is not rotated during welding.
- HORIZONTAL POSITION (FILLET WELD)
- The position in which welding is performed on the upper side of an approximately horizontal surface and against an approximately vertical surface.
- HORIZONTAL POSITION (GROOVE WELD)
- The position of welding in which the weld axis lies in an approximately horizontal plane and the weld face lies in an approximately vertical plane.
- HORIZONTAL ROLLED POSITION (PIPE WELDING)

- The position of a pipe joint in which the axis of the pipe is approximately horizontal, and welding is performed in the flat position by rotating the pipe.
- HOT CRACK
- A crack that develops during solidification.
- HOT PRESSURE WELDING (HPW)
- A solid-state welding process that produces coalescence of metals with heat and application of pressure sufficient to produce macrodeformation of the base metal. Vacuum or other shielding media may be used. See also diffusion welding and forge welding .
- HYDROGEN BRAZING
- A nonstandard term for any brazing process that takes place in a hydrogen atmosphere.
- I
- IMPULSE (RESISTANCE WELDING)
- A group of pulses occurring on a regular frequency separated only by an interpulse time.
- INCLINED POSITION
- The position of a pipe joint in which the axis of the pipe is at an angle of approximately 45° to the horizontal, and the pipe is not rotated during welding.
- INCLINED POSITION (WITH RESTRICTION RING)
- The position of a pipe joint in which the axis of the pipe is at an angle of approximately 45° to the horizontal, and a restriction ring is located near the joint. The pipe is not rotated during welding.
- INCLUDED ANGLE
- A nonstandard term for groove angle .
- INDUCTION BRAZING (IB)
- A brazing process in which the heat required is obtained from the resistance of the workpieces to induced electric current.
- INDUCTION SOLDERING (IS)
- A soldering process in which the heat required is obtained from the resistance of the workpieces to induced electric current.
- INDUCTION WELDING (IW)
- A welding process that produces coalescence of metals by the heat obtained from the resistance of the workpieces to the flow of induced high frequency welding current with or without the application of pressure. The effect of the high frequency welding current is to concentrate the welding heat at the desired location.
- INERT GAS
- A gas that normally does not combine chemically with the base metal or filler metal. See also protective atmosphere .
- INERT GAS METAL ARC WELDING
- A nonstandard term for gas metal arc welding .
- INERT GAS TUNGSTEN ARC WELDING
- A nonstandard term for gas tungsten arc welding .
- INFRARED BRAZING (IRB)
- A brazing process in which the heat required is furnished by infrared radiation.
- INFRARED SOLDERING (IRS)
- A soldering process in which the heat required is furnished by infrared radiation.
- INTERGRANULAR PENETRATION
- The penetration of a filler metal along the grain boundaries of a base metal.
- INTERPASS TEMPERATURE
- In a multipass weld, the temperature of the weld metal before the next pass is started.
- IRON SOLDERING (INS)
- A soldering process in which the heat required is obtained from a soldering iron.
- J
- J-GROOVE WELD
- A type of groove weld.
- JOINT
- The junction of members or the edges of members which are to be joined or have been joined.
- JOINT CLEARANCE
- The distance between the faying surfaces of a joint. In brazing, this distance is referred to as that which is present before brazing, at the brazing temperature, or after brazing is completed.

- JOINT EFFICIENCY
- The ratio of the strength of a joint to the strength of the base metal, expressed in percent.
- JOINT PENETRATION
- The depth a weld extends from its face into a joint, exclusive of reinforcement.
- JOINT ROOT
- That portion of a joint to be welded where the members approach closest to each other. In cross section, the joint root may be either a point, a line, or an area.
- JOINT TYPE
- A weld joint classification based on the five basic arrangements of the component parts such as butt joint, corner joint, edge joint, lap joint, and T-joint.
- K
- KERF
- The width of the cut produced during a cutting process.
- L
- LAMELLAR TEAR
- A terracelike fracture in the base metal with a basic orientation parallel to the wrought surface. It is caused by the high stress in the thickness direction that results from welding.
- LAND
- A nonstandard term for root face .
- LAP JOINT
- A joint between two overlapping members in parallel planes.
- LASER
- A device that produces a concentrated coherent light beam by stimulating electronic or molecular transitions to lower energy levels. Laser is an acronym for light amplification by stimulated emission of radiation.
- LASER BEAM CUTTING (LBC)
- A thermal cutting process that severs materials by melting or vaporizing them with the heat obtained from a laser beam, with or without the application of gas jets to augment the removal of material.
- LASER BEAM WELDING (LBW)
- A welding process that produces coalescence of materials with the heat obtained from the application of a concentrated coherent light beam impinging upon the joint.
- LEAD BURNING
- A nonstandard term for the welding of lead.
- LIQUATION
- The separation of a low melting constituent of an alloy from the remaining constituents, usually apparent in alloys having a wide melting range.
- LOCKED-UP STRESS
- A nonstandard term for residual stress .
- LONGITUDINAL CRACK
- A crack with its major axis orientation approximately parallel to the weld axis.
- M
- MACHINE WELDING
- Welding with equipment that performs the welding operation under the constant observation and control of a welding operator. The equipment may or may not load and unload the workpieces. See also automatic welding .
- MACROETCH TEST
- A test in which the specimen is prepared with a fine finish and etched to give a clear definition of the weld.
- MANUAL WELDING
- A welding operation performed and controlled completely by hand. See also automatic welding , machine welding , and semiautomatic welding .
- MASK (THERMAL SPRAYING)
- A device for protecting a substrate surface from the effects of blasting or adherence of a spray deposit.
- MECHANICAL BOND (THERMAL SPRAYING)
- The adherence of a spray deposit to a roughened surface by the mechanism of particle interlocking.
- MELT-THROUGH
- Visible root reinforcement produced in a joint welded from one side.

- METAL ARC CUTTING (MAC)
- Any of a group of arc cutting processes that serves metals by melting them with the heat of an arc between a metal electrode and the base metal. See also gas metal arc cutting and shielded metal arc cutting .
- METAL CORED ELECTRODE
- A composite filler metal electrode consisting of a metal tube or other hollow configuration containing alloying materials. Minor amounts of ingredients and fluxing of oxides may be included. External shielding gas may or may not be used.
- METAL ELECTRODE
- A filler or nonfiller metal electrode used in arc welding or cutting that consists of a metal wire or rod that has been manufactured by any method and that is either bare or covered.
- METALLIC BOND
- The principal bond that holds metals together and is formed between base metals and filler metals in all welding processes. This is a primary bond arising from the increased spatial extension of the valence electron wave functions when an aggregate of metal atoms is brought close together. See also bonding force and covalent bond .
- METALLIZING
- A nonstandard term for thermal spraying .
- METALLURGICAL BOND
- A nonstandard term for metallic bond .
- METAL POWDER CUTTING (POC)
- An oxygen cutting process that severs metals through the use of powder, such as iron, to facilitate cutting.
- MIG WELDING
- A nonstandard term for flux cored arc welding and gas metal arc welding .
- MIXING CHAMBER
- That part of a welding or cutting torch in which a fuel gas and oxygen are mixed.
- MOLTEN WELD POOL
- A nonstandard term for weld pool .
- MULTIPORT NOZZLE (PLASMA ARC WELDING AND CUTTING)
- A constricting nozzle containing two or more orifices located in a configuration to achieve a degree of control over the arc shape.
- N
- NEUTRAL FLAME
- An oxyfuel gas flame in which the portion used is neither oxidizing nor reducing. See also oxidizing flame and reducing flame .
- NONTRANSFERRED ARC (PLASMA ARC WELDING AND CUTTING, AND PLASMA SPRAYING)
- An arc established between the electrode and the constricting nozzle. The workpiece is not in the electrical circuit. See also transferred arc .
- NOZZLE
- A device that directs shielding media.
- NUGGET
- The weld metal joining the workpieces in spot, roll spot, seam, or projection welds.
- NUGGET SIZE (RESISTANCE WELDING)
- The diameter of a spot or projection weld or width of a seam weld measured in the plane of the faying surfaces.
- O
- ORIFICE GAS (PLASMA ARC WELDING AND CUTTING)
- The gas that is directed into the torch to surround the electrode. It becomes ionized in the arc to form the plasma and issues from the orifice in the torch nozzle as the plasma jet.
- OVEN SOLDERING
- A nonstandard term for furnace soldering .
- OVERHEAD POSITION
- The position in which welding is performed from the underside of the joint.
- OVERLAP
- The protrusion of weld metal beyond the weld toes or weld root.
- OVERLAP (RESISTANCE SEAM WELDING)

- The portion of the preceding weld nugget remelted by the succeeding weld.
- OVERLAYING
- A nonstandard term for surfacing
- OXIDIZING FLAME
- An oxyfuel gas flame having an oxidizing effect due to excess oxygen. See also neutral flame and reducing flame .
- OXYACETYLENE WELDING (OAW)
- An oxyfuel gas welding process that produces coalescence of metals by heating them with a gas flame or flames obtained from the combustion of acetylene with oxygen. The process may be used with or without the application of pressure and with or without the use of filler metal.
- OXYFUEL GAS CUTTING (OFC)
- A group of cutting processes used to sever metals by means of the chemical reaction of oxygen with the base metal at elevated temperatures. The necessary temperature is maintained by means of gas flames obtained from the combustion of a specified fuel gas and oxygen. See also oxygen cutting .
- OXYFUEL GAS SPRAYING
- A nonstandard term for flame spraying .
- OXYFUEL GAS WELDING (OFW)
- A group of welding processes that produces coalescence by heating materials with an oxyfuel gas flame or flames, with or without the application of pressure, and with or without the use of filler metal.
- OXYGAS CUTTING
- A nonstandard term for oxygen cutting .
- OXYGEN ARC CUTTING (AOC)
- An oxygen cutting process used to sever metals by means of the chemical reaction of oxygen with the base metal at elevated temperatures. The necessary temperature is maintained by an arc between a consumable tubular electrode and the base metal.
- OXYGEN CUTTER
- One who performs a manual oxygen cutting operation.
- OXYGEN CUTTING (OC)
- A group of cutting processes used to sever or remove metals by means of the chemical reaction between oxygen and the base metal at elevated temperatures. In the case of oxidation-resistant metals, the reaction is facilitated by the use of a chemical flux or metal powder. See also chemical flux cutting , metal powder cutting , oxyfuel gas cutting , oxygen arc cutting and oxygen lance cutting .
- OXYGEN CUTTING OPERATOR
- One who operates machine or automatic oxygen cutting equipment.
- OXYGEN GOUGING
- An application of oxygen cutting in which a bevel or groove is formed.
- OXYGEN GROOVING
- A nonstandard term for oxygen gouging .
- OXYGEN LANCE
- A length of pipe used to convey oxygen to the point of cutting in oxygen lance cutting.
- OXYGEN LANCE CUTTING (LOC)
- An oxygen cutting process used to sever metals with oxygen supplied through a consumable lance. The preheat to start the cutting is obtained by other means.
- OXYGEN LANCING
- A nonstandard term for oxygen lance cutting .
- OXYHYDROGEN WELDING (OHW)
- An oxyfuel gas welding process that produces coalescence of materials by heating them with a gas flame or flames obtained from the combustion of hydrogen with oxygen, without the application of pressure and with or without the use of filler metal.
- P
- PARALLEL WELDING
- A resistance welding secondary circuit variation in which the secondary current is divided and conducted through the workpieces and electrodes in parallel electrical paths to simultaneously form multiple resistance spot, seam, or projection welds.
- PARENT METAL
- A nonstandard term for base metal .
- PARTIAL JOINT PENETRATION

- Joint penetration that is intentionally less than complete.
- PENETRATION
- A nonstandard term for joint penetration and root penetration .
- PERCUSSION WELDING (PEW)
- A welding process that produces coalescence at the faying surface using the heat from an arc produced by a rapid discharge of electrical energy. Pressure is applied percussively during or immediately following the electrical discharge.
- PILOT ARC (PLASMA ARC WELDING)
- A low current continuous arc between the electrode and the constricting nozzle to ionize the gas and facilitate the start of the welding arc.
- PLASMA ARC CUTTING (PAC)
- An arc cutting process that severs metal by melting a localized area with a constricted arc and removing the molten material with a high velocity jet of hot, ionized gas issuing from the constricting orifice.
- PLASMA ARC WELDING (PAW)
- An arc welding process that produces coalescence of metals by heating them with a constricted arc between an electrode and the workpiece (transferred arc) or the electrode and the constricting nozzle (nontransferred arc). Shielding is obtained from the hot, ionized gas issuing from the torch which may be supplemented by an auxiliary source of shielding gas. Shielding gas may be an inert gas or a mixture of gases. Pressure may or may not be used, and filler metal may or may not be supplied.
- PLASMA METALLIZING
- A nonstandard term for plasma spraying .
- PLASMA SPRAYING (PSP)
- A thermal spraying process in which a nontransferred arc of a plasma torch is utilized to create a gas plasma that acts as the source of heat for melting and propelling the surfacing material to the substrate.
- PLENUM CHAMBER (PLASMA ARC WELDING AND CUTTING, AND PLASMA SPRAYING)
- The space between the inside wall of the constricting nozzle and the electrode.
- PLUG WELD
- A weld made in a circular hole in one member of a joint, fusing that member to another member. A fillet-welded hole is not to be construed as conforming to this definition.
- POLARITY
- See direct current electrode negative and direct current electrode positive .
- POROSITY
- Cavity type discontinuities formed by gas entrapment during solidification.
- POSTHEATING
- The application of heat to an assembly after welding, brazing, soldering, thermal spraying, or thermal cutting. See also postweld heat treatment .
- POSTWELD HEAT TREATMENT
- Any heat treatment after welding.
- POWDER CUTTING
- A nonstandard term for chemical flux cutting and metal powder cutting .
- PRECOATING
- Coating the base metal in the joint by dipping, electroplating, or other applicable means prior to soldering or brazing.
- PREFORM
- Brazing or soldering filler metal fabricated in a shape or form for a specific application.
- PREHEAT
- A nonstandard term for preheat temperature .
- PREHEAT CURRENT (RESISTANCE WELDING)
- An impulse or series of impulses that occur prior to and are separated from the welding current.
- PREHEAT TEMPERATURE
- A specified temperature that the base metal must attain in the welding, brazing, soldering, thermal spraying, or cutting area immediately before these operations are performed.
- PRESSURE-CONTROLLED WELDING
- A resistance welding process variation in which a number of spot or projection welds are made with several electrodes functioning progressively under the control of a pressure-sequencing device.
- PRESSURE GAS WELDING (PGW)

- An oxyfuel gas-welding process that produces coalescence simultaneously over the entire area of faying surfaces by heating them with gas flames obtained from the combustion of a fuel gas and oxygen and by the application of pressure, without the use of filler metal.
- PRETINNING
- A nonstandard term for precoating .
- PROCEDURE QUALIFICATION
- The demonstration that welds made by a specific procedure can meet prescribed standards.
- PROCEDURE QUALIFICATION RECORD (PQR)
- A document providing the actual welding variables used to produce an acceptable test weld and the results of tests conducted on the weld to qualify a welding procedure specification.
- PROCESS
- A grouping of basic operational elements used in welding, cutting, adhesive bonding, or thermal spraying.
- PROJECTION WELDING (PW)
- A resistance welding process that produces coalescence by the heat obtained from the resistance to the flow of the welding current. The resulting welds are localized at predetermined points by projections, embossments, or intersections.
- PROTECTIVE ATMOSPHERE
- A gas or vacuum envelope surrounding the workpieces used to prevent or facilitate removal of oxides and other detrimental surface substances.
- PUDDLE
- A nonstandard term for weld pool .
- PULL GUN TECHNIQUE
- A nonstandard term for backhand welding .
- PULSE (RESISTANCE WELDING)
- A current of controlled duration of either polarity through the welding circuit.
- R
- RANDOM INTERMITTENT WELDS
- Intermittent welds on one or both sides of a joint in which the weld increments are made without regard to spacing.
- REACTION FLUX (SOLDERING)
- A flux composition in which one or more of the ingredients reacts with a base metal upon heating to deposit one or more metals.
- REACTION STRESS
- A stress that cannot exist in a member if the member is isolated as a free body without connection to other parts of the structure.
- REDUCING ATMOSPHERE
- A chemically active protective atmosphere which at elevated temperature will reduce metal oxides to their metallic state.
- REDUCING FLAME
- A gas flame having a reducing effect due to excess fuel gas. See also neutral flame and oxidizing flame .
- REFLOWING
- A nonstandard term for flow brightening .
- REFLOW SOLDERING
- A nonstandard term for a soldering process variation in which preplaced solder is melted to produce a soldered joint or coated surface.
- RESIDUAL STRESS
- Stress present in a member that is free of external forces or thermal gradients.
- RESISTANCE BRAZING (RB)
- A brazing process in which the heat required is obtained from the resistance to electric current flow in a circuit of which the workpiece is a part.
- RESISTANCE BUTT WELDING
- A nonstandard term for flash welding and upset welding .
- RESISTANCE SEAM WELDING (RSW)
- A resistance welding process that produces coalescence at the faying surfaces of overlapped parts progressively along a length of a joint. The weld may be made with overlapping weld nuggets, a

continuous weld nugget, or by forging the joint as it is heated to the welding temperature by resistance to the flow of the welding current.

- RESISTANCE SOLDERING (RS)
- A soldering process in which the heat required is obtained from the resistance to electric current flow in a circuit of which the workpiece is a part.
- RESISTANCE SPOT WELDING (RSW)
- A resistance welding process that produces coalescence at the faying surfaces of a joint by the heat obtained from resistance to the flow of welding current through the workpieces from electrodes that serve to concentrate the welding current and pressure at the weld area.
- RESISTANCE WELDING (RW)
- A group of welding processes that produces coalescence of the faying surfaces with the heat obtained from resistance of the work to the flow of the welding current in a circuit of which the work is a part, and by the application of pressure.
- RESISTANCE WELDING ELECTRODE
- The part(s) of a resistance welding machine through which the welding current and, in most cases, force are applied directly to the work. The electrode may be in the form of a rotating wheel, rotating bar, cylinder, plate, clamp, chuck, or modification thereof.
- RESISTANCE WELDING GUN
- A manipulatable device to transfer current and provide electrode force to the weld area (usually in reference to a portable gun).
- REVERSE POLARITY
- A nonstandard term for direct current electrode positive .
- ROLL WELDING (ROW)
- A solid-state welding process that produces coalescence of metals by heating and by applying sufficient pressure with rolls to cause deformation at the faying surfaces. See also forge welding .
- ROOT
- A nonstandard term for joint root and weld root .
- ROOT BEAD
- A weld that extends into or includes part or all of the joint root.
- ROOT EDGE
- A root face of zero width. See also root face .
- ROOT FACE
- That portion of the groove face adjacent to the joint root.
- ROOT GAP
- A nonstandard term for root opening .
- ROOT OPENING
- The separation at the joint root between the workpieces.
- ROOT PENETRATION
- The depth that a weld extends into the joint root.
- ROOT RADIUS
- A nonstandard term for groove radius .
- ROOT REINFORCEMENT
- Weld reinforcement opposite the side from which welding was done.
- ROOT SURFACE
- The exposed surface of a weld opposite the side from which welding was done.
- S
- SCARF JOINT
- A form of butt joint.
- SEAL COAT
- Material applied to infiltrate the pores of a thermal spray deposit.
- SEAL WELD
- Any weld designed primarily to provide a specific degree of tightness against leakage.
- SEAM WELD
- A continuous weld made between or upon overlapping members, in which coalescence may start and occur on the faying surfaces, or may have proceeded from the outer surface of one member. The continuous weld may consist of a single weld bead or a series of overlapping spot welds. See also arc seam weld and resistance seam welding .

- SECONDARY CIRCUIT
- That portion of a welding machine that conducts the secondary current between the secondary terminals of the welding transformer and the electrodes, or electrode and workpiece.
- SELF-FLUXING ALLOYS (THERMAL SPRAYING)
- Surfacing materials that wet the substrate and coalesce when heated to their melting point, without the addition of a flux.
- SEMIAUTOMATIC ARC WELDING
- Arc welding with equipment that controls only the filler metal feed. The advance of the welding is manually controlled.
- SERIES WELDING
- A resistance welding secondary circuit variation in which the secondary current is conducted through the workpieces and electrodes or wheels in a series electrical path to simultaneously form multiple resistance spot, seam, or projection welds.
- SET DOWN
- A nonstandard term for upset .
- SHADOW MASK
- A thermal spraying process variation in which an area is partially shielded during thermal spraying, thus permitting some overspray to produce a feathering at the coating edge.
- SHEET SEPARATION (RESISTANCE WELDING)
- The gap surrounding the weld between faying surfaces, after the joint has been welded in spot, seam, or projection welding.
- SHIELDED METAL ARC CUTTING (SMAC)
- A metal arc cutting process in which metals are severed by melting them with the heat of an arc between a covered metal electrode and the base metal.
- SHIELDED METAL ARC WELDING (SMAW)
- An arc welding process that produces coalescence of metals by heating them with an arc between a covered metal electrode and the workpieces. Shielding is obtained from decomposition of the electrode covering. Pressure is not used, and filler metal is obtained from the electrode.
- SHIELDING GAS
- Protective gas used to prevent atmospheric contamination.
- SHORT CIRCUITING TRANSFER (ARC WELDING)
- Metal transfer in which molten metal from a consumable electrode is deposited during repeated short circuits. See also globular transfer and spray transfer .
- SHOULDER
- A nonstandard term for root face .
- SHRINKAGE STRESS
- A nonstandard term for residual stress .
- SHRINKAGE VOID
- A cavity type discontinuity normally formed by shrinkage during solidification.
- SILVER ALLOY BRAZING
- A nonstandard term for brazing with a silver-base filler metal.
- SILVER SOLDERING
- A nonstandard term for brazing with a silver-base filler metal.
- SINGLE-BEVEL-GROOVE WELD
- A type of groove weld.
- SINGLE-FLARE-BEVEL-GROOVE WELD
- A weld in a groove formed by a member with a curved surface in contact with a planar member.
- SINGLE-FLARE-V-GROOVE WELD
- A weld in a groove formed by two members with curved surfaces.
- SINGLE IMPULSE WELDING
- A resistance welding process variation in which spot, projection, or upset welds are made with a single impulse.
- SINGLE-J-GROOVE WELD
- A type of groove weld.
- SINGLE-PORT NOZZLE
- A constricting nozzle containing one orifice, located below and concentric with the electrode.
- SINGLE-SQUARE-GROOVE WELD

- A type of groove weld.
- SINGLE-U-GROOVE WELD
- A type of groove weld.
- SINGLE-V-GROOVE WELD
- A type of groove weld.
- SINGLE-WELDED JOINT
- A fusion welded joint that is welded from one side only.
- SKULL
- The unmelted residue from a liquated filler metal.
- SLAG INCLUSION
- Nonmetallic solid material entrapped in weld metal or between weld metal and base metal.
- SLOT WELD
- A weld made in an elongated hole in one member of a joint fusing that member to another member. The hole may be open at one end. A fillet weld slot is not to be construed as conforming to this definition.
- SLUGGING
- The act of adding a separate piece or pieces of material in a joint before or during welding that results in a welded joint not complying with design, drawing, or specification requirements.
- SOFT SOLDER
- A nonstandard term for solder .
- SOLDER
- A filler metal used in soldering that has a liquidus not exceeding 450 °C (840 °F).
- SOLDERING (S)
- A group of welding processes that produces coalescence of materials by heating them to the soldering temperature and by using a filler metal having a liquidus not exceeding 450 °C (840 °F) and below the solidus of the base metals. The filler metal is distributed between the closely fitted faying surfaces of the joint by capillary action.
- SOLDERING GUN
- An electrical soldering iron with a pistol grip and a quick heating, relatively small bit.
- SOLDERING IRON
- A soldering tool having an internally or externally heated metal bit usually made of copper.
- SOLDER INTERFACE
- The interface between filler metal and base metal in a soldered joint.
- SOLID-STATE WELDING (SSW)
- A group of welding processes that produces coalescence at temperatures essentially below the melting point of the base metal without the addition of a brazing filler metal. Pressure may or may not be used.
- SPACER STRIP
- A metal strip or bar prepared for a groove weld and inserted in the joint root to serve as a backing and to maintain the root opening during welding. It can also bridge an exceptionally wide root opening due to poor fit.
- SPIT
- A nonstandard term for flash .
- SPLIT PIPE BACKING
- Backing in the form of a pipe segment used for welding round bars.
- SPOOL
- A filler metal package consisting of a continuous length of welding wire in coil form wound on a cylinder (called a barrel) which is flanged at both ends. The flange contains a spindle hole of smaller diameter than the inside diameter of the barrel.
- SPOT WELD
- A weld made between or upon overlapping members in which coalescence may start and occur on the faying surfaces or may proceed from the outer surface of one member. The weld cross section (plan view) is approximately circular. See also arc spot weld and resistance spot welding .
- SPRAY DEPOSIT
- The coating or layer of surfacing material applied by a thermal spraying process.
- SPRAY DEPOSIT DENSITY RATIO (THERMAL SPRAYING)
- The ratio of the density of the spray deposit to the theoretical density of a surfacing material, usually expressed as a percent of theoretical density.
- SPRAY TRANSFER (ARC WELDING)

- Metal transfer in which molten metal from a consumable electrode is propelled axially across the arc in small droplets. See also globular transfer and short circuiting transfer .
- SQUARE-GROOVE WELD
- A type of groove weld.
- STACK CUTTING
- Thermal cutting of stacked metal plates arranged so that all the plates are severed by a single cut.
- STAGGERED INTERMITTENT WELD
- An intermittent weld on both sides of a joint in which the weld increments on one side are alternated with respect to those on the other side.
- STANDOFF DISTANCE
- The distance between a nozzle and the workpiece.
- STICK ELECTRODE
- A nonstandard term for covered electrode .
- STICK ELECTRODE WELDING
- A nonstandard term for shielded metal arc welding .
- STICKOUT
- A nonstandard term for electrode extension .
- STOPOFF
- A material used on the surfaces adjacent to the joint to limit the spread of soldering or brazing filler metal.
- STRAIGHT POLARITY
- A nonstandard term for direct current electrode negative .
- STRANDED ELECTRODE
- A composite filler metal electrode consisting of stranded wires that may mechanically enclose materials to improve properties, stabilize the arc, or provide shielding.
- STRESS RELIEF CRACKING
- Intergranular cracking in the heat affected zone or weld metal that occurs during the exposure of weldments to elevated temperatures during postweld heat treatment or high temperature service.
- STRESS RELIEF HEAT TREATMENT
- Uniform heating of a structure or a portion thereof to a sufficient temperature to relieve the major portion of the residual stresses, followed by uniform cooling.
- STRINGER BEAD
- A type of weld bead made without appreciable weaving motion. See also weave bead .
- STUB
- The short length of welding rod or consumable electrode that remains after its use for welding.
- STUD ARC WELDING (SW)
- An arc welding process that produces coalescence of metals by heating them with an arc between a metal stud, or similar part, and the other workpiece. When the surfaces to be joined are properly heated, they are brought together under pressure. Partial shielding may be obtained by the use of a ceramic ferrule surrounding the stud. Shielding gas or flux may or may not be used.
- STUD WELDING
- A general term for joining a metal stud or similar part to a workpiece. Welding may be accommodated by arc, resistance, friction, or other processes with or without external gas shielding.
- SUBMERGED ARC WELDING (SAW)
- An arc welding process that produces coalescence of metals by heating them with an arc or arcs between a bare metal electrode or electrodes and the workpieces. The arc and molten metal are shielded by a blanket of granular, fusible material on the workpieces. Pressure is not used, and filler metal is obtained from the electrode and sometimes from a supplemental source (welding rod, flux, or metal granules).
- SUBSTRATE
- Any material to which a thermal spray deposit is applied.
- SURFACE EXPULSION
- Expulsion occurring at an electrode-to-workpiece contact rather than at the faying surface.
- SURFACING
- The application by welding, brazing, or thermal spraying of a layer or layers of material to a surface to obtain desired properties or dimensions, as opposed to making a joint.
- SURFACING MATERIAL
- The material that is applied to a base metal or substrate during surfacing.

- SURFACING METAL
- The metal that is applied to a base metal or substrate during surfacing. See also surfacing material .
- SURFACING WELD
- A weld applied to a surface, as opposed to making a joint, to obtain desired properties or dimensions.
- SWEAT SOLDERING
- A soldering process variation in which two or more parts that have been precoated with solder are reheated and assembled into a joint without the use of additional solder.
- SYNCHRONOUS TIMING (RESISTANCE WELDING)
- The initiation of each half cycle of welding transformer primary current on an accurately timed delay with respect to the polarity reversal of the power supply.
- T
- TACKER
- A nonstandard term for a tack welder.
- TACK WELD
- A weld made to hold parts of a weldment in proper alignment until the final welds are made.
- THEORETICAL THROAT
- The distance from the beginning of the joint root perpendicular to the hypotenuse of the largest right triangle that can be inscribed within the cross section of a fillet weld. This dimension is based on the assumption that the root opening is equal to zero.
- THERMAL CUTTING (TC)
- A group of cutting processes that melts the base metal. See also arc cutting , electron beam cutting , laser beam cutting , and oxygen cutting .
- THERMAL SPRAYING (THSP)
- A group of processes in which finely divided metallic or non-metallic surfacing materials are deposited in a molten or semimolten condition on a substrate to form a spray deposit. The surfacing material may be in the form of powder, rod, or wire. See also arc spraying , flame spraying , and plasma spraying .
- THERMAL SPRAYING GUN
- A device for heating, feeding, and directing the flow of a surfacing material.
- THERMAL STRESS
- Stress resulting from nonuniform temperature distribution.
- THERMIT CRUCIBLE
- The vessel in which the thermit reaction takes place.
- THERMIT MIXTURE
- A mixture of metal oxide and finely divided aluminum with the addition of alloying metals as required.
- THERMIT MOLD
- A mold formed around the workpieces to receive the molten metal.
- THERMIT REACTION
- The chemical reaction between metal oxide and aluminum that produces superheated molten metal and a slag containing aluminum oxide.
- THERMIT WELDING (TW)
- A welding process that produces coalescence of metals by heating them with superheated liquid metal from a chemical reaction between a metal oxide and aluminum, with or without the application of pressure. Filler metal is obtained from the liquid metal. (*Note*: The *ASM Handbook* uses the spelling "thermit*e* welding.")
- THERMOCOMPRESSION BONDING
- A nonstandard term for hot pressure welding .
- THROAT OF A FILLET WELD
- See actual throat , effective throat , and theoretical throat .
- THROAT OF A GROOVE WELD
- A nonstandard term for groove weld size .
- TIG WELDING
- A nonstandard term for gas tungsten arc welding .
- TINNING
- A nonstandard term for precoating .
- T-JOINT
- A joint between two members located approximately at right angles to each other in the form of a T.
- TOE CRACK

- A crack in the base metal at the toe of a weld.
- TORCH BRAZING (TB)
- A brazing process in which the heat required is furnished by a fuel gas flame.
- TORCH SOLDERING (TS)
- A soldering process in which the heat required is furnished by a fuel gas flame.
- TORCH TIP
- See cutting tip and welding tip .
- TRANSFERRED ARC (PLASMA ARC WELDING)
- A plasma arc established between the electrode and the workpiece.
- TRANSVERSE CRACK
- A crack with its major axis oriented approximately perpendicular to the weld axis.
- TWIN CARBON ARC BRAZING
- A nonstandard term for carbon arc brazing .
- U
- U-GROOVE WELD
- A type of groove weld.
- ULTRASONIC COUPLER (ULTRASONIC SOLDERING AND ULTRASONIC WELDING)
- Elements through which ultrasonic vibration is transmitted from the transducer to the tip.
- ULTRASONIC SOLDERING
- A soldering process variation in which high frequency vibratory energy is transmitted through molten solder to remove undesirable surface films and thereby promote wetting of the base metal. This operation is usually accomplished without a flux.
- ULTRASONIC WELDING (USW)
- A solid-state welding process that produces coalescence of materials by the local application of high frequency vibratory energy as the workpieces are held together under pressure.
- UNDERBEAD CRACK
- A crack in the heat affected zone generally not extending to the surface of the base metal.
- UNDERCUT
- A groove melted into the base metal adjacent to the weld toe or weld root and left unfilled by weld metal.
- UNDERFILL
- A depression on the weld face or root surface extending below the adjacent surface of the base metal.
- UPSET
- Bulk deformation resulting from the application of pressure in welding. The upset may be measured as a percent increase in interface area, a reduction in length, a percent reduction in lap joint thickness, or a reduction in cross wire weld stack height.
- UPSET BUTT WELDING
- A nonstandard term for upset welding .
- UPSET DISTANCE
- The total loss of axial length of the workpieces from the initial contact to the completion of the weld. In flash welding, the upset distance is equal to the platen movement from the end of flash time to the end of upset.
- UPSET WELDING (UW)
- A resistance welding process that produces coalescence over the entire area of faying surfaces or progressively along a butt joint by the heat obtained from the resistance to the flow of welding current through the area where those surfaces are in contact. Pressure is used to complete the weld.
- V
- VACUUM BRAZING
- A nonstandard term for various brazing processes that take place in a chamber or retort below atmospheric pressure.
- VERTICAL POSITION
- The position of welding in which the weld axis is approximately vertical.
- VERTICAL POSITION (PIPE WELDING)
- The position of a pipe joint in which welding is performed in the horizontal position and the pipe may or may not be rotated.
- V-GROOVE WELD
- A type of groove weld.
- W

- WAVE SOLDERING (WS)
- An automatic soldering process where workpieces are passed through a wave of molten solder. See also dip soldering .
- WAX PATTERN (THERMIT WELDING)
- Wax molded around the workpieces to the form desired for the completed weld.
- WEAVE BEAD
- A type of weld bead made with transverse oscillation.
- WELD
- A localized coalescence of metals or non-metals produced either by heating the materials to the welding temperature, with or without the application of pressure, or by the application of pressure alone, with or without the use of filler metal.
- WELDABILITY
- The capacity of a material to be welded under the imposed fabrication conditions into a specific, suitably designed structure and to perform satisfactorily in the intended service.
- WELD AXIS
- A line through the length of the weld, perpendicular to and at the geometric center of its cross section.
- WELD BEAD
- A weld resulting from a pass. See also stringer bead and weave bead .
- WELD BONDING
- A resistance spot welding process variation in which the spot weld strength is augmented by adhesive at the faying surfaces.
- WELD BRAZING
- A joining method that combines resistance welding with brazing.
- WELD CRACK
- A crack located in the weld metal or heat affected zone.
- WELDER
- One who performs manual or semiautomatic welding operation.
- WELDER PERFORMANCE QUALIFICATION
- The demonstration of a welder's ability to produce welds meeting prescribed standards.
- WELD FACE
- The exposed surface of a weld on the side from which welding was done.
- WELDING
- A materials joining process used in making welds.
- WELDING BLOWPIPE
- A nonstandard term for welding torch.
- WELDING CURRENT
- The current in the welding circuit during the making of a weld.
- WELDING CYCLE
- The complete series of events involved in the making of a weld.
- WELDING ELECTRODE
- A component of the welding circuit through which current is conducted and that terminates at the arc, molten conductive slag, or base metal. See also arc welding electrode , flux cored electrode , metal cored electrode , metal electrode , resistance welding electrode , and stranded electrode .
- WELDING GROUND
- A nonstandard term for workpiece connection .
- WELDING LEADS
- The workpiece lead and electrode lead of an arc welding circuit.
- WELDING MACHINE
- Equipment used to perform the welding operation; for example, spot welding machine, arc welding machine, and seam welding machine.
- WELDING OPERATOR
- One who operates machine or automatic welding equipment.
- WELDING POSITION
- See flat position , horizontal fixed position , horizontal position, horizontal rolled position , inclined position , overhead position , and vertical position .
- WELDING PROCEDURE

- The detailed methods and practices involved in the production of a weldment. See also welding procedure specification .
- WELDING PROCEDURE SPECIFICATION (WPS)
- A document providing in detail the required variables for a specific application to ensure repeatability by properly trained welders and welding operators.
- WELDING ROD
- A form of welding filler metal, normally packaged in straight lengths, that does not conduct electrical current.
- WELDING SEQUENCE
- The order of making the welds in a weldment.
- WELDING TIP
- That part of an oxyfuel gas welding torch from which the gases issue.
- WELDING TORCH (ARC)
- A device used in the gas tungsten and plasma arc welding processes to control the position of the electrode, to transfer current to the arc, and to direct the flow of shielding and plasma gas.
- WELDING TORCH (OXYFUEL GAS)
- A device used in oxyfuel gas welding, torch brazing, and torch soldering for directing the heating flame produced by the controlled combustion of fuel gases.
- WELDING WHEEL
- A nonstandard term for resistance welding electrode .
- WELDING WIRE
- A form of welding filler metal, normally packaged as coils or spools, that may or may not conduct electrical current depending upon the welding process with which it is used. See also welding electrode and welding rod .
- WELD INTERFACE
- The interface between weld metal and base metal in a fusion weld, between base metals in a solid-state weld without filler metal or between filler metal and base metal in a solid-state weld with filler metal, and in a braze.
- WELD LINE
- A nonstandard term for weld interface .
- WELDMENT
- An assembly whose component parts are joined by welding.
- WELD METAL
- That portion of a weld that has been melted during welding.
- WELDOR
- A nonstandard term for welder .
- WELD PASS
- A single progression of welding or surfacing along a joint or substrate. The result of a pass is a weld bead, layer, or spray deposit.
- WELD PASS SEQUENCE
- The order in which the weld passes are made.
- WELD PENETRATION
- A nonstandard term for joint penetration and root penetration .
- WELD POOL
- The localized volume of molten metal in a weld prior to its solidification as weld metal.
- WELD PUDDLE
- A nonstandard term for weld pool .
- WELD REINFORCEMENT
- Weld metal in excess of the quantity required to fill a joint. See also face reinforcement and root reinforcement .
- WELD ROOT
- The points, as shown in cross section, at which the back of the weld intersects the base metal surfaces.
- WELD SIZE
- See edge weld size , fillet weld size , flange weld size , and groove weld size .
- WELD TAB
- Additional material on which the weld may be initiated or terminated.
- WELD THROAT

- See actual throat , effective throat , and theoretical throat .
- WELD TOE
- The junction of the weld face and the base metal.
- WETTING
- The phenomenon whereby a liquid filler metal or flux spreads and adheres in a thin continuous layer on a solid base metal.
- WIPED JOINT
- A joint made with solder having a wide melting range and with the heat supplied by the molten solder poured onto the joint. The solder is manipulated with a hand-held cloth or paddle so as to obtain the required size and contour.
- WORK CONNECTION
- A nonstandard term for workpiece connection .
- WORK LEAD
- A nonstandard term for workpiece lead .
- WORKPIECE
- The part being welded, brazed, soldered, or cut.
- WORKPIECE CONNECTION
- The connection of the workpiece lead to the workpiece.
- WORKPIECE LEAD
- The electrical conductor between the arc welding current source and the workpiece connection.

Note

* THIS GLOSSARY IS REPRINTED BY PERMISSION OF THE AMERICAN WELDING SOCIETY FROM THE *WELDING HANDBOOK*, 8TH EDITION, VOLUME 1, AMERICAN WELDING SOCIETY, 1987. IT WAS PREPARED BY THE AWS COMMITTEE ON DEFINITIONS AND SYMBOLS CONSISTING OF G.E. METGER, *CHAIRMAN*, AFWAL/MLLS; J.T. BISKUP, CANADIAN WELDING BUREAU; W.F. BROWN, WESTINGHOUSE HANFORD; C.D. BURNHAM, CONSULTANT; R.J. CHRISTOFFEL, GENERAL ELECTRIC COMPANY; G.B. COATES, GENERAL ELECTRIC COMPANY; MICHAEL D. COOPER, HOBART SCHOOL OF WELDING TECHNOLOGY; W.L. GREEN, OHIO STATE UNIVERSITY; J.E. GREER, GENERAL ELECTRIC RAILROAD; M.J. GRYCO, PACKER ENGINEERING ASSOCIATES; D.E. HAMILTON, TRINITY ENGINEERING TESTING CORPORATION; E.A. HARWART, CONSULTANT; A. RAY HOLLINS, JR., DUKE POWER COMPANY; M.J. HOULE, NATIONAL BOARD OF BOILER AND PRESSURE VESSEL INSPECTORS; STEPHEN R. MORSE, DEERE AND COMPANY; L.C. NORTHARD, TENNESSEE VALLEY AUTHORITY; D.H. ORTS, ARMCO, INCORPORATED; E.J. SEEL, AMERICAN WELDING SOCIETY; J.J. STANCZAK, STEEL DETAILERS & DESIGNERS; J.J. VAGI, BABCOCK AND WILCOX; J.L. WILK, COAST TO COAST CONSTRUCTION COMPANY; UNDER THE DIRECTION OF AWS WELDING HANDBOOK COMMITTEE CHAIRMEN J.H. HANNAHS, MIDMARK CORPORATION, AND M.J. TOMSIC, PLASTRONICS INCORPORATED (AFFILIATIONS CIRCA 1987).

Abbreviations, Symbols, and Tradenames

- ABBREVIATIONS AND SYMBOLS
- A
- austenite; ampere
- Å
- angstrom
- AA
- Aluminum Association
- AAR

- Association of American Railroads
- AASHTO
- American Association of State Highway and Transportation Officials
- ABS
- American Bureau of Shipping
- AC
- alternating current
- AC
- air cool; aligned carbide
- AC_{CM}
- in hypereutectoid steel, temperature at which cementite completes solution in austenite
- AC_1
- temperature at which austenite begins to form during heating
- AC_3
- temperature at which transformation of ferrite to austenite is completed during heating
- AE_{CM}, AE_1, AE_3
- equilibrium transformation temperatures in steel
- AES
- Auger electron spectroscopy; acoustic emission spectroscopy
- AF
- acicular ferrite
- AFM
- atomic force microscopy
- AI
- artificial intelligence
- AISC
- American Institute of Steel Construction
- AISI
- American Iron and Steel Institute
- AMS
- Aerospace Material Specification
- ANSI
- American National Standards Institute
- AOD
- argon-oxygen decarburization
- API
- American Petroleum Institute
- AR_{CM}
- temperature at which cementite begins to precipitate from austenite upon cooling
- AR_1
- temperature at which transformation to ferrite or to ferrite plus cementite is completed on cooling
- AR_3
- temperature at which transformation of austenite to ferrite begins on cooling
- AREA
- American Railway Engineers Association
- ASM
- American Society for Metals (now ASM International)
- ASME
- American Society of Mechanical Engineers
- ASTM
- American Society for Testing and Materials
- AT.%
- atomic percent
- ATM
- atmospheres (pressure)
- AWS
- American Welding Society

- B
- bainite
- BAL
- balance
- BCC
- body-centered cubic
- BCT
- body-centered tetragonal
- C
- edge length in crystal structure; speed of light; specific heat; constant
- C
- cementite; coulomb; heat capacity
- CAC
- carbon arc cutting
- CAC-A
- air carbon arc cutting
- CAD/CAM
- computer-aided design/computer-aided manufacturing
- CAFE
- Corporate Average Fuel Economy (standard)
- CAW
- carbon arc welding
- CAW-G
- gas carbon arc welding
- CAW-S
- shielded carbon arc welding
- CBN
- cubic boron nitride
- CCD
- charge-coupled device
- CCT
- continuous-cooling transformation
- CD
- candela
- CE
- carbon equivalent
- CGS
- centimeter-gram-second (system of units)
- CM
- centimeter
- CMC
- ceramic-matrix composite
- CNC
- computer numerical control
- COD
- crack-opening displacement
- C_P
- specific heat at constant pressure
- CP
- centipoise
- CP
- commercially pure
- CPT
- critical pitting temperature
- CR
- corrosion resistant
- CRT

- cathode-ray tube
- CST
- centistokes
- CTE
- coefficient of thermal expansion
- CTOD
- crack tip opening displacement
- CVD
- chemical vapor deposition
- CVN
- Charpy V-notch (impact test or specimen)
- *D*
- diameter
- *DA*/*DN*
- fatigue crack growth rate
- DARPA
- Defense Advanced Research Projects Agency
- DB
- decibel
- DB
- diffusion bonding; dip brazing
- DBTT
- ductile-to-brittle transition temperature
- DC
- direct current
- DCEN
- direct current, electrode negative
- DCEP
- direct current, electrode positive
- DFB
- diffusion brazing
- DFW
- diffusion welding
- DHC
- delayed hydride cracking
- DIAM
- diameter
- DIN
- Deutsche Industrie-Normen (German Industrial Standards)
- DPH
- diamond pyramid hardness
- DRA
- discontinuously reinforced aluminum
- DS
- dip soldering
- DTA
- differential thermal analysis
- *E*
- natural log base, 2.71828; charge of an electron
- EB
- electron beam
- EBC
- electron-beam cutting
- EBW
- electron-beam welding
- EDM
- electrical discharge machining

- EDXA
- energy-dispersive x-ray analysis
- EELS
- electron energy loss spectroscopy
- EERC
- Earthquake Engineering Research Center
- EGW
- electrogas welding
- ELI
- extra-low interstitial
- EMF
- electromotive force
- EPA
- Environmental Protection Agency
- EPFM
- elastic plastic fracture mechanics
- EPRI
- Electric Power Research Institute
- EQ
- equation
- ESW
- electroslag welding
- ***ET AL.***
- and others
- ETP
- electrolytic tough pitch
- EV
- electron volt
- EXB
- exothermic brazing
- EXP
- base of the natural logarithm
- EXW
- explosion welding
- ***F***
- frequency
- F
- ferrite
- FAA
- Federal Aviation Administration
- FAD
- failure-assessment diagram; fracture-assessment diagram
- FB
- furnace brazing
- FCAW
- flux-cored arc welding
- FCC
- face-centered cubic
- FCM
- fracture critical tension member
- FCT
- face-centered tetragonal
- FEA
- finite-element analysis
- FEM
- finite-element method
- FHA

- Federal Highway Administration
- FIG.
- figure
- FM
- frequency modulation
- FMVSS
- Federal Motor Vehicle Safety Standards
- FN
- ferrite number
- FRW
- friction welding
- FS
- furnace soldering
- FT
- foot
- FW
- flash welding
- G
- gram; acceleration due to gravity
- G
- graphite; gauss
- GAL
- gallon
- GBF
- grain-boundary ferrite
- GF
- gram force
- GMA
- gas-metal arc
- GMAC
- gas-metal arc cutting
- GMAW
- gas-metal arc welding
- GPA
- gigapascal
- GTA
- gas-tungsten arc
- GTAC
- gas-tungsten arc cutting
- GTAW
- gas-tungsten arc welding
- H
- hour; Planck's constant (6.626×10^{-27} erg · s)
- H
- Henry
- *H*
- enthalpy; hardness; magnetic field
- HAZ
- heat-affected zone
- HB
- Brinell hardness
- HCP
- hexagonal close-packed
- HHC
- hot-hollow cathode
- HIC
- hydrogen-induced cracking

- HIP
- hot isostatic pressing
- HK
- Knoop hardness
- HP
- horsepower
- HR
- Rockwell hardness (requires scale designation, such as HRC for Rockwell C hardness)
- HREM
- high-resolution electron microscopy
- HSLA
- high-strength low-alloy (steel)
- HSS
- high-speed steel(s)
- HTLA
- heat-treatable low-alloy (steel)
- HV
- Vickers hardness
- HZ
- hertz
- *I*
- intensity; electrical current
- IA
- inorganic acid
- ID
- inside diameter
- IGA
- intergranular attack
- IGSCC
- intergranular stress-corrosion cracking
- IIW
- International Institute of Welding
- I/M
- ingot metallurgy
- IMO
- International Maritime Organization
- IN.
- inch
- IPTS
- International Practical Temperature Scale
- IR
- infrared
- IRS
- infrared soldering
- IS
- induction soldering
- ISCC
- intergranular stress-corrosion cracking
- ISO
- International Organization for Standardization
- J
- joule
- K
- equilibrium distribution coefficient; thermal conductivity; Boltzmann constant
- K
- Kelvin
- KG

- kilogram
- KGF
- kilogram force
- K_{IC}
- plane-strain fracture toughness
- K_{ISCC}
- threshold stress intensity to produce stress-corrosion cracking
- KM
- kilometer
- KN
- kilonewton
- KPA
- kilopascal
- KSI
- kips (1000 lbf) per square inch
- KV
- kilovolt
- KW
- kilowatt
- L
- longitudinal, liter
- LB
- pound
- LBF
- pound force
- LBW
- laser-beam welding
- LCL
- lower control limit
- LEED
- low-energy electron diffraction
- LEFM
- linear elastic fracture mechanics
- LME
- liquid-metal embrittlement
- LMP
- Larson-Miller parameter
- IN
- natural logarithm (base *e*)
- LNG
- liquefied natural gas
- LOG
- common logarithm (base 10)
- LPG
- liquefied petroleum gas
- LSI
- large-scale integrated (circuit)
- LT
- long transverse (direction)
- LTE
- local thermodynamic equilibrium
- LTS
- low-temperature sensitization
- LVDT
- linear variable differential transformer
- M
- meter

- MA
- milliampere
- MC
- metal carbide
- MCL
- maximum crack length
- MEV
- megaelectronvolt
- M_F
- temperature at which martensite formation finishes during cooling
- MG
- milligram
- MG
- megagram (metric tonne, or kg × 10^3)
- MIC
- microbiologically influenced corrosion
- MIN
- minute; minimum
- ML
- milliliter
- MM
- millimeter
- MO
- multiple operator
- MPA
- millipascal
- MPA
- megapascal
- MPG
- miles per gallon
- MPH
- miles per hour
- MRDA
- man-rated demonstration vehicle
- MRR
- material removal rate
- MS
- millisecond
- M_S
- temperature at which martensite starts to form from austenite on cooling
- MS
- megasiemens
- MT
- millitesla
- MV
- millivolt
- MV
- megavolt
- MVC
- most vulnerable component
- N
- newton
- N
- number of cycles; normal solution; normal force
- NACE
- National Association of Corrosion Engineers
- NASA

- National Aeronautics and Space Administration
- NBS
- National Bureau of Standards (former name of NIST)
- NDE
- nondestructive examination
- NDE
- nondestructive evaluation
- NEC
- National Electric Code
- NEMA
- National Electrical Manufacturers Association
- NIST
- National Institute of Standards and Technology
- NM
- nanometer
- NMMA
- National Marine Manufacturers Association
- NNS
- neural network system
- NO.
- number
- NS
- nanosecond
- OA
- organic acid
- OAW
- oxyacetylene welding
- OCV
- open-circuit voltage
- OE
- oersted
- OFG
- oxyfuel gas
- OFW
- oxyfuel gas welding
- ORNL
- Oak Ridge National Laboratory
- OSHA
- Occupational Safety and Health Administration
- OZ
- ounce
- P
- page
- P
- pearlite
- PA
- pascal
- PAW
- plasma arc welding
- PEEM
- photoemission electron microscopy
- PH
- negative logarithm of hydrogen-ion activity
- PH
- precipitation hardenable; precipitation hardening
- PID
- proportional-integral-differential

- PM
- planar-magnetron
- PPB
- parts per billion
- PPM
- parts per million
- PPT
- parts per trillion
- PRE
- pitting resistance equivalent
- PRR
- pulse repetition rates
- PSI
- pounds per square inch
- PSIA
- pounds per square inch absolute
- PSIG
- gage pressure (pressure relative to ambient pressure) in pounds per square inch
- PSTM
- photon scanning tunneling microscopy
- PW
- projection welding
- PWAA
- postweld artificial aging
- PWB
- printed wiring board
- PWHT
- postweld heat treatment
- PWM
- pulse width modulation
- Q&T
- quenched and tempered
- R
- roentgen
- R_A
- surface roughness in terms of arithmetic average
- RA
- rosin fully activated; roughness average
- *RA*
- reduction in area
- RE
- rare earth
- REF
- reference
- REF
- relative erosion factor
- RF
- radio frequency
- RH
- relative humidity
- RMA
- rosin mildly activated
- RMS
- root mean square
- RPF
- relative potency factor
- RPM

- revolutions per minute
- R_Q
- rms (root mean square) roughness
- RS
- resistance soldering
- RSA
- rosin superactivated
- RSEW
- seam welding
- RSW
- resistance spot welding
- RT
- room temperature
- RW
- resistance welding
- RWMA
- Resistance Welder Manufacturers Association
- R_Y
- maximum peak-to-valley height
- R_Z
- ten-point height
- S
- second
- S
- siemens
- SA
- synthetic activated
- SACP
- selected-area channeling patterns
- SAE
- Society of Automotive Engineers
- SAM
- scanning acoustic microscope/microscopy
- SAW
- submerged arc welding
- SCC
- stress-corrosion cracking
- SCPM
- scanning chemical potential microscopy
- SCR
- silicon-controlled rectifier
- SEM
- scanning electron microscope/microscopy
- SFM
- surface feet per minute
- SHE
- standard hydrogen electrode
- SI
- Système International d'Unités
- SIR
- surface insulation resistance
- SLAM
- scanning laser acoustic microscope/microscopy
- SLEEM
- scanning low-energy electron microscopy
- SMA
- shielded metal arc

- SMAW
- shielded metal arc welding
- SPA-LEED
- spot profile analysis-low-energy electron diffraction
- SPC
- statistical process control
- SPF
- sideplate ferrite
- SQC
- statistical quality control
- SRA
- stress-relief annealing
- SSW
- solid-state welding
- STA
- solution-treated and aged
- STEM
- scanning transmission electron microscope/microscopy
- STM/S
- scanning tunneling microscopy/spectroscopy
- SUS
- Saybolt Universal Seconds (viscosity)
- SV
- sievert
- SW
- stud arc welding
- T
- thickness; time
- T
- tesla
- *T*
- temperature
- TB
- torch brazing
- TCP
- topologically close packed
- TEM
- transmission electron microscope/microscopy
- TGA
- thermogravimetric analysis
- TGSCC
- transgranular stress-corrosion cracking
- TIG
- tungsten inert gas (welding)
- TMCP
- thermomechanically controlled process
- TS
- torch soldering
- TTT
- time-temperature transformation
- TW
- thermit welding; thermite welding
- TZP
- tetragonal zirconia polycrystals
- UCL
- upper control limit
- UNS

- Unified Numbering System
- USW
- ultrasonic welding
- UTS
- ultimate tensile strength
- UW
- upset welding
- V
- velocity
- V
- volt
- VIM-VAR
- vacuum induction melted-vacuum arc remelted
- VOL
- volume
- VOL%
- volume percent
- VPPA
- variable polarity plasma arc
- W
- watt
- WI
- wettability index
- WRC
- Welding Research Council
- WS
- wave soldering
- WSN
- weld set number
- WT%
- weight percent
- XPS
- x-ray photoelectron spectroscopy
- YR
- year
- Z
- atomic number
- °
- angular measure; degree
- °C
- degree Celsius (centigrade)
- °F
- degree Fahrenheit
- €
- direction of reaction
- ÷
- divided by
- =
- equals
- ≅
- approximately equals
- ≠
- not equal to
- ≡
- identical with
- >
- greater than

- ?
- much greater than
- [GES]
- greater than or equal to
- ∞
- infinity
- ∝
- is proportional to; varies as
- ∫
- integral of
- <
- less than
- =
- much less than
- ≤
- less than or equal to
- ±
- maximum deviation
- -
- minus; negative ion charge
- ×
- diameters (magnification); multiplied by
- ·
- multiplied by
- /
- per
- %
- percent
- +
- plus; positive ion charge
- √
- square root of
- ~
- approximately; similar to
- ∂
- partial derivative
- α
- Stefan-Boltzmann constant
- γ
- shear strain rate
- γ_E
- elastic strain
- γ_T
- total strain
- Δ
- change in quantity; an increment; a range
- ε
- strain
- $\dot{e}$
- strain rate
- θ
- angle
- λ
- wavelength
- μ
- friction coefficient; magnetic permeability

- μ_S
- static coefficient of friction
- μ F
- microfarads
- μ IN.
- microinch
- μ M
- micrometer (micron)
- μS
- microsecond
- *n*
- Poisson's ratio
- π
- pi (3.141592)
-
- density
- σ
- stress; standard deviation
- Σ
- summation of
- *t*
- applied stress
- Ω
- angular velocity; frequency
- Ω
- ohm

- GREEK ALPHABET

- **GREEK ALPHABET**

- **A, A**
  - ALPHA
- **B, B**
  - BETA
- **Γ , Γ**
  - GAMMA
- **Δ, Δ**
  - DELTA
- **E, E**
  - EPSILON
- **Z,** *z*
  - ZETA
- **H, H**
  - ETA
- **Θ , Θ**
  - THETA
- **I,** *i*
  - IOTA
- **K, K**
  - KAPPA
- **Λ , LAMBDA;**
  - LAMBDA
- **M, M**
  - MU
- **N,** *u*
  - NU

- Ξ, *x*
  - XI
- **O, O**
  - OMICRON
- Π, **Π**
  - PI
- **P, P**
  - RHO
- Σ, **Σ**
  - SIGMA
- **T,** *t*
  - TAU
- ϒ, *u*
  - UPSILON
- Φ, *f*
  - PHI
- **X, X**
  - CHI
- **Ψ,**
  - PSI
- **Ω, Ω**
  - OMEGA

o TRADENAMES
o ACTIVATED DIFFUSION BONDING
o is a registered trademark of General Electric Company.
o ACTIVATED DIFFUSION HEALING
o is a trademark of General Electric Company.
o AD-85
o is a trademark of Coors.
o AD-988
o is a tradename of McDanel.
o ALLOY 52
o is a trademark of Carpenter Technology Corporation.
o ALLOY 42
o is a trademark of Carpenter Technology Corporation.
o BETA C
o is a tradename of RMI, Inc.
o CORONA 5
o is a tradename of Crucible, Inc.
o CUSIL ABA
o is a tradename of GTE Wesgo.
o FM73
o is a tradename of American Cyanimide Company.
o FM300K
o is a tradename of American Cyanimide Company.
o HAYNES AND HASTELLOY
o are registered trademarks of Haynes International, Inc.
o HEXOLOY SA
o is a tradename of Carborundum.
o 230 AND HR160
o are trademarks of Haynes International, Inc.
o INCOLOY 909
o is a tradename of Inco Alloys International, Inc.
o INCONEL AND NIMONIC

- registered trademarks of Inco Family of Companies.
- KOVAR
- is a trademark of Carpenter Technology Corporation.
- MAR-M
- is a trademark of Martin Marietta.
- MP35N AND MP159
- are registered trademarks of SPS Technologies.
- MULTIPHASE
- is a registered trademark of SPS Technologies.
- NICHROME
- is a registered trademark of Harris Co., Inc.
- NICROBRAZ
- is a tradename of Wall Colmonoy Corporation.
- NOCOLOK
- is a tradename of Alcan Aluminum.
- PAD-AS30W
- is a tradename of Cercom.
- POCO AXF-5Q
- is a tradename of Unocal Chemicals Div./Nitrogen Group.
- PYROMET
- is a registered trademark of Carpenter Technology.
- RA 333
- is a registered trademark of Rolled Alloys, Inc.
- RENÉ
- is a registered trademark of Teledyne Industries, Inc.
- SNW-1000
- is a registered trademark of GTE.
- THRESHOLD LIMIT VALUE
- is a registered trademark of the American Conference of Governmental and Industrial Hygienists.
- TICUNI
- is a registered tradename of GTE Wesgo.
- TRANSIENT LIQUID-PHASE BONDING
- is a trademark of Pratt & Whitney.
- UDIMET
- is a registered trademark of Special Metals, Inc.
- ULTEM
- is a tradename of General Electric Company.
- ULTIMET
- is a registered trademark of Haynes International, Inc.
- WASPALOY
- is a trademark of United Technologies.
- WELDALITE
- is a registered trademark of Martin Marietta Corporation.